1983
Volume 72

JOURNAL OF PHARMACEUTICAL SCIENCES

A publication of the American Pharmaceutical Association

The *Journal of Pharmaceutical Sciences* (ISSN 0022-3549) is published monthly by the American Pharmaceutical Association (APhA) at 2215 Constitution Ave., N.W., Washington, DC 20037. Second-class postage paid at Washington, D.C. and at additional mailing office.

All expressions of opinion and statements of supposed fact appearing in articles or editorials carried in this journal are published on the authority of the writer over whose name they appear and are not to be regarded as necessarily expressing the policies or views of APhA.

Offices—Editorial, Advertising, and Subscription: 2215 Constitution Ave., N.W., Washington, DC 20037. All Journal staff may be contacted at this address. Printing: 20th & Northampton Streets, Easton, PA 18042.

Annual Subscriptions—United States and foreign, industrial and government institutions $75; educational institutions $75; individuals *for personal use only* $40; single copies $10. APhA and SAPhA members may subscribe to *J. Pharm. Sci.* for $20.00 per year. All foreign subscriptions add $10 for postage. Subscription rates are subject to change without notice.

Claims—Missing numbers will not be supplied if dues or subscriptions are in arrears for more than 60 days or if claims are received more than 60 days after the date of the issue, or if loss was due to failure to give notice of change of address. APhA cannot accept responsibility for foreign delivery when its records indicate shipment was made.

Change of Address—Members and subscribers should notify at once both the Post Office and APhA of any change of address.

Photocopying—The code at the foot of the first page of an article indicates that APhA has granted permission for copying of the article beyond the limits permitted by Sections 107 and 108 of the U.S. Copyright Law provided that the copier sends the per copy fee stated in the code to the Copyright Clearance Center, Inc., 21 Congress St., Salem, MA 01970. Copies may be made for personal or internal use only and not for general distribution.

Microfilm—Available from University Microfilms International, 300 N. Zeeb Road, Ann Arbor, MI 48106.

Scientists Respond to Tylenol Crisis

Surely, all of the writers who prepare "year-end wrap-up articles," in which they list and summarize the big news stories of 1982, will include the Tylenol incident and related product tampering as one of the most notorious events of the year.

The episode constituted a major "happening" just in itself. But beyond the effect it had on the victims and their families and friends, the tragic incident has had a profound impact that is far broader. For example, it is little exaggeration to say that (*a*) it has affected human behavior for many, if not most, Americans; (*b*) it has shaken public confidence in the quality and reliability of many common products; and (*c*) it has revolutionized the packaging of consumer products and particularly nonprescription drug products.

Consequently, considerable attention has been devoted to the reaction and performance of the health care professions in the days and weeks following the initial Tylenol news reports.

Almost without exception, all those involved—from individual practitioners to the overall drug industry—behaved admirably. Virtually everyone kept "calm, cool, and collected," as per the standard recommendation for dealing with emergencies. Suitable advice, in keeping with the degree of information available at the time, was generally given by pharmacists and other practitioners. Panic was avoided despite the fertile conditions that prevailed.

The American Pharmaceutical Association issued a statement entitled "The Tylenol Issue in Perspective," and it seemed to go a long way toward helping to generate rational thinking and sensible reaction. Many other organizations undertook comparable or analogous efforts.

But what about scientists? Where were they? What did they do? And how well did they perform?

To date, we have not heard nor read of any effort to analyze or assess such performance by the scientists involved. Hence, it seems timely and appropriate to do so in this column.

Initially, it was medical scientists who made the diagnosis and clinical laboratory scientists who confirmed cyanide as the causative agent. Unquestionably, this prompt detective work was instrumental in holding down the number of deaths by enabling the authorities to issue bulletins and warnings expeditiously and for the press and broadcast media to communicate that alarming information so quickly on a nationwide basis.

Secondly, scientists effectively participated in the testing and analytical phases of the massive screening and monitoring program to assess the extent of the tampering in terms of geography, product line, manufacturers involved, and so on. No drug, cosmetic, or packaged food distributor could feel secure in those early days of the tragedy, and the responsibility for decisions as to what testing was needed, as well as the burden of conducting the testing itself, fell squarely on scientists in industry. Similarly, comparable decisions and follow-up testing were expeditiously handled by regulatory scientists in government service.

Thirdly, scientists quickly and correctly pointed out that any effort to make products "tamper-proof," or to require such product packaging through legislation, was doomed to failure. They convincingly explained that it is impossible to achieve such a result in any way that approaches being pragmatic.

Finally, scientists and engineers have quickly come up with workable designs and the necessary technology to implement them, whereby millions upon millions of individual packages can be made tamper-resistant—and at an extremely high level of reliability.

Hence, scientists not only participated and responded in this time of crisis, but they have made critical contributions in minimizing the tragedy itself as well as in proceeding toward workable, prompt, and effective solutions to avoid the possibility of any reoccurrences.

Indeed, through it all, we are aware of only one disappointing action on the part of the scientific community.

A prominent toxicologist sent off a letter calling "for legislation restricting and controlling the availability of potent poisons." But since (*a*) the letter was personally addressed to U.S. President Ronald Reagan, (*b*) it urged the President "to appoint a Presidential Task Force to study the situation and recommend appropriate restrictive legislation," and (*c*) it was publicly distributed with a news release to the press, we suspect that it was done more as a grandstand publicity play than as a serious recommendation.

Cyanide salts alone are widely used in many industrial processes, as well as in medical, scientific, and manufacturing laboratories. And beyond cyanide, there are numerous poisonous substances used to produce common, everyday, important products; in many instances, these poisonous substances may be an ingredient or even the sole ingredient of those products. Household cleaners—such as bleach, ammonia, and drain cleaners containing sodium hydroxide—are just a few examples. Garden products such as pesticides, herbicides, and fertilizers; and fuels such as gasoline, kerosene, and methyl alcohol are several others.

Obviously, it is totally impractical to restrict and control all poisons. The approach being implemented by the Food and Drug Administration with regard to requiring tamper-resistant packaging seems to be well conceived and carefully balanced. And again, it was scientists—this time government regulatory scientists—who assisted the legal people in drafting the proposed regulations.

The bottom line is that all scientists can be proud of the contributions their scientific colleagues have made in resolving one of the major crises of recent times.

—EDWARD G. FELDMANN
American Pharmaceutical Association
Washington, DC 20037

0022-3549/83/0100-0001$01.00/0

JOURNAL OF PHARMACEUTICAL SCIENCES

JANUARY 1983
VOLUME 72 NUMBER 1

Literature Survey

Physical and Biological Properties of Pyrilamine

THOMAS J. HALEY

Received December 7, 1981, from the *Department of Health and Human Services, Food and Drug Administration, National Center for Toxicological Research, National Toxicology Program, Jefferson, AR 72079.*

Keyphrases □ Pyrilamine—antihistamine, chemistry, pharmacology, metabolism, toxicology, mutagenicity, teratogenicity, carcinogenicity, literature survey □ Antihistamine—pyrilamine, chemistry, pharmacology, metabolism, toxicology, mutagenicity, teratogenicity, carcinogenicity, literature survey □ Structure–activity relationships—pyrilamine, chemistry, pharmacology, metabolism, toxicology, mutagenicity, teratogenicity, carcinogenicity, literature survey

When metapyrilene was found to be an animal carcinogen a search was begun to obtain another drug for use in nonprescription sleeping aids (1). It appeared that a related compound, pyrilamine, an antihistamine with sedative properties, could be used (2). This resulted in pyrilamine, which is structurally related to methapyrilene, being nominated for a National Toxicology Program carcinogenesis bioassay. As a result the chemistry, pharmacology, metabolism, toxicology, mutagenicity, teratogenicity, and carcinogenicity of pyrilamine was reviewed.

CHEMISTRY

Background—Production of antihistamines in the United States in 1976 was 217.2×10^3 kg, but data on pyrilamine production is unknown (3).

Pyrilamine has not been found in U.S. drinking water supplies (4), industrial effluents (5), or European water supplies (6).

It has been used as an antihistamine in treatment of allergies (7).

Synthesis—Table I (2, 8–10) gives the structure and physical and chemical properties of pyrilamine. This chemical is prepared by condensing 2-(*N*-*p*-methoxybenzyl)aminopyridine with dimethylaminoethyl chloride or by condensing *N*,*N*-dimethylaminoethyl-α-aminopyridine with *p*-methoxybenzyl chloride in the presence of sodamide or lithamide (11–14).

Analysis—Pyrilamine was separated by TLC on silica gel G plates using benzene–dioxane–diethylamine–absolute ethanol (50:40:5:5) as a solvent system, and several identifying agents (15). It was determined using silica gel G plates, 18 different solvent systems, and 8 chromogenic reagents (5). Another technique used the following solvent systems containing 0.1 *M* NaBr: methanol–butanol (60:40); chloroform–methanol (90:10); and ethyl acetate–cyclohexane–methanol (70:15:5). The use of these ion-paired adsorption systems gave improved, more reproducible separations (16). Celite columns acidified with tosic acid, 0.1 or 1.0 *M* HCl, 10.0 *M* H_2SO_4, or 1.0 *M* H_3PO_4 were used in ion-pair extraction followed by partition chromatography to separate pyrilamine and codeine (17). Other inorganic ions such as Cl^-, Br^-, I^-, NO_3^-, ClO_4^-, SCN^-, and SO_4^{2-} were also used (18).

Chromatographic columns[1] were used as anion and cation exchangers to separate pyrilamine from other amines (19). Thin-layer plates composed of silica $60F_{254}$[2], silica $60F_{254}$[2] sprayed with 0.1 *N* NaOH, silica G-25, alumina[2] $F_{254}E$, and cellulose type F[2] sprayed with 5% sodium dihydrogen citrate were used to separate pyrilamine from other amines and to determine recovery percentages (20). TLC was systematized by relating R_f values and solvent systems of five to seven test substances and coding the results into tables for rapid identification (21). This approach was applied to 76 prescription drugs (22) and other therapeutically significant organic bases (23).

TLC using plates[3] and extraction with 1,2-dichloroethane was used to identify 32 basic poisons (24). Pyrilamine was identified using nine color reagents (25), silica gel microfiber sheets[4] and the following solvent systems:

[1] Sephadex SPC 25 or QAE 25.
[2] Merck.
[3] Keiselgel.
[4] ITLC type SA.

0022-3549/83/0100-0003$01.00/0

Table I—Structure and Physical and Chemical Properties of Pyrilamine[a]

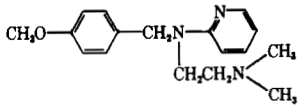

Physical State	Oily liquid
Boiling Point	201°(5 mm); 168–172°(0.06 mm)
Solubility	Soluble in acids
Refractive Index	n_D^{25} 1.5760–1.5765
CAS Number	91849
Molecular Weight	285.58
Spectroscopic Data	IR spectra 2940, 2780, 1590, 1520, 1490, 1450, 1350, 1320, 1250 1180, 1040, 980, 760, 730; UV spectra 310, 247; pH 0.1 316, 238; pH 1.0 314, 238; pH 4.1 308, 239; pH 5.7 306, 244 nm.
Volatility	Slightly volatile
Stability	Turns brown on exposure to light
Reactivity	Reacts with acids to form salts
Synonyms	*N*-[(4-methoxyphenyl)methyl]-*N'*,*N'*-dimethyl-*N*-2-pyridinyl-1,2-ethanediamine; 2[(2-dimethylaminoethyl-*p*-methoxybenzyl)amine] pyridine; *N*-*p*-methoxybenzyl-*N'*,*N'*-dimethyl-*N*-α-pyridylethylenediamine; Mepyramine; Pyranisamine; Neo-Antergan.

[a] References 2–5.

ethyl acetate–cyclohexane–ammonia–methanol–water (70:15:2:7:0.5); ethyl acetate–cyclohexane–methanol–ammonia, (50:40:0.7:0.4); ethyl acetate–cyclohexane–methanol–ammonia (70:15:10:5); ethyl acetate–cyclohexane–ammonia (50:40:0.1). Correlations between R_f values from five systems and chemical groups indicated that steric hindrance around the group responsible for the bonding to silica in a particular system, compound basicity, and the presence or absence of a pyridyl group influenced the R_f values to the greatest extent (26).

Carboxylmethylcellulose ion exchange paper (CM82) and the solvent system of water–acetone–formamide (10:1:1) easily separated pyrilamine from other antihistamines (27). Thin-layer electrophoresis on silica gel G plates was used to separate 23 basic drugs (28). Using chromatographic sheets[5] pyrilamine was separated with methanol and identified with Dragendorff's reagent or 0.3% aqueous sodium nitrate (29). Separation on silica gel $60F_{254}$ plates was reported (30) using the following solvent systems: chloroform–methanol (9:1); methanol–concentrated ammonium hydroxide (100:1.5); and chloroform–acetone (9:1); and identified under UV light (254 nm) followed by spraying with either iodine in methanol, modified Ludy–Tenger reagent, or iodine in methanol and copper chloride. Colorimetric determination of pyrilamine was performed using the pyrocatechol violet method (31). The drug was allowed to react with aniline and cyanogen bromide reagent and then was determined at 410 nm (32). Pyrilamine has been spectrophotometrically determined using the Δpi method at 236 nm with an accuracy of 100.2 ±0.8% (33). Various pharmaceutical preparations were analyzed by UV spectrophotometry to determine the pyrilamine content (34). After separation on a cation-exchange resin, alginic acid, pyrilamine was determined by UV spectrometry with an accuracy of 98.97% (35). Difference spectrophotometry at 320 nm (36) and by GC using a column[6] with a flame ionization detector were used in another study (37). Pyrilamine was determined by GC using columns of 20% GESF-96 on 45–60 mesh Chromosorb P and 5% SE-30 on 80–100 mesh Chromosorb A with cyclohexanedimethanol succinate and a thermoconductive detector (38).

A column of 1% cyclohexanedimethanol succinate on 100–120 mesh silanized GC P and a flame ionization detector were also used to determine pyrilamine after acetone–ether extraction of blood (39). A column of 200 mg of cyclohexanedimethanol succinate and 2.0 g of methylphenyl silicone on 80–100 mesh diatomaceous earth was used (40) and columns of OV-1 and OV-17 were employed under isothermal conditions (41). Retention indexes for 230 chemicals including pyrilamine were reported for analyses on SE-30, OV-1, and OV-17 columns under isothermal conditions at 180° (42). Discriminating power analysis for GC showed that columns of either SE-30 or OV-17 possessed the highest discriminating powers for separation and determination of 62 basic drugs (43). GC analysis using a column of 3% OV-17 on high-performance Chromosorb W was used to separate pyrilamine from other street drugs (44).

Columns of either 2.1 or 4.1 g of Dexsil 300 on 18 g of 80–100 mesh Chromosorb W (HP) with a flame ionization detector and an automatic sample injector were used to determine pyrilamine in pharmaceutical preparations (45). Detection in blood from cases of overdosage was possible using columns of 3% OV-17 on 100–200 mesh screens or 1% SP-1000 on 100–200 mesh screens[7] using a nitrogen–phosphorus detector (46).

GC analysis of stored blood samples indicated that the drug was stable for at least 7 months (47). Gas chromatography–mass spectrometry (GC–MS), was used to detect pyrilamine in blood plasma (48), and it was found (49) for pyrilamine and its deuterated analogs that single-ion monitoring at *m/z* 121 gave more precise ratios than multiple-ion monitoring at *m/z* 121 and 124 (49).

Direct thin-layer chromatography–mass spectrometry (TLC–MS) was applied to pyrilamine and 30 μg was detected (50). Isocratic multi-column HPLC with a variable wavelength UV detector was found useful to characterize pyrilamine eluted from columns of silica, silica treated with 3-mercaptopropyltrimethoxysilane, or a strong aliphatic cation exchange (51). A phenyl column[8], using a UV detector set at 254 nm, could detect 18 ng of pyrilamine (52). Use of a column consisting of a monomolecular layer of octadecyltrichlorosilane permanently bonded to Si—C, and a UV detector set at 254 nm, enabled the HPLC separation of pyrilamine from various other drugs (53). HPLC was used to separate pyrilamine from pentobarbital in polyethylene glycol-based suppositories (54).

After testing 15 HPLC systems, it was found that the best separations were obtained with acetonitrile–water–propylamine[9] (90:10:0.01) and CN-10, heptane–methylene chloride–acetonitrile–propylamine (50:50:25:0.1) using commercially available columns[10] (55).

METABOLISM AND STRUCTURE-ACTIVITY RELATIONSHIPS

Metabolism and Metabolic Products—One study suggested that pyrilamine can be *N*-demethylated but that

[5] Eastman 6061.
[6] 15% Dexsil 300 on Chromosorb W.
[7] Supelcocort.
[8] μBondapak.
[9] Micropak CN-10.
[10] Micropak CN-10.

more information is needed on cellular distribution, metabolism, and excretion (56). Intravenous injection of pyrilamine in rabbits did not increase the urinary excretion of histamine but did significantly increase the excretion of histamine metabolites (57). Pyrilamine increased brain histamine by blockade of central histaminergic receptors and the inhibition of histamine-*N*-methyltransferase (58) but was ineffective in decreasing histamine uptake in the heart and stomach of rats (59).

In rats, intraventricular injection of histamine affected dopamine metabolism by increasing the amount of homovanillic acid in the striatum. This effect was blocked by pyrilamine (60). Pyrilamine inhibited the activity of histamine-*N*-methyltransferase in the brain, ileum, atrium and stomach of the guinea pig *in vivo* and *in vitro* (61). Histamine-*N*-methyltransferase from pig atrium was inhibited by pyrilamine when the substrate was histamine but not when the substrate was *N'*-methylhistamine (62). Purified guinea pig histamine-*N*-methyltransferase was inhibited by pyrilamine (63). It inhibited rat liver phosphatidate phosphohydrolyase but had no effect on glycerol phosphate acyltransferase or diacylglycerol acyltransferase (64).

In another study, pyrilamine inhibited rat liver phosphatidate cytidylyltransferase, glycerol phosphate acyltransferase, and phosphatidate phosphohydrolyase (65). This inhibition had a marked effect on lipid metabolism (66). Pyrilamine blocked guinea pig adenylcyclase activity induced by tolazoline and to a lesser extent that induced by histamine (67).

Structure–Activity Relationships—Pyrilamine is a derivative of ethylenediamine and modifications in this moiety can cause extreme changes in antihistaminic potency. The terminal nitrogen atom must be tertiary; replacement of the dimethyl group with a diethyl group decreased potency as did quaternization; the chain between the nitrogen atoms must be two carbon atoms and it should not be branched; the replacement of the pyridyl group with pyrimidyl or halogenated phenyl groups did not affect potency, but substituting an additional pyridyl group for the benzyl group decreased potency, while substituting a *para*-methoxy group increased potency (68).

Pharmacodynamics and Kinetics—Pyrilamine blocked the hypotensive action of both histamine and 5-hydroxytryptamine in the rat (69). It markedly potentiated the depressor response of isoproterenol in the dog, had no effect on the isolated rat seminal vesicle preparation but antagonized epinephrine and norepinephrine, reduced the inhibitory effects of these latter drugs on the guinea pig tracheal chain, and relaxed the isolated rabbit ileum. Pyrilamine had no effect on the hind limb preparation of the rat and potentiated the positive inotropic and chronotropic effects of isoproterenol on the rabbit heart *in situ* (70). Pyrilamine was shown to be a noncompetitive antagonist to epinephrine and norepinephrine when tested on the rabbit aortic strip, rat seminal vesicle, and dog blood pressure. It reduced the response of the dog retractor penis muscle and the rat fundal strip to catecholamines (71). When applied topically (72), pyrilamine was a potent constrictor of the mammalian capillary bed of the rat. Pyrilamine significantly attenuated the baroreceptor reflex vasoconstrictor and the vasoconstrictor effect of intra-arterial histamine, but had no effect on such responses induced by intra-arterial norepinephrine in the isolated, perfused gracilis muscle of the dog (73).

Pyrilamine blocked the pressor response and potentiated the depressor response in rabbits given intravenous histamine (74). It also blocked the constrictor response of the isolated rabbit ear artery but had no effect on the perfused human temporal artery (75). Intra-arterial histamine caused a dose-dependent vasodilatation in the carotid vascular bed of the dog which was only partially blocked by pyrilamine (76, 77). In monkeys, pyrilamine only partially blocked the histamine response in the external carotid circulation but had a greater effect on the internal carotid circulation (78). The histamine depressor response in the monkey was partially blocked (79). Increases in blood flow in the left circumflex coronary artery of the dog induced by histamine infusion were only partially blocked by pyrilamine (80). Perfusion of pyrilamine from the lateral ventricle to the cisterna magna in dogs gave a hypertensive followed by a hypotensive response (81). Pyrilamine did not block the hypotension induced by venom from the green mamba (*Dendroaspis angusticeps*) in the cat, dog, rat, and guinea pig (82). Injection of histamine into the pulmonary artery circulation of the isolated perfused guinea pig lung caused increases in pulmonary perfusion pressure which were converted into decreases upon injection of pyrilamine (83, 84). Pyrilamine added to the perfusion fluid used in isolated cat lung perfusions prevented histamine and anoxia pressor responses but greatly increased the resistance of the lungs to air flow (85). Pyrilamine noncompetitively inhibited the positive ionotropic effect of histamine on the isolated guinea pig papillary muscle (86). Using the isolated spontaneously beating rabbit atria, pyrilamine was shown to have antimuscarinic and antinicotinic effects and to have a cocaine-like effect unrelated to local anesthesia (87). Pyrilamine blocked the typical cardiovascular responses, hyperkalemia and hyperglycemia, induced by histamine (88).

Pyrilamine reversed the airway constriction of the isolated guinea pig trachea and bronchus induced by histamine and honey bee venom (89), but relaxation of isolated cat tracheal rings caused by histamine was only partially inhibited (90). Pyrilamine prevented the bronchoconstrictor effect of histamine and increased bronchial motility in the gallamine paralyzed unanesthetized rabbit (91). It had no effect on the preconvulsion time in guinea pigs exposed to aerosolized propranolol (92), but it elevated the total blood carbon dioxide and decreased the blood pH in dogs (93). Histamine-induced modifications of airway resistance, respiratory frequency, pulmonary blood volume, alveolar tensio-active substances for pulmonary compliance, P_aO_2, P_aCO_2, blood pressure, and pulmonary compliance for respiratory frequency in dogs and guinea pigs were all blocked by pyrilamine (94). In the isolated perfused guinea pig lung preparation, pyrilamine inhibited the pressor response to histamine but not that of prostaglandin $F_2\alpha$, and it blocked the histamine induced contraction of guinea pig pulmonary artery strips (95). Aerosolized pyrilamine attenuated the histamine induced nasal airway resistance in the dog (96), but aerosolized histamine or sulfur dioxide inhalation increased airway resistance in humans and only the former was blocked by pyrilamine (97).

Rhythmic contractions in the isolated vas deferans of the guinea pig and rat with or without intact intramural nerves (98) were induced by pyrilamine, and it blocked the responses of the neonatal rabbit ileum to histamine (99). The acetylcholine induced contraction of the isolated toad rectus abdominalis muscle was blocked by pyrilamine (100). While the drug had no effect on the synthesis of prostaglandin E_2 from arachidonic acid by bull seminal vesicle homogenates (101), it blocked the peristaltic reflex induced by increasing the intraluminal pressure in the isolated frog stomach and guinea pig ileum (102). It did not antagonize the acid secretion induced by histamine in the isolated guinea pig gastric fundus (103), but it inhibited the responses in the fundus and antrum of isolated guinea pig stomach to histamine, cholecystokinin, and gastrin and partially inhibited the antral response to acetylcholine (104).

Pyrilamine did not antagonize gastric acid secretion induced in rats and guinea pigs by gastrin, bethanechol, and histamine (105), failed to inhibit histamine stimulation, but did suppress aminopyrine accumulation in histamine stimulated isolated rabbit gastric glands (106). Pyrilamine counteracted the inhibitory effect of supramaximal doses of histamine on gastric acid secretion in conscious gastric fistula cats (107), but failed to protect guinea pigs from histamine induced duodenal ulceration (108). In pylorus ligated rats, pyrilamine failed to prevent aspirin plus hydrochloric acid gastric ulcerations (109). It prevented the fall in diastolic blood pressure but did not prevent gastric secretion induced by histamine in dogs (110).

Histamine stimulation of gastric acid secretion and mucosal blood flow in dogs was not prevented (111), production of gastric lesions by stress in rats was inhibited (112), and gastric lesions produced by cold-restraint stress in rats were not antagonized by the drug (113). The activation of adenylate cyclase in broken-cell preparations of guinea pig gastric mucosa by histamine, sodium fluoride, or 5-guanylylimidophosphate was inhibited by pyrilamine (114). It was shown that pyrilamine had no real effect in treating gastric hyperacidity and peptic ulcers in humans (115).

Pyrilamine blocked the histamine mediated vascular exudation response to mild but not strong cold injury to rat skin (116). Intramuscular injection in sheep prevented the vascular permeability produced by intradermal injection of histamine, hyaluronidase, adenosine, guanosine, inosine, or xanthosine (117). It was reported to release histamine and as a result increased the permeability of sheep skin (118). Compound 48/80 was used to deplete histamine stores in sheep but resulted in a biphasic response in which the first phase could be blocked by pyrilamine (119). Pyrilamine blocked the vascular permeability evoked in sheep by histamine and 5-hydroxytryptamine but not that evoked by bradykinin (120). Pulmonary exudation and histamine release was induced in rats by intrapleural injection of turpentine, silver nitrate, or carrageen, and pyrilamine decreased both parameters for turpentine and silver nitrate but had an irregular effect on carrageen (121). Pyrilamine had no influence on rat mast cell histamine release mediated by cyclic adenosine phosphate or cyclic 5′-guanylic acid (122), however, it released 5-hydroxytryptamine from rat peritoneal mast cells (123) as well as from cow enterochromaffin granules *in vitro* (124). It caused a large release of histamine and stimulation of salivary secretion in the submaxillary gland of the dog (125).

Pyrilamine was used to identify two histamine binding sites in the isolated guinea pig ileum (126), and was identified as an H_1-receptor antagonist through its histamine blocking effects on guinea pig atria and ileum *in vitro* and on rat stomach contractions *in vivo* (127). It only partially antagonized the effects of histamine on the isolated cat tracheal rings and did not affect isolated sheep bronchial strips indicating very few H_1-receptors in the former and none in the latter (128). It was used to identify the histamine H_1-receptors in the cardiovascular system of the chicken (129). One study showed that pyrilamine had no effect on the microcirculation of the dog's synovial membrane, which indicated a lack of histamine H_1-receptors (130).

Pyrilamine appears to have a pseudo-dualist effect on the histamine H_1-receptors of the guinea pig ileum and trachea *in vitro* (131). [^{3}H]Pyrilamine was shown to bind specifically to guinea ilial histamine H_1-receptors *in vitro* (132). Brain membranes from rats, calves, and guinea pigs specifically bind [^{3}H]pyrilamine *in vitro* indicating the presence of histamine H_1-receptors (133), which has been confirmed in the guinea pig brain (134).

Pyrilamine did not bind to γ-aminobutyric acid receptors in the rat brain synaptosomal membrane (135), but it did bind to the histamine H_1-receptors in cultured mouse neuroblastoma cells (136). Pyrilamine was used to block H_1-receptors and had a slight immunosuppressive effect when combined with an H_2-receptor blocker in rat heart allografting (137). [^{3}H]Pyrilamine binds with high affinity to brain membranes from humans, rats, guinea pigs, rabbits, and mice indicating an association with H_1-receptors (138). Differences in [^{3}H]pyrilamine binding in guinea pig and rat brains has been attributed to an actual difference between the H_1-receptors or the presence of a relatively large number of secondary binding sites in the rat (139). Pyrilamine exhibited a noncompetitive binding to the histamine H_1-receptors in the rabbit coronary artery (140) but was only weakly bound to the tricyclic antidepressant binding sites in the rat brain (141). The binding sites in the guinea pig brain have been localized by autoradiography (142). Specific and nonspecific binding of [^{3}H]pyrilamine was studied in the brain, lung, adrenal, heart, aorta, and ileum of the guinea pig, rat, and rabbit and in the lung of the mouse and monkey. There were significant differences in the number of high affinity binding sites in the lung and adrenal gland depending upon species.

In the bovine adrenal gland, it was shown that binding was more abundant and had a higher affinity in the medulla than in the cortex (143). The H_1-receptor involved in hypotension is only partially attenuated by pyrilamine in the dog (144). [^{3}H]Pyrilamine was used to label the H_1-histamine receptors in the hypothalamus, midbrain, cortex, brain stem, cerebellum, striatum, and hippocampus of the mouse *in vivo* (145). The potencies of H_1-antihistamines in reducing [^{3}H]pyrilamine binding *in vivo* corresponded with their pharmacological activities and their affinities for [^{3}H]pyrilamine binding sites in isolated brain membranes (146). The positive inotropic effects of histamine in the dog were unmasked by injection of both H_1-

and H_2-histamine receptor antagonists (147).

Pyrilamine had an inhibitory effect on human platelet aggregation and adhesiveness *in vitro* (148), but had no effect on rubidium-86 uptake by erythrocytes (149). Pyrilamine caused red cell agglutination *in vitro* (150), but had no influence on digitalis toxicity in cats and guinea pigs (151). Histamine-induced sleepiness in chicks was counteracted by pyrilamine (152), and it inhibited development of physical dependence but not tolerance to morphine, in mice (153). Histamine potentiates the sedative action of chloral hydrate in mice and pyrilamine counteracted this effect (154). Pyrilamine had no effect on the *in vitro* hydroxylation of protocollagen by protocollagen proline hydroxylase (155) but antagonized the release of Ca^{2+} from skeletal muscle induced by scorpion venom (156). When administered alone the drug had no effect on the lipolysis of rat adipose tissue *in vitro*, but in the presence of epinephrine, it stimulated or inhibited lipolysis depending upon dose (157). Whereas pyrilamine suppressed turpentine induced pleural exudate in adult rats, it had little effect in 7-day-old rats (158).

Pyrilamine blocked the decrease in patency in the eustachian tube of the dog caused by topical or intra-arterial histamine (159), accelerated wound healing in the rat when given in conjunction with a histamine liberator, 48/80 (160), but did not antagonize reserpine induced hypothermia in mice (161). It antagonized the hypothermia produced in mice by oxotremorine, but when administered in a high dose also produced hypothermia (162). Pyrilamine antagonized posthistamine catalepsy in rats (163). Pyrilamine reduced the mortality from tourniquet shock in rats from 75 to 35% (164), but only partially reduced the edema and vascular permeability changes produced by prostaglandin E, in the rat paw (165). The binding of spleen cells[11] to beads[12] was inhibited *in vitro* (166). It did not modify the pituitary production of prolactin in patients with Parkinson's disease (167), but did reduce the tremor (168).

No information is available on the pharmacokinetics of pyrilamine (169).

TOXICOLOGY

Acute Toxicity in Animals—The acute LD_{50} in the mouse is 30 mg/kg iv; 102 ± 11 mg/kg ip (68); 150 mg/kg sc (170); 36 mg/kg orally in the rat. Symptoms of acute toxicity include generalized tremor, increased activity, incoordination of movement, Straub tail phenomenon, squeaking, restlessness, chronic convulsions, and death by asphyxia (68). Pyrilamine did not counteract lantana poisoning in buffalo calves (171). Pyrilamine and antischistosomal agents released histamine from the rat's mesentary (172). It only partially counteracted the hypotension produced by quinuronium in sheep (173), did not prevent brain edema in rats induced by intra-arterial injection of ^{85}S-microspheres (174), and not only did not protect against paracetamol-induced hepatic necrosis in rats but actually increased mortality (175).

Chronic Toxicity in Animals—Subcutaneous injection of 35 mg/kg of pyrilamine twice daily in rats arrested growth by the 7th day and normal growth ensued when the drug was discontinued. Daily subcutaneous injections of 20 mg/kg had no effect on weight gain in weanling mice. Rats receiving 10 mg/kg daily for 6 months or 200 mg/kg daily for 32 days showed no signs of chronic toxicity nor was there any evidence of gross or histological abnormalities due to the drug. Similar results were obtained in dogs receiving 20 mg/kg five times weekly for 6 months, and in monkeys receiving 50 mg/kg daily for 35 days (68). Pyrilamine, 50 mg/kg sc daily, caused leukocytosis after 14–23 days, and rupture and enlargement of the gall bladder and common duct in guinea pigs (176).

Acute Toxicity in Humans—Subcutaneous injections of pyrilamine in humans produced a 6–12-fold increase in blood histamine levels for 24 hr. Symptoms of acute toxicity included dizziness, jitteriness, somnolence, dry nose, nausea, weakness, palpitation, insomnia, abdominal cramping, numbness, cold extremities, fatigue, tendency to hemorrhage, chloroform taste, faintness, acute hysterical reaction, mydriasis, narcolepsy, sore tongue, hot flushes, early menses, and dermatitis medicamentosa (68).

Immunotoxicology—Pyrilamine completely blocked the acute inflammatory response induced in the rat skin by histamine but only partially blocked that induced by bradykinin, 5-hydroxytryptamine, and prostaglandin E_1 (177). The acute pinnal inflammation induced in mice by intravenous dextran was blocked (178). It did not inhibit the inflammatory response in hairless mice induced by photosensitization (179). The passive cutaneous anaphylactic reaction evoked in mice and rats by injection of immunoglobulin antibody was only partially blocked (180). The estradiol induced edematous response in the immature rat uterus was not inhibited (181) but pressure induced edema in the rat foot was reduced by 13% (182). It inhibited the paw edema elicited in rats and guinea pigs by local injection of histamine (183), and blocked the 4-hr passive cutaneous anaphylactic reaction in rats injected with rabbit antirat mast cell antiserum (184).

The drug inhibited the active bronchial anaphylactic response in the rat elicited by reagin-type antibodies (185), and completely antagonized the histamine released when carrageenin was injected into the rat's paw and prevented the inflammatory response (186). It reduced the volume of the rat's paw induced by injection of Freund's complete adjuvant only between days 1 and 4 (187). Pyrilamine protected rats against anaphylactic shock evoked by sensitization to egg albumin (188), but had no effect on the direct Arthus reaction elicited in the hind paw of the rat (189). Rats were not protected from horse serum induced anaphylactic shock at 10 days and only protected 20% at 20 days (190). Pyrilamine blockade of histamine's effect on the guinea pig tracheobronchial muscle and ileum *in vitro* was abolished by slow reacting substance of anaphylaxis (191). It protected against the liberation of histamine *in vivo* and *in vitro* by chloroplatinate (192), but did not inhibit the response to ovalbumin in tracheal strips from sensitized guinea pigs (193). Histamine, inhibited by pyrilamine, evoked contractions of ovalbumin sensitized guinea pig lung parenchymal strips, but was only weakly active against ovalbumin (194). The antigen–antibody reaction of the isolated guinea pig ileum was not inhibited by pyrilamine (195), and there was no effect on the rise of cyclic adenosine phosphate and 5′-guanylic acid in the

[11] BALB/c.
[12] HRS.

sensitized guinea pig lung stimulated with antigen (196). Cyclic adenosine phosphate release was suppressed in normal and sensitized guinea pig lung slices when stimulated by either histamine or antigen (197). These results have been confirmed (198).

Anaphylactic response in sensitized guinea pigs is not modified by the drug (199). Pretreatment of guinea pigs with pyrilamine and papaverine to prevent death from anaphylactic shock showed that the histaminolytic activity of the liver and plasma increased under such conditions (200). Pretreatment with pyrilamine prevented anaphylactic death in guinea pigs and increased the time before the appearance of dyspnea and cough (201). Pyrilamine suppressed the histamine-induced bronchoconstrictor component of the anaphylactic response in sensitized guinea pigs (202), but had no effect on slow-reacting substance of anaphylaxis induced bronchoconstriction in the sensitized guinea pig (203). It inhibited the increase in potassium in the blood of guinea pigs in histamine shock and anaphylaxis but not in Forssman shock (204). It prevented death in guinea pigs from anaphylatoxin and histamine and at high doses from anaphylactic shock, and also inhibited bronchoconstriction and emphysema formation from antigen (206–207).

In isolated perfused hearts of sensitized guinea pigs, pyrilamine did not affect the coronary dilating, heart stimulating, and antianaphylactic effects of released histamine or prevent anaphylaxis (208). It reduced cardiac output in the heart–lung preparation of guinea pigs and histamine, injected or antigen released, counteracts this effect (209). Pyrilamine had little effect on anaphylactic bronchospasm in the guinea pig heart–lung preparation or on the increased pulmonary vascular resistance. However, when histamine caused the above effects, pyrilamine completely counteracted them (210). In the isolated perfused sensitized guinea pig lung, pyrilamine was effective in counteracting the bronchospastic effect of antigen (211).

Pyrilamine prevented early shock death in acute anaphylaxis in guinea pigs and this effect could be abolished by propranolol (212). It significantly reduced the lipid-mobilization and hyperlipoproteinemia induced in rabbits by endotoxin (213). In horse serum sensitized rabbits, it antagonized the vasoconstrictor action of histamine on the pulmonary vessels and the right ventricular vasoconstriction caused by the administration of antigen (214). It counteracted the increased vascular permeability produced by histamine in the monkey but had no effect against prostaglandin E vascular effects (215).

Pyrilamine inhibited the skin reaction to histamine in the monkey but had no effect on the *Ascaris* antigen reaction (216). It had only a small effect against the capillary damaging effects of passive cutaneous anaphylaxis in sheep (217) and did not prevent the changes in the lymph nodes, spleen, and intestinal lymphoid tissues of sensitized sheep injected with antigen (218). Pyrilamine selectively inhibited responses to histamine and raised the threshold antibody required to elicit a passive cutaneous anaphylactic response in calves (219). It incompletely blocked depressor changes in carotid blood pressure elicited in calves by histamine and anaphylaxis (220). Pyrilamine had no effect in blocking the photobiologic increase in blood content of the pig skin sensitized to anthracene and long-wave UV radiation but inhibited the increased vascular permeability to [^{125}I]albumin (221).

Pyrilamine had little effect in causing histamine release from human leukocytes *in vitro* and little activity against antigen induced histamine release (222). It relaxed human bronchial muscle contracted by histamine or antigen *in vitro* (223). Histamine release induced by antigen in sensitized human lung mince *in vitro* was inhibited by pyrilamine (224). Intradermal injection inhibited the histamine evoked wheal and flare reaction in human skin (225). The drug had no protective effect in fog provocation of bronchoconstriction in bronchitis patients but had some protective effect against inhaled allergen in asthmatics (226).

Chloroplatinate exposure gives rise to pruritis, erythema, urticaria, eczema, mild lymphocytosis, cough, dyspnea, conjunctival vasodilatation, and asthma. All of these symptoms were successfully treated with pyrilamine, aminophylline, and corticoid therapy (227). The wheal and flare reaction induced by histamine and kallikrein were reduced (228). Pyrilamine inhibited the histamine skin reaction induced by pollen in skin testing for allergies (229).

Neurotoxicology—Injection of histamine into the endonerium of the rat sciatic nerve resulted in a markedly increased permeability of the endoneural blood vessels. This effect was blocked by pretreatment with pyrilamine. The permeability changes caused by compound 48/80, a histamine liberator, could be only partially inhibited by pyrilamine (230). Histamine caused both stimulation and inhibition of the spontaneous electrical activity of neurons in the isolated brain of the snail (*Helix asperse*) and both actions were blocked by the drug (231). Pyrilamine blockade of the motor action of histamine on the guinea pig plexus containing longitudinal muscle preparations from the ileum could still be electrically stimulated into tetanic spasms which were inhibited by histamine (232). Pyrilamine reduced potassium ion permeability in the sartorius muscle of *Rana pipiens* in a chlorine ion-free medium and increased the electrical potential change (233).

The drug did not abolish neuromuscular transmission or decrease the lingui-mandibular reflex in dogs treated with cannabis resin, tetrahydrocannabinol, or parahexyl (234). When injected into the preoptic/anterior hypothalamic nuclei, the lateral ventricle, or the third ventricle it did not block the hypothermic response elicited by systemic injection of histamine in rats (235). It reduced the contractions of the stomach of *Rana temporaria* induced by vagal stimulation (236) and the uptake of [^{3}H]γ-amino-*n*-butyric acid by the rat cerebral cortex *in vitro* (237). The postganglionic action potential of the isolated rabbit superior cervical ganglion *in vitro* was depressed in the presence of histamine and further depressed by the addition of pyrilamine (238). Pyrilamine blocked the calcium ion-related hyperpolarization of *Amphiuma* erythrocyte membrane (239).

Pyrilamine blocked the atropine-resistant responses elicited by electrical stimulation of an area located ventrally in the anterior hypothalamus and rising dorsally toward the optic tegmentum (240). Intraventrical injection of pyrilamine in cats blocked the pressor response induced by intraventricular histamine. Pyrilamine alone produced

a depressor response and blocked both reflex as well as direct excitability of the medullary vasomotor center (241), but had no effect on toothpulp nociceptive thresholds in conscious dogs (242). Pyrilamine had no effect on the biphasic response evoked by transmural stimulation of the guinea pig distal colon *in vitro* (243).

CARCINOGENICITY

Animal Carcinogenicity—No information is available on short term tests on the carcinogenicity of pyrilamine (169), but it is scheduled for a National Toxicology Program carcinogenesis bioassay (244).

Human Carcinogenicity—No epidemiological studies or case reports relating pyrilamine to human neoplasia were found in the literature (169).

MUTAGENICITY

Pyrilamine caused unscheduled DNA synthesis in primary adult rat hepatocytes in culture (245). Mitosis was inhibited 68% by histamine in human keratinocytes in culture, pyrilamine blocked this effect (246). No information is available on *in vivo* mutagenesis (247).

TERATOGENICITY

Pregnant mice given pyrilamine in their drinking water produced resorptions, abortions, premature parturitions, decreased weight of the neonates, decrease in survival rate at 44 days, alterations in skin and fur, delayed eye opening, pneumoperitoneum, and delayed opening of the external auditory meatus and vagina (248). Pyrilamine was not teratogenic in the rat (249). It caused stromal edema to be inhibited but increased the number of blastocytes recovered from the uterus of the pregnant rat on day 5 (250). Injection of histamine into the right ventricle of the rat brain produced hypokinesis and catalepsy, and pyrilamine reduced these effects (251). Pyrilamine significantly decreases motor activity in mice (252). No information is available concerning pyrilamine with the production of human malformations (253).

CONCLUSIONS

The chemistry, metabolism, structure–activity relationships, pharmacology, toxicology, mutagenicity, teratogenicity, and carcinogenicity of pyrilamine have been reviewed. More mutagenic studies using cells in culture are required to establish the drug's mutagenicity potential. Teratogenic and three generation studies employing both mice and rats are necessary to understand pyrilamine's effects on the reproductive process. A chronic toxicology study is necessary to determine the long-term effects of pyrilamine. A pharmacokinetic study coupled with *in vitro* metabolism would assist in showing the exact metabolic pathways used in biotransformation of pyrilamine.

REFERENCES

(1) W. Lijinski, M. D. Reuber, and B. N. Blackwell, *Science*, **209**, 817 (1980).

(2) "The Merck Index," 9th ed., M. Windholz, Ed., Merck and Co., Rahway, N.J., 1976, p. 1036.

(3) "Synthetic Organic Chemicals, U.S. Production and Sales," U.S. International Trade Commission, U.S. Government Printing Office, Washington, D.C., 1977, p. 131.

(4) "Drinking Water and Health," National Academy of Sciences, Washington, D.C., 1977.

(5) "Identification of Organic Compounds in Industrial Effluent Discharges," EPA Environmental Research Laboratory, Athens, Ga., EPA-600/4-79-016, Feb. 1979.

(6) CEC, European Cooperation and Coordination in the Field of Scientific and Technical Research, COST-Project 64b, A comprehensive list of polluting substances which have been identified in various fresh waters, effluent discharges, aquatic plants and animals, and bottom sediments, 2nd ed., 1976.

(7) "AMA Drug Evaluations," 1st ed., American Medical Association, Chicago, Ill, 1971, pp. 367, 370.

(8) "Registry of Toxic Effects of Chemical Substances," H. E. Christensen, Ed., US Government Printing Office, Washington, D.C., 1976, p. 1016.

(9) "CRC Atlas of Spectral Data and Physical Constants for Organic Compounds," Vol. IV, 2nd ed., J. G. Grasselli and W. M. Ritchey, Ed., CRC Press, Cleveland, Oh., 1975, p. 3735.

(10) S. N. Tewari, *Zbl. Pharm.*, **116**, 1123 (1977).

(11) D. Bovet, R. Horclois, R. Walthert, and F. Walthert, *C. R. Seances Soc. Biol.*, **68**, 99 (1944).

(12) C. P. Huttrer, C. Djerassi, W. L. Beears, R. L. Mayer, and C. R. Scholz, *J. Am. Chem. Soc.*, **68**, 1999 (1946).

(13) P. Viaud, *Prod. Pharm.*, **2**, 53 (1947).

(14) R. J. Horclois, U.S. Pat. 2,502,151, March 28, 1950.

(15) M. L. Bastos, G. E. Kananen, J. R. Monforte, and I. Sunshine, in "Methodology of Analytical Toxicology," I. Sunshine, Ed., CRC Press, Cleveland, Ohio, 1975, pp. 434–442.

(16) R. A. deZeeuw, P. Schepers, J. F. Greving, and J.-P. Franke, *Proc. Intl. Symp. Forensic Drug Chem. 1979*, pp. 167–179.

(17) T. D. Doyle and J. Levine, *Anal. Chem.*, **39**, 1282 (1967).

(18) B.-A. Persson and G. Schill, *Acta Pharm. Suec.*, **3**, 281, (1966).

(19) A. Lauvent and R. Bourdon, *Ann. Pharm. Fr.*, **33**, 171 (1975).

(20) T. M. Holdstock and H. M. Stevens, *Forensic Sci.*, **6**, 187 (1975).

(21) E. Vidic and E. Klug, *Z. Rechtmed.*, **76**, 283 (1975).

(22) R. J. Armstrong, *N. Z. J. Sci.*, **17**, 15 (1974).

(23) I. Sunshine, W. W. Fike, and H. Landesman, *J. Forensic Sci.*, **11**, 428 (1966).

(24) R. H. Drost and J. F. Reith, *Pharm. Weekbl.*, **102**, 1379 (1967).

(25) K. K. Kaistha, R. Tadrus, and R. Janda, *J. Chromatogr.*, **107**, 359 (1975).

(26) W. W. Fike, *Anal. Chem.*, **38**, 1697 (1966).

(27) Z. I. El-Darawy and Z. M. Mobarak, *Pharmazie*, **28**, 37 (1973).

(28) S. N. Tewari, *Z. Anal. Chem.*, **275**, 31 (1975).

(29) S. L. Kidman, *J. Am. Pharm. Assoc.*, **9**, 24 (1971).

(30) V. J. McLinden and A. M. Stenhouse, *Forensic Sci. Intl.*, **13**, 71 (1979).

(31) T. J. Janjie, G. A. Milovanovic, and M. B. Celap, *Bull. Soc. Chim. Beograd*, **40**, 329 (1975).

(32) J. P. Ganatra, M. R. Shastri, and R. C. Mehta, *Ind. J. Pharm*, **30**, 67 (1968).

(33) A. M. Wahbi, H. Abdine, and S. M. Blaih, *Pharmazie*, **33**, 96 (1978).

(34) S. Demir and H. Amal *Istanbul Ecz. Fak. Mec.*, **6**, 14 (1970).

(35) F. DeFabrizio, *J. Pharm. Sci.*, **57**, 644 (1968).

(36) T. D. Doyle and F. R. Fazzari, *ibid.*, **63**, 1921 (1974).

(37) B. Kaempe, *Arch. Pharm. Chem. Sci. Ed.*, **2**, 145 (1974).

(38) F. Pellerin and H. El-Makkawi, *Ann. Pharm. Fr.*, **29**, 421 (1971).

(39) N. C. Jain and P. L. Kirk, *Microchem. J.*, **12**, 242 (1967).

(40) B. R. Rader, *J. Pharm. Sci.*, **58**, 1535 (1969).

(41) E. Marozzi, V. Gambaro, F. Lodi, and A. Pariali, *Il Farmaco Ed. Pr.*, **32**, 330 (1977).

(42) *Ibid.*, **31**, 180 (1975).

(43) A. C. Moffat, A. H. Stead, and K. W. Smalldon, *J. Chromatogr.*, **90**, 19 (1974).

(44) R. C. Gupta and G. D. Lundberg, *Clin. Toxicol.*, **11**, 437 (1977).

(45) F. L. Fricke, *JAOAC*, **55**, 1162 (1972).

(46) A. W. Missen, A gas–liquid chromatographic procedure for the determination of drugs in small blood samples. Rept. N. Z. Dept. Sci. Ind. Res. Chem. Div. (CD 2282) 1979.

(47) J. C. Garriott and J. Dempsey, *Forensic Sci. Gaz.*, **8**, 1 (1977).

(48) B. J. Millard., *GC-MS News*, **6**, 80 (1975).
(49) G. J. Downs and S. A. Gwyn, *J. Chromatogr.*, **103**, 208 (1975).
(50) M. G. Lee and M. G. Millard, *Adv. Mass Spectrom.*, **7B**, 1551 (1978).
(51) B. B. Wheals, *J. Chromatogr.*, **187**, 65 (1980).
(52) T. R. Koziol, J. T. Jacobs, and R. G. Achari, *J. Pharm. Sci.*, **68**, 1135 (1979).
(53) V. Das Gupta and A. G. Ghanekar, *ibid.*, **66**, 895 (1977).
(54) J. H. Block, H. L. Levine, and J. W. Ayres, *ibid.*, **68**, 605 (1979).
(55) D. L. Massart and M. R. Detaevernier, *J. Chromatogr. Sci.*, **18**, 139 (1980).
(56) D. T. Witiak, in "Medicinal Chemistry, Vol III," 3rd ed., A. Burger, Ed., Wiley–Interscience, New York, N.Y. 1970, pp. 1643–1668.
(57) T. H. Lippert and U. Quastholff, *J. Physiol.* (London), **206**, 335 (1970).
(58) H. Pollard, S. Bischoff, and J. C. Schwartz, *Agents Actions*, **3**, 190 (1973).
(59) R. W. Shayer, *ibid.*, **3**, 191 (1973).
(60) J. Z. Nowak, *Acta Physiol. Pol.*, **28**, 101 (1977).
(61) K. M. Taylor, *Biochem. Pharmacol.*, **22**, 2775 (1973).
(62) H. Barth, I. Neimeyer, and W. Lorenz, *Proc. Symp. Histamine H-2 Receptor Antagonists*, 1973, pp. 115–125.
(63) A. Thithapandha and V. H. Cohn, *Biochem. Pharmacol.*, **27**, 263 (1978).
(64) D. N. Brindley and M. Bowley, *Biochem. J.*, **148**, 461 (1975).
(65) R. G. Sturton and D. N. Brindley, *ibid.*, **162**, 25 (1977).
(66) D. N. Brindley, D. Allan, and R. H. Mitchell, *J. Pharm. Pharmacol.*, **27**, 462 (1975).
(67) I. Weinryb and I. M. Michel, *J. Med. Chem.*, **18**, 23 (1975).
(68) T. J. Haley, *J. Am. Pharm. Assc., Sci. Ed.*, **37**, 383 (1948).
(69) J. Lecomte, *C. R. Soc. Belge Biol.*, **160**, 1972 (1966).
(70) C. T. Chpe, D. M. Brahmankar, M. A. Samra, Z. Husain, and A. K. Doyle, *Indian J. Med. Res.*, **63**, 201 (1975).
(70) O. P. Sethi, O. D. Gulati, S. D. Gokhale, and A. D. Joseph, *Arch. Int. Pharmacodyn.*, **168**, 64 (1966).
(72) T. J. Haley and D. H. Harris, *J. Pharmacol. Exp. Ther.*, **95**, 293 (1949).
(73) R. C. Boerth, *Eur. J. Pharmacol.*, **20**, 312 (1972).
(74) P. R. Carroll, W. E. Glover, and N. Latt, *Aust. J. Exp. Biol. Med. Sci.*, **52**, (Pt. 3), 477 (1974).
(75) W. E. Glover, P. R. Carroll, and N. Latt, *Proc. Symp. Histamine H-2 Receptor Antagonists*, 1973, pp. 169–174.
(76) P. R. Saxena, *Neurology*, **25**, 681 (1975).
(77) P. R. Saxena, *Proc. Symp. Vasoactive Substances Relevant to Migrain*, **11**, 34 (1975).
(78) E. J. Mylecharane, G. D. A. Lord, J. W. Duckworth, and J. W. Lance, *Proc. Aust. Physiol. Pharmacol. Soc.*, **6**, 93 (1975).
(79) T. J. Doyle and T. A. Stricke, *Experientia*, **32**, 1428 (1976).
(80) R. W. Giles, G. Heise, and D. E. L. Wilchen, *Circ. Res.*, **40**, 541 (1977).
(81) P. S. R. K. Haranath, G. Indira-Narayan, and H. Venkatakrisna-Bhatt, *Br. J. Pharmacol.*, **55**, 3 (1975).
(82) O. H. Osman, M. Ismail, and M. F. El-Asmar, *Toxicon*, **11**, 185 (1973).
(83) P. Goadby and E. A. Phillips, *Br. J. Pharmacol.*, **49**, 368 (1973).
(84) D. T. Okpake, *ibid.*, **44**, 311 (1972).
(85) H. N. Duke, *J. Physiol.* (*London*), **200**, 122 (1969).
(86) G. Bertaccini, G. Coruzzi, and T. Vitali, *Pharmacol. Res. Commun.*, **10**, 747 (1978).
(87) R. E. Osterberg and T. Koppanyi, *J. Pharm. Sci.*, **58**, 1313 (1969).
(88) H.-G. Classen and M. Spath, *Med. Exp.*, **18**, 13 (1968).
(89) N. Chand and L. DeRoth, *Toxicon*, **17**, 583 (1979).
(90) G. D. Maengwyn-Davis, *J. Pharm. Pharmacol.*, **20**, 72 (1968).
(91) E. C. Savini, M. A. Moulin, and M. J. F. Herrou, *Terapia*, **XXIII**, 1147 (1968).
(92) H. Herxheimer, *J. Physiol.* (*London*), **190**, 41 (1967).
(93) P. Duchene-Marullaz, J. Talvard, and N. Bret, *C. R. Seances Soc. Biol.*, **163**, 406 (1969).
(94) J.-R. Boissier and C. Advenier, *Arch. Int. Pharmacodyn.*, **187**, 394 (1970).
(95) D. T. Okpako, *J. Pharm. Pharmacol.*, **24**, 40 (1972).
(96) C. J. Matson, A. N. Welter, and R. C. Kvam, *Arch. Int. Pharmacodyn.*, **232**, 68 (1978).
(97) K. deVries, H. Booy-Noord, R. van der Lende, G. J. Tammeling, H. J. Sluiter, and N. G. M. Orie, *Progr. Resp. Res.*, **6**, 66 (1971).
(98) G. S. Cliff, *J. Pharm. Pharmacol.*, **20**, 579 (1968).
(99) J. H. Botting, *Br. J. Pharmacol.*, **54**, 428 (1975).
(100) J. N. Neogi, *Indian Physiol. Allied. Sci.*, **20**, 80 (1966).
(101) H. O. J. Collier, "Prostaglandin Synthetase Inhibitors," H. J. Robinson and J. R. Vane, Eds., Raven, New York, 1974, pp. 121–133.
(102) M. L. Sharma, M. D. Khapre, and K. N. Ingle, *Mater. Med. Pol.* (Eng. Ed.), **10**, 191 (1978).
(103) M. Impicciatore, G. Morini, and G. Bertaccini, *Eur. J. Pharmacol.*, **48**, 249 (1978).
(104) T. Gerner, J. F. W. Haffner, and J. Norstein, *Scand. J. Gastroenterol.*, **14**, 65 (1979).
(105) M. Albinus and K.-Fr. Sewing, *J. Pharm. Pharmacol.*, **21**, 656 (1969).
(106) C. S. Chew, S. J. Hersey, G. Sachs, and T. Berglindl, *Am. J. Physiol.*, **238**, G312 (1980).
(107) M. Albinus and S. Malinski, *Agents Actions*, **9**, 76 (1979).
(108) G. B. Eagleton and J. Watt, *J. Pharm. Pharmacol.*, **18**, 835 (1966).
(109) P. H. Guth, D. Aures, and G. Paulsen, *Gastroenterology*, **76**, 88 (1979).
(110) M. J. Daley, J. M. Humphray, and R. Stables, *Br. J. Pharmacol.*, **67**, 414 (1979).
(111) S. E. Knight, R. L. McIsaac, and C. D. Rennie, *ibid.*, **66**, 458 (1979).
(112) L. J. Hayden, G. Thomas, and G. B. West, *J. Pharm. Pharmacol.* **30**, 244 (1978).
(113) D. Beattie, *ibid.*, **29**, 748 (1977).
(114) P. Anttila, C. Lucke, and E. Westermann, *Naunyn-Schmiedeberg's Arch. Pharmacol.*, **296**, 31 (1976).
(115) W. Krol and K. Moczurad, *Pol. Tyg. Lek.*, **24**, 678 (1969).
(116) R. Cummings and A. W. J. Lykke, *Pathology*, **5**, 117 (1973).
(117) J. L. Vegad, *Indian J. Exp. Biol.*, **8**, 141 (1970).
(118) J. L. Vegad, *Indian J. Anim. Sci.*, **41**, 689 (1971).
(119) *Ibid.*, **41**, 368 (1971).
(120) *Ibid.*, **42**, 517 (1972).
(121) J. Godlewski, J. Fontagne, M. Tissot, M. Loizeau, and P. Lechat, *Arch. Int. Pharmacodyn.*, **223**, 142 (1976).
(122) V. A. Tomilets and T. S. Cho, *Agents Actions*, **9**, 67 (1979).
(123) S.-E. Jansson, *Acta Physiol. Scand.*, **78**, 420 (1970).
(124) A. Penttila and N.-E. Saris, *ibid.*, **74**, 426 (1968).
(125) W. Lorenz, G. Haubensak, M. Hutzel, and E. Werle, *Naunyn-Schmeideberg's Arch. Pharmakol. Exp. Pathol.*, **260**, 416 (1968).
(126) M. Mares-Guia, L. Rezende, Jr., and C. Ribeiro, *Cieneie e Cultura*, **23**, 519 (1971).
(127) J. W. Black, W. A. M. Duncan, C. J. Durant, C. R. Ganellin, and E. M. Parsons, *Nature* (*London*), **236**, 385 (1972).
(128) P. Eyre, *Br. J. Pharmacol.*, **48**, 321 (1973).
(129) N. Chand and P. Eyre, *Arch. Int. Pharmacodyn.*, **216**, 197 (1975).
(130) D. M. Grennan, P. J. Rooney, R. A. St. Onge, P. M. Brooks, I. J. Zeitlin, and W. C. Dick, *Eur. J. Clin. Invest.*, **5**, 75 (1975).
(131) C. Labird, G. Dureng, P. Duchene-Marzulla, and J. Moleyre, *Jpn J. Pharmacol.*, **27**, 491 (1977).
(132) S. J. Hill, J. M. Young, and D. H. Marrian, *Nature* (*London*), **270**, 361 (1977).
(133) V. T. Tran, R. S. L. Chang, and S. H. Snyder, *Proc. Natl. Acad. Sci., USA*, **75**, 6290 (1978).
(134) S. J. Hill, P. C. Emson, and J. M. Young, *J. Neurochem.*, **31**, 997 (1978).
(135) J. Hyttel, *Psychopharmacol.*, **65**, 211 (1979).
(136) E. Richelson, "Biological Psychiatry Today," J. Obiols, C. Ballus, E. Gonzales-Monicius, and J. Pujol, Eds., Elsevier/North Holland Biomedical Press, 1979, pp. 106–109.
(137) T. C. Moore and T. Ohtama, *IRCS Med. Sci. Libr. Compend.* **7**, 147 (1979).
(138) R. S. L. Chang, V. T. Tran, and S. H. Snyder, *J. Neurochem.*, **32**, 1653 (1979).
(139) S. J. Hill and J. M. Young, *Br. J. Pharmacol.*, **66**, 93 (1979).
(140) G. Coruzzi, S. Bongrani, and G. Bertaccini, Pharmacol. Res. Commun., **11**, 517 (1979).
(141) R. Raisman, M. Briley, and S. Z. Langer, *Nature* (*London*), **281**, 148 (1979).
(142) J. M. Palacios, W. S. Young, III, and M. J. Kuhar, *Eur. J. Pharmacol.*, **58**, 295 (1979).
(143) R. S. L. Chang, V. T. Tran, and S. H. Snyder, *J. Pharmacol. Exp. Ther.*, **209**, 437 (1979).

(144) J. R. Powell and M. J. Brody, *J. Pharmacol. Exp. Ther.*, **196,** 1 (1976).
(145) T. T. Quach, A. M. Duchemin, C. Rose, and J. C. Schwartz, *Neurosci. Lett.*, **17,** 49 (1980).
(146) D. Diffley, V. T. Tran, and S. H. Snyder, *Eur. J. Pharmacol.*, **64,** 177 (1980).
(147) D. Reinhardt, R. Walkenhorst, and G. Arnold, *Agents Actions*, **10,** 152 (1980).
(148) C. Thomson, C. D. Forbes, and C. R. M. Prentice, *Thromb. Diath. Haemorrh.*, **30,** 547 (1973).
(149) K. O. Vollmer, J. H. Wissler, and G. G. Betz, *Eur. J. Clin. Pharmacol.*, **4,** 99 (1972).
(150) B. Tait, *J. Pharm. Pharmacol.*, **22,** 738 (1970).
(151) B. Denes and K. Greeff, *Eur. J. Pharmacol.*, **57,** 417 (1979).
(152) B. Delbarre, *C. R. Seances Soc. Biol.*, **164,** 1619 (1970).
(153) K.-S. Hui and M. B. Roberts, *Life Sci.*, **17,** 819 (1975).
(154) B. Delbarre, *C. R. Seances Soc. Biol.*, **161,** 1441 (1967).
(155) N. Blumenkratz and G. Asboe-Hansen, *Scand. J. Rheumatol.*, **7,** 123 (1978).
(156) F. Tazieff-Depierre and M. Czajka, *C. R. Hebd. Seances Acad. Sci. Ser. D.*, **268,** 1228 (1969).
(157) P. J. Neuvonen and P. Torsti, *Ann. Med. Exp. Biol. Fenn.*, **46,** 63 (1968).
(158) C. J. Dunn and D. A. Willoughby, *J. Pathol.*, **116,** 165 (1975).
(159) R. F. Shotts and R. T. Jackson, *Arch. Otolaryngol.*, **96,** 57 (1972).
(160) N. Sandberg, *Experientia*, **31,** 580 (1975).
(161) H. van Riezen and A. Delver, *Arzneim.-Forsch.*, **21,** 1562 (1971).
(162) M. C. Gerald, K. A. Skau, and R. P. Maickel, *Eur. J. Pharmacol.*, **17,** 189 (1972).
(163) J. Z. Nowak and A. Pilc, *Acta Physiol. Pol.*, **XXVI,** 596 (1975).
(164) P. K. Mukherjee, *Indian Med. J.*, **67,** 431 (1973).
(165) K. Hyires and J. Knoll, *Pol. J. Pharmacol. Pharm.*, **27,** 257 (1975).
(166) R. P. Schleimer and E. Benjamini, *Proc. West. Pharmacol. Soc.* **22,** 251 (1979).
(167) S. Ruggieri, P. Falaschi, M. Baldassarre, R. D'Urso, G. Frajese, and A. Agnoli, in "Neuroendocrine Correlated in Neurology and Psychiatry," vol. 2, E. E. Muller and A. Agnoli, Eds., Elsevier/North Holland Biomedical Press, 1979, pp. 127–137.
(168) G. Cerone, S. Ruggieri, P. Aloisi, L. Cappenberg, and A. Agnoli, *Boll. Soc. Ital. Biol. Sper.*, **LIII,** 354 (1977).
(169) Medline/Toxline/Cancerlit, National Library of Medicine, Nov. 17, 1980.
(170) H. E. Christensen, Ed., "Registry of Toxic Effects of Chemical Substances," U.S. Government Printing Office, Washington, D.C. 1976, p. 1016.
(171) R. Hari, G. A. Shivnani, and H. C. Joshi, *Indian J. Anim. Sci.*, **43,** 829 (1973).
(172) R. Zeitoun, A. Ghazal, and N. Bakry, *J. Drug Res.*, **5,** 41 (1973).
(173) P. Eyre, *J. Pharm. Pharmacol.*, **19,** 509 (1967).
(174) J. Bralet, P. Beley, A. M. Bralet, and A. Beley, *Stroke*, **10,** 653 (1979).
(175) J. Nimmo, M. F. Dixon, and L. F. Prescott, *Clin. Toxicol.*, **6,** 75 (1973).
(176) T. J. Haley and D. H. Harris, *Stanford Med. Bull.*, **8,** 1 (1950).
(177) G. Kaley and R. Weiner, *Ann. N.Y. Acad. Sci.*, **180,** 338 (1971).
(178) S. I. Ankier and M. L. Neat, *Int. Arch. Allergy*, **42,** 264 (1972).
(179) L. W. Argenbright, P. D. Forbes, and G. J. Stewart, *Fed. Proc. Fed. Am. Soc. Exp. Biol.*, **39,** 389 (1980).
(180) R. J. Perper, A. L. Oronsky, and V. Blancuzzi, *J. Pharmacol. Exp. Ther.*, **193,** 594 (1975).
(181) J. M. Brandon, *J. Endocrinol.*, **73,** 42 (1977).
(182) R. Suchert, *Wien Klin. Wochenschnr.*, **82,** 281 (1970).
(183) O. Forster and E. Stoklaska, *Arch. Int. Pharmacodyn.*, **174,** 144 (1968).
(184) R. P. Orange, M. D. Valentine, and K. F. Austen, *Proc. Soc. Exp. Biol. Med.*, **127,** 127 (1967).
(185) L. M. Stotland and N. N. Share, *Can. J. Physiol. Pharmacol.*, **52,** 1119 (1974).
(186) P. Crunknorn and S. C. R. Meacock, *Br. J. Pharmacol.*, **42,** 392 (1971).
(187) H. A. Al-Haboubi and I. J. Zeitlin, *ibid.*, **67,** 446 (1979).
(188) K. Kizuki, H. Moriya, and C. Moriwaki, *Chem. Pharm. Bull.*, **27,** 2424 (1979).
(189) O. Forster and E. Stoklaska, *Z. Immunitaetsforsch Allerg. Klin. Immunol.*, **133,** 68 (1967).
(190) M. S. Starr and G. B. West, *Br. J. Pharmacol.*, **37,** 178 (1969).
(191) H. V. Huidobro and M. Propker, *Cien. Cultura*, **23,** 189 (1971).
(192) A. Saindelle, F. Ruff, R. Hebert, and J.-L. Parrot, *Rev. Fr. Allergy*, **8,** 205 (1968).
(193) J. M. Hand and C. K. Buckner, *Int. J. Immunopharmacol.*, **1,** 189 (1979).
(194) N. Chand, *Lung*, **156,** 271 (1979).
(195) M. Cirstea and G. Suhaciu, *Arch. Int. Physiol. Biochem.*, **76,** 344 (1968).
(196) M. J. Schmidt, L. L. Turex, C. S. Hooker, S. M. Spaethe, and J. H. Fleisch, *Life Sci.*, **24,** 2321 (1979).
(197) J. Wohnlich, F. Ruff, and J.-L. Parrot, *Biochem. Soc. Trans.*, **1,** 720 (1973).
(198) A. A. Mathe, L. Volicer, and S. K. Puri, *Res. Commun. Chem. Pathol. Pharmacol.*, **8,** 635 (1974).
(199) G. E. Davies and T. P. Johnson, *Int. Arch. Allergy*, **41,** 648 (1971).
(200) F. Hahn, F. Prohle, R. Mitze, and L. Degand, *ibid.*, **40,** 340 (1971).
(201) P. Goadby and M. A. Little, *Br. J. Pharmacol.*, **58,** 330 (1976).
(202) P. Miller and P. Robson, *ibid.*, **58,** 444 (1976).
(203) F. P. Nijkamp and A. G. M. Ramakers, *Eur. J. Pharmacol.*, **62,** 121 (1980).
(204) H. Giertz and K. Krako, *Arch. Int. Pharmacodyn.*, **181,** 424 (1969).
(205) W. Bernauer, F. Hahn, and H. Giertz, *Arch. Int. Pharmacodyn.*, **178,** 137 (1969).
(206) H. Giertz and F. Hahn, *Nauyn-Schmiedberg's Arch. Pharmakol. Exp. Pathol.*, **258,** 11 (1967).
(207) F. Hahn, K. Somorjai, R. Mitze, and H. P. Zahradnik, *Arch. Int. Pharmacodyn.*, **199,** 108 (1972).
(208) F. Hahn and W. Bernauer, *ibid.*, **184,** 129 (1970).
(209) W. Bernauer and F. Hahn, *ibid.*, **181,** 232 (1969).
(210) F. Hahn, W. Bernauer, J. Mahlstedt, S. Resch-Bollhagen, and E. Beck, *Naunyn-Schmiedberg's Arch. Pharmakol. Exp. Pathol.*, **267,** 224 (1970).
(211) W. Bernauer, U. Gossow, and F. Hahn, *Int. Arch. Allergy*, **37,** 311 (1970).
(212) W. Bernauer and P. Filipowski, *Naunyn-Schmiedberg's Arch. Pharmakol. Exp. Pathol.*, **276,** 35 (1973).
(213) K. Huth, H. Ruwisch, F. W. Schmahl, G. Blumel, and B. Ureaschek, *Verh. Dtsch. Ges. Kreislaufforsch.*, **36,** 319 (1970).
(214) G. B. Fregnan and A. H. Glasser, *Proc. Eur. Soc. Study Drug Toxic.*, **11,** 230 (1970).
(215) E. Roesch and A. Roesch, *Monogr. Allergy*, **12,** 164 (1977).
(216) R. J. Perper, M. Sanda, and L. M. Lichtenstein, *Int. Arch. Allergy*, **43,** 837 (1972).
(217) P. Eyre, *J. Pharm. Pharmacol.*, **22,** 104 (1970).
(218) F. Alexander, P. Eyre, and K. W. Head, *J. Comp. Pathol.*, **80,** 19 (1970).
(219) P. W. Wells and P. Eyre, *Can. J. Physiol. Pharmacol.*, **50,** 255 (1972).
(220) P. Eyre and P. W. Wells, *Br. J. Pharmacol.*, **49,** 364 (1973).
(221) L. W. Argenbright, P. D. Forbes, and G. J. Stewart, *Exp. Mol. Pathol.*, **32,** 154 (1980).
(222) L. M. Lichtenstein and E. Gillespie, *J. Pharmacol. Exp. Ther.*, **192,** 441 (1975).
(223) L. S. Dunlop and A. P. Smith, *Br. J. Pharmacol.*, **59,** 475 (1977).
(224) M. K. Church and C. F. Gradidge, *ibid.*, **66,** 68 (1979).
(225) O. Hagermark, K. Strandberg, and R. Gronneberg, *Acta Dermatol.*, **59,** 297 (1979).
(226) H. Booij-Noord, M. G. M. Orie, W. C. Berg, and K. deVries, *Proc. 3rd Int. Symp. on Bronchitis*, 1970, pp. 316–330.
(227) J.-L. Parrot, R. Hebert, A. Saindelle, and F. Ruff, *Arch. Environ. Health*, **19,** 685 (1969).
(228) G. Michaelsson, *Acta Dermatol.*, **50,** 31 (1970).
(229) P. Wodniansky and F. X. Wohlzogen, *Wein Klin. Wochenschnr.*, **80,** 249 (1968).

(230) Y. Olsson, *Acta Physiol. Scand. Suppl. 284*, **69**, 3 (1966).
(231) G. S. Kerkut, R. J. Walker and G. N. Woodruff, *Br. J. Pharmacol.*, **32**, 241 (1968).
(232) N. Ambache and M. B. Zar, *J. Physiol.* **204**, 20 (1969).
(233) E. J. Harris and S. Ochs, *ibid.*, **187**, 5 (1966).
(234) C. A. M. Sampaio, A. J. Lapa, and J. R. Valle, *J. Pharm. Pharmacol.*, **19**, 552 (1967).
(235) M. D. Green, B. Cox, and P. Lomax, *J. Neurosci. Res.*, **1**, 353 (1975).
(236) S. Rashid, *Arch. Int. Pharmacodyn.*, **195**, 247 (1972).
(237) M. Harris, J. M. Hopkin, and M. J. Neal, *Br. J. Pharmacol.*, **47**, 229 (1973).
(238) M. J. Brimble and D. I. Wallis, *Nature (London)*, **246**, 156 (1973).
(239) G. Gardos, U. V. Lassen, and L. Pape, *Biochim. Biophys. Acta*, **448**, 599 (1976).
(240) C. Bell, W. J. Lang, and C. Tsilemanis, *Brain Res.*, **56**, 392 (1973).
(241) J. N. Sinha, M. L. Gupta, and K. P. Bhargawa, *Eur. J. Pharmacol.*, **5**, 235 (1969).
(242) M. Skingle and M. B. Tyers, *J. Pharmacol. Methods*, **2**, 71 (1979).
(243) C. C. Eagleson and I. J. Zeitlin, *J. Physiol. (London)*, **275**, 68 (1978).
(244) National Toxicology Program, Carcinogenesis Testing Program, June 8, 1981.
(245) G. S. Probst and S. B. Neal, *Cancer Lett.*, **10**, 67 (1980).
(246) R. A. Harper and B. A. Flaxman, *J. Invest. Dermatol.*, **65**, 400 (1975).
(247) EMIC, Oak Ridge National Laboratory, Nov. 17, 1980.
(248) P. Naranjo and E. deNaranjo, *Arzneim.-Forsch.*, **18**, 188 (1968).
(249) F. Bovet-Nitti, G. Bignani, and D. Bovet, *Life Sci.*, **5**, 303 (1963).
(250) J. M. Brandon and R. M. Wallis, *J. Reprod. Fert.*, **50**, 251 (1977).
(251) J. Z. Nowak and A. Pilc, *Proc. 2nd Congress of Hungarian Pharmacol. Soc.*, Budapest, 1976, pp. 193–196.
(252) C.-I. Wong and M. B. Roberts, *IRCR Med. Sci.*, **3**, 618 (1975).
(253) ETIC, Oak Ridge National Laboratory, Nov. 17, 1980.

RESEARCH ARTICLES

Diffusion of Phenol in the Presence of a Complexing Agent, Tetrahydrofuran

J. B. DRESSMAN *§, K. J. HIMMELSTEIN *‡§x, and T. HIGUCHI *

Received October 29, 1981, from the **Department of Pharmaceutical Chemistry* and the ‡*Department of Chemical and Petroleum Engineering, The University of Kansas, Lawrence, KS 66045.* Accepted for publication February 19, 1982. §Present address: Inter$_x$ Research Corporation, Lawrence, KS 66044.

Abstract □ The effect of a complexing agent, tetrahydrofuran, on the diffusion of phenol across a stagnant fluid layer has been studied. At a given activity of free phenol, the steady-state flux of phenol appearing in an acceptor phase was greatly enhanced. However, as the fraction of phenol associated with the complexing agent increased, the flux of phenol decreased, since the transport was then controlled by the diffusion of the complex, a larger structure. A mathematical model of simultaneous association and diffusion was derived to determine whether the diffusional behavior of two associating species could be accounted for in terms of the association equilibrium constant and Fick's second law. Experimental results supported the model. It was concluded that the presence of a complexing agent tends to reduce the rate of diffusion, the effect being more pronounced at high concentrations of complexing agent.

Keyphrases □ Phenol—diffusion in a complexing agent, tetrahydrofuran □ Diffusion—phenol in a complexing agent, tetrahydrofuran □

The purpose of this study was to investigate the influence of complexing agents on the diffusional behavior of drugs. The ability of most drugs to undergo association interactions is intrinsically related to their activity, since most drugs exert their action by complexing to a receptor site. Some dosage forms are designed to take advantage of this associative tendency by using a complexing agent to increase the solubility of the drug in the formulation (1, 2). In other cases, complexing agents are used to modify the dissolution rate of a drug at the site of administration (3, 4), as it is known that the dissolution rate can be greatly affected by association in the diffusion layer (5).

In a previous study (6), the importance of associative interaction on mass transport of drugs was exemplified by the case of simultaneous self-association and diffusion of phenol through an immobilized layer of isooctane. The results of this analysis showed that the self-association of phenol can significantly alter the rate of transport of phenol. The case of simultaneous complexation and diffusion has also been investigated (7). However, those results relied on accurate determination of the forward and reverse rate constants for the associative interaction, parameters which may prove difficult to obtain. It was also assumed that for association equilibrium to be attained within the diffusion layer, it was necessary for the con-

0022-3549/83/0100-0012$01.00/0

(230) Y. Olsson, *Acta Physiol. Scand. Suppl. 284*, **69**, 3 (1966).
(231) G. S. Kerkut, R. J. Walker and G. N. Woodruff, *Br. J. Pharmacol.*, **32**, 241 (1968).
(232) N. Ambache and M. B. Zar, *J. Physiol.* **204**, 20 (1969).
(233) E. J. Harris and S. Ochs, *ibid.*, **187**, 5 (1966).
(234) C. A. M. Sampaio, A. J. Lapa, and J. R. Valle, *J. Pharm. Pharmacol.*, **19**, 552 (1967).
(235) M. D. Green, B. Cox, and P. Lomax, *J. Neurosci. Res.*, **1**, 353 (1975).
(236) S. Rashid, *Arch. Int. Pharmacodyn.*, **195**, 247 (1972).
(237) M. Harris, J. M. Hopkin, and M. J. Neal, *Br. J. Pharmacol.*, **47**, 229 (1973).
(238) M. J. Brimble and D. I. Wallis, *Nature (London)*, **246**, 156 (1973).
(239) G. Gardos, U. V. Lassen, and L. Pape, *Biochim. Biophys. Acta*, **448**, 599 (1976).
(240) C. Bell, W. J. Lang, and C. Tsilemanis, *Brain Res.*, **56**, 392 (1973).
(241) J. N. Sinha, M. L. Gupta, and K. P. Bhargawa, *Eur. J. Pharmacol.*, **5**, 235 (1969).
(242) M. Skingle and M. B. Tyers, *J. Pharmacol. Methods*, **2**, 71 (1979).
(243) C. C. Eagleson and I. J. Zeitlin, *J. Physiol. (London)*, **275**, 68 (1978).
(244) National Toxicology Program, Carcinogenesis Testing Program, June 8, 1981.
(245) G. S. Probst and S. B. Neal, *Cancer Lett.*, **10**, 67 (1980).
(246) R. A. Harper and B. A. Flaxman, *J. Invest. Dermatol.*, **65**, 400 (1975).
(247) EMIC, Oak Ridge National Laboratory, Nov. 17, 1980.
(248) P. Naranjo and E. deNaranjo, *Arzneim.-Forsch.*, **18**, 188 (1968).
(249) F. Bovet-Nitti, G. Bignani, and D. Bovet, *Life Sci.*, **5**, 303 (1963).
(250) J. M. Brandon and R. M. Wallis, *J. Reprod. Fert.*, **50**, 251 (1977).
(251) J. Z. Nowak and A. Pilc, *Proc. 2nd Congress of Hungarian Pharmacol. Soc.*, Budapest, 1976, pp. 193–196.
(252) C.-I. Wong and M. B. Roberts, *IRCR Med. Sci.*, **3**, 618 (1975).
(253) ETIC, Oak Ridge National Laboratory, Nov. 17, 1980.

RESEARCH ARTICLES

Diffusion of Phenol in the Presence of a Complexing Agent, Tetrahydrofuran

J. B. DRESSMAN *§, K. J. HIMMELSTEIN *‡§x, and T. HIGUCHI *

Received October 29, 1981, from the **Department of Pharmaceutical Chemistry* and the ‡*Department of Chemical and Petroleum Engineering, The University of Kansas, Lawrence, KS 66045.* Accepted for publication February 19, 1982. §Present address: Inter$_x$ Research Corporation, Lawrence, KS 66044.

Abstract □ The effect of a complexing agent, tetrahydrofuran, on the diffusion of phenol across a stagnant fluid layer has been studied. At a given activity of free phenol, the steady-state flux of phenol appearing in an acceptor phase was greatly enhanced. However, as the fraction of phenol associated with the complexing agent increased, the flux of phenol decreased, since the transport was then controlled by the diffusion of the complex, a larger structure. A mathematical model of simultaneous association and diffusion was derived to determine whether the diffusional behavior of two associating species could be accounted for in terms of the association equilibrium constant and Fick's second law. Experimental results supported the model. It was concluded that the presence of a complexing agent tends to reduce the rate of diffusion, the effect being more pronounced at high concentrations of complexing agent.

Keyphrases □ Phenol—diffusion in a complexing agent, tetrahydrofuran □ Diffusion—phenol in a complexing agent, tetrahydrofuran □

The purpose of this study was to investigate the influence of complexing agents on the diffusional behavior of drugs. The ability of most drugs to undergo association interactions is intrinsically related to their activity, since most drugs exert their action by complexing to a receptor site. Some dosage forms are designed to take advantage of this associative tendency by using a complexing agent to increase the solubility of the drug in the formulation (1, 2). In other cases, complexing agents are used to modify the dissolution rate of a drug at the site of administration (3, 4), as it is known that the dissolution rate can be greatly affected by association in the diffusion layer (5).

In a previous study (6), the importance of associative interaction on mass transport of drugs was exemplified by the case of simultaneous self-association and diffusion of phenol through an immobilized layer of isooctane. The results of this analysis showed that the self-association of phenol can significantly alter the rate of transport of phenol. The case of simultaneous complexation and diffusion has also been investigated (7). However, those results relied on accurate determination of the forward and reverse rate constants for the associative interaction, parameters which may prove difficult to obtain. It was also assumed that for association equilibrium to be attained within the diffusion layer, it was necessary for the con-

0022-3549/83/0100-0012$01.00/0

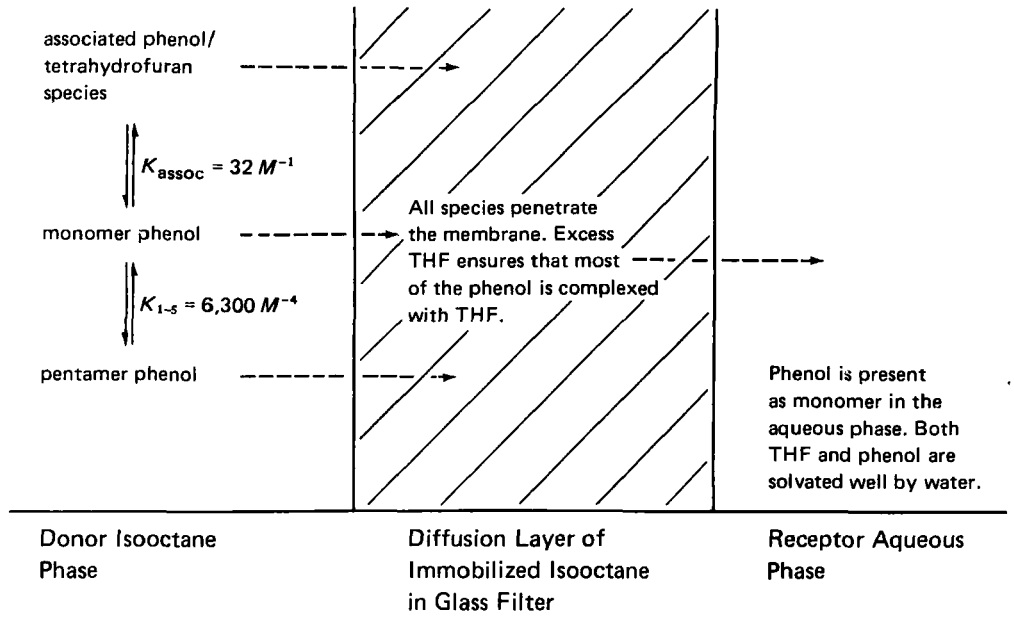

Figure 1—*The influence of tetrahydrofuran on the diffusion of phenol through an unstirred layer of isooctane.*

centration of the complexing agent to be the same at all points in the system.

In the present study, the model system used was the diffusion of phenol from a donor phase solution in isooctane, through a diffusion layer consisting of immobilized isooctane, into an aqueous receptor phase (Fig. 1). The complexing agent used was tetrahydrofuran which, as a cyclic ether, was capable of associating strongly with phenol *via* hydrogen bond formation. A mathematical model of this system was derived to determine whether the experimental diffusional behavior of the two associating species could be accounted for in terms of their association equilibrium constant and Fick's second law. The derivation was based on the following assumptions: (*a*) coupling of the fluxes of free phenol, free tetrahydrofuran, and the complex occurs; (*b*) equilibrium is rapidly attained compared with the rate of diffusion; and (*c*) diffusion of each kind of species is governed by Fick's laws.

THEORETICAL

A silanized sintered glass filter was used in the experimental portion of the present investigation to create an immobilized layer of isooctane between the donor isooctane phase and the receptor aqueous phase, a procedure described previously (6). The immobilized isooctane layer thus formed a stagnant diffusion layer. This arrangement allowed both the phenol and the tetrahydrofuran in the donor isooctane phase to diffuse across the diffusion layer. The association equilibria which occur in the donor phase and the diffusion layer are shown in Fig. 1.

The self-association of phenol in isooctane can be described by the equilibrium (8):

$$5P_m \rightleftharpoons P_5 \text{ with } K_{1-5} \approx 6{,}300\ M^{-4} \text{ at } 25° \qquad \text{(Eq. 1)}$$

where P_m is the concentration of free (monomer) phenol, P_5 is the concentration of self-associated (pentamer) phenol, and K_{1-5} is the equilibrium constant for self-association. The equilibrium governing the association between phenol and tetrahydrofuran is given by:

$$P_m + T \rightleftharpoons [P - T] \text{ with } K_{assoc} = 32\ M^{-1} \text{ at } 25° \qquad \text{(Eq. 2)}$$

where $[P - T]$ is the concentration of associated phenol–tetrahydrofuran species and K_{assoc} is the equilibrium constant for association of phenol and tetrahydrofuran in isooctane. The total concentration of phenol in the presence of tetrahydrofuran is represented by:

$$P_T = P_m + [P - T] + 5P_5 \qquad \text{(Eq. 3)}$$

The total concentration of tetrahydrofuran is given by:

$$T_T = T + [P - T] \qquad \text{(Eq. 4)}$$

where T_T is the total concentration of tetrahydrofuran, similarly expressed. Association in the aqueous phase is assumed to be negligible, since the concentrations of both phenol and tetrahydrofuran in the aqueous phase remained low over the duration of the experiment. Under these conditions, self-association also appears to be negligible[1]. Applying Fick's second law:

$$\frac{\partial C}{\partial t} = D\frac{\partial^2 C}{\partial x^2}$$

to each species of phenol present, one obtains:

$$\frac{\partial P_T}{\partial t} = D_M\frac{\partial^2 P_m}{\partial x^2} + 5D_5\frac{\partial^2 P_5}{\partial x^2} + D_{P-T}\frac{\partial^2[P - T]}{\partial x^2} \qquad \text{(Eq. 5)}$$

where D is diffusivity, t is time, C is the concentration of a given species, x is equal to distance, D_m is the diffusivity of free phenol, D_5 is the diffusivity of pentamer phenol, and P_T is expressed as molarity of monomeric phenol.

Assuming that the association equilibria are established quickly compared with the rate of diffusion, P_5 and $[P - T]$ can be substituted in Eq. 3 by the equilibrium expressions:

$$P_5 = K_{1-5}P_m{}^5 \qquad \text{(Eq. 6)}$$

$$[P - T] = K_{assoc}TP_m \qquad \text{(Eq. 7)}$$

resulting in:

$$\frac{\partial P_T}{\partial t} = D_M\frac{\partial^2 P_m}{\partial x^2} + 5D_5K_{1-5}\frac{\partial^2 P_m{}^5}{\partial x^2} + D_{P-T}K_{assoc}\frac{\partial^2(TP_m)}{\partial x^2} \qquad \text{(Eq. 8)}$$

The second term in Eq. 8 can be reexpressed as:

$$\frac{\partial^2(P_m{}^5)}{\partial x^2} = 5P_m{}^4\frac{\partial^2 P_m}{\partial x^2} + 20\,P_m{}^3\left(\frac{\partial P_m}{\partial x}\right)^2 \qquad \text{(Eq. 9)}$$

The third term in Eq. 8 can be reexpressed as:

$$\frac{\partial(TP_m)}{\partial x^2} = P_m\frac{\partial^2 T}{\partial x^2} + T\frac{\partial^2 P_m}{\partial x^2} + 2\frac{\partial P_m}{\partial x}\frac{\partial T}{\partial x} \qquad \text{(Eq. 10)}$$

Also, by substituting Eqs. 6 and 7 into Eq. 3:

$$P_T = P_m + 25K_{1-5}P_m{}^5 + K_{assoc}TP_m \qquad \text{(Eq. 11)}$$

Taking the derivative of both sides with respect to time one obtains the expression:

$$\frac{\partial P_T}{\partial t} = \frac{\partial P_m}{\partial t} + 25K_{1-5}P_m{}^4\frac{\partial P_m}{\partial t} + K_{assoc}T\frac{\partial P_m}{\partial t} + K_{assoc}P_m\frac{\partial T}{\partial t}$$

[1] Personal communication, M. Tobin.

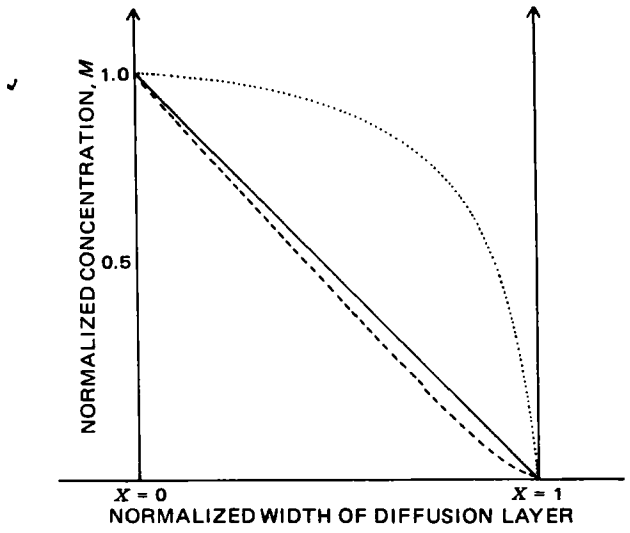

Figure 2—*Normalized steady-state concentration profiles in the diffusion layer, at total phenol concentration of 0.1403* M *and total tetrahydrofuran concentration of 4.76% (v/v) in the donor phase. Key: (——) free tetrahydrofuran concentration scaled up by a factor of 2.194; (- - - - -) associated phenol concentration scaled up by a factor of 7.616; (. . . . .) concentration of free phenol scaled up by a factor of 111.11.*

This expression can be rearranged to give:

$$\frac{\partial P_T}{\partial t} = \frac{\partial P_m}{\partial t}(1 + 25K_{1\text{-}5}P_m^4 + K_{assoc}T) + K_{assoc}P_m\frac{\partial T}{\partial t} \quad \text{(Eq. 12)}$$

By substituting Eqs. 9, 10, and 12 into Eq. 8 the following is derived:

$$\frac{\partial P_m}{\partial t}[1 + 25K_{1\text{-}5}P_m^4 + K_{assoc}T] = D_M\frac{\partial^2 P_m}{\partial x^2} + D_5K_{1\text{-}5}5P_m^4\frac{\partial^2 P_m}{\partial x^2} + 20P_m^3\left(\frac{\partial P_m}{\partial x}\right)^2 + P_m\frac{^2T}{\partial x^2} + T\frac{\partial^2 P_m}{\partial x^2} + 2\frac{\partial P_m}{\partial x}\frac{\partial T}{\partial x}D_{P\text{-}T}K_{assoc} - K_{assoc}P_m\frac{\partial T}{\partial t} \quad \text{(Eq. 13)}$$

Equation 13 can be rearranged to produce the following in terms of monomer phenol only:

$$\frac{\partial P_m}{\partial t} = \frac{\left[D_M\frac{\partial^2 P_m}{\partial x^2} + D_5K_{1\text{-}5}5P_m^4\frac{\partial^2 P_m}{\partial x^2} + 20P_m^3\left(\frac{\partial P_m}{\partial x}\right)^2 - K_{assoc}P_m\frac{\partial T}{\partial t} + D_{P\text{-}T}K_{assoc}P_m\frac{\partial^2 T}{\partial x^2} + T\frac{\partial^2 P_m}{\partial x^2} + 2\frac{\partial P_m}{\partial x}\frac{\partial T}{\partial x}\right]}{[1 + 25K_{1\text{-}5}P_m^4 + K_{assoc}T]} \quad \text{(Eq. 14)}$$

An expression for diffusion of tetrahydrofuran can be derived in a similar manner. The concentration of tetrahydrofuran in associated form can be calculated using Eq. 15:

$$[P - T] = K_{assoc}TP_m \quad \text{(Eq. 15)}$$

By applying Fick's second law to the species of tetrahydrofuran present, an expression for flux of tetrahydrofuran across a small distance within the diffusion layer can be obtained:

$$\frac{\partial T_T}{\partial t} = D_T\frac{\partial^2 T}{\partial x^2} + D_{P\text{-}T}\frac{\partial^2[P - T]}{\partial x^2} \quad \text{(Eq. 16)}$$

By appropriate substitution and rearrangement, the following expression is derived:

$$\frac{\partial T}{\partial t} = \frac{\left[\frac{\partial^2 T}{\partial x^2}[D_T + D_{P\text{-}T}K_{assoc}P_m] + D_{P\text{-}T}K_{assoc}T\frac{\partial^2 P_m}{\partial x^2} + 2\frac{\partial P_m}{\partial x}\frac{\partial T}{\partial x} - K_{assoc}T\frac{\partial P_m}{\partial t}\right]}{[1 + K_{assoc}P_m]} \quad \text{(Eq. 17)}$$

In view of the great excess of tetrahydrofuran present in all experiments

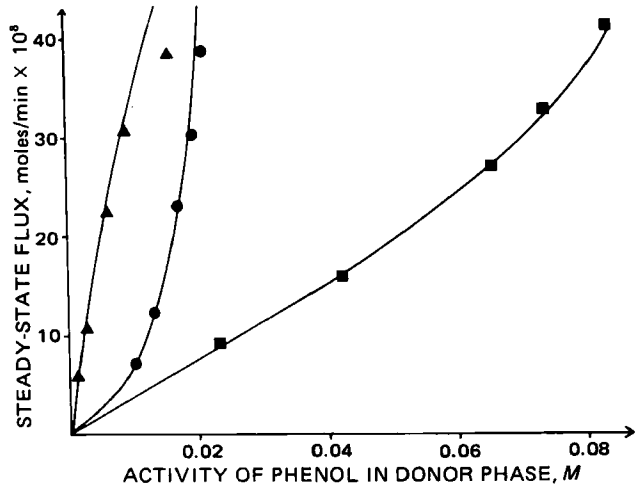

Figure 3—*Steady-state flux* versus *activity of phenol (free concentration) in the donor phase. Solid lines represent computer-generated results. Key: (▲) data from experiments in which 4.76% (v/v) tetrahydrofuran was used; (●) data from experiments in which an approximately 2:1 ratio of tetrahydrofuran to phenol was used; (■) control experiments in which no tetrahydrofuran was used.*

in which this complexing agent was used and also the magnitude of the association constant between phenol and tetrahydrofuran, it is reasonable to assume that the self-association of phenol was negligible in these experiments. For example, at $T_T = 0.5872\ M$ and $P_T = 0.1403\ M$, $[P_5] = 3.7 \times 10^{-7}\ M$.

Neglecting the contribution of the pentamer allowed the terms for diffusion of the self-associated species to be omitted. Eq. 13 is then simplified to give the following expression:

$$\frac{\partial P_m}{\partial t} = \frac{\left[\frac{\partial^2 P_m}{\partial x^2}[D_P + D_{P\text{-}T}K_{assoc}T] + D_{P\text{-}T}K_{assoc}P_m\frac{\partial^2 T}{\partial x^2} + 2\frac{\partial P_m}{\partial x}\frac{\partial T}{\partial x} - K_{assoc}P_m\frac{\partial T}{\partial t}\right]}{[1 + K_{assoc}T]} \quad \text{(Eq. 18)}$$

Since Eq. 18 is in the same form as Eq. 17, these two interdependent equations can then be solved simultaneously to determine the concentration profiles of phenol and tetrahydrofuran in the diffusion layer at a given time. Owing to the complexity of the equations involved, it was convenient to use numerical methods to obtain the required solutions. The computer program, based on the approaches described previously (9), used an implicit method of solution of differential equations of similar form. Approximate algebraic expressions, written on the $(n + 1)$ time step, were found by applying the central difference approximation to the derivative term which were thus converted to finite difference expressions. Equations 17 and 18 are nonlinear and coupled equations. To linearize and effectively decouple the equations, the following approximations were used for Eq. 17:

$$T\frac{\partial^2 P_m}{\partial x^2} = \frac{P_{n,i-1} - 2P_{n,i} + P_{n,i+1}}{\Delta x^2}T_{n+1,i}$$

$$\frac{\partial P_m}{\partial x}\frac{\partial T}{\partial x} = \frac{P_{n,i} - P_{n,i-1}}{\Delta x}\frac{T_{n+1,i} - T_{n+1,i-1}}{\Delta x}$$

$$T\frac{\partial P_m}{\partial t} = T_{n+1,i}\frac{P_{n,i} - P_{n-1,i}}{\Delta t}$$

Analogous approximations were made for the equivalent expressions in the equation governing phenol transport (Eq. 18). Since the tetrahydrofuran concentration profile was solved first for a given time step, the current values of $T_{n,i}$ were retained rather than substituting those from the previous time step:

$$P\frac{\partial T}{\partial t} = P_{n+1,i}\frac{T_{n+1,i} - T_{n,i}}{\Delta t}$$

From these expressions, it can be seen that the dependent variable on which the equation was written, *e.g.*, T in Eq. 17, was always taken to be the variable on which the terms were written implicitly. This effectively decoupled Eqs. 17 and 18, allowing them to be solved separately as sets of linear algebraic expressions to give the concentration profiles for phenol and tetrahydrofuran in the diffusion layer at a given time.

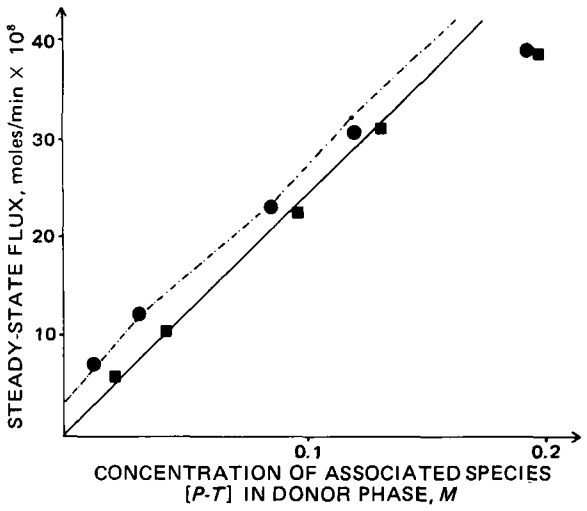

Figure 4—*Steady-state flux* versus *concentration of associated phenol in the donor phase for experiments in which 4.76% (v/v) tetrahydrofuran was used. Key: (■) the experimental data and (——) the computer-generated results. For experiments in which an approximate 2:1 ratio of tetrahydrofuran to phenol was used; (●) the experimental data and (- - -) joins computer-generated data points. Standard deviations for experimental data are incorporated into the size of the symbol.*

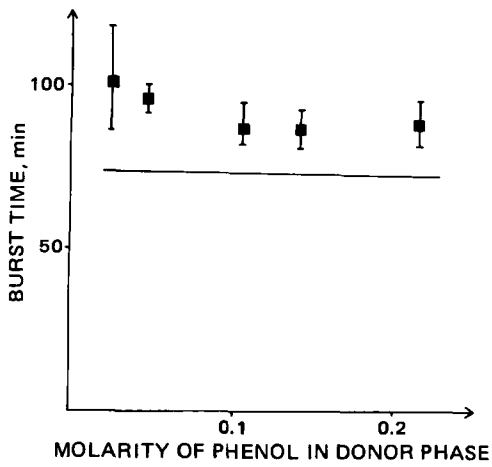

Figure 5—*Burst time* versus *concentration of phenol in the donor phase, for experiments in which 4.76% (v/v) tetrahydrofuran was used. Key: (——) computer-generated results; (■) average values observed; (⊥) ranges observed.*

It should be noted that the sets of linearized decoupled equations for Eqs. 17 and 18 can be solved iteratively for T_{n+1}^{j+1} and P_{n+1}^{j+1} such that the jth solution of the two sets of equations allows for the more accurate approximations of the nonlinear portions of the expressions. However, by choosing sufficiently small values of t, the assumed and calculated values of the derivatives differed only by a tolerably small amount after the first iteration, and therefore, iterative solutions were not required.

The coefficients of the set of linear equations for tetrahydrofuran were arranged in a matrix and solved by a method equivalent to Gaussian elimination using the subroutine TRIDAG (9) to give the current diffusion layer concentration profile of tetrahydrofuran. The same method was then applied to determine current concentrations of phenol in the diffusion layer.

From the gradients of phenol and tetrahydrofuran concentrations at the interface between the immobilized isooctane layer and the aqueous phase, the flux into the aqueous phase and subsequently the cumulative concentration in the aqueous phase was determined for each species at successive times. Since the concentrations in the aqueous phase remained consistently low, sink conditions were applied at the isooctane–aqueous phase interface for the purpose of calculating flux into the aqueous phase. This assumption may have introduced some error into the calculated steady-state flux predictions, especially at the higher donor phase concentration of phenol, and into the burst time calculations.

Typical computer-generated concentration profiles within the membrane at steady state are shown in Fig. 2 for donor phase concentrations of 0.1043 M phenol and 0.5872 M tetrahydrofuran. The gradient of the free tetrahydrofuran is linear due to the large excess of tetrahydrofuran present, but the profiles of both the associated and free phenol are nonlinear owing to the association equilibrium with tetrahydrofuran.

EXPERIMENTAL

Materials—Commercially obtained analytical reagent grade phenol[2] was fractionally distilled under vacuum to remove the preservative and other contaminants and then stored under nitrogen in a desiccator.

Tetrahydrofuran[3], containing 0.025% butylated hydroxytoluene as a preservative, was distilled from benzophenone and sodium under nitrogen, and then collected over activated 4-Å molecular sieves[4]. Batches were discarded 4 days after distillation.

Certified ACS isooctane (2,2,4-trimethylpentane)[3] was used without further purification.

Diffusion Apparatus and Study—The diffusion apparatus and the analytical procedure for phenol were described in a previous paper (6). The cutoff point for tetrahydrofuran in the UV region was 220 nm. It did not interfere with the assay of samples for phenol. Three different solution compositions were used at each concentration of phenol studied:

1. Fifty milliliters of the phenol in isooctane solution plus 2.5 ml of isooctane were used. Experiments in which solutions of this composition were used provided control data for comparison with diffusion data from experiments in which tetrahydrofuran was used.
2. Fifty milliliters of the phenol in isooctane solution, sufficient tetrahydrofuran to provide a ratio of ~ 2:1 tetrahydrofuran to phenol, and 2.5 ml (less the volume of tetrahydrofuran used) of isooctane were used.
3. Fifty milliliters of the phenol in isooctane solution plus 2.5 ml of tetrahydrofuran were used. The concentration of tetrahydrofuran present in these solutions was 0.5872 M (4.76% v/v).

The solutions required were prepared and added immediately to the tube containing the silanized sintered glass filter. Each solution was allowed to equilibrate with the filter for 3 min, enabling an immobilized layer of solution to be established within the filter. At the end of 3 min, the lower face of the filter was carefully wiped dry and the tube lowered into the jacketed beaker containing the aqueous phase, the temperature of which was maintained at 25°. When overhead and aqueous phase stirrers were turned on, the study was begun. Samples were taken from the aqueous phase at convenient times, replacing the volume removed with distilled, deoxygenated water. At the conclusion of the experiment the samples were analyzed for phenol. Further experimental details were presented in a previous study (6).

RESULTS AND DISCUSSION

Diffusion of phenol from the donor isooctane phase, through an immobilized layer of isooctane within the silanized sintered glass filter, into an aqueous receptor phase was followed by determination of the cumulative concentration of phenol in the aqueous phase at times ≤300 min. When tetrahydrofuran was used, it was present initially in both the donor phase solution and the diffusion layer. It was assumed that the association equilibrium between phenol and tetrahydrofuran was established in both the diffusion layer and the donor phase and that all species were capable of diffusing through the immobilized isooctane layer into the aqueous phase. For each type of experiment, four runs were made at each of the five phenol concentrations studied. Steady-state flux was calculated from the slope of the concentration *versus* time plot using vaues obtained at times of 100 min or longer. Runs were rejected if the linear regression correlation coefficient for the data used to calculate the slope fell below 0.999, to minimize variation in the steady-state flux and burst time values.

Steady-State Flux—When simultaneous association and diffusion occur, the rate of diffusion may increase, decrease, or remain the same. The change in the diffusion rate depends on the size of the associated species formed, its ability to penetrate or partition into the diffusion layer, and the extent to which complexation occurs.

Figure 3 shows a plot of steady-state flux *versus* concentration of free phenol (defined as activity) present in the donor phase. In the control experiments, there was a positive deviation from linearity at high phenol activities. This was accounted for by the contribution of the diffusion of

[2] Mallinckrodt.
[3] Fisher Scientific Co.
[4] Linde.

Table I—Concentrations of Various Species in Solution at Given Total Concentrations of Phenol and Tetrahydrofuran (Molar)

$[T_T]$	$[P_T]$	P	$5P_5$	$[P-T]$	$[T]$	$[T_T]:[P_T]$
0.5872	0.0233	0.0012	8.5×10^{-11}	0.0220	0.5651	-
0.5872	0.0461	0.0025	3.0×10^{-9}	0.0436	0.5435	-
0.5872	0.1034	0.0062	2.9×10^{-7}	0.0972	0.4900	-
0.5872	0.1403	0.0090	1.9×10^{-6}	0.1313	0.4559	-
0.5872	0.2130	0.0158	3.3×10^{-5}	0.1988	0.3900	-
0.0534	0.0233	0.0102	3.5×10^{-6}	0.0131	0.04026	2.29
0.1100	0.0461	0.0133	1.3×10^{-5}	0.0328	0.0772	2.39
0.2460	0.1034	0.0170	4.5×10^{-5}	0.0867	0.1493	2.39
0.3160	0.1403	0.0193	8.4×10^{-5}	0.1206	0.1954	2.25
0.4834	0.2130	0.0207	1.2×10^{-4}	0.1926	0.2908	2.27

the self-associated pentameric phenol to the overall rate of flux. In the presence of tetrahydrofuran, the steady-state flux at a given activity of phenol was greatly enhanced. The effect was more pronounced when 4.76% (v/v) tetrahydrofuran was present than when a 2:1 ratio of tetrahydrofuran to phenol was added. In both cases the increase in steady-state flux could be attributed to diffusion of the phenol–tetrahydrofuran-associated species. When 4.76% (v/v) tetrahydrofuran was used, the extent of association was greater owing to the larger excess of complexing agent present. This led to a greater enhancement of the steady-state flux values than observed for the 2:1 excess experiments, in which a significant proportion of phenol present remained unassociated.

In the 4.76% (v/v) tetrahydrofuran experiments, almost all of the phenol was expected to be associated with tetrahydrofuran (Table I). Therefore, the steady-state flux was expected to have an approximately linear relationship to the concentration of associated species present as shown in Fig. 4. Except at the highest concentration of phenol, the 4.76% (v/v) tetrahydrofuran data fall along a straight line within experimental error. This deviation at the higher donor phase phenol concentrations may arise from changes in the composition of the neighborhood of molecules surrounding each molecule. Since the theoretical development does not account for changes in the activity coefficient of the free phenol, a deviation of this nature is not surprising.

For a given concentration of associated phenol, a higher steady-state flux was predicted and observed when a 2:1 ratio of tetrahydrofuran to phenol was used than when 4.76% (v/v) tetrahydrofuran was present. This result was accounted for by the following model. In the 4.76% (v/v) tetrahydrofuran experiments virtually all flux was due to diffusion of the associated species. However, in the 2:1 ratio experiments, a significant proportion of phenol was present as free phenol. Since free phenol was able to diffuse across the immobilized isooctane layer at a faster rate than that of the larger associated species, it was able to contribute significantly to the overall flux into the aqueous phase. This resulted in a larger steady-state flux than would be predicted by considering only the contribution of the associated phenol. The differences in the steady-state flux data were most pronounced at low total concentrations of phenol. At those concentrations, the disparity in percentage of phenol present in unassociated form was also greatest (Table I), supporting the arguments derived from the model.

Overall, the steady-state flux results showed that for a system in which the associated species can penetrate the diffusion layer, the flux for a given total concentration of drug decreases as the concentration of complexing agent present increases. This is accounted for by the lower diffusivity of the larger associated species.

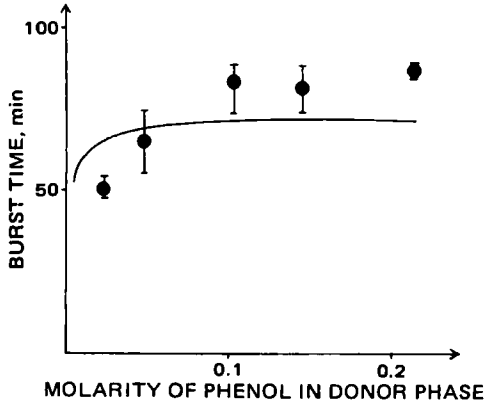

Figure 6—*Burst time* versus *concentration of phenol in the donor phase for experiments in which an approximate 2:1 ratio of tetrahydrofuran of phenol was used. Key: (——) computer-generated results; (●) experimentally observed results; (⊥) ranges.*

Transient Behavior (Burst Time)—As for the more commonly reported time lag, the burst time is inversely proportional to the diffusivity of the diffusing species. When diffusion of one species accounts for the entire flux observed, the burst time is related to the diffusivity of that species. In such cases, the burst time is independent of the donor phase concentration of the diffusing species.

Figure 5 shows the plot of burst time *versus* concentration of phenol in the donor phase in the presence of 4.76% (v/v) tetrahydrofuran. Burst time was calculated by extrapolating the steady-state portion of the concentration *versus* time plot back to zero concentration. Although there is considerable scatter in the results, the burst time was essentially independent of concentration, indicating that one species accounted for most of the mass transport observed. The excess of tetrahydrofuran was large enough in these experiments to ensure that virtually all phenol (93–98%) present was associated with tetrahydrofuran. It was proposed, therefore, that the diffusion of the associated species accounted for the greater fraction of the flux. The large value for the burst time observed in the 4.76% tetrahydrofuran experiments supported this proposal. Since large molecules have lower diffusivities, burst time tends to increase with molecular size. The average burst time observed in these experiments was ~90 min. This time was much greater than the burst time of ~35 min which was calculated for a diffusion system in which only monomer phenol was present (6).

Figure 6 depicts the burst time *versus* the donor phase concentration data for experiments in which a 2:1 ratio of tetrahydrofuran to phenol was used. The theory predicted that the burst time would be shorter at low donor phase phenol concentrations, since in those cases the percentage of phenol in the associated form was considerably lower than at high phenol concentrations (Table I). The smaller free phenol molecules were able to diffuse faster than the associated species so that when free phenol was present in significant quantities, the system came to steady state more rapidly and exhibited a shorter burst time. The observed burst times were similar to the predicted relationship. However, the effects were magnified somewhat.

The failure of the numerical solution of the derived equations to predict exactly the overall burst time was probably due partly to the boundary condition used for the aqueous phase–diffusion layer interface in the computer program (*i.e.*, sink conditions) and partly to an artifact of the experimental method. As in the phenol experiments described previously (7), small amounts of phenol on the lower face of the sintered glass filter may have been released immediately upon contact with the aqueous phase. This would result in high values for cumulative concentration in the aqueous phase and higher burst times than predicted. Build-up of tetrahydrofuran in the aqueous phase may also have affected partitioning of phenol between the diffusion layer and the aqueous phase, which would again alter the concentration of phenol attained in the aqueous phase.

Despite the great reduction in activity of phenol caused by the addition of a complexing agent, the overall transport rate of phenol for a given total concentration of phenol was almost as fast as in a complexing agent-free system. This consistency in transport rates was attributed to the ability of the associated tetrahydrofuran–phenol complex to form in and diffuse through the diffusion layer. A set of equations derived in terms of readily obtainable parameters were found to adequately account for all the data except that obtained at high concentration of phenol. Thus, it was possible to explain the seemingly complicated relationship between steady-state flux diffusional behavior and donor-phase concentration of phenol in the presence of a codiffusing species using the familiar concept of associative interactions.

In the system studied, all species formed were capable of penetrating the diffusion layer. Comparing the results of the 4.76% (v/v) tetrahydrofuran and the twofold excess tetrahydrofuran experiments, it appears

that the excessive use of an excipient capable of complexing with a drug could result in a markedly reduced rate of delivery of that drug by simultaneously lowering the drug's activity and apparent diffusivity. Although such an effect is undesirable in most circumstances, it may be possible to use this effect to advantage in the design of slow-release preparations.

REFERENCES

(1) T. Higuchi and M. Ikeda, *J. Pharm. Sci.*, **63**, 809 (1974).

(2) B. Kreilgaard, T. Higuchi, and A. J. Repta, *ibid.*, **64**, 1850 (1975).

(3) J. W. McGinity and J. L. Lach, *ibid.*, **66**, 63 (1977).

(4) W. L. Hayton, D. E. Guttman, and G. Levy, *ibid.*, **59**, 575 (1970).

(5) M. Donbrow and E. Touitou, *ibid.*, **67**, 95 (1978).

(6) J. B. Dressman, K. J. Himmelstein, and T. Higuchi, *ibid.*, **71**, 1226 (1982).

(7) V. S. Vaidhyanathan, *ibid.*, **61**, 894 (1972).

(8) B. D. Anderson, J. H. Rytting, and T. Higuchi, *J. Am. Chem. Soc.*, **101**, 5194 (1979).

(9) B. Carnahan, H. A. Luther, and J. O. Wilkes, "Applied Numerical Methods," Wiley, New York, N.Y., 1969, pp. 440–442, 464.

ACKNOWLEDGMENTS

This work was supported by Grant GM-22357 from the National Institutes of Health.

Zero-Order Controlled-Release Polymer Matrices for Micro- and Macromolecules

DEAN S. T. HSIEH *, WILLIAM D. RHINE, and ROBERT LANGER ˣ

Received May 20, 1981, from the *Department of Nutrition and Food Science, Massachusetts Institute of Technology, Cambridge, MA 02139,* the *Department of Surgery, Children's Hospital Medical Center, Boston, MA 02115,* and the *Harvard Medical School, Boston, MA 02115.* Accepted for publication February 26, 1982. *Present address: Department of Pharmaceutics, Rutgers University, Piscataway, N.J.

Abstract □ Theoretical and experimental analyses demonstrate that a hemispheric polymer–drug matrix laminated with an impermeable coating, except for an exposed cavity in the center face, can be used to achieve zero-order release kinetics. Hemispheric systems for low molecular weight drugs were prepared by heating and compressing polyethylene and drug (sodium salicylate) in a brass mold. Hemispheric systems for high molecular weight drugs were prepared by casting ethylene–vinyl acetate copolymer and protein in a hemispheric mold at −80°, followed by a two-step drying procedure (−20 and 20°). In both systems, cavities were made in the center face of the hemispheres and the remainder of the matrices coated with an impermeable material. Zero-order release for 60 days at a rate of 0.5 mg/day was achieved from polymer matrices containing bovine serum albumin (mol. wt. 68,000).

Keyphrases □ Drug delivery system—zero-order controlled-release polymer matrices, micro- and macromolecules □ Controlled-release delivery—zero-order, polymer matrices, micro- and macromolecules □ Polymers—matrices, zero-order controlled-release, micro- and macromolecules □ Sustained-release delivery—zero-order controlled-release polymer matrices, micro- and macromolecules

Diffusion-controlled matrix devices have been among the most widely used drug delivery systems, but a disadvantage frequently cited is their inability to achieve zero-order release kinetics (1–3). Most matrix devices have been designed in the form of a rectangular slab, and it has been observed that the cumulative release of drug is inversely proportional to the square root of time (4–8).

One possible means of altering release kinetics from matrix systems is to vary the matrix geometry. The influence of shape on kinetics of drug release from matrix tablets in spherical, cylindrical, and biconvex shapes has been evaluated (9, 10). It was predicted (11) that a matrix in the shape of a sector of a right circular cylinder would release drug at a zero-order rate. This analysis was more critically evaluated, and it was found that true zero-order kinetics were not achieved in practical cases but that this shape resulted in release rates that were initially high and then began to approach, but not achieve, linearity (12). A limitation cited in both studies was the need for effective procedures to fabricate these delivery systems and the requirement for further experimental testing.

In a previous study, a theoretical analysis suggested that a hemisphere with all portions laminated with an impermeable coating, except for a small cavity cut into the center of the flat surface, could achieve zero-order release kinetics (13).

In the present study, experimental results have been obtained that provide support for the theoretical analysis. Two types of fabrication procedures are presented here to demonstrate that the hemisphere design is universally suitable for either low or high molecular weight drugs.

THEORETICAL

Assuming that the drug is released from a solid matrix device by diffusion, a steady-state condition exists, and the area for mass transport,

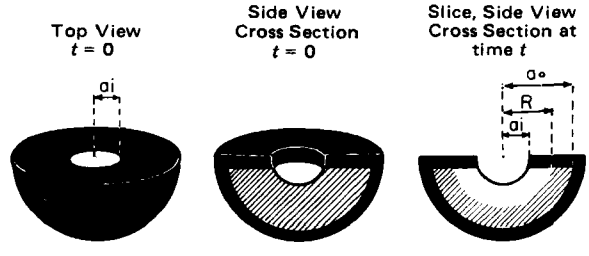

Figure 1—*Diagram of an inwardly-releasing hemisphere;* a_i *is the inner radius,* a_o *is the outer radius, and* R *is the distance to the interface between the dissolved region (white area) and the dispersed zone (diagonal lines). Black represents laminated regions through which release cannot occur.*

that the excessive use of an excipient capable of complexing with a drug could result in a markedly reduced rate of delivery of that drug by simultaneously lowering the drug's activity and apparent diffusivity. Although such an effect is undesirable in most circumstances, it may be possible to use this effect to advantage in the design of slow-release preparations.

REFERENCES

(1) T. Higuchi and M. Ikeda, *J. Pharm. Sci.*, **63**, 809 (1974).

(2) B. Kreilgaard, T. Higuchi, and A. J. Repta, *ibid.*, **64**, 1850 (1975).

(3) J. W. McGinity and J. L. Lach, *ibid.*, **66**, 63 (1977).

(4) W. L. Hayton, D. E. Guttman, and G. Levy, *ibid.*, **59**, 575 (1970).

(5) M. Donbrow and E. Touitou, *ibid.*, **67**, 95 (1978).

(6) J. B. Dressman, K. J. Himmelstein, and T. Higuchi, *ibid.*, **71**, 1226 (1982).

(7) V. S. Vaidhyanathan, *ibid.*, **61**, 894 (1972).

(8) B. D. Anderson, J. H. Rytting, and T. Higuchi, *J. Am. Chem. Soc.*, **101**, 5194 (1979).

(9) B. Carnahan, H. A. Luther, and J. O. Wilkes, "Applied Numerical Methods," Wiley, New York, N.Y., 1969, pp. 440–442, 464.

ACKNOWLEDGMENTS

This work was supported by Grant GM-22357 from the National Institutes of Health.

Zero-Order Controlled-Release Polymer Matrices for Micro- and Macromolecules

DEAN S. T. HSIEH *, WILLIAM D. RHINE, and ROBERT LANGER ˣ

Received May 20, 1981, from the *Department of Nutrition and Food Science, Massachusetts Institute of Technology, Cambridge, MA 02139,* the *Department of Surgery, Children's Hospital Medical Center, Boston, MA 02115,* and the *Harvard Medical School, Boston, MA 02115.* Accepted for publication February 26, 1982. *Present address: Department of Pharmaceutics, Rutgers University, Piscataway, N.J.

Abstract □ Theoretical and experimental analyses demonstrate that a hemispheric polymer–drug matrix laminated with an impermeable coating, except for an exposed cavity in the center face, can be used to achieve zero-order release kinetics. Hemispheric systems for low molecular weight drugs were prepared by heating and compressing polyethylene and drug (sodium salicylate) in a brass mold. Hemispheric systems for high molecular weight drugs were prepared by casting ethylene–vinyl acetate copolymer and protein in a hemispheric mold at −80°, followed by a two-step drying procedure (−20 and 20°). In both systems, cavities were made in the center face of the hemispheres and the remainder of the matrices coated with an impermeable material. Zero-order release for 60 days at a rate of 0.5 mg/day was achieved from polymer matrices containing bovine serum albumin (mol. wt. 68,000).

Keyphrases □ Drug delivery system—zero-order controlled-release polymer matrices, micro- and macromolecules □ Controlled-release delivery—zero-order, polymer matrices, micro- and macromolecules □ Polymers—matrices, zero-order controlled-release, micro- and macromolecules □ Sustained-release delivery—zero-order controlled-release polymer matrices, micro- and macromolecules

Diffusion-controlled matrix devices have been among the most widely used drug delivery systems, but a disadvantage frequently cited is their inability to achieve zero-order release kinetics (1–3). Most matrix devices have been designed in the form of a rectangular slab, and it has been observed that the cumulative release of drug is inversely proportional to the square root of time (4–8).

One possible means of altering release kinetics from matrix systems is to vary the matrix geometry. The influence of shape on kinetics of drug release from matrix tablets in spherical, cylindrical, and biconvex shapes has been evaluated (9, 10). It was predicted (11) that a matrix in the shape of a sector of a right circular cylinder would release drug at a zero-order rate. This analysis was more critically evaluated, and it was found that true zero-order kinetics were not achieved in practical cases but that this shape resulted in release rates that were initially high and then began to approach, but not achieve, linearity (12). A limitation cited in both studies was the need for effective procedures to fabricate these delivery systems and the requirement for further experimental testing.

In a previous study, a theoretical analysis suggested that a hemisphere with all portions laminated with an impermeable coating, except for a small cavity cut into the center of the flat surface, could achieve zero-order release kinetics (13).

In the present study, experimental results have been obtained that provide support for the theoretical analysis. Two types of fabrication procedures are presented here to demonstrate that the hemisphere design is universally suitable for either low or high molecular weight drugs.

THEORETICAL

Assuming that the drug is released from a solid matrix device by diffusion, a steady-state condition exists, and the area for mass transport,

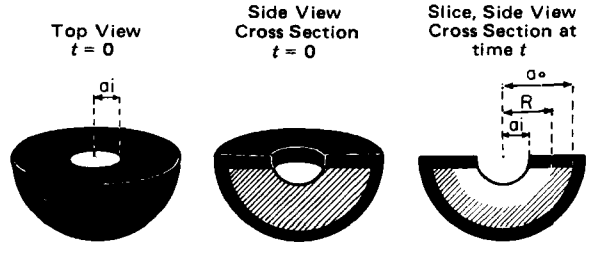

Figure 1—*Diagram of an inwardly-releasing hemisphere;* a_i *is the inner radius,* a_o *is the outer radius, and* R *is the distance to the interface between the dissolved region (white area) and the dispersed zone (diagonal lines). Black represents laminated regions through which release cannot occur.*

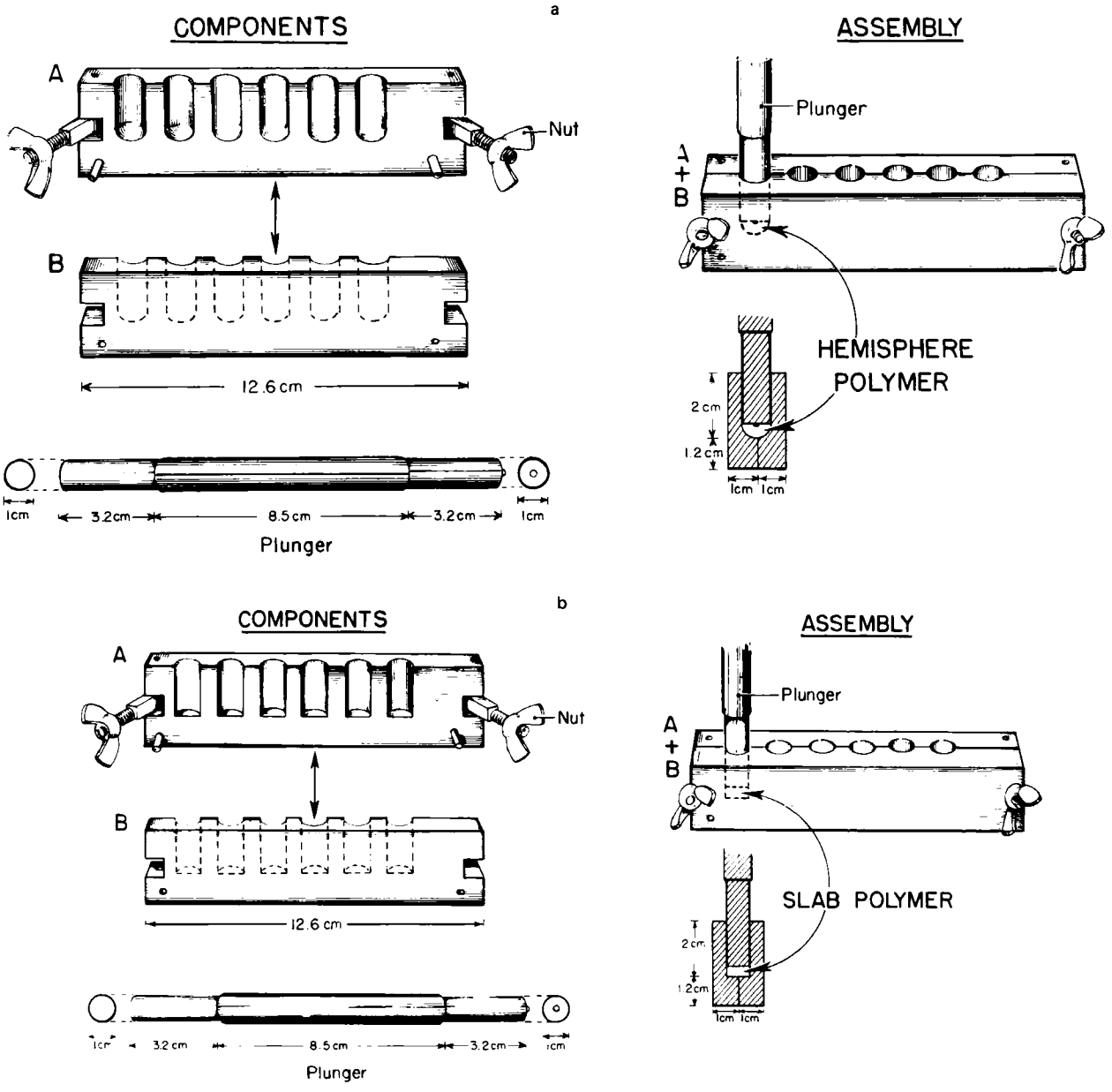

Figure 2—*Diagram of brass molds and plungers for making hemispheres and slabs containing low molecular weight drugs. (a) The brass mold (12.6 × 3.2 × 2 cm) had two halves (components A and B) fastened together with wing nuts (assembly). The mold had six hollowed cylinders (1-cm diameter and 11.4-cm length) with hemispheric bottoms (1-cm diameter). The brass plunger (1-cm diameter × 14.9-cm length) had two ends: one end was flat and the other end was press-fitted with a 2-mm (diameter) steel bead in the center in such a way that one-half of the bead was exposed and the other half was buried within the plunger. The plunger end containing the bead was used for making hemispheres. (b) The brass mold, with the same dimensions as those shown in Fig. 2a, had six hollowed cylinders with flat bottoms. The same plunger in Fig. 2a was used; however, this time the flat end was used for slabs.*

A, and drug diffusion coefficient, D, remain constant, then Fick's law of diffusion can be applied and is represented by:

$$\frac{dQ}{dt} = -DA\frac{dc}{dr} \qquad \text{(Eq. 1)}$$

where Q is the mass of drug being transferred, t is the time, c is the drug concentration, and r is the distance from the diffusion source to the release surface. From Eq. 1 it can be seen that the release rate decreases as the distance r increases; that is, the release rate is inversely proportional to the distance which the drug must travel from within the matrix to the matrix surface. The purpose of altering matrix geometry is to increase the available area of drug so as to compensate for the increase in diffusion distance of drug transport.

In a previous study (13), a theoretical analysis was conducted to derive release equations for a hemispheric device in which release only occurs through a cavity in the flat surface; all other surfaces would be laminated with an impermeable coating (Fig. 1). In the theoretical analysis (13), it was assumed as in a previous study (4) that the amount of drug present per unit volume, C_0, is substantially greater than the solubility of drug per unit volume of the vehicle, C_s. It was further assumed, as previously (4), that the solid drug dissolves from the surface layer of the device first; when this layer is depleted of drug, the next layer begins to be depleted. The interface between the region containing dissolved drug and dispersed drug moves into the interior as a front. Infinite sink conditions, no boundary layer effects, as well as other assumptions originally made (4) were considered applicable. The following notation is used:

a_i = inner radius or radius of the cavity
a_o = outer radius of device
R = radial distance to interface between dissolved and dispersed drug within the matrix (Fig. 1)
C_s = drug solubility in the release media [this also equals the concentration of drug at the interface between dissolved and dispersed drug (4)]
$Q(t)$ = drug released (wt) from the pellet at time t
D = diffusion coefficient of drug in matrix

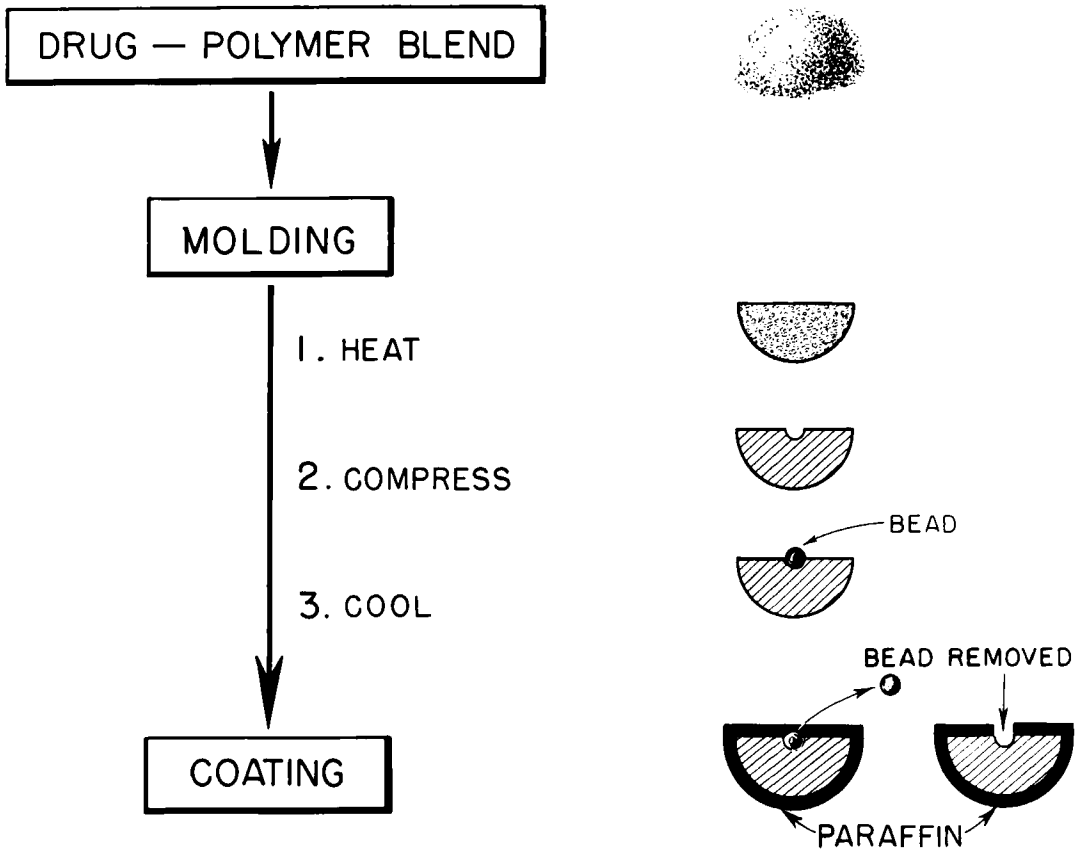

Figure 3—*Flow chart for preparing hemisphere-shaped devices for the release of small molecules. (Detailed procedures were recorded in the text.)*

Then, the release rate for the hemisphere can be derived as described previously (13) resulting in:

$$\frac{dQ}{dt} = 2\P C_s D a_i \left(\frac{R}{R - a_i}\right) \qquad \text{(Eq. 2)}$$

The approach to zero-order kinetics can be observed by examination of Eq. 2. In this equation, when $R \gg a_i$, $R - a_i$ becomes equal to R and:

$$\frac{dQ}{dt} = 2\P D C_s a_i \qquad \text{(Eq. 3)}$$

Each of the terms in Eq. 3 is a constant. Thus, for a hemispheric device with small a_i, release rates will be essentially constant. It can be calculated that for hemispheric devices designed so that the outer radius (a_o) is at least three times greater than the inner radius (a_i) zero-order kinetics will be achieved after a short burst and maintained for the duration of release (13).

Release rate expressions have been derived for several different shaped devices (13). In comparing such devices, the following statement provides a useful guideline: The hemisphere will more closely approximate zero-order release than other shapes (*e.g.*, a cylinder sector), if the inner radii (a_i) of both shapes are similar; if, however, the inner radius of the other device is much smaller than that of the hemisphere, the second device will more closely approximate zero-order release.

EXPERIMENTAL

To experimentally test the zero-order release concept for hemispheres, a polyethylene–sodium salicylate matrix was used. This matrix has been shown to follow the Higuchi model (6). For reference, release kinetics from a slab (in the present report any shape that has cross sections which were identical throughout the matrix was considered a slab) were also studied. In these studies a drug–polymer blend was molded into the different shapes; however, both the hemisphere and the slab were designed with dimensions such that similar apparatuses could be used and so that each would release approximately the same quantity of drug after the same time period.

Materials Used for Matrices Containing Low Molecular Weight Compounds—Sodium salicylate[1] and polyethylene[2] were passed through a 60-mesh screen[3] separately. These ingredients (30% sodium salicylate and 70% polyethylene) were then mixed together in a cube blender[4] for 5 min. The brass[5] mold[6] (Fig. 2) had two halves fastened together with wing nuts. The molds had six hollow cylinders (1-cm diameter, 11.4-cm long) that were either round-bottomed (with a 0.5-cm radius) for making hemispheres (Fig. 2a) or flat-bottomed for making slabs (Fig. 2b).

Hemisphere-Shaped Systems for Low Molecular Weight Compounds—A summary of the steps involved in the fabrication procedure for making hemispheres is shown in Fig. 3 and described in detail as follows. In the first step, each hollow cylinder mold (Fig. 2a) was loaded with 220 mg of a sodium salicylate–polyethylene blend and placed into a preheated oven[7] at 150° for 30 min. After heating, a brass plunger[6] (1-cm diameter) was forcefully inserted into each cylinder. Compression was complete within 30 sec. This plunger was flat-bottomed except for a central depression into which a 2-mm (diameter) steel bead[8] was press-fitted (press-fitting involves molding one metal object to another so that they are permanently attached) in such a way that half of the bead was exposed and the other half was buried within the plunger (Fig. 2a). By using this type of plunger to compress the polymer–drug matrix, a small cavity in the face of the hemisphere was formed. After compression the plunger was immediately removed. The mold containing hemispheric pellets was cooled at room temperature for 20 min. Then, the mold was disassembled. The hemispheric polymer–drug pellets were removed from the mold and trimmed with a scalpel[9] containing a surgical blade[10] to eliminate any irregular edges. The average weight of the hemisphere after trimming was 208 ± 3 mg.

[1] Fisher Scientific Co., Fair Lawn, N.J.
[2] PEP-315, Union Carbide Co., New York, N.Y.
[3] Dual Mfg. Co., Chicago, Ill.
[4] Type UG No. 16643, Erweka-G.M.B.H., Frankfurt am Main, West Germany.
[5] Admiral Metals Servicenter Co., Inc., Woburn, Mass.
[6] Mold and plunger made in machine shop of the Department of Nutrition and Food Science, M.I.T., Cambridge, Mass.
[7] Model 10, Precision Scientific Co., Bedford, Mass.
[8] Type 440C, Ultraspherics Co., Inc., Ann Arbor, Mich.
[9] Healthco, Inc., Medical Supply Division, Boston, Mass.
[10] No. 10 blade, Bard-Parker, Rutherford, N.J.

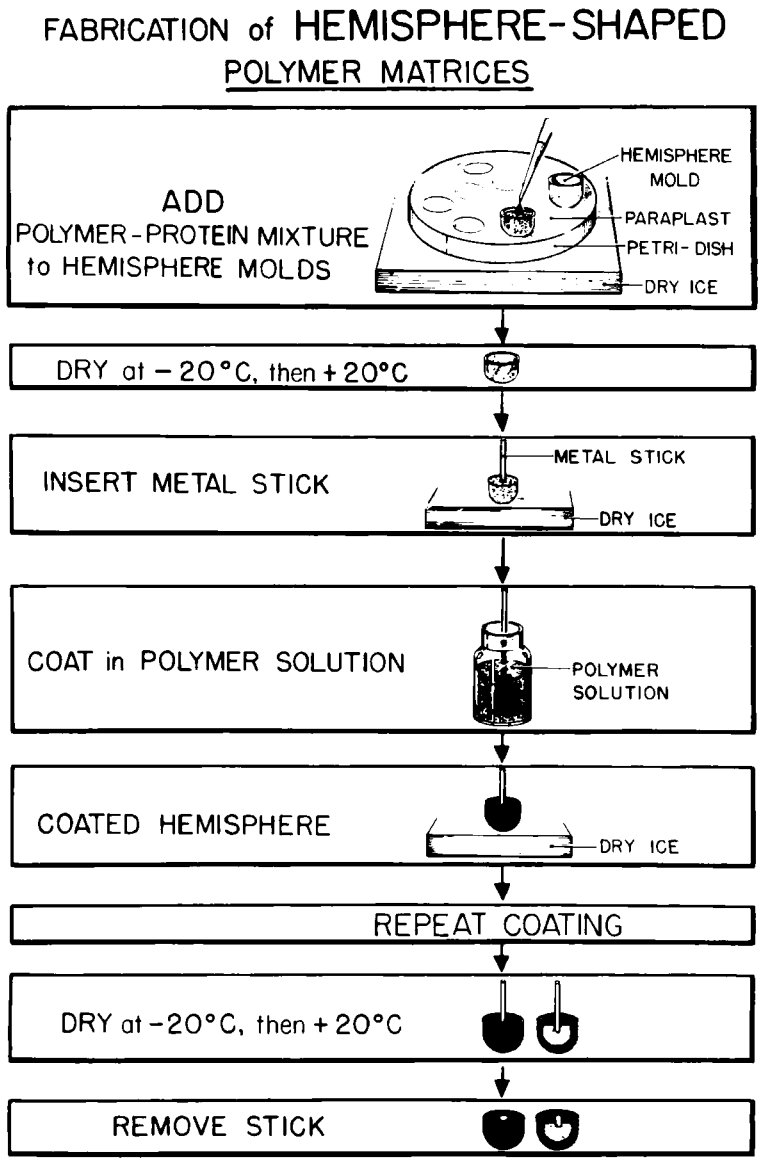

Figure 4—*Flow sheet for preparing hemisphere-shaped devices for the release of macromolecules. (Detailed procedures were recorded in the text.) In the last two blocks of the flow sheet, both the top view and a cross-sectional view of the same hemisphere device are shown.*

To protect the cavity within the hemisphere pellet during coating, a steel bead[8], 2 mm in diameter, was inserted (Fig. 3) into it with forceps[11]. The flat face of the hemisphere pellet containing the steel bead was then placed face down against a lid of a petri dish[12]. A total of nine pellets was placed in each dish. To coat the matrix, paraffin[13] was first melted in a glass beaker on a hot plate[14] until the temperature[15] of the paraffin was 50 ± 2°. Approximately 15 ml of melted paraffin was pipeted[16] onto the petri dish surrounding the pellets. This resulted in a block of paraffin[13] containing nine pellets. This block was removed with a laboratory spatula[11] and cut into nine pieces with a scalpel blade; each piece thus contained one hemisphere pellet. A drop of the melted paraffin was then layered over the flat surface of each of the hemisphere pellets, causing the pellets to be completely coated.

The final step in achieving the hemispheric design (Fig. 1) was to expose the cavity, yet leave the remainder of the pellet coated. This was accomplished by gently scraping off the paraffin covering the steel bead and removing the bead with a pair of forceps[11].

Slab Systems for Low Molecular Weight Compounds—The procedures to fabricate slabs followed methods similar to those described above. A sodium salicylate–polyethylene blend (800 mg) was loaded in the flat-bottomed brass mold[6], followed by heating in the oven and compressing with the flattened part of the plunger[6] (Fig. 2b). After compression, the resultant cylinder was cut lengthwise into two halves and trimmed to lengths of 7.4 ± 0.2 mm. The average weight was 210 ± 5 mg. The resultant pellet was placed with one of its flat faces down on the surface of a petri dish[12] and coated with melted paraffin. About 15 ml of the melted paraffin was poured over 10 pellets. The resultant slabs thus were coated on all sides except the flat faces. Each face had an exposed area of ~56 mm^2.

Hemisphere-Shaped Systems for Macromolecules—The molds used for fabricating hemisphere-shaped systems for macromolecules were composed of glass and had hemispheric bottoms[17] (13-mm diameter × 11-mm height). To prevent these molds from falling over, an embedding platform was made. This platform was constructed by pouring 15 ml of molten paraffin[13] into a bacterial petri dish[12], and then placing empty glass molds[17] into the paraffin so that they touched the bottom. After allowing the paraffin to harden, the molds were removed and the indentations left behind in the paraffin could be used to subsequently support the molds.

[11] Forceps and spatula were purchased from Healthco Inc., Medical Supply Division, Boston, Mass.
[12] Falcon 3003, Div. Becton, Dickinson and Co., Ornard, Calif.
[13] Paraplast tissue embedding medium, Lancer Co., St. Louis, Mo.
[14] PC-351, set at LO position, Corning Glass Works, Corning, N.Y.
[15] The thermometer was purchased from Fisher Scientific Co., Fair Lawn, N.J.
[16] Pasteur capillary pipets—disposable, Cat. No. 3575, Rochester Scientific Co., Rochester, N.Y.
[17] Glass molds were made using the bottoms of test tubes. These were cut in the Glass Shop, Surgical Research, Children's Hospital Medical Center, Boston, Mass.

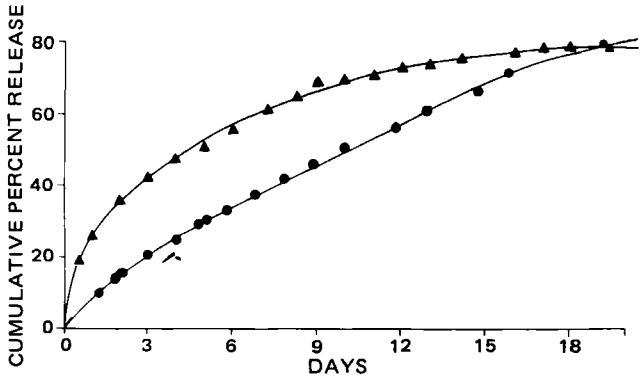

Figure 5—*Cumulative release of sodium salicylate* versus *time for the geometric shapes made as described in the text. Key: (●) hemisphere, (▲) slabs. Each point represents the mean of 10 samples for slabs and nine samples for hemispheres.* SEM *was 2% for slabs and 4% for hemispheres.*

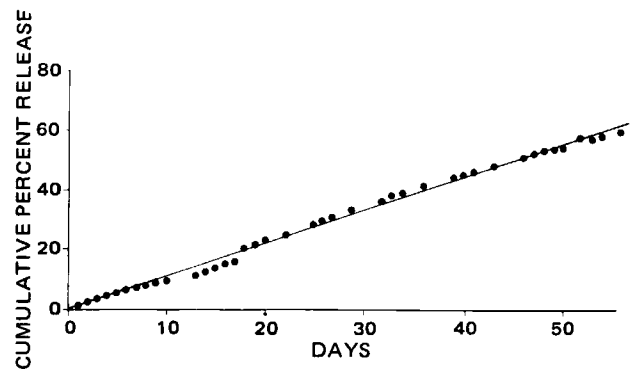

Figure 6—*Cumulative release of bovine serum albumin* versus *time. The matrix was made of ethylene–vinyl acetate copolymer and bovine serum albumin. Standard error of the mean of the cumulative release at each time point was within 12%.*

To make the hemisphere polymer systems, earlier methods of preparing polymer–macromolecule slabs (8) were adapted. The procedure is illustrated in Fig. 4 and described in detail as follows. First, empty glass molds were positioned in the indentations in the paraffin-embedding platform. Then, 6 ml of 20% ethylene–vinyl acetate copolymer[18] solution in methylene chloride[19] and 514 mg of bovine serum albumin[20] powder [particle size range (8) from 150 to 180 μm] were mixed in a glass vial at room temperature and vortexed[21] for 1 min to yield a uniform suspension. Into each hemispheric glass mold[17], 0.8 ml of the protein–polymer dispersion was pipeted[22]. The petri dish containing these samples was then transferred onto a block of dry ice for 10 min. The samples gelled within 1 min. The petri dish containing the samples was then dried first at −20° for 2 days and then at 20° for another 2 days as reported previously (8).

The hemisphere pellets were coated twice with 20% ethylene–vinyl acetate copolymer solution (containing no macromolecules) to form an impermeable barrier. The coating procedure is described as follows: (*a*) The tip of a cylindrical metal stick[23] (1.8-mm diameter × 30-mm length) was inserted into the center of the flat surface of each hemisphere pellet to a depth of ~3 mm. (*b*) Using the uninserted portion of the stick as a handle, the hemisphere pellets were placed directly on the surface of a block of dry ice for 10 min. (The round bottoms of the pellets were touching the dry ice.) (*c*) Again using the metal stick as a handle, the cooled hemisphere then was immersed into 20% ethylene–vinyl acetate copolymer solution at 20° for 10 sec, removed, and then placed immediately on the same dry ice for 10 min. (*d*) A second layer of coating was done in the same manner as described above. (*e*) The hemispheres were then put in the freezer[24] (−20°) for 2 days followed by further drying at 20° for 2 days in a desiccator[25] under a houseline vacuum (600 mtorr) to remove residual solvent (8). (*f*) Finally, to create the exposed cavity in the face of the hemisphere pellet, the metal stick[23] was removed by gently encircling the polymer surface immediately surrounding the stick with a scalpel blade.

Kinetic Studies—Studies were conducted to measure the release of salicylate into saline from polymer matrices. For these studies, each matrix was immersed in a scintillation vial[26] containing 10 ml of saline solution (0.154 *M* NaCl[27]). Each matrix was weighted down with five 9-mm stainless steel standard wound clips[28] stuck onto the wax coating. Any bubbles present on the uncoated, releasing surface were removed by aspiration with a pasteur pipet. The vials were placed on a shaker[29] at 20°. (Preliminary experiments have shown no significant difference between the release rates obtained with this mild shaking and those obtained using vigorous stirring.) At each time point, the matrices were transferred using a pair of forceps into 10-ml fresh saline-containing vials. During these transfers, excess solution on the matrix surface was removed by gentle blotting on a tissue. The released sodium salicylate concentration was determined spectrophotometrically[30] by measuring absorbance at 294 nm.

As controls, hemispheres of pure polyethylene were prepared uncoated and completely coated (including the cavity). Similarly, uncoated and completely coated hemispheres with the 30% salicylate–polyethylene blend were prepared. Identical controls were conducted for the ethylene–vinyl acetate copolymer system. All of these controls were tested for release kinetics.

The kinetics of albumin release from the hemisphere-shaped systems were followed by methods described previously (8). Albumin concentrations were measured spectrophotometrically[30] by determining absorbance at 280 or 220 nm (8).

RESULTS

The cumulative percentage release of sodium salicylate *versus* time from polyethylene matrices of these hemispheres and slabs is compared in Fig. 5. The hemisphere-shaped device closely approximates zero-order release. Standard error of the mean of cumulative release at each time point was within 2% for slabs and 4% for hemispheric devices.

Control matrices of coated and uncoated pure polyethylene hemispheres, as well as the completely coated sodium salicylate–polyethylene hemispheres, showed no material exhibiting spectrophotometric absorbance in the saline solution. The uncoated hemisphere-shaped device containing sodium salicylate prepared in the same manner as those used in the above study showed a rapid, nonlinear release and was nearly exhausted of its drug within 3 days.

To determine if the hemispheric design was applicable to macromolecules such as proteins as well as low molecular weight drugs, ethylene–vinyl acetate copolymer matrices containing bovine serum albumin were tested. Figure 6 shows the release kinetics of albumin from the hemisphere-shaped systems. Each point represented eight samples. A linear relationship between cumulative percentage release and the time of release was observed for 60 days. The release rate was ~0.5 mg of albumin/day. Standard error of the mean of cumulative release at each time point was within 12%. Control hemisphere-shaped devices completely coated twice with 20% ethylene–vinyl acetate copolymer solution did not release any protein. The media collected in the release experiments of the control hemisphere-shaped devices prepared from pure ethylene–vinyl acetate copolymer solution (without albumin) showed no spectrophotometric absorbance.

DISCUSSION

These studies demonstrate that hemispheric matrices can act as constant release systems for both low molecular weight drugs (Fig. 5) and high molecular weight compounds (Fig. 6). The fabrication procedures for these systems are relatively simple and can be performed without expensive apparatus. To fabricate the hemisphere-shaped devices, two different methods were employed: the fusion of polyethylene and drug

[18] Ethylene–vinyl acetate copolymer beads (Elvax 40, 40% vinyl acetate content w/w) manufactured by DuPont Chemical Co., Wilmington, Del., and extracted with hot water if the beads were clay coated.
[19] HPLC grade, Fisher Scientific Co., Fair Lawn, N.J.
[20] Sigma Chemical Co., St. Louis, Mo.
[21] Vortex-Genie, Fisher Scientific Co., Fair Lawn, N.J.
[22] Pipetman, Gilson Co., France.
[23] Becton, Dickinson and Co., Ornard, Calif.
[24] SciChem. Co., Howe & French Division, Boston, Mass.
[25] Bel-Art Co., Peguannock, N.J.
[26] No. 986548, Wheaton Scientific Co., Millville, N.J.
[27] USP grade, Mallinckrodt, St. Louis, Mo.
[28] No. 7032, Clay Adams, Paisippang, N.J.
[29] Clinical Rotating Apparatus, set at speed 4, Arthur H. Thomas Co., Philadelphia, Pa.
[30] Model 2400-S, Gilford Instrument Laboratories, Oberlin, Ohio.

by heating (14), and the gelation of ethylene–vinyl acetate copolymer by freezing at −80° (8). The selection of the fabrication procedure depended on the nature of the drugs. For example, the gelation of polymer at low temperature is more suitable for proteins or peptides because they may be denatured at high temperature.

It should be noted that reservoir systems, in which a core of drug is surrounded by a membrane, can also be used as a zero-order release system. In these systems, if the drug is loaded above its solubility, the drug concentration at the inside of the membrane wall will be a constant (*i.e.*, the drug solubility); furthermore, the drug will always traverse the same diffusion distance (*i.e.*, the membrane thickness). Thus, the release rate will be constant. However, such systems have disadvantages such as expense, undesirable release properties for large molecular weight drugs, and danger in the case of leaks (1–3). The reservoir system principle also was applied to polymer matrices (15), where the rectangular matrices of polymer–drug were coated with pure polymer. Under appropriate conditions, the rate-limiting step for release was diffusion through the pure polymer coating rather than through the polymer–drug matrix, and constant release was observed. To ensure that the constant release rates observed for the experimental devices in this report were not due to a similar effect (caused perhaps by drug sedimentation towards the center of the matrix during fabrication leaving a film of pure polymer at the surface), a microscopic examination of the drug–polyethylene hemisphere was conducted. In this case, a colored compound, bromcresol green[1], was incorporated into the matrix, due to its ease of optical examination under a light microscope. The matrix was sectioned using a scalpel blade. The examination of the sections confirmed the assumption that the drug particles were evenly distributed in the polyethylene matrix. A similar microscopic examination was conducted for the ethylene–vinyl acetate copolymer–protein system using previously described methods (16). These matrices also showed a uniform drug distribution. Both tests ruled out the possibility that these matrices could act in any way as a reservoir type device.

In *Theoretical*, it was assumed that no boundary layer effects were present and that infinite sink conditions prevailed. In practice there may be significant drug concentration gradients between the matrix release surface and the surrounding media. However, the resultant bulk flow has been shown to bring the release kinetics even closer to zero order (12).

In matrix systems, the factors controlling release rates can be classified into two groups: the matrix parameters such as porosity and tortuosity and the properties of drugs such as solubility and diffusion coefficient. The former are closely related to the loadings and drug particle sizes; the latter are the inherent properties of the incorporated drugs and polymers. Higuchi (4, 5) was the first to design a mathematical model to predict the release kinetics for low molecular weight drugs from a matrix system; the theoretical predictions were proven (6) by measuring the porosity and tortuosity of the matrix from a model system consisting of polyethylene and sodium salicylate. It was also found that the porosity and tortuosity of the matrix were affected by the loading and particle size of the incorporated drugs (6). In a hemisphere-shaped matrix system, it is conceivable that release rates can be varied by a similar manipulation of these fabrication parameters. Additionally, the size of the opening is another governing factor. In situations where Eq. 3 applies, it can be seen that the release rate is directly proportional to the radius of the cavity, a_i.

The release rate of macromolecules or proteins, such as bovine serum albumin, from ethylene–vinyl acetate copolymer matrix slabs can be varied by as much as 2000-fold by manipulating three fabrication parameters, (*i.e.*, drug loadings, aggregate sizes, and matrix coating) (8). The release rate of macromolecules from a hemisphere-shaped device conceivably can be changed by manipulating the same fabrication parameters and the size of the opening. Although the hemisphere design resulted in zero-order release kinetics for macromolecules such as albumin, the release mechanism for these systems has not yet been fully established. However, evidence continues to indicate that the release of macromolecules from polymeric matrices occurs *via* diffusion through interconnecting pores (16). The present study is consistent with such a mechanism. However, a mathematical model that can be used to predict release kinetics from macromolecular release systems has not yet been developed.

Although only bovine serum albumin was used as a model macromolecule in the present study, initial results have also indicated that zero-order release rates were obtained for over 1 month for lysozyme and β-lactoglobulin when they were incorporated into hemispheric matrices. The hemisphere systems have not yet been tested *in vivo*. However, initial studies have demonstrated good correlation between *in vivo* and *in vitro* release rates of macromolecules from ethylene–vinyl acetate copolymer slabs (17).

The major problems encountered in the fabrication procedures in the present study are the techniques of both coating the matrix and opening the cavity uniformly. Paraffin was used to coat the hemispheres for small molecules; however, it may not be suitable as a coating material for an *in vivo* implant because of its brittleness and incompatibility with the tissue. A search is being conducted to find an appropriate coating material to replace paraffin. On the other hand, the ethylene–vinyl acetate copolymer system used for macromolecules has been shown to be highly biocompatible (18). The development of a technique for opening the hole on the flat face of the hemisphere is very critical to achieve reproducibility. Besides the methods practiced in these studies, improved techniques to create holes on the flat face of the hemisphere-shaped device should be explored. Techniques such as computer-aided drilling may prove useful in future studies.

In summary, both theoretical and experimental analyses have demonstrated that a hemisphere can act as a zero-order release system for both micro- and macromolecules. The achievement of constant release rates for macromolecules is particularly significant, since other approaches (*e.g.*, reservoir systems) have not yet been able to release macromolecules in a controlled fashion. This study appears to be the first demonstration that macromolecules can be released at a zero-order rate for long time periods from controlled-release polymer systems.

REFERENCES

(1) D. R. Paul, in "Controlled Release Polymeric Formulations," D. R. Paul and F. W. Harris, Eds., American Chemical Society Press, Washington, D.C., 1976, p. 1.

(2) R. W. Baker and H. K. Lonsdale, in "Controlled Release of Biologically Active Agents," Advances in Experimental Medicine and Biology Series, vol. 47, A. C. Tanquary and R. E. Lacey, Eds., Plenum, New York, N.Y., 1974, pp. 15–72.

(3) R. Langer, *Chem. Eng. Commun.*, **6**, 1 (1980).

(4) T. Higuchi, *J. Pharm. Sci.*, **50**, 874 (1961).

(5) *Ibid.*, **52**, 1145 (1963).

(6) S. J. Desai, A. P. Simonelli, and W. I. Higuchi, *ibid.*, **54**, 1459 (1965).

(7) Y. Samulov, M. Donbrow, and M. Friedman, *ibid.*, **68**, 325 (1979).

(8) W. Rhine, D. S. T. Hsieh, and R. Langer, *ibid.*, **69**, 265 (1980).

(9) J. Cobby, M. Mayersohn, and G. C. Walker, *ibid.*, **63**, 725 (1974).

(10) *Ibid.*, **63**, 732 (1974).

(11) D. Brooke and F. J. Washkuhn, *J. Pharm. Sci.*, **66**, 159 (1977).

(12) R. A. Lipper and W. I. Higuchi, *ibid.*, **66**, 163 (1977).

(13) W. Rhine, V. Sukhatme, D. S. T. Hsieh, and R. Langer, in "Controlled Release of Bioactive Materials," R. Baker, Ed., Academic, New York, N.Y., 1980, pp. 177–188.

(14) G. S. Garvin, in "Polymer Processes: Chemical Technology of Plastics, Resins, Rubbers, Adhesives and Fibers," C. E. Schildknecht, Ed., Wiley-Interscience, New York, N.Y., 1956, p. 679.

(15) S. Borodkin and F. E. Tucker, *J. Pharm. Sci.*, **64**, 1289 (1975).

(16) R. Langer, W. Rhine, D. S. T. Hsieh, and R. Bawa, in "Controlled Release of Bioactive Materials," R. Baker, Ed., Academic, New York, N.Y., 1980, pp. 83–98.

(17) L. Brown, C. Wei, and R. Langer, *J. Pharm. Sci.*, in press.

(18) R. Langer, H. Brem, and D. Tapper, *J. Biomed. Mat. Res.*, **15**, 267 (1981).

ACKNOWLEDGMENTS

Preliminary reports of this work were presented at the 6th and 7th International Symposiums on the Controlled Release of Bioactive Materials.

This work was supported by NIH Grant GM 26698.

S. T. Hsieh is recipient of a starter grant from the Pharmaceutical Manufacturers Association and a fellow of the Juvenile Diabetes Foundation.

The authors thank Brian Marasca, Vikas Sukhatme, Sung Wan Kim, Robert Lipper, Argeris Karabelas, Robert W. Mendes, and Larry Brown for their assistance.

^{60}Co-Irradiation as an Alternate Method for Sterilization of Penicillin G, Neomycin, Novobiocin, and Dihydrostreptomycin

KIYOSHI TSUJI [x], PAUL D. RAHN, and KATHY A. STEINDLER

Received August 26, 1981, from *Control Analytical Research and Development, The Upjohn Co., Kalamazoo, MI 49001.* Accepted for publication February 26, 1982.

Abstract □ The effects of the use of ^{60}Co-irradiation to sterilize antibiotics were evaluated. The antibiotic powders were only occasionally contaminated with microorganisms. The *D*-values of the products and environmental isolates were 0.028, 0.027, 0.015, 0.046, 0.15, 0.018, and 0.19 Mrads for *Aspergillus* species (UC 7297, 7298), *A. fumigatus* (UC 7299), *Rhodotorula* species (UC 7300), *Penicillium oxalicum* (UC 7269), *Pseudomonas maltophilia* (UC 6855), and a biological indicator microorganism, *Bacillus pumilus* spores (ATCC 27142). An irradiation dose of 1.14 Mrads, therefore, was sufficient to achieve a six-log cycle destruction of *B. pumilus* spores. Based on the bioburden data, a minimum irradiation dose of 1.05 Mrads was calculated to be sufficient to obtain a 10^{-6} probability of sterilizing the most radioresistant isolate, *Pen. oxalicum*. To determine the radiolytic degradation scheme and the stability of the antibiotics following irradiation, high-performance liquid chromatographic (HPLC) methods were developed. The resulting rates of degradation for the antibiotics were 0.6, 1.2, 2.3, and 0.95%/Mrad for penicillin G, neomycin, novobiocin, and dihydrostreptomycin, respectively. Furthermore, radiolytic degradation pathways for the antibiotics were identified and found to be similar to those commonly encountered when antibiotics are subjected to acidic, basic, hydrolytic, or oxidative treatments. No radiolytic compounds unique to ^{60}Co-irradiation were found.

Keyphrases □ Irradiation—cobalt-60, alternate method for antibiotic sterilization □ Antibiotics—^{60}Co-irradiation as an alternate method for sterilization □ Sterilization—use of ^{60}Co-irradiation as an alternate method □ High-performance liquid chromatography—determination of radiolytic degradation scheme and stability of antibiotics following irradiation

The majority of pharmaceutical compounds are thermolabile. Sterilization of these compounds, therefore, is performed with the use of an ethylene oxide treatment. However, such a process has a low sterility assurance (1) and is quite costly. Moreover, the efficiency and safety of ethylene oxide as a sterilization agent are being questioned by both the Food and Drug Administration (FDA) (2) and the Environmental Protection Agency (3). ^{60}Co-Irradiation has been recognized as the preferred method for sterilization of medical devices and has been accepted for terminal sterilization of ophthalmic ointment (4). In many countries, products irradiated at 2.5 Mrads can be released for marketing as sterile without final sterility testing.

Recently the FDA proposed a guideline to regulate the irradiation of foods for human consumption (5). This proposal is based on a quantitative estimate of the projected daily human consumption of unique radiolytic compounds in irradiated foods (6). The daily dose of pharmaceutical products is substantially less than the amount of food intake. Thus, the feasibility of ^{60}Co-irradiation for the sterilization of antibiotics has been examined by assessing the resistance of product and environmental isolates to ^{60}Co-irradiation, determining stability, and identifying radiolytic compounds of ^{60}Co-treated antibiotics.

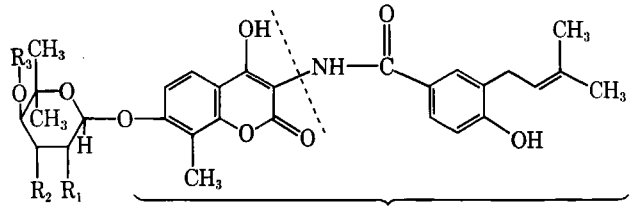

Novobiocic acid

Novenamine

	R_1	R_2	R_3
Novobiocin	OH	$OCONH_2$	CH_3
Isonovobiocin	$OCONH_2$	OH	CH_3
Descarbamylnovobiocin	OH	OH	CH_3
Desmethyldescarbamylnovobiocin	OH	OH	H
Dihydronovobiocin (reduction of isopent-2-enyl side chain to isopentyl)			

EXPERIMENTAL

^{60}Co-Irradiation—All irradiations were carried out[1], by raising the irradiation source, consisting of several rods containing ^{60}Co-pellets mounted on a plaque, from a pool of water into a stationary position for irradiation. Samples were placed in totes on two tiers surrounding the cobalt-60 source. A shuffle–dwell system averaged the radiation gradient around the source by periodically shifting the tote horizontally and vertically. Other samples were stationed at calibrated points where the radiation intensity was more precisely known.

Absorbed irradiation doses were measured potentiometrically using a ceric-cerous dosimeter[2] (7, 8) and spectrophotometrically using a red perspex dosimeter[3].

High-Performance Liquid Chromatography—The modular liquid chromatographic system consisted of a variable wavelength UV monitor[4] or a fixed wavelength UV monitor[5], a high pressure pump[6], a 20-μl fixed-loop injector[7], or a sample processor[8].

Chromatographic Conditions—*Penicillin G*—The chromatographic conditions were as described previously (9) using a reversed-phase column[9] with a mobile phase of acetonitrile, water, and 0.2 *M* ammonium acetate (50:40:10) at pH 4.0. The column effluent was monitored at 254 nm.

Neomycin—The chromatographic conditions were as described previously (10), which consisted of a precolumn derivatization of neomycin with 1-fluoro-2,4-dinitrobenzene at 100° for 40 min, followed by chromatography using a silica column[10] with a mobile phase of chloroform, tetrahydrofuran, methanol, and acetic acid (598:392:8:2). The column effluent was monitored at 254 nm.

[1] Conducted at a facility of Isomedix Inc., Morton Grove, Ill.
[2] Atomic Energy of Canada Limited, Ottawa, Canada.
[3] United Kingdom Atomic Energy Authority, Harwell, Oxon, U.K.
[4] Model 1201, Spectra Monitor I, Laboratory Data Control, Riviera Beach, Fla.
[5] 254 nm, model 1203, UV III Monitor, LDC.
[6] Milton Roy Mini Pump, LDC.
[7] Model 7010, Rheodyne, Berkeley, Calif.
[8] Intelligent Sample Processor (WISP), model 710B, Waters Associates, Milford, Mass.
[9] Partisil PXS 10/25 ODS, 10-μm particle size, or Partisil-10 ODS-3, 250 × 2.1-mm i.d., Whatman Inc., Clifton, N.J.
[10] SI-5A, Lichrosorb SI-100, 5-μm particle size, 250 × 4.6-mm i.d., Brownlee Labs, Santa Clara, Calif.

0022-3549/83/0100-0023$01.00/0

Table I—Destruction of Microorganisms by ^{60}Co-Irradiation

Microorganism	*D*-Value, Mrads
Aspergillus species	
UC 7297	0.028
UC 7298	0.027
A. fumigatus (UC 7299)	0.015
Rhodotorula species (UC 7300)	0.046
Pen. oxalicum (UC 7269)	0.15
Pseud. maltophilia (UC 1885)	0.018
B. pumilus spore (ATCC 27142)	0.19

Novobiocin—The HPLC methods were as described previously (11). The normal-phase chromatography employed a silica column[10] with a mobile phase of 50% water-saturated butyl chloride, tetrahydrofuran, methanol, and acetic acid (88:5:4:3). A C_{18} column[11] was used for reversed-phase chromatography with 0.005 *M* 1-heptanesulfonate in methanol–water (80:20). The column effluent was monitored at 254 and 340 nm.

Dihydrostreptomycin—A reversed-phase RP-8 column[12] was maintained at 30°. A linear gradient elution program changed from mobile phase A to B in 30 min. Mobile phase A was 6% methanol; mobile phase B was 20% methanol, both contained hexanesulfonic acid, sodium sulfate, and acetic acid. The postcolumn oxidation and derivatization with hypochlorite and orthophthaldehyde (12) was applied for fluorometric detection of dihydrostreptomycin. A fluorometer[13] was used to monitor the column effluent.

Microbial Resistance to ^{60}Co-Irradiation—The resistance of microorganisms, isolated from the products and environment, to ^{60}Co-irradiation was investigated. The microorganisms examined were: *Aspergillus* species (UC 7297, 7298), *A. fumigatus* (UC 7299), *Rhodotorula* species (UC 7300), *Penicillium oxalicum* (UC 7269), and *Pseudomonas maltophilia* (UC 6888). Spores of *Bacillus pumilus* (ATCC 27142) were also used as biological indicator microorganisms.

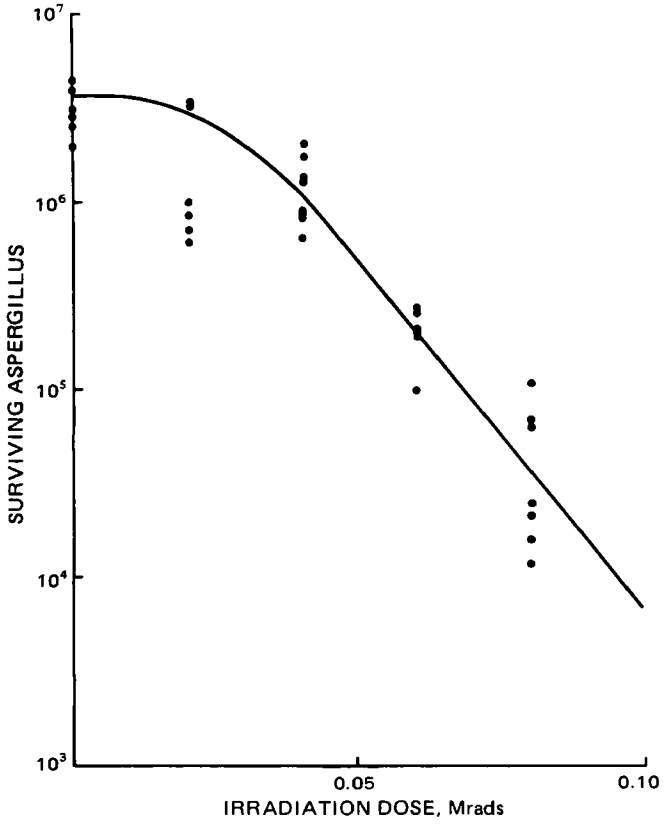

Figure 1—*Survival curve of* Aspergillus *species (UC 7298) when irradiated by cobalt-60 (D = 0.027).*

[11] Microparticulate Zorbax ODS, 250 × 4.6-mm i.d., DuPont Instrument, Wilmington, Del.

[12] RP-5A, 5-μm particle size, 250 × 4.6-mm i.d., Brownlee Labs, Santa Clara, Calif.

[13] Excitation at 360 nm, emission at 440 nm, Fluorichrom Varian, Palo Alto, Calif.

Table II—Stability of Neomycin Sulfate Powder to ^{60}Co-Irradiation

Irradiation Dose, Mrads	Neomycin B, μg/mg	Neomycin C, μg/mg
0	682.2	88.6
0.9	675.1	81.7
2.3	661.0	81.7
3.2	654.9	82.7
4.1	649.0	82.7
4.5	643.7	81.2

Table III—Stability of Penicillin G Procaine to ^{60}Co-Irradiation

Irradiation Dose, Mrads	Potency, Units
0	110.800
1.5	108.800
2.5	107.000
4.0	108.600

B. pumilus received doses of 0.0, 0.15, 0.3, 0.5, 0.7, and 0.93 Mrads, while all other microorganisms received 0, 0.02, 0.04, 0.06, and 0.08 Mrads of irradiation.

***D*-Value Determination**—Microbial resistance to ^{60}Co-irradiation was determined by the *D*-value, the irradiation dose in megarads required to achieve 90% reduction in the microbial population. The *D*-value was calculated using:

$$D = \frac{U}{\log a - \log b} \qquad \text{(Eq. 1)}$$

where *U* is the radiation in megarads, *a* is the initial microbial population prior to radiation treatment, and *b* is the microbial population surviving after treatment with *U* amount of radiation.

To determine the number of microorganisms surviving after receiving *U* amount of radiation, the samples were serially diluted, and 1.0 ml of the appropriate dilutions were plated in duplicate in trypticase soy agar[14].

RESULTS AND DISCUSSION

Microbial Resistance to ^{60}Co-Irradiation—Environmental and occasional microbial contaminants were isolated and used to examine resistance to ^{60}Co-irradiation. The survival curves of microorganisms irradiated followed first-order kinetics: when the log of survivors are plotted against the absorbed dose, a straight line is obtained. A typical

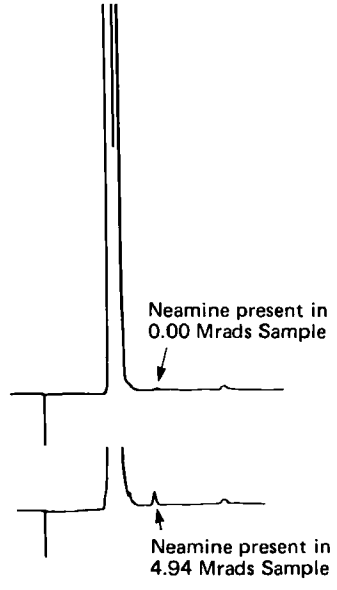

Figure 2—*HPLC indicating the increase in neamine when neomycin was irradiated by cobalt-60.*

[14] BBL, Division of Becton, Dickinson and Co., Cockeysville, Md.

Table IV—Effect of ^{60}Co-Irradiation on Stability of Sodium Novobiocin and Dihydrostreptomycin Sulfate Powder

Irradiation Dose, Mrads	Novobiocin, %	Dihydrostreptomycin, %
0	100	100
0.6	96.2	98.2
1.8	93.0	97.6
2.9	91.5	95.0
3.5	90.3	95.6
4.8	88.3	96.0
5.9	88.8	93.4

survival curve of an isolate, *Aspergillus* species (UC 7298), is shown in Fig. 1. Table I summarizes the *D*-values for *Aspergillus* species (UC 7297, 7298), *A. fumigatus* (UC 7299), *Rhodotorula* species (UC 7300), *Pen. oxalicum* (UC 7269), *Pseud. maltophilia* (UC 6888), and a biological indicator, *B. pumilus* (ATCC 27142) spores. The *D*-values of these microorganisms do not differ significantly from those values appearing in the literature (13–15).

Minimum Irradiation Dose (MID)—The highest *D*-value obtained in this study was 0.19 Mrads for the biological indicator microorganism, *B. pumilus*. Thus, 1.14 Mrads is sufficient to achieve a six-log cycle destruction of *B. pumilus* spores (0.19 × 6).

Bioburden data accumulated for 2 years indicated that <25% of a product contained >10 microorganisms/g of powder. The detection limit of the test is $\sim 10^1$ cells/g of sample. The MID required to achieve a 10^{-6} probability of sterility assurance was calculated by:

$$\text{MID} = D \times (6+1) \qquad \text{(Eq. 2)}$$

The most resistant isolate was *Pen. oxalicum* with a *D*-value of 0.15 Mrads (Table I). The MID for the product thus was calculated to be 1.05 Mrads. The 2.5-Mrads irradiation dose preferred by many countries for sterilization would result in an ~17-log cycle destruction of the most resistant isolate.

Stability of Antibiotics to ^{60}Co-Irradiation—To determine the feasibility of ^{60}Co-irradiation for the sterilization of antibiotics, stability to ^{60}Co-irradiation must be demonstrated and any unique radiolytic compounds identified.

The stability of neomycin sulfate, penicillin G procaine, sodium novobiocin, and dihydrostreptomycin following irradiation with cobalt 60 was examined by HPLC (Tables II–IV). The correlation between the HPLC and microbiological assay data was well established (9–11). The rates of degradation of penicillin G, neomycin, novobiocin, and dihydrostreptomycin by cobalt-60 were 0.6, 1.2, 2.3, and 0.95%/Mrad, respectively. If the ratio of maximum to minimum irradiation dose levels of a product is 1.3 (14), then the maximum irradiation dose that a product receives would be 1.37 Mrads (1.05 × 1.3), since the MID is 1.05. At 1.37 Mrads of irradiation, the expected percentages of degradation for penicillin G, neomycin, novobiocin, and dihydrostreptomycin are 0.8, 1.6, 3.2, and 1.3%, respectively. The rates of degradation for neomycins B and C were not statistically different (Table II).

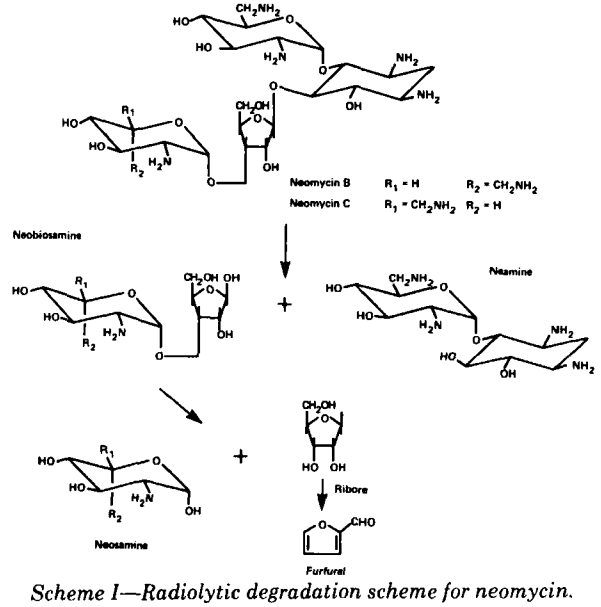

Scheme I—Radiolytic degradation scheme for neomycin.

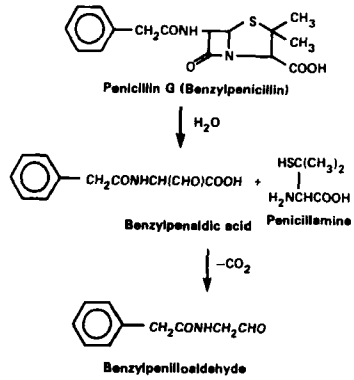

Scheme II—Radiolytic degradation scheme for penicillin G.

Identification of Radiolytic Degradation Compounds—Irradiated antibiotic powders were analyzed by stability-indicating HPLC to isolate, identify, and quantify radiolytic degradation compounds.

For positive identification, samples containing radiolytic compounds were extracted with solvents to enrich the compounds. Compounds were then purified using semipreparative scale HPLCs. The column effluents corresponding to the radiolytic compounds were collected and freeze dried. The identification of the radiolytic compounds was confirmed by a comparison of their mass spectra with those of authentic samples.

Neomycin—A nonirradiated sample and one irradiated at 5.0 Mrads were analyzed by HPLC. The nonirradiated sample contained 39.3 mg of total neomycin (neomycins B and C)/g of a product, while the 5.0-Mrads irradiated sample contained 34.8 mg/g: a decrease of 4.5 mg of neomycin/g. An inspection of HPLC chromatograms indicated an increase in the neamine peak (Fig. 2). The nonirradiated sample contained 0.8 mg of neamine/g of the product, while the irradiated sample contained 3.3 mg/g: a difference of 2.5 mg of neamine/g. A degradation of 4.5 mg of

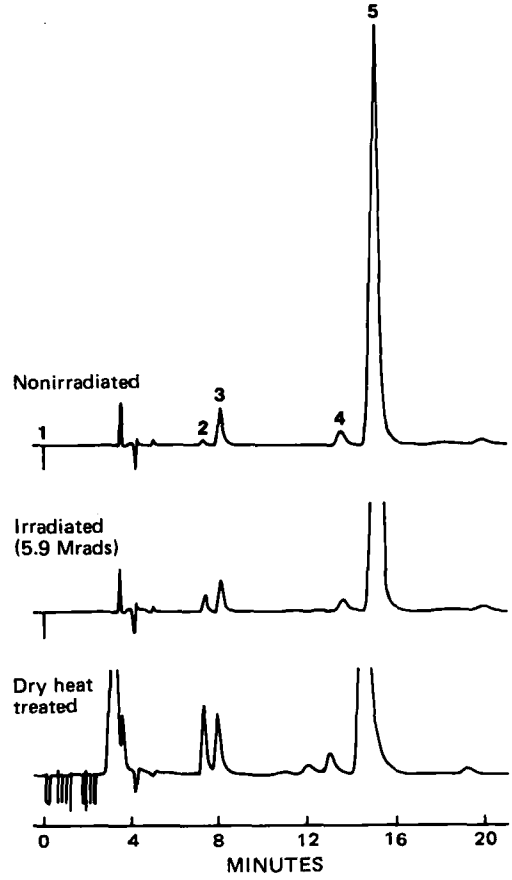

Figure 3—*Normal phase HPLC of novobiocin. Key: (1) injection; (2) radiolytic compound; (3) descarbamyl novobiocin; (4) isonovobiocin; (5) novobiocin.*

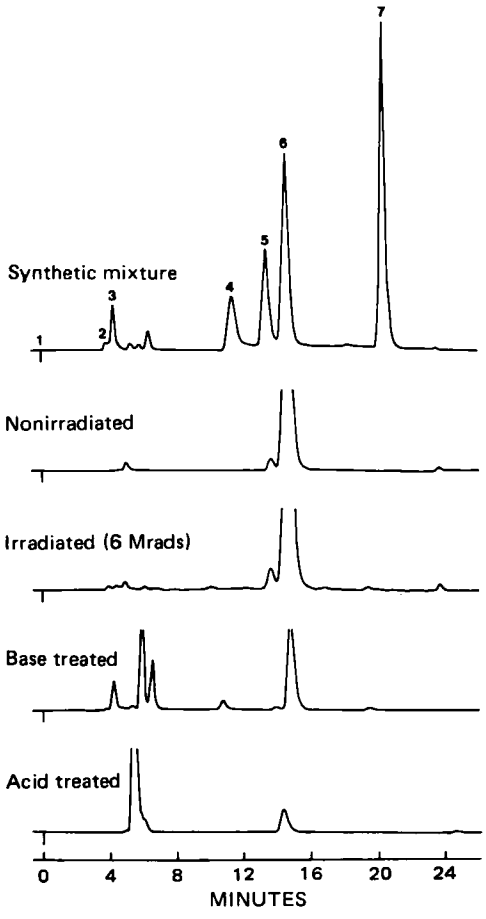

Figure 4—*HPLC of dihydrostreptomycin treated with irradiation, base, and acid. Peak identification: (1) injection; (2) streptamine; (3) D-glucosamine; (4) streptomycin; (5) dideguanyldihydrostreptomycin; (6) dihydrostreptomycin; (7) β-methyldihydrostreptobiosaminide.*

neomycin theoretically yields 2.4 mg of neamine. This calculated quantity of neamine is not statistically different from the observed value of 2.5 mg. Furthermore, a peak corresponding to neosamine increased, but no significant increase of the neobiosamine peak was observed. Thus, it may be concluded that neomycin, upon irradiation, undergoes hydrolytic cleavage at a glycosidic bond to form neamine and neobiosamine. Neobiosamine further degrades to neosamine and ribose; the latter likely yields furfural. A postulated radiolytic degradation scheme is shown in Scheme I. This is the common, hydrolytic degradation pathway for neomycin (16).

Penicillin G—The radiolytic degradation scheme for penicillin G was similarly identified and is shown in Scheme II (9). Penicillin G underwent hydrolytic cleavage to form benzylpenillic acid and benzylpenicilaldehyde. These degradation compounds may also be formed through alkaline treatment (17). Benzylpenicilloic acid, benzylpenilloic acid, and hydroxybenzylpenicillin, reported to form when penicillin G is irradiated in an aqueous solution (18), were not detected.

Novobiocin—Upon examination of the HPLC chromatogram of irradiated and nonirradiated novobiocin powder (Fig. 3), it became evident that one peak, which was originally present in the bulk powder, increased upon irradiation. This degradation compound can easily form upon dry heat treatment of novobiocin powder (Fig. 3). No new peak unique to ^{60}Co-irradiation was detected. Relative chromatographic retention of this peak (0.50) is close to but not identical to that of novobiocic acid (0.44); moreover this peak lacks absorptivity at 340 nm. Novobiocic acid strongly absorbs at 340 nm. The column fraction corresponding to this unknown peak was collected and analyzed by mass spectrometry. The mass spectrometric data clearly identified the unknown compound as the ring A amide (11). The site of the radiolytic cleavage of the novobiocin molecule is shown in the structure of novobiocin.

Dihydrostreptomycin—Identification of degradation compounds and the radiolytic pathway for dihydrostreptomycin are in progress. However, as shown in Fig. 4, the compounds that increase by irradiation were either inherently present in commercially available, nonirradiated lots or can easily be formed by acidic or basic treatment. No new compounds peculiar to irradiation were found.

^{60}Co-Irradiation has been shown to be an effective means of sterilizing antibiotics. The minimum irradiation dose required to achieve 10^{-6} probability of sterilizing the most resistant isolate, *Pen. oxalicum*, is 1.05 Mrads, degradation of antibiotics from ^{60}Co-irradiation is minimal, and the radiolytic degradation schemes are similar to those commonly encountered when antibiotics are subjected to acidic, basic, hydrolytic, or oxidative treatment. No radiolytic compounds unique to irradiation have been found.

REFERENCES

(1) "Sterility and Sterility Testing of Pharmaceutical Preparations and Biological Substances," World Health Organization, WHO/BS/73:1062 + WHO/PHARM/73:474, Washington D.C., 1973.

(2) *Fed. Reg.*, **43,** (No. 122), 411-03, June 23 (1978) p. 27,474.

(3) *Fed. Reg.*, **43,** (No. 19). 6560-01, Jan. 27 (1978).

(4) R. A. Nash, *Bull. Parenter. Drug. Assoc.*, **28,** 181 (1974).

(5) *Fed. Reg.*, **46** (No. 59), 81N-0004, March 27, (1981), pp. 18,992–18,994.

(6) "Recommendations for Evaluating the Safety of Irradiated Foods," Food and Drug Administration, Bureau of Foods, Irradiated Food Committee Report, July 1980.

(7) R. W. Matthews, *Int. J. Appl. Rad. Isotopes*, **22,** 199 (1971).

(8) R. W. Matthews, *Ratiat. Res.*, **55,** 242 (1973).

(9) K. Tsuji, J. F. Goetz, and W. M. VanMeter, *J. Pharm. Sci.*, **68,** 1075 (1979).

(10) K. Tsuji, J. F. Goetz, W. VanMeter, and K. A. Gusciora, *J. Chromatogr.*, **175,** 141 (1979).

(11) K. Tsuji, P. D. Rahn, and M. P. Kane, *ibid.*, **235,** 205 (1982).

(12) H. V. Myers and J. V. Rindler, *ibid.*, **176,** 103 (1979).

(13) H. N. Prince, *Appl. Env. Microbiol.*, **36,** 392 (1978).

(14) D. G. Pope, K. Tsuji, J. H. Robertson, and M. V. DeGeeter, *Pharm. Technol.*, **2,** (10), 30 (1978).

(15) K. Tsuji, M. P. Kane, P. D. Rahn, and K. A. Steinder, "Radiation Physics and Chemistry," Pergamon, Oxford, England, in press.

(16) T. Z. Korzybski, Korzyk-Gindiffer, and W. Kurylowicz, "Antibiotics Origin, Nature, and Properties," vol. 7, American Society of Microbiology, Washington, D.C., 1978, p. 664.

(17) P. P. Regna, in "Antibiotics, Their Chemistry and Non-Medical Uses," H. S. Goldberg, Ed., D. VanNostrand, New York, N.Y., 1959, pp. 59–66.

(18) D. M. Power, in "Sterilization of Medical Products by Ionizing Irradiation," vol. II, R. L. Ganghran and A. J. Goudie, Eds., Multi Science Publishing, Montreal, Canada, 1978, pp. 237–246.

Morphine Radioimmunoassay Specificity Before and After Extraction of Plasma and Cerebrospinal Fluid

PATRICIA Y. GRABINSKI *, ROBERT F. KAIKO *x, T. D. WALSH §, KATHLEEN M. FOLEY ‡, and RAYMOND W. HOUDE *

Received December 2, 1981, from the *Analgesic Studies Section, Sloan-Kettering Institute for Cancer Research and ‡Department of Neurology, Pain Service, Memorial Hospital, New York, NY 10021 and §St. Christopher's Hospice, Sydenham, England. Accepted for publication March 1, 1982.

Abstract □ Currently available morphine radioimmunoassays, using antiserum to 3-*O*-carboxymethylmorphine, lack sufficient specificity for clinical pharmacokinetic studies following repeated oral doses due to the relatively high plasma concentrations of cross-reacting metabolites. A procedure is described for the recovery of the drug and removal of its polar metabolites. The single-step solvent extraction recovered 97% (*CV* 6.9%) morphine and none of the major inactive metabolite, morphine-3-glucuronide. Extracted and nonextracted morphine radioimmunoassay standard curves had comparable slopes, precision, and I_{50} values. Cross reactivity between morphine-3-glucuronide and the antiserum was eliminated when the radioimmunoassay was preceded by extraction. Without prior extraction, the apparent plasma morphine concentration following repeated oral doses was dilution dependent. In contrast, concentration was dilution independent when the radioimmunoassay was preceded by extraction. The plasma morphine concentration in 23 cancer patients at 4 hr following their previous dose (calculated to 10 mg of base) was 26 ng/ml (95% confidence interval (CI), 20–33 ng/ml) with prior extraction, as compared with the apparent concentration of 80 ng/ml (95% CI, 64–96 ng/ml) without extraction. These data indicate that by combining prior extraction with radioimmunoassay, specific, steady-state plasma morphine levels can be obtained following repeated oral doses. However, no significant differences were observed between extracted and nonextracted morphine concentrations in ventricular cerebrospinal fluid from four patients who had received a single intravenous dose. The extraction procedure, prior to radioimmunoassay, provides the specificity required for the measurement of morphine in biofluids that contain relatively high concentrations of cross-reacting metabolites.

Keyphrases □ Morphine—radioimmunoassay specificity before and after extraction of plasma and cerebrospinal fluid □ Radioimmunoassay—morphine, specificity before and after extraction of plasma and cerebrospinal fluid

While the development of a sensitive morphine radioimmunoassay (1) has allowed measurement of clinical pharmacokinetic parameters following single parenteral morphine dosing (2–9), there is limited pharmacokinetic information available following repeated and oral dosing (10). Morphine-3-glucuronide, the major biotransformation product, cross reacts with morphine antisera (1, 11–13). Cross reactivity does not appear to be a significant factor following single parenteral dosing due to the limited amount of metabolite present in plasma and to its relatively low affinity for morphine antisera (3). However, with repeated and oral dosing, the ratio of plasma morphine-3-glucuronide to morphine is likely to be much higher due to the first-pass effect (14) and consequent accumulation of the inactive metabolite. Under these circumstances, most currently available morphine radioimmunoassays are lacking in specificity. While there are other methods available for the measurement of morphine, such as those employing derivatization followed by GLC (15, 16) and that employing extraction followed by scintillation counting of radiolabeled drug (14), an appropriately specific radioimmunoassay would be desirable to many investigators for further studies of the clinical pharmacokinetics of morphine.

The objective of the studies reported here was to demonstrate that an extraction procedure, preceding an otherwise nonspecific radioimmunoassay, provides the specificity required for the measurement of unconjugated morphine in plasma following repeated oral dosing. The utility of the method is demonstrated by the measurement of extracted and nonextracted steady-state plasma morphine concentrations in hospice patients who had been receiving oral morphine doses for the relief of pain due to advanced cancer. These results are contrasted with those obtained by the morphine radioimmunoassay of extracted and nonextracted serial samples of cerebrospinal fluid from cancer patients with chronic pain who had received single intravenous injections of morphine.

EXPERIMENTAL

The extraction procedure is a modification of the first step in a previously reported multistep procedure (17).

Solutions—Glassware for morphine extraction and for storage of morphine standard solutions was siliconized[1]. Morphine standards[2] were added to control plasma in concentrations of 0.31, 0.62, 1.2, 2.5, 5.0, 10, and 20 ng of free base/ml. The extraction buffer, pH 8.6–8.7, contained 40% (w/v) K_2HPO_4 and was sodium chloride saturated. The extraction organic solvent was chloroform–2-propanol (3:1). The extract was reconstituted with 0.1% (w/v) gelatin[3] in 0.01 *M* phosphate-buffered saline, pH 7.3 (assay buffer).

Procedure—An aliquot (0.5 ml) of each plasma standard and of the patient's plasma (up to 0.5 ml) was added to distilled water (1.0 ml) and extraction buffer (1.0 ml) in 15-ml screw-top centrifuge tubes. The varied volumes of the patients' plasma were adjusted to a common volume (0.5 ml) by the addition of control plasma. Each tube was vortexed. The organic solvent (6 ml) was added, and the tubes were capped and shaken for 10 min. The tubes were then centrifuged for 5 min at 300×*g*. The upper aqueous phase and the lipid interphase were aspirated off, and an aliquot (3.0 ml) of the lower organic phase was transferred to a 12-ml conical centrifuge tube. The organic phase was evaporated to dryness in a water bath at 83°. The dry extract was reconstituted with assay buffer (0.5 ml). The tubes were vortexed, and the reconstituted extract was frozen until radioimmunoassay.

Morphine and Morphine-3-glucuronide Recovery Studies—[6-^{3}H]morphine[4] (1.0, 2.0, 4.0, 5.0, 8.0, and 25 ng) was added to control plasma and extracted. Results from scintillation[5] counting of these samples at full tritium window were compared with those of identical amounts of tritiated morphine which had been added directly to the organic phase (3 ml, which had been previously shaken with buffered control plasma and water), evaporated to dryness, and reconstituted. Extracted and nonextracted [^{14}C]morphine-3-glucuronide[6] (40 μg) was also treated as described above.

The radioimmunoassay is a modification of a previously reported procedure (1, 3).

Solutions—A suspension of 0.1% (w/v) dextran[7] and 1.0% (w/v)

[1] Prosil-28, PCR Research Chemicals, Inc., Gainsville, Fla.
[2] Applied Science Labs, Inc., State College, Pa.
[3] J. T. Baker Chemical Co., Phillipsbur;, N.J.
[4] NET-445, New England Nuclear Corp., Boston, Mass.
[5] Riaflour, New England Nuclear Corp., Boston, Mass.; model LS-3133P, Beckman Instruments, Fullerton, Calif.
[6] Supplied by Dr. Amand Misra, Narcotic and Drugs Research, Inc., Brooklyn, N.Y.
[7] Dextran T70, Pharmacia Chemicals, Uppsala, Sweden.

0022-3549/83/0100-0027$01.00/0

Table I—Influence of Morphine-3-glucuronide Cross Reactivity on the Measurement of Unconjugated Morphine

Parts Morphine-3-glucuronide: Morphine Added to Control Plasma		Ratio of Morphine Equivalents Measured by Radioimmunossay to Morphine Added	
Parts	N	Extracted	Nonextracted
0:1	9	1.00 ± 0.03	1.01 ± 0.05
10:1	9	1.08 ± 0.07	1.79 ± 0.11
40:1	9	1.02 ± 0.06	2.51 ± 0.21

charcoal[8] in assay buffer was used for the adsorption of unbound morphine. The radioligand, [7,8-^{3}H]dihydromorphine[9] with a specific activity of 49 Ci/mmole at a concentration of 1.0 mCi/ml of ethanol, was diluted (1:2000) in ethanol to obtain ~20,000 cpm/50 μl. Morphine antiserum[10] was prepared from the blood of New Zealand white rabbits immunized by the administration of 3-carboxymethyl-morphine–bovine serum albumin every 2–3 months for 1 year (18). Antibody dilution studies resulted in 50% binding of the radioligand at an antibody dilution of 1:6000 in 0.01 *M* phosphate-buffered saline (pH 7.3) when 100 μl of diluted antibody was incubated in a final assay volume of 450 μl.

Procedure—Diluted antiserum (100 μl) was added to assay tubes (10 × 75-mm disposable culture tubes) containing the reconstituted plasma extract (200 μl of the original 0.50 ml for standards and 50–200 μl of the original 0.50 ml for patients' samples), radioligand (50 μl), and control plasma (100 μl) to yield a final volume of 450 μl. If necessary for patients' samples, assay buffer was added to yield the 450-μl final volume. Two sets of duplicate background tubes containing no antibody or unlabeled morphine and two sets of triplicate maximum-binding tubes containing no unlabeled morphine were included. Standards and unknowns were assayed in duplicate. The tubes were incubated at room temperature for 1 hr. After incubation, the dextran–charcoal suspension (0.50 ml), which was kept stirring in an ice bath, was added to each tube. The tubes were vortexed and placed in an ice bath for 10 min. The tubes were then centrifuged at 4° and 1500×*g* for 15 min. An aliquot (0.50 ml) of the supernatant was removed from each tube for scintillation counting. A logit-log transformation[11] was used for the linearization of the standard curve and the calculation of the amount of morphine in patients' samples.

Nonextracted radioimmunoassay conditions were identical to those described above for the extracted radioimmunoassay except that 100-μl aliquots of the plasma morphine standards were added to the assay buffer (200 μl) along with the usual amounts of radioligand and antibody solutions. Patients' plasma samples were added in 10–100-μl volumes with any volume differences adjusted by the addition of control plasma to yield a final plasma volume of 100 μl and a final incubation volume of 450 μl as in the extracted radioimmunoassay. Morphine concentrations in cerebrospinal fluid were determined by radioimmunoassays before and following extraction as described for plasma.

Specificity Studies—*Morphine-3-glucuronide Affinity Study*—A morphine-3-glucuronide[12] standard curve was generated by the substitution of the metabolite for morphine in plasma standards which were prepared in 10 times the concentrations (weight basis) as the morphine plasma standards. Conditions of the radioimmunoassay were identical to those described above for the nonextracted morphine standard curve.

Morphine-3-glucuronide Cross Reactivity Study—Three different sets of standards in control plasma were prepared as follows: set I, morphine standards in concentrations of 0.62, 5, and 20 ng/ml; set II, morphine standards as in set I with 10-fold amounts of morphine-3-glucuronide added; set III, morphine standards as in set I with 40-fold amounts of morphine-3-glucuronide added. Triplicates of each standard were assayed before and after extraction as described above for patients' plasma.

Variable Dilutions Study—Plasma samples from two hospice patients (described in the following section) were assayed prior to extraction in graded dilutions of 1:10, 1:50, and 1:250 and following extraction in graded dilutions of none, 1:5, and 1:25.

[8] Norit-A Decolarizing Carbon, Fisher Scientific Co., Fair Lawn, N.J.
[9] New England Nuclear Corp., Boston, Mass.
[10] Supplied by Drs. S. Spector and B. Berkowitz, Roche Institute of Molecular Biology, Nutley, N.J.
[11] Radioimmunoassay Program of Clinical Lab and Nuclear Medicine Pac for HP-97 calculator, Hewlett-Packard Co., Cupertino, Calif.
[12] Supplied by Dr. R. Willette, National Institute on Drug Abuse, Rockville, Md.

Table II—Morphine Equivalents Determined by Radioimmunoassay in Varied Dilutions of Patients' Plasma Before and Following Extraction

	Extracted Plasma		Nonextracted Plasma	
Patient	Dilution	Morphine, ng/ml	Dilution	Morphine, ng/ml
1	None	19.0	1:10	65
	1:5	17.8	1:50	122
	1:25	17.4	1:250	226
2	None	17.0	1:10	74
	1:5	19.6	1:50	130
	1:25	18.6	1:250	226

Applications—Extracted and nonextracted radioimmunoassay procedures were applied to the measurement of morphine equivalents in two sets of biofluids: a set of plasma samples in which the ratio of morphine-3-glucuronide to morphine might be expected to be relatively high and a set of cerebrospinal fluid samples in which the ratio would be expected to be considerably lower.

Plasma Morphine after Repeated Oral Dosing—The patients[13] (Group I) were being treated with morphine for relief of pain due to advanced cancer. There were 23 patients (10 men and 13 women) ranging in age from 42 to 84 years. They had been receiving oral doses of either 5, 10, 20, 30, 45, or 60 mg of morphine sulfate every 4 hr for at least 48 hr and had been receiving oral morphine for at least 1 week before being stabilized at their given doses. Blood samples were obtained at 4 hr following their previous medication. The plasma was recovered and assayed for morphine equivalents prior to and following extraction.

Cerebrospinal Morphine after a Single Intravenous Dose—The patients[14] (Group II) were being treated for the relief of chronic pain. There were four men (34, 45, 56, and 67 years old) who had received a single intravenous injection of 10 mg of morphine sulfate. An indwelling intraventricular catheter and Ommaya reservoir had been implanted in these patients for the introduction of chemotherapeutic agents as part of their treatment for cancer. This allowed the collection of ventricular cerebrospinal fluid samples (5, 10, 15, and 30 min and 1, 2, 4, 8, and 24 hr postdrug). Samples were assayed for morphine prior to and following extraction. The results of an initial nonextracted assay of these samples were previously reported (19).

RESULTS AND DISCUSSION

The extraction of added radiolabeled morphine (1.0–25 ng) to plasma resulted in a mean recovery of 97% (range, 88–104%; *CV*, 6.9%), with no indication of any trend between the amount of morphine added to plasma and the amount recovered. The extraction of 40 μg of radiolabeled morphine-3-glucuronide from plasma resulted in a consistent recovery of 0%. These data indicate that the extraction procedure effectively eliminates the metabolite while recovering the parent drug with acceptable loss and variation. The consistency of morphine recovery is more important than the absolute percentage recovery, since the assay is designed to treat the standards and unknowns in the same manner. Any losses of morphine in the extraction procedure would be reflected in the standards and unknowns to the same extent. High and consistent recovery is achieved, however, with thorough siliconization of the extraction tubes.

Assuming 100% recovery of extracted morphine and taking aliquot losses into consideration, the assays had been designed to yield the same amounts of morphine in each of the standard curves (0.031, 0.062, 0.12, 0.25, 0.50, 1.0, and 2.0 ng). Extracted and nonextracted standard curves were comparable with respective mean slopes of 2.4 ± 3.3% (*CV* from day to day) and 2.6 ± 6.7%, regression correlation coefficients of 0.996 ± 0.3% and 0.997 ± 0.1%, and amounts of morphine which inhibit 50% of radioligand binding equivalent to 0.16 ng ± 3.0% and 0.18 ng ± 14%. The intra-assay variation (*CV*) for duplicate standards was 4.5 and 2.8% for extracted and nonextracted assays, respectively. These data demonstrate that the assays are quite reproducible with acceptable variations in the various parameters for both standard curves. In addition, the data for extracted assays support the consistency of extraction recovery results obtained with radiolabeled morphine standards.

When morphine-3-glucuronide was substituted for morphine in the nonextracted standard curve, a slope of 1.2 was obtained as compared with the slope of 2.6 for morphine. At 25, 50, and 75% displacement of

[13] Inpatients at St. Christopher's Hospice in Sydenham, England.
[14] Inpatients at Memorial Sloan-Kettering Cancer Center, New York, N.Y.

Table III—Morphine Equivalents in Plasma after Repeated Oral Dosing (Group I) and in Cerebrospinal Fluid after a Single Intravenous Dose (Group II) Before and Following Extraction

Patient Group	N	Extracted Samples Morphine, ng/ml	Nonextracted Samples Morphine, ng/ml
Group I	23	26 ± 3.2	80 ± 7.6
Group II	4		
5 min	3	3.2 ± 1.4	3.3 ± 2.1
10 min	4	3.9 ± 1.0	3.8 ± 1.5
15 min	3	5.9 ± 1.6	7.0 ± 2.3
30 min	4	7.1 ± 0.8	7.4 ± 2.0
1 hr	4	7.8 ± 0.8	7.6 ± 1.8
2 hr	4	5.1 ± 1.1	5.2 ± 1.1
4 hr	4	4.8 ± 0.9	5.2 ± 1.4
8 hr	4	3.6 ± 1.2	4.1 ± 1.2
24 hr	2	0.4 ± 0.3	1.1 ± 0.4

radioligand binding, 9.4, 28, and 84 times as much glucuronide as morphine (weight basis) was required. Thus, the ratio of metabolite to parent drug which displaces equivalent amounts of radioligand from the antibody is dependent on the total extent of radioligand displacement. It has previously been reported that standard curves for morphine and its major metabolite (when substituted for morphine in a morphine radioimmunoassay) are not parallel (13), and that the commonly used index of cross reactivity, the ratio of the amounts of two compounds at I_{50}, can be misleading (13).

A more direct approach to examining the cross reactivity of two compounds is to assay varying combinations of them. When morphine-3-glucuronide was added to selected plasma morphine standards in 10- and 40-fold amounts, significantly higher morphine equivalents were obtained as compared with when no metabolite was added in the assays not preceded by extraction (Table I). Ten- and 40-fold amounts of the metabolite resulted in overestimates of 1.8 and 2.5 times as much morphine, respectively. The degrees of overestimation of morphine, when graded amounts of metabolite are added and assayed without prior extraction, are reasonably consistent with what would be predicted on the basis of the ratio of amounts of compounds at I_{50} derived from separate standard curves. However, when the assay was preceded by extraction of duplicate samples of the above, no significant differences were observed among morphine equivalents. These data indicate that the extraction effectively removes morphine-3-glucuronide and are consistent with the results of the recovery study.

One of the methods employed for the validation of the specificity of a radioimmunoassay is the demonstration that the final concentration of the component being measured in a particular sample is independent of the dilution at which it is assayed (20). Table II illustrates that this criterion is fulfilled when the assay is preceded by extraction, but that this is not the case when the assay is performed without prior extraction. These data indicate that the extraction removes morphine metabolites from plasma which cross react with the morphine antibody. The higher dilutions resulted in higher morphine equivalents in the nonextracted assay. This is consistent with the greater degree of cross reactivity between morphine and its metabolite at lower degrees of label displacement observed in the comparison of their standard curves.

The mean morphine concentration (calculated as a common dose of 10 mg of base) in the 23 hospice patients' plasma was 26 ng/ml (95% confidence internal (CI), 20–33 ng/ml) when assayed following extraction as compared to 80 ng/ml (95% CI, 64–96 ng/ml) when assayed without extraction (Table III). Nonextracted morphine equivalents ranged from ~1 to 10 times the extracted levels, but since these ratios are highly dependent upon the dilution of nonextracted plasma, which varied, they cannot be taken as an estimation of the actual ratios of metabolite to parent drug. Nevertheless, the average threefold difference ($p < 0.001$) indicates considerable cross-reacting metabolite(s) in plasma as compared with unconjugated morphine. These data are consistent with the significant first-pass effect for oral morphine, which results in 20–33% bioavailability (14). A molar ratio of glucuronide to unconjugated morphine of 1.8 has been reported at 4 hr following a single intravenous dose of morphine (3).

Steady-state 4-hr trough plasma levels of morphine in a comparable patient group receiving morphine according to a comparable dosing regimen have been reported to be 34 ng/ml (95% CI, 21–48 ng/ml) when adjusted to a common dose of 10 mg of morphine base (10). A nonextracted radioimmunoassay was employed in these latter studies. The mean morphine concentration was significantly ($p < 0.05$) higher (31%) than the concentration reported here. The earlier report used morphine antiserum which had been raised against 6-succinyl morphine–bovine serum albumin, rather than against a 3-position antigen. Thus, the antiserum would have a lower affinity for morphine-3-glucuronide as compared with the antiserum used in this study. While they reported a cross-reactivity of <10% in their radioimmunoassay, even this degree of specificity would not be acceptable for situations in which there is a high ratio of glucuronide to free morphine.

Table III details the results of the radioimmunoassay of extracted and nonextracted cerebrospinal fluid samples which had been obtained from four cancer patients with chronic pain following the intravenous injection of 10 mg of morphine sulfate. In contrast to the extracted and nonextracted plasma levels of patients receiving repeated oral morphine doses, there is no significant ($p > 0.3$; n, 32; paired t test) difference (5.9%) between extracted and nonextracted morphine equivalents in the cerebrospinal fluid following a single intravenous dose. These data are consistent with reports of the limited access of morphine metabolites to the cerebrospinal fluid (21).

A most specific morphine antiserum, raised against *N*-carboxymethylmorphine, has a morphine-3-glucuronide–morphine ratio of ~350–I_{50} (22). This antiserum, however, is not readily available. But even the same antigen in the same individual animal can result in batches of morphine antisera of widely differing specificity (13). Thus, short of the generation of a readily available monoclonal antibody specific for morphine, it is not likely that the numerous investigators of the clinical pharmacokinetics of morphine will be able to employ a common antiserum. While radioimmunoassays may be sufficient for accurate determination of plasma morphine following single parenteral doses, studies of the clinical pharmacokinetics of morphine following repeated and/or oral dosing should incorporate more specific methodology. Because the sensitivity and relative ease of carrying out the radioimmunoassay has made this method more acceptable to many investigators than the use of other methods, the single-step extraction procedure, prior to radioimmunoassay, provides an alternative to the adaptation of other methods for morphine measurement in human biofluids.

REFERENCES

(1) S. J. Spector, *J. Pharmacol. Exp. Ther.*, **178**, 253 (1971).

(2) S. Spector and E. S. Vesell, *Science*, **174**, 421 (1972).

(3) B. A. Berkowitz, S. H. Ngai, J. C. Yang, J. Hempstead, and S. Spector, *Clin. Pharmacol. Ther.*, **17**, 629 (1975).

(4) L. Laitinen, J. Kanto, M. Vapaavuori, and M. K. Viljamem, *Br. J. Anaesth.*, **47**, 1265 (1975).

(5) D. R. Stanski, D. J. Greenblatt, D. G. Lappas, J. Koch-Weser, and E. Lowenstein, *Clin. Pharmacol. Ther.*, **19**, 752 (1976).

(6) D. R. Stanski, D. J. Greenblatt, and E. Lowenstein, *ibid.*, **24**, 52 (1978).

(7) J. R. A. Rigg, *Br. J. Anaesth.*, **50**, 759 (1978).

(8) J. R. A. Rigg, R. A. Browne, C. Davis, J. K. Khandelwal, and C. H. Goldsmith, *ibid.*, **50**, 1125 (1978).

(9) R. F. Kaiko, R. W. Houde, A. Rogers, C. E. Inturrisi, S. L. Wallenstein, P. Grabinski, and K. M. Foley, Proceedings of the 40th Meeting of the Committee on Problems of Drug Dependence, 1978, pp. 194–216.

(10) G. Wynne Aherne, E. M. Piall, and R. G. Twycross, *Br. J. Clin. Pharmacol.*, **8**, 577 (1979).

(11) B. A. Berkowitz, C. V. Cerreta, and S. Spector, *J. Pharmacol. Exp. Ther.*, **191**, 527 (1974).

(12) J. H. Hill, *J. Immunol.*, **114**, 1363 (1975).

(13) D. H. Catlin, *J. Pharmacol. Exp. Ther.*, **200**, 224 (1977).

(14) S. F. Brunk and M. Delle, *Clin. Pharmacol. Ther.*, **16**, 51 (1974).

(15) J. E. Wallace, J. D. Biggs, and K. Blum, *Clin. Chem. Acta*, **36**, 85 (1972).

(16) B. Dahlstrom and L. Paalzow, *J. Pharmacokinet. Biopharm.*, **6**, 505 (1978).

(17) S. Y. Yeh, *J. Pharmacol. Exp. Ther.*, **192**, 201 (1975).

(18) S. Spector and C. W. Parker, *Science*, **168**, 1347 (1970).

(19) R. F. Kaiko, K. M. Foley, R. W. Houde, and C. E. Inturrisi, in "Characteristics and Function of Opioids, Developments in Neurosciences IV," J. M. Van Ree and L. Terenius, Eds., Elsevier/North Holland Biomedical Press, Amsterdam, The Netherlands, 1978, pp. 221–222.

(20) R. S. Yalow, *Circ. Res.*, **33**, Suppl. 1, 1–116 (1973).

(21) C. C. Hug, M. R. Murphy, E. P. Rigel, and W. A. Olson, *Anesthesiology*, **54**, 38 (1981).

(22) A. R. Gintzler, E. Mohacsi, and S. Spector, *Eur. J. Pharmacol.*, 38, 149 (1976).

ACKNOWLEDGMENTS

Supported in part by grants from the National Institute on Drug Abuse (DA 01707) and the National Institute on Aging (AG 01441) and by a Core Grant (CA 08748) from the National Cancer Institute.

The authors are indebted to the patients who participated in these studies; to Ada G. Rogers, clinical coordinator, and the nurse observers, Ginger Boyle, George Heidrich, III, Elizabeth Smith, and Judy Som. The authors also thank Elise Frank for typing this manuscript.

Radiolytic Degradation Scheme for ^{60}Co-Irradiated Corticosteroids

MICHAEL P. KANE and KIYOSHI TSUJI ˣ

Received August 26, 1981, from *Control Analytical Research and Development, The Upjohn Co., Kalamazoo, MI 49001.* Accepted for publication February 26, 1982.

Abstract □ The cobalt 60 radiolytic degradation products have been identified in the following corticosteroids: cortisone, cortisone acetate, hydrocortisone, hydrocortisone acetate, hydrocortisone sodium succinate, isoflupredone acetate, methylprednisolone, methylprednisolone acetate, prednisolone, prednisolone acetate, and prednisone. Two major types of degradation processes have been identified: loss of the corticoid side chain on the D-ring to produce the C-17 ketone and conversion of the C-11 alcohol, if present, to the C-11 ketone. Minor degradation products derived from other changes affecting the side chain are also identified in several corticosteroids. These compounds are frequently associated in corticosteroids as process impurities or degradation compounds. No new radiolytic compounds unique to ^{60}Co-irradiation have been found. The majority of corticosteroids have been shown to be stable to ^{60}Co-irradiation. The rates of radiolytic degradation ranged from 0.2 to 1.4%/Mrad.

Keyphrases □ Corticosteroids—^{60}Co-irradiated, radiolytic degradation scheme □ Degradation—scheme for ^{60}Co-irradiated corticosteroids □ Irradiation—radiolytic degradation of corticosteroids

The U.S. Food and Drug Administration (FDA) has proposed strict limits on allowable residual quantities of ethylene oxide and its major reaction products in drugs because of possible mutagenic and carcinogenic properties of ethylene oxide (1). Faced with the possibility of increased regulatory pressure, the replacement of ethylene oxide with steam or ^{60}Co-irradiation is a major goal of a sterilization alternative program. One phase of this program is to conduct the experimental work required to demonstrate the feasibility of sterilizing bulk drugs and formulated products with ^{60}Co-irradiation.

Recently, the FDA published a proposal regulating irradiated foods for human consumption (2). The proposal permits irradiation of any food at a dose not >100 Krads without the additional safety data. The proposal also permits irradiation of foods at a dose of ≤5 Mrads if the foods comprise only a minor portion (NMT 0.01%) of the daily diet. The proposal includes guidelines for toxicological testing of other foods irradiated at a dose >100 Krads. The proposal is based on projected daily human consumption of radiolytic degradation compounds (3).

The daily dose of pharmaceutical products is substantially less than the amount of foods consumed. Information determining the rate of degradation and identifying degradation compounds unique to irradiation, therefore, should be sufficient to examine the feasibility of ^{60}Co-irradiation as an alternate method for sterilizing pharmaceutical materials and products. The present report provides such information for corticosteroids.

EXPERIMENTAL

^{60}Co-Irradiation—The irradiation source[1], consisting of several rods containing ^{60}Co-pellets mounted on a plaque, was raised from a pool of water into a stationary position for irradiation. Samples were placed in totes on two tiers surrounding the cobalt 60 source. A shuffle–dwell system averaged the radiation gradient around the source by periodically shifting the tote horizontally and vertically. Other samples were stationed at calibrated points where the radiation intensity was more precisely known.

Absorbed irradiation doses were measured potentiometrically using a ceric-cerous dosimeter[2] (4, 5) and spectrophotometrically using a red perspex dosimeter[3].

High-Performance Liquid Chromatography (HPLC) Appara-

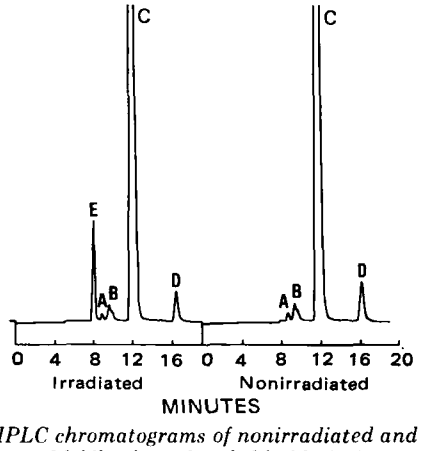

Figure 1—*HPLC chromatograms of nonirradiated and irradiated (6 Mrads) cortisone. Mobile phase: butyl chloride (50% water saturated)–tetrahydrofuran–methanol–glacial acetic acid (950:70:35:30). Column: Brownlee SI-100. Peak identification: (A) cortisone acetate; (B) hydrocortisone acetate; (C) cortisone; (D) hydrocortisone; (E) 4-androstene-3,11,17-trione.*

[1] All irradiations were conducted at a facility of Isomedix Inc., Morton Grove, Il.

[2] Atomic Energy of Canada Limited, Ottawa, Canada.

[3] United Kingdom Atomic Energy Authority, Harwell, Oxon, U.K.

0022-3549/83/0100-0030$01.00/0

(22) A. R. Gintzler, E. Mohacsi, and S. Spector, *Eur. J. Pharmacol.*, 38, 149 (1976).

ACKNOWLEDGMENTS

Supported in part by grants from the National Institute on Drug Abuse (DA 01707) and the National Institute on Aging (AG 01441) and by a Core Grant (CA 08748) from the National Cancer Institute.

The authors are indebted to the patients who participated in these studies; to Ada G. Rogers, clinical coordinator, and the nurse observers, Ginger Boyle, George Heidrich, III, Elizabeth Smith, and Judy Som. The authors also thank Elise Frank for typing this manuscript.

Radiolytic Degradation Scheme for ^{60}Co-Irradiated Corticosteroids

MICHAEL P. KANE and KIYOSHI TSUJI ˣ

Received August 26, 1981, from *Control Analytical Research and Development, The Upjohn Co., Kalamazoo, MI 49001.* Accepted for publication February 26, 1982.

Abstract □ The cobalt 60 radiolytic degradation products have been identified in the following corticosteroids: cortisone, cortisone acetate, hydrocortisone, hydrocortisone acetate, hydrocortisone sodium succinate, isoflupredone acetate, methylprednisolone, methylprednisolone acetate, prednisolone, prednisolone acetate, and prednisone. Two major types of degradation processes have been identified: loss of the corticoid side chain on the D-ring to produce the C-17 ketone and conversion of the C-11 alcohol, if present, to the C-11 ketone. Minor degradation products derived from other changes affecting the side chain are also identified in several corticosteroids. These compounds are frequently associated in corticosteroids as process impurities or degradation compounds. No new radiolytic compounds unique to ^{60}Co-irradiation have been found. The majority of corticosteroids have been shown to be stable to ^{60}Co-irradiation. The rates of radiolytic degradation ranged from 0.2 to 1.4%/Mrad.

Keyphrases □ Corticosteroids—^{60}Co-irradiated, radiolytic degradation scheme □ Degradation—scheme for ^{60}Co-irradiated corticosteroids □ Irradiation—radiolytic degradation of corticosteroids

The U.S. Food and Drug Administration (FDA) has proposed strict limits on allowable residual quantities of ethylene oxide and its major reaction products in drugs because of possible mutagenic and carcinogenic properties of ethylene oxide (1). Faced with the possibility of increased regulatory pressure, the replacement of ethylene oxide with steam or ^{60}Co-irradiation is a major goal of a sterilization alternative program. One phase of this program is to conduct the experimental work required to demonstrate the feasibility of sterilizing bulk drugs and formulated products with ^{60}Co-irradiation.

Recently, the FDA published a proposal regulating irradiated foods for human consumption (2). The proposal permits irradiation of any food at a dose not >100 Krads without the additional safety data. The proposal also permits irradiation of foods at a dose of ≤5 Mrads if the foods comprise only a minor portion (NMT 0.01%) of the daily diet. The proposal includes guidelines for toxicological testing of other foods irradiated at a dose >100 Krads. The proposal is based on projected daily human consumption of radiolytic degradation compounds (3).

The daily dose of pharmaceutical products is substantially less than the amount of foods consumed. Information determining the rate of degradation and identifying degradation compounds unique to irradiation, therefore, should be sufficient to examine the feasibility of ^{60}Co-irradiation as an alternate method for sterilizing pharmaceutical materials and products. The present report provides such information for corticosteroids.

EXPERIMENTAL

^{60}Co-Irradiation—The irradiation source[1], consisting of several rods containing ^{60}Co-pellets mounted on a plaque, was raised from a pool of water into a stationary position for irradiation. Samples were placed in totes on two tiers surrounding the cobalt 60 source. A shuffle–dwell system averaged the radiation gradient around the source by periodically shifting the tote horizontally and vertically. Other samples were stationed at calibrated points where the radiation intensity was more precisely known.

Absorbed irradiation doses were measured potentiometrically using a ceric-cerous dosimeter[2] (4, 5) and spectrophotometrically using a red perspex dosimeter[3].

High-Performance Liquid Chromatography (HPLC) Appara-

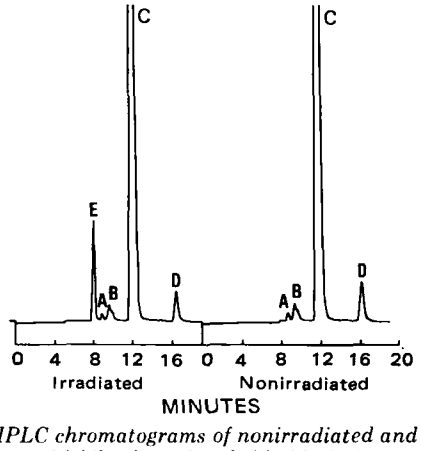

Figure 1—*HPLC chromatograms of nonirradiated and irradiated (6 Mrads) cortisone. Mobile phase: butyl chloride (50% water saturated)–tetrahydrofuran–methanol–glacial acetic acid (950:70:35:30). Column: Brownlee SI-100. Peak identification: (A) cortisone acetate; (B) hydrocortisone acetate; (C) cortisone; (D) hydrocortisone; (E) 4-androstene-3,11,17-trione.*

[1] All irradiations were conducted at a facility of Isomedix Inc., Morton Grove, Il.

[2] Atomic Energy of Canada Limited, Ottawa, Canada.

[3] United Kingdom Atomic Energy Authority, Harwell, Oxon, U.K.

0022-3549/83/0100-0030$01.00/0

Table I—Conditions for Isolation of Cobalt 60 Radiolytic Degradation Products

Corticosteroid	Enrichment Solvent	Column[a]	Mobile Phase
Cortisone	Butyl chloride	1	Butyl chloride–tetrahydrofuran–methanol–acetic acid (950:70:35:30)
Cortisone acetate	Butyl chloride	1	Butyl chloride–tetrahydrofuran–methanol–acetic acid (880:25:25:25)
Hydrocortisone	Methyl chloride	1	Butyl chloride–tetrahydrofuran–methanol–acetic acid (950:70:35:30)
Hydrocortisone acetate	Methyl chloride	2	Acetonitrile water (35:65)
Hydrocortisone sodium succinate	Methyl chloride	2	Methanol–water (55:45)
Isoflupredone acetate	Methyl chloride	2	Acetonitrile–water (40:60)
Methylprednisolone	Methyl chloride	1	Butyl chloride–tetrahydrofuran–methanol–acetic acid (950:70:35:30)
Methylprednisolone acetate[b]	Methyl chloride	1	Butyl chloride–tetrahydrofuran–methanol–acetic acid (880:25:25:25)
Prednisolone	Methyl chloride	2	Methanol–water (55:45)
Prednisolone acetate	Methyl chloride	1	Butyl chloride–tetrahydrofuran–methanol–acetic acid (880:25:25:25)
Prednisone	Butyl chloride	2	Acetonitrile–water (40:60)
17α-Hydroxyprogesterone	Butyl chloride	2	Methanol–acetonitrile–water (30:30:40)

[a] Column: (1) Brownlee SI-100 (4.6 × 250 mm) silica gel (2) Brownlee RP-18 (4.6 × 250 mm) C_{18} bonded phase. [b] A minor degradation product was isolated by chromatography on an RP-18 column using a methanol–water (55:45) mobile phase.

Table II—Mass Balance for Methylprednisolone Peak Response[a]

Irradiation Dose, Mrads	Sample No.	Methyl-prednisolone	Methyl-prednisone	6α-Methyl-11β-hydroxy-1,4-androstadiene-3,17-dione	11β,17α-Dihydroxy-6α-methyl 1,4-androstadiene-3-one
0	1	320,060	261	986	112
	2	322,815	760	1128	214
	3	323,134	252	919	401
	$\bar{x}$	322,003	424	1011	292
2.5	1	311,492	1657	3658	805
	2	322,993	1747	3724	889
	3	316,754	1629	3932	1017
	$\bar{x}$	317,080	1681	3771	904
Difference		−4923	+1257	+2760	+662
Relative Molar Absorptivity		1.00	0.88	1.06	1.00
Corrective for Relative Molar Absorptivity[b]		−4923	+1428	+2604	+662
Relative Change, %		−1.5	+0.4	+0.8	+0.1

[a] Methylprednisolone is USP micronized, and peak response is in area per milligram. [b] An equimolar response was assumed for 11β,17α-dihydroxy-6α-methyl-1,4-androstadiene-3-one due to lack of an authentic sample.

tus—The modular liquid chromatographic system consisted of a fixed wavelength UV monitor[4], a high pressure pump[5], and a 20-μl fixed-loop injector[6] or a sample processor[7].

Chromatographic Conditions—The normal-phase chromatographic conditions used for the HPLC analysis of corticosteroids were similar to those described in another report (6). The mobile phase consisted of butyl chloride (50% water saturated)–tetrahydrofuran–methanol–glacial acetic acid (970:70:35:30) for the C-21 alcohols and 880:25:25:25 for the C-21 acetates of corticosteroids. A silica column[8] was used to chromatograph corticosteroids.

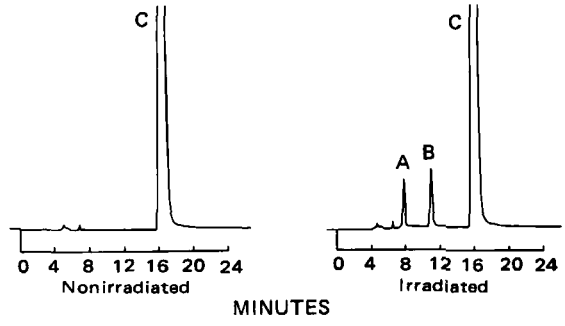

Figure 2—*HPLC chromatograms of nonirradiated and irradiated (2.5 Mrads) hydrocortisone. Mobile phase: butyl chloride (50% water saturated)–tetrahydrofuran–methanol–glacial acetic acid (950:70:35:30). Column: Brownlee SI-100. Peak identification: (A) 11β-hydroxy-4-androstene-3,17-dione; (B) cortisone; (C) hydrocortisone.*

To ensure that all major degradation products were separated, the samples were also analyzed by reversed-phase HPLC using various mixtures of acetonitrile or methanol with water on an octadecylsilane column[9]. Reversed-phase chromatographic methods for analysis of steroids have been reported (7, 8). Normal-phase conditions proved inadequate in only two cases. In hydrocortisone acetate, two degradation compounds eluted at the same retention time, but they were easily separated by reversed-phase chromatography using methanol and water (55:45) as the mobile phase. No degradation product could be eluted by normal phase HPLC for prednisone, but it was detected by reversed-

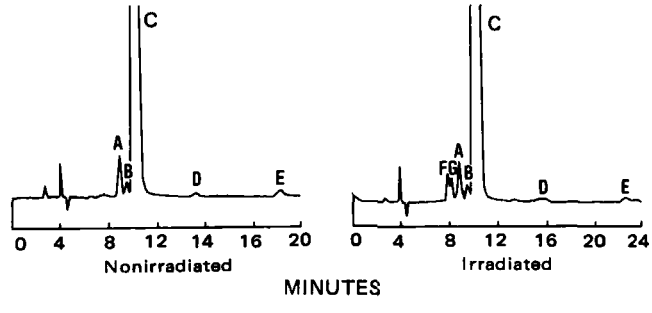

Figure 3—*HPLC chromatograms of nonirradiated and irradiated (6 Mrads) isoflupredone acetate (USP micronized). Mobile phase: butyl chloride (50% water saturated)–tetrahydrofuran–methanol–glacial acetic acid (880:25:25:25). Column: Brownlee SI-100. Peak identification: (A) 9β,11β-epoxy-17α,21-dihydroxy-1,4-pregnadiene-3,20-dione 21-acetate U-6833; (B) 9α-bromoprednisolone acetate U-6429; (C) isoflupredone acetate; (D) isoflupredone; (E) prednisolone; (F) 9α-fluoro-11β-hydroxy-1,4-androstadiene-3,17-dione; (G) 9α-fluoroprednisone acetate.*

[4] 254 nm, model 1203, UV III Monitor, Laboratory Data Control, Riviera Beach, Fla.
[5] Milton Roy Mini Pump, LDC.
[6] Model 7010, Rheodyne, Berkeley, Calif.
[7] Intelligent Sample Processor (WISP) model 710B, Waters Associates, Milford, Mass.
[8] SI-5A, 5-μm particle size, 250 × 4.6-mm i.d., Brownlee Labs., Santa Clara, Calif.
[9] RP-18, 5-μm particle size, 250 × 4.6-mm i.d., Brownlee Labs, Santa Clara, Calif.

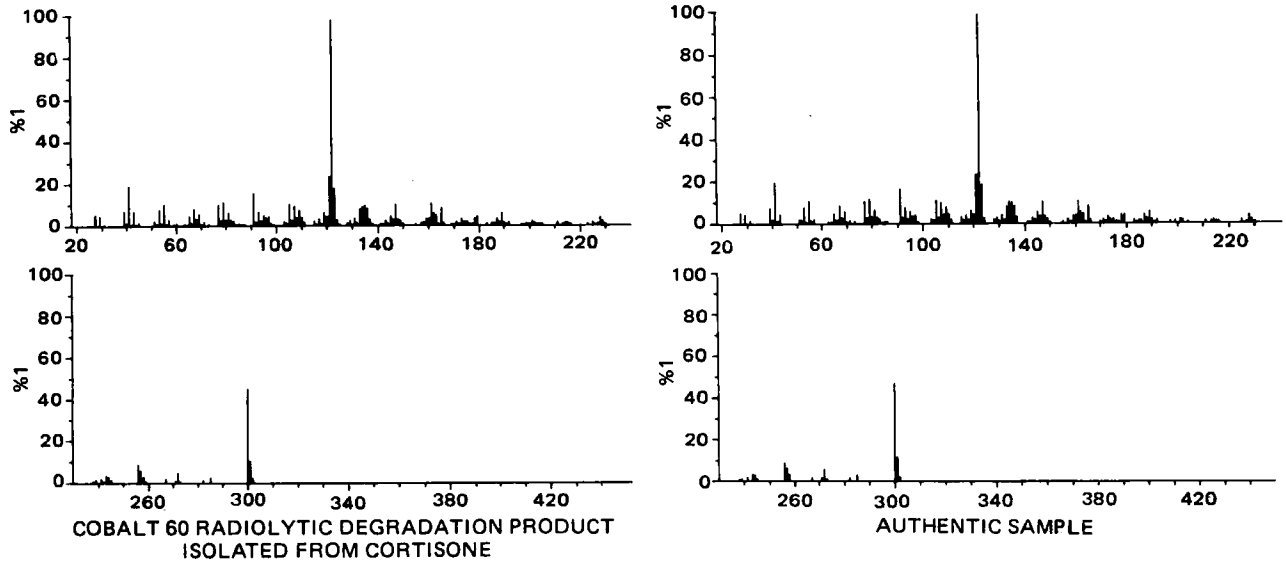

Figure 4—*Mass spectrum of 4-androstene-3,11,17-trione (M^+ m/z 300). (The authentic sample is available from the Upjohn Co.)*

phase chromatography using acetonitrile–water (40:60) as the mobile phase.

The semipreparative scale HPLC methods used to purify the radiolytic degradation compounds for identification are listed in Table I.

Corticosteroids—The following corticosteroids were examined: cortisone, cortisone acetate, hydrocortisone, hydrocortisone acetate, hydrocortisone sodium succinate, isoflupredone acetate, methylprednisolone, methylprednisolone acetate, prednisolone, prednisolone acetate, and prednisone. 17α-Hydroxyprogesterone was also examined.

RESULTS AND DISCUSSION

Identification of Radiolytic Degradation Compounds—The identities of the radiolytic degradation products are based in part on the comparison of the HPLC retention times by both normal- and reversed-phase HPLC of the degradation products with the retention times of the reference standards or authentic samples.

The identities of the degradation products were confirmed by comparison of the mass spectra (electron impact at 250°) of samples of the degradation products obtained by preparative HPLC with the mass spectra of the reference standards or authentic samples. The degradation products were isolated by preparative HPLC from enriched samples. In most cases samples could be enriched by refluxing in butyl chloride or methylene chloride. This process is, in principle, the same as recrystallization, where the mother liquor hopefully contains the impurities. For example, the degradation products of prednisolone were enriched by refluxing 2.5 g of irradiated corticosteroid in 10 ml of methylene chloride for 30 min. The methylene chloride was collected by filtration and evaporated to dryness. In the case of hydrocortisone sodium succinate, the sample was first hydrolyzed by treating a solution of 5 g in 10 ml of water with one drop of 40% NaOH. The hydrolysis products, which precipitated within minutes as the reaction proceeded, were collected by filtration and air dried prior to enrichment by refluxing in methylene chloride. The residues obtained after evaporation were then dissolved in ~20 ml of the appropriate mobile phase and chromatographed either by a normal-[7] or reversed-phase column[8]. Between 10 and 20 100-μl injections normally were made. The mobile phase was removed from the collected fractions by freeze drying.

Although this process was successful in enriching the C-11 and C-17 ketone degradation products in methylprednisolone acetate, the process failed to enrich the third minor product. An enriched sample containing this component was obtained from a normal-phase chromatographic column[10] using butyl chloride (50% water saturated)–tetrahydrofuran–methanol–glacial acetic acid (950:70:35:30). A 2-g solution of the irradiated corticosteroid was dissolved in 10 ml of acetonitrile; twelve 280-μl injections were made. Fractions containing the third component of interest were combined and freeze dried. The freeze-dried material was dissolved in 2 ml of mobile phase and rechromatographed.

The choice of whether to use a normal- or reversed-phase for preparative chromatography was made on the basis of which system provided the best separation from existing process impurities. The chromatographic conditions used in the isolation of the degradation products of each corticosteroid are listed in Table I.

Authentic samples were available for HPLC and mass spectra comparison with all degradation products isolated except the C-17 ketone derived from isoflupredone acetate and the C-17α alcohol derived from methylprednisolone. In the former case, the mass spectrum shows the expected molecular parent ion and is sufficiently similar to related compounds to establish the identification. In the latter case, the C-17β epimer was available for comparison purposes. Although the HPLC retention times of the two epimers were clearly distinctive, the mass spectra

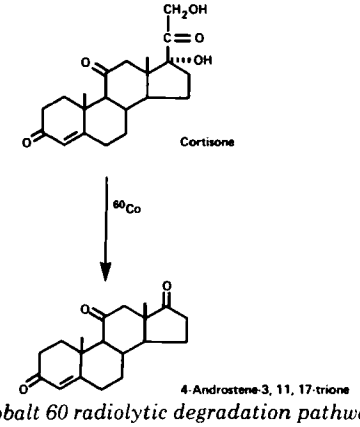

Scheme I—Cobalt 60 radiolytic degradation pathway of cortisone.

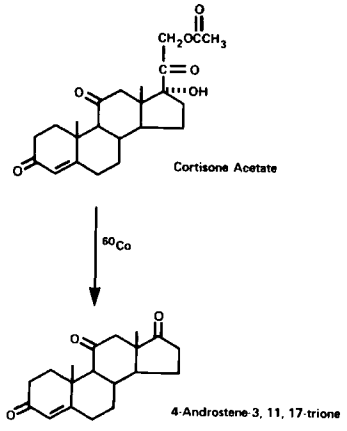

Scheme II—Cobalt 60 radiolytic degradation pathway of cortisone acetate.

[10] Porasil A 37-75 μm, 7.8 mm × 122 cm, Waters Associates, Milford, Mass.

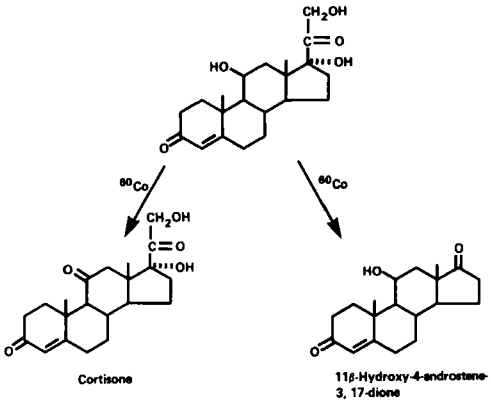

Scheme III—Cobalt 60 radiolytic degradation pathway of hydrocortisone.

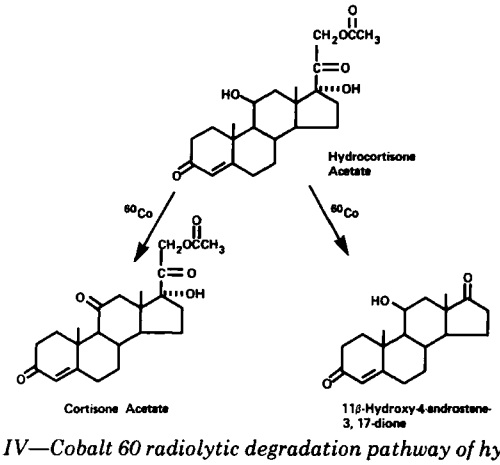

Scheme IV—Cobalt 60 radiolytic degradation pathway of hydrocortisone acetate.

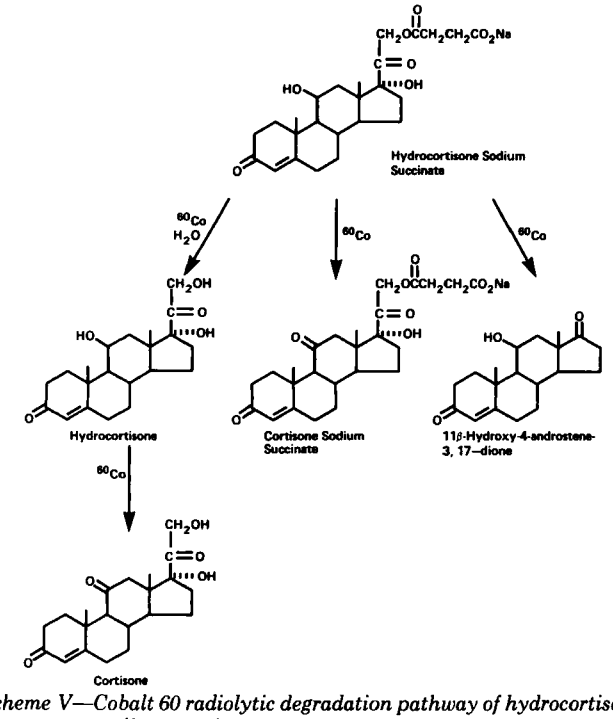

Scheme V—Cobalt 60 radiolytic degradation pathway of hydrocortisone sodium succinate.

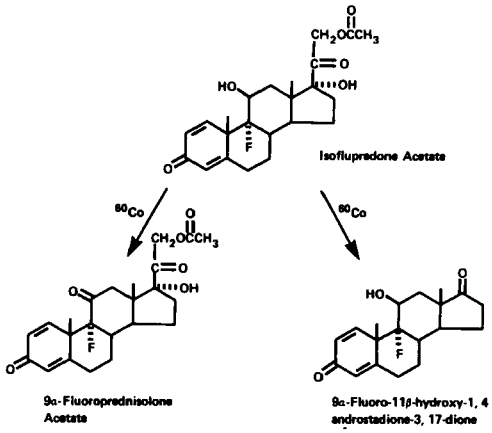

Scheme VI—Cobalt 60 radiolytic degradation pathway of isoflupredone acetate.

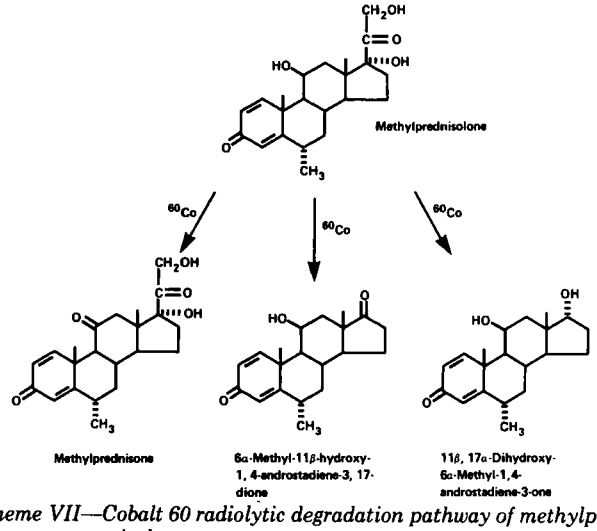

Scheme VII—Cobalt 60 radiolytic degradation pathway of methylprednisolone.

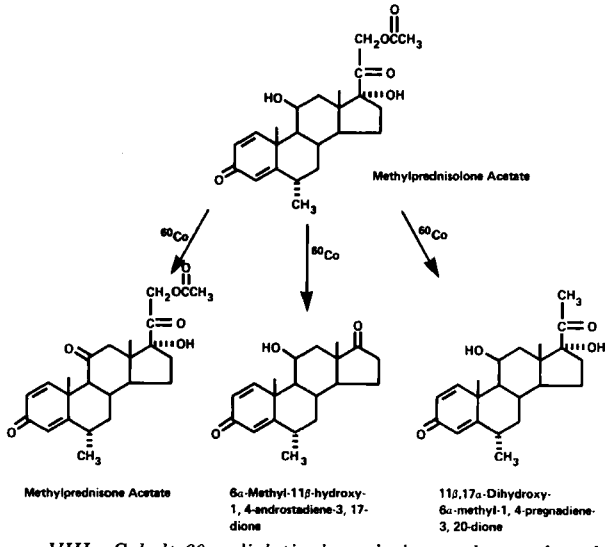

Scheme VIII—Cobalt 60 radiolytic degradation pathway of methylprednisolone acetate.

were nearly identical. It is not unusual for stereoisomers, especially epimers, to have indistinguishable mass spectra.

As examples, HPLC chromatograms of irradiated and nonirradiated cortisone, hydrocortisone, and isoflupredone acetate are shown in Figs. 1–3. The mass spectrum of a radiolytic compound in cortisone used to positively identify it as 4-androstene-3,11,17-trione is shown in Fig. 4.

Mass Balances—The mass balances were determined for the majority of the corticosteroids investigated to ascertain how much of the total degradation could be accounted for by the observed degradation process. The mass balances were obtained by comparing samples irradiated at high dose (2.5 or 6 Mrads) with nonirradiated or low dose (0.5 Mrads) samples. Using carefully dried and accurately weighed samples, the dif-

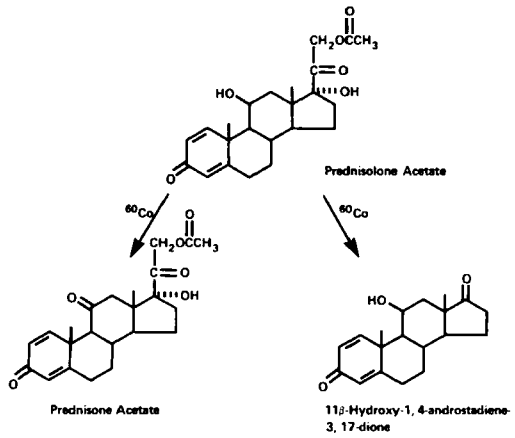

Scheme IX—Cobalt 60 radiolytic degradation pathway of prednisolone acetate.

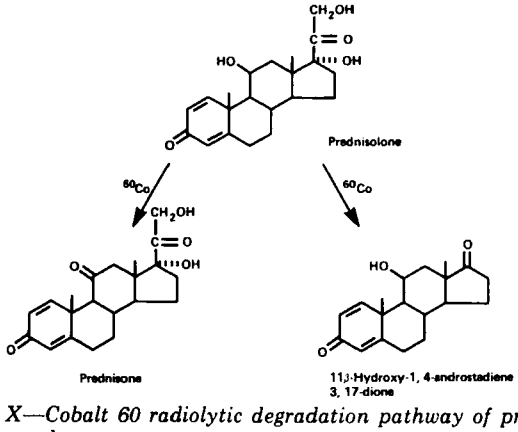

Scheme X—Cobalt 60 radiolytic degradation pathway of prednisolone.

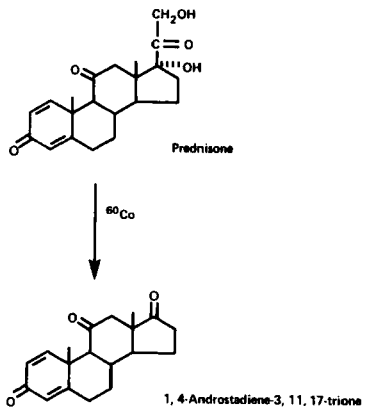

Scheme XI—Cobalt 60 radiolytic degradation pathway of prednisone.

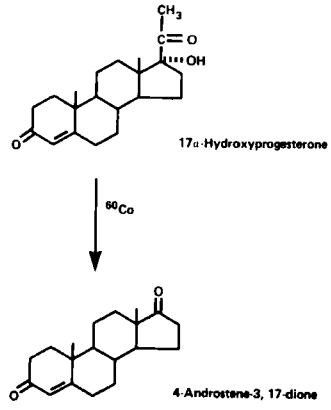

Scheme XII—Cobalt 60 radiolytic degradation pathway of 17α-Hydroxyprogesterone.

ferences in peak response (are per weight ratio) were determined for the corticosteroid and each degradation product. The differences in peak response for the degradation products were then corrected for differences in relative molar absorptivity and are reported on a percentage basis relative to the response of the corticosteroid in the nonirradiated or low-dose sample. An equimolar response was assumed when an authentic sample was not available for determination of relative molar absorptivity. As an example, the mass balance data for methylprednisolone is shown in Table II. The data support the conclusion that all of the degradation by ^{60}Co-irradiation has been accounted for.

Major Cobalt 60 Radiolytic Degradation Products—The major cobalt 60 radiolytic degradation products were identified in the following corticosteroids: cortisone, cortisone acetate, hydrocortisone, hydrocortisone acetate, hydrocortisone sodium succinate, isoflupredone acetate, methylprednisolone, methylprednisolone acetate, prednisolone, prednisolone acetate, and prednisone. Radiolytic degradation of corticosteroids are shown in Schemes I–XI. A structurally related steroid, 17α-hydroxyprogesterone, was also examined (Scheme XII).

Two major types of degradation processes were found to occur by ^{60}Co-irradiation: loss of the C-17 side chain to produce the C-17 ketone and oxidation of the C-11 alcohol, if present, to the C-11 ketone. Several degradation processes have been reported to occur in corticosteroids without irradiation: they include air oxidation of the C-11 alcohol to the C-11 ketone (9, 10), stepwise air oxidation of the D-ring corticoid side chain to the C-17 ketone, hydrolysis of C-21 esters, acyl migration of C-21 hemisuccinate to C-17 hemisuccinate, and loss of the corticoid side chain to produce the C-17 ketone by thermal treatment (11). Thus, the radiolytic degradation products were found to be identical to existing process impurities or known degradation products. A similar loss of the C-17 acyl side chain in 17α-hydroxyprogesterone to produce the C-17 ketone was also found to occur.

Table III—Rate of Radiolytic Degradation for Corticosteroids

Corticosteroids	Radiolytic Degradation, %/Mrad
Cortisone acetate	0.6
Hydrocortisone	1.0
Hydrocortisone acetate	0.3
Hydrocortisone sodium succinate	1.4
Isoflupredone acetate	0.4
Methylprednisolone	0.7
Methylprednisolone acetate	0.6
Prednisolone	0.7
Prednisolone acetate	0.4
Prednisone	0.2

Minor Cobalt 60 Radiolytic Degradation Products—Additional minor degradation products derived from processes affecting the C-17 side chain were identified in methylprednisolone and methylprednisolone acetate (Schemes VII, VIII). Loss of the C-17 side chain in methylprednisolone was also found to result in formation of the C-17α alcohol (11β,17α-dihydroxy-6α-methyl-1,4-androstadiene-3-one) in addition to the C-17 ketone. The C-21 desoxy derivative (11β,17α-dihydroxy-6α-methyl-1,4-pregnadiene-3,20-dione) was produced in methylprednisolone acetate. Hydrocortisone was identified as an additional degradation product of hydrocortisone sodium succinate (Scheme V). Sufficient water is present in the formulation to allow some hydrolysis to occur during irradiation.

Although similar minor degradation products derived from the C-17 side chain were not observed in the other corticosteroids investigated, the possibility of their formation below the detection limit of HPLC methods cannot be ruled out. The minor degradation products detected in methylprednisolone acetate and methylprednisolone were only present at 0.1 and 0.2%, respectively, at 6 Mrads.

Mechanism of Degradation—Two major types of radiolytic degradation processes for corticosteroids have been identified to occur: loss of the C-17 side chain to form the C-17 ketone and oxidation of the C-11 alcohol to form the C-11 ketone. When considering a mechanism to explain these degradation processes, the fact that the reactions involved occur in the solid state must be considered. Molecular packing within the crystal lattice and the amount of surface area could have an influence on degradation. One possible mechanism that accounts for the formation of C-17 ketones as well as the minor products derived from changes in

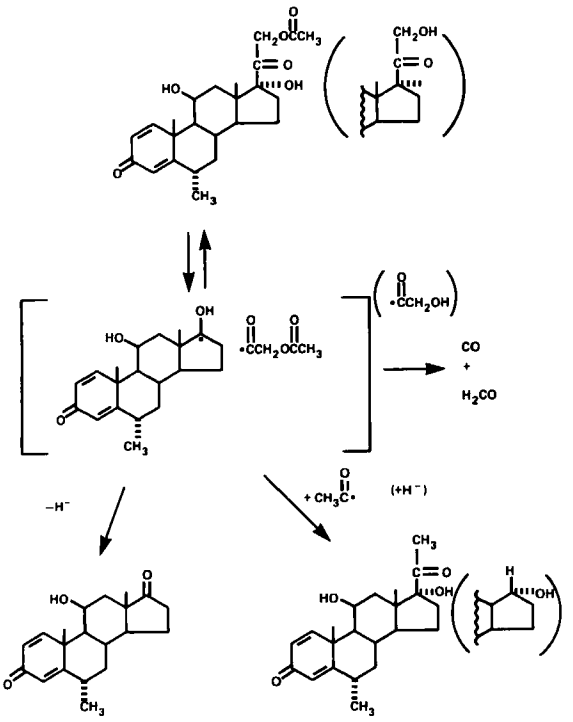

Scheme 13—Postulated mechanism for cobalt 60 radiolytic degradation of C-17 side chain of corticosteroids (example: methylprednisolone and methylprednisolone acetate).

the C-17 side chain of methylprednisolone and methylprednisolone acetate is shown in Scheme XIII. By this mechanism, reaction is initiated by homolytic cleavage between C-17 and C-20. Subsequent loss of a proton from the steroidal fragment would lead to the C-17 ketone. Recombination of the initially formed radicals could also occur. Alternatively, further disintegration of the side chain radical could lead to other radicals. Recombination with any of these radicals could also occur. For example, the C-21 acetate substituted side chain in methylprednisolone acetate could produce carbon monoxide, formaldehyde, and an acetyl radical. Recombination would generate the C-21 desoxy derivative. By a similar process, the side chain in methylprednisolone would produce a radical. Recombination in that case would form the C-21α alcohol. Preservation of the original stereochemistry at C-21 in these degradation products is attributed to the crystal lattice structure which would trap the radical intermediates in close proximity. In addition to formation of carbon monoxide and formaldehyde, other possible products derived from the C-17 side chain include methanol, methyl acetate, acetaldehyde, methane, and hydrogen. Formation of C-11 ketones could proceed by a similar mechanism initiated by loss of the C-11 proton with hydrogen produced as the other product.

Rate of Degradation—The rates of radiolytic degradation for corticosteroids were determined by analyzing irradiated and nonirradiated steroid powders using HPLC methods. The rates of degradation, expressed as percentage per megrad, are shown in Table III. The rates of degradation ranged from 0.2 to 1.4%/Mrad, thus, the majority of corticosteroids are stable to ^{60}Co-irradiation.

REFERENCES

(1) *Fed. Reg.*, **43** (No. 122), 4110-03, June 23 (1978), p. 27,474.

(2) *Fed. Reg.*, **46** (No. 59), 81N-0004, March 27 (1981), pp. 18,992–18,994.

(3) "Recommendations for Evaluating the Safety of Irradiated Foods," Irradiated Food Committee Report, Department of Health, Education, and Welfare, Food and Drug Administration, Washington, D.C., 1980.

(4) R. W. Matthews, *Int. J. Appl. Radiat. Iso.*, **22**, 199 (1971).

(5) R. W. Matthews, *Radiat. Res.*, **55**, 242 (1973).

(6) W. F. Beyer, Presented at 27th National Meeting of the American Pharmaceutical Association, Kansas City, Mo, Nov. 1979.

(7) M. Amin and P. W. Schneider, *Analyst*, **103**, 1076 (1978).

(8) A. R. Lea, J. M. Kennedy, and G. K. C. Low, *J. Chromatogr.*, **198**, 41 (1980).

(9) G. Brenner, F. E. Roberts, A. Hoinowski, J. Budavari, B. Powell, D. Hinkley, and E. Schoenewaldt, *Angew. Chem., Inter. Ed.*, **8**, 975 (1969).

(10) M. L. Lewbart, *Nature (London)*, **222**, 663 (1963).

(11) T. O. Oesterling, in "GLC and HPLC Determination of Therapeutic Agents," part 2, K. Tsuji Ed., Dekker, New York, N.Y., 1978, p. 865.

Difficulties in Applying the Scatchard Model of Ligand Binding to Proteins—Proposal of New Mathematical Tools—Application to Salicylates

C. MONOT *x, P. NETTER ‡, M. C. STALARS ‡, J. MARTIN *, R. J. ROYER ‡, A. GAUCHER §

Received December 21, 1981, from the **Inserm U 115*, ‡*Laboratoire de Pharmacologie* and the §*Clinique Rhumatologique, Université de Nancy 1 France.* Accepted for publication February 26, 1982.

Abstract □ Ill-considered use of the Scatchard model often leads to unjustified deductions. Since the main difficulty of this model is its number of parameters, new models are proposed that have only two parameters. After checking the models on simulated data, they were applied to real data on the binding of salicylates to albumin.

Keyphrases □ Scatchard model—difficulties in application to ligand binding to proteins, new mathematical tools, application to salicylates □ Salicylates—application of Scatchard model, difficulties in application to ligand binding to proteins, new mathematical tools □ Binding—ligand to proteins, difficulties in applying the Scatchard model, new mathematical tools, application to salicylates □ Proteins—ligand binding, difficulties in applying the Scatchard model, new mathematical tools, application to salicylates

The binding of ligands to proteins is most often analyzed in terms of the model proposed by Scatchard (1), in which proteins are considered to possess binding sites divided into independent classes according to their affinities. From estimations of the free and bound fractions of the ligand, it is in principle possible to determine the number of

0022-3549/83/0100-0035$01.00/0

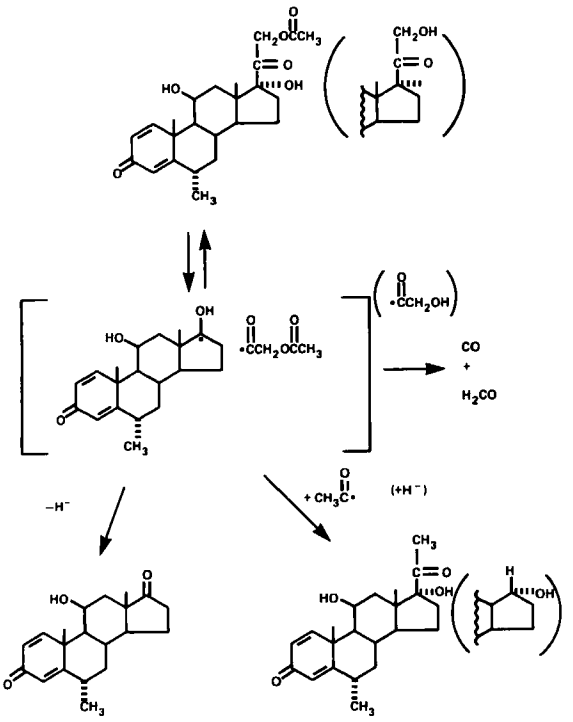

Scheme 13—Postulated mechanism for cobalt 60 radiolytic degradation of C-17 side chain of corticosteroids (example: methylprednisolone and methylprednisolone acetate).

the C-17 side chain of methylprednisolone and methylprednisolone acetate is shown in Scheme XIII. By this mechanism, reaction is initiated by homolytic cleavage between C-17 and C-20. Subsequent loss of a proton from the steroidal fragment would lead to the C-17 ketone. Recombination of the initially formed radicals could also occur. Alternatively, further disintegration of the side chain radical could lead to other radicals. Recombination with any of these radicals could also occur. For example, the C-21 acetate substituted side chain in methylprednisolone acetate could produce carbon monoxide, formaldehyde, and an acetyl radical. Recombination would generate the C-21 desoxy derivative. By a similar process, the side chain in methylprednisolone would produce a radical. Recombination in that case would form the C-21α alcohol. Preservation of the original stereochemistry at C-21 in these degradation products is attributed to the crystal lattice structure which would trap the radical intermediates in close proximity. In addition to formation of carbon monoxide and formaldehyde, other possible products derived from the C-17 side chain include methanol, methyl acetate, acetaldehyde, methane, and hydrogen. Formation of C-11 ketones could proceed by a similar mechanism initiated by loss of the C-11 proton with hydrogen produced as the other product.

Rate of Degradation—The rates of radiolytic degradation for corticosteroids were determined by analyzing irradiated and nonirradiated steroid powders using HPLC methods. The rates of degradation, expressed as percentage per megrad, are shown in Table III. The rates of degradation ranged from 0.2 to 1.4%/Mrad, thus, the majority of corticosteroids are stable to ^{60}Co-irradiation.

REFERENCES

(1) *Fed. Reg.*, **43** (No. 122), 4110-03, June 23 (1978), p. 27,474.

(2) *Fed. Reg.*, **46** (No. 59), 81N-0004, March 27 (1981), pp. 18,992–18,994.

(3) "Recommendations for Evaluating the Safety of Irradiated Foods," Irradiated Food Committee Report, Department of Health, Education, and Welfare, Food and Drug Administration, Washington, D.C., 1980.

(4) R. W. Matthews, *Int. J. Appl. Radiat. Iso.*, **22**, 199 (1971).

(5) R. W. Matthews, *Radiat. Res.*, **55**, 242 (1973).

(6) W. F. Beyer, Presented at 27th National Meeting of the American Pharmaceutical Association, Kansas City, Mo, Nov. 1979.

(7) M. Amin and P. W. Schneider, *Analyst*, **103**, 1076 (1978).

(8) A. R. Lea, J. M. Kennedy, and G. K. C. Low, *J. Chromatogr.*, **198**, 41 (1980).

(9) G. Brenner, F. E. Roberts, A. Hoinowski, J. Budavari, B. Powell, D. Hinkley, and E. Schoenewaldt, *Angew. Chem., Inter. Ed.*, **8**, 975 (1969).

(10) M. L. Lewbart, *Nature (London)*, **222**, 663 (1963).

(11) T. O. Oesterling, in "GLC and HPLC Determination of Therapeutic Agents," part 2, K. Tsuji Ed., Dekker, New York, N.Y., 1978, p. 865.

Difficulties in Applying the Scatchard Model of Ligand Binding to Proteins—Proposal of New Mathematical Tools—Application to Salicylates

C. MONOT *x, P. NETTER ‡, M. C. STALARS ‡, J. MARTIN *, R. J. ROYER ‡, A. GAUCHER §

Received December 21, 1981, from the **Inserm U 115*, ‡*Laboratoire de Pharmacologie* and the §*Clinique Rhumatologique, Université de Nancy 1 France.* Accepted for publication February 26, 1982.

Abstract □ Ill-considered use of the Scatchard model often leads to unjustified deductions. Since the main difficulty of this model is its number of parameters, new models are proposed that have only two parameters. After checking the models on simulated data, they were applied to real data on the binding of salicylates to albumin.

Keyphrases □ Scatchard model—difficulties in application to ligand binding to proteins, new mathematical tools, application to salicylates □ Salicylates—application of Scatchard model, difficulties in application to ligand binding to proteins, new mathematical tools □ Binding—ligand to proteins, difficulties in applying the Scatchard model, new mathematical tools, application to salicylates □ Proteins—ligand binding, difficulties in applying the Scatchard model, new mathematical tools, application to salicylates

The binding of ligands to proteins is most often analyzed in terms of the model proposed by Scatchard (1), in which proteins are considered to possess binding sites divided into independent classes according to their affinities. From estimations of the free and bound fractions of the ligand, it is in principle possible to determine the number of

0022-3549/83/0100-0035$01.00/0

Table I—Simulations of the Equilibrium Bound Concentration Using the Scatchard Model with Two or Three Classes of Sites

Binding Parameters	Number of Classes (1) $m = 2$	(2) $m = 3$	(3) $m = 3$
K_1	0.0284	0.03954	0.04527
K_2	0.0021	0.00482	0.00959
K_3	—	0.00153	0.00181
n_1	1.46	1.00	0.76
n_2	4.10	2.00	1.30
n_3	—	2.56	3.50
Total Drug μg/ml	Total Drug μmoles/liter	Bound Drug μmoles/liter	Bound Drug μmoles/liter	Bound Drug μmoles/liter
50	362	346	346	346
100	725	680	679	679
200	1449	1290	1291	1292
300	2174	1807	1811	1809
400	2898	2211	2211	2210
500	3623	2494	2490	2489
600	4348	2679	2672	2672
800	5797	2881	2872	2873
1000	7246	2979	2971	2973
2000	14,493	3126	3122	3123
3000	21,739	3164	3161	3162
4000	28,985	3180	3178	3179
5000	36,232	3190	3188	3189
8000	57,971	3204	3203	3203
10,000	72,464	3208	3207	3207

classes, the number of sites in each class, and the affinity constant of each class. Before computers became available, graphical methods of solving the nonlinear equations introduced by this problem were proposed (2–4). Discrepancies in the results could be attributed to the imprecisions of graphical methods, and the emergence of computers should then have caused the results to become more consistent. The results of various graphical methods were compared (4) with the results obtained by computer methods, while taking care not to adopt the algorithm of these graphical methods for the computer. Despite the extremely powerful methods available in large computing centers (5–11) difficulties remained. It was shown (8) that the results for binding of dicumarol to albumin were doubtful when errors became as large as 2%, even when based on 50 experimental measurements, and that the results obtained from 200 experimental measurements with a precision of 5% had no significance. In addition, 50 publications were reviewed (12) that contained various errors of graphical construction. However, many authors continue to use this model and to calculate the classical parameters (universally called n_i, K_i, and m).

This model is habitually used since most scientists accept it as a good representation of the real phenomenon. A study of the discussions of the independence and the initial existence of all the sites (the basic hypothesis of Scatchard), and the introduction of an interaction between sites (13–20) may provide an understanding of how efficiently this model represents reality.

Problems are encountered in the study of this model. If available experimental data do not allow determination of all parameters of the model, it becomes simply a mathematical tool whose parameters have no significance. If the experimental data do not allow an accurate determination of the parameters, then a question arises as to whether the use of other mathematical functions would provide better results.

An attempt was made in this study to solve these problems using the binding of salicylate to albumin. Other models are proposed using simulated and real data.

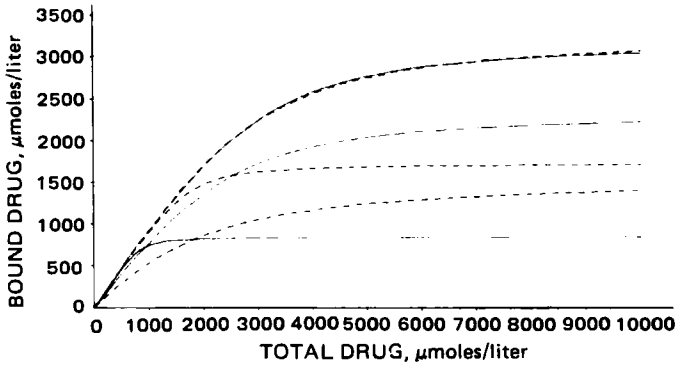

Figure 1—*Scatchard model with two classes of sites: curve of ligand binding to each class and to both classes taken as a whole, with two different combinations of parameters. Key: (—)* $K_1 = 0.00210$ *μmole/liter,* $K_2 = 0.02840$ *μmoles/liter,* $n_1 = 4.10$, $n_2 = 1.46$; *(- - - -)* $K_1 = 0.00109$ *μmoles/liter,* $K_2 = 0.01103$ *μmoles/liter,* $n_1 = 2.68$, $n_2 = 3.00$.

EXPERIMENTAL

To analyze and test different models, simulated and real data are used. Simulated data are the values of a published example on the binding of salicylate to albumin (21, 22). Real data are obtained *in vitro* by equilibrium dialysis on an apparatus[1], equipped with membranes[2] (with a molecular weight cutoff of 14,000), separating two 1.0-ml cells. The dialysis cells were placed in a water bath thermostated at 37°. Salicylate was estimated by spectrofluorimetry (excitation at 300 nm, emission at 410 nm).

Classical Scatchard Model—This model is deduced from the law of mass action and from the probability of binding to a carrier protein (1). It is based on a classification of independent sites of binding to the protein:

$$\frac{B}{P} = \sum_{i=1}^{m} \frac{n_i K_i F}{1 + K_i F} \qquad \text{(Eq. 1)}$$

where B is the concentration of the bound substance, F is the concentration of the unbound substance, P is the concentration of the protein, m is the number of classes of sites, and K_i and n_i are, respectively, the affinity constant and the number of sites of the ith class of sites.

Proposed Models—These are mathematical functions that must have the same shape as the amount of ligand bound at equilibrium expressed as a function of the total ligand concentration present. These functions have only two parameters:

$$\text{trigonometric model: } B = a_1 \arctan(a_2 T) \qquad \text{(Eq. 2)}$$

$$\text{exponential model: } B = b_1[1 - \exp(-b_2 T)] \qquad \text{(Eq. 3)}$$

where T is the total concentration of the ligand present, B is the concentration of the bound fraction at equilibrium, and a_1 and a_2, b_1 and b_2 are the two parameters of the models that are determined from the experimental data. These parameters are not totally meaningless, since in each case a_1 and b_1 are directly related to the saturating values B_∞ of the quantity of ligand bound to the protein:

$$B_\infty = a_1 \frac{\pi}{2} \qquad \text{(Eq. 4)}$$

$$B_\infty = b_1 \qquad \text{(Eq. 5)}$$

The two models proposed make it possible to study the equilibrium binding of the ligand either to binding proteins, where the protein concentration must be specified, or per unit concentration of binding protein:

$$\frac{B}{P} = \frac{a_1}{P} \arctan(a_2 T) \qquad \text{(Eq. 6)}$$

$$\frac{B}{P} = \frac{b_1}{P}[1 - \exp(-b_2 T)] \qquad \text{(Eq. 7)}$$

[1] Dianorm.
[2] Spectrapor 2.

Table II—Comparison of the Results of Simulations Using the Scatchard Model with Two Classes of Sites and Various Combinations of Parameters

		(1)	(2)	(3)	(4)	(5)	(6)	(7)
	K_1	0.00210	0.00210	0.00267	0.00170	0.00109	0.00055	0.00007
	n_1	4.10000	4.10080	4.46524	3.60528	2.68335	1.79370	1.36566
Binding	K_2	0.02840	0.02843	0.04407	0.01863	0.01103	0.00740	0.00494
Parameters	n_2	1.46000	1.45899	1.00000	2.00000	3.00000	4.00000	5.00000

Total Drug		Bound Drug	Bound Drug	Bound Drug	Bound Drug	Bound Drug	Bound Drug	Bound Drug
μg/ml	μmoles/liter	μmoles/liter	μmoles/liter	μmoles/liter	μmoles/liter	μmoles/liter	μmoles/liter	μmoles/liter
50	362	346	346	346	345	343	340	336
100	725	680	680	680	679	677	673	665
200	1449	1290	1290	1288	1295	1300	1299	1289
300	2174	1807	1807	1814	1810	1820	1831	1835
400	2898	2211	2211	2226	2207	2208	2220	2248
500	3623	2494	2494	2508	2486	2478	2479	2514
600	4348	2679	2679	2686	2672	2661	2653	2675
800	5797	2881	2881	2872	2879	2873	2862	2856
1000	7246	2979	2979	2959	2983	2985	2980	2962
1250	9060	3045	3045	3017	3054	3064	3068	3051
W		—	0.109	1788	266	1337	2615	3845
Max. limit of bound drug								
Class 1 + Class 2			3225	3170	3251	3296	3360	3692
Class 1			2379	2590	2091	1556	1040	792
Class 2			846	580	1160	1740	2320	290

In this case the parameters a_1 and b_1 are divided by the protein concentration P, whereas other parameters, a_2 and b_2, are independent of the protein concentration.

The Scatchard model, when limited to a single class of sites, can be used in certain cases and more precisely when the zone being studied is more limited (in the case of therapeutic or toxic doses of salicylates, up to or exceeding 400 μg/ml.)

The model (Eq. 1) is then written:

$$B = \frac{nPKF}{1 + KF} \quad \text{or} \quad B = \frac{nPK(T - F)}{1 + K(T - F)} \qquad \text{(Eq. 8)}$$

This model has only two parameters and occasionally gives good results, but it is disadvantageous because it is also a mere mathematical tool requiring solution of a nonlinear equation.

RESULTS AND DISCUSSION

General Applications of the Model—The usual procedure is to use a computer (or graph paper) to determine the parameters n_i, K_i, and sometimes m starting from the experimental data that has been obtained.

There are, however, problems encountered with this procedure. The study of the binding phenomenon itself, while assuming that the model is a true reflection of reality, is one problem. It must be possible to determine the parameters m, n_i, and K_i, and each must have a unique value. Other problems encountered are the study of the influence of a pathological condition on the quantity of ligand bound (which leads to a comparison of groups) and the study of a particular region of the curve of binding to a protein, such as therapeutic or toxic doses, or the saturation value of binding.

Difficulties Encountered—Difficulties are not related to the theoretical model itself but are related to the number of unknown parameters whose estimation is often incompatible with the quantity and quality of the experimental data (8). The determination of these parameters is considered from simulated data, thus eliminating experimental errors, taking as an example published data on the binding of salicylate (^{14}C-labeled COOH-salicylic acid) to albumin (21, 22).

It is essential to know the number (m) of classes of sites if one wishes the model to reflect the real phenomenon. The number m, determined only from estimations of the concentrations at equilibrium of free and bound ligand as a function of the total ligand concentration, is in reality only the minimum possible number of classes compatible with the experimental data.

As an example, Table I represents the concentrations of salicylate bound at equilibrium throughout the whole concentration range (0–10 mg/ml). The results were obtained by simulation for three cases. The first case (Table I, column 1) assumed two classes of sites (m = 2); using the values of the parameters for the binding of salicylate generally accepted in published sources. The second and third cases assumed three classes

Table III—Simulations Using the Two Proposed Models over the Concentration Range 0 to 1250 μg/ml (0 to 9060 μmole/liter [a])

		Scatchard Model— Two Classes Reference	Trigonometric Model a_1 = 2370.00 a_2 = 0.000449	Exponential Model b_1 = 3210.57 b_2 = 0.000386
Total Drug		Bound Drug	Bound Drug	Bound Drug
μg/ml	μmoles/liter	μmoles/liter	μmoles/liter	μmoles/liter
50	362	346	382	419
100	724	680	746	783
200	1449	1290	1369	1375
300	2174	1807	1835	1823
400	2898	2211	2172	2162
500	3623	2494	2418	2418
600	4348	2679	2602	2611
700	5072	2800	2744	2757
800	5797	2881	2855	2868
900	6522	2938	2944	2951
1000	7246	2979	3017	3015
1250	9060	3045	3152	3113
W		—	42743	44562

[a] Comparison with the reference values derived from the Scatchard model with two classes of sites. W Represents the residual sum of squares.

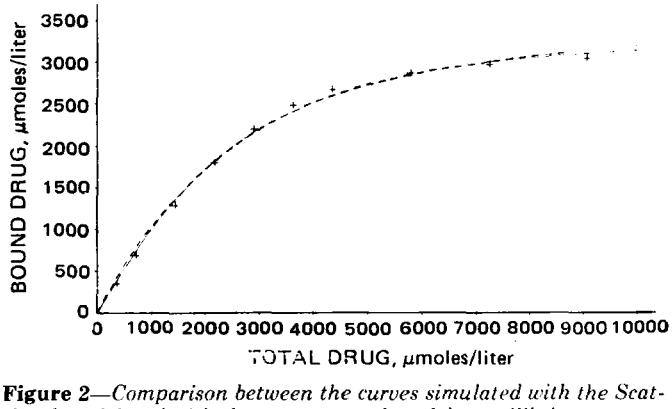

Figure 2—*Comparison between the curves simulated with the Scatchard model and with the two proposed models: equilibrium concentration <1250 μg/ml (9060 μmoles/liter). Key: (—) trigonometric model; (- - - -) exponential model; (+) Scatchard model with two classes of sites.*

Table IV—Therapeutic Concentrations [a]

		Scatchard Model Two Classes Reference	Trigonometric Model $a_1 = 2783.6$ $a_2 = 0.000347$	Exponential Model $b_1 = 3858.4$ $b_2 = 0.000285$	Scatchard Model One Class $K = 0.006972$ $n = 4.3964$
Total Drug		Bound Drug	Bound Drug	Bound Drug	Bound Drug
μg/ml	μmoles/liter	μmoles/liter	μmoles/liter	μmoles/liter	μmoles/liter
25	181	174	175	194	171
50	362	346	348	379	340
75	543	514	519	554	508
100	724	679	686	721	673
125	906	840	848	879	836
150	1087	995	1005	1029	995
175	1268	1145	1155	1172	1150
200	1449	1290	1298	1307	1300
225	1630	1429	1435	1436	1443
250	1811	1561	1563	1558	1579
275	1993	1688	1686	1674	1704
300	2174	1807	1801	1784	1818
325	2355	1919	1909	1888	1918
350	2536	2024	2011	1988	2007
W		—	806	11,544	1445

[a] Simulations using the trigonometric model, the exponential model, and the Scatchard model with one class of binding sites. Comparison with the reference values derived from the Scatchard model with two classes of sites. W represents the residual sum of squares.

of sites ($m = 3$) (Table I, columns 2 and 3), with two combinations of the six parameters n_i and K_i. However, in practice there is an infinite number of these combinations, since they were obtained by simple identification of the parameters K_i. The values of n_i were chosen arbitrarily as:

$$(n_1 + n_2 + n_3)_{m=3} = (n_1 + n_2)_{m=2} \qquad \text{(Eq. 9)}$$

so that the bound fractions reached the same limit at saturation (Eq. 1).

The exact number of classes of sites may be confused with the minimum number compatible with the available experimental results. This does not matter if the model is used simply as a mathematical tool (for example for smoothing), but it becomes a problem if the phenomenon itself is to be used and a real significance is to be given to the parameters.

Suppose that the number of classes of sites is known (or is accepted to be equal to the minimum number defined above). Difficulties have already been reported with the determination of other parameters such as n_i and K_i from the results of equilibrium estimations (4) as shown in Table II. Again the data used are the 12 values of the bound fraction simulated from published parameters (21, 22) for the binding of salicylate to albumin (Table II, column 1). The parameters (n_i and K_i are calculated in several cases: For the four parameters, n_1, n_2, K_1, and K_2, even starting the iterations from remote initial values, the results are not much different from the correct values (Table II, column 2); for the three parameters, n_1, K_1, and K_2, to the fourth parameter (n_2) we attribute the values 1, 2, 3, 4, and 5, successively (Table II, columns 3–7). The results yield combinations for the values of the parameters that are naturally very different; the quantity of ligand bound, however, remains similar from one of these groups of values to another. Figure 1 represents this phenomenon. The curves represented correspond to the two combinations:

$$K_1 = 0.00109\ K_2 = 0.01103\ n_1 = 2.6833\ n_2 = 3.0000$$
$$\text{and } K_1 = 0.0021\ K_2 = 0.0284\ n_1 = 4.1000\ n_2 = 1.4600 \qquad \text{(Eq. 10)}$$

where K_1 and K_2 are given in micromoles per liter.

In both cases the curves drawn represent the quantity bound to each site and the overall quantity for the whole of the two sites, respectively. These two curves, representing the total quantity bound to albumin, are practically identical (Fig. 1), which shows that it cannot be determined how much ligand is bound to each site; that is, the four parameters n_1, n_2, K_1, and K_2 cannot be determined.

Conclusions About Current Application of the Scatchard Model—The difficulties encountered at the various stages of the application of the model to simulated cases have been shown, in the total absence of experimental errors, for the determination of the various parameters of binding to proteins. The problem of the number of classes of sites alone destroys any significance of the parameters.

Therefore, this model should not at present be used except as a mathematical tool. It requires that a nonlinear equation be solved at each point; this drawback, which was the reason for the various graphical methods, makes it difficult to use. The large number of these parameters that cause this practical indetermination that has been reviewed previously prohibits any direct interpretation of the results (such as comparison of the parameters from two groups of patients). One solution is to arbitrarily fix the values of certain parameters (for example n_1 and n_2), as suggested previously (8). Other mathematical models are proposed here as mathematical tools but they are easier to manipulate, and have

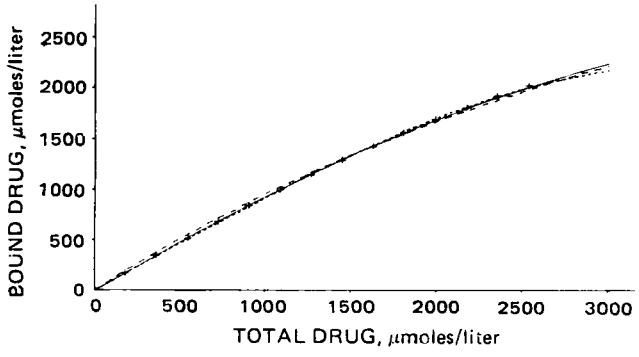

Figure 3—*Comparison of the models over the therapeutic range of concentration (<350 μg/liter, or 2536 μmoles/liter). Key: (—) trigonometric model; (- - - -) exponential model; (- · - · -) Scatchard model with one class of sites; (+) Scatchard model with two classes of sites.*

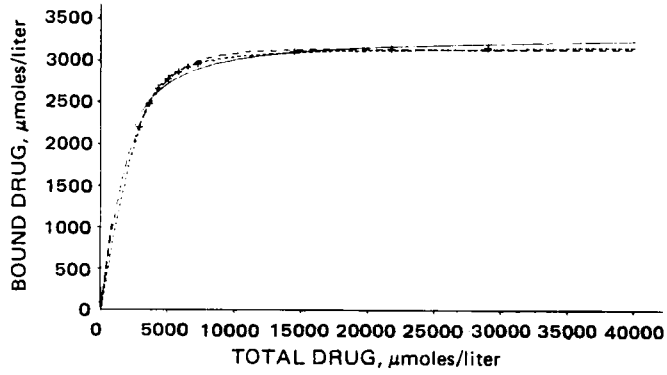

Figure 4—*Comparison of models over the high range of concentrations (>400 μg/ml, or 2900 μmoles/liter). Key: (—) trigonometric model; (- - -) exponential model; (- · - · -) Scatchard model with one class of sites; (+) Scatchard model with two classes of sites.*

Table V—Toxic and High Concentrations [a]

Total Drug		Scatchard Model Two Classes Reference	Scatchard Model One Class $K = 0.003104$ $n = 5.536$	Exponential Model $b_1 = 3161$ $b_2 = 0.000421$	Trigonometric Model $a_1 = 2125$ $a_2 = 0.000682$
μg/ml	μmoles/liter	Bound Drug μmoles/liter	Bound Drug μmoles/liter	Bound Drug μmoles/liter	Bound Drug μmoles/liter
400	2899	2210	2190	2229	2343
500	3623	2494	2497	2474	2521
600	4348	2679	2689	2655	2647
700	5072	2800	2811	2788	2740
800	5797	2881	2891	2886	2811
900	6522	2938	2946	2959	2868
1000	7246	2979	2985	3012	2914
2000	14493	3126	3122	3154	3124
3000	21739	3164	3156	3161	3195
4000	28985	3180	3171	3161	3230
5000	36232	3190	3180	3161	3251
W		—	1091	4974	44,053

[a] Simulation using the trigonometric model, the exponential model, and the Scatchard model with one class of sites; comparison with the reference values of the Scatchard model with two classes of sites. W represents the residual sum of squares.

been used during a study of the variation of the binding of salicylate in rheumatoid arthritis.

Application of the Proposed Models—In the current state of interpretation, no physiological significance should be sought in the calculated parameters. The models proposed are merely mathematical tools. They are the trigonometric model in Eq. 2 and the exponential model in Eq. 3. These equations make it possible to represent the variation in the quantity of ligand bound at equilibrium as a function of a total quantity present, while using the minimum number of parameters. The choice is not exhaustive, but the models have been tested in various circumstances: a broad-range study of the phenomenon, a detailed study of therapeutic doses over a narrowed region of study, and a study of high doses with an attempt to determine the saturating value of the quantity of ligand bound. These models can also be used to compare groups of patients.

Checking Models with Simulated Data—Simulated input data values of the equilibrium fraction of salicylate bound to albumin (Table III), derived from the Scatchard model (Eq. 1) were used for two classes of sites whose parameters have the published values (21, 22):

$$m = 2 \quad n_1 = 1.46 \quad K_1 = 0.0284\ \mu\text{moles/liter}$$
$$n_2 = 4.10 \quad K_2 = 0.0021\ \mu\text{moles/liter} \qquad \text{(Eq. 11)}$$

These data were approached as closely as possible by adjusting the parameters a_1, a_2, b_1, b_2, and perhaps n and K of the various models proposed (Eqs. 2, 3, and 8).

The proposed models were tested at equilibrium in three zones of total concentration of ligand; <1250 μg/ml (9060 μmoles/liter); <350 μg/ml (therapeutic doses); and >400 μg/ml (high concentrations).

Doses <1250 μg/ml (i.e., 9060 μmoles/liter)—This is the concentration generally studied because it covers therapeutic doses, and also approaches the limit of saturation of binding. It is more difficult to approximate a function while minimizing the number of parameters to be adjusted over a wide range of a variable (0–1250 μg/ml) than over a narrow range. However, the differences between the theoretical curve (4-Parameter Scatchard model) and the curves from the proposed models (with two parameters) remain small and less than the experimental errors encountered (Fig. 2, and Table III). The values obtained for the parameters of the two models were:

trigonometric model (Eq. 2): $a_1 = 2370.00$ μmoles/liter and $a_2 = 0.00044979$ liter/μmoles

exponential model (Eq. 3): $b_1 = 3210.57$ μmoles/liter and $b_2 = 0.00038606$ liter/μmoles (Eq. 12)

The last line of Table III represents the sum of squares of the differences between the results from the Scatchard model and from the proposed models:

$$W = \sum_{i=1}^{p} (B1_i - B2_i)^2 \qquad \text{(Eq. 13)}$$

where $B1_i$ and $B2_i$ are the fractions of ligand bound at point i at equilibrium from, respectively, the Scatchard model with two classes of sites (Eqs. 1 and 11, the input data) and one of the proposed models, p is the number of data points.

Comparison of the values obtained for W with each of the two proposed models shows that the trigonometric model gives the better results. The exponential model is a poor fit at low salicylate concentrations (of the order of 50–100 μg/ml)—at the first two points it gives an unacceptable

Table VI–Application of the Models to Real Data at Equilibrium [a]

Experimental Data			Trigonometric Model $a_1 = 2865.7$ $a_2 = 0.00284$	Exponential Model $b_1 = 3909.8$ $b_2 = 0.0002397$
Total Drug		Bound Drug	Bound Drug	Bound Drug
μg/ml	μmoles/liter	μmoles/liter	μmoles/liter	μmoles/liter
46.68	291.7	271	237	264
91.60	572.5	520	462	501
176.20	1101.2	952	869	907
380.08	2375.5	1626	1701	1697
518.01	3237.5	2100	2131	2110
650.94	4068.4	2511	2458	2435
718.99	4493.6	2737	2598	2578
938.08	5863.0	2632	2952	2951
1160.92	7255.7	3261	3206	3223
1273.95	7962.2	3424	3309	3330
W			158,000	150,000

[a] Total concentrations <1250 μg/ml (8000 μmoles/liter). Comparison of the trigonometric and exponential models with the reference Scatchard model with two classes of sites.

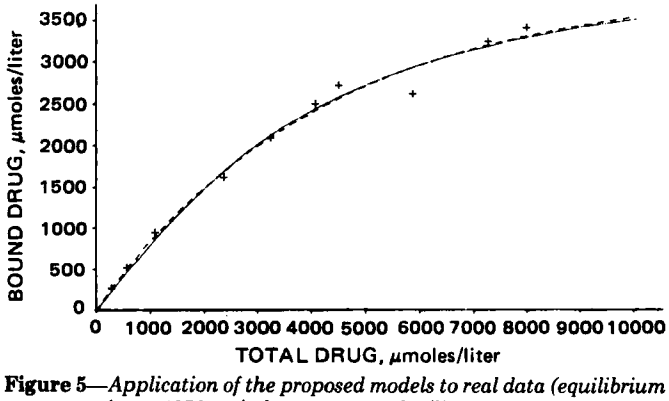

Figure 5—*Application of the proposed models to real data (equilibrium concentration <1250 μg/ml, or 8000 μmoles/liter). Key: (—) trigonometric model; (– – –) exponential model; (+) experimental values.*

Table VII—Application of the Models to Real Data at Therapeutic Concentrations [a]

Experimental Data			Trigonometric Model $a_1 = 1720.68$ $a_2 = 0.000565$	Exponential Model $b_1 = 3142.97$ $b_2 = 0.000317$	Scatchard Model One Class $K = 0.009100$ $n = 3.4784$
Total Drug		Bound Drug	Bound Drug	Bound Drug	Bound Drug
μg/ml	μmoles/liter	μmoles/liter	μmoles/liter	μmoles/liter	μmoles/liter
47.18	294.9	277.2	284	280	274
65.74	410.9	384.2	393	384	380
91.02	568.9	512.7	535	518	522
135.74	848.4	759.2	769	741	763
178.39	1114.9	979.9	968	936	976
219.01	1368.8	1175.1	1133	1106	1154
253.33	1583.3	1291.6	1256	1246	1281
282.59	1766.2	1344.9	1350	1347	1428
307.41	1921.3	1342.6	1422	1433	1543
380.37	2377.3	1629.6	1602	1664	1563
W			11,050	19,121	52,200

[a] Comparison of the trigonometric model, the exponential model, the Scatchard model with one class of sites, and the reference Scatchard model with two classes of sites.

value for the bound fraction, greater than the total concentration. The Scatchard model with a single class of sites is inapplicable over this wide range of variation of total salicylate concentration.

Therapeutic Zone of Concentrations <350 μg/ml (2500 μmoles/liter)—Over this limited zone the approximation is easier. Table IV and the curves in Fig. 3 represent the results obtained from the 14 data points from the first two columns of the table. The values of the parameters obtained with the two proposed models are:

trigonometric model (Eq. 2):

$$a_1 = 2783.6\ \mu\text{moles/liter} \quad a_2 = 0.000347\ \text{liter}/\mu\text{mole}$$

exponential model (Eq. 3):

$$b_1 = 3858.4\ \mu\text{moles/liter} \quad b_2 = 0.000285\ \text{liter}/\mu\text{mole} \quad \text{(Eq. 14)}$$

Here again the trigonometric model gives better results than does the exponential model, which has three unacceptable points where more than the total salicylate concentration is bound. A weighting of the first points in the computation remedied this disadvantage, but the differences then became greater at the points for higher concentrations.

The Scatchard model with one class of sites (Eq. 8) is applicable over this region (Fig. 3 and Table IV) and gave good results with the values $K = 0.006972$ μmoles/liter and $n = 4.3964$.

High Concentrations >400 μg/ml, 2900 μmoles/liter—The 11 points lying between 400 and 5000 μg/ml in Table V were used. The exponential model gave better results than the trigonometric model (Table V and Fig. 4):

trigonometric model (Eq. 2):

$$a_1 = 2124.92\ \mu\text{moles/liter} \quad a_2 = 0.000682\ \text{liter}/\mu\text{mole}$$

exponential model (Eq. 3):

$$b_1 = 3161.30\ \mu\text{moles/liter} \quad b_2 = 0.000421\ \text{liter}/\mu\text{mole} \quad \text{(Eq. 15)}$$

However, for high concentrations the best results were obtained with the Scatchard model limited to a single class of sites (Eq. 8). The corresponding curve was then similar to the curve from the model with two classes of sites used as data (Fig. 4 and Table V). The parameters obtained had the values $n = 5.536$ and $K = 0.003104$ μmole/liter.

Application of the Proposed Models to Real Data—The models were applied to experimental results on the binding of sodium salicylate to albumin and studied over the various zones mentioned.

Total Salicylate Concentration Lying Between 0 and 1200 μg/ml—Table VI and Fig. 5 show the bound fraction at equilibrium obtained with the trigonometric model having parameters a_1 (2865 μmoles/liter) and a_2 (0.000284 liter/μmole) and with the exponential model having parameter b_1 (3910 μmoles/liter) and b_2 (0.000240 liter/μmole).

This first zone is too broad for application of the Scatchard model limited to a single class of sites (Eq. 8).

Note that the two curves are almost identical (Fig. 5). This figure shows also that the saturation limit was still not reached and any extrapolation to estimate the value of this limit would be dangerous, whatever model is used.

Therapeutic Concentrations <350 μg/ml—Table VII and Fig. 6 show the results obtained with the trigonometric model with a_1 (1720.68 μmoles/liter) and a_2 (0.0005654 liter/μmole), and with the exponential model with b_1 (3142.97 μmoles/liter) and b_2 (0.000317 liter/μmole). Over this relatively narrow zone the single-class Scatchard model (Eq. 8) can be applied with n equal to 3.4784 and K equal to 0.00910 μmole/liter. Of the three models, the trigonometric model gave the best results (Table VII).

High Concentrations (from 400–500 μg/ml)—This zone can be of interest for example in studies of toxic doses or to estimate the saturation limit of bound fraction of substance (the plateau of the curve). The coefficients, a_1 and b_1, here have an important role since they are directly related to the value of this limit (Eqs. 4 and 5). But the experimental

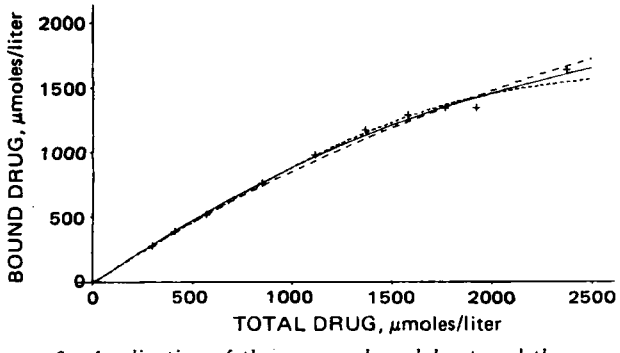

Figure 6—*Application of the proposed models at real therapeutic concentrations (<400 μg/ml, or 2500 μmoles/liter). Key: (—) trigonometric model; (- - - -) exponential model; (- - - - -) Scatchard model with one class of sites; (+) experimental values.*

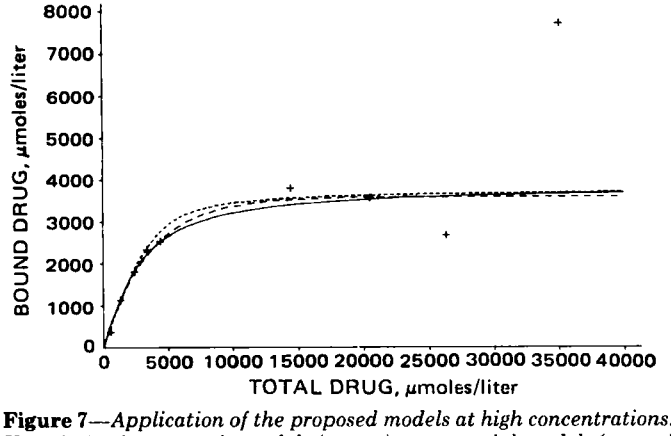

Figure 7—*Application of the proposed models at high concentrations. Key: (—) trigonometric model; (- - - -) exponential model; (- - - - -) Scatchard model with one class of sites; (+) experimental values.*

Table VIII—Application of the Models to Real Data at High Concentrations; Comparison of the Two Models

Experimental Data			Trigonometric Model $a_1 = 2466.2$ $a_2 = 0.000377$	Exponential Model $b_1 = 3618.2$ $b_2 = 0.000279$	Scatchard Model One Model $K = 0.00171$ $n = 6.00$
Total Drug		Bound Drug	Bound Drug	Bound Drug	Bound Drug
μg/ml	μmoles/liter	μmoles/liter	μmoles/liter	μmoles/liter	μmoles/liter
93.98	587	549	537	547	498
216.67	1354	1146	1163	1138	1111
396.30	2477	1829	1851	1805	1892
537.04	3356	2338	2223	2199	2373
703.70	4398	2546	2534	2557	2780
2305.83	14,411	3823	3425	3553	3591
3286.90	20,543	3586	3557	3606	3658
4214.90	26,343	2687	3626	3615	3689
5619.05	35,119	7744	3688	3618	3715
W			17.10^6	18.10^6	17.10^6

difficulties are greater at high concentrations; there are problems of dilution and precision of the measurements. The curves in Fig. 7 represent our first results in this zone (Table VIII). They were obtained with the following parameter values:

trigonometric model:

$$a_1 = 2466.2\ \mu\text{moles/liter} \quad a_2 = 0.000377\ \text{liter}/\mu\text{mole}$$

exponential model:

$$b_1 = 3618.2\ \mu\text{moles/liter} \quad b_2 = 0.000279\ \text{liter}/\mu\text{mole}$$

single-class Scatchard model: $K = 0.00171\ \mu\text{moles/liter} \quad n = 6.0$ (Eq. 16)

The basis of the Scatchard model is not questioned, but rather its quasi-automatic application in studies of the binding of a substrate to a protein. Even if this model is an accurate reflection of a real biochemical phenomenon, there may be insufficient experimental data to determine the values of the parameters unambiguously. The indistinguishability of the true number of binding classes and the minimum number of classes compatible with experimental data is sufficient to show that this model can be used only as a mathematical tool, for example, to interpolate data, or to calculate derivatives of curves or areas under them. This tool is difficult to manipulate, since it requires that a nonlinear equation be solved at each point. In addition, the practical indeterminacy of these parameters prevents them from being used separately as elements of reference for comparing groups of patients. Therefore, other models with only two parameters that have been used to study the influence of a pathological condition on the binding of a substance to a protein have been proposed.

REFERENCES

(1) G. Scatchard, *Ann. N.Y. Acad. Sci.*, **51**, 660 (1949).

(2) I. M. Klotz and D. L. Hunston, *Biochemistry*, **10**, 3065 (1971).

(3) K. Thakur and D. Rodbard, *J. Theor. Biol.*, **80**, 383 (1979).

(4) J. J. Vallner, J. H. Perrin, and S. Wold, *J. Pharm. Sci.*, **65**, 1182 (1976).

(5) O. Fischer, *M.I.T. Press*, 1285 (1969).

(6) J. Kreuzer, "GPM/GPM NLC Reference Manual," Academic Computer Center, University of Wisconsin, Madison, WI, Aug. 1971.

(7) C. M. Metzler, G. L. Elfering, and A. J. McEwen, *Biometrics*, September, 562 (1974).

(8) J. H. Perrin, J. Vallner, and S. Wold, *Biochim. Biophys. Acta*, **371**, 482 (1974).

(9) J. Wahrendorf, *Int. J. Biomed. Comput.*, **10**, 75 (1979).

(10) H. L. Behm and J. G. Wagner, *J. Pharm. Sci.*, **70**, 802 (1981).

(11) A. Faure, C. Memoz, B. Claustrat, and J. Site, *Comput. Programs Biomed.*, **12**, 19 (1980).

(12) J. G. Norby, P. Ottolenghi, and J. Jensen, *Anal. Biochem.*, **102**, 318, (1980).

(13) J. E. Fletcher and A. A. Spector, *Mol. Pharmacol.*, **13**, 387 (1977).

(14) M. Katsumata, M. K. Baker, and A. S. Goldmann, *Biochemistry*, **86**, 963, (1979).

(15) R. A. McPherson and A. Zettner, *Clin. Lab. Sci.*, **8**, 483 (1978).

(16) D. L. Parsons and J. J. Vallner, *Math. Biosci.*, **41**, 189 (1978).

(17) T. D. Sokoloski and B. A. Hoener, *J. Pharm. Sci.*, **64**, 11, 1892 (1975).

(18) M. Schoneshofer, *Clin. Chim. Acta*, **77**, 101 (1977).

(19) D. L. Parsons, and J. J. Vallner, *Math. Biosci.*, **41**, 217 (1978).

(20) K. G. Wagner, *Eur. J. Biomed.*, **10**, 261 (1969).

(21) W. D. Wosilait, *Eur. J. Clin. Pharmacol.*, **9**, 285, (1976).

(22) J. F. Zarolinski, S. Kerestes-Nagy, R. F. Mais, and Y. T. Oester, *Biochem. Pharmacol.*, **23**, 1767 (1974).

ACKNOWLEDGMENTS

This research was supported by grants from the "Institut National de la Santé et de la Récherche Medicale": ATP 78-101 and CRL 828016 and from Conseil Scientifique Université de Nancy 1.

We are grateful for the excellent technical assistance of B. Sirantoine (I.N.S.E.R.M. laboratory technician).

Evaluation of Basket and Paddle Dissolution Methods Using Different Performance Standards

VADLAMANI K. PRASAD ˣ, VINOD P. SHAH, JOHN HUNT, EDWARD PURICH, PATRICK KNIGHT, and BERNARD E. CABANA

Received January 6, 1982, from the *Division of Biopharmaceutics, Bureau of Drugs, Food and Drug Administration, Washington, DC 20204.* Accepted for publication March 2, 1982.

Abstract □ Dissolution studies using both basket and paddle methods were carried out to evaluate two prednisone standards. Results of the experiments showed that the USP prednisone calibrator is sensitive to perturbations by the basket method but not to perturbations by the paddle method. However, the National Center for Drug Analysis (NCDA) prednisone performance standard is sensitive to perturbations by the paddle method but not to perturbations by the basket method. These results suggest that no single standard can predict the suitability of the dissolution equipment by the basket and paddle methods.

Keyphrases □ Dissolution—evaluation of basket and paddle methods using different performance standards, prednisone □ Prednisone—evaluation of basket and paddle dissolution methods using different performance standards □ Basket dissolution method—prednisone, evaluation using different performance standards □ Paddle dissolution method—prednisone evaluation using different performance standards

Dissolution analysis of pharmaceutical solid dosage forms has emerged as the single most important test that will ensure the quality of the product when carried out appropriately. In several instances, the dissolution results have been correlated with the bioavailability of the product, in which case the dissolution test can also ensure the bioavailability of the product between batches that meet the dissolution criteria. The dissolution test is generally carried out by either the basket or paddle method, both of which are official in USP XX, and are referred to as USP methods I and II (1). Important variables that play a major role in the dissolution methodology include dissolution medium and intensity of agitation. In addition, before the methodology can be used, it is imperative that the instrument be properly aligned and tuned to achieve reproducible and reliable dissolution results. A system suitability test is carried out using USP prednisone and salicylic acid calibrators to check alignment and fine tuning of the dissolution unit. Deficiencies in the equipment, such as the looseness of the chain, tilt of the stirring motor (tilt), misalignment of the flasks with respect to the stirring rod (off-centering), *etc.*, have been shown (2) to be easily detectable from the dissolution results of the basket method using the USP prednisone calibrator. The results obtained using the paddle method under the same conditions did not show significant differences in the dissolution results, although the equipment was judged as being not in good operating condition. These observations led to the conclusion that the basket method was superior to the paddle method. These are worthy conclusions, yet they do not lend support to the superiority of the basket method because of the lack of reproducibility (3, 4) and problems identified with mixing (5–8).

The National Center for Drug Analysis[1] (NCDA) has identified a prednisone tablet (NCDA prednisone performance standard II) that is highly sensitive to the aberrations of the equipment when the dissolution studies are carried out by the paddle method (9). However, no systematic study has been carried out to evaluate these two standards (USP prednisone calibrator and NCDA prednisone performance standard II) using the basket as well as paddle methods.

The purpose of this report is to evaluate the basket and paddle methods using both the USP calibrator and NCDA performance standard II, and to study the influence of various perturbations of the apparatus on the results.

EXPERIMENTAL

Method—The studies were carried out using commercially available dissolution equipment[2] and employing the basket method at 100 rpm and the paddle method at 50 rpm as previously described (1). The experimental directions provided with the official calibrator were followed in performing the study.

Instrument Operating Conditions—*Normal*—The instrument was aligned properly, finely tuned, and standardized according to a previous procedure (10).

Perturbed—The following perturbations were made to the dissolution apparatus, and the dissolution test was carried out under these conditions:

1. Tilt: The dissolution head (stirring motor) was tilted by raising the back rest of the unit. This produced deviations in shaft perpendicularity. The tilt produced was accurately measured by a universal protractor[3] at 1.5°.
2. Off-center: The dissolution head was moved to one side to displace the paddle or the basket from the exact center in the vessel by 3 mm.
3. Tilt with off-centering: A 1.5° tilt was produced with 3 mm off-centering.

Standards—Two prednisone standards, USP[4] 50-mg prednisone calibrator and NCDA 10-mg prednisone performance standard II, were used in this study.

Dissolution tests were carried out in deaerated water. Six tablets were used for each dissolution run. For the USP prednisone calibrator, 900 ml of the dissolution medium was used, and for the NCDA performance standard, 500 ml of the dissolution medium was used. The amount of the drug dissolved in 30 min was determined by comparing the absorbance of the sample with the USP prednisone reference standard at 242 nm in a spectrophotometer[5].

RESULTS AND DISCUSSION

The dissolution study results obtained by the basket and paddle methods, using a USP prednisone calibrator and an NCDA prednisone performance standard under normal standardized conditions and different perturbations, are summarized in Tables I–IV.

In the dissolution studies using the basket method, an agitation of 100 rpm was used. This agitation speed was used previously in different collaborative studies (4, 11). It was also used in a study where the influence of different perturbations on the dissolution characteristics of the

[1] National Center for Drug Analysis, Food and Drug Administration, Market Street, St. Louis, MO 63101.

[2] Easilift Dissolution Test Station Model 63-734-100, Hanson Research Corp., Northridge, Calif.

[3] Sears Roebuck & Co., Chicago, Ill.

[4] Batch F.

[5] Beckman Model 25/7 spectrophotometer, Beckman Instruments, Fullerton, Calif., or Variscan spectrophotometer, Varian Associates, Palo Alto, Calif.

0022-3549/83/0100-0042$01.00/0

Table I—USP Prednisone Calibrator (Basket Method) Dissolution in 900 ml of Water at 100 rpm

Unit Operating Condition[a]	Mean ($N = 6$)	$\pm SD$	Range
Normal	68.3	0.9	67.2–69.3
	68.5	7.6	57.1–76.4
	68.9	3.2	63.2–73.7
Tilt	39.9	3.3	34.6–44.6
	40.6	0.6	39.5–41.2
Off-center	46.1	5.9	41.2–57.8
	48.9	1.0	47.7–49.9
Tilt with Off-center	36.3	1.1	34.2–37.1
	37.8	1.6	36.0–40.2

[a] ANOVA for conditions: $p = 0.0034$. Duncan's multiple range test ($\alpha = 0.05$): N O T T/O.

USP prednisone calibrator were examined (2). For normal conditions, the instrument was aligned, and all precautions were taken as described previously (10).

The basket method using the USP prednisone calibrator under normal conditions gave mean dissolution results of 68% (Table I). It is important to note that this value is very nearly identical to the normal mean value for the USP prednisone calibrator using the paddle method (4). However, when the equipment is perturbed, such as tilting the gear plate by 1.5°, the results are decreased to 40%. This is a substantial decrease. The off-centering of the basket (*i.e.*, from the center of the dissolution vessel) also produced a reduction in the mean dissolution value to 47%, which was similar to tilting. Both tilt and off-centering decreased the dissolution to ~37%, which although lower, did not suggest that these effects were additive.

This dramatic influence (*i.e.*, drop in the dissolution value, from 68 to 37% between normal and perturbed conditions) on the results of the basket method substantiates the findings reported earlier (2). The reason for the substantial decrease may partly be attributed to the decrease in the effective stirring of the dissolution medium under these perturbed conditions. The particles of the disintegrated tablet (USP prednisone calibrator) were observed to drop and collect at the center of the flask. Under tilt and off-center conditions, the particles are not sufficiently agitated because the rotating basket is not directly above the particles. These perturbed conditions, therefore, effectively lower the intensity of agitation resulting in lower dissolution value.

The intensity of agitation should not be confused with mixing, *i.e.*, uniform mixing. It was clearly established (12) that the basket method produces uniform mixing of the dissolution medium. This conclusion was based on the observation that samples drawn from different positions in the flask gave very similar results. In the cement investigation under tilt condition, the basket is positioned such that one side of the basket is close to the wall of the dissolution flask, whereas the other side is at the most distant position. Dissolution samples drawn from either side of the basket, at the same time using two probes, resulted in identical dissolution values, further indicating that there is no problem with mixing in the basket method.

The dissolution results using the USP prednisone calibrator and paddle method under normal and perturbed conditions are nearly the same (~70%, Table II). These results indicate that the paddle method cannot differentiate between the normal and perturbed conditions when the USP prednisone calibrator is used. A plausible explanation for the insensitivity of the USP prednisone calibrator to the perturbations in the paddle method is that the intensity of agitation (effective stirring) is adequate to disperse the tablet fragments throughout the medium under normal,

Table II—USP Prednisone Calibrator (Paddle Method) Dissolution in 900 ml of Water at 50 rpm

Unit Operating Condition[a]	Mean ($N = 6$)	$\pm SD$	Range
Normal	68.6	4.3	62.0–73.1
Tilt	71.7	0.8	70.7–72.8
	71.6	1.6	68.7–73.1
Off-center	64.1	2.7	60.1–67.7
	69.4	2.6	67.2–74.3

[a] ANOVA for conditions: $p = 0.72$. Duncan's multiple range test ($\alpha = 0.05$): T N O.

Table III—NCDA Prednisone Performance Standard (Paddle Method) Dissolution in 500 ml of Water at 50 rpm

Unit Operating Condition[a]	Mean ($N = 6$)	$\pm SD$	Range
Normal	41.0	2.5	36.2–43.2
	40.5	3.1	38.1–45.0
	39.2	3.8	35.4–44.5
Tilt	50.9	3.0	45.4–54.3
	53.8	4.4	49.0–59.5
Off-center	49.4	4.4	44.4–55.3
	48.9	6.0	39.6–56.8

[a] ANOVA for conditions: $p = 0.00005$. Duncan's multiple range test ($\alpha = 0.05$): T O N.

tilt, and off-center conditions, thus overcoming the inadequacies noticed in the basket method.

The results from several collaborative studies (3, 4, 11) indicate that the basket method always results in a wide range of dissolution values, where the paddle method has a narrow range of dissolution values. To establish the ruggedness and sensitivity of the paddle method, NCDA has identified a prednisone product (NCDA prednisone performance standard II) that can detect perturbations in the paddle method and that can be used for system suitability tests (9).

The dissolution results using the NCDA performance standard by the paddle method under normal and perturbed conditions are summarized in Table III. Under normal conditions, the dissolution results are ~40%, whereas under perturbed conditions they are ~ 50%. These values are significantly different when compared to normal conditions. The results thus indicate that the paddle method is sensitive to minor perturbations in the system and can differentiate between equipment that has been properly set up (normal) as opposed to a system that is improperly aligned, tilted, *etc.*, (perturbed) when NCDA performance standard II is used. The results of the NCDA performance standard using the paddle method were influenced by perturbations, and the reason might have been that after rapid disintegration, the particles are not very well dispersed, but form a mount (or cone) in the bottom of the flask. Because the particles are dense and settle down, the drug diffuses from the mound and not by dispersion throughout the medium.

NCDA prednisone performance standard II using the basket method resulted in a mean dissolution of 74% under normal conditions (Table IV). The dissolution results under perturbed conditions are also shown in Table IV. Different perturbations do not influence the results of NCDA performance standard II when the basket method is used. The tablet components of this standard, after disintegration, remained inside the basket longer, whereas the USP prednisone calibrator rapidly disintegrated and settled to the bottom of the flask. These observations partly explain the anomaly observed in the results of these two prednisone tablets when tested by the basket method. If one notices the USP calibrator results by the basket procedure, the differences between the normal and perturbed conditions are dramatic. Thus, one can reasonably conclude that the USP prednisone calibrator is sensitive to perturbations in the basket procedure, whereas the NCDA prednisone performance standard II is insensitive to any unanticipated aberrations in the equipment. The differences in the physical state of the deaggregated tablet matrix as well as the differences in the density of the particles (as observed in the flask) can, at the present time, explain these differences in the results.

The dissolution data on both standards using both methods are summarized in Fig. 1. It is interesting to note that identical perturbations

Table IV—NCDA Prednisone Performance Standard (Basket Method) Dissolution in 500 ml of Water at 100 rpm

Unit Operating Condition[a]	Mean ($N = 6$)	$\pm SD$	Range
Normal	77.4	2.6	74.7–80.5
	72.1	6.1	65.4–78.2
Tilt	81.5	3.1	77.6–85.9
	80.3	2.6	77.0–84.7
Off-center	77.9	2.1	77.0–80.6
	81.9	1.4	80.0–83.5

[a] ANOVA for conditions: $p = 0.20$. Duncan's multiple range test ($\alpha = 0.05$). T O N.

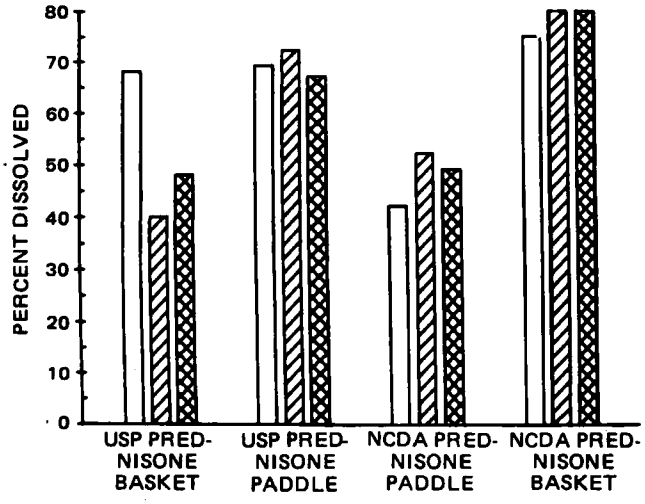

Figure 1—*Evaluation of the basket and paddle method using the USP prednisone calibrator and the NCDA prednisone performance standard. Key = (□) Normal; (▨) Tilt; (▩) Off-center.*

result in increased dissolution of the NCDA performance standard by the paddle method but decreased dissolution of USP prednisone calibrator by the basket method. The conclusion that one method (basket or paddle) is better than the other is, therefore, largely dependent on the standard product used in the system suitability test. At the present time neither the USP prednisone calibrator nor NCDA prednisone performance standard II alone can predict the suitability of a dissolution system when both the basket and paddle methods as described in the USP, are to be used.

All the dissolution results were statistically analyzed using ANOVA and Duncan's Multiple Range Test. The statistical results indicate that the dissolution results of the basket method using the USP prednisone calibrator and the dissolution results by paddle method using NCDA performance standard II under normal conditions were significantly different from the results obtained under perturbed conditions. It is therefore concluded that the USP prednisone calibrator is sensitive to perturbations by the basket method, and can be used as a calibrator in the system suitability test by the basket method only. Similarly, NCDA prednisone performance standard II is sensitive to perturbations by the paddle method and can be used as a calibrator for the system suitability test of the paddle method only. From the ANOVA it is also concluded that the USP prednisone calibrator is insensitive to perturbations by the paddle method, and NCDA performance standard II is insensitive to perturbations by the basket method. These results are summrized in Table V and indicate the necessity of an official calibrator similar to NCDA prednisone performance standard II to perform the system suitability test when the paddle method is used.

Table V—Statistical Analysis of Dissolution Data between Methods, Conditions, and Calibrators

Method	Calibrator	ANOVA[a]
Basket	USP Prednisone	$p = 0.0008$
	NCDA Prednisone	Not Significant
Paddle	USP Prednisone	Not Significant
	NCDA Prednisone	$p = 0.0001$

[a] Comparison of the dissolution data between the normal and perturbed (tilt, off-center, and tilt with off-center) conditions.

REFERENCES

(1) "The United States Pharmacopeia," 20th rev., United States Pharmacopeial Convention, Inc., Rockville, Md., 1980, p. 959.

(2) K. D. Thakkar, N. C. Naik, V. A. Gray, and S. Sun, *Pharmacopeial Forum*, **1980**, 177.

(3) B. E. Cabana and R. O'Neill, *ibid.*, **1980**, 71.

(4) D. Schuirmann, *ibid.*, **1980**, 75.

(5) R. J. Withey, *J. Pharm. Pharmacol.*, **23**, 573 (1971).

(6) R. J. Withey and A. J. Bowker, *ibid.*, **24**, 345 (1972).

(7) J. T. Carstensen, T. Lai, and V. K. Prasad, *J. Pharm. Sci.*, **66**, 607 (1977).

(8) J. E. Tingstad, *Pharmacopeial Forum*, **1981**, 1025.

(9) "Abstract," vol. 11, no. 2, APhA Academy of Pharmaceutical Sciences annual meeting, American Pharmaceutical Association, Washington, D.C., (1981), p. 129.

(10) D. C. Cox, C. Douglas, W. B. Furman, R. D. Kirchhoefer, J. W. Myrick, and C. E. Wells, *Pharm. Technol.*, **2**, 41 (1978).

(11) S. Fusari, M. F. Grostic, A. R. Lewis, J. Poole, and A. C. Sarapu, *ibid.*, **5**, 135 (1981).

(12) A. C. Cartwright, *Drug Dev. Ind. Pharm.*, **5**, 277 (1979).

ACKNOWLEDGMENTS

The authors sincerely acknowledge the following personnel of the Bureau of Drugs, Food and Drug Administration: Mr. Gene Knapp for his valuable and constructive suggestions and Mr. D. Schuirman for his guidance in statistical analysis of the data.

Potential Broad Spectrum Anthelmintics IV: Design, Synthesis, and Antiparasitic Screening of Certain 3,6-Disubstituted-(7*H*)-*s*-triazolo-[3,4-*b*][1,3,4]thiadiazine Derivatives

M. A. El-DAWY *, A.-MOHSEN M. E. OMAR ‡x, ABLA M. ISMAIL *, and A. A. B. HAZZAA ‡

Received December 4, 1980, from the *Department of Pharmaceutical Chemistry, Faculty of Pharmacy, *University of Tanta and ‡University of Alexandria, Egypt.* Accepted for publication December 29, 1981.

Abstract □ A series of 3,6-disubstituted-(7*H*)-*s*-triazolo[3,4-*b*][1,3,4]-thiadiazine derivatives were prepared. The compounds were designed to obtain structural similarities and/or bear isosteric relation with certain fused systems encountered in some well-known antiparasitic drugs. The substituents in all products were selected according to the Topliss scheme. Preliminary screening for antiparasitic activity, using *Ascaris vitulorum*, showed that the 6-substituted derivatives were generally more active than the 3-substituted ones and that the π effect is more pronounced than the σ effect.

Keyphrases □ Anthelmintics—potential broad spectrum, design, synthesis, antiparasitic screening of certain 3,6-disubstituted-(7*H*)-*s*-triazolo[3,4-*b*][1,3,4]thiadiazine derivatives □ Antiparasitic screening—potential broad spectrum anthelmintics, design, synthesis of certain 3,6-disubstituted-(7*H*)-*s*-triazolo[3,4-*b*][1,3,4]thiadiazine derivatives □ Thiadiazine, derivatives—potential broad spectrum, design, synthesis, antiparasitic screening of certain 3,6-disubstituted-(7*H*)-*s*-triazolo[3,4-*b*][1,3,4]thiadiazine derivatives

In the past few years, studies have been concerned with the design, synthesis, and screening for anthelmintic activity of several fused systems bearing structural and isosteric relationships with (±) 6-phenyl-2,3,5,6-tetrahydroimidazo[2,1-*b*]thiazone (tetramisole) (1), the well-known broad spectrum anthelmintic. As a result, a variety of compounds derived from imidazo[1,2-*b*]thiazole (2, 3), imidazo[1,2-*b*][1,3,4]thiadiazole, thiazolo[2,3-*b*]thiadiazole (4), thiazolo[2,3-*c*]tetrazole (5) as well as their open-ring counterparts were developed.

In view of the recently reported antiparasitic activity of some derivatives of triazole (6, 7), a novel series of potential anthelmintics were prepared in which the triazole is a part of the fused heterocyclic system. The compounds of interest, namely 3,6-disubstituted-(7*H*)-*s*-triazolo[3,4-*b*]-[1,3,4]thiadiazines (III–XLIV), Scheme I, were designed to contain various substituents selected according to the Topliss scheme (8). The purpose was to study the effect of the different possible variations of π and σ on the biological activity of the parent compound.

RESULTS AND DISCUSSION

Chemistry—Compounds III–XLIV were prepared in accordance with the sequence of reactions presented in Scheme I. The potassium salts of N^1-acyl-N^2-dithiocarbazates (I), synthesized from the reaction of the corresponding acylhydrazines (9–13) with carbon disulfide and potassium hydroxide, were treated with hydrazine hydrate in refluxing ethanol to give the 3-substituted-4-amino-*s*-triazolo-5-thiones (II) (14). The IR spectra of these triazoles indicated their existence in thione form *A* rather than in thiol form *B*. Condensation of the triazoles (II) with the appropriately substituted phenacylbromides (15, 16) in refluxing ethanol gave the required 3,6-disubstituted-(7*H*)-*s*-triazolo[3,4-*b*][1,3,4]thiadiazines (III–XLIV). The yields and physical constants of the products are recorded in Table I.

Unlike earlier claims (18, 19), the trials to synthesize the noncyclic analogs of compounds III–XLIV, namely the 3-(4-substituted aryl)-4-amino -5- [*S*-(4-substituted-phenacyl)mercapto]-(4*H*)-1,3,4-triazoles (XLV), which bear the same spatial arrangement as the triazolothiadiazines (III–XLIV), were fruitless. The reactions, even under the mildest conditions, always yielded the cyclized products.

The IR spectra of the products (III–XLIV) were compatible with the structures assigned. In particular, the thioureido (I, II, III, and IV) bands located for the C=S and —NH mixed vibrational coupling in the triazole (II) were greatly affected. The bands contributing to the —NH moiety of the —CSNH function at 1515 and 1090 cm^{-1} completely disappeared while those at 1315 and 950 cm^{-1}, characteristic for the C=S function (20), became weaker in intensity. The absence of the carbonyl absorbance at 1660–1630 cm^{-1} has also confirmed the cyclic structures. The PMR spectra showed the signals at the expected chemical shifts. The compounds containing the methyl groups in the aryl substituents showed a singlet in the region of 2.37–2.50 ppm, while those containing the methoxy functions showed the singlet at 3.73–3.87 ppm. The C_7-methylinic protons appeared as a singlet in the region of 4.42–4.43 ppm. The chemical shifts of the aromatic protons of the 3- and 6-aryl functions were dependent on the nature of the *p*-substituents in these groups.

For more concerted evidence, the mass spectra of compounds XXVII and XXX, as representative examples, were run, and the structure of the ions formed, under electron impact, was assigned. The spectrum of 3-*p*-methoxyphenyl-6-*p*-bromophenyl-(7*H*)-*s*-triazolo[3,4-*b*][1,3,4]thiadiazine (XXX) showed the molecular ion peak at *m/z* 400 (402 for M+2). Its

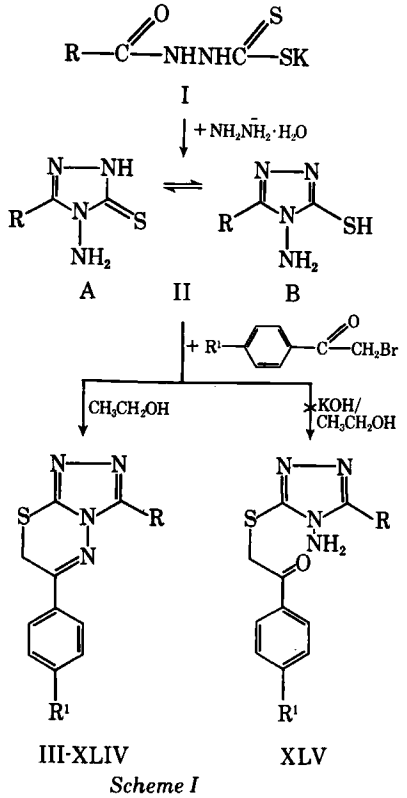

Scheme I

0022-3549/83/0100-0045$01.00/0

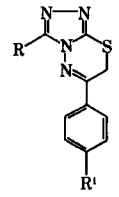

Table I—Yields, Physical Constants, Microanalytical Data, and Antiparasitic Activity of the Synthesized 3,6-Disubstituted-(7*H*)-*s*-triazolo[3,4-b][1,3,4]thiadiazine Derivatives.

Compound No.	*R*	R^1	Melting Point	Yield, %	Molecular Formula	Analysis, % Calc.	Found	π or $\Sigma\pi$	σ or $\Sigma\sigma$	Antiparasitic Activity Time[a]	Observed Effect
III	C_6H_5	H	113–114[b]	70				0.00	0.00	15–25	D[c]
IV	C_6H_5	NO_2	305	72	$C_{16}H_{11}N_5O_2S$	C 56.97 H 3.26 N 20.77 S 9.49	56.50 3.50 21.00 9.30	0.24	0.78	30–35	R[d]
V	C_6H_5	Cl	239–240	92	$C_{16}H_{11}ClN_4S$	C 58.89 H 3.37 Cl 10.73 S 9.81	59.00 3.50 10.80 9.50	0.70	0.23	7–12	D
VI	C_6H_5	Br	244–245	94	$C_{16}H_{11}BrN_4S$	C 51.75 H 2.96 Br 21.56 N 15.09 S 8.62	51.70 3.20 21.30 14.70 8.30	1.19	0.23	7–10	D
VII	C_6H_5	CH_3	192–194	78	$C_{17}H_{14}N_4S$	C 66.67 H 4.57 N 18.30 S 10.45	66.60 4.10 18.60 10.80	0.60	−0.17	20–30	R
VIII	C_6H_5	OCH_3	216–217	50	$C_{17}H_{14}N_4OS$	C 63.35 H 4.34 N 17.39	62.90 4.49 17.50	−0.04	−0.27	20–30	R
IX	$C_6H_4Cl(p)$	H	260–261	94	$C_{16}H_{11}ClN_4S$	C 58.89 H 3.37 Cl 10.73 N 17.17 S 9.81	58.80 3.40 11.10 17.50 9.60	0.70	0.23	20	D
X	$C_6H_4Cl(p)$	NO_2	246–247	63	$C_{15}H_{10}ClN_5O_2S$	C 51.75 H 2.69 Cl 9.43 S 8.60	51.50 3.10 9.10 8.20	0.94	1.01	35	R
XI	$C_6H_4Cl(p)$	Cl	276–278	56	$C_{16}H_{10}Cl_2N_4S$	C 53.33 H 2.77 Cl 19.44 N 15.55 S 8.88	53.00 3.10 18.90 15.90 9.20	1.40	0.46	7	D
XII	$C_6H_4Cl(p)$	Br	275–276	79	$C_{16}H_{10}BrClN_4S$	C 47.40 H 2.46 Br 19.75 N 13.82 S 7.90	47.70 2.40 19.40 14.00 7.70	1.89	0.46	7–10	D
XIII	$C_6H_4Cl(p)$	CH_3	253–254	71	$C_{17}H_{13}ClN_4S$	C 60.00 H 3.82 Cl 10.29	59.90 3.80 10.40	1.30	0.06	35	D
XIV	$C_6H_4Cl(p)$	OCH_3	235–236	62	$C_{17}H_{13}ClN_4OS$	C 57.30 H 3.65 Cl 9.80 N 15.73 S 8.98	57.60 3.80 10.10 15.30 9.40	0.66	−0.04	30	D
XV	$C_6H_4Br(p)$	H	258–259	90	$C_{16}H_{11}BrN_4S$	C 51.75 H 2.96 Br 21.56 N 15.09 S 8.62	51.60 2.95 22.00 15.50 8.80	1.19	0.23	10	D
XVI	$C_6H_4Br(p)$	NO_2	247–249	73	$C_{16}H_{10}BrN_5O_2S$	C 46.15 H 2.40 Br 19.23 N 16.82 S 7.69	46.10 2.50 19.00 17.20 7.30	1.43	1.01	50	R
XVII	$C_6H_4Br(p)$	Cl	271–273	83	$C_{16}H_{10}BrClN_4S$	C 47.40 H 2.46 Br 19.75 Cl 8.64 N 13.82	47.30 2.80 19.00 8.40 14.00	1.89	0.46	12–15	D
XVIII	$C_6H_4Br(p)$	Br	266–267	94	$C_{16}H_{10}Br_2N_4S$	C 42.66 H 2.22 Br 35.55 N 7.11	42.30 2.30 35.10 7.30	2.38	0.46	5–10	D

Continued

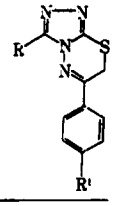

Table I–*Continued*

Compound No.	R	R^1	Melting Point	Yield, %	Molecular Formula	Analysis, %		π or $\Sigma\pi$	σ or $\Sigma\sigma$	Antiparasitic Activity	
						Calc.	Found			Time[a]	Observed Effect
XIX	$C_6H_4Br(p)$	CH_3	262–263	70	$C_{17}H_{13}BrN_4S$	C 52.98 H 3.37 Br 20.77 N 14.54 S 8.31	53.10 3.70 20.50 14.25 8.00	1.79	0.06	25	D
XX	$C_6H_4Br(p)$	OCH_3	258–260	82	$C_{17}H_{13}BrN_4OS$	C 50.87 H 3.27 Br 19.95 S 7.96	50.40 3.25 19.60 8.30	1.15	−0.04	25	D
XXI	$C_6H_4CH_3(p)$	H	200–201	81	$C_{17}H_{14}N_4S$	C 66.67 H 4.57 N 18.30	66.70 4.80 18.00	0.60	−0.71	25–35	R
XXII	$C_6H_4CH_3(p)$	NO_2	300	62	$C_{17}H_{13}N_5O_2S$	C 58.11 H 3.70 N 19.94 S 9.11	58.40 3.80 19.70 9.40	0.84	0.61	85	R
XXIII	$C_6H_4CH_3(p)$	Cl	210–212	76	$C_{17}H_{13}ClN_4S$	C 60.00 H 3.82 Cl 10.29 S 9.41	59.90 3.80 10.70 9.50	1.30	0.06	20	D
XXIV	$C_6H_4CH_3(p)$	Br	185–187	86	$C_{17}H_{13}BrN_4S$	C 52.98 H 3.37 Br 20.77 N 14.54 S 8.31	53.30 3.70 20.50 14.25 8.00	1.79	0.06	25	D
XXV	$C_6H_4CH_3(p)$	CH_3	170–172	76	$C_{18}H_{16}N_4S$	C 67.50 H 5.00 N 17.50 S 10.00	67.20 4.70 17.10 10.40	1.20	−0.34	70	R
XXVI	$C_6H_4CH_3(p)$	OCH_3	181–183	80	$C_{18}H_{16}N_4OS$	C 64.82 H 4.76 S 9.52	63.93 4.90 9.40	0.56	−0.44	40–50	R
XXVII	$C_6H_4OCH_3(p)$	H	200–203	81	$C_{17}H_{14}N_4OS$	C 63.35 H 4.34 N 17.39	63.60 4.50 17.00	−0.04	−0.27	30–35	D
XXVIII	$C_6H_4OCH_3(p)$	NO_2	251–253	39	$C_{17}H_{13}N_5O_3S$	C 55.58 H 3.54 N 19.07 S 8.71	55.60 3.90 19.40 8.30	0.20	−0.51	90	R
XXIX	$C_6H_4OCH_3(p)$	Cl	211–213	59	$C_{17}H_{13}ClN_4OS$	C 57.30 H 3.65 Cl 9.83 N 15.73	57.50 3.70 9.80 15.80	0.66	−0.04	20–25	R
XXX	$C_6H_4OCH_3(p)$	Br	217–218	80	$C_{17}H_{13}BrN_4OS$	Br 19.95 N 13.96 S 7.98	19.60 14.30 8.30	1.15	−0.44	15–25	D
XXXI	$C_6H_4OCH_3(p)$	CH_3	164–166	51	$C_{18}H_{16}N_4OS$	C 64.28 H 4.76 N 16.66 S 9.52	64.40 4.90 17.00 9.10	0.56	−0.44	45	R
XXXII	$C_6H_4OCH_3(p)$	OCH_3	172–173	72	$C_{18}H_{16}N_4O_2S$	C 61.36 H 4.54 N 15.90 S 9.09	61.00 4.70 16.20 9.20	−0.08	−0.54	60–65	R
XXXIII	$C_6H_4NH_2(p)$	H	244–245	59	$C_{16}H_{13}N_5S$	C 62.54 H 4.23 S 10.42	62.10 4.30 10.00	−1.23	−0.66	30	R
XXXIV	$C_6H_4NH_2(p)$	NO_2	251–253	43	$C_{16}H_{12}N_6O_2S$	N 23.86 S 9.09	23.50 9.50	−0.99	0.12	50–60	R
XXXV	$C_6H_4NH_2(p)$	Cl	239–241	44	$C_{16}H_{12}ClN_5S$	C 56.22 H 3.51 Cl 10.39 N 20.49 S 9.37	56.20 3.60 10.40 20.60 8.90	−0.53	−0.43	15–20	R
XXXVI	$C_6H_4NH_2(p)$	Br	237–238	64	$C_{16}H_{12}BrN_5S$	C 49.74 H 3.10 Br 20.72 S 8.29	49.70 3.30 21.00 8.50	−0.04	−0.43	15–20	R

Continued on next page

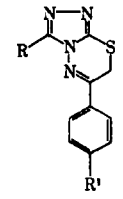

Table I–*Continued*

Compound No.	R	R[1]	Melting Point	Yield, %	Molecular Formula	Analysis, %		π or Σπ	σ or Σσ	Antiparasitic Activity	
						Calc.	Found			Time[a]	Observed Effect
XXXVII	$C_6H_4NH_2$(p)	CH_3	254–255	59	$C_{17}H_{15}N_5S$	C 63.50 H 4.30 S 9.69	63.80 4.80 9.70	−0.63	−0.83	25–35	R
XXXVIII	$C_6H_4NH_2$(p)	OCH_3	182–184	50	$C_{17}H_{15}N_5OS$	C 60.51 H 4.45 N 20.77	60.32 4.90 20.90	−1.27	−0.93	25–30	R
XXXIX	4-pyridyl	H	230–231[e]	81						20–25	R
XXXX	4-pyridyl	NO_2	250–252	59	$C_{15}H_{10}N_6O_2S$	C 53.25 H 2.95 S 9.46	52.98 2.60 9.80			30	R
XLI	4-pyridyl	Cl	254–255	75	$C_{15}H_{10}ClN_5S$	C 55.04 H 3.05 S 9.78	54.90 3.30 9.40			7–10	D
XLII	4-pyridyl	Br	262–264	79	$C_{15}H_{10}BrN_5S$	C 48.38 H 2.68 Br 21.50 S 8.60	48.20 3.10 21.20 8.30			7–10	D
XLIII	4-pyridyl	CH_3	237–239	78	$C_{16}H_{13}N_5S$	C 62.54 H 4.23 S 10.42	62.60 4.10 10.30			25	R
XLIV	4-pyridyl	OCH_3	230–231	62	$C_{16}H_{13}N_5OS$	C 59.07 H 4.16 N 21.53 S 9.84	59.30 4.60 21.20 10.00			25–30	R

[a] Time in minutes for 100% deaths or relaxation. [b] The compound is reported in Ref. 18. [c] D = Death. [d] R = Relaxation. [e] Reference 17.

fragmentation as shown in Scheme II followed four different pathways. In accordance with pathway 1, the molecule eliminated sulfur giving ion *A* at *m/z* 368 (370). In pathway 2, a *p*-bromophenyl ion was removed from compound XXX giving ion *B*, *m/z* 245, which on elimination of a nitrogen molecule and a cyanide group yielded ion *C* at *m/z* 191. This ion in turn eliminated cyanide and methylene fragments to give the phenoxyethylenesulfide ion *D* at *m/z* 151, or underwent successive cleavage of carbon monosulfide, methylene, cyanide, methyl, carbon monoxide moieties, and hydrogen producing ions *E* and *F* at *m/z* 133 and 63, respectively. The *p*-methoxyphenylcyanide ion *E* was shown as the base peak. In alternative fragmentation pathway 3, the product cleaved ion *E* and nitrogen to produce *p*-bromophenylthiazole ion *G* at *m/z* 241 (243). This on further elimination of carbon monosulfide, methylene, and cyanide fragments gave *p*-bromophenylcyanide ion *H* at *m/z* 181 (183) and *p*-bromophenyl ion *I* at *m/z* 155 (157). In pathway 4, however, the molecule eliminated ions *H* and *E* leading to ion *J* at *m/z* 219 and ion *N* at *m/z* 90. Ion *J* either eliminated a hydrogen sulfide and a methyl group giving ion *M* at *m/z* 158 or cleaved a methylene and accepted two hydrogens to produce ion *K* at *m/z* 207. Further cleavage of a *p*-methoxyphenyl ion or ion *E* from ion *K* gave ion *L* at *m/z* 102 and the pseudothiourea ion at *m/z* 75. The mass spectrum of compound XXVII showed the molecular ion peak at *m/z* 322 and the ion at 133, corresponding to *p*-methoxyphenylcyanide, as the base peak. The additional ions shown were indicative that the fragmentation of the compound followed the fragmentation pattern proposed for compound XXX.

Antiparasitic Screening—The effect of the synthesized compounds III–XLIV on *Ascaris vitulorum* worms was evaluated in accordance with a method developed previously (21). As shown in Table I, the products containing substituted phenyl groups in the 3 position were generally less active than those having the same type of substituents at the 6 position. In addition, due to increased π effect, the biological activity was higher for compounds containing 4-chloro and 4-bromophenyl substituents relative to the nonsubstituted ones.

The tolyl derivatives were found to be less potent compared with the phenyl derivatives. This finding, as well as the fact that compounds containing the nitro group ($\sigma = 0.78$) or the methoxyl group ($\sigma = 0.27$) were less active than the substituted derivatives, led to the assumption that the π effect is more predominating in this series of compounds. Moreover, the equipotent activity of the products containing 4-pyridyl and phenyl functions has been attributed to the isostericity of both functional groups.

EXPERIMENTAL[1]

Potassium Salts of 3-Aroyl Dithiocarbazates (I)—Compound I was prepared, as reported (14), starting from the corresponding acid hydrazides. They were obtained in nearly quantitative yield and employed in the following reactions without further purification.

3-Substituted-4-amino-5-mercapto-(4*H*)-1,2,4-triazoles (II)—Compound II was prepared by reaction of potassium salts of 3-aroyl dithiocarbazates with 98% hydrazine hydrate according to the reported method (14).

3,6-Disubstituted - (7*H*)-*s*-triazolo[3,4 - *b*][1,3,4]thiadiazines (III–XLIV)—Equimolar amounts of the triazoles (II) and the appropriate phenacyl bromide derivative in anhydrous ethanol were heated under reflux for 2 hr. After cooling, the mixtures were neutralized with ammonium hydroxide to separate the free base. Filtration, washing with water, and crystallization from boiling ethanol separated the products as white or pale yellow crystals. The physical constants of the products are recorded in Table I. Mass spectra for compound XXVII, *m/z* (relative abundance percent): M^+ at 322 (97), 293 (3), 290 (4), 288 (2), 245 (2), 219 (8), 191 (4), 177 (4), 161 (40), 158 (8), 151 (7), 145 (16), 133 (97), 132 (26), 130 (7), 118 (10), 117 (16), 103 (100), 90 (29), 77 (48), 63 (13), 58 (36), 51 (2); and for compound XXX: 402 (M+2) and 400 (M^+) (63), 370 (13), 368 (13), 245 (3), 241 (5), 239 (5), 219 (10), 207 (10), 197 (8), 195 (6), 191 (4), 183 (31), 181 (36), 161 (39), 158 (8), 157 (8), 155 (8), 151 (5), 145 (13), 133 (100), 118 (8), 116 (8), 103 (26), 102 (49), 90 (27), 76 (3), 75 (21), 63 (13), 58 (36), 51 (17), 50 (17).

3-Substituted-4-amino-5-[*S*-(substituted phenacyl)mercapto]-(4*H*)-1,2,4-triazole (XLV) (Attempted Preparation)—A solution of 3-(4-methoxyphenyl)-4-amino-5-mercapto-*s*-triazole (0.1 mole) in 1 *N* methanolic potassium hydroxide (20 ml) was stirred while cooling in an

[1] All melting points were uncorrected. IR spectra were measured for Nujol Mulls on a Beckmann 4210 IR Spectrophotometer. PMR spectra were measured for dimethyl sulfoxide-d_6 solutions on a high resolution T-60A Varian NMR Spectrometer. The mass spectra were taken to 70 eV on an AEIMS 902 Mass Spectrometer attached to an AEIDS 30 data system.

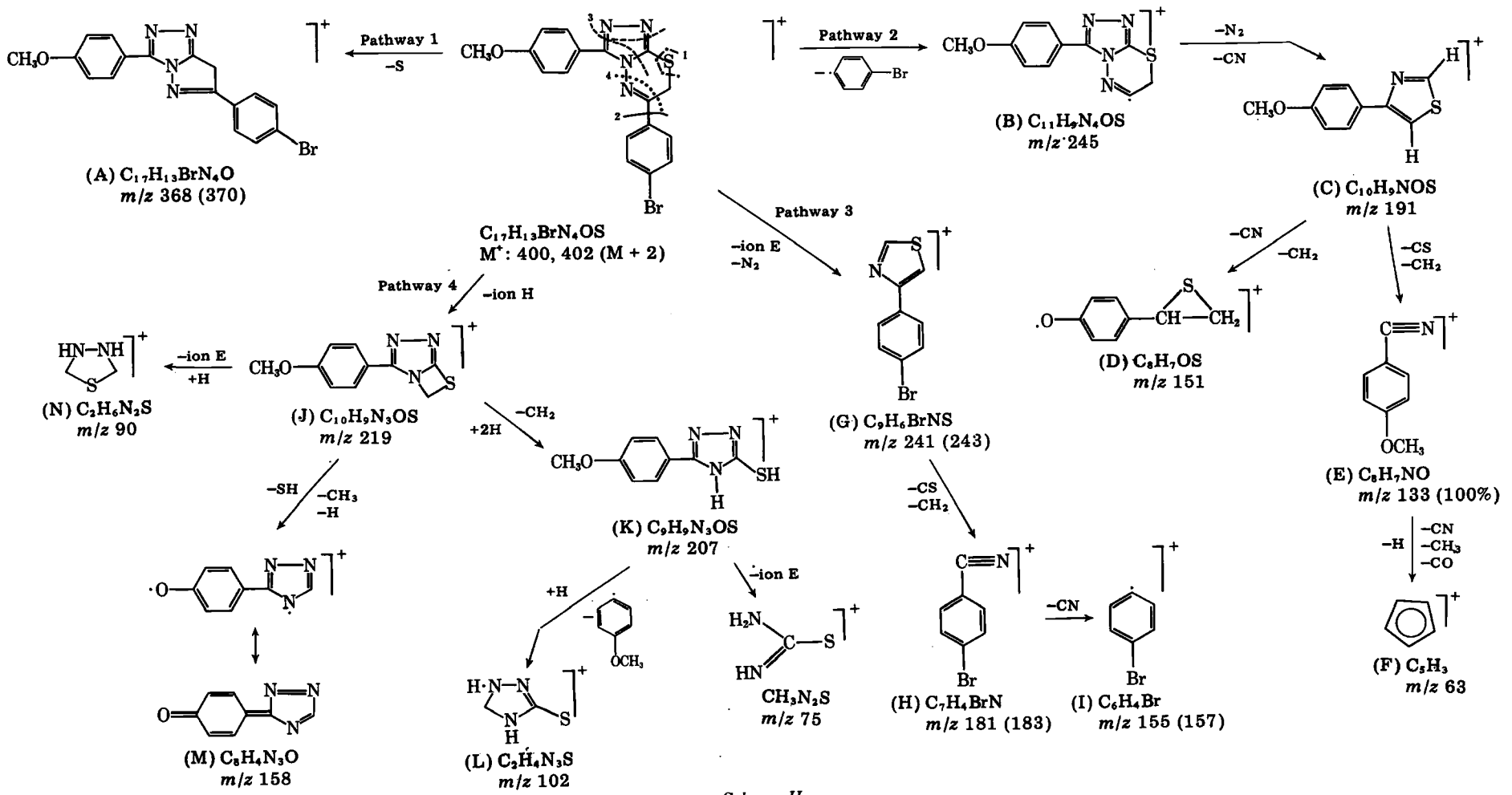
Pathway 1
–S
Pathway 2
–N₂
–CN
Pathway 3
–ion E
–N₂
Pathway 4
–ion H
–ion E
+H
–CH₂
+2H
–SH
–CH₃
–H
–CN
–CH₂
–CS
–CH₂
–CN
–H
–CN
–CH₃
–CO
+H
–ion E
(A) C₁₇H₁₃BrN₄O
m/z 368 (370)
C₁₇H₁₃BrN₄OS
M⁺: 400, 402 (M + 2)
(B) C₁₁H₉N₄OS
m/z 245
(C) C₁₀H₉NOS
m/z 191
(D) C₈H₇OS
m/z 151
(E) C₈H₇NO
m/z 133 (100%)
(F) C₅H₃
m/z 63
(G) C₉H₆BrNS
m/z 241 (243)
(H) C₇H₄BrN
m/z 181 (183)
(I) C₆H₄Br
m/z 155 (157)
(J) C₁₀H₉N₃OS
m/z 219
(K) C₉H₉N₃OS
m/z 207
(L) C₂H₄N₃S
m/z 102
(M) C₈H₄N₃O
m/z 158
(N) C₂H₆N₂S
m/z 90
CH₃N₂S
m/z 75

Scheme II

ice bath until a precipitate developed. This was dissolved by addition of methanol and the solution was treated by a dropwise addition of a solution of 4-chlorophenacyl bromide (0.2 mole) in methanol (20 ml) while maintaining the pH at 7–7.5 by 1 *N* methanolic potassium hydroxide. The final mixture was stirred for 1 hr while cooling in ice and for an additional hour at room temperature. Dilution with cold water (60 ml) caused complete separation of the product, which was found to be the cyclized product (XXIX) as evidenced by mixed melting point determination and superimposability of IR. Repeating the reaction for a shorter period of time (15 min) in aqueous methanol again gave the cyclized product (XXIX).

REFERENCES

(1) P. Andrews, H. Dorn, M. Federman, and H. Voege, *Ger. Offen.*, **2,** 614, 841 (1977); through *Chem. Abstr.*, **88,** 65976j (1978).

(2) M. A. El-Dawy, M. A. Abdel-Kader, G. M. El-Naggar, and M. A. El-Gendy, *Proc. XIII Conf. Pharm. Sci.*, Cairo, Egypt, 87 (1974).

(3) M. A. El-Dawy, M. A. Abdel-Kader, and A. N. Ahmed, *Proc. XIV Conf. Pharm. Sci.*, Cairo, Egypt, 33 (1975). M. A. El-Dawy, M. A. Abdel-Kader, and A. N. Ahmed, *Bull. Pharm. Sci.*, (Assuit Univ.), **I,** 1 (1978).

(4) M. A. El-Dawy, S. Abo-Elazm, and K. M. El-Berembally, *Pharmazie*, **34,** 144 (1979).

(5) A. S. Mehanna, Master of Science Degree Thesis, Tanta University, Egypt (1978).

(6) L. Gsell and W. Meyer, *Ger. Offen.*, **2,** 749, 753 (1978); through *Chem.Abstr.*, **89,** 43495r (1978).

(7) L. Gsell and W. Meyer, *Ger. Offen.*, **2,** 739, 084 (1978); through *Chem. Abstr.*, **88,** 190844r (1978).

(8) J. Topliss, *J. Med. Chem.*, **15,** 1006 (1972).

(9) R. Stolle, *J. Prakt. Chem.*, **69,** 145 (1904).

(10) S. Shih, *Chem. Zentralbl.*, **1,** 56 (1935).

(11) P. Curtius, *J. Prakt. Chem.*, **58,** 190 (1898).

(12) R. Kahl, *Chem. Zentralbl.*, **II,** 1493 (1904).

(13) T. Curtius, *J. Prakt. Chem.*, **51,** 168 (1895).

(14) J. R. Raid and N. D. Heindek, *J. Heterocycl. Chem.*, **13,** 925 (1976).

(15) R. M. Couper and L. H. Davidson, *Org. Synth. Coll.*, **II,** 480 (1943).

(16) C. F. Reynold, "Reactions of Organic Compounds," Wiley, New York, N.Y., 1962, p. 134.

(17) L. Giarmmanco, *Atti Acad. Sci., Lett. Arti. Palermo*, Part 1, **33,** 235 (1973); through *Chem. Abstr.*, **83,** 97228e (1975).

(18) T. George, R. Tahilramani, and D. A. Dabholkar, *Indian J. Chem.*, **49,** 057 (1969).

(19) S. Somasekhara, R. K. Thakkar, and G. F. Shah, *J. Indian Chem. Soc.*, **49,** 1057 (1972).

(20) A.-Mohsen M. E. Omar and S. A. Osman, *Pharmazie*, **28,** 30 (1973).

(21) W. A. Abdoulla, H. K. Kadry, and S. C. Mahran, *Sci. Pharm.*, **47,** 114 (1979).

Influence of Environment and Substituents on the Stability of the Radical Cations of Several Phenothiazine Derivatives

A. ORTIZ[x], I. POYATO, and J. I. FERNANDEZ-ALONSO

Received December 24, 1980, from the *Departamento de Química-Física y Química Cuántica, Centro Coordinador CSIC-UAM, Facultad de Ciencias C-XIV, Cantoblanco, Madrid 34, Spain.* Accepted for publication March 1, 1982.

Abstract □ The UV decay spectra of the radical cations of several phenothiazine derivatives in different environments was studied. The influence of the substituents on the reference spectrum could be seen, as well as a relationship between the stability of such radicals and the acidity of the environment. There is also an influence of the substituents on the stability of the radicals in the different environments studied. The instability of the radicals in solution has been studied to relate to the pharmacological activity of neuroleptics.

Keyphrases □ Phenothiazine—derivatives, influence of environment and substituents on the stability of the radical cation □ Neuroleptics—phenothiazine derivatives, influence of environment and substituents on the stability of the radical cations □ Radical cations—influence of environment and substituents on stability, phenothiazine derivatives

The physicochemical study of phenothiazines has increased in recent years. One of the most common properties of phenothiazine and its derivatives is that they are oxidized easily (1–3). The fact that various oxidized compounds were found (4) among metabolic degradation products suggested that the phenothiazines could act in humans in their oxidized form or produce a redox reaction. Based on this, it was proposed (5) that certain products could act in humans by means of an energy or electron transfer. The phenothiazines, then, can act as electron donors if there are adequate acceptors. Evidence has been presented that the drugs interact with dopamine receptors, and a good correlation has been found between drug potency and the strength of this interaction (6, 7). Several investigators have proposed that the cation radical formed by the oxidation of a phenothiazine derivative (8) such as chlorpromazine, could be an intermediate of the metabolism of the drug and may be the active pharmacological entity (8, 9).

In the present report a study of the kinetics of decay of the first oxidation product of several phenothiazine derivatives in different environments is described, and their instability is related to the substituents and their pharmacological activity.

BACKGROUND

The influence of the R_2 substituents and the structure of the R_{10} side chain on the antipsychotic activity of phenothiazines has been studied (10). However, information about substituent effects on the radical cation behavior is less prevalent due to the difficulty in studying the reactive cation radicals; therefore, it is useful to investigate the behavior of the radicals as a function of structure, given the possible involvement of the radicals in the metabolism of the drugs and in their activity.

The cation radicals of phenothiazine were first obtained in 1913 (11). It was stated that the phenothiazine oxidation proceeds by two steps (12):

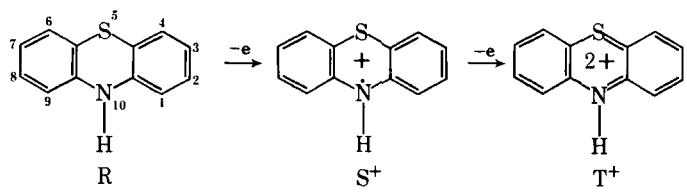

Scheme I

0022-3549/83/0100-0050$01.00/0

ice bath until a precipitate developed. This was dissolved by addition of methanol and the solution was treated by a dropwise addition of a solution of 4-chlorophenacyl bromide (0.2 mole) in methanol (20 ml) while maintaining the pH at 7–7.5 by 1 *N* methanolic potassium hydroxide. The final mixture was stirred for 1 hr while cooling in ice and for an additional hour at room temperature. Dilution with cold water (60 ml) caused complete separation of the product, which was found to be the cyclized product (XXIX) as evidenced by mixed melting point determination and superimposability of IR. Repeating the reaction for a shorter period of time (15 min) in aqueous methanol again gave the cyclized product (XXIX).

REFERENCES

(1) P. Andrews, H. Dorn, M. Federman, and H. Voege, *Ger. Offen.*, **2,** 614, 841 (1977); through *Chem. Abstr.*, **88,** 65976j (1978).

(2) M. A. El-Dawy, M. A. Abdel-Kader, G. M. El-Naggar, and M. A. El-Gendy, *Proc. XIII Conf. Pharm. Sci.*, Cairo, Egypt, 87 (1974).

(3) M. A. El-Dawy, M. A. Abdel-Kader, and A. N. Ahmed, *Proc. XIV Conf. Pharm. Sci.*, Cairo, Egypt, 33 (1975). M. A. El-Dawy, M. A. Abdel-Kader, and A. N. Ahmed, *Bull. Pharm. Sci.*, (Assuit Univ.), **I,** 1 (1978).

(4) M. A. El-Dawy, S. Abo-Elazm, and K. M. El-Berembally, *Pharmazie*, **34,** 144 (1979).

(5) A. S. Mehanna, Master of Science Degree Thesis, Tanta University, Egypt (1978).

(6) L. Gsell and W. Meyer, *Ger. Offen.*, **2,** 749, 753 (1978); through *Chem.Abstr.*, **89,** 43495r (1978).

(7) L. Gsell and W. Meyer, *Ger. Offen.*, **2,** 739, 084 (1978); through *Chem. Abstr.*, **88,** 190844r (1978).

(8) J. Topliss, *J. Med. Chem.*, **15,** 1006 (1972).

(9) R. Stolle, *J. Prakt. Chem.*, **69,** 145 (1904).

(10) S. Shih, *Chem. Zentralbl.*, **1,** 56 (1935).

(11) P. Curtius, *J. Prakt. Chem.*, **58,** 190 (1898).

(12) R. Kahl, *Chem. Zentralbl.*, **II,** 1493 (1904).

(13) T. Curtius, *J. Prakt. Chem.*, **51,** 168 (1895).

(14) J. R. Raid and N. D. Heindek, *J. Heterocycl. Chem.*, **13,** 925 (1976).

(15) R. M. Couper and L. H. Davidson, *Org. Synth. Coll.*, **II,** 480 (1943).

(16) C. F. Reynold, "Reactions of Organic Compounds," Wiley, New York, N.Y., 1962, p. 134.

(17) L. Giarmmanco, *Atti Acad. Sci., Lett. Arti. Palermo*, Part 1, **33,** 235 (1973); through *Chem. Abstr.*, **83,** 97228e (1975).

(18) T. George, R. Tahilramani, and D. A. Dabholkar, *Indian J. Chem.*, **49,** 057 (1969).

(19) S. Somasekhara, R. K. Thakkar, and G. F. Shah, *J. Indian Chem. Soc.*, **49,** 1057 (1972).

(20) A.-Mohsen M. E. Omar and S. A. Osman, *Pharmazie*, **28,** 30 (1973).

(21) W. A. Abdoulla, H. K. Kadry, and S. C. Mahran, *Sci. Pharm.*, **47,** 114 (1979).

Influence of Environment and Substituents on the Stability of the Radical Cations of Several Phenothiazine Derivatives

A. ORTIZ[x], I. POYATO, and J. I. FERNANDEZ-ALONSO

Received December 24, 1980, from the *Departamento de Química-Física y Química Cuántica, Centro Coordinador CSIC-UAM, Facultad de Ciencias C-XIV, Cantoblanco, Madrid 34, Spain.* Accepted for publication March 1, 1982.

Abstract □ The UV decay spectra of the radical cations of several phenothiazine derivatives in different environments was studied. The influence of the substituents on the reference spectrum could be seen, as well as a relationship between the stability of such radicals and the acidity of the environment. There is also an influence of the substituents on the stability of the radicals in the different environments studied. The instability of the radicals in solution has been studied to relate to the pharmacological activity of neuroleptics.

Keyphrases □ Phenothiazine—derivatives, influence of environment and substituents on the stability of the radical cation □ Neuroleptics—phenothiazine derivatives, influence of environment and substituents on the stability of the radical cations □ Radical cations—influence of environment and substituents on stability, phenothiazine derivatives

The physicochemical study of phenothiazines has increased in recent years. One of the most common properties of phenothiazine and its derivatives is that they are oxidized easily (1–3). The fact that various oxidized compounds were found (4) among metabolic degradation products suggested that the phenothiazines could act in humans in their oxidized form or produce a redox reaction. Based on this, it was proposed (5) that certain products could act in humans by means of an energy or electron transfer. The phenothiazines, then, can act as electron donors if there are adequate acceptors. Evidence has been presented that the drugs interact with dopamine receptors, and a good correlation has been found between drug potency and the strength of this interaction (6, 7). Several investigators have proposed that the cation radical formed by the oxidation of a phenothiazine derivative (8) such as chlorpromazine, could be an intermediate of the metabolism of the drug and may be the active pharmacological entity (8, 9).

In the present report a study of the kinetics of decay of the first oxidation product of several phenothiazine derivatives in different environments is described, and their instability is related to the substituents and their pharmacological activity.

BACKGROUND

The influence of the R_2 substituents and the structure of the R_{10} side chain on the antipsychotic activity of phenothiazines has been studied (10). However, information about substituent effects on the radical cation behavior is less prevalent due to the difficulty in studying the reactive cation radicals; therefore, it is useful to investigate the behavior of the radicals as a function of structure, given the possible involvement of the radicals in the metabolism of the drugs and in their activity.

The cation radicals of phenothiazine were first obtained in 1913 (11). It was stated that the phenothiazine oxidation proceeds by two steps (12):

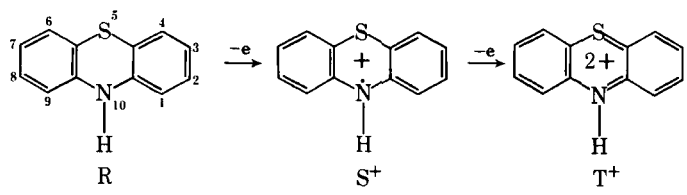

Scheme I

0022-3549/83/0100-0050$01.00/0

where R produces an uncolored solution, S^+ produces a colored solution, and T^+ an intense red solution.

The radical in solution is stable only in a concentrated acid environment, otherwise disproportionation occurs in three steps:

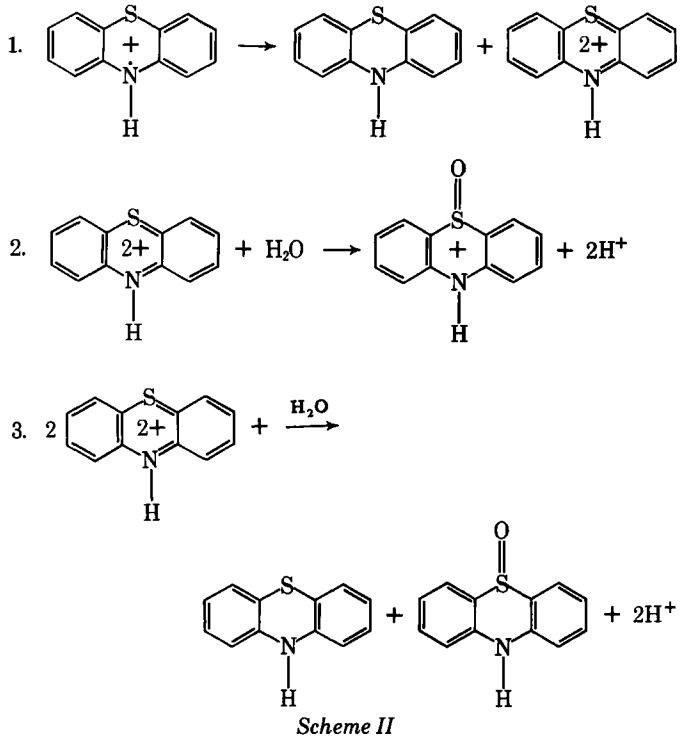

Scheme II

The first and second steps can be eliminated by acidifying the environment. The third step does not occur in the case of substituted R_{10} derivatives. Therefore, the reaction ends at step 2 and it can be expressed (13):

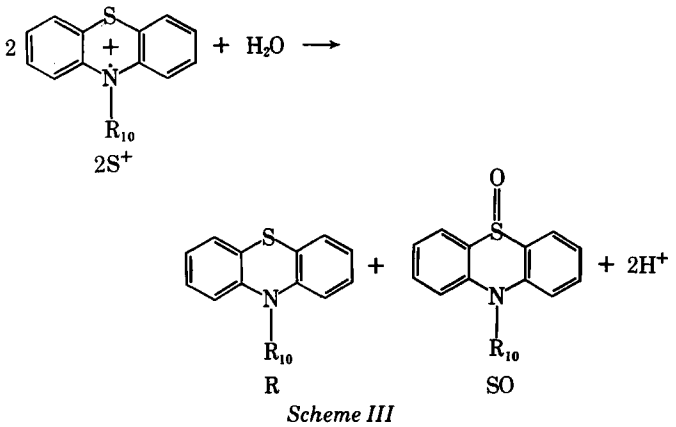

Scheme III

While the S^+ produces a colored solution, the R and sulfoxide solution are decolorized.

EXPERIMENTAL

Materials—Phenothiazine derivatives with R_2 and R_{10} substituents were used (Table I). The products were pharmacologically pure and were used without further purification. Perchloric acid (70%) was the oxidizing agent.

The solvents were bidistilled water, sulfuric acid (9 *N* and 2 *N*), and solutions with different pH values (pH 1, 2.2, and 3.5). UV and visible spectrophotometers were used to obtain the spectra to which the kinetic decay of the radicals in solution adjust.

Method—A method reported previously was used to obtain the cation radicals in the solid state (14). Analysis for phenothiazine derivative radical perchlorates were calculated.

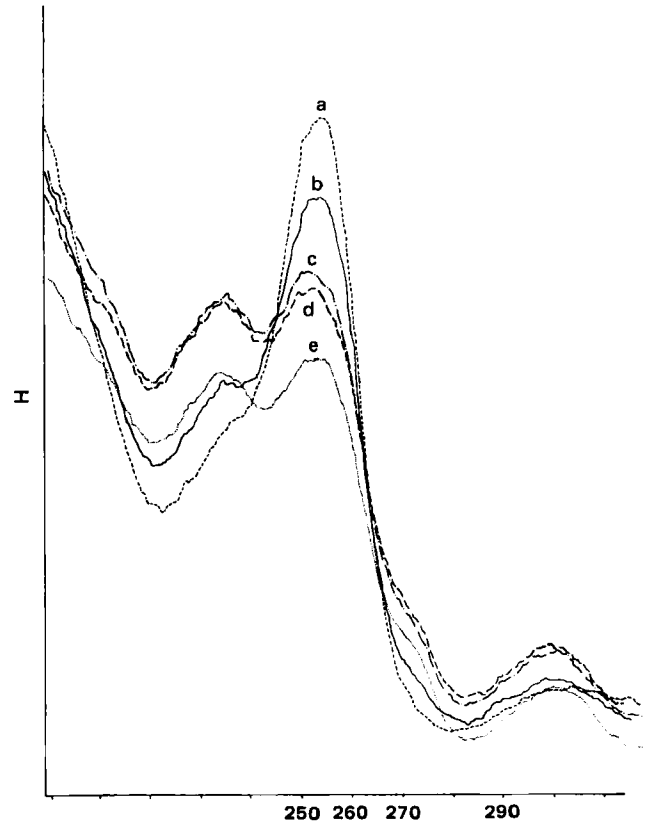

Figure 1—*Decay of the trifluoperazine radical cation in the following solutions (350–200 nm* versus *absorption) (a) water; (b) sulfuric acid pH 3.5; (c) sulfuric acid, pH 2.2; (d) sulfuric acid, pH 1; (e) 2 N sulfuric acid.*

Perazine—Anal.—Calc.: C, 43.80; H, 4.96; S, 5.84; N, 7.66; Cl, 12.93. Found: C, 43.14; H, 4.91; S, 5.92; N, 7.66; Cl, 12.91.

Trifluoperazine—Anal.—Calc.: C, 40.88; H, 4.25; N, 6.81; S, 5.20; Cl, 11.50; F, 9.24. Found: C, 40.28; H, 4.21; N, 7.05; S, 5.29; Cl, 11.6; F, 9.38.

Prochlorperazine—Anal.—Calc.: C, 41.21; H, 4.49; N, 7.20; S, 5.50; Cl, 18.25. Found: C, 41.21; H, 4.43; N, 7.35; S, 5.18; Cl, 17.84.

Thiethylperazine—Anal.—Calc.: C, 43.42; H, 5.05; N, 6.90; S, 10.53; Cl, 11.65. Found: C, 43.7; H, 5.20; N, 7.01; S, 11.0; Cl, 10.92.

Promazine—Anal.—Calc.: C, 41.38; H, 4.49; S, 6.49; N, 5.67; Cl, 14.37. Found: C, 41.15; H, 4.35; S, 6.53; N, 5.61; Cl, 14.52.

These values agreed with the proposed formula given in an earlier report for chlorpromazine perchlorate (14): (phenothiazine derivative) + $ClO_4^-.ClO_4H.\frac{1}{2}H_2O$. The melting points of these compounds ranged from 170 to 224°.

RESULTS AND DISCUSSION

The radicals dissolved in all solvents used. An intense coloration appeared which corresponded to the oxidized form. The radicals remained indefinitely stable only in 9 *N* sulfuric acid solution because of its high acidity. Disproportionation of the cation radicals occurred in all other solvents employed, with the characteristic coloration of the cation radical disappearing.

To study the kinetics of these compounds, the cation radical perchlorates were used as the oxidized form in the solid state. For each radical a control in 9 *N* sulfuric acid solution, the acid-stabilized solution, was used as a comparison standard of fixed concentration.

To determine the concentration of the radical, electron-spin resonance (ESR) spectroscopy was employed. As a reference, a benzene solution of 1,1-diphenyl-2-picrylhydrazyl, as free radical standard was used. An acid-stabilized control sample of each compound with *concentrations* of 10^{-2}–10^{-3} *M* served as the reference.

The characteristic superfine structure of the molecular structure of phenothiazine was suppressed; consequently, the ESR spectra of the radical cations consisted of a single line. The proportion of the ESR signal height with respect to the radical concentration gave a concentration measurement accurate to 3%. The comparison with the free radical

Table I—UV Spectra Data for the Radical Cations of the Phenothiazine Derivatives in 9 *N* Sulfuric Acid

Compounds[a]	R_2	Concentration	λ_{max}, nm (log ϵ)	λ_{max}, nm (log ϵ)	λ_{max}, nm (log ϵ)
I Perazine[b]	—H	4×10^{-4} mole/liter	271(3.50)	265(3.48)	212(3.25)
II Promazine[c]	—H	4×10^{-4} mole/liter	271(3.51)	265(3.48)	212(3.25)
III Thiethylperazine[d]	$-SC_2H_5$	6×10^{-4} mole/liter	296(3.29)	267(3.12) 245–236(2.98)	205(2.95)
IV Prochlorperazine[e]	—Cl	5.14×10^{-4} mole/liter	275(3.39)	268(3.37)	216(3.20)
V Trifluoperazine[f]	$-CF_3$	4×10^{-4} mole/liter	271(3.60)	—	213(3.24)

[a] For I, III–V R_{10} = $-CH_2-CH_2-CH_2-N\langle(H)\rangle N-CH_3$; for II R_{10} = $-CH_2-CH_2-CH_2-N-(CH_3)_2$. [b] Rhodia. [c] Promonta. [d] Upjohn. [e] Sandoz. [f] Squibb.

standard showed that, within the accuracy of the method, the acid-stabilized control was entirely in the free radical cation form.

The promazine and perazine cation radicals decayed slowly enough so that successive passes through the UV region (350–200 nm) could be made, and it was possible to study the entire spectrum with respect to time. For the other products, only the λ_{max}, which refers to the oxidized form, were taken, and the time dependence of the absorbance was recorded.

Influence of the Substituents of the Radical Cations in 9 *N* Sulfuric Acid Solution—Table I presents the transitions corresponding to the cation radicals in 9 *N* sulfuric acid solution (15). The reference used to study the substituent effects was perazine.

Perazine (I) and promazine (II) generate no change from the reference spectrum with R_2 = H and different substituents at R_{10}.

The radical cations with different substituents at R_2 and the same at R_{10} give different changes. Thus, the —Cl and $-SCH_2CH_3$ substituents show a resonance effect upon the π structure of the nucleus of the phenothiazine derivative which manifests itself in bathochromic shifts of the peaks (16). However, R_2= $-CF_3$, with a strong electron-withdrawing effect, seems not to affect the transitions corresponding to the radical cation.

In the perazine spectrum, it can be seen that the —Cl substituent shows a bathochromic shift in all bands.

The $-SCH_2CH_3$ caused an intense bathochromic shift in the first band, the second remained at 265 nm, and a transition peak appeared at 245–228 nm, which represents a vibratory structure. This transition peak could be caused by the sulfur atom in the R_2 substituent [the same transitions also appeared at the same wavelength in the spectra of an identical neutral compound (17)].

The $-CF_3$ derivative produces no shift in the bands; however, the second maximum at 265 nm disappeared.

Through log ϵ, a relationship can also be established between the intensity of the bands of each radical cation and the substituents. Thus, the R_{10} substituent does not exert any influence on the intensity of the bands; with perazine, however, derivatives with R_2 substituents such as —Cl or $-SC_2H_5$ seem to exert a negative influence on such bands showing a hypochromic effect. On the contrary, the $-CF_3$ substituent affects the π electronic structure of the tricyclic nucleus producing hyperchromic shifts on its maxima (16).

Decay of the Radicals—Figures 1 and 2 show the final spectra of the decay of the radical cation in the different solutions used. The corresponding λ_{max} and log ϵ values are given in Table II. The values of λ for the sulfoxide are on the right side of the table and the values for λ corresponding to neutral phenothiazine derivatives are on the left. The neutral form and sulfoxide of each radical cation were identified from earlier reports (18–20).

From these spectra the following can be seen. (*a*) The radical cations stay stable only in 9 *N* sulfuric acid; (*b*) The radicals are not stable in 2

Table II—UV Spectra of the Phenothiazine Derivatives in Sulfuric Acid Solutions of Different Acidity

Product (concentration)	Solvent	Neutral form λ_{max} (log ϵ)	Sulfoxide λ_{max} (log ϵ)
Promazine (4×10^{-4} mole/liter)	2 *N* H_2SO_4	250 (3.21) 298s (2.72)	270 (2.91) 235s (3.14) 222s (3.09)
	H_2SO_4 pH 1	251 (3.32) 298s (2.79)	270.5s (2.88) 238 (3.24) 224 (3.18)
	H_2SO_4 pH 3.5	250.5 (3.21) 298s (2.71)	271 (2.78) 236 (3.14) 225 (3.10)
	distilled water	250.5 (3.18) 298s (2.54)	270 (2.48) 235 (3.06) 224 (3.03)
Perazine (4×10^{-4} mole/liter)	2 *N* H_2SO_4	251s (3.04) 295s (2.48)	270 (2.95) 234 (3.15)
	H_2SO_4 pH = 1	251s (3.09) 297s (2.62)	271s (2.92) 234 (3.16) 243 (3.13)
	H_2SO_4 pH = 3.5	251 (3.06) 297 (2.48)	271 (2.88) 234 (3.05)
	distilled water	251 (3.12) 297 (2.52)	271s (2.85) 235 (3.03)
Thiethylperazine[a] (6×10^{-4} mole/liter)	2 *N* H_2SO_4	267 (3.25)	260 (3.25) 222–225s (3.07)
	distilled water	267 (3.25)	260 (3.23) 221–225 (3.06)
Trifluoperazine (4×10^{-4} mole/liter)	2 *N* H_2SO_4	251.5 (3.16) 300s (2.54)	271s (2.70) 234.5 (3.15)
	H_2SO_4 pH 1	252.5 (3.22) 301s (2.68)	270s (2.76) 234 (3.21)
	H_2SO_4 pH 2.2	251.5 (3.22) 301s (2.65)	270s (2.72) 235 (3.21)
	H_2SO_4 pH 3.5	251.5 (3.21) 300 (2.62)	271s (2.72) 235.5 (3.17)
	distilled water	254 (3.36) 302s (2.54)	235s (3.10)
Prochlorperazine (5.35×10^{-4} mole/liter)	2 *N* H_2SO_4	250 (3.17) 300 (2.53)	275s (2.60) 240s (3.13)
	distilled water	250 (3.15) 300s (2.54)	240 (3.05)

[a] There is an intense overlap of the bands corresponding to the sulfoxide and to the neutral derivative.

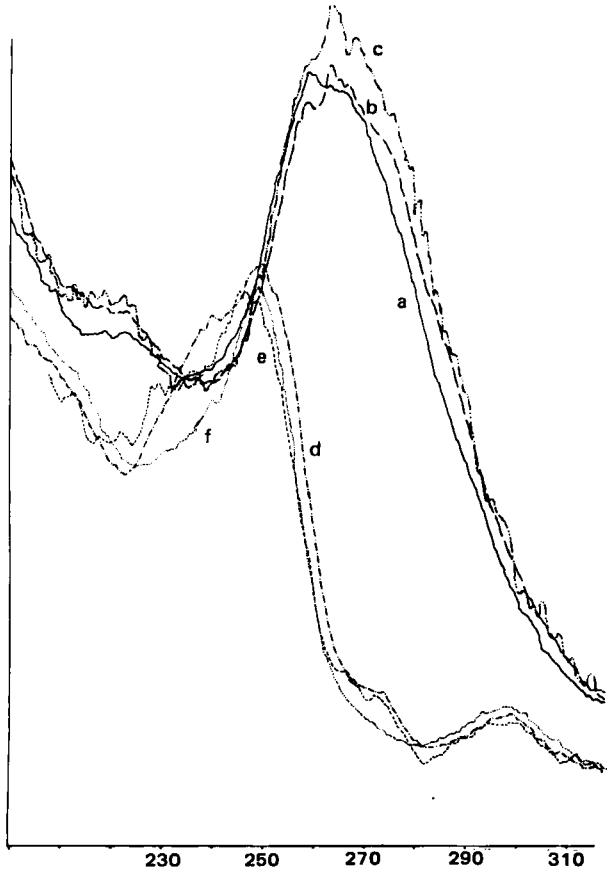

Figure 2—*Final decay spectra of prochlorperazine and thiethylperazine radical cations in the following solutions: 350–200 nm* versus *absorption) thiethylperazine in (a) 2* N *sulfuric acid; (b) water; (c) sulfuric acid, pH 1. Prochlorperazine in (d) 2* N *sulfuric acid; (e) pH 1 sulfuric acid; (f) water.*

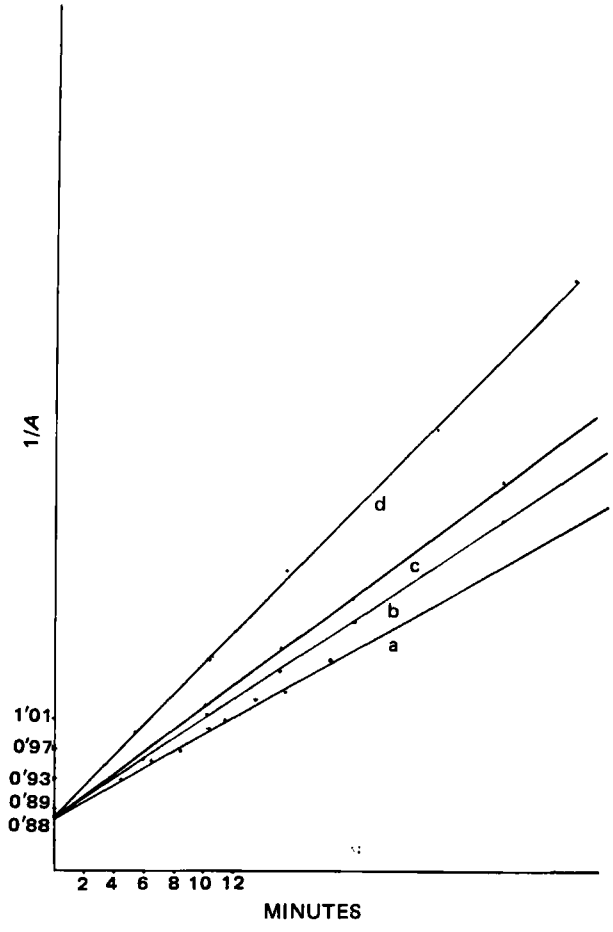

Figure 3—*1/*A versus *time (minutes) for promazine acid; in (a) 2* N *sulfuric acid; (b) pH 1 sulfuric acid; (c) pH 3.5 sulfuric acid; (d) water.*

N sulfuric acid, decoloration occurs, and new bands appear, which are different from those of the radical cation. The sulfoxide coexists with the neutral form, with the sulfoxide being more important. (*c*) In solutions of pH 1 and 3.5 decoloration goes fast, and it can be seen that the band corresponding to the neutral phenothiazine derivative is of a stronger intensity than the one corresponding to the sulfoxide. (*d*) In solutions in distilled water, the decay is almost simultaneous and decoloration is practically immediate. There is a strong prevalence of the band corresponding to the neutral phenothiazine derivative over the one corresponding to the sulfoxide. However, upon observing the spectra, an overlapping of some bands can be noticed (Fig. 2). Nevertheless, the decay of the radical cations depends upon the acidity concentration of the environment and substituents R_2 and R_{10}.

There is a correlation between the bands characteristic of each compound with the environment. Thus, in solutions with higher acidity, the sulfoxide dominates; in solutions with lower acidity, the neutral derivative dominates; and in solutions at pH 2.2 and 3.5, the proportion between these two forms is similar.

Kinetics—The decay velocity of the radicals in each solution studied was obtained from spectral data on the assumption that the absorbance was linearly related to the free radical concentration, representing $1/A$ *versus* time. In this way the initial absorbance was computed from the intercept of zero time with $1/A$. The velocity constant was obtained from:

$$K = (1/t)\,(1/A - 1/A_0) \qquad \text{(Eq. 1)}$$

where A_0 is the initial, extrapolated absorbance, A is the absorbance at time t, and t is time in minutes.

In all cases the data produced a straight line (Figs. 3 and 4) indicating a second-order decay of the semiquinone or oxidated form S^+, which agrees with 2 S+ - - - - R + SO, as proposed in other reports (13, 21).

Since the oxidized form is unstable in insufficiently acidic solutions, the initial concentration is no longer 100% but is lower from the beginning. This makes it necessary to extrapolate at time 0 to calculate A_0, which can be compared with the absorbance of the coresponding radical in 9 *N* sulfuric acid, taken as the reference, in which the concentration is 100%, because the radical stays stable indefinitely. Thus, in 2 *N* sulfuric acid the calculated initial concentration of the radicals studied are between 85 and 100% of the same compound in 9 *N* sulfuric acid.

In the less acidic solutions, the measurements are even less accurate because of the speed of the radical decay, and at lower pHs, the extrapolated initial concentrations were still lower than for 2 *N* sulfuric acid. However, it can be considered sufficient for obtaining relative reaction rates on the disproportionation of the radicals.

Effect of the Environment pH on K Decay—Least-square fits were made to obtain constants for K, experimental errors, ϵ, coefficients of regression, R^2, and $1/A_0$ data for every compound in the different media employed (Table III).

In Fig. 3 it can be seen that, as for any of the compounds studied, K increases as the acidity of the solvent decreases.

Compounds I and II with R_2 = H and a Side Chain at R_{10}—Compounds I and II differ by their R_{10} substituents and from the values obtained it could be pointed out that the chain of I, which is longer than that of II, is capable of producing a more stable radical.

It can be seen from Table III that for compound I the K decay values are very similar, in spite of the different solutions employed. This appears to indicate that acidity has little influence on the stability of this radical in solution.

However, for II, K-values depend more on the solutions used, and the relation of the K decay of these two compounds in water is double for II than for I, that is, II decays two times faster than I in water.

Effects of R_2 Substituents—A clear influence of R_2 on K is observed; thus, it can be seen that the K-values for the same solution, 2 *N* sulfuric acid, (Fig. 4) or distilled water, follow the sequence: —H < —SCH_2CH_3 < —Cl < —CF_3. Similar to the first case with R_2 = H, the K-values increase as the acidity of the solution decreases; however, this K increase is stronger for compounds with $R_2 \neq$ H.

The strongest increase of the decay constant of the radicals can be seen in the product with the electron-withdrawing substituent, R_2 = —CF_3.

Table III—$K(10^{-3})$ [a] of the Cation Radicals in Sulfuric Acid

Parameters	Products I	II	III	IV	V
$1/A_0$	0.82	0.884	1.072	0.958	0.798
K	7.12	11.82	30.01	37.03	46.72
2 N					
ϵ	±0.046	±0.446	±1.65	±0.60	±0.22
R^2	0.9997	0.991	0.993	0.998	0.9997
$1/A_0$	0.89	0.989	1.04	1.216	1.464
K	7.88	13.85	32.45	36.55	50.55
pH 1					
ϵ	±0.060	±0.33	±1.79	±0.86	±0.71
R^2	0.998	0.998	0.987	0.997	0.9990
$1/A_0$	—	—	—	—	1.500
K	—	—	—	—	55.86
pH 2.2					
ϵ	—	—	—	—	±0.24
R^2	—	—	—	—	0.99992
$1/A_0$	0.93	1.227	—	—	0.909
K	8.58	14.36	—	—	56.73
pH 3.5					
ϵ	±0.02	±0.44	—	—	±0.51
R^2	0.9998	0.980	—	—	0.909
$1/A_0$	0.938	1.34	1.21	1.426	1.003
K	8.97	18.6	49.29	56.66	60.04
Water					
ϵ	±0.65	±0.91	±1.51	±0.70	±0.72
R^2	0.979	0.992	0.994	0.9997	0.9995
$E^{1/2}$, mV	503[c]	525[b]	540[b]	570[b]	680[b]

[a] In moles/liter minute. [b] Reference 19. [c] Reference 20.

The introduction of an R_2 substituent, activated or deactivated, is capable of increasing considerably the decay of the radicals. It could have been expected that the electron-donating substituents, such as $-SCH_2CH_3$, would tend to stabilize the cation radicals in solution (22); however, in this case this was not so.

The constant decay can be related also to the $E_{1/2}$ (23, 24). The R_2 and R_{10} substituents affect the halfwave potentials as given in Table III. It is observed that a higher $E_{1/2}$ corresponds to a higher constant decay of the compound or at higher halfwave potential, less stability of the radical.

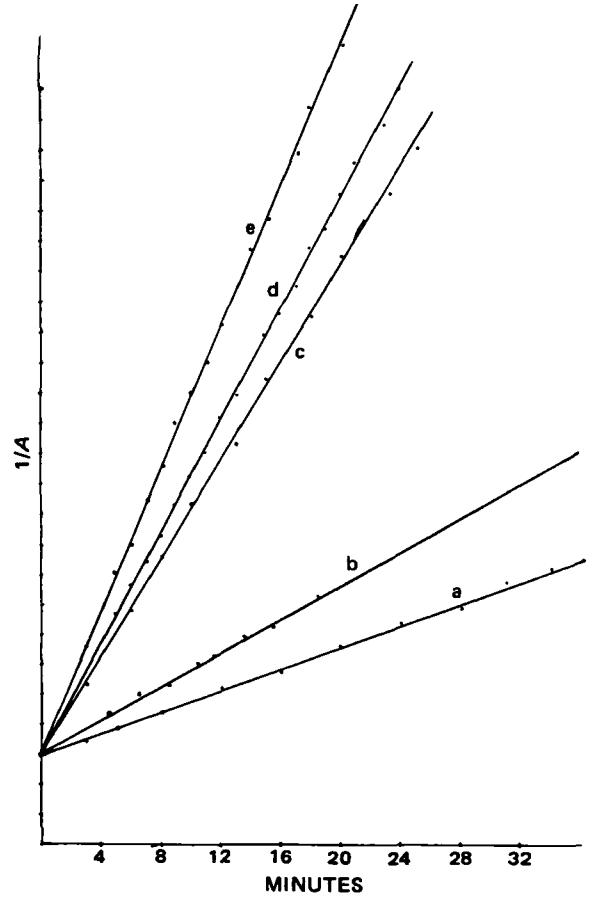

Figure 4—1/A versus *time for (a) perazine; (b) promazine; (c) thiethylperazine; (d) prochlorperazine; (e) trifluoperazine, in 2 N sulfuric acid.*

Relative Stability and Pharmacological Activity of the Radicals—It has been suggested that the phenothiazine derivative radical cation may be of some importance in the biological activity of phenothiazine (25), and in some cases it has been related to the stability of these radicals.

Since the pharmacological activity of the compounds studied, such as neuroleptics, depends on the R_2 substituents as: $-CF_3 > -Cl > -SCH_2CH_3 > -H$, and as it has been determined that the stability of their radicals varies inversely with the activity as neuroleptics, then the activity of these compounds cannot be related to the stability of the corresponding radical. However, the activity of these compounds could be related to the ability to form (CTC) charge transfer complexes whenever there are adequate receptors, with the cation radical as an intermediate in the biological action as has been suggested (26).

CONCLUSIONS

It can be concluded that the R_{10} substituents seem not to affect the transitions corresponding to the radical cation, but the R_2 substituents considerably affect such transitions in two ways: first, on the λ characteristics of the reference spectrum by bathochromic shifts (—Cl, and $-SCH_2CH_3$) and second, increasing (the $-CF_3$) or decreasing (—Cl and $-SCH_2CH_3$) the intensity of the corresponding bands.

From the final decay spectra of the radicals it can be seen that there exists a correlation between the band characteristics of the sulfoxide and the neutral form of each radical cation with the milieu, depending on the prevalence of one of the forms on the acidity of the solution employed. Thus, the neutral derivative dominates over the sulfoxide in water; however, this last compound seems to dominate the former in acidic solutions.

From the K-values obtained, it can be concluded that for each compound studied the radicals are only stable in high acidic solutions, and their stability decreases as the acidity of the environment decreases. Here it can be seen that the R_2 and R_{10} substituents' effect on the stability of radicals with longer chains are capable of producing a more stable radical. On the contrary, none of the R_2 substituents studied different than $R_2 \neq H$ are capable of generating a more stable radical. All substituents affect considerably the stability of the corresponding radicals. The more unstable the product with a strong electron-withdrawing effect ($-CF_3$), the more the other compounds (—Cl and $-SCH_2CH_3$) will also decrease the stability of their radicals but less than $-CF_3$.

This seems to indicate that the stability of the radicals can not be related to the activity of these compounds as neuroleptics, for the more

active (trifluoperazine) seems to be the less stable, and as soon as the radical is free and independent in solution, it suffers disproportionation and disappears as that radical.

REFERENCES

(1) J. P. Billon, *Bull. Soc. Chim., Fr.*, **1960**, 1784.

(2) *Idem.*, **1960**, 1923.

(3) J. E. Bloor and B. R. Gilson, *J. Med. Chem.*, **18**, 922 (1970).

(4) I. S. Forrest and M. Berger, *Biochim. Biophys. Acta*, **29**, 442 (1958).

(5) A. Szent-Gyorgy "Introduction to Submolecular Biology," Academic, New York, N.Y., 1960.

(6) I. S. Forrest, C. J. Carr, and E. Usdin, *Adv. Biochem. Psychopharmacol.*, **9**, 275 (1974).

(7) I. Creese, D. R. Burt, and S. H. Snyder, *Science*, **192**, 481 (1976) and S.J.J. Enna, J. P. Bennet, Jr., D. R. Burt, I. Creese, and S. H. Snyder, *Nature (London)*, **263**, 338 (1976).

(8) I. S. Forrest and D. E. Creen, *J. Forensic Sci.*, **17**, 592 (1972).

(9) G. M. Gooley, H. Keiser, and F. Setchel, *Nature (London)*, **21**, 948 (1972).

(10) D. Hawkins and L. Pauling, Eds., "Orthomolecular Psychiatry," W. H. Freeman, San Francisco, Calif., 1973.

(11) R. Pummerer and S. Gassner, *Chem. Ber.*, **46**, 2310 (1913).

(12) J. P. Billon, G. Gouquis, and J. Combrinson, *Bull. Soc. Chim. Fr.*, **1962**, 2062.

(13) B. C. Gilbert, P. Hanson, R. O. C. Norman, and B. T. Sutcliffe, *Chem. Commun.*, **1966**, 161.

(14) F. H. Merkle, D. A. Discher, and A. Felmeister, *J. Pharm. Sci.*, **53**, 965 (1964).

(15) A. Ortiz, A. Pardo, and J. I. Fernàndez-Alonso, *ibid.*, **69**, 378 (1980).

(16) "Ultraviolet and Visible Spectroscopy," 2nd ed., C. N. R. Rao, Ed., Butterworths, chap. 5, 1967 p. 18.

(17) J. Gonzalez and J. I. Fernàndez-Alonso, *Ann. Fis. y Quim.*, **56B**, 919 (1970).

(18) F. J. Warren, J. B. Eisdorfer, W. E. Thompson, and J. E. Zarembo, *J. Pharm. Sci.*, **55**, 144 (1966).

(19) A. Leenheer, *J. Assoc. Off. Anal. Chem.*, **56**, 105 (1973).

(20) H. J. Shine and E. E. Mach, *J. Org. Chem.*, **30**, 2130 (1965).

(21) T. N. Tozer and T. L. Dallas, *J. Pharm. Sci.*, **54**, 1169 (1965).

(22) S. C. Creason, J. Wheeler, and R. F. Nelson, *J. Org. Chem.*, **37**, 4440 (1972).

(23) J. Gonzalez and J. I. Fernàndez-Alonso, *Ann. Fis y Quim.*, **56B**, 931 (1970).

(24) P. Kabasakalina and J. Mcglotten. *Anal. Chem.*, **31**, 431 (1959).

(25) H. M. Swartz, J. R. Bolton, and D. C. Borg, "Biological Applications of Electron Spin Resonance," Wiley Interscience, New York, N.Y., 1972, chap. 7.

(26) I. Bley, *J. Pharm. Sci.*, **66**, 1577 (1977).

Simultaneous Stability-Indicating Determination of Phenylephrine Hydrochloride, Phenylpropanolamine Hydrochloride, and Guaifenesin in Dosage Forms by Reversed-Phase Paired-Ion High-Performance Liquid Chromatography

GARY W. SCHIEFFER ˣ and DAVID EMLYN HUGHES

Received December 4, 1981, from *Norwich-Eaton Pharmaceuticals, Norwich, NY 13815.* Accepted for publication March 5, 1982.

Abstract □ A method for the quantitative determination of phenylephrine hydrochloride, phenylpropanolamine hydrochloride, and guaifenesin in commercial formulations was developed. A reversed-phase paired-ion high-performance liquid chromatographic technique resolves the active from degradation products, colorings, and flavor and was found applicable to seven commercial dosage forms.

Keyphrases □ Phenylephrine hydrochloride—simultaneous determination with phenylpropanolamine hydrochloride and guaifenesin, reversed-phase paired-ion high-performance liquid chromatography □ Phenylpropanolamine hydrochloride—simultaneous determination with phenylephrine hydrochloride and guaifenesin, reversed-phase paired-ion high-performance liquid chromatography □ Guaifenesin—simultaneous determination with phenylephrine hydrochloride and phenylpropanolamine hydrochloride, reversed-phase paired-ion high-performance liquid chromatography □ High-performance liquid chromatography—reversed-phase paired-ion, simultaneous determination of phenylephrine hydrochloride, phenylpropanolamine hydrochloride, and guaifenesin

The simultaneous determination of the active components in a specific dosage form offers advantages to separate analyses. Simultaneous GLC determinations are typically successful in assaying for phenylpropanolamine hydrochloride and other amines (1–8). At least one GLC assay for guaifenesin (glyceryl guaiacolate) is available in which guaifenesin is extracted and derivatized (9). Simple and reliable procedures for the simultaneous GLC determination of the underivatized phenylephrine hydrochloride and other amines are absent from the chemical literature. Studies are available in which 71 drugs were determined using nitrogen-selective and flame-ionization (FID) detectors (2); 50 amines of pharmaceutical interest (5) and 23 physiologically active amines (8) were determined. None of these methods were responsive to phenylephrine hydrochloride.

To overcome problems arising from the presence of phenylephrine hydrochloride in pharmaceutical formulations, high-performance liquid chromatographic (HPLC) procedures have been developed for simultaneous assay. The desired chromatographic separation involves phenylephrine hydrochloride (I), phenylpropanolamine hydrochloride (II), and guaifenesin (III). The only HPLC method reported in the literature separating I, II, and III with high resolution used a bonded phase cation exchange column (10). A reversed-phase HPLC method employing ion-pairing was preferred, since bonded-phase ion-exchange columns tend to have short lifetimes and poor reproducibility from column to column (11).

Numerous reversed-phase ion-pairing methods have been reported for various combinations of I, II, and III and other drugs. A previous report (12) used a nitrile column

0022-3549/83/0100-0055$01.00/0

active (trifluoperazine) seems to be the less stable, and as soon as the radical is free and independent in solution, it suffers disproportionation and disappears as that radical.

REFERENCES

(1) J. P. Billon, *Bull. Soc. Chim., Fr.*, **1960**, 1784.

(2) *Idem.*, **1960**, 1923.

(3) J. E. Bloor and B. R. Gilson, *J. Med. Chem.*, **18**, 922 (1970).

(4) I. S. Forrest and M. Berger, *Biochim. Biophys. Acta*, **29**, 442 (1958).

(5) A. Szent-Gyorgy "Introduction to Submolecular Biology," Academic, New York, N.Y., 1960.

(6) I. S. Forrest, C. J. Carr, and E. Usdin, *Adv. Biochem. Psychopharmacol.*, **9**, 275 (1974).

(7) I. Creese, D. R. Burt, and S. H. Snyder, *Science*, **192**, 481 (1976) and S.J.J. Enna, J. P. Bennet, Jr., D. R. Burt, I. Creese, and S. H. Snyder, *Nature (London)*, **263**, 338 (1976).

(8) I. S. Forrest and D. E. Creen, *J. Forensic Sci.*, **17**, 592 (1972).

(9) G. M. Gooley, H. Keiser, and F. Setchel, *Nature (London)*, **21**, 948 (1972).

(10) D. Hawkins and L. Pauling, Eds., "Orthomolecular Psychiatry," W. H. Freeman, San Francisco, Calif., 1973.

(11) R. Pummerer and S. Gassner, *Chem. Ber.*, **46**, 2310 (1913).

(12) J. P. Billon, G. Gouquis, and J. Combrinson, *Bull. Soc. Chim. Fr.*, **1962**, 2062.

(13) B. C. Gilbert, P. Hanson, R. O. C. Norman, and B. T. Sutcliffe, *Chem. Commun.*, **1966**, 161.

(14) F. H. Merkle, D. A. Discher, and A. Felmeister, *J. Pharm. Sci.*, **53**, 965 (1964).

(15) A. Ortiz, A. Pardo, and J. I. Fernàndez-Alonso, *ibid.*, **69**, 378 (1980).

(16) "Ultraviolet and Visible Spectroscopy," 2nd ed., C. N. R. Rao, Ed., Butterworths, chap. 5, 1967 p. 18.

(17) J. Gonzalez and J. I. Fernàndez-Alonso, *Ann. Fis. y Quim.*, **56B**, 919 (1970).

(18) F. J. Warren, J. B. Eisdorfer, W. E. Thompson, and J. E. Zarembo, *J. Pharm. Sci.*, **55**, 144 (1966).

(19) A. Leenheer, *J. Assoc. Off. Anal. Chem.*, **56**, 105 (1973).

(20) H. J. Shine and E. E. Mach, *J. Org. Chem.*, **30**, 2130 (1965).

(21) T. N. Tozer and T. L. Dallas, *J. Pharm. Sci.*, **54**, 1169 (1965).

(22) S. C. Creason, J. Wheeler, and R. F. Nelson, *J. Org. Chem.*, **37**, 4440 (1972).

(23) J. Gonzalez and J. I. Fernàndez-Alonso, *Ann. Fis y Quim.*, **56B**, 931 (1970).

(24) P. Kabasakalina and J. Mcglotten. *Anal. Chem.*, **31**, 431 (1959).

(25) H. M. Swartz, J. R. Bolton, and D. C. Borg, "Biological Applications of Electron Spin Resonance," Wiley Interscience, New York, N.Y., 1972, chap. 7.

(26) I. Bley, *J. Pharm. Sci.*, **66**, 1577 (1977).

Simultaneous Stability-Indicating Determination of Phenylephrine Hydrochloride, Phenylpropanolamine Hydrochloride, and Guaifenesin in Dosage Forms by Reversed-Phase Paired-Ion High-Performance Liquid Chromatography

GARY W. SCHIEFFER ˣ and DAVID EMLYN HUGHES

Received December 4, 1981, from *Norwich-Eaton Pharmaceuticals, Norwich, NY 13815.* Accepted for publication March 5, 1982.

Abstract □ A method for the quantitative determination of phenylephrine hydrochloride, phenylpropanolamine hydrochloride, and guaifenesin in commercial formulations was developed. A reversed-phase paired-ion high-performance liquid chromatographic technique resolves the active from degradation products, colorings, and flavor and was found applicable to seven commercial dosage forms.

Keyphrases □ Phenylephrine hydrochloride—simultaneous determination with phenylpropanolamine hydrochloride and guaifenesin, reversed-phase paired-ion high-performance liquid chromatography □ Phenylpropanolamine hydrochloride—simultaneous determination with phenylephrine hydrochloride and guaifenesin, reversed-phase paired-ion high-performance liquid chromatography □ Guaifenesin—simultaneous determination with phenylephrine hydrochloride and phenylpropanolamine hydrochloride, reversed-phase paired-ion high-performance liquid chromatography □ High-performance liquid chromatography—reversed-phase paired-ion, simultaneous determination of phenylephrine hydrochloride, phenylpropanolamine hydrochloride, and guaifenesin

The simultaneous determination of the active components in a specific dosage form offers advantages to separate analyses. Simultaneous GLC determinations are typically successful in assaying for phenylpropanolamine hydrochloride and other amines (1–8). At least one GLC assay for guaifenesin (glyceryl guaiacolate) is available in which guaifenesin is extracted and derivatized (9). Simple and reliable procedures for the simultaneous GLC determination of the underivatized phenylephrine hydrochloride and other amines are absent from the chemical literature. Studies are available in which 71 drugs were determined using nitrogen-selective and flame-ionization (FID) detectors (2); 50 amines of pharmaceutical interest (5) and 23 physiologically active amines (8) were determined. None of these methods were responsive to phenylephrine hydrochloride.

To overcome problems arising from the presence of phenylephrine hydrochloride in pharmaceutical formulations, high-performance liquid chromatographic (HPLC) procedures have been developed for simultaneous assay. The desired chromatographic separation involves phenylephrine hydrochloride (I), phenylpropanolamine hydrochloride (II), and guaifenesin (III). The only HPLC method reported in the literature separating I, II, and III with high resolution used a bonded phase cation exchange column (10). A reversed-phase HPLC method employing ion-pairing was preferred, since bonded-phase ion-exchange columns tend to have short lifetimes and poor reproducibility from column to column (11).

Numerous reversed-phase ion-pairing methods have been reported for various combinations of I, II, and III and other drugs. A previous report (12) used a nitrile column

0022-3549/83/0100-0055$01.00/0

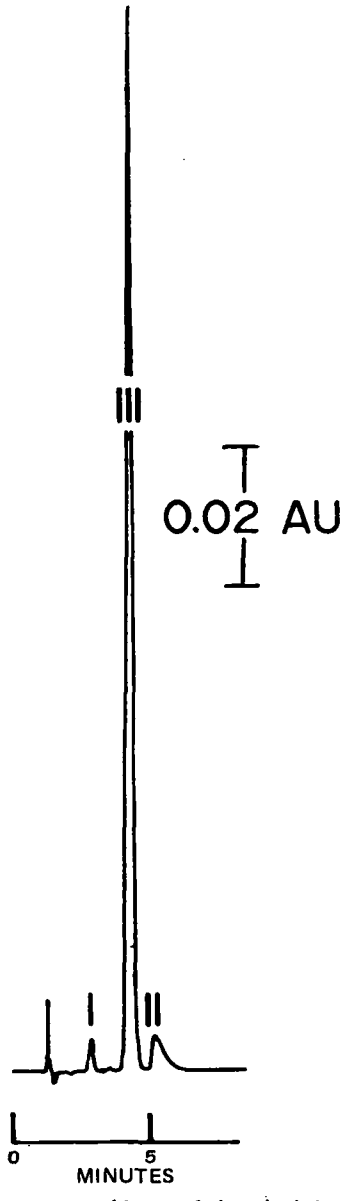

Figure 1—*Chromatogram of 0.8 μg of phenylephrine hydrochloride (I), 8 μg of phenylpropanolamine hydrochloride (II), and 36 μg of guaifenesin (III) with a C_{18} column packed in the lab. See text for chromatographic conditions.*

and an aqueous acetonitrile, acetic acid, heptanesulfonic acid salt ion-pair eluent to barely resolve I and II. Although the hydrophobic C_{18}-bonded phase has not been extensively used for this separation, the more polar phenyl bonded phase has been employed with a methanol, water, acetic acid, heptanesulfonic acid salt ion pair to yield a separation of I, II, and III with k' values of 1.2, 1.9, and 1.4, respectively (13); and to separate II and III at retention times of 15–18 min (14).

Another report (15) separated phenylephrine hydrochloride from other active compounds using a C_{18} column and an aqueous methanol and acetic acid eluent containing heptanesulfonic acid. Determinations involving guaifenesin on C_{18} columns have been characterized by the absence of an ion-pairing agent (16, 17). Phenylephrine hydrochloride and phenylpropanolamine hydrochloride were assayed (18) using a silica gel column with a methylene chloride, methanol, and aqueous ammonia eluent. The purpose of the present work was to improve the separation

Table I—Linearity Area Ratios

Parameter	Phenylephrine hydrochloride	Phenylpropanolamine hydrochloride	Guaifenesin
Correlation coefficient	0.9993	0.99987	0.99988
Standard error of the estimate ($S_{y/x}$)	0.0009	0.001	0.018
Intercept[a], %	−0.5	−0.7	−1.1
Variation[b], %	1.6	0.7	0.7

[a] (y intercept/$\bar{y}$) × 100, where $\bar{y}$ is the average y (22). [b] ($S_{y/x}/\bar{y}$) × 100.

of I, II, and III with a reversed-phase column and ion pairing to yield a method with simplified sample handling (leaching followed by direct injection) and sufficient specificity for stability-indicating analysis.

The specificity requirement dictates knowledge of the known and expected degradation products of I, II, and III. However, II and III have been reported to be stable in dosage form (15, 19) and require extreme conditions for degradation: III can be hydrolyzed to guaiacol with hot

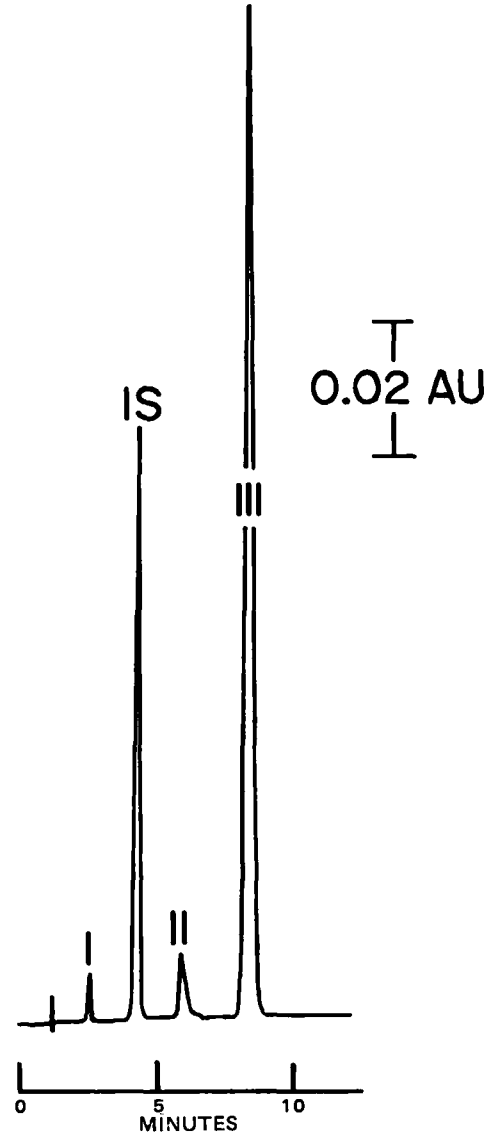

Figure 2—*Chromatogram of 0.8 μg of phenylephrine hydrochloride (I), 8 μg of phenylpropanolamine hydrochloride (II), and 36 μg of guaifenesin (III), and 2,5-dihydroxybenzoic acid internal standard (IS) with a C_8 column. See text for chromatographic conditions.*

Table II—Assay of Thermally Degraded Capsule Samples

Sample	Phenylephrine hydrochloride			Phenylpropanolamine hydrochloride			Guaifenesin		
	mg/g	Label[a], %	Initial, %	mg/g	Label[a], %	Initial, %	mg/g	Label[a], %	Initial, %
Oven at 95°, 9 days	9.42	99.9	97.0	81.5	96.0	97.9	377	100.0	100.5
0.5 *M* HCl RT, 9 days	9.85	104.4	101.4	81.3	95.8	97.6	373	98.8	99.3
0.5 *M* NaOH RT, 9 days	9.31	98.7	95.8	82.5	97.1	99.0	373	98.8	99.3
0.5 *M* NaOH 90°, 3 days	0	0	0	49.3	58.1	59.2	357	94.6	94.8
Initial[b]	9.72	103.0		83.3	98.1		376	99.5	

[a] Label is 9.43 mg/g for phenylephrine hydrochloride, 84.9 mg/g for phenylpropanolamine hydrochloride, and 377 mg/g for guaifenesin. [b] From Table III.

Table III—HPLC Assay of Capsule Sample[a]

Sample Weight, mg	Phenylephrine hydrochloride	Phenylpropanolamine hydrochloride	Guaifenesin
0.6014	9.81	83.8	375
0.6011	9.58	83.4	376
0.6021	9.62	83.3	375
0.8009	9.74	83.3	373
0.8018	9.46	85.8	372
0.8007	9.54	82.0	370
0.9990	10.01	82.2	372
1.0004	9.59	82.9	376
1.0002	9.69	82.6	379
1.2503	10.00	82.3	379
1.2498	9.71	84.4	379
1.2503	9.86	84.3	380
Mean	9.72 mg/g	83.3 mg/g	376 mg/g
RSD (1σ)	1.8%	1.3%	0.9%
Spectrophotometric control assays (average of two)	9.67 mg/g	84.1 mg/g	382 mg/g

[a] Label is 9.43 mg/g for phenylephrine hydrochloride, 84.9 mg/g for phenylpropanolamine hydrochloride, and 377 mg/g for guaifenesin.

concentrated hydrochloric acid (16) and II can be oxidized to benzaldehyde with periodate (20). Analyte I, however, has been reported to readily undergo decomposition in aqueous buffer solutions at 85° to 1,2,3,4-tetrahydro-4,6 (and 4,8)-dihydroxy-2-methylisoquinoline and other minor products with *m*-hydroxybenzaldehyde as an intermediate (21).

EXPERIMENTAL

Reagents and Chemicals—All reagents and chemicals were ACS, USP, or NF quality and were used without further purification. Phenylephrine hydrochloride, phenylpropanolamine hydrochloride, and guaifenesin were used as received[1].

Apparatus—A high-performance liquid chromatograph[2] equipped with a reciprocating pump[3], an absorbance detector at 254 nm[4] (analytical wavelength), and an injector[5] with a 20-μl loop was used. The detector was monitored with a strip-chart recorder and integrator[6]. A variable-wavelength detector[7] set at 270 nm and a fixed-wavelength detector[4] at 280 nm were used for absorbance ratio studies.

Columns—The octadecylsilane columns used were packed[8] in the lab (25 cm × 4-mm i.d.) and commercially packed[8] (30 cm × 4-mm i.d.). The more polar octyl columns examined were a commercially packed column[9] (25 cm × 4.6-mm i.d.) and two columns packed in the lab (25 cm × 4.6-mm i.d. and 30 cm × 4.0-mm i.d.) of the same material[9]. Particle size was 10 μm in all cases.

Chromatographic Conditions—For the C_8 columns, the mobile phase consisted of 300 ml of methanol, 675 ml of water, and 25 ml of pentanesulfonic acid sodium salt in glacial acetic acid[10] to yield an eluent that was 5 m*M* in ion-pairing salt and 1.7% in acetic acid. For the C_{18} columns, the basic mobile phase was 350 ml of methanol, 625 ml of water, and 25 ml of pentanesulfonic acid sodium salt in glacial acetic acid[10]. The methanol concentration had to be adjusted to between 25 and 40% for the different C_{18} columns. Readjusting the eluent for different C_8 columns was not necesary. The flow rate was 2.0 ml/min in all cases.

Standard Solution Preparation—The final method (C_8 column) used a standard solution containing 0.04 mg/ml of I, 0.4 mg/ml of II, 1.8 mg/ml of III, and 0.4 mg/ml of 2,5-dihydroxybenzoic acid internal standard with water as solvent.

Sample Preparation—For the capsule and tablet samples, 1 g of the ground sample was leached with ~250 ml of water containing a controlled amount of 2,5-dihydroxybenzoic acid internal standard (~0.4 mg/ml). The sample was injected directly after a 10-min sonication and 5-min centrifugation at 2500 rpm. For the liquid samples, 4.0–25.0 ml (depending on label claim) was diluted to ~250 ml with water containing the internal standard. The sample was then injected directly.

Thermally Degraded Samples—One-gram samples of a well-mixed capsule material containing I, II, and III as active ingredients were

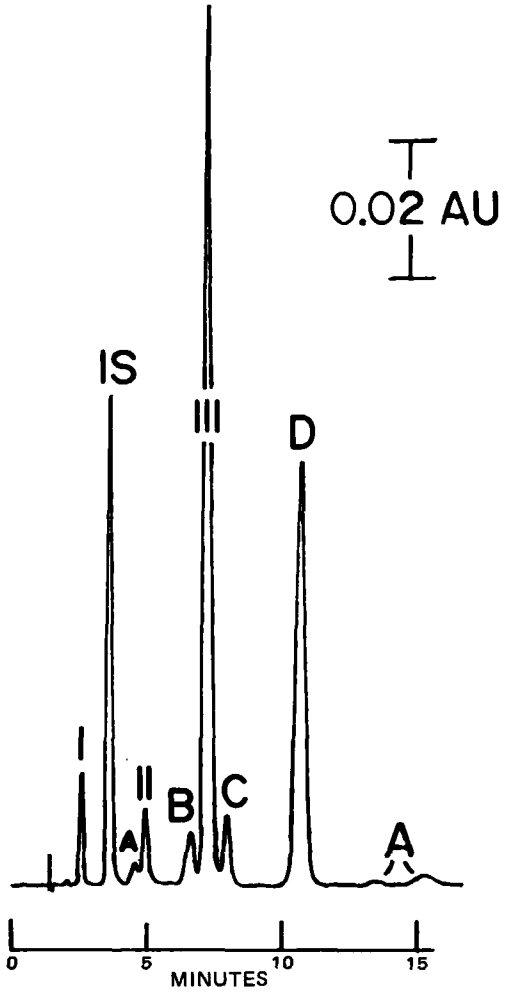

Figure 3—*Chromatogram of phenylephrine hydrochloride (I), phenylpropanolamine hydrochloride (II), and guaifenesin (III), and 2,5-dihydroxybenzoic acid internal standard (IS), and possible degradation products: phenylephrine forced degraded decomposition products (A); m-hydroxybenzaldehyde (B); guaiacol (C); benzaldehyde (D).*

[1] Norwich-Eaton Pharmaceuticals, Norwich, N.Y.
[2] Waters ALC 204, Waters Associates, Milford, Mass.
[3] Waters model 6000A.
[4] Waters model 440.
[5] Rheodyne model 725, Berkeley, Calif.
[6] Hewlett-Packard model 3352B, Avondale, Pa.
[7] Laboratory Data Control model III, Riviera Beach, Fla.
[8] Waters μ-Bondapak C_{18}.
[9] Whatman Partisil-10 C_8.
[10] Waters PIC B-5.

Table IV—HPLC Assay of Various Commercial Dosage Forms

Dosage Form	Sample	Phenylephrine hydrochloride		Phenylpropanolamine hydrochloride		Guaifenesin	
		mg/ml	Label, %	mg/ml	Label, %	mg/ml	Label, %
Syrup	1	—	—	12.3	98.8	99.9	99.9
Syrup	2	—	—	8.3	92.2	31.6	105.2
Syrup	3	—	—	8.7	96.6	97.9	97.9
Syrup	4	—	—	12.5	100.2	95.6	95.6
Eye Drop	5	2.53	101.1	—	—	—	—
Capsule	6[a]	9.72	103.0	83.3	98.1	376	99.7
Tablet	7	—	—	96.0	97.0	518	98.1

[a] From Table III.

weighed into several 500-ml Erlenmeyer flasks. One flask was placed in the oven at 95° for 9 days. Twenty milliliters of 0.5 *M* HCl and 20 ml of 0.5 *M* NaOH were added to two other separate flasks, and both were stored at room temperature for 9 days. In addition, one container was stored in direct sunlight for 13 days, and one container containing sample and 20 ml of 0.5 *M* NaOH was stored at 90° for 3 days. At the end of the required time period, the acidic and basic solutions were neutralized, internal standard added, and all the samples assayed. The analyte and internal standard peaks were also examined for homogeneity by absorbance ratios at 254 and 270 nm, except for the sample stored in 0.5 *M* NaOH at 90°, which was examined at 254 and 280 nm. Analyte I was degraded by the literature method (21) by dissolving 100 mg of standard I in 50 ml of a pH 6.8, 0.04 *M* ammonium acetate buffer and storing the solution in a 95° oven for 13 days.

Calculations—Results for I, II, and III, were calculated from their integrated peak areas and the peak area of the internal standard using the appropriate dilution factors.

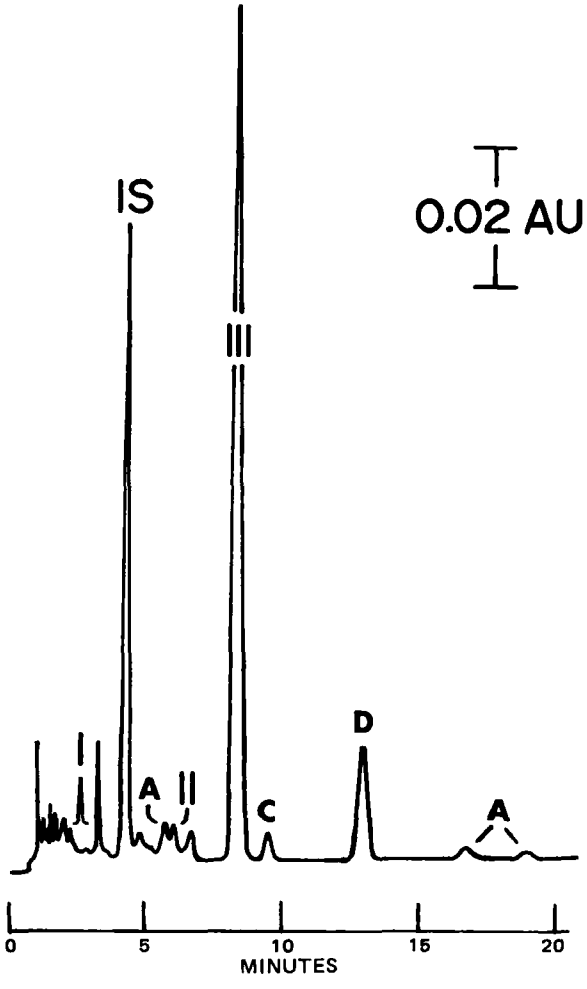

Figure 4—*Chromatogram of forced degraded (0.5 M NaOH at 90°) capsule sample: phenylpropanolamine hydrochloride (II); guaifenesin (III); 2,5-dihydroxybenzoic acid internal standard (IS): phenylephrine hydrochloride degradants (A); guaiacol (B); benzaldehyde (C). The peak for phenylephrine hydrochloride (I), which is totaly degraded, is drawn above the chromatogram.*

RESULTS AND DISCUSSION

Initial attempts to develop a reversed-phase simultaneous determination employed a C_{18} column with a methanol, water, and pentanesulfonic acid eluent yielded an assay that resolved I, II, and III from each other (Fig. 1). The chromatographic system lacked the retention and efficiency to meet the specificity requirement for guaiacol to be resolved from III. Additionally, relative retention appeared to change from column to column, often with packing from the same manufacturer. For example, II eluted after III with column packed in the lab and before III with a commercially packed column.

Exploratory experiments with a more polar octyl column were initiated and good results were obtained. The three analytes were well separated with k' values of 0.9, 2.4, and 3.7 for I, II, and III, respectively (Fig. 2). Identical chromatograms were obtained for a commercially packed column and several columns packed in the lab.

The linearity data for I, II, and III, determined by plotting peak area ratios *versus* standard weight ratios, are presented in Table I. Linearity was observed over the range studied: 0.5–1.5 μg for I; 4.8–14.4 μg for II; and 21–64 μg for III.

Assays of 11 synthetic capsule samples made by spiking placebo with solutions containing known amounts of standard I, II, and III at levels of 50–125% of theoretical yielded average recoveries and relative standard deviations of 100.9 ± 2.1%, 100.3 ± 1.3%, and 100.7 ± 0.8%, respectively.

A chromatogram of a solution containing 2.0 ml of the degraded standard solution of I (after 13 days at 95°), 20 mg of 2,5-dihydroxybenzoic acid, 2 mg of I, 20 mg of II, 89 mg of III, <5 mg of guaiacol (not completely soluble in water), 0.2 mg of *m*-hydroxybenzaldehyde, and <2 mg of benzaldehyde (not completely soluble in water) in 50 ml of water is shown in Fig. 3. All of the actual and postulated degradants were resolved. When the degraded standard solution of I was examined after only one day in the oven, a peak with the same retention time as *m*-hydroxybenzaldehyde was observed. This compound was postulated as an intermediate in a previous report (21), but was not observed.

Assay values for the thermally degraded capsule samples are listed in Table II. Except for the sample stored in 0.5 *M* NaOH at 90°, no extra peaks were noted and no significant degradation was observed. Examination of absorbance ratios indicated homogeneous peaks within experimental error.

A chromatogram (Fig. 4) of the sample solution stored in sodium hydroxide at 90° yielded several additional peaks and low assay values for I, II, and III, as shown in Table II. The difference in retention observed between Figs. 3 and 4 is caused by use of extensively used and freshly packed columns, respectively. Absorbance ratios (254/280 nm) and retention times of pure standards indicated peaks C and D, Fig. 4 were guaiacol and benzaldehyde, respectively. The internal standard and III peaks were also indicated to be homogeneous (II yielded no signal at 280 nm).

α-Aminopropiophenone, a precursor and possible trace impurity in II (23, 24), was found to elute immediately following the II peak. Although not quite baseline resolved, it could be detected down to at least 0.1% of the II concentration. It was not observed in any of the samples.

The assay results for several commercial dosage forms representing liquid, tablet, and capsule preparations are presented in Tables III and IV. None of the excipients in the formulations coeluted with the active ingredients or the internal standard.

The actives I, II, and III in the capsule sample were also determined spectrophotometrically. Analyte I was assayed colorimetrically by the

characteristic reaction of phenols with 4-aminoantipyrine described previously (25). The order of addition of reagents was altered to achieve acceptable precision. With these samples, it was necessary to add the bicarbonate buffer first. Analyte II in an aqueous solution of the sample was quantitatively oxidized to benzaldehyde with alkaline periodate by the procedure described previously (20). The benzaldehyde was then extracted from the solution with chloroform and determined spectrophotometrically. Guaifenesin was extracted from the samples with chloroform and determined by its UV absorbance. As the data in Table III indicate, the spectrophotometric assays are in good agreement with the HPLC assay presented here.

REFERENCES

(1) L. Neelakantan and H. B. Kostenbauder, *J. Pharm. Sci.*, **65**, 740 (1976).

(2) J. K. Baker, *Anal. Chem.*, **49**, 906 (1977).

(3) R. E. Madsen and D. F. Magin, *J. Pharm. Sci.*, **65**, 924 (1976).

(4) H. Kinsum, H. A. Moulin, and E. C. Savini, *ibid.*, **67**, 118 (1978).

(5) B. R. Rader and E. S. Aranda, *ibid.*, **57**, 847 (1968).

(6) D. E. Van Zwol, *J. Chromatogr.*, **24**, 26 (1966).

(7) A. C. Celeste and M. V. Polito, *J. Assoc. Off. Anal. Chem.*, **49**, 541 (1966).

(8) K. D. Parker, C. R. Fontan, and P. L. Kirk, *Anal. Chem.*, **34**, 1345 (1962).

(9) W. R. Maynard and R. B. Bruce, *J. Pharm. Sci.*, **59**, 1346 (1970).

(10) G. B. Cox, C. R. Loscombe, and K. Sugden, *Anal. Chim. Acta*, **92**, 345 (1977).

(11) R. M. Cassidy and S. Elchuk, *J. Chromatogr. Sci.*, **18**, 217 (1980).

(12) A. G. Ghanekar and V. Das Gupta, *J. Pharm. Sci.*, **67**, 873 (1978).

(13) T. R. Koziol, J. T. Jacob, and R. G. Achari, *ibid.*, **68**, 1135 (1979).

(14) N. Muhammad and J. A. Bodnar, *J. Liq. Chromatogr.*, **3**, 113 (1980).

(15) A. G. Ghanekar and V. Das Gupta, *J. Pharm. Sci.*, **67**, 1247 (1978).

(16) D. R. Heidemann, *ibid.*, **68**, 530 (1979).

(17) W. O. McSharry and I. V. E. Savage, *ibid.*, **69**, 212 (1980).

(18) R. G. Achari and E. E. Theimar, *J. Chromatogr. Sci.*, **15**, 320 (1977).

(19) S. Hugosson, L. Nyberg, and L. Nilsson, *Acta Pharm. Suec.*, **9**, 249 (1972).

(20) N. H. Brown and G. A. Portman, *J. Pharm. Sci.*, **60**, 1229 (1971).

(21) B. J. Millard, D. J. Priaulx, and E. Skotton, *J. Pharm. Pharmacol.*, **25**, 24 (1973).

(22) M. J. Cardone, P. J. Palermo, and L. B. Sybrandt, *Anal. Chem.*, **52**, 1187 (1980).

(23) "The United States Pharmacopeia," 20th rev., U.S. Pharmacopeial Convention, Rockville, Md., 1980, pp. 619–620.

(24) D. R. Heidemann, *J. Pharm. Sci.*, **70**, 820 (1981).

(25) K. T. Koshy and H. Mitchner, *ibid.*, **52**, 802 (1963).

Kinetics and Mechanism of Degradation of Cefotaxime Sodium in Aqueous Solution

S. M. BERGE ˣ, N. L. HENDERSON, and M. J. FRANK

Received January 13, 1982, from the *Pharmaceutical Development Department, Hoechst-Roussel Pharmaceuticals Inc., Somerville, NJ 08876.* Accepted for publication March 15, 1982.

Abstract □ The degradation kinetics and mechanism of a potent new cephalosporin, cefotaxime sodium, in aqueous solution were investigated at pH 0–10 at 25° and an ionic strength of 0.5. The degradation rates were determined by high-pressure liquid chromatography and were observed to follow pseudo first-order kinetics with respect to cefotaxime sodium concentration. The data suggested that the rate of degradation was influenced significantly by solvolytic, hydrogen ion, and hydroxide ion catalysis. No primary salt effects were observed in the acid or neutral regions; however, a positive salt effect was observed at pH 8.94. Buffer catalysis due to the buffer species employed was not seen during the kinetic studies. The pH–rate profile at 25° indicated that the maximum stability of cefotaxime sodium occurred in the pH 4.5–6.5 region. In aqueous solution, cefotaxime was shown to degrade by two parallel reactions: de-esterification at the C-3 position and β-lactam cleavage. Good agreement between the theoretical pH–rate profile and the experimental data support the proposed degradation process.

Keyphrases □ Kinetics—mechanism of degradation of cefotaxime sodium in aqueous solution □ Degradation—kinetics and mechanism, cefotaxime sodium in aqueous solution □ Cefotaxime sodium—kinetics and mechanism of degradation in aqueous solution □ Cephalosporins—cefotaxime sodium, kinetics and mechanism of degradation in aqueous solution

Cefotaxime sodium (I) is a potent new third generation cephalosporin possessing a broad spectrum of activity. Chemically, it is characterized by a 2-amino-4-thiazolyl ring which, in comparison to other cephalosporins, increases antibacterial activity against Gram-negative strains, and by an α-methoximino group which enhances

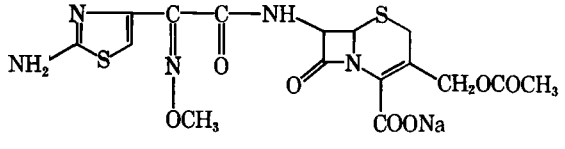

I

stability to β-lactamases (1–4). Compound I is active against Gram-positive and Gram-negative organisms, especially multiresistant strains, including many aminoglycoside-resistant strains. *In vitro*, its activity against Gram-negative organisms has been shown to be 10–200 times greater than that of the recently developed second generation cephalosporins (5).

The present report describes the stability kinetics of I in aqueous solution. The investigation was initiated to elucidate the mechanism by which I decomposes and to determine those kinetic parameters that will be of value in predicting the stability of the reconstituted antibiotic under a wide range of conditions.

EXPERIMENTAL

Materials—Cefotaxime sodium (I)[1] and desacetylcefotaxime (II)[2] were used without further purification. Desacetylcefotaxime lactone (III) was prepared using a modification of the method for cephalothin de-

[1] Claforan, Hoechst-Roussel Pharmaceuticals Inc., Somerville, N.J.
[2] Hoechst AG, Frankfurt, West Germany.

0022-3549/83/0100-0059$01.00/0

characteristic reaction of phenols with 4-aminoantipyrine described previously (25). The order of addition of reagents was altered to achieve acceptable precision. With these samples, it was necessary to add the bicarbonate buffer first. Analyte II in an aqueous solution of the sample was quantitatively oxidized to benzaldehyde with alkaline periodate by the procedure described previously (20). The benzaldehyde was then extracted from the solution with chloroform and determined spectrophotometrically. Guaifenesin was extracted from the samples with chloroform and determined by its UV absorbance. As the data in Table III indicate, the spectrophotometric assays are in good agreement with the HPLC assay presented here.

REFERENCES

(1) L. Neelakantan and H. B. Kostenbauder, *J. Pharm. Sci.*, **65**, 740 (1976).

(2) J. K. Baker, *Anal. Chem.*, **49**, 906 (1977).

(3) R. E. Madsen and D. F. Magin, *J. Pharm. Sci.*, **65**, 924 (1976).

(4) H. Kinsum, H. A. Moulin, and E. C. Savini, *ibid.*, **67**, 118 (1978).

(5) B. R. Rader and E. S. Aranda, *ibid.*, **57**, 847 (1968).

(6) D. E. Van Zwol, *J. Chromatogr.*, **24**, 26 (1966).

(7) A. C. Celeste and M. V. Polito, *J. Assoc. Off. Anal. Chem.*, **49**, 541 (1966).

(8) K. D. Parker, C. R. Fontan, and P. L. Kirk, *Anal. Chem.*, **34**, 1345 (1962).

(9) W. R. Maynard and R. B. Bruce, *J. Pharm. Sci.*, **59**, 1346 (1970).

(10) G. B. Cox, C. R. Loscombe, and K. Sugden, *Anal. Chim. Acta*, **92**, 345 (1977).

(11) R. M. Cassidy and S. Elchuk, *J. Chromatogr. Sci.*, **18**, 217 (1980).

(12) A. G. Ghanekar and V. Das Gupta, *J. Pharm. Sci.*, **67**, 873 (1978).

(13) T. R. Koziol, J. T. Jacob, and R. G. Achari, *ibid.*, **68**, 1135 (1979).

(14) N. Muhammad and J. A. Bodnar, *J. Liq. Chromatogr.*, **3**, 113 (1980).

(15) A. G. Ghanekar and V. Das Gupta, *J. Pharm. Sci.*, **67**, 1247 (1978).

(16) D. R. Heidemann, *ibid.*, **68**, 530 (1979).

(17) W. O. McSharry and I. V. E. Savage, *ibid.*, **69**, 212 (1980).

(18) R. G. Achari and E. E. Theimar, *J. Chromatogr. Sci.*, **15**, 320 (1977).

(19) S. Hugosson, L. Nyberg, and L. Nilsson, *Acta Pharm. Suec.*, **9**, 249 (1972).

(20) N. H. Brown and G. A. Portman, *J. Pharm. Sci.*, **60**, 1229 (1971).

(21) B. J. Millard, D. J. Priaulx, and E. Skotton, *J. Pharm. Pharmacol.*, **25**, 24 (1973).

(22) M. J. Cardone, P. J. Palermo, and L. B. Sybrandt, *Anal. Chem.*, **52**, 1187 (1980).

(23) "The United States Pharmacopeia," 20th rev., U.S. Pharmacopeial Convention, Rockville, Md., 1980, pp. 619–620.

(24) D. R. Heidemann, *J. Pharm. Sci.*, **70**, 820 (1981).

(25) K. T. Koshy and H. Mitchner, *ibid.*, **52**, 802 (1963).

Kinetics and Mechanism of Degradation of Cefotaxime Sodium in Aqueous Solution

S. M. BERGE ˣ, N. L. HENDERSON, and M. J. FRANK

Received January 13, 1982, from the *Pharmaceutical Development Department, Hoechst-Roussel Pharmaceuticals Inc., Somerville, NJ 08876.* Accepted for publication March 15, 1982.

Abstract □ The degradation kinetics and mechanism of a potent new cephalosporin, cefotaxime sodium, in aqueous solution were investigated at pH 0–10 at 25° and an ionic strength of 0.5. The degradation rates were determined by high-pressure liquid chromatography and were observed to follow pseudo first-order kinetics with respect to cefotaxime sodium concentration. The data suggested that the rate of degradation was influenced significantly by solvolytic, hydrogen ion, and hydroxide ion catalysis. No primary salt effects were observed in the acid or neutral regions; however, a positive salt effect was observed at pH 8.94. Buffer catalysis due to the buffer species employed was not seen during the kinetic studies. The pH–rate profile at 25° indicated that the maximum stability of cefotaxime sodium occurred in the pH 4.5–6.5 region. In aqueous solution, cefotaxime was shown to degrade by two parallel reactions: de-esterification at the C-3 position and β-lactam cleavage. Good agreement between the theoretical pH–rate profile and the experimental data support the proposed degradation process.

Keyphrases □ Kinetics—mechanism of degradation of cefotaxime sodium in aqueous solution □ Degradation—kinetics and mechanism, cefotaxime sodium in aqueous solution □ Cefotaxime sodium—kinetics and mechanism of degradation in aqueous solution □ Cephalosporins—cefotaxime sodium, kinetics and mechanism of degradation in aqueous solution

Cefotaxime sodium (I) is a potent new third generation cephalosporin possessing a broad spectrum of activity. Chemically, it is characterized by a 2-amino-4-thiazolyl ring which, in comparison to other cephalosporins, increases antibacterial activity against Gram-negative strains, and by an α-methoximino group which enhances

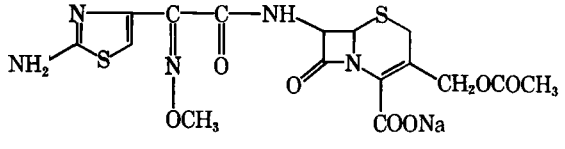

I

stability to β-lactamases (1–4). Compound I is active against Gram-positive and Gram-negative organisms, especially multiresistant strains, including many aminoglycoside-resistant strains. *In vitro*, its activity against Gram-negative organisms has been shown to be 10–200 times greater than that of the recently developed second generation cephalosporins (5).

The present report describes the stability kinetics of I in aqueous solution. The investigation was initiated to elucidate the mechanism by which I decomposes and to determine those kinetic parameters that will be of value in predicting the stability of the reconstituted antibiotic under a wide range of conditions.

EXPERIMENTAL

Materials—Cefotaxime sodium (I)[1] and desacetylcefotaxime (II)[2] were used without further purification. Desacetylcefotaxime lactone (III) was prepared using a modification of the method for cephalothin de-

[1] Claforan, Hoechst-Roussel Pharmaceuticals Inc., Somerville, N.J.
[2] Hoechst AG, Frankfurt, West Germany.

0022-3549/83/0100-0059$01.00/0

Cefotaxime

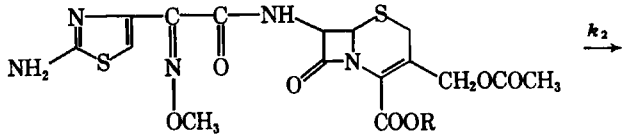

I

k_1

β-Lactam Ring Opened Products

Desacetylcefotaxime

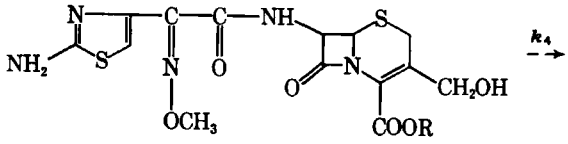

II

k_3

β-Lactam Ring Opened Products

Desacetylcefotaxime Lactone

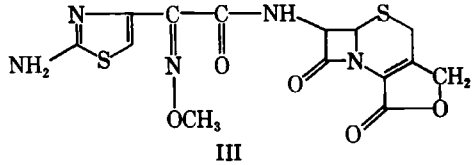

III

k_5

β-Lactam Ring Opened Products

R = H, Na

Scheme I—Reaction pathways for the degradation of I in aqueous solution.

scribed previously (6). Buffers and all other chemicals were reagent grade.

Buffers—The buffers used in the kinetic studies were hydrochloric acid–potassium chloride (pH −0.10, 0.48, 1.15, and 2.23), citrate buffer (pH 2.83), acetate buffer (pH 3.93, 4.58, 5.07, and 5.52), phosphate buffer (pH 5.85, 6.51, 6.90, 7.57, and 7.93), borate buffer (pH 8.41, 8.93, and 9.06), and carbonate buffer (pH 9.89). The buffers were 0.1 *M* with respect to hydrochloric acid, citrate, acetate, phosphate, borate, and carbonate ions (except when a buffer effect was investigated), and they were adjusted to an ionic strength of 0.5 with potassium chloride, except when primary salt effects were studied. They were prepared by dissolving specific molar ratios of the buffer pair together with potassium chloride in water or by dissolving the acidic member of the buffer pair together with potassium chloride and adjusting the pH with 1.0 *N* NaOH. The pH of each solution was measured using a pH meter[3] equipped with a combination electrode[3].

Kinetic Procedure—Approximately 100 mg of I was accurately weighed and dissolved in 100 ml of the appropriate buffer to produce a solution having a concentration of 2.09×10^{-3} *M*. All buffers were preheated to the temperature of the study. The flasks were maintained at a constant temperature (±0.2°) in a thermostatically controlled water bath. Aliquots were withdrawn at desired time intervals, diluted, and immediately analyzed.

Analytical Procedure—Residual I was determined using a high-pressure liquid chromatographic (HPLC) method. The liquid chromatograph[4] was equipped with a variable wavelength UV detector[5] set at 235 nm; the separation was carried out using a 300 × 3.9-mm octadecylsilane column[6] with a methanol–phosphate buffer (pH 7.5) (12:88) mobile phase. The column pressure was 1700–1800 psi at a flow rate of 1.2–1.3 ml/min. Peak areas, which were calculated by a programmable integrator[7], were used to quantitate the amount of I remaining. Standard curves of the peak area of I *versus* concentration exhibited linear response in the working concentration range of 10–100 μg/ml. The sample peak areas were converted to concentrations by comparison with a standard curve which was obtained daily.

[3] Corning Glass Works.
[4] Waters Associates, Milford, Mass.
[5] Perkin-Elmer LC-75.
[6] μ Bondapak C_{18}, Waters Associates, Milford, Mass.

Table I—Buffer Systems, Observed Rate Constants, and $t_{90\%}$ for the Degradation of I at 25°

pH	Buffer System	k_{obs}, $hr^{-1} \times 10^3$	$t_{90\%}$, hr
−0.10	HCl	488.2	0.2
0.48	HCl	140.0	0.8
1.15	HCl–KCl	35.5	3.0
2.23	HCl–KCl	7.82	13.4
2.83	Citrate	4.96	21.2
3.93	Acetate	3.67	28.6
4.58	Acetate	2.72	38.6
5.07	Acetate	2.85	36.9
5.52	Acetate	3.24	32.4
5.85	Phosphate	3.08	34.2
6.51	Phosphate	3.23	32.5
6.90	Phosphate	3.44	30.5
7.57	Phosphate	4.23	24.8
7.93	Phosphate	5.73	18.3
8.41	Borate	8.27	12.7
8.94	Borate	25.5	4.1
9.06	Borate	27.0	3.9
9.89	Carbonate	177.0	0.6

RESULTS AND DISCUSSION

Degradation Reactions, Reaction Order, and Observed Rate Constants—Compound I, a 3-acetoxymethylcephalosporin, has three possible sites at which degradation can occur: the amide side chain, the β-lactam ring, and the acetoxy ester group. Under conditions of pharmaceutical interest, the β-lactam ring opening and acetoxy hydrolysis predominate. The degradation reactions for I have been proposed and are shown in Scheme I. Such a scheme has been shown to be valid for other 3-acetoxymethylcephalosporins (6–10) and is supported by the experimental results observed in this study. Compound I undergoes two parallel reactions simultaneously: β-lactam ring opening (k_1) and deesterification at the C-3 position (k_2). At pH values <4, II can undergo an internal ring closure (k_4) to form III. Both II and III are susceptible to β-lactam hydrolysis (k_3,k_5). Figure 1 shows typical chromatograms

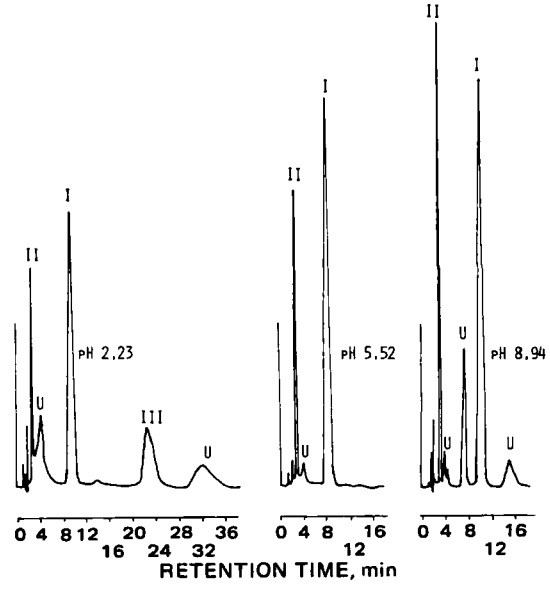

Figure 1—*High-pressure liquid chromatographs of 40–70% degraded I at 25°, μ = 0.5, and several pH values. Key: (I) cefotaxime; (II) desacetylcefotaxime; (III) desacetylcefotaxime lactone; (U) unknown peak.*

[7] Hewlett-Packard HP 3388.

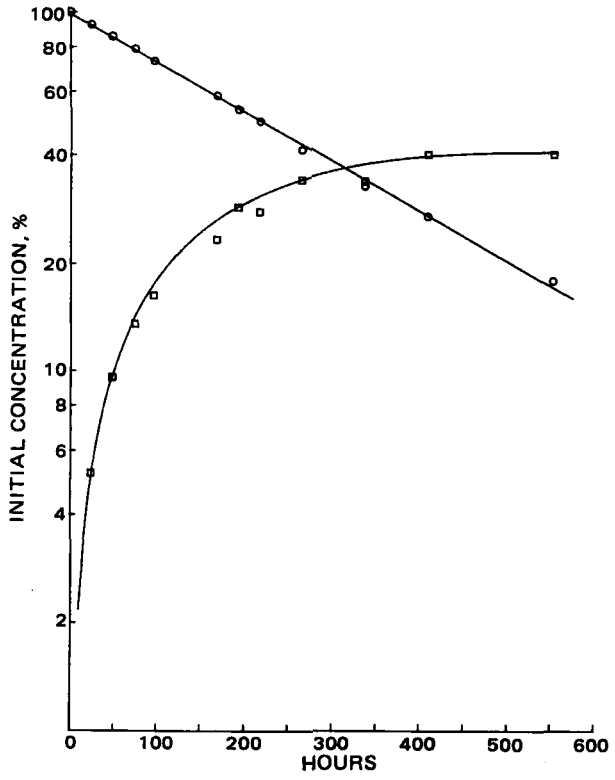

Figure 2—*Time courses for I (○) and II (□) during the degradation of I at pH 5.52, 25°, and μ = 0.5.*

of acidic (pH 2.23), neutral (pH 5.52), and basic (pH 8.94) reaction mixtures of I, which illustrate the formation of the degradation products described in Scheme I. The de-esterification reaction (k_2) occurs more rapidly, being ~1.8 times faster than the β-lactam ring opening (k_1) at pH 5.52. Figure 2 illustrates the kinetics of the disappearance of I and the formation of II at pH 5.52. The observed rate constants, k_{obs}, determined in this study are actually the sum of k_1 and k_2.

The degradation of I followed pseudo first-order kinetics at constant pH, temperature, and ionic strength over the pH range studied. This first-order dependence on the concentration of I is illustrated in Fig. 3, which shows that at pH 5.52, the log concentration *versus* time plots are

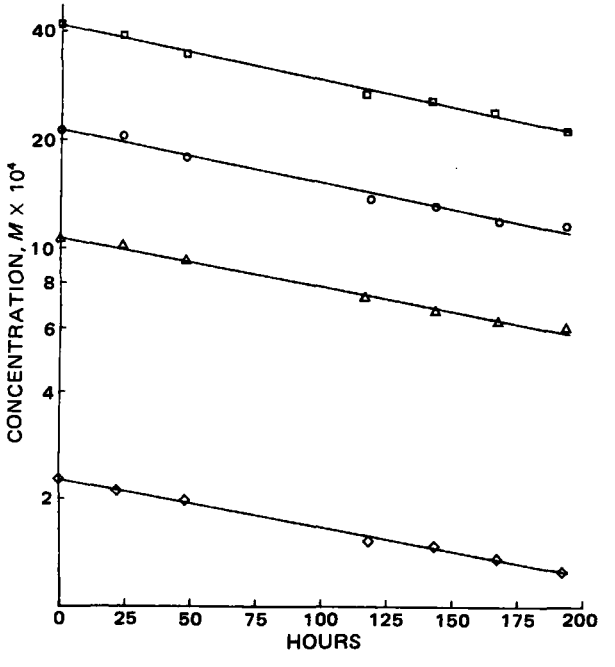

Figure 3—*Plots illustrating first-order dependence on the concentration of I at pH 5.52, 25°, and μ = 0.5. Key: (□) 2.0 mg/ml; (○) 1.0 mg/ml; (△) 0.5 mg/ml; (◇) 0.1 mg/ml.*

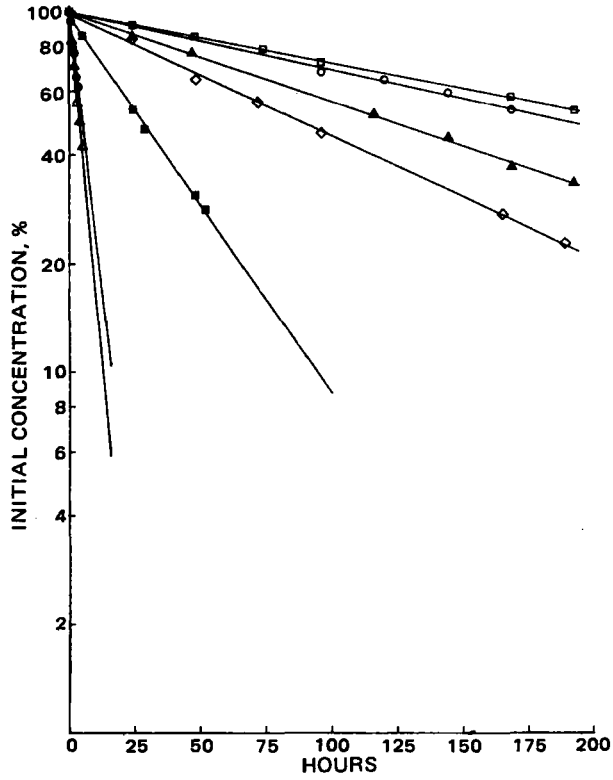

Figure 4—*Observed pseudo first-order plots for the degradation of I at various pH values, 25°, and μ = 0.5. Key: (□) pH 5.52; (○) pH 3.93; (▲) pH 7.93; (◇) pH 2.23; (■) pH 8.94; (●) pH 0.48; (△) pH 9.89.*

linear and parallel over a 20-fold concentration range (2.09×10^{-4}–4.19×10^{-3} *M*). Similar results were observed at pH 2.23 and 8.94. Further evidence of first-order kinetics is that semilogarithmic plots of the percent residual I *versus* time are linear over the pH range studied as shown in Fig. 4. The observed rate constants and the buffer systems employed are listed in Table I.

Catalytic Effect of Buffer Systems—The catalytic effect of the buffer systems used in the kinetic studies was determined at constant pH, temperature, ionic strength (μ = 0.5), and drug concentration, with only the buffer concentration varying (0.05–0.2 *M*). This experiment was done at several pH values within the effective range for each buffer employed. No appreciable effect on the degradation of I was observed for any of the buffer species used in the study.

Primary Salt Effect—The primary salt effect on the hydrolysis of

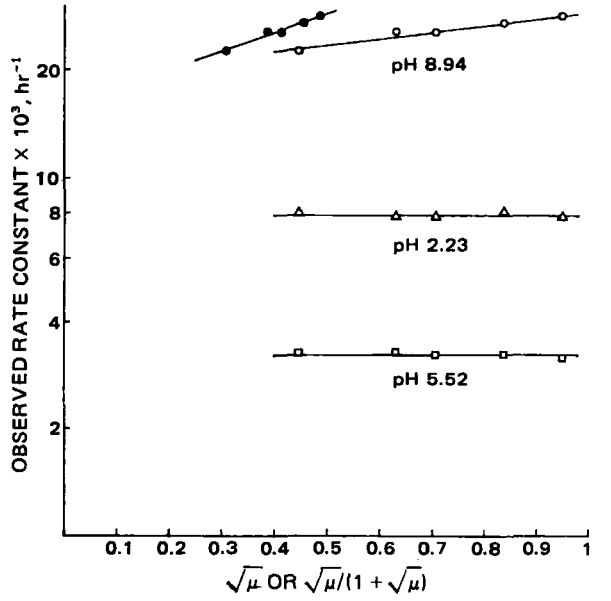

Figure 5—*Plots of log* k_{obs} versus $\sqrt{\mu}$ (○, △, and □) or $\sqrt{\mu}/(1+\sqrt{\mu})$ (●) *for the degradation of I at several pH values and 25°.*

Table II—Effect of Ionic Strength on Pseudo First-Order Rate Constants for the Degradation of I at pH 2.23, 5.52, and 8.94

Ionic Strength	k_{obs}, $hr^{-1} \times 10^3$		
	pH 2.23	pH 5.52	pH 8.94
0.2	7.99	3.28	22.6
0.4	7.82	3.30	25.6
0.5	7.82	3.24	25.5
0.7	8.07	3.25	27.1
0.9	7.79	3.17	28.3

I was studied at constant pH, temperature, and drug concentration, but the ionic strength was varied by potassium chloride addition. Studies were conducted at pH 2.23, 5.52, and 8.94 for ionic strength values ranging from 0.2 to 0.9. The data at these pH values and differing ionic strengths are given in Table II.

Within limits of the Debye-Huckel expressions, plots of k_{obs} *versus* $\sqrt{\mu}$ or $\sqrt{\mu}/(1+\sqrt{\mu})$ should yield slopes theoretically equal to $2AZ_AZ_B$, where A is a constant for the solvent at a given temperature ($A = 0.509$ at 25°, water) and Z_A and Z_B are the charges on reaction species A and B, respectively (11). Plots of k_{obs} *versus* $\sqrt{\mu}/(1+\sqrt{\mu})$ are perhaps preferred in that it has been pointed out that the use of $\sqrt{\mu}/(1+\sqrt{\mu})$ instead of $\sqrt{\mu}$ at higher ionic strengths more frequently produces values of $2AZ_AZ_B$ that are in agreement with the predicted values (12).

Figure 5 is a plot of the log k_{obs} *versus* $\sqrt{\mu}$ and $\sqrt{\mu}/(1+\sqrt{\mu})$ from the data in Table II. No kinetic salt effects were observed at pH 2.23 or 5.52, indicating that at least one of the reacting molecules is uncharged, while at pH 8.94 plots of $\sqrt{\mu}$ and $\sqrt{\mu}/(1+\sqrt{\mu})$ give positive slopes of +0.19 and +0.52, respectively. This result can be used as evidence that two negatively charged ions are reacting.

pH–Rate Profile—The pH dependence of the overall first-order rate constant for the degradation of I at 25° and an ionic strength of 0.5 is shown in Fig. 6. The pH–rate profile exhibits a U-shape which is typical of cephalosporins without an α-amino group in the C-7 side chain (7–9). This type of curve is characteristic of reactions that are susceptible to specific acid–base catalysis and that obey the general rate law:

$$k_{obs} = k_H a_{H^+} + k_w + k_{OH}[OH^-] \qquad \text{(Eq. 1)}$$

where k_H and k_{OH} are the second-order rate constants for the hydrogen ion-catalyzed degradation and hydroxide ion-catalyzed degradation, respectively; k_w is the first-order rate constant of spontaneous or water catalyzed degradation; a_{H^+} is the activity of hydrogen ion as measured by the glass electrode; and $[OH^-]$ is the hydroxide ion concentration.

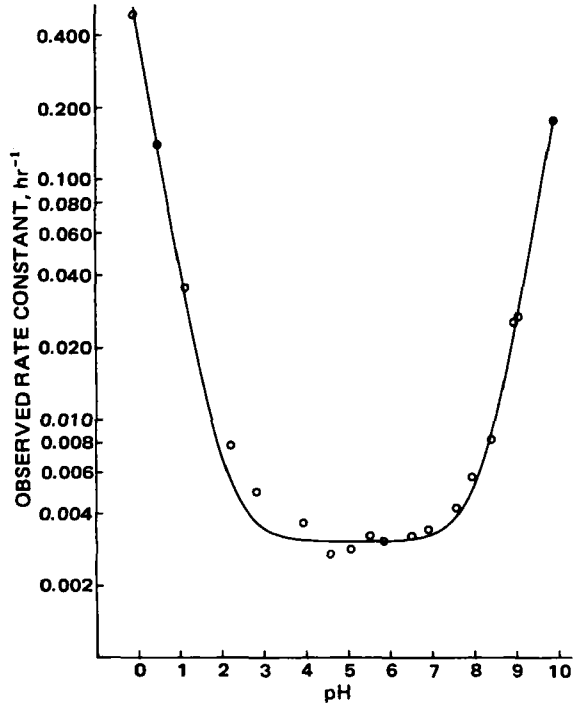

Figure 6—*Log k_{obs}–pH profile for the degradation of I in aqueous solution at 25° and $\mu = 0.5$. The points are experimental values, and the solid line is the theoretical curve calculated from Eq. 1.*

Table III—Effect of Temperature on the Degradation of I in Buffer Solutions at $\mu = 0.5$

pH	Temperature	k_{obs}, $hr^{-1} \times 10^3$	E_a, kcal/mole	log A, hr^{-1}	$k_{25°}$, $hr^{-1} \times 10^3$ (theoretical)	$k_{25°}$, $hr^{-1} \times 10^3$ (observed)
2.23	35	24.0	21.1	13.4	7.46	7.82
	45	71.2				
	55	196.7				
5.52	35	13.2	24.7	15.6	3.30	3.24
	45	44.7				
	55	154.2				
8.94	35	87.2	9.4[a]	15.2	24.50	25.50
	45	279.8				
	55	851.4				

[a] The calculated energy of activation E_a, was 22.9 kcal/mole, but this value includes the heat of ionization of water, which at 25° equals 13.5 kcal/mole (13).

Estimates of k_H, k_w, and k_{OH} were obtained from a simultaneous solution of k_{obs} (Eq. 1) at pH 0.48, 5.85, and 9.89. The hydroxide ion concentration was calculated according to:

$$[OH^-] = K_{w(exp)}/a_{H^+}\gamma\pm \qquad \text{(Eq. 2)}$$

where $K_{w(exp)} = 1.008 \times 10^{-14}$ and $\gamma\pm$ is the mean ionic activity coefficient product of water which is equal to 0.73, both at 25° and $\mu = 0.5$ (13). The resulting rate constants were $k_H = 0.4137\ M^{-1}\ hr^{-1}$, $k_w = 3.064 \times 10^{-3}\ hr^{-1}$ and $k_{OH} = 1616.5\ M^{-1}\ hr^{-1}$. The theoretical profile generated using these constants adequately describes the behavior of I and can be interpreted kinetically as follows:

Acid catalysis is important <pH 4 and base catalysis occurs >pH 8. The linear portions of the curve >pH 1.2 and 8.9 have slopes of −0.92 and +0.92, respectively, indicating that specific acid and specific base catalysis is occurring in these pH regions. The horizontal portion between pH 4 and 7 is pH independent, suggesting that the predominating reaction is the attack of water on the ionized species of I. The positive deviation in the pH 2–4 range can be postulated as being due to an intramolecular general acid catalysis of the carboxyl group on the deacetylation reaction. Such an explanation is logical in view of the facts that the pKa of I at 25° is 3.4[8] and that the drug concentration is significant in relation to the

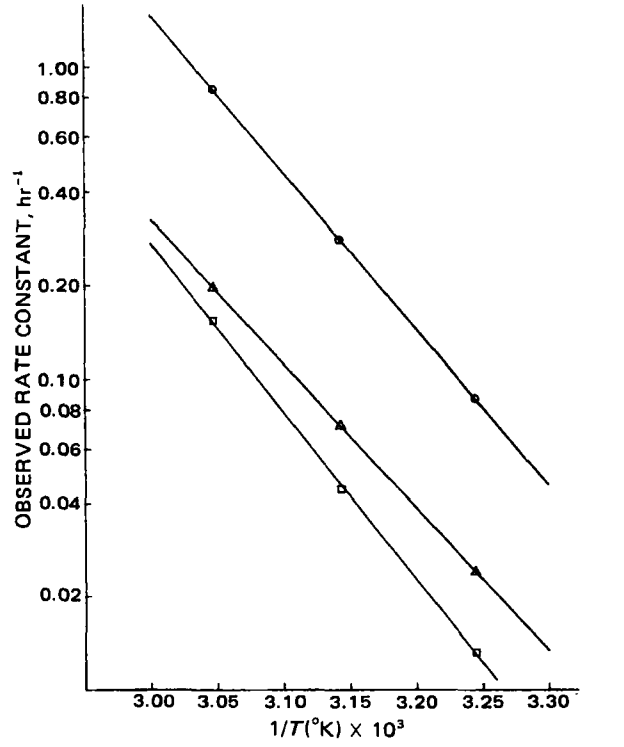

Figure 7—*Arrhenius plots for the degradation of I at several pH values and $\mu = 0.5$. Key: (△) pH 2.23; (□) pH 5.52; (○) pH 8.94.*

[8] Personal communication.

hydrogen ion concentration in this pH region. Ionic strength effects support this interpretation.

The theoretical pH minimum for the degradation of I obtained by taking the derivative of Eq. 1 and equating it to zero was pH 5.13.

Temperature Dependency—The dependence of degradation of I on temperature was determined by measuring the rate of decomposition at 35, 45, and 55° at pH 2.23, 5.52, and 8.94 and ionic strength is 0.5. The values of k_{obs}, E_a, and log A are given in Table III, and the corresponding Arrhenius plots are shown in Fig. 7. The theoretical $k_{25°}$ calculated using the energy of E_a, activation was in good agreement with the experimentally determined $k_{25°}$ at each of the three pH values, indicating that the data can be used to predict the stability of I over a wide range of pH and temperature conditions.

REFERENCES

(1) R. Heymes, A. Lutz, and E. Schrinner, 10th International Congress of Chemotherapy, Washington, D.C., Proceedings 823 (1978).

(2) H. C. Neu, N. Aswapokee, P. Aswapokee, and K. P. Fu, *Antimicrob. Agents Chemother.*, **15**, 273 (1979).

(3) M. Ochiai, O. Aki, A. Moriomoto, T. Okada, and Y. Matsushia, *Chem. Pharm. Bull.*, **25**, 3115 (1977).

(4) F. Kees, E. Strehl, K. Seeger, G. Seidel, P. Dominiak, and H. Grobecker, *Arzneim.-Forsch.*, **31**, 362 (1981).

(5) F. W. H. M. Merkus, *Pharm. Int.*, **1**, 1 (1981).

(6) S. C. Neidleman, S. C. Pan, J. A. Last, and J. E. Dolfini, *J. Med. Chem.*, **13**, 386 (1970).

(7) T. Yamana and A. Tsuji, *J. Pharm. Sci.*, **65**, 1563 (1976).

(8) K. A. Conners, G. L. Amidon, and L. Kennon, "Chemical Stability of Pharmaceuticals: A Handbook for Pharmacists," Wiley, New York, N.Y., 1979, pp. 195–200.

(9) J. Konecny, E. Felber, and J. Gruner, *J. Antibiot.*, **26**, 135 (1973).

(10) S. Kukolja, *J. Med. Chem.*, **11**, 1067 (1968).

(11) A. Frost and R. Pearson, "Kinetics and Mechanisms," 2nd ed., Wiley, New York, N.Y., chap. 7, 1971.

(12) J. T. Carstensen, *J. Pharm. Sci.*, **59**, 1140 (1970).

(13) H. S. Harned and W. J. Hamer, *J. Am. Chem. Soc.*, **55**, 2194 (1933).

ACKNOWLEDGMENTS

Presented at the Basic Pharmaceutics Section, APhA Academy of Pharmaceutical Sciences, Orlando, Fla., November 1981.

Synthesis and Biological Activity of an Amino Analogue of a Tripeptide Inhibitor of Angiotensin-Converting Enzyme

RONALD G. ALMQUIST ˣ, PAMELA H. CHRISTIE, WAN-RU CHAO, and HOWARD L. JOHNSON

Received September 8, 1980, from the *Bio-Organic Chemistry Laboratory, SRI International, Menlo Park, CA 94025.* Accepted for publication February 25, 1982.

Abstract □ An amino analogue of *N*-benzoyl-phenylalanyl-glycyl-proline, a tripeptide inhibitor of angiotensin-converting enzyme, was synthesized. The analogue (III) has the phenylalanyl-glycine amide linkage of *N*-benzoyl-phenylalanyl-glycyl-proline reduced to a methylene amine. Compound III was tested as an inhibitor of porcine plasma angiotensin-converting enzyme and has an I_{50} of 620 μM compared with an I_{50} of 9.6 μM for its parent tripeptide. These results are explained in terms of a proposed model of the converting-enzyme active site.

Keyphrases □ Angiotensin-converting enzyme—synthesis and biological activity of an amino analogue of *N*-benzoyl-phenylalanyl-glycyl-proline, a tripeptide inhibitor □ *N*-Benzoyl-phenylalanyl-glycyl-proline—tripeptide inhibitor of angiotensin-converting enzyme, synthesis and biological activity of an amino analogue

In a previous paper (1) work on a ketomethylene analogue I of the tripeptide inhibitor Bz-Phe-Gly-Pro (II) of angiotensin-converting enzyme was described:

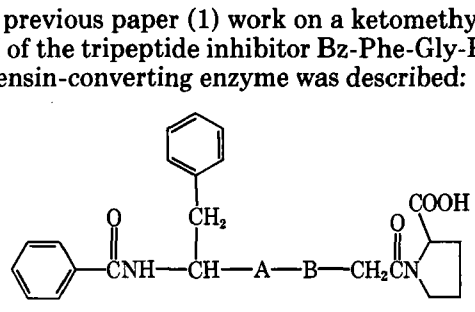

I: A = CO, B = CH_2
II: A = CO, B = NH
III: A = CH_2, B = NH

The replacement of the peptide amide linkage in II with a ketomethylene group was designed to stabilize this portion of the peptide molecule to peptidase cleavage. This substitution yielded a peptide analogue (I) with >100 times the inhibition activity against angiotensin-converting enzyme of the parent peptide.

A second approach to stabilizing this same peptide amide linkage in II to peptidase cleavage would be to reduce it to the corresponding methyleneamino compound (III). This compound has been synthesized and its inhibition activity against angiotensin-converting enzyme will be discussed.

BACKGROUND

A method for the synthesis of III was desired which would maintain the same stereochemistry around the optical centers as that found in the tripeptide (II). Initially, numerous attempts were made to selectively reduce the amide, but not the ester, group of *N*-benzyloxycarbonyl-phenylalanyl-glycine ethyl ester with borane, as reported previously (2), with *N*-benzyloxycarbonyl-glycyl-leucine methyl ester as the starting material. In contrast to those results the ester group of *N*-benzyloxycarbonyl-phenylalanyl-glycine ethyl ester was reduced more rapidly than the amide group by borane.

Because selective reduction of the desired amide functionality did not seem possible in this case, the dipeptide acid *N*-benzyloxycarbonyl-phenylalanyl-glycine (IV) was used as a starting material for the synthesis of III (Scheme I). The 9-fluorenyl-methoxycarbonyl amino blocking group (3) was used because of its stability to acidic conditions such as the Jones oxidation (4).

The low yield obtained for the transformation of VI to VIII was

0022-3549/83/0100-0063$01.00/0

hydrogen ion concentration in this pH region. Ionic strength effects support this interpretation.

The theoretical pH minimum for the degradation of I obtained by taking the derivative of Eq. 1 and equating it to zero was pH 5.13.

Temperature Dependency—The dependence of degradation of I on temperature was determined by measuring the rate of decomposition at 35, 45, and 55° at pH 2.23, 5.52, and 8.94 and ionic strength is 0.5. The values of k_{obs}, E_a, and log A are given in Table III, and the corresponding Arrhenius plots are shown in Fig. 7. The theoretical $k_{25°}$ calculated using the energy of E_a, activation was in good agreement with the experimentally determined $k_{25°}$ at each of the three pH values, indicating that the data can be used to predict the stability of I over a wide range of pH and temperature conditions.

REFERENCES

(1) R. Heymes, A. Lutz, and E. Schrinner, 10th International Congress of Chemotherapy, Washington, D.C., Proceedings 823 (1978).

(2) H. C. Neu, N. Aswapokee, P. Aswapokee, and K. P. Fu, *Antimicrob. Agents Chemother.*, **15**, 273 (1979).

(3) M. Ochiai, O. Aki, A. Moriomoto, T. Okada, and Y. Matsushia, *Chem. Pharm. Bull.*, **25**, 3115 (1977).

(4) F. Kees, E. Strehl, K. Seeger, G. Seidel, P. Dominiak, and H. Grobecker, *Arzneim.-Forsch.*, **31**, 362 (1981).

(5) F. W. H. M. Merkus, *Pharm. Int.*, **1**, 1 (1981).

(6) S. C. Neidleman, S. C. Pan, J. A. Last, and J. E. Dolfini, *J. Med. Chem.*, **13**, 386 (1970).

(7) T. Yamana and A. Tsuji, *J. Pharm. Sci.*, **65**, 1563 (1976).

(8) K. A. Conners, G. L. Amidon, and L. Kennon, "Chemical Stability of Pharmaceuticals: A Handbook for Pharmacists," Wiley, New York, N.Y., 1979, pp. 195–200.

(9) J. Konecny, E. Felber, and J. Gruner, *J. Antibiot.*, **26**, 135 (1973).

(10) S. Kukolja, *J. Med. Chem.*, **11**, 1067 (1968).

(11) A. Frost and R. Pearson, "Kinetics and Mechanisms," 2nd ed., Wiley, New York, N.Y., chap. 7, 1971.

(12) J. T. Carstensen, *J. Pharm. Sci.*, **59**, 1140 (1970).

(13) H. S. Harned and W. J. Hamer, *J. Am. Chem. Soc.*, **55**, 2194 (1933).

ACKNOWLEDGMENTS

Presented at the Basic Pharmaceutics Section, APhA Academy of Pharmaceutical Sciences, Orlando, Fla., November 1981.

Synthesis and Biological Activity of an Amino Analogue of a Tripeptide Inhibitor of Angiotensin-Converting Enzyme

RONALD G. ALMQUIST ˣ, PAMELA H. CHRISTIE, WAN-RU CHAO, and HOWARD L. JOHNSON

Received September 8, 1980, from the *Bio-Organic Chemistry Laboratory, SRI International, Menlo Park, CA 94025.* Accepted for publication February 25, 1982.

Abstract □ An amino analogue of *N*-benzoyl-phenylalanyl-glycyl-proline, a tripeptide inhibitor of angiotensin-converting enzyme, was synthesized. The analogue (III) has the phenylalanyl-glycine amide linkage of *N*-benzoyl-phenylalanyl-glycyl-proline reduced to a methylene amine. Compound III was tested as an inhibitor of porcine plasma angiotensin-converting enzyme and has an I_{50} of 620 μM compared with an I_{50} of 9.6 μM for its parent tripeptide. These results are explained in terms of a proposed model of the converting-enzyme active site.

Keyphrases □ Angiotensin-converting enzyme—synthesis and biological activity of an amino analogue of *N*-benzoyl-phenylalanyl-glycyl-proline, a tripeptide inhibitor □ *N*-Benzoyl-phenylalanyl-glycyl-proline—tripeptide inhibitor of angiotensin-converting enzyme, synthesis and biological activity of an amino analogue

In a previous paper (1) work on a ketomethylene analogue I of the tripeptide inhibitor Bz-Phe-Gly-Pro (II) of angiotensin-converting enzyme was described:

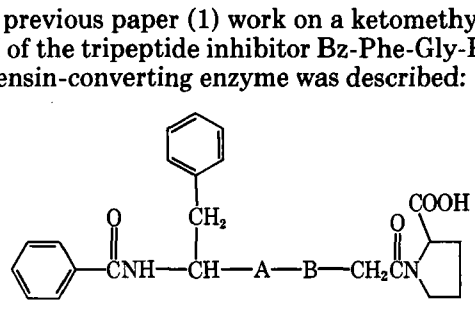

I: A = CO, B = CH_2
II: A = CO, B = NH
III: A = CH_2, B = NH

The replacement of the peptide amide linkage in II with a ketomethylene group was designed to stabilize this portion of the peptide molecule to peptidase cleavage. This substitution yielded a peptide analogue (I) with >100 times the inhibition activity against angiotensin-converting enzyme of the parent peptide.

A second approach to stabilizing this same peptide amide linkage in II to peptidase cleavage would be to reduce it to the corresponding methyleneamino compound (III). This compound has been synthesized and its inhibition activity against angiotensin-converting enzyme will be discussed.

BACKGROUND

A method for the synthesis of III was desired which would maintain the same stereochemistry around the optical centers as that found in the tripeptide (II). Initially, numerous attempts were made to selectively reduce the amide, but not the ester, group of *N*-benzyloxycarbonyl-phenylalanyl-glycine ethyl ester with borane, as reported previously (2), with *N*-benzyloxycarbonyl-glycyl-leucine methyl ester as the starting material. In contrast to those results the ester group of *N*-benzyloxycarbonyl-phenylalanyl-glycine ethyl ester was reduced more rapidly than the amide group by borane.

Because selective reduction of the desired amide functionality did not seem possible in this case, the dipeptide acid *N*-benzyloxycarbonyl-phenylalanyl-glycine (IV) was used as a starting material for the synthesis of III (Scheme I). The 9-fluorenyl-methoxycarbonyl amino blocking group (3) was used because of its stability to acidic conditions such as the Jones oxidation (4).

The low yield obtained for the transformation of VI to VIII was

0022-3549/83/0100-0063$01.00/0

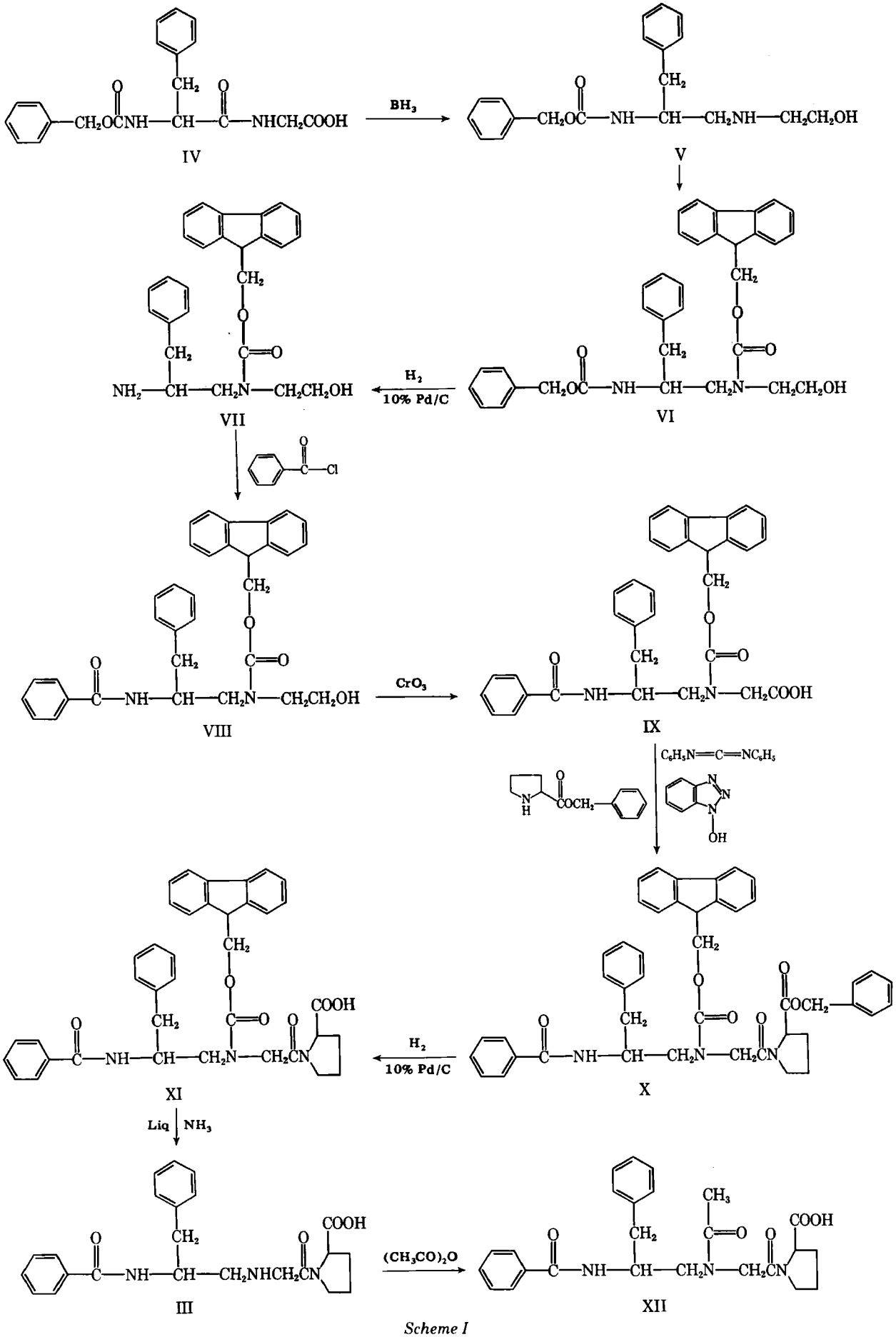

Scheme I

Table I—Inhibition of Porcine Plasma Angiotensin-Converting Enzyme

Compound	I_{50} (μM)[a]
Captopril	0.30
I	0.07
II	9.40
III	620.00
XII	2500.00

[a] Concentration required for 50% enzyme inhibition. All values are the average of results obtained in two or more experiments.

probably due to partial removal of the 9-fluorenylmethoxycarbonyl group during the hydrogenolysis step (5).

RESULTS AND DISCUSSION

The results of testing some of the compounds for inhibition of angiotensin-converting enzyme are shown in Table I. The amino analog (III) has 1/66th the inhibition activity of its parent tripeptide (II) but is about four times more active than the *N*-acetyl derivative (XII). Kinetic studies on III (Figs. 1 and 2) show it to be a competitive inhibitor of converting enzyme with either hippuryl-histidyl-leucine or angiotensin I as substrates.

The low activity of III is interesting in light of its structural similarities to the potent inhibitors (Table II) reported previously (6). Table II shows structure–activity data for some of these compounds that exhibit inhibition of the angiotensin-converting enzyme. One noteworthy conclusion from this table is that a phenethyl group in the R_1 position (*i.e.*, compound XV) yielded a more potent inhibitor than that obtained with other alkyl R_1 substituents. In previous studies on peptides (7) and tripeptide inhibitors (1), optimum activity was also obtained when the inhibitor contained an aromatic group (*i.e.*, compound II) that was the same distance from the carboxylic acid group of proline as was the phenyl group in XV. It was also found that an aromatic acyl group at the amino terminus yielded a more active inhibitor than tripeptides with either a nonaromatic or no acyl group in this position (1). Therefore, there appear to be binding points within the converting enzyme active site for groups located at the amino terminal portion of III.

Examination of the hypothetical active site of the angiotensin-converting enzyme (Fig. 3) proposed previously (8) might explain the low activity of III. One important binding functionality that all the known potent inhibitors and substrates of the angiotensin-converting enzyme have in common is a functionality that is positioned properly to interact with the enzyme-bound zinc ion. Such functionalities vary from a carbonyl (as in II) or a carboxylic acid (as in XIII–XV) to a thiol (as in captopril). The amino group in III must not be positioned properly to fulfill the role of a zinc-binding functionality. The low enzyme-inhibition activity of III exemplifies the major importance of the zinc interaction for good enzyme inhibition.

EXPERIMENTAL[1]

***N*-(2*S*-2-Benzyloxycarbonylamino-3-phenylpropyl)aminoethanol (V)**—To an ice-cold solution of *N*-benzyloxycarbonyl-L-phenylalanyl-glycine (5) (IV, 700 mg, 1.96 mmoles) in 8 ml of dry (lithium aluminum hydride-distilled) tetrahydrofuran was added 8.50 ml (8.50 mmoles) of 1 *M* borane under a nitrogen atmosphere. The solution was refluxed for 1 hr, then cooled in ice and treated dropwise with 0.5 *N* ethanolic HCl to pH 4. The mixture was stirred at room temperature for 2 hr, then cooled in ice, and filtered to give 408 mg (56% yield) of the hydrochloride as a white solid, mp 183–184°.

[1] Melting points were determined on a Thomas-Hoover Uni-melt and are uncorrected. Optical rotations were measured using a Perkin-Elmer 141 automatic polarimeter. Mass spectra were taken on an LKB 9000 GC–MS spectrometer. The ^{1}H-NMR spectra were taken on a Varian EM390 spectrometer. TLC was carried out on Uniplates from Analtech coated with 250 μm of silica gel GF. Evaporations were performed at 40° under house vacuum on a Buchi Rotavapor unless otherwise stated. Elemental analyses were conducted by Mr. Eric Meier, Stanford University, Stanford, California. Preparative high-pressure liquid chromatography (HPLC) was performed using the Waters Prep LC/System 500 and silica gel cartridges. The existence of solvents of crystallization was confirmed by ^{1}H-NMR whenever possible. Many of the compounds in this series had a strong tendency to trap solvents within their solid structure. Heating these compounds at 60–100° under 0.1-mm Hg vacuum for 24 hr would not completely remove the last traces of solvent. Continued heating under vacuum beyond this point began to decompose the compounds. All of these compounds were homogeneous by TLC and had spectra (mass spectra and/or ^{1}H-NMR) characteristics of the desired compounds. Elemental analyses have, therefore, been reported with solvents of crystallization.

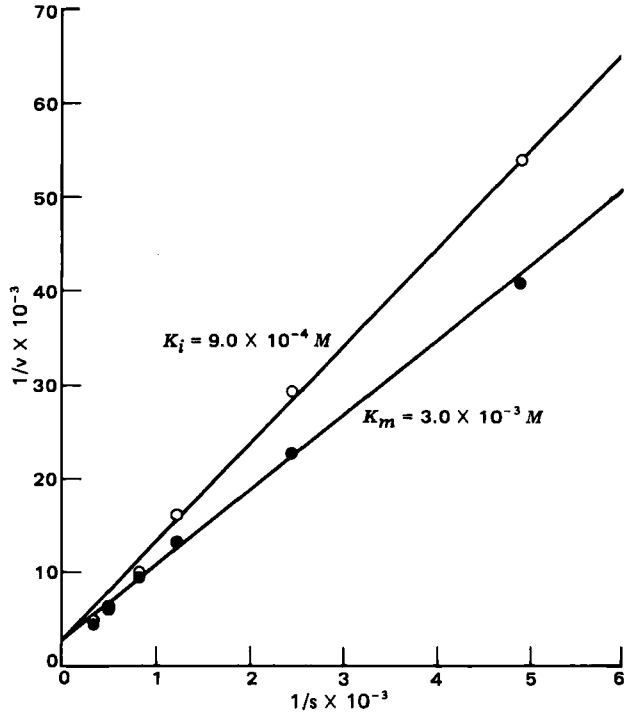

Figure 1—*Double-reciprocal plots of the effect of compound III as an inhibitor of porcine plasma angiotensin-converting emzyme with hippuryl-histidyl-leucine as substrate. Key: (●) no inhibitor; (○) with compound III at a concentration of 0.33 m*M. *Lines were drawn by the method of least squares.*

The hydrochloride was mixed with water (20 ml) and chloroform (20 ml). The aqueous layer was adjusted to pH 11 with 1 *N* NaOH while stirring vigorously. The chloroform layer was separated and the aqueous phase was extracted twice with chloroform (2 × 20 ml). The combined chloroform extracts were dried with calcium sulfate and evaporated to dryness to give 298 mg (46%) of the free base as a white solid, mp 93–95°; IR (mineral oil): 3300 and 3250 (amide NH), 1695 (CO), 1550 (amide CNH).

Anal.—Calc. for $C_{19}H_{24}N_2O_3$: C, 69.49; H, 7.37; N, 8.53. Found: C, 69.16; H, 7.26; N, 8.70.

***N*-(2*S* - 2-Benzyloxycarbonylamino-3-phenylpropyl) - *N* - (9-fluorenylmethyloxy-carbonyl)aminoethanol (VI)**—To an ice-cold solution of V (1.68 g, 5.12 mmoles) in 49 ml of 4Å sieve-dried acetone was added sodium bicarbonate (2.24 g, 26.7 mmoles) followed dropwise by a solution of 9-fluorenylmethyl chloroformate (1.98 g, 7.63 mmoles) in 5 ml of dry acetone. The mixture was stirred at 0° for 5 hr, then at room temperature for 1.5 hr, and finally stored at 4° for 64 hr.

The solid was removed by filtration. The filtrate was treated with methanol (20 ml) and evaporated to dryness. The residue was redissolved in methanol (20 ml) and again evaporated to dryness. This oil was dissolved in 20 ml of 50% ether in chloroform and added dropwise with rapid stirring to 400 ml of petroleum ether (bp 30–60°). The mixture was cooled at 4° for 20 hr. The solvent was decanted and the residual oil was dissolved in chloroform (50 ml), washed twice with water (2 × 50 ml), dried with calcium sulfate, and evaporated to dryness to give 2.54 g of a foam. This was chromatographed on silica gel preparative plates with 2% methanol in chloroform. The UV absorbing band at R_f 0.40 was extracted with 20% methanol in chloroform to give 2.07 g (73% yield) of VI as a foam; ^{1}H-NMR ($CDCl_3$): δ 4.90 (2 H, s, benzyloxy CH_2), 7.13 (18 H, m, aromatic).

Anal.—Calc. for $C_{34}H_{34}N_2O_5 \cdot 0.40\ CHCl_3$: C, 69.05; H, 5.79; N, 4.68. Found: C, 69.13; H, 6.04; N, 4.41. Subsequent larger runs were purified by HPLC with 20% ethyl acetate in chloroform.

***N*-(2*S*-2-Benzamido-3-phenylpropyl)-*N*-(9-fluorenylmethyloxy-carbonyl)aminoethanol (VIII)**—A solution of VI (3.09 g, 5.62 mmoles) in 300 ml of glacial acetic acid was hydrogenated at atmospheric pressure with 2.90 g of 10% palladium-on-carbon for 2 hr. The mixture was filtered through diatomaceous earth. The filtrate was evaporated to dryness to give the crude amine (VII) as an oil (2.65 g).

Sodium bicarbonate (1.13 g, 13.5 mmoles) was added to an ice-cold solution of the amine in 360 ml of 4Å sieve-dried dichloromethane fol-

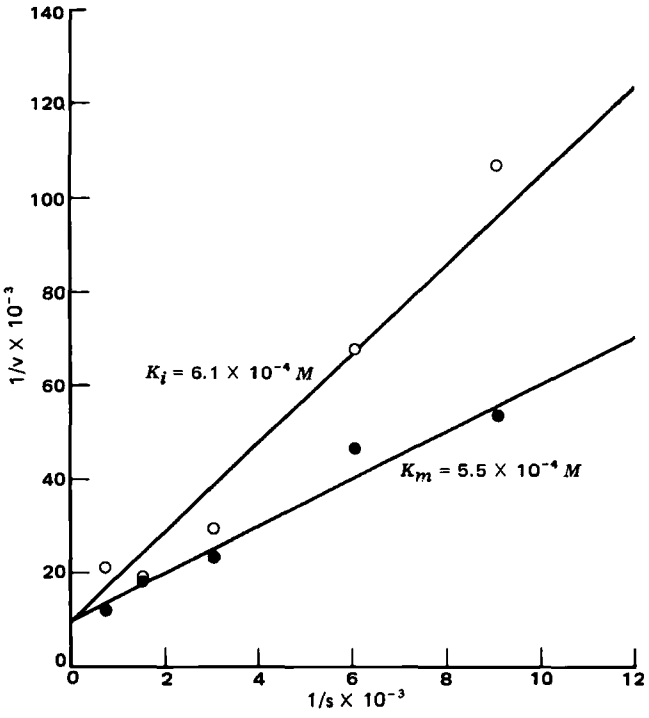

Figure 2—*Double-reciprocal plots of the effect of III as an inhibitor of porcine plasma angiotensin-converting enzyme with angiotensin I as substrate. Key: (●) no inhibitor; (○) with compound III at a concentration of 0.66 mM. Lines were drawn by the method of least squares.*

lowed dropwise by benzoyl chloride (0.785 ml, 6.74 mmoles). The mixture was stirred at room temperature for 18 hr. Another 0.523 ml of benzoyl chloride was added and stirring was continued for an additional 3 hr.

The solid was removed by filtration. The filtrate was treated with methanol (50 ml) and evaporated to dryness. The residue was redissolved in methanol (50 ml) and again evaporated to dryness. This oil was dissolved in 10 ml of chloroform and added dropwise with rapid stirring to 500 ml of petroleum ether (bp 30–60°). The mixture was cooled at 4° for 64 hr. The solvent was decanted and the residual oil was dissolved in chloroform (50 ml), washed with 0.2 *N* HCl (2 × 50 ml), saturated sodium bicarbonate solution (50 ml), and water (50 ml). The chloroform extract was dried with calcium sulfate and evaporated to dryness to give 2.06 g of a foam. This was purified by preparative HPLC using 1:1 chloroform–ethyl acetate, which afforded 1.05 g of VIII (36% yield from VI) as a white solid foam; R_f 0.5 (1:1 chloroform–ethyl acetate): mass spectrum 593 (M^+ + trimethylsilyl + H).

Anal.—Calc. for $C_{33}H_{32}N_2O_4 \cdot 0.10\ CHCl_3$: C, 74.65; H, 6.08; N, 5.26. Found: C, 74.50; H, 6.44; N, 5.16.

***N*-(2*S*-2-Benzamido-3-phenylpropyl)-*N*-(9-fluorenylmethyloxycarbonyl)aminoacetic Acid (IX)**—To an ice-cold solution of compound VIII (1.01 g, 1.94 mmoles) in 38 ml of acetone was added dropwise a solution of chromium trioxide (457 mg, 4.57 mmoles) in 9.7 ml of 35% H_2SO_4. The reaction was stirred at room temperature for 1 hr and then added to 200 ml of water and extracted with chloroform (3 × 100 ml). The chloroform extracts were washed with water (100 ml), dried with sodium sulfate, and evaporated to dryness to give compound IX as a foam (1.07 g), which was used directly in the next step.

An analytical sample was obtained in an earlier, small-scale run by crystallization from chloroform–ether following chromatography on a preparative silica gel plate with 10% methanol in chloroform. The tan solid softened at 139–142° and melted at 167–171°; R_f 0.4 (10% methanol chloroform): mass spectrum 606 (M^+ + trimethylsilyl).

Anal.—Calc. for $C_{33}H_{30}N_2O_5 \cdot 0.25\ CHCl_3$: C, 70.22; H, 5.40; N, 4.96. Found: C, 70.06; H, 5.37; N, 4.98.

***N*-[*N*-(2*S*-2-Benzamido-3-phenylpropyl)-*N*-(9-fluorenylmethyloxycarbonyl)aminoacetyl]-L-proline Benzyl Ester (X)**—To a stirred ice-cold solution of compound IX (1.07 g, 2.01 mmoles), L-proline benzyl ester hydrochloride (0.485 g, 2.01 mmoles), 1-hydroxybenzotriazole (0.300 g, 2.01 mmoles), and triethylamine (0.280 ml, 2.01 mmoles, distilled from phthalic anhydride) in 34 ml of 4Å sieve-dried dichloromethane was added a solution of dicyclohexylcarbodiimide (0.415 g, 2.01 mmoles) in 10 ml of dry dichloromethane. The mixture was stirred at 5° for 0.5 hr, then at room temperature for 45 hr.

Table II—Inhibition of Porcine Plasma Angiotensin Converting Enzyme

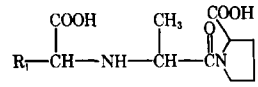

R_1	Compound	I_{50} (μM)[a]
H	XIII	2.4 (36)
CH_3	XIV	0.09 (1.3)
$-(CH_2)_2C_6H_5$	XV	0.0038 (0.057)
	Captopril	0.02 (0.30)

[a] Concentration required for 50% enzyme inhibition (1, 6). The numbers in parentheses are relative to a captopril I_{50} of 0.30 μM as reported in Table I.

The reaction mixture was cooled and filtered. The filtrate was washed with ice-cold 2 *N* HCl (25 ml), 0.3 *N* NaOH (25 ml), and water (25 ml), then dried with calcium sulfate and evaporated to dryness. The light yellow solid foam was purified by preparative HPLC with chloroform as solvent. The yield of white solid foam X was 1.06 g (73%); ^{1}H-NMR ($CDCl_3$): 7.00–7.85 (23 H, m, aromatic), 1.85 (4 H, m, proline CH_2, s); R_f 0.30 (chloroform).

Anal.—Calc. for $C_{45}H_{43}N_3O_6 \cdot 0.20\ CHCl_3$: C, 72.48; H, 5.84; N, 5.63. Found: C, 72.81; H, 5.82; N, 5.60.

***N*-[*N*-(2*S*-2-Benzamido-3-phenylpropyl)-*N*-(9-fluorenylmethyloxycarbonyl)aminoacetyl]-L-proline (XI)**—A solution of X (1.01 g, 1.40 mmoles) in 100 ml of glacial acetic acid was hydrogenated at atmospheric pressure with 1 g of 10% palladium on carbon for 2 hr. The reaction was filtered through diatomaceous earth and evaporated to dryness to give 0.900 g of crude compound XI as a gum. A white solid (mp 151–152°) analytical sample of compound XI was obtained by chromatography on a silica gel preparative plate with 7% methanol in chloroform followed by crystallization from chloroform–ether; ^{1}H-NMR ($CDCl_3$): 7.00–7.85 (18 H, m, aromatic), 1.95 (4 H, m, proline CH_2, s); R_f 0.2 (7% methanol in chloroform).

Anal.—Calc. for $C_{38}H_{37}N_3O_6 \cdot 0.60\ CHCl_3$: C, 65.92; H, 5.39; N, 5.97. Found: C, 65.52; H, 5.41; N, 5.90.

***N*-[*N*-(2*S*-2-Benzamido-3-phenylpropyl)aminoacetyl]-L-proline (III)**—Crude compound XI (836 mg, 1.32 mmoles) was stirred in 40 ml of liquid ammonia under nitrogen atmosphere for 3 hr. The ammonia was evaporated and the residue was stirred vigorously for 10 min in a mixture of 20 ml of water and 20 ml of ethyl acetate. The water layer was separated and evaporated to dryness to give a white solid. This was triturated with methanol (10 ml) to give 280 mg (52% yield) of III, mp 200–201°; mass spectrum 553 (M^+ + 2 trimethylsilyl); $[\alpha]_D^{31}$ −92.4° (*c* = 0.953, 1 *N* NH_4OH).

Anal.—Calc. for $C_{23}H_{27}N_3O_4 \cdot 0.25\ CH_3OH$: C, 66.82; H, 6.76; N, 10.06. Found: C, 66.94; H, 6.64; N, 10.00.

***N*-[*N*-Acetyl-*N*-(2*S*-2-benzamido-3-phenylpropyl)aminoacetyl]-L-proline (XII)**—The amino acid (III) (100 mg, 0.244 mmoles) was stirred in 10 ml of water and 10 ml of acetic anhydride for 2-⅓ hr at room temperature. The reaction was evaporated to dryness at 35°. Another 10 ml of water was added to the residue and the mixture was again evaporated to dryness. The residue was dissolved in chloroform (20 ml) and washed with cold 2 *N* HCl (20 ml) and water (20 ml), dried with calcium sulfate, and evaporated to dryness. The gummy residue was crystallized from chloroform–ether to give 58 mg (53% yield) of compound XII as a white solid, mp 156–158°; ^{1}H-NMR ($CDCl_3$–methanol-d_4 2:1): δ 2.01 (3 H, d, acetamide CH_3); mass spectrum 523 (M^+ + trimethylsilyl).

Anal.—Calc. for $C_{25}H_{29}N_3O_5 \cdot 0.25\ H_2O$: C, 65.85; H, 6.52; N, 9.21. Found: C, 65.88; H, 6.39; N, 9.20.

Fluorometric Assay of Angiotensin-Converting Enzyme—Materials used were porcine plasma-converting enzyme[2], hippuryl-histidyl-leucine[3], histidyl-leucine[3], *o*-phthaldehyde[3], and angiotensin I[4]. All chemicals used were reagent grade.

The enzyme assay (9) activity was conducted with fluorometric determination of histidyl-leucine, a product of the enzyme reaction. The substrate used was hippuryl-histidyl-leucine or angiotensin I. The concentration ranges were 2.6×10^{-4}–2.04×10^{-3} *M* and 1.1×10^{-4}–1.4×10^{-3} *M* for hippuryl-histidyl-leucine and angiotensin I, respectively. The

[2] Miles Laboratories.
[3] Sigma Chemical Co., St. Louis, Mo.
[4] Bachem Fine Chemicals, Marina Del Rey, Calif.

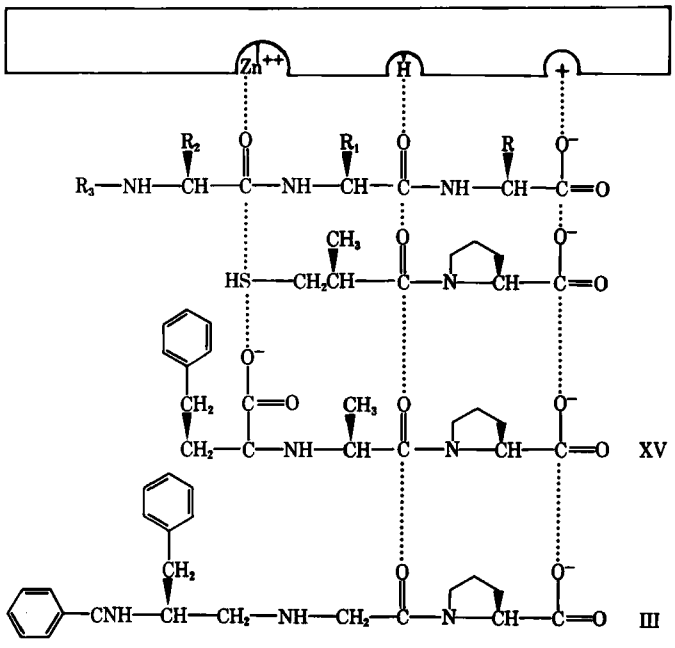

Figure 3—*Schematic representation of the binding of inhibitors and substrates at the hypothetical active site of angiotensin-converting enzyme as proposed previously (8).*

assay was carried out by mixing 10 μl of phosphate buffer (0.1 *M*, pH 7.6, containing 0.3 *M* NaCl) containing the testing inhibitor with substrate dissolved in 10 μl of phosphate buffer. Then 1 mg of porcine plasma-converting enzyme in 50 μl of buffer was added. The mixture was incubated at 37° for 90 min with constant shaking, and the reaction was stopped by adding 50 μl of 10% trichloroacetic acid. The samples were then diluted with 0.7 ml of water followed by 0.4 ml of 2 *N* NaOH. To the alkalized mixture, 0.1 ml of 1% (w/v) *o*-phthaldehyde in methanol was added. After exactly 4 min, 0.2 ml of 6 *N* HCl was added. The contents of all tubes were thoroughly mixed after each addition. The samples were then centrifuged at 10,000×*g* for 10 min, and the fluorescence of the supernatant was measured[5] with excitation at 365 nm and emission at 495 nm. The fluorescent product of histidyl-leucine with *o*-phthaldehyde is not stable in alkaline solution, but is stabilized upon acidification. The fluorescence of the acidified solution is stable up to 1 hr, so all readings should be made within that period (10).

A standard curve of histidyl-leucine was prepared for each assay by mixing various amounts of histidyl-leucine with 1 mg of enzyme in 70 μl of phosphate buffer. The tubes containing the standards were treated identically to those containing the samples. A reagent blank containing all reagents but no substrate was also run for each assay.

Test for the Effect of Inhibitors—For testing the effect of inhibitors on angiotensin-converting enzyme, two assays were run in parallel. One contained the substrate (2 m*M*), enzyme (1 mg), and various concentrations (1 n*M* to 10 m*M*) of an inhibitor; the other contained only the substrate and enzyme. The assay conditions were the same as described above. The product formed with an inhibitor relative to that without an inhibitor was calculated to give the percent of inhibition. By plotting the percent inhibition *versus* various concentrations of an inhibitor, the I_{50} was obtained.

For determination of the kinetics and the K_i of an inhibitor, the enzyme assay was carried out as described above using various concentrations of substrate with and without inhibitor. When hippuryl-histidyl-leucine was used as substrate, the concentrations were 2×10^{-4}–3×10^{-3} *M*. When angiotensin I was used as substrate, the concentrations were 1.1×10^{-4}–1.3×10^{-3} *M*. By using the Michaelis–Menten equation (11) and double-reciprocal plot (12), the K_m and K_i can be calculated.

[5] Aminco Bowman fluorometer.

REFERENCES

(1) R. G. Almquist, W.-R. Chao, M. E. Ellis, and H. L. Johnson, *J. Med. Chem.*, **23**, 1392 (1980).

(2) R. W. Roeske, F. L. Weitl, K. U. Prasad, and R. M. Thompson, *J. Org. Chem.*, **41**, 1260 (1976).

(3) L. A. Carpino and G. Y. Han, *J. Org. Chem.*, **37**, 3404 (1972).

(4) A. Bowers, T. G. Halsall, E. R. H. Jones, and A. J. Lemin, *J. Chem. Soc.*, **1953**, 2555.

(5) E. Atherton, C. Bury, R. C. Sheppared, and B. J. Williams, *Tetrahedron Lett.*, 3041 (1979).

(6) A. A. Patchett *et al.*, *Nature (London)*, **288**, 280 (1980).

(7) D. W. Cushman, J. Pluscec, N. J. Williams, E. R. Weaver, E. F. Sabo, O. Kocy, H. S. Cheung, and M. A. Ondetti, *Experientia*, **29**, 1032 (1973).

(8) M. A. Ondetti, B. Rubin, and D. W. Cushman, *Science*, **196**, 441 (1977).

(9) B. A. Tsai and M. J. Peach, *J. Med. Chem.*, **18**, 1180 (1975).

(10) Y. Piquilloud, A. Reinharz, and M. Roth, *Biochim. Biophys. Acta*, **206**, 136 (1970).

(11) L. Michaelis and M. L. Menten, *Biochem. Z.*, **49**, 333 (1913).

(12) I. H. Segel, in "Biochemical Calculations," 2nd ed., Wiley, New York, N.Y., 1976, p. 250.

ACKNOWLEDGMENTS

Supported by Grant HL 19538 from the Heart, Lung and Blood Institute of the National Institutes of Health.

The authors wish to thank Mr. Lewis Cary for the NMR results and Dr. David Thomas for the mass spectral results. The helpful discussions with Dr. Joseph DeGraw on various aspects of this work are gratefully acknowledged.

Synthesis of Sulfanilamido-Naphthoquinones as Potential Antituberculous Agents

S. A. A. OSMAN ˣ, A. A. ABDALLA, and M. O. ALAIB

Received May 12, 1981, from the *Pharmaceutical Chemistry Department, Faculty of Pharmacy, University of Khartoum. Khartoum, Sudan.* Accepted for publication March 3, 1982.

Abstract □ *p*-Aminobenzoic acid, the acid hydrazides of benzoic acid, salicylic acid and isonicotinic acid, and 4,4′-diaminodiphenyl sulfone were condensed with *p*-aminobenzenesulfonyl chloride to give the corresponding N^1-substituted sulfanilamides. These molecules were then treated with 1,4-naphthoquinone to yield 2-substituted-1,4-naphthoquinones. The partition coefficient for the substituted quinones showed, in some cases, high diffusion rates to the organic phase, benzene, from physiological Tyrode's solution. These compounds are effective in low concentration in dioxane against the human sensitive strain of *Mycobacterium tuberculosis* H_{37} Rv. Sulfanilamides obtained from *p*-aminosalicylic acid and thiosemicarbazide failed to react with 1,4-naphthoquinone. These sulfanilamides also showed high activity against the same *Mycobacterium*.

Keyphrases □ Antituberculous agents—potential, synthesis of sulfanilamido-naphthoquinones □ Sulfanilamides—synthesis of sulfanilamido-naphthoquinones as potential antituberculous agents

It has been postulated that the penetration through the Tubercle bacilli cell wall is a limiting factor in the effectiveness of the tuberculostatic agents. Consequently, trials were made to improve the cell penetration of these drugs. Surface active agents (1, 2), used to promote cell penetration, were found to be effective through modification of the surface lipids of the bacilli (3, 4).

The isolation of phthiocol (2-hydroxy-3-methyl-1,4-naphthoquinone) from the human bacilli (5, 6), indicated that the compound could be a natural metabolite of the organism; thus showing the tolerance of the latter to the *p*-quinonoid structure. Earlier reports have also indicated the use of *p*-quinonoid moieties as carriers for certain tuberculostatic agents (7, 8). These facts, beside the high lipid solubility of naphthoquinone suggested using 1,4-naphthoquinone as a carrier of certain sulfonamides, with the objective that the *p*-quinonoid moiety will facilitate the diffusion of the compounds through the cell wall giving them a better opportunity to exert their effects on the organism. The present work is concerned with the synthesis of 2-(substituted sulfanilamido)-1,4-naphthoquinones:

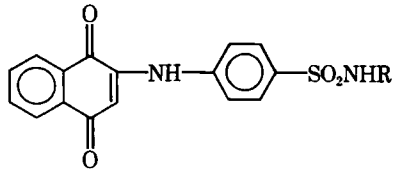

The routes by which these compounds were synthesized are shown in Scheme I.

RESULTS AND DISCUSSION

Chemistry—The key intermediates, sulfanilamide compounds, were prepared by adding *p*-acetamidobenzenesulfonyl chloride to *p*-aminobenzoic acid, *p*-aminosalicylic acid, isonicotinic acid hydrazide, benzoic acid hydrazide, salicylic acid hydrazide, and 4,4′-diaminodiphenyl sulfone according to a previously used technique (9). The products were then deacetylated. The sulfanilamide compounds obtained were allowed to react with 1,4-naphthoquinone. The 2-substituted-1,4-naphthoquinones were obtained, where the sequence of the reaction could follow the same route proposed for the reaction of the arylamine and 1,4-naphthoquinone (10, 11). The sulfanilamides obtained from *p*-aminosalicylic acid and thiosemicarbazide (II, VII) did not react with the quinone, while (VI) the ethyl ester of (II) underwent the reaction successfully. The sulfanilamide obtained from *p*-aminobenzoic acid was esterified after combining it with the 1,4-naphthoquinone (XVI, XVII). The unsubstituted 4,4′-diaminodiphenyl sulfone reacted with one molecule of 1,4-naphthoquinone (XV) and the same compound, condensed as sulfanilamide derivative, reacted with two molecules of the quinone (XIV).

Table I—Partition Coefficient $\left(\frac{A_2}{A_1 - A_2}\right)$ between Benzene and Tyrode's Solution [a]

Compound	A_1	A_2	$\frac{A_2}{A_1 - A_2}$
IX	0.085	0.050	1.43
X	0.050	0.010	0.25
XI	0.390	0.345	7.67
XII	0.650	0.640	64.00
XIII	0.055	0.030	1.20
XIV	0.620	0.600	30.00
XV	0.380	0.380	α
XVI	0.065	0.055	5.50
XVII	0.030	0.010	0.50

[a] Absorbance measured at wavelength 450 nm.

Table II—Sensitivity Pattern of *Mycobacterium tuberculosis* H_{37} Rv Against Tested Compounds

Compound	Concentrations in μg/ml in Dioxane I	II	III
II	1.0 R[a]	1.5 S	2.0 S
VII	1.0 S[b]	1.5 S	2.0 S
IX	0.5 S	1.0 S	2.0 S
X	0.06 R	0.12 S	0.24 S
XI	0.06 R	0.12 S	0.24 S
XII	0.03 S	0.06 S	0.12 S
XIII	1.0 R	1.5 S	2.0 S
XIV	1.0 R	1.5 R	2.0 S
XV	1.0 R	1.5 S	2.0 S
XVI	1.0 R	1.5 R	2.0 S
XVII	1.0 R	1.5 R	2.0 S

[a] Resistant. [b] Sensitive.

The purity and the identity of the compounds were determined by TLC on silica gel using different solvent systems, melting points (uncorrected), IR spectra using a spectrophotometer[1] as nujol mull on sodium chloride plates and elemental microanalysis.

A number of the compounds prepared (IX–XVII) showed high diffusion rates to the organic solvent, benzene, from physiological Tyrode's solution. The values of the partition coefficient between the solvents were calculated using the ratio $A_2/A_1 - A_2$, where A_1 and A_2 are the absorbances in benzene before and after extraction with the Tyrode's solution at wavelength 450 nm (Table I).

Biology—Most of the prepared compounds proved to be effective in low concentrations against the human strain of *Mycobacterium tuberculosis* H_{37} Rv[2].

A concentration of 0.1 μg/ml wet weight of 3-week-old cultures of the *Mycobacterium* was found suitable. Lowenstein–Jensen medium without

[1] Unicam 2000.
[2] Received from National Collection of Type Cultures, UK.

0022-3549/83/0100-0068$01.00/0

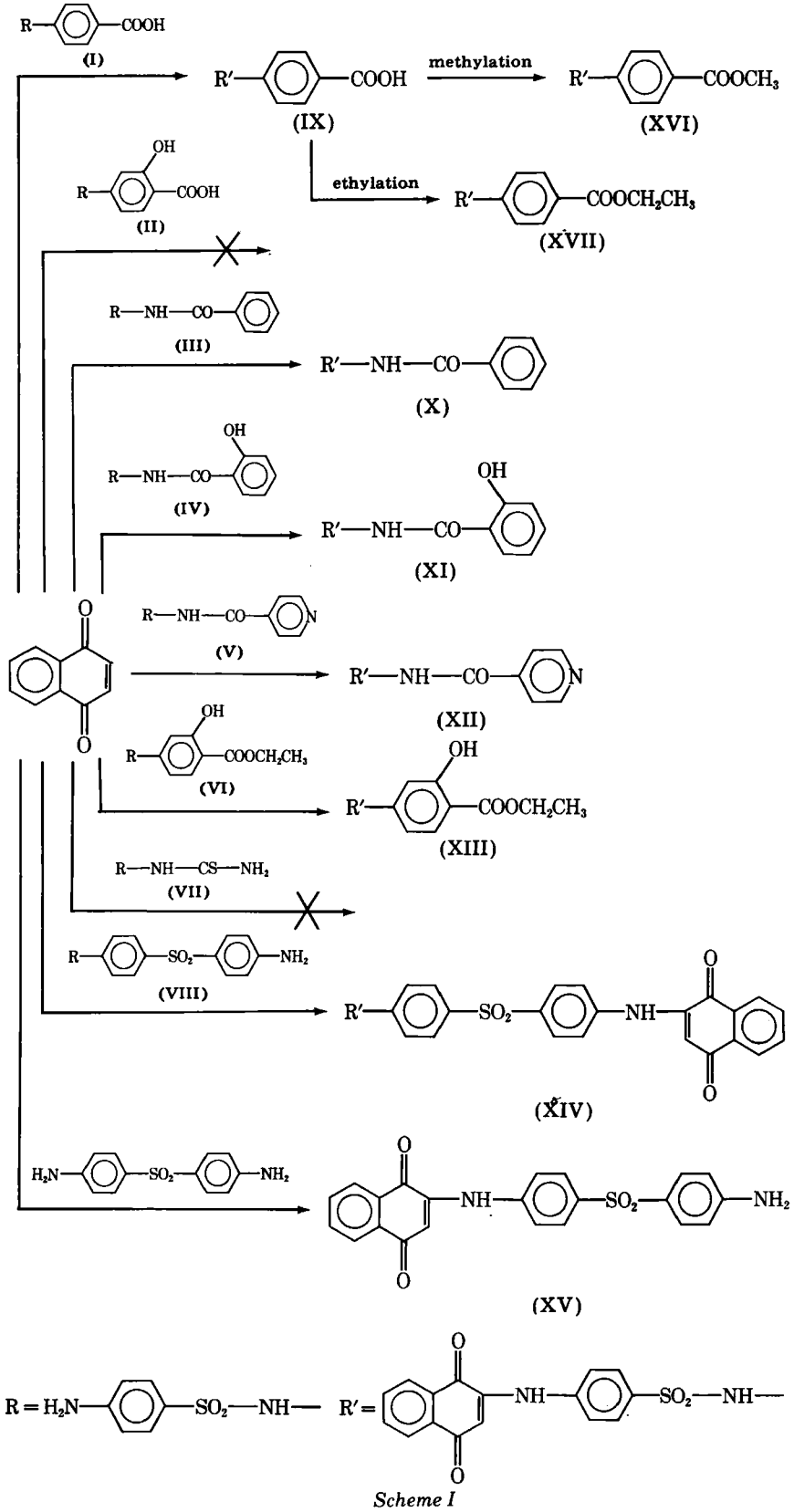

Scheme I

potato was used. No growth or growth of <20 colonies indicated that the strain was sensitive to the compounds in the given concentrations, provided that the compound-free control yielded >100 colonies.

All compounds tested were found effective against the human sensitive strain of the *Mycobacterium* in concentrations of 1–2 μg/ml. However, compounds IX–XII gave the same effect in lesser concentrations (Table II).

On comparing data from Tables I and II, structural variations of the compounds appear to show uncorrelated effects on the activities and the rates of diffusion of the compounds into the organic phase. Some of the highly active compounds were also highly diffusible, *e.g.*, compounds XI and XII. Such a relationship does not hold with the other compounds. A detailed comparative study of the effect of the structural variations involving quinonoid and unquinonoid compounds on both activities and

Table III—The *p*-Aminobenzenesulfonamide Derivatives

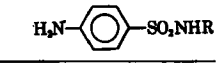

Compound	R	mp°	Yield, %	Molecular Formula	Analysis Calc.	Analysis Found
I	*p*-Carboxyphenyl	158	52	$C_{13}H_{12}N_2O_4S$	C: 53.42	53.09
					H: 4.14	4.05
					N: 9.58	9.36
					S: 10.97	11.08
II	*p*-Carboxy-*m*-hydroxyphenyl	165—166	38	$C_{13}H_{12}N_2O_5S$	C: 50.64	50.40
					H: 3.89	3.97
					N: 9.09	9.01
					S: 10.38	10.73
III	Benzamido	185–186	52	$C_{13}H_{13}N_3O_3S$	C: 53.60	53.23
					H: 4.50	4.63
					N: 14.43	14.24
					S: 11.01	10.68
IV	*o*-Hydroxybenzamido	164–165	46	$C_{13}H_{13}N_3O_4S$	C: 50.81	50.80
					H: 4.26	4.34
					N: 13.67	13.62
					S: 10.43	10.52
V	*p*-Pyridoylamino	210–211	59	$C_{12}H_{12}N_4O_3S$	C: 49.31	49.39
					H: 4.14	4.30
					N: 19.17	19.08
					S: 10.97	10.83
VII	Thiouriedo	223	42	$C_7H_{10}N_4O_2S_2$	C: 34.14	34.14
					H: 4.06	4.14
					N: 22.76	22.81
					S: 26.01	26.03
VIII	[*p*(*p*-Aminobenzene) sulfonyl]phenyl	194–195	90	$C_{18}H_{17}N_3O_4S_2$	C: 53.58	53.08
					H: 4.25	4.17
					N: 10.42	10.53
					S: 15.86	15.45

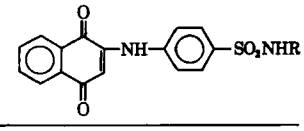

Table IV—The Sulfanilamido-1,4-naphthoquinone Derivatives

Compound	R	mp°	Yield, %	Molecular Formula	Analysis Calc.	Analysis Found
IX	*p*-Carboxyphenyl	245–245	93	$C_{23}H_{16}N_2O_6S$	C: 61.60	62.03
					H: 3.57	3.70
					N: 6.25	6.06
					S: 7.41	6.98
X	Benzamido	258–259	38	$C_{23}H_{17}N_3O_5S$	C: 61.75	62.10
					H: 3.80	3.71
					N: 8.39	7.97
					S: 7.15	7.26
XI	*o*-Hydroxybenzamido	263–264	50	$C_{23}H_{17}N_3O_6S$	C: 59.61	60.03
					H: 3.67	3.89
					N: 9.09	8.86
					S: 6.91	6.76
XII	*p*-Pyridolyamino	248–249	40	$C_{22}H_{16}N_4O_5S$	C: 58.93	58.59
					H: 3.56	3.81
					N: 12.50	12.08
					S: 7.14	6.74
XIII	*p*-Carboethoxy-*m*-hydroxyphenyl	268–269	30	$C_{25}H_{20}N_2O_7S$	C: 60.77	60.27
					H: 4.06	3.98
					N: 5.69	5.66
					S: 6.50	6.86
XIV	(*p*-{*p*-[2-(1,4-naphthoquinonyl)]aminobenzene}sulfonyl)phenyl	310–311	92	$C_{38}H_{25}N_3O_8S_2$	C: 63.98	64.25
					H: 3.49	3.92
					N: 5.87	6.03
					S: 8.25	7.84

rates of diffusion and their relationship to each other is presently being conducted.

EXPERIMENTAL

All compounds mentioned in Tables III and IV were prepared by the following general procedures. All the figures of analysis and the IR spectra of the compounds were in agreement with the structures.

***p*-Acetamidobenzenesulfanilamido Derivatives**—*p*-Acetamidobenzenesulfonyl chloride (10 mmoles) was added gradually to a solution of the appropriate derivative (20 mmoles) in 2 *N* NaOH solution (30 ml) with constant stirring. The stirring continued for 10–15 min. The alkaline solution was extracted with ether, then acidified with hydrochloric acid, when the *p*-acetamidobenzenesulfonamido compound separated. The compound was then filtered and crystalized from 95% ethyl alcohol. The IR spectra of the pure compounds showed absorption bands at 1740 cm^{-1} (C=O in $COCH_3$), 1600—1590 cm^{-1} (C=C aromatic), 1680 cm^{-1}, 1570 cm^{-1} (CONH amides I & II), 1370–1335 cm^{-1}, 1180 cm^{-1} (SO_2NH) beside others for different compounds.

Benzenesulfanilamido Derivatives—The hydrolysis (deacetylation) of the *p*-acetamidobenzene derivatives was carried out either by heating with alkali on a steam bath or by gently refluxing for 30 min with twice its weight of diluted hydrochloric acid. The IR spectra of the hydrolyzed compounds showed the disappearance of the C=O band of the $COCH_3$ group at 1740 cm^{-1} and the appearance of a typical primary N—H pair of bands at 3300 and 3130 $cm.^{-1}$ (Table III).

***N*¹-(*p*-Carboethoxy-*m*-hydroxyphenyl) Sulfanilamide (VI)**—A solution of II (10 mmoles) was esterified by warming with excess 95% ethyl alcohol in the presence of concentrated sulfuric acid. The ethyl ester, mp 230–231° was obtained in a 60% yield. The IR spectrum marked the disappearance of the bands at 1690 cm^{-1} (C=O in COOH) and 3000 cm^{-1}

(OH carboxylic) and the appearance of the band at 1665 cm^{-1} (C=O in $COOC_2H_5$).

Anal.—Calc. for $C_{15}H_{16}N_2O_5S$: C, 53.56; H, 4.79; N, 8.33; S, 9.53. Found: C, 53.06; H, 4.71; N, 8.30; S, 9.66.

Sulfanilamido-1,4-naphthoquinone Derivatives—A solution of 1,4-naphthoquinone (20 mmoles in 40 ml of 95% ethyl alcohol) was gradually added over a period of 30 min to a solution of the appropriate sulfanilamido derivative (10 mmoles in 10–30 ml of glacial acetic acid). Sodium acetate (20 mg) was added with constant stirring at 60°. Stirring was continued for 30 min, then refluxed for 1 hr, and left overnight at room temperature. A black precipitate was separated and filtered. Water was added to the filtrate when a brownish material separated. It was then filtered, washed with hot water, dried at 80°, and crystallized from 95% ethyl alcohol as light crystals. The IR spectra of the compounds showed the appearance of two bands at 1650 and 1630 cm^{-1} for the C=O of the naphthoquinone. The pair of bands of the primary NH_2 at 3300 and 3130 cm^{-1} disappeared, while the N—H stretching absorption was shown at 3245 cm^{-1} (Table IV).

4-Amino-4′-[2-(1,4-naphthoquinonyl)]aminodiphenylsulfone (XV)—This was obtained by the same procedure for the preparation of the sulfanilamido-1,4-naphthoquinone derivatives, from 1,4-naphthoquinone (20 mmoles in 40 ml of 95% ethyl alcohol) and 4,4′-diaminodiphenyl sulfone (10 mmoles in 35 ml of glacial acetic acid). The product was crystallized from 95% ethyl alcohol. Yield: 91%, mp 306–307°.

Anal.—Calc. for $C_{22}H_{16}N_2O_4S$: C, 65.34; H, 3.96; N, 6.93; S, 7.92. Found: C, 65.25; H, 4.14; N, 6.72; S, 7.71.

2-{N^4-[N^1-(*p*-Carbomethoxy)phenyl]sulfanilamido}-1,4-naphthoquinone (XVI)—A solution of IX (10 mmoles) was esterified by warming with excess methyl alcohol in the presence of concentrated sulfuric acid. The methyl ester recrystallized from glacial acetic acid was obtained in 37% yield, mp 253°. In the IR spectrum the bands at 1700 cm^{-1} (C=O in COOH) and 3245 cm^{-1} (OH carboxyl) disappeared and a band at 1750 cm^{-1} (C=O in $COOCH_3$) appeared.

Anal.—Calc. for $C_{24}H_{18}N_2O_6S$: C, 62.34; H, 3.89; N, 6.06; S, 6.90. Found: C, 61.93; H, 3.67; N, 5.64; S, 6.68.

2-[N^4-[N^1-(*p*-Carboethoxy)phenyl]sulfanilamido}-1,4-naphthoquinone (XVII)—Obtained as XVI from IX by esterification with 95% ethyl alcohol. Yield: 35%, mp 261–262°. In the IR spectrum the bands at 1700 cm^{-1} (C=O in the carboxyl group) and 3245 cm^{-1} (OH carboxyl) disappeared, and a band at 1665 cm^{-1} (C=O in $COOC_2H_5$) appeared. appeared.

Anal.—Calc. for $C_{25}H_{20}N_2O_6S$: C, 63.02; H, 4.20; N, 5.88; S, 6.72. Found: C, 62.68; H, 3.90; N, 5.48; S, 6.82.

REFERENCES

(1) H. J. Copper and M. L. Cohn, *Am. Rev. Tuber.*, **63**, 108 (1951).

(2) J. W. Cornforth, P. DA. Hart, R. J. W. Rees, and J. A. Stock, *Nature (London)*, **168**, 150 (1951).

(3) G. B. Mackaness, *Am. Rev. Tuber.*, **69**, 690 (1954).

(4) J. E. Lovelock and R. J. W. Rees, *Nature (London)*, **175**, 161 (1955).

(5) E. R. Long and F. B. Seibert, *Am. Rev. Tuber.*, **13**, 393 (1926); through *Chem. Abstract*, **20**, 2535 (1926).

(6) R. J. Anderson and M. S. Newman, *J. Biol. Chem.*, **103**, 197 (1933); through *Chem. Abstracts*, **28**, 194 (1934).

(7) A. D. Marco, B. Zachi, and V. Zavaglis, *Sperimentales*, **102**, 218 (1952); through *Chem. Abstracts*, **46**, 10435 h (1952).

(8) F. G. Valdecases, *Med. Clin. (Barcelona)*, **4**, 275 (1952); through *Chem. Abstracts*, **47**, 13084 d (1953).

(9) R. C. Denney, "Named Organic Reactions," Butterworth, London, 1969, p. 86.

(10) L. F. Fieser and M. Fieser, "Advanced Organic Chemistry," Rienhold, New York, N.Y., 1961, p. 853.

(11) J. H. Wilfred, "Reaction of Organic Compounds," 3rd ed. Longmans, London, 1957, p. 284.

High-Performance Liquid Chromatographic Determination of Alizapride, a New Antiemetic Compound, and Its Application to a Dose-Dependent Pharmacokinetic Study

G. HOUIN *, F. BREE *, N. LERUMEUR ‡, and J. P. TILLEMENT *x

Received November 20, 1980, from the **Department of Pharmacology, Faculty of Medicine of Paris XII, 8 Rue du Général Sarrail—94000 Creteil*, and the ‡*Department of Medical Statistics, Hopital du Bocage—21000 Dijon, France.* Accepted for publication March 4, 1982.

Abstract □ An assay was developed to measure alizapride (a new antiemetic compound) in biological specimens. The method involved reversed-phase high-performance liquid chromatography and fluorescence detection. The detection limit was 5 ng/ml in plasma or urine samples. The value of the assay was demonstrated with a dose-dependent pharmacokinetic study. It showed a two-phase decrease in plasma concentrations, after intravenous injection, with half-lives of 7.5-min and 2.5-hr, respectively. From plasma and urine results, pharmacokinetic parameters remained constant in the dose range of 50–200 mg.

Keyphrases □ High-performance liquid chromatography—determination and dose-dependent pharmacokinetic application of alizapride, new antiemetic compound □ Alizapride—new antiemetic compound, high-performance liquid chromatographic determination and dose-dependent pharmacokinetic application □ Antiemetic compound—high-performance liquid chromatographic determination and dose-dependent pharmacokinetic application of alizapride □ Pharmacokinetic application—dose-dependent, alizapride, new antiemetic compound, high-performance liquid chromatographic determination

Alizapride[1], *N*-[(1-allyl-2-pyrrolidinyl)methyl]-6-methoxy-1*H*-benzotriazole-5-carboxamide (I), is a new compound with antiemetic properties (1, 2). For bioavailability studies a sensitive and specific assay for plasma and urine concentrations was needed. According to the physicochemical properties of the compound, a high-performance liquid chromatographic (HPLC) assay with a fluorescence detector was selected. This study describes the procedure used for the analysis of biological samples and the preliminary results on pharmacokinetic parameters calculated in a dose-dependency study.

EXPERIMENTAL

Materials—Alizapride was obtained from commercial suppliers and showed no impurities in two different TLC systems. Methanol, chloroform, and tris(hydroxymethyl)aminomethane buffer (pH 8.1) were commercially available analytical grades and used without further purification.

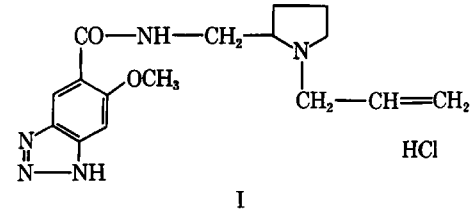

I

[1] Plitican, Delagrange Laboratories, Paris, France.

0022-3549/83/0100-0071$01.00/0

(OH carboxylic) and the appearance of the band at 1665 cm^{-1} (C=O in $COOC_2H_5$).

Anal.—Calc. for $C_{15}H_{16}N_2O_5S$: C, 53.56; H, 4.79; N, 8.33; S, 9.53. Found: C, 53.06; H, 4.71; N, 8.30; S, 9.66.

Sulfanilamido-1,4-naphthoquinone Derivatives—A solution of 1,4-naphthoquinone (20 mmoles in 40 ml of 95% ethyl alcohol) was gradually added over a period of 30 min to a solution of the appropriate sulfanilamido derivative (10 mmoles in 10–30 ml of glacial acetic acid). Sodium acetate (20 mg) was added with constant stirring at 60°. Stirring was continued for 30 min, then refluxed for 1 hr, and left overnight at room temperature. A black precipitate was separated and filtered. Water was added to the filtrate when a brownish material separated. It was then filtered, washed with hot water, dried at 80°, and crystallized from 95% ethyl alcohol as light crystals. The IR spectra of the compounds showed the appearance of two bands at 1650 and 1630 cm^{-1} for the C=O of the naphthoquinone. The pair of bands of the primary NH_2 at 3300 and 3130 cm^{-1} disappeared, while the N—H stretching absorption was shown at 3245 cm^{-1} (Table IV).

4-Amino-4′-[2-(1,4-naphthoquinonyl)]aminodiphenylsulfone (XV)—This was obtained by the same procedure for the preparation of the sulfanilamido-1,4-naphthoquinone derivatives, from 1,4-naphthoquinone (20 mmoles in 40 ml of 95% ethyl alcohol) and 4,4′-diaminodiphenyl sulfone (10 mmoles in 35 ml of glacial acetic acid). The product was crystallized from 95% ethyl alcohol. Yield: 91%, mp 306–307°.

Anal.—Calc. for $C_{22}H_{16}N_2O_4S$: C, 65.34; H, 3.96; N, 6.93; S, 7.92. Found: C, 65.25; H, 4.14; N, 6.72; S, 7.71.

2-{N^4-[N^1-(*p*-Carbomethoxy)phenyl]sulfanilamido}-1,4-naphthoquinone (XVI)—A solution of IX (10 mmoles) was esterified by warming with excess methyl alcohol in the presence of concentrated sulfuric acid. The methyl ester recrystallized from glacial acetic acid was obtained in 37% yield, mp 253°. In the IR spectrum the bands at 1700 cm^{-1} (C=O in COOH) and 3245 cm^{-1} (OH carboxyl) disappeared and a band at 1750 cm^{-1} (C=O in $COOCH_3$) appeared.

Anal.—Calc. for $C_{24}H_{18}N_2O_6S$: C, 62.34; H, 3.89; N, 6.06; S, 6.90. Found: C, 61.93; H, 3.67; N, 5.64; S, 6.68.

2-[N^4-[N^1-(*p*-Carboethoxy)phenyl]sulfanilamido}-1,4-naphthoquinone (XVII)—Obtained as XVI from IX by esterification with 95% ethyl alcohol. Yield: 35%, mp 261–262°. In the IR spectrum the bands at 1700 cm^{-1} (C=O in the carboxyl group) and 3245 cm^{-1} (OH carboxyl) disappeared, and a band at 1665 cm^{-1} (C=O in $COOC_2H_5$) appeared. appeared.

Anal.—Calc. for $C_{25}H_{20}N_2O_6S$: C, 63.02; H, 4.20; N, 5.88; S, 6.72. Found: C, 62.68; H, 3.90; N, 5.48; S, 6.82.

REFERENCES

(1) H. J. Copper and M. L. Cohn, *Am. Rev. Tuber.*, **63**, 108 (1951).

(2) J. W. Cornforth, P. DA. Hart, R. J. W. Rees, and J. A. Stock, *Nature (London)*, **168**, 150 (1951).

(3) G. B. Mackaness, *Am. Rev. Tuber.*, **69**, 690 (1954).

(4) J. E. Lovelock and R. J. W. Rees, *Nature (London)*, **175**, 161 (1955).

(5) E. R. Long and F. B. Seibert, *Am. Rev. Tuber.*, **13**, 393 (1926); through *Chem. Abstract*, **20**, 2535 (1926).

(6) R. J. Anderson and M. S. Newman, *J. Biol. Chem.*, **103**, 197 (1933); through *Chem. Abstracts*, **28**, 194 (1934).

(7) A. D. Marco, B. Zachi, and V. Zavaglis, *Sperimentales*, **102**, 218 (1952); through *Chem. Abstracts*, **46**, 10435 h (1952).

(8) F. G. Valdecases, *Med. Clin. (Barcelona)*, **4**, 275 (1952); through *Chem. Abstracts*, **47**, 13084 d (1953).

(9) R. C. Denney, "Named Organic Reactions," Butterworth, London, 1969, p. 86.

(10) L. F. Fieser and M. Fieser, "Advanced Organic Chemistry," Rienhold, New York, N.Y., 1961, p. 853.

(11) J. H. Wilfred, "Reaction of Organic Compounds," 3rd ed. Longmans, London, 1957, p. 284.

High-Performance Liquid Chromatographic Determination of Alizapride, a New Antiemetic Compound, and Its Application to a Dose-Dependent Pharmacokinetic Study

G. HOUIN *, F. BREE *, N. LERUMEUR ‡, and J. P. TILLEMENT *x

Received November 20, 1980, from the **Department of Pharmacology, Faculty of Medicine of Paris XII, 8 Rue du Général Sarrail—94000 Creteil*, and the ‡*Department of Medical Statistics, Hopital du Bocage—21000 Dijon, France.* Accepted for publication March 4, 1982.

Abstract □ An assay was developed to measure alizapride (a new antiemetic compound) in biological specimens. The method involved reversed-phase high-performance liquid chromatography and fluorescence detection. The detection limit was 5 ng/ml in plasma or urine samples. The value of the assay was demonstrated with a dose-dependent pharmacokinetic study. It showed a two-phase decrease in plasma concentrations, after intravenous injection, with half-lives of 7.5-min and 2.5-hr, respectively. From plasma and urine results, pharmacokinetic parameters remained constant in the dose range of 50–200 mg.

Keyphrases □ High-performance liquid chromatography—determination and dose-dependent pharmacokinetic application of alizapride, new antiemetic compound □ Alizapride—new antiemetic compound, high-performance liquid chromatographic determination and dose-dependent pharmacokinetic application □ Antiemetic compound—high-performance liquid chromatographic determination and dose-dependent pharmacokinetic application of alizapride □ Pharmacokinetic application—dose-dependent, alizapride, new antiemetic compound, high-performance liquid chromatographic determination

Alizapride[1], *N*-[(1-allyl-2-pyrrolidinyl)methyl]-6-methoxy-1*H*-benzotriazole-5-carboxamide (I), is a new compound with antiemetic properties (1, 2). For bioavailability studies a sensitive and specific assay for plasma and urine concentrations was needed. According to the physicochemical properties of the compound, a high-performance liquid chromatographic (HPLC) assay with a fluorescence detector was selected. This study describes the procedure used for the analysis of biological samples and the preliminary results on pharmacokinetic parameters calculated in a dose-dependency study.

EXPERIMENTAL

Materials—Alizapride was obtained from commercial suppliers and showed no impurities in two different TLC systems. Methanol, chloroform, and tris(hydroxymethyl)aminomethane buffer (pH 8.1) were commercially available analytical grades and used without further purification.

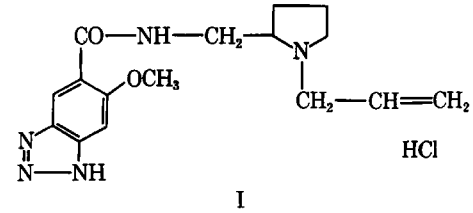

I

[1] Plitican, Delagrange Laboratories, Paris, France.

0022-3549/83/0100-0071$01.00/0

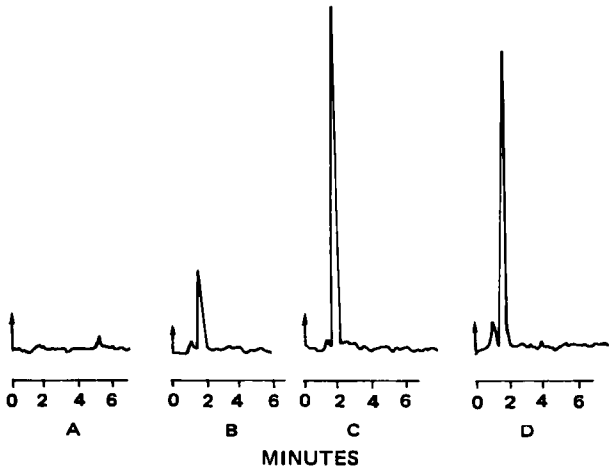

Figure 1—*High-performance liquid chromatograms of alizapride. Graph A corresponds to plasma free of alizapride, graphs B and C to plasma spiked with 50 and 250 ng of alizapride respectively, and graph D to plasma samples obtained during pharmacokinetic study.*

Apparatus—A liquid chromatograph[2] equipped with a fluorescence detector[3] and a continuous flow cell of 8-μl capacity was used. According to the fluorescence spectrum of alizapride, excitation and emission wavelengths were 323 and 380 nm, respectively. A 250-mm steel column was used, packed with a monomolecular layer of octadecyltrichlorosilane chemically bonded to Porasil beads with an average particle size of 10 μm[4]. The chromatographic solvent, methanol–pH 8.1 buffer (80:20, v/v), was delivered at a 2-ml/min flow rate.

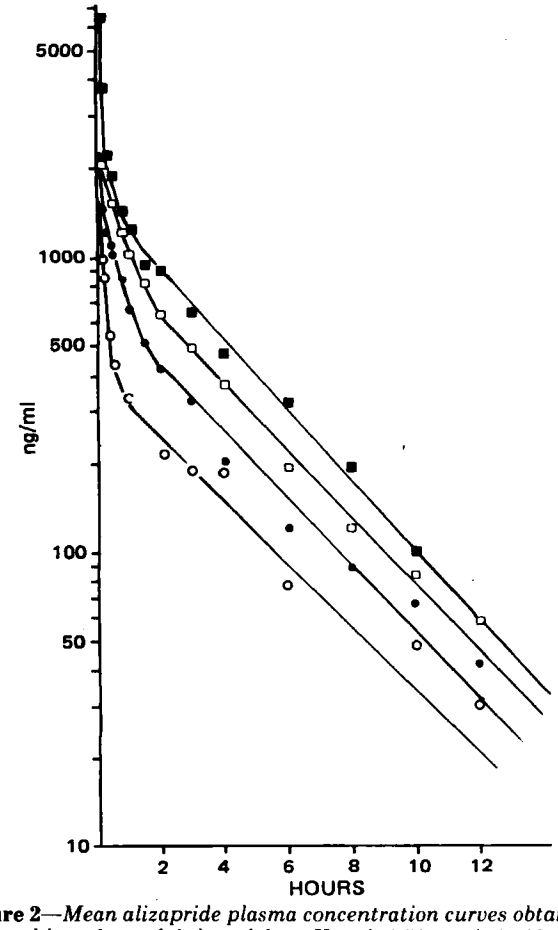

Figure 2—*Mean alizapride plasma concentration curves obtained in three subjects for each injected dose. Key: (○) 50 mg; (●) 100 mg; (□) 150 mg; (■) 200 mg.*

[2] Waters Associates, Paris, France.
[3] JY3, Jobin et Yvon, Paris, France.
[4] Bondapak C-18, Waters Associates, Paris, France.

Table I—Alizapride Recovery from Spiked Plasma Samples[a]

Recovered, ng	Added, ng						
	25	50	100	250	500	1000	2000
$\bar{m}$	25.5	49.5	99.8	248.6	501.2	1001.3	2003.0
SD	1.6	3.0	6.2	7.0	8.5	14.7	64.0
CV%	6.1	6.0	6.2	2.8	1.7	1.5	3.2

[a] Total of five assays.

Sample Preparation Procedure—For statistical analysis, human plasma was spiked with known amounts of alizapride to reach 5–2000 ng/ml and equilibrated by shaking for 30 min. In human experiments, blood samples were immediately centrifuged, and the plasma was stored at −20° until analysis.

Extraction Procedure—To a 1-ml plasma sample, 1 ml of pH 8.1 buffer and 5 ml of chloroform were added. The mixture was shaken at room temperature for 1 min on a vortex-type mixer and centrifuged at 3000 rpm for 10 min. A 4.8-ml volume of the organic phase was evaporated to dryness under a smooth nitrogen stream. The residue was reconstituted with 35 μl of the chromatographic solvent; 25 μl of the mixture was injected onto the HPLC column.

Quantitation—Calibration curves were calculated using peak height and amounts of drug added to plasma, using the least-squares method.

Human Experiments—Six subjects gave informed consent to participate in the study. They were free from cardiac, renal, hepatic, and respiratory diseases and allergies according to clinical and biological examinations. None of the subjects received any drugs for at least 15 days prior to the study. Each subject received four doses (50, 100, 150, and 200 mg) at one-week intervals, three of them intravenously and the others orally, in tablet form.

A 7-ml heparinized blood sample was withdrawn at 0, 3, 6, 10, 15, 20, 30, 45, 60, 90, and 120 min and 3, 4, 6, 8, 10, 12, and 24 hr after administration. Urine samples were collected every 2 hr during the first 12 hr, once during the next 12 hr, and every 24 hr during the next 4 days.

Calculation—Statistical and pharmacokinetic calculations were performed with a table microcomputer[5] using programs developed previously (3).

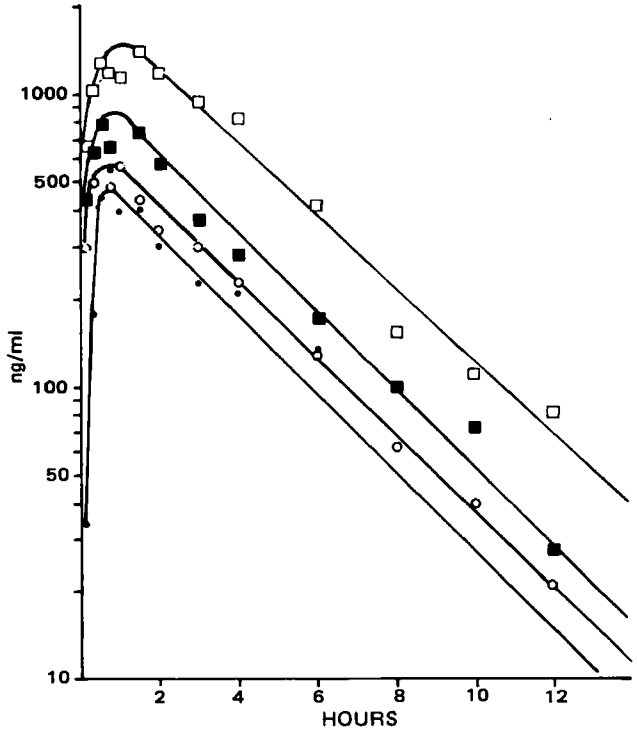

Figure 3—*Mean alizapride plasma concentration curves obtained in three subjects for each orally administered dose. Key: (●) 50 mg; (○) 100 mg; (■) 150 mg; (□) 200 mg.*

[5] Model 4051, Tektronix, Paris, France.

Table II—Mean Pharmacokinetic Parameters Obtained After Intravenous Administration of Alizapride

Parameter	Dose, mg			
	50	100	150	200
$T_{1/2\alpha}$, hr	0.135 ± 0.065	0.149 ± 0.109	0.092 ± 0.029	0.111 ± 0.055
$T_{1/2\beta}$, hr	3.453 ± 2.919	2.046 ± 0.698	1.810 ± 0.056	2.497 ± 0.081
K_{1-3}, hr^{-1}	0.915 ± 0.449	0.843 ± 0.375	1.177 ± 0.087	2.275 ± 2.458
K_{1-2}, hr^{-1}	3.291 ± 1.299	3.037 ± 4.526	4.544 ± 1.669	2.047 ± 1.071
K_{2-1}, hr^{-1}	0.978 ± 0.842	1.362 ± 1.396	2.606 ± 0.929	1.382 ± 0.428
V_1, liter	36.473 ± 8.745	29.760 ± 7.757	27.895 ± 0.177	27.486 ± 21.059
V_2, liter	73.073 ± 39.400	50.023 ± 11.548	48.540 ± 0.877	58.270 ± 10.784
AUC, mg hr/liter	1.977 ± 0.729	3.533 ± 0.899	4.660 ± 0.198	7.587 ± 2.693
Cl, ml/min	457.5 ± 148.3	495.2 ± 141.03	537.0 ± 22.2	472.6 ± 141.1
U_∞, mg	36.8 ± 5.77	61.2 ± 8.6	117.7 ± 4.95	157.6 ± 7.2
U_∞, %	73.6 ± 11.5	61.2 ± 8.6	78.5 ± 3.3	78.8 ± 3.3
$T_{1/2el}$, hr	1.98 ± 0.58	3.20 ± 0.45	2.51 ± 0.36	2.52 ± 0.14

RESULTS AND DISCUSSIONS

Figure 1 shows examples of chromatographic tracings. No peak corresponding to endogenous compounds interferes with the drug. A standard curve obtained with eight points had a mean slope of 0.0528 (1.12% *SD*), a mean correlation coefficient of 0.9998, and a mean *y*-intercept of 0.0146 (0.1% *SD*). These data indicate that the peak height at the origin is not significantly different from zero, which correlates with the absence of endogenous interfering peaks, and a linearity between 5 and 2000 ng of alizapride/ml of plasma.

Recovery of the drug from spiked plasma samples (n = 5) was determined (Table I) at several concentrations. Mean results appear to be very close to the theoretical concentrations, which show reasonable recovery and accuracy. The standard deviation decreased to a minimum of 1.5% obtained when the analyzed concentration was ~1 μg/ml. Under these conditions, assay sensitivity of alizapride in plasma was 5 ng/ml.

Blood Sample Analysis—*Intravenous Administration*—Mean alizapride concentrations obtained from the three subjects receiving intravenous doses are shown in Fig. 2. Individual concentrations have been systematically interpreted according to three different pharmacokinetic models, *i.e.*, one-, two-, or three-compartment open models. At each step, a statistical Fischer test using the least-squares criterion was performed to evaluate the benefit of increasing the number of compartments. After intravenous administration a two-compartment open model was chosen. Mean pharmacokinetic parameters are presented in Table II. It shows a very rapid distribution phase corresponding to a 0.125 ± 0.07-hr half-life (range: 0.057–0.210 hr) and an elimination phase with a 2.51 ± 1.49-hr mean half-life (range: 1.25–6.79 hr). Volumes of distribution are large: 3.9–44.5 liters (mean: 30.4 ± 4.2 liters) for the central compartment and 37.0–115.1 liters (mean: 57.5 ± 11.2 liters) for the peripheral compartment.

Oral Administration—Mean alizapride concentrations obtained from the three subjects receiving oral doses are shown in Fig. 3. With this route of administration, the better fit was obtained with the one-compartment open model with first-order absorption. However, the two curves observed after the 200-mg administration in two subjects were better described with a two-compartment open model with first-order absorption. Results are presented in Table III, and it can be seen that the apparent elimination half-life is in the same range as that obtained after intravenous administration. The area under the plasma concentration curves are lower, with the systemic availability calculated in this preliminary study being 72.5%.

Urine Sample Analysis—*Intravenous Administration*—Sigma-minus plots of the urinary excretion of unchanged alizapride is shown in Fig. 4. Corresponding pharmacokinetic parameters are presented in Table II, and it can be seen that they are remarkably constant. Two parameters are of particular interest. The first is the urinary elimination half-life of alizapride (2.60 ± 0.57 hr) compared with the terminal half-life of plasma concentration decay $t_{1/2}$ = 2.51 ± 1.49 hr. The paired t test failed to show differences in these values. The overall urinary elimination of unchanged drug, 73.0 ± 9.9% of the administered dose, shows that urinary excretion is the mean phenomenon responsible for plasma alizapride decay. About 30% of the administered dose was not recovered

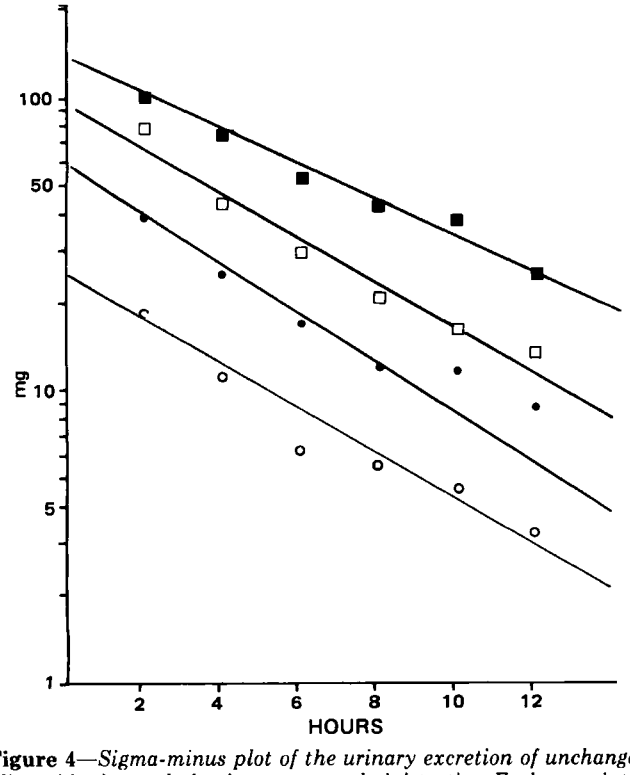

Figure 4—*Sigma-minus plot of the urinary excretion of unchanged alizapride observed after intravenous administration. Each curve is the mean of three subjects (○) 50 mg; (●) 100 mg; (□) 150 mg; (■) 200 mg.*

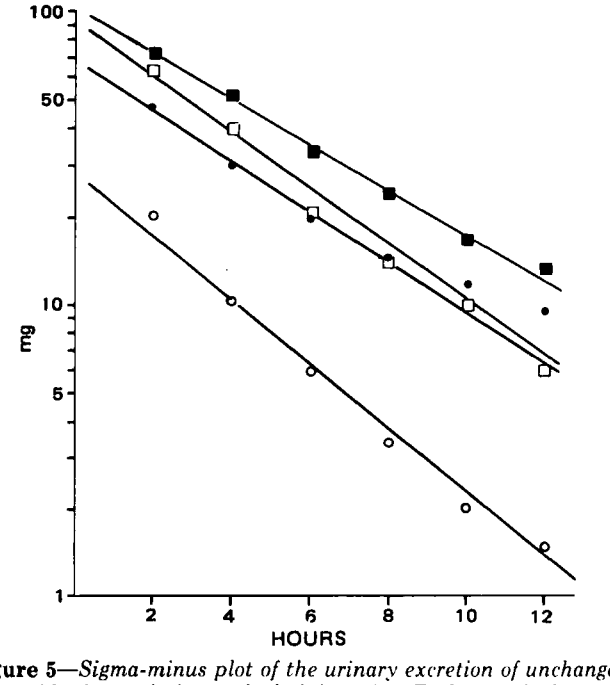

Figure 5—*Sigma-minus plot of the urinary excretion of unchanged alizapride observed after oral administration. Each curve is the mean of three subjects. Key: (○) 50 mg; (●) 100 mg; (□) 150 mg; (■) 200 mg.*

Table III—Mean Pharmacokinetic Parameters Obtained After Oral Administration of Alizapride

Parameter	Dose, mg			
	50	100	150	200
Lag time, hr	0.245 ± 0.021	0.285 ± 0.205	0.160 ± 0.169	0.513 ± 0.690
Kr, hr^{-1}	3.765 ± 1.859	6.495 ± 3.387	3.865 ± 2.567	6.060 ± 4.803
$T_{1/2r}$, hr	0.210 ± 0.099	0.125 ± 0.064	0.230 ± 0.155	1.133 ± 1.824
$T_{1/2\alpha}$, hr	—	—	—	2.240 ± 0.297
$T_{1/2\beta}$, hr	1.707 ± 0.962	2.750 ± 0.151	2.110 ± 0.532	2.817 ± 0.756
K_{1-3}, hr^{-1}	0.522 ± 0.326	0.982 ± 1.279	0.436 ± 0.091	0.303 ± 0.026
K_{1-2}, hr^{-1}	—	—	—	0.003 ± 1.10^{-5}
K_{2-1}, hr^{-1}	—	—	—	0.239 ± 0.061
V_1, liters	92.0 ± 56.1	217.3 ± 49.2	123.8 ± 21.4	101.2 ± 15.6
V_2, liters	—	—	—	1.33 ± 0.55
AUC, mghr/liter	1.706 ± 1.757	3.760 ± 3.166	3.170 ± 0.276	6.573 ± 0.464
Cl_T, ml/min	1099 ± 1006	895 ± 242	785 ± 107	472 ● 42
U_∞, mg	33.5 ± 47	80.3 ± 7.8	98.5 ± 16.5	144.9 ± 29.5
U_∞, %	67.0 ± 94	80.3 ± 78	65.7 ± 110	72.5 ± 14.8
$T_{1/2el}$, hr	2.17 ± 0.52	3.14 ± 1.56	2.26 ± 0.80	3.22 ± 1.25

during this study. Since urine was collected for 5 days and the elimination half-life is ~2.5 hr, a good approximation of the amount excreted in the urine at infinity exists. So the difference must be accounted for in the metabolism. The metabolic pathway of alizapride is unknown in humans. No extra peaks appeared on the chromatographic plots of the urine fractions collected. Furthermore, an attempt was made to see if one or more of the metabolites was eluted from the column simultaneously with the parent drug. For this reason, urine extracts have been chromatographed using different solvent systems, *i.e.*, methanol–pH 8.1 buffer from 20:80 (v/v) to 80:20 (v/v). No extra peak separated from the main peak. Either the metabolites are not extracted in chloroform or the solvent is unable to elute them from the HPLC column.

Oral Administration—Sigma-minus plots of the urinary excretion of unchanged alizapride are shown in Fig. 5, and corresponding pharmacokinetic parameters are presented in Table III. The urinary elimination half-life was 2.45 ± 1.38 hr, which is comparable to that observed after intravenous administration.

The unchanged urinary alizapride recovery amounted to 65.5 ± 22.7% of the administered dose. Compared with intravenous administration, a greater individual variation is observed after oral administration. This leads to a mean apparent systemic availability of 89.7%. This value is higher than the value found with corresponding AUC. However, the two values are not statistically different. This is probably due to the small number of subjects studied and the variations observed in urinary excretion after oral administration.

Dose-Dependency Analysis—From plasma results, dose-dependency has been checked by three methods. An example of the superposition method is shown in Fig. 6. Plasma concentrations divided by the administered dose as a function of time show reasonable superposition for the four doses tested. According to Dost's law (4), if pharmacokinetic parameters are independent of the dose, the area under the plasma concentration curve must be linearly related to the injected dose. The mean correlation coefficient was 0.9999, 0.9997, and 0.9928 for each subject. Despite the good correlation observed, there is little confidence in the results of this analysis because of the small amount of data used for the least-squares regression analysis. Accordingly, an ANOVA (5) was carried out for AUC, normalized to a 100-mg dose with the total amount of data available, obtained after either intravenous or oral administration. It failed to show a significant difference among the subjects ($^5_{16}F = 2.54$) and between administered doses ($^3_{16}B\ F = 0.74$), but, a significant difference at the 0.01 level was found between intravenous and oral administration. This must be related to the absolute availability of the oral form, which was calculated to be 72.5%.

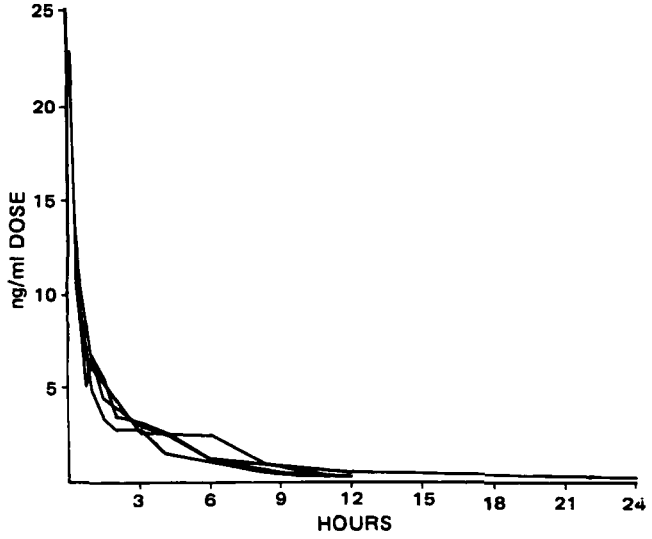

Figure 6—*Superposition of the plasma concentration curve divided by the injected dose in function of time, in subject C.*

Similarly, the same ANOVA analysis failed to show any difference between administered doses ($^3_{16}F = 0.61$) when considering urinary unchanged alizapride percentages. Nevertheless, it showed significant differences among individuals ($p < 0.05$) and between intravenous and oral administrations ($p < 0.01$).

From these three methods, it can be concluded that, in the range of administered doses, pharmacokinetic parameters of alizapride are not sensitive to dose variations.

Accordingly, variance analysis of the values of unchanged eliminated drug found for the different doses is unable to show any difference in drug elimination. The relationship between drug elimination and administered dose shows highly significant mean correlation coefficients in each subject.

The fluorescent HPLC method for biological sample analysis of alizapride has been shown to be sensitive enough to allow human pharmacokinetic studies of the drug. Preliminary results show a very rapid distribution phase with a mean half-life of 7.5 min followed by an elimination phase with a mean half-life of 2.5 hr. Urinary excretion represents the major phenomenon responsible for this elimination. In the range of tested doses, pharmacokinetic parameters of alizapride are linear.

REFERENCES

(1) P. Casanova, *Hépatol*, **16**, 381 (1980).

(2) J. M. Segrestaa, J. Gueris, D. Julien, and M. Tiar, *Thérapie*, **34**, 437 (1979).

(3) Ph. D'Athis, M. O. Richard, D. Delauture, E. Rey, M. Bouvier-D'Yvoire, E. Clement, and G. Olive, *ibid.*, **36**, 443 (1981).

(4) F. H. Dost, "Grundlagen der Pharmakokinetik," 2nd. ed., Stuttgart, Gearg Thieme Verlag, 1968, pp. 156–158.

(5) J. G. Wagner, "Fundamentals of Clinical Pharmacokinetics," Drug Intelligence Publications, Hamilton, Ill, 1975.

ACKNOWLEDGMENTS

We gratefully acknowledge Mr. L. Balant from the Department of Clinical Pharmacology, Faculty of Medicine, Geneva, Switzerland for his careful revision of the manuscript.

Vaginal Absorption of a Potent Luteinizing Hormone-Releasing Hormone Analogue (Leuprolide) in Rats II: Mechanism of Absorption Enhancement with Organic Acids

HIROAKI OKADA ˣ, IWAO YAMAZAKI, TAKATSUKA YASHIKI, and HIROYUKI MIMA

Received June 17, 1981, from the *Central Research Division, Takeda Chemical Industries, Ltd., 2-17-85 Juso, Yodogawa, Osaka 532, Japan.* Accepted for publication March 1, 1982

Abstract □ Organic acids such as citric acid enhance the vaginal absorption of luteinizing hormone-releasing hormone, the potent analogue (leuprolide), and insulin. The mechanism of this absorption enhancement was investigated with leuprolide and hydrophilic markers such as phenol red and Evan's blue. The absorption of the analogue was increased by lowering the pH of the solution and increased more by adding citric, succinic, tartaric, and malonic acids. The absolute bioavailability after vaginal administration of the 5% citric acid solution was 16.7% at pH 3.5 and 38.4% at pH 1.8. The enhancing potency of the absorption correlated well with the chelating ability of the organic acids. The vaginal absorption of phenol red was also enhanced with citric acid and edetic acid, but the enhancing effect of edetic acid was eliminated by adding equimolar calcium ion. These results suggest that the acidifying and chelating abilities of the acids may result in a potent enhancement of the vaginal absorption of leuprolide. A leakage experiment using Evan's blue on the vaginal membrane indicated that the blood–vaginal epithelium barrier was loosened with the administration of citric acid; this change was overcome rapidly.

Keyphrases □ Leuprolide—vaginal absorption, potent luteinizing hormone-releasing hormone analogue in rats, mechanism of absorption enhancement with organic acids □ Absorption, vaginal—potent luteinizing hormone-releasing hormone analogue in rats, mechanism of absorption enhancement with organic acids □ Hormones—potent luteinizing hormone-releasing hormone analogue (leuprolide) in rats, vaginal absorption, enhancement with organic acids

In a previous study (1), an investigation on the administration routes of leuprolide (I), a potent luteinizing hormone-releasing hormone (II) analogue, was carried out in rats to establish a self-administration method for antitumor therapy in humans:

(Pyro)Glu-His-Trp-Ser-Tyr-D-Leu-Leu-Arg-Pro-NH-CH_2CH_3
I

(Pyro)Glu-His-Trp-Ser-Tyr-Gly-Leu-Arg-Pro-Gly-NH_2
II

Good absorption of the analogue was observed with vaginal suppositories containing organic acids such as citric acid and succinic acid, and the vaginal application was proposed as a rational dosage method of the analogue for long-term therapy.

A series of investigations on the vaginal absorption of alcohols and alkanoic acids have been reported (2–6), but a few studies on the hydrophilic compounds and their absorption enhancement have been reported (7).

Most of the organic acids, which enhanced the vaginal absorption in the previous study, have a chelating ability. On the other hand, compounds possessing strong chelating ability, such as edetic acid (8–10) and tetracyclines (11), have been known to enhance the intestinal absorption of hydrophilic compounds, and the enhancement was supposedly due to the direct interaction with calcium or magnesium ions in the intestinal membrane.

In the present study, the mechanism of the vaginal absorption enhancement by the organic acids was investigated with leuprolide and hydrophilic marker compounds (phenol red and Evan's blue). The vaginal absorption-enhancing effect of citric acid was also confirmed on other hydrophilic, high-molecular compounds, II and insulin.

EXPERIMENTAL

Animals and Materials—Sexually mature female Sprague-Dawley rats[1] aged 120–150 days and weighing 250–330 g were used. Animals exhibiting two or more consecutive 4-day estrous cycles on daily morning examination of vaginal smears were used at diestrus.

Leuprolide [2]and II[2] were used after dehydration (1). Chemicals of reagent quality were used without further purification.

Vaginal Absorption of Leuprolide—The vaginal absorption of leuprolide was evaluated by determining the ovulation-inducing activity (1). The analogue was dissolved in 0.1 *M* glycine buffer (pH 2.02 and 3.47), 0.2 *M* phthalate buffer (pH 4.76), 0.2 *M* phosphate buffer (pH 6.70), 0.01 *N* HCl (pH 2.08), and 0.9% NaCl solution (pH 5.13) and administered vaginally with cotton balls at doses of 0.2–2 μg/kg/0.2 ml. Tonicity of the solution was measured by an osmometer[3] and adjusted to be isotonic with sodium chloride. Bovine serum albumin[4] and aprotinin[5] were added to each solution of leuprolide to prevent the loss by adsorption or proteolysis (1). After administration of the solution, the vaginal orifice was closed with a surgical adhesive.

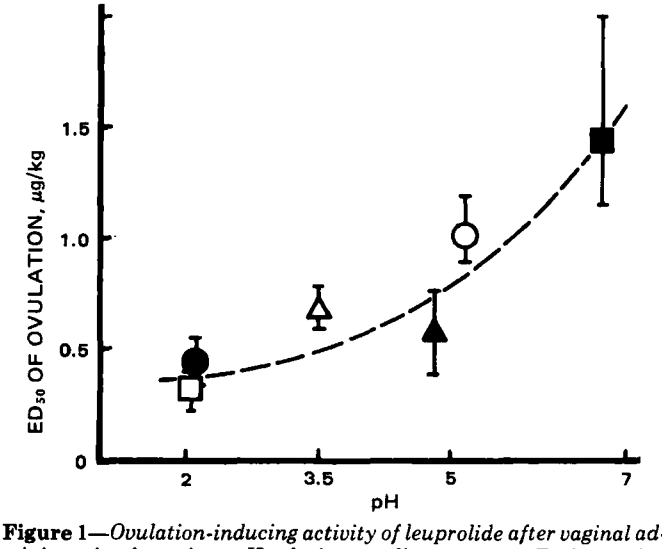

Figure 1—*Ovulation-inducing activity of leuprolide after vaginal administration in various pH solutions to diestrous rats. Each solution was adjusted to be isotonic with sodium chloride. Bars represent the 95% fiducial limits. Key: (○) 0.9% NaCl; (●) 0.012 N HCl; (□) 0.1 M glycine buffer (pH 2.02); (△) 0.1 M glycine buffer (pH 3.47); (▲) 0.2 M phthalate buffer (pH 4.76); (■) 0.2 M phosphate buffer (pH 6.70).*

[1] Clea Japan, Inc., Tokyo, Japan.
[2] These peptides were synthesized in Central Research Division of Takeda Chemical Ind., Ltd., Osaka, Japan.
[3] Fiske Osmometer, Model G-66, Fiske Associates, Inc., Uxbridge, Mass.
[4] Wako Pure Chemical, Ind., Ltd., Osaka, Japan.
[5] Trasylol, Bayer A. G., Leverkusen-Bayerwerk, West Germany.

0022-3549/83/0100-0075$01.00/0

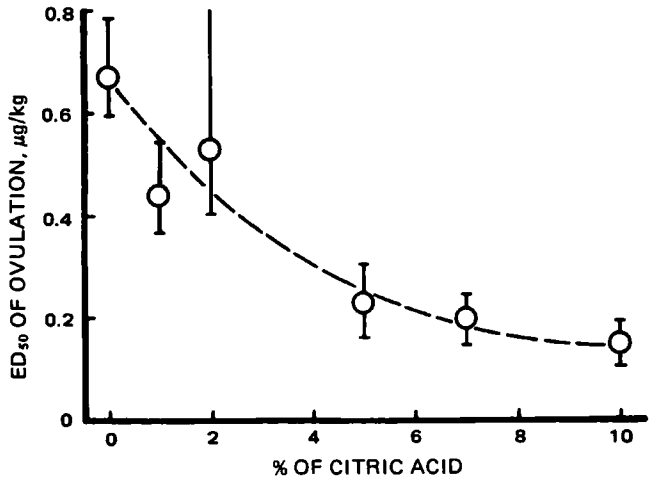

Figure 2—*Ovulation-inducing activity of leuprolide after vaginal administration in the aqueous solutions containing different concentrations of citric acid to diestrous rats. Each solution was adjusted to pH 3.5 with 10* N *NaOH or 2* N *HCl and to be isotonic with sodium chloride. Bars represent the 95% fiducial limits.*

Citric, succinic, tartaric, malonic, malic, acetic, lactic, and ascorbic acids were used at a concentration of 0.238 *M* to enhance the vaginal absorption of the analogue. The analogue dose was 400 ng/kg/0.2 ml. Each solution was adjusted to pH 3.5 with 10 *N* NaOH or 2 *N* HCl to be isotonic with sodium chloride.

The concentration effect of citric acid on the absorption enhancement was determined at 1, 2, 5 (0.238 *M*), 7, and 10% of the acid at pH 3.5. The enhancing effect of 5% dipotassium edetate solution (pH 3.5) and 5% citric acid solution (pH 1.8) were also examined.

Vaginal Absorption of Phenol Red—Phenol red was administered vaginally at a dose of 2 mg/kg/0.2 ml in the buffer (pH 2.0, 3.5, 5.0, and 6.7), 5 and10% citric acid (pH 3.5), 5% citric acid (pH 6.6), 0.12 *M* edetic acid (pH 6.7), and 0.12 *M* edetic acid and calcium chloride (pH 6.7) solutions under pentobarbital (50 mg/kg) and phenobarbital (100 mg/kg) anesthesia. Urine was collected at 3-hr intervals by a polyethylene tube[6] cannula and the collection was completed by washing the bladder with 1 ml of 0.9% NaCl solution through the catheter. Phenol red in the urine was determined by a modified method (12). Statistical evaluation of the data was performed using Student *t* test.

Effect of Citric Acid on the Leakage of Evan's Blue—To examine the time-course of the local reaction with citric acid, leakage of Evan's blue from the blood capillary on the vaginal membrane was evaluated. Evan's blue (10 mg/kg/ml) was intravenously injected immediately, or 0.5, 1.5, and 3.5 hr after vaginal administration of 5 or 10% citric acid solution, and the rats were sacrificed by decapitation 30 min later to examine the vaginal membrane. For the recovery examination, the vaginal membrane was treated with 10% citric acid solution for 1 hr, then washed with 10 ml of 0.9% NaCl solution. Evan's blue was injected immediately, 0.5, and 1.5 hr after washing.

Vaginal Absorption of II and Insulin—The ovulation-inducing activity of II after vaginal administration of a suppository consisting of an oleaginous base[7] with or without 10% citric acid was estimated in rats as described previously (1).

For evaluation of vaginal absorption of insulin, plasma glucose levels were determined using *o*-toluidine–boric acid (13). Insulin at doses of 0.5–20 U/kg iv was administered in 0.9% NaCl solution and vaginally by means of a cotton ball (~12 mg) soaked with 0.05 *M* KCl–HCl buffer solution (pH 1.70) or 10% citric acid solution (pH 1.72) to rats under anesthesia. Blood was taken from the tail vein 0.5, 1, 2, 3, 4, and 6 hr after the administration. The decrease of plasma glucose level (percent × hour) was expressed by integrating the decrease to the initial level from 0 to 6 hr.

RESULTS

Vaginal Absorption of Leuprolide—The ovulation-inducing activity of leuprolide after vaginal administration in the various pH solutions is shown in Fig. 1. The activity was increased by acidification to a level ~4 times greater at pH 2.02 than at pH 6.70.

[6] PE-50, Clay Adams Co., Parsippany, N.J.
[7] WITEPSOL S55, Dynamit Nobel Aktiengesellshaft, West Germany.

Table I—Ovulation-Inducing Activity of Leuprolide after Vaginal Administration in Aqueous Solution Containing Organic Acids to Diestrous Rats

Organic Acid	Ovulation[a]	Chelating Ability[b]
None	0/10	—
Citric	9/10	1.21
Succinic	10/10	0.80
Tartaric	2/10	0.37
Malonic	7/10	0.25
Malic	3/10	0.13
Acetic	5/10	—
Lactic	1/10	0.06
Ascorbic	0/10	—

[a] Number of rats induced ovulation per number of rats examined. Each solution containing 0.238 *M* of the organic acid was adjusted to pH 3.5 with 10 *N* NaOH or 2 *N* HCl to be isotonic with sodium chloride. Leuprolide was administered at a dose of 400 ng/kg/0.2 ml. [b] Gram ions of calcium ion sequestered by 1 *M* of organic acids at pH 10 and 30° (Ref. 7). The value of edetic acid was 1.75.

The activity of the analogue after vaginal administration in a pH 3.5 aqueous solution containing 0.238 *M* organic acids is shown in Table I. Polybasic carboxylic acids such as citric, succinic, malic, and malonic acids markedly enhanced the absorption. The enhancing effect was also recognized with acetic acid but not with lactic and ascorbic acids.

The concentration effect of citric acid on the ovulation-inducing activity of the analogue is shown in Fig. 2. The activity was potentiated with increasing concentration and approached a maximum level at >7% of the acid.

In addition, marked enhancing effects were obtained with 5% citric acid solution (pH 3.5 and 1.8) or 5% dipotassium edetate solution (pH 3.5) (Table II). Acidification of the solution from pH 3.5 to 2.0 doubled the activity of the analogue, and a further addition of 5% citric acid increased the activity by 3 times at both pH 3.5 and 1.8. Edetic acid showed a slightly stronger enhancing effect.

Vaginal Absorption of Phenol Red—Vaginal absorption of phenol red was evaluated by the urinary excretion (Fig. 3). After intramuscular injection, phenol red was rapidly excreted into the urine at 90.1 ± 3.0% (mean ±*SE*) of dose in 3 hr, and 96.3 ± 3.2% in 6 hr. After vaginal administration, excretion was sustained during 6 hr. Urinary excretion after vaginal administration in pH 2.0–6.7 buffer solutions was 28.9–38.4% of the dose in 6 hr and tended to decrease slightly with reduced pH.

Vaginal absorption of phenol red was also increased by the addition of 5 or 10% citric acid in pH 3.5 solution but was not affected by the addition of 5% citric acid in pH 6.6 solution. Although edetic acid significantly enhanced the absorption ($p < 0.01$), further addition of equimolar calcium chloride cancelled the enhancement effect.

Effect of Citric Acid on the Leakage of Evan's Blue—The time-course of the local reaction of citric acid on the vaginal membrane and its recovery from the reaction were evaluated by a leakage experiment of Evan's blue. Five percent citric acid solution induced faint staining after only 30 min, whereas 10% citric acid solution induced deep staining after 30 min and 1 hr, which gradually faded 2 and 4 hr after administration. Change of the vaginal membrane induced by 1-hr treatment with 10% citric acid solution was rapidly recovered by washing the lumen with 0.9% NaCl solution; there was a faint staining at 1 hr but none 2 hr after washing.

Vaginal Absorption of II and Insulin—Ten percent citric acid enhanced the ovulation-inducing activity of II by 30 times after the vaginal administration (Table III).

The decreased plasma levels of glucose (percent × hour) after intravenous and vaginal administration of insulin are shown in Fig. 4. A 1.1-U/kg intravenous dose of insulin caused a 125% × hr plasma glucose level decrease in 6 hr. The comparably effective doses for the vaginal administration were 30.0 U/kg in the buffer solution (pH 1.70) and 6.0 U/kg in 10% citric acid solution (pH 1.72). Absolute bioavailability, estimated by the effective doses of the latter, was 18%.

DISCUSSION

Our previous study (1) revealed that good absorption of leuprolide occurred after vaginal administration, and this absorption was enhanced by the addition of some carboxylic acids. In the present study, to establish the mechanism of absorption enhancement, the effects of pH and organic acids on the vaginal absorption of the analogue as well as a few hydrophilic compounds were determined.

The vaginal absorption of leuprolide was enhanced by a pH reduction in the solution, whereas that of phenol red tended to decrease with

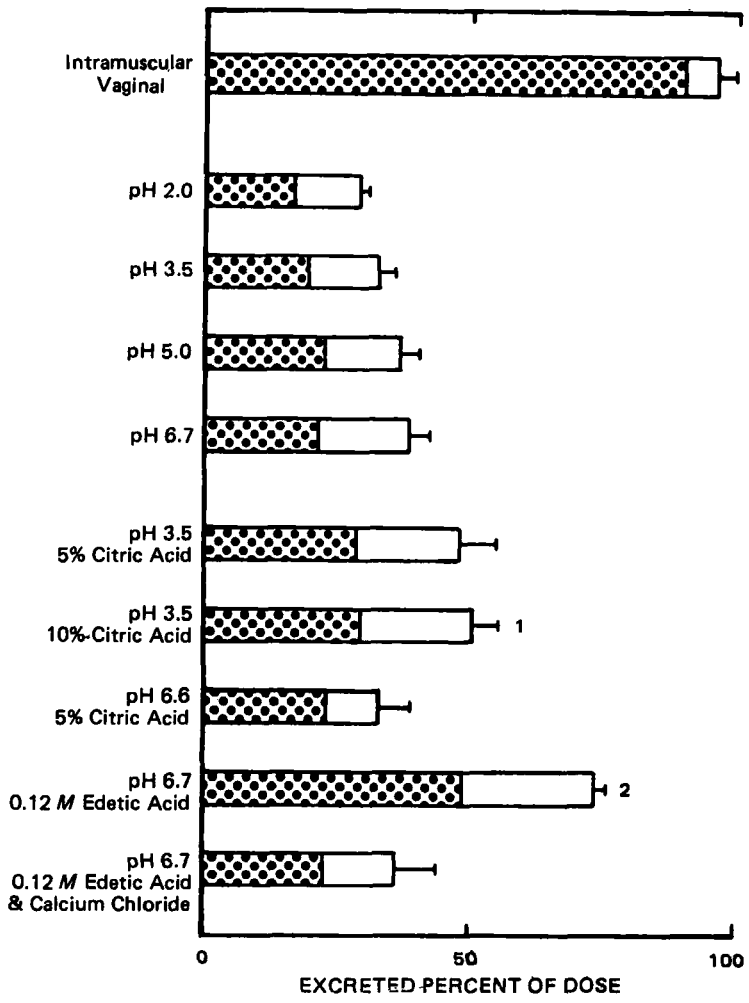

Figure 3—*Effects of pH, citric acid, and edetic acid on vaginal absorption of phenol red in diestrous rats. Each solution was adjusted to be isotonic with sodium chloride. Bars represent the mean ±SE of five rats. Significant in comparison with the same pH buffer solution: (1)* $p < 0.05$; *(2)* $p < 0.01$. *Key: (▨) 0–3 hr; (□) 3–6 hr.*

acidification. Leakage of Evan's blue on the vaginal epithelium was not induced by a moderate pH change, but it was slightly induced by a strong acid or alkali solution[8]. It can be assumed that the effect of pH on the vaginal absorption of leuprolide is due mainly to structural changes of the epithelial membrane but is also due to the self-association and conformational change of the peptide or to the change of electric charge on the epithelial surface. It is known that the pH of the vaginal tract of normal women is 3.5–3.9 (14) and that of the vaginal fluid is 4.0–4.7 (15). Therefore, an acid preparation of pH 3–4 should not disturb the normal condition of the vaginal tract. Surface of the vaginal membrane of rats exhibited a pH close to that of the applied bulk solution[8] [this is also true in rabbits (5)].

The polybasic carboxylic acids enhanced the vaginal absorption of leuprolide from aqueous solution (adjusted to pH 3.5) as well as from an oleaginous suppository, whereas lactic and ascorbic acids did not elicit the effect. The enhancing effect with 5% citric acid solution was of the same degree at both pH 1.8 and 3.5 (Table II). Bioavailability of the analogue after vaginal administration of the 5% citric acid solution (pH 1.8) was 38.5 and 58.8% of that after intravenous and subcutaneous injection, respectively.

The chelating ability of the organic acids given by gram ions of calcium ion sequestered is summarized in Table I (16). Edetic acid with the strongest ability (1.75) is followed successively by citric, succinic, tartaric, malonic, and malic acids. Lactic acid has the weakest ability. It is likely that the enhancing effect of the carboxylic acids on vaginal absorption of leuprolide, which has a good correlation with the chelating ability of the acids, is due to chelating ability as well as to the acidification of the solution. Acetic acid, which has negligible chelating ability, also enhanced vaginal absorption. This may be due to the fact that acetic acid is known to corrode mucous membranes and to have a strong interaction with peptides. The 0.12 *M* edetic acid solution enhanced the absorption of phenol red by 2 times ($p < 0.01$); the enhancement was cancelled by the addition of equimolar calcium ion. This result also supports the assumption that the chelating ability of carboxylic acids causes the enhancement of vaginal absorption. The vaginal absorption of phenol red

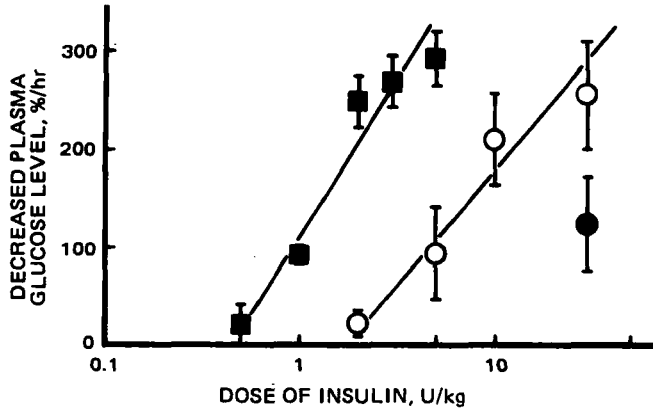

Figure 4—*Decreased plasma levels of glucose after subcutaneous and vaginal administration of insulin to diestrous rats. The decreased plasma level of glucose (percent per hour) was exhibited by integrating the decreased percent against the initial level for 6 hr. Each point represents the mean ±SE of five rats. Key: (■) subcutaneous; (○) vaginal in 10% citric acid (pH 1.72); (●) vaginal in 0.05 M KCl–hydrochloric acid buffer (pH 1.70).*

[8] Unpublished results.

Table II—Ovulation-Inducing Activity of Leuprolide after Vaginal Administration in Buffered Solutions Containing Citric Acid or Edetic Acid to Diestrous Rats

Buffered Solution	Dose of Leuprolide, ng/kg										ED_{50}, ng/kg
	60	80	100	200	300	400	500	600	800	1000	
0.1 *M* Glycine buffer (pH 3.47)						0/10	2/10	3/13	8/10	5/5	669 (596–785)[b]
5% Citric acid (pH 3.5)			1/10[a]	4/10	6/10	9/10					227 (161–305)
5% Dipotassium edetate (pH 3.5)			1/10	6/10	9/10						176 (128–229)
0.1 *M* Glycine buffer (pH 2.02)				2/10	5/10	6/10	7/10	10/10			320 (232–395)
5% Citric acid (pH 1.8)	1/10	0/10	7/10	10/10							99 (85–132)

[a] Number of rats induced ovulation per number of rats examined. [b] 95% fiducial limits.

Table III—Ovulation-Inducing Activity of Luteinizing Hormone-Releasing Hormone (II) after Vaginal Administration to Diestrous Rats

Additives	Dose of II, μg/rat	Ovulation[a]	ED_{50}, μg/rat
None	10	1/10	24.4 (17.3–32.1)[b]
	20	2/10	
	40	10/10	
	60	9/10	
	80	10/10	
Citric acid (10%)	0.4	1/10	0.82 (0.68–1.14)
	0.6	1/10	
	0.8	4/10	
	1.0	8/10	
	10.0	4/4	

[a] Number of rats induced ovulation per number of rats examined. [b] 95% fiducial limits.

was also enhanced with citric acid at pH 3.5 but only slightly enhanced at pH 6.6. This was also observed with leuprolide (1).

The vaginal absorption of leuprolide was enhanced by an increase in citric acid concentration but reached a maximum level at >7% of the acid. The vaginal absorption of phenol red was also enhanced with 5% citric acid but increased less with 10% citric acid. The hypertonic solution with sodium chloride showed a tendency to decrease the absorption[8]. The leakage of Evan's blue on the vaginal epithelium was obviously enhanced by an increase in acid concentration. These results indicate that the enhancement of permeability of the membrane for the hydrophilic compounds is caused by an increase in the acid concentration, but the apparent absorption most likely is suppressed by exudation of body fluid from the vaginal membrane due to hypertonicity of the acid solutions.

A time-course study on the change of vaginal epithelial membrane with citric acid revealed that faint staining by Evan's blue injected intravenously was observed in the early stage after treatment with 5% citric acid solution and deep staining 30 min and 1 hr after treatment with 10% citric acid solution; even in the latter, the stain gradually faded. The change in vaginal membrane treated with 10% citric acid solution recovered rapidly following washing with physiological saline solution, and the stain was barely visible 1 hr later. It is suggested that the 5% acid concentration in aqueous solution or jelly, sufficient to exert an enhancement on vaginal absorption of the analogue, will produce only a slight change and, hence, a rapid recovery of the vaginal epithelium.

The vaginal absorption of II and insulin, which are hydrophilic and high molecular compounds, was also enhanced markedly by adding citric acid.

It appears that the acidification and chelating abilities of organic acids result in their potent absorption-enhancing activity on the vaginal absorption of leuprolide. Changes in the vaginal epithelial membrane induced with citric acid are slight and recovery of the epithelium is relatively rapid.

REFERENCES

(1) H. Okada, I. Yamazaki, Y. Ogawa, S. Hirai, T. Yashiki, and H. Mima, *J. Pharm. Sci.*, **71**, 1367 (1982).

(2) T. Yotsuyanagi, A. Molokhia, S. Hwang, N. F. H. Ho, G. L. Flynn, and W. I. Higuchi, *ibid.*, **64**, 71 (1975).

(3) S. Hwang, E. Owada, T. Yotsuyanagi, L. Suhardja, N. F. H. Ho, G. L. Flynn, and W. I. Higuchi, *ibid.*, **65**, 1574 (1976).

(4) E. Owada, C. R. Behl, S. Hwang, L. Suhardja, G. L. Flynn, N. F. H. Ho, and W. I. Higuchi, *ibid.*, **66**, 216 (1977).

(5) S. Hwang, E. Owada, L. Suhardja, N. F. H. Ho, G. L. Flynn, and W. I. Higuchi, *ibid.*, **66**, 778 (1977).

(6) *Idem.*, **66**, 781 (1977).

(7) E. Touitou, M. Donbrow, and E. Azaz, *J. Pharm. Pharmacol.*, **30**, 662 (1978).

(8) E. Windsor and G. E. Cronheim, *Nature*, **190**, 263 (1961).

(9) L. S. Schanker and J. M. Johnson, *Biochem. Pharmacol.*, **8**, 421 (1961).

(10) W. D. Erdmann and S. Okonek, *Arch. Toxikol.*, **24**, 91 (1969).

(11) T. Nadai, K. Nishii, and A. Tatematsu, *Yakugaku Zasshi*, **90**, 262 (1970).

(12) K. Kakemi, H. Sezaki, T. Kimura, and M. Murakami, *Chem. Pharm. Bull.*, **18**, 275 (1970).

(13) A. Hyvärienen and E. A. Nikkilä, *Clin. Chim. Acta*, **7**, 140 (1962).

(14) W. H. Masters, *Ann. N.Y. Acad. Sci.*, **83**, 301 (1959).

(15) "Remington's Pharmaceutical Science," 15th ed., Mack Publishing Co., Easton, Pa., 1975, p. 1544.

(16) K. Ogino and N. Hayashi, *Yukagaku*, **26**, 278 (1977).

ACKNOWLEDGMENTS

The authors are grateful to Mr. H. Nakagawa and Miss T. Yamashita for assistance with the experiments, to Dr. T. Shimamoto and Dr. S.Hirai for valuable discussion, and to Dr. J. R. Miller for comments on the manuscript.

Hydration and Percutaneous Absorption IV: Influence of Hydration on *n*-Alkanol Permeation Through Rat Skin; Comparison with Hairless and Swiss Mice

CHARANJIT RAI BEHL *x, ABDEL AZIZ EL-SAYED ‡, and GORDON L. FLYNN §

Received November 6, 1981 from the *Roche Laboratories, *Pharmaceutical Research, Hoffmann-LaRoche, Inc., Nutley, NJ 07110*, the ‡*Department of Pharmaceutical Chemistry, The University of Kansas, Lawrence, KS 66044*, and the §*University of Michigan, College of Pharmacy, Ann Arbor, MI 48109.* Accepted for publication, March 15, 1982.

Abstract □ The effect of protracted aqueous contact of rat skin on its permeability to methanol, *n*-butanol, and *n*-hexanol was investigated. With the aid of small diffusion cells, sets of intermittent permeation experiments, each ~7 hr in duration, were performed on excised rat skin sections over periods lasting several days, and permeability coefficients were calculated as a function of the duration of the hydration. The permeability coefficient of methanol increased gradually to an asymptote 2.5 times higher than the initial value over the first 80 hr of immersion and then remained essentially invariant through an additional 70 hr. In contrast, the butanol permeability coefficient increased by only a small fraction (~25%) through the first 5 hr of hydration, and it remained at the higher value through to the end of the experiment at 80 hr. For more hydrophobic hexanol, the permeability coefficient increased by ~40% over the first 10 hr and then declined, returning to near the initial value by the second day. It was relatively constant past this point—up to 150 hr. When these data were compared with similarly obtained data from earlier studies involving two strains of mice, the Swiss mouse and a hairless mouse mutant, parallelism was noted in the behavior of the rat and Swiss mouse skins, which set them both apart from the behavior of the skin of the hairless mouse. The comparison suggests that, irrespective of animal species, the development of a thick coat of hair occurs with commensurate functional changes in the chemical barrier properties of the epidermis.

Keyphrases □ Permeability—hydration and percutaneous absorption, influence on *n*-alkanol through rat skin, Swiss and hairless mice comparison □ Hydration—percutaneous absorption, influence on *n*-alkanol permeation through rat skin, Swiss and hairless mice comparison □ Absorption—hydration, influence on *n*-alkanol through rat skin, Swiss and hairless mice comparison

The relative influences of moisture absorption and retention on different animal skins serves as one point of comparison of the skins and, therefore, is a factor to be considered when animals are to be used instead of human subjects in percutaneous absorption research. In recent studies the permeabilities of the skins of two strains of laboratory mice affected by protracted immersion in an isotonic saline medium were explored (1–3). Permeability, and its alteration by these extreme hydrating conditions, was shown to be dependent on the strain of mouse chosen and, within a strain, on the chemical structure of the permeant. This had mechanistic implications with regard to the functioning of the Swiss mouse and the hairless mouse ($SKh\text{-}hr^{-1}$) skins as chemical barriers. The strikingly different behaviors noted between these two strains were presumed primarily to be related to the disparity in abundance and prominance of hair and, possibly, to a change in the relative importance of the transepidermal and transfollicullar routes. It could be assumed further that the absorption behaviors of animal skins may be related more to the similarity of their coats than to the species involved, but this has yet to be proven.

Therefore, the present study was undertaken to assess the effect of hydration on the permeability of rat skin using several of the same reference permeants and under identical conditions as in the mouse experiments. The diffusional behaviors of the hairy skins of the Swiss mouse and Sprague-Dawley rat proved to be somewhat similar and set apart from that of the hairless mouse. This has implications for the choice of animals used for certain dermatological research.

EXPERIMENTAL

Chemicals—[^{3}H]methanol[1], [^{14}C]butanol[2], and [^{14}C]hexanol[2] were used as received. The radiochemicals were diluted with 0.9% sodium chloride irrigation medium[3] (saline) for the permeation experiments. The final chemical concentrations in the diffusional medium were $\leq 10^{-4}$ *M*.

Animals—Sprague-Dawley adult male rats (~300 g) were used. They had free access to food and water. All skins used in the permeation experiments were denuded of hair by the nondestructive and nonirritating procedure of close cropping with a pair of surgical scissors (2). Rats have a relatively large skin area, considering that the opening between diffusion cell compartments is on the order of 0.6 cm^2. Therefore, it was possible to take nine or more separate sections of skin from the dorsal surface of the animal, as indicated in the sketch in Table I. Differences in skin site were minimized by this technique, and only a few rats were needed to complete the study.

Permeation Procedure—Two-compartment glass diffusion cells (1) were employed to determine skin permeability. Ten skin sections were excised from the dorsal surface of one rat, sacrificed by administering sodium pentobarbital. The external medium of the diffusion cell was saline. The half-cell contents were stirred at 150 rpm. All experiments were carried out at 37°. Permeation was followed by monitoring the receiver chamber concentration for ~2 hr. The half-cell facing the stratum corneum was always the donor compartment, and the half-cell facing the dermis was always the receiver compartment. Therefore, net diffusion occurred from the stratum corneum to the dermis side. Complete hydration profiles were obtained on each piece of skin by running eight sequential experiments covering up to 150 hr of conditioning, with thorough rinsing done between the runs (1).

Radioisotopic Assay—The concentration of the radiolabeled permeant was determined by placing discrete samples in a scintillation solution[4] and assaying on a liquid scintillation counter[5]. Using the technique of dual labels, methanol–butanol and methanol–hexanol were paired. Methanol thus served as a common solute in both sets of the experiments providing a means of assuring membrane integrity.

Data Analysis—The data were plotted as receiver chamber concentration (in terms of counts per minute) as a function of time. The permeability coefficient was calculated from (3):

$$P = \frac{V}{A}\frac{(dc/dt)}{\Delta C} \qquad \text{(Eq. 1)}$$

where P is the permeability coefficient in centimeters per hour, A is the diffusional area (~0.6 cm^2), ΔC is the concentration difference across

[1] New England Nuclear Corp., Boston, Mass.
[2] International Chemical and Nuclear Corp., Irvine, Calif.
[3] Abbott Laboratories, North Chicago, Ill.
[4] Aquasol, New England Nuclear Corp., Boston, Mass.
[5] Beckman Liquid Scintillation Counter, Model LS 9000, Beckman Instruments, Inc., Fullerton, Calif.

0022-3549/83/0100-0079$01.00/0

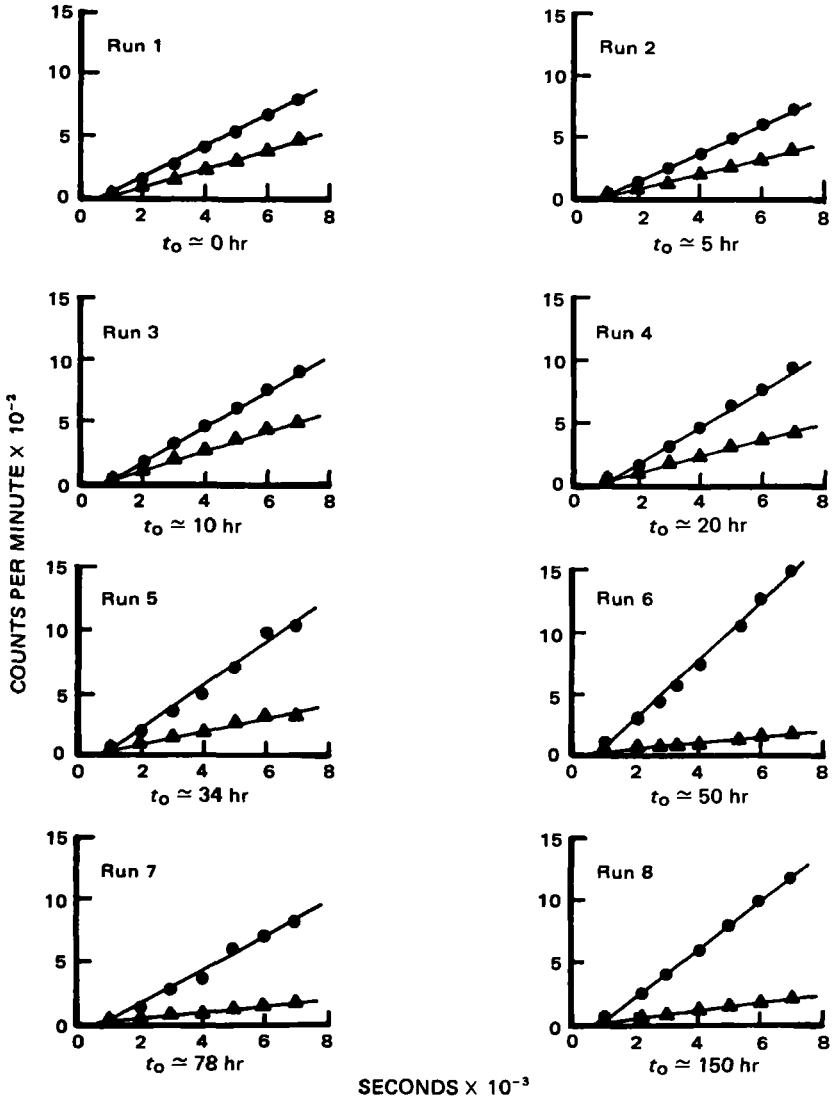

Figure 1—*Series of receiver compartment concentration (cpm)* versus *time profiles for a set of eight sequential runs on a single skin. This is one set of data from the methanol–hexanol series (see text). The initial time of hydration (t_0) for each run is indicated in the lower left-hand corner of each plot. Key: (●) methanol; (▲) hexanol.*

the membrane, which was taken to be equal to the donor concentration (cpm), V is the half-cell volume (1.4 ml), and dc/dt is the quasi steady-state slope (cpm/cm^3/hr).

RESULTS

Figure 1 contains a representative set of eight subplots obtained in sequential permeation experiments carried out on one piece of skin over 150 hr of hydration using [^{3}H]methanol and [^{14}C]hexanol as dual permeants. A linear relationship between the receiver concentration *versus* time is indicative of good approximation of steady-state transport conditions. Also, the lag times do not seem to change with hydration time. This is consistent with the permeation behavior reported for hairless (1, 3) and Swiss (2) mice. Slopes of these linear plots were used to compute permeability coefficients.

Table I contains the individual and average permeability coefficients of methanol as a function of hydration time. Both sets of methanol data, one run with butanol as the copermeant and the second run with hexanol as the copermeant, are presented. Tables II and III contain similar data for butanol and hexanol, respectively.

From data reported in Tables I–III, the percent change in permeability at any time relative to the permeability at time zero was computed (2). (The first diffusional run began immediately after placing a skin section in the diffusion cell.) These changes are reported in Figs. 2–4 for each of the permeants in terms of the percent change as a function of hours of hydration.

DISCUSSION

Effect of Hydration on Alkanol Permeation—The permeability coefficient of methanol through rat skin approaches an asymptote 2.5 times the initial value (150% hydration influence) as a function of time, with the limiting value essentially obtained at the 80-hr point (Fig. 2).

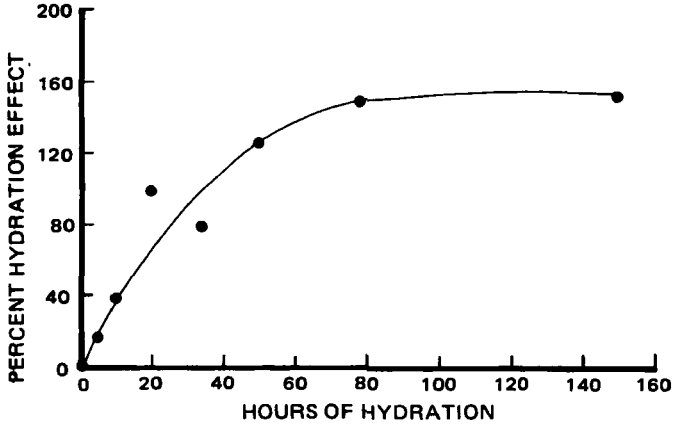

Figure 2—*Plot of percent hydration effects* versus *hydration time for methanol.*

Table I—Hydration Effect Data for Methanol

Hydration time, hr	$P \times 10^3$, cm/hr Skin Section No.[a] 1	2	3	4	5	Average ±*SD*
	Set 1 (butanol copermeant)					
~0	2.7	2.3	1.6	4.2	2.2	2.6 ±1.0
5	2.5	2.4	2.2	4.5	1.9	2.7 ±1.0
10	3.0	3.1	2.1	5.3	2.0	3.1 ±1.3
20	3.3	3.2	2.4	5.5	2.3	3.3 ±1.3
34	3.4	3.2	2.6	7.1	3.0	3.9 ±1.8
50	5.6	3.7	2.7	11.0	3.6	5.3 ±3.3
78	9.5	4.7	2.5	13.5	5.4	7.1 ±4.4
	Set 2 (hexanol copermeant)					
	6	7	8	9		
~0	1.6	1.6	3.8	2.1		2.1 ±0.8
5	1.6	1.7	5.1	2.4		2.7 ±1.6
10	2.0	2.0	6.2	2.8		3.3 ±2.0
20	2.1	2.2	7.0	2.9		3.6 ±2.3
34	2.5	2.5	7.6	4.8		4.4 ±2.4
50	—	—	7.4	3.0		5.2 ±3.1
78	3.3	3.6	7.2	—		4.7 ±2.2
150	5.8	4.7	—	—		5.3 ±0.8

[a] 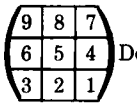

Dorsal surface of the rat.

With hairless mouse skin, the methanol permeability coefficient was unaffected by such conditioning (1). The behavior of rat skin to methanol, however, is qualitatively similar to that previously seen for the Swiss mouse (2). In the latter strain of mouse, the methanol permeability coefficient was increased by 80% (1.8 times) by hydration, with the effect leveling out by ~20 hr.

In the rat, the butanol permeability coefficient appeared to be increased marginally by hydration (20–25%) with the effect noted as early as 5 hr (Fig. 3). The permeability coefficient then appeared invariant up to 78 hr. This contrasts with the hairless mouse where a doubling of the parameter took place over the first 10 hr of experimentation (1) and with the Swiss mouse where a slightly greater than twofold increase was noted by 15 hr (2). In the Swiss mouse skin, the permeability coefficient appears to gradually and linearly decrease past 15 hr, so that the increase at the end of the second full day measured only 85%.

In the rat, hexanol permeation appears to have a unique hydration dependency (Fig. 4). Over the first 10 hr of saline immersion, the permeability coefficient appears to increase. There is, on the average, a 44% enlargement at the 10-hr point. The trend then reverses, with a systematic return to the initial, baseline value by 78 hr. In the hairless mouse hexanol behaves as butanol; there is a twofold increment which is largely complete by 10 hr. No data were obtained for hexanol passing through Swiss mouse skin.

The up and down type of pattern, apparent for butanol in the Swiss mouse and for hexanol in the rat, surfaces in the hairless mouse skin at an alkanol alkyl chain length of 8 (*n*-octanol). The absolute values of the alkanol permeability coefficients through rat skin increase from methanol to hexanol. Taking the permeability coefficients after 10 hr of conditioning as representative, the average values are 3.2×10^{-3} cm/hr for methanol, 6.4×10^{-3} cm/hr for butanol, and 13.5×10^{-3} cm/hr for hexanol. The ratio of the hexanol and methanol values of ~4 indicates a marginal dependency of permeation on hydrophobicity through the series. By way of comparison, the factor at 10 hr of hydration in the hairless mouse is >20, pointing to a more acute lipid–water partitioning reliance of the permeation process in this tissue (1).

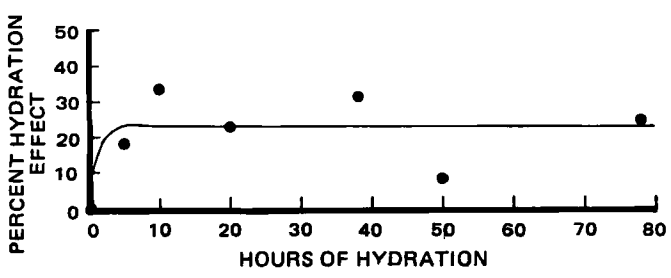

Figure 3—*Plot of percent hydration effects* versus *hydration time for butanol.*

Table II—Hydration Effect Data for Butanol

Hydration time, hr	$P \times 10^3$, cm/hr Skin Section No.[a] 1	2	3	4	5	Average ±*SD*
~0	4.2	5.0	3.7	7.1	4.0	4.8 ±1.4
5	4.8	5.9	4.9	8.6	4.2	5.7 ±1.7
0	7.3	7.1	6.6	7.3	3.6	6.4 ±1.6
20	5.9	6.1	7.7	6.2	3.8	5.9 ±1.4
34	4.7	6.6	6.8	8.5	5.0	6.3 ±1.5
50	4.9	5.8	5.9	5.9	3.7	5.2 ±1.0
78	5.0	8.7	5.5	4.8	6.1	6.0 ±1.6

[a] See Table I.

Table III—Hydration Effect Data for Hexanol

Hydration time, hr	$P \times 10^3$, cm/hr Skin Section No.[a] 6	7	8	9	Average ±*SD*
~0	9.0	8.3	10.5	9.8	9.4 ±1.0
5	8.8	11.2	15.0	13.0	12.0 ±2.6
10	11.2	11.9	18.4	12.6	13.5 ±3.3
20	9.4	10.8	14.6	13.1	12.0 ±2.3
34	8.3	10.5	14.0	11.0	11.0 ±2.3
50	7.8	8.8	12.0	7.8	9.1 ±2.0
78	6.3	9.6	10.1	10.6	9.6 ±1.9
150	10.0	10.3	—	—	10.2 ±0.2

[a] See Table I.

Significance of the Findings—It is difficult to interpret these collective observations, but the following factors affect the permeation process. The development of a coat of hair generally is accompanied by thickening of the skin, especially its dermal elements in which the follicles are anchored. This magnifies the diffusional importance of the living and functionally aqueous strata beneath the stratum corneum when these are a part of the membrane mounted in the diffusion cell. Thus, it is to be expected that the thicker skins of the furry animals will have earlier onset of rate control by the viable epidermal and the dermal strata with increasing hydrophobicity (as the alkyl chain is extended) and that the limiting rate of diffusion as aqueous tissue control is approached will also be lower; each appears to be the case.

This in part explains the more compressed range of permeability coefficient values for the alkanols in the full thickness Swiss mouse and rat skins. This influence of the thickened subcorneal elements creates a false impression of permeability of the skin in that in the living animal the peripheral blood flow collects permeant at the immediate undersurface of the epidermis, eliminating much of the diffusional resistance experienced in the nonblood perfused skins of *in vitro* measurement.

Strata thickness variations cannot explain the different hydration sensitivities of methanol permeation through the skin of the hairless mouse and the furry integuments as the permeability coefficients are small, signifying rate control by strata elsewhere in the skins. For the hairless mouse, stripping (4) and other experiments (5–7) establish the stratum corneum as the principal source of diffusional resistance for methanol. Also, both the alkanol alkyl chain length profile and the hydration effect data for the hairless mouse tissue indicate that this solute finds some pathway through the skin which is around rather than through the lipid domains of the horny layer. Thus, it is possible to conclude that the hairy epidermises function differently as barriers to methanol. The

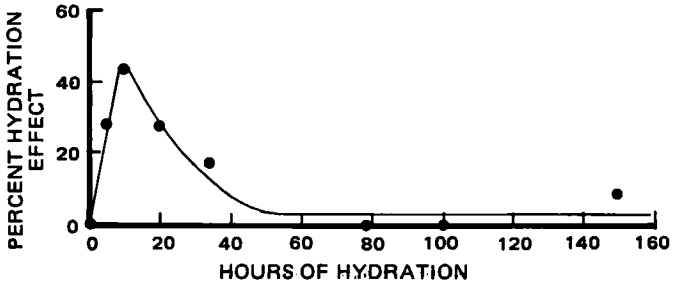

Figure 4—*Plot of percent hdyration effects* versus *hydration time for hexanol.*

difference centers around the increased prominence and number of hair follicles. Probably diffusion across the transfollicular shunt is greatly enhanced, to the point where it becomes the principal pathway. The horny layer of the epidermis is also affected by the formation of a thick coat of hair. Since the hairy mat restricts insensible perspiration, the stratum corneum associated with furry skin need not be as impermeable to water, and it is typically thinner and less well formed than when the surface is hairless. Thus, structural and compositional changes in the horny layer also provide a basis for explaining the differing hydration sensitivities. It is likely that both factors are important.

This study provides further evidence of intra- and interspecies complexities of animal skins as mass transport regulators. To a degree it demonstrates that skins covered with thick coats of hair do not behave diffusionally as hairless skins, whether of mouse or humans. Previous work (1–8) indicates a high degree of parallelism in the chemical barrier properties of hairless mouse and human skins. This study adds support for the use of hairless animals for research on percutaneous absorption, primary irritancy, topical drug delivery, *etc.*, when it is not possible or practicable to use human subjects.

REFERENCES

(1) C. R. Behl, G. L. Flynn, T. Kurihara, N. Harper, W. M. Smith, W. I. Higuchi, N. F. H. Ho, and C. L. Pierson, *J. Invest. Derm.*, **75**, 346 (1980).

(2) C. R. Behl and M. Barrett, *J. Pharm. Sci.*, **70**, 212 (1981).

(3) C. R. Behl, M. Barrett, G. L. Flynn, T. Kurihara, K. A. Walters, O. G. Gatmaitan, N. Harper, W. I. Higuchi, N. F. H. Ho, and C. L. Pierson, *ibid.*, **71**, 229 (1982).

(4) G. L. Flynn, H. H. Durrheim, and W. I. Higuchi, *ibid.*, **70**, 52 (1981).

(5) C. R. Behl, G. L. Flynn, T. Kurihara, W. Smith, O. Gatmaitan, W. I. Higuchi, N. F. H. Ho, and C. L. Pierson, *J. Invest. Derm.*, **75**, 340 (1980).

(6) G. L. Flynn, C. R. Behl, K. Walters, O. G. Gatmaitan, J. Kurihara, N. F. H. Ho, W. I. Higuchi, and C. L. Pierson, *Burns*, **8**, 47 (1981).

(7) C. R. Behl, E. E. Linn, G. L. Flynn, C. L. Pierson, W. I. Higuchi, and N. F. H. Ho, *J. Pharm. Sci.*, in press.

(8) R. B. Stroughton, in "Animal Models in Dermatology," H. Maibach, Ed., Churchill Livingstone, New York, N.Y., 1975, p. 121.

ACKNOWLEDGMENTS

This study was supported in part by Grant 5-R01GM24611 from the National Institutes of Health.

NOTES

In Vitro Adsorption of Phenobarbital onto Activated Charcoal

KARAMAT A. JAVAID ˣ **and BUTHAINA H. EL-MABROUK**

Received June 15, 1981, from the *Department of Pharmaceutics, Faculty of Pharmacy, Al-Fateh University, Tripoli, Libya (SPLAJ).* Accepted for publication January 29, 1982.

Abstract □ *In vitro* experiments were performed to determine the extent and duration of adsorption and desorption of phenobarbital onto and from activated charcoal in solutions of various pHs. The results of studies supported the evidence of the effectiveness of charcoal as an adsorbent. Adsorption was dependent upon the quantity of charcoal used. With amounts of charcoal ≥0.5 g, adsorption was complete within 60 min. Desorption was rapid, quantity dependent, and pH independent. The results of adsorption isotherms indicated no change in binding capacity of the drug from solutions of different pH.

Keyphrases □ Phenobarbital—*in vitro* adsorption onto activated charcoal, desorption, binding □ Adsorption, *in vitro*—phenobarbital onto activated charcoal, desorption, binding

The importance of activated charcoal cannot be overemphasized as an emergency treatment in drug poisoning. Activated charcoal given orally as a slurry can effectively adsorb and hold many drugs such as alkaloids, glycosides, and barbiturates (1). Acute barbiturate poisoning is common and it accounts for ~1500 deaths annually in the United States (2). Barbiturates are the second most frequent cause of poisoning in children (3).

Phenobarbital is one of the major barbiturates used in many products as a sedative–hypnotic and antiepileptic agent. It has a therapeutic range of 0.03–0.6 g daily in divided doses, and its potential for poisoning is great, having a fatal range of 1–10 g (4). Data collected on the use of phenobarbital in adsorption studies with activated charcoal can be useful.

A slurry of activated charcoal given 30 min after hypnotic doses of phenobarbital or glutethimide resulted in a plasma drug concentration at least 50% lower in treated than in untreated dogs, even when charcoal was allowed to pass through the entire GI tract (5). Adsorbed material is retained tenaciously throughout passage in the gut. There is a concern that part of the poison in the intestine may later be released because of less favorable pH conditions. It was found that the reduction in the amount of available poison is markedly high as compared to insignificant elution of the poison in the intestine (6). Administration of large amounts of activated charcoal is considered to be a routinely useful procedure. In view of the delayed emetic action of ipecac syrup, there is an increasing speculation that activated charcoal may be of more importance as an emergency treatment for accidental poisoning. Recent studies (7–9) have shown the importance of adsorption of different drugs onto activated charcoal.

The purpose of this study was to investigate and understand the extent of adsorption of phenobarbital sodium

0022-3549/83/0100-0082$01.00/0

difference centers around the increased prominence and number of hair follicles. Probably diffusion across the transfollicular shunt is greatly enhanced, to the point where it becomes the principal pathway. The horny layer of the epidermis is also affected by the formation of a thick coat of hair. Since the hairy mat restricts insensible perspiration, the stratum corneum associated with furry skin need not be as impermeable to water, and it is typically thinner and less well formed than when the surface is hairless. Thus, structural and compositional changes in the horny layer also provide a basis for explaining the differing hydration sensitivities. It is likely that both factors are important.

This study provides further evidence of intra- and interspecies complexities of animal skins as mass transport regulators. To a degree it demonstrates that skins covered with thick coats of hair do not behave diffusionally as hairless skins, whether of mouse or humans. Previous work (1–8) indicates a high degree of parallelism in the chemical barrier properties of hairless mouse and human skins. This study adds support for the use of hairless animals for research on percutaneous absorption, primary irritancy, topical drug delivery, *etc.*, when it is not possible or practicable to use human subjects.

REFERENCES

(1) C. R. Behl, G. L. Flynn, T. Kurihara, N. Harper, W. M. Smith, W. I. Higuchi, N. F. H. Ho, and C. L. Pierson, *J. Invest. Derm.*, **75**, 346 (1980).

(2) C. R. Behl and M. Barrett, *J. Pharm. Sci.*, **70**, 212 (1981).

(3) C. R. Behl, M. Barrett, G. L. Flynn, T. Kurihara, K. A. Walters, O. G. Gatmaitan, N. Harper, W. I. Higuchi, N. F. H. Ho, and C. L. Pierson, *ibid.*, **71**, 229 (1982).

(4) G. L. Flynn, H. H. Durrheim, and W. I. Higuchi, *ibid.*, **70**, 52 (1981).

(5) C. R. Behl, G. L. Flynn, T. Kurihara, W. Smith, O. Gatmaitan, W. I. Higuchi, N. F. H. Ho, and C. L. Pierson, *J. Invest. Derm.*, **75**, 340 (1980).

(6) G. L. Flynn, C. R. Behl, K. Walters, O. G. Gatmaitan, J. Kurihara, N. F. H. Ho, W. I. Higuchi, and C. L. Pierson, *Burns*, **8**, 47 (1981).

(7) C. R. Behl, E. E. Linn, G. L. Flynn, C. L. Pierson, W. I. Higuchi, and N. F. H. Ho, *J. Pharm. Sci.*, in press.

(8) R. B. Stroughton, in "Animal Models in Dermatology," H. Maibach, Ed., Churchill Livingstone, New York, N.Y., 1975, p. 121.

ACKNOWLEDGMENTS

This study was supported in part by Grant 5-R01GM24611 from the National Institutes of Health.

NOTES

In Vitro Adsorption of Phenobarbital onto Activated Charcoal

KARAMAT A. JAVAID ˣ **and BUTHAINA H. EL-MABROUK**

Received June 15, 1981, from the *Department of Pharmaceutics, Faculty of Pharmacy, Al-Fateh University, Tripoli, Libya (SPLAJ).* Accepted for publication January 29, 1982.

Abstract □ *In vitro* experiments were performed to determine the extent and duration of adsorption and desorption of phenobarbital onto and from activated charcoal in solutions of various pHs. The results of studies supported the evidence of the effectiveness of charcoal as an adsorbent. Adsorption was dependent upon the quantity of charcoal used. With amounts of charcoal ≥0.5 g, adsorption was complete within 60 min. Desorption was rapid, quantity dependent, and pH independent. The results of adsorption isotherms indicated no change in binding capacity of the drug from solutions of different pH.

Keyphrases □ Phenobarbital—*in vitro* adsorption onto activated charcoal, desorption, binding □ Adsorption, *in vitro*—phenobarbital onto activated charcoal, desorption, binding

The importance of activated charcoal cannot be overemphasized as an emergency treatment in drug poisoning. Activated charcoal given orally as a slurry can effectively adsorb and hold many drugs such as alkaloids, glycosides, and barbiturates (1). Acute barbiturate poisoning is common and it accounts for ~1500 deaths annually in the United States (2). Barbiturates are the second most frequent cause of poisoning in children (3).

Phenobarbital is one of the major barbiturates used in many products as a sedative–hypnotic and antiepileptic agent. It has a therapeutic range of 0.03–0.6 g daily in divided doses, and its potential for poisoning is great, having a fatal range of 1–10 g (4). Data collected on the use of phenobarbital in adsorption studies with activated charcoal can be useful.

A slurry of activated charcoal given 30 min after hypnotic doses of phenobarbital or glutethimide resulted in a plasma drug concentration at least 50% lower in treated than in untreated dogs, even when charcoal was allowed to pass through the entire GI tract (5). Adsorbed material is retained tenaciously throughout passage in the gut. There is a concern that part of the poison in the intestine may later be released because of less favorable pH conditions. It was found that the reduction in the amount of available poison is markedly high as compared to insignificant elution of the poison in the intestine (6). Administration of large amounts of activated charcoal is considered to be a routinely useful procedure. In view of the delayed emetic action of ipecac syrup, there is an increasing speculation that activated charcoal may be of more importance as an emergency treatment for accidental poisoning. Recent studies (7–9) have shown the importance of adsorption of different drugs onto activated charcoal.

The purpose of this study was to investigate and understand the extent of adsorption of phenobarbital sodium

0022-3549/83/0100-0082$01.00/0

Table I—Percent of Phenobarbital Desorbed at the End of 2 hr from Various Concentrations of Activated Charcoal [a] by Solutions of Various pH

pH	Charcoal Concentration, g			
	0.1	0.5	0.7	1.0
1.2	54.0	4.61	0.88	0.59
4.0	52.3	4.55	1.64	1.69
8.0	51.5	3.87	1.82	0.91

[a] For prior adsorption, different charcoal amounts were equilibrated for 2 hr with standard solution of phenobarbital sodium at pH 1.2.

onto activated charcoal as related to the effect of time, duration of equilibrium, extent of desorption, and the pH of the medium.

EXPERIMENTAL

Materials—Phenobarbital sodium BP[1] solutions, 1 mg/ml, were prepared with the following vehicles: simulated gastric fluid, USP, without pepsin, pH 1.2; McIlvaine's citrate–phosphate buffer, pH 4.0; phosphate buffer USP, pH 6.0; alkaline borate buffer USP, pH 8.0 and 9.6.

Analysis—Concentrations of phenobarbital calculated as phenobarbital sodium were determined by diluting the samples with alkaline borate buffer pH 9.6 and reading them on a spectrophotometer[2] at 240 nm.

Adsorption—Various amounts of activated charcoal[3] (0.1–1.0 g) were shaken for different time intervals, each with 50 ml of the standard phenobarbital sodium solution with pH values of 1.2, 4.0, 6.0, and 8.0. The suspensions were shaken at 44 rpm in a water bath at 37.5°. Samples were periodically removed, filtered through a double filter, and assayed. For adsorption isotherms, suspensions of 50 mg of charcoal were shaken with 50 ml of 0.02, 0.03, 0.05, 0.075, 0.09, and 0.1% solutions of the drug for 24 hr. Suspensions were filtered and the filtrate assayed.

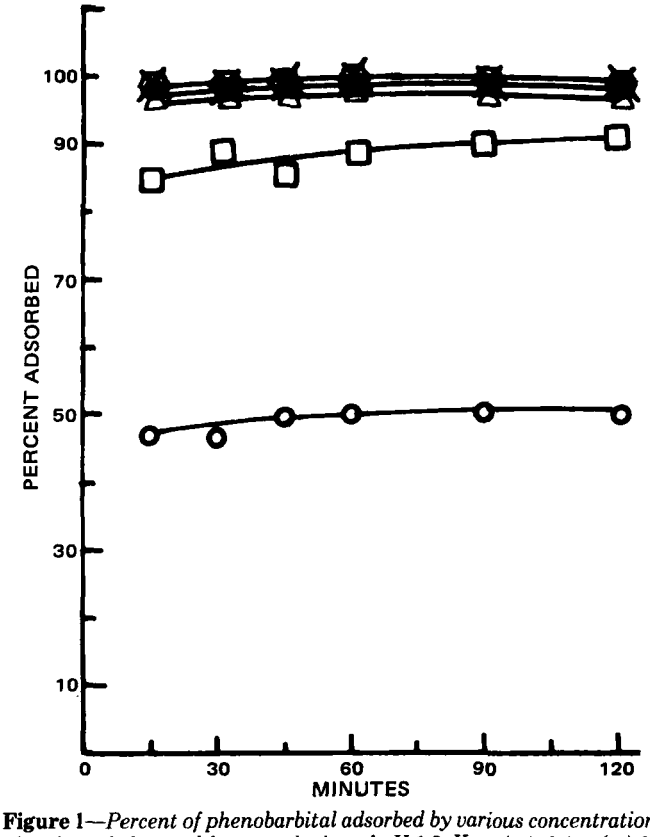

Figure 1—*Percent of phenobarbital adsorbed by various concentrations of activated charcoal from a solution of pH 1.2. Key: (○), 0.1 g; (□) 0.3 g; (△) 0.5 g; (●) 0.7 g; (×) 0.9 g; (○) 1.0 g.*

[1] Koch-Light Laboratories Ltd., Colnbrook Bucks, England.
[2] Spectrophotometer UV, Model 150-02, Shimadzu Seisakusho Ltd., Kyoto, Japan.
[3] BDH Chemicals Ltd., Poole, England.

Table II—Value of Constants of Langmuir Adsorption Isotherms at 37.5° in Solutions of Various pH

pH	Slope (n)	Adsorption Capacity $\left(\frac{1}{n}\right)$, mg	Intercept (b)	Correlation Coefficient (r)
1.2	3.42	292	0.62	1.00
4.0	3.76	265	0.65	1.00
6.0	3.86	259	0.86	1.00
8.0	3.83	261	1.17	1.00

Desorption—Various amounts of charcoal powder were equilibrated for 2 hr with the standard solution of phenobarbital sodium at pH 1.2. Two hours was selected for equilibrium during adsorption studies. This time period was found to be sufficient for adsorption to be complete. The samples were centrifuged at 2500 rpm; supernatants were aspirated and assayed. Fifty milliliters of fresh buffers without phenobarbital sodium at pH 1.2, 4.0, and 8.0 was added as an eluting medium to transfer the sediments to the flasks. The suspensions were shaken for 15, 30, 60, and 120 min. The samples were periodically removed, filtered, and assayed.

Particle Size—Average particle diameter for the activated charcoal powder used was 5.1 μm. It was determined by an air permeability device[4].

RESULTS AND DISCUSSION

Activated charcoal is a potent adsorbent that rapidly inactivates many poisons if administered before much absorption of poison has taken place. The rapid and marked effectiveness of activated charcoal *in vivo* emphasizes the potential usefulness of this antidote in the management of acute poisoning due to a rapidly absorbed chemical agent. Adsorption

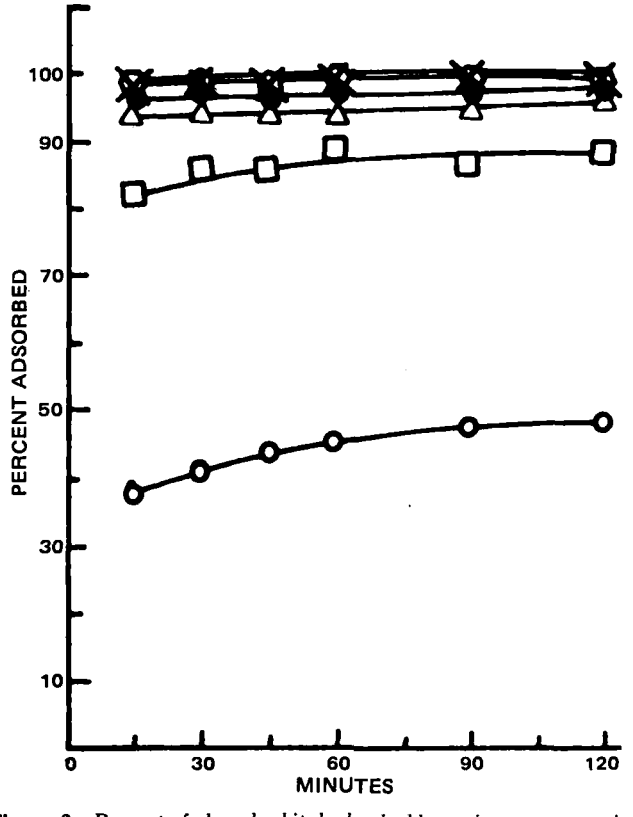

Figure 2—*Percent of phenobarbital adsorbed by various concentrations of activated charcoal from a solution of pH 4.0. Key: (○) 0.1 g; (□) 0.3 g; (△) 0.5 g; (●) 0.7 g; (×) 0.9 g; (○) 1.0 g.*

[4] Fisher-Sub-Sieve Sizer, Model 95, Fisher Scientific Co., Pittsburg, Pa.

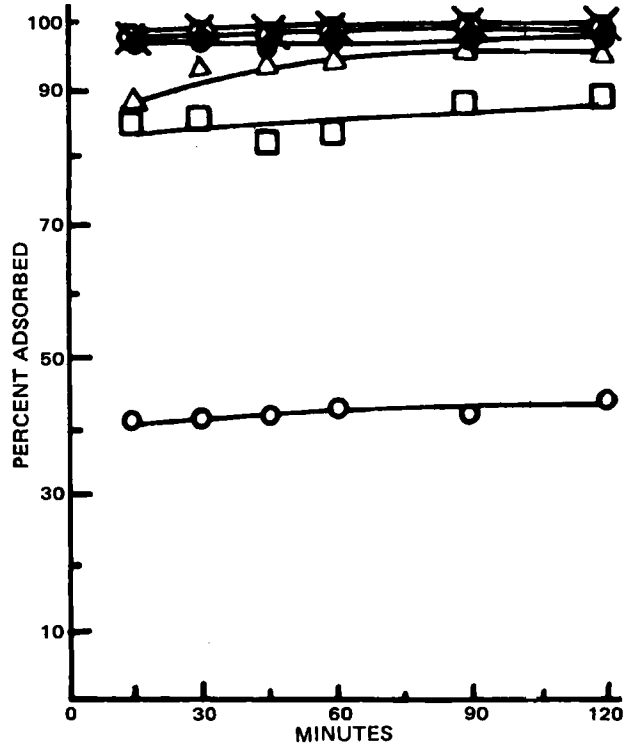

Figure 3—*Percent of phenobarbital adsorbed by various concentrations of activated charcoal from a solution of pH 6.0. Key: (○) 0.1 g; (□) 0.3 g; (△) 0.5 g; (●) 0.7 g; (×) 0.9 g; (◇) 1.0 g.*

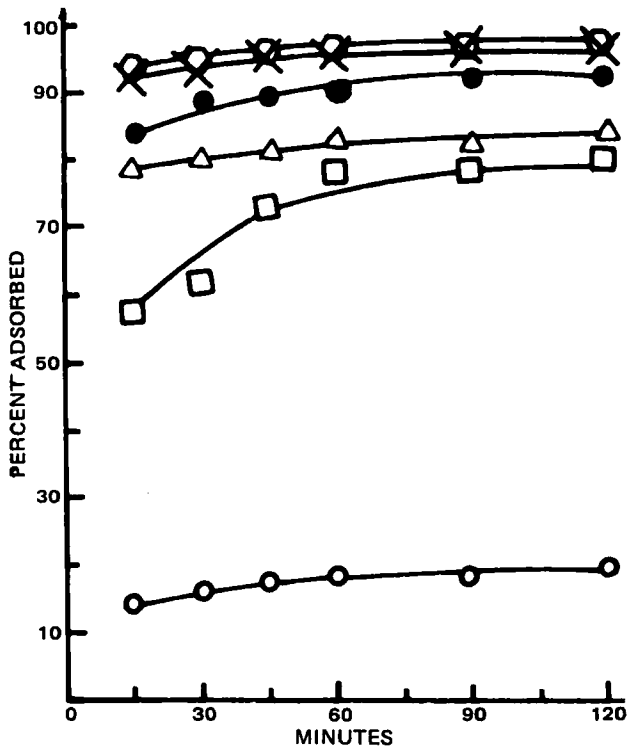

Figure 4—*Percent of phenobarbital adsorbed by various concentrations of activated charcoal from a solution of pH 8.0. Key: (○) 0.1 g; (□) 0.3 g; (△) 0.5 g; (●) 0.7 g; (×) 0.9 g; (◇) 1.0 g.*

experiments were performed to see the amounts of phenobarbital adsorbed onto activated charcoal as a function of time and hydrogen ion concentration.

Figures 1–3 show that an increase in the amount of activated charcoal resulted in higher amounts of phenobarbital adsorbed from solutions of pH 1.2, 4.0, and 6.0. A sudden rise was noted when the amount of charcoal was increased from 0.1 to 0.3 g. In solutions of pH 1.2, 4.0, and 6.0, 0.5 g of charcoal resulted in a moderate increase in the amount of drug adsorbed. As seen in Figs. 1–3, the amount of drug adsorbed by 0.5–1.0 g of charcoal is approximately the same.

As observed from Fig. 4, the amount of phenobarbital adsorbed by 0.1 g of charcoal from a solution of pH 8.0 is significantly lower than from solutions of pH 1.2, 4.0, and 6.0. Even though 0.3 g of charcoal recorded a significantly higher increase in the amount of drug adsorbed from a solution of pH 8.0, the increase was not as high as from solutions of pH 1.2, 4.0, and 6.0. For other amounts of charcoal as 0.5, 0.7, 0.9, and 1.0 g in solutions of pH 8.0, the increase was gradual and about equally distributed as far as the increment in the amount of charcoal is concerned. At pH 8.0, most of the drug exists as ionized molecules. Since adsorption onto charcoal is greater for nonionized compounds, low adsorption values obtained from a solution of pH 8.0 may be due to this reason.

It is evident that most of the phenobarbital was adsorbed onto charcoal within 60 min and adsorption was practically complete with all amounts of charcoal (except 0.1 and 0.3 g) over the pH range tested. Hpwever, the percent of phenobarbital adsorbed was dependent upon the quantity of charcoal used. The adsorption by 0.1 and 0.3 g of charcoal was not complete even at the end of 120 min, but at the 0.5-g level the adsorption was almost complete at the end of 60 min. Further increments of 0.2 g above 0.5 g did not appreciably increase the extent of adsorption in adsorbing the phenobarbital from 50 ml of standard phenobarbital sodium solution.

Desorption studies were performed in solutions of various pHs containing different amounts of charcoal to determine how much of the phenobarbital once adsorbed would be desorbed as a result of a change in the pH of the eluting medium. Table I illustrates the effect of variation of the eluting media pH on the extent of desorption at the end of 2 hr from various concentrations of charcoal. It is evident that 0.1 g of charcoal was not sufficient to hold all of the drug, and ~50% of the drug was eluted. But with 0.5 g and higher amounts of charcoal, the extent of desorption was <5%. These findings substantiate previous results (10, 11) which suggested that the charcoal–poison complex remains stable throughout the GI tract. In general, desorption from lower amounts of charcoal was essentially complete within 15 min, decreased with increasing amounts of charcoal, and was independent of pH. Therefore, it can be summarized that 0.5–0.7 g of charcoal seems to be the optimum quantity at which minimum desorption takes place. Further increments in the amount of charcoal did not significantly contribute to holding the drug particles.

Langmuir adsorption isotherms for the adsorption of phenobarbital calculated as phenobarbital sodium onto charcoal were determined from solutions of various pH. The Langmuir isotherm may simply be defined as:

$$c/(x/m) = nc + b \qquad \text{(Eq. 1)}$$

where c is the concentration of phenobarbital sodium in milligrams per milliliter at equilibrium, x is the amount of drug adsorbed in milligrams per m milligrams of charcoal. The isotherm constants n and b were determined by linear regression analysis at each pH value. Parameters presented in Table II substantiate the theory that no change in binding is indicated at different pH levels (with the numbers under the adsorption capacity column being practically the same), and that these results can possibly be construed to indicate the stability of the charcoal–drug complex throughout the physiological pH range.

REFERENCES

(1) C. H. Thienes and T. J. Haley, in "Clinical Toxicology," 5th ed., Lea and Febiger, Philadelphia, Pa., 1972, p. 252.

(2) R. E. Gosselin, H. C. Hodge, R. P. Smith, and M. N. Gleason, in "Clinical Toxicology of Commercial Products," Section III, Therapeutic Index, 4th ed., Williams and Wilkins, Baltimore, Md., 1976, p. 49.

(3) C. H. Thienes and T. J. Haley, in "Clinical Toxicology," 5th ed., Lea and Febiger, Philadelphia, Pa., 1972, p. 62.

(4) *Idem.*, p. 61

(5) R. H. Fiser, H. M. Maetz, J. J. Treuting, and W. J. Decker, *J. Pediat.*, **78**, 1045 (1971).

(6) J. M. Arena, "Poisoning," 3rd ed., Charles C Thomas, Springfield, Ill., 1976, p. 27.

(7) C. A. Bainbridge, E. L. Kelly, and W. D. Walkling, *J. Pharm. Sci.*, **66**, 480 (1977).

(8) E. M. Sellers, V. Khouw, and L. Dolman, *ibid.*, **66**, 1640 (1977).

(9) F. Ganjian, A. J. Cutie, and T. Jochsberger, *ibid.*, **69**, 352 (1980).
(10) W. J. Decker, R. A. Shpall, D. G. Corby, H. F. Combs, and C. E. Pyne, *Clin. Pharmacol. Ther.*, **10**, 710 (1969).
(11) A. L. Picchioni, *Pediat. Clin. N. Am.*, **17**, 535 (1970).

ACKNOWLEDGMENTS

The authors greatly appreciate the assistance of Mr. Asad in statistical analysis, Mr. M. Hassan for drawing the figures, and Mr. M. El-Khabouli for his help in experimentation.

Determination of Ciramadol in Plasma by Gas–Liquid Chromatography

SAMUEL F. SISENWINE ˣ, HAZEL B. KIMMEL, CESARIO O. TIO, ANN L. LIU, and HANS W. RUELIUS

Received December 14, 1981, from the *Drug Metabolism Subdivision, Wyeth Laboratories, Inc., Philadelphia, PA 19101.* Accepted for publication February 25, 1982.

Abstract □ An analytical method for determining ciramadol concentrations in plasma was developed and evaluated for its specificity, precision, linearity, and sensitivity. GLC–electron capture detection of a dipentafluorobenzoyl derivative of the drug was used for quantitation. An isomer of the drug served as an internal standard. Resulting mean ratios of the peak height of derivatized drug to that of derivatized internal standard varied with a coefficient of variation that ranged from 3.8 to 11.1%. The mean ratio was linearly related to ciramadol content (8.75–175 ng) with a correlation coefficient >0.999. The minimum quantifiable concentration was 4 ng/ml with a 2-ml specimen. An application of this method is presented.

Keyphrases □ Ciramadol—analgesics, GLC determination in plasma □ GLC—determination of ciramadol in plasma, analgesics □ Analgesics—GLC determination of ciramadol in plasma

Ciramadol [(−)*cis*-2-(α-dimethyl (I) amino-*m*-hydroxybenzyl)cyclohexanol hydrochloride] is a potent analgesic when administered to animals, and indications of its effectiveness in relieving mild to moderate pain in malignant disease and moderate to severe postoperative pain in humans have been reported (1–3). During previous metabolic disposition studies (4), it was recognized that a very sensitive assay for the drug in biological fluids would be required during preclinical studies and especially when clinical bioavailability studies were performed. Maximum concentrations in the plasma of rats given single 1-mg/kg intragastric doses of the drug were highest (105 ng/ml) at the earliest sampling time (15 min), and when studies were conducted in rhesus monkeys, maximum concentrations in plasma never exceeded 4 ng/ml after a similar dose. In the current report, an assay for ciramadol, which meets the desired requirements, is presented. It is based on the electron-capturing capability of a dipentafluorobenzoylated derivative following a GLC separation.

EXPERIMENTAL

Standards and Reagents—Ciramadol (I) and the internal standard [*trans*-2-(α-dimethylamino-*p*-hydroxybenzyl)cyclohexanol hydrochloride hemiethanolate, II] were synthesized in these laboratories[1]. Deionized water was prepared by passing distilled water through an ion-exchange system[2]. Pentafluorobenzoyl chloride and all other reagents and solvents were purchased from commercial sources.

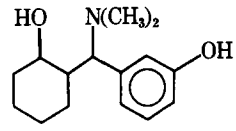

I

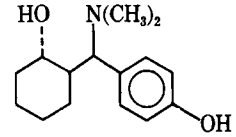

II

Pentafluorobenzoyl chloride was purified by distillation prior to use. The fraction boiling at 158–159° was collected and stored in a sealed container at 5°.

Calibration standards were prepared from a stock solution containing 1 mg of drug/ml of deionized water. Subsequently, solutions containing 0.01, 0.02, 0.05, 0.1, and 0.2 μg of drug/100 μl, or, respectively, 8.75, 17.5, 43.75, 87.5, and 175 ng of free base/100 μl were prepared. All concentrations of ciramadol in biological fluids are expressed as free base.

The concentration of the internal standard solution prepared in water was 100 ng/100 μl.

Preparation of Pentafluorobenzoyl Derivatives—One gram of ciramadol (as free base) was dissolved in 80 ml of benzene and 30 ml of pyridine. To the solution, 2.5 g of pentafluorobenzoyl chloride was added dropwise with stirring at 25° for 2 hr. The reaction mixture was washed with 100 ml each of water, 10% Na_2CO_3, water, 0.5 *N* H_2SO_4, 10% Na_2CO_3, and water. The organic layer was separated, dried over anhydrous sodium sulfate, treated with 2 g of charcoal[3], filtered, and evaporated. A pale yellow syrup was obtained. After treating again with charcoal the syrup was analyzed.

Anal.—Calc. for $C_{29}H_{21}NO_4F_{10}$: C, 54.64; H, 3.32; N, 2.20. Found: C, 54.64; H, 3.44; N, 2.27.

Compound II (200 mg) was dissolved in 16 ml of benzene and 6 ml of pyridine. To the solution, 0.5 g of pentafluorobenzoyl chloride was added dropwise with stirring at 25° for 2 hr. The reaction mixture then was washed sequentially (20-ml portions) and treated with charcoal as described above. After the solvent was removed under reduced pressure, a syrup was obtained. A pale yellow crystalline product precipitated after the syrup was dissolved in warm ethanol and cooled at 4°. The precipitate was collected, recrystallized from ethanol, and dried in air. Yield: 75 mg.

Anal.—Calc. for $C_{29}H_{21}NO_4F_{10}$: C, 54.64; H, 3.32; N, 2.20. Found: C, 54.43; H, 3.49; N, 2.65.

Mass Spectrometry—Mass spectrometric analysis of the two derivatives was performed on a mass spectrometer[4] (electron beam, 70 eV; source temperature, 200°) equipped with a data system[5]. Samples were examined by direct introduction in the electron-impact mode.

Analysis of Ciramadol in Plasma—*Extraction and Derivatization*—Standards (0.01, 0.02, 0.05, 0.1, and 0.2 μg of ciramadol) were added to a series of 16 × 125-mm culture tubes (polytef lined[6] screw cap) containing 1 ml of control (drug free) dog plasma. To each sample was added

[1] Dr. J. P. Yardley, Medicine Chemistry Section II, Wyeth Labs., Inc., Radnor, Pa.
[2] Bion Exchanger System, Pierce Chemical Co., Rockford, Ill.
[3] Norit, Fisher Scientific Co., Fair Lawn, NJ 07416.
[4] AEI-MS 902, Associated Electronic Ind., Ltd., U.K.
[5] Nova 3 Computer system with DS-50S software, Data General Corp., Southboro, Mass.
[6] Teflon, DuPont Co., Wilmington, Del.

0022-3549/83/0100-0085$01.00/0

(9) F. Ganjian, A. J. Cutie, and T. Jochsberger, *ibid.*, **69**, 352 (1980).
(10) W. J. Decker, R. A. Shpall, D. G. Corby, H. F. Combs, and C. E. Pyne, *Clin. Pharmacol. Ther.*, **10**, 710 (1969).
(11) A. L. Picchioni, *Pediat. Clin. N. Am.*, **17**, 535 (1970).

ACKNOWLEDGMENTS

The authors greatly appreciate the assistance of Mr. Asad in statistical analysis, Mr. M. Hassan for drawing the figures, and Mr. M. El-Khabouli for his help in experimentation.

Determination of Ciramadol in Plasma by Gas–Liquid Chromatography

SAMUEL F. SISENWINE ˣ, HAZEL B. KIMMEL, CESARIO O. TIO, ANN L. LIU, and HANS W. RUELIUS

Received December 14, 1981, from the *Drug Metabolism Subdivision, Wyeth Laboratories, Inc., Philadelphia, PA 19101.* Accepted for publication February 25, 1982.

Abstract □ An analytical method for determining ciramadol concentrations in plasma was developed and evaluated for its specificity, precision, linearity, and sensitivity. GLC–electron capture detection of a dipentafluorobenzoyl derivative of the drug was used for quantitation. An isomer of the drug served as an internal standard. Resulting mean ratios of the peak height of derivatized drug to that of derivatized internal standard varied with a coefficient of variation that ranged from 3.8 to 11.1%. The mean ratio was linearly related to ciramadol content (8.75–175 ng) with a correlation coefficient >0.999. The minimum quantifiable concentration was 4 ng/ml with a 2-ml specimen. An application of this method is presented.

Keyphrases □ Ciramadol—analgesics, GLC determination in plasma □ GLC—determination of ciramadol in plasma, analgesics □ Analgesics—GLC determination of ciramadol in plasma

Ciramadol [(−)*cis*-2-(α-dimethyl (I) amino-*m*-hydroxybenzyl)cyclohexanol hydrochloride] is a potent analgesic when administered to animals, and indications of its effectiveness in relieving mild to moderate pain in malignant disease and moderate to severe postoperative pain in humans have been reported (1–3). During previous metabolic disposition studies (4), it was recognized that a very sensitive assay for the drug in biological fluids would be required during preclinical studies and especially when clinical bioavailability studies were performed. Maximum concentrations in the plasma of rats given single 1-mg/kg intragastric doses of the drug were highest (105 ng/ml) at the earliest sampling time (15 min), and when studies were conducted in rhesus monkeys, maximum concentrations in plasma never exceeded 4 ng/ml after a similar dose. In the current report, an assay for ciramadol, which meets the desired requirements, is presented. It is based on the electron-capturing capability of a dipentafluorobenzoylated derivative following a GLC separation.

EXPERIMENTAL

Standards and Reagents—Ciramadol (I) and the internal standard [*trans*-2-(α-dimethylamino-*p*-hydroxybenzyl)cyclohexanol hydrochloride hemiethanolate, II] were synthesized in these laboratories[1]. Deionized water was prepared by passing distilled water through an ion-exchange system[2]. Pentafluorobenzoyl chloride and all other reagents and solvents were purchased from commercial sources.

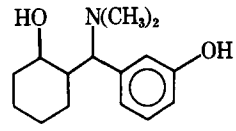

I

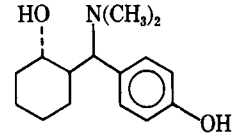

II

Pentafluorobenzoyl chloride was purified by distillation prior to use. The fraction boiling at 158–159° was collected and stored in a sealed container at 5°.

Calibration standards were prepared from a stock solution containing 1 mg of drug/ml of deionized water. Subsequently, solutions containing 0.01, 0.02, 0.05, 0.1, and 0.2 μg of drug/100 μl, or, respectively, 8.75, 17.5, 43.75, 87.5, and 175 ng of free base/100 μl were prepared. All concentrations of ciramadol in biological fluids are expressed as free base.

The concentration of the internal standard solution prepared in water was 100 ng/100 μl.

Preparation of Pentafluorobenzoyl Derivatives—One gram of ciramadol (as free base) was dissolved in 80 ml of benzene and 30 ml of pyridine. To the solution, 2.5 g of pentafluorobenzoyl chloride was added dropwise with stirring at 25° for 2 hr. The reaction mixture was washed with 100 ml each of water, 10% Na_2CO_3, water, 0.5 *N* H_2SO_4, 10% Na_2CO_3, and water. The organic layer was separated, dried over anhydrous sodium sulfate, treated with 2 g of charcoal[3], filtered, and evaporated. A pale yellow syrup was obtained. After treating again with charcoal the syrup was analyzed.

Anal.—Calc. for $C_{29}H_{21}NO_4F_{10}$: C, 54.64; H, 3.32; N, 2.20. Found: C, 54.64; H, 3.44; N, 2.27.

Compound II (200 mg) was dissolved in 16 ml of benzene and 6 ml of pyridine. To the solution, 0.5 g of pentafluorobenzoyl chloride was added dropwise with stirring at 25° for 2 hr. The reaction mixture then was washed sequentially (20-ml portions) and treated with charcoal as described above. After the solvent was removed under reduced pressure, a syrup was obtained. A pale yellow crystalline product precipitated after the syrup was dissolved in warm ethanol and cooled at 4°. The precipitate was collected, recrystallized from ethanol, and dried in air. Yield: 75 mg.

Anal.—Calc. for $C_{29}H_{21}NO_4F_{10}$: C, 54.64; H, 3.32; N, 2.20. Found: C, 54.43; H, 3.49; N, 2.65.

Mass Spectrometry—Mass spectrometric analysis of the two derivatives was performed on a mass spectrometer[4] (electron beam, 70 eV; source temperature, 200°) equipped with a data system[5]. Samples were examined by direct introduction in the electron-impact mode.

Analysis of Ciramadol in Plasma—*Extraction and Derivatization*—Standards (0.01, 0.02, 0.05, 0.1, and 0.2 μg of ciramadol) were added to a series of 16 × 125-mm culture tubes (polytef lined[6] screw cap) containing 1 ml of control (drug free) dog plasma. To each sample was added

[1] Dr. J. P. Yardley, Medicine Chemistry Section II, Wyeth Labs., Inc., Radnor, Pa.
[2] Bion Exchanger System, Pierce Chemical Co., Rockford, Ill.
[3] Norit, Fisher Scientific Co., Fair Lawn, NJ 07416.
[4] AEI-MS 902, Associated Electronic Ind., Ltd., U.K.
[5] Nova 3 Computer system with DS-50S software, Data General Corp., Southboro, Mass.
[6] Teflon, DuPont Co., Wilmington, Del.

0022-3549/83/0100-0085$01.00/0

Table I—Precision of the Ciramadol Assay

Concentration[a], Ciramadol ng/ml			Intra-assay Replications of Standards			
Hydrochloride Salt	Free Base	*N*	Mean Ratio ± *SD* I/II	*CV*, %	Slope[b]	Correlation[b] Coefficient
Experiment A						
10	8.75	5	0.160 ± 0.006	3.8		
20	17.5	5	0.307 ± 0.025	8.1		
50	43.75	5	0.805 ± 0.051	6.3		
100	87.5	5	1.544 ± 0.144	9.3		
200	175	5	3.273 ± 0.215	6.6		
					0.0187	0.9996
Experiment B						
10	8.75	5	0.126 ± 0.014	11.1		
20	17.5	4	0.232 ± 0.021	9.1		
50	43.75	5	0.610 ± 0.037	6.1		
100	87.5	5	1.151 ± 0.096	8.3		
200	175	5	2.433 ± 0.179	7.4		
					0.0138	0.9995
Experiment C						
10	8.75	5	0.153 ± 0.015	9.8		
20	17.5	5	0.294 ± 0.022	7.5		
50	43.75	5	0.757 ± 0.067	8.9		
100	87.5	5	1.522 ± 0.109	7.2		
200	175	5	2.988 ± 0.180	6.0		
					0.0172	1.0000

[a] Internal standard (100 ng) was added to a 1-ml sample of control dog plasma. [b] Values were obtained by linear regression analysis of known concentrations of ciramadol (as free base) *versus* mean ratios of peak heights.

100 ng of the internal standard in 0.10 ml of water, 1 ml of 5 *N* NH_4OH, and 5 ml of ether. Each sample was mixed thoroughly and centrifuged, and 4 ml of the ether extract was transferred to another tube. The aqueous phase was extracted once more with 5 ml of ether, and the ether phase was combined with the original extract. One ml of 5 *N* acetic acid was added to the combined ether extracts, and the contents were mixed thoroughly and centrifuged. The ether phase was aspirated, and the aqueous extract was washed with 5 ml of ethyl acetate. After aspirating the ethyl acetate wash, any remaining ethyl acetate was removed by heating the aqueous extract in a water bath at 60° for 5 min under flowing nitrogen. Sodium chloride (800 mg), 1 ml of 5 *N* NH_4OH, and 1 ml of toluene were added to each sample. The contents were mixed and centrifuged, and then 0.7 ml of the toluene extract was transferred to a 12 × 75-mm test tube and reacted with 0.10 ml of pyridine and 0.05 ml of pentafluorobenzoyl chloride at 25° for 30 min with shaking after 15 min. The reaction tube containing the mixture was washed with 1 ml of 10% Na_2CO_3, 1 ml of 0.2 *N* H_2SO_4, 1 ml of 10% Na_2CO_3, and 1 ml of water, successively, and refrigerated until analysis by GLC.

GLC Conditions—GLC analyses were performed with a gas–liquid chromatograph[7] equipped with a 1.8 m × 2-mm glass column containing 2% OV-101 Chromosorb W-HP (80/100 mesh)[8]. The column was maintained at 230°, the injection port at 260°, and the electron detector (nickel 63) at 340°. The carrier gas was ultra-high pure nitrogen. The column was pretreated by injecting 4 μl of a toluene–lecithin solution (1 mg/ml).

Calculations—The ratio of the peak heights for derivatized ciramadol to derivatized internal standard at each concentration of the drug in plasma was determined. The line of best fit relating the ratio of peak heights to ciramadol concentration was calculated by a linear regression analysis.

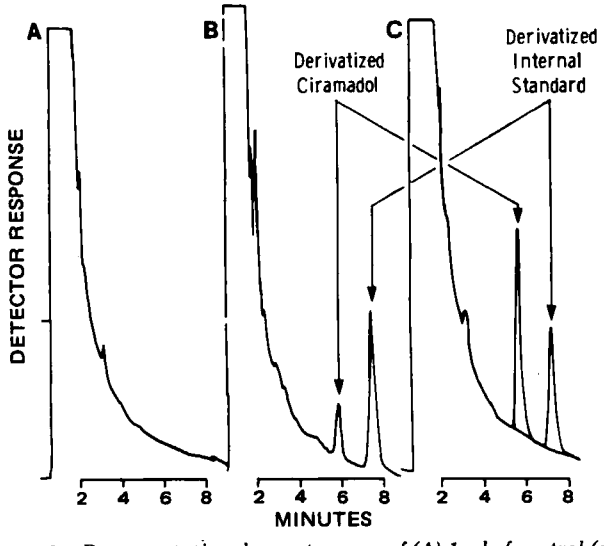

Figure 1—*Representative chromatograms of (A) 1 ml of control (drug free) plasma; (B) plasma sample (1 ml) from a dog given ciramadol; (C) 100 ng of ciramadol and 100 ng of internal standard added to 1 ml of control dog plasma.*

RESULTS

Mass Spectrometry—A mass ion at *m/z* 637 in the mass spectrum of derivatized ciramadol demonstrated that a dipentafluorobenzoyl derivative, which is consistent with the elemental analysis, occurred. The most predominant fragment was observed at *m/z* 344 and represented

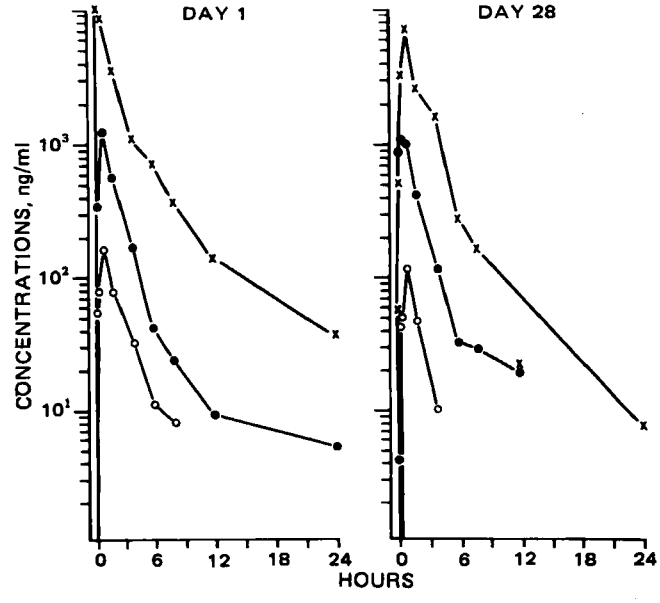

Figure 2—*Mean concentrations of ciramadol in plasma of dogs on day 1 and day 28 following the administration of daily 2- (○), 12- (●), and 72-mg/kg (×) oral doses of ciramadol.*

[7] Varian 3700, Varian Instrument Group, Palo Alto, Calif.

[8] Supelco, Inc., Bellefonte, Pa.

the facile cleavage of the derivative to the fragment $(CH_3)_2\dot{N}{=}CH{-}C_6H_4{-}OCOC_6F_5$. A fragment observed at m/z 195 indicated the loss of a pentafluorobenzoyl moiety. The mass spectrum of the derivatized internal standard was similar.

GLC—The retention time of the derivatized drug and internal standard was 5.8 and 7.6 min, respectively. A representative chromatogram is shown in Fig. 1. No interfering peaks were observed in control (drug free) plasma.

The mean ratio of the peak height for derivatized ciramadol to derivatized internal standard and its coefficient of variation at each concentration of drug added to control plasma (three experiments) is shown in Table I. The coefficient of variation for each mean ratio ranged from 3.8 to 11.1%. Standard curves relating ciramadol concentration to peak height ratio were linear with correlation coefficients ranging from 0.9995 to 1.0000. With a 2-ml plasma sample, the minimum quantifiable concentration was 4 ng/ml (as free base).

DISCUSSION

The results of the present study demonstrate that the specificity, linearity, precision, and sensitivity of the GLC assay for ciramadol is satisfactory for measuring the drug in plasma in concentrations >4 ng/ml. This method has been applied to samples obtained in studies on ciramadol disposition in rhesus monkeys, dogs, and humans. Urine specimens have also been analyzed by this procedure. An example of the application of the assay, which demonstrates its utility in a multiple dose study in dogs, is presented in Fig. 2. The assay permitted the observation that multiple dosing did not affect the metabolic disposition of ciramadol in dogs. No peaks interfered with the detection of drug or internal standard in samples obtained from other investigated species.

Other methods of analysis have been attempted but were not pursued for various reasons. These included GLC and HPLC analysis of underivatized ciramadol as well as other nonfluorinated derivatives of ciramadol. None proved to be as sensitive as the described procedure.

REFERENCES

(1) J. P. Yardley, H. Fletcher III, and P. B. Russell, *Experientia*, **34**, 1124 (1978).

(2) A. D. Cochrane, R. Bell, J. R. Sullivan, and J. Shaw, *Med. J. Aust.*, **2**, 501 (1979).

(3) F. Camu, *Eur. J. Clin. Pharmacol.*, **19**, 259 (1981).

(4) S. F. Sisenwine, C. O. Tio, and H. W. Ruelius, *Drug Metab. Dispos.*, **10**, 161 (1982).

ACKNOWLEDGMENTS

The authors wish to thank Mrs. G. White for the GLC analysis and Mr. P. Berger, Mrs. M. Burka, Mrs. H. Ruthenberg, and Mr. J. Politowski for their technical assistance.

GLC–Mass Fragmentographic Determination of Mannitol and Sorbitol in Plasma

TERUYOSHI MARUNAKA ˣ, EIJI MATSUSHIMA, YUKIHIKO UMENO, and YOSHINORI MINAMI

Received September 18, 1981, from the *Research Laboratory, Taiho Pharmaceutical Co., Ltd., Kawauchi-cho, Tokushima, 771-01, Japan.* Accepted for publication February 25, 1982.

Abstract □ A GLC–mass fragmentographic method was developed for the simultaneous determination of mannitol and sorbitol as their *n*-butyldiboronate derivatives in plasma. The plasma sample was deproteinized, and the subsequent supernatant was concentrated to dryness; the resulting residue was then dissolved in pyridine containing *n*-butylboronic acid to allow derivation. An aliquot of this solution was injected into the gas chromatograph–mass spectrometer and analyzed by a selected-ion monitoring method using galactitol as the internal standard. Detection was limited to 20 ng/0.1 ml of plasma for both mannitol and sorbitol. A rapid, precise, and sensitive assay for the determination of mannitol and sorbitol in plasma was established.

Keyphrases □ Mannitol—GLC–mass fragmentographic analysis in plasma □ Sorbitol—GLC–mass fragmentographic analysis in plasma □ GLC–mass fragmentography—analysis, mannitol and sorbitol in plasma □ Hexiol—mannitol and sorbitol in plasma, GLC–mass fragmentographic analysis

Mannitol and sorbitol (glucitol) have been used as artificial sweeteners in pharmaceutical preparations.

Many methods employing GLC with a flame ionization detector have been reported for the determination of common hexitols. Authentic samples of mannitol and sorbitol have been analyzed by this GLC method in studying the acetyl (1–7), trifluoroacetyl (8, 9), trimethylsilyl (10), phenyldiboronate (11), and *n*-butyldiboronate derivatives (12). However, the mannitol and sorbitol contents were determined (13) in pharmaceuticals as their *n*-butyldiboronate derivatives. Mannitol, sorbitol, and other polyols were assayed (14) in human plasma or cerebrospinal fluid as their acetyl derivatives. Furthermore, mannitol was measured (15) in body fluids as an *n*-butyldiboronate derivative.

However, these GLC methods indicate several problems in determining mannitol and sorbitol in plasma samples, such as poor sensitivity or the influence of glucose pooled in plasma. Thus, a GLC–mass fragmentographic determination of mannitol and sorbitol in plasma was examined, and a rapid, precise, and sensitive analytical method for their assay was established. The present method was also found applicable to other human biological fluids.

EXPERIMENTAL

Materials—Mannitol[1], sorbitol[1], galactitol[1] (dulcitol), zinc sulfate[1], barium hydroxide[1], and other chemicals used were obtained commercially. *n*-Butylboronic acid[2] and pyridine[3] were derivating agents for *n*-butyldiboronate formation.

GLC–Mass Fragmentographic Conditions—A mass spectrometer[4] with an electron-impact ion source connected to a gas chromatograph[5] was used.

The coiled glass column (1 m × 2-mm i.d.) of the gas chromatograph was packed with 3% OV-17 on Chromosorb W-AW, 80–100 mesh[6] and conditioned at 280° for 24 hr. The temperatures of the injector, column,

[1] Wako Pure Chemical Co., Osaka, Japan.
[2] Aldrich Chemical Co., Milwaukee, Wis.
[3] Pierce Chemical Co., Rockford, Ill.
[4] Model JMS-D 300, JEOL, Tokyo, Japan.
[5] Model JGC-20kP, JEOL, Tokyo, Japan.
[6] Gaschro Kogyo Co., Tokyo, Japan.

0022-3549/83/0100-0087$01.00/0

the facile cleavage of the derivative to the fragment $(CH_3)_2\dot{N}{=}CH{-}C_6H_4{-}OCOC_6F_5$. A fragment observed at m/z 195 indicated the loss of a pentafluorobenzoyl moiety. The mass spectrum of the derivatized internal standard was similar.

GLC—The retention time of the derivatized drug and internal standard was 5.8 and 7.6 min, respectively. A representative chromatogram is shown in Fig. 1. No interfering peaks were observed in control (drug free) plasma.

The mean ratio of the peak height for derivatized ciramadol to derivatized internal standard and its coefficient of variation at each concentration of drug added to control plasma (three experiments) is shown in Table I. The coefficient of variation for each mean ratio ranged from 3.8 to 11.1%. Standard curves relating ciramadol concentration to peak height ratio were linear with correlation coefficients ranging from 0.9995 to 1.0000. With a 2-ml plasma sample, the minimum quantifiable concentration was 4 ng/ml (as free base).

DISCUSSION

The results of the present study demonstrate that the specificity, linearity, precision, and sensitivity of the GLC assay for ciramadol is satisfactory for measuring the drug in plasma in concentrations >4 ng/ml. This method has been applied to samples obtained in studies on ciramadol disposition in rhesus monkeys, dogs, and humans. Urine specimens have also been analyzed by this procedure. An example of the application of the assay, which demonstrates its utility in a multiple dose study in dogs, is presented in Fig. 2. The assay permitted the observation that multiple dosing did not affect the metabolic disposition of ciramadol in dogs. No peaks interfered with the detection of drug or internal standard in samples obtained from other investigated species.

Other methods of analysis have been attempted but were not pursued for various reasons. These included GLC and HPLC analysis of underivatized ciramadol as well as other nonfluorinated derivatives of ciramadol. None proved to be as sensitive as the described procedure.

REFERENCES

(1) J. P. Yardley, H. Fletcher III, and P. B. Russell, *Experientia*, **34**, 1124 (1978).

(2) A. D. Cochrane, R. Bell, J. R. Sullivan, and J. Shaw, *Med. J. Aust.*, **2**, 501 (1979).

(3) F. Camu, *Eur. J. Clin. Pharmacol.*, **19**, 259 (1981).

(4) S. F. Sisenwine, C. O. Tio, and H. W. Ruelius, *Drug Metab. Dispos.*, **10**, 161 (1982).

ACKNOWLEDGMENTS

The authors wish to thank Mrs. G. White for the GLC analysis and Mr. P. Berger, Mrs. M. Burka, Mrs. H. Ruthenberg, and Mr. J. Politowski for their technical assistance.

GLC–Mass Fragmentographic Determination of Mannitol and Sorbitol in Plasma

TERUYOSHI MARUNAKA ˣ, EIJI MATSUSHIMA, YUKIHIKO UMENO, and YOSHINORI MINAMI

Received September 18, 1981, from the *Research Laboratory, Taiho Pharmaceutical Co., Ltd., Kawauchi-cho, Tokushima, 771-01, Japan.* Accepted for publication February 25, 1982.

Abstract □ A GLC–mass fragmentographic method was developed for the simultaneous determination of mannitol and sorbitol as their *n*-butyldiboronate derivatives in plasma. The plasma sample was deproteinized, and the subsequent supernatant was concentrated to dryness; the resulting residue was then dissolved in pyridine containing *n*-butylboronic acid to allow derivation. An aliquot of this solution was injected into the gas chromatograph–mass spectrometer and analyzed by a selected-ion monitoring method using galactitol as the internal standard. Detection was limited to 20 ng/0.1 ml of plasma for both mannitol and sorbitol. A rapid, precise, and sensitive assay for the determination of mannitol and sorbitol in plasma was established.

Keyphrases □ Mannitol—GLC–mass fragmentographic analysis in plasma □ Sorbitol—GLC–mass fragmentographic analysis in plasma □ GLC–mass fragmentography—analysis, mannitol and sorbitol in plasma □ Hexiol—mannitol and sorbitol in plasma, GLC–mass fragmentographic analysis

Mannitol and sorbitol (glucitol) have been used as artificial sweeteners in pharmaceutical preparations.

Many methods employing GLC with a flame ionization detector have been reported for the determination of common hexitols. Authentic samples of mannitol and sorbitol have been analyzed by this GLC method in studying the acetyl (1–7), trifluoroacetyl (8, 9), trimethylsilyl (10), phenyldiboronate (11), and *n*-butyldiboronate derivatives (12). However, the mannitol and sorbitol contents were determined (13) in pharmaceuticals as their *n*-butyldiboronate derivatives. Mannitol, sorbitol, and other polyols were assayed (14) in human plasma or cerebrospinal fluid as their acetyl derivatives. Furthermore, mannitol was measured (15) in body fluids as an *n*-butyldiboronate derivative.

However, these GLC methods indicate several problems in determining mannitol and sorbitol in plasma samples, such as poor sensitivity or the influence of glucose pooled in plasma. Thus, a GLC–mass fragmentographic determination of mannitol and sorbitol in plasma was examined, and a rapid, precise, and sensitive analytical method for their assay was established. The present method was also found applicable to other human biological fluids.

EXPERIMENTAL

Materials—Mannitol[1], sorbitol[1], galactitol[1] (dulcitol), zinc sulfate[1], barium hydroxide[1], and other chemicals used were obtained commercially. *n*-Butylboronic acid[2] and pyridine[3] were derivating agents for *n*-butyldiboronate formation.

GLC–Mass Fragmentographic Conditions—A mass spectrometer[4] with an electron-impact ion source connected to a gas chromatograph[5] was used.

The coiled glass column (1 m × 2-mm i.d.) of the gas chromatograph was packed with 3% OV-17 on Chromosorb W-AW, 80–100 mesh[6] and conditioned at 280° for 24 hr. The temperatures of the injector, column,

[1] Wako Pure Chemical Co., Osaka, Japan.
[2] Aldrich Chemical Co., Milwaukee, Wis.
[3] Pierce Chemical Co., Rockford, Ill.
[4] Model JMS-D 300, JEOL, Tokyo, Japan.
[5] Model JGC-20kP, JEOL, Tokyo, Japan.
[6] Gaschro Kogyo Co., Tokyo, Japan.

0022-3549/83/0100-0087$01.00/0

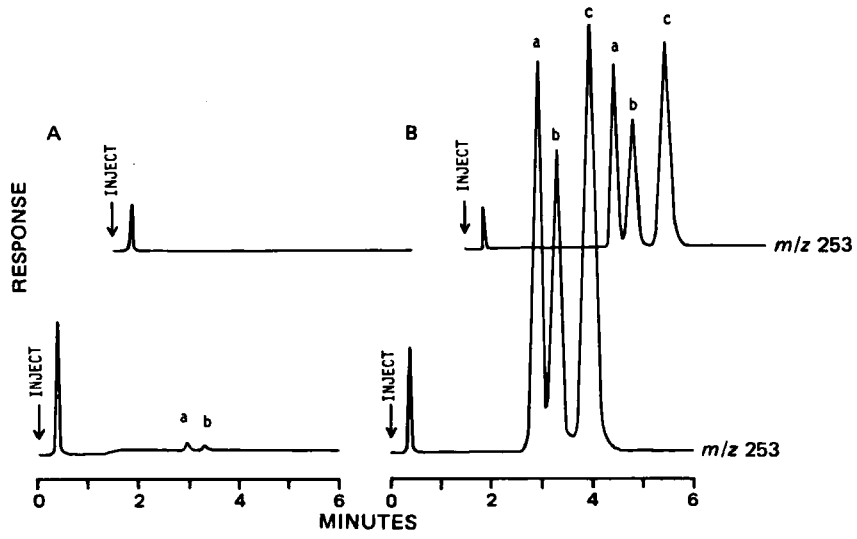

Figure 1—*GLC–mass fragmentograms of human control plasma (A) and human plasma prepared following addition of authentic samples at 500 ng/0.1 ml for each compound (B). Results are for the n-butyldiboronate derivatives and are recorded under two different attenuators. Key: (a) mannitol; (b) sorbitol; and (c) galactitol (internal standard).*

and ion source were 280, 270, and 250°, respectively. Helium was used as the carrier gas at a flow rate of 30 ml/min.

For mass fragmentography the mass spectrometer was set at the following conditions: ionization energy, 70 eV; ionization current, 300 μA; accelerating voltage, 3.0 kV; and ion multiplier voltage, 1.2–1.4 kV. The peak of *m/z* 253 for each *n*-butyldiboronate derivative of mannitol, sorbitol, and the internal standard galactitol was selected for mass fragmentographic analysis. The chromatograms were recorded under four different attenuators (1, 2, 5, and 10×10^2).

The mass spectra of the *n*-butyldiboronate derivatives of mannitol, sorbitol, and galactitol were measured under the same GLC–MS conditions.

Analytical Procedure—Blood samples were collected in heparinized containers and centrifuged to separate the plasma. The plasma then was frozen until analysis.

The plasma (0.1 ml) was diluted with 1.0 ml of 0.13 *M* $ZnSO_4$ and 0.1 ml of aqueous solution containing 100 ng of galactitol (internal standard) and mixed well. To this suspension 1.0 ml of 0.125 *M* $Ba(OH)_2$ was then added, mixed again, and centrifuged at 2000×*g* for 15 min to remove the precipitates. The supernatant was concentrated to dryness under nitrogen gas at 50° or in a freezing desiccator. The residue was dried thoroughly over phosphorus pentoxide under reduced pressure and subjected to *n*-butyldiboronate derivation at room temperature for a few minutes by the addition of ~10–15 mg of *n*-butylboronic acid and 100 μl of pyridine. Analyses by GLC–mass fragmentography were carried out on 1–3-μl samples of the resultant solution.

Calibration Curves—Calibration curves were prepared by adding known amounts of mannitol and sorbitol to plasma and then assaying the mixture by the same extraction procedure.

The calibration curves for the determination of mannitol and sorbitol by GLC–mass fragmentography were obtained by plotting the ratio of the peak heights of the respective *n*-butyldiboronate derivatives to that of the *n*-butyldiboronate derivatives of the internal standard, galactitol, against the concentration of each compound. These calibration curves were linear.

Table I—Recoveries of Mannitol and Sorbitol from Human Plasma

Drug Added, ng/0.1 ml	Recovery from Plasma[a], %	
	Mannitol	Sorbitol
50,000	93.4	93.0
10,000	92.8	93.1
5,000	93.4	92.9
1,000	92.7	93.4
500	93.4	93.2
100	93.5	93.1
50	92.9	92.9
Mean ± *SD*	93.1 ± 0.3	93.1 ± 0.2

[a] Each value is the mean of three determinations.

RESULTS AND DISCUSSION

To obtain suitable derivatives of mannitol and sorbitol for GLC separation with a flame ionization detector, various derivation procedures were examined on the basis of previous reports (1–15). The silylation procedure enabled rapid progress, but this method did not provide a good chromatographic separation. Although the acetylation procedures gave a suitable chromatographic separation, it was somewhat time consuming. The *n*-butyldiboronate derivation procedure, however, was completed almost immediately, gave excellent chromatographic separation, and was capable of providing quantitative results as reported previously (12, 13, 15). Consequently, the derivation procedure of *n*-butyldiboronate was used in the present experiments.

Since the *n*-butyldiboronate derivatives of mannitol and sorbitol are poorly separated from those of glucose and fructose on a gas-liquid chromatograph, two methods for removing glucose and fructose from plasma were examined (12, 15). One method involved a complicated procedure by transforming the glucose and fructose to their phosphate derivatives (14); however, the excess phosphoric acid hindered the formation of the *n*-butyldiboronate derivative of mannitol and sorbitol. Another method using hydrogenation of glucose and fructose with sodium borohydride (15) or sodium amalgam converted glucose to sorbitol, while fructose produced equal amounts of mannitol and sorbitol. As these methods were not suitable to remove the glucose and fructose, these two sugars were not removed from the plasma samples.

Plasma samples containing glucose and fructose were deproteinized with zinc sulfate followed by the addition of barium hydroxide to remove the surplus zinc sulfate. The supernatant obtained by centrifugation without removing glucose and fructose was dried and subjected to the *n*-butyldiboronate derivation with *n*-butylboronic acid and pyridine. An aliquot of the resultant solution was then injected into the gas chromatograph–mass spectrometer.

Galactitol, a hexitol, was chosen as the internal standard for the simultaneous determination of mannitol and sorbitol by a selected-ion detection technique. This internal standard can also form an *n*-butyl-

Table II—Changes in the Concentrations of the *n*-Butyldiboronate Derivatives of Mannitol and Sorbitol Prepared from Plasma at Various Conditions

Conditions	Concentration Changed[a], μg/ml	
	Mannitol	Sorbitol
Control	5.031	5.101
Room temperature, 12 hr	5.032	5.098
Room temperature, 24 hr	5.001	5.073
Room temperature, 3 days	4.980	5.050
Room temperature, 7 days	4.955	5.025
5°, 12 hr	5.033	5.110
5°, 24 hr	5.005	5.095
5°, 3 day	5.000	5.060
5°, 7 day	4.998	5.056

[a] Average of three determinations.

Table III—Mannitol and Sorbitol Pooled in the Plasma of Healthy Males

Subject	Concentration in Plasma: Mannitol, μg/ml (nmole/ml)	Concentration in Plasma: Sorbitol, μg/ml (nmole/ml)
A	1.385 (7.60)	1.231 (6.76)
B	1.096 (6.02)	1.030 (5.65)
C	0.741 (4.07)	0.814 (4.47)
D	0.872 (4.79)	0.902 (4.95)
E	0.793 (4.35)	0.961 (5.27)
F	0.720 (3.95)	0.788 (4.33)
G	1.055 (5.79)	1.019 (5.59)
H	1.098 (6.02)	1.159 (6.36)
I	0.546 (3.00)	0.729 (4.00)
J	0.614 (3.37)	0.596 (3.27)
Mean ± *SD*	0.892 ± 0.248 (4.90 ± 1.61)	0.923 ± 0.186 (5.06 ± 1.01)

diboronate derivative in the same way as mannitol and sorbitol (12), and the mass spectrum of this derivative is similar to that of the mannitol or sorbitol derivative. The mass fragment ion detected for GLC–mass fragmentography was the *m/z* 253 ion $[C_4H_5O_4B_2(C_4H_9)_2]^+$, since no influence of glucose, fructose, or other plasma constituents could be observed. This *m/z* 253 ion is a characteristic fragment ion formed from the molecular ion, *m/z* 380 $[C_6H_8O_6B_3(C_4H_9)_3]^+$, of each compound by loss of $C_2H_3O_2BC_4H_9$ and is not observed in the mass spectra of glucose and fructose. The GLC–mass fragmentography monitoring molecular ions or base peaks, *m/z* 127 $[C_2H_3O_2BC_4H_9]^+$, showed poor sensitivity and was mainly affected by glucose in certain samples.

To overcome the difficulties in the determination of samples containing high concentrations of mannitol and sorbitol, the ion multiplier voltage of the mass spectrometer was run at ranges from 1.2 to 1.4 kV, or the reactive solution was diluted. On the other hand, the method of simultaneous detection by a combination of GLC–mass fragmentography and GLC–mass spectrometry for total ion monitoring could not be adopted, since the latter method provided poor sensitivity, as was also the case for the GLC method with a flame ionization detector.

Known amounts of mannitol and sorbitol were added to human plasma, and the samples were analyzed. The chromatogram by GLC–mass fragmentography of the *n*-butyldiboronate derivatives of mannitol, sorbitol, and the internal standard, galactitol, prepared from human plasma following addition of authentic samples at 500 ng/0.1 ml for each compound and the chromatogram of the extract of human plasma control are shown in Fig. 1. The retention times of mannitol, sorbitol, and galactitol as their *n*-butyldiboronate derivatives were 3.0, 3.3, and 4.0 min, respectively, and the time required for the assay was ~5.0 min. As summarized in Table I, the recoveries from plasma were 93.1 ± 1.3% for mannitol and 93.2 ± 1.4% for sorbitol.

The detection limit for both mannitol and sorbitol using this GLC–mass fragmentographic method was 20 ng/0.1 ml for plasma. The reproducibility of this method was ±1.7–2.3%.

In addition, the following experiment was conducted. The *n*-butyldiboronate derivatives of mannitol, sorbitol, and galactitol prepared from human plasma were examined at room temperature and 5° under nitrogen gas for stability. As shown in Table II, it was found that no significant difference between the concentrations of the hexitol derivatives in the control and test samples could be observed over a period of several days.

The present method was also applied to other human biological fluids (*e.g.*, urine, cerebrospinal fluid, ascites fluid, bile, or lymph). The results obtained for the GLC–mass fragmentographic separations, recoveries, and sensitivities were in good agreement with those obtained with plasma. This method may also find application in the biological fluids of animals.

Table III shows the results obtained by the present GLC–mass fragmentography for the concentrations of mannitol and sorbitol present in the plasma of 10 healthy males. The quantitative results are the scope of this study.

The present method utilizing GLC–mass fragmentography for the simultaneous determination of mannitol and sorbitol in plasma is rapid and precise and has higher sensitivity than the GLC method with a flame ionization detector (1–15). Furthermore, small amounts of samples (0.1 ml) can be assayed.

Thus, this method should be useful or helpful for clinical profiling of various patients (*e.g.*, uremic, diabetic, or neurological) and for clinicopharmacological studies on therapy with mannitol, sorbitol, or mannitol plus fructose, which is an osmotherapeutic agent for treating increased intracranial pressure (16, 17) and urinary disorders (18).

REFERENCES

(1) J. A. Hause, J. A. Hubicki, and G. G. Hazen, *Anal. Chem.*, **34**, 1567 (1962).

(2) J. S. Sawardeker, J. H. Sloneker, and A. Jeanes, *ibid.*, **37**, 1602 (1965).

(3) D. H. Shaw and G. W. Moss, *J. Chromatogr.*, **41**, 350 (1969).

(4) L. J. Griggs, A. Post, E. R. White, J. A. Finkelstein, W. E. Moeckel, K. G. Holden, J. E. Zarembo, and J. A. Weisbach, *Anal. Biochem.*, **43**, 369 (1971).

(5) G. Manius, F. P. Mahn, V. S. Venturella, and B. Z. Senkowski, *J. Pharm. Sci.*, **61**, 1831 (1972).

(6) I. M. Morrison, *J. Chromatogr.*, **108**, 361 (1975).

(7) W. H. Porter, *Anal. Biochem.*, **63**, 27 (1975).

(8) J. P. Zanetta, W. C. Breckenridge, and G. Vincendon, *J. Chromatogr.*, **69**, 291 (1972).

(9) M. M. Wrann and C. W. Todd, *ibid.*, **147**, 309 (1978).

(10) F. Loewus, *Carbohyd. Res.*, **3**, 130 (1966).

(11) H. G. Kuivila, A. H. Keough, and E. J. Soboczenski, *J. Org. Chem.*, **19**, 780 (1954).

(12) F. Eisenberg, *Carbohyd. Res.*, **19**, 135 (1971).

(13) D. L. Sondack, *J. Pharm. Sci.*, **64**, 128 (1975).

(14) C. Servo, J. Palo and E. Pitkanen, *Acta Neurol. Scand.*, **56**, 104 (1977).

(15) C. Schweickhardt, *J. Clin. Chem. Clin. Biochem.*, **16**, 675 (1978).

(16) Y. Miyazaki and N. Matsumoto, *J. Neurosurg.*, **26**, 306 (1967).

(17) Y. Miyazaki, H. Ando, M. Imai, O. Miyoshi, and K. Takigawa, *Yakuri To Chiryo*, **4**, 46 (1976).

(18) *Idem.*, **4**, 67 (1976).

A Simple Radiometric *In Vitro* Assay for Acetylcholinesterase Inhibitors

TOMAS R. GUILARTE, H. DONALD BURNS *x, ROBERT F. DANNALS, and HENRY N. WAGNER, JR.

Received August 10, 1981, from the *Division of Radiation Health Sciences, Department of Environmental Health Sciences, The Johns Hopkins Medical Institutions, Baltimore, MD 21205.* Accepted for publication February 24, 1982. * Present address: Johns Hopkins University, Baltimore, MD 21211.

Abstract □ A radiometric method for screening acetylcholinesterase inhibitors has been described. The method is based on the production of [^{14}C]carbon dioxide from the hydrolysis of acetylcholine. The inhibitory concentration at 50% (IC_{50}) values for several known acetylcholinesterase inhibitors were in agreement with literature values. The new radiometric method is simple, inexpensive, and has the potential for automation.

Keyphrases □ Acetylcholinesterase inhibitors—a simple radiometric *in vitro* assay □ Radiometric method—*in vitro* assay for acetylcholinesterase inhibitors

Acetylcholinesterase activity and the effect of its inhibitors is measured by the rate of hydrolysis of acetylcholine, its natural substrate (1). The rate of acetylcholine hydrolysis can be measured in a variety of ways; the separation and quantitation of [^{14}C]acetic acid from [^{14}C]-acetylcholine is currently the most commonly used method (2–5). However, this method although sensitive and specific, requires some manual manipulation (*e.g.*, extraction of [^{14}C]acetic acid) in measuring acetylcholinesterase activity or in screening compounds exhibiting an inhibitory effect.

In the present report, an alternative radiometric method that is simple, fast, and has the potential for automation is presented.

EXPERIMENTAL

Materials and Methods—Electric eel (1200 U/ml solid) acetylcholinesterase[1] (acetylcholine acetylhydrolase, EC 3.1.1.7), acetylcholine chloride, neostigmine bromide, physostigmine bromide, and decamethonium bromide were obtained from a commercial source[2]. Phenyltrimethylammonium iodide was synthesized by methylation of *N,N*-dimethylaniline with iodomethane and characterized by melting point, elemental analysis, and IR and PMR spectroscopy. *d*-Tubocurarine chloride[3] and edrophonium chloride[4] were obtained from commercial pharmaceutical sources. [^{14}C]Sodium bicarbonate[5] with a specific activity of 56 mCi/mmole was diluted with deionized water to a specific concentration of 1 μCi/0.1 ml. All other reagents were of reagent chemical grade and commercially available. Twenty-milliliter assay vials[6], aluminum seals[7], and rubber liners[8] were obtained from commercial sources. The electric eel acetylcholinesterase was diluted in 5 m*M* $NaHCO_3$ buffer (pH 8.4) to yield a 0.1 U/μl concentration. This enzyme preparation was stable for several days if stored at −20°. Acetylcholine chloride and the various inhibitors were diluted with 5 m*M* bicarbonate buffer (pH 8.4) prior to assay.

Effect of Acetylcholine Concentration on Acetylcholinesterase Activity—The effect of acetylcholine on acetylcholinesterase activity was studied by varying the acetylcholine concentration, as all other variables were fixed. Acetylcholine standard solutions (4 and 15 m*M*) were made with 5 m*M* sodium bicarbonate buffer (pH 8.4). To 20-ml assay vials, 0.25, 0.5, 1, 0, 2.0, and 3.0 ml of the 4 m*M* acetylcholine standard solution and 1.0, 2.0, 3.0, 4.0, and 5.0 ml of the 15 m*M* acetylcholine standard solution were added. The volume was brought to 5 ml with 5 m*M* sodium bicarbonate (pH 8.4). The final pH of vial contents was 8.0. This gave a 1–75 μmole of acetylcholine/vial range. All vials were capped with aluminum seals, which were fitted with rubber liners, and chilled in ice after which 1 μCi (0.1 ml) of [^{14}C]sodium bicarbonate and 10 μliters of acetylcholinesterase (1 U) were injected. Incubation was carried out at 37° for 30 min. After incubation vials were chilled in ice water prior to measuring [^{14}C]carbon dioxide production. Figure 1 represents the effect of increasing concentration of acetylcholine on acetylcholinesterase activity.

An acetylcholinesterase activity *versus* time curve was obtained to check for linearity. To four 20-ml assay vials, 2 ml of a 30 m*M* acetylcholine solution was added and volume made up to 5 ml with 5 m*M* sodium bicarbonate buffer (pH 8.4). One unit of actylcholinesterase and 1 μCi of [^{14}C]sodium bicarbonate were used. Test vials were incubated at 37° for 15-min intervals after which they were chilled in ice and the [^{14}C]carbon dioxide was measured (Fig. 2).

***In Vitro* Inhibition of Acetylcholinesterase**—To screen each of the known acetylcholinesterase inhibitors, the following experiment was performed.

Control Vials—To 2 ml of a 30 m*M* acetylcholine chloride solution, 3 ml of a 5 m*M* bicarbonate buffer (pH 8.4) was added to make a volume of 5 ml.

Test Vials—To test for the inhibitory effect of the various compounds, a series of vials containing the same amount of acetylcholine as the controls with varying concentrations of inhibitor were prepared and the volume made up to 5 ml with 5 m*M* bicarbonate buffer (pH 8.4). All vials

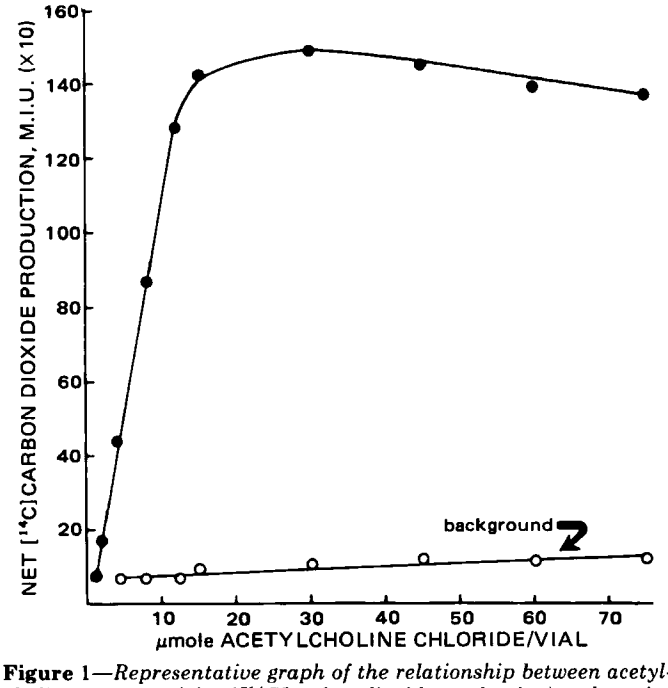

Figure 1—*Representative graph of the relationship between acetylcholinesterase activity ([^{14}C]carbon dioxide production) and varying concentrations of acetylcholine. One microcurie of [^{14}C]sodium bicarbonate and 1 U of electric eel acetylcholinesterase were used. Incubation was done at 37° for 30 min.*

[1] Acetycholinesterase type V-S, Sigma Chemical Co., St. Louis, Mo.
[2] Sigma Chemical Co., St. Louis, Mo.
[3] Squibb, Princeton, N.J.
[4] Roche, Belvidere, N.J.
[5] Amersham/Searle, Arlington Heights, Ill.
[6] Arthur H. Thomas, Philadelphia, Pa.
[7] Wheaton, Millville, N.J.
[8] Johnston Laboratories, Cockeysville, Md.

0022-3549/83/0100-0090$01.00/0

Table I—Inhibitory Potency of Known Acetylcholinesterase Inhibitors as Ranked by the Radiometric Method

Compound	IC_{50} Value	
	Radiometric, *M*	Literature, *M*
Phenyltrimethylammonium Iodide	2.7×10^{-3}	4.4×10^{-4} (9)
d-Tubocurarine Chloride	1.1×10^{-4}	9.0×10^{-4} (10)
Decamethonium Bromide	3.6×10^{-5}	2.5×10^{-5} (11)
Neostigmine Bromide	6.6×10^{-6}	3.0×10^{-6} (12)
Edrophonium Chloride	1.9×10^{-6}	1.3×10^{-5} (13)
Physostigmine Chloride	2.5×10^{-6}	10^{-6}–10^{-8} (9)

were capped with aluminum seals, which were fitted with rubber liners, and chilled in ice. One microcurie of ^{14}C-labeled sodium bicarbonate followed by 1 U (10 μl) of electric eel acetylcholinesterase were injected into each vial. Appropriate blanks (*i.e.*, background) to account for nonenzymatic hydrolysis of acetylcholine were prepared. The background vials contained all ingredients as test and control vials with the exception that no enzyme was added, thus, measuring nonenzymatically hydrolyzed acetylcholine. All vials were incubated at 37° for 30 min. The concentration of inhibitor which reduced the control value by 50% was defined as inhibitory concentration 50% (IC_{50}). This value was determined from the net [^{14}C]carbon dioxide production *versus* inhibitor concentration curve (Fig. 3).

Measurement of [^{14}C]Carbon Dioxide Produced—The amount of [^{14}C]carbon dioxide generated was quantified using a bacteriological detection system[9] which contained an ionization chamber. [^{14}C]Carbon dioxide activity was expressed as metabolic index units (miu.), where 100 miu. equals 0.031 μCi of [^{14}C]carbon dioxide. This instrument is widely used in clinical laboratories as well as in industry. Technical details have been described elsewhere (6, 7).

RESULTS AND DISCUSSION

A new and simple radiometric method was developed to screen potential acetylcholinesterase inhibitors. This technique is based on the hydrolysis of acetylcholine by acetylcholinesterase to acetic acid and choline. The acetic acid formed from the enzymatic hydrolysis of acetylcholine reacts with [^{14}C]sodium bicarbonate to generate [^{14}C]carbon dioxide, which is measured using the ionization chamber system. The

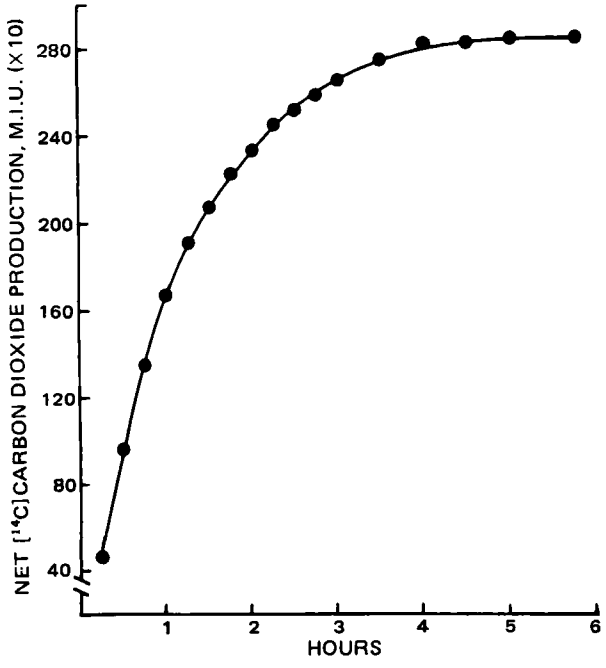

Figure 2—*Representative graph of electric eel acetylcholinesterase activity (1 U) versus time. One microcurie of [^{14}C]sodium bicarbonate and a 30 mM acetylcholine solution was used as substrate. Test vials were incubated for 15-min intervals at 37° after which [^{14}C]carbon dioxide production was quantified.*

[9] Bactec R301, Johnston Laboratories, Cockeysville, Md.

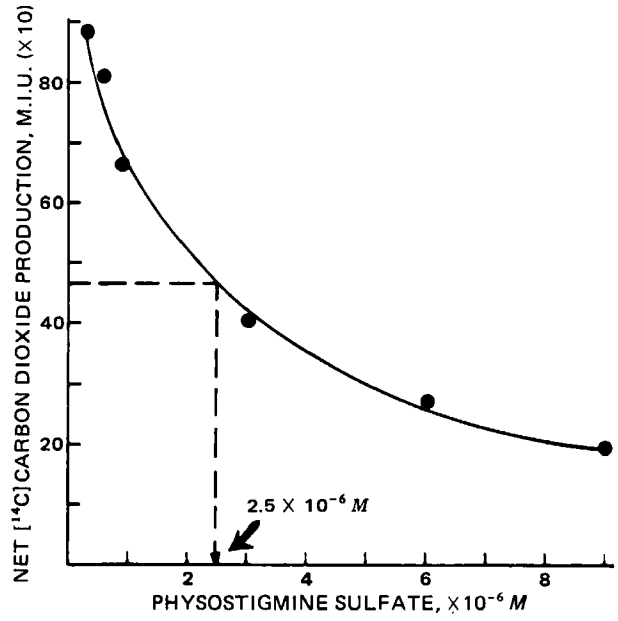

Figure 3—*Effect of increasing concentration of physostigmine sulfate on the activity of 1 U of electric eel acetylcholinesterase. IC_{50} represents the concentration of inhibitor which reduces the production of [^{14}C]-carbon dioxide by 50% of control vial containing no inhibitor. Incubation time was 30 min at 37°. (Control = 928; IC_{50} = 928/2 = 464.)*

[^{14}C]carbon dioxide evolved is proportional to the amount of acetylcholine hydrolyzed (Fig. 1).

The effect of increasing concentrations of acetylcholine on acetylcholinesterase activity was studied. Figure 1 indicates that for 30-min incubation at 37° there was a linear response of acetylcholinesterase activity from 1 to 15 μmoles of acetylcholine/vial followed by saturation at 3×10^{-3} *M* acetylcholine concentration and an actual decrease in activity as the substrate concentration increases. The decrease on acetylcholinesterase activity is a result of substrate inhibition (8). An acetylcholinesterase activity *versus* time curve was obtained to determine the incubation time of test vials (Fig. 2).

Preliminary studies with known acetylcholinesterase inhibitors have shown that the new radiometric method can be used to rank such compounds according to their inhibitory potency on acetylcholinesterase (Table I). Even though comparison of absolute IC_{50} values cannot be made between the described method and those obtained by other methods due to different experimental conditions, the results presented are in general agreement with those reported in the literature (Table I).

The new radiometric method is simple, fast, and inexpensive and has the potential for automation. Many samples can be prepared and analyzed in a few hours. It can be applied as a rapid test in the screening of such compounds as pesticides and chemicals of medical interest.

The method is not only applicable for assaying acetylcholinesterase activity and the effect of its inhibitors, but it can be extended to other enzyme systems in which a proton is generated as a result of the enzymatic action.

REFERENCES

(1) A. R. Main, in "Biology of Cholinergic Function," A. M. Goldberg and I. Hanin Eds., Raven, New York, N.Y., 1976, pp. 269–353.

(2) F. Fonnum, *Biochem. J.*, **115**, 465 (1969).

(3) M. W. McCaman, L. R. Tomey, and R. E. McCaman, *Life Sci.*, **7**, 233 (1968).

(4) L. T. Potter, *J. Pharm. Exp. Ther.*, **156**, 500 (1967).

(5) D. J. Reed, K. Goto, and C. H. Wang, *Anal. Biochem.*, **16**, 59 (1966).

(6) F. H. DeLand, in "Nuclear Medicine In-Vitro," P. Rothfeld, Ed., J. P. Lippincott, Philadelphia, Pa., 1974, pp. 384–403.

(7) J. R. Waters and A. A. Zwarun, in "Developments in Industrial Microbiology," vol. XIV, American Institute of Biological Sciences, Washington, D.C., 1973, pp. 80–89.

(8) K. B. Augustinsson, *Arch. Biochem.*, **23**, 111 (1949).

(9) J. P. Long, in "Handbuch der Experimenteelen Pharmakologie," Suppl. 15, Springer-Verlag, Berlin, West Germany, 1963, pp. 377–384.

(10) F. Bergmann, F. B. Wilson, and D. Nachmansohn, *Biochem. Biophys. Acta*, **6**, 217 (1950).
(11) F. Bergmann, I. B. Wilson, and D. Nachmansohn, *J. Biol. Chem.*, **186**, 693 (1950).
(12) C. M. Smith, S. L. Cohen, E. W. Pelikan, and K. R. Unna, *J. Pharmacol.*, **105**, 391 (1952).
(13) H. L. Cohen and K. R. Unna, *ibid.*, **103**, 340 (1951).

ACKNOWLEDGMENTS

This work was supported by the U.S. Public Health Service Research Grant GM-10548.
The authors thank Dr. Alan Goldberg from the Division of Toxicology, Department of Environmental Health Sciences for his encouragement and advice.

Microbial Metabolism Studies on the Major Microbial and Mammalian Metabolite of Primaquine

CHARLES D. HUFFORD *x, ALICE M. CLARK *, IRIS N. QUINONES *, JOHN K. BAKER ‡, and J. D. McCHESNEY *

Received December 12, 1981, from the **Department of Pharmacognosy* and the ‡*Department of Medicinal Chemistry, School of Pharmacy, the University of Mississippi, University MS 38677.* Accepted for publication February 26, 1982.

Abstract □ The microbial metabolism of 8-(3-carboxy-1-methylpropylamino)-6-methoxyquinoline (II), a known microbial and mammalian metabolite of the antimalarial drug primaquine (I), was investigated using selected organisms. *Streptomyces rimosus* produced a single metabolite that was identified as an amide derivative of II (V) by spectroscopic methods. The amide (V) was synthesized by ammonia treatment of the methyl ester (IV). The lactam derivative (VI) was also prepared by treatment of II with *N*-ethoxycarbonyl-2-ethoxy-1,3-dihydroquinoline.

Keyphrases □ Primaquine—microbial studies on the major microbial and mammalian metabolite, high-performance liquid chromatography □ High-performance liquid chromatography—microbial metabolism studies on the major microbial and mammalian metabolite of primaquine

The utilization of microorganisms as models for studying mammalian metabolism is a concept that has been advocated as an aid for future metabolic studies (1). Recent studies with phencyclidine (2) and imipramine (3) have shown that microorganisms do produce the same metabolites as mammalian systems. Primaquine (I), an antimalarial drug, has also been subjected to a microbial metabolic study since little or no information has been reported regarding its mammalian metabolism (4). The two major microbial metabolites identified were the carboxylic acid derivative (II) and the *N*-acetyl derivative of the primary amine (III). In parallel studies, the mammalian metabolism of I using rats has been studied, and II has been identified as the major mammalian metabolite as well (5). The tissue distribution of I has been studied, and even though substantial evidence indicated that I was rapidly metabolized by the rat, no mammalian metabolites were identified (6). Having microbial metabolites as reference standards for conducting mammalian metabolic studies can be useful. The purpose of this investigation was to study further the biotransformations of the major mammalian metabolite (II) of primaquine using microbial systems.

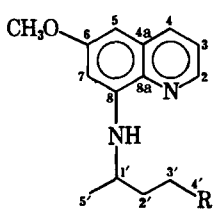

I: R = $-CH_2NH_2$
II: R = $-CO_2H$
III: R = $-CH_2NHCOCH_3$
IV: R = $-CO_2CH_3$
V: R = $-CONH_2$

RESULTS AND DISCUSSION

A total of 60 microorganisms typical of those used previously (3, 7) were used in the screening of 8-(3-carboxy-1-methylpropylamino)-6-methoxyquinoline (II) for microbial metabolites. Of these, *Streptomyces rimosus*[1] was chosen for preparative scale fermentations, since TLC indicated complete conversion in 3 days to one major metabolite. Other microorganisms showing this same metabolite as determined by TLC were *Streptomyces flocculus*[2], *Polyporus sanguineus*[3], and *Fusarium oxysporum* f. sp. *cepae*[4] although large amounts of II were also present even after 7–10 days.

Incubation of 300 mg of II with submerged cultures of *S. rimosus* for 4 days and extraction of the entire culture with ethyl acetate resulted in 700 mg of ethyl acetate solubles. Chromatography of a 400-mg sample of this residue using preparative layer silica gel and alumina plates resulted in the isolation of 18 mg of the pure metabolite by TLC and HPLC (overall yield, 12%).

The ^{1}H-NMR spectrum of the metabolite showed the aromatic protons to have nearly the same δ positions and J values as reported for II (4). The spectrum also confirmed that the methoxyl group and the secondary methyl were present. This suggested that the biotransformation had occurred in the side chain. The mass spectrum was consistent for $C_{15}H_{19}O_2N_3$ (M^+ 273, 10%) and showed significant fragments at m/z 215 (51%) and 201 (100%), further confirming that the aromatic nucleus had not been transformed (4). The IR spectrum indicated absorption at 3400, 3510, and 1760 cm^{-1}. The ^{13}C-NMR spectral data (Table I) was nearly identical to that of the methyl ester of II (IV). The collective spectroscopic data suggested the microbial metabolite was an amide derivative represented by V. This was confirmed by treating IV with methanol saturated with ammonia in a sealed tube at 140°. The product of this reaction was identical in all respects to the metabolite (V). No evidence of the lactam derivative (VI) was noted in this reaction, although VI was noted as a product of heating IV in the gas chromatograph (5). Attempts to prepare

[1] American Type Culture Collection (ATCC), 23955, Rockville, Md.
[2] ATCC 25453.
[3] ATCC 14622.
[4] ATCC 11711.

0022-3549/83/0100-0092$01.00/0

(10) F. Bergmann, F. B. Wilson, and D. Nachmansohn, *Biochem. Biophys. Acta*, **6**, 217 (1950).
(11) F. Bergmann, I. B. Wilson, and D. Nachmansohn, *J. Biol. Chem.*, **186**, 693 (1950).
(12) C. M. Smith, S. L. Cohen, E. W. Pelikan, and K. R. Unna, *J. Pharmacol.*, **105**, 391 (1952).
(13) H. L. Cohen and K. R. Unna, *ibid.*, **103**, 340 (1951).

ACKNOWLEDGMENTS

This work was supported by the U.S. Public Health Service Research Grant GM-10548.
The authors thank Dr. Alan Goldberg from the Division of Toxicology, Department of Environmental Health Sciences for his encouragement and advice.

Microbial Metabolism Studies on the Major Microbial and Mammalian Metabolite of Primaquine

CHARLES D. HUFFORD *x, ALICE M. CLARK *, IRIS N. QUINONES *, JOHN K. BAKER ‡, and J. D. McCHESNEY *

Received December 12, 1981, from the **Department of Pharmacognosy* and the ‡*Department of Medicinal Chemistry, School of Pharmacy, the University of Mississippi, University MS 38677.* Accepted for publication February 26, 1982.

Abstract □ The microbial metabolism of 8-(3-carboxy-1-methylpropylamino)-6-methoxyquinoline (II), a known microbial and mammalian metabolite of the antimalarial drug primaquine (I), was investigated using selected organisms. *Streptomyces rimosus* produced a single metabolite that was identified as an amide derivative of II (V) by spectroscopic methods. The amide (V) was synthesized by ammonia treatment of the methyl ester (IV). The lactam derivative (VI) was also prepared by treatment of II with *N*-ethoxycarbonyl-2-ethoxy-1,3-dihydroquinoline.

Keyphrases □ Primaquine—microbial studies on the major microbial and mammalian metabolite, high-performance liquid chromatography □ High-performance liquid chromatography—microbial metabolism studies on the major microbial and mammalian metabolite of primaquine

The utilization of microorganisms as models for studying mammalian metabolism is a concept that has been advocated as an aid for future metabolic studies (1). Recent studies with phencyclidine (2) and imipramine (3) have shown that microorganisms do produce the same metabolites as mammalian systems. Primaquine (I), an antimalarial drug, has also been subjected to a microbial metabolic study since little or no information has been reported regarding its mammalian metabolism (4). The two major microbial metabolites identified were the carboxylic acid derivative (II) and the *N*-acetyl derivative of the primary amine (III). In parallel studies, the mammalian metabolism of I using rats has been studied, and II has been identified as the major mammalian metabolite as well (5). The tissue distribution of I has been studied, and even though substantial evidence indicated that I was rapidly metabolized by the rat, no mammalian metabolites were identified (6). Having microbial metabolites as reference standards for conducting mammalian metabolic studies can be useful. The purpose of this investigation was to study further the biotransformations of the major mammalian metabolite (II) of primaquine using microbial systems.

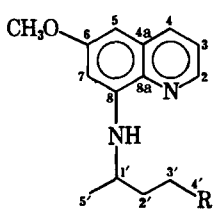

I: R = $-CH_2NH_2$
II: R = $-CO_2H$
III: R = $-CH_2NHCOCH_3$
IV: R = $-CO_2CH_3$
V: R = $-CONH_2$

RESULTS AND DISCUSSION

A total of 60 microorganisms typical of those used previously (3, 7) were used in the screening of 8-(3-carboxy-1-methylpropylamino)-6-methoxyquinoline (II) for microbial metabolites. Of these, *Streptomyces rimosus*[1] was chosen for preparative scale fermentations, since TLC indicated complete conversion in 3 days to one major metabolite. Other microorganisms showing this same metabolite as determined by TLC were *Streptomyces flocculus*[2], *Polyporus sanguineus*[3], and *Fusarium oxysporum* f. sp. *cepae*[4] although large amounts of II were also present even after 7–10 days.

Incubation of 300 mg of II with submerged cultures of *S. rimosus* for 4 days and extraction of the entire culture with ethyl acetate resulted in 700 mg of ethyl acetate solubles. Chromatography of a 400-mg sample of this residue using preparative layer silica gel and alumina plates resulted in the isolation of 18 mg of the pure metabolite by TLC and HPLC (overall yield, 12%).

The ^{1}H-NMR spectrum of the metabolite showed the aromatic protons to have nearly the same δ positions and J values as reported for II (4). The spectrum also confirmed that the methoxyl group and the secondary methyl were present. This suggested that the biotransformation had occurred in the side chain. The mass spectrum was consistent for $C_{15}H_{19}O_2N_3$ (M^+ 273, 10%) and showed significant fragments at m/z 215 (51%) and 201 (100%), further confirming that the aromatic nucleus had not been transformed (4). The IR spectrum indicated absorption at 3400, 3510, and 1760 cm^{-1}. The ^{13}C-NMR spectral data (Table I) was nearly identical to that of the methyl ester of II (IV). The collective spectroscopic data suggested the microbial metabolite was an amide derivative represented by V. This was confirmed by treating IV with methanol saturated with ammonia in a sealed tube at 140°. The product of this reaction was identical in all respects to the metabolite (V). No evidence of the lactam derivative (VI) was noted in this reaction, although VI was noted as a product of heating IV in the gas chromatograph (5). Attempts to prepare

[1] American Type Culture Collection (ATCC), 23955, Rockville, Md.
[2] ATCC 25453.
[3] ATCC 14622.
[4] ATCC 11711.

0022-3549/83/0100-0092$01.00/0

Table I—^{13}C-NMR Data for IV, V, and VI [a]

Carbon No.	IV	V	VI [b]
2	144.4d	144.4d	147.7d
3	121.9d	121.9d	121.8d
4	134.8d	134.9d	134.0d
4a	130.1s	130.0s	130.3s
5	92.3d	92.3d	105.6d
6	159.7s	159.6s	157.4s
7	97.1d	97.2d	123.0d
8	145.2s	145.2s	140.8s[1]
8a	135.6s	135.5s	136.4s[1]
1′	47.7d	47.7d	57.1d
2′	31.0t[1]	32.4t	31.3t[2]
3′	32.0t[1]	32.4t	28.0t[2]
4′	174.0s	175.3s	175.8s
5′	20.6q	20.7q	20.6q
OCH_3	55.3q	55.2q	55.7q
CO_2CH_3	51.5q	—	—

[a] Data were obtained in deuterochloroform. The data and assignments for IV have been reported (4) and are listed here for comparison with V and VI. Signals bearing the same numerical superscript may be reversed. [b] The assignments listed for VI are based on comparison with IV and V and SFORD.

V from II by using such reagents as thionyl chloride and ethyl chloroformate followed by ammonia treatment were unsuccessful. The major product appeared to be VI (TLC). The lactam (VI) could be efficiently prepared by treatment of II with *N*-ethoxycarbonyl-2-ethoxy-1,3-dihydroquinoline (VII).

Similar biotransformations of carboxylic acids to primary amides have been reported for biotin and desthiobiotin (8, 9), but they do not appear to be common microbial reactions. The conversion of mycophenolic acid to amide derivatives of glycine and alanine have also been reported (10). Whether these biotransformations play a role in the mammalian metabolism of II remains to be established, but conjugation of glycine with similar compounds is common (11).

EXPERIMENTAL[5]

Fermentation Procedures—Initial screening studies to identify microorganisms capable of metabolizing 8-(3-carboxy-1-methylpropylamino)-6-methoxyquinoline (II) were accomplished using the usual two-stage fermentation procedure (2–4, 7). Cultures were grown in 25 ml of dextrose–yeast extract–peptone medium (4) held in 125-ml Erlenmeyer flasks equipped with stainless steel tops. The substrate (II) was added to 24-hr-old second-stage cultures (0.2 mg of substrate/milliliter of culture medium) as a 5% solution in dimethylformamide. Cultures were incubated on a rotary shaker[6] at 250 rpm and room temperature.

Culture controls consisted of fermentation blanks, in which organisms were grown under identical conditions but without the substrate. Substrate controls consisted of sterilized 24-hr-old second-stage cultures containing the substrate and incubated at 250 rpm and room temperature.

The cultures were sampled at periodic intervals by homogenizing 5 ml of the culture, adjusting to pH 7–8, and extracting with 5 ml of ethyl acetate. The ethyl acetate layer was evaporated to dryness, the residue redissolved in 100 μl of ethyl acetate, and 20 μl of the solution was spotted on silica gel G TLC plates. The plates were developed in either acetone (solvent A), ether–acetone (1:1, solvent B), or 10% methanol in chloroform (solvent C). In solvent A the R_f values were 0.6 (II) and 0.56 (V); in solvent B, R_f = 0.58 (II), and 0.49 (V); and in solvent C, R_f = 0.45 (II) and 0.39 (V). Visualization was accomplished with UV light and by spraying with diazotized *p*-nitroaniline followed by spraying with concentrated hydrochloric acid. All spots were dull yellow after spraying. HPLC analyses were carried out using a C_{18}-reversed-phase column[7] and a mobile phase consisting of 6.6 g of K_2HPO_4, 8.4 g or KH_2PO_4, 4.0 g of *N,N*-dimethyl-*n*-octylamine, 2.4 liters of water, and 1.6 liters of methanol at a flow rate of 1.0 ml/min. An HPLC pump[8] and a microsyringe-loaded loop injector[9] were used with a dual wavelength UV detector[10] (254 and 280 nm). Extracts were dissolved in 1.0 ml of methanol and 40 μl was injected for analysis. In this system, the metabolite (V) has a relative retention time (relative to II) of 0.73 and an A_{254}/A_{280} value equal to 4.73.

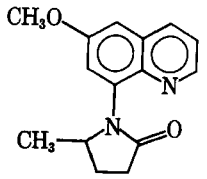

VI

Microbiological Preparation of 8-(3-Carboxamido-1-methylpropylamino)-6-methoxyquinoline (V)—*Streptomyces rimosus*[1] was grown in 1.5 liters of medium held in fifteen 500-ml Erlenmeyer flasks. A total of 300 mg of II was distributed evenly among the cultures. The cultures were incubated at room temperature and 250 rpm for 4 days after substrate addition. The cultures were pooled and extracted with ethyl acetate (2 × 700 ml, 1 × 1000 ml). The combined ethyl acetate layers were dried (sodium sulfate) and evaporated *in vacuo* to leave an oily residue (702 mg). Preparative layer chromatography of 400 mg of the residue was carried out using precoated silica gel G plates[11] (2.0 mm thick, 20 × 20 cm) developed in ether–acetone (1:1). The major band, corresponding to metabolite V, was located by UV light, scraped off, and the silica gel was extracted with ethyl acetate. Evaporation of the solvent afforded 66 mg of a crystalline residue. Crystallization from ether yielded a crystalline material, which was shown by ^{1}H-NMR to be unrelated to the primaquine nucleus. It appeared to be a simple organic constituent that was not further characterized. This substance could be separated from the metabolite on TLC alumina plates[11] using benzene–ethyl acetate–ammonium hydroxide (50:45:5). It could be visualized under UV light but it did not react with the spray reagent.

The mother liquor residue was subjected to another preparative layer chromatography over alumina plates (1.0 mm thick, 20 × 20 cm) using benzene–ethyl acetate–ammonium hydroxide (50:45:5). The metabolite band was extracted with ethyl acetate and after evaporation yielded 18 mg of the metabolite V pure by TLC and HPLC as an oily residue; IR ($CHCl_3$) ν_{max} 3510, 3490, 3400, 1670, 1612, 1595, 1575, and 1520 cm^{-1}, ^{1}H-NMR ($CDCl_3$) δ 8.53 (1H, dd, *J* = 1.5, 4.5 Hz, C-2 H), 7.93 (1H, dd, *J* = 1.5, 9.0 Hz, C-4 H), 7.30 (1H, dd, *J* = 4.5, 9.0 Hz, C-3 H), 6.34 (2H, s, C-5 H, and H-7), 6.0 (1H, br, NH), 5.6 (2H, br, NH_2), 3.87 (3H, s, OCH_3), 3.7 (1H, m, H-1′), 2.4 (2H, m, H-3′), 2.1 (2H, m, H-2′), and 1.30 (3H, d, *J* = 6.0 Hz, CH_3); CD (0.005% methanol) $[\theta]_{350-210}$ = 0; mass spectrum: M^+ at *m/z* 273 (10%), 257 (1%), 215 (51%), and 201 (100%). The metabolite sample was identical to that prepared from IV (TLC, cobalt-TLC, HPLC, IR, ^{1}H- and ^{13}C-NMR).

Synthesis of 8-(3-Carboxamido-1-methylpropylamino)-6-methoxyquinoline (V) from IV—8-(3-Carbomethoxy-1-methylpropylamino)-6-methoxyquinoline (IV, 80 mg) (4) was dissolved in a few drops of methanol and placed in a glass tube (2-mm thick, 3-mm i.d. × 30 cm) and treated with 0.5 ml of methanol saturated with anhydrous ammonia gas. Additional ammonia was bubbled into the tube while cooling in an ice bath. The tube was then sealed and heated in an oven at 140° for 4 days. The reaction mixture was evaporated *in vacuo* to leave a brown oily residue (98 mg). TLC analysis of the mixture showed the presence of two major components corresponding to starting material (IV) and the amide product (V). There was no evidence (TLC) of the presence of the lactam derivative (VI) [solvent B, R_f = 0.69 (IV), 0.22 (VI)[12], 0.49 (V)]. The reaction mixture was purified by preparative layer chromatography on alumina plates[11] (20 × 20 cm, 1.0-mm thick) using benzene–ethyl acetate–ammonium hydroxide (50:45:5) as the developing solvent. The band corresponding to the product (R_f = 0.30) was located under UV light, scraped off, and extracted with 25% methanol–ether. Filtration and evaporation of the solvent afforded 17 mg of an oily residue that was pure by TLC, HPLC, and ^{1}H-NMR. For ^{13}C-NMR data see Table I; mass spectrum: M^+ at *m/z* 273 (14%), 257 (2%), 215 (48%), 201 (100%).

Synthesis of VI From II—A 50-mg sample of II (4) was dissolved in 1 ml of methylene chloride containing 0.03 ml (1.1 eq.) of triethylamine to which was added 75 mg of VII (1.5 eq.). The clear solution was allowed to stand at room temperature for 3 days, after which time the solution was extracted with 1 ml of 1 *N* sodium hydroxide to remove traces of II. The methylene chloride layer was filtered through cotton, evaporated,

[5] IR spectra were run in chloroform using a Perkin-Elmer 281b spectrophotometer. The ^{1}H-NMR spectra (90 MHz) were recorded in deuterochloroform on a Varian EM 390 spectrometer using tetramethylsilane as an internal standard. The ^{13}C-NMR spectra (15.03 MHz) were recorded on a JEOL-FX60 FT spectrometer using tetramethylsilane as internal standard.

[6] New Brunswick Model G10-21.

[7] μBondapak, Waters Associates, Milford, Mass.

[8] Model M-6000, Waters Associates, Milford, Mass.

[9] Model U6-K, Waters Associates, Milford, Mass.

[10] Model 440, Waters Associates, Milford, Mass.

[11] Brinkmann Instruments, Westbury, N.Y.

[12] The lactam VI does not react with the spray reagent but can be visualized under UV light.

and the residue (142 mg) was purified using flash chromatography (12) (silica gel, ether, then ether–acetone, 1:1). A total of 24 mg of VI was obtained, mp 109–110° (*iso*-propyl ether); IR (KBr) ν_{max} 1690, 1615, 1590, and 1490 cm^{-1}; ^1H-NMR ($CDCl_3$) δ 8.75 (1H, dd, J = 1.5, 4.5 Hz, C-2 H), 8.06 (1H, dd, J = 1.5, 8.5 Hz, C-4 H), 7.35 (1H, dd, J = 4.2, 8.5 Hz, C-3 H), 7.29 (1H, d, J = 2.7 Hz, C-7 H), 7.07 (1H, d, J = 2.7 Hz, C-5 H), 4.72 (1H, ddq, J = 6.0, 6.0, 6.0 Hz, C-1′ H), 3.90 (3H, s OCH_3), 2.6, and 1.8 (3H and 1H, m, C-3′ H, C-2′ H), 1.03 (3H, d, J = 6.0 Hz, CH_3); mass spectrum M^+ at m/z 256 (18%), 228 (18%), 213 (21%), 200 (81%), 187 (52%), 186 (51%), 159 (100%); ^{13}C-NMR data (Table I); TLC, solvent B, R_f 0.22[12].

Anal.—Calc. for $C_{15}H_{16}N_2O_2$: C, 70.29; H, 6.29; N, 10.93. Found: C, 70.32; H, 6.40; N, 10.86.

REFERENCES

(1) J. P. Rosazza and R. V. Smith, *Adv. Appl. Microbiol.*, **25,** 169 (1979).

(2) C. D. Hufford, J. K. Baker, and A. M. Clark, *J. Pharm. Sci.*, **70,** 155 (1981).

(3) C. D. Hufford, G. A. Capiton, A. M. Clark, and J. K. Baker, *ibid.*, **70,** 151 (1981).

(4) A. M. Clark, C. D. Hufford, and J. D. McChesney, *Antimicrob. Agents Chemother.*, **19,** 337 (1981).

(5) J. K. Baker, J. D. McChesney, C. D. Hufford, and A. M. Clark, *J. Chromatogr.*, **230,** 69 (1982).

(6) D. J. Holbrook, Jr., J. B. Griffin, L. Fowler, and B. R. Gibson, *Pharmacology*, **22,** 330 (1981).

(7) C. D. Hufford, C. C. Collins, and A. M. Clark, *J. Pharm. Sci.*, **68,** 1239 (1979).

(8) C. Sekijo, T. Tsuboi, and Y. Yoshimura, *Agr. Biol. Chem.*, **33,** 683 (1969).

(9) *Idem.*, **32,** 1181 (1968).

(10) D. F. Jones, R. H. Moore, and G. C. Crowley, *J. Chem. Soc.*, **1970,** 1725.

(11) B. Testa and P. Jenner, "Drug Metabolism: Chemical and Biochemical Aspects," Dekker, New York, N.Y., 1976.

(12) W. C. Still, M. Kahn, and A. Mitra, *J. Org. Chem.*, **43,** 2923 (1978).

ACKNOWLEDGMENTS

Supported by the UNDP–World Bank–World Health Organization Special Programme for Research and Training in Tropical Diseases.

Iris N. Quinones acknowledges the National Science Foundation for a grant for Undergraduate Research Participation, SPI-8026335.

Synthesis and Anticonvulsant Activity of Some 2-Methyl-3-phenylcarbamoyl-2,3-diazabicyclo-[2.2.1]heptanes

MILTON J. KORNET ˣ and JOHN YEOU-RUOH CHU

Received January 25, 1982, from the *College of Pharmacy, University of Kentucky, Lexington, KY 40506.* Accepted for publication March 12, 1982.

Abstract □ A series of 2-methyl-3-phenylcarbamoyl-2,3-diazabicyclo[2.2.1]heptanes were obtained by treating aryl isocyanates with 2-methyl-2,3-diazabicyclo[2.2.1]heptane. The compounds showed only minimal anticonvulsant activity.

Keyphrases □ 2-Methyl-3-phenylcarbamoyl-2,3-diazabicyclo[2.2.1]-heptanes—synthesis and anticonvulsant activity □ Anticonvulsants—synthesis of some 2-methyl-3-phenylcarbamoyl-2,3-diazabicyclo[2.2.1]-heptanes

A previous report (1) describes the synthesis and anticonvulsant activity of a series of 1-methyl-2-phenylcarbamoylpiperidazines. Four members of this series showed significant activity. The present report describes the synthesis and anticonvulsant activity of a series of 2-methyl-3-phenylcarbamoyl-2,3-diazabicyclo[2.2.1]heptanes (III). The series of III, with their cage structure, would be expected to provide different steric and basic properties in comparison with the monocyclic compounds (1).

BACKGROUND

The synthesis of 2-methyl-2,3-diazabicyclo[2.2.1]heptane (II) was accomplished in two steps from 2,3-dicarboethoxy-2,3-diazabicyclo[2.2.1]heptane (IV) (2). Partial saponification of IV gave 2-carboethoxy-2,3-diazabicyclo[2.2.1]heptane (V), which underwent reduction with lithium aluminum hydride to afford the base, II (Scheme I). Compound II reacted with aryl isocyanates (I) to produce III in good yields (Scheme II; Table I).

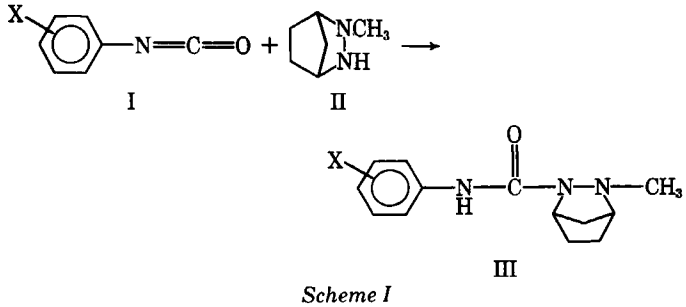

Scheme I

Compounds III*a–j* were tested in the maximal electroshock seizure and subcutaneous pentylenetetrazol seizure threshold tests for anticonvulsant activity and in the rotorod test for neurotoxicity in male mice[1] by reported procedures (3). None of the compounds showed activity in either test at 100 mg/kg.

In the maximal electroshock seizure test, compounds III*a*, *d*, *g*, *i*, and *j* exhibited activity at 300 mg/kg at 30 min. Compounds III*a* and *i* showed no toxicity at this dose level, whereas III*d*, *g*, and *j* displayed some toxicity. Two compounds were active in the subcutaneous pentylenetetrazol seizure test at 300 mg/kg. Compound III*j* was active at 30 min; compound III*b* showed activity at 4 hr with no toxicity. Apparently, the introduction

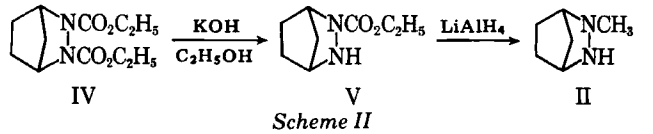

Scheme II

[1] Carworth Farms No. 1 mice.

0022-3549/83/0100-0094$01.00/0

and the residue (142 mg) was purified using flash chromatography (12) (silica gel, ether, then ether–acetone, 1:1). A total of 24 mg of VI was obtained, mp 109–110° (*iso*-propyl ether); IR (KBr) ν_{max} 1690, 1615, 1590, and 1490 cm^{-1}; ^1H-NMR ($CDCl_3$) δ 8.75 (1H, dd, J = 1.5, 4.5 Hz, C-2 H), 8.06 (1H, dd, J = 1.5, 8.5 Hz, C-4 H), 7.35 (1H, dd, J = 4.2, 8.5 Hz, C-3 H), 7.29 (1H, d, J = 2.7 Hz, C-7 H), 7.07 (1H, d, J = 2.7 Hz, C-5 H), 4.72 (1H, ddq, J = 6.0, 6.0, 6.0 Hz, C-1′ H), 3.90 (3H, s OCH_3), 2.6, and 1.8 (3H and 1H, m, C-3′ H, C-2′ H), 1.03 (3H, d, J = 6.0 Hz, CH_3); mass spectrum M^+ at m/z 256 (18%), 228 (18%), 213 (21%), 200 (81%), 187 (52%), 186 (51%), 159 (100%); ^{13}C-NMR data (Table I); TLC, solvent B, R_f 0.22[12].

Anal.—Calc. for $C_{15}H_{16}N_2O_2$: C, 70.29; H, 6.29; N, 10.93. Found: C, 70.32; H, 6.40; N, 10.86.

REFERENCES

(1) J. P. Rosazza and R. V. Smith, *Adv. Appl. Microbiol.*, **25,** 169 (1979).

(2) C. D. Hufford, J. K. Baker, and A. M. Clark, *J. Pharm. Sci.*, **70,** 155 (1981).

(3) C. D. Hufford, G. A. Capiton, A. M. Clark, and J. K. Baker, *ibid.*, **70,** 151 (1981).

(4) A. M. Clark, C. D. Hufford, and J. D. McChesney, *Antimicrob. Agents Chemother.*, **19,** 337 (1981).

(5) J. K. Baker, J. D. McChesney, C. D. Hufford, and A. M. Clark, *J. Chromatogr.*, **230,** 69 (1982).

(6) D. J. Holbrook, Jr., J. B. Griffin, L. Fowler, and B. R. Gibson, *Pharmacology*, **22,** 330 (1981).

(7) C. D. Hufford, C. C. Collins, and A. M. Clark, *J. Pharm. Sci.*, **68,** 1239 (1979).

(8) C. Sekijo, T. Tsuboi, and Y. Yoshimura, *Agr. Biol. Chem.*, **33,** 683 (1969).

(9) *Idem.*, **32,** 1181 (1968).

(10) D. F. Jones, R. H. Moore, and G. C. Crowley, *J. Chem. Soc.*, **1970,** 1725.

(11) B. Testa and P. Jenner, "Drug Metabolism: Chemical and Biochemical Aspects," Dekker, New York, N.Y., 1976.

(12) W. C. Still, M. Kahn, and A. Mitra, *J. Org. Chem.*, **43,** 2923 (1978).

ACKNOWLEDGMENTS

Supported by the UNDP–World Bank–World Health Organization Special Programme for Research and Training in Tropical Diseases.

Iris N. Quinones acknowledges the National Science Foundation for a grant for Undergraduate Research Participation, SPI-8026335.

Synthesis and Anticonvulsant Activity of Some 2-Methyl-3-phenylcarbamoyl-2,3-diazabicyclo-[2.2.1]heptanes

MILTON J. KORNET ˣ and JOHN YEOU-RUOH CHU

Received January 25, 1982, from the *College of Pharmacy, University of Kentucky, Lexington, KY 40506.* Accepted for publication March 12, 1982.

Abstract □ A series of 2-methyl-3-phenylcarbamoyl-2,3-diazabicyclo[2.2.1]heptanes were obtained by treating aryl isocyanates with 2-methyl-2,3-diazabicyclo[2.2.1]heptane. The compounds showed only minimal anticonvulsant activity.

Keyphrases □ 2-Methyl-3-phenylcarbamoyl-2,3-diazabicyclo[2.2.1]-heptanes—synthesis and anticonvulsant activity □ Anticonvulsants—synthesis of some 2-methyl-3-phenylcarbamoyl-2,3-diazabicyclo[2.2.1]-heptanes

A previous report (1) describes the synthesis and anticonvulsant activity of a series of 1-methyl-2-phenylcarbamoylpiperidazines. Four members of this series showed significant activity. The present report describes the synthesis and anticonvulsant activity of a series of 2-methyl-3-phenylcarbamoyl-2,3-diazabicyclo[2.2.1]heptanes (III). The series of III, with their cage structure, would be expected to provide different steric and basic properties in comparison with the monocyclic compounds (1).

BACKGROUND

The synthesis of 2-methyl-2,3-diazabicyclo[2.2.1]heptane (II) was accomplished in two steps from 2,3-dicarboethoxy-2,3-diazabicyclo[2.2.1]heptane (IV) (2). Partial saponification of IV gave 2-carboethoxy-2,3-diazabicyclo[2.2.1]heptane (V), which underwent reduction with lithium aluminum hydride to afford the base, II (Scheme I). Compound II reacted with aryl isocyanates (I) to produce III in good yields (Scheme II; Table I).

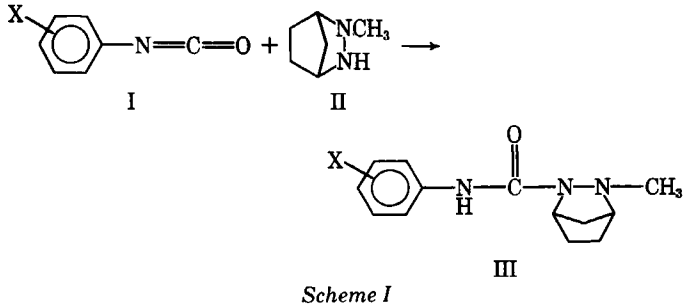

Scheme I

Compounds III*a–j* were tested in the maximal electroshock seizure and subcutaneous pentylenetetrazol seizure threshold tests for anticonvulsant activity and in the rotorod test for neurotoxicity in male mice[1] by reported procedures (3). None of the compounds showed activity in either test at 100 mg/kg.

In the maximal electroshock seizure test, compounds III*a*, *d*, *g*, *i*, and *j* exhibited activity at 300 mg/kg at 30 min. Compounds III*a* and *i* showed no toxicity at this dose level, whereas III*d*, *g*, and *j* displayed some toxicity. Two compounds were active in the subcutaneous pentylenetetrazol seizure test at 300 mg/kg. Compound III*j* was active at 30 min; compound III*b* showed activity at 4 hr with no toxicity. Apparently, the introduction

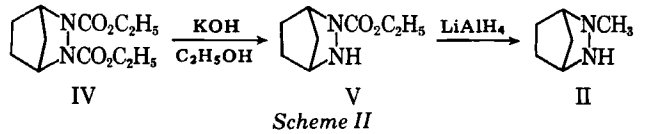

Scheme II

[1] Carworth Farms No. 1 mice.

0022-3549/83/0100-0094$01.00/0

Table I—Physical Properties of 2-Methyl-3-phenylcarbamoyl-2,3-diazabicyclo[2.2.1]heptanes

Compound	X	Melting Point	Yield, %	Recrystallization Solvent[a]	Formula		Analysis, % Calc.	Found
						C	67.51	67.65
IIIa	H	84–86	73	B	$C_{13}H_{17}N_3O$	H	7.41	7.23
						N	18.17	18.43
						C	58.76	58.76
IIIb	p-Cl	125–126.5	67	B	$C_{13}H_{16}ClN_3O$	H	6.07	5.95
						N	15.81	15.54
						C	62.64	62.67
IIIc	p-F	95.5–97	72	A	$C_{13}H_{16}FN_3O$	H	6.47	6.56
						N	16.86	16.83
						C	68.54	68.71
IIId	o-CH_3	81.5–83.5	57	C	$C_{14}H_{19}N_3O$	H	7.81	7.77
						N	17.13	17.21
						C	68.54	68.61
IIIe	m-CH_3	88–88.5	75	D	$C_{14}H_{19}N_3O$	H	7.81	7.73
						N	17.13	17.13
						C	68.54	68.72
IIIf	p-CH_3	123.5–125	56	B	$C_{14}H_{19}N_3O$	H	7.81	7.89
						N	17.13	17.34
						C	64.35	64.65
IIIg	p-CH_3O	95.5–97	82	B	$C_{14}H_{19}N_3O_2$	H	7.33	7.24
						N	16.08	16.08
						C	52.02	52.20
IIIh	3,4-Cl_2	113–115	67	B	$C_{13}H_{15}Cl_2N_3O$	H	5.04	5.01
						N	14.00	14.28
						C	60.11	60.09
IIIi	2-Cl,6-CH_3	92–94	77	B	$C_{14}H_{18}ClN_3O$	H	6.49	6.56
						N	15.02	14.98
						C	69.47	69.65
IIIj	2,6-$(CH_3)_2$	131.5–132.5	64	A	$C_{15}H_{21}N_3O$	H	8.16	8.12
						N	16.20	16.43

[a] A, cyclohexane; B, benzene–cyclohexane; C, cyclohexane–ether; D, ether.

of a methylene bridge into the 1,2-diazacyclohexane ring (1) leads to compounds with reduced anticonvulsant activity.

EXPERIMENTAL[2]

2-Carboethoxy-2,3-diazabicyclo[2.2.1]heptane (V)—This compound was prepared by saponification of 2,3-dicarboethoxy-2,3-diazabicyclo[2.2.1]heptane (IV) (2) according to the methods (4, 5) used in the preparation of 1-ethoxycarbonylpiperidazine. It was obtained as a colorless oil in 50% yield, bp 116–120° (1.3 mm). The NMR showed contamination by the starting material, and a satisfactory carbon analysis could not be obtained. Since the purity of this compound was ~95%, it was used directly in the next step.

2-Methyl-2,3-diazabicyclo[2.2.1]heptane (II)—This compound (6) was obtained from the lithium aluminum hydride reduction of V according to the same procedure (1) used for the preparation of 1-methylpiperidazine. It distilled as a colorless oil in 78% yield, bp 151–153°. This base was used directly in the preparation of III.

[2] Melting points were determined on a Thomas-Hoover melting point apparatus and are uncorrected. The IR spectra were taken on a Perkin-Elmer 700 spectrophotometer as either liquid films or as potassium bromide pellets. NMR spectra were recorded on a Varian EM-360 or T-60 spectrometer using tetramethylsilane as the internal reference. Mass spectra were obtained on a RMU-7 double focusing spectrometer by Hitachi/Perkin-Elmer. Elemental analyses were performed by Micro-Analysis, Inc., Wilmington, Del., and Dr. Kurt Eder, Geneva, Switzerland. All compounds exhibited PMR and mass spectra consistent with the structures shown.

2-Methyl-3-phenylcarbamoyl-2,3-diazabicyclo-[2.2.1]heptanes (III)—Compound IIIj was prepared from 2.0 g (0.0178 mole) of 2-methyl-2,3-diazabicyclo[2.2.1]heptane (II) and 2.38 g (0.0162 mole) of 2,6-dimethylphenyl isocyanate (I) in 35 ml of dry benzene according to the procedure previously described (3). Workup gave 2.7 g (64%) of white solid, mp 130–132°. Recrystallization from cyclohexane afforded analytically pure material, mp 131.5–132.5°.

REFERENCES

(1) M. J. Kornet and J. Chu, *J. Heterocycl. Chem.*, **18**, 293 (1981).
(2) O. Diels, J. H. Blom, and W. Koll, *Ann. Chem.*, **443**, 242 (1925).
(3) M. J. Kornet, *J. Pharm. Sci.*, **67**, 1471 (1978).
(4) K. Alder and H. Niklas, *Ann. Chem.*, **585**, 81 (1954).
(5) P. Baranger and J. Levisalles, *Bull. Soc. Chim. Fre.*, **1957**, 704.
(6) S. F. Nelsen and W. P. Parmelee, *J. Am. Chem. Soc.*, **102**, 2732 (1980).

ACKNOWLEDGMENTS

The authors thank Mr. Gill Gladding for arranging anticonvulsant testing through the Antiepileptic Drug Development Program of the National Institutes of Health. This investigation was supported by a grant from the National Institute of Neurological and Communicative Disorders and Stroke.

A New Method for Assaying Propantheline and Its Degradation Product, Xanthene-9-carboxylic Acid Using High-Performance Liquid Chromatography

B. G. CHARLES ˣ **and P. J. RAVENSCROFT**

Received November 3, 1981, from the *Department of Clinical Pharmacology, Princess Alexandra Hospital, Woolloongabba, Q. 4102 Australia.* Accepted for publication March 10, 1982.

Abstract □ A rapid, specific, and precise high-performance liquid chromatographic method is described for the simultaneous analysis of propantheline bromide and its hydrolysis product, xanthene-9-carboxylic acid. Reversed-phase chromatography was conducted using a mobile phase of 40:60, acetonitrile–0.05 *M* phosphate buffer (pH 2.5) delivered at 2 ml/min. Detection was at 254 nm. Methantheline bromide (internal standard), propantheline bromide, and xanthene-9-carboxylic acid gave retention times of 4.1, 5.4, and 8.3 min, respectively. Within-day, between-day, and total precision (*CV*) for assay of 15 mg/10 ml propantheline bromide are 1.2, 1.1, and 1.6%, respectively ($n = 20$). Similar precision was obtained for xanthene-9-carboxylic acid. The limit of detection was 2 ng. The assay is useful for routine quality assurance of propantheline in dosage forms and for stability and kinetic studies.

Keyphrases □ Propantheline—new method of high-performance liquid chromatographic assay, degradation product, xanthene-9-carboxylic acid □ Xanthene-9-carboxylic acid—degradation product, new method of high-performance liquid chromatographic assay of propantheline □ High-performance liquid chromatography—new method for assaying propantheline and its degradation product, xanthene-9-carboxylic acid

Propantheline bromide [(2-hydroxyethyl)diisopropylmethylammonium bromide xanthene-9-carboxylate] is a parasympatholytic agent which has been used to treat conditions such as urinary incontinence and GI ulceration. The development of efficient methods to measure propantheline in dosage formulations has received little attention in recent times. Some of the compendial methods to assay the drug are time consuming, often requiring several extractions followed by nonaqueous titration (1, 2). The measurement of propantheline by direct UV assay is not specific for the drug with the risk of interference from formulation excipients, drug impurities, or decomposition products of propantheline. Several organic dye–salt partition techniques have been used to assay propantheline in biological fluids (3, 4) and in pharmaceuticals (5). Various modifications of these procedures are used in the pharmaceutical industry for the quality assurance of propantheline. Most of these methods are lengthy and complex, requiring multiple extractions with one or more organic solvents before the dye–propantheline complex is measured by visible or fluorescence spectroscopy.

Propantheline has also been measured in plasma and urine by gas chromatography–mass spectroscopy (6); however, this requires highly expensive and specialized instrumentation and is unsuitable for routine assay of the drug in dosage forms.

A method for assaying propantheline by reversed-phase, high-performance liquid chromatography (HPLC) is reported here. The assay requires minimal sample preparation and has the ability to codetermine xanthene-9-carboxylic acid, a major degradation product of propantheline.

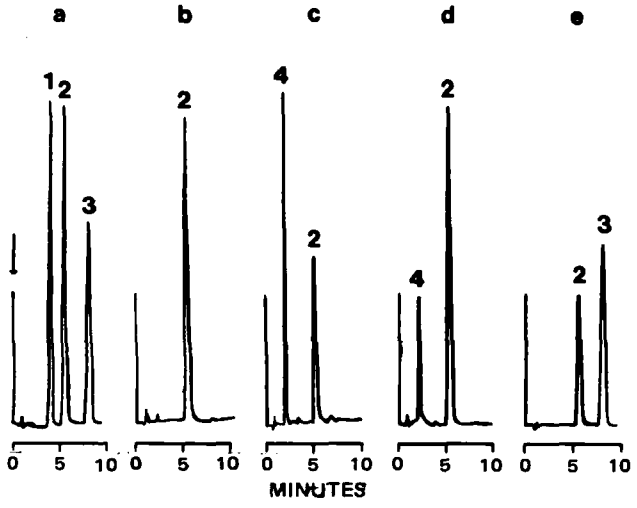

Figure 1—*Representative chromatograms for the HPLC assay of: (a) methantheline bromide, propantheline bromide, and xanthene-9-carboxylic acid reference compounds; (b) propantheline bromide tablet, 15 mg (brand A); (c) propantheline bromide tablet, 15 mg (brand B); (d) propantheline bromide ampule, 30 mg (brand A); (e) propantheline bromide hydrolysis reaction, (pH 10.1, 0.05* M *carbonate buffer, room temperature, 25 min). Key: (1) methantheline bromide; (2) propantheline bromide; (3) xanthene-9-carboxylic acid; (4) unidentified peak (see text). The injection event is represented by the arrow.*

EXPERIMENTAL

Apparatus—High-performance liquid chromatography was performed on a modular system consisting of pump[1], injector[2], bonded-phase microparticulate column[3], fixed wavelength detector[4], and chart recorder[5].

Reagents—Methantheline bromide[6], propantheline bromide[6], and xanthene-9-carboxylic acid[7] were used as received. Potassium dihydrogen orthophosphate, orthophosphoric acid, sodium carbonate, and sodium bicarbonate were analytical grade. Acetonitrile and methanol, HPLC grade[8], and reagent grade water[9] were used throughout the study.

Liquid Chromatography—Phosphate buffer (0.05 *M*) was prepared by dissolving potassium dihydrogen orthophosphate (6.805 g) in 900 ml of water, adjusting to pH 2.5 with orthophosphoric acid, and making up to 1 liter with water. The mobile phase was prepared by slowly adding 400 ml of acetonitrile to 600 ml of rapidly stirred phosphate buffer. Solutions were routinely filtered[10] and vacuum deoxygenated before chromatography. The mobile phase was delivered at 2 ml/min at a pressure of 1500 psi. Injections were made with a special high-performance liquid chromatographic (HPLC) syringe[11], and the column eluent

[1] Model 6000A, Waters Associates, Milford, Mass.
[2] Model 7120, Rheodyne Inc., Berkeley, Calif.
[3] μBondapak C_{18}, Waters Associates.
[4] Model 440, Waters Associates.
[5] Omniscribe, Houston Instruments, Austin, Tex.
[6] G.D. Searle & Co., Chicago, Ill.
[7] Aldrich Chemical Co., Ltd., Gillingham, Dorset, U.K.
[8] Waters Associates.
[9] Milli-Q System, Millipore Corp., Bedford, Mass.
[10] 0.5-μm FH filter pads, Millipore Corp.
[11] 10 μl, Hamilton Corp., Reno, Nev.

0022-3549/83/0100-0096$01.00/0

Table I—Estimates of the Precision of the Assay of Propantheline Bromide [a] and Xanthene-9-carboxylic Acid [a] by High-Performance Liquid Chromatography

Source of Variation	Propantheline Bromide		Xanthene-9-Carboxylic Acid	
	SD	*CV*, %	*SD*	*CV*, %
Between-day	0.0116	1.1	0.0148	0.8
Within-day	0.0121	1.2	0.0230	1.2
Total	0.0168	1.6	0.0273	1.4

[a] 15 mg/10 ml.

was monitored at 254 nm with the detector set at 0.05 or 0.1 aufs. Chromatograms were obtained with the recorder set for a 10-mV input and a chart speed of 2.5 mm/min. All chromatography was conducted at ambient temperature (~22°).

Analytical Procedure—*Calibration Standards*—Methanolic stock solutions (100 mg in 10 ml) of propantheline bromide, methantheline bromide, and xanthene-9-carboxylic acid were prepared daily. Working standards were prepared by pipetting 3, 2, 1, and 0.5 ml of the propantheline and xanthene-9-carboxylic acid stock solutions into four 10-ml volumetric flasks. One milliliter of methantheline bromide stock solution was added to each flask and the solutions were adjusted to volume with methanol. Thus, the working standards contained 30, 20, 10, and 5 mg of both propantheline bromide and xanthene-9-carboxylic acid in 10 ml, with 10 mg of methantheline bromide as the internal standard. These standards were analyzed by HPLC. Calibration graphs were constructed daily by plotting the ratios of the peak heights of both propantheline and xanthene-9-carboxylic acid to methantheline *versus* the weights of propantheline and xanthene-9-carboxylic acid in the standards. The calibration data were analyzed by standard, linear least-squares regression methods.

Quality Assurance—For determination of the propantheline bromide content of tablets, the following procedure was followed: A 15-mg tablet of propantheline bromide was pulverized and a 10-ml solution of methanol containing 10 mg of the internal standard was added. The solution was stirred for at least 15 min and filtered or centrifuged to obtain a particle-free solution. One microliter of the solution was injected onto the liquid chromatograph. Alternatively, intact tablets may be dissolved in 0.1 *M* hydrochloric acid or an aqueous buffer of <pH 5.0 containing the internal standard. For the assay of freeze-dried ampules of propantheline bromide (30 mg), 1 ml of methanol (containing 20 mg of internal standard) was injected into the vial. The solution was dissolved by shaking, and 0.5 ml was withdrawn and diluted to 10 ml with methanol. One microliter was injected.

Assay Precision—Methanolic stock solutions of both propantheline bromide and xanthene-9-carboxylic acid (75 mg in 5 ml) and the internal standard (50 mg in 5 ml) were prepared. Four replicate dilutions of the stocks were made in methanol so that each contained 15 mg of both propantheline bromide and xanthene-9-carboxylic acid and 10 mg of the internal standard in 10 ml. The four replicates were analyzed by HPLC, as described previously. The entire procedure was repeated daily, for 5 days, using fresh mobile phase each day. The data were treated statistically using one-way ANOVA.

Propantheline Hydrolysis—One hundred microliters of a methanolic stock solution of propantheline bromide (15 mg/10 ml) was dried under a stream of air and reconstituted in 1.0 ml of carbonate buffer (0.05 *M*, pH 10.1). A sample (1.0 μl) was withdrawn after 25 min and injected into the liquid chromatograph.

RESULTS AND DISCUSSION

Figure 1 shows chromatograms obtained following the HPLC analysis of propantheline bromide, methantheline bromide, and xanthene-9-carboxylic acid reference compounds, commercially available propantheline bromide tablets and ampules, and a propantheline hydrolysis reaction. Retention times of 4.1, 5.4, and 8.3 min were obtained for methantheline, propantheline, and xanthene-9-carboxylic acid, respectively, as seen in Fig. 1(a). For each compound, sharp, symmetrical peaks were obtained with baseline resolution and minimal tailing. Methantheline bromide served as an ideal internal standard, since it has similar spectral and chromatographic properties to propantheline. Interestingly, methantheline bromide and propantheline bromide belong to the quaternary nitrogen class of compounds, the members of which often require the presence of heptane- or pentanesulfonic acid counterions in the mobile phase for reversed-phase HPLC analysis. With the present method, paired-ion chromatography is unnecessary for the assay of propantheline bromide. The minimum detectable amount of propantheline bromide and xanthene-9-carboxylic acid was ~100 ng, although this could be decreased to ~2 ng using a 50-μl injection with the detector set to 0.01 aufs.

The chromatograms in Fig. 1(b, c) were obtained during the analysis of two commercially available brands of propantheline bromide tablets (15 mg). The peak height obtained with brand A (Fig. 1b) was similar to that obtained when a standard solution of propantheline bromide (15 mg/10 ml) was assayed. However, the results in Fig. 1(c) indicate that only half the nominal amount of the drug was present in the brand B tablets. Repeated assays of tablets from different batches of this preparation confirmed that the propantheline content was consistently <15 mg. Furthermore, an extra peak with a retention time of 2 min appeared in these chromatograms, indicating the presence of a breakdown product or impurity. As seen in Fig. 1(d), a peak with similar retention time appeared when propantheline bromide ampules (brand A) were assayed, although the height in this case was considerably less than found in the brand B tablets. While the identity of the unknown peak is yet to be established, it is interesting to note that all products tested were from new stock.

A previous study (7) has shown that propantheline is hydrolyzed to xanthene-9-carboxylic acid in aqueous solutions of pH >5.0. In this regard, the present assay may be useful when the stability of propantheline is under investigation, particularly since both the substrate and hydrolysis product can be measured in a single chromatographic run. To support this, the results in Fig. 1(e) show the decrease in propantheline concentration and appearance of xanthene-9-carboxylic acid following exposure of propantheline bromide (15 mg/10 ml) to pH 10.1 carbonate buffer for 25 min at room temperature.

The analysis of standard solutions of propantheline bromide and xanthene-9-carboxylic acid gave calibration graphs which were linear from 5 mg/10 ml to at least 30 mg/10 ml. The average of five replicate sets of standards (one replicate per day) gave calibration graphs of $y = 0.066x + 0.026$ ($r > 0.999$) for propantheline and $y = 0.122x + 0.052$ ($r > 0.999$) for xanthene-9-carboxylic acid, where y is the peak height ratio and x is the analyte concentration. Methanolic stock solutions of methantheline bromide, propantheline bromide, and xanthene-9-carboxylic acid were stable for at least 3 weeks when stored at room temperature.

The precision of the assay was assessed by analyzing solutions of propantheline bromide and xanthene-9-carboxylic acid, four times daily, on each of 5 days using new stock solutions and mobile phase each day. We chose a solution of 15 mg in 10 ml, since this is the nominal concentration obtained when a 15-mg propantheline bromide tablet is assayed by the recommended procedure. Estimates of the day-to-day, within-day, and total precision of the assay were calculated from ANOVAs of the data as described previously (8). These results appear in Table I. Coefficients of variation for the assay were determined from the mean peak height ratio for all assays of propantheline (1.021) and xanthene-9-carboxylic acid (1.903) and the appropriate standard deviation. It is preferable to use an internal standard in the assay, since the injection volume (1 μl) is less than the maximum volumes accommodated by commercially available sample loops. If samples >1 μl are to be injected, it is recommended that the samples be diluted appropriately, otherwise nonlinearity in the calibration graphs may result. Moreover, if the internal standard is not used, it is advisable that at least two duplicate injections be made per sample.

In conclusion, the present assay provides a rapid, specific, and precise method for the simultaneous determination of propantheline bromide and xanthene-9-carboxylic acid by HPLC.

This novel assay would be useful for the routine, quality assurance of propantheline and for assessing the stability and reaction kinetics of the drug.

REFERENCES

(1) "The United States Pharmacopeia," 20th rev., U.S. Pharmacopeial Convention, Rockville, Md., 1980, p. 671.

(2) "The British Pharmacopeia," Her Majesty's Stationery Office, London, 1980, p. 814.

(3) M. Pfeffer, J. M. Schor, S. Bolton, and R. Jacobsen, *J. Pharm Sci.*, **57**, 1375 (1968).

(4) D. Westerlund and K. H. Karset, *Anal. Chim. Acta*, **67**, 99 (1973).

(5) L. G. Chatten and K. O. Okamura, *J. Pharm. Sci.*, **62**, 1328

(1973).
(6) G. C. Ford, S. J. W. Grigson, N. J. Haskins, R. F. Palmer, M. Prout, and C. W. Vose, *Biomed. Mass Spectrom.*, **4**, 94 (1977).
(7) B. Beermann, K. Hollström, and A. Rosen, *Clin. Pharmacol. Ther.*, **13**, 212 (1972).
(8) J. S. Krouwer, *Clin. Chem.*, **27**, 202 (1981).

ACKNOWLEDGMENTS

Propantheline bromide and methantheline bromide were donated by Searle Research and Development Division of G.D. Searle and Co., Chicago, through Searle Laboratories Division of Searle Australia, Sydney.

COMMUNICATIONS

Assessment of 75/75 Rule: FDA Viewpoint

Keyphrases □ Bioavailability—studies involving subjects with intersubject coefficient of variation, assessment of 75/75 Rule, FDA viewpoint □ Bioequivalence—bioavailability studies involving subjects with intersubject coefficient of variation, assessment of 75/75 Rule, FDA viewpoint.

To the Editor:

Recently, the new 75/75 specification proposed by the FDA for Bioequivalency Studies came under criticism (1) as being scientifically invalid and unpredictable in bioavailability studies involving subjects with intersubject coefficient of variation (*CV*) of 60% and intrasubject *CV* of 20–30%. Similar criticism also has been launched at the FDA for application of the 75/75 Rule in establishing an *in vitro–in vivo* correlation. Although the FDA does not disagree with the calculated results on hypothetical problems in the published article and the application of the Pittman–Morgan test when appropriate, the authors of the proposed FDA rule do disagree with the underlying assumptions of the author, *i.e.*, that such large variations are the norm in bioequivalency studies.

It has been observed by the FDA that for the large majority of drugs for which bioavailability bioequivalence data are submitted as part of a New Drug Application, the coefficient of variation is generally <40%, assuming that a properly validated analytical assay is employed. To substantiate the latter claims, a review of FDA reports over a 5-year period by a primary FDA contractor (2) is summarized in Table I. The FDA review reveals that the coefficients of variation among 106 total drug products involving 12 drug entities were generally well within the 40% range. Only in the case of diphenhydramine (Table I) was

Table I—Summary of Bioavailability Studies [a]

Drug	Number of Products Tested	*CV*, % (C_{max})[b]	*CV*, % (*AUC*)[b]	Number of Products with *CV* >40%
Phenytoin	a. 6	14–33	16–45	1
	b. 6	19–24	19–26	0
Meprobamate	a. 6	6–21	12–26	0
	b. 6	15–24	22–37	0
Chlorothiazide	6	—	30–46[c]	1
Acetazolamide	4	19–36	17–30	0
Propylthiouracil	6	16–23	16–29	0
Warfarin	5	10–20	9–13	0
Griseofulvin	a. 6	21–40	14–26	0
	b. 6	27–46	24–30	1
Diphenhydramine	a. 6	14–54	35–67	4
	b. 6	36–48	40–62	5
Tolbutamide	7	12–20	18–24	0
Phenobarbital	6	16–23	21–34	0
Sulfisoxazole	a. 6	5–13	7–16	0
	b. 6	15–25	20–32	0
Trichlormethiazide	a. 5	30–35	26–35	0
	b. 5	17–25	11–26	0

[a] Studies performed under FDA Contract 223-77-3011. The total number of drug products tested was 106. The total number of drug products exceeding 40% *CV* was 12. [b] Range of *CV* values for peak plasma level (C_{max}) and area under the curve (*AUC*). [c] Range of *CV* for total cumulative urinary excretion.

Table II—Proportion of 1000 Simulated Studies with 12 Hypothetical Drugs Meeting 75/75 Rule [a]

Drug	N[b]	Intersubject *CV* TP[c]	Intersubject *CV* RP[d]	Intrasubject *CV*	Proportion of 1000 Studies Meeting 75/75 Criterion							
					p[e] = 0	p = 0.3	p = 0.4	p = 0.5	p = 0.6	p = 0.7	p = 0.8	p = 0.9
Case 1	24	60	60	30	0.15	0.19	0.22	0.26	0.30	0.35	0.43	0.52
Case 2	24	40	40	30	0.72	0.78	0.79	0.81	0.84	0.86	0.88	0.90
Case 3	24	60	40	30	0.29	0.32	0.34	0.36	0.38	0.39	0.41	0.43
Case 4	12	60	60	20	0.24	0.29	0.32	0.35	0.40	0.47	0.54	0.66
Case 5	12	40	40	20	0.55	0.63	0.66	0.69	0.73	0.79	0.82	0.88
Case 6	12	60	40	20	0.38	0.44	0.45	0.47	0.51	0.53	0.56	0.59
Case 7	12	30	30	15	0.74	—	—	0.87	—	0.91	—	0.98
Case 8	12	15	15	13	1.00	1.00	—	1.00	—	1.00	—	1.00
Case 9	12	30	15	13	0.84	—	—	0.86	—	0.88	—	0.89
Case 10	12	30	30	10	0.68	—	—	0.86	—	0.94	—	0.99
Case 11	12	15	15	10	1.00	1.00	—	1.00	—	1.00	—	1.00
Case 12	12	30	15	10	0.80	—	—	0.86	—	0.89	—	0.91

[a] Portion of Table II, *i.e.*, drugs 1–6, published by Haynes (1) drugs 7–12 was generated by Dr. Haynes at the request of Dr. Purich for presentation at the 1981 International Industrial Pharmacy Conference, Austin, Tex. [b] N is the number of subjects. [c] TP is the test product. [d] RP is the reference product. [e] Correlation coefficients between *AUC* values for test and reference products in the same individual.

0022-3549/83/0100-0098$01.00/0

(1973).
(6) G. C. Ford, S. J. W. Grigson, N. J. Haskins, R. F. Palmer, M. Prout, and C. W. Vose, *Biomed. Mass Spectrom.*, **4**, 94 (1977).
(7) B. Beermann, K. Hollström, and A. Rosen, *Clin. Pharmacol. Ther.*, **13**, 212 (1972).
(8) J. S. Krouwer, *Clin. Chem.*, **27**, 202 (1981).

ACKNOWLEDGMENTS

Propantheline bromide and methantheline bromide were donated by Searle Research and Development Division of G.D. Searle and Co., Chicago, through Searle Laboratories Division of Searle Australia, Sydney.

COMMUNICATIONS

Assessment of 75/75 Rule: FDA Viewpoint

Keyphrases □ Bioavailability—studies involving subjects with intersubject coefficient of variation, assessment of 75/75 Rule, FDA viewpoint □ Bioequivalence—bioavailability studies involving subjects with intersubject coefficient of variation, assessment of 75/75 Rule, FDA viewpoint.

To the Editor:

Recently, the new 75/75 specification proposed by the FDA for Bioequivalency Studies came under criticism (1) as being scientifically invalid and unpredictable in bioavailability studies involving subjects with intersubject coefficient of variation (*CV*) of 60% and intrasubject *CV* of 20–30%. Similar criticism also has been launched at the FDA for application of the 75/75 Rule in establishing an *in vitro–in vivo* correlation. Although the FDA does not disagree with the calculated results on hypothetical problems in the published article and the application of the Pittman–Morgan test when appropriate, the authors of the proposed FDA rule do disagree with the underlying assumptions of the author, *i.e.*, that such large variations are the norm in bioequivalency studies.

It has been observed by the FDA that for the large majority of drugs for which bioavailability bioequivalence data are submitted as part of a New Drug Application, the coefficient of variation is generally <40%, assuming that a properly validated analytical assay is employed. To substantiate the latter claims, a review of FDA reports over a 5-year period by a primary FDA contractor (2) is summarized in Table I. The FDA review reveals that the coefficients of variation among 106 total drug products involving 12 drug entities were generally well within the 40% range. Only in the case of diphenhydramine (Table I) was

Table I—Summary of Bioavailability Studies [a]

Drug	Number of Products Tested	*CV*, % (C_{max})[b]	*CV*, % (*AUC*)[b]	Number of Products with *CV* >40%
Phenytoin	a. 6	14–33	16–45	1
	b. 6	19–24	19–26	0
Meprobamate	a. 6	6–21	12–26	0
	b. 6	15–24	22–37	0
Chlorothiazide	6	—	30–46[c]	1
Acetazolamide	4	19–36	17–30	0
Propylthiouracil	6	16–23	16–29	0
Warfarin	5	10–20	9–13	0
Griseofulvin	a. 6	21–40	14–26	0
	b. 6	27–46	24–30	1
Diphenhydramine	a. 6	14–54	35–67	4
	b. 6	36–48	40–62	5
Tolbutamide	7	12–20	18–24	0
Phenobarbital	6	16–23	21–34	0
Sulfisoxazole	a. 6	5–13	7–16	0
	b. 6	15–25	20–32	0
Trichlormethiazide	a. 5	30–35	26–35	0
	b. 5	17–25	11–26	0

[a] Studies performed under FDA Contract 223-77-3011. The total number of drug products tested was 106. The total number of drug products exceeding 40% *CV* was 12. [b] Range of *CV* values for peak plasma level (C_{max}) and area under the curve (*AUC*). [c] Range of *CV* for total cumulative urinary excretion.

Table II—Proportion of 1000 Simulated Studies with 12 Hypothetical Drugs Meeting 75/75 Rule [a]

Drug	N[b]	Intersubject *CV* TP[c]	Intersubject *CV* RP[d]	Intrasubject *CV*	Proportion of 1000 Studies Meeting 75/75 Criterion							
					p[e] = 0	p = 0.3	p = 0.4	p = 0.5	p = 0.6	p = 0.7	p = 0.8	p = 0.9
Case 1	24	60	60	30	0.15	0.19	0.22	0.26	0.30	0.35	0.43	0.52
Case 2	24	40	40	30	0.72	0.78	0.79	0.81	0.84	0.86	0.88	0.90
Case 3	24	60	40	30	0.29	0.32	0.34	0.36	0.38	0.39	0.41	0.43
Case 4	12	60	60	20	0.24	0.29	0.32	0.35	0.40	0.47	0.54	0.66
Case 5	12	40	40	20	0.55	0.63	0.66	0.69	0.73	0.79	0.82	0.88
Case 6	12	60	40	20	0.38	0.44	0.45	0.47	0.51	0.53	0.56	0.59
Case 7	12	30	30	15	0.74	—	—	0.87	—	0.91	—	0.98
Case 8	12	15	15	13	1.00	1.00	—	1.00	—	1.00	—	1.00
Case 9	12	30	15	13	0.84	—	—	0.86	—	0.88	—	0.89
Case 10	12	30	30	10	0.68	—	—	0.86	—	0.94	—	0.99
Case 11	12	15	15	10	1.00	1.00	—	1.00	—	1.00	—	1.00
Case 12	12	30	15	10	0.80	—	—	0.86	—	0.89	—	0.91

[a] Portion of Table II, *i.e.*, drugs 1–6, published by Haynes (1) drugs 7–12 was generated by Dr. Haynes at the request of Dr. Purich for presentation at the 1981 International Industrial Pharmacy Conference, Austin, Tex. [b] N is the number of subjects. [c] TP is the test product. [d] RP is the reference product. [e] Correlation coefficients between *AUC* values for test and reference products in the same individual.

0022-3549/83/0100-0098$01.00/0

a significant problem encountered in utilizing the 75/75 Rule. Of 106 drug products tested in 18 bioavailability studies, 94 products had <40% *CV*.

The author of the original article pointed out that given a true correlation coefficient, $\rho = 0.90$, the probability of success utilizing the 75/75 Rule was 90% in bioavailability trials involving 24 subjects where the intersubject *CV* is 40% for both the test and reference drug, and the intrasubject *CV* is 30%. The probability of success of applying the 75/75 Rule will significantly increase when the inter- and intrasubject variations are reduced to <40 and 30%, respectively (Table II) (2). The proportion of 1000 studies involving as few as 12 subjects meeting the 75/75 Rule utilizing drugs with an intersubject *CV* of <40% and an intrasubject *CV* of <20% is >88%, and 98% with inter- and intrasubject *CV*s of 30 and 15%, respectively.

The application of the 75/75 Rule is only valid for drugs having a well-defined reference standard that has reproducible pharmacokinetic properties in terms of absorption and clearance. Drugs having a large coefficient of variation associated with extensive first-pass metabolism are often required to undergo multiple-dose steady-state study comparisons or other more appropriate study design as a basis of drug approval. To achieve these results, the FDA often utilizes an oral solution as a basis of comparison where the reference drug has poor bioavailability. Also, the 75/75 Rule is only applied in conjunction with a proper analysis of variance and the FDA relies on additional data analyses.

(1) J. D. Haynes, *J. Pharm. Sci.*, **70**, 673 (1981).
(2) M. C. Meyer, FDA Contract No. 223-77-3011 (Univ. of Tennessee A1975-1981 Reports).

Bernard E. Cabana
Director, Division of Biopharmaceutics
Food and Drug Administration
Rockville, MD 20857

Received April 2, 1982.
Accepted for publication September 9, 1982.

FDA 75/75 Rule: A Response

Keyphrases □ Bioavailability—studies involving subjects with intersubject coefficient of variation, FDA 75/75 Rule □ Bioequivalance—studies involving subjects with intersubject coefficient of variation, FDA 75/75 Rule

To the Editor:

Dr. Cabana's communication (1) refers to an article (2) that is critical on statistical grounds of the FDA Division of Biopharmaceutic's proposed 75/75 Rule for bioequivalency studies. We emphasize that the point deserving discussion here is not the rigor of the 75/75 Rule, but rather, the fatal flaws inherent in its form. The same flaws would exist even if the rule were less rigorous (50/50) or more rigorous (90/90), because it would retain the same undesirable form: the dispersion of certain ratios. We applaud the vast majority of the pharmacokinetic–bioavailability–bioequivalency regulations and guidelines as contributing to the improvement of health care; we also are glad to see that the FDA accepts the Pitman–Morgan *F*-test as the proper test for equality of test-product and reference-product variation in crossover bioavailability–bioequivalency studies. This *F*-test is described in the statistical literature as "uniformly most powerful" (3); therefore, no other test of variation in a study can have as much statistical power for detection of true differences in standard deviations. The word uniform indicates that this superiority holds for differences of all magnitudes.

In essence we agree with the communication (1) which states that the intersubject coefficient of variation (*CV*) of 40% used previously (2) is not the norm. The choice of 40% per se is not critical; however, the question is whether the results would be much different at a 35% *CV*. Such large coefficients of variation reflect the skewness of the distributions. It also should be noted that the intrasubject *CV* is 20 or 30%, common values for the error term in the analysis of variance (ANOVA).

The performance in a certain region of a proposed statistical test, such as the 75/75 Rule, generally is not very interesting to the statistician designers and the users of such a rule. The main interest in the performance of the proposed test centers on how the more variable drug products are treated by the test—whether they are treated fairly in this respect. The number of such drug products is not negligible, accounting for ≥10% (depending on a cutoff *CV* of 35 or 40%) of drugs studied, according to Dr. Cabana's Table I (1). (If other parameters for a test product have unacceptable values, they should not obscure the point under consideration.) "Are they treated fairly?" is the question addressed earlier (2) for the case of equal averages, and the answer is that they are not. For example, according to the 75/75 Rule, a test product for chlorothiazide with a variation of *AUC* values that is 50% greater than the variation of the reference product *AUC* values usually has a greater chance of being declared bioequivalent than does a test product for phenytoin with the same variation as its reference product.

The main flaw of the 75/75 Rule lies in the fact that the degree of dispersion of the ratio depends on the dispersion or both products, test and reference, without distinction. Thus, a test product which fails the 75/75 Rule in a study may do so because the reference product standard deviation is relatively large—the reference product should fail the dispersion test in that study. For example, for the 12 drugs in Dr. Cabana's Table I (1), suppose that in each study a test product always had the smallest coefficient of variation shown for that drug and the reference product had the largest coefficient of variation—both products with the same average. The unadjusted *F*-values would be, for the *AUC* columns of Table I (1): 7.9, 1.9, 4.7, 2.8, 2.4, 3.1, 3.3, 2.1, 3.4, 1.6, 3.7, 2.4, 1.8, 2.6, 5.2, 2.6. 1.8, and 5.6. Superior uniformity would be indicated for such test products but probably many would fail the 75/75 Rule falsely, because the greater variability is that of the reference products.

The statement that the 75/75 Rule "is only applied in conjunction with a proper analysis of variance" (1) implies a remedy, probably subjective, but the fatal flaws remain; the rule should be withdrawn. Furthermore, since the performance of the 75/75 Rule is affected by differences in the two mean *AUC*s (for test and reference materials),

0022-3549/83/0100-0099$01.00/0

a significant problem encountered in utilizing the 75/75 Rule. Of 106 drug products tested in 18 bioavailability studies, 94 products had <40% *CV*.

The author of the original article pointed out that given a true correlation coefficient, $\rho = 0.90$, the probability of success utilizing the 75/75 Rule was 90% in bioavailability trials involving 24 subjects where the intersubject *CV* is 40% for both the test and reference drug, and the intrasubject *CV* is 30%. The probability of success of applying the 75/75 Rule will significantly increase when the inter- and intrasubject variations are reduced to <40 and 30%, respectively (Table II) (2). The proportion of 1000 studies involving as few as 12 subjects meeting the 75/75 Rule utilizing drugs with an intersubject *CV* of <40% and an intrasubject *CV* of <20% is >88%, and 98% with inter- and intrasubject *CV*s of 30 and 15%, respectively.

The application of the 75/75 Rule is only valid for drugs having a well-defined reference standard that has reproducible pharmacokinetic properties in terms of absorption and clearance. Drugs having a large coefficient of variation associated with extensive first-pass metabolism are often required to undergo multiple-dose steady-state study comparisons or other more appropriate study design as a basis of drug approval. To achieve these results, the FDA often utilizes an oral solution as a basis of comparison where the reference drug has poor bioavailability. Also, the 75/75 Rule is only applied in conjunction with a proper analysis of variance and the FDA relies on additional data analyses.

(1) J. D. Haynes, *J. Pharm. Sci.*, **70**, 673 (1981).
(2) M. C. Meyer, FDA Contract No. 223-77-3011 (Univ. of Tennessee A1975-1981 Reports).

Bernard E. Cabana
Director, Division of Biopharmaceutics
Food and Drug Administration
Rockville, MD 20857

Received April 2, 1982.
Accepted for publication September 9, 1982.

FDA 75/75 Rule: A Response

Keyphrases □ Bioavailability—studies involving subjects with intersubject coefficient of variation, FDA 75/75 Rule □ Bioequivalance—studies involving subjects with intersubject coefficient of variation, FDA 75/75 Rule

To the Editor:

Dr. Cabana's communication (1) refers to an article (2) that is critical on statistical grounds of the FDA Division of Biopharmaceutic's proposed 75/75 Rule for bioequivalency studies. We emphasize that the point deserving discussion here is not the rigor of the 75/75 Rule, but rather, the fatal flaws inherent in its form. The same flaws would exist even if the rule were less rigorous (50/50) or more rigorous (90/90), because it would retain the same undesirable form: the dispersion of certain ratios. We applaud the vast majority of the pharmacokinetic–bioavailability–bioequivalency regulations and guidelines as contributing to the improvement of health care; we also are glad to see that the FDA accepts the Pitman–Morgan *F*-test as the proper test for equality of test-product and reference-product variation in crossover bioavailability–bioequivalency studies. This *F*-test is described in the statistical literature as "uniformly most powerful" (3); therefore, no other test of variation in a study can have as much statistical power for detection of true differences in standard deviations. The word uniform indicates that this superiority holds for differences of all magnitudes.

In essence we agree with the communication (1) which states that the intersubject coefficient of variation (*CV*) of 40% used previously (2) is not the norm. The choice of 40% per se is not critical; however, the question is whether the results would be much different at a 35% *CV*. Such large coefficients of variation reflect the skewness of the distributions. It also should be noted that the intrasubject *CV* is 20 or 30%, common values for the error term in the analysis of variance (ANOVA).

The performance in a certain region of a proposed statistical test, such as the 75/75 Rule, generally is not very interesting to the statistician designers and the users of such a rule. The main interest in the performance of the proposed test centers on how the more variable drug products are treated by the test—whether they are treated fairly in this respect. The number of such drug products is not negligible, accounting for ≥10% (depending on a cutoff *CV* of 35 or 40%) of drugs studied, according to Dr. Cabana's Table I (1). (If other parameters for a test product have unacceptable values, they should not obscure the point under consideration.) "Are they treated fairly?" is the question addressed earlier (2) for the case of equal averages, and the answer is that they are not. For example, according to the 75/75 Rule, a test product for chlorothiazide with a variation of *AUC* values that is 50% greater than the variation of the reference product *AUC* values usually has a greater chance of being declared bioequivalent than does a test product for phenytoin with the same variation as its reference product.

The main flaw of the 75/75 Rule lies in the fact that the degree of dispersion of the ratio depends on the dispersion or both products, test and reference, without distinction. Thus, a test product which fails the 75/75 Rule in a study may do so because the reference product standard deviation is relatively large—the reference product should fail the dispersion test in that study. For example, for the 12 drugs in Dr. Cabana's Table I (1), suppose that in each study a test product always had the smallest coefficient of variation shown for that drug and the reference product had the largest coefficient of variation—both products with the same average. The unadjusted *F*-values would be, for the *AUC* columns of Table I (1): 7.9, 1.9, 4.7, 2.8, 2.4, 3.1, 3.3, 2.1, 3.4, 1.6, 3.7, 2.4, 1.8, 2.6, 5.2, 2.6. 1.8, and 5.6. Superior uniformity would be indicated for such test products but probably many would fail the 75/75 Rule falsely, because the greater variability is that of the reference products.

The statement that the 75/75 Rule "is only applied in conjunction with a proper analysis of variance" (1) implies a remedy, probably subjective, but the fatal flaws remain; the rule should be withdrawn. Furthermore, since the performance of the 75/75 Rule is affected by differences in the two mean *AUC*s (for test and reference materials),

0022-3549/83/0100-0099$01.00/0

as well as differences in the two standard deviations, and since the means themselves are tested for equality in the ANOVA, the 75/75 Rule also might be said to place the test product in double jeopardy.

The stress placed previously (1) on a "well-defined reference standard which has reproducible pharmacokinetic properties in terms of absorption and clearance" or "an oral solution" makes us ask just where the criterion of acceptable reproducibility of a reference standard is set down?

(1) B. E. Cabana, *J. Pharm. Sci.*, **72**, 98 (1983).
(2) J. D. Haynes, *ibid*, **70**, 673 (1981).
(3) M. G. Kendall, "The Advanced Theory of Statistics," 3rd ed., vol. 2, Hafner, New York, N.Y., 1973, p. 531.

John D. Haynes
Medical Research Division
Lederle Laboratories,
American Cyanamid Co.
Pearl River, NY 10965

Received May 25, 1982.
Accepted for publication September 9, 1982.

Radioimmunoassay for the New Antiarrhythmic Agent Cibenzoline in Human Plasma

Keyphrases □ Cibenzoline—new antiarrhythmic agent, radioimmunoassay in human plasma □ Antiarrhythmic agent—cibenzoline, radioimmunoassay in human plasma □ Radioimmunoassay—cibenzoline, a new antiarrhythmic agent, human plasma

To the Editor:

Cibenzoline [*dl*-4,5-dihydro-2-(2,2-diphenylcyclopropyl)-1H-imidazole] (I), a new oral antiarrhythmic agent with a novel chemical structure, is presently undergoing clinical evaluation. The present report describes the development and characteristics of a radioimmunoassay for cibenzoline which permits its quantitation directly in human plasma.

To obtain antibodies to cibenzoline, an immunogen was first prepared by covalently coupling the N_1-acetic acid derivative of cibenzoline[1] (II), as a hapten, to bovine serum albumin using a mixed anhydride procedure (1). Rabbits were immunized with the resulting conjugate, and the antiserum with the highest titer of antibodies of cibenzoline was used.

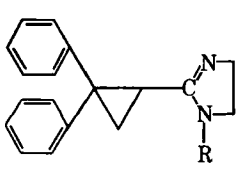

I: R = —H
II: R = CH_2CO_2H

The radioligand used for the assay was [^{3}H]cibenzoline with a specific activity of 10.8 Ci/m*M*[2]. Prior to use, radiochemical purity was established by TLC on silica gel using ethyl acetate–methanol–ammonia (80:15:5) as the solvent system.

The radioimmunoassay was carried out in 12 × 75-mm disposable glass tubes using 0.1 *M* phosphate buffered saline (pH 7.4) containing 0.1% gelatin and 0.1% sodium azide as the assay buffer. Plasma samples (0.02–0.1 ml) containing standard or unknown concentrations of cibenzoline were mixed with 0.2 ml of [^{3}H]cibenzoline in buffer (10,000 cpm) followed by 0.2 ml of diluted antiserum (1:600), and the mixture was incubated at 4° for 30 min. Then, 1 ml of a stirred suspension of a polymer-bound second antibody (goat anti-rabbit IgG)[3] was added and the tube contents were vortexed briefly and allowed to stand at 4° for 1 hr. Following centrifugation at 2000 rpm for 10 min, each supernatant was aspirated off, the pellet suspended in 0.4 ml of 1 *M* acetic acid, and mixed with 3 ml of scintillation fluid[4]. The tube was capped and radioassayed directly in a liquid scintillation counter[5] modified as described previously (2). A calibration curve was generated using a four-parameter logistic curve-fitting program for a desktop calculator[6] (3).

The logit-log calibration curve for cibenzoline was linear from 4 to 200 ng/ml using a 0.1-ml sample of plasma. Such sensitivity is adequate for the quantitation of cibenzoline following administration of therapeutic doses of the drug. The intra- and interassay coefficients of variation (n = 6) did not exceed 6.5 and 10%, respectively, over a range of 38–219 ng/ml of cibenzoline in a selection of random clinical samples. Although the antiserum was found to cross-react almost 100% with the 4,5-dehydro derivative of cibenzoline, a known metabolite of the drug in the dog[7], the specificity of the radioimmunoassay for the analysis of human plasma samples was evaluated by comparison with a specific electron-capture GLC method which was developed and utilized at another research institution[8]. For 57 clinical samples analyzed by both procedures (radioimmunoassay = y), the correlation coefficient, regression line slope, and y-intercept were 0.98, 0.93, and 16, respectively, over a range of 12–287 ng/ml. Although the slope and intercept were significantly different than 1 and 0, only 4 of the 57 highly correlated (r = 0.98) observed data points lay outside the 95% confidence limits of the fitted regression line, which indicates that the radioimmunoassay is in reasonable agreement with a specific chromatographic procedure for the quantitation of cibenzoline. It has been shown by high-performance liquid chromatography (4) that only trace amounts of the 4,5-dehydro metabolite of cibenzoline are present in human plasma, and the metabolite is separated from the parent drug in the electron-capture GLC assay.

In subjects who had received 65 mg of the drug three times a day for 6 days, the peak plasma concentrations at steady-state were ~300 ng/ml of cibenzoline.

A simple radioimmunoassay procedure with adequate sensitivity and specificity was developed for the quanti-

[1] The hapten was prepared from cibenzoline by alkylation with ethyl chloroacetate in ethanol followed by base hydrolysis and crystallized from isopropanol–ether as a partial hydrate, mp 202–204°. The MS and NMR spectra were compatible with the proposed structure.
[2] Prepared by Chemical Research Division, Hoffmann-La Roche Inc.
[3] Roche Diagnostics, Nutley, NJ 07110.
[4] Aquasol, New England Nuclear Corp., Boston, MA 02118.
[5] Packard Tri-Carb model 3255.
[6] TI-59, Texas Instruments, Lubbock, TX 79408.
[7] Data on file, Hoffmann-La Roche Inc.
[8] Personal communication, Laboratoires UPSA, Rueil Malmaison, France.

0022-3549/83/0100-0100$01.00/0

as well as differences in the two standard deviations, and since the means themselves are tested for equality in the ANOVA, the 75/75 Rule also might be said to place the test product in double jeopardy.

The stress placed previously (1) on a "well-defined reference standard which has reproducible pharmacokinetic properties in terms of absorption and clearance" or "an oral solution" makes us ask just where the criterion of acceptable reproducibility of a reference standard is set down?

(1) B. E. Cabana, *J. Pharm. Sci.*, **72**, 98 (1983).
(2) J. D. Haynes, *ibid*, **70**, 673 (1981).
(3) M. G. Kendall, "The Advanced Theory of Statistics," 3rd ed., vol. 2, Hafner, New York, N.Y., 1973, p. 531.

John D. Haynes
Medical Research Division
Lederle Laboratories,
American Cyanamid Co.
Pearl River, NY 10965

Received May 25, 1982.
Accepted for publication September 9, 1982.

Radioimmunoassay for the New Antiarrhythmic Agent Cibenzoline in Human Plasma

Keyphrases □ Cibenzoline—new antiarrhythmic agent, radioimmunoassay in human plasma □ Antiarrhythmic agent—cibenzoline, radioimmunoassay in human plasma □ Radioimmunoassay—cibenzoline, a new antiarrhythmic agent, human plasma

To the Editor:

Cibenzoline [*dl*-4,5-dihydro-2-(2,2-diphenylcyclopropyl)-1H-imidazole] (I), a new oral antiarrhythmic agent with a novel chemical structure, is presently undergoing clinical evaluation. The present report describes the development and characteristics of a radioimmunoassay for cibenzoline which permits its quantitation directly in human plasma.

To obtain antibodies to cibenzoline, an immunogen was first prepared by covalently coupling the N_1-acetic acid derivative of cibenzoline[1] (II), as a hapten, to bovine serum albumin using a mixed anhydride procedure (1). Rabbits were immunized with the resulting conjugate, and the antiserum with the highest titer of antibodies of cibenzoline was used.

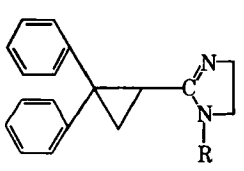

I: R = —H
II: R = CH_2CO_2H

The radioligand used for the assay was [^{3}H]cibenzoline with a specific activity of 10.8 Ci/m*M*[2]. Prior to use, radiochemical purity was established by TLC on silica gel using ethyl acetate–methanol–ammonia (80:15:5) as the solvent system.

The radioimmunoassay was carried out in 12 × 75-mm disposable glass tubes using 0.1 *M* phosphate buffered saline (pH 7.4) containing 0.1% gelatin and 0.1% sodium azide as the assay buffer. Plasma samples (0.02–0.1 ml) containing standard or unknown concentrations of cibenzoline were mixed with 0.2 ml of [^{3}H]cibenzoline in buffer (10,000 cpm) followed by 0.2 ml of diluted antiserum (1:600), and the mixture was incubated at 4° for 30 min. Then, 1 ml of a stirred suspension of a polymer-bound second antibody (goat anti-rabbit IgG)[3] was added and the tube contents were vortexed briefly and allowed to stand at 4° for 1 hr. Following centrifugation at 2000 rpm for 10 min, each supernatant was aspirated off, the pellet suspended in 0.4 ml of 1 *M* acetic acid, and mixed with 3 ml of scintillation fluid[4]. The tube was capped and radioassayed directly in a liquid scintillation counter[5] modified as described previously (2). A calibration curve was generated using a four-parameter logistic curve-fitting program for a desktop calculator[6] (3).

The logit-log calibration curve for cibenzoline was linear from 4 to 200 ng/ml using a 0.1-ml sample of plasma. Such sensitivity is adequate for the quantitation of cibenzoline following administration of therapeutic doses of the drug. The intra- and interassay coefficients of variation (n = 6) did not exceed 6.5 and 10%, respectively, over a range of 38–219 ng/ml of cibenzoline in a selection of random clinical samples. Although the antiserum was found to cross-react almost 100% with the 4,5-dehydro derivative of cibenzoline, a known metabolite of the drug in the dog[7], the specificity of the radioimmunoassay for the analysis of human plasma samples was evaluated by comparison with a specific electron-capture GLC method which was developed and utilized at another research institution[8]. For 57 clinical samples analyzed by both procedures (radioimmunoassay = y), the correlation coefficient, regression line slope, and y-intercept were 0.98, 0.93, and 16, respectively, over a range of 12–287 ng/ml. Although the slope and intercept were significantly different than 1 and 0, only 4 of the 57 highly correlated (r = 0.98) observed data points lay outside the 95% confidence limits of the fitted regression line, which indicates that the radioimmunoassay is in reasonable agreement with a specific chromatographic procedure for the quantitation of cibenzoline. It has been shown by high-performance liquid chromatography (4) that only trace amounts of the 4,5-dehydro metabolite of cibenzoline are present in human plasma, and the metabolite is separated from the parent drug in the electron-capture GLC assay.

In subjects who had received 65 mg of the drug three times a day for 6 days, the peak plasma concentrations at steady-state were ~300 ng/ml of cibenzoline.

A simple radioimmunoassay procedure with adequate sensitivity and specificity was developed for the quanti-

[1] The hapten was prepared from cibenzoline by alkylation with ethyl chloroacetate in ethanol followed by base hydrolysis and crystallized from isopropanol–ether as a partial hydrate, mp 202–204°. The MS and NMR spectra were compatible with the proposed structure.
[2] Prepared by Chemical Research Division, Hoffmann-La Roche Inc.
[3] Roche Diagnostics, Nutley, NJ 07110.
[4] Aquasol, New England Nuclear Corp., Boston, MA 02118.
[5] Packard Tri-Carb model 3255.
[6] TI-59, Texas Instruments, Lubbock, TX 79408.
[7] Data on file, Hoffmann-La Roche Inc.
[8] Personal communication, Laboratoires UPSA, Rueil Malmaison, France.

0022-3549/83/0100-0100$01.00/0

tation of cibenzoline in clinical plasma samples and shown to be specific for the drug in human plasma.

(1) B. F. Erlanger, F. Borek, S. M. Beiser, and S. Lieberman, *J. Biol. Chem.*, **234**, 1090 (1959).

(2) R. Dixon and E. Cohen, *Clin. Chem.*, **22**, 1746 (1976).

(3) M. L. Jaffe, P. J. Munson, and D. Rodbard, "Four Parameter Logistic Curve-Fitting Program for the TI-59 Calculator," National Institute of Child Health, National Institutes of Health, Bethesda, MD 20014.

(4) M. R. Hackman, T. L. Lee, and M. Brooks, *J. Chromatogr.*, in press.

Ross Dixon[x]
John Carbone
Jeff Tilley
Yu-Ying Liu
Hoffmann-La Roche Inc.
Nutley, NJ 07110

Received May 3, 1982.
Accepted for publication September 28, 1982.

BOOKS

Pharmaceutics and Pharmacy Practice. Edited by GILBERT S. BANKER and ROBERT K. CHALMERS. Lippincott, East Washington Square, Philadelphia, PA 19105. 1981, 421 pp. 18 × 25 cm. Price $27.50.

Pharmaceutics and Pharmacy Practice, for the most part, is well written, with each chapter containing much good information, with 23 authors contributing some interesting chapters.

The preface states that the book represents a new approach by interrelating pharmaceutical and clinical pharmacy knowledge about drugs and their delivery systems; however, it contains a standard chapter on physical–chemical principles and another on basic biopharmaceutics. Since the later chapters on drug-delivery systems (oral, topical, parenteral, *etc.*) relate appropriate physical–chemical and biopharmaceutics to their specific subjects, there would be no loss if the physical–chemical chapter were deleted. The chapter on biopharmaceutics could be shortened, except for the portion relative to proper interpretation of blood level curves and evaluation of bioequivalence, which could have been expanded.

The chapter, "Drug Development and Quality Evaluation," would benefit from an expansion of the discussion of selection of multisource drug products and a condensation of federal drug regulatory matters. Similarly, the chapter, "Patient Factors that Influence Dosage Form Selection," should have been edited to remove dosage, patient acceptance (also covered in "Oral Drug-Delivery Systems") and biopharmaceutic matters, while the chapter, on patient education could have been expanded in order to more closely approach the interrelation of knowledge. The style of the chapter on literature resources appears to be better suited to a work book and is repetitious.

The last six chapters are gems. Each one contains relevant anatomy and physiology, routes of drug delivery, drug-delivery systems (dosage forms), and therapeutic considerations. They also contain appropriate physical–chemical considerations and biopharmaceutical aspects. In this manner are covered the drug-delivery systems for oral, parenteral, topical (skin), topical (eye, ear, nose), inhalation, and rectal, vaginal, and urethral administration. A few considerations of extemporaneous preparation of delivery systems are to be found in all of these chapters.

While the book is described as being intended for adult professionals, the preface refers to the book's predecessor as being *Prescription Pharmacy*, which would indicate that one concern would be the dispensing function (the pharmacy practice of the title). Noticeably lacking is any information about processing the prescription, maintenance of prescription files or records, legal aspects of dispensing controlled substances, hospital pharmacy, or the use of computers in pharmacy. While the chapter on parenteral drug-delivery systems contains good material on TPN and electrolyte therapy, no mention is made of aseptic methods appropriate for making intravenous admixtures, *etc.* Thus, the book appears to be written from the aspect of pharmaceutical technology rather than pharmacy practice.

Although the editors were only partly successful in their attempt to interrelate pharmaceutical and clinical pharmacy to pharmacy practice, this book contains much excellent information presented in a highly readable manner.

Reviewed by Noel O. Nuessle
School of Pharmacy
University of Missouri-Kansas City
Kansas City, MO 64110

Analytical Profiles of Drug Substances, Vol. 10. Edited by KLAUS FLOREY, *et al.* Academic, 111 Fifth Ave., New York, NY 10003. 1981. 735 pp. 14 × 23 cm.

Analytical Profiles of Drug Substances, Vol. 10 continues the successful series of complete monographs for important drug substances. This series is compiled under the auspices of the Pharmaceutical Analysis and Control Section of the Academy of Pharmaceutical Sciences. Volume 10 contains monographs on aminosalicylic acid, azathioprine, benzyl benzoate, clindamycin hydrochloride, codeine phosphate, colchicine, cyanocobalamin, emetine hydrochloride, glibenclamide, heroin, hydrochlorothiazide, ketoprofen, methylphenidate hydrochloride, nabilone, natamycin, oxytocin, penicillamine, probenecid, salbutamol, succinylcholine chloride, and trioxsalen. There also are *errata* for cefamandole nafate, fluphenazine decanoate, gentamicin sulfate, and nadolol.

The typical monograph contains the following information: First, there is an initial description including nomenclature, formula, and other physical descriptions followed by a physical properties section which usually covers crystal properties, melting point characteristics, solubility, and spectral properties including reproductions of IR, UV, NMR, and mass spectra. Usually there is a discussion on the drug's synthesis or biosynthesis followed by the drug's metabolism. The monographs usually conclude with a literature review of different methods for analyzing the drug.

There is no question that this series fills a need. The surprising fact is, that after nine previous volumes, the editors still have not developed a standard format for the monographs. Here are some examples of inconsistencies. The Chemical Abstracts Service (CAS) Registry Number is given in 11 of the 21 monographs. When present, it may be in Section 1.1 1, 1.23, 1.2.3, 2.1, 1.2.1, 1.12, or 1.14. Wiswesser Line Notation is present in five of the monographs, and the elemental composition will be found in only eight monographs. Six of the monographs open with one or more introductory paragraphs containing information on the drug's history and use. When this is present, the nomenclature material found in Section 1 now goes into Section 2.

Section 5.5, when present, can be UV spectrometry, proton magnetic resonance spectrometry, radioassay, phosphorimetry, colorimetry, and other unrelated topics. Putting it another way: suppose an analytical chemist wishes to examine the applicability of high-pressure liquid chromatography for a drug analysis whose monograph has been published in this series. Where does he or she look? Answer: Somewhere near the end of the monograph, but be careful, because the material on chromatography may be divided between methodology, analysis of dosage forms, and analysis from biological fluids.

Make no mistake, *Analytical Profiles of Drug Substances* belongs in the personal libraries of drug analysts. Teachers in the field should purchase it as well as school, university, and company libraries. In addition, the publishers and editors should be encouraged to investigate a student rate for graduate students in pharmaceutical analysis. At the same time, some active editing would correct glaring inconsistencies and deficiencies and make the *Analytical Profiles* series reflect the care and consistency expected of the profession and the Academy.

Reviewed by John H. Block
School of Pharmacy
Oregon State University
Corvallis, OR 97331

tation of cibenzoline in clinical plasma samples and shown to be specific for the drug in human plasma.

(1) B. F. Erlanger, F. Borek, S. M. Beiser, and S. Lieberman, *J. Biol. Chem.*, **234**, 1090 (1959).

(2) R. Dixon and E. Cohen, *Clin. Chem.*, **22**, 1746 (1976).

(3) M. L. Jaffe, P. J. Munson, and D. Rodbard, "Four Parameter Logistic Curve-Fitting Program for the TI-59 Calculator," National Institute of Child Health, National Institutes of Health, Bethesda, MD 20014.

(4) M. R. Hackman, T. L. Lee, and M. Brooks, *J. Chromatogr.*, in press.

Ross Dixon[x]
John Carbone
Jeff Tilley
Yu-Ying Liu
Hoffmann-La Roche Inc.
Nutley, NJ 07110

Received May 3, 1982.
Accepted for publication September 28, 1982.

BOOKS

Pharmaceutics and Pharmacy Practice. Edited by GILBERT S. BANKER and ROBERT K. CHALMERS. Lippincott, East Washington Square, Philadelphia, PA 19105. 1981, 421 pp. 18 × 25 cm. Price $27.50.

Pharmaceutics and Pharmacy Practice, for the most part, is well written, with each chapter containing much good information, with 23 authors contributing some interesting chapters.

The preface states that the book represents a new approach by interrelating pharmaceutical and clinical pharmacy knowledge about drugs and their delivery systems; however, it contains a standard chapter on physical–chemical principles and another on basic biopharmaceutics. Since the later chapters on drug-delivery systems (oral, topical, parenteral, *etc.*) relate appropriate physical–chemical and biopharmaceutics to their specific subjects, there would be no loss if the physical–chemical chapter were deleted. The chapter on biopharmaceutics could be shortened, except for the portion relative to proper interpretation of blood level curves and evaluation of bioequivalence, which could have been expanded.

The chapter, "Drug Development and Quality Evaluation," would benefit from an expansion of the discussion of selection of multisource drug products and a condensation of federal drug regulatory matters. Similarly, the chapter, "Patient Factors that Influence Dosage Form Selection," should have been edited to remove dosage, patient acceptance (also covered in "Oral Drug-Delivery Systems") and biopharmaceutic matters, while the chapter, on patient education could have been expanded in order to more closely approach the interrelation of knowledge. The style of the chapter on literature resources appears to be better suited to a work book and is repetitious.

The last six chapters are gems. Each one contains relevant anatomy and physiology, routes of drug delivery, drug-delivery systems (dosage forms), and therapeutic considerations. They also contain appropriate physical–chemical considerations and biopharmaceutical aspects. In this manner are covered the drug-delivery systems for oral, parenteral, topical (skin), topical (eye, ear, nose), inhalation, and rectal, vaginal, and urethral administration. A few considerations of extemporaneous preparation of delivery systems are to be found in all of these chapters.

While the book is described as being intended for adult professionals, the preface refers to the book's predecessor as being *Prescription Pharmacy*, which would indicate that one concern would be the dispensing function (the pharmacy practice of the title). Noticeably lacking is any information about processing the prescription, maintenance of prescription files or records, legal aspects of dispensing controlled substances, hospital pharmacy, or the use of computers in pharmacy. While the chapter on parenteral drug-delivery systems contains good material on TPN and electrolyte therapy, no mention is made of aseptic methods appropriate for making intravenous admixtures, *etc.* Thus, the book appears to be written from the aspect of pharmaceutical technology rather than pharmacy practice.

Although the editors were only partly successful in their attempt to interrelate pharmaceutical and clinical pharmacy to pharmacy practice, this book contains much excellent information presented in a highly readable manner.

Reviewed by Noel O. Nuessle
School of Pharmacy
University of Missouri-Kansas City
Kansas City, MO 64110

Analytical Profiles of Drug Substances, Vol. 10. Edited by KLAUS FLOREY, *et al.* Academic, 111 Fifth Ave., New York, NY 10003. 1981. 735 pp. 14 × 23 cm.

Analytical Profiles of Drug Substances, Vol. 10 continues the successful series of complete monographs for important drug substances. This series is compiled under the auspices of the Pharmaceutical Analysis and Control Section of the Academy of Pharmaceutical Sciences. Volume 10 contains monographs on aminosalicylic acid, azathioprine, benzyl benzoate, clindamycin hydrochloride, codeine phosphate, colchicine, cyanocobalamin, emetine hydrochloride, glibenclamide, heroin, hydrochlorothiazide, ketoprofen, methylphenidate hydrochloride, nabilone, natamycin, oxytocin, penicillamine, probenecid, salbutamol, succinylcholine chloride, and trioxsalen. There also are *errata* for cefamandole nafate, fluphenazine decanoate, gentamicin sulfate, and nadolol.

The typical monograph contains the following information: First, there is an initial description including nomenclature, formula, and other physical descriptions followed by a physical properties section which usually covers crystal properties, melting point characteristics, solubility, and spectral properties including reproductions of IR, UV, NMR, and mass spectra. Usually there is a discussion on the drug's synthesis or biosynthesis followed by the drug's metabolism. The monographs usually conclude with a literature review of different methods for analyzing the drug.

There is no question that this series fills a need. The surprising fact is, that after nine previous volumes, the editors still have not developed a standard format for the monographs. Here are some examples of inconsistencies. The Chemical Abstracts Service (CAS) Registry Number is given in 11 of the 21 monographs. When present, it may be in Section 1.1 1, 1.23, 1.2.3, 2.1, 1.2.1, 1.12, or 1.14. Wiswesser Line Notation is present in five of the monographs, and the elemental composition will be found in only eight monographs. Six of the monographs open with one or more introductory paragraphs containing information on the drug's history and use. When this is present, the nomenclature material found in Section 1 now goes into Section 2.

Section 5.5, when present, can be UV spectrometry, proton magnetic resonance spectrometry, radioassay, phosphorimetry, colorimetry, and other unrelated topics. Putting it another way: suppose an analytical chemist wishes to examine the applicability of high-pressure liquid chromatography for a drug analysis whose monograph has been published in this series. Where does he or she look? Answer: Somewhere near the end of the monograph, but be careful, because the material on chromatography may be divided between methodology, analysis of dosage forms, and analysis from biological fluids.

Make no mistake, *Analytical Profiles of Drug Substances* belongs in the personal libraries of drug analysts. Teachers in the field should purchase it as well as school, university, and company libraries. In addition, the publishers and editors should be encouraged to investigate a student rate for graduate students in pharmaceutical analysis. At the same time, some active editing would correct glaring inconsistencies and deficiencies and make the *Analytical Profiles* series reflect the care and consistency expected of the profession and the Academy.

Reviewed by John H. Block
School of Pharmacy
Oregon State University
Corvallis, OR 97331

tation of cibenzoline in clinical plasma samples and shown to be specific for the drug in human plasma.

(1) B. F. Erlanger, F. Borek, S. M. Beiser, and S. Lieberman, *J. Biol. Chem.*, **234**, 1090 (1959).

(2) R. Dixon and E. Cohen, *Clin. Chem.*, **22**, 1746 (1976).

(3) M. L. Jaffe, P. J. Munson, and D. Rodbard, "Four Parameter Logistic Curve-Fitting Program for the TI-59 Calculator," National Institute of Child Health, National Institutes of Health, Bethesda, MD 20014.

(4) M. R. Hackman, T. L. Lee, and M. Brooks, *J. Chromatogr.*, in press.

Ross Dixon[x]
John Carbone
Jeff Tilley
Yu-Ying Liu
Hoffmann-La Roche Inc.
Nutley, NJ 07110

Received May 3, 1982.
Accepted for publication September 28, 1982.

BOOKS

Pharmaceutics and Pharmacy Practice. Edited by GILBERT S. BANKER and ROBERT K. CHALMERS. Lippincott, East Washington Square, Philadelphia, PA 19105. 1981, 421 pp. 18 × 25 cm. Price $27.50.

Pharmaceutics and Pharmacy Practice, for the most part, is well written, with each chapter containing much good information, with 23 authors contributing some interesting chapters.

The preface states that the book represents a new approach by interrelating pharmaceutical and clinical pharmacy knowledge about drugs and their delivery systems; however, it contains a standard chapter on physical–chemical principles and another on basic biopharmaceutics. Since the later chapters on drug-delivery systems (oral, topical, parenteral, *etc.*) relate appropriate physical–chemical and biopharmaceutics to their specific subjects, there would be no loss if the physical–chemical chapter were deleted. The chapter on biopharmaceutics could be shortened, except for the portion relative to proper interpretation of blood level curves and evaluation of bioequivalence, which could have been expanded.

The chapter, "Drug Development and Quality Evaluation," would benefit from an expansion of the discussion of selection of multisource drug products and a condensation of federal drug regulatory matters. Similarly, the chapter, "Patient Factors that Influence Dosage Form Selection," should have been edited to remove dosage, patient acceptance (also covered in "Oral Drug-Delivery Systems") and biopharmaceutic matters, while the chapter, on patient education could have been expanded in order to more closely approach the interrelation of knowledge. The style of the chapter on literature resources appears to be better suited to a work book and is repetitious.

The last six chapters are gems. Each one contains relevant anatomy and physiology, routes of drug delivery, drug-delivery systems (dosage forms), and therapeutic considerations. They also contain appropriate physical–chemical considerations and biopharmaceutical aspects. In this manner are covered the drug-delivery systems for oral, parenteral, topical (skin), topical (eye, ear, nose), inhalation, and rectal, vaginal, and urethral administration. A few considerations of extemporaneous preparation of delivery systems are to be found in all of these chapters.

While the book is described as being intended for adult professionals, the preface refers to the book's predecessor as being *Prescription Pharmacy*, which would indicate that one concern would be the dispensing function (the pharmacy practice of the title). Noticeably lacking is any information about processing the prescription, maintenance of prescription files or records, legal aspects of dispensing controlled substances, hospital pharmacy, or the use of computers in pharmacy. While the chapter on parenteral drug-delivery systems contains good material on TPN and electrolyte therapy, no mention is made of aseptic methods appropriate for making intravenous admixtures, *etc.* Thus, the book appears to be written from the aspect of pharmaceutical technology rather than pharmacy practice.

Although the editors were only partly successful in their attempt to interrelate pharmaceutical and clinical pharmacy to pharmacy practice, this book contains much excellent information presented in a highly readable manner.

Reviewed by Noel O. Nuessle
School of Pharmacy
University of Missouri-Kansas City
Kansas City, MO 64110

Analytical Profiles of Drug Substances, Vol. 10. Edited by KLAUS FLOREY, *et al.* Academic, 111 Fifth Ave., New York, NY 10003. 1981. 735 pp. 14 × 23 cm.

Analytical Profiles of Drug Substances, Vol. 10 continues the successful series of complete monographs for important drug substances. This series is compiled under the auspices of the Pharmaceutical Analysis and Control Section of the Academy of Pharmaceutical Sciences. Volume 10 contains monographs on aminosalicylic acid, azathioprine, benzyl benzoate, clindamycin hydrochloride, codeine phosphate, colchicine, cyanocobalamin, emetine hydrochloride, glibenclamide, heroin, hydrochlorothiazide, ketoprofen, methylphenidate hydrochloride, nabilone, natamycin, oxytocin, penicillamine, probenecid, salbutamol, succinylcholine chloride, and trioxsalen. There also are *errata* for cefamandole nafate, fluphenazine decanoate, gentamicin sulfate, and nadolol.

The typical monograph contains the following information: First, there is an initial description including nomenclature, formula, and other physical descriptions followed by a physical properties section which usually covers crystal properties, melting point characteristics, solubility, and spectral properties including reproductions of IR, UV, NMR, and mass spectra. Usually there is a discussion on the drug's synthesis or biosynthesis followed by the drug's metabolism. The monographs usually conclude with a literature review of different methods for analyzing the drug.

There is no question that this series fills a need. The surprising fact is, that after nine previous volumes, the editors still have not developed a standard format for the monographs. Here are some examples of inconsistencies. The Chemical Abstracts Service (CAS) Registry Number is given in 11 of the 21 monographs. When present, it may be in Section 1.1 1, 1.23, 1.2.3, 2.1, 1.2.1, 1.12, or 1.14. Wiswesser Line Notation is present in five of the monographs, and the elemental composition will be found in only eight monographs. Six of the monographs open with one or more introductory paragraphs containing information on the drug's history and use. When this is present, the nomenclature material found in Section 1 now goes into Section 2.

Section 5.5, when present, can be UV spectrometry, proton magnetic resonance spectrometry, radioassay, phosphorimetry, colorimetry, and other unrelated topics. Putting it another way: suppose an analytical chemist wishes to examine the applicability of high-pressure liquid chromatography for a drug analysis whose monograph has been published in this series. Where does he or she look? Answer: Somewhere near the end of the monograph, but be careful, because the material on chromatography may be divided between methodology, analysis of dosage forms, and analysis from biological fluids.

Make no mistake, *Analytical Profiles of Drug Substances* belongs in the personal libraries of drug analysts. Teachers in the field should purchase it as well as school, university, and company libraries. In addition, the publishers and editors should be encouraged to investigate a student rate for graduate students in pharmaceutical analysis. At the same time, some active editing would correct glaring inconsistencies and deficiencies and make the *Analytical Profiles* series reflect the care and consistency expected of the profession and the Academy.

Reviewed by John H. Block
School of Pharmacy
Oregon State University
Corvallis, OR 97331

Handbook of Chemical Property Estimation Methods, Edited by W. J. LYMAN, W. REEHL, and D. ROSENBLATT, McGraw-Hill, 1221 Avenue of the Americas, New York, NY 10020. 1982. 960 pp., 71 illustrations. 19 × 24 cm. Price $42.50.

This handbook of chemical property estimation methods is an outgrowth of a combined U.S. Army–Arthur D. Little project to assess properties of organic chemicals that are of environmental concern. Much basic physical and chemical data needed to perform a proper assessment of the risk of these chemicals to humans and the environment is evidently lacking in existing literature. Therefore, an estimation of the most important properties for selected chemicals would aid in this assessment and, thus, is the basis for this scientific contribution.

A review of existing literature reveals that approximately 50 physicochemical properties of organic compounds are of interest, but estimation methods are only available for about half of these properties. A total of 26 properties and their estimation methods are included in the handbook. Two or more estimation methods were selected for each property. These estimation methods were chosen for their range of applicability, ease of use, minimum input data requirements, and accuracy. Among the physicochemical properties covered that would be of pharmaceutical interest are octanol–water partition coefficient, solubility in water, solubility in various solvents, acid dissociation constant, rate of hydrolysis, rate of biodegradation, vapor pressure, densities of vapors, liquids and solids, surface tension, dipole moment, and index of refraction. The handbook is divided into chapters with each property covered in a given chapter. The Editors have maintained some degree of uniformity in style and content in each chapter. For each property, there is introductory material describing the property, background data on available estimation methods, a description of the recommended estimation method(s) with specific instructions for calculation, examples of each method, a listing of symbols and definitions associated with the method, and pertinent literature references.

Aside from deficiencies and errors in the handbook, the basic limitation is that only single-component organic chemicals are covered. There are plans to cover organic mixtures in future editions. A definite plus for the handbook is that the chapters were rigorously reviewed by individual scientists connected with the U.S. Army, the Environmental Protection Agency, Arthur D. Little, various universities, and other organizations.

The Handbook should be beneficial to those who need to estimate selected physicochemical properties where such data are either unavailable or nonexistent. The user should be able to obtain the estimation quickly using only a hand calculator and the handbook instructions. The price is not too prohibitive to prelude addition to an individual's library. It is not meant to be used as a course textbook, but could be easily utilized as a reference text, especially for courses in pharmaceutics and medicinal chemistry. I do not especially recommend the handbook for acquisition by a School of Pharmacy Library or Reading Room facility, but feel that it should be available for use on campus in a Science Library.

Reviewed by James T. Stewart
School of Pharmacy
University of Georgia
Athens, GA 30602

Pharmaceutical Dosage Forms: Tablets Vol. 3. Edited by HERBERT A. LIEBERMAN and LEON LACHMAN. Dekker, 270 Madison Avenue, New York, NY 10016. 1982. 472 pp. 18 × 25.5 cm. Price $59.75 (20% higher outside U.S. and Canada).

This volume, the concluding volume of this treatise, empathizes the final stages in the evolution of a finished tablet product. As with the earlier volumes, each chapter is a logical self-contained entity, not critically dependent on familiarity with preceding chapters. In spite of this, the editors have continued to skillfully prevent any repetition by the various authors of the redevelopment of information for processes completed prior to those covered in their chapter describing the next stage of tablet production.

The first four chapters of this volume are specific to the unit processes involved. They are Principles of Improved Tablet Production System Design, Pan Coating of Tablets and Granules, Particles Coating Methods, and Sustained Drug Release from Tablets and Particles through Coating. Each is clearly, logically, and completely developed.

The next two chapters, entitled Stability/Kinetics and Quality Assurance, review the testing of the final product and the documentation of the adherence to GMP throughout every processing step.

As with the previous volumes, the indexing is good. With computer type-setting it is unfortunate that an additional cumulative index for the three volumes was not compiled.

Each chapter in this set is written by qualified experts and clearly represents the state-of-the-art for the immediate future. It is hoped that to create a complete treatise the editors will soon move on to additional volumes to cover other pharmaceutical dosage forms.

Reviewed by John H. Wood
School of Pharmacy
Medical College of Virginia Campus
Virginia Commonwealth University
Richmond, VA 23298

CRC Handbook of Chromatography Drugs. Vols. I and II. Edited by RAM N. GUPTA with series Editors-in-chief, GUNTER ZWEIG and JOSEPH SHERMA, CRC Press Inc., Boca Raton, FL 33431. 1981. Vol. I: 340 pp., Vol. II: 404 pp. 17.5 × 25.5 cm. Price Vol. I: $59.95, Vol. II: $59.95.

Earlier editions of this handbook attempted to cover a wider range of compounds in two volumes, but the growth of the literature demanded a new approach resulting in a series of separate books more selective in scope. These two volumes are intended as a reference source of the different chromatographic techniques available for the analysis of drugs, except steroids which are to be treated separately. Coverage embraces specimens from pharmaceutical dosages to biological matrixes. There is a brief, useful introductory section on collection, storage and processing of samples. The comments on interferences from commercial blood sampling containers are marred, however, by incorrect figure legends and a missing reference (No. 78).

The major part of the volumes presents useful tables listing separately the main features of gas, high-pressure liquid, and thin-layer chromatographic methods available for each drug listed. Key chromatographic conditions are cited, together with type of method, *e.g.*, *D* = dosage form, sample size, and sensitivity on a scale of 1–3. (The latter would be more useful if a concentration were estimated.)

This book would be a useful desk reference for those who do not have ready access to a library. However, its utility is compromised by the incomplete (or selective) compilation of methods with no explanation of the criteria for choice of the particular methods tabulated. Thus, methods for such drugs as allopurinol, digoxin, oxyphenbutazone, quinine, and promethazine—among others in this reviewer's files—are not cited.

It would also be useful in such handbooks if the date of literature coverage (apparently to the end of 1979) were quoted, as some methods cited have already become outdated by later advances, *e.g.*, GLC of isosorbide, HPLC of chlorpromazine, naproxen, and propanolol, an inevitable consequence of the advances with useful technique. One is left with the impression that this handbook would be more useful for those analysts involved with biological samples rather than raw materials or formulations.

Reviewed by Iain J. McGilveray
Bureau of Drug Research
Health & Welfare Canada
Ottawa, Ontario
K1A 0L2

Handbook of Chemical Property Estimation Methods, Edited by W. J. LYMAN, W. REEHL, and D. ROSENBLATT, McGraw-Hill, 1221 Avenue of the Americas, New York, NY 10020. 1982. 960 pp., 71 illustrations. 19 × 24 cm. Price $42.50.

This handbook of chemical property estimation methods is an outgrowth of a combined U.S. Army–Arthur D. Little project to assess properties of organic chemicals that are of environmental concern. Much basic physical and chemical data needed to perform a proper assessment of the risk of these chemicals to humans and the environment is evidently lacking in existing literature. Therefore, an estimation of the most important properties for selected chemicals would aid in this assessment and, thus, is the basis for this scientific contribution.

A review of existing literature reveals that approximately 50 physicochemical properties of organic compounds are of interest, but estimation methods are only available for about half of these properties. A total of 26 properties and their estimation methods are included in the handbook. Two or more estimation methods were selected for each property. These estimation methods were chosen for their range of applicability, ease of use, minimum input data requirements, and accuracy. Among the physicochemical properties covered that would be of pharmaceutical interest are octanol–water partition coefficient, solubility in water, solubility in various solvents, acid dissociation constant, rate of hydrolysis, rate of biodegradation, vapor pressure, densities of vapors, liquids and solids, surface tension, dipole moment, and index of refraction. The handbook is divided into chapters with each property covered in a given chapter. The Editors have maintained some degree of uniformity in style and content in each chapter. For each property, there is introductory material describing the property, background data on available estimation methods, a description of the recommended estimation method(s) with specific instructions for calculation, examples of each method, a listing of symbols and definitions associated with the method, and pertinent literature references.

Aside from deficiencies and errors in the handbook, the basic limitation is that only single-component organic chemicals are covered. There are plans to cover organic mixtures in future editions. A definite plus for the handbook is that the chapters were rigorously reviewed by individual scientists connected with the U.S. Army, the Environmental Protection Agency, Arthur D. Little, various universities, and other organizations.

The Handbook should be beneficial to those who need to estimate selected physicochemical properties where such data are either unavailable or nonexistent. The user should be able to obtain the estimation quickly using only a hand calculator and the handbook instructions. The price is not too prohibitive to prelude addition to an individual's library. It is not meant to be used as a course textbook, but could be easily utilized as a reference text, especially for courses in pharmaceutics and medicinal chemistry. I do not especially recommend the handbook for acquisition by a School of Pharmacy Library or Reading Room facility, but feel that it should be available for use on campus in a Science Library.

Reviewed by James T. Stewart
School of Pharmacy
University of Georgia
Athens, GA 30602

Pharmaceutical Dosage Forms: Tablets Vol. 3. Edited by HERBERT A. LIEBERMAN and LEON LACHMAN. Dekker, 270 Madison Avenue, New York, NY 10016. 1982. 472 pp. 18 × 25.5 cm. Price $59.75 (20% higher outside U.S. and Canada).

This volume, the concluding volume of this treatise, empathizes the final stages in the evolution of a finished tablet product. As with the earlier volumes, each chapter is a logical self-contained entity, not critically dependent on familiarity with preceding chapters. In spite of this, the editors have continued to skillfully prevent any repetition by the various authors of the redevelopment of information for processes completed prior to those covered in their chapter describing the next stage of tablet production.

The first four chapters of this volume are specific to the unit processes involved. They are Principles of Improved Tablet Production System Design, Pan Coating of Tablets and Granules, Particles Coating Methods, and Sustained Drug Release from Tablets and Particles through Coating. Each is clearly, logically, and completely developed.

The next two chapters, entitled Stability/Kinetics and Quality Assurance, review the testing of the final product and the documentation of the adherence to GMP throughout every processing step.

As with the previous volumes, the indexing is good. With computer type-setting it is unfortunate that an additional cumulative index for the three volumes was not compiled.

Each chapter in this set is written by qualified experts and clearly represents the state-of-the-art for the immediate future. It is hoped that to create a complete treatise the editors will soon move on to additional volumes to cover other pharmaceutical dosage forms.

Reviewed by John H. Wood
School of Pharmacy
Medical College of Virginia Campus
Virginia Commonwealth University
Richmond, VA 23298

CRC Handbook of Chromatography Drugs. Vols. I and II. Edited by RAM N. GUPTA with series Editors-in-chief, GUNTER ZWEIG and JOSEPH SHERMA, CRC Press Inc., Boca Raton, FL 33431. 1981. Vol. I: 340 pp., Vol. II: 404 pp. 17.5 × 25.5 cm. Price Vol. I: $59.95, Vol. II: $59.95.

Earlier editions of this handbook attempted to cover a wider range of compounds in two volumes, but the growth of the literature demanded a new approach resulting in a series of separate books more selective in scope. These two volumes are intended as a reference source of the different chromatographic techniques available for the analysis of drugs, except steroids which are to be treated separately. Coverage embraces specimens from pharmaceutical dosages to biological matrixes. There is a brief, useful introductory section on collection, storage and processing of samples. The comments on interferences from commercial blood sampling containers are marred, however, by incorrect figure legends and a missing reference (No. 78).

The major part of the volumes presents useful tables listing separately the main features of gas, high-pressure liquid, and thin-layer chromatographic methods available for each drug listed. Key chromatographic conditions are cited, together with type of method, *e.g.*, *D* = dosage form, sample size, and sensitivity on a scale of 1–3. (The latter would be more useful if a concentration were estimated.)

This book would be a useful desk reference for those who do not have ready access to a library. However, its utility is compromised by the incomplete (or selective) compilation of methods with no explanation of the criteria for choice of the particular methods tabulated. Thus, methods for such drugs as allopurinol, digoxin, oxyphenbutazone, quinine, and promethazine—among others in this reviewer's files—are not cited.

It would also be useful in such handbooks if the date of literature coverage (apparently to the end of 1979) were quoted, as some methods cited have already become outdated by later advances, *e.g.*, GLC of isosorbide, HPLC of chlorpromazine, naproxen, and propanolol, an inevitable consequence of the advances with useful technique. One is left with the impression that this handbook would be more useful for those analysts involved with biological samples rather than raw materials or formulations.

Reviewed by Iain J. McGilveray
Bureau of Drug Research
Health & Welfare Canada
Ottawa, Ontario
K1A 0L2

Handbook of Chemical Property Estimation Methods, Edited by W. J. LYMAN, W. REEHL, and D. ROSENBLATT, McGraw-Hill, 1221 Avenue of the Americas, New York, NY 10020. 1982. 960 pp., 71 illustrations. 19 × 24 cm. Price $42.50.

This handbook of chemical property estimation methods is an outgrowth of a combined U.S. Army–Arthur D. Little project to assess properties of organic chemicals that are of environmental concern. Much basic physical and chemical data needed to perform a proper assessment of the risk of these chemicals to humans and the environment is evidently lacking in existing literature. Therefore, an estimation of the most important properties for selected chemicals would aid in this assessment and, thus, is the basis for this scientific contribution.

A review of existing literature reveals that approximately 50 physicochemical properties of organic compounds are of interest, but estimation methods are only available for about half of these properties. A total of 26 properties and their estimation methods are included in the handbook. Two or more estimation methods were selected for each property. These estimation methods were chosen for their range of applicability, ease of use, minimum input data requirements, and accuracy. Among the physicochemical properties covered that would be of pharmaceutical interest are octanol–water partition coefficient, solubility in water, solubility in various solvents, acid dissociation constant, rate of hydrolysis, rate of biodegradation, vapor pressure, densities of vapors, liquids and solids, surface tension, dipole moment, and index of refraction. The handbook is divided into chapters with each property covered in a given chapter. The Editors have maintained some degree of uniformity in style and content in each chapter. For each property, there is introductory material describing the property, background data on available estimation methods, a description of the recommended estimation method(s) with specific instructions for calculation, examples of each method, a listing of symbols and definitions associated with the method, and pertinent literature references.

Aside from deficiencies and errors in the handbook, the basic limitation is that only single-component organic chemicals are covered. There are plans to cover organic mixtures in future editions. A definite plus for the handbook is that the chapters were rigorously reviewed by individual scientists connected with the U.S. Army, the Environmental Protection Agency, Arthur D. Little, various universities, and other organizations.

The Handbook should be beneficial to those who need to estimate selected physicochemical properties where such data are either unavailable or nonexistent. The user should be able to obtain the estimation quickly using only a hand calculator and the handbook instructions. The price is not too prohibitive to prelude addition to an individual's library. It is not meant to be used as a course textbook, but could be easily utilized as a reference text, especially for courses in pharmaceutics and medicinal chemistry. I do not especially recommend the handbook for acquisition by a School of Pharmacy Library or Reading Room facility, but feel that it should be available for use on campus in a Science Library.

Reviewed by James T. Stewart
School of Pharmacy
University of Georgia
Athens, GA 30602

Pharmaceutical Dosage Forms: Tablets Vol. 3. Edited by HERBERT A. LIEBERMAN and LEON LACHMAN. Dekker, 270 Madison Avenue, New York, NY 10016. 1982. 472 pp. 18 × 25.5 cm. Price $59.75 (20% higher outside U.S. and Canada).

This volume, the concluding volume of this treatise, empathizes the final stages in the evolution of a finished tablet product. As with the earlier volumes, each chapter is a logical self-contained entity, not critically dependent on familiarity with preceding chapters. In spite of this, the editors have continued to skillfully prevent any repetition by the various authors of the redevelopment of information for processes completed prior to those covered in their chapter describing the next stage of tablet production.

The first four chapters of this volume are specific to the unit processes involved. They are Principles of Improved Tablet Production System Design, Pan Coating of Tablets and Granules, Particles Coating Methods, and Sustained Drug Release from Tablets and Particles through Coating. Each is clearly, logically, and completely developed.

The next two chapters, entitled Stability/Kinetics and Quality Assurance, review the testing of the final product and the documentation of the adherence to GMP throughout every processing step.

As with the previous volumes, the indexing is good. With computer type-setting it is unfortunate that an additional cumulative index for the three volumes was not compiled.

Each chapter in this set is written by qualified experts and clearly represents the state-of-the-art for the immediate future. It is hoped that to create a complete treatise the editors will soon move on to additional volumes to cover other pharmaceutical dosage forms.

Reviewed by John H. Wood
School of Pharmacy
Medical College of Virginia Campus
Virginia Commonwealth University
Richmond, VA 23298

CRC Handbook of Chromatography Drugs. Vols. I and II. Edited by RAM N. GUPTA with series Editors-in-chief, GUNTER ZWEIG and JOSEPH SHERMA, CRC Press Inc., Boca Raton, FL 33431. 1981. Vol. I: 340 pp., Vol. II: 404 pp. 17.5 × 25.5 cm. Price Vol. I: $59.95, Vol. II: $59.95.

Earlier editions of this handbook attempted to cover a wider range of compounds in two volumes, but the growth of the literature demanded a new approach resulting in a series of separate books more selective in scope. These two volumes are intended as a reference source of the different chromatographic techniques available for the analysis of drugs, except steroids which are to be treated separately. Coverage embraces specimens from pharmaceutical dosages to biological matrixes. There is a brief, useful introductory section on collection, storage and processing of samples. The comments on interferences from commercial blood sampling containers are marred, however, by incorrect figure legends and a missing reference (No. 78).

The major part of the volumes presents useful tables listing separately the main features of gas, high-pressure liquid, and thin-layer chromatographic methods available for each drug listed. Key chromatographic conditions are cited, together with type of method, *e.g.*, *D* = dosage form, sample size, and sensitivity on a scale of 1–3. (The latter would be more useful if a concentration were estimated.)

This book would be a useful desk reference for those who do not have ready access to a library. However, its utility is compromised by the incomplete (or selective) compilation of methods with no explanation of the criteria for choice of the particular methods tabulated. Thus, methods for such drugs as allopurinol, digoxin, oxyphenbutazone, quinine, and promethazine—among others in this reviewer's files—are not cited.

It would also be useful in such handbooks if the date of literature coverage (apparently to the end of 1979) were quoted, as some methods cited have already become outdated by later advances, *e.g.*, GLC of isosorbide, HPLC of chlorpromazine, naproxen, and propanolol, an inevitable consequence of the advances with useful technique. One is left with the impression that this handbook would be more useful for those analysts involved with biological samples rather than raw materials or formulations.

Reviewed by Iain J. McGilveray
Bureau of Drug Research
Health & Welfare Canada
Ottawa, Ontario
K1A 0L2

1983
Volume 72

JOURNAL OF PHARMACEUTICAL SCIENCES

A publication of the American Pharmaceutical Association

The *Journal of Pharmaceutical Sciences* (ISSN 0022-3549) is published monthly by the American Pharmaceutical Association (APhA) at 2215 Constitution Ave., N.W., Washington, DC 20037. Second-class postage paid at Washington, D.C. and at additional mailing office.

All expressions of opinion and statements of supposed fact appearing in articles or editorials carried in this journal are published on the authority of the writer over whose name they appear and are not to be regarded as necessarily expressing the policies or views of APhA.

Offices—Editorial, Advertising, and Subscription: 2215 Constitution Ave., N.W., Washington, DC 20037. All Journal staff may be contacted at this address. Printing: 20th & Northampton Streets, Easton, PA 18042.

Annual Subscriptions—United States and foreign, industrial and government institutions $75; educational institutions $75; individuals *for personal use only* $40; single copies $10. APhA and SAPhA members may subscribe to *J. Pharm. Sci.* for $20.00 per year. All foreign subscriptions add $10 for postage. Subscription rates are subject to change without notice.

Claims—Missing numbers will not be supplied if dues or subscriptions are in arrears for more than 60 days or if claims are received more than 60 days after the date of the issue, or if loss was due to failure to give notice of change of address. APhA cannot accept responsibility for foreign delivery when its records indicate shipment was made.

Change of Address—Members and subscribers should notify at once both the Post Office and APhA of any change of address.

Photocopying—The code at the foot of the first page of an article indicates that APhA has granted permission for copying of the article beyond the limits permitted by Sections 107 and 108 of the U.S. Copyright Law provided that the copier sends the per copy fee stated in the code to the Copyright Clearance Center, Inc., 21 Congress St., Salem, MA 01970. Copies may be made for personal or internal use only and not for general distribution.

Microfilm—Available from University Microfilms International, 300 N. Zeeb Road, Ann Arbor, MI 48106.

Maintaining Excellence in Pharmacy Education

In "The Merchant of Venice," William Shakespeare wrote that "The quality of mercy is not strained . . . ." That may be true for mercy, but it is not true for education. Pharmacy education, in particular, is being subjected to stresses and strains that are expected to intensify and grow worse in the years immediately ahead.

The best facilities, the best students, and the best curricula will rarely produce high-quality graduates in the absence of a teaching faculty that is of comparable talent. And it is in that area of faculty quality that a growing number of individuals and groups are beginning to express serious concern.

Current faculties are generally competent and adequate. The great majority of faculty members received their advanced training when new graduate students regularly constituted "the cream of the crop" from the previous year's graduating class. Following advanced study and after taking advanced degrees, a major portion of these select graduate students chose teaching as a career. As a consequence, each new generation of students received its training from the very best of the previous generation's crop.

In recent years, however, this pattern has been changing, and it is this change that is arousing concern.

APhA Academy of Pharmaceutical Sciences President Kenneth R. Heimlich addressed the matter in his November 1982 interim report.

". . . graduate education in the pharmaceutical sciences received considerable discussion (by the APS Executive Committee). Concern was raised over both the ability to attract talented students to graduate studies in the pharmaceutical sciences and to obtain funding for those students who do apply."

Dr. Heimlich went on to describe specific actions taken by the APS and several of its sections in an effort to focus attention on the problem of declining graduate student quality.

Pharmacy students themselves have noted this trend of declining interest in graduate study; the Student APhA has gone so far as to pass a resolution regarding the problem, and to sponsor several programs in an effort to identify remedies for it.

Years ago, when the undergraduate program in pharmacy was being shifted to a minimum five-year curriculum, many educators expressed concern that it would ultimately have an adverse effect on pharmacy graduate degree programs. Acknowledging the benefits of a five-year program for professional practice, many of these same educators suggested a "two-track" undergraduate program in which the student could opt either for a five-year professional degree or a four-year degree as preparation for graduate school studies and an advanced academic degree—generally as preparation for a career in research and/or teaching.

But even that "two-track" approach was not without its problems. In particular, many young people do not know clearly what their career objectives are when they finish four or five years of college. To expect them to make such specific choices at the beginning of their college work would be an unrealistic expectation.

Consequently, no simple or readily apparent answer appears currently available to resolve this dilemma.

In the meantime, a very large proportion of the applicants to graduate studies in the pharmaceutical sciences are graduates of four-year nonpharmacy programs or from four-year foreign pharmacy schools. And the admission standards for the five-year graduate of American pharmacy schools are much lower than in the past. The cummulative result of these factors is that the overall talent reflected in the present and recent graduate student bodies is not of the traditional select caliber that was the norm until about 10 years ago.

Gradually, the composite excellence of those granted M.S. and, in particular, Ph.D. degrees has been declining. In turn, the same erosion of high quality is beginning to occur within pharmacy faculty and research ranks as these recent graduates have emerged to take their place in the classroom and research laboratory.

Unfortunately, we have no ready solution to offer. At this time, we can only join Dr. Heimlich and his colleagues in the APS in noting the existence of the problem and in urging that prompt attention be devoted to it by appropriate groups. In particular, this would appear to be a key issue for review and study by the APhA Task Force on Pharmacy Education. As discussed above, it is an issue that will have an ultimate impact on the very heart of the quality of pharmacy education.

—EDWARD G. FELDMANN
American Pharmaceutical Association
Washington, DC 20037

0022-3549/83/0200-0103$01.00/0

JOURNAL OF PHARMACEUTICAL SCIENCES

FEBRUARY 1983
VOLUME 72 NUMBER 2

RESEARCH ARTICLES

Nonlinear Pharmacokinetics of the New Positive Inotropic Agent Sulmazole in the Dog

EDWARD R. GARRETT ˣ **and WILLY ROTH** *

Received December 14, 1981, from *The Beehive, College of Pharmacy, J. Hillis Miller Health Center, University of Florida, Gainesville, FL 32610.* Accepted for publication April 15, 1982. *Present address: Department of Biochemistry, Dr. Karl Thomae GmbH, 795 Biberach, Federal Republic of Germany.

Abstract □ Sulmazole (I) 2-[2-methoxy-4-(methylsulfinyl)phenyl]-1*H*-imidazo[4,5-*b*]pyridine, a new positive inotropic agent, is based on a pyridoimidazole nucleus. Sulmazole pharmacokinetics were monitored in plasma and urine by a specific, sensitive reverse-phase fully automated HPLC system with fluorimetric detection. The hydroxylated metabolite, III, was also monitored in the urine, and unusual pharmacokinetics were observed. Sulmazole disappeared and metabolite II appeared in plasma by zero-order rates for most of their time courses in the 2–15-mg/kg range with a 75% conversion to II. Pure Michaelis–Menten pharmacokinetics were not applicable, and the v_{max} value increased with increasing dose. Pharmacokinetics of sulmazole and II at 0.7-mg/kg iv doses were characterized by a first-order two-compartment body model. Metabolite III at 0.7- and 2-mg/kg iv doses showed no dose-dependent pharmacokinetics. The unchanged drug and its major metabolite, II, were negligibly excreted renally (0.5–2%). Their renal clearance showed urine flow rate dependencies. The plasma protein bindings were: sulmazole, 40.8 ± 1.0%; II, 54 ± 2%; III, 43 ± 1%, and they were concentration independent.

Keyphrases □ Pharmacokinetics—nonlinear, sulmazole, in the dog □ Models, pharmacokinetic—nonlinear, sulmazole, in the dog □ Sulmazole—nonlinear pharmacokinetics in the dog

Sulmazole[1] (I) has shown positive inotropic activity in an isolated dog heart preparation and in intact dogs (1–4). The onset and magnitude of cardiovascular response of this new nonglycosidic cardiotonic drug was studied in humans (5–10). The drug's action started immediately after intravenous administration, indicating that action was due to the parent compound (5) on the presumption that the time course of pharmacological action was related to the time course of the active drug in the central circulation.

Pharmacokinetic studies of radiolabeled I have been conducted in the rat (11, 12), baboon (13), rabbit and dog (14), and rhesus monkey (15), but only total radioactivity was measured. These studies did not reveal the pharmacokinetic behavior of the extensively metabolized I (16).

The present paper reports on the pharmacokinetics of I as a function of dose using specific and sensitive high-performance liquid chromatographic (HPLC) assays (17, 18). The stability, protein binding, and red blood cell partitioning of I, administered intravenously in dogs, and its metabolites, excreted in the urine, were also studied. Various methods of challenging the possible Michaelis–Menten pharmacokinetics of sulmazole were developed and applied to the data.

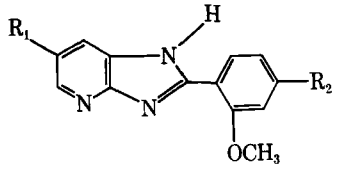

Compound	R_1	R_2	Name
I	H	$-SOCH_3$	2-[2-methoxy-4(methylsulfinyl)-phenyl]-1*H*-imidazo[4,5-*b*]pyridine; Sulmazole[1], mol. wt. 287.3
II	H	$-SO_2CH_3$	2-[2-methoxy-4-(methylsulfonyl)-phenyl]-1*H*-imidazo[4,5-*b*]pyridine[2] mol. wt. 303.3
III	OH	$-SOCH_3$	6′-hydroxy-2-[(2-methoxy-4-methylsulfinyl)phenyl]-1*H*-imidazo[4,5-*b*]pyridine; metabolite M2; mol. wt. 303.3

[1] AR-L 115 BS, Lot No. Ch.-B 00718, Dr. Karl Thomae GmbH, 7950 Biberach/Riss, West Germany.

0022-3549/83/0200-0105$01.00/0

EXPERIMENTAL

Materials—Sulmazole, 2-[2-methoxy-4-(methylsulfinyl)phenyl]-1*H*-imidazo[4,5-*b*]pyridine, I, was obtained in ampules of 1000 mg/10 ml[1]. Synthesized (19) ^{14}C-I had >99% chromatographic purity by TLC with subsequent liquid scintillation counting of extracted material and by radioscanning. This purity was substantiated by HPLC analysis. Reference compounds II and III were also obtained[2]. The solvents and reagents used were anhydrous dibasic sodium phosphate[3], 85% phosphoric acid[4], acetonitrile HPLC grade[4], 30% hydrogen peroxide[4], and phenobarbital sodium USP XIV granular[5]. A toluene base scintillation fluid[6] was used for the radioactive counting with a liquid scintillation counter[7]. Standard catheters were used for catheterization of the jugular[8] and the foreleg[9] veins. Blood was withdrawn into heparinized containers[10].

Pharmacokinetic Studies in Dogs—Three healthy male mongrel dogs (23–27 kg) were used for the pharmacokinetic investigations. Their blood analysis showed no pathogenic abnormality or presence of microfilaria. The dogs were fasted at least 17–20 hr before each study and were given water *ad libitum*. The animals were supported by a dog sling in a frame[11] placed on a laboratory table. The dogs were given 120 ml of water, 30–45 min prior to the experiments, followed by intravenous saline infusion (35 drops/min) until drug administration when the intravenous drip was reduced to 20 drops/min. One day before the experiment, the animals were catheterized with a 30.5-cm standard catheter in the jugular vein after local anesthesia with mepivacaine hydrochloride[12]. A second catheter was also implanted in a foreleg vein (vena brachialis). On the following day, the drugs were injected directly into the jugular catheter (1–4 sec) followed by flushing of the catheter with 20 ml of physiological saline. Then, the catheter was connected by a three-way stopcock[13] to the saline infusion bottle[14]. Blood samples (4 ml) were taken into a heparinized vacutainer[10] after filling the dead volume of the catheter with blood by aspirating with an extra syringe. These samples were discarded. During the first hour, blood was taken from the foreleg vein with subsequent sampling from the jugular. In several studies, samples were taken simultaneously from both sites in the first hour. The heparinized blood was centrifuged immediately for 5–8 min at 3000 rpm, and plasma was removed with sterile glass pipets. The red blood cells were suspended in 2 ml of physiological saline and stored in an ice bath for reinfusion at the end of the study. Plasma was injected directly and immediately into an HPLC system after appropriate dilution and recentrifugation. Urine was collected from the dogs through a urinary catheter[15] at 15–30-min intervals up to 10–24 hr. Withdrawal time, volumes, and urinary pH were recorded, and aliquots of each sample were frozen until analyzed.

One 24-kg dog, previously studied at several intravenous doses, was administered orally 16 mg/kg/day of phenobarbital in gelatin capsules[8] for 13 days. Subsequently, the pharmacokinetics of an intravenous bolus of 2 mg/kg of I were studied in this dog.

HPLC Assays—A fully automated HPLC system (18) permitted the direct injection of body fluids. The drugs and metabolites were trapped on either of two alternately working enrichment precolumns and dry-filled with reverse-phase material[16], while nonlipophilic material was separated by flushing the precolumns for 3 min with deionized water with a 2-ml/min flow rate. Backflush elution with the mobile phase was used to desorb the drugs from the precolumns to the analytical column in order to chromatographically separate and quantify. The equipment consisted of an autosampler[17], two HPLC pumps[18], a fluorescence detector[19], a chromatographic data station[20], and a self-made precolumn switching system activated by pressurized air (18). The mobile phase for I and II was acetonitrile–0.05 *M* dibasic sodium phosphate buffer (1:2.3, mobile phase A) apparent pH 6.8, with respective retention times of 2.40 and 3.01 min. The mobile phase for III (mobile phase B) had a retention time of 5.74 min and was mobile phase A diluted 1:1.13 with deionized water when urine was assayed after administration of I. When III was administered intravenously, there were no interferences at its 2.03-min retention time, and mobile phase A was used. A self-packed steel column[21] with reverse-phase material[22] was used with a working pressure of 8.5 megapascals at 49° (flow rate: 2 ml/min for mobile phase A; 2.5 ml/min for mobile phase B). The wavelengths (excitation/emission) in urine and plasma were 330 and 370 nm for compounds I and II and 345 and 515 nm for III. These wavelength selections permitted no mutual interferences of III with I and II. The slit width was adjusted to 10 nm (excitation) and 5 and 10 nm (emission) for I, II, and III, respectively. Calibration curves were established in the biological fluid as concentration *versus* peak area (19).

Stability Studies—Solutions of ~100 and 1000 ng/ml of I, II, and III were prepared in 1.0 *N* NaOH[23] and 1.0 *N* HCl[23], and the concentrations were monitored by specific HPLC assay after 0, 4, and 20 hr at 20 and 47°. Similar studies were conducted in fresh dog plasma and urine at 20 and 37.5°.

Protein Binding—Protein binding was studied by ultrafiltration (20) and ultracentrifugation in freshly prepared dog plasma obtained by centrifugation of heparinized dog blood (5000 U of heparin[24]/50 ml of blood) for 20 min at 2000 rpm. [^{14}C]-I and metabolites II and III were used.

Ultrafiltration—Ultrafiltration membrane cones[25] were immersed for 5 hr in refrigerated deionized water, and excess liquid was removed by centrifugation for 5 min at 1000 rpm. Since I showed markedly unspecific binding to the filter cones in the range of 17.6–33% at concentrations of 3.5×10^{-3}–3.5×10^{-5} *M*, all cones were presaturated with appropriate concentrations prior to the experiment, which reduced the unspecific binding to 0–4.3% (20). The fraction bound was calculated from the HPLC and liquid scintillation counting assay of the total concentration prior to the ultrafiltration of 2.5–3 ml of plasma and in the plasma water filtrate after 30% filtration.

Ultracentrifugation—Drug concentrations between 10^{-6} and 10^{-8} *M* in dog plasma were centrifuged[26] for 20 hr at 45,000 rpm at 20°. Initial and supernatant concentrations were determined by liquid scintillation counting for I and by HPLC for I, II, and III.

Red Blood Cell Partitioning—The time dependency of red blood cell partitioning of I (1.02 μg/ml) was investigated in prepared heparinized dog blood with a previously determined hematocrit. The blood (5 ml) was maintained at 37.5°, and 200-μl aliquots were removed at 2-min time intervals and digested for 5 hr with 2 ml of a mixture of 2-propanol[4]–commercial solvent[27] (1:1.5). Decoloration was effected with 0.2 ml of hydrogen peroxide for 30 min, then 10 ml of scintillation fluid[6] was added. After an adaptation period of 6 hr at 10°, liquid scintillation counting was performed. The centrifuged plasma was assayed similarly, and the red blood cell–plasma water partition coefficients were determined similarly. Freshly prepared red blood cells, obtained by centrifugation of heparinized dog blood at 1500 rpm, were washed four times with plasma water with subsequent centrifugation and were then resuspended in plasma water. They were also resuspended in iso-osmolar physiological buffer (5.52 g of Na_2HPO_4, 0.86 g of KH_2PO_4, and 32 g of NaCl/liter). The hematocrit was determined and the suspension was spiked with eight different concentrations of I in the range of 9.8×10^{-6}–9.6×10^{-8} *M*. After 20 min of incubation at 37.5° under gentle mixing, aliquots were taken, the hematocrit determined, and the partition coefficient calculated (21).

RESULTS AND DISCUSSION

HPLC Assays—The described automated system permits direct injection of urine and plasma (diluted at least 1:1.5 with deionized water) from an automatic injection system for assays of I, II, and III. The sample adsorbed on the reverse-phase material of the precolumn was washed

[2] AR-L 114 BS, DR. Karl Thomae GmbH, 7950 Biberach/Riss, West Germany.
[3] Mallinckrodt, Inc., Paris, KY 40361.
[4] Fisher Scientific Co., Fair Lawn, NJ 07410.
[5] Mallinckrodt Chemical Works, St. Louis, MO.
[6] Scinti-Verse, Fisher Scientific Co., Fair Lawn, NJ 07410.
[7] Packard Tri Carb 460 CD Liquid Scintillation System, Packard Instrument Co. Inc., Downers Grove, IL 60515.
[8] Intracath intravenous catheter placement unit 30.48 cm (12 in), 16 gauge, The Deseret Co., Sandy, UT 84070.
[9] 30.48 cm (12 in) catheter, 17 gauge 0.031 in. i.d., The Deseret Co., Sandy, UT 84070.
[10] Becton Dickinson Vacutainer, heparinized, Rutherford, NJ 07070.
[11] Alice King Chatham Medical Arts, Los Angeles, CA 90043.
[12] Carbocaine, Winthrop Laboratories, New York, NY 10016.
[13] Pharmaseal, Toa Alta, PR 00758.
[14] McGaw Laboratories, Irvine, CA 92714.
[15] Monojet, Division of Sherwood Co., A Brunswick Co., St. Louis, MO 63103.
[16] Bondapak C_{18}-Corasil, Waters Associates, Milford, MA 01757.
[17] Model 420B, Perkin-Elmer, Norwalk, CT 06856.
[18] Series 3B, Perkin-Elmer, Norwalk, CT 06856.
[19] Model 650S, Perkin-Elmer, Norwalk, CT 06856.
[20] Data Station Sigma 15, Perkin-Elmer, Norwalk, CT 06856.
[21] Herbert Knauer, 6370 Ober Ursel, West Germany.
[22] Hypersil ODS particle size 5 μm, Shandon Southern Products, United Kingdom, Astmore, Runcorn WA 71 PR.
[23] Ricca Chemical Co., Arlington, TX 76012.
[24] Heparin Sodium, 10,000 U/ml, The Upjohn Co., Kalamazoo, MI 49001.
[25] Membrane filter cones 2100 CF 50, Amicon Co., Lexington, MA 02173.
[26] Beckman Ultracentrifuge model LS-50 with rotor Ti 50, Beckman Instruments, Norcross, GA 30092.
[27] Biosolv, Beckman Inc., Fullerton, CA 92634.

for 3 min with deionized water to remove water soluble substances in the plasma and urine. Subsequently, the mobile phase backflushed the adsorbed material into the analytical column for HPLC assay, and the printer-plotter was activated to record the chromatogram 3 min after injection on the precolumn. The automated system of switching valves permitted injection and flushing of water soluble substances on one precolumn, while the second precolumn was backflushed for assay. The total time for a single assay was 12–15 min and 64–80 assays can be performed automatically in an 8-hr period.

In the assays of I (2.40 min) and II (3.01 min) in urine with mobile phase A, a peak due to an unknown metabolite was observed at 2.20 min that did not interfere with these fluorimetric assays at 330-nm excitation and 370-nm emission. In the assay of III (5.74 min) in dog urine with mobile phase B, peaks due to unknown metabolites were observed at 2.21, 3.63, 6.85, and 9.05 min with the fluorimetric assay at 345-nm excitation and 515-nm emission. These peaks did not appear in blank urine when III was administered intravenously, and mobile phase A could be used for a retention time of 2.03 min at 345-nm excitation and 515-nm emission.

The regression statistics (22) of calibration curves (n = 13–27) of concentrations *versus* peak area in the range of 20–1000 ng/ml for I and II and 40–1000 ng/ml for III gave analytical sensitivities (2 times the standard error of the estimate of concentration on peak area) of 15–18 ng/ml for plasma and 12–26 ng/ml for urine. All curves showed intercepts not significantly different from zero, correlation coefficients >0.990, standard errors of regression coefficient of 0.4–0.9% of the coefficient, and standard errors of the intercept within ±4.1 ng/ml.

Protein Binding—Plasma protein binding percentages (percent of 100 times the concentration in plasma–water/concentration in plasma) for different concentrations of drug and metabolites showed no apparent dose dependencies of protein binding. The percent protein bindings of I in the plasma concentration range of 50–15,000 ng/ml were consistent by both ultrafiltration (41.5 ± 1.2%, n = 6) and ultracentrifugation (40.5 ± 1.5%, n = 11) techniques, and the overall average was 40.8 ± 1.0% (*SEM*). The percent protein binding of II and III were 54 ± 2% (n = 3) and 43 ± 1% (n = 3), respectively, as determined by the ultracentrifugation technique in the 140–1500-ng/ml plasma range.

Red Blood Cell–Plasma Water Partitioning—The red blood cell–plasma water partition coefficient is the ratio of concentrations in the red blood cell to that in the plasma water. It can be calculated from the drug concentrations in plasma before and after equilibration with red blood cells with a known hematocrit, $H = V_{RBC}/V_{blood}$, and when the fraction, f, of the drug bound to plasma proteins is known, by means of an equation developed previously (21, Eq. 9). The time-dependent studies showed that red blood cell–plasma equilibration was achieved within 10 min (n = 7), since there was no significant difference in radioactivity counts of the supernatant, 2246 ± 36 cpm/ml (*SD*) of plasma water after that time. The partition coefficients, D, calculated from studies in whole blood and for red blood cells suspended in plasma–water showed no significant dose dependencies. The calculated partition coefficients averaged 3.10 ± 0.05 (*SEM*) in whole blood in the range of 67–6000 ng/ml (n = 6) and 2.72 ± 0.30 in red blood cell suspensions in plasma water in the range of 28–2820 ng/ml (n = 7). There was no significant difference when physiological buffer was used for the red blood cell suspensions. At 157 ng/ml, D was 3.20 ± 0.09 and 3.10 ± 0.13 from plasma–water and buffer, respectively.

Studies at 200 ng of I/ml also were conducted with the use of the HPLC assay for nonradiolabeled compound, where D = 2.59 for 6.9×10^{-7} M in blood and 5.52×10^{-7} M in plasma and D = 2.07 for 200 ng/ml in the red blood cell suspension and 140 ng/ml in the plasma water.

Stability of Compounds—The concentrations from the HPLC assays of I after appropriate dilution when subjected to 1.0 N NaOH and 1.0 N HCl for 20 hr were no different than when assayed at time zero. The maximum decrease in concentrations of I, II, and III at 100 and 1000 ng/ml of fresh dog plasma after 24 hr at 37.5° was 4 and 0.5% for I; 0.0 and 0.1% for II; and 0.1 and 0.0% for III. The values were the same when the samples were incubated in fresh dog urine. Thus, there was no significant degradation within 1 day for I, II, and III in strong acid, strong alkali, or in plasma or urine.

Nonlinear Plasma Pharmacokinetics of Sulmazole: Data Analysis on the Presumption of Michaelis–Menten Kinetics—The semilogarithmic plots of plasma levels of I *versus* time (Fig. 1) are given for several studies at different doses in dogs. Data was obtained from blood taken from the foreleg vein during the first hour and from the jugular after that. The concentrations of sulmazole in jugular blood were up to 3.0 times higher than that of foreleg blood in the first 15 min during the 2 mg/kg iv study in dog 1. Subsequently, the values coincided. The S-shapes of such curves are indicative of primarily saturable elimination processes

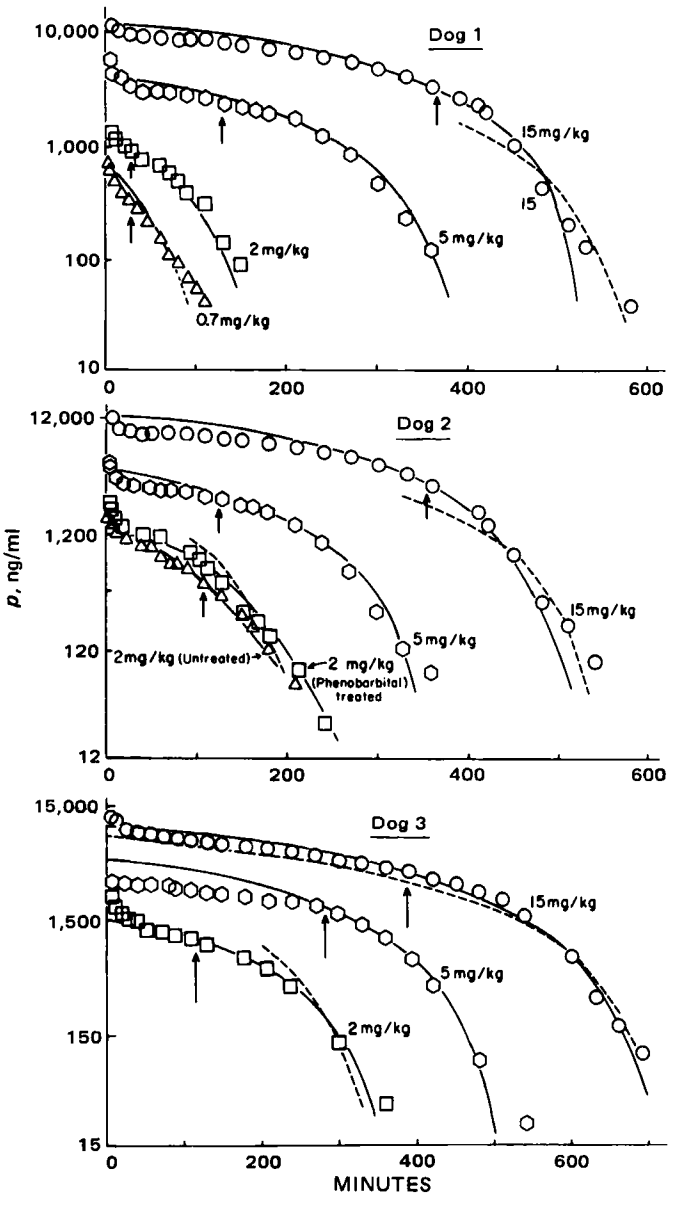

Figure 1—*Semilogarithmic plots of plasma levels of sulmazole on intravenous bolus administration of the labeled dose to dogs. The solid curves through the experimental values were calculated by Eq. 6 from the parameters given in Table I for each dog study. The squared symbols for dog 2 are for a study at 2 mg/kg after the dog had been treated daily with 16 mg/kg of oral phenobarbital over 13 days. The dashed lines for each dog study were plotted by Eq. 6 using the parameters for the 5-mg/kg dose study for each dog (Table I). The arrows designate the plasma level (p_1) values taken at time t_1 for the calculation of t_2 for any plasma level p_2. The initial estimation of Michaelis–Menten parameters by application of Eq. 5 were made from paired values subsequent to that time, t_1.*

in the disposition phase (23). The initial sharp decrease can be assigned to distribution and the subsequent increasing slopes with time to disposition. If there were only one saturable process and no significant parallel first-order elimination, the rate of plasma concentration (p) decrease subsequent to equilibration of the drug in the body would be characterized by:

$$-dp/dt = \frac{v_{max}\, p}{K_m + p} \qquad \text{(Eq. 1)}$$

where v_{max} is the maximum possible rate of decrease of plasma concentration (ng/ml/min) at maximal plasma levels, and v_{max}/K_m is the apparent first-order rate constant for terminal first-order elimination of drug when plasma levels approach zero:

$$\lim_{p \to \infty} -dp/dt = v_{max} \qquad \text{(Eq. 2)}$$

Table I—Parameters for Apparent Nonlinear Pharmacokinetics of Sulmazole and the Formation of Its Major Metabolite II

Parameter	Dog 1			Dog 2			Dog 3			Averages[a]			Overall average[a]
Weight, kg	22.4	25.4	23.4	25.4	25.0	24.6	26.5	25.2	25.0				
Dose, mg (mg/kg)	336(15)	127(5)	46.8(2)	381(15)	125(5)	49.2(2)	398(15)	126(5)	50(2)	(15)	(5)	(2)	
v_{max}[b], ng/ml/min	23.9 ± 0.6	12.8 ± 0.8	10.9 ± 0.4	30.8 ± 1.3	13.9 ± 1.0	10.4 ± 1.0	17.2 ± 0.6	13.1 ± 0.8	4.9 ± 0.3	23.9 ± 3.9	13.3 ± 0.3	8.7 ± 1.9	15.3 ± 2.6
$10^3 v_{max}/K_m$[b], min^{-1}	153 ± 65	73 ± 31	48 ± 3	79 ± 19	88 ± 45	33 ± 3	47 ± 7	54 ± 12	74 ± 63	93 ± 31	72 ± 10	52 ± 12	72 ± 12
$(t_{1/2})v_{max}/K_m$, min	4.5 ± 1.5	9.5 ± 3.4	14.5 ± 1.0	8.8 ± 2.0	7.8 ± 3.0	21.1 ± 1.0	14.7 ± 2.2	12.8 ± 3.6	9.3 ± 5.0	9.7 ± 1.5	10.0 ± 1.5	15.0 ± 3.4	11.4 ± 1.6
K_m[c], ng/ml	156 ± 60	175 ± 67	228 ± 24	391 ± 107	157 ± 85	313 ± 51	364 ± 68	242 ± 66	66 ± 35	304 ± 74	191 ± 26	202 ± 72	232 ± 36
k_0^I/V_I[d], ng/ml/min	20.8	11.0	8.0	23.6	12.1	6.4	12.7	5.1	4.5	19.0 ± 3.3	8.9 ± 1.9	6.3 ± 1.0	11.4 ± 2.2
V_I[e], liters	31.4	32.6	36.0	31.7	34.7	42.8	46.0	40.0	33.3	36.4 ± 4.8	35.8 ± 2.2	37.4 ± 2.8	36.5 ± 1.7
V_I'[f] liters	40.0	43.8	42.5	43.5	41.7	39.4	44.5	40.0	33.3	42.7 ± 1.4	41.8 ± 1.1	38.4 ± 2.7	41.0 ± 1.1
k_0^I[g], ng/min	6.53	3.58	2.88	7.48	4.21	2.74	5.84	2.04	1.50	6.62 ± 0.48	3.10 ± 0.53	2.37 ± 0.44	4.03 ± 0.70
$(k_0^I)'$[h], ng/min	8.32	4.81	3.40	10.26	5.05	2.52	5.65	2.04	1.50	8.08 ± 1.34	3.97 ± 0.97	2.47 ± 0.55	4.92 ± 0.88
10^{-3} AUC_∞^I/dose[i], (ml/min)/(mg/kg)	177	134	42	260	120	56	200	177	130	213 ± 25	144 ± 17	76 ± 27	144 ± 23
k_0^{II}/V_{II}[j], ng/ml/min	11.14	6.48	11.06	11.02	8.22	11.14	9.20	3.13	2.02	10.45 ± 0.63	5.94 ± 1.49	8.07 ± 3.03	8.16 ± 1.19
10^3 Cl^{II}/V_{II}[j], min^{-1}	4.0	6.7	39.7	6.2	12.7	4.0	7.5	4.5	4.6	5.9 ± 1.0	8.0 ± 2.5	16.1 ± 11.8	10.0 ± 3.8
10^3 β_{II}[k], min^{-1}	29.0	27.1	24.6	24.7	24.7	25.1	34.3	26.6	22.2	29.3 ± 2.8	26.1 ± 0.7	24.0 ± 0.9	26.5 ± 1.2
$(t_{1/2})\beta_{II}$[k], min	23.4	25.6	28.2	28.0	28.0	27.7	20.2	26.0	31.1	23.9 ± 2.3	26.5 ± 0.7	29.0 ± 1.1	26.5 ± 1.1
C_0^{II}[k], ng/ml	1.02×10^9	1.77×10^6	5.01×10^3	5.24×10^7	4.16×10^5	1.30×10^4	1.08×10^{12}	3.49×10^7	1.16×10^5				
k_0^{II}[l], ng/min	5.41	3.15	5.37	5.35	3.99	5.41	4.46	1.52	0.981	5.07 ± 0.31	2.89 ± 0.73	3.92 ± 1.47	3.96 ± 0.58
$k_{0_{corr}}^{II}/k_0^I$[m]	0.783	0.834	(1.77)	0.677	0.898	(1.87)	0.724	0.706	0.620	0.728 ± 0.031	0.813 ± 0.056	(1.42 ± 0.4)	0.749 ± 0.036
10^{-3} AUC_∞^{II}/dose of I[n], (ml/min)/(mg/kg)	47.7	37.0	17.5	34.7	28.6	22.3	38.4	36.4	31.0	40.3 ± 3.9	34.0 ± 2.7	23.6 ± 4.0	32.6 ± 3.0

[a] The ± values for the averages are the *SEM* for the values averaged. [b] $1/v_{max}$ and K_m/v_{max} values were determined from the slopes and intercepts, respectively, of the statistical regression of $(t_2 - t_1)/\ln(p_1/p_2)$ against $(p_1 - p_2)/\ln(p_1 - p_2)$ in accordance with Eq. 5 for all pairs of I plasma levels, p_1 and p_2, at their respective times, t_1 and t_2, in the postdistributive phases. The correlation coefficients ranged between 0.9559 and 0.9888. The values of v_{max} and v_{max}/K_m and their error estimates were calculated from the respective reciprocals of the slope ± s slope, and of the intercept ±s intercept. [c] Intercept, K_m/v_{max}, divided by slope, $1/v_{max}$. [d] Best estimate of slope of plasma level of I against time on the presumption of zero-order kinetics in the disposition phase. [e] $V_I = D_0/C_0$ where D_0 is dose of I in milligrams and C_0 is the extrapolated intercept of the estimated zero-order loss, k_0^I/V_I (ng/ml/min). [f] $V_I = D_0/C_0$ where C_0 was obtained from the extrapolated intercept of a line through the plateau values in the 40–100-min interval (Fig. 3) after intravenous administration. [g] $k_0^I = V_I \times k_0^I/V_I$. [h] $(k_0^I)' = V_I \times k_0^I/V_I$. [i] Total area (ng/ml/min) under plasma level–time curve of I per mg/kg of I dose. [j] The apparent zero-order rates of formation of II, k_0^{II}/V_I, and its subsequent clearance per unit volume, Cl^{II}/V_{II}, were determined from the respective slopes and intercepts of plots (Fig. 7) in accordance with Eq. 16. [k] Parameters for first-order elimination of II after cessation of formation from I in accordance with $C_0^{II} = e^{-\beta_{II}t}$ where C_0^{II} is the extrapolated value to zero time. [l] Nanograms of II formed/min from I calculated from $V_{II}(k_0^{II}/V_{II})$ where V_{II} was taken as the 48,558-ml apparent overall volume of distribution determined from the study after administration of 0.7 mg/kg iv of II. [m] Fraction of rate of loss of I transformed to II, *i.e.*, $k_0^{II}(corr)/k_0^I = (k_0^{II}/k_0^I)$ mol. wt. I/mol. wt. II = 0.9473 (k_0^{II}/k_0^I). The overall average is given with the values for 2-mg/kg doses in dogs 1 and 2 omitted. [n] AUC_∞^{II} is by trapezoidal rule of area under plasma level of II *versus* time on intravenous administration of I plus $[II]_n/\beta_{II}$ where $[II]_n$ is the terminal plasma level at t_n used to estimate $AUC_{t_n}^{II}$ up to that time. This value is divided by the dose of I (mg/kg).

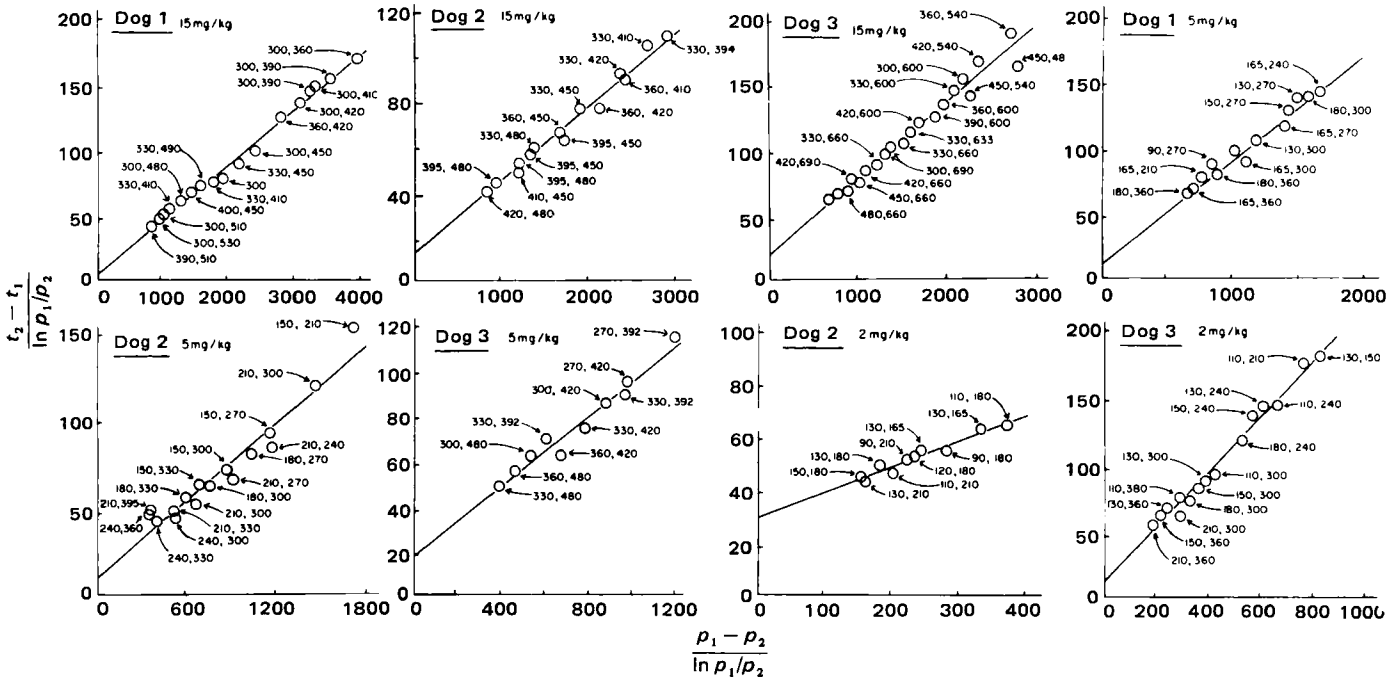

Figure 2—*Plots of paired sulmazole plasma level–time data after the time given by the arrow in Fig. 1 in accordance with Eq. 5 to estimate* $1/v_{max}$ *from the slope and* K_m/v_{max} *from the intercept. Each data point is labeled with the times after administration of the data pair used (*p_1 *at* t_1 *and* p_2 *at* t_2*).*

and

$$\lim_{p \to 0} -dp/dt = (v_{max}/K_m)p \qquad \text{(Eq. 3)}$$

If the elimination process can be attributed to saturable metabolism, K_m can be interpreted as the affinity constant for the available enzymes where the metabolic rate is proportional to the amount of drug–enzyme complex. When all enzymes are complexed in the steady state, the maximal zero-order rate, v_{max}, would be achieved. The data for all doses appeared to approach a final first-order loss of drug from the plasma (Fig. 1) with visually estimated apparent half-lives of 30.0 ± 5.9 (*SD*) ± 2.9 min (*SEM*) for dog 1 (n = 4), 27.2 ± 7.0 (*SD*) ± 4.0 min (*SEM*) for dog 2 (n = 3), and 30.8 ± 1.0 (*SD*) ± 0.6 min (*SEM*) for dog 3 (n = 3).

These estimates of the terminal half-lives are approximate and likely overestimate $0.693/(v_{max}/K_m)$, since they may be based on an estimated linearity of a slightly curving semilogarithmic plot of the terminal plasma concentrations against time (Fig. 1).

The saturable disposition phase after complete equilibration of the drug among the tissues of the body can be characterized by the integrated form (24) of Eq. 1:

$$(p_1 - p_2) - K_m \ln \frac{p_2}{p_1} = v_{max}(t_2 - t_1) \qquad \text{(Eq. 4)}$$

where p_1 and p_2 are plasma concentrations in the postdistribution phase taken at times t_1 and t_2, respectively. This transcendental equation has no explicit solution for plasma concentration with time. Equation 4 can be rearranged to:

$$\frac{t_2 - t_1}{\ln (p_1/p_2)} = \frac{p_1 - p_2}{\ln (p_1/p_2)} \frac{1}{v_{max}} + \frac{K_m}{v_{max}} \qquad \text{(Eq. 5)}$$

where $1/v_{max}$ and K_m/v_{max} are the respective slopes and intercepts that can be estimated from linear plots of $(t_2 - t_1)/\ln(p_1/p_2)$ against $(p_1 - p_2)/\ln(p_1/p_2)$ for any pair of plasma levels, p_1 and p_2, at their respective times, t_1 and t_2, in the postdistributive phase. Examples of such plots are given in Fig. 2 and the resulting calculated values of K_m and v_{max} are listed in Table I. Such plots must be restricted to plasma levels subsequent to the achievement of pseudo steady-state equilibration among the tissues of the body, *i.e.*, the establishment of a one-compartment body model. Also, they are only valid for estimation of parameters (Table I) when there is only one saturable elimination process and no significant amount of drug is eliminated by any parallel first-order process. Thus, p_1-values were not taken at earlier times. The p_1-values, taken after body equilibration of drug was assumed (arrows in Figs. 1 and 3), were then paired with later p_2-values, not too close in time, to produce the plots of Fig. 2 in accordance with Eq. 5. The v_{max}- and K_m-values were then substituted into a rearranged Eq. 4:

$$t_2 = \frac{p_1 - p_2}{v_{max}} - \frac{K_m}{v_{max}} \ln \frac{p_2}{p_1} + t_1 \qquad \text{(Eq. 6)}$$

An experimental value for p_1 at a known time t_1 (designated by the arrows in Figs. 1 and 3) in the presumed pseudosteady-state phase was assumed to be valid, and t_2-values were calculated for various p_2-values. The solid curves in Fig. 1 and the dashed curves in Fig. 3 were calculated in this manner.

Although the parameters v_{max} and K_m (Table I) for Eqs. 4 and 6 obtained in this manner permit good fit to the experimental plasma level–time data (Figs. 1 and 3) subsequent to the time when pseudo steady-state equilibrations among body tissues are probably established, the calculated plasma level values significantly overestimate the experimental values in the early time periods subsequent to the usual relatively rapid (α-phase) tissue distribution.

Table II—Parameters for Apparent Linear Pharmacokinetics of Sulmazole and Metabolites II and III in the 24.2-kg Dog 1

Parameter	Compound I	II	III	
Dose, mg/kg	0.7	0.7	1.0	2.0
mg	16.94	16.73	24.4	48.8
a^a, ng/ml	325	500	2000	4600
b^a	573	302	272	552
α^a, min^{-1}	0.384	0.384	0.221	0.271
($t_{1/2}$, min)	(1.80)	(1.81)	(3.13)	(2.56)
β^a	0.0235	0.0326	0.0186	0.0186
	(29.5)	(21.2)	(37.3)	(37.3)
$Cl_{tot}{}^b$, ml/min	671	1583	1031	1046
$Cl_{ren}{}^c$	13.9	3.00	0.25	0.25
$Cl_{met}{}^d$	657	1580	1031	1046
$V_c{}^e$, liters	18.9	20.9	10.7	9.5
$V_d{}^f$	28.6	48.6	55.5	56.2
$V_{extrap}{}^g$	29.6	55.4	9.0	8.8

[a] Parameter description of time course of plasma concentrations, $p = ae^{-\alpha t} + be^{-\beta t}$. [b] $Cl_{tot} = AUC_\infty$/dose (ng) where the total area under the plasma level–time curve is $AUC_\infty = A/\alpha + b/\beta$. [c] Slope of plot of cumulative drug *excreted at time* t, ΣU_t, against the area under the plasma level–time curve until that time, where $AUC_t = (a/\alpha)(1 - e^{\alpha t}) + (b/\beta)(1 - e^{-\beta t})$. [d] $Cl_{met} = Cl_{tot} - Cl_{ren}$. [e] Apparent volume of distribution of central compartment referenced to plasma concentration, $V_c = p_0$/dose (ng) = $(a + b)$/dose (ng). [f] Apparent overall pseudo steady-state volume of distribution referenced to plasma concentration, $V_d = Cl_{tot}/\beta$. [g] Apparent overall volume of distribution on the assumption of the one-compartment body model, V_{extrap} = b/dose (ng).

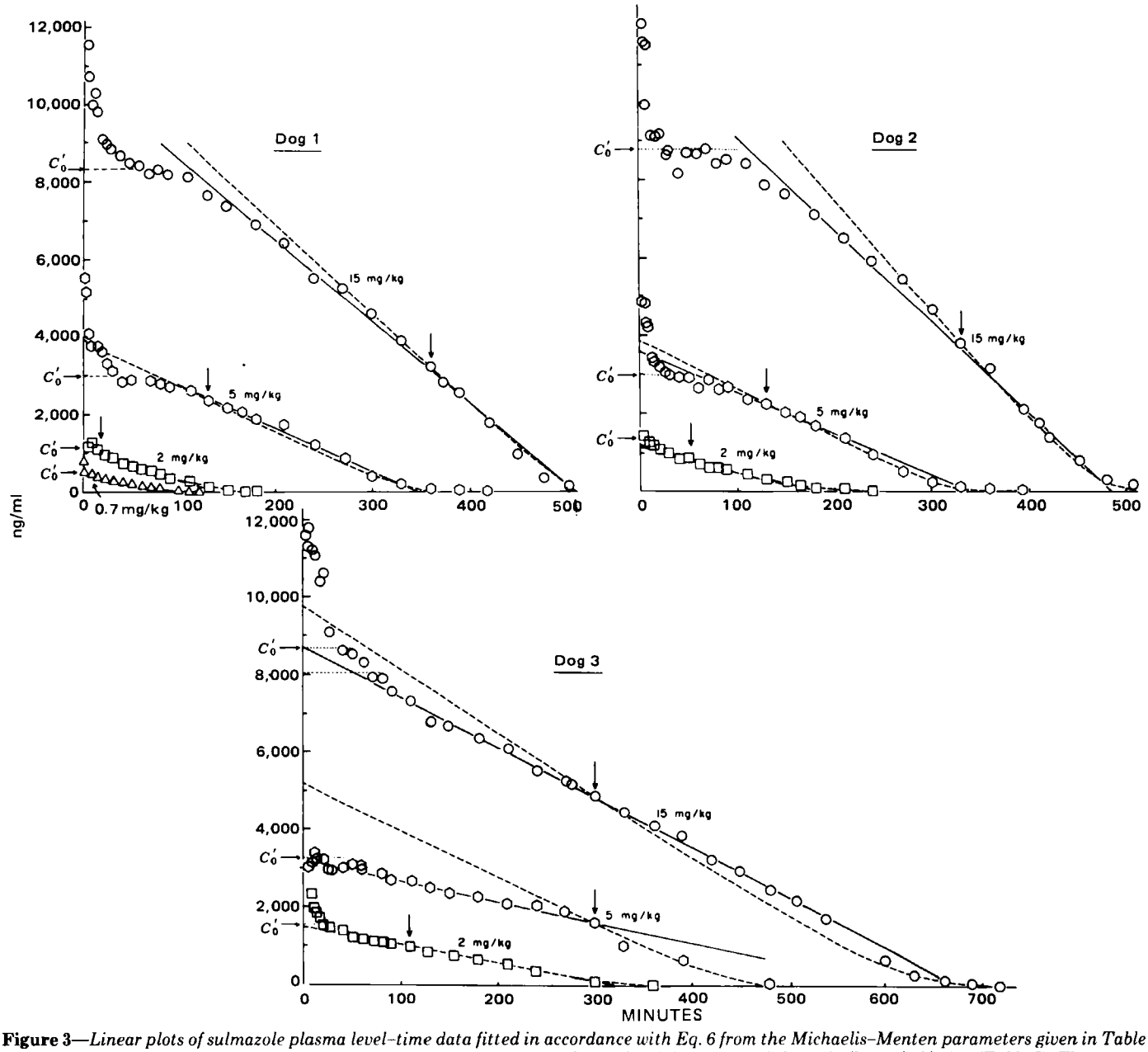

Figure 3—*Linear plots of sulmazole plasma level–time data fitted in accordance with Eq. 6 from the Michaelis–Menten parameters given in Table I (- - -) and fitted on the presumption of constant zero-order rates of plasma level decay (—) of slopes* k_0/V *(ng/ml/min) (Table I). The arrows designate the plasma level* (p_1) *values taken at time* t_1 *for the calculation of* t_2 *for any plasma level* p_2 *by Eq. 6.*

This can be seen at the 15-mg/kg dose but less so at the 2-mg/kg dose. One possible explanation of the constantly recurring plateau or increase in plasma levels for all three dogs at 40–100 min after drug administration may be the presence of enterohepatic recirculation, the delayed continuous reabsorption of biliary excreted sulmazole from the GI tract.

The v_{max}-values of Table I have reasonable precision that average ±7% and show a decided dose effect: 23.9 ± 3.9, 13.3 ± 0.3, and 8.7 ± 1.9 ng/ml/min (*SEM*) at the 15-, 5-, and 2-mg/kg iv doses of sulmazole, respectively. The estimated K_m-values with their much higher variability averaging ±32% do not permit any conclusion as to dose dependencies. The overall average of 232 ± 36 ng/ml (*SEM*) is relatively small and does not disturb the linearities of the concentration–time plots of sulmazole for the greatest portion of the time course.

The fact that one set of v_{max}/K_m-values fails to characterize the plasma level–time values of sulmazole for all doses is apparent when the set of values for the 5-mg/kg dose was used to attempt to fit the data at all doses (dashed lines in Fig. 1).

The v_{max}/K_m-values and the derived $(t_{1/2})_{v_{max}}/K_m$-values (Table I) provide estimates of the apparent first-order rate constant effective at low drug concentrations in plasma in accordance with the postulation of one saturable elimination process directing the elimination that conforms to Michaelis–Menten kinetics.

Although there appears to be a systematic decrease in the averages of the v_{max}/K_m-values and an accompanying systematic increase in the averages of the apparent half-lives with decreasing dose (0.7 ± 1.5, 10.0 ± 1.5,and 15.0 ± 3.4 min (*SEM*) at 15, 5, and 2 mg/kg of sulmazole, respectively), the standard errors do not permit an absolute decision. The data for dog 3 were contrary to those of the averages.

The plasma level–time curve for sulmazole at the lowest dose studied, 0.70 mg/kg, is plotted semiliogarithmically in Fig. 4. At this dose the pharmacokinetics appear to be linear; the drug appears to be eliminated by first-order processes from a two-compartment body model. The pharmacokinetic parameters are listed in Table II. The terminal half-life of 29.5 min confirms the indicated increase of the terminal half-life with decreasing dose.

Data Analyses on the Presumption of Zero-Order Pharmacokinetics—Constant slopes k_0^I/V_I (ng/ml/min) can be obtained from the slopes of the plotted data in Fig. 3 and can reasonably characterize the plasma level–time data of sulmazole. These are given in Table I and are close to the estimated v_{max}-values. Considering that they give less weight to the terminal data, they show similar dose dependencies.

The dose dependencies of k_0/V_I and v_{max} permit the conclusion that the simple model of a Michaelis–Menten single saturable elimination process with a constant v_{max} cannot describe the sulmazole plasma

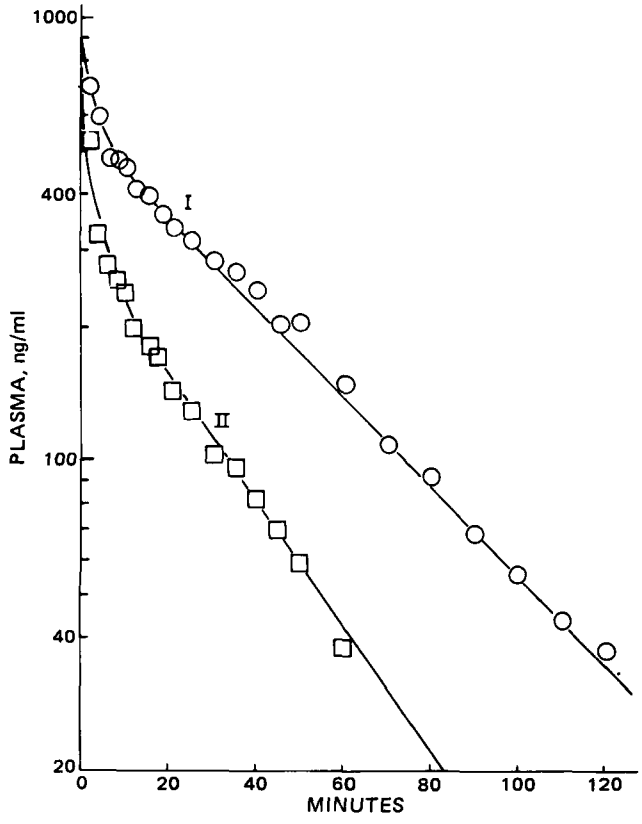

Figure 4—*Semilogarithmic plots of plasma levels of sulmazole (I) and II after intravenous administration of 0.7 mg/kg of each to dog 1. The curves through the data were constructed from the parameters given in Table II in accordance with* $p = ae^{-\alpha t} + be^{-\beta t}$.

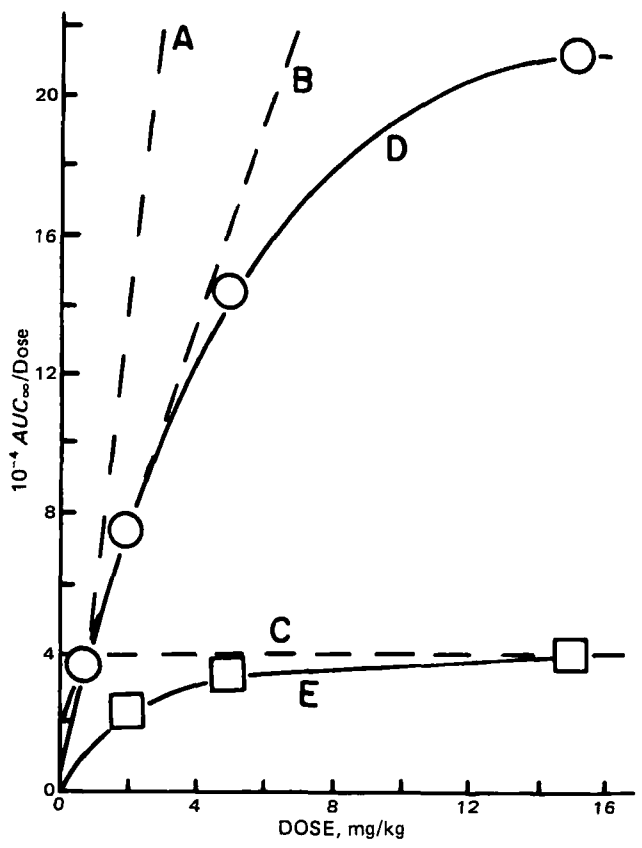

Figure 5—*Plots of ratios of total area under the curve (ng/min/ml^{-1}) to dose (mg/kg) against dose for sulmazole (○), curve D, and metabolite II (□), curve E. The anticipated forms of curves expected are given as dashed lines for (A) zero-order kinetics with constant elimination rates at all doses, (B) saturable pharmacokinetics with constant Michaelis–Menten parameters at all doses, and (C) first-order elimination rates.*

level–time data at all doses, even though it may give a reasonable fit at a given dose. The linearities of the plasma level–time data (Fig. 3) over such long time periods deny the existence of significant parallel first-order processes of elimination. Such processes could increase elimination rates at higher doses and plasma concentrations.

The apparent zero-order rate constants, k_0^I/V_I (ng/ml/min) in the 2–15-mg/kg dose range can be well characterized by the linear plot of their average values *versus* dose of sulmazole (mg/kg), $r = 0.9996$, to give:

$$k_0^I/V_I(\pm 0.26) = 0.985(\pm 0.027) \times \text{Dose} + 4.17 \pm 0.25 \quad \text{(Eq. 7)}$$

The apparent overall volumes of distribution referenced to plasma concentration of sulmazole apparently were dose independent and were obtained from the intercept, C_0, obtained from the extrapolation of the *straight line* of best fit through the plasma level–time data and averaged V_I = dose (ng)/C_0 (ng/liter) = 36.5 ± 1.7 liters. The value of V_I by this method was 30 liters for the 0.7-mg/kg dose (Table II, Fig. 4). These volumes could also be estimated from the intercept, C_0', obtained from extrapolation of the plateau in the 40–100-min interval (Fig. 3) after intravenous administration and a V_I' = dose (ng)/C_0' (ng/liter) = 41.0 ± 1.1 liters. The latter equation may be the more valid estimate if enterohepatic circulation did exist. Its existence would cause an overestimation of C_0 in the equilibrated fluids of the body and an underestimation of the apparent volume of distribution by the former method. The lower standard error of the mean of the latter (V_I') with respect to the former (V_I) at several doses confirms this. The values are listed in Table I. The averages of the $(k_0^I)' = V_I'(k_0/V_I)$ of sulmazole eliminated from the body are correlated well with the dose in milligrams per kilogram in the 2–15-mg/kg range, $r = 0.9982$, by:

$$k_0^I \pm 0.161 = (0.426 \pm 0.167) \times \text{Dose} + 1.71 \pm 0.15 \quad \text{(Eq. 8)}$$

Areas Under Plasma Sulmazole Level–Time Curves and Possible Relations to Doses—The total area under the plasma level–time curve for saturable (Michaelis–Menten) disposition pharmacokinetics for the one-compartment body model (23) of volume V with an intravenous bolus is:

$$AUC_\infty^{sat} = \frac{D}{v_{max}V}\left(\frac{D}{2V} + K_m\right) = \frac{D}{k_0}\left(\frac{D}{2V} + K_m\right) \quad \text{(Eq. 9)}$$

Thus:

$$AUC_\infty^{sat} = \frac{D^2}{2v_{max}V^2} + \frac{K_mD}{v_{max}V} = \frac{D^2}{2k_0V} + \frac{K_mD}{k_0} \quad \text{(Eq. 10)}$$

The ratio of the total area under the plasma level–time curve for zero-order elimination (k_0) to dose (D) for the one-compartment body model with an intravenous bolus is:

$$\frac{AUC_\infty^0}{D} = \frac{D}{2v_{max}V^2} = \frac{D}{2k_0V} \quad \text{(Eq. 11)}$$

where $v_{max} = k_0/V$.

In Eqs. 10 and 11 plots of the ratio of total area–dose should be linear functions of dose with a positive slope. In the saturable case (Eq. 10), the intercept should be positive; in the zero-order case (Eq. 11), the intercept should be zero.

The ratio of the total AUC for first-order elimination to the doses is a constant:

$$AUC_\infty^I/D = 1/\beta V = 1/Cl_{tot} \quad \text{(Eq. 12)}$$

where the total clearance (Cl_{tot}) is a product of the terminal rate constant (β) and the apparent overall volume of distribution (V).

Such ratios of AUC–dose in milligrams per kilogram are given in Table I for sulmazole, AUC_∞^I/D. The ratio for the 0.7-mg/kg dose was 36,000. A plot of the ratio *versus* dose is given in Fig. 5 for sulmazole. The ratio increases with dose to indicate nonlinear pharmacokinetics, but it does not increase linearly. Sulmazole does not conform to the patterns anticipated for true saturable or zero-order pharmacokinetics in the one-compartment body model. This is a consequence of the apparent increases of v_{max} or k_0^I/V (Fig. 3, Table I) with the initial dose, where k_0^I/V, the zero-order rate of elimination, persists throughout the major time course of the drug in the plasma.

Pharmacokinetics of the Formation of II from Sulmazole—The time courses of formation of II in the plasma on intravenous administration of sulmazole at 2, 5, and 15 mg/kg are plotted in Fig. 6 for the

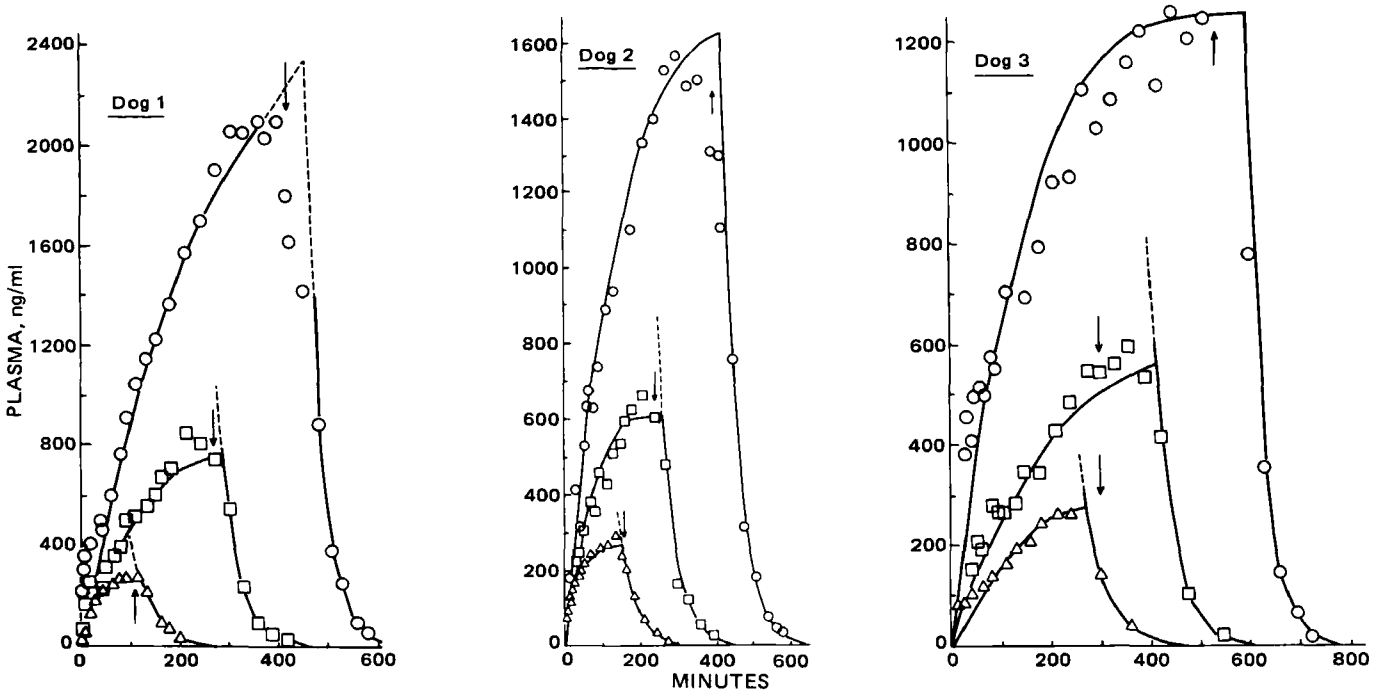

Figure 6—*Linear plots of plasma levels of metabolite II as formed with time after intravenous administration of 2 (△), 5 (□), and 15 (○) mg/kg of sulmazole to dogs 1–3. The arrows designate the approximate times of cessation of zero-order depletion of sulmazole in the plasma. The curves drawn through the points prior to the maxima were calculated from [II] = $(k_0^{II}/V_{II})t - (Cl^{II}/V_{II})AUC_{II}$. The curves drawn through the points subsequent to the maxima were calculated from $C_0^{II}e^{-\beta_{II}t}$ where the pertinent parameters are given in Table I.*

studies in dogs 1, 2, and 3. The shapes of the curves imply a zero-order formation of II up to the times marked by the arrows, where sulmazole was depleted from the plasma and a subsequent first-order elimination. This hypothesis was challenged.

If first-order formation and elimination existed, the amount of II formed could be expressed as:

$$II = Cl^{I\to II}AUC^{I} - Cl^{II}AUC^{II} \qquad \text{(Eq. 13)}$$

where AUC^{I} and AUC^{II} are the respective areas under plasma level–time curves for I and II, and $Cl^{I\to II}$ and Cl^{II} are the clearances of I–II and of II, respectively. Since the amount of II = V_{II} [II], where V_{II} is the apparent overall volume of distribution of II, and [II] is the plasma level, Eq. 13 can be rearranged to:

$$[II]/AUC^{I} = Cl^{I\to II}/V_{II} - (Cl^{II}/V_{II})AUC^{II}/AUC^{I} \qquad \text{(Eq. 14)}$$

However, plots of the ratio of the plasma level [II] at a time t to the area under the plasma sulmazole–time curve up to that time t (AUC^{I}) against the ratio of the areas of plasma metabolite–time to plasma sulmazole–time (AUC^{II}/AUC^{I}) were decidedly nonlinear, contraindicating the validity of the postulation of first-order formation of II from sulmazole with a constant clearance $Cl^{I\to II}$ with subsequent first-order elimination or constant clearance of II, Cl^{II}.

A zero-order formation of the amount of II from sulmazole with subsequent first-order elimination can be expressed as:

$$II = k_0^{II}t - Cl^{II}AUC^{II} \qquad \text{(Eq. 15)}$$

This expression can be rearranged to:

$$[II]/AUC^{II} = (k_0^{II}/V_{II})(t/AUC^{II}) - Cl^{II}/V_{II} \qquad \text{(Eq. 16)}$$

and plots of the ratio of plasma levels of the metabolite [II] at a given time (t) to that of the area under the plasma metabolite concentration (AUC^{II}) to that time against the ratio of the time (t) to the AUC^{II} should be linear with a slope k_0^{II}/V_{II} (ng/ml/min) and a negative intercept of Cl^{II}/V_{II} (min^{-1}), the apparent overall rate constant of elimination of the metabolite from its equilibrated tissues. These plots (Fig. 7) were linear to confirming the postulation of zero-order formation of the metabolite, II, with its subsequent first-order elimination. The obtained zero-order rates of formation of II from sulmazole, k_0^{II}/V_{II} (ng/ml/min), and the apparent clearance per unit volume of II, Cl^{II}/V_{II} (min^{-1}), are given in Table I.

The plasma values of II with time were calculated with these parameters and plotted as the curves through the data before the maximal values in Fig. 6. The values of maximum time corresponded to the cessation times of the zero-order rate of depletion of sulmazole in the plasma (Figs. 3 and 4).

Subsequent to the maximal values, metabolite plasma levels of II decreased by an apparent first-order process which could be characterized by:

$$[II] = C_0^{II}e^{-\beta II t} \qquad \text{(Eq. 17)}$$

where the values for C_0^{II}, the apparent plasma level extrapolated to zero time, and β_{II}, the apparent overall first-order elimination rate constant of II, are listed in Table I. These latter values appear to be dose-independent for plasma concentrations <2000 ng/ml of II, and the half-lives average 26.5 ± 1.2 min, consistent with the terminal half-life of 21.2 min when 0.7 mg/kg of II was administered (Fig. 4, Table II), a dose when the pharmacokinetics of II appear to conform to a two-compartment body model with first-order processes. The plasma values of II on sulmazole administration, subsequent to the maximal values, were calculated from the obtained C_0^{II} and β_{II}-values of Table I and were plotted through the experimental data in Fig. 6.

The rate of appearance of II (ng/min), k_0^{II}, was calculated from the product of the k_0^{II}/V_{II}-values (Table I) and the apparent overall volume of distribution, V_{II} = 48,558 ml, obtained from the administration of 0.7 mg/kg iv of II (Table II). Although the k_0^{II}-values of II appearance decreased consistently (5.07 ± 0.31–2.89 ± 0.73 ng/min) with the decrease of sulmazole dose from 15 to 5 mg/kg, the values at 2 mg/kg of sulmazole were high for dogs 1 and 2 (>1). A possible reason is that the volume of distribution for II (V_{II}) obtained from the single 0.7-mg/kg iv bolus study of II and used to convert k_0^{II}/V_{II}, the zero-order rate of II appearance per unit of volume, to k_0^{II} was not valid in these particular studies. If these values were not included, the ratio of k_0^{II} (corrected to sulmazole equivalents) to k_0^{I}, the apparent zero-order rates of II appearance and sulmazole disappearance, respectively, averaged 0.75 ± 0.04 (Table I) and were reasonably consistent among doses and dogs. The two anomalous values at 2 mg/kg for dogs 1 and 2 showed ratios of 1.77 and 1.87, respectively. It is concluded that 75% of the sulmazole is transformed to its major metabolite, II, by the zero-order process, 73 ± 3% at 15 mg/kg and 81 ± 6% at 5 mg/kg of sulmazole.

If, as shown in Table I, a relatively constant fraction of II was formed from I and if II were eliminated only by first-order processes or dose-independent clearances, the ratio of the area under the plasma level–time curve for II to the dose would not change with dose in accordance with Eq. 12. The fact that there is an increase of the ratio AUC_{∞}^{II}/dose with dose (Table I, Fig. 5), although not as significantly great as the comparable

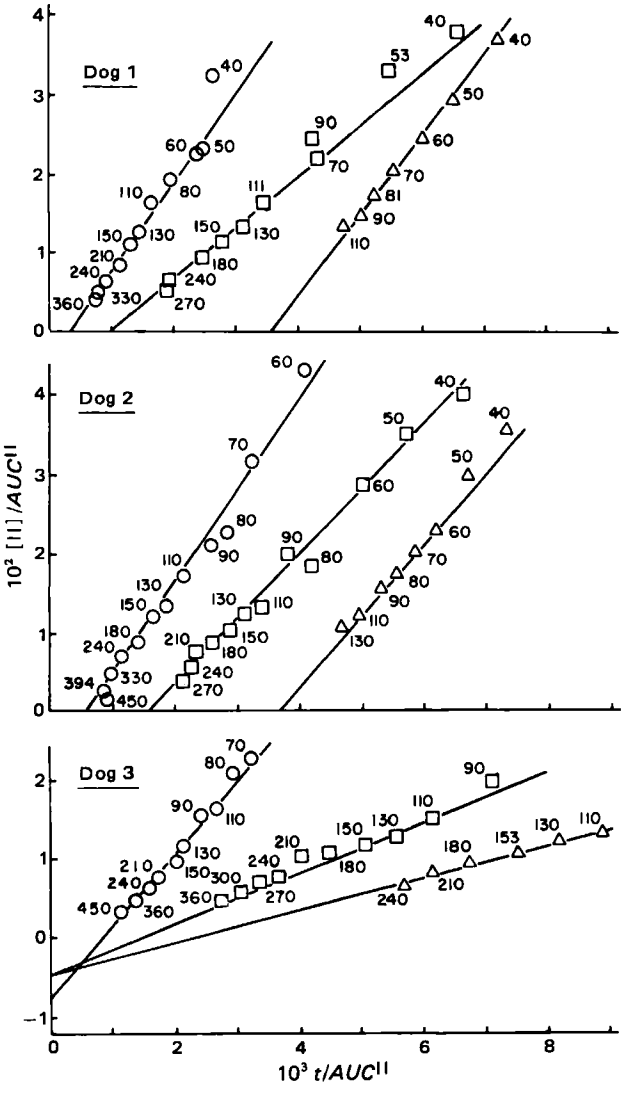

Figure 7—*Plots in accordance with Eq. 16 for the estimation of the zero-order appearance of metabolite II (slope = k_0^{II}/V_{II}, ng/ml/min^{-1}) and its first-order disappearance (intercept = $-Cl^{II}/V_{II}$, min^{-1}) for intravenous doses of 2 (△), 5 (□), and 15 (○) mg/kg of sulmazole.*

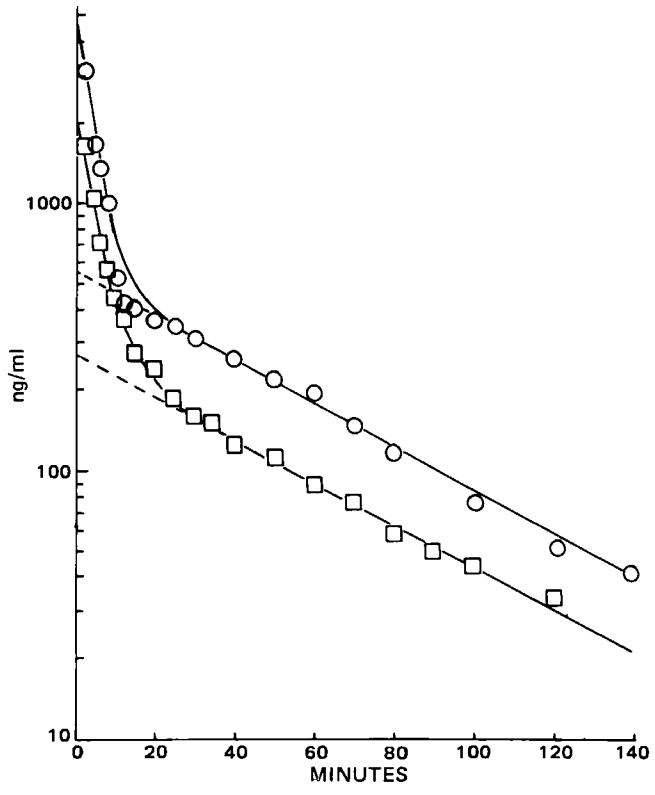

Figure 8—*Semilogarithmic plots of plasma levels of metabolite III against time when III was administered intravenously at 1 (□) and 2 (○) mg/kg. The curves through the data are drawn in accordance to* $p = ae^{-\alpha t} + be^{-\beta t}$ *where the pharmacokinetic parameters are given in Table II.*

ratio for sulmazole, indicates some degree of nonlinear pharmacokinetics for II at the higher sulmazole doses.

Pharmacokinetics of III—There was negligible renal excretion of unchanged I, II, and III. A possible route of metabolism of sulmazole, in addition to its oxidation to II, is its hydroxylation to III, since III is observed in the urine, although plasma III levels, even at 15 mg/kg of sulmazole, were below the analytical sensitivities.

The pharmacokinetics of III were studied at 1.0 and 2.0 mg/kg after intravenous administration of III and conformed to a two-compartment body model with apparent first-order transferences (Table II, Fig. 8). There were no apparent dose dependencies. Total clearances (1040 ml/min), terminal half-lives (37.3 min), and volumes of the central compartment (10 liters) and overall volumes (56 liters) were not significantly different for the two doses.

The lack of significant plasma levels and the fact that a week-long phenobarbital regimen did not increase sulmazole elimination rates significantly over the prephenobarbital regimen study at a dose of 2 mg/kg of sulmazole (Fig. 1) indicates that the hydroxylated compound is not a major product in sulmazole elimination. Phenobarbital is a well-known inducer of phenyl ring hydroxylation.

Renal Elimination of I and Metabolite II—Unchanged I was excreted renally at an average of 2.3 ± 0.4% of the administered dose (Table III) with no apparent statistically significant dose effects. Similarly, an average of 0.27 ± 0.05% of the administered sulmazole dose was excreted renally as metabolite II. Typical plots of cumulative amounts excreted with time are given in Fig. 9.

When there were narrow ranges of urine flow rates (Table III) reasonably constant renal clearances could be obtained from the regressions:

$$\Delta U/\Delta t = Cl_{ren} p_{t_{mid}} \quad \text{(Eq. 18)}$$

where $\Delta U/\Delta t$ is the amount (ΔU) of material excreted in a time interval (Δt), where $p_{t_{mid}}$ is the plasma level at the mid time of that interval, and:

$$\Sigma U = Cl_{ren} AUC \quad \text{(Eq. 19)}$$

where ΣU is the cumulative amount of material excreted at a time when AUC is the area under the plasma level–time curve up to that time.

In those cases where the urine flow rates varied over wider ranges, it was not possible to obtain reasonable correlations for Eqs. 18 and 19. The apparent renal clearance (Cl_{ren}^{app}) showed significant functional dependence on urine flow rate ($\Delta V/\Delta t$):

$$Cl_{ren}^{app} = (\Delta U/\Delta t)/p_{t_{mid}} = a \pm s_a + (b \pm s_b)(\Delta V/\Delta t) \quad \text{(Eq. 20)}$$

Examples of this dependence are shown in Fig. 10. Fittings of cumulative amounts of materials excreted into the urine with time are shown in Fig. 9 for the premises of constant renal clearance and renal clearances varying with urine flow rates using the parameters of Eq. 20 listed in Table III.

The apparent renal clearances of sulmazole varied between 1.6 and 7.4, except for the 13.8 ml/min of the 0.7-mg/kg dose with an overall average of 3.9 ± 0.8 ml/min. The apparent renal clearance of metabolite II varied between 1.0 and 3.4 ml/min, except for the 6.4 ml/min from the 0.7-mg/kg dose of sulmazole, with an overall average of 1.8 ± 0.3 ml/min. Even when corrected for protein binding, the respective renal clearance referenced to free drug in plasma of I and II did not exceed 6.6 and 3.91 ml/min. This is strong evidence for a high excess of tubular reabsorption which is supported by the dependence of apparent renal clearance on urine flow rate (Eq. 20).

The renal clearance of 0.7 mg/kg of intravenously administered II was 3.0 ml/min from the plot in accordance with Eq. 18 (Fig. 11). The renal clearance of 1.0 and 2.0 mg/kg of intravenously administered III was independent of dose (0.25 ml/min) (Fig. 11). The plots of cumulative urinary excretion against time of III are given in Fig. 12 and conformed to the values calculated in accordance with Eq. 19.

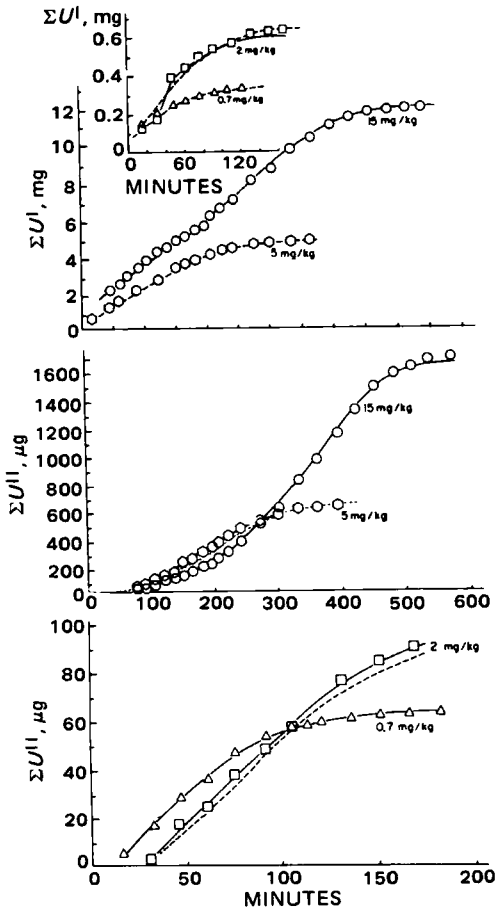

Figure 9—*Plots of cumulative amounts of unchanged sulmazole and metabolite II excreted in urine for the labeled amounts of sulmazole administered intravenously to dog 1. The dashed lines are plotted for an assumed sulmazole constant renal clearance, Cl^{I}_{ren}, of 7.4, 7.77, and 13.8 ml/min for the 5-, 2-, and 0.7-mg/kg doses, respectively, in accordance with $\Sigma U^{I} = Cl^{I}_{ren} AUC^{I}$. Dashed lines are plotted for an assumed metabolite II constant renal clearance, Cl^{II}_{ren}, of 3.35 and 2.77 ml/min for the sulmazole doses of 5 and 2 mg/kg, respectively, in accordance with $\Sigma U^{II} = Cl^{II}_{ren} AUC^{II}$. The solid lines are calculated for a urine flow-dependent renal clearance, $Cl_{ren} = a + b(\Delta V/\Delta t)$ where the a and b constants are given in Table III.*

Possible Rationales for the Unusual Nonlinear Pharmacokinetics of Sulmazole—The higher maximal zero-order rates of sulmazole elimination and transformation over large sulmazole concentration ranges at higher initial doses of sulmazole cannot be described by simple Michaelis–Menten kinetics. It is possible to speculate why. The hypothesis of product-inhibited processes (as by hydroxylated metabolite) (25) cannot explain this phenomenon, since this factor would lower maximal zero-order rates with the higher dose. In addition, it has been shown that *p*-hydroxylation of the phenyl ring is not the major metabolic route.

It was recently argued (25) that the Michaelis–Menten model for nonlinear processes has definite limitations, in that its basic premise is the establishment of a quasi-equilibrium process; *i.e.*, the validity of Eq. 1 is based on the premise of ready establishment of an equilibrium between the drug and the metabolizing enzyme where the subsequent rate-determining step depends on the concentrations of enzyme-bound substrate. A general unsteady-state model was proposed which denies the steady-state postulate underlying Michaelis–Menten kinetics. These concepts were applied to the simulation of plasma level–time curves on the premise of competition of metabolic products with substrate for plasma-, enzymes-, and tissue-binding sites to demonstrate that product-inhibited transformations would not necessarily conform to Michaelis–Menten kinetics.

The unsteady state concept may be useful to model this system, where the apparent zero-order elimination rate of sulmazole disappearance and metabolite II appearance seems to be dose- and initial plasma concentration-dependent. Speculation on the basis of an unsteady state possibly could lead to explanations of the unusual nonlinear pharmacokinetics

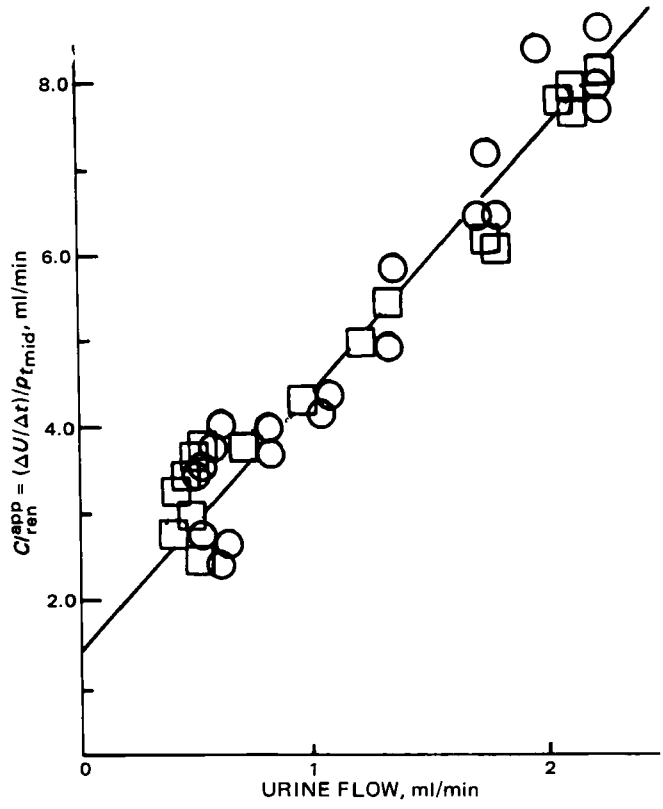

Figure 10—*Example of the dependence of the apparent renal clearance, Cl^{app}_{ren}, of sulmazole (○) and II (□) for a urine collection interval on the urine flow rate, $\Delta V/\Delta t$, in that interval for dog 1 (15-mg/kg dose study).*

of sulmazole where the major route of sulmazole substrate metabolism to II can be postulated as:

$$S + R \underset{k_2}{\overset{k_1}{\rightleftharpoons}} (SR) \xrightarrow{k_3} (MR) \xrightarrow{k_4} M + R \qquad \text{(Eq. 21)}$$

and it can be conjectured that substrate (S) has noninstantaneous but high affinity to large numbers (R) of receptor sites.

If the rate of transformation of receptor-bound substrate (SR) to receptor-bound metabolite (RM) and the subsequent regeneration of free receptor sites by dissociation of metabolite (M) were not instantaneous processes, there could be a preliminary interval when few free receptor sites would be available to bind to the substrate. This would explain the existence of initial plateaus in the plasma level–time curves of Fig. 3 subsequent to an initial drop in plasma levels and provide an alternative explanation to enterohepatic circulation as their cause.

Also, if the transformation of receptor-bound substrate (SR) to receptor-bound metabolite (RM) and its subsequent dissociation were rate-determining and time-dependent processes, the release of receptor-bound metabolite and the removal of substrate by available receptor sites would be greater for initially higher doses (or concentrations) of

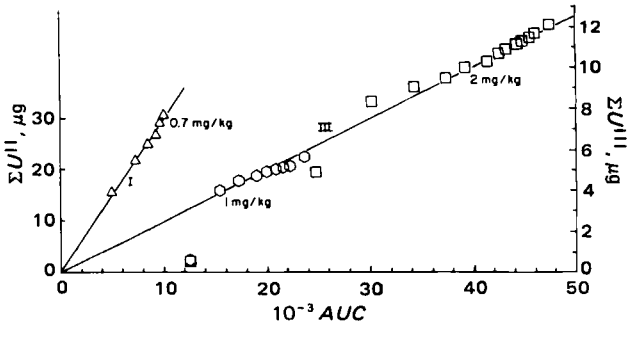

Figure 11—*Renal clearance plots in accordance with Eq. 19 for intravenous administration to dog 1 of 0.7 mg/kg of II (△, left ordinate, Cl^{II}_{ren} = 3.0 ml/min) and 1.0 (□) and 2.0 (○) mg/kg of III (right ordinate, Cl^{III}_{ren} = 0.25 ml/min).*

Table III—Parameters of Renal Elimination of Sulmazole and Metabolite II on Intravenous Administration of Sulmazole

Dog	mg/kg	ΣU_∞, mg I	ΣU_∞, mg II	Dose, %[a] I	Dose, %[a] II	Estimated Average Renal Clearances, ml/min: ΣU versus AUC[b] I	ΣU versus AUC[b] II	$\Delta U/\Delta t$ versus $p_{t_{mid}}$[c] I	$\Delta U/\Delta t$ versus $p_{t_{mid}}$[c] II
	15	12.0	1.686	3.6	0.48	—[d]	—[d]	—[d]	—[d]
	5	4.8	0.602	3.8	0.45	7.4 ± 0.1	2.4 ± 0.1	7.3 ± 0.4	3.4 ± 0.6
1	2	0.64	0.091	1.4	0.18	6.4 ± 0.3	2.8 ± 0.1	5.2 ± 0.9	—[d]
	0.7	0.34	0.065	2.0	0.36	13.8 ± 0.16	6.4 ± 0.4	—[d]	—[d]
	15	5.4	0.501	1.4	0.13	1.6 ± 0.1	1.2 ± 0.2	—[d]	—[d]
2	5	1.5	0.195	1.2	0.15	2.0 ± 0.1	—[d]	—[d]	1.0 ± 0.2
	2	0.32	0.048	0.65	0.10	1.6 ± 0.2	1.2 ± 0.1	1.9 ± 0.1	—[d]
	15	14.2	1.586	3.6	0.38	4.5 ± 0.1	1.8 ± 0.2	—[d]	1.4 ± 0.7
3	5	5.4	0.403	4.3	0.31	5.9 ± 0.2	2.1 ± 0.1	4.3 ± 0.9	2.3 ± 0.4
	2	0.52	0.062	1.0	0.11	2.2 ± 0.1	1.0 ± 0.1	2.0 ± 0.2	1.2 ± 0.1

Dog	mg/kg	$a + s_a$[e] I	$a + s_a$[e] II	$b + s_b$[e] I	$b + s_b$[e] II	r[g] I	r[g] II	Urine Flow, ml/min
	15	1.27 ± 0.22	0.8 ± 0.2	3.1 ± 0.2	1.2 ± 0.1	0.97	0.90	0.5–2.5
1	5	—[f]	1.7 ± 0.3	—[f]	1.4 ± 0.2	—[f]	0.85	0.6–2.4
	2	0.7 ± 2.1	−0.9 ● 0.3	3.8 ± 1.5	2.6 ± 0.2	0.72	0.98	0.6–2.0
	0.7	5.4 ± 3.0	0.1 ± 0.1	4.7 ± 0.7	3.4 ± 0.4	0.94	0.97	0.7–3.0
	15	0.5 ± 0.1	−0.1 ± 0.1	2.7 ± 0.4	0.6 ± 0.1	0.97	0.93	0.3–2.0
2	5	0.4 ± 0.3	0.0 ± 0.3	2.5 ± 0.4	1.9 ± 0.3	0.87	0.85	0.3–0.8
	2	—[f]	—[f]	—[f]	—[f]	—[f]	—[f]	0.4–0.7
	15	—[f]	—[f]	—[f]	—[f]	—[f]	—[f]	0.4–0.6
3	5	2.2 ± 0.3	0.8 ± 0.1	3.2 ± 0.3	1.5 ± 0.1	0.95	0.93	0.3–2.0
	2	—[f]	—[f]	—[f]	—[f]	—[f]	—[f]	0.1–0.3

[a] $100 \times \Sigma U_\infty$/dose (mg) where ΣU^{II} is converted to weight equivalents of I, *i.e.*, multiplied by mol. wt. I/mol. wt. II = 0.95. [b] Regression coefficient and its standard error of estimate for plots of cumulative amount excreted against the area under the plasma level–time curve for the respective compound at the time of cumulative excretion. [c] Regression coefficient and its standard error of estimate for plots of rate of excretion in an interval against the plasma level at the midtime of that interval. [d] Specified plots were nonlinear due to Cl_{ren} dependence on urine flow. [e] Constants for the linear regression and their standard errors (22) of apparent renal clearances [$Cl_{ren} = (\Delta U/\Delta t)/p_{t_{mid}}$ (ml/min)], the ratio of amount of compound excreted in a time interval, Δt, divided by the plasma level of compound at the midtime of that interval, on the urine flow rate [$\Delta V/\Delta t$, ml urine/the collection interval (ml/min)] in accordance with $Cl_{ren} = (b \pm s_b)(\Delta V/\Delta t) + a \pm s_a$. [f] Insufficient variation in urine flow ($\Delta V/\Delta t$) to warrant attempted regression of Cl_{ren} or no significant regression. [g] Correlation coefficient for dependence of apparent renal clearance on urine flow rate.

sulmazole when the plasma levels reach those initially obtained from lower doses than when the lower doses were administered. Thus, a dose-dependent rate of loss of sulmazole would be observed, since there would be slower overall rates of metabolism at lower doses where the available sites would be occupied by metabolites for greater fractions of the time course and not available for the depletion of plasma levels.

This model has been confirmed by simulation on the analogue computer. The conformity of the simulations with the observed data will be presented in detail in the future.

Summary—The experimental data indicate that the higher dose and initial concentration give the greater constant rate of sulmazole loss from plasma. The proposed nonsteady-state model would account for these unusual nonlinear pharmacokinetics if it is speculated that all receptor sites can be potentially occupied by substrate, but not instantaneously, that there is a time- and plasma concentration-dependent rate of occupation of receptor sites and a time-dependent release of metabolite to provide unreacted receptor sites.

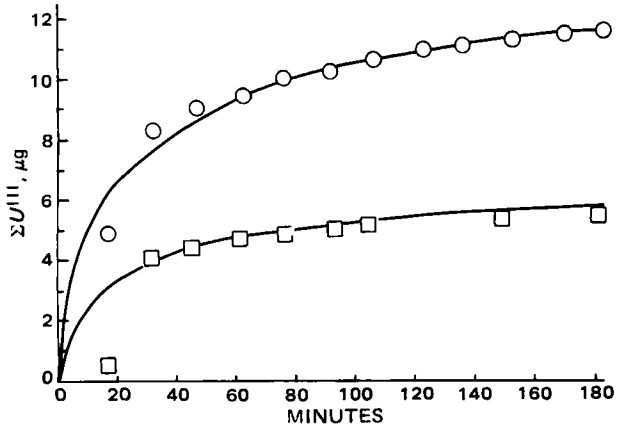

Figure 12—*Cumulative plots of III excreted with time at 1.0 (□) and 2.0 (○) mg/kg iv of III administered to dog 1. The curves drawn through the data were plotted in accordance with* $\Sigma U^{III} = Cl^{III}_{ren}AUC$ *where* $Cl^{III}_{ren} = 0.25$ *ml/min.*

An alternative explanation can be based on the hypothesis that high concentrations of sulmazole, metabolite II, and/or another metabolite can cause an irreversible, allotropic modification of the receptor so that binding of substrate, transformation to metabolite, and/or release of metabolite are enhanced.

REFERENCES

(1) W. Diederen and R. Kadatz, *Arzneim.-Forsch. (Drug Res.)*, **31**, 146 (1981).

(2) J. Dämmgen, R. Kadatz, and W. Diederen, *ibid.*, **31**, 151 (1981).

(3) G. Hellige, D. Baller, F. B. M. Ensick, J. Zipfel, H. G. W. Wolpers, and H. J. Bretschneider, *ibid.*, **31**, 155 (1981).

(4) Th. Hockerts, B. Höcht, R. Broll, K. Trenkel, J. Sieber, A. Kilian, and B. Brendle, *ibid.*, **31**, 157 (1981).

(5) L. Benedikter and T. Mey, *ibid.*, **31**, 239 (1981).

(6) G. F. Hauf, P. Bubenheimer, and H. Roskamm, *ibid.*, **31**, 253 (1981).

(7) H. Drexler, H. Wollschläger, H. Löllgen, and H. Just, *ibid.*, **31**, 259 (1981).

(8) M. Stauch and W. Nechwatal, *ibid.*, **31**, 267 (1981).

(9) K. D. Ruffmann, H. C. Mehmel and W. Kübler, *ibid.*, **31**, 271 (1981).

(10) J. Thormann, W. Kramer,and M. Schlepper, *ibid.*, **31**, 273 (1981).

(11) U. Busch, *ibid.*, **31**, 204 (1981).

(12) *Idem.*, **31**, 209 (1981).

(13) B. D. Cameron, G. H. Draffan, J. P. Dunsire, and A. Zimmer, Arneim.-Forsch. (Drug Res.), **31**, 217 (1981).

(14) A. Zimmer and R. Hammer, *ibid.*, **31**, 212 (1981).

(15) J. Mierau, *ibid.*, **31**, 221 (1981).

(16) W. Roth, A. Prox, A. Reuter, J. Schmid, A. Zimmer, and H. Zipp, *ibid.*, **31**, 232 (1981).

(17) W. Roth, A. Zimmer, and U. Busch, *ibid.*, **31**, 236 (1981).

(18) W. Roth, K. Beschke, R. Jauch, A. Zimmer, and F. W. Koss, *J. Chromatogr. Biomed. Appl.*, **222**, 13 (1981).

(19) H. Zipp, W. Roth, and A. Zimmer, *Arzneim.-Forsch. (Drug Res.)*, **31**, 200 (1981).
(20) P. H. Hinderling, J. Bres, and E. R. Garrett, *J. Pharm. Sci.*, **63**, 1684 (1974).
(21) E. R. Garrett and H. J. Lambert, *ibid.*, **62**, 550 (1973).
(22) HP-65, STAT-PAC-1 "Linear Regression," Hewlett-Packard, Corvallis, Ore., p. 49.
(23) E. R. Garrett, J. Bres, Kurt Schnelle, and L. L. Rolf, Jr., *J. Pharmacokinet. Biopharm.*, **2**, 43 (1974).
(24) J. G. Wagner, *ibid.*, **1**, 103 (1973).
(25) M. T. Smith and T. C. Smith, *Eur. J. Clin. Pharmacol.*, **20**, 387 (1981).

ACKNOWLEDGMENTS

Supported in part by an unrestricted grant from Dr. Karl Thomae GmbH, Biberach, West Germany.

The technical assistance of Mrs. Kathleen Eberst was greatly appreciated as was the discussion with Dr. Paul Altmayer and his analogue and digital computer simulations.

Effect of Insulin and Dinoprostone on D-Glucose and 2-Deoxy-D-Glucose Uptake by Normal and Diabetic Rat Hepatocytes

A. B. BIKHAZI *x, H. M. NUBANI, and E. L. COE ‡

Received July 17, 1981, from the **Department of Physiology and the* ‡*Department of Biochemistry, Faculty of Medicine, American University of Beirut, Beirut, Lebanon.* Accepted for publication November 25, 1981.

Abstract □ Suspensions of deaggregated hepatocytes were prepared by a collagenase perfusion technique from livers of both normal rats and rats rendered diabetic by streptozocin treatment. Uptake of D-glucose and 2-deoxy-D-glucose was estimated by adding ^{14}C- or ^{3}H-labeled hexose to a stirring suspension of cells in Krebs–Henseleit buffer at 37°, separating the cells by rapid centrifugation, and measuring radioactivity in the packed cell pellet. Uptake, calculated after correction for entrapped extracellular fluid, includes any hexose bound to, transported into, or otherwise immobilized in the cells. High concentrations of glucose (5–20 m*M*) establish an intracellular–extracellular distribution ratio near 1.0 within 1 min, indicating a facilitated diffusion transport system. In contrast, a low level of glucose (71 n*M*) almost immediately (<15 sec) establishes ratios of between 3 and 4, which suggests a significant amount of glucose binding to cell membrane. Such binding would not be detected at the high glucose levels because of its small magnitude. Hepatocytes from diabetic rats exhibit a decrease in this apparent binding to ~60% of normal; preincubation with 0.1 IU/ml insulin increases this toward normal values, although it does not affect the binding by normal hepatocytes themselves. Preincubation with 0.1 μ*M* dinoprostone depresses glucose binding in cells from both normal and diabetic rats. A low concentration (1.2 n*M*) of 2-deoxy-D-glucose establishes even higher intracellular–extracellular distribution ratios of between 4 and 6, but the apparent binding of this sugar is identical in normal and diabetic rat hepatocytes and is not affected by preincubation with either insulin or dinoprostone alone. However, combined treatment with both agents causes a significant increase in 2-deoxyglucose binding. The results suggest that insulin promotes formation of hexose-binding sites and conversion of these to specific glucose-binding sites while dinoprostone may act by blocking the latter conversion.

Keyphrases □ Insulin—effect on D-glucose and 2-deoxy-D-glucose uptake, normal and diabetic rat hepatocytes, dinoprostone □ Dinoprostone—effect on D-glucose and 2-deoxy-D-glucose uptake, normal and diabetic rat hepatocytes, insulin □ Hepatocytes—rat, normal and diabetic, effect of insulin, dinoprostone on D-glucose, 2-deoxy-D-glucose uptake

The roles of insulin and prostaglandins on glucose retention by adipocytes, muscle cells, and hepatocytes have been the subject of contention in the literature. Although some have denied the existence of any stimulatory action of insulin on sugar retention by normal hepatocytes (1, 2), others have demonstrated an increase in liver glycogen deposition in response to this hormone (3, 4). Treatment of diabetic animals with insulin is reported to augment glucose uptake by liver (5, 6), and insulin may also enhance sugar uptake by adipocytes (7) and muscle cells (8, 9). Dinoprostone stimulates glucose uptake and oxidation by adipocytes (10) and intravenous infusion of dinoprostone in humans increases blood glucose levels (11). The present study demonstrates that insulin specifically enhances binding of low levels of glucose to hepatocytes and that dinoprostone inhibits this binding

EXPERIMENTAL

Preparation of Rat Hepatocytes—Liver parenchymal cells were isolated and prepared by the procedure of Bikhazi *et al.* (12), which modified procedures previously described by Berry and Friend (13) and Ingebretsen and Wagle (14).

Tests for Cell Viability—Trypan blue exclusion test for cellular viability was routinely performed before and after the experiments and preparations showing 90% viable cells or more were used.

The metabolic state of the hepatocytes during the incubation period was examined by following the respiration rate of cell suspensions in several separate experiments. Oxygen tension was recorded continuously with the aid of a biological oxygen monitor[1]. Rates were determined from the slopes of the oxygen tension curves and were calculated in terms of μl of oxygen/mg of cell protein. Protein was determined by the biuret reaction, using bovine serum albumin as a standard on centrifuged cell pellets dissolved in 1 *N* NaOH to minimize possible interference from medium components.

Preparation of Diabetic Rats—Rats were rendered diabetic by streptozocin treatment following the procedure of Chandramouli and Carter (15) as modified by Bikhazi *et al.* (12).

Isotopically Labeled Hexose—In all experiments with labeled glucose, 10 μCi of [1-^{14}C]D-glucose (58 mCi/mmole) was added to 226 ml of buffer to give a final concentration of 71 n*M*. In experiments with labeled 2-deoxyglucose, 5 μCi of [1-^{3}H]-2-deoxy-D-glucose (18.8 Ci/mmole) was added to the same volume to give a final concentration of 1.2 n*M*.

Determination of Hepatocyte Count and Mean Diameter—Hepatocyte count (1.2×10^8 cells per liver) and mean diameter (20 μm) were estimated by the procedure of Bikhazi *et al.* (12) using an automated counting machine[2].

Uptake of D-Glucose and 2-Deoxy-D-glucose by Hepatocytes—In general, 15×10^6 cells obtained from one rat liver were added to 225 ml of stirred Krebs–Henseleit solution in a water-jacketed beaker at 37° (the data in Tables I and II represent results from six different animals). After 45 min a small volume of isotopically labeled hexose was added, and 1.5 ml aliquots of suspension were periodically withdrawn, transferred to

[1] Yellow Springs Instruments, Yellow Springs, Ohio.
[2] Coulter Counter model A, Coulter Electronics, Hialeah, Fla.

0022-3549/83/0200-0116$01.00/0

(19) H. Zipp, W. Roth, and A. Zimmer, *Arzneim.-Forsch. (Drug Res.)*, **31**, 200 (1981).
(20) P. H. Hinderling, J. Bres, and E. R. Garrett, *J. Pharm. Sci.*, **63**, 1684 (1974).
(21) E. R. Garrett and H. J. Lambert, *ibid.*, **62**, 550 (1973).
(22) HP-65, STAT-PAC-1 "Linear Regression," Hewlett-Packard, Corvallis, Ore., p. 49.
(23) E. R. Garrett, J. Bres, Kurt Schnelle, and L. L. Rolf, Jr., *J. Pharmacokinet. Biopharm.*, **2**, 43 (1974).
(24) J. G. Wagner, *ibid.*, **1**, 103 (1973).
(25) M. T. Smith and T. C. Smith, *Eur. J. Clin. Pharmacol.*, **20**, 387 (1981).

ACKNOWLEDGMENTS

Supported in part by an unrestricted grant from Dr. Karl Thomae GmbH, Biberach, West Germany.

The technical assistance of Mrs. Kathleen Eberst was greatly appreciated as was the discussion with Dr. Paul Altmayer and his analogue and digital computer simulations.

Effect of Insulin and Dinoprostone on D-Glucose and 2-Deoxy-D-Glucose Uptake by Normal and Diabetic Rat Hepatocytes

A. B. BIKHAZI *x, H. M. NUBANI, and E. L. COE ‡

Received July 17, 1981, from the **Department of Physiology and the* ‡*Department of Biochemistry, Faculty of Medicine, American University of Beirut, Beirut, Lebanon.* Accepted for publication November 25, 1981.

Abstract □ Suspensions of deaggregated hepatocytes were prepared by a collagenase perfusion technique from livers of both normal rats and rats rendered diabetic by streptozocin treatment. Uptake of D-glucose and 2-deoxy-D-glucose was estimated by adding ^{14}C- or ^{3}H-labeled hexose to a stirring suspension of cells in Krebs–Henseleit buffer at 37°, separating the cells by rapid centrifugation, and measuring radioactivity in the packed cell pellet. Uptake, calculated after correction for entrapped extracellular fluid, includes any hexose bound to, transported into, or otherwise immobilized in the cells. High concentrations of glucose (5–20 m*M*) establish an intracellular–extracellular distribution ratio near 1.0 within 1 min, indicating a facilitated diffusion transport system. In contrast, a low level of glucose (71 n*M*) almost immediately (<15 sec) establishes ratios of between 3 and 4, which suggests a significant amount of glucose binding to cell membrane. Such binding would not be detected at the high glucose levels because of its small magnitude. Hepatocytes from diabetic rats exhibit a decrease in this apparent binding to ~60% of normal; preincubation with 0.1 IU/ml insulin increases this toward normal values, although it does not affect the binding by normal hepatocytes themselves. Preincubation with 0.1 μ*M* dinoprostone depresses glucose binding in cells from both normal and diabetic rats. A low concentration (1.2 n*M*) of 2-deoxy-D-glucose establishes even higher intracellular–extracellular distribution ratios of between 4 and 6, but the apparent binding of this sugar is identical in normal and diabetic rat hepatocytes and is not affected by preincubation with either insulin or dinoprostone alone. However, combined treatment with both agents causes a significant increase in 2-deoxyglucose binding. The results suggest that insulin promotes formation of hexose-binding sites and conversion of these to specific glucose-binding sites while dinoprostone may act by blocking the latter conversion.

Keyphrases □ Insulin—effect on D-glucose and 2-deoxy-D-glucose uptake, normal and diabetic rat hepatocytes, dinoprostone □ Dinoprostone—effect on D-glucose and 2-deoxy-D-glucose uptake, normal and diabetic rat hepatocytes, insulin □ Hepatocytes—rat, normal and diabetic, effect of insulin, dinoprostone on D-glucose, 2-deoxy-D-glucose uptake

The roles of insulin and prostaglandins on glucose retention by adipocytes, muscle cells, and hepatocytes have been the subject of contention in the literature. Although some have denied the existence of any stimulatory action of insulin on sugar retention by normal hepatocytes (1, 2), others have demonstrated an increase in liver glycogen deposition in response to this hormone (3, 4). Treatment of diabetic animals with insulin is reported to augment glucose uptake by liver (5, 6), and insulin may also enhance sugar uptake by adipocytes (7) and muscle cells (8, 9). Dinoprostone stimulates glucose uptake and oxidation by adipocytes (10) and intravenous infusion of dinoprostone in humans increases blood glucose levels (11). The present study demonstrates that insulin specifically enhances binding of low levels of glucose to hepatocytes and that dinoprostone inhibits this binding

EXPERIMENTAL

Preparation of Rat Hepatocytes—Liver parenchymal cells were isolated and prepared by the procedure of Bikhazi *et al.* (12), which modified procedures previously described by Berry and Friend (13) and Ingebretsen and Wagle (14).

Tests for Cell Viability—Trypan blue exclusion test for cellular viability was routinely performed before and after the experiments and preparations showing 90% viable cells or more were used.

The metabolic state of the hepatocytes during the incubation period was examined by following the respiration rate of cell suspensions in several separate experiments. Oxygen tension was recorded continuously with the aid of a biological oxygen monitor[1]. Rates were determined from the slopes of the oxygen tension curves and were calculated in terms of μl of oxygen/mg of cell protein. Protein was determined by the biuret reaction, using bovine serum albumin as a standard on centrifuged cell pellets dissolved in 1 *N* NaOH to minimize possible interference from medium components.

Preparation of Diabetic Rats—Rats were rendered diabetic by streptozocin treatment following the procedure of Chandramouli and Carter (15) as modified by Bikhazi *et al.* (12).

Isotopically Labeled Hexose—In all experiments with labeled glucose, 10 μCi of [1-^{14}C]D-glucose (58 mCi/mmole) was added to 226 ml of buffer to give a final concentration of 71 n*M*. In experiments with labeled 2-deoxyglucose, 5 μCi of [1-^{3}H]-2-deoxy-D-glucose (18.8 Ci/mmole) was added to the same volume to give a final concentration of 1.2 n*M*.

Determination of Hepatocyte Count and Mean Diameter—Hepatocyte count (1.2×10^8 cells per liver) and mean diameter (20 μm) were estimated by the procedure of Bikhazi *et al.* (12) using an automated counting machine[2].

Uptake of D-Glucose and 2-Deoxy-D-glucose by Hepatocytes—In general, 15×10^6 cells obtained from one rat liver were added to 225 ml of stirred Krebs–Henseleit solution in a water-jacketed beaker at 37° (the data in Tables I and II represent results from six different animals). After 45 min a small volume of isotopically labeled hexose was added, and 1.5 ml aliquots of suspension were periodically withdrawn, transferred to

[1] Yellow Springs Instruments, Yellow Springs, Ohio.
[2] Coulter Counter model A, Coulter Electronics, Hialeah, Fla.

0022-3549/83/0200-0116$01.00/0

Table I—Uptake of Very Low Concentrations of Glucose by Normal and Diabetic Hepatocytes [a]

Additions	Total Uptake, p moles 10^6 cells	Calculated Intracellular Concentration, n*M*	Excess Uptake, n*M*	Binding, % of Normal	Exp
Normal					
	1.128 ± 0.044	268	205	(100)	a
+I	1.150 ± 0.039	274	211	103	b
+P	0.972 ± 0.022	232	169	82	c
+I+P	0.983 ± 0.006	234	171	83	d
Diabetic					
	0.761 ± 0.011	181	118	58	e
+I	0.894 ± 0.017	213	150	73	f
+P	0.733 ± 0.033	174	111	54	g
+I+P	0.800 ± 0.017	190	127	62	h

[a] Significant differences ($N = 6$). $0.01 < p < 0.02$ (b,c), (b,d), (f,g); $p < 0.01$ (e,f), (f,h), (a,e), (b,f), (c,g), (d,h). No other combinations show significant differences.
Extracellular concentration of glucose: 71 n*M*. Expected intracellular concentration of glucose based on uptake at high concentration (Table III): 63 n*M*. Intracellular concentration was calculated as described in Table III and 63 n*M* was subtracted to obtain excess uptake. Excess uptake for the normal control was set equal to 100% to obtain percent binding.
Conditions: (+I), preincubated in the presence of 0.10 IU/ml of insulin for 45 min; (+P), preincubated in the presence of 0.10 μM of dinoprostone for 45 min; (+I+P) preincubated in the presence of both insulin and dinoprostone. The error given is the *SEM*.

Table II—Uptake of Very Low Concentrations of 2-Deoxyglucose by Normal and Diabetic Hepatocytes [a]

Additions	Total Uptake, p moles 10^6 cells	Calculated Intracellular Concentration, n*M*	Excess Uptake, n*M*	Binding, % of Normal	Exp
Normal					
	0.0168 ± 0.0013	4.00	3.00	(100)	a
+I	0.0188 ± 0.0005	4.48	3.48	116	b
+P	0.0187 ± 0.0008	4.45	3.45	115	c
+I+P	0.0298 ± 0.0015	7.10	6.10	205	d
Diabetic					
	0.0181 ± 0.0004	4.30	3.30	110	e
+I	0.0188 ± 0.0004	4.48	3.48	116	f
+P	0.0178 ± 0.0002	4.24	3.24	108	g
+I+P	0.0257 ± 0.0008	6.12	5.12	172	h

[a] Significant differences ($N = 6$). $p < 0.01$ (a,d), (b,d), (c,d), (e,h), (f,h), (g,h). No other combinations show significant differences. Extracellular concentration of 2-deoxyglucose: 1.18 n*M*. Expected intracellular concentration based on Table III: 1.00 n*M*. Other calculations and conditions are as described in Table I.

a 1.5-ml plastic centrifuge tube, and centrifuged at 10,000×*g* for 30 sec in a microcentrifuge[3]. The supernatant solution was removed, the sedimented cell pellet was rinsed 2–3 times with phosphate buffer, and the tip of the plastic tube containing the pellet was cut with a knife and placed in a scintillation vial. The pellet was solubilized with 1 ml of 1% papain solution, 5 ml of scintillation fluid was added, and radioactivity measured using a three-channel liquid scintillation spectrometer[4]. The amount of hexose retained in the pellet was estimated from the radioactivity measured in standard samples of the hexose.

The effects of insulin and dinoprostone and a combination of these two substances were evaluated with a series of four incubations carried out in parallel. A concentrated cell suspension was divided into 4 aliquots, each containing ~15 × 10^6 cells. The first aliquot was added to 225 ml of buffer solution; the second was added to the same volume of buffer solution containing 0.10 IU of insulin/ml; the third to the buffer solution containing 0.10 μM dinoprostone; and the fourth to the buffer solution containing both insulin and dinoprostone. After 45 min of preincubation, labeled hexose was added and the procedure described above was followed.

Uptake of high concentrations (5, 10, and 20 m*M*) of glucose was measured after addition of normal hepatocytes to 225 ml of buffer containing the indicated concentrations of glucose plus a tracer dose of [1-^{14}C]D-glucose.

Measurement of Extracellular Space in the Packed Pellet—The general procedure for uptake of hexoses was applied, as described above, except that labeled hexose was replaced by 5 μCi of [^{3}H]inulin. The radioactivity retained in a packed cell pellet of known volume was used to calculate the volume of medium contained within the pellet, assuming that inulin is excluded from the intracellular space. The inulin space (extracellular space) in the packed cell pellet ranged from 35 to 40%, and averaged 38%, a value consistent with the extracellular space around closely packed spheres. All estimates of uptake were corrected for inclusion of 38% of extracellular fluid in the packed cell pellet.

Statistical Treatment—Data were statistically treated and the tests of significance were checked by the standard error of the mean (*SEM*) using the Student's *t* test distribution table.

RESULTS

Viability of Hepatocytes During the Course of the Experiments—The trypan blue exclusion test indicates that almost all cells retain their ability to exclude the dye over the 45-min period of incubation. Moreover, the mean cell diameter remains constant during the incubation in either insulin or dinoprostone. A QO_2 of ~1.0 μl/mg dry weight/hr is estimated which is lower than that reported for liver slices, but is within the range of normal mammalian cells (16). The protein content of hepatocytes is ~16% of the wet weight, near the value reported for whole liver (16). The usual hexose uptake experiments were conducted after the steady-state rate of respiration had been established.

Uptake of High Concentrations of Glucose by Hepatocytes of Normal Rats—The data in Fig. 1 and Table III indicate a carrier-mediated facilitated mode of transport for glucose as expected with most mammalian cells. The intracellular concentration of glucose reaches an equilibrium value near the extracellular concentration within 1.0 min. The initial velocity of transport is too great to be estimated by the procedure used; hence, calculation of a K_M for glucose transport is impossible, although it is known to be in the millimolar range for other cell types (3).

Uptake of a Low Concentration of Glucose—Table I summarizes the uptake of glucose by hepatocytes from both normal and diabetic rats in the presence and absence of insulin and dinoprostone. Several features were evident:

1. The uptake exceeded that expected of a facilitated diffusion transport. Instead of a ratio of near 1.0 (0.885 in Table III), ratios between 2.5 and 3.5 were obtained for the intracellular–extracellular distribution.
2. Uptake was greatly reduced in hepatocytes from diabetic animals under all conditions. In terms of percent binding, untreated cells from

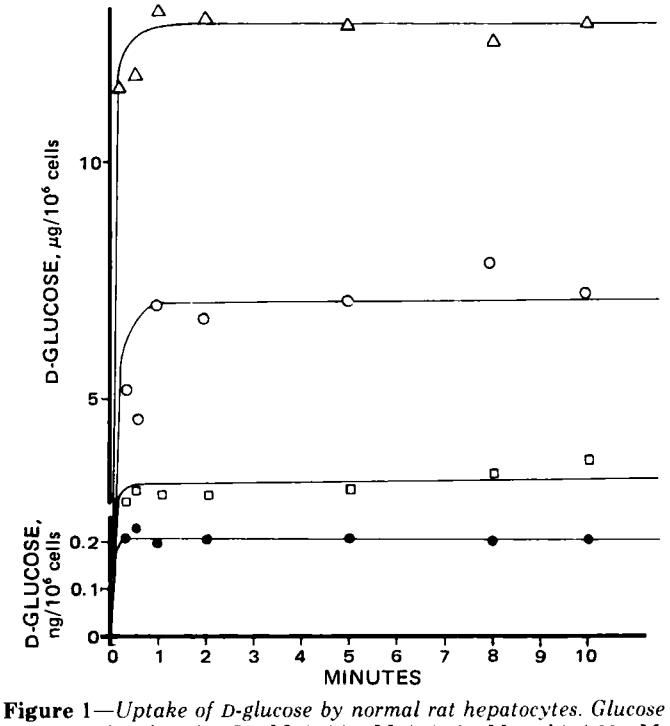

Figure 1—*Uptake of D-glucose by normal rat hepatocytes. Glucose concentrations key: (●) 71 n*M*, (□) 5 m*M*, (○) 10 m*M*, and (△) 20 m*M*. Note that the scale used for the low concentration differs from the scale for the three high concentrations.*

[3] Eppendorf Microcentrifuge, model 5412, Brinkmann Instruments, Westbury, N.Y.
[4] Tricarb, model 3320, Packard Instrument Co., Downers Grove, Ill.

Table III—Uptake of High Concentrations of Glucose by Normal Hepatocytes [a]

Extracellular Concentration, m*M*	Uptake, nmoles / 10^6 cells	Intracellular Concentration, m*M*	Concentration Ratio, Intracell / Extracell
5.0	18	4.3	0.87
10.0	39	9.3	0.93
19.9	72	17.1	0.86
		Mean	0.885

[a] Uptake was estimated from the levels shown in Fig. 1. Intracellular concentration was based on cell volume estimated from a mean cell diameter of 20 μm, which gave a volume of 4.2 μl/10^6 cells. All values for uptake have been corrected for an estimated 38% inclusion of extracellular fluid in the packed cell pellet (see text).

diabetic rats were found to bind only 58% as much glucose as their normal counterparts.

3. Insulin significantly increased (but not to the normal value) the uptake by the cells from diabetic animals, but had no effect on hepatocytes from normal rats.

4. Dinoprostone tended to depress glucose uptake in both normal hepatocytes and in insulin-treated cells from diabetic rats.

Uptake of a Low Concentration of 2-Deoxyglucose—As in the case of glucose, the uptake of 2-deoxyglucose considerably exceeded the uptake expected from facilitated diffusion and gave even higher intracellular–extracellular distribution ratios (Table II). However, there are several striking differences between the glucose and 2-deoxyglucose uptake patterns.

1. There was no difference in the uptake of 2-deoxyglucose with or without insulin when cells from normal and diabetic animals were compared.

2. Dinoprostone had no depressing effect on 2-deoxyglucose uptake.

3. The only significant effect of any treatment was the marked increase in uptake and apparent binding when either cell type was exposed to a combination of insulin and dinoprostone.

DISCUSSION

A previous report (2) showed that insulin had no effect on the uptake of sugars by enzymatically dispersed normal hepatocytes. The effect of insulin in the present study was rendered evident by two factors: first, the use of hepatocytes from diabetic rats, which had a depressed glucose uptake responsive to insulin, in contrast to hepatocytes from normal rats which may already have been maximally stimulated; and second, the use of an extremely low level of glucose, much less than the physiological concentrations (~5 m*M*) usually employed in such experiments.

The excess uptake detected by the use of a very low glucose concentration probably reflects some change in the glucose binding sites in the cell. The possibility that this excess uptake is attributable to an active transport system cannot be ruled out absolutely, although it appears unlikely because of the speed of equilibration which appears within 15 sec (Fig. 1). Assuming that the excess does indeed represent glucose binding, the question remains as to what relationship this binding has to the transport mechanism and whether it indicates some change in a transport carrier protein.

The most striking difference between the excess uptake of a low level of glucose and an even lower level of 2-deoxyglucose was the lack of effect of diabetes and insulin on the 2-deoxyglucose uptake. This may indicate that different sites and/or some differential change in relative affinities of the same sites are involved in the binding of the two sugars. In either case, it appeared that the insulin effect is specific for glucose.

In conclusion insulin increases the uptake of glucose by hepatocytes from diabetic rats and not by those from normal rats, possibly because the normal cells are already maximally stimulated as is evident at low concentrations (<100 n*M*) of glucose. The insulin effect is specific for glucose since the hormone does not enhance binding of 2-deoxy-D-glucose. The results suggest that insulin promotes formation of hexose binding sites and conversion of these to specific glucose binding sites, while dinoprostone may act by blocking the latter conversion.

REFERENCES

(1) P. O. Seglen, *FEBS Lett.*, **30,** 25 (1973).

(2) H. Baur and H. W. Heldt, *Eur. J. Biochem.*, **74,** 397 (1977).

(3) W. Bachmann and D. Challoner, *Biochim. Biophys. Acta*, **443,** 254 (1976).

(4) L. L. Madison, *Arch. Intern. Med.*, **123,** 284 (1969).

(5) D. F. Steiner and R. H. Williams, *J. Biol. Chem.*, **234,** 1342 (1959).

(6) H. C. Lequin and E. P. Steyn Parvé, *Biochim. Biophys. Acta*, **58,** 439 (1962).

(7) J. M. Olefsky, *Biochem. J.*, **172,** 137 (1978).

(8) M. Berger, S. A. Hagg, M. N. Goodman, and N. B. Ruderman, *Biochem. J.*, **158,** 191 (1976).

(9) W. Y. Fujimoto and R. Williams, *Diabetes*, **23,** 443 (1974).

(10) H. A. Haessler and J. D. Crawford, *J. Clin. Invest.*, **46,** 1065 (1967).

(11) R. P. Robertson and M. Chen, *ibid.*, **60,** 747 (1977).

(12) A. B. Bikhazi, E. H. Abboud, S. K. Agulian, and C. F. Nassar, *Pfluegers Arch.*, **386,** 245 (1980).

(13) M. N. Berry and D. S. Friend, *J. Cell Biol.*, **43,** 506 (1969).

(14) W. R. Ingebretsen and S. R. Wagle, *Biochem. Biophys. Res. Commun.*, **47,** 403 (1972).

(15) V. Chandramouli and J. R. Carter, *Diabetes*, **24,** 257 (1975).

(16) P. L. Altman and D. S. Dittmer, "Metabolism," Fed. Am. Soc. Exp. Biol., Bethesda, Md, 1968, p. 389.

ACKNOWLEDGMENTS

This work is supported in part, by Grant 38-5706 from the Lebanese Council for Scientific Research and by Grant 18-5205 from the University Medical Research Fund.

Method for Predicting Fill Weight Variation When Packing Powders Using Vacuum/Purge Fillers

R. C. LIJANA [x] **and J. D. TAULBEE**

Received December 18, 1981, from the *Procter & Gamble Co., Miami Valley Laboratories, Cincinnati, OH 45247.* Accepted for publication March 15, 1982.

Abstract □ The present report demonstrates that for at least four pharmaceutical powders, the variation in fill weight associated with a vacuum/purge filling port is correlated with the length–diameter ratio of that port. This relationship has been mathematically modeled, and a design curve based on production data is presented, which depicts this relationship over a wide range of length–diameter ratios. For powders with properties similar to those presented, the design curve may be used to determine the dimensions of the port which will yield acceptable process weight control. Fill weight variances also can be predicted given a fixed port diameter. For other powders, the model can be used to create design curves with a few data points.

Keyphrases □ Vacuum/purge fillers—method for predicting fill weight variation when packing powders □ Pharmaceutical powders—method for predicting fill weight variation when packing powders using vacuum/purge fillers □ Models, mathematical—method for predicting fill weight variation when packing powders using vacuum/purge fillers

Industry employs a variety of methods to fill containers with measured amounts of solids (1–6). The pharmaceutical industry most frequently uses vacuum/purge filling: the powder to be filled is drawn under vacuum from a hopper into a cylindrical port of preset dimensions. The powder is held against a piston under vacuum until a container is available for loading, then light air pressure replaces the vacuum and discharges the powder.

The weight of the powder slug is determined by the bulk density of the powder and the geometry of the filling port. The diameter of the port (d) is determined by the choice of a filling wheel and can be varied only by changing wheels. The depth of the port, or the length (l), can be adjusted at any time but is generally set before a filling run begins. The choices of filling wheels and port length settings to achieve the proper powder weight delivery are normally determined by trial and error, requiring a large number of determinations. Since variability around the desired weight is an important consideration in pharmaceutical solid dose preparation, selecting the combination of settings yielding the minimum variation is desirable.

Design curves, *i.e.*, mathematical models fitted to empirical data and correlating equipment variables with desired results, frequently have been used in the chemical process industries to reduce dependence on trial and error adjustments. Unfortunately, the literature is lacking convenient mathematical relationships by which the operation and precision of filling equipment for the pharmaceutical industry can be predicted and optimized. Piston compaction/ejection equipment was studied (7), and the compaction forces needed to achieve the required fill weight, given powder bed height, and piston height were tested. Earlier, a mathematical model was developed (8) for filling gelatin capsules. Similar fillers were studied (9) but there was only an interest in the packing properties of various powders as a source of fill-weight variation. Thus, none of these contributions are directly applicable to the stated problem.

The object of the present work, therefore, was to develop a design curve relating the variance of powder fill weights to equipment variables for a specific set of vacuum/purge fillers and a specific set of pharmaceutically useful powders. It was hoped that the technique and the design curve used might also be shown to be more generally useful.

THEORETICAL

The variance in powder fill weights can be transformed into a dimensionless parameter and normalized by a new variable, CV, the coefficient of variation, defined as:

$$CV = \frac{S}{\overline{W}} \times 100\% \qquad \text{(Eq. 1)}$$

where S is the standard deviation of fill-weight data, and $\overline{W}$ is the average fill weight.

The independent variable for the model can incorporate both equipment and component effects as follows. Assuming the walls of an individual cylindrical port to be smooth, then the variation in the weight of a powder plug is proportional to the exposed lateral surface area and to the pressure drop across the cylinder. Assuming further that the pressure drop is constant across the length of the powder plug (distance) and time, then the pressure drop is solely a function of component properties and the integrity of the piston/filler which is used to set port length: $\Delta p = f$ (crystallinity, particle size, particle shape, piston integrity).

The component properties can be related to the bulk density of a material. Piston integrity can decrease during the course of routine filling due to blinding, but measured port pressure changes alert the operator to the need for piston replacement. Thus, $\Delta p = f$ may be reduced to:

$$\Delta p \propto \rho \qquad \text{(Eq. 2)}$$

where ρ is the material bulk density.

Viewed from another perspective, the bulk density of a material determines the length of a contained powder plug and, therefore, the length of exposed cylinder for a specified fill weight and port diameter. This diameter, in turn, is an equipment parameter which determines the exposed lateral surface areas. Therefore, the independent dimensionless variable for the design curve may be:

$$\frac{l}{d} \qquad \text{(Eq. 3)}$$

where l is the length of the powder plug and d is the diameter of the port.

Consideration of certain boundary conditions, which will be more fully discussed, suggests that the model should have both vertical and horizontal asymptotes. Such a model can be constructed as follows:

$$y = A + B_1/(x - v) + B_2/(x - v)^2 + \ldots + B_n/(x - v)^n \qquad \text{(Eq. 4)}$$

where y is CV, x is the l/d ratio, A is the horizontal asymptote, and v is the vertical asymptote.

The vertical asymptote should be fixed at zero, otherwise the model has the unrealistic characteristic that once the l/d ratio is less than v, the CV begins to decrease with decreasing l/d ratio.

The model of choice to attempt to fit the design curve, then, is:

$$y = A + B_1/x + B_2/x^2 + \ldots + B_n/x^n \qquad \text{(Eq. 5)}$$

where terms are added until the parameter for the last term is not statistically different from zero.

The interpretation of Eq. 5 is that A is the smallest value of CV, which can be attained by varying the l/d ratio. Implied also is that CV will increase as the l/d ratio becomes small. This is reasonable, because with

0022-3549/83/0200-0119$01.00/0

Table I—Filler Dimensions and Calculated Packed Densities for Zinc Acetate Powder Filling

	Plug Diameter	Plug Length	Density g/cm³	*l/d*
d	0.95 cm	1.3 cm	0.650	1.3
constant	0.95 cm	2.5 cm	0.664	2.7
	0.95 cm	3.8 cm	0.656	4.0
	0.95 cm	5.0 cm	0.659	5.3
l	0.48 cm	2.5 cm	0.666	5.3
constant	0.79 cm	2.5 cm	0.640	3.2
	0.79 cm	2.5 cm	0.638	3.2
	0.95 cm	2.5 cm	0.664[a]	2.7
	0.95 cm	2.5 cm	0.664	2.7
	0.95 cm	2.5 cm	0.643	2.7
	1.3 cm	2.5 cm	0.678	2.0
	1.3 cm	2.5 cm	0.660	2.0

[a] This measurement was repeated from the first section of Table I.

l/d ratio decreasing, the cylinder is becoming shorter and wider, and large surface area effects would contribute to a more variable fill. Conversely, if the cylinder becomes very long in relation to its diameter, pressure drop effects would add to variability and *CV* would be expected to rise. Therefore, the minimum *CV* would be expected to occur at an *l/d* ratio between the extremes.

The model (Eq. 5) does not provide for increasing *CV* with very high *l/d* values, because this phenomenon did not occur in this work. If necessary, the model (Eq. 5) can easily be modified by adding a term Ce^x, where *C* would be a small positive number. The parameter Ce^x would not contribute noticeable amounts to the expression until *x* (the *l/d* ratio) became quite large.

EXPERIMENTAL

Materials—Two vacuum/purge powder fillers were used. When small quantities of containers were packed, a semi-automatic portable powder filler[1] was used at a rate of ~5–10 containers/min. Larger quantities of containers were filled at a rate of 15–65 containers/min using an automatic powder filler[2].

Use of these two units provided port diameters ranging from 0.48 to 1.3 cm and lengths ranging from 0.19 to 9.5 cm.

Four powders currently used in marketed or investigational pharmaceutical finished-dose forms were available for study. The four materials are listed with their bulk densities. All are fine powders (<15-μm average particle size), low and constant in moisture content, and nonfree-flowing.

Material	g/cm³
1. Erythromycin base[3]	0.520
2. Zinc acetate[4]	0.655
3. Tetracycline hydrochlorides[5] and sodium bisulfite[6]	0.745
4. Similar to 3, but with different proportions	0.732

Methods—Since the first purpose of this work was to develop design curves for two fillers in use, actual production conditions and data were used. Values of *l/d* commonly used were selected and fill weights were measured. For each unique combination of product, filler, filling port diameter, and filling port *l/d* ratio, 10–60 weight measurements were taken. In all, four materials, seven port diameters, and 39 *l/d* ratios from 0.20 to 10.0 were tested. Eighty-eight coefficients of variation were calculated.

In addition to measuring fill weights, packed densities were calculated for a number of the combinations. These densities were used to test the implicit assumption of constant density in the model.

RESULTS AND DISCUSSION

Figure 1 shows the design curve relating *CV* to the *l/d* ratio for all collected data. The equation for this curve is:

$$CV = 0.35 + \frac{1.3}{l/d} \qquad \text{(Eq. 6)}$$

[1] Model LM-14, Perry Industries, Inc., Hicksville, N.Y.
[2] Model E-1200, Perry Industries, Inc., Hicksville, N.Y.
[3] Abbott Laboratories, Chicago, Ill.
[4] J. T. Baker, Phillipsburg, N.J.
[5] Ankerfarm, Milan, Italy.
[6] Virginia Chemical, Portsmouth, Va.

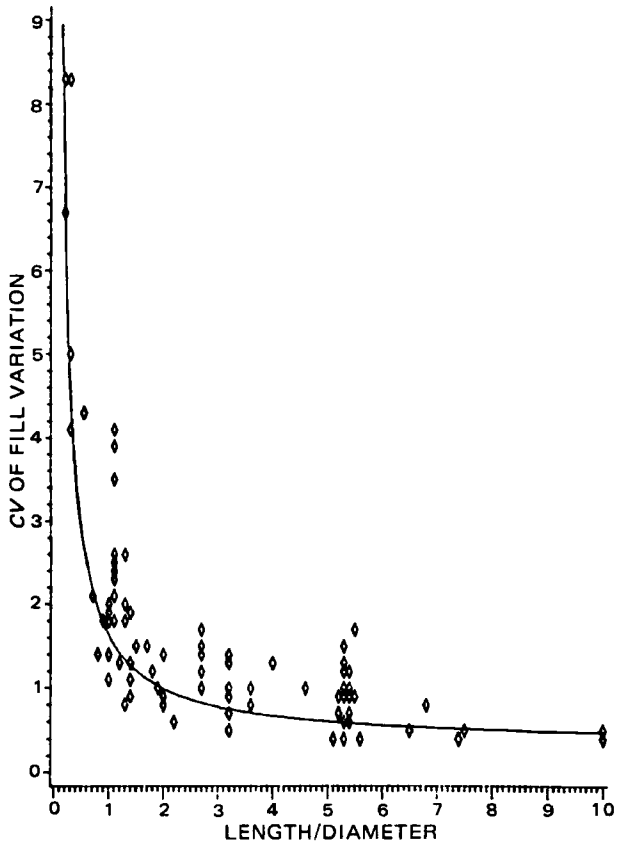

Figure 1—*Powder filling precision* versus *port size (powder plug and port dimensions) for vacuum/purge filling of four pharmaceutical powders.*

Table I shows the packed densities for samples taken during filling of zinc acetate powder.

The model was fit for each separate component using a weighted least-squares procedure with weights $1/y^2$.

Weighting was thought desirable for two reasons: the estimated *CV*s for low *l/d* ratios were expected to have higher variability, and the estimate of *A*, the minimum achievable *CV*, is an important result of curve fitting and weighting the lower *CV* values gives a better picture of the true minimum.

This proved to be reasonable, since the sum of squared deviations of the data about the model was less when the weighting procedure was used.

In all cases, the actual version of the model (Eq. 5) derived was:

$$y = A + B_1/x \qquad \text{(Eq. 7)}$$

because terms in higher powers of $1/x$ did not have coefficients that were statistically significantly different from zero, as seen in Table II. (All tests of statistical significance were done at a two-sided, 5% level.)

To examine whether another form of model might provide a better fit to the data, another fit was examined:

$$y = a \exp(b/x) \qquad \text{(Eq. 8)}$$

where *a* and *b* are the parameters of interest.

This model, like the other model (Eq. 7), has a horizontal asymptote, *a*, and a vertical asymptote, $x = 0$. The model (Eq. 8) was fitted to the zinc acetate powder data. The sum of weighted squared deviations about the model was 8.29, >1.5 times that obtained with the model (Eq. 7) for the same data (Table II). The chosen model (Eq. 7) gives a better fit than the (Eq. 8) model.

The curve in Fig. 1 is the result of combining the data for all materials. To test the validity of combining the data, statistics of the two largest blocks of data were examined. A comparison of the estimates of *A* and B_1 (Table II) of the zinc acetate data with those of erythromycin showed no statistically significant differences between them (*p*-values of 0.50 and 0.95 for *A* and B_1, respectively). There is no statistical evidence to indicate a difference in design curves for the types of powders or equipment used. Thus, it is concluded that one general physical phenomenon underlies these data and dictates the shape of the curve.

Table II—Results of Fitting Model [a] to the *CV versus l/d* Data for Four Powders and Two Fillers

Powder	Estimate of A	Estimate of B_1	p-Value for H_0:$B_1 = 0$	p-Value for H_0:$B_2 = 0$	Sum of Squared Observations	Sum of Weighted Squared Deviations about the Model
Zinc acetate [b]	0.361	1.43	0.0001	0.83	145.50	4.99
Erythromycin [b]	0.277	1.40	0.0016	0.91	19.97	2.91
Pooled data from zinc acetate and erythromycin [b]	0.294	1.47	0.0001	0.76	187.96	8.09
All four [c]	0.408	0.94	0.0001	0.37	2.63	0.55
All four [d]	0.347	1.29	0.0001	0.73	195.84	10.86

[a] Model from Eq. 5. [b] Filled with Model LM-14, Perry Industries, Inc., Hicksville, N.Y. [c] Filled with Model E-1200, Perry Industries, Inc., Hicksville, N.Y. [d] Combinations of powders filled with Model LM-14 or Model E-1200, Perry Industries, Inc., Hicksville, N.Y.

The shape of the curve describes several things about the characteristics of vacuum/purge fillers. It indicates that, in most cases, a powder plug l/d ratio ≥ 1.5 will yield acceptably small fill-weight variances. It indicates, further, that as the l/d ratio decreases to <1.5, powder-filling precision rapidly becomes worse and is extremely sensitive to l/d ratio changes. This is logical since the exposed surface area becomes a much greater percentage of the total surface areas as the l/d ratio decreases. It also indicates that when the l/d ratio rises >1.5, precision approaches a nonzero limiting value. This asymptote predicts that efforts to increase weight control through port (or component) changes in this region will go unrewarded.

It could be speculated that the validity of the entire approach rests on the assumption of a constant packed powder density. A variable packed density could lead to random variation in fill weight which would confound any model. To examine this, data in Table I were used. These density data are shown in two sections: one with a constant d value and one when l is constant. When d is constant and l increases, density does not significantly change. When l is constant and d increases, density does not change either. Thus, the implicit assumption of constant density used in the model development is valid.

This provides a basis for selecting the length for a filling port of preset diameter from a design curve, thereby eliminating the necessity for large-scale experimental testing of different port sizes. Given the bulk density of a powder or a mixture of powders and the required fill weight, one may use the design curve to determine the port length yielding acceptable process weight control for any preset port diameter (l/d ratio of ~ 1.5 is a good general choice). In addition, the curve allows prediction of fill-weight variances given a fixed port length. The model has been established with a large data base, it fits the data well, and it satisfies engineering constraints.

For powders similar to those used in this work, the design curve can be used as is. For powders with significantly different characteristics, a few data points will allow the curve to be established. In any such operation, various l/d ratios producing the desired fill weight should be established, then the model (Eq. 5) fitted to the data with nonsignificant terms deleted. If very high l/d ratios are used, Ce^x should be added to the model, where C is to be estimated. A plot of the data with the fitted curve will then allow a reasonable choice of the l/d ratio.

REFERENCES

(1) P. Moxey, *Soap, Perfum. Cosmet.*, **51**, 9 (1978).

(2) G. C. Cole and G. May, *J. Pharm. Pharmacol.*, **27**, 353 (1975).

(3) D. P. McDonald, *Manuf. Chem. Aerosol News*, **31**, (July, 1972).

(4) *Food Process Ind.*, **38**, (458), 37 (1969).

(5) W. Ruf and H. E. Rothmann, U.S. pat. 4,074,507 (Feb. 21, 1978).

(6) G. J. Raymus and E. H. Steymann, "Chemical Engineers' Handbook," 5th ed., R. H. Perry and C. H. Chilton, Eds., McGraw-Hill, New York, N.Y., 1973, pp. 7-1–7-50.

(7) L. E. Small and L. L. Augsburger, *Drug Dev. Ind. Pharm.*, **4**, 345 (1978).

(8) G. Reier, R. Cohn, S. Rock, and F. Wagenblast, *J. Pharm. Sci.*, **57**, 660 (1968).

(9) Y. Miyake, A. Shinoda, T. Nasu, M. Furukawa, K. Vesugi, and K. Hoshi, *Yakuzaigaku*, **34**, 32 (1974).

ACKNOWLEDGMENTS

The authors thank E. G. Helton for technical writing assistance.

Antacid Effects on the Gastrointestinal Absorption of Riboflavin

STUART FELDMAN[x] and WYATT HEDRICK

Received November 14, 1977, from the *Department of Pharmaceutics, University of Houston, Houston, TX 77030.* Accepted for publication March 17, 1982.

Abstract □ The effect of aluminum hydroxide, magnesium hydroxide, and a combination of aluminum–magnesium hydroxide suspensions on the oral absorption of riboflavin was examined in five subjects. Coadministration of aluminum hydroxide or magnesium hydroxide suspension with riboflavin (30 mg) resulted in an increase in time of peak urinary excretion rate of riboflavin when compared with control studies. There was no increase in the peak excretion rate or total urinary excretion of riboflavin when the antacid-treated subjects were compared to the control studies. *In vitro* experiments indicated that significant binding of riboflavin to the aluminum hydroxide and magnesium hydroxide suspensions occurred. The results of the present investigation are consistent with the reported effect of aluminum ion on GI motility and the known influence of gastric emptying on the absorption of riboflavin from the GI tract.

Keyphrases □ Absorption, GI—antacid effects on riboflavin □ Riboflavin—antacid effects on GI absorption □ Antacids—effects on the GI absorption of riboflavin

Antacids are a therapeutic class of drugs which have great potential for drug absorption interactions. Since they may be purchased over-the-counter, they are widely used by the public and may be taken concurrently with many other drugs. Antacids have been reported to alter the GI absorption of a number of drugs through the formation of

Table II—Results of Fitting Model [a] to the *CV versus l/d* Data for Four Powders and Two Fillers

Powder	Estimate of A	Estimate of B_1	p-Value for H_0:$B_1 = 0$	p-Value for H_0:$B_2 = 0$	Sum of Squared Observations	Sum of Weighted Squared Deviations about the Model
Zinc acetate [b]	0.361	1.43	0.0001	0.83	145.50	4.99
Erythromycin [b]	0.277	1.40	0.0016	0.91	19.97	2.91
Pooled data from zinc acetate and erythromycin [b]	0.294	1.47	0.0001	0.76	187.96	8.09
All four [c]	0.408	0.94	0.0001	0.37	2.63	0.55
All four [d]	0.347	1.29	0.0001	0.73	195.84	10.86

[a] Model from Eq. 5. [b] Filled with Model LM-14, Perry Industries, Inc., Hicksville, N.Y. [c] Filled with Model E-1200, Perry Industries, Inc., Hicksville, N.Y. [d] Combinations of powders filled with Model LM-14 or Model E-1200, Perry Industries, Inc., Hicksville, N.Y.

The shape of the curve describes several things about the characteristics of vacuum/purge fillers. It indicates that, in most cases, a powder plug l/d ratio ≥ 1.5 will yield acceptably small fill-weight variances. It indicates, further, that as the l/d ratio decreases to <1.5, powder-filling precision rapidly becomes worse and is extremely sensitive to l/d ratio changes. This is logical since the exposed surface area becomes a much greater percentage of the total surface areas as the l/d ratio decreases. It also indicates that when the l/d ratio rises >1.5, precision approaches a nonzero limiting value. This asymptote predicts that efforts to increase weight control through port (or component) changes in this region will go unrewarded.

It could be speculated that the validity of the entire approach rests on the assumption of a constant packed powder density. A variable packed density could lead to random variation in fill weight which would confound any model. To examine this, data in Table I were used. These density data are shown in two sections: one with a constant d value and one when l is constant. When d is constant and l increases, density does not significantly change. When l is constant and d increases, density does not change either. Thus, the implicit assumption of constant density used in the model development is valid.

This provides a basis for selecting the length for a filling port of preset diameter from a design curve, thereby eliminating the necessity for large-scale experimental testing of different port sizes. Given the bulk density of a powder or a mixture of powders and the required fill weight, one may use the design curve to determine the port length yielding acceptable process weight control for any preset port diameter (l/d ratio of ~ 1.5 is a good general choice). In addition, the curve allows prediction of fill-weight variances given a fixed port length. The model has been established with a large data base, it fits the data well, and it satisfies engineering constraints.

For powders similar to those used in this work, the design curve can be used as is. For powders with significantly different characteristics, a few data points will allow the curve to be established. In any such operation, various l/d ratios producing the desired fill weight should be established, then the model (Eq. 5) fitted to the data with nonsignificant terms deleted. If very high l/d ratios are used, Ce^x should be added to the model, where C is to be estimated. A plot of the data with the fitted curve will then allow a reasonable choice of the l/d ratio.

REFERENCES

(1) P. Moxey, *Soap, Perfum. Cosmet.*, **51**, 9 (1978).

(2) G. C. Cole and G. May, *J. Pharm. Pharmacol.*, **27**, 353 (1975).

(3) D. P. McDonald, *Manuf. Chem. Aerosol News*, **31**, (July, 1972).

(4) *Food Process Ind.*, **38**, (458), 37 (1969).

(5) W. Ruf and H. E. Rothmann, U.S. pat. 4,074,507 (Feb. 21, 1978).

(6) G. J. Raymus and E. H. Steymann, "Chemical Engineers' Handbook," 5th ed., R. H. Perry and C. H. Chilton, Eds., McGraw-Hill, New York, N.Y., 1973, pp. 7-1–7-50.

(7) L. E. Small and L. L. Augsburger, *Drug Dev. Ind. Pharm.*, **4**, 345 (1978).

(8) G. Reier, R. Cohn, S. Rock, and F. Wagenblast, *J. Pharm. Sci.*, **57**, 660 (1968).

(9) Y. Miyake, A. Shinoda, T. Nasu, M. Furukawa, K. Vesugi, and K. Hoshi, *Yakuzaigaku*, **34**, 32 (1974).

ACKNOWLEDGMENTS

The authors thank E. G. Helton for technical writing assistance.

Antacid Effects on the Gastrointestinal Absorption of Riboflavin

STUART FELDMAN[x] and WYATT HEDRICK

Received November 14, 1977, from the *Department of Pharmaceutics, University of Houston, Houston, TX 77030.* Accepted for publication March 17, 1982.

Abstract □ The effect of aluminum hydroxide, magnesium hydroxide, and a combination of aluminum–magnesium hydroxide suspensions on the oral absorption of riboflavin was examined in five subjects. Coadministration of aluminum hydroxide or magnesium hydroxide suspension with riboflavin (30 mg) resulted in an increase in time of peak urinary excretion rate of riboflavin when compared with control studies. There was no increase in the peak excretion rate or total urinary excretion of riboflavin when the antacid-treated subjects were compared to the control studies. *In vitro* experiments indicated that significant binding of riboflavin to the aluminum hydroxide and magnesium hydroxide suspensions occurred. The results of the present investigation are consistent with the reported effect of aluminum ion on GI motility and the known influence of gastric emptying on the absorption of riboflavin from the GI tract.

Keyphrases □ Absorption, GI—antacid effects on riboflavin □ Riboflavin—antacid effects on GI absorption □ Antacids—effects on the GI absorption of riboflavin

Antacids are a therapeutic class of drugs which have great potential for drug absorption interactions. Since they may be purchased over-the-counter, they are widely used by the public and may be taken concurrently with many other drugs. Antacids have been reported to alter the GI absorption of a number of drugs through the formation of

Table I—Time to Peak Riboflavin [a] Excretion Rate in Control and Antacid-Treated Subjects

Subject	Control, hr	Aluminum–Magnesium Hydroxide, hr	Aluminum Hydroxide, hr	Magnesium Hydroxide, hr
A	2.25	1.75	2.25	1.75
B	0.75	2.25	2.25	2.25
C	1.25	1.25	2.25	2.75
D	0.75	1.25	2.25	1.75
E	2.25	0.75	2.75	2.25
Mean	1.45	1.45	2.35[b]	2.15[b]
SD	0.75	0.57	0.22	0.41

[a] The riboflavin dose was 30 mg. [b] $p < 0.05$, ANOVA and Dunnett multiple comparison test (8).

Table II—Peak Excretion Rate of Riboflavin [a] in Control and Antacid-Treated Subjects

Subject	Control, μg/hr	Aluminum–Magnesium Hydroxide, μg/hr	Aluminum Hydroxide, μg/hr	Magnesium Hydroxide, μg/hr
A	2394	2811	2826	2337
B	673	1476	822	1391
C	1247	653	1301	1512
D	787	1437	1010	2176
E	631	552	968	800
Mean	1146	1386	1386	1643
SD	739	904	824	624

[a] The riboflavin dose was 30 mg.

complexes (1), alterations in gastric pH (2), and changes in the rate of gastric emptying (2, 3).

It was shown (2) that aluminum hydroxide gel delayed the GI absorption of pentobarbital sodium in the rat by retarding gastric emptying. A similar effect of aluminum hydroxide gel has been shown (4) to alter the rate of disappearance of [^{51}Cr]sodium chromate from the stomach of leukemic children. In the five patients studied, administration of aluminum hydroxide gel slowed the mean maximal emptying rate from 5.1 to 1.8%/min. Effects of other antacids or combinations of antacids on gastric emptying have not been well documented.

The present investigation examines the influence of commercially available preparations of aluminum hydroxide, magnesium hydroxide, and an aluminum–magnesium hydroxide combination on the GI absorption of riboflavin in humans. The suitability of riboflavin to study the effect of antacids on gastric emptying stems from the fact that riboflavin is absorbed by a specialized transport system (5) in the proximal portion of the small intestine, and alterations in gastric emptying can produce significant changes in the rate and extent of riboflavin absorption from the GI tract (6, 7).

EXPERIMENTAL

Subjects—Five healthy male subjects (age 22–30 years; weight, 66–81 kg) volunteered for the study and gave written, informed consent. No vitamin preparations were taken for at least 1 month prior to and during the course of the study. The study was conducted over a period of 4 consecutive weeks in a randomized, crossover manner with each subject receiving riboflavin[1] control, riboflavin with aluminum–magnesium hydroxide oral suspension[2], riboflavin with aluminum hydroxide gel[3], or riboflavin with magnesium hydroxide oral suspension[4].

Riboflavin Absorption Study—After an overnight fast, each subject ingested 50 ml of water 1 and 0.5 hr prior to the administration of the drug. At the time of riboflavin administration, the bladder was voided and 30 mg of riboflavin was suspended in water and ingested in a total volume of 100 ml. This dose of riboflavin was utilized in other studies of riboflavin absorption in humans (5) and reflected alterations in gastric emptying patterns. Total urine samples were collected in plastic bags[5] at 0.5, 1, 1.5, 2, 2.5, 3, 4, 5, 6, 8, 10, 12, and 16 hr after administration of riboflavin and at convenient intervals up to 36 hr after taking the drug. Food was not ingested for 4 hr following administration of the riboflavin dose. Fifty milliliters of water was ingested after each urine sample for as long as necessary to maintain adequate urinary output. Glacial acetic acid (3 ml/100 ml of urine) was added for stability purposes. The urine samples were stored in a refrigerator or freezer until assayed. Blank urinary excretion rates of riboflavin were obtained from 2- to 4-hr urine samples collected on the day prior to the experiment.

Antacid–Riboflavin Absorption Study—One hour before administration of riboflavin, 50 ml of water was ingested. One-half hour before administration of the drug, 20 ml of either aluminum hydroxide gel or aluminum–magnesium hydroxide suspension, or 10 ml of magnesium hydroxide suspension was ingested with either 30 or 40 ml of water. At the time of riboflavin ingestion, 20 ml of aluminum hydroxide or aluminum–magnesium hydroxide or 10 ml of magnesium hydroxide followed by 30 mg of riboflavin suspended in a total volume of 100 ml of water was ingested. The collection procedure was identical to that followed for the riboflavin control samples. The antacid dose was chosen to represent minimum dosages according to label directions. A lower dose of magnesium hydroxide was necessary to minimize the possibility of a laxative effect from magnesium hydroxide. At least 1 week separated each of the riboflavin absorption studies.

Assay—After suitable dilution, the urine samples were assayed using a modified USP assay for riboflavin (5), and fluorescence was measured on a filter fluorimeter[6].

Binding Studies—Various volumes of each antacid suspension were added to two different concentrations (1.6 and 4.9 μg/ml) of riboflavin in glass bottles. These concentrations reflected the low solubility of riboflavin in aqueous solution and represented only an approximation of *in vivo* levels. The resulting suspensions were shaken in a water bath[7] at 37° for at least 30 min. Equilibrium was established by repetitive sampling. The suspensions were centrifuged[8] in warm (40°) centrifuge tubes for 2 min at 3000 rpm, and the supernatant solution was assayed for riboflavin content by the described assay method.

RESULTS AND DISCUSSION

One measure of gastric emptying rate is the time to peak urinary excretion rate of an oral dose of riboflavin. Peak excretion rate data for the five subjects studied are presented in Table I. The data, when analyzed by ANOVA and the Dunnett test (8), reveal that coadministration of aluminum hydroxide gel or magnesium hydroxide suspension with the riboflavin suspension results in a significant ($p < 0.05$) increase in the time to peak excretion rate.

The data for the peak urinary excretion rate of riboflavin in the control- and antacid-treated subjects are presented in Table II. The coadministration of the antacid mixtures with the riboflavin suspension results in a slight increase in the mean peak urinary excretion rates of riboflavin, but these data were not significantly different from control values.

The percent urinary recovery of riboflavin for the control and in the presence of each antacid studied for each subject is presented in Table III. Control riboflavin urinary recovery ranged from 12.1 to 38.0% of the 30-mg dose with a mean value of 21.4 ± 9.3%. Examination of the data in Table III reveals no change in the percent of riboflavin dose excreted in urine following concomitant administration of the antacids.

Typical plots of the urinary excretion rate of riboflavin *versus* time in one subject for each experiment are presented in Fig. 1. Administration of aluminum hydroxide gel results in a significant delay in the excretion peak time rate of riboflavin when compared with control values. This is consistent with the reported activity of Al^{3+} as a smooth muscle relaxant (9). The smooth muscle relaxing effect of aluminum hydroxide would reduce the gastric emptying rate and, therefore, result in a delay in the time until riboflavin reached its absorption site in the small intestine.

[1] Eastman Kodak Co.
[2] Maalox, W.H. Rorer Co.
[3] Amphojel, Wyeth Laboratories.
[4] Milk of Magnesia, C. H. Phillips Co.
[5] Whirl-Pak, 18 oz., Nasco Co.
[6] Turner Fluorimeter, model 111, G. K. Turner Associates Inc.
[7] Precision model 25 Water Bath Shaker, Precision Scientific.
[8] IEC, model HN-S centrifuge.

Table III—Percent Dose of Riboflavin [a] Excreted in Urine in Control and Antacid-Treated Subjects [b]

Subject	Control	Aluminum–Magnesium Hydroxide	Aluminum Hydroxide	Magnesium Hydroxide
A	38.0	43.7	29.1	31.1
B	12.1	23.2	15.6	24.9
C	24.0	12.5	20.1	28.7
D	13.6	23.4	16.1	23.8
E	19.4	21.8	24.1	19.9
Mean	21.4	24.9	21.0	25.7
SD	9.3	10.2	5.1	3.9

[a] The riboflavin dose was 30 mg. [b] Cumulative amount of riboflavin excreted per dose × 100.

Under these conditions, coadministration of aluminum hydroxide gel should result in a significant increase in the peak urinary excretion rate of riboflavin, since decreased gastric emptying would lead to a decrease in the rate in which the vitamin reaches the absorption site in the small intestine and, thereby, result in an increase in peak absorption rate (5–7). If this were the case, an increase in riboflavin bioavailability in the presence of aluminum hydroxide gel would be expected. Table III indicates that this is not the case. The mean percent riboflavin urinary recovery in control studies was 21.4%, while the percent recovery in aluminum hydroxide treated subjects was 21.0%. A possible explanation for this occurrence is presented in Table IV, which lists the percent riboflavin bound as a function of antacid and riboflavin concentration in the *in vitro* studies. As can be seen from this table, in the *in vitro* experiment, riboflavin binding to the aluminum hydroxide suspension (50%) at an initial riboflavin concentration of 1.6 μg/ml was 30.9% and was 26.9% at a riboflavin concentration of 4.9 μg/ml. If binding occurs *in vivo*, it could potentially reduce the total amount of riboflavin available for absorption and result in no apparent net change in the amount of riboflavin excreted in urine in the presence of aluminum hydroxide suspension when compared with control experiments.

Administration of magnesium hydroxide suspension to the five subjects also resulted in a significant alteration in the time to peak excretion rate,

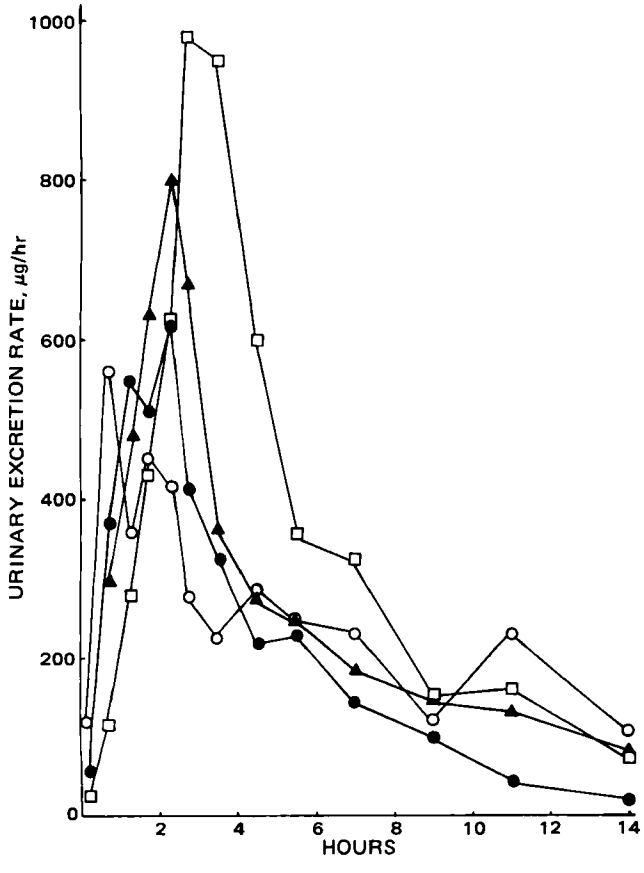

Figure 1—*Urinary excretion rate of riboflavin as a function of time in subject E for control (●), aluminum–magnesium hydroxide (○), magnesium hydroxide (▲), and aluminum hydroxide (□) treatments.*

Table IV—Percent Riboflavin Bound as a Function of Riboflavin and Antacid Concentration

Antacid [a]	Initial Concentration of Riboflavin, μg/ml 1.6	4.9
Aluminum–magnesium hydroxide (50)	10.9 ± 1.4 [b]	11.8 ± 1.0
Aluminum–magnesium hydroxide (17)	2.7 ± 0.7	2.4 ± 0.5
Aluminum hydroxide (50)	30.9 ± 0.8	26.9 ± 1.6
Aluminum hydroxide (17)	4.1 ± 0.4	5.7 ± 0.4
Magnesium hydroxide (50)	83.0 ± 0.8	80.8 ± 0.4
Magnesium hydroxide (17)	53.3 ± 1.7	68.3 ± 0.9

[a] Numbers in parentheses are the percent of v/v liquid antacid used. The total volume was 30 ml. [b] Percent riboflavin bound; mean ± *SD* of five determinations.

with no change in peak excretion rate and the amount of riboflavin excreted in the urine. However, an increase in peak rate and extent of riboflavin excretion was noted in four of the five subjects studied. It was shown in rats (3) that magnesium hydroxide suspension can decrease gastric emptying through an effect on gastric fluid volume. Of additional interest is the percent riboflavin bound to magnesium hydroxide suspension in the *in vitro* studies presented in Table IV. In a 50% magnesium hydroxide suspension, ~83% of a 1.6-μg/ml riboflavin solution was bound, while 81% of a 4.9-μg/ml solution was bound. This high percentage of binding could reduce substantially the dose of riboflavin available at the GI absorption site. Further experiments would be necessary to support this possibility.

There was no apparent effect of coadministration of the magnesium–aluminum hydroxide combination suspension on riboflavin absorption from the GI tract. This was surprising in view of the effects of both aluminum hydroxide and magnesium hydroxide on the pattern of riboflavin absorption in humans. One possible explanation is the Al^{3+} dose contained in each dosage form. The total dose of aluminum hydroxide gel administered contained 2.56 g of aluminum hydroxide (10), while the aluminum–magnesium hydroxide combination contained 1.8 g of aluminum hydroxide (10). However, the magnesium hydroxide dose was identical (1.6 g) in both the combination antacid and magnesium hydroxide suspension (10). Since no dose–effect relationship of the antacid dose to riboflavin absorption has been studied, other possibilities cannot be ruled out. However, it was shown (3) that of a series of aluminum-containing antacids studied, only aluminum hydroxide gel produced significant concentrations of aluminum ion capable of altering gastric emptying after reaction with acid. This reportedly is due to the relatively low pH (4.5) of the aluminum hydroxide antacid compared with the pH (7.2) of the aluminum–magnesium hydroxide combination. The relatively low degree of binding (~11%) of riboflavin to the combination antacid product (Table IV) should be noted.

The results of the present investigation reveal an alteration in the absorption profile of a drug that is reported to be absorbed by a specialized process in the upper portion of the small intestine when the drug is administered with aluminum hydroxide gel or magnesium hydroxide suspension. While additional work needs to be done in relation to the effect of dose and dosing regimen, it is apparent that antacids can influence the absorption pattern of a specialized transport drug, the effect being dependent upon type of antacid or product administered and the degree of drug binding.

REFERENCES

(1) C. M. Kunin and M. Finland, *Clin. Pharmacol. Ther.*, **2**, 51 (1961).

(2) A. Hurwitz and M. B. Sheehan, *J. Pharmacol. Exp. Ther.*, **179**, 124 (1971).

(3) A. Hurwitz, R. G. Robinson, T. S. Vats, F. C. Whittier, and W. F. Herrin, *Gastroenterology*, **71**, 268 (1976).

(4) T. S. Vats, A. Hurwitz, R. G. Robinson, and W. Herrin, *Pediat. Res.*, **22**, 340 (1973).

(5) G. Levy and W. J. Jusko, *J. Pharm. Sci.*, **55**, 285 (1966).

(6) G. Levy and R. R. Hewitt, *Am. J. Clin. Nutr.*, **24**, 401 (1971).

(7) G. Levy, M. Gibaldi, and J. A. Procknal, *J. Pharm Sci.*, **61**, 798 (1972).

(8) C. W. Dunnett, *Am. Stat. Assoc. J.*, **50**, 1096 (1955).

(9) M. Hava and H. Hurwitz, *Eur. J. Pharmacol.*, **22**, 156 (1973).

(10) W. R. Garnett, in "Handbook of Nonprescription Drugs," 5th ed., American Pharmaceutical Association, Washington, D.C., 1977, Chap. 1.

Validation of High-Performance Liquid Chromatographic Methods for Analysis of Sustained-Release Preparations Containing Nitroglycerin, Isosorbide Dinitrate, or Pentaerythritol Tetranitrate

LOREN GELBER[x] and ANDREW N. PAPAS

Received December 14, 1981, from the *Winchester Engineering and Analytical Center, Food and Drug Administration, Winchester MA 01890.* Accepted for publication March 16, 1982.

Abstract □ The assay of sustained-release tablets or capsules containing nitroglycerin, isosorbide dinitrate, or pentaerythritol tetranitrate by high-performance liquid chromatography is described. Acetonitrile was found to be the sample preparation solvent with the most general applicability to these products. Anisole was used as an internal standard for nitroglycerin and pentaerythritol tetranitrate, while 4-chloroacetanilide was used for isosorbide dinitrate. The method, which uses a C_{18} bonded-phase column, a methanol–water mobile phase, and 214-nm detection, was shown to be accurate, linear, and reproducible.

Keyphrases □ High-performance liquid chromatography—analysis of sustained-release preparations containing nitroglycerin, isosorbide dinitrate, or pentaerythritol tetranitrate □ Sustained-release preparations—high-performance liquid chromatographic analysis of preparations containing nitroglycerin, isosorbide dinitrate, or pentaerythritol tetranitrate □ Nitroglycerin—high-performance liquid chromatographic analysis of sustained-release preparation □ Isosorbide dinitrate—high-performance liquid chromatographic analysis of sustained-release preparation □ Pentaerythritol tetranitrate—high-performance liquid chromatographic analysis of sustained-release preparation

Recently, the analysis of nitroglycerin ointment was reported by this laboratory (1). Nitroglycerin and the related drugs, isosorbide dinitrate and pentaerythritol tetranitrate, are also formulated as sustained-release capsules and tablets. Pharmaceutical glaze and/or various cellulosic polymers are used to delay release of the active ingredient. Sustained-release nitroglycerin tablet analysis by column partition chromatography (2), sustained-release isosorbide dinitrate by GLC (3), and sustained-release pentaerythritol tetranitrate analysis by color development with phenoldisulfonic acid (4) have been reported. However, high-performance liquid chromatography (HPLC) has advantages over all of these, since it is less time consuming than column chromatography, more specific than phenoldisulfonic acid, and does not subject the samples to heat, which may cause thermal decomposition (5).

The chromatography used for nitroglycerin ointment was based on a previously described method (6) and was adapted to the sustained-release preparations by varying the methanol content of the mobile phase to achieve the desired separation. A study was made of the ability of various solvents to extract the drug from the sustained-release matrix, since this is the most critical step in the analysis.

EXPERIMENTAL

Materials—The water[1] and acetonitrile[2] used were HPLC grade; methanol[3] was distilled in glass; dimethyl sulfoxide, dicalcium phosphate, calcium sulfate, stearic acid, and ferric oxide[4] were ACS reagent grade; and magnesium stearate[4] was laboratory grade. Intestinal fluid was simulated intestinal fluid T.S. (7) without enzymes. Ethyl cellulose, carnauba wax[4], povidone[5], talc[6], colloidal silica[7], pharmaceutical glaze[8], nonpareil seeds[9], starch[10], lactose, polyethylene glycol, guar gum[11], carboxypolymethylene, hydrogenated vegetable oil[12], hydroxymethylpropylcellulose[13], zein[14], microcrystalline cellulose[15], sodium starch glycolate[16], dried malt syrup[17], FD&C blue No. 1, FD&C yellow No. 5, and D&C yellow No. 10[18] were used as received without further purification.

Standard nitroglycerin was as described previously (1), standard isosorbide dinitrate triturate[19] assayed at 25.06% by the compendial method (8), and standard pentaerythritol tetranitrate triturate[20] assayed at 18.52% by the compendial method (9).

Instrumentation—Instrumentation was as reported previously (1). For Table I, HPLC column 1 was μBondapak C_{18}[21] and column 2 was Ultrasphere ODS[22]. In addition, for analysis of authentic mixtures an electronic integrator[23] was used.

Chromatographic Conditions—Typical chromatographic parameters [calculated as reported previously (1)] are summarized in Table I.

Procedure—Twenty tablets or the pellet contents of 20 capsules from the sample to be analyzed were accurately weighed and ground until just reduced to a fine powder. An appropriate weight of composite was transferred to a glass-stoppered Erlenmeyer flask or centrifuge tube and 10.0 or 20.0 ml of the solvent being tested, containing internal standard (except as noted) was added. Flasks or tubes were stoppered, sealed with paraffin film and vigorously shaken with a wrist-action mechanical shaker for 1 hr. The following concentrations were used: nitroglycerin, 0.1 mg/ml in intestinal fluid, 1 mg/ml in dimethyl sulfoxide, and 0.5 mg/ml in acetonitrile; isosorbide dinitrate, 0.25 mg/ml in water, 0.5 mg/ml in dimethyl sulfoxide, and 0.5 mg/ml in acetonitrile; pentaerythritol tetranitrate, 1 mg/ml in dimethyl sulfoxide, and 0.5 mg/ml in acetonitrile. For nitroglycerin and pentaerythritol tetranitrate, anisole, as reported previously (1), was used as an internal standard, except for the intestinal fluid trials, where no internal standard was used. For isosorbide dinitrate, 4-chloroacetanilide was used as an internal standard in all solvents. Internal standards were selected for suitable retention parameters; it was not considered desirable to use compounds of similar chemistry as internal standards due to the difficulties in handling polynitro compounds. The solutions were filtered[24] except for dimethyl sulfoxide solutions, which were centrifuged. The clarified solutions were injected onto the liquid chromatograph. All detection was at 214 nm.

[1] J. T. Baker, Phillipsburg, N.J.
[2] Fisher Scientific Co., Fairlawn, N.J.
[3] Burdick and Jackson Laboratories Inc., Muskegon, Mich.
[4] Pfaltz and Bauer Inc., Stamford, Conn.
[5] GAF Corp., New York, N.Y.
[6] Whittaker, Clark and Daniels Inc., Plainfield, N.J.
[7] Syloid 244, W. R. Grace and Co., Davison Chemical Division, Baltimore, Md. and Cab-o-sil, Cabot Corp., Cab-o-sil Division, Boston, Mass.
[8] William Zinser and Co. Inc., Somerset, N.J.
[9] SCM SnowCrest, Salem, Mass.
[10] Colorcon Inc., West Point, Pa.
[11] Sigma Chemical Co., St. Louis, Mo.
[12] Bolar Pharmaceutical Co., Copaigue, N.Y.
[13] Forest Labs, New York, N.Y.
[14] Eastman Kodak Co., Rochester, N.Y.
[15] Avicel pH 101, FMC Corp., Philadelphia, Pa.
[16] Explotab, Generichem Corp., Little Falls N.J.
[17] Stanofill, Standard Brands, New York, N.Y.
[18] Division of Colors, Bureau of Foods, Food and Drug Administration, Washington, D.C.
[19] Barr Laboratories, Northvale, N.C.
[20] Bolar Pharmaceutical Company, Copaigue, N.Y.
[21] Waters Associates, Milford, Mass.
[22] Altex Scientific Inc., Berkeley, Calif.
[23] Model 3390A, Hewlett-Packard, Avondale, Pa.
[24] Grade 1, Whatman Ltd., England, followed by AAWP or FHLP, Millipore Corp., Bedford, Mass.

0022-3549/83/0200-0124$01.00/0

Table I—Typical Chromatographic Parameters

Compound	Sample Solvent[a]	Mobile Phase Percent Methanol	k'	Plate Count	Resolution
Nitroglycerin	Dimethyl sulfoxide	50	5.1	2240	1.95
Anisole	Dimethyl sulfoxide	50	6.0	2850	1.95
Nitroglycerin	Acetonitrile	60	2.6	1745	3.8
Anisole	Acetonitrile	60	3.6	2570	3.8
Isosorbide dinitrate	Dimethyl sulfoxide	40	4.9	1370	3.9
4-Chloroacetanilide	Dimethyl sulfoxide	40	7.7	1140	3.9
Isosorbide dinitrate	Acetonitrile	55	2.8	1270	2.3
4-Chloroacetanilide	Acetonitrile	55	3.7	1290	2.3
Pentaerythritol tetranitrate	Dimethyl sulfoxide	50	7.4	1770	3.9
Anisole	Dimethyl sulfoxide	50	5.2	840	3.9
Pentaerythritol tetranitrate	Acetonitrile	60	5.5	1725	1.8
Anisole	Acetonitrile	60	4.6	2130	1.8

[a] Dimethyl sulfoxide sample solvent runs on column 1, acetonitrile sample solvent runs on column 2.

Table II—Comparison of Sample Preparation Solvents for Nitroglycerin

Manufacturer	Dosage Form	Intestinal Fluid (pH 8)		Dimethyl Sulfoxide		Acetonitrile	
		A[a]	R[b]	A	R	A	R
1	6.5-mg capsule	n.d.[c]	n.d.	100.0	100.5	103.4	99.4
	2.5-mg capsule	83.8	n.d.	92.9	99.3	90.0	102.7
2	6.5-mg capsule	107.2	98.8	98.2	102.5	94.5	97.7
	2.5-mg capsule	92.6	110.4	n.d.	n.d.	94.4	101.2
3	6.5-mg tablet	n.d.	n.d.	86.8	119.4	116.9	102.4
4	2.6-mg tablet	n.d.	n.d.	84.0	94.7	79.8	99.3

[a] A is the percent of the declared assay. [b] R is the percent recovery from the spiked sample. [c] n.d. is not determined.

Table III—Comparison of Sample Preparation Solvents for Isosorbide Dinitrate

Manufacturer	Dosage Form	Water		Dimethyl Sulfoxide		Acetonitrile	
		A[a]	R[b]	A	R	A	R
3	40-mg tablet	105.0	104.8	n.d.[c]	n.d.	100.6	96.3
5	40-mg tablet	87.7	97.2	98.6	97.4	99.7	99.4
6	40-mg tablet	101.0	101.0	n.d.	n.d.	94.6	99.8
7	40-mg tablet	73.5	88.6	96.9	98.3	99.8	98.2

[a] A is the percent of the declared assay. [b] R is the percent recovery from spiked sample. [c] n.d. is not determined.

Spiked samples were prepared from one-half the appropriate composite weight and one-half the appropriate standard weight and treated as described. Authentic samples were prepared by combining individual weighings of the appropriate excipients and standards and analyzing them according to the method.

RESULTS AND DISCUSSION

The results of solvent comparison (reported as the average of two determinations) are presented in Tables II–IV. Solvents were selected to span a range of polarities consistent with the solubility properties of the analytes and compatability with reverse-phase HPLC. Preliminary trials with methanol and water–methanol gave poor recoveries for isosorbide dinitrate. Since a single sample solvent for all products was considered desirable, no further consideration was given to methanol. The data indicate that acetonitrile is the solvent with the most general applicability to these products. Aqueous solvents gave good extraction of the active ingredient in only about one-half of the cases in which they were tried. In addition, an interfering excipient peak was observed when 2.5-mg nitroglycerin capsules from manufacturer No. 2 were prepared with intestinal fluid. Since pentaerythritol tetranitrate is practically insoluble in water (8) aqueous extraction was not attempted for this drug. Due to their solubility in dimethyl sulfoxide, cellulose derivative excipients caused interference (a broad peak between dimethyl sulfoxide and nitroglycerin in samples from manufacturer No. 3) when dimethyl sulfoxide was the solvent. Acetonitrile has further advantages over dimethyl sulfoxide, since it can be filtered through nylon or perfluoroelastomer membranes and does not give a large solvent peak, allowing a more polar mobile phase to be used. The most serious disadvantage of dimethyl sulfoxide is that the solvent peak obscures the presence of any incompletely nitrated impurities, which are reported to elute before the fully nitrated product (6). These impurities can be detected if acetonitrile is the extracting solvent.

Since acetonitrile was the best solvent, the methods in which it was used were subjected to further validation. Authentic mixtures containing the excipients and drug expected in these products at the levels most likely to be used in commercial formulations were analyzed. In the case of manufacturers No. 1 and No. 2, where two potency levels were under consideration, authentic samples were prepared corresponding to the lower potency. Since the formulations of the two potencies are similar, the lower potency is more likely to reveal any possible interferences. For nitroglycerin the excipients used were nonpareil seeds, talc, colloidal silica, povidone, pharmaceutical glaze, magnesium stearate, dicalcium phosphate, ferric oxide, ethyl cellulose, hydroxymethylpropylcellulose, and D&C yellow No. 10. The excipients used for isosorbide dinitrate were starch, lactose, talc, pharmaceutical glaze, ethylcellulose carboxypolymethylene, magnesium stearate, stearic acid, colloidal silica, hydroxymethylpropylcellulose, hydrogenated vegetable oil, povidone, FD&C blue No. 1, and FD&C yellow No. 5. For pentaerythritol tetranitrate the excipients studied were carnauba wax, hydrogenated vegetable oil, zein,

Table IV—Comparison of Sample Preparation Solvents for Pentaerythritol Tetranitrate

Manufacturer	Dosage Form	Dimethyl Sulfoxide		Acetonitrile	
		A[a]	R[b]	A	R
6	80-mg tablet	100.2	100.8	104.1	102.1
7	80-mg capsule	101.3	101.6	107.2	101.5
8	80-mg tablet	104.6	100.0	107.0	101.8

[a] A is the percent of the declared assay. [b] R is the percent recovery from spiked sample. [c] n.d. is not determined.

Table V—Authentic Recoveries, Acetonitrile Sample Preparation Solvent

Formulation Type[a]	Recovery of Label Claim, %	
Nitroglycerin		
1	97.5	100.8
2	101.1	100.5
3	100.3	100.4
4	98.3	101.8
5	101.3	99.7
	average	100.1
	CV[b] 1.25%	
Isosorbide Dinitrate		
3	100.6	101.6
5	97.8	98.3
6	102.0	100.6
7	100.0	99.2
	average	100.0
	CV 1.50%	
Pentaerythritol Tetranitrate		
6	99.0	99.2
7	99.9	100.1
8	98.2	99.8
	average	99.4
	CV 0.72%	

[a] Formulation types correspond by number to manufacturer numbers in previous tables. [b] Coefficient of variation.

magnesium stearate, talc, dried malt syrup, microcrystalling cellulose, sodium starch glycolate, calcium sulfate, stearic acid, starch, colloidal silica, lactose, polyethylene glycol, guar gum, FD&C blue No. 1 and FD&C yellow No. 5. Placebo mixtures without active ingredient or internal standard gave no peaks past the solvent front. Excipient peaks would not interfere with the detection of incompletely nitrated impurities.

The results of assays of authentic mixtures containing active ingredient are given in Table V. The average recoveries of 99.4–100.1% with 0.72–1.50% *CV* indicate that the accuracy and reproducibility of the method are acceptable for the analysis of this type of product. The results of the spiked authentic samples demonstrate that 60-min shaking time is adequate to extract the drug. Since this is compatible with requirements of chromatograph start-up and equilibration, shorter times were not investigated.

Linearity was tested using authentic mixtures. For nitroglycerin linearity was demonstrated from 0.2 to 0.8 mg/ml, representing 40–160% of label declaration. A correlation coefficient of 0.9990 was obtained (10) from the analysis of 0.2-, 0.4-, 0.5-, 0.6-, and 0.8-mg/ml samples. For isosorbide dinitrate linearity was demonstrated from 0.27 to 0.8 mg/ml, representing 54–160% of label declaration. A correlation coefficient of 0.9998 was obtained (10) by measuring 0.27, 0.45, 0.55, 0.63, and 0.80 mg/ml. For pentaerythritol tetranitrate linearity was demonstrated from 0.5 to 1.5 mg/ml, representing 50–150% of label declaration. A correlation coefficient of 0.9999 was obtained (10) by measuring 0.5, 0.78, 1.0, 1.24, and 1.5 mg/ml.

It appears that reverse-phase HPLC, after sample preparation with acetonitrile, is a useful method for the analysis of nitroglycerin, isosorbide dinitrate, and pentaerythritol tetranitrate sustained-release tablets and capsules. Since nitroglycerin hydrolysis products were recently demonstrated to elute substantially prior to nitroglycerin in this system (11), the method is anticipated to be stability indicating for nitroglycerin.

REFERENCES

(1) L. Gelber, *J. Pharm. Sci.*, **69**, 1084 (1980).

(2) A. M. Soeterboet and M. VanThiel, *Pharm. Weekbl.*, **110**, 169 (1975).

(3) D. G. Prue, R. N. Johnson, and B. T. Kho, *J. Assoc. Off. Anal. Chem.*, **60**, 1341 (1977).

(4) V. D. Gupta, *J. Pharm. Sci.*, **67**, 717 (1978).

(5) P. Vouros, B. A. Petersen, L. Colwell, and B. L. Karger, *Anal. Chem.*, **49**, 1039 (1977).

(6) W. G. Crouthmal and B. Dorsch, *J. Pharm. Sci.*, **68**, 237 (1979).

(7) "The United States Pharmacopeia," 19th rev., U.S. Pharmacopeial Convention, Rockville, Md., 1975, p. 765.

(8) *Idem.*, p. 276.

(9) "The National Formulary," 14th ed., U.S. Pharmacopeial Convention, Rockville, Md., 1975, p. 539.

(10) R. G. D. Steel and J. H. Torrie, "Principles and Procedures of Statistics," McGraw-Hill, New York, N.Y., 1960, p. 188.

(11) C. C. Wu, T. D. Sokoloski, A. M. Burkman, and L. S. Wu, *J. Chromatogr.*, **216**, 1981, p. 239.

ACKNOWLEDGMENTS

The authors thank Mary-Ann Jarski, Bureau of Drugs, Food and Drug Administration and Mathew Dow and Yvonne Juhn, National Center for Drug Analysis, Food and Drug Administration, for assistances in identifying and locating appropriate excipients; and Dr. Michael Delaney, Boston University, Winchester Engineering and Analytical Center Science Advisor, for continuing support and encouragement.

Titrimetric Determination of Ascorbic Acid with 2,6-Dichlorophenol Indophenol in Commercial Liquid Diets

DAVID EMLYN HUGHES

Received November 9, 1981, from the *Analytical Chemistry Division, Norwich Eaton Pharmaceuticals, Inc., Norwich, NY 13815.* Accepted for publication March 18, 1982.

Abstract □ The titrimetric determination of ascorbic acid in the presence of a variety of potentially physically and chemically interfering species in commercial liquid diets is presented. The titrant and indicator was a solution of 2,6-dichlorophenol indophenol. Iron(II), copper(II), cysteine, glutathione, sulfite, and tin(II) do not interfere.

Keyphrases □ Ascorbic acid—titrimetric determination with 2,6-dichlorophenol indophenol in commercial liquid diets □ 2,6-Dichlorophenol indophenol—titrimetric determination of ascorbic acid in commercial liquid diets □ Titrimetric determination—ascorbic acid determination with 2,6-dichlorophenol indophenol in commercial liquid diets

Ascorbic acid frequently appears in multicomponent media, except in simple synthetic preparations such as ascorbic acid injection (1). In commercial liquid diets, for example, it is accompanied by proteins, amino acids, saccharides, lipids, and minerals (2). Methods involving oxidation of ascorbic acid are complicated by oxidizable metal ions, notably iron(II) and tin(II) (3).

The titrimetric oxidation of the two enolic groups of

0022-3549/83/0200-0126$01.00/0

Table V—Authentic Recoveries, Acetonitrile Sample Preparation Solvent

Formulation Type[a]	Recovery of Label Claim, %	
Nitroglycerin		
1	97.5	100.8
2	101.1	100.5
3	100.3	100.4
4	98.3	101.8
5	101.3	99.7
	average	100.1
	CV[b] 1.25%	
Isosorbide Dinitrate		
3	100.6	101.6
5	97.8	98.3
6	102.0	100.6
7	100.0	99.2
	average	100.0
	CV 1.50%	
Pentaerythritol Tetranitrate		
6	99.0	99.2
7	99.9	100.1
8	98.2	99.8
	average	99.4
	CV 0.72%	

[a] Formulation types correspond by number to manufacturer numbers in previous tables. [b] Coefficient of variation.

magnesium stearate, talc, dried malt syrup, microcrystalling cellulose, sodium starch glycolate, calcium sulfate, stearic acid, starch, colloidal silica, lactose, polyethylene glycol, guar gum, FD&C blue No. 1 and FD&C yellow No. 5. Placebo mixtures without active ingredient or internal standard gave no peaks past the solvent front. Excipient peaks would not interfere with the detection of incompletely nitrated impurities.

The results of assays of authentic mixtures containing active ingredient are given in Table V. The average recoveries of 99.4–100.1% with 0.72–1.50% *CV* indicate that the accuracy and reproducibility of the method are acceptable for the analysis of this type of product. The results of the spiked authentic samples demonstrate that 60-min shaking time is adequate to extract the drug. Since this is compatible with requirements of chromatograph start-up and equilibration, shorter times were not investigated.

Linearity was tested using authentic mixtures. For nitroglycerin linearity was demonstrated from 0.2 to 0.8 mg/ml, representing 40–160% of label declaration. A correlation coefficient of 0.9990 was obtained (10) from the analysis of 0.2-, 0.4-, 0.5-, 0.6-, and 0.8-mg/ml samples. For isosorbide dinitrate linearity was demonstrated from 0.27 to 0.8 mg/ml, representing 54–160% of label declaration. A correlation coefficient of 0.9998 was obtained (10) by measuring 0.27, 0.45, 0.55, 0.63, and 0.80 mg/ml. For pentaerythritol tetranitrate linearity was demonstrated from 0.5 to 1.5 mg/ml, representing 50–150% of label declaration. A correlation coefficient of 0.9999 was obtained (10) by measuring 0.5, 0.78, 1.0, 1.24, and 1.5 mg/ml.

It appears that reverse-phase HPLC, after sample preparation with acetonitrile, is a useful method for the analysis of nitroglycerin, isosorbide dinitrate, and pentaerythritol tetranitrate sustained-release tablets and capsules. Since nitroglycerin hydrolysis products were recently demonstrated to elute substantially prior to nitroglycerin in this system (11), the method is anticipated to be stability indicating for nitroglycerin.

REFERENCES

(1) L. Gelber, *J. Pharm. Sci.*, **69**, 1084 (1980).

(2) A. M. Soeterboet and M. VanThiel, *Pharm. Weekbl.*, **110**, 169 (1975).

(3) D. G. Prue, R. N. Johnson, and B. T. Kho, *J. Assoc. Off. Anal. Chem.*, **60**, 1341 (1977).

(4) V. D. Gupta, *J. Pharm. Sci.*, **67**, 717 (1978).

(5) P. Vouros, B. A. Petersen, L. Colwell, and B. L. Karger, *Anal. Chem.*, **49**, 1039 (1977).

(6) W. G. Crouthmal and B. Dorsch, *J. Pharm. Sci.*, **68**, 237 (1979).

(7) "The United States Pharmacopeia," 19th rev., U.S. Pharmacopeial Convention, Rockville, Md., 1975, p. 765.

(8) *Idem.*, p. 276.

(9) "The National Formulary," 14th ed., U.S. Pharmacopeial Convention, Rockville, Md., 1975, p. 539.

(10) R. G. D. Steel and J. H. Torrie, "Principles and Procedures of Statistics," McGraw-Hill, New York, N.Y., 1960, p. 188.

(11) C. C. Wu, T. D. Sokoloski, A. M. Burkman, and L. S. Wu, *J. Chromatogr.*, **216**, 1981, p. 239.

ACKNOWLEDGMENTS

The authors thank Mary-Ann Jarski, Bureau of Drugs, Food and Drug Administration and Mathew Dow and Yvonne Juhn, National Center for Drug Analysis, Food and Drug Administration, for assistances in identifying and locating appropriate excipients; and Dr. Michael Delaney, Boston University, Winchester Engineering and Analytical Center Science Advisor, for continuing support and encouragement.

Titrimetric Determination of Ascorbic Acid with 2,6-Dichlorophenol Indophenol in Commercial Liquid Diets

DAVID EMLYN HUGHES

Received November 9, 1981, from the *Analytical Chemistry Division, Norwich Eaton Pharmaceuticals, Inc., Norwich, NY 13815.* Accepted for publication March 18, 1982.

Abstract □ The titrimetric determination of ascorbic acid in the presence of a variety of potentially physically and chemically interfering species in commercial liquid diets is presented. The titrant and indicator was a solution of 2,6-dichlorophenol indophenol. Iron(II), copper(II), cysteine, glutathione, sulfite, and tin(II) do not interfere.

Keyphrases □ Ascorbic acid—titrimetric determination with 2,6-dichlorophenol indophenol in commercial liquid diets □ 2,6-Dichlorophenol indophenol—titrimetric determination of ascorbic acid in commercial liquid diets □ Titrimetric determination—ascorbic acid determination with 2,6-dichlorophenol indophenol in commercial liquid diets

Ascorbic acid frequently appears in multicomponent media, except in simple synthetic preparations such as ascorbic acid injection (1). In commercial liquid diets, for example, it is accompanied by proteins, amino acids, saccharides, lipids, and minerals (2). Methods involving oxidation of ascorbic acid are complicated by oxidizable metal ions, notably iron(II) and tin(II) (3).

The titrimetric oxidation of the two enolic groups of

0022-3549/83/0200-0126$01.00/0

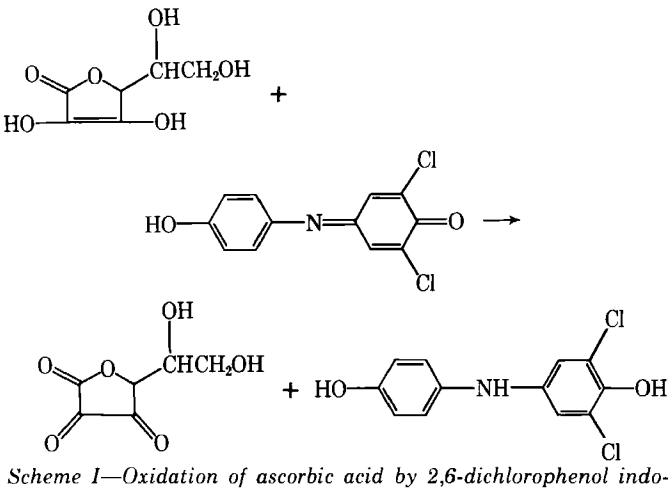

Scheme I—Oxidation of ascorbic acid by 2,6-dichlorophenol indophenol

ascorbic acid to the two keto groups of dehydroascorbic acid by 2,6-dichlorophenol indophenol (Scheme I) lacks specificity in all but the most chemically inert systems. Other traditional methods are available. Microbiological assays are specific, but they are lengthy and suffer from poor precision. A popular colorimetric procedure (4) and a modification using *p*-nitroaniline are sensitive to impurities and unresponsive at low ascorbic acid concentrations. An existing microfluorometric assay (5) does not distinguish between ascorbic acid and dehydroascorbic acid; this may be a serious shortcoming in stability studies, since dehydroascorbic acid is the principal degradation product of ascorbic acid. Methods for selective ascorbic acid determination appear to require extensive sample clean-up (6) or a sophisticated chromatographic system with selective detection such as high-performance liquid chromatography (HPLC) (7, 8), ion-exchange chromatography (9), electrochemical detection (10), amperometric detection (11), or differential-pulse polarography (12).

Although the HPLC methods mentioned are sensitive, frequently they are unable to resolve ascorbic acid from the water-soluble B vitamins. The more sophisticated detectors may not be available in many laboratories. The speed and accuracy of a titrimetric method is especially attractive where ascorbic acid analysis is done on a large number of samples or on a routine basis. The purpose of this report is to present a modification of the standard 2,6-dichlorophenol indophenol titration such that it may be run in the presence of a large number of potential physical and chemical interferences present in commercial liquid diets.

BACKGROUND

Almost 50 years ago, the desirability of increasing the specificity of the 2,6-dichlorophenol indophenol titration to exclude the ferrous ion and glutathione was well understood (13–15). The titrimetric method was then sufficiently well developed to spawn its use in an impressive list of media including fruit and vegetable juice, milk, body tissues, cerebral fluid, plant extracts, and animal organs (16, 17). The animal and vegetable media offer few interferences, but biological systems often contain enough oxidizable metal ions, notably ferrous ions, to interfere. Since the 1940s, the 2,6-dichlorophenol indophenol titration has been unearthed and the ferrous ion interference eliminated by carrying out the titration in acid. Hence, the ferrous ion interference was eliminated by titrating in acetic acid (18). The interference also was removed by titrating in hydrochloric acid solution (19), and hydrochloric acid–acetate mixtures (20). Aqueous acetic acid solutions also were used to eliminate ferrous ion interference

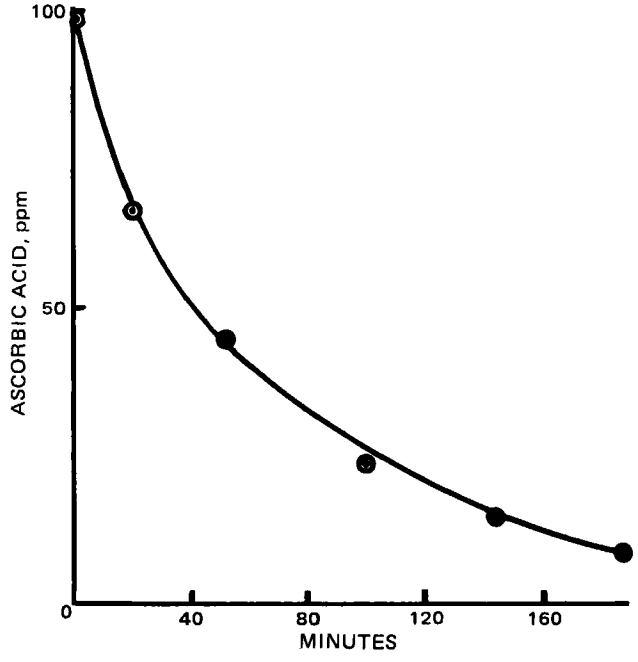

Figure 1—*Degradation of ascorbic acid in an unmasked sample (pH 5.0).*

(21, 22). In a two-step titration of ferrous ion and ascorbic acid, the ferrous ion was masked by an aqueous succinic or adipic acid solution (23). Despite these successful attempts to mask the ferrous ion during the ascorbic acid determination, extension of the method to include other redox interferences is absent from the chemical literature.

An example of a redox interference is the presence of a reducible species in the sample such as cupric or ferric ions. The metal ions are reduced, and the ascorbic acid is oxidized yielding erroneously low ascorbic acid values. The reaction, $e^- + Cu^{2+} \rightarrow Cu^+$, occurs stoichiometrically with the ascorbic acid oxidation, and the cupric ion has been used to determine ascorbic acid (24). The ferric ion interference may be masked in some samples with the tartrate ion.

Oxidizable metal ions and organic species, notably the mercaptans, cysteine and glutathione, interfere and yield high ascorbic acid assay values. The 2,6-dichlorophenol indophenol reacts with both the ascorbic acid and the oxidizable mercaptan. These interferences may be avoided by low pH solutions, and weak organic acids may be preferred since ascorbic acid is destroyed in very acidic solutions.

Sulfur dioxide interference has been eliminated by addition of acetone, hydrogen peroxide, or formaldehyde. Strongly colored solutions have been decolorized with tablets[1] (25) to allow a visual endpoint.

The standard 2,6-dichlorophenol indophenol titration is seen to be usable when other species in solution are not easily oxidized or reduced. Prevention of one oxidation reaction, $Fe^{2+} \rightarrow Fe^{3+} + e^-$, may be accomplished by dissolving the sample in a solution of a weak acid. The standard titration is not selective enough for analysis of biological fluids (since they often contain oxidizable species such as cysteine and glutathione), soft drinks that contain the sulfite ion, and vitamin formulations containing the stannous ion. None of the previous reports (18–23) attempted to modify the 2,6-dichlorophenol indophenol titration to select ascorbic acid in the presence of any oxidizable species except ferrous ion. The present report investigates sample handling conditions which would mask cysteine, glutathione, sulfite, and tin(II) and, hence, extend the utility of 2,6-dichlorophenol indophenol titration to systems where selectivity is important.

EXPERIMENTAL

Reagents—All chemicals were analytical reagent grade unless otherwise noted.

Procedure—A sample containing ~10 mg of ascorbic acid was weighed and transferred to a 125-ml Erlenmeyer flask having a ground-glass stopper. In addition to ascorbic acid, the samples contained glucose oligosaccharides, L-glutamine, L-aspartic acid, glycine, L-phenylalanine,

[1] Boehringer.

Table I—Titrimetric Assay of Various Commercial Liquid Diets

Sample	Ascorbic Acid[a], ppm	Colorimetric Assay[b]
1	347	325
2	285	277
3	251	240
4	237	240
5	160	
6	166	

[a] Label value for all products was 160 ppm of ascorbic acid. [b] Ref. 30.

L-proline, L-leucine, L-lysine hydrochloride, L-alanine, L-arginine hydrochloride, magnesium gluconate dihydrate, sodium citrate dihydrate, L-methionine, L-valine, L-threonine, L-isoleucine, L-serine, calcium glycerophosphate, L-histidine hydrochloride monohydrate, sodium glycerophosphate, potassium citrate monohydrate, safflower oil, L-tryptophan, potassium chloride, potassium sorbate, L-tyrosine, polyoxyethylene sorbitan monooleate, ferrous gluconate dihydrate, choline bitartrate, zinc acetate dihydrate, α-tocopherol acetate, niacinamide, manganese glycerophosphate, D-calcium pantothenate, cupric citrate, ascorbyl palmitate, pyridoxine hydrochloride, riboflavin phosphate sodium salt, vitamin A acetate, thiamine hydrochloride, folic acid, *d*-biotin, potassium iodide, phytonadione, ergocalciferol, and cyanocobalamin. About 20–40 ml of 1.5 *N* acetic acid was added. The sample was titrated immediately with the titrant consisting of 0.2 g of 2,6-dichlorophenol indophenol and 0.2 g of sodium bicarbonate and distilled water sufficient to make 1000 ml of solution. The endpoint was a distinct pink color which lasted for 30 sec and was more intensely colored than a phenolphthalein endpoint. Similarly, a semimicro titration was performed. For a 5-ml buret, the titrant was prepared from 1.2 g of 2,6-dichlorophenol indophenol and 1.2 g of sodium bicarbonate to make 1 liter of solution. The titrant was standardized by titration against a standard solution of 100 mg of USP ascorbic acid[2] in 100 ml of 1.5 *N* aqueous acetic acid. Two milliliters of this standard solution was pipeted and titrated for the titrant standardization in both the macro and semimicro titrations.

Wet additions of cysteine, glutathione, sodium sulfite, and tin(II) chloride were made to a final concentration in the sample solutions of 66.6–333 μg/ml. The samples were then assayed for ascorbic acid using the semimicro titration procedure.

RESULTS AND DISCUSSION

Some confusion exists in the literature over the nomenclature for the determination of ascorbic acid by oxidation to dehydroascorbic acid. Some investigators choose ascorbic acid, L-ascorbic acid, vitamin C, or total vitamin C as the species determined. Since the 2,6-dichlorophenol indophenol oxidation does not distinguish between D and L forms, and since vitamin C is defined (26) as L-ascorbic acid, the generic term ascorbic acid may be less misleading. Total vitamin C is defined as the arithmetic sum of the L-ascorbic acid plus dehydroascorbic acid content of the sample. Dehydroascorbic acid has the same molar biological (antiscorbutic) activity as ascorbic acid (26), and, hence, assays of biological origin usually attempt to determine total vitamin C. Any assay specific for ascorbic acid does not necessarily measure the biological activity, since some or all of the ascorbic acid in the sample may have been oxidized to dehydroascorbic acid. Conforming to official USP nomenclature, the species determined by the described procedure is ascorbic acid (D and L forms). Dehydroascorbic acid (and, therefore, the total vitamin C or biological activity) is neither determined nor does its presence interfere. If an assay for total vitamin C is desired, prior reduction of dehydroascorbic acid with hydrogen sulfide may be possible (27, 28).

In many solid samples, the formation of dehydroascorbic acid follows dissolution in water. In standard solutions, the aerial ascorbic acid to dehydroascorbic acid conversion is slow, requiring 24 hr for 0.3% dehydroascorbic acid to be formed (29). Inert atmospheres of carbon dioxide, nitrogen, and hydrogen have been employed to slow degradation further. Although it would appear that no special sample handling is required, even minute amounts of ferric and cupric ions present in samples, strongly catalyze the ascorbic acid oxidation (2). In Fig. 1, considerable oxidation of ascorbic acid is seen to occur in the samples used in this study, even in an acidic medium. Even when the ferric ion has been eliminated by complexation or masking as a direct interference, the ion is still capable of catalysis of the ascorbic acid to dehydroascorbic acid conversion. When the dissolution medium is 1.5 *N* acetic acid, no degradation is observed for at least the first 5 min.

[2] Aldrich Chemical Co., Milwaukee, Wis.

Table II—Dry Recoveries of Ascorbic Acid from Placebo

Milligrams Added	Milligrams Found	Recovery,[a] %
0.500	0.500	100
0.500	0.520	104
1.00	1.02	102
1.00	1.00	100
1.50	1.47	98
1.50	1.46	97
1.56	1.53	98
1.56	1.53	98
1.56	1.53	98
1.56	1.52	97
1.95	1.92	98
1.95	1.91	98
1.95	1.92	98
1.95	1.90	97
2.34	2.36	101
2.34	2.37	101
2.34	2.35	100
2.34	2.35	100

[a] Average = 99.2%. *SD* = 1.95. *RSD* = 1.96%.

Initial attempts to increase the specificity of the 2,6-dichlorophenol indophenol oxidation of ascorbic acid using 0.1 *M* hydrochloric, nitric, and sulfuric acid media for dissolution were unsuccessful. The samples containing the ferrous ion yielded an assay equal to ascorbic acid plus the ferrous ion content. Five percent aqueous trichloroacetic acid was then used to dissolve some of the samples. The assay values were time-dependent, *i.e.*, the longer the titration time, the lower the ascorbic acid content. *m*-Phosphoric acid (0.1 *M*), sulfuric acid, and oxalic acid were tested, since they have been reported to increase the specificity of the reaction (28). None yielded satisfactory recoveries when sulfite was present. After trials with several mixed solvent and weak organic acid combinations, aqueous acetic acid was found to be the most applicable sample medium. The most dilute solution, which consistently masked ferrous ions, stannous ions, sulfite, cysteine, and glutathione was 1.5 *N* CH_3CO_2H. This dissolution medium was also found to mask cupric ions and other excipients listed in *Experimental*. Several commercial liquid diets were assayed titrimetrically and the results appear in Table I. Since commercial liquid diets frequently contain a large excess of ascorbic acid, some formulations were also assayed by the colorimetric determination of the 2,4-dinitrophenylhydrazine derivative of dehydroascorbic acid (30). The two methods are in good agreement.

The selectivity of the titrimetric procedure presented here compares favorably with other oxidative titrations. Titration with *N*-bromosuccinimide, for example, is complicated by cysteine, glutathione, and sulfite (31). The selectivity of the basic chloramine T procedure (32) is limited to samples without sulfite and sulfhydryl compounds, thiosulfates, sulfides, or tin(II). The modified 2,6-dichlorophenol indophenol determination is seen to be highly selective when compared with other titrimetric procedures.

The utility of the 2,6-dichlorophenol indophenol titration of ascorbic acid has been extended to systems of a biological composition in the presence of iron(II), copper(II), cysteine, glutathione, sulfite, tin(II), and other redox interferences. The data for 18 dry recovery samples are presented in Table II. The ascorbic acid was introduced to the placebo at six levels ranging from 0.5–2.34 mg. The average recovery was 99.2% with a relative standard deviation of 1.96%. For the precision of the procedure, 11 samples ranging from 4.34–6.48 g were assayed. All samples

Table III—Precision of Ascorbic Acid Titrimetric Assay

Sample, g	μg of Ascorbic Acid/g,[a]
4.34	101.0
4.17	97.5
4.34	101.0
5.37	99.9
5.25	98.1
5.47	102.0
5.48	102.0
6.56	102.0
6.53	102.0
6.51	101.0
6.48	101.0

[a] Label value was 97.5 μg ascorbic acid/g sample; mean = 101 μg/g. *SD* = 1.57 μg/g. *RSD* = 1.56 μg/g.

Table IV—Recoveries of Ascorbic Acid in the Presence of Known Interferences

	μg/ml	Ascorbic Acid Added, μg[a]	Found, μg[a]	Recovery, %
Cysteine	66.6	666	663	99.6
	133.0	666	672	101.0
	200.0	666	667	100.0
	266.0	666	673	101.0
	333.0	666	671	101.0
Glutathione	66.6	666	669	100.0
	133.0	666	665	100.0
	200.0	666	660	99.2
	266.0	666	661	99.3
	333.0	666	672	101.0
Sulfite	66.6	666	666	100.0
	133.0	666	668	100.0
	200.0	666	671	99.2
	266.0	666	660	99.2
	333.0	666	663	99.6
Tin(II)	66.6	666	656	98.5
	133.0	666	667	100.0
	200.0	666	660	99.0
	266.0	666	662	99.4
	333.0	666	667	100.0

[a] Mean = 665 μg. *SD* = 5.0 μg. *RSD* = 0.75%.

were obtained from the same lot and the theoretical ascorbic acid content was 97.5 μg/g. The samples displayed good homogeneity and assayed at an average of 101 μg of ascorbic acid/g of sample or 104% of label value. The data appear in Table III. In Table IV data are presented for the recovery of ascorbic acid in the presence of known redox interferences. In each case a wet spike of the interference was made to a standard containing 666 μg of ascorbic acid. The resulting solution was then 333 μg/ml in ascorbic acid and from 66.6–333 μg/ml (20–100% of the ascorbic acid concentration) interference. The titration was also performed without the acetic acid masking solution, and in each case, the recoveries were markedly <100%. Dissolution of samples in 1.5 *M* acetic acid masks commonly encountered interferences and allows the use of a titrimetric procedure where more sophisticated methods were previously required.

The simplicity of the method cannot be overstated. The titrant is the only reagent required for the titration (since the titrant is also the indicator) and is stable for at least 1 month. The sample preparation consists of shaking with 1.5 *M* acetic acid for several seconds. Other titrimetric procedures not only are more time consuming for the determination itself, but require special procedures or unstable reagent. Reduction of the 1,2-enediol group by *N*-bromosuccinimide, for example, requires titration with an unstable reagent. Titration of ascorbic acid with chloramine T in some cases requires a carefully prepared sodium tetrathionate solution which is thermally and photochemically degradable. Although a recent report (32) describes the determination of ascorbic acid with chloramine T in the presence of sulfhydryl compounds or sulfite, it does not outline a procedure for safely distilling the acrylonitrile. Some analysts may be unwilling to distill as highly toxic, flammable, and explosive (33) a liquid as acrylonitrile. The oxidation of the 1,2-enediol group by 2,6-dichlorophenol indophenol appears to be the fastest and safest titrimetric determination of ascorbic acid presently available.

REFERENCES

(1) "United States Pharmacopeia," Vol. XX, U.S. Pharmacopeial Convention, Inc., Rockville, Md., 1980, p. 55.

(2) P. Gyrogy and W. N. Pearson, "The Vitamins," Academic, New York, N.Y., 1967, pp. 138–142.

(3) "Official Methods of Analysis," 13th ed., Association of Official Analytical Chemists, Washington, D.C., 1980, p. 746.

(4) C. E. Weeks and M. Deutsch, *J. Assoc. Off. Anal. Chem.*, **48**, 1245 (1965).

(5) *Idem.*, **48**, 1248 (1965).

(6) P. György and W. N. Pearson, "The Vitamins," Academic, New York, N.Y., 1967, pp. 83–126.

(7) R. B. H. Wills, C. G. Shaw, and W. R. Day, *J. Chromatogr. Sci.*, **15**, 262 (1977).

(8) S. O. Sood, L. E. Sartori, D. P. Wittmer, and W. G. Haney, *Anal. Chem.*, **48**, 796 (1976).

(9) R. C. Williams, D. R. Baker, and J. A. Schmit, *J. Chromatogr. Sci.*, **11**, 618 (1973).

(10) L. A. Pachla and P. T. Kissinger, *Anal. Chem.*, **48**, 364 (1976).

(11) *Ibid.*, *Methods Enzymol.*, **62**, 15 (1979).

(12) G. Sowtag and G. Kainz, *Mikrochim. Acta*, **I(1–2)**, 1975 (1978).

(13) J. Tillmans, P. Hirsch, and W. Hirsch, *Z. Unters. Lebensm.*, **63**, 1 (1932).

(14) T. W. Birch, L. J. Harris, and S. N. Ray, *Biochem. J.*, **26**, 187 (1932).

(15) L. J. Harris and S. N. Ray, *ibid.*, **27**, 303 (1933).

(16) M. R. F. Ashworth, "Titrimetric Organic Analysis," Part I, Interscience, New York, N.Y., 1964, pp. 434–439.

(17) A. Emmerie and M. van Eekelen, *Biochem. J.*, **28**, 1153 (1934).

(18) O. Gawron and R. Berg, *Ind. Eng. Chem.*, **16**, 757 (1944).

(19) M. Ott and E. Meisenburg, *Chemie*, **58**, 22 (1945).

(20) F. Brown and W. B. Adam, *J. Sci. Food Agr.*, **1**, 1951 (1950).

(21) D. Glick, *J. Biol. Chem.*, **109**, 433 (1935).

(22) W. L. Hall and M. J. Deutsch, *J. Assoc. Off. Anal. Chem.*, **48**, 1236 (1965).

(23) W. Müller-Mulot, *Z. Anal. Chem.*, **226**, 266 (1967).

(24) B. C. Verma and S. Kumar, *Talanta*, **24**, 694 (1977).

(25) G. Schumann, *Mschr. Brau*, **23**, 218 (1970); *Anal. Abstr.*, **21**, 595 (1970).

(26) P. G. Stecher, "The Merck Index," 9th ed., Merck, Rahway, N.J., 1976, p. 110.

(27) J. Toothill, S. Y. Thompson, and J. Edwards-Webb, *J. Dairy Res.*, **37**, 29 (1970).

(28) H. Vallant, *Mikrochim. Acta*, **1969**, 436.

(29) I. M. Kolthoff and R. Belcher, "Volumetric Analysis," Interscience, New York, N.Y., 1957, p. 626.

(30) J. H. Roe and C. A. Kuether, *J. Bio. Chem.*, **147**, 399, (1943).

(31) K. K. Verma and S. Z. Bose, *Anal. Chem.*, **274**, 126 (1975).

(32) K. K. Verma and A. K. Gulati, *ibid.*, **52**, 2336 (1980).

(33) P. G. Steecher, "The Merck Index," 9th ed., Merck, Rahway, N.J., 1976, p. 17.

External Scintigraphy in Monitoring the Behavior of Pharmaceutical Formulations *In Vivo* I: Technique for Acquiring High-Resolution Images of Tablets

MICHAEL C. THEODORAKIS *§x, DAVID R. SIMPSON *, DOMINIC M. LEUNG *, and MICHAEL DEVOUS, Sr. *‡

Received February 18, 1981, from the *University of Illinois at Urbana-Champaign, *Section of Nuclear Medicine and Radiopharmacology and ‡Department of Bioengineering, Colleges of Veterinary Medicine and Engineering, Urbana, IL 61801.* Accepted for publication March 16, 1982. §Present address: College of Pharmacy, Department of Pharmaceutics, University of Florida, Gainesville, FL 32610.

Abstract □ A new method for monitoring tablet disintegration *in vivo* was developed. In this method, the tablets were labeled with a short-lived radionuclide, technetium 99m, and monitored by a gamma camera. Several innovations were introduced with this method. First, computer reconstruction algorithms were used to enhance the scintigraphic images of the disintegrating tablet *in vivo*. Second, the use of a four-pinhole collimator to acquire multiple views of the tablet resulted in high count rates and reduced acquisition times of the scintigraphic images. Third, the magnification of the scintigraphic images achieved by pinhole collimation led to significant improvement in resolution. Fourth, the radioinuclide was incorporated into the granulation so that the whole mass of the tablet was uniformly labeled with high levels of activity. This technique allowed the continuous monitoring of the disintegration process of tablets *in vivo* in experimental animals. Multiple pinhole collimation and the labeling process permitted the acquisition of quality scintigraphic images of the labeled tablet every 30 sec. The resolution of the method was tested *in vitro* and *in vivo*.

Keyphrases □ Disintegration—external scintigraphy in monitoring the behavior of pharmaceutical formulations *in vivo*, technique for acquiring high-resolution images of tablets □ Tablet formulation—external scintigraphy in monitoring the behavior *in vivo*, technique for acquiring high-resolution images of tablets □ Scintigraphy—external, monitoring the behavior of pharmaceutical formulations *in vivo*, technique for acquiring high-resolution images of tablets □ Radionuclides—^{99m}Tc-labeled tablets, external scintigraphy in monitoring the behavior of pharmaceutical formulations *in vivo*, technique for acquiring high-resolution images of tablets

Several techniques have been developed that permit the direct observation *in vivo* of pharmaceutical formulations such as tablets and capsules. The advantages and shortcomings of these techniques have been reviewed in a number of reports (1–3). Although at the present time the pharmaceutical scientists evaluate the formulation work by *in vitro* disintegration and dissolution studies coupled with *in vivo* blood studies, there are instances where the formulations of locally acting chemotherapeutic agents, antibiotics, antacids, and endogenous substances such as iron, potassium, and calcium salts do not provide distinguishable blood levels. Therefore, in such cases it is necessary to observe the *in vivo* disintegration time of the formulation in order to confirm the *in vitro* findings (2, 4). Furthermore, questions regarding the site of disintegration in the GI tract, the completeness of disintegration, the effectiveness of different enteric coatings, the rate of transition of the formulation through the different segments of the GI tract with respect to the age of the individual, the gastric and intestinal malfunctions, and diseases can be only answered by direct observation of the formulation within the GI tract. However, examination of the scientific literature during the last 50 years has revealed that only limited information is available on disintegration of formulations *in vivo*. This can be attributed to the fact that the previous techniques were difficult to perform and were invasive to both animal and human subjects. The development of the gamma scintillation camera coupled with the availability of short-lived gamma-ray emitting nuclides and devices for fast acquisition, processing, and storage of digital data has provided an opportunity to develop a useful method for performing such *in vivo* studies on tablets or capsules (3, 5–8). Furthermore, the development of mathematical methods of image reconstruction and enhancement of objects emitting gamma radiation has made it possible to enhance the resolution of the images of small objects acquired by the gamma scintillation camera (5, 6, 9).

The present report addresses further the application of external scintigraphy and image reconstruction in the acquisition of high-resolution scintigraphic images of labeled tablets *in vitro* and *in vivo*.

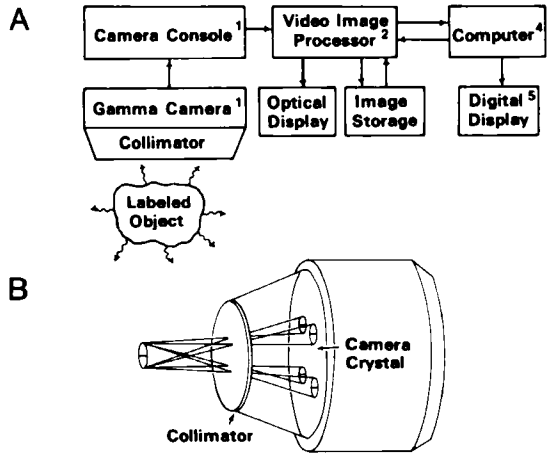

Figure 1—*(A) Block diagram of the image acquisition and data processing system; (B) projection of the four images using a four-pinhole collimator.*

EXPERIMENTAL

Image Acquisition and Processing—A standard gamma camera[1] with a sodium iodide–thallium iodide crystal (diameter 25.4 cm; thickness 1.25 cm) optically connected to 19 photomultiplier tubes was used to acquire the scintigraphic images of the labeled tablet phantoms and tablets *in vitro* and *in vivo*. The images were digitized and stored on magnetic tape[2] of the video image processor[3] prior to transmission to another computer[4] where the four pinhole images were back-projected

[1] Pho Gamma/HP, Siemens Gammasonics (formerly Searle Radiographics), Des Plaines, Ill.
[2] Primus, 9-Track Magnetic Tape, 9 in Reel, Wabash Tape Co., Huntley, Ill.
[3] Video Image Processor 460 (VIP-460), Technicare Inc. (formerly Ohio-Nuclear), Solon, Ohio.
[4] Eclipse S/140, Data General Corp., Southboro, Mass.

0022-3549/83/0200-0130$01.00/0

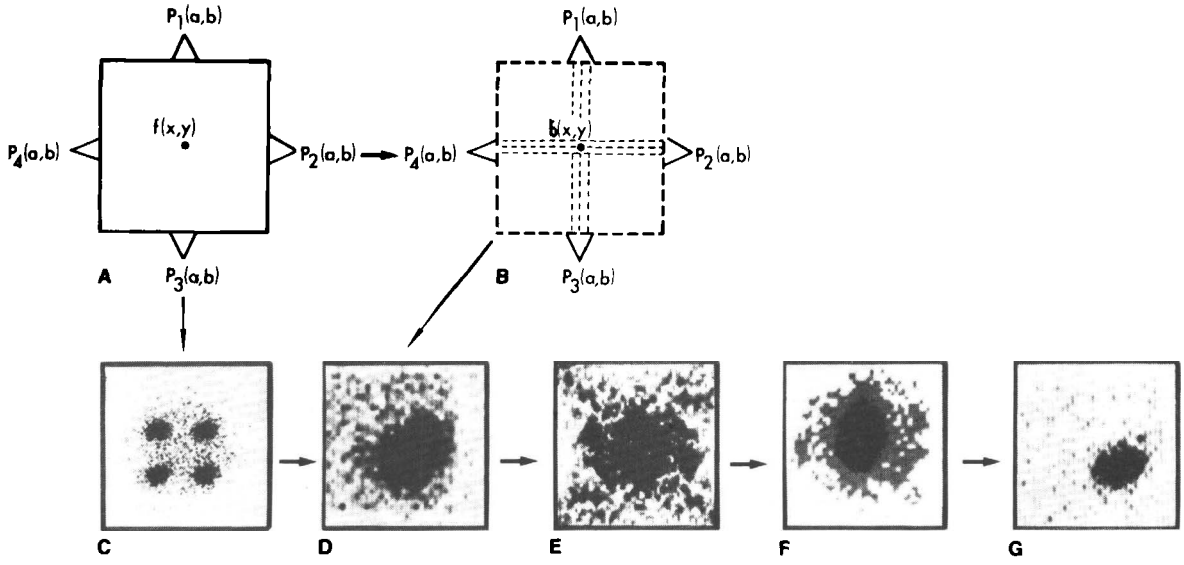

Figure 2—*Schematic illustration of the back-projection process (A and B) and the actual images of the back-projection and Fourier enhancement of a ^{99m}Tc-labeled tablet (C–G). (A) Four projections (images), $P_i(a,b)$, of a ^{99m}Tc-labeled tablet, f(x,y); (B) the images are back projected to form the back-projected image of the tablet, b(x,y); (C) original images, $P_i(a,b)$, of a tablet from a four-pinhole collimator; (D) back-projected image of the tablet, b(x,y); (E) Fourier spectrum of back-projected image of the tablet; (F) Fourier spectrum of the tablet's back-projected image after filtering the very high frequency components (noise); and (G) the enhanced back-projected image of the tablet after inverse Fourier transformation was applied on F.*

into one image which was enhanced by using filtered back-projection (Figs. 1B and 2). The final image was either displayed on the CRT screen of the video image processor, which also has photographic capability, or printed on a printer[5] using a 32-level gray scale display. The different interfaced devices and the flow of data are shown as a block diagram in Fig. 1A. A four-pinhole collimator was used to acquire four images of the labeled object. The distance between tablet and camera was optimized to provide the maximum magnification while all four images remained within the field of view of the camera. Serial images of the tablet were recorded at 30-sec intervals on the video image processor. The duration of data acquisition for each image was 30 sec.

Pinhole Collimator—A pinhole collimator was used to magnify and create four images of the tablet phantoms. The detachable pinhole assembly of a standard single-pinhole collimator was replaced by a lead cap of uniform thickness (0.3 cm) bearing four pinholes 0.119 cm in diameter, equally spaced on the periphery of a circle 3.8 cm in diameter (Figs. 1B and 3).

Pinhole Collimator Optimization—The diameter of the pinholes was optimized by imaging a ^{99m}Tc-labeled tablet (0.4 mCi). Images were taken with the tablet placed flat under the collimator and with the tablet placed on its edge. The counting time needed to accumulate 50,000 counts was plotted *versus* the pinhole diameter (Fig. 4).

Labeling of Tablets and Tablet Phantoms—Sodium [^{99m}Tc]pertechnetate (I) in saline (10 mCi/ml) received from a molybdenum-99–technetium-99m generator[6] was sprayed on the tablet granulation. The granulation was mixed, dried, and compressed[7] in tablets of specified hardness. Each tablet was labeled with 50,000–500,000 cpm as determined by the gamma camera detector. The diameter of the tablet was 1.04 cm and the thickness was 0.40 cm.

Five tablet phantoms were made of leather (Fig. 5A). Each phantom has a diameter of 0.8 cm and a thickness of 0.3 cm. Defects representing 0–9.9% of the weight of the phantom were artificially created (Table I). The phantoms were labeled by exposure to an aqueous solution of I. Each phantom was labeled with 100,000–200,000 cpm as determined by the gamma camera detector.

Back-Projection—The four images of the labeled phantom were back-projected into a single image by the following process. The distance between phantom and collimator was determined either by direct measurement or by the displacement of the images on the gamma camera crystal. This constant was used to determine the location of the four images on the crystal of the gamma camera. Then a two-dimensional array consisting of 64 × 64 picture elements (pixels[8]) was established around the center of each image. The four arrays were added together to form the back-projection image (Figs. 2A and B). The flow chart of the computer program used in back-projection is shown in Fig. 6A.

Image Enhancement—Pixels in the back-projected image were transformed into the Fourier domain first by rows then by columns, filtered (as will be described) and retransformed to the spatial domain. Image enhancement was completed when every pixel of the back-projected image was filtered. An example is given in Fig. 2. The flow chart of the computer algorithms used is shown in Fig. 6B.

Filter Optimization—To enhance the edges of the tablet and therefore increase the resolution, a modified ramp frequency filter[9] was used to filter the back-projected image of the tablet. This modified ramp frequency filter was derived by multiplying a basic ramp frequency filter with different frequency filters[9]. Several filters were constructed (Fig. 7). The best modified ramp frequency filter[9] was selected by evaluating the image–noise ratio (Table II). The image–noise ratio was established

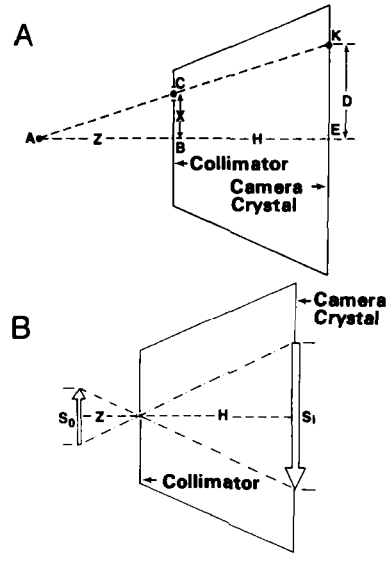

Figure 3—*(A) The location of the image (K) of tablet A, at distance D from the center of the gamma camera's sodium iodide–thallium iodide crystal was determined by the use of similar triangles ABC and AEK; (B) demonstration of image magnification and inversion by pinhole imaging.*

[5] Decwriter III, Digital Equipment, Marlboro, Mass.
[6] Mallinckrodt Nuclear Co., St. Louis, Mo.
[7] Hydraulic Press, model C, Fred S. Carver, Inc., Menomonee Falls, Wis.
[8] Pixel is an acronym for picture element.
[9] Butterworth.

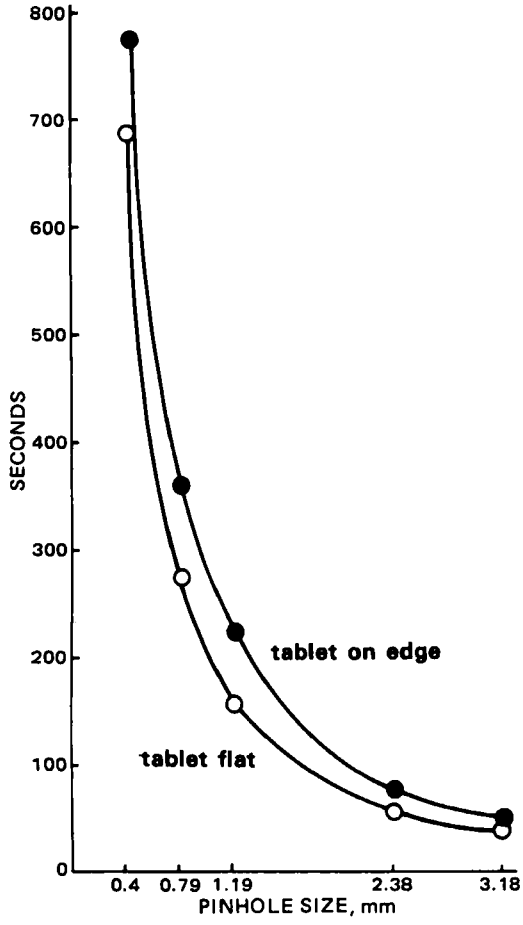

Figure 4—*Relationship between counting time and pinhole size.*

by dividing the number of counts in the pixels of the back-projected image of phantom tablet 1 (Fig. 5A) by the number of counts in an equal number of pixels in the background. The same frequency ramp filter was also evaluated in terms of image–defect ratio, which was established by dividing the average of the number of counts in the pixels corresponding to three intact portions, a, b, c, of the phantom tablet by the number of counts in the pixels corresponding to the defective area, d, of the tablet phantom 5 (Figs. 5A and B). All four areas, a, b, c, d, had an equal number of pixels.

Sensitivity to Defect Size—The labeled tablet phantoms, 2–5, were placed at different distances from the collimator, and their images were acquired and enhanced. The image–defect ratio was calculated for each defective phantom at different distances (Fig. 8). The image–defect ratio was used as a measure of evaluating the resolution of the technique with regard to the defect size of the tablet phantom and its distance from the collimator.

***In Vitro* Imaging Studies**—The *in vitro* imaging studies involved two parts. In the first part, ^{99m}Tc-labeled intact or defective tablet phantoms (Fig. 5A) were placed 6 cm in front of the collimator of the

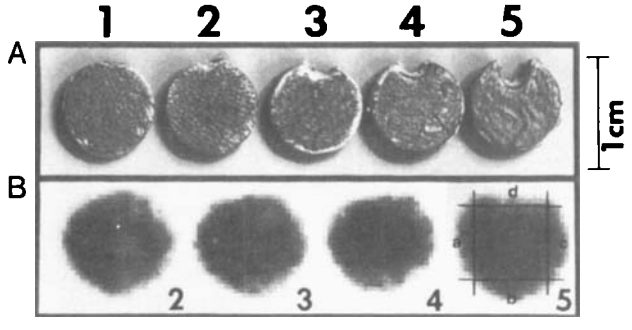

Figure 5—*(A) Tablet phantoms with various defects. (B) Enhanced scintigraphic images of the tablet phantoms with various size defects magnified five times by computer. Scale applies only to tablet phantoms.*

Table I—Size of Defects in Tablet Phantoms

Phantom No.	A[a], mm^2	B[b], %
1	0.0	0.0
2	0.62	1.2
3	1.4	2.8
4	2.6	5.2
5	5.0	9.9

[a] A is the area of defect in square millimeters. [b] B is the defect size expressed as the percent of the total weight of the phantom.

gamma camera and their images were acquired and reconstructed (Fig. 5B) according to the process described previously. The second part involved ^{99m}Tc-labeled tablets which were left to disintegrate in a shallow dish covered with distilled water. The water was lightly agitated occasionally. Scintigraphic images as well as photographs of the disintegrating tablet were taken every 30 sec (Fig. 9). The acquired images were reconstructed and enhanced.

***In Vivo* Imaging Studies**—The labeled tablet was administered orally to a dog weighing 13 kg. The animal was tranquilized[10] for imaging, placed in a supine position on a table, and the abdomen then was positioned under the collimated detector of the gamma camera. Data were accumulated for up to 75 min. During that period, scintigraphic images of the abdominal area were taken, back-projected, and enhanced (Fig. 10).

RESULTS

The acquisition and processing of the scintigraphic images are illustrated in Fig. 1A. The signal from the gamma camera console to the video image processor consisted of an x,y grid location of each detected emission within the specified energy range. Each of the images was digitized into a matrix of 64 × 64 pixels and stored on magnetic tape. The digitized images were transmitted to a general purpose computer[4] (16 bit, 512K) where the back projection and filtering of the scintigraphic image was conducted. The enhanced image was then displayed on the video image processor. The flow charts of the algorithms used for back-projecting and filtering the scintigraphic images are illustrated in Fig. 6.

The optimum diameter of the pinhole was determined experimentally by plotting the time needed to acquire 50,000 cpm from a ^{99m}Tc-labeled tablet *versus* the pinhole diameter size (Fig. 4). The optimum diameter was chosen to be 0.119 cm. The four pinholes were arranged equidistantly on the periphery of a cycle with a 3.8-cm diameter. The diameter was determined by using Eq. A1 (see *Appendix*) which was derived by geometric consideration of Fig. 3A. Distance (H) was constant at 16.7 cm. When a ^{99m}Tc-labeled tablet or tablet phantom placed at distance (Z) ranging from 3.3 to 7.5 cm, the image (K) was formed 11.5 and 6.1 cm from the center (E) of the crystal. The magnification was determined by Eq. A2, which was also derived by geometric consideration of Fig. 3. For instance, a tablet phantom with a 0.8-cm diameter placed 3.3 cm away from the collimator was magnified five times.

The back-projected image, $b(x,y)$, was in a sense the sum of the four images, $P_i(a,b)$, of the labeled tablet, $f(x,y)$, which were created by the four-pinhole collimator (Figs. 2A, B, and C). This back-projected image contained the true image in a single plane, and it was marked by interference due to natural background radioactivity, loss of small amounts of radioactivity because of the disintegration and dissolution process, and electronic noise (Fig. 2D). Each row and column of the 4096 pixel matrix (64 × 64) of each back-projected image was transformed from the spatial domain to the frequency domain by means of a Fourier transformation (Eq. A4). This is shown in Fig. 2E. The resulting frequencies from each column and row of pixels were filtered by the use of a modified ramp frequency filter[9], $f(k_x,k_y)$, which had been optimized experimentally (Eq. A5). The use of a frequency filter in the Fourier domain improved the image created by the process of back-projection by minimizing the very high-frequency components which were associated with the background interference and yet enchanced the frequency component of the back-projected image corresponding to the edges of the tablet. Each point of the filtered Fourier frequency spectrum (Fig. 2F) was transformed back to the spatial domain by means of an inverse Fourier transformation (Eq. A6), and the enhanced image of the tablet was obtained (Fig. 2G).

The modified ramp frequency filter[9], $f(k_x,k_y)$ (Eq. A5), was constructed by multiplying the relative magnitude of the ramp filter with the relative magnitude of another filter[9] at the same distance from the

[10] Rompun (Xylazine), 1.1 mg/kg, Bagvet, Division of Cutter Laboratories, Shawnee, Kan.

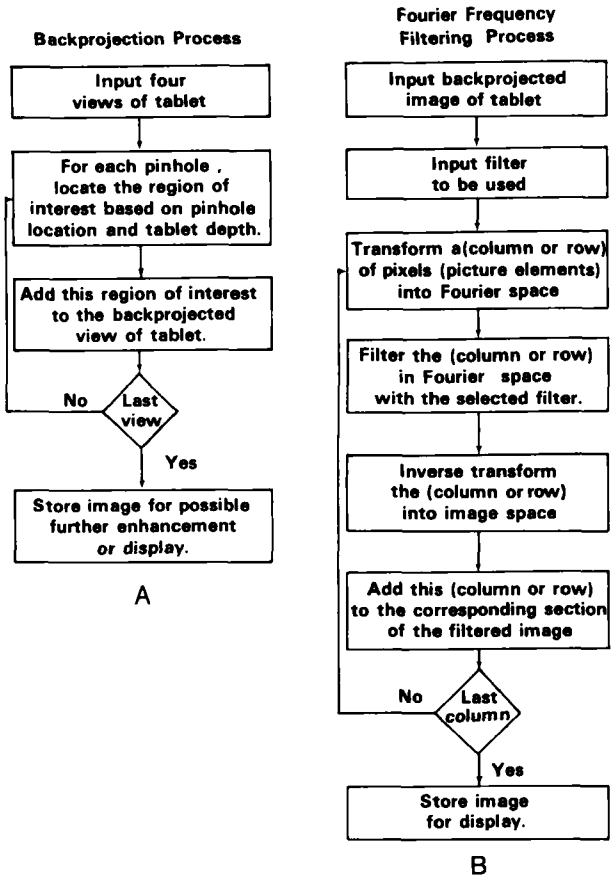

Figure 6—*Flow charts of the computer programs for back-projection (A) and for the filtering process (B).*

origin in the Fourier domain (Fig. 7). Several modified ramp frequency filters were used to enhance the images of the ^{99m}Tc-labeled tablets and tablet phantoms (Fig. 7). The image–noise ratio increased from filter 2 to 5 and then decreased gradually; on the other hand, the image–defect ratio declined rapidly from filter 2 to 5 and then leveled off (Table II). Frequency filter 3 (Fig. 7) was chosen for image enhancement and reconstruction as a reasonable compromise between image–noise and image–defect ratios.

The resolution of the method was tested *in vitro* by imaging a series of ^{99m}Tc-labeled tablet phantoms bearing artificial defects on the periphery (Fig. 5A). The labeled tablet phantoms were imaged at different distances from the collimator and the image–defect ratio was calculated (Fig. 8). When the image–defect ratio was ≥5, the defect was visible in the reconstructed image. The 0.62-mm^2 defect could not be resolved because it was smaller than the area of the pinhole (1.11 mm^2). Defect sizes as small as 1.42 mm^2 were discernible at a distance of 4.0 cm from the collimator. As the distance from the collimator increased and the magnification decreased, the resolution decreased rapidly (Fig. 8). For larger defects (5 mm^2), the resolution was independent of the magnification for distances ranging from 3.3 to 7.5 cm. The filtered back-projected images of each phantom are illustrated in Fig. 5B.

The resolution of the method was further tested *in vitro* with a series of experiments in which a rapidly disintegrating tablet labeled with

Table II—Image–Noise and Image–Defect Ratios for Various Frequency Filters

Filter	Image–Noise	Image–Defect
1	87.8	39.9
2	151.0	33.7
3	246.0	21.0
4	264.0	14.6
5	252.0	11.7
6 ramp filter	238.0	10.2
7	233.0	9.77
8	228.0	9.37
9	225.0	9.15
10	224.0	9.02

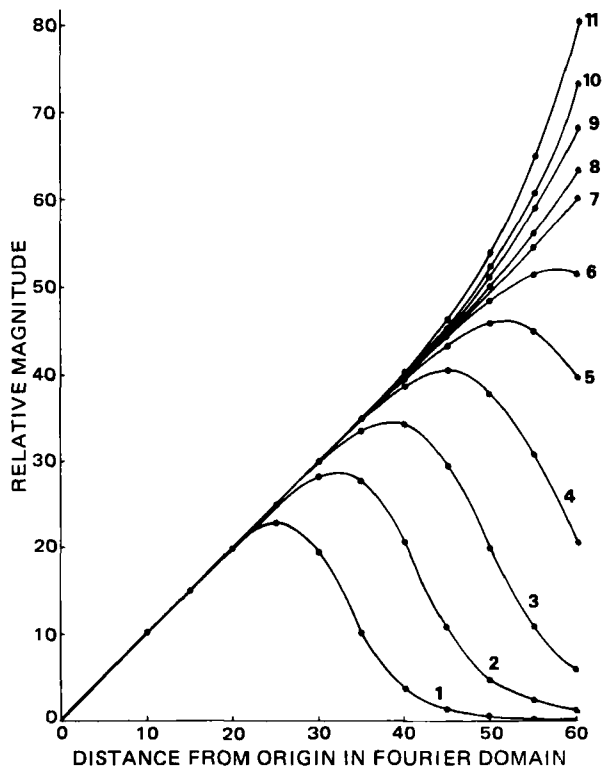

Figure 7—*Modified ramp frequency filters tested.*

technetium-99m was monitored with a gamma camera. The acquired scintigraphic images were processed and compared with photographs of the disintegrating tablet taken simultaneously with the images (Fig. 9). The disintegration started at 120 sec after the labeled tablet came in contact with the water and terminated 300 sec later (Fig. 9A). The scintigraphic images showed that the onset of the disintegration process was 180 sec after contact with the water (Fig. 9C).

The resolution of the technique was tested *in vivo* in the dog (Fig. 10). From the scintigraphs of the unprocessed image (Fig. 10A) and the corresponding back-projected and enhanced images (Fig. 10B), the onset of disintegration was evident 30 min postingestion, while at 75 min postingestion the tablet had undergone extensive disintegration.

DISCUSSION

The size of the pinhole was chosen to be 0.119 cm which was a compromise between the desired counting time (<60 sec) for a tablet labeled with 0.4 mCi of technetium-99m and the desired resolution which cannot be smaller than the diameter of the pinhole itself (10). The counting time was inversely proportional to the square of the radius of the pinhole and proportional to the square of the distance between labeled tablet and the collimator.

The spacing of the pinholes on the collimator was also critical. If the pinholes were very close together, then the four images formed on the camera crystal overlapped as the labeled tablet moved away from the camera. However, if the pinholes were spaced far apart, then the images were formed outside of the crystal as the labeled tablet moved closer to the collimator. Therefore, with an established pinhole size of 0.119 cm in diameter as optimum and with the equidistant spatial arrangement of the four pinholes on a circle 3.8 cm in diameter, the imaging of a tablet was feasible in distances ranging from 3.3 to 7.5 cm away from the collimator. The advantage of using a four-pinhole collimator was that four images were collected simultaneously. This increased the efficiency of detection by increasing the total counts collected in a certain time or by decreasing the time needed to acquire an image with a certain number of counts. In turn, short times of image acquisition minimized the effect of the slight perturbations of the tablet due to GI motility. Also, the interference of background was reduced by increasing the count rate. Finally, the pinhole magnified the image thereby improving the resolution (Fig. 3B).

The back-projection process (Figs. 2A–D) made the use of the four-pinhole collimator beneficial, while the process of Fourier enhancement (Figs. 2E–G) improved the resolution by eliminating the high-frequency

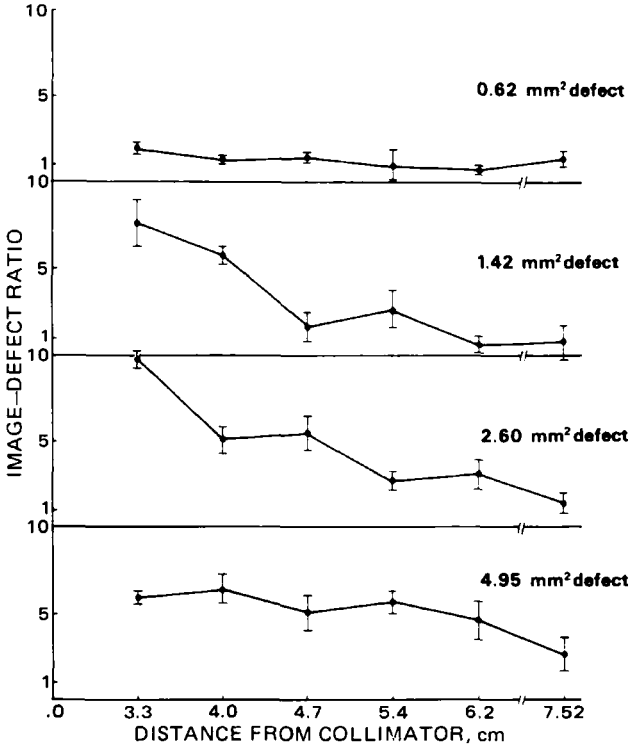

Figure 8—*The image-defect ratio as a function of distance and defect size. Image-defect ratio, larger than five yields observable defects.*

components (interference) of the back-projected image (Fig. 2). The reconstructed image (Fig. 2G) had more sharply defined edges than the back-projected image (Fig. 2D).

The resolution of the technique depended on the size of the pinhole diameter (10) and the type of frequency filter used to filter the Fourier spectrum of the back-projected image of the tablet (Figs. 2E and F). Every pixel of the back-projected image was transformed from the spatial domain to the frequency domain by Eq. A4, and then the modified ramp frequency filter was applied to eliminate the background interference and sharpen the edges of the tablet (Eq. A5). The image-noise and image-defect ratios (Table II) are a good measure for testing the resolution of the technique and selecting the optimum modified ramp frequency filter from other alternatives (Fig. 7). Defects of 5 mm^2 were readily recognizable at distances ranging from 3.3 to 7.5 cm. The *in vitro* experiments using ^{99m}Tc-labeled tablets with a 1.04-cm diameter showed that the resolution was improved by the enhancement process and the onset of disintegration became evident 60 sec after the process had started (Fig. 9). In the *in vivo* experiments, the onset of disintegration became evident ~30 min postingestion. This was because the resolution was compromised due to the interference of the abdominal and stomach tissue; therefore, the observable defect was probably >5 mm^2. The disintegration *in vivo* was slower than *in vitro*, thus, confirming observations of previous investigators (11).

The incorporation of the radioisotope, technetium-99m, into the tablet granulation in the form of spray of a saline solution of I ensured the uniform distribution of the label throughout the entire mass of the tablet. This method of labeling gave better results than a previously reported method where the labeling was achieved by exposing the tablet itself to vapors of iodine-131 (3). In that method, the surface of the tablet was uniformly coated with iodine-131; however, the penetration of the label into the core was inadequate. The mass of I that was incorporated into the tablet was negligible (~10^{-11} g of I/tablet), and, therefore, the physical or chemical integrity or characteristics of the formulation remained unaffected. The radioactivity of the labeled tablets ranged from 50,000 to 500,000 cpm/tablet. Finally, in instances where the formulation is sensitive to moisture, the technetium-99m can be added in the form of a dry powder derived by lyophilization of a solution of I in saline or [^{99m}Tc]-methylene disphosphonate in saline.

The technique of external scintigraphy has been applied before for the purpose of monitoring the disintegration *in vivo* of tablets and capsules (3, 7, 8). However, in both instances the technique did not involve enhancement of the scintigraphic images, and thus, the detection of small defects that would signify the onset of the disintegration process could

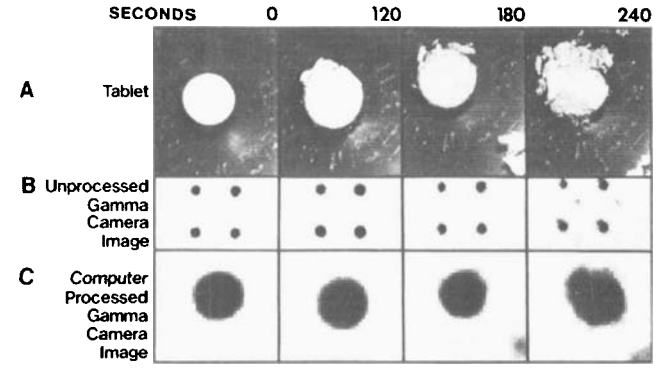

Figure 9—*Photographs (A) and* in vitro *scintigraphic images of a ^{99m}Tc-labeled tablet before (B) and after enhancement (C).*

not be evidenced due to the lower resolution of the technique. On the other hand, the present technique, which combines external scintigraphy with image enhancement, increased the resolution of the system so that small defects on the formulation can be detected, and it reduced the interference of the background activity, which may be attributed either to natural radioactivity, dissolution of the label to the dispersal of the fine labeled granules, or to a combination of these factors. This reduction of the background interference facilitates the monitoring of disintegration of small fragments of the formulation and, thus, enables the observer to determine the end of the disintegration process. Furthermore, reduction of the background interference will be useful when the determination of the transition times of the disintegrating formulation through the GI tract will be attempted, especially at the stages where considerable portions of the formulation have disintegrated.

A similar technique which also involved labeling of the formulation with gamma ray emitters such as iron-59, technetium-99m or chromium 51 and made use of two simple sodium iodide–thallium iodide crystal detectors has been applied in evaluating the disintegration and dissolution of tablets and capsules *in vivo* (4, 12). However, this technique did not allow direct observation of the formulation; thus, the onset and end of the disintegration *in vivo* could not be determined with any reasonable accuracy.

In the past, most of the techniques that were developed for determining the disintegration time of tablets *in vivo* were based on the use of roentgenography or fluoroscopy with or without the inclusion of radiopaque materials in the formulation (1, 2, 11, 13). Those techniques exposed the animal or human subject to high radiation doses of X-rays; they did not allow magnification or enhancement of the tablet's image; they could not be used for continuous monitoring of the formulation in the GI tract; and finally, rendering a nonradiopaque formulation radiopaque required inclusion of large amounts of radiopaque substances relative to the mass of the formulation, thus, effectively altering the composition of the formulation. In contrast, the proposed technique is free of the aforementioned shortcomings. The main feature of this method is the high resolution. The high resolution was achieved by using a four-pinhole collimator, which magnified the four scintigraphic images of the labeled tablet phantom or tablet, and by image enhancement of the back-projected image using Fourier transformation and filtering.

APPENDIX

Initial testing of image reconstruction and enhancement algorithms were performed with scintigraphic images of tablet phantoms. The method of image acquisition and enhancement applied in this study involved three separate steps. First, the determination of the location of the four pinhole projections of the tablet phantom on the crystal of the gamma camera; second, the back-projection of the four projected images to form a single back-projected image; and third, the enhancement of the back-projected image using filtering techniques based on Fourier transformations.

The determination of the location of the phantom's images on the crystal of the gamma camera involved simple Euclidean geometry (Fig. 3A). The displacement D of the tablet's image K from the center of the camera crystal is given by:

$$D/(Z + H) \approx X/Z \qquad \text{(Eq. A1)}$$

where Z is the distance from center of the collimator to tablet A, H is the distance from center of the collimator to the center of camera crystal (16.7

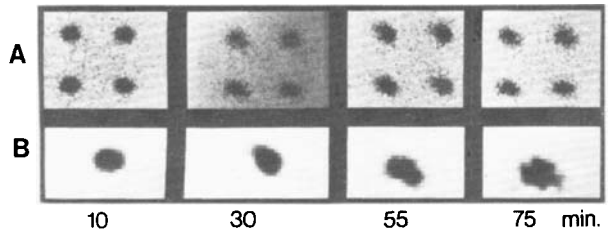

Figure 10—*Scintigraphs of a disintegrating tablet* in vivo *before (A) and after processing (B).*

cm), and X is the distance from the center of the collimator to the pinhole (1.9 cm).

The image magnification (Fig. 3B) is given by the size relationship between tablet phantom, S_o, and its image S_i, described by:

$$S_o/S_i = Z/H \qquad \text{(Eq. A2)}$$

The four images (projections), $P_i(a,b)$, of the tablet phantom were then combined to form the back-projected image, $b(x,y)$. Mathematically, the process is described by:

$$b(x,y) = \sum_{i=1}^{m} P_i(a,b) \qquad \text{(Eq. A3)}$$

where $b(x,y)$ was a point in the back-projected image, $P_i(a,b)$ was the point on the ith image corresponding to $b(x,y)$, and m was the number of images obtained. The back-projection process is described diagrammatically in Figs. 2A and B. Four images (P_1–P_4) of the labeled tablet phantom $f(x,y)$ were taken (Fig. 2A). The four images were then combined (back-projected) to form the back-projected image, $b(x,y)$ (Fig. 2B). The back-projected image actually contained the true image of the labeled tablet which was masked by background interference (noise artifacts) during the process of back-projection (Fig. 2D).

The back-projected image of the tablet phantom was improved by frequency domain filtering using Fourier transformations. It was based on the fact that both edges and noise artifacts in the image were represented by very high frequencies when the image was transformed into the frequency domain. Thus, by transforming the image from its spatial domain into its frequency domain, filtering can be performed to enhance the edges and, at the same time, try to reduce the background interference by filtering out the very high-frequency components.

The process of frequency filtering of the back-projected image involved three steps. In the first step, each row and column of pixels in the image was transformed into the Fourier domain, $F(k_x k_y)$, by performing two-dimensional Fourier transformation as given by:

$$F(k_x,k_y) = \int_{-\infty}^{\infty}\int_{-\infty}^{\infty} b(x,y)\exp(-2_\pi i(k_x x + k_y y)dxdy) \qquad \text{(Eq. A4)}$$

where $b(x,y)$ is the back-projection image pixel values, k_x and k_y are variables representing distances from the origin in the Fourier domain, and $i = \sqrt{-1}$ (14, 15).

In the second step, each Fourier coefficient $F(k_x k_y)$ was multiplied by a modified ramp frequency filter[9] $f(k_x,k_y)$, and thereby converted to the Fourier coefficients $F_I(k_x,k_y)$ of the final image:

$$F_I(k_x,k_y) = F(k_x,k_y) \times f(k_x,k_y) \qquad \text{(Eq. A5)}$$

In the third step, the Fourier coefficients of the final image, $F_I(k_x,k_y)$, were transformed back to the spatial domain by application of the inverse Fourier transformation:

$$b'(x,y) = \int_{-\infty}^{\infty}\int_{-\infty}^{\infty} F_I(k_x,k_y)\exp(2_\pi i(k_x x + k_y y)dxdy) \qquad \text{(Eq. A6)}$$

where $b'(x,y)$ was the pixel value in the final image.

The process of Fourier transformation and filtering is shown in Figs. 2B, E, and F. In Fig. 2C the four images taken from the four-pinhole collimator are shown. The four images are then back-projected to form the back-projected image (Fig. 2D). Discrete Fourier transformation is performed on the image (Fig. 2E). The origin of the frequency domain is in the middle of the image. The components around the four corners represented random noise. The frequency domain was then filtered, and the filtered spectrum is shown in Fig. 2F. The very high-frequency components, which represent noise, are filtered out, and the high frequencies are enhanced. The filtered frequency domain is then transformed back to the spatial domain and the enhanced, back-projected image is shown in Fig. 2G.

REFERENCES

(1) J. G. Wagner, "Biopharmaceutics and Relevant Pharmacokinetics," 1st ed., Drug Intelligence Publications, Hamilton, Ill., 1971, p. 72.

(2) W. H. Steinberg, G. H. Frey, J. N. Masci, and H. H. Hutchins, *J. Pharm. Sci.*, **54**, 747 (1965).

(3) M. C. Theodorakis, M. D. Devous, Sr., and D. R. Simpson, *ibid.*, **69**, 1107 (1980).

(4) M. Alpsten, G. Ekenved, and L. Solvell, *Acta Pharm. Suec.*, **13**, 107 (1976).

(5) M. C. Theodorakis, M. D. Devous, Sr., and D. R. Simpson, "Abstracts," vol. 10, No. 1, APhA Academy of Pharmaceutical Sciences, Washington, D.C., 1980, p. 79.

(6) M. C. Theodorakis, M. D. Devous, Sr., and D. R. Simpson, in "Radionuclide Imaging in Drug Research," C. G. Wilson, J. G. Hardy, M. Frier, and S. S. Davis, Eds., Croom and Helm, Ltd., London, England, 1982, pp. 153–169.

(7) D. L. Casey, R. M. Beihn, G. A. Digenis, and M. B. Shambhu, *J. Pharm. Sci.*, **65**, 1412 (1976).

(8) G. A. Digenis, in "Radionuclide Imaging in Drug Research," C. G. Wilson, J. G. Hardy, M. Frier, and S. S. Davis, Eds., Croom and Helm, Ltd., London, England, 1982, pp. 103–143.

(9) R. A. Vogel, D. Kirch, M. LeFree, and P. Steele, *J. Nucl. Med.*, **19**, 648 (1978).

(10) W. L. Rogers, "Update on Multiple Pinhole Tomography," Third Annual Conference on Advances in Emission Tomography at Andover, Mass., October 1979.

(11) G. Levy, *J. Pharm. Sci.*, **52**, 1039 (1963).

(12) M. Alpsten, C. Bogentoft, G. Ekenved, and L. Solvell, *J. Pharm. Pharmacol.*, **31**, 480 (1979).

(13) J. G. Wagner, W. Veldkamp, and S. Long, *J. Am. Pharm. Assoc., Sci. Ed.*, **47**, 681 (1958).

(14) R. L. Gonzalez and P. Wintz, "Digital Image Processing," 1st ed., Addison-Wesley, Reading, Mass., 1979, p. 36.

(15) T. F. Budinger, *J. Nucl. Med.*, **21**, 579 (1980).

ACKNOWLEDGMENTS

Supported by Grant CA 09067 awarded by the National Cancer Institute, Department of Health, Education, and Welfare (Department of Health and Human Services).

Part of this work was presented at the annual meeting of the American Pharmaceutical Association in Washington, D.C. in April 1980, and at the 2nd International Symposium on "Applications of Radionuclides in Drug Formulation Studies," Department of Pharmacy, University of Nottingham, Nottingham, England, April 1–3, 1981.

Systemic Absorption of Δ^9-Tetrahydrocannabinol after Ophthalmic Administration to the Rabbit

CHIA-WHEI N. CHIANG *x, GENE BARNETT *, and DOLORES BRINE ‡

Received December 2, 1981, from the **Division of Research, National Institute on Drug Abuse, Rockville, MD 20857* and ‡*Research Triangle Institute, Research Triangle Park, NC 27709.* Accepted for publication March 18, 1982.

Abstract □ Δ^9-Tetrahydrocannabinol was given by ophthalmic administration to the rabbit. Plasma concentrations were measured for two strengths of ophthalmic solution and compared with intravenous data to establish bioavailability. Absorption was variable, while maximum plasma levels were sustained for several hours.

Keyphrases □ Absorption—systemic, Δ^9-tetrahydrocannabinol after ophthalmic administration, rabbits □ Bioavailability—systemic absorption of Δ^9-tetrahydrocannabinol after ophthalmic administration, rabbits □ Pharmacokinetics—intravenous administration, half-lives systemic absorption of Δ^9-tetrahydrocannabinol after ophthalmic administration, rabbits □ Δ^9-Tetrahydrocannabinol—systemic absorption after ophthalmic administration, rabbits

Marijuana has been shown to reduce intraocular pressure in humans when smoked in the form of a cigarette (1). Δ^9-Tetrahydrocannabinol (I), the primary psychoactive ingredient of marijuana, has also been shown to reduce intraocular pressure in clinical studies when given either by the intravenous (2) or oral (3) route of administration. Although efficacy for topical application in clinical studies has not been established (4), dosage form development should be undertaken as this route of administration is expected to minimize the undesired psychotropic side effects.

Studies with the rabbit indicate that I in light mineral oil is an efficient dosage form to allow penetration of I into the eye (5). Related studies have also demonstrated that I applied topically to one eye lowers intraocular pressure in both eyes (6). Since the rabbit has become one of the animal models used to evaluate the therapeutic potential of I for treatment of glaucoma, studies have been carried out to determine the systemic absorption of I after topical ophthalmic application.

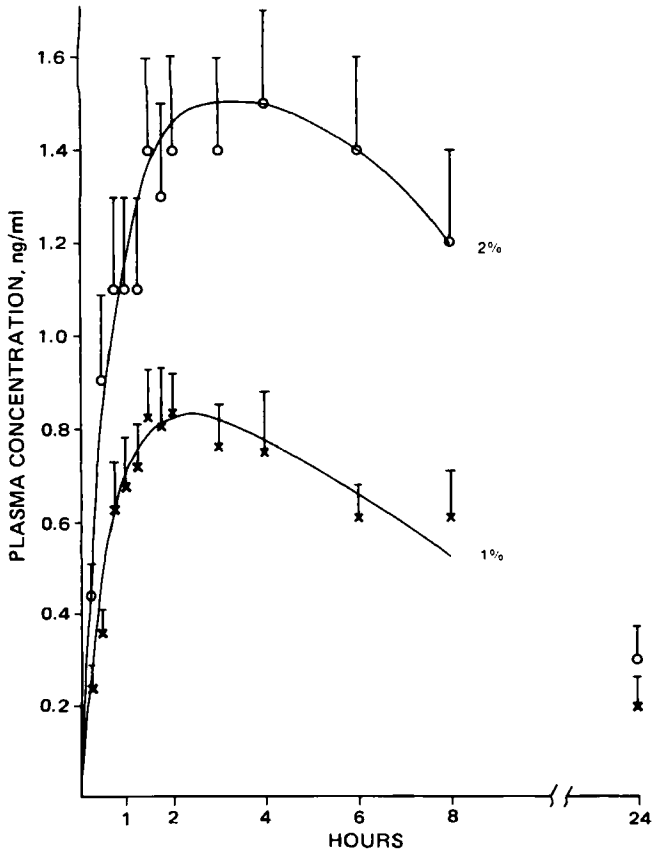

Figure 1—*Plasma concentration of I after ophthalmic administration to rabbits.*

EXPERIMENTAL

Adult albino rabbits weighing 3.4–4.8 kg were given [1′,2′-$^3H_2$]-I, which was used for intravenous and ophthalmic dosage forms. The intravenous solution, containing 170 μCi/mg of [^{3}H]-I, was prepared by dissolving [^{3}H]-I in ethanol, which was then added to a solution of 25% rabbit serum albumin. The solution was sterilized by filtering through a 0.22-μm membrane filter[1] before administration. An intravenous dose of a 0.2-ml solution contained 15 μg of I and 2 μl of ethanol.

Ophthalmic solutions were prepared in light mineral oil NF[2] viscosity of 9.5 centistokes at 21.5° (50–60 Saybolt Universal Seconds) to a strength of 1% I, 138 μCi/mg, and 2% I, 165 μCi/mg. The animals were dosed by ophthalmic topical application with 25 μl of I solution, which was applied to both eyes simultaneously to ensure measurable plasma levels of I. Each animal was dosed with 1 and 2% solutions on *separate occasions*, and four of the animals were also given a dose of 15 μg iv of I through an ear vein. A washout period of 1 month was allowed between all studies.

Blood samples were collected from an ear notch at 15, 30, 45, 60, 75, 90, 105, 120, 180, 240, 360, 480, and 1440 min after ophthalmic dosing and at 1.5, 5, 10, 20, 30, 45, 60, 90, 120, 240, 360, and 480 min after intravenous dosing. Blood samples of 2 ml were drawn, centrifuged, separated, and the plasma was immediately frozen until the assay was carried out. The ophthalmic administration, carried out with a syringe[3], yielded such small losses (≤7% of the dose) that no corrections were made.

Quantitative analysis of plasma for the concentration of I was carried out by TLC according to a previously described method (7, 8). Plasma samples were extracted twice with petroleum ether containing 1.5% isoamyl alcohol. The extracts were then concentrated and chromatographed on silica gel plates[4]. Developing solvents were acetone–*tert*-butyl alcohol–chloroform (3:5:92). Zones of I were scraped and counted. The TLC method was shown to correlate well with electron-capture GLC and with GLC–MS methods of analysis.

RESULTS

Plasma concentrations of I after ophthalmic administration of 1 and 2% solutions are reported as average values for eight animals in Fig. 1. The concentration increases to maximum values over the first 1–2 hr and then declines very slowly up to 24 hr. Variability in the data is indicated by the standard errors which are also given in the figure. Data for individual animals are presented in Table I for the maximum plasma concentration, C_{max}, which is actually a limited range of values, the time of these peak values t_{peak}, the time interval over which the C_{max} range extends, and the area under the plasma curve from t = 0 to 24 hr,

[1] Millipore Corp., Bedford, Mass.
[2] Klearol, Witco Co., New York, N.Y.
[3] Wiretrel, Bolab Inc., Derry, N.H.
[4] Brinkmann Inc., Westbury, N.Y.

0022-3549/83/0200-0136$01.00/0

Table I—Pharmacokinetic Data Following Ophthalmic Administration of I to Rabbits

Animal No.	C_{max} ng/ml		t_{peak}, min		$AUC_{0-24\ hr}$ hr ng/ml		F, %	
	1%	2%	1%	2%	1%	2%	1%	2%
1	1.0–1.3	1.8–2.3	60–240	240–480	14	30	33	36
2	0.8–1.5	1.2–1.6	60–480	90–480	24	23	—	—
3	0.7–1.2	1.0–1.5	45–180	30–240	14	17	—	—
4	0.4–0.5	0.4–0.6	60–480	30–480	7	11	13	10
5	0.7–1.3	1.4–2.3	45–480	45–480	17	33	40	38
6	0.3–0.6	1.2–1.7	45–480	30–360	6	18	6	8
7	0.3–0.9	0.4–0.7(1.4)[a]	15–480	30–480(180)[a]	13	11	—	—
8	1.6–1.2(2.2)[a]	—	30–180(105)[a]	—	8	—	—	—
9	—	1.9–2.6	—	30–480	—	37	—	—

[a] The values in parentheses are single points above the C_{max} range which occurred within the t_{peak} range.

Table II—Pharmacokinetic Parameters of I Following Intravenous Administration[a] to Rabbits[b]

Animal No.	k_{12} hr^{-1}	k_{21} hr^{-1}	k_{10} hr^{-1}	V_1^{-1}, liter^{-1}	$t_{1/2\alpha}$ min	$t_{1/2\beta}$ hr	AUC, ng/ml hr
1	6.12(48)	1.50(25)	2.76(57)	0.27(65)	4	1.7	1.25
4	0.85(15)	0.47(31)	1.46(13)	0.15(10)	17	2.6	1.65
5	0.97(20)	0.82(21)	1.61(9)	0.13(9)	14	1.5	1.30
6	3.55(18)	1.08(10)	1.65(13)	0.31(14)	7	2.3	3.27

[a] Administration of a 15-μg dose. [b] The percent coefficient of variation of each parameter is given in parentheses. The half-life values are calculated from α and β which are calculated from: $1/2[(k_{12} + k_{21} + k_{10}) \pm (k_{12} + k_{21} + k_{10})^2 - 4\,k_{21}k_{10})^{1/2}]$.

$AUC_{0-24\ hr}$. Inspection of the individual data shows that the plasma concentration increases relatively rapidly to a maximum value, which then varies very little for the next several hours as a plasma plateau exists over an extended period of time. Animal 1 in the 1% study had a C_{max} which varied in a range from 1.0 to 1.3 ng/ml during the time t_{peak} from 60 to 240 min postdose. Similarly, the 2% solution for the same animal gave a C_{max} range of 1.8–2.3 ng/ml for the plasma plateau, which existed during the 240–480-min period, and showed higher plasma levels as compared with the 1% data during the plateau. The dose-normalized AUC values for animal 1 were approximately the same for both doses. Table I shows that the plasma maxima were higher for the 2% dose but were usually not double the lower values. The time plateau, which always extended over several hours, usually showed no difference between doses for most animals. The AUC ratio for the 2:1% solutions was >1 for the four of the animals and ~1 for the other animals.

For the intravenous studies, the average plasma data for four animals is shown in Fig. 2. The curve is biphasic for each animal in agreement with work reported earlier (9). The pharmacokinetic parameters were obtained by nonlinear regression analysis to solve the standard two-compartment open model (10) in terms of:

$$dC_1/dt = -(k_{10} + k_{12})C_1 + k_{21}C_2 \quad \text{(Eq. 1)}$$

$$dC_2/dt = k_{12}C_1 - k_{21}C_2 \quad \text{(Eq. 2)}$$

with the initial condition:

$$V_1^{-1} = C_{1(t=0)}/\text{Dose} \quad \text{(Eq. 3)}$$

Table II presents the micro rate constants k_{12}, k_{21}, k_{10}, the reciprocal volume V_1^{-1}, and the respective coefficients of variation (CV) for the four parameters. For animal 1 the CV values are so large as to render the computer fit questionable, but for the remaining three animals the CVs indicate a good computer estimate of the pharmacokinetic parameters. For the three animals the value for k_{12} has a range of 1.0–3.6 hr^{-1}, while the value for k_{21} is in closer agreement (0.5–1.1 hr^{-1}). The elimination rate constant k_{10} was well estimated with a small range, 1.5–1.7 hr^{-1}. The computer estimate of V_1^{-1} ranges from 0.1 to 0.3 liters^{-1}. The calculated half-lives are 4–17 min for $t_{1/2\alpha}$ and 1.5–2.6 hr for $t_{1/2\beta}$.

The bioavailability for the two ophthalmic solutions relative to the intravenous dose calculated by AUC ratios reported for the four animals

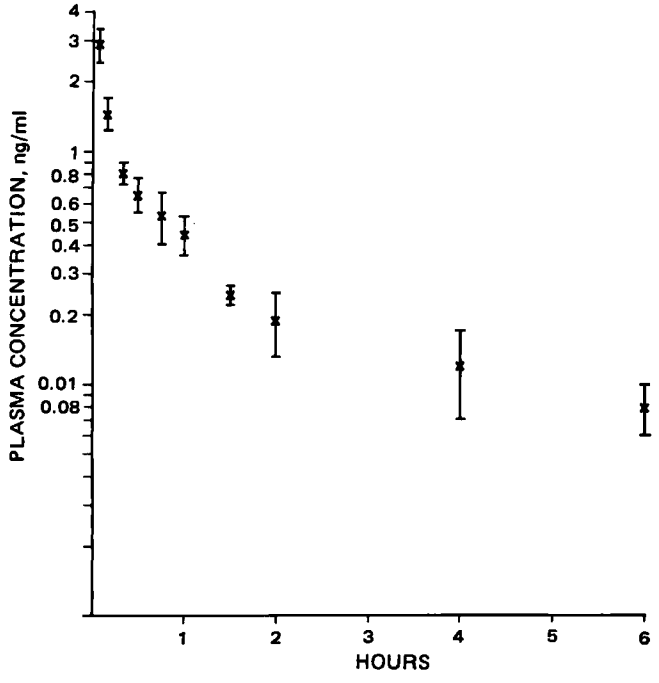

Figure 2—*Plasma concentration of I after intravenous administration of a 15-μg dose to rabbits.*

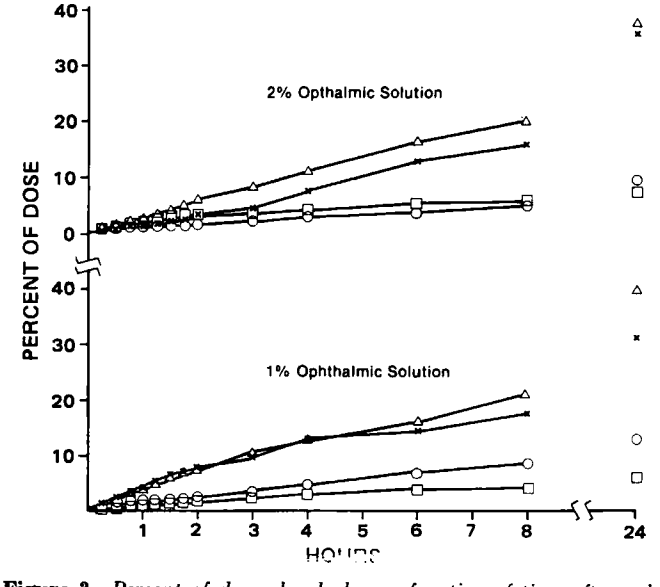

Figure 3—*Percent of dose absorbed as a function of time after ophthalmic administration to rabbits. Key: (X) rabbit 1; (○) rabbit 4; (△) rabbit 5; (□) rabbit 6.*

in Table I is approximately constant. An estimate of the fraction of dose absorbed as a function of time after opthalmic administration can be obtained from (10):

$$A_t/\text{Dose} = [C_t + k_1 AUC_{(0-t)} + (X_t)V_1^{-1}] \times V_1/\text{Dose} \quad \text{(Eq. 4)}$$

This equation was applied to the experimental data from t = 0–8 hr only, and the 24-hr points were determined separately from the dose-normalized AUC ratios. The fraction of dose absorbed as a function of time is presented in Fig. 3 for the 1 and 2% ophthalmic doses for the four animals using the parameters reported in Table II. From Fig. 3 it can be seen that absorption continues until at least 8 hr after administration for all animals at both doses. Furthermore, the fraction absorbed as a function of time does not appear to change for the two doses. The curves for animals 4 and 6 indicate a slower rate of absorption and appear to be flattening out at 8 hr, suggesting that absorption is essentially complete. The curves for animals 1 and 5 suggest that both the rate and extent of absorption is considerably greater.

The present study indicates that systemic absorption of I in the rabbit is slow and highly variable after ophthalmic administration. Prior work with rabbits demonstrates the possibility that both local and systemic mechanisms are involved in ocular pressure lowering (5, 6, 11). It would be desirable to have more detailed effect–time data together with plasma–time data in order to investigate possible I plasma–effect relationships. Clinical studies with glaucoma patients using both oral I and smoking marijuana cigarettes also show effective lowering of intraocular pressure. The pharmacodynamics is consistent with the clinical pharmacokinetics for both routes of administration, since the effect has a much slower onset and considerably longer duration for the oral study than occurs in the smoking study. The studies reported here do not differentiate local and systemic mechanisms. For ophthalmic administration, which should minimize systemic side effects, further work is needed to develop an effective dosage form (4).

REFERENCES

(1) J. C. Merritt, W. J. Crawford, P. C. Alexander, A. L. Anduze, and S. S. Belbart, *Ophthalmology*, **87**, 222 (1980).

(2) P. Cooler and J. M. Gregg, in "The Therapeutic Potential of Marijuana," S. Cohen and R. C. Stillman, Eds., Plenum, New York, N.Y., 1976. p. 77.

(3) J. C. Merritt, S. McKinnon, J. R. Armstrong, G. Hatem, and L. A. Reid, *Ann. Ophthalmol.*, **12**, 947 (1980).

(4) J. C. Merritt, D. D. Perry, D. N. Russell, and B. F. Jones, *J. Clin. Pharmacol.*, **21**, 467S (1981).

(5) K. Green, J. F. Bigger, K. King, and K. Bowman, *Exp. Eye Res.*, **24**, 197 (1977).

(6) K. Green and K. Bowman, in "The Pharmacology of Marijuana," M. C. Braude and S. Szara, Eds., Raven, New York, N.Y., 1976, p. 803.

(7) M. E. Wall, D. R. Brine, and M. Perez-Reyes, in "The Pharmacology of Marijuana," M. C. Braude and S. Szara, Eds. Raven, New York, N.Y., 1976, p. 93.

(8) M. E. Wall, D. R. Brine, J. T. Bursey, and D. Rosenthal, in "Cannabinoid Analysis in Physiological Fluids," J. A. Vinson, Ed., American Chemical Society, Washington, D.C., 1979, Chap. 3.

(9) J. D. Teale, J. M. Clough, E. M. Piall, L. J. King, and V. Marks, *Res. Commun. Chem. Pathol. Pharmacol.*, **11**, 339 (1975).

(10) M. Gibaldi and D. Perrier, "Pharmacokinetics," Marcel, New York, N.Y., 1975, Chap. 4.

(11) T. Krupin, C. Fritz, J. J. Dutton, and B. Becker, *Exp. Eye Res.*, **30**, 345 (1980).

ACKNOWLEDGMENTS

The experimental work was carried out at the Research Triangle Institute with funds from the National Institute on Drug Abuse under contracts HSM 42-71-95 to M. E. Wall and D. R. Brine, and N01-MH-1-0092 to K. H. Davis and J. Olsen.

Use of Metzler's NONLIN Program for Fitting Discontinuous Absorption Profiles

JAMES J. ZIMMERMAN

Received July 13, 1981, from the *Department of Pharmaceutics, School of Pharmacy, Temple University, Philadelphia, PA 19140.* Accepted for publication March 17, 1982. Present address: Clinical Research Department, Stuart Pharmaceuticals, Wilmington, DE 19897.

Abstract □ An alternative to the use of integral hybrid flow/compartmental model (HFCM) equations in fitting cases I and II discontinuous absorption profiles is presented. It is proposed that HFCM-integral equations be replaced by a system of differential equations in which sequential sets of equations describe the absorption profile from time zero to infinity. The required sets of differential equations for these two cases are presented as they apply to a two-compartment drug, potentially undergoing multiple absorption steps. It was shown that the use of the NONLIN program in the differential equation mode provides good fits for some unusually shaped absorption profiles of buformin, sulfisoxazole, and griseofulvin. The values of the parameter estimates and the sum of squared deviations, ΣSD, obtained with NONLIN were almost identical to those obtained with the FITSI2 program utilizing HFCM equations. While HFCM-integral equations required less computer time, they introduced the potential for negative absorption times. This problem is avoided by use of the differential equations method.

Keyphrases □ Absorption—fitting discontinuous profiles, use of NONLIN program □ NONLIN program—use for fitting discontinuous absorption profiles

Recently, discontinuous absorption processes in relation to linear pharmacokinetic models were reported (1). Integral equations for hybrid flow/compartmental models (HFCM) were derived for application to single- and multicompartment drugs exhibiting two special cases of discontinuous absorption.

In case I, absorption is assumed to begin at time t_1 and end at time t_2. The mathematical treatment of this case allows for a negative, zero, or positive value of t_1. Zero and positive values of t_1 have been used universally up to the present time in fitting data to equations for the extravascular administration of drugs exhibiting continuous absorption profiles (2). A positive t_1-value indicates the presence of an absorption lag time, while $t_1 = 0$ indicates the absence of a lag time. Negative values of t_1, however, have not been used previously and are difficult to rationalize. It was suggested that negative t_1 values obtained from computer fits using HFCM equations signify a rapid initial absorption phase (1). The absorption rate constant for this phase, however, is not estimable from these equations. Values of t_2 are always positive. When t_2 approximates the time to peak concentration, the absorption profile exhibits a discontinuity or sharp break, at which point the subsequent shape of the profile is governed only by the dispo-

0022-3549/83/0200-0138$01.00/0

in Table I is approximately constant. An estimate of the fraction of dose absorbed as a function of time after opthalmic administration can be obtained from (10):

$$A_t/\text{Dose} = [C_t + k_1 AUC_{(0-t)} + (X_t)V_1^{-1}] \times V_1/\text{Dose} \quad \text{(Eq. 4)}$$

This equation was applied to the experimental data from t = 0–8 hr only, and the 24-hr points were determined separately from the dose-normalized AUC ratios. The fraction of dose absorbed as a function of time is presented in Fig. 3 for the 1 and 2% ophthalmic doses for the four animals using the parameters reported in Table II. From Fig. 3 it can be seen that absorption continues until at least 8 hr after administration for all animals at both doses. Furthermore, the fraction absorbed as a function of time does not appear to change for the two doses. The curves for animals 4 and 6 indicate a slower rate of absorption and appear to be flattening out at 8 hr, suggesting that absorption is essentially complete. The curves for animals 1 and 5 suggest that both the rate and extent of absorption is considerably greater.

The present study indicates that systemic absorption of I in the rabbit is slow and highly variable after ophthalmic administration. Prior work with rabbits demonstrates the possibility that both local and systemic mechanisms are involved in ocular pressure lowering (5, 6, 11). It would be desirable to have more detailed effect–time data together with plasma–time data in order to investigate possible I plasma–effect relationships. Clinical studies with glaucoma patients using both oral I and smoking marijuana cigarettes also show effective lowering of intraocular pressure. The pharmacodynamics is consistent with the clinical pharmacokinetics for both routes of administration, since the effect has a much slower onset and considerably longer duration for the oral study than occurs in the smoking study. The studies reported here do not differentiate local and systemic mechanisms. For ophthalmic administration, which should minimize systemic side effects, further work is needed to develop an effective dosage form (4).

REFERENCES

(1) J. C. Merritt, W. J. Crawford, P. C. Alexander, A. L. Anduze, and S. S. Belbart, *Ophthalmology*, **87**, 222 (1980).

(2) P. Cooler and J. M. Gregg, in "The Therapeutic Potential of Marijuana," S. Cohen and R. C. Stillman, Eds., Plenum, New York, N.Y., 1976. p. 77.

(3) J. C. Merritt, S. McKinnon, J. R. Armstrong, G. Hatem, and L. A. Reid, *Ann. Ophthalmol.*, **12**, 947 (1980).

(4) J. C. Merritt, D. D. Perry, D. N. Russell, and B. F. Jones, *J. Clin. Pharmacol.*, **21**, 467S (1981).

(5) K. Green, J. F. Bigger, K. King, and K. Bowman, *Exp. Eye Res.*, **24**, 197 (1977).

(6) K. Green and K. Bowman, in "The Pharmacology of Marijuana," M. C. Braude and S. Szara, Eds., Raven, New York, N.Y., 1976, p. 803.

(7) M. E. Wall, D. R. Brine, and M. Perez-Reyes, in "The Pharmacology of Marijuana," M. C. Braude and S. Szara, Eds. Raven, New York, N.Y., 1976, p. 93.

(8) M. E. Wall, D. R. Brine, J. T. Bursey, and D. Rosenthal, in "Cannabinoid Analysis in Physiological Fluids," J. A. Vinson, Ed., American Chemical Society, Washington, D.C., 1979, Chap. 3.

(9) J. D. Teale, J. M. Clough, E. M. Piall, L. J. King, and V. Marks, *Res. Commun. Chem. Pathol. Pharmacol.*, **11**, 339 (1975).

(10) M. Gibaldi and D. Perrier, "Pharmacokinetics," Marcel, New York, N.Y., 1975, Chap. 4.

(11) T. Krupin, C. Fritz, J. J. Dutton, and B. Becker, *Exp. Eye Res.*, **30**, 345 (1980).

ACKNOWLEDGMENTS

The experimental work was carried out at the Research Triangle Institute with funds from the National Institute on Drug Abuse under contracts HSM 42-71-95 to M. E. Wall and D. R. Brine, and N01-MH-1-0092 to K. H. Davis and J. Olsen.

Use of Metzler's NONLIN Program for Fitting Discontinuous Absorption Profiles

JAMES J. ZIMMERMAN

Received July 13, 1981, from the *Department of Pharmaceutics, School of Pharmacy, Temple University, Philadelphia, PA 19140.* Accepted for publication March 17, 1982. Present address: Clinical Research Department, Stuart Pharmaceuticals, Wilmington, DE 19897.

Abstract □ An alternative to the use of integral hybrid flow/compartmental model (HFCM) equations in fitting cases I and II discontinuous absorption profiles is presented. It is proposed that HFCM-integral equations be replaced by a system of differential equations in which sequential sets of equations describe the absorption profile from time zero to infinity. The required sets of differential equations for these two cases are presented as they apply to a two-compartment drug, potentially undergoing multiple absorption steps. It was shown that the use of the NONLIN program in the differential equation mode provides good fits for some unusually shaped absorption profiles of buformin, sulfisoxazole, and griseofulvin. The values of the parameter estimates and the sum of squared deviations, ΣSD, obtained with NONLIN were almost identical to those obtained with the FITSI2 program utilizing HFCM equations. While HFCM-integral equations required less computer time, they introduced the potential for negative absorption times. This problem is avoided by use of the differential equations method.

Keyphrases □ Absorption—fitting discontinuous profiles, use of NONLIN program □ NONLIN program—use for fitting discontinuous absorption profiles

Recently, discontinuous absorption processes in relation to linear pharmacokinetic models were reported (1). Integral equations for hybrid flow/compartmental models (HFCM) were derived for application to single- and multicompartment drugs exhibiting two special cases of discontinuous absorption.

In case I, absorption is assumed to begin at time t_1 and end at time t_2. The mathematical treatment of this case allows for a negative, zero, or positive value of t_1. Zero and positive values of t_1 have been used universally up to the present time in fitting data to equations for the extravascular administration of drugs exhibiting continuous absorption profiles (2). A positive t_1-value indicates the presence of an absorption lag time, while $t_1 = 0$ indicates the absence of a lag time. Negative values of t_1, however, have not been used previously and are difficult to rationalize. It was suggested that negative t_1 values obtained from computer fits using HFCM equations signify a rapid initial absorption phase (1). The absorption rate constant for this phase, however, is not estimable from these equations. Values of t_2 are always positive. When t_2 approximates the time to peak concentration, the absorption profile exhibits a discontinuity or sharp break, at which point the subsequent shape of the profile is governed only by the dispo-

0022-3549/83/0200-0138$01.00/0

Table I—Differential Equations Required in the DFUNC Subroutine of Metzler's NONLIN Program for Scheme I in Cases I and II Discontinuous Absorption Processes

Value of t_1[a]	Time Interval	Differential Equations	
		Case I: Absorption ceases at t_2	
<0	t_0–t_1'	$dX_a/dt = -k_{a1}X_a$	(Eq. 1)
		$dC_c/dt = k_{a1}X_a/V_c + k_{21}X_p/V_c - (k_{12} + k_{10})X_c/V_c$	(Eq. 2)
		$dC_p/dt = k_{12}X_c/V_c - k_{21}X_p/V_c$	(Eq. 3)
	t_1'–t_2	$dX_a/dt = -k_{a2}X_a$	(Eq. 4)
		$dC_c/dt = k_{a2}X_a/V_c + k_{21}X_p/V_c - (k_{12} + k_{10})X_c/V_c$	(Eq. 5)
		Eq. 3	
	t_2–t_∞	$dC_c/dt = k_{21}X_p/V_c - (k_{12} + k_{10})X_c/V_c$	(Eq. 6)
		Eq. 3	
0	t_1–t_2	Eqs. 1–3	
	t_2–t_∞	Eqs. 3 and 6	
>0	t_0–t_1	$dX_a/dt = 0$	(Eq. 7)
	t_1–t_2	Eqs. 1–3	
	t_1–t_∞	Eqs. 3 and 6	
		Case II: Absorption rate changes at t_2	
<0	t_0–t_1'	Eqs. 1–3	
	t_1–t_2	Eqs. 3–5	
	t_2–t_∞	$dX_a/dt = -k_{a3}X_a$	(Eq. 8)
		$dC_c/dt = k_{a3}X_a/V_c + k_{21}X_p/V_c - (k_{12} + k_{10})X_c/V_c$	(Eq. 9)
		Eq. 3	
0	t_1–t_2	Eqs. 1–3	
	t_2–t_∞	Eqs. 3–5	
>0	t_0–t_1	Eq. 7	
	t_1–t_2	Eqs. 1–3	
	t_2–t_∞	Eqs. 3–5	
		Combination of Cases I and II: Absorption rate changes at t_2 and ceases at t_3	
<0	t_0–t_1'	Eqs. 1–3	
	t_1–t_2	Eqs. 3–5	
	t_2–t_3	Eqs. 3, 8 and 9	
	t_3–t_∞	Eqs. 3 and 6	
0	t_1–t_2	Eqs. 1–3	
	t_2–t_3	Eqs. 3–5	
	t_3–t_∞	Eqs. 3 and 6	
>0	t_0–t_1	Eq. 7	
	t_1–t_2	Eqs. 1–3	
	t_2–t_3	Eqs. 3–5	
	t_3–t_∞	Eqs. 3 and 6	

[a] The parameter t_1 corresponds to the t_1-value permitted in the integral equations described previously (1).

sition of the drug. When t_2 is very large compared with absorption half-life, then the general equations reduce to those for the more typical case for continuous absorption (2).

In case II, t_1 may also assume a negative, zero, or positive value, but absorption does not end at t_2; it merely proceeds at a new rate. Consequently, two absorption rate constants are generated from the computer fit for the two sequential absorption phases. The absorption profile again shows a discontinuity at t_2, at which point there is a change in slope in the ascending region of the profile.

From a mechanistic point of view, case I discontinuities may represent situations where the absorption efficiency of the intestine reduces to zero at some location in the GI tract or where the release of drug from the dosage form abruptly ceases. Case II discontinuities may result from the existence of intestinal segments with different absorption efficiencies, or alternatively, from a change in the release characteristics of the formulation or from a pH-induced change in the concentration of absorbable drug species at the membrane site (1).

The usefulness of the HFCM equations was demonstrated (1) by obtaining nearly perfect fits for some unusual absorption profiles of griseofulvin (3), buformin (4), and sulfisoxazole (5). For each of these drugs, less exact fits were obtained when equations for continuous absorption were used in the fitting process.

The present report describes an alternative approach for the computer fitting of discontinuous absorption profiles. An alternative approach is needed that does not produce potentially negative absorption times as a result of the mathematical analysis. It is proposed that HFCM integral equations be replaced by a system of differential equations in which sequential sets of equations describe the absorption profile from time zero to infinity. It was shown that Metzler's NONLIN program (6), utilized in the differential equation mode, may be used to implement the proposed approach[1].

THEORETICAL

The use of Metzler's NONLIN program for implementing the proposed method for fitting discontinuous absorption profiles requires that a DFUNC subroutine be written employing differential equations[2]. Prior to writing the subroutine, however, it is necessary to choose an appropriate kinetic model, write differential equations for each species in the model, and correctly order the equations within the subroutine. The choice of kinetic model requires decisions with respect to both the compartmental and absorption characteristics of the drug. The compartmental characteristics may usually be obtained from previous studies or from a graphical treatment of the experimental data. Discontinuous absorption characteristics may be inferred from a graphical representation of the experimental data or from poor computer fits obtained using continuous absorption models. A correct ordering of the equations within

[1] The NONLIN program is available for use on (*a*) IBM (C. M. Metzler, The Upjohn Co., Kalamazoo, MI 40991) and (*b*) CDC (M. Rowland, Department of Pharmacy, University of Manchester, Manchester, M139PL, England) computers with the CDC version having the added advantage of providing residual plots and statistics for the residuals.

[2] While differential equations require more computer time than integral equations, the writing of DFUNC subroutines for discontinuous absorption processes is greatly simplified, particularly for complex models, when differential equations are used.

Table II—Parameter Values For The Fitting of Buformin Data [a]

Parameters	Values: HFCM Ref. 1 [b]	Values: HFCM FITSI2 [c]	Values: NONLIN [c]
k_{a1}, hr^{-1}	—	—	0.2509
k_{a2}, hr^{-1}	0.1836	0.1611	0.1580
k_{21}, hr^{-1}	0.05106	0.08804	0.07970
α, hr^{-1}	0.2362	0.2834	0.2719
β, hr^{-1}	0.0202	0.03441	0.03132
t_1, hr	−0.3016	−0.3119	—
t_1', hr [d]	—	—	0.50
t_2, hr	3.722	3.734	3.716
V_c/F, liters [e]	3203.4	79.582	79.343
D_0, μg [f]	100,000.0	100,000.0	100,000.0
ΣD^2	—	160.6	163.7
CP, sec [g]	—	2.58	4.93

[a] Data from Ref. 4. [b] Run on a PDP 11/10 computer. [c] Run on a CDC Cyber 174/2550 computer. [d] The parameter t_1' was a constant in NONLIN, and 0.50 hr is the time of the first blood sample after drug administration; $t_0 = 0$. [e] The parameter F is the systemic availability. [f] The parameter D_0 is the dose. [g] Fortran execution time without line printer plots and statistics for residuals.

the subroutine requires that the user follow instructions given in the NONLIN manual regarding the use of differential equations and that selected Fortran IF statements be employed to provide a logical kinetic flow while stressing the discontinuities. The development of a functional DFUNC subroutine is illustrated using Scheme I for a drug exhibiting known two-compartment characteristics and potential multiple absorption steps. The approach could be applied equally well to a drug characterized by either a fewer or a greater number of compartments.

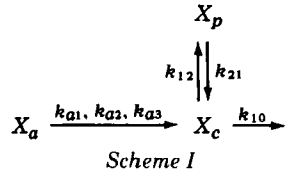

Scheme I

where X_a is the amount of drug at the absorption site; X_c is the amount of drug in the central compartment; X_p is the amount of drug in the peripheral compartment; k_{a1}, k_{a2}, and k_{a3} are the first-order absorption constants for the first, second, and third absorption steps, respectively; k_{12} and k_{21} are the first-order rate constants for the transfer of drug between compartments; and k_{10} is the first-order elimination constant.

Table I presents a summary of the systems of differential equations (Eqs. 1–9) associated with Scheme I for case I, case II, and combined cases I and II discontinuous absorption processes. For each of the cases, the differential equations are subgrouped further according to values of $t_1 < 0$, $= 0$, and > 0 and according to the time interval involved. The time-interval grouping introduces discontinuity into the model. Each time interval for a given initial value of t_1 corresponds to a different set of differential equations. For example, in case I ($t_1 < 0$), Eqs. 1–3 define absorption, distribution, and elimination (ADE) during the initial rapid absorption phase for the time interval, t_0–t_1', and Eqs. 3–5 describe the same events for the slower absorption phase from t_1' to t_2. Equations 3 and 6 describe the disposition of the drug after cessation of all absorption during the time interval, t_2–t_∞. The intervals, t_0–t_1' and t_1'–t_2, replace the single interval, t_1–t_2, reported previously (1). Since $t_0 = 0$, all absorption times are positive, and an absorption rate constant for the initial rapid absorption phase replaces a negative time constant. When data are scarce for the early absorption period, t_1' usually will be a constant taking on the time for the first blood sample after drug administration. For case I ($t_1 = 0$), the required set of differential equations includes Eqs. 1–3 for a single ADE cycle from t_1 to t_2 and Eqs. 3 and 6 for disposition for t_2 to t_∞. The required set of equations for case I ($t_1 > 0$) include those for case I ($t_1 = 0$) and Eq. 7, which accounts for the lag time from t_0 to t_1. For case II ($t_1 < 0$), Eqs. 1–3 and 3–5 represent the ADE processes for the first two absorption phases during the time intervals, t_0–t_1' and t_1'–t_2, respectively. These two intervals again replace the single interval, t_1–t_2. Equations 3, 8, and 9 represent the ADE processes for the third absorption phase from t_3 to t_∞. For case II ($t_1 = 0$) and case II ($t_1 > 0$), the required sets of differential equations involve an appropriate combination selected from Eqs. 1–5 and 7. Similarly, for the combination of cases I and II ($t_1 < 0$, $t_1 = 0$, $t_1 > 0$), the required sets of differential equations are chosen from Eqs. 1–9.

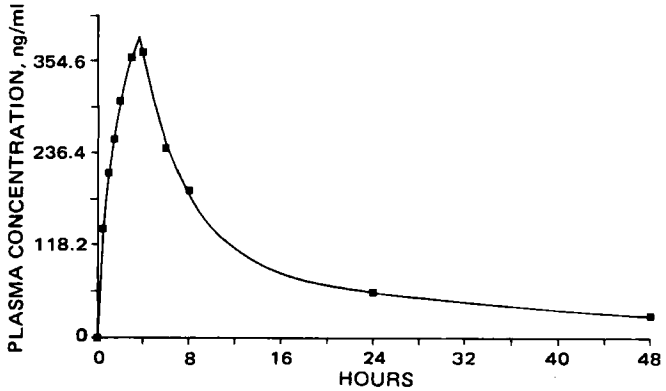

Figure 1—*Plasma concentration–time plot for the discontinuous fit of buformin data obtained with NONLIN. Key: theoretical (—); data points (■).*

Table III—Parameter Values For The Fitting of Sulfisoxazole Data [a]

Parameters	Values: HFCM Ref. 1 [b]	Values: HFCM FITSI2 [c]	Values: NONLIN [c]
k_{a1}, hr^{-1}	—	—	0.4082
k_{a2}, hr^{-1}	0.1080	0.1054	0.1063
k_{a3}, hr^{-1}	1.6788	1.5285	1.5363
k_{21}, hr^{-1}	0.1941	0.1833	0.1855
α, hr^{-1}	0.2938	0.2874	0.2879
β, hr^{-1}	0.08086	0.07853	0.07875
t_1, hr	−1.6656	−1.7104	—
t_1', hr [d]	—	—	0.50
t_2, hr	2.0807	2.000	2.000
V_c/F, liters [e]	10.749	10.604	10.907
D_0, mg [f]	2000.0	2000.0	2000.0
ΣD^2	—	0.83572	0.85284
CP, sec [g]	—	4.02	8.95

[a] Data from Ref. 5. [b] Run on a PDP 11/10 computer. [c] Run on a CDC Cyber 174/2550 computer. [d] The parameter t_1' was a constant in NONLIN, and 0.50 hr is the time of the first blood sample after drug administration; $t_0 = 0$. [e] The parameter F is the systemic availability. [f] The parameter D_0 is the dose. [g] Fortran execution time without line printer plots and statistics for residuals.

Equations 1–6 are written in a form consistent with the actual input quantities. Thus, Eqs. 2, 3, 5, and 6 are written in terms of concentrations. The latter conversions are made by dividing the rate expressions for X_c and X_p in Scheme I by V_c, the apparent volume of distribution for the central compartment. The concentration of drug in the peripheral compartment is also referred to the central compartment, since V_p, the apparent volume of distribution for the peripheral compartment, can only be estimated when experimental data for that compartment are available.

The ordering of differential equations within the DFUNC subroutine is accomplished by using the required NONLIN format (7) and selected IF statements for discontinuity[3].

EXPERIMENTAL

The version (*b*) of Metzler's NONLIN program[1] and a version of the FITSI2 program[4] for fitting discontinuous absorption data were obtained and made operational on a computer[5] by the university computer staff.

The data sets used in the computer fits were those used previously (1): griseofulvin (3), rat 11; buformin (4), patient 1; and sulfisoxazole (5) subject 3. Plots of the NONLIN computer fits were obtained with a plotter[6] and are reproduced as tracings in Figs. 1–3.

The initial estimates of the parameters used with both FITSI2 and

[3] The DFUNC subroutines used in fitting the data in Figs. 1–3 are available from the author upon request.

[4] R. Süverkrüp, Pharmazeutische Technologie, Pharmazeutisches Institut der Universität Bonn, Bonn, West Germany.

[5] CDC Cyber 174/2550.

[6] Calcomp.

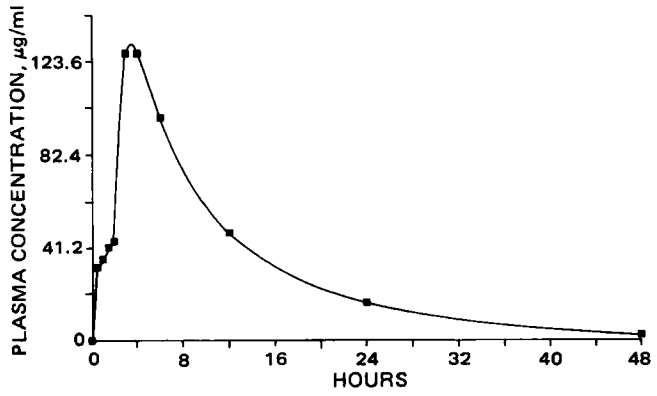

Figure 2—*Plasma concentration–time plot for the discontinuous fit of sulfisoxazole data obtained with NONLIN. Key: theoretical (—); data points (■).*

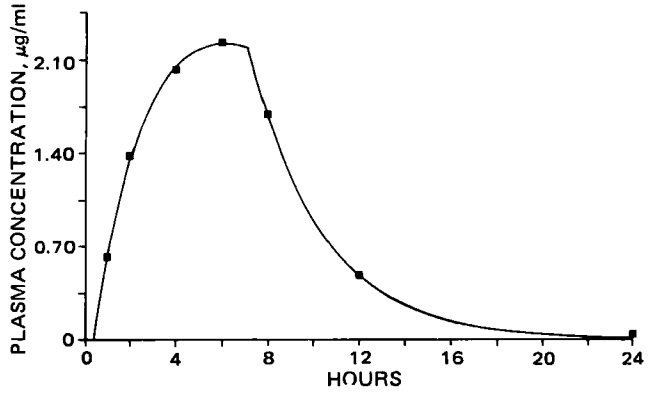

Figure 3—*Plasma concentration–time plot for the discontinuous fit of griseofulvin data obtained with NONLIN. Key: theoretical (—); data points (■).*

NONLIN were published values (1). The final estimates of the parameters were obtained by repeatedly entering the computed parameter values as initial estimates until the values stabilized.

In computer fits with NONLIN, the program default values for the parameters, DELINT, SSSTOP, and DELDER, were utilized. The DIG(I) parameter was set at 0.01, 0.001, and 0.001 to obtain the best fits for buformin, sulfisoxazole, and griseofulvin, respectively. All the data points shown in Figs. 1–3 were weighted equally.

RESULTS AND DISCUSSION

The results of the computer analyses of the three data sets are summarized in Tables II–IV and Figs. 1–3. In Tables II and III, parameter estimates obtained from NONLIN and FITSI2 are compared with those described previously (1). In both of these tables, values of α and β listed under NONLIN were calculated from quadratic relationships (8) using the NONLIN estimates of k_{12}, k_{21}, and k_{10}. In Table IV parameter estimates obtained from NONLIN are compared with those described previously (1). Less than perfect agreement between the two methods is expected since different algorithms are used in the two computer solutions and because Scheme I is not exactly the same model used previously (1).

Buformin (Case I: $t_1 < 0$)—The plasma data for buformin (4) in Fig. 1 was obtained in a diabetic patient after the oral administration of 100 mg of [^{14}C]buformin hydrochloride in a wax matrix. Based on first-order *in vitro* release characteristics of the dosage unit and two-compartment disposition characteristics *in vivo* (9), the data were fitted with NONLIN using a DFUNC subroutine for Scheme I, case I: $t_1 < 0$. The NONLIN estimates of k_{12} and k_{10} needed for calculating α and β were 0.116659 and 0.106853 hr^{-1}, respectively.

The model used in fitting the buformin data predicts two distinct absorption phases with absorption abruptly ending during the second and longer absorption time period. Accordingly, use of HFCM equations yields a negative value of t_1 and a positive value of t_2 as shown in columns 2 and 3 of Table II. An absorption rate constant, k_{a2}, is given for the second absorption phase but not for the short initial absorption phase. Use of the proposed differential equations method, however, provides absorption rate constants for both absorption phases and values for t_1' and t_2 as observed in column 4 of Table II. The estimated values of k_{12}, k_{21}, α, β, t_2, and V_c/F obtained with NONLIN (column 4) show closer agreement with values obtained with FITSI2 (column 3) run on a computer b^1 than with the published values (1) (column 2). However, the agreement in these parameters is not perfect for the described reasons. The extreme value of V_c/F in column 2 is apparently in error, since both NONLIN and FITSI2 gave much lower and almost identical estimates for this parameter.

Table IV—Parameter Values For The Fitting of Griseofulvin Data [a]

Parameters	Values HFCM[b] (Ref. 1)	Values NONLIN[c]
k_{a1}, hr^{-1}	0.09066	0.08944
k, hr^{-1} [d]	0.3090	0.3096
V_c/F, liters[e]	3.9393	3.9224
t_1, hr	0.3612	0.3308
t_2, hr	7.168	7.192
D_0, mg[f]	50.0	50.0
ΣD^2	—	0.001979
CP, sec[g]	—	2.43

[a] Data from Ref. 3. [b] Run on a PDP 11/10 computer. [c] Run on a CDC Cyber 174/2550 computer. [d] The parameter k is the elimination constant. [e] The parameter F is the systemic availability. [f] The parameter D_0 is the dose. [g] Fortran execution time without line printer plots and statistics for residuals.

Based upon the sum of squared deviations, ΣD^2, NONLIN and FITSI2 yielded almost identical fits to the data. It was observed, however, that NONLIN required more computer time for obtaining the parameter estimates than did FITSI2. The increased execution time with NONLIN is expected, since curve-fitting procedures using differential equations are inherently more time consuming than those using integral equations. The good fit provided by NONLIN is illustrated in Fig. 1.

Sulfisoxazole (Case II: $t_1 < 0$)—The plasma data for sulfisoxazole (5) in Fig. 2 was obtained from a healthy male subject after the oral administration of a 2.0-g tablet of sulfisoxazole. Because of the reported two-compartment behavior after intravenous administration (5), the data were fit with NONLIN using a DFUNC subroutine for Scheme I, case II: $t_1 < 0$. The NONLIN estimates of k_{12} and k_{10} required in calculating α and β were 0.0589257 and 0.122213 hr^{-1}, respectively.

The model used in fitting the sulfisoxazole data predicts three distinct absorption phases with absorption continuing sequentially throughout the three phases. The discontinuities in this case are incurred only by abrupt changes in the absorption rate, not by termination of absorption during the usual absorption period. Consequently, the use of HFCM equations yields a negative value for t_1 and a positive value for t_2, as listed in columns 2 and 3 of Table III. Columns 2 and 3 list estimates only of k_{a2} and k_{a3} for the second and third absorption phases. By contrast, the differential equations method (column 4) provides estimates of the absorption rate constants for all three absorption phases, together with values for t_1' and t_2.

The parameters in Table III estimated with NONLIN (column 4) show closer agreement with those obtained with FITSI2 (column 3) than those described previously (1) (column 2). For this data set, NONLIN yielded almost identical parameter estimates, but again, required more execution time for the discussed reasons. Based on the ΣD^2, almost identical fits were obtained with NONLIN and FITSI2. The exactness of the fit obtained with NONLIN is illustrated in Fig. 2.

The potential mechanisms for the irregular absorption profile for sulfisoxazole were discussed (5) (Fig. 2). Apparently, a small fraction of the 2.0-g dose dissolves rapidly to saturate the existing gastric fluid. A large fraction of the dose, however, remains as undissolved solid during its time in the stomach because of the small volume of fluid available for dissolution and the low membrane surface area available for absorption. Therefore, a rapid but limited absorption of this weak organic acid is possible from the stomach. Unabsorbed sulfisoxazole emptied into the small intestine undergoes a more rapid and complete absorption because of a more favorable pH for dissolution and an increased membrane surface area for absorption. Absorption phases 1 and 2 reflect gastric absorption, while absorption phase 3 reflects intestinal absorption.

Griseofulvin (Case I: $t_1 > 0$)—The plasma data for griseofulvin (3) in Fig. 3 was obtained in a rat after the oral intubation of 50 mg/kg of griseofulvin in a corn oil suspension. This data was fit with NONLIN using a modified DFUNC subroutine for Scheme I, case I: $t_1 > 0$, in which k_{12} and k_{21} equal zero.

The model used in fitting the data predicts a lag time before absorption begins and a single absorption phase that abruptly ends before absorption ceases. Accordingly, the use of HFCM equations yields positive values for both t_1 and t_2 and a value for the single absorption rate constant, k_{a1}, as observed in column 2 of Table IV. The proposed method in this case provides estimates of the same parameters, and there is good agreement between the estimates given in columns 2 and 3. The close-fitting plot obtained using NONLIN is given in Fig. 3.

REFERENCES

(1) R. Süverkrüp, *J. Pharm. Sci.*, **68**, 1395 (1979).

(2) M. Gibaldi and D. Perrier, "Pharmacokinetics," Dekker, New York, N.Y., 1975, Chaps. 1 and 2.

(3) P. J. Carrigan and T. R. Bates, *J. Pharm. Sci.*, **62**, 1477 (1973).

(4) V. H. Gutsche, L. Blumenbach, W. Losert, and H. Wiemann, *Arzneim.-Forsch.*, **26**, 1227 (1976).

(5) S. A. Kaplan, R. E. Weinfield, C. W. Abruzzo, and M. Lewis, *J. Pharm. Sci.*, **61**, 773 (1972).

(6) C. M. Metzler, G. L. Elfring, and A. J. McEwen, *Biometrics*, **30**, 562 (1974).

(7) C. M. Metzler, G. L. Elfring, and A. J. McEwen, "A Users Manual For NONLIN and Associated Programs," The Upjohn Co., Kalamazoo, Mich., 1976.

(8) M. Gibaldi and D. Perrier, "Pharmacokinetics," Dekker, New York, N.Y., 1975, Chap. 2.

(9) P. Botterman, A. Sovatzoglou, and U. Schweigart, in "Proceedings of the Second International Bigaunid Symposium," K. Oberdisse, H. Daweke, and G. Michael, Eds., Thieme, Stuttgart, West Germany, 1968.

ACKNOWLEGMENTS

The author acknowledges the assistance of the following members of the Temple University computer staff: Roslyn Gorin for procuring NONLIN; Liliane Clever for implementing NONLIN; Drusilla Gifford for implementing the Calcomp plots; and Bridget Peezick for implementing FITSI2.

The suggestion of Dr. C. M. Metzler for increasing the efficiency of the DFUNC subroutines used in this study is appreciated.

Kinetics and Thermodynamics of Interfacial Transfer

ROBERT FLEMING *, RICHARD H. GUY * § ×, and JONATHAN HADGRAFT ‡

Received January 13, 1981, from the **Department of Pharmaceutical Chemistry, The School of Pharmacy, University of London, London, WC1N 1AX, UK.* and the ‡*Department of Pharmacy, University of Nottingham, University Park, Nottingham, NG7 2RD, UK.* Accepted for publication March 25, 1982. §Present address: School of Pharmacy, University of California, San Francisco, CA 94143.

Abstract □ The kinetic barrier against the transport of methyl and ethyl nicotinates across the water–isopropyl myristate interface has been studied as a function of temperature using a rotating diffusion cell. The temperature dependence of the interfacial transfer kinetics has enabled calculation of the thermodynamic parameters for the process. It is evident from the results that, for the transferring solutes considered, the activation energy barrier is enthalpic, because there is a large positive entropy for transfer into the interfacial region.

Keyphrases □ Interfacial transfer—kinetics and thermodynamics, water–isopropyl myristate interface, methyl and ethyl nicotinates □ Kinetics—interfacial transfer thermodynamics, water–isopropyl myristate interface, methyl and ethyl nicotinates □ Thermodynamics—interfacial transfer kinetics, water–isopropyl myristate interface, methyl and ethyl nicotinates

An important physical process, common to all systems in which a solute transports from a high concentration aqueous phase across an organic membrane barrier into a low concentration aqueous phase, is the interfacial transfer of the substrate at the aqueous–organic and organic–aqueous interfaces. Few investigations into the kinetics and thermodynamics of interfacial transfer have been made, and the contribution of the phenomenon to overall membrane permeation has generally been assumed insignificant. However, recent studies have shown that transfer across the interfacial barrier can require a significant free energy input (1–3), and it is possible to identify circumstances for which the rate of interfacial transfer becomes the rate-determining step in membrane transport. For example, in the simplest case, consider the transport of drug molecules from an aqueous reservoir across an organic membrane into a perfect sink. Assuming that there is no stagnant diffusion layer in the aqueous reservoir phase, then the drug molecules must overcome two barriers so as to reach the sink on the far side of the membrane. These barriers are present due to interfacial transfer at the aqueous phase–membrane interface and due to diffusion through the organic membrane. The interfacial transfer is characterized by a heterogeneous rate constant k_{-1} (m/sec), which is related to the aqueous–organic partition coefficient of the drug (K) by the rate constant k_1 for interfacial transfer in the opposite direction (organic → aqueous), $K = k_1/k_{-1}$. Diffusion through the membrane is dependent upon the thickness of the membrane (l) and the diffusion coefficient of the drug in the membrane (D_{org}). Both processes also depend upon the cross-sectional area of the membrane. The relative contributions of the two components of the barrier may be compared by their reciprocal permeabilities [or resistivities (4)] and for interfacial transfer kinetics to have a significant effect on the overall rate of transport therefore requires:

$$1/Kk_{-1} \geq l/D_{org} \qquad \text{(Eq. 1)}$$

For certain small organic drug molecules, Kk_{-1} has been shown (1–3) to be $\sim 10^{-6}$ m/sec, and, taking a typical D_{org} of 10^{-10} m^2/sec, the inequality (Eq. 1) is satisfied by $l \leq 100$ μm. This degree of thickness is relevant not only to many biological membranes but also to emulsion systems and sustained-release formulations. Therefore, in neglecting slow interfacial transfer, it is possible that a major contribution to the transport rate-determining process in these systems is being ignored.

In this study, the kinetic barrier against interfacial transfer was investigated as a function of temperature. The

0022-3549/83/0200-0142$01.00/0

The model used in fitting the data predicts a lag time before absorption begins and a single absorption phase that abruptly ends before absorption ceases. Accordingly, the use of HFCM equations yields positive values for both t_1 and t_2 and a value for the single absorption rate constant, k_{a1}, as observed in column 2 of Table IV. The proposed method in this case provides estimates of the same parameters, and there is good agreement between the estimates given in columns 2 and 3. The close-fitting plot obtained using NONLIN is given in Fig. 3.

REFERENCES

(1) R. Süverkrüp, *J. Pharm. Sci.*, **68**, 1395 (1979).

(2) M. Gibaldi and D. Perrier, "Pharmacokinetics," Dekker, New York, N.Y., 1975, Chaps. 1 and 2.

(3) P. J. Carrigan and T. R. Bates, *J. Pharm. Sci.*, **62**, 1477 (1973).

(4) V. H. Gutsche, L. Blumenbach, W. Losert, and H. Wiemann, *Arzneim.-Forsch.*, **26**, 1227 (1976).

(5) S. A. Kaplan, R. E. Weinfield, C. W. Abruzzo, and M. Lewis, *J. Pharm. Sci.*, **61**, 773 (1972).

(6) C. M. Metzler, G. L. Elfring, and A. J. McEwen, *Biometrics*, **30**, 562 (1974).

(7) C. M. Metzler, G. L. Elfring, and A. J. McEwen, "A Users Manual For NONLIN and Associated Programs," The Upjohn Co., Kalamazoo, Mich., 1976.

(8) M. Gibaldi and D. Perrier, "Pharmacokinetics," Dekker, New York, N.Y., 1975, Chap. 2.

(9) P. Botterman, A. Sovatzoglou, and U. Schweigart, in "Proceedings of the Second International Bigaunid Symposium," K. Oberdisse, H. Daweke, and G. Michael, Eds., Thieme, Stuttgart, West Germany, 1968.

ACKNOWLEGMENTS

The author acknowledges the assistance of the following members of the Temple University computer staff: Roslyn Gorin for procuring NONLIN; Liliane Clever for implementing NONLIN; Drusilla Gifford for implementing the Calcomp plots; and Bridget Peezick for implementing FITSI2.

The suggestion of Dr. C. M. Metzler for increasing the efficiency of the DFUNC subroutines used in this study is appreciated.

Kinetics and Thermodynamics of Interfacial Transfer

ROBERT FLEMING *, RICHARD H. GUY * § ×, and JONATHAN HADGRAFT ‡

Received January 13, 1981, from the **Department of Pharmaceutical Chemistry, The School of Pharmacy, University of London, London, WC1N 1AX, UK.* and the ‡*Department of Pharmacy, University of Nottingham, University Park, Nottingham, NG7 2RD, UK.* Accepted for publication March 25, 1982. §Present address: School of Pharmacy, University of California, San Francisco, CA 94143.

Abstract □ The kinetic barrier against the transport of methyl and ethyl nicotinates across the water–isopropyl myristate interface has been studied as a function of temperature using a rotating diffusion cell. The temperature dependence of the interfacial transfer kinetics has enabled calculation of the thermodynamic parameters for the process. It is evident from the results that, for the transferring solutes considered, the activation energy barrier is enthalpic, because there is a large positive entropy for transfer into the interfacial region.

Keyphrases □ Interfacial transfer—kinetics and thermodynamics, water–isopropyl myristate interface, methyl and ethyl nicotinates □ Kinetics—interfacial transfer thermodynamics, water–isopropyl myristate interface, methyl and ethyl nicotinates □ Thermodynamics—interfacial transfer kinetics, water–isopropyl myristate interface, methyl and ethyl nicotinates

An important physical process, common to all systems in which a solute transports from a high concentration aqueous phase across an organic membrane barrier into a low concentration aqueous phase, is the interfacial transfer of the substrate at the aqueous–organic and organic–aqueous interfaces. Few investigations into the kinetics and thermodynamics of interfacial transfer have been made, and the contribution of the phenomenon to overall membrane permeation has generally been assumed insignificant. However, recent studies have shown that transfer across the interfacial barrier can require a significant free energy input (1–3), and it is possible to identify circumstances for which the rate of interfacial transfer becomes the rate-determining step in membrane transport. For example, in the simplest case, consider the transport of drug molecules from an aqueous reservoir across an organic membrane into a perfect sink. Assuming that there is no stagnant diffusion layer in the aqueous reservoir phase, then the drug molecules must overcome two barriers so as to reach the sink on the far side of the membrane. These barriers are present due to interfacial transfer at the aqueous phase–membrane interface and due to diffusion through the organic membrane. The interfacial transfer is characterized by a heterogeneous rate constant k_{-1} (m/sec), which is related to the aqueous–organic partition coefficient of the drug (K) by the rate constant k_1 for interfacial transfer in the opposite direction (organic → aqueous), $K = k_1/k_{-1}$. Diffusion through the membrane is dependent upon the thickness of the membrane (l) and the diffusion coefficient of the drug in the membrane (D_{org}). Both processes also depend upon the cross-sectional area of the membrane. The relative contributions of the two components of the barrier may be compared by their reciprocal permeabilities [or resistivities (4)] and for interfacial transfer kinetics to have a significant effect on the overall rate of transport therefore requires:

$$1/Kk_{-1} \geq l/D_{org} \qquad \text{(Eq. 1)}$$

For certain small organic drug molecules, Kk_{-1} has been shown (1–3) to be $\sim 10^{-6}$ m/sec, and, taking a typical D_{org} of 10^{-10} m^2/sec, the inequality (Eq. 1) is satisfied by $l \leq 100$ μm. This degree of thickness is relevant not only to many biological membranes but also to emulsion systems and sustained-release formulations. Therefore, in neglecting slow interfacial transfer, it is possible that a major contribution to the transport rate-determining process in these systems is being ignored.

In this study, the kinetic barrier against interfacial transfer was investigated as a function of temperature. The

0022-3549/83/0200-0142$01.00/0

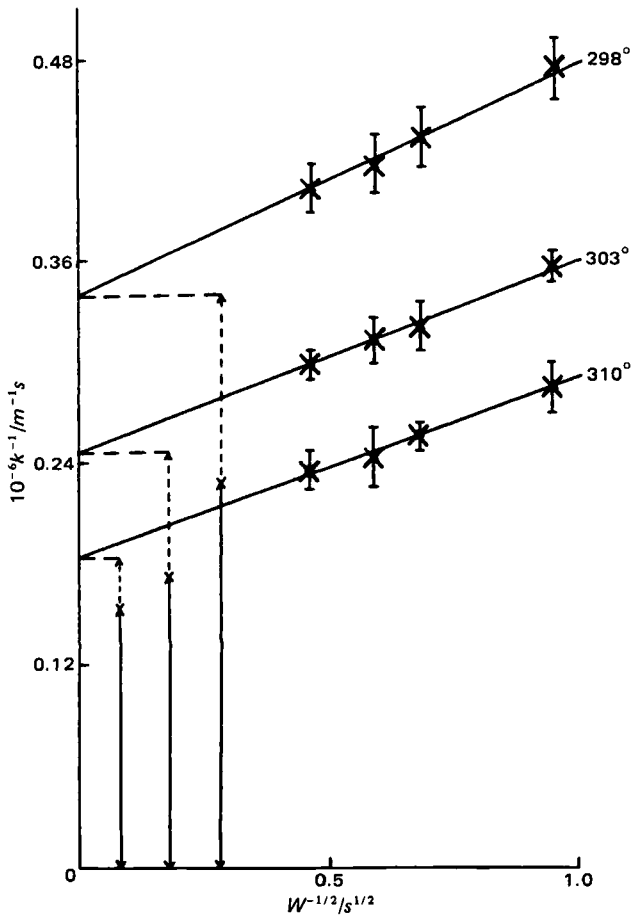

Figure 1—*Methyl nicotinate: Plots of* k^{-1} *as a function of rotation speed at the three temperatures (°K) indicated. Each experimental point is the mean of at least 10 separate determinations; the error bars indicate the standard deviations about the mean. The lines through the data are the theoretical gradients calculated from the Levich equation (Eq. 5) and given in Table I. The contributions to the intercepts of interfacial transfer* ($I_t = 2/a'k_{-1}$) *and diffusion through the filter* ($D_f = Kl/a'D_{org}$) *are indicated. Key: (⟷) D_f; (←→) I_t.*

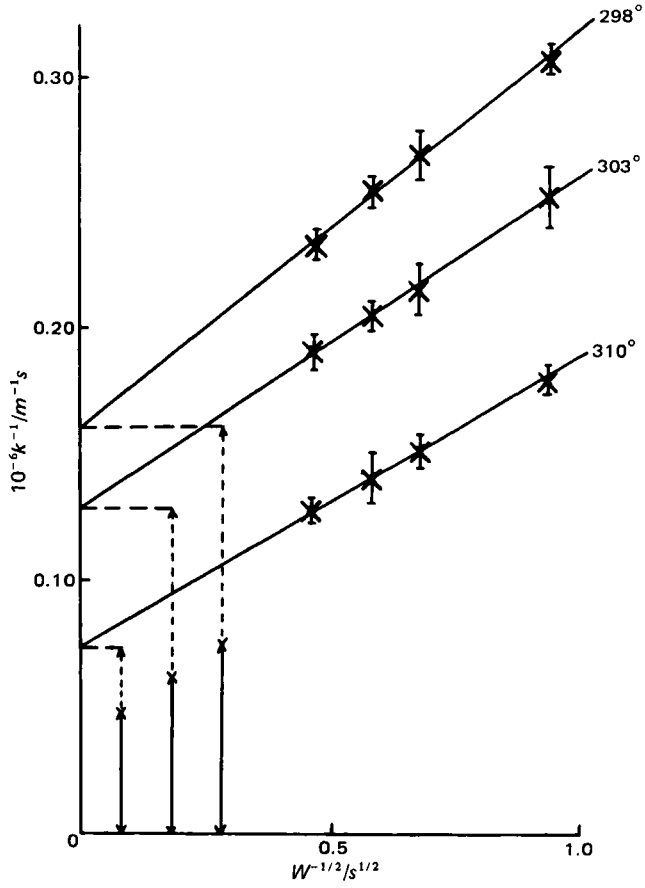

Figure 2—*Ethyl nicotinate: The corresponding plots for the ethyl ester. Temperature in °K. Key: (⟷) D_f; (←→) I_t.*

transport of the methyl and ethyl esters of nicotinic acid across the water–isopropyl myristate (I) interface has been followed using a rotating diffusion cell (1). This cell uses the hydrodynamics of the rotating disk system (5) to impose a known pattern of convective diffusion on either side of a filter[1]. The rotation of the cell produces a stagnant diffusion layer of known thickness on both sides of the filter. In the experiments reported here, two interfaces were established with the aqueous phase above and below the filter which was saturated with the organic phase. The choice of I as the organic liquid reflected the suggestion by several workers that it is a good model compound for skin lipids (6). The rate constants for interfacial transfer were determined at three temperatures and converted to free energies of activation. An Arrhenius relationship has enabled the enthalpic contribution to the energy barrier to be found and the entropic component was obtained by difference. The data indicate that the free energy barrier to transfer is essentially enthalpic, there being a large positive entropy for transfer into the interfacial region. The results show the same pattern as that recently found for salicylic acid crossing the same aqueous–organic interface (3). Finally, the thermodynamic parameters for interfacial transfer are compared with those corresponding to solute transfer between the bulk IPM and bulk aqueous phases (the values being determined from the temperature dependence of the partition coefficient), and the marked differences are discussed.

[1] Millipore Corp., Bedford, Mass.

EXPERIMENTAL

Comprehensive descriptions of the rotating diffusion cell and its method of operation have been given previously (1, 2, 7). The transport of methyl and ethyl nicotinates at 25, 30, and 37° was followed from an aqueous inner compartment across a filter[1] saturated with I into a larger aqueous outer compartment. The flux of ester into the receptor phase was determined as a function of rotation speed by periodically sampling the outer compartment and analyzing the nicotinate concentration using UV spectrophotometry.

Partition coefficients were found by continuously shaking an aqueous solution of nicotinate with an equal volume of I for a period of ~48 hr and then analyzing for the substrate spectrophotometrically.

Diffusion coefficients for the two nicotinates in water and in I were determined at 25° using the Goüy interferometric technique. The results for methyl nicotinate were found to be in good agreement with the published values (1). Diffusion coefficients at the higher temperatures were obtained using the Stokes–Einstein relation and a ratio technique previously described (1–3, 7).

All chemicals were supplied commercially at least 99% pure and were used without further purification. Solutions were prepared with distilled water from an all-glass apparatus.

THEORETICAL

For the experiments described in this paper, the flux (J/mole/sec) of diffusing species from the inner compartment of the rotating diffusion cell to the outer is given by

$$J = kA(C_I - C_O) \qquad \text{(Eq. 2)}$$

Table I—Experimental Results from Figs. 1 and 2 and the Associated Solute Diffusion Coefficients [a]

°K	$10^9 D_{aq}$/ $m^2 s^{-1}$	$10^9 D_{org}$/ $m^2 s^{-1}$	10^{-6}Gradient[b]/ $s^{1/2} m^{-1}$	10^{-6}Intercept/ $m^{-1} s$
		Methyl Nicotinate		
298	0.88	0.41	0.137	0.341
303	1.13	0.48	0.114	0.246
310	1.20	0.51	0.107	0.184
		Ethyl Nicotinate		
298	0.76	0.37	0.151	0.161
303	0.89	0.42	0.134	0.129
310	1.06	0.46	0.116	0.074

[a] Diffusion coefficient values at 298°K were measured experimentally using a high precision Goüy diffusiometer (Ref. 9). The Stokes–Einstein relationship and a ratio technique were used to determine the values at the two higher temperatures. [b] These values were calculated using the corresponding aqueous diffusion coefficients and kinematic viscosities (Ref. 10). The gradients have then been forced through the experimental points in Figs. 1 and 2 to obtain the intercepts given in the final columns of this table.

where A is the area of the filter and C_I and C_O are the bulk concentrations in the inner and outer compartments, respectively. Detailed treatment of this expression has been presented previously (1) and the variation of the concentrations with time was shown to be:

$$[(C_{O,t} - C_{O,0})(1 + V_O/V_I)]/(C_{I,0} - C_{O,0}) = 1 - \exp[-kA(V_I^{-1} + V_O^{-1})t] \quad \text{(Eq. 3)}$$

where V_I and V_O refer to the respective volumes of the inner and outer compartments and the second subscripts on C refer to time. Furthermore, analysis of the flux equations for the double interface systems of this study indicates that the rate constant k be interpreted as follows (1):

$$k^{-1} = 2Z_D/D_{aq} + Kl/a'D_{org} + 2/a'k_{-1} \quad \text{(Eq. 4)}$$

In this equation, $2Z_D/D_{aq}$ describes the diffusion through the aqueous stagnant diffusion layers established on either side of the filter by the rotating disk hydrodynamics. The thickness of these layers (Z_D) is given by the equation (8):

$$Z_D = 0.643\, \upsilon^{1/6} D_{aq}^{1/3} W^{-1/2} \quad \text{(Eq. 5)}$$

where υ is the kinematic viscosity of water, D_{aq} the aqueous diffusion coefficient of the solute, and $W(s^{-1})$ the rotation speed of the filter. The second term in Eq. 4 describes the diffusion of the solute through the organic liquid filled filter of length l; K is the aqueous–organic partition coefficient of the substrate, and D_{org} its diffusion coefficient in the organic phase. The factor a' is the area of the pores of the filter divided by A. The final term $2/a'k_{-1}$ describes the interfacial transfer of the solute, the factor of two arising because there are two interfaces. For transfer of a substrate M, the forward and backward interfacial transfer rate constants (k_1 and k_{-1}) have the following significance:

$$M_{org} \underset{k_{-1}}{\overset{k_1}{\rightleftharpoons}} M_{aq}: \qquad K = k_1/k_{-1} \quad \text{(Eq. 6)}$$

The largest of the three terms in Eq. 4 wil be the most important in determining the rate of the overall transfer process.

RESULTS AND DISCUSSION

The samples periodically removed from the outer compartment of the rotating diffusion cell enable values of k^{-1} to be calculated using Eq. 3. Figures 1 and 2 show that the linear relationship, predicted by Eqs. 4 and 5, between k^{-1} and $W^{-1/2}$ is experimentally verified for both methyl and ethyl nicotinates at each of the three temperatures considered. In these figures, the theoretical gradients calculated using Eq. 5 are forced through the experimental points to obtain the intercepts on the k^{-1} axis. Experimental data lie very close to the theoretical slopes, indicating that the correct hydrodynamics are indeed set up by the rotation of the diffusion cell. The aqueous diffusion coefficients and theoretical gradients together with the derived intercepts at $W^{-1/2} = 0$ are given in Table I for both nicotinic acid esters.

The intercepts in Table I and Figs. 1 and 2 correspond to the flux at infinite rotation speed when the Z_D term in Eq. 4 is zero. The remaining two terms describing diffusion through the filter and interfacial transfer may be separated using known values of K, D_{org}, l, and a': the partition coefficients for both esters at the three temperatures were determined and are presented in Table II; values for D_{org} were also found and are given in Table I; and the parameters[2] l and a' are 150 μm and 0.75, respectively, for the 0.22-μm pore size filters used. Independent verifications of the values of l and a' have been reported (11, 12). Hence, the intercepts provide direct measurements of k_{-1} for both esters at three temperatures. These rate constants, and the corresponding k_1 values calculated from Eq. 6, are given in Table II, and the interfacial transfer contributions to the intercepts are shown in Figs. 1 and 2. Furthermore, in Table II, the kinetic terms have been converted to free energy barriers using Eq. 7 (1)

Table II—Interfacial Transfer Parameters

°K	K	$10^6 k_1$/ m/sec	$10^6 k_{-1}$/ m/sec	$\Delta G°_{1,\#}$/kJ mole^{-1}	$\Delta G°_{-1,\#}$/kJ mole^{-1}
			Methyl Nicotinate		
298	0.45	9.9	22	39.7	37.8
303	0.42	16	38	39.4	37.2
310	0.39	34	86	38.4	36.0
			Ethyl Nicotinate		
298	0.14	4.4	31	42.0	37.1
303	0.13	5.2	40	42.2	37.1
310	0.11	11	102	41.3	35.5

$$\Delta G°_{\pm 1,\#} = -RT \ln(k_{\pm 1}/Z) \quad \text{(Eq. 7)}$$

which includes a frequency factor (Z) of 10^2 m/sec (13).

Because the interfacial transfer rate constants have been determined as a function of temperature, the enthalpy of transfer into the interfacial region may be estimated using an Arrhenius relation:

$$\ln k_{\pm 1} = \text{constant} - \Delta H°_{\pm 1,\#}/RT \quad \text{(Eq. 8)}$$

Plots of the natural logarithm of the $k_{\pm 1}$ values in Table II against $1/T$ were constructed and the enthalpy changes obtained from the gradients are given in the first columns of Tables III and IV for methyl and ethyl nicotinates, respectively. The magnitude of the entropy changes for interfacial transfer may then be calculated by difference using:

$$\Delta S°_{\pm 1,\#} = (\Delta H°_{\pm 1,\#} - \Delta G°_{\pm 1,\#})/T \quad \text{(Eq. 9)}$$

The results obtained for the two nicotinates at 298°K are again given in the left-hand columns of Tables III and IV.

The thermodynamic parameters for solute transfer between the bulk phases, *i.e.*, the energy difference between molecules in the bulk I and in the bulk aqueous phase, have been calculated from the partition coefficients in Table II. The results at 298°K are summarized in the second columns of Tables III and IV for methyl and ethyl nicotinates, respectively.

Consideration of the thermodynamic data in Tables II–IV provides the following observations:

1. The free energy of activation for interfacial transfer in either direction (organic ⇌ aqueous) is always in the region of 39 kJ/mole. The free energy differences between the molecules in the bulk phases, however, are comparatively small at 298°K.
2. For interfacial transfer in both directions, there is a reasonably large positive enthalpy of activation. The temperature dependence of the nicotinates water–I partition coefficients, though, indicates that transfer from the bulk I phase to the bulk aqueous phase is an exothermic process $\Delta H \simeq$ 10–15 kJ/mole. The transfer between the bulk phases in the opposite direction has a correspondingly positive ΔH.
3. For both solutes, in either direction, there is a large significant positive entropy for transfer into the interfacial region. This implies that the free energy barrier to interfacial transfer discussed above is essentially enthalpic rather than entropic. For solute transfer from the bulk I to the bulk aqueous phase, on the other hand, ΔS is negative. Furthermore, in this situation, the negative entropy changes are responsible for the positive free energy changes calculated from the partition coefficients.

The constancy of the interfacial transfer free energy of activation has been reported previously (1, 3), and the results of this study are in good agreement with the data in the literature. The values also compare favorably with a result for $\Delta G°_{\#}$ determined using a Stokes cell (14). In

[2] Millipore Corp., Bedford, Mass., Cat. no. MC 179/u, pp. 3–4, 13.

Table III—Methyl Nicotinate: Thermodynamic Values at 298°K

I → Water

	I (interface) $\xrightarrow{k_1}$ Water (interface)	I (bulk) $\xrightarrow{K}$ Water (bulk)[a]
$\Delta G/kJ$ mole^{-1}	39.7	2.0
$\Delta H/kJ$ mole^{-1}	75.9	−9.1
$\Delta S/J$ mole$^{-1}K^{-1}$	121	−37

Water → I

	Water (interface) $\xrightarrow{k_{-1}}$ I (interface)	Water (bulk) $\xrightarrow{1/K}$ I (bulk)[b]
$\Delta G/kJ$ mole^{-1}	37.8	−2.0
$\Delta H/kJ$ mole^{-1}	85.1	9.1
$\Delta S/J$ mole$^{-1}K^{-1}$	159	37

[a] ΔG in this column is calculated using $\Delta G = -RT \ln K$, ΔH is found from the slope of an Arrhenius plot of ln K *versus* $1/T$, and ΔS is determined by difference. [b] In this case, $\Delta G = +RT \ln K$, ΔH is found by plotting ln K^{-1} against $1/T$, and ΔS is again determined by difference.

Table IV—Ethyl Nicotinate: Thermodynamic Values at 298°K

I → Water

	I (interface) $\xrightarrow{k_1}$ Water (interface)	I (bulk $\xrightarrow{K}$ Water (bulk)[a]
$\Delta G/kJ$ mole^{-1}	42.0	4.9
$\Delta H/kJ$ mole^{-1}	67.2	−15.6
$\Delta S/J$ mole$^{-1}K^{-1}$	85	−69

Water → I

	Water (interface) $\xrightarrow{k_{-1}}$ I (interface)	Water (bulk) $\xrightarrow{1/K}$ I (bulk)[b]
$\Delta G/kJ$ mole^{-1}	37.1	−4.9
$\Delta H/kJ$ mole^{-1}	84.1	15.6
$\Delta S/J$ mole$^{-1}K^{-1}$	158	69

[a] ΔG in this column is calculated using $\Delta G = -RT \ln K$, ΔH is found from the slope of an Arrhenius plot of ln K *versus* $1/T$, and ΔS is determined by difference. [b] In this case, $\Delta G = +RT \ln K$, ΔH is found by plotting ln K^{-1} against $1/T$, and ΔS is again determined by difference.

this case, the system contained only one interface (set up on the surface of the sinter of the cell) between I and water, and the transferring substrate was *p*-methyl benzyl chloride. It seems unlikely that the technique of this earlier determination and the rotating diffusion cell suffer from the same experimental errors or artifacts. The good agreement between the two sets of results is believed (1), therefore, to provide confirmation of both the existence of the interfacial transfer process and of the reliability of the rotating diffusion cell.

Investigations of the temperature dependence of the interfacial transfer process have produced somewhat disparate results. For example, the interfacial barrier for *p*-methyl benzyl chloride crossing the water–I interface (14) was found to be almost totally enthalpic, with little or no entropic contribution. However, an earlier investigation of methyl nicotinate traversing the same interface (1), indicated that the interfacial transfer rate constants passed through a minimum as the temperature was raised from 11 to 37°. The data obtained at 21 and 37° support the trend in values found in this work. The discrepancy arises because of the enhanced rate of transfer measured at 11°, for which there appears to be no straightforward explanation. Most recently, the transfer of salicylic acid across the water–I interface has been considered (3), and substantially the same pattern of results was obtained as reported for the nicotinates in this paper; *i.e.*, the entropy of transfer across the interfacial region acts so as to reduce the overall free energy barrier, to which there exists a large positive enthalpic contribution.

The large positive entropy of activation found for interfacial transfer in either direction warrants further consideration. For both nicotinates [and salicylic acid (3)], transfer from the bulk I to the bulk aqueous phase involves a negative entropy change. This seems reasonable, since it is undoubtedly true that the solvation of the solute molecules will be more efficient in water than in I. The transfer from bulk I to bulk water will, therefore, produce an increase in the order of the system. However, this is not true in the region of the interface where nicotinate transfer causes a large increase in disorder. It is possible that this observation reflects the absence of any solvation sheath around the solutes as they traverse the interfacial regions. Alternatively it seems reasonable to suggest that a I–water interface possesses a well-ordered structure in which the ester groups of the I moieties will be oriented toward and solvated by the adjacent water molecules. The transport of a solute molecule through this rather ordered structure must destroy the I–water interactions, thereby contributing toward a positive entropy charge.

Further conclusions from the kinetic and thermodynamic parameters reported here cannot be drawn until more experiments are performed in which the nature of the solutes and solvents used are systematically varied. Like most two-phase and solvation phenomena, a variety of behavior may be expected. However, it has been demonstrated that the role of interfacial transfer in the permeation of organic barriers by the solutes described in this and other work should be considered significant to the overall transport process taking place in these systems.

REFERENCES

(1) W. J. Albery, J. F. Burke, E. B. Leffler, and J. Hadgraft, *J. Chem. Soc. Faraday Trans. I*, **72**, 1618 (1976).

(2) W. J. Albery and J. Hadgraft, *J. Pharm. Pharmacol.*, **31**, 65 (1979).

(3) R. H. Guy and J. Hadgraft, *J. Colloid Interface Sci.*, **81**, 69 (1981).

(4) G. L. Flynn, S. M. Yalkowsky, and T. J. Roseman, *J. Pharm. Sci.*, **63**, 479 (1974).

(5) A. C. Riddiford, *Adv. Electrochem. Electrochem. Eng.*, **4**, 47 (1966).

(6) B. J. Poulsen, E. Young, V. Coquilla, and M. Katz, *J. Pharm. Sci.*, **57**, 928 (1968).

(7) R. H. Guy and R. Fleming, *Int. J. Pharm.*, **3**, 143 (1979).

(8) V. G. Levich, "Physicochemical Hydrodynamics," Prentice-Hall, Englewood Cliffs, N.J., 1962, p. 69.

(9) A. A. Deshmukh and R. Fleming, *J. Phys. Ec.*, **3**, 976 (1970).

(10) "Chemical Rubber Company Handbook of Chemistry and Physics," 61st ed., CRC Press, Boca Raton, Fla., 1980–1981.

(11) Y. W. Chien, C. L. Olson, and T. D. Sokoloski, *J. Pharm. Sci.*, **62**, 435 (1973).

(12) W. J. Albery and P. R. Fisk, in "Hydrometallurgy 81," Society of Chemical Industry, London, 1981, FS1/FS15.

(13) R. A. Marcus, *J. Phys. Chem.*, **67**, 853 (1963).

(14) W. J. Albery, A. M. Couper, J. Hadgraft, and C. Ryan, *J. Chem. Soc. Faraday Trans. I*, **70**, 1124 (1974).

Kinetic Study and Analytical Application of the Hexadecyltrimethylammonium Bromide-Catalyzed Reaction of 1-Fluoro-2,4-dinitrobenzene with Amines

MICHELLE P. WONG and KENNETH A. CONNORS ˣ

Received March 9, 1982, from the *School of Pharmacy, University of Wisconsin, Madison, WI 53706.* Accepted for publication April 1, 1982.

Abstract □ Arylation of amines by reaction with 1-fluoro-2,4-dinitrobenzene is catalyzed by micelles of cetrimonium bromide. This catalysis has been exploited to reduce the analysis time in the spectrophotometric determination of amines as their dinitrophenyl derivatives. The kinetics of the catalysis were studied for the five amines: alanine, phenylalanine, aniline, 4-methylaniline, and 4-methoxyaniline. The dependence of rate constant on surfactant concentration can be quantitatively accounted for by Berezin's model, in which uptake of the amine and the 1-fluoro-2,4-dinitrobenzene by the micelle is described as a partitioning phenomenon for both species. An alternative model is developed in which one reactant partitions into the micellar phase and the other binds to the micelle with 1:1 stoichiometry; the two models are formally equivalent. Intrinsic catalytic rate constants and binding constants were evaluated. About one-third to one-half of the maximum observed micellar acceleration is attributed to a true micellar catalysis, the remainder being ascribed to an increase in local reactant concentrations in the micelle.

Keyphrases □ 1-Fluoro-2,4-dinitrobenzene—hexadecyltrimethylammonium bromide-catalyzed reaction with amines, kinetics, analytical application □ Hexadecyltrimethylammonium bromide-catalyzed reaction—1-fluoro-2,4-dinitrobenzene with amines, kinetics, analytical application □ Kinetics—hexadecyltrimethylammonium bromide-catalyzed reaction of 1-fluoro-2,4-dinitrobenzene with amines, analytical application

1-Fluoro-2,4-dinitrobenzene undergoes nucleophilic aromatic substitution by amines to give dinitrophenylamines, which are useful derivatives for the spectrophotometric analysis of amines (1–5). Typical reaction times are 10–20 min at 65°. The catalysis of this reaction by the surfactant cetrimonium bromide was previously described (6). It was later suggested (7, 8) that this catalysis could be applied to the analytical system to reduce the reaction times. A preliminary communication showed that this was practical, and described analytical conditions making use of the micellar catalysis (9). The present paper extends the investigation of this analytical application and reports kinetic studies, and their interpretation, of the cetrimonium bromide-catalyzed reaction of 1-fluoro-2,4-dinitrobenzene with five amines.

EXPERIMENTAL

Materials—Cetrimonium bromide[1] was purified by a previous procedure (10). 1-Fluoro-2,4-dinitrobenzene was distilled under reduced pressure. Aniline[2] was distilled; bp 181°. 4-Methylaniline[3] (*p*-toluidine) was distilled under reduced pressure; bp 61.5°/2 mm Hg, mp 44.5–45° [lit. mp 44.8° (11)]. 4-Methoxyaniline[3] (*p*-anisidine) was distilled under reduced pressure; bp 98°/2 mm Hg, mp 56.5–57° [lit. mp 57° (12)]. Other chemicals were used directly.

Product Identification—Alanine and 1-fluoro-2,4-dinitrobenzene were reacted in pH 9.2 borate buffer in the presence of cetrimonium bromide. The solution was acidified to below pH 3 with concentrated HCl and was extracted with diethyl ether. The ether layer was dried, redissolved in ether, and then spotted on silica gel TLC plates[4]. This was developed with a mixed solvent of ether–glacial acetic acid–water (100:3:3). The product (2,4-dinitrophenylalanine) isolated in this way was recrystallized from 50% ethanol, and its IR spectrum was determined in solid potassium bromide for comparison with the spectrum of an authentic sample of 2,4-dinitrophenylalanine[5]. UV spectra were also measured.

The hydrolysis of 1-fluoro-2,4-dinitrobenzene was studied in pH 9.2 borate buffer containing cetrimonium bromide, but no amine. After hydrolysis the solution was acidified, extracted with ethyl acetate, the extract was evaporated to dryness, and the residue was dissolved in methanol for spotting on TLC plates. The development solvent was chloroform–methanol–glacial acetic acid (40:10:0.5). The spot was scraped off, dissolved in methanol, and centrifuged. The supernatant was dried, and the residue was compressed with potassium bromide for IR spectroscopy[6]. An authentic sample of 2,4-dinitrophenol was carried through the same procedure.

Kinetic Studies—For reactions in which the reagent (1-fluoro-2,4-dinitrobenzene) concentration was higher than the amine concentration, typical initial conditions were: 5×10^{-4} *M* amine and 0.035 *M* cetrimonium bromide in 0.065 *M* pH 9.2 borate buffer; the reaction was initiated by adding 1.0 ml of 1.3% v/v 1-fluoro-2,4-dinitrobenzene (dissolved in acetone) to 19 ml of thermostated aqueous solution. Samples of 1.0 ml were removed at recorded times and were added to 9.0 ml of a 1:100 dilution of concentrated HCl in dioxane (4). The absorbance was measured[7] at the wavelength of maximum absorption (usually 350 nm) in a 1.0-cm cell against a reagent blank carried through the same procedure.

For reactions in which the amine concentration exceeded the 1-fluoro-2,4-dinitrobenzene concentration, the reaction was monitored directly in the thermostated spectrophotometer cell compartment.

Proposed Analytical Method—To a 25-ml volumetric flask 0.25 g of cetrimonium bromide and enough of the amine sample should be added so that its final concentration will be 10^{-4} *M*; the solution brought to 19 ml with 0.065 *M* pH 9.2 borate buffer; the flask brought to the desired reaction temperature (25–45°); and the reaction initiated by adding 1.0 ml of 1.3% v/v 1-fluoro-2,4-dinitrobenzene in acetone. After ~5 half-lives at the experimental temperature, a 1.0-ml portion should be added to 9.0 ml of a 1:100 dilution of concentrated hydrochloric acid in dioxane, and the absorbance immediately measured at the absorption maximum against a reagent blank carried through the same procedure. A standard curve should be prepared by subjecting known concentrations of the same amine to the procedure.

RESULTS

Analytical Method—Analytical conditions require that the concentration of reagent (1-fluoro-2,4-dinitrobenzene) should be greater than that of the amine. Under these conditions, light absorption by the 2,4-dinitrophenolate produced through concurrent hydrolysis of the reagent interferes with direct observation of the dinitrophenylated amine. It is, therefore, necessary to withdraw samples and to acidify them, which stops the reaction and concomitantly alters the spectrum of the phenol so that it does not interfere with the detection of the amine derivative (4).

Figure 1 shows the extent of the catalysis by cetrimonium bromide in the reaction of alanine with 1-fluoro-2,4-dinitrobenzene. The apparent first-order plots were linear for two or more half-lives in both the presence and absence of surfactant. Table I lists half-lives for numerous amines subjected to this procedure, and the rate enhancement produced by the surfactant is given in the final column. Rate enhancements for aliphatic amino acids and peptides are in the range of 10–20, whereas aromatic amino acids show much greater enhancements. The neutral aniline has

[1] Baker Analyzed Reagent.
[2] Mallinckrodt.
[3] Aldrich.
[4] Eastman Kodak.
[5] Sigma Chemical Co.
[6] Perkin-Elmer 599B IR spectrophotometer.
[7] Cary models 14 or 16, or Perkin-Elmer 559 spectrophotometers.

0022-3549/83/0200-0146$01.00/0

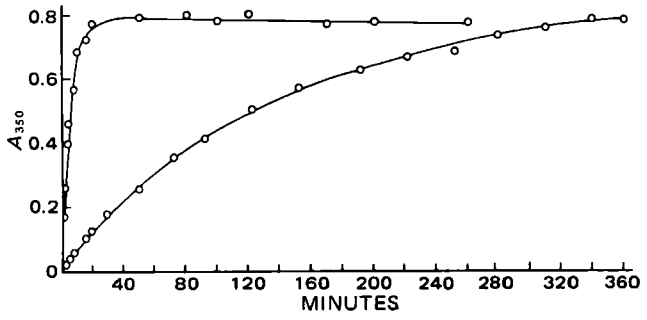

Figure 1—*Change of absorbance at 350 nm with time for the arylation of alanine at 23°: 5 × 10⁻⁴ M alanine, 3.5 × 10⁻³ M 1-fluoro-2,4-dinitrobenzene, pH 9.2. Upper curve, 0.035 M cetrimonium bromide; lower curve, no surfactant.*

the lowest relative rate in the table. These data suggest that the catalysis by the cationic micelle is assisted by anionic and hydrophobic sites on the amine. When both features are present, as in 11-aminoundecanoic acid, a very large rate enhancement can occur. The half-lives in Table I can guide the analyst in selecting appropriate reaction times.

The effect of temperature on the reaction rate was studied in the presence and absence of 0.0175 *M* surfactant to learn the extent of the analytical advantage to be gained by working at a higher temperature. The reaction was studied at 15, 25, 35, and 45°; the Arrhenius plots were linear. In the absence of surfactant, the activation enthalpy $\Delta H^{\ddagger}$ was 16.1 (*SD* 0.5) Kcal/mole and the activation entropy $\Delta S^{\ddagger}$ was −11.2 (*SD* 0.5) EU (entropy units). In the presence of surfactant, $\Delta H^{\ddagger}$ was 13.7 (*SD* 0.4) Kcal/mole and $\Delta S^{\ddagger}$ was −14.6 (*SD* 1.3) EU. No mechanistic interpretation is given to these results, because they include several effects (the micellar rate effect and the uptake of the two reactants by the micelle). However, the analytical reaction time can be reduced by a factor of ~3 by raising the temperature from 25 to 45°. The slopes of the concentration-absorbance curves were identical for reactions run at 25 and 45°.

The product identification studies showed, by means of TLC, IR spectroscopy, and UV spectroscopy, that the products of the reaction of 1-fluoro-2,4-dinitrobenzene with alanine in the presence of cetrimonium bromide were 2,4-dinitrophenylalanine and 2,4-dinitrophenol.

Reaction Order—In the analytical studies the reagent was in excess by necessity, but for studying the reaction kinetics it is more convenient to have the amine in excess. This permits the reaction to be monitored directly in the spectrophotometer. However, 1-fluoro-2,4-dinitrobenzene undergoes two reactions in this system, yielding the two products, a 2,4-dinitrophenylamine and 2,4-dinitrophenol. The following kinetic treatment takes this into account. Scheme I is the kinetic scheme, where *R* represents 1-fluoro-2,4-dinitrobenzene, *D* is the dinitrophenylamine derivative, *P* is dinitrophenol, k_D is an apparent first-order rate constant for the production of *D*, and k_P is an apparent first-order rate constant for the production of *P*.

$$R \xrightarrow{k_D} D$$

$$R \xrightarrow{k_P} P$$

Scheme I

Then $-d[R]/dt = (k_D + k_P)[R] = k[R]$, where $k = k_D + k_P$; the loss of *R* is a first-order process, and $[R] = [R]_0 \exp(-kt)$. The rate of formation of *D* is $d[D]/dt = k_D[R] = k_D[R]_0 \exp(-kt)$. Integrating this with the initial condition $[D] = 0$ at $t = 0$ gives:

$$[D] = \frac{k_D[R]_0}{k}(1 - e^{-kt}) \qquad \text{(Eq. 1)}$$

In the same way, Eq. 2 is obtained:

$$[P] = \frac{k_P[R]_0}{k}(1 - e^{-kt}) \qquad \text{(Eq. 2)}$$

The absorbance of the solution (in a 1-cm cell) at any time is given by:

$$A = \epsilon_R[R] + \epsilon_D[D] + \epsilon_P[P] \qquad \text{(Eq. 3)}$$

Combining Eqs. 1–3 gives:

$$A = \frac{[R]_0}{k}(\epsilon_D k_D + \epsilon_P k_P) + \frac{[R]_0}{k}(\epsilon_R k - \epsilon_D k_D - \epsilon_P k_P)e^{-kt} \qquad \text{(Eq. 4)}$$

Table I—Micellar Catalysis of Amine–1-Fluoro-2,4-dinitrobenzene Reactions by Cetrimonium Bromide [a]

Amine	Half-life/min: No Surfactant	Half-life/min: 0.035 *M* Surfactant	Rate Enhancement
Glycine	36.0	2.0	18.0
Alanine	87.4	4.7	18.6
Phenylalanine	32.0	<0.3	>94
Tyrosine	22.0	<0.5	>44
Tryptophan	9.0	<0.1	>90
Glycylglycine	63.5	5.4	11.8
Glycylglycylglycine	94.0	7.5	12.5
Glutamic acid	72.0	<0.3	>240
p-Aminobenzoic acid	137.5	3.0	45.8
11-Aminoundecanoic acid	133.0	<0.1	>1330
Aniline	60.0	7.5	8.0

[a] At pH 9.2 and 23°; 0.0035 *M* 1-fluoro-2,4-dinitrobenzene.

If the absorbance is measured at a wavelength where $\epsilon_D = \epsilon_P = \epsilon$, Eq. 4 simplifies to:

$$\epsilon[R]_0 - A = (\epsilon - \epsilon_R)[R]_0 e^{-kt} \qquad \text{(Eq. 5)}$$

But $\epsilon[R]_0 = A_\infty$, the absorbance when reaction is complete. Therefore, a conventional plot of $\log(A_\infty - A)$ against *t* should be linear, the slope yielding $k = k_D + k_P$. Since k_P can be measured in a separate experiment in the absence of amine, the desired rate constant (k_D) is accessible. Absorbance measurements were made at 350 nm, where $\epsilon_D = \epsilon_P$, and the first-order plots were linear for over three half-lives.

At pH 9.2 with alanine serving as the amine substrate, the kinetic dependence on the amine and the reagent was established. In the presence of 0.035 *M* cetrimonium bromide, the rate was directly dependent on the concentrations of amine and 1-fluoro-2,4-dinitrobenzene, confirming the first-order dependence upon each of these reactants in the presence of the surfactant.

Kinetic Dependence on Surfactant Concentration—The kinetics of the reaction of five amines (alanine, phenylalanine, aniline, 4-methylaniline, and 4-methoxyaniline) were studied in the presence of varying concentrations of surfactant at 25° and pH 9.2; the amine concentrations were 0.001–0.1 *M*, and the 1-fluoro-2,4-dinitrobenzene concentration was 6.32×10^{-5} *M*. Figure 2 is a plot of the first-order rate constant (k_D) against the total surfactant concentration (C_T) for phenylalanine. The general pattern in Fig. 2 was seen with all amines, namely an increase in rate at low surfactant concentrations with a saturation-type effect setting in at high concentrations. However, instead of an invariant plateau level, a maximum is observed in the plot (13).

At very low surfactant concentrations, the rate constant depends linearly on surfactant concentration, as shown in Fig. 3 for three concentrations of alanine. The discontinuity in the plot marks the effective critical micelle concentration (*CMC*); below this concentration the surfactant exists solely as the monomer.

DISCUSSION

The Partitioning–Partitioning Model—The kinetic dependence of micellar catalysis on surfactant concentration is often described by means of a kinetic scheme analogous to the Michaelis–Menten model of enzyme kinetics (14). This description is appropriate for a first-order reaction (*i.e.*, one in which a single substrate is taken up by the micelle), for which it predicts a saturation curve with an invariant plateau value at high surfactant concentrations. Evidently, the Michaelis–Menten model cannot provide a quantitative treatment of a reaction like the nucleophilic substitution described here, for the concentration dependence of the rate reveals a maximum. It is necessary to take into account the uptake of two reactants by the micelle in this second-order reaction, and this leads to a quantitative description of the experimental curve. This was accomplished previously (15–18) by workers who investigated (among other systems) the acceleration of the aminolysis of 1-fluoro-2,4-dinitrobenzene with *N*-benzoyl-L-histidine methyl ester in the presence of cetrimonium bromide. To account for the dependence of rate on surfactant concentration they proposed a model in which both the 1-fluoro-2,4-dinitrobenzene (designated *R*) and the amine (*S*) are distributed between the micellar (*M*) and aqueous (*W*) phases in conformity with the simple distribution law. This model is referred to here as the partitioning–partitioning model, since it postulates a partitioning mechanism for the uptake of both solutes.

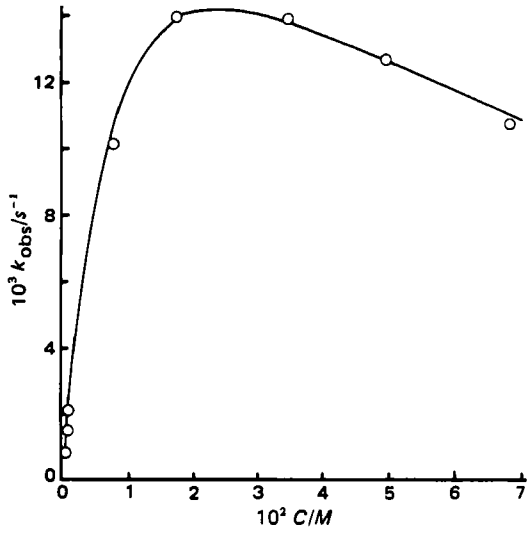

Figure 2—*Plot of first-order rate constant for the phenylalanine–1-fluoro-2,4-dinitrobenzene system at 25° and pH 9.2 as a function of surfactant concentration. The phenylalanine concentration is 1.04 × 10^{-3} M. The smooth line was drawn with Eq. 33.*

If V_T, V_M, and V_W represent the total volume of the system, the volume of the micellar phase, and the volume of the aqueous phase, respectively, then $V_T = V_M + V_W$, and:

$$\frac{V_W}{V_T} = 1 - \frac{V_M}{V_T} \qquad \text{(Eq. 6)}$$

A mass balance on R yields:

$$[R]_T V_T = [R]_M V_M + [R]_W V_W \qquad \text{(Eq. 7)}$$

and similarly for S. Substituting into Eq. 2 from Eq. 1:

$$[R]_T = [R]_M \frac{V_M}{V_T} + [R]_W \left(1 - \frac{V_M}{V_T}\right) \qquad \text{(Eq. 8)}$$

The molar concentration of surfactant present as micelles, C, is defined:

$$C = C_T - (CMC) \qquad \text{(Eq. 9)}$$

Letting V be the molar volume of surfactant, it follows that the product CV is the liters of surfactant present as micelles per liter of solution, or the volume fraction of the micellar phase, hence:

$$CV = V_M/V_T \qquad \text{(Eq. 10)}$$

which, combined with Eq. 8, gives:

$$[R]_T = [R]_M CV + [R]_W(1 - CV) \qquad \text{(Eq. 11)}$$

The distribution equilibria, according to this model, are:

$$R_W \rightleftharpoons R_M$$

$$S_W \rightleftharpoons S_M$$

Scheme II

The partition coefficient for R is defined:

$$P_R = \frac{[R]_M}{[R]_W} \qquad \text{(Eq. 12)}$$

and similarly for S. Eqs. 11 and 12 are combined to yield:

$$\frac{[R]_T}{[R]_W} = 1 + (P_R - 1)CV \qquad \text{(Eq. 13)}$$

The quantity K_R is defined:

$$K_R = (P_R - 1)V \qquad \text{(Eq. 14)}$$

Then Eq. 15 is written for R, and Eq. 16 is the analogous equation for S:

$$\frac{[R]_T}{[R]_W} = 1 + K_R C \qquad \text{(Eq. 15)}$$

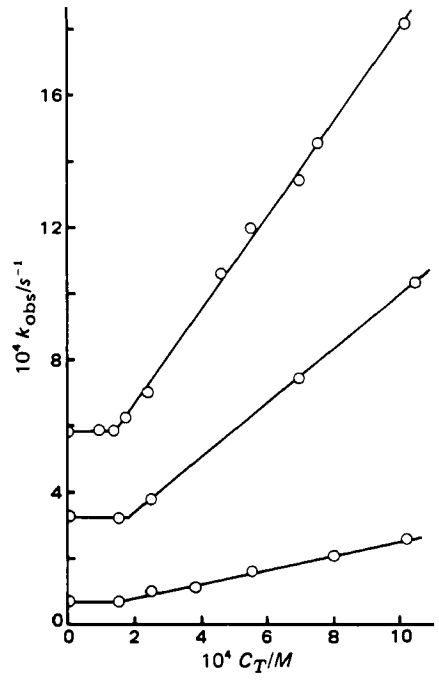

Figure 3—*Plot of first-order rate constant for the alanine–1-fluoro-2,4-dinitrobenzene system as a function of total surfactant concentration. Alanine concentrations, top to bottom: 0.025* M, *0.0125* M, *0.00267* M.

$$\frac{[S]_T}{[S]_W} = 1 + K_S C \qquad \text{(Eq. 16)}$$

In these equations K_R and K_S have the units of M^{-1}; *i.e.*, they have the character of 1:1 binding constants.

The bimolecular reaction between R and S can occur in both phases, with corresponding rate equations:

$$v_M = k_M[R]_M[S]_M \qquad \text{(Eq. 17)}$$

$$v_W = k_W[R]_W[S]_W \qquad \text{(Eq. 18)}$$

The observed velocity (v) is equal to the sum of the products of the velocities in the individual phases and the volume fractions of the phases:

$$v = v_M CV + v_W(1 - CV) \qquad \text{(Eq. 19)}$$

An experimentally observed second-order rate constant can be defined:

$$v = k_{exp}[R]_T[S]_T \qquad \text{(Eq. 20)}$$

Equations 19 and 20 are combined with 15 and 16 and the partition coefficient definitions:

$$k_{exp} = \frac{k_M P_R P_S CV + k_W(1 - CV)}{(1 + K_R C)(1 + K_S C)} \qquad \text{(Eq. 21)}$$

Equation 21 can be simplified for the present purpose. When partitioning into the micelle is favored, as with anionic and hydrophobic species, P is much larger than unity, and the binding constants from Eq. 14 can be written as $K_R = P_R V$ and $K_S = P_S V$. Moreover, when $CV \ll 1$, Eq. 21 becomes:

$$k_{exp} = \frac{k'_M K_R K_S C + k_W}{(1 + K_R C)(1 + K_S C)} \qquad \text{(Eq. 22)}$$

where $k'_M = k_M/V$.

This model can account for the appearance of a maximum in the dependence of k_{exp} on C. As Berezin points out (17), to account for this maximum it is necessary to describe the uptake of both solutes, making the model, and the corresponding equation, qualitatively different from the Michaelis–Menten model.

A Binding–Partitioning Model—It is now shown that a result formally equivalent to the Berezin partitioning–partitioning model can be obtained with a different physical picture of the process. It is postulated that one of the reactants, the one in large excess (S in this case) partitions

between the micellar and aqueous phases, whereas the other reactant binds to the micelle with 1:1 stoichiometry. These equilibria are:

$$S_W \rightleftarrows S_M$$

$$R + MS \rightleftarrows MSR$$

Scheme III

In this formulation, $[S]_M$ is the concentration of S in the micellar phase, and $[MS]$ is the solution concentration of S-containing micelles. There are no micelles without S, but there can be micelles without R. This is physically reasonable when $[S]_T >$ [micelles] $> [R]_T$. By arguments given above, Eq. 16 applies to S, whereas Eq. 23 defines the binding constant for R.

$$K'_M = \frac{[MSR]}{[R]_W[MS]} \qquad \text{(Eq. 23)}$$

The rate equation for loss of R is given by:

$$-\frac{d[R]}{dt} = k_W[R]_W[S]_W + k_M[MSR][S]_M \qquad \text{(Eq. 24)}$$

The mass balance on surfactant is:

$$C_T = [CMC] + n[MS] + n[MSR] \qquad \text{(Eq. 25)}$$

where n is the micelle aggregation number. Combining Eqs. 9, 23, and 25:

$$[MS] = \frac{C}{n + nK'_M[R]_W} \qquad \text{(Eq. 26)}$$

The mass balance on R is:

$$[R]_T = [R]_W + [MSR] \qquad \text{(Eq. 27)}$$

since $[MSR]$ is the concentration of micelles each containing an R. This leads to:

$$[R]_W = \frac{[R]_T}{1 + K'_M[MS]} \qquad \text{(Eq. 28)}$$

Combining the partition coefficient $P_S = [S]_M/[S]_W$ with Eqs. 23, 24, and 28 gives the rate equation:

$$-\frac{d[R]_T}{dt} = \left[\frac{k_M K'_M P_S[MS] + k_W}{1 + K'_M[MS]}\right][S]_W[R]_T \qquad \text{(Eq. 29)}$$

This is first-order in $[R]_T$, with the apparent first-order rate constant k_{obs}:

$$k_{obs} = \left[\frac{k_M K'_M P_S[MS] + k_W}{1 + K'_M[MS]}\right][S]_W \qquad \text{(Eq. 30)}$$

Eq. 26 is combined with Eq. 30 to give:

$$k_{obs} = \left[\frac{\dfrac{k_M K'_M P_S C}{n + nK'_M[R]_W} + k_W}{1 + \dfrac{K'_M C}{n + nK'_M[R]_W}}\right][S]_W \qquad \text{(Eq. 31)}$$

Equation 31 is simplified by using the reasonable assumption $K'_M[R]_W \ll 1$, substituting $K_S = P_S V$, and replacing $[S]_W$ from Eq. 16 to give:

$$k_{exp} = \frac{k'_M K_M K_S C + k_W}{(1 + K_M C)(1 + K_S C)} \qquad \text{(Eq. 32)}$$

where $k'_M = k_M/V$, $K_M = K'_M/n$, and $k_{exp} = k_{obs}/[S]_T$. Equation 32 for the binding-partitioning model is identical in form with Eq. 22 for the partitioning-partitioning model. In these equations the quantity K_S has the same significance, but K_R in Eq. 22 is interpreted as K'_M/n in Eq. 32 as a consequence of the different assumptions concerning the uptake of R into the micelle.

Estimation of the Model Parameters—Equations 22 and 32 can be written in the equivalent form:

$$k_{obs} = \left[\frac{k'_M K_M K_S C + k_W}{(1 + K_M C)(1 + K_S C)}\right][S]_T \qquad \text{(Eq. 33)}$$

The parameters can be estimated in several ways from the dependence of k_{obs} on C.

A plot of k_{obs} against C_T, at very low C_T, will give $k_W[S]_T$ as the value of k_{obs} below the CMC. Above the CMC, the slope of the straight line is equal to $k'_M K_M K_S[S]_T$, from which the product $k'_M K_M K_S$ is found. The intersection of the straight line segments marks the CMC. Figure 3 shows plots of this type.

A plot of k_{obs} against C over the full range of C, as shown in Figure 2,

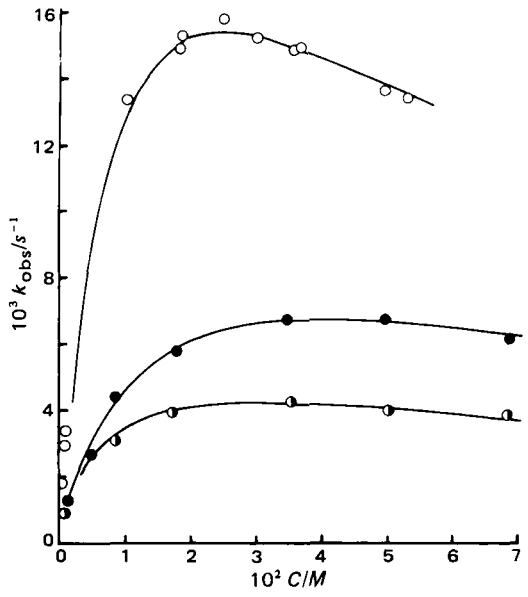

Figure 4—*Dependence of* k_{obs} *on surfactant concentration for aniline (○), 4-methylaniline (●), and 4-methoxyaniline (◑). The smooth curves were drawn with Eq. 33 and the parameters in Table II. The amine concentrations were: aniline, 0.0988* M; *4-methylaniline, 0.00807* M; *4-methoxyaniline, 0.0243* M.

exhibits a maximum if Eq. 33 describes the system. The concentration C_{max} corresponding to this maximum is found by setting the derivative dk_{obs}/dC equal to zero:

$$C_{max} = (K_M K_S)^{-1/2} \qquad \text{(Eq. 34)}$$

This result yields the product $K_M K_S$, and k'_M is obtained from this and the estimate of $k'_M K_M K_S$.

Inserting Eq. 34 into Eq. 32, and neglecting k_W, leads to Eq. 35, where k_{exp}^{max} is the value of k_{exp} when $C = C_{max}$:

$$\left[\frac{k_{max}^{exp}}{k'_M}\right]^{-1/2} = K_M^{-1/2} + K_S^{-1/2} \qquad \text{(Eq. 35)}$$

With these relationships, the four parameters k_W, k'_M, K_M, and K_S can be evaluated. Because Eq. 33 is symmetrical in K_M and K_S, it is not possible to assign these quantities unambiguously.

Another approach is a modification of a method described previously (18). Eq. 32 can be rearranged to:

$$k_{exp} - k_W = \left[\frac{K_M C}{1 + K_M C}\right]\left[\frac{k'_M K_S}{1 + K_S C} - k_W\right] \qquad \text{(Eq. 36)}$$

From this, Eq. 37 is obtained:

$$\frac{C}{k_{exp} - k_W} = \frac{1}{A} + \frac{(K_M + K_S)}{A}C + \frac{K_M K_S}{A}C^2 \qquad \text{(Eq. 37)}$$

where $A = k'_M K_M K_S - k_W K_M(1 + K_S C)$. A plot of $C/(k_{exp} - k_W)$ against C is a curve, whose intercept at $C = 0$ is $1/(k'_M K_M K_S - k_W K_M)$. If the k_W term is negligible, this gives an estimate of $k'_M K_M K_S$.

Equation 32 is then rearranged to:

$$\frac{k'_M K_M K_S C + k_W - k_{exp}}{k_{exp} C} = K_M K_S C + (K_M + K_S) \qquad \text{(Eq. 38)}$$

A plot of the left side against C yields $K_M K_S$ and $(K_M + K_S)$ from the slope and intercept.

By either of these methods K_M and K_S are found by solving the quadratic formula. In some instances the solution is indeterminate—that is, the estimates $K_M K_S$ and $(K_M + K_S)$ are mutually inconsistent, because of experimental error. The individual constants are then evaluated by a curve-fitting method, in which Eq. 33 is fitted to the experimental points. This is a straightforward process, because the quantities $k'_M K_M K_S$ and $K_M K_S$ serve as constraints. Figures 2 and 4 show some of these curves.

Interpretation of the Micellar Catalysis—Table II gives the values of K_M, K_S, k_W, k'_M, and k_M for the cetrimonium bromide-catalyzed reaction of 1-fluoro-2,4-dinitrobenzene with five amines. The second-order rate constant k_M was obtained from the relationship $k_M = k'_M/V$, where V is the molar volume of surfactant; in this calculation V was taken as 0.35 liter/mole, as estimated by Berezin and coworkers (15, 18), who have

Table II—Parameters for the Cetrimonium Bromide-Catalyzed Reaction of 1-Fluoro-2,4-dinitrobenzene with Some Amines at 25° [a,b]

Amine	K_S, M^{-1}	K_M, M^{-1}	k'_M, s^{-1}	k_M, $M^{-1}s^{-1}$	k_W, $M^{-1}s^{-1}$	k_M/k_{exp}^{max}
Alanine	9.5	70.	0.091	0.26	0.025	0.56
	(0.7)	(5.2)	(0.012)			
Phenylalanine	25.9	66.	1.39	3.98	0.093	0.29
	(1.1)	(2.8)	(0.19)			
Aniline	9.2	113.	0.0075	0.0213	0.005	0.50
	(0.4)	(4.3)	(0.0018)			
4-Methylaniline	27.0	55.5	0.20	0.57	0.143	0.30
	(1.8)	(3.6)	(0.024)			
4-Methoxyaniline	13.7	43.8	0.048	0.138	0.0223	0.50
	(1.0)	(3.3)	(0.0063)			

[a] Symbols refer to Eq. 33. [b] Standard deviations in parentheses.

also discussed the uncertainty involved in estimating V (17). The assignment of K_M and K_S to the binding constant estimates is based on two chemical factors: (*a*) it is expected that phenylalanine will be taken up by the micelle more extensively than will alanine; (*b*) the K_S values for the three anilines vary roughly as their partition coefficients in the octanol–water system (19). K_M represents binding of 1-fluoro-2,4-dinitrobenzene to the micelle; the variation in this quantity is greater than expected, indicating that the nature of the amine taken up by the micelle influences binding of the second reactant.

The uncertainties assigned to the K_S, K_M, and k'_M values in Table II are based upon the uncertainties in the products $k'_M K_M K_S$ and $K_M K_S$, which are the quantities directly evaluated from the data. Division of the uncertainty in $K_M K_S$ between K_M and K_S was based on the assumption that the uncertainty was weighted by the value of the constant, according to the relationship $s_{K_M}/s_{K_S} = K_M/K_S$, where s represents standard deviation.

Table II includes the k_W values, and it is seen that the ratio of k_M/k_W is substantially greater than unity for all of the amines. The last column of the table gives the ratio of k_M to k_{exp}^{max}, the maximum value of the observed second-order rate constant. This ratio is a measure of the fraction of true *micellar catalysis* contributing to the total micellar acceleration effect, as suggested:

$$\frac{k_M}{k_{exp}^{max}} = \frac{k_M/k_W}{k_{exp}^{max}/k_W}$$

That is, approximately one-third to one-half of the maximum observed acceleration is a consequence of catalysis by the micelle, the remainder being a concentration effect, through which the micelle increases the local concentrations of the reactants.

A previous study (18) carried out a similar analysis for the cetrimonium bromide-catalyzed reaction of 1-fluoro-2,4-dinitrobenzene with *N*-benzoyl-L-histidine methyl ester. These authors found that k_M/k_W was in the range of 1–2, and they concluded that most of the micellar acceleration was a result of the concentration of the reactants in the micellar phase. They also measured the binding constants by an independent solubility method, finding the value of 27 M^{-1} at 18° for 1-fluoro-2,4-dinitrobenzene. This value will be smaller at 25° because the heat of binding is negative. This result is not in good agreement with the K_M assignment in Table II, and this assignment is therefore in some doubt[8].

[8] One factor that may influence the binding constants is the composition of the solvent, which in the present studies contained 5% acetone. Another possible factor may be the buffer species.

REFERENCES

(1) F. Sanger, *Biochem. J.*, **39**, 507 (1945).

(2) F. C. McIntire, L. W. Clements, and M. Sproull, *Anal. Chem.*, **25**, 1757 (1953).

(3) S. M. Rosenthal and C. W. Tabor, *J. Pharmacol. Exp. Ther.*, **116**, 131 (1956).

(4) D. T. Dubin, *J. Biol. Chem.*, **235**, 783 (1960).

(5) M. Pesez and J. Bartos, "Colorimetric and Fluorimetric Analysis of Organic Compounds and Drugs," Dekker, New York, N.Y., 1974, p. 129.

(6) C. A. Bunton and L. Robinson, *J. Am. Chem. Soc.*, **92**, 356 (1970).

(7) K. A. Connors, "Reaction Mechanisms in Organic Analytical Chemistry," Wiley-Interscience, New York, N.Y., 1973, p. 284.

(8) C. A. Bunton, in "Applications of Biochemical Systems in Organic Chemistry," Vol. X, Part 2 of "Techniques of Chemistry," J. B. Jones, C. J. Sih, and D. Perlman, Eds., Wiley-Interscience, New York, N.Y., 1976, p. 806.

(9) K. A. Connors and M. P. Wong, *J. Pharm. Sci.*, **68**, 1470 (1979).

(10) P. Murkerjee and K. J. Mysels, *J. Am. Chem. Soc.*, **77**, 2937 (1955).

(11) J. F. T. Berlinear and O. E. May, *ibid.*, **49**, 1007 (1927).

(12) D. D. Perrin, W. L. F. Armarego, and D. R. Perrin, "Purification of Laboratory Chemicals," Pergamon, Long Island City, N.Y., 1966.

(13) M. P. Wong, Ph.D. Thesis, University of Wisconsin-Madison, 1981.

(14) J. H. Fendler and E. J. Fendler, "Catalysis in Micellar and Macromolecular Systems," Academic, New York, N.Y., 1975, Chap. 4.

(15) A. K. Yatsimirskii, K. Martinek, and I. V. Berezin, *Dokl. Akad. Nauk SSSR*, **194**, 840 (1970).

(16) *Idem.*, *Tetrahedron*, **27**, 2855 (1971).

(17) *Idem.*, *Russ. Chem. Revs.*, **42**, 787 (1973).

(18) A. K. Yatsimirskii, Z. A. Strel'tsova, K. Martinek, and I. V. Berezin, *Kinet. Katal.*, **15**, 354 (1974).

(19) A. Leo, C. Hansch, and D. Elkins, *Chem. Rev.*, **71**, 525 (1971).

ACKNOWLEDGMENTS

The contribution of Professor Pasupati Mukerjee, who brought to our attention the work of the Berezin group, is gratefully acknowledged. The experimental assistance of Dr. Yang Shude is also acknowledged.

Interaction of Cyclazocine and the Sympathetic Nervous System

GARY D. RUSSI * and F. GENE MARTIN ˣ

Received November 30, 1981, from the *Department of Pharmacology and Toxicology, School of Pharmacy, University of Kansas, Lawrence, KS 66045.* Accepted for publication March 29, 1982. * Present address: Drake University, Department of Pharmacology, College of Pharmacy, Des Moines, IA 50311.

Abstract □ Cyclazocine, a benzomorphan derivative narcotic agonist–antagonist, reduced the uptake of tritiated norepinephrine and reduced the recovery of [^{3}H]3,4-dihydroxymandelic acid, but did not significantly alter the recovery of [^{3}H]normetanephrine in the rat heart *in vivo*. Cyclazocine also reduced endogenous levels of norepinephrine in the rat heart. Comparatively, desipramine reduced the uptake of [^{3}H]norepinephrine, the recovery of [^{3}H]3,4-dihydroxymandelic acid, and the recovery of [^{3}H]normetanephrine in the rat heart *in vivo*. Further, cyclazocine added to the perfusion medium or administered systemically reduced the uptake of radiolabeled norepinephrine by the isolated rat heart. The cyclazocine-induced decrease in the accumulation of [^{3}H]norepinephrine in the rat heart *in vivo* and *in vitro* presumably is due to an alteration of sympathetic function through the inhibition of neuronal uptake. It is further suggested that cyclazocine has other actions on the sympathetic nervous system, such as promoting neurotransmitter release.

Keyphrases □ Cyclazocine—interaction with the sympathetic nervous system □ Sympathetic nervous system—interaction with cyclazocine

Cyclazocine was first synthesized in the search for nonaddicting analgesics. Although cyclazocine is an effective analgesic in animals (1) and humans (2, 3), it has been shown to be a potent narcotic antagonist (4, 5). Consequently, it has been employed in the treatment of narcotic addiction (6–9). In these patients, a cyclazocine-induced euphorigenic and antidepressant action was noticed (7). Subsequently, the clinical evaluation of cyclazocine in depressed patients was reported (10, 11). It was concluded that cyclazocine exhibited a clinical antidepressant action with a range of activity very similar to imipramine.

Support for clinical data (10) was found by demonstrating that the cyclazocine-induced electroencephalogram changes were similar to those induced by imipramine in depressed patients. Likewise, electroencephalogram changes induced by cyclazocine and imipramine have been reported to be similar in the rabbit (12, 13).

Tricyclic antidepressants (imipramine and related compounds) have been shown to potentiate certain cardiovascular responses to norepinephrine in cats (14) and humans (15), presumably by preventing the uptake of norepinephrine by sympathetic neuronal structures (16, 17). Likewise, cyclazocine potentiates certain actions of norepinephrine *in vivo* and *in vitro* (18).

Since these studies suggest that cyclazocine may possess pharmacological actions similar to tricyclic antidepressants, the possibility that cyclazocine may alter sympathetic nervous system function was investigated.

EXPERIMENTAL

Cannulation of Vessels—The animals (male Sprague-Dawley rats, 200–350 g) were anesthetized with ether, and the right femoral vein was cannulated to facilitate intravenous drug injections. Each injection was washed into the vein with a 0.2-ml solution of normal saline.

Perfusion of the Rat Heart—All rats were given 1000 U ip of heparin 5 min prior to decapitation to reduce intravascular clotting. The hearts were removed and perfused by the Langendorff technique (19). After a 10-min perfusion of amine-free modified Krebs-bicarbonate solution at 60 mm Hg, the hearts were perfused until a constant volume was reached (~10 min), with modified Krebs-bicarbonate solution containing 3.3 nCi of [^{3}H]norepinephrine, diluted with nonradioactive norepinephrine to a final concentration of 10 ng/ml. Following the amine perfusion, the extraneuronal norepinephrine was removed by a 2-min wash with amine-free medium. This washing technique has been reported to remove 95% of the extracellular norepinephrine (20). The heart was removed from the perfusion apparatus, blotted, weighed, and assayed for [^{3}H]norepinephrine.

Each liter of bathing medium, continuously bubbled with a mixture of 5% carbon dioxide in oxygen, contained (m*M*): NaCl (118); $NaHCO_3$ (25); KCl (4.75); $MgSO_4$ (1.19); KH_2PO_4 (1.19); $CaCl_2 \cdot 2H_2O$ (2.5); glucose, 2 g; disodium edetate, 0.010 g.

Norepinephrine and Metabolite Assay—The isolation procedure for radioactive and endogenous norepinephrine and its metabolites was carried out by the use of ion-exchange resins and alumina (21).

Norepinephrine was made to fluoresce by the trihydroxyindole technique (22). The fluorescence was read on a spectrofluorometer[1]. Efficiency of the assay was determined by the use of a standard carried completely through the assay. Reagent fluorescence was determined after carrying each reagent used for elution through the assay. Mean recovery rates were: norepinephrine, 90%; normetanephrine, 72%; dihydroxymandelic acid, 85%.

For estimation of the tritiated catecholamine and the tritiated metabolites, 1 ml of the appropriate eluate containing the tritiated norepinephrine or metabolite was added to 10 ml of a commercial counting cocktail[2] and counted in a liquid scintillation counter[3]. Efficiency and quench were determined by using a tritium external standard.

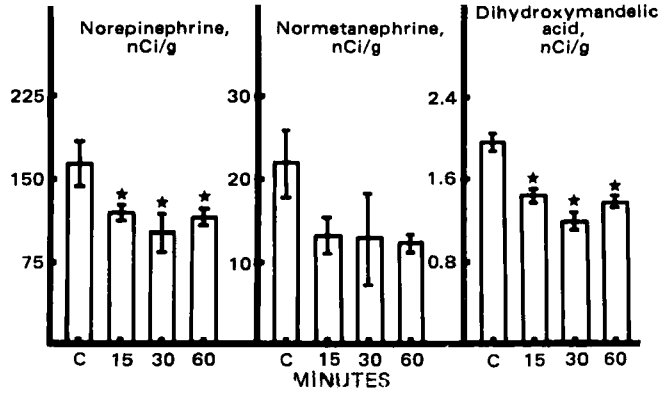

Figure 1—*The effect of cyclazocine on the uptake and metabolism of tritiated norepinephrine in rat hearts* in vivo. *Rats were given cyclazocaine (5 mg/kg iv) 15, 30, and 60 min prior to an infection of 10 μCi iv % tritiated norepinephrine. Control animals received an intravenous injection of saline. The hearts were removed 30 min later and assayed for the radiolabeled compounds, norepinephrine, normetanephrine, and 3,4-dihyroxymandelic acid. All values represent the means (horizontal bar) ± SEM (vertical bar) from four rats. Key: (*), postcyclazocine values significantly different from control values (C) at* $p < 0.05$.

[1] Aminco-Bowman model XLS IA M2.
[2] Aquasol, New England Nuclear Corp., Boston, Mass.
[3] Beckman model 230.

0022-3549/83/0200-0151$01.00/0

Table I—Effect of Cyclazocine on Endogenous Heart Norepinephrine in the Rat [a]

Time, hr	Heart Norepinephrine, μg/g			
	Cyclazocine, mg/kg			
	5	10	20	40
Control	0.87 ± 0.07	0.91 ± 0.03	0.93 ± 0.03	0.95 ± 0.05
1	0.79 ± 0.09	0.79 ± 0.02[b]	0.70 ± 0.08[b]	0.80 ± 0.07
2	0.87 ± 0.04	0.70 ± 0.02[b]	0.65 ± 0.05[b]	0.69 ± 0.03[b]
4	0.88 ± 0.08	0.57 ± 0.01[b]	0.83 ± 0.04	0.79 ± 0.11

[a] $n = 4$; all values represent the mean ± *SEM*. [b] $p < 0.05$.

Drugs and Solutions—Cyclazocine[4] was dissolved in acidic aqueous solution prior to use. In the perfused heart studies, cyclazocine was dissolved using 10% polysorbate 80[5] as a cosolvent in water and added directly to the bathing medium. The medium containing no cyclazocine received an equivalent amount of polysorbate 80.

[7-^{3}H]DL-Norepinephrine (5.0 or 15.8 Ci/m*M*)[6] solutions were made by diluting a proportion of the commercial stock solution with 0.1 *N* HCl containing 0.85% NaCl and norepinephrine bitartrate[7] to the desired specific activity.

Desipramine hydrochloride[8] was dissolved in double distilled water containing 0.85% NaCl.

Statistical Analysis—The data presented as means ± *SE* were analyzed with a randomized complete block analysis of variance with Duncan's new multiple range test (23). Values of $p < 0.05$ were considered significant.

RESULTS

Influence of Cyclazocine on the Uptake and Metabolism of [^{3}H]norepinephrine *In Vivo*—Cyclazocine significantly altered the uptake and metabolism of tritiated norepinephrine in the rat heart. After an intravenous injection of cyclazocine (15, 30, and 60 min) (5 mg/kg) the uptake of [^{3}H]norepinephrine (10 μCi) was significantly reduced (Fig. 1). Cyclazocine did not significantly alter the catechol-*O*-methyltransferase metabolite, normetanephrine, although there appeared to be some reduction. The monoamine oxidase metabolite, 3,4-dihyroxymandelic acid, was significantly reduced by cyclazocine at all three time periods measured.

An evaluation was made of the effect of three doses of cyclazocine, 2.5, 5.0, or 10 mg/kg iv on the uptake of the tritiated amine at the 30-min interval. The uptake of [^{3}H]norepinephrine was significantly reduced at doses of 2.5, 5.0, and 10 mg/kg (Fig. 2).

Effect of Desipramine on the Uptake and Metabolism of [^{3}H]-Norepinephrine *In Vivo*—Intravenous desipramine (5 mg/kg) significantly reduced the uptake of [^{3}H]norepinephrine and altered the formation of radiolabeled dihydroxymandelic acid at all time periods tested (Fig. 3). Unlike cyclazocine, desipramine significantly altered tritiated normetanephrine at all time periods measured.

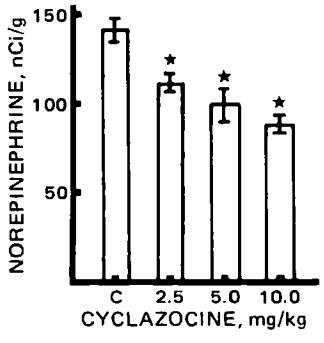

Figure 2—*The effect of various doses of cyclazocine on the uptake of tritiated norepinephrine in the rat heart* in vivo. *Rats were given cyclazocine 2.5, 5.0, or 10.0 mg/kg 30 min prior to an injection of 10 μCi iv of tritiated norepinephrine. Control animals received an intravenous injection of saline. The hearts were removed 30 min later and assayed for tritiated norepinephrine. All values represent the mean (horizontal bar) ± SEM (vertical bar) from four rats. Key: (*), postcyclazocine values significantly different from control values (C) at* $p < 0.05$.

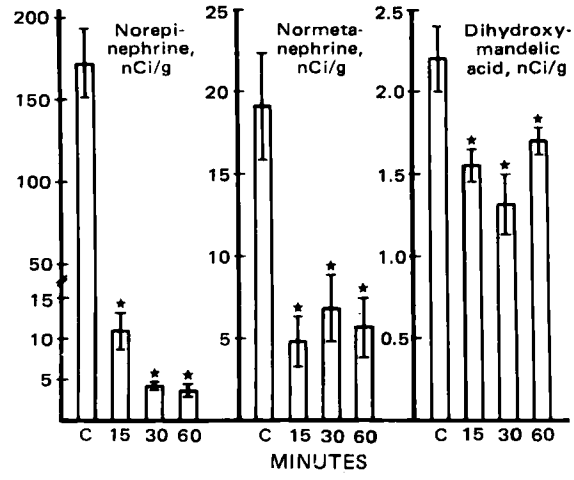

Figure 3—*The effect of desipramine on the uptake and metabolism of tritiated norepinephrine in rat hearts* in vivo. *Rats were given desipramine (5 mg/kg iv) 15, 30, and 60 min prior to an injection of 10 μCi of [^{3}H]norepinephrine. Control animals received an intravenous injection of saline. The hearts were removed 30 min later and assayed for the radiolabeled compounds, norepinephrine, normetanephrine, and 3,4-dihydroxymandelic acid. All values represent the mean (horizontal bar) ± SEM (vertical bar) from four rats. Key: (*), postdesipramine values significantly different from control values (C) at* $p < 0.05$.

Influence of Cyclazocine on the Uptake of Tritiated Norepinephrine *In Vitro*—The intraperitoneal injection of cyclazocine, 2.5, 5, or 10 mg/kg, 1 hr before the removal of the rat heart and subsequent perfusion with radiolabeled norepinephrine significantly reduced the uptake of the tritiated norepinephrine (Fig. 4). Cyclazocine added directly to the bathing medium in concentrations of 10^{-5} and 10^{-4} *M*, likewise, significantly reduced the uptake of [^{3}H]norepinephrine by the isolated perfused rat heart (Fig. 5).

Effect of Cyclazocine on Heart Endogenous Norepinephrine—Table I shows the influence of cyclazocine, *5, 10, 20, or 40 mg/kg ip on rat* heart norepinephrine 1, 2, or 4 hr after cyclazocine. Cyclazocine significantly reduced rat heart norepinephrine levels at doses of 10, 20, and 40 mg/kg, but did not alter the levels at 5 mg/kg.

DISCUSSION

These results support the hypothesis that cyclazocine produces alterations in sympathetic nervous system function by virtue of changes in uptake processes at adrenergic nerve endings.

A reduced recovery of [^{3}H]norepinephrine in rat heart *in vivo* produced by cyclazocine could be related to an altered uptake of norepinephrine

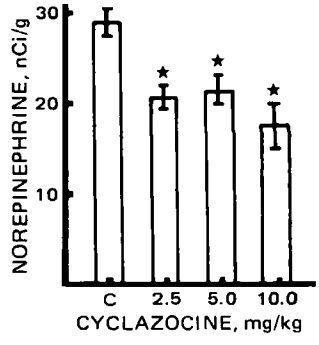

Figure 4—*The effect of systemic cyclazocine on the uptake of tritiated norepinephrine by the isolated perfused rat heart. Rats were given cyclazocine 2.5, 5.0, or 10.0 mg/kg ip 1 hr prior to removal of the heart. Control rats received an intraperitoneal injection of saline. The hearts were perfused with tritiated norepinephrine (10 ng/ml, 3.3 nCi/ml). All values represent the mean (horizontal bar) ± SEM (vertical bar) from four rats. Key: (*), postcyclazocine values significantly different from control values (C) at* $p < 0.05$.

[4] Sterling Winthrop Research Institute, Rensselaer, N.Y.
[5] Tween 80, Atlas Powder Co., Wilmington, Del.
[6] New England Nuclear Corp., Boston, Mass.
[7] Sigma Chemical Co., St. Louis, Mo.
[8] Geigy Pharmaceuticals, Ardsley, N.Y.

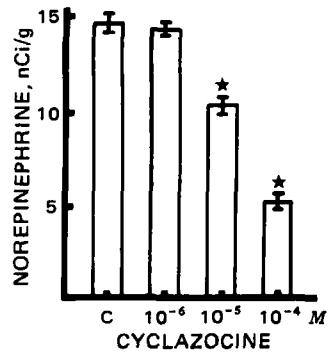

Figure 5—*The effect of various concentrations of cyclazocine on the uptake of tritiated norepinephrine by the isolated perfused rat heart. Hearts were removed and perfused with tritiated norepinephrine (10 ng/ml, 3.3 nCi/ml) in the absence (control C) and presence of 10^{-6}, 10^{-5}, or 10^{-4} M cyclazocine ± SEM (vertical bar) from four rats. Key: (*), cyclazocine-treated values significantly different from control values (C) at $p < 0.05$.*

into sympathetic nerves. Such an inference is supported by a significant cyclazocine-induced decrease in the formation of [^{3}H]dihydroxymandelic acid. Since monoamine oxidase appears to be principally located in the adrenergic neuron and has been shown to catalyze the oxidative deamination of intraneuronal norepinephrine, a decrease in neural uptake would be expected to result in a decrease in the deaminated metabolite of norepinephrine, dihydroxymandelic acid. In comparing the effect of desipramine, a compound that has been reported to decrease neuronal uptake in the rat heart (24), cyclazocine was less active in suppressing the accumulation of tritiated norepinephrine by the rat heart and did not produce a significant decrease in the formation of [^{3}H]normetanephrine (Figs. 1 and 3).

The observed changes in the recovery of radiolabeled normetanephrine from the heart induced by cyclazocine and desipramine were of interest in light of the reported increases in normetanephrine accumulation produced by agents that inhibit neuronal uptake in brain tissue (25, 26). These results are consistent with those presented previously (27, 28). It was shown that agents that inhibit adrenergic neuronal uptake (cocaine or imipramine) reduce the recovery of tritiated normetanephrine from heart tissue when [^{3}H]norepinephrine is administered intravenously. One explanation for the difference in the recovery of normetanephrine in brain and heart tissue produced by an agent that impedes neural uptake might be that the diffusion rate of the *O*-methylated metabolite out of the tissues varies markedly (29).

Since the *in vivo* results suggested a cyclazocine-induced inhibition of neuronal uptake, the effect of cyclazocine on the uptake of [^{3}H]norepinephrine was examined in isolated rat heart perfused with a concentration of norepinephrine (10 ng/ml) that when recovered would be indicative of neuronal uptake (19, 26). Cyclazocine added directly to the medium or given to the animal significantly decreased the uptake of tritiated norepinephrine into the isolated perfused heart, presumably at the level of the sympathetic nerve terminals.

Cyclazocine caused a depletion of endogenous cardiac norepinephrine at 10, 20, and 40 mg/kg. Cyclazocine has been shown to decrease levels of norepinephrine in brain tissue (30). It could be suggested that the depletion of endogenous cardiac norepinephrine was due to an inhibition of uptake; however, such a conclusion is not warranted, since tricyclic antidepressants with potent neuronal uptake inhibitory actions do not deplete catecholamine stores (31, 32). One possible mechanism is that cyclazocine releases norepinephrine, thereby, reducing stores of the catechol in the rat heart.

An earlier study (33) can be cited in support of such an alternate hypothesis. It was theorized that pentazocine, a chemically related compound to cyclazocine, produces a calcium-dependent action on vasculature and that the ability of pentazocine to decrease norepinephrine concentrations is related to an enhanced calcium influx into the nerve terminal, causing a release and subsequent depletion of the neurotransmitter.

Although the results presented in this paper suggest that cyclazocine interacts with the sympathetic nervous system by impeding neuronal uptake, they do not negate the possibility that cyclazocine alters sympathetic neural activity by other actions, *e.g.*, by enhancing release of neurotransmitter.

Furthermore, the results add support to the hypothesis that cyclazocine can induce central nervous system effects by not only interacting with opiate receptors but by altering adrenergic nerve function (34, 35).

REFERENCES

(1) E. Weiss and V. G. Laties, *J. Pharmacol. Exp. Ther.*, **143**, 169 (1964).

(2) L. Lasagna, J. J. DeKornfeld, and J. W. Pearson, *ibid.*, **144**, 12 (1964).

(3) L. S. Harris and A. K. Pierson, *ibid.*, **143**, 141 (1964).

(4) W. R. Martin, *Pharmacol. Rev.*, **19**, 367 (1967).

(5) W. R. Martin, *Res. Publ. Assoc, Res. Nerv. Ment. Dis.*, **46**, 367 (1968).

(6) W. R. Martin, C. W. Gorodetzke, and T. K. McClaine, *Clin. Pharmacol. Ther.*, **7**, 455 (1966).

(7) A. M. Freedman and M. Fink, *Br. J. Addict.*, **63**, 59 (1968).

(8) E. S. Petursson and E. Preble, *Dis. Nerv. Syst.*, **31**, 549 (1970).

(9) M. J. Goldstein, *Int. J. Addict.*, **15**, 939 (1980).

(10) M. Fink and T. Itil, in "Psychopharmacology: A Review of Progress 1956–67," D. H. Efron, J. O. Cole, J. Levine, and J. R. Wittenform, Eds., U.S. Government Printing Office, Washington, D.C., 1968, p. 671.

(11) M. Fink, J. Simeon, J. M. Itil, and A. M. Freedman, *Clin. Pharmacol. Ther.*, **11**, 41 (1970).

(12) R. P. White, W. G. Drew, and M. Fink, in "Recent Advances in Biological Psychiatry," J. Wortis, Ed., Plenum, New York, N.Y., 1969, p. 317.

(13) W. G. Drew and R. P. White, *Pharmacology*, **9**, 65 (1973).

(14) E. B. Sigg, *Can. Psychiatr. Assoc. J.*, **4**, 575 (1959).

(15) A. J. Prange, Jr., E. Postrom, and R. M. Cochrane, *Psychiatry Dig.*, **25**, 27 (1964).

(16) H. J. Dengler, H. E. Speigel, and E. O. Titus, *Nature (London)*, **191**, 816 (1961).

(17) J. Glowinski and J. Axelrod, *ibid.*, **204**, 1318 (1964).

(18) G. D. Russi and F. G. Martin, *Eur. J. Pharmacol.*, **24**, 321 (1973).

(19) L. L. Iversen, *Br. J. Pharmacol. Chemother.*, **25**, 18 (1965).

(20) *Idem.*, **21**, 523 (1963).

(21) K. M. Taylor and R. Laverty, *J. Neurochem.*, **16**, 1361 (1969).

(22) *Ibid.*, *Proc. Univ. Otago Med. Sch.*, **45**, 8 (1967).

(23) R. G. D. Steel and J. H. Torrie, "Principles and Procedures of Statistics," McGraw-Hill, New York, N.Y., 1960, p. 132.

(24) B. A. Callingham, in "Antidepressant Drugs," S. Garattini and M. N. G. Dukes, Eds., Excerpta Medica, Amsterdam, 1967, p. 35.

(25) J. J. Schildkraut, A. Winokur, and C. W. Applegate, *Science*, **168**, 867(1970).

(26) J. J. Schildkraut, A. Winokur, P. R. Draskoczy, and J. H. Hensle, *Am. J. Psychiat.*, **127**, 8 (1971).

(27) J. Axelrod, L. G. Whitby, and G. Hertting, *Science*, **133**, 383 (1961).

(28) G. Hertting, J. Axelrod, and L. G. Whitby, *J. Pharmacol. Exp. Ther.*, **134**, 146 (1961).

(29) S. L. Lightman and L. L. Iversen, *Br. J. Pharmacol.*, **37**, 638 (1969).

(30) S. G. Holtzman and R. E. Jewett, *J. Pharmacol. Exp. Ther.*, **187**, 380 (1973).

(31) D. E. Schwartz, W. P. Burkard, M. Roth, K. F. Gey, and A. Pletscher, *Arch. Int. Pharmacodyn.*, **141**, 135 (1963).

(32) H. Nyback, Z. Borzecki, and G. Sedvall, *Eur. J. Pharmacol.*, **4**, 395 (1968).

(33) C. Lee and B. A. Berkowitz, *J. Pharmacol. Exp. Ther.*, **198**, 347 (1976).

(34) S. G. Holtzman and R. E. Jewett, *ibid.*, **187**, 380 (1973).

(35) J. J. Teal and S. G. Holtzman, *ibid.*, **212**, 368 (1980).

ACKNOWLEDGMENTS

Supported in part by grants from the University of Kansas and The Kansas Heart Association.

Dependence of Renal Clearance on Urine Flow: A Mathematical Model and its Application

D. DAN-SHYA TANG-LIU, THOMAS N. TOZER ˣ, and SIDNEY RIEGELMAN†

Received August 21, 1981, from the *Department of Pharmaceutical Chemistry, School of Pharmacy, University of California, San Francisco, CA 94143.* Accepted for publication March 29, 1982. † Deceased.

Abstract □ A mathematical model is developed to explain the dependence of renal clearance on urine flow rate. The model is tested using human data from the literature on compounds that are neither secreted nor reabsorbed by active or pH-sensitive mechanisms. The physiologically derived model explains and predicts the relationship between renal clearance and urine flow for a broad spectrum of compounds (*i.e.*, butabarbital, chloramphenicol, creatinine, ethanol, theophylline, and urea) for which appropriate data are available.

Keyphrases □ Excretion, renal—dependence of renal clearance on urine flow, mathematical model, application, reabsorption (□) Urine flow—dependence of renal clearance, mathematical model, application, reabsorption □ Reabsorption—dependence of renal clearance on urine flow, mathematical model, application

Passive reabsorption is a major process controlling the renal excretion of many organic substances (1, 2). The magnitude of passive reabsorption depends on the nature of the substance, *i.e.*, its lipophilicity and its extent of ionization. It also depends on the urine flow rate and the pH of the luminal fluid in the renal tubule. For a compound readily undergoing reabsorption, its rate of urinary excretion can be elevated by increasing the urine flow (2–4). This dependence on urine flow leads to problems in clinically or pharmacokinetically assessing urine data, because of a large variability in renal clearance or excretion rate–plasma concentration. However, the dependence can be used beneficially. For example, forced diuresis hastens the elimination of drugs and shortens the time required to detoxify patients overdosed on certain drugs (5–7). Experiments have demonstrated this flow dependence of renal excretion (8–11).

In this work a model based upon physiological considerations was derived. Literature data on the renal clearance–urine flow relationship for representative compounds were fitted to the model. Factors determining the urine flow dependence are discussed and exemplified by computer simulation.

BACKGROUND

The functional unit of the kidney, the nephron, is composed of the glomerulus, the proximal tubule, the loop of Henle, the distal tubule, and the collecting duct, each of varying dimensions [Table I, (12)]. The glomerulus receives the arterial blood and a portion of the plasma water is filtered. About two thirds of the glomerular filtrate is reabsorbed isoosmotically in the proximal tubule (13). The wall of the ascending loop of Henle is thought to be relatively impermeable to water. Further reabsorption of water occurs in the distal tubule and collecting ducts. The volume of plasma water filtered per unit of time at the glomerulus, the glomerular filtration rate, is ~120 ml/min in an average 20-year-old male. Because of the extensive reabsorption of water, the urine flow rate averages ~1–2 ml/min. The renal plasma flow, ~650 ml/min, and the glomerular filtration rate are reasonably constant, but because of the variable reabsorption of water in the distal tubule and collecting duct, the urine flow rate is quite variable.

Table I—Dimensions of Renal Tubule in Humans

Segment of Renal Tubule	Length, mm[a]	Outside Diameter, μm[a]	Outer Surface Area,[b] M^2
Proximal	12–24	50–65	6.6
Loop of Henle, thin	0–14	14–22	1.0
thick	6–18	—	
Distal	2–9	20–50	1.2
Collecting duct	22	up to 200	20.7

[a] Obtained from R. F. Pitts (12). [b] π(average outer diameter)(average length) × 2(number of nephrons per kidney) (Ref. 25).

The renal excretion rate of a drug is the net result of filtration, secretion, and reabsorption:

$$\text{rate of excretion} = \text{rate of filtration} + \text{rate of secretion} - \text{rate of reabsorption} \quad \text{(Eq. 1)}$$

Because only drug in plasma water (the unbound drug) is filtered at the glomerulus:

$$\text{rate of filtration} = F\alpha C_p \quad \text{(Eq. 2)}$$

For definition of symbols, see the Appendix.

Substituting Eq. 2 into Eq. 1 and dividing by plasma drug concentration, the renal clearance, a proportionality constant relating the rate of excretion to the plasma drug concentration, is obtained:

$$CL_r = \alpha F + \frac{\text{rate of secretion} - \text{rate of reabsorption}}{C_p} \quad \text{(Eq. 3)}$$

A renal clearance of less than αF, therefore, indicates that reabsorption occurs. If a drug is secreted, reabsorption must then be greater than secretion.

The renal clearance of a nonpolar compound that is nonionized at physiological conditions shows flow dependence. The extent of the dependence is determined by its lipophilicity and the membrane permeability. For drugs that are not secreted, the renal clearance is expressed by:

$$CL_r = \alpha F - \frac{\text{rate of reabsorption}}{C_p} \quad \text{(Eq. 4)}$$

The following model applies to a drug that is neither secreted nor ionized at physiological pH.

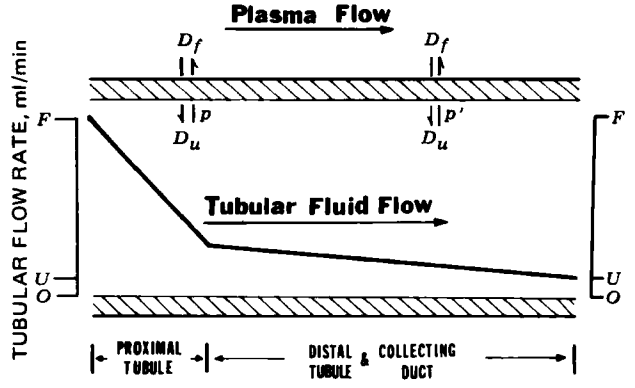

Figure 1—*Schematic diagram of drug and water reabsorption in an average functional nephron. The exchange of drug in luminal fluid (D_u) and free drug in plasma (D_f) is characterized by the permeability constant, P or P′, of each region of the nephron. The decline of the luminal fluid flow rate is assumed to be linear within the proximal and post proximal parts of the tubule. The glomerular filtration rate (F), the urine flow (U), and the origin (O) are also shown on the y-axes.*

0022-3549/83/0200-0154$01.00/0

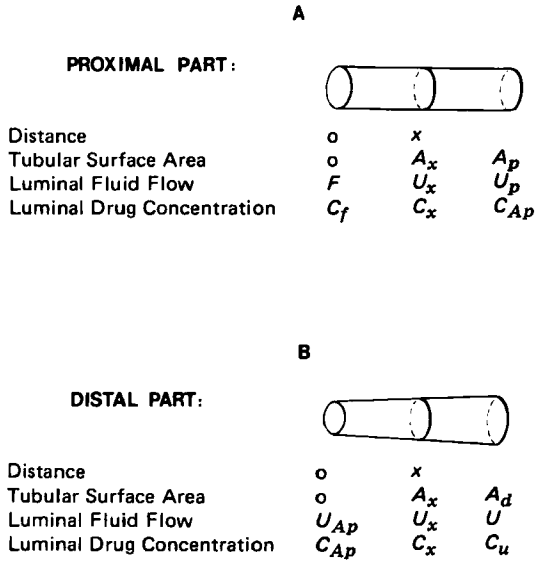

Figure 2—*Scheme for symbols used in model derivation. Proximal part of the renal tubule (A); and distal part of the renal tubule (B).*

THEORETICAL

To develop a model for the urine flow rate dependence of renal clearance for a nonsecreted, poorly ionized drug, the following assumptions are made:

1. Each nephron behaves, on average, as a single functional unit as depicted in Fig. 1.
2. There is a constant reabsorption flux of water within the proximal and distal regions of the tubule. The net rate of the change of luminal fluid volume per unit of surface area of membrane is P_w in the proximal and P'_w in the rest of the nephron. Urine flow alterations reflect a physiological change in P'_w.
3. The rate of reabsorption of a compound at any point in the tubule is proportional to the difference between the concentrations in luminal fluids and in plasma and depends on the permeability of the drug in the tubular membrane. The permeability of the membrane per unit of surface area for a given compound is assumed to be constant within each of the regions of the tubule.

Reabsorption in the Proximal Tubule—At point x, the rate of change of luminal fluid flow is:

$$\frac{dU_x}{dA_x} = -P_w \qquad \text{(Eq. 5)}$$

and the proximal luminal fluid flow, U_x, in the model (Fig. 2A), is described by:

$$U_x = F - P_w A_x \qquad \text{(Eq. 6)}$$

Thus, the luminal fluid flow rate declines from F to $F - P_w A_p$, or U_{Ap}. The rate of reabsorption of drug depends on the permeability constant, P, and the concentration gradient of the exchangeable drug (unbound) across the membrane at point x. Therefore:

$$\text{rate of reabsorption} = P(C_x - \alpha C_p)dA_x \qquad \text{(Eq. 7)}$$

The rate of loss of the drug from the tubule is:

$$-d(U_x C_x) = -U_x dC_x - C_x dU_x \qquad \text{(Eq. 8)}$$

Because these two rates must be the same, it follows that:

$$U_x \frac{dC_x}{dA_x} + C_x \frac{dU_x}{dA_x} = -P(C_x - \alpha C_p) \qquad \text{(Eq. 9)}$$

By substituting Eqs. 5 and 6 into Eq. 9:

$$(F - P_w A_x)\frac{dC_x}{dA_x} + C_x(P - P_w) = \alpha C_p P \qquad \text{(Eq. 10)}$$

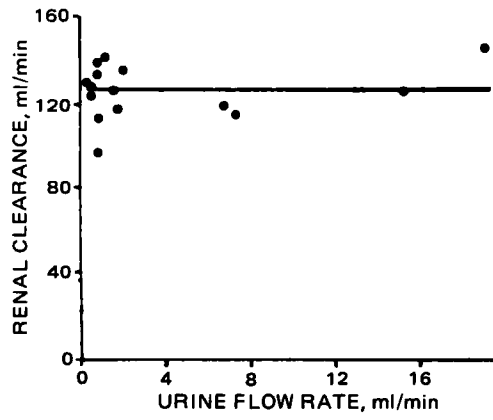

Figure 3—*Relationship between renal clearance of creatinine and urine flow rate. Data from Ref. 14. The solid line is the computer fit using the model.*

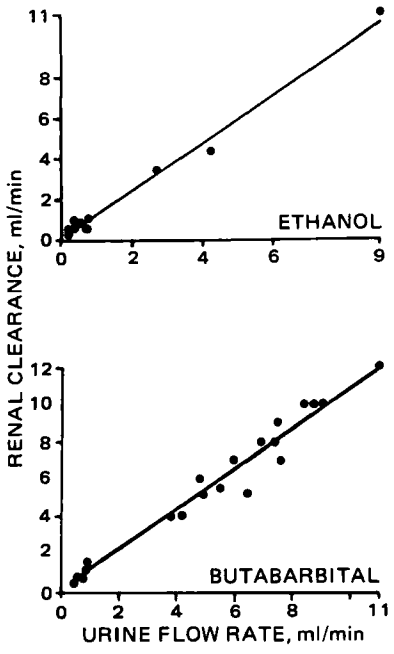

Figure 4—*Urine flow-dependence of renal clearance for ethanol and butabarbital. Data from Refs. 14 and 7, respectively. Solid lines are the computer fits of the model.*

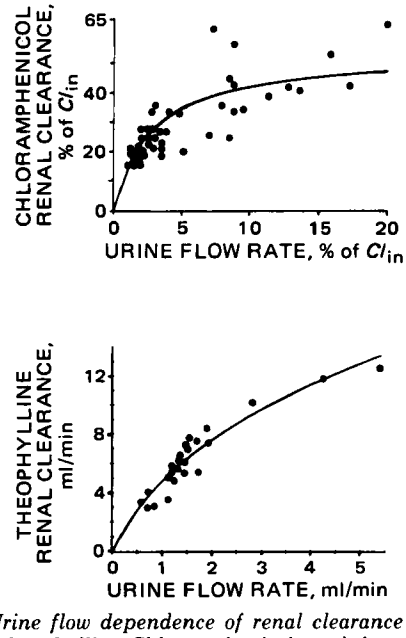

Figure 5—*Urine flow dependence of renal clearance for chloramphenicol and theophylline. Chloramphenicol renal clearance and urine flow were normalized by inulin clearance (CL_{in}). Data for chloramphenicol are from Ref. 15. The theophylline data are unpublished (17). Solid lines are the computer fits of the model.*

Table II—Parameter Values of Model[a]

Parameter	Urea[b] A	Urea[b] B	Urea[b] C	Creatinine	Ethanol	Butabarbital	Chloramphenicol	Theophylline
ϵ, ml/min	6.7	8.0	9.1	0	665	120	13.9	27.5
δ	0.013	0.016	0.018	0	5	1.01	0.028	0.25
α	1	1	1	1	1	0.72[c]	0.47[d]	0.47[e]
F, ml/min	125	85	145	125	140	120	133	118

[a] ϵ, δ, and F values from fit of Eq. 28 to data (7, 14–18). [b] From three subjects. [c] Ref. 19. [d] Ref. 20. [e] Ref. 17.

On rearrangement:

$$\frac{dC_x}{dA_x} + \left(\frac{P - P_w}{F - P_w A_x}\right) C_x = \frac{\alpha C_p P}{F - P_w A_x} \qquad \text{(Eq. 11)}$$

Integration of this first-order linear differential equation gives:

$$C_x = \frac{\alpha C_p \delta}{\delta - 1} + \beta (F - P_w A_x)^{-W} \qquad \text{(Eq. 12)}$$

where $W = 1 - \delta$, δ is P/P_w, and β is the constant of integration. Because only the unbound drug is filtered at the glomerulus, the drug concentration in the initial filtrate, where A_x is zero, is αC_p. Accordingly, the integration constant is:

$$\beta = -\alpha C_p \left(\frac{1}{\delta - 1}\right) F^W \qquad \text{(Eq. 13)}$$

and the luminal drug concentration at any point x within the proximal tubule is:

$$C_x = \frac{\alpha C_p}{\delta - 1}\left[\delta - \left(\frac{F}{F - P_w A_x}\right)^W\right] \qquad \text{(Eq. 14)}$$

At the end of the proximal tubule, the luminal concentration becomes:

$$C_{Ap} = \frac{\alpha C_p}{\delta - 1}\left[\delta - \left(\frac{F}{F - P_w A_p}\right)^W\right] \qquad \text{(Eq. 15)}$$

Because ~70% of the glomerular filtrate is reabsorbed in the proximal tubule (13), $P_w A_p$ can be approximated by $0.7F$. Therefore:

$$C_{Ap} = \frac{\alpha C_p}{\delta - 1}(\delta - 0.3^{-W}) \qquad \text{(Eq. 16)}$$

Reabsorption in the Distal Tubule and the Collecting Duct—The luminal flow through an annulus at point x in the distal part of the nephron (Fig. 2B) is:

$$U_x = 0.3F - P'_w A_x \qquad \text{(Eq. 17)}$$

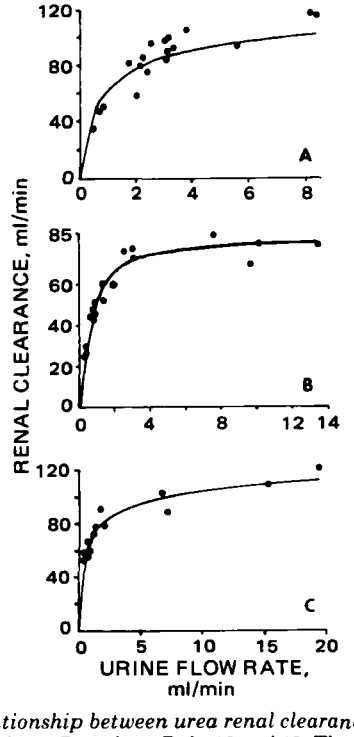

Figure 6—*Relationship between urea renal clearance and urine flow rate in three subjects. Data from Refs. 16 and 18. The solid lines are the computer fits of the model.*

The rate of reabsorption of luminal fluid at any annulus is obtained from the derivative of Eq. 17, *i.e.*:

$$\frac{dU_x}{dA_x} = -P'_w \qquad \text{(Eq. 18)}$$

The rate of reabsorption of the drug within the annulus at point x is:

$$\text{rate of reabsorption} = P'(C_x - \alpha C_p) dA_x \qquad \text{(Eq. 19)}$$

By equating Eqs. 8 and 19, with substitution of Eqs. 17 and 18, and rearranging, we obtain:

$$\frac{dC_x}{dA_x} + \left(\frac{P' - P'_w}{0.3F - P'_w A_x}\right) C_x = \frac{\alpha C_p P'}{0.3F - P'_w A_x} \qquad \text{(Eq. 20)}$$

On integrating:

$$C_x = \frac{\alpha C_p P'}{P' - P'_w} + \gamma (0.3F - P'_w A_x)^{-Z} \qquad \text{(Eq. 21)}$$

where $Z = 1 - P'/P'_w$, and γ is the constant of integration. The drug concentration at the entry of distal tubule ($A_x = 0$) is that at the end of the proximal tubule (Eq. 16). Therefore, solving for the integration constant using Eqs. 16 and 21 (when $A_x = 0$), the luminal drug concentration at any point x within the distal part of the nephron is:

$$C_x = \alpha C_p \left[\frac{P'}{P' - P_w'} + \left(\frac{\delta}{\delta - 1} - \frac{0.3^{-W}}{\delta - 1} - \frac{P'}{P' - P'_w}\right)(0.3F)^Z (0.3F - P'_w A_x)^{-Z}\right] \qquad \text{(Eq. 22)}$$

At the end of the collecting duct ($A_x = A_d$) the luminal concentration is the observed urine concentration (C_u), therefore:

$$C_u = \alpha C_p \left[\frac{P'}{P' - P'_w} + \left(\frac{\delta}{\delta - 1} - \frac{0.3^{-W}}{\delta - 1} - \frac{P'}{P' - P'_w}\right)\left(\frac{0.3F}{U}\right)^Z\right] \qquad \text{(Eq. 23)}$$

The ratio of urine and plasma concentrations becomes:

$$\frac{C_u}{C_p} = \alpha \left[\frac{P'}{P' - P'_w} + \left(\frac{\delta}{\delta - 1} - \frac{0.3^{-W}}{\delta - 1} - \frac{P'}{P' - P'_w}\right)\left(\frac{0.3E}{U}\right)^Z\right] \qquad \text{(Eq. 24)}$$

The value of P'_w is related to the luminal flow rates at two boundaries, $0.3F$ and U, *i.e.*, at the end of the distal region, P'_w is $(0.3F - U)/Ad$ (from Eq. 17). To minimize the number of parameters and to simplify the final form of the model, let:

$$\epsilon = P'Ad \qquad \text{(Eq. 25)}$$

and therefore:

$$\frac{P'}{P'_w} = \frac{\epsilon}{0.3F - U} \qquad \text{(Eq. 26)}$$

Renal clearance relates the urinary excretion rate to the plasma drug concentration. Experimentally, the excretion rate is calculated from urine flow and drug concentration in urine:

$$Cl_r = U\frac{C_u}{C_p} \qquad \text{(Eq. 27)}$$

and from Eqs. 24 and 26, the dependence of renal clearance on urine flow, α, δ, ϵ, and F is obtained:

$$Cl_r = \alpha U \left[\frac{\epsilon}{\epsilon - 0.3F + U} + \left(\frac{0.3^{-W} - \delta}{W} - \frac{\epsilon}{\epsilon - 0.3F + U}\right)\left(\frac{0.3F}{U}\right)^Z\right] \qquad \text{(Eq. 28)}$$

where $W = 1 - \delta$, and $Z = 1 - \epsilon/0.3F - U$.

Renal clearance and urine flow data for compounds demonstrating various degrees of urine flow dependence, namely, alcohol (14), chlor-

amphenicol (15), creatinine (16), butabarbital (7), theophylline (17), and urea (16, 18) were used to test the validity of the model. When tables of data were not available (*i.e.*, chloramphenicol and butabarbital), renal clearance and urine flow values were estimated from figures in the respective references using a ruler with a millimeter scale. Intraindividual values were used except for chloramphenicol, for which renal clearance and urine flow were normalized to inulin clearance (CL_{in}), *i.e.*, CL_r/CL_{in} and U/CL_{in}. Data analysis and graphical examination of the urine flow dependencies were performed by nonlinear regression of Eq. 28 using the PROPHET computer system. The best-fits of the parameters were determined by the minimized residual sum of squares.

RESULTS AND DISCUSSION

The passive diffusion of a drug across the tubular membrane proceeds toward an equilibrium state in which the diffusible species attains the same concentration in both luminal and plasma fluids. The reabsorption of water along the renal tubule produces disequilibrium with an increased concentration of drug in the luminal fluid. The greater the reabsorption of water, the more the drug is concentrated and, perhaps, the longer it stays in the tubule. Drugs can be classified into three categories: one in which no drug is reabsorbed, one in which drug is reabsorbed to equilibrium, and one in which drug is reabsorbed but equilibrium is not achieved.

If a drug is not reabsorbed at all (*e.g.*, creatinine, inulin, gentamicin, and kanamycin), the δ and ϵ values approach zero and the urinary excretion rate is the filtration rate. Under these conditions, the renal clearance is αF (Eq. 4) and is independent of urine flow. This relationship is demonstrated by creatinine (Fig. 3). If a drug is reabsorbed to equilibrium, its ability to diffuse must be equal to or greater than that of water. This category is exemplified by alcohol and butabarbital (Fig. 4), compounds with high δ and ϵ values (Table II). Because of the rapid exchange of the drugs, their plasma unbound and urine concentrations are identical at all urine flow conditions. As the values of δ and ϵ approach infinity (Eq. 28), the renal clearance becomes:

$$CL_r = \alpha U \qquad \text{(Eq. 29)}$$

Within the range of plasma concentrations in which there is a constant fraction unbound, a linear relationship between CL_r and U is observed (Fig. 4).

For many drugs with medium δ and ϵ values, equilibrium is not achieved, because the diffusional rate of the drug (*e.g.*, theophylline, chloramphenicol, and urea) is less than that of water. Various degrees of water reabsorption in the distal portion of the tubule result in various urine flow rates and different disequilibrium states. For theophylline and similar drugs, a convex-ascending relationship can be observed for flow-dependent renal clearance (Fig. 5). Among compounds in this group, urea has received the most attention. Urea clearance increases markedly with urine flow, up to ~3 ml/min, and thereafter increases only slightly if at all (Fig. 6). The model visually fits the urea data well and predicts an asymptotic value of αF; *i.e.*, at higher urine flow rates virtually all the filtered urea is excreted into the urine. This is a classic example of urine flow dependence of renal clearance.

Changes in renal clearance with urine flow predicted by the model for compounds of varied permeability are shown in Fig. 7. The larger the permeability as reflected by δ and ϵ, the greater the dependence on urine flow, and the smaller the value of renal clearance.

It is the unbound drug in plasma that is filtered at the glomerulus. Consequently, the greater the value of α, the larger the filtered load (Eq. 2) for a given plasma concentration. For two compounds of the same permeability, the one with the higher value of α is expected to have the higher renal clearance. This conclusion applies to drugs in all three categories.

There are three more factors to be considered to complete a general model for flow-dependent renal clearance of all drugs. They are: secretion, active reabsorption, and the change of pH in the tubular fluid along the nephron. The present model does not incorporate these factors. The compounds discussed here were chosen because they are neither secreted nor extensively ionized at physiological pH.

Secretion is an active process. If a drug is highly secreted into the lumen, its plasma concentration along the tubule may decline dramatically even if highly bound to plasma proteins. This leads to a perfusion limitation in the excretion of the drug and difficulty in estimating the concentration gradient along the tubule. Furthermore, only a portion of the renal blood flow reaches the distal part of the nephron. These considerations make prediction of urine flow dependence difficult.

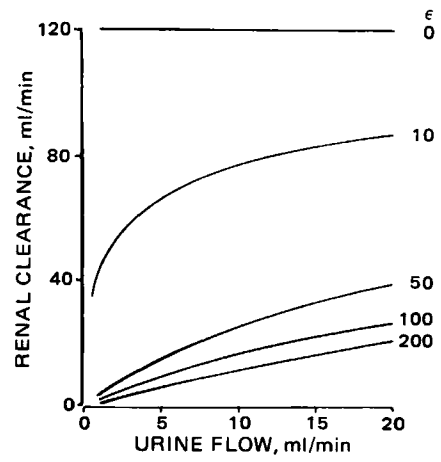

Figure 7—*Simulation of the effect of permeability on the urine flow-dependence of drug renal clearance. Values of parameters used in simulation were: drug unbound fraction in plasma, 1.0; glomerular filtration rate, 120 ml/min; $\epsilon/\delta = 100$.*

Active reabsorption usually occurs for endogenous compounds, *e.g.*, vitamins, electrolytes, glucose, and amino acids. However, the reabsorption process for drugs, mostly exogenous compounds, is mainly passive diffusion. Therefore, the model was restricted to the passive processes.

The luminal fluid starts with a pH of 7.4 at the glomerulus and ends its journey at a pH of 4.5–8.0 (1). Usually, the urine pH is 6.25 ± 0.36 (mean ±*SD*). There is evidence that the greater change of pH occurs in the distal part of the nephron, *i.e.*, mostly in the collecting ducts (21–23). For acidic and basic compounds with pKa values sensitive to physiologic pH changes, their fractions nonionized vary with their location in the tubule. Of the compounds tested, only butabarbital (pK_a = 7.9) and theophylline (pK_a = 8.8) are slightly ionizable at physiologic pHs. The urine pH was not reported with the data of butabarbital. It was assumed that samples were collected under these conditions and the pH sensitivity of butabarital renal clearance is not expected. In one theophylline study, subjects took ammonium chloride orally to maintain acidic urine. The urine pH was successfully maintained below 5.5 under normal urine flow conditions. However, the urine pH increased when urine flow rate was increased (due to the diuretic effect of theophylline). Presumably, at high urine flow rates, the controlling mechanism (located mainly in the collecting ducts) has less effect on the pH of the fluid. Therefore, the pH of the tubular fluid not only varies with the distance the luminal fluid travels in the tubule, but also is a function of urine flow rate.

The model explains and predicts the dependence of renal clearance on permeability and urine flow. The model was tested using literature data for compounds that are apparently not secreted, actively reabsorbed, or pH sensitive, but represent a wide spectrum of lipophilicity. From the fits of the model, it can be concluded that the urine flow dependence of renal clearance can be adequately described and predicted by our physiologically derived model.

APPENDIX

A_d = Surface area of the distal tubule and collecting ducts, centimeter squared
A_p = Surface area of the proximal tubule, centimeter squared
A_x = Surface area of membrane from the integration starting point to point x, centimeter squared
C_{Ap} = Concentration of the drug in luminal fluid at the end of the proximal tubule, micrograms per milliliter
C_f = Free drug concentration in plasma, micrograms per milliliter
CL_r = Renal clearance of the drug, milliliter per minute
C_p = Total drug concentration in plasma, micrograms per milliliter
C_u = Drug concentration in urine, micrograms per milliliter
C_x = Luminal drug concentration in annulus at point x, micrograms per milliliter
F = Glomerular filtration rate, milliliter per minute
P = Permeability constant of the drug in the proximal tubule, centimeters per minute

P' = Permeability constant of the drug in the distal tubule and collecting ducts, centimeter per minute
P_w = Reabsorption flux of water in the proximal tubule, centimeter per minute
P'_w = Reabsorption flux of water in the distal tubule and collecting duct, centimeter per minute
pK_a = The dissociation constant of the drug
U = Urine flow rate, millimeter per minute
U_{Ap} = Luminal fluid flow rate at the end of the proximal tubule, milliliter per minute
U_x = Luminal fluid flow rate in annulus at point x, millimeter per minute
α = Unbound fraction of drug in plasma
δ = Ratio of P/P_w
ϵ = Product of $P'A_d$, ml/min

REFERENCES

(1) M. Rowland and T. N. Tozer, "Clinical Pharmacokinetics, Concepts and Applications," Lea and Febiger, Philadelphia, Pa., 1980.

(2) I. M. Weiner, in "Handbook of Physiology, Section 8: Renal Physiology," J. Orloff and R. W. Berliner, Eds., American Physiological Society, Bethesda, Md., 1973, p. 521.

(3) M. Cohen and R. Pocelinko, *J. Pharmacol. Exp. Ther.*, **185,** 703 (1973).

(4) E. R. Garrett, *Int. J. Clin. Pharmacol.*, **16,** 155 (1973).

(5) A. Giotti and E. W. Maynert, *J. Pharmacol. Exp. Ther.*, **101,** 296 (1951).

(6) L. W. Henderson and J. P. Merrill, *Ann. Int. Med.*, **64,** 876 (1976).

(7) A. L. Linton, P. G. Luke, and J. D. Briggs, *Lancet*, **2,** 377 (1967).

(8) D. W. Barfuss and J. A. Schafer, *Am. J. Physiol.*, F163 (1979).

(9) G. Levy and R. Koysooko, *J. Clin. Pharmacol.* **6,** 329 (1976).

(10) G. H. Mudge, P. Silva, and G. R. Stibitz, *Med. Clin. N. Am.*, **59,** 681 (1975).

(11) I. M. Weiner and G. H. Mudge, *Am. J. Med.*, **36,** 743 (1964).

(12) R. F. Pitts, "Physiology of the Kidney and Body Fluid," Year Book Medical Publishers, Chicago, Ill., 1964, p. 16.

(13) E. Koushanpour, "Renal Physiology: Principles and Functions," W. B. Saunders, Philadelphia, Pa., 1976.

(14) H. W. Haggard, L. A. Greenberg, and R. P. Carroll, *J. Pharmacol. Exp. Ther.*, **71,** 348 (1941).

(15) O. Schück, H. Nádvorniková, J. Grafuetterová, and V. Prát, *Int. J. Clin. Pharmacol.*, **15,** 201 (1977).

(16) J. H. Austin, E. Stillman, and D. D. Van Slyke, *J. Biol. Chem.*, **46,** 91 (1921).

(17) D. D.-S. Tang-Liu, T. N. Tozer, and S. Riegelman, *J. Pharmacokinet. Biopharm.*, in press.

(18) P. B. Rehberg, *Biochem. J.*, **20,** 461 (1926).

(19) L. R. Boldbaum and P. K. Smith, *J. Pharmacol. Exp. Ther.*, **111,** 197 (1954).

(20) L. S. Goodman and A. Gilman (Eds), in "The Pharmacological Basis of Therapeutics," 6th ed., MacMillan, New York, N.Y., 1980, p. 1695.

(21) C. M. Bennett, B. M. Brenner, and R. W. Berliner, *J. Clin. Invest.*, **47,** 203 (1968).

(22) C. W. Gottschalk, W. E. Lassiter, and M. Mylle, *Am. J. Physiol.*, **198,** 581 (1960).

(23) F. L. Vieira and G. Malnic, *ibid.*, **214,** 710 (1968).

(24) W. F. Raub, *Proc. Natl. Comput. Conf. Exposition*, **43,** 457 (1974).

(25) B. M. Brenner and F. C. Rector (Eds.), in "The Kidney," W. B. Saunders, Philadelphia, Pa., 1976, p. 8.

ACKNOWLEDGMENTS

The authors wish to thank Dr. Svein Øie for his review of the manuscript.

Data analyses and graphical examination of the results were performed with the PROPHET system, a specialized resource developed by the Chemical/Biochemical Information Handling Program of the National Institutes of Health.

Absorption Kinetics and Steady-State Plasma Concentrations of Theophylline Following Therapeutic Doses of Two Sustained-Release Preparations

O. ANDERSEN, M. K. NIELSEN, P. B. ERIKSEN, M. FENGER, and P. J. KNUDSEN ˣ

Received October 5, 1981, from the *Department of Clinical Chemistry, Centralsygehuset i Naestved, DK 4700 Naestved, Denmark.* Accepted for publication March 19, 1982.

Abstract □ Ten healthy volunteers received two sustained-release preparations as a single and multiple dose regimen in an open crossover study. Plasma theophylline concentrations were measured by an enzyme immunoassay. The limited fluctuation of the theophylline levels at steady state, with twice daily administration, clearly demonstrated the marked sustained release properties of both preparations. Results indicate similar properties for the two preparations. Significant correlations between the single dose period and steady state were found for C_{max} and AUC (r = 0.76 and 0.87, respectively) with one formulation, whereas this was not the case for the other (r = 0.27 and 0.49). The daily dose necessary to keep the plasma concentration within the therapeutic range of 55–110 μmole/liter varied from 7.9 to 22.9 mg/kg. Only mild side effects were recorded, but they were not correlated to the plasma theophylline concentration.

Keyphrases □ Absorption—kinetics and steady-state plasma concentrations of theophylline following therapeutic doses of two sustained-release preparations □ Kinetics—absorption and steady-state plasma concentrations of theophylline following therapeutic doses of two sustained-release preparations □ Theophylline—absorption kinetics and steady-state plasma concentrations following therapeutic doses of two sustained-release preparations

Theophylline produces relaxation of bronchial smooth muscles and is widely used in the treatment of reversible obstructive lung disease. The bronchodilator effect of theophylline increases with serum concentrations over a range of 28–110 μmoles/liter (5–20 μg/ml), but at levels of >110 μmoles/liter there is an increased risk of serious toxicity (1). Maximal bronchodilation with minimal toxicity occurs at levels between 55–110 μmoles/liter (10–20 μg/ml), and this is therefore normally considered the therapeutic range (2). It is very difficult to maintain serum

0022-3549/83/0200-0158$01.00/0

P' = Permeability constant of the drug in the distal tubule and collecting ducts, centimeter per minute
P_w = Reabsorption flux of water in the proximal tubule, centimeter per minute
P'_w = Reabsorption flux of water in the distal tubule and collecting duct, centimeter per minute
pK_a = The dissociation constant of the drug
U = Urine flow rate, millimeter per minute
U_{Ap} = Luminal fluid flow rate at the end of the proximal tubule, milliliter per minute
U_x = Luminal fluid flow rate in annulus at point x, millimeter per minute
α = Unbound fraction of drug in plasma
δ = Ratio of P/P_w
ϵ = Product of $P'A_d$, ml/min

REFERENCES

(1) M. Rowland and T. N. Tozer, "Clinical Pharmacokinetics, Concepts and Applications," Lea and Febiger, Philadelphia, Pa., 1980.

(2) I. M. Weiner, in "Handbook of Physiology, Section 8: Renal Physiology," J. Orloff and R. W. Berliner, Eds., American Physiological Society, Bethesda, Md., 1973, p. 521.

(3) M. Cohen and R. Pocelinko, *J. Pharmacol. Exp. Ther.*, **185,** 703 (1973).

(4) E. R. Garrett, *Int. J. Clin. Pharmacol.*, **16,** 155 (1973).

(5) A. Giotti and E. W. Maynert, *J. Pharmacol. Exp. Ther.*, **101,** 296 (1951).

(6) L. W. Henderson and J. P. Merrill, *Ann. Int. Med.*, **64,** 876 (1976).

(7) A. L. Linton, P. G. Luke, and J. D. Briggs, *Lancet*, **2,** 377 (1967).

(8) D. W. Barfuss and J. A. Schafer, *Am. J. Physiol.*, F163 (1979).

(9) G. Levy and R. Koysooko, *J. Clin. Pharmacol.* **6,** 329 (1976).

(10) G. H. Mudge, P. Silva, and G. R. Stibitz, *Med. Clin. N. Am.*, **59,** 681 (1975).

(11) I. M. Weiner and G. H. Mudge, *Am. J. Med.*, **36,** 743 (1964).

(12) R. F. Pitts, "Physiology of the Kidney and Body Fluid," Year Book Medical Publishers, Chicago, Ill., 1964, p. 16.

(13) E. Koushanpour, "Renal Physiology: Principles and Functions," W. B. Saunders, Philadelphia, Pa., 1976.

(14) H. W. Haggard, L. A. Greenberg, and R. P. Carroll, *J. Pharmacol. Exp. Ther.*, **71,** 348 (1941).

(15) O. Schück, H. Nádvorniková, J. Grafuetterová, and V. Prát, *Int. J. Clin. Pharmacol.*, **15,** 201 (1977).

(16) J. H. Austin, E. Stillman, and D. D. Van Slyke, *J. Biol. Chem.*, **46,** 91 (1921).

(17) D. D.-S. Tang-Liu, T. N. Tozer, and S. Riegelman, *J. Pharmacokinet. Biopharm.*, in press.

(18) P. B. Rehberg, *Biochem. J.*, **20,** 461 (1926).

(19) L. R. Boldbaum and P. K. Smith, *J. Pharmacol. Exp. Ther.*, **111,** 197 (1954).

(20) L. S. Goodman and A. Gilman (Eds), in "The Pharmacological Basis of Therapeutics," 6th ed., MacMillan, New York, N.Y., 1980, p. 1695.

(21) C. M. Bennett, B. M. Brenner, and R. W. Berliner, *J. Clin. Invest.*, **47,** 203 (1968).

(22) C. W. Gottschalk, W. E. Lassiter, and M. Mylle, *Am. J. Physiol.*, **198,** 581 (1960).

(23) F. L. Vieira and G. Malnic, *ibid.*, **214,** 710 (1968).

(24) W. F. Raub, *Proc. Natl. Comput. Conf. Exposition*, **43,** 457 (1974).

(25) B. M. Brenner and F. C. Rector (Eds.), in "The Kidney," W. B. Saunders, Philadelphia, Pa., 1976, p. 8.

ACKNOWLEDGMENTS

The authors wish to thank Dr. Svein Øie for his review of the manuscript.

Data analyses and graphical examination of the results were performed with the PROPHET system, a specialized resource developed by the Chemical/Biochemical Information Handling Program of the National Institutes of Health.

Absorption Kinetics and Steady-State Plasma Concentrations of Theophylline Following Therapeutic Doses of Two Sustained-Release Preparations

O. ANDERSEN, M. K. NIELSEN, P. B. ERIKSEN, M. FENGER, and P. J. KNUDSEN ˣ

Received October 5, 1981, from the *Department of Clinical Chemistry, Centralsygehuset i Naestved, DK 4700 Naestved, Denmark.* Accepted for publication March 19, 1982.

Abstract □ Ten healthy volunteers received two sustained-release preparations as a single and multiple dose regimen in an open crossover study. Plasma theophylline concentrations were measured by an enzyme immunoassay. The limited fluctuation of the theophylline levels at steady state, with twice daily administration, clearly demonstrated the marked sustained release properties of both preparations. Results indicate similar properties for the two preparations. Significant correlations between the single dose period and steady state were found for C_{max} and AUC (r = 0.76 and 0.87, respectively) with one formulation, whereas this was not the case for the other (r = 0.27 and 0.49). The daily dose necessary to keep the plasma concentration within the therapeutic range of 55–110 μmole/liter varied from 7.9 to 22.9 mg/kg. Only mild side effects were recorded, but they were not correlated to the plasma theophylline concentration.

Keyphrases □ Absorption—kinetics and steady-state plasma concentrations of theophylline following therapeutic doses of two sustained-release preparations □ Kinetics—absorption and steady-state plasma concentrations of theophylline following therapeutic doses of two sustained-release preparations □ Theophylline—absorption kinetics and steady-state plasma concentrations following therapeutic doses of two sustained-release preparations

Theophylline produces relaxation of bronchial smooth muscles and is widely used in the treatment of reversible obstructive lung disease. The bronchodilator effect of theophylline increases with serum concentrations over a range of 28–110 μmoles/liter (5–20 μg/ml), but at levels of >110 μmoles/liter there is an increased risk of serious toxicity (1). Maximal bronchodilation with minimal toxicity occurs at levels between 55–110 μmoles/liter (10–20 μg/ml), and this is therefore normally considered the therapeutic range (2). It is very difficult to maintain serum

0022-3549/83/0200-0158$01.00/0

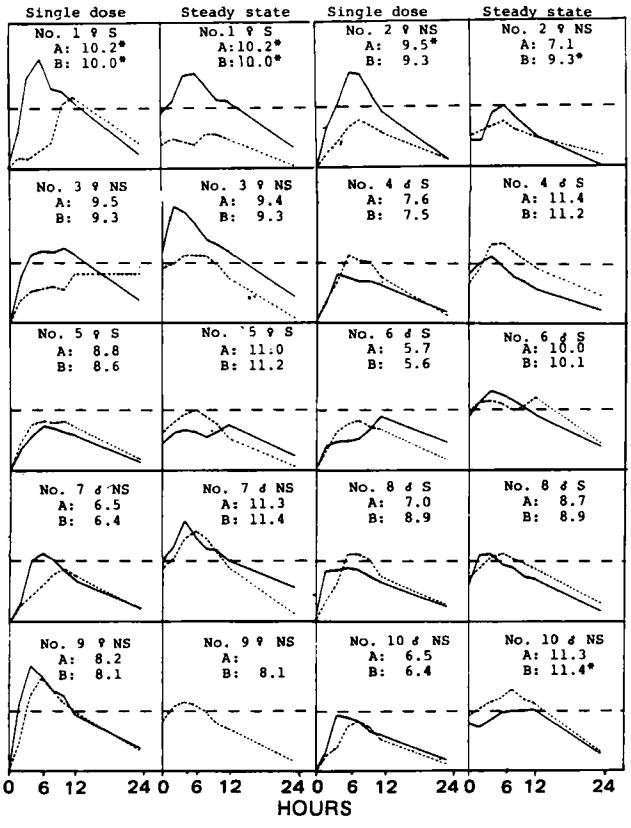

Figure 1—*Plasma concentration–time relationship for all subjects. Ordinate gives plasma concentration. The odd numbers (left in figure) received tablet B in the first period, the even numbers received tablet A. Figures in each frame are doses in milligrams per kilogram (single dose experiments) and milligram per kilogram per day (steady-state experiment). Key: (---) 55 μmoles/liter; (—) tablet A; (·····) tablet B; (S) smoker; (NS) nonsmoker; (*) occurrence of side-effects during the administration of this dose or at the next higher dose according to the dose schedule.*

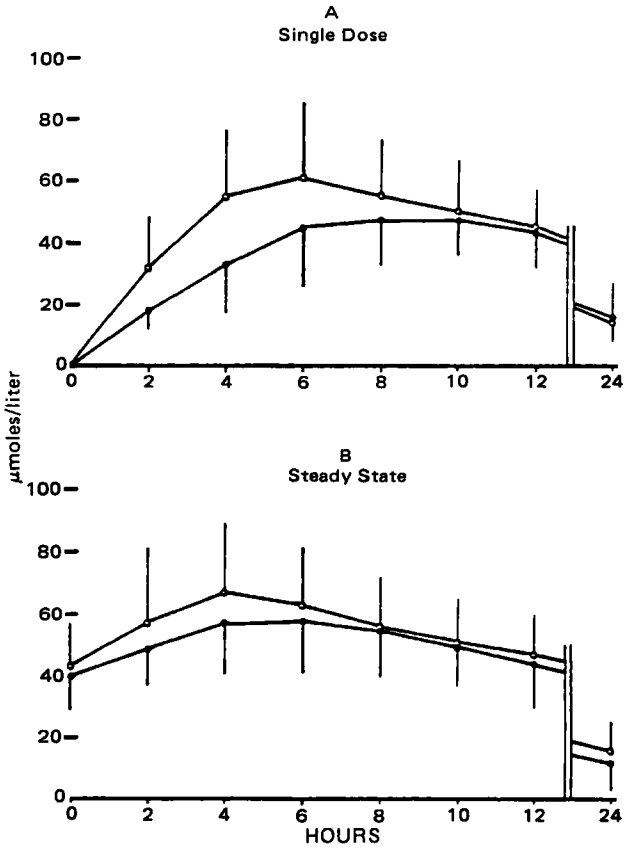

Figure 2—*(A) Plasma concentrations after administration of a single dose of tablet A (dose equivalent to 510 mg of theophylline), or tablet B (dose equivalent to 500 mg of theophylline). Mean of 10 healthy adults ±SD. Key: (○) tablet A; (●) tablet B. (B) Plasma concentrations at steady state. Tablet A (mean dose; 10.0, range: 7.1–11.4 mg/kg/day as theophylline). Tablet B (mean dose; 10.1, range: 8.1–11.4 mg/kg/day as theophylline). Mean of 10 healthy adults ±SD. Key: (○) tablet A; (●) tablet B.*

theophylline concentrations within this narrow therapeutic range during treatment with conventional tablets, due to the large interindividual variation in theophylline clearance, fast absorption, and relatively short half-life. A growing interest in sustained-release preparations has appeared during recent years and a number of different preparations are now on the market in several countries. This report deals with a comparison of two sustained-release preparations, containing theophylline–ethylenediamine and theophylline, respectively, after single dose administration, as well as repeated dosage to give levels within the therapeutic range. The theophylline dosage form was studied previously (3), and it was shown that a mean C_{max} value of 41 μmoles/liter (7.5 μg/ml) was obtained with 8 mg/kg every 12 hr. Levels of theophylline–ethylenediamine within the therapeutic range have only been investigated in single dose studies (4, 5) and the preparation has not been compared with other sustained-release preparations.

EXPERIMENTAL

Preparations—Tablet A[1] was a theophylline–ethylenediamine formulation with 350 mg of theophylline–ethylenediamine (equivalent to 255 mg of anhydrous theophylline) given as whole or half tablets. Tablet B[2] was a theophylline formulation with 200 or 300 mg of anhydrous theophylline, given as whole tablets only.

Subjects—Ten healthy volunteers (5 females and 5 males), age 26–54 years, mean 38, were included in the study. Their heights ranged from 160 to 192 cm, mean 175, and they weighed from 50 to 89 kg, mean 67. Five were smokers and five nonsmokers. All were found healthy by physical examination and laboratory testing for functions of liver, heart, kidney, and bone marrow.

Study Design and Dosage—The study was an open crossover study in which half of the subjects were randomly allocated to start on one preparation and the other half on the other preparation. The subjects received only one dose (510 mg of theophylline for tablet A and 500 mg for tablet B) for the first 24 hr. From the second day on the dose was gradually increased, starting with ~400 mg of theophylline daily and increasing in steps of 25% every 3 days (6). The final dose for each individual subject was determined by the occurrence of one of the following criteria: (*a*) The next increase in dose gave rise to side effects; (*b*) the plasma theophylline concentration 6 hr after the morning dose was within the therapeutic range (55–110 μmoles/liter); or (*c*) the dose had reached 13 mg/kg or 900 mg/day. The dosage used in the first period was used in the second period. Each preparation was given for 13 days with an 8-day wash-out period in between. The subjects were instructed not to take methylxanthine-containing beverages or food 12 hr before and on the day of blood sampling. They were also instructed to make notes on side effects during the study.

Blood Sampling—On day 1 of each period 10-ml blood samples were drawn before, and 2, 4, 6, 8, 10, 12, and 24 hr after drug administration. On the last day of each period the same sequence of blood sampling was followed after the morning dose, the maximum dose having been administered for at least 3 days. Blood samples were drawn from a cubital

[1] Tablet A: Euphyllin retard, H. Lundbeck & Co., A/S, Batch No. 2218-2.

[2] Tablet B: Theo-Dur, Draco, Batch Nos. 055889 and 056481.

Table I—Comparison of the Parameters Obtained with Two Sustained-Release Preparations

	Single Dose Period					Steady-State Period				
	Tablet A		Tablet B			Tablet A		Tablet B		
	mean	*SD*	mean	*SD*	*p*-value	mean	*SD*	mean	*SD*	*p*-value
C_{max}[a], μmoles/liter/mg	0.13	0.04	0.11	0.03	0.25	0.20	0.11	0.15	0.03	0.21
C_{min}[a], μmoles/liter/mg	—	—	—	—	—	0.13	0.06	0.11	0.02	0.30
T_{max}, hours	6.4	2.6	9.1	3.6	0.03	6.0	3.6	7.1	2.2	0.44
C_{max}–C_{min}	—	—	—	—	—	1.51	0.28	1.41	0.20	0.39
$AUC_{0\to\infty}$[a], μmoles/liter/mg hr	2.01	0.57	1.84	0.44	0.19	—	—	—	—	—
$AUC_{0\to12}$[a], μmoles/liter/mg hr	—	—	—	—	—	1.95	1.00	1.58	0.33	0.28

[a] Normalized by division by dose in milligrams of theophylline.

vein using an evacuated heparinized container[3] and using stasis times of <1 min. Within 1 hr the plasma was separated from blood cells by centrifugation and transferred to a clean vial. The theophylline concentrations were determined immediately or after storage at −20° for <24 hr. No significant decrease was found in plasma samples stored at −20° for 6 months.

Drug Estimation—Plasma theophylline was measured by an enzyme immunoassay[4] (7) adapted for use with a biochromatic analyzer[5]. Comparative analyses of patient samples analyzed by the enzyme immunoassay and HPLC methods have confirmed the lack of interference from metabolites or structurally related molecules in the enzyme immunoassay (8). The accuracy of this enzyme immunoassay is the same as the HPLC methods usually used in clinical pharmacological studies of theophylline (9). In the present study the within-day coefficient of variation was 1.4% and the between-day coefficient of variation was 3.9%.

Data Treatment—The elimination rate constant (β) was calculated from the slope of the concentration line, from 12 to 24 hr after administration, in a semilogarithmic plot as $\beta = -2.303$ slope. The area under the plasma concentration curve after the first dose ($AUC_{0\to\infty}$) was calculated by the trapezoidal rule in the time period of 0–24 hr ($AUC_{0\to24}$) and by the formula C_{24}/β in the period 24 hr to infinity ($AUC_{24\to\infty}$). In the steady-state period, the area under the curve in a dosage interval ($AUC_{0\to12}$) was calculated by the trapezoidal rule. The different parameters (concentrations dose corrected) obtained with the two preparations were compared by a paired-sample *t* test (10). The regression line illustrating the correlation of the parameters from the single dose period with those from the steady-state period with the same preparation was calculated by the least-square method [Pearson's product moment correlation (11)].

RESULTS

Plasma concentration–time curves obtained during the study are shown in Fig. 1. The plasma concentration curves show a rather large variation between the individual subjects, but do not indicate that one preparation gives more consistent plasma levels than the other.

The single (first) dose periods are compared in Fig. 2A. The curves show that the maximum plasma concentration after tablet A appeared earlier than after tablet B. This was confirmed by a statistically significant difference found by a paired *t* test (Table I). The curves also show a higher maximum plasma concentration and a larger area under the curve (AUC) after tablet A, but the statistical analysis showed no difference.

Mean plasma theophylline concentrations after repeated administration to steady state appear in Fig. 2B. The mean dose (±*SD*) on repeated administration was 10.0 (±1.5) mg/kg for tablet A, and 10.1 (±1.2) mg/kg for tablet B, giving mean peak plasma concentrations at 4 hr after administration for tablet A (67 μmoles/liter) and at 6 hr after tablet B (58 μmoles/liter). The corresponding minimum values (mean of 0 and 12 hr) were 45 μmoles/liter and 42 μmoles/liter, respectively. There was a tendency toward an earlier maximum with tablet A, but the difference was not significant (Table I). Also, values for C_{max}, C_{min} (mean of C_0 and C_{12}), and $AUC_{0\to12}$ tended to be higher for tablet A but with no significant difference. The fluctuations in the dosage interval expressed as the C_{max}–C_{min} ratio, are similar for the two preparations being a mean of 1.5 and 1.4 for tablets A and B, respectively (Table I).

The dosage, *giving* a concentration within the therapeutic range of 55–110 μmoles/liter throughout the entire period, can be calculated from the minimum concentration measured during steady state in each subject. For tablet A this dose was a mean (range) 12.8 (7.9–18.3) mg/kg/day, and for tablet B 14.1 (9.3–22.9) mg/kg/day.

A correlation analysis on the different parameters shows, that C_{max} and AUC (both normalized by division by dose) are significantly correlated in the single dose and steady-state periods ($r = 0.76$ and 0.87, respectively) during administration of tablet A, but not with tablet B ($r = 0.27$ and 0.49) (Fig. 3). Time of maximum, T_{max}, did not show correlation between single dose and repeated administration for either of the preparations.

The reports on side effects are shown in Fig. 1; it appears that the frequency of side effects was similar from the two preparations. The symptoms reported include palpitations, tremor, vomiting, nausea, headache, and insomnia, subjectively estimated as ranging from mild to severe.

DISCUSSION

The present investigation clearly demonstrates the marked sustained-release properties of the two preparations. This is in accordance with earlier investigations in which the two preparations were compared to conventional tablets (3–5, 9). The limited fluctuation seen during the steady-state dosage interval of 12 hr shows that this frequency of dosing would be reasonable during maintenance therapy with any one of these two sustained-release preparations. As expected, the dose necessary to keep the plasma theophylline concentration within the therapeutic range varied considerably between individuals (7.9–22.9 mg/kg/day).

The preparations did not differ significantly as to maximum plasma concentration, minimum plasma concentration, fluctuation in plasma concentration during the dosage interval, and area under the plasma concentration curve. This indicated that the amount of theophylline absorbed from the two preparations was the same, and that the absorption took place at almost the same rate. The significantly earlier average time of individual peak occurrence seen with tablet A in the single dose period may indicate that absorption is slightly faster with this preparation, but it does not significantly influence the steady-state plasma concentration curve. Tablet B contained theophylline only, whereas tablet A, in addition to theophylline, contained ethylenediamine to increase the solubility of theophylline. This difference does not seem to influence absorption considerably.

There is a difference, however, between the two preparations on one point. The plasma levels for tablet A after the first dose (expressed as dose normalized C_{max} or AUC) correlated significantly with those found at steady state, whereas no such correlation was found with tablet B. This indicates less intraindividual variation with tablet A possibly because of more stable release of drug from this preparation. Moreover it means that in subjects receiving tablet A it is possible to perform measurements on the first dose (C_{max} or AUC), and from these obtain a guideline for choosing the dose for further treatment. This does not, however, render a later monitoring of the drug level unnecessary. The present results do not indicate that it would be of any help to measure plasma levels after the first dose with tablet B.

In connection with the calculation of the AUC values after single dose administration, an elimination rate constant, β, has been calculated. As this value is only based on two concentrations, C_{12} and C_{24}, and one cannot be sure that absorption is complete at 12 hr after administration, β is encumbered with some uncertainty. However, the values obtained (0.06–0.18) give half-lives in the range of 3.9–11.6 hr, which are in agreement with the half-lives normally found for theophylline (1). Moreover it supports the view that the steady state can be reached with 3 days of constant dosage. A difference in half-lives between smokers and nonsmokers as demonstrated by others (12–14), could not be found, but the reason for this may be that none of the volunteers were heavy smokers. A comparison of $AUC_{0\to\infty}$ after single dose and $AUC_{0\to12}$ after dosing to steady state shows that the AUC values are not significantly different. This means that the pharmacokinetics of theophylline have not changed during treatment.

[3] Venoject.
[4] EMIT, Syva Corp., Palo Alto, CA 94304.
[5] ABA 100.

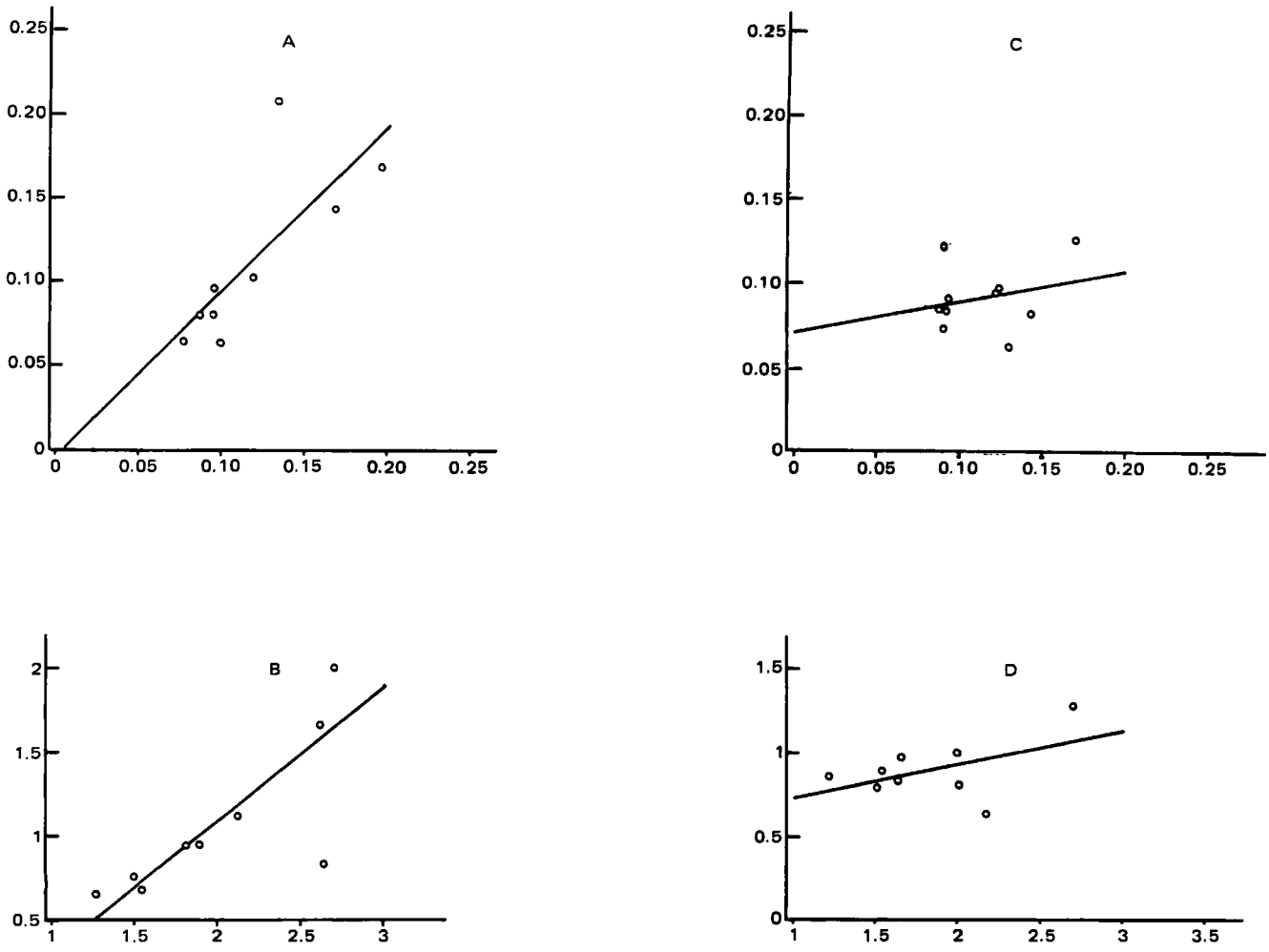

Figure 3—*Correlations between single dose (abscissa) and steady state (ordinate). Key: (A) Tablet A,* C_{max}, $y = 0.972x - 0.005$, $r = 0.76$; *(B) Tablet A,* AUC, $y = 0.799x - 0.511$, $r = 0.87$; *(C) Tablet B,* C_{max}, $y = 0.189x + 0.070$, $r = 0.27$; *(D) Tablet B,* AUC, $y = 0.199x + 0.529$, $r = 0.49$. C_{max} *values are μmoles/liter/mg of theophylline.* AUC *values are μmole hr/liter/mg of theophylline.*

The design of this investigation does not allow conclusions considering side-effects. Appearance of side-effects was not related to plasma theophylline concentrations in the range investigated. Some subjects experienced more side-effects from one preparation than from the other, whereas the opposite was experienced by others. Similarly for some, the first period seemed to be worse than the second and *vice versa.* Some subjects did not experience any adverse side-effects at all. Thus, it seems that each individual patient must be allowed to try whichever preparation is most suitable.

REFERENCES

(1) R. I. Ogilvie, *Clin Pharmacokinet.*, **3,** 267 (1978).

(2) R. G. van Dellen, *Mayo Clin. Proc.*, **54,** 733 (1978).

(3) D. L. Spangler, D. D. Kalof, F. L. Bloom, and H. J. Wittig, *Ann. Allergy*, **40,** 6 (1978).

(4) J. Ahrens, *Dtsch. Med. Wochenschr.*, **102,** 482 (1977).

(5) A. Somogyi and R. Gugler, *Fortschr. Med.*, **98,** 1707 (1980).

(6) L. Hendeles, M. Weinberger, and R. Wyatt, *Am. J. Dis. Child*, **132,** 876 (1978).

(7) J. B. Gushaw, M. W. Hu, P. Singh, J. G. Miller, and R. S. Schneider, *Clin. Chem.*, **23,** 1144 (1977).

(8) J. R. Koup and B. Brodsky, *Am. Rev. Resp. Dis.*, **117,** 1135 (1978).

(9) M. Weinberger, L. Hendeles, and L. Bighley, *N. Engl. J. Med.*, **299,** 852 (1978).

(10) J. Miller and J. E. Freund, "Probability and Statistics for Engineers," Prentice-Hall, Englewood Cliffs, N.J., 1965, p. 169.

(11) M. G. Kendall and A. Stuart, "The Advanced Theory of Statistics," vol. 2, Charles Griffin, London, 1973.

(12) J. Jenne, H. Nagasawa, R. McHugh, F. MacDonald, and E. Wyse, *Life Sci.*, **17,** 195 (1975).

(13) S. N. Hunt, W. J. Jusko, and A. M. Yurchak, *Clin. Pharmacol. Ther.*, **19,** 546 (1976).

(14) B. Cusack, J. G. Kelly, L. Lavan, J. Noel, and K. O'Malley, *Br. J. Clin. Pharmacol.*, **10,** 109 (1980).

ACKNOWLEDGMENTS

This study was supported by H. Lundbeck & Co. A/S, Copenhagen, Denmark.

Dissolution of a Soluble Drug Substance from Vinyl Polymer Matrices

C. BROSSARD *‡, D. LEFORT DES YLOUSES §, D. DUCHÊNE *, F. PUISIEUX *, and J. T. CARSTENSEN *x

Received July 30, 1980, from the *Faculté de Pharmacie, Laboratoire Galénique, Université de Paris-Sud, 92290 Châtenay-Malabry, France, the ‡School of Pharmacy, University of Wisconsin, Madison, WI 53706, and the §Faculté de Medecine et de Pharmacie, 87032, Limoges, France. Accepted for publication March 19, 1982.

Abstract □ It was shown that vinyl polymers form good bases for *in vitro* sustained-release matrices, and that the character of the release curves is basically in line with their pH–solubility profiles. For a flow cell, the release curves may be approximated by the equation: $\ln (m/m_0) = -K(t - t_i)$, where m is the amount not dissolved, m_0 is the initial drug content, K is a dissolution constant, t is time, and t_i is a lag time. Furthermore, it was shown that K is a function of tablet hardness (H) and polymer content (Q, percent). This functionality is well represented by the equation: $\ln K = \alpha H + \gamma \ln Q + \epsilon$, where α, γ, and ϵ are polymer-dependent parameters. Matrix erosion is represented by an exponential decay: $(p/p_0) = \exp(-Dt + a)$, where p is the amount not eroded, p_0 is the initial weight, D is an erosion constant, and a is a soluble polymer-dependent parameter. In the case of these soluble polymers, K is not solely a function of D.

Keyphrases □ Dissolution—soluble drug substances from vinyl polymer matrices □ Polymers—vinyl polymer matrices, dissolution of a soluble drug substance □ Matrices—vinyl polymer, dissolution of a soluble drug substance

The fundamental dissolution relationship from sustained-release preparations have been studied extensively. Matrix formulations are based on a published model (1), and the ensuing square root law has been well established (2). In these formulas, the matrix is completely insoluble.

BACKGROUND

Several reports (3–13) have appeared describing dissolution from rapidly disintegrating dosage forms. The dissolution frequently appears to follow an exponential decay law. It would be expected that the dissolution should adhere to a cube root law; that it does not is due to the effect of disintegration of the tablet in the dissolution apparatus. This effect (3) gives rise to a dissolution equation of the form:

$$\ln (p/p_0) = -Dt \qquad \text{(Eq. 1)}$$

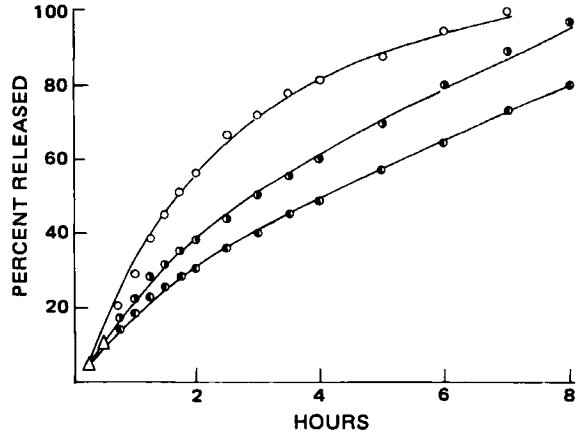

Figure 1—*Example of release curves by half-change method in flow cell under sink conditions of polyvinyl phthalate acetate, 60% directly compressed. Key: (○) 5-kg hardness; (◑) 10-kg hardness; (◐) 15-kg hardness; (△) points that are graphically indistinguishable between the three hardnesses.*

where p is the amount not disintegrated at time t (p_0 at time zero) and D is a disintegration constant. For a tablet where disintegration is rapid, Eq. 1 in conjunction with a cube root equation leads to a dissolution curve of the type:

$$\ln (m/m_0) = -K(t - t_i) \qquad \text{(Eq. 2)}$$

where m is the amount not dissolved, m_0 is the amount of drug present in the tablet, K is a dissolution constant, and t_i is a lag time. The parameter is frequently a function of D by the relation:

$$\ln K = a' + n \ln D \qquad \text{(Eq. 3)}$$

where a' and n are constants.

Contrary to previous studies, many sustained-release preparations can be formulated where the matrix is not completely insoluble, *i.e.*, the tablets disintegrate or erode to some extent during the dissolution process. The word erosion is preferred over the word disintegration, although at times a sharp distinction between the two is not possible.

One of the purposes of the present report is to examine matrices that are not completely insoluble, and to (*a*) elucidate the general dissolution profile, (*b*) estimate the effect of formulation and processing parameters on the dissolution profile, and (*c*) estimate the disintegration or erosion profile in the dissolution apparatus to assess its effect on the dissolution profile.

The conditions of study are such that a half-change method is used. Long-acting tablets were prepared with polymers of different types such that they: (*a*) are acid soluble, but alkali insoluble (giving an initial phase where dissolution is correlated to disintegration and where the final phase should be by diffusion), (*b*) are alkali soluble but acid insoluble (giving the reverse effect), (*c*) are soluble over the entire pH range, and (*d*) are insoluble over the entire pH range.

Since flow methods (11) are commonly used in Europe, one of the purposes of the work reported in this study was to investigate erosion and dissolution behavior in such an apparatus. Erosion profiles in flow cells are not well understood. Some reports on disintegration time (6) have appeared, but elucidation of erosion time curves have not been attempted previously.

The present investigation also reports on formulas that possess *in vitro* release characteristics making them good candidates for sustained-release preparations. The empirical equations serve as a means of obtaining optimum operating conditions for producing the sustained-release tablets and for obtaining the most desirable tablet formula for a given set of specifications for the amount released at two time points.

The drug selected was especially chosen because its solubility is not particularly pH dependent. This allows study of the dissolution behavior to be aimed at the effect of the matrix. The rationale for sustained-release preparations of the compound and its biopharmaceutical characteristics have been described (13).

Table I—Formulas Used [a]

	Direct Compression			Wet
	I	II	III	Granulation
Dyphylline	20	20	20	20
Polymer[b]	15	30	60	15
Dicalcium phosphate[c]	60	45	15	62
Talc	3	3	3	1
Magnesium stearate	1.5	1.5	1.5	2
Pyrogenic silica[d]	0.5	0.5	0.5	
Solvent[e]				(22.5)[c]

[a] Quantities listed are percent by weight, and quantities in parentheses are the percent lost on drying. [b] See Table II. [c] Encompress, Edward Mendell Co., Carmel, NY 10512, (S.P.C.I., 93212, La Plaine-St. Denis, France). Encompress was used in the direct compression formula only. [d] Aerosil 200, Degussa-France, 92100, Neuilly, France. [e] The solvents used are listed in Table II.

0022-3549/83/0200-0162$01.00/0

Table II—Polymers Used

Polymer	Formula (Monomer Unit)	Solvent for Granulation	Characteristics
Polyvinyl acetal diethylamino acetate[a] (I)	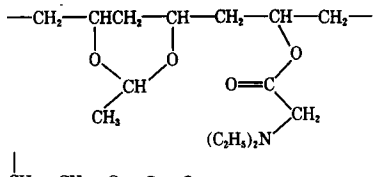	Absolute ethanol	Acid soluble; alkali insoluble; *pK* 5.8–6.1; Mol. wt., 20,000
Polyvinyl acetate phthalate[b] (II)	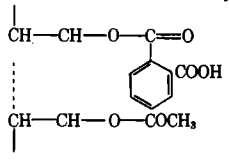	Absolute ethanol	55–65% phthalate groups; 1.2% free acid; acid insoluble, alkali soluble
Polyvinyl acetate[c] (III)	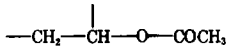	Water	Insoluble at low and high pHs
Povidone[d] (IV)	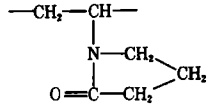	Water	Soluble at all pHs; Mol. wt., 40,000
Povidone–vinyl acetate[e] (V)	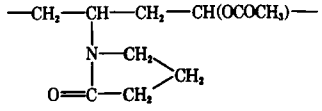	Water	Povidone–vinyl acetate (60:40); soluble at all pHs; Mol. wt., 60,000 ± 15,000
Polyvinyl alcohol–acetate[f] (VI)	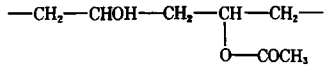	Water	Soluble at all pHs; 12% acetate groups

[a] Sankyo, Marcel Quarré, 75009, Paris, France, designation PADAA 5. [b] Colorcon, Seppic, Elysées, 75008 Paris, France. [c] Rhodopas, BB_3 used for direct compression. Emulsion A 010 Rhodopas readymade aqueous suspension used for wet granulation. Rhône-Poulenc polymères, 92408 Courbevoie, France. [d] Plasdone K 29-32, General Aniline and Film, 95380, Louvres, France. [e] PVP/VA S-630, General Aniline and Film, 95380, Louvres, France. [f] Mowiol, 4-88, Hoechst—France, 75008 Paris, France.

The use of polyvinyl polymers for sustained-release matrices has been reported in general (14–17). Polyvinyl alcohol has been used extensively for pharmaceutical purposes: in coating (18–23) and as a binder in granulation (24). Povidone has also been used extensively for coating (18, 21, 24–27), as a binder in granulation (28–31), and for sustained-release matrices (32). Polyvinyl acetate has been used in coating (18, 33–37), in matrices (17, 38–40), and in sustained-release capsule beads (41, 42). Povidone–vinyl acetate has been used in coating (43, 44) in granulations (45), and in cast films (46–48). Polyvinyl acetate phthalate has been used for coating (49–53), and polyvinyl acetal diethylaminoacetate has been used in coating (54, 55), studied in cast films (56, 57), and used in matrices (14).

EXPERIMENTAL

Dyphylline was selected for study in the sustained-release preparations because of its high solubility (~25% w/v in water at 25°) and the ease of assay (spectrophotometric). Tablets were made by both direct compression and wet granulation.

Direct Compression—The formulas used for direct compression are shown in Table I. The polymer and dyphylline were sieved, and the fraction finer than 315 μm was used. The powders were mixed in a turbulent action mixer[1] for 10 min and were compressed at three pressures, giving hardnesses of 5, 10, and 15 kg.

The experimental conditions (punch pressures) giving these conditions had been established, and hardness was within 5%. All experiments were carried out immediately after manufacture of the tablets. Tablets were compressed on a single-punch tablet machine[2], at a tablet weight of 500 mg using a flat, nonbeveled punch, 12-mm diameter. The machine was instrumented with strain gauges to record upper and lower punch forces.

Wet Granulation—The chemical properties and the granulation solvents are listed in Table II. The general formula for the wet granulation

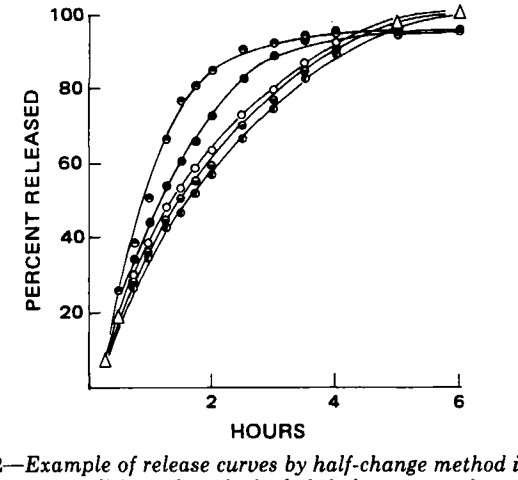

Figure 2—*Example of release curves by half-change method in flow cell under sink conditions of a polyvinyl phthalate acetate formulation (15%) made by wet granulation and compressed to three hardnesses. Key: (○) 5 kg; (◒) 10 kg; (◐) 15 kg; (△) points that are graphically indistinguishable; (◓) povidone–vinyl acetate, 15% at 10 kg; (●) polyvinyl acetate, 15% at 15 kg.*

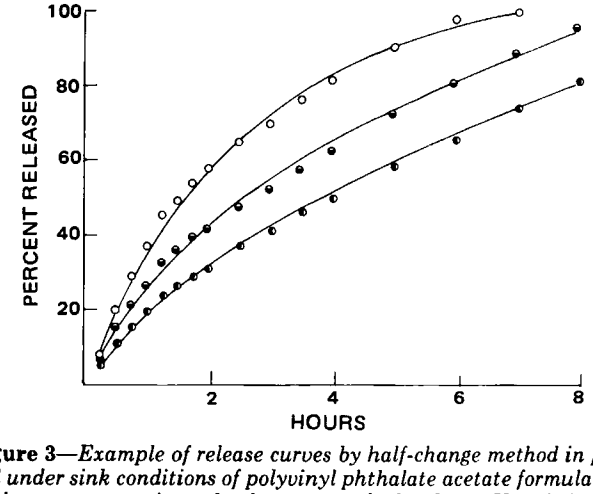

Figure 3—*Example of release curves by half-change method in flow cell under sink conditions of polyvinyl phthalate acetate formulation at three concentrations of polymer at 15-kg hardness. Key: (○) 15%; (◒) 30%; (◐) 60%. All formulas were directly compressed.*

[1] Turbula mixer, Prolabo, 75011 Paris, France.
[2] Model AO Machine, Frogerais, 94400, Vitry-sur-Seine, France.

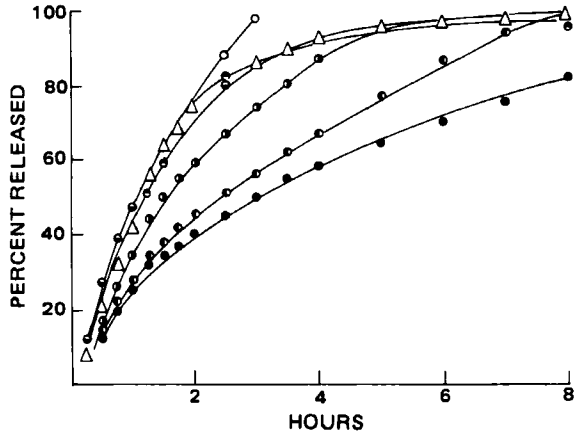

Figure 4—*Release curves at a particular pressure for each of the directly compressed polymer formulas tested, shown for general comparison. Key: (○) polyvinyl alcohol–acetate, 60% at 5 kg; (◒) povidone–vinyl acetate, 15% at 10 kg; (◒) povidone, 30% at 15 kg; (◑) polyvinyl acetal diethylamino acetate, 60% at 15 kg; (◐) polyvinyl acetate phthalate, 30% at 10 kg; (●) polyvinyl acetate, 60% at 5 kg, (△) graphically indistinguishable points.*

is in the last column of Table I. The sieved dyphylline was mixed with the dibasic calcium phosphate for 5 min in a planetary mixer[3]. A 50% w/w solution of the polymer in the solvent was added to the mixture in the planetary mixer, and kneading was carried out for 5 min. The remaining solvent was added and kneading was performed for an additional 5 min. The wet mass was passed through an oscillating granulator[4] equipped with a 2-mm screen. The granulation was dried at 60° in a fluid bed dryer[5] to a moisture content of 2% (loss on drying in an IR moisture balance[6]). Drying time was ~30 min for alcohol wet granulations and ~1 hr for water wet product. The dried granulation was passed through an oscillating granulator with a 1-mm screen, lubricated for 5 min in the turbulent action mixer, and compressed.

Testing—Dissolution was carried out at 37° in a continuous flow apparatus with a flow cell[7], under sink conditions, using the half-change method. One tablet was placed in the cell, and simulated gastric fluid without enzymes was added; after 1 hr this was changed to a 50% mix of simulated gastric fluid and simulated intestinal fluid, both without enzymes. After 2 hr the acid concentration was reduced to 25%. The pH values recorded were: 0–1 hr, 1.2; 1–2 hr, 2.0; 2–3 hr, 6.4; 3–4 hr, 7.0; 4–5 hr, 7.2; 5–6 hr, 7.3; 6–7 hr, 7.4; and 7–8 hr, 7.5. The test was carried out under sink conditions, *i.e.*, fluid was not returned to the cell once it had passed. The assays were carried out spectrophotometrically at 274 nm. The results were converted to amount of drug, m (in milligrams or percent), not released at time t. The testing intervals were typically as shown in Figs. 1 and 2. The hardness of the tablets was tested using a moving-stationary anvil fracture strength tester[8].

The disintegration mode was studied by a described method (4, 9) and yielded the weight of tablet, p (on a dry basis), not disintegrated at time

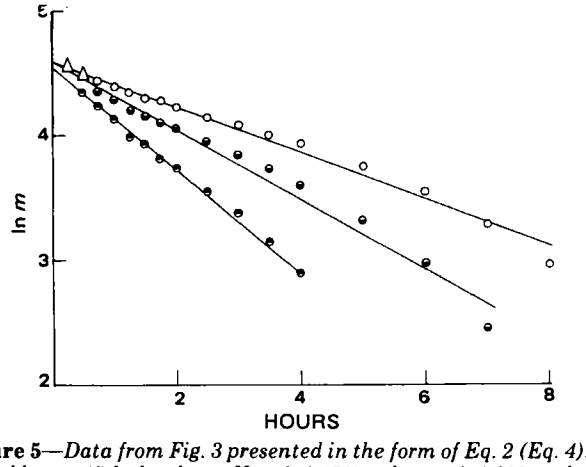

Figure 5—*Data from Fig. 3 presented in the form of Eq. 2 (Eq. 4). All are tablets at 15-kg hardness. Key: (◒) 15% polymer; (◒) 30% polymer; (○) 60% polymer; (△) graphically indistinguishable points.*

Table III—Least-Squares Fit Values for All Dissolution Data Treated According to Eq. 4

Polymer	Percent	Hardness, kg	Correlation Coefficient, r^2	Intercept a	Negative Slope K
I	15	5	0.988	4.89	1.23
	15	10	0.996	4.80	1.01
	15	15	0.998	4.74	0.89
	15g[a]	5	0.999	4.71	0.82
	15g[a]	10	0.998	4.78	0.96
	15g[a]	15	0.998	4.76	0.82
	30	5	0.999	4.69	0.75
	30	10	0.999	4.63	0.57
	30	15	0.995	4.60	0.53
	60	5	0.987	4.84	0.77
	60	10	0.997	4.68	0.61
	60	15	0.991	4.68	0.50
II	15	5	0.999	4.69	0.71
	15	10	0.985	4.59	0.45
	15	15	0.996	4.56	0.45
	30	5	0.997	4.63	0.45
	30	10	0.982	4.61	0.30
	30	15	0.978	4.62	0.27
	60	5	0.997	4.67	0.44
	60	10	0.971	4.69	0.30
	60	15	0.977	4.61	0.18
	15g[a]	5	0.993	4.60	0.58
	15g[a]	10	0.988	4.73	0.56
	15g[a]	15	0.973	4.74	0.54
III	15	5	0.989	4.80	0.90
	15	10	0.975	4.77	0.81
	15	15	0.984	4.73	0.76
	30	5	0.990	4.75	0.62
	30	10	0.988	4.76	0.65
	30	15	0.995	4.71	0.59
	60	5	0.993	4.51	0.19
	60	10	0.990	4.50	0.15
	60	15	0.981	4.48	0.12
	15g[a]	5	0.996	4.78	1.18
	15g[a]	10	0.997	4.66	0.75
	15g[a]	15	0.990	4.74	0.76
IV	15	5	0.961	4.76	0.90
	15	10	0.973	4.72	0.76
	15	15	0.976	4.77	0.74
	30	5	0.958	4.99	1.32
	30	10	0.984	4.85	0.98
	30	15	0.994	4.67	0.70
	60	5	0.974	4.77	1.03
	60	10	0.987	4.91	1.17
	60	15	0.984	4.97	1.31
	15g[a]	5	0.992	4.73	0.79
	15g[a]	10	0.983	4.78	0.81
	15g[a]	15	0.996	4.76	0.88
V	15	5	0.999	4.69	0.70
	15	10	0.999	4.61	0.65
	15	15	0.996	4.73	0.85
	15g[a]	5	0.978	4.91	1.27
	15g[a]	10	0.987	4.81	1.08
	15g[a]	15	0.989	4.74	0.98
	30	5	0.990	4.91	1.41
	30	10	0.997	4.85	1.35
	30	15	0.994	4.59	0.76
	60	5	0.992	4.75	1.80
	60	10	0.975	5.00	1.58
	60	15	0.981	4.89	1.51
VI[b]	15	5	0.989	4.92	1.55
	15	10	0.991	4.87	1.15
VI[b]	30	5	0.992	4.86	1.06
VI[b]	60	5	0.960	4.86	0.85
	15g[a]	5	0.978	4.84	0.91
	15g[a]	10	0.992	4.74	0.84
	15g[a]	15	0.992	4.81	0.95

[a] g stands for wet granulated. [b] Even at very high compression pressures it was not possible to make tablets harder than those shown.

[3] Hobart Mixer, 1-kg capacity, Hobart Manufacturing Co., Troy, Ohio.
[4] Erweka, model F.G.S., Euraf, 75018 Paris, France.
[5] Glatt, model TR2, Chimie-Plastique, BP 664, 95004, Cergy, France.
[6] Mettler, LP12, Sofranie, Levallois-Perret, France.
[7] Desaga flow cell.

[8] Heberlein Hardness Tester, Grogerais, 94400 Vitry-sur-Seine, France.

Table IV—Least-Squares Fit Parameter Values According to Eq. 5

Polymer	Percent	α	β	Correlation Coefficient, r
I	15	−0.032	+0.357	−0.992
I	15g[a]	−0.031	+0.273	−1.0
I	30	−0.035	−0.148	−0.948
I	60	−0.043	−0.051	−0.999
II	15	−0.055	−0.127	−0.935
II	15g[a]	−0.007	−0.509	−0.999
II	30	−0.051	−0.593	−0.947
II	60	−0.089	−0.353	−0.997
III	15	−0.018	−0.018	−0.996
III	15g[a]	−0.091	+0.618	−1
III	30	−0.019	−0.237	−1
III	60	−0.046	−1.434	−0.999
IV	15	−0.020	−0.031	−0.922
IV	15g[a]	+0.011	−0.300	+0.955
IV	30	−0.063	+0.602	−0.999
IV	60	0.024	−0.089	0.999
V	15	0.054	−0.969	1.0
V	15g[a]	−0.026	+0.358	−0.990
V	30	−0.062	+0.741	−0.896
V	60	−0.018	0.662	−0.962
VI	15	−0.060	0.736	−1.0
VI	15g[a]	−0.016	−0.014	−1.0

[a] g is wet granulated.

t. Testing intervals were typically 1, 2, 3, 4, 6, and 8 hr, except for periods during dissolution in particular cases where disintegration was rapid. In these cases the intervals were shortened.

RESULTS AND DISCUSSION

The dissolution curves obtained are all of the shape shown in Figs. 1–4, which is a type profile frequently encountered in dissolution work. The general, mutual position of the curves is in good agreement with the physical characteristics of the polymers, the most soluble giving rise to the most rapid release and the least soluble giving rise to the slowest. This is illustrated in Fig. 4, where all formulas are shown at one hardness (per polymer). It is seen from Fig. 2 that wet granulation causes a marked increase in dissolution rate.

It is to be expected that hardness (H) and polymer content (Q) would affect the rate of release. Figures 1–3 demonstrate this in a qualitative way. In a more quantitative fashion, the dissolution constant (K, hr^{-1}) would have to be a function of both Q and H.

To establish a function that could describe this dependence, the effect of hardness will first be examined, and then the effect of both hardness and polymer concentration will be scrutinized.

It is conventional to fit dissolution data to one of several types of functions (11), an exponential decay (Eq. 2) being one such relationship. In this case the plotting should follow:

$$\ln (m/m_0) = -Kt + a \qquad \text{(Eq. 4)}$$

where m_0 is the initial drug content. Figure 5 shows this type of plotting to be well adhered to, and the least-squares fit parameters for all the preparations are shown in Table III. From the correlation coefficients, the empirical choice of Eq. 4 is well justified.

Table V—Amount Disintegrated as a Function of Time for Three Polymers

Polymer	Percent	Hardness	Fraction Not Disintegrated at Time t, hr			
			0.5	1.0	1.5	2
IV	15	15	0.55	0.36	0.40	0.40
	30	15	0.50	0.30		
	60	15	0.36	0.10	0.05	
	15g[a]	15	0.65	0.47	0.50	0.46
V	15	15	0.56	0.43	0.51	0.37
	30	15	0.45	0.14		
	60	15	0.46	0.19	0.04	
	15g[a]	15	0.49	0.29	0.11	0.14
VI	15	10	0.45	0.24	0.20	
	30	5	0.44	0.24	0.21	0.07
	60	5	0.66	0.46	0.37	
	15g[a]	15	0.47	0.32	0.24	0.20

[a] g is wet granulated.

Table VI—Multiple Regression Treatment of the Data According to Eq. 7 (Direct Compression Formulas)

Polymer	ϵ	α	γ	Average α from Table IV for Direct Compression Formulas
I	1.32	−0.037	−0.37	−0.037
II	1.04	−0.065	−0.41	−0.065
III	3.36	−0.011	−1.22	−0.027
IV	−0.77	−0.020	+0.27	−0.019
V	−1.93	−0.034	+0.683	−0.009
VI	+1.86	−0.054	−0.434	−0.048

It was mentioned earlier that K decreases with increasing hardness, H, and inspection of Table III leads to the plausibility of a relation of the type:

$$\ln K = \alpha H + \beta \qquad \text{(Eq. 5)}$$

The least-squares values for K for all the preparations in Table III have been treated according to Eq. 5, and for each polymer (i), the least-squares fit parameters β_i and α_i are listed in Table IV. A dimensionless plot, as described previously (10, 12), is shown in Fig. 6; the ordinate values are the individual values of $y = \ln K_i - \beta_i$, and the abscissa values are $x = \alpha_i H_i$, and since according to Eq. 5:

$$(\ln K_i) - \beta_i = \alpha_i H \qquad \text{(Eq. 6)}$$

a line with unity slope and zero intercept should follow. Figure 6 indicates that this is the case, showing that Eq. 5 is a reasonable choice of function representing the dependence of K on H, and all values for all the preparations are included.

Table IV shows that the wet granulated preparations are less sensitive to hardness (tableting pressure) than the directly compressed tablets.

The parameter K is not only a function of H but also of the drug content, Q (percent), of the polymer. There are four of the cases where K decreases with increasing polymer concentration, and two cases (povidone and povidone–vinyl acetate) where K increases with increasing polymer concentration. These latter two cases are in accord with previously reported findings where povidone (58–61) and providone–vinyl acetate (45) have been found to increase dissolution rates. However, as seen in Table V, erosion rates also increase with increasing concentration of these two polymers, so that dissolution (diffusion) rate increase or erosion rate increase (or both) could account for the increase in K with an increase in the polymer concentration. Table V shows that K probably approaches a limiting value (K') as Q increases. This requires four parameter fits (*i.e.*, $K = F(H,Q,K')$, where F denotes function of. Since K' would have to be obtained by iteration, the resulting statistics would be of questionable robustness. Instead, it has been assumed here that K for a given hardness

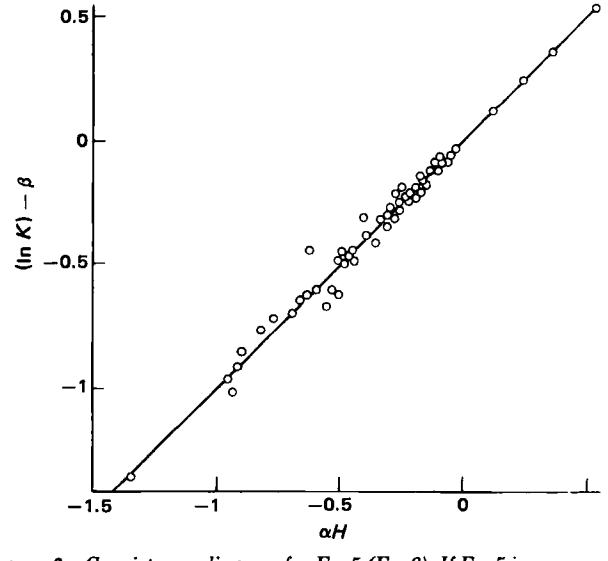

Figure 6—*Consistency diagram for Eq. 5 (Eq. 6). If Eq. 5 is a reasonable fit, then* y = x, *where* x = αh *and* y = ln K − β. *The least-squares fit of the line is* y = 1.002x − 0.0004, i.e., *the slope is close to unity, the intercept is close to zero, and the equation is close to* y = x.

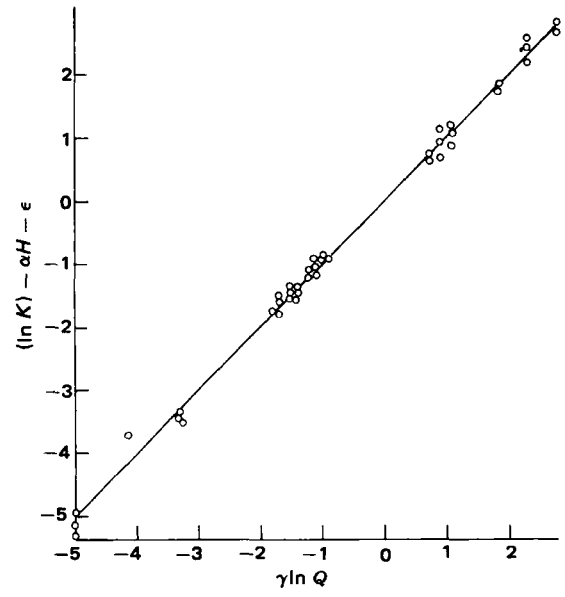

Figure 7—*Data treated according to Eq. 7. The abscissa is* x = γln Q *and the ordinate is* y = (ln K) − αH − ϵ. *The least-squares fit is* y = $(1 \times 10^{-5})x + 5 \times 10^{-4}$, *so that the slope is close to unity and the intercept close to zero as required for Eq. 7 to be a reasonable function* (r = 0.997).

changes in log–log fashion with Q, *i.e.*, retaining the format of Eq. 5 for the H-dependence:

$$\ln K = \alpha H + \epsilon + \gamma \ln Q \qquad \text{(Eq. 7)}$$

The data have been treated by multiple regression, and the least-squares fit values are shown in Table VI. The data are shown in dimensionless presentation in Fig. 7. The ordinate is $y = \ln K - \alpha_i H - \epsilon_i$, where the subscript i is the individual parameter values for the ith polymer. The abscissa is $\gamma_i \ln Q$, so the line, $y = x$, should have unity slope and zero intercept, which is the case. Equation 7, therefore, is a reasonable overall empirical function for the data. The values of α in Tables IV and VI should be close to one another, and as shown in the last column of Table VI, they are.

The value of the phenomonological approach is as follows. For development of sustained-release products, it is usually the intent to obtain a certain *in vitro* release curve. This is often of the military specification type with a range of percent release after (for example) 1 hr, and a range of percent released after 4 hr. At this starting point there is already a benefit from knowing the release equation. If the specifications were, *e.g.*, 25–30% after 1 hr and 40–60% after 4 hr, then the type release found here

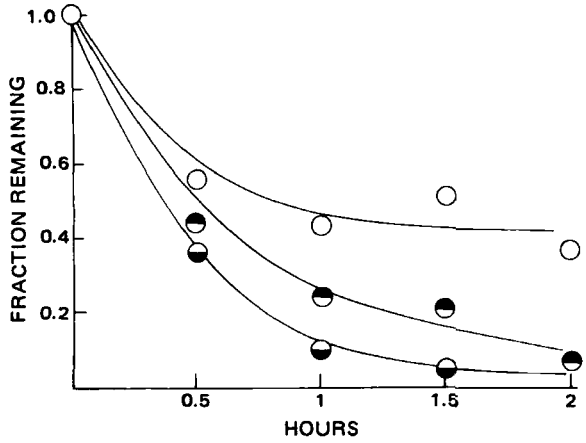

Figure 8—*Disintegration data for polymers with non pH-dependent solubilities. The ordinate is fraction not disintegrated (eroded) at time* t. *Key: (○) providone–vinyl acetate, 15%, 15-kg hardness; (◒) povidone, 60%, 15-kg hardness; (◓) polyvinyl alcohol–acetate, 30%, 5-kg hardness.*

Table VII—Disintegration Data for Tablets Made with Polyvinyl Acetal Diethylaminoacetate

Polymer, %	Parameters for Eq. 15			
	P_∞ (Fraction)	a	D	Correlation Coefficient, r
15g[a]	0.16	−0.318	1.076	−0.98
15	0.18	−0.244	−0.973	−0.99
30	0.26	−0.30	−1.36	−1.0
60	0.33	−0.40	−1.50	−1.0

[a] g is wet granulated.

Table VIII—Values of (p/p_0) for Polyvinyl Acetate Phthalate Formulations

Time, hr	Formula (Polymer, %; Hardness, kg)				
	15%, 15 kg	30%, 15 kg	60%, 15 kg	60%, 10 kg	60%, 5 kg
0	1	1	1	1	1
1	0.7	0.81	0.97	0.98	0.96
2	0.7	0.79	0.97	0.98	0.97
4	0.62	0.66	0.93	0.81	0.77
6	0.34	0.55	0.78	0.63	0.63
8	0.27	0.39	0.54	0.47	0.39
D	0.208	0.130	0.138	0.135	0.170
a	0.289	0.126	0.512	0.340	0.470
$t_i = a/D$	1.39	1.97	3.72	2.49	2.75
r	−0.97	−0.98	−0.97	−0.99	0.97

(Eq. 2) would not be adequate[9]. It should be pointed out that most sustained-release patterns are of this type. That it would not be adequate is seen from the following. The K-value calculated from the 4- and 1-hr restrictions must be in the range:

$$\text{1 hr: } -\ln 0.75 < K < -\ln 0.70 \text{ or } 0.29 < K < 0.35 \qquad \text{(Eq. 8)}$$

$$\text{4 hr: } -0.25 \ln 0.6 < K < -0.25 \ln 0.4 \text{ or } 0.13 < K < 0.23 \qquad \text{(Eq. 9)}$$

Since the two intervals do not overlap, it is not possible to meet the specification range requirements. Without knowing the dissolution pattern, it would be possible to spend considerable time attempting to obtain a formulation which could not possibly meet the given requirements.

If, instead, the required release ranges were 25–35% after 1 hr and 55–75% after 4 hr, then similar calculations would give:

$$\text{1 hr: } 0.29 < K < 0.43 \qquad \text{(Eq. 10)}$$

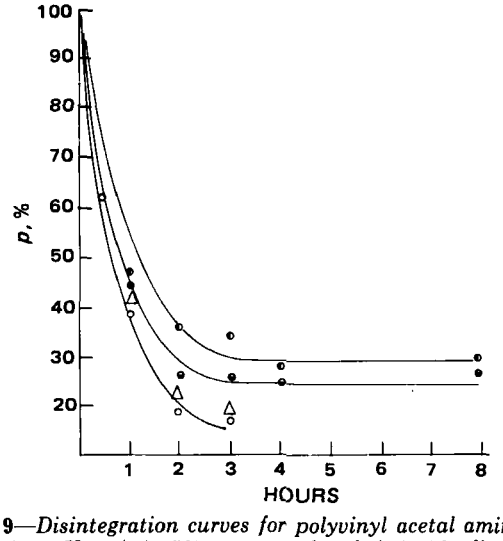

Figure 9—*Disintegration curves for polyvinyl acetal aminoacetate preparations. Key: (○) 15% wet granulated; (△) 15% directly compressed; (◒) 30% directly compressed; (◐) 60% directly compressed. The parameter* p *is the amount not disintegrated in percent.*

[9] It should be noted that an immediate release component in the formulation might solve this. An extension of the argument is that if a specification is set in addition at, *e.g.*, 8 hr, a similar impossible situation might arise.

Table IX—Disintegration Data Treated According to Eq. 17

Polymer	Percent (Q)	Hardness (H)	Correlation Coefficient, r	a	D	ln D	ln K^c
V	15	15	−0.92	−0.408	0.365	−1.01	0.162
	30	15	−1.0[b]	0.243	1.832	0.605	−0.274
	60	15	0.98	0.644	2.455	0.898	0.412
	15g[a]	15	−0.95	−0.208	0.987	−0.013	−0.020
IV	15	15	−0.84	−0.489	0.270	−1.309	−0.301
	30	15	−1.0[b]	−0.155	0.860	−0.151	−0.357
	60	15	−0.99	0.079	1.837	0.608	0.270
	15g[a]	15	−0.93	−0.320	0.307	−1.181	−0.128
VI	15	10	−0.99	−0.267	0.910	−0.094	0.140
	30	5	−0.97	−0.069	1.138	0.129	0.058
	60	5	−0.99	−0.105	0.586	−0.534	−0.163
	15g[a]	15	−0.99	−0.343	0.661	−0.414	−0.051

[a] g is wet granulated. [b] Only two points were available and were not included in Fig. 12. [c] From Table III.

$$4 \text{ hr: } 0.20 < K < 0.35 \qquad \text{(Eq. 11)}$$

i.e., K must be in the interval: $0.29 < K < 0.35$.

If polymer II is used, and a 8–11-kg hardness is required, then (Table VI, line 2):

$$\ln K = -0.065\,H - 0.41 \ln Q + 1.04 \qquad \text{(Eq. 12)}$$

Inserting lower limits for K and H gives:

$$\ln 0.29 + (0.065 \times 8) - 1.04 = -0.41 \ln Q \text{ or } Q = 73 \qquad \text{(Eq. 13)}$$

and inserting upper limits for K and H:

$$\ln 0.35 + (0.065 \times 11) - 1.04 = -0.41 \ln Q \text{ or } Q = 29 \qquad \text{(Eq. 14)}$$

Therefore, in this case, Q must be between 30 and 73, and narrowing the specification limits or the hardness limits would produce a narrower range of Q, but the example gives a starting point for the final phase of product development for a product of this type. Other factors may affect release (*e.g.*, moisture content and machine speed) and such factors can (at increased experimentation) be included in a multivariable phenomonological equation. Preliminary factorial experimentation on two levels may sort out the variables of importance prior to model experimentation. If many variables are included, then it is best, as suggested previously (62) to assume that all the relations can be described by two-power polynomials and approach the problem by fractional factorials. In this case there is no experimental testing of the actual functionality: it is assumed to be a two-power polynomial.

Erosion Curves—Disintegration is presumably erosion due to dissolution of the polymer. If this is so, then the erosion is a function of polymer solubility. It should follow a cube root law if the solubility is absolutely pH independent; as pointed out previously (63), cube root relations often resemble exponential decays. Because of the differences in solubility profiles as a function of pH, the cases will be discussed individually in the following, but typical examples of disintegration patterns for polymers with pH-insensitive solubility are shown in Fig. 8, and the erosion figures are given in Table V.

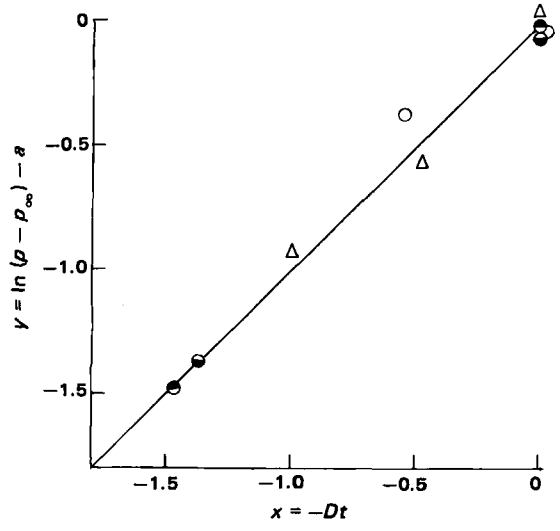

Figure 10—*Consistency diagram in dimensionless units for Eq. 8, using data in Table VII. The parameter* p *is here in fraction. For Eq. 8 to be a reasonable function, the data should be linear and the line should go through the origin (*y = x *as shown). Key: (Δ) 15% wet granulated; (○) 15% directly compressed; (◒) 30% directly compressed; (◓) 60% directly compressed.*

Table X—Disintegration Data (p/p_0) for Polyvinyl Acetate Preparations

Time, hr	Fraction disintegrated at the time indicated (Polymer, %; Hardness, kg)			
	15%, 15 kg	30%, 15 kg	60%, 15 kg	15%, 15 kg, g[a]
0	1	1	1	1
0.5				0.8
1	0.77	0.81	0.94	0.75
1.5				0.74
2	0.69	0.77	0.96	0.72
4	0.74	0.81	0.95	
6	0.76	0.79	0.93	
8	0.69	0.78	0.91	

[a] g is wet granulated.

Polyvinyl Acetal Diethylaminoacetate (I)—Polyvinyl acetal diethylaminoacetate is acid soluble and alkali insoluble; therefore, it should be subject to erosion (dissolution) only in the first 2 hr, as seen in Table VII. The value of p in Eq. 2 should approach an asymptotic value different from zero (unless erosion were complete within 2 hr, which is not the case). The erosion equation should reflect this as:

$$\ln (p - p_\infty) = -Dt + a \qquad \text{(Eq. 15)}$$

where p_∞ is the amount of matrix not disintegrated at infinite time, p is the matrix, and the data in Table VI, referring to polyvinyl acetal diethylamino acetate have been subjected to this adjustment. The data are shown in Fig. 9. Reasonable asymptote values can be estimated from the figure, and the data have been subjected to dimensionless plotting in Table VII. The dimensionless plot is shown in Fig. 10 and establishes that Eq. 8 is a reasonable function for treating the erosion data.

The erosion constant is of the same order of magnitude in the first 2

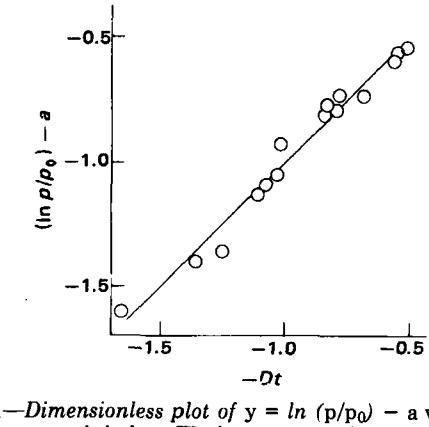

Figure 11—*Dimensionless plot of* y = *ln* (p/p0) − a versus −Dt *for polyvinyl acetate phthalate. The least-squares fit is* y = *0.998*x − *0.002, i.e., a straight line with close to unity slope and close to zero intercept, showing applicability of Eq. 1 to this system (*r = *0.99).*

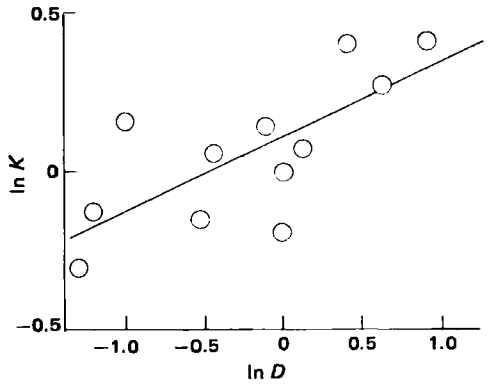

Figure 12—*ln* K *as a function of ln* D *(Table IX). The least-squares fit line is ln* K = *0.229 ln* D + *0.105 (r = 0.79).*

hr as the dissolution constant in the remainder of the dissolution period, so that the overall dissolution curve will be well represented by Eq. 4. It may be concluded that the rate-controlling process is twofold: erosion in the first 2 hr and diffusion in the remainder of the dissolution period (during this latter period the matrix weight remains constant and the dissolution is log-linear).

Polyvinyl Acetate Phthalate—In this case the polymer is acid insoluble and alkali soluble. Dissolution of the polymer should not occur until after the second hour. It is seen in Table VIII that in the case of the two lower polymer concentrations (15 and 30%) there is a certain amount of erosion immediately. Apparently this is an effect of the excipients and does not occur at the high concentration. After this immediate erosion the weight remains constant for 2 hr (during which time the pH is low and the polymer does not dissolve), and after 2 hr the increase in pH causes the solubility of the polymer to increase and erosion to begin. It is seen in Table VIII that the erosion after the 2-hr point appears to follow Eq. 1, and the least-squares fit values are listed. Since the disintegration actually does not occur substantially until a certain time, t_i (presumably between 2 and 4 hr), the correct form of Eq. 1 would be:

$$\ln (p/p_0) = -D(t - t_i) \qquad \text{(Eq. 16)}$$

so that a is equal to Dt_i. Values of t_i calculated in this fashion are shown in Table VIII and are in the correct range for the higher concentration.

The data in Table VIII are shown in dimensionless presentation in Fig. 11, and the adherence of this plot to linearity with unity slope and zero intercept shows that the disintegration is well represented by Eq. 16.

Povidone, Povidone–Vinyl Acetate, and Polyvinyl Alcohol–Acetate—These three polymers have solubilities that are not pH dependent. The disintegration of the formulas follow Eq. 1 fairly well, and the least-squares fit parameters are shown in Table IX. The effect of flow cells on disintegration has been reported for povidone (6).

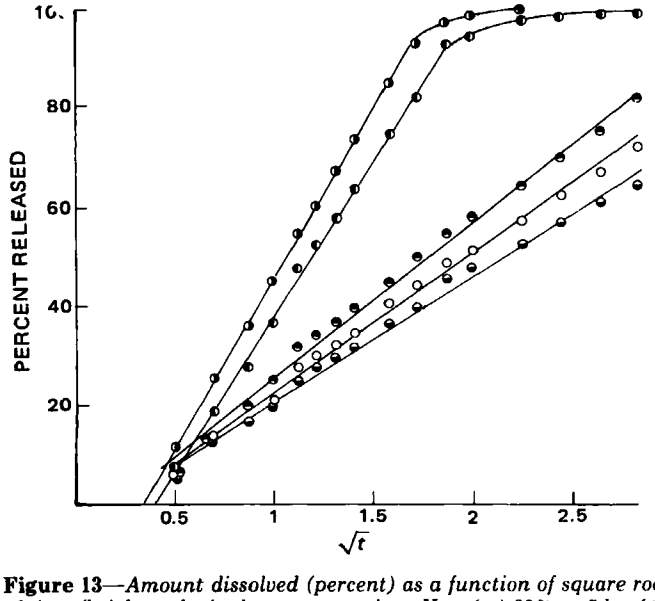

Figure 13—*Amount dissolved (percent) as a function of square root of time (hr) for polyvinyl acetate matrices. Key: (●) 60% at 5 kg; (○) 60% at 10 kg; (◒) 60% at 5 kg; (◐) 30% at 15 kg; (◑) 15% at 15 kg.*

In addition, the disintegration behavior in rotating baskets (2–5, 64–66) has been shown to lead to exponential decay dissolution profiles (Eq. 2) with lag time when disintegration is the rate-limiting factor. Therefore, correlations between K and D frequently occur in rotating dissolution apparatuses (4, 9–11) when rapidly disintegrating formulas are tested. Such a correlation is not necessarily to be expected in the case of the polymers reported here; however, the data in Table IX imply a correlation of the type:

$$\ln D = q \ln K + j \qquad \text{(Eq. 17)}$$

where q and j are constants. The data in Table IX are shown by a dimensionless representation in Fig. 12 using Eq. 17. There is fair linearity, the slope is close to unity, and the intercept is close to zero, so that Eq. 17 is not an unacceptable function, but the scatter about the line is such that other effects might be expected. Presumably, the amount, m, not released at time t, would be a complex function of both K and D, where K and D are not entirely independent of one another.

Polyvinyl Acetate—In this case there should be insolubility throughout the pH range. As shown earlier, only the 60% preparation is free from some initial disintegration (erosion). In the case of the two lower concentrations, the amount of weight lost is in excess of drug released, *e.g.*, for the 30% polymer concentration 30 mg (6% of the tablet weight) of drug is dissolved after 1 hr as opposed to the fact that the weight loss is 23%. In the case of polyvinyl acetate, the matrix should be insoluble, and the release pattern should come close to being a square root of time dependence (1). Figure 13 and Table X shows this to be the case, although the deviations from the line are first negative, then positive, then negative (+ − +) so that [Durbin–Watson statistics (67)] the fit is not exact. The initial lag time and the end effect is to be expected (2). It is apparent that the release is also well represented by a semilogarithmic relationship (Eq. 2). These latter frequently simulate square root in time functions (68).

REFERENCES

(1) T. Higuchi, *J. Pharm. Sci.*, **52**, 1145 (1963).

(2) H. Fessi, J.-P. Marty, F. Puisieux, and J. T. Carstensen, *Int. J. Pharm.*, **1**, 265 (1978).

(3) J. T. Carstensen, J. L. Wright, K. W. Blessel, and J. Sheridan. *J. Pharm. Sci.*, **67**, 48 (1978).

(4) *Idem*, **67**, 982 (1978).

(5) K. G. Nelson and L. Y. Wang, *J. Pharm. Sci.*, **66**, 1758 (1977).

(6) M. J. Groves and M. H. Alkan, *Int. J. Pharmaceutics*, **3**, 81 (1979).

(7) J. T. Carstensen, in "Dissolution Technology," L. Leeson and J. T. Carstensen, Eds., IPT Section, American Pharmaceutical Association, Washington, D.C., 1974.

(8) J. T. Carstensen, T. Lai, and V. K. Prasad, *J. Pharm. Sci.*, **66**, 607 (1977).

(9) J. T. Carstensen, R. Kothari, V. K. Prasad, and J. Sheridan, *ibid.*, **69**, 290 (1980).

(10) J. T. Carstensen, R. Kothari, and Z. Chowhan, *Drug. Dev. Ind. Pharmacy*, **6**, 569 (1980).

(11) J. T. Carstensen, "Mechanical Properties and Rate Processes in Solid Pharmaceutics," Academic, New York, N.Y., 1980, pp. 224–229.

(12) O. Cruaud, D. Duchêne, F. Puisieux, and J. T. Carstensen, *J. Pharm. Sci.*, **69**, 607 (1980).

(13) K. J. Simons, F. E. R. Simons, and C. W. Bierman, *J. Clin. Pharmacol.*, **17**, 237 (1977).

(14) D. Lefort des Ylouses and C. Brossard, *Sci. Techn. Pharm.*, **5**, 341 (1976).

(15) M. Roland and A. Tamba Vemba, *Labo-Pharma*, **22**, 935 (1974).

(16) R. C. Rowe, *Manuf. Chem. Aerosol News*, **46**, 23 (1975).

(17) W. A. Ritschel, *Pharma. Internat.*, **3**, 18 (1971).

(18) G. S. Banker, *J. Pharm. Sci.*, **55**, 81 (1966).

(19) T. Kuriyama, M. Nobutoki, and M. Nakanishi, *ibid.*, **59**, 1341 (1970).

(20) *Idem.*, **59**, 1344 (1970).

(21) D. Dreher, *Pharm. Ind.*, **1420**(1), (1975).

(22) R. Huttenrauch and S. Fricke, *Pharmazie*, **30**, 305 (1975).

(23) H. Moldenhauer, H. Kala, G. Zessin, and G. Nauenburg, *Pharmazie*, **29**, 26 (1974).

(24) C. R. Willis, G. S. Banker, and H. G. DeKay, *J. Pharm. Sci.*, **54**, 366 (1965).

(25) S. S. Ahsan and S. M. Blaug, *Drug. Standards*, **26**, 29 (1958).
(26) A. S. Alam and E. L. Parrott, *J. Pharm. Sci.*, **61**, 265 (1972).
(27) J. L. Kanig and H. Goodman, *ibid.*, **51**, 77 (1962).
(28) P. Prioux, D. Lefort des Ylouses, M. Seiller, and D. Duchêne, *J. Pharm. Belg.*, **30**, 132 (1975).
(29) C. F. Harwood and N. Pilpel, *J. Pharm. Sci.*, **57**, 478 (1968).
(30) L. Krowczynski and T. Stozek, *Dis. Pharm. Pharmacol.*, **20**, 685 (1968).
(31) A. Dakkuri, L. D. Butler, and P. P. Deluca, *J. Pharm. Sci.*, **67**, 357 (1978).
(32) H. Lapidus and N. G. Lordi, *ibid.*, **57**, 1292 (1968).
(33) M. Seiller and D. Duchêne, *Ann. Pharm. Fr.*, **26**, 291 (1968).
(34) B. J. Munden, H. G. DeKay, and G. S. Banker, *J. Pharm. Sci.*, **53**, 396 (1964).
(35) S. Borodkin and F. E. Tucker, *ibid.*, **64**, 1289 (1975).
(36) *Ibid.*, **63**, 1359 (1974).
(37) R. J. Nessel, H. G. DeKay, and G. S. Banker, *ibid.*, **53**, 790 (1964).
(38) L. E. Dahlinder, C. Graffner, and J. Sjögren, *Acta Pharm. Suecica*, **10**, 323 (1973).
(39) W. A. Ritschel, *J. Pharm. Sci.*, **60**, 1683 (1971).
(40) J. C. Etter, *Labo-Pharma*, **20**, 63 (1972).
(41) A. Widmann, F. Eiden, and J. Tenczer, *Arzneim.-Forsch.*, **20**, 283 (1970).
(42) S. C. Khanna, T. Jecklin, and P. Speiser, *J. Pharm. Sci.*, **59**, 614 (1970).
(43) A. Tamba Vemba, J. Gillard, and M. Roland, Premier Congres Internat. Techn. Pharm., June 1977, Paris (A.P.G.I.), Proceedings, vol. 3, pg, 109.
(44) L. Feigenbaum and D. Lefort des Ylouses, *Labo-Pharma*, **19**, 68 (1971).
(45) G. Suren, *Acta Pharm. Suecica*, **7**, 483 (1970).
(46) J. L. Zatz, *J. Pharm. Sci.*, **67**, 1464 (1978).
(47) J. L. Zatz and B. Knowles, *ibid.*, **60**, 1731 (1971).
(48) J. L. Zatz and B. Knowles, *J. Colloid Interface Sci.*, **40**, 475 (1972).
(49) J. P. Delporte, *Pharm. Acta Helv.*, **45**, 525 (1970).
(50) S. C. Porter and K. Ridgway, Premier Congres Internat. Techn. Pharm. June 1977, Paris (A.P.G.I.), Proceedings, vol. 3, pg 75.
(51) S. C. Porter and K. Ridgway, *J. Pharm. Pharmacol.*, **29**, 42S (1977).
(52) J. Sajvera, *Czek. Farm.*, **18**, 114 (1969).
(53) S. Akagi, K. Matsui, M. Okamoto, and Y. Ikegami, *Sankyo Kentyusha Nempa*, **19**, 71 (1967).
(54) T. Kuriyama, M. Nobutoki, and M. Nakanishi, *J. Pharm. Sci.*, **59**, 1341 (1970).
(55) H. Negoro, E. Awada, Y. Ikegami, S. Akagi, and K. Matsui, *Ind. Chim. Belg.*, **32**, 241 (1967).
(56) C. Mony and D. Lefort des Ylouses, *J. Pharm. Belg.*, **33**, 77 (1978).
(57) *Idem.*, **33**, 86 (1978).
(58) A. P. Simonelli, S. C. Mehta, and W. I. Higuchi, *J. Pharm. Sci.*, **65**, 355 (1976).
(59) G. H. Svoboda, M. J. Sweeney, and W. D. Walkling, *ibid.*, **60**, 333 (1971).
(60) E. J. Stupak and T. R. Bates, *ibid.*, **61**, 400 (1972).
(61) *Idem.*, **62**, 1806 (1973).
(62) J. B. Schwartz, J. R. Flamholz, and R. H. Press, *ibid.*, **62**, 1165 (1973).
(63) M. Bamba, F. Puisieux, J.-P. Marty, and J. T. Carstensen, *Int. J. Pharm.*, **2**, 307 (1979).
(64) K. G. Nelson and L. Y. Wang, *J. Pharm. Sci.*, **67**, 87 (1978).
(65) N. Kitamori and T. Shimamoto, *Chem. Pharm. Bull.*, **24**, 1789 (1976).
(66) N. Kitamori and K. Iga, *J. Pharm. Sci.*, **67**, 1436 (1978).
(67) J. Durbin and G. Watson, *Biometrika, Part II*, **58**, 1 (1971).
(68) E. Nelson, D. Eppich, and J. Carstensen, *J. Pharm. Sci.*, **63**, 755 (1974).

Evaluation of Mosquito Repellent Formulations

WILLIAM G. REIFENRATH ˣ **and LOUIS C. RUTLEDGE**

Received December 21, 1981, from the *Division of Cutaneous Hazards, Letterman Army Institute of Research, The Presidio of San Francisco, CA 94129.* Accepted for publication April 7, 1982.

Abstract □ *N,N*-Diethyl-*m*-toluamide was formulated with several acrylate polymers in ethanol solution and various silicone polymers in 2-propanol suspension; the ratio of polymer to *N,N*-diethyl-*m*-toluamide (I) was varied. Formulations that had drying times of <10 min were evaluated for film hardness and elasticity. Contact angles made by water on films cast from the formulations were measured when such films were uniform. For the acrylate formulations, containing polymers that are solid at room temperature, the presence of I increased drying times; decreased film hardness and elasticity resulted from decreasing the ratio of polymers to I. Lower contact angle with water resulted from decreasing the ratio of acrylate polymer to I. However, this effect was less pronounced with the lower molecular weight acrylate polymer formulations. Films cast from the silicone formulations had low contact angles with water. In addition, formulations of repellents, ethohexadiol and *N,N*-diethyl-*p*-toluamide, each in combination with a silicone polymer, were evaluated. Films with short drying times, high contact angle, and measurable hardness could be cast from the *N,N*-diethyl-*p*-toluamide–silicone formulations due to the film-forming ability of the repellent itself. The physical properties of the ethohexadiol–silicone formulations were similar to the I–silicone formulations. Selected formulations received preliminary evaluation for duration of effectiveness against *Aedes aegypti* mosquitoes *in vitro* and in animal test systems. Except for one formulation of I with a lower molecular weight acrylate polymer, these formulations did not enhance the duration of effectiveness of I on hairless dogs. The *in vitro* ED_{50} of the test repellent for *A. aegypti* was significantly enhanced in 5 of 15 formulations tested. The 4-hr ED_{50} of the test repellent on white mice was significantly enhanced in 6 of 15 formulations tested.

Keyphrases □ Repellents, mosquito—film hardness and elasticity evaluation for *N,N*-diethyl-*m*-toluamide–acrylate polymer formulations □ *N,N*-Diethyl-*m*-toluamide—formulation with acrylate polymer, evaluation for film hardness and elasticity in mosquito repellents □ Polymers—*N,N*-diethyl-*m*-toluamide formulations, evaluation for film hardness and elasticity in mosquito repellents

The duration of protection afforded by a mosquito repellent is limited by the ways it can be lost from the skin surface, such as abrasion and removal by water immersion (1) and excessive evaporation and penetration into the skin (2, 3). Many efforts have been made to improve the persistance of mosquito repellents by incorporating the active ingredient (usually *N,N*-diethyl-*m*-toluamide, I) with a variety of materials such as polysaccharide esters or silicone and acrylic polymers (4), clay (5), zinc oxide (6), vanillin (7), and others. However, there remains to be found a repellent formulation which has acceptable cosmetic and toxicologic properties and has significantly

0022-3549/83/0200-0169$01.00/0

(25) S. S. Ahsan and S. M. Blaug, *Drug. Standards*, **26**, 29 (1958).
(26) A. S. Alam and E. L. Parrott, *J. Pharm. Sci.*, **61**, 265 (1972).
(27) J. L. Kanig and H. Goodman, *ibid.*, **51**, 77 (1962).
(28) P. Prioux, D. Lefort des Ylouses, M. Seiller, and D. Duchêne, *J. Pharm. Belg.*, **30**, 132 (1975).
(29) C. F. Harwood and N. Pilpel, *J. Pharm. Sci.*, **57**, 478 (1968).
(30) L. Krowczynski and T. Stozek, *Dis. Pharm. Pharmacol.*, **20**, 685 (1968).
(31) A. Dakkuri, L. D. Butler, and P. P. Deluca, *J. Pharm. Sci.*, **67**, 357 (1978).
(32) H. Lapidus and N. G. Lordi, *ibid.*, **57**, 1292 (1968).
(33) M. Seiller and D. Duchêne, *Ann. Pharm. Fr.*, **26**, 291 (1968).
(34) B. J. Munden, H. G. DeKay, and G. S. Banker, *J. Pharm. Sci.*, **53**, 396 (1964).
(35) S. Borodkin and F. E. Tucker, *ibid.*, **64**, 1289 (1975).
(36) *Ibid.*, **63**, 1359 (1974).
(37) R. J. Nessel, H. G. DeKay, and G. S. Banker, *ibid.*, **53**, 790 (1964).
(38) L. E. Dahlinder, C. Graffner, and J. Sjögren, *Acta Pharm. Suecica*, **10**, 323 (1973).
(39) W. A. Ritschel, *J. Pharm. Sci.*, **60**, 1683 (1971).
(40) J. C. Etter, *Labo-Pharma*, **20**, 63 (1972).
(41) A. Widmann, F. Eiden, and J. Tenczer, *Arzneim.-Forsch.*, **20**, 283 (1970).
(42) S. C. Khanna, T. Jecklin, and P. Speiser, *J. Pharm. Sci.*, **59**, 614 (1970).
(43) A. Tamba Vemba, J. Gillard, and M. Roland, Premier Congres Internat. Techn. Pharm., June 1977, Paris (A.P.G.I.), Proceedings, vol. 3, pg, 109.
(44) L. Feigenbaum and D. Lefort des Ylouses, *Labo-Pharma*, **19**, 68 (1971).
(45) G. Suren, *Acta Pharm. Suecica*, **7**, 483 (1970).
(46) J. L. Zatz, *J. Pharm. Sci.*, **67**, 1464 (1978).
(47) J. L. Zatz and B. Knowles, *ibid.*, **60**, 1731 (1971).
(48) J. L. Zatz and B. Knowles, *J. Colloid Interface Sci.*, **40**, 475 (1972).
(49) J. P. Delporte, *Pharm. Acta Helv.*, **45**, 525 (1970).
(50) S. C. Porter and K. Ridgway, Premier Congres Internat. Techn. Pharm. June 1977, Paris (A.P.G.I.), Proceedings, vol. 3, pg 75.
(51) S. C. Porter and K. Ridgway, *J. Pharm. Pharmacol.*, **29**, 42S (1977).
(52) J. Sajvera, *Czek. Farm.*, **18**, 114 (1969).
(53) S. Akagi, K. Matsui, M. Okamoto, and Y. Ikegami, *Sankyo Kentyusha Nempa*, **19**, 71 (1967).
(54) T. Kuriyama, M. Nobutoki, and M. Nakanishi, *J. Pharm. Sci.*, **59**, 1341 (1970).
(55) H. Negoro, E. Awada, Y. Ikegami, S. Akagi, and K. Matsui, *Ind. Chim. Belg.*, **32**, 241 (1967).
(56) C. Mony and D. Lefort des Ylouses, *J. Pharm. Belg.*, **33**, 77 (1978).
(57) *Idem.*, **33**, 86 (1978).
(58) A. P. Simonelli, S. C. Mehta, and W. I. Higuchi, *J. Pharm. Sci.*, **65**, 355 (1976).
(59) G. H. Svoboda, M. J. Sweeney, and W. D. Walkling, *ibid.*, **60**, 333 (1971).
(60) E. J. Stupak and T. R. Bates, *ibid.*, **61**, 400 (1972).
(61) *Idem.*, **62**, 1806 (1973).
(62) J. B. Schwartz, J. R. Flamholz, and R. H. Press, *ibid.*, **62**, 1165 (1973).
(63) M. Bamba, F. Puisieux, J.-P. Marty, and J. T. Carstensen, *Int. J. Pharm.*, **2**, 307 (1979).
(64) K. G. Nelson and L. Y. Wang, *J. Pharm. Sci.*, **67**, 87 (1978).
(65) N. Kitamori and T. Shimamoto, *Chem. Pharm. Bull.*, **24**, 1789 (1976).
(66) N. Kitamori and K. Iga, *J. Pharm. Sci.*, **67**, 1436 (1978).
(67) J. Durbin and G. Watson, *Biometrika, Part II*, **58**, 1 (1971).
(68) E. Nelson, D. Eppich, and J. Carstensen, *J. Pharm. Sci.*, **63**, 755 (1974).

Evaluation of Mosquito Repellent Formulations

WILLIAM G. REIFENRATH ˣ **and LOUIS C. RUTLEDGE**

Received December 21, 1981, from the *Division of Cutaneous Hazards, Letterman Army Institute of Research, The Presidio of San Francisco, CA 94129.* Accepted for publication April 7, 1982.

Abstract □ *N,N*-Diethyl-*m*-toluamide was formulated with several acrylate polymers in ethanol solution and various silicone polymers in 2-propanol suspension; the ratio of polymer to *N,N*-diethyl-*m*-toluamide (I) was varied. Formulations that had drying times of <10 min were evaluated for film hardness and elasticity. Contact angles made by water on films cast from the formulations were measured when such films were uniform. For the acrylate formulations, containing polymers that are solid at room temperature, the presence of I increased drying times; decreased film hardness and elasticity resulted from decreasing the ratio of polymers to I. Lower contact angle with water resulted from decreasing the ratio of acrylate polymer to I. However, this effect was less pronounced with the lower molecular weight acrylate polymer formulations. Films cast from the silicone formulations had low contact angles with water. In addition, formulations of repellents, ethohexadiol and *N,N*-diethyl-*p*-toluamide, each in combination with a silicone polymer, were evaluated. Films with short drying times, high contact angle, and measurable hardness could be cast from the *N,N*-diethyl-*p*-toluamide–silicone formulations due to the film-forming ability of the repellent itself. The physical properties of the ethohexadiol–silicone formulations were similar to the I–silicone formulations. Selected formulations received preliminary evaluation for duration of effectiveness against *Aedes aegypti* mosquitoes *in vitro* and in animal test systems. Except for one formulation of I with a lower molecular weight acrylate polymer, these formulations did not enhance the duration of effectiveness of I on hairless dogs. The *in vitro* ED_{50} of the test repellent for *A. aegypti* was significantly enhanced in 5 of 15 formulations tested. The 4-hr ED_{50} of the test repellent on white mice was significantly enhanced in 6 of 15 formulations tested.

Keyphrases □ Repellents, mosquito—film hardness and elasticity evaluation for *N,N*-diethyl-*m*-toluamide–acrylate polymer formulations □ *N,N*-Diethyl-*m*-toluamide—formulation with acrylate polymer, evaluation for film hardness and elasticity in mosquito repellents □ Polymers—*N,N*-diethyl-*m*-toluamide formulations, evaluation for film hardness and elasticity in mosquito repellents

The duration of protection afforded by a mosquito repellent is limited by the ways it can be lost from the skin surface, such as abrasion and removal by water immersion (1) and excessive evaporation and penetration into the skin (2, 3). Many efforts have been made to improve the persistance of mosquito repellents by incorporating the active ingredient (usually *N,N*-diethyl-*m*-toluamide, I) with a variety of materials such as polysaccharide esters or silicone and acrylic polymers (4), clay (5), zinc oxide (6), vanillin (7), and others. However, there remains to be found a repellent formulation which has acceptable cosmetic and toxicologic properties and has significantly

0022-3549/83/0200-0169$01.00/0

Table I—Composition and Water Contact Angle Measurement of Mosquito Repellent–Acrylate Polymer Formulations

Formulation No.	*N,N*-Diethyl-*m*-toluamide concentration, % (w/v)	Polymer concentration, % (w/v)	Contact angle, degree[a]
N,N-Diethyl-*m*-toluamide–Polymer I Formulations			
36	3.9	0.4	10 ± 1
28	3.9	2.0	17 ± 1
37	3.9	3.9	31 ± 2
38	3.9	7.8	33 ± 2
39	3.9	11.8	—[b]
63	0.0	3.9	46 ± 1
N,N-Diethyl-*m*-toluamide–Polymer II Formulations			
32	3.9	0.4	10 ± 1
27	3.9	0.6	12 ± 2
33	3.9	3.9	12 ± 1
34	3.9	7.8	19 ± 1
35	3.9	11.8	25 ± 1
64	0.0	3.9	14 ± 4
N,N-Diethyl-*m*-toluamide–Polymer III Formulations			
11	6.1	3.1	32 ± 1
44	3.9	0.4	25 ± 1
25	3.9	2.0	42 ± 4
17	3.9	3.9	51 ± 1(2)
18	3.9	7.8	65 ± 2
19	3.9	11.8	70 ± 4(2)
61	0.0	3.9	71 ± 1
N,N-Diethyl-*m*-toluamide–Polymer IV Formulations			
40	3.9	0.4	14 ± 1
26	3.9	2.0	41 ± 4
41	3.9	3.9	47 ± 0
42	3.9	7.8	79 ± 4
43	3.9	11.8	71 ± 3
62	0.0	3.9	75 ± 1

[a] Contact angle measurements were replicated three times, except where number of replicates are indicated in parentheses following value, mean ± *SD*. [b] Film surface was too irregular to allow measurement.

Table II—Composition and Water Contact Angle Measurement of Mosquito Repellent–Silicone Polymer Formulations

Formulation No.	Repellent concentration, % (w/v)	Polymer concentration, % (w/v)	Contact angle, degree[a]
N,N-Diethyl-*m*-toluamide–Polymer V Formulations			
15	6.1	3.1	8 ± 2
50	3.9	0.4	10 ± 1
30	3.9	2.0	8 ± 1
24	3.9	3.9	—[b]
N,N-Diethyl-*m*-toluamide–Polymer VI Formulations			
16	6.1	3.1	—[b]
53	3.9	0.4	11 ± 1
31	3.9	2.0	—[b]
N,N-Diethyl-*m*-toluamide–Polymer VII Formulations			
14	6.1	3.1	7 ± 2
47	3.9	0.4	13 ± 1
29	3.9	2.0	10 ± 1
23	3.9	3.9	23 ± 4(5)
N,N-Diethyl-*m*-toluamide–Polymer VIII Formulations			
57	3.9	0.4	10 ± 1
58	3.9	2.0	16 ± 1
22	3.9	3.9	18 ± 1
Ethohexadiol–Polymer VIII Formulation			
12	3.9	2.0	19 ± 1
N,N-Diethyl-*p*-toluamide–Polymer VIII Formulation			
13	3.9	2.0	72 ± 1

[a] Contact angle measurements were replicated three times, except where the number of replicates are indicated in parentheses following value, mean ± *SD*. [b] Film surface was too irregular for determination of contact angle with water.

better duration of protection than unformulated I. In an effort to understand better the results obtained by adding I to various polymers, I was formulated in varying ratios to several commercially available silicone and acrylate polymers, some of which have been used extensively by the cosmetic industry.

EXPERIMENTAL

Materials—The materials used for the preparation of mosquito repellent formulations were acrylate polymers[1] I–IV, silicone polymers[2] V–VIII, and the mosquito repellents *N,N*-diethyl-*m*-toluamide[3], *N,N*-diethyl-*p*-toluamide[4], and ethohexadiol[5]. The composition of the formulations is listed in Tables I and II. Acrylate polymers III and IV required heating to effect solution in ethanol.

Determination of Drying Times—Films were cast on glass microscope slides by using a mechanical drive[6] and an applicator[7] with 0.19-mm wet film thickness and allowed to dry at ambient conditions (40% relative humidity and 23°). Using a cotton ball, the slide was checked for a dry tack-free surface every 2 min up to 15 min, every 10 min up to 1 hr, and then every hour up to 8 hr. Drying times were done in duplicate.

Film Hardness, Film Thickness, and Modulus of Elasticity—These were determined by published procedures (8). Films were cast as for drying time determinations; however, the substrate was a polished aluminum plate. Films were tested 4 hr after they were cast. The modulus of elasticity (E) was calculated by:

$$E = \frac{KR^3}{T^3}$$

where R is the Sward hardness (number of rocks) and K is a constant for thickness (T) determined by extrapolation from data in the literature (9).

Contact Angle—Films were cast on a glass microscope slide cut in half lengthwise, by the same procedure as for drying time determinations. Fifteen minutes after the film was cast, the slide was inserted in the contact angle viewer[8]. A drop of distilled water was placed on the film, and the angles, formed by the base of the drop on its left and right sides, were read. The volume of the drop was then increased by small increments until the left and right side angles were the same and remained constant. This final angle is reported as the contact angle. The determination was replicated three times.

Protection Time—The protection time of the formulations was determined on hairless dogs using a published procedure (10). After all the application sites on the dog's skin had failed, the skin was scrubbed with soap[9] and water to remove residual polymer. Dogs were usually rested 3–4 days between tests.

Median Effective Dosage—The median effective doses (ED_{50}) of 19 formulations for the yellow fever mosquito, *Aedes aegypti*, were determined by a previous method (11). This method utilizes an *in vitro* mosquito blood-feeding system having test surfaces of goldbeater's skin (the prepared outside membrane of the large intestine of cattle used for separating the leaves of metal in goldbeating).

Four-Hour Median Effective Dose—Four-hour ED_{50} values of 19 formulations for *A. aegypti* were determined on 7–10-day-old white mice. Four mice were wetted with serial dilutions of the test formulation, and a fifth (the control) was wetted with a corresponding solvent (ethanol or 2-propanol). The mice were held at 27° for 4 hr, after which they were transferred to a 30 × 30 × 30-cm mosquito cage containing 100 nulliparous, 5–15-day-old female *A. aegypti*. The number of mosquitoes feeding on each mouse was recorded at 2 min intervals for a period of 30 min. The totals of the 10 feeding counts obtained for each of the mice were combined with the corresponding totals from subsequent replicates of the test, and the totals for each dose were then converted to percentages of

[1] Acrylate polymer I is Carboset 515, II is Carboset 514, III is Carboset 526, and IV is Carboset 525. Polymers were obtained from B. F. Goodrich Chemical Co., Cleveland, Ohio.
[2] Silicone polymer V is 200 fluid, 350 centistoke; VI is 200 fluid, 1000 centistoke; VII is QF13593A; and VIII is MDX 4-4142. Polymers were obtained from Dow Corning Corp., Midland, Mich.
[3] Eastman Kodak Co., Rochester, N.Y.
[4] Hercules, Inc., Wilmington, Del.
[5] Niagara Chemical Division, FMC, Middleport, N.Y.
[6] Gardner mechanical drive, Gardner Laboratory, Bethesda, Md.
[7] Gardner film casting knife, Gardner Laboratory, Bethesda, Md.
[8] Contact angle viewer (No. D-1060), Gardner Laboratory, Bethesda, Md.
[9] Ivory soap, Proctor & Gamble Corp., Cincinnati, Ohio.

Table III—Film Characteristics of Polymers and Mosquito Repellent Formulations with Short Drying Times [a]

Formulation No.	Repellent–Additive ratio	Drying time, min	Film thickness, μm	Sward hardness, No. of rocks	Modulus of elasticity, ×10⁴ dyne/cm²
		Polymer II			
64	0	9	3	6	430
	N,N-Diethyl-*m*-toluamide–Polymer III Formulations				
18	1/2	7	15	5	590
19	1/3	7	18	9	3700
61	0	5	9	11	4800
		Polymer IV			
62	0	6	7	11	4100
	N,N-Diethyl-*p*-toluamide–Polymer VIII Formulation				
13	2/1	5	4	4	149

[a] Film characteristics were not measured for formulations with drying times >10 min.

the total for the control. The 4-hr ED_{50} was computed from the percentages and the logarithm doses by probit analysis.

RESULTS AND DISCUSSION

The composition and contact angle measurements of the acrylate formulations are given in Table I and of the silicone formulations in Table II. Film thickness, Sward hardness, and modulus of elasticity of the acrylate and silicone formulations with drying times <10 min are given in Table III. The protection times determined on the hairless dog of the acrylate formulations are given in Table IV and of the silicone formulations in Table V. The ED_{50}s and 4-hr ED_{50}s are given in Tables VI and VII and VIII and IX, respectively.

The acrylate polymers are derived from acrylic acid esters, methacrylic acid esters, and α,β-unsaturated carboxylic acids. The mean molecular weight of polymer I is 7000, II is 30,000, III is 200,000, and IV is 260,000. Polymer I is a viscous liquid at room temperature, while polymer II was obtained as a 30% solution of polymer in ammonia water with a final pH of 7.5; percentages of polymer II in Table I are based on the weight of polymer in solution.

For the I–acrylate formulations containing the higher molecular weight polymers, III and IV, increasing the ratio of polymer to a constant amount of I resulted in higher contact angles (Table I). The same trend was observed with Compound I–polymer I and II formulations, although it was less pronounced. The low contact angles for polymer II formulations were probably the result of the presence of water in polymer II and salt formation between the ammonia present and carboxylic acid functional groups.

Table IV—Protection Times Against *A. aegypti* Mosquitoes for Selected Repellent–Acrylate Polymer Formulations Tested on the Hairless Dog

Formulation No.	Repellent dose, mg/cm²[a]	Protection time, hr mean ± *SD*	*N*[b]	Significance[c]
	N,N-Diethyl-*m*-toluamide–Polymer I Formulations			
28	0.32	10.6 ± 1.1	7	S
Control[d]	0.32	6.4 ± 1.6	7	—
	N,N-Diethyl-*m*-toluamide–Polymer II Formulations			
27	0.32	6.5 ± 1.9	16	NS
Control[d]	0.32	6.5 ± 1.9	16	—
	N,N-Diethyl-*m*-toluamide–Polymer III Formulation			
11	0.5	9.6 ± 2.9	16	NS
Control[d]	0.5	8.5 ± 1.8	16	—
25	0.32	7.5 ± 2.4	16	NS
Control[d]	0.32	8.2 ± 2.1	16	—
17	0.32	9.8 ± 1.6	8	NS
Control[d]	0.32	9.4 ± 1.8	8	—
	N,N-Diethyl-*m*-toluamide–Polymer IV Formulations			
26	0.32	7.3 ± 1.8	16	NS
Control[d]	0.32	6.9 ± 1.9	16	—

[a] Dose obtained when 0.4 ml of formulation is spread over a 49-cm² skin area. [b] Number of replicates. [c] Significance was tested at the 95% confidence level using Dunnett's test for comparing *K* means with a control. [d] *N,N*-Diethyl-*m*-toluamide, dissolved in alcohol, was applied to the skin using the same volume as was used for application of the formulation to give the same dose of *N,N*-diethyl-*m*-toluamide.

Table V—Protection Time Against *A. aegypti* Mosquitoes for Selected Repellent–silicone Polymer Formulations Tested on the Hairless Dog

Formulation No.	Repellent, mg/cm²[a]	Protection time, hr mean ± *SD*	*N*[b]	Significance[c]
	N,N-Diethyl-*m*-toluamide–Polymer V Formulations			
15	0.50	4.8 ± 2.4	8	NS
Control[d]	0.50	6.8 ± 3.0	8	—
30	0.32	6.0 ± 0.8	8	NS
Control[d]	0.32	5.4 ± 0.8	8	—
24	0.32	8.1 ± 3.9	16	NS
Control[d]	0.32	8.3 ± 2.4	16	—
	N,N-Diethyl-*m*-toluamide–Polymer VI Formulations			
16	0.50	4.8 ± 1.5	8	NS
Control[d]	0.50	6.8 ± 3.0	8	—
31	0.32	6.0 ± 0.8	8	NS
Control[d]	0.32	5.4 ± 0.8	8	—
	N,N-Diethyl-*m*-toluamide–Polymer VII Formulations			
14	0.50	6.1 ± 2.3	8	NS
Control[d]	0.50	6.8 ± 3.0	8	—
29	0.32	5.9 ± 1.2	8	NS
Control[d]	0.32	5.4 ± 0.8	8	—
23	0.32	8.8 ± 2.9	16	NS
Control[d]	0.32	8.3 ± 2.9	16	—
	N,N-Diethyl-*m*-toluamide–Polymer VIII Formulation			
22	0.32	9.2 ± 2.8	16	NS
Control[d]	0.32	8.3 ± 2.4	16	—
	Ethohexadiol–Polymer VIII Formulation			
12	0.50	5.5 ± 2.2	16	S
Control[d]	0.50	8.5 ± 1.8	16	—
	N,N-Diethyl-*p*-toluamide–Polymer VIII Formulation			
13	0.50	5.4 ± 2.9	16	S
Control[d]	0.50	8.5 ± 1.8	16	—

[a] Dose obtained when 0.4 ml of formulation is spread over a 49-cm² skin area. [b] Number of replicates. [c] Significance was tested at the 95% confidence level using Dunnett's test for comparing *K* means with a control. [d] *N,N*-Diethyl-*m*-toluamide, dissolved in alcohol, was applied to the skin using the same volume as was used for application of the formulation to give the same dose of *N,N*-diethyl-*m*-toluamide.

The silicone polymers, V and VI, are linear polydimethylsiloxanes. Polymer V has ~200 dimethylsiloxane units and a molecular weight of ~15,000. Polymer VI has a molecular weight of ~25,000, which corresponds to 336 dimethylsiloxane units. Polymer VII is composed of a linear polydimethylsiloxane (~100 dimethylsiloxane units) and a highly crosslinked trimethylsiloxysilicate resin. Polymer VIII is related to polymer VII and is made by a slightly different manufacturing procedure[10].

Contact angles of water with the silicone formulations were generally low relative to those of the acrylate formulations and bore little apparent relationship to the ratio of repellent to polymer. The exception was formulation 13. In this case the *N,N*-diethyl-*p*-toluamide (which is a solid at room temperature, in contrast to the *meta* isomer) itself forms a film (visible films of *N,N*-diethyl-*p*-toluamide sometimes can be observed after the repellent is applied in alcoholic solution to human skin).

For each silicone polymer tested, formulations containing higher ratios of polymer to I than those in Table II were prepared along with suspensions of silicone polymers alone in 2-propanol. Films cast from these suspensions did not dry, and the surface of the films were too irregular for measurement of the contact angle with water.

With the exception of formulations 13, 18, and 19 (Table III), all of the mosquito repellent polymer formulations had drying times >8 hr (formulations containing silicone polymers or acrylate polymer I were not expected to dry, because the polymers are liquid at room temperature), and films cast from these formulations were not tested for hardness because of a probable change in component ratios due to evaporation of the repellent during the drying period required. The plasticizing effect of I on the acrylate polymers III and IV was shown by comparing formulation

[10] Personal communication, Mike Starch, Dow Corning Corp., Midland, Mich.

Table VI—*In Vitro* ED_{50}s of Selected Repellent–Acrylate Polymer Formulations for *A. aegypti*

Formulation No.	N[a]	ED_{50}, mg/cm^2[b]	95% Confidence interval	Significance[c]
N,N-Diethyl-*m*-toluamide–Polymer I Formulation				
28	2	0.013	0.006–0.019	S
N,N-Diethyl-*m*-toluamide–Polymer II Formulation				
27	2	0.030	0.020–0.046	NS
N,N-Diethyl-*m*-toluamide–Polymer III Formulations				
11/25[d]	4	0.017	0.012–0.022	NS
17	2	0.031	0.024–0.041	NS
18	2	0.009	0.004–0.013	S
19	2	0.019	0.011–0.027	NS
N,N-Diethyl-*m*-toluamide–Polymer IV Formulation				
26	2	0.021	0.013–0.029	NS
N,N-Diethyl-*m*-toluamide in Ethanol				
—	6	0.031	0.020–0.041	—

[a] Number of replicates. [b] Refers to the dosage of active ingredient (*N,N*-diethyl-*m*-toluamide). [c] The ED_{50}s of formulated and unformulated *N,N*-diethyl-*m*-toluamide are significantly different if their respective confidence intervals do not overlap. [d] Formulations having the same active ingredient–polymer ratio (Tables I and II) are equivalent in the ED_{50} test.

Table VIII—Four-hour ED_{50}s of Selected Repellent–Acrylate Polymer Formulations on White Mice Against *A. aegypti*

Formulation No.	N[a]	4-hr ED_{50}, % concentration[b]	95% Confidence interval	Significance[c]
N,N-Diethyl-*m*-toluamide–Polymer I Formulation				
28	8	0.05	0.002–0.12	NS
N,N-Diethyl-*m*-toluamide–Polymer II Formulation				
27	6	0.03	0.006–0.06	S
N,N-Diethyl-*m*-toluamide–Polymer III Formulations				
11/25[d]	14	0.03	0.002–0.06	S
17	3	0.06	0.000–0.12	NS
18	3	0.07	0.000–0.15	NS
19	6	0.20	0.000–0.47	NS
N,N-Diethyl-*m*-toluamide–Polymer IV Formulation				
26	6	0.03	0.010–0.06	S
N,N-Diethyl-*m*-toluamide in Ethanol				
—	6	0.16	0.108–0.22	—

[a] Number of replicates. [b] Refers to the concentration of active ingredient (*N,N*-diethyl-*m*-toluamide). [c] The 4-hr ED_{50}s of formulated and unformulated *N,N*-diethyl-*m*-toluamide are significantly different if their respective confidence intervals do not overlap. [d] Formulations having the same active ingredient–polymer ratio (Tables I and II) are equivalent in the 4-hr ED_{50} test.

61 with 17 for polymer III and comparing formulation 62 with 41 for polymer IV. The contact angle with water was higher, drying time was shorter, and films cast from the formulations were harder when I was absent. A similar observation can be made for polymer II (compare formulation 64 with 33); however, in this case, the presence of ammonia and water in the polymer obscures the effect of I on the contact angle. Since polymer I is a liquid, the effects of Compound I on drying time and film hardness are irrelevant. The plasticizing effect of I is not limited to the acrylate polymers. This effect occurs with a variety of polymers, which causes user acceptability problems (*e.g.*, softening or marring of plastics and painted surfaces).

The effect of the increasing modulus of elasticity (Table III) with higher ratios of polymer III to constant levels of I is illustrated in the following observations. Formulations 17–19 were applied to hairless dogs along with a I–ethanol control which gave the same dose of I per unit area (0.32 mg/cm^2). Four hours after application, the sites were observed. As expected, the I–ethanol treated sites were not noted to be any different than the surrounding nonapplication areas of skin. A film was visible on five of the eight sites to which formulation 17 was applied; however, there was no evidence of cracking or peeling. With formulation 18, a film had peeled from two of the application sites. With formulation 19, six sites were peeling, and on another site the film had cracked.

The results of the longer drying times associated with lower ratios of polymer III to compound I were the production of sticky, cosmetically unacceptable films when formulation 25 was tested on human subjects (4).

If the contact angle to water by films cast from the formulations is an indication of the wash resistance of the formulation, then the acrylate

Table VII—*In Vitro* ED_{50}s of Selected Repellent–Silicone Polymer Formulations for *A. aegypti*

Formulation No.	N[a]	ED_{50}, mg/cm^2[b]	95% Confidence interval	Significance[c]
N,N-Diethyl-*m*-toluamide–Polymer V Formulations				
15/30[d]	4	0.019	0.014–0.025	NS
24	2	0.027	0.020–0.037	NS
N,N-Diethyl-*m*-toluamide–Polymer VI Formulation				
16/31[d]	4	0.015	0.011–0.019	
N,N-Diethyl-*m*-toluamide–Polymer VII Formulations				
14/29[d]	4	0.017	0.013–0.020	NS
23	2	0.005	0.002–0.008	S
N,N-Diethyl-*m*-toluamide–Polymer VIII Formulation				
22	2	0.021	0.013–0.028	NS
Ethohexadiol–Polymer VIII Formulation				
12	2	0.027	0.019–0.036	S
N,N-Diethyl-*p*-toluamide–Polymer VIII Formulation				
13	2	0.015	0.010–0.020	[e]
N,N-Diethyl-*m*-toluamide in Ethanol				
—	6	0.031	0.020–0.041	—
Ethohexadiol in Ethanol				
—	4	0.113	0.081–0.197	—

[a] Number of replicates. [b] Refers to the dosage of active ingredient (*N,N*-diethyl-*m*-toluamide, ethohexadiol, or *N,N*-diethyl-*p*-toluamide). [c] The ED_{50}s of formulated and unformulated *N,N*-diethyl-*m*-toluamide or ethohexadiol are significantly different if their respective confidence intervals do not overlap. [d] Formulations having the same active ingredient–polymer ratio (Tables I and II) are equivalent in the ED_{50} test. [e] Unformulated *N,N*-diethyl-*p*-toluamide not tested.

Table IX—Four-hour ED_{50}s of Selected Repellent–Silicone Polymer Formulations on White Mice Against *A. aegypti*

Formulation No.	N[a]	4-hr ED_{50}, % concentration[b]	95% Confidence interval	Significance[c]
N,N-Diethyl-*m*-toluamide–Polymer V Formulations				
15/30[d]	9	0.03	0.000–0.06	S
24	9	0.02	0.001–0.05	S
N,N-Diethyl-*m*-toluamide–Polymer VI Formulation				
16/31[d]	15	0.02	0.002–0.05	S
N,N-Diethyl-*m*-toluamide–Polymer VII Formulations				
14/29[d]	11	0.01	(not determined)	NS
23	4	0.08	0.003–0.16	NS
N,N-Diethyl-*m*-toluamide–Polymer VIII Formulation				
22	6	0.04	0.000–0.11	NS
Ethohexadiol–Polymer VIII Formulation				
12	3	0.08	0.061–0.10	NS
N,N-Diethyl-*p*-toluamide–Polymer VIII Formulation				
13	9	0.05	0.004–0.10	—[e]
N,N-Diethyl-*m*-toluamide in Ethanol				
—	6	0.16	0.108–0.22	—
Ethohexadiol in Ethanol				
—	12	0.15	0.030–0.26	—

[a] Number of replicates. [b] Refers to the concentration of active ingredient (*N,N*-diethyl-*m*-toluamide, ethohexadiol, or *N,N*-diethyl-*p*-toluamide). [c] The ED_{50}s of formulated and unformulated *N,N*-diethyl-*m*-toluamide or ethohexadiol are significantly different if their respective confidence intervals do not overlap. [d] Formulations having the same active ingredient–polymer ratio (Tables I and II) are equivalent in the 4-hr ED_{50} test. [e] Unformulated *N,N*-diethyl-*p*-toluamide not tested.

formulations such as those made from polymers III or IV would be expected to provide greater wash resistance than the I–silicone formulations. In tests on human subjects, acrylate formulations such as 25, but not silicone formulations, enhanced I wash resistance (4). However, the contact angles would not necessarily reflect a difference in wash resistance due to a difference in film adhesion to the skin or a difference between a solid flexible film and a liquid film with similar contact angles.

In a preliminary test on hairless dogs, only one of the I formulations (28) appeared to provide greater duration of protection against *A. aegypti* mosquitoes than unformulated I. Results obtained by the ED_{50} and 4-hr test methods were more promising. The ED_{50} of the test repellent was significantly enhanced in two of the seven repellent–acrylate polymer formulations and in three of the eight repellent–silicone polymer formulations (Tables VI and VII). The 4-hr ED_{50}, which measures the combined effects of repellency and persistence on the skin of the test animal, was enhanced significantly in three of the seven repellent–acrylate polymer formulations and in three of the eight repellent–silicone polymer formulations (Tables VIII and IX). Both ED_{50} and 4-hr ED_{50} were enhanced in only one formulation (16, Tables VII and IX). This demonstrates that repellency and persistence on the skin are fundamentally different properties of the repellent formulation. As has been pointed out (12), these two properties of topical repellents have usually been confounded in the past.

In future studies with mosquito repellent formulations, the release kinetics of the repellent (either to evaporation or penetration) will be examined using an *in vitro* skin evaporation–penetration apparatus. Additional knowledge will permit more than an empirical approach to the design of longer lasting mosquito repellent formulations.

REFERENCES

(1) A. A. Khan, H. I. Maibach, and D. L. Skidmore, *Mosquito News*, **37**, 123 (1977).

(2) T. S. Spencer, J. A. Hill, R. J. Feldmann, and H. I. Maibach, *J. Invest. Dermatol.*, **72**, 317 (1979).

(3) H. I. Maibach, A. A. Khan, and W. A. Akers, *Arch. Dermatol.*, **109**, 32 (1974).

(4) A. P. Kurtz, J. A. Logan, and W. A. Akers, Report No. 13, Letterman Army Institute of Research, Presidio of San Francisco, Calif., 1973.

(5) S. R. Christophers, *J. Hyg.*, **45**, 176 (1947).

(6) C. N. Smith, *Misc. Publ. Entomol. Soc. Am.*, **7**, 99 (1970).

(7) T. S. Spencer, J. A. Hill, W. A. Akers, and G. Bjorkland, *Proc. Calif. Mosq. Control Assoc.*, **45**, 121 (1977).

(8) B. V. Iyer and R. C. Vasavada, *J. Pharm. Sci.*, **68**, 782 (1979).

(9) R. A. Cass, *J. Paint Technol.*, **38**, 281 (1966).

(10) J. A. Hill, P. B. Robinson, D. L. McVey, W. A. Akers, and W. G. Reifenrath, *Mosquito News*, **39**, 307 (1979).

(11) L. C. Rutledge, M. A. Moussa, and C. J. Belletti, *ibid.*, **36**, 283 (1976).

(12) J. R. Busvine, "A Critical Review of the Techniques for Testing Insecticides," 2nd ed., Commonwealth Agricultural Bureaux, Farnham Royal, Slough, England, 1971, p. 333.

Vaginal Absorption of a Potent Luteinizing Hormone–Releasing Hormone Analogue (Leuprolide) in Rats III: Effect of Estrous Cycle on Vaginal Absorption of Hydrophilic Model Compounds

HIROAKI OKADA ˣ, TAKATSUKA YASHIKI, and HIROYUKI MIMA

Received February 2, 1982, from the *Central Research Division, Takeda Chemical Industries, Ltd., 2-17-85 Juso, Yodogawa, Osaka 532, Japan.* Accepted for publication April 1, 1982.

Abstract □ The effect of estrous cycle stages on vaginal absorption was determined by the use of insulin, phenolsulfonphthalein, and salicylic acid as hydrophilic model compounds. Absorption of these compounds was markedly affected by the stage, possibly due to the change of transport rate through the pore-like pathways. The absorption of phenolsulfonphthalein during proestrus and estrus is roughly one-tenth of that during metestrus and diestrus. An increase of the nonionized form of salicylic acid, produced by a lowered pH, resulted in an enhancement of absorption during proestrus and diestrus; higher contribution of the transport through the cell membrane possibly reduced an effect of the estrous cycle. However, consecutive daily administration of leuprolide halted the cycle at diestrus and reduced the cycle effect on the vaginal absorption of phenolsulfonphthalein; when the treatment was started at any of the four stages of the cycle, vaginal absorption was enhanced ~20%, with less variance than that observed in normal diestrous rats.

Keyphrases □ Absorption, vaginal—luteinizing hormone–releasing hormone, leuprolide, effect of estrous cycle on vaginal absorption of hydrophilic model compounds □ Leuprolide—effect of estrous cycle on vaginal absorption of hydrophilic model compounds □ Luteinizing hormone–releasing hormone analogue—effect of estrous cycle on vaginal absorption of hydrophilic model compounds □ Releasing hormone analogue—luteinizing hormone, effect of estrous cycle on vaginal absorption of hydrophilic model compounds

In previous studies (1, 2), vaginal application was proposed as a rational dosage method for long-term self-administration of hydrophilic drugs, because leuprolide (I), a potent luteinizing hormone–releasing hormone (II) analogue, and several hydrophilic compounds (phenolsulfonphthalein, insulin, and II) are well absorbed through the vaginal membrane of diestrous rats.

(Pyro)Glu-His-Trp-Ser-Tyr-D-Leu-Leu-Arg-Pro-NH-CH_2CH_3

I

(Pyro)Glu-His-Trp-Ser-Tyr-Gly-Leu-Arg-Pro-Gly-NH_2

II

In those studies, vaginal absorbability was estimated at the diestrus only, since the ovulation-inducing activity of leuprolide could be examined during other stages.

The estrous cycle of the rat is completed in 4–5 days, and during this cycle changes in the vaginal mucosal membrane, the ovaries, and the uterus occur (3). Similar, but not as remarkable, changes of the vaginal mucosa occur in women during the menstrual cycle (4).

In the present study, the effect of estrous cycle stages on vaginal absorption was determined with phenolsulfonphthalein, insulin, and salicylic acid in rats. Furthermore, as continuous administration of leuprolide halts the estrous cycle of rats at diestrus (5), the vaginal absorption of phenolsulfonphthalein following consecutive subcutaneous injection of the analogue over a 10-day period was also estimated.

0022-3549/83/0200-0173$01.00/0

formulations such as those made from polymers III or IV would be expected to provide greater wash resistance than the I–silicone formulations. In tests on human subjects, acrylate formulations such as 25, but not silicone formulations, enhanced I wash resistance (4). However, the contact angles would not necessarily reflect a difference in wash resistance due to a difference in film adhesion to the skin or a difference between a solid flexible film and a liquid film with similar contact angles.

In a preliminary test on hairless dogs, only one of the I formulations (28) appeared to provide greater duration of protection against *A. aegypti* mosquitoes than unformulated I. Results obtained by the ED_{50} and 4-hr test methods were more promising. The ED_{50} of the test repellent was significantly enhanced in two of the seven repellent–acrylate polymer formulations and in three of the eight repellent–silicone polymer formulations (Tables VI and VII). The 4-hr ED_{50}, which measures the combined effects of repellency and persistence on the skin of the test animal, was enhanced significantly in three of the seven repellent–acrylate polymer formulations and in three of the eight repellent–silicone polymer formulations (Tables VIII and IX). Both ED_{50} and 4-hr ED_{50} were enhanced in only one formulation (16, Tables VII and IX). This demonstrates that repellency and persistence on the skin are fundamentally different properties of the repellent formulation. As has been pointed out (12), these two properties of topical repellents have usually been confounded in the past.

In future studies with mosquito repellent formulations, the release kinetics of the repellent (either to evaporation or penetration) will be examined using an *in vitro* skin evaporation–penetration apparatus. Additional knowledge will permit more than an empirical approach to the design of longer lasting mosquito repellent formulations.

REFERENCES

(1) A. A. Khan, H. I. Maibach, and D. L. Skidmore, *Mosquito News*, **37**, 123 (1977).

(2) T. S. Spencer, J. A. Hill, R. J. Feldmann, and H. I. Maibach, *J. Invest. Dermatol.*, **72**, 317 (1979).

(3) H. I. Maibach, A. A. Khan, and W. A. Akers, *Arch. Dermatol.*, **109**, 32 (1974).

(4) A. P. Kurtz, J. A. Logan, and W. A. Akers, Report No. 13, Letterman Army Institute of Research, Presidio of San Francisco, Calif., 1973.

(5) S. R. Christophers, *J. Hyg.*, **45**, 176 (1947).

(6) C. N. Smith, *Misc. Publ. Entomol. Soc. Am.*, **7**, 99 (1970).

(7) T. S. Spencer, J. A. Hill, W. A. Akers, and G. Bjorkland, *Proc. Calif. Mosq. Control Assoc.*, **45**, 121 (1977).

(8) B. V. Iyer and R. C. Vasavada, *J. Pharm. Sci.*, **68**, 782 (1979).

(9) R. A. Cass, *J. Paint Technol.*, **38**, 281 (1966).

(10) J. A. Hill, P. B. Robinson, D. L. McVey, W. A. Akers, and W. G. Reifenrath, *Mosquito News*, **39**, 307 (1979).

(11) L. C. Rutledge, M. A. Moussa, and C. J. Belletti, *ibid.*, **36**, 283 (1976).

(12) J. R. Busvine, "A Critical Review of the Techniques for Testing Insecticides," 2nd ed., Commonwealth Agricultural Bureaux, Farnham Royal, Slough, England, 1971, p. 333.

Vaginal Absorption of a Potent Luteinizing Hormone–Releasing Hormone Analogue (Leuprolide) in Rats III: Effect of Estrous Cycle on Vaginal Absorption of Hydrophilic Model Compounds

HIROAKI OKADA ˣ, TAKATSUKA YASHIKI, and HIROYUKI MIMA

Received February 2, 1982, from the *Central Research Division, Takeda Chemical Industries, Ltd., 2-17-85 Juso, Yodogawa, Osaka 532, Japan.* Accepted for publication April 1, 1982.

Abstract □ The effect of estrous cycle stages on vaginal absorption was determined by the use of insulin, phenolsulfonphthalein, and salicylic acid as hydrophilic model compounds. Absorption of these compounds was markedly affected by the stage, possibly due to the change of transport rate through the pore-like pathways. The absorption of phenolsulfonphthalein during proestrus and estrus is roughly one-tenth of that during metestrus and diestrus. An increase of the nonionized form of salicylic acid, produced by a lowered pH, resulted in an enhancement of absorption during proestrus and diestrus; higher contribution of the transport through the cell membrane possibly reduced an effect of the estrous cycle. However, consecutive daily administration of leuprolide halted the cycle at diestrus and reduced the cycle effect on the vaginal absorption of phenolsulfonphthalein; when the treatment was started at any of the four stages of the cycle, vaginal absorption was enhanced ~20%, with less variance than that observed in normal diestrous rats.

Keyphrases □ Absorption, vaginal—luteinizing hormone–releasing hormone, leuprolide, effect of estrous cycle on vaginal absorption of hydrophilic model compounds □ Leuprolide—effect of estrous cycle on vaginal absorption of hydrophilic model compounds □ Luteinizing hormone–releasing hormone analogue—effect of estrous cycle on vaginal absorption of hydrophilic model compounds □ Releasing hormone analogue—luteinizing hormone, effect of estrous cycle on vaginal absorption of hydrophilic model compounds

In previous studies (1, 2), vaginal application was proposed as a rational dosage method for long-term self-administration of hydrophilic drugs, because leuprolide (I), a potent luteinizing hormone–releasing hormone (II) analogue, and several hydrophilic compounds (phenolsulfonphthalein, insulin, and II) are well absorbed through the vaginal membrane of diestrous rats.

(Pyro)Glu-His-Trp-Ser-Tyr-D-Leu-Leu-Arg-Pro-NH-CH_2CH_3

I

(Pyro)Glu-His-Trp-Ser-Tyr-Gly-Leu-Arg-Pro-Gly-NH_2

II

In those studies, vaginal absorbability was estimated at the diestrus only, since the ovulation-inducing activity of leuprolide could be examined during other stages.

The estrous cycle of the rat is completed in 4–5 days, and during this cycle changes in the vaginal mucosal membrane, the ovaries, and the uterus occur (3). Similar, but not as remarkable, changes of the vaginal mucosa occur in women during the menstrual cycle (4).

In the present study, the effect of estrous cycle stages on vaginal absorption was determined with phenolsulfonphthalein, insulin, and salicylic acid in rats. Furthermore, as continuous administration of leuprolide halts the estrous cycle of rats at diestrus (5), the vaginal absorption of phenolsulfonphthalein following consecutive subcutaneous injection of the analogue over a 10-day period was also estimated.

0022-3549/83/0200-0173$01.00/0

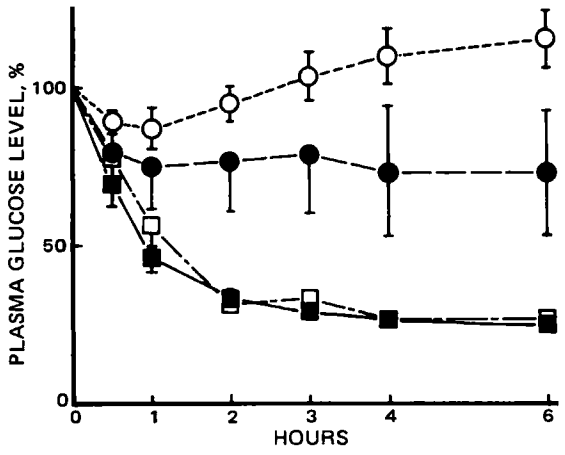

Figure 1—*Plasma glucose levels after vaginal administration of insulin during different stages of the estrous cycle in rats. Insulin was administered vaginally at a dose of 20 U/rat in an oleaginous suppository containing 10% citric acid. The glucose level is shown as a percentage against the initial level. Each point represents the mean ± SE of five rats. Key: (○) proestrus; (●) estrus; (□) metestrus; (■) diestrus.*

EXPERIMENTAL

Animals and Materials—Mature female Sprague-Dawley rats[1] (age, 120–150 days; weighing 250–330 g) exhibiting two or more consecutive 4-day estrous cycles were used.

Leuprolide and insulin were of the same quality used previously (1, 2), and the other chemicals were of reagent grade.

Effect of Estrous Cycle on Vaginal Absorption of Insulin and Phenolsulfonphthalein—Twenty units of porcine insulin (26.29 U/mg) in an oleaginous base[2] containing 10% citric acid was administered vaginally to proestrous, estrous, metestrous, and diestrous rats under pentobarbital (50 mg/kg) and phenobarbital (100 mg/kg) anesthesia. Blood was collected from the tail vein 0.5, 1, 2, 3, 4, and 6 hr after the administration, and 30 μl of the plasma was used for the assay of glucose levels (2).

Phenolsulfonphthalein was administered vaginally at a dose of 2 mg/kg/0.2 ml in pH 6.68, 0.03 *M* phosphate buffer solution (isotonic) to rats exhibiting the four different stages of the estrous cycle. Phenolsulfonphthalein in the urine collected for 6 hr by cannula was determined (2).

Vaginal Absorption of Salicylic Acid at Various pHs in Diestrous and Proestrous Rats—Salicylic acid dissolved at 1% in 0.2 *M* phthalate–hydrochloric acid buffer (pH 3.49), 0.2 *M* phthalate–sodium hydroxide buffer (pH 4.08 and 4.80), 0.1 *M* glycine–hydrochloric acid buffer (pH 3.53 and 4.53), and 0.03 *M* phosphate buffer (pH 5.73), and at 0.4% in 0.2 *M* potassium chloride–hydrochloric acid buffer (pH 2.29), was

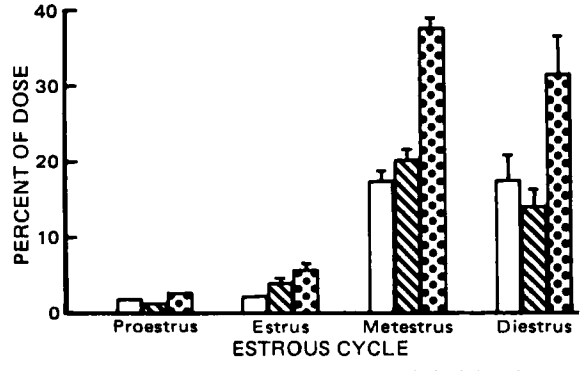

Figure 2—*Urinary excretion of phenolsulfonphthalein after vaginal administration at different stages of the estrous cycle in rats. Phenolsulfonphthalein was administered at a dose of 2 mg/kg/0.2 ml in the pH 6.68 phosphate buffer solution. Each bar represents the mean ± SE of five rats. Key: (□) 0–3 hr; (▨) 3–6 hr; (□) total.*

[1] Clea Japan, Inc., Tokyo, Japan.
[2] Witepsol S55, Dynamit Nobel Aktiengesellschaft, West Germany.

Table I—Remaining Percentage of Salicylic Acid [a] 1 hr after Vaginal Administration in Various pH Solutions to Diestrous and Proestrous Rats

$pH_{observed}$ (buffer)	Diestrus	Proestrus
2.29 (KCl–HCl)	7.1(1.5)[b]	10.4(2.5)
3.49 (phthalate)	18.2(2.1)	28.9(10.0)
3.53 (glycine)	44.0(1.8)	80.7(0.7)
4.08 (phthalate)	32.0(2.8)	58.3(2.9)
4.53 (glycine)	55.8(5.2)	82.1(11.4)
4.80 (phthalate)	35.2(2.1)	71.4(1.1)
5.73 (phosphate)	32.1(3.5)	71.3(12.2)

[a] Salicylic acid was administered at a dose of 2 mg/kg/0.2 ml, except at pH 2.29 (0.8 mg/kg/0.2 ml). [b] Each value represents the mean ± *SE* of three rats.

administered vaginally at a dose of 0.2 ml/kg with cotton balls to diestrous and proestrous rats under anesthesia. Each solution was adjusted to be isotonic with sodium chloride. Rats were decapitated 1 hr after administration, and the salicylic acid remaining in the vaginal tract was determined by a modified method (6). The vaginal tract was homogenized[3] in 5 ml of 0.9% NaCl solution and extracted with 8 ml of ethylene dichloride after acidification by the addition of 1 ml of 6 *N* HCl. Six milliliters of the organic layer was re-extracted with 4 ml of iron reagent [0.05% $Fe(NO_3)_3$–0.0035 *N* HNO_3 solution]. Absorbance of the aqueous layer was determined spectrophotometrically at 530 nm.

Vaginal Absorption of Phenolsulfonphthalein after Consecutive Subcutaneous Injection of Leuprolide—Leuprolide (100 μg/kg) was administered subcutaneously once a day for 10 consecutive days to rats exhibiting four different stages of estrous cycle on the initial day, and the vaginal smear was examined during administration. Phenolsulfonphthalein was administered vaginally at a dose of 2 mg/kg/0.2 ml in 5% citric acid solution (pH 3.5) with cotton balls to the pretreated animals, and the urinary excretion was determined (2).

RESULTS

Effect of Estrous Cycle on Vaginal Absorption of Insulin and Phenolsulfonphthalein—The plasma levels of glucose after vaginal administration of insulin to rats at different stages of the estrous cycle are shown as a percentage against the initial level (100%) in Fig. 1. A slight decrease of glucose level was observed only at an early period during proestrus; whereas, a distinct decrease was obtained during estrus and a more remarkable decrease during metestrus and diestrus. The integrated values (mean ± *SE*) of decreased plasma glucose level from 0 to 6 hr were −14.2 ± 38.2% hr for proestrus, 142.1 ± 94.2% hr for estrus, 364.2 ± 12.7% hr for metestrus, and 378.8 ± 9.3% hr for diestrus.

Vaginal absorption of phenolsulfonphthalein during the estrous cycle is shown by the urinary excretion in Fig. 2. The percentage excreted

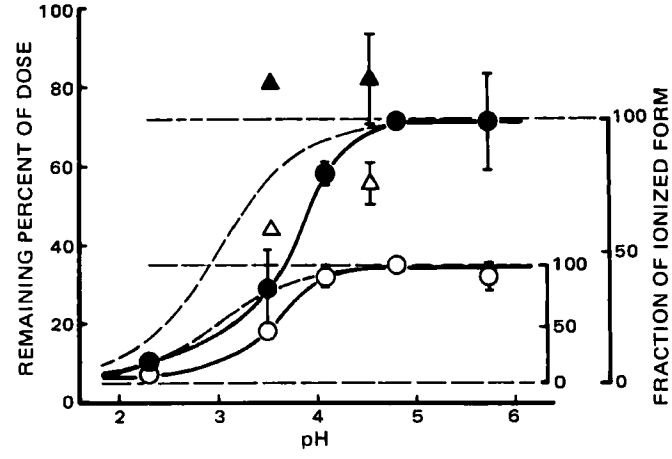

Figure 3—*Remaining percentage of salicylic acid 1 hr after vaginal administration in various pH solutions to diestrous and proestrous rats and fraction of ionized form of the acid. Salicylic acid was administered at a dose of 2 mg/kg/0.2 ml in the buffer solutions, except at pH 2.29 (0.8 mg/kg/0.2 ml). Key: (○) diestrus; [(△) in glycine buffer]; (●) proestrus [(▲) in glycine buffer]; (- -) fraction of the ionized form.*

[3] Polytron, Typ. PT10/35, Kinematica GmbH, Luzern, Switzerland.

Table II—Change in Estrous Cycle of Rats during 10 Daily Subcutaneous Injections of Leuprolide [a]

Rat No.	Day 1	2	3	4	5	6	7	8	9	10	11
1	I	III	IV	V	—[b]	V	V	V	V	V	V
2	I	III	IV	V	—	V	V	V	V	V	V
3	I	III	IV	V	—	V	V	V	V	V	V
4	III	IV	V	V	—	V	V	V	V	V	V
5	III	IV	V	V	—	V	V	V	V	V	V
6	III	IV	V	V	—	V	V	V	V	V	V
7	IV	V	V	V	—	V	V	V	V	V	V
8	IV	V	V	V	—	V	V	V	V	V	V
9	IV	V	V	V	—	V	V	V	V	V	V
10	V	I	III	IV	—	V	V	V	V	V	V
11	V	I	III	IV	—	V	V	V	V	V	V
12	V	I	III	IV	—	V	V	V	V	V	V

[a] (I) proestrus; (III) estrus; (IV) metestrus; (V) diestrus. The analogue was administered once a day at a dose of 100 μg/kg, and the stage of estrous cycle was determined by an examination of vaginal smears each morning. [b] (—) not determined.

(mean ± *SE*) of dose in 6 hr after vaginal administration of phenolsulfonphthalein was 31.4 ± 5.3% during diestrus, 37.5 ± 1.6% during metestrus, 5.5 ± 1.1% during estrus, and 2.4 ± 0.3% during proestrus.

The estrous cycle stage affects vaginal absorption of both insulin and phenolsulfonphthalein.

Vaginal Absorption of Salicylic Acid at Various pHs in Diestrous and Proestrous Rats—The remaining percentage of salicylic acid 1 hr after vaginal administration at various pHs to diestrous and proestrous rats (Table I) are plotted together with the calculated fraction of the ionized form (pK_a of the acid, 3.00) against the pH of the solution in Fig. 3. The disappearance of the acid from the vaginal tract during diestrus was relatively rapid even at pHs where most of the acid was ionized (pH 4.08, 4.80, and 5.73), and the disappearance rate increased at lower pH (pH 3.49 and 2.29). During proestrus the disappearance rate was reduced in nonionized form, but at lower pHs it approached the rate observed during diestrus. The disappearance rate of the ionized form was 66%/hr for diestrus and 29%/hr for proestrus. The absorption from the glycine buffer solutions (pH 3.53 and 4.53) was reduced during both stages.

Vaginal Absorption of Phenolsulfonphthalein after Consecutive Subcutaneous Injection of Leuprolide—After one normal estrous cycle, all rats treated with leuprolide settled in the diestrous stage (Table II). No matter at which stage of the estrous cycle the pretreatment began, the urinary excretion of phenolsulfonphthalein was enhanced ~20% with less variance compared to excretion in the untreated diestrous rats, especially during the 3 hr immediately following vaginal administration (Fig. 4).

DISCUSSION

Vaginal absorption of insulin and phenolsulfonphthalein in rats was dependent on the stage of estrous cycle: absorption was poor during proestrus, slightly improved during estrus, and good during metestrus and diestrus. These results can be explained by changes in vaginal epithelium (3) as follows. The epithelium during metestrus and diestrus is thin and highly porous, so many leukocytes can migrate through it. During proestrus, the superficial layers consist of tightly bound fresh cells and the epithelium is at its thickest. During estrus, the superficial layers become squamous, cornified, and are exfoliated into the vaginal lumen.

To estimate the absorption pathway of hydrophilic and hydrophobic compounds, vaginal absorption for the nonionized and ionized form of salicylic acid was also investigated during proestrus and diestrus. The disappearance of the nonionized acid from the vagina was increased markedly, and similar rates occurred during both stages. The disappearance of the ionized form was different: 66% of the dose in 1 hr during diestrus and 29% during proestrus. In a previous study (1), it was postulated that transport through pore-like pathways, such as intercellular channels, rather than permeation by partition to the cell membrane should cause good absorption of hydrophilic compounds. Thus, the postulation may be supported by the fact that the vaginal absorption of hydrophilic compounds highly depend on the estrous cycle stages which dominate the change of porosity of the membrane. The results also reveal the possibility of vaginal application of hydrophilic compounds during diestrus and metestrus. The high disappearance rate at lowered pHs during both stages possibly are caused by the increased permeation of the nonionized form through the cell membrane, and, in the case of salicylic acid, by the enhancing effect on the mucosal absorption of the drug (7). Since such an enhancing effect was not observed with phenolsulfonphthalein, the vaginal absorption would be more dependent on transport through pore-like pathways. Thus, the apparent porosity during diestrus is presumed to be more than 10 times that during proestrus and estrus (Fig. 2).

In addition, the correlation curve of the remaining percent of salicylic acid with pH during diestrus and proestrus shifted in the direction of higher pH than the theoretical ionized fraction *versus* pH curve (Fig. 3). This phenomenon may be ascribed to the pH difference between bulk solution and the unstirred layer on the membrane or the absorption-enhancing effect of the acid itself. The absorption from glycine buffer was significantly reduced during both proestrus and diestrus. Glycine also reduced the ovulation-inducing activity of leuprolide applied vaginally in an oleaginous base (1). The effects may be due to the stabilizing activity of glycine on the epithelial membrane.

The vaginal epithelium of a mature woman is known to change during the menstrual cycle, and changes of surface ultrastructure have been reported (4). In the follicular phase, the surface of the epithelium consists of a cluster of proliferated, nonkeratinized squamous cells. In the luteal phase, desquamation takes place on the superficial epithelial layer, proceeded by loosening of the intercellular grooves. After ovulation, intercellular porosity is confirmed by the observation of pore-like intercellular crevices and open intercellular connections (dissociated desmosomes). Thus, a similar effect of the reproductive cycle on the vaginal absorption may be expected as observed in rats. The vaginal epithelium is also subject to change with aging (neonate, prepuberty, adult, and senescence), pregnancy, and hormonal disorder. These specific structural changes of vaginal epithelium would influence vaginal absorption, and must be taken into account as a significant factor in the vaginal application of drugs, especially of hydrophilic compounds.

Previously, the continuous administration of leuprolide was found to affect the estrous cycle of rats (5). In the present study, it was confirmed by daily cytological examination of vaginal smears that the cycle was halted at the subsequent diestrus by consecutive treatment with the analogue. During the treatment, the vaginal mucosa was thin and similar to that of normal diestrus except that the smear contained more mucilage.

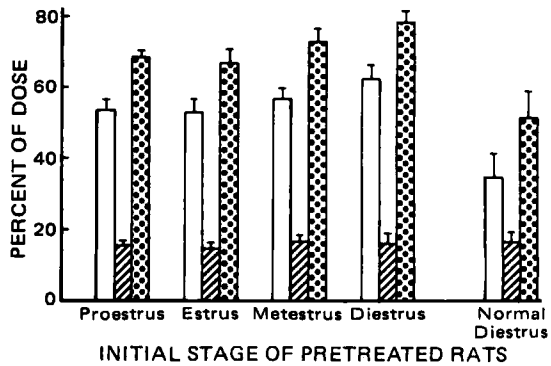

Figure 4—*Urinary excretion of phenolsulfonphthalein after vaginal administration to rats pretreated subcutaneously with leuprolide for 10 days. Phenolsulfonphthalein was administered vaginally at a dose of 2 mg/kg/0.2 ml in 5% citric acid solution (pH 3.5) to rats pretreated with 100 μg/kg/day of the analogue. Each bar represents the mean ± SE of four or five (normal) rats. Key: (□) 0–3 hr; (▨) 3–6 hr; (▩) total.*

Furthermore, the vaginal absorption of phenolsulfonphthalein after the consecutive administration resulted in an enhanced absorption with less variance, regardless of the initial stage of the estrous cycle (Fig. 4). The better absorption supports the halt of the cycle at diestrus and possibly reveals the thinner epithelial membrane.

In long-term therapy with vaginal application of leuprolide, the reproductive cycle effects would be leveled off by continuous administration, either parenterally or vaginally, although some fluctuation in absorption may be unavoidable at the initial period of administration. The authors' previous proposal of the vaginal application of leuprolide as a rational method for long-term anticancer therapy was supported by the findings of the present study.

REFERENCES

(1) H. Okada, I. Yamazaki, Y. Ogawa, S. Hirai, T. Yashiki, and H. Mima, *J. Pharm. Sci.*, **71**, 1367 (1982).

(2) H. Okada, I. Yamazaki, T. Yashiki, and H. Mima, *ibid.*, **72**, 75 (1983).

(3) C. D. Turner and J. T. Bagnara, "General Endocrinology," 6th ed., Saunders, 1970, p. 470.

(4) K. A. Walz, H. Metzger, and H. Ludwig, in "The Human Vagina," Human Reproductive Medicine, vol. 2, E. S. E. Hafez and T. N. Evans, Eds., Elsevier/North-Holland Biochemical Press, 1978, p. 55.

(5) E. S. Johnson, R. L. Gendrich, and W. F. White, *Fertil. Steril.*, **27**, 853 (1976).

(6) P. K. Smith, H. L. Gleason, C. G. Stoll, and S. Ogorzalek, *J. Pharmacol. Exp. Ther.*, **87**, 237 (1946).

(7) T. Nishihata, J. H. Rytting, and T. Higuchi, *J. Pharm. Sci.*, **70**, 71 (1981).

ACKNOWLEDGMENTS

The authors thank Miss T. Yamashita for assistance with the experiments; Dr. T. Shimamoto, Dr. I. Yamazaki, and Dr. S. Hirai for valuable discussion; and Dr. J. R. Miller for comments on the manuscript.

Methaqualone–Diphenhydramine Interaction Study in Humans

K. W. HINDMARSH *x, S. M. WALLACE *, C. B. SCHNEIDER *, and E. D. KORCHINSKI ‡

Received November 3, 1981, from the **College of Pharmacy and* ‡*College of Medicine, University of Saskatchewan, Saskatoon, Saskatchewan, Canada S7N 0W0.* Accepted for publication April 12, 1982.

Abstract □ Twelve healthy subjects received three single oral doses (250 mg) of methaqualone alone or in combination with diphenhydramine (25 mg). Blood samples were collected for a 48-hr period after each dose and analyzed for methaqualone and its major metabolite, 2-methyl-3-(2′-hydroxymethylphenyl)-4(3H)-quinazolinone. Peak blood concentrations ranging from 1.0 to 2.7 μg/ml occurred ~1–2 hr after the oral dose. The area under the blood level–time curve, peak plasma level, and elimination half-life for methaqualone were not significantly different (three-way ANOVA, $p > 0.05$) when methaqualone was administered alone, in combination with a diphenhydramine elixir or as a commercial product (capsule) containing both methaqualone and diphenhydramine. Statistically significant intersubject differences in the area under the curve were eliminated if the area was corrected for subject differences in elimination. Blood levels of the metabolite reached an average peak of 314 ng/ml (±107) between 4 and 8 hr after the dose and remained elevated for the 48-hr sampling period. The areas under the blood level time curve of the metabolite were not significantly different for the three treatments. Diphenhydramine administered at the dosage level used in therapeutic combination products did not alter the blood levels of methaqualone or its metabolite. In addition, no significant differences in methaqualone availability from the two commercial formulations tested could be detected.

Keyphrases □ Methaqualone—interaction study with diphenhydramine in humans, elimination, metabolism □ Diphenhydramine—interaction study with methaqualone in humans, elimination, metabolism □ Elimination—methaqualone–diphenhydramine interaction study in humans, metabolism □ Metabolism—methaqualone–diphenhydramine interaction study in humans, elimination

Although the therapeutic use of the methaqualone–diphenhydramine combination has declined, abuse continues to flourish (1–3). The reasons for the enhanced CNS effects claimed by drug abusers is not clearly understood.

Metabolism of methaqualone by the 10,000-g supernatant fraction of rat liver homogenates is inhibited *in vitro* by diphenhydramine (4). Concurrent oral administration of methaqualone and diphenhydramine to rats increases the blood and brain levels of methaqualone (3), whereas concurrent intravenous administration has no significant effect (5).

In humans, diphenhydramine has been credited with increasing the sedative-hypnotic effect of methaqualone (6), although the mechanism has not been elucidated. A previous study (7) compared methaqualone plasma concentrations achieved after administration of two commercially available diphenhydramine–methaqualone combination products and three methaqualone products. Differences in plasma levels were noted and attributed to formulation factors. An earlier study (8), comparing plasma levels after single dose administration of commercial products containing methaqualone, methaqualone hydrochloride, and methaqualone plus diphenhydramine, is difficult to interpret since no subject appears to have received more than one formulation. In a subsequent study (9) reduction of buccal absorption was reported when methaqualone powder was administered with diphenhydramine powder, but there was no difference in plasma levels after oral administration of the combination.

The objective of the present study was to compare, in healthy subjects, the concentrations of methaqualone and its major metabolite in blood (2-methyl-3-(2′-hydroxymethylphenyl)-4(3H)-quinazolinone), after administration of methaqualone alone and in combination with diphenhydramine. The possibility of a formulation effect was anticipated by including in the study design administration of diphenhydramine–methaqualone as a commercial combination product and as a mixture of a methaqualone capsule and diphenhydramine elixir.

0022-3549/83/0200-0176$01.00/0

Furthermore, the vaginal absorption of phenolsulfonphthalein after the consecutive administration resulted in an enhanced absorption with less variance, regardless of the initial stage of the estrous cycle (Fig. 4). The better absorption supports the halt of the cycle at diestrus and possibly reveals the thinner epithelial membrane.

In long-term therapy with vaginal application of leuprolide, the reproductive cycle effects would be leveled off by continuous administration, either parenterally or vaginally, although some fluctuation in absorption may be unavoidable at the initial period of administration. The authors' previous proposal of the vaginal application of leuprolide as a rational method for long-term anticancer therapy was supported by the findings of the present study.

REFERENCES

(1) H. Okada, I. Yamazaki, Y. Ogawa, S. Hirai, T. Yashiki, and H. Mima, *J. Pharm. Sci.*, **71**, 1367 (1982).

(2) H. Okada, I. Yamazaki, T. Yashiki, and H. Mima, *ibid.*, **72**, 75 (1983).

(3) C. D. Turner and J. T. Bagnara, "General Endocrinology," 6th ed., Saunders, 1970, p. 470.

(4) K. A. Walz, H. Metzger, and H. Ludwig, in "The Human Vagina," Human Reproductive Medicine, vol. 2, E. S. E. Hafez and T. N. Evans, Eds., Elsevier/North-Holland Biochemical Press, 1978, p. 55.

(5) E. S. Johnson, R. L. Gendrich, and W. F. White, *Fertil. Steril.*, **27**, 853 (1976).

(6) P. K. Smith, H. L. Gleason, C. G. Stoll, and S. Ogorzalek, *J. Pharmacol. Exp. Ther.*, **87**, 237 (1946).

(7) T. Nishihata, J. H. Rytting, and T. Higuchi, *J. Pharm. Sci.*, **70**, 71 (1981).

ACKNOWLEDGMENTS

The authors thank Miss T. Yamashita for assistance with the experiments; Dr. T. Shimamoto, Dr. I. Yamazaki, and Dr. S. Hirai for valuable discussion; and Dr. J. R. Miller for comments on the manuscript.

Methaqualone–Diphenhydramine Interaction Study in Humans

K. W. HINDMARSH *x, S. M. WALLACE *, C. B. SCHNEIDER *, and E. D. KORCHINSKI ‡

Received November 3, 1981, from the **College of Pharmacy and* ‡*College of Medicine, University of Saskatchewan, Saskatoon, Saskatchewan, Canada S7N 0W0.* Accepted for publication April 12, 1982.

Abstract □ Twelve healthy subjects received three single oral doses (250 mg) of methaqualone alone or in combination with diphenhydramine (25 mg). Blood samples were collected for a 48-hr period after each dose and analyzed for methaqualone and its major metabolite, 2-methyl-3-(2′-hydroxymethylphenyl)-4(3H)-quinazolinone. Peak blood concentrations ranging from 1.0 to 2.7 μg/ml occurred ~1–2 hr after the oral dose. The area under the blood level–time curve, peak plasma level, and elimination half-life for methaqualone were not significantly different (three-way ANOVA, $p > 0.05$) when methaqualone was administered alone, in combination with a diphenhydramine elixir or as a commercial product (capsule) containing both methaqualone and diphenhydramine. Statistically significant intersubject differences in the area under the curve were eliminated if the area was corrected for subject differences in elimination. Blood levels of the metabolite reached an average peak of 314 ng/ml (±107) between 4 and 8 hr after the dose and remained elevated for the 48-hr sampling period. The areas under the blood level time curve of the metabolite were not significantly different for the three treatments. Diphenhydramine administered at the dosage level used in therapeutic combination products did not alter the blood levels of methaqualone or its metabolite. In addition, no significant differences in methaqualone availability from the two commercial formulations tested could be detected.

Keyphrases □ Methaqualone—interaction study with diphenhydramine in humans, elimination, metabolism □ Diphenhydramine—interaction study with methaqualone in humans, elimination, metabolism □ Elimination—methaqualone–diphenhydramine interaction study in humans, metabolism □ Metabolism—methaqualone–diphenhydramine interaction study in humans, elimination

Although the therapeutic use of the methaqualone–diphenhydramine combination has declined, abuse continues to flourish (1–3). The reasons for the enhanced CNS effects claimed by drug abusers is not clearly understood.

Metabolism of methaqualone by the 10,000-g supernatant fraction of rat liver homogenates is inhibited *in vitro* by diphenhydramine (4). Concurrent oral administration of methaqualone and diphenhydramine to rats increases the blood and brain levels of methaqualone (3), whereas concurrent intravenous administration has no significant effect (5).

In humans, diphenhydramine has been credited with increasing the sedative-hypnotic effect of methaqualone (6), although the mechanism has not been elucidated. A previous study (7) compared methaqualone plasma concentrations achieved after administration of two commercially available diphenhydramine–methaqualone combination products and three methaqualone products. Differences in plasma levels were noted and attributed to formulation factors. An earlier study (8), comparing plasma levels after single dose administration of commercial products containing methaqualone, methaqualone hydrochloride, and methaqualone plus diphenhydramine, is difficult to interpret since no subject appears to have received more than one formulation. In a subsequent study (9) reduction of buccal absorption was reported when methaqualone powder was administered with diphenhydramine powder, but there was no difference in plasma levels after oral administration of the combination.

The objective of the present study was to compare, in healthy subjects, the concentrations of methaqualone and its major metabolite in blood (2-methyl-3-(2′-hydroxymethylphenyl)-4(3H)-quinazolinone), after administration of methaqualone alone and in combination with diphenhydramine. The possibility of a formulation effect was anticipated by including in the study design administration of diphenhydramine–methaqualone as a commercial combination product and as a mixture of a methaqualone capsule and diphenhydramine elixir.

0022-3549/83/0200-0176$01.00/0

Figure 1—*Gas chromatograms of extracts of blood. Key: (A) control blood sample with imipramine added; (B) blood from subject receiving methaqualone (Peak I) with imipramine (Peak II) added.*

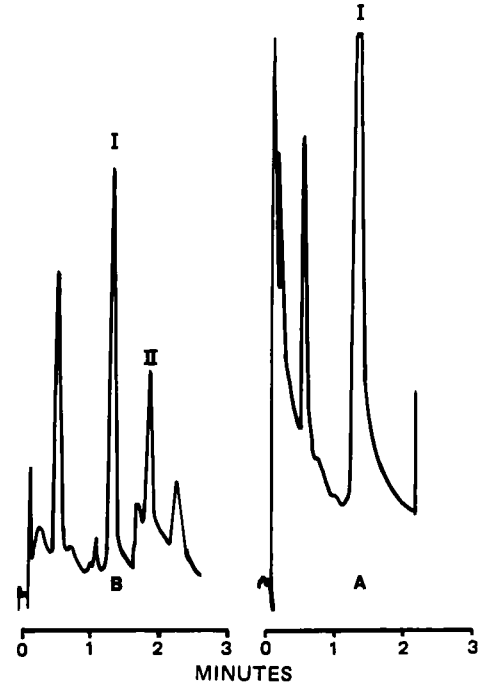

Figure 2—*Gas chromatograms of silylated extracts of blood. Key: (A) control blood sample with imipramine (Peak I) added; (B) blood from subject receiving methaqualone, Peak I imipramine, Peak II 2-methyl-3-(2'-hydroxymethylphenyl)-4(3H)-quinazolinone.*

EXPERIMENTAL

Materials—Methaqualone hydrochloride[1], 1-chlorobutane[2], ammonium carbonate[3], imipramine hydrochloride[4], bis-(trimethylsilyl)-trifluroacetamide with trimethylchlorosilane (1%)[5], dichloromethane[6], ethyl acetate[6], and glacial acetic acid[7] were obtained commercially and appropriate aqueous or methanolic solutions were prepared as required. The solvent used for extracting biological fluids was prepared by mixing dichloromethane with ether (11:14 v/v) (10). An acetate buffer (pH 5.2) was prepared by mixing 21 ml of 0.1 *M* acetic acid with 79 ml of 0.1 *M* sodium acetate.

***In Vitro* Blood–Plasma Distribution Studies**—Methaqualone hydrochloride (1 μg/ml of solution in methanol) was added to Erlenmyer flasks in sufficient quantity to produce a final methaqualone hydrochloride concentration of 1–20 μg/ml (0.87–17.5 μg/ml of methaqualone). The methanol was evaporated and 20 ml of blood[8] added. The flasks were covered[9] and incubated[10] for 2 hr (37°). Two hours had been established previously as sufficient time to ensure equilibration. A portion of the blood from each flask was centrifuged[11] to separate plasma. Aliquots (1 ml) of blood and plasma were extracted and methaqualone concentrations were determined by GLC. Hematocrits were determined[12] and red blood cell concentrations were calculated (11).

Study Design—Twelve volunteers (4 female, 8 male) weighing between 50.2 and 83.9 kg each and ranging in age from 21 to 38 years participated in the study. All subjects received a medical examination and a series of standard laboratory tests prior to entering the study. All subjects gave their written informed consent according to an approved[13] *protocol.*

Each subject received a single dose each of methaqualone hydrochloride in a 250-mg capsule[14], methaqualone hydrochloride capsule[14] plus 25 mg of diphenhydramine hydrochloride [elixir][15] and a methaqualone (250 mg)–diphenhydramine hydrochloride (25 mg) capsule[16]. The order of treatments was randomized according to a Latin-square design with a minimum period of 2 weeks between each treatment (*i.e.*, each drug administration). Drugs were administered with water after a 12-hr fast. Food was not consumed until at least 4 hr after the drugs had been administered. One subject received a fourth treatment of methaqualone hydrochloride and 50 mg of diphenhydramine hydrochloride[17].

Blood samples (7 ml) were collected[18] at 0, 0.5, 1, 2, 4, 8, 24, 32, and 48 hr after each drug administration, and were refrigerated until extracted and analyzed for methaqualone concentration by GLC. For 9 of the 12 subjects, blood samples were also analyzed for 2-methyl-3-(2'-hydroxymethylphenyl)-4(3H)-quinazolinone by GLC. All samples were extracted within 48 hr of collection.

A portion of the blood collected for five of the subjects, after one of the drug doses, was centrifuged[11] to separate plasma. Both plasma and blood samples were analyzed for methaqualone by GLC.

GLC–mass spectrometry was performed on a GLC-mass spectrometer linked to a data system[19].

Extraction of Biological Fluids—For samples from *in vitro* studies, aliquots (1 ml) of blood and plasma were added to centrifuge tubes containing the internal standard, imipramine (4 μg). The samples were diluted with distilled water (1 ml), basified (10 *M* NaOH) and extracted[20] twice with 1-chlorobutane (5 ml) for 1.0 min. The pooled organic layers were evaporated[21] (at 85°) to dryness under a flow of air. The residue was quantitatively transferred to glass vials (1 ml)[22] using small portions of methanol. The methanol was evaporated[23]. The residue was dissolved in methanol (20 μl) and 1–2 μl injected onto the GLC.

[1] William H. Rorer (Canada) Ltd., Bramalea, Ontario, Canada.
[2] J. T. Baker Chemical Co., Phillipsburg, NJ.
[3] British Drug Houses (Canada) Ltd., Toronto, Ontario, Canada.
[4] Geigy Pharmaceuticals, Division of Ciba-Geigy Canada Ltd., Dorval, Quebec, Canada.
[5] Pierce Chemical Co., Rockford, Ill.
[6] Caledon Laboratories Ltd., Georgetown, Ontario, Canada.
[7] Fisher Scientific Co., Fair Lawn, NJ.
[8] Canadian Red Cross Society Blood Bank, Saskatoon, Saskatchewan, Canada.
[9] Parafilm, American Can Co., Greenwich, Conn.
[10] Model G-76, Gyrotory Water bath shaker, New Brunswick Scientific Co., Inc., New Brunswick, NJ.
[11] Model IEC-HN-S centrifuge, Damon/IEC Division, Needham Heights, Mass.
[12] Readacrit centrifuge, Clay Adams Division of Becton, Dickinson and Co., Parsippany, NJ.
[13] President's Committee on Ethics in Human Experimentation, University of Saskatchewan, Saskatoon, Saskatchewan, Canada.
[14] Mequelon capsules, 250 mg, Charles E. Frosst and Co., Pointe Claire-Dorval, Quebec, Canada.
[15] Benadryl elixir, 12.5 mg/5 ml, Parke-Davis and Co. Ltd., Scarborough, Ontario, Canada.
[16] Mandrax capsules, Roussel (Canada) Ltd., Montreal, Quebec, Canada.
[17] Benadryl capsule, 50 mg, Parke-Davis and Co. Ltd., Scarborough, Ontario, Canada.
[18] Venoject, heparinized, evacuated blood collection tubes, Kimble-Terumo, Elkton, Md.
[19] Model 3300, Finnigan GC–MS and Model 2300, Incos Data System, Finnigan Corp., Honeyville, Calif.
[20] Vortex Genie, Fisher Scientific Co., Montreal, Quebec, Canada.
[21] Thermolyne Dri-Bath, Thermolyne Corp., Dubuque, Iowa.
[22] Reacti-vials, 1 ml, Pierce Chemical Co., Rockford, Ill.
[23] Extracted at a speed setting of 10, Evapomix, Buchler Instruments, Fort Lee, NJ.

Table I—*In Vitro* Distribution of Methaqualone Between Plasma and Erythrocytes

Methaqualone Concentration, μg/ml			
Blood[a], C_B	Plasma, C_P	Erythrocytes[b], C_{RBC}	Blood–Plasma Ratio
1.0	1.25	0.60	0.80
2.0	2.37	1.41	0.84
3.0	3.30	2.52	0.91
4.0	4.71	2.87	0.85
5.0	4.47	5.72	1.12
10.0	6.20	15.1	1.61
15.0	8.20	24.2	1.83
20.0	9.03	34.8	2.21

[a] Concentration added to blood. [b] Calculated from $C_B = C_P(1 - H) + C_{RBC}(H)$, where the hematocrit (H) is 38.5% for concentrations of 1–4 μg/ml and 42.5% for concentrations of 5–20 μg/ml.

Table II—*In Vivo* Distribution of Methaqualone in Blood[a]

Time after Administration, hr	Methaqualone Concentration, μg/ml		Blood–Plasma Ratio
	Blood	Plasma	
0	0	0	
0.5	0.44 ± 0.46	0.47 ± 0.31	0.95 ± 0.03[b]
1	1.10 ± 0.64	1.21 ± 0.69	0.90 ± 0.14
2	1.18 ± 0.14	1.32 ± 0.22	0.90 ± 0.09
4	0.66 ± 0.12	0.80 ± 0.10	0.82 ± 0.09
8	0.42 ± 0.09	0.50 ± 0.07	0.82 ± 0.05
24	0.24 ± 0.02	0.25 ± 0.02	0.97 ± 0.05
32	0.21 ± 0.02	0.23 ± 0.02	0.92 ± 0.06
48	0.17 ± 0.01	0.19 ± 0.02	0.93 ± 0.09

[a] Values are the mean ± *SD* for 5 subjects (1, 6, 8, 10, and 12) with hematocrits of 0.45, 0.48, 0.52, 0.42, and 0.47, respectively. [b] Two of five blood and plasma concentrations had a value of zero at 0.5 hr.

For analysis of samples from the *in vivo* study, 1-ml aliquots of blood or plasma were diluted with 1 ml of distilled water containing 3 μg/ml of imipramine hydrochloride. Ammonium carbonate (1 g) was added, and the samples were extracted twice with 4 ml of ether–dichloromethane (14:11) for 10 min[23]. The tubes were centrifuged at 2000 rpm[11] for 10 min. The pooled organic layers were evaporated[21] at 85° under a gentle flow of nitrogen. The residue was dissolved in 500 μl of methanol. For analysis of methaqualone concentrations, 2–5-μl aliquots were injected onto the GLC. For analysis of the methaqualone metabolite in blood the remaining methanol was evaporated under a flow of nitrogen. Silyl ether derivatives were prepared by adding ethyl acetate (300 μl dried over molecular sieves) and bis-(trimethylsilyl)trifluoroacetamide with 1% trimethylchlorosilane (50 μl) to the residue in each tube. The tubes were capped and incubated[21] at 85° for 1 hr. The solvent was evaporated under a flow of nitrogen. The residue was dissolved in ethyl acetate (500 μl), and 2–5-μl aliquots were injected onto the GLC.

GLC Analysis—For analysis of samples from *in vitro* studies, a GLC[24] equipped with a flame-ionization detector was used. The chromatographic column was 1.2-m × 3.2-mm o.d. coiled, stainless-steel tubing packed with 3% methyl silicone coated on a high-performance diatomite support (80–100 mesh)[25]. The column was conditioned by maintaining the oven at 290° with low carrier gas flow for 18 hr. Operating temperatures were: injection port, 270°; column, 220°; detector, 265°.

The nitrogen flow was 30 ml/min. Hydrogen and compressed air flow rates were adjusted to give maximum response. Methaqualone concentrations were determined from a standard curve plotted as the peak height ratio (methaqualone–internal standard) against methaqualone concentration.

For analysis of methaqualone and its metabolite in blood obtained during the *in vivo* study, a GLC[26] equipped with a nitrogen–phosphorus detector was used. The chromatographic column was 1.2-m × 2.0-mm i.d. coiled-glass tubing packed with 2% methyl silicone on a high-performance diatomite support (100–120 mesh)[25]. Operating temperatures were: injection and detector ports, 300°; column, 240° (for methaqualone) or 220° (for the methaqualone metabolite). The helium flow rate was 30 ml/min, and the hydrogen and compressed air flow rates were adjusted to 3 ml/min and 50 ml/min, respectively. Concentrations of methaqualone and its metabolite were calculated from standard curves plotted as peak area (methaqualone) or peak height (metabolite) ratio (compound–internal standard) against concentration. All standard curves for analysis of samples were prepared as extracted standard curves by adding known amounts of methaqualone (or metabolite) to blood and extracting the standards as previously described.

Data Analysis—Slope and intercept of standard curves were calculated by least-squares linear regression[27]. The disposition rate constant (β) for methaqualone was determined by log-linear regression[27] of the last 3–4 data points of the blood level–time curve. The biological half-life ($t_{1/2\beta}$) was calculated as $0.693/\beta$. The area under the blood level time curve for methaqualone (AUC_0^{48}) and its metabolite ($AUC_{0\,met}^{48}$) was estimated using the trapezoidal rule. To obtain the total area under the curve for methaqualone (AUC_0^∞), the area from the last sampling point to infinity (plasma level at 48 hr/β) was added to AUC_0^{48}. All parameters, except the time of peak plasma levels (t_{max}) and $t_{1/2\beta}$, were corrected for subject differences in the milligram per kilogram dose (*i.e.*, by dividing by the ratio of the dose of methaqualone base to the subject's weight) (12). The AUC_0^∞ was corrected for changes in elimination by multiplying by β ($AUC_0^\infty\,\beta$). All parameters (AUC_0^{48}, AUC_0^∞, $AUC_0^\infty\beta$, $AUC_{0\,met}^{48}$, t_{max}, C_{max}, and $t_{1/2\beta}$) were then analyzed statistically by three-way ANOVA[28] for treatment, period (*i.e.*, order of treatment), and subject effects; effects were considered significant if $p \leq 0.05$.

RESULTS AND DISCUSSION

GLC analysis of blood extracts revealed a well-defined peak (I, Fig. 1B) adequately separated from the internal standard, imipramine, (Peak II, Fig. 1B) and endogenous material (Fig. 1A). Peak I was identified, by GLC–mass spectrometry, as methaqualone. A molecular ion at m/z 250 and the base peak at m/z 235 due to the loss of the methyl group at the 2-position of the molecular ion were noted. A column temperature of 240° gave a relative retention time (with respect to imipramine) of 0.86 min for methaqualone. The standard curve for the GLC analysis of methaqualone was linear (r^2, coefficient of determination = 0.996) over a concentration range of 0.15–2.40 μg/ml.

Chromatography of silylated blood samples revealed one major peak (Peak II, Fig. 2B) not found in control blood extracts (Fig. 2A). Peak II (Fig. 2B) had a relative retention time of 1.39 min with respect to the internal standard, imipramine (Peak I, 2B). GLC–MS confirmed that Peak II was the trimethylsilyl derivative of the monohydroxy methaqualone metabolite, 2-methyl-3-(2′-hydroxymethylphenyl)-4(3H)-quinazolinone. Similar fragment ions to those previously reported for this metabolite (13, 14) were detected. The standard curve for GLC analysis of the metabolite was linear (r^2, coefficient of determination = 0.99) over a concentration range of 0.06–0.96 μg/ml. Mean recoveries of methaqualone and the metabolite from blood were 89.4 ± 6.6 (*SD*) and 87.2 ± 11.2%, respectively.

While forensic studies of methaqualone overdosage tend to report blood levels of the drug (15–17), pharmacokinetic studies measure the concentration of the drug in plasma or serum (18–20). Erythrocyte concentrations at <50% of the corresponding plasma concentration have been reported (9, 21). Another study (22) claimed >90% of the methaqualone in plasma phase with little, if any, bound to the cellular elements of blood. In the present report, however, concentrations of methaqualone in blood and plasma did not differ greatly except for blood concentrations of 5 μg/ml or greater (Table I).

After administration of a single 250-mg dose of methaqualone to healthy subjects, the blood–plasma ratio of methaqualone concentrations ranged from 0.82 to 0.97 over the 48-hr period studied (Table II). *In vitro* distribution studies yielded similar results for the concentration range of 1–4 μg/ml of blood. At higher blood concentrations, *in vitro*, erythrocyte concentrations of methaqualone were significantly greater than plasma concentrations (Table I). A larger fraction free in plasma would not account for the changing blood–plasma ratios, since a relatively constant fraction (95%) of methaqualone is bound *in vitro* to human plasma proteins over the concentration range of 5–20 μg/ml plasma (unpublished observations).

One may speculate that larger blood–plasma ratios result from a cooperative binding to erythrocytes at higher methaqualone concentrations. The reasons for the apparent accumulation in erythrocytes were not investigated. Blood and plasma concentrations appear to be approximately equivalent at the lower methaqualone concentrations encountered in pharmacokinetic studies. However, in overdose cases, blood and plasma

[24] Model 5750B, Hewlett-Packard, Avondale, Pa.
[25] OV-101 on Chromosorb W, Chromatographic Specialties, Brockville, Ontario, Canada.
[26] Model 5840, Hewlett-Packard, Avondale, Pa.
[27] TI-59 Programmable Calculator, Texas Instruments Inc., Dallas, Tex.
[28] SPSS program package, University of Pittsburgh, and DEC-20 computer.

Table III—Comparison of Parameters for Methaqualone after Administration of a Single Oral Dose with and without Diphenhydramine

Parameter	Treatment[d] Methaqualone HCl Capsule	Methaqualone HCl plus Diphenhydramine Elixir	Methaqualone–Diphenhydramine Capsule	p Value for Subject Effect[a]
AUC_0^{48} μg/ml × hr[b]	5.29 ± 0.99	5.33 ± 0.97	5.22 ± 0.97	<0.001
AUC_0^{∞} μg/ml × hr[b]	8.16 ± 2.67	7.82 ± 2.20	7.81 ± 1.47	<0.001
$AUC_0^{\infty}\beta$ μg/ml[b]	0.15 ± 0.03	0.16 ± 0.02	0.15 ± 0.03	0.06
C_{max}, μg/ml[b]	0.51 ± 0.11	0.46 ± 0.11	0.50 ± 0.10	0.04
t_{max}, hr	1.5 ± 0.5	1.3 ± 0.5	1.8 ± 0.9	0.30
$t_{1/2\beta}$, hr	37.7 ± 14.1	33.4 ± 8.7	36.6 ± 11.5	0.01
$AUC_{0\,met}^{48}$[b,c] μg/ml × hr	3.47 ± 1.04	3.19 ± 1.44	3.05 ± 0.61	0.12
Dose/kg, methaqualone base	3.26 ± 0.53	3.26 ± 0.53	3.74 ± 0.61	

[a] p values >0.05 for treatment and period effects for all parameters. [b] Corrected for dose–kilogram of body weight (divide all units by mg/kg). [c] Determined for 9 of the 12 subjects. [d] Mequelon, Charles E. Frosst & Co.; Mequelon and Benadryl elixir, Parke Davis & Co. Ltd.; Mandrax, Roussel (Canada) Ltd.

levels may not be equivalent and the difference should perhaps be considered when evaluating a patient. For the purposes of the present investigation, blood was chosen as the biological fluid for analysis, because cleaner extracts with less GLC baseline interference were obtained.

To determine whether methaqualone blood levels differed when methaqualone was administered orally with diphenhydramine, blood was sampled over a 48-hr period in 12 healthy subjects. Data from subject 6 are presented as representative of methaqualone blood levels achieved with oral administration of a single dose of methaqualone with and without diphenhydramine (Fig. 3). The time of blood collection (48 hr) was too short to obtain a pharmacokinetically accurate value for the elimination half-life, but the estimates for $t_{1/2}$ were within the range previously reported for methaqualone (19.6–41.5 hr) (18). Peak blood levels ranged from 1.0–2.7 μg/ml at 1–2 hr after oral administration (Table IV). The t_{max} and $t_{1/2\beta}$ values were not significantly different for the three treatments (methaqualone HCl capsule, methaqualone HCl capsule plus diphenhydramine elixir, methaqualone–diphenhydramine capsule). All other parameters were corrected for the mg/kg dose of methaqualone administered. No treatment or formulation effect was evident for AUC_0^{48}, AUC_0^{∞}, $AUC_0^{\infty}\beta$, or C_{max} (p for treatments >0.05) (Table III). The power of the statistical test was such that a difference of 20% would have been detected (23). Significant intersubject differences (p <0.05) were noted for AUC_0^{48}, AUC_0^{∞}, C_{max}, and $t_{1/2\beta}$. No significant intersubject differences in $AUC_0^{\infty}\beta$ were apparent, thus suggesting the major factor contributing to intersubject differences in the AUC value for methaqualone was the elimination of the drug.

Maximum blood levels of the methaqualone metabolite, 2-methyl-3(2′-hydroxymethylphenyl)-4(3H)-quinazolinone), occurred between 4 and 8 hr after methaqualone administration and remained elevated over the 48-hr sampling time (Fig. 4). The average maximum metabolite level was 314 ng/ml ± 107 (SD). The $AUC_{0\,met}^{48}$ values after administration of methaqualone with and without diphenhydramine were not significantly different.

No major differences in blood levels could be detected between the methaqualone HCl capsule and methaqualone–diphenhydramine HCl capsule formulation. Diphenhydramine administered at the dosage level

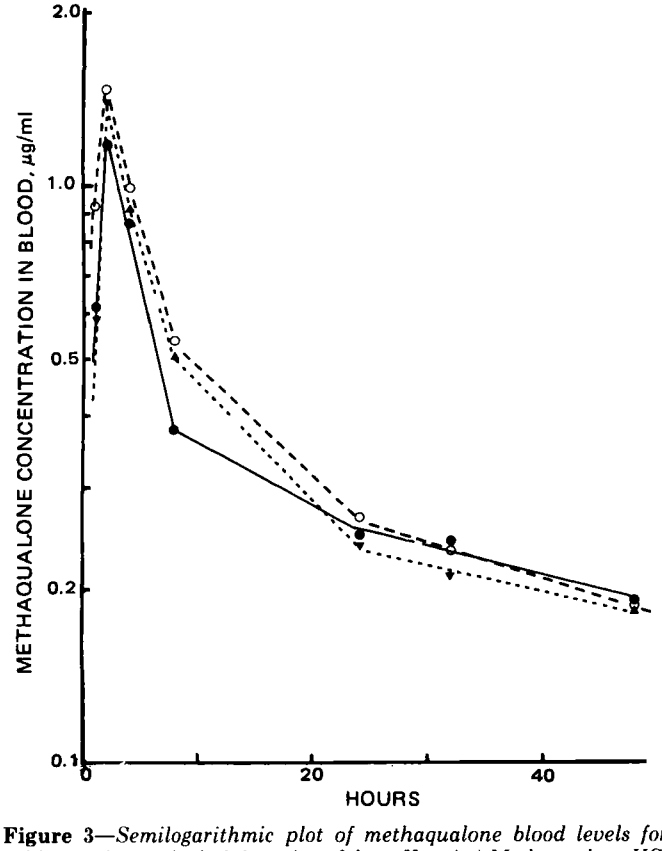

Figure 3—*Semilogarithmic plot of methaqualone blood levels for subject 6 after oral administration of drug. Key: (●) Methaqualone HCl (250 mg); (○) methaqualone HCl (250 mg) and diphenhydramine HCl (25 mg) elixir; (▼) methaqualone diphenhydramine HCl capsule (250:25 mg).*

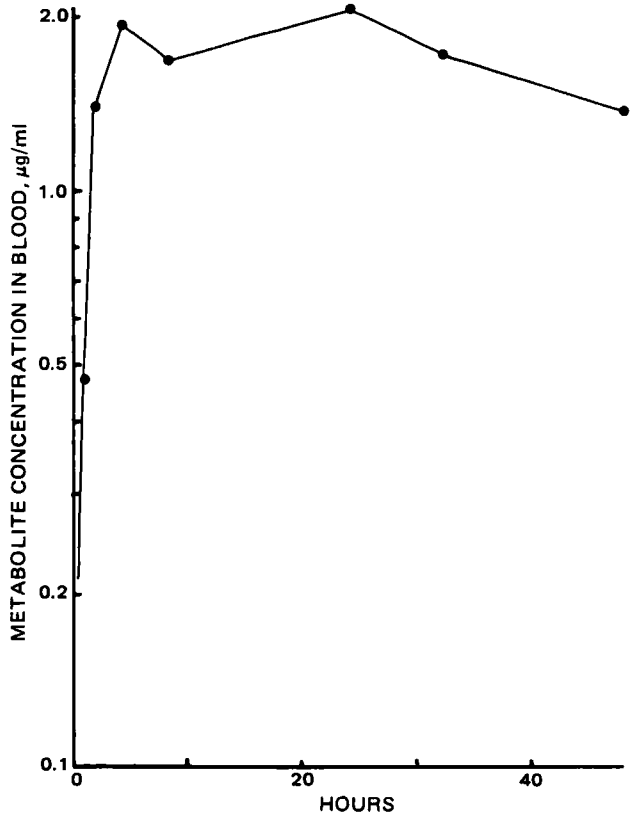

Figure 4—*Semilogarithmic plot of 2-methyl-3-(2′-hydroxymethylphenyl)-4(3H)-quinazolinone blood levels for subject 6 after administration of a methaqualone HCl (250 mg) capsule.*

Table IV—Methaqualone Concentrations in Blood [a] at Various Times after Administration of a Single Oral Dose with and without Diphenhydramine

Time[b], hr	Treatment: Methaqualone HCl Capsule	Methaqualone HCl plus Diphenhydramine Elixir	Methaqualone–Diphenhydramine Capsule
0.5	0.38 ± 0.44	0.24 ± 0.25	0.60 ± 0.50
1	1.39 ± 0.68	1.34 ± 0.53	1.54 ± 0.53
2	1.38 ± 0.35	1.26 ± 0.31	1.56 ± 0.48
4	0.79 ± 0.23	0.81 ± 0.23	0.92 ± 0.35
8	0.49 ± 0.15	0.51 ± 0.20	0.54 ± 0.17
24	0.24 ± 0.07	0.25 ± 0.08	0.30 ± 0.10
32	0.21 ± 0.08	0.21 ± 0.08	0.26 ± 0.09
48	0.16 ± 0.07	0.16 ± 0.07	0.18 ± 0.06

[a] Values (μg/ml) are the mean ± *SD* for 12 subjects. [b] Means were calculated using the approximate time of blood collection; exact collection times were recorded and used for *AUC* and $t_{1/2}$ determinations.

used in therapeutic combination products (25 mg) did not affect blood levels of methaqualone or its major metabolite.

An important consideration, in comparing the present study conducted in healthy humans to previous studies conducted in the rat (3), may be the relative doses of diphenhydramine and methaqualone hydrochloride administered. Although the ratio of methaqualone–diphenhydramine doses were similar (8:1 for rats and 10:1 for humans), the doses administered per kilogram of body weight were higher in animal studies (40 mg/kg for methaqualone HCl; 5 mg/kg for diphenhydramine HCl) than in human studies (3.7 mg/kg for methaqualone HCl and 0.4 mg/kg for diphenhydramine HCl). For the one subject who received a fourth dose of methaqualone in combination with a larger dose of diphenhydramine (50 mg), the $t_{1/2}$ for methaqualone increased and the urinary metabolite excretion decreased with increasing diphenhydramine dosage. While the AUC_0^∞ had increased, after correction for the increase in $t_{1/2}$, the $AUC_0^\infty\beta$ had decreased with the larger diphenhydramine dosage. Thus, larger doses of diphenhydramine, as might be favored by drug abusers, may elicit a pharmacokinetic interaction. The possibility of a dose-dependent interaction was not specifically investigated and would require further study.

This study was concerned only with investigating a pharmacokinetic interaction, and therefore does not preclude the possibility of a pharmacological interaction between methaqualone and diphenhydramine.

REFERENCES

(1) K. C. Dube, A. Kumar, and S. P. Gupta, *Bull. Narc.*, **29**, 47 (1977).

(2) N. L. Rock and H. D. Selsby, *Int. J. Addict.*, **13**, 327 (1978).

(3) K. W. Hindmarsh, S. M. Wallace, and D. F. LeGatt, *Can. J. Pharm. Sci.*, **14**, 74 (1978).

(4) K. W. Hindmarsh, N. W. Hamon, D. F. LeGatt, and S. M. Wallace, *J. Pharm. Sci.*, **67**, 1547 (1978).

(5) D. F. LeGatt, K. W. Hindmarsh, S. M. Wallace, and D. D. Johnson, *Can. J. Pharm. Sci.*, **15**, 64 (1980).

(6) M. G. Kelly, *J. Ir. Med. Assoc.*, **66**, 456 (1973).

(7) M. E. Williams, M. J. Kendall, M. Mitchard, S. S. Davis, and R. Poxon, *Br. J. Clin. Pharmacol.*, **1**, 99 (1974).

(8) S. Goenechea, S. S. Brown, and M. M. Ferguson, *Arch. Toxikol.*, **31**, 25 (1973).

(9) M. E. Williams, S. S. Davis, R. Poxon, M. J. Kendall, and M. Mitchard, *Br. J. Clin. Pharmacol.*, **1**, 259 (1974).

(10) K. K. Midha, I. J. McGilveray, and J. K. Cooper, *J. Chromatogr.*, **87**, 491 (1973).

(11) S. M. Wallace, V. P. Shah, and S. Riegelman, *J. Pharm. Sci.*, **66**, 527 (1977).

(12) J. G. Wagner, "Fundamentals of Clinical Pharmacokinetics," Drug Intelligence Publications, Hamilton, Ill., 1975.

(13) R. Bonnischen, C. G. Fri, C. Negoita, and R. Ryhage, *Clin. Chim. Acta*, **40**, 309 (1972).

(14) K. W. Hindmarsh, N. W. Hamon, and D. F. LeGatt, *Can. J. Pharm. Sci.*, **12**, 103 (1977).

(15) R. Bonnischen, Y. Marde, and R. Ryhage, *Clin. Chem.*, **20**, 230 (1974).

(16) R. Bonnischen, R. Dimberg, Y. Marde, and R. Ryhage, *Clin. Chim. Acta*, **60**, 67 (1975).

(17) L. Kazyak, *J. Anal. Toxicol.*, **3**, 67 (1979).

(18) G. Alvan, J. E. Lindgren, C. Bogentoft, and O. Ericsson, *Eur. J. Clin. Pharmacol.*, **6**, 187 (1973).

(19) G. Alvan, O. Ericsson, S. Levander, and J. E. Lindgren, *ibid.*, **7**, 449 (1974).

(20) R. G. Stoll, G. C. Chao, H. J. Hoyt, and A. Yacobi, *J. Pharm. Sci.*, **67**, 1328 (1978).

(21) M. E. Williams, M. J. Kendall, and M. Mitchard, *J. Clin. Pharm.*, **1**, 63 (1976).

(22) R. D. Smyth, *et al.*, *J. Int. Med. Res.*, **212**, 85 (1974).

(23) W. J. Westlake, "Current Concepts in Pharmaceutical Sciences," J. Swarbrick, Ed., Lea and Febiger, Philadelphia, Pa., 1973, Chap. 5.

ACKNOWLEDGMENTS

The assistance of the Medical Research Council in the form of an operating grant (MA-6599) and studentship (CBS) is greatly appreciated.

Photolytic Decomposition of Hydrochlorothiazide

SWASONO R. TAMAT and DOUGLAS E. MOORE ˣ

Received January 25, 1982, from the *Department of Pharmacy, The University of Sydney, Sydney 2006, Australia.* Accepted for publication April 9, 1982.

Abstract □ Hydrochlorothiazide decomposes upon irradiation with near-UV light ($\lambda > 310$ nm) both in methanol and aqueous solutions. In the photolysis the chlorine substituent is removed to be replaced by either —H or —OR from the solvent ROH. Hydrolysis of the thiadiazine ring is superimposed upon the dechlorination. The presence of oxygen inhibits the decomposition. The mechanism of the photolysis is suggested to involve cation radical formation which facilitates the hydrolysis step. 5-Chloro-2,4-disulphonamido-aniline, the normal hydrolysis product from hydrochlorothiazide, is also susceptible to photolytic dechlorination by a similar mechanism.

Keyphrases □ Hydrochlorothiazide—photolytic decomposition, irradiation, dechlorination, hydrolysis □ Decomposition, photolytic—hydrochlorothiazide, irradiation, dechlorination, hydrolysis □ Hydrolysis—photolytic decomposition of hydrochlorothiazide, dechlorination, irradiation

Hydrochlorothiazide [6-chloro-3,4-dihydro-1,2,4-benzothiadiazine-7-sulphonamido-1,1-dioxide] (I) is a widely used diuretic effective in small doses. Within a few years of its introduction there were reports of its implication in skin photosensitization (1). From oxygen uptake measurements and free radical polymerization (2), I and some

0022-3549/83/0200-0180$01.00/0

Table IV—Methaqualone Concentrations in Blood [a] at Various Times after Administration of a Single Oral Dose with and without Diphenhydramine

Time[b], hr	Treatment: Methaqualone HCl Capsule	Methaqualone HCl plus Diphenhydramine Elixir	Methaqualone–Diphenhydramine Capsule
0.5	0.38 ± 0.44	0.24 ± 0.25	0.60 ± 0.50
1	1.39 ± 0.68	1.34 ± 0.53	1.54 ± 0.53
2	1.38 ± 0.35	1.26 ± 0.31	1.56 ± 0.48
4	0.79 ± 0.23	0.81 ± 0.23	0.92 ± 0.35
8	0.49 ± 0.15	0.51 ± 0.20	0.54 ± 0.17
24	0.24 ± 0.07	0.25 ± 0.08	0.30 ± 0.10
32	0.21 ± 0.08	0.21 ± 0.08	0.26 ± 0.09
48	0.16 ± 0.07	0.16 ± 0.07	0.18 ± 0.06

[a] Values (μg/ml) are the mean ± *SD* for 12 subjects. [b] Means were calculated using the approximate time of blood collection; exact collection times were recorded and used for *AUC* and $t_{1/2}$ determinations.

used in therapeutic combination products (25 mg) did not affect blood levels of methaqualone or its major metabolite.

An important consideration, in comparing the present study conducted in healthy humans to previous studies conducted in the rat (3), may be the relative doses of diphenhydramine and methaqualone hydrochloride administered. Although the ratio of methaqualone–diphenhydramine doses were similar (8:1 for rats and 10:1 for humans), the doses administered per kilogram of body weight were higher in animal studies (40 mg/kg for methaqualone HCl; 5 mg/kg for diphenhydramine HCl) than in human studies (3.7 mg/kg for methaqualone HCl and 0.4 mg/kg for diphenhydramine HCl). For the one subject who received a fourth dose of methaqualone in combination with a larger dose of diphenhydramine (50 mg), the $t_{1/2}$ for methaqualone increased and the urinary metabolite excretion decreased with increasing diphenhydramine dosage. While the AUC_0^∞ had increased, after correction for the increase in $t_{1/2}$, the $AUC_0^\infty\beta$ had decreased with the larger diphenhydramine dosage. Thus, larger doses of diphenhydramine, as might be favored by drug abusers, may elicit a pharmacokinetic interaction. The possibility of a dose-dependent interaction was not specifically investigated and would require further study.

This study was concerned only with investigating a pharmacokinetic interaction, and therefore does not preclude the possibility of a pharmacological interaction between methaqualone and diphenhydramine.

REFERENCES

(1) K. C. Dube, A. Kumar, and S. P. Gupta, *Bull. Narc.*, **29**, 47 (1977).

(2) N. L. Rock and H. D. Selsby, *Int. J. Addict.*, **13**, 327 (1978).

(3) K. W. Hindmarsh, S. M. Wallace, and D. F. LeGatt, *Can. J. Pharm. Sci.*, **14**, 74 (1978).

(4) K. W. Hindmarsh, N. W. Hamon, D. F. LeGatt, and S. M. Wallace, *J. Pharm. Sci.*, **67**, 1547 (1978).

(5) D. F. LeGatt, K. W. Hindmarsh, S. M. Wallace, and D. D. Johnson, *Can. J. Pharm. Sci.*, **15**, 64 (1980).

(6) M. G. Kelly, *J. Ir. Med. Assoc.*, **66**, 456 (1973).

(7) M. E. Williams, M. J. Kendall, M. Mitchard, S. S. Davis, and R. Poxon, *Br. J. Clin. Pharmacol.*, **1**, 99 (1974).

(8) S. Goenechea, S. S. Brown, and M. M. Ferguson, *Arch. Toxikol.*, **31**, 25 (1973).

(9) M. E. Williams, S. S. Davis, R. Poxon, M. J. Kendall, and M. Mitchard, *Br. J. Clin. Pharmacol.*, **1**, 259 (1974).

(10) K. K. Midha, I. J. McGilveray, and J. K. Cooper, *J. Chromatogr.*, **87**, 491 (1973).

(11) S. M. Wallace, V. P. Shah, and S. Riegelman, *J. Pharm. Sci.*, **66**, 527 (1977).

(12) J. G. Wagner, "Fundamentals of Clinical Pharmacokinetics," Drug Intelligence Publications, Hamilton, Ill., 1975.

(13) R. Bonnischen, C. G. Fri, C. Negoita, and R. Ryhage, *Clin. Chim. Acta*, **40**, 309 (1972).

(14) K. W. Hindmarsh, N. W. Hamon, and D. F. LeGatt, *Can. J. Pharm. Sci.*, **12**, 103 (1977).

(15) R. Bonnischen, Y. Marde, and R. Ryhage, *Clin. Chem.*, **20**, 230 (1974).

(16) R. Bonnischen, R. Dimberg, Y. Marde, and R. Ryhage, *Clin. Chim. Acta*, **60**, 67 (1975).

(17) L. Kazyak, *J. Anal. Toxicol.*, **3**, 67 (1979).

(18) G. Alvan, J. E. Lindgren, C. Bogentoft, and O. Ericsson, *Eur. J. Clin. Pharmacol.*, **6**, 187 (1973).

(19) G. Alvan, O. Ericsson, S. Levander, and J. E. Lindgren, *ibid.*, **7**, 449 (1974).

(20) R. G. Stoll, G. C. Chao, H. J. Hoyt, and A. Yacobi, *J. Pharm. Sci.*, **67**, 1328 (1978).

(21) M. E. Williams, M. J. Kendall, and M. Mitchard, *J. Clin. Pharm.*, **1**, 63 (1976).

(22) R. D. Smyth, *et al.*, *J. Int. Med. Res.*, **212**, 85 (1974).

(23) W. J. Westlake, "Current Concepts in Pharmaceutical Sciences," J. Swarbrick, Ed., Lea and Febiger, Philadelphia, Pa., 1973, Chap. 5.

ACKNOWLEDGMENTS

The assistance of the Medical Research Council in the form of an operating grant (MA-6599) and studentship (CBS) is greatly appreciated.

Photolytic Decomposition of Hydrochlorothiazide

SWASONO R. TAMAT and DOUGLAS E. MOORE ˣ

Received January 25, 1982, from the *Department of Pharmacy, The University of Sydney, Sydney 2006, Australia.* Accepted for publication April 9, 1982.

Abstract □ Hydrochlorothiazide decomposes upon irradiation with near-UV light ($\lambda > 310$ nm) both in methanol and aqueous solutions. In the photolysis the chlorine substituent is removed to be replaced by either —H or —OR from the solvent ROH. Hydrolysis of the thiadiazine ring is superimposed upon the dechlorination. The presence of oxygen inhibits the decomposition. The mechanism of the photolysis is suggested to involve cation radical formation which facilitates the hydrolysis step. 5-Chloro-2,4-disulphonamido-aniline, the normal hydrolysis product from hydrochlorothiazide, is also susceptible to photolytic dechlorination by a similar mechanism.

Keyphrases □ Hydrochlorothiazide—photolytic decomposition, irradiation, dechlorination, hydrolysis □ Decomposition, photolytic—hydrochlorothiazide, irradiation, dechlorination, hydrolysis □ Hydrolysis—photolytic decomposition of hydrochlorothiazide, dechlorination, irradiation

Hydrochlorothiazide [6-chloro-3,4-dihydro-1,2,4-benzothiadiazine-7-sulphonamido-1,1-dioxide] (I) is a widely used diuretic effective in small doses. Within a few years of its introduction there were reports of its implication in skin photosensitization (1). From oxygen uptake measurements and free radical polymerization (2), I and some

0022-3549/83/0200-0180$01.00/0

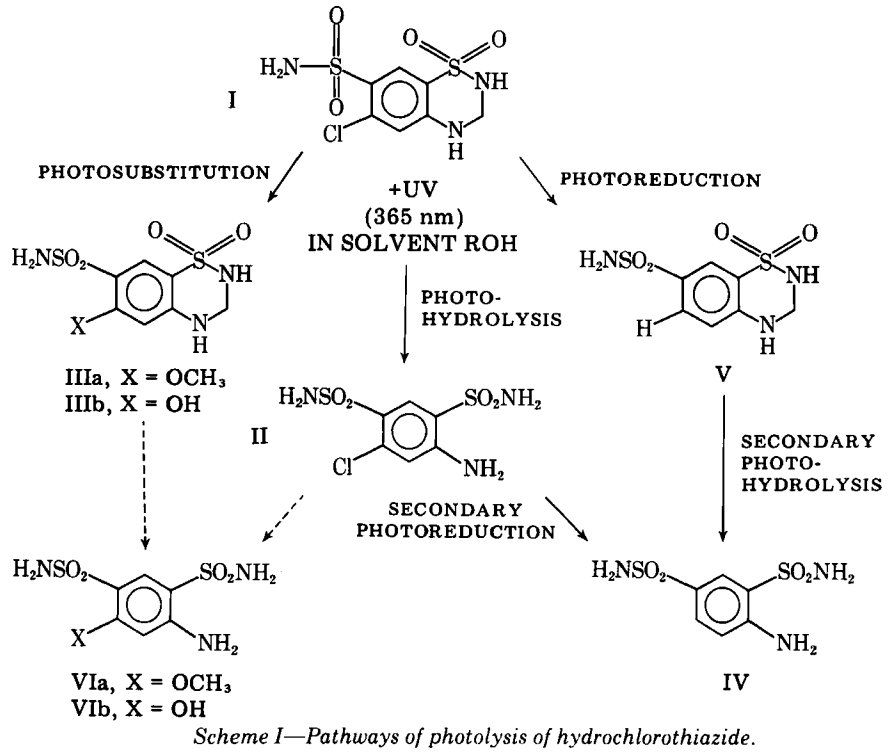

Scheme I—Pathways of photolysis of hydrochlorothiazide.

thiazide derivatives were found to be capable of acting as photosensitizers by both free radical and excited singlet molecular oxygen mechanisms. Subsequently, it was reported (3) that the chlorine substituent in I is photolabile.

In a study to determine the mutagenic activity of a number of drugs, I proved to be weakly mutagenic (4). Mutagenicity appeared to depend on the presence of an aromatic chlorine substituent and required activation by light. This study suggests that the drugs undergo photodehalogenation, yielding a reactive form, which can damage DNA. The nature of the photolysis products of I has now been examined and found to involve ring opening (hydrolysis) as well as dechlorination.

The chlorine substituent in 5-chloro-2,4-disulphonamidoaniline II, the normal hydrolysis product of I, has also been found to be photolabile.

EXPERIMENTAL

Materials—Hydrochlorothiazide (I)[1] and 5-chloro-2,4-disulphonamidoaniline (II)[2] were indicated to be >99% pure by high-performance liquid chromatography (HPLC).

2,4-Disulphonamidoaniline (IV) and 2,4-disulphonamido-5-methoxyaniline (VIa) were prepared by the action of chlorosulphonic acid on aniline and *m*-anisidine, respectively, followed by hydrolysis with ammonium hydroxide, by analogy to a previous method (5). Colorless crystals, mp 233–235° for IV and 252–253° for VIa, were obtained after recrystallization from water.

Cyclization of VIa with paraformaldehyde to 6-methoxy-3,4-dihydro-1,2,4-benzothiadiazine-7-sulphonamido-1,1-dioxide (referred to as methoxyhydrothiazide) (IIIa) was based on the method for I (6). Colorless crystals, mp 273–275°, were obtained after recrystallization from water. All compounds synthesized gave the expected NMR and mass spectra.

Trimethylanilinium hydroxide, a methylating agent for GC, was obtained as 2 *M* solution in methanol[3]. Acrylamide[4] was twice recrystallized from redistilled chloroform. All other chemicals and solvents were of analytical grade[5]. Doubly distilled water was used in aqueous systems.

Methods—A solution of I was irradiated at a concentration of 5×10^{-4} *M* in either methanol or water containing 5% methanol (to assist in dissolution). A medium pressure mercury lamp and a glass reaction vessel were used as previously described (3), so that the solution was exposed to UV light of >310-nm wavelength. The solution was presaturated with nitrogen or oxygen as required by bubbling for 90 min, and the gas flow was maintained to stir the solution during the irradiation. The product mixture was sampled at various times and analyzed by:

1. HPLC[6] with a fixed-wavelength UV detector at 254 nm and a reverse-phase 10-μm column (0.4 × 25 cm)[7] (mobile phase: 10% methanol in water);
2. GC[8] with hydrogen flame-ionization detector, nitrogen carrier gas, and phenyl methyl silicone stationary phase[9]. Following a previous method (7) the irradiated solution of I was concentrated 10-fold, and to 100 μl was added 2.5 μl of 2 *M* trimethylanilinium hydroxide. Methylation of I occurred in the heated injection port at 290°. The column and detector temperatures were 260° and 310°, respectively;
3. GC–chemical-ionization mass spectrometry[10] using the column as above and methane carrier gas.

Photopolymerization of acrylamide (0.125 *M*) initiated by I, II, IIIa, or chlorpromazine (8×10^{-5} *M*) was performed using the apparatus and procedures described previously (2).

RESULTS AND DISCUSSION

Photolysis of Hydrochlorothiazide in Methanol Solution—The photolysis of I dissolved in methanol saturated with nitrogen leads to dechlorination and hydrolysis of the thiadiazine ring in approximately equal proportions as shown in Scheme I. The quantum yield for Cl^- production was 0.18 ± 0.05, as previously reported (3). Under the conditions of irradiation used, the dechlorination was complete in ~6 hr, as determined by potentiometric titration. Other product formation is shown in Fig. 1 as a function of time from HPLC analysis of aliquots withdrawn at various times. For the major products the relative peak areas have been corrected by subsequent calibration with authentic samples of the compound. Confirmation of the identity of the major

[1] Ciba-Geigy, Sydney, Australia.
[2] A gift from Dr. J. A. Mollica, Ciba-Geigy Research and Development, Suffern, N.Y.
[3] Pierce Chemical Co., Rockford, Ill.
[4] BDH Chemicals, Poole, England.
[5] Ajax Chemicals, Sydney, Australia.
[6] Altex model 330.
[7] Hewlett-Packard Model 5720A.
[8] Brownlee RP-8.
[9] 100–120 mesh Gas Chrom Q, coated with 3% OV-1 packed in a 3 mm × 1-m silanized glass column.
[10] Finnigan 6110-9500 system.

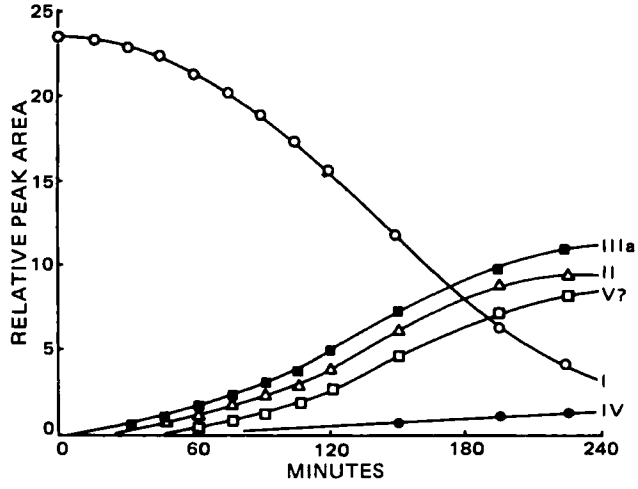

Figure 1—*Photodegradation of hydrochlorothiazide (0.5 mM) in oxygen-free methanol solution at 30° from HPLC analysis of aliquots withdrawn at various times.*

products was achieved by comparison of the chromatographic behavior of authentic samples of the hydrolysis product, 5-chloro-2,4-disulphonamidoaniline (II) and the reduced and substituted derivatives of I and II, namely, methoxyhydrothiazide (IIIa) and 2,4-disulphonamidoaniline (IV). On the basis of reported photoreactions of chloroaromatic compounds in methanol (8), coupled with the hydrolysis of I, other expected products were hydrothiazide (V) and 5-methoxy-2,4-disulphonamidoaniline (VIa). The latter compound was synthesized but its HPLC retention did not correspond to any of the photolysis products. Compound V, however, proved difficult to synthesize.

GC–MS analysis of trimethylanilinium hydroxide-treated samples of the photolysis mixture was complicated by the existence of such a large number of active protons in I and the photolysis products. Nevertheless, molecular ions corresponding to permethylated derivatives of II, IIIa, IV, and V were detected. For each one the GC peak height correlated approximately with the amounts detected by HPLC.

Figure 1 shows that dechlorination and hydrolysis occur simultaneously upon irradiation, where the concentrations of both II and IIIa build up to a maximum level after ~4 hr. Thereafter, II diminished as dechlorination proceeded as a secondary reaction. There was no hydrolysis detected in an unirradiated methanol solution of I after 6 hr at 30°, although complete hydrolysis can be achieved in ~1 hr by refluxing in 1 *M* NaOH, as reported previously (9).

Direct photolysis of II was also examined under the same conditions with the observation of dechlorination occurrence, leading predominantly to IV (~85%). A minor product was found, but its HPLC retention did not correspond to that of VIa. This correlated with the fact that VIa was not observed as a product from photolysis of I. In the GC–MS analysis of irradiated II a minor peak with *m/z* 319 was observed. This value

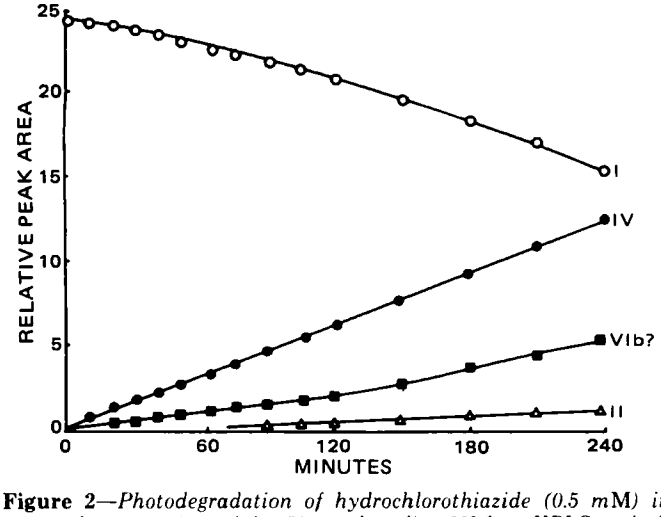

Figure 2—*Photodegradation of hydrochlorothiazide (0.5 mM) in oxygen-free water (containing 5% methanol) at 30° from HPLC analysis of aliquots withdrawn at various times.*

Table I—Rates of Photosensitized Polymerization of Acrylamide at 30°

Sensitizer, 8.3×10^{-5} *M*	Rate of Polymerization[a], mmoles liter^{-1} min^{-1}	
	pH 7.0 Buffer	Methanol
Hydrochlorothiazide (I)	1.58	0.39
5-Chloro-2,4-disulphonamido-aniline (II)	1.29	0.32
Methoxyhydrothiazide (IIIa)	3.47	0.16
Chlorpromazine	5.70	0.40

[a] Error in rate data ±5%.

corresponded to tetramethyl-V, suggesting that ring closure to form the thiadiazine ring had occurred to a small extent under irradiation. This assignment was confirmed by TLC separation, followed by solid-probe MS of the separated compounds without derivatization. That ring closure is a possibility comes from the observation that the hydrolysis of I is reversible (9).

When the methanol solution of I was saturated with oxygen before irradiation, both dechlorination and hydrolysis reactions were markedly inhibited. Loss of I and formation of II and IIIa occur at ~one-tenth the rate seen in the absence of oxygen. This is in agreement with the chloride yields already reported (3). Similarly, when II was irradiated in an oxygen-saturated solution, the dechlorination was inhibited, and only product IV was detected.

Photolysis of Hydrochlorothiazide in an Aqueous System—The solubility of I in pure water is relatively low, and the addition of 5% methanol was necessary to achieve the concentration of 0.5 m*M* used for the irradiation. Under these conditions and in the absence of oxygen, photodecomposition of I occurred at ~50% the rate in oxygen-free methanol, as shown in Fig. 2. It should be noted that the chloride ion appeared at the same rate in both solvents (3). The product distribution is seen to be different, with the hydrolyzed and dechlorinated IV as the dominant product. A relatively minor amount of the intermediate II was found, suggesting that dechlorination of I was occurring first followed by rapid hydrolysis. The other significant product was suspected of being VIb on the basis of its chromatographic retention, but samples collected were insufficient for direct MS confirmation. Molecular ions corresponding to permethylated compounds II, IV, and VIb were found by GC–MS analysis.

When the system was saturated with oxygen before irradiation, IV was the only product detected following a much slower reaction.

When the direct photolysis of II was examined in the aqueous system in the absence of oxygen, IV and the compound suspected of being VIb were found in the approximate ratio of 3:1.

Mechanism of the Photodegradation—The dechlorination step in the photolysis of both I and II leads to either reduction (Aryl-H) or substitution (Aryl-OR) involving the solvent ROH, as observed for other chloroaromatic compounds (8, 10). Additionally, photohydrolysis of the thiadiazine ring of I occurs, as has been observed for some other drugs susceptible to alkaline hydrolysis such as pentobarbitone (11) and indapamide (12).

It was proposed (8, 13) that photoreduction and photosubstitution of simple chloroaromatic compounds in methanol involves the formation of a pair of radical ions from the triplet state. The precursor of the reduction product (Aryl-H) is suggested to be a radical anion (Aryl-Cl^{-}), while a radical cation (Aryl-Cl^{+}) is postulated as the precursor of the substitution product (Aryl-OR). Alternatively, flash photolysis experiments with chlorpromazine in 2-propanol (10) led to the suggestion that a direct homolysis of the C–Cl bond occurs from the triplet state. We have observed (3) that chlorpromazine is moderately active as a triplet state photosensitizer in methanol solution, while in aqueous solution the predominance of photoionization as the primary photochemical event with phenothiazines (14) results in a significantly lower rate for this type of reaction.

Photoionization is reported for other heteroaromatic compounds not containing chlorine substituents *e.g.*, 4-hydroxybenzothiazole (15). The cation radical of chlorpromazine was postulated as the main initiating species of the photopolymerization of acrylamide following studies in cationic and anionic surfactants (16).

In view of the information available on the photochemistry of chlorpromazine, it was used as a standard against which the reactivity of other drugs might be compared. Hydrochlorothiazide was found to react in the same manner as chlorpromazine in triplet state photosensitization (3). The rates of photopolymerization of acrylamide in aqueous buffer and methanol solutions, sensitized by I, II, IIIa, and chlorpromazine were

measured, as shown in Table I. Since these four compounds have similar UV absorption characteristics, the rates of polymerization should provide an approximate indication of relative radical yields and reactivity. In aqueous solution the values of the rates suggest that cation radical production does not depend upon loss of chloride, as evidenced by the comparatively high rate sensitized by IIIa. However, in methanol solution the three compounds that lose chlorine show about the same rate of polymerization, a higher value than that for IIIa.

On the basis of the above results, the primary photochemical processes occurring on irradiation of hydrochlorothiazide appear similar to those found for chlorpromazine, with photoionization predominating in aqueous solution and triplet state formation mainly in methanol. However, it is possible that the polymerization technique is not an adequate indicator of radical ion formation in methanol where ion recombination or reaction with solvent may occur more readily than in water. A phenomenon that is indicative of excited state electron transfer is the quenching of fluorescence by an electron donor (17). We have observed that the fluorescence of I (50 μM in methanol) is quenched to 50% by 6 mM triethylamine. In contrast, the fluorescence of chlorpromazine is unaffected (18).

The fact that hydrolysis of I is stimulated by irradiation implies the formation of a cation radical in the thiadiazine ring, thereby rendering it more susceptible to attack by nucleophiles. This is most evident in the aqueous system where the expected intermediate IIIb was not detected. The dechlorination is presumably effected by the solvated electron formed in the photoionization.

In methanol the formation of cation radicals is indicated by the presence of significant amounts of the hydrolyzed compound II. However it is not clear if the cation radicals result from photoionization or radical-ion-pair formation from the triplet state. Flash photolysis experiments are needed to clarify the primary photochemical events. However, as pointed out elsewhere (10, 16), it is believed that the formation of free radicals following absorption of UV radiation is the significant factor in the initiation of a photobiological effect.

REFERENCES

(1) I. A. Magnus, "Dermatological Photobiology," Blackwell, Oxford, 1976, pp. 213–215.

(2) D. E. Moore, *J. Pharm. Sci.*, **66,** 1282 (1977).

(3) D. E. Moore and S. R. Tamat, *J. Pharm. Pharmacol.*, **32,** 172 (1980).

(4) J. G. Jose, *Proc. Natl. Acad. Sci. USA*, **76,** 469 (1979).

(5) F. C. Novello and J. M. Sprague, *J. Am. Chem. Soc.*, **79,** 2028 (1957).

(6) L. H. Werner, A. Halamandaris, S. Ricca, L. Dorfman, and G. de Stevens, *J. Am. Chem. Soc.*, **82,** 1161 (1960).

(7) W. J. A. Vandenheuvel, *J. Pharm. Sci.*, **64,** 1309 (1975).

(8) J. P. Soumillion and B. De Wolf, *J. Chem. Soc. Chem. Commun.*, **1981,** 436.

(9) C. R. Rehm and J. B. Smith, *J. Am. Pharm. Assoc., Sci. Ed.*, **49,** 386 (1960).

(10) A. K. Davies, S. Navaratnam, and G. O. Phillips, *J. Chem. Soc. Perkin Trans. 2*, **1976,** 25.

(11) H. Barton, J. Mokrosz, J. Bojarski, and M. Klimczak, *Pharmazie*, **35,** 155 (1980).

(12) R. Davis, C. H. J. Wells, and A. R. Taylor, *J. Pharm. Sci.*, **68,** 1063 (1979).

(13) N. J. Bunce and L. Ravanal, *J. Am. Chem. Soc.*, **99,** 4150 (1977).

(14) S. Navaratnam, B. J. Parsons, G. O. Phillips, and A. K. Davies, *J. Chem. Soc. Faraday Trans. 1*, **74,** 1811 (1978).

(15) M. R. Chedekel, E. J. Land, R. S. Sinclair, D. Tait, and T. G. Truscott, *J. Am. Chem. Soc.*, **102,** 6587 (1980).

(16) D. E. Moore and C. D. Burt, *Photochem. Photobiol.*, **34,** 431 (1981).

(17) S. P. Van and G. S. Hammond, *J. Am. Chem. Soc.*, **100,** 3895 (1978).

(18) N. J. Bunce, Y. Kumar, and L. Ravanal, *J. Med. Chem.*, **22,** 202 (1979).

ACKNOWLEDGMENTS

This work was made possible by the award of a Colombo Plan Scholarship to Swasono R. Tamat, and the generous assistance of Ciba-Geigy, Sydney.

NOTES

Evaluation of Various *N*-Substituted Azaspiranedione Derivatives as Potential Antimicrobial Agents

K. R. SCOTT *x, POLEDI G. KENNEDY *, MURRAY KEMP *, VASANT G. TELANG *, and H. W. MATTHEWS ‡

Received September 28, 1981, from the **College of Pharmacy and Pharmacal Sciences, Department of Biomedicinal Chemistry, Howard University, Washington, DC 20059*, and the ‡*Southern School of Pharmacy, Department of Biomedical Sciences, Mercer University, Atlanta, GA 30312.* Accepted for publication March 3, 1982.

Abstract □ A series of *N*-substituted hydrazines were condensed with various spiro[4.5] and [5.5]anhydrides and the resultant *N*-substituted azaspiranediones were evaluated for antimicrobial activity. None displayed any significant activity in a variety of organisms tested.

Keyphrases □ Antimicrobial agents—potential, evaluation of various *N*-substituted azaspiranedione derivatives □ Azaspiranedione—evaluation of various derivatives as potential antimicrobial agents

Previous works (1, 2) have shown a wide variety of biological effects for the azaspiro nucleus. It was of interest to extend this work to various 2-substituted-2-azaspiro-[4.5]decane-1,3-diones (I) and 3-substituted-3-azaspiro-[5.5]undecane-2,4-diones (II) and to evaluate these hydrazinoimides as potential antimicrobial agents.

It has been demonstrated (3–6) that in the fused 4-azacholestane ring various 4-alkyl-substituted derivatives

0022-3549/83/0200-0183$01.00/0

measured, as shown in Table I. Since these four compounds have similar UV absorption characteristics, the rates of polymerization should provide an approximate indication of relative radical yields and reactivity. In aqueous solution the values of the rates suggest that cation radical production does not depend upon loss of chloride, as evidenced by the comparatively high rate sensitized by IIIa. However, in methanol solution the three compounds that lose chlorine show about the same rate of polymerization, a higher value than that for IIIa.

On the basis of the above results, the primary photochemical processes occurring on irradiation of hydrochlorothiazide appear similar to those found for chlorpromazine, with photoionization predominating in aqueous solution and triplet state formation mainly in methanol. However, it is possible that the polymerization technique is not an adequate indicator of radical ion formation in methanol where ion recombination or reaction with solvent may occur more readily than in water. A phenomenon that is indicative of excited state electron transfer is the quenching of fluorescence by an electron donor (17). We have observed that the fluorescence of I (50 μM in methanol) is quenched to 50% by 6 mM triethylamine. In contrast, the fluorescence of chlorpromazine is unaffected (18).

The fact that hydrolysis of I is stimulated by irradiation implies the formation of a cation radical in the thiadiazine ring, thereby rendering it more susceptible to attack by nucleophiles. This is most evident in the aqueous system where the expected intermediate IIIb was not detected. The dechlorination is presumably effected by the solvated electron formed in the photoionization.

In methanol the formation of cation radicals is indicated by the presence of significant amounts of the hydrolyzed compound II. However it is not clear if the cation radicals result from photoionization or radical-ion-pair formation from the triplet state. Flash photolysis experiments are needed to clarify the primary photochemical events. However, as pointed out elsewhere (10, 16), it is believed that the formation of free radicals following absorption of UV radiation is the significant factor in the initiation of a photobiological effect.

REFERENCES

(1) I. A. Magnus, "Dermatological Photobiology," Blackwell, Oxford, 1976, pp. 213–215.

(2) D. E. Moore, *J. Pharm. Sci.*, **66,** 1282 (1977).

(3) D. E. Moore and S. R. Tamat, *J. Pharm. Pharmacol.*, **32,** 172 (1980).

(4) J. G. Jose, *Proc. Natl. Acad. Sci. USA*, **76,** 469 (1979).

(5) F. C. Novello and J. M. Sprague, *J. Am. Chem. Soc.*, **79,** 2028 (1957).

(6) L. H. Werner, A. Halamandaris, S. Ricca, L. Dorfman, and G. de Stevens, *J. Am. Chem. Soc.*, **82,** 1161 (1960).

(7) W. J. A. Vandenheuvel, *J. Pharm. Sci.*, **64,** 1309 (1975).

(8) J. P. Soumillion and B. De Wolf, *J. Chem. Soc. Chem. Commun.*, **1981,** 436.

(9) C. R. Rehm and J. B. Smith, *J. Am. Pharm. Assoc., Sci. Ed.*, **49,** 386 (1960).

(10) A. K. Davies, S. Navaratnam, and G. O. Phillips, *J. Chem. Soc. Perkin Trans. 2*, **1976,** 25.

(11) H. Barton, J. Mokrosz, J. Bojarski, and M. Klimczak, *Pharmazie*, **35,** 155 (1980).

(12) R. Davis, C. H. J. Wells, and A. R. Taylor, *J. Pharm. Sci.*, **68,** 1063 (1979).

(13) N. J. Bunce and L. Ravanal, *J. Am. Chem. Soc.*, **99,** 4150 (1977).

(14) S. Navaratnam, B. J. Parsons, G. O. Phillips, and A. K. Davies, *J. Chem. Soc. Faraday Trans. 1*, **74,** 1811 (1978).

(15) M. R. Chedekel, E. J. Land, R. S. Sinclair, D. Tait, and T. G. Truscott, *J. Am. Chem. Soc.*, **102,** 6587 (1980).

(16) D. E. Moore and C. D. Burt, *Photochem. Photobiol.*, **34,** 431 (1981).

(17) S. P. Van and G. S. Hammond, *J. Am. Chem. Soc.*, **100,** 3895 (1978).

(18) N. J. Bunce, Y. Kumar, and L. Ravanal, *J. Med. Chem.*, **22,** 202 (1979).

ACKNOWLEDGMENTS

This work was made possible by the award of a Colombo Plan Scholarship to Swasono R. Tamat, and the generous assistance of Ciba-Geigy, Sydney.

NOTES

Evaluation of Various *N*-Substituted Azaspiranedione Derivatives as Potential Antimicrobial Agents

K. R. SCOTT *x, POLEDI G. KENNEDY *, MURRAY KEMP *, VASANT G. TELANG *, and H. W. MATTHEWS ‡

Received September 28, 1981, from the **College of Pharmacy and Pharmacal Sciences, Department of Biomedicinal Chemistry, Howard University, Washington, DC 20059*, and the ‡*Southern School of Pharmacy, Department of Biomedical Sciences, Mercer University, Atlanta, GA 30312.* Accepted for publication March 3, 1982.

Abstract □ A series of *N*-substituted hydrazines were condensed with various spiro[4.5] and [5.5]anhydrides and the resultant *N*-substituted azaspiranediones were evaluated for antimicrobial activity. None displayed any significant activity in a variety of organisms tested.

Keyphrases □ Antimicrobial agents—potential, evaluation of various *N*-substituted azaspiranedione derivatives □ Azaspiranedione—evaluation of various derivatives as potential antimicrobial agents

Previous works (1, 2) have shown a wide variety of biological effects for the azaspiro nucleus. It was of interest to extend this work to various 2-substituted-2-azaspiro-[4.5]decane-1,3-diones (I) and 3-substituted-3-azaspiro-[5.5]undecane-2,4-diones (II) and to evaluate these hydrazinoimides as potential antimicrobial agents.

It has been demonstrated (3–6) that in the fused 4-azacholestane ring various 4-alkyl-substituted derivatives

0022-3549/83/0200-0183$01.00/0

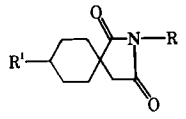

Table I—2-Substituted-2-azaspiro[4.5]decane-1,3-diones

Compound	R	R¹	Yield, %	Isolation Procedure[a]	Melting Point	Boiling Point, mm	Formula	Analysis, % Calc.	Found
XIII	H	H	77	D, C	144–145° [b,c]	199–205° (1.75)	$C_9H_{13}NO_2$	C 64.64 H 7.84 N 8.38	64.82 7.82 8.40
XIV	NH_2	H	57	C	116–117° [b]	—	$C_9H_{14}N_2O_2$	C 59.30 H 7.75 N 15.38	59.59 7.80 15.40
XV	—N⬡	H	73	C	132–133° [d]	—	$C_{14}H_{22}N_2O_2$	C 67.15 H 8.86 N 11.19	67.25 8.90 11.31
XVI	—N⬡O	H	64	C	151–153° [e]	—	$C_{13}H_{20}N_2O_3$	C 61.87 H 8.00 N 11.11	61.90 8.10 11.21
XVII	NH_2	CH_3	72	D, C	130–131° [b]	109–219° (1.75)	$C_{10}H_{16}N_2O_2$	C 61.19 H 8.22 N 14.28	61.30 8.18 14.19
XVIII	—N⬡	CH_3	82	D, C	143–144° [f]	154–155° (3.75)	$C_{15}H_{24}N_2O_2$	C 68.13 H 9.16 N 10.60	68.31 9.22 10.70
XIX	—N⬡O	CH_3	79	D, C	166–167° [f]	174–184° (2.25)	$C_{14}H_{22}N_2O_3$	C 63.12 H 8.33 N 10.52	63.13 8.40 10.50

[a] Legend: D is distillation; C is chromatography (alumina, neutral; solvent benzene–methanol, 4:1). [b] Ethanol–Water. [c] Lit. (15) mp 145°. [d] Hexane. [e] Benzene. [f] Methanol.

(III, IV) possessed antimicrobial activity. Thus, it was of interest to determine whether this activity could be extended to the spiro nucleus as well.

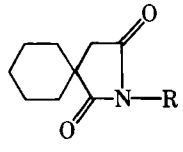

(I)

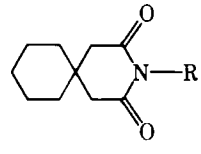

(II)

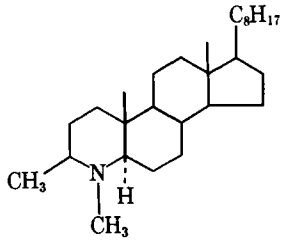

(III)

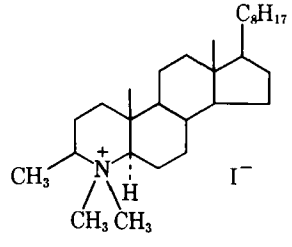

(IV)

The reaction sequence for the 2-azaspiro[4.5]decane series is shown in Scheme I:

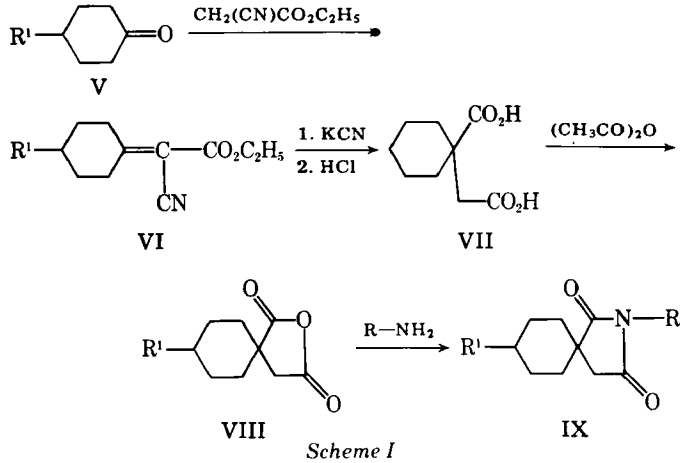

Scheme I

The ketone (V) is subjected to a Cope procedure (7) using ammonium acetate and acetic acid as catalysts. The resultant alkylidene cyanoacetic ester (VI) was obtained in purified form on distillation. (This ester should be used within several days as decomposition is noted even under the most careful conditions.) Addition of potassium cyanide followed by acid hydrolysis produced the 1-carboxy-1-acetic acid derivative (VII), which was quantitatively converted to the anhydride (VIII), with excess acetic anhydride. Condensation of the anhydride with substituted hydrazines in the presence of a high-boiling solvent and molecular sieves followed by distillation produced the desired 2-substituted-2-azaspiro[4.5]decane (IX). The reaction sequence for the 3-azaspiro[5.5]undecane series is shown in Scheme II:

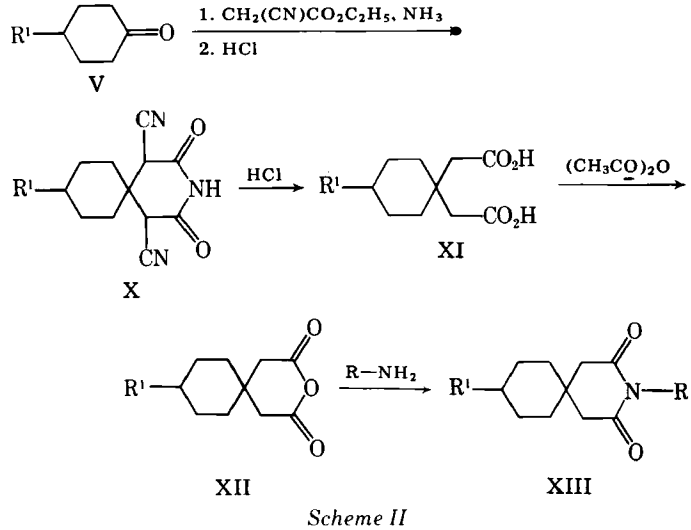

Scheme II

In this sequence, the ketone was subjected to 2.0 moles of ethyl cyanoacetate in the presence of anhydrous ammonia to yield the ammonium salt of the Guareschi imide (8) which was converted to the imide (X), on acidification

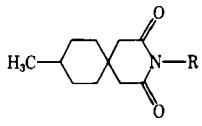

Table II—3-Substituted-3-azaspiro-9-methyl[5.5]undecane-2,4-diones

Compound	R	Yield, %	Isolation Procedure[a]	Melting Point	Boiling Point, mm	Formula	Analysis, % Calc.	Found
XX	H	82	C	161–162° [b,c]	—	$C_{11}H_{17}NO_2$	C 67.65	67.75
							H 8.78	8.89
							N 7.18	7.20
XXI	NH_2	83	C	162–163° [c]	—	$C_{11}H_{18}N_2O_2$	C 62.82	62.90
							H 8.63	8.73
							N 13.33	13.46
XXII	—N⟨⟩	73	D, C	110–111° [d]	179° [f]	$C_{16}H_{26}N_2O_2$	C 69.02	69.00
							H 9.42	9.54
							N 10.07	10.00
XXIII	—N⟨O⟩	82	C	132–133° [e]	—	$C_{15}H_{24}N_2O_3$	C 62.24	62.20
							H 8.63	8.50
							N 10.00	10.10

[a] Legend (Table I). [b] Lit. (16): 162°. [c] Methanol. [d] Benzene. [e] Hexane. [f] Ref. 1.

with hydrochloric acid. Sulfuric acid hydrolysis converted the imide into the 1,1-bisacetic acid compound (XI). Acetic anhydride, followed by hydrazine condensation as in the previous scheme, produced the anhydride (XII) and the 3-azaspiro[5.5]undecane-2,4-dione derivative (XIII), respectively. The imides were tested against a variety of microorganisms for antibacterial activity.

EXPERIMENTAL

Instruments—Melting points were obtained using a capillary melting point apparatus[1] and are uncorrected. Observed boiling points were also uncorrected. IR spectra were obtained on a spectrophotometer[2] as a Nujol mull or neat. NMR spectra were determined on a 60-MHz spectrometer[3] with tetramethylsilane as the internal reference. Elemental analyses were also performed[4].

Reagents—All ketones, ethyl cyanoacetate, and hydrazine[5], *N*-aminopiperidine, and *N*-aminomorpholine[6] were distilled before use.

Ethyl α-Cyclohexylidene-α-cyanoacetate (VI, R¹=H)—The general procedure (7) was followed using 1.0 mole of cyclohexanone and 1.0 mole of ethyl cyanoacetate with 7.7 g of ammonium acetate and 12 g of acetic acid in a 500-ml flask. Yield: 125 g (65%), bp 104–107° (0.25 mm). [lit. 150–151° (9 mm) (7), 151° (12 mm) (9), 163° (15 mm) (10), 151° (10 mm) (11–13)] IR (neat) 4.45μ (Sharp, C≡N).

Ethyl α-(4-Methylcyclohexylidene)-α-cyanoacetate (VI, R¹=CH₃)—Using the above procedure and the same molar quantities, 145 g (70%) was obtained, bp 98–104° (0.7 mm) [lit. 165–168° (14 mm), 175° (20 mm), 167° (14 mm)].

Cyclohexane-1-carboxy-1-acetic Acid (VII, R¹=H)—Using a previous procedure (9) employing 0.18 mole of ester and 0.36 mole of potassium cyanide, after solvent removal and 16 hr of refluxing in 250 ml of concentrated hydrochloric acid, 14 g (42%) of the acid was obtained, mp 132–133° (ligroin–ethyl acetate). The yield was improved to 50% by chilling the acid filtrate overnight and collecting the additional crude acid [lit. 134° (9, 14), 132° (10, 15)]. IR(Nujol) 5.75μ (Sharp, C=O).

4-Methylcyclohexane-1-carboxy-1-acetic Acid (VII, R¹=CH₃)—The same method (9) was employed on the same molar quantities of ester and cyanide as with compound VII above. Yield: 19 g (53%) mp 173–174° (ligroin–ethyl acetate).

Anal.—Calc. for $C_{10}H_{16}O_4$: C, 59.97, H, 8.00. Found: C, 59.73, H, 7.90.

Cyclohexane-1-carboxy-1-acetic Acid Anhydride (VIII, R¹=H)—Using a previous procedure (9), from 0.05 mole of acid 8.1 g (90%) of anhydride was obtained, bp 112° (1.75 mm), which slowly solidified on standing, mp 57° [lit. 56° (9), 57° (14)]. IR(Nujol) 5.50μ (Sharp, C=O).

4-Methylcyclohexane-1-carboxy-1-acetic Acid Anhydride (VIII, R¹=CH₃)—As previously indicated, the title compound was quantitatively prepared, bp 124–126° (3 mm), solidifying on standing, mp 60–61°.

Anal.—Calc. for $C_{10}H_{14}O_3$: C 65.90; H, 7.76. Found: C, 65.90; H, 7.64.

The Guareschi Imide-9-methyl-1,5-dicyano-3-azaspiro[5.5]-undecane-2,4-dione (X, R¹=CH₃)—A general procedure (16) was modified using 1.0 mole of ketone and 2.0 moles of ethyl cyanoacetate in a 1.5-liter thick-wall flask. After cooling to −5°, 400 ml of absolute ethanol saturated with anhydrous ammonia and cooled to −5° was added, the flask stoppered, taped securely, and stored at 0° for 1 week. The crude ammonium salt of the Guareschi imide (8, 17) was filtered, washed with alcohol and then ether, and air dried. The product was dissolved in 1 liter of boiling water, filtered, and the hot solution acidified with excess concentrated hydrochloric acid. The product, on cooling, was filtered, washed with water, and dried at 100° to give 115 g (47%), mp 217–218° (methanol) [lit. 217–218° (16)].

4-Methylcyclohexane-1,1-diacetic Acid (XI, R¹=CH₃)—Using a previous procedure (16), 0.5 mole of imide, 240 ml of concentrated sulfuric acid, which after standing overnight at room temperature, was diluted with 225 ml of water and refluxed for 24 hr, resulting in a product, 140 g (65%), mp 157–158° [lit. 158° (16)].

4-Methylcyclohexane-1,1-diacetic Acid Anhydride (XII, R¹=CH₃)—The previous procedure produced the desired product, bp 152–154° (1.25 mm), which solidified on standing, mp 53° [lit. bp 212° (20 mm), mp 53° (16)].

General Procedure for the Preparation of Azaspiranediones—The anhydride, 0.05 mole, and the substituted hydrazine were added to 10 ml of xylene (distilled from sodium) in a 50-ml flask containing molecular sieves[7]. The mixture was stirred magnetically and refluxed for 2–8 hr. The product precipitated on cooling overnight, and after separation, the residual oil was seeded and chilled. The entire residue was combined and either chromatographed or distilled. The distillate was then either chromatographed or recrystallized (Tables I and II). As previously reported (2), azaspiro[5.5]undecane-2,4-diones formed unstable hydrochloride salts. This was also observed with the undecanes synthesized in this study as well as the azaspiro[4.5]decane-1,3-diones.

RESULTS AND DISCUSSION

In addition to the potential antimicrobial activity of various *N*-substituted azasteroids (3–6), adamantane spiro compounds (18, 19) have been evaluated for antiviral activity and spirofluorene (20) and spiroperimidines (21) have been tested for antineoplastic activity. Compounds XIV–XVI and XXI–XXIII were thus submitted for antimicrobial screening. The analyses were performed by the use of the Kirby–Bauer technique (22) with the following organisms: *Escherichia coli*, *Staphylococcus aureus*, *Sarcina lutea*, *Bacillus subtilis*, and *Pseudomonas aeruginosa* (23). The compounds showed no activity at concentrations up to 100 μm/ml.

[1] Thomas-Hoover.
[2] Beckman IR-18A.
[3] Varian EM 360A.
[4] Performed by the Schwarzkopf Microanalytical Laboratory, Woodside, NY 11377.
[5] Eastman Chemicals.
[6] Columbia Organics, Inc.
[7] Molecular sieves, type 4A, Fisher Scientific Co.

REFERENCES

(1) L. M. Rice, C. F. Geschickter, and C. H. Grogan, *J. Med. Chem.* **6**, 388 (1963).

(2) C. H. Grogan, C. F. Geschickter, and L. M. Rice, *ibid.*, **7**, 78 (1964).

(3) R. F. Smith, D. E. Shay, and N. J. Doorenbos, *J. Bacteriol.*, **85**, 1295 (1963).

(4) R. F. Smith, D. E. Shay, and N. J. Doorenbos, *Proc. Pa. Acad. Sci.*, **36**, 113 (1962).

(5) R. F. Smith, D. E. Shay, and N. J. Doorenbos, *Appl. Microbiol.*, **11**, 542 (1963).

(6) R. F. Smith, D. E. Shay, and N. J. Doorenbos, *J. Pharm. Sci.*, **53**, 1214 (1964).

(7) A. C. Cope, C. M. Hofmann, C. Wyckoff, and E. Hardenbergh, *J. Am. Chem. Soc.*, **63**, 3452 (1941).

(8) I. Guareschi, *Atti. Accad. Sci. Torino*, **36**, 443 (1900/1901).

(9) I. Vogel, *J. Chem. Soc.*, **1928**, 2010.

(10) A. Lapworth and J. A. McRae, *ibid.*, **121**, 2741 (1922).

(11) S. F. Birch, G. A. R. Kon, and W. S. G. P. Norris, *ibid.*, **123**, 1361 (1923).

(12) V. J. Harding, W. N. Haworth, and W. H. Perkin, *ibid.*, **93**, 1943 (1908).

(13) A. C. Cope, *J. Am. Chem. Soc.*, **59**, 2327 (1937).

(14) W. S. G. P. Norris and J. F. Thorpe, *J. Chem. Soc.*, **119**, 1199 (1921).

(15) F. Dickens, L. Horton, and J. F. Thorpe, *ibid.*, **124**, 1830 (1924).

(16) J. F. Thorpe and A. S. Wood, *ibid.*, **103**, 1586 (1913).

(17) G. A. R. Kon and J. F. Thorpe, *ibid.*, **115**, 693 (1919).

(18) K. Lundahl, J. Schut, J. L. M. A. Schlatmann, G. B. Paerels, and A. Peters, *J. Med. Chem.*, **15**, 129 (1972).

(19) R. VanHes, A. Smit, T. Kralt, and A. Peters, *ibid.*, **15**, 132 (1972).

(20) H.-L. Pan and T. L. Fletcher, *ibid.*, **10**, 957 (1967).

(21) W. Wasulko, A. C. Noble, and F. D. Popp, *ibid.*, **9**, 599 (1966).

(22) A. W. Bauer, W. M. M. Kirby, J. C. Sherris, and M. Turck, *Am. J. Clin. Pathol.*, **45**, 493 (1966).

(23) D. Perlman, K. L. Perlman, M. Bodanszky, A. Bodanszky, R. L. Foltz, and H. W. Matthews, *Bioorgan. Chem.*, **6**, 263 (1977).

ACKNOWLEDGMENTS

The authors wish to thank Dr. Peter E. Frankenberg and Mr. C. H. Roberts of the Du Pont Company, Wilmington, Del., for the NMR analyses.

Dissolution Apparatus for Gels

HO-LUN WENG and EUGENE L. PARROTT ˣ

Received January 11, 1982, from the *Division of Pharmaceutics, College of Pharmacy, University of Iowa, Iowa City, IA 52242.* Accepted for publication March 11, 1982.

Abstract □ A modification of the USP Dissolution Apparatus 2 is presented for use in the measurement of the release of a medicinal compound from a pharmaceutical gel.

Keyphrases □ Dissolution—apparatus for gels, modification of the USP Dissolution Apparatus 2 □ Pharmaceutical gels—dissolution apparatus, modification of the USP Dissolution Apparatus 2

The *in vitro* test methods for measuring the dissolution of a medicinal compound from a tablet or a capsule are defined in the United States Pharmacopeia (USP) (1). Mathur *et al.* (2) appear to be the first to have reported *in vitro* dissolution testing of suspensions. It seems that dissolution testing of any dosage form that may restrict the delivery of molecules of the medicinal compound to the GI epithelium is advisable.

This report presents a modification of the USP Dissolution Apparatus 2, that can be used to measure dissolution profiles from pharmaceutical gels.

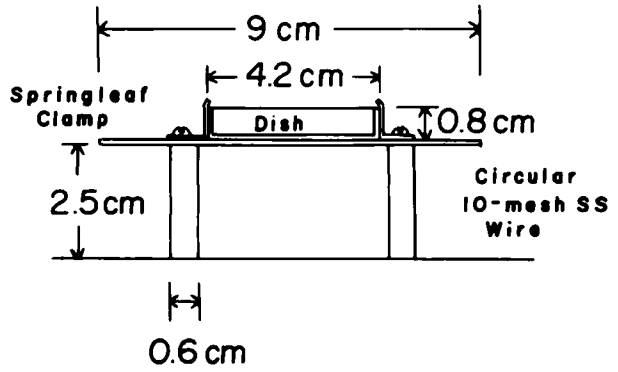

Figure 1—*Modification of the USP Dissolution Apparatus 2 for gels.*

EXPERIMENTAL

Dissolution Apparatus—A circular, 10-mesh stainless-steel cloth with a 9.0-cm diameter was fitted with four 2.5-cm plastic legs (diameter 0.6 cm) so that, as it rested on the bottom of the reaction vessel, the wire cloth was at the point of curvature of the base of the vessel. Four springleaf clamps were affixed to the upper surface of the wire cloth to hold the glass dish in the center of the platform (Fig. 1). The dish was cut from a 50-ml beaker and had 3.9-cm i.d. and an outer height of 0.8 cm.

A 5-g sample of the gel was weighed in the dish on an analytical balance, and using forceps the dish was gently lowered through the dissolution medium in the assembled apparatus and was inserted into the clamps. The time required by an experienced operator was ~30 sec. With thin gels, the level spontaneously adjusted to the horizontal plane; with very viscous gels, the surface may be leveled by use of a spatula prior to weighing. In the gels investigated, the 5-g samples completely filled the dish to the rim. If a particular gel had a high density, it would be advisable to use a greater weight, which would fill the dish. The dissolution medium was 900 ml of distilled water or 0.1 *N* HCl at 37 ± 0.5°. The paddle of the modified USP Dissolution Apparatus 2 was centrally positioned 2.5 cm above the rim of the dish. The apparatus was then started. Samples were withdrawn by a pipet through a glass filter. Ephedrine sulfate was assayed using a previously described method (3).

Dosage Forms—Tablets containing 25 mg of ephedrine sulfate was prepared by direct compression in a single-punch tablet machine. A portion of the batch was compressed to a hardness of 4 kg; the remainder was compressed to an 8-kg hardness. The formulation was:

Ephedrine sulfate[1]	25 mg
Microcrystalline cellulose[2]	190 mg
Lactose[3]	382 mg
Magnesium stearate[4]	3 mg

[1] USP.
[2] Avicel PH 101.
[3] USP, spray dried.
[4] NF.

0022-3549/83/0200-0186$01.00/0

REFERENCES

(1) L. M. Rice, C. F. Geschickter, and C. H. Grogan, *J. Med. Chem.* **6**, 388 (1963).

(2) C. H. Grogan, C. F. Geschickter, and L. M. Rice, *ibid.*, **7**, 78 (1964).

(3) R. F. Smith, D. E. Shay, and N. J. Doorenbos, *J. Bacteriol.*, **85**, 1295 (1963).

(4) R. F. Smith, D. E. Shay, and N. J. Doorenbos, *Proc. Pa. Acad. Sci.*, **36**, 113 (1962).

(5) R. F. Smith, D. E. Shay, and N. J. Doorenbos, *Appl. Microbiol.*, **11**, 542 (1963).

(6) R. F. Smith, D. E. Shay, and N. J. Doorenbos, *J. Pharm. Sci.*, **53**, 1214 (1964).

(7) A. C. Cope, C. M. Hofmann, C. Wyckoff, and E. Hardenbergh, *J. Am. Chem. Soc.*, **63**, 3452 (1941).

(8) I. Guareschi, *Atti. Accad. Sci. Torino*, **36**, 443 (1900/1901).

(9) I. Vogel, *J. Chem. Soc.*, **1928**, 2010.

(10) A. Lapworth and J. A. McRae, *ibid.*, **121**, 2741 (1922).

(11) S. F. Birch, G. A. R. Kon, and W. S. G. P. Norris, *ibid.*, **123**, 1361 (1923).

(12) V. J. Harding, W. N. Haworth, and W. H. Perkin, *ibid.*, **93**, 1943 (1908).

(13) A. C. Cope, *J. Am. Chem. Soc.*, **59**, 2327 (1937).

(14) W. S. G. P. Norris and J. F. Thorpe, *J. Chem. Soc.*, **119**, 1199 (1921).

(15) F. Dickens, L. Horton, and J. F. Thorpe, *ibid.*, **124**, 1830 (1924).

(16) J. F. Thorpe and A. S. Wood, *ibid.*, **103**, 1586 (1913).

(17) G. A. R. Kon and J. F. Thorpe, *ibid.*, **115**, 693 (1919).

(18) K. Lundahl, J. Schut, J. L. M. A. Schlatmann, G. B. Paerels, and A. Peters, *J. Med. Chem.*, **15**, 129 (1972).

(19) R. VanHes, A. Smit, T. Kralt, and A. Peters, *ibid.*, **15**, 132 (1972).

(20) H.-L. Pan and T. L. Fletcher, *ibid.*, **10**, 957 (1967).

(21) W. Wasulko, A. C. Noble, and F. D. Popp, *ibid.*, **9**, 599 (1966).

(22) A. W. Bauer, W. M. M. Kirby, J. C. Sherris, and M. Turck, *Am. J. Clin. Pathol.*, **45**, 493 (1966).

(23) D. Perlman, K. L. Perlman, M. Bodanszky, A. Bodanszky, R. L. Foltz, and H. W. Matthews, *Bioorgan. Chem.*, **6**, 263 (1977).

ACKNOWLEDGMENTS

The authors wish to thank Dr. Peter E. Frankenberg and Mr. C. H. Roberts of the Du Pont Company, Wilmington, Del., for the NMR analyses.

Dissolution Apparatus for Gels

HO-LUN WENG and EUGENE L. PARROTT ˣ

Received January 11, 1982, from the *Division of Pharmaceutics, College of Pharmacy, University of Iowa, Iowa City, IA 52242.* Accepted for publication March 11, 1982.

Abstract □ A modification of the USP Dissolution Apparatus 2 is presented for use in the measurement of the release of a medicinal compound from a pharmaceutical gel.

Keyphrases □ Dissolution—apparatus for gels, modification of the USP Dissolution Apparatus 2 □ Pharmaceutical gels—dissolution apparatus, modification of the USP Dissolution Apparatus 2

The *in vitro* test methods for measuring the dissolution of a medicinal compound from a tablet or a capsule are defined in the United States Pharmacopeia (USP) (1). Mathur *et al.* (2) appear to be the first to have reported *in vitro* dissolution testing of suspensions. It seems that dissolution testing of any dosage form that may restrict the delivery of molecules of the medicinal compound to the GI epithelium is advisable.

This report presents a modification of the USP Dissolution Apparatus 2, that can be used to measure dissolution profiles from pharmaceutical gels.

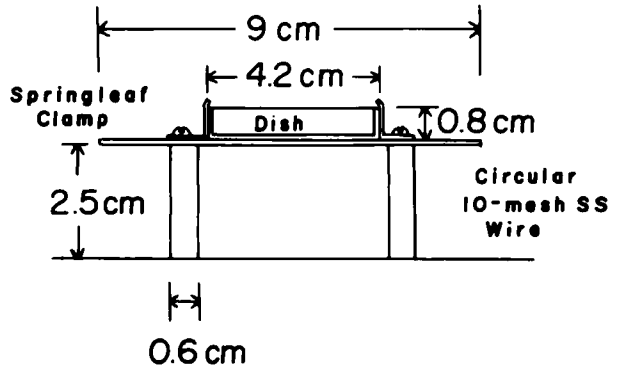

Figure 1—*Modification of the USP Dissolution Apparatus 2 for gels.*

EXPERIMENTAL

Dissolution Apparatus—A circular, 10-mesh stainless-steel cloth with a 9.0-cm diameter was fitted with four 2.5-cm plastic legs (diameter 0.6 cm) so that, as it rested on the bottom of the reaction vessel, the wire cloth was at the point of curvature of the base of the vessel. Four springleaf clamps were affixed to the upper surface of the wire cloth to hold the glass dish in the center of the platform (Fig. 1). The dish was cut from a 50-ml beaker and had 3.9-cm i.d. and an outer height of 0.8 cm.

A 5-g sample of the gel was weighed in the dish on an analytical balance, and using forceps the dish was gently lowered through the dissolution medium in the assembled apparatus and was inserted into the clamps. The time required by an experienced operator was ~30 sec. With thin gels, the level spontaneously adjusted to the horizontal plane; with very viscous gels, the surface may be leveled by use of a spatula prior to weighing. In the gels investigated, the 5-g samples completely filled the dish to the rim. If a particular gel had a high density, it would be advisable to use a greater weight, which would fill the dish. The dissolution medium was 900 ml of distilled water or 0.1 *N* HCl at 37 ± 0.5°. The paddle of the modified USP Dissolution Apparatus 2 was centrally positioned 2.5 cm above the rim of the dish. The apparatus was then started. Samples were withdrawn by a pipet through a glass filter. Ephedrine sulfate was assayed using a previously described method (3).

Dosage Forms—Tablets containing 25 mg of ephedrine sulfate was prepared by direct compression in a single-punch tablet machine. A portion of the batch was compressed to a hardness of 4 kg; the remainder was compressed to an 8-kg hardness. The formulation was:

Ephedrine sulfate[1]	25 mg
Microcrystalline cellulose[2]	190 mg
Lactose[3]	382 mg
Magnesium stearate[4]	3 mg

[1] USP.
[2] Avicel PH 101.
[3] USP, spray dried.
[4] NF.

0022-3549/83/0200-0186$01.00/0

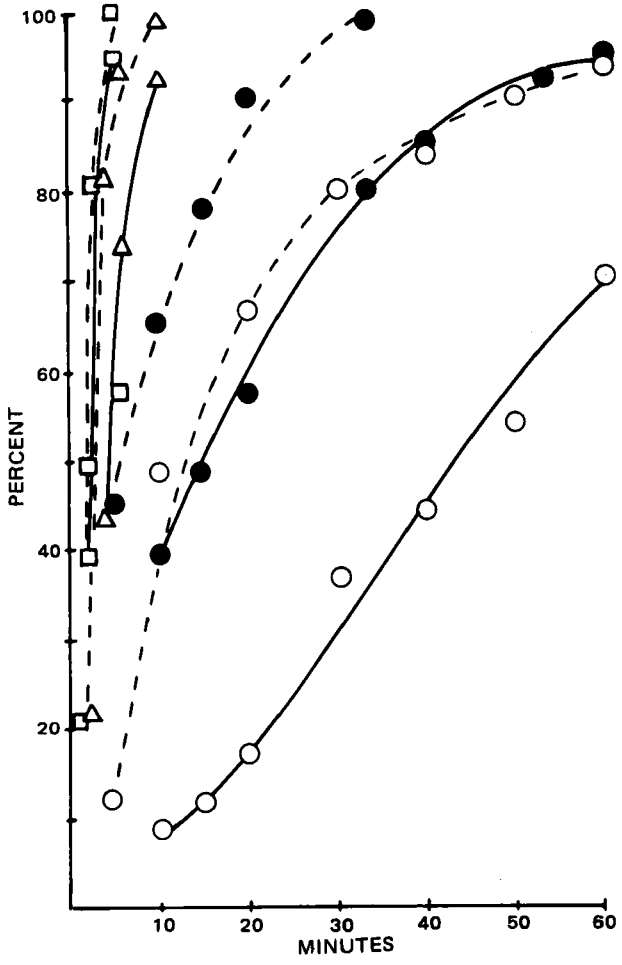

Figure 2—*Comparison of percent of ephedrine sulfate released from tablets having a hardness of 8 kg as determined by the USP Dissolution Apparatus 2 and a modification for gels at various speeds. Key: (- - -) USP; (—) modified for gel apparatus; (○) 12 rpm; (●) 30 rpm; (△) 60 rpm; (□) 100 rpm.*

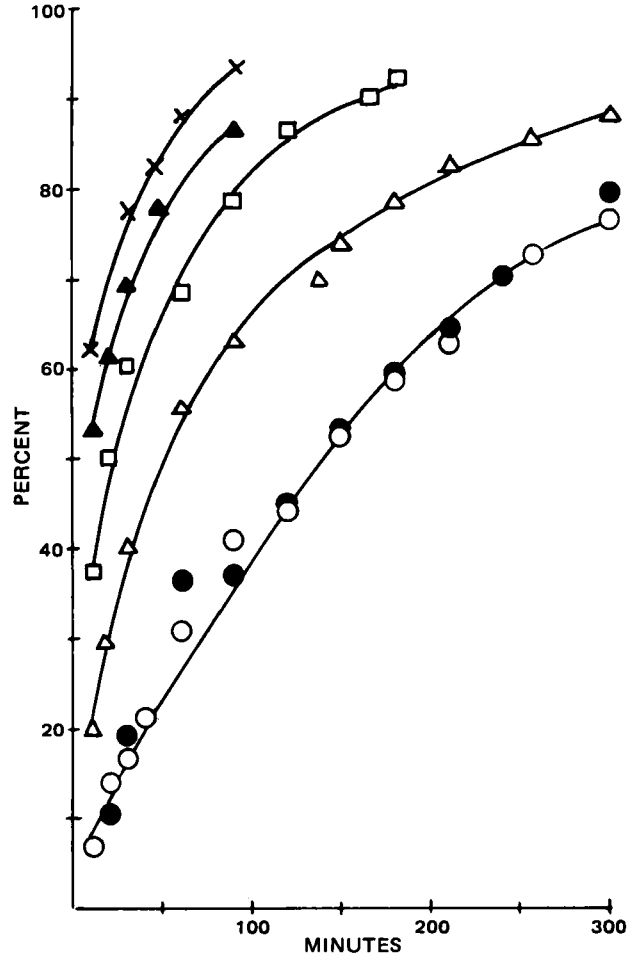

Figure 3—*Release profile of ephedrine sulfate from a methylcellulose gel at various speeds. Key: (○) 12 rpm; (●) 30 rpm; (△) 60 rpm; (□) 70 rpm; (▲) 80 rpm; (×) 90 rpm.*

The formulation of the gel used as a model was:

Ephedrine sulfate	20 mg
Methylcellulose[5]	200 mg
Distilled water	4780 mg

RESULTS AND DISCUSSION

Gels are semisolid systems consisting of either suspensions made up of small inorganic particles or large organic molecules interpenetrated by a liquid (4). Gels with wide viscosities may be used as vehicles for a dissolved or a suspended medicinal compound. The wide range of viscosities of pharmaceutical gels limits the use of the USP dissolution apparatus. For example, with USP Dissolution Apparatus 1, a gel of low viscosity may drip from the basket assembly, and a gel of high viscosity will tend to clog the wire mesh.

It is desirable to have an apparatus for all dosage forms that is not markedly different than the officially accepted dissolution apparatus. To compare the agitation and the dissolution profiles obtained by the USP Dissolution Apparatus 2 and the modification, dissolution from tablets of ephedrine sulfate was studied at 12, 30, 60, and 100 rpm in 900 ml of distilled water. The dissolution profiles are given in Fig. 2 for tablets with a hardness of 8 kg. From Fig. 2, and a similar plot for tablets with a hardness of 4 kg, the times required for 50% ($t_{1/2}$) and 66.7% ($t_{2/3}$) of the ephedrine sulfate to dissolve from the tablets were determined and are listed in Table I.

At 60 and 100 rpm (speeds frequently utilized in official tests) there is no apparent difference in the dissolution profiles as obtained by the USP Dissolution Apparatus 2 and the modification suggested for de-

[5] USP, type 400 cps.

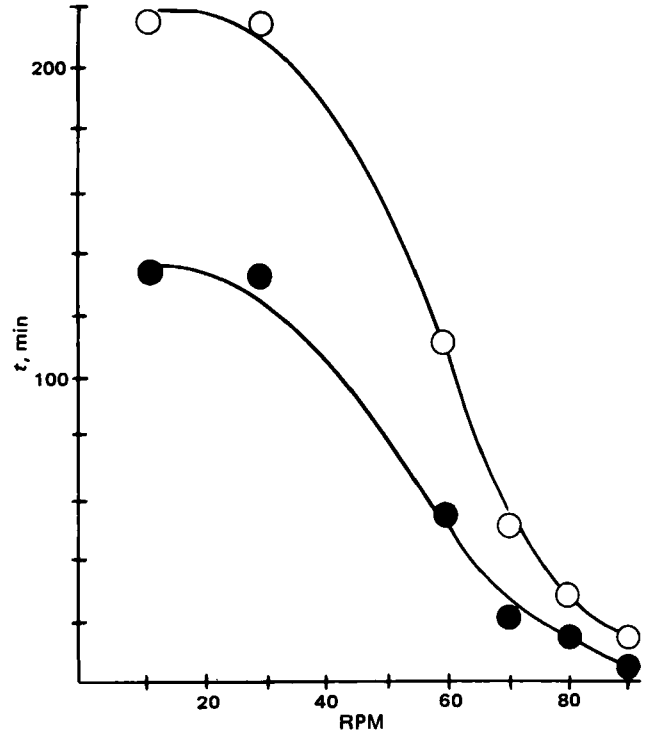

Figure 4—*Influence of speed on dissolution. Key: (○) $t_{2/3}$; (●) $t_{1/2}$.*

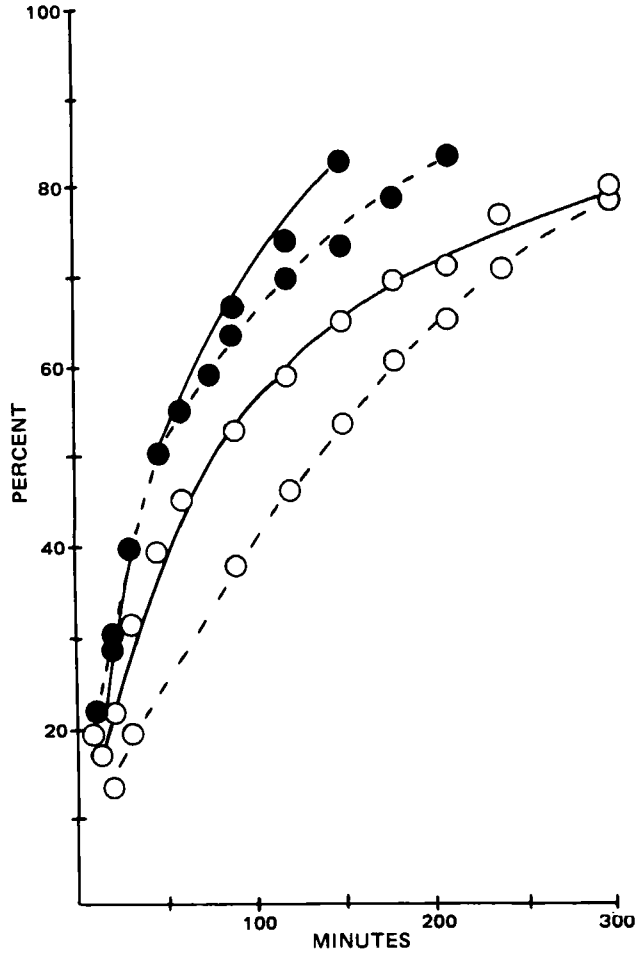

Figure 5—*Release profile of ephedrine sulfate from a methylcellulose gel in water and 0.1 N HCl. Key: (- - -) water; (—) 0.1 N HCl; (○) 30 rpm; (●) 60 rpm.*

termining the release profile from gels. Thus, at these speeds the factors contributing to dissolution are similar, and a comparison of release from a solid dosage form (tablet) and the release from a gel would be valid.

The release of ephedrine sulfate from the model gel was studied at 12, 30, 60, 70, 80, and 90 rpm as shown in Fig. 3. At the higher speeds, the agitation moves portions of the gel in a random manner so that filaments

Table I—Comparison of Dissolution as Measured by the USP Dissolution Apparatus 2 and by the Apparatus Modified for a Gel Using Compressed Tablets Containing 25 mg of Ephedrine Sulfate

Speed, rpm	$t_{1/2}$, min[a]		$t_{2/3}$, min[a]	
	USP Apparatus 2	Gel Apparatus	USP Apparatus 2	Gel Apparatus
		Hardness (4 kg)		
12	9	35	15	47
30	5	5	7	11
60	~1	2	~1	3
100	~1	1	~1	2
		Hardness (8 kg)		
12	10	43.5	19	59
30	6.5	15	11	22
60	~2	~4	~2	5
100	2	~3	~3	4

[a] Rounded to the nearest 0.5 min.

and masses of the gel may move away from the gel in the dish and at times become entwined around the shaft of the paddle. At lowest speeds, the release from the gel to the bulk of the dissolution medium is slow and requires an inconveniently long testing period (>4 hr). Intermediate speeds did not grossly disturb the gel in the dish and did not unduly prolong the release of the ephedrine sulfate; thus, 30 and 60 rpm appear to be practical speeds. The influence of speed on dissolution is shown in Fig. 4.

The release of the ephedrine sulfate from the model gel was determined in distilled water and in 0.1 *N* HCl at 30 and 60 rpm and is plotted in Fig. 5. At 30 rpm the values of $t_{1/2}$ are 135 and 80 min in water and 0.1 *N* HCl, respectively. At 60 rpm the values of $t_{1/2}$ are ~45 min in water and 0.1 *N* HCl.

REFERENCES

(1) "The United States Pharmacopeia," 20th rev., United States Pharmacopeial Convention, Rockville, Md., 1980, p. 959.

(2) L. K. Mathur, J. M. Jaffe, R. I. Poust, H. Barry, III, T. J. Goehl, V. P. Shah, and J. L. Colaizzi, *J. Pharm. Sci.*, **68**, 699 (1979).

(3) W. N. French and B. A. Reidel, *Can. J. Pharm. Sci.*, *1*, *80* (1966).

(4) "The United States Pharmacopeia," 20th rev., United States Pharmacopeial Convention, Rockville, Md., 1980, p. 1026.

ACKNOWLEDGMENTS

Supported in part by Johnson & Johnson Baby Products Co., Skillman, NJ 08558.

^{1}H- and ^{13}C-NMR Spectra of Fenobam

G. PELLIZER *x and F. RUBESSA ‡

Received October 7, 1981, from the **Istituto di Chimica and the* ‡*Istituto di Chimica Farmaceutica, Università di Trieste, Italy.* Accepted for publication March 12, 1982.

Abstract □ ^{1}H- and ^{13}C-NMR data and spectral assignments are reported for fenobam using noise modulated gated, single frequency off resonance, and single frequency selective proton decoupling techniques.

Keyphrases □ Fenobam—^{1}H- and ^{13}C-NMR spectroscopic analysis □ ^{1}H- and ^{13}C-NMR spectroscopy—analysis of fenobam

Fenobam (I), *N*-(3-chlorophenyl)-*N'*-(4,5-dihydro-1-methyl-4-oxo-1*H*-imidazol-2-yl)urea monohydrate, has been shown to possess selective anxiolytic properties in animals and in clinical trials, with a mode of action different from that of the benzodiazepines (1, 2).

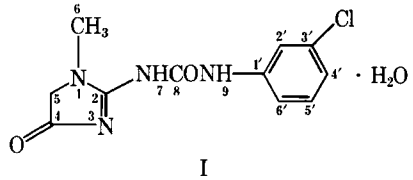

I

NMR parameters, especially ^{13}C-chemical shifts, are being widely used to establish structure–activity relationships. As a part of a study on psychoactive molecules, the ^{1}H- and natural abundance ^{13}C-NMR spectra of I are reported. Their assignments are accomplished by gated, single frequency off resonance, and single frequency selective proton decoupling, and by comparison with other structurally related compounds.

EXPERIMENTAL

The NMR spectra were recorded at room temperature from 0.3 *M* solutions of I in $^2H_6$-dimethyl sulfoxide in 5 mm (^{1}H-NMR) and 10-mm (^{13}C-NMR) tubes[1]. Tetramethylsilane was used as the internal standard for ^{1}H-NMR spectra, while the ^{13}C-multiplet of the deuterated solvent served as the internal reference. Chemical shifts were converted to tetramethylsilane scale using:

$$\delta = \delta\ (^2H_6\text{-dimethyl sulfoxide}) + 39.6\ \text{ppm}$$

^{1}H-NMR spectra were measured at 80 MHz using 90° pulse, sweep widths of 800 and 400 Hz, and single-scan and Fourier transform. ^{13}C-NMR spectra were obtained at 20.1 MHz using 2-μsec pulses (a 90° tip angle required a pulse width of 6.5 μsec), acquisition time 0.9102 sec (corresponding to a sweep width of 4500 Hz), accumulation of free induction decays, and Fourier transform. No delay was given between the end of acquisition and the next pulse. Line broadening (0.5 Hz) was introduced in the spectrum by exponential multiplication of free induction decays. The decoupler was used in broad band, broad band gated, single frequency off resonance, and single frequency selective decoupling modes. Carbon–proton coupling constants were measured from undecoupled spectra and gated proton decoupled spectra.

Monohydrated I was dissolved in $^2H_6$-dimethyl sulfoxide without further purification. A dehydrated sample was prepared by heating at 85° and 1 torr. In the final IR spectrum the water peak disappeared. This sample was dissolved in anhydrous $^2H_6$-dimethyl sulfoxide.

RESULTS AND DISCUSSION

Anhydrous and monohydrated fenobam show identical ^{1}H-NMR spectra. A detailed interpretation of the spectrum was made in order to use single frequency proton decoupling for carbon assignments. The results are presented in Table I.

Table I—Proton Chemical Shifts and Coupling Constants of Fenobam

Protons	δ^a	Hz
5	4.01	—
6	3.00	—
7	9.52[b]	—
9	10.90[b]	—
2′	7.89	—
4′	6.99	—
5′	7.26	—
6′	7.53	—
$J_{H\text{-}2',H\text{-}4'}$	—	2.07
$J_{H\text{-}2',H\text{-}5'}$	—	0.25
$J_{H\text{-}2',H\text{-}6'}$	—	1.99
$J_{H\text{-}4',H\text{-}5'}$	—	7.96
$J_{H\text{-}4',H\text{-}6'}$	—	0.97
$J_{H\text{-}5',H\text{-}6'}$	—	8.60

[a] Parts per million from tetramethylsilane. [b] Values may be interchanged.

The values for the aromatic protons were obtained through iterative simulation[2]. Assignments of H-2′ and H-5′ are straightforward from spectral pattern. The peaks of the multiplet at 7.53 ppm are appreciably broader than those at 6.99 ppm, indicating that the former are due to H-6′ (*ortho* to nitrogen). Assuming additivity in the substituent effect on the aromatic protons chemical shifts and using the values reported previously (3) for the chlorine atom, it turns out from the above assignment that the ureido group has relevant deshielding effects only on the two protons, H-2′ and H-6′, which are in *ortho* positions.

The broad band proton decoupled ^{13}C spectrum consists of 11 well-separated peaks (Table II).

In the gated proton decoupled spectrum, the resonances centered at 30.3 and 51.1 ppm appear as a quartet and a broadened triplet and are attributed to C-6 and C-5, respectively. The resonances centered at 117.1, 118.1 and 121.5 ppm appear as doublets of multiplets reflecting couplings with two *meta* protons and are ascribed to C-6′, C-2′, and C-4′, respectively. In particular, C-4′ originates a doublet of quartets (the two J_{meta} are ~6 and 8 Hz), while the doublet of 1:3:3:1 quartets associated with C-2′ and the doublet of unresolved multiplets assigned to C-6′ indicate a relevant coupling with proton 9. For C-6′, there is also a significant coupling with H-5′. Centered at 130.3 ppm there is a doublet due to C-5′. These assignments are further confirmed by single frequency proton decoupling experiments. The resonances centered at 133.2, 142.3, 157.3, 160.8, and 171.6 ppm belong to quaternary carbons and appear, respectively, as a doublet of unresolved multiplets, another broad doublet, an unresolved multiplet, a slightly broadened singlet, and a triplet.

Selective irradiation of H-2′ causes the complete collapse of the multiplet centered at 118.1 ppm which, therefore, is unambiguously assigned to C-2′. As expected, all the aromatic carbon resonances are strongly affected, *i.e.*, all long-range couplings collapse while the direct C—H bond couplings are strongly reduced in magnitude. The residual splitting decreases in the order C-4′ > C-5′ > C-6′, *i.e.*, as the resonance frequency of the attached proton approaches the decoupling frequency (Table I). This observation and single frequency off resonance experiments support the assignment here reported for C-4′, C-5′, and C-6′. Decoupling of H-2′ has much weaker effects on the resonances at 157.3, 160.8, and 171.6 ppm.

However, irradiation of methylene protons transforms the triplet at 171.6 ppm into a sharp singlet and the unresolved multiplet at 157.3 ppm into a broad singlet, indicating that these resonances are due to imidazolinone ring carbons C-4 and C-2, respectively, the former being coupled only with H-5 protons and the latter with both H-5 and methyl protons. Irradiation of the methyl protons confirms these assignments. Further-

[1] Bruker WP 80 spectrometer equipped with a BNC 28 computer with 8K data memory.

[2] Bruker ITRCAL program.

0022-3549/83/0200-0189$01.00/0

Table II—^{13}C-NMR Data

Assignment	δ^a	Multiplicity
C-2	157.3 (169.5[b], 156.7[c])	Unresolved multiplet
C-4	171.6 (188.8[b], 172.0[c])	Triplet, $^2J_{CH}$ = 5 Hz
C-5	51.1 (56.4[b], 54.1[c])	Triplet, $^1J_{CH}$ = 147 Hz
C-6	30.3 (30.2[b], 31.2[c])	Quartet, $^1J_{CH}$ = 140 Hz
C-8	160.8	Singlet
C-1′	142.3	Broad doublet, $^3J_{CH} \simeq 9$ Hz
C-2′	118.1	Doublet of 1:3:3:1 quartets $^1J_{CH}$ = 168 Hz; $^3J_{CH\text{-}4'} \simeq {}^3J_{CH\text{-}6'} \simeq {}^3J_{CH\text{-}9} \simeq 5$ Hz
C-3′	133.2	Doublet of unresolved multiplets, $^3J_{CH} \simeq 11$ Hz
C-4′	121.5	Doublet of quartets, $^1J_{CH}$ = 168.5 Hz, $^3J_{CH} \simeq 6$ and 8 Hz
C-5′	130.3	Doublet, $^1J_{CH}$ = 163 Hz
C-6′	117.1	Doublet of unresolved multiplets, $^1J_{CH}$ = 165 Hz

[a] Chemical shifts in parts per million relative to tetramethylsilane. [b] Values of 2-amino-1,5-dihydro-1-methyl-4*H*-imidazol-4- one. [c] Values for its corresponding monohydrochloride.

more, these decouplings, apart from the collapse of C-5 and methyl carbon resonances, have weak effects on the aromatic carbon resonances, and the splittings due to small C—H couplings are still observable.

The assignment of 142.2 and 133.2 ppm resonances was made by comparison with similar compounds. Assuming that the substituent effects on the shifts of the aromatic carbons are additive and using the data reported previously (4) for the chlorine atom, the values calculated for the ureido group are very close to those determined for other aromatic ureas (5) and acetanilide (4).

The chemical shifts of C-2, C-4, C-5, and C-6 are close to those of 2-amino-1,5-dihydro-1-methyl-4*H*-imidazol-4-one hydrochloride in $^2H_6$-dimethyl sulfoxide (Table II) (6). The ureido ^{13}C-chemical shift (160.8 ppm) is nearer to urea (160.5 ppm) (7) than diphenylurea (152.7 ppm) or di-*p*-anisylurea (153.0 ppm) (5).

REFERENCES

(1) T. M. Itil, P. A. Seaman, M. Hugue, S. Mukhopadhyay, D. Biasucci, Kung Tat NQ, and P. E. Ciccone, *Curr. Ther. Res.*, **24**, 708 (1978).

(2) F. L. Fabre, *Clin. Res.*, **25**, 269A (1977).

(3) R. J. Abraham and P. Loftus "Proton and Carbon-13 NMR Spectroscopy," Heyden, London, 1978, p. 28.

(4) F. W. Wehrli and T. Wirthlin "Interpretation of Carbon-13 NMR Spectra," Heyden, New York, N.Y., 1976, p. 47.

(5) G. Trickes, V. Plucken, and H. Meier, *Z. Naturforsch. B*, **32**, 956 (1977).

(6) R. L. Smith, D. W. Cochran, P. Gund, and E. J. Cagroe, *J. Am. Chem. Soc.*, **101**, 191 (1979).

(7) B. Coxon, A. Fatiadi, L. Sniegoski, and H. Hertz, *J. Org. Chem.*, **42**, 3132 (1977).

ACKNOWLEDGMENTS

The authors thank the McNeill Laboratory for the generous gift of fenobam and Mr. L. Stoppari for technical assistance.

Dissolution Profiles for Finely Divided Drug Suspensions

JOHN W. MAUGER ˣ, STEPHEN A. HOWARD, and KIRIT AMIN

Received September 3, 1981, from the *School of Pharmacy, West Virginia University, Morgantown, WV 26506.* Accepted for publication March 16, 1982.

Abstract □ A suspension of micronized prednisolone acetate was separated into four fractions by the technique of centrifugal elutriation. Data showed that each fraction had a narrow particle size. The dissolution experiments were carried out under sink conditions (<10% of saturation concentration) in a dissolution apparatus with a rotating filter assembly and a continuous circulation of filtered fluid samples through a recording spectrophotometer. The dissolution profile was highly reproducible and substantially different for each fraction. As expected, fractions with the smallest and largest particles showed the fastest and slowest dissolution, respectively. Almost the entire dissolution profiles for four small particle size fractions can be satisfactorily described by the Higuchi–Hiestand model with the dissolution rate constant, K, in the range of 1.5–2.0 × 10^{-9}cm^2/sec. This is ~3.5 times greater than the value for K calculated on the basis of reported reasonable values for diffusion coefficient, density, and solubility.

Keyphrases □ Dissolution—profiles for drug suspensions, prednisolone acetate, centrifugal elutriation □ Drug suspensions—dissolution profiles, prednisolone acetate, centrifugal elutriation □ Prednisolone acetate—dissolution profiles for drug suspensions, centrifugal elutriation

Dissolution models for multisized drug particles have been proposed and studied experimentally. However, few studies deal specifically with finely divided drug particles (micrometer range). There were notable exceptions (1, 2) published more than a decade ago which showed approximate agreement between diffusional model theory and experimental data for micronized methylprednisolone particles. A more recent study (3) of the dissolution kinetics of micronized steroid particles was unable to confirm the application of the diffusion-based law for the decay of particle size used in those earlier studies (1, 2). To date, the relationship between diffusional-based dissolution theory for finely divided drug particles, and its experimental justification remains fragile.

One of the reasons for the inability to relate the theory with experimental data may be the difficulties encountered in obtaining very small particles with known narrow particle size distributions. The aforementioned studies used multisized drug particle populations in which the dissolution kinetics for the largest and smallest particles may have differed. This possibility has been discussed (4) and an interpolation formula provided which mixes the diffusion kinetics for large and small particles. Therefore, the possibility of mixed models makes critical testing of a specific model difficult. With recent advances in centrifugal elutriation separation and particle size measurement techniques (5) in conjunction with the spin filter dissolution apparatus, it has become possible to test the dissolution models with more rigorously controlled experiments.

0022-3549/83/0200-0190$01.00/0

Table II—^{13}C-NMR Data

Assignment	δ^a	Multiplicity
C-2	157.3 (169.5[b], 156.7[c])	Unresolved multiplet
C-4	171.6 (188.8[b], 172.0[c])	Triplet, $^2J_{CH}$ = 5 Hz
C-5	51.1 (56.4[b], 54.1[c])	Triplet, $^1J_{CH}$ = 147 Hz
C-6	30.3 (30.2[b], 31.2[c])	Quartet, $^1J_{CH}$ = 140 Hz
C-8	160.8	Singlet
C-1′	142.3	Broad doublet, $^3J_{CH} \simeq 9$ Hz
C-2′	118.1	Doublet of 1:3:3:1 quartets $^1J_{CH}$ = 168 Hz; $^3J_{CH\text{-}4'} \simeq {}^3J_{CH\text{-}6'} \simeq {}^3J_{CH\text{-}9} \simeq 5$ Hz
C-3′	133.2	Doublet of unresolved multiplets, $^3J_{CH} \simeq 11$ Hz
C-4′	121.5	Doublet of quartets, $^1J_{CH}$ = 168.5 Hz, $^3J_{CH} \simeq 6$ and 8 Hz
C-5′	130.3	Doublet, $^1J_{CH}$ = 163 Hz
C-6′	117.1	Doublet of unresolved multiplets, $^1J_{CH}$ = 165 Hz

[a] Chemical shifts in parts per million relative to tetramethylsilane. [b] Values of 2-amino-1,5-dihydro-1-methyl-4*H*-imidazol-4- one. [c] Values for its corresponding monohydrochloride.

more, these decouplings, apart from the collapse of C-5 and methyl carbon resonances, have weak effects on the aromatic carbon resonances, and the splittings due to small C—H couplings are still observable.

The assignment of 142.2 and 133.2 ppm resonances was made by comparison with similar compounds. Assuming that the substituent effects on the shifts of the aromatic carbons are additive and using the data reported previously (4) for the chlorine atom, the values calculated for the ureido group are very close to those determined for other aromatic ureas (5) and acetanilide (4).

The chemical shifts of C-2, C-4, C-5, and C-6 are close to those of 2-amino-1,5-dihydro-1-methyl-4*H*-imidazol-4-one hydrochloride in $^2H_6$-dimethyl sulfoxide (Table II) (6). The ureido ^{13}C-chemical shift (160.8 ppm) is nearer to urea (160.5 ppm) (7) than diphenylurea (152.7 ppm) or di-*p*-anisylurea (153.0 ppm) (5).

REFERENCES

(1) T. M. Itil, P. A. Seaman, M. Hugue, S. Mukhopadhyay, D. Biasucci, Kung Tat NQ, and P. E. Ciccone, *Curr. Ther. Res.*, **24**, 708 (1978).

(2) F. L. Fabre, *Clin. Res.*, **25**, 269A (1977).

(3) R. J. Abraham and P. Loftus "Proton and Carbon-13 NMR Spectroscopy," Heyden, London, 1978, p. 28.

(4) F. W. Wehrli and T. Wirthlin "Interpretation of Carbon-13 NMR Spectra," Heyden, New York, N.Y., 1976, p. 47.

(5) G. Trickes, V. Plucken, and H. Meier, *Z. Naturforsch. B*, **32**, 956 (1977).

(6) R. L. Smith, D. W. Cochran, P. Gund, and E. J. Cagroe, *J. Am. Chem. Soc.*, **101**, 191 (1979).

(7) B. Coxon, A. Fatiadi, L. Sniegoski, and H. Hertz, *J. Org. Chem.*, **42**, 3132 (1977).

ACKNOWLEDGMENTS

The authors thank the McNeill Laboratory for the generous gift of fenobam and Mr. L. Stoppari for technical assistance.

Dissolution Profiles for Finely Divided Drug Suspensions

JOHN W. MAUGER ˣ, STEPHEN A. HOWARD, and KIRIT AMIN

Received September 3, 1981, from the *School of Pharmacy, West Virginia University, Morgantown, WV 26506.* Accepted for publication March 16, 1982.

Abstract □ A suspension of micronized prednisolone acetate was separated into four fractions by the technique of centrifugal elutriation. Data showed that each fraction had a narrow particle size. The dissolution experiments were carried out under sink conditions (<10% of saturation concentration) in a dissolution apparatus with a rotating filter assembly and a continuous circulation of filtered fluid samples through a recording spectrophotometer. The dissolution profile was highly reproducible and substantially different for each fraction. As expected, fractions with the smallest and largest particles showed the fastest and slowest dissolution, respectively. Almost the entire dissolution profiles for four small particle size fractions can be satisfactorily described by the Higuchi–Hiestand model with the dissolution rate constant, K, in the range of 1.5–2.0 × 10^{-9}cm^2/sec. This is ~3.5 times greater than the value for K calculated on the basis of reported reasonable values for diffusion coefficient, density, and solubility.

Keyphrases □ Dissolution—profiles for drug suspensions, prednisolone acetate, centrifugal elutriation □ Drug suspensions—dissolution profiles, prednisolone acetate, centrifugal elutriation □ Prednisolone acetate—dissolution profiles for drug suspensions, centrifugal elutriation

Dissolution models for multisized drug particles have been proposed and studied experimentally. However, few studies deal specifically with finely divided drug particles (micrometer range). There were notable exceptions (1, 2) published more than a decade ago which showed approximate agreement between diffusional model theory and experimental data for micronized methylprednisolone particles. A more recent study (3) of the dissolution kinetics of micronized steroid particles was unable to confirm the application of the diffusion-based law for the decay of particle size used in those earlier studies (1, 2). To date, the relationship between diffusional-based dissolution theory for finely divided drug particles, and its experimental justification remains fragile.

One of the reasons for the inability to relate the theory with experimental data may be the difficulties encountered in obtaining very small particles with known narrow particle size distributions. The aforementioned studies used multisized drug particle populations in which the dissolution kinetics for the largest and smallest particles may have differed. This possibility has been discussed (4) and an interpolation formula provided which mixes the diffusion kinetics for large and small particles. Therefore, the possibility of mixed models makes critical testing of a specific model difficult. With recent advances in centrifugal elutriation separation and particle size measurement techniques (5) in conjunction with the spin filter dissolution apparatus, it has become possible to test the dissolution models with more rigorously controlled experiments.

0022-3549/83/0200-0190$01.00/0

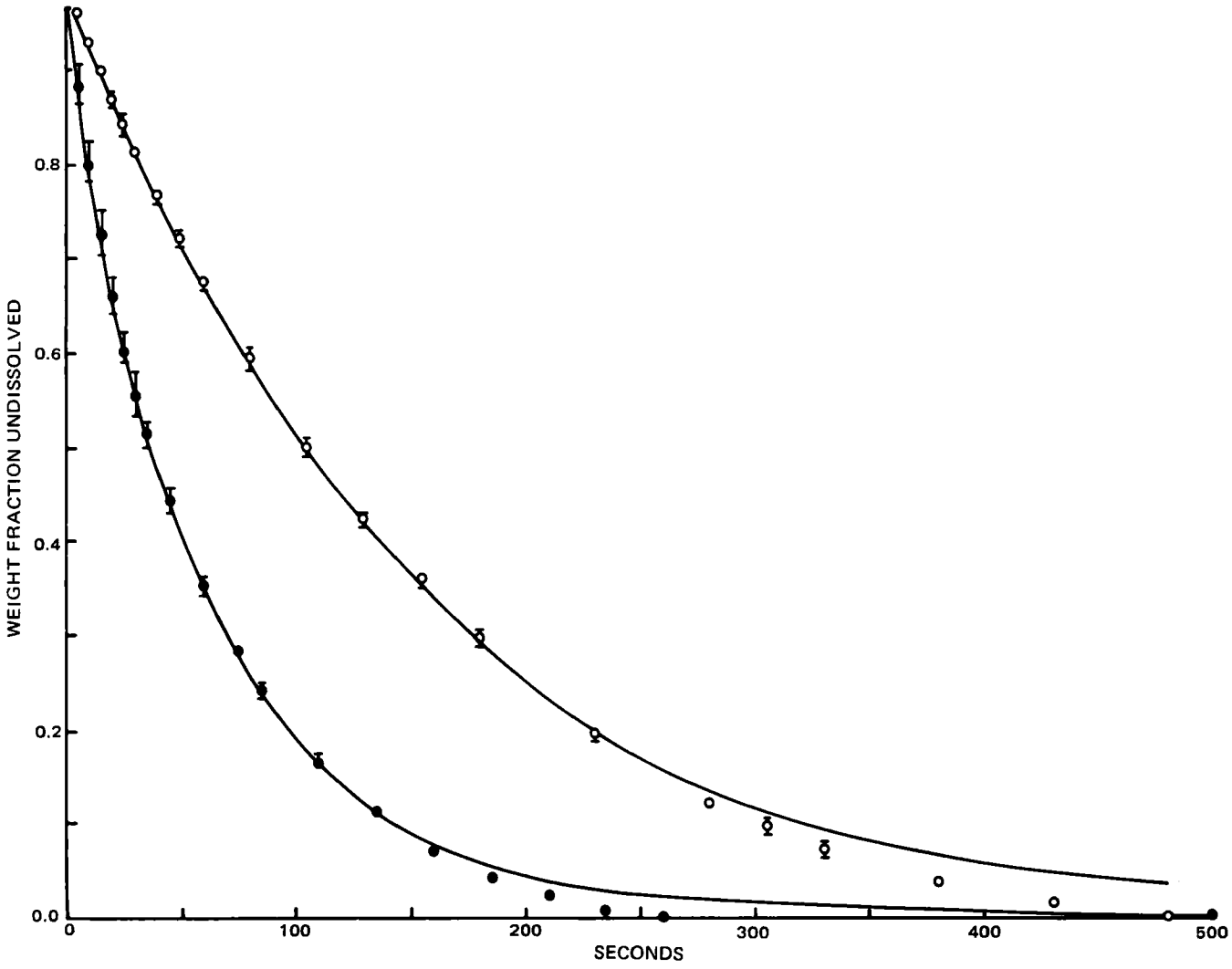

Figure 1—*Dissolution profiles for first and second prednisolone acetate fractions. Key: (●) experimental values for fraction 1, solid line calculated using theory with* K = 1.85×10^{-9} *cm²/sec; (○) experimental values for fraction 2, calculated using theory with* K = 1.50×10^{-9} *cm²/sec.*

EXPERIMENTAL

Particle Separation—A previous study (5) demonstrated that centrifugal elutriation[1,2] is capable of separating fractions of small particles with very narrow particle size distributions. In this study a 0.6% suspension of micronized prednisolone acetate in 0.9% sodium chloride solution presaturated with drug was separated into four fractions by the technique of centrifugal elutriation. Four fractions were obtained. Pump speeds of 30 and 52 ml/min and centrifuge speeds of 2000, 1000, and 500 rpm were utilized.

Particle Sizing—An electronic particle sizing device[3] with either a 50- or 200-μm aperture tube was used for particle size analysis. An electrolyte solution[4] presaturated with micronized prednisolone acetate was used as a vehicle. This multichannel instrument provides detailed information about particle size distribution. The particles were classified and counted into one of 14 channels. The first two channels were not used. Almost all of the particles in each fraction were distributed over not more than three to four consecutive channels indicating a narrow particle size distribution.

Dissolution—All dissolution experiments were carried out in an apparatus reported previously (6) which is well-suited for monitoring the dissolution of suspended particles. The rotating filter assembly used in this device provides a variable intensity of mild liquid agitation, and it also functions as an *in situ* nonclogging filter to allow continuous filtration of the dissolution fluid without removing the dissolving particles during the dissolution process.

Procedure—A prednisolone acetate suspension was prepared and elutriated as described, and then a measured sample of each fraction was dissolved in water for 24 hr and assayed. The concentrations thus obtained were utilized in adjusting the suspension concentration of each fraction so that a 5-ml sample would allow for perfect sink conditions to exist in the dissolution test.

Immediately prior to dissolution testing the sample was sized electronically as described, and within 5 min of sizing dissolution testing was initiated. The dissolution experiments were initiated by injecting 5 ml of the desired fraction of prednisolone acetate suspension in a liter of distilled water. The temperature was maintained at 37° and the stirring speed of the filter assembly was set at 600 rpm. Filtered fluid samples were continuously circulated through a spectrophotometer[5] and back into the dissolution flask at the rate of 100 ml/min. The absorbance at 247 nm was continuously recorded as a function of time. The final concentration of prednisolone acetate in the dissolution medium was kept below 10% of saturation.

RESULTS

Four size fractions of prednisolone acetate were obtained, sized, and dissolution tested. The results were then compared to the multisize form of the Higuchi–Hiestand model (1). Weight fraction remaining undissolved, $W(F)$, as a function of time, t, was calculated from the dissolution data in the following manner. The time scale was first corrected for the lag time by subtracting lag time (~15 sec), and the absorbances were corrected by subtracting absorbance due to dilution of the saturated solution (5 ml of saturated solution used in the dissolution experiment).

[1] Model JEG, Beckman Instrument Co., Fullerton, Calif.
[2] Model J-21B, Beckman Instrument Co., Fullerton, Calif.
[3] Model TAII, Coulter Electronics, Hialeah, Fla.
[4] Isoton, Coulter Diagnostics Inc., Hialeah, Fla.
[5] Cary 118, Varian Instruments, Palo Alto, Calif.

Table I—Particle Size Distributions for Fractions 1 and 2 with 50-μm Aperture Tube

Channel No. I	Diameter, μm	Fraction of Total Volume, F_I 1	2
3	0.897	0.0310	0.0094
4	1.130	0.0182	0.0045
5	1.425	0.0298	0.0049
6	1.795	0.0315	0.0052
7	2.260	0.0408	0.0084
8	2.845	0.0597	0.0114
9	3.585	0.1178	0.0218
10	4.520	0.2214	0.0709
11	5.695	0.2617	0.2373
12	7.175	0.1375	0.3693
13	9.040	0.0380	0.1915
14	11.390	0.0083	0.0426
15	14.350	0.0049	0.0062
16	18.100	0.0026	0.0166

Table II—Particle Size Distributions for Fractions 3 and 4 with 200-μm Aperture Tube

Channel No. I	Diameter, μm	Fraction of Total Volume, F_I 3	4
3	3.58	0.0087	0.0058
4	4.52	0.0168	0.0103
5	5.69	0.0502	0.0321
6	7.17	0.1549	0.0690
7	9.04	0.2907	0.1508
8	11.39	0.2780	0.2473
9	14.35	0.1400	0.2652
10	18.10	0.0395	0.1565
11	22.80	0.0081	0.0413
12	28.70	0.0071	0.0059
13	36.15	0.0058	0.0065
14	45.55	0.0000	0.0046
15	57.40	0.0000	0.0033
16	72.32	0.0000	0.0013

After corrections, the absorbance at each time, $A(T)$, was divided by the maximum absorbance, A_{max}, to obtain weight fraction dissolved at time, T, $W(DT)$. Thus, $W(DT) = A(T)/A_{max}$ and $[1 - W(DT)] = W(F)$, weight fraction undissolved at time T.

According to the Higuchi–Hiestand model for micronized range size, spherical particles dissolving under sink conditions by a diffusion controlled process the diameter, A, of a single particle at time T is given by

$$A(T) = (A_0^2 - KT)^{1/2} \qquad \text{(Eq. 1)}$$

where $A(T)$ is the diameter in centimeters at time T (sec); A_0 is the diameter at time zero; K is $(8DC)/\rho$, (cm²/sec); D is the diffusion coefficient for solute (5×10^{-6} cm²/sec); C is the solubility of solute (1.5×10^{-5} g/cm³); and ρ is the density of solute (1.3 g/cm³).

The weight fraction, $W(F)$, of a particle remaining undissolved at time T is:

$$W(F) = A(T)^3/A_0^3 = [(A_0^2 - KT)/A_0^2]^{3/2} \qquad \text{(Eq. 2)}$$

The weight fraction, $W(F)$, of multisized particles remaining undissolved at time T is:

$$W(F) = [(A_{0I}^2 - KT)/A_{0I}^2]^{3/2}(F_I) \qquad \text{(Eq. 3)}$$

where I is the channel number corresponding to the particle size range on the electronic particle size measurement instrument; A_{0I} is the initial diameter of particles in the Ith channel; and F_I is the fraction of the total volume (weight) of particles in the Ith channel.

The dissolution rate constant, K, in the above equation was varied to obtain the best fit for the dissolution profile. The calculated value for K would be $8DC/\rho = 4.6 \times 10^{-10}$ cm²/sec. Particle size distributions based on volume fraction in each channel obtained from the electronic counter were used to generate theoretical curves for $W(F)$ as a function of time.

Particle size distributions of the two small particle size fractions (fractions 1 and 2) are presented in Table I. These data represent an average of results of three experiments. Fraction 1 with the smallest particles has a mean particle diameter of 4.9 μm. Fraction 2 consists of slightly larger particles with a mean particle diameter of 7.1 μm. The narrowness of each fraction is noteworthy. For fraction 1, over 80% of the population, based on volume, is located in only 6 channels (channels 8–13), and 73% is located in only 4 channels (channels 9–12). For fraction 2, over 90% of the population, based on volume, is located in only 5 channels (channels 10–14), and 79% is located in only 3 channels (channels 11–13).

Dissolution profiles for fractions 1 and 2 are given in Fig. 1, and $W(F)$ as a function of time is plotted in this figure. Each point on these graphs represents an average of at least three experiments.

As expected, fraction 1 with smaller particles dissolves considerably faster than the one with larger particles. As can be seen from Fig. 1, almost the entire dissolution profile for each of the two fractions can be satisfactorily described by the Higuchi–Hiestand model with the dissolution rate constant, K, being 1.50×10^{-9} cm²/sec and 1.85×10^{-9} cm²/sec for fractions 1 and 2, respectively. This is ~3.5 times larger than the calculated values for K of 4.6×10^{-10} cm²/sec.

The particle size data for fractions 3 and 4 are shown in Table II. The mean for fraction 3 is 10.6 μm and the mean for fraction 4 is 13.5 μm. The narrowness for each fraction is again demonstrated with 86% of the population for fraction 1 found in 4 channels (channels 6–9), and 82% of the population for fraction 2 also found in 4 channels (channels 7–10).

Dissolution profiles for fractions 3 and 4 are presented in Fig. 2. Fraction 3, as anticipated, dissolved more rapidly than fraction 4. The dissolution profile for each fraction could be adequately described theoretically with K values of 2.0×10^{-9} and 1.7×10^{-9} cm²/sec for fractions 3 and 4, respectively. However, as with fractions 1 and 2 the K values from the experimental data are about four times larger than the theoretical value of 4.6×10^{-10} cm²/sec. It has been concluded from the previous data that the Higuchi–Hiestand model describes a relationship between particle size and dissolution rate but that the K values obtained were approximately four times the theoretical value.

DISCUSSION

It is noteworthy that the K values obtained from the dissolution profiles of four distinct narrow particle size distributions of prednisolone acetate are very similar. This finding suggests that particles ranging in average size from ~5–14 μm in diameter dissolve with one mechanism predominating. This is in keeping with the simulated data reported (7) in which it was demonstrated that a narrow distribution of drug particles, where the smallest and largest particles in the population were 2 and 20 μm in diameter, obeyed a single diffusional model. The suggestion that one mechanism predominates is further substantiated with the recognition that theory and the experimental data agree over the entire dissolution profile and not just during the initial portions of the profile.

Important to a test of this model is recognition that the shape of each experimental dissolution profile is very similar to the shape of the profile generated by the model. This observation suggests that the model is physically realistic.

While the experimental data and theory agree quite well, certain limitations must be recognized. A major finding of this study is that the theory cannot be used to predict actual dissolution profiles, since the calculated K value is ~3.5–4 times greater than the theoretical one. Part of the discrepancy may be related to the physical–chemical data used to calculate the theoretical value for K. In particular, the diffusion coefficient value is only approximate. Further, the particle size data are artificially put into discrete distribution form by the electronic counting device. The resulting histogram of particle sizes may not exactly represent the underlying distribution. However, the K value calculated in connection with Eq. 3 is dependent on the fraction of the total weight of particles in any particular channel.

As previously mentioned (2), the theory assumes that the particles are spheres, and a shape factor may account to some extent for the difference between the calculated and theoretical value for K. However, it is not expected that inclusion of a shape factor would correct for the magnitude of differences found in this study.

One other reason for the discrepancy may be related to a fundamental property of the diffusion-based model. The differential equation for the steady-state form of the model as previously used (1) is:

$$\frac{dm}{dt} = \frac{-D\Delta CA}{a} \qquad \text{(Eq. 4)}$$

where m is the weight of a solid particle, a is the particle radius at time t, and A is the area ($4\pi a^2$). Thus, one can see the similarity between this expression and the commonly used form of Fick's first law, with the particle radius, a, replacing h as the apparent diffusion layer thickness. If the value for the diffusion layer thickness was changed, albeit arbi-

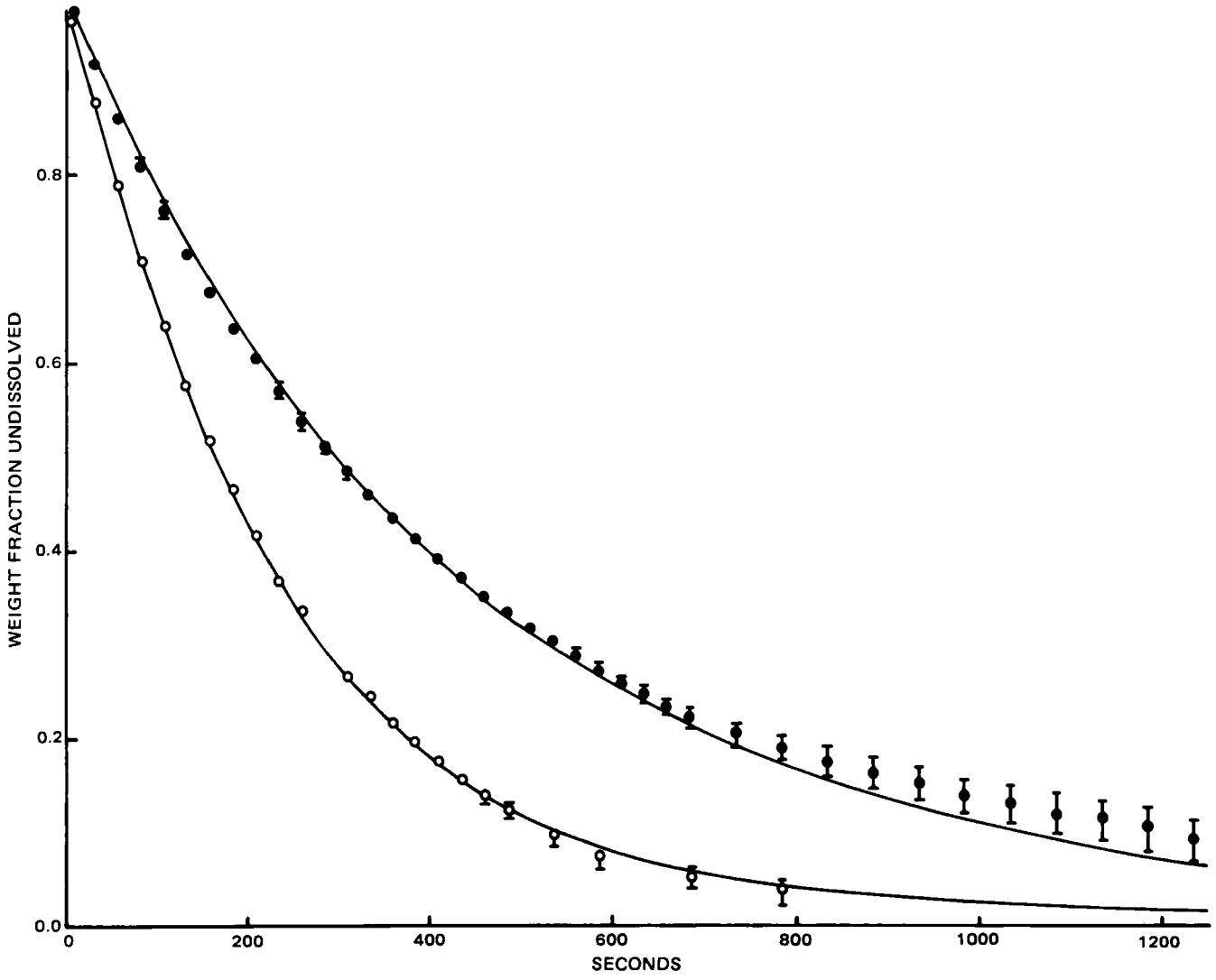

Figure 2—*Dissolution profiles for third and fourth prednisolone acetate fractions. Key: (○) experimental values for fraction 3, solid line calculated from theory with* $K = 2.0 \times 10^{-9}$ *cm²/sec; (●) experimental values for fraction 4, solid line calculated from theory with* $K = 1.7 \times 10^{-9}$ *cm²/sec.*

trarily, then the value for K calculated from the experimental data set could easily be rationalized. Unfortunately, an arbitrarily chosen proportionality constant does not provide any mechanistic insight.

The fact that the calculated value for K is greater than the theoretical one poses a question as to whether or not the diffusion layer thickness for small particles is a function of stirring. While this relationship is not predicted from convective diffusion theory for particles in the size range in this study (7), experimental verification of the actual hydrodynamic effects remains untested.

In summary, excellent correlation exists between a diffusion-based dissolution model and the experimental dissolution profiles for four narrow distributions of prednisolone acetate particles. It is noteworthy that the correlation exists over the entire dissolution profile. Similar rate constants, K, were used to fit the dissolution profile for each prednisolone acetate fraction, indicating a similar dissolution mechanism for each particle size distribution. The rate constants used to fit the experimental data are ~3–4 times greater than the theoretical rate constant calculated using independently determined or calculated values for the solute diffusion coefficient, solubility, and density.

REFERENCES

(1) W. Higuchi and E. Hiestand, *J. Pharm. Sci.*, **52,** 67 (1963).

(2) W. Higuchi, E. Rowe, and E. Hiestand, *ibid.*, **52,** 162 (1963).

(3) M. P. Short, W. P. Sharkey, and C. T. Rhodes, *Colloid Polym. Sci.*, **253,** 544 (1975).

(4) V. G. Levich, "Physicochemical Hydrodynamics," Prentice-Hall, Engelwood Cliffs, N.J., 1962, p. 87.

(5) S. Howard, J. Mauger, A. Khwangsopha, and P. Lee, *J. Pharm. Sci.*, **67,** 673 (1978).

(6) A. C. Shah, C. B. Pest, and J. F. Ocks, *ibid.*, **62,** 671 (1973).

(7) J. Mauger and S. Howard, *ibid.*, **65,** 1042 (1976).

High-Performance Liquid Chromatographic Assay for Partially Nitrated Glycerins in Nitroglycerin

DAVID M. BAASKE ˣ, NANCY N. KARNATZ, and JAMES E. CARTER *

Received December 18, 1981, from the *Analytical Development Group, Product Development Section, Pharmaceutical Development Department, Research and Development Division, American Critical Care, Division of American Hospital Supply Corporation, McGaw Park, IL 60085.* Accepted for publication March 17, 1982. * Present address: Drug Characterization, Ortho Pharmaceutical Corporation, Raritan, NJ 08869.

Abstract □ A high-performance liquid chromatographic method for determining the concentration of mononitroglycerins and dinitroglycerins in the commonly used pharmaceutical raw material nitroglycerin (10% w/w) on lactose USP is presented. A coefficient of variation of <5% for the partially nitrated glycerins was achieved over the range examined (0–4.0 μg/mg). Thirteen lots of raw material were examined and found to contain a total of <0.13% w/w partially nitrated glycerins. A variable wavelength detector (λ = 218 nm) and a microphenyl column were employed. The mobile phase was acetonitrile–water (36:64) pumped at 2 ml/min. The internal standard was isosorbide dinitrate. Total analysis time was 12 min.

Keyphrases □ High-performance liquid chromatography—assay for partially nitrated glycerins in nitroglycerin □ Nitroglycerin—high-performance liquid chromatographic assay for partially nitrated glycerins □ Glycerin—partially nitrated, high-performance liquid chromatographic assay for nitroglycerin

Nitroglycerin has been used orally and topically for many years for the treatment of angina pectoris. Recently, research has led to several new indications for nitroglycerin, all of which take advantage of the benefits of intravenous administration (1–3). The increase in the use of intravenous administration of nitroglycerin has prompted the FDA to seek additional data on the stability and purity of the raw materials used in the manufacture of drugs. To supply this data, a rapid and accurate assay for the partially nitrated glycerins (1,2-dinitroglycerin, 1,3-dinitroglycerin, 1-mononitroglycerin, and 2-mononitroglycerin) in nitroglycerin is needed.

BACKGROUND

Nitroglycerin is the triester of nitric acid and glycerol and is synthesized from glycerol and nitric acid using sulfuric acid as a catalyst. The addition of the nitro groups presumably proceeds in a stepwise manner. Metabolism and the nonexplosive chemical degradation occur by an opposite process—a stepwise loss of nitro groups. Partial completion of any of these processes would result in the contamination of nitroglycerin with partially nitrated glycerins (Scheme I).

Another potential source of partially nitrated glycerins in nitroglycerin is contamination. Most of the nitroglycerin made is intended for use as explosives. Pharmaceutical nitroglycerin is a small proportion of the production. Several explosive mixtures contain significant quantities of partially nitrated glycerins by design, and since they are made by the same manufacturer as the nitroglycerin intended for pharmaceutical use, the potential for cross contamination exists.

There are two widely used colorimetric methods for quantitating nitroglycerin which can be made stability indicating (4, 5). One is the basis for compendial monographs (4). However, the colorimetric methods and a published kinetic assay (6) do not allow the direct quantitation of partially nitrated glycerins.

Gas chromatographic (GC) and high-performance liquid chromatographic (HPLC) methods offer the potential to quantitate the partially nitrated glycerins in nitroglycerin. However, all GC methods require a tedious extraction into an organic phase (7–13), and only two have been employed for dosage-form types of solutions (7, 13), while the rest were designed for blood level assays. The HPLC methods are faster since they do not employ an extraction step (14–17). Of all the chromatographic methods only four demonstrate the potential quantitation of partially nitrated glycerins (12–15) and none specifically do so.

A sensitive HPLC method is described here that specifically allows the rapid direct quantitation of partially nitrated glycerins in nitroglycerin raw materials.

EXPERIMENTAL

Materials—Nitroglycerin[1] (10% w/w on lactose, USP) and isosorbide dinitrate[2] (25% w/w on lactose) were used as received. 1,2-Dinitroglycerin (10% w/w on lactose), 1,3-dinitroglycerin (10% w/w on lactose), 1-mononitroglycerin, and 2-mononitroglycerin were synthesized using literature methods (18). All standards were calibrated by the USP phenoldisulfonic acid assay for nitroglycerin (19). Glass-distilled acetonitrile and methanol were used for all procedures[3]. Purified water was further purified[4] prior to use.

Instrumentation—The liquid chromatographic system consisted of a solvent pumping system[5], an automatic fixed-loop sample injector[6], a variable wavelength detector[7], and a 10-mv recorder[8]. A 30 cm × 3.9-mm column packed with alkylphenyl-bonded silica gel[9] (10 μm), a detector wavelength of 218 nm (AUFS = 0.05), and a chart speed of 20 cm/hr were employed. Sample injections of 100 μl were used.

Mobile Phase—Approximately 1 liter of mobile phase was prepared fresh daily by thoroughly mixing 360 ml of acetonitrile and 640 ml of water. The mobile phase was always filtered through a 0.5-μm filter[4] prior to use. The mobile phase was pumped at a constant rate of 2 ml/min which yielded a pressure of <2000 psi.

Standard Curve—Stock standard solutions were prepared by transferring an accurately weighed sample of partially nitrated glycerin equivalent to 25 mg of active ingredient to a 50-ml volumetric flask. They were then dissolved in 5 ml of alcohol (USP) and brought to volume with water.

Working standard concentrations of ~20, 10, 5, and 2.5 μg/ml in both a mononitroglycerin and a dinitroglycerin were prepared from the stock standards by diluting in water 2-mononitroglycerin (or 1-mononitroglycerin) stock standard solution and 1,2-dinitroglycerin (or 1,3-dinitroglycerin) stock standard solution.

An accurately weighed sample of isosorbide dinitrate (25% w/w on lactose) of 500 mg was placed into a 250-ml volumetric flask, dissolved in 25 ml of alcohol and swirled for 5 min. It was brought to volume with water and mixed well. Ten milliliters of this solution was diluted to 100 ml to yield a final concentration of 50 μg/ml.

An accurately weighed sample of nitroglycerin (10% w/w on lactose), equivalent to 50 mg of active ingredient, was placed in a 100-ml volumetric flask, dissolved in 10 ml of alcohol, and brought to volume with water.

To 1.0 ml of each standard or sample was added 500 μl of isosorbide dinitrate (50 μg/ml) internal standard. Each solution was vortexed[10] for 5 sec and chromatographed. Peak heights for the partially nitrated glycerins and isosorbide dinitrate were measured manually. The peak areas were measured by a laboratory data system[11]. The peak area ratios

[1] ICI Americas, Wilmington, Del.
[2] Napp Chemicals, Inc., Lodi, N.J.
[3] Burdick and Jackson, Muskegon, Mich., or J. T. Baker, Phillipsburg, N.J.
[4] Millipore Corp., Bedford, Mass.
[5] System 2/2, Perkin-Elmer Corp., Norwalk, Conn.
[6] Model 420 Perkin-Elmer Corp., Norwalk, Conn.
[7] LC-55B, Perkin-Elmer Corp., Norwalk, Conn.
[8] Model 023, Perkin-Elmer Corp., Norwalk, Conn.
[9] μBondapak Phenyl, Waters Associates, Milford, Mass.
[10] Vortex Genie Mixer, American Scientific Products, McGaw Park, Ill.
[11] Model 3354, Hewlett-Packard Corp., Avondale, Pa.

0022-3549/83/0200-0194$01.00/0

$$\text{GLYCEROL} \underset{\text{metabolism or degradation}}{\overset{\text{syn}}{\rightleftharpoons}} \text{MONONITROGLYCERIN} \underset{\text{metabolism or degradation}}{\overset{\text{syn}}{\rightleftharpoons}} \text{DINITROGLYCERIN} \underset{\text{metabolism or degradation}}{\overset{\text{syn}}{\rightleftharpoons}} \text{TRINITROGLYCERIN}$$

Scheme I

were then plotted *versus* concentration to yield a calibration curve. Identical results were obtained using peak height ratios.

RESULTS AND DISCUSSION

The direct quantitation of the partially nitrated glycerins in nitroglycerin (10% w/w on lactose) is reported for the first time. It is based on a modification of an HPLC procedure for nitroglycerin which has been used successfully for over 3 years on almost 10,000 samples (14). Alcohol has been used to speed the dissolution of the various nitrates but is not required.

This procedure does not resolve the dinitroglycerins from one another, nor does it resolve the mononitroglycerins from one another. For the purpose of quantitating partially nitrated glycerins in nitroglycerin raw material the resolution of the isomers is unnecessary. It was demonstrated that not only do the pairs of isomers coelute, but they yield superimposable calibration lines. Thus, it is simpler and more practical to quantitate the isomers employing only one mononitroglycerin and one dinitroglycerin standard. Chromatograms illustrating the obtainable separations are shown in Fig. 1.

The described procedure, using 1 ml of sample or standard and 0.5 ml of internal standard, allows an accurate assay of partially nitrated glycerins over the concentration range commonly encountered in nitroglycerin raw materials (0.0–4.0 μg/mg). It is possible to detect the partially nitrated glycerins down to a level of 0.02 μg/mg by using the maximum detector sensitivity of AUFS 0.002. Even greater sensitivities are theoretically achievable using greater sample sizes or an extraction, but were not required for this study.

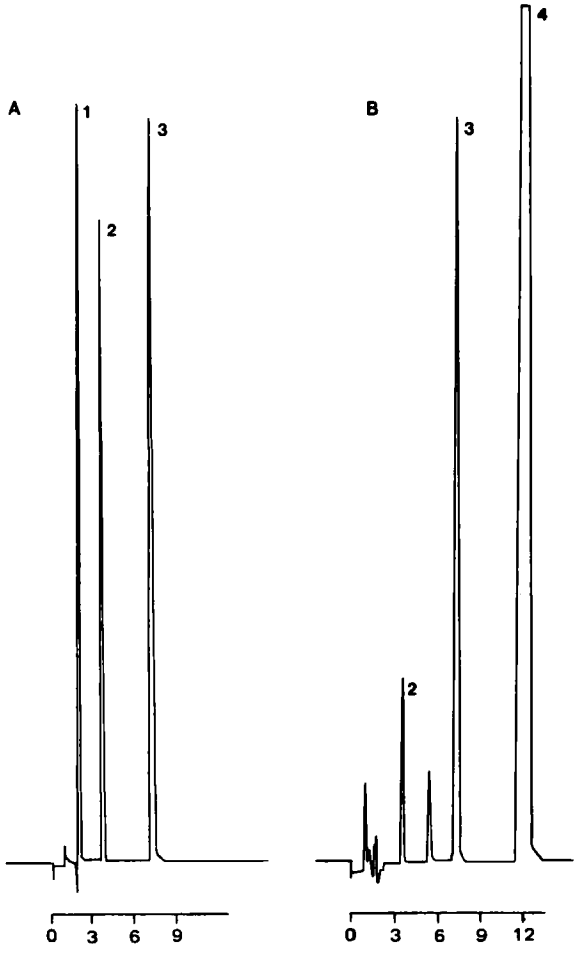

Figure 1—*A—Typical chromatogram of a partially nitrated glycerin standard. Combined partially nitrated glycerin concentration equal to ~0.6% w/w in raw material. Key: (1) mononitroglycerins peak of 14.15 μg/ml; (2) dinitroglycerins peak of 16.40 μg/ml; (3) isosorbide dinitrate. B—Typical chromatogram of a nitroglycerin on lactose raw material sample. No mononitroglycerins detected. Key: (2) dinitroglycerins peak of ~0.1% w/w in raw material; (3) isosorbide dinitrate; (4) trinitroglycerin.*

Table I—Levels of Partially Nitrated Glycerins [a]

Lot	Mononitroglycerins, % w/w in Sample [b]	Dinitroglycerins, % w/w in Sample
A		0.12
B	0	0.10
C	0	0.10
D	0	0.11
E	0	0.11
F	0	0.08
G	0	0.09
H	0	0.09
I	0	0.08
J	0	0.08
K	0	0.07
L	0	0.09
M	0	0.09

[a] Thirteen lots of nitroglycerin (10% w/w on lactose), raw material in percent. [b] 0 = < 0.001%.

Accuracy and Precision—Four replicate, partially nitrated glycerin standards (20, 10, 5, and 2.5 μg/ml) were chromatographed. A correlation coefficient of >0.99 was consistently obtained for both partially nitrated glycerins, as was a coefficient of variation of <3% for the dinitroglycerins and 5% for the mononitroglycerins. Finally, accuracy for the mono- and dinitroglycerins of >95 and 98%, respectively, were found.

Applicability—The method has been applied to nitroglycerin in alcohol, nitroglycerin in propylene glycol (USP), and nitroglycerin (10% w/w on lactose). The practicality of the method was demonstrated by the analysis of 13 lots of nitroglycerin triturate (Table I). In all instances the level of mononitroglycerins was zero. Under the conditions of the experiment this was equivalent to <0.05 μg/ml in the assay solution or 0.001% w/w in the raw material. The dinitroglycerins were present at levels of <0.15% (w/w) in all samples, even after storage at room temperature for 4 years.

REFERENCES

(1) J. B. Stetson, *Int. Anesthesiol. Clin.*, **16**, 261 (1978).

(2) J. R. Parratt, *J. Pharm. Pharmacol.*, **31**, 801 (1979).

(3) N. S. Hill, E. M. Antman, L. H. Green, and J. S. Alpert, *Chest*, **79**, 69 (1981).

(4) J. R. Hohman and J. Levine, *J. Assoc. Off. Anal. Chem.*, **47**, 471 (1964).

(5) F. K. Bell, *J. Pharm. Sci.*, **53**, 752 (1964).

(6) H.-L. Fung, P. Dalecki, E. Tse, and C. T. Rhodes, *ibid.*, **62**, 696 (1973).

(7) J. K. Sturek, T. D. Sokoloski, W. T. Winsley, and P. E. Stach, *Am. J. Hosp. Pharm.*, **35**, 537 (1978).

(8) Y. Givant and F. G. Sulman, *Experientia*, **34**, 643 (1978).

(9) P. W. Armstrong, J. A. Armstrong, and G. S. Marks, *Circulation*, **59**, 585 (1979).

(10) J. Y. Wei and P. R. Reid, *ibid.*, **59**, 588 (1979).

(11) P.-H. Yuen, S. L. Denman, T. D. Sokoloski, and A. M. Burkman, *J. Pharm. Sci.*, **68**, 1163 (1979).

(12) M. T. Rosseel and M. G. Bogaert, *ibid.*, **62**, 754 (1973).

(13) P. S. K. Yap, E. F. McNiff, and H.-L. Fung, *ibid.*, **67**, 582 (1978).

(14) D. M. Baaske, J. E. Carter, and A. H. Amann, *ibid.*, **68**, 481 (1979).

(15) W. G. Crouthamel and B. Dorsch, *ibid.*, **68**, 237 (1979).

(16) L. Gelber, *ibid.*, **69**, 1084 (1980).

(17) T. D. Sokoloski, C.-C. Wu, and M. Burkman, *Int. J. Pharm.*, **6**, 63 (1980).

(18) I. Dunstan, J. V. Griffiths, and S. A. Harvey, *J. Chem. Soc.*, **1965**, 1319.

(19) "The United States Pharmacopeia XX, The National Formulary XV," U.S. Pharmacopeial Convention, Inc., Rockville, Md., 1980, p. 552.

ACKNOWLEDGMENTS

The authors wish to thank Dr. David M. Stout for the synthesis of the dinitroglycerins and Ms. Martine Bunting for assistance in the preparation of this manuscript.

Simultaneous Determination of Acetaminophen, Guaifenesin, Pseudoephedrine, Pholcodine, and Paraben Preservatives in Cough Mixture by High-Performance Liquid Chromatography

LAURA CARNEVALE

Received August 3, 1981, from the *Quality Control Department, Fisons Pty. Ltd., Sydney, Australia.* Accepted for publication March 25, 1982.

Abstract □ The separation and simultaneous determination, by high-performance liquid chromatography, of acetaminophen (I), guaifenesin (II), pseudoephedrine hydrochloride (III), and pholcodine (IV), together with a series of parabens (methyl to butyl, V–VIII) in a cough mixture, has been demonstrated using a chemically bonded octadecylsilane stationary phase with a mobile phase of methanol–water–acetic acid (45:55:2) containing the ion-pairing agent octanesulfonic acid. Retention volumes for the active ingredients were 3.8 ml, 5.4 ml, 9.4 ml, and 15.6 ml for compounds I–IV, respectively. Corrected retention volumes for the parabens [5.4 ml for methyl (V), 9.6 ml for ethyl (VI), 18.5 ml for propyl (VII), and 37.9 ml for butyl (VIII)] showed an exponential relationship with chain length of the esterifying alcohols. Excipients did not interfere with the estimation of any of the compounds, hence pretreatment of the sample was unnecessary. Average recoveries of the active ingredients and of the parabens from laboratory prepared samples were essentially 100% of theoretical with standard deviations of 1.7, 0.3, 1.5, 0.3, 0.3, 3.3, 0.7, and 2.7% for I–VIII, respectively.

Keyphrases □ Acetaminophen—simultaneous determination of guaifenesin, pseudoephedrine, pholcodine, and paraben preservatives in cough mixture by high-performance liquid chromatography □ Pseudoephedrine—simultaneous determination of acetaminophen, guaifenesin, pholcodine, and paraben in preservatives in cough mixture by high-performance liquid chromatography □ Paraben—simultaneous determination of acetaminophen, guaifenesin, pseudoephedrine, and pholcodine in preservatives in cough mixture by high-performance liquid chromatography □ High-performance liquid chromatography—simultaneous determination of acetaminophen, guaifenesin, pseudoephedrine, pholcodine, and paraben preservatives in cough mixture

High-performance liquid chromatography (HPLC) has become a powerful tool for the analysis of pharmaceutical products. Mixtures used for the treatment of coughs and colds may be complexes containing several active ingredients including a decongestant, an antihistamine, frequently an analgesic, preservatives, dyes, and flavors. The active materials cover a range of structures with widely varying polarities and include both acidic and basic compounds.

A number of conventional methods have been applied to the present series. Pholcodine has been estimated by UV spectrophotometry following separation by TLC and colorimetry (1, 2). Pseudoephedrine and acetaminophen have been determined spectrophotometrically (3, 4) and by GLC (5, 6). Guaifenesin has been determined in pharmaceutical preparations by GLC (7, 8). The parabens may be assayed by GLC (9) or by UV spectroscopy following sample clean-up by column chromatography (10).

Spectrophotometric, GLC, or methods requiring TLC separation when applied to samples such as cough mixtures can be lengthy and/or subject to interferences by the matrix of the sample, and they are generally not suitable for simultaneous assay. The simultaneous assay of the drugs and preservatives described in this report cannot be achieved by any of the techniques mentioned here.

The application of HPLC procedures to various combinations of drugs and parabens has been reported (11–19), and some attention has been given to the effect of carbon chain length of the alkylsulfonic acid ion-pairing agents on retention times of several drugs (20, 21). The effect of chain length on resolution of mixtures of materials with varying polarity was tested, and a procedure was developed by which eight components, four active materials and four preservatives, may be determined with one injection.

EXPERIMENTAL

Materials—All active ingredients and paraben preservatives were of BP quality except guaifenesin which conformed to BPC standard. All were used without further purification.

Mobile Phase—The mobile phase, methanol[1]–water–glacial acetic acid (45:55:2) containing 0.005 *M* octanesulfonic acid[2], was filtered through a 0.45-μm filter[3]. The flow rate was 2.5 ml/min.

Instrumentation—The liquid chromatograph consisted of a constant flow pump[4], a low-pressure injector[5], a dual channel absorbance detector[6] set at 254 and 280 nm, and a 30-cm × 4-mm i.d. octadecylsilane column[7]. Outputs from the 280-[8] and 254-nm[9] channels were quantitated. Separate monitoring at 254 nm was required for pseudoephedrine which is not detected on the 280-nm channel.

Standard Solutions—The stock solution of analytes in methanol contained 25.00, 5.00, 5.00, 0.75, 0.61, 0.20, 0.33, and 0.20 mg/ml of I–VIII, respectively. Aliquots (2, 3, 4, 5, 6, and 7 ml) of this solution were diluted to 100 ml with water and filtered through a 0.45-μm filter[10]. A calibration

[1] Methanol BDH, redistilled in glass.
[2] PIC B8, Waters Associates, Milford, Mass.
[3] Millipore Type FH organic.
[4] Model 6000A, Waters Associates, Milford, Mass.
[5] Model U6K, Waters Associates, Milford, Mass.
[6] Model 440, Waters Associates, Milford, Mass.
[7] μ-Bondapak C-18, Waters Associates, Milford, Mass.
[8] Data Module, Waters Associates, Milford, Mass.
[9] Varian CDS III integrator.
[10] Millipore Type HA aqueous.

0022-3549/83/0200-0196$01.00/0

(18) I. Dunstan, J. V. Griffiths, and S. A. Harvey, *J. Chem. Soc.*, **1965**, 1319.

(19) "The United States Pharmacopeia XX, The National Formulary XV," U.S. Pharmacopeial Convention, Inc., Rockville, Md., 1980, p. 552.

ACKNOWLEDGMENTS

The authors wish to thank Dr. David M. Stout for the synthesis of the dinitroglycerins and Ms. Martine Bunting for assistance in the preparation of this manuscript.

Simultaneous Determination of Acetaminophen, Guaifenesin, Pseudoephedrine, Pholcodine, and Paraben Preservatives in Cough Mixture by High-Performance Liquid Chromatography

LAURA CARNEVALE

Received August 3, 1981, from the *Quality Control Department, Fisons Pty. Ltd., Sydney, Australia.* Accepted for publication March 25, 1982.

Abstract □ The separation and simultaneous determination, by high-performance liquid chromatography, of acetaminophen (I), guaifenesin (II), pseudoephedrine hydrochloride (III), and pholcodine (IV), together with a series of parabens (methyl to butyl, V–VIII) in a cough mixture, has been demonstrated using a chemically bonded octadecylsilane stationary phase with a mobile phase of methanol–water–acetic acid (45:55:2) containing the ion-pairing agent octanesulfonic acid. Retention volumes for the active ingredients were 3.8 ml, 5.4 ml, 9.4 ml, and 15.6 ml for compounds I–IV, respectively. Corrected retention volumes for the parabens [5.4 ml for methyl (V), 9.6 ml for ethyl (VI), 18.5 ml for propyl (VII), and 37.9 ml for butyl (VIII)] showed an exponential relationship with chain length of the esterifying alcohols. Excipients did not interfere with the estimation of any of the compounds, hence pretreatment of the sample was unnecessary. Average recoveries of the active ingredients and of the parabens from laboratory prepared samples were essentially 100% of theoretical with standard deviations of 1.7, 0.3, 1.5, 0.3, 0.3, 3.3, 0.7, and 2.7% for I–VIII, respectively.

Keyphrases □ Acetaminophen—simultaneous determination of guaifenesin, pseudoephedrine, pholcodine, and paraben preservatives in cough mixture by high-performance liquid chromatography □ Pseudoephedrine—simultaneous determination of acetaminophen, guaifenesin, pholcodine, and paraben in preservatives in cough mixture by high-performance liquid chromatography □ Paraben—simultaneous determination of acetaminophen, guaifenesin, pseudoephedrine, and pholcodine in preservatives in cough mixture by high-performance liquid chromatography □ High-performance liquid chromatography—simultaneous determination of acetaminophen, guaifenesin, pseudoephedrine, pholcodine, and paraben preservatives in cough mixture

High-performance liquid chromatography (HPLC) has become a powerful tool for the analysis of pharmaceutical products. Mixtures used for the treatment of coughs and colds may be complexes containing several active ingredients including a decongestant, an antihistamine, frequently an analgesic, preservatives, dyes, and flavors. The active materials cover a range of structures with widely varying polarities and include both acidic and basic compounds.

A number of conventional methods have been applied to the present series. Pholcodine has been estimated by UV spectrophotometry following separation by TLC and colorimetry (1, 2). Pseudoephedrine and acetaminophen have been determined spectrophotometrically (3, 4) and by GLC (5, 6). Guaifenesin has been determined in pharmaceutical preparations by GLC (7, 8). The parabens may be assayed by GLC (9) or by UV spectroscopy following sample clean-up by column chromatography (10).

Spectrophotometric, GLC, or methods requiring TLC separation when applied to samples such as cough mixtures can be lengthy and/or subject to interferences by the matrix of the sample, and they are generally not suitable for simultaneous assay. The simultaneous assay of the drugs and preservatives described in this report cannot be achieved by any of the techniques mentioned here.

The application of HPLC procedures to various combinations of drugs and parabens has been reported (11–19), and some attention has been given to the effect of carbon chain length of the alkylsulfonic acid ion-pairing agents on retention times of several drugs (20, 21). The effect of chain length on resolution of mixtures of materials with varying polarity was tested, and a procedure was developed by which eight components, four active materials and four preservatives, may be determined with one injection.

EXPERIMENTAL

Materials—All active ingredients and paraben preservatives were of BP quality except guaifenesin which conformed to BPC standard. All were used without further purification.

Mobile Phase—The mobile phase, methanol[1]–water–glacial acetic acid (45:55:2) containing 0.005 *M* octanesulfonic acid[2], was filtered through a 0.45-μm filter[3]. The flow rate was 2.5 ml/min.

Instrumentation—The liquid chromatograph consisted of a constant flow pump[4], a low-pressure injector[5], a dual channel absorbance detector[6] set at 254 and 280 nm, and a 30-cm × 4-mm i.d. octadecylsilane column[7]. Outputs from the 280-[8] and 254-nm[9] channels were quantitated. Separate monitoring at 254 nm was required for pseudoephedrine which is not detected on the 280-nm channel.

Standard Solutions—The stock solution of analytes in methanol contained 25.00, 5.00, 5.00, 0.75, 0.61, 0.20, 0.33, and 0.20 mg/ml of I–VIII, respectively. Aliquots (2, 3, 4, 5, 6, and 7 ml) of this solution were diluted to 100 ml with water and filtered through a 0.45-μm filter[10]. A calibration

[1] Methanol BDH, redistilled in glass.
[2] PIC B8, Waters Associates, Milford, Mass.
[3] Millipore Type FH organic.
[4] Model 6000A, Waters Associates, Milford, Mass.
[5] Model U6K, Waters Associates, Milford, Mass.
[6] Model 440, Waters Associates, Milford, Mass.
[7] μ-Bondapak C-18, Waters Associates, Milford, Mass.
[8] Data Module, Waters Associates, Milford, Mass.
[9] Varian CDS III integrator.
[10] Millipore Type HA aqueous.

0022-3549/83/0200-0196$01.00/0

Table I—Percent Recovery of Compounds I–IV from Prepared Mixtures

Amount added as Percent of Theoretical	Acetaminophen (I)	Guaifenesin (II)	Pseudoephedrine Hydrochloride (III)	Pholcodine (IV)
80	103.8	98.5	96.4	100.0
100	99.7	98.5	98.7	99.3
120	100.9	99.1	99.9	99.9
Mean	101.5	98.7	98.3	99.7
SD	2.1	0.3	1.8	0.4

curve for each compound was prepared from triplicate, 20-μl injections of these solutions.

Quantitation of the Actives and Preservatives in Synthetic and Commercial Cough Mixtures—For the determination of recoveries, small laboratory batches of a cough mixture were prepared containing 80, 100, and 120% of the theoretical amount of each of the active ingredients and the four parabens: 500.0, 100.0, 30.0, 15.0, 13.4, 4.0, 6.6, and 4.0 mg of I–VIII/20 ml, respectively.

A control sample containing all ingredients except the actives and parabens was also prepared. Sample analysis was carried out by diluting 5–100 ml with water and filtering through a 0.45-μm filter.

Duplicate, 20-μl injections were made of each filtered sample solution and the results were calculated by reference to a standard containing the theoretical sample concentration. The response of the standard was determined by making four replicate injections, two before and two after the samples were run.

Commercial mixtures were assayed by diluting 5–100 ml with water, filtering with a 0.45-μm filter, and injecting 20 μl. The results were calculated by reference to a single standard containing the theoretical sample level of actives and preservatives.

RESULTS

A typical chromatogram from a cough syrup prepared with the four actives and the four preservatives is shown in Fig. 1. Detector response was linear for all eight compounds between 40 and 140% of the theoretical sample level. Deviations of points from linearity for compounds I–VIII were ≤3.9%.

Preparation of the control sample (*i.e.*, without I–VIII) permitted checking on the possibility of the presence of interfering peaks. The results of the recoveries, shown in Tables I and II, indicate satisfactory

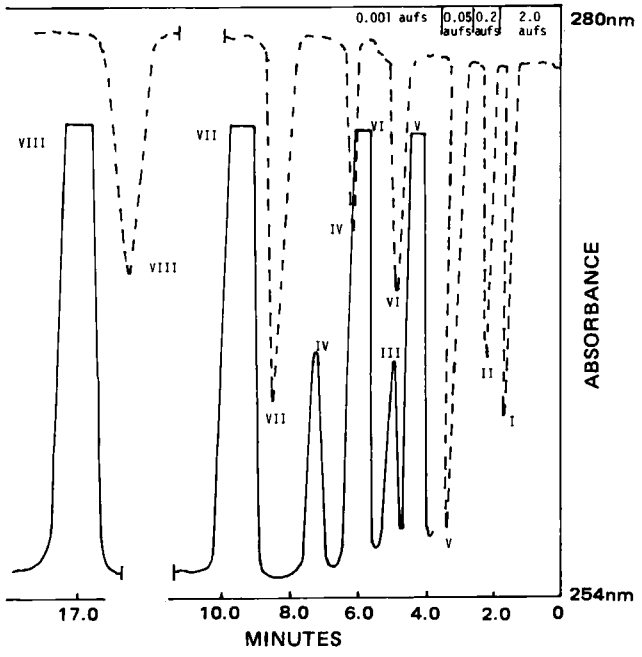

Figure 1—*High-performance liquid chromatogram of a cough preparation. Peaks I–VIII are acetaminophen, guaifenesin, pseudoephedrine hydrochloride, pholcodine, methyl–butyl paraben, respectively.*

Table II—Percent Recovery of Compounds V–VIII from Prepared Mixtures

Amount added as Percent of Theoretical	Methyl Paraben (V)	Ethyl Paraben (VI)	Propyl Paraben (VII)	Butyl Paraben (VIII)
80	99.3	103.1	99.4	105.0
100	99.3	98.0	100.2	100.0
120	99.9	104.2	98.5	104.2
Mean	99.5	101.8	99.4	103.1
SD	0.3	3.3	0.9	2.7

method precision and accuracy, the highest standard deviation for the recovery of any one compound being 3.3% and the average recoveries for all eight compounds lying within the range of 98.3–103.1%.

A result emerging coincidentally from this work was the determination of the structure–retention volume relationship for the parabens. A plot of corrected retention volume *versus* chain length of the esterifying alcohol shows the exponential type relationship which reduces to a semilog linear plot (Fig. 2).

The overall accuracy was evaluated by making a single injection of each of nine commercial preparations of known composition and calculating the results by comparison with nine replicate injections of a single standard solution (Table III).

DISCUSSION

The simultaneous analysis of this group of compounds presented several problems. The difference in polarity between I and VIII rendered separation of I–VI difficult, if VII and VIII were to be eluted within a reasonable time. The large differences in detector response and concentration between acetaminophen and the other components restricted the amount of sample that could be injected without overloading the detector on both channels. Even at the concentration described, maximum absorbance of acetaminophen on the 280-nm channel approaches 2.0. However, this concentration was necessary in order to obtain quantifiable peaks for pseudoephedrine and pholcodine. Difficulties were encountered because there were three classes of compounds [acidic (I), basic (III, IV) and nonpolar (II, V–VIII)] undergoing analysis simultaneously. Ideally, two types of chromatography would be required to achieve the desired separation: reverse-phase with ion-pairing reagents for acidic and basic compounds and ordinary reverse-phase for nonpolar compounds. An alkylsulfonic acid was added to the mobile phase to obtain retention and separation of the two basic compounds (III and IV) present in the mixture. The acetaminophen elutes close to the solvent front but does not suffer from interference by coeluting impurities from the sample matrix.

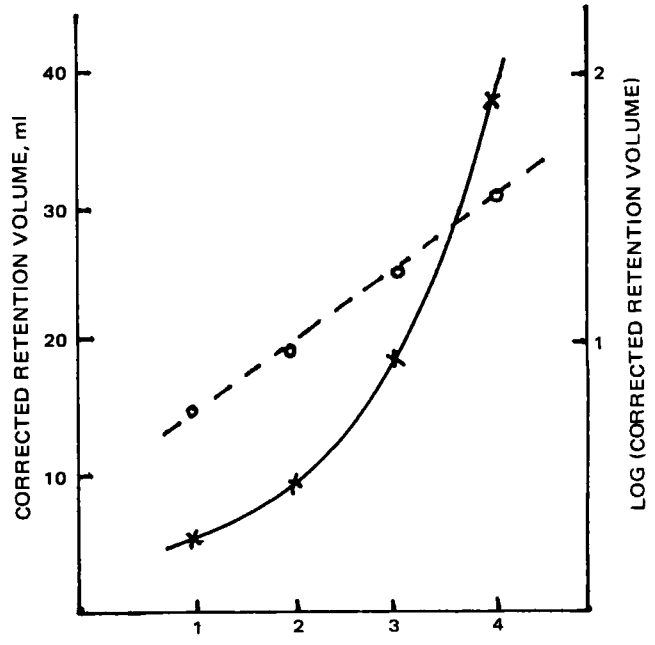

Figure 2—*Carbon chain length of esterifying alcohol of parabens.*

Table III—Typical Assay Results of Commercial Preparations

Sample[a]	Acetaminophen (I)	Guaifenesin (II)	Pseudoephedrine Hydrochloride (III)	Pholcodine (IV)	Methyl Paraben (VI)	Propyl Paraben (VII)
1	100.0	100.1	100.3	100.0	101.5	101.2
2	102.4	98.8	99.2	98.3	100.0	101.8
3	98.9	98.5	101.0	99.5	100.5	97.3
4	100.0	97.0	98.2	101.1	97.7	98.5
Mean Recovery[b]	100.6	98.1	100.0	100.6	99.2	99.9
SD[c]	1.5	1.6	1.5	2.3	1.8	2.1

[a] Recoveries expressed as percent of theoretical. [b] Calculated from nine replicates. [c] Standard deviations of a single determination calculated from nine replicates.

Initially hexanesulfonic acid[11] was chosen with a water–methanol ratio of 70:30, but this resulted not only in a long retention time for VIII, as its retention is not dependent on the ion-pairing agent, but also gave a poor separation of III and V. By using octanesulfonic acid as the ion-pairing agent and changing the water–methanol–acetic acid ratio of the mobile phase to 55:45:2, a satisfactory separation was achieved. Addition of acetic acid reduced tailing of III and peak broadening of IV.

The analytical results demonstrate the ability of ion-pair reverse-phase HPLC to simultaneously assay four actives and four paraben preservatives. A particular advantage of the method is the minimum time required for sample preparation and analysis of the complete separation requiring only 18 min. The method has been successfully used on a routine basis for over 6 months. Special column clean-up procedures have not been required during this time and no significant loss of column performance has been observed.

REFERENCES

(1) H. Wullen and E. Stainer, *J. Pharm. Belg.*, **21**, 505 (1966).

(2) J. S. Shohet, *J. Pharm. Sci.*, **64**, 1011 (1975).

(3) J. Wallace, *Anal. Chem.*, **39**, 531 (1967).

(4) S. F. Belal, M. Abdel-Hady Elsayed, A. Elwalily, and H. Abdine, *Analyst*, **104**, 919 (1979).

(5) A. H. Beckett and G. R. Wilkinson, *J. Pharm. Pharmacol. Suppl.*, **17**, 104S (1965).

(6) F. M. Plakogiannis and A. M. Saad, *J. Pharm. Sci.*, **66**, 604 (1977).

(7) J. Hudanick, *ibid.*, **59**, 238 (1970).

(8) E. Mario and L. G. Meehan, *ibid.*, **59**, 538 (1970).

(9) J. L. Lach and J. S. Sawardeker, *ibid.*, **54**, 424 (1965).

(10) M. Batchelder, H. I. Tarlin, and G. Williamson, *ibid.*, **61**, 252 (1972).

(11) V. Das Gupta, *ibid.*, **69**, 110 (1980).

(12) D. R. Heidemann, *ibid.*, **68**, 530 (1979).

(13) H. Y. Mohammed and F. F. Cantwell, *Anal. Chem.*, **50**, 491 (1978).

(14) M. K. Chao, I. J. Holcomb, and S. A. Fusari, *J. Pharm. Sci.*, **68**, 1463 (1979).

(15) W. O. McSharry and I. V. E. Savage, *ibid.*, **69**, 212 (1980).

(16) A. Yacobi, Z. M. Look, and C. Lai, *ibid.*, **67**, 1668 (1978).

(17) K. L. Austin and L. E. Mather, *ibid.*, **67**, 1510 (1978).

(18) F. F. Cantwell, *Anal. Chem.*, **48**, 1854 (1976).

(19) F. A. Fitzpatrick, A. F. Summa, and A. D. Cooper, *J. Soc. Cosmet. Chem.*, **26**, 377 (1975).

(20) T. R. Koziol, J. T. Jacob, and R. G. Achari, *J. Pharm. Sci.*, **68**, 1135 (1979).

(21) E. J. Kubiac and J. W. Munson, *ibid.*, **69**, 152 (1980).

[11] PIC B6, Waters Associates, Milford, Mass.

ACKNOWLEDGMENTS

The author thanks Mr. Alan Wright for many useful discussions and Fisons Pty. Ltd., for granting permission to publish this manuscript.

Synthesis and Pharmacological Activity of Benzo[*b*]thiophene-3-carboxylic Acid Derivatives

A. SHAFIEE * ×, M. A. HEDAYATI *, M. M. SALIMI ‡, and S. M. FAGHIHI ‡

Received December 7, 1981, from the **Department of Chemistry, College of Pharmacy* and the ‡*Department of Animal Physiology and Pharmacology, School of Veterinary Medicine, Tehran University, Tehran, Iran.* Accepted for publication March 31, 1982.

Abstract □ Several dialkylaminoethyl benzo[*b*]thiophene-3-carboxylates, *N*-(2-dialkylaminoethyl)benzo[*b*]thiophene-3-carboxamides, 2-dialkylaminoethyl benzo[*b*]thiophene-3-carbamates, and substituted ureas with benzo[*b*]thiophene moiety, were prepared and tested for local anesthetic, anticholinergic, and antihistaminic activities. Several of the compounds showed significant activity

Keyphrases □ Benzo[*b*]thiophene-3-carboxylic acid derivatives—synthesis and pharmacological activity, local anesthetic, anticholinergic, and antihistaminic activity □ Anesthetics, local—synthesis and pharmacological activity of benzo[*b*]thiophene-3-carboxylic acid derivatives □ Anticholinergics—synthesis and pharmacological activity of benzo[*b*]thiophene-3-carboxylic acid derivatives □ Antihistamines—synthesis and pharmacological activity of benzo[*b*]thiophene-3-carboxylic acid derivatives

Many of the clinically active local anesthetics are dialkylaminoalkyl esters and dialkylaminoalkylamides of carboxylic acids (1). Some dialkylaminoalkylesters of 2- or 3-benzo[*b*]thiophenecarboxylic acid have been reported to have hypotensive, antiviral, and antifungal activities (2), as have some benzo[*b*]thiophene-2-carboxamides (3). It

0022-3549/83/0200-0198$01.00/0

Table III—Typical Assay Results of Commercial Preparations

Sample[a]	Acetaminophen (I)	Guaifenesin (II)	Pseudoephedrine Hydrochloride (III)	Pholcodine (IV)	Methyl Paraben (VI)	Propyl Paraben (VII)
1	100.0	100.1	100.3	100.0	101.5	101.2
2	102.4	98.8	99.2	98.3	100.0	101.8
3	98.9	98.5	101.0	99.5	100.5	97.3
4	100.0	97.0	98.2	101.1	97.7	98.5
Mean Recovery[b]	100.6	98.1	100.0	100.6	99.2	99.9
SD[c]	1.5	1.6	1.5	2.3	1.8	2.1

[a] Recoveries expressed as percent of theoretical. [b] Calculated from nine replicates. [c] Standard deviations of a single determination calculated from nine replicates.

Initially hexanesulfonic acid[11] was chosen with a water–methanol ratio of 70:30, but this resulted not only in a long retention time for VIII, as its retention is not dependent on the ion-pairing agent, but also gave a poor separation of III and V. By using octanesulfonic acid as the ion-pairing agent and changing the water–methanol–acetic acid ratio of the mobile phase to 55:45:2, a satisfactory separation was achieved. Addition of acetic acid reduced tailing of III and peak broadening of IV.

The analytical results demonstrate the ability of ion-pair reverse-phase HPLC to simultaneously assay four actives and four paraben preservatives. A particular advantage of the method is the minimum time required for sample preparation and analysis of the complete separation requiring only 18 min. The method has been successfully used on a routine basis for over 6 months. Special column clean-up procedures have not been required during this time and no significant loss of column performance has been observed.

REFERENCES

(1) H. Wullen and E. Stainer, *J. Pharm. Belg.*, **21**, 505 (1966).

(2) J. S. Shohet, *J. Pharm. Sci.*, **64**, 1011 (1975).

(3) J. Wallace, *Anal. Chem.*, **39**, 531 (1967).

(4) S. F. Belal, M. Abdel-Hady Elsayed, A. Elwalily, and H. Abdine, *Analyst*, **104**, 919 (1979).

(5) A. H. Beckett and G. R. Wilkinson, *J. Pharm. Pharmacol. Suppl.*, **17**, 104S (1965).

(6) F. M. Plakogiannis and A. M. Saad, *J. Pharm. Sci.*, **66**, 604 (1977).

(7) J. Hudanick, *ibid.*, **59**, 238 (1970).

(8) E. Mario and L. G. Meehan, *ibid.*, **59**, 538 (1970).

(9) J. L. Lach and J. S. Sawardeker, *ibid.*, **54**, 424 (1965).

(10) M. Batchelder, H. I. Tarlin, and G. Williamson, *ibid.*, **61**, 252 (1972).

(11) V. Das Gupta, *ibid.*, **69**, 110 (1980).

(12) D. R. Heidemann, *ibid.*, **68**, 530 (1979).

(13) H. Y. Mohammed and F. F. Cantwell, *Anal. Chem.*, **50**, 491 (1978).

(14) M. K. Chao, I. J. Holcomb, and S. A. Fusari, *J. Pharm. Sci.*, **68**, 1463 (1979).

(15) W. O. McSharry and I. V. E. Savage, *ibid.*, **69**, 212 (1980).

(16) A. Yacobi, Z. M. Look, and C. Lai, *ibid.*, **67**, 1668 (1978).

(17) K. L. Austin and L. E. Mather, *ibid.*, **67**, 1510 (1978).

(18) F. F. Cantwell, *Anal. Chem.*, **48**, 1854 (1976).

(19) F. A. Fitzpatrick, A. F. Summa, and A. D. Cooper, *J. Soc. Cosmet. Chem.*, **26**, 377 (1975).

(20) T. R. Koziol, J. T. Jacob, and R. G. Achari, *J. Pharm. Sci.*, **68**, 1135 (1979).

(21) E. J. Kubiac and J. W. Munson, *ibid.*, **69**, 152 (1980).

[11] PIC B6, Waters Associates, Milford, Mass.

ACKNOWLEDGMENTS

The author thanks Mr. Alan Wright for many useful discussions and Fisons Pty. Ltd., for granting permission to publish this manuscript.

Synthesis and Pharmacological Activity of Benzo[*b*]thiophene-3-carboxylic Acid Derivatives

A. SHAFIEE * ×, M. A. HEDAYATI *, M. M. SALIMI ‡, and S. M. FAGHIHI ‡

Received December 7, 1981, from the **Department of Chemistry, College of Pharmacy* and the ‡*Department of Animal Physiology and Pharmacology, School of Veterinary Medicine, Tehran University, Tehran, Iran.* Accepted for publication March 31, 1982.

Abstract □ Several dialkylaminoethyl benzo[*b*]thiophene-3-carboxylates, *N*-(2-dialkylaminoethyl)benzo[*b*]thiophene-3-carboxamides, 2-dialkylaminoethyl benzo[*b*]thiophene-3-carbamates, and substituted ureas with benzo[*b*]thiophene moiety, were prepared and tested for local anesthetic, anticholinergic, and antihistaminic activities. Several of the compounds showed significant activity

Keyphrases □ Benzo[*b*]thiophene-3-carboxylic acid derivatives—synthesis and pharmacological activity, local anesthetic, anticholinergic, and antihistaminic activity □ Anesthetics, local—synthesis and pharmacological activity of benzo[*b*]thiophene-3-carboxylic acid derivatives □ Anticholinergics—synthesis and pharmacological activity of benzo[*b*]thiophene-3-carboxylic acid derivatives □ Antihistamines—synthesis and pharmacological activity of benzo[*b*]thiophene-3-carboxylic acid derivatives

Many of the clinically active local anesthetics are dialkylaminoalkyl esters and dialkylaminoalkylamides of carboxylic acids (1). Some dialkylaminoalkylesters of 2- or 3-benzo[*b*]thiophenecarboxylic acid have been reported to have hypotensive, antiviral, and antifungal activities (2), as have some benzo[*b*]thiophene-2-carboxamides (3). It

0022-3549/83/0200-0198$01.00/0

Table I—Physical Constants of 2-Dialkylaminoethyl Benzo[*b*]thiophene-3-carboxylates

Compound	R_1	R_2	R_3	Yield, %	Melting Point[a]	Formula[b]	Analysis, % Calc.	Found
IIIa	H	CH_3	CH_3	85	131–132°	$C_{13}H_{16}ClNO_2S$	C 54.64	54.58
							H 5.60	5.76
							N 4.90	5.08
IIIb	H	C_2H_5	C_2H_5	90	151–152°	$C_{15}H_{20}ClNO_2S$	C 57.42	57.35
							H 6.38	6.19
							N 4.47	4.65
IIIc	H	n-C_4H_9	n-C_4H_9	80	101–102°	$C_{19}H_{28}ClNO_2S$	C 61.71	61.90
							H 7.58	7.76
							N 3.79	3.96
IIId	H	CH_3	$CH_2C_6H_5$	80	194–195°	$C_{19}H_{20}ClNO_2S$	C 63.07	62.91
							H 5.53	5.35
							N 3.87	4.05
IIIe	H	—$(CH_2$—$CH_2)_2O$		70	198–199°	$C_{15}H_{18}ClNO_3S$	C 54.96	55.09
							H 5.50	5.75
							N 4.27	4.45
IIIf	CH_3	CH_3	CH_3	70	170–171°	$C_{15}H_{20}ClNO_2S$	C 57.42	57.26
							H 6.38	6.57
							N 4.47	4.65

[a] All compounds were crystallized as hydrochlorides and the recrystallization solvent was ethanol–ethyl acetate. [b] IR, NMR, and mass spectra of all compounds were consistent with the structural assignment.

Table II—Physical Constants of *N*-(2-Dialkylaminoethyl)benzo[*b*]thiophene-3-carboxamides

Compound	R	Yield, %	Melting Point[a]	Formula[b]	Analysis, % Calc.	Found
IV*a*	CH_3	70.	134–135°	$C_{13}H_{17}ClN_2OS$	C 54.83	54.95
					H 5.98	6.05
					N 9.84	9.98
IV*b*	C_2H_5	65	78–79°	$C_{15}H_{21}ClN_2OS$	C 57.60	57.76
					H 6.72	6.91
					N 8.96	8.79
IV*c*	—$(CH_2)_2O(CH_2)_2$—	75	176–177°	$C_{15}H_{19}ClN_2O_2S$	C 55.13	55.01
					H 5.82	5.95
					N 8.58	8.73
V		70	235–236°	$C_{14}H_{17}ClN_2OS$	C 56.66	56.49
					H 5.73	5.54
					N 9.44	9.62

[a] All compounds were crystallized as hydrochlorides and the recrystallization solvent was ethanol–ethyl acetate. [b] IR, NMR, and mass spectra of all compounds were consistent with the structural assignment.

has been demonstrated that some dialkylaminoalkylesters and dialkylaminoalkylamides of benzo[*b*]thiophene-2-carboxylic acid have local anesthetic activity (4). Recently, antibacterial and antifungal activities of alkyl and polyhalophenyl esters of benzo[*b*]thiophene-3-carbamic acid have been reported (5).

In a continuing effort to find a potent pharmacologically active compound with low toxicity (6), a series of dialkylaminoethyl benzo[*b*]thiophene-3-carboxylates, *N*-(2-dialkylaminoethyl)benzo[*b*]thiophene-3-carboxamide, 2-dialkylaminoethyl benzo[*b*]thiophene-3-carbamates, and substituted ureas with the benzo[*b*]thiophene moiety were prepared and the efficacy was determined.

DISCUSSION

Chemistry—Dialkylaminoethyl benzo[*b*]thiophene-3-carboxylates were synthesized using readily available benzo[*b*]thiophene-3-carboxylic acid (I) (5). Reaction of I with thionyl chloride and the subsequent reaction of the acyl halide with dialkylaminoethanol gave the desired compound III (Scheme I).

Benzo[*b*]thiophene-3-carboxamide derivatives (IV or V) were obtained through the reaction of benzo[*b*]thiophene-3-carbonyl chloride (II) with 2-dialkylaminoethylamine or *N*-methylpiperazine (Scheme I).

2-Dialkylaminoethyl benzo[*b*]thiophene-3-carbamates (VII) were prepared through the reaction of benzo[*b*]thiophene-3-carboxazide (VI) (5) with 2-dialkylaminoethanol (Scheme II).

Substituted ureas with the benzo[*b*]thiophene moiety (VIII or IX) were obtained through the reaction of VI with a dialkylaminoalkylamine or *N*-methylpiperazine (Scheme II).

The physical data for the prepared compounds are summarized in Tables I–IV.

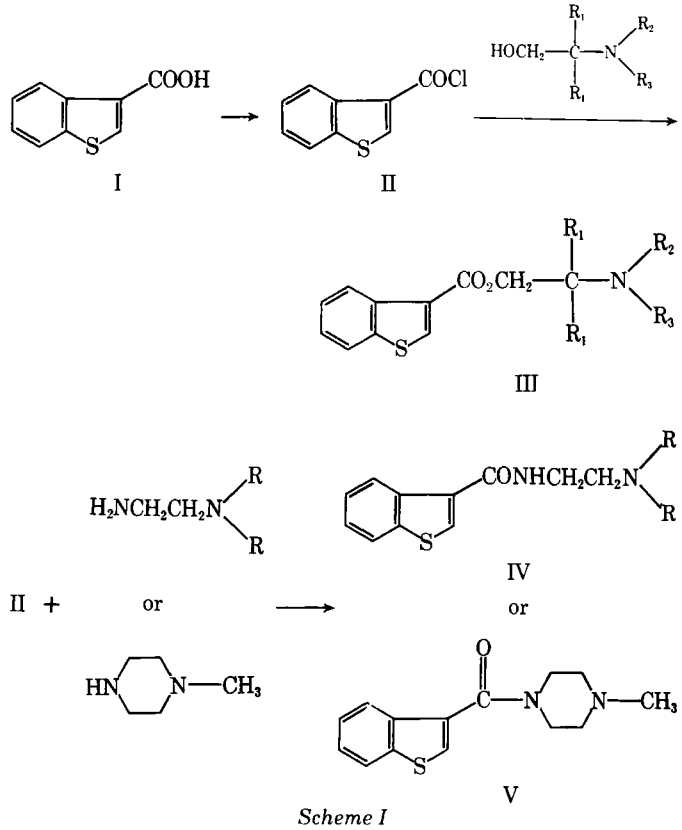

Scheme I

Table III—Physical Constants of 2-Dialkylaminoethyl Benzo[*b*]thiophene-3-carbamates

Compound	R_1	R_2	R_3	Yield, %	Melting Point[a]	Formula[b]	Analysis, % Calc.	Found
VII*a*	H	CH_3	CH_3	78	174–175°	$C_{13}H_{17}ClN_2O_2S$	C 51.91	52.10
							H 5.66	5.47
							N 9.32	9.51
VII*b*	H	C_2H_5	C_2H_5	75	155–156°	$C_{15}H_{21}ClN_2O_2S$	C 54.79	54.96
							H 6.39	6.58
							N 8.52	8.71
VII*c*	H	*n*-C_4H_9	*n*-C_4H_9	70	140–141°	$C_{19}H_{29}ClN_2O_2S$	C 59.30	59.15
							H 7.54	7.36
							N 7.28	7.11
VII*d*	H	$-(CH_2\text{-}CH_2)_2O$		75	161–162°	$C_{15}H_{19}ClN_2O_3S$	C 52.55	52.73
							H 5.55	5.71
							N 8.18	8.06
VII*e*	CH_3	CH_3	CH_3	80	194–195°	$C_{15}H_{21}ClN_2O_2S$	C 54.79	54.61
							H 6.39	6.54
							N 8.52	8.34

[a] All compounds were crystallized as hydrochlorides and the recrystallization solvent was ethanol–ethyl acetate. [b] IR, NMR, and mass spectra of all compounds were consistent with the structural assignments.

Pharmacological Assay—The compounds listed in Tables I–IV were screened for surface anesthetic, anticholinergic, and antihistaminic activities. For surface anesthetic activity, a rabbit conjunctival sac was kept filled with the aqueous solution of the hydrochloric salt of the compounds for 60 sec. The cornea was tested once every minute, and the duration of anesthesia was followed for 18 min. Lidocaine hydrochloride was used for comparison. The results are presented in Table V.

Compounds III*e*, III*f*, IV*b*, and VIII*d* were the most potent. The LD_{50} values of compounds III*e*, III*f*, and IV*b* in mice, estimated by the moving average method (7), were 424.7 (395.9–455.6), 274.2 (255.2–294.8), and 179.5 (158.3–204.2) mg/kg, respectively, when injected intraperitoneally.

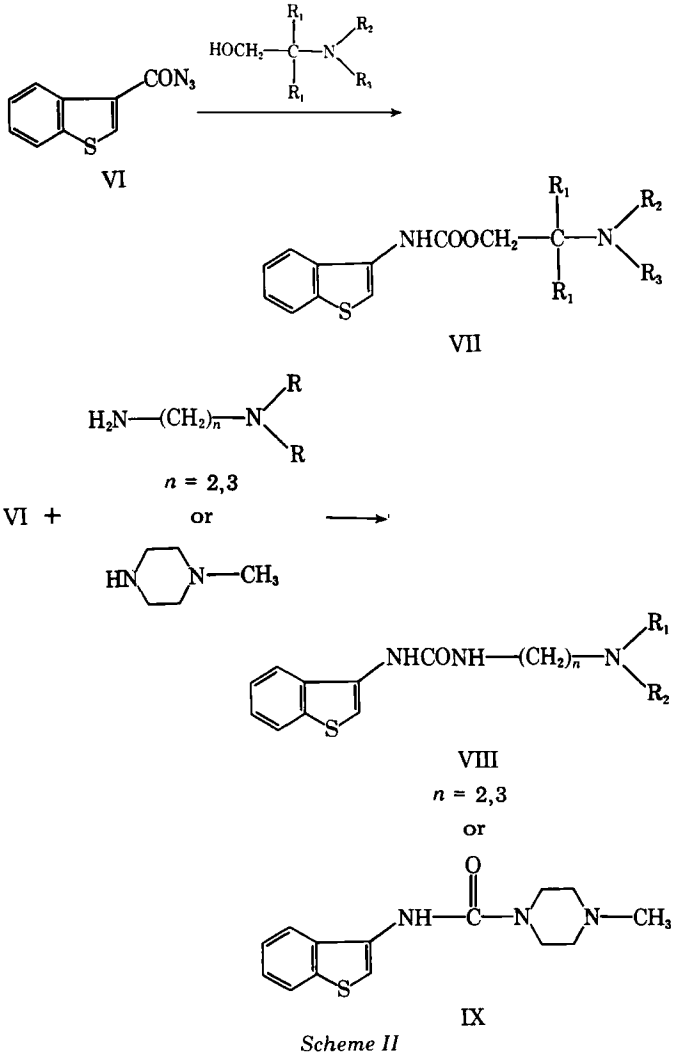

Scheme II

Apart from transient irritation, no conjunctival intolerance or corneal opalescene was observed 24 and 48 hr and 1 week after drug application.

Anticholinergic and antihistaminic activities were tested on isolated guinea pig ileum. The results are presented in Table V.

Compounds III*a*, III*f*, IV*b*, VII*c*, and VIII*d* were the most potent as anticholinergics; and compounds III*a*, V, VII*c*, and VIII*d* were the most potent as antihistamines.

EXPERIMENTAL[1]

Benzo[*b*]thiophene-3-carbonyl Chloride (II)—A mixture of the acid, I (17.8 g, 0.1 mole), and thionyl chloride (35 ml) was refluxed for 4 hr. Excess thionyl chloride was removed under reduced pressure, and the residue was fractionated to give 17.7 g (90%) of the desired compound, bp 149–150°; 4 mm Hg [lit. (11) bp 296–298°, 758 mm Hg].

Anal.—Calc. for C_9H_5ClOS: C, 54.96; H, 2.54. Found: C, 55.07; H, 2.39.

2-Dimethylaminoethyl Benzo[*b*]thiophene-3-carboxylate (III*a*)—A solution of 2-dimethylaminoethanol (0.89 g, 0.01 mole) and II (1.965 g, 0.01 mole) in 20 ml of dry benzene was refluxed for 4 hr. The solvent was evaporated, and the residue was crystallized from ethanol–ethyl acetate to give III*a* (2.43 g, 88%), mp 131–132°; IR (potassium bromide): 1710 and 1195 (ester) cm^{-1}; NMR (deuterochloroform, as free base): 8.67 (m, 1H, H_4), 8.43 (s, 1H, H_2), 7.90 (m, 1H, aromatic), 7.50 (m, 2H, aromatic), 4.47 (t, 2H, OCH_2), 2.73 (t, 2H, CH_2N), and 2.33 (s, 6H, NCH_3) ppm; *m/z* 249.

Compounds III*b–f* were prepared similarly (Table I).

***N*-(2-Dimethylaminoethyl)benzo[*b*]thiophene-3-carboxamide (IV*a*)**—A solution of II (1.965 g, 0.01 mole) and 2-dimethylaminoethylamine (0.88 g, 0.01 mole) in 30 ml of dry benzene was refluxed for 2 hr. The solvent was evaporated and the residue was crystallized from ethanol–ethyl acetate to give IV*a* (1.74 g, 70%), mp 134–135°; IR (potassium bromide): 3260 (NH) and 1640 (amide) cm^{-1}; NMR (deuterochloroform, as free base): 8.45 (m, 1H, H_4), 7.95 (s, 1H, H_2), 7.86 (m, 1H, aromatic), 7.45 (m, 2H, aromatic), 6.96 (bs, 1H, NH), 3.56 (q, 2H, $CONCH_2$), 2.46 (q, 2H, CH_2N), and 1.26 (s, 6H, NCH_3) ppm; *m/z* 248.

Compounds IV*b*, IV*c*, and V were prepared similarly (Table II).

2-Dimethylaminoethyl Benzo[*b*]thiophene-3-carbamate (VII*a*)—A solution of benzo[*b*]thiophene-3-carboxazide (VI, 2.03 g, 0.01 mole) (5) in 20 ml of dry benzene was refluxed for 2 hr, 2-dimethylaminoethanol (0.89 g, 0.01 mole) was added, and reflux was continued for an additional 2 hr. The solvent was evaporated and the residue was crystallized as a hydrochloride from ethanol–ethyl acetate to give VII*a* (2.34 g, 78%), mp 174–175°; IR (potassium bromide): 3180 (NH), 1710 (carbonyl) cm^{-1}; NMR (deuterochloroform, as free base): 8.06–7.40 (m, 6H, aromatic and NH), 4.42 (t, 2H, OCH_2), 2.70 (t, 2H, CH_2N), and 2.36 (s, 6H, NCH_3) ppm; *m/z* 264.

Compounds VII*b–e* were prepared similarly (Table III).

***N*$_1$-(Dimethylaminoethyl)-*N*$_3$-(benzo[*b*]thiophene-3-yl)urea (VIII*a*)**—A solution of VI (2.03 g, 0.01 mole) in 20 ml of dry benzene was refluxed for 2 hr, 2-dimethylaminoethylamine (0.88 g, 0.01 mole) was

[1] Melting points were taken on a Kofler hot-stage microscope and are uncorrected. IR spectra were recorded using a Perkin-Elmer model 267 spectrograph. NMR spectra were determined using a Varian T-60 spectrometer and chemical shifts (δ) are in parts per million relative to internal tetramethylsilane. Mass spectra were recorded on a Varian MAT-311 instrument.

Table IV—Physical Constants of N_1-(Dialkylaminoalkyl)-N_3-(benzo[*b*]thiophene-3-yl)ureas

Compound	*n*	R_1	R_2	Yield, %	Melting Point[a]	Formula[b]	Analysis, % Calc.	Found
VIII*a*	2	CH_3	CH_3	75	207–208°	$C_{13}H_{18}ClN_3OS$	C 52.09	51.95
							H 6.01	5.87
							N 14.02	14.15
VIII*b*	3	CH_3	CH_3	80	205–206°	$C_{14}H_{20}ClN_3OS$	C 53.59	53.77
							H 6.38	6.56
							N 13.40	13.25
VIII*c*	3	C_2H_5	C_2H_5	95	209–210°	$C_{16}H_{24}ClN_3OS$	C 56.22	56.04
							H 7.03	6.91
							N 12.30	12.05
VIII*d*	3	n-C_4H_9	n-C_4H_9	80	179–180°	$C_{20}H_{32}ClN_3OS$	C 60.38	60.19
							H 8.05	7.87
							N 10.57	10.38
VIII*e*	2	$-(CH_2\text{-}CH_2)_2O$		90	222–223°	$C_{15}H_{20}ClN_3O_2S$	C 52.71	52.87
							H 5.86	6.04
							N 12.30	12.14
IX				75	235–236°	$C_{14}H_{18}ClN_3OS$	C 53.93	53.99
							H 5.78	5.88
							N 13.48	13.29

[a] All compounds were crystallized as hydrochlorides and the recrystallization solvent was ethanol–ethyl acetate. [b] IR, NMR, and mass spectra of all compounds were consistent with the structural assignments.

Table V—Local Anesthetic, Anticholinergic, and Antihistaminic Activities of Benzo[*b*]thiophene Derivatives

Compound	Local Anesthetic Activity[a] Concentration, %	Potency	Duration, min	Concentration, μg/ml	Anticholinergic[b]	Antihistaminic[b]
III*a*	2	0.55(0.39–0.71)	6–12	1	100	93.7
				5	100	97.2
				10	100	97.2
III*b*	2	0.32(0.2–0.44)	2–8	5	33.3	21.3
				10	33.3	30.3
III*c*	2	0.0	—	5	56.9	34.1
				10	60.8	34.1
III*d*	2	0.41(0.25–0.57)	4–8	5	0.0	49.4
				10	0.0	64.7
III*e*	1	0.67(0.56–0.78)	9–14	5	15.1	13.9
	2	0.83(0.74–0.92)	14–16	10	15.1	13.9
III*f*	1	0.55(0.44–0.66)	9–12	1	94.3	4.5
	2	0.88(0.78–0.98)	15–18	5	100	61.8
				10	100	73.1
IV*a*	2	0.0	—	10	0.0	0.0
IV*b*	1	0.54(0.43–0.65)	7–12	5	63.8	18
	2	0.61(0.50–0.72)	10–14	10	96.6	40.9
IV*c*	2	0.0	—	10	0.0	0.0
V	2	0.17(0.05–0.22)	1–5	5	0.0	85.7
				10	0.0	89.6
VII*a*	2	0.22(0.09–0.35)	2–6	5	9.5	26.4
				10	9.5	63.1
VII*b*	2	0.13(0.04–0.22)	1–4	5	26.5	33.3
				10	26.5	70.8
VII*c*	2	0.22(0.09–0.35)	3–6	1	20.4	77.8
				5	81.5	100
				10	83.3	100
VII*d*	2	0.26(0.15–0.37)	4–6	5	0.0	17.1
				10	0.0	22.0
VII*e*	2	0.15(0.06–0.24)	1–5	1	10.2	0.0
				5	40.5	22.9
				10	57.3	33.7
VIII*a*	2	0.11(0.03–0.19)	1–4	5	14.0	13.6
				10	14.0	17.0
VIII*b*	2	0.0	—	5	0.0	9.1
				10	0.0	10.0
VIII*c*	1	0.05(0.00–0.10)	0–2	5	15.1	33.3
	2	0.13(0.04–0.22)	1–4	10	16.8	56.4
VIII*d*	1	0.50(0.34–0.66)	6–11	5	73.0	97.3
	2	0.77(0.65–0.89)	11–15			
VIII*e*	2	0.38(0.25–0.51)	4–8	5	21.1	0.0
				10	21.1	0.0
IX	2	0.36(0.23–0.49)	3–6	10	0.0	0.0
Lidocaine hydrochloride	1	0.33(0.18–0.48)	3–7			
	2	0.86(0.57–0.97)	15–16			

[a] Surface anesthesia was tested according to a previously described method (8). Anesthetic potency was calculated for the first 18 min (9). A potency of 1.00 indicates an onset of anesthesia in 1 min and a duration of at least 18 min. [b] Reduction of contraction (percent) against acetylcholine (0.01 μg/ml) and histamine dihydrochloride (0.01 μg/ml). Assay was carried out on isolated guinea pig ileum according to a previous method (10).

added, and reflux was continued for an additional 3 hr. The solvent was evaporated, and the residue was crystallized as a hydrochloride from ethanol–ethyl acetate to give VIII*a* (2.25 g, 75%), mp 207–208°; IR (potassium bromide): 3300 (NH), 1685 (carbonyl) cm^{-1}; NMR (deuterochloroform): 8.80 (bs, 1H, NH), 7.87–7.50 (m, 2H, aromatic), 7.57 (s, 1H, H_2), 6.40 (bs, 1H, NH), 3.37 (q, 2H, $CONCH_2$), 2.47 (q, 2H, CH_2N), and 2.13 (s, 6H, NCH_3) ppm; *m/z* 263.

Compounds VIII*b–e* and IX were prepared similarly (Table IV).

REFERENCES

(1) R. F. Doerge, in "Textbook of Organic Medicinal and Pharmaceutical Chemistry," C. O. Wilson, O. Gisvold, and F. R. Doerge, Eds., 6th ed., J. B. Lippincott, Philadelphia, Pa., 1971, p. 649.

(2) W. Voegtli, U.S. pat. 2,857,383 (1958); *Chem. Abstr.*, **53**, 6249h (1959).

(3) R. W. Goettsch and G. A. Wiese, *J. Am. Pharm. Assoc., Sci. Ed.*, **47**, 319 (1958).

(4) E. Campaigne and T. Bosin, *J. Med. Chem.*, **10**, 945 (1967).

(5) A. Shafiee, M. Vossoghi, J. Wossooghi, and S. Yazdani, *J. Pharm. Sci.*, **70**, 566 (1981).

(6) A. Shafiee, F. Savabi, A. Rezvani, M. Farrokhsiar, and A. Khoyi, *ibid.*, **67**, 125 (1978).

(7) C. S. Weil, *Biometrics*, **8**, 243 (1952).

(8) M. R. A. Chance and H. J. Lobstein, *J. Pharmacol. Exp. Ther.*, **82**, 203 (1944).

(9) A. H. Campbell, J. A. Strasse, G. H. Lord, and J. E. Wilson, *J. Pharm. Sci.*, **57**, 2045 (1968).

(10) J. Magnus, *Pflugers Arch. Ges. Physiol.*, **102**, 123 (1904).

(11) G. Komppa and S. Weckman, *J. Prakt. Chem.*, **138**, 109 (1933).

ACKNOWLEDGMENTS

Supported by a grant from the Research Council of the University Crusade of Tehran University.

The authors thank Drs. M. A. Khoyi and K. Mohammad for their fruitful discussion.

Binding of Several Phenothiazine Neuroleptics to a Common Binding Site of α_1-Acid Glycoprotein, Orosomucoid

SAFAA EL-GAMAL *§, UWE WOLLERT *†, and WALTER E. MÜLLER ‡ ×

Received December 14, 1981, from the **Pharmakologie und Toxikologie für Naturwissenschaftler, Fachgereich Pharmazie, Universität Mainz* and the ‡*Pharmakologisches Institut der Universität Mainz, Obere Zahlbacher Strasse 67, D-6500 Mainz, West Germany.* Accepted for publication April 1, 1982. §Present address: Department of Pharmaceutics, Faculty of Pharmacy, Alexandria University, Alexandria, Egypt. †Deceased.

Abstract □ The interaction of several phenothiazine neuroleptics with α_1-acid glycoprotein was investigated using circular dichroism and equilibrium dialysis techniques. For chlorpromazine only, one high-affinity binding site of the protein was found. The binding of the drug to this single site generated typical polyphasic extrinsic Cotton effects. Since several other phenothiazine neuroleptics gave qualitatively comparable extrinsic Cotton effects in the presence of α_1-acid glycoprotein and potently inhibited the binding of chlorpromazine to the single site, it was concluded that all phenothiazine derivatives investigated bound preferentially to only one common binding site of the α_1-acid glycoprotein molecule.

Keyphrases □ Phenothiazines—neuroleptics, binding to a common binding site of α_1-acid glycoprotein, orosomucoid □ Neuroleptic agents—binding of phenothiazines to a common binding site of α_1-acid glycoprotein, orosomucoid □ α_1-Acid glycoproteins—binding of several phenothiazine neuroleptics to a common binding site, orosomucoid □ Orosomucoid—binding of several phenothiazine neuroleptics to a common binding site of α_1-acid glycoprotein

While for most neutral or anionic drugs the predominating role of the albumin fraction as the major binding component in human blood is established, increasing evidence has been presented during recent years that this is not the case for several basic drugs where other proteins also contribute considerably to the plasma binding. Out of these, orosomucoid (α_1-acid glycoprotein) received the most attention because of its possible significance for the pharmacokinetic pattern of basic drugs (1). Thus, large variations in the blood levels of α_1-acid glycoprotein observed in patients suffering from various disease states could have been responsible for similarly large variations of the free plasma levels of some basic drugs measured in the same patients (1–3). Since the average plasma levels of α_1-acid glycoprotein are rather low, usually between 10 and 40 μmole/liter (2, 3), a fairly strong drug binding to this protein has to be assumed if variations of its plasma levels were to contribute considerably to the free fraction of a drug. Some recent work shows that several basic drugs are bound very strongly to α_1-acid glycoprotein (4–8). An example of this is the phenothiazine derivative, perazine, which is bound with very high affinity to mainly one site of the α_1-acid glycoprotein molecule (5–7).

The present study reports similar findings for chlorpromazine. Evidence is presented that a variety of phenothiazine neuroleptics, including perazine and chlorpromazine, are preferentially, if not exclusively, bound to only one common binding site of the α_1-acid glycoprotein molecule.

EXPERIMENTAL

Materials—α_1-Acid glycoprotein[1] (orosomucoid) had an electrophoretic purity >99%. [^{14}C]Chlorpromazine[2] had a specific activity of 80 mCi/mmole and a radiochemical purity >99%. All chlorpromazine derivatives were gifts from the manufacturers[3]. All other chemicals were obtained from commercial suppliers. All solutions were prepared with deionized water.

Circular Dichroism Measurements—Circular dichroism measurements were carried out with a spectropolarimeter[4] calibrated with *d*-camphorsulfonic acid. All spectra were recorded in cylindrical cells with 10-mm path length using a full-scale deflection of 0.02° θ and a spectral band width of 2 nm. All measurements were made in 0.07 *M* phosphate buffer (pH 7.4). Results are expressed as molar ellipticity ($[\theta]$) calculated with reference to the α_1-acid glycoprotein concentration (25 μM).

Equilibrium Dialysis—Binding of [^{14}C]chlorpromazine to α_1-acid glycoprotein was determined by equilibrium dialysis using a protein concentration of 12.5 μM and varying concentrations of the drug. All solutions were prepared in 0.07 *M* phosphate buffer (pH 7.4); 0.9 ml of the protein solution was dialyzed for 16 hr in the dark against 0.9 ml of buffer containing [^{14}C]chlorpromazine. One-milliliter dialysis cells and

[1] Behringwerke, Marburg, West Germany.

[2] Amersham Buchler, Braunschweig, West Germany.

[3] Perazine from Promonta, Hamburg, West Germany, promazine from Wyeth, Münster, West Germany; prothipendyl from Homburg, Frankfurt, West Germany; trifluopromazine from Heyden, Munich, West Germany; acepromazine from Clin-Comar, Paris, France.

[4] Cary 61.

0022-3549/83/0200-0202$01.00/0

REFERENCES

(1) R. F. Doerge, in "Textbook of Organic Medicinal and Pharmaceutical Chemistry," C. O. Wilson, O. Gisvold, and F. R. Doerge, Eds., 6th ed., J. B. Lippincott, Philadelphia, Pa., 1971, p. 649.

(2) W. Voegtli, U.S. pat. 2,857,383 (1958); *Chem. Abstr.*, **53**, 6249h (1959).

(3) R. W. Goettsch and G. A. Wiese, *J. Am. Pharm. Assoc., Sci. Ed.*, **47**, 319 (1958).

(4) E. Campaigne and T. Bosin, *J. Med. Chem.*, **10**, 945 (1967).

(5) A. Shafiee, M. Vossoghi, J. Wossooghi, and S. Yazdani, *J. Pharm. Sci.*, **70**, 566 (1981).

(6) A. Shafiee, F. Savabi, A. Rezvani, M. Farrokhsiar, and A. Khoyi, *ibid.*, **67**, 125 (1978).

(7) C. S. Weil, *Biometrics*, **8**, 243 (1952).

(8) M. R. A. Chance and H. J. Lobstein, *J. Pharmacol. Exp. Ther.*, **82**, 203 (1944).

(9) A. H. Campbell, J. A. Strasse, G. H. Lord, and J. E. Wilson, *J. Pharm. Sci.*, **57**, 2045 (1968).

(10) J. Magnus, *Pflugers Arch. Ges. Physiol.*, **102**, 123 (1904).

(11) G. Komppa and S. Weckman, *J. Prakt. Chem.*, **138**, 109 (1933).

ACKNOWLEDGMENTS

Supported by a grant from the Research Council of the University Crusade of Tehran University.

The authors thank Drs. M. A. Khoyi and K. Mohammad for their fruitful discussion.

Binding of Several Phenothiazine Neuroleptics to a Common Binding Site of α_1-Acid Glycoprotein, Orosomucoid

SAFAA EL-GAMAL *§, UWE WOLLERT *†, and WALTER E. MÜLLER ‡ ×

Received December 14, 1981, from the **Pharmakologie und Toxikologie für Naturwissenschaftler, Fachgereich Pharmazie, Universität Mainz* and the ‡*Pharmakologisches Institut der Universität Mainz, Obere Zahlbacher Strasse 67, D-6500 Mainz, West Germany.* Accepted for publication April 1, 1982. §Present address: Department of Pharmaceutics, Faculty of Pharmacy, Alexandria University, Alexandria, Egypt. †Deceased.

Abstract □ The interaction of several phenothiazine neuroleptics with α_1-acid glycoprotein was investigated using circular dichroism and equilibrium dialysis techniques. For chlorpromazine only, one high-affinity binding site of the protein was found. The binding of the drug to this single site generated typical polyphasic extrinsic Cotton effects. Since several other phenothiazine neuroleptics gave qualitatively comparable extrinsic Cotton effects in the presence of α_1-acid glycoprotein and potently inhibited the binding of chlorpromazine to the single site, it was concluded that all phenothiazine derivatives investigated bound preferentially to only one common binding site of the α_1-acid glycoprotein molecule.

Keyphrases □ Phenothiazines—neuroleptics, binding to a common binding site of α_1-acid glycoprotein, orosomucoid □ Neuroleptic agents—binding of phenothiazines to a common binding site of α_1-acid glycoprotein, orosomucoid □ α_1-Acid glycoproteins—binding of several phenothiazine neuroleptics to a common binding site, orosomucoid □ Orosomucoid—binding of several phenothiazine neuroleptics to a common binding site of α_1-acid glycoprotein

While for most neutral or anionic drugs the predominating role of the albumin fraction as the major binding component in human blood is established, increasing evidence has been presented during recent years that this is not the case for several basic drugs where other proteins also contribute considerably to the plasma binding. Out of these, orosomucoid (α_1-acid glycoprotein) received the most attention because of its possible significance for the pharmacokinetic pattern of basic drugs (1). Thus, large variations in the blood levels of α_1-acid glycoprotein observed in patients suffering from various disease states could have been responsible for similarly large variations of the free plasma levels of some basic drugs measured in the same patients (1–3). Since the average plasma levels of α_1-acid glycoprotein are rather low, usually between 10 and 40 μmole/liter (2, 3), a fairly strong drug binding to this protein has to be assumed if variations of its plasma levels were to contribute considerably to the free fraction of a drug. Some recent work shows that several basic drugs are bound very strongly to α_1-acid glycoprotein (4–8). An example of this is the phenothiazine derivative, perazine, which is bound with very high affinity to mainly one site of the α_1-acid glycoprotein molecule (5–7).

The present study reports similar findings for chlorpromazine. Evidence is presented that a variety of phenothiazine neuroleptics, including perazine and chlorpromazine, are preferentially, if not exclusively, bound to only one common binding site of the α_1-acid glycoprotein molecule.

EXPERIMENTAL

Materials—α_1-Acid glycoprotein[1] (orosomucoid) had an electrophoretic purity >99%. [^{14}C]Chlorpromazine[2] had a specific activity of 80 mCi/mmole and a radiochemical purity >99%. All chlorpromazine derivatives were gifts from the manufacturers[3]. All other chemicals were obtained from commercial suppliers. All solutions were prepared with deionized water.

Circular Dichroism Measurements—Circular dichroism measurements were carried out with a spectropolarimeter[4] calibrated with *d*-camphorsulfonic acid. All spectra were recorded in cylindrical cells with 10-mm path length using a full-scale deflection of 0.02° θ and a spectral band width of 2 nm. All measurements were made in 0.07 *M* phosphate buffer (pH 7.4). Results are expressed as molar ellipticity ($[\theta]$) calculated with reference to the α_1-acid glycoprotein concentration (25 μM).

Equilibrium Dialysis—Binding of [^{14}C]chlorpromazine to α_1-acid glycoprotein was determined by equilibrium dialysis using a protein concentration of 12.5 μM and varying concentrations of the drug. All solutions were prepared in 0.07 *M* phosphate buffer (pH 7.4); 0.9 ml of the protein solution was dialyzed for 16 hr in the dark against 0.9 ml of buffer containing [^{14}C]chlorpromazine. One-milliliter dialysis cells and

[1] Behringwerke, Marburg, West Germany.

[2] Amersham Buchler, Braunschweig, West Germany.

[3] Perazine from Promonta, Hamburg, West Germany, promazine from Wyeth, Münster, West Germany; prothipendyl from Homburg, Frankfurt, West Germany; trifluopromazine from Heyden, Munich, West Germany; acepromazine from Clin-Comar, Paris, France.

[4] Cary 61.

0022-3549/83/0200-0202$01.00/0

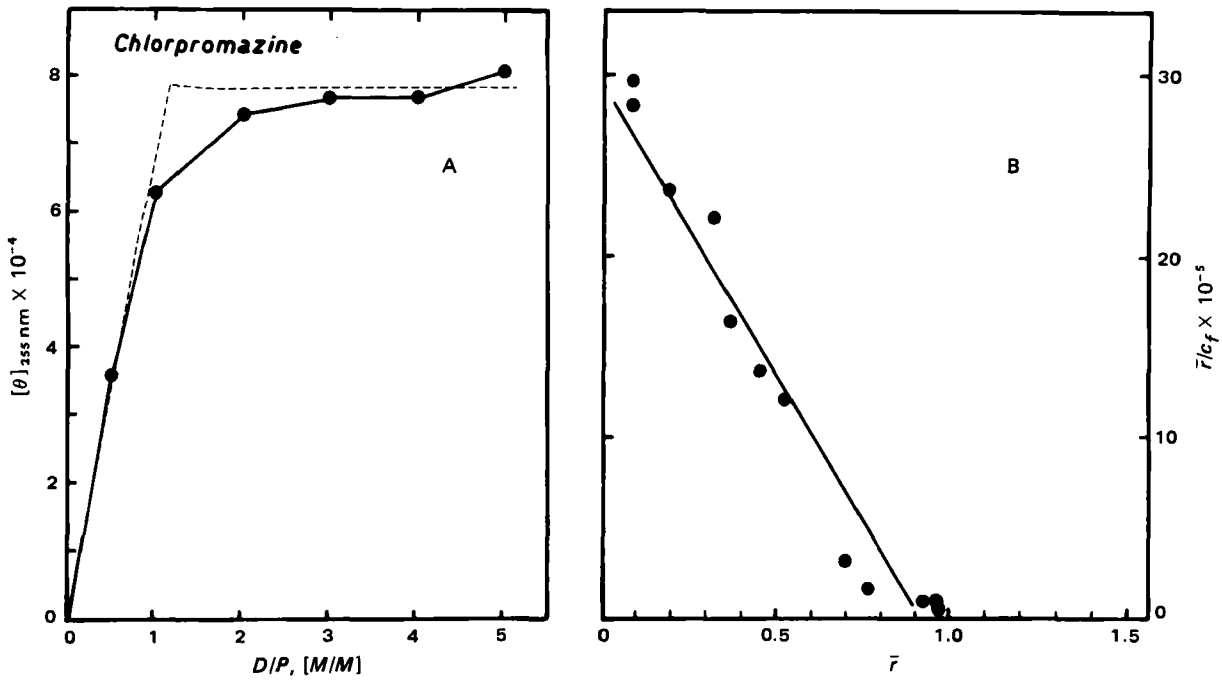

Figure 1—*The interaction of chlorpromazine with only one binding site of α_1-acid glycoprotein. (A) The relationship between the molar chlorpromazine–α_1-acid glycoprotein ratio (D/P) and the intensity of the induced circular dichroism band at 255 nm ($[\theta]_{255}$). (B) Scatchard plot of the interaction of [^{14}C]chlorpromazine with α_1-acid glycoprotein; k is the association constant (2.94×10^5); n is the number of binding sites per α_1-acid glycoprotein molecule (0.91); and r is the correlation coefficient of the calculated regression line (0.96).*

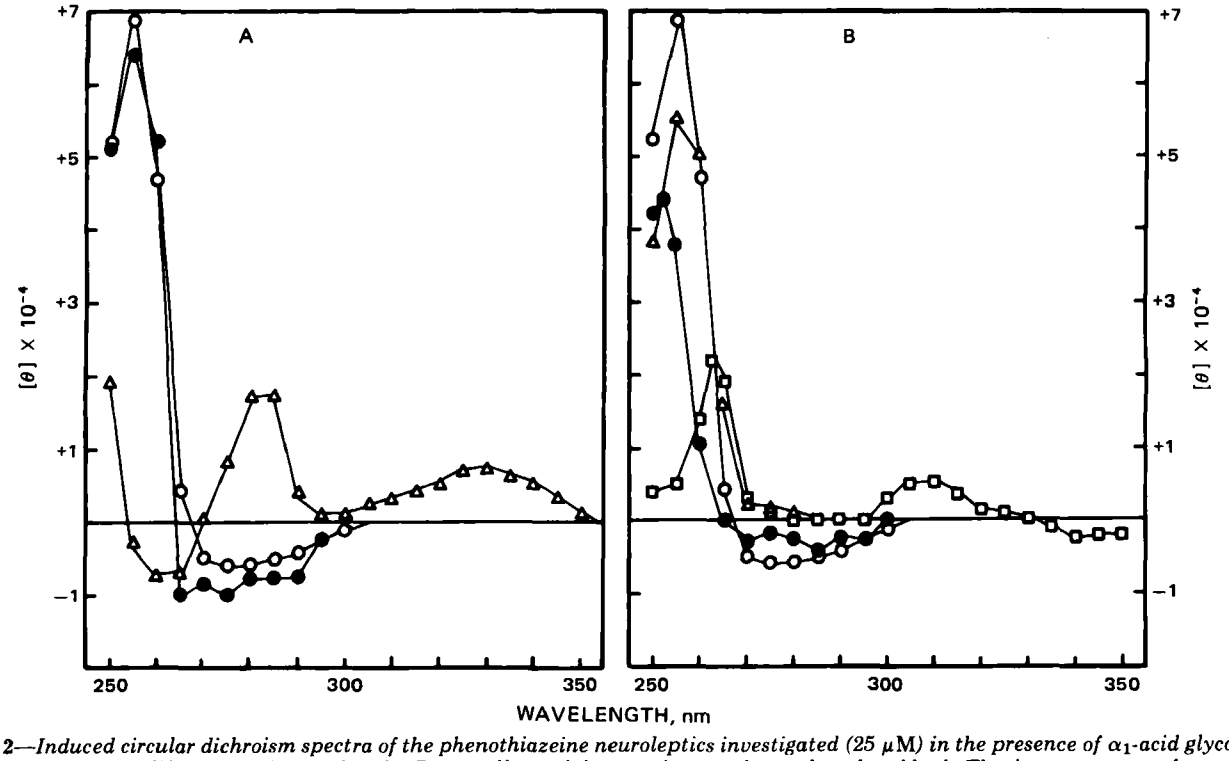

Figure 2—*Induced circular dichroism spectra of the phenothiazeine neuroleptics investigated (25 μM) in the presence of α_1-acid glycoprotein (25 μM). The data are difference values, using the Cotton effects of the protein at each wavelength as blank. The data are means of two different runs. Key: (A) (●) chlorpromazine; (○) promazine; (△) acepromazine; (B) (○) promazine; (●) prothipendyl; (△) perazine; (□) trifluoperazine.*

cellophane dialysis membranes[5] were used. The radioactivity at both sides of the membrane was determined by liquid scintillation spectrometry[6].

RESULTS AND DISCUSSION

Plotting the binding data obtained by the equilibrium dialysis experiments for the interaction of [^{14}C]chlorpromazine with α_1-acid glycoprotein according to Scatchard (9) revealed a straight line with an abscissa intercept of 0.9, indicating that [^{14}C]chlorpromazine binds within the concentration range investigated (up to a molar drug–protein ratio of 5) to only one site of the α_1-acid glycoprotein moleculer (Fig. 1B). As indicated by the association constant, k, $\sim 3 \times 10^6\ M^{-1}$, the affinity of this single site for chlorpromazine is very high and within the range of the strongest drug interactions with human serum albumin (10–12).

The binding of chlorpromazine to α_1-acid glycoprotein profoundly

[5] Union Carbide.
[6] Packard model 3255.

Table I—Structural Requirements for the High-Affinity Binding of Phenothiazine Neuroleptics to α_1-Acid Glycoprotein

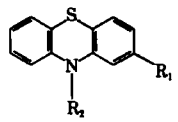

I-VI

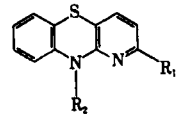

VII

Compound	R_1	R_2	log P^a	$\Delta\alpha^b$, %	λ_{max}^c, nm	$[\theta] \times 10^{4d}$ $D/P, M/M$ 1	2	3
Promazine (I)	—H	—CH_2—CH_2—CH_2—N(CH_3)(CH_3)	2.6	19	255	+6.8	+8.3	+8.6
Chlorpromazine (II)	—Cl	—CH_2—CH_2—CH_2—N(CH_3)(CH_3)	3.3	30	255	+6.3	+7.8	+8.2
Acepromazine (III)	—OC—CH_3	—CH_2—CH_2—CH_2—N(CH_3)(CH_3)	2.3	16	260	−0.8	−1.0	−1.0
Trifluopromazine (IV)	—CF_3	—CH_2—CH_2—CH_2—N(CH_3)(CH_3)	3.4	23	—	—	—	—
Perazine (V)	—H	—CH_2—CH_2—CH_2—N(piperazine)—CH_3	2.9	14	255	+5.2	+6.8	+7.6
Trifluoperazine (VI)	—CF_3	—CH_2—CH_2—CH_2—N(piperazine)—CH_3	4.75[e]	21	263	+2.4	+3.5	+3.8
Prothipendyl (VII)	—H	—CH_2—CH_2—CH_2—N(CH_3)(CH_3)	2.2	24	253	+4.1	+4.8	+5.4

[a] The partition coefficients P between n-octanol and buffer were taken from Refs. 14 and 15. [b] Increase of the percentage free (α) of [^{14}C]chlorpromazine (6.3 μM) in the presence of the unlabeled neuroleptics (25 μM). Without displacer the percentage free (α) was 9.0 ± 0.9 (n = 6). [c] Wavelength of the induced circular dichroism band. [d] Intensity of the induced circular dichroism band at various molar drug–protein (D/P) ratios. [e] Calculated from a linear relationship between partition coefficients of n-octanol and buffer and R_M values obtained from a reverse-phase thin-layer technique, Ref. 15.

changes the native intrinsic circular dichroism spectrum of the protein between 250 and 350 nm (4, 13). In the difference spectrum, when the intrinsic Cotton effects of the protein alone have been subtracted, typical polyphasic extrinsic Cotton effects can be seen (Fig. 2). For chlorpromazine, a large positive band around 255 nm and two weaker negative bands around 27 nm can be seen (Fig. 2). The change in intensity of all three bands depends on the drug–protein concentration ratio in a similar fashion which can be demonstrated using the data for the strong positive band at 255 nm (Fig. 1A). The results show that maximum induction of the Cotton effects occurs when the drug–protein ratio reaches 1, indicating that the induction of Cotton effects is associated with the binding of chlorpromazine to only one site.

Several other phenothiazine neuroleptics also generate extrinsic Cotton effects in the presence of α_1-acid glycoprotein which are qualitatively similar to those of chlorpromazine (Fig. 2). The two most pronounced exceptions are the presence of an additional positive band >300 nm in the case of acepromazine and trifluoperazine and the positive sign of the band of acepromazine around 270 nm, instead of the negative sign observed for all other derivatives (Fig. 2). For trifluopromazine no extrinsic Cotton effects up to a molar excess of five were observed. The extrinsic Cotton effects of all phenothiazine derivatives depend on the drug concentration in a manner similar to that of chlorpromazine as shown for the positive band around 260 nm (Table I). Thus, the induced Cotton effects of the five chlorpromazine derivatives may also be associated with one preferential binding site. Moreover, the qualitatively comparable spectra suggest that the steric parameters of these interactions are similar for the drugs investigated, which might indicate that all phenothiazine derivatives investigated share the same high-affinity binding site with chlorpromazine. In agreement with these assumptions are the findings that all derivatives investigated inhibit the binding of [^{14}C]chlorpromazine to the single binding site; however, there are different potencies (Table I). Thus, considering these observations and the findings of only one high-affinity binding site of perazine (5–7), the assumption of one common high-affinity binding site of α_1-acid glycoprotein for most phenothiazine neuroleptics is justified.

In contrast to the rather unspecific binding of phenothiazine neuroleptics to serum albumin where good correlations between hydrophobic character and binding have been reported (14, 15) there is neither a clear correlation between lipophilicity (indicated by the partition coefficients in Table I) and the potencies of the derivatives as inhibitors of [^{14}C]-chlorpromazine binding nor between lipophilicity and the intensities of the induced Cotton effects (Table I). Structural parameters other than the lipophilicity are more important. As far as it is possible with the limited data available at the present state, it seems that for the intensity of the extrinsic Cotton effects and for the binding itself (indicated by the increase of the free fraction of [^{14}C]chlorpromazine) the substituent —R_1 on the phenothiazine nucleus is much more important than the aliphatic side chain (—R_2). This is best seen when comparing the data for promazine with either the data of acepromazine or trifluopromazine or comparing promazine with perazine. However, to draw final conclusions about the structural parameters leading to high-affinity binding and strong induced Cotton effects in the case of the interaction of phenothiazine derivatives with α_1-acid glycoprotein, more data using more derivatives are needed.

In conclusion, the data reported indicate that for the phenothiazine neuroleptics investigated in this study, binding to α_1-acid glycoprotein is mediated mainly by only one common high-affinity binding site of the protein.

REFERENCES

(1) K. M. Piafsky, *Clin. Pharmacokinet.*, **5**, 246 (1980).

(2) K. M. Piafsky and O. Borga, *Clin. Pharmacol. Ther.*, **22**, 545 (1977).

(3) M. K. Romach, K. M. Piafsky, J. G. Abel, V. Khouw, and E. M. Sellers, *Ibid.*, **29**, 211 (1981).

(4) S. El-Gamal, U. Wollert, and W. E. Müller, *J. Pharm. Pharmacol.*, **34**, 152 (1982).

(5) J. Schley, M. Siegert, and B. Müller-Oerlinghausen, *Eur. J. Clin. Pharmacol.*, **18**, 501 (1980).

(6) J. Schley, M. Nündel, M. Siegert, E. Riedel, and B. Müller-Oerlinghausen, *Pharmacopsychiatry*, **13**, 144 (1980).

(7) M. Brinkschulte and U. Breyer-Pfaff, *Naunyn-Schmiedeberg Arch. Pharmacol.*, **314**, 61 (1980).

(8) M. L. Kornguth, L. G. Hutchins, and B. S. Eichelman, *Biochem. Pharmacol.*, **30**, 2435 (1981).

(9) G. Scatchard, *Ann. N. Y. Acad. Sci.*, **51**, 660 (1949).

(10) J. Koch-Weser and E. M. Sellers, *N. Engl. J. Med.*, **294**, 311 and 526 (1976).
(11) W. E. Müller and U. Wollert, *Pharmacology*, **19**, 59 (1979).
(12) U. Kragh-Hansen, *Pharmacol. Rev.*, **33**, 17 (1981).
(13) B. Jirgenssons, *Biochim. Biophys. Acta*, **434**, 58 (1976).
(14) H. Glaser and J. Krieglstein, *Naunyn-Schmiedebergs Arch. Pharmacol.*, **265**, 321 (1970).
(15) A. Hulshoff and J. P. Perrin, *J. Med. Chem.*, **20**, 430 (1977).

ACKNOWLEDGMENTS

This study was supported by a grant of the Deutsche Forschungsgemeinschaft and a fellowship grant of the Alexander von Humboldt-Stiftung.

The excellent technical assistance of A. Stillbauer is gratefully acknowledged.

Complexation of Procainamide with Hydroxide-Containing Compounds

V. DAS GUPTA

Received September 18, 1981, from the *University of Houston, College of Pharmacy, Houston, TX 77030.* Accepted for publication April 2, 1982.

Abstract □ The complexation of procainamide with hydroxide-containing compounds, ethanol, fructose, glucose, glycerin, lactose, maltose, propylene glycol, sorbitol, and sucrose, have been studied. Procainamide formed a complex with glucose, lactose, and maltose, all of which contain a hemiacetal group, whereas fructose and sucrose do not. The percent of complex formed was dependent on the pH of the solution, with an optimum range of ~4–5.2. As with glucose, the percent of complex formed was directly related to the concentration of lactose in the solution. In dry mixtures, procainamide did not form a complex with glucose or lactose. The complex formed with lactose or maltose could be completely reversed by adding hydrochloric acid. A similar observation with glucose was reported earlier. In the optimum pH range, equilibrium was established in ~24 hr, and the process of complexation followed the equation for reversible reactions.

Keyphrases □ Complexation—procainamide with hydroxide-containing compounds □ Procainamide—complexation with hydroxide-containing compounds □ Hydroxide-containing compounds—complexation with procainamide

An earlier report (1) reviewed the literature concerning stability and complexation problems of procainamide in the presence of glucose. The report also presented the results of a study on the complexation of procainamide with glucose. (These two compounds are often mixed in hospitals for intravenous infusion for the treatment of cardiovascular diseases.)

Since procainamide oral dosage forms also are used widely, the formation of complex with some of the excipients seemed possible. The present report investigated the formation of procainamide complexes with hydroxide-containing compounds, ethanol, fructose, glucose, glycerin, lactose, maltose, propylene glycol, sorbitol, and sucrose.

EXPERIMENTAL

Materials—All chemicals and reagents were USP, NF, or ACS grade and were used as received. Procainamide hydrochloride[1] (I) was used without further purification.

A high-performance liquid chromatograph[2], equipped with a multiple wavelength detector[3], a recorder[4] and digital integrator[5], was used.

A semipolar column[6] (30 cm long × 4-mm i.d.) consisting of a monomolecular layer of cyanopropylsilane permanently bonded to silica gel was used.

Chromatographic Conditions—The mobile phase was 40% (v/v) acetonitrile in water containing 0.02 *M* ammonium acetate (pH ~7)[7], and the flow rate was 2.0 ml/min. The detector was set at 280 nm (the wavelength of maximum absorption), the sensitivity was 0.04, the temperature was ambient, and the chart speed was 30.5 cm/hr.

Methods—The stock solutions of procainamide hydrochloride (1.0 mg/ml) and the internal standard, methapyrilene hydrochloride (5.0 mg/ml) in water, were prepared fresh daily. A standard solution was prepared by transferring a 1.5-ml quantity of the stock solution of I and a 4.0-ml quantity of the stock solution of methapyrilene hydrochloride (II) to a 100-ml volumetric flask and then diluting with water to volume.

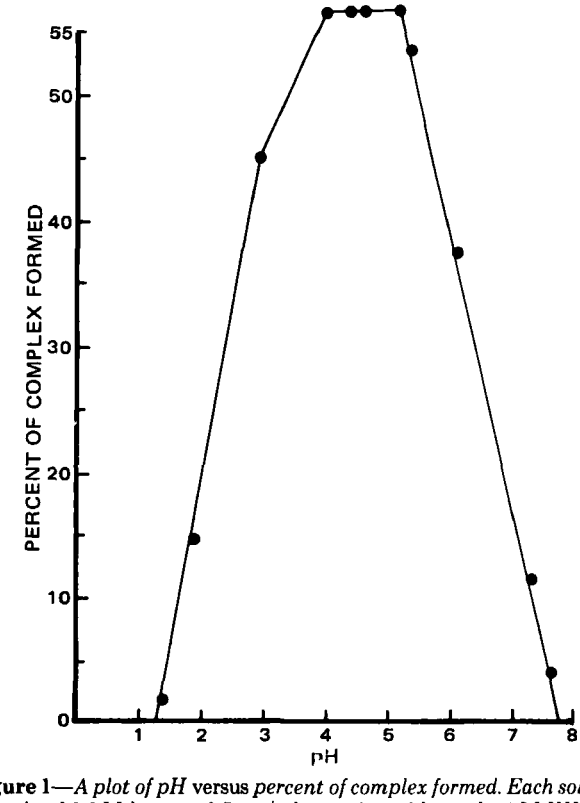

Figure 1—*A plot of pH* versus *percent of complex formed. Each solution contained 0.2* M *lactose, 0.5 mg/ml procainamide, and 0.2* M KH_2PO_4. *Solution of pH 1.4 was buffered with ~1* N *HCl. A similar plot was obtained with glucose.*

[1] Supplied by E. R. Squibb & Sons, Princeton, N.J.
[2] Waters ALC 202 equipped with U6K universal injector, Milford, Mass.
[3] Schoeffel SF770, Westwood, N.J.
[4] Omniscribe 1513-12, Houston Instruments, Austin, Tex.
[5] Autolab minigrator, Spectra Physics, Santa Clara, Calif.
[6] Waters, μBondapak/CN.
[7] Beckman Zeromatic (SS-3) pH meter.

0022-3549/83/0200-0205$01.00/0

(10) J. Koch-Weser and E. M. Sellers, *N. Engl. J. Med.*, **294**, 311 and 526 (1976).
(11) W. E. Müller and U. Wollert, *Pharmacology*, **19**, 59 (1979).
(12) U. Kragh-Hansen, *Pharmacol. Rev.*, **33**, 17 (1981).
(13) B. Jirgenssons, *Biochim. Biophys. Acta*, **434**, 58 (1976).
(14) H. Glaser and J. Krieglstein, *Naunyn-Schmiedebergs Arch. Pharmacol.*, **265**, 321 (1970).
(15) A. Hulshoff and J. P. Perrin, *J. Med. Chem.*, **20**, 430 (1977).

ACKNOWLEDGMENTS

This study was supported by a grant of the Deutsche Forschungsgemeinschaft and a fellowship grant of the Alexander von Humboldt-Stiftung.

The excellent technical assistance of A. Stillbauer is gratefully acknowledged.

Complexation of Procainamide with Hydroxide-Containing Compounds

V. DAS GUPTA

Received September 18, 1981, from the *University of Houston, College of Pharmacy, Houston, TX 77030.* Accepted for publication April 2, 1982.

Abstract □ The complexation of procainamide with hydroxide-containing compounds, ethanol, fructose, glucose, glycerin, lactose, maltose, propylene glycol, sorbitol, and sucrose, have been studied. Procainamide formed a complex with glucose, lactose, and maltose, all of which contain a hemiacetal group, whereas fructose and sucrose do not. The percent of complex formed was dependent on the pH of the solution, with an optimum range of ~4–5.2. As with glucose, the percent of complex formed was directly related to the concentration of lactose in the solution. In dry mixtures, procainamide did not form a complex with glucose or lactose. The complex formed with lactose or maltose could be completely reversed by adding hydrochloric acid. A similar observation with glucose was reported earlier. In the optimum pH range, equilibrium was established in ~24 hr, and the process of complexation followed the equation for reversible reactions.

Keyphrases □ Complexation—procainamide with hydroxide-containing compounds □ Procainamide—complexation with hydroxide-containing compounds □ Hydroxide-containing compounds—complexation with procainamide

An earlier report (1) reviewed the literature concerning stability and complexation problems of procainamide in the presence of glucose. The report also presented the results of a study on the complexation of procainamide with glucose. (These two compounds are often mixed in hospitals for intravenous infusion for the treatment of cardiovascular diseases.)

Since procainamide oral dosage forms also are used widely, the formation of complex with some of the excipients seemed possible. The present report investigated the formation of procainamide complexes with hydroxide-containing compounds, ethanol, fructose, glucose, glycerin, lactose, maltose, propylene glycol, sorbitol, and sucrose.

EXPERIMENTAL

Materials—All chemicals and reagents were USP, NF, or ACS grade and were used as received. Procainamide hydrochloride[1] (I) was used without further purification.

A high-performance liquid chromatograph[2], equipped with a multiple wavelength detector[3], a recorder[4] and digital integrator[5], was used.

A semipolar column[6] (30 cm long × 4-mm i.d.) consisting of a monomolecular layer of cyanopropylsilane permanently bonded to silica gel was used.

Chromatographic Conditions—The mobile phase was 40% (v/v) acetonitrile in water containing 0.02 *M* ammonium acetate (pH ~7)[7], and the flow rate was 2.0 ml/min. The detector was set at 280 nm (the wavelength of maximum absorption), the sensitivity was 0.04, the temperature was ambient, and the chart speed was 30.5 cm/hr.

Methods—The stock solutions of procainamide hydrochloride (1.0 mg/ml) and the internal standard, methapyrilene hydrochloride (5.0 mg/ml) in water, were prepared fresh daily. A standard solution was prepared by transferring a 1.5-ml quantity of the stock solution of I and a 4.0-ml quantity of the stock solution of methapyrilene hydrochloride (II) to a 100-ml volumetric flask and then diluting with water to volume.

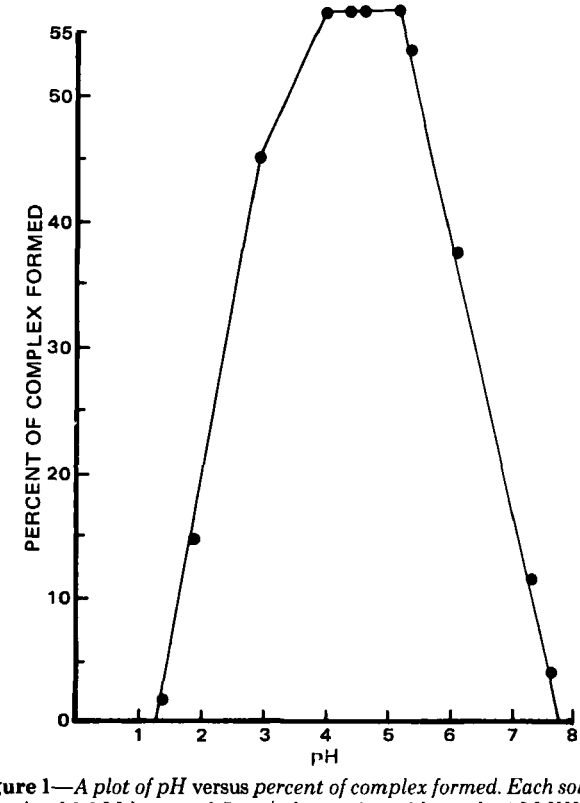

Figure 1—*A plot of pH* versus *percent of complex formed. Each solution contained 0.2* M *lactose, 0.5 mg/ml procainamide, and 0.2* M KH_2PO_4. *Solution of pH 1.4 was buffered with ~1* N *HCl. A similar plot was obtained with glucose.*

[1] Supplied by E. R. Squibb & Sons, Princeton, N.J.
[2] Waters ALC 202 equipped with U6K universal injector, Milford, Mass.
[3] Schoeffel SF770, Westwood, N.J.
[4] Omniscribe 1513-12, Houston Instruments, Austin, Tex.
[5] Autolab minigrator, Spectra Physics, Santa Clara, Calif.
[6] Waters, μBondapak/CN.
[7] Beckman Zeromatic (SS-3) pH meter.

0022-3549/83/0200-0205$01.00/0

Table I—List of Procainamide Aqueous Solutions Prepared

Solution Number	Other Ingredients[a] If Any (Final Concentration)	pH Initial (+0.1)	pH After 1 Day	Percent Retained After 1 Day
1	0.5 *M* Ethanol	6.0	6.3	98.2
2	0.5 *M* Glucose	6.1	6.2	90.3
3	0.5 *M* Glycerin	6.0	6.2	97.1
4	0.5 *M* Lactose	4.2	4.1	32.8
5	0.5 *M* Propylene Glycol	6.0	6.2	99.1
6	0.5 *M* Sorbitol	6.2	6.3	97.4
7	0.5 *M* Sucrose	5.1	5.2	98.6
8	0.2 *M* Ethanol[b]	4.6	4.6	100.3
9	0.2 *M* Glucose[b]	4.6	4.6	45.3
10	0.2 *M* Glycerin[b]	4.6	4.6	101.0
11	0.2 *M* Lactose[b]	4.6	4.6	42.6
12	0.2 *M* Lactose[b]	4.6	4.6	42.4
13	0.2 *M* Propylene[b] glycol	4.6	4.6	99.1
14	0.2 *M* Sorbitol[b]	4.6	4.6	99.7
15	0.2 *M* Sucrose[b]	4.6	4.6	98.9
16	0.2 *M* Lactose and 0.5 *M* KH_2PO_4	4.6	4.6	42.4
17	0.025 *M* Lactose[b]	4.5	4.5	88.3
18	0.05 *M* Lactose[b]	4.5	4.5	76.2
19	0.075 *M* Lactose[c]	4.5	4.5	67.4
20	0.1 *M* Lactose[c]	4.5	4.5	60.8
21	0.1 *M* Lactose[d]	4.4	4.4	59.8
22	0.2 *M* Lactose[d]	4.4	4.4	41.7
23	0.3 *M* Lactose[d]	4.4	4.4	31.4
24	0.4 *M* Lactose[d]	4.4	4.4	25.1
25	0.2 *M* Lactose and enough ~1 *N* HCl	1.0	1.0	100.5
26	0.2 *M* Lactose and enough ~1 *N* HCl	1.4	1.4	97.7
27	0.2 *M* Lactose[d]	1.9	1.9	85.1
28	0.2 *M* Lactose[d]	2.9	2.9	55.0
29	0.2 *M* Lactose[d]	4.0	4.0	42.6
30	0.2 *M* Lactose[d,e]	4.0	4.0	42.9
31	0.2 *M* Lactose[d]	5.2	5.2	42.8
32	0.2 *M* Lactose[d]	6.1	6.1	62.4
33	0.2 *M* Lactose[d]	7.3	7.3	88.8
34	0.2 *M* Glucose[d]	3.0	3.0	59.0
35	0.2 *M* Glucose[d]	4.2	4.2	43.2
36	0.2 *M* Glucose[d,e]	4.2	4.2	42.4
37	0.2 *M* Glucose[d]	4.4	4.4	42.7
38	0.2 *M* Glucose[d]	5.4	5.4	46.2
39	0.2 *M* Glucose[d]	6.2	6.2	71.7
40	0.2 *M* Glucose[d]	7.6	7.6	95.9
41	0.1 *M* Fructose[d]	4.4	4.4	99.7
42	0.1 *M* Maltose[d]	4.4	4.4	59.1

[a] All solutions contained 0.5 mg/ml of procainamide except solutions 1–7, which contained 1.0 mg/ml. [b] Each solution also contained 0.05% of sodium edetate and 0.5 *M* KH_2PO_4 as buffering agent except solution 12, which did not contain sodium edetate. [c] Each solution also contained 0.1 *M* KH_2PO_4. [d] Each solution also contained 0.2 *M* KH_2PO_4. In solutions 27–40, enough hydrochloric acid (~1 *N*) or NaOH (~1 *N*) was added to adjust the pH. More solutions of different pH values in both lactose and glucose were studied (Fig. 1). [e] The solution also contained 0.1 *M* KCl to study the effect of ionic strength.

Table II—Assay Results of Dry Mixtures and some Selected Solutions

Storage duration, hr	Solution Number[a] 9[b]	12	17	18	19	20	Dry Mixture With Glucose	Dry Mixture With Lactose
0	99.7	100.4	—	—	—	—	99.8	99.5
1	73.3	70.5	—	—	—	—	—	—
2	58.4	56.8	—	—	—	—	—	—
4	46.4	46.2	—	—	—	—	—	—
6	43.8	42.2	—	—	—	—	—	—
24	42.7	41.7	88.3	76.2	67.4	60.8	99.5	98.9
144	42.3	41.8	84.4	76.8	67.4	60.2	—	—

[a] See Table I. [b] Without sodium edetate.

All solutions prepared for the investigations of procainamide complexes are reported in Table I. All were prepared using a simple solution method. The solutions were assayed, transferred to amber-colored bottles[8], and stored at room temperature (24 ± 1°). They were assayed after appropriate intervals, and pH values were also determined.

All solutions were diluted with water to contain 15.0 μg/ml of I (based on the label claim) and 200.0 μg/ml of II (internal standard).

A 20.0-μl aliquot of the assay solution was injected into the chromatograph using the described conditions. For comparison, an identical volume of the standard solution was injected after the assay solution eluted.

[8] Brockway Glass Co., Brockway, Pa.

Calculations—The results were calculated using:

$$\frac{(Ph)_a}{(Ph)_s} \times 100 = \text{Percent of the label claim} \qquad \text{(Eq. 1)}$$

where $(Ph)_a$ is the ratio of the peak heights of procainamide and methapyrilene of the assay solution and $(Ph)_s$ is that of the standard solution of identical concentrations.

Other Experiments—A 1.5-ml quantity of 1-day-old solution in 0.2 *M* lactose (solution 12 in Table I) or in 0.1 *M* maltose (solution 42 in Table I) was mixed with 1.5 ml of ~5 *N* HCl. The mixture was allowed to stand for ~15 min, then 4.0 of the stock solution of the internal standard was added, the mixture brought to volume (100.0 ml) with water, and assayed.

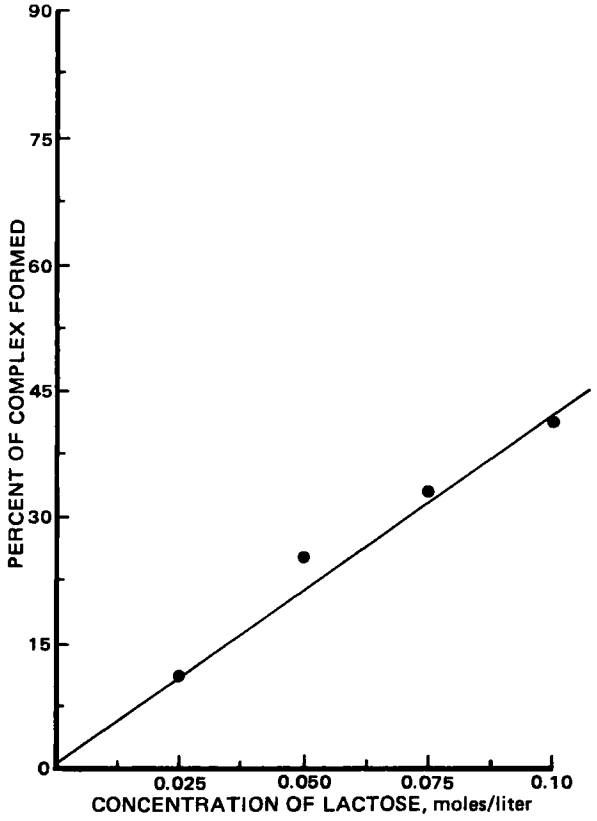

Figure 2—*A plot of lactose concentration (moles/liter)* versus *percent of complex formed.*

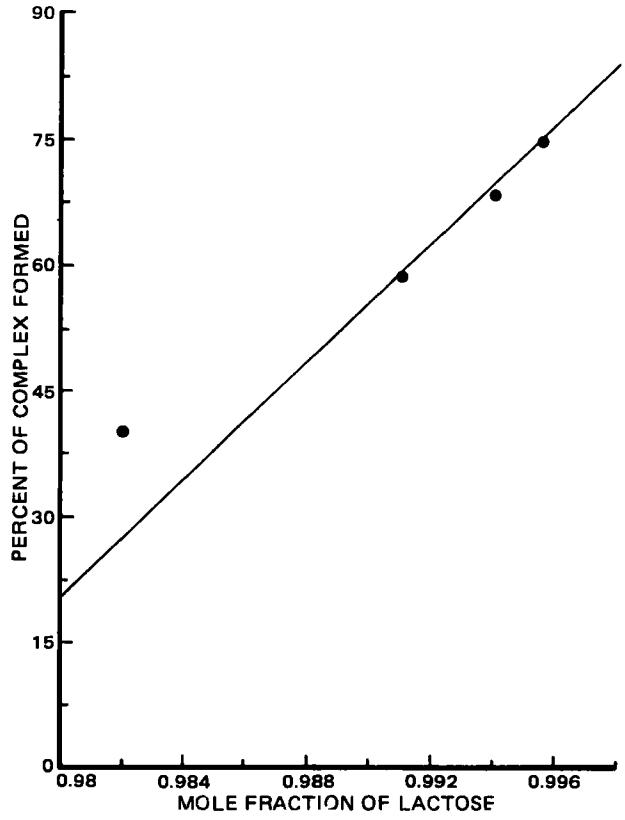

Figure 3—*A plot of lactose concentration (mole fraction)* versus *percent of complex formed.*

A 25.0-mg quantity of procainamide was mixed thoroughly with either 1.8 g of glucose or 3.6 g of lactose; the dry mixtures were allowed to stand overnight and assayed.

The solutions containing 0.2 *M* glucose/lactose, 0.2 *M* KH_2PO_4, and 0.5 mg/ml of procainamide were prepared and assayed at appropriate intervals up to 144 hr.

RESULTS AND DISCUSSION

The results indicate (Table I) that procainamide forms complexes with glucose, lactose (solutions 1–15, Table I), and maltose (solution 42 in Table I). The other hydroxide-containing compounds, ethanol, fructose, glycerin, propylene glycol, sorbitol, and sucrose, did not form complexes with procainamide (Table I). Therefore, it appears that a hemiacetal group is necessary for the formation of a complex. This group is present only in glucose, lactose, and maltose and not in other hydroxide-containing compounds.

The percent of procainamide complexed with lactose (as with glucose) was dependent on the initial pH value of the solution (solutions 25–40, Table I). For both glucose and lactose, the optimum pH range for the formation of complex appears to be ~4–5.2 (Fig. 1). The percent of complex formed with lactose and maltose were similar (solutions 21 and 42, Table I).

In a biologically useful pH range (7.3–7.5), the formation of complex was low (solutions 33 and 40, Table I). For example, only 11.2% of procainamide was complexed with lactose at pH 7.3, whereas almost 57% complexed between pH 4 and 5.2. Similar results were obtained with glucose.

Initially, when solution 2 in Table I was compared with solution 4, the percent of complex formed with lactose appeared much higher than with glucose. Nevertheless, in buffered solutions of identical pH (solutions 9 and 11, Table I), the difference was negligible.

The formation of complex was not affected by the addition of sodium edetate (solutions 11 and 12, Table I) or potassium chloride (solutions 29 and 30 and 35 and 36, Table I). As in glucose, the percent of complex formed was directly related to the concentration of lactose in the solution. At lower concentrations, molar concentrations of lactose were related and higher concentration mole fractions were related (Figs. 2 and 3). The formation of the complex could be completely reversed by adding hydrochloric acid (a similar observation was reported earlier with glucose). For example, solution 12 in Table I had only 42.4% of free procainamide after 24 hr of storage. On treatment with hydrochloric acid (*Other Experiments*), the concentration of free procainamide was 100.3%.

When solutions 17–20 (Table I) were reassayed after 6 days, there was only slight change in the concentration of free procainamide in solution 17 (Table II). In others, no significant change was noted (Table II). In solutions 9 and 12, the equilibrium was established in ~24 hr (Table II). The process of complexation followed the equation of reversible reactions as explained previously (1) for glucose.

In dry mixtures (*Other Experiments*), procainamide did not form a complex with glucose or lactose (Table II). Apparently, water is necessary for the formation of the complex.

REFERENCES

(1) V. D. Gupta, *J. Pharm. Sci.*, **71**, 994 (1982).

Correlation between Dissolution and Disintegration in Dissolution Apparatuses

Keyphrases □ Dissolution—disintegration, mathematical model linking dissolution and disintegration □ Disintegration—dissolution, mathematical model linking dissolution and distintegration

To the Editor:

El-Yazigi (1) in a recent article has proposed a model that links dissolution and disintegration in a dissolution apparatus. In deriving a convenient mathematical presentation mode, he assumes that the rate of appearance of dissolved material (A_s) is proportional to the mass of undissolved particles (A_p):

$$\frac{dA_s}{dt} = k_s A_p \qquad \text{(Eq. 1)}$$

where t is time and k_s is a dissolution rate constant (obviously in units of reciprocal time). He correctly cautions that this is not necessarily correct. The reason for using the mass dependence ($k_s A_p$ in Eq. 1) rather than a surface dependence:

$$\frac{dA_s}{dt} = k' \cdot \Gamma \cdot (A_p)^{2/3} \qquad \text{(Eq. 2)}$$

in which Γ is a shape factor (2), is presumably a mathematical convenience. It is an interesting approach, and it is the intent of this communication to compare the conclusion of El-Yazigi with those of previous investigators (3, 4). In the latter case the conditions of Eq. 2 and sink conditions were employed (*i.e.*, a cube root law was assumed) for the dissolution of drug from particles. The equations arrived at were for a basket apparatus, but a similar approach with similar conclusions can be arrived at for the simpler paddle apparatus.

The equations in the previous report (1) predict a biphasic exponential decay of undissolved mass, where the exponential term in the later phase depends on k_s. Several previously published treatments (3–6) have dealt with this problem. Carstensen *et al.* (3, 4) predicted (and demonstrated experimentally) that the undissolved mass should decay in a biphasic manner in the (often encountered) particular cases where disintegration (k_d in reciprocal time units) is rate determining. The latter phase is an exponential decay, but with the exponent dependent on k_d, *i.e.*, being a function of disintegration. This, however, is not universally applicable and only holds if the disintegration is rate limiting. A similar model has been developed (5) using (and demonstrating) a cube root dissolution model for the powder in a tablet, and for an established dissolution curve the disintegration curve was back calculated (6). This latter approach was found to be of a power exponential type [$\exp(-tb/a)$, where a and b are Weibull constants]. Other reports supporting surface dependent models have appeared in the literature (7).

In any event, the approach (1) is interesting and contains some supporting data which allow for some comparisons. Eq. 11 of Ref. 1 states:

$$DT_{calc} = 6 \cdot 0.693/k_d \qquad \text{(Eq. 3)}$$

where DT_{calc} is the calculated disintegration time obtained from the exponent of the initial phase of the dissolution plot. It is, as shown, based on the assumption that 1.56% of the tablet weight remaining (6 half-lives) constitutes complete disintegration. This is as good a conservative termination point as any, but it should be pointed out that there is nothing magical about it, and that, for instance, five half-lives would have been a good estimate as well. From a physical point of view, it might be rational to assume that the point where the tablet has been reduced to the size of a granule (8) (either the one used in producing the tablet or the one produced by disintegration) might be the cutoff point.

If, on the other hand, the number of half-lives, n, is assumed unknown than Eq. 3 takes the form:

$$DT = n\ 0.693/k_d \qquad \text{(Eq. 4)}$$

where DT stands for disintegration time. In logarithmic form this becomes:

$$\ln(DT) = \ln n + \ln 0.693 - \ln k_d \qquad \text{(Eq. 5)}$$

If this is equated to the experimentally determined disintegration time (DT), then $\ln(DT)$ should be linear in $\ln k_d$ with a slope of -1. The data from Table II of Ref. 1 are repeated in this form in Table I, and $\ln(DT)$ is shown as a functon of $\ln k_d$ in Fig. 1. It is seen that there is fair

Table I—Data from Table II of Reference 1

$\ln DT_{exp}$	$\ln k_d$
2.64	−1.136
2.34	−0.774
1.91	−0.785
2.43	−1.008
2.29	−0.884
3.20	−1.595
Slope[a]	−1.314
Intercept[a]	1.114
Correlation Coefficient[a]	−0.994

[a] Regression of $\ln DT$ on $\ln k$.

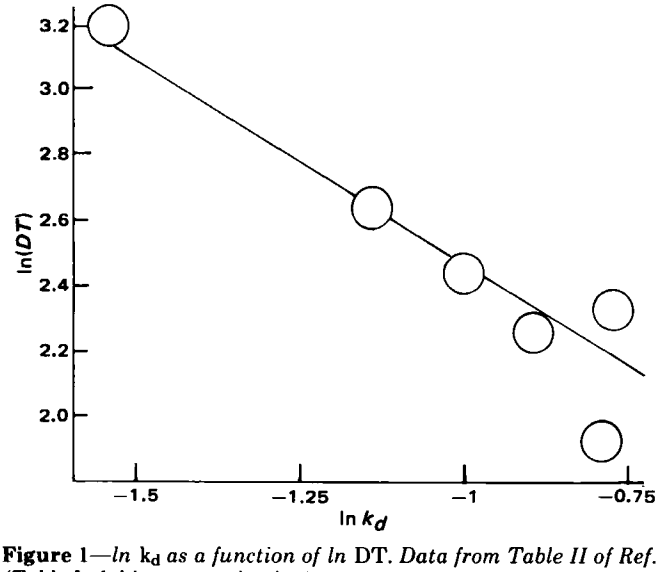

Figure 1—*ln* k_d *as a function of ln* DT. *Data from Table II of Ref. 1 (Table I of this communication).*

0022-3549/83/0200-0208$01.00/0

linearity (the correlation coefficient being 0.994 as shown in Table I). The least-squares fit is:

$$\ln(DT) = -1.32 \ln k_d + 1.114 \qquad \text{(Eq. 6)}$$

Although the slope is (significantly) different from −1, it is of the same order of magnitude so that this fact in no way disproves the utility of the previous method[1]. From the intercept it can be concluded that $\ln(0.693n) = 1.114$, *i.e.*, $n = 3.0/0.693 = 4.4$ half lives.

It is seen that further analysis of the data (1) do not disprove the hypothesis put forth. Whether the model of El-Yazigi is more applicable than previously proposed models (3, 4) is a point for future experimentors to verify.

(1) Adnan El-Yazigi, *J. Pharm. Sci.*, **70**, 535 (1981).
(2) T. Y-F. Lai and J. T. Carstensen, *Int. J. Pharm.*, **1**, 33 (1978).
(3) J. T. Carstensen, J. L. Wright, K. W. Blessel, and J. Sheridan, *J. Pharm. Sci.*, **67**, 48 (1978).
(4) *Idem.*, **67**, 982 (1978).
(5) K. G. Nelson and L. Y. Wang, *J. Pharm. Sci.*, **67**, 1758 (1977).
(6) *Idem.*, **67**, 86 (1978).
(7) J. T. Carstensen, R. Kothari, and Z. T. Chowhan, *Drug. Dev. Ind. Pharm.*, **6**, 569 (1980).
(8) K. A. Khan and C. T. Rhodes, *J. Pharm. Sci.*, **64**, 166 (1975).

J. T. Carstensen[x]
School of Pharmacy
University of Wisconsin,
Madison, WI 53706

Ashok Mehta
Formby's Inc.
Olive Branch,
Miss. 38654

M. A. Zoglio
Merrell-Dow Laboratories
Cincinnati, OH 45215

Received March 19, 1982.
Accepted for publication July 9, 1982.

[1] Equation 6 is approximate in the sense that different formulations are being compared.

BOOKS

Annual Review of Pharmacology and Toxicology. Vol. 22. Edited by ROBERT GEORGE, RONALD OKUN, and ARTHUR K. CHO. Annual Reviews Inc., 4139 El Camino Way, Palo Alto, CA 94306. 1982. 739 pp. 16 × 23 cm. Price $22.00 ($25.00 outside USA).

Traditionally, the first chapter of each volume of this annual review has been devoted to a historical/philosophical/autobiographical topic. This year it is an autobiographical statement by Thomas H. Maren. Traditionally also, the last chapter has been reserved for Chauncey Leake's "Review of Reviews." Since Leake's death, that feature has been continued in a very creditable fashion by E. Leong Way, although with a somewhat narrower perspective. The remainder of the book consists of 23 reviews of the literature, which have been sorted into 13 sections with 1–4 chapters each.

The sections of this year's review are titled: Mechanisms of Action of Drugs and Chemicals; Perinatal Pharmacology; Antimicrobial, Antiviral, and Antiparasite Chemotherapy; Cardiovascular Pharmacology; Renal Pharmacology; Neuropharmacology and Neurochemistry; Behavioral and Psychopharmacology; Anesthetics, Analgesics, and Anti-Inflammatory Agents; Endocrine Pharmacology; Comparative Pharmacology; Environmental and Industrial Pharmacology and Toxicology; Clinical Pharmacology and Drug Interaction; and Techniques.

One would presume that the chapters within each section would be clumped together but, in actuality, they are randomly distributed among the chapters of other sections. Therefore, the practice of dividing the table of contents into sections seems to be an unnecessary gesture since the readers of this volume will be quite capable of grasping the general content of each chapter from the titles themselves.

Individuals in the pharmaceutical sciences will find the review by H. H. Szeto on "Pharmacokinetics in the Ovine Maternal–Fetal Unit" to be of interest and the review on "Food and Drug Interactions" by C. Jelleff Carr to be useful but rudimental. Especially effective literature reviews are M. J. Antonaccio's "Angiotensin Converting Enzyme (ACE) Inhibitors," J. Torretti's "Sympathetic Control of Renin Release," and H. E. Brezenoff and R. Giuliano's "Cardiovascular Control by Cholinergic Mechanisms in the Central Nervous System." Perhaps the most provocative review is "Neurochemical Basis of Acupuncture Analgesia" by J. S. Han and L. Terenius, while the most debatable offering is "Sociopharmacology" by M. T. McGuire, M. J. Raleigh, and G. L. Brammer.

This reviewer has a standing order for this series and considers it essential as a continuing education tool and as a quick reference source. The number of primary references per review ranges from 67 to 318 for this volume. Considering the current prices for technical books, this series is a bargain by any standard that might be applied.

Reviewed by Marvin H. Malone
Physiology and Pharmacology Unit
School of Pharmacy
University of the Pacific
Stockton, CA 95207

Topics in Pharmaceutical Sciences Edited by D. D. BREIMER and P. SPEISER. Elsivier/North Holland Biomedical Press, Amsterdam, The Netherlands 1981. 535 pp. 16 × 24 cm. Price $69.74 U.S., 150 Dfl.

The book, which contains over thirty chapters, is the proceedings of the 41st International Congress of FIP, held in Vienna, Austria, Sept. 1981. There chapters are divided into seven symposia which cover some of the major areas of thrust in the pharmaceutical sciences. The symposium titles are:

Advances in Pharmacokinetics;
Pharmaceutical Aspects of Anti-Cancer Drug Treatment;
Biopharmaceutics: Advances in Drug Delivery
Drug Stability *in vitro* and *in vivo;*
Analysis and Drug Metabolites in the 80s;
Pharmaceutical Technology;
Gene Manipulation, Cell Cultures, and Pharmaceutical Sciences.

An author index is provided but, unfortunately, there is no subject index. The price is rather high for a symposium proceeding produced from camera-ready copy.

Since *Topics in Pharmaceutical Sciences* covers a very broad spectrum of subjects, it cannot be recommended for anyone seeking an in-depth discussion on any particular subject. (It averages less than 80 pages per symposium.) It can, however, be recommended for those who want an overview of the current thinking in the subjects covered.

Reviewed by S. H. Yalkowsky
The Upjohn Co.
Kalamazoo, MI 49001

linearity (the correlation coefficient being 0.994 as shown in Table I). The least-squares fit is:

$$\ln(DT) = -1.32 \ln k_d + 1.114 \qquad \text{(Eq. 6)}$$

Although the slope is (significantly) different from −1, it is of the same order of magnitude so that this fact in no way disproves the utility of the previous method[1]. From the intercept it can be concluded that $\ln(0.693n) = 1.114$, *i.e.*, $n = 3.0/0.693 = 4.4$ half lives.

It is seen that further analysis of the data (1) do not disprove the hypothesis put forth. Whether the model of El-Yazigi is more applicable than previously proposed models (3, 4) is a point for future experimentors to verify.

(1) Adnan El-Yazigi, *J. Pharm. Sci.*, **70**, 535 (1981).
(2) T. Y-F. Lai and J. T. Carstensen, *Int. J. Pharm.*, **1**, 33 (1978).
(3) J. T. Carstensen, J. L. Wright, K. W. Blessel, and J. Sheridan, *J. Pharm. Sci.*, **67**, 48 (1978).
(4) *Idem.*, **67**, 982 (1978).
(5) K. G. Nelson and L. Y. Wang, *J. Pharm. Sci.*, **67**, 1758 (1977).
(6) *Idem.*, **67**, 86 (1978).
(7) J. T. Carstensen, R. Kothari, and Z. T. Chowhan, *Drug. Dev. Ind. Pharm.*, **6**, 569 (1980).
(8) K. A. Khan and C. T. Rhodes, *J. Pharm. Sci.*, **64**, 166 (1975).

J. T. Carstensen[x]
School of Pharmacy
University of Wisconsin,
Madison, WI 53706

Ashok Mehta
Formby's Inc.
Olive Branch,
Miss. 38654

M. A. Zoglio
Merrell-Dow Laboratories
Cincinnati, OH 45215

Received March 19, 1982.
Accepted for publication July 9, 1982.

[1] Equation 6 is approximate in the sense that different formulations are being compared.

BOOKS

Annual Review of Pharmacology and Toxicology. Vol. 22. Edited by ROBERT GEORGE, RONALD OKUN, and ARTHUR K. CHO. Annual Reviews Inc., 4139 El Camino Way, Palo Alto, CA 94306. 1982. 739 pp. 16 × 23 cm. Price $22.00 ($25.00 outside USA).

Traditionally, the first chapter of each volume of this annual review has been devoted to a historical/philosophical/autobiographical topic. This year it is an autobiographical statement by Thomas H. Maren. Traditionally also, the last chapter has been reserved for Chauncey Leake's "Review of Reviews." Since Leake's death, that feature has been continued in a very creditable fashion by E. Leong Way, although with a somewhat narrower perspective. The remainder of the book consists of 23 reviews of the literature, which have been sorted into 13 sections with 1–4 chapters each.

The sections of this year's review are titled: Mechanisms of Action of Drugs and Chemicals; Perinatal Pharmacology; Antimicrobial, Antiviral, and Antiparasite Chemotherapy; Cardiovascular Pharmacology; Renal Pharmacology; Neuropharmacology and Neurochemistry; Behavioral and Psychopharmacology; Anesthetics, Analgesics, and Anti-Inflammatory Agents; Endocrine Pharmacology; Comparative Pharmacology; Environmental and Industrial Pharmacology and Toxicology; Clinical Pharmacology and Drug Interaction; and Techniques.

One would presume that the chapters within each section would be clumped together but, in actuality, they are randomly distributed among the chapters of other sections. Therefore, the practice of dividing the table of contents into sections seems to be an unnecessary gesture since the readers of this volume will be quite capable of grasping the general content of each chapter from the titles themselves.

Individuals in the pharmaceutical sciences will find the review by H. H. Szeto on "Pharmacokinetics in the Ovine Maternal–Fetal Unit" to be of interest and the review on "Food and Drug Interactions" by C. Jelleff Carr to be useful but rudimental. Especially effective literature reviews are M. J. Antonaccio's "Angiotensin Converting Enzyme (ACE) Inhibitors," J. Torretti's "Sympathetic Control of Renin Release," and H. E. Brezenoff and R. Giuliano's "Cardiovascular Control by Cholinergic Mechanisms in the Central Nervous System." Perhaps the most provocative review is "Neurochemical Basis of Acupuncture Analgesia" by J. S. Han and L. Terenius, while the most debatable offering is "Sociopharmacology" by M. T. McGuire, M. J. Raleigh, and G. L. Brammer.

This reviewer has a standing order for this series and considers it essential as a continuing education tool and as a quick reference source. The number of primary references per review ranges from 67 to 318 for this volume. Considering the current prices for technical books, this series is a bargain by any standard that might be applied.

Reviewed by Marvin H. Malone
Physiology and Pharmacology Unit
School of Pharmacy
University of the Pacific
Stockton, CA 95207

Topics in Pharmaceutical Sciences Edited by D. D. BREIMER and P. SPEISER. Elsivier/North Holland Biomedical Press, Amsterdam, The Netherlands 1981. 535 pp. 16 × 24 cm. Price $69.74 U.S., 150 Dfl.

The book, which contains over thirty chapters, is the proceedings of the 41st International Congress of FIP, held in Vienna, Austria, Sept. 1981. There chapters are divided into seven symposia which cover some of the major areas of thrust in the pharmaceutical sciences. The symposium titles are:

Advances in Pharmacokinetics;
Pharmaceutical Aspects of Anti-Cancer Drug Treatment;
Biopharmaceutics: Advances in Drug Delivery
Drug Stability *in vitro* and *in vivo;*
Analysis and Drug Metabolites in the 80s;
Pharmaceutical Technology;
Gene Manipulation, Cell Cultures, and Pharmaceutical Sciences.

An author index is provided but, unfortunately, there is no subject index. The price is rather high for a symposium proceeding produced from camera-ready copy.

Since *Topics in Pharmaceutical Sciences* covers a very broad spectrum of subjects, it cannot be recommended for anyone seeking an in-depth discussion on any particular subject. (It averages less than 80 pages per symposium.) It can, however, be recommended for those who want an overview of the current thinking in the subjects covered.

Reviewed by S. H. Yalkowsky
The Upjohn Co.
Kalamazoo, MI 49001

linearity (the correlation coefficient being 0.994 as shown in Table I). The least-squares fit is:

$$\ln(DT) = -1.32 \ln k_d + 1.114 \qquad \text{(Eq. 6)}$$

Although the slope is (significantly) different from −1, it is of the same order of magnitude so that this fact in no way disproves the utility of the previous method[1]. From the intercept it can be concluded that $\ln(0.693n) = 1.114$, *i.e.*, $n = 3.0/0.693 = 4.4$ half lives.

It is seen that further analysis of the data (1) do not disprove the hypothesis put forth. Whether the model of El-Yazigi is more applicable than previously proposed models (3, 4) is a point for future experimentors to verify.

(1) Adnan El-Yazigi, *J. Pharm. Sci.*, **70**, 535 (1981).
(2) T. Y-F. Lai and J. T. Carstensen, *Int. J. Pharm.*, **1**, 33 (1978).
(3) J. T. Carstensen, J. L. Wright, K. W. Blessel, and J. Sheridan, *J. Pharm. Sci.*, **67**, 48 (1978).
(4) *Idem.*, **67**, 982 (1978).
(5) K. G. Nelson and L. Y. Wang, *J. Pharm. Sci.*, **67**, 1758 (1977).
(6) *Idem.*, **67**, 86 (1978).
(7) J. T. Carstensen, R. Kothari, and Z. T. Chowhan, *Drug. Dev. Ind. Pharm.*, **6**, 569 (1980).
(8) K. A. Khan and C. T. Rhodes, *J. Pharm. Sci.*, **64**, 166 (1975).

J. T. Carstensen[x]
School of Pharmacy
University of Wisconsin,
Madison, WI 53706

Ashok Mehta
Formby's Inc.
Olive Branch,
Miss. 38654

M. A. Zoglio
Merrell-Dow Laboratories
Cincinnati, OH 45215

Received March 19, 1982.
Accepted for publication July 9, 1982.

[1] Equation 6 is approximate in the sense that different formulations are being compared.

BOOKS

Annual Review of Pharmacology and Toxicology. Vol. 22. Edited by ROBERT GEORGE, RONALD OKUN, and ARTHUR K. CHO. Annual Reviews Inc., 4139 El Camino Way, Palo Alto, CA 94306. 1982. 739 pp. 16 × 23 cm. Price $22.00 ($25.00 outside USA).

Traditionally, the first chapter of each volume of this annual review has been devoted to a historical/philosophical/autobiographical topic. This year it is an autobiographical statement by Thomas H. Maren. Traditionally also, the last chapter has been reserved for Chauncey Leake's "Review of Reviews." Since Leake's death, that feature has been continued in a very creditable fashion by E. Leong Way, although with a somewhat narrower perspective. The remainder of the book consists of 23 reviews of the literature, which have been sorted into 13 sections with 1–4 chapters each.

The sections of this year's review are titled: Mechanisms of Action of Drugs and Chemicals; Perinatal Pharmacology; Antimicrobial, Antiviral, and Antiparasite Chemotherapy; Cardiovascular Pharmacology; Renal Pharmacology; Neuropharmacology and Neurochemistry; Behavioral and Psychopharmacology; Anesthetics, Analgesics, and Anti-Inflammatory Agents; Endocrine Pharmacology; Comparative Pharmacology; Environmental and Industrial Pharmacology and Toxicology; Clinical Pharmacology and Drug Interaction; and Techniques.

One would presume that the chapters within each section would be clumped together but, in actuality, they are randomly distributed among the chapters of other sections. Therefore, the practice of dividing the table of contents into sections seems to be an unnecessary gesture since the readers of this volume will be quite capable of grasping the general content of each chapter from the titles themselves.

Individuals in the pharmaceutical sciences will find the review by H. H. Szeto on "Pharmacokinetics in the Ovine Maternal–Fetal Unit" to be of interest and the review on "Food and Drug Interactions" by C. Jelleff Carr to be useful but rudimental. Especially effective literature reviews are M. J. Antonaccio's "Angiotensin Converting Enzyme (ACE) Inhibitors," J. Torretti's "Sympathetic Control of Renin Release," and H. E. Brezenoff and R. Giuliano's "Cardiovascular Control by Cholinergic Mechanisms in the Central Nervous System." Perhaps the most provocative review is "Neurochemical Basis of Acupuncture Analgesia" by J. S. Han and L. Terenius, while the most debatable offering is "Sociopharmacology" by M. T. McGuire, M. J. Raleigh, and G. L. Brammer.

This reviewer has a standing order for this series and considers it essential as a continuing education tool and as a quick reference source. The number of primary references per review ranges from 67 to 318 for this volume. Considering the current prices for technical books, this series is a bargain by any standard that might be applied.

Reviewed by Marvin H. Malone
Physiology and Pharmacology Unit
School of Pharmacy
University of the Pacific
Stockton, CA 95207

Topics in Pharmaceutical Sciences Edited by D. D. BREIMER and P. SPEISER. Elsivier/North Holland Biomedical Press, Amsterdam, The Netherlands 1981. 535 pp. 16 × 24 cm. Price $69.74 U.S., 150 Dfl.

The book, which contains over thirty chapters, is the proceedings of the 41st International Congress of FIP, held in Vienna, Austria, Sept. 1981. There chapters are divided into seven symposia which cover some of the major areas of thrust in the pharmaceutical sciences. The symposium titles are:

Advances in Pharmacokinetics;
Pharmaceutical Aspects of Anti-Cancer Drug Treatment;
Biopharmaceutics: Advances in Drug Delivery
Drug Stability *in vitro* and *in vivo;*
Analysis and Drug Metabolites in the 80s;
Pharmaceutical Technology;
Gene Manipulation, Cell Cultures, and Pharmaceutical Sciences.

An author index is provided but, unfortunately, there is no subject index. The price is rather high for a symposium proceeding produced from camera-ready copy.

Since *Topics in Pharmaceutical Sciences* covers a very broad spectrum of subjects, it cannot be recommended for anyone seeking an in-depth discussion on any particular subject. (It averages less than 80 pages per symposium.) It can, however, be recommended for those who want an overview of the current thinking in the subjects covered.

Reviewed by S. H. Yalkowsky
The Upjohn Co.
Kalamazoo, MI 49001

Molecular Basis of Drug Action. Edited by THOMAS P. SINGER and RAUL N. ONDARZA. Elsevier/North-Holland, New York, NY 10017. 1981. 408 pp. 16 × 24 cm. Price $55.00.

This book contains the proceedings of the International Symposium on the Molecular Basis of Drug Action held in Queretaro, Mexico in October 1980. The editors have dedicated the book to the memory of Dr. Eugene C. Jorgensen. The warmth of the picture of Gene in the front of the book and the clear sparkling quality of his chapter brings us poignant reminders of the humanistic and scientific qualities of this man.

The book is divided into five sections; each section having three to six chapters. The section topics are: Drugs Against Microbial Invaders, Suicide Inhibitors, New Directions in Molecular Pharmacology, Ionic Channels and Pumps, and Mechanisms of Drug Resistance.

The book is unusual for a symposium volume for several reasons. The chapters have been carefully guided and edited so that there is more than the usual background information found in symposia volumes. Most chapters are mini reviews. The tables, schemes, figures, and art work are well-designed and attractive. Most importantly, they enrich the information content of the chapter. The choice of sections and articles covers quite thoroughly most of the current work in this dynamic approach. The distinguished contributors bring together in one volume a valuable collection of articles on the molecular basis of drug action.

The book is of such significant quality that individual drug scientists may want to purchase it for their libraries. It is certainly a fitting memorial to Gene Jorgensen, one of the pioneers in this field.

Reviewed by Lemont B. Kier
Department of Pharmaceutical Chemistry
School of Pharmacy
Medical College of Virginia
Virginia Commonwealth University
Richmond, Virginia 23298

The Alkaloids. Chemistry and Physiology, Vol. 19. Founding Editor, R. H. F. MANSKE, Edited by R. G. A. RODRIGO. Academic Press, Inc., New York, NY 10003 1981. 227 pp. 15 × 23 cm. Price $39.00.

Volume 19 of *The Alkaloids* marks the continuation of this classic series, which reviews advances in alkaloid chemistry. Included in this volume are groups of alkaloids which have not been reviewed for over 10 years. These new groups are *Sceletium*, *Solanum* steroids, and phenanthroindolizidine and phenanthroquinolizidine alkaloids.

Peter W. Jeffs has written an excellent comprehensive review of the *Sceletium* (Fam. *Aizoaceae*) alkaloids. The number of alkaloids from this genus has increased to more than 25. They fall into four structural classes based on four different ring systems: the mesembrine, joubertiamine, pyridine-dihydropyridone, and tortuosamine. Detailed descriptions are given of chemical and spectral methods of structure elucidation, synthetic methods, chemical transformations, and biosynthetic studies.

A chapter by Helmut Ripperger and Klaus Schreiber reviews the *Solanum* steroid alkaloids. This well-organized chapter presents work since 1966 in tables which supplement similar surveys in Volume 10. There are tables of the occurrence of *Solanum* glycoalkaloids and alkamines, composition of the glycoalkaloids, and physical constants of all the glycosides, alkamines, and their derivatives (over 500) described since 1967. The physical constants are arranged by tables according to the five different C_{27}-carbon skeletons comprising the *Solanum* steriodal alkamines. The structure elucidation of new alkamines, syntheses, and chemical degradations are described in detail. Interest has been renewed in these alkaloids as a source of starting material for making hormonal steroid drugs.

In another chapter Ralph C. Bick and Wannee Sinchai review all 16 phenanthroindolizidine and two phenanthroquinolizidine alkaloids that are known. The phenanthroindolizidines are often called *Tylophora* alkaloids, since they frequently occur in this genus (Fam. *Asclepiadaceae*). Spectral methods are described in separate sections with specific examples of how the techniques are used for structure characterization. The chapter also features a section on the various synthetic schemes which have been developed for these alkaloids. The large interest in syntheses stems from reported biological activities of these compounds, including antitumor activity.

This volume of *The Alkaloids* maintains the high quality of the series and should be added to the collections of alkaloid chemists.

Reviewed by Susan Tafur
Philip Morris Research Center
P.O. Box 26583
Richmond, VA 23261

The Alkaloids. Chemistry and Physiology, Volume 20. Founding Editor, R. H. F. MANSKE, Edited by R. G. A. RODRIGO. Academic Press, Inc., New York, NY 10003. 1981. 341 pp. 15 × 23 cm. Price $59.50.

This 20th volume of the excellent series on advances in alkaloid chemistry is devoted to bisindole and eburnamine–vincamine alkaloids. The exacting thoroughness with which these groups of alkaloids are covered is characteristic of the reviews in this series.

Geoffrey A. Cordell and J. Edwin Saxton have combined discussions of various bisindole alkaloids into a single review, whereas in previous volumes the dimeric alkaloids have been a part of more specific reviews on alkaloids of a particular genus or structural type. The unifying factor of the bisindoles lies in their containing two tryptophan-derived nuclei. The sections of the review are organized based on progressing biosynthetic pathways from simple tryptamine units to two monoterpenoid indoles. Special sections on ^{13}C-NMR data or various synthetic schemes of particular groups of alkaloids are also included. References for plant sources and physical data of all structurally identified bisindoles are summarized by table.

The other group of alkaloids covered in this volume is the eburnamine–vincamine type which is reviewed by Werner Döpke. Much of the recent work on these pentacyclic indole alkaloids is in the area of establishing absolute configurations. New stereoselective syntheses have been achieved, especially for vincamine, which has recently been found to have medicinal uses. Extensive discussions on specific alkaloids are restricted mainly to the new alkaloids of this type which have been isolated since the last review in Volume 11.

Volume 20 continues the well-organized style of this outstanding series. It should be of particular interest to indole alkaloid chemists and others who wish to have exceptional reviews of these important classes of alkaloids.

Reviewed by Susan Tafur
Philip Morris Research Center
P.O. Box 26583
Richmond, VA 23261

Molecular Basis of Drug Action. Edited by THOMAS P. SINGER and RAUL N. ONDARZA. Elsevier/North-Holland, New York, NY 10017. 1981. 408 pp. 16 × 24 cm. Price $55.00.

This book contains the proceedings of the International Symposium on the Molecular Basis of Drug Action held in Queretaro, Mexico in October 1980. The editors have dedicated the book to the memory of Dr. Eugene C. Jorgensen. The warmth of the picture of Gene in the front of the book and the clear sparkling quality of his chapter brings us poignant reminders of the humanistic and scientific qualities of this man.

The book is divided into five sections; each section having three to six chapters. The section topics are: Drugs Against Microbial Invaders, Suicide Inhibitors, New Directions in Molecular Pharmacology, Ionic Channels and Pumps, and Mechanisms of Drug Resistance.

The book is unusual for a symposium volume for several reasons. The chapters have been carefully guided and edited so that there is more than the usual background information found in symposia volumes. Most chapters are mini reviews. The tables, schemes, figures, and art work are well-designed and attractive. Most importantly, they enrich the information content of the chapter. The choice of sections and articles covers quite thoroughly most of the current work in this dynamic approach. The distinguished contributors bring together in one volume a valuable collection of articles on the molecular basis of drug action.

The book is of such significant quality that individual drug scientists may want to purchase it for their libraries. It is certainly a fitting memorial to Gene Jorgensen, one of the pioneers in this field.

Reviewed by Lemont B. Kier
Department of Pharmaceutical Chemistry
School of Pharmacy
Medical College of Virginia
Virginia Commonwealth University
Richmond, Virginia 23298

The Alkaloids. Chemistry and Physiology, Vol. 19. Founding Editor, R. H. F. MANSKE, Edited by R. G. A. RODRIGO. Academic Press, Inc., New York, NY 10003 1981. 227 pp. 15 × 23 cm. Price $39.00.

Volume 19 of *The Alkaloids* marks the continuation of this classic series, which reviews advances in alkaloid chemistry. Included in this volume are groups of alkaloids which have not been reviewed for over 10 years. These new groups are *Sceletium*, *Solanum* steroids, and phenanthroindolizidine and phenanthroquinolizidine alkaloids.

Peter W. Jeffs has written an excellent comprehensive review of the *Sceletium* (Fam. *Aizoaceae*) alkaloids. The number of alkaloids from this genus has increased to more than 25. They fall into four structural classes based on four different ring systems: the mesembrine, joubertiamine, pyridine-dihydropyridone, and tortuosamine. Detailed descriptions are given of chemical and spectral methods of structure elucidation, synthetic methods, chemical transformations, and biosynthetic studies.

A chapter by Helmut Ripperger and Klaus Schreiber reviews the *Solanum* steroid alkaloids. This well-organized chapter presents work since 1966 in tables which supplement similar surveys in Volume 10. There are tables of the occurrence of *Solanum* glycoalkaloids and alkamines, composition of the glycoalkaloids, and physical constants of all the glycosides, alkamines, and their derivatives (over 500) described since 1967. The physical constants are arranged by tables according to the five different C_{27}-carbon skeletons comprising the *Solanum* steriodal alkamines. The structure elucidation of new alkamines, syntheses, and chemical degradations are described in detail. Interest has been renewed in these alkaloids as a source of starting material for making hormonal steroid drugs.

In another chapter Ralph C. Bick and Wannee Sinchai review all 16 phenanthroindolizidine and two phenanthroquinolizidine alkaloids that are known. The phenanthroindolizidines are often called *Tylophora* alkaloids, since they frequently occur in this genus (Fam. *Asclepiadaceae*). Spectral methods are described in separate sections with specific examples of how the techniques are used for structure characterization. The chapter also features a section on the various synthetic schemes which have been developed for these alkaloids. The large interest in syntheses stems from reported biological activities of these compounds, including antitumor activity.

This volume of *The Alkaloids* maintains the high quality of the series and should be added to the collections of alkaloid chemists.

Reviewed by Susan Tafur
Philip Morris Research Center
P.O. Box 26583
Richmond, VA 23261

The Alkaloids. Chemistry and Physiology, Volume 20. Founding Editor, R. H. F. MANSKE, Edited by R. G. A. RODRIGO. Academic Press, Inc., New York, NY 10003. 1981. 341 pp. 15 × 23 cm. Price $59.50.

This 20th volume of the excellent series on advances in alkaloid chemistry is devoted to bisindole and eburnamine–vincamine alkaloids. The exacting thoroughness with which these groups of alkaloids are covered is characteristic of the reviews in this series.

Geoffrey A. Cordell and J. Edwin Saxton have combined discussions of various bisindole alkaloids into a single review, whereas in previous volumes the dimeric alkaloids have been a part of more specific reviews on alkaloids of a particular genus or structural type. The unifying factor of the bisindoles lies in their containing two tryptophan-derived nuclei. The sections of the review are organized based on progressing biosynthetic pathways from simple tryptamine units to two monoterpenoid indoles. Special sections on ^{13}C-NMR data or various synthetic schemes of particular groups of alkaloids are also included. References for plant sources and physical data of all structurally identified bisindoles are summarized by table.

The other group of alkaloids covered in this volume is the eburnamine–vincamine type which is reviewed by Werner Döpke. Much of the recent work on these pentacyclic indole alkaloids is in the area of establishing absolute configurations. New stereoselective syntheses have been achieved, especially for vincamine, which has recently been found to have medicinal uses. Extensive discussions on specific alkaloids are restricted mainly to the new alkaloids of this type which have been isolated since the last review in Volume 11.

Volume 20 continues the well-organized style of this outstanding series. It should be of particular interest to indole alkaloid chemists and others who wish to have exceptional reviews of these important classes of alkaloids.

Reviewed by Susan Tafur
Philip Morris Research Center
P.O. Box 26583
Richmond, VA 23261

Molecular Basis of Drug Action. Edited by THOMAS P. SINGER and RAUL N. ONDARZA. Elsevier/North-Holland, New York, NY 10017. 1981. 408 pp. 16 × 24 cm. Price $55.00.

This book contains the proceedings of the International Symposium on the Molecular Basis of Drug Action held in Queretaro, Mexico in October 1980. The editors have dedicated the book to the memory of Dr. Eugene C. Jorgensen. The warmth of the picture of Gene in the front of the book and the clear sparkling quality of his chapter brings us poignant reminders of the humanistic and scientific qualities of this man.

The book is divided into five sections; each section having three to six chapters. The section topics are: Drugs Against Microbial Invaders, Suicide Inhibitors, New Directions in Molecular Pharmacology, Ionic Channels and Pumps, and Mechanisms of Drug Resistance.

The book is unusual for a symposium volume for several reasons. The chapters have been carefully guided and edited so that there is more than the usual background information found in symposia volumes. Most chapters are mini reviews. The tables, schemes, figures, and art work are well-designed and attractive. Most importantly, they enrich the information content of the chapter. The choice of sections and articles covers quite thoroughly most of the current work in this dynamic approach. The distinguished contributors bring together in one volume a valuable collection of articles on the molecular basis of drug action.

The book is of such significant quality that individual drug scientists may want to purchase it for their libraries. It is certainly a fitting memorial to Gene Jorgensen, one of the pioneers in this field.

Reviewed by Lemont B. Kier
Department of Pharmaceutical Chemistry
School of Pharmacy
Medical College of Virginia
Virginia Commonwealth University
Richmond, Virginia 23298

The Alkaloids. Chemistry and Physiology, Vol. 19. Founding Editor, R. H. F. MANSKE, Edited by R. G. A. RODRIGO. Academic Press, Inc., New York, NY 10003 1981. 227 pp. 15 × 23 cm. Price $39.00.

Volume 19 of *The Alkaloids* marks the continuation of this classic series, which reviews advances in alkaloid chemistry. Included in this volume are groups of alkaloids which have not been reviewed for over 10 years. These new groups are *Sceletium*, *Solanum* steroids, and phenanthroindolizidine and phenanthroquinolizidine alkaloids.

Peter W. Jeffs has written an excellent comprehensive review of the *Sceletium* (Fam. *Aizoaceae*) alkaloids. The number of alkaloids from this genus has increased to more than 25. They fall into four structural classes based on four different ring systems: the mesembrine, joubertiamine, pyridine-dihydropyridone, and tortuosamine. Detailed descriptions are given of chemical and spectral methods of structure elucidation, synthetic methods, chemical transformations, and biosynthetic studies.

A chapter by Helmut Ripperger and Klaus Schreiber reviews the *Solanum* steroid alkaloids. This well-organized chapter presents work since 1966 in tables which supplement similar surveys in Volume 10. There are tables of the occurrence of *Solanum* glycoalkaloids and alkamines, composition of the glycoalkaloids, and physical constants of all the glycosides, alkamines, and their derivatives (over 500) described since 1967. The physical constants are arranged by tables according to the five different C_{27}-carbon skeletons comprising the *Solanum* steriodal alkamines. The structure elucidation of new alkamines, syntheses, and chemical degradations are described in detail. Interest has been renewed in these alkaloids as a source of starting material for making hormonal steroid drugs.

In another chapter Ralph C. Bick and Wannee Sinchai review all 16 phenanthroindolizidine and two phenanthroquinolizidine alkaloids that are known. The phenanthroindolizidines are often called *Tylophora* alkaloids, since they frequently occur in this genus (Fam. *Asclepiadaceae*). Spectral methods are described in separate sections with specific examples of how the techniques are used for structure characterization. The chapter also features a section on the various synthetic schemes which have been developed for these alkaloids. The large interest in syntheses stems from reported biological activities of these compounds, including antitumor activity.

This volume of *The Alkaloids* maintains the high quality of the series and should be added to the collections of alkaloid chemists.

Reviewed by Susan Tafur
Philip Morris Research Center
P.O. Box 26583
Richmond, VA 23261

The Alkaloids. Chemistry and Physiology, Volume 20. Founding Editor, R. H. F. MANSKE, Edited by R. G. A. RODRIGO. Academic Press, Inc., New York, NY 10003. 1981. 341 pp. 15 × 23 cm. Price $59.50.

This 20th volume of the excellent series on advances in alkaloid chemistry is devoted to bisindole and eburnamine–vincamine alkaloids. The exacting thoroughness with which these groups of alkaloids are covered is characteristic of the reviews in this series.

Geoffrey A. Cordell and J. Edwin Saxton have combined discussions of various bisindole alkaloids into a single review, whereas in previous volumes the dimeric alkaloids have been a part of more specific reviews on alkaloids of a particular genus or structural type. The unifying factor of the bisindoles lies in their containing two tryptophan-derived nuclei. The sections of the review are organized based on progressing biosynthetic pathways from simple tryptamine units to two monoterpenoid indoles. Special sections on ^{13}C-NMR data or various synthetic schemes of particular groups of alkaloids are also included. References for plant sources and physical data of all structurally identified bisindoles are summarized by table.

The other group of alkaloids covered in this volume is the eburnamine–vincamine type which is reviewed by Werner Döpke. Much of the recent work on these pentacyclic indole alkaloids is in the area of establishing absolute configurations. New stereoselective syntheses have been achieved, especially for vincamine, which has recently been found to have medicinal uses. Extensive discussions on specific alkaloids are restricted mainly to the new alkaloids of this type which have been isolated since the last review in Volume 11.

Volume 20 continues the well-organized style of this outstanding series. It should be of particular interest to indole alkaloid chemists and others who wish to have exceptional reviews of these important classes of alkaloids.

Reviewed by Susan Tafur
Philip Morris Research Center
P.O. Box 26583
Richmond, VA 23261

1983
Volume 72

JOURNAL OF PHARMACEUTICAL SCIENCES

A publication of the American Pharmaceutical Association

The *Journal of Pharmaceutical Sciences* (ISSN 0022-3549) is published monthly by the American Pharmaceutical Association (APhA) at 2215 Constitution Ave., N.W., Washington, DC 20037. Second-class postage paid at Washington, D.C. and at additional mailing office.

All expressions of opinion and statements of supposed fact appearing in articles or editorials carried in this journal are published on the authority of the writer over whose name they appear and are not to be regarded as necessarily expressing the policies or views of APhA.

Offices—Editorial, Advertising, and Subscription: 2215 Constitution Ave., N.W., Washington, DC 20037. All Journal staff may be contacted at this address. Printing: 20th & Northampton Streets, Easton, PA 18042.

Annual Subscriptions—United States and foreign, industrial and government institutions $75; educational institutions $75; individuals *for personal use only* $40; single copies $10. APhA and SAPhA members may subscribe to *J. Pharm. Sci.* for $20.00 per year. All foreign subscriptions add $10 for postage. Subscription rates are subject to change without notice.

Claims—Missing numbers will not be supplied if dues or subscriptions are in arrears for more than 60 days or if claims are received more than 60 days after the date of the issue, or if loss was due to failure to give notice of change of address. APhA cannot accept responsibility for foreign delivery when its records indicate shipment was made.

Change of Address—Members and subscribers should notify at once both the Post Office and APhA of any change of address.

Photocopying—The code at the foot of the first page of an article indicates that APhA has granted permission for copying of the article beyond the limits permitted by Sections 107 and 108 of the U.S. Copyright Law provided that the copier sends the per copy fee stated in the code to the Copyright Clearance Center, Inc., 21 Congress St., Salem, MA 01970. Copies may be made for personal or internal use only and not for general distribution.

Microfilm—Available from University Microfilms International, 300 N. Zeeb Road, Ann Arbor, MI 48106.

Restoring the Oracle of Science

When the APhA member pays his or her annual membership dues, that member is helping to support or "buy"—among other benefits, services, and programs—a certain amount of representation in the halls of Congress and the offices of the federal executive agencies. Such representation includes offering advice, technical counsel, and scientific persuasion to those in government.

We recently read an article in the Sunday magazine section of *The Washington Post*, the thesis of which is that no one in Washington really has "power" in the usual sense of the word. What they do have is "access," and "access" translates into "influence," which is the true common denominator in politics as practiced in Washington, D.C. Consequently, the success of organizations in the nation's capital is largely dependent upon how well those organizations are able to establish access to the right people and, in turn, exert influence over those people *via* that access.

In the case of APhA—as with other national health care and scientific membership societies—representation at the national political level is only one of several equally important purposes or objectives of the organization. And, within that sphere, representation and influence regarding scientific matters and technical issues constitutes an even more limited scope of activity and basis for APhA's existence.

In contrast, the geographic "next-door neighbor" to APhA on Constitution Avenue is the National Academy of Sciences–National Research Council (NAS–NRC). This venerable institution was chartered by Congress and President Abraham Lincoln in 1863 with the express purpose of serving as a, if not "the," private-sector science advisory body for the federal government. But many things have changed over the past 120 years.

The federal government itself has grown immensely and in that growth has added all sorts of technical, scientific, and research groups to its regulatory agencies, to the cabinet executive departments, and in the support services provided to Congress as the legislative wing of the United States government. For example, in the health area, these groups range from the Food and Drug Administration's National Center for Drugs and Biologics, to the National Institutes of Health, to the Congressional Office of Technology Assessment. Moreover, a host of independent or quasi-independent bodies have also sprung up including the National Science Foundation, The Brookings Institute, the Carnegie Institution, the Rand Corporation, and so on. Finally, since approximately the end of the World War II era, most U.S. Presidents have recognized the value of appointing a special Science Advisor to the President or having a Presidential Office of Science Policy.

So no longer is there any shortage of science advice and willing and eager science advisors on the Washington political scene. Indeed, they often agressively compete among and between themselves for attention, visibility, and the opportunity to be heard even if their advice may not be accepted or followed.

All of this has spelled trouble—with a capital "T"—for the prestigious NAS–NRC. Its prominence and reputation went unchallenged for many years, and, as in the case with many venerable and stodgy institutions of a by-gone era, it was ill-prepared to meet the onslaught of competition from younger, more vigorous, and more aggressive purveyors of scientific counsel and technical advice. Unsurprisingly, the result is that NAS–NRC has gone into at least a partial eclipse as its once undisputed position suddenly declined.

Thirteen years ago, an effort to reverse this situation was started when Philip Handler was named NAS–NRC President. Although he happened to be a distinguished biochemist, that facet of his background was incidental to his new assignment. Basically, what was needed was a skilled administrator—which Handler generally proved to be—and his past reputation as a research biochemist was simply a bonus that helped him to open doors, gain attention, and win the respect of his scientific peers.

But years of benign neglect and an activist and often hostile climate of operation limited what any one leader could accomplish. Due to economic considerations, the NAS–NRC day-to-day operation was forced to undertake fee-for-service activities numbering in the hundreds but almost all of extremely narrow scope. The hundreds of committees, panels, and boards were all diligently studying and dissecting the trees while ignoring the forest.

Science and Government Report, a Washington-based publication that describes itself as "The Independent Bulletin of Science Policy," devoted much of one of its 1982 issues to a close look at the NAS–NRC in an article titled "Academy of Sciences Stakes Out a New Role." Editor Daniel S. Greenberg reviewed and analyzed what he characterized as the "institutional shaking, headrolling, and reorganizing that's going on at the venerable NAS."

It is Greenberg's thesis that Handler's successor, former Presidential Science Advisor Frank Press, is trying to reshape the Academy and to restore it to its former position "as the high temple of science." Greenberg sees the new NAS president as having a markedly different agenda than that followed during the Handler era.

"In Press's vision of the Academy of the future, the institution would focus its scholarly resources on big issues and eventually get out of the role of job shop for any government agency that wants to hire its prestige . . . . Press would like to see the Academy revert to its early role as a staging area for science's political interests in Washington. Lots of wheeling and dealing aimed at starting or stopping something on the federal scene used to go on at the Academy."

But the key to being able to pull off such a change is money. It was the "job shop" projects that paid the bills for the Academy to operate over the past generation or longer. Without the infusion of a lot of financial donations from some philanthropic source, there will not be the wherewithal to do what Press is described as trying to accomplish.

And in a budget-tight economy, with an Administration looking for every place to cut further on expenditures, the prospect of Uncle Sam becoming Santa Claus is extremely remote.

Moreover, to date the Reagan Administration has shown little desire, need, or interest in tapping any outside source for the purpose of major shaping of science policy.

Collectively, all of this projects a relatively dismal prognosis for the NAS. Academy President Press will need to muster not only his considerable personal administrative talents, but also the strong and unified support of the entire scientific community, if the NAS is to regain its former exalted position as the pinnacle of science policy.

—EDWARD G. FELDMANN
American Pharmaceutical Association
Washington, DC 20037

0022-3549/83/0300-0211$01.00/0

JOURNAL OF PHARMACEUTICAL SCIENCES

MARCH 1983
VOLUME 72 NUMBER 3

RESEARCH ARTICLES

Renal Clearance of Inorganic Sulfate in Rats: Effect of Acetaminophen-Induced Depletion of Endogenous Sulfate

JIUNN HUEI LIN and GERHARD LEVY ˣ

Received February 4, 1982, from the *Department of Pharmaceutics, School of Pharmacy, State University of New York at Buffalo, Amherst, NY 14260.* Accepted for publication May 14, 1982.

Abstract □ Certain drugs that are eliminated partly by conjugation with sulfate cause appreciable depletion of endogenous inorganic sulfate in animals and humans. The limited availability of endogenous inorganic sulfate contributes to, or is responsible for, dose-dependent elimination kinetics and can cause pronounced time-dependent changes in the disposition of drugs that are metabolized to sulfate conjugates. A comprehensive characterization of the pharmacokinetics of such drugs requires, therefore, an interdigitation with the kinetics of endogenous inorganic sulfate. The latter is cleared from the body primarily by renal excretion. The purpose of this investigation was to determine the relationship between the renal clearance and the serum concentration of inorganic sulfate, particularly in the subnormal concentration range during acetaminophen-induced sulfate depletion. Administration of acetaminophen, 150 mg/kg iv, to adult male rats reduced their serum inorganic sulfate concentration from $\simeq$1 m*M* to <0.1 m*M* without affecting the renal clearance of creatinine. The renal clearance ratio, sulfate–creatinine, decreased from between 0.2 and 0.3 at $\simeq$1 m*M* serum sulfate to $\simeq$ 0.05 at <0.1 m*M* serum sulfate concentration. When serum sulfate concentration was increased to $\simeq$1.5 m*M* by iv infusion of sodium sulfate, the sulfate–creatinine renal clearance ratio increased abruptly to $\simeq$1 without affecting creatinine renal clearance. Acetaminophen had no effect on the high renal clearance of inorganic sulfate during hypersulfatemia. The pronounced serum concentration dependence of sulfate renal clearance facilitates inorganic sulfate homeostasis. A survey of the literature indicates that the relatively low endogenous serum sulfate concentration ($\simeq$0.3–0.4 m*M*) in humans (compared with dogs, rabbits, and rats) is due primarily to low formation rate rather than high renal clearance of inorganic sulfate.

Keyphrases □ Inorganic sulfate—renal clearance in rats, effect of acetaminophen-induced depletion of endogenous sulfate □ Renal clearance—inorganic sulfate in rats, effect of acetaminophen-induced depletion of endogenous sulfate □ Acetaminophen—renal clearance of inorganic sulfate in rats, effect of induced depletion of endogenous sulfate

Conjugation with sulfate is an important biotransformation pathway for certain phenolic drugs and for many endogenous compounds including certain steroids and biogenic amines (1). Administration of therapeutic or pharmacologic doses of acetaminophen or salicylamide results in depletion of endogenous sulfate, as reflected by decreased serum concentrations and urinary excretion of inorganic sulfate in humans and animals (2–6). This depletion of inorganic sulfate, and the consequent decrease in the availability of activated sulfate (3′-phosphoadenosine-5′-phosphosulfate) as a cosubstrate for sulfate conjugation, can cause or contribute to pronounced dose dependency in the pharmacokinetics of drugs that are eliminated by conjugation with sulfate and can also cause the pharmacokinetics of such drugs to exhibit marked time-dependency (7, 8). A comprehensive characterization of the pharmacokinetics of these drugs requires, therefore, mathematical models that include a description of the kinetics of endogenous sulfate formation and elimination.

Endogenous sulfate is derived primarily from oxidation of sulfur-containing amino acids and, partly, from inorganic sulfate contained in the diet (9–11). Thus, previous researchers (9) were able to demonstrate a strong correlation between the urinary excretion of sulfate and the dietary intake of methionine and cystine in human subjects. The urinary excretion of sulfate by children with kwashiorkor is only about one-third of normal due to their protein-deficient diet and the resultant reduced intake of sulfur-containing amino acids (10). Inorganic sulfate is eliminated from the body predominantly by urinary excretion as such (12). In nonmedicated humans on a normal diet and with normal renal function, only ~7–20% of total sulfate is excreted in bound form, *i.e.*, as endogenous sulfate conjugates (3,13). The ratio of bound to free sulfate excretion by normal rats is similar to (14) or even lower than in humans (3). Reduced or absent renal function is associated with pronounced retention of inorganic sulfate; there is a strong, positive correlation between the serum concentrations of creatinine and inorganic sulfate in hu-

0022-3549/83/0300-0213$01.00/0

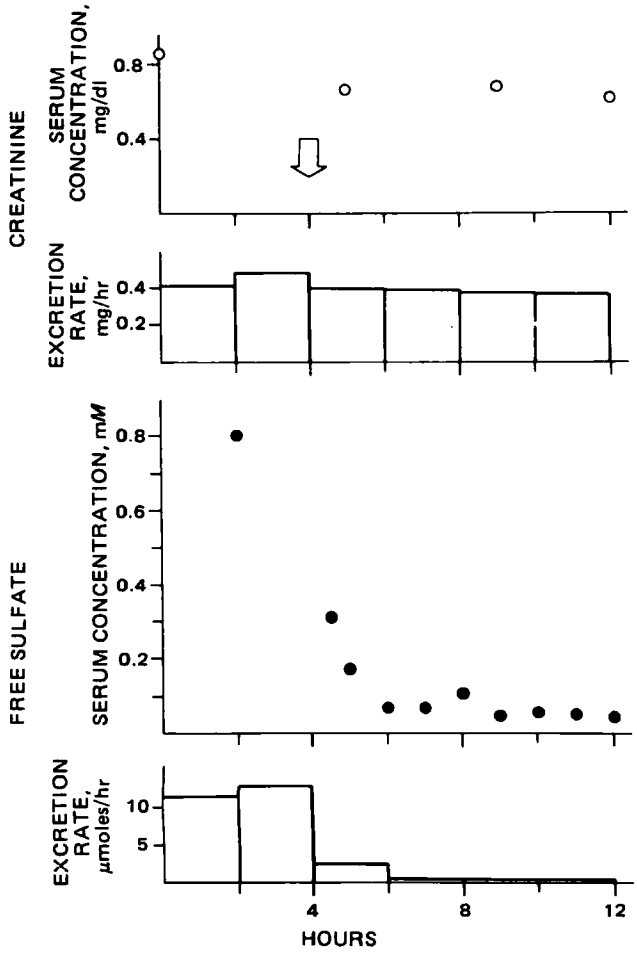

Figure 1—*Effect of an iv injection of acetaminophen (time of injection shown by arrow), 150 mg/kg, on creatinine concentration in serum and urinary excretion rate, and on inorganic sulfate concentration in serum and urinary excretion rate in a rat. This figure shows the experimental design used to determine the renal clearance and renal clearance ratio of inorganic sulfate as a function of sulfate concentration in serum in the normal and subnormal serum concentration range.*

mans (15) and rats (8) with renal dysfunction. Thus, renal clearance is the major determinant of inorganic sulfate elimination kinetics.

Studies on healthy humans and animals (dogs, rabbits, and rats) have shown that the renal clearance of inorganic sulfate is ~10–35% of glomerular filtration rate (GFR) under normal physiological conditions and increases to a rate approximately equal to GFR when serum sulfate concentrations are increased substantially by administration of sodium sulfate (15–20). This renal clearance–serum concentration profile is consistent with glomerular filtration of inorganic sulfate and partial renal tubular reabsorption by a capacity-limited process (19, 20). However, more recent studies have revealed also the presence of a tubular secretory process for sulfate ion in mammals, but it is quite clear that net reabsorption is predominant (21,22). To date, *in vivo* investigations of sulfate renal clearance have been performed under conditions in which serum sulfate concentrations were in the physiological range or elevated by administration of inorganic sulfate. For considerations of the role of endogenous sulfate levels in the elimination of drugs that are subject to sulfate conjugation, the renal clearance of inorganic sulfate at subnormal serum sulfate concentrations

Table I—Urinary Excretion Rate of Inorganic Sulfate, Acetaminophen Sulfate, and Total Conjugated Sulfate Before and After Injection of Acetaminophen [a]

Time Period, hr	Urinary Excretion Rate[b], μmoles/hr/kg		
	Inorganic Sulfate	Acetaminophen Sulfate	Total Conjugated Sulfate
0–4	23.2 ± 4.1	0	1.1 ± 1.9
4–8	5.6 ± 0.5	43.5 ± 8.8	46.9 ± 8.3
8–12	0.4 ± 0.2	28.4 ± 1.2	31.6 ± 2.1

[a] Acetaminophen, 150 mg/kg iv, at 4 hr. [b] Mean ± *SD*, $n = 3$.

is more relevant. This investigation has been designed particularly to determine the concentration dependence of inorganic sulfate renal clearance during sulfate depletion, *i.e.*, in the subnormal serum sulfate concentration range.

EXPERIMENTAL

Adult, male Sprague-Dawley rats (330–380 g) had a cannula implanted in the right jugular vein (23) and another in the urinary bladder, under light ether anesthesia 1 day before the experiment. The animals were kept unrestricted in individual plastic metabolism cages. Food and water were withdrawn in the morning and withheld for the duration of the experiment, which was started in the morning.

The general experimental design is illustrated in Fig. 1. Urine was collected at 2-hr intervals, usually for 12 hr. Each time, the bladder was

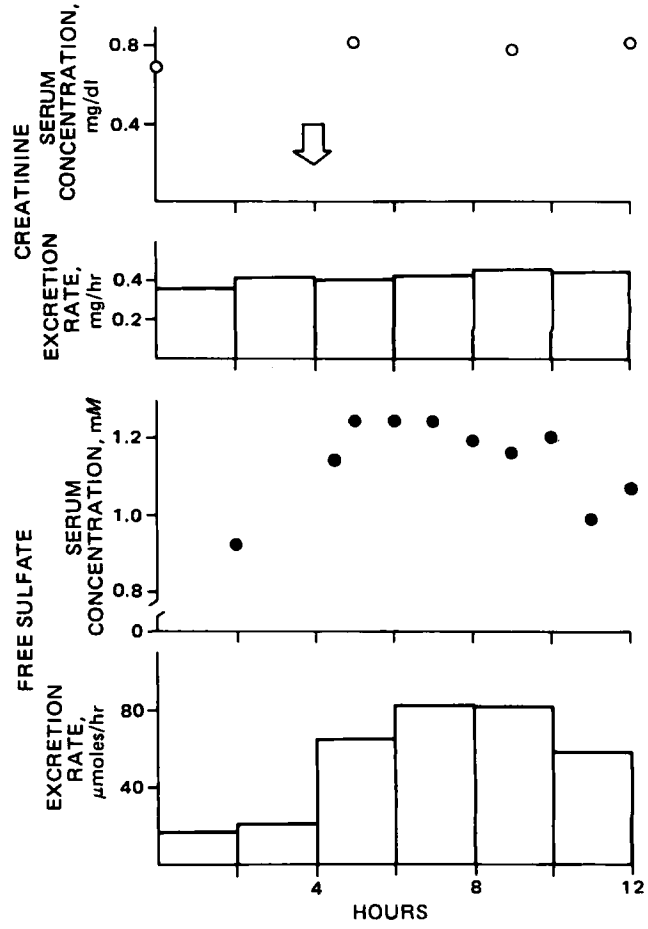

Figure 2—*Effect of an 8-hr infusion of sodium sulfate (start of infusion shown by arrow), 9.6 mg/hr, on creatinine concentration in serum and urinary excretion rate, and on inorganic sulfate concentration in serum and urinary excretion rate in a rat. The figure shows the experimental design used to determine the renal clearance and renal clearance ratio of inorganic sulfate as a function of sulfate concentration in serum in the normal and supernormal serum concentration range.*

Table II—Effect of Acetaminophen or Sodium Sulfate on Serum Concentrations and Renal Clearance of Creatinine in Rats[a]

Time, hr	Acetaminophen[b]		Sodium Sulfate[c]	
	Creatinine Concentration in Serum, mg/100 ml	Creatinine Renal Clearance, ml/min/kg	Creatinine Concentration in Serum, mg/100 ml	Creatinine Renal Clearance, ml/min/kg
0	0.67 ± 0.22	3.14 ± 1.22	0.55 ± 0.08	3.41 ± 0.84
5	0.59 ± 0.13	3.49 ± 1.75	0.59 ± 0.13	3.19 ± 0.85
7	0.63 ± 0.15	3.29 ± 1.35	0.59 ± 0.17	3.48 ± 1.26
12	0.59 ± 0.22	2.96 ± 1.22	0.64 ± 0.13	3.40 ± 1.28

[a] Results are expressed as mean ± *SD*, $n=11$ (for acetaminophen) or $n=6$ (for sodium sulfate). [b] 150 mg/kg iv at 4 hr. [c] 9.6 mg/hr was infused for 8 hr starting at the 4th hour of the experiment.

washed with three 1-ml portions of normal saline solution and these were combined with the collected urine. Blood samples were obtained at frequent intervals, as shown in Fig. 1. After a 4-hr control period for collection of two 2-hr urine samples and two blood samples (one for creatinine and the other for inorganic sulfate determination), the animals received an injection of acetaminophen, 150 mg/kg iv, through the cannula. The drug was administered as a 2.5% solution in 40% propylene glycol–normal saline. Blood samples (0.35 or 0.60 ml) were collected in plastic syringes, and serum was separated by centrifugation. To ensure that mainstream blood was obtained, the saline solution (without heparin) in the cannula and a small volume of blood were aspirated into another syringe before sample collection and then reinjected. One milliliter of normal saline solution was also injected after each blood withdrawal, to replace blood volume, fill the cannula, and stimulate urine flow.

Another group of rats had an additional cannula implanted in the left carotid artery for sodium sulfate infusion. These animals received 9.6 mg/hr/rat, as an isotonic solution containing 0.8% sodium sulfate and 0.45% sodium chloride in water. The solution was infused at a rate of 1.2 ml/hr from the 4th to the 12th hour of the experiment. The urine and blood collection schedule for this experiment is shown in Fig. 3. Some rats received both acetaminophen and sodium sulfate, the former as an injection at 4 hr and the latter as an infusion from the 8th to the 12th hour.

The concentration of inorganic sulfate in serum or urine was determined by the turbidimetric method of Berglund and Sörbo (24) as modified by Krijgsheld *et al.* (25). The method was scaled down for serum assays to a serum volume of 0.15 ml. The concentration of bound sulfate in urine was determined as the difference in sulfate concentrations before and after acid hydrolysis (diluted urine–10 *N* hydrochloric acid, 10:1, v/v, heated for 2 hr at 100°).

Creatinine concentrations in serum and urine were determined with a commercial kit[1], which is based on a modification of a previous assay procedure (26).

Acetaminophen sulfate in urine was assayed by high-performance liquid chromatography (HPLC) based on a previous method (27,28).

Renal clearances of inorganic sulfate and creatinine in the control periods were determined as excretion rate divided by serum concentration, and were normalized for body weight. During periods of changing serum sulfate concentrations, (after acetaminophen injection and during sodium sulfate infusion), the renal clearance of inorganic sulfate was calculated as the amount excreted in the urine divided by the area under the serum concentration–time curve during the urine collection interval. Some of the results are reported as clearance ratio, *i.e.*, the renal clearance of sulfate divided by the renal clearance of creatinine.

RESULTS

Control renal clearance determinations were made on 32 animals. The serum sulfate concentration was 0.89 ± 0.08 m*M*, urinary excretion of inorganic sulfate averaged 0.55 ± 0.26 μmole/min/kg, and renal clearance of inorganic sulfate was 0.64 ± 0.24 ml/min/kg. Serum creatinine concentrations were 0.72 ± 0.24 mg/dl, and creatinine clearance was 3.0 ± 1.2 ml/min/kg. The renal clearance ratio of inorganic sulfate was 0.24 ± 0.14. All of these results are mean values ±*SD*.

Injection of acetaminophen, 150 mg/kg, produced a rapid, pronounced, and persistent decline of serum concentrations and urinary excretion of inorganic sulfate (Fig. 1). A separate study showed that under these conditions, acetaminophen concentrations in plasma average ~150 μg/ml initially and decline with an apparent half-life of ~1 hr (7).

The urinary excretion of sulfate before acetaminophen administration consisted mostly of inorganic (free) sulfate; <10% of total sulfate was of the bound form (*i.e.*, sulfate conjugated with endogenous substances). The pronounced reduction of inorganic sulfate excretion after acetaminophen administration was accompanied by a very large increase in the excretion rate of bound (conjugated) sulfate, mostly in the form of acetaminophen sulfate (Table I).

Acetaminophen had no apparent effect on the serum concentration and urinary excretion rate of creatinine and, therefore, on the renal clearance of endogenous creatinine (Fig. 1 and Table II). This lack of effect became apparent in preliminary experiments and justified a reduction of serum creatinine determinations (which required an extra 0.25-ml of blood per sample) to four during 12 hr, to minimize blood volume depletion. Sulfate renal clearance ratios were, therefore, determined on the basis of an average creatinine clearance for each animal, calculated by dividing the 12-hr creatinine excretion rate by the average of the four successive serum creatinine concentrations.

Control experiments were performed to determine the possible effects of normal saline solution and propylene glycol on the renal clearances of creatinine and inorganic sulfate in otherwise unmedicated rats. Seven rats were studied during a 4-hr control period and during 4 hr of normal saline infusion at a rate of 1.2 ml/hr. The ratios, control–treatment, of individual creatinine and sulfate clearance values were 1.00 ± 0.18 (*SD*) and 0.93 ± 0.15, respectively. The effect of propylene glycol was determined in an experiment identical to that described in Fig. 1 except for the omission of acetaminophen. The injection solution consisted of 40% propylene glycol in normal saline, 6 ml/kg. Again, there was no effect on the renal clearance of creatinine or sulfate; the control–treatment ratios were 0.92 ± 0.15 for creatinine and 1.02 ± 0.18 for sulfate renal clearance.

Infusion of sodium sulfate caused a significant increase of serum concentrations and urinary excretion rates of inorganic sulfate, without any apparent effect on the serum concentrations and renal clearance of creatinine (Fig. 2 and Table II).

Depletion of endogenous inorganic sulfate by acetaminophen and supplementation by sodium sulfate administration permitted determination of the relationship between serum concentration and renal clearance of sulfate over a wide concentration range (Fig. 3). To rule out a possible direct effect of acetaminophen on sulfate clearance (*i.e.*, an

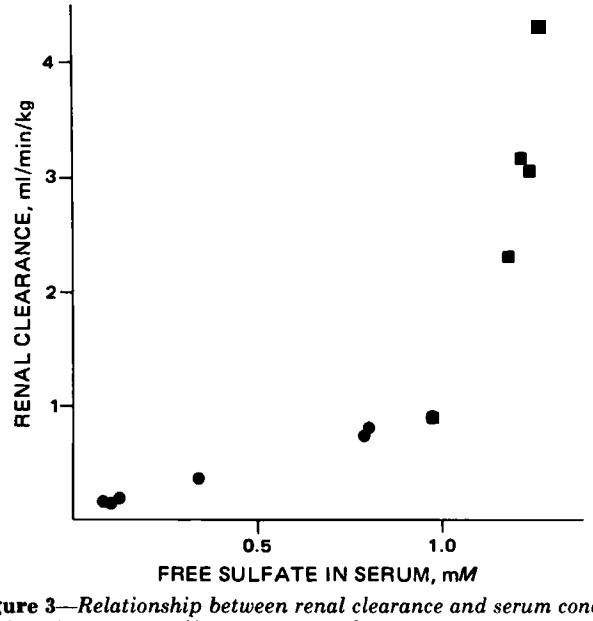

Figure 3—*Relationship between renal clearance and serum concentration of inorganic sulfate in two rats. One animal received acetaminophen (●); the other received sodium sulfate (■).*

[1] Creatinine Kit, No. 555-A, Sigma Chemical Co., St. Louis, Mo.

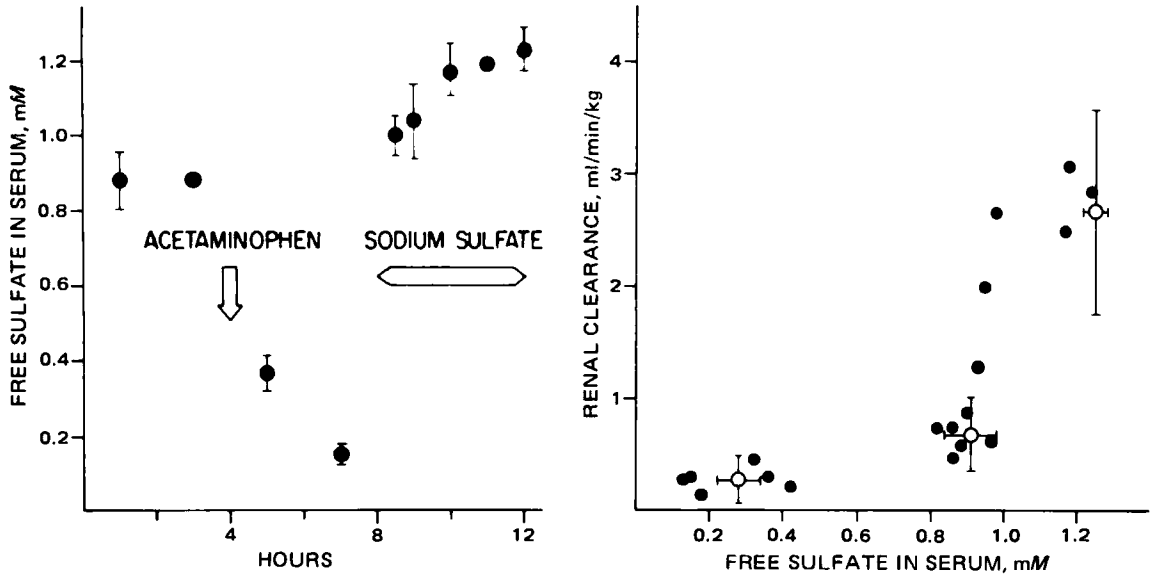

Figure 4—*Effect of acetaminophen on the renal clearance of inorganic sulfate at subnormal and supernormal serum sulfate concentrations in rats. Left panel: Inorganic sulfate concentrations (mean ±SD) in serum of 3 rats during a 4-hr control period and after intravenous injection of acetaminophen at 4 hr followed by a 4-hr infusion of sodium sulfate, 9.6 mg/hr, from 8 to 12 hr. Right panel: Renal clearance of inorganic sulfate as a function of sulfate concentration in serum, derived from the experiment shown in the left panel (●). Also shown (○) are results obtained, at selected concentration ranges, from animals who received either only acetaminophen or only sodium sulfate, or neither (mean ±SD).*

effect unrelated to the acetaminophen-induced diminished serum sulfate concentrations), sulfate depletion following acetaminophen administration was reversed by infusion of sodium sulfate. The renal clearance of inorganic sulfate at elevated serum sulfate concentrations was unaffected by acetaminophen (Fig. 4).

A summary of all renal clearance data obtained over a wide range (<0.1–1.5 m*M*) of serum sulfate concentrations is presented in Fig. 5. Excluded from that figure are data from two rats with some evidence of renal dysfunction. To facilitate the presentation of the combined results of experiments on 15 rats, the data were normalized with respect to creatinine clearance by being expressed as clearance ratios. The clearance ratio of inorganic sulfate is very low (<0.1 on the average) at serum sulfate concentrations <0.1 m*M* and increases to ≃1 when serum sulfate concentration is ~1.5 m*M*. There is a very steep increase of the clearance ratio when serum sulfate concentration slightly exceeds 1 m*M*, *i.e.*, the usual physiological level of inorganic sulfate in rats. In the serum concentration range from <0.1 to 1 m*M* (*i.e.*, during hyposulfatemia in rats), the renal clearance of sulfate also increases with increasing serum concentration, albeit not as steeply as between serum concentrations from 1 to 1.5 m*M*. The serum concentration dependence of sulfate renal clearance in the subnormal concentration range was established by the following objective criteria, applied to the group of animals that received acetaminophen: (*a*) comparison of renal clearance values at serum sulfate concentrations <0.25 m*M* to those at >0.5 m*M* indicated the latter to be significantly higher ($p < 0.001$ by paired t test), and (*b*) analysis of data for each animal separately showed a strong positive correlation between renal clearance and serum concentration of sulfate for every rat in the study ($r > 0.85$, $p < 0.05$).

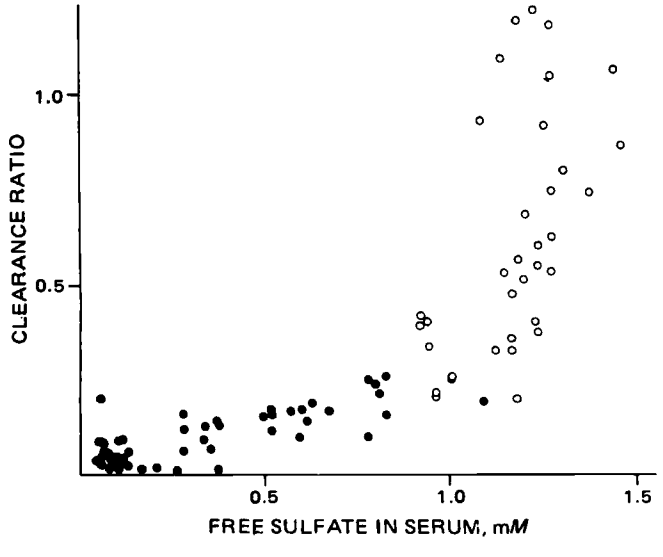

Figure 5—*Renal clearance ratio of inorganic sulfate (sulfate clearance–creatinine clearance) as a function of sulfate concentration in serum of nine rats before and after acetaminophen injection (●) and six rats before and during sodium sulfate infusion (○).*

DISCUSSION

Baseline data obtained during the control periods in this investigation are in excellent agreement with literature values. This includes serum inorganic sulfate concentration (11, 19, 29), urinary excretion rate of inorganic sulfate (3, 11), serum creatinine concentration (30), and renal clearance of creatinine (31) in rats. Previous researchers (14) observed a circadian rhythm with respect to serum concentration and urinary excretion rate of inorganic sulfate in rats; serum sulfate concentration decreased rapidly from ≃0.9 to ≃0.6 m*M* in the evening while sulfate excretion increased. Apparently, this phenomenon does not occur consistently, since the same investigators reported essentially constant serum sulfate concentrations in rats during a 24-hr period in another study (11). Experiments in this investigation were always started in the morning and lasted 12 hr; serum concentrations and urinary excretion of inorganic sulfate remained essentially constant during this time in unmedicated rats.

It appears that the renal tubular reabsorption of sulfate is coupled to active transport of sodium through a sodium–sulfate cotransport system (32, 33). Under certain conditions, administration of sodium chloride causes a transient decrease of serum sulfate concentrations in rats (5, 25). The use of sodium chloride in this investigation to adjust the tonicity of the sodium sulfate infusion solution and, as normal saline solution, to replace blood volume and stimulate urine flow, had no apparent effect on the serum concentration and urinary excretion of endogenous inorganic sulfate. Propylene glycol, used as a solvent for acetaminophen, also had no effect on endogenous sulfate serum concentration and urinary excretion under the experimental conditions.

Under normal physiological conditions, the renal clearance of sulfate is considerably below GFR even though sulfate in plasma is completely ultrafiltrable (34). Thus, inorganic sulfate undergoes considerable renal tubular reabsorption. This process is saturable, causing sulfate renal clearance to increase with increasing serum sulfate concentration. This concentration dependence is strikingly apparent in the rat when serum sulfate concentrations are increased by infusion of sodium sulfate (Figs. 3 and 5). More problematical has been the search for the existence of a

Table III—Interspecies Comparison of Free Sulfate Kinetics

	Humans[a]	Dog[b]	Rabbit[c]	Rat[d]
Reported or assumed body weight, kg	70	12	2.5	0.35
Serum-free sulfate concentration, m*M*	0.44	1.40	1.21	0.89
Renal clearance of creatinine, ml/min/kg	1.7	3.4	4.3	3.0
Renal clearance of sulfate, ml/min/kg	0.54	0.35	0.57	0.64
Renal clearance ratio, sulfate/creatinine	0.33	0.10	0.13	0.24
Urinary excretion rate of free sulfate, μmoles/min/kg	0.24	0.48	0.76	0.55

[a] Reference 13. [b] Reference 38. [c] Reference 15. [d] This study.

renal tubular secretory process for sulfate. Studies in several species, including humans and dogs, have failed to demonstrate that renal clearance of sulfate can exceed GFR (18, 20, 35). While sulfate renal clearance ratios in the present investigation have occasionally exceeded unity at high serum sulfate concentrations (Fig. 5), these values have all been close to unity. Clearance ratio determinations are based on four measurements (sulfate and creatinine in serum and urine) and are therefore subject to some error. The results of our renal clearance experiments at elevated serum sulfate concentrations provide no definitive evidence of renal secretion of sulfate and are consistent with the experiences of other investigators who have not been able to demonstrate conclusively, by conventional clearance determinations in mammals, that inorganic sulfate is subject to renal tubular secretion (22). However, a renal secretory process for sulfate has been found by tubular microperfusion techniques but appears to be rudimentary (21, 22). In any event, the focus of this investigation has been on the concentration dependence of sulfate in the subnormal serum concentration range where the secretory process is overshadowed by the reabsorption process.

The use of a drug to deplete endogeneous sulfate has permitted, apparently for the first time, the determination of sulfate renal clearance at subnormal serum sulfate concentrations. This information is important for the comprehensive characterization of the pharmacokinetics of drugs that are subject to sulfate conjugation and whose biotransformation is associated with a depletion of endogenous sulfate. It was found that the renal clearance of sulfate decreases continuously with decreasing serum sulfate concentrations. When endogenous sulfate is severely depleted, there occurs almost complete reabsorption of sulfate from the glomerular filtrate. Thus, the serum concentration dependence of renal sulfate clearance in rats facilitates sulfate homeostasis by retaining sulfate when this ion is depleted and by excreting it rapidly when serum concentrations are elevated above normal. These conclusions apply also to humans, as is evident from the results of an ongoing investigation[2].

There are very large species differences in serum sulfate concentrations; the goat and rooster have concentrations $\simeq$2.5 m*M*, the rat and mouse $\simeq$1 m*M*, and the monkey and humans are at the lower extreme with concentrations $\simeq$0.3 m*M* (14). The two most likely reasons for these species differences are variations in the formation rate (or dietary intake) of sulfate and in the renal sulfate clearance. Volume of distribution differences are much less likely; sulfate ion is not protein bound and distributes almost exclusively in extracellular space (36, 37). A survey of the literature shows that, based on body weight, the renal clearance of sulfate in humans under physiological conditions is similar to that of rats, rabbits, and dogs (Table III). The low serum sulfate concentration in humans under these conditions suggests that their sulfate formation rate is relatively low, perhaps due to lower dietary intake of precursors. This conclusion is supported by the fact that the urinary excretion rate of free sulfate (which is a good approximation of the formation rate since tracer doses of sulfate-S^{35} are excreted largely as such), is much less in humans than in the other three species (Table III).

[2] M. E. Morris and G. Levy, to be published.

REFERENCES

(1) G. J. Mulder, "Sulfation of Drugs and Related Compounds," CRC Press, Boca Raton, Fla., 1981, chap. 5.

(2) H. Greiling and B. Schular, *Z. Rheumaforsch.*, **22,** 47 (1963).

(3) H. Büch, W. Rummel, K. Pfleger, Ch. Eschrich, and N. Texter, *Naunyn-Schmiedebergs Arch. Pharmakol. Exp. Pathol.*, **259,** 276 (1968).

(4) J. H. Lin and G. Levy, *Biochem. Pharmacol.*, **30,** 2723 (1981).

(5) K. R. Krijgsheld, E. Scholtens, and G. J. Mulder, *ibid.*, **30,** 1973 (1981).

(6) M. Koike, K. Sugeno, and M. Hirata, *J. Pharm. Sci.*, **70,** 308 (1981).

(7) R. E. Galinsky and G. Levy, *J. Pharmacol. Exp. Ther.*, **219,** 14 (1981).

(8) J. H. Lin and G. Levy, *ibid.*, **221,** 80 (1982).

(9) Z. I. Sabry, S. B. Shadarevian, J. W. Cowan, and J. A. Campbell, *Nature*, **206,** 931 (1965).

(10) T. R. Ittyerah, *Clin. Chim. Acta*, **25,** 365 (1969).

(11) K. R. Krijgsheld, E. Z. Glazenburg, E. Scholtens, and G. J. Mulder, *Biochim. Biophys. Acta*, **677,** 7 (1981).

(12) D. M. Cocchetto and G. Levy, *J. Pharm. Sci.*, **70,** 331 (1981).

(13) P. Lundquist, J. Mårtensson, B. Sörbo, and S. Öhman, *Clin. Chem.*, **26,** 1178 (1980).

(14) K. R. Krijgsheld, E. Scholtens, and G. J. Mulder, *Comp. Biochem. Physiol.*, **67A,** 683 (1980).

(15) R. M. Freeman and C. J. Richards, *Kidney Int.*, **15,** 167 (1979).

(16) J. M. Hayman, Jr., *J. Clin. Invest.*, **11,** 607 (1932).

(17) P. Schou, *Acta Physiol. Scand.*, **7,** 183 (1944).

(18) W. D. Lotspeich, *Am. J. Physiol.*, **151,** 311 (1947).

(19) F. Berglund, *Acta Physiol. Scand.*, **62,** 336 (1964).

(20) E. L. Becker, H. O. Heinemann, K. Igarashi, J. E. Hodler, and H. Gershberg, *J. Clin. Invest.*, **39,** 1909 (1960).

(21) K. J. Ullrich, G. Rumrich and S. Klöss, *Pfluegers Arch.*, **387,** 127 (1980).

(22) P. C. Brazy and V. W. Dennis, *Am. J. Physiol.*, **241,** F300 (1981).

(23) J. R. Weeks and J. D. Davis, *J. Appl. Physiol.*, **19,** 540 (1964).

(24) F. Berglund and B. Sörbo, *Scand. J. Clin. Lab. Invest.*, **12,** 147 (1960).

(25) K. R. Krijgsheld, H. Frankena, E. Scholtens, J. Zweens, and G. J. Mulder, *Biochim. Biophys. Acta*, **586,** 492 (1979).

(26) D. Heinegard and G. Tiderstrom, *Clin. Chim. Acta*, **43,** 305 (1973).

(27) P. I. Adriaenssens and L. F. Prescott, *Br. J. Clin. Pharmacol.*, **6,** 87 (1978).

(28) R. E. Galinsky, J. T. Slattery, and G. Levy, *J. Pharm. Sci.*, **68,** 803 (1979).

(29) J. G. Weitering, K. R. Krijgsheld, and G. J. Mulder, *Biochem. Pharmacol.*, **28,** 757 (1979).

(30) K. M. Giacomini, S. M. Roberts, and G. Levy, *J. Pharm. Sci.*, **70,** 117 (1981).

(31) J. Strassberg, J. Paule, H. C. Gonick, M. H. Maxwell, and C. R. Kleeman, *Nephron*, **4,** 384 (1967).

(32) K. J. Ullrich, G. Rumrich, and S. Klöss, *Pfluegers Arch.*, **383,** 159 (1980).

(33) H. Lücke, S. Stange, and H. Murer, *Biochem. J.*, **182,** 223 (1979).

(34) F. Berglund, *Acta Physiol. Scand. Suppl.*, **49,** 1 (1960).

(35) K. Hierholzer, R. Cade, R. Gurd, R. Kessler, and R. Pitts, *Am. J. Physiol.*, **198,** 833 (1960).

(36) M. Walser, D. W. Seldin, and A. Grollman, *J. Clin. Invest.*, **32,** 299 (1953).

(37) J. H. Bauer, *J. Appl. Physiol.*, **40,** 648 (1976).

(38) W. J. O'Connor and R. A. Summerill, *J. Physiol.*, **260,** 597 (1976).

ACKNOWLEDGMENTS

Supported in part by Grant GM 19568 from the National Institute of General Medical Sciences, National Institutes of Health.

Effects of Breed, Season, Temperature, and Solvents on the Permeability of Frozen and Reconstituted Cattle Skin to Levamisole

IAN H. PITMAN ˣ, SUSAN J. ROSTAS, and LEANNE M. DOWNES

Received October 13, 1981, from the *Victorian College of Pharmacy Ltd., Parkville, 3052, Australia.* Accepted for publication April 8, 1982.

Abstract □ *In vitro* measurements have been made of the permeability of frozen and reconstituted cattle skins to levamisole. Breeds used were Red Poll cross, Hereford/Shorthorn cross, Hereford/Santa Gatrudis cross (or Brahman), Friesian (or Friesian/Jersey cross), and Hereford cattle killed in early fall, early summer, or winter. Inter- and intrabreed differences in skin permeability were small, but skin permeability in summer and fall was appreciably greater than in winter. Increases in skin temperature also increased skin permeability. The solvent properties of the skin toward neutral molecules appeared to be similar to those of water, suggesting that skin is a relatively polar barrier.

Keyphrases □ Levamisole—effects of breed, season, temperature, and solvents on permeability, frozen and reconstituted cattle skin □ Permeability—frozen and reconstituted cattle skin, effects of breed, season, temperature, and solvents, levamisole □ Skin, cattle—frozen and reconstituted, effects of breed, season, temperature, and solvents on permeability to levamisole

It has been shown recently (1) that the outer 1 mm of frozen and reconstituted skin from a Hereford calf (*i.e.*, stratum corneum, viable epidermis, papillary layer of the dermis, and associated appendages) acts as a homogenous barrier to the diffusion of molecules of levamisole (I). This observation highlights a significant difference between the barrier properties of cattle skin and those of similarly treated human skin in which the stratum corneum is the rate-determining barrier to diffusing molecules (2, 3). Consequently, it is probable that different mechanisms are involved in the transport of molecules across cattle and human skin, and different steps must be taken when formulating topical products for cattle than those taken when formulating topical products for humans.

Steps that can be taken to control topical absorption of drugs by humans have been reviewed previously (4, 5).

The effects of breed, season, skin temperature, and solvents on the *in vitro* permeability of frozen and reconstituted[1] cattle skin to I are reported here.

It is anticipated that the results of this study will be directly applicable to the development of liquid dosage forms that are intended to promote systemic drug delivery [*i.e.*, pour-ons (6)] to cattle.

EXPERIMENTAL

The methods used to harvest and store cattle skins were identical to those described earlier (1). Details of the cattle used and of the times when skins were harvested are in Table I.

Materials—Compound I (mp 61°), I hydrochloride (mp 228°), polyoxypropylene-15-stearyl ether, sorbitan sesquioleate, the nonaromatic hydrocarbon fraction, and 2-ethoxyethanol were used as received[2] as was formulation C (Table II). All other chemicals were analytical reagents unless otherwise stated. Formulations are listed in Table II.

Measurement of Skin Permeability—The procedures, including analytical methods, described previously (1, 7) were employed to determine the permeability of the skins to I. Skin penetration was followed for 300 min, and lag times varied from 4 min (for penetration from toluene) to 120 min (for penetration from aqueous and alcoholic solutions). In two studies, measurements were made of the penetration of tritiated water (^3H_2O) through cattle skin. Approximately 0.5 μCi of tritiated water was added to either the aqueous pH 8.9 solution or the pH 6.0 solution of I, and 1.0 ml of the mixture was applied to the epidermal surface of the skin. Samples (0.2 ml) of the donor solutions were taken at 0 and 300 min, and samples (1.0 ml) of the receptor solutions were taken at 300 min. The samples were adjusted to 1 ml with water and to each was added 10 ml of scintillation liquid (0.4% 2,5-diphenyloxazole in toluene–tyloxopol[3], 2:1 v/v). After thorough mixing, the samples were counted on a liquid scintillation spectrometer[4].

The temperature of the water bath in which all experiments, except those carried out to study variation of permeability with temperature, was 37.0 ± 0.1°. Thermistor measurements indicated that the temperature of the outer surface of the skin in these experiments was 30.6 ± 0.5°.

Statistical Analysis—Unless otherwise stated, a multiple comparison statistical technique previously described (8) and modified[5] was used to analyze the experimental results.

RESULTS AND DISCUSSION

As a consequence of the finding (1) that the outer 1 mm of cattle skin behaves as an homogenous barrier to the diffusion of molecules of I, it follows that:

1. The product of the permeability constant (k_p, cm min^{-1}) and the thickness of the skin specimen (r, cm, *i.e.*, $k_p r$ cm^2 min^{-1}) is a constant for diffusion through skin specimens with thicknesses in the range of 0.3–1.0 mm;
2. The diffusion coefficient (D, cm^2 min^{-1}) of I in skin specimens with thicknesses in the range of 0.3–1.0 mm can be calculated from the lag time for diffusion (L, min) by:

$$D = r^2/6L \qquad \text{(Eq. 1)}$$

3. The partition coefficient (PC) for I from the formulation into skin specimens with thicknesses up to 1.0 mm can be calculated from:

$$PC = k_p r/D \qquad \text{(Eq. 2)}$$

The derivations of Eqs. 1 and 2 are discussed in a previous report (1).

Values of $k_p r$, D, and PC for penetration of I through the skins of a number of cattle from a single formulation and from several formulations are in Tables III and IV, respectively. The skin specimens used in all experiments had thicknesses in the range of 0.3–1.0 mm.

Intra- and Interbreed Variation in Skin Permeability—Table III contains mean values of $k_p r$, D, and PC for penetration of I through skins of four Hereford calves from formulation A. The calves were about the same age, and the skin was harvested in early fall.

Statistical analysis of the data indicates that there was no significant difference at the 1% level between the permeability of the four skins and suggests that intrabreed differences are likely to be small for animals with similar histories treated during the same season.

Two pieces of evidence suggest that interbreed differences (involving mainly European breeds) in skin permeability are also likely to be small for animals of similar ages that are treated during the same seasons.

Thus, the permeability of the skin of a Friesian calf to I from formu-

[1] Results to be published shortly from this laboratory establish that there are no significant differences at the 5% level in the permeability of fresh, frozen, and reconstituted cattle skin.

[2] ICI Australia Ltd.

[3] Triton X-100.

[4] Packard Tri-carb #544.

[5] Personal Communication, B. H. Kellett, Victorian College of Pharmacy.

0022-3549/83/0300-0218$01.00/0

Table I—Details of Cattle and Time of Skin Harvesting

Calf Number	Approximate Age, months	Breed	Time of Harvesting
115	6	Red Poll Cross	Late August (winter)
110	9–11	Hereford/Shorthorn cross	Late August (winter)
109	6–8	Hereford/Santa cross Gatrudis or Brahman	
F1	4–6	Friesian (or Friesian/Jersey cross)	Early December (early Summer)
16	10–12	Hereford	Mid March (early fall)
21	8	Hereford	Mid March (early fall)
29	8–10	Hereford	Mid March (early fall)
34	8–9	Hereford	Mid March (early fall)

lation A in early summer was similar (there was no significant difference at the 1% level) to that of skins of the four Hereford calves in early fall (Table III). Similarly, the results in Table IV show that interbreed differences for the permeability of the winter skins of a Red Poll (No. 115), a Hereford/Shorthorn cross (No. 110), and a Hereford/Santa Gatrudis cross or Brahman (No. 109) to I from formulation A and of those of calves Nos. 110 and 109 to formulations B and C, aqueous pH 8.9 and 6.0 solutions, were not significant at the 1% level.

Seasonal Variation—Comparison of the results in Table III for the permeability to I from formulation A of the skin of the four Hereford calves killed in early fall (Nos. 16, 21, 29, and 34) with similar data in Table IV for skins of calves killed in winter (Nos. 115, 110, and 109) indicate that the skin is significantly more permeable to I in the fall than in the winter (a two-tailed t test on the means for each group of results indicated that $p < 10^{-7}$).

This result is consistent with an observation that greater blood levels of I were achieved in cattle following application of a pour-on in summer than were achieved in winter[6].

Furthermore, while the values of both the diffusion coefficient and partition coefficient for I were greater in fall skin than in winter skin ($p < 10^{-2}$ and $p < 10^{-4}$, respectively), inspection of the data reveals that the increase in the value of the partition coefficient is much larger. The greater partition coefficient in fall indicates that for I fall skin is a better solvent than winter skin.

The solvent properties of the skin will be discussed further after considering the effect that different formulations and different temperatures have on skin permeability.

Formulation Variation—A noticeable feature of the data in Table IV is that I penetrated the skins of calves 110 and 109 ~30 times faster ($p < 10^{-2}$) from the aqueous pH 8.9 solution (where I existed to the extent of 90% as a neutral molecule[7]) than from the aqueous pH 6.0 solution (where I existed to the extent of 99% as a cation).

To test whether the pH value of aqueous buffers affected the intrinsic permeability of the skin, experiments were conducted using aqueous solutions of I buffered at pH 8.9 and 6.0 and containing tritiated water. Measurements were made of the rate at which both tritiated water and I penetrated the skin from each formulation. The results in Table V indicate that the percent of the applied amount of tritiated water penetrating the skin in 300 min was essentially the same at pH 8.9 and 6.0. This result is consistent with the conclusion that the variation of pH values from 8.9 to 6.0 does not significantly alter the intrinsic permeability of the cattle skin. In the same experiments, the percent of the applied dose of I that penetrated the skin in 300 min was ~ 10 times higher than the pH 8.9 buffer than from the pH 6.0 buffer.

The data in Table IV indicate that whereas the value of the diffusion coefficient for I in cattle skin is essentially the same from aqueous pH 8.9 and 6.0 solutions (differences are not significant at the 1% levels), the value of the partition coefficient of I from pH 8.9 solution into the skin is >10 times that from the pH 6.0 solution ($p < 10^{-2}$).

This result suggests that the skin has similar solvent properties to water for neutral molecules for I but is an inferior solvent for I cations.

Comparison of the data in Table IV for penetration of neutral molecules of I through the skins of calves Nos. 110 and 109 from formulations A (largely 2-ethoxyethanol), B (largely 2-ethoxyethanol), and C (largely 2-propanol) and water indicates that for I the skin permeability is greatest from water. Also, while the values of the diffusion coefficient for I from each of the above formulations are similar, the value of the partition coefficient for I into the skin is significantly greater from water than from the organic solvents ($p < 10^{-2}$).

Table IV also includes data for the penetration of neutral molecules of I through the skin of calf No. 109 from 80% dimethyl sulfoxide (in water) and from toluene. These results differ from those from the other formulations studied, in that the values of the diffusion coefficients of I in the skin were significantly larger ($p < 10^{-2}$) when 80% dimethyl sulfoxide and toluene were used as solvents. These results arose because the lag times for diffusion from these solvents were much less than those from aqueous pH 8.9 solution, aqueous pH 6.0 solution, or from formulations A, B, and C.

In the case of penetration from 80% dimethyl sulfoxide, the value of $k_p r$ was six times less than that from aqueous pH 8.9 solution, although the value of the diffusion coefficient in the former system was 8.6 times larger. The determining factor in this case was the fact that the value of the partition coefficient of I between the aqueous pH 8.9 solution and skin was ~60 times that between 80% dimethyl sulfoxide and skin.

The value of $k_p r$ for penetration from toluene was comparable to that from aqueous pH 8.9 solutions at the 1% level. In this case, although the partition coefficient of I from toluene into skin was 0.06 that from aqueous pH 8.9 solution, the value of the diffusion coefficient in the former case was 18.7 times that in the latter.

These results are difficult to explain at the present time, but it is probable that they arise because dimethyl sulfoxide and toluene dissolve away or displace certain components of the skin and thereby change its permeability characteristics. It is known (9) that the application of ether removes a significant proportion of the lipid and stratum corneum from cattle skin.

An important conclusion that can be drawn from these observations is that dimethyl sulfoxide may not be a universal promoter of penetration of neutral molecules through cattle skin to the same extent as it is for human skin penetration (10, 11). It has previously been shown (7) that dimethyl sulfoxide impedes rather than promotes the absorption of I through sheep skin.

Table II—Formulations

Designation	% w/v I	Formulation
Aqueous pH 8.9 solution	0.85	I HCl 1% Borate Buffer to 100% Final pH 8.9
Aqueous pH 6.0 solution	0.85	I HCl 1% Phosphate Buffer to 100% Final pH 6.0
80% Dimethyl sulfoxide	1	I 1% Water 20% Dimethyl Sulfoxide to 100%
Toluene	0.85	I to 0.85% Toluene to 100%
Formulation A[a]	10	I 10% Poloxypropylene-15-stearyl ether 12% Nonaromatic Hydrocarbons 15% 2-Ethoxyethanol to 100%
Formulation B	10	I 10% Sorbitan Sesquioleate 10% Nonaromatic Hydrocarbons 20% 2-Ethoxyethanol to 100%
Formulation C[a]	10	I 10% Spindle Oil 10% Isopropanol to 100%

[a] Bayer.

Table III—Comparative Data[a] for Penetration of I from Formulation A through Hereford[b] and Friesian[c] Skins

Calf Number	Formulation	$10^6 k_p r$ ($\pm SD$) $cm^2\ min^{-1}$	$10^6 D$ ($\pm SD$) $cm^2\ min^{-1}$	Partition Coefficient ($\pm SD$)
16	A	17.8(4.5)	17(4)	1.13(0.42)
21	A	15.7(2.1)	28(3)	0.58(0.14)
29	A	20.8(7.2)	21(8)	1.19(0.79)
34	A	19.6(5.5)	19(5)	1.12(0.60)
F1	A	24.0(3.7)	23(6)	1.09(0.35)

[a] Mean values of $k_p r$, D, and PC from at least four experiments with skin sample thicknesses between 0.3 and 1 μm, together with standard deviations (SD). [b] Calves 16, 21, 29, and 34 harvested in early fall. [c] Calf F1 harvested in early summer.

[6] Personal Communication, D. Taylor, I.C.I. Limited, United Kingdom.
[7] The pK_a value of I is 7.94 at 37° (7).

Table IV—Comparative Data for Penetration of I from a Variety of Solvents through Winter Skin of Three Breeds of Cattle [a]

Calf Number	Formulation	$10^6 k_p r$ (±SD) $cm^2\ min^{-1}$	$10^6 D$ (±SD) $cm^2\ min^{-1}$	Partition Coefficient (± SD) $cm^2\ min^{-1}$
115	A	1.8(0.2)	14(7)	0.15(0.05)
110	A	2.0(0.01)	10(4)	0.22(0.09)
109	A	1.8(0.5)	11(3)	0.18(0.10)
110	B	2.3(0.4)	10(3)	0.25(0.10)
109	B	1.2(0.3)	11(3)	0.11(0.02)
110	C	0.8(0.2)	14(5)	0.07(0.04)
109	C	0.6(0.1)	20(15)	0.05(0.03)
110	Aqueous pH 8.9 solution	11.3(3.6)	15(3)	0.79(0.24)
109	Aqueous pH 8.9 solution	10.2(3.1)	10(4)	1.10(0.47)
110	Aqueous pH 6.0 solution	0.4(0.1)	11(7)	0.04(0.05)
109	Aqueous pH 6.0 solution	0.3(0.1)	12(13)	0.06(0.06)
109	80% Dimethyl Sulfoxide [b]	1.6	86	0.02
109	Toluene	13.1(1.1)	188(14)	0.07

[a] As described in Table I. [b] Only one experiment was performed.

Table V—Relative Rates of Penetration of I and Tritiated Water through the Skin of Calf No. 115 at 37°

Formulation	Applied Dose of I Penetrating in 300 min, % (1)	Applied Dose of Tritiated Water Penetrating in 300 min, % (2)	(1)/(2)
Aqueous pH 8.9 solution + tritiated water	1.6	2.6	0.6
Aqueous pH 8.9 solution + tritiated water	1.7	1.3	1.3
Aqueous pH 6.0 solution + tritiated water	0.1	2.1	0.05
Aqueous pH 6.0 solution + tritiated water	0.2	2.0	0.08

Temperature Variation—Table VI contains values of $k_p r$, diffusion coefficient (D), and partition coefficient (PC) for penetration of I from formulation A through the skin of calf No. F1 at different temperatures.

As expected for a diffusional process, the rate of penetration, as reflected in the value of $k_p r$, increased with an increase in temperature. (Differences between values of $k_p r$ at the two lower temperatures and at the two higher temperatures were not significant at the 5% level, but $k_p r$ values at the higher temperatures were greater than those at lower temperatures.)

This result is important when taken in conjunction with the observation that the permeability of animal skin in early fall (and presumably summer) is greater than that in winter. Hence, the higher ambient temperatures that are likely to exist in fall as compared with winter are likely to contribute to very much greater permeability in fall (and summer) as compared with winter.

The complexity of the effect of temperature on skin permeability is highlighted by the fact that at both the 1 and 5% level there was no significant difference in values of D and PC as the skin temperature was raised from 24.1 to 32.7°.

Diffusion Model and Solvent Properties of Cattle Skin—It was postulated (1) that the major mechanism by which I, and presumably other neutral molecules, is transported across cattle skin involves diffusion into and down the hair follicles and into their associated sweat and sebaceous ducts to a capillary bed, at which point they enter the blood. It was also suggested (1) that the emulsified sebum [which is expelled from the common sweat and sebaceous ducts into the infundibulae of the hair follicles and which seeps up through the outer layers of the stratum corneum and down the hair follicle (12)] has a profound influence on skin permeability.

A potentially useful model for cattle skin penetration involves the following steps:

1. Drug molecules rapidly partition from applied topical formulations into the emulsified sebum which is associated with the skin. The partition coefficient for this step is the PC value calculated from *in vitro* diffusion experiments.
2. Drug molecules diffuse through the emulsified sebum and eventually pass down the hair follicles and reach the capillary beds where they pass into the blood. The parameter (D) that is calculated from *in vitro* experiments would be the diffusion coefficient for this process.

Results to date indicate that the value of D is not significantly affected by solvents such as water, 2-ethoxyethanol, and 2-propanol, but is affected by toluene and 80% dimethyl sulfoxide. It was suggested earlier that those latter solvents might modify the diffusion barrier (the emulsion) by dissolving or displacing a component.

A rationalization of the solvent properties of emulsified sebum, and consequently of values of PC, can be achieved by considering those features that determine what is a good or a poor solvent for I.

Table VII contains values of the partition coefficients for neutral molecules of I from aqueous pH 8.9 solution into liquid paraffin, toluene, and dimethyl sulfoxide. These results indicate that I is less soluble in water than in each of the other solvents, but that a complex relationship exists between the solubility of I and the polarity (dielectric constant ϵ) or solubility parameter (δ) of the solvent. For the purposes of these comparisons, liquid paraffin has been assigned the same values of ϵ and δ that are possessed by n-hexane (1.89 at 20° and 7.3 hr (13), respectively).

Hence, although the solubility of I in liquid paraffin, toluene, and dimethyl sulfoxide increases as both the dielectric constant increases [1.89 at 20° (13), 2.38 at 25° (13), and 45 (14)] and the solubility parameter increases [7.3 H, 8.9 H, 12.0 H (13)], it is least soluble in water, the solvent with the highest dielectric constant [78.54 at 25° (13)] and solubility parameter [23.4 H (13)]. It appears that specific dipole–dipole or other solvent–solute interactions are of at least equal importance to polarity in determining the solubility of I in a given solvent.

The PC values in Table IV that relate to partitioning of I between various solvents and the barrier (*i.e.*, the emulsion) suggest that the latter has similar solvent properties to water toward I, but that it is poorer than the alcohol-based solvents in formulations A, B, and C as well as toluene or 80% dimethyl sulfoxide. The results also show that while the barrier has similar solvent properties to water toward neutral molecules of I, it is a poorer solvent than water toward cations.

Table VI—Effect of Temperature on the Permeability of Cattle Skin [a] to I from Formulation A

Bath Temperature	Skin Temperature	No. Experiments	$10^6 k_p r$, $cm^2\ min^{-1}$	$10^6 D$, $cm^2\ min^{-1}$	Partition Coefficient
25.0°	24.1°(0.2)	6	8.2(1.7)	16(5)	0.59(0.29)
30.0°	27.3°(0.5)	5	13.2(3.1)	16(4)	0.90(0.39)
37.0°	30.6°(0.5)	11	24.0(3.7)	23(6)	1.09(0.35)
40.0°	32.7°(0.5)	2	22.6(1.1)	21(6)	1.19(0.40)

[a] The skin was from the dorsal region of calf F1. [b] The temperature of the skin was measured periodically using a thermistor.

Table VII—Partition Coefficients[a,b] for I at 37°

Solvent 2	Solvent 1	Partition Coefficient (*PC*), (±*SD*)
Liquid paraffin	aqueous pH 8.9 solution	2.3(0.6)
Toluene	aqueous pH 8.9 solution	5.2(2.1)
Dimethyl sulfoxide	aqueous pH 8.9 solution	14.4[c]

[a] *PC* = [I] solvent 2/[I] solvent 1. [b] Data are from Ref. 7. [c] Calculated by dividing *PC* from aqueous pH 8.9 solution into liquid paraffin (2.3) by *PC* from dimethyl sulfoxide into liquid paraffin (0.16).

The results in Tables III and IV reveal that the solvent properties of the skin toward I increase in the fall as compared with winter.

The complex nature of the solubility of I does not allow simplistic statements to be made. However, it is very likely that changes in the composition of the emulsified sebum, perhaps even phase changes, led to the observed changes in permeability.

There appears to be very little difference between the skin permeabilities of European breeds of cattle at any particular time, and intrabreed differences are small.

Because the permeability of cattle skin appears to be 10 times greater in early fall as compared with winter and to increase with increasing temperature, it can be predicted that the skin permeability of cattle in the field in mid-summer will be substantially higher than that in mid-winter. Cattle skin is a relatively polar solvent with properties similar to water towards neutral organic molecules. Consequently, water or poorer solvents than water for particular drugs should be selected for topical formulations in preference to better solvents than water in order to maximize the rate of drug penetration.

Studies aimed at characterizing the solvent properties of domestic animal skins are currently underway.

REFERENCES

(1) I. H. Pitman and S. J. Rostas, *J. Pharm. Sci.*, **71**, 427 (1982).

(2) R. J. Scheuplein and I. H. Blank, *Physiol. Rev.*, **51**, 702 (1971).

(3) I. H. Blank and R. J. Scheuplein, *Br. J. Dermatol.*, **81**, 4 (1964).

(4) B. J. Poulsen, in "Drug Design," vol. 4, E. J. Ariens, Eds., Academic, New York, N.Y., 1973, pp. 149, 192.

(5) T. Higuchi, in "Design of Biopharmaceutical Properties Through Pro-drugs and Analogues," E. B. Roche, Ed., American Pharmaceutical Association, Washington, D.C., 1977.

(6) I. H. Pitman and S. J. Rostas, *J. Pharm. Sci.*, **70**, 1181 (1981).

(7) L. M. Ponting and I. H. Pitman, *Aust. J. Pharm. Sci.*, **8**, 15 (1979).

(8) R. G. Miller, "Simultaneous Statistical Inference," McGraw-Hill, New York, N.Y., 1966.

(9) D. H. Lloyd, W. D. B. Dick, and D. M. Jenkinson, *Res. Vet. Sci.*, **26**, 250 (1979).

(10) R. B. Stoughton and W. Fritsch, *Arch. Dermatol.*, **90**, 512 (1964).

(11) H. I. Maibach and R. J. Feldmann, *Ann. N.Y. Acad. Sci.*, **141**, 423 (1967).

(12) D. M. Jenkinson, *Proc. R. S. Edenburgh, Sect. B: Biol.* **79**, 3 (1980).

(13) "Handbook of Chemistry and Physics," 57th ed., R. C. Weast, Ed., CRC Press, Cleveland, Ohio, 1976.

(14) "The Merck Index," 9th ed., M. Windolz, Ed., Merck, Rahway, N.J. 1976.

ACKNOWLEDGMENTS

This work was supported by a grant from ICI Ltd. and ICI Australia, Ltd.

The authors wish to acknowledge the help of Dr B.H. Kellett (statistics) and Mr. Ian Ray (technical assistance).

Determination of Antimicrobial Preservatives in Pharmaceutical Formulations Using Reverse-Phase Liquid Chromatography

THOMAS P. RADUS * and GRETCHEN GYR ˣ

Received November 20, 1981, from *The Upjohn Company, Kalamazoo, MI 49001.* Accepted for publication April 15, 1982. *Present address: Westinghouse Electric Corporation, Bettis Atomic Power Laboratory, West Mifflin, PA 15122.

Abstract □ A specific stability-indicating reverse-phase high-performance liquid chromatographic analytical method has been developed to quantitate the antimicrobial preservatives methylparaben, propylparaben, butylparaben, sorbic acid, and benzoic acid in a series of typical pharmaceutical formulations. The mobile phase of this system is a water–acetonitrile mixture, modified by various acids and buffers. The proportions of water and acetonitrile as well as the type and amounts of modifiers are varied in order to achieve optimum chromatography. This method has been used successfully to quantitate preservatives in solutions, suspensions, creams, lotions, and ointments, and can be readily adapted to routine automated assays, either for routine product evaluation or stability programs.

Keyphrases □ Preservatives, antimicrobial—determination in pharmaceutical formulations using reverse-phase liquid chromatography □ Reverse-phase liquid chromatography—determination of antimicrobial preservatives in pharmaceutical formulations

Antimicrobial preservatives are materials added to formulations to protect the product from microbial contamination. A given preservative material can be used in a wide variety of products and also may be used in combinations with other preservatives. Separate testing methods for each product–preservative combination would not make efficient use of laboratory resources if the tests are to be performed frequently; thus a method which is generally applicable is desirable. However, the analytical methods should be specific to ensure that decomposition products and impurities are not inadvertently measured. Regulatory agencies have also shown interest in specific test methods for preservatives (1, 2). The challenge for the methods developer is to come up with a method that satisfies both criteria of assay efficiency and specificity.

It is currently of interest within the pharmaceutical industry to assure that specific, stability-indicating, and validated testing methods are available for antimicrobial preservatives. This study reports the development of a reverse-phase high-performance liquid chromatographic (HPLC) assay system that, with minor modifications in

0022-3549/83/0300-0221$01.00/0

Table VII—Partition Coefficients[a,b] for I at 37°

Solvent 2	Solvent 1	Partition Coefficient (*PC*), (±*SD*)
Liquid paraffin	aqueous pH 8.9 solution	2.3(0.6)
Toluene	aqueous pH 8.9 solution	5.2(2.1)
Dimethyl sulfoxide	aqueous pH 8.9 solution	14.4[c]

[a] *PC* = [I] solvent 2/[I] solvent 1. [b] Data are from Ref. 7. [c] Calculated by dividing *PC* from aqueous pH 8.9 solution into liquid paraffin (2.3) by *PC* from dimethyl sulfoxide into liquid paraffin (0.16).

The results in Tables III and IV reveal that the solvent properties of the skin toward I increase in the fall as compared with winter.

The complex nature of the solubility of I does not allow simplistic statements to be made. However, it is very likely that changes in the composition of the emulsified sebum, perhaps even phase changes, led to the observed changes in permeability.

There appears to be very little difference between the skin permeabilities of European breeds of cattle at any particular time, and intrabreed differences are small.

Because the permeability of cattle skin appears to be 10 times greater in early fall as compared with winter and to increase with increasing temperature, it can be predicted that the skin permeability of cattle in the field in mid-summer will be substantially higher than that in mid-winter. Cattle skin is a relatively polar solvent with properties similar to water towards neutral organic molecules. Consequently, water or poorer solvents than water for particular drugs should be selected for topical formulations in preference to better solvents than water in order to maximize the rate of drug penetration.

Studies aimed at characterizing the solvent properties of domestic animal skins are currently underway.

REFERENCES

(1) I. H. Pitman and S. J. Rostas, *J. Pharm. Sci.*, **71**, 427 (1982).

(2) R. J. Scheuplein and I. H. Blank, *Physiol. Rev.*, **51**, 702 (1971).

(3) I. H. Blank and R. J. Scheuplein, *Br. J. Dermatol.*, **81**, 4 (1964).

(4) B. J. Poulsen, in "Drug Design," vol. 4, E. J. Ariens, Eds., Academic, New York, N.Y., 1973, pp. 149, 192.

(5) T. Higuchi, in "Design of Biopharmaceutical Properties Through Pro-drugs and Analogues," E. B. Roche, Ed., American Pharmaceutical Association, Washington, D.C., 1977.

(6) I. H. Pitman and S. J. Rostas, *J. Pharm. Sci.*, **70**, 1181 (1981).

(7) L. M. Ponting and I. H. Pitman, *Aust. J. Pharm. Sci.*, **8**, 15 (1979).

(8) R. G. Miller, "Simultaneous Statistical Inference," McGraw-Hill, New York, N.Y., 1966.

(9) D. H. Lloyd, W. D. B. Dick, and D. M. Jenkinson, *Res. Vet. Sci.*, **26**, 250 (1979).

(10) R. B. Stoughton and W. Fritsch, *Arch. Dermatol.*, **90**, 512 (1964).

(11) H. I. Maibach and R. J. Feldmann, *Ann. N.Y. Acad. Sci.*, **141**, 423 (1967).

(12) D. M. Jenkinson, *Proc. R. S. Edenburgh, Sect. B: Biol.* **79**, 3 (1980).

(13) "Handbook of Chemistry and Physics," 57th ed., R. C. Weast, Ed., CRC Press, Cleveland, Ohio, 1976.

(14) "The Merck Index," 9th ed., M. Windolz, Ed., Merck, Rahway, N.J. 1976.

ACKNOWLEDGMENTS

This work was supported by a grant from ICI Ltd. and ICI Australia, Ltd.

The authors wish to acknowledge the help of Dr B.H. Kellett (statistics) and Mr. Ian Ray (technical assistance).

Determination of Antimicrobial Preservatives in Pharmaceutical Formulations Using Reverse-Phase Liquid Chromatography

THOMAS P. RADUS * and GRETCHEN GYR ˣ

Received November 20, 1981, from *The Upjohn Company, Kalamazoo, MI 49001.* Accepted for publication April 15, 1982. *Present address: Westinghouse Electric Corporation, Bettis Atomic Power Laboratory, West Mifflin, PA 15122.

Abstract □ A specific stability-indicating reverse-phase high-performance liquid chromatographic analytical method has been developed to quantitate the antimicrobial preservatives methylparaben, propylparaben, butylparaben, sorbic acid, and benzoic acid in a series of typical pharmaceutical formulations. The mobile phase of this system is a water–acetonitrile mixture, modified by various acids and buffers. The proportions of water and acetonitrile as well as the type and amounts of modifiers are varied in order to achieve optimum chromatography. This method has been used successfully to quantitate preservatives in solutions, suspensions, creams, lotions, and ointments, and can be readily adapted to routine automated assays, either for routine product evaluation or stability programs.

Keyphrases □ Preservatives, antimicrobial—determination in pharmaceutical formulations using reverse-phase liquid chromatography □ Reverse-phase liquid chromatography—determination of antimicrobial preservatives in pharmaceutical formulations

Antimicrobial preservatives are materials added to formulations to protect the product from microbial contamination. A given preservative material can be used in a wide variety of products and also may be used in combinations with other preservatives. Separate testing methods for each product–preservative combination would not make efficient use of laboratory resources if the tests are to be performed frequently; thus a method which is generally applicable is desirable. However, the analytical methods should be specific to ensure that decomposition products and impurities are not inadvertently measured. Regulatory agencies have also shown interest in specific test methods for preservatives (1, 2). The challenge for the methods developer is to come up with a method that satisfies both criteria of assay efficiency and specificity.

It is currently of interest within the pharmaceutical industry to assure that specific, stability-indicating, and validated testing methods are available for antimicrobial preservatives. This study reports the development of a reverse-phase high-performance liquid chromatographic (HPLC) assay system that, with minor modifications in

0022-3549/83/0300-0221$01.00/0

Table I—Data for the Preservative Assays for Pharmaceutical Products Containing Only the Parabens as Preservatives

Product Type	Preservatives	Internal Standard	Mobile Phase	Average Recovery, %	*RSD*, %	Concentration Range Validated
Ointment (5)[a]	Methylbaraben	Calusterone	1	100.3	1.4	0.1–0.3 mg/g
	Butylparaben			100.0	1.4	0.9–2.7 mg/g
Cream A (2)	Methylparaben	Calusterone	1	100.5	1.2	0.5–2.0 mg/g
	Butylparaben			100.1	1.2	2.0–6.0 mg/g
Cream B (1)	Methylparaben	Calusterone	1	98.0	1.2	0.5–2.0 mg/g
	Butylparaben			99.8	1.8	2.0–6.0 mg/g
Cream C (2)	Methylparaben	Calusterone	1	100.9	1.3	2.0–6.0 mg/g
	Butylparaben			101.7	1.5	1.5–4.5 mg/g
Lotion (2)	Methylparaben	Calusterone	1	98.7	0.8	1.0–3.0 mg/g
	Butylparaben			99.7	1.0	1.5–4.5 mg/g
Sterile Suspension D (1)	Methylparaben	Butylparaben	1	98.3	1.0	0.8–3.2 mg/ml
	Propylparaben			102.7	1.5	0.09–0.36 mg/ml
Fluid E (1)	Methylparaben	Butylparaben	1	99.8	1.0	0.5–2.0 mg/ml
Sterile Suspension F (1)	Methylparaben	Butylparaben	1A	99.6	1.8	0.4–1.6 mg/ml
	Propylparaben			99.3	1.3	0.04–0.18 mg/ml
Fluid G (1)	Methylparaben	Ethylparaben	1B	100.2	1.4	0.35–1.5 mg/ml
	Propylparaben			98.1	1.3	0.10–0.5 mg/ml

[a] Number of products in parentheses.

the mobile phase, is capable of quantitating the preservatives methylparaben, propylparaben, butylparaben, sorbic acid, and benzoic acid in a wide range of pharmaceutical formulations.

BACKGROUND

Validation criteria have been developed for the potency assays for pharmaceutically active ingredients (3). This system was used as the starting point for the criteria that would be applied to the preservative assays. However, it was realized that in several important aspects, quantitating preservatives is significantly different from quantitating the active pharmaceutical ingredient, and that consideration of these aspects will influence the criteria used to judge the validity of the test method. If appropriate criteria are established before development work begins, it should be possible for both the developer and the ultimate user of the testing methods to utilize their resources as effectively as possible. These aspects will now be considered in more detail.

Preservatives are neither pharmacologically active, nor are they inert formulation excipients. They are, however, considered essential ingredients because they are active in maintaining product integrity (1).

Efficiency in a Routine Environment—A completely new testing method may be required for a new product, or even for an old drug in a new formulation, to satisfy requirements for potency or impurity quantitation methods. A given preservative material may, however, be used in a wide range of products and types of formulations. To have a different testing method for each different occurrence of the preservative would not be very efficient for laboratory operations but would allow the flexibility of developing a highly precise, accurate assay method. However, the highest laboratory efficiency would be gained if only one automated assay system were needed for all products containing the given preservative, but accuracy and precision would suffer, considering the wide variety of samples to be processed. An automated system is not available for preservatives, and the most reasonable compromise would involve a minimum number of testing methods with assay variabilities between the two extremes, and with only minimal detrimental effects on efficiency. The method reported here is an example of such a system.

Table II—Data for the Preservative Assays for Pharmaceutical Products Containing Sorbic Acid and the Parabens as Preservatives ●

Product Type	Preservatives	Average Recovery, %	*RSD*, %	Concentration Range Validated, mg/ml
Suspension H (2)[b]	Sorbic Acid	100.1	0.5	0.5–2.0
	Methylparaben	100.7	1.0	1.0–4.0
Solution J (2)	Sorbic Acid	98.8	0.8	0.5–2.0
	Methylparaben	99.3	0.7	0.3–1.5
	Propylparaben	99.8	1.1	0.1–0.4
Cream K (1)	Sorbic Acid	99.4	0.5	1.0–4.0

[a] The mobile phase used was mobile phase 2; the internal standard was ethylparaben. [b] Number of products in parentheses.

Preservative Concentrations—Preservatives are generally formulated at concentrations of 1 mg/ml, which can be as much as two orders of magnitude less than the active ingredient. This can put preservatives in the sample at the approximate levels of impurities or degradation products. This can cause problems of interferences from these extra materials leading to poor reproducibility and/or assay bias.

Variation with Time–Degradation Products—The concentration of preservatives may decrease over the shelf-life of a product at a rate faster than that of the drug itself. The analytical testing method must be validated well below the usual preservative concentration to quantitate these amounts, and must be specific for degradation products. (Although in most cases it is not known what contribution, if any, to the preservative capacity of the system could be made by these compounds.) To quantitate these lower levels demands analytical methods that are accurate, linear, and which have acceptable slope and intercept values (ideally one and zero, respectively, within experimental error for plots of amounts added *versus* amounts recovered).

Assay Variability—For a drug in a product, the lowest acceptable concentration is frequently specified by a compendial limit. For preservatives, the lowest acceptable concentration is stated implicitly as the minimum amount which will allow the formulation to pass preservative efficacy tests. Because of the nature of these microbiological tests, this concentration cannot be accurately specified. The analytical method which measures that concentration need not be any more accurate than required by the normal variability of the microbial tests. Since the coefficient of variation of liquid chromatographic analytical methods of the type used here is less than the variability of the microbial tests, liquid chromatographic methods are more than suitable for this purpose.

The approach used in the development of these analytical methods was to start with a water–acetonitrile binary system and add other modifiers as necessary to achieve satisfactory chromatography. However, any mobile phase not otherwise modified was made to contain 2% acetic acid to be in agreement with the mobile phase previously suggested for quantitating parabens[1]. In all cases reported here, satisfactory chromatography could be achieved by adjusting the water–acetonitrile ratio and/or the buffer–pH combinations.

EXPERIMENTAL

The equipment used in these studies included standard HPLC pumping systems[2], injector[3], columns[4], and UV detectors[5]. Sample injections were made by an autosampler system[6], which also actuated the injector valve (4). Solvent[7] flow rates were typically 2 ml/min, and in-

[1] Unpublished communication, Analytical Research Department, Pharmaceutical Products Division, Abbott Laboratories, North Chicago, Ill.
[2] Milton-Roy minipump; Waters model 6000A pump.
[3] Rheodyne model 7126.
[4] Waters C-18 μBondapak.
[5] Waters Model 440; LDC model 1203.
[6] The Upjohn Co.
[7] Burdick and Jackson.

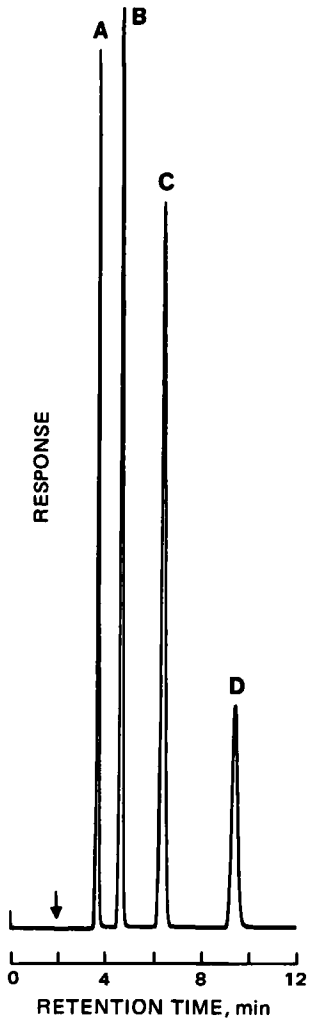

Figure 1—*Chromatogram of a mixture of methylparaben (A), ethylparaben (B), propylparben (C), and butylparaben (D) using mobile phase 1. The solvent front is indicated by the arrow. The mixture was prepared by dissolving 7 mg of methylparaben, 13 mg of ethylparaben, 15 mg of propylparaben, and 7 mg of butylparaben in 100 ml of mobile phase.*

jection volumes were 10 μl. Quantitation was performed by measuring peak heights. The mobile phase compositions referenced later in the text by number are: 1, water–acetonitrile–glacial acetic acid (58:40:2); 1A, water–acetonitrile (70:30) 0.2 *M* ammonium acetate, pH 7.2; 1B, water–acetonitrile (65:35) 0.01 *M* ammonium dihydrogen phosphate, pH 2.2 with concentrated phosphoric acid; and 2, water–acetonitrile (70:30) 0.01 *M* potassium acetate, pH 5.4 with glacial acetic acid.

Recovery Studies—For each product type a sample was prepared containing all ingredients (including active ingredients) in their proper proportion except for the preservatives. Reference standard preservative material was then added to portions of the sample in amounts ranging from 50 to 150% of the normal preservative concentration. These spiked samples were quantitated against the reference standard to determine recovery and linearity for the analytical method. Replicate assay results on several production lots were pooled to determine the relative standard deviation (*RSD*). All analytical methods reported here showed acceptable linearity and have a slope of 1.00 within experimental error for plots of amounts recovered *versus* amount added. Tables I–III list the product type, number of individual products within each type, preservatives, internal standard used, mobile phase, average recovery as a percentage of the amount added, *RSD* calculated for the method, and range of concentrations validated. All recoveries and *RSD*s satisfied the validation criteria.

Sample Preparation for Products Containing Only Parabens (Table I)—*Ointments*—The four ointment products[8] studied make use

[8] Cortaid, Neo-Cortef, Mycitracin, Neo-Oxylone.

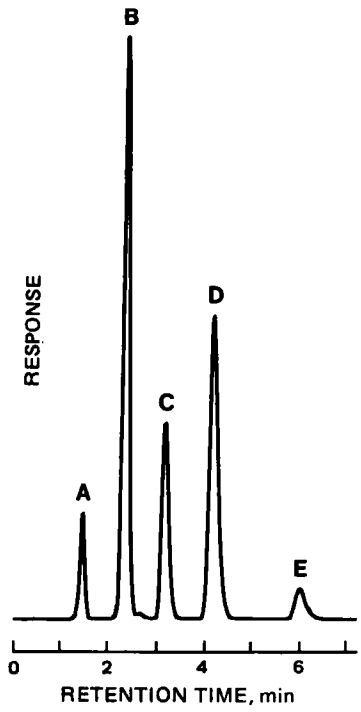

Figure 2—*Chromatogram of a production lot of fluid product J using mobile phase 2. The peaks are: (A) Solvent front and excipients, (B) sorbic acid, (C) methylparaben, (D) ethylparaben, and (E) propylparaben.*

of a typical hydrocarbon ointment base. This base would not dissolve in any solvents that were compatible with the mobile phase. Quantitative recovery was achieved by extraction into dimethylformamide. A 10.0-ml volume of this solvent was added to 1.0 g of ointment and 20.0 ml of the internal standard in a water–acetonitrile solution. The mixture was shaken in a hot water shaker bath at 50° and then centrifuged. The undissolved base congealed at the top and an aliquot of the clear lower layer was assayed.

Creams—The three cream product types[9] (five products) were all variations of typical oil-in-water emulsions. A measure of 0.5 g of each cream was added to 100.0 ml of tetrahydrofuran and 5.0 ml of the internal standard in a water–acetonitrile solution. The samples were shaken for 15 min and then chromatographed.

Lotions—The two lotions[10] were very similar to the cream formulations. The sample preparation was the same as for the cream products.

Sterile Product—Sterile suspension D[11] (1.0 ml) was diluted with 30 ml of water containing the internal standard, mixed, centrifuged to remove the undissolved drug, and chromatographed.

Nonsterile Fluid—The fluid formulation E[12] was an oral antibiotic suspension. One milliliter of this fluid was added to 30.0 ml of an acidified (acetic acid) acetonitrile–water solution of the internal standard to increase solubility and prevent the formation of an emulsion. The sample was then mixed, centrifuged, and chromatographed.

Sample Preparation for Products Containing Sorbic Acid and Parabens (Table II)—One milliliter of fluid samples H and J[13] was added to 30.0 ml of a solution of the internal standard in mobile phase, mixed, and chromatographed. Cream product K[14] (1.0 g) was dissolved in 100 ml of tetrahydrofuran. Five milliliters of this solution was added to 5.0 ml of internal standard in mobile phase, mixed, and chromatographed.

RESULTS AND DISCUSSION

Products Containing Parabens Only—Methyl, propyl, and butyl paraben can occur in these products either singly or in pairs. Ethyl par-

[9] (Cream A) Cortaid, oxylone; (Cream B) Neo-Cortef; (Cream C) Neo-Medrol, medrol.
[10] Cortaid, Neo-Cortef.
[11] Depo-Provera.
[12] Panmycin syrup.
[13] Kaopectate, Kaopectate concentrate.
[14] Florone.

Table III—Data for the Preservative Assays for Pharmaceutical Products Containing Benzoic Acid as the Preservative

Product	Internal Standard	Mobile Phase	Average Recovery, %	*RSD*, %	Concentration Range Validated, mg/ml
Fluid L	Ethylparaben	1B	100.1	0.5	0.5–2.0
Fluid M	Ethylparaben	1B	100.3	0.7	0.5–2.0

aben was not used as a preservative in the formulations studied and, thus, could serve as an internal standard. Figure 1 shows a chromatogram obtained by injecting a solution of these four materials dissolved in mobile phase 1. Excellent resolution was obtained between all four materials. The primary degradation product of all of these compounds was *p*-hydroxybenzoic acid, which eluted with the solvent front under these conditions. The total chromatographic time was ~10 min.

As previously suggested[1], the majority of the products containing only parabens as the preservative could be chromatographed using this mobile phase. The sample preparations were described earlier. The products successfully chromatographed by this method are creams, ointments, lotions, and sterile solutions and suspensions. The products are grouped in Table I by product type, where a product type is a group of products of essentially identical composition except for the active ingredient.

Products Requiring Different Mobile Phases—Two products containing only parabens as preservatives could not be chromatographed successfully by this system: a sterile penicillin suspension (F) and an oral tetracycline suspension (G). In both cases the active ingredient interfered with the preservatives. For the penicillin product it was found that the acidic mobile phase produced decomposition products which could not be adequately separated from the preservatives. By reducing the acetonitrile concentration and buffering mobile phase IA at an apparent pH of 7.2, decomposition could be avoided and all components were resolved. The sample preparation was identical to that for sterile suspension D.

For the oral tetracycline product (fluid G) it was found that the drug eluted as a broad, tailing peak with mobile phase 1. Lowering the pH narrowed the peak and moved it toward the solvent front. At pH 2.3 the tetracycline tail no longer interfered in the quantitation of the methyl paraben. Below pH 2.2, however, no improvement in peak shape was seen. Mobile phase IB was developed with the adjustment to an apparent pH of 2.2 with concentrated phosphoric acid. The sample was prepared by adding 1.0 ml of the fluid to 1.0 ml of a 0.2 *M* $NH_4H_2PO_4$ solution adjusted to pH 1.6. This solution was then diluted with 20.0 ml of an acetonitrile–water solution containing the internal standard. The sample was then mixed and chromatographed.

Recovery data for both products are included in Table I.

Products Containing Sorbic Acid With or Without Parabens—Several products were evaluated which use sorbic acid, either alone or in combination with methylparaben or methyl- and propylparaben. When these samples were chromatographed using mobile phase 1, the sorbic acid and methylparaben coeluted. Since it is well known that the retention times of weak acids are dependent on the pH of the system, it was decided to adjust the pH in an attempt to achieve optimum resolution. An acetic acid–acetate buffer at pH 5.4 was found to give the best chromatography and to separate all formulation excipients as well as *p*-hydroxybenzoic acid. The mobile phase used was mobile phase 2. The apparent pH was adjusted to 5.4 with acetic acid. This system allowed the use of ethylparaben as the internal standard. Products included suspensions (H), solutions (J), and a cream (K).

The results are listed in Table II. All recoveries and *RSD*s satisfy the validation criteria. Figure 2 shows a chromatogram of the solution product (J) and indicates the separation achieved between the three preservatives (sorbic acid, methylparaben, and propylparaben) and the internal standard (ethylparaben). The total chromatographic time was 8 min.

Benzoic Acid—Benzoic acid is used in two fluid products[15] (L and M). Mobile phase 1 was not able to resolve all excipients from the benzoic acid peak. Adopting the same approach as for sorbic acid, it was found that changing the pH could improve peak resolution. Optimum separation was achieved at pH values of ~2.5. Since this value was close to the pH used for mobile phase 1B, that system was tried. Mobile phase 1B did resolve the components sufficiently, and this offered the opportunity to consolidate several products on one analytical system, which would improve laboratory efficiency. The samples were prepared by diluting 1.0 ml of the fluids in 20.0 ml of an acetonitrile–water internal standard solution and chromatographing. The results are shown in Table III.

This paper has reported on a reverse-phase HPLC method which has been used successfully to quantitate antimicrobial preservatives in typical pharmaceutical formulations. The mobile phase used was basically an acetonitrile–water mixture, with various modifiers added as necessary to optimize the chromatography. This method was used successfully on five preservative materials: methylparaben, propylparaben, butylparaben, sorbic acid, and benzoic acid. This system can be easily adapted for automated sample analysis.

REFERENCES

(1) Joel S. Davis, *Pharma. Tech.*, **4**, 103 (1980).

(2) E. C. Juenge, D. F. Gurka, and M. A. Kreienbau, *J. Pharm. Sci.*, **70**, 589 (1981).

(3) A. J. Vanderwielen and E. A. Hardwidge, *Pharma. Tech.*, **6**, 66 (1982).

(4) W. F. Beyer and D. D. Gleason, *J. Pharm. Sci.*, **64**, 1557 (1975).

[15] Cheracol D, Cheracol Syrup.

Immobilization of Urokinase on Agarose Matrices

HYUN PYO KIM, SI MYUNG BYUN, YOUNG IL YEOM, and SUNG WAN KIM *x

Received October 9, 1981, from the *Department of Biological Science & Engineering, Korea Advanced Institute of Science & Technology, Seoul, Korea*, and the **Department of Pharmaceutics, University of Utah, Salt Lake City, UT, 84112.* Accepted for publication April 20, 1982.

Abstract □ Immobilization of urokinase, a plasminogen activator, was carried out to determine the effect of spacer length used on the immobilized enzyme activity. The enzyme was covalently coupled to agarose gel, both directly to the matrix and also *via* interposing different lengths of spacer groups. The specific activity of immobilized urokinase increased as the spacer length (n') increased to a certain length and tended to decrease thereafter. The maximal activity was shown when the value of n' was 7 for the agarose-NH-$(CH_2)_n$-CO-NH-$(CH_2)_2$-CO-NH-urokinase series. The coupling yield of the enzyme activity was from 33 to 68% depending on various forms of immobilized urokinase. The immobilized urokinase was characterized with regard to pH, temperature, storage, and thermal stabilities.

Keyphrases □ Urokinase—immobilization on agarose matrices, effect on spacer length, enzyme activity □ Agarose—immobilization of urokinase on matrices, effect of spacer length, enzyme activity □ Immobilization—urokinase on agarose matrices, effect of spacer length, enzyme activity

Urokinase, a plasminogen activator, has been used for the treatment of thrombosis and/or vascular obstruction. For the purpose of thrombolytic therapy the immobilization of urokinase was attempted (*a*) to increase the *in vivo* half life, (*b*) to obtain local fibrinolytic activity for thromboembolic disorders, and (*c*) to develop antithrombogenic materials (1–6). Previous results suggested the potential clinical application of the immobilized urokinase (2–6).

Urokinase has been immobilized (1, 2) onto agarose matrices using the cyanogen bromide activation technique. Polyamide has been used as a matrix for the immobilization of urokinase (3, 5, 6) and other studies have utilized polyamide, polyester, polyvinyl chloride, polyurethane, and polydimethyl siloxane for this purpose (4, 6). The results demonstrated that the immobilized urokinase activated plasminogen. In a previous study streptokinase, a metabolic product of β-hemolytic *Streptococci* was immobilized for this purpose (7).

Steric considerations in the immobilization of bioactive agents appear to be important. It has been reported that urokinase immobilized onto a polyethyleneimine copolymer *via* a nitrophthalic acid spacer group showed better fibrinolytic activity than urokinase immobilized directly onto polyamide (4). Recently, researchers (8) immobilized heparin on polymers using different spacer group lengths. When immobilized, heparin activity increases rapidly, beginning with 8 carbon diaminoalkane spacer groups. In this work, the immobilization of urokinase onto an agarose surface was carried out by varying the spacer length between the enzyme and substrate.

EXPERIMENTAL

Materials—Crude urokinase was prepared from fresh human urine and human Cohn fraction III[1]. Crude urokinase, adsorbed onto silica gel, was extracted with 30% ethanol followed by dialysis and freeze-drying. Human plasminogen was purified from human Cohn fraction III according to a previous method (9) by using a lysyl-agarose affinity column. Human plasmin was prepared by eluting plasminogen into the column containing immobilized urokinase. One hundred milliliters of plasminogen solution, consisting of 0.5 CTA[2] units/ml of 0.1 *M* tromethamine hydrochloride buffer (pH 7.5), was passed through the column at a flow rate of 0.3 ml/min. The eluted plasmin was used for the standard curve calibration of the urokinase assay. Bovine serum albumin, α-casein, α-aminobutyric acid, ε-aminocaproic acid, and ω-aminocaprylic acid[3] were used as received. Glycine, *N*-hydroxysuccinimide, β-alanine[4], 1-cyclohexyl-3-(2-morpholinoethyl)carbodiimide metho-*p*-toluenesulfonate (I), and 1-ethyl-3-(3-dimethylaminopropyl)carbodiimide hydrochloride[5] (II) were used as received. Agarose beads (III)[6] were used as the substrate for urokinase immobilization. (All other reagents were commercially available reagent grades.)

Urokinase Immobilization—*Direct Coupling of Urokinase on the Matrix*—Compound III was activated with cyanogen bromide according to a previously described procedure (11). A 10-ml slurry of washed III, consisting of equal volumes of the gel and water, was added to 10 ml of 2 *M* sodium carbonate and gently mixed. One gram of cyanogen bromide in 0.5 ml of acetonitrile was then added, and the slurry was stirred for 2 min. The cyanogen bromide-activated beads were then collected by filtration on a glass filter and washed successively with 100 ml each of cold 0.1 *M* sodium bicarbonate and 0.1 *M* sodium borate buffer.

To 10 ml of an activated slurry of III was added 50 mg of urokinase (1500 CTA units) in 20 ml 0.1 *M* sodium borate buffer (pH 7.5) containing 0.05 *M* HCl and 50 m*M* $CaCl_2$, which was then gently swirled overnight at 4°. The beads were collected on a coarse glass filter and washed with 300 ml each of cold water, 0.5 *M* NaCl, 2 *M* urea, and 0.1 *M* sodium borate buffer.

Coupling of Diaminoalkanes to Cyanogen Bromide-Activated III—Ten milliliters of activated III, prepared as previously described, was suspended in 10 ml of cold 0.1 *M* sodium bicarbonate, pH 9.0, and mixed with 10 ml of the various 1 *M* α,ω-diaminoalkane solutions which had been previously adjusted to pH 9.0 with 6 *N* HCl. The coupling was carried out overnight at 4° by stirring with a synchronized stirrer. After the reaction was completed, III was again sequentially washed with cold water, 0.1 *M* $NaHCO_3$, 0.05 *M* NaOH, water, 0.1 *M* CH_3COOH, and water.

Coupling of Urokinase to ω-Aminoalkyl-III with I and II—Ten milliliters of each of the above aminoalkyl-III beads was suspended in 10 ml of 0.1 *M* borate buffer solution, pH 7.5, containing 40 mg of I or II and 50 mg of urokinase (1500 CTA units). The reaction was continued overnight at 4°. Compound III was filtered and thoroughly washed with cold water, 0.5 *M* NaCl, and 2 *M* urea. The final immobilized urokinase was stored in 0.9% NaCl solution at 4° until use.

Coupling of Aminoalkyl Carboxylic Acids to Cyanogen Bromide-Activated III—Aminoalkyl carboxylic acid-coupled III was prepared according to the procedure for diaminoalkane coupling described above. Ten milliliters of the various 1 *M* aminoalkyl carboxylic acids was added to 10 ml of cyanogen bromide-activated III. The other procedures were similar to those described for diaminoalkane coupling.

Coupling of Urokinase to Carboxylic Alkyl-III with N-hydroxysuccinimide—The ω-carboxylic alkyl-III beads were activated with *N*-hydroxysuccinimide according to previous procedures (12, 13).

Ten milliliters of each washed carboxylic alkyl-III, which was prepared as previously described, was washed with anhydrous dioxane extensively to obtain anhydrous conditions. Compound III was suspended in dioxane to make a total volume of 30 ml. The *N*-hydroxysuccinimide, 346 mg, was

[1] Korea Green Cross Corp., Seoul, Korea.

[2] As defined by the Committee on Thrombolytic Agents from Ref. 10.
[3] Sigma Chemical Co., St. Louis, MO 63178.
[4] Aldrich Chemical Co., Inc., Milwaukee, WI 53233.
[5] Pierce Chemical Co., Rockford, IL 61105.
[6] Sepharose 4B, Pharmacia Fine Chemicals, Piscataway, NJ 08854.

0022-3549/83/0300-0225$01.00/0

Table I—Comparative Results of Various Immobilized Urokinases on III

	Spacer length, n'	Activity, CTA units/ml, wet gel	Specific Activity, CTA units/mg, bound urokinase
Direct-coupled urokinase (III-urokinase)	0	56	14.4
III—NH—$(CH_2)_n$—C(=O)—NH-urokinase			
$n = 2$	3	49	33.6
$n = 3$	4	52	37.0
$n = 5$	6	112	45.0
$n = 7$	8	89	31.6
III—NH—$(CH_2)_n$—C(=O)—NH—$(CH_2)_2$—C(=O)—NH-urokinase			
$n = 2$	6	78	56.2
$n = 3$	7	102	64.0
$n = 5$	9	93	42.4
$n = 7$	11	84	41.4

added to the gel suspension to obtain 0.1 *M* concentration, an equal molar quantity of dicyclohexylcarbodiimide was then added and the suspension was stirred gently for 70 min at room temperature. Activated III was washed with dioxane, followed by washing with methanol and dioxane. After drying the gels briefly in air, slightly moist cakes of the activated gels were subjected to coupling. Each gel was added rapidly to 10 ml of 0.1 *M* sodium borate buffer, pH 7.5, which contained 50 mg of urokinase. After stirring for 8 hr at 4°, 750 mg of glycine was added to react any remaining *N*-hydroxysuccinimide-activated spacer groups. After 2 hr, the gels were sequentially washed with cold deionized water, 2 *M* urea, and 0.5 *M* NaCl.

Coupling of β-Alanine to Carboxylic Alkyl-III—β-Alanine-coupling reaction was conducted for 8 hr as described in the previously mentioned experiment. β-Alanine (890 mg) was mixed with 10 ml of each *N*-hydroxysuccinimide-activated alkyl-III.

Coupling of Urokinase to β-Alanine-Linked III—Ten milliliters of each β-alanine-linked III was activated with *N*-hydroxysuccinimide as previously described. Urokinase (10 mg) was coupled to 2 ml of each β-alanine-linked III.

Determination of Urokinase Bound to III—To determine the amount of the immobilized urokinase on III[6] the amino acid content was determined by an auto amino acid analyzer after the immobilized urokinase, on the various gel matrices, was hydrolyzed with 6 *N* HCl (13). Soluble urokinase was also subjected to amino acid determination for reference purposes.

One milliliter of packed gel volume of the various immobilized urokinase gels was filtered on a glass filter and washed thoroughly with distilled water, followed by amino acid hydrolysis with 2 ml of 6 *N* HCl in a sealed tube at 110° for 24 hr. After hydrolysis, the hydrogen chloride was neutralized with 0.1 *M* sodium citrate, and the amino acid solutions were concentrated by rotoevaporatization. The amounts of amino acids were determined with a fully automated amino acid analyzer[7]. With a comparison to soluble urokinase, the amount of urokinase bound to the various gels was calculated based on quantities of alanine, lysine, and arginine.

Procedures for Enzyme Activity Assays—The activities of urokinase, plasminogen, and plasmin were determined by the caseinolytic assay method (10). Thirty CTA units of urokinase was used in the experiment. The activity of the immobilized urokinase was also determined by the same methods, constantly stirring the immobilized enzyme with the incubation mixture using a water-immersed magnetic stirrer. Protein concentrations were determined according to a previous method (14) using bovine serum albumin as a standard. The medium in which the immobilized enzyme was stored was assayed and showed no urokinase activity due to possible leakage.

RESULTS

Immobilization of Urokinase—To minimize steric hinderance for improved plasminogen accessibility to the coupled urokinase, various immobilized systems were prepared interposing different spacer group

[7] Beckman Model 118-BL, Mountain View, CA 94043.

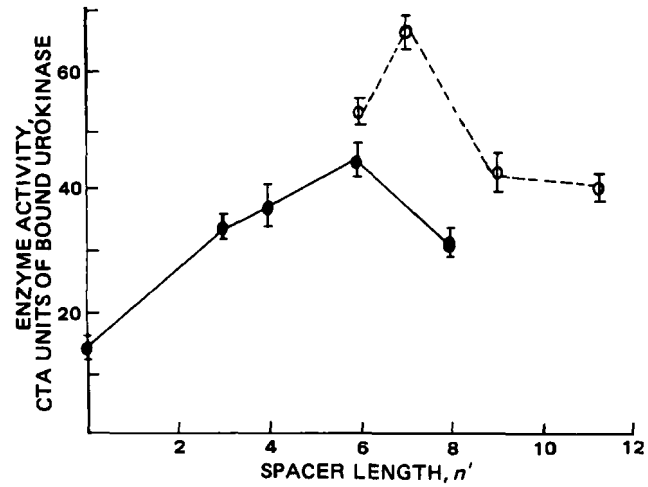

Figure 1—*Effect of spacer length on the activity of the immobilized urokinase. The length of spacer is represented by n' corresponding to: [—$(CH_2)_n$—C(=O)—] for III—NH—$(CH_2)_n$—C(=O) NH-urokinase series and [—$(CH_2)_n$—C(=O)—NH—$(CH_2)_2$—C(=O)—] for III—NH—$(CH_2)_n$—C(=O)—NH—$(CH_2)_2$—C(=O)—NH—urokinase series, respectively; (●—●) III—NH—$(CH_2)_n$—C(=O)—NH—urokinase series; (○ . . . ○) III—NH—$(CH_2)_n$—C(=O)—NH—$(CH_2)_2$—NH-urokinase series.*

lengths between III and the immobilized urokinase, as described. The results are summarized in Table I.

In the III—NH—$(CH_2)_n$—C(=O)—NH-urokinase series, the activity of immobilized urokinase increased as the length of spacer increased up to $n = 5$ ($n' = 6$). However, the highest activity was observed when $n = 3$ ($n' = 7$) in the III—NH—$(CH_2)_n$—C(=O)—NH—$(CH_2)_2$—C(=O)—NH-urokinase series. Above $n = 3$ ($n' = 7$) the activity decreased.

In immobilized urokinase activity experiments where it was immobilized onto diaminoalkane-derivatized III through carboxylic groups on the enzyme, it was found that the immobilized urokinase retained no activity. The loss in activity was found to be due to urokinase cross-linking by the carbodiimides during the immobilization step, resulting in the complete loss of enzyme activity.

The directly coupled urokinase ($n' = 0$) showed higher immobilization yields than those for III—NH—$(CH_2)_n$—C(=O)—NH-urokinase, when $n' = 3$ or 4. However, the enzymatic activity was much lower for the directly coupled urokinase relative to spacer arm mediated immobilized urokinase.

Figure 1 illustrates the effects of increasing spacer length (n') between the matrix and enzyme on the activities of the immobilized urokinase. The activity per milligram of bound enzyme was calculated from the data obtained by amino acid analysis of the immobilized urokinase. The enzymatic activity increased as spacer lengths extended to a certain length and tended to decrease thereafter. The maximum enzymatic activity was observed when $n' = 7$ for the III—NH—$(CH_2)_n$—C(=O)—NH—$(CH_2)_2$—C(=O)—NH-urokinase series.

Properties of the Immobilized Urokinase—Properties of the immobilized urokinase in terms of activity *versus* pH and temperature and the thermal stability were measured for III-urokinase and III—$(CH_2)_5$—C(=O)—NH-urokinase ($n' = 6$). Figure 2 illustrates the pH effects on the activity of urokinase in solution and the immobilized urokinase. The optimum pH of the soluble urokinase and III-urokinase was between 7.5 and 8.0, while III—$(CH_2)_5$—C(=O)—NH-urokinase was most active over a pH range from 7.5 to 9.0.

The effect of temperature on the activity of the immobilized urokinase was compared with that of the solution. The result indicated that the optimal temperature was 40° for both enzymes (Fig. 3).

Figure 4 shows the retention of the activity of immobilized urokinase in 0.9% NaCl solution at 4°. Both urokinase solution and III—NH—$(CH_2)_5$—C(=O)—NH-urokinase are stable in these storage conditions for 10 days without loss of activity, while III-urokinase (direct coupled urokinase) lost almost 40% of its original activity within 10 days. The urokinase immobilized with aminoalkane carboxylic acid spacer groups maintained well over 90% activity even after 60 days.

After heat treatment at 70° for 30 min, the urokinase solution lost activity completely, while III—NH—$(CH_2)_5$—C(=O)—NH-urokinase retained 45% of its activity by the same treatment.

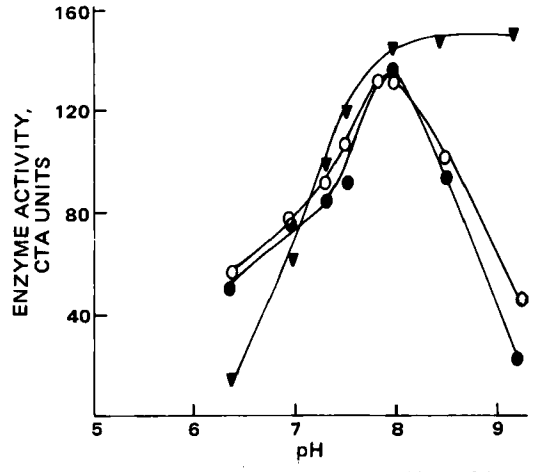

Figure 2—*Effects of pH on the activity of soluble and immobilized urokinase at 40°. Key: (○—○) soluble urokinase; (●—●) direct coupled urokinase (III-urokinase); (▼—▼) III—NH—$(CH_2)_5$—C(=O)—NH-urokinase.*

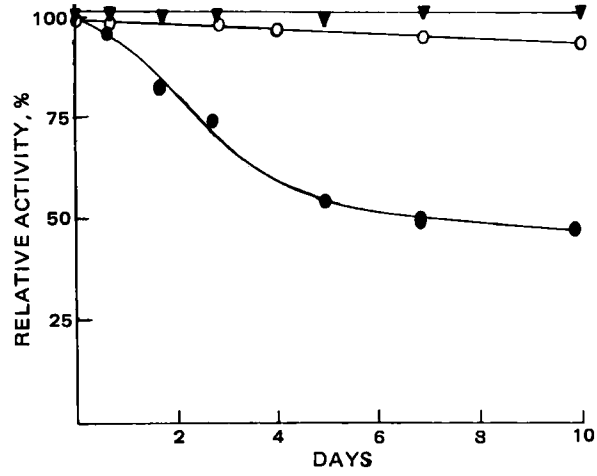

Figure 4—*Storage stability of soluble and immobilized urokinase. Key: (○—○) soluble urokinase; (●—●) direct coupled urokinase (III-urokinase); (▼—▼) III—NH—$(CH_2)_5$—C(=O)—NH-urokinase.*

DISCUSSION

Urokinase has been immobilized onto various matrices, and the results suggest a potential clinical use for thrombolytic therapy (2–6). Among them, polyamide, polyesters, and polyurethane-immobilized urokinase are useful clinically (3–6). Nevertheless, it can be said that an immobilized urokinase may experience steric hindrance from the polymer matrix. This has been postulated previously (4), where the polyamide–spacer–urokinase showed better fibrinolytic activity than the directly coupled polyamide–urokinase.

We first immobilized urokinase onto aminoalkyl-III which was prepared by a previously described method (13, 15). Unfortunately, unlike pronase (13), aminoalkyl-III-urokinase and III—NH—$(CH_2)_n$—NH—C(=O)-urokinase retained <5% of the initial urokinase enzymatic activity. It appears that urokinase was inactivated due to cross-linking by the carbodiimide I or II, which was used as a condensing agent in the immobilization step. We tested the inactivation of urokinase by treating free urokinase in solution with I or II in the presence or absence of aminoalkyl-III. In either case it was shown that urokinase retained no activity, whereas pronase activity remained when treated in a similar way.

Interposing spacer lengths (n') from 0 to 11, we have observed that the enzymatic activity of the immobilized urokinase increased as the spacer length (n') increased to a certain length, and tended to decrease thereafter (Table I, Fig. 1).

For a series of III—NH—$(CH_2)_n$—NH—C(=O)-urokinase, the highest activity was observed when $n' = 6$ (6.4 Å), while $n' = 7$ (9 Å) for a series of III—NH—$(CH_2)_n$—NH—C(=O)—$(CH_2)_2$—C(=O)—NH-urokinase resulted in maximum activity. Alternatively, direct attachment

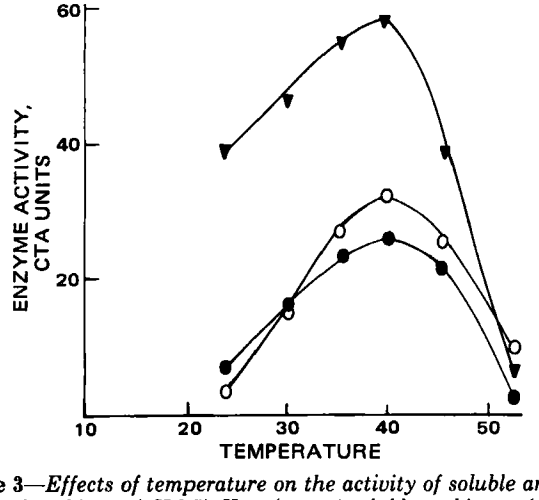

Figure 3—*Effects of temperature on the activity of soluble and immobilized urokinase (pH 8.5). Key: (○—○) soluble urokinase; (●—●) direct coupled urokinase (III-urokinase); (▼—▼) III—NH—$(CH_2)_5$—C(=O)—NH-urokinase.*

of urokinase to the matrix resulted in lower activity for plasminogen as shown in Table I. Differences of maximum enzymatic activity for the above two series of spacer arms are not clear and may be due to the different microenvironment of the hydrophilic polymers. An additional group from β-alanine provides a more hydrophilic environment which may introduce better accessibility of plasminogen to the immobilized urokinase.

As previously suggested (16), the dramatic effects associated with increasing the spacer length may in part be explained by relief of steric restrictions imposed by the matrix and in part by the increased flexibility and mobility of the urokinase as it protrudes further into the solvent phase. Plasminogen could then approach more readily the immobilized urokinase. This flexibility and folding of the spacer could also account for an apparent decrease in urokinase activity observed when the spacer lengths (n') >6 or 7 were interposed between the matrix and urokinase bond. This decreasing trend may be caused by the increased hydrophobicity of the spacer arms and/or rapid folding within immobilized urokinase by cohesive interactions.

The critical role of the matrix in the determination of accessibility of the coupled molecules to interacting macromolecule has been especially emphasized for affinity chromatography (15–17). A previous study (15) reported that a spacer length from 4 to 8 of interposed methylene groups (5–10 Å) elicited a substantial increase in enzyme binding affinities for kinases and pyrimidine nucleotide-dependent dehydrogenases with insoluble derivatives of adenosine triphosphate and nicotinamide adenine dinucleotide.

In conclusion, steric considerations appeared to be important in urokinase immobilization and maximum enzymatic activity was observed when the length of the spacer group was in the region of 6.4–9.0 Å.

The optimum pH with regard to the activity of soluble urokinase and III-urokinase was between 7.5 and 8.5. However, III—NH-$(CH_2)_5$—C(=O)—NH-urokinase showed maximum activity over a pH range from 7.5 to 9.0 (Fig. 2). The unchanged maximum activity for immobilized urokinase over the alkaline pH range may be due to unreacted carboxylic groups from aminoalkyl carboxylic spacers, which could neutralize the alkaline pH at the solvent–immobilized urokinase interface.

After heat treatment at 70° for 30 min, III—NH—$(CH_2)_5$—C(=O)—NH-urokinase retained activity. Activities of the soluble urokinase and III—NH—$(CH_2)_5$—C(=O)—NH-urokinase proved to be stable during storage in 0.9% NaCl at 4°, whereas III-urokinase was unstable under the same conditions (Fig. 4).

Since urokinase immobilized on matrices such as polyamide, polyester, and polyurethane had a proven antithrombotic action *in vivo*, steric problems in urokinase immobilization should be considered to improve immobilized urokinase activity with *in vivo* systems.

REFERENCES

(1) B. Wilman and P. Wallen, *Eur. J. Biochem.*, **36**, 25 (1973).

(2) T. Ohshiro, A. Sugitachi, S. D. Hong, K. Mukai, F. Murakami, G. Kosaki, and S. Motoi, *Blood and Vessel (Japan)*, **9**, 72 (1978).

(3) A. Sugitachi, T. Kawahara, J. Kodama, Y. Kikkawa, and K. Takagi, *Blut*, **37**, 31 (1978).

(4) T. Ohshiro and G. Kosaki, *Int. J. Artif. Organs*, **4**, 58 (1980).
(5) A. Sugitachi, K. Takagi, S. Imaoka, and G. Kosaki, *Thromb. Haemostasis*, **39**, 426 (1978).
(6) A. Sugitachi and K. Takagi, *Int. J. Artif. Organs*, **1**, 88 (1978).
(7) L. C. Mercer, K. E. Everse, A. W. Holmes, and J. Everse, *Throm. Res.*, **13**, 931 (1978).
(8) C. D. Ebert and S. W. Kim, *ibid.*, **26**, 43 (1982).
(9) P. J. Walther, H. M. Steinman, R. L. Hill, and P. A. McKee, *J. Biol. Chem.*, **249**, 1178 (1974).
(10) A. J. Johnson, D. L. Kline, and N. Alkjaersig, *Thromb. Diath. Haemorrh.*, **21**, 259 (1969).
(11) S. C. March, I. Parikh, and P. Cuatrecasas, *Anal. Biochem.*, **60**, 149 (1974).
(12) P. Cuatrecasas and I. Parikh, *Biochemistry*, **11**, 2291 (1972).
(13) S. M. Byun and F. Wold, *Korean J. Food Sci. Technol.*, **8**, 253 (1976).
(14) D. H. Lowry, W. J. Rosenbrough, A. L. Farr, and R. J. Randall, *J. Biol. Chem.*, **193**, 265 (1951).
(15) C. R. Lowe, M. J. Harvey, D. B. Craven, and P. D. G. Dean, *Biochem. J.*, **133**, 499 (1973).
(16) P. Cuatrecasas, *J. Biol. Chem.*, **245**, 3059 (1970).
(17) E. Steers, P. Cuatrecasas, and H. Pollard, *J. Biol. Chem.*, **246**, 196 (1971).

ACKNOWLEDGMENTS

This work was partly supported by National Institutes of Health Grant HL-20251. The authors wish to thank Dr. C. D. Ebert and Dr. J. Feijen for their comments.

Prevention of Insulin Self-Association and Surface Adsorption

SHUJI SATO, CHARLES D. EBERT, and SUNG WAN KIM ˣ

Received November 30, 1982, from the *Department of Pharmaceutics, University of Utah, Salt Lake City, UT 84112.* Accepted for publication April 14, 1982.

Abstract □ The self-association of insulin monomers into oligomers and macromolecular aggregates leads to complications in the administration of insulin, both in conventional administration and in the development of long-term insulin delivery systems. These problems are aggravated by the tendency of insulin to adsorb onto the surface of solution containers and infusion devices. Furthermore, with insulin infusion devices, shear rates can be generated which can accelerate the self-association and surface adsorption processes. The effects of urea on shear-induced insulin self-association and surface adsorption were investigated. It was found that the addition of a certain concentration range of urea to insulin solutions greatly reduces both insulin self-association and surface adsorption. Circular dichroic studies established that these concentrations of urea also preserve insulin conformation under high shear rates, where conformations are altered without urea. Higher urea concentrations lead to insulin denaturation and accelerated self-association.

Keyphrases □ Insulin—prevention of self-association and surface adsorption, circular dichroism □ Adsorption, surface—insulin, prevention of self-association □ Self-association—insulin, prevention of surface adsorption

The self-association of insulin molecules into dimers, tetramers, hexamers, and macromolecular aggregates has been studied by numerous groups, and in general, is a multiparameter process dependent upon insulin concentration, pH, solvent composition, ionic strength, and solvent dielectric properties (1–3). This self-association process leads to complications in the administration of insulin for the control of diabetes, both in the conventional administration and in the development of long-term insulin delivery systems. These problems are further complicated by the tendency for insulin to adsorb onto the surfaces of insulin solution containers and infusion devices, perhaps by mechanisms similar to those inducing aggregation.

Investigations have attempted to overcome the self-association and surface adsorption phenomena by the addition of various agents to the insulin preparations. These additives include various organic solvents (1), autologous serum (2), and amino acids (3). This report focuses on the effects of additives on insulin conformation, self-association, and adsorption onto various polymeric surfaces. In addition to the effects on insulin aggregation caused by the additives, the effects of shear stresses on macromolecular aggregation were studied. Depending on the infusion device, substantial shear rates can be developed during insulin infusions which can influence insulin self-association and macromolecular aggregation and limit the effective duration of such devices. These effects must also be considered in the development of insulin delivery systems.

This report studies the effects of additives on the insulin conformation–self-association process under constant shear, solvent pH, and ionic strength. The adsorption of insulin onto various polymers was also studied under the above conditions as a prerequisite to the development of a diffusion controlled, self-regulating insulin delivery system presently under development.

EXPERIMENTAL

Reagents—Bovine zinc–insulin[1] was used without further treatment. This insulin preparation had an activity of 25.5 IU/mg. Gentamicin sulfate[1] was used at a concentration of 25 μg/ml in all insulin aggregation and polymer adsorption studies to prevent bacterial growth. A pH 8.0 phosphate-buffered saline, containing 0.0945 *M* Na_2HPO_4, 0.0055 *M* KH_2PO_4, and 0.015 *M* NaCl, was used as the buffer solution in all studies. Hydroxyethyl methacrylate[2] was polymerized with azobisisobutyronitrile[3]. Poly(dimethylsiloxane)[4] was cured with 0.5% (w/w) stannous octoate. Cellulose sheets were obtained from a hemodialyzer[5] and soxhlet extracted for 24 hr, with double-distilled water. A segmental poly(urethane ether) copolymer[6], was dissolved in dimethylformamide and cast

[1] Sigma Chemical Co., St. Louis, MO 63178.
[2] Polyscience, Inc., Warrington, PA 18976.
[3] Aldrich Chemical Co., Milwaukee, WI 53201.
[4] Silastic 382, Dow Corning Corp., Midland, MI 48640.
[5] Lundia major hemodialyzer, Gambro Inc., Newport News, VA 23605.
[6] Biomer, Ethicon, Somerville, NJ 08876.

0022-3549/83/0300-0228$01.00/0

(4) T. Ohshiro and G. Kosaki, *Int. J. Artif. Organs*, **4**, 58 (1980).
(5) A. Sugitachi, K. Takagi, S. Imaoka, and G. Kosaki, *Thromb. Haemostasis*, **39**, 426 (1978).
(6) A. Sugitachi and K. Takagi, *Int. J. Artif. Organs*, **1**, 88 (1978).
(7) L. C. Mercer, K. E. Everse, A. W. Holmes, and J. Everse, *Throm. Res.*, **13**, 931 (1978).
(8) C. D. Ebert and S. W. Kim, *ibid.*, **26**, 43 (1982).
(9) P. J. Walther, H. M. Steinman, R. L. Hill, and P. A. McKee, *J. Biol. Chem.*, **249**, 1178 (1974).
(10) A. J. Johnson, D. L. Kline, and N. Alkjaersig, *Thromb. Diath. Haemorrh.*, **21**, 259 (1969).
(11) S. C. March, I. Parikh, and P. Cuatrecasas, *Anal. Biochem.*, **60**, 149 (1974).
(12) P. Cuatrecasas and I. Parikh, *Biochemistry*, **11**, 2291 (1972).
(13) S. M. Byun and F. Wold, *Korean J. Food Sci. Technol.*, **8**, 253 (1976).
(14) D. H. Lowry, W. J. Rosenbrough, A. L. Farr, and R. J. Randall, *J. Biol. Chem.*, **193**, 265 (1951).
(15) C. R. Lowe, M. J. Harvey, D. B. Craven, and P. D. G. Dean, *Biochem. J.*, **133**, 499 (1973).
(16) P. Cuatrecasas, *J. Biol. Chem.*, **245**, 3059 (1970).
(17) E. Steers, P. Cuatrecasas, and H. Pollard, *J. Biol. Chem.*, **246**, 196 (1971).

ACKNOWLEDGMENTS

This work was partly supported by National Institutes of Health Grant HL-20251. The authors wish to thank Dr. C. D. Ebert and Dr. J. Feijen for their comments.

Prevention of Insulin Self-Association and Surface Adsorption

SHUJI SATO, CHARLES D. EBERT, and SUNG WAN KIM ˣ

Received November 30, 1982, from the *Department of Pharmaceutics, University of Utah, Salt Lake City, UT 84112.* Accepted for publication April 14, 1982.

Abstract □ The self-association of insulin monomers into oligomers and macromolecular aggregates leads to complications in the administration of insulin, both in conventional administration and in the development of long-term insulin delivery systems. These problems are aggravated by the tendency of insulin to adsorb onto the surface of solution containers and infusion devices. Furthermore, with insulin infusion devices, shear rates can be generated which can accelerate the self-association and surface adsorption processes. The effects of urea on shear-induced insulin self-association and surface adsorption were investigated. It was found that the addition of a certain concentration range of urea to insulin solutions greatly reduces both insulin self-association and surface adsorption. Circular dichroic studies established that these concentrations of urea also preserve insulin conformation under high shear rates, where conformations are altered without urea. Higher urea concentrations lead to insulin denaturation and accelerated self-association.

Keyphrases □ Insulin—prevention of self-association and surface adsorption, circular dichroism □ Adsorption, surface—insulin, prevention of self-association □ Self-association—insulin, prevention of surface adsorption

The self-association of insulin molecules into dimers, tetramers, hexamers, and macromolecular aggregates has been studied by numerous groups, and in general, is a multiparameter process dependent upon insulin concentration, pH, solvent composition, ionic strength, and solvent dielectric properties (1–3). This self-association process leads to complications in the administration of insulin for the control of diabetes, both in the conventional administration and in the development of long-term insulin delivery systems. These problems are further complicated by the tendency for insulin to adsorb onto the surfaces of insulin solution containers and infusion devices, perhaps by mechanisms similar to those inducing aggregation.

Investigations have attempted to overcome the self-association and surface adsorption phenomena by the addition of various agents to the insulin preparations. These additives include various organic solvents (1), autologous serum (2), and amino acids (3). This report focuses on the effects of additives on insulin conformation, self-association, and adsorption onto various polymeric surfaces. In addition to the effects on insulin aggregation caused by the additives, the effects of shear stresses on macromolecular aggregation were studied. Depending on the infusion device, substantial shear rates can be developed during insulin infusions which can influence insulin self-association and macromolecular aggregation and limit the effective duration of such devices. These effects must also be considered in the development of insulin delivery systems.

This report studies the effects of additives on the insulin conformation–self-association process under constant shear, solvent pH, and ionic strength. The adsorption of insulin onto various polymers was also studied under the above conditions as a prerequisite to the development of a diffusion controlled, self-regulating insulin delivery system presently under development.

EXPERIMENTAL

Reagents—Bovine zinc–insulin[1] was used without further treatment. This insulin preparation had an activity of 25.5 IU/mg. Gentamicin sulfate[1] was used at a concentration of 25 μg/ml in all insulin aggregation and polymer adsorption studies to prevent bacterial growth. A pH 8.0 phosphate-buffered saline, containing 0.0945 *M* Na_2HPO_4, 0.0055 *M* KH_2PO_4, and 0.015 *M* NaCl, was used as the buffer solution in all studies. Hydroxyethyl methacrylate[2] was polymerized with azobisisobutyronitrile[3]. Poly(dimethylsiloxane)[4] was cured with 0.5% (w/w) stannous octoate. Cellulose sheets were obtained from a hemodialyzer[5] and soxhlet extracted for 24 hr, with double-distilled water. A segmental poly(urethane ether) copolymer[6], was dissolved in dimethylformamide and cast

[1] Sigma Chemical Co., St. Louis, MO 63178.
[2] Polyscience, Inc., Warrington, PA 18976.
[3] Aldrich Chemical Co., Milwaukee, WI 53201.
[4] Silastic 382, Dow Corning Corp., Midland, MI 48640.
[5] Lundia major hemodialyzer, Gambro Inc., Newport News, VA 23605.
[6] Biomer, Ethicon, Somerville, NJ 08876.

0022-3549/83/0300-0228$01.00/0

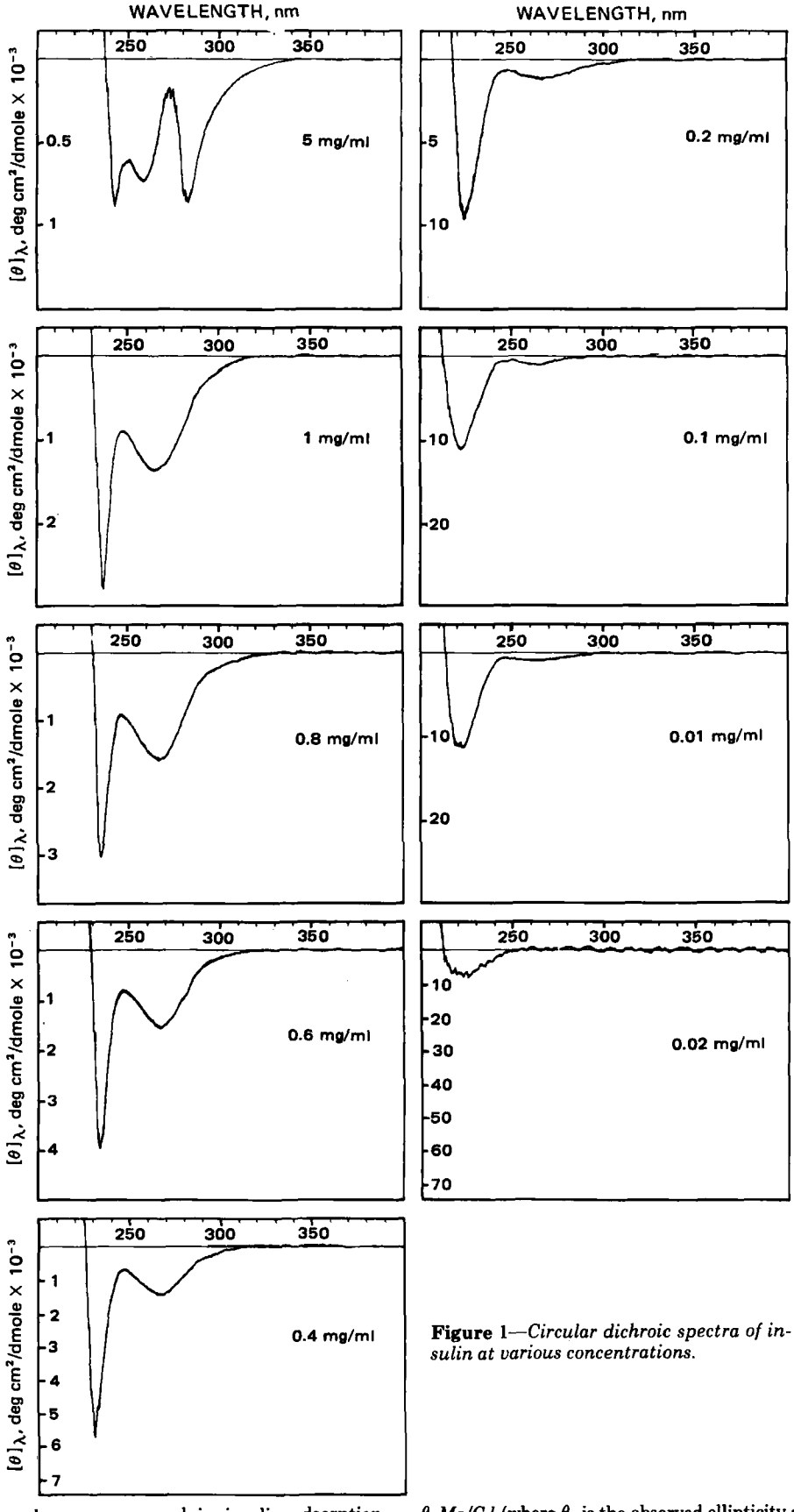

Figure 1—*Circular dichroic spectra of insulin at various concentrations.*

into sheets. The above polymers were used in insulin adsorption studies.

Circular Dichroic (CD) Studies—All CD spectra were obtained with a CD spectrophotometer[7] at 25°. Mean residue ellipticities, $[\theta]_\lambda = \theta_\lambda Mo/C \cdot l$ (where θ_λ is the observed ellipticity at wavelength λ, Mo is the mean residue molecular weight for insulin (112 g/residue), C is the insulin concentration in grams per milliliter, and l is the pathlength in centimeters) were calculated for the various wavelengths and insulin concentrations.

Effects of Shear on Insulin Self-Association and Adsorption—To

[7] JASCO model 40A, Japan Spectroscopy Co., Tokyo, Japan.

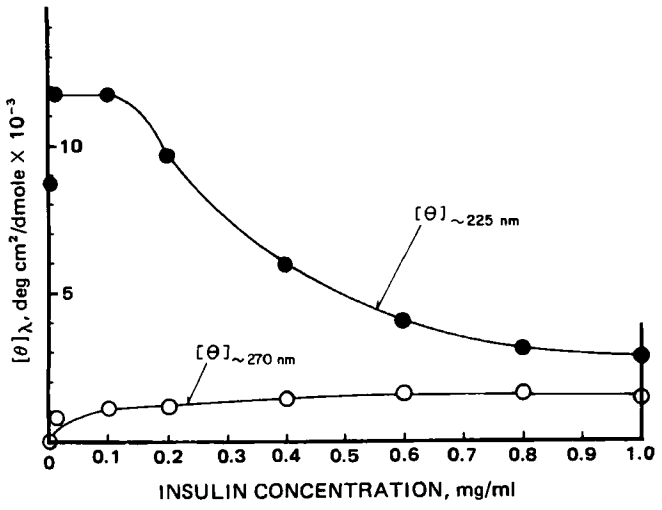

Figure 2—*Mean residual ellipticities at ~225 and ~270 nm* versus *insulin concentration.*

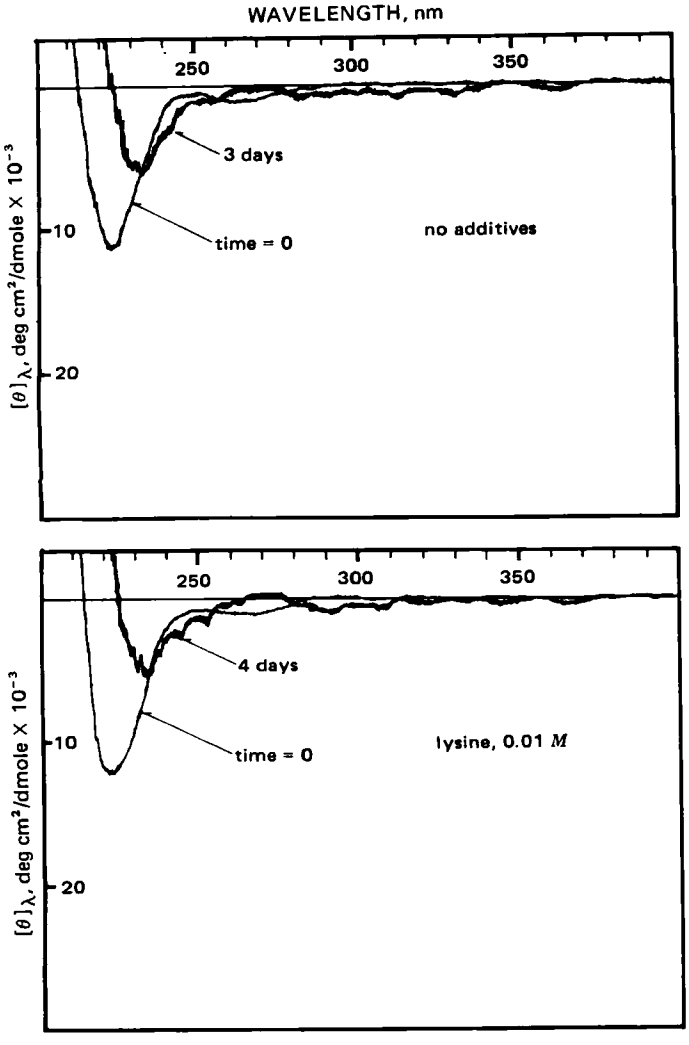

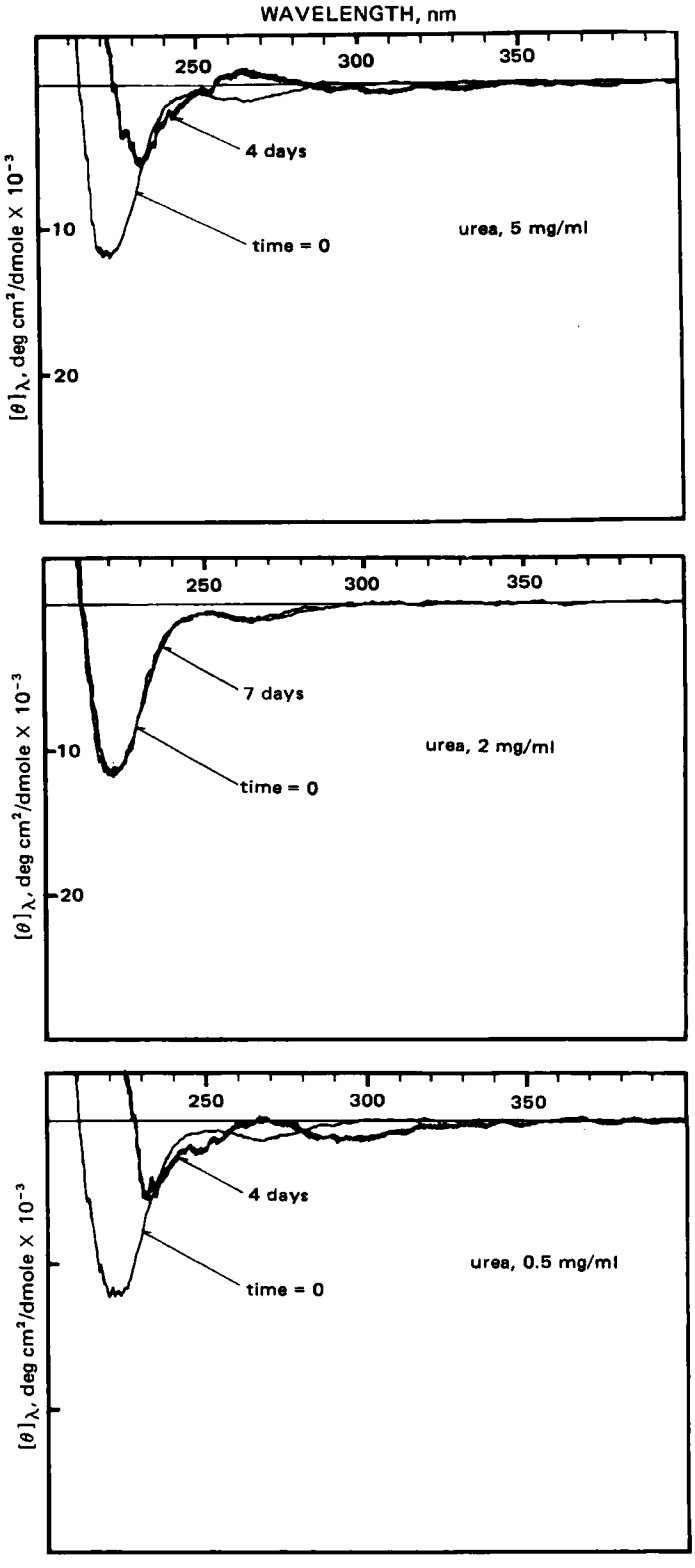

Figure 3—*Effects of additives on changes of the circular dichroic spectra of insulin subjected to high shear rates. All insulin concentrations were set at 0.1 mg/ml.*

evaluate the effects of shear on insulin macromolecular aggregation, 100-ml portions of various concentrations of insulin were stirred at 1550 rpm with a mechanical stirrer. This stirring velocity was selected because it represents an extreme case for shears that could be developed with infusion devices, and because these conditions will be utilized in current insulin–polymer diffusion experiments for the development of the self-regulating insulin delivery system previously described. Periodic samples were withdrawn and visibly evaluated for macroaggregation. Approximately 1-cm^2 disks of poly(hydroxyethyl methacrylate), cellulose, poly(dimethylsiloxane), and poly(urethane ether) were placed in the above insulin solutions and withdrawn after 7 days. These polymer samples were vacuum dried, gold coated, and a scanning electron microscopy[8] of the resultant polymer surfaces was conducted.

[8] Cambridge Stereo Scan Mark IIA, Cambridge, England.

Table I—The Effect of Additives on Insulin Aggregation Time[a]

Additive	Concentration of Additive	Time for Aggregation
No Additive	—	2–3 days
Lysine	0.01 *M*	3–4 days
Lysine	0.002 *M*	3–4 days
+ I[b]	0.005 *M*	
I[b]	0.005 *M*	2–3 days
Urea	0.5 mg/ml	3–4 days
Urea	1.0 mg/ml	7 days
Urea	2.0 mg/ml	7 days
Urea	3.0 mg/ml	7 days
Urea	5.0 mg/ml	3–4 days

[a] Insulin concentration set at 0.1 mg/ml in all cases. [b] EDTA (I).

Effects of Additives on Insulin Self-Association and Adsorption Under High Shear—The effects of various concentrations of lysine[1], urea[1], and disodium edetate (I)[1] on insulin circular dichroism, macromolecular aggregation, and adsorption on polymer surfaces were evaluated under high shear conditions as described.

RESULTS AND DISCUSSION

The CD spectra of insulin at various concentrations is presented in Fig. 1, where mean residue ellipticity, $[\theta]_\lambda$ in deg cm^2/*d*mol × 10^{-3}, is plotted *versus* wavelength. At an insulin concentration of 5 mg/ml, negative maxima were observed at 245, 262, and 283 nm, the trough at 262 nm having been assigned to phenylalanine at B24 and/or B25 residues, while the trough at 283 nm was assigned to tyrosine at B26 (4).

Two negative maxima at ~245 and 270 nm were observed between 1.0 and 0.4 mg/ml. The trough at ~270 nm was assigned to tyrosine and phenylalanine aromatic residues in the B23–28 region of the antiparallel β-structure formed between insulin monomers in insulin aggregated states. Attenuation of this band has been associated with disaggregation of insulin (5), while strengthening of the band is associated with conditions that enhance insulin aggregation (6). The optical activity of the aromatic residues contributing to this band is, therefore, dependent upon the state of insulin self-association. As insulin concentration decreased, the strength of this band progressively decreased indicating reduced insulin self-association. At 0.2 mg/ml the 270-nm trough was greatly diminished and a negative maxima at ~225 nm was the dominant band. This trough was the predominant feature of the insulin CD spectra for 0.2, 0.1, and 0.01 mg/ml insulin concentration. The appearance of this trough at ~225 nm was assigned to the antiparallel β-structure of insulin dimers (7). This band was the predominant feature of the insulin dimer. Furthermore, this peak was not attenuated upon dilution from 0.2 to 0.01 mg/ml, suggesting that insulin dimers are the prominent species in that concentration range. At an insulin concentration of 0.02 mg/ml, mean residue ellipticity at 225 nm decreased and the trough was broadened, demonstrating negative ellipticity at ~210 nm. Negative ellipticity at ~210 nm has long been associated with an α-helical structure. The attenuation of negative ellipticity at 225 nm combined with the appearance of negative ellipticity at 210 nm suggests that insulin dimers are less prevalent at this concentration.

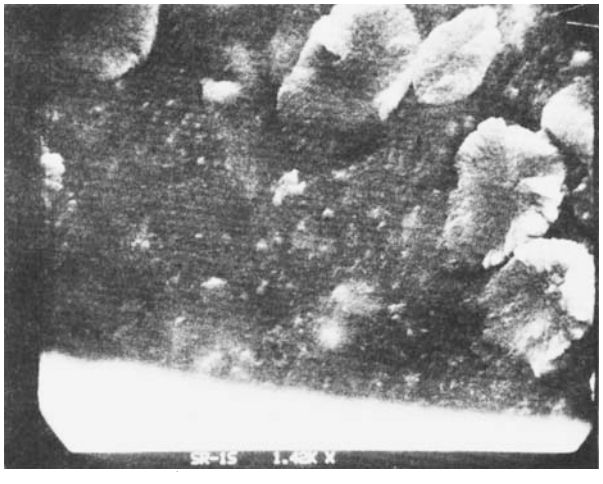

Figure 4—*Insulin adsorbed onto silicone rubber under high shear, 1600 ×.*

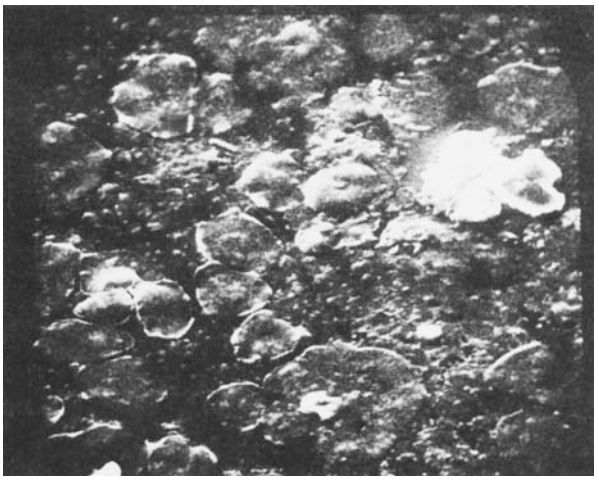

Figure 5—*Insulin adsorbed onto the segmental poly(urethane ether) copolymer under high shear, 600 ×.*

Results from the data reported here and studies by others (4, 7) suggest that the ~225- and 270-nm bands provide an indication of insulin self-association. When mean residue ellipticity is plotted *versus* insulin concentration, Figure 2, it is evident that the ~225-nm band is the more sensitive indicator of insulin self-association, insulin self-association into dimers, tetramers, hexamers, *etc.*, in turn having previously been correlated by others with insulin concentration (4, 8).

Using insulin CD as the indicator of insulin self-association, the effects of various additives on insulin self-association under high shear rate conditions were evaluated. These results are presented in Fig. 3, where the lighter tracing represents the CD spectra at time 0 and the darker tracing represents the CD spectra for the same insulin solution at the indicated time. The insulin concentration was set at 0.1 mg/ml for all spectra presented. At a urea concentration of 2.0 mg/ml, no changes in the 225-nm peak were observed even after 7 days under high shear rate conditions. Changes in the CD spectra were observed for higher and lower concentrations of urea at ~4 days providing spectra similar to aggregated insulin without additives. Interestingly, the small trough at 270-nm disappears under high shear rates indicating a loss in optical activity for the B23–28 aromatic residues.

Table I summarizes the effects of additives on shear-induced insulin macromolecular aggregation, all data obtained at an insulin concentration of 0.1 mg/ml where insulin dimers were the prevalent species. Macromolecular aggregation was observed without additives within 2–3 days. The same aggregation time was observed for 0.005 *M* EDTA (I). The addition of 0.01 *M* lysine or a combination of 0.01 *M* lysine and 0.005 *M* I prolonged macromolecular aggregation of insulin by ~2 days. The addition of 0.5 mg/ml of urea produced aggregation times similar to the lysine–I combination; however, aggregation times were >7 days

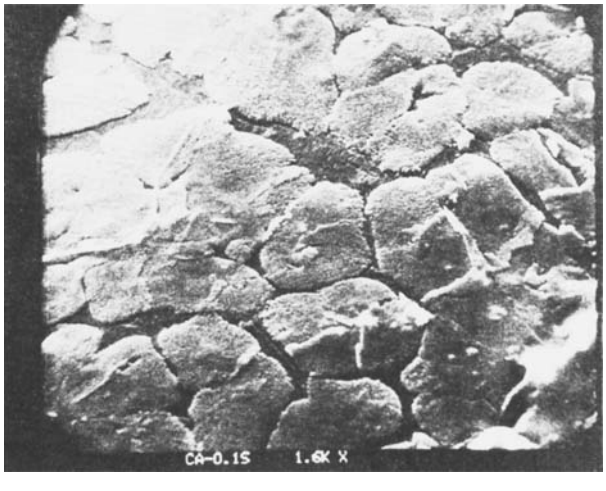

Figure 6—*Insulin adsorbed onto cellulose under high shear, 1600 ×.*

Figure 7—*Insulin adsorbed onto the segmental poly(urethane ether) copolymer under high shear with 2.0 mg/ml urea, 2100 ×.*

for urea concentrations ranging from 1.0 to 3.0 mg/ml. At higher urea concentration, aggregation times were ~4 days.

Scanning microscopy revealed that insulin adsorption onto various polymer surfaces was substantially greater under high shear as compared with static conditions. The morphology of the adsorbed insulin was found also to be dependent on shear conditions. Scanning electron micrographs of insulin adsorbed under high shear onto poly(dimethylsiloxane), poly(urethane ether), and cellulose are presented in Figs. 4–6, respectively. Under high shear, insulin adsorbs onto all of the polymers evaluated as disk-like structures. Without high shear rates, such disk-like insulin adsorbates were not observed over the time frame evaluated. Under high shear, the morphology of the adsorbed insulin appears independent of the polymer nature, disk-like adsorbates were observed on all types of polymer surfaces. However, under static conditions the morphology may be dependent upon the polymer substrate.

Concentrations of urea that prolonged insulin macromolecular aggregation times were found also to inhibit insulin adsorption onto polymer surfaces. Disk-like insulin adsorbates were not observed on the various polymer surfaces with the addition of 2.0 mg/ml urea under high shear, as shown for poly(urethane ether) in Fig. 7 as a representative case.

The self-association of insulin molecules in solution and the adsorption of insulin onto container surfaces pose complications in the administration of insulin. These problems are of particular importance with long-term insulin infusion devices where insulin crystals on the various surfaces of such devices have been observed by several investigators (9, 10). With such systems, insulin can be subjected to shear rates that can greatly effect and potentiate this process.

The addition of urea in a limited concentration range (*i.e.*, 1–3 mg/ml of urea) inhibits both insulin self-association and surface adsorption. It has been suggested that the initial step in insulin self-association is the hydrophobic association of the B23–28 regions on insulin monomers to form insulin dimers which further associate into larger oligomers. Urea, a water structure-breaking solute, was found to greatly inhibit insulin self-association and surface adsorption presumably by decreasing interactions between dimers to prevent further self-association. Higher urea concentrations were found to denature insulin, leading to rapid macromolecular aggregation times. The concentration range of urea that inhibits these processes poses little to no toxicity risks and can stabilize insulin preparations for extended periods, both for conventional administration preparations and for the development of long-term insulin delivery systems.

REFERENCES

(1) E. Fredericq, *Org. Biol. Chem.*, **79**, 599, 1957.

(2) A. M. Albisser, W. Lougheed, K. Perlman, and A. Bahoric, *Diabetes*, **29**, 241, 1980.

(3) J. Bringer, A. Heldt, and G. M. Grodsky, *ibid.*, **30**, 83, 1981.

(4) J. Goldman and F. H. Carpenter, *Biochemistry*, **13**, 4566, 1974.

(5) E. Fredericq, *Nature (London)*, **171**, 570, 1953.

(6) J. Goldman, Ph.D. Thesis, University of California, Berkeley, Calif.

(7) F. Quadrifoglio and P. W. Urry, *J. Am. Chem. Soc.*, **90**, 2760, 1968.

(8) P. D. Jeffrey and J. H. Coates, *Biochemistry*, **5**, 489, 1966.

(9) W. D. Lougheed, H. Woulfe-Hanagan, J. R. Clement, and A. M. Albisser, *Diabetologia*, **19**, 1, 1980.

(10) M. V. Sefton and E. Nishimura, *J. Pharm. Sci.*, **69**, 1, 1980.

ACKNOWLEDGMENTS

This work was supported by National Institutes of Health Grant AM 27929.

Conformational Study of Two Polymorphs of Spiperone: Possible Consequences on the Interpretation of Pharmacological Activity

M. AZIBI *, M. DRAGUET-BRUGHMANS *, R. BOUCHE *x, B. TINANT ‡, G. GERMAIN ‡, J. P. DECLERCQ ‡, and M. VAN MEERSSCHE ‡

Received December 18, 1981, from the **Laboratoire d'Analyse des Médicaments, Institut de Pharmacie UCL 7340, 1200, Bruxelles, Belgium*, and the ‡*Laboratoire de Chimie physique et de Cristallographie, Université de Louvain, Place Louis Pasteur, 1348, Louvain-la-Neuve, Belgium.* Accepted for publication April 15, 1982.

Abstract □ A second polymorph of spiperone, 8-[3-(*p*-fluorobenzoyl)-propyl]-1-phenyl-1,3,8-triazaspiro[4,5]decan-4-one, has been isolated and characterized by thermal analysis and IR spectrometry. Its structure was solved by X-ray diffraction analysis. The results are compared with those previously obtained on spiperone, the main difference being in the conformation of the side chain and in the nature of the hydrogen bonding.

Keyphrases □ Spiperone—polymorphs, conformational study, possible consequences on interpretation of pharmacological activity □ Pharmacological activity—conformational study of two polymorphs of spiperone, possible consequences of interpretation □ Polymorphs—spiperone, conformational study, possible consequences on interpretation of pharmacological activity

Complete data about the crystal structure and solid-state molecular conformation of different polymorphs of the same drug are rarely available. The main reason lies in the difficulty in obtaining single crystals of good quality from the different polymorphs. Studies of drug polymorphism are generally restricted to determination of IR

0022-3549/83/0300-0232$01.00/0

Figure 7—*Insulin adsorbed onto the segmental poly(urethane ether) copolymer under high shear with 2.0 mg/ml urea, 2100 ×.*

for urea concentrations ranging from 1.0 to 3.0 mg/ml. At higher urea concentration, aggregation times were ~4 days.

Scanning microscopy revealed that insulin adsorption onto various polymer surfaces was substantially greater under high shear as compared with static conditions. The morphology of the adsorbed insulin was found also to be dependent on shear conditions. Scanning electron micrographs of insulin adsorbed under high shear onto poly(dimethylsiloxane), poly(urethane ether), and cellulose are presented in Figs. 4–6, respectively. Under high shear, insulin adsorbs onto all of the polymers evaluated as disk-like structures. Without high shear rates, such disk-like insulin adsorbates were not observed over the time frame evaluated. Under high shear, the morphology of the adsorbed insulin appears independent of the polymer nature, disk-like adsorbates were observed on all types of polymer surfaces. However, under static conditions the morphology may be dependent upon the polymer substrate.

Concentrations of urea that prolonged insulin macromolecular aggregation times were found also to inhibit insulin adsorption onto polymer surfaces. Disk-like insulin adsorbates were not observed on the various polymer surfaces with the addition of 2.0 mg/ml urea under high shear, as shown for poly(urethane ether) in Fig. 7 as a representative case.

The self-association of insulin molecules in solution and the adsorption of insulin onto container surfaces pose complications in the administration of insulin. These problems are of particular importance with long-term insulin infusion devices where insulin crystals on the various surfaces of such devices have been observed by several investigators (9, 10). With such systems, insulin can be subjected to shear rates that can greatly effect and potentiate this process.

The addition of urea in a limited concentration range (*i.e.*, 1–3 mg/ml of urea) inhibits both insulin self-association and surface adsorption. It has been suggested that the initial step in insulin self-association is the hydrophobic association of the B23–28 regions on insulin monomers to form insulin dimers which further associate into larger oligomers. Urea, a water structure-breaking solute, was found to greatly inhibit insulin self-association and surface adsorption presumably by decreasing interactions between dimers to prevent further self-association. Higher urea concentrations were found to denature insulin, leading to rapid macromolecular aggregation times. The concentration range of urea that inhibits these processes poses little to no toxicity risks and can stabilize insulin preparations for extended periods, both for conventional administration preparations and for the development of long-term insulin delivery systems.

REFERENCES

(1) E. Fredericq, *Org. Biol. Chem.*, **79**, 599, 1957.

(2) A. M. Albisser, W. Lougheed, K. Perlman, and A. Bahoric, *Diabetes*, **29**, 241, 1980.

(3) J. Bringer, A. Heldt, and G. M. Grodsky, *ibid.*, **30**, 83, 1981.

(4) J. Goldman and F. H. Carpenter, *Biochemistry*, **13**, 4566, 1974.

(5) E. Fredericq, *Nature (London)*, **171**, 570, 1953.

(6) J. Goldman, Ph.D. Thesis, University of California, Berkeley, Calif.

(7) F. Quadrifoglio and P. W. Urry, *J. Am. Chem. Soc.*, **90**, 2760, 1968.

(8) P. D. Jeffrey and J. H. Coates, *Biochemistry*, **5**, 489, 1966.

(9) W. D. Lougheed, H. Woulfe-Hanagan, J. R. Clement, and A. M. Albisser, *Diabetologia*, **19**, 1, 1980.

(10) M. V. Sefton and E. Nishimura, *J. Pharm. Sci.*, **69**, 1, 1980.

ACKNOWLEDGMENTS

This work was supported by National Institutes of Health Grant AM 27929.

Conformational Study of Two Polymorphs of Spiperone: Possible Consequences on the Interpretation of Pharmacological Activity

M. AZIBI *, M. DRAGUET-BRUGHMANS *, R. BOUCHE *x, B. TINANT ‡, G. GERMAIN ‡, J. P. DECLERCQ ‡, and M. VAN MEERSSCHE ‡

Received December 18, 1981, from the **Laboratoire d'Analyse des Médicaments, Institut de Pharmacie UCL 7340, 1200, Bruxelles, Belgium*, and the ‡*Laboratoire de Chimie physique et de Cristallographie, Université de Louvain, Place Louis Pasteur, 1348, Louvain-la-Neuve, Belgium.* Accepted for publication April 15, 1982.

Abstract □ A second polymorph of spiperone, 8-[3-(*p*-fluorobenzoyl)-propyl]-1-phenyl-1,3,8-triazaspiro[4,5]decan-4-one, has been isolated and characterized by thermal analysis and IR spectrometry. Its structure was solved by X-ray diffraction analysis. The results are compared with those previously obtained on spiperone, the main difference being in the conformation of the side chain and in the nature of the hydrogen bonding.

Keyphrases □ Spiperone—polymorphs, conformational study, possible consequences on interpretation of pharmacological activity □ Pharmacological activity—conformational study of two polymorphs of spiperone, possible consequences of interpretation □ Polymorphs—spiperone, conformational study, possible consequences on interpretation of pharmacological activity

Complete data about the crystal structure and solid-state molecular conformation of different polymorphs of the same drug are rarely available. The main reason lies in the difficulty in obtaining single crystals of good quality from the different polymorphs. Studies of drug polymorphism are generally restricted to determination of IR

0022-3549/83/0300-0232$01.00/0

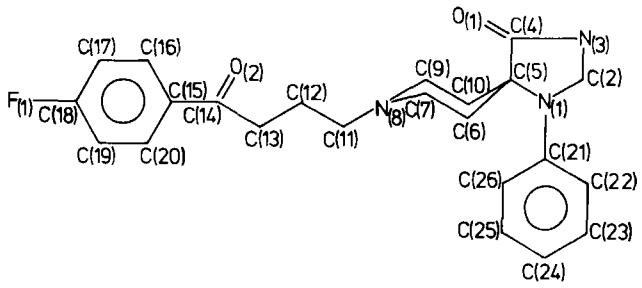

Figure 1—*Chemical structure and atom numbering of spiperone.*

Table I—Crystal Data of Spiperone I and II

	Form I	Form II[a]
Molecular formula	$C_{23}H_{26}FN_3O_2$	$C_{23}H_{26}FN_3O_2$
Molecular weight	395.46	395.46
Space group	$P2_1/a$	$P2_1/c$
System	Monoclinic	Monoclinic
Unit cell dimensions, Å or degrees		
a	12.722	18.571
b	7.510	6.072
c	21.910	20.681
β	95.08	118.69
Unit cell volume, Å^3	2085.1	2045.7
Number of formula Unit per cell = Z	4	4

[a] Data from ref. 5.

spectra and thermal properties, determination of dissolution characteristics, and recording of X-ray powder diffraction spectra (1–3).

Many crystal and molecular structures of neuroleptics belonging to the family of butyrophenones have been published, without reference to possible polymorphism (4–13). Among those was the crystal structure of spiperone[1] (Fig. 1), one of the most potent neuroleptic drugs (5). The structure of spiperone is mainly characterized by its unique conformation of the side chain and is often used as reference in studies of the structure–activity relationship for testing the conformational resemblance of neuroleptics to dopamine (14, 15).

This paper characterizes the crystal structure of a second polymorph of spiperone, compares this polymorph with the known structure, and discusses the possible consequences on the interpretation of the pharmacological activity.

EXPERIMENTAL

IR Spectrometry[2]—IR spectra were recorded in potassium bromide pellets (0.5%, w/w).

X-Ray Diffraction[3]—The intensities of 2551 reflections were measured on a four-circle diffractometer by the ω-scan technique up to $2\theta = 44°$. Incident radiation was graphite-monochromatized Mo$K\alpha$: $\lambda = 0.7107$ Å. Only 921 reflections with $I > 2.5\sigma(I)$ were considered as observed and retained for the resolution and refinement of the structure. The structure was solved by direct methods using the MULTAN 80 computer system[4]. The refinement was carried out by the SHELX 76[5] program with anisotropic thermal parameters. The positions of the hydrogen atoms were calculated by SHELX. The final conventional R index was 0.079. For crystal data see Table I.

[1] Janssen Pharmaceutica, Beerse, Belgium, U.S. Patent no. 3,155,669 (1964 J. Ph.).

[2] Perkin-Elmer model 580 IR spectrophotometer.

[3] Enraf Nonius CAD-4 four-circle diffractometer.

[4] P. Main, S. J. Fiske, S. E. Hull, L. Lessinger, M. M. Woolfson, G. Germain, and J. P. Declercq (1980). MULTAN 80. A system of computer programs for the automatic solution of crystal structures from X-ray diffraction data. Universities of York (England) and Louvain-la-Nueve (Belgium).

[5] G. M. Sheldrick, SHELX 76, Program for crystal structure determination, University of Cambridge, England, 1976.

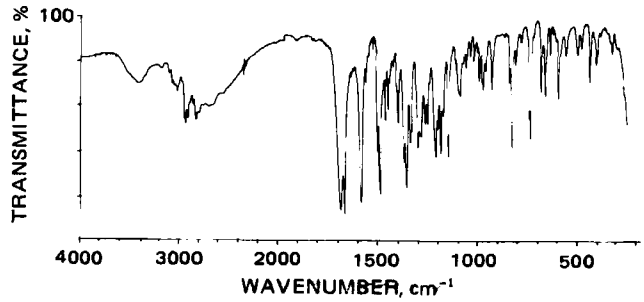

Figure 2—*IR spectrum of polymorph I.*

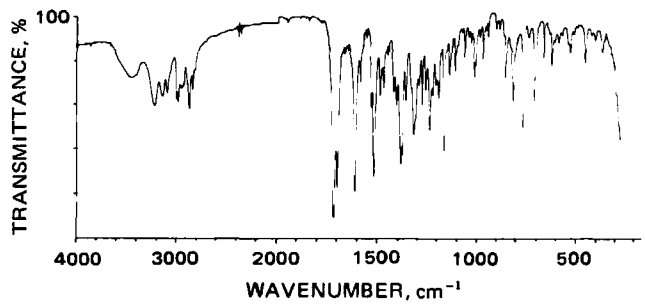

Figure 3—*IR spectrum of polymorph II.*

Table II—Atomic Coordinates ($\times 10^4$) and B_{eq} Values (Å^2)

	X/A	Y/B	Z/C	B_{eq}
N(1)	8679 (8)	515 (15)	6455 (5)	4.26
C(2)	9766 (8)	−79 (18)	6412 (7)	4.38
N(3)	10380 (8)	1076 (15)	6820 (6)	4.98
C(4)	9800 (11)	2318 (21)	7086 (7)	4.10
O(1)	10176 (7)	3445 (14)	7424 (5)	6.16
C(5)	8643 (9)	2087 (15)	6871 (6)	3.11
C(6)	8258 (9)	3742 (16)	6496 (6)	4.16
C(7)	8090 (11)	5339 (17)	6920 (6)	4.36
N(8)	7382 (7)	4909 (14)	7365 (5)	4.08
C(9)	7830 (9)	3462 (17)	7769 (6)	3.88
C(10)	8001 (10)	1773 (16)	7397 (6)	4.02
C(11)	7172 (11)	6560 (19)	7725 (7)	5.75
C(12)	6326 (14)	6434 (22)	8133 (8)	7.22
C(13)	6078 (13)	8242 (19)	8416 (8)	6.68
C(14)	5101 (14)	8185 (28)	8722 (9)	7.13
O(2)	4559 (13)	6812 (18)	8718 (8)	11.62
C(15)	4732 (14)	9765 (25)	9016 (7)	5.50
C(16)	3831 (14)	9648 (29)	9370 (8)	7.22
C(17)	3469 (18)	11124 (36)	9628 (9)	7.17
C(18)	3970 (18)	12651 (37)	9586 (9)	8.22
F(1)	3546 (11)	14138 (18)	9826 (7)	14.73
C(19)	4817 (14)	12836 (22)	9232 (9)	8.14
C(20)	5229 (12)	11402 (21)	8973 (6)	5.14
C(21)	7875 (10)	−278 (18)	6066 (6)	3.94
C(22)	8103 (11)	−1620 (18)	5677 (6)	3.87
C(23)	7321 (14)	−2400 (19)	5321 (6)	5.59
C(24)	6266 (13)	−1925 (22)	5343 (7)	5.76
C(25)	6012 (11)	−655 (22)	5731 (7)	5.67
C(26)	6788 (10)	172 (18)	6091 (6)	4.58

Thermal Analysis[6]—Thermal behavior was studied on a differential scanning calorimeter at a heating rate of 5°/min. Temperatures of fusion were measured at the onset point of each peak.

Preparation of Crystals[7]—Good quality crystals were obtained by slow evaporation at 60° of n-heptane (form I) and by slow evaporation at 60° of 2-propanol (form II).

RESULTS AND DISCUSSION

Two polymorphs of the title compound were isolated and characterized by differential scanning calorimetry. Form I[8] melted at 209.8° (heat of fusion: 52.3 kJ/mole), whereas form II melted at 207.0° (heat of fusion 51.8 kJ/mole). These two forms showed an equivalent stability at room

[6] Perkin-Elmer DSC-model 2.

[7] Spiperone, Janssen Pharmaceutica, Beerse, Belgium.

[8] Polymorphs are numbered I and II in decreasing order of their melting points.

Table III—Interatomic Distances, Å

C(2) —N(1)	1.464 (13)
C(5) —N(1)	1.494 (14)
C(21)—N(1)	1.404 (14)
N(3) —C(2)	1.426 (14)
C(4) —N(3)	1.353 (15)
O(1) —C(4)	1.197 (14)
C(5) —C(4)	1.515 (16)
C(6) —C(5)	1.545 (14)
C(10)—C(5)	1.490 (14)
C(7) —C(6)	1.543 (15)
N(8) —C(7)	1.421 (13)
C(9) —N(8)	1.484 (13)
C(11)—N(8)	1.505 (15)
C(10)—C(9)	1.533 (15)
C(12)—C(11)	1.462 (18)
C(13)—C(12)	1.536 (18)
C(14)—C(13)	1.465 (21)
O(2) —C(14)	1.240 (17)
C(15)—C(14)	1.448 (20)
C(16)—C(15)	1.441 (20)
C(20)—C(15)	1.389 (18)
C(17)—C(16)	1.345 (22)
C(18)—C(17)	1.319 (24)
F(1) —C(18)	1.366 (21)
C(19)—C(18)	1.390 (23)
C(20)—C(19)	1.344 (17)
C(22)—C(21)	1.367 (15)
C(26)—C(21)	1.430 (16)
C(23)—C(22)	1.343 (16)
C(24)—C(23)	1.394 (18)
C(25)—C(24)	1.337 (18)
C(26)—C(25)	1.357 (16)

Table IV—Bond Angles, Degrees

C(5) —N(1) —C(2)	111.0 (1.0)	C(14)—C(13)—C(12)	111.8 (1.5)
C(21)—N(1) —C(2)	118.3 (1.1)	O(2) —C(14)—C(13)	121.0 (1.9)
C(21)—N(1) —C(5)	130.2 (1.1)	C(15)—C(14)—C(13)	120.1 (1.8)
N(3) —C(2) —N(1)	104.1 (1.0)	C(15)—C(14)—O(2)	118.9 (1.8)
C(4) —N(3) —C(2)	113.6 (1.1)	C(16)—C(15)—C(14)	119.6 (2.0)
O(1) —C(4) —N(3)	123.5 (1.3)	C(20)—C(15)—C(14)	121.8 (1.8)
C(5) —C(4) —N(3)	109.8 (1.2)	C(20)—C(15)—C(16)	118.6 (1.6)
C(5) —C(4) —O(1)	126.7 (1.4)	C(17)—C(16)—C(15)	119.7 (1.9)
C(4) —C(5) —N(1)	101.5 (1.0)	C(18)—C(17)—C(16)	120.0 (2.3)
C(6) —C(5) —N(1)	109.7 (1.0)	F(1) —C(18)—C(17)	118.3 (2.0)
C(6) —C(5) —C(4)	109.1 (1.0)	C(19)—C(18)—C(17)	122.0 (2.1)
C(10)—C(5) —N(1)	113.3 (0.9)	C(19)—C(18)—F(1)	119.0 (2.4)
C(10)—C(5) —C(4)	111.2 (1.0)	C(20)—C(19)—C(18)	120.4 (1.8)
C(10)—C(5) —C(6)	111.6 (1.1)	C(19)—C(20)—C(15)	118.9 (1.5)
C(7) —C(6) —C(5)	111.1 (1.1)	C(22)—C(21)—N(1)	120.5 (1.3)
N(8) —C(7) —C(6)	111.5 (1.0)	C(26)—C(21)—N(1)	122.1 (1.3)
C(9) —N(8) —C(7)	110.0 (1.0)	C(26)—C(21)—C(22)	117.2 (1.2)
C(11)—N(8) —C(7)	108.9 (1.0)	C(23)—C(22)—C(21)	119.8 (1.3)
C(11)—N(8) —C(9)	111.5 (1.0)	C(24)—C(23)—C(22)	122.3 (1.5)
C(10)—C(9) —N(8)	110.7 (1.0)	C(25)—C(24)—C(23)	119.5 (1.5)
C(9) —C(10)—C(5)	113.2 (1.0)	C(26)—C(25)—C(24)	119.5 (1.5)
C(12)—C(11)—N(8)	116.2 (1.2)	C(25)—C(26)—C(21)	121.7 (1.4)
C(13)—C(12)—C(11)	112.2 (1.4)		

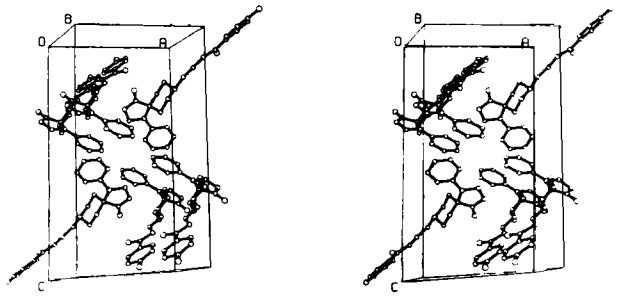

Figure 4—*Stereoscopic view of crystal packing of spiperone I*[10].

temperature, in the presence of water, and under high pressure required for preparation of potassium bromide pellets.

The IR spectrum in the solid state of form I corresponded to that obtained from the commercial product[9] (Figs. 2 and 3) and was different from that of form II.

[9] Janssen Pharmaceutica specification report number 598 (760317).

Table V—Selected Torsion Angles, Degrees

C(9)	—N(8)	—C(11)	—C(12)	−68
C(7)	—N(8)	—C(11)	—C(12)	170
N(8)	—C(11)	—C(12)	—C(13)	−173
C(11)	—C(12)	—C(13)	—C(14)	169
C(12)	—C(13)	—C(14)	—C(15)	180
C(12)	—C(13)	—C(14)	—O(2)	−2
C(4)	—C(5)	—C(6)	—C(7)	−76
C(10)	—C(5)	—C(6)	—C(7)	47
C(6)	—C(5)	—C(10)	—C(9)	−47
C(5)	—C(6)	—C(7)	—N(8)	−56
C(6)	—C(7)	—N(8)	—C(9)	63
C(6)	—C(7)	—N(8)	—C(11)	−175
C(7)	—N(8)	—C(9)	—C(10)	−61
N(8)	—C(9)	—C(10)	—C(5)	54
C(2)	—N(1)	—C(21)	—C(22)	3
C(2)	—N(1)	—C(21)	—C(26)	178
C(5)	—N(1)	—C(21)	—C(22)	174
C(5)	—N(1)	—C(21)	—C(26)	−11

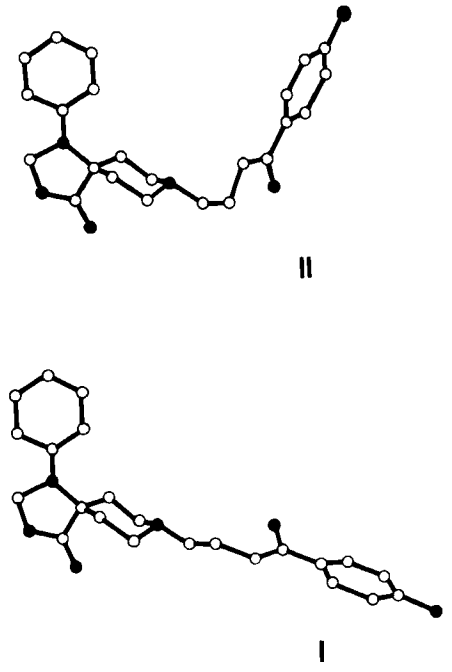

Figure 5—*Molecular conformation of spiperone I and II.*

Unit cell parameters of form II corresponded to those published earlier (5), while the crystal lattice of form I was different (Table I). Complete crystal structure of form I was thus determined and compared with that of form II (Tables II–V, Fig. 4).

The main difference between the molecular conformation of the polymorphs was found to be in the conformation of the side chain. Form I was shown to have the same side-chain conformation as aceperone[11], azaperone[12] I, benperidol[13] I, moperone[14] I, III (R1838)[15,19]-I, pipamperone[16], IV (R1616 hydrochloride)[17,19], haloperidol hydrobromide[18],

[10] S. Motherwell and W. Clegg, PLUTO, University of Cambridge, England, 1978.

[11] Aceperone—4 - [4-(acetamidomethyl) -4- phenylpiperidino]-4′-fluorobutyrophenone. Belgian Patent no. 606,849 (1961), Janssen Pharmaceutica.

[12] Azaperone—1-(4-fluorophenyl)-4-[4-(2-pyridinyl)-1-piperazinyl]-1-butanone. U.S. Patent no. 2,979,508 (1961), Janssen Pharmaceutica.

[13] Benperidol—1-{1-[3 - (*p*-fluorobenzoyl)propyl] -4- piperidol}-2-benzimidazolinone. Belgian Patent no. 626,307 (1963), Janssen Pharmaceutica.

[14] Moperone—4′ - fluoro -4- (4 - hydroxy-4-*p*-tolylpiperidino)butyrophenone, British Patent no. 881,893 (1961), Janssen Pharmaceutica.

[15] R 1838—4-(4 - hydroxy -4- phenyl -1- piperidinyl)-1-(4-fluorophenyl)-1-butanone.

[16] Pipamperone—1′-[4-(4 - fluorophenyl) -4- oxobutyl]-[1,4′ - bipiperidine]-4′-carboxamide. Belgian Patent no. 610,830 (1962), Janssen Pharmaceutica.

[17] R 1616 hydrochloride—4 - [4 - (4-fluorophenyl) -4- hydroxy-1-piperidinyl] -1- (4-fluorophenyl)-1-butanone hydrochloride.

[18] Haloperidol hydrobromide—4-[4 - (4 - chlorophenyl)-4-hydroxy -1- piperidinyl] -1- (4-fluorophenyl)-1-butanone hydrobromide.

[19] Names to be published.

Table VI—Intermolecular Bond Characteristics [a] of Spiperone I and II

	Hydrogen Bonding			Other Short Intermolecular Contacts		
	Contact	Position	Distance, Å	Contact	Position	Distance, Å
Spiperone I	N(8)—N(3)	−2(0,1,0)	2.81	C(20)-O(1)	−2(0,2,0)	3.39
	N(3)—N(8)	−2(1,1,0)	2.81	F—C(17)	2(0,0,2)	3.28
Spiperone II [b]	O(1)—N(3)	−1(1,1,0)	2.87	C(23)—C(2)	2(1,1,0)	3.36
	N(3)—O(1)	−1(1,1,0)	2.87	O(2)—C(13)	2(0,0,1)	3.30
				O(1)—C(23)	−2(0,1,0)	3.33
				F—C(26)	−1(0,1,0)	3.26

[a] Hydrogens are not positioned. [b] Calculated from ref. 5 data.

moperone hydrobromide (4, 6, 7, 9, 11, 12, 14, 15) (Fig. 5). The side-chain conformation of form II was found to be different from the compounds described above.

This modification of the conformation between the two polymorphs of spiperone is not surprising since PCILO (16) calculations have showed the possible existence of five isoenergetic minima for the propyl chain of butyrophenones (5, 14–17). The piperidine ring of form I is in the usual chair form encountered in most butyrophenones.

The angle between the mean plane of the piperidine and phenyl rings, and the corresponding torsion angles, are nearly identical in the two polymorphs (Table V). This fact may be explained by the coplanarity of the phenyl and five-membered rings that are attached by a $C(sp_2)$-$N(sp_3)$ single bond with lengths of 1.404 Å (I) and 1.394 Å (II), respectively (18). As a result the rotation of the phenyl ring is not allowed. The PCILO potential energy curve of the phenyl ring-containing moiety of spiperone leads to an identical interpretation (15, 17). Experimental values of torsion angles of spiperone I fall in the same minimum of the PCILO curve as those of spiperone II, thus confirming the existence of a potential barrier.

The two polymorphs differ entirely from one another in the nature and the force of hydrogen bonding. Indeed, in form II, each molecule is bonded to another by two hydrogen bonds, [N(3) to O(1)], and the crystal is made up of dimers which are held together by packing forces only (5). On the other hand, in form I only one type of hydrogen bond, [N(3) to N(8)] contributes to the building of a polymeric lattice (Table VI). Differences between intermolecular bonding of the two forms are visible in IR spectra. In form I, the stretching of the NH—N polymeric bond appears in the 3000–3100 cm^{-1} region as a broad peak, whereas the narrow bands observed at 3190 and 3110 cm^{-1} in form II indicate that the NH vibrator included has a more localized bond, such as a dimeric structure. Nevertheless, the shift of the C=O(1) vibration frequency (1705 cm^{-1}) is not visible because the N(3)H to O(1)C hydrogen bond taken individually is not very strong; intensity of the corresponding absorption band is only increased.

The two polymorphs of spiperone exhibit different crystal structures. Their molecular conformation and intermolecular bonds in solid state differ entirely.

The study of molecular conformation of the two polymorphs confirms the flexibility of the side chain of butyrophenone derivatives claimed previously by PCILO calculations (15, 17). Moreover, existence of two conformations of the side chain for the same compound proves definitively that this conformation is not influenced by the nature of the phenyl ring-containing moiety and by the substituents on that ring.

Several authors have attempted to explain the high level of activity of spiperone by relatively high local concentrations in brain regions, caused by dimerization *in vivo*, considering that spiperone preferentially forms dimers (14). The structure of form I proves that a stable nondimerized form of spiperone can exist with a high probability of occurrence.

REFERENCES

(1) M. L. Huang and S. Miazi, *J. Pharm. Sci.*, **66**, 609 (1977).

(2) H. G. Ibrahim, F. Pisano, and A. Bruno, *ibid.*, **66**, 669 (1977).

(3) W. G. Wagner and J. K. Guillory, *ibid.*, **68**, 1005 (1979).

(4) M. H. J. Koch and G. Germain, *Acta Crystallogr.*, **B28**, 121 (1972).

(5) M. H. J. Koch, *ibid.*, **B29**, 379 (1973).

(6) L. L. Reed and J. P. Schaefer, *ibid.*, **B29**, 1886 (1973).

(7) J. P. Declercq, G. Germain, and M. H. J. Koch, *ibid.*, **B29**, 2311 (1973).

(8) M. H. J. Koch and G. Evrard, *ibid.*, **B30**, 237 (1974).

(9) J. P. Declercq, G. Germain, and M. H. J. Koch, *ibid.*, **B31**, 628 (1975).

(10) A. G. Michel, G. Evrard, M. Schiltz, F. Durant, and M. H. J. Koch, *ibid.*, **B32**, 2507 (1976).

(11) N. Van Opdenbosch, G. Evrard, C. Dorval, and F. Durant, *ibid.*, **B33**, 171 (1977).

(12) M. H. J. Koch, G. Germain, J. P. Declercq and M. Van Meerssche, *ibid.*, **B33**, 1975 (1977).

(13) N. M. Blaton, O. M. Peeters, and C. T. De Ranter, *ibid.*, **B36**, 2828 (1980).

(14) M. H. J. Koch, *Mol. Pharmacol.*, **10**, 425 (1974).

(15) J. P. Tollenaere, H. Moereels, and M. H. J. Koch, *Eur. J. Med. Chem.*, **12**, 199 (1977).

(16) J. L. Courbeils and B. Pullman, *Theoret. Chem.* Acta, **24**, 35 (1972).

(17) J. P. Tollenaere and H. Moereels, *Gaz. Chim. Ital.*, **108**, 419 (1978).

(18) G. Gilli and V. Bertolosi, *J. Am. Chem. Soc.*, **101**, 7704 (1979).

ACKNOWLEDGMENTS

The authors wish to thank the Fonds de la Recherche Scientifique Médicale (FRSM) for supporting the project, Janssen Pharmaceutica (Beerse, Belgium) for providing spiperone, and the Department of Chemistry, University of Antwerp, U.I.A., for collecting the crystallographic data.

Analysis of Theophylline by Automated Multidimensional High-Performance Liquid Chromatography Involving Direct Plasma Injection

SHAW F. CHANG ˣ, TERESA M. WELSCHER, and ROBERT E. OBER

Received November 23, 1981, from the *Drug Metabolism Department, Riker Laboratories, Inc., Subsidiary of 3M, St. Paul, MN 55144.* Accepted for publication April 20, 1982.

Abstract □ A procedure of direct injection of whole plasma for the analysis of theophylline by an automated multidimensional high-performance liquid chromatographic (HPLC) technique is described. The procedure requires as little as 30 μl of plasma sample and has a linear range of 0.25–30 μg/ml. Unknown plasma samples, after the addition of internal standard, are directly injected into the HPLC system. The chromatographic procedure is fully automated, thus the attention and time required from the analyst is reduced to a minimum. About 70 samples can be analyzed per day with ~3 hr of analyst time.

Keyphrases □ Theophylline—analysis by automated multidimensional high-performance liquid chromatography involving direct plasma injection □ High-performance liquid chromatography—automated multidimensional analysis of theophylline involving direct plasma injection □ Direct plasma injection—analysis of theophylline by automated multidimensional high-performance liquid chromatography

Multidimensional high-performance liquid chromatography (HPLC) has been in use for quite some time. However, the majority of the applications do not involve the direct injection of plasma samples (1–5).

The purpose of the present investigation was to test the concept of analyzing drugs in plasma by the multidimensional column chromatography technique and to determine if the technique could be completely automated. The test compound in this case was theophylline. After the investigation was completed, an abstract outlining the feasibility of the concept for theophylline was published (6). In the present report, the successful application of a fully automated multidimensional HPLC technique for the routine analysis of theopnylline is described.

BACKGROUND

Monitoring plasma levels of drugs in clinical management of patients or studying pharmacokinetic parameters for a marketed or developmental drug both require the quantitative determination of the drug in biological fluids, most often in plasma. Generally used procedures require the separation of the drug from the plasma proteins by a solvent extraction or protein precipitation technique prior to quantitation. With the recently available gel permeation columns designed to separate water soluble polymers, it is possible to employ a gel permeation column in place of the normal extraction procedure for the purpose of separating the drug from the plasma proteins. Thus, a coupled-column or multidimensional column chromatography technique can be used. In this technique, the drug is first separated from the plasma proteins on a gel permeation column based on molecular size difference, then the drug is selectively transferred *via* a switching valve onto a reverse-phase column where, on the basis of partition characteristics, it is further separated from any endogenous material with a similar range of molecular weight. The first step eliminates the plasma proteins, and the second step separates and quantitates small molecular weight substances.

EXPERIMENTAL

Reagents and Apparatus—The tetrahydrofuran was distilled in glass[1], and the methanol was suitable for liquid chromatographic use[2]. All chemicals were analytical reagent grade. All HPLC analyses were performed using a liquid chromatograph equipped with two solvent delivery systems[3], an automatic liquid sampler[4], and a detector[5] with a 280-nm filter. Peak heights were measured by an integrator[6]. The two columns used were a gel permeation column[7] and a 25-cm × 4.6-mm i.d. reverse-phase column[8]. A 4-port switching valve with air actuator[9] was placed in line, and the valve switching was controlled by the integrator through an external relay. The integrator was programmed to turn the valve at a certain time during each sample run. Figure 1 shows the arrangement of apparatus.

Standard Solutions—Standard solutions of theophylline and β-hydroxyethyl theophylline[10] were prepared by diluting 400-μg/ml stock solutions of each compound. Concentrations used were 0.3, 0.6, 1.8, 4.2, 9.0, 18.0, and 36.0 μg of theophylline/ml for the theophylline standard and 8.0 μg of β-hydroxyethyl theophylline/ml for the internal standard. All solutions were made in 0.05 *M* sodium phosphate buffer, pH 7.0, and were kept refrigerated.

Mobile Phase—Mobile phase A consisted of 0.05 *M* sodium phosphate buffer, pH 7.0. The phosphate buffer was prepared from 0.1 *M* dibasic sodium phosphate and 0.1 *M* monobasic sodium phosphate. Mobile phase B was prepared by mixing 70 ml of methanol, 10 ml of tetrahydrofuran, 92 ml of 0.1 *M* sodium acetate buffer pH 5.0, and 828 ml of distilled water. The final composition was methanol–tetrahydrofuran–0.01 *M* sodium acetate buffer pH 5.0 (7:1:92, v/v/v). This mobile phase was reported previously for the analysis of theophylline by HPLC (7). The mobile

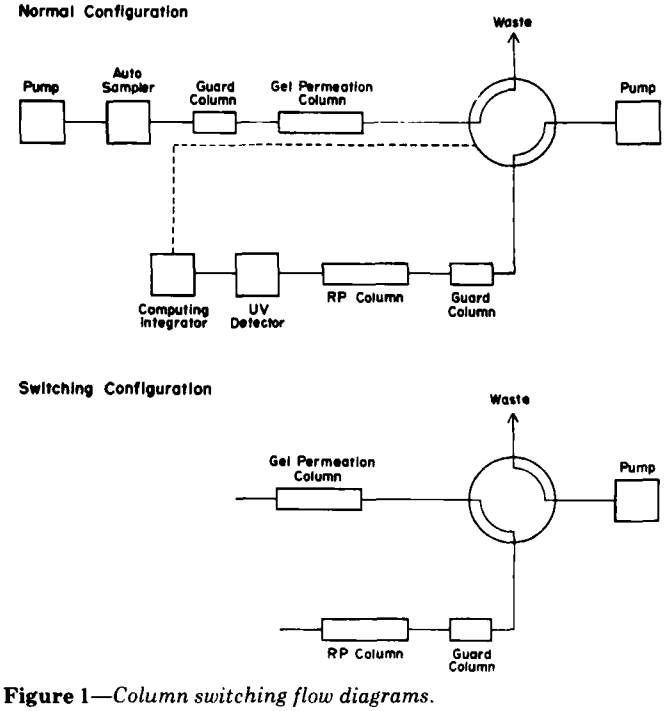

Figure 1—*Column switching flow diagrams.*

[1] Burdick-Jackson.
[2] Omnisolv, MCB.
[3] Model 6000, Waters Associates.
[4] Model 710A, Waters Associates.
[5] Model 440, Waters Associates.
[6] Model 4100, Spectra-Physics.
[7] I-125, Waters Associates.
[8] Ultrasphere-ODS, Altex, Inc.
[9] Helical Drive Air Actuator, Valco Instruments Co.
[10] Pierce Chemical Company.

0022-3549/83/0300-0236$01.00/0

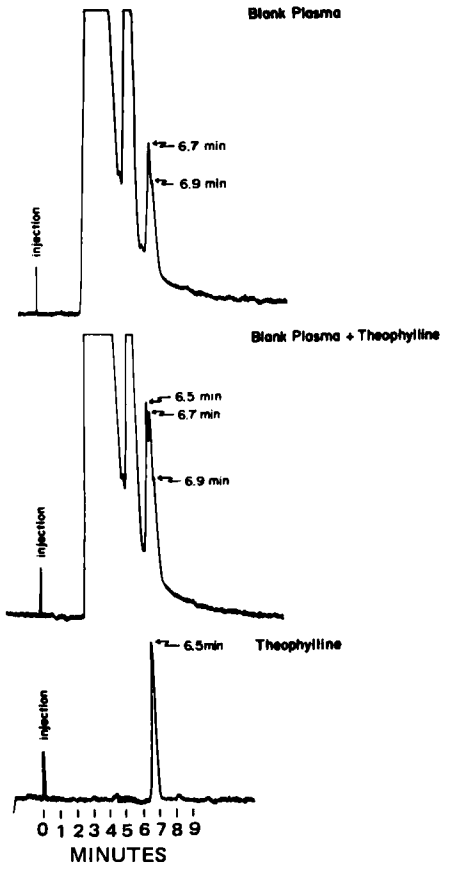

Figure 2—*Separation of theophylline from human plasma proteins on the gel permeation column.*

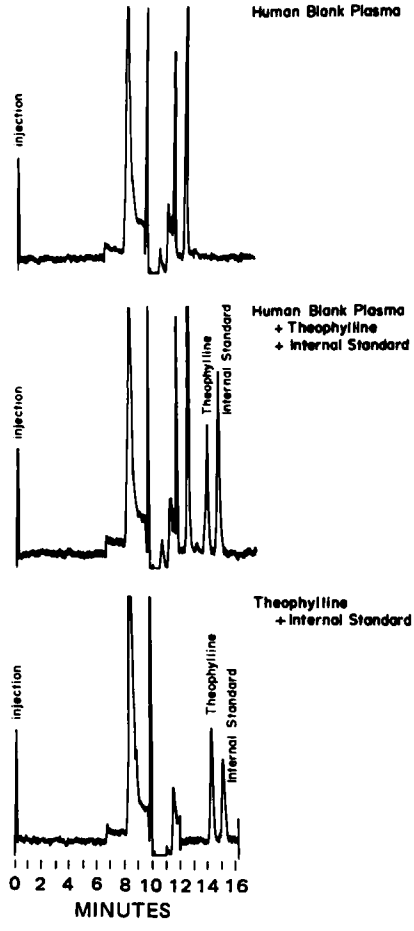

Figure 3—*Determination of theophylline in human plasma by a multidimensional technique.*

phases were filtered through a membrane filter[11] (pore size 0.45 μm) and deoxygenated prior to use.

Sample Preparation and Injection—Plasma, internal standard, and phosphate buffer (0.05 *M*, pH 7.0) were mixed in the ratio 30:25:25 (v/v/v). The minimum volume of plasma used was 30 μl. Eight theophylline standards were prepared by mixing blank plasma, internal standard, and the theophylline standard in the same ratio as above. The standard concentrations were 0, 0.25, 0.5, 1.5, 3.5, 7.5, 15, and 30 μg/ml plasma. To prevent overloading the gel permeation column, no more than 53 μl of the mixture (equal to 20 μl plasma) was injected into the liquid chromatograph. If duplicate injections are desired, the volumes for mixing should be doubled.

At 0 min, the valve was positioned so that mobile phase A flowed through the gel permeation column to the waste. Simultaneously, mobile phase B flowed through the reverse-phase column to the UV detector. The sample was injected onto the gel permeation column which separated the plasma proteins from the lower molecular weight materials, including theophylline. At the beginning of the theophylline peak the valve was switched so that effluent from the gel permeation column was directed onto the reverse-phase column. Mobile phase B then flowed directly to waste. The theophylline was concentrated at the head of the reverse-phase column by the aqueous mobile phase A. At 2 min after the switching, the valve was turned back to the original position. Mobile phase B was then flowing through the reverse-phase column where further separation of theophylline and the other lower molecular weight materials occurred. Actual switching times can vary by ±0.4 min, depending upon the retention time of theophylline on different gel permeation columns.

Method of Calculation—The construction of a standard curve, and subsequent calibration of unknown samples with the standard curve, was fully automated and was performed by a computing integrator. The integrator collected the peak height ratios (theophylline–internal standard) from the standards during a run, and the slope (A) and intercept (B) for the least-squares line between the peak height ratios (*x*-axis) and the theophylline concentrations (*y*-axis) were determined. The slope and intercept were automatically entered into the integrator's memory. For the unknown samples, the integrator determined the peak height ratio for each sample, retrieved the slope and intercept from the memory, and calculated the theophylline concentration in the following manner: theophylline concentration = peak height ratio × A + B. The final result of each unknown is reported in micrograms per milliliter.

[11] Millipore Corp.

RESULTS AND DISCUSSION

Determination of Valve-Switching Time—The purpose of the multidimensional technique was to separate the plasma proteins from the drug. This was accomplished through the switching valve. Thus, the time and duration that the valve is switched become a critical part of the overall procedure. An early switch will result in the transfer of plasma proteins onto the reverse-phase column and the rapid deterioration of that column. A late switch will result in the loss of the drug to waste. The duration of the time the valve was in the switching configuration controlled the quantitative transfer of the drug onto the reverse-phase column. For each drug studied and each gel permeation column used, the time and duration of the valve switching were predetermined. Figure 2 shows a set of typical chromatographic profiles of the gel permeation column alone. The majority of the UV-absorptive materials were eluted before 6 min. The theophylline started eluting at 6.3 min and peaked at 6.5 min; thus 6 min after the injection was chosen as the switching time of the valve. The peaks at 6.7 and 6.9 min from the blank plasma were also transferred onto the reverse-phase column, but were separated from theophylline and the internal standard and constitute no interference with the assay. Based on experimental results for theophylline, it was found that if the valve remained in the switching configuration for at least 2 min, a quantitative transfer of theophylline onto the reverse-phase column resulted.

Separation—The separation of theophylline and internal standard from endogenous materials in the plasma by the multidimensional technique is shown in Fig. 3. Baseline separation was achieved between theophylline and the internal standard. The retention times were 14.3 and 15.1 min, respectively, under the experimental conditions. There were

Table I—Intraday Precision and Accuracy

Sample Concentration[a], μg/ml	Mean ± *SD*, μg/ml	*RSD*, %	Relative Error, %
0.38	0.35 ± 0.01	2.9	−9.2
2.5	2.48 ± 0.05	2.0	1.0
11.3	11.35 ± 0.26	2.3	0.4
22.5	22.75 ± 0.70	3.1	1.1

[a] Four samples were used at each concentration.

two major peaks from the plasma which were also transferred onto the reverse-phase column during the switch; their retention times were 12 and 12.8 min, respectively, and constituted no interference with theophylline and the internal standard. The results clearly indicated that for theophylline, adaptation of an existing HPLC separation (7) to the multidimensional technique presented no chromatographic problems.

The application of the multidimensional technique did not prolong the elution time in comparison with the reported retention times of theophylline and the internal standard with the use of the same mobile phase and the same reverse-phase column alone; 15 and 17.5 min were reported for theophylline and the internal standard, respectively (7). The reason that this elution process with a rather long elution time was chosen for the multidimensional technique was that the procedure provided better specificity than most of the other HPLC methods for theophylline. The caffeine metabolite, 1,7-dimethylxanthine, was also separated from theophylline. The other major peaks seen in the chromatogram were due to the change of pressure and mobile phase on the reverse-phase column at the valve-switching step of the procedure. For repeated injections, the next injection was made before the last sample was completely eluted from the system. Under the experimental conditions, a sample was injected every 11 min. About 70 samples can be analyzed per day with ~3 hr of analyst time. This procedure is ideal for maximum utilization of the liquid chromatographic equipment for overnight runs with minimum requirement of an analyst's time for sample preparation.

Calibration Curve and Linearity—Daily calibration curves were prepared by spiking blank human plasma with theophylline standards resulting in final concentrations of 0, 0.25, 1.5, 3.5, 7.5, 15, and 30 μg/ml. The theophylline concentrations and the peak height ratios for theophylline and internal standard were fitted by the computing integrator to a straight line by the least-squares method. The mathematical representation of the line was y (theophylline concentration) = 0.2186x (response ratio) + 0.0182. The correlation coefficient was 0.9999. A linear relationship was demonstrated between response and theophylline concentration over a range of 0.25–30 μg/ml. The relationship was not tested beyond 30 μg/ml. At the 0.25 μg/ml concentration level, the response was 3–5 times the noise level of the system.

Precision and Accuracy—Intraday precision and accuracy were established by spiking blank human plasma in quadruplicate with theophylline at four concentration levels: 0.38, 2.5, 11.3, and 22.5 μg/ml. These spiked samples were analyzed by the procedure outlined in *Experimental*. The results are shown in Table I. The intraday precision, expressed as the relative standard deviation, was 2.9, 2.0, 2.3, and 3.1% for 0.38, 2.5, 11.3, and 22.5 μg/ml levels, respectively. The accuracy, expressed as relative error, was −9.2, 1.0, 0.4, and 1.1% for the four concentrations. The intraday precision and accuracy were excellent and certainly adequate for the monitoring of theophylline levels in clinical therapeutic settings and for more research-oriented pharmacokinetic studies. The interday precision was established by analyzing seven theophylline standards, 0.25, 0.5, 1.5, 3.5, 7.5, 15.0, and 30.0 μg/ml plasma, five separate times over an 8-month period. During this time, different

Table II—Interday Precision

Sample Concentration[a], μg/ml	Mean ± *SD*, μg/ml	*RSD*, %
0.25	0.31 ± 0.04	12.9
0.5	0.58 ± 0.11	19.0
1.5	1.52 ± 0.04	2.6
3.5	3.52 ± 0.08	2.3
7.5	7.44 ± 0.18	2.4
15.0	14.68 ± 0.24	1.6
30.0	30.16 ± 0.17	0.6

[a] Five samples were used at each concentration.

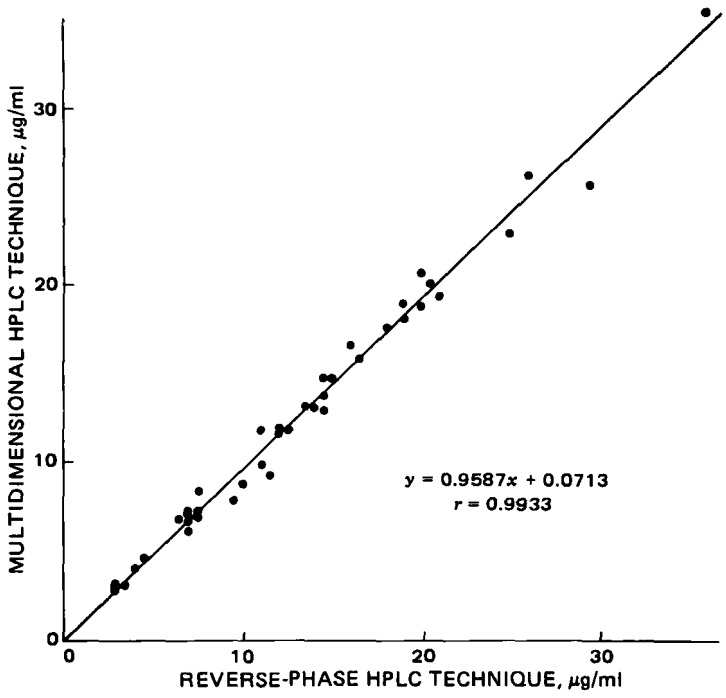

Figure 4—*Comparison of the multidimensional HPLC technique with an established reverse-phase HPLC method.*

theophylline standard solutions, gel permeation columns, and reverse-phase columns were used. The results are tabulated in Table II. Excellent day-to-day reproducibility over the concentration range of 1.5–30.0 μg/ml of plasma was demonstrated with the relative standard deviation ≤2.6% in each case. At lower concentrations, 0.25 and 0.5 μg/ml of plasma, larger relative standard deviations were obtained.

Comparison with Other Methods—Plasma samples were obtained from a local hospital. These samples were initially analyzed by the hospital using an HPLC method (8), and were reanalyzed using the multidimensional technique. Both results are presented in Fig. 4 and exhibit excellent correlation (slope = 0.96, r = 0.99) between methods for these 42 samples over a concentration range of 2.9–36 μg/ml.

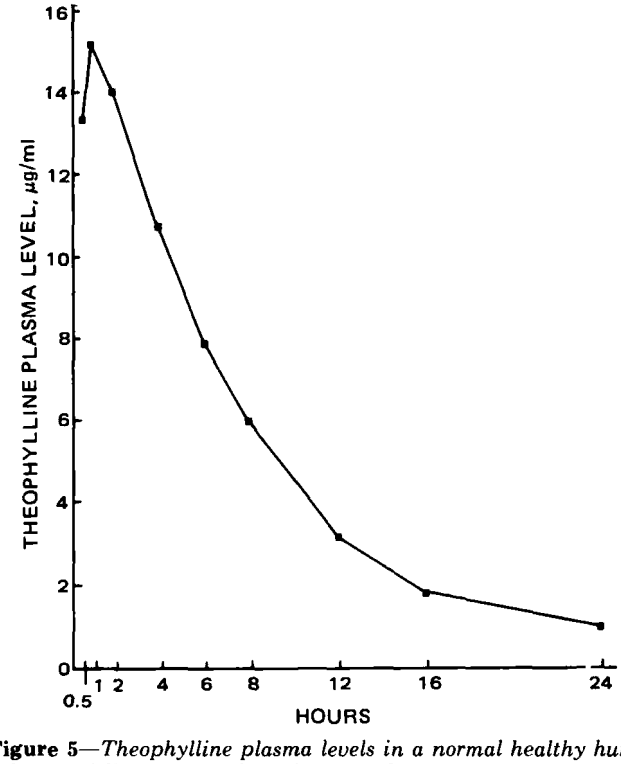

Figure 5—*Theophylline plasma levels in a normal healthy human volunteer following a single oral 500-mg dose.*

Interferences—Dietary xanthines, theophylline and caffeine metabolites, and several drugs that could be administered with theophylline in a therapeutic situation, were tested for interference. The compounds that were tested and found not to interfere with the assay procedure are: acetaminophen, ampicillin, caffeine, ceforamide, cephalothin sodium, cephloridine, corticosterone, dilantin, 1,3-dimethyluric acid, 1,7-dimethylxanthine, ephedrine, hypoxanthine, isoproterenol, 1-methyluric acid, 3-methyluric acid, 1-methylxanthine, 3-methylxanthine, 7-methylxanthine, phenobarbital, theobromine, uric acid, and xanthine.

Applicability—This method has been used in the evaluation of new theophylline formulations in dogs and in bioavailability studies of theophylline formulations in healthy human volunteers. Figure 5 is a typical theophylline plasma level–time profile following the oral administration of a 500-mg theophylline dose to a human volunteer.

It has been demonstrated that theophylline can be efficiently analyzed by the automatic multidimensional HPLC technique, thus, totally eliminating the extraction step. With the use of a computing integrator (as described in this report) to automate the data reduction step, the total analysis of plasma theophylline has been reduced to manually mixing the unknown plasma sample with the internal standard solution in a small glass tube of the autosampler; the rest of the procedure is performed automatically by instruments.

REFERENCES

(1) D. H. Freeman, *Anal. Chem.*, **53**, 2 (1981).

(2) E. Erni and R. W. Feri, *J. Chromatogr.*, **149**, 561 (1978).

(3) F. W. Willmott, I. MacKenzie, and R. J. Dolphin, *J. Chromatogr.*, **167**, 31 (1978).

(4) E. J. Johnson, R. Gloor, and R. E. Majors, *ibid.*, **149**, 571 (1978).

(5) A. Yamatodani and H. Wada, *Clin. Chem.*, **27**, 1983 (1981).

(6) J. A. Apffel, T. V. Alfredson, and R. E. Majors, International Symposium on Chromatography, Cannes, France, June, 1980.

(7) J. R. Miksic and B. Hodes, *J. Pharm. Sci.*, **68**, 1200 (1979).

(8) J. J. Orcutt, P. P. Kozak, S. A. Gillman, and L. H. Cummins, *Clin. Chem.*, **23**, 599 (1977).

ACKNOWLEDGMENTS

The results were presented in part at the Pittsburg Conference and Exposition on Analytical Chemistry and Applied Spectroscopy, Atlantic City, N.J., March 1981.

The authors thank Sue Price, Toxicology Laboratories, St. Paul Ramsey Medical Center for providing patient plasma samples for cross checking theophylline methods, and Jeanne Fox for her critical review of the manuscript.

Esterase Activities in Adult Rabbit Eyes

VINCENT H. L. LEE

Received January 11, 1982, from the *School of Pharmacy, University of Southern California, Los Angeles, CA 90033.* Accepted for publication April 14, 1982.

Abstract □ The rational design of prodrugs to improve the therapeutic efficacy of existing drugs would be expedited if the nature of the *in vivo* enzymatic conditions that regenerate the drugs from their prodrugs is known. Using albino and pigmented rabbits as models, this research seeks to delineate the esterase activities in their corneas, irises, ciliary bodies, and aqueous humor, which are intimately involved in the disposition of drugs from topical dosing. This was achieved by monitoring the hydrolysis kinetics of α-naphthyl acetate, both in the presence and absence of esterase inhibitors, upon incubation with aqueous humor and homogenates of cornea, iris, and ciliary body. It was found that in both breeds of rabbits, esterase activity was the highest in the iris–ciliary body followed by the cornea and then the aqueous humor, and that multiple esterases probably existed in the aqueous humor and the ocular tissues studied. However, the esterase activity in the cornea and iris–ciliary body of the pigmented rabbit was greater when compared with the albino rabbit. Based on these results, drugs and prodrugs containing ester linkages can undergo varying extents of esterase-mediated hydrolysis while permeating the cornea and upon entering the aqueous humor, iris, and ciliary body. Moreover, in view of the differences in esterase activity that exist between the albino and pigmented rabbits, it would be necessary to employ both breeds of rabbits in evaluating the rate and extent to which ocular ester prodrugs would be converted to their parent compounds.

Keyphrases □ Esterase activities—adult rabbit eyes, disposition, hydrolysis kinetics □ Eyes, adult rabbits—esterase activities, disposition, hydrolysis kinetics □ Disposition—esterase activities in adult rabbit eyes, hydrolysis kinetics □ Kinetics, hydrolysis—esterase activities in adult rabbit eyes, disposition

Until recently, there have been few reports on drug metabolism in the eye (1). Invariably, they are concerned with polycyclic aromatic compounds entering the uveal circulation and reaching the photoreceptor cells through the choriocapillaries. Because of its dual capability to terminate the pharmacological activities of inherently active drugs and to transform inactive drugs to their active moieties, drug metabolism in the eye is an important aspect of drug action. In view of the necessarily close association between esterase activities in the various segments of the eye and the extent of metabolic alterations of drugs containing ester linkages, knowledge of esterase activities in the eye would allow a first estimation of the clinical efficacy of such drugs as pilocarpine, atropine, and dipivefrin.

During the past 5 years, the prodrug approach (2) of preparing bioreversible derivatives of existing drugs has been successfully extended to the topical ophthalmic drug epinephrine (3). In principle, several other topical ophthalmic drugs that are currently available should also benefit from this approach, since they, like epinephrine, contain functional groups amenable to ester prodrug derivatization.

For these ester prodrugs to be useful clinically, esterase activity must be available in the ocular tissues to regenerate the parent compounds. Several investigators (4–10) have evidence to support the presence of esterases predominantly in innervated ocular tissues. They include the cornea, iris–ciliary body, retina, and optic nerve. However, the level of esterase activities in each tissue and the biochemical properties of these esterases remain to be determined. It is reasonable to expect that when such information is available, the rational design of ester prodrugs would follow.

The first step in the eventual characterization of esterases present in the various ocular tissues of both albino and pigmented rabbits is the determination of esterase activities in their corneas, irises, ciliary bodies, and aqueous humor, and this is the subject of this report. The rationale for studying esterases in both albino and pigmented rabbit

0022-3549/83/0300-0239$01.00/0

Interferences—Dietary xanthines, theophylline and caffeine metabolites, and several drugs that could be administered with theophylline in a therapeutic situation, were tested for interference. The compounds that were tested and found not to interfere with the assay procedure are: acetaminophen, ampicillin, caffeine, ceforamide, cephalothin sodium, cephloridine, corticosterone, dilantin, 1,3-dimethyluric acid, 1,7-dimethylxanthine, ephedrine, hypoxanthine, isoproterenol, 1-methyluric acid, 3-methyluric acid, 1-methylxanthine, 3-methylxanthine, 7-methylxanthine, phenobarbital, theobromine, uric acid, and xanthine.

Applicability—This method has been used in the evaluation of new theophylline formulations in dogs and in bioavailability studies of theophylline formulations in healthy human volunteers. Figure 5 is a typical theophylline plasma level–time profile following the oral administration of a 500-mg theophylline dose to a human volunteer.

It has been demonstrated that theophylline can be efficiently analyzed by the automatic multidimensional HPLC technique, thus, totally eliminating the extraction step. With the use of a computing integrator (as described in this report) to automate the data reduction step, the total analysis of plasma theophylline has been reduced to manually mixing the unknown plasma sample with the internal standard solution in a small glass tube of the autosampler; the rest of the procedure is performed automatically by instruments.

REFERENCES

(1) D. H. Freeman, *Anal. Chem.*, **53**, 2 (1981).

(2) E. Erni and R. W. Feri, *J. Chromatogr.*, **149**, 561 (1978).

(3) F. W. Willmott, I. MacKenzie, and R. J. Dolphin, *J. Chromatogr.*, **167**, 31 (1978).

(4) E. J. Johnson, R. Gloor, and R. E. Majors, *ibid.*, **149**, 571 (1978).

(5) A. Yamatodani and H. Wada, *Clin. Chem.*, **27**, 1983 (1981).

(6) J. A. Apffel, T. V. Alfredson, and R. E. Majors, International Symposium on Chromatography, Cannes, France, June, 1980.

(7) J. R. Miksic and B. Hodes, *J. Pharm. Sci.*, **68**, 1200 (1979).

(8) J. J. Orcutt, P. P. Kozak, S. A. Gillman, and L. H. Cummins, *Clin. Chem.*, **23**, 599 (1977).

ACKNOWLEDGMENTS

The results were presented in part at the Pittsburg Conference and Exposition on Analytical Chemistry and Applied Spectroscopy, Atlantic City, N.J., March 1981.

The authors thank Sue Price, Toxicology Laboratories, St. Paul Ramsey Medical Center for providing patient plasma samples for cross checking theophylline methods, and Jeanne Fox for her critical review of the manuscript.

Esterase Activities in Adult Rabbit Eyes

VINCENT H. L. LEE

Received January 11, 1982, from the *School of Pharmacy, University of Southern California, Los Angeles, CA 90033.* Accepted for publication April 14, 1982.

Abstract □ The rational design of prodrugs to improve the therapeutic efficacy of existing drugs would be expedited if the nature of the *in vivo* enzymatic conditions that regenerate the drugs from their prodrugs is known. Using albino and pigmented rabbits as models, this research seeks to delineate the esterase activities in their corneas, irises, ciliary bodies, and aqueous humor, which are intimately involved in the disposition of drugs from topical dosing. This was achieved by monitoring the hydrolysis kinetics of α-naphthyl acetate, both in the presence and absence of esterase inhibitors, upon incubation with aqueous humor and homogenates of cornea, iris, and ciliary body. It was found that in both breeds of rabbits, esterase activity was the highest in the iris–ciliary body followed by the cornea and then the aqueous humor, and that multiple esterases probably existed in the aqueous humor and the ocular tissues studied. However, the esterase activity in the cornea and iris–ciliary body of the pigmented rabbit was greater when compared with the albino rabbit. Based on these results, drugs and prodrugs containing ester linkages can undergo varying extents of esterase-mediated hydrolysis while permeating the cornea and upon entering the aqueous humor, iris, and ciliary body. Moreover, in view of the differences in esterase activity that exist between the albino and pigmented rabbits, it would be necessary to employ both breeds of rabbits in evaluating the rate and extent to which ocular ester prodrugs would be converted to their parent compounds.

Keyphrases □ Esterase activities—adult rabbit eyes, disposition, hydrolysis kinetics □ Eyes, adult rabbits—esterase activities, disposition, hydrolysis kinetics □ Disposition—esterase activities in adult rabbit eyes, hydrolysis kinetics □ Kinetics, hydrolysis—esterase activities in adult rabbit eyes, disposition

Until recently, there have been few reports on drug metabolism in the eye (1). Invariably, they are concerned with polycyclic aromatic compounds entering the uveal circulation and reaching the photoreceptor cells through the choriocapillaries. Because of its dual capability to terminate the pharmacological activities of inherently active drugs and to transform inactive drugs to their active moieties, drug metabolism in the eye is an important aspect of drug action. In view of the necessarily close association between esterase activities in the various segments of the eye and the extent of metabolic alterations of drugs containing ester linkages, knowledge of esterase activities in the eye would allow a first estimation of the clinical efficacy of such drugs as pilocarpine, atropine, and dipivefrin.

During the past 5 years, the prodrug approach (2) of preparing bioreversible derivatives of existing drugs has been successfully extended to the topical ophthalmic drug epinephrine (3). In principle, several other topical ophthalmic drugs that are currently available should also benefit from this approach, since they, like epinephrine, contain functional groups amenable to ester prodrug derivatization.

For these ester prodrugs to be useful clinically, esterase activity must be available in the ocular tissues to regenerate the parent compounds. Several investigators (4–10) have evidence to support the presence of esterases predominantly in innervated ocular tissues. They include the cornea, iris–ciliary body, retina, and optic nerve. However, the level of esterase activities in each tissue and the biochemical properties of these esterases remain to be determined. It is reasonable to expect that when such information is available, the rational design of ester prodrugs would follow.

The first step in the eventual characterization of esterases present in the various ocular tissues of both albino and pigmented rabbits is the determination of esterase activities in their corneas, irises, ciliary bodies, and aqueous humor, and this is the subject of this report. The rationale for studying esterases in both albino and pigmented rabbit

0022-3549/83/0300-0239$01.00/0

eyes comes from an earlier observation (11) that the extent and rate of hydrolysis of pilocarpine to pilocarpic acid are one to two orders of magnitude greater in the eyes of pigmented rabbits than in the eyes of albino rabbits. The cause underlying this apparent disparity is unclear, although it could be related to differences in the concentration, activities, or perhaps type of esterases.

α-Naphthyl acetate was chosen as the model substrate, since it has been shown to be a substrate for most esterases (12), and because at this stage of the study screening for esterase activity was of primary concern. The advantage offered by this substrate is that at an excitation wavelength of 317 nm and emission wavelength of 470 nm, it is practically nonfluorescent when compared with its hydrolytic product α-naphthol. Consequently, the progress of esterase-mediated hydrolysis, and therefore esterase activity, can be monitored by noting the increase in fluorescence with time. Scheme I presents the stoichiometry of the reaction.

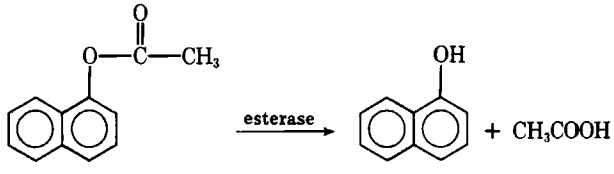

α-naphthyl acetate α-naphthol

Scheme I—Hydrolysis of α-naphthyl acetate.

Recognizing that multiple esterases are likely to be present in each ocular tissue and in the fluid and that each esterase may possess its own ester substrate specificity, the esterase activities reported here, at best, represent mean values. During preliminary investigation two other esterase substrates, ethyl *p*-aminobenzoate and dipivefrin, were also considered, but for a variety of reasons were found to be unsuitable to screen for esterase activity.

EXPERIMENTAL

Male albino rabbits[1], weighing ~2.4 kg, were used throughout the study. All chemicals were either reagent or analytical grade and were used as received.

Preparation of Substrate Solutions—*α-Naphthyl Acetate*—A 2×10^{-3} *M* solution of α-naphthyl acetate[2] was prepared by first dissolving 0.0372 g of the compound in 10 ml of 95% ethyl alcohol followed by dilution to 100 ml with an isotonic tromethamine buffer at pH 7.4. From this stock solution 1.5×10^{-5} *M* and 5.85×10^{-5} *M* solutions were prepared for the enzymatic hydrolysis studies. These concentrations covered the range of drug concentrations typically achieved in ocular tissues.

The 10 ml of alcohol was found to be necessary to maintain the α-naphthyl acetate in solution. Two other solutions, one in 15% and the other in 20% alcohol, were also prepared to study the effect of alcohol on esterase activity. The cornea was the only tissue whose esterase activity showed statistically significant ($p < 0.05$) reduction as the ethyl alcohol concentration was varied 10–20%. Nonetheless, there was a tendency toward reduced esterase activity in the presence of ethyl alcohol. Provided a given concentration of ethyl alcohol inhibited esterase activity in the aqueous humor, cornea, iris, and ciliary body to roughly the same extent, a comparison of the relative esterase activities in them should still be valid. The remaining experiments, unless otherwise indicated, were conducted using α-naphthyl acetate solutions in 10% ethyl alcohol.

L-Leucyl-β-Naphthylamide Solutions—A solution of L-leucyl-β-naphthylamide[2], a peptidase substrate, was selected to screen for the presence of peptidases and to correct for their contribution to the esterase activity observed using α-naphthyl acetate. The peptidases, cathepsins, have been found in the eye (13) and shown to possess esterase activity (14).

A 4.67×10^{-4} *M* solution of L-leucyl-β-naphthylamide was prepared by first dissolving 0.0114 g of the compound in 10 ml of 95% ethyl alcohol followed by dilution to 100 ml with a 0.0612 *M* tromethamine buffer at pH 8.2.

Fluorescence Intensities of α-Naphthol, α-Naphthyl Acetate, β-Naphthylamine and L-Leucyl-β-Naphthylamide—The wavelengths of maximum excitation and emission were determined for each compound using a spectrophotometer[3] and a spectrofluorometer[4], respectively. They were found to be as follows:

Compound	λ_{ex}, nm	λ_{em}, nm
α-naphthol	317	470
β-naphthylamine	277.5	412

The corresponding esters were found to be nonfluorescent at the wavelengths chosen. The fluorescence intensity varied linearly with α-naphthol[5] concentration in the range of 10^{-7}–10^{-5} *M*, and with β-naphthylamine[5] concentration in the range of 6×10^{-8}–5×10^{-5} *M*. Potential interference of the fluorescence intensity of α-naphthol by α-naphthyl acetate was determined by spiking 1×10^{-6} *M* solutions of α-naphthyl acetate with α-naphthol (concentrations: $0.1–1 \times 10^{-6}$ *M*). This procedure was repeated with a 1.5×10^{-5} *M* L-leucyl-β-naphthylamide solution to which was added 1.5×10^{-4} *M* β-naphthylamine. At these concentrations, neither α-naphthyl acetate nor L-leucyl-β-naphthylamide quenched the fluorescence due to α-naphthol and β-naphthylamine, respectively. Thus, the increase in fluorescence intensity in subsequent enzymatic hydrolysis experiments could only be due to the hydrolytic products.

Preparation of Ocular Tissues for Enzymatic Hydrolysis Studies—Albino and pigmented rabbits, approximately 10 of each, were kept in restraining boxes in a normal upright posture. They were sacrificed by a rapid injection of a 30% sodium phenobarbital solution into a marginal ear vein. After withdrawing 10 to 15 ml of blood through intracardiac puncture, the corneal surfaces were rinsed with saline and blotted dry. About 150 μl of aqueous humor was aspirated using a 27-gauge × 1.27 cm needle attached to a 1-ml tuberculin syringe, and the cornea, iris, and ciliary body[6] were removed in sequence using a surgical scalpel.

Immediately following their removal, the tissues were transferred to homogenization vessels and the aqueous humor and blood to culture tubes. All were placed in an ice bath. The tissues were homogenized in ~10 ml of ice-cold isotonic potassium chloride solution for ~80 sec using a motor-driven tissue grinder[7]. The homogenate was centrifuged at 755×*g* in a refrigerated (4°) centrifuge[8], and the supernatant was saved for enzymatic hydrolysis studies. The blood was allowed to coagulate, and the fibrin clot and blood cells were removed by centrifugation under the same conditions as for ocular tissue homogenates. The protein content of each supernatant was then determined using a protein–dye binding assay[9] (15) with rabbit serum albumin as the standard.

During aspiration it was possible that the aqueous humor was contaminated with esterases from the cornea and the iris–ciliary body. However, the probability of this occurring was low. This was suggested by the different response to modulators of esterase activity by aqueous humor samples as compared with cornea and iris–ciliary body samples (Fig. 1). The complicating factors, of course, were that the esterases might not partition into the aqueous humor in exact proportion to their concentrations in the tissues, and that homogenization of the tissues might release other enzymes or proteins which altered the esterases.

Enzymatic Hydrolysis of Various Substrates in the Absence of Their Inhibitors—Prior to initiating enzymatic hydrolysis studies, the presence of esterases in selected ocular tissues/fluids was ascertained by electrophoresis on 7.5% polyacrylamide gels[9] and staining proteins (16), esterases (12), and peptidases (17).

α-Naphthyl Acetate—To 3 ml of a 1.5×10^{-5} *M* or 5.85×10^{-5} *M* α-naphthyl acetate solution in a fluorescence cuvet was added 100 μl of ocular tissue supernatant, aqueous humor, or serum. After mixing, the

[1] ABC Rabbitry, Pomona, Calif.
[2] United States Biochemical, Cleveland, Ohio.
[3] Cary 219 spectrophotometer, Varian Instruments, Downey, Calif.
[4] Aminco-Bowman spectrofluorometer, American Instrument Co., Silver Spring, Md.
[5] Sigma Chemical Co., St. Louis, Mo.
[6] The iris and ciliary body were removed as one structure and hereafter will be referred to as the iris–ciliary body.
[7] Polytron, Brinkmann Instruments, Inc., Westburg, N.Y.
[8] Sorvall RC-5B refrigerated superspeed centrifuge, DuPont Instruments, Newtown, Conn.
[9] Bio-Rad Laboratories, Richmond, Calif.

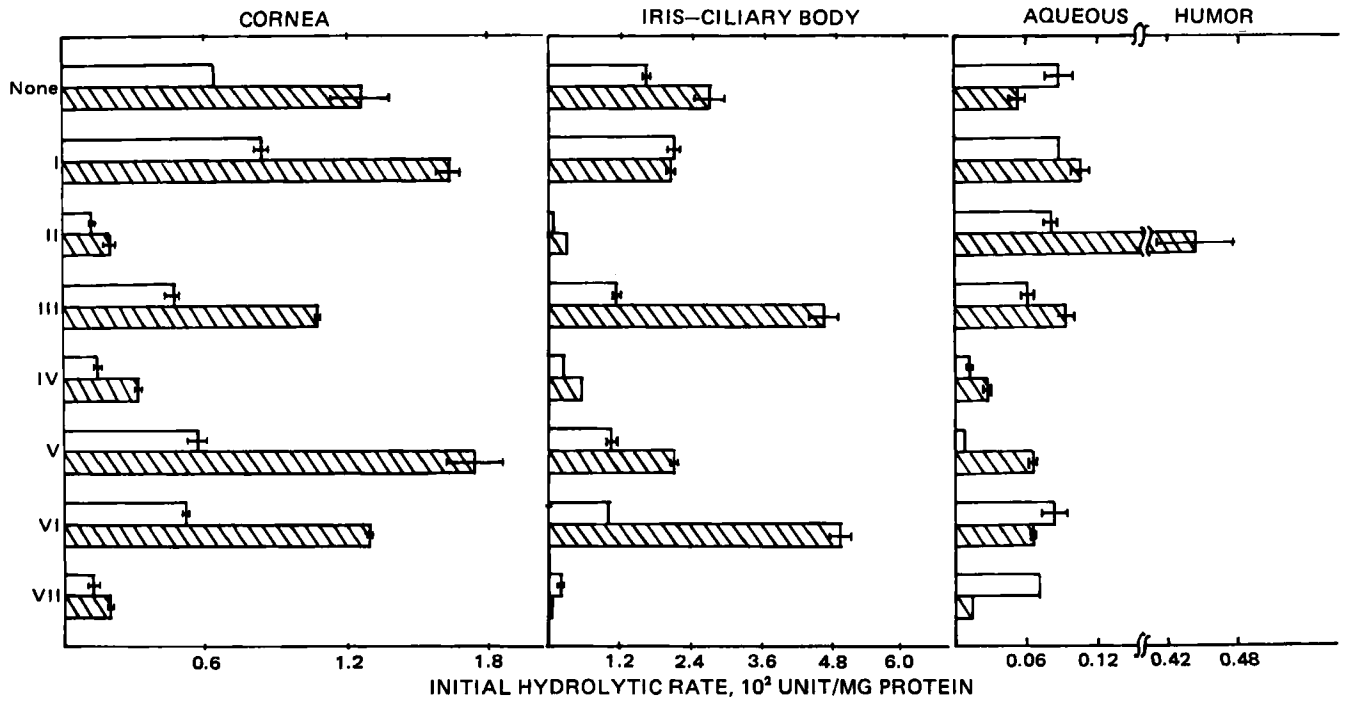

Figure 1—*Esterase activity, expressed as initial hydrolytic rate, in the cornea, iris–ciliary body, and aqueous humor of albino (□) and pigmented (▨) rabbits. Determinations were made in the presence of various inhibitors. The data for each tissue–fluid were obtained from at least 20 eyes. Error bars represent standard error of the mean. Key: I, acetazolamide; II, physostigmine sulfate; III, neostigmine bromide; IV, isofluorophate; V, p-chloromercuribenzoate; VI, edetic acid; VII, preheating supernatants at 45°.*

fluorescence intensity was monitored at ambient temperature every 25 sec for the first 200 sec, then every 100 sec for the next 400 sec. By applying suitable conversions, the initial hydrolysis rate in unit[10] per milligram of protein was calculated from the initial slope of a plot of fluorescence intensity *versus* time. Because no attempt was made to free membrane-bound esterases, the esterase activity thus determined should only be interpreted as that due to soluble esterases. The implicit assumption was that the fraction of soluble proteins that was esterases paralleled the total protein. As demonstrated by the lack of increase in fluorescence intensity with time in the control solution, which contained 3 ml of α-naphthyl acetate and 100 μl of 1.17% KCl, no chemical hydrolysis of α-naphthyl acetate occurred during enzymatic hydrolysis. Between three and four determinations were made for each ocular tissue or fluid of a rabbit.

The purpose of determining esterase activity in serum was to estimate the contribution of esterases in the blood, which perfuses the iris and ciliary body, to the total activity found in the iris and ciliary body. As shown in Fig. 2, this amounted to ~15% in the albino rabbit and ~25% in the pigmented rabbit.

L-Leucyl-β-Naphthylamide—One hundred microliters of tissue supernatant, aqueous humor, or serum was incubated with 2.6 ml of an activator solution[11] at 45° for 5 min. After cooling the mixture to room temperature, 300 μl of 95% ethyl alcohol was added. Hydrolysis was initiated by adding 100 μl of the amide solution to this mixture. The fluorescence intensity was monitored at ambient temperature every 100 sec for 600 sec. By applying suitable conversions, the initial hydrolysis rate in unit[10] per milligram of soluble proteins was calculated from the initial slope of a plot of fluorescence intensity *versus* time. No chemical hydrolysis of the amide occurred during enzymatic hydrolysis, as demonstrated by the lack of increase in fluorescence intensity with time in the control solution, which contained 3 ml of L-leucyl-β-naphthylamide and 100 μl of 1.17% KCl. Between three and four determinations were made for each ocular tissue/fluid of a rabbit.

The preceding procedure was also repeated with a 1.5×10^{-5} *M* α-naphthyl acetate solution to study the effect of heat on esterase activity. As shown in Fig. 1, except for the aqueous humor of the albino rabbit, the ocular esterase activity at 45° was significantly lower than that at 25°, suggesting that ocular esterases, like dermal esterases (19), were temperature sensitive.

Enzymatic Hydrolysis of α-Naphthyl Acetate in the Presence of Inhibitors—To ensure that the observed esterase activity was due to true esterases, the hydrolysis of α-naphthyl acetate was conducted in the presence of various inhibitors. They were acetazolamide[5], a carbonic anhydrase inhibitor; physostigmine sulfate[2], neostigmine bromide[2], and isofluorophate[12], all cholinesterase inhibitors; and *p*-chloromercuribenzoate[2] and edetic acid[2], modulators of carboxylesterase and aryl esterase activity. With the exception of acetazolamide, which was employed at a concentration of 2×10^{-5} *M*, the concentration of each inhibitor solution was 1×10^{-3} *M*. None of these concentrations altered the fluorescence intensity due to α-naphthol.

One hundred microliters of tissue supernatant was incubated with 2.9 ml of an inhibitor solution for 15 min prior to initiation of hydrolysis by adding 100 μl of a 4.5×10^{-5} *M* α-naphthyl acetate solution, thus generating 1.5×10^{-5} *M* α-naphthyl acetate solution. The fluorescence intensity was monitored as a function of time in the same manner as those experiments that did not involve inhibitors. This substrate concentration, 1.5×10^{-5} *M*, was well below the concentration where substrate inhibition occurred. This was demonstrated by the fact that the initial hydrolytic rate continued to increase as the α-naphthyl acetate concentration was increased to 5.85×10^{-5} *M*.

RESULTS AND DISCUSSION

The presence of esterases or esterase activity in the cornea has been implied by the hydrolysis of pilocarpine to pilocarpic acid (11) and by the conversion of the prodrugs dipivefrin (3, 8, 9) and pivenfrine (10, 20) to their corresponding parent compounds. This study demonstrated this to be the case. As shown in Fig. 3, when α-naphthyl acetate, the model substrate, was incubated with aqueous humor and the supernatant derived from the cornea, iris, and ciliary body, the fluorescence intensity increased with time, indicating that esterase activity was present in ocular tissues and fluids aside from the cornea. This esterase activity can be derived from true esterases like acetylcholinesterase, peptidases like cathepsins (14) and carbonic anhydrase (21), all of which are known or said to be present in the eye (6, 13, 22). With L-leucyl-β-naphthylamide as the substrate, peptidase activity could only be detected in the iris–ciliary body of the albino rabbit, one of the few ocular tissues enriched

[10] Unit is defined as μmoles of substrate hydrolyzed per minute.

[11] The activator solution was 0.0768 *M* in tromethamine, 1.28×10^{-4} *M* in $CoCl_2 \cdot 6H_2O$, 0.128 *M* in $MgSO_4 \cdot 7H_2O$ and 2.01×10^{-4} *M* in $MnCl_2$. It was adjusted to pH 8.2 with 3 *N* HCl. This solution was reported by Wolff and Resnick (18) to be optimal for peptidase activity.

[12] Calbiochem-Behring Corp., San Diego, Calif.

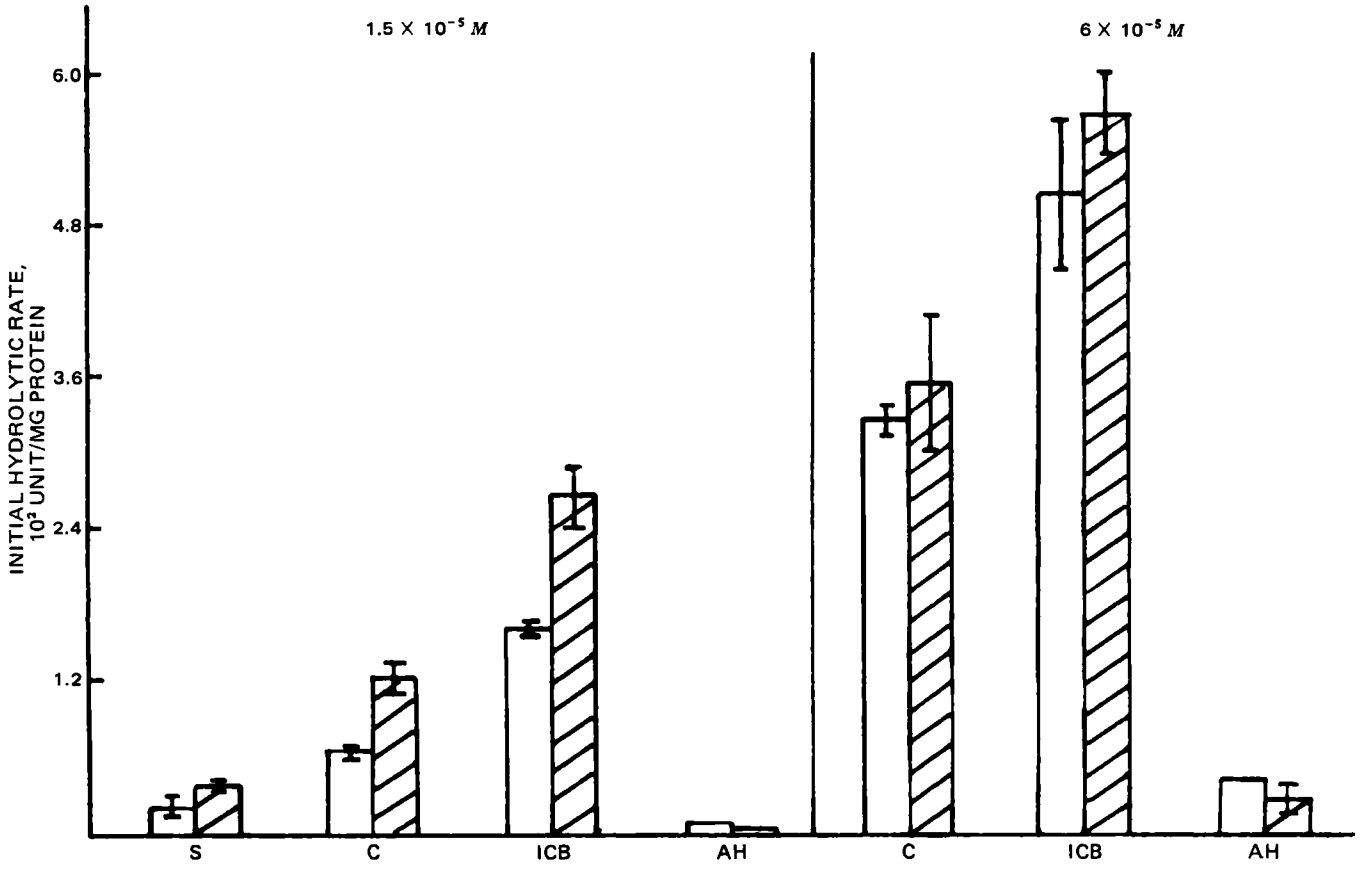

Figure 2—*Esterase activity, expressed as initial hydrolytic rate, in the serum (S), cornea (C), iris–ciliary body (ICB), and aqueous humor (AH) of albino (□) and pigmented (▨) rabbits. All determinations were made in the absence of inhibitors. The data for each tissue/fluid were obtained from at least 20 eyes. Error bars represent standard error of the mean.*

in cathepsins (13). This peptidase activity was calculated to be 3.95 ± 0.24 × 10^{-5} U/mg of protein[10], which was ~1/400 of the esterase activity in the same tissue determined under similar incubation conditions. This result, which was in agreement with previous findings (23), suggests that peptidases contributed insignificantly to total esterase activity. For unknown reasons the iris–ciliary body of the pigmented rabbit did not hydrolyze L-leucyl-β-naphthylamide and on this basis was judged to be devoid of peptidase activity.

Besides peptidases, carbonic anhydrase is another enzyme that possesses esterase activity (21), and this was verified in our laboratory[13] by incubating rabbit erythrocyte carbonic anhydrase with α-naphthyl acetate. Based on the reduction in esterase activity when acetazolamide, a specific carbonic anhydrase inhibitor that has little or no effect on true esterases (24), was included in the incubation medium, the iris–ciliary body of the pigmented rabbit was the only ocular tissue of both breeds of rabbits in which a percentage of total esterase activity could be ascribed to carbonic anhydrase. This was estimated to be 24% of total esterase activity.

Thus, true esterases were principally responsible for the esterase activity observed in the cornea, iris–ciliary body, and aqueous humor of albino and pigmented rabbits. Their behavior towards modulators of esterase activity suggested that they were a heterogeneous group of enzymes, in accord with the heterogeneity known of other esterases such as hepatic esterases (25). For the time being, two of the possible members in this group could be acetylcholinesterase and pseudocholinesterase. Their presence was suggested by the reduction in esterase activity, seen in the cornea and iris–ciliary body only (Fig. 1), in the presence of physostigmine sulfate, neostigmine bromide, and isofluorophate. Because *p*-chloromercuribenzoate, an agent that acts on free sulfhydryl groups in a noncompetitive fashion, also altered esterase activity in the iris–ciliary body, and also because free sulfhydryl groups have been shown to be nonessential for acetylcholinesterase activity, other esterases like arylesterase could also be present in the iris–ciliary body. As suggested by the results shown in Fig. 1, at least some of the esterases present in the aqueous humor were different from those in the cornea, iris, and ciliary body.

Taking the albino and pigmented rabbits as a group, the net effect of these esterases in the aqueous humor, cornea, iris, and ciliary body was to generate a rank order of esterase activity such that the activity was the highest in the iris–ciliary body followed by the cornea and then the aqueous humor. Specifically, the esterase activity in the cornea and aqueous humor was, respectively, 50 and 2–5% of that seen in the iris–ciliary body. The higher level of esterase activity in the iris and ciliary body may be due to the fact that these tissues are more cellular than both the cornea and the aqueous humor and, therefore, are more abundant in esterases. It may also be due to the presence of intrinsically more active esterases in the iris and ciliary body. Further work is needed to distinguish between these two possibilities as well as to identify additional ones. Nonetheless, the presence of esterase activity in the iris and ciliary body ensures that drugs containing ester linkages reaching this tissue from the systemic circulation will be hydrolyzed to some extent prior to distribution to the remaining ocular tissues.

Even though the cornea is not as enzymatically active as the iris and ciliary body, it is still in a strategic position to determine the amount of intact drug ultimately reaching the internal eye from topical dosing. The reason is that the major pathway of drug entry into the eye following topical dosing is permeation through the cornea. Partly because of this requirement, the cornea may fortuitously appear to be the primary site of hydrolysis when in fact the iris and ciliary body are enzymatically more

Table I—Michaelis–Menten Parameter Estimates for Esterases in the Cornea and Iris–Ciliary Body of Albino and Pigmented Rabbits

Tissue	K_m, ×10^5 M		V_{max}, 10^2 Unit[a]/mg protein	
	Albino	Pigmented	Albino	Pigmented
Cornea	26.2	10.6	1.98	1.14
Iris–Ciliary body	15.7	3.8	1.86	0.96

[a] Unit = μmoles of substrate hydrolyzed per minute.

[13]Unpublished data.

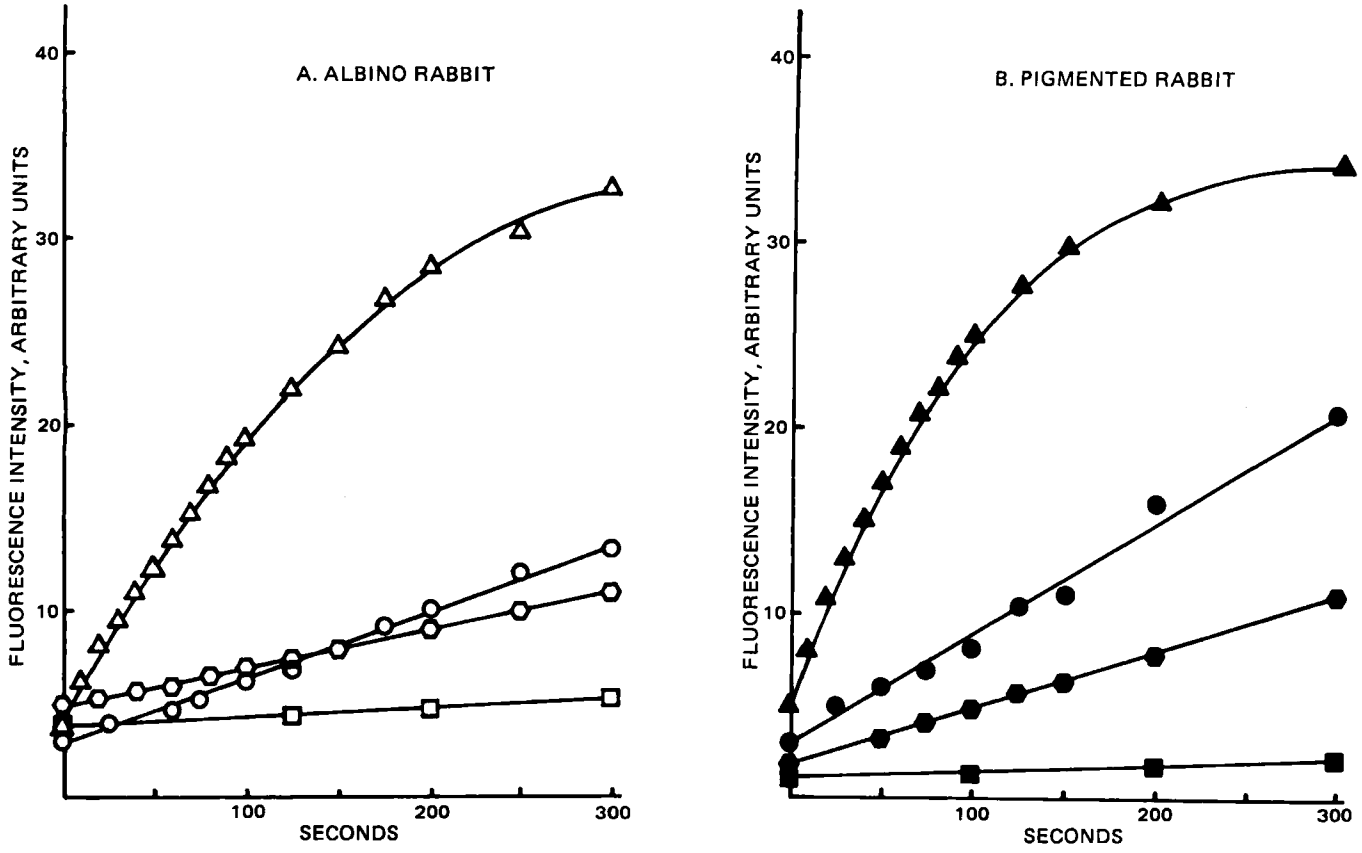

Figure 3—*Hydrolysis of α-naphthyl acetate (1.5 × 10^{-5} M) in the supernatants of the cornea (○, ●), iris–ciliary body (△, ▲), aqueous humor (□, ■), and serum (○, ●). The fluorescence intensity was determined at ambient temperature in a spectrofluorometer[4] with λex at 317 nm and λem at 470 nm, multiplier = 0.1 and sensitivity = 40. Plot A is shown for an albino rabbit, and B for a pigmented rabbit.*

active. This would be observed for drugs like dipivefrin (9) which are extensively hydrolyzed during permeation through the cornea.

The preceding discussion was presented in general terms, without emphasizing the possible variation of ocular esterase activity, as suggested previously (11), with rabbit strain. Based on the more extensive hydrolysis of pilocarpine to pilocarpic acid in the eye of the pigmented rabbit as compared with the albino rabbit, it was speculated (11) that the pigmented rabbit possessed greater esterase activity in the ocular tissues. This study confirmed this speculation for the cornea, iris, and ciliary body, but not for the aqueous humor. Thus, the faster rate of pilocarpine hydrolysis reported for the pigmented rabbit's cornea was more likely the result of greater esterase activity in the cornea rather than a fast permeation rate and the resultant greater accessibility of the drug to the esterases in the cornea. At an α-naphthyl acetate concentration of 1.5 × 10^{-5} M, the esterase activity in the pigmented rabbit's cornea and iris–ciliary body was ~2.0 and 1.6 times that in these tissues of the albino rabbit, respectively. However, such differences ceased to exist at a slightly higher substrate concentration of 5.85 × 10^{-5} M, suggesting that the apparent differential rate of pilocarpine hydrolysis in the two breeds of rabbits could be a substrate concentration or dose-dependent phenomenon.

Crude estimates on the Michaelis–Menten parameters associated with the ocular esterases of the rabbits, presented in Table I, suggest that the esterases in the cornea and iris–ciliary body of the pigmented rabbit show a higher affinity for the substrate than those found in the albino rabbit, but suffer from a lower maximum initial velocity. Conceivably, at a certain substrate concentration, these two factors offset one another, thereby giving identical initial rates of hydrolysis, and the esterase activity in the two breeds of rabbits would then appear to be equal. However, so long as the substrate concentration in a given ocular tissue is much less than the Michaelis–Menten constant (K_m), not at all an unlikely situation, the pigmented rabbit will appear to have a higher esterase activity than the albino rabbit.

In light of the different values obtained for the Michaelis–Menten parameters for the esterases in the cornea and iris–ciliary body of the two breeds of rabbits, it is possible that several of these esterases are unique to either the albino or the pigmented rabbit. This is further supported by the manner in which the esterase activity in the ocular tissues of the albino and pigmented rabbits responded to modulators of esterase activities, as shown in Fig. 1. Thus, in the albino rabbit, a reduction in esterase activity of the cornea and iris–ciliary body was observed with physostigmine sulfate and isofluorophate only; with the other esterase inhibitors, either an increase or no change in activity was observed. In addition, esterases which require polyvalent ions for their activity appeared to be present in the albino but absent in the pigmented rabbit.

In summary, several esterases, probably heterogeneous with respect to their substrate specificities, are present in the cornea, iris, ciliary body, and aqueous humor of albino and pigmented rabbits. In both types of rabbits, the iris and ciliary body possess twice the esterase activity detected in the less cellular cornea and 20–50 times the esterase activity detected in the acellular aqueous humor. At the concentration of α-naphthyl acetate used, the cornea and iris–ciliary body of the pigmented rabbit exhibit an esterase activity approximately double that in the same tissues of the albino rabbit. Extrapolating this observation to humans, it is probable that the greater drug requirement in brown-eye as compared to blue-eye subjects, a well-known phenomenon, can be attributed to both greater propensity of the drug for esterase-mediated hydrolysis and binding of the drug to the pigments in the iris and ciliary body.

Studies are now underway to fractionate these esterases and to characterize them with respect to substrate specificity and stereospecificity, susceptibility to substrate and product inhibition, the nature of their catalytic sites, and the pH for optimal enzymatic action. The effect of chain length on the rate of ester hydrolysis catalyzed by each esterase will also be investigated, and this information will be combined with that on the effect of chain length on tissue permeation to allow the judicial selection of a prodrug that gives the desired rate of release and even site localization. It is hoped that in so doing the bioavailability and therapeutic efficacy of drugs for such disease states as glaucoma will be improved.

REFERENCES

(1) H. Shichi and D. W. Nebert, in "Extra-hepatic Metabolism of Drugs and Other Foreign Compounds," T. E. Gram, Ed., S. P. Medical and Scientific Books, New York, N.Y., 1980, pp. 333–363.

(2) S. H. Yalkowsky and W. Morozowich, in "Drug Design," vol. 9, E. J. Ariens, Ed., Academic, New York, N.Y., 1980, pp. 121–185.
(3) P. D. Krause, in "Ophthalmic Drug Delivery Systems," J. R. Robinson, Ed., American Pharmaceutical Association, Washington, D.C., 1980, pp. 91–104.
(4) A. de Roetth, Jr., *Arch Ophthalmol.*, **43**, 1004 (1950).
(5) G. B. Koelle and J. S. Friedenwald, *Am. J. Ophthalmol.*, **33**, 253 (1950).
(6) R. A. Peterson, K. J. Lee, and A. Donn, *Arch Ophthalmol.*, **73**, 370 (1965).
(7) A. A. Swanson, *Invest. Ophthalmol.*, **13**, 466 (1974).
(8) C.-P. Wei, J. A. Anderson, and I. H. Leopold, *Invest. Ophthalmol. Vis. Sci.*, **17**, 315 (1978).
(9) J. A. Anderson, W. L. Davis, and C.-P. Wei, *ibid.* **19**, 817 (1980).
(10) W. D. Staatz, H. F. Edelhauser, R. Lehner, and D. L. Van Horn, *Arch. Ophthalmol.*, **98**, 1279 (1980).
(11) V. H.-L. Lee, H.-W. Hui, and J. R. Robinson, *Invest. Ophthalmol. Vis. Sci.*, **19**, 210 (1980).
(12) D. J. Ecobichon and W. Kalow, *Biochem. Pharmacol.*, **11**, 573 (1962).
(13) S. Hayasaka and I. Hayasaka, *Albrecht von Graefes Arch Klin. Exp. Ophthalmol.*, **206**, 163 (1978).
(14) M. L. Bender and F. T. Kezdy, *Annu. Rev. Biochem.*, **34**, 49 (1965).
(15) M. Bradford, *Anal. Biochem.*, **72**, 248 (1976).
(16) S. Fazekas de St. Groth, R. G. Webster, and A. Datyner, *Biochim. Biophys. Acta*, **71**, 377 (1963).
(17) K. Felgenhauer and G. G. Glenner, *J. Histochem. Cytochem.*, **14**, 401 (1966).
(18) J. B. Wolff and R. A. Resnick, *Biochim. Biophys. Acta*, **73**, 588 (1963).
(19) A. Pannatier, B. Testa, and J.-C. Etter, *Int. J. Pharm.*, **8**, 167 (1981).
(20) S.-S. Yuan and N. Bodor, *J. Pharm. Sci.*, **65**, 929 (1976).
(21) J. M. Armstrong, D. V. Meyers, J. A. Verpoorte, and J. T. Edsall, *J. Biol. Chem.*, **241**, 5137 (1966).
(22) G. Lönnerholm, *Acta Physiol. Scand.*, **90**, 143 (1974).
(23) J. K. Stoops, D. J. Horgan, M. T. C. Runnegar, J. de Jersey, E. C. Webb, and B. Zerner, *Biochemistry*, **8**, 2026 (1969).
(24) Y. Pocker and J. T. Stone, *ibid.*, **7**, 3021 (1968).
(25) G. Maksay, Z. Tegyey, E. Simon-Trompler, and L. Ötvös, *Eur. J. Drug Metab. Pharmacokinet.*, **5**, 193 (1980).

ACKNOWLEDGMENTS

Supported by a grant from Allergan Pharmaceuticals, Inc., Irvine, California, and by Grant EY-03816 from the National Eye Institute, Bethesda, Maryland.

Monolayer Studies of Insulin–Lipid Interactions

DAVID L. SCHWINKE, M. G. GANESAN, and N. D. WEINER ˣ

Received December 28, 1981, from the *College of Pharmacy, University of Michigan, Ann Arbor, MI 48109.* Accepted for publication April 30, 1982.

Abstract □ The interactions between insulin and various lipids were studied by monolayer penetration experiments at constant surface area. The increase in surface pressure, $\Delta\Pi$, of a lipid film depended upon the particular lipid used and the concentration of insulin in the subphase. For all lipids studied, $\Delta\Pi$ was dependent on the initial surface pressure of the lipid film. Evidence of the interaction between insulin and the lipids was found in the ability of insulin to penetrate lipid films with initial pressures >16 dynes/cm, the maximum surface pressure obtained by insulin alone. For phospholipids, both the nonpolar and polar regions influenced the degree of interaction with insulin. Saturated chain lecithins exhibited less penetration than phospholipids with unsaturated hydrocarbon chains. The net charge of the lipid was not found to be an important determinant of penetration; however, the structure of the polar group can have a dramatic effect. Insulin penetration of mixed lipid films cannot be predicted by the penetration characteristics of the pure components. The possible role of these interactions in determining the geography of the insulin molecule within the liposome and its resultant effects on the stability is discussed.

Keyphrases □ Insulin—monolayer studies of interactions with lipids □ Monolayer studies—insulin–lipid interactions □ Lipids—monolayer studies of interactions with insulin

Monolayer interactions between proteins and lipids are of much interest in the study of cell membrane structure (1, 2), hormonal action (3, 4), and enzyme activity (5). Early studies (6) established the technique of injecting a protein into the subphase beneath a lipid film at constant surface area. Since then modifications of this procedure have been used in an effort to gain a more detailed understanding of the nature of these interactions.

Recent attempts to develop an oral dosage form of insulin have utilized liposomal entrapment in order to protect the hormone from proteolytic degradation in the GI tract. In theory, to achieve the necessary degree of protection, the entrapped insulin should not penetrate or decrease the stability of the lipid bilayer. The geography of the insulin molecule within the liposome should be dependent upon the degree and type of its interactions with the lipid components. This report investigates the interactions of insulin with cholesterol, stearylamine, and various phospholipids through the use of monolayer penetration studies.

BACKGROUND

The increase in surface pressure of a lipid film with the addition of protein has been termed penetration, although the exact nature of this phenomenon remains unclear. For example, as more protein is added to the subphase, the increase in surface pressure may be attributed to an increase in the number of protein molecules at the surface, enhanced interaction between the surface components, or protein–protein interactions just below the surface, which may alter molecular orientation at the surface. Although the various mechanisms cannot always be differentiated, the results of such penetration studies are still of value in determining the criteria that affect lipid–protein interactions.

The great variation in the behavior of lipid–protein films reported in the literature can be ascribed to the wide range of physical properties of the proteins used. The unique characteristics of each protein or polypeptide prevent accurate predictions of the nature and magnitude of its interactions with lipids. Also, relative protein penetration does not show consistent results based on the type of lipid involved. Therefore, it is necessary to individually assess the effect of insulin on films of pure lipids or lipid mixtures in order to better understand their interactions.

0022-3549/83/0300-0244$01.00/0

(2) S. H. Yalkowsky and W. Morozowich, in "Drug Design," vol. 9, E. J. Ariens, Ed., Academic, New York, N.Y., 1980, pp. 121–185.
(3) P. D. Krause, in "Ophthalmic Drug Delivery Systems," J. R. Robinson, Ed., American Pharmaceutical Association, Washington, D.C., 1980, pp. 91–104.
(4) A. de Roetth, Jr., *Arch Ophthalmol.*, **43**, 1004 (1950).
(5) G. B. Koelle and J. S. Friedenwald, *Am. J. Ophthalmol.*, **33**, 253 (1950).
(6) R. A. Peterson, K. J. Lee, and A. Donn, *Arch Ophthalmol.*, **73**, 370 (1965).
(7) A. A. Swanson, *Invest. Ophthalmol.*, **13**, 466 (1974).
(8) C.-P. Wei, J. A. Anderson, and I. H. Leopold, *Invest. Ophthalmol. Vis. Sci.*, **17**, 315 (1978).
(9) J. A. Anderson, W. L. Davis, and C.-P. Wei, *ibid.* **19**, 817 (1980).
(10) W. D. Staatz, H. F. Edelhauser, R. Lehner, and D. L. Van Horn, *Arch. Ophthalmol.*, **98**, 1279 (1980).
(11) V. H.-L. Lee, H.-W. Hui, and J. R. Robinson, *Invest. Ophthalmol. Vis. Sci.*, **19**, 210 (1980).
(12) D. J. Ecobichon and W. Kalow, *Biochem. Pharmacol.*, **11**, 573 (1962).
(13) S. Hayasaka and I. Hayasaka, *Albrecht von Graefes Arch Klin. Exp. Ophthalmol.*, **206**, 163 (1978).
(14) M. L. Bender and F. T. Kezdy, *Annu. Rev. Biochem.*, **34**, 49 (1965).
(15) M. Bradford, *Anal. Biochem.*, **72**, 248 (1976).
(16) S. Fazekas de St. Groth, R. G. Webster, and A. Datyner, *Biochim. Biophys. Acta*, **71**, 377 (1963).
(17) K. Felgenhauer and G. G. Glenner, *J. Histochem. Cytochem.*, **14**, 401 (1966).
(18) J. B. Wolff and R. A. Resnick, *Biochim. Biophys. Acta*, **73**, 588 (1963).
(19) A. Pannatier, B. Testa, and J.-C. Etter, *Int. J. Pharm.*, **8**, 167 (1981).
(20) S.-S. Yuan and N. Bodor, *J. Pharm. Sci.*, **65**, 929 (1976).
(21) J. M. Armstrong, D. V. Meyers, J. A. Verpoorte, and J. T. Edsall, *J. Biol. Chem.*, **241**, 5137 (1966).
(22) G. Lönnerholm, *Acta Physiol. Scand.*, **90**, 143 (1974).
(23) J. K. Stoops, D. J. Horgan, M. T. C. Runnegar, J. de Jersey, E. C. Webb, and B. Zerner, *Biochemistry*, **8**, 2026 (1969).
(24) Y. Pocker and J. T. Stone, *ibid.*, **7**, 3021 (1968).
(25) G. Maksay, Z. Tegyey, E. Simon-Trompler, and L. Ötvös, *Eur. J. Drug Metab. Pharmacokinet.*, **5**, 193 (1980).

ACKNOWLEDGMENTS

Supported by a grant from Allergan Pharmaceuticals, Inc., Irvine, California, and by Grant EY-03816 from the National Eye Institute, Bethesda, Maryland.

Monolayer Studies of Insulin–Lipid Interactions

DAVID L. SCHWINKE, M. G. GANESAN, and N. D. WEINER ˣ

Received December 28, 1981, from the *College of Pharmacy, University of Michigan, Ann Arbor, MI 48109.* Accepted for publication April 30, 1982.

Abstract □ The interactions between insulin and various lipids were studied by monolayer penetration experiments at constant surface area. The increase in surface pressure, $\Delta\Pi$, of a lipid film depended upon the particular lipid used and the concentration of insulin in the subphase. For all lipids studied, $\Delta\Pi$ was dependent on the initial surface pressure of the lipid film. Evidence of the interaction between insulin and the lipids was found in the ability of insulin to penetrate lipid films with initial pressures >16 dynes/cm, the maximum surface pressure obtained by insulin alone. For phospholipids, both the nonpolar and polar regions influenced the degree of interaction with insulin. Saturated chain lecithins exhibited less penetration than phospholipids with unsaturated hydrocarbon chains. The net charge of the lipid was not found to be an important determinant of penetration; however, the structure of the polar group can have a dramatic effect. Insulin penetration of mixed lipid films cannot be predicted by the penetration characteristics of the pure components. The possible role of these interactions in determining the geography of the insulin molecule within the liposome and its resultant effects on the stability is discussed.

Keyphrases □ Insulin—monolayer studies of interactions with lipids □ Monolayer studies—insulin–lipid interactions □ Lipids—monolayer studies of interactions with insulin

Monolayer interactions between proteins and lipids are of much interest in the study of cell membrane structure (1, 2), hormonal action (3, 4), and enzyme activity (5). Early studies (6) established the technique of injecting a protein into the subphase beneath a lipid film at constant surface area. Since then modifications of this procedure have been used in an effort to gain a more detailed understanding of the nature of these interactions.

Recent attempts to develop an oral dosage form of insulin have utilized liposomal entrapment in order to protect the hormone from proteolytic degradation in the GI tract. In theory, to achieve the necessary degree of protection, the entrapped insulin should not penetrate or decrease the stability of the lipid bilayer. The geography of the insulin molecule within the liposome should be dependent upon the degree and type of its interactions with the lipid components. This report investigates the interactions of insulin with cholesterol, stearylamine, and various phospholipids through the use of monolayer penetration studies.

BACKGROUND

The increase in surface pressure of a lipid film with the addition of protein has been termed penetration, although the exact nature of this phenomenon remains unclear. For example, as more protein is added to the subphase, the increase in surface pressure may be attributed to an increase in the number of protein molecules at the surface, enhanced interaction between the surface components, or protein–protein interactions just below the surface, which may alter molecular orientation at the surface. Although the various mechanisms cannot always be differentiated, the results of such penetration studies are still of value in determining the criteria that affect lipid–protein interactions.

The great variation in the behavior of lipid–protein films reported in the literature can be ascribed to the wide range of physical properties of the proteins used. The unique characteristics of each protein or polypeptide prevent accurate predictions of the nature and magnitude of its interactions with lipids. Also, relative protein penetration does not show consistent results based on the type of lipid involved. Therefore, it is necessary to individually assess the effect of insulin on films of pure lipids or lipid mixtures in order to better understand their interactions.

0022-3549/83/0300-0244$01.00/0

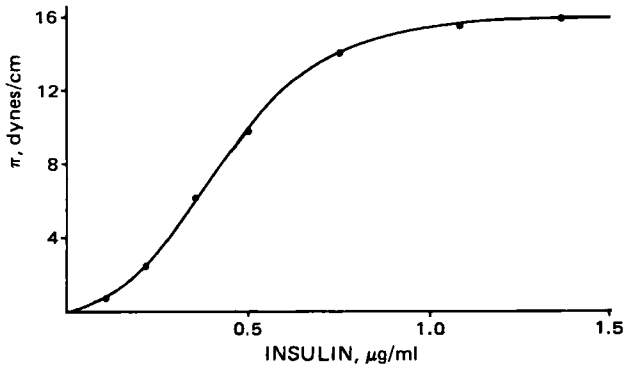

Figure 1—*The surface pressure–concentration profile of insulin upon injection into 0.05* M N-*2-hydroxyethylpiperazine-*N′*-2-ethanesulfonic acid in 0.9% NaCl buffer, pH 7. The surface pressure was measured 30 min after each insulin addition. A limiting or collapse pressure for insulin of 16 dynes/cm was observed.*

EXPERIMENTAL

Phosphatidylcholine[1] (I) was purified on an activated alumina column. Cholesterol[2] was purified by recrystallizing three times from ethanol solution. All other lipids were used as supplied[2] and stored at 0°. TLC of all lipids revealed a single spot.

The subphase buffer was prepared from triple-distilled water, the second distillation was from alkaline permanganate. An all-glass distillation apparatus was used to prevent contamination. Sodium chloride, reagent grade, was heated to 600° to remove organic impurities. All other chemicals were reagent grade.

Research grade crystalline porcine insulin[3] with an activity of 28.5 units/mg and containing 0.6% zinc was used. The only impurity noted by polyacrylamide gel electrophoresis and high-performance liquid chromatographic (HPLC) analysis was 1–2% monodesamido insulin. Stock solutions of 4.0 mg/ml were prepared in 0.01 *N* HCl and stored at 4°. Further dilutions were prepared in 0.05 *M* *N*-2-hydroxyethylpiperazine-*N*′-2-ethanesulfonic acid in 0.9% NaCl buffer, pH 7. The glass vials used for these dilutions were rinsed twice with the insulin solution to avoid loss of insulin due to adsorption.

The monolayer penetration studies were a modification of previous studies (6). The experiments were performed at 25 ± 1° on a surface tensiometer[4] having a sensitivity of 0.04 dynes/cm, using a sandblasted platinum Wilhelmy plate. The subphase consisted of 90 ml of 0.05 *M* *N*-2-hydroxyethylpiperazine-*N*′-2-ethanesulfonic acid in 0.9% NaCl buffer, pH 7, contained in a circular polytetrafluoroethylene dish having an area of 46 cm^2. A polytetrafluoroethylene-coated magnetic stirrer was used for mixing of the subphase. The entire apparatus was enclosed to reduce airborne contamination.

All lipids were spread from solutions of hexane–ethanol (9:1) in a micrometer syringe[5] in amounts sufficient to produce the desired initial surface pressure. Each mixed lipid film was spread from a single solution in which the appropriate lipids were dissolved. The addition of the spreading solvent alone to a clean buffer surface produced no measurable change in surface tension. The dissolved lipids were stored below 0° under a dry nitrogen atmosphere for no longer than 5 days.

A stationary needle with a removable glass syringe was used to deliver concentrated insulin solutions beneath the surface into the subphase. Insulin was added in 1–2-ml increments, and an equal volume of the subphase was discarded prior to the additions. The needle and syringe were rinsed three times after each addition of insulin by withdrawing and reinjecting 1–2 ml of the subphase. A magnetic stirrer (10 rpm) mixed the subphase for 15 min, and the mixture was allowed to settle for 15 min for the monolayer to equilibrate before recording the surface tension. Surface pressure changes due to insulin addition were found to be virtually complete within 30 min.

Surface pressure (Π) was calculated as the difference in surface tension in the absence of the film (γ_0 = 72.3 dynes/cm) and that of the film-covered surface (γ). The change in surface pressure ($\Delta\Pi$) was calculated as the difference in pressure of the lipid film upon injection of insulin into the subphase (Π) and that of the film in the absence of insulin, *i.e.*, at its initial surface pressure (Π_0).

[1] Egg lecithin, Type IX-E, Sigma Chemical Co., St. Louis, Mo.
[2] Sigma Chemical Co., St. Louis, Mo.
[3] Lilly Research Laboratories, Indianapolis, Ind.
[4] Rosano Surface Tensiometer, VWR Scientific.
[5] Agla; Wellcome Reagents Ltd., Beckenham, U.K.

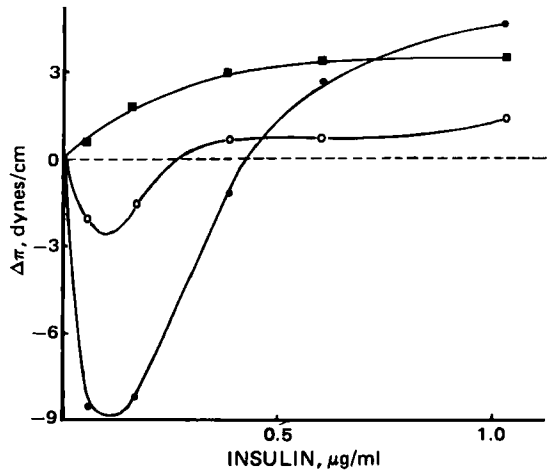

Figure 2—*The time-dependent changes in surface pressure of phosphatidic acid (II) monolayers upon the injection of insulin into the subphase. Each curve represents a film with an apparent initial surface pressure of ~13 dynes/cm. The delay times that followed the spreading of the films before the start of the experiments are as follows: (●) no delay; (○) 60 min; (■) 120 min. In control studies the surface pressure of films of II required 120 min to attain a stable value, which then remained constant for at least 3 hr.*

RESULTS

The insulin protein, although soluble in aqueous solutions, is a surface-active molecule denaturing at the air–water interface to give rise to surface pressures as high as 20 dynes/cm (7). Under the conditions of these experiments, the surface pressure–concentration (Π–*C*) curve of insulin approached a limiting or collapse pressure of 16 dynes/cm at pH 7, as seen in Fig. 1. This is in agreement with the collapse pressure obtained from the Π–*A* isotherms in a previous study (7) for insulin at pH 7.4.

The stability of the lipid films for the duration of the experiments (~3 hr) was confirmed by measuring the surface pressure as a function of time. With most of the lipids studied, a constant surface pressure was obtained within 15 min after spreading. However, with phosphatidic acid (II), phosphatidylserine (III), dipalmitoylphosphatidylcholine (VI), and distearoylphosphatidylcholine (VII) a slow decrease in surface pressure was observed for 1–2 hr, followed by constant values for at least 3 hr thereafter. Recognizing this time effect is important in obtaining accurate

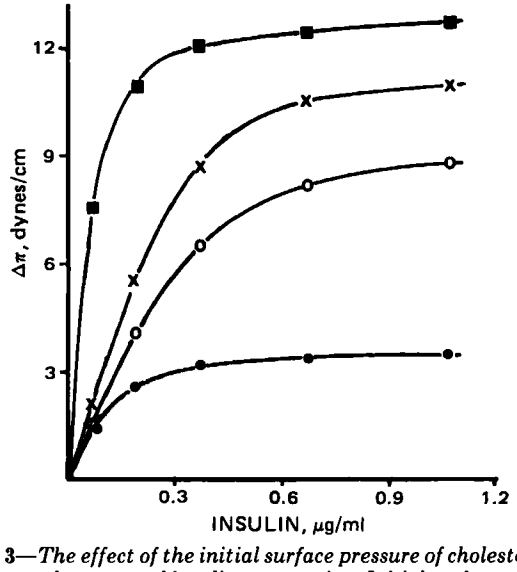

Figure 3—*The effect of the initial surface pressure of cholesterol monolayers on the extent of insulin penetration. Initial surface pressures (dynes/cm) are: (■) 4.8; (×) 11.1; (○) 15.8; (●) 19.5. This set of curves is qualitatively similar to those of all lipids studied in these experiments.*

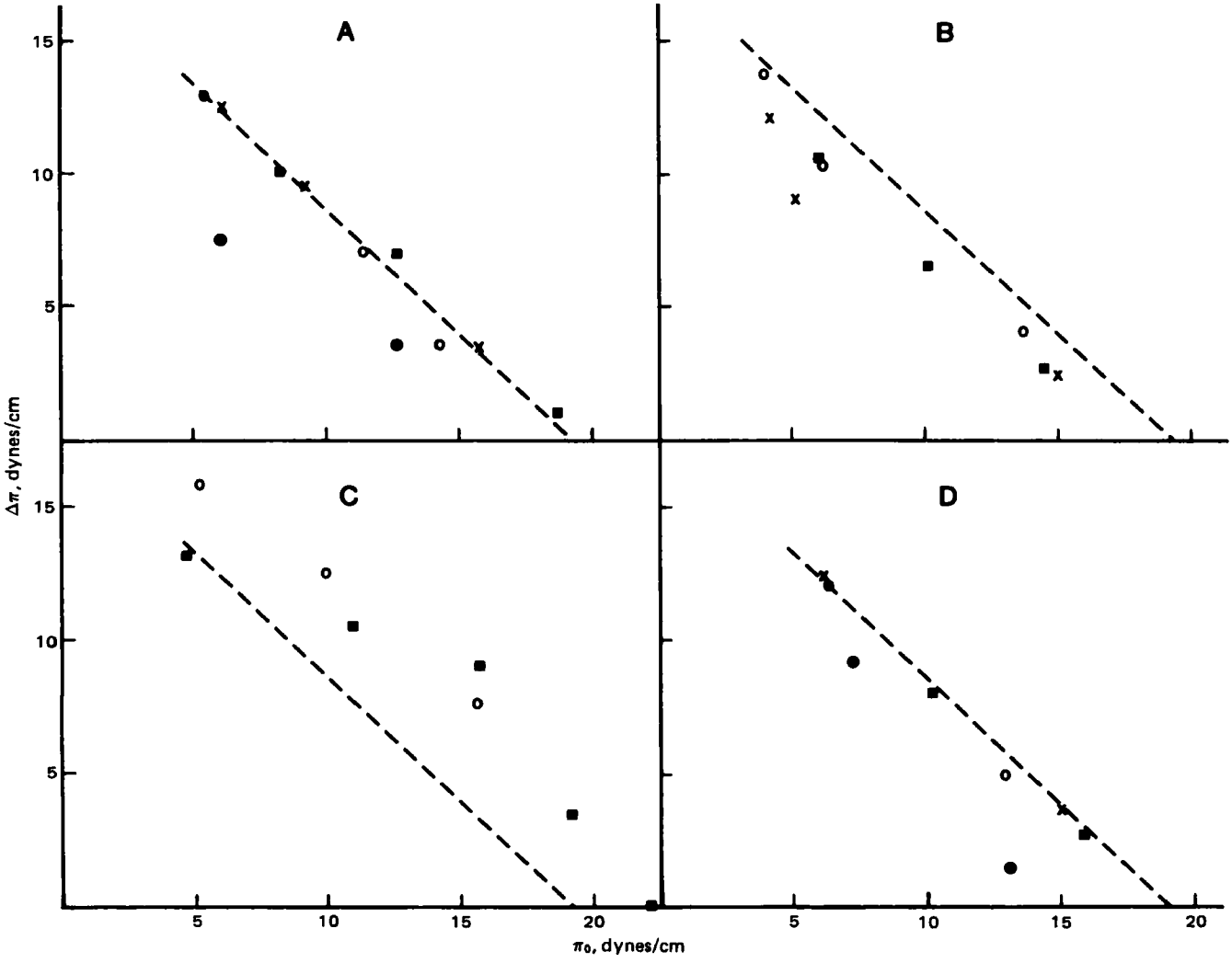

Figure 4—*Penetration of insulin (1.0 μg/ml) into monolayers of various lipids. Key: (A) unsaturated phospholipids: (■) phosphatidylcholine (I); (●) phosphatidic acid (II); (○) phosphatidylserine (III); (×) phosphatidylinositol (IV); (B) saturated lecithins: (■) dimyristoyl-(V); (×) dipalmitoyl-(VI); (○) distearoylphosphatidylcholine (VII); (C) other lipids: (■) cholesterol; (○) stearylamine; (D) mixed lipid films: (■) phosphatidylcholine–cholesterol (2:1) (VIII), (×) phosphatidylcholine–cholesterol–phosphatidic acid (4:2:1) (IX); (○) phosphatidylcholine–cholesterol–stearylamine (4:2:1) (×); (●) dipalmitoylphosphatidylcholine–cholesterol (2:1) (XI).*

results. The most dramatic pressure drop was observed with II. Figure 2 depicts three $\Delta\Pi$–C curves for films of II, each of which had an apparent initial surface pressure of ~13 dynes/cm. As can be seen, if the lipid film is not given sufficient time to equilibrate prior to addition of insulin to the subphase, both the magnitude and the shape of the curve is affected. For example, at 0- and 60-min delays, an initial condensation effect was observed (decrease in surface pressure), whereas with a 120-min delay, only an expansion effect (increase in surface pressure) was seen.

Placing additional pure spreading solvent on a film of II after its pressure had stabilized resulted in virtually no pressure change after 10 min, indicating that solvent retention in the lipid film was not a problem. Another study (8) also reported no evidence of solvent retention with a hexane–ethanol (9:1) solvent in lecithin and phosphatidylethanolamine films when $\Pi_0 > 2$ dynes/cm.

Two of the saturated lecithins, VI and VII, also showed a slow decrease in surface pressure during the first hour after spreading. With respect to the equilibrium-spreading pressure, Πe, which is defined as the pressure at which the monolayer is in equilibrium with the bulk lipid phase (9), films of both of these lipids may be considered thermodynamically unstable. For lecithins, it has been determined that spreading from the bulk phase does not occur below the gel–liquid crystal transition temperature (T_c), hence, $\Pi_e = 0$ at temperatures below T_c (10). The values of T_c for VI and VII are 41 and 60°, respectively (11); therefore, their solvent-spread films at 25° are not at true thermodynamic equilibrium. The spread films, however, do maintain a constant surface pressure and thus can be considered metastable (8–10), since the attainment of equilibrium (collapsing of the monolayer to the gel state) is a slow process and does not occur within the time frame of the experiments.

For all lipids studied the degree of penetration or association of insulin into the monolayer, as measured by the magnitude of $\Delta\Pi$ (6), was very dependent on the initial surface pressure, Π_0, as is generally expected with insulin (12) and other proteins (6, 13–18). A greater degree of penetration was observed at lower Π_0 values as indicated both by the magnitude of $\Delta\Pi$ and the initial slope of the $\Delta\Pi$–C curves. Figure 3 shows a set of typical $\Delta\Pi$–C curves.

Plots of $\Delta\Pi$ *versus* Π_0 for the single component and mixed lipid films are shown in Fig. 4A–D. The data were obtained from $\Delta\Pi$–C curves for the various lipids at an insulin concentration of 1.0 μg/ml. For all lipids, the changes in $\Delta\Pi$ were virtually complete at this concentration of insulin. It was found that the lipids fell into three distinct groups based on the magnitude of $\Delta\Pi$. The first group (Fig. 4A, D), consisting of the unsaturated lipids I, III, and phosphatidylinositol (IV), and the mixed lipid films phosphatidylcholine–cholesterol (2:1) (VIII), phosphatidylcholine–cholesterol–phosphatidic acid (4:2:1) (IX), and phosphatidylcholine–cholesterol–stearylamine (4:2:1) (X), showed an intermediate degree of penetration by insulin. Their behaviors, as indicated by the dashed line, is included as a reference in these four plots. Cholesterol and stearylamine (Fig. 4C) form a second group of lipids characterized by enhanced penetration by insulin. The third group of lipids, those showing reduced or inhibited penetration, consists of the saturated lecithins dimyristoylphosphatidylcholine (V), VI, and VII (Fig. 4B), the unsaturated phospholipid II (Fig. 4A), and the mixed film of dipalmitoylphosphatidylcholine–cholesterol (2:1) (XI) (Fig. 4D). In all cases, $\Delta\Pi$ de-

creases with increasing values of Π_0 until at a critical Π_0 value, no pressure change is observed. This value of Π_0, where $\Delta\Pi = 0$ is termed the limiting Π (18). For the lipids in the second group a limiting Π of 19.2 dynes/cm was in close agreement with the value obtained previously (12) of 19 dynes/cm for phosphatidylcholine, stearyl alcohol, and stearic acid monolayers. For cholesterol, however, our limiting Π value of ~22 dynes/cm is lower than that of a previously derived value of 27 dynes/cm (12). Repeated trials with cholesterol films at pressures between 22 and 24 dynes/cm failed to show any response to insulin under our conditions.

Insulin, which is soluble in the subphase, is able to penetrate monolayers with an initial surface pressure greater than the collapse pressure of insulin alone (16 dynes/cm). This indicates that insulin is interacting in some manner with the lipids, and that the observed behavior is not merely competition for the surface by two different surface-active molecules.

The combined data for the three saturated lecithins (Fig. 4B) indicate a limiting Π value of 17.7 dynes/cm. The absence of double bonds in the acyl chains in these lecithins results in closer packing of their molecules at the air–water interface (15, 19) as compared with unsaturated lecithin (I). As a result, insulin penetration is reduced. The temperature at which the experiments were performed (25°) is above the gel–liquid crystal transition temperature of V (T_c = 23°) (11), but is below that of VI and VII as previously mentioned. The influence of this parameter alone was not found to be of great importance in determining the degree of insulin penetration in this monolayer system.

Of the three lipids (II, III, and IV) with a net negative charge, only II showed decreased penetration (Fig. 4A). Since all three lipids, like I, are unsaturated, it is likely that the structure of the polar group, not the charge, is a more important determinant of penetration. The positively charged stearylamine films enhanced penetration by insulin, which has a net negative charge of pH 7; this effect may be due to electrostatic interactions. However, direct comparisons between stearylamine and lecithin films are inappropriate due to gross structural differences.

The mixed lipid films showed some interesting behavior and, as expected, were unique with respect to their individual components. Although cholesterol is strongly interactive with both I and VI as shown by monolayer studies (19, 20), the addition of cholesterol to films of I did not change the degree of insulin penetration, whereas incorporation of cholesterol into films of VI significantly reduced the penetration of insulin into the mixed monolayer. In both negatively (IX) and positively (X) charged mixed films, the individual behavior of the charged lipid was not apparent and the films demonstrated penetration similar to that of films of VIII or I.

DISCUSSION

Previously published results on the penetration or association of various proteins with lipid monolayers have yielded few consistent patterns of behavior based on the type of lipid involved. Since proteins encompass a wide range of physical properties including net charge, structure, and hydrophobicity, it is reasonable to expect that their interactions with lipids will be dependent on the structure and orientation of the lipid. The present results, which indicate decreased penetration by insulin into films of saturated lecithins as compared with I were also observed for α-lactalbumin (14) and delipidated high-density lipoprotein (21). However, a previous study (22) reported that I and fully hydrogenated I showed identical penetration by rabbit IgG. With β-casein (17, 21) and a fraction of delipidated lipoprotein (17), more penetration was observed into saturated lecithins than into I. Cholesterol films have consistantly allowed greater penetration than films of I (12, 13, 22), which is also apparent from the results of the present study.

It is widely recognized that properties of the subphase can affect the interactions of proteins with lipid films. Variations in pH (6, 14, 16, 18), temperature (13), ionic strength (18, 23), and the method of introducing the lipid and protein at the surface (13) all determine, in part, the changes in the interfacial region.

The mechanism of protein penetration and interaction with lipid films remains a topic of current research. The structure of proteins in lipid films and bilayers is also receiving more attention as new and more powerful analytic methods become available. Early work (24, 25) suggested that various proteins, including insulin, formed two distinct layers under a lipid film. The first layer was said to consist of fully denatured protein interacting by an ionic mechanism with the choline residue of lecithins, with penetration into the film by hydrophobic side chains of the protein producing a change in surface pressure. Beneath this was adsorbed a second layer of native protein. A monolayer study of insulin (12) stressed that hydrophobic interactions control penetration. However, results here indicate that this is not the only factor.

Several mechanisms of monolayer and membrane interactions have been proposed (1, 13, 22, 26) with proteins dependent upon the nature of both the lipid and protein. In these studies the role of many factors, including protein hydrophobicity and flexibility, lipid compressibility, electrostatic interactions, and water structuring about the lipid polar groups, are discussed. Other reports (16–18, 21, 27) also conclude that lipid–protein interactions cannot be explained on the basis of hydrophobic or electrostatic mechanisms alone. The importance of lipid compressibility (6) has also been discussed in reports of film penetration experiments with β-casein and apoprotein (17). However, the contention that decreased compressibility due to the incorporation of cholesterol in a lecithin film (2, 15) should lead to decreased penetration was not apparent in several of the mixed films which were studied. Measurements of the surface concentration of proteins indicate that $\Delta\Pi$ is not necessarily a measure of the amount of penetrating protein (22), and protein continues to adsorb beneath a film after a maximum in $\Delta\Pi$ has been attained (18, 27).

Monolayer penetration experiments are a valuable tool for exploring the interactions between lipids and proteins and can, with limitations, provide insight into the interactions occurring in liposomal systems (2, 8, 16, 17). We can conclude from our data that insulin is capable of some degree of penetration into lipid films, which can be controlled by the choice of lipid. Such penetration into the bilayer of a liposome may render the hormone susceptible to attack by proteases present in the external medium and also change the bilayer integrity. Saturated lecithins alone or in combination with cholesterol, which exhibit inhibited penetration, would be good candidates for liposomal delivery systems of insulin. These lipids would be better able to confine insulin within the aqueous compartments of the liposome than lipids that allow greater penetration.

Adsorption of insulin on the external and internal faces of the bilayer is also variable and can greatly affect the degree of entrapment. The incubation of liposomes in solutions of free insulin can result in the irreversible binding of the protein on the vesicle surface (28). Many reports of oral administration (29, 30) include externally bound insulin when calculating entrapped insulin and the administered dose. Upon oral administration, such insulin would be expected to undergo rapid destruction.

A better understanding of the underlying insulin–lipid interactions may aid in the design of an effective and reliable oral insulin dosage form.

REFERENCES

(1) G. Colacicco, *N.Y. Acad. Sci.*, **195**, 224 (1972).

(2) M. C. Phillips, D. E. Grahm, and H. Hauser, *Nature*, **254**, 154 (1975).

(3) M. S. Kafka and C. Y. C. Pak, *J. Colloid Interface Sci.*, **41**, 148 (1972).

(4) R. S. Snart and N. N. Sanyal, *Biochem. J.*, **108**, 369 (1968).

(5) D. G. Dervichian and J. P. Barque, *J. Lipid Res.*, **20**, 437 (1979).

(6) P. Doty and J. Schulman, *Discuss. Faraday Soc.*, **6**, 21 (1949).

(7) J. D. Arnold and C. Y. C. Pak, *J. Colloid Sci.*, **17**, 348 (1962).

(8) M. C. Phillips and D. Chapman, *Biochim. Biophys. Acta*, **163**, 301 (1968).

(9) G. L. Gaines, "Insoluble Monolayers at Liquid-Gas Interfaces," Interscience, New York, N.Y., 1966, p. 147.

(10) M. C. Phillips and H. Hauser, *J. Colloid Interface Sci.*, **49**, 31 (1974).

(11) D. Chapman, R. M. Williams, and B. D. Ladbrooke, *Chem. Phys. Lipids*, **1**, 445 (1967).

(12) K. S. Birdi, *J. Colloid Interface Sci.*, **57**, 228 (1976).

(13) G. Colacicco, M. M. Rapport, and D. Shapiro, *ibid.*, **25**, 5 (1967).

(14) I. Hanssens and F. H. VanCauwelaert, *Biochem. Biophys. Res. Commun.*, **84**, 1088 (1978).

(15) E. D. Goddard, "Monolayers," American Chemical Society, Washington, D.C., 1975, pp. 217–230.

(16) H. K. Kimelberg and D. Papahadjopolous, *Biochim. Biophys. Acta*, **233**, 805 (1971).

(17) M. C. Phillips, H. Hauser, R. B. Leslie, and D. Oldani, *ibid.*, **406**, 402 (1975).

(18) P. J. Quinn and R. M. C. Dawson, *Biochem. J.*, **113**, 791 (1969).

(19) R. A. Demel, L. L. M. Van Deenen, and B. A. Pethica, *Biochim. Biophys. Acta*, **135**, 11 (1967).
(20) F. Muller-Landau and D. A. Cadenhead, *Chem. Phys. Lipids*, **25**, 315 (1979).
(21) M. A. F. Davis, H. Hauser, R. B. Leslie, and M. C. Phillips, *Biochim. Biophys. Acta*, **317**, 214 (1973).
(22) G. Colacicco, *Lipids*, **5**, 636 (1970).
(23) A. Khaiat and R. Miller, *Biochim. Biophys. Acta*, **183**, 309 (1969).
(24) D. D. Eley and D. G. Hedge, *J. Colloid Sci.*, 11, 445 (1956).
(25) D. D. Eley and D. G. Hedge, *Discuss. Faraday Soc.*, **21**, 221 (1956).
(26) G. Colacicco, *J. Colloid Interface Sci.*, **29**, 345 (1969).
(27) P. J. Quinn and R. M. C. Dawson, *Biochem. J.*, **116**, 671 (1970).
(28) B. Solomon, S. Inserpi, and I. R. Miller, *Biochim. Biophys. Acta*, **600**, 931 (1980).
(29) H. M. Patel and B. E. Ryman, *FEBS Lett.*, **62**, 60 (1976).
(30) G. Dapergolas and G. Gregoriadis, *Lancet*. **ii**, 824 (1976).

ACKNOWLEDGMENTS

This research was supported by the Michigan Diabetes Research Training Center, sponsored by the NIH National Institute of Arthritis, Diabetes, and Digestive and Kidney Disease, Grant No. 5 P60 AM20572.

Dr. David L. Schwinke wishes to thank the American Foundation for Pharmaceutical Education for their gracious support of his graduate studies. The authors also wish to thank Dr. George Zografi for his valuable suggestions during the preparation of this manuscript.

Bilirubin-Displacing Effect of Ampicillin, Indomethacin, Chlorpromazine, Gentamicin, and Parabens *In Vitro* and in Newborn Infants

ROLF BRODERSEN *x **and FINN EBBESEN** ‡

Received November 23, 1981, from the *Department of Biochemistry, University of Aarhus, DK-8000 Aarhus C, and the ‡Department of Neonatology, Rigshospitalet, DK-2100 Copenhagen φ, Denmark. Accepted for publication April 30, 1982.

Abstract □ Displacement of bilirubin bound to human serum albumin by ampicillin, indomethacin, chlorpromazine, gentamicin, methylparaben, and propylparaben was investigated quantitatively. Two methods were used *in vitro*: measurement of bilirubin displacement by studying the rate of bilirubin oxidation with hydrogen peroxide and peroxidase and determination of the albumin reserve for binding of bilirubin by observation of the dialysis rate of an added trace amount of a deputy ligand monoacetyldapsone (*p*-acetamido-*p'*-aminodiphenyl sulfone). The latter method was also used for the determination of the albumin reserve in sera from treated newborn infants. The following doses were given: ampicillin, 100 mg/kg iv; indomethacin, 0.2 mg/kg iv; chlorpromazine hydrochloride, 0.7 mg/kg im; gentamicin sulfate, 2.5 mg/kg im. The parabens were present in injectable preparations of chlorpromazine and gentamicin and were therefore given in the following doses: methylparaben, 0.35 mg/kg, and propylparaben, 0.05 mg/kg. All drugs were given in a single dose. A few additional additives and metabolites were studied *in vitro*. Ampicillin, given to 19 infants, produced a small, significant decrease in plasma albumin reserve, to 82% of the pretreatment level and, thus, had a slight bilirubin-displacing effect, quantitatively consistent with a weak displacing effect measured *in vitro*. None of the other substances showed any measurable displacement *in vivo*, likewise in agreement with the results from *in vitro* studies.

Keyphrases □ Bilirubin—displacing effect of ampicillin, indomethacin, chloropromazine, gentamicin, and parabens, *in vitro* and in newborn infants □ Ampicillin—bilirubin-displacing effects of indomethacin, chlorpromazine, gentamicin, and parabens, *in vitro* and in newborn infants □ Indomethacin—bilirubin-displacing effects of ampicillin, chlorpromazine, gentamicin, and parabens, *in vitro* and in newborn infants □ Chlorpromazine—bilirubin-displacing effects of ampicillin, indomethacin, gentamicin, and parabens, *in vitro* and in newborn infants □ Gentamicin—bilirubin-displacing effects of ampicillin, indomethacin, chlorpromazine, and parabens, *in vitro* and in newborn infants □ Parabens—bilirubin-displacing effects of ampicillin, indomethacin, chlorpromazine, and gentamicin, *in vitro* and in newborn infants

A few drugs, notably sulfonamides, are capable of occupying the bilirubin-binding capacity of albumin in plasma, thereby increasing the risk of kernicterus in icteric human neonates (1, 2) as well as in experimental animals (3). Studies of such binding interactions *in vitro* have indicated displacing effects of ampicillin (4), indomethacin (4), some antimicrobial additives (parabens and sodium benzoate) (4–6) and chlorpromazine (7). Gentamicin in itself does not interfere with binding of bilirubin to albumin but is marketed with displacing additives (8). Measurement of the rate of dialysis of an added trace amount of monoacetyldapsone (I) into an otherwise identical plasma sample without this additive has recently been introduced as a technique for quantitative studies of occupation of albumin by drugs (9). Compound I serves as a deputy ligand for bilirubin, since one molecule of I competes selectively with binding of one molecule of bilirubin to human albumin (10). Determinations in undiluted sera at 37° are possible with this technique. Drug effects can thus be studied quantitatively *in vivo* as well as *in vitro*.

Previous work (11, 12) has shown that the concentration of free bilirubin in plasma may return quickly to the pretreatment level after administration of a bilirubin-displacing drug. Since there are no suitable methods for measuring the free bilirubin concentration in undiluted samples of infant serum (often hemolytic) at body temperature, it was decided to base the present *in vivo* studies on a combination of three measurements: determinations of albumin, bilirubin (bound), and albumin reserve in serum samples obtained before giving a single dose of the drug and at one point of time thereafter. The theoretical basis for this principle will be discussed, and the drugs mentioned will be tested accordingly.

EXPERIMENTAL

Human serum albumin[1] was obtained in the lyophilized state with its natural content of fatty acids and was used as a standard in albumin and

[1] AB Kabi, Stockholm, Sweden.

0022-3549/83/0300-0248$01.00/0

(19) R. A. Demel, L. L. M. Van Deenen, and B. A. Pethica, *Biochim. Biophys. Acta*, **135**, 11 (1967).
(20) F. Muller-Landau and D. A. Cadenhead, *Chem. Phys. Lipids*, **25**, 315 (1979).
(21) M. A. F. Davis, H. Hauser, R. B. Leslie, and M. C. Phillips, *Biochim. Biophys. Acta*, **317**, 214 (1973).
(22) G. Colacicco, *Lipids*, **5**, 636 (1970).
(23) A. Khaiat and R. Miller, *Biochim. Biophys. Acta*, **183**, 309 (1969).
(24) D. D. Eley and D. G. Hedge, *J. Colloid Sci.*, 11, 445 (1956).
(25) D. D. Eley and D. G. Hedge, *Discuss. Faraday Soc.*, **21**, 221 (1956).
(26) G. Colacicco, *J. Colloid Interface Sci.*, **29**, 345 (1969).
(27) P. J. Quinn and R. M. C. Dawson, *Biochem. J.*, **116**, 671 (1970).
(28) B. Solomon, S. Inserpi, and I. R. Miller, *Biochim. Biophys. Acta*, **600**, 931 (1980).
(29) H. M. Patel and B. E. Ryman, *FEBS Lett.*, **62**, 60 (1976).
(30) G. Dapergolas and G. Gregoriadis, *Lancet*. **ii**, 824 (1976).

ACKNOWLEDGMENTS

This research was supported by the Michigan Diabetes Research Training Center, sponsored by the NIH National Institute of Arthritis, Diabetes, and Digestive and Kidney Disease, Grant No. 5 P60 AM20572.

Dr. David L. Schwinke wishes to thank the American Foundation for Pharmaceutical Education for their gracious support of his graduate studies. The authors also wish to thank Dr. George Zografi for his valuable suggestions during the preparation of this manuscript.

Bilirubin-Displacing Effect of Ampicillin, Indomethacin, Chlorpromazine, Gentamicin, and Parabens *In Vitro* and in Newborn Infants

ROLF BRODERSEN *x **and FINN EBBESEN** ‡

Received November 23, 1981, from the *Department of Biochemistry, University of Aarhus, DK-8000 Aarhus C, and the ‡Department of Neonatology, Rigshospitalet, DK-2100 Copenhagen φ, Denmark. Accepted for publication April 30, 1982.

Abstract □ Displacement of bilirubin bound to human serum albumin by ampicillin, indomethacin, chlorpromazine, gentamicin, methylparaben, and propylparaben was investigated quantitatively. Two methods were used *in vitro*: measurement of bilirubin displacement by studying the rate of bilirubin oxidation with hydrogen peroxide and peroxidase and determination of the albumin reserve for binding of bilirubin by observation of the dialysis rate of an added trace amount of a deputy ligand monoacetyldapsone (*p*-acetamido-*p'*-aminodiphenyl sulfone). The latter method was also used for the determination of the albumin reserve in sera from treated newborn infants. The following doses were given: ampicillin, 100 mg/kg iv; indomethacin, 0.2 mg/kg iv; chlorpromazine hydrochloride, 0.7 mg/kg im; gentamicin sulfate, 2.5 mg/kg im. The parabens were present in injectable preparations of chlorpromazine and gentamicin and were therefore given in the following doses: methylparaben, 0.35 mg/kg, and propylparaben, 0.05 mg/kg. All drugs were given in a single dose. A few additional additives and metabolites were studied *in vitro*. Ampicillin, given to 19 infants, produced a small, significant decrease in plasma albumin reserve, to 82% of the pretreatment level and, thus, had a slight bilirubin-displacing effect, quantitatively consistent with a weak displacing effect measured *in vitro*. None of the other substances showed any measurable displacement *in vivo*, likewise in agreement with the results from *in vitro* studies.

Keyphrases □ Bilirubin—displacing effect of ampicillin, indomethacin, chloropromazine, gentamicin, and parabens, *in vitro* and in newborn infants □ Ampicillin—bilirubin-displacing effects of indomethacin, chlorpromazine, gentamicin, and parabens, *in vitro* and in newborn infants □ Indomethacin—bilirubin-displacing effects of ampicillin, chlorpromazine, gentamicin, and parabens, *in vitro* and in newborn infants □ Chlorpromazine—bilirubin-displacing effects of ampicillin, indomethacin, gentamicin, and parabens, *in vitro* and in newborn infants □ Gentamicin—bilirubin-displacing effects of ampicillin, indomethacin, chlorpromazine, and parabens, *in vitro* and in newborn infants □ Parabens—bilirubin-displacing effects of ampicillin, indomethacin, chlorpromazine, and gentamicin, *in vitro* and in newborn infants

A few drugs, notably sulfonamides, are capable of occupying the bilirubin-binding capacity of albumin in plasma, thereby increasing the risk of kernicterus in icteric human neonates (1, 2) as well as in experimental animals (3). Studies of such binding interactions *in vitro* have indicated displacing effects of ampicillin (4), indomethacin (4), some antimicrobial additives (parabens and sodium benzoate) (4–6) and chlorpromazine (7). Gentamicin in itself does not interfere with binding of bilirubin to albumin but is marketed with displacing additives (8). Measurement of the rate of dialysis of an added trace amount of monoacetyldapsone (I) into an otherwise identical plasma sample without this additive has recently been introduced as a technique for quantitative studies of occupation of albumin by drugs (9). Compound I serves as a deputy ligand for bilirubin, since one molecule of I competes selectively with binding of one molecule of bilirubin to human albumin (10). Determinations in undiluted sera at 37° are possible with this technique. Drug effects can thus be studied quantitatively *in vivo* as well as *in vitro*.

Previous work (11, 12) has shown that the concentration of free bilirubin in plasma may return quickly to the pretreatment level after administration of a bilirubin-displacing drug. Since there are no suitable methods for measuring the free bilirubin concentration in undiluted samples of infant serum (often hemolytic) at body temperature, it was decided to base the present *in vivo* studies on a combination of three measurements: determinations of albumin, bilirubin (bound), and albumin reserve in serum samples obtained before giving a single dose of the drug and at one point of time thereafter. The theoretical basis for this principle will be discussed, and the drugs mentioned will be tested accordingly.

EXPERIMENTAL

Human serum albumin[1] was obtained in the lyophilized state with its natural content of fatty acids and was used as a standard in albumin and

[1] AB Kabi, Stockholm, Sweden.

0022-3549/83/0300-0248$01.00/0

Table I—Pretreatment Data of the Patients [a]

	Number of Patients	Birth Weight, g	Gestational Age, days	Age at Injection, days	Plasma Concentrations, μM		
					Unconjugated Bilirubin	Reserve Albumin for Binding of I	Albumin
Ampicillin	19	2100 (1300–3680)	241 (218–286)	5 (1–27)	94 (12–160)	67 (23–141)	472 (365–531)
Indomethacin	6	1490 (810–2130)	222 (198–237)	15 (11–21)	72 (14–178)	44 (13–103)	509 (437–638)
Chlorpromazine, Methylparaben	6	3230 (2630–3620)	287 (274–307)	2 (1–28)	64 (11–130)	149 (88–307)	546 (495–604)
Gentamicin, Methylparaben, Propylparaben	14	2240 (1250–3350)	243 (199–291)	5 (1–23)	74 (14–172)	128 (34–278)	515 (399–592)

[a] Median; number in parentheses is the range.

albumin reserve determinations. Bilirubin[2] was purified according to a previous study (13). The drugs for *in vitro* studies were obtained commercially. The following solutions were used for injections: ampicillin[3], 1.0 g of the sodium salt was dissolved in 5 ml of sterile water. Indomethacin[4]; 20 mg dissolved in 2 ml of sterile water. Chlorpromazine[5] was obtained as an injectable solution containing 2.0 mg of chlorpromazine hydrochloride and 1.0 mg/ml of methylparaben. Gentamicin[6] injectable solution contained 10 mg of gentamicin sulfate, 1.3 mg of methylparaben, 0.2 mg of propylparaben, and 3.2 mg of sodium pyrosulfite/ml.

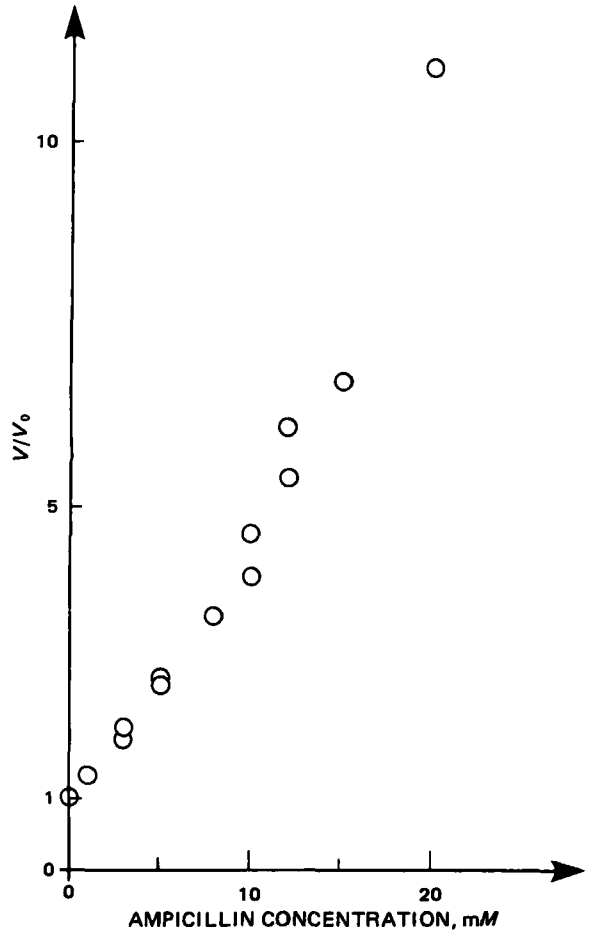

Figure 1—*Rate of oxidation of bilirubin with hydrogen peroxide and horseradish peroxidase in a solution containing 30 μM of human serum albumin and 15 μM of bilirubin as a function of varying concentrations of ampicillin (abscissa). The ordinates are oxidation rates relative to the rate without ampicillin. Sodium phosphate buffer, 66 mM, pH 7.4, 37°.*

[2] Sigma Chemical Co., St. Louis, Mo.
[3] Anhypen, Gist-Brocades, Delft, Netherlands.
[4] Indometacin, Dumex Ltd., Copenhagen, Denmark.
[5] Klorpromazin, DAK Laboratories, Copenhagen, Denmark.
[6] Garamycin, Schering Corp., Kenilworth, N.J.

Bilirubin-displacing effects of the drugs were studied *in vitro* by the following two techniques. The increase of free bilirubin dianion concentration in pure solutions of albumin and bilirubin with the addition of varying concentrations of the drugs was measured by the rate of bilirubin oxidation with hydrogen peroxide and horseradish peroxidase, as previously described (14) at pH 7.4, 37°. None of the drugs studied inhibited the peroxidase process in the absence of albumin. The amount of available albumin after addition of the drug was measured by the rate of dialysis of I, added in low concentration, into an identical volume of the same solution without added I (9). This method was used in its micromodification (10) with ^{14}C-labeled I and with 20-μl compartment volumes of the dialysis chambers. One volume of 0.53 *M* sodium phosphate buffer was added to 15 volumes of the sample to obtain a pH close to 7.4. The temperature was 37°, dialysis time was 10 min. The latter technique was used for studies with pure solutions of albumin as well as with infant serum, in both cases with drugs added in varying concentrations.

The following patients were used for investigations *in vivo*. Nineteen newborn infants suspected of having sepsis were given ampicillin, 100 mg iv/kg of body weight. Six newborn, preterm infants with patent ductus arteriosus received indomethacin, 0.2 mg/kg iv. Six newborns with narcotic withdrawal syndrome were given chlorpromazine hydrochloride, 0.7 mg/kg im. Fourteen newborn infants suspected of having sepsis were

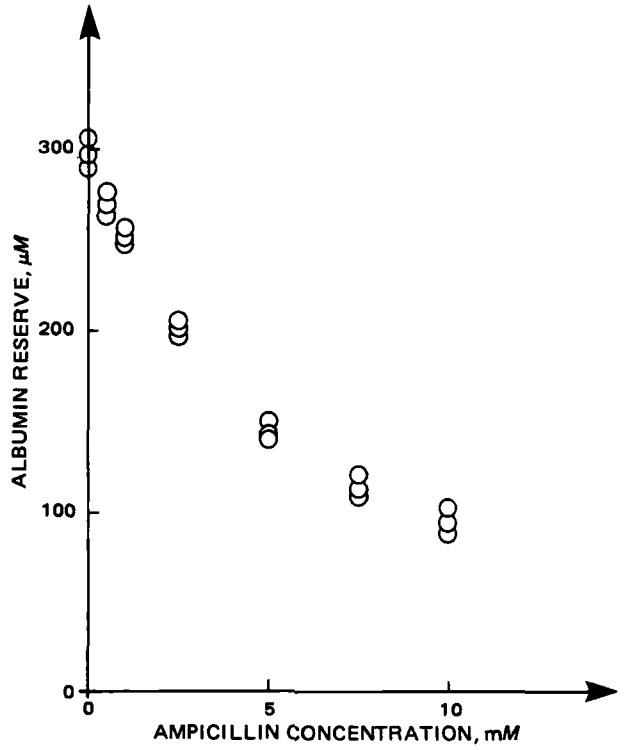

Figure 2—*Reserve albumin concentration for binding of I (ordinates), determined by measuring the rate of dialysis of an added trace amount of [^{14}C]I through a membrane into another compartment containing the same sample without added I. The sample was a solution of human serum albumin, 300 μM, varying concentrations of ampicillin (abscissa). Buffer and temperature as in Fig. 1.*

Table II—Displacing Effects *In Vitro*

	Displacing Drug Concentration					
	Peroxidase Method[a]		Monoacetyldapsone (I) Method[b]		Maximum Drug Concentration in Plasma[c]	
	μM	mg/liter	μM	mg/liter	μM	mg/liter
Ampicillin	3100	1100	4800	1700	5600	1950
Indomethacin	30	11	350	125	11	4
Chlorpromazine	5	1.6	1200	380	39	12
Gentamicin	>5000	>2000	>5000	>2000	111	50
Methyl *p*-hydroxybenzoate	18	2.7	1200	180	44	7
Propyl *p*-hydroxybenzoate	19	3.4	350	65	5	0.9
Sodium *p*-hydroxybenzoate	13	2.1	>2000	>320	44	7
Benzyl alcohol	4000	432	20,000			
Sodium benzoate	600	90	2200			
Sodium hippurate	500	100	750			
Sulfisoxazole	52	14	450			

[a] Concentration doubling rate of oxidation of bilirubin with H_2O_2 and peroxidase (test system contains human serum albumin, 30 μM, and bilirubin, 15 μM). [b] Drug concentration doubling rate of dialysis of I (test system contains human serum albumin, 300 μM, and I, 3 μM). [c] Drug concentration if dose were distributed in infant's plasma volume.

given gentamicin sulfate, 2.5 mg/kg im. Pretreatment data of the patients are summarized in Table I.

Capillary blood samples were obtained by heel prick. One sample was taken immediately before the administration of a single dose of the drug. A second sample was obtained 15 min after giving the intravenously injected drugs and 30 min after those given intramuscularly.

Total unconjugated bilirubin was determined in serum by a modification (15) of a previous method (16). This method was chosen under the assumption that it is more specific than the diazo method. Fifty microliters of serum and 1250 μl of acetone were mixed and centrifuged, thereafter the absorbance of the supernatant was measured at absorption maximum 454 nm[7]. Purified bilirubin (13), dissolved in 0.1*M* potassium cyanide in formamide (17) and added to human serum, was used for the standardization. The coefficient of variation of the analysis was 2% by duplicate determinations.

Albumin was determined in serum by an electrophoretic method (18). The coefficient of variation of the analysis was 3% by duplicate determinations.

The concentration of reserve albumin for binding of I was determined in serum samples from the patients as mentioned above. By triplicate determinations, the coefficient of variation of the analysis was 5–6%, the intraday coefficient of variation being 4–5%.

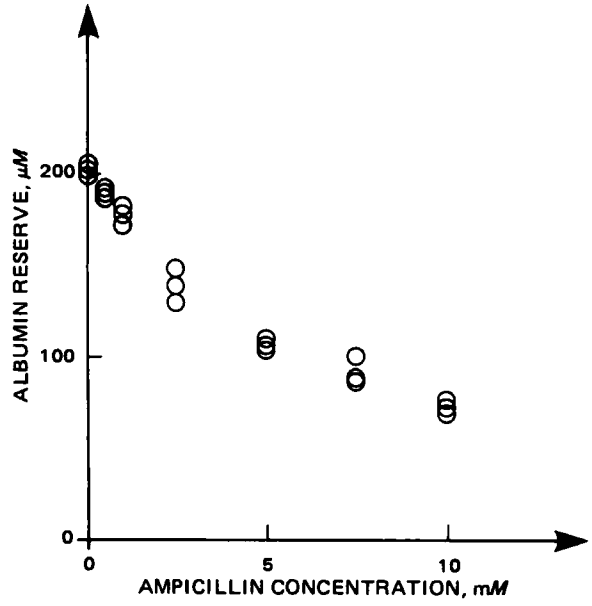

Figure 3—*Reserve albumin concentration for binding of I, determined as in Fig. 2 but in pooled infant (umbilical cord) sera with varying concentrations of added ampicillin, pH 7.4, 37°. Albumin concentration in the infant serum was 500 μM, nonesterified fatty acids, 460 μM. Note that the albumin reserve for binding of I, and thereby for binding of bilirubin, is only 40% of the total albumin concentration and in agreement with previous findings (19).*

[7] Zeiss PM2D spectrophotometer.

Statistical analyses were performed using the *t* test for paired observations. Ninety-five percent confidence limits for the true change in the plasma concentrations of unconjugated bilirubin, reserve albumin, and albumin, have been calculated from the formula: Confidence limits = $\bar{x} \pm t_{0.975} \times SD/\sqrt{n}$, where $t_{0.975}$ is the 97.5 percentile of the *t* distribution with $n - 1$ degrees of freedom.

Informed consent was obtained from the mothers of all infants included in the study.

RESULTS

***In Vitro* Studies**—All drugs and additives except gentamicin, showed some degree of bilirubin displacement (Table II, Figs. 1–3). Drug concentrations giving a twofold increase of oxidation rate in the peroxidase method, and a twofold increase of dialysis rate in the I method, are reported. In both techniques this ideally should be the concentration of drug needed to establish a binding equilibrium in which half of the vacant albumin capacity for binding of bilirubin is occupied by bound drug, increasing the free bilirubin concentration twofold. Major discrepancies are seen between the two methods and will be discussed later.

***In vivo* Studies**—Table III shows the observed changes in plasma concentrations of unconjugated bilirubin, reserve albumin for binding of I, and albumin, caused by a single injection of the four preparations studied.

Ampicillin, injected intravenously in a dose of 100 mg/kg, resulted in a significant decrease of average reserve albumin for binding of I by 18% in samples taken 15 min after the injection. The plasma albumin concentration remained unchanged, indicating that the decrease of reserve albumin was not caused by dilution of the infants' blood. It is noteworthy that the concentration of unconjugated bilirubin in the plasma was not influenced by injection of ampicillin. Individual values of reserve albumin concentrations for binding of I, obtained from plasma samples before and 15 min after giving ampicillin to 19 infants, are plotted in Fig. 4. The albumin reserve after treatment ranged from 62 to 100% of pretreatment levels. Unconjugated bilirubin and albumin concentrations remained unchanged.

The other preparations examined, indomethacin, chlorpromazine with methylparaben, and gentamicin with methylparaben and propylparaben, did not cause any change of the measured parameters.

DISCUSSION

Choice of Analytical Methods—Methods for the study of bilirubin-displacing effects of drugs *in vitro* and *in vivo* should measure either the free bilirubin dianion concentration or the reserve albumin for binding of bilirubin. Results should be obtained in quantitative terms, measurements should be performed in undiluted serum or plasma and at a pH and temperature the same as that of the patient. Techniques should be avoided in which the parameter to be measured is shifted by the addition of large amounts of binding dyes, by removal of bilirubin to agarose, or by attempted titration of albumin binding capacity with bilirubin, as previously discussed (20). The peroxidase method, whereby changes of free bilirubin dianion concentration are estimated by variations of the rate of oxidation with hydrogen peroxide and peroxidase (14), can be used for *in vitro* studies in pure solutions of albumin in low concentrations. False indications of displacement are, however, obtained

Table III—Changes in the Plasma Concentrations of Unconjugated Bilirubin, Reserve Albumin for Binding of I, and Albumin After a Single Dose of Ampicillin, Indomethacin, Gentamicin with Additives, and Chlorpromazine with Additive

	Changes in Plasma Concentrations					
	Unconjugated Bilirubin		Reserve Albumin for Binding of I		Albumin	
	Percent	μM[a]	Percent	μM[a]	Percent	μM[a]
Ampicillin	−2	−2 (−7, +2)	−18	−12 (−16, −8)[b]	0	0 (−12, +12)
Indomethacin	0	0 (−7, +7)	0	0 (−4, +3)	+1.0	+5 (−24, +33)
Chlorpromazine Methylparaben	0	0 (−6, +5)	+3	+5 (−12, +23)	−1.5	−8 (−21, +6)
Gentamicin Methylparaben Propylparaben	+1	+1 (−1, +3)	−1	−1 (−6, +4)	−0.6	−3 (−16, +10)

[a] Mean (95% confidence limits). [b] $p < 0.001$; all other changes are insignificant, $p > 0.05$.

with certain drugs, forming free radicals on oxidation, especially with some derivatives of phenol and phenothiazine (5, 7), as exemplified by the parabens and chlorpromazine. Also, due to the presence of hemoglobin, which has a peroxidase effect, the peroxidase method cannot be used in infant sera.

An alternative approach is determination of the concentration of albumin available for binding of bilirubin. In the presence of a displacing drug, the albumin reserve is generally decreased in the same proportion as the free bilirubin concentration is increased. A trace amount of a deputy ligand for bilirubin, I, is added to the sample, and the binding of this ligand is assessed by observing its rate of dialysis into a compartment containing the same sample without added I. The difficulties connected with determination of free bilirubin are obviated. On the other hand, individual drugs may displace I and bilirubin to different degrees due to differences of allosteric effects, a difficulty avoided in the peroxidase method where displacement of bilirubin itself is studied.

Results Obtained *In Vitro*—Table II shows considerable differences between results obtained for displacement of bilirubin with either of the two methods. These are explained by the above-mentioned free-radical effects, by possible differences of allosteric effects upon binding of bilirubin and I, and by the differences of albumin concentrations.

At equilibrium, half of the available albumin molecules will be occupied by a drug at a specific site when the concentration of free drug is equal to the inverse binding constant. The total drug concentration needed to obtain this comprises the concentrations of free drug, of drug bound to the specific site, and of drug bound to other sites on the albumin molecule. A higher albumin concentration was used in the I method than in the peroxidase test, and it was expected that half-saturation of the bilirubin site required a higher concentration of the drug in the former technique. The discrepancy could be avoided if equal concentrations of albumin were employed. This is not practical for routine purposes, since increased concentrations in the peroxidase method cause increased rates of unspecific oxidation reactions (7), while decreased concentrations in the I technique resulted in poor precision due to weak binding of I. Previous experience with sodium benzoate and other substances has shown, however, that identical results may be obtained if equal concentrations of albumin are used in both methods (9).

Ampicillin gave fairly consistent results in the two methods (Table II); the somewhat higher concentration of ampicillin needed to occupy half of the albumin in the I method is explained by the higher concentration of albumin. The dose of ampicillin injected during the *in vivo* studies would, if it were evenly distributed in the plasma volume of the infant, give a slightly higher concentration, as seen in the last column of Table II, and would thus occupy slightly more than half of the total amount of circulating albumin. Due to distribution of the drug into tissues, smaller degrees of occupation of albumin would be expected at 15 min after the injection. Distribution volumes for ampicillin, calculated from literature data (21), range from 8 to 12 times the plasma volume. It is thus theoretically conceivable that ampicillin, in a dose of 100 mg/kg iv, would occupy a fraction of the plasma albumin somewhere between 5 and 50%.

Indomethacin is bound firmly to albumin, and it seems likely that the higher concentration needed to occupy half of the albumin in the I method, when compared with the peroxidase results, can be explained by the higher albumin concentration in the former technique. The I method gave a more reliable basis for an estimate of the displacing effect *in vivo* and showed that larger amounts of indomethacin than given would be needed to occupy an appreciable fraction of the albumin. It was concluded that the dose of indomethacin was too small to cause any considerable bilirubin displacement.

Chlorpromazine gave a false indication of displacement in the peroxidase method, as previously reported (7), and again the I method must be relied upon. The dose given was too small to produce a significant displacement.

Gentamicin, in agreement with previous reports (8), did not occupy bilirubin-binding loci on the albumin molecule in any of the two tests and, therefore, was not expected to cause displacement.

The parabens, and their metabolite, *p*-hydroxybenzoic acid, again gave falsely high displacements in the peroxidase method. The doses given were apparently too low to cause displacement.

Benzyl alcohol and sodium benzoate are sometimes used as antimicrobial additives in injection medicines, and sodium benzoate is present in many foods, naturally or added. These substances and their metabolite, sodium hippurate, must be added in fairly high concentrations in the I technique in order to occupy half of the albumin. Excessive doses would probably be needed to produce a significant displacement. This is in agreement with results published previously (22).

Sulfisoxazole has been tested for comparison. Therapeutic plasma concentrations of this drug are in the range of ~800 μM, considerably in excess of the concentrations needed to occupy half of the albumin in both techniques. Sulfisoxazole should thus be capable of producing displacement *in vivo*, in agreement with clinical experience (1, 2).

Procedure for Testing *In Vivo*—Due to shortcomings in the *in vitro* methods, as discussed above, and due to possible displacing effects of drug metabolites, it may be necessary sometimes to test a drug *in vivo*. Some information can be obtained from experiments in Gunn rats, observing displacement by a fall of total bilirubin concentration in plasma after drug administration (3, 23) or by damage to Purkinje cells after drug-induced displacement of bilirubin into the central nervous system (24). However, species differences of drug metabolism and of binding to albumin prevent final conclusions from animal experiments. The ultimate test must be conducted in human patients.

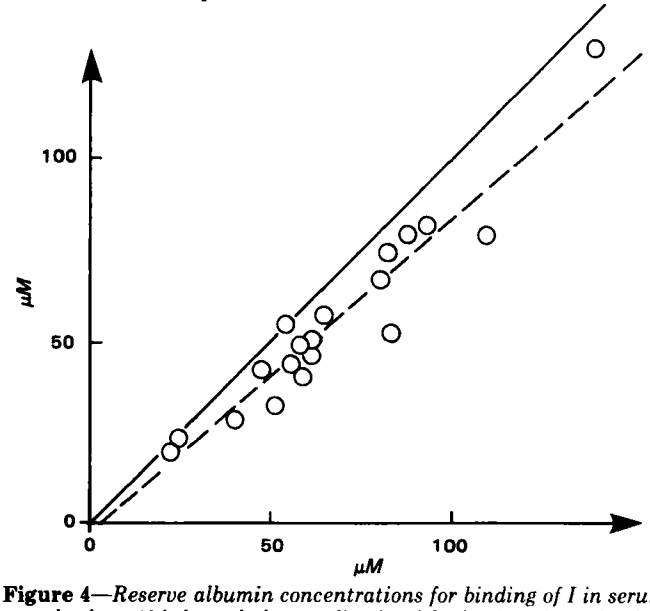

Figure 4—*Reserve albumin concentrations for binding of I in serum samples from 19 infants, before medication (abscissa), and 15 min after giving ampicillin (ordinate) by intravenous injection, dose 100 mg/kg. pH 7.4, 37°. A full line, x = y, is shown. The regression line, stippled, is y = 0.87x − 3 μM. The average decrease of reserve albumin concentration was 18% of the pretreatment level with 95% confidence limits, 12 and 24%. The average decrease was significant, p < 0.001, by paired t test.*

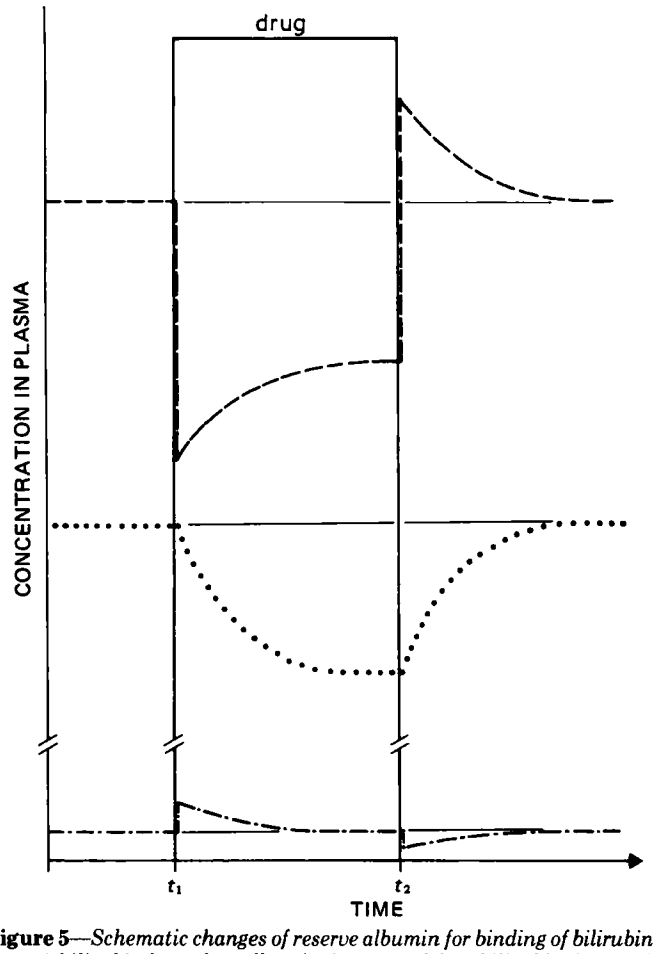

Figure 5—*Schematic changes of reserve albumin for binding of bilirubin (- - -) bilirubin bound to albumin (····), and free bilirubin (- · - · -) resulting from administration of a drug. A constant plasma concentration of the drug is hypothetically established during the interval of time from* t_1 *to* t_2.

The pharmacokinetic consequences of giving a displacing drug should be considered before a final choice of technique for *in vivo* studies is made. Wennberg and Rasmussen (25) have pointed out that "kernicterus may develop from bilirubin displaced during transient high serum concentrations of a competing drug." A theory has been worked out by Levy and Yacobi (11). As a consequence, the following train of events may be envisioned (Fig. 5). A steady state is thought to be present before the drug is given, with constant plasma concentrations of bound bilirubin, free bilirubin, and reserve albumin with a vacant capacity for binding of bilirubin. A constant concentration of the drug is established at the time t_1. The concentration of reserve albumin decreases immediately, since the binding capacity is partially occupied by the drug. This causes an immediate increase of free bilirubin concentration followed more slowly by transfer of bilirubin from plasma into tissues or to red blood cells, whereby the bound bilirubin concentration in plasma decreases. The reserve albumin increases with the decrease of bilirubin until a new steady state is established with the pretreatment level of free bilirubin and with decreased bound bilirubin and reserve albumin.

Such changes of free and bound bilirubin have been experimentally verified (12) after giving sulfisoxazole to rats, in which it was found that the free bilirubin concentration, after a sharp, transient increase, returned to its pretreatment value in spite of continued infusion of the displacing drug. If the drug is now removed instantly (time t_2), the concentration of reserve albumin will increase to above pretreatment level, resulting in a fall of free bilirubin which again will cause back-diffusion of bilirubin from tissues to plasma, leading to re-establishment of the original steady state.

These changes have not been experimentally verified and will be less acute when the drug level recedes gradually. It will, however, be theoretically possible to have normal or increased levels of reserve albumin when the drug concentration is declining. In this case, the bound bilirubin concentration will be below pretreatment value.

In conclusion, if a single blood sample is obtained after giving the drug, as in the present study, it will be possible to observe an unchanged level, either of bound bilirubin or of reserve albumin, even if the drug has caused displacement of bilirubin. However, unchanged concentrations of both bilirubin and reserve albumin cannot occur at the same time if a displacing drug was given. The concentration of bound bilirubin[8] as well as that of reserve albumin should be measured accordingly. In addition to this, determination of albumin should be done, since hemodilution by injection of the drug theoretically may cause low values of bound bilirubin and reserve albumin, imitating displacement of bilirubin. The sample should be obtained while the drug level is high. If all three concentrations (bound bilirubin, albumin, and reserve albumin), under these circumstances are unchanged by the medication, it may be concluded that bilirubin displacement was not observed.

Results Obtained *In Vivo*—After giving ampicillin, a small, statistically significant decrease of reserve albumin was observed (Table III, Fig. 4), indicating that a fraction of the available albumin binding capacity for bilirubin was occupied by this drug. The average occupancy observed, 18%, and the range of individual values is in good agreement with those expected from the *in vitro* tests.

Indomethacin, chlorpromazine, gentamicin, and the parabens did not cause any change of reserve albumin, total unconjugated bilirubin, or albumin concentrations and did not show displacing effects in the doses given (Table III). This again is consistent with expectations from *in vitro* results.

The practical significance of the bilirubin-displacing effect of ampicillin may be evaluated as follows. Effective plasma concentrations of ampicillin are usually considered to be in the range of 120–180 μM (40–60 μg/ml). These concentrations would cause a 3–5% increase of free bilirubin concentration, as measured by the peroxidase method (Fig. 1), using a low albumin concentration of 30 μM. The real displacement of bilirubin in plasma would be less. The I technique, applied to infant sera with varying added concentrations of ampicillin, shows that the reserve albumin concentrations would be decreased by 1.5–2.5% (Fig. 3), and the free bilirubin concentration would be increased by a similar percentage. This latter estimate seems to indicate a very small or insignificant increase of the risk of bilirubin encephalopathy, if weighted against the benefit obtained from the antibacterial effect of the drug. Somewhat higher degrees of displacement were seen in the present study; in one patient as much as 38% of available albumin for binding of I was occupied, presumably indicating an increase of free bilirubin concentration by a percentage of the same order of magnitude. In cases of threatening kernicterus, when such an increase of free bilirubin concentration may be unwanted, ampicillin could be given by slow injection, or by continuous infusion, thus avoiding significant occupation of albumin by the drug (26).

In previous rat experiments (12) the plasma concentration of unconjugated bilirubin dropped acutely to a lower level in <5 min after intravenous administration of a displacing drug. No change of bilirubin concentration was observed in the patients, in a sample taken 15 min after giving ampicillin. It might appear as if this finding could be taken as evidence against a bilirubin-displacing effect of ampicillin in human infants. Considerations of the rate of the expected decline of plasma bilirubin concentration show, however, that a measurable change could not be anticipated within 15 min, even after administration of a drug occupying half of the available albumin. The rats received a continuous infusion of bilirubin, regulated after a larger initial dose to a continuous rate of 100-fold that of normal bilirubin turnover in the rat, resulting in a high, constant concentration of unconjugated bilirubin in the plasma. The rate of infusion of bilirubin was 0.55 μmole/kg/min, the plasma bilirubin pool of the rats in the stationary state was ~7 μmoles/kg, and the turnover time of plasma bilirubin was thus ~13 min. However, in the infants, bilirubin turnover was of the order of 0.005 μmole/kg/min, and the total plasma bilirubin pool in the average patient was ~5 μmoles/kg (total unconjugated plasma bilirubin concentration, 94 μM, and plasma volume, 55 ml/kg), which gives a turnover time of ~1000 min for plasma bilirubin of the infants.

If a drug that occupies half of the available albumin is given to the infant one can expect that the free bilirubin concentration is doubled and that the rate of bilirubin removal from the plasma is doubled. This will result in a decline of the bound (and total) bilirubin concentration to a final value of ~50% of the pretreatment level. This decline would proceed slowly, with a rate constant of 0.001/min. In 15 min, the total bilirubin concentration would thus decline from 100 to 99.2 μM, an immeasurable

[8] The concentration of bound bilirubin for practical purposes is measured as that of total, unconjugated bilirubin, since the concentration of the free pigment is very low compared with the bound.

change. In addition, observation of such a slow change is precluded by the fact that the bound bilirubin concentration in these infants increases by an average of 2 μM/hr when no treatment is given. Observation of total plasma bilirubin concentrations alone, in consequence, cannot be used for estimating bilirubin-displacing effects of drugs, given to human infants. Measurement of the albumin reserve should be the main tool for this purpose. As shown above, plasma bilirubin and albumin concentrations should be measured in parallel. Unchanged values of all three parameters, observed at a point in time when the drug concentration in plasma is high, constitute evidence against a bilirubin-displacing effect.

These results underline the necessity of using quantitative methods for evaluation of bilirubin-displacing effects. Drugs cannot be rated as displacing or nondisplacing; dosage and plasma concentrations should be related to the displacing effect, expressed in quantitative terms. This method using monoacetyldapsone (I) seems feasible for such studies *in vitro* and *in vivo*.

REFERENCES

(1) W. A. Silverman, D. H. Anderson, W. A. Blanc, and D. N. Crozier, *Pediatrics*, **18**, 614 (1956).

(2) R. C. Harris, J. F. Lucey, and J. R. MacLean, *ibid.*, **20**, 875 (1958).

(3) L. Johnson, M. L. Garcia, E. Figueroa, and F. Sarmiento, *Am. J. Dis. Child.*, **101**, 322 (1961).

(4) R. Brodersen, in "Intensive Care in the Newborn," vol. 2, L. Stern, Ed., Masson, New York, N.Y., 1978, p. 331.

(5) L. F. Rasmussen, C. E. Ahlfors, and R. P. Wennberg, *J. Pediatr.*, **89**, 475 (1976).

(6) D. Schiff, G. Chan, and L. Stern, *Pediatrics*, **48**, 139 (1971).

(7) R. Brodersen, W. J. Cashore, R. P. Wennberg, C. E. Ahlfors, L. F. Rasmussen, and D. Shusterman, *Scand. J. Clin. Lab. Invest.*, **39**, 143 (1979).

(8) R. P. Wennberg and L. F. Rasmussen, *J. Pediatr.*, **86**, 611 (1975).

(9) R. Brodersen, *Acta Pharmacol. Toxicol.*, **42**, 153 (1978).

(10) R. Brodersen, S. Andersen, C. Jacobsen, O. Sønderskov, F. Ebbesen, W. J. Cashore, and S. Larsen, *Anal. Biochem.*, **121**, 395 (1982).

(11) G. Levy and A. Yacobi, *J. Pharm. Sci.*, **63**, 805 (1974).

(12) S. Øie and G. Levy, *ibid.*, **68**, 6 (1979).

(13) A. F. McDonagh and F. Assisi, *Biochem. J.*, **129**, 797 (1972).

(14) R. Brodersen, *J. Clin. Invest.*, **54**, 1353 (1974).

(15) R. Brodersen and J. Jacobsen, *Methods Biochem. Anal.*, **17**, 31 (1954).

(16) J. E. Mertz and C. D. West, *Am. J. Dis. Child.*, **91**, 19 (1956).

(17) R. Dybkær and H. Hertz, *Scand. J. Clin. Lab. Invest.*, **25**, 151 (1970).

(18) C. B. Laurell, *Anal. Biochem.*, **15**, 45 (1966).

(19) F. Ebbesen, *Acta Paediatr. Scand.*, **70**, 223 (1981).

(20) R. Brodersen, *Crit. Rev. Clin. Lab. Sci.*, **11**, 305 (1979).

(21) J. M. Kaplan, G. H. McCracken, and L. S. Horton, *J. Pediatr.*, **84**, 517 (1974).

(22) G. Nathenson, M. I. Cohen, and H. McNamara, *ibid.*, **86**, 799 (1975).

(23) R. Schmid, I. Diamond, L. Hammaker, and C. B. Gundersen, *Nature (London)*, **204**, 1041 (1965).

(24) W. A. Blanc and L. Johnson, *J. Neuropathol. Exp. Neurol.*, **18**, 165 (1959).

(25) R. P. Wennberg and L. F. Rasmussen, *J. Pediatr.*, **87**, 1007 (1975).

(26) S. Øie and G. Levy, *J. Pharm. Sci.*, **68**, 1 (1979).

ACKNOWLEDGMENTS

This study was supported by the Danish Medical Research Council (Grants Nos. 512-10626, 512-10767, and 512-15538), Nordisk Gjenforsikrings Selskabs Jubilæumsfond, and by Købmand i Odense Johann og Hanne Weimanns Legat.

The authors wish to thank Professor B. Friis-Hansen for advice and guidance during the study. [^{14}C]I was synthesized by C. Jacobsen. Inger Bonnevie, Signe Andersen, and Birthe Lindgaard are thanked for skillful technical assistance, and the staffs of the departments of Neonatology and Clinical Chemistry are thanked for helpful assistance.

Elementary Osmotic Pump for Indomethacin

F. THEEUWES *[x], D. SWANSON *, P. WONG *, P. BONSEN *, V. PLACE *, K. HEIMLICH [‡], and K. C. KWAN [‡]

Received January 22, 1982, from the **ALZA Corporation, Palo Alto, CA 94304* and [‡]*Merck Sharp & Dohme, Inc., West Point, PA.* Accepted for publication April 14, 1982.

Abstract □ Based on the principles of an elementary osmotic pump, systems were designed to deliver indomethacin in solution at a constant rate, Z, to contain a total amount of drug, M_t, and to deliver 80% of their content at time t_{80}. To allow selection of the optimal delivery rate into the body, three different prototypes were prepared with respective values for Z, M_t, and t_{80} of: 7 mg/hr, 85 mg, 11 hr; 9 mg/hr, 85 mg, 8 hr; and 12 mg/hr, 85 mg, 6 hr. These systems were found to deliver 70% of each system's contents at zero-order rates. Delivery rates were independent of pH, method of measurement, and stirring rate. In keeping with these results, the systems in the GI tract of dogs delivered at the same rate as *in vitro*, which qualifies the *in vitro* test as a bioanalogous method predictive of the *in vivo* performance of the dosage forms. Preliminary results in normal volunteers yielded similar urinary recoveries, while plasma profiles were different from each other and distinct from those following conventional capsules.

Keyphrases □ Indomethacin—design and preliminary evaluation of an oral osmotic delivery system, zero-order drug delivery □ Osmotic pump—oral, design and preliminary evaluation, indomethacin □ Drug delivery—design and preliminary evaluation of an oral osmotic delivery system containing indomethacin □ Anti-inflammatory agents—indomethacin, design and preliminary evaluation of an oral osmotic delivery system

The concept of continuous drug delivery that maintains the lowest delivery rate and that will elicit a therapeutic effect has much appeal. Intuitively, such a situation should represent the most efficacious use of the drug, while presenting a minimal risk of adverse reactions. Within certain prescribed constraints, theoretical analyses (1, 2) appear to favor dosing patterns that approach a constant *infusion*. However, direct experimental support for this hypothesis is limited (3). In part, this shortcoming may result from a lack of a practical way to deliver a suitable drug chronically and at a constant rate.

The recent development of an oral dosage form, based

0022-3549/83/0300-0253$01.00/0

change. In addition, observation of such a slow change is precluded by the fact that the bound bilirubin concentration in these infants increases by an average of 2 μM/hr when no treatment is given. Observation of total plasma bilirubin concentrations alone, in consequence, cannot be used for estimating bilirubin-displacing effects of drugs, given to human infants. Measurement of the albumin reserve should be the main tool for this purpose. As shown above, plasma bilirubin and albumin concentrations should be measured in parallel. Unchanged values of all three parameters, observed at a point in time when the drug concentration in plasma is high, constitute evidence against a bilirubin-displacing effect.

These results underline the necessity of using quantitative methods for evaluation of bilirubin-displacing effects. Drugs cannot be rated as displacing or nondisplacing; dosage and plasma concentrations should be related to the displacing effect, expressed in quantitative terms. This method using monoacetyldapsone (I) seems feasible for such studies *in vitro* and *in vivo*.

REFERENCES

(1) W. A. Silverman, D. H. Anderson, W. A. Blanc, and D. N. Crozier, *Pediatrics*, **18**, 614 (1956).

(2) R. C. Harris, J. F. Lucey, and J. R. MacLean, *ibid.*, **20**, 875 (1958).

(3) L. Johnson, M. L. Garcia, E. Figueroa, and F. Sarmiento, *Am. J. Dis. Child.*, **101**, 322 (1961).

(4) R. Brodersen, in "Intensive Care in the Newborn," vol. 2, L. Stern, Ed., Masson, New York, N.Y., 1978, p. 331.

(5) L. F. Rasmussen, C. E. Ahlfors, and R. P. Wennberg, *J. Pediatr.*, **89**, 475 (1976).

(6) D. Schiff, G. Chan, and L. Stern, *Pediatrics*, **48**, 139 (1971).

(7) R. Brodersen, W. J. Cashore, R. P. Wennberg, C. E. Ahlfors, L. F. Rasmussen, and D. Shusterman, *Scand. J. Clin. Lab. Invest.*, **39**, 143 (1979).

(8) R. P. Wennberg and L. F. Rasmussen, *J. Pediatr.*, **86**, 611 (1975).

(9) R. Brodersen, *Acta Pharmacol. Toxicol.*, **42**, 153 (1978).

(10) R. Brodersen, S. Andersen, C. Jacobsen, O. Sønderskov, F. Ebbesen, W. J. Cashore, and S. Larsen, *Anal. Biochem.*, **121**, 395 (1982).

(11) G. Levy and A. Yacobi, *J. Pharm. Sci.*, **63**, 805 (1974).

(12) S. Øie and G. Levy, *ibid.*, **68**, 6 (1979).

(13) A. F. McDonagh and F. Assisi, *Biochem. J.*, **129**, 797 (1972).

(14) R. Brodersen, *J. Clin. Invest.*, **54**, 1353 (1974).

(15) R. Brodersen and J. Jacobsen, *Methods Biochem. Anal.*, **17**, 31 (1954).

(16) J. E. Mertz and C. D. West, *Am. J. Dis. Child.*, **91**, 19 (1956).

(17) R. Dybkær and H. Hertz, *Scand. J. Clin. Lab. Invest.*, **25**, 151 (1970).

(18) C. B. Laurell, *Anal. Biochem.*, **15**, 45 (1966).

(19) F. Ebbesen, *Acta Paediatr. Scand.*, **70**, 223 (1981).

(20) R. Brodersen, *Crit. Rev. Clin. Lab. Sci.*, **11**, 305 (1979).

(21) J. M. Kaplan, G. H. McCracken, and L. S. Horton, *J. Pediatr.*, **84**, 517 (1974).

(22) G. Nathenson, M. I. Cohen, and H. McNamara, *ibid.*, **86**, 799 (1975).

(23) R. Schmid, I. Diamond, L. Hammaker, and C. B. Gundersen, *Nature (London)*, **204**, 1041 (1965).

(24) W. A. Blanc and L. Johnson, *J. Neuropathol. Exp. Neurol.*, **18**, 165 (1959).

(25) R. P. Wennberg and L. F. Rasmussen, *J. Pediatr.*, **87**, 1007 (1975).

(26) S. Øie and G. Levy, *J. Pharm. Sci.*, **68**, 1 (1979).

ACKNOWLEDGMENTS

This study was supported by the Danish Medical Research Council (Grants Nos. 512-10626, 512-10767, and 512-15538), Nordisk Gjenforsikrings Selskabs Jubilæumsfond, and by Købmand i Odense Johann og Hanne Weimanns Legat.

The authors wish to thank Professor B. Friis-Hansen for advice and guidance during the study. [^{14}C]I was synthesized by C. Jacobsen. Inger Bonnevie, Signe Andersen, and Birthe Lindgaard are thanked for skillful technical assistance, and the staffs of the departments of Neonatology and Clinical Chemistry are thanked for helpful assistance.

Elementary Osmotic Pump for Indomethacin

F. THEEUWES *[x], D. SWANSON *, P. WONG *, P. BONSEN *, V. PLACE *, K. HEIMLICH [‡], and K. C. KWAN [‡]

Received January 22, 1982, from the **ALZA Corporation, Palo Alto, CA 94304* and [‡]*Merck Sharp & Dohme, Inc., West Point, PA.* Accepted for publication April 14, 1982.

Abstract □ Based on the principles of an elementary osmotic pump, systems were designed to deliver indomethacin in solution at a constant rate, Z, to contain a total amount of drug, M_t, and to deliver 80% of their content at time t_{80}. To allow selection of the optimal delivery rate into the body, three different prototypes were prepared with respective values for Z, M_t, and t_{80} of: 7 mg/hr, 85 mg, 11 hr; 9 mg/hr, 85 mg, 8 hr; and 12 mg/hr, 85 mg, 6 hr. These systems were found to deliver 70% of each system's contents at zero-order rates. Delivery rates were independent of pH, method of measurement, and stirring rate. In keeping with these results, the systems in the GI tract of dogs delivered at the same rate as *in vitro*, which qualifies the *in vitro* test as a bioanalogous method predictive of the *in vivo* performance of the dosage forms. Preliminary results in normal volunteers yielded similar urinary recoveries, while plasma profiles were different from each other and distinct from those following conventional capsules.

Keyphrases □ Indomethacin—design and preliminary evaluation of an oral osmotic delivery system, zero-order drug delivery □ Osmotic pump—oral, design and preliminary evaluation, indomethacin □ Drug delivery—design and preliminary evaluation of an oral osmotic delivery system containing indomethacin □ Anti-inflammatory agents—indomethacin, design and preliminary evaluation of an oral osmotic delivery system

The concept of continuous drug delivery that maintains the lowest delivery rate and that will elicit a therapeutic effect has much appeal. Intuitively, such a situation should represent the most efficacious use of the drug, while presenting a minimal risk of adverse reactions. Within certain prescribed constraints, theoretical analyses (1, 2) appear to favor dosing patterns that approach a constant *infusion*. However, direct experimental support for this hypothesis is limited (3). In part, this shortcoming may result from a lack of a practical way to deliver a suitable drug chronically and at a constant rate.

The recent development of an oral dosage form, based

0022-3549/83/0300-0253$01.00/0

Table I—Properties of Drug Core-Determining Shape of Release Rate Profile

Property	Symbol	Value
Mutual solubility of indomethacin sodium trihydrate	S_d	201.2 mg/ml
Total osmotic pressure	π_t	140 atm
Tablet core surface area	A	1.6 cm^2
Membrane density	ρ_m	1.3 g/ml

on the principles of an elementary osmotic pump, permits a close approximation to zero-order drug delivery (4). The present report describes the design and preliminary evaluation of an oral osmotic delivery system containing indomethacin, a potent anti-inflammatory agent used chronically 2–4 times daily in various forms of arthritis. Indomethacin (I) has a relatively short biological half-life (~4 hr) but is well absorbed throughout the GI tract (5–7).

THEORETICAL

Delivery of any agent in solution from the elementary osmotic pump can be achieved at a rate proportional to the solubility of the agent inside the system (S_d) and the osmotic pressure of the formulation inside the system (π_t). Given a tablet size with surface area, A, and given the membrane permeability and thickness, the desired rate can be obtained by incorporating into the core formulation substances that affect either S_d or π_t. Such a formulation can be called the composite core.

Delivery of potent agents may require the incorporation of formulating agents to permit fabrication of a system of acceptable size. (These agents are also added during the formulation of conventional tablets.) If these agents are water soluble, system performance can be predicted from the knowledge of certain parameters and the theoretical considerations presented here. The zero-order release rate of drug, $(dm_d/dt)_z$, from such a system, assuming a negligible osmotic pressure of the environmental fluid, is then given by:

$$Z \equiv \left(\frac{dm_d}{dt}\right)_z = k\frac{A}{h}\pi_t S_d \qquad \text{(Eq. 1)}$$

where k is the osmotic permeability coefficient of the membrane, A is the membrane area, h is the membrane thickness, and π_t and S_d are as defined above. The zero-order rate will persist from time $t = 0$ to $t = t_z$, at which time the solids—drug and osmotic agent—have gone into solution. The nonzero-order rate will decline parabolically as a function of time (4).

Table II—Average Zero-Order Release Rate and Membrane Weight for Three Lots of EOP-Indomethacin

System Designation[a]	Average Zero-order Rate, mg/hr	Rate-controlling Membrane Weight, mg[b]
7/85	7.2	16.9
9/85	9.6	11.9
12/85	12	8.4

[a] Nominal release rate (milligrams per hour)/total drug content (milligrams). [b] Estimated from total solids applied and coating efficiency factor (see *Experimental*).

Equation 1 provides a convenient way of calculating the membrane permeability (k) for a set of systems with the same release rate. Alternatively, for systems with different membrane thicknesses and release rates, the slope of the line of the release rate *versus* the inverse of the membrane thickness provides a means of calculating the membrane permeability. Consequently, the release rate can be expressed as a function of membrane weight (W), since this weight is related to membrane thickness:

$$W = \rho_m A h \qquad \text{(Eq. 2)}$$

where ρ_m is the membrane density, and A and h are as specified above. By substituting Eq. 2 into Eq. 1, one obtains:

$$Z_d = k\frac{A^2}{W}\rho_m \pi_t S_d \qquad \text{(Eq. 3)}$$

The membrane permeability, therefore, can be obtained from the slope of the line Z_d *versus* $1/W$.

Equation 3 indicates the parameters to which the average zero-order release rate will be sensitive. These parameters are: membrane permeability (k), tablet core surface area (A), membrane weight (W) and density (ρ_m), total osmotic pressure (π_t), and drug solubility (S_d). When a composite composition is chosen, π_t and S_d become fixed for the zero-order release period. The fixed composition also determines the total surface area (A) of the tablet core. When the membrane is chosen and applied reproducibly, values for k and π_m are fixed. Therefore, when testing is conducted at a constant temperature, the average zero-order release rate should be a function of the weight of the membrane applied.

To designate the zero-order release rate and total drug content of a system, the following convention was developed. Each system is described by a release rate (x) and total content (y) of indomethacin and designated as EOP-indomethacin x/y. Therefore, a system designed to deliver sodium indomethacin at 7 mg/hr (expressed as equivalents of indomethacin-free acid) from a system that contains 85 mg total (expressed as free

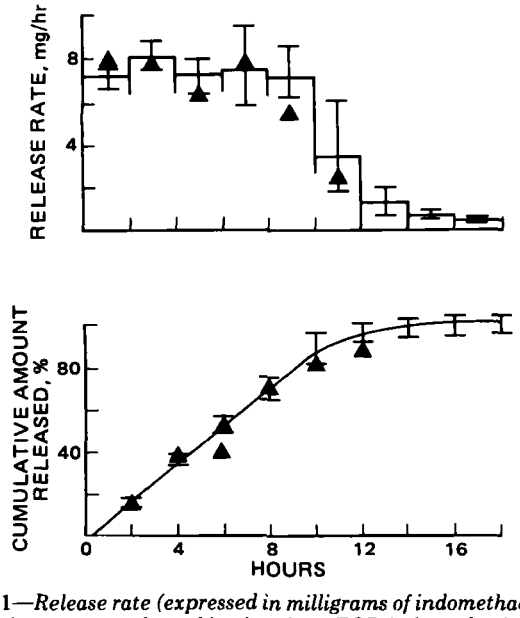

Figure 1—*Release rate (expressed in milligrams of indomethacin) and cumulative amount released* in vitro *from EOP-indomethacin 7/85,* N = 10. *Key: (▲) USP intestinal fluid (I) range (0–4 hr: gastric USP; 4–18: intestinal USP).*

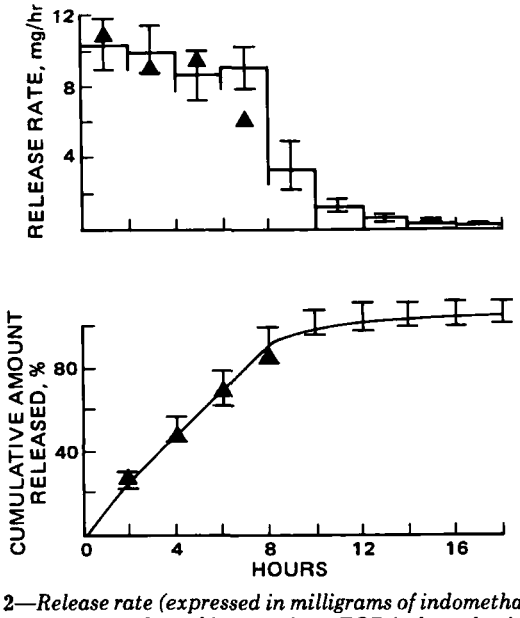

Figure 2—*Release rate (expressed in milligrams of indomethacin) and cumulative amount released* in vitro *from EOP-indomethacin 9/85,* N = 10. *Key: (▲) USP intestinal fluid (I) range (0–4 hr: gastric USP; 4–18: intestinal USP).*

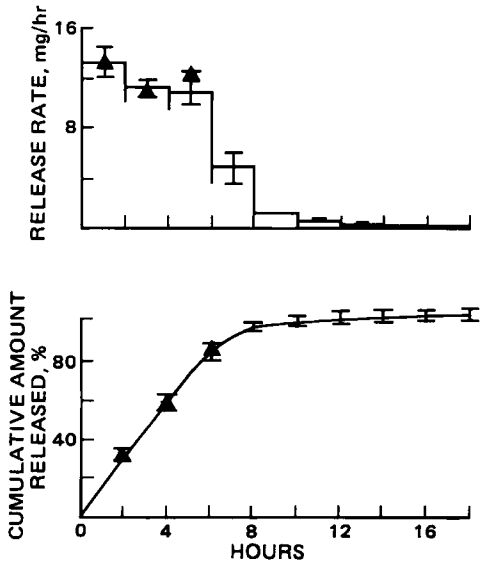

Figure 3—*Release rate (expressed in milligrams of indomethacin) and cumulative amount released* in vitro *from EOP-indomethacin 12/85, N = 10. Key: (▲) USP intestinal fluid (I) range (0–4 hr: gastric USP; 4–18: intestinal USP).*

acid) is designated EOP-indomethacin 7/85. This convention is used throughout the present report for three systems with different release rates but the same indomethacin content (85 mg) designated as EOP-indomethacin 7/85, 9/85, and 12/85.

EXPERIMENTAL

Materials—The tablet, membrane, and laboratory reagents for these studies were USF, NF, or ACS grades and were used without further purification. Sodium indomethacin trihydrate (II) was a gift[1].

Potassium bicarbonate was selected as the osmotic driving agent because of its high osmotic pressure and buffer capacity. In addition, when the dosage form operates in an acid environment, such as the stomach, carbon dioxide bubbles are produced that disperse the indomethacin acid formed. This process produces a finely dispersed drug formulation that readily redissolves and remains available for absorption. Details of the formulation are discussed elsewhere (8).

Determination of Solubilities and Osmotic Pressures—The solubility at 37° was determined for sodium indomethacin trihydrate in the presence of potassium bicarbonate. Excess amounts of each material were added to water in glass vials; the vials were capped tightly and equilibrated at 37° in a water bath for 24 hr. Aliquots of the resulting solutions were withdrawn from the vials using a preheated syringe and 0.2-μm filter. The sodium indomethacin content was determined by UV analysis after appropriate dilution.

Osmotic pressures of these same solutions were determined[2] at 37°.

Fabrication of System—Tablet cores were compressed on a rotary press[3] using 7.9-mm diameter, standard concave (IPT) tooling.

The membranes were applied by an air suspension coater[4], and membrane densities were obtained from volume and weight measurements.

Coated systems were dried in a forced-air oven at 50° until the residual solvent levels were <500 ppm. Systems were then equilibrated at ambient conditions to obtain the equilibrium trihydrate form of sodium indomethacin.

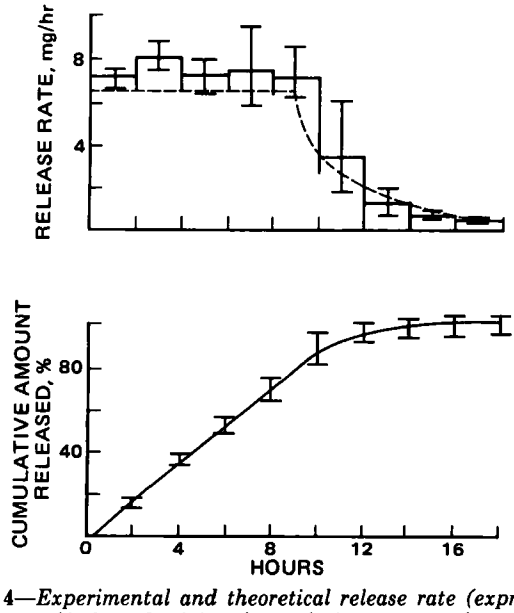

Figue 4—*Experimental and theoretical release rate (expressed in milligrams of indomethacin) and cumulative amount released* in vitro *from EOP-indomethacin 7/85. Key: (- - -) theoretical (I) range.*

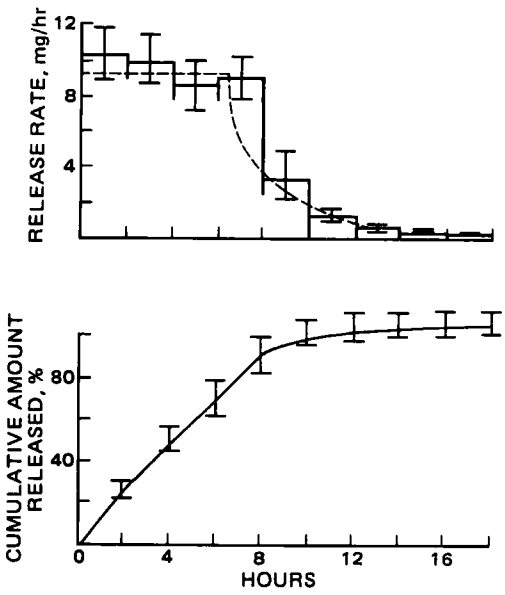

Figure 5—*Experimental and theoretical release rate (expressed in milligrams of indomethacin) and cumulative amount released* in vitro *from EOP-indomethacin 9/85. Key: (- - -) theoretical (I) range.*

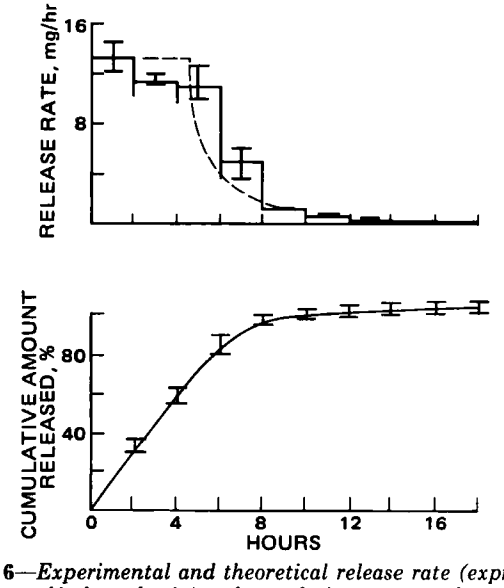

Figure 6—*Experimental and theoretical release rate (expressed in milligrams of indomethacin) and cumulative amount released* in vitro *from EOP-indomethacin 12/85. Key: (- - -) theoretical (I) range.*

[1] Merck Sharp & Dohme Laboratories.

[2] Hewlett-Packard model 302B, Vapor Pressure Osmometer.

[3] Manesty D3B.

[4] Wurster.

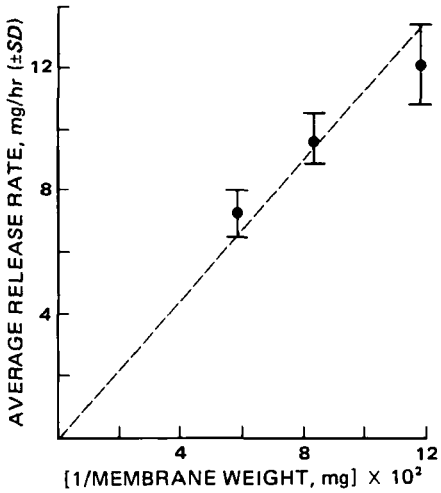

Figure 7—*Relation between weight of the membrane coating and average release rate from the EOP-indomethacin.*

Exit ports were drilled in each system by a high-speed mechanical drill or by an automated laser.

Release Rates—Differential release rates were determined by placing a finished system in a loose mesh bag and attaching the bag to a glass or plastic rod. The rod was attached to a horizontal arm connected to a vertically reciprocating shaker. The arms containing several systems were then positioned over a water bath (37°) that contained several test tubes. Each tube contained a known amount of release rate receptor media—simulated gastric or intestinal fluid without enzymes with 0.2% polysorbate 20. When the shaker started, the systems were immersed in the release rate media and stirred vertically at an amplitude of 3 cm and frequency of 0.25–0.5 cycle/sec. After 2 hr, the systems were removed from the first receptor container and moved to a second receptor; the stirring then was resumed. This procedure continued until the systems had been tested for 12 hr. Each receptor solution then was analyzed for sodium indomethacin content. The release rate in milligrams per hour for each system for each interval was determined by dividing the amount released in each receptor by 2 hr. The cumulative amount released was determined by taking the sum of the amount released by each system in each interval.

Cumulative amounts released were measured in the USP Dissolution Apparatus 1 (basket) or 2 (paddle); 900 ml of simulated intestinal fluid without enzyme with 0.2% polysorbate 20, pre-equilibrated to 37°, was used. For Apparatus 2, each system was placed in a loose mesh bag weighted with a few small glass beads. Samples were withdrawn from the receptor container at appropriate intervals for analysis, and the amount released was calculated after solution volume corrections were made.

Average zero-order differential release rates for each system were determined by averaging the rates into and including the periods up to the point where 70% of the drug was released.

After the average rate for each system was calculated, an average batch rate was determined using the average rates for all individual systems. The standard deviation obtained from this calculation was the between-system variation. Averaging the rates for all systems in all zero-order intervals provided the same batch average as before but also provided the overall standard deviation. Subtracting the variation between systems from the overall variation provided the variation within systems. This standard analysis of variance is routinely incorporated into all differential release rate determinations.

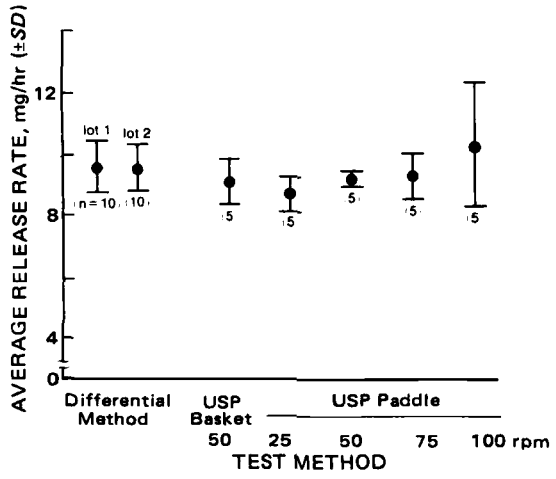

Figure 8—*Average release rate from EOP-indomethacin as a function of the test method (SD between-system variation).*

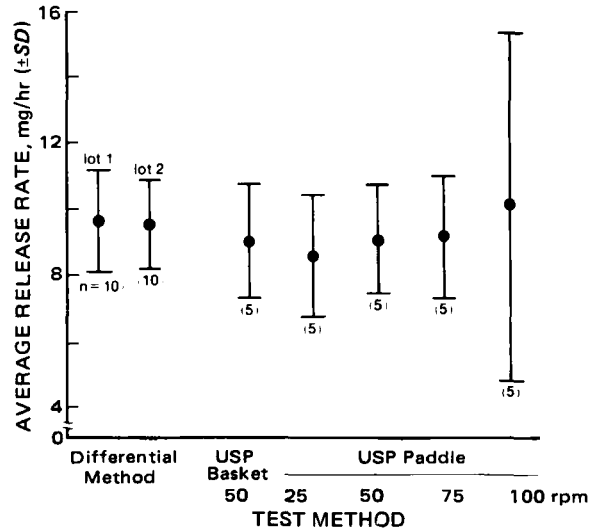

Figure 9—*Average release rate from EOP-indomethacin as a function of test method (SD within-system variation).*

Calculations were made as follows:

$$\text{standard deviation between systems} = \sqrt{\frac{\sum_{j=1}^{S}(\bar{Z}_j - \bar{Z})^2}{(S-1)}} \quad \text{(Eq. 4)}$$

$$\text{standard deviation within systems} = \sqrt{\frac{\sum_{j=1}^{S}\sum_{i=1}^{I}(Z_{ij} - \bar{Z}_j)^2}{(N-S)}} \quad \text{(Eq. 5)}$$

$$\text{standard deviation overall} = \sqrt{\frac{\sum_{j=1}^{S}\sum_{i=1}^{I}(Z_{ij} - \bar{Z})^2}{(N-1)}} \quad \text{(Eq. 6)}$$

where S is the number of systems tested, I is the number of zero-order intervals, $\bar{Z}$ is the average batch rate, $\bar{Z}_j$ is the average rate for system j, and $N = SI$.

Cumulative Amounts Released *In Vivo* and *In Vitro*—The release rate performance of these systems *in vitro* was compared with their performance *in vivo* using a dog model. Forty systems were individually weighed and marked with a number in indelible ink. The height (thickness) and diameter of each were measured. These were divided into two groups of 20.

Four mongrel dogs were used after a 3-week quarantine. They were fasted the night before and the day of the study but were allowed water *ad libitum*.

One system was administered orally to each dog 10, 8, 6, 4, and 2 hr before sacrifice, and the time of administration was recorded. Each dog was monitored each hour throughout the study, and all fecal and regurgitated material was examined for the presence of a system. If one was found, the time of recovery was recorded, and the system was washed and stored for analysis. Two hours after the last administration, each dog received an appropriate dose of euthanasia solution[5]. The entire GI tract was removed and opened. Each system was recovered and its recovery location in the tract and time of recovery recorded. All fecal and intestinal material adhering to the systems was carefully rinsed away. Each system was analyzed for its residual drug content.

Concurrent with administration to the dogs, systems were placed in

[5] T-61 euthanasia solution.

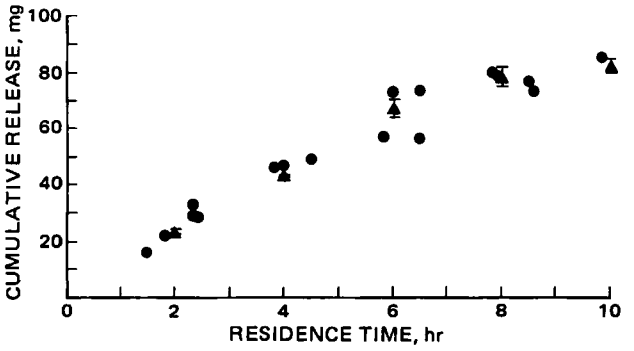

Figure 10—*Cumulative amount of indomethacin released by EOP-indomethacin 9/85 (expressed as milligrams of indomethacin)* in vitro *and in the GI tract of dogs. Key: (●) in vivo (dog); (▲) mean in vitro.*

release rate receptor medium. Each system remained in one container of medium for the study. All systems were attached to the vertically reciprocating shaker mechanism. At the end of the study, all systems were removed from the receptor media and each analyzed for residual drug content.

Separately, 10 systems were weighed and analyzed for total drug content; their average fractional drug content (Q) was then determined. The parameter Q was then multiplied by the weight of the 20 systems studied *in vivo* and the 20 systems studied *in vitro* to determine the initial drug content of each system. By subtracting the analyzed residual amount from the calculated initial content, the amount of drug released for various time intervals could be determined *in vivo* (dog) and *in vitro*. The data were plotted on the same graph (amount released as a function of residence time) for comparison.

Preliminary Assessment of Extent of Drug Absorption in Humans—Two four-way crossover studies were designed to determine the total urinary excretion and temporal pattern of plasma indomethacin concentrations in healthy volunteers. Six fasting subjects received single doses of EOP-indomethacin[6] 7/85, 9/85, 12/85 and indomethacin capsules[7] (3 × 25 mg) in randomized crossover fashion at weekly intervals. In a multiple-dose study, a total of eight doses of the four different formulations were administered at twelve 1-hr intervals to three other subjects. There was a 2-week period between the first dose of each treatment.

During the single-dose study, blood samples were collected at one-half hr preadministration and 1, 2, 4, 6, 12, and 24 hr postadministration; timed urine samples were collected incrementally. During the multiple-dose study, urine samples were collected over 120 hr at 10 equal intervals. The plasma and urine samples were analyzed by HPLC (9).

RESULTS AND DISCUSSION

Release rate data are expressed as milligrams per hour of indomethacin acid, the pharmacologically active drug moiety. Release rate performance, however, as it relates to the physicochemical constants discussed in *Theoretical*, depends on properties of the drug salt, sodium indomethacin trihydrate, contained in the core (Table I). Molecular weights of indomethacin and its trihydrate salt are 357.8 and 433.8, respectively. The solubility of indomethacin is then obtained from the solubility of its salt, S_d, by dividing the solubility (Table I) by the ratio of the molecular weights (1.212). The content of indomethacin per system was selected at 85 mg, which is equivalent to 103 mg of salt.

Table II lists the three dosage forms by their nominal release rate–total drug content and shows their actual zero-order release rates and membrane weights.

pH Independent Release Rate *In Vitro*—Release rates of three different types of systems (Figs. 1–3) were measured by the differential method from which the cumulative amounts released were calculated and expressed as percent of total drug content. The data, with bars expressing the range of data, were obtained from measurements in gastric fluid for the first 4 hr and in intestinal fluid for the remainder of the test. In a separate experiment, release rates of systems from the same batch were studied in intestinal fluid. Average release rates obtained in this fashion are represented by the triangle. The release rates in either gastric or intestinal fluid were the same.

[6] ALZA Corp.
[7] INDOCIN, Merck Sharp & Dohme.

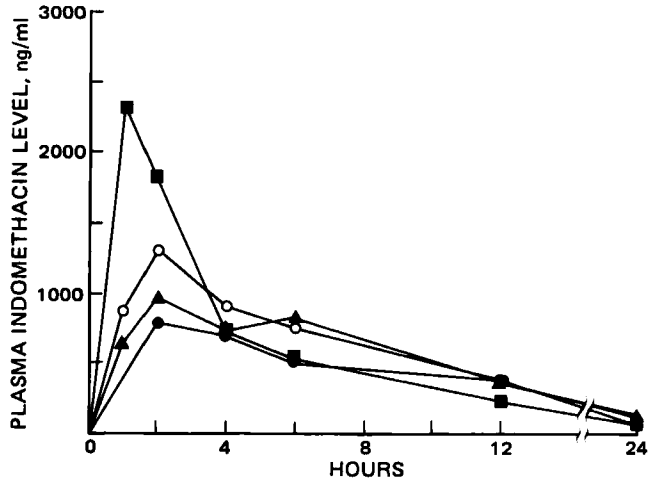

Figure 11—*Average (n = 6) indomethacin plasma profiles after single doses of indomethacin capsules (3 × 25 mg) and the EOP-indomethacin 7/85, 9/85, and 12/85. Key: (■) Indomethacin capsules (3 × 25 mg), (●) EOP-indomethacin 7/85, (▲) EOP-indomethacin 9/85, (○) EOP-indomethacin 12/85.*

Predictable Release Rates—The relationship between the release rate and membrane permeability for this type of system has been treated elsewhere (4). The purpose of this section, then, is not intended to prove the validity of Eqs. 1 and 3 but to use them as a tool to correlate the data of three sets of experiments on the release rate from systems 7/85, 9/85, and 12/85 (Figs. 4–6). These three systems were coated with the same membrane formulation of which only the thickness and, therefore, weight differed. The average zero order rates (Z_d) of these systems can be plotted *versus* $1/W$, the inverse of the average membrane weight (Fig. 7). From the slope of the best straight line through the origin, the membrane permeability constant (k) is estimated to be 1.4×10^{-6} cm^3/hr atm according to Eq. 3.

This estimate is used to calculate the total release rate profile in Figs. 4–6. The theoretical and actual release rates agree to within 10%.

Release Rate Independent of Stirring Rate—The effect of stirring rates on the average zero-order rate was studied on a second lot of the 9/85 system using the three different methods listed. Results are shown in Figs. 8 and 9. Average zero-order release rates, calculated as previously described, are the same for lots 1 and 2 of the 9/85 system. Standard deviations between and within those systems, calculated according to Eqs. 4 and 5, are comparable (Figs. 8 and 9). A two-tailed Student's t-test of these data indicated no significant differences ($p > 0.1$) between the two lots of systems in rates determined by the differential method. As seen from Figs. 8 and 9, the average rates obtained by the differential method and USP Apparatus 1 (50 rpm) (basket) and 2 (25–75 rpm) (paddle) demonstrate no differences in averages or in deviations from average values. Release rates were measured in artificial intestinal fluid containing 0.2% polysorbate 20.

Comparison of the average release rate for lot 2, determined by the differential method, to the average rates obtained from the USP Apparatus 1 (50 rpm) and 2 (25–100 rpm), showed that no significant differences exist as determined by a Student's t-test ($p > 0.1$). When the overall variance for lot 2 is compared to those for the USP methods, only method 2 at 100 rpm is significantly different ($p < 0.05$), as determined by a variance ratio (f) test. That deviation was due to rupture of the membrane by the vigorous stirring, making the results at this stirring rate invalid. In all other cases, overall agreement exists between the various *in vitro* methods reported here.

Release Rate *In Vivo versus* Release Rate *In Vitro*—The release rate *in vivo* cannot readily be measured with the differential method used *in vitro*. Cumulative amounts released *in vivo* were obtained instead and compared (Fig. 10) with cumulative amounts released *in vitro* and also measured directly. The ranges of experimental *in vitro* data are indicated with error bars, while amounts released from individual systems in the GI tract of four dogs are listed as separate data points. The systems studied were of the 9/85 type and were obtained from the batch for which data are given in Fig. 2. The average release rate for each separate system, *in vitro* or *in vivo*, which released an amount Δm_i in a residence time Δt_i is found as:

$$Z_i = \Delta m_i / \Delta t_i \qquad \text{(Eq. 7)}$$

Table III—Mean Urinary Recovery and Renal Clearance (±*SD*) of Indomethacin Following Single Doses in Six Subjects

Treatment	Renal Clearance, ml/min	Percent Recovered in Urine
Capsules	32.4 ± 14.3	17.3 ± 12.5
EOP-7/85	33.9 ± 11.9	22.3 ± 7.7
EOP-9/85	35.1 ± 11.4	23.8 ± 5.9
EOP-12/85	42.1 ± 14.2	28.1 ± 7.1

The average zero-order rate for systems that delivered for a time period ≤6 hr was found to be:

In vitro:

$$\bar{Z}_1 = \frac{\sum_i^{12} Z_i}{12} = 10.8 \pm 9.4\% \qquad \text{(Eq. 8)}$$

In vivo:

$$\bar{Z}_2 = \frac{\sum_i^{12} Z_i}{12} = 10.6 \pm 16\% \qquad \text{(Eq. 9)}$$

The *in vitro* and *in vivo* rates are equal and are not significantly different from the rate obtained by the differential method.

Plasma Concentrations and Extent of Drug Absorption from Two Limited Studies in Humans—Plasma profiles from the single-dose study illustrated the controlled-release properties of the EOP-indomethacin dosage forms. Compared with the indomethacin capsules, they produced more constant and prolonged plasma levels (Fig. 11); renal clearance and total urinary recoveries of indomethacin and conjugates are shown in Table III. Relative to capsules of indomethacin, which are known to be completely absorbed (5, 7), the bioavailability of the 7/85, 9/85, and 12/85 systems were estimated to be 0.80, 0.84, and 0.88, respectively (10, 11).

Total 120-hr urinary recovery of indomethacin (free and conjugated) for the multiple-dose study was 130.2 ± 26.7, 139.4 ± 8.9, and 147.7 ± 23.1 mg, respectively, following EOP-indomethacin 7/85, 9/85, and 12/85, and was 128.8 ± 39.1 mg following indomethacin capsules. Similar urinary recovery of indomethacin suggests comparable bioavailability.

Summary—Preliminary studies in humans showed that the extent of absorption from EOP-indomethacin systems 7/85, 9/85, and 12/85 is similar to that after 75 mg of indomethacin in capsules. Plasma concentration profiles are consistent with the planned differences in drug delivery rate and the anticipated effects of enterohepatic circulation (5–7).

REFERENCES

(1) S. E. DeJongh and M. Wijnans, *Acta Physiol. Pharmacol. Neerlandica*, **1**, 237 (1950).

(2) A. G. M. Van Gemert and J W. Duyff, *ibid.*, **1**, 256 (1950).

(3) A. C. Wood, G. A. Glaubiger, and T. N. Chase, *Lancet*, **i**, 1391 (1973).

(4) F. Theeuwes, *J. Pharm. Sci.*, **64**, 1987 (1975).

(5) K. C. Kwan, G. O. Breault, E. R. Umbenhauer, F. G. McMahon, and D. E. Duggan, *J. Pharmacokinet. Biopharm.*, **4**, 225 (1976).

(6) J. Alvan, M. Orme, L. Bertilsson, R. Ekstrand, and L. Palmer, *Clin. Pharmacol. Ther.*, **18**, 364 (1975).

(7) K. C. Kwan, G. O. Breault, R. L. Davis, B. W. Lei, A. W. Czerwinski, G. H. Besselaar, and D. E. Duggan, *J. Pharmacokinet. Biopharm.*, **6**, 451 (1978).

(8) P. Bonsen, P. S. Wong, F. Theeuwes, U.S. Pat. 4,265,874 (1981).

(9) W. F. Bayne, T. East, and D. Dye, *J. Pharm. Sci.*, **70**, 458 (1981).

(10) K. C. Kwan and A. E. Till, *ibid.*, **62**, 1499 (1973).

(11) S. Hwang and K. C. Kwan, *ibid.*, **69**, 77 (1980).

Prediction of Stability in Pharmaceutical Preparations XX: Stability Evaluation and Bioanalysis of Cocaine and Benzoylecgonine by High-Performance Liquid Chromatography

EDWARD R. GARRETT ˣ and KAZIMIERZ SEYDA

Received December 7, 1981 from *The Beehive, College of Pharmacy, J. Hillis Miller Health Center, University of Florida, Gainesville, FL 32610.* Accepted for publication April 22, 1982.

Abstract □ Specific, sensitive, reverse-phase high-performance liquid chromatographic (HPLC) assays of cocaine (I) and its hydrolysis products, benzoylecgonine (II) and benzoic acid (III), have been devised with analytical sensitivities as low as 15 ng/ml of plasma for I using spectrophotometric detection at 232 nm. Cocaine can be separated from its hydrolysis products by extraction at pH 7.5 with haloalkanes. Benzoylecgonine and benzoic acid can be extracted at pH 3.0 with 1-butanol. The evaporated residues were reconstituted in acetonitrile–water for HPLC assay. The assay was used to determine the stabilities of I and II in aqueous solutions, to establish log k–pH profiles at various temperatures, and to evaluate Arrhenius' parameters. Hydrolyses were by specific acid–base catalysis. Cocaine showed hydrogen and hydroxyl ion attack on protonated I with 40 and 90% proceeding through the benzoylecgonine route, respectively, as well as hydroxyl ion attack on neutral cocaine, with only 6% proceeding through the benzoylecgonine route. Cocaine is relatively unstable in the neutral pH range with a half-life of 5 hr in buffer at pH 7.25 and 40°. Similar half-lives were observed in fresh dog plasma at 300 and 30 μg/ml, although one study at 0.5 μg/ml indicated a doubling of the rate.

Keyphrases □ Cocaine—stability evaluation and bioanalysis, hydrolysis products, high-performance liquid chromatography □ High-performance liquid chromatography—cocaine, benzoylecgonine, and benzoic acid in buffers in biological fluids □ Stability—prediction and bioanalysis of cocaine and benzoylecgonine in plasma and buffers, high-performance liquid chromatography □ Benzoylecgonine—hydrolysis product of cocaine, stability evaluation and bioanalysis by high-performance liquid chromatography □ Protein binding—cocaine and its hydrolysis products, benzoylecgonine and benzoic acid, stability evaluation and bioanalysis, high-performance liquid chromatography

Cocaine (I) is metabolized *in vivo*, principally to its solvolytic products (1, 2), with an apparent terminal half-life in humans ranging between 40 and 91 min (3). Although available data on the stability of I in plasma *in vitro* is sparse (3), a rough estimate of the half-life in human plasma of 150 min at 25° can be made.

0022-3549/83/0300-0258$01.00/0

Table III—Mean Urinary Recovery and Renal Clearance (±*SD*) of Indomethacin Following Single Doses in Six Subjects

Treatment	Renal Clearance, ml/min	Percent Recovered in Urine
Capsules	32.4 ± 14.3	17.3 ± 12.5
EOP-7/85	33.9 ± 11.9	22.3 ± 7.7
EOP-9/85	35.1 ± 11.4	23.8 ± 5.9
EOP-12/85	42.1 ± 14.2	28.1 ± 7.1

The average zero-order rate for systems that delivered for a time period ≤6 hr was found to be:

In vitro:

$$\bar{Z}_1 = \frac{\sum_i^{12} Z_i}{12} = 10.8 \pm 9.4\% \qquad \text{(Eq. 8)}$$

In vivo:

$$\bar{Z}_2 = \frac{\sum_i^{12} Z_i}{12} = 10.6 \pm 16\% \qquad \text{(Eq. 9)}$$

The *in vitro* and *in vivo* rates are equal and are not significantly different from the rate obtained by the differential method.

Plasma Concentrations and Extent of Drug Absorption from Two Limited Studies in Humans—Plasma profiles from the single-dose study illustrated the controlled-release properties of the EOP-indomethacin dosage forms. Compared with the indomethacin capsules, they produced more constant and prolonged plasma levels (Fig. 11); renal clearance and total urinary recoveries of indomethacin and conjugates are shown in Table III. Relative to capsules of indomethacin, which are known to be completely absorbed (5, 7), the bioavailability of the 7/85, 9/85, and 12/85 systems were estimated to be 0.80, 0.84, and 0.88, respectively (10, 11).

Total 120-hr urinary recovery of indomethacin (free and conjugated) for the multiple-dose study was 130.2 ± 26.7, 139.4 ± 8.9, and 147.7 ± 23.1 mg, respectively, following EOP-indomethacin 7/85, 9/85, and 12/85, and was 128.8 ± 39.1 mg following indomethacin capsules. Similar urinary recovery of indomethacin suggests comparable bioavailability.

Summary—Preliminary studies in humans showed that the extent of absorption from EOP-indomethacin systems 7/85, 9/85, and 12/85 is similar to that after 75 mg of indomethacin in capsules. Plasma concentration profiles are consistent with the planned differences in drug delivery rate and the anticipated effects of enterohepatic circulation (5–7).

REFERENCES

(1) S. E. DeJongh and M. Wijnans, *Acta Physiol. Pharmacol. Neerlandica*, **1**, 237 (1950).

(2) A. G. M. Van Gemert and J W. Duyff, *ibid.*, **1**, 256 (1950).

(3) A. C. Wood, G. A. Glaubiger, and T. N. Chase, *Lancet*, **i**, 1391 (1973).

(4) F. Theeuwes, *J. Pharm. Sci.*, **64**, 1987 (1975).

(5) K. C. Kwan, G. O. Breault, E. R. Umbenhauer, F. G. McMahon, and D. E. Duggan, *J. Pharmacokinet. Biopharm.*, **4**, 225 (1976).

(6) J. Alvan, M. Orme, L. Bertilsson, R. Ekstrand, and L. Palmer, *Clin. Pharmacol. Ther.*, **18**, 364 (1975).

(7) K. C. Kwan, G. O. Breault, R. L. Davis, B. W. Lei, A. W. Czerwinski, G. H. Besselaar, and D. E. Duggan, *J. Pharmacokinet. Biopharm.*, **6**, 451 (1978).

(8) P. Bonsen, P. S. Wong, F. Theeuwes, U.S. Pat. 4,265,874 (1981).

(9) W. F. Bayne, T. East, and D. Dye, *J. Pharm. Sci.*, **70**, 458 (1981).

(10) K. C. Kwan and A. E. Till, *ibid.*, **62**, 1499 (1973).

(11) S. Hwang and K. C. Kwan, *ibid.*, **69**, 77 (1980).

Prediction of Stability in Pharmaceutical Preparations XX: Stability Evaluation and Bioanalysis of Cocaine and Benzoylecgonine by High-Performance Liquid Chromatography

EDWARD R. GARRETT ˣ and KAZIMIERZ SEYDA

Received December 7, 1981 from *The Beehive, College of Pharmacy, J. Hillis Miller Health Center, University of Florida, Gainesville, FL 32610.* Accepted for publication April 22, 1982.

Abstract □ Specific, sensitive, reverse-phase high-performance liquid chromatographic (HPLC) assays of cocaine (I) and its hydrolysis products, benzoylecgonine (II) and benzoic acid (III), have been devised with analytical sensitivities as low as 15 ng/ml of plasma for I using spectrophotometric detection at 232 nm. Cocaine can be separated from its hydrolysis products by extraction at pH 7.5 with haloalkanes. Benzoylecgonine and benzoic acid can be extracted at pH 3.0 with 1-butanol. The evaporated residues were reconstituted in acetonitrile–water for HPLC assay. The assay was used to determine the stabilities of I and II in aqueous solutions, to establish log k–pH profiles at various temperatures, and to evaluate Arrhenius' parameters. Hydrolyses were by specific acid–base catalysis. Cocaine showed hydrogen and hydroxyl ion attack on protonated I with 40 and 90% proceeding through the benzoylecgonine route, respectively, as well as hydroxyl ion attack on neutral cocaine, with only 6% proceeding through the benzoylecgonine route. Cocaine is relatively unstable in the neutral pH range with a half-life of 5 hr in buffer at pH 7.25 and 40°. Similar half-lives were observed in fresh dog plasma at 300 and 30 μg/ml, although one study at 0.5 μg/ml indicated a doubling of the rate.

Keyphrases □ Cocaine—stability evaluation and bioanalysis, hydrolysis products, high-performance liquid chromatography □ High-performance liquid chromatography—cocaine, benzoylecgonine, and benzoic acid in buffers in biological fluids □ Stability—prediction and bioanalysis of cocaine and benzoylecgonine in plasma and buffers, high-performance liquid chromatography □ Benzoylecgonine—hydrolysis product of cocaine, stability evaluation and bioanalysis by high-performance liquid chromatography □ Protein binding—cocaine and its hydrolysis products, benzoylecgonine and benzoic acid, stability evaluation and bioanalysis, high-performance liquid chromatography

Cocaine (I) is metabolized *in vivo*, principally to its solvolytic products (1, 2), with an apparent terminal half-life in humans ranging between 40 and 91 min (3). Although available data on the stability of I in plasma *in vitro* is sparse (3), a rough estimate of the half-life in human plasma of 150 min at 25° can be made.

0022-3549/83/0300-0258$01.00/0

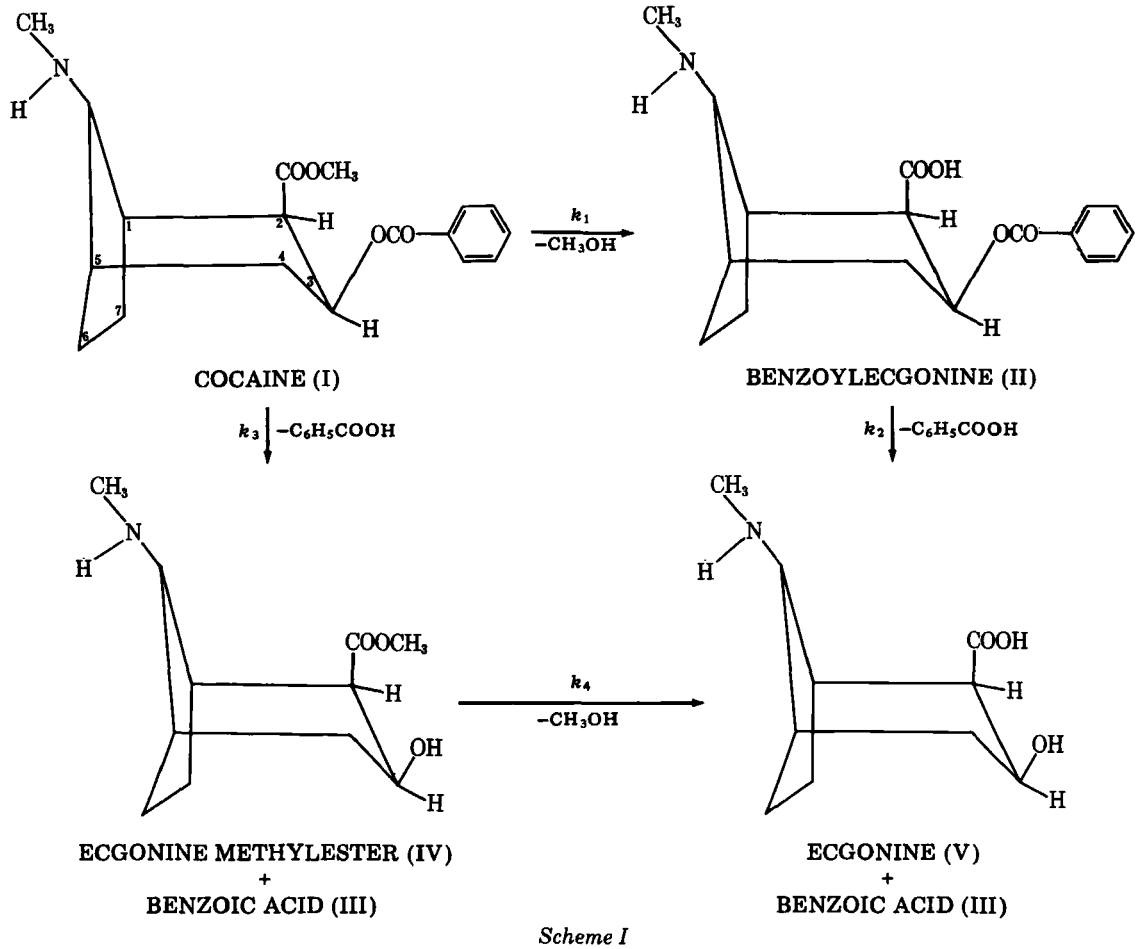

Scheme I

The aqueous solvolysis of 10 mg of I/ml was studied by assaying unchanged drug with time between pH 1 and 8.8 (5). Cocaine was extracted with ether from 5% sodium bicarbonate solutions and spectrophotometrically assayed after reextraction into 0.01 *N* HCl. The maximum stability was stated to be at pH 1.95 and benzoylecgonine (II) was claimed to be the solvolytic product (5).

The present study develops and applies specific and sensitive HPLC assays of I and its solvolytic products (Scheme I) to kinetic studies of stability and mechanisms of solvolyses of both I and II in aqueous and biological fluids, and establishes complete log k–pH profiles at several temperatures in preparation of systematic pharmacokinetic investigations of the drug and its metabolites. The validity of the use of basic physicochemical relations in predicting the stability of drugs under all conditions and optimizing valid assays has been demonstrated (6–9).

An HPLC assay has been claimed to detect I and II at 200 and 235 nm for ~100 ng/ml from 5 ml of urine after selective pH extraction. A valid linear calibration curve was claimed to exist over a range of 0.5–10 μg/ml of urine, although no quantitative assays were given (10). A more

Table I—Typical Statistics of HPLC Calibration Curves of I, II, and III in Aqueous Solutions and Plasma [a]

HPLC Procedure, nm of detection	Compound	Range, μg/ml	$s_{C\cdot PHR}$	m	s_m	b	s_b	n	r
I(254)[b]	I	15–111	0.88	88.6	1.0	−4.4	0.8	6	0.9997
	II	7–50	0.34	31.1	0.3	−0.4	0.3	6	0.9998
	III	6–45	0.25	32.2	0.2	−1.9	0.2	6	0.9999
II(254)[c]	I	15–90	1.64	75.5	2.1	−0.3	1.6	5	0.9989
	II	14–81	0.77	55.2	0.8	0.2	0.7	5	0.9997
	III	6–37	0.55	51.3	1.1	−1.5	0.6	5	0.9993
II(232)[c]	I	0.4–2.8	0.038	4.90	0.09	−0.08	0.03	6	0.9990
	II	0.3–2.5	0.065	3.49	0.13	−0.21	0.06	6	0.9971
	III	0.2–1.1	0.035	2.07	0.09	−0.13	0.04	6	0.9969
III(254)[d]	I	4–36	1.16	114.4	5.2	0.88	0.91	5	0.9969
	II	3–31	0.90	63.8	2.5	−0.25	0.73	5	0.9976
IV(232)[e]	I	0.36–2.68	0.049	1.88	0.05	−0.018	0.046	5	0.9989
IV′(232)[e]	I	0.05–0.40	0.0073	0.282	0.008	−0.0026	0.0069	5	0.9989

[a] Statistics are in accordance with $C(\mu g/ml) \pm s_{C\cdot PHR} = (m \pm s_m)\ PHR + b \pm s_b$ from aqueous solutions (HPLC procedure I) and plasma (HPLC procedures II–IV). All values are for concentrations in the final assayed solutions except for IV′ which is for concentrations in the original plasma. The constants m and b are the slope and intercept, respectively, of the regression of concentration (C, μg/ml) on peak height ratio to internal standard (PHR) where $s_{C\cdot PHR}$, s_m, and s_b are standard errors of estimate (μg/ml) (14) of concentration on peak height ratio, of the slope (m), and of the intercept (b), respectively. [b] Degrading buffered solutions of I were diluted to one-sixth the original concentration before assaying in mobile phase solution. [c] Plasma (0.5 ml) denatured with 0.5 ml acetonitrile and the supernatant assayed. [d] Evaporated chloroform extracts of 1.0 ml of plasma were reconstituted in 0.5 ml of aqueous acetonitrile and assayed for I at twice the original plasma concentration. Evaporated 1-butanol extracts of the plasma were reconstituted similarly, and II and III were assayed at twice the original plasma concentration. [e] As in footnote *d* except the compounds were 6.7 times the original 2.0-ml plasma concentration. Plasma components at these low II and III concentrations and at 232-nm detection interfered with their assays.

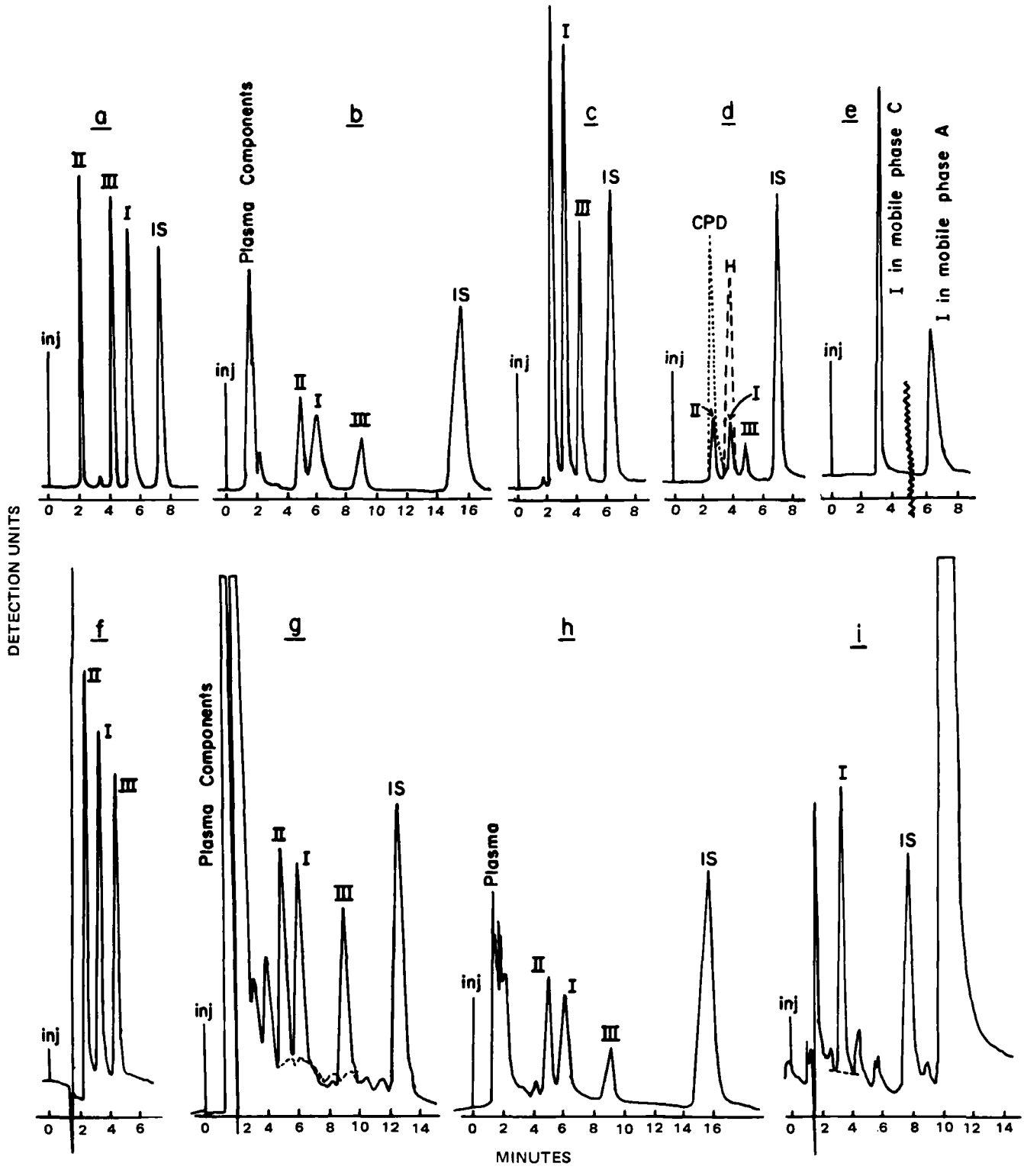

Figure 1—*Examples of reverse-phase HPLC chromatograms at 254-nm detection with 25 μl injected: (a) Aqueous solution containing 2.98 × 10^{-4} M (90.4 μg/ml) I, 1.415 × 10^{-4} M (42.92 μg/ml) II, 3.034 × 10^{-4} M (37 μg/ml) III, and 3.517 × 10^{-4} M (48 μg/ml)* m-*toluic acid (IS) in mobile phase A. (b) Heparinized plasma solution denatured (1:1) with acetonitrile in mobile phase B. The mixture contained 1.98 × 10^{-4} M (60 μg/ml) I, 1.864 × 10^{-4} M (56.5 μg/ml) II, 2.044 × 10^{-4} M (25 μg/ml) III, and 1.057 × 10^{-3} M (144 μg/ml)* o-*toluic acid (IS). (c) Aqueous solution containing 1.65 × 10^{-4} M (50 μg/ml) I, 1.553 × 10^{-4} M (45 μg/ml) II, 1.703 × 10^{-4} M (20.8 μg/ml) III, and 2.968 × 10^{-4} M (40.4 μg/ml)* o-*toluic acid (IS) into mobile phase C. (d) Aqueous solution containing 2.475 × 10^{-5} M (7.5 μg/ml) I, 2.33 × 10^{-5} M (7.07 μg/ml) II, 2.555 × 10^{-5} M (3.12 μg/ml) III, and 2.968 × 10^{-5} M (4.04 μg/ml)* o-*toluic acid (IS) in mobile phase C. The dashed line is the chromatogram for the same composition with heparin (H). The dotted line is the chromatogram for the same composition with citrate phosphate dextrose (CPD) solution USP (5 μl in 2 ml of injected solution. (e) Effect of tetrabutylammonium hydroxide in mobile phase on chromatogram of I. Aqueous solutions of 1.65 × 10^{-4} M (50 μg/ml) I injected into mobile phases A and C, acetonitrile–0.085 M acetate buffer (25:75) (pH 3.6) without and with 0.002 M tetrabutylammonium hydroxide in the acetate buffer, respectively. Examples of reverse-phase HPLC chromatograms at 232 nm detection with 25 μl injected: (f) Aqueous solution*

continued on next page

recent paper claims an HPLC detection limit for I, II, and norcocaine of 1.0 μg/ml of biological fluid from 0.5 ml of sample at 235 nm after extraction at pH 9.0 and reconstitution of the evaporated organic extract in 250 μl of water (11).

In a recent guide to I and metabolite analysis in biological material (12), it was stated that "surprisingly very few papers utilizing this technique for the determination of cocaine and its metabolites have appeared . . ."

One of the HPLC methods presented has an analytical sensitivity in plasma of 15 ng/ml for I.

EXPERIMENTAL

Materials—The following analytical grade materials were used: cocaine hydrochloride[1], benzoylecgonine·4H_2O[1], benzoic acid[2], *m*-toluic acid[3], *o*-toluic acid[3], glacial acetic acid[2], sodium acetate[2], boric acid[4], sodium borate[4], sodium chloride[2], monobasic sodium phosphate[4], dibasic sodium phosphate[2], 1 *M* hydrochloric acid[5], 1 *M* sodium hydroxide[5], 0.4 *M* tetrabutylammonium hydroxide in water[6], acetonitrile[6], chloroform[2], and 1-butanol[4].

Apparatus—A high-performance liquid chromatograph[7] equipped with fixed[8] and variable[9] wavelength UV detectors was used with a reverse-phase μBondapak C_{18} column.

HPLC Procedures—*Procedure I: Kinetics in Aqueous Solution*—The mobile phase (A) acetonitrile–0.085 *M* acetate buffer (25:75) (pH 3.6) with UV detection at 254 nm was used to assay degrading aqueous solutions of I and II with 4.22×10^{-4} *M* *m*-toluic acid as the internal standard. All reaction samples were diluted with acetonitrile and acetate buffer (pH 3.6) which contained the internal standard to give the same composition as the mobile phase, and 25 μl was injected into the chromatograph.

Procedure II: Acetonitrile Denaturation for Higher Concentrations of I in Plasma—Plasma (0.5 ml) was denatured with 0.5 ml of acetonitrile containing 2.113×10^{-4} *M* *o*-toluic acid as internal standard, with vortexing after subsequent centrifugation at 3000 rpm for 10 min. A 25-μl aliquot of the supernatant was injected into the chromatograph with a mobile phase (B) of acetonitrile–0.0002 *M* tetrabutylammonium hydroxide in 0.085 *M* acetate buffer (15:85) (pH 3.63) and UV detection at 254 or 232 nm.

Procedure III: Extraction Procedure for Higher Concentrations of I in Plasma—Plasma (1.0 ml) was extracted twice with 1.00 ml of chloroform. The combined organic extract was evaporated to dryness under nitrogen, reconstituted in 0.5 ml of acetate buffer (pH 3.6)–acetonitrile (1:1) which contained 1.187×10^{-3} *M* *o*-toluic acid as internal standard. Then, 25 μl was injected into the chromatograph to assay I with a mobile phase (C) at 254 nm detection of acetonitrile–0.0002 *M* tetrabutylammonium hydroxide in 0.085 *M* acetate buffer (25:75) (pH 3.63). The extracted plasma was adjusted to pH 3 and again extracted with 10 ml of 1-butanol. The organic extract was evaporated to dryness under nitrogen, reconstituted as above, and 25 μl was injected into the chromatograph to assay II and benzoic acid (III) with mobile phase B at 254 nm detection.

Procedure IV: Extraction Procedure for Lower Concentrations of I in Plasma—Plasma (2.0 ml) was extracted with 3.0 ml of chloroform. The extract (2.0 ml) was evaporated to dryness under nitrogen and reconstituted with 0.2 ml of acetonitrile–acetate buffer (1:3) (pH 3.6) mixture which contained 1.665×10^{-5} *M* *p*-chloroaniline as internal standard. A 25-μl injection was used with mobile phase C for analysis of I at 232 nm detection. Once extracted, the plasma was adjusted to pH 3 and extracted twice with 5 ml of 1-butanol. The combined extracts were taken to dryness, reconstituted as above, and 25 μl was assayed with mobile phase B for II and III. At the low drug concentrations, extracted plasma components interfered with the assay of II. All procedures used flow rates of 2.0 ml/min which gave back pressures of 1800–2100 psi.

Kinetics of Hydrolytic Degradation of I and II—*Acid Hydrolyses*—Aliquots of aqueous solutions of a drug were mixed with appropriate amounts of standardized concentrate to give 0.1, 0.04, and 0.02 *M* HCl solutions that were 1.32×10^{-3} *M* in I or 8.518×10^{-4} *M* in II (Table I). Aliquots (1.5 ml) were put in tightly closed 10-ml vials that were placed in 90, 80, or 70° thermostated oil baths. The vials were withdrawn periodically, ice-cooled, and 0.5 ml of the reaction mixtures was mixed with 2.5 ml of quenching solution containing 4.22×10^{-4} *M* *m*-toluic acid as internal standard. The rates were sufficiently slow such that the time of thermal equilibration did not affect the studies significantly. The quenching solution was an appropriate mixture of acetate buffer–acetonitrile to yield the same ultimate composition of the used mobile phase A in HPLC procedure I.

Alkaline Hydrolyses—Aliquots of aqueous stock solutions of a drug were mixed with thermally preequilibrated appropriate sodium hydroxide solutions (Table I) prepared from a standardized concentrate to obtain 2.472×10^{-3} *M* of I or 8.518×10^{-4} *M* of II. Aliquots (0.5 ml) of the thermostated samples were pipeted periodically into 2.5 ml of a quenching solution that contained acetate buffer, acetonitrile, and hydrochloric acid for neutralization of excess sodium hydroxide and internal standard and was 4.22×10^{-4} *M* in *m*-toluic acid. The HPLC procedure I was used for the assay.

Solvolysis Studies at Intermediate pH-Values—Acetate (pH 3.98–5.67), phosphate (pH 6.22–7.25), and borate (pH 7.72–11.85) buffers were prepared with ionic strengths of 0.1 adjusted with sodium chloride. The buffer solutions were preequilibrated in a constant-temperature bath before addition of appropriate amounts of stock solutions of I or II to obtain concentrations of 1.32×10^{-3} *M* and 8.51×10^{-4} *M* for I and II, respectively. Aliquots (0.5 ml) were removed periodically into 2.5 ml of quenching solution which contained 4.22×10^{-4} *M* *m*-toluic acid as internal standard to obtain the same composition as the HPLC mobile phase A. HPLC Procedure I was used for the assay.

Buffer Catalysis—Kinetic studies were conducted at several concentrations of buffers at a pH equal to the pK_a of appropriate buffer and constant ionic strength 0.1 (Table I). Additional studies at different pH values and concentrations of acetate buffer were effected. No significant buffer catalysis was observed in any of the buffers.

Potentiometric Determination of $pK_{a'}$ Values of I and II—Compound I or II (0.00017 mole) was dissolved in 5 ml of 0.1 *M* HCl, diluted with 20 ml of deionized water, and titrated potentiometrically with 0.1 *M* NaOH. The blank solutions, without I or II, were titrated similarly. The $pK_{a'}$ values were estimated from the plots of the difference between the number of milliliters of titer necessary to bring both blank solutions and solutions containing a drug to the same pH value (13). The $pK_{a'}$ values of I were estimated at several temperatures by half neutralizing solutions of I maintained at those temperatures and measuring the pH values as a function of time and extrapolating pH values back to time zero. This method was complicated by the 10–20 sec necessary to obtain electrode equilibration and the relatively fast degradation of I at these pH values and higher temperatures.

Kinetics of Degradation of Higher Concentrations of I in Plasma—An aliquot (0.4 ml) of an aqueous solution of 3.3×10^{-3} *M* I hydrochloride was evaporated under nitrogen to dryness, and the residue was mixed with 15 ml of heparinized fresh dog plasma, thermally equil-

[1] NIDA, 1140 Rockville Pike, Rockville, MD 20852.
[2] Malinckrodt Chemical Works, St. Louis, MO 63160.
[3] Eastman Kodak Co., Rochester, NY 14650.
[4] J. T. Baker Chemical Co., Phillipsburg, NJ 08865.
[5] Ricca Chemical Co., Arlington, TX 76012.
[6] Fisher Scientific Co., Chemical Manufacturing Division, Fair Lawn, NJ 07410.
[7] Model M-6000 A solvent delivery system and model U6K injector, Waters Associates, Milford, MA 01757.
[8] Model 440 absorbance detector, Waters Associates, Milford, MA 01757.
[9] Model 450 variable-wavelength UV detector, Waters Associates, Milford, MA 01757.

continued
containing 9.075×10^{-6} M (2.75 μg/ml) I, 8.54×10^{-6} M (2.6 μg/ml) II, and 9.368×10^{-6} M (1.14 μg/ml) III into mobile phase C. (g) Plasma obtained with citrate phosphate dextrose USP as anticoagulant and denatured 1:1 with acetonitrile. The mixture containing 9.075×10^{-6} M (2.75 μg/ml) I, 8.54×10^{-6} M (2.6 μg/ml) II, 9.368×10^{-6} M (1.14 μg/ml) III, and 4.14×10^{-5} M (5.28 μg/ml) p-chloroaniline (IS) was injected into mobile phase B after denaturation (1:1) with acetonitrile. (h) Plasma (1.0 ml) with 1.087×10^{-4} M II, 1.155×10^{-4} M I, and 1.192 M III was extracted with 2 ml of chloroform, adjusted to pH 3, and extracted with 10 ml butanol. The combined extracts were evaporated, reconstituted in 1.0 ml of mobile phase containing 5.94×10^{-4} M o-toluic acid (IS) and 25 μl was injected with mobile phase B. (i) Plasma (2.0 ml) at 0.50 μg/ml of I was extracted with 3.0 ml chloroform. An aliquot (2.0 ml) of extract was evaporated, the residue reconstituted in 0.2 ml of mobile phase, and 25 μl of 7.58×10^{-6} M solution (2.3 μg/ml) injected into mobile phase C (Procedure IV). The dashed line is for a sample treated similarly without I. The internal standard (IS) was 2.22×10^{-5} M p-chloroaniline in the injected sample.

Table II—Apparent Partition Coefficients for I (C_{org}/C_{buffer}) with Various Organic Phases

pH	Diethyl Ether	Hexane	Benzene	Methylene Chloride	Chloroform
10.7	161	46	—	220	>200
9.0	159	32	212	>200	237
8.2	22	7.5	135	—	185
5.9	0.023	0.07	1.6	4.0	5.5
3.9	—	—	0.04	0.22	0.30

ibrated at the body temperature of the dog (38.9°) to give an 8.8×10^{-3} *M* (299 μg/ml) or 8.8×10^{-4} *M* (29.9 μg/ml) solution. The residues were assayed with time by Procedures II and III, respectively.

Kinetics of Degradation of Lower Concentrations of I in Plasma—Since heparin interfered with the use of Procedure IV for the assay of low concentrations of cocaine, a citrate, phosphate, and dextrose solution USP[10] was used as the anticoagulant for assays of I in plasma at an initial concentration of 1.471×10^{-6} *M* (0.5 μg/ml) and 38.9° by this procedure. The spiked plasma was prepared in the same manner as described earlier.

Kinetics of Degradation of II in Plasma—An aliquot (0.35 ml) of an acetonitrile solution of 3.105×10^{-2} *M* II·4H_2O was evaporated under nitrogen to dryness, and the residue was mixed with 15 ml of heparinized fresh dog plasma to give a 7.245×10^{-4} *M* solution. Aliquots (0.5 ml) at 38.9° were periodically mixed with 0.5 ml of acetonitrile supernatant to be assayed by Procedure II.

Partition Studies as Function of pH—Partition studies between appropriate volume ratios of water-saturated organic solvent and buffer solutions of various pH values were effected by shaking mixtures containing I·HCl or II. Higher relative volumes of organic phase were used at the lower pH values of the buffer and lower volumes of organic solvent at higher pH values in the cocaine studies. Higher relative volumes of organic phase were used in the studies of II in each experiment. Aliquots of the separated organic phases were evaporated under nitrogen to dryness and assayed by HPLC Procedure I after reconstitution in the mobile phase. The aqueous phases were adjusted to the composition of the mobile phase and assayed similarly.

Red Blood Cell–Plasma and Buffer Partitioning—Aliquots of a stock solution of I hydrochloride (0.02 mg/ml) were evaporated to dryness and reconstituted with whole blood with an hematocrit of 41.5 or with a red blood cell suspension in plasma–water or buffer with an hematocrit of 32.5 and maintained at 38.9°. After 1 and 2 hr, the vials were centrifuged at 3000 rpm, and 0.5 ml of plasma or buffer layer was extracted with 1.0 ml of chloroform. An aliquot of the chloroform (0.75 ml) was evaporated and reconstituted in 1 ml of acetonitrile–0.085 *M* acetate buffer (25:75) (pH 3.6), and 25 μl was injected into mobile phase C for HPLC detection at 232 nm.

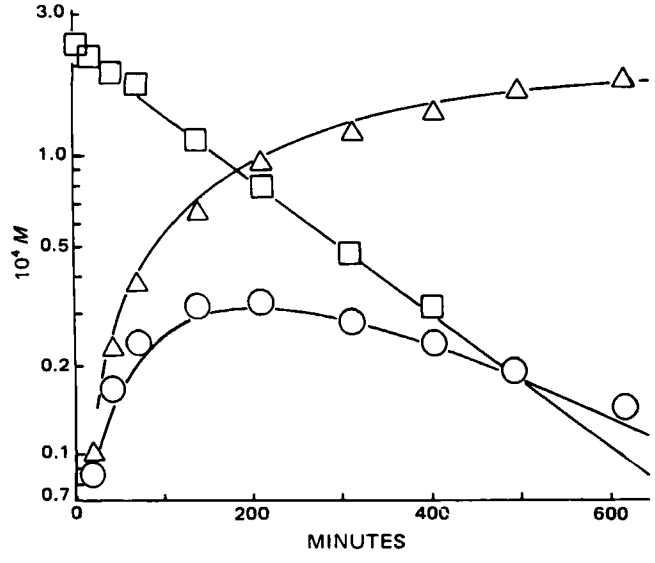

Figure 2—*Semilogarithmic plots of I, II, and III against time on I solvolysis in hydrochloric acid solutions. The curves through the data were calculated from the equations given in the text based on the kinetic constants given in the tables. The specific conditions of the kinetic study were for an initial concentration of 1.32×10^{-3} M I at 80.1° in 0.04 M HCl (pH 1.48). The initial theoretical concentration of the assayed quenched solution was 2.21×10^{-4} M in I. Key: (□) I; (○) II; (△) III.*

[10] McGaw Blood Products, McGaw Laboratories, Division of American Hospital Supply Corporation, Irvine, CA 92714.

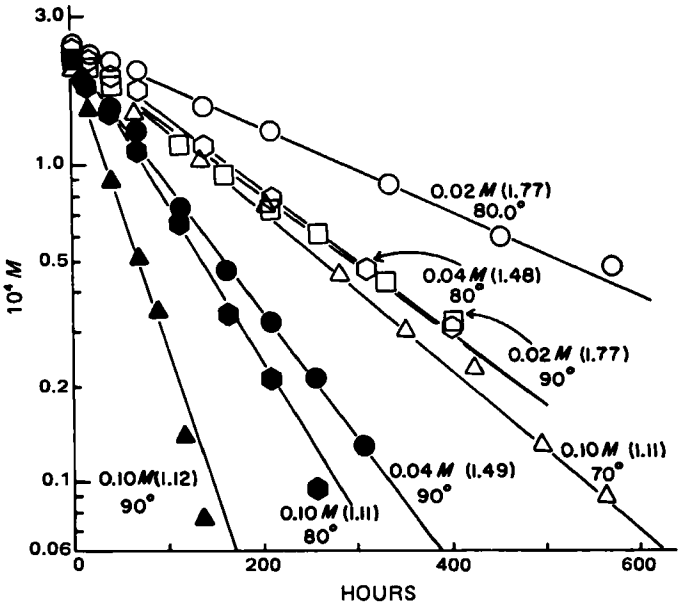

Figure 3—*Semilogarithmic plots of I in its quenched solution against time for its solvolysis in the labeled hydrochloric acid solutions. Calculated pH values are given in parentheses.*

Protein Binding by Ultrafiltration—Fresh ultrafiltration membrane cones[11] were used to filter 4 ml of plasma–water and plasma containing 1 μg/ml of I with centrifugation at 1000 rpm. The solutions were

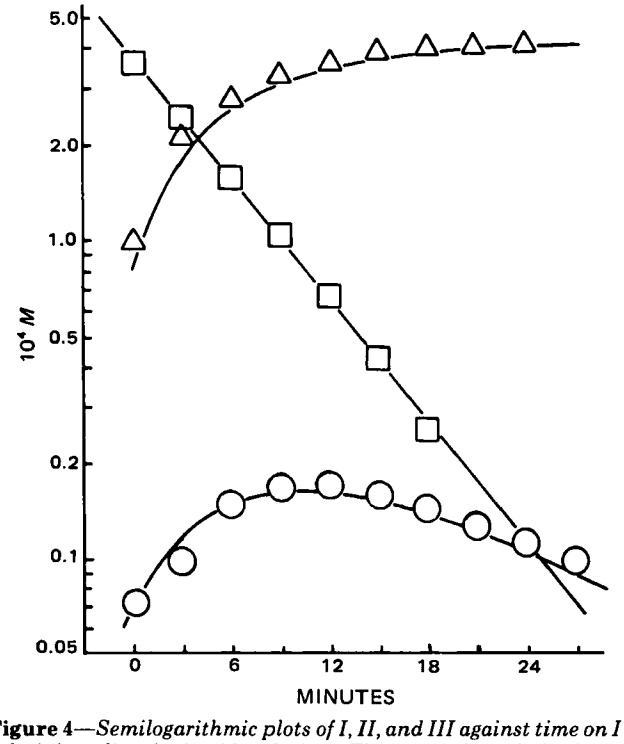

Figure 4—*Semilogarithmic plots of I, II, and III against time on I solvolysis in sodium hydroxide solutions. The curves through the data were calculated from the equations given in the text based on the kinetic constants given in the tables. The specific conditions of the kinetic study were for an initial concentration of 2.70×10^{-3} M I at 30.0° in 0.0373 M NaOH (pH 12.25). The initial theoretical concentration of the assayed quenched solution was 4.50×10^{-4} M in I. Key: (□) I; (○) II; (△) III.*

[11] Membrane filter cones 2100 CF 50, Amicon Co., Lexington, MA 02173.

Table III—First-Order Rate Constants (k, sec^{-1}) [a]

[NaOH][b]	Temperature	pH[c]	10^5k	10^5k_1	10^5k_2	10^5k_3
0.0884	15.1	13.18	208	12.5	80.0	195
0.0884	19.6	13.01	268	16.1	96.0	252
0.0884	30.0	12.67	534	32.1	160	502
0.0773	30.0	12.61	451	—	—	—
0.0573	30.0	12.50	382	20.2	115	362
0.0373	30.0	12.33	242	17.0	92.5	225
0.0170	30.0	12.02	101	12.7	61.0	87.1
0.0884	39.7	12.37	984	59.1	300	925
[HCl]						
0.100	70.0	1.11	0.161	0.0643	0.126	0.0965
0.020	80.0	1.77	0.0847	0.0381	0.0836	0.0467
0.040	80.0	1.48	0.144	0.0576	0.127	0.0864
0.100	80.0	1.11	0.319	0.128	0.246	0.192
0.020	90.0	1.77	0.140	0.0629	0.165	0.0768
0.040	90.0	1.49	0.265	0.111	0.240	0.154
0.100	90.0	1.12	0.588	0.223	0.491	0.335

[a] Rate constants for overall hydrolysis of I, for hydrolysis to II (k_1, sec^{-1}), and to IV (k_3, sec^{-1}) and for the hydrolysis of II (k_2, sec^{-1}) to ecgonine in hydrochloric acid and sodium hydroxide solutions (Scheme I). [b] Final compositions. Sufficient alkali was added to neutralize the added I hydrochloride. [c] The pH values for [NaOH] and [HCl] solutions were calculated from $pH = pK_w + \log f_{NaOH}[NaOH]$ and $pH = -\log f_{HCl}[HCl]$, respectively, from the pK_w values and activity coefficients, f_{NaOH} and f_{HCl}, available in the literature (15) for the designated temperatures, $pK_w = 2715(1/T) + 4.87$.

filtered, and the filtrates were assayed by the described HPLC procedures. Cones pre-equilibrated by filtering 2.5 ml of 6.0 ml of phosphate buffer (pH 7.5) containing 1 and 2 μg/ml, respectively, of I were also used. The same amount of plasma with the same concentrations of I were filtered through the respective cones, and the filtrate was assayed.

RESULTS AND DISCUSSION

HPLC Assays—The specific HPLC assays developed for cocaine (I) and its solvolysis products, benzoylecgonine (II) and benzoic acid (III), were applied to kinetic studies of the solvolysis of I and II and to partition studies of these compounds. Statistics of typical calibration curve regressions are given in Table I; HPLC chromatograms are given in Fig. 1. The analytical sensitivities ($2 \times s_{C\text{-}PHR}$) of 0.5–1.6 μg/ml (Procedure I, Table I; Fig. 1a) with UV detection at 254 nm with mobile phase A, of 1.0–3.0 μg/ml (Procedure II, Table I; Fig. 1b) were modified to 70–120 ng/ml by the use of a variable wavelength detector of 232 nm with a modified mobile phase B (Fig. 1g) or C (Fig. 1f; Procedure II, Table I) containing 0.0002 M tetrabutylammonium hydroxide in the 0.085 M acetate buffer.

Tetrabutylammonium hydroxide in mobile phase C increased the peak height sensitivity of the assay of I by decreasing its retention time (Fig. 1e). A concentration of 0.0002 M tetrabutylammonium hydroxide decreased the retention time of I from 6.6 to 3.2 min and 0.0004 M to 2.4 min. The tetrabutylammonium cation blocks adsorption sites on the column from I and effectively lowers the retention volume of I. The peak heights and retention times of the acidic II (2.3 min) and III (4 min) at pH 3.63 of the mobile phases, close to the pH of maximum stability of I and II, were not significantly affected by the tetrabutylammonium hydroxide.

Mobile phase B (Figs. 1b, 1g, and 1h) was advantageous in the assay of plasma solutions, in that plasma component peaks did not interfere with those of I and II in this system as they did in mobile phases A and C (Fig. 1i). The plasma component peaks did not interfere with the cocaine assay using mobile phase C in the extraction HPLC procedures III and IV (Fig. 1i), although some interferences were observed in C but not B at low concentrations of II. The sequential extraction procedures of III and methylecgonine (IV) permitted the selective assay of II in mobile phase B where there was no interference.

The retention times of heparin and I were similar in mobile phases B and C (Fig. 1d shows mobile phase C). Thus, the noninterfering citrate phosphate dextrose solution USP was used as the anticoagulant in plasma studies for the assay of low concentrations of I in mobile phase C (Fig. 1d). In this mobile phase, the anticoagulant, citrate phosphate dextrose solution USP, interfered with the peak of II (Fig. 1d) but did not interfere when mobile phase B was used (Fig. 1h).

The use of the developed extraction procedures with reconstitution into small volumes of the dried extracts gives analytical sensitivities from plasma of 15 ng/ml (Procedure IV and IV′, Table I) for I.

The apparent partition coefficients for I into several organic solvents are given in Table II for several pH values. All of the solvents listed showed potential complete extractions of I above pH 8.0. Chloroform appeared best suited for extraction at plasma pH values.

Compound II, at a pH of 6.32 where it exists as the zwitterion, had the following partition coefficients in the designated solvents: 0.4, ethyl acetate–acetonitrile (1:1); 0.79, isobutyl alcohol; and 0.87, *sec*-butyl alcohol. The partition coefficients for 1-butanol at pH 7.67, 6.32, and 3.89 were 1.02 ± 0.02 and were 0.30 ± 0.1 for *n*-butyl alcohol–chloroform (1:3). The partition coefficients for chloroform and methylene dichloride extraction of II were 0.12 ± 0.01 at pH 4, 6, 8, 9, and 11. Thus, 1-butanol was the most effective solvent for extraction of II.

These partition studies served as the basis for designing the sequential extraction of I and its metabolites. A primary extraction of I with limited amounts of chloroform at >pH 7 would remove negligible amounts of II, which could be reasonably extracted subsequently with 1-butanol. At pH 3, III would be readily extracted as well.

Kinetics of Solvolysis of I and II—At constant pH, I degrades by an apparent first-order process. Representative semilogarithmic plots of concentrations, C, against time are given for hydrochloric acid solutions (Figs. 2 and 3), sodium hydroxide solutions (Figs. 4 and 5), and buffers (Figs. 6 and 7), where the apparent first-order rate constants, k, were obtained from the slopes in accordance with:

$$\log C = -\frac{k}{2.303}t + \log C_0 \qquad \text{(Eq. 1)}$$

where C and C_0 are the concentrations at time t and time zero, respectively. These k-values are listed in Tables III and IV.

The pH values of the degrading buffer solutions were determined experimentally at the temperature of the study. The pH values for hydrochloric acid solutions were calculated from:

$$pH = -\log \gamma[HCl] \qquad \text{(Eq. 2)}$$

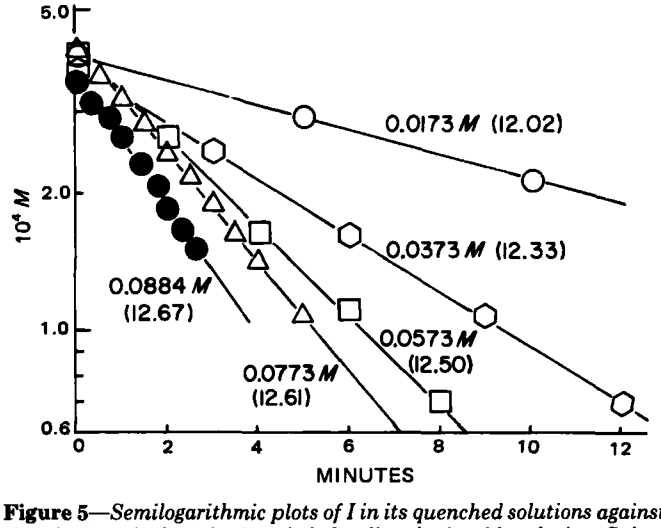

Figure 5—*Semilogarithmic plots of I in its quenched solutions against time for its solvolysis in the labeled sodium hydroxide solution. Calculated pH values at 30.0° are given in parentheses.*

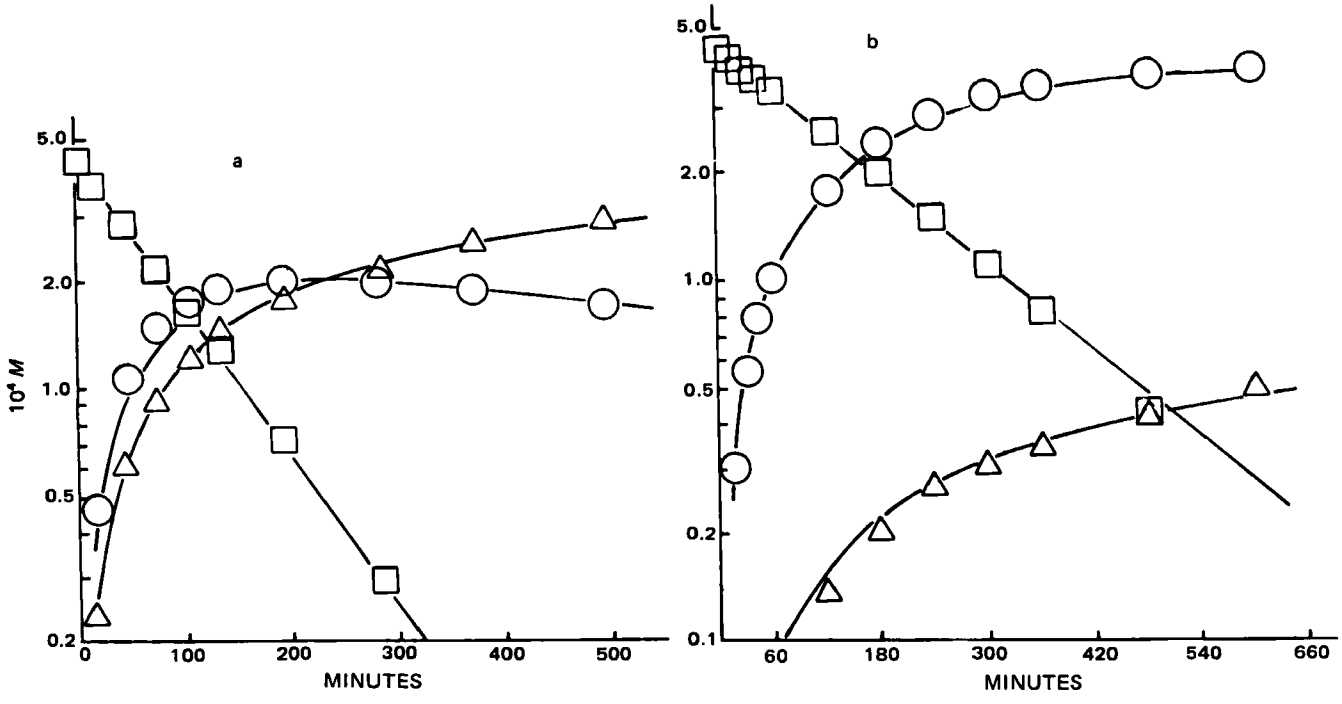

Figure 6—*Example of semilogarithmic plots of I, II, and III against time on I solvolysis in buffered solutions. The curves through the data were calculated from the equations given in the text based on the kinetic constants given in the tables. The specific conditions of the kinetic studies were for initial concentration of 2.65 × 10^{-3} M I at 30.0° at a) pH 10.33 and b) pH 9.09. The initial theoretical concentrations of the assayed quenched solutions were 4.41 × 10^{-4} M in I. Key: (□) I; (○) II; (△) III.*

where γ is the mean activity coefficient for the hydrochloric acid solutions. For sodium hydroxide solutions:

$$\text{pH} = pK_w - \text{pOH} = pK_w + \log \gamma[\text{NaOH}] \qquad \text{(Eq. 3)}$$

where γ is the mean activity coefficient for the sodium hydroxide solution (15) and values of pK_w are $-\log K_w$ where K_w is the hydrolysis constant for water.

In a similar manner, some direct measurements of the first-order rate constants, k_2, for II solvolysis to ecgonine (V) and III, (Scheme I) were determined. Examples of the semilogarithmic plots of concentrations, C, against time are given in Fig. 8, and the determined rate constants k_2 at the specified conditions are given in Table V.

Determination of Rate Constants in the Sequential Hydrolysis of I—The overall rate constant, k, for the hydrolysis of I is the sum of the separate constants, k_1 and k_3, for the routes to II and III plus IV, respectively (Scheme I):

$$k = k_1 + k_3 \qquad \text{(Eq. 4)}$$

If I were hydrolyzed solely to II, *i.e.*, $k_3 = 0$, the concentration of generated II would be (16):

$$[\text{II}]' = [\text{I}]_0 \frac{k}{k_2 - k}(e^{-kt} - e^{-k_2 t}) \qquad \text{(Eq. 5)}$$

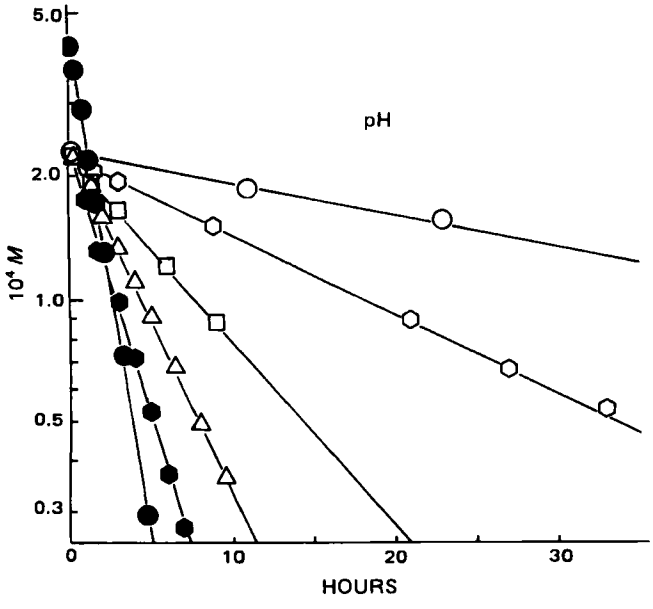

Figure 7—*Semilogarithmic plots of I in its quenched solutions against time for its solvolysis in the buffer at 30.0°. Key: (●) pH 10.33; (●) pH 8.94; (△) pH 8.55; (□) pH 8.15; (○) pH 7.72; (○) pH 7.25.*

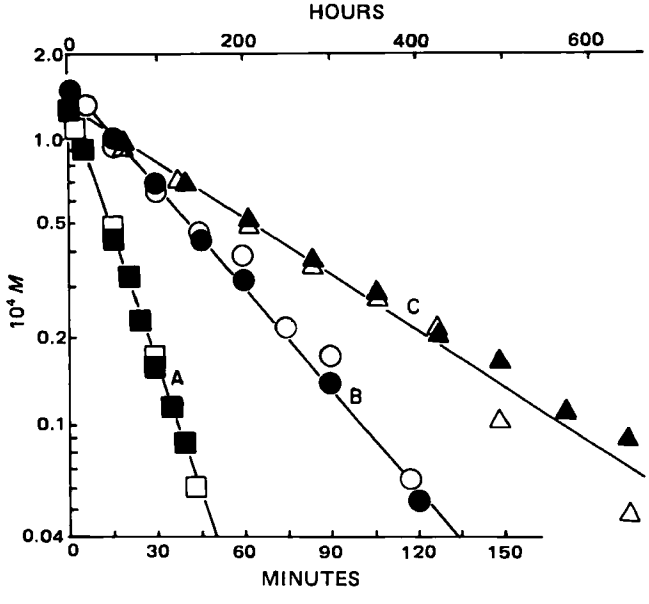

Figure 8—*Semilogarithmic plots of II concentrations (c_0 = 1.42 × 10^{-4} M) in quenched solutions against time. The solid symbols are for plots of II against time. The open symbols are for the difference plots of III, $[III]_\infty - [III]$ against time: A) 0.060 M NaOH, pH 12.32 at 30.0° against time scale in minutes; B) borate buffer, pH 8.92 at 80.0° against time scale in minutes; C) 0.04 M HCl solution, pH 1.41 at 80.0° against time scale in hours. The initial concentration of II in the reaction mixture was 8.52 × 10^{-4} M.*

Table IV—First-Order Rate Constants (k, sec^{-1}) [a]

Buffer	Temperature	pH	10^5k	10^5k_1	10^5k_2	10^5k_3
Borate	30.0	11.85	105	—	—	—
Borate	30.0	11.38	52.7	10.5	27.0	42.2
Borate	30.0	10.33	15.6	9.53	2.08	6.10
Borate	30.0	9.63	10.2	9.15	0.417	1.02
Borate	30.0	9.09	7.74	7.12	0.133	0.619
Borate[b]	30.0	9.14	10.1	8.96	0.150	1.11
Borate[c]	30.0	9.15	10.2	—	—	—
Borate[d]	30.0	9.14	9.81	—	—	—
Borate	30.0	8.94	8.26	7.43	0.0980	0.826
Borate	30.0	8.55	5.83	5.13	0.0400	0.700
Borate	30.0	8.15	2.92	2.63	0.0160	0.292
Borate	30.0	7.72	1.25	1.12	0.0054	0.125
Phosphate[e]	30.0	7.25	0.497	0.447	0.0019	0.50
Phosphate[f]	30.0	7.26	0.500	—	—	—
Phosphate[g]	30.0	7.27	0.507	—	—	—
Phosphate	70.0	6.22	4.37	3.94	0.0833	0.43
Phosphate	80.0	6.26	11.4	10.2	0.136	1.2
Phosphate	90.0	6.25	37.1	33.4	0.250	3.71
Acetate	80.0	5.23	1.78	1.60	0.0540	0.18
Acetate	80.0	4.70	0.362	—	—	—
Acetate	80.0	4.38	0.241	0.224	0.039	0.017
Acetate[h]	90.0	5.65	7.37	6.34	0.0917	1.03
Acetate[i]	90.0	5.65	7.22	—	—	—
Acetate	90.0	5.24	3.64	3.20	0.0840	0.44
Acetate[j]	90.0	4.70	1.30	1.14	0.0833	0.16
Acetate[k]	90.0	4.69	0.985	—	—	—
Acetate[l]	90.0	4.69	0.966	—	—	—
Acetate[l]	90.0	4.69	0.812	—	—	—
Acetate	90.0	4.37	0.640	0.557	0.0833	0.083
Acetate[m]	90.0	4.06	0.293	0.258	0.080	0.035
Acetate[n]	90.0	4.05	0.275	—	—	—
Acetate[o]	90.0	4.04	0.242	—	—	—
Acetate[p]	90.0	4.06	0.201	—	—	—

[a] Rate constants for overall hydrolysis of I, for hydrolysis to II (k_1, sec^{-1}) and IV (k_3, sec^{-1}) and for the hydrolysis of III (k_2, sec^{-1}) to ecgonine in buffer solutions at 0.1 ionic strength (Scheme I). [b] The composition of the borate buffer in the reaction mixture was 0.1 *M* NaH_2BO_3 + 0.1 *M* H_3BO_3. [c] The borate buffer in footnote *b* was diluted 1:1 with 0.1 *M* NaCl. [d] The borate buffer in footnote *b* was diluted 1:3 with 0.1 *M* NaCl. [e] The composition of the phosphate buffer in the reaction mixture was 0.017 *M* NaH_2PO_4 + 0.017 *M* Na_2HPO_4 + 0.033 *M* NaCl. [f] The phosphate buffer of footnote *e* was diluted 1:1 with 0.1 *M* NaCl. [g] The phosphate buffer of footnote *e* was diluted 1:3 with 0.1 *M* NaCl. [h] The composition of the acetate buffer in the reaction mixture was 0.011 *M* CH_3COOH + 0.089 *M* CH_3COONa + 0.011 *M* NaCl. [i] The acetate buffer of footnote *h* was diluted 4:1 with 0.1 *M* NaCl. [j] The composition of the acetate buffer in the reaction mixture was 0.05 *M* CH_3COOH + 0.05 *M* CH_3COONa + 0.05 *M* NaCl. [k] The acetate buffer of footnote *j* was diluted 1:1 with 0.1 *M* NaCl. [l] The acetate buffer of footnote *j* was diluted 1:3 with 0.1 *M* NaCl. [m] The composition of the acetate buffer in the reaction mixture was 0.083 *M* CH_3COOH + 0.017 *M* CH_3COONa + 0.083 *M* NaCl. [n] The acetate buffer of footnote *m* was diluted 4:1 with 0.1 *M* NaCl. [o] The acetate buffer of footnote *m* was diluted 1:1 with 0.1 *M* NaCl. [p] The acetate buffer of footnote *m* was diluted 1:4 with 0.1 *M* NaCl.

where $[I]_0$ is the initial concentration of I and [II]′ is the predicted concentration of II on the presumption that the sole route of hydrolysis is:

$$I \xrightarrow{k} II + CH_3OH \xrightarrow{k_2} III + IV$$

However, if IV and III were also products of the hydrolysis of I, the actual concentration of II, would be (9, 17):

$$[II] = [I]_0 \frac{k_1}{k_2 - k}(e^{-kt} - e^{-k_2t}) \qquad \text{(Eq. 6)}$$

where

$$k_1/k = [II]/[II]' \qquad \text{(Eq. 7)}$$

Thus, the ratios of the observed experimental concentrations of II, [II], to the concentrations generated by Eq. 5 for a given time [II]′, will be constant, and the k_1 and k_3 values can be estimated from Eqs. 7 and 4, respectively.

The apparent first-order rate constant, k_2, for the hydrolysis of II could be obtained from the terminal slope of the semilogarithmic plots of its generation from I with time (Figs. 2, 4, and 6) or from the direct kinetic studies of II (Fig. 7, Table V).

An alternate method to deduce k_1 and k_2 values is to best fit Eq. 6 to the time-course data of experimentally determined concentrations of II with appropriate adjustments of k_1 and k_2 as was done in Figs. 2, 4, and 6 where the curves drawn through the data were drawn in accordance with Eqs. 1 and 6 for I and II, respectively. The appropriate constants are listed in Tables III–V. The calculated time curve for [III] was calculated from:

$$[III] = [I]_0 - [II] \qquad \text{(Eq. 8)}$$

The data show that, contrary to prior implications (5), the route to II is not the only route of hydrolysis of I at pH >1.0.

The fraction through the route for II on hydrogen ion attack on protonated I <pH 2.0 is 0.4 (Fig. 2 and Table III). The fraction through this route for hydroxide ion attack on neutral I >pH 11.5 is only 0.06 (Fig. 4, Table III), whereas the hydroxide attack on protonated I between pH 4 and 10 gives a fraction of 0.90 (Fig. 6, Table IV). There are intermediate fractions between the stated pH ranges.

Log k–pH Profiles for I—The log k–pH profiles (6) for the overall hydrolysis of I (Fig. 9), the log k_1–pH profiles for the hydrolysis of I through II (Fig. 10), and the log k_3–pH profiles for the hydrolysis of I through IV and III (Fig. 11) are fitted in accordance with:

$$k_i = (k'_{OH})_i\, a_{OH}\, [I] + (k_{OH})_i\, a_{OH}[IH^+] + (k_H)_i\, a_{H^+}\, [IH^+] \qquad \text{(Eq. 9)}$$

where k_i is k, k_1, or k_3; a_{H^+} and a_{OH^-} are the respective activities of the hydrogen and hydroxyl ions; [I] and $[IH^+]$ are the respective concentrations of neutral and protonated I; $(k'_{OH})_i$ is the specific bimolecular rate constant for hydroxide ion attack on neutral I; $(k_{OH})_i$ is the specific bimolecular rate constant for hydroxide ion attack on protonated I; and $(k_H)_i$ is the specific bimolecular rate constant for hydrogen ion attack on protonated I.

The acid branches of the log k_i–pH profiles can be fitted to:

$$\log k_i = \log (k_H)_i - pH \qquad \text{(Eq. 10)}$$

to obtain estimates of $(k_{H^+})_i$.

The alkaline branches are characterized by:

$$k_i = (k'_{OH})_i\, f_I\, a_{OH} + (k_{OH})_i\, f_{(IH^+)}\, a_{OH} \qquad \text{(Eq. 11)}$$

where f_I is the fraction of I concentration that is the neutral species, and $f_{(IH^+)}$ is the fraction that is the protonated species. These fractions can be calculated from the known pH, pK'_a, and pK_w values from:

$$f_I = \frac{K'_a}{K'_a + a_{H^+}} \qquad \text{(Eq. 12)}$$

$$f_{(IH^+)} = \frac{a_{H^+}}{K'_a + a_{H^+}} \qquad \text{(Eq. 13)}$$

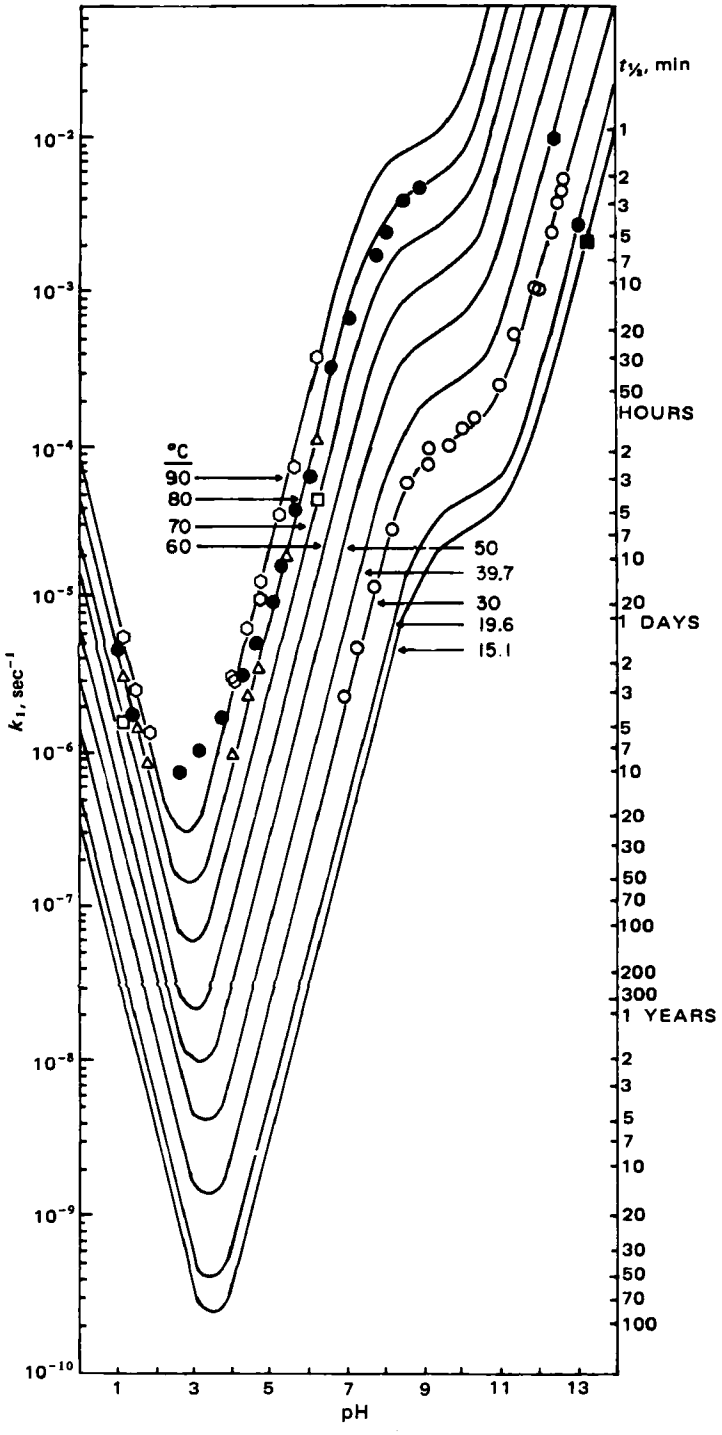

Figure 9—*Fitted and predicted log* k–*pH profiles for the overall hydrolyses of I at the designated temperatures. The fits and predictions are in accordance with:* $k = k_{H}a_{H^+} + k_{OH}\,[K_w/(K'_a + a_{H^+})] + k'_{OH}\,[K'_aK_w/(K'_a + a_{H^+})]$ *and* $\ln k_j = \ln P - 10^3\,(\Delta H_a/R)(1/T)$ *where the pertinent parameters are listed in Table VI,* ΔH_a *is in kcal/mole,* $a_{H^+} = 10^{-pH}$ *and* T *is in degrees Kelvin. The solid symbols are previously reported data (Ref. 5) for rate constants obtained at 80° plotted against the stated pH values for the various buffer solutions.*

where $a_{H^+} = 10^{-pH}$, $K_w = 10^{-pK_w}$ and $K'_a = 10^{-pK'_a}$. Since $K_w = a_{H^+}a_{OH^-}$, Eq. 11 can be modified to:

$$k_i = (k'_{OH})_i \frac{K'_a K_w}{(K'_a + a_{H^+})a_{H^+}} + (k_{OH})_i \frac{K_w}{(K'_a + a_{H^+})} \qquad \text{(Eq. 14)}$$

which was used to fit the alkaline branches of the log k_i–pH profiles of Figs. 9–11 with the parameters listed in Table VI.

The potentiometrically determined pK'_a of I was 8.81 at 25°. The apparent pK'_a values obtained by extrapolation of the pH-values of half-neutralization back to time zero were 8.81 at 25°, 8.70 at 30°, 8.30 at 60°, 8.19 at 70°, 8.04 at 80°, and 7.95 at 90°. These pK'_a values can be characterized by $1429(1/T) + 4.02$, where T is degress Kelvin but are suspect, since degradation of I at these pH-values and temperatures were fast. When the kinetic pK'_a values of best fit at 30 and 80° were used to esti-

Table V—First-Order Rate Constants (k_2, sec^{-1}) from Direct Studies of the Hydrolysis of II

[NaOH]	Temperature	pH[a]	10^5k_2
0.0992	30.0	12.71	154
0.0592	30.0	12.51	113
0.0392	30.0	12.34	95.0
0.0192	30.0	12.06	64.2
0.0192	40.0	11.76	132
0.0192	50.0	11.49	280
0.0192	60.0	11.24	516
[HCl]			
0.0992	70.0	1.12	0.126
0.0992	80.0	1.12	0.249
0.0392	80.0	1.49	0.127
0.0192	80.0	1.79	0.0836
0.0992	90.0	1.12	0.491
0.0392	90.0	1.50	0.256
0.0192	90.0	1.79	0.165
Buffer			
Borate	30.0	10.33	1.65
Borate	30.0	9.59	0.474
Borate	30.0	9.25	0.190
Borate	30.0	9.09	0.126
Borate	80.0	8.92	45.2
Borate	90.0	8.94	93.9
Acetate	90.0	5.27	0.883
Acetate	90.0	4.43	0.695

[a] The pH-values for [NaOH] and [HCl] solutions were calculated from $pH = pK_w + \log f_{NaOH}[NaOH]$ and $pH = -\log f_{HCl}[HCl]$, respectively, from the pK_w values and activity coefficients, f_{NaOH} and f_{HCl}, available in the literature (15) for the designated temperatures.

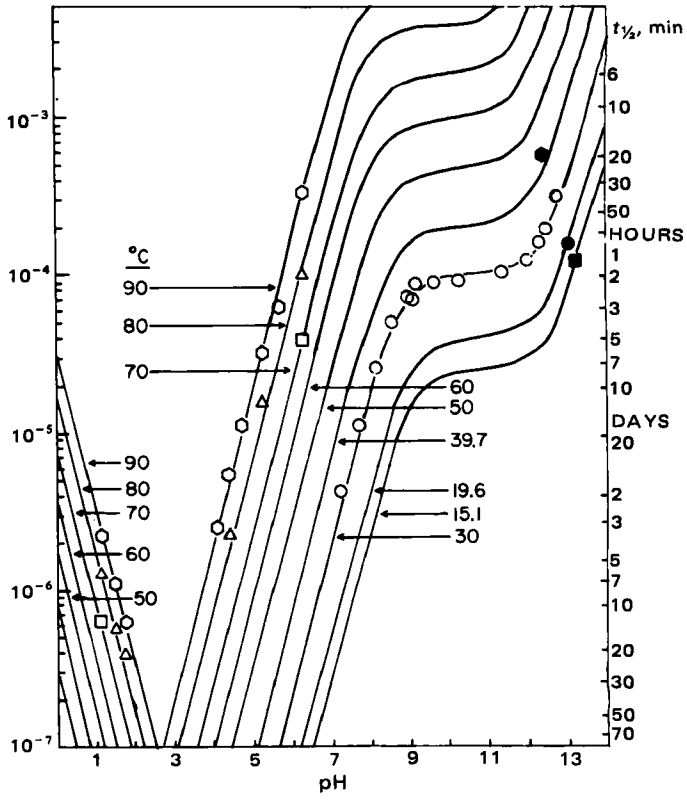

Figure 10—*Fitted and predicted log* k_1–*pH profiles for the hydrolysis of I to II at the designated temperatures. The fits and predictions are in accordance with:* $k_1 = (k_H)_1a_{H^+} + (k_{OH})_1\,[K_w/(K'_a + a_{H^+})] + (k'_{OH})_1\,K'_aK_w/[(K'_a + a_{H^+})a_{H^+}]$ *and* $\ln k_j = \ln P - 10^3(\Delta H_a/R)(1/T)$ *where the pertinent parameters are listed in Table VI,* ΔH_a *is in kcal/mole,* $a_{H^+} = 10^{-pH}$ *and* T *is in degrees Kelvin.*

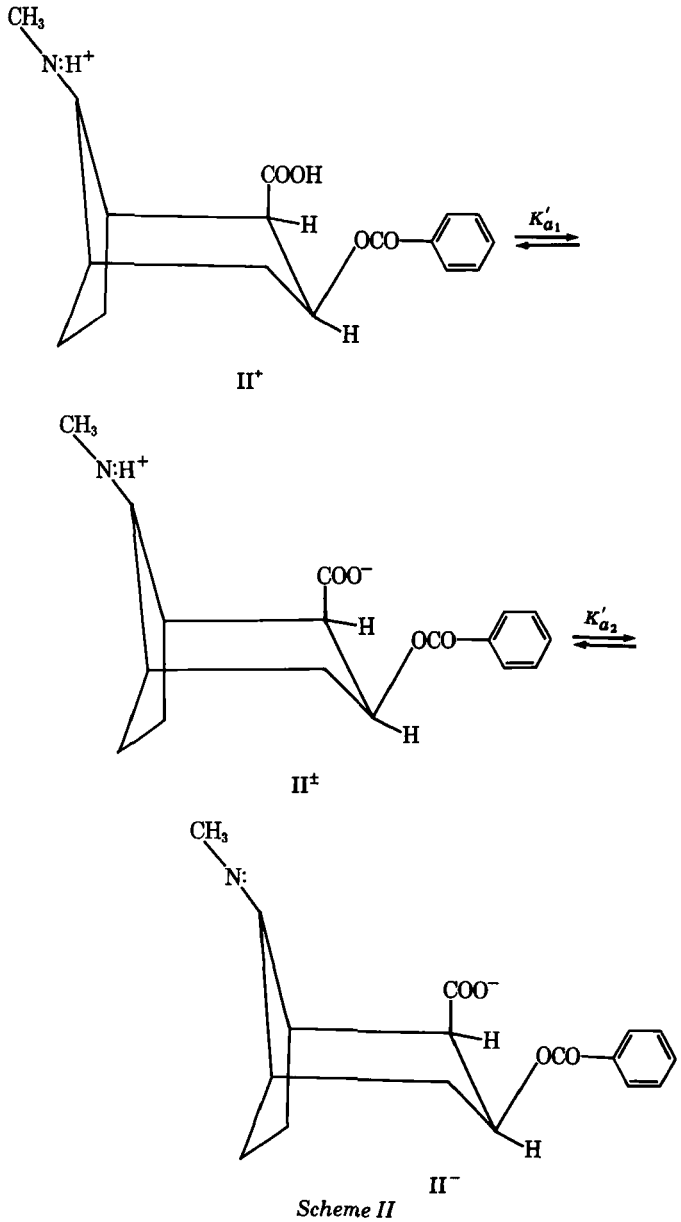

Scheme II

mate temperature dependency, the expression was $1938(1/T) + 2.22$. These values were used in the predicted log k–pH profiles of Figs. 9–11 and are listed in Table VI. The kinetic pK'_a of 7.7 at 80° was estimated from previously reported data (5) on the assumption that the given pH values were measured at the temperature of the reaction. Unfortunately, it was not stated (5) whether or not this was true, so that the possibility of erroneously chosen pH values at 80° cannot be excluded.

The apparent first-order rate constants given previously (5) for studies conducted at 80° and at concentrations tenfold higher than those studied here agreed with the predicted values (Fig. 9) in the 5–6.5 and 0–2 pH ranges. The values were significantly higher than the predicted values in the 2.5–4.5 range. It was probably due to the observed (5) enhancing buffer effects on rate by the citric acid–potassium citrate buffer solution used in the pH 2.2–4.8 range. No general acid–base effects were observed with the buffers used in these present studies.

Log k_2–pH Profiles for II—The log k_2–pH profiles for the solvolysis of II are given in Fig. 12 and were fitted with the estimated parameters given in Table V. The two pK'_a values for II (Scheme II) at room temperature were determined potentiometrically and were 11.75 and 2.1. In this case the acid branch (Eq. 10) of the log k–pH profile would be for the attack of hydrogen ion on the protonated II, whereas below the pK'_{a2} of 11.75, the alkaline branch would be for the hydroxide ion attack on the zwitterion. Above this value, the attack of hydroxide ion would be on the negatively charged compound, and:

$$k_2 = (k'_{OH})_2 f_{II^+} a_{OH} + (k_{OH})_2 f_{II^\pm} a_{OH} \qquad \text{(Eq. 15)}$$

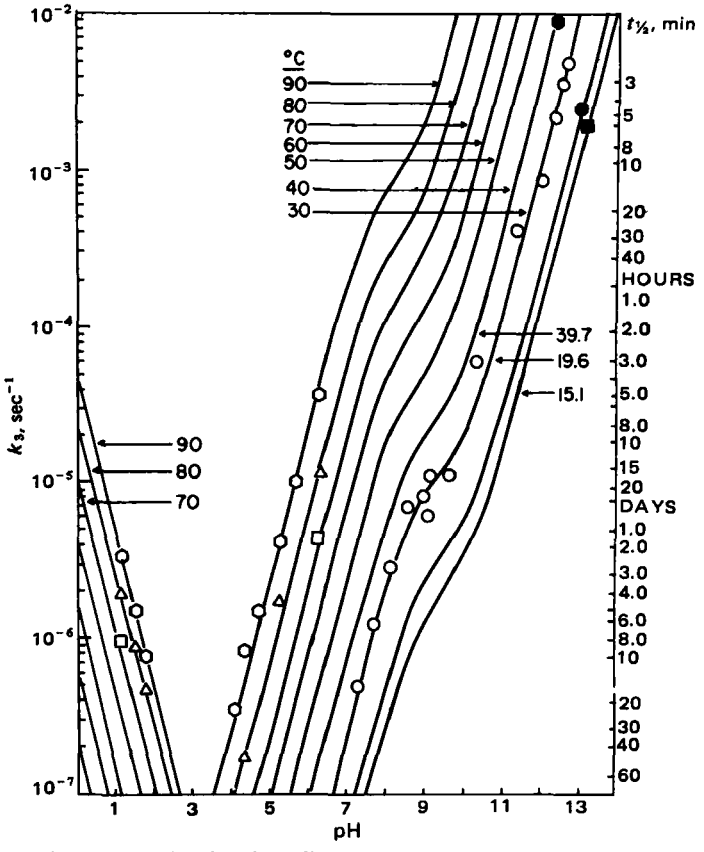

Figure 11—*Fitted and predicted log* k_3*–pH profiles for the hydrolysos of I to IV at the designated temperatures. The fits and predictions are in accordance with:* $k_3 = (k_H)_3 a_{H^+} + (k_{OH})_3 [K_w/(K'_a + a_{H^+})] + (k'_{OH})_3 K'_a K_w/[(K'_a + a_{H^+})a_{H^+}]$ *and ln* $k_j = ln\ P - 10^3(\Delta H_a/R)(1/T)$ *where the pertinent parameters are listed in Table VI,* ΔH_a *is in kcal/mole,* $a_{H^+} = 10^{-pH}$ *and T is in degrees Kelvin.*

where the respective fractions of anionic II (f_{II^-}) and zwitterionic II ($f_{II^\pm}$) >pH 3 are:

$$f_{II^+} = \frac{(K'_{a2})_{II}}{(K'_{a2})_{II} + a_{H^+}} \qquad \text{(Eq. 16)}$$

and:

$$f_{II^\pm} = \frac{a_{H^+}}{(K'_{a2})_{II} + a_{H^+}} \qquad \text{(Eq. 17)}$$

where the pertinent charged structures are given in Scheme II.

Thus, the alkaline branch above pH 6 can be fitted to:

$$k_2 = \frac{(k'_{OH})_2 (K'_{a2})_{II} K_w}{[(K'_{a2})_{II} + a_{H^+}]a_{H^+}} + \frac{(k_{OH})_2 K_w}{(K'_{a2})_{II} + a_{H^+}} \qquad \text{(Eq. 18)}$$

and the acid branch $<pK'_{a1}$ of 2.1 can be fitted to:

$$k_2 = (k_{H^+})_2 f_{II^+} a_{H^+} \qquad \text{(Eq. 19)}$$

where the fraction of protonated II (Scheme II) is:

$$f_{II^+} = \frac{a_{H^+}}{(K'_{a1})_{II} + a_{H^+}} \qquad \text{(Eq. 20)}$$

The fact that there is a pH-independent segment of the log k_2–pH profile at pH 4–5 at the studied temperatures of 80 and 90°, indicates an additional functional dependency for the first-order rate constant, k_2. This additional factor can be rationalized by an hydroxyl ion attack on positively charged II or its kinetic equivalent of water attack on the zwitterion ($II^\pm$):

$$(k_0)_2 f_{II^\pm} = (k''_{OH})_2 a_{OH} f_{II^+} = (k_0)_2 \frac{K'_{a1}}{a_{H^+} + K'_{a1}}$$

$$= (k''_{OH})_2 a_{OH} \frac{a_{H^+}}{a_{H^+} + K'_{a1}} = \frac{(k''_{OH})_2 K_w}{a_{H^+} + K'_{a1}} \qquad \text{(Eq. 21)}$$

where $(k''_{OH})_2 K_w = (k_0)_2 K'_{a1}$.

Thus, an additional dip ~pH 2–4 in the log k_2–pH profile of II can be

Table VI—Parameters for the log k_i^a–pH Profiles for the Hydrolyses of I

Temperature	$10^7 k_H$	k_{OH}	$10^2 k'_{OH}$	$10^7(k_H)_1$	$(k_{OH})_1$	$10^3(k'_{OH})_1$	$10^7(k_H)_3$	$(k_{OH})_3$	$10^2(k'_{OH})_3$	pK'^b_a
15.1	4.0	6.6	2.74	0.75	6.0	0.99	0.82	0.57	2.57	8.94
19.6	6.0	8.8	3.70	1.4	8.4	1.34	1.29	0.78	3.48	8.84
30.0	14.0	18.6	7.65	3.3	17.0	2.33	3.25	1.70	7.76	8.61
39.7	30.0	34.0	15.2	8.0	29.8	4.60	8.00	3.0	14.3	8.41
50.0	64.0	64.0	31.5	18.3	56	7.00	18.0	5.4	28.8	8.22
60.0	130	114	58.5	41.0	98	11.9	40.5	9.5	56.5	8.04
70.0	240	196	100	84.0	160	19.0	83.0	16.0	95.0	7.87
80.0	450	330	170	170	280	29.0	180	26.0	163	7.71
90.0	800	537	290	320	424	45.0	330	54.9	270	7.55
ΔH_a	15.1	12.3	13.0	16.9	11.8	10.6	16.8	11.8	13.1	
ln P	11.52	23.30	19.14	13.05	22.47	11.64	13.03	20.05	19.17	
$\Delta S^\ddagger$	−35.8	−12.3	−20.6	−32.7	−14.0	−35.5	−32.7	−18.8	−20.5	

[a] Log k_i–pH profiles are from Figs. 9–11; the apparent first-order rate constants (k, k_1, and k_3) for the routes of Scheme I are in sec^{-1}, where the given bimolecular rate constants are in liter/mole/sec, ΔH_a is in kcal/mole, and $\Delta S^\ddagger$ is in entropy units (eu) where $\Delta S^\ddagger = R[\ln P - (\ln k_B T/k)]$, the Boltzmann constant $k_B = 1.387 \times 10^{-16}$ erg/deg and the Planck constants $h = 6.623 \times 10^{-27}$ erg sec, and T is 313°K. [b] Values at 30 and 80° were obtained from the best log k–pH fit at these temperatures. Values at other temperatures were calculated from $pK'_a = 1938(1/T) + 2.22$.

predicted (dashed line in Fig. 12). This could be calculated exactly if the K'_{a1} values of Eq. 20 were known at all temperatures. The total dependency would be:

$$k_2 = (k_H)_2 a_{H^+} \frac{a_{H^+}}{a_{H^+} + K'_{a1}} + (k_0)_2 \frac{K'_{a1}}{a_{H^+} + K'_{a1}} + (k_{OH})_2 \frac{K_w}{K'_{a2} + a_{H^+}} + (k'_{OH})_2 \frac{K'_{a2} K_w}{[K'_{a2} + a_{H^+}] a_{H^+}} = (k_H)_2 a_{H^+} f_{II^+} + [(k_0)_2 + (k_{OH})] f_{II^\pm} + (k'_{OH})_2 f_{II^-} \quad \text{(Eq. 22)}$$

Temperature Dependency and Strategy for Stability Prediction—Studies of this nature delineate stabilities or reaction rates at all temperatures and pH-values with a minimum of experimental effort. An appropriate strategy is to determine first the functional kinetic dependencies from the dependence of the apparent first-order rate constant, k, on pH at a given temperature. If this were accomplished, pH regions could be ascertained where the only significant reaction was due to the attack of one ion on only one ionic species of substrate, *e.g.*, hydroxyl ion attack on protonated I with a bimolecular rate constant of k_{OH}. Similarly, the k_H bimolecular rate constant (Eq. 22) for hydrogen ion catalysis could be determined in the highly acidic pH region.

The specific bimolecular rate constant for hydroxyl ion catalysis, k_{OH}, of a unique ionic substrate species can be determined readily, since:

$$\log k_{OH} = \log k + pK_w - \text{pH} \quad \text{(Eq. 23)}$$

and k_{OH} can be estimated from any k–pH pair in the region where a linear positive slope of unity exists in the log k–pH profile. Similarly, the bimolecular rate constant for hydrogen ion catalysis, k_H, of a unique ionic substrate species can be determined from:

$$\log k_H = \log k + \text{pH} \quad \text{(Eq. 24)}$$

and k_H can be estimated from any k–pH pair where a linear negative slope of unity exists in the log k–pH profile.

Such bimolecular rate constants, k_j, which may be either k_{OH}, k'_{OH}, or k_H, can be related to temperature by the Arrhenius rule:

$$\ln k_j = \ln P - \left(\frac{10^3 \Delta H_a}{R}\right)\frac{1}{T} \quad \text{(Eq. 25)}$$

where ΔH_a is the heat of activation (kcal/mole) and T is the absolute temperature (degrees Kelvin). The k_j-values at several temperatures could be estimated from a single k–pH pair obtained at a given temperature in the pH region, where only one catalytic process was extant. Arrhenius plots of such bimolecular rate constants for the solvolysis of I and II in accordance with Eq. 25 are given in Fig. 13, and the determined Arrhenius parameters, ΔH_a and ln P, are listed in Tables VI and VII. For the experimental convenience of limiting the times of kinetic studies without being excessively fast, Arrhenius parameters were obtained at high temperatures (70–90°) for hydrogen ion (k_H) and hydroxyl ion (k_{OH}) attack on protonated I ($I{\cdot}H^+$) and at low temperatures (15–40°) for hydroxyl ion attack (k'_{OH}) on neutral I (Figs. 9–11). Similar choices of appropriate temperatures and pH ranges were made in the studies of II (Fig. 12) for appropriate calculations of bimolecular rate constants (k_j) and subsequent estimations of their Arrhenius parameters (Fig. 13, Table VII).

If pK'_a values were known at several temperatures, as from independent potentiometric titrations, the apparent first-order rate constants, k_i, could be calculated readily in the intermediate pH regions where several rate processes exist concomitantly, from expressions such as Eq. 14 for the solvolysis of I and Eqs. 18 and 22 for the solvolysis of II. The respective bimolecular rate constants, k_j, at the respective temperatures as listed in Tables VI and VII could be calculated from Eq. 25 using the determined Arrhenius parameters.

If apparent first-order rate constants were obtained in the pH region of transition from one rate process to another (*e.g.*, at pH 7–11 where solvolytic dependencies of I change from hydroxyl ion attack on the protonated species to that on a neutral species as in Figs. 9–11), the pK'_a for the dissociation of the substrate as an acid can be obtained by fitting the more complex dependency of the apparent first-order rate constant, k, on pH on K'_a. In the case of I, Eq. 14 was fitted with a best-estimated pK'_a in this transition region at 30°, where k_{OH} and k'_{OH} had been determined from linear segments of the log k–pH profiles from application of Eq. 23.

In the case of II, Eq. 18 could be fitted with a best-estimated K'_{a2} in the transition pH region where reaction dependency changes from hydroxyl ion attack on the zwitterion to hydroxyl ion attack on the anion of II if the $(k_{OH})_2$ and $(k'_{OH})_2$ values were known. Unfortunately, the high pK'_{a2} (11.75 at room temperature) of the zwitterion of II (Scheme III) does not

Table VII—Parameters for the log k_2^a–pH Profiles for the Hydrolyses of II

Temperature	$10^7(k_H)_2$	$10^9(k_0)_2^a$	$10^2(k_{OH})_2$	$10^3(k'_{OH})_2$	pK'_{a2}	pK_w
15.1	0.68	0.93	2.4	5.53	12.5	14.30
19.6	1.11	1.50	3.4	7.98	12.2	14.15
30.0	3.52	4.60	7.4	12.5	11.7	13.83
39.7	9.50	13.0	15.2	34.7	11.3	13.56
50.0	26.0	32.0	29.5	112	10.8	13.28
60.0	67.0	80.3	57.0	253	10.3	13.03
70.0	150	180	100	410	9.9	12.79
80.0	350	400	202	750	9.6	12.57
90.0	700	800	241	1300	9.2	12.35
ΔH_a	19.4	18.9	13.8	15.2		
ln P	17.39	12.26	20.30	21.34		
$\Delta S^\ddagger$	−24.1	−34.3	−18.3	−16.2		

[a] The log k_2 profiles are from Fig. 12; the given bimolecular rate constants are in liter/mole/sec, ΔH_a is in kcal/mole, $\Delta S^\ddagger$ is in entropy units (eu) where $\Delta S^\ddagger = R[\ln P - (\ln k_B T/k)]$ and the Boltzmann constant $k_B = 1.387 \times 10^{-16}$ erg/deg, and the Planck constant $h = 6.623 \times 10^{-27}$ erg/sec, and T is 313°K. The apparent first-order rate constants k_2 and k_0 are in sec^{-1}.

Table VIII—Arrhenius Parameters [a] for Apparent First-Order Rate Constants for Solvolysis of I Under Different Conditions

Medium	pH	k		k_1		k_2		k_3	
		ΔH_a	$\ln P$	ΔH_a	$\ln P$	ΔH_a	$\ln P$	ΔH_a	$\ln P$
0.1 *M* HCl	1.11	15.9	10.00	16.5	9.97	17.2	11.65	14.6	7.68
Phosphate buffer	6.25	26.2	11.15	26.5	28.8	13.9	6.31	27.3	27.62
0.0884 *M* NaOH	12.17	11.2	13.31	11.6	11.2	8.76	8.17	11.4	13.55

[a] The parameter $\ln k_i = \ln P - (10^3\,\Delta H_a/R)(1/T)$ where R = 1.987 cal/deg and ΔH_a is in kcal/mole.

permit the immediate determination of $(k'_{OH})_2$ from a linear segment of the pH profile (Fig. 12) above a pH equal to pK'_{a2}. The experimentally determined apparent first-order rate constants (k_2) for the solvolysis of II in strong alkali were still in the region of the pK'_{a2} value. Estimates of both pK'_{a2} and $(k'_{OH})_2$ that were consistent with the first-order rate constants, k_2 in this transition region, were made in accordance with Eq. 18 and are given in Table VII. These pK'_{a2} values can be characterized by $4556(1/T) - 3.33$. The pK'_{a2} values calculated accordingly were used in the predicted log k_2–pH profiles of Fig. 12 and are listed in Table VII.

There is a caveat for those who wish to use these strategies in prediction of stabilities. Prediction at temperatures other than those studied should not be made based on Arrhenius parameters (Eq. 25, Table VIII, Fig. 14) for studies conducted in the same buffer solutions at several temperatures. Comparison of apparent heats of activation for the bimolecular rate constants (Table VI) and the apparent first-order rate constants (Table VIII) shows wide discrepancies in many instances. For example, the estimated $(\Delta H_a)_{k_j}$ (kcal/mole) for the apparent first-order rate constants of solvolysis of I in pH 6.25 phosphate buffer were 26.2, k; 26.5, k_1; and 27.3, k_3; whereas the $(\Delta H_a)_{k_j}$ values for the bimolecular rate constants representative of hydroxyl ion attack on protonated I were 12.3, k_{OH}; 11.8, $(k_{OH})_1$; and 11.8, $(k_{OH})_3$. These latter values are typical of hydroxyl ion-catalyzed solvolysis of esters.

The reason for these discrepancies are simple. Since:

$$k = k_{OH}a_{OH} = k_{OH}K_w/a_{H^+} \qquad \text{(Eq. 26)}$$

or in general:

$$k_i = k_j a_{OH} = k_j K_w/a_{H^+}$$

then:

$$\ln k = \ln k_{OH} - \text{pOH} = \ln k_{OH} + \text{pH} - pK_w \qquad \text{(Eq. 27)}$$

Each apparent logarithm of the rate constant and that of the K_w can be expressed by a relation such as Eq. 25, and therefore:

$$\ln P_{k_i} - (\Delta H_a)_{k_i}/RT = \ln P_{k_j} - (\Delta H_a)_{k_j}/RT + \text{pH} - (\ln P_{K_w} + \Delta E_{K_w}/RT) = \ln P_{k_j} - \ln P_{K_w} + \text{pH} - [(\Delta H_a)_{k_j} - (\Delta E)_{K_w}]/RT \qquad \text{(Eq. 28)}$$

Table IX—Red Blood Cell Partitioning of I

	$[I]_0$, μg/ml	Equilibration time, min	D
Whole blood	10	60	0.754
	10	120	0.752
Red blood cell–phosphate buffer (pH 7.4)	10	60	0.789
	10	120	0.612
Red blood cell–plasma water	4	35	0.758
	3	35	0.902
	2	35	0.753

Table X—Red Blood Cell Partitioning of II [a]

		D	
$[II]_0$	Blood	Red Blood Cell–Phosphate Buffer (pH 7.4)	Red Blood Cell–Plasma Water
10	0.91	0.88	—
5	1.18	1.34	1.34
1	0.88	0.66	0.95, 0.84
0.5	0.85	0.98	—
2.5	0.88, 0.67, 0.74	—	—

[a] After 25-min equilibration.

Thus:

$$\ln P_{k_i} = \ln P_{k_j} - \ln P_{K_w} + \text{pH} \qquad \text{(Eq. 29)}$$

and entropies of activation calculated from $\ln P_{k_i}$ are pH dependent and are not valid estimates. Also:

$$(\Delta H_a)_{k_i} = (\Delta H_a)_{k_j} - \Delta E_{K_w} \qquad \text{(Eq. 30)}$$

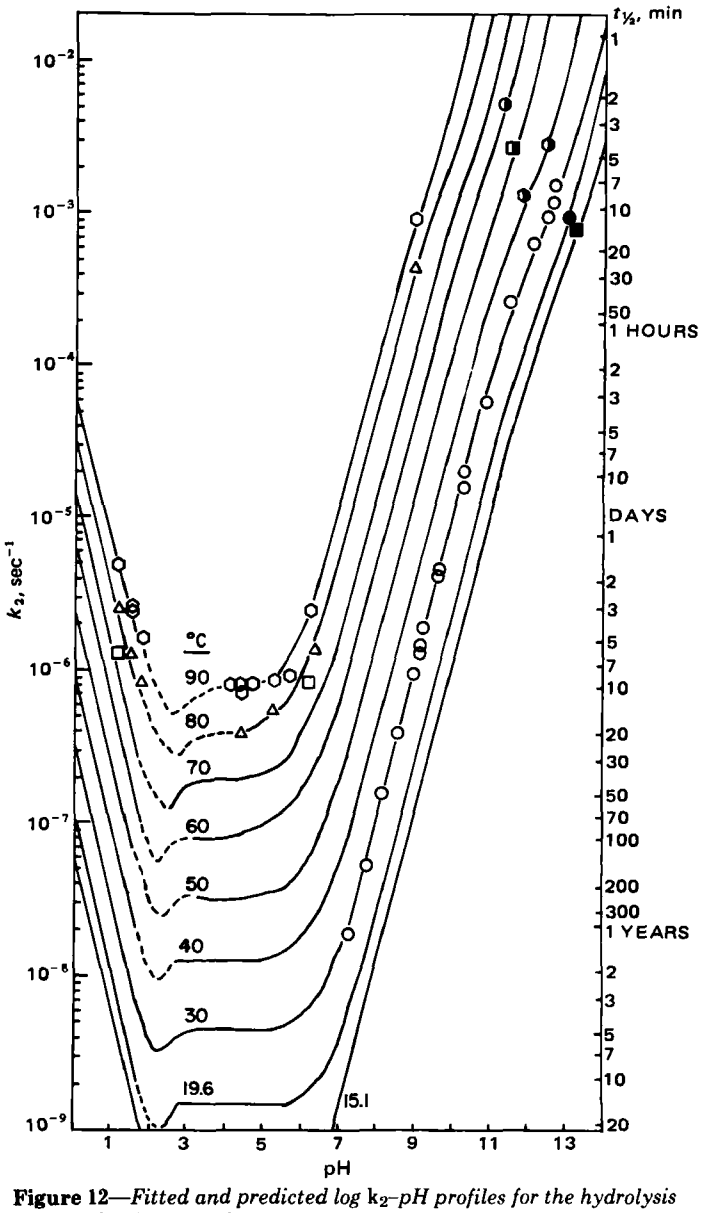

Figure 12—*Fitted and predicted log* k_2*–pH profiles for the hydrolysis of II at the designated temperatures. The fits and predictions are in accordance with:* $k_2 = (k_H)_2 a_{H^+}\,[a_{H^+}/(a_{H^+} + K'_{a_2})] + (k_0)_2\,[(K'_a)_1/(a_{H^+} + K'_{a_1})] + (k_{OH})_2\,[K_w/(K'_{a2} + a_{H^+})] + (k'_{OH})_2\,[K'_{a2}K_w/(K'_{a2} + a_{H^+}a_{H^+})]$ *and* $\ln k_j = \ln P - 10^3(\Delta H_a/R)(1/T)$ *where the pertinent parameters are listed in Table VII,* ΔH_a *is in kcal/mole,* $a_{H^+} = 10^{-pH}$ *and T is in degrees Kelvin. Since the* $p(K'_a)_1 = 2.1$ *was only estimated at room temperature, the given dashed segments of the profiles at other temperatures are only estimates of the dependencies.*

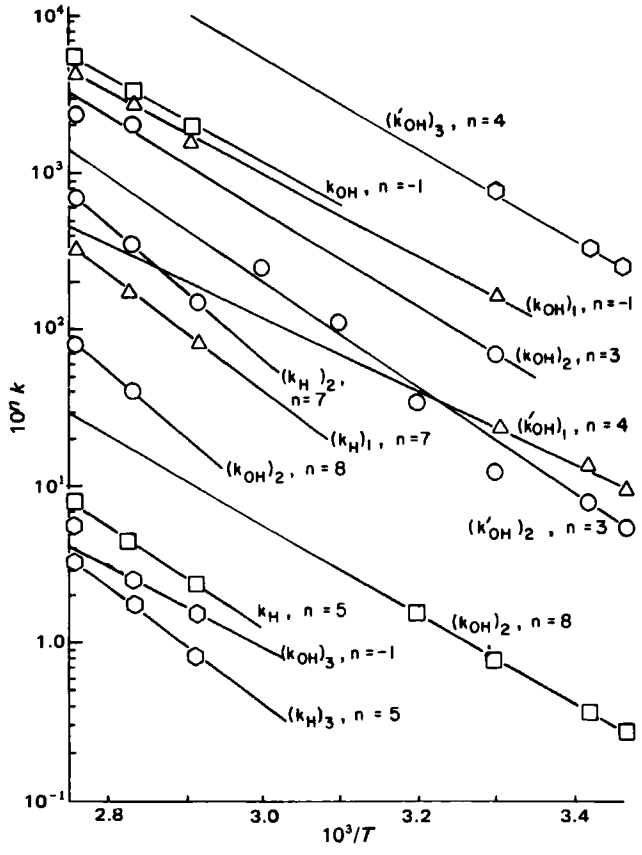

Figure 13—*Arrhenius plots (ln* k_j, *liters mole*$^{-1}$ *sec*$^{-1}$, versus *1/T where T is in degrees Kelvin) for the bimolecular rate constants for hydrogen ion-catalyzed solvolyses of I: overall,* k_H; *to II* $(k_H)_1$; *to IV* $(k_H)_3$; *and for the acid-catalyzed solvolysis of II,* $(k_H)_2$. *Also, for the hydroxyl ion-catalyzed solvolysis of protonated and neutral I, respectively: overall,* k_{OH} *and* k'_{OH}; *to II,* $(k_{OH})_1$ *and* $(k'_{OH})_1$; *to IV,* $(k_{OH})_3$ *and* $(k'_{OH})_3$; *and for the respective hydroxyl ion-catalyzed solvolysis of zwitterionic and anionic II,* $(k_{OH})_2$ *and* $(k'_{OH})_2$. *The* $(k_0)_2$ *is for the attack of water on the zwitterion of II.*

and heats of activation calculated from the apparent first-order rate constants obtained from the same buffer solutions studied at different temperatures always exceed the heats of activation calculated from the bimolecular rate constants and are not valid estimates.

The assertions (5) that the maximum stability of I was pH 1.95 and that II was the solvolytic product needs to be modified in light of these present studies; compound IV is also produced (Tables III and IV, Fig. 11). The maximum stabilities of I are at the minima of the log-pH profiles of Fig. 9 and vary between pH 3.2 and 3.8 from 15 to 90°. The maximum stabilities of II (Fig. 12) are ~pH 1.8.

The apparent heats of activation of the apparent first-order rate constants for solvolysis of I were given previously (5) as 22.9 kcal/mole at pH 6.8, 25.6 kcal/mole at pH 5.0, and 23.4 kcal/mole at pH 2.2. The values were not inconsistent with that of 26.2 kcal/mole determined at pH 6.25 in this investigation.

Applications of Plasma Assays to Stabilities of I in Fresh Plasma—The stability of I was monitored by HPLC assay in fresh dog plasma. A study of 8.8×10^{-3} *M* (299 μg/ml) I at 38.9° (Fig. 15) by HPLC Procedure II showed an apparent half-life of 5.44 hr ($k = 3.54 \times 10^{-5}$ sec^{-1}), close to the half-life of I in phosphate buffer at that temperature (Table IV, Fig. 9). The data for II in Fig. 15 could be well-fitted by the procedures outlined relative to Eqs. 4–8 and were consistent with 90% of I being hydrolyzed through the route for hydrolysis of II, the same product of aqueous solvolysis at this pH. An approximate estimate of hydrolysis of II could be estimated with a half-life of >100 hr ($k_2 = 1.9 \times 10^{-6}$ sec^{-1}).

An additional study at an initial concentration of 8.8×10^{-4} *M* I in dog plasma (30 μg/ml) using HPLC procedure III showed a similar apparent half-life (Fig. 15) for I of $t_{1/2}$ = 6.0 hr and demonstrated no significant change for this tenfold dilution of substrate. However, the fraction hydrolyzing through the route for II was only 0.5 under these conditions.

Additional studies on plasma stability of I were conducted at 1000, 500, and 250 ng/ml in the same fresh dog plasma by HPLC procedure IV (Fig. 15) and showed half-lives of 1.98, 2.08, and 1.9 hr, respectively. This signified a more than doubling of the plasmolysis rate at the lower concentrations of I to indicate a possible saturation of hydrolyzing enzymes at the higher concentrations of I. The possible increase in hydrolysis rates (dashed lines, Fig. 15) at high initial cocaine concentrations was confirmed.

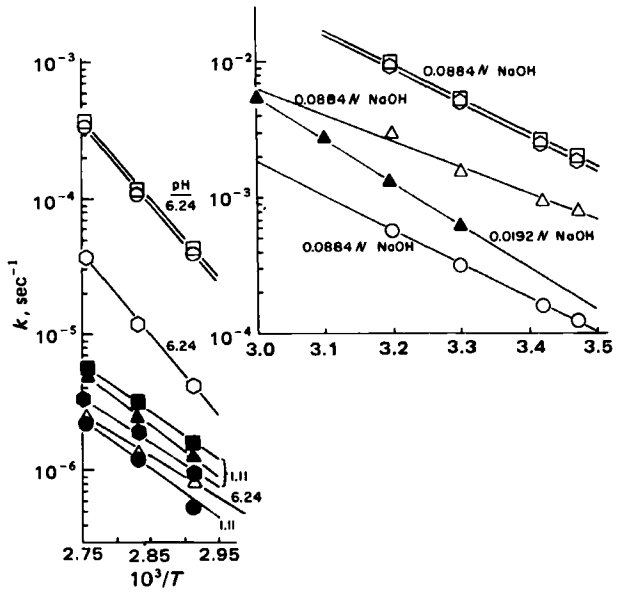

Figure 14—*Arrhenius plots (ln* k_i *sec*$^{-1}$ versus *1/T where T is in degrees Kelvin) for (□)* k, *(○)* k_1, *(△)* k_2, *and* k_3 *(○) rate constants at the labeled specified conditions.*

Red Blood Cell–Plasma and –Buffer and –Plasma Water Partitioning and Protein Binding of I and II—The assayed plasma or plasma water concentrations of I, $[I]_p$, were substituted into the following

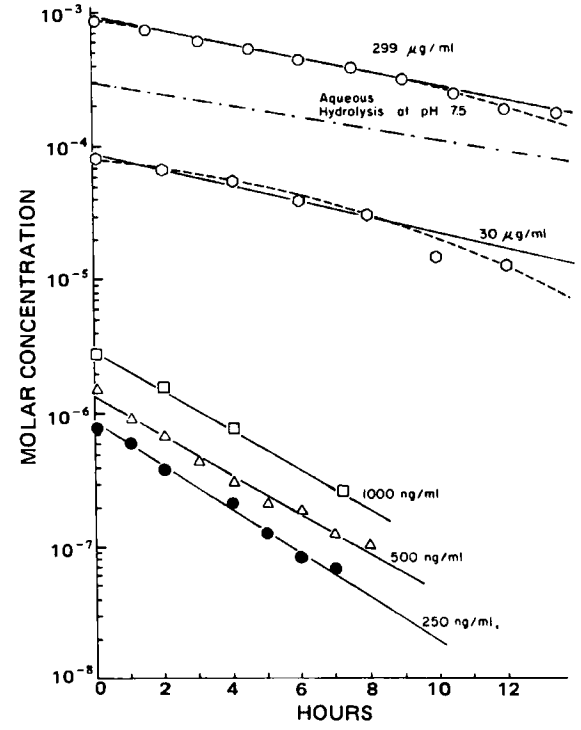

Figure 15—*Semilogarithmic plots of I in fresh dog plasma against time at 38.9° with the designated initial concentrations of I* (I_0). *The solid lines were drawn on the premise of first-order disappearance of I, although accelerating rates with time (dashed lines) are possible at the higher concentrations. The time course of hydrolysis of I in aqueous pH 7.5 buffers is also given (---) for comparison. Key: (●) 250 ng/ml; (△) 500 ng/ml; (□) 1000 ng/ml; (○) 30 μg/ml; (○) 299 μg/ml.*

equation to determine the concentration of I in red blood cells ($[I]_{RBC}$):

$$[I]_{RBC} = \frac{I - [I]_p V(1 - H)}{VH} \quad \text{(Eq. 31)}$$

where I is the amount of cocaine added to a volume (V) of blood or synthetic blood with an H fraction of this volume as red blood cells. The I-values used were calculated from $I = I_0 e^{-kt}$ where I_0 is the amount of I added at t minutes before assay, and k is the apparent first-order rate constant of degradation of I in the system. The apparent red blood cell–plasma partition coefficient was $D = [I]_{RBC}/[I]_p$; values are given in Table IX. The fact that there is no significant difference among systems with and without plasma proteins is indicative of no significant protein binding of I.

Similar studies were conducted with II (Table X). Although the data are more variable than in the case for I, the reasonable consistency of red blood cell–plasma and red blood cell–buffer or plasma water coefficients (D) in parallel studies at a given concentration of II ($[II]_0$) is indicative of negligible plasma protein binding of II.

Since I has relatively high solvolysis rates in plasma and buffers, plasma protein binding studies by equilibrium dialysis or ultracentrifugation are not applicable, since they take relatively long periods of time. An attempt to use ultrafiltration through filter cones (17) was not satisfactory, since I was variable and highly bound to the filter cones. When 4 ml of plasma and 4 ml of plasma–water were filtered to the same extent through individual fresh cones, the percent of the filtered 1-μg/ml solution recovered was 32 ± 1% for plasma–water and 23 ± 1% for plasma to indicate a possible plasma protein binding of 8% for I. The filter cones were pre-equilibrated with buffer containing the same concentrations of I in plasma that were to be filtered through those same cones. The percent concentration recovered in the filtrate in the same cone from buffer filtration and subsequent plasma filtration, respectively, was 46.3 and 54.6 at 2 μg/ml and 48.8 and 54.6 at 1 μg/ml.

However, when the same two filtrations in the same cone were effected using only buffer, the percent concentration of I recovered in the same cone was 43.8 and 56.2 at 1 μg/ml and 38.8 and 61.3 at 0.5 μg/ml. This mimicked the situation when the second filtration was of I-spiked plasma to show that the loss of I in the filtrate was due to its binding to the cones on successive filtrations and that it could not be assigned to plasma protein binding.

REFERENCES

(1) R. L. Foltz, A. F. Fentiman, and R. B. Foltz, NIDA Research Monograph 32, Aug. 1980, pp. 90–109.

(2) P. I. Jatlow and D. N. Bailey, *Clin. Chem.*, **21**, 1918 (1975).

(3) G. Barnett, R. Hawks, and R. Resnick, *J. Ethnopharmacol.*, **3**, 353 (1981).

(4) J. I. Javaid, H. Dekirmenjian, J. M. Davis, and C. R. Schuster, *J. Chromatogr.*, **152**, 105 (1978).

(5) J. B. Murray and H. I. Al-Shora, *J. Clin. Pharmacy*, **3**, 1 (1978).

(6) E. R. Garrett, in "Advances in Pharmaceutical Sciences" vol. II, H. S. Bean, A. H. Beckett, and J. E. Carless, Eds., Academic, New York, N.Y., 1967, pp. 1–94.

(7) E. R. Garrett, *J. Pharm. Educ.*, **44**, 347 (1980).

(8) E. R. Garrett and R. Barbhaiya, *J. Pharm. Sci.*, **70**, 39 (1981).

(9) E. R. Garrett and M. R. Gardner, *ibid.*, **71**, 14 (1982).

(10) P. I. Jatlow, C. Van Dyke, P. Barash, and R. Byck, *J. Chromatogr.*, **152**, 115 (1978).

(11) M. A. Evans and T. Morarity, *J. Anal. Toxicol.*, **4**, 19 (1980).

(12) J. E. Lindgren, *J. Ethnopharmacol.*, **3**, 337 (1981).

(13) T. V. Parke and W. W. Davis, *Anal. Chem.*, **26**, 642 (1954).

(14) Stat-1-22A "Linear Regression" HP-65 Stat Pac I, Hewlett-Packard, Cupertino, Calif., pp. 49–51.

(15) H. S. Harned and B. B. Owen, "The Physical Chemistry of Electrolytic Solutions," 3rd ed. Reinhold, New York, N.Y., 1958.

(16) S. Glasstone, "Textbook of Physical Chemistry," 2nd ed., D. Van Nostrand, New York, N.Y., 1946, p. 1075.

(17) P. H. Hinderling, J. Bres, and E. R. Garrett, *J. Pharm. Sci.*, **63**, 1684 (1974).

ACKNOWLEDGMENTS

Supported in part by Grant 2-R01-DA-00743 from the National Institute of Drug Abuse, Rockville, MD 20852.

Spectral Analysis of the Configuration and Solution Conformation of Dihydrodigoxigenin Epimers

HOWARD N. BOCKBRADER * and RICHARD H. REUNING ˣ

Received November 21, 1980, from the *College of Pharmacy, The Ohio State University, Columbus, OH 43210.* Accepted for publication May 12, 1982.

*Present address: Pharmaceutical Research Division, Warner-Lambert/Parke-Davis, Ann Arbor, MI 48106.

Abstract □ The C_{20} configuration and solution conformation of each epimer of dihydrodigoxigenin has been studied by circular dichroism (CD) and NMR spectroscopy. Results from the CD spectra indicate that the two epimers have opposite orientations of the β-carbon in the lactone ring. This finding, together with X-ray crystallographic data from a separate study on the minor epimer, establishes the C_{20} configuration of the minor epimer as *S* and of the major epimer as *R*. NMR evidence indicates that the average lactone rotamer for the minor epimer has the C_{22} position located on the C_{12} side of the steroid nucleus, whereas the average lactone rotamer for the major epimer has the C_{21} position located on the C_{12} side of the steroid nucleus. Molecular models indicate that these are the least-hindered positions for the respective rotamers. Physical data characterizing the two epimers are provided.

Keyphrases □ Dihydrodigoxigenin—epimers, spectral analysis of the configuration and solution conformation □ Spectral analysis—configuration and solution conformation of dihydrodigoxigenin epimers □ Epimers, dihydrodigoxigenin—spectral analysis of the configuration and solution conformation

Since the discovery of dihydrodigoxigenin (I) in the urine of a patient requiring large doses of digoxin (1) and the discovery of the metabolite dihydrodigoxin (II) in the plasma samples of three different subjects (2), a significant amount of research has been carried out on the digoxin cardanolide metabolites that are reduced at the C_{20}—C_{22} bond. Previous studies (3, 4) found 0.2–2% of the total radioactivity in urine as II in seven subjects after an oral dose of tritiated digoxin. Excretion of 12–20% of the digoxin maintenance dose as II in the urine of nine patients has also been reported (5, 6). Others (7) have found an average of 13% (range 1–47%) of the total glycosides in the meth-

0022-3549/83/0300-0271$01.00/0

equation to determine the concentration of I in red blood cells ($[I]_{RBC}$):

$$[I]_{RBC} = \frac{I - [I]_p V(1 - H)}{VH} \quad \text{(Eq. 31)}$$

where I is the amount of cocaine added to a volume (V) of blood or synthetic blood with an H fraction of this volume as red blood cells. The I-values used were calculated from $I = I_0 e^{-kt}$ where I_0 is the amount of I added at t minutes before assay, and k is the apparent first-order rate constant of degradation of I in the system. The apparent red blood cell–plasma partition coefficient was $D = [I]_{RBC}/[I]_p$; values are given in Table IX. The fact that there is no significant difference among systems with and without plasma proteins is indicative of no significant protein binding of I.

Similar studies were conducted with II (Table X). Although the data are more variable than in the case for I, the reasonable consistency of red blood cell–plasma and red blood cell–buffer or plasma water coefficients (D) in parallel studies at a given concentration of II ($[II]_0$) is indicative of negligible plasma protein binding of II.

Since I has relatively high solvolysis rates in plasma and buffers, plasma protein binding studies by equilibrium dialysis or ultracentrifugation are not applicable, since they take relatively long periods of time. An attempt to use ultrafiltration through filter cones (17) was not satisfactory, since I was variable and highly bound to the filter cones. When 4 ml of plasma and 4 ml of plasma–water were filtered to the same extent through individual fresh cones, the percent of the filtered 1-μg/ml solution recovered was 32 ± 1% for plasma–water and 23 ± 1% for plasma to indicate a possible plasma protein binding of 8% for I. The filter cones were pre-equilibrated with buffer containing the same concentrations of I in plasma that were to be filtered through those same cones. The percent concentration recovered in the filtrate in the same cone from buffer filtration and subsequent plasma filtration, respectively, was 46.3 and 54.6 at 2 μg/ml and 48.8 and 54.6 at 1 μg/ml.

However, when the same two filtrations in the same cone were effected using only buffer, the percent concentration of I recovered in the same cone was 43.8 and 56.2 at 1 μg/ml and 38.8 and 61.3 at 0.5 μg/ml. This mimicked the situation when the second filtration was of I-spiked plasma to show that the loss of I in the filtrate was due to its binding to the cones on successive filtrations and that it could not be assigned to plasma protein binding.

REFERENCES

(1) R. L. Foltz, A. F. Fentiman, and R. B. Foltz, NIDA Research Monograph 32, Aug. 1980, pp. 90–109.

(2) P. I. Jatlow and D. N. Bailey, *Clin. Chem.*, **21**, 1918 (1975).

(3) G. Barnett, R. Hawks, and R. Resnick, *J. Ethnopharmacol.*, **3**, 353 (1981).

(4) J. I. Javaid, H. Dekirmenjian, J. M. Davis, and C. R. Schuster, *J. Chromatogr.*, **152**, 105 (1978).

(5) J. B. Murray and H. I. Al-Shora, *J. Clin. Pharmacy*, **3**, 1 (1978).

(6) E. R. Garrett, in "Advances in Pharmaceutical Sciences" vol. II, H. S. Bean, A. H. Beckett, and J. E. Carless, Eds., Academic, New York, N.Y., 1967, pp. 1–94.

(7) E. R. Garrett, *J. Pharm. Educ.*, **44**, 347 (1980).

(8) E. R. Garrett and R. Barbhaiya, *J. Pharm. Sci.*, **70**, 39 (1981).

(9) E. R. Garrett and M. R. Gardner, *ibid.*, **71**, 14 (1982).

(10) P. I. Jatlow, C. Van Dyke, P. Barash, and R. Byck, *J. Chromatogr.*, **152**, 115 (1978).

(11) M. A. Evans and T. Morarity, *J. Anal. Toxicol.*, **4**, 19 (1980).

(12) J. E. Lindgren, *J. Ethnopharmacol.*, **3**, 337 (1981).

(13) T. V. Parke and W. W. Davis, *Anal. Chem.*, **26**, 642 (1954).

(14) Stat-1-22A "Linear Regression" HP-65 Stat Pac I, Hewlett-Packard, Cupertino, Calif., pp. 49–51.

(15) H. S. Harned and B. B. Owen, "The Physical Chemistry of Electrolytic Solutions," 3rd ed. Reinhold, New York, N.Y., 1958.

(16) S. Glasstone, "Textbook of Physical Chemistry," 2nd ed., D. Van Nostrand, New York, N.Y., 1946, p. 1075.

(17) P. H. Hinderling, J. Bres, and E. R. Garrett, *J. Pharm. Sci.*, **63**, 1684 (1974).

ACKNOWLEDGMENTS

Supported in part by Grant 2-R01-DA-00743 from the National Institute of Drug Abuse, Rockville, MD 20852.

Spectral Analysis of the Configuration and Solution Conformation of Dihydrodigoxigenin Epimers

HOWARD N. BOCKBRADER * and RICHARD H. REUNING ˣ

Received November 21, 1980, from the *College of Pharmacy, The Ohio State University, Columbus, OH 43210.* Accepted for publication May 12, 1982.

*Present address: Pharmaceutical Research Division, Warner-Lambert/Parke-Davis, Ann Arbor, MI 48106.

Abstract □ The C_{20} configuration and solution conformation of each epimer of dihydrodigoxigenin has been studied by circular dichroism (CD) and NMR spectroscopy. Results from the CD spectra indicate that the two epimers have opposite orientations of the β-carbon in the lactone ring. This finding, together with X-ray crystallographic data from a separate study on the minor epimer, establishes the C_{20} configuration of the minor epimer as *S* and of the major epimer as *R*. NMR evidence indicates that the average lactone rotamer for the minor epimer has the C_{22} position located on the C_{12} side of the steroid nucleus, whereas the average lactone rotamer for the major epimer has the C_{21} position located on the C_{12} side of the steroid nucleus. Molecular models indicate that these are the least-hindered positions for the respective rotamers. Physical data characterizing the two epimers are provided.

Keyphrases □ Dihydrodigoxigenin—epimers, spectral analysis of the configuration and solution conformation □ Spectral analysis—configuration and solution conformation of dihydrodigoxigenin epimers □ Epimers, dihydrodigoxigenin—spectral analysis of the configuration and solution conformation

Since the discovery of dihydrodigoxigenin (I) in the urine of a patient requiring large doses of digoxin (1) and the discovery of the metabolite dihydrodigoxin (II) in the plasma samples of three different subjects (2), a significant amount of research has been carried out on the digoxin cardanolide metabolites that are reduced at the C_{20}—C_{22} bond. Previous studies (3, 4) found 0.2–2% of the total radioactivity in urine as II in seven subjects after an oral dose of tritiated digoxin. Excretion of 12–20% of the digoxin maintenance dose as II in the urine of nine patients has also been reported (5, 6). Others (7) have found an average of 13% (range 1–47%) of the total glycosides in the meth-

0022-3549/83/0300-0271$01.00/0

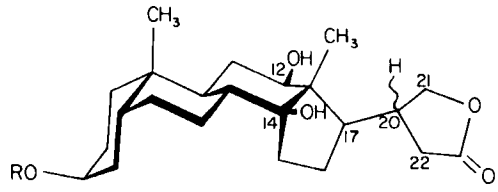

I R = H
II R = digitoxose$_3$

ylene chloride extract of urine present as II. Of the 50 subjects in this study, 48 had detectable urinary levels of II. Urine samples of 100 patients taking oral digoxin for the control of heart disease were investigated more recently (8, 9). The average percent of cardanolides present in the 0–24-hr urine was 12% (range 2–52%) based on the total methylene chloride extractable cardiac glycoside content. Out of the 100 patients, 53 excreted >10% while seven excreted >35% as the cardanolide metabolites.

Reduction of the 20,22-unsaturated lactone ring of digoxin introduces a center of asymmetry at C_{20} and generates three aspects of stereochemistry that must be investigated in order to determine the conformation of any epimers of I or II. First, the resulting saturated γ-lactone has the β-carbon out of plane, thus creating the possibility of the enantiomeric pair illustrated in Fig. 1 (10, 11). Second, the chiral center at C_{20} can have either an *R* or *S* configuration. Finally, the overall asymmetry of the steroid nucleus and the likely steric hindrance to free rotation of the lactone ring about the C_{17}—C_{20} bond results in the possibility of preferred rotamers for the lactone.

Research on the C_{20} configuration and the lactone conformation of the reduced metabolites of digoxin has been inhibited by the lack of methodology for effective separation of any epimers that may be formed either biologically or chemically. Most of the metabolic studies (1–9, 12, 13) have utilized either TLC or GC techniques which have yielded only a single peak for either reference or biologically produced I or II. In an investigation of the crystallographic conformation, C_{20} configuration, and biological activity of various cardanolides (14–17), a TLC procedure was recently reported capable of separating certain 20*R* and 20*S* cardanolide epimers (18). However, this method has not yet been applied to the epimers of I or II.

Since II is an important metabolite of digoxin, it is critical that the stereochemical properties of this metabolite be determined. Essential to this determination is the

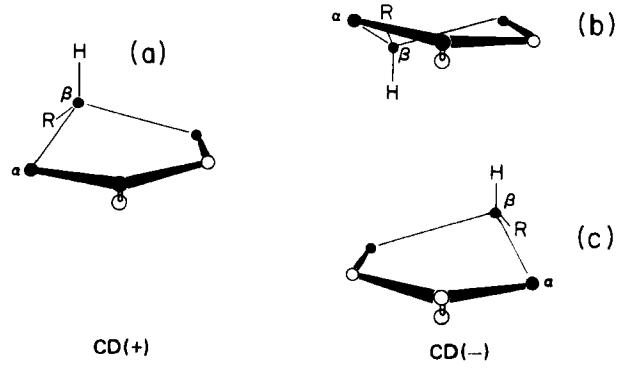

Figure 1—*Perspective representation of the two stable conformations of the γ-lactone. A positive CD spectrum is associated with conformation (a) and a negative CD spectrum with (b). Representation (c) is rotated 180° about the β carbon compared with (b) and* R *represents the steroid nucleus shown in I.*

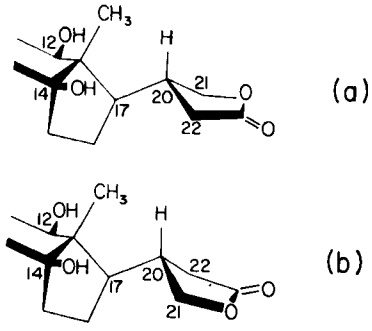

Figure 2—*Perspective representation of the relationships of the γ-lactone to the steroid nucleus wherein the 17—20 bond is pseudoequatorial, and the lactone rotamer has the oxygens oriented away from the methyl substituent at C_{13}. Structure (a) has the* R *configuration at C_{20}, and structure (b) has the* S *configuration.*

identification of suitable synthetic references with known stereochemistry so that subsequent comparisons to biologically produced metabolites may be made. Previous researchers (19) hydrogenated digoxigenin and fractionally crystallized the product yielding two epimers. However, that stereochemical assignment was based only on melting point and optical rotation values. The purpose of the present investigation was to define the C_{20} configuration and solution conformation of the epimers of synthetic I, the aglycone of II. It was not possible to carry out a definitive study on II because of interference from the sugar moieties in the interpretation of the various spectra.

RESULTS AND DISCUSSION

Catalytic hydrogenation of either digoxin or digoxigenin yielded two components that were separable as the 3,5-dinitrobenzoyl esters on high-performance liquid chromatography (HPLC). The component with the longer retention time on a normal phase system was present in larger amount and is designated the major fraction. Isolation of the derivatized major and minor fractions of I was accomplished by collecting the HPLC eluate. The corresponding underivatized fractions were then obtained by base hydrolysis. It was also possible to isolate the major underivatized fraction of I by fractional crystallization, but not the minor underivatized fraction. These major and minor fractions were each then subjected to spectral analysis for information concerning the conformation of the lactone ring, the configuration at C_{20}, and the preferred average rotamer of the lactone in relation to the steroid backbone.

Lactone Conformation and C_{20} Configuration—Associated with the optically active lactone is the $n \rightarrow \pi^*$-absorption band in the region of 214–219 nm. Circular dichroism studies have shown that a lactone ring will have a CD curve whose sign and magnitude are determined by the interactions within the lactone ring structure (10). Previous evidence (10, 11, 20, 21) has shown that the sign of the lactone CD curve for γ-lactones is associated with the location of the β-carbon relative to the planar lactone ring. The orientation of the plane is such that the α- and γ-carbons and the lactone moiety form the plane, the carbonyl function faces forward, and the ring oxygen is located to the right (Fig. 1a and b). The CD curve is positive when the conformation of the γ-lactone has the β-carbon above the plane and negative when the β-carbon is below the plane.

Results of the CD study of I revealed that the underivatized major component had a positive CD curve ($[\theta]_{218} = 136$) and the underivatized minor component had a negative CD curve ($[\theta]_{216} = -206$). These results indicate that the β-carbon of the lactone (C_{20} of I) is oriented as in Fig. 1a for the major component of I and as in Fig. 1b for the minor component. The energetically preferred position for the steroid substituent on the β-carbon would appear to be pseudoequatorial as shown in Fig. 1. In support of this viewpoint, the 22-methylene analogue of dihydrodigitoxigenin has been shown by X-ray crystallographic data (16) to have the steroid part of the molecule in a pseudoequatorial position at C_{20}. If this is the case for dihydrodigoxigenin, then the configuration at C_{20} (β-carbon of the lactone) is 20*R* for the major component and 20*S* for the minor component of I. This interpretation of the spectral data with respect to lactone conformation and C_{20} configuration has been confirmed by direct

X-ray crystallographic determination of the structure of the minor epimer (22).

Preferred Rotamer For Lactone—When either the 20*R* or 20*S* epimer of I is illustrated with Dreiding models and the molecule is rotated about the C_{17}—C_{20} bond, the conformation having the least steric hindrance with the C_{18}-methyl is that rotamer in which the lactone is oriented away from the C_{18}-methyl. This is illustrated for the 20*R* epimer of I in Fig. 2a. To orient the lactone away from the C_{18}-methyl in the 20*S* epimer it is necessary to rotate the lactone conformation shown in Fig. 1b by ~180° to that shown in Fig. 1c. The result for the dihydrodigoxigenin 20*S* epimer is shown in Fig. 2b.

A strategy was developed for testing the hypothesis that the two epimers of I have the lactones oriented as shown in Fig. 2. Advantage was taken of the fact that the tertiary 14-hydroxyl group does not form esters (23). Thus, esterification with 3,5-dinitrobenzoyl chloride at the 3 and 12 positions of I yields a derivative that should have the added aromatic moiety at the 12 position sufficiently close to the C_{21} protons in the *R* epimer (Fig. 2a) to influence the NMR spectrum of these protons. For the *S* epimer (Fig. 2b) the NMR of the C_{22} protons should be influenced by their proximity to the C_{12} aromatic moiety.

The NMR spectra of the underivatized major and minor components of I lacked similarity in the regions of the C_{21} protons (3.9–4.5 ppm) and the C_{22} protons (2.1–2.7 ppm, Fig. 3, spectra b and d). Differences in the chemical shifts occurring in these two regions were compared in the underivatized and derivatized forms of each component. A comparison of the NMR spectrum of the underivatized major component of I with that of the derivatized major component (Fig. 3, spectra b and a) reveals that the 3,5-dinitrobenzoate ester at the C_{12} position induces significant chemical shift changes in the C_{21} protons (underivatized major component of I apparent triplets at 4.00 and 4.40 ppm, derivatized major component at 3.76 and 4.53 ppm). However, the results are different with respect to the C_{22} protons. Overlap of the apparent triplets in the region of 2.2–2.5 ppm makes this segment of the NMR spectrum difficult to interpret, but only minor differences exist in this region when the underivatized major component of I is compared with the derivatized major component (suspected location of apparent triplets for C_{22} protons, underivatized major component at 2.34 and 2.48 ppm, derivatized major component at 2.35 and 2.57 ppm).

In comparing the NMR spectrum of the underivatized minor component of I with that of the derivatized minor component, the reverse effect was observed for the C_{21} and C_{22} protons (Fig. 3, spectra d and c). Minimal differences occurred in the chemical shift locations of the C_{21} protons when the underivatized minor component (4.05 and 4.35 ppm) was compared with the derivatized minor component (4.02 and 4.40 ppm). Again, the NMR spectra are difficult to interpret in the C_{22} region; however, significant differences do exist in this region between the underivatized minor component of I and the derivatized minor component (Fig. 3). The suspected location of the C_{22} protons for the underivatized minor component is 2.29–2.53 ppm and for the derivatized minor component 2.02–2.64 ppm.

The results of the NMR studies indicate that the major and minor components of I are opposite rotamers at the C_{17}—C_{20} bond. The influence of derivatization on the chemical shift of the C_{21} protons of the major component of I but not the C_{22} protons confirms the predictions from the Dreiding model of the preferred average rotamer for the *R* epimer, as illustrated in Fig. 2a. The opposite effect of derivatization on the chemical shift of the C_{21} and C_{22} protons of the minor component is consistent with the predicted average rotamer for the *S* epimer, as shown in Fig. 2b.

Determination of the Influence of the Isolation Procedure on the Spectral Observations—The major and minor components of I were separated by derivatization with 3,5-dinitrobenzoyl chloride, HPLC of the derivatives yielding separate peaks for the two components and then base hydrolysis of the separated components. As a control to determine the influence of the isolation procedure on the structure of I, the major component was also prepared by fractional crystallization. Attempts to purify the minor component by fractional crystallization were not successful. Comparison of the NMR spectrum of the recrystallized major component with the NMR of the same component isolated by derivatization, HPLC, and base hydrolysis revealed that the spectra were essentially the same. Thus, the derivatization and base hydrolysis procedures required for the isolation of the two components of I did not alter the starting material, dihydrodigoxigenin (I).

Conclusion—The agreement for the minor epimer of I between the CD results and the results of a separate X-ray crystallography study (22) establishes the C_{20} configuration as *S* and the lactone conformation as shown in Fig. 2b. NMR evidence suggests that the average lactone rotamer in solution is approximately as shown in Fig. 2b for the minor epimer. The CD results for the major epimer indicate the opposite conformation of the β-carbon in the lactone compared with the minor epimer. This result, together with the X-ray crystallography data for the minor epimer, establishes the *R* configuration at C_{20} for the major epimer. NMR evidence suggests that the average lactone rotamer for the major epimer is approximately as shown in Fig. 2a.

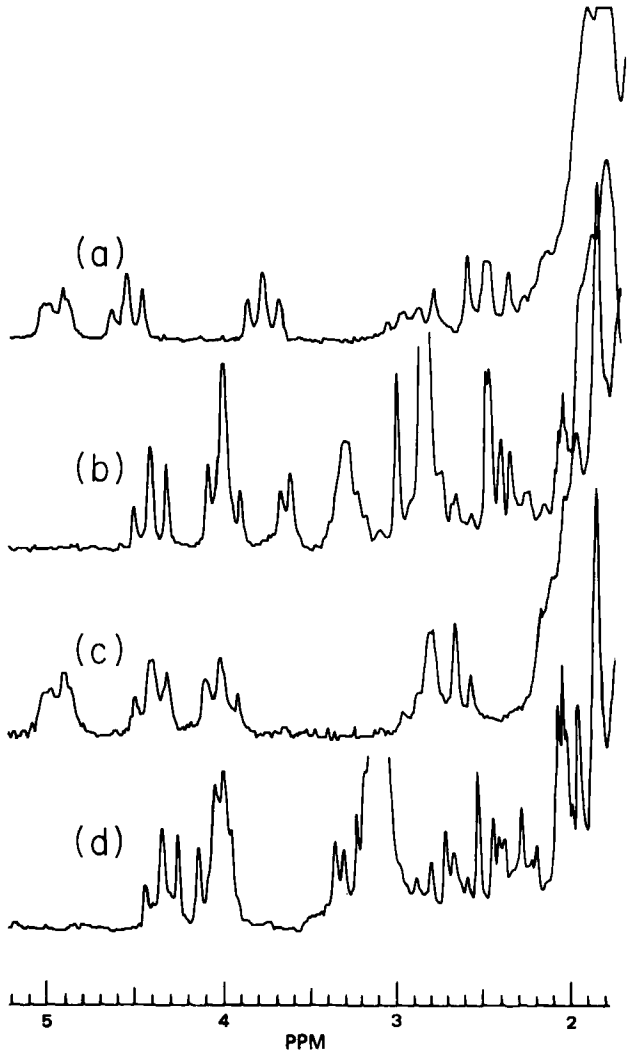

Figure 3—*Partial proton NMR spectrum of (a) derivatized major component of I (in deuterated chloroform), (b) underivatized major component of I (in deuterated acetone), (c) derivatized minor component of I (in deuterated chloroform), and (d) underivatized minor component of I (in deuterated acetone). The derivatizing agent was 3,5-dinitrobenzoyl chloride.*

EXPERIMENTAL

Hydrogenation of Digoxigenin to Dihydrodigoxigenin (I)—Digoxigenin[1] (500 mg) was added to a hydrogenation bottle containing 60 ml of ethanol and 85 mg of platinum oxide catalyst. The digoxigenin was hydrogenated for 12 hr at 30 psi. The platinum oxide was removed by filtering the ethanol solution through a fritted glass filter, and the ethanol was evaporated under a stream of nitrogen at 50°.

Fractional Crystallization of I—Five hundred mg of I was recrystallized from ethyl acetate. The resulting crystals were recrystallized four additional times from ethyl acetate to yield 23 mg. *Less than 4% contamination of the major component of I with the minor component was* detected based on high-performance liquid chromatography (HPLC): mp 189–213°; NMR (CD_3COCD_3) integration (35.4 protons, theoretical 36 protons) δ 4.40 (t J = 8 Hz, 1, C_{21}—H), 4.00 (s, 1, C_3—H), 4.00 (t, one

[1] Boehringer Mannheim Biochemicals, Indianapolis, Ind.

peak under the 4.00 s, J = 8 Hz, 1, C_{21}—H), 2.26–2.65 (m, with major peaks at 2.26, 2.34, 2.39, 2.46, 2.65, 2, C_{22}—H), 0.90, and 0.93 (each s, 6, C_{18}—H, and C_{19}—H).

Derivatization and Liquid Chromatography of (I) to Isolate the Major and Minor Components—One g of I was derivatized with 3,5-dinitrobenzoyl chloride by taking 10-mg aliquots of I and dissolving in 13 ml of pyridine which had been distilled and stored over sodium hydroxide pellets. Next, 1.077 g of 3,5-dinitrobenzoyl chloride[2] (recrystallized from petroleum ether) was added and the solution was heated for 30 min in a water bath (50°). After the major portion of pyridine was removed under vacuum (60°), 10 ml of 5% $NaHCO_3$ solution containing 20 mg of 4-dimethylaminopyridine[2] was added to hydrolyze the excess derivatizing agent and 10 ml of chloroform was added to solubilize and extract the derivatized I. Following the removal of the aqueous phase, the organic phase was washed with 10 ml of 5% $NaHCO_3$ followed by four 30-ml washings with a 0.05 N HCl solution containing 5% NaCl. The chloroform solution from each aliquot was concentrated to a total of 10 ml by evaporating the chloroform under a nitrogen stream at 50°. This solution was washed eight times with the acid wash to remove any residual pyridine, and the final volume of 2 ml was achieved by evaporation under nitrogen (50°). Aliquots of this solution were chromatographed by HPLC using a mobile phase of hexane–methylene chloride–acetonitrile (3:1:1) and a silica gel stationary phase[3]. Appropriate fractions were collected to isolate the derivatized major and minor components of I. Purity with respect to the opposite component was determined by HPLC. Derivatized major component of I, <1% cross-contamination from derivatized minor component; NMR[4] ($CDCl_3$) δ 9.12–9.28 (m, with major peaks at 9.12, 9.14, 9.21, 9.23, 9.25, 9.28, 6, aromatic H), 5.49 (s, 1, C_3—H), 4.88 (m, 1, C_{12}—H), 4.52 (t, J = 8 Hz, 1, C_{21}—H), 3.75 (t, J = 8 Hz, 1, C_{21}—H), 2.25–2.76 (m, with major peaks at 2.34, 2.44, 2.56, 2, C_{22}—H), 1.22 (s, 3, C_{19}—H), 1.09 (s, 3, C_{18}—H). Derivatized minor component of I, <1% cross-contamination from derivatized major component; NMR ($CDCl_3$) δ 9.12–9.24 (m, with major peaks at 9.12, 9.14, 9.24, 6, aromatic-H), 5.48 (s, 1, C_3—H), 4.90 (m, 1, C_{12}—H), 4.40 (t, J = 8 Hz, 1, C_{21}—H), 4.02 (t, J = 8 Hz, 1, C_{21}—H), 2.64 (t, J = 8 Hz, 1, C_{22}—H), 2.02 (t, J = 8 Hz, 1, C_{22}—H), 1.23 (s, 3, C_{19}—H), 1.10 (s, 3, C_{18}—H).

Base Hydrolysis of the Derivatized Major and Minor Components of I—A mixture of chloroform (1.5 ml), methanol (13.5 ml), and 5% $KHCO_3$ (1.5 ml) containing either 100 mg of the derivatized major component of I or 131 mg of the derivatized minor component was refluxed for 90 min. After increasing the volume of the aqueous phase with 3 ml of distilled water, the aqueous phase was extracted three times with methylene chloride (40 ml). To ensure against opening of the lactone ring from the base hydrolysis procedure (24), the aqueous phase was acidified to ~pH 2 with 0.2 N HCl. Twelve hours later the solution was adjusted to pH 10 with 5% $KHCO_3$ and extracted three times with methylene chloride (40 ml). After combining like fractions and evaporating the methylene chloride, each component was crystallized from ethyl acetate. Purity was determined by HPLC. Major component of I (37.3 mg, 37.3% yield) <1% contamination from minor component; mp 235–237°; NMR (CD_3COCD_3) integration (35.1 protons, theoretical 36 protons), δ 4.41 (t, J = 8 Hz, 1, C_{21}—H), 4.00 (s, 1, C_3—H), 4.00 (t, one peak under the 4.00 s, J = 8 Hz, 1, C_{21}—H), 2.24–2.54 (m, with major peaks at 2.24, 2.34, 2.40, 2.46, 2.48, 2.54, 2, C_{22}—H), 0.90 and 0.93 (each s, 6, C_{18}—H and C_{19}—H); $[\alpha]_D^{21}$ + 20.2° (C 0.436); CD $[\theta]_{218}$ 136[5].

Anal.—Calc. for $C_{23}H_{36}O_5$: C, 70.38; H, 9.24. Found: C, 70.02; H, 9.46.

Minor component of I (41.6 mg, 31.8% yield), <1% contamination from major component; mp 209.5–211.5°; NMR (CD_3COCD_3) integration (35.9 protons, theoretical 36 protons), δ 4.35 (t, J = 8 Hz, 1, C_{21}—H), 4.01 (s, 1, C_3—H), 4.05 (t, J = 8 Hz, 1, C_{21}—H), 2.20–2.62 (m, with major peaks at 2.20, 2.29, 2.38, 2.45, 2.53, 2.62, 2, C_{22}—H), 0.92 (s, 6, C_{18}—H and C_{19}—H); $[\alpha]_D^{21}$ + 17.9° (C 0.29); CD $[\theta]_{216}$–206.

Anal.—Calc. for $C_{23}H_{36}O_5$: C, 70.38; H, 9.24. Found: C. 70.10; H, 9.38.

[2] Purum grade, Fluka A.G., Buchs, Switzerland.
[3] Partisil 10, Whatman Inc., Clifton, NJ.
[4] Bruker HX-90 NMR spectrometer.
[5] Durrum-Jasco ORD-CD spectrometer.

REFERENCES

(1) R. J. Luchi and J. W. Gruber, *Am. J. Med.*, **45**, 322 (1968).

(2) E. Watson, D. R. Clark, and S. M. Kalman, *J. Pharmacol. Exp. Ther.*, **184**, 424 (1973).

(3) D. Sugden, M. Ahmed, C. Maloney, and M. H. Gault, *Clin. Res.*, **23**, 610A (1975).

(4) D. Sugden, M. Ahmed, and M. H. Gault, *J. Chromatogr.*, **121**, 401 (1976).

(5) H. Greenwood, W. Snedden, R. P. Hayward, and J. Landon, *Clin. Chim. Acta*, **62**, 213 (1975).

(6) H. Greenwood and W. Snedden, in "Mass Spectrometry in Drug Metabolism," A. Frigeris and E. Ghisalberti, Eds., Plenum, New York, N.Y., 1977, p. 179.

(7) D. R. Clark and S. M. Kalman, *Drug Metab. Dispos.*, **2**, 148 (1974).

(8) U. Peters, L. C. Falk, and S. M. Kalman, *Arch. Intern. Med.*, **138**, 1074 (1978).

(9) U. Peters and S. M. Kalman, *Z. Kardiol.*, **67**, 342 (1978).

(10) A. F. Beecham, *Tetrahedron Lett.*, **19**, 2355 (1968).

(11) *Idem.*, **32**, 3591 (1968).

(12) E. Watson and S. M. Kalman, *J. Chromatogr.*, **56**, 209 (1971).

(13) E. Watson, P. Tramell, and S. M. Kalman, *ibid.*, **69**, 157 (1972).

(14) D. S. Fullerton, T. M. Gilman, M. C. Pankaskic, K. Ahmed, A. H. L. From, W. Duax, and D. C. Rohrer, *J. Med. Chem.*, **20**, 841 (1977).

(15) D. S. Fullerton, K. Yoshioka, D. C. Rohrer, A. H. L. From, and K. Ahmed, *ibid.*, **22**, 529 (1979).

(16) D. C. Rohrer, W. L. Duax, and D. S. Fullerton, *Acta Crystallogr. Sect. B.*, **32**, 2893 (1976).

(17) D. S. Fullerton, K. Yoshioka, D. C. Rohrer, A. H. L. From, and K. Ahmed, *Science*, **205**, 917 (1979).

(18) K. Yoshioka, D. S. Fullerton, and D. C. Rohrer, *Steroids*, **32**, 511 (1978).

(19) B. T. Brown and S. E. Wright, *J. Pharm. Pharmacol.*, **13**, 262 (1961).

(20) A. F. Beecham, *Tetrahedron Lett.*, **55**, 4897 (1969).

(21) *Idem.*, **55**, 4763 (1970).

(22) A. Mostad, *Acta Chem. Scand. Ser. B*, **36**, 635 (1982).

(23) H. W. Voigtländer and G. Balsam, *Arch. Pharm.*, **301**, 208 (1968).

(24) N. Heinz and H. Flasch, *Nauyn Schmiedeberg's Arch. Pharmacol.*, **303**, 181 (1978).

ACKNOWLEDGMENTS

Presented before the Medicinal Chemistry Section at the 26th National Meeting of the APhA Academy of Pharmaceutical Sciences, Anaheim, Calif., April 1979.

The financial assistance of Central Ohio Heart Chapter Inc. (grant 78-41) and NIH (Training grant no. GM07622-HNB) is gratefully acknowledged. The authors wish to thank Susan B. Ashcraft and Brent E. Morrison for technical assistance and Drs. Raymond W. Doskotch, Duane D. Miller, and H. B. Bhat for their encouragement and expert advice.

Sensitive High-Performance Liquid Chromatographic Method for the Determination of Etodolac in Serum

L. COSYNS, M. SPAIN *, and M. KRAML ˣ

Received February 5, 1982, from *Ayerst Research Laboratories, Montreal, Quebec, H3C 3J1 Canada.* Accepted for publication April 30, 1982. *Present address: Chromatography Sciences Co., Montreal, Quebec, Canada.

Abstract □ A sensitive high-performance liquid chromatographic method for the determination of etodolac in serum was developed. The limit of detection was 0.2 μg/ml. The specificity of the method was demonstrated by the lack of response obtained with a variety of control sera, sera spiked with etodolac congeners, and sera obtained from rats treated with a variety of other drugs.

Keyphrases □ Etodolac—sensitive high-performance liquid chromatographic method for determination in serum □ High-performance liquid chromatography—sensitive method for the determination of etodolac in serum □ Serum specificity—sensitive high-performance liquid chromatographic method for the determination of etodolac □ Analgesics—etodolac, sensitive high-performance liquid chromatographic method for determination in serum □ Anti-inflammatory agents—etodolac, sensitive high-performance liquid chromatographic method for determination in serum

Experiments in laboratory animals have demonstrated that etodolac [1,8-diethyl-1,3,4,9-tetrahydropyrano[3,4-*b*]indole-1-acetic acid[1], (I)] is a potent nonsteroidal, anti-inflammatory and analgesic agent (1, 2). To carry out pharmacokinetic studies in both animals and humans, a

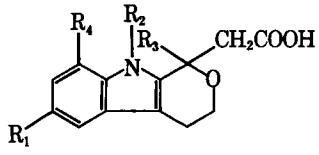

I

sensitive and reliable analytical method was needed. Etodolac can be quantitated by a fluorometric method that has been developed for its 1-propyl congener, prodolic acid (3); however, because of endogenous fluorescent substances, the limit of detection is only 2–3 μg/ml. Therefore, a specific and sensitive (0.2 μg/ml) high-performance liquid chromatographic (HPLC) method has been developed.

EXPERIMENTAL

Reagents—Isopentyl alcohol[2], hexane[3], methanol[3], and acetonitrile[4] were used as supplied. All other chemicals, monobasic potassium phosphate, hydrochloric acid, phosphoric acid, and glycine, were analytical reagent grade. Etodolac and its 1-propyl, 1-phenyl, 1,9-dimethyl, and 6-hydroxy congeners were synthesized as described previously (4, 5) as was [^{14}C]etodolac (6). Drugs used for specificity studies were purchased from commercial sources.

Instrumentation—The liquid chromatographic system employed consisted of an automatic variable-volume injector[5], a high-pressure pump[6], a variable wavelength spectrophotometer[7], and a recorder[8].

Column Preparation—Two 250 × 4.6-mm stainless steel HPLC columns were employed in the experiments: Chromosorb LC-7[9] (ODS, 10 μm; column A) and Spherisorb[10] (ODS, 5 μm; column B). Using 2-propanol slurries, the columns were packed at 6000 psi with a compressed air pump[11]. The columns were mounted with a glass water-jacket to provide temperature control. At a flow rate of 1.8 ml/min and a temperature of 50°, typical back pressures of 750 and 1680 psi were obtained for columns A and B, respectively.

Extraction and Mobile Phases—For both columns, the mobile phase was a mixture of 0.1 *M* potassium phosphate (pH 6.0) and acetonitrile. To provide similar retention times, the concentration of acetonitrile was varied from 30% (column B) to 38% (column A). The extraction phase was prepared by mixing isopentyl alcohol and hexane in a ratio of 1:19 (v/v).

Standards—A stock standard of 1.0 mg/ml of etodolac was prepared by dissolving 10.0 mg in 1.0 ml of methanol and completing to 10.0 ml with distilled water. Dilute, nonextracted test-tube standards were prepared at the desired concentration by appropriate dilution in 0.1 *M* glycine buffer (pH 11.0). In recovery studies and in actual analytical runs, working standards were prepared by diluting the stock standard in pooled rat, dog, or human control serum.

Procedure—Solutions of 4.0 ml of 1.0 *N* HCl and 5.0 ml of isopentyl alcohol–hexane were added to 1.0 ml of serum (or plasma) in a 15-ml screw-capped glass[12] tube. The tube was capped and agitated mechanically for 15 min. The two phases were separated by low-speed centrifugation (5 min, 1000 rpm), and 4.0 ml of the upper phase was transferred to a clean tube, and 1.0 ml of 0.1 *M* glycine buffer[13] was added. The tube was agitated for an additional 15 min, and a 0.8-ml aliquot of the aqueous phase was transferred to a clean tube. Prior to injection onto the HPLC column, 20 μl of 2.5 *M* phosphoric acid was added to partially neutralize the glycine buffer. With each analytical run, column performance was monitored by injecting test-tube standards. Control serum blanks and control serum, spiked with the appropriate concentration of etodolac (in triplicate), were carried through the method.

Chromatographic conditions were as follows: injected sample volume, 50–150 μl; temperature, 50°; flow rate, 1.8 ml/min; mobile phase, acetonitrile–phosphate buffer (30 or 38% for columnns B or A, respectively); UV detector settings, 226 nm and 0.05 AUFS (running at high sensitivity). Quantitation was based on peak height of the unknowns relative to that of the spiked control serum standards.

Recovery—Human serum spiked with 1.0–10.0 and 5.0–50.0 μg/ml of etodolac was carried through the procedure, in triplicate, to provide data on the linearity and reproducibility. Recovery was based on the response of test-tube standards injected concurrently. Recovery from a variety of aqueous media, *i.e.*, rat, dog, or human serum, and distilled water was also carried out on replicate samples at concentrations of 1.0, 10.0, and 50.0 μg/ml.

Sensitivity and Specificity—The specificity of the procedure was evaluated using three criteria: (*a*) interference due to similar chromatographic characteristics (retention times) and spectral properties (UV absorption at 226 nm) of endogenous constituents of serum, (*b*) the potential for interference from etodolac metabolites (or congeners), and (*c*) interference from other drugs that may be administered concurrently.

Typical serum blanks were measured by processing replicate (10–23) samples of rat, dog, and human control sera through the method.

Interference from etodolac congeners was estimated by injecting the pure compounds and evaluating their retention times relative to that of etodolac.

[1] Ultradol, Ayerst Laboratories, Inc., New York, N.Y.
[2] Fluorometric grade, A & C American Chemicals.
[3] Spectrograde, A & C American Chemicals.
[4] Lichrosolv, BDH Chemicals.
[5] Waters Associates, WISP model 710.
[6] Altex Scientific, Inc., model 110A.
[7] Perkin-Elmer, model LC-55B.
[8] Perkin-Elmer, model 56.
[9] Johns-Manville.
[10] Phase Separation Ltd.
[11] Haskel Eng. and Supply Co., model DST-1220.
[12] Pyrex tube.
[13] Due to complex formation with an impurity in some grades of glycine, etodolac may chromatograph as a split peak. The glycine buffer can be replaced with 0.1 *M* THAM [tris(hydroxymethyl)amino methane] (Fisher Scientific Co.) (pH 11.0).

0022-3549/83/0300-0275$01.00/0

Table I—Recovery of Etodolac [a] from Water and Rat, Dog, and Human Sera

Medium	n	Mean ± SE
Water	18	93.1 ± 1.0
Sera		
Rat	17	86.2 ± 1.7
Dog	18	88.0 ± 1.2
Human	18	91.5 ± 2.1

[a] Six replicates of 1.0, 10.0, and 50.0 μg/ml.

In random serum samples from rats and dogs given etodolac orally at a 50-mg/kg dose, etodolac concentrations were estimated by the fluorometric procedure (3) and in a second aliquot by the HPLC procedure (using a 5 μm Lichrosorb RP-2 column).

In selected studies in rats and dogs (7), [^{14}C]etodolac was administered orally in doses of 10 and 50 mg/kg, and total carbon 14 and unchanged etodolac were estimated at 0.25, 0.5, 1, and 3 hr postdosing.

Interference from a concurrently administered drug, or its metabolite(s), was estimated by treating rats with a high dose of the drug, obtaining a blood sample 2 hr postdosing, and processing the serum through the etodolac method. Interference was estimated from the response, at the retention time of etodolac, compared to that of serum from saline-treated control rats. Drugs tested and dose administered, in milligrams per kilogram, were: ethacrynic acid (300), salicylic acid (400), acetominophen (400), niacin (300), propoxyphene (60), phenobarbital (100), hydrochlorothiazide (100), tolbutamide (200), glyburide (200), indomethacin (25), phenylbutazone (200), phenytoin (100), dicumarol (250), and diazepam (350).

Stability—The stability of etodolac in serum was determined by analyzing serum samples spiked at 60.0 μg/ml after 1-, 3-, and 7-day storage at 20° or in the refrigerator at 4°.

RESULTS AND DISCUSSION

Chromatography—Typical liquid chromatograms of an etodolac standard, a control serum extract, and an extract of control serum spiked with etodolac are presented in Fig. 1. Using column B (250 × 4.6-mm) and a mobile phase of 30% acetonitrile–phosphate buffer, etodolac had a retention time of 5.0 min (flow rate, 1.8 ml/min). No interfering peaks were seen in the scan obtained with control serum. With column A a similar retention time is obtained if the concentration of acetonitrile is increased to 38%.

The linearity in the peak height response of the detector was demonstrated for low (1–10 μg/ml) and high (5–50 μg/ml) concentrations of etodolac. The regression line for the low test-tube standards was: $y = 21.4x - 1.23$ ($R = 0.9999$). For the high concentration standards the regression line was: $y = 4.79x - 3.93$ ($R = 0.9996$).

Recovery Studies—The linearity of recovery of etodolac from pooled human serum was also tested at two concentration ranges. For triplicate samples, covering the range of 1.0–10.0 μg/ml, the recovery was independent of etodolac concentration. The regression line for the recovery was: $y = 10.28x - 0.39$ ($R = 0.9984$). At high concentrations (5–50 μg/ml), linearity was maintained [regression line: $y = 2.57x - 3.55$ ($R = 0.9970$)]. In separate experiments small differences were noted when recoveries from rat, dog, and human sera and distilled water were evaluated at concentrations of 1.0, 10.0, and 50.0 μg/ml (Table I). The highest recovery (93.1%) was obtained with water, and with the sera recoveries varied from 86.2 (rat) to 91.5% (humans). Over a period of 6 months to 1 year, recovery of etodolac from pooled human serum varied from a low of 70 to a high of 94% [mean ± SE, 81.0 ± 1.6%]. The variations in day-to-day recovery from the same pooled serum were of the same order of magnitude as the differences found for various sera.

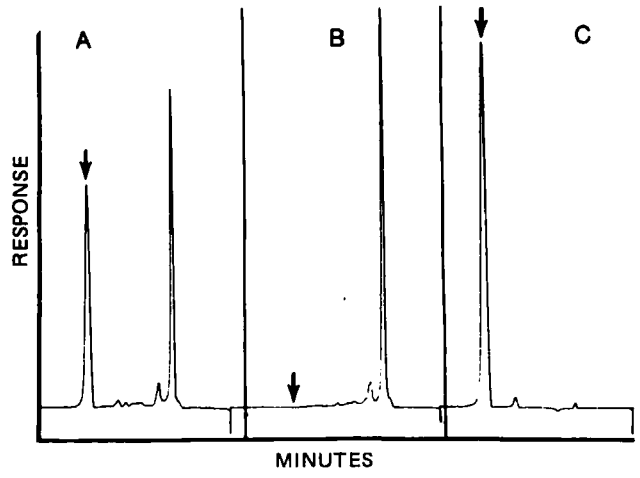

Figure 1—*HPLC chromatograms of: (A) extract of control serum spiked with etodolac (5 μg/ml); (B) extract of human control serum; and (C) etodolac standard (5 μg/ml), retention time (↓) 5.0 min, column 5 μm Spherisorb ODS.*

In the course of these experiments, it became apparent that variations in recovery were to a large extent due to instability of the etodolac test-tube standards (see *Stability*). To ensure that the small day-to-day and species-to-species variations in recovery do not result in an error in the estimation of etodolac, in actual analytical runs, standardization is based on appropriate serum standards spiked and run concurrently.

Sensitivity and Specificity—Control sera from rats ($n = 10$), dogs ($n = 23$), and humans ($n = 17$) were processed through the method and injected on the liquid chromatograph, operating at its highest sensitivity (0.05 AUFS). With the exception of one spurious sample (the apparent etodolac concentration was 0.7 μg/ml) none of the extracts revealed any UV absorption in the region of emergence of etodolac. The limit of detection of the method, consistent with baseline noise, was conservatively taken as 0.2 μg/ml. In contrast to the fluorometric procedure (3) with respect to endogenous substances, the HPLC method is specific.

When randomly selected serum samples were analyzed by both the fluorometric (3) and HPLC procedures, a good correlation was found. The mean etodolac concentrations in dog serum were estimated as 20.8 (fluorometric) and 18.3 μg/ml (HPLC). For rats the corresponding values were 78.7 and 80.2 μg/ml. The differences of 2.2 ± 1.2 and −1.5 ± 1.1 μg/ml were within the limit of reproducibility of the fluorometric method. When higher concentrations of etodolac are being measured, the more rapid fluorometric procedure can be employed, as long as the values are corrected for the 2–3 μg/ml of apparent etodolac found in control sera.

When sera from rats and dogs treated with [^{14}C]etodolac were analyzed for unchanged drug and total carbon 14 (Table II), 85–95% of the carbon 14 was accounted for by unchanged etodolac. In serum extracts used for chemical analysis, the percentage would be even higher. This explains why the inherently more specific HPLC method and the fluorometric method provide similar values. Finally, the ready separation of etodolac from its congeners, especially the phenolic analogue (Table III), suggests that the method is specific with regard to potential metabolites.

The potential for interference from selected drugs or their metabolites with the HPLC method was tested as follows. Rats were given high doses of each drug, bled 2 hr postdosing, and the serum was processed through the etodolac procedure. The HPLC chromatograms were examined for the presence of interfering peaks. Serum from control rats served as reference. The sample extracts were injected on both columns A and B. When ethacrynic acid, niacin, propoxyphene, phenobarbital, hydro-

Table II—Serum Concentrations of Unchanged Etodolac [a] and Total Carbon 14 in Rats and Dogs Given [^{14}C]Etodolac Orally

	Rat [b]			Dog [c]		
Postdose, hr	Etodolac, μg/ml	Carbon 14, μg/ml	Ratio	Etodolac, μg/ml	Carbon 14, μg/ml	Ratio
0.25	17.2	18.0	0.96	64.0	71.0	0.90
0.50	23.8	24.6	0.97	111.3	121.5	0.92
1.00	30.0	30.9	0.97	141.3	157.4	0.90
3.00	23.0	25.7	0.89	41.3	53.5	0.75
Mean			0.95			0.87

[a] *Fluorimetric* analysis. [b] $n = 4$, dose = 10 mg/kg po. [c] $n = 4$, dose = 50 mg/kg po.

Table III—Relative Retention Times [a] of Etodolac Congeners

Compound	Substituents R_1	R_2	R_3	R_4	Relative Retention Time
Etodolac	H	H	C_2H_5	C_2H_5	1.00
I	H	H	n-C_3H_7	H	0.80
II	H	H	phenyl	H	0.94
III	H	CH_3	CH_3	H	0.62
IV	OH	H	CH_3	H	0.44

[a] Chromosorb column; mobile phase: 38% acetonitrile–phosphate buffer; etodolac retention time, 5.0 min.

Table IV—Stability of Etodolac in Serum [a]

Temperature	Recovery (%) on day 1	3	7
20°	100.5 ± 0.5	97.6 ± 0.4	100.2 ± 0.5
4°	98.6 ± 0.5	97.4 ± 0.5	100.4 ± 0.6

[a] Pooled serum spiked with 60 μg/ml of etodolac.

chlorothiazide, glyburide, or diazepam were administered, no peaks were seen in the HPLC scans. Phenylbutazone and dicumarol produced strong interfering peaks with either column. With indomethacin, acetominophen, and salicylate, peaks separate from etodolac were noted, but due to tailing, these peaks partially overlapped the etodolac peak when injected on column A. A better separation was achieved on column B. Because concomitant administration of salicylate or acetominophen is likely to occur clinically, pooled rat serum spiked with etodolac was supplemented with 50–500 μg/ml of salicylate or 20–250 μg/ml of acetominophen, carried through the HPLC procedure, and analyzed on column B. No interference could be demonstrated, nor was there any adverse effect on the recovery of etodolac. In the presence of coadministered drugs, column B is preferred.

Stability—When etodolac was added to pooled serum and kept for up to 7 days at room temperature (20°) or in the refrigerator (4°), no significant loss of etodolac was detected at either temperature (Table IV).

Because of day-to-day variations in recovery, the stability of the test-tube standards and the extracted spiked control serum standards was also investigated. The peak height response of the test-tube standards (n = 12) declined from 100.0 ± 1.3 to 91.5 ± 1.2% in 1 hr. In contrast, the extracts from spiked control serum remained unchanged: 100.0 ± 1.3 *versus* 100.7 ± 2.2%. For this reason, the test-tube standard is used only to adjust mobile phase concentrations when the method is being set up. Quantitation is based on the stable extracts from spiked control sera, and no recovery factor is needed.

Application of the method—Initial studies in humans have indicated that activity is achieved with 100-mg etodolac doses given twice daily. At these doses the peak concentrations of etodolac varied between 4.0 and 14.3 μg/ml, and the daily minima between 0.3 and 3.5 μg/ml. Thus, the HPLC procedure possesses the specificity and sensitivity required to monitor etodolac concentrations in humans.

REFERENCES

(1) R. R. Martel and J. Klicius, *Can. J. Physiol.*, **54**, 245 (1976).

(2) *Ibid.*, *Agents Actions*, **12**, 295 (1982).

(3) W. T. Robinson, M. Kraml, E. Greselin, and D. Dvornik, *Xenobiotica*, **7**, 329 (1977).

(4) C. A. Demerson, L. G. Humber, T. A. Dobson, and I. L. Jirkovsky, U.S. Pat. 3,843,681 (Oct. 22, 1974).

(5) C. A. Demerson, L. G. Humber, A. H. Philipp, and R. R. Martel, *J. Med. Chem.*, **19**, 391 (1976).

(6) E. S. Ferdinandi, D. R. Hicks, W. Verbestel, and P. Raman, *J. Labelled Compd. Radiopharm.*, **14**, 411 (1978).

(7) M. N. Cayen, M. Kraml, E. S. Ferdinandi, E. Greselin, and D. Dvornik, *Drug Metab. Rev.*, **12**, 339 (1981).

Analysis of Chlorobutanol in Ophthalmic Ointments and Aqueous Solutions by Reverse-Phase High-Performance Liquid Chromatography

DANNY L. DUNN ˣ, WILLIAM J. JONES, and EDWIN D. DORSEY

Received March 3, 1982, from the *Analytical Chemistry Department, Alcon Laboratories, Inc., Fort Worth, TX 76134.* Accepted for publication May 6, 1982.

Abstract □ A reverse-phase high-performance liquid chromatographic assay for chlorobutanol was developed and found suitable for the routine analysis of ophthalmic ointments and aqueous solutions. The method utilized a column packed with 10-μm octadecylsilane with a mobile phase of methanol–water (50:50). Peak detection was by UV absorption at 210 nm. In this chromatographic system, chlorobutanol had a capacity factor (K') of 4.1. Standard curves obtained in the presence of ointment vehicle containing an aminoglycoside were linear, intercepted at zero, and averaged 99.4% recovery. Degradation studies indicated that the method was stability indicating. The analytical results for a complete experimental ophthalmic ointment and an aqueous ophthalmic diluent are presented. This high-performance liquid chromatographic method of analysis represents an alternative to GC procedures for determining chlorobutanol.

Keyphrases □ Chlorobutanol—analysis in opthalmic ointments and aqueous solutions by reverse-phase high-performance liquid chromatography □ High-performance liquid chromatography—reverse-phase, analysis of chlorobutanol in ophthalmic ointments and aqueous solutions □ Ophthalmic ointments—aqueous solutions, chlorobutanol, analysis by reverse-phase high-performance liquid chromatography □ GC—alternative method for analysis of chlorobutanol in opthalmic ointments and aqueous solutions, reverse-phase high-performance liquid chromatography

Chlorobutanol (1,1,1-trichloro-2-methyl-2-propanol) is a commonly used preservative in ophthalmic medications. It is readily degraded by base as shown in Scheme I to form acetone, carbon monoxide, and chloride ion (1). Chlorobutanol is also highly volatile, and loss by evaporation from ophthalmic solutions was reported through porous plastic bottles and closures (2).

BACKGROUND

A variety of analytical methods were developed for the analysis of chlorobutanol. Originally, analysis consisted of decomposing chlorobutanol by heating with base and then analyzing for chloride ion. This was done titrametrically (3, 4) iodometrically (5), gravimetrically (6), and amperometrically (7). Degradation using a known amount of base and determination of excess base by acid titration and degradation followed by an iodometric determination of acetone (8) also were used. These

0022-3549/83/0300-0277$01.00/0

Table III—Relative Retention Times [a] of Etodolac Congeners

Compound	Substituents R_1	R_2	R_3	R_4	Relative Retention Time
Etodolac	H	H	C_2H_5	C_2H_5	1.00
I	H	H	n-C_3H_7	H	0.80
II	H	H	phenyl	H	0.94
III	H	CH_3	CH_3	H	0.62
IV	OH	H	CH_3	H	0.44

[a] Chromosorb column; mobile phase: 38% acetonitrile–phosphate buffer; etodolac retention time, 5.0 min.

Table IV—Stability of Etodolac in Serum [a]

Temperature	Recovery (%) on day 1	3	7
20°	100.5 ± 0.5	97.6 ± 0.4	100.2 ± 0.5
4°	98.6 ± 0.5	97.4 ± 0.5	100.4 ± 0.6

[a] Pooled serum spiked with 60 μg/ml of etodolac.

chlorothiazide, glyburide, or diazepam were administered, no peaks were seen in the HPLC scans. Phenylbutazone and dicumarol produced strong interfering peaks with either column. With indomethacin, acetominophen, and salicylate, peaks separate from etodolac were noted, but due to tailing, these peaks partially overlapped the etodolac peak when injected on column A. A better separation was achieved on column B. Because concomitant administration of salicylate or acetominophen is likely to occur clinically, pooled rat serum spiked with etodolac was supplemented with 50–500 μg/ml of salicylate or 20–250 μg/ml of acetominophen, carried through the HPLC procedure, and analyzed on column B. No interference could be demonstrated, nor was there any adverse effect on the recovery of etodolac. In the presence of coadministered drugs, column B is preferred.

Stability—When etodolac was added to pooled serum and kept for up to 7 days at room temperature (20°) or in the refrigerator (4°), no significant loss of etodolac was detected at either temperature (Table IV).

Because of day-to-day variations in recovery, the stability of the test-tube standards and the extracted spiked control serum standards was also investigated. The peak height response of the test-tube standards (n = 12) declined from 100.0 ± 1.3 to 91.5 ± 1.2% in 1 hr. In contrast, the extracts from spiked control serum remained unchanged: 100.0 ± 1.3 *versus* 100.7 ± 2.2%. For this reason, the test-tube standard is used only to adjust mobile phase concentrations when the method is being set up. Quantitation is based on the stable extracts from spiked control sera, and no recovery factor is needed.

Application of the method—Initial studies in humans have indicated that activity is achieved with 100-mg etodolac doses given twice daily. At these doses the peak concentrations of etodolac varied between 4.0 and 14.3 μg/ml, and the daily minima between 0.3 and 3.5 μg/ml. Thus, the HPLC procedure possesses the specificity and sensitivity required to monitor etodolac concentrations in humans.

REFERENCES

(1) R. R. Martel and J. Klicius, *Can. J. Physiol.*, **54**, 245 (1976).

(2) *Ibid.*, *Agents Actions*, **12**, 295 (1982).

(3) W. T. Robinson, M. Kraml, E. Greselin, and D. Dvornik, *Xenobiotica*, **7**, 329 (1977).

(4) C. A. Demerson, L. G. Humber, T. A. Dobson, and I. L. Jirkovsky, U.S. Pat. 3,843,681 (Oct. 22, 1974).

(5) C. A. Demerson, L. G. Humber, A. H. Philipp, and R. R. Martel, *J. Med. Chem.*, **19**, 391 (1976).

(6) E. S. Ferdinandi, D. R. Hicks, W. Verbestel, and P. Raman, *J. Labelled Compd. Radiopharm.*, **14**, 411 (1978).

(7) M. N. Cayen, M. Kraml, E. S. Ferdinandi, E. Greselin, and D. Dvornik, *Drug Metab. Rev.*, **12**, 339 (1981).

Analysis of Chlorobutanol in Ophthalmic Ointments and Aqueous Solutions by Reverse-Phase High-Performance Liquid Chromatography

DANNY L. DUNN ˣ, WILLIAM J. JONES, and EDWIN D. DORSEY

Received March 3, 1982, from the *Analytical Chemistry Department, Alcon Laboratories, Inc., Fort Worth, TX 76134.* Accepted for publication May 6, 1982.

Abstract □ A reverse-phase high-performance liquid chromatographic assay for chlorobutanol was developed and found suitable for the routine analysis of ophthalmic ointments and aqueous solutions. The method utilized a column packed with 10-μm octadecylsilane with a mobile phase of methanol–water (50:50). Peak detection was by UV absorption at 210 nm. In this chromatographic system, chlorobutanol had a capacity factor (K') of 4.1. Standard curves obtained in the presence of ointment vehicle containing an aminoglycoside were linear, intercepted at zero, and averaged 99.4% recovery. Degradation studies indicated that the method was stability indicating. The analytical results for a complete experimental ophthalmic ointment and an aqueous ophthalmic diluent are presented. This high-performance liquid chromatographic method of analysis represents an alternative to GC procedures for determining chlorobutanol.

Keyphrases □ Chlorobutanol—analysis in opthalmic ointments and aqueous solutions by reverse-phase high-performance liquid chromatography □ High-performance liquid chromatography—reverse-phase, analysis of chlorobutanol in ophthalmic ointments and aqueous solutions □ Ophthalmic ointments—aqueous solutions, chlorobutanol, analysis by reverse-phase high-performance liquid chromatography □ GC—alternative method for analysis of chlorobutanol in opthalmic ointments and aqueous solutions, reverse-phase high-performance liquid chromatography

Chlorobutanol (1,1,1-trichloro-2-methyl-2-propanol) is a commonly used preservative in ophthalmic medications. It is readily degraded by base as shown in Scheme I to form acetone, carbon monoxide, and chloride ion (1). Chlorobutanol is also highly volatile, and loss by evaporation from ophthalmic solutions was reported through porous plastic bottles and closures (2).

BACKGROUND

A variety of analytical methods were developed for the analysis of chlorobutanol. Originally, analysis consisted of decomposing chlorobutanol by heating with base and then analyzing for chloride ion. This was done titrametrically (3, 4) iodometrically (5), gravimetrically (6), and amperometrically (7). Degradation using a known amount of base and determination of excess base by acid titration and degradation followed by an iodometric determination of acetone (8) also were used. These

0022-3549/83/0300-0277$01.00/0

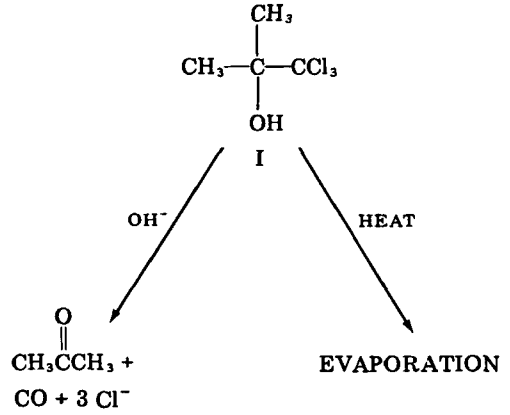

Scheme I—Potential routes for the loss of chlorobutanol (I) from ophthalmic formulations.

methods are not specific, because they are unable to differentiate from excipient chloride sources such as electrolytes or other organic compounds which also contain chlorine. In addition, tedious sample preparation such as steam distillation is often required.

Two colorimetric procedures were developed. The Fujiwara alkali–pyridine colorimetric reaction for chloroform has been used successfully to analyze for chlorobutanol (9, 10). By using 3-substituted pyridines, increased sensitivity to chlorobutanol was reported (11). Reaction of hydroxylamine and chlorobutanol in basic solution forms a product which produces a colored complex with ferric ion (12). Both colorimetric reactions lack specificity, and colors are produced with a variety of organic moieties.

Instrumental methods of analysis include polarography, which is sensitive but requires separation of chlorobutanol from excipients by steam distillation (13), and NMR spectrometry (14), which is difficult to justify for a routine analysis. IR spectrophotometry has also been used for samples eluted through a diatomaceous earth column to remove excipients (15, 16). Because of the high volatility of chlorobutanol, the most successful method of analysis has been gas chromatography (GC). Flame ionization detection is satisfactory with a large number of different stationary phases (2, 15, 16). In one reported GC method, electron capture detection was used (17).

The official USP analytical method for chlorobutanol is a GC procedure utilizing flame ionization detection, a 5% polyethylene glycol 20M stationary phase, and a benzaldehyde internal standard (18). However, attempts to analyze chlorobutanol in an experimental ointment formulation containing an aminoglycoside using a similar GC procedure yielded results which slowly increased according to the length of time samples were allowed to stand at room temperature before analysis. Evidence indicated that the benzaldehyde was slowly reacting with the vehicle, and the resulting variance in internal standard concentration was causing variance in the results.

A high-performance liquid chromatographic (HPLC) method of analysis for chlorobutanol is discussed, which uses an octadecylsilane column with UV peak detection at 210 nm. This reversed-phase system was found to be satisfactory for the routine analysis of chlorobutanol in ophthalmic ointments and aqueous solutions. Data is included to demonstrate that the procedure gives a linear response and reproducible recoveries from an ointment vehicle. The actual analyses of a complete bulk experimental ointment formulation and an aqueous ophthalmic diluent are presented. The results for the aqueous diluent are compared with the results obtained from a GC method using a cyclohexanol internal standard instead of benzaldehyde.

Table I—GC Analysis of a Chlorobutanol Vehicle Standard Using a Benzaldehyde Internal Standard

Time Left Standing Before Analysis, min	Ratio of Chlorobutanol Peak Height to Benzaldehyde Peak Height	Recovery, %[a]
0	1.13	100.9
10	1.17	104.9
21	1.19	106.1
31	1.22	109.4
40	1.26	112.7
50	1.29	115.4
59	1.35	120.6
69	1.37	122.3
78	1.40	125.0

[a] The vehicle standard contained 0.57 mg of chlorobutanol/ml and ~4.0 g of ointment vehicle which contained an aminoglycoside.

Table II—HPLC Analysis of Chlorobutanol Vehicle Standards Containing 4.0 g of Ointment Vehicle

Chlorobutanol Concentration, mg/ml	Chlorobutanol Peak Height, cm	Chlorobutanol Concentration Found[a], mg/ml	Recovery, %
0.281	8.70	0.281	100.0
0.281	8.70	0.281	100.0
0.328	10.20	0.330	100.5
0.328	10.20	0.330	100.5
0.375	11.50	0.372	99.1
0.375	11.45	0.370	98.7
0.422	12.90	0.417	98.8
0.422	12.90	0.417	98.8
0.469	14.45	0.467	99.6
0.469	14.45	0.467	99.6

[a] A standard containing 0.375 mg of chlorobutanol/ml was extracted and used to calculate these concentrations.

EXPERIMENTAL

Reagents and Solvents—Chlorobutanol hemihydrate[1], USP grade, was used without further purification. Its absolute purity on an anhydrous basis was established by titration of total chloride (3), and all subsequent calculations were corrected using this factor. Methanol[2] and hexane[2] were reagent grade.

Gas Chromatography—The gas chromatograph[3] was equipped with a flame ionization detector and a 91.4-cm × 6.4-mm glass column packed with 5% polyethylene glycol 20M[4] coated on 100–120 mesh diatomaceous earth[5]. The temperatures of the injector, column, and detector were 140, 80, and 250°, respectively. The gas flow rates of helium, hydrogen, and compressed air were 20, 20, and 350 ml/min, respectively.

Preparation of GC Ointment Samples—A sample of ointment equivalent to ~25 mg of chlorobutanol was weighed into a 60-ml separatory funnel. After dissolving in hexane (35 ml), the cloudy solution was extracted with three 7-ml portions of methanol. Each time the lower (methanol) layer was drained into a 50-ml volumetric flask. A 1.0-ml al-

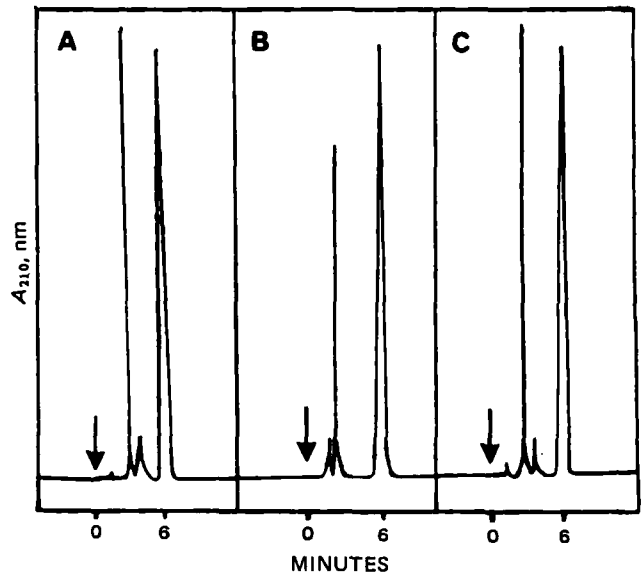

Figure 1—*Typical chromatograms for chlorobutanol analysis. Key: (A) a methanol standard; (B) sample extracted from an ophthalmic ointment; (C) a diluted sample of an aqueous ophthalmic diluent.*

[1] Stauffer Chemical Co.
[2] 'Baker Analyzed' Reagent, Baker Chemical Co.
[3] Model 402, Hewlett-Packard.
[4] Carbowax 20M, Supelco.
[5] Gas Chrom Q, Supelco.

Table III—HPLC Analysis of Complete Ophthalmic Samples

Sample (Age)	Chlorobutanol Analysis, Percent Label[a]
Experimental bulk ointment sample (14 days)	111.8, 112.1, 112.4, 111.2, 111.2
Experimental bulk ointment sample (15 days)	109.0, 111.7, 112.6, 112.5, 112.7
Aqueous diluent (5 months)	107.8, 107.8, 107.8, 108.3, 107.8, 107.5, 107.9, 107.9, 107.9

[a] The chlorobutanol concentrations were labeled 5.0 mg/g; however, since a 15% excess was added, the theoretical content is 115% of label.

iquot of a 7-mg/ml methanolic benzaldehyde solution was added, and the mixture was diluted to volume with methanol. A 1.0-μl injection of this solution was made directly into the gas chromatograph.

High-Performance Liquid Chromatography—A liquid chromatograph, equipped with a high-pressure pump[6], a variable-wavelength UV detector[7], an autoinjector[8], and a strip-chart recorder[9] was used with a 25-cm × 4.0-mm i.d. column packed with 10-μm octadecylsilane[10]. A 10-cm × 2.0-mm i.d. precolumn packed with 47-μm octadecylsilane[11] was used to protect the analytical column from the absorption of ointment vehicle.

Mobile Phase—Methanol (500 ml) and water (500 ml) were mixed and filtered through a 0.47-μm filter[12] before use.

Analysis Conditions—The mobile phase was pumped through the column at a flow rate of 1.8 ml/min. UV detection was at 210 nm, and the injection size was 100 μl. A sample was injected every 6 min. The plate count for the column, determined at a chart speed of 5.08 cm/min with a 0.37-mg/ml chlorobutanol solution, was 3000 plates/m[13]. After completion of the analysis, methanol was pumped through the column prior to storage.

Preparation of Standard Curves—The following were prepared using a methanolic 2.35 mg/ml of chlorobutanol stock solution:

Chlorobutanol Standard Curve—Five aliquots, giving final concentrations in the range of 0.28–0.48 mg of chlorobutanol/ml, were added to different 125-ml separatory funnels. Hexane (50 ml) was added and the methanolic layer adjusted to 15 ml with methanol–water (75:25). After shaking, the lower (methanolic) layer was drained into a 50-ml volumetric flask. The mixture was extracted twice more with 15 ml of methanol–water (75:25), and the lower layers were collected each time. The extracts in the volumetric flask were diluted to volume with methanol–water (75:25), and the resulting solution was injected directly into the HPLC.

Chlorobutanol Vehicle Standard Curve—The same series of aliquots used for the standard curve was added to different 125-ml separatory funnels which contained 4.0 g of ointment vehicle. The samples were dissolved in hexane and extracted with a methanol–water (75:25) solution as described above.

Preparation of Ophthalmic Ointment Samples—A sample of ointment equivalent to ~20 mg of chlorobutanol was weighed into a 125-ml separatory funnel. After dissolving in hexane (50 ml) the sample was extracted as described above. A standard was prepared by extracting 8.0 ml of a methanolic 2.5 mg of chlorobutanol/ml stock solution in a similar manner.

Preparation of Ophthalmic Aqueous Solutions—The sample was diluted with methanol to a final concentration of 0.5 mg of chlorobutanol/ml. A chlorobutanol standard of similar concentration was prepared in methanol.

RESULTS AND DISCUSSION

The chlorobutanol analysis of an experimental ointment formulation containing an aminoglycoside by gas chromatography was found to change if the samples were allowed to stand before being analyzed. In an attempt to isolate the problem, a vehicle standard containing 0.57 mg of chlorobutanol/ml was prepared and injected into a gas chromatograph every 10 min. The results presented in Table I show an apparent increase in chlorobutanol concentration with time at room temperature. This is probably due to a slow removal of the benzaldehyde internal standard caused either by oxidation to benzoic acid or reaction with the aminoglycoside present. A methanol chlorobutanol standard similarly injected showed no increase in concentration with time.

Since long automated runs were clearly impossible using this GC procedure, a reverse-phase HPLC system was developed. Using the HPLC conditions described under *Experimental*, chlorobutanol eluted at ~6 min, which corresponds to a capacity factor (K') of 4.1. Typical chromatograms are given in Fig. 1.

Table IV—HPLC Analysis of Forcibly Degraded Chlorobutanol Vehicle Standards Containing 4.0 g of Ointment Vehicle

Method of Degradation[a]	Theoretical Chlorobutanol Concentration, mg/ml	Chlorobutanol Peak Height, cm	Chlorobutanol Concentration Found, mg/ml	Recovery, %[b]
Heat alone	0.3773	2.20	0.0722	19.1
Heat + Acid	0.3773	5.00	0.1641	43.5
Heat + Base	0.3773	4.60	0.1509	40.0
Heat + Peroxide	0.3773	2.85	0.0935	24.8

[a] All samples were heated at 110° overnight. [b] No interfering HPLC peaks were observed.

Five chlorobutanol standards prepared in methanol over the concentration range of 0.28–0.48 mg/ml were extracted with hexane, as if they were ointment samples, and analyzed. A least-squares regression analysis of these results yielded a coefficient of determination (R^2) of 0.9983, a y-intercept of −0.24 cm, a slope of 29.54 cm/mg/ml, and a standard error of 0.093. Five vehicle standards containing ~4.0 g of ointment vehicle were also prepared over approximately the same concentration range and analyzed (Table II). A coefficient of determination (R^2) of 0.9990, a y-intercept of 0.19 cm, a slope of 30.28 cm/mg/ml, and a standard error of 0.070 were calculated. These statistics indicate that the HPLC analysis gives a linear response, and a single point standard may be used. The recoveries from 10 vehicle standards containing ointment vehicle averaged 99.4 ± 0.2%[14].

Two complete ophthalmic formulations were analyzed for chlorobutanol content (Table III). One was an experimental ophthalmic ointment which contained an aminoglycoside, mineral oil, and petrolatum as excipients. The other formulation was an aqueous ophthalmic diluent[15] which contained boric acid and polysorbate 80.

The ointment was analyzed on 2 consecutive days to check assay reproducibility. Fourteen days after manufacture, the chlorobutanol analysis of five samples taken from the bulk ointment averaged 111.7 ± 0.5%[14]. On the next day, five new samples were analyzed. The results were 111.7 ± 1.6%[14]. Fifteen percent excess chlorobutanol had been added, so the theoretical content was 115% of label. These data indicate that the HPLC assay has good day-to-day reproducibility with a standard deviation for each set of samples in the range acceptable for the analysis of a preservative.

Nine samples of the aqueous ophthalmic diluent were diluted with methanol and analyzed for chlorobutanol. Theoretical content was 115% of label. The results averaged 107.9 ± 0.2%[14]. These samples were also later analyzed using a GC method similar to the one described under *Experimental*, but utilizing a cyclohexanol internal standard instead of benzaldehyde and a 3% polyethylene glycol 20M stationary phase. By this procedure, the chlorobutanol content averaged 107.4% label, which is in good agreement with the HPLC results.

Four vehicle standard samples of chlorobutanol containing ~4.0 g of ointment vehicle were forcibly degraded to ensure that chlorobutanol or excipient degradation products did not interfere with the HPLC assay. To the first sample several drops of concentrated hydrochloric acid was added, to the second several drops of concentrated ammonium hydroxide was added, to the third several drops of 30% hydrogen peroxide was added, and to the fourth nothing was added. The vials were tightly capped and heated at 110° overnight. These samples correspond to the potential degradation pathways catalyzed by acid, base, oxidation, and heat.

[6] Model 110 A, Altex Scientific Co.
[7] Model SF 770, Schoeffel Instruments.
[8] WISP 710 B, Waters Associates.
[9] Omniscribe Model A 5111-1, Houston Instruments.
[10] ODS-10 (10 μm), Bio-Rad Laboratories.
[11] Bondapak C_{18}/Corasil (47 μm), Waters Associates.
[12] Fluoropore, Millipore Corp.
[13] Theoretical plates per meter (N) = 16 $(T/T_w)^2(100/L)$, where T is the retention time of chlorobutanol, T_w is the peak width of chlorobutanol measured along the baseline, and L is the column length in centimeters (19).
[14] Mean ± SD.
[15] Echodide Diluent, Alcon Laboratories.

Degradation was observed (Table IV), but no interfering HPLC peaks were present. The HPLC method thus appears to be stability indicating.

Analysis of chlorobutanol by HPLC using UV detection at 210 nm is a reasonable alternative to the GC methods of analysis. Several years ago, the HPLC analysis of 'non-UV absorbers,' such as chlorobutanol, was thought to be difficult if not impossible (20); however, modern UV detectors can readily operate at the lower wavelengths (*i.e.*, 200–220 nm), and the quantitation of 'non-UV absorbers' has now become routine.

REFERENCES

(1) A. Nair and J. Lach, *J. Am. Pharm. Assoc., Sci. Ed.*, **48**, 390 (1959).

(2) K. Koshy, R. Conwell, and R. Duvall, *J. Pharm. Sci.*, **56**, 269 (1967).

(3) "The United States Pharmacopeia," 20th rev., United States Pharmacopeial Convention, Rockville, Md., 1980, p. 1221.

(4) E. Brennan, *Am. J. Hosp. Pharm.*, **26**, 53 (1969).

(5) N. Ray and U. Basu, *Indian J. Pharm.*, **12**, 6 (1950).

(6) F. Sinton, *J. Assoc. Off. Agr. Chem.*, **21**, 557 (1938).

(7) L. Lach, D. Nair, and S. Blaug, *J. Am. Pharm. Assoc., Sci. Ed.*, **47**, 46 (1958).

(8) H. Jensen and P. Jannke, *ibid.*, **37**, 37 (1948).

(9) L. Chafetz and R. Mahoney, *J. Pharm. Sci.*, **54**, 1805 (1965).

(10) J. Reith, W. Van Ditmarsch, and T. DeRiciter, *Analysis (London)*, **99**, 652 (1974); through *Chem. Abstr.*, **82**, 80134.

(11) A. Taha, N. El-Rabbat, and M. El-Kommos, *J. Pharm. Belg.*, **35**, 107 (1980).

(12) C. Rehm and W. Mader, *J. Am. Pharm. Assoc., Sci. Ed.*, **46**, 621 (1957).

(13) J. Birner, *J. Anal. Chem.*, **33**, 1955 (1961).

(14) J. Fabregas, *Ann. Pharm. Fr.*, **36**, 485 (1978); through *Chem. Abstr.*, **90**, 174755.

(15) D. Healton and A. Davidson, *J. Assoc. Off. Anal. Chem.*, **49**, 850 (1966).

(16) A. Davidson, *ibid.*, **50**, 669 (1967).

(17) H. Smith and J. Thorpe, *J. Chromatogr.*, **134**, 178 (1977).

(18) "The United States Pharmacopeia," 20th rev., United States Pharmacopeial Convention, Rockville, Md., 1980, p. 914.

(19) L. Snyder and J. Kirkland, "Introduction to Modern Liquid Chromatography," 2nd ed., Wiley, New York, N.Y., 1979, pp. 27–28.

(20) J. Nelson, in "GLC and HPLC Determination of Therapeutic Agents," Part 2, K. Tsuji, Ed., Dekker, New York, N.Y., 1978, p. 821.

ACKNOWLEDGMENTS

Presented in part at the 37th Southwest Regional American Chemical Society Meeting, San Antonio, Texas, December 1981.

The authors greatly appreciate the technical assistance of Diane Loesch and Karen Haggard. Thanks are also due Britt Scott and Linda Brammer for proofreading the final manuscript and much helpful advice.

Adjuvant Effects of Glyceryl Esters of Acetoacetic Acid on Rectal Absorption of Insulin and Inulin in Rabbits

TOSHIAKI NISHIHATA *¶ˣ, SUNI KIM *, SHIGEYOSHI MORISHITA *, AKIRA KAMADA *, NOBORU YATA ‡ and TAKERU HIGUCHI §

Received January 28, 1982, from the **Faculty of Pharmaceutical Sciences, Osaka University, 133-1 Yamada-Kami, Suita, Osaka, 565, Japan;* the ‡*Institute of Pharmaceutical Sciences, University of Hiroshima School of Medicine, 1-2-3 Kasumi, Hiroshima, 734, Japan;* and the §*Department of Pharmaceutical Chemistry, University of Kansas, Lawrence, KS 66045.* Accepted for publication May 4, 1982. ¶Present address: Department of Pharmaceutical Chemistry, University of Kansas, Lawrence, KS 66045.

Abstract □ The promoting effect of glyceryl esters of acetoacetic acid on the rectal absorption of insulin and inulin was studied. A decrease in the serum glucose level was observed in rabbits following the administration of an insulin suppository containing glyceryl-1,3-diacetoacetate (adjuvant II) or 1,2-isopropylideneglycerine-3-acetoacetate (adjuvant IV). The promoting effects of adjuvants II and IV on the rectal absorption of insulin and inulin were suppressed by the addition of calcium and magnesium to the suppository. This indicates that adjuvant interaction with the calcium and magnesium ion located in the rectal membrane is involved in the enhanced absorption of insulin and inulin. Adjuvant release from the suppository formulation in addition to adjuvant lipid solubility were found to be other important factors for enhanced absorption of insulin and inulin.

Keyphrases □ Insulin—adjuvant effects of glyceryl esters of acetoacetic acid on rectal absorption, rabbits, inulin □ Inulin—adjuvant effects of glyceryl esters of acetoacetic acid on rectal absorption, rabbits, insulin □ Glyceryl esters—acetoacetic acid, adjuvant effects on rectal absorption of insulin and inulin, rabbits

In a previous paper (1), the effect of enamine derivatives of DL-phenylglycine on the rectal absorption of insulin was reported. It was suggested that rectal absorption of insulin was enhanced due to an interaction between the enamine derivatives and the calcium ions in the membrane. This interaction caused a temporary change in the integrity of the membrane allowing the insulin to pass more easily through the barrier. The active forms of the phenylglycine enamines are considered to be predominantly anionic. The interaction of these adjuvants with calcium and magnesium may be through the carboxylate moiety and/or the enamine moiety.

It has been reported (2) that intravenous administration of acetoacetic acid enhanced the distribution of chloropropamide and sulfadimetoxide to the red blood cells, indicating some change in erythrocyte membrane permeability. In the present paper, the glyceryl esters of acetoacetic acid were examined as adjuvants for promoting the rectal absorption of insulin and inulin. The ability of these nonionic compounds to be released from the suppository formulations, to permeate the rectal membrane, and to interact with divalent metal ions was examined.

EXPERIMENTAL

Materials—Glyceryl esters of acetoacetic acid were routinely synthesized by adding acetoacetic acid to glycerol or 1,2-isopropylideneglycerol in the presence of potassium acetoacetate (a catalyst) at

0022-3549/83/0300-0280$01.00/0

Degradation was observed (Table IV), but no interfering HPLC peaks were present. The HPLC method thus appears to be stability indicating.

Analysis of chlorobutanol by HPLC using UV detection at 210 nm is a reasonable alternative to the GC methods of analysis. Several years ago, the HPLC analysis of 'non-UV absorbers,' such as chlorobutanol, was thought to be difficult if not impossible (20); however, modern UV detectors can readily operate at the lower wavelengths (*i.e.*, 200–220 nm), and the quantitation of 'non-UV absorbers' has now become routine.

REFERENCES

(1) A. Nair and J. Lach, *J. Am. Pharm. Assoc., Sci. Ed.*, **48**, 390 (1959).

(2) K. Koshy, R. Conwell, and R. Duvall, *J. Pharm. Sci.*, **56**, 269 (1967).

(3) "The United States Pharmacopeia," 20th rev., United States Pharmacopeial Convention, Rockville, Md., 1980, p. 1221.

(4) E. Brennan, *Am. J. Hosp. Pharm.*, **26**, 53 (1969).

(5) N. Ray and U. Basu, *Indian J. Pharm.*, **12**, 6 (1950).

(6) F. Sinton, *J. Assoc. Off. Agr. Chem.*, **21**, 557 (1938).

(7) L. Lach, D. Nair, and S. Blaug, *J. Am. Pharm. Assoc., Sci. Ed.*, **47**, 46 (1958).

(8) H. Jensen and P. Jannke, *ibid.*, **37**, 37 (1948).

(9) L. Chafetz and R. Mahoney, *J. Pharm. Sci.*, **54**, 1805 (1965).

(10) J. Reith, W. Van Ditmarsch, and T. DeRiciter, *Analysis (London)*, **99**, 652 (1974); through *Chem. Abstr.*, **82**, 80134.

(11) A. Taha, N. El-Rabbat, and M. El-Kommos, *J. Pharm. Belg.*, **35**, 107 (1980).

(12) C. Rehm and W. Mader, *J. Am. Pharm. Assoc., Sci. Ed.*, **46**, 621 (1957).

(13) J. Birner, *J. Anal. Chem.*, **33**, 1955 (1961).

(14) J. Fabregas, *Ann. Pharm. Fr.*, **36**, 485 (1978); through *Chem. Abstr.*, **90**, 174755.

(15) D. Healton and A. Davidson, *J. Assoc. Off. Anal. Chem.*, **49**, 850 (1966).

(16) A. Davidson, *ibid.*, **50**, 669 (1967).

(17) H. Smith and J. Thorpe, *J. Chromatogr.*, **134**, 178 (1977).

(18) "The United States Pharmacopeia," 20th rev., United States Pharmacopeial Convention, Rockville, Md., 1980, p. 914.

(19) L. Snyder and J. Kirkland, "Introduction to Modern Liquid Chromatography," 2nd ed., Wiley, New York, N.Y., 1979, pp. 27–28.

(20) J. Nelson, in "GLC and HPLC Determination of Therapeutic Agents," Part 2, K. Tsuji, Ed., Dekker, New York, N.Y., 1978, p. 821.

ACKNOWLEDGMENTS

Presented in part at the 37th Southwest Regional American Chemical Society Meeting, San Antonio, Texas, December 1981.

The authors greatly appreciate the technical assistance of Diane Loesch and Karen Haggard. Thanks are also due Britt Scott and Linda Brammer for proofreading the final manuscript and much helpful advice.

Adjuvant Effects of Glyceryl Esters of Acetoacetic Acid on Rectal Absorption of Insulin and Inulin in Rabbits

TOSHIAKI NISHIHATA *¶ˣ, SUNI KIM *, SHIGEYOSHI MORISHITA *, AKIRA KAMADA *, NOBORU YATA ‡ and TAKERU HIGUCHI §

Received January 28, 1982, from the **Faculty of Pharmaceutical Sciences, Osaka University, 133-1 Yamada-Kami, Suita, Osaka, 565, Japan;* the ‡*Institute of Pharmaceutical Sciences, University of Hiroshima School of Medicine, 1-2-3 Kasumi, Hiroshima, 734, Japan;* and the §*Department of Pharmaceutical Chemistry, University of Kansas, Lawrence, KS 66045.* Accepted for publication May 4, 1982. ¶Present address: Department of Pharmaceutical Chemistry, University of Kansas, Lawrence, KS 66045.

Abstract □ The promoting effect of glyceryl esters of acetoacetic acid on the rectal absorption of insulin and inulin was studied. A decrease in the serum glucose level was observed in rabbits following the administration of an insulin suppository containing glyceryl-1,3-diacetoacetate (adjuvant II) or 1,2-isopropylideneglycerine-3-acetoacetate (adjuvant IV). The promoting effects of adjuvants II and IV on the rectal absorption of insulin and inulin were suppressed by the addition of calcium and magnesium to the suppository. This indicates that adjuvant interaction with the calcium and magnesium ion located in the rectal membrane is involved in the enhanced absorption of insulin and inulin. Adjuvant release from the suppository formulation in addition to adjuvant lipid solubility were found to be other important factors for enhanced absorption of insulin and inulin.

Keyphrases □ Insulin—adjuvant effects of glyceryl esters of acetoacetic acid on rectal absorption, rabbits, inulin □ Inulin—adjuvant effects of glyceryl esters of acetoacetic acid on rectal absorption, rabbits, insulin □ Glyceryl esters—acetoacetic acid, adjuvant effects on rectal absorption of insulin and inulin, rabbits

In a previous paper (1), the effect of enamine derivatives of DL-phenylglycine on the rectal absorption of insulin was reported. It was suggested that rectal absorption of insulin was enhanced due to an interaction between the enamine derivatives and the calcium ions in the membrane. This interaction caused a temporary change in the integrity of the membrane allowing the insulin to pass more easily through the barrier. The active forms of the phenylglycine enamines are considered to be predominantly anionic. The interaction of these adjuvants with calcium and magnesium may be through the carboxylate moiety and/or the enamine moiety.

It has been reported (2) that intravenous administration of acetoacetic acid enhanced the distribution of chloropropamide and sulfadimetoxide to the red blood cells, indicating some change in erythrocyte membrane permeability. In the present paper, the glyceryl esters of acetoacetic acid were examined as adjuvants for promoting the rectal absorption of insulin and inulin. The ability of these nonionic compounds to be released from the suppository formulations, to permeate the rectal membrane, and to interact with divalent metal ions was examined.

EXPERIMENTAL

Materials—Glyceryl esters of acetoacetic acid were routinely synthesized by adding acetoacetic acid to glycerol or 1,2-isopropylideneglycerol in the presence of potassium acetoacetate (a catalyst) at

0022-3549/83/0300-0280$01.00/0

Table I—Glyceryl Esters of Acetoacetic Acid

Adjuvants		Physical State	IR, cm^{-1} [a] C=O	IR, cm^{-1} [a] O—H	NMR, ppm
Glyceryl-1-monoacetoacetate	I[b]	Oil	1720, 1705	3400	2.18 (s, 3H, $-CH_3$), 3.39 (b, 2H, $-CH_2OH$), 3.53 (s, 2H, $-COCH_2CO-$), 4.03 (m, 2H, $-CH_2OC-$), 4.30 (b, 1H, $CH-OH$), 4.65 (b, 2H, $-OH$).
Glyceryl-1,3-diacetoacetate	II[b]	Oil	1720, 1705	3450	2.01 (s, 6H, $-CH_3 \times 2$), 3.55 (s, 4H, $-COCH_2CO- \times 2$), 4.15 (s, 4H, $-CH_2O- \times 2$), 4.25 (b, 2H, $CH-OH$).
Glyceryl-1,2,3-triacetoacetate	III[b]	Oil	1722, 1707		2.00 (s, 9H, $-CH_3 \times 3$), 3.55 (s, 6H, $-COCH_2CO- \times 3$), 4.33 (d, J = 6.0Hz, 4H, $-CH_2O- \times 2$), 5.30 (quintet, J = 6.0 Hz, 1H, $-CH-O-$).
1,2-Isopropylidene glyceryl-3-acetoacetate	IV[c]	Oil	1720, 1709		1.28 (s, 3H, $-CH_3$), 1.33 (s, 3H, CH_3). 2.19 (s, 3H, $-CH_3$), 3.37 (s, 2H, $-COCH_2CO-$), 3.70 (m, 2H, H), 4.07 (s, 2H, $-CH_2OC-$), 4.10 (m, 1H, $CH-O$).

[a] Liquid form. [b] Compounds I, II, and III were purified by chromatographic method: silica gel (70 ~ 325 mesh) was the column material; a mixture of benzene and ethylacetoacetate (2:1) was the mobile phase. [c] Compound IV was purified by a vacuum distillation method.

Table II—Suppository Formulations [a]

Formula	Adjuvant (50 mg)	Silicon Dioxide (5 mg)	Insulin (3 IU)	Inulin (25 mg)	Triglyceride Base, q.s.	Calcium Gluconate (7.5 mg)	Magnesium Chloride (3.5 mg)
1	II or III	X	X	—	X	—	—
2	I or IV	—	X	—	X	—	—
3	II or IV	Added only with adjuvant II	X	—	X	X	—
4	II or IV	Added only with adjuvant II	X	—	X	—	X
5	I, II, III or IV	Added only with adjuvants II or III	—	X	X	—	—
6	II or IV	Added only with adjuvant II	—	X	X	X	—
7	II or IV	Added only with adjuvant II	—	X	X	—	X

[a] X indicates compounds present.

100–110° while stirring. The insolubles, if necessary, were removed from the mixture by filtration. The crude products obtained were purified by liquid chromatographic methods (Table I). Commercially available crystalline beef insulin (zinc content 0.5% w/w on dry basis, 24.5 IU/mg) was used throughout the experiments[1]. Other reagents used were of analytical grade.

Preparation of Suppositories—Suppositories were prepared by combining the adjuvant, silicon dioxide[2], and either insulin or inulin with a triglyceride suppository base[3] (melted on a hot plate at 40°) according to the formulas in Table II. Silicon dioxide was added to the suppositories prepared with adjuvants II and III to disperse each adjuvant in the suppository base. The molten liquid was poured into disposable plastic molds[4]. The suppositories were allowed to stand for 2 hr at room temperature and were then stored in a refrigerator until used. Each suppository was slightly conical in shape with a rounded apex, measured 25 mm in length and 7 mm in maximum diameter, and weighed ~1 g.

***In Vivo* Studies**—Male white rabbits (2.5–3.0 kg) were fasted (with water available) for 16 hr prior to experimentation. One-milliliter control blood samples were collected from a marginal vein before the rectal administration of the suppository. After rectal administration of the suppository, the anus was closed with a plastic clip to prevent leakage of the rectal contents during the experiments. Blood samples were collected at specific time intervals for 3 hr. Each sample was frozen until assays of glucose and insulin were made.

***In Vitro* Studies**—Male Sprague-Dawley rats (250–300 g) were fasted (with water available) for 24 hr prior to the experiments. After decapitation and excision of the gut, the rectum and anus were washed with a Krebs-Ringer's solution containing 0.3% glucose (pH 7.4). The rectal segment was ligated at the anus, a 0.1-g liquified suppository was placed

Table III—Control Experiments in Rabbits without Insulin [a]

Triglyceride as Suppository Base	Serum Glucose Level mg/100 ml, 0	0.5	1.0	1.5	2.0	2.5, hr
+ I	108.6 (12.6)	127.4 (6.9)	113.5 (14.8)	120.3 (12.6)	117.2 (18.3)	114.8 (13.9)
+ II	102.9 (10.5)	129.7 (18.9)	124.6 (16.5)	112.8 (5.7)	106.4 (11.7)	109.3 (8.4)
+ III	112.1 (7.3)	119.3 (12.7)	119.5 (17.1)	112.7 (9.3)	117.1 (12.4)	109.7 (9.7)
+ IV	99.7 (4.1)	107.4 (8.5)	103.2 (9.2)	105.1 (9.3)	103.8 (12.4)	108.2 (6.0)
Base alone[b]	102.9 (11.4)	135.8 (21.4)	127.0 (16.3)	119.3 (20.1)	120.0 (8.5)	109.2 (10.2)

[a] Each figure is the mean ± standard deviation of six rabbits. [b] No significant differences in the serum glucose level resulted from suppositories administered with adjuvant compared to suppositories administered without adjuvant.

[1] Common Wealth Serum Laboratories, Australia.
[2] Aerosil 200, Colloidsilica Begussa, Germany.
[3] Witepsol H-15, Chemishe Werk, Witten, Germany.
[4] Nichii Packing Co., Ltd., Osaka, Japan.

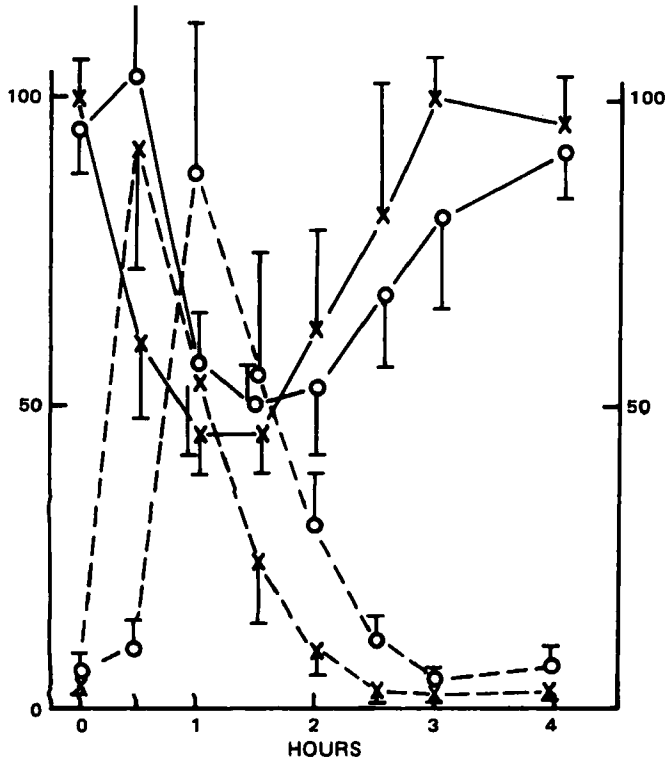

Figure 1—*Changes in serum glucose levels (—) (mg/100 ml) and serum insulin levels (---) (μIU/ml) in rabbits after administration of insulin suppositories containing 3 IU of insulin and 50 mg of adjuvant II (○) or adjuvant IV (×). The suppositories administered were prepared following formulas 1 and 2 (Table II). Each value in the figure indicates the mean and standard deviation of six rabbits.*

inside, and the other end of the segment was closed by ligation. The sac was placed into a test tube containing 40 ml of Krebs-Ringer's solution. The solution was held at 37° and aerated with an oxygen–carbon dioxide mixture (95:5). The concentration of glycerine esters in solution was determined by the assay described below.

Interaction of Glyceryl Esters with Calcium—The interaction of glyceryl esters with calcium was studied following a turbidimetric titration method previously described (3) with modifications (1).

Release of Adjuvants from Suppositories—The release of adjuvants from suppositories was studied using a previous method (4). A special apparatus[5] and a membrane filter (pore size 3.0 μm)[6] were used in the study of drug release from suppositories.

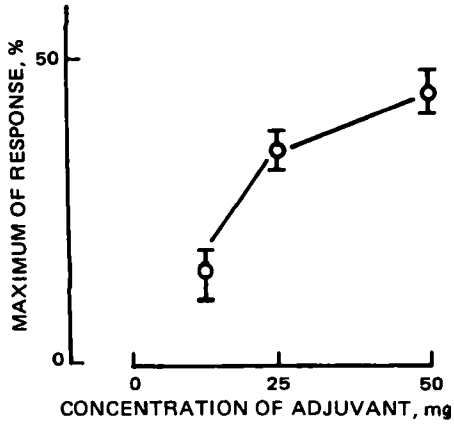

Figure 2—*Concentration effect of adjuvant II in suppositories containing 3 IU/body of insulin. The maximum response expressed in terms of the maximum change in glucose level as a percent of the initial level. Each value indicates the mean and standard deviation of six rabbits.*

[5] Toyama Sangyo Co., Ltd., Japan.
[6] Type SM, Sartorius Membranefilter GmbH, Germany.

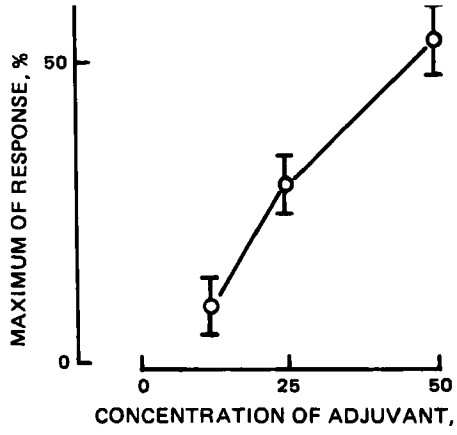

Figure 3—*Concentration effect of adjuvant IV in suppositories containing 3 IU/body of insulin. The maximum response is expressed in terms of the maximum change in glucose level as a percent of the initial level. Each value indicates the mean and standard deviation of six rabbits.*

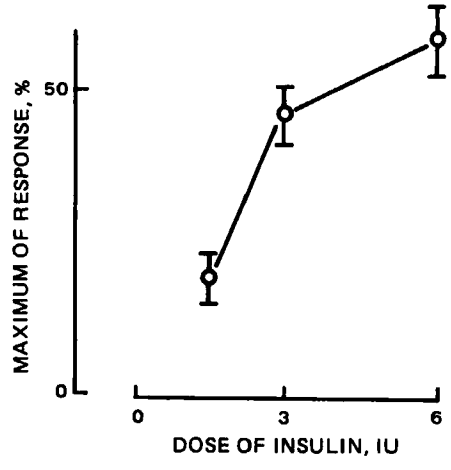

Figure 4—*Dose-response profile of insulin in rabbits administered suppositories containing 1.5–6 IU of insulin and 50 mg of adjuvant II. Response was expressed in terms of the maximum change in glucose levels as a percent of the initial level. Each value indicates the mean and standard deviation of six rabbits.*

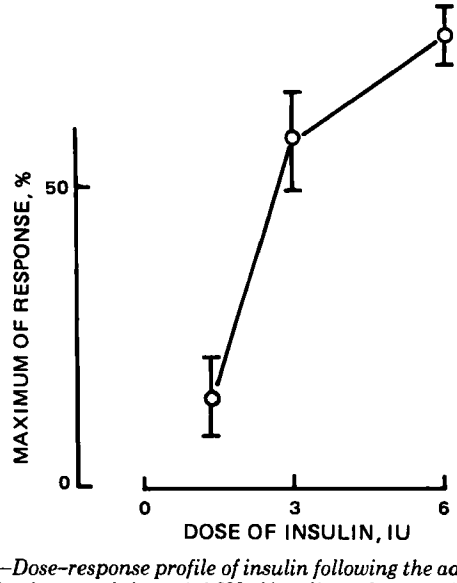

Figure 5—*Dose-response profile of insulin following the administration of suppositories containing 1.5–6 IU of insulin and 50 mg of the adjuvant IV. Response was expressed in terms of the maximum change in glucose level as a percent of the initial level. Each value indicates the mean and standard deviation of six rabbits.*

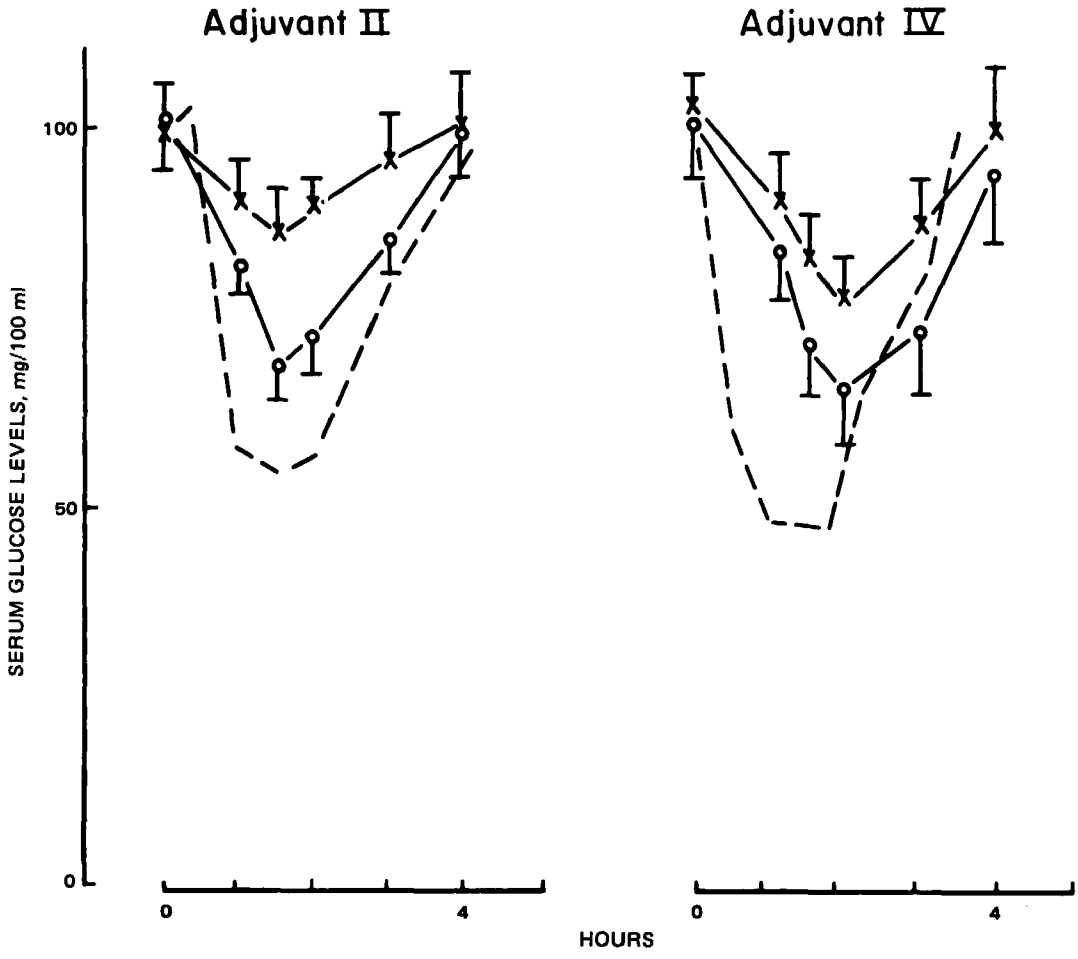

Figure 6—*Effect of calcium (O) and magnesium (X) on the promotive efficacy of adjuvants II or IV. Suppositories made according to formulas 3 and 4 (Table II) were administered at 1.0-g doses. The broken line indicates the change in serum glucose levels following the administration of an insulin suppository without calcium and magnesium. Each value indicates the mean and standard deviation of six rabbits.*

Assays—The serum glucose level was determined with the *o*-toluidine boric acid method (5) with a modification using a glucose test kit[7]. Serum insulin levels of rats were determined by a radioimmunoassay method described previously (5) using an insulin assay kit containing an agarose-bound antibody[8]. Inulin was determined as previously described (6) with the following slight modifications. A 0.5-ml sample was mixed with 1 ml of 0.1% resorcinol in 95% ethanol and 2.5 ml of 30% hydrochloric acid in a glass-stoppered test tube. The test tube was kept in a water bath at a temperature of 80 ± 0.5° for 25 min. After cooling with running water for 3 min, the color of the solution was spectrophotometrically determined at 490 nm. The concentration of glyceryl esters of acetoacetic acid in solution was determined according to a previous method (1) as a function of acetoacetate.

RESULTS AND DISCUSSION

As control experiments, 1.0-g suppositories containing glyceryl-1-monoacetoacetate (adjuvant I), glycerine-1,3-diacetoacetate (adjuvant II), glyceryl-1,2,3-triacetoacetate (adjuvant III), or 1,2-isopropylidene glyceryl-3-acetoacetate (adjuvant IV) at doses of 100 mg were administered to rabbits (Tables I and III). None of these control suppositories had any effect on the rabbits' serum glucose levels.

After rectal administration of suppositories (formulas 1 and 2 in Table II) containing 3 IU of insulin and only 50 mg of adjuvant, the serum glucose and serum insulin profiles were measured (Fig. 1). The administration of the suppositories containing adjuvants II and IV caused a dramatic decrease in glucose levels with minimums at 60–120 min and 60–90 min, respectively (Table I). Concomitantly, the serum insulin concentrations increased rapidly and reached maximum levels at 60 min for the suppositories containing adjuvant II and 30 min for adjuvant IV.

[7] Wako Pure Chemical Ind. Co., Japan.
[8] Pharmacia Co., Ltd., Japan.

Adjuvants I and III failed to reduce the serum glucose and did not increase the serum insulin level in these experiments. Adjuvants I and III also failed to enhance the rectal absorption of inulin. When 1.0-g suppositories (formula 5 in Table II) containing 25 mg of inulin/g and 50 mg of the adjuvant were rectally administered to rabbits, only adjuvants II and IV promoted inulin absorption (Table IV).

To study the effect of adjuvant concentration on the serum glucose

Table IV—Recovery of Inulin in Urine After Administration of Suppositories Containing 25 mg of Inulin/g and 50 mg of the Adjuvant at a Dose of 1.0 g of Suppository [a]

Adjuvant	Recovery of Inulin in Urine, % (4.0 hr)[b]
I	—
II	28.5 ± 1.8
III	—
IV	38.7 ± 2.1

[a] See formula 5 in Table II for suppository content. [b] Each value in the table indicates the mean ± standard deviation of six rabbits.

Table V—The Effect of Calcium and Magnesium on the Recovery of Inulin in Urine After Administration of 1.0-g Suppositories [a]

Adjuvant	Recovery of Inulin in Urine, % (4.0 hr)	
	Calcium[b]	Magnesium[c]
II	11.6 ± 2.1	6.3 ± 2.4
IV	19.8 ± 4.2	10.9 ± 3.8

[a] Each value in the table indicates the mean ± standard deviation of six rabbits. [b] See formula 6 in Table II for suppository content. [c] See formula 7 in Table II for suppository content.

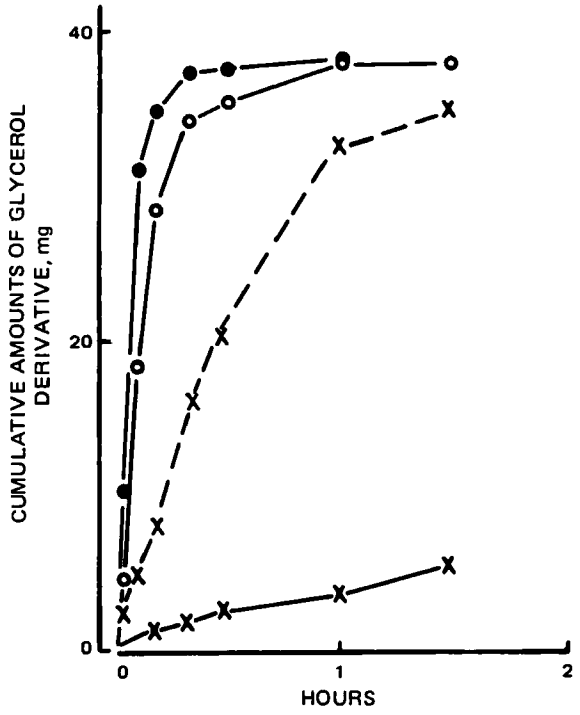

Figure 7—*Release of adjuvants I (●), II (○), III (— × —), and IV (-- × --) from triglyceride base into a saline solution.*

level, 1.0-g suppositories were prepared with concentrations ranging between 12.5 and 50 mg of adjuvant II or IV and containing 3 IU of insulin (Figs. 2 and 3). The insulin response was expressed as the maximum change in glucose relative to the initial level. With increasing adjuvant concentration in the suppositories, the maximum change in the serum glucose level increased accordingly. Rectal administration of 3 IU of insulin in the presence of 50 mg of adjuvant II or IV caused a 50% reduction in rabbit serum glucose concentration.

To study the dose–reponse profiles of insulin, 1.0-g suppositories containing 1.5–6.0 IU of insulin and 100 mg of adjuvant II were administered to rabbits (Fig. 4). The maximum response increased asymptotically with an increase in the insulin dose. Normal glucose level recovery took longer with higher concentrations of insulin. Similar results were obtained with adjuvant IV (Fig. 5).

In a previous paper (1), it was suggested that the absorption-promoting efficacy of enamine derivative was linearly related to their interacting ability with calcium ions located in the rectal membrane. In the present experiment, the addition of calcium gluconate or magnesium chloride

Table VI—Interacting Ability of Glycerol Derivatives with Calcium at pH 10.0 [a]

Adjuvant	Calcium gram per mole of compound
I	0.26
II	0.34
III	0.36
IV	0.28

[a] Gram of calcium ion interacting with 1 mole of glycerol derivative; results represent the mean of 3 determinations.

to suppositories markedly suppressed the promotive efficacy of adjuvants II and IV on the rectal absorption of insulin and inulin (Fig. 6 and Table V). The depressive effects of calcium and magnesium on the action of adjuvants were dramatically observed at doses shown in formulas 3, 4, 6, and 7 (Table II). Half doses of calcium and magnesium caused only small changes in the serum glucose compared with doses without the ions. These results appear to indicate that the promotive efficacy of glyceryl esters as well as enamine derivatives may be partly dependent on the interaction of the adjuvant with calcium and magnesium ions located in the rectal membrane. This interaction may cause transient gaps to form in the membrane allowing the insulin or inulin to permeate the rectal membrane more readily.

Even though the calcium binding ability of the four glyceryl esters was found to be similar to that of the enamine derivatives (Table VI), adjuvants I and III did not promote the rectal absorption of either insulin or inulin. Therefore, the promotive efficacy of adjuvants II and IV can not totally be explained by their ability to interact with calcium. To further explore possible absorption-enhancing mechanisms of these adjuvants, release of adjuvants from triglyceride base to water (maintained at 37° and continually stirred with a magnetic stirring bar) was studied (Fig. 7). The rates of release of the adjuvants were found to be in the order of I ($k_1 = 0.207$ min^{-1}), II ($k_1 = 0.115$ min^{-1}), IV ($k_1 = 0.029$ min^{-1}), and III (unmeasurable) as calculated by the following equation:

$$\frac{d(A_t/V)}{d_t} = k_1\left(\frac{A_0 - A_t}{V}\right) \qquad \text{(Eq. 1)}$$

where A_0 is the total amount of glycerol derivative in the system, A_t is the released amount of glycerol derivative at time t, V is the volume of the solution, and k_1 is the release rate constant.

Adjuvant III was inadequately released from the base owing to its poor water solubility. Thus, the deficiency in the promotive activity of adjuvant III may be explained by its inadequate partitioning property.

To investigate the deficiency in the promotive activity of adjuvant I, permeation of adjuvants and inulin through the excised sac of the rat rectum was studied (Fig. 8). Permeation rates were calculated using Eq. 2:

$$\frac{d(A_t/V)}{d_t} = k_2\left(\frac{A_0 - A_t}{V}\right) \qquad \text{(Eq. 2)}$$

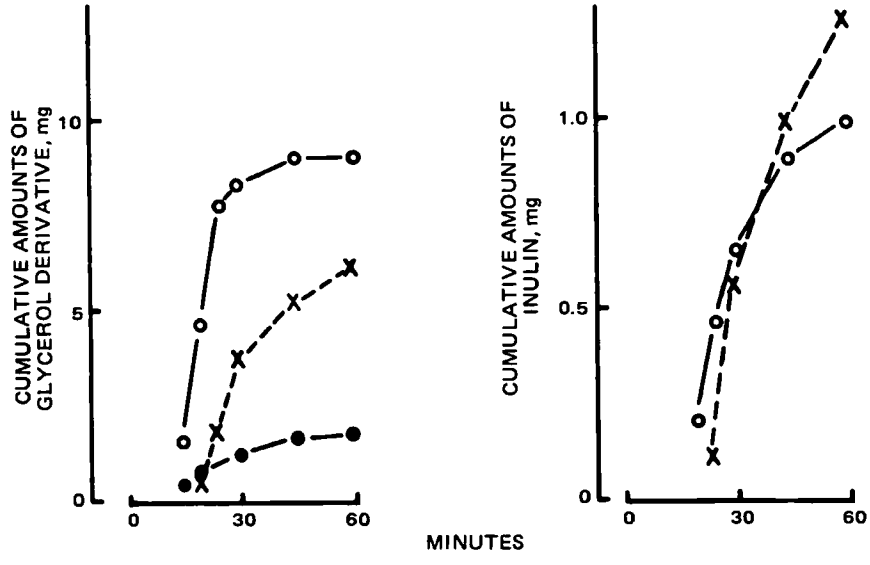

Figure 8—*Permeation of adjuvants I (●), II (○), and IV (×) with inulin through the excised sac of the rat rectum. Liquified suppositories (0.1 g) containing 10% of one of the glycerol derivatives and 30 mg of inulin/g of suppository were used.*

where all symbols are the same as before and k_2 is the permeation rate constant. Adjuvant I ($k_2 = 0.42 \times 10^2$ min^{-1}) did not readily cross the rectal membrane, possibly due to its strong lipophobicity. Adjuvants II ($k_2 = 7.29 \times 10^2$ min^{-1}) and IV ($k_2 = 1.91 \times 10^2$ min^{-1}) which are more lipophilic, easily permeated the rectal membrane and promoted the absorption of inulin.

Thus, adjuvant enhancement of rectal absorption of insulin and inulin appears to depend on at least three factors: adjuvants must be effectively released from the suppository, be able to permeate the membrane, and be able to interact with the calcium and magnesium ions in the membrane.

REFERENCES

(1) A. Kamada, T. Nishihata, S. Kim, M. Yamamoto, and N. Yata, *Chem. Pharm. Bull.*, **29**, 2012 (1981).

(2) T. Nishihata, N. Yata, and A. Kamada, *ibid.*, **27**, 1740 (1979).

(3) K. Ogino and N. Hayashi, *Yukagaku*, **32**, 88 (1979).

(4) S. Muranishi, Y. Okubo, and H. Sezaki, *Yakuzaigaku*, **39**, 1 (1980).

(5) T. Nishihata, N. Yata, and A. Kamada, *Chem. Pharm. Bull.*, **26**, 2238 (1978).

(6) E. Lunt and D. Sutcliff, *J. Biochem.*, **55**, 122 (1953).

Analysis and Prediction of Partition Coefficients of *meta*- and *para*-Disubstituted Benzenes in Terms of Substituent Effects

TOSHIO FUJITA

Received November 13, 1981, from the *Department of Agricultural Chemistry, Kyoto University, Kyoto, Japan 606.* Accepted for publication May 5, 1982.

Abstract □ The hydrophobic substituent parameter for a system of *meta*- and *para*-disubstituted benzenes, XC_6H_4Y, defined as $\pi_{X/PhY} = \log P_{XC_6H_4Y} - \log P_{C_6H_5Y}$, where P is the octanol–water partition coefficient and X and Y are variable and fixed substituents, respectively, varies from one system to another, according to the variation in substituent effects on the hydrogen bonding association of substituents with solvents. Using parameters from monosubstituted benzenes, $\pi_{X/PhH}$ as the reference, the π_X values were analyzed by such relations as $\pi_{X/PhY} = a\pi_{X/PhH} + \rho_Y\sigma_X + \rho_X\sigma_Y$, where ρ_Y and ρ_X are susceptibilities of the relative hydrogen bonding association of substituents Y and X with two partitioning solvents to the electronic effect of X and Y, respectively. For substituents incapable of hydrogen bonding such as alkyl and halogen, the ρ value is 0. The parameter a is a constant $\simeq 1$. The relationship was applied in calculating log P values of disubstituted benzenes.

Keyphrases □ Partition coefficient—octanol–water, analysis and prediction, *meta*- and *para*-disubstituted benzenes in terms of substituent effects □ Disubstituted benzenes—*meta*- and *para*-, analysis and prediction of partition coefficient, substituent effects □ Structure–activity relationships—analysis and prediction of partition coefficient of *meta*- and *para*-disubstituted benzenes in terms of substituent effects

In recent years, log P values (P is the 1-octanol–water partition coefficient) have been widely used as a parameter of the hydrophobic property of organic compounds in structure–activity studies (1). Log P values of complex molecules often can be calculated from those of suitable reference molecules and π values, where π is defined as $\pi_X = \log P_X - \log P_H$ (P_X is the coefficient value of a derivative on which the substituent X is carried and P_H is the coefficient value of a reference).

As pointed out earlier, however, the π value varies from one solute system to another (2). It was suggested that the variation in π values of aromatic substituents in various disubstituted benzene systems should be rationalized in terms of electronic interactions between substituents when no significant steric interaction is involved (2). For *meta*- and *para*-X substituents in disubstituted benzene systems of the type XC_6H_4Y, it was proposed that the variation in π relative to the value obtained for the monosubstituted benzene system, XC_6H_4H, depends on electronic interaction between each of the X-substituents and the fixed function Y, and is formulated, in general, as:

$$\Delta\pi = \pi_{X/PhY} - \pi_{X/PhH} = \rho_Y\sigma_X + \rho_X\sigma_Y \quad \text{(Eq. 1)}$$

where ρ_Y and ρ_X are the susceptibility constants of substituents Y and X to the solubility-modifying effects of substituents X and Y, respectively.

Since interest in the use of log P values in quantitative structure–activity studies is growing rapidly, it is important to clarify the composition of π values from various solute systems. The present report examines how far relations such as Eq. 1 can be applied in predicting π values for calculation of log P values.

EXPERIMENTAL

Solute Systems—Seventeen sets of π values (a total of 360 values) were used for the study. They were calculated from log P values of 17 disubstituted benzene solute systems and the corresponding reference monosubstituted benzenes. The majority of the log P values were taken from earlier reports (2, 3).

Several were determined[1] according to the reported procedure (2). Other values, *e.g.*, those for substituted benzamides (4), formanilides (5), acetanilides (6), and pyridines (7), are from the literature.

General Procedure—It was assumed that the solubility-modifying effect of substituent X on Y, as well as that of Y on X, was due primarily to the variation in hydrogen bonding association of substituents with solvents, according to the variation in the electronic environment of substituents X and Y. In actual examination of the applicability of Eq. 1, analysis was performed according to equations where $\pi_{X/PhY}$ and $\pi_{X/PhH}$ were used as dependent and independent variables, respectively. Although it should be close to 1, the slope of the $\pi_{X/PhH}$ term is not necessarily equal to 1. To avoid giving the unsubstituted solute excessive weight, an intercept term, c, has been included which should be close to 0. Equation 2 is employed when the fixed substituent Y is capable of hydrogen bonding:

$$\pi_{X/PhY} = a\pi_{X/PhH} + \rho_Y\sigma_X + \rho_X\sigma_Y(meta) + \rho_X\sigma_Y(para) + c \quad \text{(Eq. 2)}$$

[1] Agricultural Chemistry Department, Kyoto University and the Laboratory and Chemistry Department, Pomona College, Claremont, Calif.

0022-3549/83/0300-0285$01.00/0

where all symbols are the same as before and k_2 is the permeation rate constant. Adjuvant I ($k_2 = 0.42 \times 10^2$ min^{-1}) did not readily cross the rectal membrane, possibly due to its strong lipophobicity. Adjuvants II ($k_2 = 7.29 \times 10^2$ min^{-1}) and IV ($k_2 = 1.91 \times 10^2$ min^{-1}) which are more lipophilic, easily permeated the rectal membrane and promoted the absorption of inulin.

Thus, adjuvant enhancement of rectal absorption of insulin and inulin appears to depend on at least three factors: adjuvants must be effectively released from the suppository, be able to permeate the membrane, and be able to interact with the calcium and magnesium ions in the membrane.

REFERENCES

(1) A. Kamada, T. Nishihata, S. Kim, M. Yamamoto, and N. Yata, *Chem. Pharm. Bull.*, **29**, 2012 (1981).

(2) T. Nishihata, N. Yata, and A. Kamada, *ibid.*, **27**, 1740 (1979).

(3) K. Ogino and N. Hayashi, *Yukagaku*, **32**, 88 (1979).

(4) S. Muranishi, Y. Okubo, and H. Sezaki, *Yakuzaigaku*, **39**, 1 (1980).

(5) T. Nishihata, N. Yata, and A. Kamada, *Chem. Pharm. Bull.*, **26**, 2238 (1978).

(6) E. Lunt and D. Sutcliff, *J. Biochem.*, **55**, 122 (1953).

Analysis and Prediction of Partition Coefficients of *meta*- and *para*-Disubstituted Benzenes in Terms of Substituent Effects

TOSHIO FUJITA

Received November 13, 1981, from the *Department of Agricultural Chemistry, Kyoto University, Kyoto, Japan 606.* Accepted for publication May 5, 1982.

Abstract □ The hydrophobic substituent parameter for a system of *meta*- and *para*-disubstituted benzenes, XC_6H_4Y, defined as $\pi_{X/PhY} = \log P_{XC_6H_4Y} - \log P_{C_6H_5Y}$, where P is the octanol–water partition coefficient and X and Y are variable and fixed substituents, respectively, varies from one system to another, according to the variation in substituent effects on the hydrogen bonding association of substituents with solvents. Using parameters from monosubstituted benzenes, $\pi_{X/PhH}$ as the reference, the π_X values were analyzed by such relations as $\pi_{X/PhY} = a\pi_{X/PhH} + \rho_Y\sigma_X + \rho_X\sigma_Y$, where ρ_Y and ρ_X are susceptibilities of the relative hydrogen bonding association of substituents Y and X with two partitioning solvents to the electronic effect of X and Y, respectively. For substituents incapable of hydrogen bonding such as alkyl and halogen, the ρ value is 0. The parameter a is a constant $\simeq 1$. The relationship was applied in calculating log P values of disubstituted benzenes.

Keyphrases □ Partition coefficient—octanol–water, analysis and prediction, *meta*- and *para*-disubstituted benzenes in terms of substituent effects □ Disubstituted benzenes—*meta*- and *para*-, analysis and prediction of partition coefficient, substituent effects □ Structure–activity relationships—analysis and prediction of partition coefficient of *meta*- and *para*-disubstituted benzenes in terms of substituent effects

In recent years, log P values (P is the 1-octanol–water partition coefficient) have been widely used as a parameter of the hydrophobic property of organic compounds in structure–activity studies (1). Log P values of complex molecules often can be calculated from those of suitable reference molecules and π values, where π is defined as $\pi_X = \log P_X - \log P_H$ (P_X is the coefficient value of a derivative on which the substituent X is carried and P_H is the coefficient value of a reference).

As pointed out earlier, however, the π value varies from one solute system to another (2). It was suggested that the variation in π values of aromatic substituents in various disubstituted benzene systems should be rationalized in terms of electronic interactions between substituents when no significant steric interaction is involved (2). For *meta*- and *para*-X substituents in disubstituted benzene systems of the type XC_6H_4Y, it was proposed that the variation in π relative to the value obtained for the monosubstituted benzene system, XC_6H_4H, depends on electronic interaction between each of the X-substituents and the fixed function Y, and is formulated, in general, as:

$$\Delta\pi = \pi_{X/PhY} - \pi_{X/PhH} = \rho_Y\sigma_X + \rho_X\sigma_Y \quad \text{(Eq. 1)}$$

where ρ_Y and ρ_X are the susceptibility constants of substituents Y and X to the solubility-modifying effects of substituents X and Y, respectively.

Since interest in the use of log P values in quantitative structure–activity studies is growing rapidly, it is important to clarify the composition of π values from various solute systems. The present report examines how far relations such as Eq. 1 can be applied in predicting π values for calculation of log P values.

EXPERIMENTAL

Solute Systems—Seventeen sets of π values (a total of 360 values) were used for the study. They were calculated from log P values of 17 disubstituted benzene solute systems and the corresponding reference monosubstituted benzenes. The majority of the log P values were taken from earlier reports (2, 3).

Several were determined[1] according to the reported procedure (2). Other values, *e.g.*, those for substituted benzamides (4), formanilides (5), acetanilides (6), and pyridines (7), are from the literature.

General Procedure—It was assumed that the solubility-modifying effect of substituent X on Y, as well as that of Y on X, was due primarily to the variation in hydrogen bonding association of substituents with solvents, according to the variation in the electronic environment of substituents X and Y. In actual examination of the applicability of Eq. 1, analysis was performed according to equations where $\pi_{X/PhY}$ and $\pi_{X/PhH}$ were used as dependent and independent variables, respectively. Although it should be close to 1, the slope of the $\pi_{X/PhH}$ term is not necessarily equal to 1. To avoid giving the unsubstituted solute excessive weight, an intercept term, c, has been included which should be close to 0. Equation 2 is employed when the fixed substituent Y is capable of hydrogen bonding:

$$\pi_{X/PhY} = a\pi_{X/PhH} + \rho_Y\sigma_X + \rho_X\sigma_Y(meta) + \rho_X\sigma_Y(para) + c \quad \text{(Eq. 2)}$$

[1] Agricultural Chemistry Department, Kyoto University and the Laboratory and Chemistry Department, Pomona College, Claremont, Calif.

0022-3549/83/0300-0285$01.00/0

Table I—Primary Correlations of $\pi_{X/PhY}$ Using Eqs. 2 and 4 [a]

Solute System	a	ρ_Y	σ_Y^0 (*meta*)	σ_Y^0 (*para*)	c	s[b]	r[c]	n[d]	Substituents Used for Correlation	Equation
Benzoic acids	0.964 (0.071)	0.499 (0.140)			−0.021 (0.048)	0.035	0.977	12	H, *m*-F, *m*-Cl, *m*-Br, *m*-I, *m*-CH_3, *m*-CF_3, *p*-F, *p*-Cl, *p*-Br, *p*-I, *p*-CH_3	5
Phenylacetic acids	1.038 (0.155)	0.317[e] (0.304)			−0.057 (0.104)	0.076	0.987	12	H, *m*-F, *m*-Cl, *m*-Br, *m*-I, *m*-CH_3, *m*-CF_3, *p*-F, *p*-Cl, *p*-Br, *p*-I, *p*-CH_3	6
Phenoxyacetic acids	0.935 (0.051)	0.465 (0.118)			−0.007 (0.068)	0.065	0.993	24	H, *m*-F, *m*-Cl, *m*-Br, *m*-I, *m*-CH_3, *m*-C_2H_5, *m*-C_3H_7, *m*-*i*-C_3H_7, *m*-C_4H_9, *m*-*t*-C_4H_9, *m*-C_6H_5, *m*-CF_3, *m*-SF_5, *p*-F, *p*-Cl, *p*-Br, *p*-I, *p*-CH_3, *p*-*i*-C_3H_7, *p*-*s*-C_4H_9, 3,4-$(CH)_4$, 3,4-$(CH_2)_3$, 3,4-$(CH_2)_4$	7
Phenols	1.028 (0.108)	0.959 (0.202)			0.000 (0.081)	0.060	0.993	13	H, *m*-F, *m*-Cl, *m*-Br, *m*-I, *m*-CH_3, *m*-C_2H_5, *m*-CF_3, *p*-F, *p*-Cl, *p*-Br, *p*-I, *p*-CH_3	8
Benzamides	0.999 (0.077)	0.437 (0.181)			0.028 (0.085)	0.064	0.994	13	H, *m*-Br, *m*-Cl, *m*-F, *m*-CH_3, *p*-F, *p*-Cl, *p*-Br, *p*-I, *p*-CH_3, *p*-CF_3, *p*-*i*-C_3H_7, *p*-*t*-C_4H_9	9
Anilines	1.020 (0.055)	0.731 (0.082)			−0.005 (0.028)	0.015	0.999	7	H, *m*-F, *m*-Cl, *m*-CH_3, *p*-F, *p*-Cl, *p*-CH_3	10
Benzyl alcohols	0.937 (0.052)	0.486 (0.096)			0.023 (0.035)	0.046	0.998	11	H, *m*-Cl, *m*-CH_3, *m*-NO_2, *m*-OH, *m*-NH_2, *p*-Cl, *p*-CH_3, *p*-NO_2, *p*-OCH_3, *p*-OH	11
Formanilides	0.977 (0.053)	0.696 (0.068)			0.028 (0.027)	0.019	0.999	7	H, *p*-Cl, *p*-NO_2, *p*-CN, *p*-CH_3, *p*-OCH_3, *p*-$COCH_3$	12
Acetanilides	0.989 (0.058)	0.907 (0.159)			0.008 (0.060)	0.043	0.999	7	H, *p*-F, *p*-Br, *p*-I, *p*-OCH_3, *p*-NO_2, *p*-$CONH_2$	13
Benzonitriles	0.882 (0.135)		0.769 (0.264)	0.712 (0.244)	−0.095 (0.153)	0.083	0.987	11	H, *m*-OH, *m*-COOH, *m*-CH_2COOH, *m*-OCH_2COOH, *m*-$CONH_2$, *p*-OH, *p*-COOH, *p*-OCH_2COOH, *p*-$CONH_2$, *p*-NHCHO	14
Nitrobenzenes	0.920 (0.046)	−0.200 (0.109)	0.742 (0.128)	0.758 (0.132)	0.001 (0.047)	0.053	0.997	20	H, *m*-Cl, *m*-Br, *m*-CH_3, *m*-COOH, *m*-CH_2COOH, *m*-OCH_2COOH, *m*-CH_2OH, *m*-OH, *m*-NH_2, *m*-$CONH_2$, *p*-Cl, *p*-CH_3, *p*-COOH, *p*-CH_2COOH, *p*-OCH_2COOH, *p*-CH_2OH, *p*-OH, *p*-NH_2, *p*-$CONH_2$	15
Acetophenones	0.886 (0.111)	0.178[f] (0.197)	0.388 (0.212)	0.352 (0.235)	0.044 (0.084)	0.068	0.994	12	H, *m*-OCH_2COOH, *m*-OH, *m*-NO_2, *p*-OCH_2COOH, *p*-OH, *p*-NO_2, *p*-NHCHO, *m*-NH_2, *p*-NH_2, *p*-CH_3, *p*-Cl	16
Anisoles	0.911 (0.077)	0.292 (0.130)	0.011[g] (0.125)	−0.168 (0.124)	0.012 (0.082)	0.055	0.994	18	H, *m*-COOH, *m*-CH_2COOH, *m*-OCH_2COOH, *m*-OH, *m*-$CONH_2$, *m*-NH_2 *m*-NHCHO, *m*-NO_2, *p*-COOH, *p*-CH_2COOH, *p*-OCH_2COOH, *p*-OH, *p*-$CONH_2$, *p*-CH_2OH, *p*-NHCHO, *p*-$NHCOCH_3$, *p*-NO_2	17

[a] $\pi_{X/PhY} = a\pi_{X/PhH} + \rho_Y\sigma_X^0 + \rho_X\sigma_Y^0(m) + \rho_X\sigma_Y^0(p) + c$; unless noted, all of the terms except for the intercept values are justified above the 99.5% level; figures in parentheses are the 95% confidence intervals. [b] Standard deviation. [c] Correlation coefficient. [d] Number of points used for correlations. [e] Justified at the 95% level. [f] Justified at the 93% level. [g] Justified at the 50% level.

For cases when Y is incapable of association:

$$\pi_{X/PhY} = a\pi_{X/PhH} + \rho_X\sigma_Y(meta) + \rho_X\sigma_Y(para) + c \quad \text{(Eq. 3)}$$

Since the effect of Y on X is accounted for either by $\sigma_Y(meta)$ or $\sigma_Y(para)$, depending on the position of X-substituents, the term $\rho_X\sigma_Y$ in Eq. 1 should be separated as in Eqs. 2 and 3. Each of the $\rho_X\sigma_Y$ terms is only applicable to each of the corresponding *meta*- and *para*-substituents. For nonhydrogen-bonding variable substituents X, the value of ρ_X should be taken as 0. For π values derived from a set of XC_6H_4Y compounds where a fixed substituent Y is capable of hydrogen-bonding while the variable X substituents are not, Eq. 2 can be simplified as:

$$\pi_{X/PhY} = a\pi_{X/PhH} + \rho_Y\sigma_X + c \quad \text{(Eq. 4)}$$

According to recent studies on the hydrogen-bonding effect on oil–water partitioning of substituted benzene derivatives, substituents such as hydrogen, halogen, alkyl, phenyl, trifluoromethyl (CF_3), and pentafluorothio (SF_5) are discriminated as nonhydrogen bonders (8).

Values of σ^0 were used throughout this study. Preliminary examinations showed that σ^0 works better than σ^- for π values from phenols and anilines. Even π values from benzoic acids and benzamides were better correlated by σ^0 than σ. Values for $\pi_{X/PhH}$ (1) and σ^0 (9) used for correlations were taken from the literature.

The values for a, ρ_Y, σ_Y (*meta*), σ_Y (*para*), and c were determined by regression analysis. If the correlation is complete, σ_Y (*meta*) and σ_Y (*para*) values determined as regression coefficients of ρ_X terms should be equal to the respective σ values of the fixed substituent Y.

Preliminary Analysis—To carry out analyses using Eqs. 2 and 3, ρ_X values for hydrogen bonding variable substituents were needed. In the first six cases in Table I, data for only nonhydrogen bonding X substituents were fit to an equation of the form of Eq. 4 to get an approximate value for ρ_Y for such Y substituents as carboxyl, carboxylmethyl (CH_2COOH), carboxylmethoxy (OCH_2COOH), hydroxy, carbamoyl ($CONH_2$), and amino. The assumption for the first approximation was that $\rho_X = 0$. In the next three cases in Table I, σ_Y^0 values of functional groups such as *m*- and *p*-hydroxymethyl(CH_2OH), *p*-formylamido(NHCHO), and *p*-acetamido ($NHCOCH_3$) were essentially 0 (1, 9); hence, there was no electronic effect, for example, of hydroxymethyl on hydrogen bonding X substituents to affect π. Therefore, these three examples, including hydrogen bonding and nonhydrogen bonding substituents can be fit to the same type of equation as the first six. This provided the approximate ρ_Y values altogether for nine hydrogen bonding Y substituents.

For the benzonitriles, nitrobenzenes, acetophenones, and anisoles, few derivatives with nonhydrogen bonding X substituents have reported π values; therefore, in these examples, equations of the type derived for the

Table II—Final Correlation of $\pi_{X/PhY}$ Using Eqs. 2 and 3 [a]

Solute System	a	ρ_Y	$\sigma_Y^0(m)$	$\sigma_Y^0(p)$	c	s^a	r^a	n^a	Substituents used for correlation[b]	Equation
Benzoic acids	1.001 (0.042)	0.435 (0.098)	0.352 (0.126)	0.427 (0.138)	−0.024 (0.046)	0.048	0.998	22	*m*-CN, *p*-CN, *m*-OCH_3, *p*-OCH_3, *m*-NO_2, *p*-NO_2, *m*-OH, *p*-OH, *m*-OCH_2COOH, *p*-NH_2	18
Phenylacetic acids	0.954 (0.057)	0.294 (0.143)			0.012 (0.059)	0.079	0.993	20	*m*-COOH, *m*-CN, *m*-OH, *m*-OCH_3, *p*-OCH_3, *m*-NO_2, *p*-NO_2, *m*-SO_2CH_3	19
Phenoxyacetic acids	0.913 (0.026)	0.416 (0.082)			0.035 (0.035)	0.076	0.996	44	*m*-$COCH_3$, *p*-$COCH_3$ *m*-CN, *p*-CN, *m*-OCH_3, *p*-OCH_3, *m*-OCF_3, *m*-NO_2, *p*-NO_2, *m*-$NHCOCH_3$, *m*-$NHCOC_6H_5$, *m*-SCH_3, *m*-SCF_3, *m*-SO_2CH_3, *m*-COOH, *m*-OH, *p*-OH, *p*-$N{=}NC_6H_5$, *m*-$NHCONH_2$, *m*-SO_2CF_3	20
Phenols	0.967 (0.040)	0.941 (0.105)		−0.151[c] (0.138)	0.052 (0.040)	0.080	0.996	35	*m*-$COCH_3$, *p*-$COCH_3$, *m*-OCH_3, *p*-OCH_3, *m*-NO_2, *p*-NO_2, *m*-CN, *p*-CN, *m*-COOH, *p*-COOH, *m*-OH, *p*-OH, *m*-NH_2, *p*-NH_2, *m*-CH_2OH, *p*-CH_2OH, *m*-OCH_2COOH, *p*-OCH_2COOH, *m*-$CONH_2$, *p*-$CONH_2$, *m*-CH_2COOH, *m*-$N(CH_3)_2$	21
Benzamides	0.951 (0.056)	0.447 (0.132)	0.281 (0.174)	0.285 (0.170)	0.085 (0.062)	0.070	0.996	24	*m*-NO_2, *p*-NO_2, *m*-CN, *p*-CN, *p*-$NHCOCH_3$, *m*-OH, *p*-OH, *m*-NH_2, *p*-NH_2, *m*-OCH_3, *p*-OCH_3	22
Anilines	0.889 (0.100)	0.740 (0.219)	−0.255[d] (0.259)	−0.566 (0.240)	0.069 (0.089)	0.087	0.994	18	*m*-NO_2, *p*-NO_2, *m*-OCH_3, *m*-OH, *p*-OH, *m*-$COCH_3$, *p*-$COCH_3$, *p*-COOH, *m*-CH_2OH, *m*-$CONH_2$, *p*-$CONH_2$	23
Benzonitriles	0.915 (0.087)		0.757 (0.142)	0.694 (0.132)	−0.048 (0.069)	0.059	0.990	15	*m*-NO_2, *p*-NO_2, *m*-$OCONHCH_3$, *p*-$OCONHCH_3$	24
Nitrobenzenes	0.913 (0.051)	−0.139[e] (0.105)	0.751 (0.141)	0.751 (0.151)	0.018 (0.049)	0.063	0.993	28	*m*-$COCH_3$, *p*-$COCH_3$, *m*-CN, *p*-CN, *m*-OCH_3, *p*-OCH_3, *m*-NO_2, *p*-NO_2	25
Acetophenones	0.904 (0.092)	0.156[c] (0.153)	0.410 (0.179)	0.376 (0.197)	0.050 (0.065)	0.058	0.995	13	*p*-OCH_3	26
Anisoles	0.924 (0.061)	0.272 (0.099)		−0.193 (0.084)	0.037 (0.058)	0.052	0.995	20	*p*-$COCH_3$, *m*-OCH_3	27
Toluenes	0.980 (0.034)				−0.054[f] (0.029)	0.052	0.997	24	H, *m*-Cl, *p*-Cl, *m*-CH_3, *p*-CH_3, *m*-NO_2, *p*-NO_2, *m*-OCH_2COOH,	28
	0.998 (0.037)			−0.102[c] (0.096)		0.061	0.998	24	*p*-OCH_2COOH, *m*-CH_2COOH, *p*-CH_2COOH, *m*-COOH, *p*-COOH, *m*-CH_2OH, *p*-CH_2OH, *m*-OH, *p*-OH, *m*-NH_2, *p*-NH_2, *m*-$CONH_2$, *p*-$CONH_2$, *m*-$OCONHCH_3$, *p*-$OCONHCH_3$, *p*-$COCH_3$	28a
Chlorobenzenes	0.966 (0.058)		0.394 (0.137)	0.370 (0.138)	−0.088[f] (0.043)	0.066	0.994	24	H, *m*-Cl, *p*-Cl, *m*-CH_3, *p*-CH_3, *m*-NO_2, *p*-NO_2, *m*-OH, *p*-OH, *m*-	29
	0.975 (0.079)		0.269 (0.165)	0.240[g] (0.166)		0.089	0.994	24	NH_2, *p*-NH_2, *m*-COOH, *p*-COOH, *m*-CH_2COOH, *p*-CH_2COOH, *m*-OCH_2COOH, *p*-OCH_2COOH, *m*-CH_2OH, *p*-CH_2OH, *m*-$CONH_2$, *p*-$CONH_2$, *m*-$OCONHCH_3$, *p*-$OCONHCH_3$, *p*-$COCH_3$	29a
Pyridines	0.800 (0.055)		0.430 (0.173)	0.604 (0.177)	0.169[f] (0.048)	0.075	0.994	19	H, β-CH_3, β-Cl, β-Br, β-CN, γ-CH_3, γ-Br, γ-Cl, γ-C_6H_5,	30
	0.901 (0.064)	0.332 (0.138)	0.750 (0.195)	1.023 (0.194)		0.099	0.992	19	γ-CN, γ-C_3H_7, β-NO_2, β-$COCH_3$, γ-$COCH_3$, β-NH_2, γ-NH_2, β-$NHCOCH_3$, γ-$NHCOCH_3$, γ-OCH_3	30a
Phenyl *N*-methylcarbamates	0.992 (0.049)	0.602 (0.140)	0.469 (0.297)	0.481 (0.318)	0.037 (0.066)	0.079	0.994	41	H, *m*-F, *m*-Cl, *m*-Br, *m*-I, *m*-CH_3, *m*-C_2H_5, *m*-C_3H_7, *m*-*i*-C_3H_7, *m*-*t*-C_4H_9, *m*-CF_3, *p*-F, *p*-Cl, *p*-Br, *p*-I, *p*-CH_3, *p*-C_2H_5, *p*-C_3H_7, *p*-*i*-C_3H_7, *p*-*s*-C_4H_9, *p*-*t*-C_4H_9, *m*-OCH_3, *m*-CN, *m*-NO_2, *m*-$COCH_3$, *p*-OCH_3, *p*-$COCH_3$, *p*-CN, *p*-NO_2, *m*-OC_2H_5, *m*-*O*-*i*-C_3H_7, *m*-OC_4H_9, *m*-CHO, *m*-$COOCH_3$, *m*-COC_2H_5, *p*-OC_2H_5, *p*-OC_4H_9, *p*-COC_2H_5, *p*-CHO, *p*-$COOCH_3$, *p*-*O*-*i*-C_3H_7	31

[a] $\pi_{X/PhY} = a\pi_{X/PhH} + \rho_Y\sigma_X^0 + \rho_X\sigma_Y^0(m) + \rho_X\sigma_Y^0(p) + c$; see footnotes *a–d* in Table I. [b] Those already indicated in Table I are not listed. [c] Justified at the 95% level. [d] Justified at the 94% level. [e] Justified at the 97.5% level. [f] Justified above the 99.5% level. [g] Justified at the 99% level.

first nine data sets of Table I were not appropriate, so hydrogen bonding X substituents had to be included in these cases. The electronic effect of substituents from Y to X should be taken into account. The ρ_X value for each of the hydrogen bonding X substituents should be identical to the ρ_Y value for a solute system where the corresponding hydrogen bonding substituent was invariant. Values of ρ_Y, calculated for the nine

Table III—Susceptibility Constant of Relative Hydrogen Bonding Association with Solvents

Y-Substituent	ρ_Y	Y-Substituent	ρ_Y
Nonhydrogen bonder		Amphiprotic substituents	
CH_3	0	CH_2COOH	0.29(±0.14)
Cl	0	OCH_2COOH	0.42(±0.08)
		COOH	0.44(±0.10)
Hydrogen acceptor		$CONH_2$	0.45(±0.13)
NO_2	−0.14(±0.11)	CH_2OH	0.49(±0.10)
CN	0	$OCONHCH_3$	0.50(±0.14)
OCH_3	0.27(±0.10)	NHCHO	0.70(±0.07)
$COCH_3$	0.16(±0.15)	NH_2	0.74(±0.22)
—*N*=	0.33(±0.14)	$NHCOCH_3$	0.91(±0.16)
		OH	0.94(±0.11)

hydrogen bonding Y substituents, could be substituted for either of the ρ_X terms of Eq. 2 for these hydrogen bonding X substituents. The values of ρ_X for nonhydrogen bonding substituents was taken as 0. Performing the regression analysis yielded Eqs. 14–17 (Table I) with four new approximate ρ_Y values for hydrogen bonding Y substituents, nitro, cyano, acetyl, and methoxy. Values of σ_Y^0 were determined as regression coefficients of ρ_X terms. In the case of the benzonitriles, ρ_Y was essentially 0. The results of these primary correlations are shown as Eqs. 5–17 (Table I). The level of significance of all of the correlations in Table I was >99.5%, as determined by the *F* test.

Final Regression Analysis—The 13 primary ρ_Y values can now be substituted into Eq. 2 for the ρ_X values for hydrogen bonding X substituents. The regression analysis was performed by including nonhydrogen bonding as well as hydrogen bonding substituents. For π values from benzyl alcohol, formanilides, and acetanilides, it was unnecessary to refit, since σ_Y^0 is 0 in these examples, no matter what the ρ_X values were. The ρ_Y values for hydrogen bonding Y substituents determined for 10 series of π values were slightly different from the corresponding primary values; thus, this process was repeated by substituting newly derived ρ_Y values into Eq. 2 for ρ_X values until constant ρ_Y values were obtained. In the course of the calculations, ρ_X terms were found to be insignificant in the correlation equations for phenylacetic acids and phenoxyacetic acids; hence, it was possible to include hydrogen bonding X substituents for which the ρ_X values were not known in the final correlations.

Values of π_X from substituted toluenes and chlorobenzenes, where the fixed function is nonhydrogen bonding, were analyzed by means of Eq. 3 using self-consistent ρ_X values. Finally, π values from substituted phenyl *N*-methylcarbamates and pyridines were applied to Eq. 2. Since σ values of the substituent *N*-methylcarbamoyloxy ($OCONHCH_3$) were not available and, since there is some uncertainty for σ values of aza(—*N*=) function, π_X values of $OCONHCH_3$ and —*N*= as X substituents were not included in correlations, except for a few cases where the σ_X term was insignificant. In deriving Eq. 31 for those of phenyl-*N*-methylcarbamates, the ρ_X values of alkoxyl groups were approximated by that of the methoxyl group and those of acyl and carbomethoxyl groups by that of the acetyl group.

RESULTS

The results for 14 sets of π values are shown in Table II as Eqs. 18–31. All the correlations and the terms other than the intercepts are justified >99.5% by *F* and *t* tests, unless noted. Those for π values of benzyl alcohols, formanilides, and acetanilides are the same as the primary correlations, Eqs. 11–13 in Table I. Values of *a* and ρ_Y observed in Eqs. 18–23 of the correlations including hydrogen bonding substituents are practically identical with those in Eqs. 5–10 for only nonhydrogen bonding X substituents; this seems to support the assumptions made to formulate Eq. 1. The effect of X on Y and Y on X are mutually independent, and the effects are additive in determining the variation of π values.

As expected, the value of *a*, the slope of the $\pi_{X/PhH}$ term, and the *c* value (the intercept) are close to 1 and 0, respectively, in most of the equations in Tables I and II. For substituted pyridines, however, the value for *a* is considerably lower than 1 (0.80 ± 0.06) in Eq. 30. The ρ_X terms for toluenes (Eq. 28) and the σ_X^0 term for pyridines (Eq. 30) are insignificant. For substituted toluenes (Eq. 28), chlorobenzenes (Eq. 29), and pyridines (Eq. 30), the *c* value is significant, >99.5%. It was expected that the correlations without an intercept may reveal different features such as different and/or significant slope values of respective terms for these three sets from those of Eqs. 28–30; in fact, the deletion of the intercept seems to yield more reasonable results as shown in Eqs. 28*a*–30*a*, although the quality of correlations in terms of standard deviation becomes slightly poorer. In Eq. 28*a* for toluene π values, the slope of the ρ_X (*para*) term is now significant, coinciding with the authentic σ^0 (p-CH_3) value. In Eq. 30*a* for pyridine π values, the value of *a* comes close to 1, the σ_X^0 term becomes significant, and the σ_Y^0 values estimated for the β- and γ-aza (—*N*=) groups get closer to the values derived from hydrolytic rates of isonicotinic and nicotinic acid esters (10) and IR frequency studies of substituted pyridines (11). The following discussion will be made on the basis of final correlations: Eqs. 11–13 in Table I and Eqs. 18–27, 28*a*–30*a*, and 31 in Table II.

DISCUSSION

Intrinsic Hydrophobicity of Substituents—Although the values of *a* are close to 1, most of the values from 17 sets of π values are slightly <1; the average is 0.94 ± 0.03, which is attributable to the fact that the assumption leading to Eq. 1 is not entirely valid. After separating the effects due to hydrogen bond formation, the intrinsic hydrophobicity of substituents in disubstituted benzenes is lower than that in monosubstituted benzenes. When a substituent is introduced in the monosubstituted benzene ring, the extent of the iceberg formation could be slightly lower than that formed by the introduction into the unsubstituted benzene.

Susceptibility in Hydrogen Bonding Association of Fixed Substituents to Electronic Effect of Variable Substituents, ρ_Y Values—The ρ_Y values are summarized in Table III. The sign of the ρ_Y values can be explained by considering the relative hydrogen bonding effect of substituents with solvents. For hydrogen-accepting Y substituents, such as acetyl in acetophenones where the carbonyl oxygen works as a hydrogen acceptor, a type of solvation such as >C=O . . . HOR (I) is only possible where R=H or n-C_8H_{17} in each of the water and octanol phases. Water, being more acidic than 1-octanol, would effectively compete in this type of solvation; thus, the strongly electron-withdrawing substituents would not be favorable to the hydration at the basic group and raise the partition coefficient.

For amphiprotic substituents such as hydroxyl in substituted phenols, there are two types of hydrogen bonding, XC_6H_4OH . . . R—O—H (II) and XC_6H_4H—O . . . HOR (III). Octanol, being more basic and less acidic than water, would favor the association of type II, whereas water would more effectively undergo the type III association. The more electron-withdrawing the substituent X, the more the amount of type II solvation with octanol (and the less the ratio of type III hydration). This effect results in a higher partition coefficient; therefore, regardless of whether the Y group is hydrogen-accepting, -donating, or amphiprotic, the electron withdrawal of X substituents is expected to make the $\pi_{X/PhY}$ value higher than the $\pi_{X/PhH}$ value. The positive ρ values for most of the Y groups in Table III can be understood on this basis.

For amphiprotic functions, the ρ_Y value for the relative solvation effect seems to roughly depend on the distance between the ring and associable hydrogen. The higher ρ values are found for phenols, anilines, and anilides, while the lowest value is for phenylacetic acids. Almost identical ρ values are observed for carboxyl, carbamoyl, and hydroxymethyl functions where the location of the hydrogen is similar.

The ρ values for hydrogen-acceptor functions are lower than what might be anticipated from the location of the association sites; in particular, the value for the benzonitriles is insignificant. The low ρ value for the relative solvation effect at basic functions seems to reflect a difference in hydrogen-donating ability smaller than that in hydrogen-accepting ability between water and octanol; the type II solvation would be more susceptible to the substituent effect than types I and III. At the present time, no relevant rationalization can be found for the negative ρ value found for the nitro group.

Electronic Effect of Fixed Substituents on Hydrogen Bonding Association of Variable Substituents, σ_Y^0 Values—The regression coefficients of the ρ_X terms are compared with available authentic σ_Y^0 values in Table IV (12). The calculated σ_Y^0 values coincide with respective authentic values within the 95% confidence intervals. Although the sequence of magnitude of calculated σ_m^0 and σ_p^0 values for some pairs of *meta*- and *para*-substituents is reversed from that of the authentic values, the general agreement between calculated and authentic σ_Y^0 values seems good. The correlation between these values for 30 *meta*- and *para*-substituents is expressed by:

$$\sigma^0 \text{ (calculated)} = 1.058(\pm 0.091)\sigma^0 \text{ (authentic)} - 0.019(\pm 0.036) \quad \text{(Eq. 32)}$$

where *n* is 30, *r* is 0.971, and *s* is 0.081. The electronic effect of fixed substituents Y actually is represented by σ_Y^0 values and exhibited only toward hydrogen bondable variable substituents X. This is believed to

Table IV—Comparison of Calculated σ_Y^0 Values with Authentic σ_Y^0 Constants

Y-Substituent		σ_Y^0 (authentic)[a]	σ_Y^0 (calc.)	Y-Substituent		σ_Y^0 (authentic)[a]	σ_Y^0 (calc.)
COOH	*meta*	0.37	0.35(±0.13)	CN	*meta*	0.62	0.76(±0.14)
	para	0.46	0.43(±0.14)		*para*	0.69	0.69(±0.13)
CH_2COOH	*meta*	0.03	0	NO_2	*meta*	0.70	0.75(±0.14)
	para	−0.05	0		*para*	0.82	0.75(±0.15)
OCH_2COOH	*meta*	0.05	0	$COCH_3$	*meta*	0.34	0.41(±0.18)
	para	−0.21	0		*para*	0.46	0.38(±0.20)
OH	*meta*	0.04	0	OCH_3	*meta*	0.06	0
	para	−0.13	−0.15(±0.14)		*para*	−0.16	−0.19(±0.08)
$CONH_2$	*meta*	0.28	0.28(±0.17)	CH_3	*meta*	−0.07	0
	para	0.36	0.29(±0.07)		*para*	−0.12	−0.10(±0.10)
NH_2	*meta*	−0.14	−0.26(±0.26)	Cl	*meta*	0.37	0.27(±0.17)
	para	−0.38	−0.57(±0.24)		*para*	0.27	0.24(±0.17)
NHCHO	*para*	0	0	—*N*=	β	0.62[b]	0.75(±0.20)
					γ	0.93[b]	1.02(±0.19)
$NHCOCH_3$	*para*	0.03	0				
CH_2OH	*meta*	0	0				
	para	0.05	0				

[a] From Ref. 9. [b] Ref. 12.

support the fundamental assumption leading to the present procedure.

Prediction of Log *P* Values of Disubstituted Benzenes—The present work indicates that the variations in π values of *meta*- and *para*-aromatic substituents from one system to another are due primarily to variations in the extent of hydrogen bonding solvation of substituents. Practically no outliers from correlations are found using the present procedure. The substituent effects governing this variation, in general, are bidirectional. The π value of a certain substituent is modified not only by its own effect on a fixed function but also by a backward effect from the fixed function. These modifications depend on susceptibilities of substituents to relative hydrogen bond formation with solvents, and the susceptibility varies from one substituent to another. Thus, $\pi_{X/PhH}$ values could be used as fixed substituent constants in predicting log *P* values of aromatic compounds as a first approximation only when aromatic substituents are rather insensitive to and/or not influential on the relative hydrogen-bonding effect.

Had more ρ_X values been determined for hydrogen-bondable X substituents, a large number of log *P* values of disubstituted aromatic compounds could have been predicted more precisely according to the present procedure using relations such as:

$$\pi_{X/PhY} = 0.94\pi_{X/PhH} + \rho_Y\sigma_X^0 + \rho_X\sigma_Y^0 \text{ (}meta\text{ or }para\text{)} \quad \text{(Eq. 33)}$$

Furthermore, had the present procedure been combined with the recently developed method to analyze the *ortho* effect (13), it would have been possible to calculate even the log *P* values of *ortho*-disubstituted benzenes.

The full account of this study, including theoretical considerations on the bidirectional Hammett relationship governing the $\Delta\pi$ values as well as the data and parameters used for correlations, will be published elsewhere (14).

REFERENCES

(1) C. Hansch and A. Leo, "Substituent Constants for Correlation Analysis in Chemistry and Biology," Wiley, New York, N.Y., 1979, p. 13.

(2) T. Fujita, J. Iwasa, and C. Hansch, *J. Am. Chem. Soc.*, **86**, 5175 (1964).

(3) T. Fujita, K. Kamoshita, T. Nishioka, and M. Nakajima, *Agr. Biol. Chem. (Tokyo)*, **38**, 1521 (1974).

(4) C. Hansch, K. H. Kim, and R. H. Sarma, *J. Am. Chem. Soc.*, **95**, 6447 (1973).

(5) J. Fastrez and A. R. Fersht, *Biochemistry*, **12**, 1067 (1973).

(6) J. C. Dearden and E. Tomlinson, *J. Pharm. Pharmacol.*, **73**, 73S (1971).

(7) R. Mirrlees and P. Taylor, in "Substituent Constants for Correlation Analysis in Chemistry and Biology," (C. Hansch and A. Leo, Authors) Wiley, New York, N.Y., 1979, p. 171.

(8) T. Fujita, T. Nishioka, and M. Nakajima, *J. Med. Chem.*, **20**, 1071 (1977).

(9) O. Exner, "Advances in Linear Free Energy Relationships," N. B. Chapman and J. Shorter, Eds., Plenum, London, 1972, p. 1.

(10) H. H. Jaffé, *Chem. Rev.*, **53**, 191 (1953).

(11) H. Shindo, *Chem. Pharm. Bull. (Tokyo)*, **5**, 472 (1957).

(12) H. H. Jaffé and H. L. Jones, *Adv. Heterocycl. Chem.*, **3**, 226 (1964).

(13) T. Fujita and T. Nishioka, *Prog. Phys. Org. Chem.*, **12**, 49 (1976).

(14) T. Fujita, *ibid.*, **14**, in press.

ACKNOWLEDGMENTS

The author thanks Dr. Corwin Hansch for his generosity in allowing the use of newly determined π values as well as for his stimulating discussions and to Dr. Albert Leo for his invaluable suggestions. Newly determined π values were by S. Anderson, W. R. Glave, F. Helmer, P. Y. C. Jow, K. Kamoshita, D. Nikaitani, T. Nishioka, and A. Ogino to whom thanks are also extended.

Determination of Benzalkonium Chloride by Chemical Ionization Mass Spectroscopy

N. N. DAOUD*, P. A. CROOKS *§x, R. SPEAK ‡, and P. GILBERT *

Received December 28, 1981, from the *Departments of *Pharmacy and ‡Chemistry, University of Manchester, Manchester MI3 9PL, UK.* Accepted for publication May 17, 1982. § Present address: College of Pharmacy, University of Kentucky, Lexington, KY 40536-0053.

Abstract □ A new specific and sensitive method of analysis for samples of benzalkonium chlorides is presented. Chemical-ionization mass spectroscopy has been used to identify and determine the proportions of various alkyl chain lengths in commercial mixtures of benzalkonium chlorides. This method allows the direct and simultaneous determination of individual benzalkonium chlorides.

Keyphrases □ Benzalkonium chloride—determination by chemical-ionization mass spectroscopy, alkyl chain lengths □ Chemical-ionization mass spectroscopy—determination of benzalkonium chloride, alkyl chain lengths

Benzalkonium chlorides (I) USP are a mixture of benzalkonium chlorides, where R = *n*-alkyl and *n* can vary from C_{10} to C_{18}. The relative amounts of these different species greatly affects both the antimicrobial spectrum and

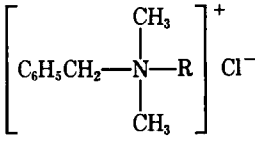

I

activity of the mixture (1–3). The current methods of identification of benzalkonium chloride solutions according to the USP (4), rely upon titrimetric analysis of total alkyl benzyldimethylammonium chloride based upon potassium iodate equivalents. Additionally, the ratio of the various *n*-alkyl components of benzalkonium chlorides can be determined by microhydrogenation followed by solvent extraction and GLC. The ratio of alkyl components is then calculated and must meet specific USP requirements. These requirements state that the C_{12} homologue must comprise at least 40% of the total benzalkonium chloride content and that the C_{14} homologue must be at least 20%. Furthermore, these two homologues must comprise together 70% of the total content. Other methods have been used for the determination of benzalkonium chlorides: ion-pairing techniques (5–8), direct titration involving tetraphenylboron (9) and iodate (10), reverse-phase HPLC (11), and pyrolytic GLC (12).

The present method directly determines the chemical composition and alkyl chain length ratios of benzalkonium chloride species in commercial samples.

EXPERIMENTAL

Apparatus—Measurements were conducted upon a spectrometer[1] fitted with an electron-impact–chemical-ionization (EI–CI) source and a DS-55 data system.

Reagents and Solvents—Individual benzalkonium chloride standards were prepared with R = C_1–C_{20}, by a previous method (13) and characterized by spectroscopic and elemental analysis. Purity was in all cases

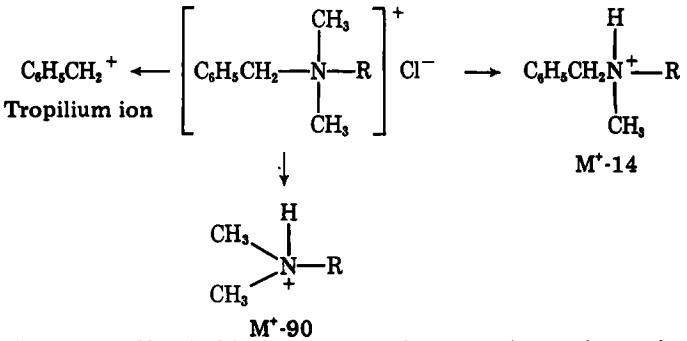

Scheme 1—Chemical-ionization mass fragmentation pathways for benzalkonium chloride (1).

>99.6%. The commercial benzalkonium chloride mixtures were obtained from three different manufacturers. Samples for analysis were prepared as millimolar solutions in methanol[2].

Assay—Standard solutions were prepared as 2 μl methanol solutions containing R = C_9 internal standard (0.01 *M*) together with pure synthetic benzalkonium chloride (0.001–0.01 *M*) with R = C_{10}, C_{12}, C_{14}, C_{16}, and C_{18}. Samples were applied as methanol solutions by the direct-inlet technique at 200° on a glass probe tip and evaporated into the chemical-ionization plasma of ammonia gas. Evaporation profiles were deter-

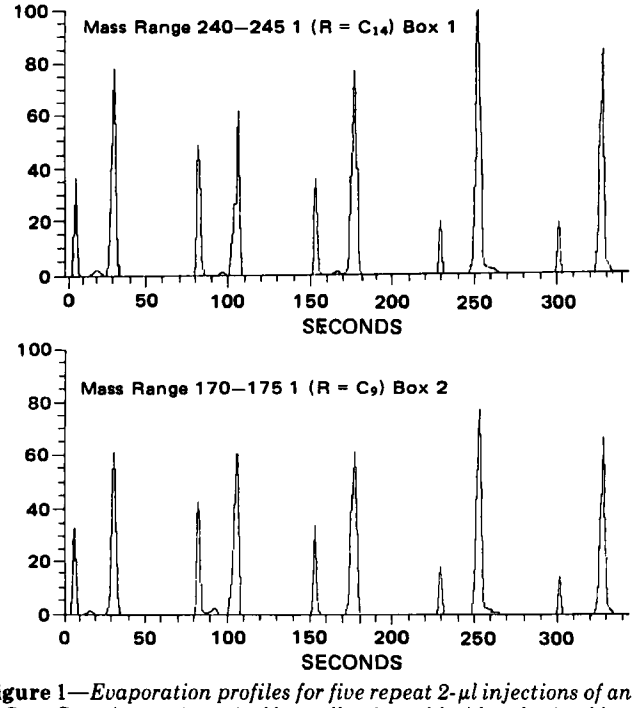

Figure 1—*Evaporation profiles for five repeat 2-μl injections of an R = C_9 + C_{14} mixture (50:50) of benzalkonium chlorides obtained by simultaneous monitoring of the M^+ −90 ions. (The first peak in each evaporation profile is observed as a result of evaporation off the probe before the heater switches in. The second peak is the main evaporation profile. Total ions were collected at one time by continuous scanning.)*

[1] Kratos MS25.

[2] British Drug Houses, Ltd., London, England.

0022-3549/83/0300-0290$01.00/0

Table I—Relative Intensities of Diagnostic Ions Obtained for a Series of Synthetic Benzalkonium Chlorides Where R = C_{10} to C_{18}

Diagnostic Ion[a]	m/z (RI) R = C_9	R = C_{10}	R = C_{12}	R = C_{14}	R = C_{16}	R = C_{18}
M^+; $C_6H_5CH_2N(CH_3)_2R^+$	262(9.1)	276(4.6)	304(5.4)	332(0.4)	360(2.8)	388(4.0)
$M^+ -14$; $C_6H_5CH_2N(H)(CH_3)R^+$	248(61.3)	262(18.6)	290(54.2)	318(10.7)	346(27.3)	374(37.4)
$M^+ -90$; $(CH_3)_2NHR^+$	172(19.4)	186(73.6)	214(94.5)	242(81.5)	270(91.9)	298(70.1)
$M^+ -91$; $(CH_3)_2NR^+$	171(14.7)	185(5.1)	213(11.7)	241(1.9)	269(5.4)	297(8.9)

[a] M^+ is equivalent to the mass of the cation and not to the molecular weight of the salt.

Table II—Total Ion-Current Ratios for the $M^+ -90$ Ions of Five Repeat Injections of Solutions of Synthetic Benzalkonium Chlorides (R = C_{10}–C_{18}) and R = C_9 Internal Standard.

R	Total Ion-Current Ratios C_n/C_9 Internal Standard Mean	CV[a], %	Mean	CV, %	Mean	CV, %	Mean	CV, %
C_{10}	0.735	±3.1	0.411	±7.4	0.185	±4.9	0.088	±4.2
C_{11}	0.867	±3.8	0.369	±2.9	0.198	±5.6	0.130	±9.7
C_{12}	1.145	±2.7	0.603	±3.03	0.246	±8.5	0.117	±6.2
C_{14}	0.969	±1.6	0.424	±4.7	0.179	±6.0	0.084	±4.5
C_{16}	0.808	±2.1	0.312	±4.3	0.137	±5.3	0.060	±9.1
C_{18}	0.852	±2.9	0.271	±6.1	0.107	±6.7	0.019	±9.5
Molar Ratio Cn/C_9	1:1		1:2		1:5		1:10	

[a] Coefficient of variation.

Table III—Relative Intensities of $M^+ -90$ Ions Obtained in Commercial Mixtures of Benzalkonium Chlorides

Commercial Mixture	Relative intensity of $M^+ -90$ ion for R C_9	C_{10}	C_{12}	C_{14}	C_{16}	C_{18}	C_{20}
Sample A	0.0	0.0	3.7	5.3	48.4	100.0	0.0
Sample B	0.0	0.0	100.0	60.0	10.6	0.0	0.0
Sample C	0.0	7.6	100.0	23.2	6.6	0.0	0.0

mined and total ions for diagnostic peaks collected by continuous scanning. Average ion currents for particular diagnostic peaks were determined as ratios to that of the R = C_9 internal standard. Calibration curves were constructed for ions of particular interest. Such calibration curves were used in the quantitative analysis of commercial benzalkonium chloride mixtures.

RESULTS AND DISCUSSION

The chemical-ionization mass spectra of pure benzalkonium chlorides have been measured, and predictable, characteristic fragmentation patterns affording diagnostic ions of use in structural identification were determined (Scheme I). Diagnostic ions were observed at $M^+ -14$ (loss of CH_3 plus addition of H) and $M^+ -90$ (loss of $C_6H_5CH_2$ plus addition of H). A low-intensity peak was also observed for the benzalkonium cation. A common peak was found at *m/z* 91 due to the tropilium ion. Table I shows the fragmentation data for a series of pure benzalkonium chloride standards where R = C_{10}, C_{12}, C_{14}, C_{16}, and C_{18}. From these data it was possible to determine the molecular weight of the individual

Table IV—Total Ion-Current Ratios for $M^+ -90$ Ions and Calculated Molar Ratios of Component Benzalkonium Chlorides in Commercial Mixtures and R = C_9 Internal Standard

Commercial Mixture	R	Total Ion-Current Ratio, C_n/C_9	Molar Ratio in Mixture, %
Sample A	C_{12}	0.021 ± 0.0024	2
	C_{14}	0.035 ± 0.0028	2
	C_{16}	0.350 ± 0.0038	26
	C_{18}	1.080 ± 0.0093	70
Sample B	C_{12}	1.812 ± 0.018	71
	C_{14}	0.529 ± 0.020	24
	C_{16}	0.121 ± 0.014	4
Sample C	C_{10}	0.438 ± 0.0157	5
	C_{12}	1.119 ± 0.0488	68
	C_{14}	0.334 ± 0.0640	23
	C_{16}	0.054 ± 0.0223	5

benzalkonium chloride, since a significant M^+ peak (2–10% relative intensity) in addition to medium intensity ions at $M^+ -14$ and $M^+ -90$ was observed. The $M^+ -90$ peak was the most intense in all the spectra examined and was chosen for quantitative investigations. Replicate 2-μl analytical samples containing varying proportions of the R = C_9 standard and the appropriate benzalkonium chloride were introduced into the mass spectrometer, and the total-ion currents for their $M^+ -90$ ions, together with their peak heights, were simultaneously determined to give relative evaporation profiles. Evaporation profiles for all the compounds were

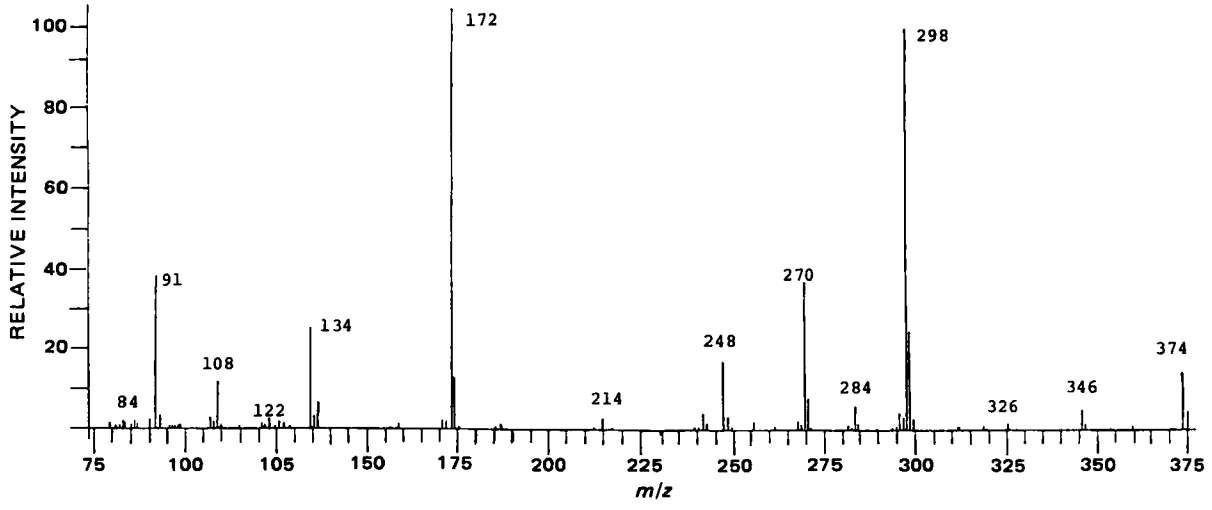

Figure 2—*Chemical-ionization mass spectrum of commercial sample A benzalkonium chloride containing C_9 internal reference from* m/z *75–400.*

similar to one another, as illustrated in Fig. 1 for R = C_{14} and R = C_9 internal standard. Results were expressed as total ion-current ratios for R = C_n/C_9. Table II gives total ion-current ratios together with coefficients of variation for repeat integrations of varying molar proportions of R = C_9 and benzalkonium chloride standards C_{10}–C_{18}. Interestingly, the integral ratios R = C_n/R = C_9 varied with alkyl chain length (Table II); consequently, it was necessary to construct calibration curves for each individual benzalkonium chloride species examined. These were constructed by assay of various dilutions of test compound, spiked with internal standard. Graphs of total ion-current ratio *versus* concentration were linear in nature for all benzalkonium chlorides examined.

Samples of commercial benzalkonium chloride mixtures were prepared as methanol solutions (1 mg/ml). Spectra were obtained for these mixtures (illustrated in Fig. 2 for sample A), and the relative intensities of their component benzalkonium chloride species were determined (Table III). As can be seen, sample A contains R = C_{12}, C_{14}, C_{16}, and C_{18}, with R = C_{18} predominating, whereas samples B and C are predominant in R = C_{12} species but are qualitatively different. Having determined the species content of the mixtures, quantitative measurements were carried out by the simultaneous monitoring of each M^+ −90 ion relative to the M^+ −90 ion of the internal standard. Concentrations of benzalkonium chloride species were obtained by relating total ion-current ratios (Table II) to those from the calibration data. From these data it can be observed that two of the three commercial samples comply with the USP limits, while the remaining sample varies quite markedly in alkyl chain compositions (See Table IV).

REFERENCES

(1) E. I. Valko and A. S. DuBois, *J. Bacteriol.*, **47**, 15 (1944).

(2) *Idem.*, **50**, 481 (1945).

(3) J. C. Hoogerheide, *J. Bacteriol.*, **49**, 277 (1945).

(4) "The United States Pharmacopeia," 19th rev., U.S. Pharmacopeial Convention, Rockville, Md., 1975, pp. 552–553.

(5) M. E. Auerbach, *Anal. Chem.*, **15**, 492 (1943).

(6) C. W. Ballard, J. Isaacs, and P. G. W. Scott, *J. Pharm. Pharmacol.*, **6**, 971 (1954).

(7) E. L. Colichman, *Anal. Chem.*, **19**, 430 (1947).

(8) L. G. Chatten and K. O. Okamura, *J. Pharm. Sci.*, **62**, 1328 (1973).

(9) L. D. Metcalfe, R. J. Martin, and A. A. Schmitz, *J. Am. Oil Chem. Soc.*, **43**, 355 (1966).

(10) E. R. Brown, *J. Pharm. Pharmacol.*, **15**, 379 (1963).

(11) R. C. Meyer, *J. Pharm. Sci.*, **69**, 1148 (1980).

(12) E. C. Jennings and H. Mitchner, *ibid.*, **56**, 1590 (1967).

(13) H. T. Clarke, H. B. Gillespie, and S. Z. Weisshaus, *J. Am. Chem. Soc.*, **55**, 4571 (1933).

Solubility in Binary Solvent Systems III: Predictive Expressions Based on Molecular Surface Areas

WILLIAM E. ACREE, JR. and J. HOWARD RYTTING ˣ

Received February 8, 1982, from the *Department of Pharmaceutical Chemistry, The University of Kansas, Lawrence, KS 66045.* Accepted for publication May 13, 1982.

Abstract □ The nearly ideal binary solvent model, which has led to successful predictive equations for the partial molar Gibbs free energy of the solute in binary solvent mixtures, was extended to include molecular surface areas as weighting factors. Two additional expressions were derived and compared to previously developed equations (based on molar volumes as weighting factors) for their ability to predict anthracene and naphthalene solubilities in mixed solvents from measurements in the pure solvents. The most successful equation in terms of goodness of fit involved a surface fraction average of the excess Gibbs free energy relative to Raoult's law and predicted experimental solubilities in 25 systems with an average deviation of 1.7% and a maximum deviation of 7.5%. Two expressions approximating weighting factors with molar volumes provided accurate predictions in many of the systems studied but failed in their ability to predict anthracene solubilities in solvent mixtures containing benzene.

Keyphrases □ Binary solvents—solubility, predictive expressions based on molecular surface areas □ Solubility—binary solvent systems, predictive expressions based on molecular surface areas □ Molecular surface area—solubility in binary solvent systems □ Anthracene—prediction of solubility in binary solvent systems based on molecular surface areas □ Naphthalene—prediction of solubility in binary solvent systems based on molecular surface areas

The use of binary solvents for influencing solubility and multiphase partitioning has many potential applications in the pharmaceutical industry. However, maximum realization of these applications depends on the development of equations that enable *a priori* prediction of solution behavior in mixed solvents from a minimum number of additional observations. Ideally, the ability to predict a drug molecule's solubility and partition coefficients based solely on a consideration of molecular structure is desired, but for more practical applications, a less fundamental approach must often suffice.

The nearly ideal binary solvent (NIBS) approach developed previously (1–6) provides a relatively simple method for estimating the excess partial molar properties of a solute, $\overline{Z}_3^{ex}$, at infinite dilution in a binary solvent (components 1 and 2):

$$\overline{Z}_3^{ex} = f_1^0(\overline{Z}_3^{ex})_1 + f_2^0(\overline{Z}_3^{ex})_2 - \Gamma_3(X_1^0\Gamma_1 + X_2\Gamma_2)^{-1}\,\overline{Z}_{12}^{ex} \quad \text{(Eq. 1)}$$

$$f_1^0 = 1 - f_2^0 = X_1^0\Gamma_1/(X_1^0\Gamma_1 + X_2^0\Gamma_2) \quad \text{(Eq. 2)}$$

in terms of a weighted mole fraction average of the properties of the solute in the two pure solvents [$(\overline{Z}_3^{ex})_1$ and $(\overline{Z}_3^{ex})_2$] and a contribution due to the unmixing of the solvent pair by the presence of the solute. This equation leads to accurate predictions of solubilities (3, 5–8), gas–liquid partition coefficients (4, 9), and enthalpies of solution (1, 2) in systems of nonspecific interactions when the weighting factors (Γ_i) are approximated with molar volumes.

A simpler approximation of equating all three weighting factors provides considerably poorer predictions for systems in which the molar volumes of the components differ appreciably. The superiority of expressions based on molar volumes suggests that the relative sizes of the molecules are an important consideration. The use of surface areas as weighting factors may be revealing, since surface area often represents a different measure of molecular size.

0022-3549/83/0300-0292$01.00/0

similar to one another, as illustrated in Fig. 1 for R = C_{14} and R = C_9 internal standard. Results were expressed as total ion-current ratios for R = C_n/C_9. Table II gives total ion-current ratios together with coefficients of variation for repeat integrations of varying molar proportions of R = C_9 and benzalkonium chloride standards C_{10}–C_{18}. Interestingly, the integral ratios R = C_n/R = C_9 varied with alkyl chain length (Table II); consequently, it was necessary to construct calibration curves for each individual benzalkonium chloride species examined. These were constructed by assay of various dilutions of test compound, spiked with internal standard. Graphs of total ion-current ratio *versus* concentration were linear in nature for all benzalkonium chlorides examined.

Samples of commercial benzalkonium chloride mixtures were prepared as methanol solutions (1 mg/ml). Spectra were obtained for these mixtures (illustrated in Fig. 2 for sample A), and the relative intensities of their component benzalkonium chloride species were determined (Table III). As can be seen, sample A contains R = C_{12}, C_{14}, C_{16}, and C_{18}, with R = C_{18} predominating, whereas samples B and C are predominant in R = C_{12} species but are qualitatively different. Having determined the species content of the mixtures, quantitative measurements were carried out by the simultaneous monitoring of each M^+ −90 ion relative to the M^+ −90 ion of the internal standard. Concentrations of benzalkonium chloride species were obtained by relating total ion-current ratios (Table II) to those from the calibration data. From these data it can be observed that two of the three commercial samples comply with the USP limits, while the remaining sample varies quite markedly in alkyl chain compositions (See Table IV).

REFERENCES

(1) E. I. Valko and A. S. DuBois, *J. Bacteriol.*, **47**, 15 (1944).

(2) *Idem.*, **50**, 481 (1945).

(3) J. C. Hoogerheide, *J. Bacteriol.*, **49**, 277 (1945).

(4) "The United States Pharmacopeia," 19th rev., U.S. Pharmacopeial Convention, Rockville, Md., 1975, pp. 552–553.

(5) M. E. Auerbach, *Anal. Chem.*, **15**, 492 (1943).

(6) C. W. Ballard, J. Isaacs, and P. G. W. Scott, *J. Pharm. Pharmacol.*, **6**, 971 (1954).

(7) E. L. Colichman, *Anal. Chem.*, **19**, 430 (1947).

(8) L. G. Chatten and K. O. Okamura, *J. Pharm. Sci.*, **62**, 1328 (1973).

(9) L. D. Metcalfe, R. J. Martin, and A. A. Schmitz, *J. Am. Oil Chem. Soc.*, **43**, 355 (1966).

(10) E. R. Brown, *J. Pharm. Pharmacol.*, **15**, 379 (1963).

(11) R. C. Meyer, *J. Pharm. Sci.*, **69**, 1148 (1980).

(12) E. C. Jennings and H. Mitchner, *ibid.*, **56**, 1590 (1967).

(13) H. T. Clarke, H. B. Gillespie, and S. Z. Weisshaus, *J. Am. Chem. Soc.*, **55**, 4571 (1933).

Solubility in Binary Solvent Systems III: Predictive Expressions Based on Molecular Surface Areas

WILLIAM E. ACREE, JR. and J. HOWARD RYTTING ˣ

Received February 8, 1982, from the *Department of Pharmaceutical Chemistry, The University of Kansas, Lawrence, KS 66045.* Accepted for publication May 13, 1982.

Abstract □ The nearly ideal binary solvent model, which has led to successful predictive equations for the partial molar Gibbs free energy of the solute in binary solvent mixtures, was extended to include molecular surface areas as weighting factors. Two additional expressions were derived and compared to previously developed equations (based on molar volumes as weighting factors) for their ability to predict anthracene and naphthalene solubilities in mixed solvents from measurements in the pure solvents. The most successful equation in terms of goodness of fit involved a surface fraction average of the excess Gibbs free energy relative to Raoult's law and predicted experimental solubilities in 25 systems with an average deviation of 1.7% and a maximum deviation of 7.5%. Two expressions approximating weighting factors with molar volumes provided accurate predictions in many of the systems studied but failed in their ability to predict anthracene solubilities in solvent mixtures containing benzene.

Keyphrases □ Binary solvents—solubility, predictive expressions based on molecular surface areas □ Solubility—binary solvent systems, predictive expressions based on molecular surface areas □ Molecular surface area—solubility in binary solvent systems □ Anthracene—prediction of solubility in binary solvent systems based on molecular surface areas □ Naphthalene—prediction of solubility in binary solvent systems based on molecular surface areas

The use of binary solvents for influencing solubility and multiphase partitioning has many potential applications in the pharmaceutical industry. However, maximum realization of these applications depends on the development of equations that enable *a priori* prediction of solution behavior in mixed solvents from a minimum number of additional observations. Ideally, the ability to predict a drug molecule's solubility and partition coefficients based solely on a consideration of molecular structure is desired, but for more practical applications, a less fundamental approach must often suffice.

The nearly ideal binary solvent (NIBS) approach developed previously (1–6) provides a relatively simple method for estimating the excess partial molar properties of a solute, $\overline{Z}_3^{ex}$, at infinite dilution in a binary solvent (components 1 and 2):

$$\overline{Z}_3^{ex} = f_1^0(\overline{Z}_3^{ex})_1 + f_2^0(\overline{Z}_3^{ex})_2 - \Gamma_3(X_1^0\Gamma_1 + X_2\Gamma_2)^{-1}\,\overline{Z}_{12}^{ex} \quad \text{(Eq. 1)}$$

$$f_1^0 = 1 - f_2^0 = X_1^0\Gamma_1/(X_1^0\Gamma_1 + X_2^0\Gamma_2) \quad \text{(Eq. 2)}$$

in terms of a weighted mole fraction average of the properties of the solute in the two pure solvents [$(\overline{Z}_3^{ex})_1$ and $(\overline{Z}_3^{ex})_2$] and a contribution due to the unmixing of the solvent pair by the presence of the solute. This equation leads to accurate predictions of solubilities (3, 5–8), gas–liquid partition coefficients (4, 9), and enthalpies of solution (1, 2) in systems of nonspecific interactions when the weighting factors (Γ_i) are approximated with molar volumes.

A simpler approximation of equating all three weighting factors provides considerably poorer predictions for systems in which the molar volumes of the components differ appreciably. The superiority of expressions based on molar volumes suggests that the relative sizes of the molecules are an important consideration. The use of surface areas as weighting factors may be revealing, since surface area often represents a different measure of molecular size.

0022-3549/83/0300-0292$01.00/0

Experimental solubilities of naphthalene (10–12) and *p*-dibromobenzene (13) are available in the literature for several binary solvent mixtures and can be used to compare the various approximations for weighting factors. However, these systems encompass a narrow two-fold range of mole fraction solubilities. The applicability of Eq. 1 is not very sensitive to errors in the relative magnitude of the weighting factors whenever the solubility of the solute is identical (or nearly identical) in both the pure solvents, but these errors become much more significant as the range of solubilities increases. For this reason, anthracene solubilities were determined in several mixtures containing benzene, which cover up to a sixfold range.

During the course of this investigation, it was noted that the NIBS model predicted a slight maximum solubility in binary solutions of cyclohexane and *n*-heptane. Such synergistic effects in simple systems are usually explained by solubility parameter theory in terms of the solubility parameter of the solute being bracketed by the solubility parameters of the two pure solvents (14, 15). However, the solubility parameter of anthracene ($\delta = 9.9$) is far greater than either the solubility parameters of cyclohexane ($\delta = 8.2$) or *n*-heptane ($\delta = 7.4$). Solubility determinations of anthracene in this binary solvent mixture will provide an additional test of the basic NIBS model.

EXPERIMENTAL

Anthracene[1] was used as received. Cyclohexane[2], *n*-heptane[3], isooctane[3], *n*-octane[4], cyclooctane[4], *n*-hexane[4], and benzene[5] were stored over molecular sieves[6]. Binary solvent mixtures were prepared by weight so that compositions could be calculated to a mole fraction of 0.0001.

Excess solute and solvent were placed in amber glass bottles and allowed to equilibrate in a constant-temperature bath at 25.0° for several days. The attainment of equilibrium was verified by repetitive measurements after several additional days and in some cases by approaching equilibrium from supersaturation by pre-equilibrating the solution at a higher temperature. Aliquots of saturated anthracene solutions were transferred through a coarse filter into a tared volumetric flask to determine the amount of sample and diluted quantitatively with methanol. Concentrations were determined spectrophotometrically[7] at 356 nm. Experimental solubilities of anthracene in several binary solvent mixtures are given in Table I, with the measurements being reproducible to within ±1%.

RESULTS AND DISCUSSION

The following three equations have been derived previously for solubility in binary solvent systems containing only nonspecific interactions:

$$RT \ln(a_3^{solid}/X_3^{sat}) = (1 - X_3^{sat})^2[X_1^0(\overline{G}_3^{ex})_1 + X_2^0(\overline{G}_3^{ex})_2 - \overline{G}_{12}^{ex}] \quad \text{(Eq. 3)}$$

$$RT \ln(a_3^{solid}/X_3^{sat}) = (1 - \phi_3^{sat})^2 [\phi_1^0(\overline{G}_3^{ex})_1 + \phi_2^0(\overline{G}_3^{ex})_2 - V_3(X_1^0V_1 + X_2^0V_2)^{-1}\,\overline{G}_{12}^{ex}] \quad \text{(Eq. 4)}$$

and:

$$RT\left[\ln(a_3^{solid}/\phi_3^{sat}) - (1 - \phi_3^{sat})\left(1 - \frac{V_3}{(X_1^0V_1 + X_2^0V_2)}\right)\right] = (1 - \phi_3^{sat})^2[\phi_1^0(\overline{G}_3^{fh})_1 + \phi_2^0(\overline{G}_3^{fh})_2 - V_3(X_1^0V_1 + X_2^0V_2)^{-1}\,\overline{G}_{12}^{fh}] \quad \text{(Eq. 5)}$$

in which V_i is the molar volume of a pure liquid, X_i is mole fraction, ϕ_i is volume fraction, $\overline{G}_{12}^{ex}$ is the molar excess Gibbs free energy of the binary solvent relative to Raoult's law, and:

$$\overline{G}_{12}^{fh} = \overline{G}_{12}^{ex} + RT[\ln(X_1^0V_1 + X_2^0V_2) - X_1^0 \ln V_1 - X_2^0 \ln V_2] \quad \text{(Eq. 6)}$$

[1] Aldrich 99.9%.
[2] Phillips 99.5 weight percent.
[3] Phillips 99 mole percent.
[4] Aldrich Chemical Co.
[5] Fischer Scientific Co.
[6] Linde Type 4A.
[7] Cary 118 Spectrophotometer.

Table I—Solubility of Anthracene in Several Binary Solvents at 25.0°

Solvent (1)	+	Solvent (2)	X_1^0	X_{Solute}^{Sat}
n-Hexane	+	Cyclohexane	0.0000	0.001574
			0.1735	0.001572
			0.3565	0.001544
			0.4498	0.001515
			0.5571	0.001478
			0.7646	0.001398
			1.0000	0.001290
n-Octane	+	Cyclohexane	0.0000	0.001574
			0.1463	0.001648
			0.3114	0.001717
			0.3954	0.001749
			0.5519	0.001774
			0.7930	0.001832
			1.0000	0.001850
Cyclooctane	+	Cyclohexane	0.0000	0.001574
			0.1746	0.001704
			0.3412	0.001824
			0.4475	0.001882
			0.5533	0.001989
			0.7580	0.002096
			1.0000	0.002258
n-Heptane	+	Cyclohexane	0.0000	0.001574
			0.1542	0.001608
			0.3283	0.001642
			0.4230	0.001640
			0.5250	0.001621
			0.7236	0.001605
			1.0000	0.001571
Isooctane	+	Cyclohexane	0.0000	0.001574
			0.1385	0.001488
			0.2988	0.001407
			0.3895	0.001362
			0.5391	0.001283
			0.7725	0.001182
			1.0000	0.001087
n-Hexane	+	Benzene	0.0000	0.007418
			0.1442	0.006274
			0.3093	0.004908
			0.3842	0.004317
			0.4963	0.003549
			0.7365	0.002242
			1.0000	0.001290
Benzene	+	*n*-Heptane	0.0000	0.001571
			0.2323	0.002283
			0.4637	0.003375
			0.5546	0.003922
			0.7103	0.005022
			0.8280	0.005987
			1.0000	0.007418
Benzene	+	Cyclohexane	0.0000	0.001574
			0.2320	0.002592
			0.4380	0.003802
			0.5427	0.004506
			0.6357	0.005154
			0.8317	0.006482
			1.0000	0.007418
Cyclooctane	+	Benzene	0.0000	0.007418
			0.1416	0.006814
			0.3045	0.005708
			0.3984	0.005282
			0.4935	0.004745
			0.6685	0.003740
			1.0000	0.002258
Benzene	+	Isooctane	0.0000	0.001087
			0.3127	0.001983
			0.5398	0.003144
			0.6354	0.003830
			0.7209	0.004571
			0.8591	0.005840
			1.0000	0.007418

Numerical values of $\overline{G}_{12}^{ex}$ can be found in the chemical literature for many common binary systems. For example, the thermodynamic excess properties of several hundred binary systems have been listed (16). The superscript (0) indicates that the solvent composition is calculated as if the solute were not present. The activity of the solid solute (a_3^{solid}), relative to the supercooled liquid, can be calculated by:

$$\ln a_3^{solid} = -\frac{\Delta H_3^{fus}(T_m - T)}{R\,T_m\,T} + \frac{\Delta C_p(T_m - T)}{RT} - \frac{\Delta C_p}{R}\ln(T_m/T) \quad \text{(Eq. 7)}$$

Table II—Comparison of Predictive Equations for the Solubilities of Naphthalene, *p*-Dibromobenzene, and Anthracene in Various Binary Solvent Mixtures at 25°

Solute	Solvent System	Data Ref.	RMS Deviations[a] (%) for the Predictive Equations 3	4	5	8	9	$\overline{G}_{12}^{ex}$ Ref.
Naphthalene	Benzene + Cyclohexane	10	−1.4	−1.2	−1.1	+0.4	+0.6	41
Naphthalene	Benzene + *n*-Hexane	10	+2.3	1.4	1.4	+1.9	+2.2	42
Naphthalene	Cyclohexane + Hexadecane	11	−4.0	+2.9	+1.4	+2.8	+1.5	43
Naphthalene	*n*-Hexane + Hexadecane	11	−6.8	+1.8	+0.8	+1.7	+0.6	44
Naphthalene	Benzene + Hexadecane	10	+9.2	+2.4	+0.7	+3.3	+2.5	45
Naphthalene	Cyclohexane + *n*-Hexane	11	0.8	0.6	0.6	0.8	0.8	28
Naphthalene	Benzene + Toluene	10	+0.5	+0.5	+0.6	+0.5	+0.7	29
Naphthalene	Cyclohexane + Toluene	12	−1.8	−0.9	−0.8	+1.0	+1.0	30
Naphthalene	Cyclohexane + Ethylbenzene	12	−1.7	0.3	0.3	+1.4	+1.5	31
p-Dibromobenzene	Hexadecane + Carbon tetrachloride	13	+5.4	+1.8	−0.8	NA	NA	45
p-Dibromobenzene	Cyclohexane + Carbon tetrachloride	13	−0.6	−1.5	−1.5	NA	NA	41
p-Dibromobenzene	*n*-Hexane + Hexadecane	13	−8.5	+1.6	0.6	+1.7	0.5	44
Anthracene	Cyclohexane + *n*-Heptane	—	1.0	0.6	0.6	0.6	+1.0	32
Anthracene	Cyclohexane + Cyclooctane	—	−1.4	0.9	0.9	+1.0	+1.2	33
Anthracene	Cyclohexane + Octane	—	−1.3	+0.6	+0.7	+0.9	+1.5	34
Anthracene	Cyclohexane + Isooctane	—	+1.9	−1.2	−1.0	+0.5	+1.1	35
Anthracene	Cyclohexane + *n*-Hexane	—	−1.2	−1.2	−1.1	0.3	0.3	28
Anthracene	Benzene + *n*-Heptane	—	+10.6	2.1	1.6	+5.9	+6.9	36
Anthracene	Benzene + *n*-Heptane	—	+7.9	−4.6	−3.8	+2.1	+3.1	37
Anthracene	Benzene + Cyclohexane	—	−6.9	−7.7	−7.5	−1.8	−1.7	41
Anthracene	Benzene + Cyclohexane	38	−6.2	−6.8	−6.6	1.1	1.1	41
Anthracene	Benzene + Carbon tetrachloride	38	−3.1	−2.1	−2.0	NA	NA	41
Anthracene	Benzene + *n*-Hexane	—	+2.7	−6.0	−5.4	+2.6	+3.1	42
Anthracene	Benzene + Cyclooctane	—	1.8	−8.3	−7.7	−3.6	3.0	39
Anthracene	Benzene + Isooctane	—	+10.5	−11.6	−10.7	+1.8	+3.0	40

[a] RMS deviations (%) = $(100/N^{1/2})\{\sum_{j=1}^{N}[\ln(X_{calc}^{sat}/X_{exp}^{sat})]^2\}^{1/2}$; the algebraic sign indicates that all deviations were of the same sign.

from the molar heat of fusion (ΔH_3^{fus}) at the normal melting point (T_m) and the differences between the molar heat capacities of the liquid and solid.

Introduction of molecular surface areas (A_i) into Eq. 1 results in the development of two more predictive expressions:

$$RT\ln(a_3^{solid}/X_3^{sat}) = (1-\theta_3^{sat})^2[\theta_1^0(\overline{G}_3^{ex})_1 + \theta_2^0(\overline{G}_3^{ex})_2 - A_3(X_1^0A_1 + X_2^0A_2)^{-1}\,\overline{G}_{12}^{ex}] \quad \text{(Eq. 8)}$$

and:

$$RT\left[\ln(a_3^{solid}/\phi_3^{sat}) - (1-\phi_3^{sat})\left(1-\frac{V_3}{(X_1^0V_1 + X_2^0V_2)}\right)\right] = (1-\theta_3^{sat})^2[\theta_1^0(\overline{G}_3^{fh})_1 + \theta_2^0(\overline{G}_3^{fh})_2 - A_3(X_1^0A_1 + X_2^0A_2)^{-1}\overline{G}_{12}^{fh}] \quad \text{(Eq. 9)}$$

depending on whether a regular solution model (Eq. 8) or a Flory–Huggins model (Eq. 9) is used to describe solution ideality. The use of these five predictive equations for solubility predictions in binary solvents is as follows: the quantities $(\overline{G}_3^{ex})_i$ or $(\overline{G}_3^{fh})_i$ are calculated from the experimental solubility of the solute in the pure solvents, then these properties are used in the appropriate equation to calculate the solubility as X_3^{sat} or ϕ_3^{sat} in the solvent mixture using a reiterative process. The quantity $(1 - f_3^{sat})$ is taken as unity in the first approximation, and convergence is rapid unless the solubility is large. A numerical example is presented in the *Appendix* illustrating the prediction of naphthalene solubility in a binary mixture containing *n*-hexane and carbon tetrachloride using Eq. 4.

The predictive abilities of these equations are compared in Table II for 25 systems for which solubility data and the excess free energy of the binary solvent are available at or near the same temperature. Surface areas of the individual molecules were taken from tabulated values presented in previous reports (17–20), with the exception that the surface area of carbon tetrachloride was provided[8]. In all cases, the surface areas exclude solvent molecules which may be located within the atomic radii. Table III lists numerical values of the surface areas and molar volumes used in these predictions.

Based on surface areas as weighting factors for the excess free energy relative to Raoult's law, Eq. 8 is seen to be the most generally applicable with an overall average (RMS) deviation[9] of 1.7% and a maximum error for a single data point of 7.5%. This maximum deviation occurs in a system (benzene–*n*-heptane) in which conflicting values of $\overline{G}_{12}^{ex}$ have been reported. As shown in Table II, deviations between predicted and observed solubilities depend to a large extent on which literature source is used for the solvent properties. This leads to two sets of predicted anthracene solubilities that differ from each other by as much as 6%. Discrepancies in the reported values of $\overline{G}_{12}^{ex}$ were not noted for the remaining 15 binary solvent systems. The primary advantage of Eq. 8 over expressions based on molar volumes, Eqs. 4 and 5, is its applicability to anthracene solubilities in solvent mixtures containing benzene. If these systems are excluded from the calculations, Eqs. 4 and 5 are slightly better than equations based on surface areas. All five equations correctly predict a maximum mole fraction solubility for anthracene in cyclohexane–*n*-heptane mixtures.

Solubility in simple binary solvents, C_3^{sat}, was described (21) as:

$$C_3^{sat} = K_1C_1 + K_2C_2 \quad \text{(Eq. 10)}$$

and:

$$K_i = (C_3^{sat})_i/C_i^* \qquad i = 1, 2$$

where C is molar concentration, and C_i^* is the concentration in a pure solvent. For solutes of limited solubility, it was demonstrated (4) that Eq. 3 is equivalent to:

$$X_3^{sat} = X_1^0(X_3^{sat})_1 + X_2^0(X_3^{sat})_2 \quad \text{(Eq. 11)}$$

While Eq. 11 gives reasonable predictions for several of the anthracene systems studied, these predictions are off by as much as 50% for *p*-benzoquinone in the *n*-heptane–carbon tetrachloride system (8) and off by a factor of two for benzil in the isooctane–carbon tetrachloride system (7)[10]. Inspection of Eq. 4 reveals that the mathematical form is incapable of completely describing systems having either a maximum or minimum mole fraction solubility. Anthracene exhibits a maximum solubility in binary mixtures of cyclohexane and *n*-heptane, and a slight minimum solubility has been observed for iodine in binary mixtures containing cyclohexane and octamethylcyclotetrasiloxane (6). It has been suggested

[8] The authors thank Robert S. Pearlman, University of Texas, for providing the surface area of carbon tetrachloride.

[9] RMS Deviations (%)

$$= (100/N^{1/2})\left\{\sum_{j=1}^{N}[\ln(X_{calc}/X_{exp})]^2\right\}^{1/2},$$

and these values are then averaged for all of the systems listed in Table II.

[10] For solutes having greater solubility $C_i = X_i/(X_1V_1 + X_2V_2 + X_3Y_3)$ and Eq. 10 can be shown to be equivalent to:

$$\frac{X_3^{sat}}{1-X_3^{sat}} = X_1^0\left(\frac{X_3^{sat}}{1-X_3^{sat}}\right)_{X_2^0=1} + X_2^0\left(\frac{X_3^{sat}}{1-X_3^{sat}}\right)_{X_2^0=1}$$

This consideration does not significantly alter the large deviations for the solubilities of *p*-benzoquinone and benzil. This extended form cannot predict either a maximum or minimum solubility.

Table III—Properties Used in Calculations

Component	$\overline{V}$, ml/mole	$\overline{A}$, Å²/mole	
Benzene	89.41	109.5	
Carbon tetrachloride	97.08	118.7	
Cyclohexane	108.76	120.8	
Hexadecane	294.12	323.2	
n-Heptane	147.48	160.3	
n-Hexane	131.51	142.1	
Cyclooctane	134.88	148.8	
Octane	163.46	178.4	
Isooctane	166.09	163.1	
Toluene	106.84	126.5	
Ethylbenzene	123.06	144.9	
Naphthalene	123.00	155.8	(a_3^{solid} = 0.312)
p-Dibromobenzene	118.00	156.6	(a_3^{solid} = 0.248)
Anthracene	150.00	202.2	(a_3^{solid} = 0.01049)

(22) that the incorporation of mixed solvates into Eq. 11 is a way to explain maximum solubilities:

$$1{\cdot}3 + 2 \rightleftharpoons 1{\cdot}2{\cdot}3$$

$$K' = \frac{C_{1\cdot2\cdot3}}{C_{1\cdot3}C_2}$$

$$C_3^{sat} = K_1C_1 + K_2C_2 + K'K_1C_1C_2 \qquad \text{(Eq. 12)}$$

Postulation of mixed solvates is not needed in the nearly ideal binary solvent model, as its predictive equations correctly predict the existence of the maximum anthracene solubility as well as the minimum iodine solubility.

The Scatchard–Hildebrand (23) equation:

$$RT \ln(a_3^{solid}/X_3^{sat}) = V_3(1 - \phi_3^{sat})^2 (\delta_{12} - \delta_3)^2 \qquad \text{(Eq. 13)}$$

$$\delta_{12} = \frac{\phi_1\delta_1 + \phi_2\delta_2}{\phi_1 + \phi_2} \qquad \text{(Eq. 14)}$$

describes solubility in simple binary solvent mixtures in terms of the solubility parameters (δ_i) of the individual pure components. For liquids, the solubility parameters are available in the literature or can be determined experimentally from the temperature dependence of vapor pressures. The solubility parameters of crystalline compounds are obtained indirectly from solubility measurements, and several calculated methods (24–26) have been suggested recently for determining the best value of δ_3. Examination of Eqs. 13 and 14 reveals that the solute should exhibit a maximum mole fraction solubility only when its solubility parameter is between the solubility parameters of the two pure solvents. Since the solubility parameter of anthracene (δ = 9.9) is greater than either the solubility parameter of cyclohexane (δ = 8.2) or *n*-heptane (δ = 7.4), a maximum anthracene solubility would not be predicted by Eq. 13. Similar failures of Eq. 6 have been observed for benzoic acid in cyclohexane–*n*-heptane and cyclohexane–*n*-hexane mixtures (5) and for anthracene in benzene–iodobenzene, benzene–iodoethane, cyclohexane–iodoethane, and cyclohexene–iodoethane mixtures (27). It was noted (5) that Eqs. 3–5 predicted the existence of maximum benzoic acid solubilities for both the monomeric and dimeric treatment of monofunctional carboxylic acids. Because of the unavailability of binary $\overline{G}_{12}^{ex}$ values, it was not possible to apply the NIBS model to the anthracene solubilities listed above. The fact that the nearly ideal binary solvent model correctly predicts maximum solubilities in three of these binary solvent mixtures suggests its greater application.

CONCLUSIONS

An important consequence of this research involves earlier contentions that the failure of Eq. 1 may be taken as an indication of specific solute–solvent or solvent–solvent interactions. While this concept is relatively straightforward in principle, its practical applications are complicated by the various weighting factor approximations. For example, does the failure of Eqs. 4 and 5 to predict anthracene solubilities in binary solvent mixtures containing benzene indicate specific solute–solvent (π–π) interactions, or does the success of Eq. 8 indicate that surface areas provide better approximations of weighting factors in systems containing both a planar solute and solvent molecule.

Unfortunately, this research does not indicate clearly whether weighting factors are better approximated with molar volumes or surface areas. From the standpoint of calculational simplicity and the ready availability of molar volumes, Eq. 4 is preferred, and some support for this form can be found in its adaptability to the Scatchard–Hildebrand solubility parameter theory. Similar support for Eq. 8 (and Eq. 9) can be found in correlations of partition coefficients with surface areas and in several semi-empirical expressions developed for predicting liquid–vapor equilibria. However, Eq. 5 is also applicable to polymer solutions, and this form often is preferred, because it is more directly related to gas–liquid chromatographic partition coefficients and to molarity-based equilibrium constants.

APPENDIX

The following example illustrates the prediction of naphthalene solubility in a binary solvent mixture containing *n*-hexane and carbon tetrachloride. For calculational purposes, the initial mole fraction composition of the solvent mixture is taken to be $X_1^0 = X_{hexane}^0 = 0.5000$. This corresponds to a volume fraction of *n*-hexane of $\phi_1^0 = 0.5753$. The naphthalene solubilities in the pure solvents, $(X_3^{sat})_1 = 0.1168$ and $(X_3^{sat})_2 = 0.2591$ are taken from a previous report (10), and the excess free energy of mixing of the solvent mixture at $X_1^0 = 0.5000$, $\overline{G}_{12}^{ex} = 35.5$ cal/mole, is taken from other reported data (46).

The NIBS prediction begins by calculating the excess partial molar Gibbs free energy of the solute $(\overline{G}_3^{ex})_i$ in the two pure solvents:
For *n*-hexane:

$$(\overline{G}_3^{ex})_1 = (1 - 0.1101)^{-2}\,(1.987)(298.15)\ln(0.312/0.1168)$$
$$= 735.02 \text{ cal/mole}$$

and for carbon tetrachloride:

$$(\overline{G}_3^{ex})_2 = (1 - 0.3070)^{-2}$$
$$(1.987)(298.15)\ln(0.312/0.2591)$$
$$= 229.2 \text{ cal/mole}$$

The properties in the two pure solvents are then combined with $\overline{G}_{12}^{ex}$ to give:

$$(1.987)(298.15)\ln(0.312/X_3^{sat}) = (1 - \phi_3^{sat})^2\,[(0.5753)(735.02)$$
$$+ (0.4247)(229.2) - (123.00)(114.30)^{-1}(35.5)]$$

In the first approximation $(1 - \phi_3^{sat}) \approx 1$, and solving for the mole fraction solubility gives:

$$X_3^{sat} = 0.1383$$

The first approximation is then used to calculate $(1 - \phi_3^{sat})$, and this quantity is then used to obtain a second approximation:

$$(1.987)(298.15)\ln(0.312/X_3^{sat}) = (1 - 0.1483)^2[(0.5753)(735.02)$$
$$+ (0.4247)(229.2) - (123.00)(114.30)^{-1}(35.5)]$$

The second approximation of X_3^{sat} (= 0.1729) is used to calculate a new value of $(1 - \phi_3^{sat})$, and the calculations are repeated until a constant mole fraction solubility is obtained. As mentioned previously, this convergence is quite rapid unless the solubility is large.

REFERENCES

(1) T. E. Burchfield and G. L. Bertrand, *J. Solution Chem.*, **4**, 205 (1975).

(2) T. E. Burchfield, PhD Dissertation, University of Missouri-Rolla, 1977.

(3) W. E. Acree, Jr. and G. L. Bertrand, *J. Phys. Chem.*, **81**, 1170 (1977).

(4) *Idem.*, **83**, 2355 (1979).

(5) W. E. Acree, Jr, and G. L. Bertrand, *J. Pharm. Sci.*, **70**, 1033 (1981).

(6) W. E. Acree, Jr., PhD Dissertation, University of Missouri-Rolla, 1981.

(7) W. E. Acree, Jr. and J. H. Rytting, *J. Pharm. Sci.*, **71**, 201 (1982).

(8) *Ibid., Int. J. Pharm.*, **10**, 231 (1982).

(9) *Ibid., Anal. Chem.*, **52**, 1764 (1980).

(10) E. L. Heric and C. D. Posey, *J. Chem. Eng. Data*, **9**, 35 (1964).

(11) *Idem.*, **9**, 161 (1964).

(12) *Idem.*, **10**, 25 (1965).

(13) J. M. Berryman and E. L. Heric, *ibid.*, **12**, 249 (1967).

(14) H. Buchowski, U. Domanska, and A. Ksiazczak, *Polish J. Chem.*, **53**, 1127 (1979).

(15) L. J. Gordon and R. L. Scott, *J. Am. Chem. Soc.*, **74**, 4138 (1952).

(16) J. Gmehling, U. Onken, and A. Arlt, in "Vapor-Liquid Equilib-

rium Data Collection," DECHEMA Chemistry Data Series, Vol. 1 (12 parts), Scholium International, New York, N.Y., 1977.
(17) S. H. Yalkowsky and S. C. Valvani, *J. Med. Chem.*, **19**, 727 (1976).
(18) S. C. Valvani, S. H. Yalkowsky, and G. L. Amidon, *J. Phys. Chem.*, **80**, 829 (1976).
(19) S. H. Yalkowsky and S. C. Valvani, *J. Chem. Eng. Data*, **24**, 127 (1979).
(20) S. H. Yalkowsky, R. J. Orr, and S. C. Valvani, *Ind. Eng. Chem. Fundam.*, **18**, 351 (1979).
(21) M. S. Sytilin, *Russ. J. Phys. Chem.*, **48**, 1091, 1353, 1500 (1974).
(22) *Idem.*, **52**, 1671 (1978).
(23) J. H. Hildebrand and R. L. Scott, "The Solubility of Nonelectrolytes," Dover, New York, N.Y., 1964.
(24) G. Cave, R. Kothari, F. Puisieux, A. Martin, and J. T. Carstensen, *Int. J. Pharm.*, **5**, 267 (1980).
(25) W. E. Acree, Jr., J. H. Rytting, and J. T. Carstensen, *ibid.*, **8**, 69 (1981).
(26) A. Martin and J. Carstensen, *J. Pharm. Sci.*, **70**, 170 (1981).
(27) G. R. Somayajulu and S. R. Palit, *J. Phys. Chem.*, **58**, 417 (1954).
(28) I. P.-C. Li, B. C.-Y. Lu, and E. C. Chen, *J. Chem. Eng. Data*, **18**, 305 (1973).
(29) J. S. Rowlinson, "Liquids and Liquid Mixtures", Academic Press, New York, N.Y., p. 150.
(30) T. Katayama, E. K. Sung, and E. N. Lightfoot, *AIChE J.*, **11**, 924 (1965).
(31) D. V. S. Jain and O. P. Yadav, *Indian J. Chem.*, **12**, 718 (1974).
(32) K. L. Young, R. A. Mentzer, R. A. Greenkorn, and K. C. Chao, *J. Chem. Thermodyn.*, **9**, 979 (1977).
(33) M. B. Ewing and K. N. Marsh, *ibid.*, **6**, 395 (1974).
(34) D. V. S. Jain and O. P. Yadav, *Indian J. Chem.*, **9**, 342 (1971).
(35) R. Battino, *J. Phys. Chem.*, **70**, 3408 (1966).
(36) D. V. S. Jain, V. K. Gupta, and B. S. Lark, *J. Chem. Thermodyn.*, **5**, 451 (1973).
(37) K. R. Harris and P. J. Dunlop, *ibid.*, **2**, 805 (1970).
(38) M. Smutek, M. Fris, and J. Fohl, *Collect. Czech. Chem. Commun.*, **32**, 931 (1967).
(39) R. C. Mitra, S. C. Guhaniyogi, and S. N. Bhattacharyya, *J. Chem. Eng. Data*, **18**, 147 (1973).
(40) S. Weissman and S. E. Wood, *J. Chem. Phys.*, **32**, 1153 (1960).
(41) J. R. Goates, R. J. Sullivan, and J. B. Ott, *J. Phys. Chem.*, **63**, 589 (1959).
(42) V. C. Smith and R. L. Robinson, Jr., *J. Chem. Eng. Data*, **15**, 391 (1970).
(43) J. D. Gomez-Ibanez and J. J. C. Shieh, *J. Phys. Chem.*, **69**, 1660 (1965).
(44) M. L. McGlashan and A. G. Williamson, *Trans. Faraday Soc.*, **57**, 588 (1961).
(45) D. V. S. Jain and B. S. Lark, *J. Chem. Thermodyn.*, **5**, 455 (1973).
(46) D. V. S. Jain, V. K. Gupta, and B. S. Lark, *Indian J. Chem.*, **8**, 815 (1970).

Transport of Prostaglandins Through Normal and Diabetic Rat Hepatocytes

ANWAR B. BIKHAZI ˣ, GHASSAN M. BAASIRI, NABIL Z. BOULOS, and RAJA N. KHURI

Received May 15, 1980, from the *Department of Physiology, Faculty of Medicine, American University of Beirut, Beirut, Republic of Lebanon.* Accepted for publication April 14, 1982.

Abstract □ Transport of alprostadil (prostaglandin E_1) and dinoprost (prostaglandin $F_{2\alpha}$) was studied in enzymatically dispersed normal and streptozocin-treated rat hepatocytes prepared by collagenase perfusion. Cell suspensions incubated at 37° were sampled at time intervals for a period of 5 min and the supernatant analyzed for prostaglandins after centrifugation. The data analysis employed a theory and a model for solute transfer at the cell membrane–water interphase. Biophysical parameters such as the effective partition and the apparent permeability constants were used to define the transport mechanism. The apparent permeability coefficient of alprostadil and dinoprost transfer through normal hepatocytes was calculated to be 5×10^{-3} and 3×10^{-3} cm/sec with a mean partition coefficient of 1345 and 764 for both solutes, respectively. The permeability coefficient of alprostadil and dinoprost transfer through diabetic hepatocytes were 3×10^{-3} and 2×10^{-3} cm/sec with partition coefficient of 572 and 206, respectively. The results showed differences in prostaglandin transport between normal and diabetic hepatocytes, resulting from morphological and lipid alteration in the cytoplasmic membrane.

Keyphrases □ Prostaglandins—transport through normal and diabetic rat hepatocytes, alprostadil and dinoprost □ Alprostadil—transport through normal and diabetic rat hepatocytes □ Dinoprost—transport through normal and diabetic rat hepatocytes □ Hepatocytes, rat—normal and diabetic, transport of alprostadil and dinoprost □ Permeability—transport of alprostadil and dinoprost through normal and diabetic rat hepatocytes □ Partition coefficient—transport of alprostadil and dinoprost through normal and diabetic rat hepatocytes

Multicomponent and multicompartment diffusional models have been used to study transport of solutes across biological membranes. For example, erythrocyte permeability (1), lymphocyte permeability (2), Ehrlich ascites tumor cell permeability (3), and Burkitt lymphoma cell permeability (4) have been reported. The majority of the studies dealt with solute transfer through blood cell components and tissue culture cell suspensions. However, few mechanistic studies were attempted on cell suspensions obtained by enzymatic dispersion, *e.g.*, embryonic heart cells (5), adipocytes (6), and hepatocytes (7, 8).

Alprostadil (prostaglandin E_1) and dinoprost were chosen as solute models to mechanistically explain the transfer of acidic lipids through normal and diabetic rat hepatocytes. Furthermore, autoradiographic studies in mice have shown high concentrations of alprostadil and dinoprost in the liver 15 min after intravenous injection (9).

The present report describes the uptake mechanism of alprostadil and dinoprost through enzymatically dispersed normal and diabetic adult rat hepatocytes. The techniques, methodology, and the theoretical model employed are well suited to characterize interfacial barriers to interface transport in biological systems.

EXPERIMENTAL

Preparation of Rat Hepatocyte Suspensions—Suspensions of isolated liver parenchymal cells were prepared by a modification of a previously described procedure (10). Male Sprague-Dawley rats weighing

0022-3549/83/0300-0296$01.00/0

rium Data Collection," DECHEMA Chemistry Data Series, Vol. 1 (12 parts), Scholium International, New York, N.Y., 1977.
(17) S. H. Yalkowsky and S. C. Valvani, *J. Med. Chem.*, **19**, 727 (1976).
(18) S. C. Valvani, S. H. Yalkowsky, and G. L. Amidon, *J. Phys. Chem.*, **80**, 829 (1976).
(19) S. H. Yalkowsky and S. C. Valvani, *J. Chem. Eng. Data*, **24**, 127 (1979).
(20) S. H. Yalkowsky, R. J. Orr, and S. C. Valvani, *Ind. Eng. Chem. Fundam.*, **18**, 351 (1979).
(21) M. S. Sytilin, *Russ. J. Phys. Chem.*, **48**, 1091, 1353, 1500 (1974).
(22) *Idem.*, **52**, 1671 (1978).
(23) J. H. Hildebrand and R. L. Scott, "The Solubility of Nonelectrolytes," Dover, New York, N.Y., 1964.
(24) G. Cave, R. Kothari, F. Puisieux, A. Martin, and J. T. Carstensen, *Int. J. Pharm.*, **5**, 267 (1980).
(25) W. E. Acree, Jr., J. H. Rytting, and J. T. Carstensen, *ibid.*, **8**, 69 (1981).
(26) A. Martin and J. Carstensen, *J. Pharm. Sci.*, **70**, 170 (1981).
(27) G. R. Somayajulu and S. R. Palit, *J. Phys. Chem.*, **58**, 417 (1954).
(28) I. P.-C. Li, B. C.-Y. Lu, and E. C. Chen, *J. Chem. Eng. Data*, **18**, 305 (1973).
(29) J. S. Rowlinson, "Liquids and Liquid Mixtures", Academic Press, New York, N.Y., p. 150.
(30) T. Katayama, E. K. Sung, and E. N. Lightfoot, *AIChE J.*, **11**, 924 (1965).
(31) D. V. S. Jain and O. P. Yadav, *Indian J. Chem.*, **12**, 718 (1974).
(32) K. L. Young, R. A. Mentzer, R. A. Greenkorn, and K. C. Chao, *J. Chem. Thermodyn.*, **9**, 979 (1977).
(33) M. B. Ewing and K. N. Marsh, *ibid.*, **6**, 395 (1974).
(34) D. V. S. Jain and O. P. Yadav, *Indian J. Chem.*, **9**, 342 (1971).
(35) R. Battino, *J. Phys. Chem.*, **70**, 3408 (1966).
(36) D. V. S. Jain, V. K. Gupta, and B. S. Lark, *J. Chem. Thermodyn.*, **5**, 451 (1973).
(37) K. R. Harris and P. J. Dunlop, *ibid.*, **2**, 805 (1970).
(38) M. Smutek, M. Fris, and J. Fohl, *Collect. Czech. Chem. Commun.*, **32**, 931 (1967).
(39) R. C. Mitra, S. C. Guhaniyogi, and S. N. Bhattacharyya, *J. Chem. Eng. Data*, **18**, 147 (1973).
(40) S. Weissman and S. E. Wood, *J. Chem. Phys.*, **32**, 1153 (1960).
(41) J. R. Goates, R. J. Sullivan, and J. B. Ott, *J. Phys. Chem.*, **63**, 589 (1959).
(42) V. C. Smith and R. L. Robinson, Jr., *J. Chem. Eng. Data*, **15**, 391 (1970).
(43) J. D. Gomez-Ibanez and J. J. C. Shieh, *J. Phys. Chem.*, **69**, 1660 (1965).
(44) M. L. McGlashan and A. G. Williamson, *Trans. Faraday Soc.*, **57**, 588 (1961).
(45) D. V. S. Jain and B. S. Lark, *J. Chem. Thermodyn.*, **5**, 455 (1973).
(46) D. V. S. Jain, V. K. Gupta, and B. S. Lark, *Indian J. Chem.*, **8**, 815 (1970).

Transport of Prostaglandins Through Normal and Diabetic Rat Hepatocytes

ANWAR B. BIKHAZI ˣ, GHASSAN M. BAASIRI, NABIL Z. BOULOS, and RAJA N. KHURI

Received May 15, 1980, from the *Department of Physiology, Faculty of Medicine, American University of Beirut, Beirut, Republic of Lebanon.* Accepted for publication April 14, 1982.

Abstract □ Transport of alprostadil (prostaglandin E_1) and dinoprost (prostaglandin $F_{2\alpha}$) was studied in enzymatically dispersed normal and streptozocin-treated rat hepatocytes prepared by collagenase perfusion. Cell suspensions incubated at 37° were sampled at time intervals for a period of 5 min and the supernatant analyzed for prostaglandins after centrifugation. The data analysis employed a theory and a model for solute transfer at the cell membrane–water interphase. Biophysical parameters such as the effective partition and the apparent permeability constants were used to define the transport mechanism. The apparent permeability coefficient of alprostadil and dinoprost transfer through normal hepatocytes was calculated to be 5×10^{-3} and 3×10^{-3} cm/sec with a mean partition coefficient of 1345 and 764 for both solutes, respectively. The permeability coefficient of alprostadil and dinoprost transfer through diabetic hepatocytes were 3×10^{-3} and 2×10^{-3} cm/sec with partition coefficient of 572 and 206, respectively. The results showed differences in prostaglandin transport between normal and diabetic hepatocytes, resulting from morphological and lipid alteration in the cytoplasmic membrane.

Keyphrases □ Prostaglandins—transport through normal and diabetic rat hepatocytes, alprostadil and dinoprost □ Alprostadil—transport through normal and diabetic rat hepatocytes □ Dinoprost—transport through normal and diabetic rat hepatocytes □ Hepatocytes, rat—normal and diabetic, transport of alprostadil and dinoprost □ Permeability—transport of alprostadil and dinoprost through normal and diabetic rat hepatocytes □ Partition coefficient—transport of alprostadil and dinoprost through normal and diabetic rat hepatocytes

Multicomponent and multicompartment diffusional models have been used to study transport of solutes across biological membranes. For example, erythrocyte permeability (1), lymphocyte permeability (2), Ehrlich ascites tumor cell permeability (3), and Burkitt lymphoma cell permeability (4) have been reported. The majority of the studies dealt with solute transfer through blood cell components and tissue culture cell suspensions. However, few mechanistic studies were attempted on cell suspensions obtained by enzymatic dispersion, *e.g.*, embryonic heart cells (5), adipocytes (6), and hepatocytes (7, 8).

Alprostadil (prostaglandin E_1) and dinoprost were chosen as solute models to mechanistically explain the transfer of acidic lipids through normal and diabetic rat hepatocytes. Furthermore, autoradiographic studies in mice have shown high concentrations of alprostadil and dinoprost in the liver 15 min after intravenous injection (9).

The present report describes the uptake mechanism of alprostadil and dinoprost through enzymatically dispersed normal and diabetic adult rat hepatocytes. The techniques, methodology, and the theoretical model employed are well suited to characterize interfacial barriers to interface transport in biological systems.

EXPERIMENTAL

Preparation of Rat Hepatocyte Suspensions—Suspensions of isolated liver parenchymal cells were prepared by a modification of a previously described procedure (10). Male Sprague-Dawley rats weighing

0022-3549/83/0300-0296$01.00/0

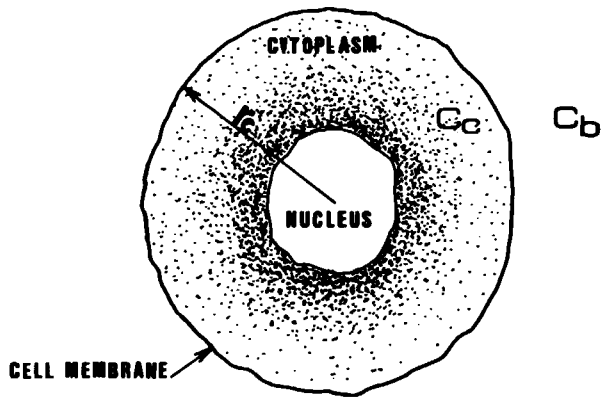

Figure 1—*Physical model describing uptake across hepatocyte–water interface.*

200–250 g and fed *ad libitum* were anesthetized by injection of 80 mg/kg ip of the sodium salt of 5-*sec*-butyl-5-ethyl-2-thiobarbituric acid[1]. The liver was initially perfused through the portal vein at a flow rate of 30–40 ml/min with 200-ml heparinized Ca^{2+}-free Krebs–Henseleit (I) solution to clear it of its blood supply. Perfusion was continued with 250 ml of I containing 0.4 mg/ml of collagenase[2] at a flow rate of 100 ml/min using a peristaltic pump[3]. All perfusion media were aereated with 95% oxygen–5% carbon dioxide throughout the experiment. After 30 min of perfusion, the fibrous tunic was scraped and the hepatocytes dispersed by gentle motion. The cells were filtered through a course 250-μm nylon-mesh filter, washed and suspended into 30 ml of Ca^{2+}- and Mg^{2+}-free phosphate buffered saline (II) (pH 7.4). Hepatocyte viability was then estimated by the trypan blue exclusion test.

Preparation of Diabetic Rats—Male rats were injected with 65 mg/kg iv streptozocin[4] in saline acidified to pH 4.5 with 0.05 *M* solution of sodium citrate. They were fed *ad libitum* and checked daily for diabetes by urine sugar analysis paper[5] and a blood glucose test (11). Animals whose blood glucose levels were >250 mg/100 ml after day 7 were used in the experiments; their livers were perfused by the same procedure mentioned above to obtain cells from diabetic rats.

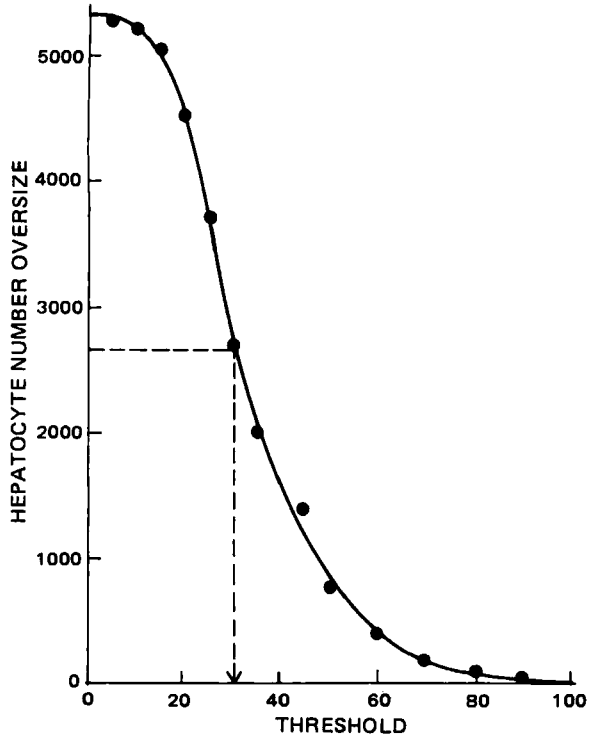

Figure 2—*Cumulative size distribution for rat hepatocytes.*

[1] Inaction, Byk Gulden, Konstanz, West Germany.
[2] Type CLS II, 140-175 U/mg, Worthington Biochemical Corporation, Freehold, N.J.
[3] Ministaltic pump, Manostat, New York, N.Y.
[4] U-9889, lot 60,273-1, Courtesy of The Upjohn Co., Kalamazoo, Mich.
[5] Eli Lilly Co., Indianapolis, Ind.

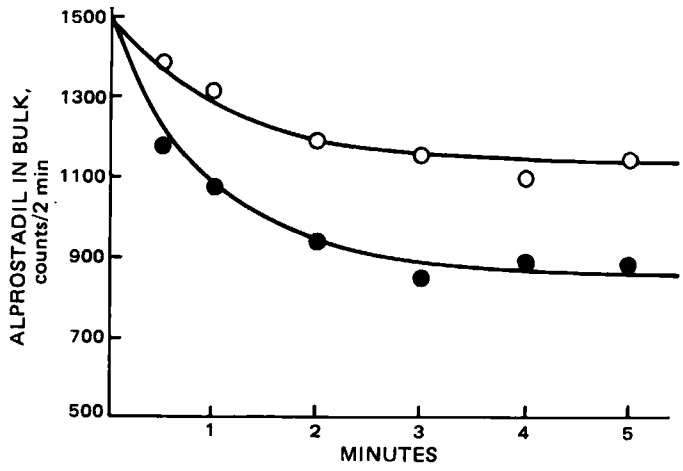

Figure 3—*Comparison of experimental data with theory for uptake of alprostadil by normal hepatocytes. Key: (○) 13,169,475 cells; (●) 27,362,137 cells;* P = 5 × 10^{-3} *cm/sec;* K = 1345.

Determination of Mean Hepatocyte Count and Diameter—An automated counter[6] was used to determine the mean hepatocyte count and diameter. The instrument was precalibrated with a suspension of polystyrene divinyl benzene latex (16.6-μm diameter).

The hepatocyte suspension (0.5 ml) was placed in a 200-ml solution of II, and cell counts were read at thresholds 2, 5, 10, 15, 20, 30, 35, 40, 60, 80, and 100, respectively.

Uptake of Alprostadil and Dinoprost by Hepatocytes from Normal and Diabetic Rats—One microcurie (~0.635 n*M*) of [5,6(*n*)-^{3}H]-alprostadil or 1 μCi (~3.81 n*M*) or [1-^{14}C]dinoprost[7] was added to 225 ml of a solution of II at 37° in a water-jacketed beaker. A 1-ml sample from time zero was withdrawn from the beaker into a liquid scintillation vial for radioactive assay in a liquid scintillation counter. Following this, a measured volume of hepatocyte suspension was added into the beaker to obtain ~1.3 × 10^{7} or 2.6 × 10^{7} cells/225 ml of a solution of II. The hepatocytes were kept in suspension throughout the experiment by stirring with a 120-rpm synchronous motor. At 0.5-, 1-, 2-, 3-, 4-, and 5-min intervals, 3-ml aliquots of the suspension were withdrawn and the cells immediately sedimented by centrifugation at 800×*g* for 15 sec. One-milliliter samples of the supernatant solutions were assayed for their radioactive content.

THEORETICAL

The selected experimental method involves the dispersion of hepatocytes in an isotonic aqueous phase. The following discussion describes a physical model with relevant interrelationships between experimental

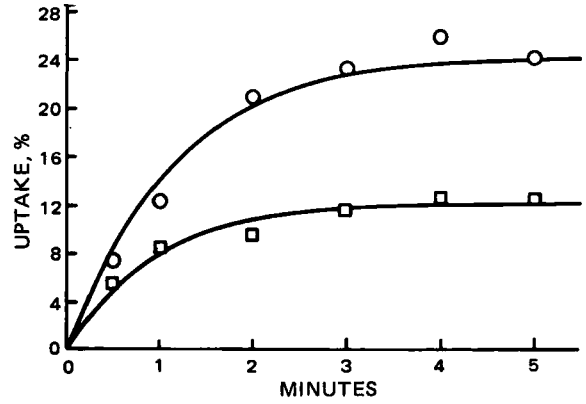

Figure 4—*Normalized plot, by percent uptake, of experimental data with theory of alprostadil by normal and diabetic hepatocytes. Key: (○) 13,169,475 normal cells;* P = 5 × 10^{-3} *cm/sec;* K = 1345; *(□) 13,450,000 diabetic cells;* P = 3 × 10^{-3} *cm/sec;* K = 572.

[6] Coulter Counter model A, Coulter Electronics, Hialeah, Fla.
[7] The Radiochemical Centre, Amersham, England.

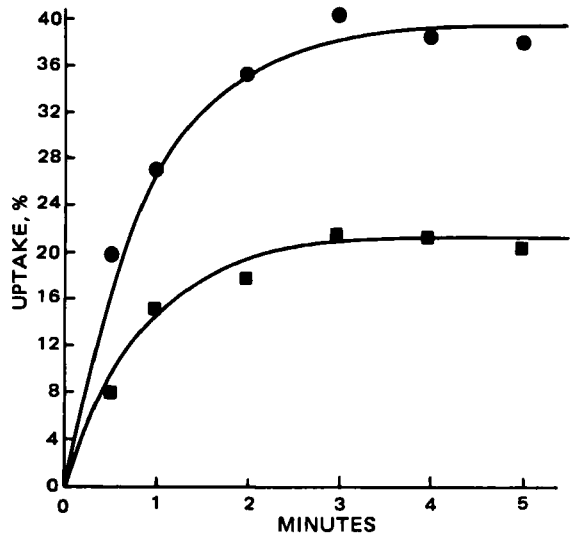

Figure 5—*Normalized plot, by percent uptake, of experimental data with theory of alprostadil by normal and diabetic hepatocytes. Key: (●) 27,362,137 normal cells;* P = 5 × 10^{-3} *cm/sec;* K = *1345; (■) 27,000,000 diabetic cells;* P = 3 × 10^{-3} *cm/sec;* K = *572.*

and theory which incorporates parameters physically describing the system.

The model shown in Fig. 1 is similar to the one proposed previously (12) for rapid equilibration in the heterogeneous cytosol with no binding of solute molecules to components outside the cell. The model describes a hepatocyte of radius r_c suspended in buffer II with C_c as the intracellular solute concentration and C_b as the aqueous bulk solute concentration. The resistance to solute transport may be described as a barrier to transfer across the cytoplasmic membrane. It is best characterized by a transport coefficient (permeability coefficient, P) which can be a function of solute and membrane characteristics.

A quasi-steady-state rate of uptake of solute by a cell was described (13) by:

$$\frac{dC_c}{dt} = \frac{4\pi r_c^2 P}{V_c}\left(C_b - \frac{C_c}{K}\right) \qquad \text{(Eq. 1)}$$

where P is the apparent permeability coefficient for the interfacial resistance, K is the effective cell-water partition coefficient, and V_c is the hepatocyte volume.

From mass balance:

$$T_{Ab} + T_{Ac} = \text{Constant} \qquad \text{(Eq. 2)}$$

can be written where T_{Ab} and T_{Ac} are the total amounts of solute in the bulk phase and in the cells at any time t. Therefore:

$$V_b C_b + 4/3\pi r_c^3 N C_c = \text{Constant} \qquad \text{(Eq. 3)}$$

where V_b is the bulk volume, and N is the number of hepatocytes in the suspension.

Differentiating C_b and C_c in Eq. 3 with respect to time and rearranging:

$$\frac{dC_b}{dt} = -\frac{4/3\pi r_c^3 N}{V_b}\frac{dC_c}{dt} \qquad \text{(Eq. 4)}$$

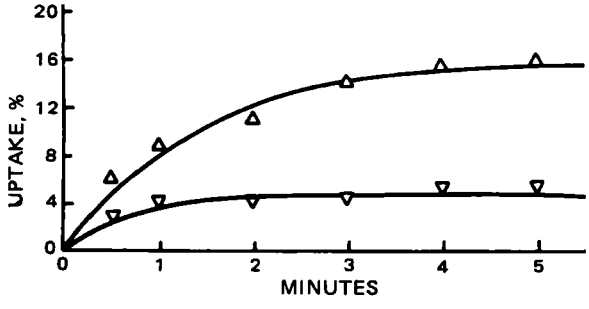

Figure 6—*Normalized plot, by percent uptake, of experimental data with theory of dinoprost by normal and diabetic hepatocytes. Key: (△) 11,948,182 normal cells;* P = 3 × 10^{-3} *cm/sec;* K = *860; (▽) 13,033,125 diabetic cells;* P = 2 × 10^{-3} *cm/sec;* K = *206.*

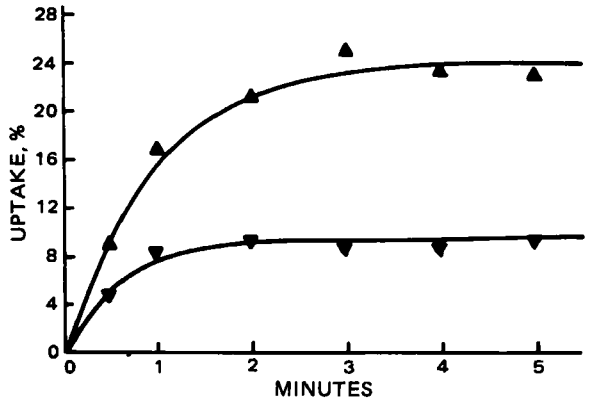

Figure 7—*Normalized plot, by percent uptake, of experimental data with theory of dinoprost by normal and diabetic hepatocytes. Key: (▲) 26,320,500 normal cells;* P = 3 × 10^{-3} *cm/sec;* K = *667; (▼), 27,169,687 diabetic cells;* P = 2 × 10^{-3} *cm/sec;* K = *206.*

Equations 1 and 4 are combined to give:

$$\frac{dC_b}{dt} = -\frac{4\pi r_c^2 NP}{V_b}\left(C_b - \frac{C_c}{K}\right) \qquad \text{(Eq. 5)}$$

Equations 1, 3, and 5 are used to solve for C_b as a function of time when V_b, K (which can be calculated from the steady-state data points and Eq. 3), r_c, P, and C_b^0 (concentration of solute in bulk phase at $t = 0$) are known. These equations can be solved analytically to yield a solution of the form:

$$C_b = Ae^{-\alpha t} + B \qquad \text{(Eq. 6)}$$

where A, α, and B are constants and are expressed as:

$$A = \frac{C_b^0 K V_c N}{(KV_c N + V_b)} \qquad \text{(Eq. 7)}$$

$$\alpha = \frac{3NP(KV_c N + V_b)}{r_c V_b K} \qquad \text{(Eq. 8)}$$

and:

$$B = \frac{C_b^0 V_b}{(KV_c N + V_b)} \qquad \text{(Eq. 9)}$$

However, to manipulate this solution is tedious and prone to errors considering the expressions for A, α, and B, especially in situations of nonuniformity in size distribution of the cells (14). A more practical approach is to resort to numerical methods using the Hamming's predictor–corrector method. The computer program calls on a subroutine which employs the fourth-order Runge–Kutta method to yield the starting values for Hamming's algorithm (15). Comparing the numerical solution with that obtained analytically for some of the data yielded a very close fit, thus, supporting the results.

RESULTS

Determination of Mean Hepatocyte Count and Diameter—The number of isolated cells per liver was ~1.2 × 10^8 hepatocytes. Hepatocyte preparations showing ≥90% viable cells were used in the experiments.

The mean hepatocyte count corresponds to threshold 17 for the calibration material polystyrene divinyl benzene latex (16.6-μm diameter). Figure 2 represents a plot of the number of normal oversize cells *versus* threshold of the suspension with mean count at threshold 30. Identical size distribution curves were observed for hepatocytes from diabetic animals. A procedure similar to the one reported previously (16) was used to calculate the mean diameter, which was estimated to be 20 μm.

Uptake Studies—Uptake studies of alprostadil and dinoprost by 6 × 10^4 and 12 × 10^4 cells/ml from normal and diabetic rats were attempted to verify that the calculated physical constants remain the same, irrespective of cell number in the uptake medium. The theoretical calculations are presented as smooth curves in Figs. 3–7 with the apparent permeability coefficient (P) experimentally determined as the value which gives the best fit to the data points.

Uptake of Alprostadil and Dinoprost by Hepatocytes from Normal Rats—Figure 3 compares the experimental data with theory for uptake of alprostadil by normal hepatocytes. A similar graph was obtained for dinoprost uptake. Steady state was observed in 5 min, and the effective cell-water partition coefficient was 1345 and 764 for alprostadil

and dinoprost, respectively. The apparent P-value for both solutes was in the range of 5×10^{-3} and 3×10^{-3} cm/sec, respectively.

Uptake of Alprostadil and Dinoprost by Hepatocytes from Diabetic Rats—Plots similar to Fig. 3 were observed with diabetic cells. The effective cell–water partition coefficient was 572 for alprostadil and 206 for dinoprost. The apparent P-value was estimated to be 3×10^{-3} and 2×10^{-3} cm/sec, respectively.

Normalized Plots of the Data—Figures 4–7 are normalized plots for alprostadil and dinoprost uptake by hepatocytes from normal and diabetic rats at almost identical cell counts. At steady state the percent uptake of alprostadil and dinoprost by normal cells was almost double that of cells from diabetic rats, because of differences in the K-values of both solutes between the two types of cells.

DISCUSSION

Diffusion- and Permeability-Controlled Transfer Through Cell Suspension Models—Solute transfer through cell suspensions is generally controlled by two physically defined situations, namely the diffusion of the solute from bulk phase to the proximity of the cell membrane, and then the permeation of the solute through the membrane. In the present study, movement of solute from the bulk phase to the hepatocyte membrane interface will be contributing minimally, if any, to the rate of solute transport. Therefore, solute transfer through the cell membrane becomes rate limiting. Membrane permeation is then physically assessed by the isolation of the apparent permeability coefficient. Since this coefficient is in the range of 10^{-3} cm/sec, then the effective diffusivities (D) of both solutes in an ~100-Å thick (d_c) hepatocyte membrane may be estimated to be in the range of 10^{-9} cm^2/sec. Therefore, the lag time for solute transport may be expressed by:

$$\tau = \frac{d_c^2}{D} \qquad \text{(Eq. 10)}$$

where τ has a value of $\sim 10^{-3}$ sec, a short lag time when compared with 5 min, the time needed to reach steady state.

Assessment of the Data—It was reported (11) that in streptozocin-treated rats, cell membranes have shown significant changes in sialic acid and cholesterol content which support the findings on concanavalin A-induced agglutination[8] that cells from diabetic rats flocculate at a slower rate than those from controls. This suggests that diabetic cells, when compared with normal cells, are either less rich in glycoprotein receptors (sialic acid-rich receptors) or the receptors are arranged differently in the cell membrane. The data on the K-values presented here show that normal cells are more lipoidal than diabetic ones. For example, the ratio of the K-values of both prostaglandins in normal cells (1345 for alprostadil and 763 for dinoprost) is 1.76, which agrees fairly well with previous data (17) on the partition coefficient ratio of alprostadil and dinoprost between n-octane and water (ratio 1.72). Furthermore, the ratio of the K-values of the same solutes in diabetic cells is 2.78, which agrees with the ratio of their partition coefficients (ratio 2.11) between 1-octanol and water as well.

The initial rate of transport of alprostadil and the apparent permeability coefficients are larger in normal as compared with diabetic hepatocytes (Figs. 4 and 5). This is also observed in Figs. 6 and 7 for dinoprost. However, alprostadil is transported faster and to a greater extent in both normal and diabetic cells than dinoprost (Figs. 4 and 6, Figs. 5 and 7, respectively). Therefore, it can be concluded that solute partitioning plays a prominant role in the transport mechanism, since the apparent permeability coefficient is a function of the effective partition coefficient.

[8] Unpublished data.

REFERENCES

(1) C. G.Winter and H. N. Christensen, *J. Biol. Chem.*, **240,** 3594 (1965).

(2) K. J. Van Den Berg and I. Betel, *FEBS Lett.*, **29,** 149 (1973).

(3) L. K. Stitzer and J. A. Jacquez, *Am. J. Physiol.*, **229,** 172 (1975).

(4) J. S. Turi, W. I. Higuchi, C. Shipman, Jr., and N. F. H. Ho, *J. Pharm. Sci.*, **61,** 1618 (1972).

(5) G. C. Gazzola, R. Franchi-Gazzola, R. P. Ronchi, and G. G. Guidotti, *Biochim. Biophys. Acta*, **311,** 292 (1973).

(6) M. Touabi and B. Jeanrenaud, *ibid.*, **173,** 128 (1969).

(7) A. Le Cam and P. Freychet, *J. Biol. Chem.*, **252,** 148 (1977).

(8) J. W. Edmondson, L. Lumeng, and T. Li, *Biochim. Biophys. Res. Commun.*, **76,** 751 (1977).

(9) E. W. Horton, in "Prostaglandins," Monographs on Endocrinology, Vol. 7, Springer-Verlag, 1972, pp. 67–86.

(10) W. R. Ingebretsen and S. R. Wagle, *Biochim. Biophys. Res. Commun.*, **47,** 403 (1972).

(11) V. Chandramouli and J. Carter, *Diabetes*, **24,** 257 (1975).

(12) J. S. Turi, Ph.D. Thesis, The University of Michigan, Ann Arbor, Mich., 1972.

(13) N. F. H. Ho, J. S. Turi, C. Shipman, Jr., and W. I. Higuchi, *J. Theor. Biol.*, **34,** 451 (1972).

(14) A. B. Bikhazi and W. I. Higuchi, *J. Pharm. Sci.*, **59,** 744 (1970).

(15) B. Carnahan, H. A. Luther, and J. O. Wilkes, in "Applied Numerical Methods," Wiley, 1969, pp. 361–404.

(16) A. B. Bikhazi and G. E. Ayyub, *J. Pharm. Sci.*, **67,** 939 (1978).

(17) A. B. Bikhazi, N. S. Nadir, and J. J. Hajjar, *ibid.*, **66,** 1308 (1977).

ACKNOWLEDGMENTS

This work was supported in part by Grant 38-5766 from the Lebanese Council for Scientific Research and by Grant 18-5205 from the American University of Beirut Medical Research Fund.

High-Performance Liquid Chromatography of Preparations of Ribonucleic Acid Inactivator(s) from Cupric Ion and Hydroquinone Before and After Treatment with Histidine

G. R. DUBES *x, A. N. MASOUD ‡¶, and M. I. AL-MOSLIH §

Received March 22, 1982, from the *Departments of Medical Microbiology and ‡Anesthesiology, University of Nebraska College of Medicine, Omaha, NE 68105, and the §Department of Microbiology, University of Baghdad College of Medicine, Baghdad, Iraq. Accepted for publication May 17, 1982. ¶Present address: Division of Toxicology, Department of Environmental Health Sciences, School of Hygiene and Public Health, Johns Hopkins University, Baltimore, MD 21205.

Abstract □ Preparations of viral RNA inactivator(s) produced during the cupric ion-catalyzed oxidation of hydroquinone were analyzed by high-performance liquid chromatography (HPLC) using UV and electrochemical (EC) detectors. In addition to hydroquinone and the main oxidation product (*p*-benzoquinone), which is known not to be the inactivator(s), the analysis showed three unidentified components (I–III). Partial UV absorption spectra of I–III were determined by HPLC with the UV detector set at various wavelengths. Components II and III, but not I, were highly unstable in the presence of L-histidine, which is an excellent chelator of cupric ion and can promptly stop ongoing viral RNA inactivation by the inactivator(s). The product *p*-benzoquinone was also highly unstable in the presence of L-histidine; the reaction between these two compounds (with or without copper) resulted in a cascade of products. The possibility that the inactivator(s) is II or III, or both, is discussed.

Keyphrases □ Hydroquinone—high-performance liquid chromatography of preparations of ribonucleic acid inactivator(s) from cupric ion after treatment with histidine □ Histidine—high-performance liquid chromatography of preparations of ribonucleic acid inactivator(s) from cupric ion and hydroquinone □ High-performance liquid chromatography—preparations of ribonucleic acid inactivator(s) from cupric ion and hydroquinone before and after treatment with histidine

Cupric ion and many lots of commercial reagent-grade phenol interact to produce a potent inactivator(s) of the naked RNA from poliovirions; even after redistillation, the purified phenol shows a strong capacity to interact with cupric ion to produce the RNA inactivator(s) (1, 2). This RNA inactivator(s) can be a serious problem when phenol is used for the isolation of RNAs.

However, phenol purified by steam distillation shows no activity, the activity being recoverable from the aqueous residue remaining after the steam distillation (1). The activity of this residue has been shown to be due, at least in part, to hydroquinone and catechol, which occur as impurities in the commercial reagent grade phenol (2, 3). In addition to hydroquinone and catechol, two other phenols have been shown to be active: pyrogallol and orcinol (2). Hydroquinone is the most active of the four phenols (2).

When cupric ion and hydroquinone are mixed together in buffer (pH 7.3) under air, the copper-catalyzed oxidation of the hydroquinone to *p*-benzoquinone starts promptly and proceeds rapidly, and inactivator activity rises in parallel with the rise in *p*-benzoquinone concentration (4). However, as shown by direct tests, *p*-benzoquinone is not the inactivator(s), nor is cuprous ion (4).

In the present report, preparations of inactivator(s) from cupric ion and hydroquinone were examined by HPLC using UV and EC detectors with the aim of detecting additional chemical species which could be candidates for the role of inactivator(s); three such species were found. Because of the effect of L-histidine, an excellent chelator of cupric ion (5), in promptly stopping ongoing inactivation of RNA by the inactivator(s) (1), the effect of L-histidine on the stability of these three species was determined.

EXPERIMENTAL

Chemicals—The following chemicals were used: *p*-benzoquinone, practical grade[1]; cupric chloride, reagent grade[2]; hydroquinone, purified[2]; 85% orthophosphoric acid, reagent grade[3]; potassium dihydrogen phosphate, reagent grade[3]; L-histidine monohydrochloride monohydrate[4]; tetramethylammonium hydroxide pentahydrate[5].

Distilled water was deionized, demineralized, and then double-distilled in glass before use.

The commercial hydroquinone was recrystallized twice from water before use. Solutions of the recrystallized hydroquinone in water were stored frozen under nitrogen.

Preparation of Viral RNA Inactivator(s)—Inactivator preparations were made by incubating cupric chloride at 1.11 m*M* and hydroquinone at 2.22 m*M* in buffer under air at 23° for 5 min (6). The buffer used was 137 m*M* NaCl, 2.69 m*M* KCl, 8.15 m*M* Na_2HPO_4, and 1.46 m*M* KH_2PO_4, pH 7.3. To obtain the UV absorption spectra, the incubation was for 20 instead of 5 min so that higher concentrations of the unknown products I–III would be obtained.

Treatment of Inactivator Preparation with L-Histidine—Solutions of buffer containing L-histidine hydrochloride at 167 m*M* and with the pH adjusted with sodium hydroxide back to 7.3 were prepared. One volume of the buffer with L-histidine, at 23°, was mixed with three volumes of fresh inactivator preparation. Samples were taken immediately and after various periods of incubation at 23°. Controls were done in the same way, except that plain buffer was used instead of buffer with L-histidine.

Treatment of *p*-Benzoquinone with L-Histidine—One volume of the above mentioned buffer with L-histidine, at 23°, was mixed with three volumes of a reference solution of 0.300 m*M* *p*-benzoquinone in buffer with cupric chloride at 1.11 m*M* or without cupric chloride. This reference solution had been preincubated under air at 23° for 5 min, in simulation of the incubation used in preparing the viral RNA inactivator(s). Samples were taken immediately and 15 min after adding the L-histidine. In the controls, plain buffer replaced the buffer with L-histidine.

HPLC—An isocratic HPLC system similar to that previously described was used (7). The fixed-volume injector[6] contained a 20-μl loop. A 250 × 4-mm reverse-phase column packed with Lichrosorb[7] RP-18, 10 μm, with a slurry packing technique was used. A guard column RP-18 MPLC[8] was incorporated into the system. An aqueous mobile phase containing 100 m*M* KH_2PO_4 and 12.5 m*M* tetramethylammonium hydroxide, pH adjusted to 3.9 using 14.7 *M* H_3PO_4, was prepared using the triple-distilled deionized demineralized water. This mobile phase was

[1] Eastman Kodak Co.
[2] Fisher Chemical Co.
[3] Mallinckrodt Chemical Works.
[4] Mann Research Laboratories.
[5] Sigma Chemical Co.
[6] Rheodyne.
[7] E. Merck Laboratories.
[8] Brownlee Laboratories.

0022-3549/83/0300-0300$01.00/0

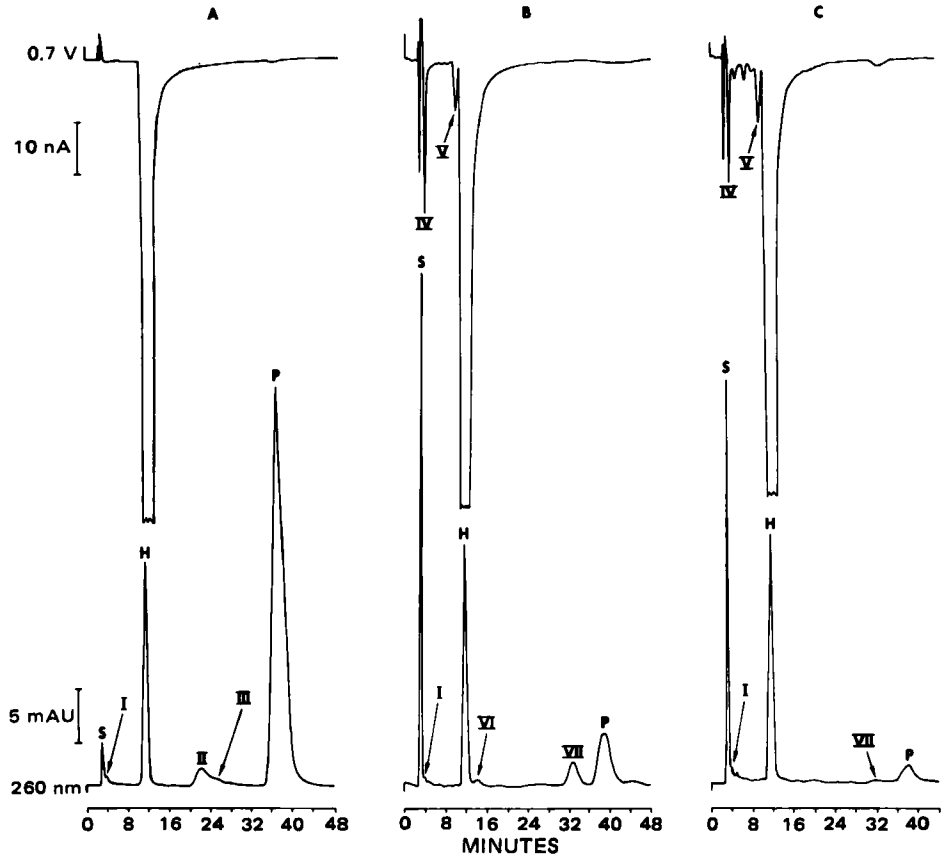

Figure 1—*Chromatograms of RNA inactivator(s) before and after treatment with L-histidine. To one volume of inactivator preparation made using the 5-min incubation was added one-third volume of either plain buffer (control) or buffer with L-histidine (experimental). Key: A, control immediately injected; B, experimental injected 15 min after adding L-histidine; C, experimental injected 3 hr after adding L-histidine. Upper and lower chromatograms: responses of EC and UV (260 nm), respectively. Key: (S) solvent front; (mAU) milliabsorbance unit; (H) hydroquinone; (P) p-benzoquinone; I–III, unknowns in inactivator preparation; IV–VII, unknowns appearing within 15 min after adding L-histidine. Offscale peaks: three H(EC) peaks and the S(UV) peak of panel B.*

filtered through a 0.2-μm porosity membrane filter[9], deaerated under vacuum, and kept at 40° during chromatography. The UV detector was set at 260 nm and 0.05 absorbance units full scale in most experiments. In some experiments, as described, the UV detector was set at wavelengths shorter or longer than 260 nm. The EC detector was set at 0.7 V and 100 nA full scale.

RESULTS

Components of Preparations of RNA Inactivator(s)—HPLC of RNA inactivator preparations made using the 5-min incubation of cupric chloride with hydroquinone showed six peaks (Fig. 1A): the solvent front peak, where cupric ion elutes; hydroquinone; *p*-benzoquinone; and three unidentified products (I–III). At the UV wavelength of 260 nm used for this chromatogram, product III appears as a trailing shoulder on the peak due to product II; but when 230-nm UV was used, II and III were seen as two peaks (Fig. 2). The peak due to component I was also more obvious when 230-nm UV was used (Fig. 2). The peak between component I and hydroquinone (Fig. 2) was due to one of the components, possibly unknown component XI (see below), appearing only after incubation of the cupric chloride and hydroquinone together for more than 5 min. Chromatograms of such inactivator preparations were found to be highly reproducible when the same conditions for production of inactivator(s), for separation, and for detection were used.

Partial UV Absorption Spectra of Components I–III—Partial UV absorption spectra of components I–III were determined from chromatograms of replicate inactivator preparations with the UV detector set at various UV wavelengths from 200 to 320 nm and are shown in Fig. 3.

Components Appearing upon Further Incubation of RNA Inactivator Preparations—In this study, attention was concentrated on components I–III, because of their presence after incubation of cupric ion with hydroquinone for only 5 min, and since previous experiments had shown that the production of RNA inactivator(s) from cupric ion and hydroquinone proceeds rapidly and without lag (4).

When the reaction between cupric chloride and hydroquinone was prolonged beyond 5 min, as in the controls where one-third volume of plain buffer was added at 5 min and the incubation continued at 23°, additional unknown products appeared. This result was shown by tests of samples that were taken after additional incubation periods of 5, 15, 30, 60, 180, and 420 min and analyzed by HPLC using both detectors with the UV detector set at 260 nm. These chromatograms showed seven additional unknown products (VIII–XIV) with retention times of <1 hr. Referred to by the earliest time of their appearance in min after starting the additional incubation, by the detector(s) *sensitive to them and by* their retention times in minutes and seconds, these seven products were: VIII, 5UV and EC5:45; IX, 5UV and EC17:15; X, 15UV4:45; XI, 15UV8:05; XII, 60EC4:15; XIII, 180UV14:15; XIV, 420UV41:35.

Effects of Histidine—The addition of L-histidine to inactivator preparations resulted in the rapid loss of components II and III but not of component I (Figs. 1 and 4). The synthesis of additional component I was, however, greatly diminished by L-histidine. The addition of L-histidine had other effects, which may be grouped in two sets.

The first set consists of effects that are connected or probably connected with the capacity of L-histidine to chelate cupric ion. One such effect was the very rapid formation of chelate complex(es) of cupric ion and L- histidine (8) (Fig. 1B); the offscale UV-absorbing peak at the solvent front (*S*) was due mainly to such complex(es), as shown by control chromatograms of L-histidine and cupric chloride chromatographed individually and after being mixed together. Another effect was the virtually immediate cessation of the oxidation of hydroquinone. A third effect was the blocking of the production of VIII, IX, XI, XIII, and XIV. Production of X was not blocked. Whether production of XII was blocked was not ascertained, due to interference from new compounds appearing after adding L-histidine (Fig. 1 and below).

The second set of effects of L-histidine consists of those which were

[9] Millipore.

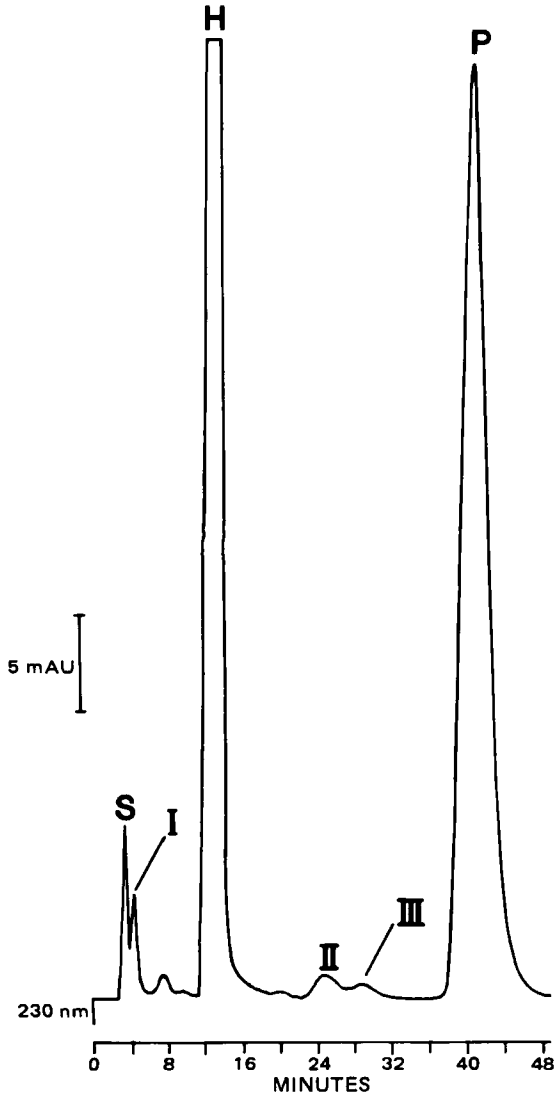

Figure 2—*Chromatogram of RNA inactivator prepared using 20-min incubation. Symbols as in Fig. 1.*

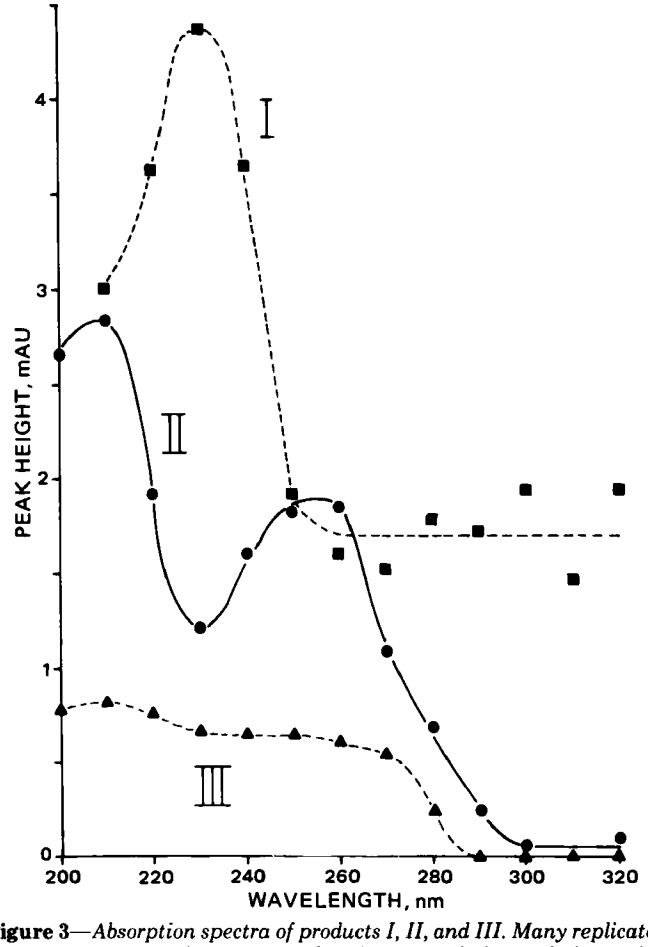

Figure 3—*Absorption spectra of products I, II, and III. Many replicate inactivator preparations were made using a 20-min instead of a 5-min incubation, the addition of plain buffer, and immediate sampling for analysis by HPLC using the UV detector, which was set at 200, 200, 220, 230, 240, 250, 260, 270, 280, 290, 300, 310, and 320 nm, respectively, for the replicate preparations. For each chromatogram, peak heights in milliabsorbance units (mAU) for unknown components I–III were estimated. The point for component I at 200 nm was missed due to interference from the offscale solvent front.*

found to be independent of the capacity of L-histidine to chelate cupric ion. These effects were (*d*) the rapid loss of *p*-benzoquinone (Figs. 1 and 4), (*e*) the increase in hydroquinone (Figs. 1 and 4), and (*f*) the appearance of a cascade of new compounds including IV–VII (Figs. 1 and 5).

Evidence of the cascade of new compounds was seen soon after the addition of L-histidine. Within 15 min after this addition, four new components, IV–VII, appeared. Components IV and V were detected by the EC detector and VI and VII by the UV detector (Fig. 1B). The kinetics of production of IV–VII and the kinetics of the later decrease or disappearance of IV, VI, and VII are shown in Fig. 5. These four components did not appear in the controls not containing L-histidine. At times > 15 min after adding L-histidine, additional new compounds appeared which did not appear in the corresponding controls that had received only plain buffer. At least four of these additional compounds are shown in Fig. 1C, where the inactivator preparation had been incubated for 3 hr after adding the L-histidine. Such chromatograms are highly reproducible. To avoid cluttering the figure, these additional unknown compounds have not been numbered.

That the above effects (*d*), (*e*), and (*f*) are independent of copper was shown by tests of the effect of L-histidine on *p*-benzoquinone with and without cupric ion. Buffer with L-histidine, or plain buffer for the controls, was added to solutions of commercial *p*-benzoquinone in buffer with and without cupric chloride; and the mixtures were analyzed either immediately or after 15 min at 23°. The chromatograms showed that L-histidine, with or without copper, caused a rapid decrease in the concentration of *p*-benzoquinone. In two experiments, after 15 min only 14 and 9.3% of the starting *p*-benzoquinone remained when cupric chloride was not added; when cupric chloride was added the corresponding figures were 17 and 21%. In the controls where plain buffer was added, there was no significant change in the concentration of *p*-benzoquinone in 15 min with or without cupric chloride. In the commercial *p*-benzoquinone used there was a very small amount of hydroquinone, detectable by the EC detector. In 15 min after adding L-histidine, the amount of hydroquinone increased five- to eightfold with or without cupric chloride. In the controls where plain buffer was added, there was no significant change in the concentration of hydroquinone in 15 min without cupric chloride; but with cupric chloride there was, as expected, a marked reduction in the concentration of hydroquinone after 15 min, due to cupric ion-catalyzed oxidation. The chromatograms of samples taken 15 min after the addition of L-histidine to the *p*-benzoquinone with and without cupric chloride showed peaks virtually identical to unknown components IV–VII both in retention time and in detector response ratios of the UV and EC detectors.

These experiments show that L-histidine reacts with *p*-benzoquinone, that direct or indirect products of the reaction are hydroquinone and unknown components IV–VII, and that copper is not necessary for this reaction or for the production of these five products. These effects of the reaction between L-histidine and *p*-benzoquinone can account for the above-described effects (*d*), (*e*), and (*f*).

DISCUSSION

The most significant aspects of this work are that components other than hydroquinone and *p*-benzoquinone were sufficiently stable to be detected by HPLC in preparations of RNA inactivator(s) and that two of these components, II and III, were unstable in the presence of L-histidine. This instability casts II and III as candidates for the role of inac-

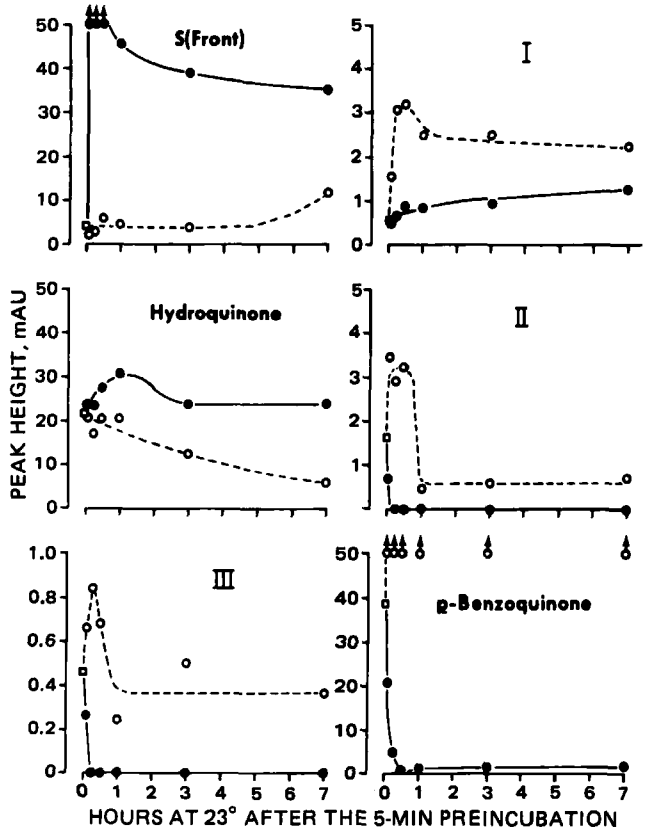

Figure 4—*Effect of L-histidine on six UV-absorbing peaks from inactivator preparation. The inactivator preparation was made and the control and experimental additions were made as in Fig. 1. A sample of the control was immediately injected for analysis by HPLC, using the same chromatographic conditions as in Fig. 1. Incubation of control and experimental continued at 23°, under air, and samples taken at the various times shown were analyzed by HPLC. Key: mAU, milliabsorbance unit; S, peak at solvent front; I–III, three unknown components shown in Fig. 1A. (□) immediate sampling of buffer control; (○) incubated buffer control; (●) incubated histidine experimental. The arrows indicate offscale peaks.*

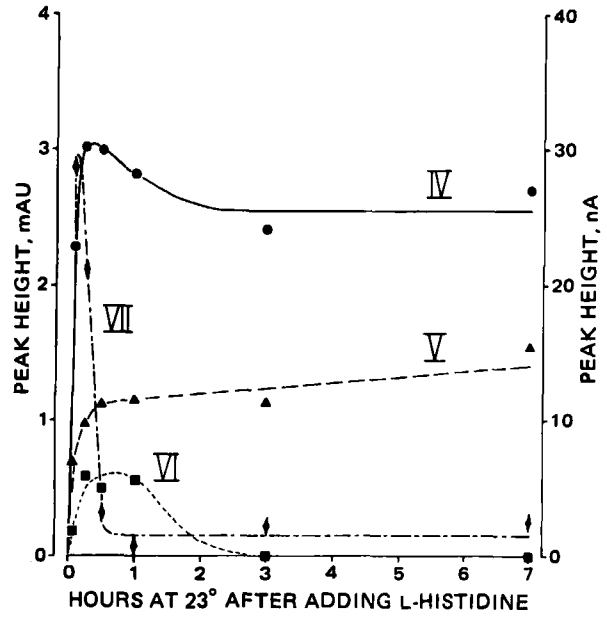

Figure 5—*Kinetics of appearance and disappearance of unknown components IV–VII after addition of L-histidine. Inactivator preparations were made and L-histidine then added, as in experimentals of Fig. 1B and C. Samples were analyzed by HPLC 5, 15, 30, 60, 180, and 420 min later. Components IV and V were analyzed by EC detector, VI and VII by UV detector, as in Fig. 1. mAU, milliabsorbance unit.*

tivator(s). What connection, if any, components II and III may have with the free radical species at the one-electron oxidation step, namely, *p*-benzosemiquinone and its anion as well as the complex of this anion with cupric ion (9), is presently unknown.

Another important aspect of the work is that it shows the multiplicity of the effects of L-histidine on RNA inactivator preparations. It appears that most or all of these effects can be attributed to just two properties of L-histidine: its capacities to chelate cupric ion and to react with *p*-benzoquinone.

For more than a century, various amines have been known to react with *p*-benzoquinone (10). The reaction leads successively to several products. For example, reaction with an aromatic amine may yield 2-arylaminohydroquinone, 2,5-diarylaminohydroquinone, and from these products the corresponding quinones through oxidation by remaining *p*-benzoquinone; moreover, this oxidation would in turn also yield hydroquinone. If the reacting amine were L-histidine, the substituent on the hydroquinone and on the quinone would be relatively polar, and the substituted compounds would be expected to show shorter retention times in the HPLC system used here than the corresponding unsubstituted compounds. Also, it would be expected that the substituted quinones would be detectable by the UV detector at 260 nm but probably not detectable by the EC detector as used here, whereas the substituted hydroquinones would probably be more readily detected by the EC detector. Thus, such a series of reactions could explain several of the observations regarding the reaction between *p*-benzoquinone and L-histidine, namely: (*a*) the rapid production of four unknown components (IV–VII), (*b*) that two of these were detected by EC, whereas the other two were detected by UV, (*c*) the retention times of IV–VII relative to the retention times of hydroquinone and *p*-benzoquinone, and (*d*) the increase in hydroquinone.

REFERENCES

(1) G. R. Dubes, R. J. Wegrzyn, and A. N. Masoud, *Arch. Virol.*, **66**, 27 (1980).

(2) G. R. Dubes and A. N. Masoud, *Biochim. Biophys. Acta*, **653**, 219 (1981).

(3) A. N. Masoud and G. R. Dubes, *J. High Resolution Chromat. Chromat. Commun.*, **3**, 133 (1980).

(4) G. R. Dubes and A. N. Masoud, "Abstracts," 18th Annual Meeting of the American Society for Microbiology, American Society of Microbiology, Washington, D.C., 1980, p. 263.

(5) L. E. Maley and D. P. Mellor, *Nature (London)*, **165**, 453 (1950).

(6) A. N. Masoud, M. I. Al-Moslih, and G. R. Dubes, *J. Environ. Pathol. Toxicol. Oncol.*, in press.

(7) M. I. Al-Moslih, G. R. Dubes, and A. N. Masoud, *J. High Resolution Chromat. Chromat. Commun.*, **4**, 173 (1981).

(8) J. L. Meyer and J. E. Bauman, Jr., *J. Am. Chem. Soc.*, **92**, 4210 (1970).

(9) I. V. Khudyakov, V. A. Kuzmin, and N. M. Emanuel, *Internat. J. Chem. Kinet.*, **10**, 1005 (1978).

(10) W. J. Hickinbottom, "Reactions of Organic Compounds," 2nd ed., Longmans Green, London, 1948, pp. 214–219.

ACKNOWLEDGMENTS

The authors thank the late Professor Rainer Fried for discussions of some of the results and Mrs. Liselotte Karnish and Mrs. Dorothy Burgin for typing the manuscript.

Synthesis and Action on the Central Nervous System of Mescaline Analogues Containing Piperazine or Homopiperazine Rings

MICHAŁ W. MAJCHRZAK *x, ANTONI KOTEŁKO *, ROMAN GURYN *, JOSEPH B. LAMBERT ‡, ANNA SZADOWSKA §, and KAZIMIERZ KOWALCZYK §

Received December 29, 1981, from the **Medical Academy, Department of Drug Technology, Narutowicza 120a, 90145 Łódź, Poland,* the ‡*Department of Chemistry, Northwestern University, Evanston, IL 60201,* and the §*Medical Academy, Department of Pharmacodynamics, Narutowicza 120a, 90145 Łódź, Poland.* Accepted for publication March 29, 1982.

Abstract □ Structural juxtaposition of the 3,4,5-trimethoxyphenyl group in the same molecule with a piperazine or homopiperazine ring has been realized in a series of mescaline analogues (I–IV) as part of an investigation into the pharmacological properties of the seven-membered perhydro-1,4-diazepines (homopiperazines). The analogous six-membered piperazines were synthesized and tested as reference substances to determine whether the seven-membered ring conveyed special properties. A variety of pharmacological tests of action on the CNS showed that replacement of the amino group in mescaline by the heterocycles significantly alters the biological activity. In particular, both the piperazine and the homopiperazine derivatives displayed sedative activity to about the same extent.

Keyphrases □ Mescaline analogues—synthesis and action on the CNS, containing piperazine or homopiperazine rings □ CNS agents—synthesis and action of mescaline analogues containing piperazine or homopiperazine rings □ Piperazine rings—mescaline analogues, synthesis and action on the CNS □ Homopiperazine rings—mescaline analogues, synthesis and action on the CNS

The 3,4,5-trimethoxyphenyl moiety attached to an amino nitrogen through a two- or three-carbon bridge is well known as a pharmacophoric group in drugs that possess sedative, hypotensive, antiarrhythmic, and vasodilating properties (1). Furthermore, there are numerous commercial drugs containing the piperazine ring, and a few with the perhydro-1,4-diazepine (homopiperazine) ring. At least two drugs contain both the homopiperazine ring and the trimethoxyphenyl group: 1-methyl-4-(3,4,5-trimethoxybenzoyloxy)methylhomopiperazine, an antihypertensive agent, and 1,4-bis[3-(3,4,5-trimethoxybenzoyloxy)propyl]homopiperazine (dilazep), a coronary vasodilator.

Mescaline, 2-(3,4,5-trimethoxyphenyl)ethylamine [3,4,5-$(CH_3O)_3C_6H_2CH_2CH_2NH_2$], a simple trimethoxyphenyl derivative, has been known as an hallucinogen and an agent on the CNS. The present study explored the biological effects on the CNS of a molecule that closely juxtaposes the trimethoxyphenyl group with the homopiperazine ring. This arrangement was obtained by replacing the amino group in mescaline with the homopiperazine ring. The piperazine analogue also was examined for comparison. These lines of inquiry were suggested by earlier investigations on the conformational (2, 3) and pharmacological (4) properties of homopiperazines.

DISCUSSION

The synthetic objective was attachment of the heterocycles, piperazine or homopiperazine, through a bismethylene fragment to the trimethoxyphenyl group. One approach attached the heterocycle to the bismethylene carbon through one nitrogen, and the second nitrogen carried a methyl group (compounds I and II, respectively). In another approach, both nitrogens of the heterocycles were supplied with the trimethoxyphenyl substrate (compounds III and IV, respectively). The synthesis of these four molecules began with 3,4,5-trimethoxyphenylacetic acid [3,4,5-$(CH_3O)_3C_6H_2CH_2CO_2H$].

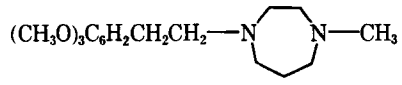

I

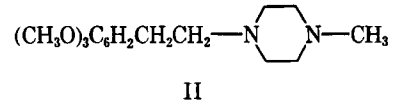

II

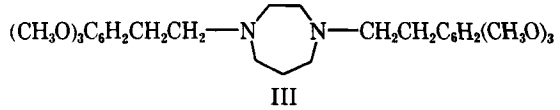

III

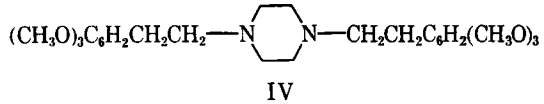

IV

Reduction of the corresponding methyl ester and treatment with thionyl chloride produced the chloride, 3,4,5-$(CH_3O)_3C_6H_2CH_2CH_2Cl$, which was allowed to react with the cyclic amines to give the four desired compounds, 1-methyl-4-[2-(3,4,5-trimethoxyphenyl)ethyl]perhydro-1,4-diazepine (I); 1-methyl-4-[2-(3,4,5-trimethoxyphenyl)ethyl]piperazine (II); 1,4-bis[2-(3,4,5-trimethoxyphenyl)ethyl]perhydro-1,4-diazepine (III); and 1,4-bis[2-(3,4,5-trimethoxyphenyl)ethyl]piperazine (IV). Alternatively, the ester, 3,4,5-$(CH_3O)_3C_6H_2CH_2CO_2CH_3$, was converted through the acid chloride to the amide containing the heterocycle, and the amide was reduced to the desired product. The structures of all products were confirmed by spectral and elemental analysis.

The four compounds were used in nine separate tests of pharmacological activity. In several tests, the dose level as a ratio of the LD_{50} was varied. No differences were found between the control group, which received doses of 0.9% NaCl, and the groups that received doses of compounds I–IV, for the following properties: body temperature, behavioral despair, central action of 3-(3,4-dihydroxyphenyl)-L-alanine (levodopa), apomorphine-induced stereotypy, or convulsant action of pentylenetetrazol. None of the compounds eliminated the aggressiveness of isolated mice. Quantitative data for apomorphine behavior are given in Table I. Other negative results are omitted. Thus, these compounds do not exhibit activity typical of tranquilizers.

Positive, dose-related results for three other tests are listed in Table I. All four tested compounds prolonged sleeping time and inhibited locomotor activity in mice. Reduction in amphetamine-induced locomotor stimulation was observed in mice for all four compounds, but the results are significant at the 95% level only for I and II, which contain a single

0022-3549/83/0300-0304$01.00/0

Table I—Pharmacological Results on Heterocyclic Analogues of Mescaline

Compound	LD_{50}, mg/kg ip	Dose, Ratio of LD_{50}	Spontaneous Locomotor Activity, Count/30 min (n = 10)	Amphetamine Hyperactivity, Counts/30 min (n = 10)	Hexobarbital Sleeping Time, min (n = 10)	Apomorphine Behavior Mean Scores (n = 6)	
						Excitation	Stereotyped Behavior
0.9% NaCl[a]			185 ± 20.1[b]	418 ± 55	18.1 ± 1.4	4.0 ± 0.85	7.6 ± 1.3
I	685 ± 170[b]	0.1	120 ± 13.3[c]	236 ± 40[c]	33.7 ± 2.2[e]	4.0 ± 0.75	7.5 ± 1.8
		0.05	175 ± 19.7	421 ± 52	23.0 ± 2.5		
II	660 ± 172	0.1	115 ± 19.0[c]	251 ± 38[c]	41.4 ± 4.0[e]	4.2 ± 0.92	6.8 ± 2.4
		0.05	181 ± 23.2	385 ± 48	28.6 ± 3.0[d]		
		0.025			17.2 ± 1.6		
III	330 ± 87	0.1	112 ± 17.0[c]	310 ± 54	38.4 ± 2.1[e]	4.3 ± 0.72	7.7 ± 2.1
		0.05	195 ± 22.3	405 ± 48	28.4 ± 3.2[d]		
		0.025			21.7 ± 2.3		
IV	305 ± 65	0.1	115 ± 20.0[c]	286 ± 40	36.5 ± 1.6[e]	4.4 ± 0.81	7.4 ± 2.2
		0.05	184 ± 22.4	398 ± 47	26.8 ± 2.9[d]		
		0.025			19.0 ± 2.0		

[a] Control group. [b] Standard error of the mean. [c] A significant difference from the control at the 95% confidence level. [d] A significant difference from the control group at the 99% confidence level. [e] A significant difference from the control at the 99.9% confidence level.

trimethoxyphenyl residue. Thus, the results of these tests indicate that I–IV exhibit sedative activity.

The presence of the piperazine or homopiperazine ring in place of the simple amino group in mescaline significantly alters the effect of the compound on the CNS. Within this group of compounds, there was little difference in sedative activity between the six- and seven-membered rings. Previously tested (5) homopiperazine-containing compounds, which were esters or amides of *p*-chlorobenzoic acids, did not exhibit a depressive effect on the CNS. Consequently, the sedative activity of I–IV is caused at least in part by the presence of the 3,4,5-trimethoxyphenylethyl moiety. Since neither mescaline nor *N,N*-dimethylmescaline (6) exhibits this behavior, it was concluded that the sedative activity requires both the trimethoxyphenyl group and the cyclic, tertiary amine.

EXPERIMENTAL

Chemistry—Melting points (uncorrected) were determined in open glass capillaries[1]. IR spectra were obtained on a scanning spectrophotometer[2], either as a neat thin film or as potassium bromide disks. NMR spectra were recorded[3] with respect to tetramethylsilane. Mass spectra[4] were obtained by direct injection. Microanalysis[5] for carbon, hydrogen, and nitrogen were within 0.4% of calculated values. Piperazine, 1-methylpiperazine, homopiperazine, and 3,4,5-trimethoxyphenylacetic acid were commercially available[6]. 1-Methylhomopiperazine was prepared according to the literature (7).

2-(3,4,5-Trimethoxyphenyl)ethanol—Trimethoxyphenylacetic acid[6] was converted to its ester, which was reduced according to a previous method (8), with a change in the ratio of lithium aluminum hydride to 1.5 moles/mole of the methyl-3,4,5-trimethoxyphenylacetate: 76% yield, bp 160–164°/0.8 mm Hg.

Anal.—Calc. for $C_{11}H_{16}O_4$: C, 62.25; H, 7.60. Found: C, 62.02; H, 7.55.

1-Chloro-2-(3,4,5-trimethoxyphenyl)ethane — 1-Chloro-2-(3,4,5-trimethoxyphenyl)ethane was prepared by treatment of the alcohol with thionyl chloride in pyridine (8): 74% yield, bp 158–160°/0.8 mm Hg.

Anal.—Calc. for $C_{11}H_{15}ClO_3$: C, 57.27; H, 6.55. Found: C, 57.01; H, 6.48.

3,4,5-Trimethoxyphenylacetyl Chloride — 3,4,5-Trimethoxyphenylacetic acid[6] (17.8 g, 0.15 mole) was added to a benzene solution (100 ml) of thionyl chloride (22.6 g, 0.1 mole). The reaction mixture was heated to reflux until evolution of sulfur dioxide ceased. Benzene and excess thionyl chloride were removed by rotary evaporation, and the residue was distilled to give 16.2 g (72.3%) of the product: bp 154–156°/1 mm Hg, mp 96–98° (from petroleum ether).

Anal.—Calc. for $C_{11}H_{13}ClO_4$: C, 53.99; H, 5.35. Found: C, 53.55; H, 5.25.

1-Methyl-4-(3,4,5-trimethoxyphenylacetyl)perhydro-1,4-diazepine—The acid chloride (4 g, 0.016 mole) was added dropwise with boiling to a benzene solution (50 ml) of 1-methylhomopiperazine (1.82 g, 0.016 mole) and sodium carbonate (2.1 g, 0.02 mole). Stirring and heating were continued for 3 hr, and the hot reaction mixture was filtered from the inorganic salts. The solvent was removed by rotary evaporation, and the residue was recrystallized from diethyl ether–benzene: 2.6 g, 50% yield, mp 111–114°; NMR (chloroform-*d*) δ 1.85 (m, 2H, CCH_2C), 2.29 (s, 3H, NCH_3), 2.50 (m, 4H, $RNCH_2$), 3.58 (m, 6H, $CONCH_2$), 3.82 (s, 9H, OCH_3), and 6.5 (s, 2H, aromatic); IR (KBr) 3050, 1670, and 1620 cm^{-1}.

Anal.—Calc. for $C_{17}H_{26}N_2O_4$: C, 63.33; H, 8.13; N, 8.69. Found: C, 63.20; H, 8.21; N, 8.90.

1-Methyl-4-[2-(3,4,5-trimethoxyphenyl)ethyl]perhydro-1,4-diazepine (I)—In a dropwise fashion, 1-chloro-2-(3,4,5-trimethoxyphenyl)ethane (10 g, 0.04 mole) in 75 ml of a 1:1 solution of toluene–dimethylformamide was added to a refluxing solution of toluene (75 ml) and dimethylformamide (75 ml) containing 1-methylhomopiperazine (4.5 g, 0.04 mole) and anhydrous potassium carbonate (11.04 g, 0.08 mole). Stirring and heating were continued for 14 hr. The inorganic salts were filtered, and the solvents were removed by rotary evaporation. The residue was distilled to give 6.5 g (52.7%) of the product: bp 175–190°/0.2 mm Hg, n_D^{20} 1.5365; NMR (chloroform-*d*): δ 1.85 (m, 2H, CCH_2C), 2.42 (s, 3H, NCH_3), 2.77 (m, 12H, CH_2), 3.88 (s, 9H, OCH_3), 6.47 (s, 2H, aromatic); IR (film) 3050, 1620, and 1520 cm^{-1}.

The dihydrochloride was prepared by acidification of I in absolute diethyl ether with an ether solution of anhydrous hydrogen chloride: mp 240–241°.

Anal.—Calc. for $C_{17}H_{30}Cl_2N_2O_3$: C, 53.54; H, 7.93; N, 7.35. Found: C, 53.23; H, 7.67; N, 7.20.

Reduction of 1-methyl-4-(3,4,5-trimethoxyphenylacetyl)perhydro-1,4-diazepine with lithium aluminum hydride in tetrahydrofuran afforded I (45%) that was identical chemically and spectroscopically to the material obtained above.

1-Methyl-4-[2-(3,4,5-trimethoxyphenyl)ethyl]piperazine (II)—Treatment of 1-chloro-2-(3,4,5-trimethoxyphenyl)ethane with piperazine[6] in a manner analogous to the preparation of I produced II: 6.3 g, 53.5% yield, bp 174–184°/0.2 mm Hg, n_D^{20} 1.5335; NMR (chloroform-*d*): δ 2.38 (m, 15H, CH_3/CH_2), 3.79 (s, 9H, OCH_3), and 6.38 (s, 2H, aromatic); IR (film) 3050, 1620, 1510, and 1150 cm^{-1}. The dihydrochloride was prepared as described for I, mp 257–258° dec.

Anal.—Calc. for $C_{16}H_{28}Cl_2N_2O_3$: C, 52.32; H, 7.68; N, 7.63. Found: C, 52.01; H, 7.61; N, 7.45.

1,4-Bis[2-(3,4,5-trimethoxyphenyl)ethyl]perhydro-1,4-diazepine (III)—To a refluxing solution of toluene (75 ml) and dimethylformamide (75 ml) containing homopiperazine[6] (1.5 g, 0.015 mole) and anhydrous potassium carbonate (8.26 g, 0.06 mole) was added 1-chloro-2-(3,4,5-trimethoxyphenyl)ethane (7.0 g, 0.03 mole) in 50 ml of 1:1 toluene–dimethylformamide, in a dropwise fashion. Stirring and heating were continued for 14 hr. The inorganic salts were filtered, and the solvents were removed by rotary evaporation. The thick, oily residue (7 g, 95% yield) appeared by spectroscopy to be pure but failed to crystallize. It was purified as the hydrochloride, which was prepared as described for I: 6 g, 75% yield, mp 198–200° (absolute methanol–diethyl ether); NMR (chloroform-*d*): δ 1.80 (m, 2H, CCH_2C), 2.68 (m, 16H, CH_2), 3.71 (s, 18H, OCH_3), and 6.32 (s, 4H, aromatic); IR (film of crude product) 3050, 1600, 1510, and 1130 cm^{-1}.

Anal.—Calc. for $C_{27}H_{42}Cl_2O_6N_2$: C, 57.75; H, 7.54; N, 4.99. Found: C, 57.55; H, 7.34; N, 4.57.

[1] Electrothermal Ltd., Deer Park, N.Y.
[2] Unicam SP 200G, England.
[3] Varian EM-360 Spectrometer, Varian Associates, Palo Alto, Calif.
[4] LKB 2091, LKB Instruments, Rockville, Md.
[5] Medical Academy, Łódź, Poland.
[6] Aldrich Chemical Co., Milwaukee, Wis.

1,4-Bis[2-(3,4,5-trimethoxyphenyl)ethyl]piperazine (IV)—Compound IV was prepared in the same manner as described for III, but with piperazine[6]. After evaporation of the solvents, the residue crystallized from 1:1 diethyl ether–petroleum ether: 2.3 g, 32% yield, mp 120–122°; NMR (chloroform-*d*): δ 2.65 (s, 16H, CH_2), 3.87 (s, 18H, OCH_3), and 6.41 (s, 4H, aromatic). IR (KBr) 3040, 1620, 1500, and 1160 cm^{-1}. The dihydrochloride was prepared as described for I: mp 259–260° dec.

Anal.—Calc. for $C_{26}H_{40}O_6N_2Cl_2$: C, 57.03; H, 7.36; N, 5.12. Found: C, 56.85; H, 7.23; N, 5.01.

Pharmacology—The experiments were performed on male Swiss white mice (18–26 g) and male Wistar rats (150–180 g). The investigated compounds were administered intraperitoneially in aqueous solutions.

The LD_{50} values were determined by a previous method (9).

The effect of I–IV on locomotor activity in normal and amphetamine-treated mice was recorded throughout 30-min sessions in photoresistant cages. The investigated compounds (administered intraperitoneally) and amphetamine (5 mg/kg sec) were administered 60 and 30 min, respectively, before testing.

The effect on the apomorphine-induced stereotypy was investigated in rats. Apomorphine (1.25 mg/kg sec) was injected 60 min after the tested compounds.

For the effect on sleeping time in mice, hexobarbital (70 mg/kg ip) was injected 60 min after the test compounds.

Anticonvulsant activity was investigated by the minimal and maximal pentylenetetrazol shock (pentylenetetrazol, 80 and 50 mg/kg sc, respectively). The number of animals protected against clonic convulsions in minimal shock or tonic extensions of limbs in maximal shock was registered.

The effect on behavioral despair in mice was examined by a previous method (10). The compounds were injected 60 min before examination.

The effect on the central action of 3-(3,4-dihydroxyphenyl)-L-alanine (levodopa) was tested on mice by modifications of a previous method (11). The alanine (100 mg/kg) was injected 4 hr after pargyline (40 mg/kg po) and 1 hr after the investigated compounds.

The effect on the aggressiveness of isolated (3 weeks) mice was examined by a previous method (12). Behavior was tested at 1-hr intervals for 4 hr.

Rectal body temperature in mice was measured with a thermometer for 3 hr after administration of the test compounds.

REFERENCES

(1) M. Negwer, "Organic-Chemical Drugs and Their Synonyms," Akademie-Verlag, Berlin, 1978.

(2) M. Majchrzak, A. Kotełko, and R. Guryn, *Pol. J. Chem.*, **53**, 2135 (1979).

(3) M. W. Majchrzak, A. Kotełko, R. Guryn, J. B. Lambert, and S. M. Wharry, *Tetrahedron*, **37**, 1075 (1981).

(4) R. Guryn, A. Kotełko, M. Majchrzak, A. Szadowska, and I. Wejman, *Acta Pol. Pharm.*, **37**, 53 (1980).

(5) A. Szadowska, M. Mazur, J. Graczyk, M. B. Kiełek, R. Guryn, H. Mikolajewska, R. Glinka, and B. Kotełko, *ibid.*, in press.

(6) J. R. Smythies and E. A. Sykes, *Psychopharmacol.*, **8**, 324 (1966); J. R. Smythies, E. A. Sykes, and C. P. Lord, *ibid.*, **9**, 434 (1966).

(7) R. Guryn, A. Kotełko, and M. Majchrzak, *ibid.*, **32**, 421 (1975).

(8) R. T. Major and K. W. Ohly, *J. Med. Pharm. Chem.*, **4**, 51 (1961).

(9) J. T. Litchfield, Jr., and F. Wilcoxon, *J. Pharmacol. Exp. Ther.*, **96**, 99 (1949).

(10) R. D. Porsolt, A. Bertin, and M. Jalfre, *Arch. Int. Pharmacodyn. Ther.*, **229**, 327 (1977).

(11) G. M. Everett, F. Will, and A. Evans, *Fed. Proc. Fed. Am. Soc. Exp. Biol.*, **23**, 198 (1968).

(12) H. D. Y. Yen, R. L. Stanger, and N. Millman, *J. Pharmacol. Exp. Ther.*, **122**, 85A (1958).

ACKNOWLEDGMENTS

This work was supported by the National Institutes of Health (Grant R01 GM26124) and by the Polish Academy of Sciences (Problem I.12).

Phenytoin I: *In Vitro–In Vivo* Correlation for 100-mg Phenytoin Sodium Capsules

VINOD P. SHAH ˣ, VADLAMANI K. PRASAD, TREVA ALSTON, BERNARD E. CABANA, RICHARD P. GURAL *, and MARVIN C. MEYER ‡

Received March 9, 1981, from the *Division of Biopharmaceutics, Food and Drug Administration, Washington, DC 20204*, and the **School of Pharmacy, University of Tennessee, Memphis, TN 37916.* Accepted for publication April 6, 1982. ‡Present Address: Clinical Drug Metabolism, Schering Corp., Bloomsfield, NJ 07003.

Abstract □ *Dissolution profiles for 11 brands of phenytoin sodium capsules were carried out by the basket and paddle methods (USP) and the spin-filter method. The results from the dissolution studies have been correlated with observed differences in in vivo parameters (C_{max} and t_{max}). The dissolution by the basket method at 50 rpm in water gave a correlation >0.9. The results suggest the existence of two types of phenytoin sodium products on the market.*

Keyphrases □ Phenytoin—*in vitro–in vivo* correlation for sodium phenytoin capsules, dissolution □ Dissolution—*in vitro–in vivo* correlation for sodium phenytoin capsules □ *In vitro–in vivo* correlation—sodium phenytoin capsules, dissolution

Increasing evidence has been presented in the scientific literature which show correlations between the *in vivo* performance of formulations and their *in vitro* dissolution behavior (1–3). To obtain an *in vitro–in vivo* correlation for any product, two criteria are essential: (*a*) the differences in *in vivo* parameters such as *AUC*, t_{max}, C_{max}, or C_p at a time among different lots tested and (*b*) differences in the *in vitro* dissolution rates of the same products. In cases where differences are observed in *in vivo* behavior, the *in vitro* parameter can be altered to optimize the correlation with *in vivo* data. This is achieved by varying such parameters as dissolution methodology, dissolution medium, rate of agitation, *etc.* In many instances, it has been possible to obtain correlations with *in vivo* data where a discriminating and reproducible *in vitro* test is employed (1–3). *In vitro–in vivo* correlations can generally be achieved with any reproducible method provided the proper selection of medium and the degree of agitation are made so as to permit discrimination among drug products. The key elements are reproducibility of the method, proper choice of medium, and degree of agitation.

Phenytoin is a commonly used anticonvulsant drug and has been classified as a drug with high risk potential with

0022-3549/83/0300-0306$01.00/0

1,4-Bis[2-(3,4,5-trimethoxyphenyl)ethyl]piperazine (IV)—Compound IV was prepared in the same manner as described for III, but with piperazine[6]. After evaporation of the solvents, the residue crystallized from 1:1 diethyl ether–petroleum ether: 2.3 g, 32% yield, mp 120–122°; NMR (chloroform-*d*): δ 2.65 (s, 16H, CH_2), 3.87 (s, 18H, OCH_3), and 6.41 (s, 4H, aromatic). IR (KBr) 3040, 1620, 1500, and 1160 cm^{-1}. The dihydrochloride was prepared as described for I: mp 259–260° dec.

Anal.—Calc. for $C_{26}H_{40}O_6N_2Cl_2$: C, 57.03; H, 7.36; N, 5.12. Found: C, 56.85; H, 7.23; N, 5.01.

Pharmacology—The experiments were performed on male Swiss white mice (18–26 g) and male Wistar rats (150–180 g). The investigated compounds were administered intraperitoneially in aqueous solutions.

The LD_{50} values were determined by a previous method (9).

The effect of I–IV on locomotor activity in normal and amphetamine-treated mice was recorded throughout 30-min sessions in photoresistant cages. The investigated compounds (administered intraperitoneally) and amphetamine (5 mg/kg sec) were administered 60 and 30 min, respectively, before testing.

The effect on the apomorphine-induced stereotypy was investigated in rats. Apomorphine (1.25 mg/kg sec) was injected 60 min after the tested compounds.

For the effect on sleeping time in mice, hexobarbital (70 mg/kg ip) was injected 60 min after the test compounds.

Anticonvulsant activity was investigated by the minimal and maximal pentylenetetrazol shock (pentylenetetrazol, 80 and 50 mg/kg sc, respectively). The number of animals protected against clonic convulsions in minimal shock or tonic extensions of limbs in maximal shock was registered.

The effect on behavioral despair in mice was examined by a previous method (10). The compounds were injected 60 min before examination.

The effect on the central action of 3-(3,4-dihydroxyphenyl)-L-alanine (levodopa) was tested on mice by modifications of a previous method (11). The alanine (100 mg/kg) was injected 4 hr after pargyline (40 mg/kg po) and 1 hr after the investigated compounds.

The effect on the aggressiveness of isolated (3 weeks) mice was examined by a previous method (12). Behavior was tested at 1-hr intervals for 4 hr.

Rectal body temperature in mice was measured with a thermometer for 3 hr after administration of the test compounds.

REFERENCES

(1) M. Negwer, "Organic-Chemical Drugs and Their Synonyms," Akademie-Verlag, Berlin, 1978.

(2) M. Majchrzak, A. Kotełko, and R. Guryn, *Pol. J. Chem.*, **53**, 2135 (1979).

(3) M. W. Majchrzak, A. Kotełko, R. Guryn, J. B. Lambert, and S. M. Wharry, *Tetrahedron*, **37**, 1075 (1981).

(4) R. Guryn, A. Kotełko, M. Majchrzak, A. Szadowska, and I. Wejman, *Acta Pol. Pharm.*, **37**, 53 (1980).

(5) A. Szadowska, M. Mazur, J. Graczyk, M. B. Kiełek, R. Guryn, H. Mikolajewska, R. Glinka, and B. Kotełko, *ibid.*, in press.

(6) J. R. Smythies and E. A. Sykes, *Psychopharmacol.*, **8**, 324 (1966); J. R. Smythies, E. A. Sykes, and C. P. Lord, *ibid.*, **9**, 434 (1966).

(7) R. Guryn, A. Kotełko, and M. Majchrzak, *ibid.*, **32**, 421 (1975).

(8) R. T. Major and K. W. Ohly, *J. Med. Pharm. Chem.*, **4**, 51 (1961).

(9) J. T. Litchfield, Jr., and F. Wilcoxon, *J. Pharmacol. Exp. Ther.*, **96**, 99 (1949).

(10) R. D. Porsolt, A. Bertin, and M. Jalfre, *Arch. Int. Pharmacodyn. Ther.*, **229**, 327 (1977).

(11) G. M. Everett, F. Will, and A. Evans, *Fed. Proc. Fed. Am. Soc. Exp. Biol.*, **23**, 198 (1968).

(12) H. D. Y. Yen, R. L. Stanger, and N. Millman, *J. Pharmacol. Exp. Ther.*, **122**, 85A (1958).

ACKNOWLEDGMENTS

This work was supported by the National Institutes of Health (Grant R01 GM26124) and by the Polish Academy of Sciences (Problem I.12).

Phenytoin I: *In Vitro–In Vivo* Correlation for 100-mg Phenytoin Sodium Capsules

VINOD P. SHAH ˣ, VADLAMANI K. PRASAD, TREVA ALSTON, BERNARD E. CABANA, RICHARD P. GURAL *, and MARVIN C. MEYER ‡

Received March 9, 1981, from the *Division of Biopharmaceutics, Food and Drug Administration, Washington, DC 20204*, and the **School of Pharmacy, University of Tennessee, Memphis, TN 37916.* Accepted for publication April 6, 1982. ‡Present Address: Clinical Drug Metabolism, Schering Corp., Bloomsfield, NJ 07003.

Abstract □ *Dissolution profiles for 11 brands of phenytoin sodium capsules were carried out by the basket and paddle methods (USP) and the spin-filter method. The results from the dissolution studies have been correlated with observed differences in in vivo parameters (C_{max} and t_{max}). The dissolution by the basket method at 50 rpm in water gave a correlation >0.9. The results suggest the existence of two types of phenytoin sodium products on the market.*

Keyphrases □ Phenytoin—*in vitro–in vivo* correlation for sodium phenytoin capsules, dissolution □ Dissolution—*in vitro–in vivo* correlation for sodium phenytoin capsules □ *In vitro–in vivo* correlation—sodium phenytoin capsules, dissolution

Increasing evidence has been presented in the scientific literature which show correlations between the *in vivo* performance of formulations and their *in vitro* dissolution behavior (1–3). To obtain an *in vitro–in vivo* correlation for any product, two criteria are essential: (*a*) the differences in *in vivo* parameters such as *AUC*, t_{max}, C_{max}, or C_p at a time among different lots tested and (*b*) differences in the *in vitro* dissolution rates of the same products. In cases where differences are observed in *in vivo* behavior, the *in vitro* parameter can be altered to optimize the correlation with *in vivo* data. This is achieved by varying such parameters as dissolution methodology, dissolution medium, rate of agitation, *etc.* In many instances, it has been possible to obtain correlations with *in vivo* data where a discriminating and reproducible *in vitro* test is employed (1–3). *In vitro–in vivo* correlations can generally be achieved with any reproducible method provided the proper selection of medium and the degree of agitation are made so as to permit discrimination among drug products. The key elements are reproducibility of the method, proper choice of medium, and degree of agitation.

Phenytoin is a commonly used anticonvulsant drug and has been classified as a drug with high risk potential with

0022-3549/83/0300-0306$01.00/0

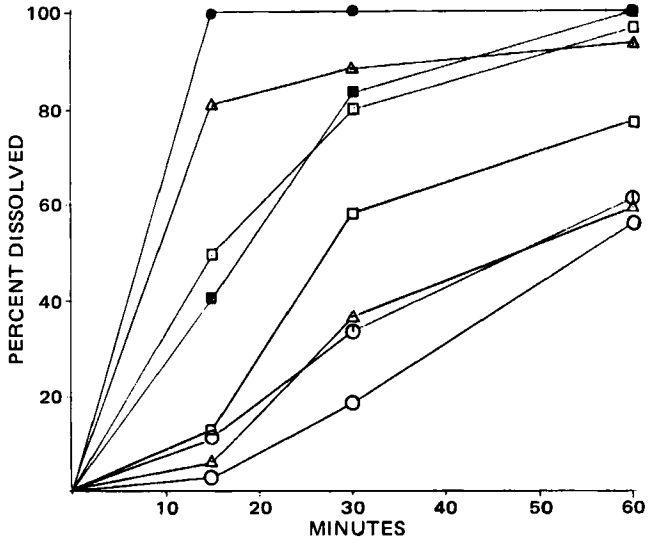

Figure 1—*Dissolution profile of phenytoin sodium products using basket method at 50 rpm in water. Key: (○) Product A; (□) Product B; (●) Product C; (⊡) Product E; (⊙) Product F; (■) Product H; (△) Project J; (▲) Product K.*

respect to bioavailability problems (4). Because of its physicochemical properties, narrow therapeutic range, and dose-dependent kinetics, phenytoin has been identified as a critical drug with a potential bioavailability–bioequivalence problem (5–9). Phenytoin sodium capsules are manufactured by several companies whose formulations have exhibited bioavailability–bioequivalence problems (4, 6, 9). It has been documented that phenytoin products of different manufacturers have pronounced influence on the rate and extent of absorption of the new drug resulting in bioinequivalence (6, 9).

A number of studies, using marketed phenytoin dosage forms were conducted to establish a correlation between the *in vivo* bioavailability and *in vitro* dissolution parameters.

EXPERIMENTAL

All dissolution studies were carried out by USP methods I and II as described in USP XX with an agitation speed of 50 rpm for both methods in distilled water (10) and by the spin-filter method with an agitation speed of 300 rpm in distilled water (11). All samples were analyzed using a spectrophotometer[1].

The studies involving human subjects were carried out after obtaining appropriate clearances and approval[2]. The study design, the analytical method, and the results are published elsewhere (12).

RESULTS AND DISCUSSIONS

The bioequivalence study was conducted in healthy volunteers using 11 lots of marketed 100-mg phenytoin sodium capsules manufactured by eight different companies[3] in two groups (six products each) using the innovator's product[4] as a reference product (12). All products were evaluated with respect to *AUC*, C_{max}, t_{max}, and plasma levels at different time intervals. The results of the previous study (12) show a significant

[1] Beckman spectrophotometer, model 25/7, Beckman Instrument Co., Fullerton, Calif.

[2] From the Risk Involving Human Subjects Committee of Food and Drug Administration, and equivalent committee of the University of Tennessee.

[3] Product A: McKesson capsules, lot no. 7E697. Product B: Westward capsules, lot no. 40981. Product C: Zenith Labs capsules, lot no. 2057-40. Product D: Zenith Labs capsules, lot no. 2057-37A. Product E: Zenith Labs capsules, lot no. 2057-35. Product F: Parke-Davis capsules, lot no. RL288. Product G: Danbury capsules, lot no. 9714. Product H: Danbury capsules, lot no. 9715. Product I: Xttrium Labs capsules, lot no. 403721A-78. Product J: Premo capsules, lot no. 8404. Product K: Kasar Labs capsules, lot no. 280564.

[4] Parke-Davis.

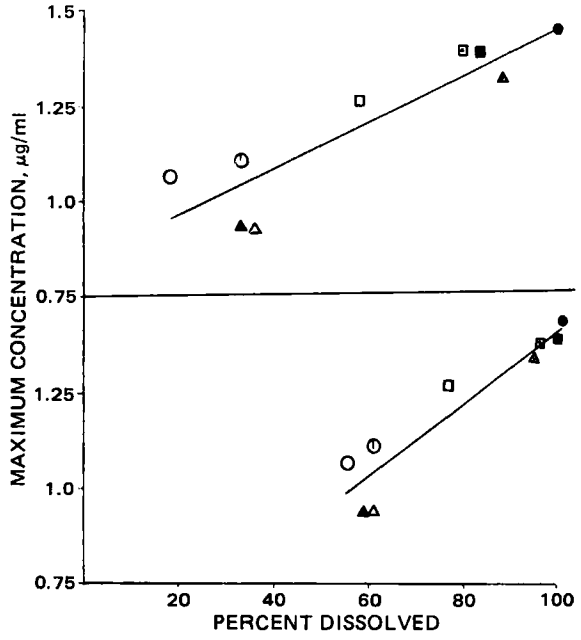

Figure 2—In vitro–in vivo *correlation between* C_{max} *and percent drug dissolved in 30 min (slope = 0.06,* r = 0.902, p < 0.001) *(A); 60 min (slope = 0.10,* r = 0.940, p < 0.001) *(B). Key: (○) Product A; (□) Product B; (●) Product C; (■) Product E; (⊙) Product F; (▲) Product G; (■) Product H; (△) Product J; (▲) Product K.*

difference in rate (C_{max} and t_{max}) and in the extent of bioavailability (*AUC*) in one group, and only a difference in C_{max} in the other group. The bioavailability of the products is defined both with respect to rate and extent. Because of a narrow therapeutic range and dose-dependent metabolism of phenytoin, even small changes in the rate of absorption may result in major changes in serum drug concentration, thus resulting in serious clinical consequences in some patients. Therefore, a clear distinction must be made between slow-absorbing and fast-absorbing phenytoin products.

The *in vitro* dissolution studies for these products were carried out under various conditions in order to obtain the correlation with *in vivo* data. The *in vivo* data obtained are invariant and are dependent on the

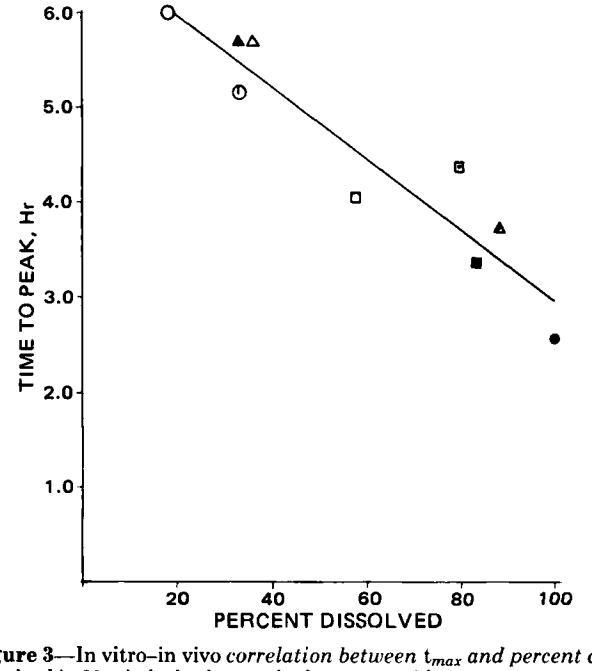

Figure 3—In vitro–in vivo *correlation between* t_{max} *and percent drug dissolved in 30 min by basket method at 50 rpm (slope =* 0.038, r = 0.944, p < 0.001). *Key: (○) Product A; (□) Product B; (●) Product C; (⊡) Product E; (⊙) Product F; (▲) Product G; (■) Product H; (△) Product J; (▲) Product K.*

Table I—Dissolution Profile of 100-mg Phenytoin Sodium Capsules in Water at 37° Using Paddle, Basket, and Spin-filter Methods

Minutes	Products A	B	C	D	E	F	G	H	I	J	K
	Percent of Drug[b] Dissolved										
	Paddle Method—50 rpm—4.5 cm-900 ml										
15	4.4	24.3	98.5	96.2	58.6	13.8	22.2	19.2	34.8	8.1	28.7
30	38.4	60.0	115.5	114.9	96.4	38.5	52.2	45.8	60.0	33.4	46.3
45	70.1	78.9	—	—	111.5	56.6	70.9	62.9	72.8	51.2	49.7
60	87.7	90.3	—	—	120.9	70.3	84.3	74.6	79.1	63.2	51.9
	Basket Method—50 rpm, 900 ml										
15	2.7	12.9	104.8	—	49.5	11.2	—	40.3	—	6.1	80.8
30	18.4	58.0	111.9	—	79.8	33.4	—	83.5	—	36.2	88.5
60	55.6	77.1	117.0	—	96.5	61.0	—	101.7	—	59.0	93.6
	Spin-filter Method—300 rpm, 1000 ml										
10	0.3	—	55.7	—	13.9	1.1	1.3	0.2	—	12.0[a]	50.9
30	29.4	—	105.0	—	103.1	28.8	95.1	87.9	—	50.0	99.5
60	72.5	—	107.5	—	105.5	62.7	101.8	98.1	—	78.9	99.6

[a] 20 min. [b] Label claim.

behavior of the dosage forms administered. The *in vitro* procedures can be altered such that correlations can be made between *in vitro* dissolution results and *in vivo* pharmacokinetic parameters. Such correlations can be statistically significant with respect to one or more of these *in vivo* parameters. Occasionally, there may be a product that exhibits an anomalous behavior with respect to an *in vitro* or *in vivo* parameter.

The *in vitro* dissolution studies were carried out by using the USP dissolution methods *I and II* (basket and paddle) with an agitation of 50 rpm and by the spin-filter method with an agitation of 300 rpm in water. A marked difference in dissolution profiles of these products was observed, both in terms of rate of extent of dissolution in 1 hr (Fig. 1, Table I). The amount of drug dissolved in 30 min (basket method, 50 rpm) varied between 18 and 100% and between 56 and 100% in 60 min. Based on the dissolution characteristics, the products could be classified in two major groups: products that dissolved slowly and achieved only 50–60% dissolution in 1 hr (*e.g.*, product F, Fig. 1) and products that dissolved rapidly and achieved >80% dissolution in 30 min (*e.g.*, product C, Fig. 1). This observed difference in the dissolution profiles of the phenytoin sodium products manifested itself in the *in vivo* performance of the product, resulting in a significantly different rate, but not the extent of bioavailability.

The correlation between C_{max} and percent drug dissolved in 30 and 60 min, and between t_{max} and percent drug dissolved in 30 and 60 min is shown in Figs. 2 and 3, respectively. Among the methods correlated, the basket method resulted in the best correlation ($r = 0.94$) followed by the spin-filter method ($r = 0.836$) and then the paddle method ($r = 0.694$).

These studies suggest that there are two types of phenytoin sodium products on the market. Because of the wide divergence in the dissolution rate of marketed phenytoin products and because of the very slow dissolution characteristics of the most commonly prescribed reference product, it is difficult to set a single dissolution standard covering all products. Therefore, a more definitive study comparing the slow-dissolving phenytoin sodium reference product and the fast-dissolving phenytoin sodium product with a phenytoin sodium solution as a reference standard was carried out. This study will be described in a subsequent report.

REFERENCES

(1) V. K. Prasad, J. P. Hunt, B. E. Cabana, and J. G. Wagner, "Abstracts," Meeting of APhA Academy of Pharmaceutical Sciences, vol. 7, no. 2, American Pharmaceutical Assoc., Washington, D.C., 1977, p. 161.

(2) V. K. Prasad, B. E. Cabana, J. P. Hunt, D. Cox, C. Wells, and J. Wood, *ibid.*, vol. 7, no. 2, p. 167.

(3) V. P. Shah, J. P. Hunt, V. K. Prasad, and B. E. Cabana, *ibid.*, vol. 7, no. 1, p. 206.

(4) Report of Ad Hoc Committee on Drug Product Selection of the Academy of General Practice of Pharmacy and the Academy of Pharmaceutical Sciences, *J. Am. Pharm. Assoc.*, NS13:278 (1973).

(5) *Fed. Reg.*, Jan. 7, 1977, p. 1624.

(6) P. J. Neuvonen, *Clin. Pharmacokinet.*, **4**, 91 (1979).

(7) A. Richens, *ibid.*, **4**, 153 (1979).

(8) E. Martin, T. N. Tozer, L. B. Sheiner, and S. Riegelman, *J. Pharmacokinet. Biopharm.*, **5**, 597 (1977).

(9) P. J. Pentikainen, P. J. Neuvonen and S. M. Elfving, *Eur. J. Clin. Pharmacokinet.*, **9**, 213 (1975).

(10) "United States Pharmacopeia" 20th rev., U.S. Pharmacopeial Convention, Rockville, Md., 1980, p. 959.

(11) A. C. Shah, C. B. Poet, and J. G. Och, *J. Pharm. Sci.*, **62**, 671 (1973).

(12) A. P. Melikian, A. B. Straughn, G. W. A. Slywka, P. L. Whyatt, and M. C. Meyer, *J. Pharmacokinet. Biopharm.*, **5**, 133 (1977).

Phenytoin II: *In Vitro–In Vivo* Bioequivalence Standard for 100-mg Phenytoin Sodium Capsules

VINOD P. SHAH ˣ, VADLAMANI K. PRASAD, CORINNE FREEMAN, JEROME P. SKELLY, and BERNARD E. CABANA

Received March 9, 1981, from the *Division of Biopharmaceutics, Bureau of Drugs, Food and Drug Administration, Washington, DC 20204.* Accepted for publication April 6, 1982.

Abstract □ A bioequivalence study was undertaken using an oral solution, a fast-dissolving capsule and a slow-dissolving phenytoin sodium capsule. The *AUC*, t_{max} and C_{max} correlated with *in vitro* dissolution data. The results of the present studies substantiate the presence of two types of phenytoin sodium products on the market. On the basis of these studies, *in vitro* specifications for fast- and slow-dissolving phenytoin sodium capsules as well as the *in vivo* bioequivalence requirements for these two types of products are recommended.

Keyphrases □ Phenytoin—*in vitro–in vivo* bioequivalence standard for phenytoin sodium capsules, dissolution □ Dissolution—*in vitro–in vivo* bioequivalence standard for phenytoin sodium capsules □ Bioequivalence—*in vitro–in vivo* standard for phenytoin sodium, capsules, dissolution

A good correlation between *in vitro* dissolution and *in vivo* parameters for phenytoin sodium (sodium salt of 5,5-diphenylhydantoin) capsules has been established (1). Previous work indicated that there are two types of phenytoin sodium products on the market, *i.e.*, fast and slow dissolving (1). It was shown that some of the marketed products including the innovator's phenytoin sodium capsules[1] dissolved slowly. Furthermore, the slow-dissolving innovator's product achieved significantly lower peak concentration at a later time (t_{max}) compared with other faster-dissolving products used in the study. Since there are differences between products, bioavailability studies using a solution as a reference standard were initiated. Two studies (single and multiple dose) were carried out using a slow-dissolving product, a fast-dissolving product, and a phenytoin sodium solution. The multiple-dose study was reported previously (2).

EXPERIMENTAL

***In-Vitro* Dissolution Studies**—The dissolution studies were carried out with distilled water using USP method I (rotating basket method) as described in USP XX with an agitation speed of 50 rpm (3).

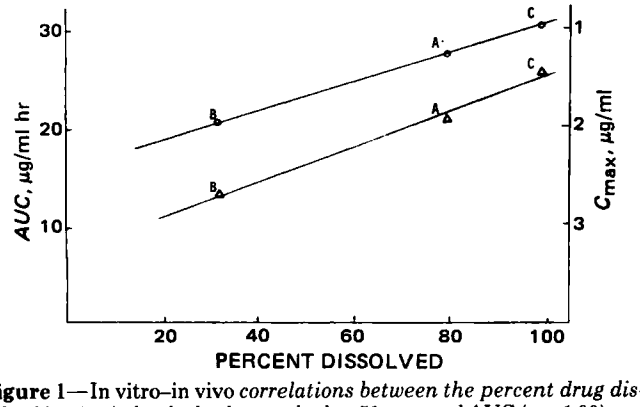

Figure 1—In vitro–in vivo *correlations between the percent drug dissolved in 30 min by the basket method at 50 rpm and* AUC (r = *1.00) and* C_{max} (r = *0.98) for products A, B, and C. Key:* (○) AUC; (△) C_{max}.

[1] Parke-Davis.

Using a randomized Latin-square design, the single-dose study was carried out in 15 healthy volunteers employing the following phenytoin sodium products: a fast-dissolving 100-mg phenytoin sodium capsule (product A); a slow-dissolving 100-mg phenytoin sodium capsule (product B); and a 100-mg phenytoin sodium solution (product C)[2,3]. Blood and saliva samples were collected over a period of 32 hr and analyzed by the published GC method with minor modifications (4).

The multiple-dose study was carried out in 24 epileptic patients using a fast-dissolving 100-mg phenytoin sodium capsule (product D), a slow-dissolving 100-mg phenytoin sodium capsule (product E), and a 100-mg phenytoin sodium solution (product F)[4,5] on a regimen of three doses per day for a 2-week period (2). Blood samples were collected and analyzed by a previous high-performance liquid chromatographic method (5).

RESULTS AND DISCUSSION

The evaluation of the data from the earlier single-dose study suggested that the reference phenytoin sodium product commonly used was slow dissolving and gave lower peak plasma concentrations (4). The C_{max} for this product was 0.93 μg/ml compared to C_{max} values of 1.06–1.44 μg/ml for other products (4).

Table I summarizes the various pharmacokinetic parameters obtained in this single-dose study. Statistical analysis of the data indicates a significant difference in *AUC*, C_{max}, and t_{max} for the three products tested. The use of a phenytoin sodium solution resulted in a higher C_{max}, higher *AUC*, and shorter t_{max} than the fast-dissolving capsule which, in turn, was higher and faster than the slow-dissolving capsule. The relative bioavailability of the slow-dissolving product was 73% compared with the solution and 80% compared with fast-dissolving product. As expected, these data correlate very well (r = 1.00 for *AUC*, and r = 0.98 for C_{max}) with the dissolution data (Fig. 1, Table I). The correlation between values of C_{max}, t_{max}, and the percent dissolved in 30 min by the basket method is shown in Fig. 1.

The results from the multiple-dose study summarized in Table II support the results of the single-dose study. The analysis of the steady-state blood level data from the multiple-dose study showed a significant difference in C_{max} and *AUC* values achieved with fast- and slow-dissolving products. The fast-dissolving phenytoin sodium product (D) and the phenytoin sodium solution resulted in significantly higher steady-state plasma levels when compared with the slow-dissolving phenytoin sodium product (E). The fast-dissolving product (D) was equivalent to the solution in C_{max} and *AUC*. Comparison of the C_{min} values revealed little, if any, difference in the three products tested. However, in 40% of the patients, therapeutically significant differences in plasma levels (> ±25%) were observed. In some instances plasma level differences of >5 μg/ml were observed (2, 6). These data substantiate the premise that the rate of dissolution is an important contributing factor in determining the rate of absorption and bioavailability of the product. The details of this study will be published elsewhere.

***In Vitro* Dissolution Studies**—The dissolution studies for products[6]

[2] Product A, Zenith capsules, lot no. 2057-35; product B, Parke-Davis capsule, lot no. RL288; and product C, Phenytoin sodium solution, Parke-Davis, lot no. RxX42884. The 100-mg phenytoin sodium solution was specially formulated and supplied by Parke-Davis Co., Dept. of Clinical Investigation, Detroit, Mich.

[3] Appropriate clearances and approvals from the Risk Involving Human Subjects Committee of the Agency and the University of Maryland were obtained before initiating the studies.

[4] Product D, Zenith capsules, lot no. 2057-40; product E, Parke-Davis capsules, lot no. TB479-RS; and product F, Phenytoin sodium solution, Parke-Davis, lot no. RxX43093.

[5] Appropriate clearances and approvals from the Risk Involving Human Subjects Committee of the Agency and the equivalent committee of University of Minnesota were obtained before initiating the studies.

[6] The dissolution of product E used in the multiple-dose study was 35% in 30 min, 62% in 60 min, and 88% in 120 min.

0022-3549/83/0300-0309$01.00/0

Table I—Pharmacokinetic Parameters After Administering a Single Dose of 100-mg Phenytoin Sodium and Dissolution Characteristics of the Products

Product	*In Vivo* Parameters[a]			*In Vitro* Parameters	
	AUC_{0-32}, μg/ml hr	C_{max}, μg/ml	t_{max}, hr	% Dissolved[c] 30 min	60 min
A	28.77 ± 6.93	2.08 ± 0.56	3.00 ± 1.12	80	97
B	22.91 ± 6.76	1.42 ± 0.53	4.67 ± 2.0	33	61
C	31.44 ± 7.04	2.68 ± 0.84	1.20 ± 0.63	100[b]	100
Statistics	C > B A > B	C > B A > B	B > A B > C A > C		

[a] Data represents mean ± *SD*. [b] Assumed as 100%. [c] Basket method, 50 rpm.

used in these bioavailability studies were carried out by the basket method in water at 50 rpm (1). The fast-dissolving product showed a dissolution of ~80% in 30 min. The slow-dissolving product showed a dissolution of ~35% in 30 min, 60% in 60 min and 85% in 120 min.

***In Vitro–In Vivo* Correlations**—A number of researchers have attempted to study the correlation between *in vitro* dissolution and *in vivo* performance of phenytoin sodium products. A good correlation has been reported (7) for a variety of phenytoin products (including free acid, sodium salt, and calcium salt in tablet or capsule dosage forms) and the percent drug dissolved in 30 min when the dissolution is carried out by the USP basket method at 150 rpm in pH 9 borate buffer. Correlations of 0.920 and 0.950 were observed between percent dissolved in 30 min and C_{max} and *AUC* values, respectively (7). In this report, correlations of 0.98, 0.97, and 1.00 were observed between percent drug dissolved in 30 min and C_{max}, t_{max}, and *AUC* values, respectively (Table I, Fig. 1).

Poor correlation between *in vivo* and *in vitro* data, in spite of observed significant differences in *AUC*, C_{max}, and t_{max} has also been reported (8). Dissolution studies were carried out by the basket method in pH 9 borate buffer at 120 rpm (9). The lack of correlation found by these researchers can be attributed to the dissolution conditions employed. However, the phenytoin products were found to be acceptable, but were not considered to be interchangeable. The *in vivo* studies described here substantiate these findings. However, because of the differences in the dissolution methodologies employed, it is possible to correlate the *in vitro* results with *in vivo*, thus substantiating previous work (7).

The studies described here and in a previous report (1) have demonstrated a wide variance in the dissolution performance of marketed phenytoin sodium products which has been correlated with significant differences in *in vivo* performance. Because of the critical nature of this drug and documented bioinequivalence of phenytoin, an approved New Drug Application is required before marketing a phenytoin or phenytoin sodium drug product. Based on dissolution data, bioavailability data from single-dose and multiple-dose studies, and *in vitro–in vivo* correlation, it appears that there are two distinct types of phenytoin sodium products on the market, a slow-dissolving phenytoin sodium capsule (or extended phenytoin sodium capsule) and a fast-dissolving phenytoin sodium capsule (or prompt phenytoin sodium capsule). Phenytoin often is administered on a long-term basis. Due to its dose-dependent metabolism and narrow therapeutic range, even small changes in bioavailability profile can cause major changes in serum phenytoin concentration and can have serious clinical implications. Because of the differences in rate of drug delivery and absorption, it is possible that a patient accustomed to the slow-dissolving product and changed over to the fast-dissolving product may achieve higher, possibly toxic, blood levels. If the patient is accustomed to the fast-dissolving product, he or she may not achieve therapeutic levels when changed over to the slow-dissolving product. These products are not interchangeable and are therefore, not therapeutically equivalent.

Based on the information available, two separate *in vitro* and *in vivo* bioequivalence requirements for the two types of phenytoin sodium products, fast- and slow-dissolving, can be established. The *in vitro* dissolution specifications have already been accepted by the USP.

For fast-dissolving or prompt phenytoin sodium products, the bioequivalence requirements are:

Table II—Steady-State Pharmacokinetic Parameters During Administration of 100-mg Phenytoin Sodium Three Times a Day

Product	C_{min}, μg/ml	C_{max}, μg/ml	*AUC*, μg/ml hr
D	12.2	14.0	100
E	10.8	11.8	86
F	12.4	14.3	103
ANOVA	No difference	D ≠ E E ≠ F D = F	D ≠ E E ≠ F D = F

1. The test product shall be deemed to meet the *in vitro* bioequivalence requirement if it dissolves ≥80% in 30 min, and 95% in 60 min when the dissolution is carried out in water using the rotating basket method at 50 rpm.
2. The test product shall be deemed to meet the *in vivo* requirement when a satisfactory single-dose bioavailability study in humans is carried out comparing the test product with phenytoin sodium solution and the reference product.

For slow-dissolving or extended phenytoin sodium products, the *in vivo* bioequivalence testing will involve satisfactory human single-dose and multiple-dose study data. The single-dose bioavailability study should compare the test product with the reference product and a phenytoin sodium solution. The multiple-dose study should compare equivalent doses of the test and reference product administered once a day in patients. The USP labeling requirement for rapidly dissolving phenytoin sodium products contains the statement "not for once a day dosing" (10). The extended-release (slow-dissolving) phenytoin sodium products can be given once a day, and the prompt-release (fast-dissolving phenytoin sodium products are for two or three times a day dosing and not for once a day.

A good correlation has been observed with *in vitro* dissolution and *in vivo* bioavailability data. Based on *in vitro* and *in vivo* data, specifications for fast- and slow-dissolving phenytoin sodium capsules have been established. These products are not interchangeable because they are not therapeutically equivalent.

REFERENCES

(1) V. P. Shah, V. K. Prasad, T. Alston, B. E. Cabana, R. Gural, and M. C. Meyer, *J. Pharm. Sci.*, **72**, 306 (1982).

(2) FDA Contract No. 223-76-3019, University of Minnesota, Minneapolis, MN.

(3) "United States Pharmacopeia" 20th rev., U.S. Pharmacopeial Convention, Rockville, Md., 1980, p. 959.

(4) A. P. Melikan, A. B. Straughn, G. W. A. Slywka, P. L. Whyatt, and M. C. Meyer, *J. Pharmacokinet. Biopharm.*, **5**, 133 (1977).

(5) R. J. Sawchuk and L. L. Carter, *Clin. Chem.*, **26**, 835 (1980).

(6) B. E. Cabana, E. Purich, J. Hunt, R. Gummit, I. Leppick, and R. Sawchuk, "Abstracts," First European Congress of Biopharmaceutics and Pharmacokinetics Imprimerie Jouve 17, rue du Louvre, 75001 Paris (1981).

(7) V. R. Brandau and H. V. Wehnert, *Arzneim-Forsch/Drug Res.*, **29(I)**, 552 (1979).

(8) S. Sved, R. D. Hossie, I. J. McGilvery, N. Beaudoin, and R. Brien, *Can. J. Pharm. Sci.*, **14**, 67 (1979).

(9) P. J. Neuvonen, P. J. Pentikainen, and S. M. Elfving, *Int. J. Clin. Pharmacol.*, **15**, 84 (1977).

(10) "United States Pharmacopeia" XX, Addendum 'a' to supplement 1, U.S. Pharmacopeial Convention, Rockville, Md., 1980, p. 144.

ACKNOWLEDGMENTS

The authors sincerely appreciate the valuable and constructive suggestions of Mr. Gene Knapp, Associate Director, Drug Monographs, Bureau of Drugs, Food and Drug Administration, and acknowledge the assistance of Dr. Richard B. Hornick and Merril J. Snyder of the Division of Infectious Disease, School of Medicine, University of Maryland, Baltimore, Maryland for their assistance in the clinical studies.

Biliary Excretion of [^{14}C]Temazepam and its Metabolites in the Rat

FRANCIS L. S. TSE ˣ, FRANCES BALLARD, and JAMES M. JAFFE

Received January 20, 1982, from the *Drug Metabolism Section, Sandoz, Inc., East Hanover, NJ 07936.* Accepted for publication April 13, 1982.

Abstract □ The excretion of temazepam and its *N*-desmethyl metabolite, oxazepam, and their respective *O*-conjugates was examined following a single intravenous dose of [^{14}C]temazepam to two groups of bile fistula rats, with and without bile replenishment to the animals *via* duodenal cannulae. During an 8-hr collection period, the two groups produced virtually identical bile volumes, and there were no significant differences between them in the amount of total radioactivity, free temazepam, or the identified metabolites in the bile, as determined by TLC and liquid scintillation counting. Elimination of the radioactive dose was rapid during 0–8 hr, with a half-life of ~1 hr. Approximately 85–90% of the administered radioactivity was recovered in the bile: <1% as free temazepam, 3% as oxazepam, and ~10% as their *O*-conjugates.

Keyphrases □ Temazepam—^{14}C-labeled, biliary excretion metabolites in the rat □ Excretion, biliary—[^{14}C]temazepam and its metabolites in the rat □ Metabolism—biliary excretion of [^{14}C]temazepam in the rat

Temazepam (7-chloro-1,3-dihydro-3-hydroxy-1-methyl-5-phenyl-2*H*-1,4-benzodiazepin-2-one) is a benzodiazepine hypnotic agent recently introduced in the United States. The pharmacokinetic profile of temazepam in humans as well as in mice, rats, and dogs have been described (1). Orally administered temazepam is well absorbed in all species studied. However, there is considerable interspecies variation with respect to drug excretion and metabolite patterns in blood and urine. In humans, temazepam is completely metabolized prior to excretion, with 80% of the dose eliminated in the urine and 12% in the feces. The major metabolite is its *O*-conjugate with glucuronic acid, while *N*-desmethyl temazepam (oxazepam) and its *O*-conjugate have also been identified. In animal models, particularly the rat, biliary excretion appears to play a more important role, with as much as 78% of the dose recovered in the rat feces. Therefore, the effect of possible enterohepatic circulation must be considered in the interpretation of pharmacokinetic data obtained from these animal species.

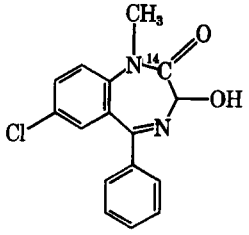

[^{14}C]temazepam

Previous studies using radiolabeled drug in the rat (1) have shown that free temazepam and oxazepam constitute ~40% of the radioactivity in blood, while neither these compounds nor their *O*-conjugates appears in more than trace quantities in the urine. Similar information on the excretion of temazepam in bile is not available. Since the rate and extent of GI reabsorption depend in part on the nature of the compound excreted in the bile, the present study was undertaken to examine the extent of biliary excretion of temazepam and its known metabolites in rats with bile fistula, following a single intravenous dose of the parent compound. Furthermore, the possible effects of bile depletion due to bile duct cannulation on bile flow and biliary excretion of the drugs were also investigated.

EXPERIMENTAL

Animal Preparation—Six male Wistar strain rats[1], average weight ~250 g, were equally divided into two groups, A and B. The bile duct of each rat was cannulated proximal to the liver under light ether anesthesia. In addition, a silicone tube[2], 0.019-cm i.d., was inserted into the duodenum of each rat in group A opposite the sphincter of Oddi and secured by ligation with a surgical silk suture. The tubings were passed subcutaneously and the distal end exteriorized through a stab incision at the back prior to closure of the abdomen with sutures.

The rats were housed individually in special metabolism cages with covers that allowed passage of the cannulae (2). The cover also served as a restraint for the rat, while allowing some freedom of movement inside the cage.

The duodenal cannulae of the rats in group A were subsequently connected *via* 0.013-cm i.d. silicone pump tubes[3] to a peristaltic pump[4]. Previously collected control rat bile was pumped into these rats at a rate of 0.9 ml/hr, approximately the rate of bile secretion of rats of this size.

Dosing and Sample Collection—The radioactive temazepam[5] (labeled at the 2-position of the benzodiazepin structure with carbon-14, specific activity 52.25 μCi/mg) was diluted with nonradioactive drug to a final specific activity of 26.13 μCi/mg. The [^{14}C]temazepam dose, 2 mg/kg, was prepared as a 2.5 mg/ml solution in a phosphate buffer (pH 7.3) containing 40% polyethylene glycol 400 and 10% ethanol. After recovering from anesthesia, each rat received 0.2 ml of the solution as a single, rapid injection *via* the tail vein. Food and a 5% solution of glucose in Ringer's solution were provided *ad libitum*.

The bile of each rat was collected quantitatively at hourly intervals for 8 hr postdosing. All bile samples were stored frozen until analyzed.

Analysis of Radioactivity—Radioactivity was measured in a liquid scintillation counter[6]; the quench correction and efficiency of the counter were determined using ^{14}C-labeled hexadecane[7] of known specific activity as an internal standard. The bile and dose preparations were assayed directly by counting aliquots in a scintillation cocktail consisting of 2,5-bis-2-(5-*tert*-butylbenzoxazolyl) thiophene[8] in toluene (8.3 g/liter).

Thin-Layer Chromatography—Free temazepam and oxazepam were determined by TLC on silica gel[9]. A 1–2 μl bile sample was applied to the chromatographic sheet, which was subsequently developed in ethyl acetate–methanol–ammonium hydroxide (15:4:1). Standard solutions obtained by adding temazepam and oxazepam to control bile were developed concurrently, and the R_f values of these two compounds were determined by visualization under UV light (254 nm)[10].

The sample strip was cut into eight 1.5-cm sections and placed indi-

[1] Royal Hart, Middletown, N.Y.
[2] Acculab, Norwood, N.J.
[3] SMA Flow-Rated Pump Tubes, Technicon Instruments Corp., Tarrytown, N.Y.
[4] Technicon Auto-Analyzer II Peristaltic Pump, Technicon Instruments Corp., Tarrytown, N.Y.
[5] Synthetic Tracer Laboratory, Sandoz, Inc., East Hanover, N.J.
[6] Model 2450, Packard Instrument Co., Downers Grove, Ill.
[7] Packard Instrument Co., Downers Grove, Ill.
[8] BBOT, scintillation grade, Packard Instrument Co., Downers Grove, Ill.
[9] Silica Gel 13181 with fluorescent indicator, Eastman Kodak Co., Rochester, N.Y.
[10] Chromato-Vue, Ultra Violet Products, San Gabriel, Calif.

0022-3549/83/0300-0311$01.00/0

Table I—Mean Bile Volume and Biliary Excretion of Administered Radioactivity in Rats with (group A) and without (group B) Bile Replenishment

Time Period, hr	Bile Volume, ml[a]		Percent of Dose[b]	
	Group A	Group B	Group A	Group B
0–1	0.93 ± 0.058[c]	0.87 ± 0.21	52.4 ± 8.7	43.9 ± 2.5
1–2	0.88 ± 0.076	0.85 ± 0.13	18.5 ± 1.6	23.3 ± 2.5
2–3	0.82 ± 0.029	0.83 ± 0.15	8.0 ± 1.1	10.8 ± 3.6
3–4	0.83 ± 0.12	0.85 ± 0.26	3.5 ± 0.62	5.5 ± 2.3
4–5	0.83 ± 0.058	0.82 ± 0.25	1.8 ± 0.57	2.9 ± 1.7
5–6	0.87 ± 0.058	0.80 ± 0.17	0.97 ± 0.23	1.6 ± 1.2
6–7	0.87 ± 0.12	0.70 ± 0.17	0.46 ± 0.11	0.93 ± 0.61
7–8	0.90 ± 0.10	0.73 ± 0.15	0.31 ± 0.076	0.57 ± 0.29
0–8	6.9 ± 0.34	6.5 ± 1.5	85.9 ± 7.7	89.5 ± 6.2

[a] No significant differences between groups, $p > 0.05$. [b] No significant differences between groups, $p > 0.05$, except the 1–2 hr period, $p < 0.05$. [c] Standard deviation, $n = 3$.

Table II—Mean Biliary Excretion (0–3 hr) of Temazepam and Some Metabolites in Rats with (group A) and without (group B) Bile Replenishment

Compound	Percent of Dose[a]	
	Group A	Group B
Temazepam	0.5 ± 0.3	0.5 ± 0.2
Temazepam Conjugate	4 ± 7	3 ± 4
Oxazepam	3 ± 0	3 ± 1
Oxazepam Conjugate	5 ± 4	7 ± 4
Total Identified Compounds	13 ± 10	12 ± 9

[a] No significant differences between groups, $p > 0.05$.

vidually in scintillation vials. The ^{14}C-labeled drug or metabolite was eluted by the addition of 5 ml of methanol. The scintillation cocktail (15 ml) was then added and the radioactivity determined by direct counting in a liquid scintillation counter. Thus, the radioactivity from the zones corresponding to temazepam and oxazepam, as well as total radioactivity in the bile sample, were obtained.

Similarly, total (free plus conjugated) temazepam and oxazepam were determined by the above procedure after enzymatic hydrolysis of the glucuronate or sulfate conjugates. Aliquots (100 μl) of bile were hydrolyzed by diluting with 100 μl of pH 5.2 acetate buffer, adding an excess (20 μl) of a mixture of enzymes including β-glucuronidase and sulfatase[11], and incubating at 37° for 2 hr.

Statistical Analysis—The effects of bile depletion on bile flow and biliary excretion of temazepam and its metabolites were examined by comparing the data obtained from the two groups of rats, using the two-tailed t test.

RESULTS

The mean bile flow and biliary excretion of administered radioactivity, together with statistical analysis, are given in Table I. There were no significant differences in the volume of bile produced by the two groups of rats during each hourly interval. The secretion rate appeared constant during 0–8 hr; total bile volumes produced in this period were 6.9 and 6.5 ml for rats with and without bile replenishment, respectively.

In the rats with bile replenishment *via* duodenal cannulae (group A), 52% of the radioactive dose was recovered in the bile in 1 hr, and the excretion rate gradually decreased to 0.3%/hr during 7–8 hr. Total biliary excretion in 8 hr was 86% of the dose. Similar results were obtained from the rats without bile replenishment (group B); comparison by t tests showed no signficant differences in the biliary excretion of the two groups during all but one (1–2 hr) collection interval. Total 8-hr biliary excretion in group B was 90% of the administered radioactivity.

Linear regression analysis of the logarithmic values of the excretion rates in Table I *versus* the midpoint of the time periods yielded overall elimination rate constants of 0.73 hr^{-1} ($r = -0.99$) for group A and 0.63 hr^{-1} ($r = -1.00$) for group B (3). These corresponded to half-lives of 1.0 and 1.1 hr, respectively, for the rats with and without bile replenishment.

Since nearly 80% of the dose in both groups was excreted in the bile during the first 3 hr postdosing, only these bile samples were analyzed for temazepam, oxazepam, and their conjugates. TLC analysis enabled separation of temazepam and oxazepam from other metabolites on the sheet; R_f values were 0.61 for temazepam and 0.50 for oxazepam. Thus, the relative amounts of temazepam, oxazepam, and their conjugates in each bile sample were calculated and, combined with the data in Table I, yielded the biliary excretion of each compound as a percent of the dose. The mean 0–3-hr cumulative excretion, together with statistical analysis, are shown in Table II.

Biliary excretion of free temazepam constituted <1% of the dose, while an additional 3–4% was found as temazepam conjugate. The *N*-desmethyl metabolite, oxazepam, and its conjugate in the bile accounted for 3 and 5–7% of the dose, respectively. Thus, only 12–13% of the dose was recovered in the bile as these four identified compounds. Again, there were no significant differences in the excretion of each compound by the two groups of rats.

DISCUSSION

Previous experiments in the rat have shown that the depletion of bile caused by bile duct cannulation could result in a 10- to 20-fold increase in bile salt synthesis and a decrease in the amount of bile excreted; these changes occurred within 1–2 weeks (4). The potential effects of such changes in the biliary excretion and recycling of drugs are well recognized, and sophisticated instruments have been designed for enterohepatic circulation studies in order to eliminate these artifacts (5). In the present study, however, comparison of data obtained from bile fistula rats without bile replenishment *versus* those from the rats with duodenal cannulae showed no significant differences between the two groups in the rate of bile secretion, probably due to the relatively short collection period. Thus, the results would suggest that the loss of bile has little effect on experiments of short duration (<1 day). Also, the excretion of total radioactivity, free temazepam, and the identified metabolites in the bile are unaffected by bile depletion.

Results of this study confirmed the biliary route as the major excretion pathway of temazepam in the rat. Furthermore, although temazepam, oxazepam, and their *O*-conjugates accounted for nearly 50% of the radioactivity in blood (1), they were present in much smaller proportions in the bile of rats. Less than 1% of the [^{14}C]temazepam dose was recovered unchanged, the rest extensively metabolized prior to rapid biliary excretion. Nevertheless, the clinically inactive metabolites (6) may be reverted, *e.g.*, through deconjugations, to the parent compound in the GI tract (7) and subsequently reabsorbed, thus contributing to the overall effectiveness of the temazepam dose. The demonstrated importance of the biliary excretion route warrants further studies to determine the significance of enterohepatic circulation for this drug.

REFERENCES

(1) H. J. Schwarz, *Br. J. Clin. Pharmacol.*, **8**, 23S (1979).

(2) F. L. S. Tse, F. Ballard, and J. M. Jaffe, *J. Pharmacol. Meth.*, **7**, 139 (1982).

(3) J. G. Wagner, "Fundamentals of Clinical Pharmacokinetics," Drug Intelligence, Hamilton, Ill., 1979, p. 76.

(4) S. Eriksson, *Proc. Soc. Exp. Biol. Med.*, **94**, 578 (1957).

(5) J. Berger, R. Redinger, and D. M. Small, *Med. Biol. Eng.*, **8**, 19 (1970).

(6) L. M. Fuccella, G. Bolcioni, V. Tamassia, L. Ferrario, and G. Tognoni, *Eur. J. Clin. Pharmacol.*, **12**, 383 (1977).

(7) H. G. Boxenbaum, I. Bekersky, M. L. Jack, and S. A. Kaplan, *Drug Metab. Rev.*, **9**, 259 (1979).

ACKNOWLEDGMENTS

The authors are grateful to Dr. Lawrence A. Kelly for helpful suggestions.

[11] Glusulase, Endo Laboratories, Garden City, N.Y.

Improved Microscopic Techniques for Droplet Size Determination of Emulsions

HANS SCHOTT ˣ and ALAN E. ROYCE

Received October 21, 1981, from the *School of Pharmacy, Temple University, Philadelphia, PA 19140.* Accepted for publication April 5, 1982.

Abstract □ A novel, disposable cell for microscopic determination of the droplet size of emulsions is described. It is made from a piece of adhesive tape in which a hole has been punched which is placed between a glass slide and a cover glass. This cell is easier to fill with emulsions thickened to reduce Brownian motion and creaming than commercial counting chambers, and it prevents field flow. Droplet size averages and distributions obtained with this cell and another counting chamber agreed, provided that the emulsion viscosity was ~20 cp or higher. The sample size required to provide arithmetic mean diameters with a specified accuracy at a preselected confidence probability was calculated.

Keyphrases □ Droplet size determination—improved microscopic techniques for emulsions □ Emulsions—improved microscopic techniques for droplet size determination

While microscopic droplet size measurements are more laborious than other methods for determining the various averages and the distribution of the droplet sizes of emulsions, the results are subject to less uncertainty (1). Experimental problems encountered in microscopic size determinations by direct visual measurements and by measurements from photomicrographs include Brownian motion, creaming, and field flow.

Field flow is the motion of the entire volume of emulsion in the field of view in a given direction. It is caused by pressure exerted on the cover glass, especially from an immersion objective, by convection currents due to heating by the light source, or by evaporation of the continuous phase from the edge of the cover glass.

The present report describes a novel, disposable cell for microscopic measurements and compares droplet size averages and distributions obtained with the cell and a counting chamber. The effect of emulsion viscosity, through its influence on the velocities of Brownian motion and creaming, on droplet size averages and distribution, is examined with both cells.

The number of droplets that must be counted to obtain estimates for the mean diameter with a specified accuracy at a given confidence probability is calculated.

EXPERIMENTAL

Materials—The oil phase was hexadecane[1], and the water was double distilled. The surfactant, octoxynol 9 NF[2], a nonionic polyoxyethylated octylphenol, has an average of 9–10 ethylene oxide units/molecule. Polyvinyl alcohol[3] was 99% hydrolyzed. Gelatin[4] was granular, USP grade.

Emulsification—Preliminary emulsification was made by adding 33.31 g of hexadecane to a solution of 0.067 g of octoxynol 9 in 66.62 g of water in a tall-form 200-ml beaker and agitating for 20 min with a stirrer equipped with two counter-rotating propellers[5] at an input of 30 V. Subsequently, the emulsion was given three passes through a stainless steel hand-operated homogenizer, applying maximum tension to the spring. The emulsion was diluted with an aqueous octoxynol 9 solution to a final composition of 25% (w/w) hexadecane and 0.1% (w/w) octoxynol 9, based on the weight of the water. All measurements were made on a single emulsion batch which had been aged for 7 months to minimize changes in droplet size during the 8-hr period required to make those measurements.

Microscope—The binocular microscope had a 100× achromatic oil immersion objective and 10× wide-field eyepieces. The eyepiece micrometer had a 5-mm scale comprising 50 divisions with each division measuring 0.976 μm.

Dilution Media—The emulsion was diluted ~600-fold for droplet size measurements. The five media employed were 0.1% octoxynol 9, glycerin, 0.1% octoxynol 9 thickened with 1–2% polyvinyl alcohol, and 5% gelatin (2), respectively. The aqueous gelatin, warmed to 40°, was a liquid of medium viscosity. Emulsion drops were blended with a 600-fold excess of this solution under gentle agitation to avoid breaking up oil droplets and changing the particle size distribution. The mixture was transferred into the cells while warm. Once it reached room temperature, it set to a soft gel.

Cells for Droplet Size Determination—Three kinds of hemacytometers and a Helber-type counting chamber[6] (H-cell) were commercial products. The chambers were filled by touching the edge of the cover glass with a capillary containing the emulsion, whereupon the liquid was drawn into the cell by capillary action without the aid of gravity.

A novel cell (T-cell) was made as follows. A circular hole with a 4.76-mm ($3/16''$) diameter was made with a one-hole paper punch in a piece of pressure-sensitive adhesive tape[7]. The tape was laid on a standard plain 7.62 × 2.54-cm (3″ × 1″) microscope slide and flattened by running the edge of another slide, held in a slanted position, across it.

The thickness of the tape was 57 ± 3, 60 ± 1, or 62 ± 4 μm when measured with a thickness gauge in cross-section with a microscope, or flat by the vertical travel of the objective when the focus was moved from the upper surface of the tape to the upper surface of the glass slide supporting the tape. Aside from its thickness, the choice of adhesive tape is probably not important. The cover glasses had a diameter of 18 mm and a thickness of 0.18 ± 0.02 mm. To fill the T-cell, a cover glass was placed flat on the slide to cover most of the hole in the tape. A small drop of diluted emulsion, extruded from the tip of a glass capillary, was positioned to touch the edge of the cover glass directly above the uncovered portion of the hole. Capillarity combined with gravity caused the emulsion to fill the hole rapidly. The cover glass was then moved sideways so that it covered the hole completely, closing the cell. Excess emulsion was squeezed out of the cell by applying gentle pressure to the cover glass.

Emulsion aliquots diluted with gelatin were also examined between a glass slide and a cover glass (S and C). The application procedure was to hold together two microscope slides, immerse them vertically into the mixture of 5% gelatin solution and emulsion held at 40°, withdrawing and separating the slides, and placing cover glasses on the gelatin film on the outer surfaces of the two slides. The purpose of holding two slides together was to minimize contamination of their bottom surfaces with the gelatin mixture. The thickness of the gelled emulsion layers between the cover glass and microscope slide ranged from 40 to 70 μm.

RESULTS AND DISCUSSION

Droplet size distributions were determined in 1-μm increments with five combinations of cells and dilution media. The five combinations and their droplet size averages are listed in Table I. Droplet size distributions, represented by frequency polygons, are shown in Fig. 1. The equations

[1] Practical grade, Eastman Organic Chemicals.
[2] Triton X-100, Rohm and Haas Co., Philadelphia, Pa.
[3] Matheson, Coleman and Bell, East Rutherford, N.J.
[4] Amend Drug and Chemical Co., Irvington, N.J.
[5] Brookfield counter-rotating mixer, Brookfield Engineering Laboratories, Stoughton, Mass.
[6] Petroff-Hausser bacteria counter, Hausser Scientific, Philadelphia, Pa.
[7] Highland Brand permanent mending tape No. 6200, $3/16''$ width, 3M Co., St. Paul, Minn.

0022-3549/83/0300-0313$01.00/0

Table I—Cells, Composition of Diluted Emulsions, and Values of Various Statistical Diameters in Micrometers

System No.	Cell	Diluent	N^a	$D_a \pm SE^b$	$D_v{}^c$	$D_{vs}{}^d$
I	T	0.1% octoxynol 9	226	3.56 ± 0.11	4.20	4.82
II	T	0.1% octoxynol 9 + 1–2% polyvinyl alcohol	261	2.73 ± 0.16	3.92	4.90
III	H	0.1% octoxynol 9 + 1–2% polyvinyl alcohol	176	2.68 ± 0.14	3.64	4.59
IV	T	5% gelatin	230	2.64 ± 0.13	3.71	4.78
V	S and C	5% gelatin	200	2.58 ± 0.14	3.66	4.78

[a] Number of droplets, representing sum of three cell fillings. [b] Arithmetic mean diameter ± *SEM*. [c] Mean volume diameter defined by Eq. 1. [d] Mean volume–surface diameter defined by Eq. 2.

used to compute the mean volume diameter D_v and the mean volume–surface diameter D_{vs} are (3–5):

$$D_v = \left(\frac{\Sigma N_i D_i^3}{\Sigma N_i}\right)^{1/3} \quad \text{(Eq. 1)}$$

$$D_{vs} = \frac{\Sigma N_i D_i^3}{\Sigma N_i D_i^2} \quad \text{(Eq. 2)}$$

where D_i is the diameter equal to the midpoint of the ith size range and N_i the number of droplets in that range. The droplets contribute to the arithmetic mean diameter only in proportion to the first power of their diameters. Therefore, the mean volume and mean volume–surface diameters are larger than the arithmetic mean diameter and, unlike it, only slightly affected by submicroscopic droplets.

Creaming and Brownian motion affect microscopic droplet size measurements adversely by overemphasizing the largest droplets. Since the velocity of creaming is proportional to the square of the droplet diameter, larger droplets rise considerably faster toward the cover glass and the focal plane than smaller droplets. Brownian motion affects especially the smallest droplets. It prevents creaming for droplets having a diameter smaller than the critical diameter given previously [(6), Eq. 25]. For hexadecane–water emulsions at 20°, this diameter is 2.24 μm for a 1-sec and 0.90 μm for a 100-sec time interval. In the present emulsion, 46 and 28% of the droplets had diameters equal to or smaller than these two critical values, respectively.

Another adverse effect of Brownian motion is that it makes the smaller droplets move randomly in and out of focus, causing them to be undercounted. The mean displacement along a given axis such as the vertical direction in water is 0.62 μm for droplets with diameters equal to the critical diameter, 2.24 μm, for an observation time of 1 sec; it is 9.8 μm for droplets having the critical diameter of 0.90 μm for an observation time of 100 sec [(6), Eq. 22].

For comparison, the visual depth of focus of an objective with numerical aperture 1.40 at a 1000× magnification is <0.5 μm, increasing with decreasing magnification and numerical aperture. The photographic depth of focus is less than one-quarter of that encountered in visual observation (7). The distance travelled in random Brownian motion in 1 sec by almost one-half of the droplets, thus, is comparable to or larger than the depth of focus, making it difficult to measure the smallest and fastest moving droplets.

Cells and Dilution Media—Glycerin, the diluting and thickening medium of choice (1, 8), could not be used because its refractive index was too close to that of hexadecane. A 69% glycerin content is required to increase the viscosity of water to 20 cp, which constitutes about the lowest useful level. The refractive index of that medium differs from that of hexadecane by only 0.015 unit, rendering the hexadecane droplets indistinct. The dilute aqueous polymer media were viscous enough to reduce or eliminate Brownian motion and creaming while changing the refractive index of water only slightly.

System I gave considerably larger mean diameter values than the other four systems (Table I) and a distinctly different droplet size distribution (Fig. 1). The remaining four frequency polygons are practically identical.

Comparison of the five arithmetic mean diameters by the variance ratio or F-test (9, 10) showed that the null hypothesis did not apply; the calculated F-value was larger than the critical value for the 1% level. However, the F-value obtained by comparing the arithmetic mean diameters of systems II–V was smaller than the critical F-value for the 25% level. System I produced a significantly larger arithmetic mean diameter while the differences between the other four values were not statistically significant. This discrepancy is ascribed to the combination of Brownian motion and creaming in the nonthickened medium.

The velocities of Brownian motion and of creaming are inversely proportional to the one-half and first powers of the viscosity of the contin-

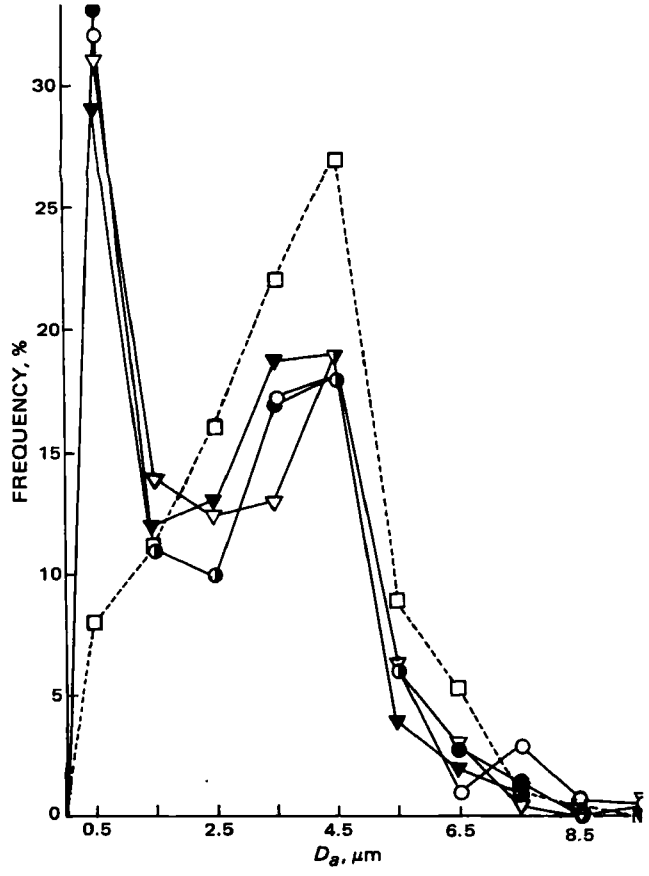

Figure 1—*Frequency polygons for the particle size distributions obtained with five systems. Key: (□) system I; (○) system II; (▼) system III; (●) system IV; (▽) system V.*

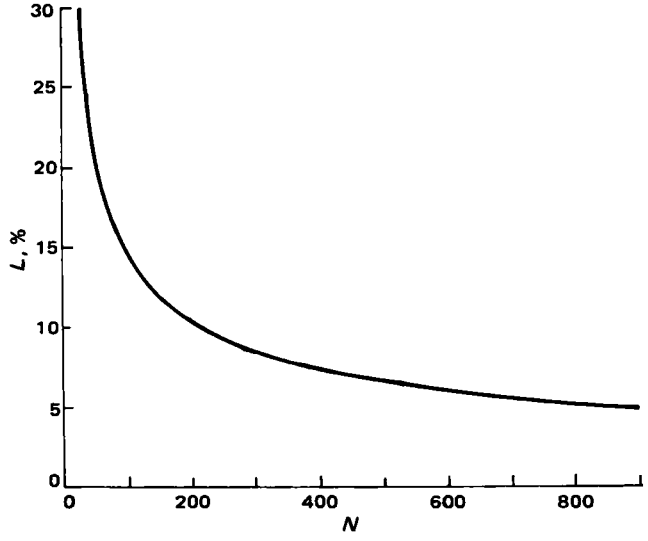

Figure 2—*Number of droplets,* N, *to be counted for the experimental arithmetic mean diameter to lie within* ±L, *the 95% confidence interval, of the true arithmetic mean diameter,* d_a. *The parameter* L *is expressed as percent of the 2.642-μm value of* d_a.

uous phase, respectively (6). The agreement of systems II and III thickened with polyvinyl alcohol to ~20 cp with IV and V, thickened with gelatin to a gel, supports the conclusion that a 20-cp viscosity reduces Brownian motion and creaming sufficiently for microscopic droplet size determinations of fine emulsions. A viscosity of 10 cp was insufficient.

The S and C cell could not be used with a polyvinyl alcohol-thickened emulsion because of field flow. While the S and C cell was used successfully with a gelatin-gelled emulsion, the variation in the thickness of the emulsion layer and the occasionally observed distorted droplets were disadvantages not met with the T-cell. Hemacytometers could not be used. The depth of their cells, ~0.1 mm, plus the thickness of their cover glasses, 0.4–0.6 mm, exceeded the working distance of the immersion objective and made focusing impossible. Furthermore, the ruling is at the bottom of the cells while the hexadecane droplets rose slowly, except in the gelatin medium.

The H-cell was only 0.02-mm deep and its cover glass 0.2-mm thick, so that it could be used with the immersion objective. Disadvantages of the H-cell were the long times required for filling it with viscous emulsions thickened with polyvinyl alcohol or gelatin and for cleaning. The T-cell could be filled faster, because the opening between the cover glass and tape hole could readily be increased for viscous emulsions while the clearance of the H-cell was narrow and constant. Being easy and inexpensive to make and disposable were added advantages of the T-cell. Moreover, it eliminated field flow even in nonthickened emulsions because it prevented evaporation of water, and the pressure exerted by the immersion objective on the cover glass was borne by the tape and the glass slide.

Sample Size—Since most emulsions have broad droplet size distributions, many investigators count several thousand droplets per sample to obtain reliable average droplet sizes (11–13). The number of droplets that must be counted to obtain estimates of the mean diameter with a predetermined accuracy is discussed.

The true arithmetic mean diameter, d_a, is the diameter that would be obtained if all droplets of the entire emulsion batch were measured. The confidence probability that the experimental arithmetic mean diameter of the sample, D_a, lies within a specified percentage limit or interval, L, of d_a, *i.e.*, the probability that D_a is correct within $\pm L$, is calculated for a sample size of $N = 200$ droplets.

Since the differences between the average droplet sizes measured with systems II–V were not statistically significant, the four sets of data, comprising a total of 767 droplets, were pooled. The overall D_a, 2.642 μm, is assumed to equal d_a. The standard deviation for the measurement of a single diameter, computed from the values of 767 droplets, 1.956 μm, is assumed to be equal to the standard deviation of the entire emulsion batch.

The pertinent expression is then (14):

$$2.642 - 1.956Z/\sqrt{N} \leq D_a \leq 2.642 + 1.956Z/\sqrt{N} \qquad \text{(Eq. 3)}$$

and the specified limit is (14):

$$L = 1.956Z/\sqrt{N} \qquad \text{(Eq. 4)}$$

The value of Z corresponding to any given confidence probability is found in a table of cumulative normal frequency distribution.

The use of such a table is predicated on an emulsion with a normal droplet size distribution. A plot of cumulative percent frequency for the pooled droplet size data of systems II–V *versus* diameter on normal probability graph paper was approximately linear, as were plots for the distributions of the four individual systems.

If the specified limit L is 10% of d_a or 0.264 μm, $Z = 1.91$ for $N = 200$. This Z-value corresponds to a 94% confidence probability that the experimental D_a lies within ±10% of d_a. The confidence probability that D_a lies within ±15% of d_a is 99.6%.

In the opposite approach, the confidence probability is set at 95%. The number of droplets that must be counted so that the experimental arithmetic mean diameter lies inside the 95% confidence interval of the true arithmetic mean diameter is calculated by Eq. 4 as a function of the size of that interval. The value of Z is 1.96. In Fig. 2, the number of droplets to be counted is plotted against the two-tailed 95% confidence limit expressed as percent of the 2.642-μm value of the true arithmetic mean diameter. This plot begins to level off in the vicinity of $L \cong 10\%$ $N \cong 200$ droplets. It shows that the increased accuracy gained by counting >400 droplets is marginal.

REFERENCES

(1) P. Becher, "Emulsions: Theory and Practice," 2nd ed., Reinhold, New York, N.Y., 1965, chap. 10.

(2) J. O. Sibree, *Trans. Faraday Soc.*, **27**, 161 (1931).

(3) J. M. DallaValle, "Micromeritics," Pitman, New York, N.Y., 1943, chap. 3.

(4) A. N. Martin, J. Swarbrick, and A. Cammarata, "Physical Pharmacy," 2nd ed., Lea & Febiger, Philadelphia, Pa., 1969, chap. 17.

(5) R. R. Irani and C. F. Callis, "Particle Size: Measurement, Interpretation, and Application," Wiley, New York, N.Y., 1963, p. 25–45.

(6) H. Schott and A. N. Martin, in "American Pharmacy," 7th ed., L. W. Dittert, Ed., Lippincott, Philadelphia, Pa., 1974, chap. 6.

(7) E. M. Chamot and C. W. Mason, "Handbook of Chemical Microscopy," 2nd ed., vol. 1, Wiley, New York, N.Y., 1944, chap. 1.

(8) J. R. Cockton and J. B. Wynn, *J. Pharm. Pharmacol.*, **4**, 959 (1952).

(9) W. J. Youden, "Statistical Methods for Chemists," Wiley, New York, N.Y., 1951, chap. 3.

(10) G. W. Snedecor and W. G. Cochran, "Statistical Methods," 6th ed., Iowa State University Press, Ames, Iowa, 1974, chap. 10.

(11) E. K. Fischer and W. D. Harkins, *J. Phys. Chem.*, **36**, 98 (1932).

(12) P. Sherman, *ibid.*, **67**, 2531 (1963).

(13) P. Sherman, "Emulsion Science," Academic, New York, N.Y., 1968, chap. 3.

(14) G. W. Snedecor and W. G. Cochran, "Statistical Methods," 6th ed., Iowa State University Press, Ames, Iowa, 1974, chap. 2.

ACKNOWLEDGMENTS

This work was supported by the National Institutes of Health under Grant GM 27802.

Effect of Different Water-Soluble Additives on Water Sorption into Silicone Rubber

V. CARELLI and G. DI COLO ˣ

Received March 24, 1981, from the *Pharmaceutical Technology Laboratory, Institute of Pharmaceutical Chemistry, University of Pisa, 56100 Pisa, Italy.* Accepted for publication April 30, 1982.

Abstract □ The ability of ethylene glycol; glycerin; polyethylene glycols 200, 400, and 6000; polysorbate 80; and lactose dispersed in silicone rubber, to promote water sorption into the polymer was investigated in water and in isotonic (pH 7.4) phosphate buffer. Polyethylene glycols 200 and 400, lactose, and, especially, glycerin were effective water carriers. Marked differences in the kinetics of rubber swelling were observed, depending on the carrier. The swelling patterns relative to ethylene glycol, glycerin, and polyethylene glycol 200 showed a maximum due to significant leaching of these additives from the polymer. Steady swelling degrees were afforded by polyethylene glycols 400 and 6000 and by polysorbate 80. The interdependent processes of polymer imbibition and carrier release were speeded up without altering their kinetic patterns by increasing the initial surface–volume ratio of the devices. A proportionality resulted between maximal swelling and initial carrier concentration, although the swelling patterns were substantially unaffected by this variable.

Keyphrases □ Silicone rubber—effect of different water-soluble additives on water sorption □ Sorption—water, effect of different water-soluble additives on water sorption into silicone rubber □ Water-soluble additives—effect on water sorption into silicone rubber □ Swelling behavior—effect of different water-soluble additives on water sorption into silicone rubber

The advantages offered by the use of silicone rubber matrices as long-acting drug delivery systems are manifest in the literature (1–9). A number of water-soluble substances recently have been shown to promote water sorption into silicone rubber pellets containing morphine sulfate, thereby enhancing both *in vitro* and *in vivo* release of this drug (2, 3). In view of their potential use for control of drug release, other hydrophilic materials should be investigated with regard to their suitability to be dispersed in silicone rubber and to act as water carriers.

The present work is concerned with a study of the swelling behavior of silicone rubber devices containing different water-soluble additives: ethylene glycol; glycerin; polyethylene glycols 200, 400, and 6000; polysorbate 80; and lactose.

EXPERIMENTAL

Materials—Polydimethylsiloxane elastomer and silica filler[1]; stannous octoate[2]; ethylene glycol[3]; glycerin[3]; polyethylene glycols 200, 400, and 6000[4]; polysorbate 80[5]; monobasic sodium phosphate[3]; and dibasic sodium phosphate[3] were used as received. Lactose[3] was passed through a 140-mesh screen prior to use.

Preparation of Devices—The additive (ethylene glycol, glycerin, lactose, polyethylene glycol 200 or 400, or polysorbate 80) or a solution of the additive in chloroform (polyethylene glycol 6000) was dispersed in polydimethylsiloxane elastomer in the desired proportion by levigating for ~3 min. Five-gram amounts of the mixture generally were used. Stannous octoate catalyst (1 drop, ~20 mg; or 2 drops with polyethylene glycol 200) was levigated into 1 g of the above dispersion for ~0.5 min (after evaporation of chloroform in the case of polyethylene glycol 6000). The mixture then was added rapidly to a plastic mold, pressed with a plastic plate into a sheet of uniform thickness (0.2 or 0.05 cm), and allowed to cure overnight at room temperature. A cylinder (0.5-cm diameter, 0.2-cm thick) or a disk (1-cm diameter, 0.05-cm thick) was cut from the polymerized sheet and immediately used for the swelling experiments. The cylinders or the disks had dry weights which were between 46.2 and 54.4 mg or 49.1 and 53.5 mg, respectively, depending on the additive and its concentration.

Swelling Determinations—The sample being studied was flushed with distilled water and then rapidly placed between filter paper to remove clinging water. Its dry weight then was determined. Next, it was immersed in 20 ml of phosphate buffer (0.13 *N*, pH 7.4), or distilled water which was maintained at 37°. At measured intervals, the swollen sample was removed from the solvent, cleared of water with filter paper, weighed in a weighing bottle, and quickly immersed in 20 ml of fresh solvent prewarmed to 37° (time zero of the next interval). Each experiment was run in triplicate, and the data were averaged. The range of the measured values was not >±5% of the mean. Shaking had practically no effect on the swelling kinetics.

RESULTS AND DISCUSSION

The swelling kinetics of silicone rubber cylinders containing 12% (w/w) carrier, determined in isotonic phosphate buffer (pH 7.4) or in pure water, is presented in Figs. 1 and 2, respectively, where the ratio of the weights of swollen–dry sample, γ, defined as swelling degree, was plotted against time. The plots in Fig. 1 relative to ethylene glycol, glycerin, and polyethylene glycol 200 went through a maximum, thus, pointing to a change in the sign of the swelling pressure. Such a pattern was indicative of significant leaching of these substances from the silicone polymer. Much slower leaching, if any, of polyethylene glycols 400 and 6000 and polysorbate 80 was suggested by the respective swelling degrees which apparently attained steady equilibrium values. At any given swelling degree, a considerably higher swelling rate in pure water than in buffer was always observed. This was in accord with a higher osmotic pressure differential in the case of the pure water.

The swelling kinetics of silicone rubber disks (1-cm diameter and 0.05-cm thick), having the same volume and carrier concentration as the cylinders in Fig. 1, was followed to study the effect of varying the surface–volume ratio of the polymeric device. Disks filled with polyethylene glycol 6000 did not swell, and their weight decreased slightly upon hy-

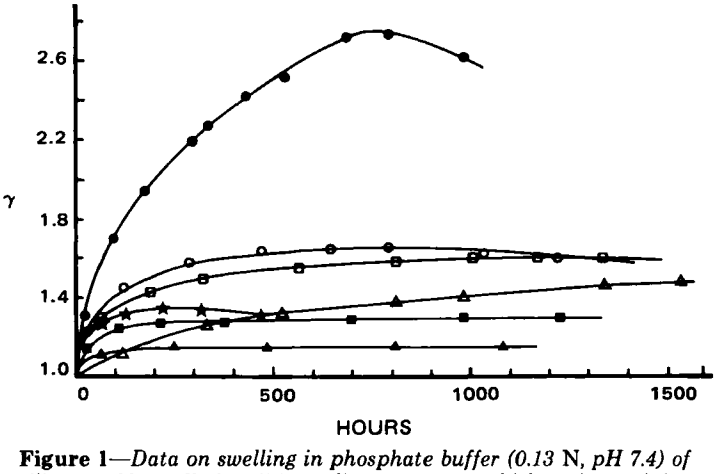

Figure 1—*Data on swelling in phosphate buffer (0.13 N, pH 7.4) of silicone rubber cylinders (0.5-cm diameter, 0.2-cm thickness) containing various water carriers (12% w/w). Key: (●) glycerin; (○) polyethylene glycol 200; (□) polyethylene glycol 400; (★) ethylene glycol; (△) lactose; (■) polyethylene glycol 6000; (▲) polysorbate 80.*

[1] Silastic 382 medical grade elastomer, Dow Corning Corp., Midland, Mich.
[2] Catalyst M, Dow Corning Corp., Midland, Mich.
[3] Carlo Erba S.p.A., Milano, Italy.
[4] Merck-Schuchardt, München, West Germany.
[5] Tween 80, Atlas Chemie GmbH, Essen, West Germany.

0022-3549/83/0300-0316$01.00/0

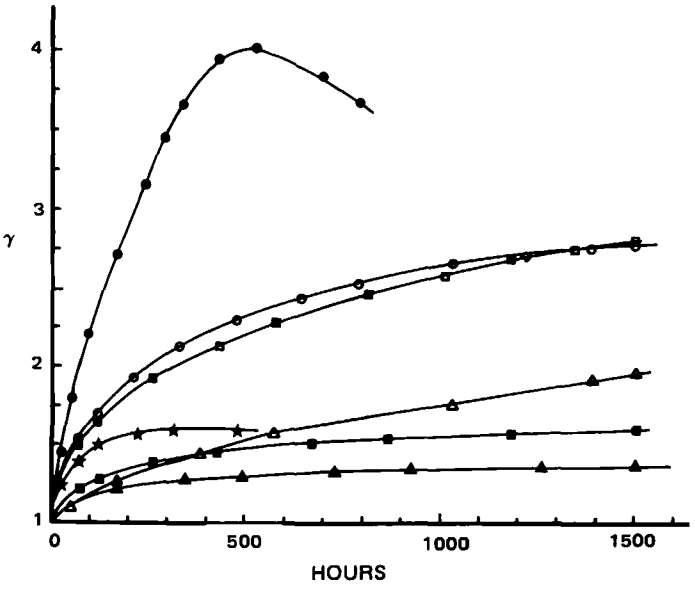

Figure 2—*Data on swelling in water of silicone rubber cylinders (0.5-cm diameter, 0.2-cm thickness) containing various water carriers (12% w/w). Key: (●) glycerin; (○) polyethylene glycol 200; (□) polyethylene glycol 400; (★) ethylene glycol; (△) lactose; (■) polyethylene glycol 6000; (▲) polysorbate 80.*

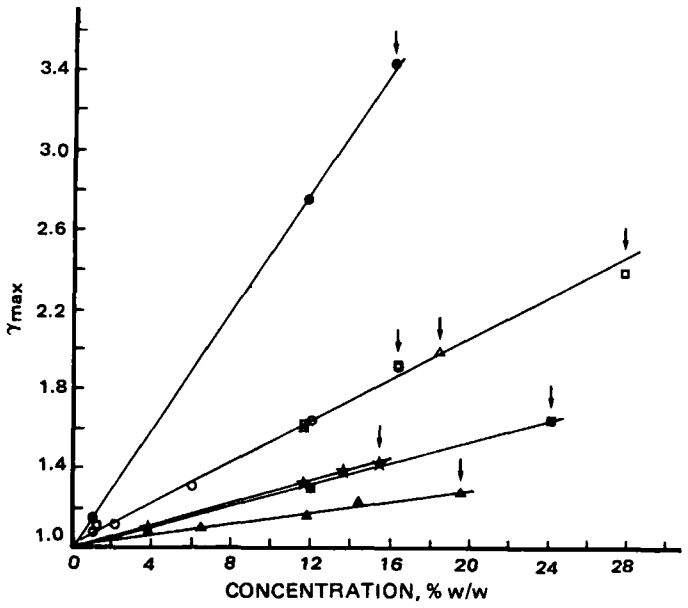

Figure 3—*Dependence of maximal swelling degree of cylinders in buffer on initial additive concentration. Key: (●) glycerin; (○) polyethylene glycol 200; (□) polyethylene glycol 400; (△) lactose; (★) ethylene glycol; (■) polyethylene glycol 6000; (▲) polysorbate 80. Concentrations substantially exceeding the values indicated for each additive by the arrows gave nonreproducible data.*

dration. The cause of this behavior could reside in an inadequate dispersion of this additive. Due to a comparatively high surface–volume ratio, the fraction of carrier undergoing a rapid dissolution from the disk surface predominated in this case over the carrier fraction in the disk core. The opposite occurred with the cylinders, which gave reproducible swelling data. The profile of the γ *versus* time plots, as well as the maximal swelling degrees of disks (not reported), remained unchanged with respect to the corresponding properties of cylinders, although the process was speeded up considerably in all cases with the disks. Since swelling was carrier driven, a similar effect of the surface–volume ratio on the release process of the leachable carriers could be inferred. The relevance of these findings to the release of water-soluble drugs embedded in silicone rubber is apparent.

Cylinders were used to study the effect of carrier concentration. Devices formulated with varying concentrations of the same additive all gave swelling plots similar in shape (not reported), although the magnitude of swelling was concentration dependent. Figure 3 shows the plots of the maximal swelling degree (γ_{max}) attained in buffer by the cylinders *versus* initial carrier concentration. Concentrations substantially exceeding the values indicated for each carrier in Fig. 3 did not yield reproducible results. A straight line with zero intercept was obtained with all of the additives studied. Such an apparent proportionality is intriguing, since the extent of swelling depended on numerous factors which in turn could be complex functions of initial carrier concentration. These are the osmotic activity of carrier (free or bound to the polymer through hydrogen or covalent bonding), the rate of carrier release from polymer, the polymer contractility, and the polymer plasticizing effect of the carrier. The slopes of the plots in Fig. 3, which can be referred to as the specific swelling power of the single carriers, appeared to be different for carriers of a similar physical and chemical nature, such as ethylene glycol and glycerin, or similar for additives of a different physical and chemical nature, such as polyethylene glycol 200 and lactose.

The variation range of all reported data was $\leq \pm 5\%$. This reproducibility is indicative of an inherent ease in additive dispersal in polydimethylsiloxane, because of the simplicity of the mixing technique. With the liquid additives, especially with polyethylene glycol 200, higher than usual catalyst concentrations were needed to crosslink the polymer. Such an interference of these additives with the action of the initiator needs further investigation because of possibility that these compounds may be part of the crosslinking reaction. Shaking of the device–solvent systems did not affect the swelling data, suggesting the absence of boundary layer effects on the swelling kinetics.

In conclusion, polyethylene glycols 200 and 400, lactose, and especially glycerin were effective water carriers. Their actual role in drug release from silicone rubber will be assessed in future studies.

REFERENCES

(1) W. Lotz and B. Syllwasschy, *J. Pharm. Pharmacol.*, **31**, 649 (1979).

(2) J. W. McGinity, L. A. Hunke, and A. B. Combs, *J. Pharm. Sci.*, **68**, 662 (1979).

(3) W. H. Riffee, R. E. Wilcox, J. A. Anderson, and J. W. McGinity, *ibid.*, **69**, 980 (1980).

(4) Y. W. Chien, L. F. Rozek, and H. J. Lambert, in "Controlled Release Polymeric Formulations," D. R. Paul and F. W. Harris, Eds., ACS Symposium Series No. 33, American Chemical Society, Washington, D.C., 1976, chap. 6.

(5) Y. W. Chien, *Chem. Pharm. Bull.*, **24**, 1471 (1976).

(6) M. Thiery, D. Vandekerckhove, M. Dhout, A. Vermeulen, and J. M. Decoster, *Contraception*, **13**, 605 (1976).

(7) D. R. Mishell, Jr., D. E. Moore, S. Roy, P. F. Brenner, and M. A. Page, *Am. J. Obstet. Gynecol.*, **130**, 55 (1978).

(8) J. H. Duenhoclter, R. S. Ramos, L. Milewich, and P. C. MacDonald, *Contraception*, **17**, 51 (1978).

(9) Y. W. Chien, in "Sustained and Controlled Release Drug Delivery Systems," J. Robinson, Ed., Dekker, New York, N.Y., 1978, chap. 4.

ACKNOWLEDGMENTS

This work was supported in part by a grant from Consiglio Nazionale delle Ricerche.

Potential Anticonvulsants VI: Condensation of Isatins with Cyclohexanone and other Cyclic Ketones

HOSSEIN PAJOUHESH, RANDY PARSON, and FRANK D. POPP ˣ

Received March 1, 1982, from the *Department of Chemistry, University of Missouri-Kansas City, Kansas City, MO 64110.* Accepted for publication April 15, 1982.

Abstract □ Cyclohexanone, substituted cyclohexanones, and other cycloalkanones have been condensed with isatin and substituted isatins to give a series of new 3-hydroxy-3-substituted oxindoles. A number of these 3-hydroxyoxindoles possess anticonvulsant activity.

Keyphrases □ Anticonvulsants—potential, condensation of isatins with cyclohexanone and other cyclic ketones □ Isatins—condensation with cyclohexanone and other cyclic ketones, potential anticonvulsants □ Cyclohexanones—condensation of isatins, potential anticonvulsants

It has been reported (1, 2) that I exhibited anticonvulsant activity in the maximal electroshock seizure test[1] with an ED_{50} of 102 mg/kg and a protective index of ~4 and that II had an ED_{50} of 40 mg/kg and a protective index of 12 in that same test. The 3-hydroxyoxindole derivative, II, was also active at 300 mg/kg in the pentylenetetrazol seizure threshold test[1]. Compound III had an ED_{50} of 56 with a protective index of 3 in the maximal electroshock seizure test, while IV had an ED_{50} of ~115 and a protective index of ~4 in both tests (2).

Compound V was derived from isatin and cyclohexanone and was active in the maximal electroshock seizure (MES) screen (2). Dehydration to VI resulted in an increase in activity. This latter observation is in contrast to the observation that the dehydration products of I and II were inactive. A number of products from isatin and cyclic ketones (3) were prepared, and it was found that VII had an ED_{50} of 171 and a protective index of 8 in the MES screen and that VIII was active in both screens.

The present investigation reports on the condensation of various alicyclic ketones with isatins to give additional analogs of V–VIII.

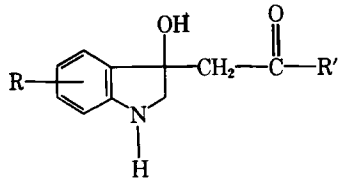

I: R = H, R′ = C_6H_5
II: R = H, R′ = CH_3
III: R = 4-Cl-7-CH_3, R′ = CH_3
IV: R = 7-CH_3, R′ = CH_3

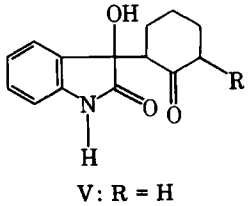

V: R = H
VII: R = CH_3

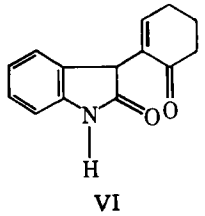

VI

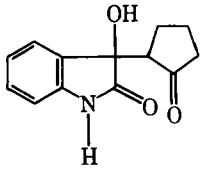

VIII

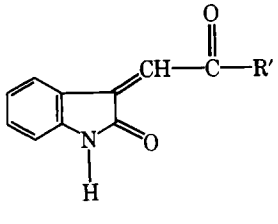

IX

EXPERIMENTAL[2]

Condensation of Isatin with Ketones—The compounds in Tables I–IV were prepared, as previously described (1–3, 5, 6), by heating on a steam bath a solution of the isatin and the appropriate ketone in absolute ethanol containing a few drops of diethylamine.

Dehydration of 3-Hydroxyoxindoles—The compounds in Table V were prepared, as previously described (1, 2, 5), by heating the 3-hydroxyoxindoles on a steam bath in acetic acid containing a small amount of hydrochloric acid.

DISCUSSION

Cyclohexanone was condensed in the presence of diethylamine with a variety of substituted isatins to give compounds of type V. These products are included in Table I. With the exception of the product derived from 4-chloro-7-methoxyisatin, none of these derivatives were as active as V in the MES screen. In contrast, a considerable number of these analogs were active in the pentylenetetrazol seizure threshold test (Met) screen. Worthy of particular note were those products formed from 7-methyl-, 4-chloro-7-methoxy-, and 6-chloro-7-methylisatin. 5-Chloro-, 5-methyl-, and 5-nitroisatin also led to compounds active in the Met test.

In view of the activity of VIII (3), a number of cycloalkanones of various ring sizes were condensed with isatins to give the compounds shown in Table II. With the exception of a high degree of Met test activity in the product from 5-bromoisatin and cyclopentadecanone, none of the compounds, including several from cyclopentanone and substituted isatins, were as active as VIII.

Although the products from isatin and 4-substituted cyclohexanones were inactive (3), compound VII had good MES activity. In view of this, a number of 2-substituted cyclohexanones and 3-methylcyclohexanone were condensed with isatins to give the products shown in Table III. In the case of VII the introduction of substituents in the isatin portion of the molecule or replacement of the methyl by phenyl or cyclohexyl led to a loss of activity. A single exception is the activity of the 5-nitro analogue of VII, which is active in the Met test. Replacement of 2-methylcyclohexanone by 3-methylcyclohexanone gave an active product both with isatin and with 1-methylisatin.

Although it has been reported that dehydration of I (1) and II (2) to IX causes a loss of activity, dehydration of V to VI leads to an increase of activity in the MES test. Unfortunately, dehydration of a number of analogues of V and VII resulted in a decrease or loss of activity. These dehydration products are shown in Table V.

Table IV includes a number of additional examples of compounds of type I. None of these compounds exhibited any significant anticonvulsant activity.

This series of investigations has reported (1–3, 5, 6) on the synthesis of a number of 3-substituted oxindoles with anticonvulsant activity.

[1] Anticonvulsant screenings were carried out through the Antiepileptic Drug Development Program of the NINCDS, National Institutes of Health. The standard screening protocol of that group was followed.

[2] All compounds exhibited IR spectra consistent with the structures shown and with those previously reported (1–3). Melting points are uncorrected, and analyses were carried out by Spang Microanalytical Laboratory.

0022-3549/83/0300-0318$01.00/0

Table I—Reaction of Isatins with Cyclohexanone

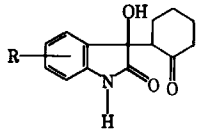

Substituent	mp°[a]	Formula	Analysis, % Calc. / Found C	H	N	Anticonvulsant Activity, mg/kg[b] MES	Met
H	198–199[c]	$C_{14}H_{15}NO_3$	—	—	—	300	NA[d]
H[e]	240–241	$C_{22}H_{20}N_2O_5$	67.34 / 67.40	5.14 / 5.25	7.14 / 7.13	—	—
1-$C_6H_5CH_2$	183–185	$C_{21}H_{21}NO_3$	75.20 / 75.22	6.31 / 6.48	4.18 / 4.18	NA[f]	NA[f]
5-Br	218–219	$C_{14}H_{14}BrNO_3$	51.87 / 52.01	4.35 / 4.42	—	NA[f]	NA[f]
5-Cl	217–218	$C_{14}H_{14}ClNO_3$	60.11 / 59.91	5.04 / 5.03	—	NA[f]	100
5-CH_3	198–199	$C_{15}H_{17}NO_3$	69.48 / 69.69	6.61 / 6.79	—	NA[f]	100
5-CH_3O	162–164[g]	$C_{15}H_{17}NO_4$	—	—	—	600[h]	300[h]
5-NO_2	228–230	$C_{14}H_{14}N_2O_5$	57.93 / 57.82	4.86 / 4.87	—	NA[f]	100
6-Cl	220–222	$C_{14}H_{14}ClNO_3$	60.11 / 59.70	5.04 / 5.22	—	NA[f]	NA[f]
7-CH_3	196–198	$C_{15}H_{17}NO_3$	69.48 / 69.44	6.61 / 6.71	—	600	30[i]
4-Cl-7-CH_3	209–211	$C_{15}H_{16}ClNO_3$	61.37 / 61.53	5.49 / 5.60	4.77 / 4.74	NA[f]	NA[f]
4-Cl-7-CH_3O	153–154	$C_{15}H_{16}ClNO_4$[j]	57.38 / 57.26	6.23 / 6.16	3.94 / 3.92	300[h]	30[h]
5-Cl-7-CH_3	200–202	$C_{15}H_{16}ClNO_3$	61.33 / 61.17	5.49 / 5.46	—	NA[f]	600
5-CH_3O-6-Cl	240–241	$C_{15}H_{16}ClNO_4$	58.16 / 58.10	5.21 / 5.09	4.52 / 4.54	NA[f]	NA[f]
6-Cl-7-CH_3	207–208	$C_{15}H_{16}ClNO_3$	61.33 / 61.22	5.49 / 5.45	—	NA[f]	30

[a] Recrystallized from ethanol, melting point uncorrected, spectral data consistent with structure. [b] Anticonvulsant screenings were carried out through the Antiepileptic Drug Development Program, National Institutes of Health. The standard screening protocol of the group was followed. [c] Described in ref. 2. [d] No activity at 300 mg/kg. [e] Product from reaction of 2 moles of cyclohexanone with 1 mole of isatin. [f] No activity at 600 mg/kg. [g] Reported (6) mp 168–171°. [h] Toxic at 600 mg/kg. [i] Met ED_{50} 550.23; TD_{50} > 900. [j] Analysis, sample $C_{15}H_{16}ClNO_4 \cdot C_2H_5OH$.

Table II—Reaction of Isatin with Cyclic Ketones

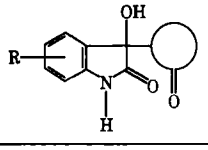

Substituent	Ketone Used	mp°,[a]	Formula	Analysis, % Calc. / Found C	H	N	Anticonvulsant Activity, mg/kg[b] MES	Met
H	Cyclopentanone	173–174[c]	$C_{13}H_{13}NO_3$	—	—	—	100[d]	300[d]
5-Br	Cyclopentanone	270–271	$C_{13}H_{12}BrNO_3$	—	—	4.52 / 4.91	600	300
5-NO_2	Cyclopentanone	200–201	$C_{13}H_{12}N_2O_5$	56.52 / 56.19	4.38 / 4.24	10.14 / 10.21	NA[e]	600
4-Cl-7-OCH_3	Cyclopentanone	196–198	$C_{14}H_{14}ClNO_4$	56.86 / 56.96	4.77 / 4.77	4.74 / 4.66	NA[e]	300
H	2-Ethylcyclopentanone	132–134	$C_{15}H_{17}NO_3$	69.48 / 69.29	6.61 / 6.64	5.40 / 5.54	300	NA[f]
H	Cycloheptanone	169–170	$C_{15}H_{17}NO_3$	69.48 / 69.42	6.61 / 6.50	5.40 / 5.43	300[g]	300[g]
5-Br	Cycloheptanone	220–221	$C_{15}H_{16}BrNO_3$	53.27 / 53.49	4.77 / 4.79	4.14 / 4.15	NA[e]	NA[e]
5-NO_2	Cycloheptanone	224–225	$C_{15}H_{16}N_2O_5$	59.20 / 58.94	5.30 / 5.24	9.21 / 9.02	NA[e]	NA[e]
4-Cl-7-OCH_3	Cycloheptanone	199–200	$C_{16}H_{18}ClNO_4$	59.35 / 59.44	5.60 / 5.72	4.33 / 4.31	NA[e]	NA[e]

Continued on next page

Table II—*Continued*

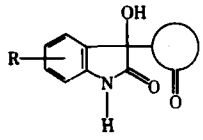

Substituent	Ketone Used	mp°,[a]	Formula	Analysis, % Calc. / Found C	H	N	Anticonvulsant Activity, mg/kg[b] MES	Met
H	Cyclooctanone	168–169	$C_{16}H_{19}NO_3$	70.30 / 70.33	7.01 / 6.96	5.12 / 5.16	600	NA[e]
5-Cl	Cyclopentanone	175–176	$C_{13}H_{12}CNO_3$	58.76 / 58.47	4.55 / 4.61	—	600[g]	600[g]
5-CH_3	Cyclopentanone	256–257	$C_{14}H_{15}NO_3$	68.55 / 68.20	6.16 / 5.73	—	NA[e]	300
6-Cl-7-CH_3	Cyclopentanone	206–207	$C_{14}H_{14}ClNO_3$	60.11 / 60.16	5.04 / 5.07	5.01 / 4.81	300	NA[e]
5-Br	Cyclooctanone	195–196	$C_{16}H_{18}BrNO_3$	54.56 / 55.00	5.50 / 5.19	3.98 / 4.09	NA[e]	NA[e]
5-NO_2	Cyclooctanone	147–149	$C_{16}H_{18}H_2O_5$	60.39 / 60.06	5.70 / 5.70	—	600	600
H	Cyclododecanone	185–186	$C_{20}H_{27}NO_3$	72.92 / 73.11	8.26 / 8.37	4.25 / 4.36	NA[e]	NA[e]
1-CH_3	Cyclopentadecanone	180–181	$C_{24}H_{35}NO_3$	74.76 / 74.80	9.15 / 9.25	3.63 / 3.79	NA[e]	NA[e]
5-Br	Cyclopentadecanone	213–215	$C_{23}H_{32}BrNO_3$	61.33 / 61.49	7.16 / 7.24	3.11 / 3.10	NA[e]	30[h]
5-NO_2	Cyclopentadecanone	233–235	$C_{23}H_{32}N_2O_5$	66.32 / 66.03	7.74 / 7.72	6.73 / 6.69	NA[e]	NA[e]
4-Cl-7-OCH_3	Cyclopentadecanone	223–225	$C_{24}H_{34}ClNO_4$	66.12 / 66.05	7.86 / 7.83	3.21 / 3.18	NA[e]	NA[e]

[a] Recrystallized from ethanol, melting point uncorrected, spectral data consistent with structure. [b] Anticonvulsant screenings were carried out through the Antiepileptic Drug Development Program, National Institutes of Health. The standard screening protocol of the group was followed. [c] Described in ref. 3. [d] MES ED_{50} 124.4; Met ED_{50} 202.4, TD_{50} 255.4. [e] No activity at 600 mg/kg. [f] No activity at 300 mg/kg, toxic at 600 mg/kg. [g] Toxic at this dose. [h] Repeated testing indicated that the subcutaneous Met activity is variable.

Table III—Reaction of Isatins with Substituted Cyclohexanones

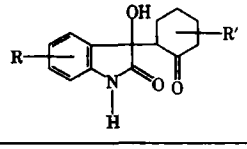

Substituent	Ketone Used	mp°,[a]	Formula	Analysis, % Calc. / Found C	H	N	Anticonvulsant Activity, mg/kg[b] MES	Met
H	2-Methylcyclohexanone	199–201[c]	$C_{15}H_{17}NO_3$	—	—	—	100[d]	600[d]
1-CH_3	2-Methylcyclohexanone	160–162	$C_{16}H_{19}NO_3$	70.30 / 70.36	7.01 / 7.11	5.12 / 5.02	300[e]	NA[f]
5-Br	2-Methylcyclohexanone	228–230	$C_{15}H_{16}BrNO_3$	53.27 / 53.36	4.77 / 4.71	—	NA[f]	600
5-NO_2	2-Methylcyclohexanone	236–237	$C_{15}H_{16}N_2O_5$	59.20 / 59.22	5.30 / 5.27	—	NA[f]	30
4-Cl-7-CH_3	2-Methylcyclohexanone	229–230	$C_{16}H_{18}ClNO_3$	62.44 / 62.39	5.90 / 5.78	4.55 / 4.64	NA[f]	NA[f]
H	2-Methylcyclohexanone	187–188	$C_{20}H_{19}NO_3$	74.74 / 74.75	5.96 / 5.95	4.36 / 4.45	NA[f]	NA[f]
5-NO_2	2-Methylcyclohexanone	235–236	$C_{20}H_{18}N_2O_5$	64.50 / 64.64	6.50 / 6.53	7.52 / 7.38	NA[f]	NA[f]
5-Br	2-Cyclohexylcyclohexanone	235–236	$C_{20}H_{24}BrNO_3$	59.12 / 59.31	5.95 / 5.99	3.45 / 3.15	NA[f]	NA[f]
H	3-Methylcyclohexanone	171–172	$C_{15}H_{17}NO_3$	69.48 / 69.38	6.61 / 6.68	5.40 / 5.35	100[g]	300[e]
1-CH_3	3-Methylcyclohexanone	167–168	$C_{16}H_{19}NO_3$	—	—	5.12 / 5.36	100	600[e]
5-Br	3-Methylcyclohexanone	219–220	$C_{15}H_{16}BrNO_3$	53.27 / 53.35	4.77 / 4.82	—	NA[f]	NA[f]
5-NO_2	3-Methylcyclohexanone	228–229	$C_{15}H_{16}N_2O_5$	59.20 / 58.88	5.30 / 4.92	—	NA[f]	NA[f]

[a] Recrystallized from ethanol, melting point uncorrected, spectral data consistent with structure. [b] Anticonvulsant screenings were carried out through the Antiepileptic Drug Development Program, National Institutes of Health. The standard screening protocol of the group was followed (see Table I). [c] Described in ref. 3. [d] MES ED_{50} 171.5; TD_{50} 1380. [e] Some toxicity at this dose. [f] No activity at 600 mg/kg. [g] MES ED_{50} 83.7; TD_{50} 323.9.

Table IV—Additional Products from Acetophenone

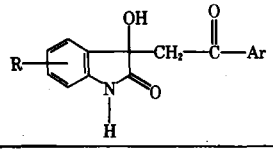

Substituent	Ar	mp°,[a]	Formula	Analysis, % Calc. / Found C	Analysis, % Calc. / Found H	Anticonvulsant Activity, mg/kg[b] Met
5-Cl	C_6H_5	212–213	$C_{16}H_{12}ClNO_3$	63.69 / 63.79	4.01 / 3.98	NA[c]
6-Cl-7-CH_3	C_6H_5	218–219	$C_{17}H_{14}ClNO_3$	64.66 / 64.53	4.47 / 4.42	600
7-Cl	C_6H_5	168–169	$C_{16}H_{12}ClNO_3$	63.69 / 63.57	4.01 / 4.15	600
4-Cl-7-CH_3O	C_6H_5	211–212	$C_{17}H_{14}ClNO_4$	61.54 / 61.60	4.25 / 4.23	600
H	3-$NO_2C_6H_4$	160–161	$C_{16}H_{12}N_2O_5$	61.54 / 61.59	3.87 / 3.91	600
H	2-HOC_6H_4	206–208	$C_{16}H_{13}NO_4$	67.84 / 67.91	4.63 / 4.61	NA[c]
H	4-$CF_3C_6H_4$	175–176	$C_{17}H_{12}F_3NO_3$	60.90 / 60.93	3.61 / 3.55	300

[a] Recrystallized from ethanol, melting point uncorrected, spectral data consistent with structure. [b] Anticonvulsant screenings were carried out through the Antiepileptic Drug Development Program, National Institutes of Health. The standard screening protocol of the group was followed (see Table I). All compounds were inactive at 600 mg/kg in the maximal electroshock seizure test. [c] No activity at 600 mg/kg.

Table V—Dehydration of Products (Table I) from Isatins and Cyclohexanone

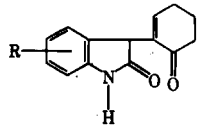

R	mp°,[a]	Formula	Analysis, % Calc. / Found C	Analysis, % Calc. / Found H	Analysis, % Calc. / Found N	Anticonvulsant Activity, mg/kg[b] MES	Met
H	207[c]	$C_{14}H_{13}NO_2$	—	—	—	100[d]	NA[e]
5-Br	245–246[f]	$C_{14}H_{12}BrNO_2$	54.92 / 54.89	3.95 / 3.58	—	600	NA[g]
5-Cl	233–234[f]	$C_{14}H_{12}ClNO_2$	64.25 / 63.78	4.62 / 4.34	5.35 / 4.96	NA[g]	NA[g]
5-CH_3	211–213	$C_{15}H_{15}NO_2$[h]	72.70 / 72.87	6.86 / 6.42	5.30 / 5.14	300	NA[g]
5-NO_2	216–217	$C_{14}H_{12}N_2O_4$	61.76 / 61.65	4.44 / 4.48	10.29 / 10.22	NA[g]	NA[g]
5-CH_3O-6-Cl	265–266	$C_{15}H_{14}ClNO_3$	61.75 / 61.86	4.84 / 4.91	—	NA[g]	NA[g]
H[i]	190–192[j]	$C_{15}H_{15}NO_2$[i]	74.66 / 74.58	6.27 / 6.25	—	300	300

[a] Recrystallized from ethanol, melting point uncorrected, spectral data consistent with structure. [b] Anticonvulsant screenings were carried out through the Antiepileptic Drug Development Program, National Institutes of Health. The standard screening protocol of the group was followed (see Table I). [c] Described in ref. 2. [d] MES ED_{50} 519. TD_{50} > 1600. [e] No activity at 300 mg/kg. [f] Vε insoluble, not recrystallized, but washed with hot solvents. [g] No activity at 600 mg/kg. [h] Analysis for $C_{15}H_{15}NO_2 \cdot 0.5C_2H_5OH$. [i] Dehydration of isatin-2-methylcyclohexanone product. [j] Reported (7) mp 185–186°.

However, to date, no consistent structure to activity pattern has become evident.

REFERENCES

(1) F. D. Popp and B. E. Donigan, *J. Pharm. Sci.*, **68**, 519 (1979).
(2) F. D. Popp, R. Parson, and B. E. Donigan, *ibid.*, **69**, 1235 (1980).
(3) F. D. Popp, R. Parson, and B. E. Donigan, *J. Heterocycl. Chem.*, **17**, 1329 (1980).
(4) S. Pietra and G. Tacconi, *Farmaco Ed. Sci.*, **20**, 891 (1965).
(5) F. D. Popp and H. Pajouhesh, *J. Pharm. Sci.*, **71**, 1052 (1982).
(6) F. D. Popp, *J. Heterocycl. Chem.*, **19**, 589 (1982).
(7) S. Pietra and G. Taconi, *Farmaco. Ed. Sci.*, **16**, 492 (1961).

ACKNOWLEDGMENTS

The authors thank the ADD program of the NINCDS, National Institute of Health making available the anticonvulsant screening tests.

Thermal Decomposition of Aspirin: Formation of Linear Oligomeric Salicylate Esters

Keyphrases □ Decomposition, thermal—aspirin, formation of linear oligomeric salicylate esters □ Aspirin—thermal decomposition, formation of linear oligomeric salicylate esters □ Salicylate esters—thermal decomposition of aspirin, formation of linear oligomeric salicylate esters

To the Editor:

Although there are numerous reports on aspirin stability or degradation described in terms of decreasing amounts of aspirin or increasing amounts of salicylic acid, few recognize the existence of decomposition products other than salicylic acid. Pyrolysis of aspirin with simultaneous distillation of products at 300–350° (15 mm) produces cyclic polymers of salicylic acid, referred to as salicylides; the *cis*-disalicylide and the trisalicylide have been isolated[1] (1–4). Salicylsalicylic acid (I*a*) (5) and acetylsalicylsalicylic acid (I*b*) (6, 7) have also been recognized as decomposition products of aspirin. Aspirin anhydride (8), salicylsalicylic acid (I*a*) (9), and acetylsalicylsalicylic acid (I*b*) (10) have been detected as impurities in aspirin tablets. Presented here is the discovery that thermal decomposition of aspirin, in the solid state or in organic solution, produces not only

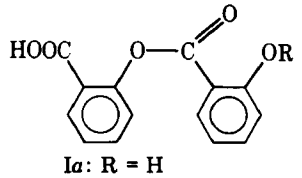

I*a*: R = H
I*b*: R = —$COCH_3$

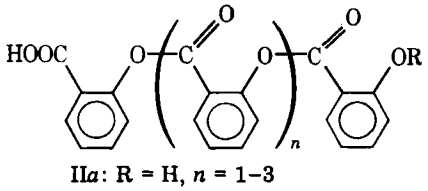

II*a*: R = H, n = 1–3
II*b*: R = —$COCH_3$, n = 1–4

I*a* and *b*, but higher linear oligomeric salicylate esters (II*a*) and their acetate derivatives (II*b*).

When a mixture of aspirin and magnesium carbonate[2] (2:1) was heated in the solid state at 85° for 2 hr, a complex mixture was obtained[3]. The reverse-phase C-18 high-performance liquid chromatogram of this mixture showed components corresponding in retention time to salicylic acid, I*a*, I*b*, and several components with longer retention times (Fig. 1). Chromatographic separation and crystallization provided several pure compounds, three of which were shown to be salicylic acid, I*a*, and I*b* by comparison with authentic compounds. Compounds with longer retention times had UV spectra characteristic of salicylates.

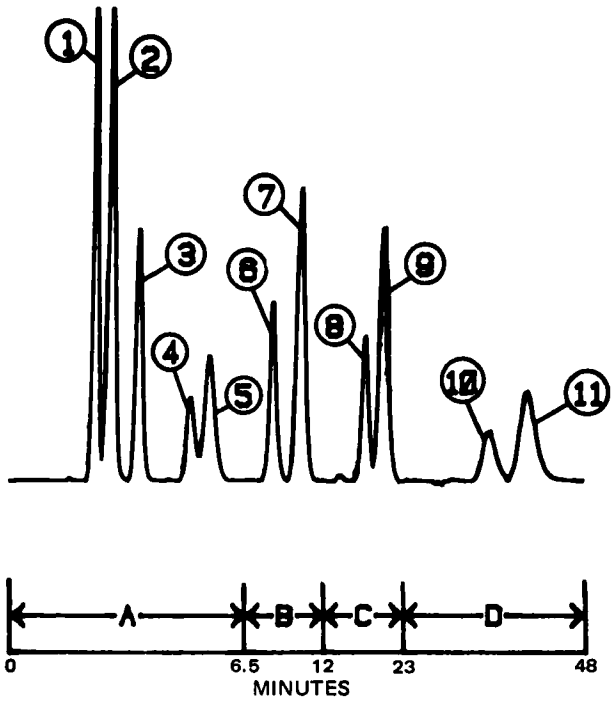

Figure 1—*Reversed-phase C-18 high-performance liquid chromatogram of decomposed aspirin. Mobile phase: water–acetic acid–methanol (420:10:570); flow rate: 2.0 ml/min; detection: UV absorbance at 254 nm. Recorder settings (att = attenuator (2↑), cs = chart speed, cm/min): (A) att 9, cs 0.5; (B) att 6, cs 0.2; (C) att 4, cs 0.1; (D) att 3, cs 0.1. Key (each compound is followed by its retention time in minutes): (1) aspirin, 2.19; (2) salicylic acid, 2.62; (3) Ib, 3.40; (4) Ia, 4.88; (5) IIb (n = 1), 5.40; (6) IIa (n = 1), 8.26; (7) IIb (n = 2), 10.18; (8) IIa (n = 2), 17.23; (9) IIb (n = 3), 19.63; (10) IIa (n = 3), 33.93; (11) IIb (n = 4), 39.13.*

Acetyl compounds (I*b* and II*b*) could be readily differentiated from free phenolic compounds (I*a* and II*a*) by a significant difference in their absorbance maxima (near 278 nm for acetyl compounds and 309 nm for free phenols) in acidic or neutral aqueous alcohol and very rapid cleavage of the acetate esters in 0.01 *N* aqueous ethanolic sodium hydroxide, a reaction completed in 2 min at room temperature, to form the corresponding free phenolic compounds, whose absorbance maxima were near 340 nm in basic solution.

Hydrolysis of the salicylate esters in 0.01 *N* aqueous ethanolic sodium hydroxide occurred over several hours, much slower than acetate ester hydrolysis, and eventually each oligomer (I*a*, I*b*, II*a*, II*b*) was completely converted to salicylic acid (λ_{max} 297 nm). This afforded a means to measure the equivalent weight of each compound in terms of the number of salicyl moieties in the molecule. This technique was suitable for the lower oligomers; however, the higher the oligomer, the closer its equivalent weight approaches those of its neighboring homologues, making it more difficult to differentiate among them.

Like aspirin, I*a* also undergoes thermal decomposition[4]. Being free of acetyl compounds, decomposed I*a* was a

[1] Tetra- and hexasalicylides were also isolated when salicylic acid was treated with phosphorus oxychloride or when salicyloyl chloride was heated (1, 2).

[2] Although aspirin itself decomposes when heated, the rate is greatly accelerated by weak bases such as magnesium carbonate.

[3] A similar mixture was obtained when aspirin was heated in benzene or toluene with or without magnesium carbonate in suspension.

[4] The rate of decomposition of I*a* is slower than that of aspirin. This is attributed to the lower reactivity of the salicylate ester relative to the acetate ester. As with aspirin decomposition, I*a* decomposition is catalyzed by magnesium carbonate.

0022-3549/83/0300-0322$01.00/0

much less complex mixture than decomposed aspirin, and its components were more easily separated. The linear trimer (II*a*, $n = 1$) was isolated from decomposed I*a* as a white crystalline solid, mp 150–152°; UV: λ_{max} (ethanol) 228 (ϵ 27,200), 281 (4350), and 310 (4900) nm; IR (chloroform): ν_{max} 1746 (strong, unassociated ester C=O stretching) and 1696 (strong, intramolecular hydrogen-bonded ester C=O stretching[5] and intermolecular hydrogen-bonded acid C=O stretching) cm^{-1}; NMR (deuterochloroform): δ 10.07 (s, 2H, COOH and OH, exchanged with deuterium), 8.43–7.87 (m, 3H, aromatic protons *ortho* to C=O), and 7.87–6.57 (m, 9H, remaining aromatic protons) ppm.

Anal.—Calc. for $C_{21}H_{14}O_7$: C, 66.67; H, 3.73. Found: C, 66.88; H, 3.92.

Compound II*a* ($n = 1$) was acetylated to provide a compound identical to II*b* ($n = 1$) isolated from decomposed aspirin. Compound II*b* ($n = 1$) was obtained as a white crystalline solid, mp 161.5–163°; UV: λ_{max} (ethanol) 227 (ϵ 29,900) and 277 (4500) nm; IR (chloroform): ν_{max} 1750 (strong, C=O stretching of three ester groups) and 1703 (weak, intermolecular hydrogen-bonded acid C=O stretching) cm^{-1}; NMR (deuterochloroform): δ 8.43–7.80 (m, 4H, COOH proton, which exchanged with deuterium, and three aromatic protons *ortho* to C=O), 7.80–6.90 (m, 9H, remaining aromatic protons), and 2.23 (s, 3H, $—CH_3$) ppm.

Anal.—Calc. for $C_{23}H_{16}O_8$: C, 65.72; H, 3.84. Found: C, 65.53; H, 4.03. Compound II*b* ($n = 1$) was also found in several samples of buffered aspirin tablets; it was isolated from one of them and identified.

The tetramer (II*a*, $n = 2$) was isolated from decomposed I*a* as white crystals, mp 177–183° (dec); IR (chloroform): ν_{max} 1744 (strong, stretching of two unassociated ester carbonyl groups) and 1693 (strong, intramolecular hydrogen-bonded ester carbonyl stretching[5] and intermolecular hydrogen-bonded acid carbonyl stretching) cm^{-1}.

Anal.—Calc. for $C_{28}H_{18}O_9$: C, 67.47; H, 3.64. Found: C, 67.63; H, 3.77.

In the aromatic region the NMR spectrum (deuterochloroform) had two multiplets that were not fully resolved until the solution was shaken with deuterium oxide, which indicated that the exchangeable phenolic and carboxylic acid protons were obscured by aromatic proton absorption.

The methyl esters of I*a*, I*b*, trimer (II*a*, $n = 1$), tetramer (II*a*, $n = 2$), and acetyl-trimer (II*b*, $n = 1$) were synthesized by treatment of the acids with methyl iodide; solid–liquid phase transfer catalysis (11) was used to avoid acetate or salicylate ester hydrolysis during methylation. IR spectra for each of the five methyl esters in carbon tetrachloride supported their structures; the following assignments were made for carbonyl stretching frequencies: ν_{max} 1735–1731 (methyl esters), 1758–1754 (unassociated carbonyl of ester groups between aromatic rings), 1700–1695 (intramolecular hydrogen-bonded ester[5]), 1780–1779 (acetate ester) cm^{-1}. The NMR spectrum (deuterochloroform) of each compound had a singlet near δ 3.7 (methyl ester protons) and two multiplets, one downfield from δ 7.8 (aromatic protons *ortho* to C=O) and the other upfield from δ 7.8 (remaining aromatic protons). In addition to these peaks, the spectra of the three phenolic compounds showed a sharp singlet near δ 10.25 (hydroxide proton, which was exchangeable with deuterium), and the spectra of the two acetyl derivatives showed a singlet at δ 2.25 ($CH_3CO_2—$). The integrals of each compound's spectrum gave the proper ratio of protons for the assigned structures.

Additional proof that these compounds were oligomers was provided by their relative retention on a reverse-phase C-18 high-performance liquid chromatogram. Plots of logarithms of capacity factors (k') for a homologous series have been shown to be linear in a number of cases (12). A plot of log k' *versus* number of salicyl moieties for each of the components in decomposed I*a* was found to be linear[6]. Two linear plots were obtained for decomposed aspirin: one for the free phenols[6], components corresponding in retention time to components in decomposed I*a*, and one for the acetyl compounds[7], the remaining components in the chromatogram. The linear oligomers, produced from aspirin at low temperatures as reported here, are undoubtedly precursors to the previously reported cyclic salicylate oligomers (1–4) produced at much higher temperatures.

Sample analyses showed that the levels of linear salicylate oligomers were generally higher in buffered than in plain aspirin tablets. Subsequent experiments revealed that the thermal decomposition reaction was catalyzed by weakly basic substances, such as magnesium hydroxide or magnesium carbonate, compounds often used in buffered aspirin formulations.

(1) R. Anschutz and K. Rupenkroger, *Justus Liebigs Ann. Chem.*, **439**, 1 (1924).

(2) W. Baker, W. D. Ollis, and T. S. Zeally, *J. Chem. Soc.*, **1951**, 201.

(3) R. Anschutz, *Chem. Ber.*, **52**, 1875 (1919).

(4) G. Schroeter, *ibid.*, **52**, 2224 (1919).

(5) V. Y. Taguchi, M. L. Cotton, C. H. Yates, and J. F. Miller, *J. Pharm. Sci.*, **70**, 64 (1981).

(6) D. Davidson and L. Auerbach, *J. Am. Chem. Soc.*, **75**, 5984 (1953).

(7) H. Bundgaard and C. Larsen, *J. Pharm. Sci.*, **65**, 776 (1976).

(8) A. L. DeWeck, *Int. Arch. Allergy Appl. Immunol.*, **41**, 393 (1971).

(9) J. C. Reepmeyer and R. D. Kirchhoefer, *J. Pharm. Sci.*, **68**, 1167 (1979).

(10) S. Patel, J. H. Perrin, and J. J. Windheuser, *ibid.*, **61**, 1794 (1972).

(11) A. Arbin, H. Brink, and J. Vessman, *J. Chromatogr.*, **170**, 25 (1979).

(12) W. R. Melander and C. Horvath, in "High-Performance Liquid Chromatography, Advances and Perspectives," vol. 2, C. Horvath, Ed., Academic, New York, N.Y., 1980, pp. 219–220.

John C. Reepmeyer

Food and Drug Administration
National Center for Drug Analysis
St. Louis, MO 63101

Received July 14, 1982.
Accepted for publication September 17, 1982.

[5] A strong intramolecular hydrogen bond exists between the ester carbonyl on the terminal aromatic ring and the phenolic group *ortho* to it.

[6] Log k' *versus* salicyl moieties was plotted for four compounds corresponding to dimer (I*a*) through pentamer (II*a*, $n = 3$); the correlation coefficient was 0.9994.

[7] Log k' *versus* salicyl moieties was plotted for five compounds corresponding to dimer (I*b*) through hexamer (II*b*, $n = 4$); the correlation coefficient was 0.9998. Each acetyl compound eluted from the C-18 column prior to its corresponding free phenol.

Biologically Reversible Phosphate-Protective Groups

Keyphrases □ Phosphate-protective groups—biologically reversible, acyloxymethyl groups □ Acyloxymethyl groups—biologically reversible phosphate-protective groups □ Chemotherapeutic agents—biologically reversible phosphate-protective groups, acyloxymethyl groups, as a means of traversing biological membranes

To the Editor:

The inability of nucleotides and other ionic organophosphate esters to traverse biological membranes (1, 2) constitutes a major impediment to the use of such compounds as chemotherapeutic agents. In an attempt to overcome this limitation, we have investigated the potential of acyloxymethyl groups as biologically reversible phosphate-protective groups. Conceivably, neutral acyloxymethyl phosphotriesters[1] could penetrate cell membranes by passive diffusion and revert, intracellularly, to the parent ionic phosphate after cleavage of the acyloxy group by carboxylate esterase and elimination of formaldehyde (Scheme I). To explore synthetic routes to bis(acyloxymethyl) phosphotriesters and to investigate the chemical properties of this class of compounds, we chose phenyl phosphate as a model organophosphate monoester.

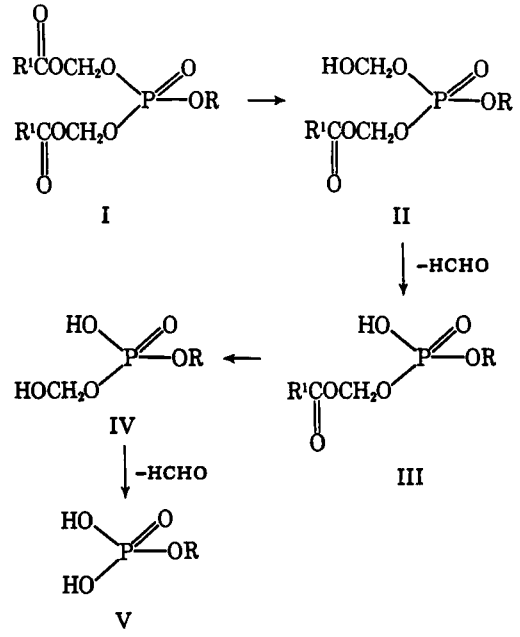

Scheme I

Reaction of disilver phenyl phosphate[2] (VI*a*) with a 2.5 mole excess of iodomethyl acetate (VII*a*) (3) in anhydrous benzene at room temperature for 5 hr gave bis(acetoxymethyl) phenyl phosphate[3,4] (I*a*) in 53% yield. Bis(pivaloyloxymethyl) phenyl phosphate[3] (I*b*) was prepared similarly from (VI*a*) and iodomethyl pivaloate (VII*b*) (3) in 54% yield (Scheme II).

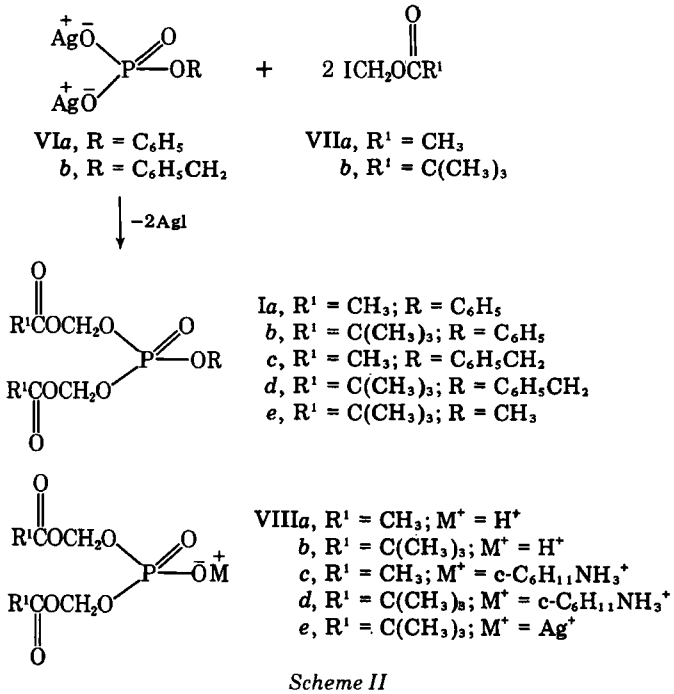

Scheme II

Compound I*a* was stable in neutral aprotic solvents (*e.g.*, benzene, diethyl ether, ethyl acetate); however, in protonic solvents (*e.g.*, ethanol, water, 0.05 *M* potassium phosphate buffer, pH 7.4) it was converted[5] slowly ($t_{1/2}$ > 4 hr) to mono(acetoxymethyl) phenyl phosphate (III, R = C_6H_5, R^1 = CH_3). This product is presumably formed by solvolysis of I*a* to the hydroxymethyl intermediate[6] (II, R = C_6H_5, R^1 = CH_3), followed by spontaneous loss of formaldehyde. When incubated at 37° in 0.05 *M* potassium phosphate buffer (pH 7.4) with hog liver carboxylate esterase[7] (E.C. No. 3.1.1.1) (1.6 mg of protein/ml) or mouse plasma (50% by volume), I*a* (2 m*M*) was rapidly degraded[8] ($t_{1/2}$ < 15 min), first to the mono(acetoxymethyl) analogue

[1] To the best of the authors' knowledge, such compounds have not previously been reported.

[2] Obtained from the corresponding disodium salt by reaction with silver nitrate in water.

[3] Obtained as a viscous oil.

[4] All compounds gave satisfactory elemental analyses and exhibited spectral characteristics (NMR, MS, IR) consistent with the assigned structures.

[5] The solutions were analyzed by high-performance liquid chromatography (HPLC) (Waters model ALC 204). The disappearance of I was monitored by reverse-phase chromatography on a column of μBondapak-C_{18} (30 cm × 4-mm i.d., 10 μm; Waters Assoc., Milford, Mass.) using solutions of 0.01 *M* potassium phosphate buffer (pH 7.0)–methanol (various proportions, typically 25–50% alcohol) as mobile phase. The formation of III and V was monitored by ion-pair chromatography on μBondapak-C_{18} using the same buffer system as described for I except that tetrabutylammonium hydroxide was added to a concentration of 2×10^{-3} *M*, or by anion-exchange chromatography on a column of Partisil SAX (25 cm × 4.6-mm i.d., 10 μm; Whatman) using a linear gradient of 0.01–0.1 *M* potassium phosphate buffer (pH 6.5) as eluent. The flow rates ranged from 1.0 to 2.0 ml/min. The column effluents were monitored at 254 nm with a Schoeffel model 450 UV detector, and the concentrations of I, III, and V were determined by comparison of the peak areas with those of reference standards.

[6] A labile intermediate was detected in some solutions by HPLC but was not characterized. The hydroxymethyl compound II (R = C_6H_5, R^1 = CH_3) is expected to facilely dissociate, probably by a six-membered cyclic transition state, to give mono(acetoxymethyl) phenyl phosphate and formaldehyde:

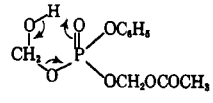

[7] Obtained from Sigma Chemical Co., St. Louis, Mo.

[8] At appropriate intervals, aliquots (100 μl) of the incubation mixtures were diluted with 3 volumes of methanol than agitated for 1 min on a Vortex shaker. The precipitated protein was separated by centrifugation at 10,000×*g* for 5 min, and the supernatants were analyzed by HPLC as described in footnote 5.

0022-3549/83/0300-0324$01.00/0

(III, R = C_6H_5, R^1 = CH_3) and then to phenyl phosphate (V, R = C_6H_5).

The bis(pivaloyloxymethyl) phosphotriester[3] (I*b*), by comparison, was much more resistant to both chemical and enzymatic hydrolysis. Thus, it was stable in protonic solvents and had a half-life ≃5 hr when incubated with mouse plasma under conditions identical to that described for I*a*. Clearly, the nature of the acyl substituent has a marked influence on the susceptibility of bis(acyloxymethyl) phosphotriesters to hydrolysis.

The benzyl phosphotriesters, I*c*[3] and I*d*[3], were prepared similarly from disilver benzyl phosphate[2] (VI*b*). Catalytic hydrogenolysis of these compounds over 5% palladium-on-charcoal Pd-C in cyclohexane gave the corresponding monobasic acids, VIII*a* and *b* which were isolated as their cyclohexylammonium salts, VIII*c* and *d*. Silver bis(pivaloyloxymethyl) phosphate (VIII*e*) was prepared from VIII*d* by successive ion-exchange[9]. Reaction of VIII*e* with benzyl bromide or methyl iodide in benzene for 5 hr at room temperature gave bis(pivaloyloxymethyl) benzyl phosphate[3] (I*d*) and bis(pivaloyloxymethyl) methyl phosphate[3] (I*e*), respectively, in nearly quantitative yield. These reactions illustrate the utility of VIII*e* in the synthesis of bis(acyloxymethyl) phosphotriesters.

Reactions of VIII*e* with 5′-deoxy-5′-iodo-3′-*O*-acetylthymidine (IX*a*) (4) in toluene under reflux for 5 hr gave bis(pivaloyloxymethyl)-3′-*O*-acetylthymidine-5′-phosphate (X*a*), 39% yield (Scheme III). Similarly, the reaction

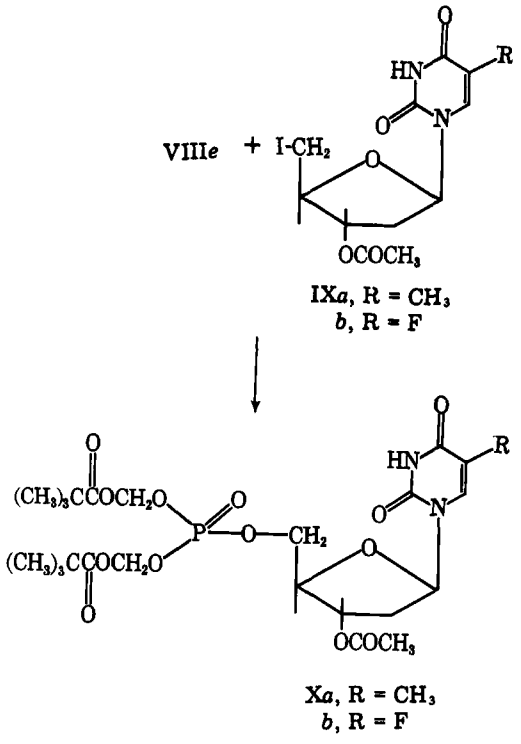

Scheme III

of VIII*e* with 2′,5-dideoxy-5′-iodo-3′-*O*-acetyl-5-fluorouridine[10] (IX*b*) gave X*b* (15% yield). Compound X*b* prevented the growth of Chinese hamster ovary cells in culture (5) at a concentration of 5.0×10^{-6} *M* (5-fluoro-2′-deoxyuridine control, 1.0×10^{-6} *M*).

Further chemical and biological studies of these compounds are in progress.

[9] Prepared on Dowex 50 Na^+ and Dowex 50 Ag^+.

[10] Prepared from 3′-*O*-acetyl-2′-deoxy-5-fluorouridine in 65% yield, according to the general procedure described previously (4).

(1) K. C. Liebman and C. Heidelberger, *J. Biol. Chem.*, **216**, 823 (1955).

(2) P. M. Roll, H. Weinfeld, E. Carroll, and G. B. Brown, *ibid.*, **220**, 439 (1956).

(3) E. K. Euranto, A. Napolen, and T. Kujanpaa, *Acta. Chem. Scand.*, **20**, 1273 (1966).

(4) J. P. H. Verheyden and J. G. Moffatt, *J. Org. Chem.*, **35**, 2319 (1970).

(5) P. P. Saunders, L.-Y. Chao, T. L. Loo, and R. K. Robins, *Biochem. Pharmacol.*, **30**, 2374 (1981).

*David Farquhar**
Devendra N. Srivastva
Nancy J. Kuttesch
Priscilla P. Saunders
Department of Developmental Therapeutics
The University of Texas M. D. Anderson Hospital and Tumor Institute at Houston
Texas Medical Center
Houston, TX 77030

This research was supported by Grant CA 14528 from the National Cancer Institute, National Institutes of Health.

Received April 5, 1982.

Accepted for publication September 9, 1982.

Estimation of the Extent of Drug–Excipient Interactions Involving Croscarmellose Sodium

Keyphrases □ Croscarmellose sodium—estimation of the extent of drug–excipient interactions □ Drug–excipient interactions—estimation of the extent involving croscarmellose sodium □ Excipients—estimation of the extent of drug–excipient interactions involving croscarmellose sodium

To the Editor:

In a recent communication (1), a pH-dependent interaction of oxymorphone derivatives with croscarmellose sodium, Type A, NF XV[1] was identified. Any drug–excipient interaction is potentially serious if it has a deleterious influence on the bioavailability of the drug from the dosage form. However, as in this case, the excipient may be responsible for certain dosage form properties which promote or at least ensure reproducible drug delivery.

There is a need to be able to assess the risk which may be involved before advocating or indicting an excipient. The objectives here are to provide a means for determining when an interaction with the disintegrant croscarmellose sodium might be expected and a means for estimating the extent of the interaction when it occurs.

Certain aspects of the interaction were presented in the previous communication (1); although, the general utility of these results is limited. Details were not given con-

[1] Ac-Di-Sol, FMC Corporation, Philadelphia, Pa.

0022-3549/83/0300-0325$01.00/0

(III, R = C_6H_5, R^1 = CH_3) and then to phenyl phosphate (V, R = C_6H_5).

The bis(pivaloyloxymethyl) phosphotriester[3] (I*b*), by comparison, was much more resistant to both chemical and enzymatic hydrolysis. Thus, it was stable in protonic solvents and had a half-life ≃5 hr when incubated with mouse plasma under conditions identical to that described for I*a*. Clearly, the nature of the acyl substituent has a marked influence on the susceptibility of bis(acyloxymethyl) phosphotriesters to hydrolysis.

The benzyl phosphotriesters, I*c*[3] and I*d*[3], were prepared similarly from disilver benzyl phosphate[2] (VI*b*). Catalytic hydrogenolysis of these compounds over 5% palladium-on-charcoal Pd-C in cyclohexane gave the corresponding monobasic acids, VIII*a* and *b* which were isolated as their cyclohexylammonium salts, VIII*c* and *d*. Silver bis(pivaloyloxymethyl) phosphate (VIII*e*) was prepared from VIII*d* by successive ion-exchange[9]. Reaction of VIII*e* with benzyl bromide or methyl iodide in benzene for 5 hr at room temperature gave bis(pivaloyloxymethyl) benzyl phosphate[3] (I*d*) and bis(pivaloyloxymethyl) methyl phosphate[3] (I*e*), respectively, in nearly quantitative yield. These reactions illustrate the utility of VIII*e* in the synthesis of bis(acyloxymethyl) phosphotriesters.

Reactions of VIII*e* with 5′-deoxy-5′-iodo-3′-*O*-acetylthymidine (IX*a*) (4) in toluene under reflux for 5 hr gave bis(pivaloyloxymethyl)-3′-*O*-acetylthymidine-5′-phosphate (X*a*), 39% yield (Scheme III). Similarly, the reaction

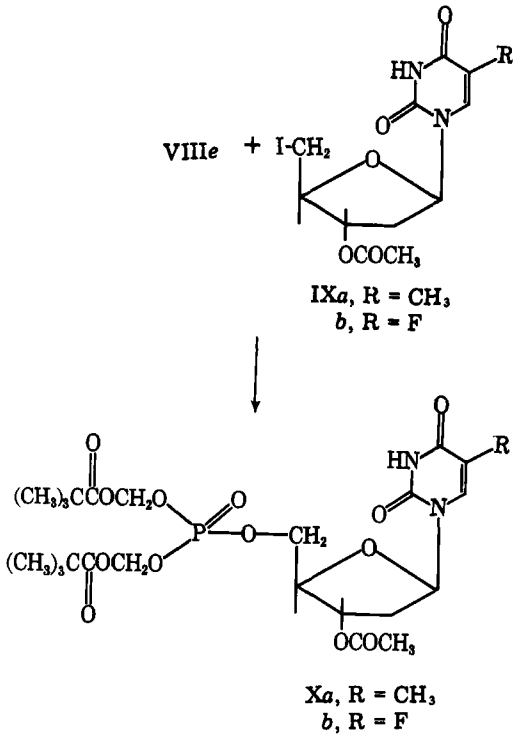

Scheme III

of VIII*e* with 2′,5-dideoxy-5′-iodo-3′-*O*-acetyl-5-fluorouridine[10] (IX*b*) gave X*b* (15% yield). Compound X*b* prevented the growth of Chinese hamster ovary cells in culture (5) at a concentration of 5.0×10^{-6} *M* (5-fluoro-2′-deoxyuridine control, 1.0×10^{-6} *M*).

Further chemical and biological studies of these compounds are in progress.

[9] Prepared on Dowex 50 Na^+ and Dowex 50 Ag^+.

[10] Prepared from 3′-*O*-acetyl-2′-deoxy-5-fluorouridine in 65% yield, according to the general procedure described previously (4).

(1) K. C. Liebman and C. Heidelberger, *J. Biol. Chem.*, **216**, 823 (1955).

(2) P. M. Roll, H. Weinfeld, E. Carroll, and G. B. Brown, *ibid.*, **220**, 439 (1956).

(3) E. K. Euranto, A. Napolen, and T. Kujanpaa, *Acta. Chem. Scand.*, **20**, 1273 (1966).

(4) J. P. H. Verheyden and J. G. Moffatt, *J. Org. Chem.*, **35**, 2319 (1970).

(5) P. P. Saunders, L.-Y. Chao, T. L. Loo, and R. K. Robins, *Biochem. Pharmacol.*, **30**, 2374 (1981).

*David Farquhar**
Devendra N. Srivastva
Nancy J. Kuttesch
Priscilla P. Saunders
Department of Developmental Therapeutics
The University of Texas M. D. Anderson Hospital and Tumor Institute at Houston
Texas Medical Center
Houston, TX 77030

This research was supported by Grant CA 14528 from the National Cancer Institute, National Institutes of Health.

Received April 5, 1982.

Accepted for publication September 9, 1982.

Estimation of the Extent of Drug–Excipient Interactions Involving Croscarmellose Sodium

Keyphrases □ Croscarmellose sodium—estimation of the extent of drug–excipient interactions □ Drug–excipient interactions—estimation of the extent involving croscarmellose sodium □ Excipients—estimation of the extent of drug–excipient interactions involving croscarmellose sodium

To the Editor:

In a recent communication (1), a pH-dependent interaction of oxymorphone derivatives with croscarmellose sodium, Type A, NF XV[1] was identified. Any drug–excipient interaction is potentially serious if it has a deleterious influence on the bioavailability of the drug from the dosage form. However, as in this case, the excipient may be responsible for certain dosage form properties which promote or at least ensure reproducible drug delivery.

There is a need to be able to assess the risk which may be involved before advocating or indicting an excipient. The objectives here are to provide a means for determining when an interaction with the disintegrant croscarmellose sodium might be expected and a means for estimating the extent of the interaction when it occurs.

Certain aspects of the interaction were presented in the previous communication (1); although, the general utility of these results is limited. Details were not given con-

[1] Ac-Di-Sol, FMC Corporation, Philadelphia, Pa.

0022-3549/83/0300-0325$01.00/0

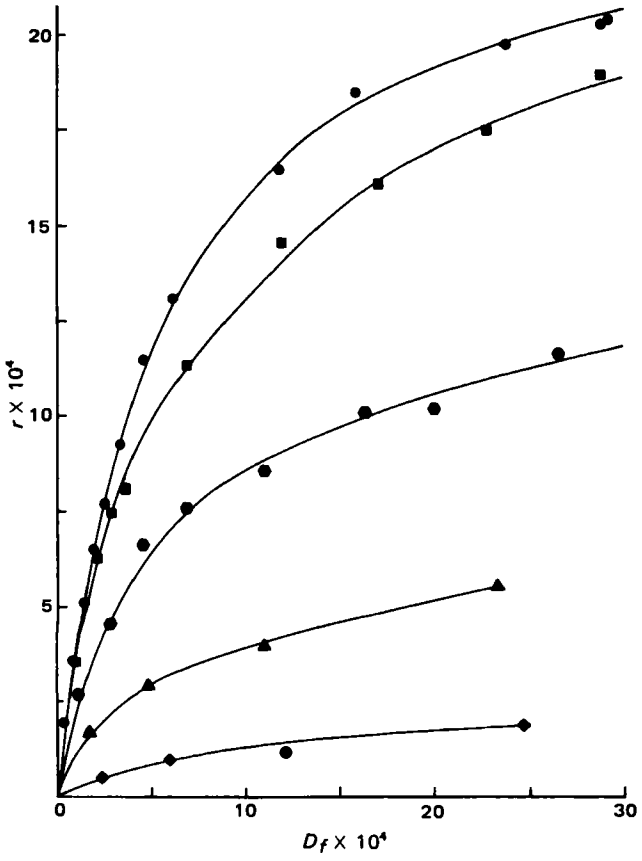

Figure 1—*Interaction isotherms of chlorpheniramine with croscarmellose sodium in aqueous dispersion at various hydrogen ion activities at 25°. (See Table I for definition of symbols, units and experimental conditions.) Key: (●) pH 7; (■) pH 6; (●) pH 5; (▲) pH 4; (◆) pH 3.*

Table I—Identification and Definition of Experimental Variables

Variable	Units	Experimental Value
D_T	Total amount of drug, moles	—
A_T	Total amount of excipient, g	0.100
V	Volume of liquid, liters	0.200
D_f	Free drug concentration, moles/liter	—
r	Moles of drug bound per gram of excipient	—

cerning analytical procedure, the method of altering pH, and the units of drug and disintegrant concentration. Without this information, it is not possible to estimate the extent of an interaction that might be expected under a different set of conditions.

An effort is underway in this laboratory to characterize the interaction of ionized weak bases with croscarmellose sodium. In light of the preceding discussion, we present a portion of our results that they may provide a qualitative and quantitative guide to these interactions. Figure 1 represents the results of a study of the interaction of chlorpheniramine maleate[2] with croscarmellose sodium at varying pHs. The experimental variables are defined in Table I, along with the values used to generate the results in Fig. 1. In an effort to keep the ionic strength low, the pH was adjusted in each case by the dropwise addition of 0.1 *N* HCl or 0.1 *N* NaOH, whichever was appropriate. After a 24-hr equilibration period, during which the drug–ex-

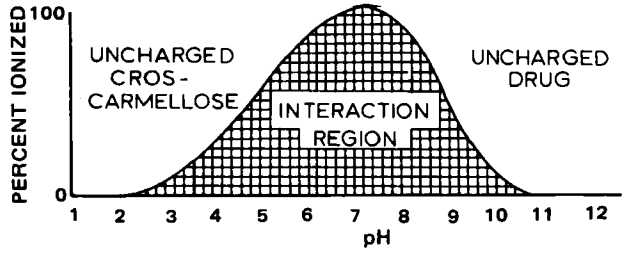

Figure 2—*Croscarmellose interaction profile for a hypothetical weakly basic drug with pKa = 9.0. (See text for details.)*

cipient suspension was maintained at 25°, the suspension was allowed to settle, and an aliquot of the supernatant was withdrawn with a syringe. The aliquot was freed of particles by rapid filtration through a borosilicate microfiber glass depth filter pad[3], and free drug concentrations were determined by UV spectrophotometric analysis of the filtrate at the pH-dependent wavelength of a maximum absorbance (261.5–264.5 nm). Free drug concentrations are presented in terms of molar concentration, because it is anticipated that these results can be extended to weak bases other than chlorpheniramine. The amount of drug adsorbed was determined by mass balance with quantitative corrections made for the slight adsorption to the filter, which occurred at high concentrations of drug.

It appears that the interaction is of electrostatic origin, involving ionized croscarmellose (negatively charged, pH >2) and cations. Thus, any weakly basic drug in an environment whose pH is >2 and near or below the pK_a of the weak base should be expected to interact with the ionized polymer. This generalization is presented graphically in Fig. 2 for a hypothetical weakly basic drug with a pK_a of 9.0. The ionization of the drug has been calculated from the pK_a assuming ideal behavior. The ionization of the drug outlines the interaction region at higher pHs. The ionization of croscarmellose has been estimated from the maximum binding data (r[max]) in Fig. 1. At pH 7, r[max] = 24×10^{-4} moles of drug/g of excipient, and the assumption is made that this value represents the maximum number of binding sites available. The fraction of croscarmellose ionized at any pH may be estimated by comparing the number of sites at that pH to the value at pH 7. At pH 4, for example, r[max] = 6×10^{-4} moles of drug/g of excipient, and the amount of croscarmellose ionized is estimated to be 25%. The outline of the interaction region at lower pHs has been generated by similar calculations.

An independent attempt to determine the pK_a of croscarmellose by titration produced spurious results, possibly due to the competitive equilibria for binding sites involving sodium and hydrogen ions. The influence of sodium ions on binding is addressed in subsequent discussion.

A diagram may be constructed for a drug with any pK_a by reconstructing the drug ionization curve. The area of the interaction region increases the higher the pK_a of the weak base. If the drug is a weak acid or nonelectrolyte, no interaction is anticipated.

Assuming that the interaction is nonspecific, reversible, and can be characterized as an equilibrium relationship, Fig. 1 can be utilized to estimate the fraction of drug bound

[2] Chlorpheniramine maleate USP, Hexagon Laboratories, Inc., Bronx, N.Y.

[3] Type AP25, Millipore Corp., Bedford, Mass.

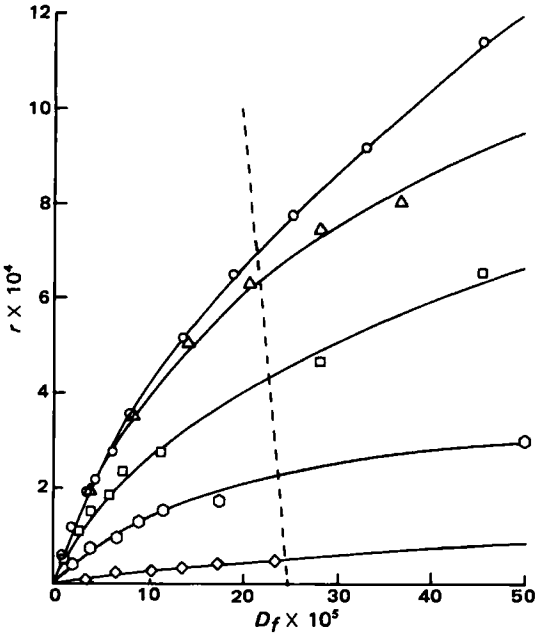

Figure 3—*Low concentration interaction isotherms of chlorpheniramine with croscarmellose sodium in aqueous dispersion at various hydrogen ion activities at 25°. Dashed line defines an interaction profile for the following conditions:* $D_T = 2.5 \times 10^{-5}$ *moles,* $A_T = 0.005$ *g,* V = *0.100 liter. (See Table I for definition of symbols and units.) Key: (○) pH 7; (△) pH 6; (□) pH 5; (○) pH 4; (◇) pH 3.*

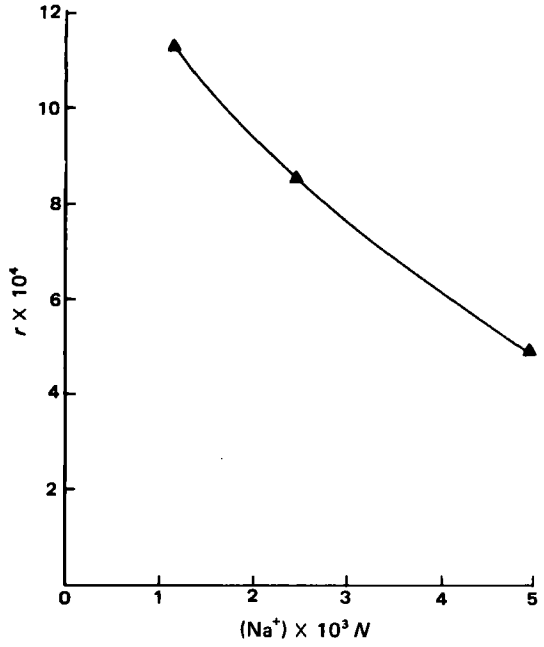

Figure 4—*Effect of added sodium ion concentration on the interaction of chlorpheniramine with croscarmellose sodium at pH 7.0 and 25°;* $D_T = 2.06 \times 10^{-4}$ *moles,* $A_T = 0.100$ *g,* V = *0.200 liter. (See Table I for definition of variables.)*

for any combination of A_T, D_T, and V, as long as the pH is ≤7 and the drug has a $pK_a \geq 9.0$. For purposes of illustration, and because there is particular concern for low dose drugs, Fig. 3 presents an expanded segment of the data from Fig. 1. For this analysis, the following mass balance will be used:

$$D_T = (D_f)V + rA_T \quad \text{(Eq. 1)}$$

where the variables are defined in Table I. By rearrangement:

$$r = \frac{D_T}{A_T} - (D_f)\frac{V}{A_T} \quad \text{(Eq. 2)}$$

It can be seen that r is a linear function of (D_f) when D_T, A_T, and V are fixed. The intercepts of this function:

$$(D_f) = \frac{D_T}{V} \quad \text{(Eq. 3)}$$

when $r = 0$ and:

$$r = \frac{D_T}{A_T} \quad \text{(Eq. 4)}$$

when $D_f = 0$ and/or the slope $(-V/A_T)$ permit construction of a specific binding profile for any set of conditions.

As an example, consider a tablet containing 10 mg of a weakly basic drug, with a pKa >9, a molecular weight of 400, containing 5 mg of croscarmellose sodium as a disintegrant, and placed in 100 ml of liquid.

Thus, $D_T = 2.5 \times 10^{-5}$ moles, $A_T = 0.005$ g, and $V = 0.100$ liter. The dashed line constructed in Fig. 3 from Eq. 2 can be used to determine a pH profile for this particular situation. The free drug concentration at any pH can be determined from the intersection of this line and the appropriate binding isotherm. At pH 7.0, for example, $D_f = 21.5 \times 10^{-5}$ M, and therefore, ~14% of the drug is bound.

The success of this approach depends upon the nonspecificity of the interaction and the validity of the binding data in Figs. 1 and 3. While we are still investigating the former, a comment about the binding results can be made at this time: Interactions in distilled water are generally higher than that predicted by this method. In retrospect, the method of elevating pH in this study, by adding sodium hydroxide, was a poor approach because of the specific competition of binding sites for sodium. Figure 4 presents the results of a simple study where total drug and excipient concentrations were held constant, and sodium ion concentration was increased by adding progressively larger quantities of sodium hydroxide and then adjusting the pH with standardized hydrochloric acid. It can be seen that increases in added sodium ion concentration significantly reduce the amount of drug bound. Thus, the data in Figs. 1 and 2 probably underestimate the extent of binding which would occur at higher pHs in the absence of added sodium ion or other competitive cations. On the other hand, the mean level of sodium ion in gastric fluid is 4.9×10^{-2} N (2), a concentration which must substantially reduce the extent of drug interaction.

Several important questions remain which we will address as further progress is made, and our studies will include *in vivo* work if there is evidence of a potential influence on bioavailability.

(1) Y. W. Chien, P. Van Nostrand, A. R. Hurwitz, and E. G. Shami, *J. Pharm. Sci.*, **70**, 709 (1981).

(2) "Scientific Tables," 7th ed., K. Diem and C. Lentner, Eds., Ciba-Geigy Limited, Basle, Switzerland.

R. Gary Hollenbeck ˣ
Krongtong T. Mitrevej
Allan C. Fan
University of Maryland
School of Pharmacy
Pharmaceutics Department
Baltimore, MD 21201

Received October 21, 1981.
Accepted for publication July 12, 1982.
Supported by a grant from the FMC Corporation.

REVIEWS

Introduction to Alkaloids—A Biogenetic Approach. By GEOFFREY A. CORDELL. Wiley-Interscience, New York, N.Y. 1981. 1055 pp. 17 × 24 cm. Price $50.00.

As the title implies, this introductory text uses the concept of biogenesis to organize a vast and heterogeneous group of natural products, the alkaloids. Comprehensive coverage of alkaloids with specific chemical nuclei have been presented in the past in the form of edited texts and an edited series of volumes. These treatises are predominantly chemically oriented.

Dr. Cordell's effort to cover many aspects of the various biogenetic classes of alkaloids was as a single author and not as an editor. He should be highly commended for his enthusiasm and dedication in the writing of this excellent work. It surely was a monumental, but necessary, task in an era where the alkaloid field is expanding at such a rapid rate.

The book consists of almost 1000 pages divided into 12 chapters. As would be expected, the first chapter involves background material with concise presentations of history, occurrence, classification, properties, detection, isolation, purification, structure elucidation, and pharmacology of the alkaloids. The second chapter focuses on alkaloid biosynthesis and biogenesis and establishes the organizational tenor for the remainder of the text. The next nine chapters deal with alkaloids derived from ornithine, lysine, nicotinic acid, polyacetate, anthranilic acid, phenylalanine and tyrosine, tryptophan, histidine, and isoprenoid metabolism. The last chapter presents several very interesting miscellaneous alkaloids. The Appendix lists formulas for many of the useful alkaloid detecting reagents. In addition to the usual subject index, the organism index provides additional utility to this book.

The individual chapters are sectioned with each section comprising a single important alkaloid or group of related compounds derived from a common biosynthetic precursor. Within each section there are discussions involving chemistry, biosynthesis, and pharmacology. In certain cases useful synthetic and spectral data are presented. Most sections conclude with a listing of selected key literature references.

Although some scientists may be disappointed in the limited coverage of certain groups of alkaloids, Dr. Cordell has done a good job in keeping relative importance in perspective. For instance, Chapters 8 (Alkaloids Derived from Phenylalanine and Tyrosine) and 9 (Alkaloids Derived from Tryptophan) constitute over half of the book. However, these compounds probably deserve this degree of attention because of the great deal of published research on their medicinal value. This perspective and unity of presentation is one important advantage of a single author covering a broad scientific topic.

In conclusion, this book is a useful reference for scientists interested in various aspects of alkaloid research. The illustrations are excellent. Grammatical, spelling, and chemical structure errors are minimal. The utility of this interesting text, however, may be limited by its price.

William J. Keller
Div. of Medicinal
Chemistry and Pharmaceutics
Northeast Louisiana University
Monroe, LA 71209

Textbook of Organic Medicinal and Pharmaceutical Chemistry, 8th Ed. Edited by ROBERT F. DOERGE. Lippincott/Harper, East Washington Square, Philadelphia, PA 19105. 1982. 876 pp. 21 × 26 cm. Price $47.50.

Because of its consistently high quality, the latest edition of this classical textbook, intended for use in undergraduate courses in Medicinal and Pharmaceutical Chemistry, was a pleasure to review. Despite the loss due to death or retirement of several of the prominent contributors to previous editions, those remaining, together with their new collaborators, have written excellent chapters. The combined effort is impressive. The first chapter is a broad overview of medicinal chemistry. This is followed by an effective summary of the basic material of the discipline, such as how structure relates to the drug–receptor interaction, and an excellent exposition of the medicinal chemistry of drug metabolism.

The anti-infectives, a specific group of therapeutical agents, is dealt with in the fourth chapter. Here, and in the remaining chapters, all treating specific groups of agents, one sees a consistent pattern of a thorough overview of the group under consideration and compact discussions of the chemical and biological properties of each of the members of the group.

Chapters dealing with sulfonamides, antimalarials, antibiotics, and antineoplastic agents are all very thorough and well written. Local anesthetics and antihistamines are also treated in well-written chapters. Excellent reviews of analgesics and steroids are also found in this text.

CNS depressants and stimulants and material from the Seventh Edition are substantially updated. Adrenergic agents and cholinergic agents are given highly competent treatment in subsequent chapters.

The chapter on diuretics is impressively updated and another chapter takes us easily through cardiovascular agents, a potentially difficult group.

Carbohydrates, proteins, and vitamins are skillfully treated. A concluding chapter effectively brings together a diverse group of agents, one example of which is diagnostic agents.

Two valuable appendixes describe properties of pharmaceutical aids and list pKa values for a number of drugs. Finally, the index is detailed and should prove to be useful.

All of the chapters of this text show signs of painstaking preparation. Revising and updating over the Seventh Edition is extensive. Literature citations are also extensive and current. Coordination between chapters is very good, and there is little redundancy. There is a high degree of consistency among the chapters in the nature of the material presented and the format for its presentation. A useful feature for pharmacy students is that pertinent chemical properties of the individual agents are given.

In summary, this is a most impressive textbook, judged for completeness, cohesiveness, and balance. The authors have used care and good judgment in making it an appropriate textbook for undergraduate pharmacy students.

Reviewed by Eugene Isaacson
Idaho State University
College of Pharmacy
Pocatello, IO 83201

Physicochemical Principles of Pharmacy. By A. T. FLORENCE and D. ATTWOOD, Chapman and Hall, New York, N.Y. 10017. 1982. 509 pp. 15 × 23 cm. Price $29.95.

The purpose of this book is to provide the physicochemical background to the design and use of pharmaceutical products. Processing technology is not discussed. Special problems of the various routes of administration and of duration of activity are presented if the mechanism is physical and not biological.

An effort is made to demonstrate that often the same forces operate in inanimate and animate systems. The authors assume that undergraduates using this book will have had a standard physical chemistry course. Since it is aimed at undergraduates, the reference lists have been kept to a minimum.

The book is divided into 11 chapters, which are entitled: Gases; Properties of the Solid State; Liquids; Solutions; Solubilty of Drugs in Liquids; Surface Chemistry; Colloidal and Coarse Lyophobic Dispersions; Polymeric Systems; Principles of Drug Absorption and Routes of Administration; Drug Interactions and Incompatibilities: a physicochemical viewpoint; and Chemical Stability of Drugs.

There is an abundance of easily comprehended figures to supplement the text. Although examples are given, perhaps the inclusion of a greater number of sample calculations would have been helpful to the student. The chapters on principles of drug absorption and drug interactions and incompatibilities are especially valuable additions to a book dealing with physicochemical principles. This is a fine text which fulfills its purpose.

Reviewed by Eugene L. Parrott
College of Pharmacy
University of Iowa
Iowa City, IA 52240

0022-3549/83/0300-0328$01.00/0

REVIEWS

Introduction to Alkaloids—A Biogenetic Approach. By GEOFFREY A. CORDELL. Wiley-Interscience, New York, N.Y. 1981. 1055 pp. 17 × 24 cm. Price $50.00.

As the title implies, this introductory text uses the concept of biogenesis to organize a vast and heterogeneous group of natural products, the alkaloids. Comprehensive coverage of alkaloids with specific chemical nuclei have been presented in the past in the form of edited texts and an edited series of volumes. These treatises are predominantly chemically oriented.

Dr. Cordell's effort to cover many aspects of the various biogenetic classes of alkaloids was as a single author and not as an editor. He should be highly commended for his enthusiasm and dedication in the writing of this excellent work. It surely was a monumental, but necessary, task in an era where the alkaloid field is expanding at such a rapid rate.

The book consists of almost 1000 pages divided into 12 chapters. As would be expected, the first chapter involves background material with concise presentations of history, occurrence, classification, properties, detection, isolation, purification, structure elucidation, and pharmacology of the alkaloids. The second chapter focuses on alkaloid biosynthesis and biogenesis and establishes the organizational tenor for the remainder of the text. The next nine chapters deal with alkaloids derived from ornithine, lysine, nicotinic acid, polyacetate, anthranilic acid, phenylalanine and tyrosine, tryptophan, histidine, and isoprenoid metabolism. The last chapter presents several very interesting miscellaneous alkaloids. The Appendix lists formulas for many of the useful alkaloid detecting reagents. In addition to the usual subject index, the organism index provides additional utility to this book.

The individual chapters are sectioned with each section comprising a single important alkaloid or group of related compounds derived from a common biosynthetic precursor. Within each section there are discussions involving chemistry, biosynthesis, and pharmacology. In certain cases useful synthetic and spectral data are presented. Most sections conclude with a listing of selected key literature references.

Although some scientists may be disappointed in the limited coverage of certain groups of alkaloids, Dr. Cordell has done a good job in keeping relative importance in perspective. For instance, Chapters 8 (Alkaloids Derived from Phenylalanine and Tyrosine) and 9 (Alkaloids Derived from Tryptophan) constitute over half of the book. However, these compounds probably deserve this degree of attention because of the great deal of published research on their medicinal value. This perspective and unity of presentation is one important advantage of a single author covering a broad scientific topic.

In conclusion, this book is a useful reference for scientists interested in various aspects of alkaloid research. The illustrations are excellent. Grammatical, spelling, and chemical structure errors are minimal. The utility of this interesting text, however, may be limited by its price.

William J. Keller
Div. of Medicinal
Chemistry and Pharmaceutics
Northeast Louisiana University
Monroe, LA 71209

Textbook of Organic Medicinal and Pharmaceutical Chemistry, 8th Ed. Edited by ROBERT F. DOERGE. Lippincott/Harper, East Washington Square, Philadelphia, PA 19105. 1982. 876 pp. 21 × 26 cm. Price $47.50.

Because of its consistently high quality, the latest edition of this classical textbook, intended for use in undergraduate courses in Medicinal and Pharmaceutical Chemistry, was a pleasure to review. Despite the loss due to death or retirement of several of the prominent contributors to previous editions, those remaining, together with their new collaborators, have written excellent chapters. The combined effort is impressive. The first chapter is a broad overview of medicinal chemistry. This is followed by an effective summary of the basic material of the discipline, such as how structure relates to the drug–receptor interaction, and an excellent exposition of the medicinal chemistry of drug metabolism.

The anti-infectives, a specific group of therapeutical agents, is dealt with in the fourth chapter. Here, and in the remaining chapters, all treating specific groups of agents, one sees a consistent pattern of a thorough overview of the group under consideration and compact discussions of the chemical and biological properties of each of the members of the group.

Chapters dealing with sulfonamides, antimalarials, antibiotics, and antineoplastic agents are all very thorough and well written. Local anesthetics and antihistamines are also treated in well-written chapters. Excellent reviews of analgesics and steroids are also found in this text.

CNS depressants and stimulants and material from the Seventh Edition are substantially updated. Adrenergic agents and cholinergic agents are given highly competent treatment in subsequent chapters.

The chapter on diuretics is impressively updated and another chapter takes us easily through cardiovascular agents, a potentially difficult group.

Carbohydrates, proteins, and vitamins are skillfully treated. A concluding chapter effectively brings together a diverse group of agents, one example of which is diagnostic agents.

Two valuable appendixes describe properties of pharmaceutical aids and list pKa values for a number of drugs. Finally, the index is detailed and should prove to be useful.

All of the chapters of this text show signs of painstaking preparation. Revising and updating over the Seventh Edition is extensive. Literature citations are also extensive and current. Coordination between chapters is very good, and there is little redundancy. There is a high degree of consistency among the chapters in the nature of the material presented and the format for its presentation. A useful feature for pharmacy students is that pertinent chemical properties of the individual agents are given.

In summary, this is a most impressive textbook, judged for completeness, cohesiveness, and balance. The authors have used care and good judgment in making it an appropriate textbook for undergraduate pharmacy students.

Reviewed by Eugene Isaacson
Idaho State University
College of Pharmacy
Pocatello, IO 83201

Physicochemical Principles of Pharmacy. By A. T. FLORENCE and D. ATTWOOD, Chapman and Hall, New York, N.Y. 10017. 1982. 509 pp. 15 × 23 cm. Price $29.95.

The purpose of this book is to provide the physicochemical background to the design and use of pharmaceutical products. Processing technology is not discussed. Special problems of the various routes of administration and of duration of activity are presented if the mechanism is physical and not biological.

An effort is made to demonstrate that often the same forces operate in inanimate and animate systems. The authors assume that undergraduates using this book will have had a standard physical chemistry course. Since it is aimed at undergraduates, the reference lists have been kept to a minimum.

The book is divided into 11 chapters, which are entitled: Gases; Properties of the Solid State; Liquids; Solutions; Solubilty of Drugs in Liquids; Surface Chemistry; Colloidal and Coarse Lyophobic Dispersions; Polymeric Systems; Principles of Drug Absorption and Routes of Administration; Drug Interactions and Incompatibilities: a physicochemical viewpoint; and Chemical Stability of Drugs.

There is an abundance of easily comprehended figures to supplement the text. Although examples are given, perhaps the inclusion of a greater number of sample calculations would have been helpful to the student. The chapters on principles of drug absorption and drug interactions and incompatibilities are especially valuable additions to a book dealing with physicochemical principles. This is a fine text which fulfills its purpose.

Reviewed by Eugene L. Parrott
College of Pharmacy
University of Iowa
Iowa City, IA 52240

0022-3549/83/0300-0328$01.00/0

REVIEWS

Introduction to Alkaloids—A Biogenetic Approach. By GEOFFREY A. CORDELL. Wiley-Interscience, New York, N.Y. 1981. 1055 pp. 17 × 24 cm. Price $50.00.

As the title implies, this introductory text uses the concept of biogenesis to organize a vast and heterogeneous group of natural products, the alkaloids. Comprehensive coverage of alkaloids with specific chemical nuclei have been presented in the past in the form of edited texts and an edited series of volumes. These treatises are predominantly chemically oriented.

Dr. Cordell's effort to cover many aspects of the various biogenetic classes of alkaloids was as a single author and not as an editor. He should be highly commended for his enthusiasm and dedication in the writing of this excellent work. It surely was a monumental, but necessary, task in an era where the alkaloid field is expanding at such a rapid rate.

The book consists of almost 1000 pages divided into 12 chapters. As would be expected, the first chapter involves background material with concise presentations of history, occurrence, classification, properties, detection, isolation, purification, structure elucidation, and pharmacology of the alkaloids. The second chapter focuses on alkaloid biosynthesis and biogenesis and establishes the organizational tenor for the remainder of the text. The next nine chapters deal with alkaloids derived from ornithine, lysine, nicotinic acid, polyacetate, anthranilic acid, phenylalanine and tyrosine, tryptophan, histidine, and isoprenoid metabolism. The last chapter presents several very interesting miscellaneous alkaloids. The Appendix lists formulas for many of the useful alkaloid detecting reagents. In addition to the usual subject index, the organism index provides additional utility to this book.

The individual chapters are sectioned with each section comprising a single important alkaloid or group of related compounds derived from a common biosynthetic precursor. Within each section there are discussions involving chemistry, biosynthesis, and pharmacology. In certain cases useful synthetic and spectral data are presented. Most sections conclude with a listing of selected key literature references.

Although some scientists may be disappointed in the limited coverage of certain groups of alkaloids, Dr. Cordell has done a good job in keeping relative importance in perspective. For instance, Chapters 8 (Alkaloids Derived from Phenylalanine and Tyrosine) and 9 (Alkaloids Derived from Tryptophan) constitute over half of the book. However, these compounds probably deserve this degree of attention because of the great deal of published research on their medicinal value. This perspective and unity of presentation is one important advantage of a single author covering a broad scientific topic.

In conclusion, this book is a useful reference for scientists interested in various aspects of alkaloid research. The illustrations are excellent. Grammatical, spelling, and chemical structure errors are minimal. The utility of this interesting text, however, may be limited by its price.

William J. Keller
Div. of Medicinal
Chemistry and Pharmaceutics
Northeast Louisiana University
Monroe, LA 71209

Textbook of Organic Medicinal and Pharmaceutical Chemistry, 8th Ed. Edited by ROBERT F. DOERGE. Lippincott/Harper, East Washington Square, Philadelphia, PA 19105. 1982. 876 pp. 21 × 26 cm. Price $47.50.

Because of its consistently high quality, the latest edition of this classical textbook, intended for use in undergraduate courses in Medicinal and Pharmaceutical Chemistry, was a pleasure to review. Despite the loss due to death or retirement of several of the prominent contributors to previous editions, those remaining, together with their new collaborators, have written excellent chapters. The combined effort is impressive. The first chapter is a broad overview of medicinal chemistry. This is followed by an effective summary of the basic material of the discipline, such as how structure relates to the drug–receptor interaction, and an excellent exposition of the medicinal chemistry of drug metabolism.

The anti-infectives, a specific group of therapeutical agents, is dealt with in the fourth chapter. Here, and in the remaining chapters, all treating specific groups of agents, one sees a consistent pattern of a thorough overview of the group under consideration and compact discussions of the chemical and biological properties of each of the members of the group.

Chapters dealing with sulfonamides, antimalarials, antibiotics, and antineoplastic agents are all very thorough and well written. Local anesthetics and antihistamines are also treated in well-written chapters. Excellent reviews of analgesics and steroids are also found in this text.

CNS depressants and stimulants and material from the Seventh Edition are substantially updated. Adrenergic agents and cholinergic agents are given highly competent treatment in subsequent chapters.

The chapter on diuretics is impressively updated and another chapter takes us easily through cardiovascular agents, a potentially difficult group.

Carbohydrates, proteins, and vitamins are skillfully treated. A concluding chapter effectively brings together a diverse group of agents, one example of which is diagnostic agents.

Two valuable appendixes describe properties of pharmaceutical aids and list pKa values for a number of drugs. Finally, the index is detailed and should prove to be useful.

All of the chapters of this text show signs of painstaking preparation. Revising and updating over the Seventh Edition is extensive. Literature citations are also extensive and current. Coordination between chapters is very good, and there is little redundancy. There is a high degree of consistency among the chapters in the nature of the material presented and the format for its presentation. A useful feature for pharmacy students is that pertinent chemical properties of the individual agents are given.

In summary, this is a most impressive textbook, judged for completeness, cohesiveness, and balance. The authors have used care and good judgment in making it an appropriate textbook for undergraduate pharmacy students.

Reviewed by Eugene Isaacson
Idaho State University
College of Pharmacy
Pocatello, IO 83201

Physicochemical Principles of Pharmacy. By A. T. FLORENCE and D. ATTWOOD, Chapman and Hall, New York, N.Y. 10017. 1982. 509 pp. 15 × 23 cm. Price $29.95.

The purpose of this book is to provide the physicochemical background to the design and use of pharmaceutical products. Processing technology is not discussed. Special problems of the various routes of administration and of duration of activity are presented if the mechanism is physical and not biological.

An effort is made to demonstrate that often the same forces operate in inanimate and animate systems. The authors assume that undergraduates using this book will have had a standard physical chemistry course. Since it is aimed at undergraduates, the reference lists have been kept to a minimum.

The book is divided into 11 chapters, which are entitled: Gases; Properties of the Solid State; Liquids; Solutions; Solubilty of Drugs in Liquids; Surface Chemistry; Colloidal and Coarse Lyophobic Dispersions; Polymeric Systems; Principles of Drug Absorption and Routes of Administration; Drug Interactions and Incompatibilities: a physicochemical viewpoint; and Chemical Stability of Drugs.

There is an abundance of easily comprehended figures to supplement the text. Although examples are given, perhaps the inclusion of a greater number of sample calculations would have been helpful to the student. The chapters on principles of drug absorption and drug interactions and incompatibilities are especially valuable additions to a book dealing with physicochemical principles. This is a fine text which fulfills its purpose.

Reviewed by Eugene L. Parrott
College of Pharmacy
University of Iowa
Iowa City, IA 52240

0022-3549/83/0300-0328$01.00/0

1983
Volume 72

JOURNAL OF PHARMACEUTICAL SCIENCES

A publication of the American Pharmaceutical Association

The *Journal of Pharmaceutical Sciences* (ISSN 0022-3549) is published monthly by the American Pharmaceutical Association (APhA) at 2215 Constitution Ave., N.W., Washington, DC 20037. Second-class postage paid at Washington, D.C. and at additional mailing office.

All expressions of opinion and statements of supposed fact appearing in articles or editorials carried in this journal are published on the authority of the writer over whose name they appear and are not to be regarded as necessarily expressing the policies or views of APhA.

Offices—Editorial, Advertising, and Subscription: 2215 Constitution Ave., N.W., Washington, DC 20037. All Journal staff may be contacted at this address. Printing: 20th & Northampton Streets, Easton, PA 18042.

Annual Subscriptions—United States and foreign, industrial and government institutions $75; educational institutions $75; individuals *for personal use only* $40; single copies $10. APhA and SAPhA members may subscribe to *J. Pharm. Sci.* for $20.00 per year. All foreign subscriptions add $10 for postage. Subscription rates are subject to change without notice.

Claims—Missing numbers will not be supplied if dues or subscriptions are in arrears for more than 60 days or if claims are received more than 60 days after the date of the issue, or if loss was due to failure to give notice of change of address. APhA cannot accept responsibility for foreign delivery when its records indicate shipment was made.

Change of Address—Members and subscribers should notify at once both the Post Office and APhA of any change of address.

Photocopying—The code at the foot of the first page of an article indicates that APhA has granted permission for copying of the article beyond the limits permitted by Sections 107 and 108 of the U.S. Copyright Law provided that the copier sends the per copy fee stated in the code to the Copyright Clearance Center, Inc., 21 Congress St., Salem, MA 01970. Copies may be made for personal or internal use only and not for general distribution.

Microfilm—Available from University Microfilms International, 300 N. Zeeb Road, Ann Arbor, MI 48106.

JOURNAL OF PHARMACEUTICAL SCIENCES

APRIL 1983
VOLUME 72 NUMBER 4

SYMPOSIUM ARTICLES

Further Studies on the Catalysis of Hydrolysis and Aminolysis of Benzylpenicillin by Metal Chelates

HISAO TOMIDA * and MICHAEL A. SCHWARTZ ˣ

Received January 15, 1982, from the *College of Pharmacy, University of Florida, Gainesville, FL 32610.* Accepted for publication, June 14, 1982. *Present address: Faculty of Pharmaceutical Sciences, Fukuyama University, Fukuyama City, Japan.

Abstract □ It was suggested previously that the very rapid catalysis of benzylpenicillin hydrolysis and aminolysis by zinc ion and tris(hydroxymethyl)aminomethane (tromethamine) was mediated by a ternary complex in which the metal ion not only held the substrate and tromethamine in close proximity but also lowered the pK_a of a bound tromethamine hydroxyl group making it a very powerful nucleophile. In this study the scope of this reaction was explored further by examining the effects of changes in substrate side chain, metal ion, and amino alcohols. All of the penicillins studied showed about the same rate of reaction. Of the other metal ions examined Cu^{2+} and Ni^{2+} showed no activity, Mn^{2+} very slight activity, and Cd^{2+} and Co^{2+} somewhat greater activity. The latter was the most effective of this group but was 40 times slower than zinc. The results with a number of amino alcohols provided additional evidence for the ternary complex mechanism. Studies with the methyl ester of benzylpenicillin indicated that the metal ion is bound to the antibiotic at the carboxylate site and that a different mechanism is involved in the slower catalysis observed with the ester. Some comparison is made with a zinc-dependent β-lactamase.

Keyphrases □ Benzylpenicillin—mechanism of hydrolysis and aminolysis, catalysis by divalent cations and amino alcohols, ternary complex formation □ Metal-ion catalysis—hydrolysis and aminolysis of benzyl penicillin, mechanism, ternary complex formation

It was previously shown that zinc ion in the presence of tromethamine buffer in the 7–10 pH range is a very facile catalyst for the hydrolysis and aminolysis of benzylpenicillin (1). Evidence was offered to show that the mechanism of this catalysis most probably involved a ternary complex in which zinc ion acts as a template to bring the reactants, tromethamine and penicillin, together. In this complex the bound hydroxyl group of tromethamine can become a very powerful nucleophile, by virtue of a lowering of its pK_a as a result of coordination of zinc ion, and attack the β-lactam carbonyl of penicillin. The resulting tromethamine ester then hydrolyzes to penicilloic acid or reacts with another molecule of tromethamine to form an amide.

The present study was undertaken to explore the scope of this reaction, *i.e.*, the activity of other metal ions and other ligands, as well as the effects of structural changes in the substrate side chain.

EXPERIMENTAL

Materials—Benzylpenicillin[1], phenethicillin[1], and methicillin[1] were used as received. Methylpenicillin was prepared by acetylating 6-aminopenicillanic acid as reported previously (2). The methyl ester of benzylpenicillin was prepared as follows.

Potassium benzylpenicillin and methyl iodide were stirred in dimethylsulfoxide for 4 hr at room temperature. The mixture was diluted with water, extracted with ether, and then the extract was dried and the solvent removed *in vacuo*. A small volume of ethyl acetate was added to the resulting oil and the solution chromatographed on silica gel 60[2] with ethyl acetate as the developing solvent. The fractions containing ester were combined and solvent removed *in vacuo*. The resulting oil crystallized on trituration with *n*-hexane and was recrystallized twice from carbon tetrachloride. Its structure was confirmed by IR and NMR spectroscopy.

Tromethamine was a very pure grade[3]; ethanolamine, diethanolamine, and triethanolamine were all reagent grade[4]; 2-amino-2-methyl-1,3-propanediol was recrystallized from ethanol; 2-methoxyethanolamine and 2-diethylaminoethanol were redistilled prior to use.

Zinc chloride solution was prepared from reagent grade zinc metal as previously described (1). The other metal ions were in the form of chloride salts and were reagent grade.

Imidazole was recrystallized twice from benzene and washed with ether.

Kinetics—All rate measurements were carried out at 35° with the ionic strength brought to 0.5 by the addition of potassium chloride. The amines normally acted as their own buffers. In some cases where buffer capacity was too low, the pH was maintained constant on a radiometer pH-stat.

Rate of loss of penicillin from solution was followed either by following the decrease in absorbance at 235 nm (3) or by sampling the reactant solution and assaying for residual penicillin by the method of Bundgaard and Ilver (4). Initial concentration of penicillin was 5×10^{-4} *M* in the

[1] Supplied by Bristol Laboratories.
[2] E. Merck, Germany.
[3] Trizma, Sigma Chemical Co.
[4] J. T. Baker Chemical Co.

0022-3549/83/0400-0331$01.00/0

Table I—Catalytic Rate Constants [a] for Aminolysis by Tromethamine and Hydrolysis of Penicillins

Penicillin	Side Chain, R	k_T [b]	k_{OH} [c]
Benzylpenicillin	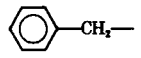	0.032 [d]	12.5
Phenethicillin	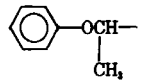	0.039	12.6
Methicillin	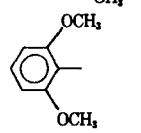	0.0263	6.5
Methyl penicillin	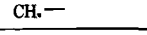	0.0294	10.6

[a] Rate constants in M^{-1} min^{-1}. [b] Reactions carried out at 35°, I = 0.5 with tromethamine alone. [c] Reactions carried out at 31.5°, I = 0.2 (2). [d] From Ref. (1)

direct spectrophotometric method and 2.75×10^{-4} *M* in the sampling method. When the methyl ester was used, the reaction mixture included 4.5% acetonitrile to keep the ester in solution.

Ionization Constants—The apparent pK_a of each of the amines was determined at 35° and ionic strength 0.5 by potentiometric titration.

RESULTS AND DISCUSSION

Effect of Penicillin Side-Chain Structure —The rates of the reaction of several penicillins with tromethamine were measured in both the absence and presence of zinc ion. Table I presents the second-order rate constants for the aminolysis of the penicillins by tromethamine in the absence of zinc ion and compares these with the alkaline hydrolysis rate constants. It can be seen that the order of reactivity is the same in both cases, reflecting the relatively small effect of the side chain on the susceptibility of the β-lactam ring to nucleophilic attack.

In Fig. 1 is shown the dependence on tromethamine concentration of the rate of loss of penicillins in the presence of zinc ion at pH 8.0. In these studies 3×10^{-6} *M* zinc ion was used, and the first-order rate constants were corrected for rate with tromethamine alone and normalized with respect to zinc ion.

It can be seen that differences in the side-chain structure exert only a very small effect on the rate of β-lactam cleavage. The rates with all the penicillins are very rapid relative to the rate in the absence of zinc ion, but there is only a less than twofold difference in rate. This result would be expected if binding of the drug to zinc ion were at the carboxyl group of the thiazolidine ring as has been proposed (5, 6). To further test this hypothesis, rates of reaction under similar conditions were carried out with the methyl ester of benzylpenicillin.

Effect of Esterification of Carboxyl Group—In the absence of zinc ion the methyl ester of benzylpenicillin reacts more rapidly with tromethamine than the free penicillin, as shown in Fig. 2. It should be noted that the reaction in both cases is at the β-lactam carbonyl. The ester is more susceptible to attack at this point than the free penicillin, because

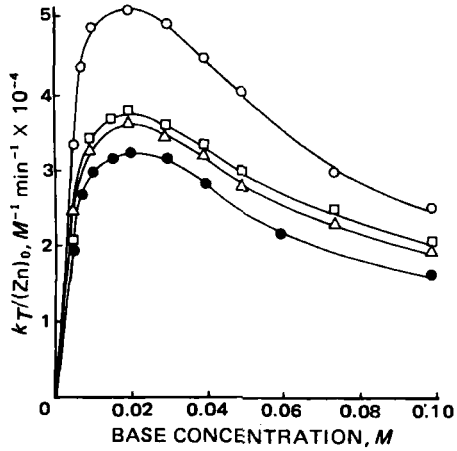

Figure 1—*Dependence on tromethamine concentration of rate constant for penicillin loss at pH 8.0. Key: (●) benzylpenicillin, (△) methicillin, (□) phenethicillin, (○) methylpenicillin.*

Table II—Effect of Zinc Ion on Rate of Loss of Benzylpenicillin and Its Methyl Ester in Tromethamine Buffer [a]

	Tromethamine-Base Concentration, *M*	$[Zn]_0$, *M*	$10^3 k_{obs}$, min^{-1}
Benzylpenicillin	0.02	0	0.526
	0.02	3×10^{-6}	110
	0.10	0	2.50
	0.10	3×10^{-6}	72.3
Methyl ester	0.02	0	2.02
	0.02	3×10^{-6}	2.33
	0.10	0	9.85
	0.10	3×10^{-6}	10.3

[a] Reactions run at pH 8.0, 35°, containing 4.5% acetonitrile with initial concentration of penicillin 2.75×10^{-4} *M*.

the negative charge on the latter tends to repel nucleophiles such as hydroxyl ion (7) and tromethamine. The presence of 3×10^{-6} *M* zinc ion causes, as shown in Table II, only a very small effect on the methyl ester of penicillin relative to the free penicillin. Again, if penicillin is coordinated to zinc ion at the carboxylate ion one would expect the result obtained.

At much higher concentrations of zinc ion there is observed a significant effect on the loss of methyl ester of penicillin in the presence of tromethamine, as shown in Fig. 3. Here the rate constant is a linear function of zinc ion concentration up to 10^{-3} *M*. The dependence of the rates of this reaction on tromethamine concentration is shown in Fig. 4, where it is compared with that of free benzylpenicillin.

Both curves show a maximum near 0.02 *M* tromethamine, but there are significant differences in slope of the curve as well as the magnitude of the rates. At the maximum, the rate constant for the ester is about 1400 times slower than that of the free penicillin. At tromethamine concentrations above 0.02 *M* the rate constant for the free penicillin decreases much more rapidly than that of the ester. These results, coupled with the great difference in rate, indicated that the reaction with the ester involves a different mechanism than the reaction with penicillin. In the latter it was proposed that catalysis is mediated by a ternary complex, in which both tromethamine and penicillin are bound to a zinc ion with nucleophilic attack by a tromethamine hydroxyl on the β-lactam carbonyl taking place within the complex. At high tromethamine concentrations a second tromethamine would compete with penicillin for the binding site of the zinc ion and reduce the reaction rate by reducing the relative amount of ternary complex that could be formed. Blocking of the penicillin carboxyl in the ester prevents the formation of this ternary complex, and, even if the ester binds to zinc it must be with a much lower affinity than the free acid, and the predominant species in solution would be chelates of tromethamine with zinc ion (ZnT and ZnT_2). With the ester one possible mechanism suggested by the tromethamine dependence is a direct intermolecular nucleophilic attack by these chelates on the β-lactam carbonyl. When tromethamine is coordinated to zinc ion through the amine and one of the hydroxyl groups, the pK_a of the coordinated hydroxyl group can be lowered substantially (*i.e.*, 3 or 4 units), but the alkoxide ion thus formed will retain the nucleophilicity of a group with the higher pK_a (8). Thus, these groups in the chelates can become relatively powerful nucleophiles at a pH close to neutrality. Also, it would be expected that the pK_a of the hydroxyl group in ZnT and ZnT_2 would

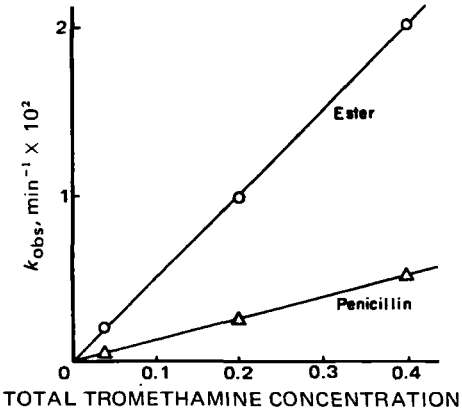

Figure 2—*Dependence of observed rate constant (k_{obs}) on tromethamine concentration, pH 8.0, EDTA 1×10^{-5} M, 4.5% acetonitrile. Key: (△) benzylpenicillin, (○) methyl ester.*

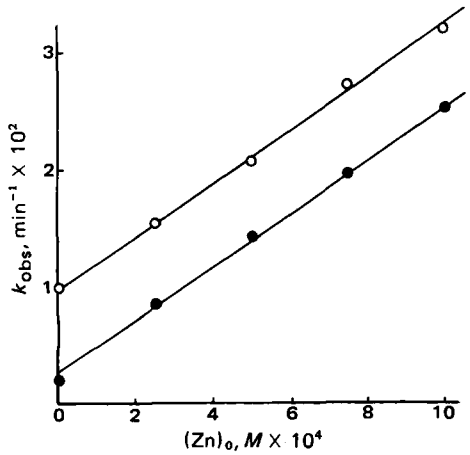

Figure 3—*Dependence of observed rate constant for loss of methyl ester of benzylpenicillin on zinc ion. Key: (○) tromethamine base 0.1* M, *(●) tromethamine base 0.02* M.

not be very different, and hence the rate constants for their reaction with the penicillin ester would be expected to be similar. That they are is evidenced by the tromethamine dependence shown in Fig. 4, where the decrease in rate at high tromethamine is relatively small. We may express the overall rate constant as follows:

$$k_T/[Zn]_0 = k_1[ZnT^{1+}] + k_2[ZnT_2^{1+}]$$

where k_T is the observed rate constant corrected for the rate with tromethamine alone, and $[Zn]_0$ is the stoichiometric total zinc ion concentration. Using values previously estimated for the affinity constants of the zinc–tromethamine chelates (1), and assuming the pK_a value for the two chelates are equal (pK_a = 8.7), values for the rate constants were calculated as $k_1 = 220\ M^{-1}\ min^{-1}$ and $k_2 = 120\ M^{-1}\ min^{-1}$. These values are in the range one would expect for nucleophiles with pK_a values ~12–13 (9), which is probably in the pK_a range of uncomplexed tromethamine.

It should be noted that this type of reaction probably also could occur with the free penicillin, but with a rate so low that it would be insignificant relative to that of the ternary complex pathway.

Effects of Other Metal Ions—It was of interest to examine the effects of other metal ions in this system. Rates of loss of benzylpenicillin in solution in the presence of Co^{2+}, Cd^{2+}, Mn^{2+}, Cu^{2+}, and Ni^{2+} were measured at pH 8, at constant tromethamine concentration. The results are shown in Fig. 5 where these are compared with Zn^{2+}. Both Cu^{2+} and Ni^{2+} showed no activity at concentrations up to 10^{-4} M. The other metal ions all show a linear dependence on metal ion concentration and much lower rates than zinc ion.

In Fig. 6 is shown the dependence of the rate of penicillin loss on tromethamine concentration in the presence of three metal ions. Here again, the rate constants were corrected for the rate with tromethamine alone and normalized with respect to metal ion concentration. While the curve for Co^{2+} ion shows a maximum similar to that of zinc ion, Cd^{2+} ion shows only a plateau, and the curve for Mn^{2+} reveals only a steady increase in

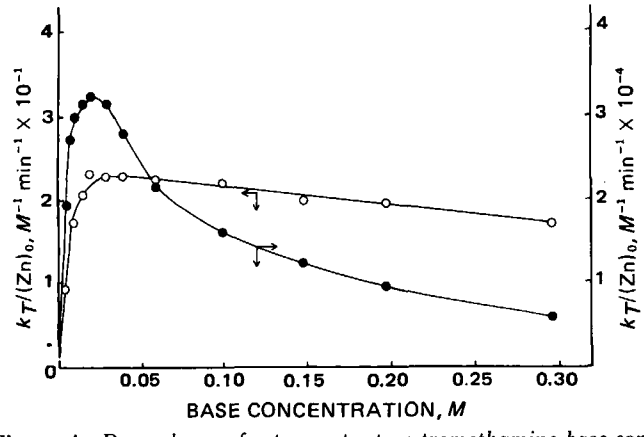

Figure 4—*Dependence of rate constant on tromethamine base concentration at pH 8.0. Key: (○) methyl ester, (●) penicillin.*

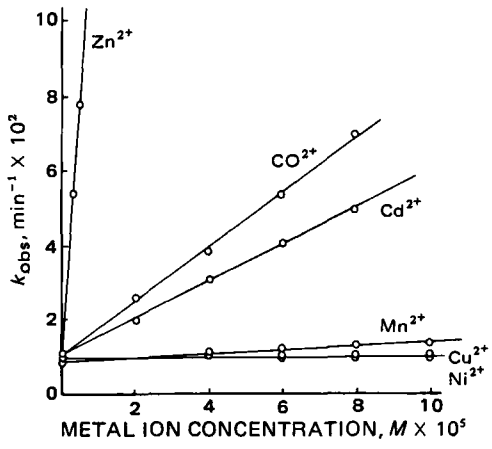

Figure 5—*Effect of concentration of metal ions on observed rate constant for penicillin loss at pH 8.0, 0.2* M *tromethamine buffer.*

rate with increasing tromethamine. Based on the mechanism proposed for zinc ion with benzylpenicillin, the differences in these curves might be thought to result from differences in the formation constants of the metal chelates with tromethamine. This appears to be the case particularly with Co^{2+}, but with Cd^{2+} the plateau suggests a different mechanism, perhaps similar to that proposed for the reaction of zinc–tromethamine chelates with penicillin methyl ester.

The rates of loss of the methyl ester of benzylpenicillin with these metal ions were also measured and are reported in Table III as the rate constant at the maximum in the tromethamine dependence curve divided by the metal ion concentration, except in the case of Mn^{2+} where no maximum was reached. Here the rates are compared at the same tromethamine concentration. In all cases the rate for the penicillin is much greater than that of the ester but these differences decrease markedly in the order shown in Table III.

Such a result may be expected if the reaction with the free penicillin, as proposed at least with zinc and cobalt, is mediated by a ternary complex in which an appropriate conformation of tromethamine and substrate would be necessary for optimum reaction rate. If an optimum fit is obtained with zinc ion, then large differences would be expected with other ions of different size. On the other hand, with the ester, where the reaction may involve bimolecular nucleophilic attack by the metal chelate, smaller differences would be expected based more on the effect of the metal ion on pK_a of the tromethamine hydroxyl, steric factors, *etc.* Thus, while these data are not inconsistent with the proposed mechanism, a good deal more information on the nature of the tromethamine complexes and the effect of pH on reaction rate would be necessary to make more definitive conclusions.

In terms of this system as a potential model for the zinc-dependent β-lactamases, it is interesting to note that other metal ions may replace zinc in the enzyme with some retention of activity (10). It has been reported that replacement with Co^{2+} ion gives an enzyme with 12.6% of the activity of the zinc-containing enzyme. With Mn^{2+} and Cd^{2+} the activity was reduced to 6.7 and 1%, respectively. No enzymic activity was noted

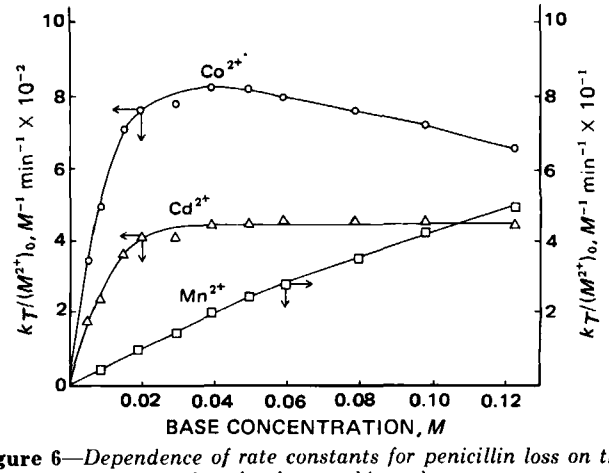

Figure 6—*Dependence of rate constants for penicillin loss on tromethamine concentrations for the metal ions shown.*

Table III—Effect of Metal Ions on Rate of Loss of Benzylpenicillin and Its Methyl Ester in Tromethamine Buffer [a] at pH 8.0

Metal Ion	Benzylpenicillin k_{max}/M_0	Benzylpenicillin Relative Activity	Methyl Ester [b] k_{max}/M_0	Methyl Ester [b] Relative Activity	Ratio of Penicillin–Ester
Zn^{2+}	3.22×10^4	100	23.6	100	1360
Co^{2+}	8.20×10^2	2.55	4.38	18.6	187
Cd^{2+}	451	1.40	8.78	37.2	51
Mn^{2+}	49.5	0.14	2.6	11.0	19
Cu^{2+}	0 [c]	0	0		
Ni^{2+}	0 [c]	0	0		

[a] Tromethamine base was 0.12 *M*. [b] Reaction solution contained 4.5% acetonitrile. [c] Up to 1×10^{-4} *M* metal ion.

Table IV—Effect of Amine Structure on Reaction Rate In Absence and Presence of Zinc Ion

Amine	pK_a	k_{amine} [a], M^{-1} min^{-1}	$k_{max}/[Zn]_0$ [b], M^{-1} min$^{-1} \times 10^{-4}$
Tromethamine	8.01	0.032	10.3
2-Amino-2-methyl-1, 3-propanediol	8.68	0.251	5.5
Ethanolamine	9.21	0.833 [c]	2.8
Diethanolamine	8.94	0.591	7.0
Triethanolamine	7.85	0.017	0.37
2-Diethylaminoethanol	9.86	0.600	10.7 [d]
2-Methoxyethylamine	9.30	—	0

[a] Rate constant in absence of Zn^{2+}. [b] Done at pH 9. [c] From Ref. (11). [d] At base conc. 0.069 *M* (no maximum observed).

with Cu^{2+} and Ni^{2+}. Thus, there is a considerable degree of similarity between the relative order of activity of metal ions in the enzyme and this model system.

Effect of Ligand Structure—As an initial approach to determining the effect of ligand structure on catalytic activity, the rates of loss of benzylpenicillin were measured in the presence of zinc ion with several amino alcohols and one in which the hydroxyl group was blocked. The results are shown in Figs. 7 and 8 and summarized in Table IV.

These data provide further evidence for the intermediacy of a ternary complex (amine–zinc ion–penicillin) in this type of reaction, as opposed to nucleophilic attack by amine on a metal ion–penicillin complex. If the latter were the predominant pathway, one would not expect to observe a great difference in rate between ethanolamine and methoxyethylamine, since their pK_a values are very close, unless the latter had a much greater affinity for the metal ion. One would expect however, that ethanolamine would show the greater affinity, because of the opportunity for a bidentate complex with the free hydroxyl group.

On the other hand, these data are entirely consistent with the ternary complex mechanism in which the hydroxyl of the ethanolamine, coupled to metal ion, is the attacking species. Methoxyethylamine cannot enter into a ternary complex, in which it can behave as a nucleophile, because of the blocked hydroxyl group.

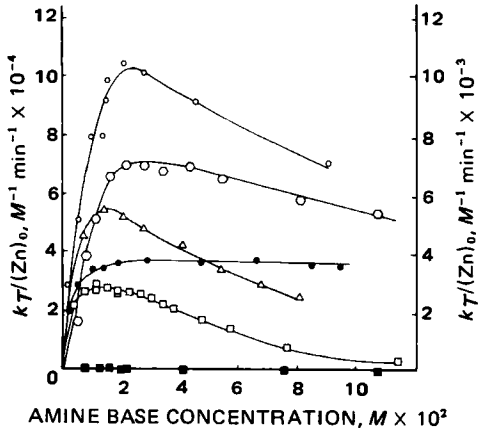

Figure 7—*Dependence of rate constant on amine concentration. Key: Left ordinate: (○) tromethamine, (△) 2-amino-2-methyl-1,3-propanediol (□) ethanolamine, (○) diethanolamine; right ordinate: (●) triethanolamine (■) 2-methoxyethylamine.*

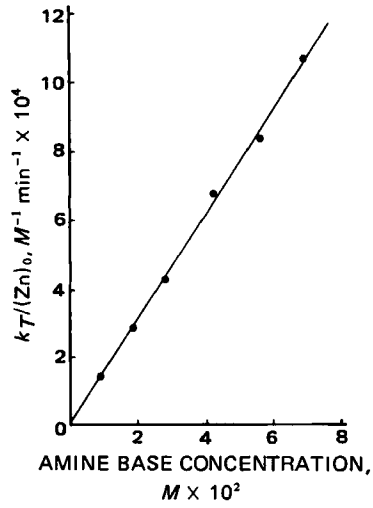

Figure 8—*Dependence of rate constant on concentration of 2-diethyl-aminoethanol.*

The relative values of the rate constants for tromethamine, 2-amino-2-methyl-1,3-propanediol and ethanolamine also lend support to the ternary complex hypothesis. If the other mechanism were predominant, one would expect the rates to increase with increasing pK_a, as they do in the absence of metal ion. The order of reactivity, however, seems to be determined more by the number of hydroxyl groups available for binding to the metal ion (*i.e.*, a statistical effect), which would be expected if the affinity for metal ion in a ternary complex was the most important factor involved.

The same general effect is seen in comparing the rate constants for diethanolamine with ethanolamine. Though the latter has a higher pK_a and reacts more rapidly with penicillin in the absence of zinc ion, its rate in the presence of zinc ion is significantly lower. Again, the rate constants with zinc ion are related more to the number of hydroxyl groups and this factor further supports the ternary complex mechanism.

With triethanolamine two factors are of interest: the relatively low rates with zinc ion and the shape of the concentration-dependence curve. The latter may indicate that triethanolamine forms only a 1:1 complex with zinc as it does with cupric ion (12). The plateau indicates either that the same species is present throughout the concentration range studied or that a higher complex has the same activity. The former seems more likely, in view of the fact that Cu^{2+} forms only a 1:1 complex with triethanolamine. The inability of triethanolamine to form higher complexes is probably due to steric inhibition. The lower rate with penicillin may reflect the same kind of steric inhibition of formation of a ternary complex with substrate.

The concentration dependence of rates with diethylaminoethanol is of interest, because it shows no maximum up to 0.1 *M*. This apparently results from formation of only a 1:1 complex perhaps due to steric inhibition or to a relatively low affinity of the compound for zinc ion. Yet the rates are relatively high, and it may be of interest to further study the concentration and pH dependence of this reaction. This type of compound may also be of more interest as a β-lactam model, since the product, with a tertiary amine, should be only penicilloic acid as with the enzyme rather than a mixture of the acid with an amine as with primary amines.

In summary, additional evidence presented here provides further support for the previously proposed mechanism for the catalysis of hydrolysis and aminolysis of penicillin by zinc ion and tromethamine, involving a ternary complex intermediate. The relative rates of reaction of other metal ions substituted for zinc are in the same general order as in a zinc-dependent β-lactamase. Thus, this system may be a model for the enzyme.

REFERENCES

(1) M. A. Schwartz, *Bioorg. Chem.*, **11**, 4 (1982).

(2) R. D. Kinget and M. A. Schwartz, *J. Pharm. Sci.*, **58**, 1102, (1969).

(3) S. G. Waley, *Biochem J.*, **139**, 789 (1974).

(4) H. Bundgaard and K. Ilver, *J. Pharm. Pharmacol.*, **24**, 790 (1972).

(5) G. V. Fazakerley and G. E. Jackson, *J. Chem. Soc. Perkin Trans.* **2**, 567 (1975).
(6) N. P. Gensmantel, P. Proctor, and M. I. Page, *ibid.*, **1980**, 1725.
(7) M. A. Schwartz, *J. Pharm. Sci.*, **54**, 1308 (1965).
(8) M. F. Dunn, *Struct. Bonding (Berlin)*, **23**, 61 (1976).
(9) M. A. Schwartz, in "Beta-Lactamases," J. M. T. Hamilton-Miller and J. T. Smith, Eds., Academic, London, 1979.
(10) G. S. Baldwin, G. F. S. Edwards, P. A. Kiener, M. J. Tully, S. G. Waley, and E. P. Abraham, *Biochem J.*, **191**, 111 (1980).
(11) T. Yamana, A. Tsuji, E. Miyamoto, and E. Kiya, *J. Pharm. Pharmacol.*, **27**, 771 (1975).
(12) L. G. Sillen and A. E. Martell "Stability Constants of Metal Ion Complexes Parts II, III," The Chemical Society, London 1964, 1970.

ACKNOWLEDGMENT

Supported in part by a grant from Merck Sharp & Dohme.

Interaction of Nitroglycerin With Human Blood Components

T. D. SOKOLOSKI ˣ, C. C. WU *, L. S. WU, and A. M. BURKMAN

Received October 6, 1981, from the *College of Pharmacy, Ohio State University, Columbus, OH 43210.* Accepted for publication December 31, 1981. * Present address: Ayerst Laboratories, Rouses Point, N.Y.

Abstract □ Nitroglycerin is rapidly lost from solution when incubated with red blood cells or whole blood. The assumption that the loss is enzymatic in nature may not be true, since no major metabolite is detected during this incubation. Explanation on the basis of a chemical reaction is also difficult, since the products of the chemical hydrolysis of nitroglycerin are the same as the metabolic products. After an initial rapid loss, nitroglycerin disappearance at 37° follows an apparent first-order process in the concentration range of 10–480 ng/ml when incubated with washed red blood cells suspended in normal saline solution. The half-life for the reaction of the apparent first-order phase varies with the initial concentration and increases as the concentration increases (4 min at 10 ng/ml, 52 min at 480 ng/ml), suggesting a mixed kinetic mechanism. Metabolites of nitroglycerin (1,2- and 1,3-dinitroglycerin) react similarly to nitroglycerin in terms of an apparent initial, fast step, a secondary first-order dependence, and concentration-dependent rate effects; however, the rate of the reaction is much slower ($t_{1/2}$ = 33 min at 10 ng/ml) for the metabolite. These data suggest the possibility of a physical mechanism for the loss of nitroglycerin. Since the loss to red blood cells can be rapid, it seems that the mechanism should be delineated, and that the rate of disappearnce be considered in an analysis of the pharmacodynamics of the drug.

Keyphrases □ Kinetics—nitroglycerin loss to red blood cells □ Nitroglycerin—rate of loss to red blood cells □ 1,2- and 1,3-Dinitroglycerin—rate of loss to red blood cells □ Disposition—reactivity of nitroglycerin and its metabolites with blood

It has been reported that when nitroglycerin is incubated with whole blood (fresh or outdated), resuspended red blood cells, serum, or plasma, the drug is lost from solution by an apparent first-order process. A relatively rapid loss occurred in blood or resuspended cells (1–3) ($t_{1/2}$ = 6 min) and rat serum ($t_{1/2}$ = 20 min) (4) with a slower loss occurring in plasma, $t_{1/2}$ = 53 (1) or 175 min (5). The rate of loss in the presence of erythrocytes approaches the biological half-life of organic nitrate (1.9 min) (1). The interaction of nitroglycerin with blood cells, serum, or plasma has been assumed by other workers to be an enzymatic reaction. However, our earlier work using an assay with resuspended red blood cells that could detect the major nitroglycerin metabolites (1,2-dinitroglycerin and 1,3-dinitroglycerin) showed that there was no metabolite in the medium over the entire time course of the loss of nitroglycerin (3). This observation led to the conclusion that the loss of nitroglycerin may not be enzymatic in nature. In this paper further studies are reported which probe the mechanism of loss of nitroglycerin when the drug is incubated with red blood cells. Since the rate of loss of nitroglycerin is rapid, it would appear that a knowledge of the mechanism of its loss would have significant impact on an analysis of the disposition kinetics of the drug and possibly its physiological activity as well.

EXPERIMENTAL

Nitroglycerin stock solutions were prepared from an alcoholic extract of a 10% aqueous solution of lactose adsorbate[1]. The major metabolites of nitroglycerin, 1,2-dinitroglycerin and 1,3-dinitroglycerin, were prepared from 2,3-dibromopropanol[2] and 1,3-dibromopropane-2-ol[3] using the method of Dunstan *et al.* (6). The purity of the compounds was determined by high-performance liquid chromatography (HPLC) and TLC and the solutions standardized as reported by Yuen *et al.* (7). All other chemicals used were obtained commercially and were reagent grade or better.

An electron capture gas chromatograph[4] was used with a data processor[5]. The GLC assay for nitroglycerin was reported earlier (9% QF-1[6] on 60–80 mesh Supelcoport[7]) (3). The column was silanized glass 2 mm × 0.915 m and the temperatures of the injection port, the column, and the detector were 150, 125, and 200°, respectively. The carrier gas was 5% methane in argon used at a flow rate of 21 ml/min. Under these conditions the retention times were: mixture of 1,2-dinitroglycerin and 1,3-dinitroglycerin, 3 min; nitroglycerin, 6.3 min; and internal standard (1-fluoro-2,4-dinitrobenzene[8]) 7.57 min. The system does not separate the two isomeric metabolites but does optimize their combined detection.

For the assay of 1,2- and 1,3-dinitroglycerin a method was used that was a slight modification of our earlier method (8). The column (silanized glass, 2 mm × 50 cm) consisted of 3% Carbowax 20M-TPA[9] on 60–80 mesh Supelcoport[7]. The injection port, column, and detector were at 150, 135, and 200°, respectively and the flow rate of the carrier gas was 20 ml/min. Using these conditions the two metabolites could be separated from each other and from nitroglycerin. The approximate retention times in minutes were: nitroglycerin, 2.7; *o*-iodobenzyl alcohol[10] (internal standard), 3.4; 1,2-dinitroglycerin, 6.5; and 1,3-dinitroglycerin, 8.2.

The concentration of nitroglycerin or its metabolite in the various

[1] Nitroglycerin 10% (w/w) in lactose, lot K17-O-H, ICI Americas, Atlas Chemical Div, Wilmington, DE 19899.
[2] Eastman Kodak, lot A5A, Rochester, NY 14650.
[3] Eastman Kodak, lot B6C, Rochester, NY 14650.
[4] 3700 Series dual column gas chromatograph, Varian Instrument Div., Palo Alto, CA 94303.
[5] Shimadzu Recording Data Processor. Chromatopac C-RIA Shimadzu Scientific Instruments, Columbia, MD 21045.
[6] Analabs, No. Haven, CT 06473.
[7] Supelco, Bellefonte, PA 16823.
[8] Eastman Organic Chemicals, Distribution Products Ind. Rochester, NY 14650.
[9] Applied Science Labs, State College, PA 16801.
[10] Aldrich Chemical Co., Milwaukee, WI 53233.

0022-3549/83/0400-0335$01.00/0

(5) G. V. Fazakerley and G. E. Jackson, *J. Chem. Soc. Perkin Trans.* **2**, 567 (1975).
(6) N. P. Gensmantel, P. Proctor, and M. I. Page, *ibid.*, **1980**, 1725.
(7) M. A. Schwartz, *J. Pharm. Sci.*, **54**, 1308 (1965).
(8) M. F. Dunn, *Struct. Bonding (Berlin)*, **23**, 61 (1976).
(9) M. A. Schwartz, in "Beta-Lactamases," J. M. T. Hamilton-Miller and J. T. Smith, Eds., Academic, London, 1979.
(10) G. S. Baldwin, G. F. S. Edwards, P. A. Kiener, M. J. Tully, S. G. Waley, and E. P. Abraham, *Biochem J.*, **191**, 111 (1980).
(11) T. Yamana, A. Tsuji, E. Miyamoto, and E. Kiya, *J. Pharm. Pharmacol.*, **27**, 771 (1975).
(12) L. G. Sillen and A. E. Martell "Stability Constants of Metal Ion Complexes Parts II, III," The Chemical Society, London 1964, 1970.

ACKNOWLEDGMENT

Supported in part by a grant from Merck Sharp & Dohme.

Interaction of Nitroglycerin With Human Blood Components

T. D. SOKOLOSKI ˣ, C. C. WU *, L. S. WU, and A. M. BURKMAN

Received October 6, 1981, from the *College of Pharmacy, Ohio State University, Columbus, OH 43210.* Accepted for publication December 31, 1981. * Present address: Ayerst Laboratories, Rouses Point, N.Y.

Abstract □ Nitroglycerin is rapidly lost from solution when incubated with red blood cells or whole blood. The assumption that the loss is enzymatic in nature may not be true, since no major metabolite is detected during this incubation. Explanation on the basis of a chemical reaction is also difficult, since the products of the chemical hydrolysis of nitroglycerin are the same as the metabolic products. After an initial rapid loss, nitroglycerin disappearance at 37° follows an apparent first-order process in the concentration range of 10–480 ng/ml when incubated with washed red blood cells suspended in normal saline solution. The half-life for the reaction of the apparent first-order phase varies with the initial concentration and increases as the concentration increases (4 min at 10 ng/ml, 52 min at 480 ng/ml), suggesting a mixed kinetic mechanism. Metabolites of nitroglycerin (1,2- and 1,3-dinitroglycerin) react similarly to nitroglycerin in terms of an apparent initial, fast step, a secondary first-order dependence, and concentration-dependent rate effects; however, the rate of the reaction is much slower ($t_{1/2}$ = 33 min at 10 ng/ml) for the metabolite. These data suggest the possibility of a physical mechanism for the loss of nitroglycerin. Since the loss to red blood cells can be rapid, it seems that the mechanism should be delineated, and that the rate of disappearnce be considered in an analysis of the pharmacodynamics of the drug.

Keyphrases □ Kinetics—nitroglycerin loss to red blood cells □ Nitroglycerin—rate of loss to red blood cells □ 1,2- and 1,3-Dinitroglycerin—rate of loss to red blood cells □ Disposition—reactivity of nitroglycerin and its metabolites with blood

It has been reported that when nitroglycerin is incubated with whole blood (fresh or outdated), resuspended red blood cells, serum, or plasma, the drug is lost from solution by an apparent first-order process. A relatively rapid loss occurred in blood or resuspended cells (1–3) ($t_{1/2}$ = 6 min) and rat serum ($t_{1/2}$ = 20 min) (4) with a slower loss occurring in plasma, $t_{1/2}$ = 53 (1) or 175 min (5). The rate of loss in the presence of erythrocytes approaches the biological half-life of organic nitrate (1.9 min) (1). The interaction of nitroglycerin with blood cells, serum, or plasma has been assumed by other workers to be an enzymatic reaction. However, our earlier work using an assay with resuspended red blood cells that could detect the major nitroglycerin metabolites (1,2-dinitroglycerin and 1,3-dinitroglycerin) showed that there was no metabolite in the medium over the entire time course of the loss of nitroglycerin (3). This observation led to the conclusion that the loss of nitroglycerin may not be enzymatic in nature. In this paper further studies are reported which probe the mechanism of loss of nitroglycerin when the drug is incubated with red blood cells. Since the rate of loss of nitroglycerin is rapid, it would appear that a knowledge of the mechanism of its loss would have significant impact on an analysis of the disposition kinetics of the drug and possibly its physiological activity as well.

EXPERIMENTAL

Nitroglycerin stock solutions were prepared from an alcoholic extract of a 10% aqueous solution of lactose adsorbate[1]. The major metabolites of nitroglycerin, 1,2-dinitroglycerin and 1,3-dinitroglycerin, were prepared from 2,3-dibromopropanol[2] and 1,3-dibromopropane-2-ol[3] using the method of Dunstan *et al.* (6). The purity of the compounds was determined by high-performance liquid chromatography (HPLC) and TLC and the solutions standardized as reported by Yuen *et al.* (7). All other chemicals used were obtained commercially and were reagent grade or better.

An electron capture gas chromatograph[4] was used with a data processor[5]. The GLC assay for nitroglycerin was reported earlier (9% QF-1[6] on 60–80 mesh Supelcoport[7]) (3). The column was silanized glass 2 mm × 0.915 m and the temperatures of the injection port, the column, and the detector were 150, 125, and 200°, respectively. The carrier gas was 5% methane in argon used at a flow rate of 21 ml/min. Under these conditions the retention times were: mixture of 1,2-dinitroglycerin and 1,3-dinitroglycerin, 3 min; nitroglycerin, 6.3 min; and internal standard (1-fluoro-2,4-dinitrobenzene[8]) 7.57 min. The system does not separate the two isomeric metabolites but does optimize their combined detection.

For the assay of 1,2- and 1,3-dinitroglycerin a method was used that was a slight modification of our earlier method (8). The column (silanized glass, 2 mm × 50 cm) consisted of 3% Carbowax 20M-TPA[9] on 60–80 mesh Supelcoport[7]. The injection port, column, and detector were at 150, 135, and 200°, respectively and the flow rate of the carrier gas was 20 ml/min. Using these conditions the two metabolites could be separated from each other and from nitroglycerin. The approximate retention times in minutes were: nitroglycerin, 2.7; *o*-iodobenzyl alcohol[10] (internal standard), 3.4; 1,2-dinitroglycerin, 6.5; and 1,3-dinitroglycerin, 8.2.

The concentration of nitroglycerin or its metabolite in the various

[1] Nitroglycerin 10% (w/w) in lactose, lot K17-O-H, ICI Americas, Atlas Chemical Div, Wilmington, DE 19899.
[2] Eastman Kodak, lot A5A, Rochester, NY 14650.
[3] Eastman Kodak, lot B6C, Rochester, NY 14650.
[4] 3700 Series dual column gas chromatograph, Varian Instrument Div., Palo Alto, CA 94303.
[5] Shimadzu Recording Data Processor. Chromatopac C-RIA Shimadzu Scientific Instruments, Columbia, MD 21045.
[6] Analabs, No. Haven, CT 06473.
[7] Supelco, Bellefonte, PA 16823.
[8] Eastman Organic Chemicals, Distribution Products Ind. Rochester, NY 14650.
[9] Applied Science Labs, State College, PA 16801.
[10] Aldrich Chemical Co., Milwaukee, WI 53233.

0022-3549/83/0400-0335$01.00/0

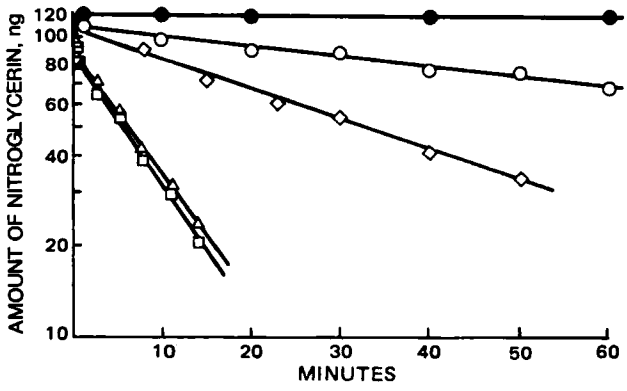

Figure 1—*Relationship between the logarithm of the amount of nitroglycerin (ng) extracted from 2 ml of several preparations initially at 60 ng/ml and the time in minutes. The preparations used at 37° together with their interpolated half-lives (in parentheses) were: (●) normal saline and protein free plasma (∞); (○) plasma (130); (◇) washed red cells diluted 1/3 of normal erythrocyte count (30); (△) red cells at normal erythrocyte count (7); (□) whole blood (6.7).*

samples used (described below) was determined relative to the internal standard (3). Using the QF-1 chromatographic system the precision was ~ ±8% at 1 ng/ml. The lower limit of nitroglycerin detection was ~50 pg/ml. The metabolites had a detector response of ~1/2 that of an equal amount of nitroglycerin, and the precision was ±10% at 3 ng/ml using the Carbowax 20 M-TPA system.

The loss of nitroglycerin or metabolite was followed in a number of different systems: whole blood, washed and resuspended red blood cells, plasma, protein-free plasma, and normal saline solution. The majority of the studies reported used resuspended cells, since the loss of nitroglycerin is the same in these systems as in whole blood (1, 3), and the resuspended cells represent more clearly defined systems that yield trouble-free reference blanks.

The various systems used in the several studies were obtained using approximately 100-ml portions of heparinized whole blood obtained from normal subjects. The blood was transferred to centrifuge tubes, centrifuged at 1200 rpm at 5° for 15 min, and then the plasma was separated from the cells. A portion of this plasma was used for a set of experiments. The remainder of the plasma was rendered protein free by ultrafiltration at 30 psi using a suitable membrane[11]. The cells obtained by centrifugation were washed three times with saline solution and reconstituted after centrifugation to 100 ml with saline solution. The cell count in such preparations was measured[12] and adjusted if necessary to a normal erythrocyte count (~5 × 10^6 cells/μl).

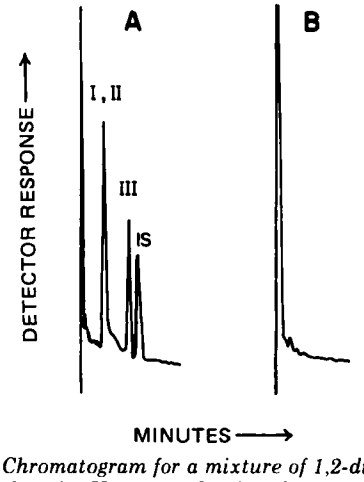

Figure 2—*(A) Chromatogram for a mixture of 1,2-dinitroglycerin, I, and 1,3-dinitroglycerin, II, 1 ng each; nitroglycerin, III (1 ng) and 1-fluoro-2,4-dinitrobenzene, IS, (internal standard) using a 9% QF-1 column. The retention times found in minutes were: I and II = 3; III = 6.3; IS = 7.6. (B) Chromatogram for red cell sample without drug.*

[11] Model 12 Ultrafiltration Cell with PM10 Membrane, Amicon Corp., Lexington, MA 02173.

[12] Micro-Computerized Elzone, Model APC-80XY, Particle Data, Inc., Elmhurst, IL 60126. Dilution procedure for red cell count accompanies the instrument manual.

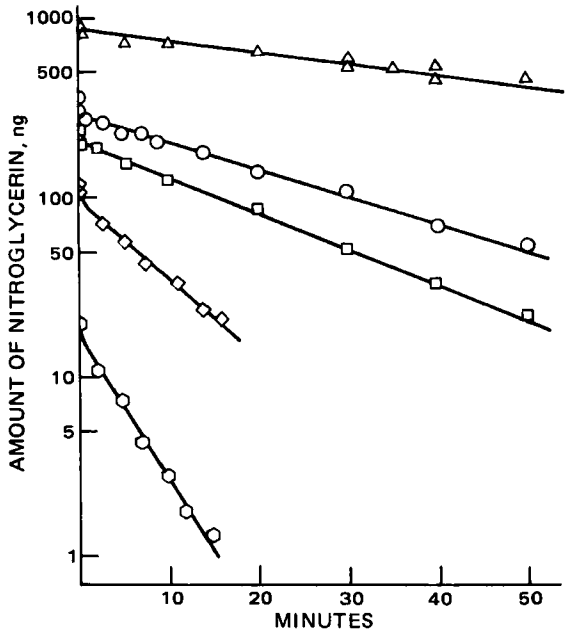

Figure 3—*Relationship between the logarithm of the amount of nitroglycerin (ng) extracted from 2 ml of washed red blood cells in normal saline and the time in minutes. The suspensions at normal erythrocyte count and at 37° were incubated with varying initial concentrations of nitroglycerin. The concentrations used and the interpolated half-lives were: (△) 480 ng/ml, 52 min; (○) 180 ng/ml, 20 min; (□) 120 ng/ml, 16 min; (◇) 60 ng/ml, 7 min; (○) 10 ng/ml, 4 min.*

In general, 2 ml of a particular preparation (whole blood, resuspended cells, plasma, protein-free plasma, or saline) was transferred to each of a series of 12-ml silanized tubes and equilibrated at 37° (~20 min). An aliquot (~50 μl) of a solution of nitroglycerin metabolite in normal saline was added to each tube to give a final concentration in each set of tubes of 10, 20, 60, 120, 180, or 480 ng/ml. The tubes were gently stirred using a rotator submerged in a water bath at 37°. Periodically over a given time interval, a tube was removed, the internal standard was added (if necessary), and the preparation was immediately extracted twice with 3 ml of ethyl acetate[13]. Both extracts were combined and concentrated or diluted for GC analysis. A portion of this solution (5 μl) was injected into the gas chromatograph for determination of the nitroglycerin and/or metabolite concentration.

The extraction efficiencies of nitroglycerin, 1,2-dinitroglycerin, and 1,3-dinitroglycerin in the red cell suspensions were previously reported: 84, 84, and 75%, respectively (3). The extraction efficiency for the metabolites from plasma was 81% (9).

RESULTS AND DISCUSSION

When nitroglycerin is incubated with whole blood or with red blood cells that are washed and suspended at a normal erythrocyte level, the loss of nitroglycerin in either preparation is the same, and after an apparent initial rapid step, it follows an apparent first-order process. Figure 1 shows the loss of nitroglycerin initially at 60 ng/ml in both whole blood and washed red cells. The half lives for the first-order loss are 7 min in whole blood and 6.7 min in red blood cells. These results are similar to those found by Armstrong *et al.* (1): 6.2 and 6.6 min, respectively, for the whole blood and suspended cell preparations at an initial nitroglycerin level of 50 ng/ml at 37°. The rate of reaction is dependent on the number of cells in the system at a constant concentration. If the initial concentration is held at 60 ng/ml and the concentration of cells is reduced threefold, the first-order half-life increases to 30 min (Fig. 1).

In whole blood and resuspended cell systems no metabolite (or hydrolysis product) accumulates in the medium. The dinitro compounds are the principal hydrolysis or metabolic products of nitroglycerin. This observation supports our earlier conclusion (3) that loss of nitroglycerin from whole blood and red cell systems may not be enzymatic, as assumed by others (1, 2). Figure 2A shows a chromatogram of a mixture of 1,2-

[13] Baker Resi-Analyzed for pesticide analysis, J. T. Baker Chem. Phillipsburg, NJ 08865.

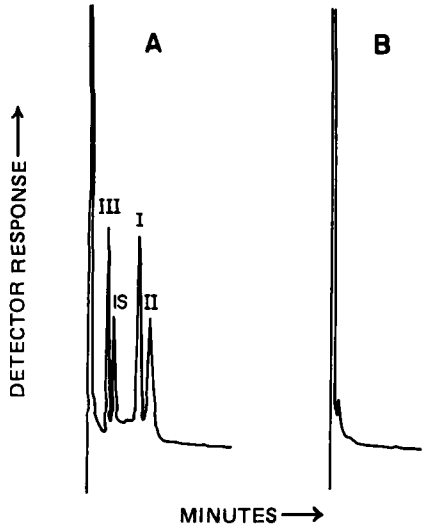

Figure 4—*(A) Chromatogram for a mixture of 2 ng of 1,2-dinitroglycerin (I), 1.6 ng of 1,3-dinitroglycerin (II), 1 ng of nitroglycerin (III), and o-iodobenzy alcohol (IS) using a 3% Carbowax 20M-TPA column. The retention times found in minutes were: I = 6.5; II = 8.2; III = 2.7; IS = 3.4. (B) Chromatogram for red cell sample without drug.*

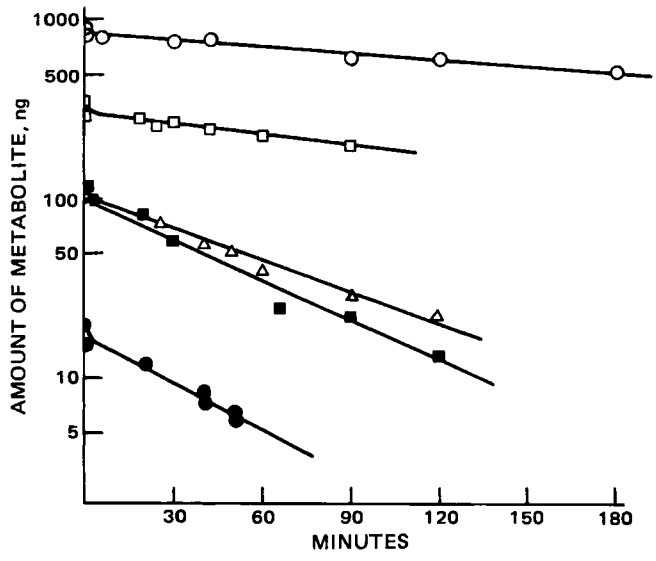

Figure 5—*Relationship between the logarithm of the amount of nitroglycerin metabolite extracted from 2 ml of red cell suspensions at normal erythrocyte count and time in minutes. The suspensions at 37° were incubated with varying initial concentrations of metabolite. The concentrations of the metabolite (I = 1,2-dinitroglycerin; II = 1,3-dinitroglycerin) used, and the interpolated half-lives were: (○) II, 480 ng/ml, 228 min; (□) II, 180 ng/ml, 141 min.; (△) I, 60 ng/ml, 51 min; (■) II, 60 ng/ml, 40 min; (●) II, 10 ng/ml, 33 min.*

dinitroglycerin (1 ng), 1,3-dinitroglycerin (1 ng), nitroglycerin (1 ng), and internal standard. The base line for a red cell blank containing no drug or metabolite is given in Fig. 2B and clearly shows no interfering materials. If metabolites were present in the blood or red cell systems, as presented in Fig. 1, the assay would have detected them.

The loss of nitroglycerin in human plasma at the same initial concentration as in whole blood or in red cell suspension follows an apparent first-order process (Fig. 1) without a detectable rapid initial phase. The reaction occurs at a much slower rate in comparison with blood studies: half-life 130 min at an initial concentration of 50 ng/ml at 37°. This slower rate in plasma was also observed by Armstrong *et al.* (1) who reported a half-life of 53 min and by Maier *et al.* (5) who reported a half-life of 175 min. The latter group used a slightly diluted sample. The decomposition of nitroglycerin in plasma may be associated with its interaction with protein, since protein-free plasma and normal saline solution containing the same initial concentration of nitroglycerin show no drug loss (Fig. 1). It is not possible to unequivocally state that the loss of nitroglycerin in plasma does not result in dinitroglycerin formation. The levels of 1,2-dinitroglycerin or 1,3-dinitroglycerin that would be expected over a 1-hr period would not be detected with any certainty. The reason for this is that the detector sensitivity for the dinitro compounds is about one-half that of nitroglycerin (8). The interaction of nitroglycerin with sulfhydryl groups (e.g., on protein) *via* a nonenzymatic process would generate denitrated compounds. This is a possibility since the nitroxyl groups of nitroglycerin should be good leaving groups. In support of this possible reactivity, Needleman reported that the interaction of nitroglycerin with sulfhydryl groups leads to the same products in the presence or absence of enzyme (10).

The effect of various initial concentrations of nitroglycerin on drug loss following its incubation with a constant level of red blood cells at 37° is given in Fig. 3. The loss of nitroglycerin initially at 10, 60, 120, 180, and 480 ng/ml follows a terminal first-order process at all concentrations. At concentrations ≤180 ng/ml an initial fast reaction phase is suggested. The first-order half-life increases as the initial concentration increases. The apparent half-lives as determined by graphical interpolation are: 4 min at 10 ng/ml, 7 min at 60 ng/ml, 16 min at 120 ng/ml, 20 min at 180 ng/ml, and 52 min at 480 ng/ml. Therapeutic levels of nitroglycerin are believed to be in the range of 1.2–11.1 ng/ml (11), and thus the interaction of the drug with red blood cells should probably be a factor to be considered in an analysis of nitroglycerin pharmacokinetics or pharmacodynamics.

At each of the several concentrations of nitroglycerin used in the studies summarized in Fig. 3, no metabolite or hydrolysis product of nitroglycerin accumulated in the medium. This led to the question of whether or not any denitrated products formed and, having reacted very rapidly with cells, did not accumulate in the medium. To get an answer to this question, the kinetics of the loss of the dinitro compounds to red blood cells was undertaken. The assay method utilizing a 3% Carbowax 20M-TPA column and an ethyl acetate extraction provided a method for accurate separation and determination of both dinitro isomers. Figure 4A shows the chromatogram for a mixture of nitroglycerin, *o*-iodobenzyl alcohol (internal standard), and the two isomeric dinitroglycerins. The amounts of components injected were: 1 ng nitroglycerin, 2 ng 1,2-dinitroglycerin, and 1.6 ng 1,3-dinitroglycerin. Figure 4B showing the chromatogram for a red cell system with no drug or metabolite added indicates that no interfering materials are extracted. The amount of metabolite extracted from samples incubated at a constant level of red cells in normal saline at 37° at various times is presented in Fig. 5. After a possible initial phase, the loss of metabolite followed an apparent first-order process at each level of 1,3-dinitroglycerin studied and the single level of 1,2-dinitroglycerin used. The half-lives for the 1,3-isomer interpolated from the plots increased as the initial concentration increased: at 10 ng/ml, 33 min; at 60 ng/ml, 40 min; at 180 ng/ml, 141 min; and at 480 ng/ml, 228 min. Although the same trend is found for the dependence of half-life on initial concentration as for nitroglycerin, the reaction at comparable concentrations is much slower for the dinitro compound. This suggests that if nitroglycerin loss results in the formation of metabolites released to the medium, the metabolites should have been detected. Figure 5 also shows that the first-order rate of loss of the 1,2-isomer is about the same as the 1,3-isomer. When both are initially present at 60 ng/ml, the half-life interpolated for 1,2-dinitroglycerin is 51 min and that for 1,3-dinitroglycerin is 40 min. Therefore, even if one isomer were preferred in the denitration of nitroglycerin, it would have been detected in the loss of the drug incubated with red blood cells. It would also seem that whatever the mechanism of loss of nitroglycerin to red blood cell is, the loss of metabolite may follow a similar mechanism since the same general kinetic behavior is found for it.

Although the mechanism of loss of nitroglycerin incubated with erythrocytes is not known, based on the observations presented here and elsewhere (3, 12) it appears that the loss of nitroglycerin to red blood cells need not be enzymatic in nature, although the possibility is not entirely eliminated. This evidence is primarily the absence of metabolite in the medium following the loss of nitroglycerin, and the inactivity toward nitroglycerin of the glutathione transferase isolated from erythrocytes as reported by Marcus *et al.* (12). The erythrocyte enzyme designated as the ρ form is quite different from the most active δ form found in the liver or indeed different from any of the liver forms, α–ϵ (12). The unusual rate dependence (Fig. 3) and the absence of metabolite or hydrolysis product suggest that the loss could be physical in nature. It would appear that a mixed kinetic process or processes occur when intervening steps involve slow and fast kinetic states. The mechanism (or mechanisms) of nitroglycerin loss in blood should be established since its elucidation will not only impinge on valid pharmacodynamic analysis but even impinge on factors such as obtaining meaningful blood level determinations. Studies are currently being undertaken to explore an adsorption/ab-

sorption mechanism. No particular mechanism is concluded, nor has an enzymatic mechanism been conclusively eliminated. If the interaction with red cells is physical in nature, it is possible that interaction with other biotissues can be quite significant and that what has been found with red blood cells is only one of many important interactive phenomena. Indeed, McNiff *et al.* have recently suggested that the target tissue (blood vessels) for nitroglycerin might have a higher concentration of drug than found in plasma (13). Furthermore, Armstrong *et al.* conclude that the intact *nitroglycerin molecule is essential* for initiation of relaxation based on dose-response curves of nitroglycerin effects on phenylephrine-contracted canine dorsal pedal arteries and medial saphenous veins (14). These workers found that relaxation occurred without the release of detectable amounts of metabolites into the incubation medium.

REFERENCES

(1) J. A. Armstrong, S. E. Slaughter, G. S. Marks, and P. A. Armstrong, *Can. J. Physiol. Pharmacol.*, **58**, 459 (1980).

(2) H. L. Lee, *Biochem. Pharmacol.*, **22**, 3122 (1973).

(3) C. C. Wu, T. D. Sokoloski, M. F. Blanford, and A. M. Burkman, *Int. J. Pharm.*, **8**, 323 (1981).

(4) F. J. DiCarlo and M. D. Melgar, *Biochem. Pharmacol.*, **19**, 1371 (1970).

(5) G. A. Maier, A. Poliszczuk, and H. L. Fung, *Int. J. Pharm.* **4**, 75 (1979).

(6) I. Dunstan, J. V. Griffiths, and S. A. Harvey, *J. Chem. Soc. Rev.*, 1319 (1965).

(7) P. H. Yuen, S. L. Denman, T. D. Sokoloski, and A. M. Burkman, *J. Pharm. Sci.*, **68**, 1163 (1979).

(8) C. C. Wu, T. D. Sokoloski, A. M. Burkman, and L. S. Wu, *J. Chromatogr.*, **216**, 239 (1981).

(9) C. C. Wu, T. D. Sokoloski, A. M. Burkman, M. F. Blanford, and L. S. Wu, *J. Chromatogr., Biomed. Appl.*, **228**, 333 (1982).

(10) P. Needleman, *Annu. Rev. Pharmacol. Toxicol.*, **16**, 81 (1976).

(11) P. A. Armstrong, J. A. Armstrong, and G. S. Marks, *La Nouvelle Presse. Medicale*, **9**, 2429 (1980).

(12) C. J. Marcus, W. H. Habig, and W. B. Jakoby, *Arch. Biochem. Biophys.*, **188**, 287 (1978).

(13) E. F. McNiff, A. Yacobi, F. M. Young-Chang, L. H. Golden, A. Goldfarb, and H. L. Fung, *J. Pharm. Sci.*, **70**, 1054 (1981).

(14) J. A. Armstrong, G. S. Marks, and P. A. Armstrong, *Mol. Pharmacol.*, **18**, 112 (1980).

ACKNOWLEDGMENTS

Supported in part by National Institutes of Health Grant HL-23303, Public Health Service, USA.

Liquid Crystal Solubilization of Cholesterol: Potential Method for Gallstone Dissolution

JOSEPH B. BOGARDUS

Received January 15, 1982 from the *College of Pharmacy, University of Kentucky, Lexington, KY 40536* Accepted for publication April 2, 1982.

Abstract □ Solubilization rate and phase equilibrium studies were conducted for cholesterol in aqueous sodium oleate solutions. The components interacted to form a lamellar liquid crystalline phase, and this phenomenon was investigated as a potential method for cholesterol gallstone dissolution. Phase equilibria data for cholesterol–sodium oleate–water showed that the mesophase contained approximately equimolar amounts of cholesterol and oleate with large amounts of water. The cholesterol solubilization rate from a static pellet in sodium oleate solutions was much faster than dissolution in sodium cholate solutions and was independent of oleate concentration from 2.5 to 10%. In these experiments, the medium became a cloudy disperson of liquid crystalline phase in the micellar solutions. The rate-limiting step in the solubilization process appears to be dispersion of fragments from the liquid crystalline layer on the cholesterol surface. This hypothesis was consistent with the kinetic effects of viscosity, stirring rate, and oleate concentration. By converting cholesterol to a liquid crystalline phase, the solubilization process avoids the limitations of micellar solubility and interfacial resistance which control cholesterol dissolution in bile salt-containing media.

Keyphrases □ Cholesterol—solubilization in fatty acid salt solutions, dissolution in bile salt solutions, potential method for gallstone dissolution □ Solubilization—cholesterol in fatty acid salt solutions, bile salt solutions, potential method for gallstone dissolution

Cholecystectomy is the primary method for elimination of gallstones, which are composed primarily of cholesterol. In ~5% of cases, because of size or location, some stones in the ductal system cannot be removed using physical extraction techniques and are retained (1). A number of approaches have been tried for *in situ* dissolution of common bile duct stones using solvents such as ether and chloroform and solutions of bile salts or heparin (2). Recent clinical studies have shown that infusion of monooctanoin (glyceryl monooctanoate), an excellent solvent for cholesterol *in vitro* (3), dissolves common duct stones in 50–70% of patients, although treatment for 2–3 weeks is required (4, 5). The solution is infused into the bile duct *via* a T-tube drain in postcholecystectomy patients or through a nasobiliary tube inserted using a duodenoscope.

This paper reports initial investigations toward development of liquid crystal solubilization as a method for cholesterol gallstone dissolution. Ekwall *et al.* (6, 7) reported the formation of liquid crystalline droplets on the surface of cholesterol monohydrate crystals suspended in fatty acid salt solutions. Longer chain-length salts interacted more strongly with cholesterol than did shorter ones. In the present study, the rate of solubilization of cholesterol was much faster than simple dissolution in sodium cholate solutions. The cholesterol was present in the medium primarily in the form of droplets of liquid crystalline phase dispersed in the micellar solution.

EXPERIMENTAL

Phase Equilibria—Mixtures of cholesterol (1.6–11.8%), sodium oleate (1.2–14.8%), and water were weighed into glass ampules. The ampules were flushed with nitrogen, sealed, warmed to 80° in a water bath, cooled to room temperatures (22–24°), and then allowed to stand for 3 weeks with periodic shaking. A sample of the contents of each ampule was ob-

0022-3549/83/0400-0338$01.00/0

sorption mechanism. No particular mechanism is concluded, nor has an enzymatic mechanism been conclusively eliminated. If the interaction with red cells is physical in nature, it is possible that interaction with other biotissues can be quite significant and that what has been found with red blood cells is only one of many important interactive phenomena. Indeed, McNiff *et al.* have recently suggested that the target tissue (blood vessels) for nitroglycerin might have a higher concentration of drug than found in plasma (13). Furthermore, Armstrong *et al.* conclude that the intact *nitroglycerin molecule is essential* for initiation of relaxation based on dose-response curves of nitroglycerin effects on phenylephrine-contracted canine dorsal pedal arteries and medial saphenous veins (14). These workers found that relaxation occurred without the release of detectable amounts of metabolites into the incubation medium.

REFERENCES

(1) J. A. Armstrong, S. E. Slaughter, G. S. Marks, and P. A. Armstrong, *Can. J. Physiol. Pharmacol.*, **58**, 459 (1980).

(2) H. L. Lee, *Biochem. Pharmacol.*, **22**, 3122 (1973).

(3) C. C. Wu, T. D. Sokoloski, M. F. Blanford, and A. M. Burkman, *Int. J. Pharm.*, **8**, 323 (1981).

(4) F. J. DiCarlo and M. D. Melgar, *Biochem. Pharmacol.*, **19**, 1371 (1970).

(5) G. A. Maier, A. Poliszczuk, and H. L. Fung, *Int. J. Pharm.* **4**, 75 (1979).

(6) I. Dunstan, J. V. Griffiths, and S. A. Harvey, *J. Chem. Soc. Rev.*, 1319 (1965).

(7) P. H. Yuen, S. L. Denman, T. D. Sokoloski, and A. M. Burkman, *J. Pharm. Sci.*, **68**, 1163 (1979).

(8) C. C. Wu, T. D. Sokoloski, A. M. Burkman, and L. S. Wu, *J. Chromatogr.*, **216**, 239 (1981).

(9) C. C. Wu, T. D. Sokoloski, A. M. Burkman, M. F. Blanford, and L. S. Wu, *J. Chromatogr., Biomed. Appl.*, **228**, 333 (1982).

(10) P. Needleman, *Annu. Rev. Pharmacol. Toxicol.*, **16**, 81 (1976).

(11) P. A. Armstrong, J. A. Armstrong, and G. S. Marks, *La Nouvelle Presse. Medicale*, **9**, 2429 (1980).

(12) C. J. Marcus, W. H. Habig, and W. B. Jakoby, *Arch. Biochem. Biophys.*, **188**, 287 (1978).

(13) E. F. McNiff, A. Yacobi, F. M. Young-Chang, L. H. Golden, A. Goldfarb, and H. L. Fung, *J. Pharm. Sci.*, **70**, 1054 (1981).

(14) J. A. Armstrong, G. S. Marks, and P. A. Armstrong, *Mol. Pharmacol.*, **18**, 112 (1980).

ACKNOWLEDGMENTS

Supported in part by National Institutes of Health Grant HL-23303, Public Health Service, USA.

Liquid Crystal Solubilization of Cholesterol: Potential Method for Gallstone Dissolution

JOSEPH B. BOGARDUS

Received January 15, 1982 from the *College of Pharmacy, University of Kentucky, Lexington, KY 40536* Accepted for publication April 2, 1982.

Abstract □ Solubilization rate and phase equilibrium studies were conducted for cholesterol in aqueous sodium oleate solutions. The components interacted to form a lamellar liquid crystalline phase, and this phenomenon was investigated as a potential method for cholesterol gallstone dissolution. Phase equilibria data for cholesterol–sodium oleate–water showed that the mesophase contained approximately equimolar amounts of cholesterol and oleate with large amounts of water. The cholesterol solubilization rate from a static pellet in sodium oleate solutions was much faster than dissolution in sodium cholate solutions and was independent of oleate concentration from 2.5 to 10%. In these experiments, the medium became a cloudy disperson of liquid crystalline phase in the micellar solutions. The rate-limiting step in the solubilization process appears to be dispersion of fragments from the liquid crystalline layer on the cholesterol surface. This hypothesis was consistent with the kinetic effects of viscosity, stirring rate, and oleate concentration. By converting cholesterol to a liquid crystalline phase, the solubilization process avoids the limitations of micellar solubility and interfacial resistance which control cholesterol dissolution in bile salt-containing media.

Keyphrases □ Cholesterol—solubilization in fatty acid salt solutions, dissolution in bile salt solutions, potential method for gallstone dissolution □ Solubilization—cholesterol in fatty acid salt solutions, bile salt solutions, potential method for gallstone dissolution

Cholecystectomy is the primary method for elimination of gallstones, which are composed primarily of cholesterol. In ~5% of cases, because of size or location, some stones in the ductal system cannot be removed using physical extraction techniques and are retained (1). A number of approaches have been tried for *in situ* dissolution of common bile duct stones using solvents such as ether and chloroform and solutions of bile salts or heparin (2). Recent clinical studies have shown that infusion of monooctanoin (glyceryl monooctanoate), an excellent solvent for cholesterol *in vitro* (3), dissolves common duct stones in 50–70% of patients, although treatment for 2–3 weeks is required (4, 5). The solution is infused into the bile duct *via* a T-tube drain in postcholecystectomy patients or through a nasobiliary tube inserted using a duodenoscope.

This paper reports initial investigations toward development of liquid crystal solubilization as a method for cholesterol gallstone dissolution. Ekwall *et al.* (6, 7) reported the formation of liquid crystalline droplets on the surface of cholesterol monohydrate crystals suspended in fatty acid salt solutions. Longer chain-length salts interacted more strongly with cholesterol than did shorter ones. In the present study, the rate of solubilization of cholesterol was much faster than simple dissolution in sodium cholate solutions. The cholesterol was present in the medium primarily in the form of droplets of liquid crystalline phase dispersed in the micellar solution.

EXPERIMENTAL

Phase Equilibria—Mixtures of cholesterol (1.6–11.8%), sodium oleate (1.2–14.8%), and water were weighed into glass ampules. The ampules were flushed with nitrogen, sealed, warmed to 80° in a water bath, cooled to room temperatures (22–24°), and then allowed to stand for 3 weeks with periodic shaking. A sample of the contents of each ampule was ob-

0022-3549/83/0400-0338$01.00/0

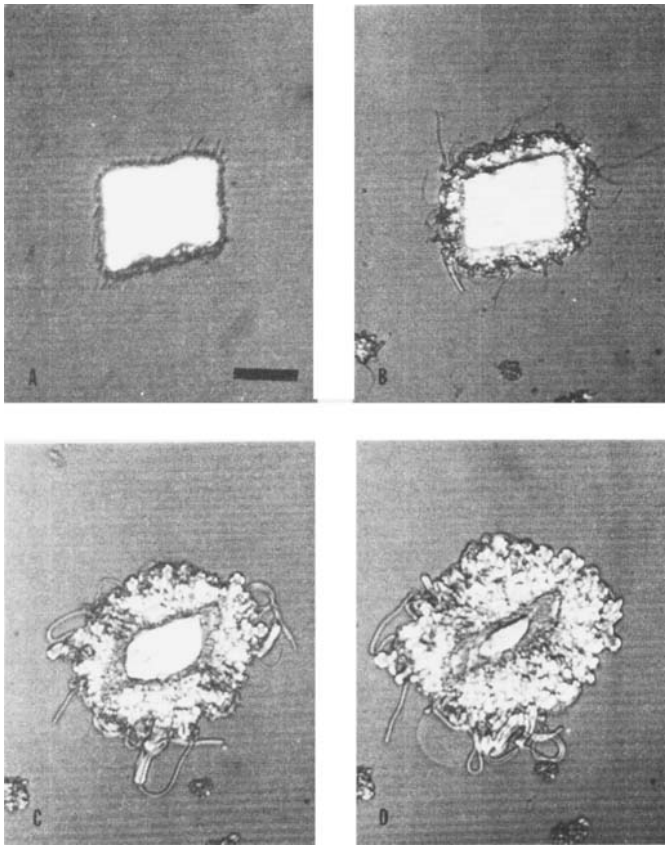

Figure 1—*Liquid crystal solubilization of cholesterol monohydrate in a 5% sodium oleate solution. Key: (A) 5–10 sec after mixing (bar = 100 μm), (B) after 1 min, (C) after 5 min, and (D) after 10 min.*

served on a polarizing microscope[1], and the remaining material was centrifuged[2] at 22–25° for 18 hr at 25,000×*g*. The phases were carefully separated using a syringe, checked microscopically for homogeneity, and analyzed by high-performance liquid chromatography (HPLC).

Solubilization Rate—Pellets of cholesterol monohydrate were compressed in a 1.27-cm diameter die with a laboratory press[3]. The pellet-die was placed in the bottom of a vessel containing 300 ml of medium thermostated at 37°. A flat-faced paddle and constant-speed stirrer[4] agitated the medium at the desired rate. Samples were periodically removed, extracted with ether, and assayed by HPLC.

HPLC—An HPLC method was developed for direct separation of cholesterol–oleic acid mixtures using a C_{18} column[5]. The compounds were detected at 205 nm[6] due to the weakly absorbing UV chromophores present. Quantitation was by peak height measurement. To obtain adequate retention of oleic acid, mobile phases previously reported for cholesterol, 100% acetonitrile (8) or 50:50 isopropyl alcohol–acetonitrile (9), were modified. Optimum separation was obtained with 3:97 methanol–acetonitrile at 1.5 ml/min. Oleic acid eluted as a doublet at 3.0 and 3.6 min followed by cholesterol at 9 min.

Samples of cholesterol–sodium oleate mixtures from equilibrium or solubilization rate experiments containing 5–50 mg of the components were weighed accurately in a screw-cap tube and 2 ml of 0.5 *M* citric acid was added. The resulting oily emulsion was then extracted with 10 ml of ether. The ether phase was appropriately diluted with acetonitrile, and this solution was analyzed by HPLC. Preliminary studies indicated that both components were quantitatively extracted by this procedure. Standards containing both compounds were prepared in ether, diluted with acetonitrile, and injected periodically for peak height standardization.

Microscopy—Samples of the phases in the equilibrium study and from the pellet surface during solubilization were examined by polarizing light microscopy. Based on the classifications of Rosevear (10), the liquid crystalline phase appears to be of the lamellar (or neat soap) type.

[1] Zetopan, Reichert.
[2] Beckman J2-21.
[3] Carver.
[4] Hanson Research Corp.
[5] Waters Associates.
[6] Varian Varichrome.

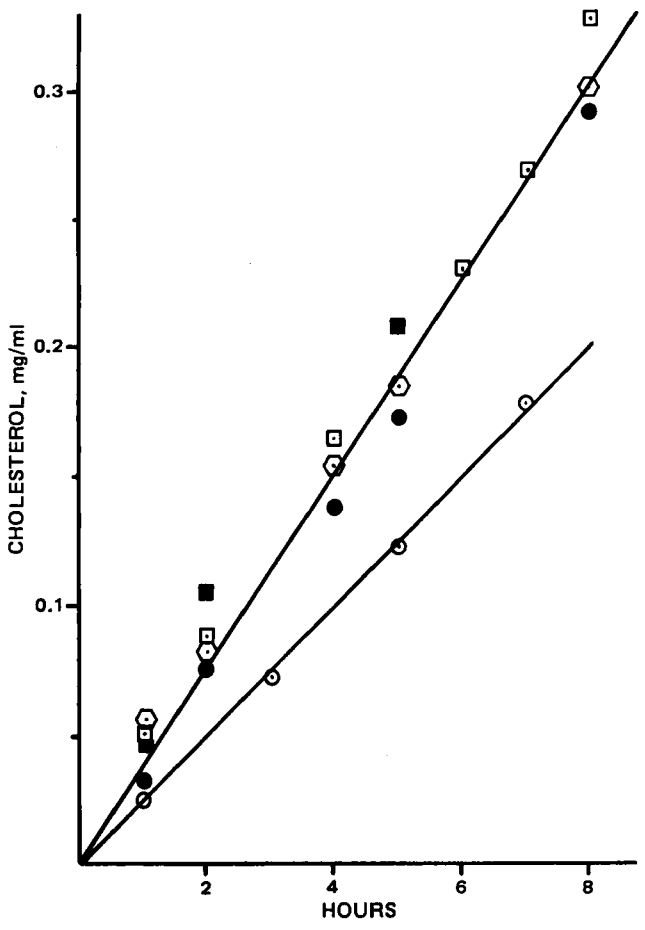

Figure 2—*Cholesterol solubilization in sodium oleate solutions at 37°, 150 rpm. The line for 2.5–10% data has slope = 25 × 10^{-4} mg cm^{-2} sec^{-1} and zero intercept. The slope for the 1% oleate data is 16 × 10^{-4} mg cm^{-2} sec^{-1}. Percent oleate key: (⊙) 1.0%, (●) 2.5%, (⊡) 5.0%, (■) 7.5%, and (⊛) 10%.*

Materials—Cholesterol USP[7], oleic acid[8], and lauric acid[7] were obtained commercially. Chromatographic solvents were HPLC grade and the source did not affect the assay.

Cholesterol was recrystallized from 10% aqueous acetone which gave the monohydrate. Problems in removal of ethanol were encountered after recrystallization from 95% ethanol. The vacuum-drying conditions needed to remove residual ethanol lowered the water content to ~1% (Karl Fischer titration) and presumably formed anhydrous cholesterol, which did not readily revert to the monohydrate in the presence of water (11). Using the acetone–water method, the solvent evaporated (air-drying for 0.5–1 hr at ambient temperature and humidity), and the water content was near the theoretical value for the monohydrate (4.4% water).

Sodium oleate and sodium laurate were prepared in ethanol from the respective acids by neutralization with 25% sodium methoxide in methanol[9]. The end point was confirmed with bromothymol blue and the solvents were removed using a rotary evaporator. Purity of the sodium oleate was checked by HPLC comparison with oleic acid.

RESULTS AND DISCUSSION

Phase Equilibria—Figure 1 is a photomicrograph of the liquid crystalline phase forming on the surface of crystalline cholesterol monohydrate. The mesophase forms rapidly upon contact with sodium oleate solutions, and smaller crystals are solubilized on the microscope slide within a few minutes. In a separate experiment, a coarse suspension of 300 mg of cholesterol with 300 mg/10 ml sodium oleate solution was solubilized within 24 hr at room temperature with occasional shaking.

[7] Sigma Chemical Co.
[8] Fisher purified grade.
[9] Aldrich Chemical Co.

Table I—Preliminary Phase Equilibrium Data for Cholesterol–Sodium Oleate–Water at 22°

Original Mixture (w/w)		Phases	Phase Composition				Molar Ratio
			Isotropic		Liquid Crystalline		
Cholesterol, %	Oleate, %	Present at Equilibrium[a]	Cholesterol, %	Oleate, %	Cholesterol, %	Oleate, %	Cholesterol–Oleate[b]
1.6	14.8	I + L	1.6	7.9	19.6	14.6	1.01
1.6	4.9	I + L	0.16	2.8	10.2	10.6	0.72
1.6	1.2	I + (L + V) + C	0.36	1.4	3.8	4.2	0.68
3.2	14.5	I + L	2.3	5.9	26.3	16.3	1.21
3.2	4.8	I + L	0.43	2.1	9.6	8.7	0.83
3.2	1.2	I + (L + V) + C	0.02	0.59	3.2	3.1	0.78
6.2	14.1	I + L	1.3	5.8	18.8	13.0	1.09
6.2	4.7	L + C	(Phase Absent)		6.9	4.0	1.30
6.2	1.2	L + C	(Phase Absent)		4.1	1.8	1.71
11.8	13.2	I + L	0.59	2.6	9.1	7.5	0.91
11.8	4.4	L + C	(Phase Absent)		9.0	5.6	1.21

[a] Abbreviations: (I) Isotropic micellar solution, (L) Liquid crystalline phase, (V) Vesicles, and (C) Cholesterol monohydrate crystals. [b] In the liquid crystalline phase.

These observations are consistent with previous work on the interaction between fatty acid salt solutions and cholesterol (6). The minimum concentration at which the mesophase was observed decreased as fatty acid chain length increased from C_9 to C_{18}. For sodium oleate, the mesophase formed at concentrations as low as 3×10^{-4} *M*; for sodium nonanoate, it was present only at concentrations >0.14 *M*. This stronger interaction of cholesterol with longer chain-length compounds was not observed in solubility studies in homologous normal alkanols or fatty acid ethyl esters (3). For these solvents, cholesterol solubility was maximum at a chain length of ~6–7 carbon atoms. However, crystalline solvates of cholesterol were observed in some of the solvents which influenced the solubility trends. In addition, the energetic and structural requirements for mesophase formation in water are likely to be quite different than those for solvation and interaction in the nonpolar solvents.

Preliminary phase equilibrium studies were conducted in the dilute solution region for cholesterol–sodium oleate–water, as shown in Table I. Additional data will be necessary before the phase diagram can be constructed. The system viscosity increased at higher component concentrations making equilibration and phase separation more difficult. The phases present at equilibrium and their composition are dependent on the amounts of cholesterol and oleate in the original mixtures. When the cholesterol–oleate ratio was <1, the cholesterol was completely solubilized, and the system consisted of isotropic micellar solution and liquid crystalline phase, which were readily separated by centrifugation. Vesicles were observed in samples with low lipid concentrations and ratios approaching 1:1. The existence of cholesterol–oleate vesicles was reported by Hargreaves and Deamer (12) who investigated the potential use of these systems for drug delivery and as model biomembranes. In Table I, the liquid crystalline phase and vesicles are considered as a single phase, since the two cannot be readily differentiated microscopically. The lipid concentrations in the isotropic solution reflect the solubilization of cholesterol in sodium oleate micelles but are generally lower than the initial amount due to presence of the mesophase or undissolved cholesterol.

As shown in Table I, the relative amounts of cholesterol–oleate in the liquid crystalline phase ranged from 0.68 to 1.71. The lower ratios in the mesophase occurred with low initial concentration of lipids; the higher ratios were observed when the isotropic phase was absent and the mesophase was saturated with cholesterol. The structure of the mesophase is likely to be a bilayer of alternating cholesterol and oleate molecules. Thus, it is not solubilization in the micellar sense in which a number of surfactant molecules are present for each substrate molecule. Small angle X-ray diffraction data would be necessary to determine the structure of the mesophase.

Solubilization Rate—Cholesterol solubilization rate plots from a static compressed disk of cholesterol monohydrate are shown in Fig. 2. After a short time, the medium became a cloudy-milky fluid dispersion of liquid crystalline phase in the isotropic micellar solution. The amount of cholesterol solubilized, and thus the approximate amount of oleate precipitated as mesophase, was much less than the original oleate concentrations in all cases. A single line was drawn through the data at 2.5–10% sodium oleate. The solubilization rate in this range was essentially independent of oleate concentration. The slower rate with 1% oleate may be indicative of a change in the rate-limiting step for the solubilization process. Microscopic observations confirm that the mesophase forms at oleate concentrations <1% (6, 7).

Least-squares analysis of individual runs showed a slight positive intercept which increased with concentration, although the terminal slopes were constant within experimental error. The apparently higher initial rates may be due to the initial dissolution of cholesterol prior to establishment of the liquid crystalline surface layer. Early in the experiment, the mesophase would be expected to dissolve in the bulk medium until its saturation level was reached. Despite the high oleate–cholesterol ratio in the bulk medium, saturation apparently occurred early in the experiments, judging from the turbidity.

Addition of electrolytes is known to increase the cholesterol dissolution rate in simulated bile solutions (13). In these systems, the salt decreases the interfacial resistance to dissolution, a dominant factor in the dissolution rate process. In sodium oleate solutions, sodium chloride decreased the solubilization rate of cholesterol, as shown in Table II. The origin of this effect may be related to the viscosity, the nature of the micellar solution, or that of the mesophase. The viscosity of sodium oleate solutions with added salt was noticeably higher at 5 and 10% oleate, although quantitative data were not obtained. The higher viscosity would be expected to decrease the shear at the pellet surface.

Since the solubilization process is physically different from dissolution, limited data were obtained on the effect of stirring rate (Table III). The ratio of the rates at the two rotational speeds was similar to the square root dependence (1.414) predicted by the Levich equation for a diffusion-controlled process (14). This result was surprising because cholesterol dissolution in bile salt or bile salt–lecithin solutions is relatively insensitive to stirring rate. In this case, interfacial resistance to micellar solubilization of cholesterol is a dominant characteristic (14, 15). The stirring rate dependence in the present experiments probably does not imply that the rate process is diffusion controlled. The presence of the liquid crystalline surface layer and the rate independence of oleate concentration also must be considered in the description of the solubilization process. Experiments using a rotating disk apparatus would be required

Table II—Effect of 0.9% NaCl on Cholesterol Monohydrate Solubilization in Sodium Oleate Solutions at 37°, 150 rpm

Oleate, %	Rate, $\times 10^4$ mg cm^{-2} sec^{-1}	
	Control	With 0.9% NaCl
2.5	23.3	15.3
5	23.6	6.8
10	23.2	8.5

Table III—Effect of Stirring Rate on Cholesterol Solubilization in Sodium Oleate Solutions at 37°

Oleate, %	Rate, $\times 10^4$ mg cm^{-2} sec^{-1}		
	75 rpm	150 rpm	Rate Ratio
2.5	14.7	23.3	1.59
5	15.1	23.6	1.56

Table IV—Comparison of Solubilization Rate in Sodium Oleate Solution with Other Media at 37°

Solution, 5%	Rate, $\times 10^4$ mg cm^{-2} sec^{-1}
Sodium oleate	23.6
Sodium laurate	28.3
Sodium cholate	0.11

to quantitatively evaluate the relative importance of diffusional, interfacial, and surface shear processes in this system.

The solubilization rate of cholesterol monohydrate, prepared by recrystallization from 10% water–acetone, was not sensitive to the compression load used to make the pellet. At loads of 1364, 2045, and 3182 kg (3000, 4500, and 7000 lb, respectively) and oleate concentrations of 2.5, 5.0, and 10%, the rate was essentially unchanged. In preliminary studies, however, problems were encountered with reproducibility at the lower pressures; therefore, 3182 kg was used as a standard compression load for this investigation.

In Table IV, the solubilization rate in 5% sodium oleate is compared with 5% sodium laurate and 5% sodium cholate. The two fatty acid salts show similar solubilization rates. Previous work (6) found that the minimum concentration of sodium laurate which formed a mesophase with cholesterol was 0.007 *M*, approximately 20-fold higher than the minimum for sodium oleate. Thus, it appears that the concentration for mesophase formation and solubilization rate cannot be directly correlated. The solubilization rates are clearly much faster than dissolution in micellar sodium cholate solutions. The sodium cholate rate is somewhat slower than that reported by Feld and Higuchi, 0.73×10^{-4} mg cm^{-2} sec^{-1}, (15) in 5% sodium cholate with 0.1 *M* phosphate buffer, pH 8.0. Buffer effects (13), different assay methods, apparatus, and method of cholesterol monohydrate preparation are potential explanations for the difference in rate. The last factor was recently found to affect strongly the dissolution rate (15). Due to these differences, further comparisons with literature data are not likely to be meaningful.

Solubilization Mechanism—The solubilization mechanism of cholesterol in fatty acid salt solutions is considerably different from dissolution in bile salt solutions. Mesophase formation generally does not occur in dilute bile salt or bile salt–lecithin solutions. Formation of a liquid crystalline phase has been observed only with ursodeoxycholate and then only after several hours of contact with cholesterol (16, 17). In dissolution studies with this bile salt, cholesterol release did not level off at the apparent micellar solubility but continued to higher values with formation of the mesophase. An equilibrium model was suggested whereby cholesterol could be dissolved in the micellar solution or directly incorporated into the mesophase (17). After several days when the micelles were saturated with cholesterol, the primary mass transport process was thought to proceed by liquid crystal solubilization. For sodium oleate, the mesophase forms immediately (Fig. 1), and the system has a lower capacity for micellar solubilization of cholesterol.

A hypothetical model for cholesterol solubilization in fatty acid salt solutions is shown in Fig. 3. Rapid formation of a multilamellar region of liquid crystalline material on the crystal surface was observed microscopically. This surface layer grows by diffusion of cholesterol away from the crystal and diffusion of oleate and water from the bulk solution. Figure 1 shows that buildup of a significant surface layer under static conditions does not strongly inhibit solubilization of additional cholesterol from the crystal. Diffusion within the mesophase layer must be rapid in both the inner (cholesterol-rich) and outer (oleate-rich) regions. Scrapings from the pellet surface during the rate studies confirmed the presence of mesophase, even at 150 rpm. The primary mode of mass transfer of cholesterol to the bulk medium is thought to be by dispersion or shearing of liquid crystalline fragments from the surface, as shown in Fig. 3. These so-called myelin figures can be composed entirely of mesophase (spherulites) or have an aqueous core (vesicles or tubules). After dispersal into the bulk solution, the fragments may either dissolve into the micellar solution (which would occur early in the experiment) or remain in the liquid crystalline state.

The solubilization mechanism in this system can be considered as two major steps: (*a*) diffusional processes involved with formation and growth of the liquid crystalline surface layer and (*b*) physical dispersion or shearing of liquid crystalline fragments into the bulk medium. The present data support the proposal that the second step is rate limiting in the 2.5–10% oleate solutions. Under these conditions, the rate of surface mesophase formation is assumed to be faster than its removal by stirring. Reasons for this proposal are:

1. The observed relationship between stirring and solubilization rates (Table III) is probably due to the effect of higher shear on the surface layer, increasing the dispersal rate of the mesophase into the bulk solution. The alternate explanation of diffusional control does not seem to be consistent with the physical system under study.

2. If the first step of the solubilization mechanism were rate limiting, a kinetic dependence on oleate concentration but independence on stirring rate would be expected. Both these conditions are in disagreement with the data. Under static conditions on the microscope, however, the rate of solubilization was clearly increased with increasing oleate concentrations. Except for viscosity effects, the rate of a hydrodynamically controlled process (step *b*) should not be dependent on oleate concentration. This assumes that the process in the surface layer occurs much faster than the mass transport of fragments away from the surface. The slower solubilization rate with 1% oleate may be indicative of a change from hydrodynamic to surface control. As the oleate concentration is reduced, the rate of step *a* should decrease until this process is similar in rate to step *b*. At this point, a crossover between the two processes would have to occur.

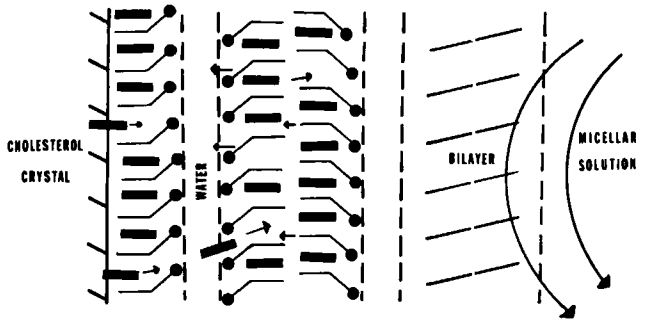

Figure 3—*Schematic diagram for the liquid crystal solubilization of cholesterol in sodium oleate solutions (bars represent cholesterol, angles represent oleate). Small arrows represent diffusion of the species within the mesophase layer. Large arrows indicate dispersion of surface material into the medium.*

3. The effect of salt (Table II) may be primarily due to the higher viscosity of the medium rather than to significant changes in the solution or the mesophase. Increased viscosity would reduce the shear on the rate-controlling surface layer.

4. Finally, the similarity in rates with oleate and laurate, but not cholate (Table IV), is consistent with a hydrodynamically controlled process. Laurate does not interact with cholesterol as strongly as oleate (6). Despite this difference in affinity, the solubilization rates were almost equal. This suggests a common rate-controlling step for both salts, which is independent of mesophase formation on the cholesterol surface.

REFERENCES

(1) F. Glenn, *Ann. Surg.*, **179**, 528 (1974).

(2) R. W. Motson, *Br. J. Surg.*, **68**, 203 (1981).

(3) G. L. Flynn, Y. Shah, S. Prakongpan, K. H. Kwan, W. I. Higuchi, and A. F. Hofmann, *J. Pharm. Sci.*, **68**, 1090 (1979).

(4) J. L. Thistle, G. F. Carlson, A. F. Hofmann, N. F. LaRusso, R. L. MacCarty, G. L. Flynn, W. I. Higuchi, and V. K. Babayan, *Gastroenterology*, **78**, 1016 (1980).

(5) J. Schenk, B. Schmack, W. Rösch, J. F. Riemann, H. Koch, and L. Demling, *Dtsch. Med. Wochenschr.*, **105**, 917 (1980).

(6) P. Ekwall, H. Baltscheffsky, and L. Mandell, *Acta Chem. Scand.*, **15**, 1195 (1961).

(7) P. Ekwall and L. Mandell, *ibid.*, **15**, 1403 (1961).

(8) E. Hansbury and T. J. Scallen, *J. Lipid Res.* **19**, 742 (1978).

(9) I. W. Duncan, P. H. Culbreath, and C. A. Burtis, *J. Chromatogr.*, **162**, 281 (1979).

(10) F. B. Rosevear, *J. Am. Oil Chem. Soc.*, **31**, 628 (1954).

(11) C. R. Loomis, G. G. Shipley, and D. M. Small, *J. Lipid Res.*, **20**, 525 (1979).

(12) W. R. Hargreaves and D. W. Deamer, *Biochemistry*, **17**, 3759 (1978).

(13) K. H. Kwan, W. I. Higuchi, A. M. Molokhia, and A. F. Hofmann, *J. Pharm. Sci.*, **66**, 1094 (1977).

(14) S. Prakongpan, W. I. Higuchi, K. H. Kwan, and A. M. Molokhia, *ibid.*, **65**, 685 (1976).

(15) K.M. Feld and W. I. Higuchi, *ibid.*, **70**, 717 (1981).

(16) O. I. Corrigan, C. C. Su, W. I. Higuchi, and A. F. Hofmann, *ibid.*, **69**, 869 (1980).

(17) C. C. Su, J. Y. Park, W. I. Higuchi, M. H. Alkan, O. I. Corrigan, and A. F. Hofmann, *ibid.*, **70**, 713 (1981).

ACKNOWLEDGMENTS

This work was supported in part by the University of Kentucky Research Foundation and by a Merck grant for faculty development.

The technical assistance of R. Perrone is gratefully acknowledged. The author thanks Dr. W. I. Higuchi for providing comments on the manuscript.

Unloading and Postcompression Viscoelastic Stress *versus* Strain Behavior of Pharmaceutical Solids

DOUGLAS W. DANIELSON *, WILLIAM T. MOREHEAD, and EDWARD G. RIPPIE ˣ

Received March 1, 1982, from the *Department of Pharmaceutics, College of Pharmacy, University of Minnesota, Minneapolis, MN 55455.* Accepted for publication June 11, 1982. *Present address: Merrell National Laboratories, Cincinnati, OH 45215.

Abstract □ The viscoelastic properties of several compacts composed of drugs and direct compression excipients have been measured during the stress unloading and postcompression phases of the tablet compression process. Measurements of applied strains and the resultant stresses, generated in the tablet structure under compaction, were made using a rotary press. The press was instrumented to measure punch and die wall stresses at normal operating speeds. The three-dimensional viscoelastic theory, used in data analysis, provides for the separate characterization of tablet behavior into its dilation and distortion components. The tablets investigated were found to behave elastically in dilation, but to have both viscous and elastic contributions to their stress/strain relaxation in distortion. This latter behavior could be modeled well as a Kelvin solid. Data derived from an elastic-in-dilation, Kelvin-in-distortion analysis of tablets, compressed at similar machine speeds but at various peak pressures, were found to vary widely depending on tablet composition. Dependence of the viscous and elastic parameters on compression conditions was found to be predictive of conditions under which capping or lamination of the compact would occur.

Keyphrases □ Viscoelastic behavior—of compacts of drugs and direct compression excipients □ Tablet formulation—viscoelastic behavior of compacts during stress unloading and postcompression, parameters predictive of capping and lamination □ Compression—viscoelastic behavior of tablets, conditions predictive of capping and lamination

The physical properties of pharmaceutical tablets are of practical interest not only because they dictate manufacturing methodology and determine resistance to physical damage in handling, but also because they can influence drug bioavailability through the processes of tablet disintegration and dissolution. These properties or physical parameters can be categorized roughly in terms of those which may be observed under either changing or static conditions, or both. Viscoelastic properties of solids can be elucidated fully only if measurements of the dynamic relationships between stress and strain are made.

BACKGROUND

Effects of the time-dependent viscoelastic behavior of compressed tablets have been observed under a variety of transient conditions (1–6) and are distinguishable from the hysteretic effects, due to plastic failure, observed in radial *versus* axial pressure cycles measured under quasistatic or equilibrium conditions (3, 7, 8).

The successful formation of a pharmaceutical tablet by the compression of solid particulate matter depends on interparticulate bonding across particle–particle interfaces. The areas of virtual contact, necessary for bonding, are both formed and destroyed during the compression and decompression phases, and possibly also during ejection from the die. The net area of such interparticulate contacts, during and after compression, is expected to depend on the time-dependent flow of material which occurs in conjunction with instantaneously responding elastic deformations. Coupling of these processes results in the viscoelastic behavior observed during the compression of tablets at normal production speeds and, often, at slower speeds. The viscoelastic parameters of tablets and their components, therefore, are expected to be indicative of the relative sensitivity of tablet formation to the rates of compression and decompression, and the rate and nature of ejection from the die. More fundamentally, these parameters provide for insight into the kinetically controlled formation and destruction of interparticulate bonds and the resultant changes in internal structure which occur during and after these periods.

THEORETICAL

The temporal relationships between stress and strain which are exhibited by many materials can be described and analyzed in terms of viscoelastic theory and its related mathematical models. The elements of such models consist of springs, representing elastic behavior, and dashpots, corresponding to viscous flow characteristics.

The simplest application of this theory is to fully dense materials, either fluids or solids, in which voids do not occur. However, the presence of crystal dislocations, grain boundaries, or other structural irregularities in such solids can have a significant effect on their mechanical properties. Provided the test process does not in itself change these material properties, the viscoelastic constants determined by a given test procedure will be independent of the test and are true material constants. In applications such as powder metallurgy or pharmaceutical tablets, however, the structure under study is not fully dense. In these cases, the nature of the pores, crevices, or other voids is a significant part of the structure and is reflected in the measured viscoelastic parameters. Thus, these parameters are a function of the architecture of the tablet as well as the characteristics of the units of which it is constructed. Further, both the nature of the architecture and the material comprising the units can be expected to depend on the strain *versus* time profile of the compaction process; *i.e.*, the compression stress *versus* strain event as a function of time, together with the material constants of the tablet components (which are themselves likely to be dependent on the compression event), determine the viscoelastic parameters of the tablet proper. In the remainder of this paper when material behavior is discussed, the material referred to is the compact and not individual particles of its component substance(s).

The theory of linear three-dimensional viscoelasticity (9, 10) permits the dynamics of tablet compression to be mathematically separated into two components: isostatic contraction/dilation and distortion at constant volume. The former process occurs because the volume occupied by the tableted material is substantially reduced during compression and then increases slightly due to rebound. Because the tablet is confined radially by the die, the majority of this volume change occurs in the axial direction causing a change in the tablet height–diameter ratio, resulting in a distortion in shape.

Several three-dimensional viscoelastic models have been developed to describe the behavior of various materials in a rotary press and were tested against experimental stress/strain data collected during and after compression. Among those tested, four models were found to provide a good statistical fit to the data: Kelvin-in-dilation/Kelvin-in-distortion, elastic-in-dilation/three parameter solid-in-distortion, elastic-in-dilation/four parameter solid-in-distortion, and elastic-in-dilation/Kelvin-in-distortion. The latter was selected since it was the simplest model that fit the data.

Three sets of equations representing this model were developed (11). The first two sets describe the time dependence of axial stress (σ_{zz}) and radial stress (σ_{xx}) during the period of stress unloading:

$$\sigma_{zz} = A_1 - A_2[(r_1 + r_2)^2 - (r_3 \sin \omega t - x_2)^2]^{1/2} + \frac{A_3 \omega r_3 \cos \omega t (r_3 \sin \omega t - x_2)}{[(r_1 + r_2)^2 - (r_3 \sin \omega t - x_2)^2]^{1/2}} \quad \text{(Eq. 1)}$$

where the macroconstants are defined by:

$$A_1 = (2/3)[(q_0'' - q_0')\epsilon_{xx} + (2q_0' + q_0'')|z_0|/L] \quad \text{(Eq. 2)}$$

$$A_2 = (2/3)(2q_0' + q_0'')/L \quad \text{(Eq. 3)}$$

$$A_3 = (4/3)q_1'/L \quad \text{(Eq. 4)}$$

0022-3549/83/0400-0342$01.00/0

Table I—Viscoelastic Constants [a] for Unloading and Postcompression Phases of Tablet Compression [b]

Viscoelastic Constant	Macroconstants [c]	Peak Punch Pressure, MPa 125	208	333
		Mannitol		
q_0'	A_1B_1	87.1 ± 4.1	152 ± 5	714 ± 12
q_0''	A_2B_2	88.9 ± 4.2	154 ± 5.1	716 ± 13
q_0''	A_1B_1	1540 ± 73	2180 ± 72	2780 ± 49
q_0''	A_2B_2	1550 ± 74	2180 ± 72	2780 ± 49
q_1'	$A_1B_1C_2$	3.35 ± 0.11	5.09 ± 0.14	10.1 ± 0.22
q_1'	$A_2B_2C_2$	3.38 ± 0.11	5.10 ± 0.14	10.1 ± 0.22
		Dextrose		
q_0'	A_1B_1	698 ± 21	1260 ± 19	1210 ± 18
q_0''	A_2B_2	700 ± 21	1270 ± 20	1220 ± 18
q_0''	A_1B_1	2070 ± 63	2920 ± 45	3340 ± 50
q_0''	A_2B_2	2070 ± 63	2920 ± 45	3350 ± 50
q_1'	$A_1B_1C_2$	6.74 ± 0.19	12.0 ± 0.22	10.1 ± 0.19
q_1'	$A_2B_2C_2$	6.75 ± 0.19	12.1 ± 0.22	10.1 ± 0.19
		Sucrose		
q_0'	A_1B_1	859 ± 24	1070 ± 17	1590 ± 21
q_0''	A_2B_2	860 ± 24	1070 ± 17	1590 ± 21
q_0''	A_1B_1	1810 ± 51	2450 ± 38	3200 ± 43
q_0''	A_2B_2	1810 ± 51	2450 ± 38	3210 ± 43
q_1'	$A_1B_1C_2$	4.23 ± 0.10	6.52 ± 0.14	8.84 ± 0.21
q_1'	$A_2B_2C_2$	4.23 ± 0.10	6.52 ± 0.14	8.85 ± 0.22
		Dextrate		
q_0'	A_1B_1	219 ± 4	652 ± 24	761 ± 16
q_0''	A_2B_2	221 ± 4	654 ± 24	765 ± 16
q_0''	A_1B_1	1160 ± 43	1950 ± 72	2580 ± 54
q_0''	A_2B_2	1160 ± 43	1960 ± 72	2590 ± 54
q_1'	$A_1B_1C_2$	3.09 ± 0.24	3.62 ± 0.15	14.0 ± 0.47
q_1'	$A_2B_2C_2$	3.09 ± 0.24	3.63 ± 0.15	14.1 ± 0.47
		Starch USP		
q_0'	A_1B_1	−23.4 ± 1.8 [d]	101 ± 8.3 [d]	−215 ± 68 [d]
q_0''	A_2B_2	−21.0 ± 1.6	104 ± 8.3	−207 ± 87
q_0''	A_1B_1	315 ± 24	364 ± 30	−76.7 ± 24
q_0''	A_2B_2	319 ± 25	370 ± 30	−61.2 ± 21
q_1'	$A_1B_1C_2$	0.766 ± 0.037	1.69 ± 0.087	−1.42 ± 0.24
q_1'	$A_2B_2C_2$	0.791 ± 0.038	1.720 ± 0.087	−1.34 ± 0.24
		Sulfanilamide		
q_0'	A_1B_1	698 ± 17	204 ± 6.4	209 ± 7.4
q_0''	A_2B_2	699 ± 17	207 ± 6.4	213 ± 7.5
q_0''	A_1B_1	2110 ± 52	1630 ± 51	1950 ± 69
q_0''	A_2B_2	2120 ± 52	1630 ± 51	1960 ± 69
q_1'	$A_1B_1C_2$	9.08 ± 0.21	5.54 ± 0.15	7.26 ± 0.19
q_1'	$A_2B_2C_2$	9.11 ± 0.21	5.55 ± 0.15	7.32 ± 0.19
		Sulfamerazine		
q_0'	A_1B_1	−374 ± 40 [e]	284 ± 10	229 ± 5.5
q_0''	A_2B_2	−372 ± 40	286 ± 10	232 ± 5.6
q_0''	A_1B_1	1300 ± 140	2320 ± 80	2410 ± 58
q_0''	A_2B_2	1300 ± 138	2330 ± 80	2410 ± 58
q_1'	$A_1B_1C_2$	0.791 ± 0.057	4.47 ± 0.20	3.45 ± 0.11
q_1'	$A_2B_2C_2$	0.797 ± 0.057	4.49 ± 0.20	3.45 ± 0.11
		Acetylsalicylic Acid		
q_0'	A_1B_1	−776 ± 38 [f]	−374 ± 12 [f]	−288 ± 9.6 [f]
q_0''	A_2B_2	−775 ± 37	−373 ± 12	−286 ± 9.4
q_0''	A_1B_1	3390 ± 164	4130 ± 130	3710 ● 124
q_0''	A_2B_2	3400 ± 163	4140 ± 128	3730 ± 123
q_1'	$A_1B_1C_2$	3.63 ± 0.11	6.26 ± 0.15	4.96 ± 0.15
q_1'	$A_2B_2C_2$	3.66 ± 0.11	6.29 ± 0.15	5.00 ± 0.14
		Salicylamide		
q_0'	A_1B_1	−632 ± 40 [f]	−252 ± 5.8 [f]	−117 ± 2.7 [f]
q_0''	A_2B_2	−631 ± 39	−251 ± 5.8	−115 ± 2.7
q_0''	A_1B_1	2820 ± 178	4610 ± 106	4310 ± 101
q_0''	A_2B_2	2820 ± 175	4620 ± 106	4320 ± 102
q_1'	$A_1B_1C_2$	3.60 ± 0.14	7.81 ± 0.14	7.78 ± 0.15
q_1'	$A_2B_2C_2$	3.61 ± 0.14	7.83 ± 0.14	7.81 ± 0.15
		Salicylic Acid		
q_0'	A_1B_1	−755 ± 185 [f]	−245 ± 8.8 [f]	−618 ± 26 [f]
q_0''	A_2B_2	−753 ± 183	−243 ± 8.7	−613 ± 25
q_0''	A_1B_1	2280 ± 560	3780 ± 136	4060 ± 173
q_0''	A_2B_2	2280 ± 553	3780 ± 136	4070 ± 169
q_1'	$A_1B_1C_2$	1.76 ± 0.23	7.55 ± 0.20	5.47 ± 0.20
q_1'	$A_2B_2C_2$	1.77 ± 0.23	7.56 ± 0.20	5.51 ± 0.20
		Acetaminophen		
q_0'	A_1B_1	−425 ± 33 [d]	136 ± 4.7	−1270 ± 28 [d,e]
q_0''	A_2B_2	−423 ± 31	138 ± 4.8	−1270 ± 27
q_0''	A_1B_1	2420 ± 188	4570 ± 158	4020 ± 894
q_0''	A_2B_2	2420 ± 179	4580 ± 158	4030 ± 854
q_1'	$A_1B_1C_2$	2.80 ± 0.13	8.84 ± 0.22	2.85 ± 0.35
q_1'	$A_2B_2C_2$	2.81 ± 0.13	8.86 ± 0.22	2.87 ± 0.34
		Phenacetin		
q_0'	A_1B_1	−629 ± 32 [d,e]	166 ± 3.0 [d]	−1320 ± 154 [d,e]
q_0''	A_2B_2	−627 ± 32	167 ± 3.1	−1320 ± 150
q_0''	A_1B_1	2890 ± 149	3920 ± 73	3700 ± 431
q_0''	A_2B_2	2900 ± 148	3920 ± 73	3720 ± 422
q_1'	$A_1B_1C_2$	3.49 ± 0.12	10.9 ± 0.18	2.51 ± 0.16
q_1'	$A_2B_2C_2$	3.52 ± 0.12	11.0 ± 0.18	2.56 ± 0.16

[a] Calculated from mean macroconstants derived from triplicate compressions. [b] Units are MPa for q_0' and q_0'' and MPa sec for q_1' (±*SE*). [c] Macroconstants used in calculation of viscoelastic constants. [d] Weak friable tablets. [e] Frequent capping and lamination on ejection. [f] Occasional capping and lamination on ejection.

and:

$$\sigma_{xx} = B_1 - B_2[(r_1 + r_2)^2 - (r_3 \sin \omega t - x_2)^2]^{1/2} - \frac{B_3 \omega r_3 \cos \omega t (r_3 \sin \omega t - x_2)}{[(r_1 + r_2)^2 - (r_3 \sin \omega t - x_2)^2]^{1/2}} \quad \text{(Eq. 5)}$$

where the macroconstants are defined by:

$$B_1 = (1/3)[(2q_0'' + q_0')\epsilon_{xx} + 2(q_0'' - q_0')|z_0|/L] \quad \text{(Eq. 6)}$$

$$B_2 = (2/3)(q_0'' - q_0')/L \quad \text{(Eq. 7)}$$

$$B_3 = (2/3)q_1'/L \quad \text{(Eq. 8)}$$

In the above equations: q_0' and q_0'' are the elastic microconstants in distortion and dilation, respectively; q_1' is the viscous microconstant in distortion; ϵ_{xx} is the radial strain; z_0 is the vertical punch displacement at separation from the tablet; ω is the turret angular velocity; x_2 is the horizontal distance between the vertical center line of the upper punch and the center of vertical curvature of the punch head rim; r_1 and r_2 are the radii of the compression roller and punch head rim, respectively; r_3 is the radial distance between the turret and punch axes; and L is the tablet thickness.

Following compression and prior to tablet ejection, the radial stress can be expressed as:

$$\sigma_{xx} = [\sigma_{xx}(0) - C_1] \exp(-C_2 t) + C_1 \quad \text{(Eq. 9)}$$

where:

$$C_1 = \frac{3q_0' q_0'' \epsilon_{xx}(0)}{2q_0' + q_0''} \quad \text{(Eq. 10)}$$

$$C_2 = (2q_0' + q_0'')/2q_1' \quad \text{(Eq. 11)}$$

and the microconstants are as defined above.

EXPERIMENTAL

Materials—Twelve substances, including drugs and popular organic excipients, were chosen to represent a broad spectrum of physical properties. Materials were selected which comprise a substantial volume fraction of tablets in which they appear, and whose tableting characteristics are generally well known. These range from brittle to plastic, from highly to poorly cohesive, and from highly crystalline to mixed partially amorphous monomers and polymers derived from natural sources.

Substances were dried in an oven for 14 hr at 70° and stored over anhydrous calcium sulfate prior to compression. Except for drying, all materials were used as received and were not mixed with a lubricant or other substance prior to compression. Because of a tendency to cake, dextrate[1] was not dried by heating. Other excipients included starch USP[2], sucrose[3], dextrose[4], mannitol[5], and sulfanilamide[6], sulfamerazine[7], salicylic acid[8], salicylamide[5], acetylsalicylic acid[4], acetaminophen[5], and phenacetin[9].

Methods—Details of the experimental setup and methodology have been reported previously (11) and are outlined here. Tablets were compressed on a rotary tablet machine[10] using 9.525-mm flat-faced punches. Punch and die wall stresses were measured using resistance strain gauges during and after compression. Signals displayed on an oscilloscope were photographed for later analysis. Because of the difficulty in mounting displacement transducers, punch displacements were calculated as a function of time from the known mechanical geometry of the machine. All tablets were compressed in the same location in the instrumented die, at the same angular velocity ($\omega = 2.76$ rad/sec) of the die table, and at the same punch settings. The die wall was lubricated prior to each compression by swabbing with a 10% slurry of magnesium stearate in ethanol. Compressions were ~70–80 msec in duration from punch contact to punch separation; experiments were conducted in triplicate at each of three peak punch pressures (125, 208, and 333 MPa). Pressures were adjusted by control of the fill weight of individually weighed charges.

Numerical data obtained by electronic digitization of scope photographs were analyzed in terms of Eqs. 1–11 using statistical regression programs (12, 13). Viscoelastic constants corresponding to elastic behavior in dilation and to Kelvin solid behavior in distortion were calculated from the regression coefficients in Eqs. 1 and 5. These equations describe punch and die stresses during the punch stress unloading phase of compression where the elastic contributions predominate. The viscous constant relating to distortion was obtained from the postcompression data using the exponential regression coefficient of Eq. 9, expressed as Eq. 11, together with previously determined elastic constants. The rationale for this method of viscoelastic microconstant calculation from the regression macroconstants has been discussed previously (11).

RESULTS AND DISCUSSION

Within the categories of drugs and excipients studied here, there was a degree of correlation between overall viscoelastic behavior and chemical composition. With the exception of starch, the carbohydrates (mannitol, dextrose, sucrose, and dextrate) were found to produce hard, well-formed tablets. As shown in Table I, all three viscoelastic parameters were seen to increase with increasing peak pressure, except for dextrose. In this latter case, the distortional constants decreased slightly at a peak pressure of 333 MPa. These compacts showed increased internal structural strength with increased pressure, as reflected by their viscoelastic properties. This is characteristic of readily compressible materials, and these carbohydrates are useful as binders when included in tablet formulations. It should be noted that the higher pressures employed in these studies were somewhat above those normally used in production. They were chosen to reveal the pressure sensitivity of viscoelasticity and to include the range of slugging pressures.

Before discussing starch and the remaining materials, it is necessary to consider the meaning of negative elastic and viscous microconstants in relation to internal tablet structure. Positive or negative elasticity can be related to the behavior of a simple spring. Consider the elastic behavior of a tablet in response to the confinement imposed on it by the die and punches. This condition corresponds to that of a spring under compression. A normal spring, *i.e.*, one having a positive modulus, would exert a decreased force on the die and punches with a decrease in its degree of compression. Conversely, a spring having a negative modulus would exert an increased force with a decrease in compression. Tablets undergoing unloading, following the application of the peak pressure, are springing back toward their final dimensions. This entails both an expansion in volume and a distortion in shape, since the diameter is held constant by the die. If, in the generation of increased voids produced by this process, sufficient interparticulate bonds are broken, internally borne stresses residing in elastically deformed particles will be transferred to the die wall. This behavior corresponds to a negative elastic modulus and reflects a disruption of internal structure. These constants are not solely a reflection of the nature of the materials comprising the tablet, but are strongly influenced by the efficiency of survival of the bonded areas within the tablet during elastic recovery. These bonds, which are formed during compaction, are a consequence of molecular forces acting across interfaces in zones of true interparticulate contact. If sufficient plastic deformation occurs at the bonded areas (or elsewhere in the structure) so that the stresses developed by elastic recovery do not exceed bond strength, the bonds will survive. However, if the disruption is sufficient, the integrity of the tablet will be destroyed.

Further, consider the case of a plastic body subjected to a shear stress sufficient to produce flow. In materials possessing positive coefficients of viscosity, an increase in the flow rate implies an increase in the applied stress. In such a system, the greater the rate of shear imposed, the greater the thrust or drag produced by the flow. Again (as seen with negative elasticity) an increasing breakdown of internal structure with increasing shear rates may be indicated. It must be emphasized that the substances which comprise compacts exhibiting negative viscoelastic parameters do not in themselves have negative elastic or viscous properties. Instead, it is the destruction of bonds within the structure of the tablet during elastic recovery that leads to such behavior. The viscoelastic constants reported here must be considered to reflect the behavior of the compact itself and are not primary constants related to the individual fully dense components only. This conclusion is supported further by the observed dependence of the viscoelastic parameters on pressure. Tablet microstructure can be expected to depend on compaction forces, and changes in structure resulting from changes in the compression process will be manifested by changes in the parameters.

Starch, as shown in Table I, exhibited all negative microconstants at a peak compaction pressure of 333 MPa. This was the only material–pressure combination of those studied which showed this behavior; an intact tablet could not be made at this pressure. A crumbled tablet also resulted at 125 MPa peak pressure, on ejection. Only at the intermediate pressure were intact, although fragile, tablets obtained. Their weak character is reflected by the very low values of the microconstants.

The sulfas are brittle crystalline materials which are noted for tablet-making difficulties due to lamination and capping. Sulfanilamide produced intact tablets at all pressures while sulfamerazine capped and laminated at 125 MPa.

Fracture and splitting of the tablets made from the salicylates was a common occurrence. Despite lubrication of the die and punches, die wall and punch face adhesion could not be avoided totally. Acetaminophen and phenacetin also are known for the difficulties experienced in forming tablets from them. Their general behavior was similar to that of the salicylates, with frequent capping and lamination.

Although the 12 materials studied exhibited diverse viscoelastic behavior, as shown by the wide range in the numerical value of their microconstants, they may be separated into two distinct groups: those having negative distortional elastic moduli and those which do not. While all tablets in the former group did not laminate on ejection, they could be laminated easily with the fingernail. Moreover, all tablets which laminated showed negative q_0' values.

The group of materials exhibiting positive microconstants, over the range of pressures reported, could be divided further into two categories: those showing increased viscoelastic parameters with increased pressure and those with decreasing or relatively constant parameters at high pressures. Of the materials reported, only sulfanilamide fell in the latter category. These materials were compressed at peak pressures above 333 MPa to observe their tendency to laminate. Because of the danger to the instrumented die posed by these pressures (up to ~425 MPa), a standard die was used, and therefore, viscoelastic data are not available. A substantial fraction of the tablets in the second category capped and/or laminated, whereas this was a rare occurrence with the first four materials listed in Table I. The rate at which the compacts relax their stresses following compaction can be seen from Eq. 11 to be dependent not only on the viscous constant but also on the elastic constants. The latter constants serve to drive the plastic flow and also, in conjunction with the lateral strain, determine the residual die wall stress.

When tablets are ejected from the die, they are subjected to a transverse shearing stress at the point where they emerge from the die. This results from externally unsupported radial stresses in the portion of the tablet above the die face. The transverse shearing stress builds to a limit as progressively more of the tablet extends above the die and the tablet is ejected. Structural failure due to this stress, coupled with an

[1] Emdex; Edward Mendell Co., Inc., Carmel, N.Y.
[2] Sta-Rx 1500; S. E. Stanley Mfg. Co., Decatur, Ill.
[3] American Crystal Sugar, East Grand Forks, Minn.
[4] Mallinckrodt Inc., St. Louis, Mo.
[5] Sigma Chemical Co., St. Louis, Mo.
[6] Eastman Organic Chemicals, Rochester, N.Y.
[7] Matheson Co., Norwood, Ohio.
[8] Fisher Scientific Co., Fair Lawn, N.J.
[9] Merck & Co., Inc., Rahway, N.J.
[10] Colton model 216; Cherry-Burrell Corp., Park Ridge, Ill.

inadequate tablet shear strength, is thought to be the principal cause of capping and lamination, although there is some disagreement on this point (7). In support of this view (4), tablet formulations found to consistently laminate or cap were satisfactorily made with a press utilizing flexible die walls which retreat from the tablet prior to ejection.

In any case, it is apparent that the ejection of the tablet from the die subjects it to significant shear stresses. It is likely, therefore, that some internal strutural changes occur even in tablets that survive ejection and appear intact. For this reason, viscoelastic microconstants, when considered together with die wall stress, indicate the mechanical properties of the tablet within the die cavity and reflect the ability of the tablet to withstand ejection. In many, if not all, cases these parameters will not apply to the ejected tablet even though it has escaped gross fracture.

Because tablets were allowed to remain in the die for an extended period (several minutes in many cases) before being ejected manually by prying up the lower punch, the ejection event was atypical and did not reproduce production conditions. Studies utilizing an instrumented ejection cam to produce normal ejections are in progress to investigate this and other aspects of tablet viscoelasticity.

REFERENCES

(1) S. Shlanta and G. Milosovich, *J. Pharm. Sci.*, **53**, 562 (1964).

(2) S. T. David and L. L. Augsburger, *ibid.*, **66**, 155 (1977).

(3) E. N. Hiestand, J. E. Wells, C. B. Peot, and J. F. Ochs, *ibid.*, **66**, 510 (1977).

(4) G. E. Amidon, D. P. Smith, and E. N. Hiestand, *ibid.*, **70**, 613 (1981).

(5) E. N. Hiestand, Proc. International Conference on Powder Technology and Pharmacy, Basel, Switzerland (1978).

(6) J. E. Rees and P. J. Rue, *J. Pharm. Pharmacol.*, **30**, 601 (1978).

(7) W. M. Long, *Powder Metall.*, **6**, 73 (1960).

(8) S. Leigh, J. E. Carless, and B. W. Burt, *J. Pharm. Sci.*, **56**, 888 (1967).

(9) D. R. Bland, "The Theory of Linear Viscoelasticity," Pergamon, New York, N.Y., 1960, p. 1.

(10) W. Flugge, "Viscoelasticity," 2nd ed., Springer-Verlag, New York, N.Y., 1975.

(11) E. G. Rippie and D. W. Danielson, *J. Pharm. Sci.*, **70**, 476 (1981).

(12) N. H. Nie, C. H. Hull, J. G. Jenkins, K. Steinbrenner, and D. H. Bent, "Statistical Package for the Social Sciences," 2nd ed., McGraw-Hill, St. Louis, Mo., 1975.

(13) "Statistical Package for the Social Sciences; NONLINEAR Regression Subprogram," Vogelback Computing Center, Northwestern University, Evanston, Ill., 1978.

ACKNOWLEDGMENTS

Presented at the Higuchi Symposium, APhA Academy of Pharmaceutical Sciences meeting at Orlando, November 1981.

Abstracted in part from a dissertation submitted by D. W. Danielson to the University of Minnesota in partial fulfillment of the Doctor of Philosophy degree requirements.

Supported in part by a grant-in-aid from The Squibb Institute for Medical Research, New Brunswick, N.J.

Inhibition of Oral Lead Absorption in Rats by Phosphate-Containing Products

BRUCE J. AUNGST and HO-LEUNG FUNG ˣ

Received January 15, 1982, from *Department of Pharmaceutics, School of Pharmacy, State University of New York at Buffalo, Amherst, NY 14260.* Accepted for publication April 30, 1982

Abstract □ Recent studies indicate that elevated blood lead levels in children are largely a result of exposure to this metal *via* the oral route. A logical approach to decrease or prevent lead intoxication would be to reduce its absorption as soon as lead ingestion is known or suspected. Presently, however, there are no readily available products recommended to accomplish this goal. It was found that a phosphate-buffered, saline laxative reduced lead absorption over 50% in rats administered a single oral lead acetate dose, presumably by promoting the formation of less soluble lead salts. A popular phosphate-containing carbonated beverage also decreased lead absorption ~30% after oral lead acetate or lead-based paint doses, possibly by decreasing solubility, dissolution rate and/or GI motility. It is possible that these household products, and those with similar ingredients, may be safely used to reduce lead absorption in humans.

Keyphrases □ Lead absorption—reduction *in vivo* in rats by administration of phosphate-containing products □ Phosphate—lowering of blood lead levels in rats after oral administration of lead acetate or lead-based paint.

Ingested lead is the major source of the body burden of lead for most people (1). Children are exposed to lead from household dust (2), paint (3), and hand-to-mouth activity (4). Because they absorb a greater percentage of ingested lead than do adults (5), children have a higher risk of lead intoxication. Children with pica may be prone to chronic and repeated lead intoxication (6). Therapeutic intervention is not initiated, however, until blood-lead concentrations become elevated or symptoms of lead toxicity appear. It is recognized that subtle effects of lead on behavior and intelligence may occur in children at levels of exposure which do not produce elevated blood-lead concentrations or symptoms of lead intoxication (7). Prevention of lead exposure is therefore extremely important. Reduction of environmental lead and maintenance of sufficient dietary mineral intake partially achieve this objective. Presently there are no methods recommended to prevent or reduce the absorption of ingested lead.

A logical biopharmaceutical approach to reduce the extent of intestinal lead absorption, and thereby lead intoxication, is to decrease its solubility and dissolution rate in the GI tract. For some compounds, the extent of oral absorption is directly related to the absorption rate (8), which in turn may be limited by the rate of dissolution of the solid compound in the gut fluids (9). Dissolution rate is proportional to solubility, among other factors (10). Since the solubility products of lead phosphate and hydroxide are very low (Ksp $Pb_3(PO_4)_2 = 8 \times 10^{-43}$, Ksp of $Pb(OH)_2 = 1.2 \times 10^{-15}$) (11), it is possible that products containing phosphate or hydroxide ions might significantly reduce the extent of lead absorption by promoting the formation of insoluble lead phosphate and hydroxide salts in the GI tract. Since several household products contain

0022-3549/83/0400-0345$01.00/0

inadequate tablet shear strength, is thought to be the principal cause of capping and lamination, although there is some disagreement on this point (7). In support of this view (4), tablet formulations found to consistently laminate or cap were satisfactorily made with a press utilizing flexible die walls which retreat from the tablet prior to ejection.

In any case, it is apparent that the ejection of the tablet from the die subjects it to significant shear stresses. It is likely, therefore, that some internal strutural changes occur even in tablets that survive ejection and appear intact. For this reason, viscoelastic microconstants, when considered together with die wall stress, indicate the mechanical properties of the tablet within the die cavity and reflect the ability of the tablet to withstand ejection. In many, if not all, cases these parameters will not apply to the ejected tablet even though it has escaped gross fracture.

Because tablets were allowed to remain in the die for an extended period (several minutes in many cases) before being ejected manually by prying up the lower punch, the ejection event was atypical and did not reproduce production conditions. Studies utilizing an instrumented ejection cam to produce normal ejections are in progress to investigate this and other aspects of tablet viscoelasticity.

REFERENCES

(1) S. Shlanta and G. Milosovich, *J. Pharm. Sci.*, **53**, 562 (1964).

(2) S. T. David and L. L. Augsburger, *ibid.*, **66**, 155 (1977).

(3) E. N. Hiestand, J. E. Wells, C. B. Peot, and J. F. Ochs, *ibid.*, **66**, 510 (1977).

(4) G. E. Amidon, D. P. Smith, and E. N. Hiestand, *ibid.*, **70**, 613 (1981).

(5) E. N. Hiestand, Proc. International Conference on Powder Technology and Pharmacy, Basel, Switzerland (1978).

(6) J. E. Rees and P. J. Rue, *J. Pharm. Pharmacol.*, **30**, 601 (1978).

(7) W. M. Long, *Powder Metall.*, **6**, 73 (1960).

(8) S. Leigh, J. E. Carless, and B. W. Burt, *J. Pharm. Sci.*, **56**, 888 (1967).

(9) D. R. Bland, "The Theory of Linear Viscoelasticity," Pergamon, New York, N.Y., 1960, p. 1.

(10) W. Flugge, "Viscoelasticity," 2nd ed., Springer-Verlag, New York, N.Y., 1975.

(11) E. G. Rippie and D. W. Danielson, *J. Pharm. Sci.*, **70**, 476 (1981).

(12) N. H. Nie, C. H. Hull, J. G. Jenkins, K. Steinbrenner, and D. H. Bent, "Statistical Package for the Social Sciences," 2nd ed., McGraw-Hill, St. Louis, Mo., 1975.

(13) "Statistical Package for the Social Sciences; NONLINEAR Regression Subprogram," Vogelback Computing Center, Northwestern University, Evanston, Ill., 1978.

ACKNOWLEDGMENTS

Presented at the Higuchi Symposium, APhA Academy of Pharmaceutical Sciences meeting at Orlando, November 1981.

Abstracted in part from a dissertation submitted by D. W. Danielson to the University of Minnesota in partial fulfillment of the Doctor of Philosophy degree requirements.

Supported in part by a grant-in-aid from The Squibb Institute for Medical Research, New Brunswick, N.J.

Inhibition of Oral Lead Absorption in Rats by Phosphate-Containing Products

BRUCE J. AUNGST and HO-LEUNG FUNG ˣ

Received January 15, 1982, from *Department of Pharmaceutics, School of Pharmacy, State University of New York at Buffalo, Amherst, NY 14260.* Accepted for publication April 30, 1982

Abstract □ Recent studies indicate that elevated blood lead levels in children are largely a result of exposure to this metal *via* the oral route. A logical approach to decrease or prevent lead intoxication would be to reduce its absorption as soon as lead ingestion is known or suspected. Presently, however, there are no readily available products recommended to accomplish this goal. It was found that a phosphate-buffered, saline laxative reduced lead absorption over 50% in rats administered a single oral lead acetate dose, presumably by promoting the formation of less soluble lead salts. A popular phosphate-containing carbonated beverage also decreased lead absorption ~30% after oral lead acetate or lead-based paint doses, possibly by decreasing solubility, dissolution rate and/or GI motility. It is possible that these household products, and those with similar ingredients, may be safely used to reduce lead absorption in humans.

Keyphrases □ Lead absorption—reduction *in vivo* in rats by administration of phosphate-containing products □ Phosphate—lowering of blood lead levels in rats after oral administration of lead acetate or lead-based paint.

Ingested lead is the major source of the body burden of lead for most people (1). Children are exposed to lead from household dust (2), paint (3), and hand-to-mouth activity (4). Because they absorb a greater percentage of ingested lead than do adults (5), children have a higher risk of lead intoxication. Children with pica may be prone to chronic and repeated lead intoxication (6). Therapeutic intervention is not initiated, however, until blood-lead concentrations become elevated or symptoms of lead toxicity appear. It is recognized that subtle effects of lead on behavior and intelligence may occur in children at levels of exposure which do not produce elevated blood-lead concentrations or symptoms of lead intoxication (7). Prevention of lead exposure is therefore extremely important. Reduction of environmental lead and maintenance of sufficient dietary mineral intake partially achieve this objective. Presently there are no methods recommended to prevent or reduce the absorption of ingested lead.

A logical biopharmaceutical approach to reduce the extent of intestinal lead absorption, and thereby lead intoxication, is to decrease its solubility and dissolution rate in the GI tract. For some compounds, the extent of oral absorption is directly related to the absorption rate (8), which in turn may be limited by the rate of dissolution of the solid compound in the gut fluids (9). Dissolution rate is proportional to solubility, among other factors (10). Since the solubility products of lead phosphate and hydroxide are very low (Ksp $Pb_3(PO_4)_2 = 8 \times 10^{-43}$, Ksp of $Pb(OH)_2 = 1.2 \times 10^{-15}$) (11), it is possible that products containing phosphate or hydroxide ions might significantly reduce the extent of lead absorption by promoting the formation of insoluble lead phosphate and hydroxide salts in the GI tract. Since several household products contain

0022-3549/83/0400-0345$01.00/0

Table I—Precipitation of Lead *In Vitro*

Test Product[a]	Phosphate–Lead Molar Ratio	Lead Remaining in Solution, %	Supernatant pH
Water	—	100	4.5[b]
Carbonated beverage	0.5	29 ± 2[c]	3.8
Phosphoric acid	0.5	14 ± 6	3.1
Laxative (1:10 dilution)	4.4	0.17 ± 0.04	5.6
Laxative (1:250 dilution)	1.8	0.19 ± 0.01	4.0
Antacid	—	4.7 ± 0.3	7.4

[a] See Footnotes 1–3 for names of test products. [b] Samples were pooled for pH determination. [c] Data represent mean ± *SE* of three determinations and are expressed as percentage of control.

high contents of phosphate or hydroxide, the feasibility of lead absorption inhibition with these products was tested.

EXPERIMENTAL

Precipitation of Lead *In Vitro*—The effects of several household products on lead solubility were examined in preliminary *in vitro* experiments. The test products included a carbonated beverage[1], a phosphoric acid solution with the same phosphate content (0.56 *M*) and pH (2.4) as the carbonated beverage, a phosphate-buffered, saline laxative[2] diluted 10-fold and 250-fold, and an antacid containing magnesium and aluminum hydroxides[3]. The carbonated beverage was stored in an open container prior to use to allow liberation of carbon dioxide. In a glass tube, 0.25 ml of a lead acetate solution (10 mg of Pb/ml, pH 4.5) was mixed with 1 ml of the test product. The pH and the amount of lead remaining in the 1000×*g* supernatant solution were measured. Lead analyses were performed using atomic absorption spectrophotometry[4].

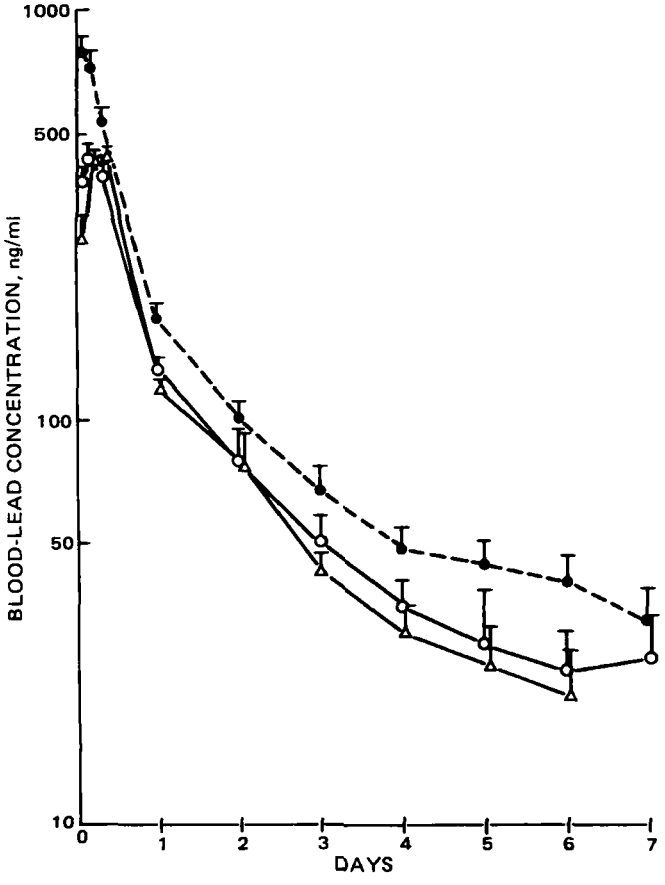

Figure 1—*Effects of a carbonated beverage (○) and a phosphoric acid solution (△) on absorption of lead after oral administration of a lead acetate solution, compared with control (●). Values represent mean* + SE.

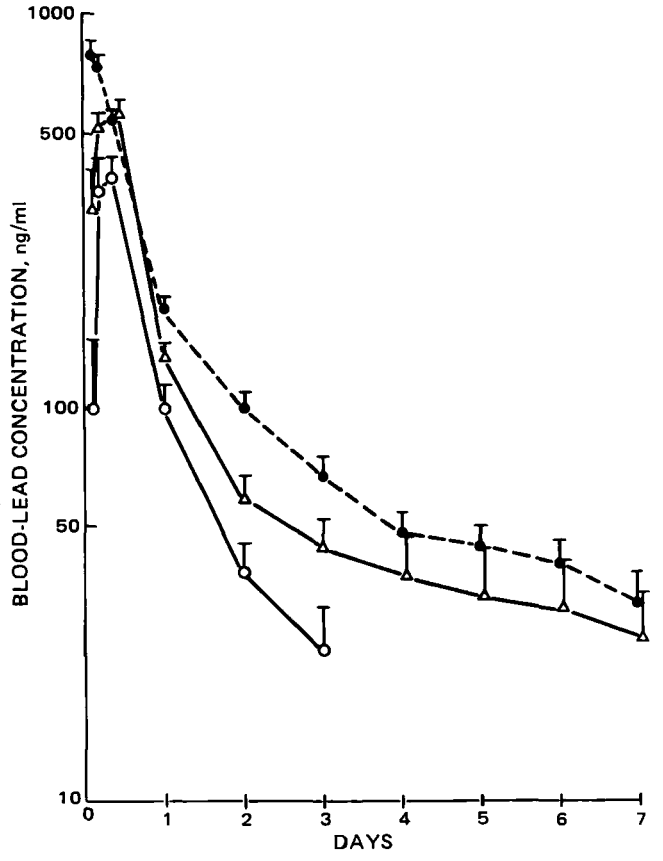

Figure 2—*Blood-lead concentrations in rats administered a 10 mg/kg oral lead dose followed by water (●), or a phosphate-buffered saline laxative diluted 1:10 (○) or 1:250 (△). Values are mean* + SE.

***In Vivo* Studies—**After an overnight fast, male Sprague-Dawley rats[5] (200–300 g) were administered, by gastric intubation, a single lead dose followed immediately by 1 ml of a test product or control treatment. Lead was administered as lead acetate (10 mg of Pb/ml, pH 4.5) or as powdered lead-based paint[6] suspended in 2% methylcellulose. The doses were 10 mg of Pb/kg, when administering lead acetate, and 50 mg of Pb/kg, when administering the lead-based paint. The amounts of lead and test product administered were similar to those used in the *in vitro* experiment. The control groups were administered 1 ml of distilled water following the lead dose. There were 5–9 rats in each group. Blood samples were collected in heparinized glass tubes by tail clipping and milking at 2, 4, and 8 hr, and every day for 7 days postdose, and were frozen immediately. Whole blood lead concentrations were determined using a previously described atomic absorption spectrophotometric method (12). During the course of the experiments the animals were housed in stainless steel cages with wire mesh floors.

Data Analysis—The area under the blood-lead concentration *versus* time curve (AUC) from 0 to 7 days was calculated for each rat. This parameter has been shown to be a good indicator of the extent of lead absorption (13). Systemic lead clearance was assumed to be unaffected by these oral treatments. Differences between any two groups were tested for significance using the Student's *t* test. All data are expressed as mean ± *SE*.

RESULTS AND DISCUSSION

Precipitation of Lead *In Vitro*—The effects of each test product on the solubility of a lead solution typical of a lead dose are shown in Table I. All test products precipitated lead from the solution, with greater precipitation at higher phosphate–lead ratios, as expected. At equal

[1] Coca-Cola.
[2] Phospho-Soda buffered saline laxative, C.B. Fleet Co., Lynchburg, Va.
[3] Maalox, W. H. Rorer, Fort Washington, Pa.
[4] Perkin-Elmer 603 with HGA 2000 Controller.
[5] Blue Spruce, Altamont, N.Y.
[6] National Bureau of Standards Reference No. 1579, 11.87 ± 0.04% Pb.

Table II—Inhibition of Lead Absorption *In Vivo*

Lead Dose	Test Product[a]	N	C_{max}, ng/ml	p	AUC, ng days/ml	p	Lead Absorption Relative to Control, %
10 mg Pb/kg Lead Acetate	Water	9	843 ± 64[b]		807 ± 71[b]		100
	Carbonated beverage	8	482 ± 36	<0.001	581 ± 57	<0.05	72
	Phosphoric acid	6	478 ± 19	<0.001	533 ± 39	<0.01	66
	Laxative (1:10)	6	433 ± 47	<0.001	359 ± 64	<0.001	44
	Laxative (1:250)	6	601 ± 42	<0.02	616 ± 79	NS	76
	Antacid	5	685 ± 77	<0.05	809 ± 115	NS	100
50 mg Pb/kg Lead-Based Paint	Water	9	871 ± 52		1095 ± 98		100
	Carbonated beverage	9	613 ± 30	<0.001	769 ± 62	<0.02	70

[a] See Footnotes 1–3 for names of test products. [b] Data are mean ± *SE* and were evaluated for statistical difference from the appropriate group administered water.

phosphate content, the carbonated beverage was not as effective as phosphoric acid in precipitating lead. The presence of other ingredients in the carbonated beverage might have altered the solubility product of lead phosphate.

Effects on Oral Lead Absorption—Decreased lead solubility *in vitro* was associated with an apparently decreased rate of *in vivo* absorption. The blood-lead concentration *versus* time profiles for those groups administered lead acetate and control, carbonated beverage, or phosphoric acid treatments are shown in Fig. 1. Similar results were observed following the administration of the phosphate laxative (Fig. 2). Although absorption rates were not calculated, the time to reach the maximum blood-lead concentration (C_{max}) was longer in each of these treatment groups than in the control group. The majority of rats administered phosphate, in either the carbonated beverage, phosphoric acid, or laxative, reached C_{max} at either 4 or 8 hr; whereas in the control group five rats reached C_{max} at 2 hr, four rats at 4 hr, and none at 8 hr. In addition to delaying absorption, each of these treatments resulted in a lower value of C_{max}, as compared with the control (Table II). The AUC, a direct index of the bioavailability of an oral lead dose, was significantly reduced when either the carbonated beverage, phosphoric acid solution, or laxative diluted 10-fold was administered after lead ingestion. The 250-fold diluted laxative also appeared to decrease the AUC, but not significantly.

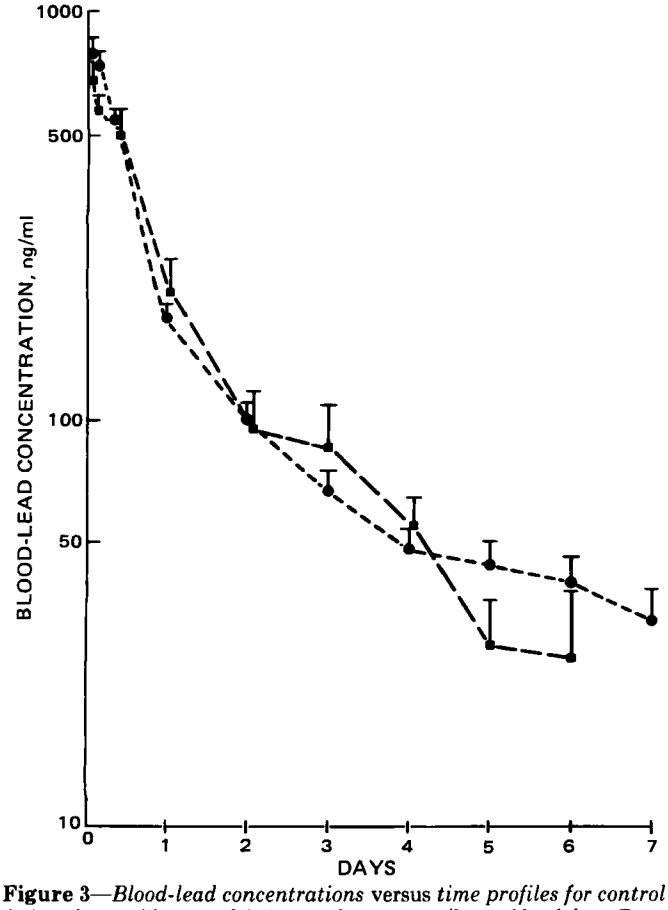

Figure 3—*Blood-lead concentrations* versus *time profiles for control (●) and antacid-treated (■) rats after a 10 mg/kg oral lead dose. Data represent mean* + SE.

Administration of the antacid after the lead dose had no apparent effect on either the blood-lead concentration *versus* time profile (Fig. 3), C_{max}, or AUC (Table II). Although the antacid caused significant precipitation of lead *in vitro*, it was ineffective in inhibiting *in vivo* lead absorption. The reasons for this lack of effect are unclear at present[7].

The effect of the carbonated beverage on lead absorption from a lead-based paint was also examined. As shown in Fig. 4, blood-lead concentrations were reduced by treatment with the carbonated beverage. The carbonated beverage again apparently decreased the rate of lead absorption, as indicated in the delay in the time C_{max} was observed (8 hr). The value of C_{max} was reduced as well (Table II). The AUC was significantly less than that observed in control rats, which were administered water after the paint dose.

The efficacies of the various treatments in reducing lead absorption were not predictable based on the amount of phosphate administered, and other effects of these treatments must be considered. Changes in gastric emptying rate, GI motility, solid particle size, and volume of fluid

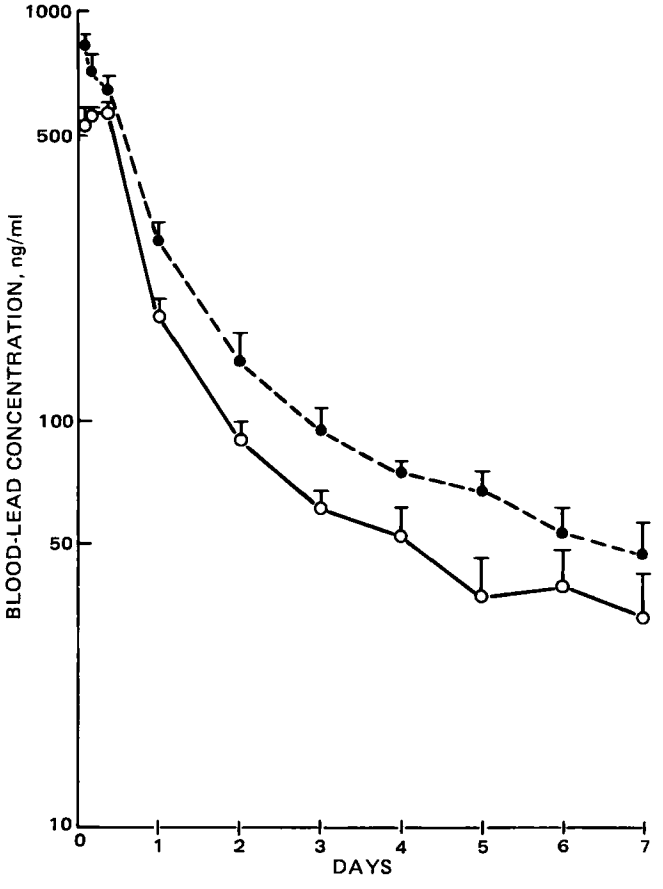

Figure 4—*Blood-level concentrations (mean* + SE*) in rats administered 50 mg of Pb/kg as a lead-based paint. Rats were also administered water (●) or a carbonated beverage (○).*

[7] In a follow-up experiment, stomach acidity was measured in three rats 20 min after dosing with the lead solution and antacid. The stomach pH in these animals was elevated to 4.5, 6.0, and 7.0, respectively, compared with control values of 2.5–3.0 in animals not treated with antacid. It appears possible that the pH effect on lead solubility might have been compensated by other effects of the antacid, *e.g.*, gastric emptying and GI motility, on lead absorption.

in the gut might also have been important. Houston and Levy reported that by inhibiting gastric emptying and GI motility, the same carbonated beverage used in this study altered the absorption rates of riboflavin and salicylamide (14). These effects were due to the phosphoric acid and carbohydrate in the carbonated beverage. In another study (15) the authors showed that propantheline bromide, an inhibitor of gastric emptying and GI motility, decreased the rate and extent of lead absorption by ~50%, suggesting that lead absorption is modified by the degree of agitation of the gut contents, among other factors. The phosphate-buffered, saline laxative functions as such by retaining water in the gut, and indirectly increases GI motility (16). Both of these actions could have counteracted the effect of decreased solubility on lead absorption.

Although abolition of lead absorption was not achieved by these products, the inhibitory effects are comparable to those shown for excess calcium and iron; administration of lead with 250-fold and 1000-fold molar excesses of calcium decreased lead absorption 46 and 43%, respectively, in rats (17, 18). Iron, at amounts 100-fold and 1000-fold greater than lead, decreased lead absorption in rats 20 and 80%, respectively (19).

Since the consequences of lead intoxication are severe (20), especially in children, prevention of undue lead exposure is very important. The household products identified here have been shown to significantly reduce lead absorption in rats when administered acutely. These agents might, therefore, also be useful in decreasing lead exposure after lead ingestion in humans. Their relatively nontoxic nature and easy accessibility make them attractive candidates for such use, particularly for children with a history of pica. Of course, the potential for use of these products is suggested only as an adjunct or supportive measure, and is not intended to replace therapeutic intervention for relief of the symptoms of lead toxicity.

REFERENCES

(1) D. Gloag, *Br. Med. J.*, **282**, 41 (1981).

(2) E. Charney, J. Sayre, and M. Coulter, *Pediatrics*, **65**, 226 (1980).

(3) P. B. Hammond, C. S. Clark, P. S. Gartside, O. Berger, A. Walker, and L. W. Michael, *Int. Arch. Occup. Environ. Health*, **46**, 191 (1980).

(4) J. W. Sayre, E. Charney, J. Vostal, and I. B. Pless, *Am. J. Dis. Child.*, **127**, 167 (1974).

(5) E. E. Ziegler, B. B. Edwards, R. L. Jensen, K. R. Mahaffey, and S. J. Somon, *Pediatr. Res.*, **12**, 29 (1978).

(6) K. R. Mahaffey, *Environ. Health Perspect.*, **19**, 285 (1977).

(7) H. L. Needleman, C. Gunnoe, A. Leviton, R. Reed, H. Peresie, C. Maher, and P. Barrett, *N. Engl. J. Med.*, **300**, 689 (1979).

(8) T. R. Bates and M. Gibaldi, in "Current Concepts in the Pharmaceutical Sciences: Biopharmaceutics," J. Swarbrick, Ed., Lea and Febiger, Philadelphia, Pa., 1971.

(9) G. Levy and B. A. Hayes, *N. Engl. J. Med.*, **262**, 1053 (1960).

(10) A. A. Noyes and W. R. Whitney, *J. Am. Chem. Soc.*, **19**, 930 (1897).

(11) "Lange's Handbook of Chemistry," J. A. Dean, Ed., McGraw-Hill, New York, N.Y., 1979, p. 5.

(12) B. J. Aungst, J. Dolce, and H.-L. Fung, *Anal. Lett.*, **13**, 347 (1980).

(13) B. J. Aungst, J. A. Dolce, and H.-L. Fung, *Toxicol. Appl. Pharmacol.*, **61**, 48 (1981).

(14) J. B. Houston and G. Levy, *J. Pharm. Sci.*, **64**, 1504 (1975).

(15) B. J. Aungst and H.-L. Fung, *Res. Commun. Chem. Pathol. Pharmacol.*, **34**, 515 (1981).

(16) E. Fingl, in "The Pharmacological Basis of Therapeutics," L. S. Goodman and A. Gilman, Eds., MacMillan, New York, N.Y., 1975.

(17) P. A. Meredith, M. Moore, and A. Goldberg, *Biochem. J.*, **166**, 531 (1977).

(18) J. C. Barton, M. E. Conrad, L. Harrison, and S. Nuby, *J. Lab. Clin. Med.*, **91**, 366 (1978).

(19) *Idem.*, **92**, 536 (1978).

(20) P. Grandjean, *Environ. Res.*, **17**, 303 (1978).

ACKNOWLEDGMENTS

Presented at the Dr. Takeru Higuchi Recognition Symposium, Academy of Pharmaceutical Sciences National Meeting, November 15–16, 1981, Orlando, Fla.

This work was supported in part by National Institutes of Health Grant ES 01317.

We thank Dr. G. Levy for valuable suggestions and James Dolce for technical assistance.

Zn(II)–Theophylline–Ethylenediamine: Structure and pH Stability

MARK J. GARDNER, FRANCIS X. SMITH, and ELI SHEFTER ˣ

Received November 27, 1981, from the *Department of Pharmaceutics, School of Pharmacy, State University of New York at Buffalo, Amherst, NY 14260.* Accepted for publication February 19, 1982.

Abstract □ A zinc-containing salt of theophylline, Zn(II)-aminophylline, was synthesized and its structure determined by X-ray diffraction techniques. The zinc ion is coordinated to two theophylline anions and a molecule of ethylenediamine in a tetrahedral arrangement. The solubility of the compound in water at 30° (0.047 mg/ml) is 180-fold lower than that of theophylline (8.40 mg/ml). The complex is relatively stable in the alkaline pH range, but it hydrolyzes, releasing theophylline in acidic environments. The rate of theophylline release is pH dependent. These properties are useful in formulating chewable tablets and liquid suspension dosage forms that overcome the characteristic bitter taste of theophylline, yet provide for efficacious treatment of diseases involving the respiratory tract.

Keyphrases □ Zn(II)–Aminophylline—structure determination by X-ray diffraction, release rate of theophylline, potential for use in oral preparation □ X-ray diffraction—Zn(II)–aminophylline, release rate of theophylline, potential for use in oral preparations □ Theophylline release rate—Zn(II)–aminophylline complex, X-ray diffraction, potential for use in oral preparations

Theophylline, a naturally occurring xanthine alkaloid derivative, possesses potent bronchodilating properties. Consequently, for nearly half a century both it and its ethylenediamine salt, aminophylline, have been used extensively in the treatment of diseases involving the respiratory tract (1). In particular, they have been shown to be efficacious in the treatment of asthma (2), exercise-induced bronchospasm (3), Cheyne-Stokes respiration (4), and chronic bronchitis/emphysema (5).

Although the pharmacologic properties of this drug are beneficial for such disorders, some of its physicochemical properties hinder totally effective therapy. First, the

0022-3549/83/0400-0348$01.00/0

in the gut might also have been important. Houston and Levy reported that by inhibiting gastric emptying and GI motility, the same carbonated beverage used in this study altered the absorption rates of riboflavin and salicylamide (14). These effects were due to the phosphoric acid and carbohydrate in the carbonated beverage. In another study (15) the authors showed that propantheline bromide, an inhibitor of gastric emptying and GI motility, decreased the rate and extent of lead absorption by ~50%, suggesting that lead absorption is modified by the degree of agitation of the gut contents, among other factors. The phosphate-buffered, saline laxative functions as such by retaining water in the gut, and indirectly increases GI motility (16). Both of these actions could have counteracted the effect of decreased solubility on lead absorption.

Although abolition of lead absorption was not achieved by these products, the inhibitory effects are comparable to those shown for excess calcium and iron; administration of lead with 250-fold and 1000-fold molar excesses of calcium decreased lead absorption 46 and 43%, respectively, in rats (17, 18). Iron, at amounts 100-fold and 1000-fold greater than lead, decreased lead absorption in rats 20 and 80%, respectively (19).

Since the consequences of lead intoxication are severe (20), especially in children, prevention of undue lead exposure is very important. The household products identified here have been shown to significantly reduce lead absorption in rats when administered acutely. These agents might, therefore, also be useful in decreasing lead exposure after lead ingestion in humans. Their relatively nontoxic nature and easy accessibility make them attractive candidates for such use, particularly for children with a history of pica. Of course, the potential for use of these products is suggested only as an adjunct or supportive measure, and is not intended to replace therapeutic intervention for relief of the symptoms of lead toxicity.

REFERENCES

(1) D. Gloag, *Br. Med. J.*, **282**, 41 (1981).

(2) E. Charney, J. Sayre, and M. Coulter, *Pediatrics*, **65**, 226 (1980).

(3) P. B. Hammond, C. S. Clark, P. S. Gartside, O. Berger, A. Walker, and L. W. Michael, *Int. Arch. Occup. Environ. Health*, **46**, 191 (1980).

(4) J. W. Sayre, E. Charney, J. Vostal, and I. B. Pless, *Am. J. Dis. Child.*, **127**, 167 (1974).

(5) E. E. Ziegler, B. B. Edwards, R. L. Jensen, K. R. Mahaffey, and S. J. Somon, *Pediatr. Res.*, **12**, 29 (1978).

(6) K. R. Mahaffey, *Environ. Health Perspect.*, **19**, 285 (1977).

(7) H. L. Needleman, C. Gunnoe, A. Leviton, R. Reed, H. Peresie, C. Maher, and P. Barrett, *N. Engl. J. Med.*, **300**, 689 (1979).

(8) T. R. Bates and M. Gibaldi, in "Current Concepts in the Pharmaceutical Sciences: Biopharmaceutics," J. Swarbrick, Ed., Lea and Febiger, Philadelphia, Pa., 1971.

(9) G. Levy and B. A. Hayes, *N. Engl. J. Med.*, **262**, 1053 (1960).

(10) A. A. Noyes and W. R. Whitney, *J. Am. Chem. Soc.*, **19**, 930 (1897).

(11) "Lange's Handbook of Chemistry," J. A. Dean, Ed., McGraw-Hill, New York, N.Y., 1979, p. 5.

(12) B. J. Aungst, J. Dolce, and H.-L. Fung, *Anal. Lett.*, **13**, 347 (1980).

(13) B. J. Aungst, J. A. Dolce, and H.-L. Fung, *Toxicol. Appl. Pharmacol.*, **61**, 48 (1981).

(14) J. B. Houston and G. Levy, *J. Pharm. Sci.*, **64**, 1504 (1975).

(15) B. J. Aungst and H.-L. Fung, *Res. Commun. Chem. Pathol. Pharmacol.*, **34**, 515 (1981).

(16) E. Fingl, in "The Pharmacological Basis of Therapeutics," L. S. Goodman and A. Gilman, Eds., MacMillan, New York, N.Y., 1975.

(17) P. A. Meredith, M. Moore, and A. Goldberg, *Biochem. J.*, **166**, 531 (1977).

(18) J. C. Barton, M. E. Conrad, L. Harrison, and S. Nuby, *J. Lab. Clin. Med.*, **91**, 366 (1978).

(19) *Idem.*, **92**, 536 (1978).

(20) P. Grandjean, *Environ. Res.*, **17**, 303 (1978).

ACKNOWLEDGMENTS

Presented at the Dr. Takeru Higuchi Recognition Symposium, Academy of Pharmaceutical Sciences National Meeting, November 15–16, 1981, Orlando, Fla.

This work was supported in part by National Institutes of Health Grant ES 01317.

We thank Dr. G. Levy for valuable suggestions and James Dolce for technical assistance.

Zn(II)–Theophylline–Ethylenediamine: Structure and pH Stability

MARK J. GARDNER, FRANCIS X. SMITH, and ELI SHEFTER ˣ

Received November 27, 1981, from the *Department of Pharmaceutics, School of Pharmacy, State University of New York at Buffalo, Amherst, NY 14260.* Accepted for publication February 19, 1982.

Abstract □ A zinc-containing salt of theophylline, Zn(II)-aminophylline, was synthesized and its structure determined by X-ray diffraction techniques. The zinc ion is coordinated to two theophylline anions and a molecule of ethylenediamine in a tetrahedral arrangement. The solubility of the compound in water at 30° (0.047 mg/ml) is 180-fold lower than that of theophylline (8.40 mg/ml). The complex is relatively stable in the alkaline pH range, but it hydrolyzes, releasing theophylline in acidic environments. The rate of theophylline release is pH dependent. These properties are useful in formulating chewable tablets and liquid suspension dosage forms that overcome the characteristic bitter taste of theophylline, yet provide for efficacious treatment of diseases involving the respiratory tract.

Keyphrases □ Zn(II)–Aminophylline—structure determination by X-ray diffraction, release rate of theophylline, potential for use in oral preparation □ X-ray diffraction—Zn(II)–aminophylline, release rate of theophylline, potential for use in oral preparations □ Theophylline release rate—Zn(II)–aminophylline complex, X-ray diffraction, potential for use in oral preparations

Theophylline, a naturally occurring xanthine alkaloid derivative, possesses potent bronchodilating properties. Consequently, for nearly half a century both it and its ethylenediamine salt, aminophylline, have been used extensively in the treatment of diseases involving the respiratory tract (1). In particular, they have been shown to be efficacious in the treatment of asthma (2), exercise-induced bronchospasm (3), Cheyne-Stokes respiration (4), and chronic bronchitis/emphysema (5).

Although the pharmacologic properties of this drug are beneficial for such disorders, some of its physicochemical properties hinder totally effective therapy. First, the

0022-3549/83/0400-0348$01.00/0

Table I—Positional Parameters [a]

Atom	x/a	y/b	z/c
Zn(II)	0000	5604(2)	2500
N(1)	−3874(11)	5243(9)	−383(6)
C(2)	−4880(12)	6247(12)	−762(7)
N(3)	−4619(10)	7302(10)	−283(6)
C(4)	−3445(11)	7676(11)	501(6)
C(5)	−2500(11)	6345(11)	843(6)
C(6)	−2666(12)	5232(11)	374(7)
N(7)	−1474(10)	6681(9)	1627(6)
C(8)	−1861(12)	7814(12)	1706(7)
N(9)	−3081(11)	8266(10)	1037(6)
C(1)	−4189(14)	4131(13)	−930(8)
O(2)	−5897(9)	6152(9)	−1458(5)
C(3)	−5613(14)	8360(12)	−631(8)
O(6)	−1873(9)	4292(9)	619(6)
N(E)	1009(11)	4192(9)	2294(6)
C(E)	772(14)	3047(13)	2594(8)

[a] Estimated standard deviations in parentheses (all times 10^4).

aqueous solubilities of theophylline and aminophylline at 25° are 8.33 and 200.00 mg/ml, respectively (6). Such solubilities lead to considerable dissolution of the compounds in human saliva. This coupled with the fact that xanthine derivatives impart a characteristic bitter taste (7), leads to palatability problems. Of special concern are chewable tablets and liquid preparations. Attempts to mask this characteristic bitter taste in the latter dosage form have not been highly successful (8), and this has resulted in noncompliance problems (8, 9). Failure to take this drug as prescribed could be exacerbated further by the characteristics of the population most likely to be medicated with these oral dosage forms. In particular, Blackwell (9) has reported that noncompliance occurs most often in the extreme age groups: the pediatric and geriatric patient populations.

Second, once ingested as a conventional tablet dosage form, theophylline is rapidly absorbed from the GI tract. This can result in a spiking effect, where theophylline serum concentrations rise very quickly. It is widely accepted that serum concentrations of theophylline should be maintained within the range of 10–20 μg/ml to facilitate effective therapy and avoid side effects (10). Such rapid

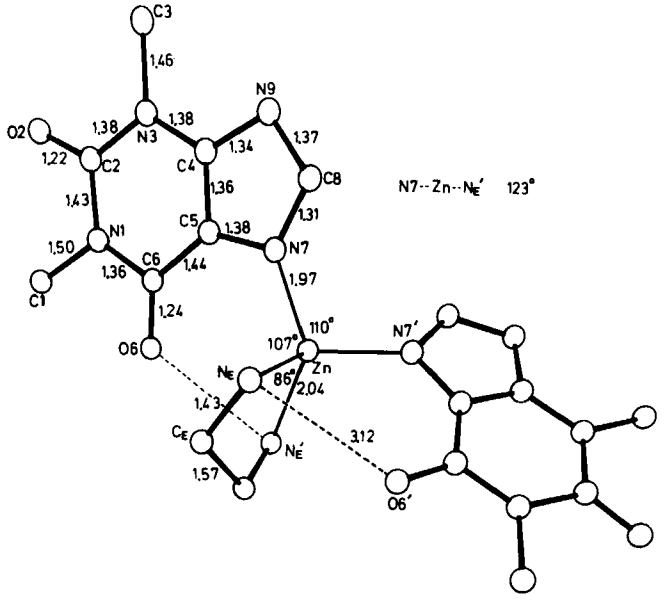

Figure 1—*Molecular structure of Zn(II)–aminophylline as determined by single-crystal X-ray diffractometry. Relevant bond angles and lengths are indicated.*

Table II—Intermolecular Contacts

Atom	Atom	Symmetry Operation Applied to Coordinates of Second Atom	Distance
N(E)	O(2)	1 + x, 1 − y, 0.5 + z	3.00(2)Å
N(E)	O(6)	x, y, z	3.12(2)Å
N(E)	N(7)	−x, y, 0.5 − z	3.23(2)Å
N(E)	N(9)	0.5 + x, y − 0.5, z	3.27(2)Å
C(8)	O(2)	0.5 + x, 1.5 − y, 0.5 + z	3.32(2)Å

absorption of theophylline can lead to serum concentrations that exceed 20 μg/ml, resulting in toxic side effects.

In an effort to overcome some of the problems associated with the use of theophylline, a zinc–aminophylline complex has been prepared. The preparation, molecular structure and physicochemical properties of this salt are discussed.

EXPERIMENTAL

Preparation—Fifty grams of anhydrous theophylline[1] was dissolved in 250 ml of an ethylenediamine solution (4.2% by volume) and subsequently diluted to 2.5 liters. It is important to maintain the pH of the solution between 8.0–9.0 to maximize the yield; it should be adjusted by the addition of ethylenediamine.

After warming the solution to approximately 60°, 250 ml of a 10% aqueous solution of $ZnSO_4 \cdot 7H_2O$[2] was added. The crystals of the zinc–aminophylline complex that formed were filtered and washed with cold water.

The initial precipitate that was formed in the reaction vessel had a colloidal appearance, but slowly transformed into octahedral prisms. The transformation could be accelerated by heat.

Recently, Zitzman *et al.* (11) used a similar procedure to prepare zinc(II) complexes of theophylline with ammonia and methylamine.

Crystal Structure Analysis—The isolated crystals were subjected to X-ray diffraction analysis to determine their molecular structure. They were found to be monoclinic, belonging to space group C 2/c based on systematic absences observed in the diffraction pattern of single-crystal crystals. The measured cell dimensions for these crystals are a = 11.222(4), b = 10.550(3), c = 19.496(10) Å, and β = 122.66(3) Å.

Intensity data were measured by the stationary counter-stationary crystal technique using balanced filters for the CuK radiation used on a diffractometer[3]. In the range of data collection ($20 \leq 110°$) 1154 reflections of the 1303 unique data had peak intensities significantly greater than background. An absorption correction, based on the anisotropy of transmission of the X-rays as a function of the diffractometer angle ϕ, was applied to the data as well as the usual Lorentz-polarization correction.

A trial structure was obtained by direct methods using the program MULTAN (12). The structure was refined by the Fourier and least-squares methods. The positions of the hydrogens could not be accurately assessed from difference electron density maps and were excluded from the refinement. The final R value (usual crystallographic reliability factor) was 0.11 for the observed data. The final positional parameters for the molecule are listed in Table I.

Solubility—The apparent aqueous solubilities of the complex and theophylline were determined at 30°. An excess quantity of material was added to a flask containing deionized water. The flasks were then placed in a water bath (30°) and allowed to equilibrate with agitation. Samples were withdrawn through a 1-μm millipore filter[4] and subsequently assayed for theophylline by a high-performance liquid chromatographic technique (13).

Hydrolysis of Complex—The hydrolysis of the complex was evaluated by placing 300 mg into 200 ml of a buffered solution (0.1 *N* HCl, pH 0.96; 0.1 *N* NaOAc, pH 4.73; 0.1 *N* Na_3PO_4, pH 7.39). These solutions were agitated by means of a magnetic stirrer and their temperature maintained at 25°. Filtered samples were withdrawn at regular intervals and assayed for theophylline spectrophotometrically at 270 nm.

[1] Ruger Chemical Co., Hillside, N.J.
[2] Fisher Scientific Co., Fair Lawn, N.J.
[3] General Electric XRD-6.
[4] Millipore Corp., Bedford, Mass.

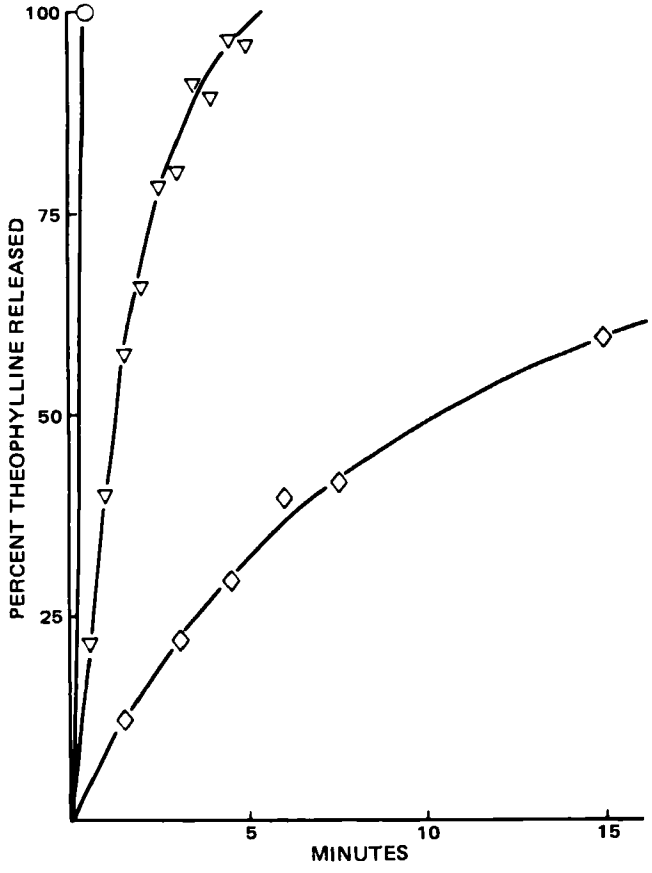

Figure 2—*Apparent hydrolysis of Zn(II)–aminophylline as a function of time at various pH values. Key: (○) 1; (▽) 4.8; (◇) 7.4.*

Though the same batch of material was used throughout these studies, its particle size distribution was not determined.

Two hundred milligrams of pure theophylline was placed in 200 ml of the appropriate buffer for each system. These solutions were sampled in tandem with the complex–buffer systems to serve as appropriate controls. The pH of the solution was monitored periodically throughout the course of these studies.

RESULTS AND DISCUSSION

Molecular Structure—The spatial disposition of theophylline and ethylenediamine around the zinc ion is shown in Fig. 1. The zinc atom is tetrahedrally coordinated. The distortion of the coordination angles from their ideal tetrahedral value of 109.5° is to a large measure due to steric factors and hydrogen-bond interactions.

Zinc is commonly found to be tetrahedrally coordinated in complexes with nitrogen ligands. The Zn—N distances in such complexes range from 1.99 to 2.10 Å (14–16). The more basic the nitrogen ligand the shorter the length; in this case the distances between theophylline and zinc are significantly shorter than those between ethylenediamine and zinc.

In general, the intramolecular bonding parameters found for the theophylline anion are quite similar to those reported for the acidic form of theophylline (17–19). There is one bond which appears to undergo a substantial change upon dissociation of the N(7) proton. The C(9)—N(9) is longer in the anionic form (1.37 Å) than the acidic form (range 1.31–1.33 Å).

The theophylline moiety exhibits a small but significant degree of distortion from planarity. This has previously been observed for theophylline (18, 19), and a wide variety of purine compounds. In most instances the purine ring is bent above the C(4)—C(5) bond. The two rings comprising the purine nucleus are only slightly tilted from planarity (0.7 Å) in this structure.

The ethylenediamine residue is in the *synclinal* conformation. The torsion angle about the ethylene bond is 53°.

Intermolecular Bonding—The ethylenediamine nitrogen atoms, N(E), are in close proximity to a number of atoms (Table II). Although the hydrogen atoms attached to N(E) were not clearly discernible from electron density maps, geometrical considerations of these short contacts suggest that they are hydrogen bond interactions. It appears that both hydrogen atoms on N(E) are involved in bifurcated hydrogen bonds: one hydrogen being shared by N(7) and O(2) and the other by N(9) and O(6). In addition to these intermolecular interactions, the hydrogen on C(8) appears to be involved in a weak hydrogen bond with O(2). This type of interaction has been observed in the other reported theophylline structures (17–19).

Apparent Hydrolysis—The hydrolysis of the Zn(II)–aminophylline complex was found to be strongly affected by changes in pH (Fig. 2). The lower the pH the faster the hydrolysis. Complete hydrolysis is accomplished in <1 min at pH 1. At pH 7.4, the apparent hydrolytic rate was markedly reduced. As noted in Fig. 2, after 15 min only 60% of the total theophylline content in the complex was released. Since this phenomenon is directly influenced by particle size, the hydrolytic rate could be slowed by increasing the particle size of the sample.

A separate solubility experiment was conducted at 30° to determine the apparent aqueous solubility of the complex in relation to that of theophylline. It was determined that the apparent aqueous solubility of the complex was 0.047 mg/ml as compared with 8.40 mg/ml for theophylline. This reflects a 180-fold difference. Apparent solubility studies for the complex alone are impossible to conduct at pH values lower than 8.2, due to hydrolysis.

Figure 2 gives some insight into the usefulness of this new salt in formulating liquids and chewable tablets. At salivary pH, 6.40–8.24 for children (20) and 5.8–7.1 for adults (21), these profiles predict relatively slow release of theophylline from the complex, and consequently a substantial reduction in the bitterness associated with theophylline therapy.

Once the complex is ingested, the pH of the gastric environment is sufficiently low to effect rapid hydrolysis. This has been borne out in some preliminary human and animal bioavailability studies[5]. The theophylline plasma concentration after oral administration of the complex was comparable to those following dosing with anhydrous theophylline. However, with the use of appropriate buffering excipients, formulations have been designed that can control the hydrolysis rate and, therefore, the release rate of theophylline from the complex in the GI tract.

REFERENCES

(1) C. D. May, *Clin. Allergy*, **4**, 211 (1974).

(2) W. R. MacLaren, *Ann. Allergy*, **17**, 729 (1959).

(3) C. W. Bierman, G. G. Shapiro, W. E. Pierson, and C. S. Dorsett, *Pediatrics*, **60**, 845 (1977).

(4) A. R. Dowell, A. Heyman, H. O. Sieker, and K. Tripathy, *N. Engl. J. Med.*, **273**, 1447 (1965).

(5) D. McIntosh, *Br. J. Clin. Prac.*, **25**, 233 (1971).

(6) "The Merck Index," 9th ed., Merck, Rahway, N.J., 1976, p. 64, 1196.

(7) A. Osol, "Remington's Pharmaceutical Sciences," 15th ed., Mack Publishing, Easton, Pa., 1975, p. 1067.

(8) W. R. Burleson, L. J. Mantlo, T. H. Self, and M. R. Ryan, *Am. J. Hosp. Pharm.*, **35**, 584 (1978).

(9) B. Blackwell, *N. Engl. J. Med.*, **289**, 249 (1973).

(10) J. W. Jenne, E. Wyze, F. S. Rood, and F. M. MacDonald, *Clin. Pharmacol. Ther.*, **13**, 349 (1972).

(11) N. S. Zitzman, R. R. Krebs, and W. J. Birdsall, *J. Inorg. Nucl. Chem.*, **40**, 571 (1978).

(12) G. Germain, P. Main, and M. M. Woolfson, *Acta. Crystallogr.*, **27**, 368 (1971).

(13) W. J. Jusko and A. Poliszczuk, *Am. J. Hosp. Pharm.*, **33**, 1193 (1976).

(14) N. C. Baenziger and R. J. Schultz, *Inorg. Chem.*, **10**, 661 (1971).

(15) B. J. Aylett, "Comprehensive Inorganic Chemistry," Pergamon, Oxford, England, 1973, p. 249.

(16) L. Nassimibeni and A. Rogers, *Acta Crystallogr.*, **B30**, 1953 (1974).

(17) D. J. Sutor, *ibid.*, **11**, 83 (1958).

(18) E. Shefter and P. Sackman, *J. Pharm. Sci.*, **60**, 282 (1971).

(19) E. Shefter, *ibid.*, **58**, 710 (1969).

(20) N. C. Turner, J. H. Scribner, and J. T. Bell, *J. Bent. Res.*, **33**, 55 (1954).

(21) V. A. Kostlin and S. Rauch, *Helv. Med. Acta*, **24**, 600 (1957).

[5] Gardner, Smith, Shefter, Jusko, unpublished data.

High-Performance Liquid Chromatography of Cisplatin

C. M. RILEY, L. A. STERNSON[x], and A. J. REPTA

Received October 13, 1981 from the *Department of Pharmaceutical Chemistry, The University of Kansas, Lawrence, KS 66045.* Accepted for publication March 19, 1982.

Abstract □ The retention behavior of cisplatin on a variety of stationary phases has been investigated using aqueous mobile phases modified by the addition of various electrolytes and methanol. Cisplatin is poorly retained on reverse-phase or silica columns but satisfactorily retained on chemically bonded or solvent-generated anion exchangers. The retention of the neutral complex on positively charged stationary phases is explained in terms of ion–dipole interactions and rationalized by the application of solvophobic theory. The use of solvent-generated anion exchangers for the analysis of cisplatin offers significant advantages over the chemically bonded system in terms of peak shape, column efficiency, and stability. By the use of column switching and off-line atomic absorption, solvent-generated anion exchange high-performance liquid chromatography (HPLC) is applicable to the determination of cisplatin in urine.

Keyphrases □ High-performance liquid chromatography—analysis for cisplatin in urine, solvent-generated anion exchange, column switching technique □ Cisplatin—analysis in urine, high-performance liquid chromatography using column-switching techniques

The demonstrated ability of platinum complexes to inhibit cell division in *Escherichia coli* (1) has led to extensive studies of their antitumor activity (2, 3). Although ~1300 platinum complexes have been investigated as potential anticancer agents (3), the prototype, *cis*-diamminedichloroplatinum(II) (cisplatin, structure I), remains the most widely used in the clinical setting.

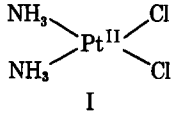

I

Cisplatin readily undergoes nucleophilic substitution (4, 5) with loss of chloride ion. These nucleophilic reactions have been implicated in its biological activity (3), biotransformation (3), and chemical degradation (3, 6, 7). Consequently, ligand selectivity is a necessary requirement of any analytical procedure for cisplatin. While X-ray fluorescence (8) and flameless atomic absorption spectrophotometry (9) provide the necessary sensitivities, these methods are nonselective. High-performance liquid chromatography (HPLC) offers the potential for good functional group selectivity (10); however, the poor solubility of cisplatin in nonaqueous media precludes the use of many conventional chromatographic techniques. Additionally, the UV absorptivity of cisplatin is low ($\epsilon = 150$ at 301 nm), and until a sensitive platinum detector is developed, off-line atomic absorption spectroscopy after separation is necessary for the determination of therapeutic drug concentrations in biological fluids. HPLC methods involving precolumn derivatization with diethyldithiocarbamate provide the required sensitivity (11, 12); however, they respond only to total platinum levels. Cisplatin has been retained on and eluted intact from strong anion exchangers (13); however, these systems suffer from poor peak shape and provide only moderate selectivities. Furthermore, the high concentrations of methanol required for adequate solute retention (>60%) are incompatible with injections of urine and efficient use of reaction detectors. This report describes the chromatographic behavior of cisplatin on anion-exchange columns and application to its analysis in biological fluid.

EXPERIMENTAL

Materials—Crystalline cisplatin was obtained from the National Cancer Institute[1] and used as received. All other chemicals were of reagent grade, except for the methanol which was HPLC grade[2]. Glass-distilled water was used throughout.

High-Performance Liquid Chromatography—The liquid chromatograph was comprised of a constant flow-rate pump[3], an injector[4] fitted with a 20-μl loop, and a fixed wavelength[5] (280 nm) UV detector. Six columns containing various stationary phases were used in the course of the study. Columns A[6], B[6], and C[7] contained reverse-phase material,

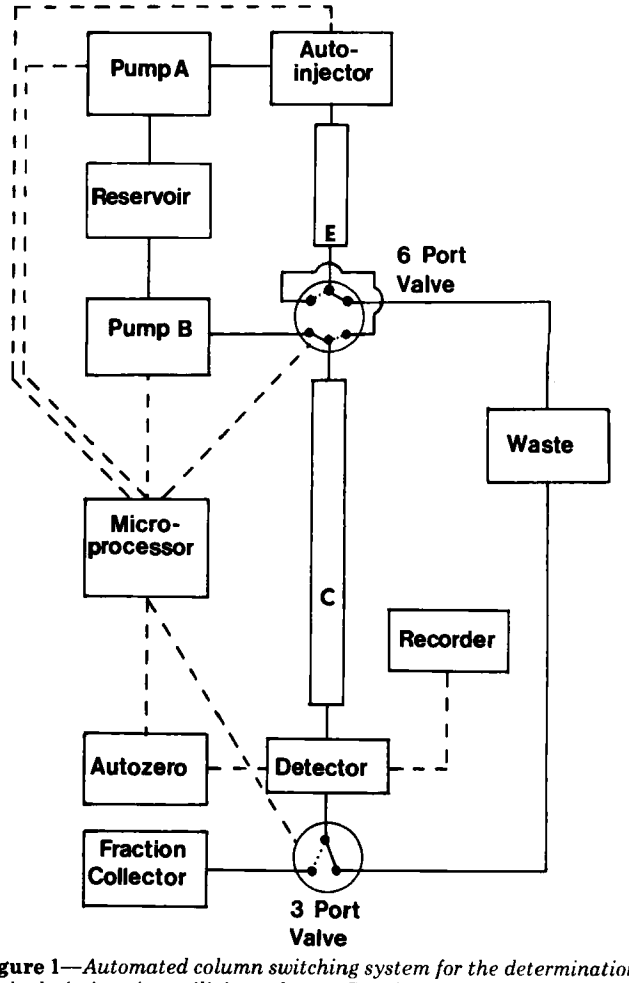

Figure 1—*Automated column switching system for the determination of cisplatin in urine utilizing columns C and E.*

[1] NCI, Bethesda, Md.
[2] Fisher Scientific Co., Fair Lawn, N.J.
[3] Altex model 110A, Beckman Instruments, Inc., Berkeley, Calif.
[4] Altex model 210, Beckman Instruments, Inc., Berkeley, Calif.
[5] Altex model 153, Beckman Instruments, Inc., Berkeley, Calif.
[6] μ-Bondapak C_{18} (10 μm, 300 mm × 3.9-mm i.d.), Waters Associates, Milford, Mass.
[7] ODS Ultrapak (10 μm, 150 mm × 4.6-mm i.d.), Beckman Instruments, Inc., Berkeley, Calif.

0022-3549/83/0400-0351$01.00/0

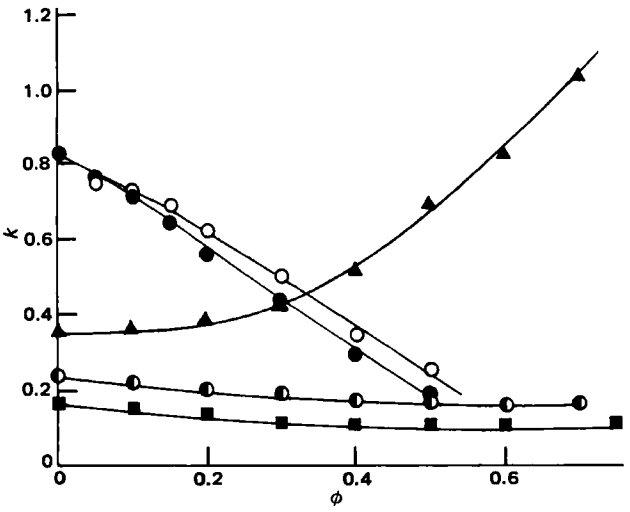

Figure 2—*The relationship between the capacity ratio of cisplatin (k) and the volume fraction (ϕ) of methanol in the mobile phase using various stationary phases at 30°. Key: (▲) column F, (■) column D, (◐) column A, (○) column A plus 0.99 μmoles/m² of 10^{-4} M hexadecyltrimethylammonium bromide, and (●) column A plus 0.99 μmoles/m² of 10^{-5} M hexadecyltrimethylammonium bromide.*

columns D[8] and E[9] contained silica gel, and column F[10] was a strong anion exchanger. Columns A, B, D, and F were obtained from commercial sources; columns C and E were slurry packed using standard procedures (14, 15).

Solute capacity ratios (k) were determined in duplicate by:

$$k = (t_r - t_0)/t_0 \qquad \text{(Eq. 1)}$$

using deuterium oxide as the unretained marker, where t_r and t_0 are the elution times of the solute and deuterium oxide, respectively.

Solvent-generated anion exchangers were prepared by the adsorption of hexadecyltrimethylammonium bromide onto the surfaces of columns A, B, C, and E. Solutions (0.5% w/v) of hexadecyltrimethylammonium bromide were pumped through the columns until a rise in baseline, attributed to equilibration of the system, was observed (16). After each working day (~10 hr) the columns were washed with water and then with successively increasing concentrations of methanol in water (up to 50%), except column F which was regenerated according to the manufacturer's specifications.

Chromatography was performed either at room temperature (~22°) or at 30° in which case the column was thermostated by the use of a water jacket[11] and a recycling water heater[12].

For the analysis of cisplatin in urine, an automated column-switching system was used (Fig. 1). Columns C and E were connected in series *via* a six-port switching valve[13], which was positioned so that the eluent from column E either could be passed to waste or transferred to column C. A three-port switching valve[14] was positioned after the detector so that the eluent from column C either could be passed to waste or transferred to the fraction collector[15]. All chromatographic events were controlled externally by the use of a microprocessor[16]. A mobile phase of 10^{-2} M citrate buffer (pH 7.0) containing 10^{-4} M hexadecyltrimethylammonium bromide was delivered from a common reservoir by two pumps[3] at a rate of 1.0 ml/min through both columns.

The urine samples were injected automatically[17] onto column E and eluted to waste for 1.6 min, after which time the valve was switched and the fractions containing cisplatin were loaded onto column C. After loading column C, the valve was returned to its original configuration and the remaining endogenous material eluting from column E was vented to waste at a high flow rate (3.0 ml/min). At the same time, cisplatin was separated on column C from the endogenous material with which it coeluted from column E. After passing through the detector, the eluent fraction containing cisplatin was collected and subsequently analyzed for platinum content by atomic absorption. The cisplatin concentration was determined by comparison with calibration curves prepared by treating standard solutions of cisplatin (2–200 μg/ml) in 0.9% NaCl (normal saline) in an identical manner.

Platinum Determination—Platinum determinations were made on an atomic absorption spectrophotometer[18] fitted with a carbon rod atomizer. A constant lamp current of 10 mA was used and the platinum line monitored at 265.95 nm. A three-stage heating program was used: 95° for 45 sec (dry), 1400° for 15 sec (ash), and 2300° for 0.5 sec (atomize) with a ramp rate of 600°/sec. Depending on concentration 2–20-μl samples were injected directly onto the carbon rod.

Clinical Urinalysis—Urine samples (10 ml) were taken from three patients treated with cisplatin (50 mg/m²) for ovarian cancer. Urine specimens were divided (providing duplicate samples), frozen rapidly, and stored over solid CO_2 prior to analysis. The samples were thawed, sonicated for 2 min, passed through 3-μm filters[19], and analyzed immediately. The cisplatin concentration was determined by the aforementioned HPLC procedure, and the total platinum concentration was determined directly by atomic absorption after appropriate dilution with normal saline.

Table I—Relationship Between τ Values of Electrolytes Added to the Mobile Phase and the Capacity Ratios of Cisplatin [a]

Electrolyte	τ [b]	k [c]
Citrate buffer (pH 7)	3.12	3.97
Sodium sulfate	2.73	3.22
Sodium nitrate	1.32	0.86
Sodium bromide	1.06	0.74

[a] Mobile phase: 10^{-4} M hexadecyltrimethylammonium bromide, 0.1 M electrolyte. Stationary phase: 1.31 μmoles/m² hexadecyltrimethylammonium bromide supported by column B. Temperature: 30°. [b] Constants describing the effect of electrolyte on the surface tension of water (Eq. 3, Ref. 21). [c] $k = (t_r - t_0)/t_0$ (Eq. 1).

RESULTS AND DISCUSSION

The Chromatography of Cisplatin—Due to its very low solubility in organic solvents, the chromatography of cisplatin is limited to systems employing aqueous mobile phases modified by polar solvents such as methanol. The retention of cisplatin on various stationary phases was investigated using aqueous methanol mobile phases (Fig. 2). Cisplatin was poorly retained (k = 0.25, Eq. 1) on both silica (column D) and hydrophobic (column A) reverse-phase columns, and its retention decreased slightly with an increase in methanol concentration. In contrast, cisplatin was significantly retained on stationary phases possessing cationic functionalities in the form of either chemically bonded (column F) or physically adsorbed (column A modified by a monolayer of hexadecyltrimethylammonium bromide) quaternary ammonium groups. By the observation of breakthrough times (16) it was found that a monolayer of 0.99 μmole/m² hexadecyltrimethylammonium bromide was adsorbed onto the hydrophobic stationary phase (column A). With a purely aqueous mobile phase, the stability of the modified stationary phase was maintained by a low concentration (10^{-4} or 10^{-5} M) of surfactant in the mobile phase. The addition of methanol to the mobile phase resulted in displacement of some of the surfactant from the stationary phase. With 10^{-5} M hexadecyltrimethylammonium bromide in the mobile phase, partial displacement of the adsorbed surfactant was observed when the methanol volume fraction ϕ exceeded 0.10, and successive increases in methanol concentration produced further displacement. With 10^{-4} M surfactant in the mobile phase no displacement of adsorbed surfactant was observed at $\phi \leq 0.15$. These observations indicate that the surface of the modified reverse-phase column consisted of a mixture of adsorbed surfactant and methanol, the proportions of which were determined by the composition of the mobile phase.

Although cisplatin was retained on both chemically bonded and solvent-generated anion exchangers, Fig. 2 indicates that the retention mechanism and the influence of methanol was different in the two systems. Initially, with a purely aqueous mobile phase, cisplatin was retained better on the solvent-generated anion exchanger than on the chemically bonded anion exchanger. Increasing the methanol concentration de-

[8] Partisil 5, (5 μm, 250 mm × 4.6-mm i.d.), Whatman, Inc., Clifton, N.J.
[9] Hypersil (5 μm, 50 mm × 4.6-mm i.d.), Shardon Southern, Sewickley, Pa.
[10] Partisil 10 SAX (10 μm, 250 mm × 4.6-mm i.d.), Whatman, Inc., Clifton, N.J.
[11] Alltech Associates, Deerfield, Ill.
[12] Haake, Saddlebrook, N.J.
[13] Rheodyne 7001, Cotati, Calif.
[14] Systech, Inc., New Brighton, Minn.
[15] Model 273, Instrument Specialties, Lincoln, Nebr.
[16] SLIC 1400, Systec, Inc., New Brighton, Minn.
[17] WISP 710, Waters Associates, Milford, Mass.
[18] Varian Techtron 175B, Varian Assoc., Palo Alto, Calif.
[19] Millipore Corp., Bedford, Mass.

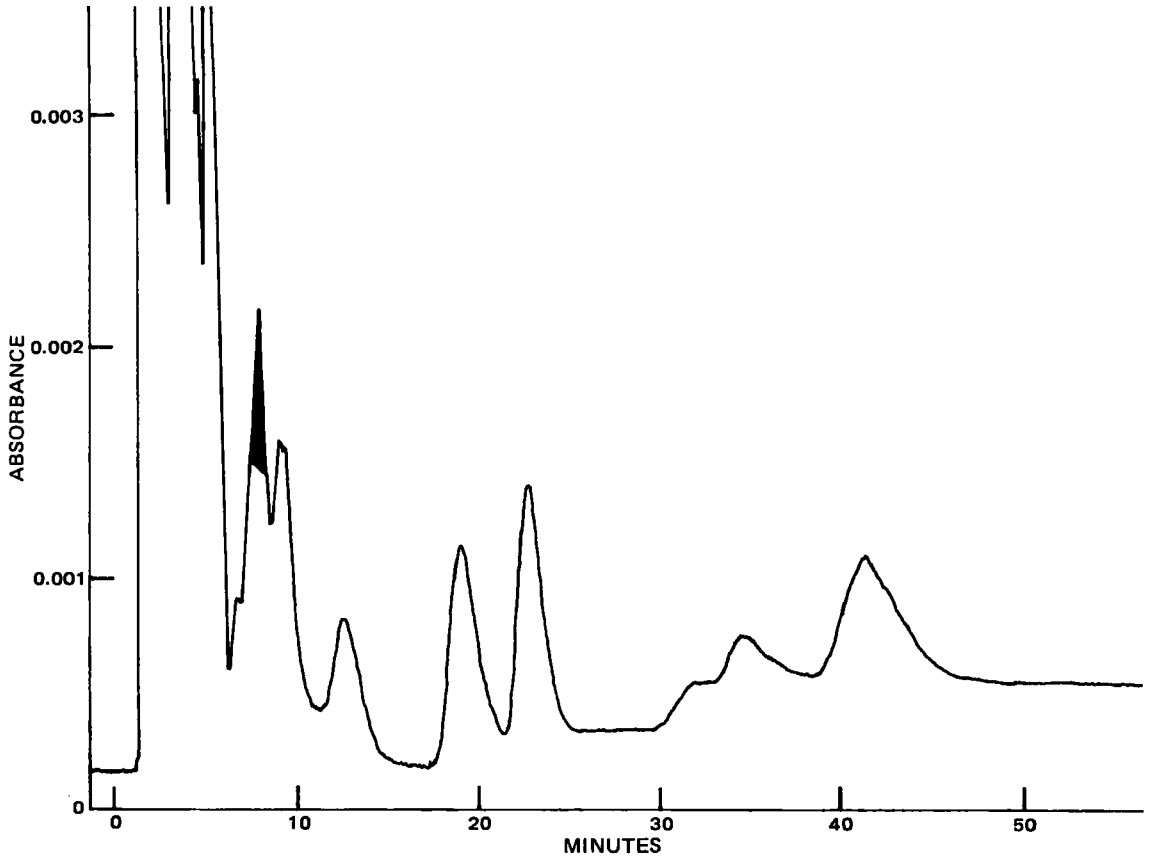

Figure 3—*Chromatogram of human urine spiked with 200 μg/ml of cisplatin on a reverse-phase column coated with 1.96 μmoles/m² of hexadecyltrimethylammonium bromide. Other chromatographic conditions were: mobile phase, 10^{-2} M citrate buffer (pH 7.0) + 10^{-4} M hexadecyltrimethylammonium bromide; flow rate, 1.0 ml/min; and ambient temperature. Arrow indicates cisplatin peak (darkened).*

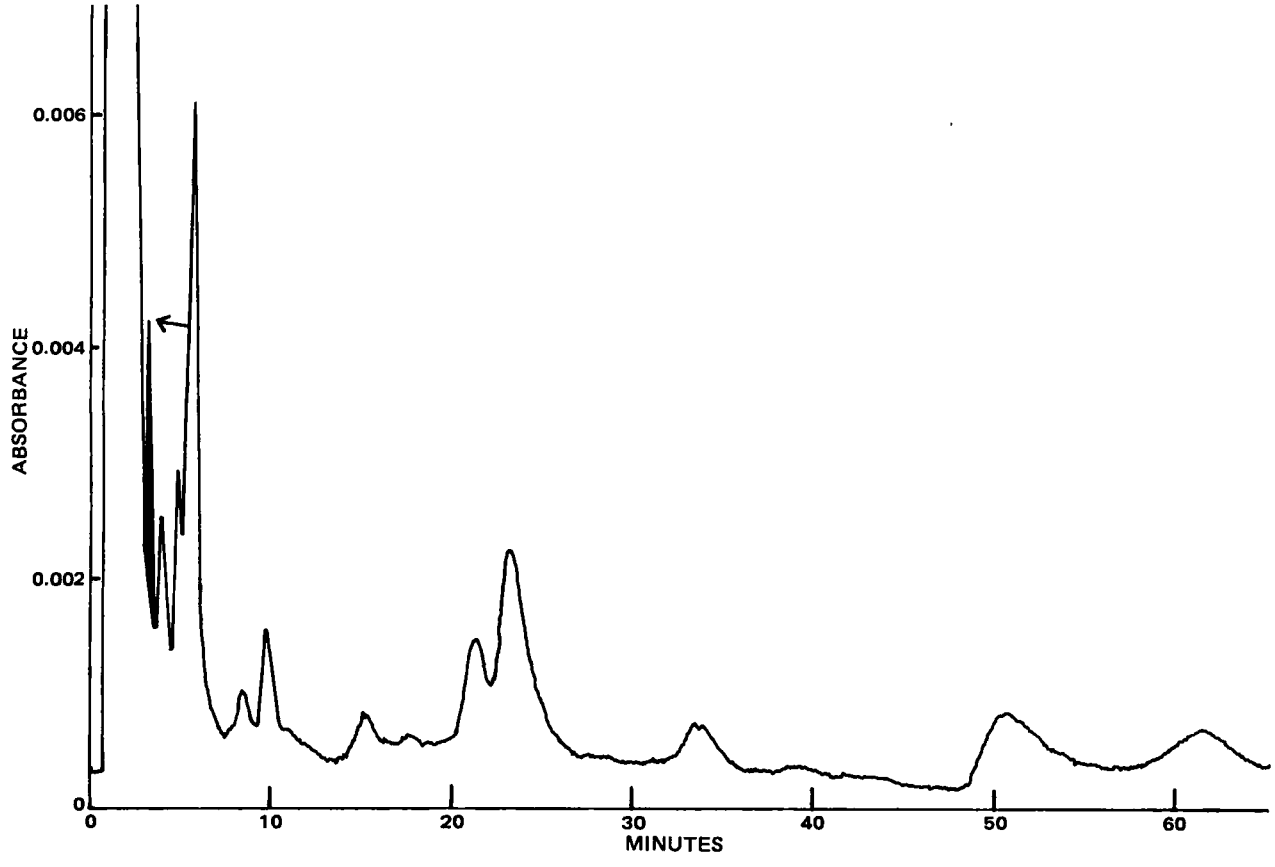

Figure 4—*Chromatogram of human urine spiked with 200 μg/ml of cisplatin on silica gel coated with 0.63 μmoles/m² of hexadecyltrimethylammonium bromide. Arrow indicates cisplatin peak (darkened). Other chromatographic conditions as Fig. 3.*

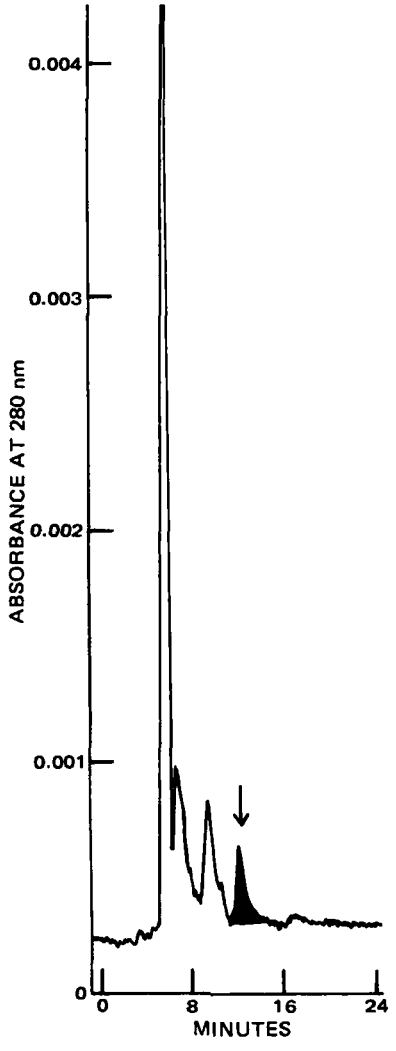

Figure 5—*Chromatogram of clinical urine sample containing 96 μg/ml of cisplatin using a column-switching configuration as in Fig. 1 and mobile phase conditions as described in Fig. 3. Arrow indicates cisplatin peak (darkened).*

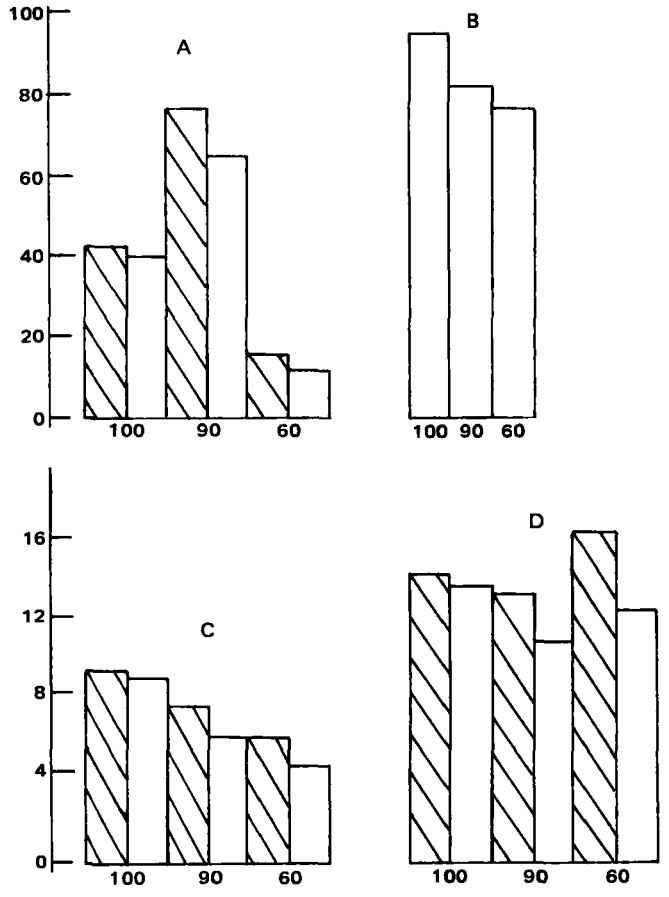

Figure 6—*Urine analysis of three patients treated with cisplatin for ovarian cancer, showing the amounts and concentrations of unchanged drug and total platinum excreted 30 min after infusion (50 mg/m² iv at 1 mg/min). Key: (A) urinary concentration of total platinum ▨ and cisplatin □ μg/ml; (B) ratio of cisplatin–total platinum for three patients, %; (C) absolute amount of total platinum ▨ and cisplatin □ present in the urine samples, μg; and (D) fraction of the administered dose excreted as total platinum ▨ and cisplatin □, %. The doses of drug administered to each patient are given under each histogram in milligrams of cisplatin; amounts and concentrations excreted are given in terms of free metal (Pt).*

creased retention on the former while increasing retention on the latter. Below $\phi = 0.10$, cisplatin retention on the modified reverse-phase column was independent of surfactant concentration in the mobile phase, which indicates that the contribution to retention of solute–surfactant interactions in the mobile phase was negligible. At higher concentrations of methanol, cisplatin retention was dependent on the concentration of hexadecyltrimethylammonium bromide in the mobile phase due to displacement of the adsorbed surfactant. However, this desorption does not explain the initial decrease in retention with increasing methanol concentration on the modified reverse-phase column.

The retention of cisplatin on either of the cationic stationary phases is explained most readily in terms of ion–dipole interactions between the neutral platinum complex and the positively charged stationary phase. The differences between the two systems may be explained in terms of the different environments in which these interactions occur and the influence of methanol on those environments. The cationic groups on column A are situated in an apolar, hydrophobic environment, whereas the quaternary ammonium groups on the chemically bonded column (F) are in a polar environment in close proximity to a silica backbone. In both systems methanol is adsorbed at the stationary phase–mobile phase interface (17, 18), which decreases the polarity of the cationic groups of column F while increasing the polarity of the corresponding groups on column A.

The effects of methanol may be further rationalized by the application of solvophobic theory. According to solvophobic theory, retention in HPLC systems employing aqueous mobile phases may be described by:

$$\ln k = a + b + \frac{\gamma \Delta A}{RT} \qquad \text{(Eq. 2)}$$

which is a summation of all the possible solute–solvent–stationary phase interactions contributing to retention (19, 20). The first term, a, is related to the properties of the mobile and stationary phases and is independent of the nature of the solute. In the present system, b may be taken as a measure of the ion–dipole interactions which contribute to retention. The third term is a measure of the hydrophobic interactions where γ is the mobile phase surface tension and ΔA is the decrease in hydrophobic surface area on binding of the solute to the stationary phase. Since the chemically bonded anion exchanger has little hydrophobic character, the contribution of the third term is probably negligible in this system, and the increased retention observed with increasing methanol concentration arises from an increase in the contribution of b.

In the solvent-generated system, increasing the methanol concentration may influence both b and the hydrophobic term ($\gamma \Delta A/RT$). The increase in polarity of the environment in which the interactions occur, due to the presence of methanol, can be expected to result in a decrease in the contribution of b and decreased retention. Also, the addition of methanol lowers the mobile phase surface tension (19), further reducing retention. As indicated previously, a third effect is introduced at higher methanol concentrations at which hexyldecyltrimethylammonium bromide is displaced from the column, reducing the contributions of both a and b.

Solvophobic theory may be applied also to the explanation of the effects of electrolyte on the retention of cisplatin on solvent-generated anion exchangers (Table I). In this study column B was used as support for the adsorbed surfactant. This column produced a higher uptake of surfactant (1.31 μmoles/m²) which resulted in a correspondingly increased retention of cisplatin. The addition of the monovalent electrolytes

sodium bromide and sodium nitrate (both 0.1 M) to the mobile phase decreased the retention of cisplatin. Conversely, the addition of the polyvalent electrolytes, sodium citrate and sodium sulfate, produced a significant enhancement of retention. These effects may be explained in terms of the effect of the added salts on the mobile phase surface tension as described by the relationship:

$$\gamma = \gamma_0 + \tau m \qquad \text{(Eq. 3)}$$

where m is the molality of the electrolyte, γ_0 is the surface tension of the pure solvent and τ is a constant for the particular electrolyte. Combining Eqs. 2 and 3 gives a prediction of the linear relationship between ln k and τ at a fixed salt concentration:

$$\ln k = a + b + \frac{(\gamma_0 + \tau m)\, A}{RT} \qquad \text{(Eq. 4)}$$

The relationship between ln k and τ (21) at an electrolyte concentration of 0.1 M for the cisplatin solvent-generated anion exchange system was found to be:

$$\ln k = 0.85\,\tau - 1.23 \quad r = 0.998,\ n = 4 \qquad \text{(Eq. 5)}$$

Increasing the ionic concentration of the mobile phase may also reduce the thermodynamic activity of the cationic stationary phase binding sites due to ion–ion interactions which in turn leads to a decreased contribution of a and b (Eq. 4) and decreased retention of cisplatin. The excellent linearity of Eq. 5 indicates that this latter contribution is constant for the different salts examined at a concentration of 0.1 M and is more than compensated for by the increase in mobile phase surface tension produced by the polyvalent electrolytes having large values of τ.

Urinalysis—The use of columns A and B was associated with short column lives and considerable batch-to-batch variation. Consequently, column C was used as the support for the cationic surfactant in the analysis of cisplatin in urine. This material produced a higher coverage of adsorbed surfactant (1.96 μmoles/m^2) and a correspondingly greater retention of cisplatin. As a result, it was possible to use a lower concentration of citrate (10^{-2} M) in the mobile phase and still maintain adequate retention of cisplatin (k = 4.68).

Despite optimal retention of cisplatin on column C coated with hexadecyltrimethylammonium bromide, the drug still coeluted with several endogenous urine components (Fig. 3). Additionally, a number of highly retained peaks were observed, resulting in long analysis times. These interfering compounds were not satisfactorily removed by the use of a silica precolumn (column E). However, it was observed that cisplatin was significantly retained (k = 2.83) on this precolumn and that on silica it coeluted with different urine components (Fig. 4). Since it has been shown that cisplatin was virtually unretained on silica (Fig. 2) it was concluded that the silica had been modified by the presence of hexadecyltrimethylammonium bromide and that it was behaving as a solvent-generated anion exchanger with a different selectivity from that produced by adsorbing the surfactant onto a reverse-phase column. This hypothesis was confirmed by uptake studies which revealed significant amounts of surfactant (0.63 μmole/m^2) adsorbed onto the silica surface.

By the application of column-switching techniques (Fig. 1) the different selectivities of the two solvent-generated anion exchangers bonded to silica and hydrophobic supports were utilized and complete resolution of cisplatin from urine was achieved (Fig. 5). The system was fully automated, under microprocessor control, and designed so that only the cisplatin-containing fraction which eluted from column E was transferred to column C. After column transfer, cisplatin was separated from the components with which it coeluted from the first column. The remaining urine components were eluted from the first column at a higher flow rate (3.0 ml/min) and vented to waste.

Due to the poor sensitivity provided by UV spectroscopy, off-line flameless atomic absorption was preferred for the analysis of urine containing cisplatin at <100 μg/ml. After chromatography, the fraction containing cisplatin was collected and determined by atomic absorption spectrophotometry. The platinum absorbance of the collected fraction A_{Pt} was linear with respect to the amount of cisplatin injected (calibration curve prepared as described in *Experimental*), as defined by:

$$A_{Pt} = 0.65\ [\text{cisplatin}] + 0.001 \quad r = 0.999,\ n = 6 \qquad \text{(Eq. 7)}$$

and offered a detection limit of 2 μg/ml. Although the use of off-line atomic absorption introduces an extra step in the analysis, it provides a specific platinum-detection system which potentiates the selectivity of the HPLC.

It was found that urine samples containing cisplatin could not be satisfactorily stored in a freezer (−11°) since >30% was lost from one sample over a period of 48 hr. No degradation of cisplatin was observed in urine stored over solid CO_2 (~ −60°) for 48 hr. The recovery of drug (50 μg/ml) from urine samples stored in this manner was 101% with a relative *SD* of 3.6% (n = 9).

The developed methodology was applied to the analysis of the urine taken from three patients treated with cisplatin for ovarian cancer (Fig. 6). The amount of unchanged cisplatin excreted was determined by HPLC, and total platinum concentration was determined directly by atomic absorption spectroscopy. There was wide variation in the concentration of cisplatin found; the amounts and percentages of the total dose excreted unchanged were similar. The ratios of cisplatin–total platinum excreted varied between 75 and 95%, indicating that the previous results (3) reporting low levels of cisplatin in urine may be due to degradation during storage, either in the bladder or after sample collection, rather than extensive biotransformation. Furthermore, the presence of high concentrations of unchanged cisplatin in urine may be related to its clinical utility in the treatment of bladder cancers (3, 22).

REFERENCES

(1) B. Rosenberg, L. Van Camp, and T. Krigas, *Nature (London)*, **205,** 698 (1965).

(2) T. A. Connors and J. J. Roberts, Eds., "Platinum Coordination Complexes in Cancer Chemotherapy," Springer-Verlag, New York, N.Y., 1974.

(3) A. W. Prestayko, S. T. Crooke, and S. K. Carter, Eds., "Cisplatin, Current Status and New Developments," Academic, New York, N.Y., 1980.

(4) F. Basolo and R. G. Pearson, "Mechanisms of Inorganic Reactions. A Study of Metal Complexes in Solution," 2nd ed., Wiley, New York, N.Y., 1967, p. 378.

(5) U. Belluco, "Organometallic and Coordination Chemistry of Platinum," Academic, London, 1974, p. 142.

(6) A. A. Hincal, D. F. Long, and A. J. Repta, *Parenter. Drug Assoc., J.* **33,** 107 (1979).

(7) A. J. Repta, D. F. Long, and A. A. Hincal, *Cancer Treat. Rep.*, **63,** 1515 (1979).

(8) S. J. Bannister, L. A. Sternson, A. J. Repta, and G. W. James, *Clin. Chem.*, **23,** 2258 (1977).

(9) S. J. Bannister, Y. Chang, L. A. Sternson, and A. J. Repta, *ibid.*, **24,** 877 (1978).

(10) C. M. Riley, E. Tomlinson, and T. M. Jefferies, *J. Chromatogr.*, **185,** 197 (1979).

(11) S. J. Bannister, L. A. Sternson, and A. J. Repta, *ibid.*, **173,** 333 (1979).

(12) R. F. Borch, J. H. Markowitz, and M. E. Pleasants, *Anal. Lett.*, **12,** 917 (1979).

(13) Y. Chang, L. A. Sternson, and A. J. Repta, *ibid.*, **11,** 449 (1978).

(14) P. A. Bristow, P. N. Brittain, C. M. Riley, and B. F. Williamson, *J. Chromatogr.*, **131,** 57 (1977).

(15) G. J. Manius and R. J. Tscherne, *Am. Lab. (Boston)*, 138 (1981).

(16) E. Tomlinson, C. M. Riley, and T. M. Jefferies, *J. Chromatogr.*, **173,** 89 (1979).

(17) R. P. W. Scott and P. Kucera, *ibid.*, **112,** 425 (1975).

(18) *Idem.*, **149,** 93 (1978).

(19) C. Horvath, W. Melander, and I. Molnar, *ibid.*, **125,** 129 (1976).

(20) C. Horvath, W. Melander, I. Molnar, and P. Molnar, *Anal. Chem.*, **49,** 2295 (1977).

(21) W. Melander and C. Horvath, *Arch. Biochem. Biophys.*, **183,** 158 (1977).

(22) M. B. Troner, *Proc. Am. Assoc. Cancer Res.*, **20,** 117 (1979).

ACKNOWLEDGMENTS

This work was supported by grants from the American Cancer Society (CH 149) and the National Institutes of Health (CA 24934).

Kinetics and Equilibrium of the Reversible Alprazolam Ring-Opening Reaction

M. J. CHO ˣ, T. A. SCAHILL, and J. B. HESTER, Jr.

Received April 9, 1981, from the *Pharmaceutical Research and Development Division, The Upjohn Company, Kalamazoo, MI 49001.* Accepted for publication June 25, 1981.

Abstract □ Alprazolam underwent a facile 1,4-benzodiazepine ring-opening reaction in an acidic aqueous solution to form a benzophenone compound. The reaction was demonstrated by means of UV, IR, and ^{1}H- and ^{13}C-NMR spectroscopy. Its reverse cyclization reaction to alprazolam occurred when an acidic solution was neutralized. Both the ring-opening and the cyclization rate constants were obtained from the overall rate constant measured at 25° over a pH range of 0.5–8.0; the latter was measured by monitoring the UV spectral change of the reaction. Although the equilibrium was favored for the benzophenone compound in acidic solutions, it was possible to directly measure the cyclization rate at three acidic pH values by providing a sink condition for the product, alprazolam, using a biphasic reaction system. The bell-shaped cyclization rate pH profile was interpreted in terms of a change in the rate-determining step. The pH profile of the ring-opening rate showed an inflection point indicating a different reactivity of mono- and dicationic alprazolam. The apparent equilibrium between alprazolam and the benzophenone compound at a given pH was estimated from the rate constants for the ring-opening and cyclization reactions. The results agree with the apparent pK_a measured by a conventional UV spectrophotometry and a titration technique. The pK_a of monocationic alprazolam, the reactive species for the covalent hydration, was determined from the pH dependence of the initial absorbance when an alprazolam solution is acidified.

Keyphrases □ Alprazolam—kinetics and equilibrium of reversible ring-opening reaction □ Kinetics—alprazolam, reversible ring-opening reaction □ Equilibrium—alprazolam, reversible ring-opening reaction

The relationship between structure and chemical reactivity is an important research subject in physical organic chemistry. In heterolytic reactions involving nucleophilic reagents, an activated electrophile is often chosen as a model substrate and its reaction with a variety of nucleophiles studied. The nucleophilicity is determined from the observed reaction rates, preferably in the form of linear free-energy relationships. Such studies are well documented for substrates containing carbonyl groups (1–7) and to a lesser extent for substrates containing imino (C=N—) bonds (8). A systematic structural change in a series of analogous substrates toward a given nucleophile such as water has not been incorporated as commonly in mechanistic studies, presumably because of a limited choice of substrates. This practice is usually the case, especially when looking for a series of substrates containing an activated imino bond (9).

BACKGROUND

Analogues of 1,4-benzodiazepine provide an excellent opportunity to investigate the structural influence on the lability of a C=N— bond toward a given nucleophile, since many 1,4-benzodiazepines undergo nucleophilic covalent hydration across the C(5)—N(4) double bond, which is followed by ring opening to the corresponding benzophenone compounds (10–21).

A detailed kinetic study on the reversible ring-opening reaction of alprazolam (8-chloro-1-methyl-6-phenyl-4*H*-*s*-triazolo[4,3-*a*][1,4]benzodiazepine)[1] was undertaken. In addition to the azomethine bond in the seven-membered ring, alprazolam contains other weakly basic centers on the 1,2,4-triazole. The opened-ring compound carries a primary amino function; thus, the observed rate constant (which is the sum of the ring opening and the cyclization rate constants) was a composite function of several microscopic rate constants. The present study attempted to determine these constants separately. Comparison of these constants with the corresponding rate constant of other benzodiazepines may eventually clarify the structure–activity relationships associated with an imino bond.

The facile reversibility of the ring-opening reaction required solution of the multiple equilibria involved. An attempt was made to solve these equilibria in terms of pH change through experimentally determined ionization constants and the apparent equilibrium between the two compounds engaged in the reversible reaction.

EXPERIMENTAL

Materials and Equipment—A buffer system of low ionic strength (0.01 *M*) (22) was used throughout the kinetic study to avoid any possible buffer catalysis. At pH <2, the ionic strength was inevitably >0.01 *M*; however, only hydrochloric acid was present in the system. For the pH ranges of 2.0–3.8, 4.0–6.0, 6.0–7.0, and 7.0–8.5, chloroacetate, succinate, phosphate, and tromethamine buffers were used, respectively. The buffer components were analytical grade.

A UV spectrophotometer[2] with a cell compartment between thermoplates was used throughout the kinetic study. A constant temperature of 25 ± 0.1° was maintained by a circulating water bath[3]. When UV scanning was necessary, a different spectrophotometer[4] equipped with an automatic repetitive scanning device was used. Titration for pK_a determination as well as pH measurement was done using an automatic titrator[5]. When continuous flow of a reaction system through a spectrophotometer was required, a two-piston pump with a low dead volume[6] was used for circulation.

NMR Studies—All spectra were reported on a 200-MHz NMR spectrometer[7] with a magnetic field strength of 4.7 tesla. The instrument was operated in the FT mode and the lock was provided by the deuterium signal from the solvent.

^{1}H-NMR spectra were run at 200 MHz at ambient probe temperature (20.5°). Typical instrument settings were: sweep width, 2600 Hz; acquisition time, 1.5 sec; data points, 8K (with zero filling); and pulse width, 5 μsec. Typically, <100 transients were needed for a good signal-to-noise ratio.

^{13}C-NMR spectra were run at 50.3 MHz at ambient probe temperature (21.5°). Typical instrument settings were: sweep width, 10,000 Hz; acquisition time, 0.720 sec; data points, 16K (with zero filling); and pulse width, 5 μsec (30° tip angle). Typically, 20,000 transients were needed for a good signal-to-noise ratio.

Samples for ^{1}H- and ^{13}C-NMR spectra were prepared by dissolving 250 mg of alprazolam (~0.8 mmole) or compound *C* (Scheme I; ~0.75 mmole) in 2.0 ml of deuterated chloroform[8]. To this was added 158 μl of trifluoroacetic acid[9] (~2 meq) and 50 μl of deuterated water[8].

Reversible Reaction Kinetics—The overall reaction was initiated either by acidifying a neutral solution of alprazolam to a desired pH or by neutralizing an acidic solution which previously had been equilibrated at a pH close to 1.0. In the former case, ~160 μl of a stock solution of alprazolam in methanol (~10 mg/25 ml) was injected directly into a 1.0-cm

[1] The numbering system is in accordance with that of *Chemical Abstracts*. In the remainder of the present report, however, the numbering system of the parent 1,4-benzodiazepine is used exclusively.

[2] Gilford model 250 spectrophotometer.
[3] Lauda model B-2 waterbath.
[4] Zeiss model DMR-21 spectrophotometer.
[5] Radiometer model PHM-26 equipped with models ABU-12, TTA 60, and TTT-116.
[6] Milton Roy minipump.
[7] Varian model XL-200 NMR spectrometer.
[8] Merck Sharp and Dohme. Deuterated chloroform containing 1% tetramethylsilane was passed through a silica column to eliminate trace hydrochloric acid.
[9] Aldrich (used as received).

0022-3549/83/0400-0356$01.00/0

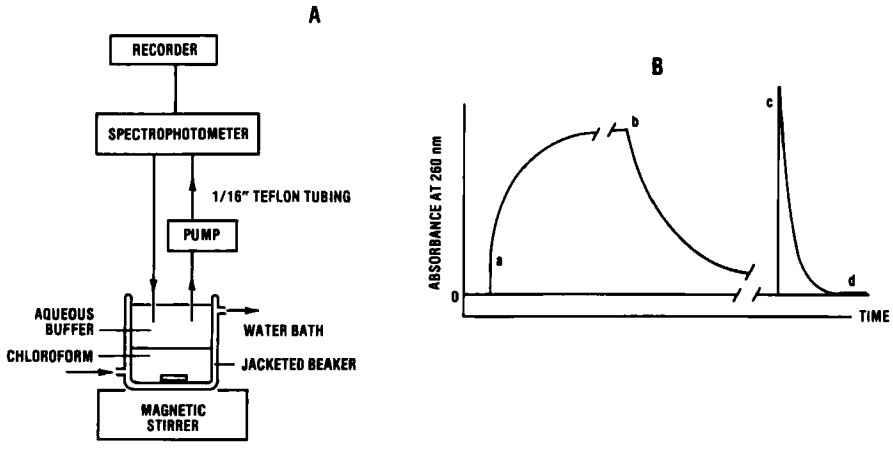

Figure 1—*(A) Experimental setup for monitoring irreversible process of cyclization of the opened-ring compound to alprazolam. (B) A typical tracing of absorbance at 260 nm as a function of time: a to b, reversible overall (largely ring-opening) reaction; b to c, cyclization reaction only (alprazolam is continuously extracted to chloroform layer); c to d, alprazolam partitioning process at given hydrodynamics.*

cell containing 3.0 ml of a given buffer. A Hamilton microsyringe (250 μl) was used for introducing the alprazolam stock solution. After rapid mixing, the absorbance increase at 260 nm was continuously monitored. The concentration of alprazolam and methanol in the final reaction system was 6.2×10^{-5} *M* and 5.0% (v/v), respectively.

At pH >3.5, the absorbance change was so small that the overall reaction rate constant was obtained by neutralizing an acidic solution. A typically acidic stock solution of alprazolam was prepared by dissolving ~10 mg of alprazolam in 25 ml of 0.2 *N* HCl containing 20% (v/v) methanol. The solution was left at room temperature for at least 10 min but not more than 30 min prior to use. This stock solution (160 μl) was introduced into a cell containing 3.0 ml buffer at the desired pH. The reaction was then initiated by rapidly injecting 160 μl of 0.2 *N* NaOH. After mixing, the absorbance increase at 240 nm was continuously recorded. The concentration of alprazolam in the final reaction mixture was the same as in the first case; however, the methanol concentration was only ~1.0% (v/v). The final ionic strength was no longer 0.01 *M*; it was calculated to be ~0.02 *M*. A separate series of experiments established that a methanol concentration of ≤5% (v/v) did not influence the observed rate constant within experimental error.

In both of the described procedures, the pH determined at the end of the reaction was considered to be the pH maintained during the reaction. The observed rate constant (k_{obs}) was calculated in a conventional manner, *i.e.*, from the slope of the plot of $\log(A_\infty - A_t)$ *versus* time, where A_t is absorbance at a given time t and A_∞ is that at equilibrium. In general, excellent first-order kinetics were observed over three half-lives. Under extremely acidic pH, however, a small but significant deviation from linearity was observed after the reaction was more than 75% completed.

Kinetics of Irreversible Cyclization Reaction—At pH 2.41, 2.75, and 3.35 the rate of cyclization of the opened-ring compound to alprazolam was measured by providing a sink condition for the product. Approximately 0.7 ml of an alprazolam stock solution in methanol (~1.38 mg/ml) was added to 50 ml of a given buffer solution which had been placed in a jacketed beaker at 25°. The absorbance change at 260 nm was followed immediately by circulating the reaction mixture through a 1.0-cm flow-through cell at a flow of ~18 ml/min. After the equilibrium was established and k_{obs} was obtained, 50 ml of chloroform previously saturated with the buffer solution and kept at 25° was gently added. The binary mixture was vigorously stirred with a magnetic stirrer while the aqueous upper layer was being continuously circulated through the spectrophotometer.

Every 5–10 min, 20 ml of the chloroform layer was replaced with fresh chloroform to make sure that a perfect sink condition for alprazolam was maintained. The decrease in UV absorption 260 nm from the aqueous layer was recorded continuously down to zero. To be sure that under the hydrodynamic conditions adoped the observed rate did not merely represent the transport rate across the interface, the following test was made at the end of a kinetic run. The pH of the aqueous layer remaining on top of chloroform was readjusted to 8.0–8.5 by adding a concentrated solution of tromethamine. To this, ~0.7 ml of the alprazolam stock solution in methanol was introduced and the disappearance was monitored. Throughout this operation, the hydrodynamics remained the same as previously. The experimental setup and a typical absorbance tracing are shown in Fig. 1.

Determination of pK_a—The pK_a of the primary amino function present in the opened-ring compound was determined from a rapidly obtained titration curve. An accurately known amount of alprazolam between 50 and 100 mg was dissolved in 2.50 ml of methanol. To this, 15

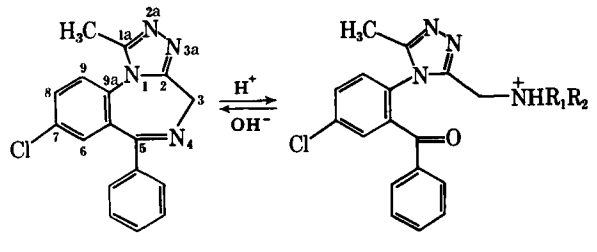

A *B*: $R_1 = R_2 = H$
C: $R_1 = CH_3$ and $R_2 = H$
D: $R_1 = R_2 = CH_3$

Scheme I

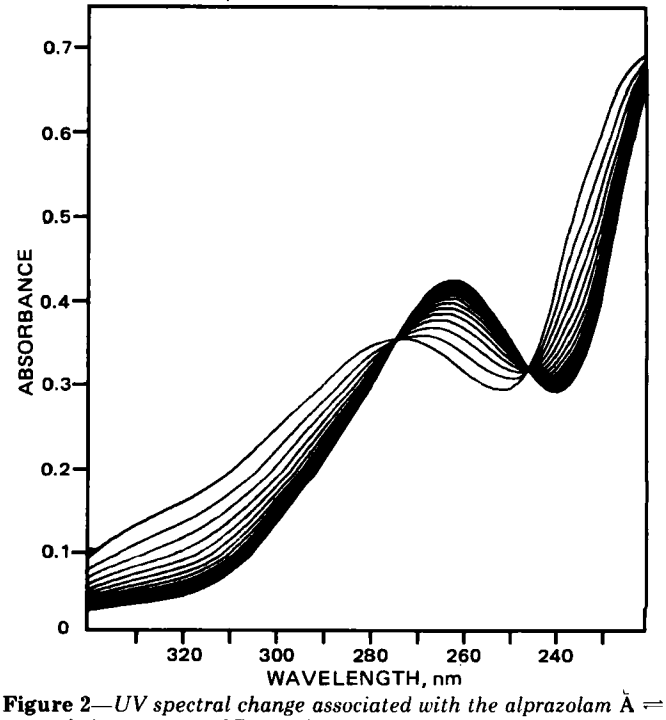

Figure 2—*UV spectral change associated with the alprazolam* A ⇌ *opened-ring-compound* B *reaction at pH 1.17 and room temperature;* A + B = 4.02×10^{-5} M; *methanol, 10% (v/v); and repetitive scanning speed, 300 nm/min.*

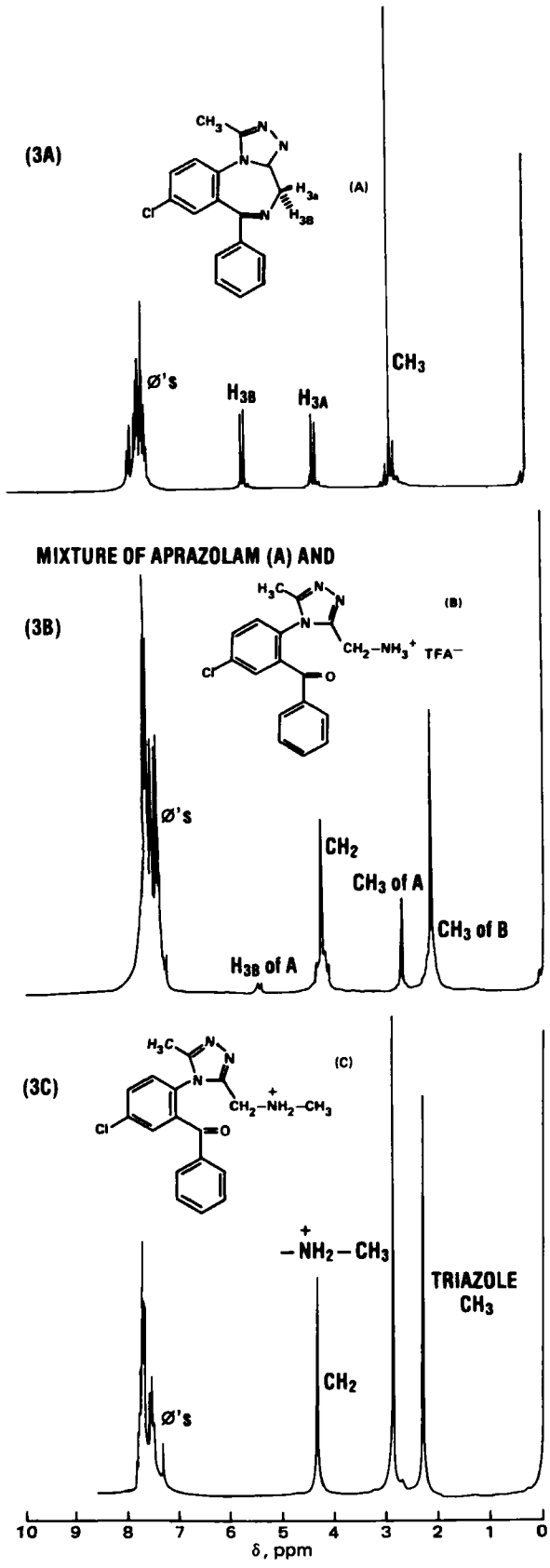

Figure 3—^1H-*NMR spectrum of alprazolam in deuterochloroform, A; a mixture in* $CDCl_3$ *of alprazolam and compound* B *(~1:3) which was formed* in situ *upon addition of trifluoroacetic acid and deuterated water, B; and compound* C *in* $CDCl_3$ *containing* TFA *and* D_2O, *C. In samples B and C, the amounts of* TFA *and* D_2O *added were 2.0 meq of alprazolam or compound* C *and 50 μl, respectively. Spectra were all obtained from a sample size in the range of 250 mg.*

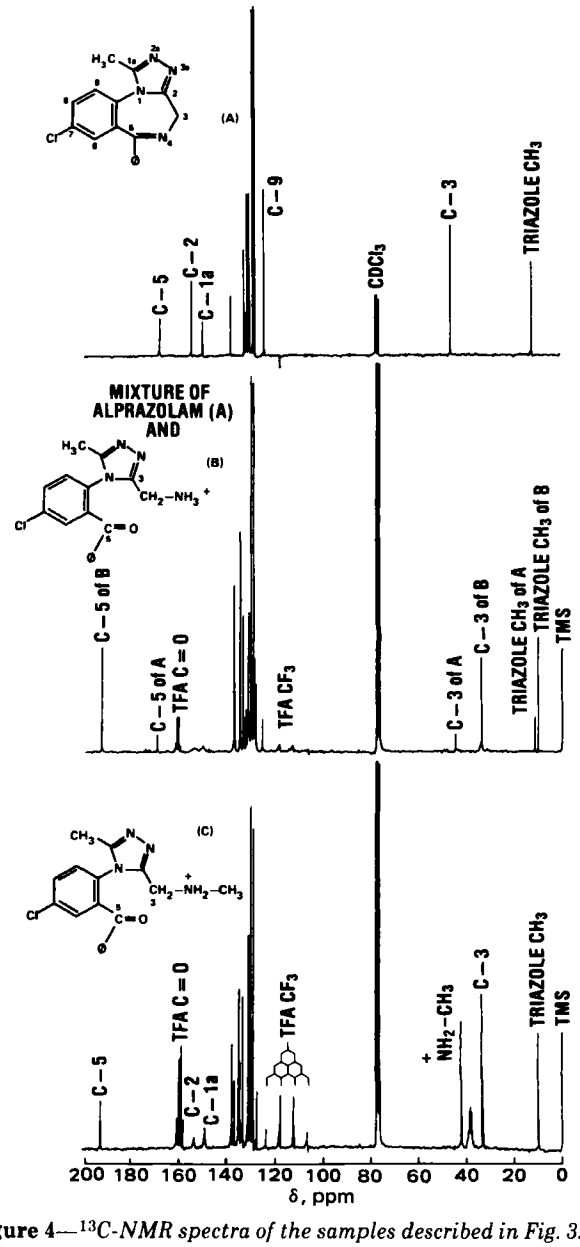

Figure 4—^{13}C-*NMR spectra of the samples described in Fig. 3.*

ml of water and 3.0 ml of 0.1 *N* HCl were added. The solution was left for at least 30 min, and the pH was accurately measured (2.0–2.5). Immediately after adding 3.0 ml of 0.1 *N* NaOH, the solution was rapidly titrated with 0.1 *N* HCl. The starting pH was ~8.5. The titration was repeated three times, and it took <4 min on the average to complete the titration. The pH observed at half of the titration end point was taken as the pKa of the primary amino group of the benzophenone compound. Since less than 2.0 ml of the titrant was consumed at the titration end point, the concentration of alprazolam and methanol near the pKa was on the order of 0.01 *M* and 10% (v/v), respectively. Although the system contained as much as 10% methanol, precipitation was observed at ~5–10 min after completion of titration (pH ~2.75), but not during the titration.

An attempt was made to measure the pKa of protonated alprazolam (the reactive species) from the pH-dependence of the initial absorbance at a given wavelength immediately after acidification of a series of alprazolam solutions at a given concentration. The experimental procedure was essentially the same as the procedure in which k_{obs} was measured. Into a 1.0-cm UV cell containing 3.0 ml of a given buffer, 100 μl of an alprazolam stock solution in methanol (0.719 mg/ml) was rapidly introduced through a 250-μl Hamilton syringe. Absorbance at 310 nm was monitored immediately and the initial absorbance value was estimated from extrapolation to the time of mixing. At a certain pH, the ring-opening reaction occurred quite rapidly (*i.e.*, $t_{1/2} \simeq 2$ min at pH 1.5). In such a case, the absorbance at the moment of mixing was estimated from the first-order kinetic plot by extrapolation to $t = 0$.

The conventional UV spectrophotometric pK_a determination (23) was carried out by scanning a series of alprazolam solutions at a given concentration (6.13×10^{-5} *M*) after the solutions were left at room temperatures for at least 30 min. The methanol concentration in these solutions was 5.0% (v/v). Each UV scan was made against the corresponding buffer as a reference.

RESULTS AND DISCUSSION

System Characterization—At an early stage of drug development, it was found that alprazolam undergoes the reversible reaction shown in Scheme I; the opened-ring compound *B* was favored in an acidic solution and alprazolam was favored in a neutral or alkaline solution. The identity of the reaction was established by means of IR, UV, and ^{1}H- and ^{13}C-NMR spectroscopy.

The solid product obtained immediately after neutralizing an acidic solution of alprazolam contained two compounds: alprazolam and a compound with an IR spectrum closely resembling that of compound *C* (benzophenone C=O absorption band at 1665 cm^{-1}). Attempts to isolate this second component in free form were not successful. Exhaustive crystallization only produced alprazolam. A similar difficulty in obtaining the opened-ring compound was reported previously for a related 1,4-benzodiazepine system (10).

On the other hand, when an alprazolam solution was acidified, the UV spectrum changed continuously and rapidly with two isosbestic points at 246 and 274 nm (Fig. 2). At pH ~1.0, the equilibrium UV spectrum (λ_{max} 262 nm and λ_{min} 239 nm) was found to be virtually identical to that of compound *C* or *D* (λ_{max} 263 nm and λ_{min} 238 nm; ϵ_{263} 1.01×10^4 and ϵ_{238} 5.80×10^3). Compounds *C* and *D* do not cyclize to form a 1,4-benzodiazapine ring. Similarly, when an acidic solution of alprazolam was neutralized with a concentrated sodium hydroxide solution, the UV spectrum slowly changed back to that of the neutral alprazolam species (λ_{max} 222 nm and λ_s 245 nm; ϵ_{222} 4.27×10^4 and ϵ_{245} 1.86×10^4).

In the ^{1}H-NMR spectrum, the nonequivalent protons at C-3 of alprazolam appeared at 5.4 and 4.10 ppm (Fig. 3A). These doublets merged into a singlet at 4.10 ppm when trifluoroacetic acid and deuterated water were added (Fig. 3B). In addition, the singlet at 2.60 ppm, which corresponds to the methyl group on the triazole moiety, underwent an upfield shift to 2.00 ppm. The resulting ^{1}H-NMR spectrum of the compound produced from alprazolam in the presence of trifluoroacetic acid and deuterated water closely resembled the ^{1}H-NMR spectrum of a model compound *C* obtained under identical conditions (s at 4.35 ppm for 2H and s at 2.32 ppm for 3H) (Fig. 3C).

Changes in the ^{13}C-NMR of alprazolam (Fig. 4A) that occurred upon addition of trifluoroacetic acid and deuterated water provided more direct evidence for the reaction shown in Scheme I. A downfield shift took place for C-5, from 168 to 192 ppm, supporting the presence of a benzophenone carbonyl carbon (Fig. 4B). The upfield shift of C-3 from 46 to 34 ppm was also in accordance with the ring-opening reaction. As expected, the signal corresponding to the methyl group on the triazole moiety changed very little with an upfield shift of ~1.5 ppm.

Finally, the overall ^{13}C-NMR spectrum of the reaction product was nearly identical to that of compound *C* (Fig. 4C), with the benzophenone carbonyl at 193 ppm, C-3 at 34 ppm, and the triazole methyl at 10 ppm. This is consistent only if the reaction product has the same benzophenone-type structure as compound *C*.

The reaction that alprazolam undergoes in an aqueous acidic solution can be further characterized based on the aforementioned spectroscopic data. IR and NMR (particularly ^{13}C-NMR) data positively identify the reaction as that in Scheme I. The product *B* is favored under acidic conditions and *A* under neutral or alkaline conditions. The reaction is similar to the ring-opening reaction of other 1,4-benzodiazepines (10–21).

The presence of isosbestic points in the UV spectral change supports the conclusion that there were no significant side reactions, during the attainment of equilibrium. Under a strongly acidic condition (pH < 0.5), however, the isosbestic points were found to drift. The nature of this slow side reaction has not been established.

The UV spectrum of alprazolam cation ($\lambda_{max} \simeq 274$ nm; Fig. 2), which rapidly changes as the ring-opening reaction takes place, is different from that of neutral alprazolam (λ_{max} 222 nm and λ_s 245 nm).

Cyclization Kinetics—The UV spectrum of alprazolam changed very little when a neutral solution was acidified to pH 5 or above, indicating that alprazolam is the predominant species at a neutral or an alkaline pH. The spectral change that occurred when an acidic solution was neutralized to pH >6 reflected the cyclization reaction exclusively. On the other hand, the rate of UV spectral change on acidification of an alprazolam solution to a pH <5 reflected the rate of both the ring-opening and the cyclization reactions. To separately determine the cyclization rate for this pH range, a sink condition for the product (alprazolam) was provided by continuously replacing chloroform in the system. A critical assumption made here was that only alprazolam partitions into the chloroform layer in a quantitative manner. This assumption appears to have been warranted by the pK_a of the primary amino function of the ring-opened compound in the range of 7.0 (see below); the benzophenone compound should exist exclusively as a cation over the pH range of the determination. Alprazolam is extremely insoluble in water (~0.1 mg/ml at 37°) but freely soluble in chloroform, and the pK_a of monocation is 2.4.

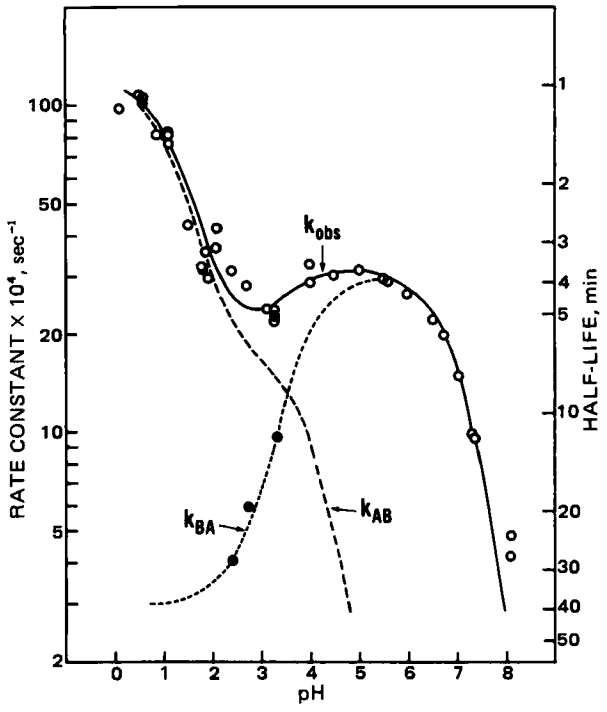

Figure 5—*pH Dependence of the overall alprazolam ring-opening and cyclization reaction rate constant (k_{obs}), ring-opening reaction rate constant (k_{AB}; dashed line), and cyclization rate constant (k_{BA}; dotted line up to pH 5.5 and descending solid line thereafter); all at 25°. The rates were also expressed in terms of half-life (right-hand side coordinate). Closed circles represent k_{BA} determined from an irreversible* B → A *reaction condition.*

The three data points (Fig. 5) obtained from the described biphasic system together with the data points at pH values >5.5 resulted in a bell-shape pH-profile of the cyclization rate constant (Fig. 5). The cyclization reaction is analogous to a Schiff-base formation reaction, the kinetics of which have been thoroughly studied (24). The bell-shape pH-profile arises from a change in the rate-determining step with the pH change. Under acidic conditions, formation of the carbinolamine intermediate (*I* in Scheme II) is rate-controlling, since the concentration of kinetically reactive —NH_2 is extremely low and the dehydration of *I* is facilitated by protonation of the —OH group to form an excellent leaving group, H_2O. However, as the pH increases, approaching the pK_a of the primary amino group, the nucleophilic attack of the —NH_2 group on the benzophenone carbonyl group becomes faster than the dehydration of the carbinolamine intermediate *I*.

Closely following the kinetic treatment developed by Jenck (24), the following expression for the overall cyclization rate constant as a function of $[H^+]$ was derived:

$$k_{BA} = \frac{k_3[H^+](k_1 + k_2[H^+])}{k_{-1} + k_{-2}[H^+] + k_3[H^+] + k_3[H^+]} \times \frac{K_a^{BH}}{K_a^{BH} + [H^+]} \quad \text{(Eq. 1)}$$

Definitions of K_a^{BH} and several microscopic rate constants in Eq. 1 are shown in Scheme II. In this treatment, the dicationic species BH_2^{2+} does not need to be differentiated from the monocationic species BH^+ and that each of the rate constants can represent a kinetically equivalent reaction pathway; *e.g.*, the specific acid-catalyzed —NH_2 attack ($k_2[H^+]$ process) is equivalent to H_2O catalyzed *I* formation from BH^+.

Crude approximates of the rate constants were first obtained as described previously (24). These, together with the experimentally deter-

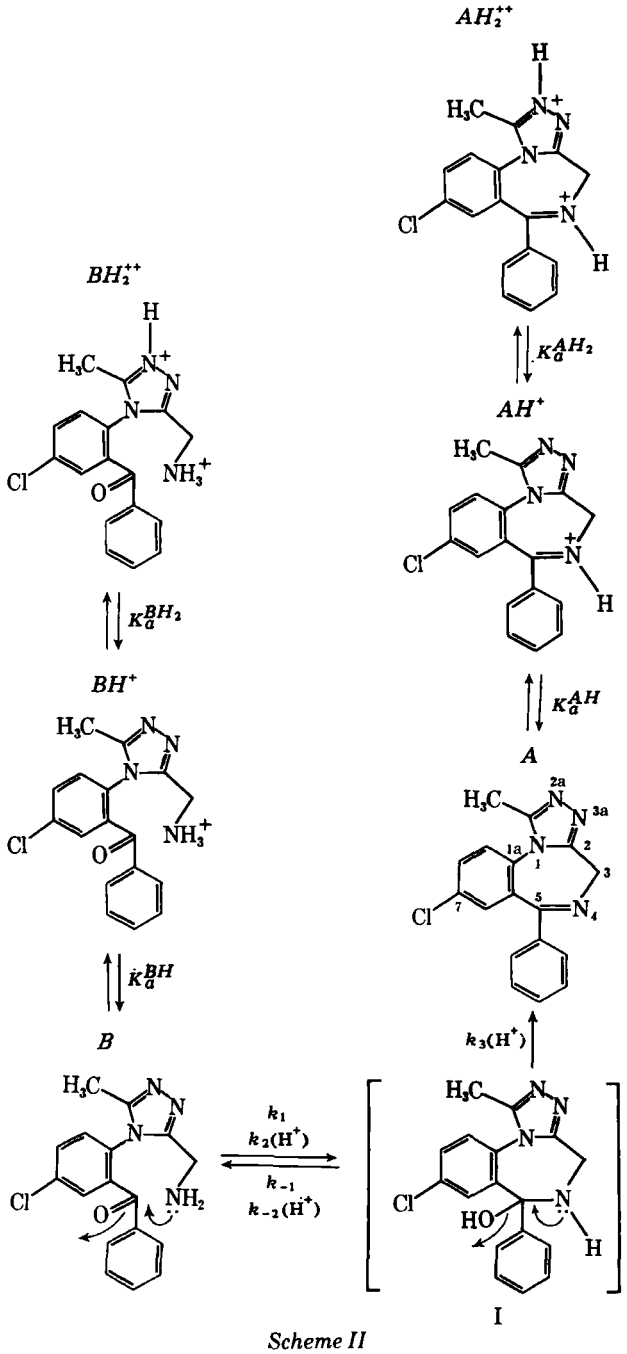

Scheme II

mined K_a^{BH} value, served as the first approximates in the final curve fitting by means of the SIMPLEX least-square computer program. Values for the individual microscopic rate constants and K_a^{BH} obtained using three data points at pH <3.4 and at 11 points at pH >5 are listed in Table I. The reliability of these values can be exemplified as follows: the experimentally determined pK_a^{BH} in the presence of 10% (v/v) methanol was 6.78 ± 0.02 (n = 3), whereas that from the numerical analysis of the pH profile was 7.02 with a range of 6.77–7.29 at a 95% confidence level. The bell-shaped curve, the dotted line up to pH 5.5 and the descending solid line thereafter (Fig. 5), was generated with the constants listed in Table I and Eq. 1. The positive deviation from a slope of +1 that one may expect on the log k_{BA}–pH profile when pH decreases from 3.5 was attributed to the steady increase in concentration of the protonated benzophenone carbonyl group, which should be extremely reactive toward the nucleophilic attack of —NH_2. This reaction pathway was implicitly included in the mathematical expression for k_{BA} (24).

Sites of Protonation on Alprazolam—Alprazolam contains four potentially basic nitrogens. It was challenging to determine the basicity ranking in an aqueous solution. In nonaqueous systems, three important pieces of evidence support that N-2*a* on the triazole ring is most basic:

Table I—Rate and Equilibrium Constants Associated with the *A* ⇌ *B* Reaction at 25°

Constants	Lower Limit[a]	Upper Limit[a]
$k_1 = 7.32\ sec^{-1}$	—	—
$k_2 = 4.26 \times 10^3\ sec^{-1}\ M^{-1}$	—	—
$k_{-1}/k_3 = 2.27 \times 10^{-4}\ M$	—	—
$k_2/k_3 = 0.343$	—	—
$K_a^{BH} = 9.51 \times 10^{-8}\ M (pK_a^{BH} = 7.02)$	5.13×10^{-8}	1.71×10^{-7}
$K_a^{BH} = 1.66 \times 10^{-7}\ M (pK_a^{BH} = 6.78)$[b]	—	—
$k_4 \cdot K \cdot K_a^{AH2}/K_a^{IH2} = 1.15 \times 10^{-2}\ sec^{-1}$	1.02×10^{-2}	1.30×10^{-2}
$k_4 \cdot K \cdot K_a^{AH2} = 9.02 \times 10^{-5}\ sec^{-1}\ M^{-1}$	2.67×10^{-5}	2.94×10^{-4}
$K_a^{IH2} = 7.84 \times 10^{-3}\ M (pK_a^{IH2} = 2.11)$	—	—
$K_a^{AH2} = 5.62 \times 10^{-2}\ M (pK_a^{AH2} = 1.25)$	3.16×10^{-2}	1.08×10^{-1}
$K_a^{AH} \cdot K_a^{AH2} = 3.95 \times 10^{-6}\ M^2$[c]	4.89×10^{-8}	4.27×10^{-5}
$K_a^{AH} = 7.03 \times 10^{-5}\ M (pK_a^{AH} = 4.15)$	—	—
$K_a^{AH} = 3.98 \times 10^{-3}\ M (pK_a^{AH} = 2.40)$[b]	—	—
$K_a^{BH2} = 3.16 \times 10^{-2}\ M (pK_a^{BH2} = 1.50)$[d]	—	—

[a] At a 95% confidence level. [b] Experimental data. [c] Not reliable (see the wide range of variation). [d] Estimated from the pKa of compound *C*.

(*a*), X-ray crystallographic study on the hydrogen bromide salt which was prepared from a nonaqueous system, indicated that a proton resides on N-2*a* (25); (*b*), ^{15}N-NMR spectrum of alprazolam in deuterated chloroform showed that N-2*a* undergoes a more profound upfield shift than any other nitrogen when trifluoroacetic acid is successively added to the system (26); and (*c*) in many chemical manipulations, N-2*a* proved to be the most nucleophilic and very likely the most basic; *e.g.*, simple alkylation preferably takes place at N-2*a* (27).

When the basicity of N-2*a* is compared with that of N-3*a*, the facts listed are in accordance with what is expected from the consideration of electronic effects; N-3*a* is linked with C(2)—CH_2(3)—N(4), whereas N-2a is linked with C(1*a*)—CH_3. The aniline N-1 should exert an identical electronic effect on both nitrogens. Thus, the electron-withdrawing effect of the aromatic azomethine bond, C(5)=N(4), should make the protonation at N-3*a* more difficult than at N-2*a*. On the other hand, N-1 is believed to be less basic than N-4 for reasons similar to that of medazepam (28). The latter is very similar to alprazolam structurally; instead of a triazole ring, a methyl group is attached to N-1. These two considerations leave either N-4 or N-2*a* to be the most basic center on the alprazolam molecule in aqueous solutions.

When alprazolam was methylated in methylene chloride at N-2*a* to form a quaternary ammonium compound, the UV spectrum hardly changed (27). Similarly, the UV spectrum of compound *C*, a compound containing a triazole ring but not a 1,4-diazepine ring, underwent a very small bathochromic shift of 4–5 nm when the pH of the sample solution was systematically changed from 4.0 to 0.3. Thus, it was apparent that protonation or methylation at N-2*a* is associated with little UV spectral change. This is perhaps because the lone-pair electrons on N-2*a* are not engaged in the aromaticity of 1,2,4-triazole. Although the opened-ring compound *C* underwent a very small bathochromic shift when dissolved in acidic solutions, it was possible to estimate the pK_a from the pH dependence of the absorbance at 280 nm. The pK_a of N-2*a* was found to be 1.5 or less.

The UV spectrum obtained immediately after acidifying an alprazolam solution to a pH below 0.5 shows an absorption maximum at 280 nm (Fig. 2). Appearance of this peak, which disappears again as the ring-opening reaction proceeds, amounts to a bathochromic shift of as much as 35 nm of the shoulder peak of alprazolam at 245 nm. The absorbance of this transient UV spectrum at a given wavelength was extrapolated to the time of acidification, and its dependence on the pH to which the alprazolam solution was acidified yielded an apparent pK_a of 2.40 (Fig. 6). This pK_a should correspond to that of N-4, and the large bathochromic shift observed reflects the resonance interaction of the positive charge with adjacent benzene rings.

The conclusion that N-4 should be more basic than N-2*a* in aqueous solutions is in contrast to many experimental evidences that N-2*a* is most basic in various nonaqueous environments. One possible explanation is based on the difference in steric hindrance that each nitrogen is subject to. In aqueous solutions, the proton donor is the relatively small hydronium ion. In nonaqueous systems in which N-2*a* was found to be more basic than N-4, the proton or alkyl group donors were all bulky: hydrogen bromide, trifluoroacetic acid, or trimethyloxonium fluoroborate (25–27). X-ray crystallographic data (25) indicate that N-1 and N-4 are subject to a higher degree of steric hindrance than the other two triazole nitrogens, making them less accessible to bulky proton donors. In this context

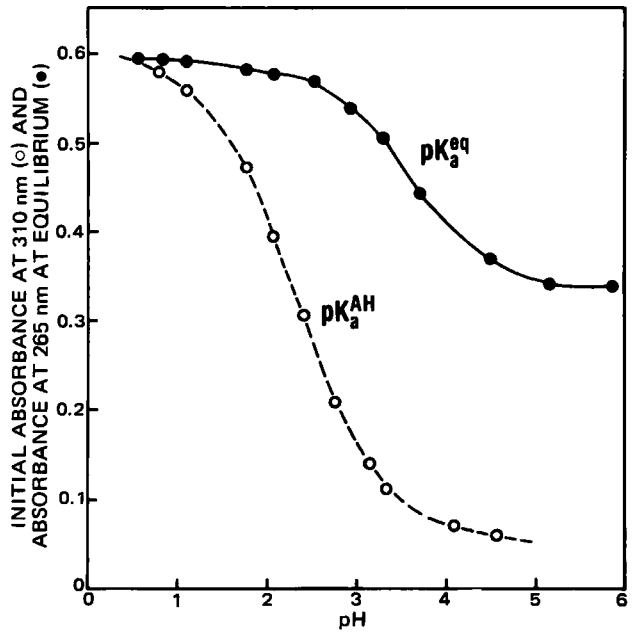

Figure 6—*Spectrophotometric determination of pK_a of monocationic alprazolam (pK_a^{AH}) and apparent equilibrium pK_a.*

it should be noted that the ^{15}N-NMR upfield shift associated with protonation of nitrogens in alprazolam with trifluoacetic acid was ordered N-2*a* > N-3*a* > N-4 > N-1 (26). It is not uncommon that the usual basicity order for a series of compounds can be completely inverted when bulky proton donors are used in the protonation (29).

Kinetics of Alprazolam Ring-Opening Reaction—The pH profiles of the ring-opening rate constant (k_{AB}) was obtained by subtracting k_{BA} from the spectrophotometrically determined overall rate constant (k_{obs}). That is, the value of k_{AB} was calculated at each pH where k_{obs} was measured in such a way that the sum of k_{BA} and k_{AB} best accommodated a total of 35 experimental data points of k_{obs}. In this manipulation, the pH dependence of k_{BA} was dictated by Eq. 2.

In deriving a mathematical expression for k_{AB} in terms of hydronium ion concentration, it was first assumed that the carbinolamine intermediate (IH^+) formation is much faster than the subsequent abstraction of a proton to form the benzophenone compound (BH^+; Scheme III) over the entire pH range studied. This is in accordance with the principle of microscopic reversibility applied to the cyclization reaction discussed earlier; however, it will create some error especially at a pH >4. The concentration of IH^+ can then be simply represented by an equilibrium constant, $K' = (I_T)/(A_T)$, and $d(B_T)/dt = k_4(I_T)$ by definition of k_4. Note that the only base which abstracts a proton from IH^+ is H_2O and, therefore, this step should be pH independent. In other words, the observed pH dependence of k_{AB} arises from the pH dependence of the apparent equilibrium constant K' in the kinetic scheme, and the equillibrium concentration of the intermediate at a given pH is ultimately governed by the reactivity of different ionic species of alprazolam present at that particular pH. This analysis simplifies the kinetic scheme tremendously, and the following expression for k_{AB} was derived, in which $K = (IH^+)/(AH^+)$, a pH independent equilibrium constant. Other constants included in the expression are all self-explanatory from Scheme III:

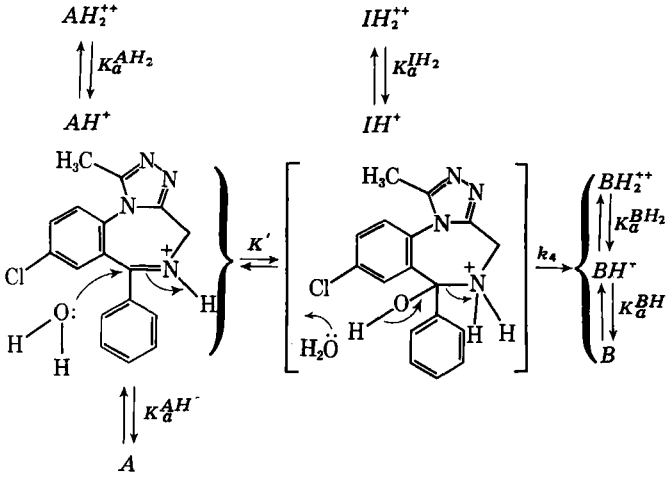

Scheme III

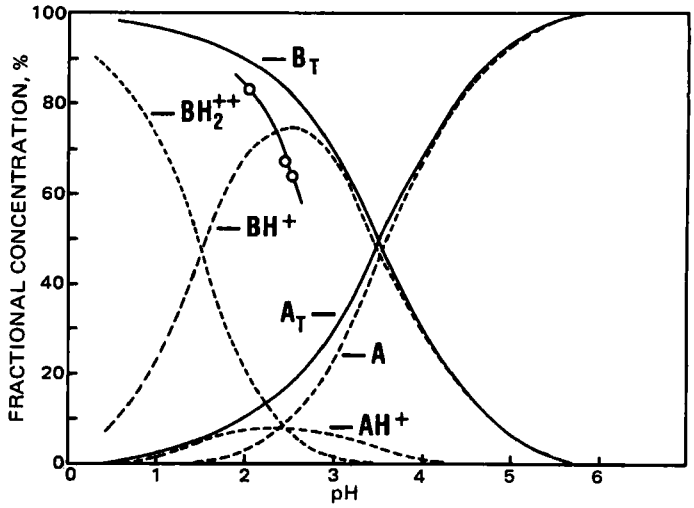

Figure 7—*Fractional concentration of various ionic species involved in the A ⇌ B reaction as a function of pH. Open circles represent the total concentration of the opened-ring compound determined by a rapid back-titration technique.*

$$k_{AB} = \frac{k_4K(K_a^{A2H}/K_a^{I2H})[H^+]^2 + k_4KK_a^{A2H}[H^+]}{[H^+]^2 + K_a^{A2H}[H^+] + K_a^{AH}K_a^{A2H}} \quad \text{(Eq. 2)}$$

Various constants present in the equation for k_{AB} were obtained from the SIMPLEX least-squares program and are listed in Table I. The dashed line on Fig. 5 was generated from these values and Eq. 2.

The presence of an inflection point on the pH profile of k_{AB} implies that the AH_2^{2+} is somewhat more reactive than AH^+. Protonation on the triazole moiety would exert an electron-withdrawing inductive effect to make the C(5)=N(4) bond more susceptible to a nucleophilic attack at C-5. However, the position of the inflection point which will determine the kinetically measurable pKa of alprazolam is subject to a significant error in the present study in that the pH-profile of k_{AB} was obtained second hand. It was not surprising that the kinetically obtained pK_a^{AH} (4.15) is very different from that obtained experimentally (2.40). The pK_a of dicationic alprazolam ($pK_a^{A2H} \simeq 1.25$) is in a fair agreement with the pK_a of compound *C* (~1.5 or below).

Over the pH range where the ring-opening reaction takes place to significant extent, the rate-determining step is largely the breakdown of intermediate IH^+, and it was not possible to isolate the reactivity of the N(4)=C(5) bond toward the H_2O attack. This is believed to be the case for other 1,4-benzodiazepines; however, the pH-dependence of K' itself should result in some interesting structure–reactivity relationships among them.

Multiple Equilibria—In the context of the present discussion, the term "equilibrium" is defined as a state of the $A \rightleftharpoons B$ system after 5–10 reaction half-lives. This restricted definition is particularly important for strongly acidic aqueous solutions in which alprazolam and/or compound *B* undergoes another slow reaction which is yet to be identified.

Equilibrium UV spectra of alprazolam at different pH values tend to produce an isosbestic point at 254 nm for pH 0.5–6.0. This finding implies that there are only two predominant species in terms of UV absorption and the apparent equilibrium concentration of these two species is identical at pH 3.50 (*i.e.*, equilibrium $pK_a = 3.50$, Fig. 6). From the values of k_{AB} and k_{BA}, the pH dependence of the apparent equilibrium of $A \rightleftharpoons B$ can also be estimated (Fig. 7). These kinetically determined equilibrium constants also showed that at pH 3.50 the total concentration of *A* is equal to that of *B*.

Fractional concentrations of different ionic species of alprazolam and the opened-ring compound are then determined by the pK_a of the species involved. Since pK_a^{BH} (6.80, determined from the rapidly obtained titration curve) is much greater than 3.5, one can safely rule out the neutral species of the opened-ring compound as an important species at any pH. Similarly, dicationic alprazolam is also not included in the present analysis. The pK_a of dicationic opened-ring compound (pK_a^{BH2}) was

assumed to be 1.5, the pK_a of compound *C*. On the other hand, the pK_a of protonated alprazolam was determined from the initial absorbance at 310 nm after a methanolic solution was diluted to a given pH (Fig. 6); the pK_a^{AH} was 2.40. Note that at 310 nm the opened-ring compound or its analogue *C* absorbed very little UV energy (Fig. 2) and the pH dependence shown on Fig. 6 should reflect the protonation at N-4. From the values of equilibrium pK_a, pK_a^{AH}, and pK_a^{BH2}, the fractional concentration of important ionic species involved in the $A \rightleftharpoons B$ equilibrium was calculated (Fig. 7).

The concentration of the opened-ring compound was also estimated experimentally. An alprazolam solution in methanol was first acidified with HCl and left to attain equilibrium. The mixture was then neutralized with an equivalent amount of hydroxide ion and immediately back-titrated. The titration end point should represent the amount of the opened-ring compound which was generated from the acid treatment. A critical assumption was that during the neutralization and the titration no significant $A \rightleftharpoons B$ reaction occurred. Since the titration end point occurs at a pH betweeen 4 and 6, alprazolam was never protonated in the titration. Three determinations of the total opened-ring compound by this rapid titration technique are shown on Fig. 7 (open circles). Since the titration system contained as much as 10% (v/v) methanol, the total concentration of the opened-ring compound recovered at a given pH was expected to be much lower than in the absence of methanol. In this particular instance, not only should the activity of water have been lower but the pK_a^{AH} was also expected to decrease significantly to result in a displacement of pH profile for the fractional concentration of opened-ring compound toward lower pH.

REFERENCES

(1) M. L. Bender, *Chem. Rev.*, **60**, 53 (1960).

(2) W. P. Jencks, *Prog. Phys. Org. Chem.*, **2**, 63 (1964).

(3) S. Johnson, *Adv. Phys. Org. Chem.*, **5**, 237 (1964).

(4) R. B. Martin, *J. Phys. Chem.*, **68**, 1369 (1964).

(5) T. C. Bruice and S. Benkovic, "Bioorganic Mechanisms," vol. 1, Benjamin, New York, N.Y., 1966, pp. 27–118.

(6) E. G. Sander and W. P. Jencks, *J. Am. Chem. Soc.*, **90**, 6154 (1968).

(7) J. Hine and R. W. Redding, *J. Org. Chem.*, **35**, 2769 (1970).

(8) M. J. Cho and I. H. Pitman, *J. Am. Chem. Soc.*, **96**, 1843 (1974).

(9) D. D. Perrin, *Adv. Heterocycl. Chem.*, **4**, 43 (1965).

(10) L. H. Sternbach, E. Reeder, and G. A. Archer, *J. Org. Chem.*, **28**, 2456 (1963).

(11) J. T. Carstensen, K. S. E. Su, P. Maddrell, J. B. Johnson, and H. N. Newark, *Bull. Parenter. Drug Assoc.*, **25**, 193 (1971).

(12) W. Mayer, S. Erbe, and R. Voight, *Pharmazie*, **27**, 32 (1972).

(13) W. Mayer, S. Erbe, G. Wolf, and R. Voight, *ibid.*, **29**, 700 (1974).

(14) H. V. Maulding, J. P. Nazareno, J. E. Pearseen, and A. F. Michaelis, *J. Pharm. Sci.*, **64**, 278 (1975).

(15) W. W. Han, G. J. Yakatan, and D. D. Maness, *ibid.*, **65**, 1198 (1976).

(16) *Idem.*, **66**, 573 (1977).

(17) *Idem.*, **66**, 795 (1977).

(18) C. H. Hassall, S. W. Holmes, W. H. Johnson, A. Krohn, C. E. Smithen, and W. A. Thomas, *Experientia*, **33**, 1492 (1977).

(19) M. Nakano, N. Inotsume, N. Kohri, and T. Arita, *Int. J. Pharm.*, **3**, 195 (1979).

(20) N. Inotsume and M. Nakano, *J. Pharm. Sci.*, **69**, 1331 (1980).

(21) N. Inotsume and M. Nakano, *Chem. Pharm. Bull.*, **28**, 2536 (1980).

(22) D. D. Perrin, *Aust. J. Chem.*, **16**, 572 (1963).

(23) A. Albert and E. P. Serjeant, "Ionization Constants," Wiley, New York, N.Y., 1962.

(24) W. P. Jencks, "Catalysis in Chemistry and Enzymology," McGraw-Hill, New York, N.Y., 1969, pp. 463–477.

(25) J. B. Hester, Jr., D. J. Duchamp, and C. G. Chidester, *Tetrahedron Lett.*, **1971**, 1609.

(26) T. A. Scahill, Ph.D. thesis, University of Kentucky, 1981.

(27) J. B. Hester, Jr., C. G. Chidester, and J. Szmuszkovicz, *J. Org. Chem.*, **44**, 2688 (1979).

(28) J. Barrett, W. F. Smyth, and I. E. Davidson, *J. Pharm. Pharmacol.*, **25**, 387 (1973).

(29) J. March, "Advanced Organic Chemistry: Reactions, Mechanisms, and Structure," McGraw-Hill, New York, N.Y., 1968, pp. 228–230, and references cited therein.

ACKNOWLEDGMENTS

A part of the text was presented at the Higuchi Symposium, Orlando, Fla., November 1981.

M. J. Cho thanks Dr. B. D. Anderson and Dr. W. C. Krueger for helpful discussions.

Factorial Designs in Pharmaceutical Stability Studies

SANFORD BOLTON

Received October 26, 1981, from the *College of Pharmacy and Allied Health Sciences, St. John's University, Jamaica, NY 11439.* Accepted for publication May 27, 1982.

ABSTRACT □ An approach to analyzing and interpreting kinetic data from stability studies using factorial designs is presented. This may be useful for screening purposes or as an aid in identifying significant effects in complex systems. A typical 2^n factorial experiment is discussed, and methods of variance estimation and statistical testing are presented. An example of simulated data is used to demonstrate how typical results may be analyzed, as well as the potential and limitations of this design in interpretation and construction of kinetic models.

Keyphrases □ Factorial designs—in pharmaceutical stability studies, kinetic models, statistical analysis □ Stability studies, pharmaceutical—factorial designs, kinetic models, statistical analysis

Factorial designs are extremely useful in a wide variety of experimental situations, and applications of these designs to pharmaceutical problems have appeared in the recent literature (1–3). Factorial designs applied to stability studies of pharmaceuticals can be used for screening purposes or to help interpret complex systems. This paper deals with an approach to the design and statistical analysis of such experiments.

BACKGROUND

A factorial experiment considers the effects of various *factors* (*e.g.*, temperature, pH, drug concentration, buffer concentration) at several *levels* (*e.g.*, 2 pHs, one high pH and one low pH) where results of all combinations of the factor levels are observed. Modifications of the complete factorial design may be used in situations where it is not convenient or possible to do all of the combinations or trials (4). For this presentation, only experiments with all factors at two levels, a 2^n factorial design (where n is the number of factors, the effects of which are to be investigated), will be considered. The *main effect* is the difference in response (*e.g.*, rate constant) caused by the change in level of a factor (pH,

0022-3549/83/0400-0362$01.00/0

assumed to be 1.5, the pK_a of compound *C*. On the other hand, the pK_a of protonated alprazolam was determined from the initial absorbance at 310 nm after a methanolic solution was diluted to a given pH (Fig. 6); the pK_a^{AH} was 2.40. Note that at 310 nm the opened-ring compound or its analogue *C* absorbed very little UV energy (Fig. 2) and the pH dependence shown on Fig. 6 should reflect the protonation at N-4. From the values of equilibrium pK_a, pK_a^{AH}, and pK_a^{BH2}, the fractional concentration of important ionic species involved in the $A \rightleftharpoons B$ equilibrium was calculated (Fig. 7).

The concentration of the opened-ring compound was also estimated experimentally. An alprazolam solution in methanol was first acidified with HCl and left to attain equilibrium. The mixture was then neutralized with an equivalent amount of hydroxide ion and immediately back-titrated. The titration end point should represent the amount of the opened-ring compound which was generated from the acid treatment. A critical assumption was that during the neutralization and the titration no significant $A \rightleftharpoons B$ reaction occurred. Since the titration end point occurs at a pH betweeen 4 and 6, alprazolam was never protonated in the titration. Three determinations of the total opened-ring compound by this rapid titration technique are shown on Fig. 7 (open circles). Since the titration system contained as much as 10% (v/v) methanol, the total concentration of the opened-ring compound recovered at a given pH was expected to be much lower than in the absence of methanol. In this particular instance, not only should the activity of water have been lower but the pK_a^{AH} was also expected to decrease significantly to result in a displacement of pH profile for the fractional concentration of opened-ring compound toward lower pH.

REFERENCES

(1) M. L. Bender, *Chem. Rev.*, **60**, 53 (1960).

(2) W. P. Jencks, *Prog. Phys. Org. Chem.*, **2**, 63 (1964).

(3) S. Johnson, *Adv. Phys. Org. Chem.*, **5**, 237 (1964).

(4) R. B. Martin, *J. Phys. Chem.*, **68**, 1369 (1964).

(5) T. C. Bruice and S. Benkovic, "Bioorganic Mechanisms," vol. 1, Benjamin, New York, N.Y., 1966, pp. 27–118.

(6) E. G. Sander and W. P. Jencks, *J. Am. Chem. Soc.*, **90**, 6154 (1968).

(7) J. Hine and R. W. Redding, *J. Org. Chem.*, **35**, 2769 (1970).

(8) M. J. Cho and I. H. Pitman, *J. Am. Chem. Soc.*, **96**, 1843 (1974).

(9) D. D. Perrin, *Adv. Heterocycl. Chem.*, **4**, 43 (1965).

(10) L. H. Sternbach, E. Reeder, and G. A. Archer, *J. Org. Chem.*, **28**, 2456 (1963).

(11) J. T. Carstensen, K. S. E. Su, P. Maddrell, J. B. Johnson, and H. N. Newark, *Bull. Parenter. Drug Assoc.*, **25**, 193 (1971).

(12) W. Mayer, S. Erbe, and R. Voight, *Pharmazie*, **27**, 32 (1972).

(13) W. Mayer, S. Erbe, G. Wolf, and R. Voight, *ibid.*, **29**, 700 (1974).

(14) H. V. Maulding, J. P. Nazareno, J. E. Pearseen, and A. F. Michaelis, *J. Pharm. Sci.*, **64**, 278 (1975).

(15) W. W. Han, G. J. Yakatan, and D. D. Maness, *ibid.*, **65**, 1198 (1976).

(16) *Idem.*, **66**, 573 (1977).

(17) *Idem.*, **66**, 795 (1977).

(18) C. H. Hassall, S. W. Holmes, W. H. Johnson, A. Krohn, C. E. Smithen, and W. A. Thomas, *Experientia*, **33**, 1492 (1977).

(19) M. Nakano, N. Inotsume, N. Kohri, and T. Arita, *Int. J. Pharm.*, **3**, 195 (1979).

(20) N. Inotsume and M. Nakano, *J. Pharm. Sci.*, **69**, 1331 (1980).

(21) N. Inotsume and M. Nakano, *Chem. Pharm. Bull.*, **28**, 2536 (1980).

(22) D. D. Perrin, *Aust. J. Chem.*, **16**, 572 (1963).

(23) A. Albert and E. P. Serjeant, "Ionization Constants," Wiley, New York, N.Y., 1962.

(24) W. P. Jencks, "Catalysis in Chemistry and Enzymology," McGraw-Hill, New York, N.Y., 1969, pp. 463–477.

(25) J. B. Hester, Jr., D. J. Duchamp, and C. G. Chidester, *Tetrahedron Lett.*, **1971**, 1609.

(26) T. A. Scahill, Ph.D. thesis, University of Kentucky, 1981.

(27) J. B. Hester, Jr., C. G. Chidester, and J. Szmuszkovicz, *J. Org. Chem.*, **44**, 2688 (1979).

(28) J. Barrett, W. F. Smyth, and I. E. Davidson, *J. Pharm. Pharmacol.*, **25**, 387 (1973).

(29) J. March, "Advanced Organic Chemistry: Reactions, Mechanisms, and Structure," McGraw-Hill, New York, N.Y., 1968, pp. 228–230, and references cited therein.

ACKNOWLEDGMENTS

A part of the text was presented at the Higuchi Symposium, Orlando, Fla., November 1981.

M. J. Cho thanks Dr. B. D. Anderson and Dr. W. C. Krueger for helpful discussions.

Factorial Designs in Pharmaceutical Stability Studies

SANFORD BOLTON

Received October 26, 1981, from the *College of Pharmacy and Allied Health Sciences, St. John's University, Jamaica, NY 11439.* Accepted for publication May 27, 1982.

ABSTRACT □ An approach to analyzing and interpreting kinetic data from stability studies using factorial designs is presented. This may be useful for screening purposes or as an aid in identifying significant effects in complex systems. A typical 2^n factorial experiment is discussed, and methods of variance estimation and statistical testing are presented. An example of simulated data is used to demonstrate how typical results may be analyzed, as well as the potential and limitations of this design in interpretation and construction of kinetic models.

Keyphrases □ Factorial designs—in pharmaceutical stability studies, kinetic models, statistical analysis □ Stability studies, pharmaceutical—factorial designs, kinetic models, statistical analysis

Factorial designs are extremely useful in a wide variety of experimental situations, and applications of these designs to pharmaceutical problems have appeared in the recent literature (1–3). Factorial designs applied to stability studies of pharmaceuticals can be used for screening purposes or to help interpret complex systems. This paper deals with an approach to the design and statistical analysis of such experiments.

BACKGROUND

A factorial experiment considers the effects of various *factors* (*e.g.*, temperature, pH, drug concentration, buffer concentration) at several *levels* (*e.g.*, 2 pHs, one high pH and one low pH) where results of all combinations of the factor levels are observed. Modifications of the complete factorial design may be used in situations where it is not convenient or possible to do all of the combinations or trials (4). For this presentation, only experiments with all factors at two levels, a 2^n factorial design (where n is the number of factors, the effects of which are to be investigated), will be considered. The *main effect* is the difference in response (*e.g.*, rate constant) caused by the change in level of a factor (pH,

0022-3549/83/0400-0362$01.00/0

for example) averaged over all levels of the other factors. This has meaning in a practical sense if the effect of pH is not dependent on the levels of the other factors. If the effect of pH is dependent on the level of another factor (buffer, for example) an interaction between pH and buffer is said to exist. In this case a description of the effect of the factor, pH, would not be complete without consideration of the buffer level. This concept may be extended to higher order interactions. Thus, if an AB interaction exists and is dependent on the level of, say, factor C, the level of C should be specified when describing the AB interaction. This latter situation describes a 3-factor ABC, interaction.

A 2^3 factorial experiment with factors A, B, and C each at two levels consists of the following eight trials using the usual notation: (1), a, b, ab, c, ac, bc, abc. In this case (1) refers to all factors at their low level, a refers to the experiment with factor A at the high level and B and C at low levels, *etc.* The main effect of A is computed as $\frac{1}{4}$ [{a + ab + ac + abc} − {(1) + b + c + bc}]; the interaction AB is $\frac{1}{4}$ [{(1) + ab + c + abc} − {a + b + ac + bc}]; *etc.* Thus, the results of all experiments are used to calculate each main effect and interaction.

A relatively simple method of calculating the effects, is described by Davies (4).

THEORETICAL

The usual approach to kinetic studies is to examine, one at a time, the factors that are thought to affect the reaction rate. In many cases this approach is sufficient, since either some fundamental relationship is to be examined, or the effect of the various factors may be fairly well understood. One disadvantage of this experimental method is that, when present, interactions of factors may not be observed. Usually, little or no extra effort is required to uncover all possible effects by use of the factorial design. Factorial experiments are particularly advantageous in situations in which (*a*) the effects of several factors (and their interactions) are to be determined simultaneously in the absence of prior information, (*b*) a relatively small preliminary screening experiment is desired to obtain an estimate of the magnitude of effects of various variables, (*c*) the effects of factors are determined in a complex experimental situation (*e.g.*, many simultaneously varied factors), and (*d*) the experimental error (*e.g.*, assay) is relatively large. Statistical techniques may then be applied to test the significance of the main effects and interactions.

In typical kinetic studies, effects are usually additive. Thus, the following might describe a kinetic model:

$$k_{obs} = k_b[B] + k_c[C] + \ldots$$

in which [B] and [C] might represent hydroxide ion and buffer concentration, respectively. One objective is to estimate the rate constants, k_b, k_c, *etc.*

Since the usual statistical analysis is based on additivity of effects, it is important to consider carefully any analyses based on a model that also shows multiplicative relationships. For example, if ionic strength were a factor, the model could be of the following form:

$$k_{obs} = f(A)\{k_b[B] + k_c[C] + \ldots\}$$

in which $f(A)$ is a function of ionic strength.

If interaction of the multiplicative factor A (*e.g.*, ionic strength) with the additive factors B and C is present[1], the usual statistical analysis will be difficult, if not impossible, to interpret. In these cases, it is recommended that two separate analyses be performed, one at each level of A. Then, the effects of B and C can be estimated under the experimental conditions, *i.e.*, A constant at either the low or high level.

If interactions with A are absent, then the usual ANOVA of the rate constants (suitably weighted as described below) would, in general, provide a valid statistical test for the significance of the BC interaction only. The effects of the additive factors will be confounded with the multiplicative effects, and the effects of the additive factors should be evaluated separately at each level of A.

The factorial analysis of ln k (if CV is small and the k values are suitably weighted) will result in approximately valid statistical tests for A, AB, AC, and ABC under the null hypothesis that AB = AC = 0 (A is assumed not to interact with the additive factors B and C). In the absence of these interactions, the antilog of the A effect approximates the multiplicative effect of A (if CV is small).

Otherwise, the usual assumptions for ANOVA are considered to hold, as discussed later in this paper.

Because of the above implications, some knowledge of the functional relationships of the factors is helpful to come to meaningful conclusions. This knowledge may come from inspection of the data or from prior experience.

Statistical Considerations—In addition to the additivity concept discussed above, other assumptions inherent in the usual analysis of factorial experiments are that the errors are normally and independently distributed, and the variance (σ^2) is the same for each observation (homoscedasticity). In general, this latter assumption does not hold for experimentally determined rate constants, and the treatment of the data needs special consideration.

The variation or error in these studies arises from several factors, among which are assay error, other manipulative errors, and, possibly, the fact that the theoretical functional relationships such as linearity are not exactly satisfied. Measurement of the variance may be checked at several points during the study. Thus, it is useful during the assay development to check the assay variation at several concentrations of intact drug. Often the standard deviation is found to be proportional to the concentration of drug, *i.e.*, CV is constant; ($CV = S/C$, where S is the standard deviation and C is the concentration.) If the CV is constant and not too large, the logarithms of the assayed concentrations will have approximately equal variance at different concentration levels of drug (see *Appendix*). In this case the slope of the ordinary least-squares fit of the line, ln C *versus* time (first-order plot), is an unbiased estimate of the rate constant, k. The remainder of the discussion will be based on the assumption that the CV is constant and the reactions follow first-order kinetics. Certain modifications of the following analysis may be necessary if the kinetics are other than first order (see *Appendix*).

The variance of concern is the variation of ln C, σ^2 (which is approximately constant). Two estimates of σ^2 are available: (*a*) an estimate of the variance of ln C from replicates of assays of intact drug and (*b*) the variance estimate obtained from the least-squares line fit. If the error is due only to assay-related variation, these two estimates should show good agreement. In general, there will be sources other than assay variation contributing to the experimental error, and the line fitting should give a more realistic estimate of the variance. Another check on the error estimate could be obtained from replicate runs. (A run consists of determining the concentration as a function of time at specified levels of the factors.) Each set of replicates will contribute $n - 1$ degrees of freedom (df) to the error estimate in which n is the number of replicates. The details of this calculation for replicate runs (*i.e.*, repeat assessments of k with factor levels the same) are described in the *Appendix*.

Other studies[2] have shown excellent agreement of the variance estimate using replicates and line fitting. The line fitting approach has distinct advantages compared with replicates, since less runs are needed and more degrees of freedom for error are available.

An independent estimate of the variance as described is particularly important in this type of study. Higher order interaction terms (third order or higher) are often assumed to be nonexistent and are used to obtain estimates of the error. This approach has the disadvantage of yielding few degrees of freedom for error and possibly making false assumptions about the existence of such interactions. Most importantly, the computation of an independent variance estimate enables us to calculate the significance of the effects and all interactions in a relatively uncomplicated manner without prior consideration of the magnitude of interaction terms. As previously mentioned, the usual analysis of factorial designs assumes the variance of the observations to be equal. Under conditions usually present in kinetic studies this will very rarely be the case. The variance of a slope (the rate constant in this case) is $\sigma^2/\Sigma(t - \bar{t})^2$, in which t is the time at which the sample is assayed. Since $\Sigma(t - \bar{t})^2$ will, in general, be different for the different runs, the situation is one of variance inequality. The variance of ln k is $\sim\sigma^2/k^2\Sigma(t - \bar{t})^2$, if σ^2/k^2 is small (see *Appendix*). Interestingly, if, for each run, the same number of equally spaced time intervals are used that go to the same point of decomposition (say, 1 half-life), $k^2\Sigma(t - \bar{t})^2$ will be constant, and the variance of the ln k values will be approximately equal. This situation could be closely realized in practice if the approximate *magnitude of the* rates were known in advance. Then the usual factorial analysis of the ln k values could be used with the variance estimated as σ^2/K, with $K = k^2\Sigma(t - \bar{t})^2$. In the more realistic case, the variances are expected to differ, and, thus, one must approach the analysis differently. Initially, the main effects and interactions may be computed in the usual way (4). This is

[1] A is defined as not interacting if the response at high A is a constant multiple of the response at low a for all combinations of the additive factors, *i.e.*, ab/b = ac/c = abc/bc = a/(1).

[2] To be reported in a subsequent publication; S. Bolton, personal data.

Table I—Results of Simulation Study for 2^3 Factorial (run in duplicate) Untransformed Values

Combination	Average Rate Constant	Average ln Rate Constant	$\frac{1}{\Sigma\Sigma(t-\bar{t})^2}$	$\frac{1}{k^2\Sigma(\Sigma t-\bar{t})^2}$
(1)	1.87	0.63	0.77	0.22
a	3.77	1.38	5.00	0.34
b	3.10	1.16	2.92	0.30
ab	7.04	1.99	40.00	0.79
c	3.07	1.20	5.00	0.50
ac	5.35	1.72	40.00	1.36
bc	3.67	1.40	8.62	0.60
abc	8.04	2.11	31.25	0.47
Average = 4.49			Total 133.56	4.58

an appropriate unweighted average of the 2^n trials. The variance of these effects is estimated as described below, and the usual t test is applied by forming the ratio:

$$t = \frac{|\text{effect}|}{\sqrt{\text{Variance (effect)}}}$$

If t exceeds the tabulated α% value with appropriate degrees of freedom, the effect is significant. Nonsignificance does not necessarily mean that the effect is not present, but rather that it cannot be dissociated from error. This is important because most factors probably will affect the rate to some extent. If the effect is so small that it cannot be dissociated from error, it would probably not be of interest from a practical standpoint. The variance estimates of an effect may be calculated as follows: a main effect or interaction is the change in the rate constant due to changes in the levels of a factor or combination of factors appropriately averaged over all runs:

$$\hat{\sigma}^2 \text{ effect} = \frac{\hat{\sigma}^2\Sigma 1/\Sigma(t-\bar{t})^2}{2^{2n-2}} \qquad \text{(Eq. 1)}$$

in which $\hat{\sigma}^2$ is the estimated variance and $1/\Sigma(t-\bar{t})^2$ is summed over all 2^n trials or runs.

For ln rate constants:

$$\hat{\sigma}^2 \text{ effect} = \frac{\hat{\sigma}^2\Sigma 1/[k^2\Sigma(t-\bar{t})^2]}{2^{2n-2}} \qquad \text{(Eq. 2)}$$

In an experiment where many factors are being investigated, it may be convenient to look at segments of the data in which some factors are kept constant, while others are allowed to vary. The same statistical analysis as above may be used, but the summation in Eqs. 1 and 2 will include only those experiments that are appropriate to that segment of the experiment.

Example of Analysis—To illustrate the analysis described above, a hypothetical experiment was simulated with three factors, each at two levels, conforming to the following model:

$$k_{obs} = 10^{k_A\sqrt{A}}(k_B[B] + k_c[C])$$

The levels of A, B, and C are as follows:

Factor	Low Level	High Level
A	0	0.09
B	10^{-3}	2×10^{-3}
C	0.1	0.2

k_a, k_b, and k_c were assumed to be equal to 1, 1000, and 10, respectively.

A constant 0.2 CV, using random normal deviates, was imposed upon concentration readings at arbitrary time intervals, and the rate constants were calculated. (Duplicate runs were made for each of the eight combinations comprising the factorial, a total of 16 runs.) It should be mentioned that this error is relatively large for kinetic work; if anything, one should expect better results with real data. Pertinent results are shown in Table I.

The average rate constants and average ln rate constants were calculated as a weighted average of the respective duplicates with the weights being equal to $\Sigma(t-\bar{t})^2$ and $k^2\Sigma(t-\bar{t})^2$, respectively. The last two columns in Table I represent the weighting factors for computing the variances of the effects for rate constants and ln rate constants respectively, as shown in Eqs. 1 and 2; here $\Sigma[\Sigma(t-\bar{t})^2]$ is the sum from the two replicates.

The variance calculated from the line fitting (16 plots of ln C *versus* time) was 0.039 with 44 *df*. The variance calculated from the duplicate runs (using rate constants) was 0.060 with 8 *df*. This latter calculation

Table II—Effects Based on Data of Simulation Study (Untransformed Values)

Source	Average Effect
A	3.12
B	1.95
AB	1.03
C	1.09
AC	0.20
BC	−0.30
ABC	0.01

is described in the *Appendix*. The theoretical value should be ~0.04 ($CV^2 = 0.2^2$) and the results are within expectation, especially in view of the approximations involved. In this case the more dependable value of 0.039 determined from the least-squares line fitting for the variance will be used.

If the usual analysis on the untransformed rate constants is performed, one may expect to obtain estimates only for the BC interaction because of the multiplicative effects of A in the model. Table II shows the average effects based on the rate constants. The variance of an effect, calculated according to Eq. 1 is:

$$\frac{1}{16}\left[\frac{1}{\Sigma[\Sigma(t-\bar{t})^2]}\right]\hat{\sigma}^2$$

where $\hat{\sigma}^2 = 0.039$ and the summation includes all runs. The square root of the variance yields the standard deviation which, in this case, is 0.57 $[\sqrt{(0.039)(133.56)/16}]$. The BC interaction (−0.30) is not significant at the 5% level (Fig. 1). Keeping the multiplicative factor (A) constant, the results can be examined separately at both levels of A. With A at the low level, Eq. 1 is used where the summation includes readings (1), b, c, and bc. The *SD* of an effect is now 0.206. The results show that the main effects, B and C (0.92 and 0.89, respectively) are significant and the BC interaction (−0.32) is not. Similarly, an analysis with A at the high level yields 0.535 *SD*. As before, both main effects, B and C, are significant (2.98 and 1.29) while, again, the interaction (−0.29) is not (Table III).

Analysis of the log rate constants gives information on the effect of A and its interactions. The calculated effects are listed in Table IV. The standard deviation of an effect is 0.106 (Eq. 2), $\sqrt{0.039(4.58)/16}$.

The main effect of A is significant, and in the absence of interaction the antilog estimates its effect. The antilog of 0.70 is 2.01, which is very close to the known effect, 2. The analysis of these results also shows that all interactions with A are not significant. The results for B, C, and BC are difficult to interpret, since the additive and multiplicative properties are now confused with these effects.

Once the significant effects have been identified, it is of interest to estimate the rate constants associated with the different factors, which may be hydrogen ion concentration, buffer concentration, ionic strength, *etc.*, in a real example. Also, it would be most useful to construct a kinetic model that can be used to predict stability under various conditions (different levels of the factors). The fitting of such a model, however, would be rather precarious in the case of a design with factors at only two levels. In this situation, responses must be assumed to be linear functions

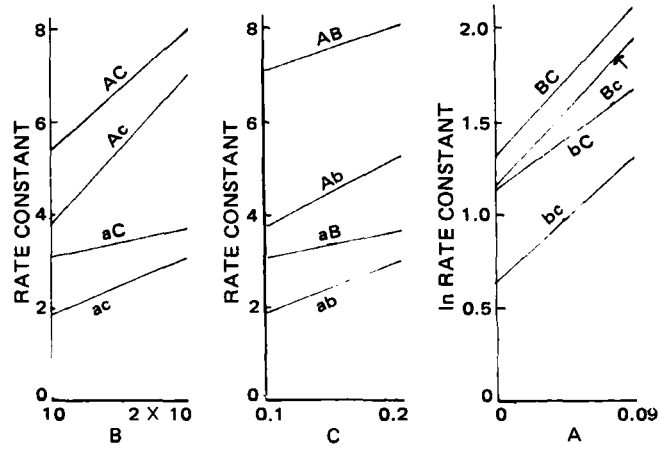

Figure 1—*Plot showing lack of interaction of factors. Capital letters are factors at high levels; lower case letters are factors at low levels. For example, aC is factor A at low level (0) with factor C at high level (0.2).*

Table III—Effects at Low and High Level of A

A = 0		A = 0.09	
Source	Average Effect	Source	Average Effect
B	0.92	B	2.98
C	0.89	C	1.29
BC	−0.32	BC	−0.29

of the factor levels. If a curved response exists, a 2^n design will not be sufficient to fit a proper model.

The rate constant associated with a factor is the slope of the observed rate constant *versus* factor level plot (Fig. 2). For example, in the case of factor B, at the low level of A (the multiplicative factor), the main effect is 0.92. The term k_B can be determined as follows: The average result at the high level of B (2×10^{-3}) is 3.39 ({3.10 + 3.67}/2), and the average result at the low level of B is 2.47 ({1.87 + 3.07}/2). The rate constant, k_B, is $(3.39 - 2.47)/(2 \times 10^{-3} - 1 \times 10^{-3}) = 920$. If interactions or multiplicative effects are not present, the rate constants can be simply calculated. If interactions exist, kinetic models may not be simply and clearly described in a single equation, and it may be preferable to describe the system at each level of the interacting factors. If a multiplicative factor is present, one may wish to include this as part of the final model. In this example the observed rate constant can be expressed as:

$$k_{obs} = 10^{k_A\sqrt{A}}(k_B[B] + k_C[C]) \qquad \text{(Eq. 3)}$$

Since interactions are nonsignificant in this example, it is convenient to express the kinetics in terms of Eq. 3.

To determine k_A, proceed as described, but use the main effect of A, expressed as $\log_{10}$:

$$k_a = \frac{0.70/2.303}{\sqrt{0.09} - \sqrt{0}} = 1.01 \qquad \text{(Eq. 4)}$$

One way to estimate k_B to satisfy Eq. 3 is to initially estimate the main effect of B, taking into account the multiplicative effect of A. From Table II, it is seen that the main effect of B is 1.95, which is the average of the main effects at low A and high A ({0.92 + 2.98}/2), as shown in Table III. Since the result of increasing the level of A is to multiply the effect of B by 2.01 (antilog of 0.70), the effect of B can be estimated: 2.01 (B $\text{effect}_{\text{low A}}$) + B $\text{effect}_{\text{low A}} \simeq 3.90$ (Note: 2.01 (B $\text{effect}_{\text{low A}}$) = B $\text{effect}_{\text{high A}}$):

$$\text{B effect}_{\text{low A}} \cong \frac{3.90}{3.01} \cong 1.30 \qquad \text{(Eq. 5)}$$

$$k_B \cong \frac{1.30}{2 \times 10^{-3} - 1 \times 10^{-3}} \cong 1300 \qquad \text{(Eq. 6)}$$

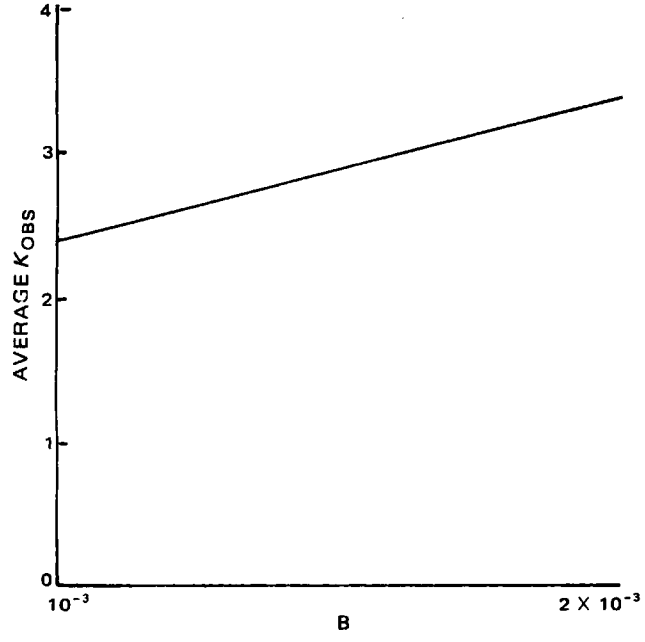

Figure 2—*Plot showing calculation of effect of factor B at low level of factor A, averaged over both levels of factor C. Slope = k_B = 920.*

Table IV—Factorial Analysis of ln Rate Constants

Source	Average Effect
A	0.70
B	0.43
AB	0.07
C	0.32
AC	−0.09
BC	−0.14
ABC	0.03

Similarly, $k_c = 7.24$, and the model (Eq. 3) can be estimated:

$$k_{obs} = 10^{\sqrt{A}}(1300[B] + 7.24[C]) \qquad \text{(Eq. 7)}$$

For example, this equation can be used to predict the rate constant with the combination, abc (A = 0.09, B = 2×10^{-3}, C = 0.2):

$$k_{obs} = 10^{\sqrt{0.09}}(1300[2 \times 10^{-3}] + 7.2[0.2]) = 8.10 \qquad \text{(Eq. 8)}$$

Without multiplicative effects, a model may also be constructed based on multiple regression techniques. In the case of a factorial design, it is convenient to use transformed (coded) values of the factor levels, where the low level equals −1 and the high level equals +1. The transformation is:

$$\frac{\text{Factor Level} - \dfrac{\text{Low Level} + \text{High Level}}{2}}{\dfrac{\text{High Level} - \text{Low Level}}{2}}$$

For Factor B, the transformation is:

$$\frac{\text{Factor Level} - 1.5 \times 10^{-3}}{0.5 \times 10^{-3}}$$

For transformed values (+1 or −1), in general, the coefficients for factors in the model are the main effects divided by 2. With the multiplicative factor A equal to 2.01, the coefficients are equal to the main effects divided by (1 + 2.01) = 3.01. For example, the coefficient for factor B is: 1.95/3.01 = 0.65. When coded values are used, an intercept value is usually calculated as the average of the rate constants, 4.49 (Table I). With the multiplicative factor A in the model, one can calculate the intercept as the average of the rate constants at the low level of A as follows:

$$\frac{2.93 + 6.05}{3.01} = \frac{\text{Average at low A + average at high A}}{3.01} = 2.98 \qquad \textit{(Eq. 11)}$$

The final equation is:

$$k_{obs} = 10^{1.0\sqrt{A}}(2.98 + 0.65[B'] + 0.36[C']) \qquad \text{(Eq. 12)}$$

where B′ and C′ are the transformed values[3], *i.e.*, the levels are transformed to equal ±1.

APPENDIX

(*a*) Approximation to the Variance of ln *y*—Using a Taylor series expansion, it can be shown that variance (ln *y*) = $CV^2(1 + \frac{1}{2}CV^2 + \ldots)$. If the *CV* is small, variance (ln *y*) = $CV^2 = \sigma^2/y^2$. Obviously, the smaller the *CV*, the better the approximation.

This result may be used to calculate the approximate variance of ln rate constant, ln *k*. The estimated variance of a rate constant is $\hat{\sigma}^2/\Sigma(t - \bar{t})^2$. Thus, the approximate variance of ln *k* is $\hat{\sigma}^2_k/k^2 = \hat{\sigma}^2/k^2\Sigma(t - \bar{t})^2$.

(*b*) The Use of Weighting in Line Fitting and Variance Estimation—The ordinary least-squares line fitting procedure assumes equal variance at each point, C. If the *CV* is constant, the variance (σ^2) is not constant, but depends on the value of C. However, in view of the above discussion, if the *CV* is constant, ln C has approximately equal variance (CV^2) and the fitting of the line, ln C *versus* time, can be computed as usual. The residual variance estimates CV^2.

[3] Note that this equation is not exactly equivalent to the equation previously constructed due to differences in calculating the multiplicative effect. If the error and interactions are small, different ways of calculating the effect of A will be very close. Here, where the error is relatively large, the results are equivocal. For example, the effect of A can be determined as the antilog of the effect of A when analyzing ln rate constants (2.01); as the ratio of the average results at high A compared with the average at low A (2.01); or as the average, in this example, of the four ratios of the rate at high level with the rate at low level of A under constant conditions of the other factors, B and C, *i.e.*, the average of a/(1), ab/b, ac/c, and abc/bc (2.06).

If the variance is constant at each point C, a fit of ln C *versus* time would require weighting each point proportional to the reciprocal of the variance, approximately C^2 in the case of constant CV. With constant variance, a zero-order plot would require no weighting.

From similar considerations, an estimate of σ^2 (equal to CV^2 in the case of constant CV and a first-order reaction) can be obtained from replicate determinations of the rate constant using the formula:

$$\Sigma w(k - \bar{k}_w)^2/(n - 1)$$

Where $\bar{k}_w$ is the weighted mean, n is the number of replications and w is $\Sigma(t - \bar{t})^2$. (Term w is equal to $k^2\Sigma(t - \bar{t})^2$ in the case of ln k). A shortcut formula for $\Sigma w(k - \bar{k})^2$ is $\Sigma wk^2 - \Sigma w(\bar{k}w)^2$.

An example of some calculations for the combination ab follows. The duplicate determinations of the rate constants were 5.86 and 8.22, and $\Sigma(t - \bar{t})^2$ was 0.0125 for each determination:

(1) The weighted average, $\bar{k}_w$, = [(0.0125)5.86 + (0.0125)8.22]/(0.025 + 0.025) = 7.04 (since the weights are equal, the weighted average equals the ordinary arithmetic average).

(2) σ^2 (One degree of freedom) from the duplicates = $[\Sigma wk^2 - \Sigma w(\bar{k}_w)^2]/(n - 1)$ = [(0.0125)(5.86)^2 + (0.0125)(8.22)^2 − 0.025 (7.04)^2]/1 = 0.0348

(3) The weighted average of ln k = ln k_w = [(5.86)^2(0.0125) ln 5.86 + (8.22)^2(0.0125)ln 8.22]/[(5.86)^2(0.0125) + (8.22)^2(0.0125)] = 1.99

The approximations inherent in the method should be kept in mind, namely the transformation to logs and the fact that observed values are used rather than true values in the weighting. However, if the CV is not large, the reliability of any conclusions from this analysis should not be in doubt.

REFERENCES

(1) J. A. Plaizier-Vercammen and R. E. De Neve, *J. Pharm. Sci.*, **69**, 1403 (1980).

(2) D. E. Fonner, Jr., J. R. Buck, and G. S. Banker, *ibid*, **59**, 1587 (1970).

(3) S. Dincer and S. Ozdurmus, *ibid*, **66**, 1070 (1977).

(4) O. L. Davies, "Design and Analysis of Industrial Experiments," Hafner, New York, N.Y., 1963.

Kinetics and Mechanism of Hydroxy Compound Cinnamoylation in Acetonitrile Catalyzed by *N*-Methylimidazole and 4-Dimethylaminopyridine

CHUKWUENWENIWE J. EBOKA and KENNETH A. CONNORS ˣ

Received March 25, 1982 from the *School of Pharmacy, University of Wisconsin, Madison, WI 53706.* Accepted for publication June 14, 1982.

Abstract □ The kinetics of reaction of the acylating agents *trans*-cinnamic anhydride and *trans*-cinnamoyl chloride with the hydroxy compounds *n*-propyl alcohol and water in the presence of *N*-methylimidazole and 4-dimethylaminopyridine were studied spectrophotometrically in acetonitrile solution at 25°. The acid chloride reacted *via* the intermediate formation of the *N*-acyl catalyst, which underwent general base-catalyzed reaction with the hydroxy compound. The anhydride did not form the *N*-acyl intermediate, but instead underwent direct general base catalysis. In the presence of water, all systems formed the *N*-acyl intermediate. The mechanistic route followed by the system was determined by the nucleophilicity of the catalyst, the ability of the leaving group, and the polarity of the solvent.

Keyphrases □ Cinnamoylation—hydroxy compounds in acetonitrile, catalyzed by *N*-methylimidazole and 4-dimethylaminopyridine, kinetics □ Kinetics—cinnamoylation of hydroxy compounds in acetonitrile □ 4-Dimethylaminopyridine catalysis—cinnamoylation of hydroxy compounds, kinetics □ *N*-Methylimidazole catalysis—cinnamoylation of hydroxy compounds, kinetics

Acylation is an important synthetic and analytical reaction. Pyridine is the classical acylation catalyst, but during the past decade more powerful catalysts have been introduced, most notably 4-dimethylaminopyridine, which has been used in synthesis (1–4) and analysis (5–8). More recently this laboratory introduced *N*-methylimidazole as an analytical acylation catalyst (9–13).

Acylation reactions are usually carried out in nonaqueous solvents. Although the mechanisms of acyl transfer in aqueous systems have been well studied (14–16), the nature of these reactions in nonhydroxylic solvents is not yet understood. Among the features that have been suggested as important in determining the kinetics and mechanisms of these reactions are the balance between nucleophilic and general base catalysis, the complex nature of rate equations (17–19), the possibility of kinetically significant ion-pair formation (3, 20, 21), competing reactions (22), and formation of molecular complexes (23). Some of these factors were addressed in a recent study on the kinetics of acetylation of alcohols by acetic anhydride and acetyl chloride, catalyzed by *N*-methylimidazole and 4-dimethylaminopyridine, in acetonitrile solution (24).

Since the cinnamoyl group, $C_6H_5CH{=}CHCO$, is a powerful UV chromophore, it is an interesting analytical acyl group (25, 26). An earlier study (27) reported the kinetics of hydrolysis of *trans*-cinnamic anhydride and of its reactions with some alcohols, catalyzed by pyridine, 4-dimethylaminopyridine, and *N*-methylimidazole, but the study was not designed to explore the detailed nature of the mechanism. In the present paper the reactions of *trans*-cinnamic anhydride and *trans*-cinnamoyl chloride with *n*-propyl alcohol and water, in acetonitrile solution, are described. The catalysts were *N*-methylimidazole and 4-dimethylaminopyridine; the reactions were studied by UV spectrophotometry.

EXPERIMENTAL

Materials—*trans*-Cinnamoyl chloride[1] was distilled under reduced pressure to give colorless crystals, mp 34–35° [lit. mp 35–36° (28)]. The molar absorptivity at 298 nm, in acetonitrile, was 2.42 × 10^4 liter/mole cm. *trans*-Cinnamic anhydride was synthesized as previously described (27), mp 136–137° [lit. mp 136° (29)]. Its molar absorptivity at 294 nm was 4.26 × 10^4 liter/mole cm. *N*-Methylimidazole[1] was distilled under

[1] Aldrich Chemical Co.

0022-3549/83/0400-0366$01.00/0

If the variance is constant at each point C, a fit of ln C *versus* time would require weighting each point proportional to the reciprocal of the variance, approximately C^2 in the case of constant CV. With constant variance, a zero-order plot would require no weighting.

From similar considerations, an estimate of σ^2 (equal to CV^2 in the case of constant CV and a first-order reaction) can be obtained from replicate determinations of the rate constant using the formula:

$$\Sigma w(k - \bar{k}_w)^2/(n - 1)$$

Where $\bar{k}_w$ is the weighted mean, n is the number of replications and w is $\Sigma(t - \bar{t})^2$. (Term w is equal to $k^2\Sigma(t - \bar{t})^2$ in the case of ln k). A shortcut formula for $\Sigma w(k - \bar{k})^2$ is $\Sigma wk^2 - \Sigma w(\bar{k}w)^2$.

An example of some calculations for the combination ab follows. The duplicate determinations of the rate constants were 5.86 and 8.22, and $\Sigma(t - \bar{t})^2$ was 0.0125 for each determination:

(1) The weighted average, $\bar{k}_w$, = [(0.0125)5.86 + (0.0125)8.22]/(0.025 + 0.025) = 7.04 (since the weights are equal, the weighted average equals the ordinary arithmetic average).

(2) σ^2 (One degree of freedom) from the duplicates = $[\Sigma wk^2 - \Sigma w(\bar{k}_w)^2]/(n - 1)$ = [(0.0125)(5.86)^2 + (0.0125)(8.22)^2 − 0.025 (7.04)^2]/1 = 0.0348

(3) The weighted average of ln k = ln k_w = [(5.86)^2(0.0125) ln 5.86 + (8.22)^2(0.0125)ln 8.22]/[(5.86)^2(0.0125) + (8.22)^2(0.0125)] = 1.99

The approximations inherent in the method should be kept in mind, namely the transformation to logs and the fact that observed values are used rather than true values in the weighting. However, if the CV is not large, the reliability of any conclusions from this analysis should not be in doubt.

REFERENCES

(1) J. A. Plaizier-Vercammen and R. E. De Neve, *J. Pharm. Sci.*, **69**, 1403 (1980).

(2) D. E. Fonner, Jr., J. R. Buck, and G. S. Banker, *ibid*, **59**, 1587 (1970).

(3) S. Dincer and S. Ozdurmus, *ibid*, **66**, 1070 (1977).

(4) O. L. Davies, "Design and Analysis of Industrial Experiments," Hafner, New York, N.Y., 1963.

Kinetics and Mechanism of Hydroxy Compound Cinnamoylation in Acetonitrile Catalyzed by *N*-Methylimidazole and 4-Dimethylaminopyridine

CHUKWUENWENIWE J. EBOKA and KENNETH A. CONNORS ˣ

Received March 25, 1982 from the *School of Pharmacy, University of Wisconsin, Madison, WI 53706.* Accepted for publication June 14, 1982.

Abstract □ The kinetics of reaction of the acylating agents *trans*-cinnamic anhydride and *trans*-cinnamoyl chloride with the hydroxy compounds *n*-propyl alcohol and water in the presence of *N*-methylimidazole and 4-dimethylaminopyridine were studied spectrophotometrically in acetonitrile solution at 25°. The acid chloride reacted *via* the intermediate formation of the *N*-acyl catalyst, which underwent general base-catalyzed reaction with the hydroxy compound. The anhydride did not form the *N*-acyl intermediate, but instead underwent direct general base catalysis. In the presence of water, all systems formed the *N*-acyl intermediate. The mechanistic route followed by the system was determined by the nucleophilicity of the catalyst, the ability of the leaving group, and the polarity of the solvent.

Keyphrases □ Cinnamoylation—hydroxy compounds in acetonitrile, catalyzed by *N*-methylimidazole and 4-dimethylaminopyridine, kinetics □ Kinetics—cinnamoylation of hydroxy compounds in acetonitrile □ 4-Dimethylaminopyridine catalysis—cinnamoylation of hydroxy compounds, kinetics □ *N*-Methylimidazole catalysis—cinnamoylation of hydroxy compounds, kinetics

Acylation is an important synthetic and analytical reaction. Pyridine is the classical acylation catalyst, but during the past decade more powerful catalysts have been introduced, most notably 4-dimethylaminopyridine, which has been used in synthesis (1–4) and analysis (5–8). More recently this laboratory introduced *N*-methylimidazole as an analytical acylation catalyst (9–13).

Acylation reactions are usually carried out in nonaqueous solvents. Although the mechanisms of acyl transfer in aqueous systems have been well studied (14–16), the nature of these reactions in nonhydroxylic solvents is not yet understood. Among the features that have been suggested as important in determining the kinetics and mechanisms of these reactions are the balance between nucleophilic and general base catalysis, the complex nature of rate equations (17–19), the possibility of kinetically significant ion-pair formation (3, 20, 21), competing reactions (22), and formation of molecular complexes (23). Some of these factors were addressed in a recent study on the kinetics of acetylation of alcohols by acetic anhydride and acetyl chloride, catalyzed by *N*-methylimidazole and 4-dimethylaminopyridine, in acetonitrile solution (24).

Since the cinnamoyl group, $C_6H_5CH{=}CHCO$, is a powerful UV chromophore, it is an interesting analytical acyl group (25, 26). An earlier study (27) reported the kinetics of hydrolysis of *trans*-cinnamic anhydride and of its reactions with some alcohols, catalyzed by pyridine, 4-dimethylaminopyridine, and *N*-methylimidazole, but the study was not designed to explore the detailed nature of the mechanism. In the present paper the reactions of *trans*-cinnamic anhydride and *trans*-cinnamoyl chloride with *n*-propyl alcohol and water, in acetonitrile solution, are described. The catalysts were *N*-methylimidazole and 4-dimethylaminopyridine; the reactions were studied by UV spectrophotometry.

EXPERIMENTAL

Materials—*trans*-Cinnamoyl chloride[1] was distilled under reduced pressure to give colorless crystals, mp 34–35° [lit. mp 35–36° (28)]. The molar absorptivity at 298 nm, in acetonitrile, was 2.42 × 10^4 liter/mole cm. *trans*-Cinnamic anhydride was synthesized as previously described (27), mp 136–137° [lit. mp 136° (29)]. Its molar absorptivity at 294 nm was 4.26 × 10^4 liter/mole cm. *N*-Methylimidazole[1] was distilled under

[1] Aldrich Chemical Co.

0022-3549/83/0400-0366$01.00/0

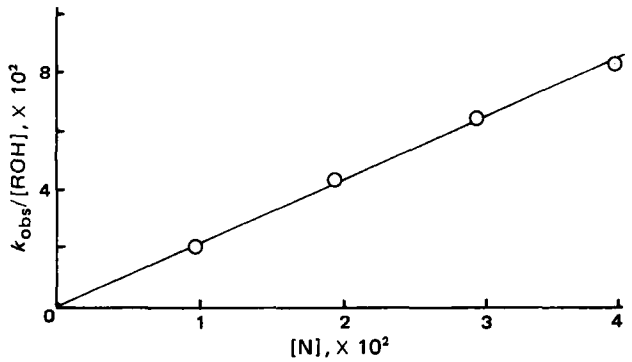

Figure 1—*Plot of Eq. 1 for the cinnamoyl chloride–dimethylaminopyridine–n-propyl alcohol system. Initial cinnamoyl chloride concentration was 2.71 × 10^{-5} M and the alcohol concentrations ranged from 0.08 to 0.61* M.

reduced pressure, bp 55° at 14–16 mm Hg. 4-Dimethylaminopyridine[1] was recrystallized from *n*-hexane, mp 113.5° [lit. 112–113° (3)]. Acetonitrile[2] was spectrophotometric grade.

Procedures—A typical kinetic run was carried out as follows. Solutions of the acylating agent, the catalyst, and the hydroxy compound were prepared in acetonitrile. Appropriate portions of the catalyst and hydroxy compound were mixed to give a volume of 4.8 ml; this solution was equilibrated at 25°. Reaction was initiated by adding 0.2 ml of the acylating agent solution. The progress of the reaction was followed by recording the absorbance, at a wavelength suitable for the particular system, as a function of time[3]. The absorbance at the completion of the reaction was measured after the lapse of at least 10 half-lives. In all cases the catalyst and hydroxy compound were in large excess to establish pseudo first-order conditions with respect to the acylating agent.

For the measurement of the rate of intermediate formation in the cinnamic anhydride–dimethylaminopyridine system in aqueous acetonitrile, 3.5 ml of a mixture of catalyst, water, and acetonitrile was equilibrated in a 1-cm spectrophotometer cell in the thermostated cell compartment. Fifty microliters of a solution of cinnamic anhydride in acetonitrile was added to the cell and the mixture was stirred. The absorbance was monitored at 350 nm; recording of the absorbance began <10 sec after adding the acylating agent. All data reported are at 25.0 ± 0.1°.

RESULTS AND DISCUSSION

Kinetic Scheme—The reactions of acetic anhydride and acetyl chloride in acetonitrile, in the presence of *N*-methylimidazole or 4-dimethylaminopyridine, were previously described (24). This same kinetic scheme (Scheme I) was used in the present study to analyze the kinetic data.

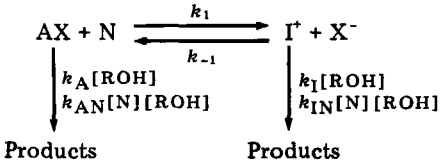

Scheme I

In Scheme I, AX represents the acylating agent (cinnamic anhydride or cinnamoyl chloride), N is the catalyst (*N*-methylimidazole or 4-dimethylaminopyridine), ROH is the hydroxy compound (*n*-propyl alcohol or water), X^- is the leaving group (cinnamate or chloride ion), and I^+ is the *N*-cinnamoylated catalyst, *i.e.*, I or II, where R is $C_6H_5CH{=}CH$.

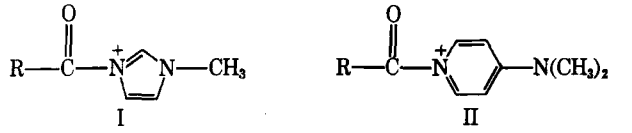

Scheme I includes several possible kinds of kinetic behavior, dependent on the relative values of the rate constants (especially the ratio k_1/k_{-1},

[2] Burdick and Jackson.

[3] Cary Model 14 spectrophotometer equipped with a thermostated cell compartment.

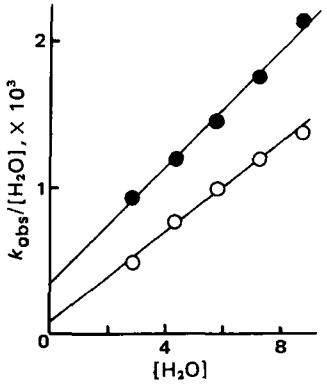

Figure 2—*Plot of Eq. 2 for the hydrolysis of cinnamoyl chloride in acetonitrile with 4-dimethylaminopyridine as catalyst. Initial cinnamoyl chloride concentration: 8.05 × 10^{-5}* M. *Catalyst concentrations: (○) 7.81 × 10^{-3}* M, *(●) 13.02 × 10^{-3}* M.

which largely determines the level of intermediate I^+ in the system). The rate constants for product formation can be described as: (k_A) the uncatalyzed reaction, (k_{AN}) general base catalysis, (k_I) nucleophilic reaction, and (k_{IN}) general base catalysis of the nucleophilic reaction.

The general experimental approach was to examine the reaction mixture spectrophotometrically for evidence of the presence of I^+. The kinetics were followed by observing the decrease in concentration of either AX or I^+ on reaction with ROH. Rate constants were evaluated from semi-logarithmic pseudo first-order plots. Derivations for those systems that can be described by the same rate equations developed for the acetylation kinetics (24) are not presented in this paper.

Cinnamoyl Chloride–Dimethylaminopyridine–*n*-Propyl Alcohol—A mixture of cinnamoyl chloride and dimethylaminopyridine exhibited UV absorption at longer wavelengths than either of the solution components. The new spectrum is ascribed to *N*-cinnamoyl dimethyl aminopyridinium chloride. In the presence of excess catalyst, the intermediate was formed very rapidly; in the presence of excess cinnamoyl chloride, up to several minutes was required. Quantitative conversion to the intermediate was demonstrated by using various amounts of catalyst and cinnamoyl chloride. The intermediate shows λ_{max} 350 nm, log ϵ_{max} 4.6. This system belongs to the special case $k_1 >>> k_{-1}$ in Scheme I; so, as shown previously (24), the kinetics may be described by:

$$\frac{k_{obs}}{[ROH]} = k_I + k_{IN}[N] \qquad \text{(Eq. 1)}$$

In Eq. 1, k_{obs} is the observed first-order rate constant and [N] is the free catalyst concentration. Since the intermediate is quantitatively formed, $[N] = [N]_0 - [AX]_0$, where the subscripted quantities are initial concentrations.

Pseudo first-order behavior was observed for >3 half-lives, with reactions monitored at 350 nm. The k_{obs} values were linearly dependent on the *n*-propyl alcohol concentration at constant $[N]_0$. Figure 1 shows the plot according to Eq. 1. The estimates $k_I = 0.14 \times 10^{-3}\ M^{-1}\ sec^{-1}$ (*SD*

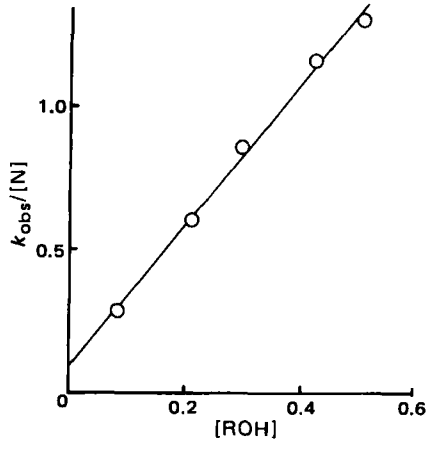

Figure 3—*Plot of Eq. 3 for the cinnamic anhydride–dimethylaminopyridine–n-propyl alcohol system. Catalyst concentration: 0.0125* M, *initial anhydride concentration: 3.50 × 10^{-4}* M.

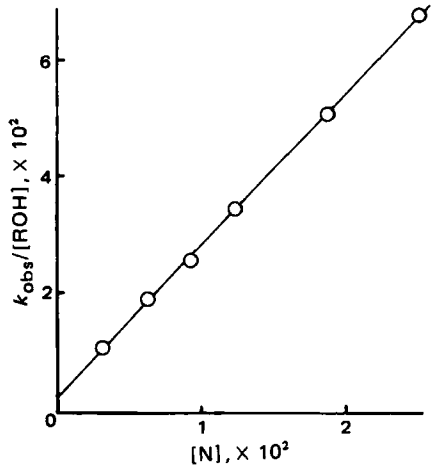

Figure 4—*Plot of Eq. 4 for the cinnamic anhydride–dimethylaminopyridine–n-propyl alcohol system. Alcohol concentration: 0.426* M.

2.6×10^{-3}) and $k_{IN} = 2.18\ M^{-2}\ sec^{-1}$ (*SD* 0.10) were obtained from this plot, thus k_I is not significantly different from zero.

Cinnamoyl Chloride–*N*-Methylimidazole–*n*-Propyl Alcohol—This system also gave quantitative intermediate formation, with λ_{max} 340 nm. The data were analyzed using Eq. 1, yielding $k_I = 5.3 \times 10^{-3}\ M^{-1}\ sec^{-1}$ (*SD* 1.6×10^{-3}) and $k_{IN} = 0.229\ M^{-2}\ sec^{-1}$ (*SD* 0.007).

Cinnamoyl Chloride–Dimethylaminopyridine–Water—Since the intermediate was formed quantitatively in this system, the loss of intermediate on reaction with water was followed at 350 nm. The water concentration ranged from 2.8 to 8.8 *M*. First-order kinetics were observed for the higher water concentrations, but significant deviations were seen at low water concentrations. The pseudo first-order rate constants were linearly dependent on the catalyst concentration, but did not vary linearly with the water concentration. The dependence suggested a rate equation both first- and second-order in water:

$$k_{obs} = (k_I + k_{IN}[N])[H_2O] + (k_I^W + k_{IN}^W[N])[H_2O]^2 \quad \text{(Eq. 2)}$$

If Eq. 2 describes the system, a plot of $k_{obs}/[H_2O]$ *versus* $[H_2O]$ should be linear and, from the dependence of the intercept and slope on [N], the individual constants can be estimated (Fig. 2). The rate constants found were $k_I = -2.8 \times 10^{-3}\ M^{-1}\ sec^{-1}$ (*SD* 3.2×10^{-3}), $k_{IN} = 0.045\ M^{-2}\ sec^{-1}$ (*SD* 0.012), $k_I^W = 7.2 \times 10^{-5}\ M^{-2}\ sec^{-1}$ (*SD* 8.1×10^{-5}), and $k_{IN}^W = 0.010\ M^{-3}\ sec^{-1}$ (*SD* 0.001). Thus k_I and k_I^W are not significantly different from zero. Scheme I requires modification for this system to include catalysis of the "IN" route by a molecule of water.

The cinnamoyl chloride–*N*-methylimidazole–water system was also examined. At low water concentrations the kinetic behavior was similar to that described for dimethylaminopyridine, but at high water concentrations serious deviations from first-order kinetics were seen. This may be a consequence of the formation of cinnamic anhydride *in situ*, as postulated for the analogous acetyl system (24).

Cinnamic Anhydride–Dimethylaminopyridine–*n*-Propyl Alcohol—The mixture of cinnamic anhydride and dimethylaminopyridine in acetonitrile exhibited an absorption spectrum that nearly could be accounted for as the sum of the spectra of the two solutes. But at high concentrations (~0.2 *M* for each solute), some absorption at longer wavelength was seen, presumably a consequence of the formation of a small amount of the intermediate. In this system, therefore, $k_1 \ll k_{-1}$. Reaction may take place *via* AX, I^+, or both. This kinetic system was described previously and (24) leads to:

$$\frac{k_{obs}}{[N]} = k_I + \left(\frac{k_A}{[N]} + k_{AN}\right)[ROH] \quad \text{(Eq. 3)}$$

and

$$\frac{k_{obs}}{[ROH]} = k_A + \left(\frac{k_1}{[ROH]} + k_{AN}\right)[N] \quad \text{(Eq. 4)}$$

If [N] is held constant and [ROH] is varied, Eq. 3 is plotted; if [ROH] is constant and [N] varies, Eq. 4 is used. From the slopes and intercepts the rate constants can be evaluated.

The reaction was followed at 320 nm, and good first-order kinetics were followed for >3 half-lives. Figures 3 and 4 show the plots according to Eqs. 3 and 4, respectively. The values found were: $k_1 = 0.096\ M^{-1}\ sec^{-1}$ (*SD* 0.039); $k_A = 0.33 \times 10^{-2}\ M^{-1}\ sec^{-1}$ (*SD* 0.16×10^{-2}); and $k_{AN} = 2.18\ M^{-2}\ sec^{-1}$ (*SD* 0.09). Evidently this reaction occurs mainly by the general base (k_{AN}) route; k_A is essentially zero, as verified in the corresponding *N*-methylimidazole system.

Table I—Mechanisms of Cinnamoylation Reactions in Acetonitrile [a]

Catalyst	Leaving Group: Chloride	Leaving Group: Cinnamate
N-Methylimidazole	*Via* I^+	*Via* AX
4-Dimethylaminopyridine	*Via* I^+	Mainly *via* AX

[a] Symbols as defined in Scheme I.

Cinnamic Anhydride–*N*-Methylimidazole–*n*-Propyl Alcohol—This system displayed the same kinetic behavior as the preceding system and Eqs. 3 and 4 were applied. The kinetics were first-order for >3 half-lives. The rate constants were $k_1 = 0.029 \times 10^{-2}\ M^{-1}\ sec^{-1}$ (*SD* 0.037×10^{-2}), $k_A = 0.69 \times 10^{-4}\ M^{-1}\ sec^{-1}$ (*SD* 0.96×10^{-4}), and $k_{AN} = 2.16 \times 10^{-2}\ M^{-2}\ sec^{-1}$ (*SD* 0.12×10^{-2}). Clearly k_1 and k_A are not significantly different from zero.

Cinnamic Anhydride–*N*-Methylimidazole–Water—On the addition of cinnamic anhydride to a solution of *N*-methylimidazole in aqueous methanol, light absorption was observed at wavelengths longer than the spectra of the added solutes, implying that the increased polarity of the medium (relative to dry acetonitrile) promotes formation of the intermediate. This behavior was seen also in the corresponding acetic anhydride system (24), which was described by:

$$k_{obs} = \left[\frac{k_I' + R'k_A'}{1 + R'}\right][H_2O] \quad \text{(Eq. 5)}$$

where $k_I' = k_1 + k_{IN}[N]$, $k_A' = k_A + k_{AN}[N]$, and $R'\ [X^-]/K[N] + k_I'[H_2O]/k_1[N]$ with $K = k_1/k_{-1}$. As the water concentration increases, both K and k_1 will increase and R' will decrease. At high water concentrations R' approaches zero and k_{obs} approaches $k_I'[H_2O]$: the reaction proceeds solely *via* the intermediate. At extremely low water concentration, R' becomes very large and k_{obs} approaches $k_A'[H_2O]$; the reaction then occurs solely *via* the anhydride. At intermediate water concentrations where R' is finite, both routes may be involved. According to Eq. 5, moreover, if R' is finite and varies during the course of a reaction, deviations from first-order kinetics may be observed.

The reaction was monitored at 340 nm. At low water concentrations (0.56–2.56 *M*) significant deviations from first-order kinetics were seen. The k_{obs} values estimated from the first half-life were linearly dependent on [N] and $[H_2O]$. At high water concentrations (11.1–27.8 *M*), the reactions were strictly first-order and k_{obs} was directly dependent on [N]. The dependence on water concentration in this region, however, was not linear, suggesting the possible involvement of a second molecule of water.

Cinnamic Anhydride–Dimethylaminopyridine–Water—This system showed spectral and kinetic behavior very similar to that observed with the *N*-methylimidazole system. During the very early stage after mixing the components, the absorbance at 350 nm (attributed to the intermediate) increased on a time scale accessible to measurement. At time zero, the concentrations $[I^+]$ and $[X^-]$ are very small, so the back-reaction (k_{-1} step) and reaction with water (k_I' step) are negligible. Hence the initial rate, measured as the absorbance change per sec, is equal to $\epsilon_I k_1[N]_0[AX]_0$, where ϵ_I is the molar absorptivity of I^+. Over the first 20 sec of reaction the absorbance was a linear function of time. Experiments were carried out at several water concentrations, with these results: $[H_2O]$ 5.65 *M*, k_1 46.5 M^{-1} sec−1; $[H_2O]$ 10.9 *M*, k_1 57.5 $M^{-1}\ sec^{-1}$; $[H_2O]$ 16.4 *M*, k_1 69.7 $M^{-1}\ sec^{-1}$; $[H_2O]$ 21.9 *M*, k_1 82.0 $M^{-1}\ sec^{-1}$; and $[H_2O]$ 27.3 *M*, k_1 106.4 $M^{-1}\ sec^{-1}$.

Catalytic Mechanisms—Table I summarizes the qualitative observations of this study. The acid chloride reacts by forming the intermediate

Table II—Comparison of Rate Constants for Some Acylation Reactions in Acetonitrile at 25°

Catalyst [a]	Alcohol	Acyl Group [b]	Acid Chloride [c] k_{IN}	Anhydride [c] k_{AN}
NMIM	*n*-Propyl Alcohol	Acetyl	0.50	0.0403
NMIM	*n*-Propyl Alcohol	Cinnamoyl	0.23	0.0216
DMAP	*n*-Propyl Alcohol	Cinnamoyl	2.18	2.18
NMIM	Isopropyl Alcohol	Acetyl	0.053	0.0041
DMAP	Isopropyl Alcohol	Acetyl	1.3	0.5

[a] NMIM = *N*-methylimidazole, DMAP = 4-dimethylaminopyridine. [b] Acetyl data from Ref. 24. [c] Units are $M^{-2}\ sec^{-1}$.

acylammonium ion (I^+ in Scheme I), whereas the anhydride does not form the intermediate unless the catalyst is very powerful. When the solvent polarity is increased by adding water, intermediate formation is favored even in the anhydride systems. These conclusions are identical with those reached in the study of acylations with acetyl chloride and acetic anhydride (24). This insensitivity of mechanistic pathway to the nature of the acyl group suggests that the mechanism is determined primarily by three factors: the catalyst nucleophilicity, the leaving group ability, and the solvent polarity. Increases in any of these factors will promote the formation of intermediate and the possibility of product formation through the k_I and k_{IN} routes. That the acid anhydrides react mainly by the general base catalyzed (k_{AN}) route, even in the presence of strong nucleophilic catalysts, has been an unexpected finding of these studies.

Table II lists rate constants for the cinnamoylation reactions reported here and includes, for comparison, some data (24) on acetylation reactions. Several patterns can be seen. In comparable systems, the general base catalysis quantities k_{AN} and k_{IN} are larger for 4-dimethylaminopyridine than for *N*-methylimidazole, reflecting the greater base strength of the former catalyst. The acetyl substrates are two-fold more reactive than the corresponding cinnamoyl compounds. For a given acyl group and alcohol, the chloride–anhydride (k_{IN}/k_{AN}) ratio is >10 for *N*-methylimidazole and close to unity for 4-dimethylaminopyridine. Since k_{IN} describes the reaction of the intermediate, this indicates that *N*-methylimidazole is a better leaving group than is a carboxylate, whereas 4-dimethylaminopyridine is about as good a leaving group as a carboxylate. These relationships are not expected on the basis of the leaving group basicities, but they may reflect a relatively greater resonance stabilization of the *N*-acyl-4-dimethylaminopyridinium intermediate.

REFERENCES

(1) W. Steglich and G. Höfle, *Angew. Chem. Int. Ed.*, **8**, 981 (1969).

(2) G. Höfle and W. Steglich, *Synthesis*, **1972**, 620.

(3) G. Höfle, W. Steglich, and H. Vorbrüggen, *Angew. Chem. Int. Ed.*, **17**, 569 (1978).

(4) S. S. Wang, J. P. Tam, B. S. Wang, and R. B. Merrifield, *Int. J. Pept. Protein Res.*, **18**, 459 (1981).

(5) K. A. Connors and K. S. Albert, *J. Pharm. Sci.*, **62**, 845 (1973).

(6) E. L. Rowe and S. M. Machkovech, *ibid.*, **66**, 273 (1977).

(7) V. Fell and C. R. Lee, *J. Chromatogr.*, **121**, 41 (1976).

(8) F. de Fabrizio, *J. Pharm. Sci.*, **69**, 854 (1980).

(9) K. A. Connors and N. K. Pandit, *Anal. Chem.*, **50**, 1542 (1978).

(10) R. Wachowiak and K. A. Connors, *ibid.*, **51**, 27 (1979).

(11) S. L. Wellons, M. A. Carey, and D. K. Eider, *ibid.*, **52**, 1374 (1980).

(12) A. S. Bittner, L. E. Harris, and W. F. Campbell, *J. Agr. Food Chem.*, **28**, 1242 (1980).

(13) N. K. Pandit, A. O. Obaseki, and K. A. Connors, *Anal. Chem.*, **52**, 1678 (1980).

(14) T. C. Bruice and S. J. Benkovic, "Bioorganic Mechanisms," Vol. I, W. A. Benjamin, New York, N.Y., 1966.

(15) W. P. Jencks, "Catalysis in Chemistry and Enzymology," McGraw-Hill, New York, N.Y., 1969.

(16) M. L. Bender, "Mechanisms of Homogeneous Catalysis from Protons to Proteins," Wiley-Interscience, New York, N.Y., 1971.

(17) S. A. Lapshin, V. A. Dadali, Y. S. Simanenko, and L. M. Litvinenko, *Zh. Org. Khim.*, **13**, 586 (1977).

(18) V. A. Dadali, I. A. Tsupilo, and L. M. Litvinenko, *ibid.*, **13**, 211 (1977).

(19) I. H. Pitman and T. Higuchi, *J. Org. Chem.*, **40**, 378 (1975).

(20) E. M. Cherkasova, S. V. Bogatkov, and Z. P. Golivina, *Russ. Chem. Rev. (Engl. Transl.)*, **46**, 246 (1977).

(21) L. M. Litvinenko, V. A. Savelova, V. A. Shatskaya, and T. N. Sadovskaya, *Dokl. Akad. Nauk SSSR*, **198**, 844 (1971).

(22) A. Hassner, L. R. Krepski, and V. Alexanian, *Tetrahedron*, **34**, 2069 (1978).

(23) E. Guibe-Jampel, G. Le Corre, and M. Wakselman, *Tetrahedron Lett.*, **1979**, 1157.

(24) N. K. Pandit and K. A. Connors, *J. Pharm. Sci.*, **71**, 485 (1982).

(25) W. H. Hong and K. A. Connors, *Anal. Chem.*, **40**, 1273 (1968).

(26) K. A. Connors and W. H. Hong, *Anal. Chim. Acta*, **43**, 334 (1968).

(27) S.-F. Lin and K. A. Connors, *J. Pharm. Sci.*, **70**, 235 (1981).

(28) R. Adams and L. H. Ulrich, *J. Am. Chem. Soc.*, **42**, 605 (1920).

(29) J. D. M. Simpson and S. S. Israelstam, *J. S. African Chem. Inst.*, **2**, 170 (1949).

ACKNOWLEDGMENT

This work was supported in part by National Science Foundation Grant CHE 78-06603.

Solvent Effects on the Cinnamoylation of *n*-Propyl Alcohol Catalyzed by *N*-Methylimidazole and 4-Dimethylaminopyridine

KENNETH A. CONNORS ˣ **and CHUKWUENWENIWE J. EBOKA**

Received April 5, 1982 from the *School of Pharmacy, University of Wisconsin, Madison, WI 53706.* Accepted for publication June 24, 1982.

Abstract □ The kinetics of reaction of *trans*-cinnamic anhydride or *trans*-cinnamoyl chloride with *n*-propyl alcohol, catalyzed by *N*-methylimidazole or 4-dimethylaminopyridine, were studied spectrophotometrically at 25° in methyl ethyl ketone, ethylene dichloride, methylene chloride, and toluene. The acid chloride reacted in all solvents *via* the intermediate formation of the *N*-acyl catalyst, which underwent reaction with the alcohol catalyzed by another molecule of the base. The anhydride did not form the intermediate in any of the solvents, but underwent direct general base catalysis. The rate of the anhydride reactions was not sensitive to solvent polarity, whereas the rate of the chloride reactions tended to increase as the solvent polarity decreased. A kinetic analysis is given of the effect of ion-pair formation on the kinetics of acyl transfer in systems where the charged *N*-acyl catalyst intermediate is formed.

Keyphrases □ Cinnamoylation—of *n*-propyl alcohol, catalysis by *N*-methylimidazole and 4-dimethylaminopyridine, solvent effects □ 4-Dimethylaminopyridine—catalyses, cinnamoylation of *n*-propyl alcohol □ *N*-methylimidazole—catalyses, cinnamoylation of *n*-propyl alcohol

Although the kinetics and mechanisms of acyl transfer reactions in water have been carefully studied (in large part because such reactions serve as models for enzyme-catalyzed reactions), acyl transfers in nonaqueous media are less well understood despite their great importance in synthesis and analysis. The relatively recent introduction of powerful acylation catalysts like 4-dimethylaminopyridine (1) and *N*-methylimidazole (2) has stimulated in-

0022-3549/83/0400-0369$01.00/0

acylammonium ion (I^+ in Scheme I), whereas the anhydride does not form the intermediate unless the catalyst is very powerful. When the solvent polarity is increased by adding water, intermediate formation is favored even in the anhydride systems. These conclusions are identical with those reached in the study of acylations with acetyl chloride and acetic anhydride (24). This insensitivity of mechanistic pathway to the nature of the acyl group suggests that the mechanism is determined primarily by three factors: the catalyst nucleophilicity, the leaving group ability, and the solvent polarity. Increases in any of these factors will promote the formation of intermediate and the possibility of product formation through the k_I and k_{IN} routes. That the acid anhydrides react mainly by the general base catalyzed (k_{AN}) route, even in the presence of strong nucleophilic catalysts, has been an unexpected finding of these studies.

Table II lists rate constants for the cinnamoylation reactions reported here and includes, for comparison, some data (24) on acetylation reactions. Several patterns can be seen. In comparable systems, the general base catalysis quantities k_{AN} and k_{IN} are larger for 4-dimethylaminopyridine than for *N*-methylimidazole, reflecting the greater base strength of the former catalyst. The acetyl substrates are two-fold more reactive than the corresponding cinnamoyl compounds. For a given acyl group and alcohol, the chloride–anhydride (k_{IN}/k_{AN}) ratio is >10 for *N*-methylimidazole and close to unity for 4-dimethylaminopyridine. Since k_{IN} describes the reaction of the intermediate, this indicates that *N*-methylimidazole is a better leaving group than is a carboxylate, whereas 4-dimethylaminopyridine is about as good a leaving group as a carboxylate. These relationships are not expected on the basis of the leaving group basicities, but they may reflect a relatively greater resonance stabilization of the *N*-acyl-4-dimethylaminopyridinium intermediate.

REFERENCES

(1) W. Steglich and G. Höfle, *Angew. Chem. Int. Ed.*, **8**, 981 (1969).

(2) G. Höfle and W. Steglich, *Synthesis*, **1972**, 620.

(3) G. Höfle, W. Steglich, and H. Vorbrüggen, *Angew. Chem. Int. Ed.*, **17**, 569 (1978).

(4) S. S. Wang, J. P. Tam, B. S. Wang, and R. B. Merrifield, *Int. J. Pept. Protein Res.*, **18**, 459 (1981).

(5) K. A. Connors and K. S. Albert, *J. Pharm. Sci.*, **62**, 845 (1973).

(6) E. L. Rowe and S. M. Machkovech, *ibid.*, **66**, 273 (1977).

(7) V. Fell and C. R. Lee, *J. Chromatogr.*, **121**, 41 (1976).

(8) F. de Fabrizio, *J. Pharm. Sci.*, **69**, 854 (1980).

(9) K. A. Connors and N. K. Pandit, *Anal. Chem.*, **50**, 1542 (1978).

(10) R. Wachowiak and K. A. Connors, *ibid.*, **51**, 27 (1979).

(11) S. L. Wellons, M. A. Carey, and D. K. Eider, *ibid.*, **52**, 1374 (1980).

(12) A. S. Bittner, L. E. Harris, and W. F. Campbell, *J. Agr. Food Chem.*, **28**, 1242 (1980).

(13) N. K. Pandit, A. O. Obaseki, and K. A. Connors, *Anal. Chem.*, **52**, 1678 (1980).

(14) T. C. Bruice and S. J. Benkovic, "Bioorganic Mechanisms," Vol. I, W. A. Benjamin, New York, N.Y., 1966.

(15) W. P. Jencks, "Catalysis in Chemistry and Enzymology," McGraw-Hill, New York, N.Y., 1969.

(16) M. L. Bender, "Mechanisms of Homogeneous Catalysis from Protons to Proteins," Wiley-Interscience, New York, N.Y., 1971.

(17) S. A. Lapshin, V. A. Dadali, Y. S. Simanenko, and L. M. Litvinenko, *Zh. Org. Khim.*, **13**, 586 (1977).

(18) V. A. Dadali, I. A. Tsupilo, and L. M. Litvinenko, *ibid.*, **13**, 211 (1977).

(19) I. H. Pitman and T. Higuchi, *J. Org. Chem.*, **40**, 378 (1975).

(20) E. M. Cherkasova, S. V. Bogatkov, and Z. P. Golivina, *Russ. Chem. Rev. (Engl. Transl.)*, **46**, 246 (1977).

(21) L. M. Litvinenko, V. A. Savelova, V. A. Shatskaya, and T. N. Sadovskaya, *Dokl. Akad. Nauk SSSR*, **198**, 844 (1971).

(22) A. Hassner, L. R. Krepski, and V. Alexanian, *Tetrahedron*, **34**, 2069 (1978).

(23) E. Guibe-Jampel, G. Le Corre, and M. Wakselman, *Tetrahedron Lett.*, **1979**, 1157.

(24) N. K. Pandit and K. A. Connors, *J. Pharm. Sci.*, **71**, 485 (1982).

(25) W. H. Hong and K. A. Connors, *Anal. Chem.*, **40**, 1273 (1968).

(26) K. A. Connors and W. H. Hong, *Anal. Chim. Acta*, **43**, 334 (1968).

(27) S.-F. Lin and K. A. Connors, *J. Pharm. Sci.*, **70**, 235 (1981).

(28) R. Adams and L. H. Ulrich, *J. Am. Chem. Soc.*, **42**, 605 (1920).

(29) J. D. M. Simpson and S. S. Israelstam, *J. S. African Chem. Inst.*, **2**, 170 (1949).

ACKNOWLEDGMENT

This work was supported in part by National Science Foundation Grant CHE 78-06603.

Solvent Effects on the Cinnamoylation of *n*-Propyl Alcohol Catalyzed by *N*-Methylimidazole and 4-Dimethylaminopyridine

KENNETH A. CONNORS ˣ **and CHUKWUENWENIWE J. EBOKA**

Received April 5, 1982 from the *School of Pharmacy, University of Wisconsin, Madison, WI 53706.* Accepted for publication June 24, 1982.

Abstract □ The kinetics of reaction of *trans*-cinnamic anhydride or *trans*-cinnamoyl chloride with *n*-propyl alcohol, catalyzed by *N*-methylimidazole or 4-dimethylaminopyridine, were studied spectrophotometrically at 25° in methyl ethyl ketone, ethylene dichloride, methylene chloride, and toluene. The acid chloride reacted in all solvents *via* the intermediate formation of the *N*-acyl catalyst, which underwent reaction with the alcohol catalyzed by another molecule of the base. The anhydride did not form the intermediate in any of the solvents, but underwent direct general base catalysis. The rate of the anhydride reactions was not sensitive to solvent polarity, whereas the rate of the chloride reactions tended to increase as the solvent polarity decreased. A kinetic analysis is given of the effect of ion-pair formation on the kinetics of acyl transfer in systems where the charged *N*-acyl catalyst intermediate is formed.

Keyphrases □ Cinnamoylation—of *n*-propyl alcohol, catalysis by *N*-methylimidazole and 4-dimethylaminopyridine, solvent effects □ 4-Dimethylaminopyridine—catalyses, cinnamoylation of *n*-propyl alcohol □ *N*-methylimidazole—catalyses, cinnamoylation of *n*-propyl alcohol

Although the kinetics and mechanisms of acyl transfer reactions in water have been carefully studied (in large part because such reactions serve as models for enzyme-catalyzed reactions), acyl transfers in nonaqueous media are less well understood despite their great importance in synthesis and analysis. The relatively recent introduction of powerful acylation catalysts like 4-dimethylaminopyridine (1) and *N*-methylimidazole (2) has stimulated in-

0022-3549/83/0400-0369$01.00/0

Table I—Rate Constants for the Reaction of Cinnamoyl Chloride with *n*-Propyl Alcohol at 25°

Solvent	Catalyst[a]	$k_I \times 10^2$ M^{-1} sec^{-1}	k_{IN}/M^{-2} sec^{-1}
Methyl ethyl ketone	NMIM	0.52(0.18)[b]	0.192(0.009)[b]
Methyl ethyl ketone	DMAP	−0.006(0.39)	3.06(0.30)
Ethylene dichloride	NMIM	1.64(0.46)	0.70(0.07)
Ethylene dichloride	DMAP	0.18(0.67)	65.1(1.42)
Methylene chloride	NMIM	0.60(0.10)	0.393(0.021)
Methylene chloride	DMAP	2.5(2.0)	47.0(4.1)
Toluene	NMIM	1.7(2.5)	6.70(0.30)

[a] NMIM = N-methylimidazole; DMAP = 4-dimethylaminopyridine. [b] Standard deviations in parentheses.

vestigations of acylation reactions in nonaqueous solvents by several laboratories. There are features of these reactions, however, that remain obscure: one of these is the effect of the solvent on the mechanism and rate of the reaction. This is the subject of the present paper.

There are two general routes available in an acyl transfer reaction when a nucleophile (base) is present. One of these is a direct reaction of the acylating agent with the acyl acceptor, either general base-catalyzed or uncatalyzed; the other is transfer of the acyl group from the acylating agent to the nucleophile to give an ionic intermediate, which then reacts with the acyl acceptor (in catalyzed or uncatalyzed reactions). Since the latter nucleophilic route presumably involves extensive charge separation in the transition state, it would be expected that high solvent polarity should favor this route. Thus, solvent polarity must be considered in any treatment of solvent kinetic effects. Unfortunately there is no single measure of solvent polarity applicable in all circumstances, so quantitative description is difficult. Many measures of polarity have been devised (3). Besides this general effect of the solvent on the mechanistic route, several specific rate effects have been implicated in acylation reactions. In solvents of low dielectric constant, ionic dissociation is less extensive than in polar solvents and ionic aggregates (particularly ion-pairs) may be present, which may have kinetic consequences. Several workers have suggested that ion-pair formation between the cationic acylated nucleophile and the anionic leaving group may be responsible for some unusual kinetic behavior in these systems (4, 5). Molecular complex formation has been proposed as a factor of importance in nonpolar solvents (6). An interesting observation is that acylation may proceed faster in nonpolar aprotic solvents than in polar protic solvents; this has been attributed to the favored collapse of the charged intermediate to uncharged products (7). The rate equations observed for acylations in solvents of low polarity sometimes are very complex (8).

Earlier work in this laboratory made use of the acid chlorides and anhydrides of acetic and cinnamic acids as acylating agents, 4-dimethylaminopyridine and *N*-methylimidazole as catalysts, and acetonitrile or aqueous acetonitrile as solvents (9, 10). The cinnamoyl group is particularly useful because of its convenient spectral properties, which permit the sensitive observation of the intermediate, if present (10). In the present study the solvent effect on the mechanism and the rate of acylation of *n*-propyl alcohol by *trans*-cinnamoyl chloride or *trans*-cinnamic anhydride, catalyzed by 4-dimethylaminopyridine or *N*-methylimidazole, has been studied in several solvents that are less polar than acetonitrile.

EXPERIMENTAL

Materials—The *trans*-cinnamic anhydride, *trans*-cinnamoyl chloride, 4-dimethylaminopyridine, and *N*-methylimidazole used were as previously described (10, 11). The solvents were of spectrophotometric grade[1] and were used as obtained.

Procedures—Reactions were followed spectrophotometrically[2] as described previously (10). All kinetics reported here are at 25.0°.

RESULTS AND DISCUSSION

Kinetic Scheme—Earlier work (9, 10) in acetonitrile and acetonitrile–water mixtures showed that Scheme I describes most of the kinetic observations.

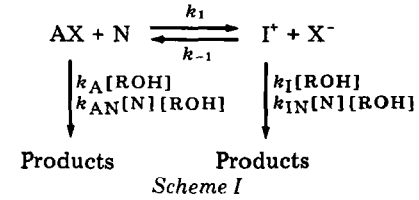

Scheme I

In this kinetic scheme, AX represents the acylating agent (cinnamic anhydride or cinnamoyl chloride), N is the catalyst (4-dimethylaminopyridine or *N*-methylimidazole), X^- is the leaving group (cinnamate or chloride ion), ROH is *n*-propyl alcohol, and I^+ is the *N*-cinnamoylated catalyst I or II, where R is $C_6H_5CH{=}CH$.

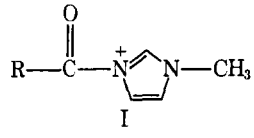

I

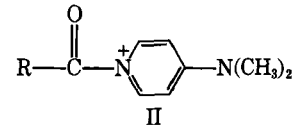

II

Although Scheme I does not include possible ion-pair formation (this phenomenon is treated in the later discussion), it was found to account for most of the observed behavior. Reaction of AX with ROH (the "A" route) may occur *via* uncatalyzed (k_A) or general base-catalyzed (k_{AN}) reactions; nucleophilic reaction of AX with N to form the intermediate I^+ may lead to reaction of I^+ with ROH (the "I" route) *via* uncatalyzed (k_I) and general base-catalyzed (k_{IN}) reactions[3].

The system was examined spectrophotometrically for evidence of the intermediate and the kinetics were measured by following the loss of AX or I^+ as appropriate. The initial concentrations of alcohol and catalyst were much larger than the acylating agent concentration and pseudo first-order rate constants were obtained from plots of log $(A_t - A_\infty)$ against time, where *A* represents absorbance. For most systems these plots were linear for >3 half-lives; exceptions are noted. Rate constants k_A, k_{AN}, k_I, and k_{IN} were determined as described in detail elsewhere (9).

Kinetics in Nonpolar Solvents—The results of these studies consist, in general terms, of two components: (*a*) demonstration of the presence or absence of the intermediate I^+ and (*b*) evaluation of the pertinent rate constants in Scheme I, *i.e.*, k_A and k_{AN} if the intermediate is absent or k_I and k_{IN} if I^+ is present. It is conceivable that these assignments of rate constants are in error because an intermediate, though present, may not be on the reaction path. On the other hand, the intermediate may be present at undetectably low concentrations even though all of the reaction occurs by this route. However, the interpretation given here is the simplest one and is consistent with the observations.

The acid chloride was studied with both catalysts; the anhydride was studied only with 4-dimethylaminopyridine. The anhydride–*N*-methylimidazole system was not studied because earlier work (9, 10) made it clear that no intermediate would be detected in this system. The solvents used were methyl ethyl ketone, ethylene dichloride, methylene chloride, and toluene.

In all solvents, the acid chloride showed evidence of intermediate formation, with both catalysts, with intense absorption in the 340–350 nm region (10). The acid chloride–*N*-methylimidazole system gave strict

[1] Burdick and Jackson.
[2] Cary 14 spectrophotometer.
[3] The k_I route in Scheme I is widely described as nucleophilic catalysis, but it should be observed that if $k_I < k_A$, diversion through this route will actually inhibit the reaction. The k_{IN} reaction can be described as general base-catalyzed nucleophilic reaction.

first-order kinetics in all solvents; however, in toluene the intermediate salt precipitated and it was necessary to increase the concentration of *n*-propyl alcohol (to at least 0.04 *M*) to solubilize the intermediate. The acid chloride–dimethylaminopyridine system gave first-order kinetics in ethylene dichloride and toluene (in toluene at least 0.2 *M* propyl alcohol was added to solubilize the intermediate). In methyl ethyl ketone this system showed first-order behavior for ~3 half-lives and then showed a slight upward curvature. In methylene this system gave more complicated kinetics: the reaction became faster with time and finally, after up to 1 half-life, became satisfactorily first order. The values of k_I and k_{IN} were obtained, for all the acid chloride systems, from the dependence of the observed first-order rate constants on the catalyst and alcohol concentrations by methods described earlier (9, 10). The first-order rate constants were linearly dependent on catalyst and alcohol concentrations[4]. Table I lists the k_I and k_{IN} values found for the acid chloride systems. Most of the k_I values are not significantly different from zero. A qualitative summary of the eight acid chloride systems shows: (*a*) first-order kinetics were observed in six systems, with minor deviations in two; (*b*) in one system the rate seemed to be independent of alcohol concentration (this system is therefore omitted from Table I); and (*c*) in two systems anomalous dependence on catalyst concentration was seen[4]. In general the kinetics appear to be fairly uncomplicated.

In all of the anhydride systems, there was no spectral evidence of intermediate formation, strict first-order kinetics were observed, and the first-order rate constant was linearly dependent on the initial concentrations of catalyst and alcohol[5]. The treatment of the kinetic data (9, 10) yields estimates of k_1, k_A, and k_{AN} (Table II). There appears to be neither high sensitivity nor direct dependence of k_1 on the solvent polarity [in acetonitrile (10) k_1 is 0.096 M^{-1} sec^{-1}], which is surprising if this assignment of k_1 is correct.

Kinetic Effects of Ion-Pairs—It was pointed out that in solvents of low dielectric constant, ion-pair formation is possible, and since in general ion-pairs and dissociated ions may have different properties, kinetic consequences of ion-pairing may be anticipated. To analyze this quantitatively, Scheme I was modified by incorporating the ion-pair I^+X^- as shown:

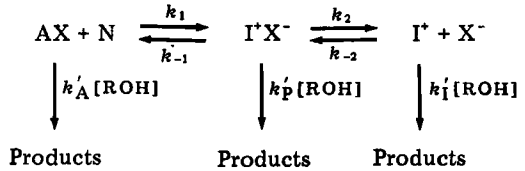

Scheme II

In Scheme II it is expected that the primed quantities have the form $k_A' = k_A + k_{AN}[N]$, *etc.*

In systems such as acid chlorides in the presence of strongly nucleophilic catalysts, intermediate formation is essentially quantitative and Scheme II can be drawn as:

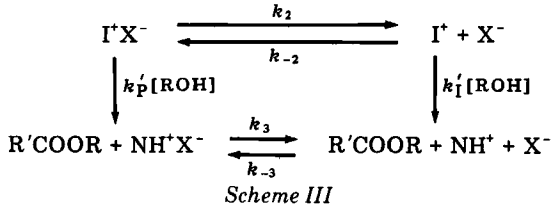

Scheme III

An expression was sought for the rate of loss of reactant. The basic rate equation is:

$$-\frac{d([I^+X^-] + [I^+])}{dt} = k_I'[ROH][I^+] + k_P'[ROH][I^+X^-] \quad \text{(Eq. 1)}$$

The ion-pair equilibrium is assumed to be much faster than the reactions with ROH, so the ion-pair dissociation constant expression (K_d^{IX}) is always satisfied. This may be expressed as:

$$K_d^{IX} = \frac{[I^+][X^-]}{[I^+X^-]} \quad \text{(Eq. 2)}$$

Setting $[X^-]/K_d^{IX} = P$ gives $[I^+X^-] = P[I^+]$, so $-d[I^+X^-]/dt = -P(d[I^+]/dt)$, and Eq. 2 may be expressed as:

$$-\frac{d([I^+X^-] + [I^+])}{dt} = -(1 + P)\frac{d[I^+]}{dt} \quad \text{(Eq. 3)}$$

Equating Eqs. 1 and 3 gives:

$$-\frac{d[I^+]}{dt} = \left(\frac{k_I' + Pk_P'}{1 + P}\right)[I^+][ROH] \quad \text{(Eq. 4)}$$

and similarly:

$$-\frac{d[I^+X^-]}{dt} = \left(\frac{k_I' + Pk_P'}{1 + P}\right)[I^+X^-][ROH] \quad \text{(Eq. 5)}$$

It follows from the above relationships:

$$-\frac{d([I^+X^-] + [I^+])}{dt} = \left(\frac{k_I' + Pk_P'}{1 + P}\right)[ROH]([I^+X^-] + [I^+]) \quad \text{(Eq. 6)}$$

Equation 6 has a first-order form, with apparent first-order rate constant k_{obs} given by:

$$k_{obs} = \left(\frac{k_I' + Pk_P'}{1 + P}\right)[ROH] \quad \text{(Eq. 7)}$$

P is inversely proportional to K_d^{IX}; in solvents of high dielectric constant, P will approach zero, whereas in low dielectric constant solvents, P will become very large. Under pseudo first-order conditions of large catalyst and alcohol concentrations, the quantity k_{obs} will be equal to $k_I'[ROH]$ in polar dissociating solvents, but k_{obs} will approach $k_P'[ROH]$ in nonpolar nondissociating solvents. In solvents whose *polarity permits* the significant coexistence of both the ion-pair and the dissociated ions, k_{obs} is given by Eq. 7.

There is a possible kinetic consequence of Eq. 7 that can be observed if P makes a finite contribution to k_{obs}. During the time course of a reaction, if P is a function of time, k_{obs} may vary detectably and deviations from first-order kinetics may be seen. (This is a possible cause of the deviations that were observed in some of the cinnamoyl chloride systems.) This variaton can be analyzed as follows. The ion Cl^- is a much weaker base than is N in these systems, where N represents 4-dimethylaminopyridine or *N*-methylimidazole. Therefore, the protons produced in the acylation of the alcohol will be accepted predominantly by the catalyst. As a consequence there are two ion-pair equilibria in the solution, as shown in Scheme III. The dissociation constant K_d^{NHX} is defined by:

$$K_d^{NHX} = \frac{[NH^+][X^-]}{[NH^+X^-]} \quad \text{(Eq. 8)}$$

It is instructive to write this in the logarithmic form:

$$pX = pK_d^{NHX} + \log\frac{[NH^+]}{[NH^+X^-]} \quad \text{(Eq. 9)}$$

which is analogous to the Henderson–Hasselbalch equation for aqueous buffer action. That is, the concentration $[X^-]$ is established by a buffer consisting of the protonated catalyst. Since P in Eq. 7 *is equal to* $[X^-]/K_d^{IX}$, evidently the buffer capacity with respect to $[X^-]$ is important in determining the constancy of k_{obs}. This buffer capacity should be maximal when $pX = pK_d^{NHX}$, and it should increase with time since the total buffer concentration ($[NH^+] + [NH^+X^-]$) increases with time. (This may explain why, in the cinnamoyl chloride–dimethylaminopyridine–methylene chloride system, the first-order plot became linear after an initial nonlinear portion.) Whether P increases or decreases with time

Table II—Rate Constants for the 4-Dimethylaminopyridine-Catalyzed Reaction of Cinnamic Anhydride with *n*-Propyl Alcohol at 25°

Solvent	k_1/M^{-1} sec^{-1}	$k_A, \times 10^4 M^{-1}/$ sec^{-1}	k_{AN}/M^{-2} sec^{-1}
Methyl ethyl ketone	0.063(0.019)[a]	19.0(13.3)[a]	1.50(0.11)[a]
Ethylene dichloride	0.274(0.049)	19.0(2.0)	2.93(0.13)
Methylene chloride	0.179(0.063)	10(40)	2.45(0.27)
Toluene	0.198(0.028)	4(10)	3.62(0.10)

[a] Standard deviations in parentheses.

[4] For the dimethylaminopyridine system in toluene the rate constants were linearly dependent on catalyst but independent of alcohol concentration. In methyl ethyl ketone the chloride–dimethylaminopyridine system, and in toluene the chloride–*N*-methylimidazole system, gave different intercepts at different catalyst concentrations when k_{obs} was plotted against alcohol concentration. This may have been caused by reaction with a second trace constituent, possibly water (12).

[5] At high alcohol concentrations the linear dependence is lost for the ethylene dichloride system.

Table III—Third-Order Rate Constants for the Cinnamoylation of *n*-Propyl Alcohol at 25°

Solvent	ϵ[a]	k_{AN} (anhydride, DMAP)[b]	k_{IN} (chloride, DMAP)[b]	k_{IN} (chloride, NMIM)[b]
Acetonitrile[c]	35.9	2.18	2.18	0.23
Methyl ethyl ketone	18.5	1.50	3.06	0.19
Ethylene dichloride	10.4	2.93	65.1	0.70
Methylene chloride	8.9	2.45	47.0	0.39
Toluene	2.4	3.62	—	6.70

[a] Dielectric constant. [b] (Acylating agent, catalyst); units of rate constants are as given in Tables I and II. [c] Data from Ref. 10.

depends on the ratio K_d^{NHX}/K_d^{IX}, because as reaction occurs the species I^+X^-/I^+ are replaced by NH^+X^-/NH^+:

$$P = \frac{[X^-]}{K_d^{IX}} = \frac{[I^+X^-]}{[I^+]} = \frac{K_d^{NHX}[NH^+X^-]}{K_d^{IX}[NH^+]} \qquad \text{(Eq. 10)}$$

Values of ion-pair dissociation constants are extremely sensitive to the solvent dielectric constant, with typical values (13) of 10^{-16}–10^{-12} at dielectric constants of 2–3 and as high as 10^{-5} at dielectric constants near 6. In solvents more polar than acetonitrile, ion-pair formation is probably kinetically negligible. In a given solvent the ratio of ion-pair dissociation constants for two ion-pairs is controlled largely by the effective ionic sizes.

Solvent Effect on Rates and Mechanism—Table III collects k_{AN} and k_{IN} values for the cinnamoylation of *n*-propyl alcohol in five solvents. The k_{AN} values, describing the general base catalysis, are not very sensitive to the nature of the solvent; this is consistent with earlier data on alcohol acetylation by acetic anhydride catalyzed by *N*-methylimidazole (14)[6]. The k_{IN} values for the acid chloride systems reveal considerable variation with solvent polarity, the less polar solvents tending to give higher rates. In solvents that are very nonpolar k_{IN} may be influenced by ion-pair formation, as discussed in connection with Scheme III; therefore, the k_{IN} in Table III may be a composite reflecting both the ion-pair and the dissociated ion routes.

[6] The titrimetrically determined third-order rate constants in these acetic anhydride systems (14) can be interpreted as k_{AN} in Scheme I.

Since the acid chloride and the anhydride react by different mechanisms, it is dangerous to compare them. Several workers have noted that an anhydride appears to be more reactive than the acid chloride in nonpolar solvents, yet (according to Table III) $k_{IN} > k_{AN}$ for a common catalyst. An explanation of these apparently contradictory observations (9) is that formation of the intermediate from the acid chloride consumes an equimolar amount of catalyst, whereas in the anhydride system this depletion of catalyst concentration does not occur, causing $k_{AN}[N]$ in the anhydride system to be greater than $k_{IN}[N]$ is in the acid chloride system.

REFERENCES

(1) W. Steglich and G. Höfle, *Angew. Chem. Int. Ed.*, **8**, 981 (1969).

(2) K. A. Connors and N. K. Pandit, *Anal. Chem.*, **50**, 1542 (1978).

(3) C. Reichardt, *Angew. Chem. Int. Ed.*, **18**, 98 (1979).

(4) L. M. Litvinenko, V. A. Savelova, V. A. Shatskaya, and T. N. Sadovskaya, *Dokl. Akad. Nauk SSSR*, **198**, 844 (1971).

(5) G. Höfle, W. Steglich, and H. Vorbrüggen, *Angew. Chem. Int. Ed.*, **17**, 569 (1978).

(6) E. Guibe-Jampel, G. Le Corre, and M. Wakselman, *Tetrahedron Lett.*, **1979**, 1157.

(7) A. Hassner, L. R. Krepski, and V. Alexanian, *Tetrahedron*, **34**, 2069 (1978).

(8) I. H. Pitman and T. Higuchi, *J. Org. Chem.*, **40**, 378 (1975).

(9) N. K. Pandit and K. A. Connors, *J. Pharm. Sci.*, **71**, 485 (1982).

(10) C. J. Eboka and K. A. Connors, *ibid.*, **72**, 366 (1983).

(11) S.-F. Lin and K. A. Connors, *ibid.*, **70**, 235 (1981).

(12) C. J. Eboka, Ph.D. Thesis, University of Wisconsin-Madison, 1981.

(13) H. S. Harned and B. B. Owen, "The Physical Chemistry of Electrolytic Solutions," 3rd ed., Reinhold, New York, N.Y., 1958, p. 295.

(14) N. K. Pandit, A. O. Obaseki, and K. A. Connors, *Anal. Chem.*, **52**, 1678 (1980).

ACKNOWLEDGMENTS

This work was supported by grants from the National Science Foundation (CHE 78-06603) and The Upjohn Company.

Prodrugs of 6-Thiopurines: Enhanced Delivery Through the Skin

K. B. SLOAN [§ x], **M. HASHIDA** [‡], **J. ALEXANDER** [*], **N. BODOR** [§], **and T. HIGUCHI** [* ‡]

Received December 21, 1981, from the **INTER$_X$ Research Corporation, Merck Sharp and Dohme Research Laboratories, Lawrence, KS 66044; the ‡Department of Pharmaceutical Chemistry, University of Kansas, Lawrence, KS 66045; and the §Department of Medicinal Chemistry, The University of Florida, Gainesville, FL 32610.* Accepted for publication February 18, 1982.

Abstract □ Soft-alkylated derivatives of 6-mercaptopurine, its riboside, and 2-amino-6-mercaptopurine riboside have been prepared and evaluated to improve the delivery of the thiopurines through the skin. The soft-alkylated derivatives were prepared by the alkylation of the thiopurines with acylheteroalkyl halides under neutral or basic conditions. The penetration of the derivatives through hairless mouse skin was measured using diffusion cells. All of the derivatives underwent extensive degradation during their diffusion through skin so that the parent thiopurine, even in the case of the ribosides, was the major product observed in the receptor phase. The pivaloyloxymethyl derivatives showed the greatest potential for enhancing the penetration of the thiopurines through the skin. Among the 6-mercaptopurine derivatives, VII and XI were the most effective; they delivered 5 and 13 times, respectively, more 6-mercaptopurine than 6-mercaptopurine itself.

Keyphrases □ Prodrugs of 6-thiopurines—soft-alkylated derivatives of 6-mercaptopurine, enhanced delivery through the skin, pivaloyloxymethyl derivatives □ Hairless mouse skin—penetration of prodrugs of 6-thiopurines, pivaloyloxymethyl derivatives. □ Pivaloyloxymethyl derivatives—prodrugs of 6-thiopurines, penetration through hairless mouse skin

Many high-melting drugs are insoluble in water and organic solvents; consequently, they have poor biphasic solubilities and are also poorly absorbed through biological membranes. The thiopurines represent one class of such drugs that exhibit these properties. One approach to increasing the solubilities of the thiopurines, while at the

0022-3549/83/0400-0372$01.00/0

Table III—Third-Order Rate Constants for the Cinnamoylation of *n*-Propyl Alcohol at 25°

Solvent	ϵ[a]	k_{AN} (anhydride, DMAP)[b]	k_{IN} (chloride, DMAP)[b]	k_{IN} (chloride, NMIM)[b]
Acetonitrile[c]	35.9	2.18	2.18	0.23
Methyl ethyl ketone	18.5	1.50	3.06	0.19
Ethylene dichloride	10.4	2.93	65.1	0.70
Methylene chloride	8.9	2.45	47.0	0.39
Toluene	2.4	3.62	—	6.70

[a] Dielectric constant. [b] (Acylating agent, catalyst); units of rate constants are as given in Tables I and II. [c] Data from Ref. 10.

depends on the ratio K_d^{NHX}/K_d^{IX}, because as reaction occurs the species I^+X^-/I^+ are replaced by NH^+X^-/NH^+:

$$P = \frac{[X^-]}{K_d^{IX}} = \frac{[I^+X^-]}{[I^+]} = \frac{K_d^{NHX}[NH^+X^-]}{K_d^{IX}[NH^+]} \qquad \text{(Eq. 10)}$$

Values of ion-pair dissociation constants are extremely sensitive to the solvent dielectric constant, with typical values (13) of 10^{-16}–10^{-12} at dielectric constants of 2–3 and as high as 10^{-5} at dielectric constants near 6. In solvents more polar than acetonitrile, ion-pair formation is probably kinetically negligible. In a given solvent the ratio of ion-pair dissociation constants for two ion-pairs is controlled largely by the effective ionic sizes.

Solvent Effect on Rates and Mechanism—Table III collects k_{AN} and k_{IN} values for the cinnamoylation of *n*-propyl alcohol in five solvents. The k_{AN} values, describing the general base catalysis, are not very sensitive to the nature of the solvent; this is consistent with earlier data on alcohol acetylation by acetic anhydride catalyzed by *N*-methylimidazole (14)[6]. The k_{IN} values for the acid chloride systems reveal considerable variation with solvent polarity, the less polar solvents tending to give higher rates. In solvents that are very nonpolar k_{IN} may be influenced by ion-pair formation, as discussed in connection with Scheme III; therefore, the k_{IN} in Table III may be a composite reflecting both the ion-pair and the dissociated ion routes.

[6] The titrimetrically determined third-order rate constants in these acetic anhydride systems (14) can be interpreted as k_{AN} in Scheme I.

Since the acid chloride and the anhydride react by different mechanisms, it is dangerous to compare them. Several workers have noted that an anhydride appears to be more reactive than the acid chloride in nonpolar solvents, yet (according to Table III) $k_{IN} > k_{AN}$ for a common catalyst. An explanation of these apparently contradictory observations (9) is that formation of the intermediate from the acid chloride consumes an equimolar amount of catalyst, whereas in the anhydride system this depletion of catalyst concentration does not occur, causing $k_{AN}[N]$ in the anhydride system to be greater than $k_{IN}[N]$ is in the acid chloride system.

REFERENCES

(1) W. Steglich and G. Höfle, *Angew. Chem. Int. Ed.*, **8**, 981 (1969).

(2) K. A. Connors and N. K. Pandit, *Anal. Chem.*, **50**, 1542 (1978).

(3) C. Reichardt, *Angew. Chem. Int. Ed.*, **18**, 98 (1979).

(4) L. M. Litvinenko, V. A. Savelova, V. A. Shatskaya, and T. N. Sadovskaya, *Dokl. Akad. Nauk SSSR*, **198**, 844 (1971).

(5) G. Höfle, W. Steglich, and H. Vorbrüggen, *Angew. Chem. Int. Ed.*, **17**, 569 (1978).

(6) E. Guibe-Jampel, G. Le Corre, and M. Wakselman, *Tetrahedron Lett.*, **1979**, 1157.

(7) A. Hassner, L. R. Krepski, and V. Alexanian, *Tetrahedron*, **34**, 2069 (1978).

(8) I. H. Pitman and T. Higuchi, *J. Org. Chem.*, **40**, 378 (1975).

(9) N. K. Pandit and K. A. Connors, *J. Pharm. Sci.*, **71**, 485 (1982).

(10) C. J. Eboka and K. A. Connors, *ibid.*, **72**, 366 (1983).

(11) S.-F. Lin and K. A. Connors, *ibid.*, **70**, 235 (1981).

(12) C. J. Eboka, Ph.D. Thesis, University of Wisconsin-Madison, 1981.

(13) H. S. Harned and B. B. Owen, "The Physical Chemistry of Electrolytic Solutions," 3rd ed., Reinhold, New York, N.Y., 1958, p. 295.

(14) N. K. Pandit, A. O. Obaseki, and K. A. Connors, *Anal. Chem.*, **52**, 1678 (1980).

ACKNOWLEDGMENTS

This work was supported by grants from the National Science Foundation (CHE 78-06603) and The Upjohn Company.

Prodrugs of 6-Thiopurines: Enhanced Delivery Through the Skin

K. B. SLOAN [§ x], **M. HASHIDA** [‡], **J. ALEXANDER** [*], **N. BODOR** [§], **and T. HIGUCHI** [* ‡]

Received December 21, 1981, from the **INTER$_X$ Research Corporation, Merck Sharp and Dohme Research Laboratories, Lawrence, KS 66044; the ‡Department of Pharmaceutical Chemistry, University of Kansas, Lawrence, KS 66045; and the §Department of Medicinal Chemistry, The University of Florida, Gainesville, FL 32610.* Accepted for publication February 18, 1982.

Abstract □ Soft-alkylated derivatives of 6-mercaptopurine, its riboside, and 2-amino-6-mercaptopurine riboside have been prepared and evaluated to improve the delivery of the thiopurines through the skin. The soft-alkylated derivatives were prepared by the alkylation of the thiopurines with acylheteroalkyl halides under neutral or basic conditions. The penetration of the derivatives through hairless mouse skin was measured using diffusion cells. All of the derivatives underwent extensive degradation during their diffusion through skin so that the parent thiopurine, even in the case of the ribosides, was the major product observed in the receptor phase. The pivaloyloxymethyl derivatives showed the greatest potential for enhancing the penetration of the thiopurines through the skin. Among the 6-mercaptopurine derivatives, VII and XI were the most effective; they delivered 5 and 13 times, respectively, more 6-mercaptopurine than 6-mercaptopurine itself.

Keyphrases □ Prodrugs of 6-thiopurines—soft-alkylated derivatives of 6-mercaptopurine, enhanced delivery through the skin, pivaloyloxymethyl derivatives □ Hairless mouse skin—penetration of prodrugs of 6-thiopurines, pivaloyloxymethyl derivatives. □ Pivaloyloxymethyl derivatives—prodrugs of 6-thiopurines, penetration through hairless mouse skin

Many high-melting drugs are insoluble in water and organic solvents; consequently, they have poor biphasic solubilities and are also poorly absorbed through biological membranes. The thiopurines represent one class of such drugs that exhibit these properties. One approach to increasing the solubilities of the thiopurines, while at the

0022-3549/83/0400-0372$01.00/0

Table I—Melting Point and UV Spectra of Selected Thiopurines and their Prodrugs

Compound	mp	UV λ_{max} (log ϵ) in Methanol				
I	>300°[a]		229 (3.88)		322 (4.35)[b]	
II	>360°[a]					
IV	221–222°[a]	217 (4.0)	226 (sh, 3.9)		282 (4.13)	288 (4.13)[c]
Va	222–223°	225 (4.19)			282 (4.13)	288 (4.12)
Vb	273.5–274.5°	225 (4.25)		287 (4.22)	296 (4.29)	
VI	189–190°	215 (4.07)	223 (sh, 4.0)		278 (4.14)	284 (4.12)
VII	87–89°	218 (4.17)	226 (sh, 4.13)		278 (4.31)	283 (4.27)
VIII	135–137°	218 (3.99)	256 (3.56)	279 (sh, 3.96)	287 (4.03)	295 (sh, 3.93)
IX	193.5–195°		227 (3.96)		326 (4.23)	
X	183–188°	218 (3.93)	244 (3.85)	300 (3.57)	337 (4.02)	
XI	Oil				276 (4.3)	282 (4.24)
XII	Oil				312 (4.0)	
XIII	255–256°[d]		236 (4.13)		309 (4.37)	
XIV	221–223°[a]				323 (4.4)	
XV	209–211°[d]		251 (3.92)		317 (4.13)	
XVI	230–231°[a]			335 (4.36)	344 (4.42)	
6-Methylthio-1-methylpurine	Free base unstable				307[b]	
6-Methylthio-3-methylpurine	163–165°[e]		238 (4.05)		312 (4.23)[c]	
6-Methylthio-7-methylpurine	212–213°[f]	220 (4.02)		285 (sh, 4.02)	293 (4.12)	301 (sh, 4.04)[c]
6-Methylthio-9-methylpurine	171–172°[g]	219 (4.10)	227 (sh, 4.04)		284 (4.32)	292 (4.2)[c]
1-Methyl-7-benzylpurine-6-thione	171°[h]		238 (4.01)		324 (4.27)[h]	
1,9-Dimethylpurine-6-thione	250°[b]		233 (3.98)		318 (4.32)[b]	
3,7-Dimethylpurine-6-thione	282–283°[b]		246 (3.77)		341 (4.38)[b]	
3,9-Dimethylpurine-6-thione	276–278°[b]		230 (4.13)		327 (4.24)[b]	
7-Methylpurine-6-thione	306–308°[f]				328 (4.31)[b]	
9-Methylpurine-6-thione	>300°[g]		229 (4.10)		321 (4.42)[b]	
3-Methylpurine-6-thione	>300°[i]		245 (3.96)		338 (4.51)[b]	
1-Methylpurine-6-thione	>300°[h]		234 (3.97)		320 (4.32)[b]	

[a] Aldrich Chemical Co. [b] UV of neutral molecule in water (Ref. 18). [c] B. Pullman, H. Berthod, F. Bergmann, Z. Neiman, H. Weiler-Feilchenfeld and E. D. Bergmann *Tetrahedron*, **26**, 1483 (1970); UV of molecule in ethanol. [d] UV of neutral molecule in water (Ref. 16). [e] Ref. 21. [f] E. Fischer, *Ber.*, 31, 431 (1898). [g] R. K. Robins and H. H. Lin, *J. Am. Chem. Soc.*, **79**, 490 (1957). [h] L. Townsend and R. K. Robins, *J. Org. Chem.*, **27**, 990 (1962). [i] F. Bergmann, G. Levin, A. Kalmus, and H. Kwietny-Govrin, *J. Org. Chem.*, **26**, 1504 (1961); UV of neutral molecule in water.

same time ensuring delivery of only the thiopurine, is to prepare prodrugs of the thiopurines.

BACKGROUND

Since cancer and psoriasis are both characterized by proliferation of cells in an uncontrolled manner, it is not surprising that a recurrent theme in psoriasis therapy has been the use of the latest cancer chemotherapeutic drugs. In fact, psoriasis has been effectively treated by the systemic administration of cancer chemotherapeutic agents such as methotrexate (1), azaribine (2), 6-mercaptopurine (3), hydroxyurea (4), and mycophenolic acid (5). Unfortunately, these same agents have generally been found to be ineffective when applied topically. However, the real possibility exists that the systemic toxicity of such agents can be either circumvented entirely or at least minimized, and efforts have been continued to find anticancer agents that are effective topically.

Until recently, the reason for the topical ineffectiveness of many anticancer agents had not been investigated. Now, it has been found that the effect of topical antiproliferative drugs on epidermal DNA synthesis in hairless mice correlates well with the clinical effectiveness of the same topical agents in humans (6), but that there is little correlation between the clinical effectiveness of a topical agent and its ability to decrease epidermal DNA synthesis in essential fatty acid-(EFA) deficient mice. Apparently, the compromised epidermal barrier in the EFA-deficient mice allows some agents to penetrate the skin that are not capable of penetrating the skin of psoriatic patients or hairless mice. For instance, methotrexate, which had failed repeatedly in clinical tests as a topical antipsoriasis agent (7) and which was ineffective in decreasing DNA synthesis in the hairless mouse, was effective in decreasing DNA synthesis by 30% in EFA-deficient mice. Similarly, 15% 6-mercaptopurine and 10% thioguanine sodium were inactive clinically in humans and in the hairless mouse but were active in the EFA-deficient mouse. Thus, the reason that a number of the topically administered anticancer agents tried have been found to be ineffective may be simply that they are not absorbed: they do not penetrate the skin in their present form.

It is easy to see why 6-mercaptopurine and thioguanine are not well absorbed topically. Both purines are high-melting solids (Table I) with very low water or lipid solubility. On the other hand, well-absorbed topical drugs exhibit good water and lipid solubilities which allow their facile penetration through the biphasic epidermal barrier. One way to improve the biphasic solubilities of 6-mercaptopurine (I) and thioguanine (II) is to use the prodrug approach. An attractive prodrug strategy in this case is alkylation rather than the more routinely employed strategy of acylation, since chemical precedent suggests that the sulfur or imidazole acylates that would result are too unstable to be practical.

Inspection of the melting points and solubilities of the products obtained from the alkylation of the pyrimidine uracil shows that a correlation exists between a decrease in melting point and an increase in aqueous solubility (8). However, *N*-alkylation is normally not an easily reversible process *in vivo*, so that the biological activity profile of the parent compound is usually drastically changed by such a modification. On the other hand, in the case of uracil (8), and other amides and imide-like molecules (9), the formation of *N*-hydroxymethyl derivatives results not only in a decrease in the melting point and an increase in the water solubility of the prodrug compared with its parent, but also results in an easily reversible derivative. These *N*-hydroxymethyl derivatives are "soft-alkylated" prodrugs[1] of amides, imides, and amines: they are reversed by chemical hydrolysis rather than initially requiring a metabolically activating oxidation step. However, the range of physical properties of hydroxymethyl derivatives is limited by the relatively small number of aldehydes that will form the hydroxyalkyl adducts and by the fact that a hydroxyl group is introduced into the molecule in each case. Thus, with hydroxymethyl derivatives there is a limit to the concomitant increase in lipid solubility that is both possible and essential for efficient penetration of the epidermal membrane by the prodrug. This difficulty has been overcome by several investigators (10–14) who have acylated the hydroxymethyl derivative to give acyloxymethyl derivatives of the general formula III. Cleavage of the acyl group by esterases gives the hydroxymethyl derivative that, in turn, liberates the parent amide or imide. The acyloxymethyl derivatives, then, are also soft-alkylated derivatives which differ from the hydroxymethyl derivatives in that they must first undergo enzymatic hydrolysis before undergoing chemical hydrolysis.

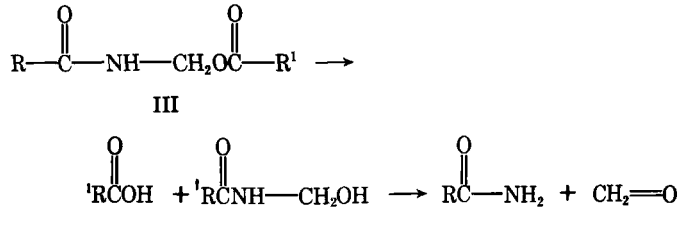

III

[1] These soft-alkylated derivatives are not soft drugs, although other soft-alkylated compounds are soft drugs. For example see N. Bodor, J. Kaminski, and S. Selk, *J. Med. Chem.*, **23**, 469 (1980).

Table II—NMR Spectra of Prodrugs [a]

Compound	(C2)H	(C8)H	SCH_2X	NCH_2X
Va	8.77	8.55	5.85 (d, J = 6Hz) [b]	
Vb	8.90	8.57	5.85 (d, J = 6Hz) [c]	
VI	8.83	8.30	6.06	
VII	8.80	8.23	6.03	6.17
VIII	8.90	8.27	6.03	6.17
IX	8.53	8.08	6.06	6.40
X	8.50	8.23		6.37, 6.63
XI	8.71	8.01	5.90	
XII		7.80	5.90	

[a] Chemical shifts in δ in $CDCl_3$. [b] Run in DMSO-d_6 + $CDCl_3$ (1:5). [c] Run in DMSO-d_6.

The advantage of this type of modification can be illustrated by the case of theophylline (12) in which prodrugs with increased water or lipid solubility or with partition coefficients of ~1 were obtained by varying the acyl group R^1 in III above. Selected derivatives in this series were also found to penetrate the epidermal barrier better than theophylline and to revert to theophylline *in vivo*. In addition, these same derivatives were found to decrease the synthesis of DNA in hairless mice after their topical administration. Thus, it is possible to reduce the melting point and increase not only the biphasic solubility but also the ability of amide and imide drugs to penetrate the epidermal barrier by acyloxyalkylation.

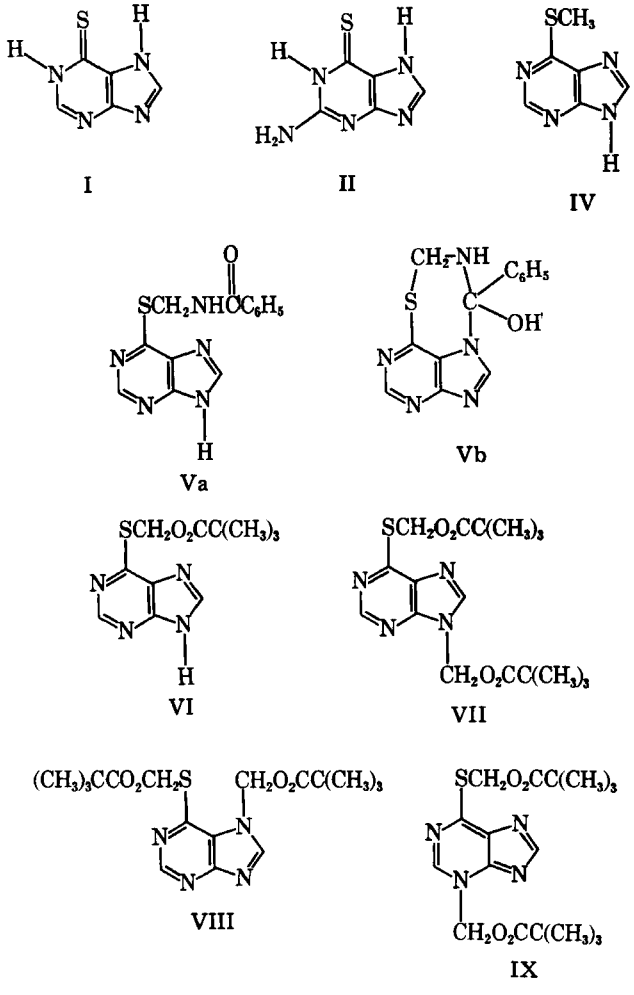

It is clear from the data listed in Table I that alkylation on nitrogen in 6-mercaptopurine does not drastically decrease the melting point of the 6-mercaptopurine derivative. This is probably because I and its 7- and 9-alkylated derivatives exist primarily in the thioamide form (15). On the other hand, S-alkylation drastically reduces the melting point of the 6-mercaptopurine derivative, either by itself or more dramatically in combination with N-alkylation; there are similar trends in the melting points of the alkylated 2-amino-6-mercaptopurine (II) series. Therefore, as a first step in determining whether the lack of clinical activity exhibited by I and II was due to their inability to penetrate the epidermis, a number of S-acylheteroalkylated derivatives of I and XVI were synthesized and their physical properties examined. The preliminary results of that work are reported here.

RESULTS AND DISCUSSION

There have not been any previous reports on the synthesis of S-acylheteroalkyl derivatives of heterocyclic thione amides such as I or II. However, the alkylations were relatively straightforward. Representatives of two types of acylheteroalkyl derivatives were prepared for I. The first type was the S-acylaminomethyl derivative V. Compound V was prepared from the reaction of chloromethylbenzamide with I in dimethylsulfoxide. Under these conditions, alkylations of I with other alkylating agents have been shown to take place exclusively on sulfur (18). In addition, the elemental analysis, and the NMR and mass spectra were consistent only with a monoalkylated derivative. Among the possible monoalkylated derivatives, the UV spectrum (Table I) was consistent only with the S-alkylated derivative (compare Va with IV).

The only unusual feature of this reaction was the formation of two monoalkylated products, which have been designated as Va and Vb. Compound Va differs significantly from Vb in its TLC, melting point, solubility, and UV and mass spectra. The NMR spectra (Table II) of the two compounds are identical except for the difference in the position of the (C2)H absorptions, which is comparable to the difference exhibited by the (C2)H absorptions in the imidazole alkylated tautomers VII and VIII. The UV spectral difference between Va and Vb is also similar to the difference between 6-methylthio-7- and 6-methylthio-9-methylpurine and between VII and VIII. In each case the S^6,7-disubstituted product exhibits a UV maximum at a longer wavelength than that of the S^6,9-disubstituted product. However, although the spectral data suggest that Va and Vb are simply 9-H and 7-H tautomers, the separation and isolation of the two tautomers should be impossible because the energy difference between the 7-H (Vb) and 9-H (Va) tautomers is only about 3.5 kcal (19). On the other hand, the 7-H tautomer can form a cyclic adduct, which is shown as Vb[2]. There is chemical precedent for the formation of similar cyclols from amide–amide adducts in small peptides (20). In this case the adduct stabilizes the less stable 7-H tautomer of V as Vb.

Only one representative of the S-acylaminoalkyl-type derivative was studied in diffusion cell experiments. Although the melting points of both derivatives (Va and Vb) were lower than that of I, only the lower melting derivative Va was studied. Derivative Va did not enhance the diffusion of I through the skin (Table III). Apparently the amide N—H group of this type of derivative introduces too much polarity into the derivative to provide much assistance to the diffusion of 6-mercaptopurine.

The second type of acylheteroalkyl derivative of I and II is the pivaloyloxymethyl derivative. The pivaloyloxymethyl group has been used previously as a protecting and reaction-steering group in some alkylation reactions of adenine examined by Rasmussen and Leonard (21). However, this is the first report of the pivaloyloxymethyl group being used as a protecting group for sulfur. In this study it was possible to condense I with chloromethyl pivalate in dimethylsulfoxide to give the monoalkylated derivative VI, albeit in very low yield especially compared with the good yields of V that were obtained above. The structure of VI followed from its UV and NMR spectra which were consistent with monoalkylation on sulfur[3]. Derivative VI was not tested in the diffusion cells because other, lower-melting representatives of this class of acylheteroalkylated I were more attractive candidates.

It was also possible to prepare dialkylated derivatives of I. Compound I was condensed with excess chloromethyl pivalate in the presence of base in dichloromethane to give a mixture of dialkylated products based on the NMR spectrum of the crude reaction product. Although chemical precedent (18) suggests that the S-alkylated product is formed as an intermediate, such as intermediate (VI) is much more soluble in dichloromethane than I and is more available than I itself for further reactions with chloromethyl pivalate. Thus, VI was not obtained as a product under these reaction conditions even when only one equivalent of chloromethyl pivalate was used; instead, unreacted I and the same mixture of the dialkylated products were obtained. Methyl iodide did not react with I in dichloromethane in the presence of triethylamine. On the other hand, chloromethylbenzamide did react to give two high-melting dialkylated products of undetermined structure. Their diffusion through skin was not studied because of their melting points.

[2] Based on mass spectral considerations, K. B. Sloan and Alice Ng, unpublished results.

[3] The UV absorption maxima for the 1-, 3-, 7-, or 9-monomethyl derivatives are all at much longer wavelengths (see Table I).

Table III—Diffusion of Prodrugs of Thiopurines Through Hairless Mouse Skin

Compound	% Prodrug Remaining in Donor Phase after 48 hr, ± *SD*	Drug in Receptor Phase 6-Mercaptopurine after 48 hr, m*M* ± *SD*	Drug in Receptor Phase as Intact Prodrug after 48 hr, m*M* ± *SD*
I		$2.6 \times 10^{-3} \pm 4.9 \times 10^{-4}$	
Va	96.5 ± 1.09	$0.3 \times 10^{-3} \pm 1.1 \times 10^{-4}$	0
VII	75.1 ± 3.0	$13 \times 10^{-3} \pm 2 \times 10^{-3}$	0
IX	89.7 ± 2.8	$3.9 \times 10^{-3} \pm 1.3 \times 10^{-3}$	$0.37 \times 10^{-3} \pm 1.3 \times 10^{-4}$
XI	61.9 ± 8.8	$33 \times 10^{-3} \pm 1 \times 10^{-2}$	$0.35 \times 10^{-3} \pm 2.1 \times 10^{-4}$
XII	38.9 ± 10.5		
XIII	92.5 ± 6.4	$2.15 \times 10^{-3} \pm 1.1 \times 10^{-3}$	$0.2 \times 10^{-3} \pm 1 \times 10^{-4}$
XIV	91.7 ± 0.33	$1.5 \times 10^{-3} \pm 3 \times 10^{-4}$	0

The structures of the dipivaloyloxymethylated products were determined by a combination of NMR and UV spectroscopy. The dialkylated products VII and VIII were assigned the S^6,9- and S^6,7-structures because their NMR spectra contained both SCH_2O and NCH_2O absorptions (Table II), and because their UV spectra were very similar to those of the corresponding S^6,9- and S^6,7-dimethyl derivatives of I (Table I);[4] the UV spectra are characteristic of the respective dialkyl substitution patterns in I.

The dialkylated product IX was assigned the S^6,3-dialkylated structure because its NMR spectrum contained the SCH_2O and NCH_2O groups and its UV spectrum contained a UV maximum at 326 nm. The only other possible sulfur, nitrogen-dialkylated I candidate which exhibits similar UV spectral properties to IX is the S^6,1-dialkylated structure. However, such structures are very unstable as the free base, while IX has been observed to be stable at room temperature for 2 years. The formation of IX is not surprising in view of the fact that the alkylation of I with methyl tosylate under neutral conditions gives S^6,3-dimethylmercaptopurine (22). Furthermore, since the reactions between triethylamine and chloromethyl pivalate and between triethylamine and VI were found to be incomplete reactions, there was ample opportunity for VI, rather than its ion, to react with chloromethyl pivalate.

The fourth product (X) that was isolated from the reaction mixture was also a dialkylated product, but its NMR spectrum lacked the SCH_2O absorption. Therefore, it was not an *S,N*-dialkylated product but rather a *N,N*-dialkylated product. The various possible *N,N*-dialkylated products arise by alkylation of a *S,N*-dialkylated product followed by *S*-dealkylation. In the case of the 3,7- or 3,9-dialkylated products, *S*-dealkylation only takes place by thio-hydrolysis and would not occur spontaneously under the above reaction conditions. On the other hand, 1,7- or 1,9-dialkylated products have been shown to form spontaneously from S^6,1,9- and S^6,1,7-trialkylated intermediates during the alkylation of 1-methyl-6-mercaptopurine (18) with methyl iodide or benzyl chloride, respectively. Thus, X is probably a 1,7- or 1,9-dialkylated product based on its NMR and UV spectra. To check the possibility that X was formed from further alkylation of the major product VII, VII was allowed to react for 2 days with chloromethyl pivalate either in excess or with triethylamine in excess; no reaction at all occurred. Since the only reactions leading to 1,7- or 1,9-dialkylated products start with 1-alkyl-6-mercaptopurine, it appears likely that in addition to initial *S*-alkylation of I some small amount of 1-alkylation also takes place under these reaction conditions and ultimately leads to the formation of X.

Compounds XI and XII were also prepared under basic conditions but in acetone using potassium carbonate as the base. The riboside hydroxyl groups in these cases were converted to their acetate esters to protect them from possible side reactions with chloromethyl pivalate. The structures of XI and XII follow from their UV and NMR spectra. The UV spectrum of XI is very similar to that of VII, which is characteristic of the S^6,9-substitution pattern of dialkylated 6-mercaptopurine. Both XI and XII exhibited an absorption at δ 5.90 in their NMR spectra, which is characteristic of the SCH_2O group.

The results from the diffusion studies with the *S*-acylheteroalkyl derivatives are shown in Table III. It is obvious that all of the *S*-alkylated prodrugs of I (except for Va) enhance the delivery of I to the receptor phase, and that in any comparison among prodrugs the lower melting prodrug is the one that produces the higher level of 6-mercaptopurine in the receptor phase (compare for instance VII and IX). Compounds VII, XI, and XII appear to be the most attractive candidates for screening in the hairless mouse model (6).

[4] The 1,9-, 1,7-, 3,7-, 3,9-, S^6,1-, and S^6,3-dimethyl derivatives all exhibit UV absorption maxima at much longer wavelengths and between the S^6,7- and S^6,9-derivatives the derivative exhibiting the shorter wavelength UV maximum is the S^6,9-dimethyl derivative.

The results from the diffusion studies also illustrate the advantage that soft alkylation enjoys over the more traditional approach, *i.e.*, esterification, to prodrug modification of the physical chemical properties of drugs. The triacetyl riboside of I (XIII), although marginally more effective than the riboside itself (XIV), is <7% as effective as the soft-alkylated prodrug based on the triacetylated riboside (XI). Thus, to significantly improve the delivery of I through the skin, it is imperative that the thione amide group be alkylated in a transient manner.

The prodrugs deliver very little if any of the intact prodrug to the receptor phase. This does not appear to be due to degradation of the prodrug in the receptor phase after diffusion of the intact prodrug, because even the earliest samples taken of the receptor phase (3 hr) show the same ratio of prodrug to 6-mercaptopurine, and the prodrugs are stable at pH 7.4 for that length of time (Table IV). The fact that primarily 6-mercaptopurine (I) and 2-amino-6-mercaptopurine (II) are found in the receptor phase after the absorption of the alkylated forms of I, its riboside, and the riboside of II, is a consequence of using fresh skin with metabolic systems that were still active and of the sensitivity of the nucleosides to nucleoside phosphorylase (23).

In the case of XII, it was impossible to determine quantitatively the amount of 2-amino-6-mercaptopurine or XII in the receptor phase. The major product appeared to be 2-amino-6-mercaptopurine (II), but there were a number of other unidentified products also formed which interfered with its analysis. Based only on the very small amount of XII remaining in the donor phase, it seems that XII is a very efficient prodrug form for the delivery of II or XVI.

It is interesting that the *S*-benzamidomethyl derivative Va hydrolyzed completely during its diffusion through the skin. Although the stability of *S*-benzamidomethyl cysteine (24) has not been reported, *S*-acetamidomethyl cysteine is reportedly completely stable at pH 13 and 1 (25). Apparently, amidomethyl derivatives of thioamides such as I are much more labile than those of aliphatic thiol groups. The mechanism for the hydrolysis of *S*-acetamidomethyl or *S*-benzamidomethyl groups is not known, but it may be similar to the mechanism proposed for the hydrolysis of amidomethylamines (26) which involves a unimolecular N—C cleavage as the rate-determining step. The relatively short $t_{1/2}$ in buffer which increases[5] with increasing methanol concentration (decreasing dielectric constant) suggests that such an interpretation has merit.

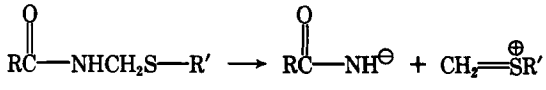

Based on the solubility data in Table IV, the prodrugs that were completely soluble in isopropyl myristate at the concentration at which they were applied were the prodrugs that gave the greatest absorption. Thus, since flux is directly proportional to concentration of the drug in the applied phase (27), it is possible, and even probable, that the reason that I and Va were not absorbed more completely was primarily that they were not soluble enough in the vehicle and, hence, not available for absorption while VII, XI, and XII were available. The prodrug approach in this case then may be considered (*a*) as a quasi-formulation approach to enhancing delivery which overcomes the poor solubility of the drug in a commonly used component of formulations or (*b*) as actually increasing the diffusivity of the prodrug in the skin. There is not enough information available to decide between these two explanations. However, this should not detract from the practical result that more I is delivered by using these *S*-acyloxymethyl prodrugs than by using I, XIII, or XIV.

There does not appear to be any linear correlation between the lipo-

[5] K. B. Sloan and Alice Ng, unpublished results.

Table IV—Physicochemical Characteristics of Thiopurines and Selected Prodrugs

Compound	Solubility, m*M*			log k' Methanol–Water 50:50	$t_{1/2}$ (hr) for Loss of Intact Prodrug at pH 7.4
	pH 7.4 Buffer	Isopropyl Myristate	Chloroform		
I	0.2	−0[a]	0.004	−0.336	
II				−1.074	
Va	0.003	0.42		0.820	0.53
VII		>10.0		1.659	
IX		0.74		1.142	
XI	0.02	>10.0	>2.0	1.260	31.2
XII	0.02	>10.0	>2.0	0.877	30.3
XIII	7.8	0.16	>2.0	0.735	25.6
XIV		0.01		−0.513	196

[a] Could not be measured.

philic index log k' (28) generated from HPLC data and the absorption of the prodrugs.

Finally, from a practical point of view, since both VII and XI primarily deliver I, which is subsequently converted to the corresponding riboside phosphate by hypoxanthine–guanine phosphoribosyltransferase (29) *in vivo*, and the riboside XIV cannot be converted to its phosphate directly, the greater cost of the starting material (XIV compared with I) for XI balances the greater efficiency of delivery of I by XI. Thus, depending on the relative activity of VII and XI in inhibiting DNA synthesis in the hairless mouse model, VII may be the more practical prodrug form of I in spite of the fact that it actually enhances the delivery of I less than XI.

EXPERIMENTAL[6]

Synthesis of 6-Benzamidomethylmercaptopurine (Va)(Vb)—To a dimethylsulfoxide solution (4 ml) containing 0.80 g (0.0047 mole) of 6-mercaptopurine hydrate was added 0.90 g (0.0053 mole) of freshly prepared chloromethylbenzamide. The solution was stirred at room temperature overnight to give a suspension which was dissolved in 10 ml of chloroform, and then stirred with 1 ml of triethylamine for 30 min. The solution was diluted to 100 ml with dichloromethane and was then extracted with 50 ml of water. The water layer was quickly separated, because a precipitate formed in the dichloromethane layer immediately after the water wash. The dichloromethane suspension was filtered. The residue was dried to give 0.60 g (mp 205–211°, 45% yield) of Vb as white crystals. A 0.21-g sample of Vb was crystallized from methanol to give an analytical sample of Vb that was identical with the crude product by TLC, NMR, and IR spectroscopy: 0.19 g, mp 273.5–274.5°, IR (KBr) 1640 and 1660 cm^{-1} (s) (C=O); TLC (silica gel, ether–methanol, 10:3) R_f 0.52 (6-mercaptopurine R_f 0.47); ^1H NMR (DMSO-d_6) δ 9.77 (t, 1, J = 6 Hz, N—*H*), 8.0–7.73 (m, 2, aromatic *H*), 7.7–7.33 (s, 3, aromatic *H*), 5.47 (s, 1, imidazole N—*H*).

Anal.—Calc. for $C_{13}H_{11}N_5OS$: C, 54.74; H, 3.88; N, 24.56. Found: C, 55.03; H, 3.88; N, 23.99.

The dichloromethane filtrate from the above isolation of Vb was concentrated to give a yellow wax which was crystallized from methanol and dichloromethane to give 0.38 g (mp 206–208°, 29% yield) of Va as yellow crystals. A 65-mg sample of Va was recrystallized from 20 ml of chloroform to give 50 mg (*foamed at* 150°; resolidified at 175°; mp 222–223°) of Va as white crystals which was identical with the crude Va by TLC, NMR, and IR spectroscopy: IR (KBr) 1660, 1650, and 1640 cm^{-1} (s) (C=O); ^1H NMR ($CDCl_3$-DMSO-d_6, 5:1) δ 8.0–7.73 (m, 2, aromatic *H*) and 7.7–7.33 (s, 3, aromatic *H*).

Anal.—Calc. for $C_{13}H_{11}N_5OS$·0.4 $CHCl_3$: C, 48.31, H, 3.45, N, 21.02 Found: C, 47.97; H, 3.05; N, 20.98.

When the chloroform solvate was heated to 200° for 2 min then cooled, the light-yellow solid (mp 215–218°) that was obtained exhibited only one spot upon TLC analysis and the same UV spectrum as the solvate.

Anal.—Calc. for $C_{13}H_{11}N_5OS$: C, 54.74; H, 3.89; N, 24.56. Found: C, 54.34; H, 3.66; N, 24.33.

6-Pivaloyloxymethylmercaptopurine (VI))—A dimethylsulfoxide solution (3 ml) containing 0.85 g (0.0057 mole) of chloromethyl pivalate was allowed to react with 0.63 g (0.00375 mole) of 6-mercaptopurine hydrate at room temperature overnight. The reaction mixture was processed as above. However, not all of the precipitate in the reaction mixture was soluble in the dichloromethane, and when that suspension was filtered 0.35 g (mp >270°, 56% recovery) of 6-mercaptopurine was obtained as a yellow solid. After the filtration, the dichloromethane solution was washed with water, but a precipitate did not form in the dichloromethane solution as above. The residue from the dichloromethane solution was chromatographed on silica AR CC-7 using ether as the eluent. An oil was obtained which was crystallized from hexane–dichloromethane to give a total of 25 mg (mp 179–182°, 2.5% yield, 5.7% conversion) of VI as white fibrous crystals: IR (KBr) 1740 cm^{-1} (s) (C=O); ^1H NMR ($CDCl_3$) δ 1.2 [s, 9, (CH_3)$_3$C]; TLC (silica gel, ether) R_f 0.12. The 25 mg which had been used for the NMR sample was recrystallized from dichloromethane–hexane to give 11 mg (mp 189–190°) of an analytical sample of VI, which was identical with the crude product by IR spectroscopy and TLC.

Anal.—Calc. for $C_{11}H_{14}N_4O_2S$: C, 49.61; H, 5.30; N, 21.04. Found: C, 49.53; H, 5.34; N, 20.99.

Reaction of Chloromethyl Pivalate with 6-Mercaptopurine Hydrate: The Preparation of VII, VIII, IX, and X—To 2.0 g (0.0118 mole) of 6-mercaptopurine hydrate suspended in 10 ml of dichloromethane and 6 ml of triethylamine was added 5.28 g (0.035 mole) of chloromethyl pivalate. The reaction was stirred at room temperature overnight to give a suspension which was diluted to 100 ml with dichloromethane to give a clear-yellow solution. The solution was washed with water (50 ml), 10% concentrated HCl (50 ml), and water (50 ml) and then was dried over sodium sulfate and concentrated. The residue was triturated with 50 ml of ether and allowed to stand overnight. The suspension was filtered to give 0.40 g of IX as a yellow solid. This material was recrystallized from dichloromethane–ether (2:8 ml) to give 0.35 g (mp 193.5–195.0°, 8% yield) of IX as yellow crystals: IR (KBr) 1735 cm^{-1} (s) (C=O); ^1H NMR ($CDCl_3$) δ 1.2 [s, 18, (CH_3)$_3$C]; TLC (silica gel, ether) R_f 0.0.

Anal.—Calc. for $C_{17}H_{24}N_4O_4S$: C, 53.66; H, 6.36; N, 14.73. Found: C, 53.68; H, 6.30; N, 14.80.

The ether filtrate described above was chromatographed on silica AR CC-7 using ether as the eluent to give three fractions. The first fraction was crystallized from petroleum ether (bp 37–42°)-heptane (20:15 ml) to give 2.05 g (mp 87–89°, 45% yield) of VII as white crystals: IR (KBr) 1735 cm^{-1} (s) (C=O); ^1H NMR ($CDCl_3$) δ 1.18 [s, 18, (CH_3)$_3$C]; TLC (silica gel, ether) R_f 0.52.

Anal.—Calc. for $C_{17}H_{24}N_4O_4S$: C, 53.66; H, 6.36; N, 14.73. Found: C, 53.88; H, 6.51; N, 14.80.

The second fraction was crystallized from ether to give 17 mg (mp 135–137°, 0.3% yield) of VIII as yellow crystals: IR (KBr) 1735 cm^{-1} (s) (C=O); ^1H NMR ($CDCl_3$) δ 1.18 [s, 18, (CH_3)$_3$C]; TLC (silica gel, ether) R_f 0.25.

Anal.—Calc. for $C_{17}H_{24}N_4O_4S$: C, 53.66, H, 6.36, N, 14.73. Found: C, 53.48; H, 6.41; N, 14.67.

The third fraction was also crystallized from ether to give 43 mg (mp 183–188°, 1% yield) of an unknown compound X: IR (KBr) 1720 and 1745 cm^{-1} (s) (C=O); ^1H NMR ($CDCl_3$) δ 1.18 [s, 18, (CH_3)$_3$C]; TLC (silica gel, ether) R_f 0.21.

Anal.—Calc. for $C_{17}H_{24}N_4O_4S$: C, 53.66; H, 6.36; N, 14.73. Found: C, 53.60; H, 6.36; N, 14.69.

[6] TLC were run on Brinkman Polygram Sil G/UV 254; ether or ether–methanol mixtures. Melting points (uncorrected) were taken with a Thomas-Hoover Capillary apparatus. NMR spectra were recorded on a Varian T-60. IR spectra were obtained on a Beckman Accu Lab 4 infrared spectrophotometer. Microanalyses were obtained by Midwest Microlab, Ltd., Indianapolis, Ind. or by Atlantic Microlab, Atlanta Ga. The benzamide, chloromethyl pivalate, formaldehyde, acetyl chloride, and thionyl chloride were obtained from Aldrich. The 6-mercaptopurine, 6-mercaptopurine-9-riboside, 6-mercapto-2-aminopurine, 6-mercapto-2-aminopurine riboside, and 6-methylmercaptopurine were obtained from Sigma. The bulk solvents were obtained from Mallinckrodt. The hairless mice (SKH-hr-1) were obtained from the Temple University Skin and Cancer Hospital and the diffusion cells were obtained from Kercso Engineering Consultants., Palo Alto, Calif. The HPLC system was a Water Associates instrument using a Chrompack C_{18} column.

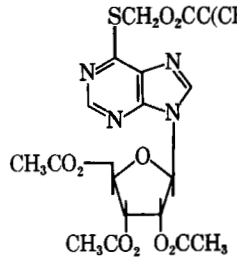

XI

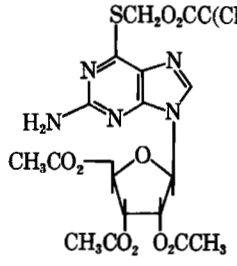

XII

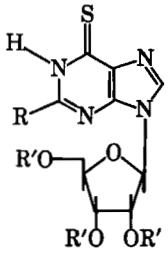

XIII: R = H; R′ = $COCH_3$
XIV: R = H; R′ = H
XV: R = NH_2; R′ = $COCH_3$
XVI: R = NH_2; R′ = H

Preparation of 9-β-D-Ribofuranosyl-6-pivaloyloxymethylthio-9H-purine 2′,3′,5′-triacetate (XI)—Chloromethyl pivalate (112 mg) in acetone (10 ml) was allowed to react with sodium iodide (135 mg) in the dark for 40 min. The solution was decanted into a solution of 9-β-D-ribofuranosyl-6-thio-9H-purine 2′,3′,5′-triacetate (16) (254 mg, 0.00062 mole) in 30 ml of acetone. Potassium carbonate (1.0 g) was added to the resulting solution and the mixture was stirred in the dark. When the reaction was complete by TLC[7], the reaction mixture was filtered and the filtrate was evaporated. The residue was dissolved in ethyl acetate, and the solution was washed with water (three times), dried over sodium sulfate, and the solvent removed to yield a residue (350 mg, contaminated with traces of pivaloyloxymethyl halides) which was dissolved in ethyl acetate and filtered through silica gel (12.5 g). Compound XI was obtained as a pale white waxy solid (296 mg 91%) and showed one spot on TLC: IR (neat) 1755, cm^{-1} (s) (C=O); ^1H NMR ($CDCl_3$)δ 1.10 [9, s, $(CH_3)_3C$], 2.03 (3, s, CH_3CO_2), 2.06 (3, s, CH_3CO_2), 2.15 (3, s, CH_3CO_2), 4.43 (3, $CH_2OAc + 4'H$), 5.70 (1, m, 3′H), 6.0 (1, 6, 2′H), 6.25 (1, d, 1′H); TLC (silica gel, ethyl acetate–chloroform, 1:1) R_f 0.32; exact mass calculated for $C_{22}H_{28}N_4O_9S$ (m/z) 524.1575 (M^+): Found, 524.1561 (m/z).

Preparation of 9-β-D-Ribofuranosyl-2-amino-6-pivaloxymethylthio-9H-purine 2′,3′,5′-triacetate (XII)—To a solution of chloromethyl pivalate (106 mg) in acetone (15 ml) was added sodium iodide (130 mg). The suspension was stirred for 35 min while protected from light. The supernatant was decanted from the precipitated sodium chloride and added to a solution of thioguanosine triacetate (16) (250 mg, 0.00059 mole) in acetone (25 ml). Potassium carbonate (1.0 g) was added to the reaction mixture, stirring was continued for 69 hr, and then the suspended solid was filtered and washed with acetone. The filtrate was evaporated to dryness. The residue was dissolved in ether, and the resulting solution washed with water (three times), dried over sodium sulfate, and then the solvent was evaporated. The residue was purified by chromatography on silica gel (12.5 g, chloroform–ethyl acetate 1:1), to give the pivaloyloxymethyl derivative XII (82 mg, 57.4%) as a foam which showed one spot on TLC: IR (film) 3380 and 3490 cm^{-1} (s) (NH) 1738 cm^{-1} (s) (C=O); ^1H NMR ($CDCl_3$) δ 1.15 [9, s, $(CH_3)_3C$] 2.05 (3, s, CH_3CO_2), 2.08 (3, s, CH_3CO_2), 2.13 (3, s, CH_3CO_2), 4.41 (3, s, $CH_2OAc + 4'H$), 5.20 (2, s, NH_2), 5.80 (1, broad, 3′H), 5.96 (1, t, 2′H), 6.0 (1, d, 1′H); exact mass calculated for $C_{22}H_{29}N_5O_9S$, 539.1683 (m/z): Found, 539.1680 (m/z); TLC (silica gel[3], ethyl acetate–chloroform, 1:1) R_f 0.32.

Diffusion Cell Studies—Full thickness dorsal skin of 12- to 14-week-old female hairless mice was used. The mice were sacrificed by snapping the spinal cord. The excised skin was gently scrapped to remove fat and visceral debris and then gently secured over the diffusion cell with a rubber gasket. The diffusion cells themselves have been previously described (17). The receptor side of the cell (43 ml) was filled with pH 7.4 isotonic phosphate buffer containing 100-ppm gentamicin, which was stirred magnetically. The compounds were applied as 0.01 *M* solutions or suspensions in 500 μl of isopropyl myristate to the donor side of skin. The cells were kept at 32° and 1-ml samples were removed at 3, 9, 24, and 48 hr; 1 ml of buffer was added to the receptor after each sample was withdrawn. Samples were frozen immediately after they were taken and stored at 0° until analyzed. Controlled studies showed that using this procedure, no change in the sample composition took place during the cold storage time. After 48 hr the donor side was washed with 25 ml of methanol, and the methanol and buffer samples were analyzed for the prodrug and its parent drug by high-performance liquid chromatography (HPLC). The HPLC analysis was performed at 25° using mixtures of methanol and distilled water as the mobile phase and a flow rate of 1–2 ml/min. The results for each compound studied are for four diffusion cells.

Solubility Studies—The lipophilic indices ($\log k' = \log [(t_r - t_0)/t_0]$, where t_r is the retention time and t_0 is the elution time of solvent) for the prodrugs were determined by HPLC using mixtures of methanol and distilled water on Chrompack C_{18} column at 25°. There was no effect of pH 3–10 of the mobile phase on the retention time of the prodrugs Va, VII, IX, XI, and XII; of pH < 7.5 on the retention time of XIII; and of pH < 4 on the retention time of I and XIV. A plot of log *k′ versus* percent methanol was linear in each case over four methanol–water concentrations. The values for log *k′* are given in Table IV along with some miscellaneous solubility data. These solubilities were obtained by suspending an excess of the drug or prodrug in the appropriate solvent and sonicating the suspension for 20 min. The suspension was then quickly equilibrated at 37° and centrifuged. The supernatant was then filtered, diluted with more of the solvent, and analyzed by HPLC using the above conditions.

Stability Studies—The rates of degradation of the thiopurines and their prodrugs were determined by adding 50 μl of a 0.025 m*M* methanol solution of the compound to 10 ml of a pH 7.4 phosphate buffer solution at 37°. The solutions were shaken vigorously and then stirred magnetically during sampling. Samples were stored at 0° until analyzed. Analysis was accomplished by HPLC using the above conditions.

[7] Analtech silica gel GHLF.

REFERENCES

(1) E. J. Van Scott, R. Auerback, and D. G. Weinstein, *Arch. Dermatol.*, **89**, 550 (1964).

(2) H. G. Milstein, R. C. Cornell, and R. B. Stoughton, *ibid.*, **108**, 43 (1973).

(3) R. E. Kravetz and T. Balsam, *ibid.*, **84**, 597 (1961).

(4) U. W. Leavell and J. W. Yarbro, *ibid.*, **102**, 144 (1970).

(5) W. S. Lynch and H. R. Roenigk, *ibid.*, **113**, 1203 (1977).

(6) N. J. Lowe, R. B. Stoughton, J. L. McCullough, and G. D. Weinstein, *ibid.*, **117**, 394 (1981).

(7) D. S. Nurse, *ibid.*, **87**, 258 (1963).

(8) P. C. Bansal, I. H. Pitman, J. N. S. Tam, M. Mertes, and J. J. Kaminski, *J. Pharm. Sci.*, **70**, 850 (1981).

(9) P. C. Bansal, I. H. Pitman, and T. Higuchi, *ibid.*, **70**, 855 (1981).

(10) C. F. Spencer and J. G. Michels, *J. Org. Chem.*, **29**, 3416 (1964).

(11) J. A. Vida, M. H. O'Dea, C. M. Samour, and J. F. Reinhard, *J. Med. Chem.*, **18**, 383 (1975).

(12) N. S. Bodor and K. B. Sloan, U.S. Pat., 4,061,753 (December 6, 1977).

(13) V. J. Stella and K. B. Sloan, U.S. Pat., 4,163,058 (July 31, 1979).

(14) S. Ozaki, Y. Ike, and H. Mori, *Chem. Abstr.*, **92**, 128964 (1980).

(15) M. T. Chenon, R. J. Pugmire, D. M. Grant, R. P. Panzica, and L. B. Townsend, *J. Am. Chem. Soc.*, **97**, 4636 (1975).

(16) J. F. Gerster, J. W. Jones, and R. K. Robins, *J. Org. Chem.*, **28**, 945 (1963).

(17) T. Loftsson and N. Bodor, *J. Pharm. Sci.*, **70**, 756 (1981).

(18) Z. Neiman and F. Bergmann, *Israel J. Chem.*, **3**, 161 (1965).

(19) B. Pullman and A. Pullman, in "Advances in Heterocyclic Chemistry," vol. 13, 1971, p. 146.

(20) S. Cerrini, W. Fedeli, and W. Mazza, *Chem. Commun.*, **1971**, 1607.

(21) M. Rasmussen and N. J. Leonard, *J. Am. Chem. Soc.*, **89**, 5439 (1967).

(22) J. W. Jones and R. K. Robins, *ibid.*, **84**, 1914 (1962).

(23) A. R. P. Paterson and A. Sutherland, *Can. J. Biochem.*, **42**, 1415 (1964).

(24) P. K. Chakravarty and R. K. Olsen, *J. Org. Chem.*, **43**, 1270 (1978).
(25) D. F. Veber, J. D. Milkowski, S. L. Varga, R. G. Denkewalter, and R. Hirschmann, *J. Am. Chem. Soc.*, **94**, 5456 (1972).
(26) H. Bundgaard and M. Johansen, *J. Pharm. Sci.*, **69**, 44 (1980).
(27) I. H. Blank, *J. Invest. Dermatol.*, **49**, 582 (1964).
(28) T. Yamana, A. Tsuji, E. Miyamoto, and O. Kubo, *J. Pharm. Sci.*, **66**, 747 (1977).
(29) L. N. Lukens and K. A. Herrington, *Biochim. Biophys. Acta*, **27**, 432 (1957).

Sustained Release of Theophylline from Hydroxypropylcellulose Tablets

MASAHIRO NAKANO *x, NAOKO OHMORI *, AKO OGATA ‡, KAZUKO SUGIMOTO *, YUKIKO TOBINO *, REIKO IWAOKU *, and KAZUHIKO JUNI *

Received November 27, 1981, from the **Department of Pharmaceutical Services, Kumamoto University Hospital, 1-1-1 Honjo, Kumamoto 860, Japan* and the ‡*Faculty of Pharmaceutical Sciences, Hokkaido University, Kita-ku, Sapporo 060, Japan.* Accepted for publication September 24, 1982.

Abstract □ Compressed tablets were prepared from theophylline and hydroxypropylcellulose. Effects of the viscosity grades of the polymer, the mixing ratios of two polymers with different viscosity grades, and the polymer contents in the tablets on release patterns of theophylline were examined *in vitro*. Release rate was decreased with increasing viscosity designation and polymer contents in the tablets. In salivary level profiles of theophylline following oral administration of sustained-release tablets to five human volunteers, a low but sustained level was noted indicating sustained release of the drug from the tablets *in vivo*.

Keyphrases □ Theophylline—hydroxypropylcellulose tablets □ Hydroxypropylcellulose—viscosity grades, mixing ratio, contents □ Compressed tablets—sustained release *in vitro*, oral administration □ Salivary levels—reverse-phase high-performance liquid chromatography

Since most of the commercially available water-soluble cellulose derivatives (1) are considered to be stable against microbial attack and safe when ingested orally, it appeared to be worthwhile to evaluate them as suitable materials for sustained-release preparations.

Although several studies have reported the sustained release of drugs from compressed hydrophilic matrices prepared from cellulose derivatives (2–8), few have examined the relationship between release rates *in vitro* and drug concentration profiles in body fluids (7).

Following the examination of representative viscosity grade polymers of methylcellulose, sodium carboxymethylcellulose, hydroxypropylmethylcellulose, and hydroxypropylcellulose, hydroxypropylcellulose was selected for further studies, since it exhibited release patterns suitable for a sustained-release preparation.

In the present study, modification of the release rate of theophylline from compressed hydroxypropylcellulose tablets was examined by changing viscosity grades of the polymer, mixing ratios of two polymers with different viscosity grades, and changing polymer contents in the tablets. Theophylline was used as a representative drug, since sustained-release formulations are desirable because of the short elimination half-life in humans, especially in children (9). To evaluate body fluid level profiles of theophylline in volunteers, saliva levels were measured, since correlation of serum and saliva theophylline concentrations after administration of a sustained-release preparation has been reported (10).

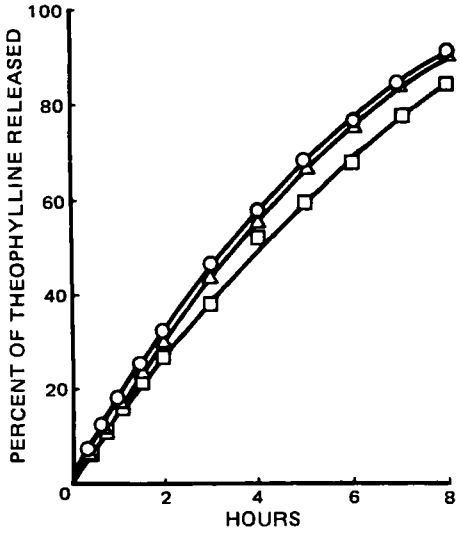

Figure 1—*Release profiles of theophylline from tablets prepared from 1:1 mixture of theophylline (250 mg) and hydroxyproylcellulose (1:1 mixture of low- and medium-viscosity grades) by compressing the drug–polymer mixture for 5 sec (○), 30 sec (△), or 120 sec (□). Average of three determinations.*

EXPERIMENTAL

Materials—Three viscosity grades of hydroxypropylcellulose[1] were used. Theophylline (anhydrous) and 7-(2-hydroxyethyl)theophylline were used as supplied [2]; and all other chemicals were of reagent grade.

Preparation of Tablets—Flat-faced tablets (500 mg, 13-mm diameter, and ~3-mm thickness) were prepared by compressing mixtures of theophylline and hydroxypropylcellulose directly under 180 kg/cm^2 for 30 sec using a potassium bromide tablet die and a hydraulic press[3].

To examine the effect of compression pressure on drug release, pressures of 60, 180, or 540 kg/cm^2 were applied to the drug–polymer mixture for 30 sec. To examine the effect of compression periods on drug release, a compression pressure of 180 kg/cm^2 was applied to the drug–polymer mixture for 5, 30, or 120 sec.

Release Studies—A tablet was suspended by means of a polyethylene net in a 200-ml release medium in a wide-mouthed bottle. Since the release rate of theophylline from hydroxypropylcellulose tablets is not very dependent on the pH values of the medium, a 0.2% NaCl solution, ad-

[1] HPC-L, M, and H from Nihon Soda Co., Tokyo. Viscosity ranges of 2% aqueous solutions at 20° are 6–10, 150–400 and 1000–4000 cps, respectively.
[2] Tokyo Kasei Kogyo Co., Tokyo.
[3] Shimadzu potassium bromide press, Shimadzu Manufacturing Co., Kyoto.

0022-3549/83/0400-0378$01.00/0

(24) P. K. Chakravarty and R. K. Olsen, *J. Org. Chem.*, **43**, 1270 (1978).
(25) D. F. Veber, J. D. Milkowski, S. L. Varga, R. G. Denkewalter, and R. Hirschmann, *J. Am. Chem. Soc.*, **94**, 5456 (1972).
(26) H. Bundgaard and M. Johansen, *J. Pharm. Sci.*, **69**, 44 (1980).
(27) I. H. Blank, *J. Invest. Dermatol.*, **49**, 582 (1964).
(28) T. Yamana, A. Tsuji, E. Miyamoto, and O. Kubo, *J. Pharm. Sci.*, **66**, 747 (1977).
(29) L. N. Lukens and K. A. Herrington, *Biochim. Biophys. Acta*, **27**, 432 (1957).

Sustained Release of Theophylline from Hydroxypropylcellulose Tablets

MASAHIRO NAKANO *x, NAOKO OHMORI *, AKO OGATA ‡, KAZUKO SUGIMOTO *, YUKIKO TOBINO *, REIKO IWAOKU *, and KAZUHIKO JUNI *

Received November 27, 1981, from the **Department of Pharmaceutical Services, Kumamoto University Hospital, 1-1-1 Honjo, Kumamoto 860, Japan* and the ‡*Faculty of Pharmaceutical Sciences, Hokkaido University, Kita-ku, Sapporo 060, Japan.* Accepted for publication September 24, 1982.

Abstract □ Compressed tablets were prepared from theophylline and hydroxypropylcellulose. Effects of the viscosity grades of the polymer, the mixing ratios of two polymers with different viscosity grades, and the polymer contents in the tablets on release patterns of theophylline were examined *in vitro*. Release rate was decreased with increasing viscosity designation and polymer contents in the tablets. In salivary level profiles of theophylline following oral administration of sustained-release tablets to five human volunteers, a low but sustained level was noted indicating sustained release of the drug from the tablets *in vivo*.

Keyphrases □ Theophylline—hydroxypropylcellulose tablets □ Hydroxypropylcellulose—viscosity grades, mixing ratio, contents □ Compressed tablets—sustained release *in vitro*, oral administration □ Salivary levels—reverse-phase high-performance liquid chromatography

Since most of the commercially available water-soluble cellulose derivatives (1) are considered to be stable against microbial attack and safe when ingested orally, it appeared to be worthwhile to evaluate them as suitable materials for sustained-release preparations.

Although several studies have reported the sustained release of drugs from compressed hydrophilic matrices prepared from cellulose derivatives (2–8), few have examined the relationship between release rates *in vitro* and drug concentration profiles in body fluids (7).

Following the examination of representative viscosity grade polymers of methylcellulose, sodium carboxymethylcellulose, hydroxypropylmethylcellulose, and hydroxypropylcellulose, hydroxypropylcellulose was selected for further studies, since it exhibited release patterns suitable for a sustained-release preparation.

In the present study, modification of the release rate of theophylline from compressed hydroxypropylcellulose tablets was examined by changing viscosity grades of the polymer, mixing ratios of two polymers with different viscosity grades, and changing polymer contents in the tablets. Theophylline was used as a representative drug, since sustained-release formulations are desirable because of the short elimination half-life in humans, especially in children (9). To evaluate body fluid level profiles of theophylline in volunteers, saliva levels were measured, since correlation of serum and saliva theophylline concentrations after administration of a sustained-release preparation has been reported (10).

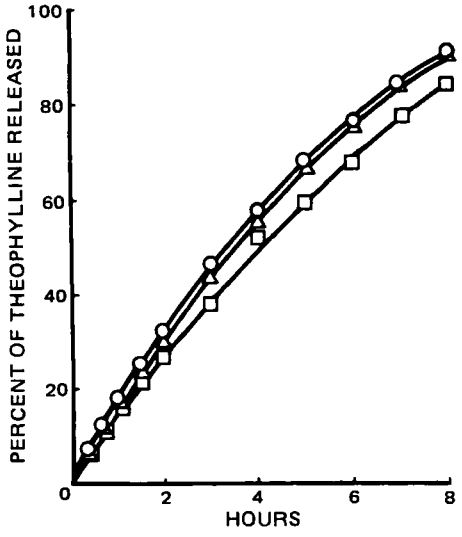

Figure 1—*Release profiles of theophylline from tablets prepared from 1:1 mixture of theophylline (250 mg) and hydroxyproylcellulose (1:1 mixture of low- and medium-viscosity grades) by compressing the drug–polymer mixture for 5 sec (○), 30 sec (△), or 120 sec (□). Average of three determinations.*

EXPERIMENTAL

Materials—Three viscosity grades of hydroxypropylcellulose[1] were used. Theophylline (anhydrous) and 7-(2-hydroxyethyl)theophylline were used as supplied [2]; and all other chemicals were of reagent grade.

Preparation of Tablets—Flat-faced tablets (500 mg, 13-mm diameter, and ~3-mm thickness) were prepared by compressing mixtures of theophylline and hydroxypropylcellulose directly under 180 kg/cm^2 for 30 sec using a potassium bromide tablet die and a hydraulic press[3].

To examine the effect of compression pressure on drug release, pressures of 60, 180, or 540 kg/cm^2 were applied to the drug–polymer mixture for 30 sec. To examine the effect of compression periods on drug release, a compression pressure of 180 kg/cm^2 was applied to the drug–polymer mixture for 5, 30, or 120 sec.

Release Studies—A tablet was suspended by means of a polyethylene net in a 200-ml release medium in a wide-mouthed bottle. Since the release rate of theophylline from hydroxypropylcellulose tablets is not very dependent on the pH values of the medium, a 0.2% NaCl solution, ad-

[1] HPC-L, M, and H from Nihon Soda Co., Tokyo. Viscosity ranges of 2% aqueous solutions at 20° are 6–10, 150–400 and 1000–4000 cps, respectively.
[2] Tokyo Kasei Kogyo Co., Tokyo.
[3] Shimadzu potassium bromide press, Shimadzu Manufacturing Co., Kyoto.

0022-3549/83/0400-0378$01.00/0

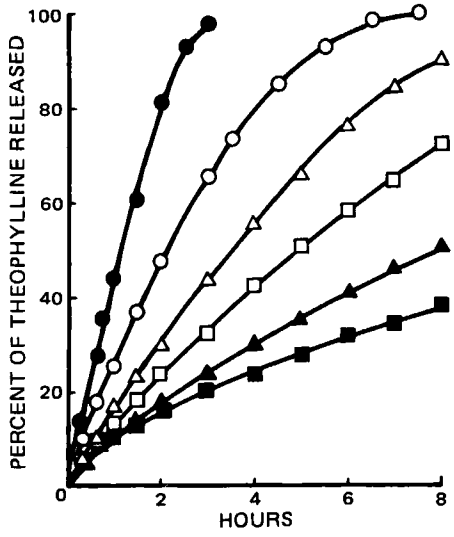

Figure 2—*Release profiles of theophylline from tablets prepared from 1:1 mixture of theophylline (250 mg) and hydroxypropylcellulose of various compositions. Average of three determinations. Key: Viscosity grades of the polymer: (●) low; (▲) medium; (■) high-viscosity grade polymer, and (○) (3:1) (△), 1:1, and (□) 1:2 mixtures of low- and medium-viscosity grade polymers.*

justed to pH 1.2 was used as a release medium. The medium was kept at 37° and stirred with a magnetic stirrer. At predetermined intervals, 1-ml portions of the medium were pipetted for the spectrophotometric determination of the theophylline concentration at 272 nm after dilution with 0.2 *M* acetate buffer, pH 5.0.

Measurement of Salivary Levels in Human Volunteers—Five healthy volunteers, two males and three females (23–31 years of age), participated in the study. To eliminate ingestion of theophylline from other sources and possible formation of theophylline *in vivo* following intake of caffeine (11), the subjects were told to abstain from any drinks containing caffeine. Blank saliva samples were collected a few minutes before administering the preparation. After overnight fasting, a single 250-mg dose of theophylline powder (as a fast-dissolving preparation) or a hydroxypropylcellulose tablet (as a sustained-release preparation) containing the same amount of the drug was administered, with 100-ml water, wrapped in a wafer sheet to eliminate possible contact of the drug with mucosa of the mouth. Saliva samples were collected at appropriate intervals up to 24 hr. A small amount (~10 mg) of citric acid, a salivary flow stimulant, was put on the tongue and held in the mouth for 1–2 min, then a 2-ml sample of the saliva was collected in a test tube and kept frozen until analysis. No food was taken for 4 hr postdose. A crossover design was used and a minimum interval of 1 week was allowed between trials.

Analysis of Theophylline Levels in Saliva—Reverse-phase high-performance liquid chromatography for theophylline in saliva (12) was employed using 7-(2-hydroxyethyl)theophylline as an internal standard. A liquid chromatograph[4] equipped with UV detector set at 270 nm and a reverse-phase-type column (Zorbax ODS, 4.6 ϕ × 0.25 m) was used.

RESULTS AND DISCUSSION

Effect of Compression Pressure and Compression Period on Drug Release—Figure 1 shows the release patterns of theophylline from tablets prepared by compressing the drug–polymer mixture for various periods. Only a slight decrease in release rate was observed with 6- and 24-fold increases in compression period.

In the examination of the effect of compression pressure on release rate, three pressure levels covering a ninefold change in pressure were applied to the mixture. Release patterns (not shown) of theophylline from tablets thus prepared were practically superimposable. Thus, compression pressure and compression period are not important factors in modifying the release pattern of the drug.

Effect of Viscosity Grades of the Polymer—Figure 2 shows the release patterns of theophylline from tablets with 250 mg of theophylline and 250 mg of one of three viscosity grades of hydroxypropylcellulose.

[4] Model LC-3A, Shimadzu Manufacturing Co., Kyoto.

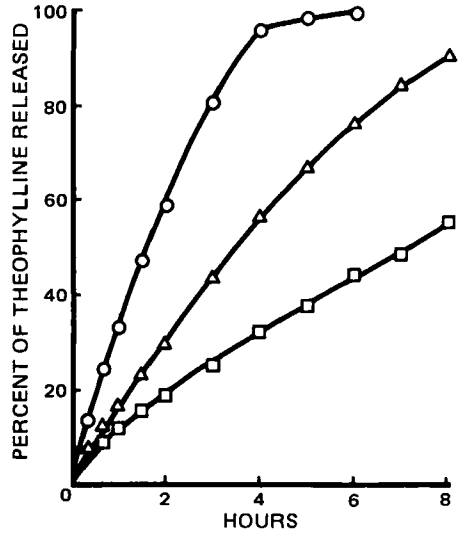

Figure 3—*Release profiles of theophylline from tablets prepared from (○) 1:1/3, (△) 1:1 and (□) 1:3 mixtures of theophylline (250 mg) and hydroxypropylcellulose (1:1 mixture of low- and medium-viscosity grade polymers). Average of three determinations.*

The drug release rate was fast from the tablets made of the low-viscosity grade polymer, while the release rate was slow from tablets made of the polymers of medium- and high-viscosity grades. Therefore, tablets made from mixtures of low-viscosity grade polymer and medium-viscosity grade polymer in the mixing ratios, as shown in Fig. 2, were examined to obtain an appropriate release rate. With an increase in the contents of the medium-viscosity grade polymer, the release rate was decreased. Therefore, the drug release rate can be modified by changing the mixing ratio of two polymers with different viscosity grades depending on the required sustained period.

To examine a release mechanism of theophylline from compressed hydrophilic tablets, the amount of the drug released was plotted (not shown) against square root of time according to the Higuchi equation (13). The lines obtained were upward curves, indicating a different release mechanism from that expected from the Higuchi equation for release of drug from solid matrices. The tablet expanded as water penetrated forming a layer of gel on the surface of the tablet, but it gradually eroded afterward. Thus the following processes are likely to operate: penetration of water through matrices to form a gel in the outer layer, dissolution of a drug in the gel, permeation of the drug through the gel, release of the drug from the gel to a release medium, and slow dissolution of the gelled polymer in the outermost layer in the release medium.

Effect of Polymer Contents—Figure 3 shows the release patterns of theophylline from three tablets containing the same amount of the drug

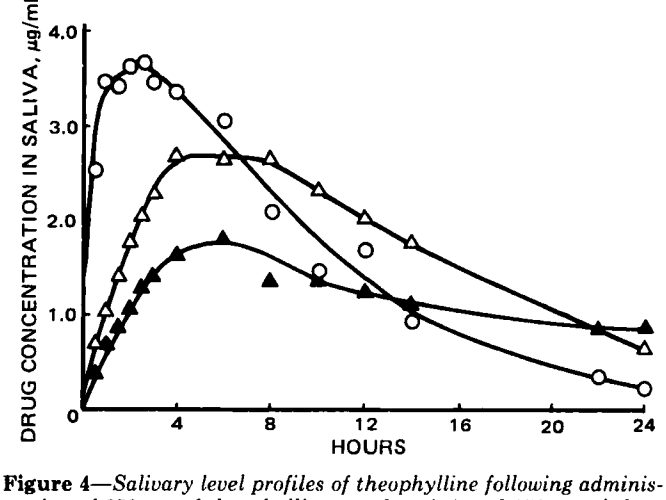

Figure 4—*Salivary level profiles of theophylline following administration of 250 mg of theophylline powders (○) and 250 mg of theophylline–250 mg of hydroxypropylcellulose [1:1 mixture of low- and medium-grade polymers (△) or medium-viscosity grade polymer alone (▲)] tablets to volunteers. Average of five subjects.*

but different amounts of the polymer. The polymer mixture used in the test was a 1:1 mixture of the low-viscosity grade polymer and the medium-viscosity grade polymer. As expected, the drug was released from tablets more slowly with an increase in polymer contents; therefore, the release rate of the drug can be modified by changing the polymer contents in the tablets.

Salivary Levels Following Oral Administration—In Fig. 4, the average salivary levels of theophylline following oral administration of two kinds of sustained-release tablets were compared with those of fast-dissolving powders. After the administration of the tablets, salivary levels were lower at earlier hours but higher afterward compared with salivary levels following administration of powders. The lowest salivary levels observed after administration of the tablet prepared from the medium-viscosity grade polymer reflect a slow release rate, as shown in Fig. 2, demonstrating that different drug level profiles in body fluids are obtainable by modifying the release patterns of drug. Although it is shown that the rate of bioavailability is decreased with a decrease in release rate *in vitro*, the effect of release rate on the extent of bioavailability has to be examined by extending sampling periods to 36–48 hr.

The present study demonstrated that the release of theophylline from compressed tablets prepared from hydroxypropylcellulose can be modified by changing viscosity grades of the polymer, mixing ratios of two polymers with different viscosity grades, and changing polymer contents in the tablets. Sustained-release *in vitro* is reflected in drug level curves after oral administration of sustained-release tablets.

REFERENCES

(1) R. L. Davidson, Ed., "Handbook of Water-Soluble Gums and Resins," McGraw-Hill, New York, N.Y., 1980.

(2) H. Lapidus and N. G. Lordi, *J. Pharm. Sci.*, **55**, 840 (1966).

(3) H. E. Huber, L. B. Dale, and G. L. Christenson, *ibid.*, **55**, 974 (1966).

(4) H. E. Huber and G. L. Christenson, *ibid.*, **57**, 164 (1968).

(5) H. Lapidus and N. G. Lordi, *ibid.*, **57**, 1292 (1968).

(6) Y. Machida and T. Nagai, *Chem. Pharm. Bull.*, **26**, 1652 (1978).

(7) H. Schneider, C. H. Nightingale, R. Quintiliani, and D. R. Flanagan, *J. Pharm. Sci.*, **67**, 1620 (1978).

(8) Y. Machida and T. Nagai, *Chem. Pharm. Bull.*, **28**, 1082 (1980).

(9) D. E. Zaske, K. W. Mitler, E. L. Strem, S. Austrian, and P. B. Johnson, *J. Am. Med. Assoc.*, **237**, 1453 (1979).

(10) J. H. G. Jonkman, G. H. Koëter, R. Schoenmaker, K. de Vries, J. E. Greving, and R. A. de Zeeuw, *Eur. J. Clin. Pharmacol.*, **20**, 73 (1981).

(11) F. L. S. Tse, K. H. Valia, D. W. Szeto, T. J. Raimondo, and B. Koplowitz, *J. Pharm. Sci.*, **70**, 395 (1981).

(12) M. Nakano, Y. Nakamura, K. Juni, and T. Tomitsuka, *J. Pharm. Dyn.*, **3**, 702 (1980).

(13) T. Higuchi, *J. Pharm. Sci.*, **52**, 1145 (1963).

ACKNOWLEDGMENTS

The authors are grateful to Nihon Soda Co., for generous gifts of hydroxypropylcellulose samples.

Characterization of Spray Patterns of Inhalation Aerosols Using Thin-Layer Chromatography

ERIC J. BENJAMIN, JOSEPH J. KROETEN, and EFRAIM SHEK ˣ

Received November 27, 1981 from the *Institute of Pharmaceutical Sciences, Syntex Research, Palo Alto, CA 94304.* Accepted for publication May 5, 1982.

Abstract □ The spray pattern of an inhalation aerosol was characterized using photography and by observing the impaction pattern on a TLC plate. The aerosol plume was conical in shape, and its cross section increased with increasing distance from the actuator. Three puffs of the aerosol, at a distance of 3 cm between actuator and the TLC plate, produced a spot that had approximately the same diameter as the cross section of the aerosol plume at that distance from the actuator. The TLC technique with these parameters was selected to develop an assay characterizing the spray pattern of an inhalation aerosol because of its specificity, simplicity, and speed.

Keyphrases □ Aerosols, inhalation—spray pattern characterizations using photography and TLC □ TLC—characterization of spray patterns for inhalation aerosols □ Spray patterns—of inhalation aerosols, characterized by TLC and photography

Pressurized inhalation aerosols are generally used for drug administration into the lower respiratory tract. Only a minor part of the dose administered reaches the lung directly (1–3). Recently, using an *in vivo* radioactive technique, it was estimated directly that an average 8.8% of the administered dose was deposited in the lungs with 80% deposited in the mouth (4). The remainder of the drug (9.8%) was either exhaled or deposited in the aerosol actuator. Various test methods for the control of aerosol products have been developed (5–7). These include tests for net contents, medication delivered per dose, particle size distribution, valve delivery, vapor pressure, leakage rate, moisture contents, and spray pattern.

One of the important objectives in developing an aerosol product is to obtain the spray pattern best suited for the intended application. Various factors can affect the spray pattern. These factors are the design of the valve and the actuator, the pressure in the container, and its content composition (8, 9). The spray pattern is affected by the size and shape of the actuator orifice as well as by the valve (10). Therefore, characterization of spray patterns is important for evaluating the valve and actuator performances. In addition to its pattern, other tests generally used to characterize the spray are particle size distribution of the drug substance delivered and spray angle (11).

Several methods have been devised to record and compare the spray pattern of aerosol products. One method is based on the impingement of the spray on a piece of paper, glass, silica gel, or paper that has been treated with a dye–talc mixture (12, 13). Photographic (14) and laser holographic[1] methods also have been used. Miszuk *et al.* (15) recently described a technique that utilizes two orthogonal video images. These methods are best suited for solution aerosols in which the active ingredient is dissolved

[1] Laser Photographic Laboratories, Arlington Heights, Ill.

0022-3549/83/0400-0380$01.00/0

but different amounts of the polymer. The polymer mixture used in the test was a 1:1 mixture of the low-viscosity grade polymer and the medium-viscosity grade polymer. As expected, the drug was released from tablets more slowly with an increase in polymer contents; therefore, the release rate of the drug can be modified by changing the polymer contents in the tablets.

Salivary Levels Following Oral Administration—In Fig. 4, the average salivary levels of theophylline following oral administration of two kinds of sustained-release tablets were compared with those of fast-dissolving powders. After the administration of the tablets, salivary levels were lower at earlier hours but higher afterward compared with salivary levels following administration of powders. The lowest salivary levels observed after administration of the tablet prepared from the medium-viscosity grade polymer reflect a slow release rate, as shown in Fig. 2, demonstrating that different drug level profiles in body fluids are obtainable by modifying the release patterns of drug. Although it is shown that the rate of bioavailability is decreased with a decrease in release rate *in vitro*, the effect of release rate on the extent of bioavailability has to be examined by extending sampling periods to 36–48 hr.

The present study demonstrated that the release of theophylline from compressed tablets prepared from hydroxypropylcellulose can be modified by changing viscosity grades of the polymer, mixing ratios of two polymers with different viscosity grades, and changing polymer contents in the tablets. Sustained-release *in vitro* is reflected in drug level curves after oral administration of sustained-release tablets.

REFERENCES

(1) R. L. Davidson, Ed., "Handbook of Water-Soluble Gums and Resins," McGraw-Hill, New York, N.Y., 1980.

(2) H. Lapidus and N. G. Lordi, *J. Pharm. Sci.*, **55**, 840 (1966).

(3) H. E. Huber, L. B. Dale, and G. L. Christenson, *ibid.*, **55**, 974 (1966).

(4) H. E. Huber and G. L. Christenson, *ibid.*, **57**, 164 (1968).

(5) H. Lapidus and N. G. Lordi, *ibid.*, **57**, 1292 (1968).

(6) Y. Machida and T. Nagai, *Chem. Pharm. Bull.*, **26**, 1652 (1978).

(7) H. Schneider, C. H. Nightingale, R. Quintiliani, and D. R. Flanagan, *J. Pharm. Sci.*, **67**, 1620 (1978).

(8) Y. Machida and T. Nagai, *Chem. Pharm. Bull.*, **28**, 1082 (1980).

(9) D. E. Zaske, K. W. Mitler, E. L. Strem, S. Austrian, and P. B. Johnson, *J. Am. Med. Assoc.*, **237**, 1453 (1979).

(10) J. H. G. Jonkman, G. H. Koëter, R. Schoenmaker, K. de Vries, J. E. Greving, and R. A. de Zeeuw, *Eur. J. Clin. Pharmacol.*, **20**, 73 (1981).

(11) F. L. S. Tse, K. H. Valia, D. W. Szeto, T. J. Raimondo, and B. Koplowitz, *J. Pharm. Sci.*, **70**, 395 (1981).

(12) M. Nakano, Y. Nakamura, K. Juni, and T. Tomitsuka, *J. Pharm. Dyn.*, **3**, 702 (1980).

(13) T. Higuchi, *J. Pharm. Sci.*, **52**, 1145 (1963).

ACKNOWLEDGMENTS

The authors are grateful to Nihon Soda Co., for generous gifts of hydroxypropylcellulose samples.

Characterization of Spray Patterns of Inhalation Aerosols Using Thin-Layer Chromatography

ERIC J. BENJAMIN, JOSEPH J. KROETEN, and EFRAIM SHEK ˣ

Received November 27, 1981 from the *Institute of Pharmaceutical Sciences, Syntex Research, Palo Alto, CA 94304.* Accepted for publication May 5, 1982.

Abstract □ The spray pattern of an inhalation aerosol was characterized using photography and by observing the impaction pattern on a TLC plate. The aerosol plume was conical in shape, and its cross section increased with increasing distance from the actuator. Three puffs of the aerosol, at a distance of 3 cm between actuator and the TLC plate, produced a spot that had approximately the same diameter as the cross section of the aerosol plume at that distance from the actuator. The TLC technique with these parameters was selected to develop an assay characterizing the spray pattern of an inhalation aerosol because of its specificity, simplicity, and speed.

Keyphrases □ Aerosols, inhalation—spray pattern characterizations using photography and TLC □ TLC—characterization of spray patterns for inhalation aerosols □ Spray patterns—of inhalation aerosols, characterized by TLC and photography

Pressurized inhalation aerosols are generally used for drug administration into the lower respiratory tract. Only a minor part of the dose administered reaches the lung directly (1–3). Recently, using an *in vivo* radioactive technique, it was estimated directly that an average 8.8% of the administered dose was deposited in the lungs with 80% deposited in the mouth (4). The remainder of the drug (9.8%) was either exhaled or deposited in the aerosol actuator. Various test methods for the control of aerosol products have been developed (5–7). These include tests for net contents, medication delivered per dose, particle size distribution, valve delivery, vapor pressure, leakage rate, moisture contents, and spray pattern.

One of the important objectives in developing an aerosol product is to obtain the spray pattern best suited for the intended application. Various factors can affect the spray pattern. These factors are the design of the valve and the actuator, the pressure in the container, and its content composition (8, 9). The spray pattern is affected by the size and shape of the actuator orifice as well as by the valve (10). Therefore, characterization of spray patterns is important for evaluating the valve and actuator performances. In addition to its pattern, other tests generally used to characterize the spray are particle size distribution of the drug substance delivered and spray angle (11).

Several methods have been devised to record and compare the spray pattern of aerosol products. One method is based on the impingement of the spray on a piece of paper, glass, silica gel, or paper that has been treated with a dye–talc mixture (12, 13). Photographic (14) and laser holographic[1] methods also have been used. Miszuk *et al.* (15) recently described a technique that utilizes two orthogonal video images. These methods are best suited for solution aerosols in which the active ingredient is dissolved

[1] Laser Photographic Laboratories, Arlington Heights, Ill.

0022-3549/83/0400-0380$01.00/0

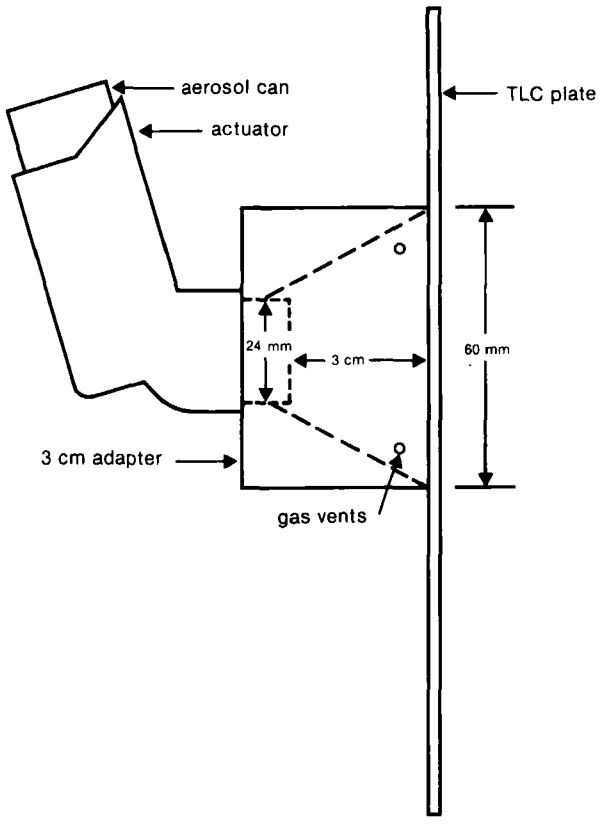

Figure 1—*Equipment and setup used to test the plume of corticosteroid aerosol by TLC method.*

in the solvent/propellant. In the case of heterogeneous aerosols (*e.g.*, suspensions), a major portion of the resulting spray consists only of the propellants. In such cases the aforementioned methods, being nonselective, do not provide sufficient information about distribution of the solid drug particles in various regions of the spray. The purpose of this study was to develop a specific method to characterize the spray pattern with respect to drug distribution in a plume pattern of an heterogeneous inhalation aerosol system.

EXPERIMENTAL

Materials—The aerosol formulations consisted of a suspension of micronized corticosteroid in a chlorofluorocarbon propellant system containing a surfactant. Dosage was controlled by a metered aerosol valve[2], with a 50-μl metering chamber and stainless steel stem. The valve gave a metered puff of formulation upon each actuation. The actuation of the valve was effected by a plastic actuator[2], also serving as a mouthpiece.

Four actuators were selected for this study. Three of them were modified as follows: the orifice diameter of actuator 2 was reduced to 0.483 mm; the orifice diameter of actuator 3 was enlarged to 0.864 mm; and the orifice exit angle with respect to the axis of the delivery tube for actuator 4 was changed and the orifice diameter was reduced to 0.406 mm. Actuator 1 was used as manufactured, with an orifice size of 0.533 mm.

Photography—Photographs of the spray were taken using a camera[3] with a 127-mm lens which was loaded with black and white film[4]. The aperture was set at f/16 and the shutter speed set at 0.5 sec. A flood light[5] was used to illuminate the aerosol plume from below. The actuator and shutter release were coordinated manually.

TLC Method—A plastic adapter was attached to the actuator. These were used to actuate an aerosol can to deliver a spray on a 20 × 20-cm silica gel TLC plate[6] from a fixed distance. The resulting spot was observed and outlined under UV light. Both the long and the short diameters of the spot were measured. The equipment and setup used is diagrammed in Fig. 1.

Corticosteroid Contents—In addition to measuring the diameters of the spots, corticosteroid contents in the spot were also determined. This was accomplished by scraping the silica gel corresponding to the spot from the plate and transferring it quantitatively into a test tube. This was followed by extraction of the corticosteroid with ethanol and quantitation by blue tetrazolium colorimetry (16).

Particle Size Distribution—The actuator was connected to the air sampler[7] by a stainless steel tubular throat. The nozzle of the aerosol can was inserted into the actuator, and a fixed number of puffs were sprayed into the eight-stage air sampler. The airflow through the air sampler was set at 28.5 liters/min. The acutator, throat, and the various stages were rinsed with ethanol. The corticoid deposited on the various stages was quantitated by reverse-phase high-performance liquid chromatography (HPLC) using an octadecylsilane column[8]. The mobile phase was water–acetonitrile (65:35) containing 1% acetic acid.

Table I—Cross Sections of Aerosol Plumes at Various Distances from the Actuator [a]

Distance from the Actuator, cm	Cross Section of Plume, mm							
	Actuator 1A			Actuator 1B			Mean	*SD*
1	15	14	14	15	14	17	14.8	1.2
2	18	18	16	17	15	18	17.0	1.3
3	22	20	18	20	19	20	19.8	1.3
4	25	23	23	24	22	25	23.7	1.2
5	30	27	27	28	25	28	27.5	1.6
6	34	31	30	33	30	33	31.8	1.7
7	38	35	34	37	35	37	36.0	1.5
15	75	80	75	80	82	80	78.7	2.9

[a] Measurements were taken from photographs.

RESULTS AND DISCUSSION

Photography—The photograph of an aerosol plume generated using actuator 1 (unaltered) shows that the plume is conical, symmetrical, and ~31–33 cm in length (Fig. 2). Photographs of six sprays using two actuators (1A and B) were taken. The widths of the aerosol plumes at various distances from the actuator were measured from these photographs. The data are given in Table I, and a plot of the plume width *versus* distance from actuator is shown in Fig. 3.

An ideal aerosol plume is considered to be a symmetrical cone of optimum apical angle to provide considerable clearance from the mouthpiece of the actuator (15). In addition, there should be only a few large particle dropouts from the spray cone (14). Actuator 1 yielded a plume consistent with the above criteria. However, the plumes produced by actuators 2, 3, and 4 (modified) had one or more deviations from such an ideal plume (Fig. 2). The actuator with the small orifice (actuator 2) yielded a misty and irregular-shaped spray with considerable amounts of streaks (dropouts). The apical angle appeared to be large and resulted in inadequate clearance from the actuator nozzle. The plume yielded by actuator 4 had about the same characteristics as 2. In addition, there was a displacement of the plume from the center and more dropouts. The effect of actuator 3 on the plume shape was not very obvious; however, the plume had a slightly larger apical angle and more dropouts than the regular actuator. This demonstrates that photography is capable of differentiating some defects in the actuators.

TLC Method—The spots effected by spraying the aerosol onto a TLC plate using the regular actuator (actuator 1) were circular in shape (Fig. 4). They consisted of an inner dark area surrounded by an outer diffused zone. The size of the spot varied with the number of puffs sprayed and the distance between the TLC plate and the actuator. The average diameter of the spot as a function of the number of puffs sprayed and the distance from the actuator is given in Table II, and graphical representations are shown in Fig. 3. For any fixed distance between the TLC plate and the actuator, the diameter of the spot increased with increasing number of puffs.

[2] Riker Laboratories, Northridge, Calif.
[3] Polaroid Land Camera CU-5, Cambridge, Mass.
[4] Landfilm type 107, ASA 3000, Polaroid Corp., Cambridge, Mass.
[5] Photoflood lamp G, G.E., Cleveland, Ohio.
[6] Analtech, Newark, Del.
[7] Andersen 2000 Inc., Atlanta, Ga.
[8] μBondapak, Waters Associates, Milford, Mass.

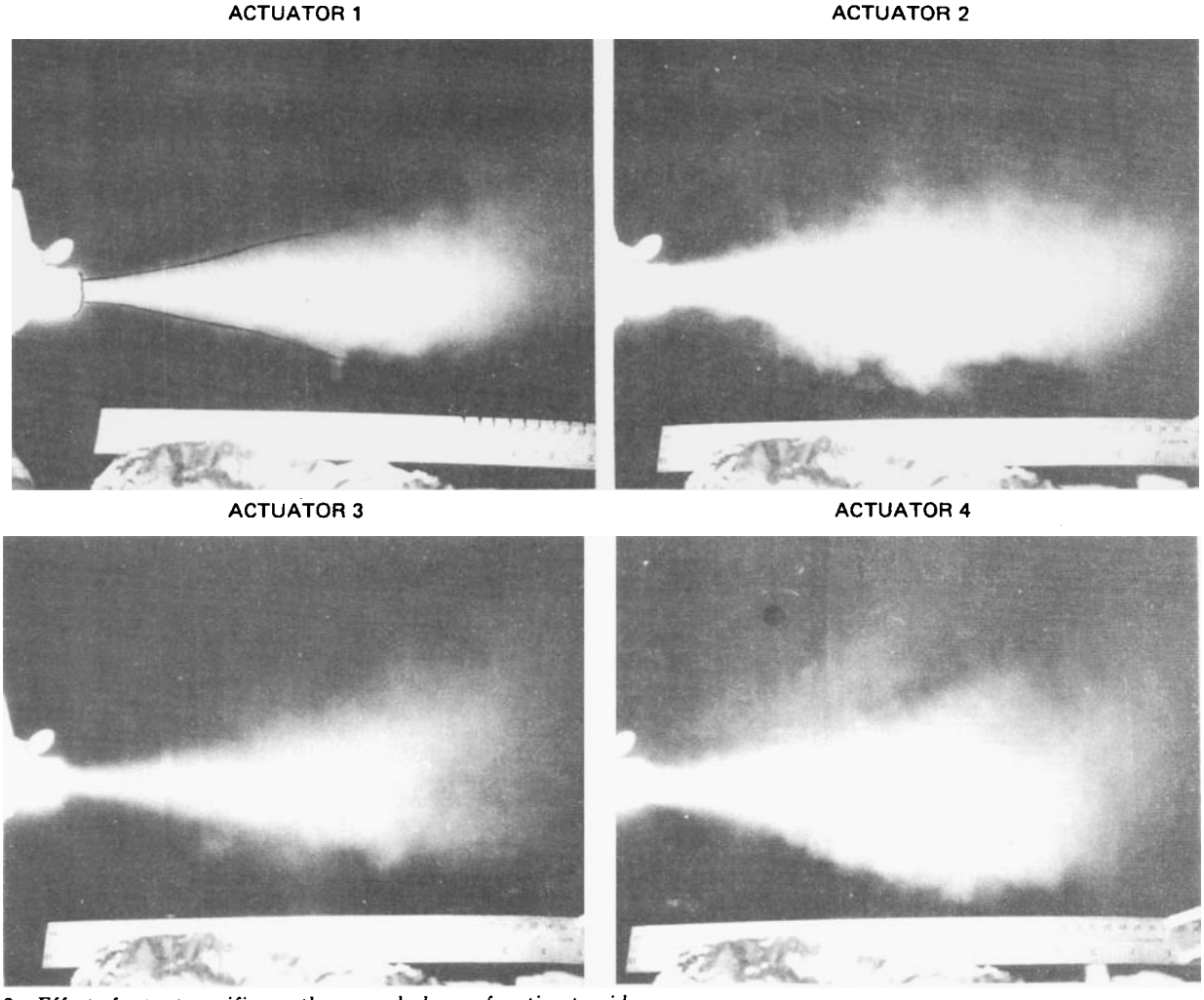

Figure 2—*Effect of actuator orifice on the aerosol plume of corticosteroid.*

Examination of the effect of varying this target distance, however, yielded some interesting facts. When three or fewer puffs were used, the diameter of the spot decreased with increasing distance from the actuator. On the other hand, the use of five or more puffs resulted in larger spot size with increase in distance from the actuator. Assuming that the aerosol plume has a conical shape (as shown by photography, Fig. 2), one would expect an increase in the size of the spot with increasing distance of the TLC plate from the actuator, irrespective of the number of puffs sprayed. This discrepancy could be due to the fact that photography does not distinguish between drug substance particles and propellant droplets in the plume. Thus, photography gives no indication of the drug substance density gradient in the aerosol plume (*i.e.*, between the center and outer part). On the other hand, the TLC method directly examines drug substance particles in the cross section of the plume, as the spot on the TLC plate (being the only UV absorbing species) is mainly produced by the drug. It is possible that the effective plume (containing the drug substance) is really a narrow jet burst rather than an expanding conical spray. Thus, the drug substance might be denser, to some extent, in the center of the plume cross section than at its outer zone. As more puffs are sprayed onto the TLC plate the concentration of the drug in the outer zone now increases and contributes to the observable diameter of the spot. This is consistent with the increase in the diameter of the TLC spot with increasing number of puffs sprayed.

The shapes of the spots (outlines) produced from the aerosol unit using four different experimental actuators are shown in Fig. 4. Using the regular actuator (actuator 1) a circular spot was produced. The modified actuators produced distinctly distorted spots. Actuator 3 with the largest orifice produced a slightly oval or kidney-shaped spot. Actuators 2 and 4 gave crescent-shaped spots indicating deflection of the spray from the actuator nozzle due to its displacement from the center. This information indicates that the TLC method is equal or better than photography in detecting defects in the size and shape of the actuator orifice. Moreover,

Table II—Diameters of the TLC Spots Produced by Spraying Various Puffs of the Inhalation Aerosol at Various Distances from the Actuator

Distance from the Actuator, cm	Mean Diameter[a] ± *SD*, mm				
	1 Puff	2 Puffs	3 Puffs	5 Puffs	10 Puffs
1.7	12.3 ± 0.37 (6)	14.3 ± 0.74 (6)	17.4 ± 0.64 (6)	20.4 ± 1.5 (10)	23.3 ± 1.85 (10)
2.8	11.9 ± 0.50 (6)	15.38 ± 1.13 (6)	17.57 ± 1.61 (6)	21.6 ± 1.8 (10)	
3.5	9.85 ± 0.22 (6)	13.8 ± 0.76 (6)	16.75 ± 0.69 (6)		
3.7	11.12 ± 0.88 (14)	15.0 ± 1.1 (12)	17.5 ± 1.25 (28)	24.3 ± 1.6 (10)	29.35 ± 2.17 (10)
5	7.6 ± 0.53 (6)	11.83 ± 0.75 (6)	16.36 ± 0.66 (6)	23.9 ± 1.3 (10)	30.7 ± 2.22 (10)
6	9.54 ± 0.48 (10)	12.6 ± 1.46 (12)	16.3 ± 1.1 (30)	24.8 ± 1.8 (10)	
7.5	5.92 ± 0.24 (6)	10.46 ± 0.32 (6)	15.2 ± 0.58 (6)	25.0 ± 1.7 (10)	33.27 ± 1.69 (10)

[a] The mean includes height and width for all the spots. The number of measurements is given in parentheses.

Table III—Effect of Distance Between the TLC Plate and Actuator on the Dimension and Drug Contents of the TLC Spot [a]

Distance from the Actuator, cm	Drug Recovered		Dimensions of Spot [b]	
	Mean, μg	Recovery, %[c]	Diameter, mm	Surface Area, mm²
1.7	671	89	17.43	238
3.7	633	85	17.50	240
5.0	542	72	16.36	210
6.0	538	72	16.30	209
7.5	446	60	15.20	181

[a] Spots produced by spraying three puffs from the aerosol unit onto the TLC plate. [b] Mean measurements of 3–15 spots. [c] Based on 250 μg/puff.

Table IV—Effect of the Number of Puffs Used on the Dimension and Drug Contents of the TLC Spots [a]

Number of Puffs	Drug Recovered		Dimensions of Spot [b]	
	Mean, μg	Recovery, %[c]	Diameter, mm	Surface Area, mm²
1	240	96	12	113
2	425	85	13.5	143
3	664	89	16.4	211
5	1207	97	20.2	322
10	2402	96	26	531

[a] Spots produced by spraying various puffs from the aerosol unit onto a TLC plate at a distance of 3 cm from the actuator. [b] Mean measurements of three spots. [c] Based on 250 μg/puff.

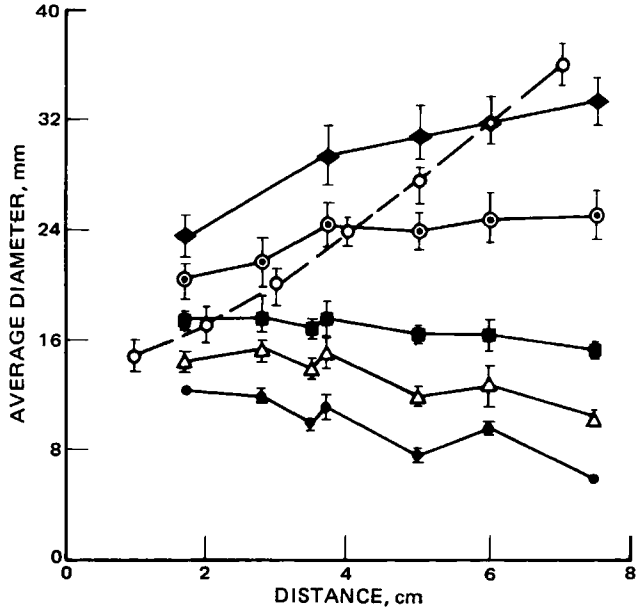

Figure 3—*TLC spot size and cross section of the aerosol plume as a function of distance from the actuator and number of puffs sprayed. Key: (○) cross section of plume by photography; diameter of the TLC spot using (●) one puff, (△) two puffs, (■) three puffs, (⊙) five puffs, and (◆) 10 puffs.*

the TLC method being specific for the drug substance itself provides direct information about the spray pattern of the latter rather than the propellant or solvent.

Correlation of Drug Contents and Dimensions of the TLC Spot—The contents of the drug substance in the TLC spot produced by spraying three puffs of the aerosol at various distances between the TLC plate and the actuator were quantified using blue tetrazolium colorimetry. The data are presented in Table III, and the correlation of the surface area of the spot with the drug recovered is shown in Fig. 5. The data indicate that the surface area of the spot appears to be a good indicator of the drug content in various sections of the observed plume. Table IV shows the recoveries of drug substances from TLC spots that were produced by spraying various puffs of aerosol from a distance of 3 cm from the TLC plate. The recovery of the drug appears to have a reasonably linear correlation (Table V) with the number of puffs, as shown in Fig. 6. This indicates that the drug is quantitatively deposited in the observed spot on the TLC plate under the conditions of the plume geometry test.

Usually a portion of the drug emitted from the valve deposits on the inside of the actuator and is unavailable to the patient. The medication delivered to the patient therefore, is, the amount of drug actually available at the mouthpiece of the actuator. This and other delivery characteristics of the regular (actuator 1) and the defective (actuators 2, 3, and 4) actuators were compared utilizing an air sampler. The air sampler consisted of seven stages. These stages can separate the aerosol particles into seven fractions ranging from an 11.0 to a 0.44-μm aerodynamic diameter. This sampling device can be used as an *in vitro* model for the respiratory tract. As such it simulates, to a reasonable extent, the distribution and retention of inhaled drug particles in the human lungs. The total recovery of the drug, medication delivered to the patient, and percent of drug deposited on the actuator, the tubular throat, and various stages of the air sampler are presented in Table VI. The total recovery of the drug substance was about the same for each actuator. The percent of drug substance deposited on the actuator was considerably higher using the defective actuators; consequently, the amount of medication delivered to the patient was markedly less for these defective actuators. These results are in excellent agreement with those obtained using the TLC method to define the spray pattern. Actuators 2, 3, and 4 produced distorted spots (Fig. 4), and therefore, it was expected that a greater portion of the drug emitted from the aerosol unit in these cases would be deposited on the actuator.

Another parameter of interest was the particle size distribution of the drug substance in the emitted aerosol. This is important since the indi-

Table V—Linear Correlation of Drug Recovered from the TLC Spot with the Surface Area of the TLC Spot and the Number of Puffs Sprayed

Parameters Correlated	Slope ± 90% Confidence Limits	Intercept ± 90% Confidence Limits	Standard Error of Regression	Correlation Coefficient
Drug contents and surface area of the spot [a]	0.270 ± 0.094	62.5 ± 54.0	5.2	0.98260
Drug content of the spot and number of puffs sprayed [b]	244 ± 0.0	−37.1 ± 0.0	82.4	0.99555

[a] From data in Table III and Fig. 5. [b] From data in Table IV and Fig. 6.

Table VI—Various Drug Delivery Parameters [a] of the Aerosol Unit Using Various Actuators

Actuator	Total Recovery, %[c]	Amount Delivered to Patient, %[d]	Drug Substance Recovery, %[b]			
			Actuator	Throat, Sampler Top, Stage 0 and Stage 1	Stages 2 and 3[e]	Stages 4–6[f]
1	109.0 ± 1.1	98.7 ± 2.0	23.0 ± 1.0	50.7 ± 0.6	21.0 ± 1.0	5.6 ± 0.6
2	105.6 ± 4.0	78.0 ± 4.5	37.6 ± 1.1	30.3 ± 2.1	25.0 ± 1.0	7.0 ± 0.0
3	110.3 ± 4.5	85.3 ± 4.5	34.3 ± 1.2	57.0 ± 2.6	6.3 ± 2.8	3.0 ± 0.0
4	110.3 ± 6.4	90.3 ± 6.6	30.6 ± 1.5	46.7 ± 2.3	16.6 ± 1.5	6.0 ± 0.0

[a] Average of three determinations. [b] Drug substance recovery on various stages of an air sampler. [c] Assuming 294 μg/puff. [d] Assuming 250 μg/puff. [e] Estimate to represent aerodynamic particle size in the range of 3.3–7.0 μm. [f] Estimate to represent aerodynamic particle size <3.3 μm.

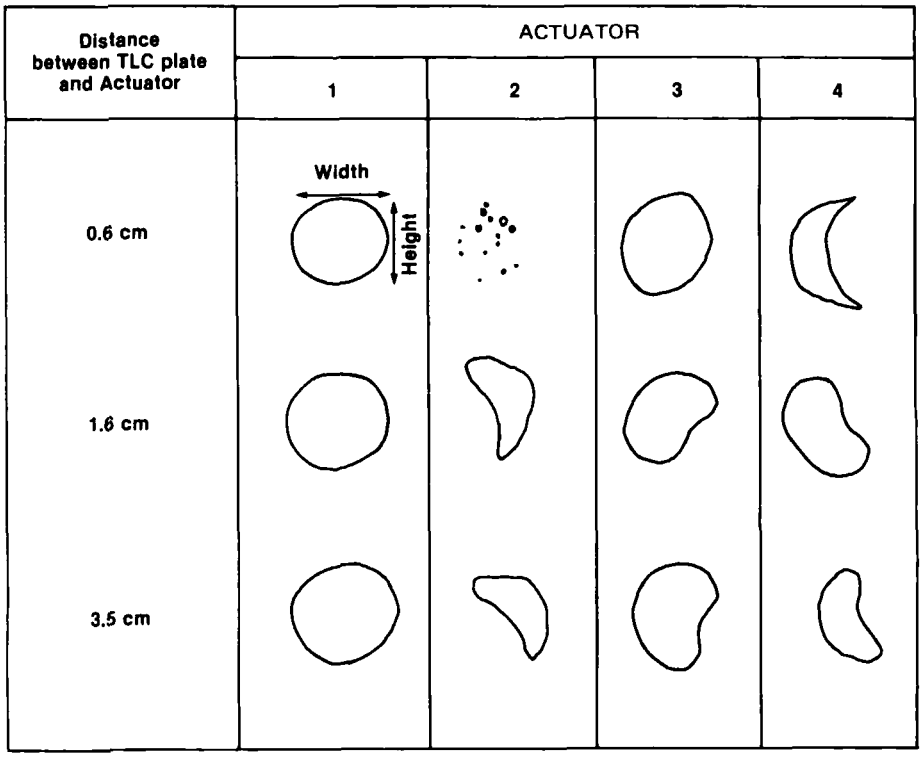

Figure 4—*Spot shapes produced by spraying from the aerosol unit on a TLC plate using the various actuators.*

vidual drug particles are destined for delivery to the lung, and efficiency of the bronchial delivery is dependent on the effective aerodynamic particle size. It was suggested that the effective aerodynamic particle size of drugs for delivery into the lung is <5 μm (17). The percent of drug substance deposited on the various stages of air sampler is included in Table VI. The effective aerodynamic size of particles deposited on stages 2–6 of the air sampler is considered to be <7 μm[9]. Actuator 3 delivered substantially fewer particles <7-μm aerodynamic size because of higher depositions on the throat and actuator. When actuator 2 was used a crescent-shaped spot was observed on the TLC plate (Fig. 4), and the largest amount of the drug substance was deposited on the actuator while the least amount was deposited on the throat. However, this did not affect the amount of particles expected to reach the lungs. Actuator 4, which also yielded a crescent-shaped spot on the TLC plate, showed slightly lower recoveries of particles <7 μm due to larger deposit on the actuator (compared with actuator 1) as well as on the throat stage (compared with actuator 2).

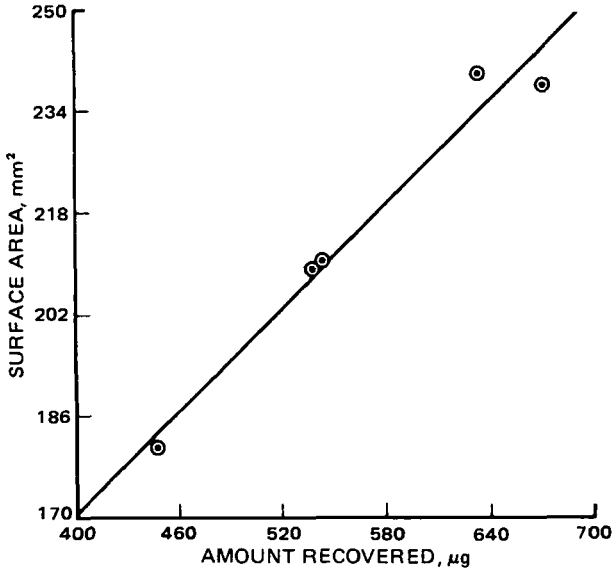

Figure 5—*Correlation of surface area and drug substance content recovered from TLC spots produced by spraying three puffs from the aerosol unit.*

[9] "Particle Fractionating Sampler Bulletin 176-3" Andersen 2000 Inc., Atlanta, Ga.

CONCLUSIONS

The TLC method for characterization of the spray pattern of inhalation aerosols is specific for the drug substance. Therefore, this method provides direct information about the distribution of the drug particles in the spray rather than the general pattern of the propellant or solvent in the spray. Such information is extremely useful in cases of heterogeneous aerosols. In addition, the TLC method is capable of detecting defects in the size and shape of the actuator orifice. Thus, the TLC technique, because of its specificity, simplicity, and speed, can be used as a good incoming quality control tool to evaluate actuators and valve performances.

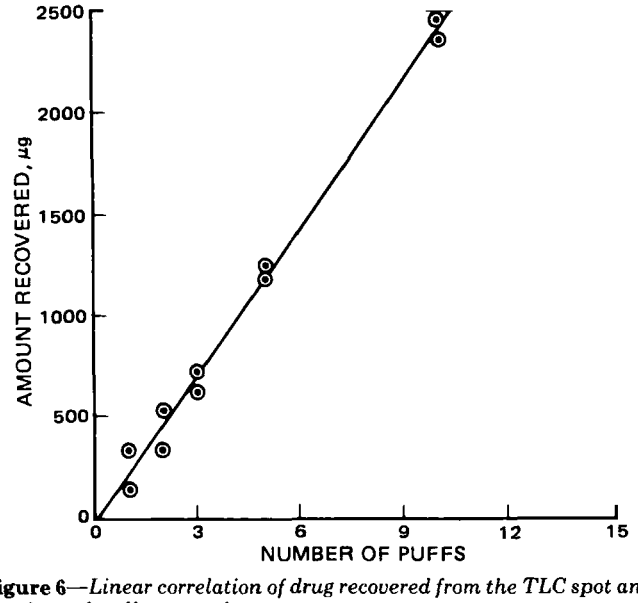

Figure 6—*Linear correlation of drug recovered from the TLC spot and numbers of puffs sprayed.*

REFERENCES

(1) H. T. Nilsson, B. G. Simonsson, and B. Strom, *Eur. J. Clin. Pharmacol.*, **10**, 1 (1976).

(2) E. W. Blackwell, M. E. Conolly, D. S. Davis, and C. T. Dollery, *Br. J. Pharmacol.*, **39**, 194 (1970).

(3) S. R. Walker, M. E. Evans, A. J. Richards, and J. W. Paterson, *Clin. Pharmacol. Ther.*, **13**, 861 (1972).

(4) S. P. Newman, D. Pavia, F. Moren, N. F. Sheahan, and S. W. Clarke, *Thorax*, **36**, 52 (1981).

(5) I. Porush, C. Thiele, and J. Young, *J Am. Pharm. Assoc., Sci. Ed.*, **49**, 70 (1960).

(6) "Aerosol Guide," Chemical Specialties Manufacturers Association, Washington, D.C., 1971, p. 47.

(7) J. G. Young, I. Porush, C. G. Thiel, S. Cohen, and C. H. Stimmel, *J. Am. Pharm. Assoc., Sci. Ed.*, **49**, 72 (1960).

(8) M. V. Wiener, *J. Soc. Cosmet. Chem.*, **9**, 289 (1958).

(9) V. M. Tsetlin, *Aerosol Age*, **14**, 57 (1969).

(10) W. C. Beard, Jr., "Aerosols: Science and Technology," H. R. Shepherd, Ed., Interscience, New York, N.Y., 1960, p. 148.

(11) M. J. Root, *ibid.*, p. 281.

(12) ASTM Standard, Part 46, American Society for Testing and Materials, Philadelphia, Pa. 1978, D 3077-72.

(13) B. Hunerbein, H. Kala, and H. Moldenhauer, *Pharmazie*, **33**, 12 (1978).

(14) K. J. Turner, *Aerosol Age*, **25**, 24 (1980).

(15) S. Miszuk, B. M. Gupta, F. C. Chen, C. Clawans, and J. Z. Knapp, *J. Pharm. Sci.*, **69**, 713 (1980).

(16) W. J. Mader and R. R. Buck, *Anal. Chem.*, **24**, 666 (1952).

(17) A. B. Dobkin, "Ventilators and Inhalation Therapy," *2nd. ed.*, Little, Brown, Boston, Mass., 1972.

ACKNOWLEDGMENTS

The authors acknowledge Dr. R. Jones' and Mrs. G. Harringer's contributions in adapting the Andersen Air Sampler to determine particle size distribution of the corticosteroid in the inhaled aerosol.

Esterase-Like Activity of Human Serum Albumin II: Reaction with *N-trans*-Cinnamoylimidazoles

NAOKO OHTA, YUKIHISA KURONO, and KEN IKEDA ˣ

Received March 1, 1982 from the *Faculty of Pharmaceutical Sciences, Nagoya City University, Tanabe-dori, Mizuho-ku, Nagoya, 467, Japan.* Accepted for publication September 17, 1982.

Abstract □ To elucidate the details of the esterase activity of human serum albumin, the reaction of *N-trans*-cinnamoylimidazoles with albumin was investigated kinetically at various pHs at 25°. The reaction consisted of the acylation of albumin (probably the tyrosine-411 residue) by the substrate and the deacylation of cinnamoyl-albumin. The acylation was ~10–100-fold faster than the spontaneous hydrolysis of the substrate over the pH range examined. The pH profile for the deacylation rate constant indicated the participation of a group having a pK_a of ~9.4. The deacylation was subjected to the effect of deuterium oxide. The electron-withdrawing substituent facilitated the deacylation; the Hammett ρ value was 1.63. These results suggest that the deacylation proceeded *via* general base catalysis by this group.

Keyphrases □ Albumin, human serum—esterase-like activity, acylation with *N-trans*-cinnamoylimidazoles, kinetics □ Cinnamoylimidazoles—acylation of albumin, kinetics □ Kinetics—acylation of albumin with *N-trans*-cinnamoylimidazoles at the tyrosine-411 residue binding site

Studies involving the binding of drugs to human serum albumin are pharmacologically and clinically important, since this binding influences the *in vivo* distribution, availability, and elimination of drugs (1). Localization of drug binding sites on the albumin molecule and the classification of drugs with respect to the binding sites can be used to predict the displacement of one drug by another when two or more drugs are administered concurrently (2). It was reported previously that albumin exhibits esterase activity toward phenyl esters (3, 4). The active site involved when the substrate is *p*-nitrophenyl acetate was found to be one of the most important drug binding sites on albumin, and was named the R site (5–7). The R site is located near the reactive tyrosine-411 residue (5, 8–12). Previous studies (5–7) examined the inhibition of the esterase activity by several drugs, and led to the classification and identification of the various binding sites involved.

The details of the esterase activity of albumin have not been described. The activity of albumin toward amide substrates as well as the mechanisim of the deacylation of the acyl-albumin are not known. Since many drugs possess the amide linkage, we have investigated the activity of

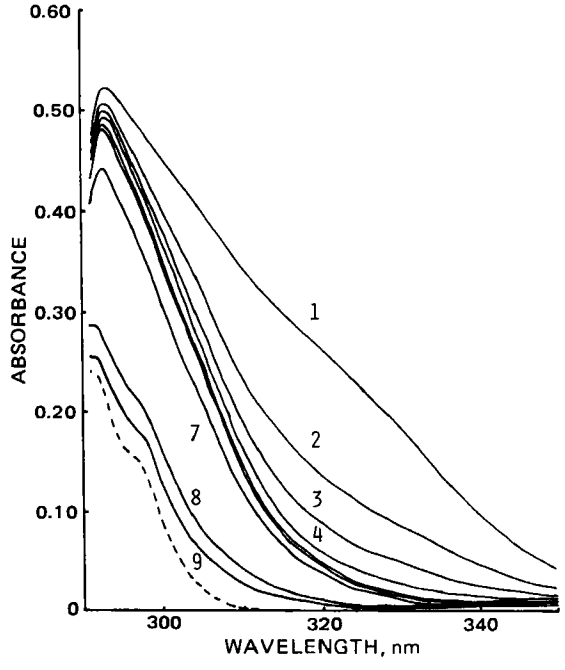

Figure 1—*Periodic difference spectrum of the reaction mixture (albumin + I)* versus *albumin at pH 8.41 and 25°. The dotted line is the spectrum of the mixture of* trans-*cinnamic acid and imidazole. Key: (1) 1.0, (2) 3.0, (3) 5.0, (4) 9.0, (5) 30, (6) 60, (7) 240, (8) 1440, and (9) 2580 min. The initial concentrations of I and albumin are 4.00 × 10^{-5} M and 2.00 × 10^{-4} M, respectively.*

0022-3549/83/0400-0385$01.00/0

REFERENCES

(1) H. T. Nilsson, B. G. Simonsson, and B. Strom, *Eur. J. Clin. Pharmacol.*, **10**, 1 (1976).

(2) E. W. Blackwell, M. E. Conolly, D. S. Davis, and C. T. Dollery, *Br. J. Pharmacol.*, **39**, 194 (1970).

(3) S. R. Walker, M. E. Evans, A. J. Richards, and J. W. Paterson, *Clin. Pharmacol. Ther.*, **13**, 861 (1972).

(4) S. P. Newman, D. Pavia, F. Moren, N. F. Sheahan, and S. W. Clarke, *Thorax*, **36**, 52 (1981).

(5) I. Porush, C. Thiele, and J. Young, *J Am. Pharm. Assoc., Sci. Ed.*, **49**, 70 (1960).

(6) "Aerosol Guide," Chemical Specialties Manufacturers Association, Washington, D.C., 1971, p. 47.

(7) J. G. Young, I. Porush, C. G. Thiel, S. Cohen, and C. H. Stimmel, *J. Am. Pharm. Assoc., Sci. Ed.*, **49**, 72 (1960).

(8) M. V. Wiener, *J. Soc. Cosmet. Chem.*, **9**, 289 (1958).

(9) V. M. Tsetlin, *Aerosol Age*, **14**, 57 (1969).

(10) W. C. Beard, Jr., "Aerosols: Science and Technology," H. R. Shepherd, Ed., Interscience, New York, N.Y., 1960, p. 148.

(11) M. J. Root, *ibid.*, p. 281.

(12) ASTM Standard, Part 46, American Society for Testing and Materials, Philadelphia, Pa. 1978, D 3077-72.

(13) B. Hunerbein, H. Kala, and H. Moldenhauer, *Pharmazie*, **33**, 12 (1978).

(14) K. J. Turner, *Aerosol Age*, **25**, 24 (1980).

(15) S. Miszuk, B. M. Gupta, F. C. Chen, C. Clawans, and J. Z. Knapp, *J. Pharm. Sci.*, **69**, 713 (1980).

(16) W. J. Mader and R. R. Buck, *Anal. Chem.*, **24**, 666 (1952).

(17) A. B. Dobkin, "Ventilators and Inhalation Therapy," *2nd. ed.*, Little, Brown, Boston, Mass., 1972.

ACKNOWLEDGMENTS

The authors acknowledge Dr. R. Jones' and Mrs. G. Harringer's contributions in adapting the Andersen Air Sampler to determine particle size distribution of the corticosteroid in the inhaled aerosol.

Esterase-Like Activity of Human Serum Albumin II: Reaction with *N-trans*-Cinnamoylimidazoles

NAOKO OHTA, YUKIHISA KURONO, and KEN IKEDA ˣ

Received March 1, 1982 from the *Faculty of Pharmaceutical Sciences, Nagoya City University, Tanabe-dori, Mizuho-ku, Nagoya, 467, Japan.* Accepted for publication September 17, 1982.

Abstract □ To elucidate the details of the esterase activity of human serum albumin, the reaction of *N-trans*-cinnamoylimidazoles with albumin was investigated kinetically at various pHs at 25°. The reaction consisted of the acylation of albumin (probably the tyrosine-411 residue) by the substrate and the deacylation of cinnamoyl-albumin. The acylation was ~10–100-fold faster than the spontaneous hydrolysis of the substrate over the pH range examined. The pH profile for the deacylation rate constant indicated the participation of a group having a pK_a of ~9.4. The deacylation was subjected to the effect of deuterium oxide. The electron-withdrawing substituent facilitated the deacylation; the Hammett ρ value was 1.63. These results suggest that the deacylation proceeded *via* general base catalysis by this group.

Keyphrases □ Albumin, human serum—esterase-like activity, acylation with *N-trans*-cinnamoylimidazoles, kinetics □ Cinnamoylimidazoles—acylation of albumin, kinetics □ Kinetics—acylation of albumin with *N-trans*-cinnamoylimidazoles at the tyrosine-411 residue binding site

Studies involving the binding of drugs to human serum albumin are pharmacologically and clinically important, since this binding influences the *in vivo* distribution, availability, and elimination of drugs (1). Localization of drug binding sites on the albumin molecule and the classification of drugs with respect to the binding sites can be used to predict the displacement of one drug by another when two or more drugs are administered concurrently (2). It was reported previously that albumin exhibits esterase activity toward phenyl esters (3, 4). The active site involved when the substrate is *p*-nitrophenyl acetate was found to be one of the most important drug binding sites on albumin, and was named the R site (5–7). The R site is located near the reactive tyrosine-411 residue (5, 8–12). Previous studies (5–7) examined the inhibition of the esterase activity by several drugs, and led to the classification and identification of the various binding sites involved.

The details of the esterase activity of albumin have not been described. The activity of albumin toward amide substrates as well as the mechanisim of the deacylation of the acyl-albumin are not known. Since many drugs possess the amide linkage, we have investigated the activity of

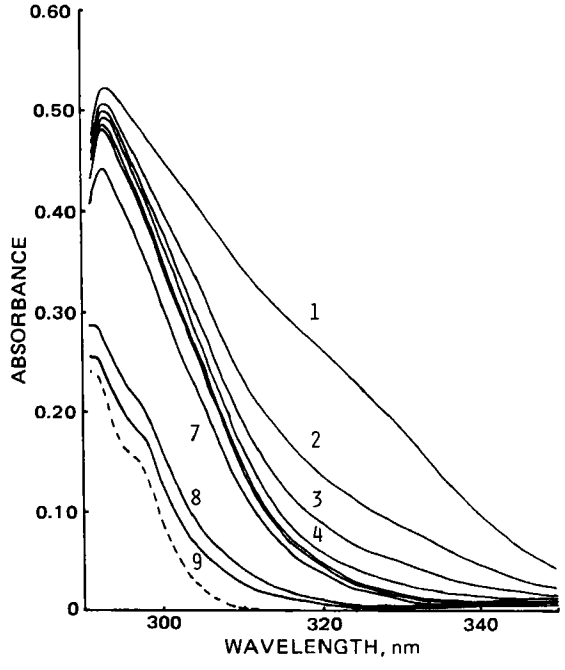

Figure 1—*Periodic difference spectrum of the reaction mixture (albumin + I)* versus *albumin at pH 8.41 and 25°. The dotted line is the spectrum of the mixture of* trans-*cinnamic acid and imidazole. Key: (1) 1.0, (2) 3.0, (3) 5.0, (4) 9.0, (5) 30, (6) 60, (7) 240, (8) 1440, and (9) 2580 min. The initial concentrations of I and albumin are 4.00 × 10^{-5} M and 2.00 × 10^{-4} M, respectively.*

0022-3549/83/0400-0385$01.00/0

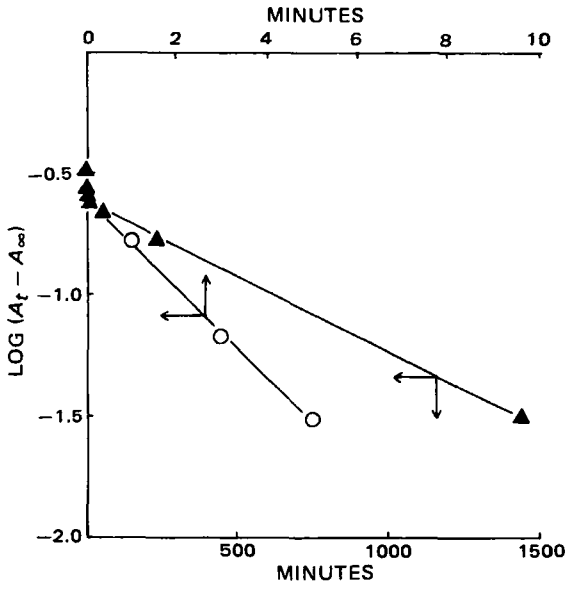

Figure 2—*First-order plots for the spectral changes in Fig. 1.* A_t *and* A_∞ *are the absorbances at time* t *and at completion of the reaction, respectively. Key: (○) at 330 nm and (▲) at 300 nm.*

albumin toward potential model substrates, the substituted *N-trans*-cinnamoylimidazoles. The pH dependence, isotope effect (deuterium oxide), and substituent effects for both the acylation and deacylation were examined using spectrophotometric methods.

EXPERIMENTAL

Materials—Albumin[1] was used after purification by the method of Chen (13). The molecular weight of the albumin was assumed to be 69,000 and the concentration was determained using an extinction coefficient $E^{0.1\%}_{1\,cm}$ of 0.531 at 278 nm (4). *N-trans*-Cinnamoylimidazole (I) was prepared by the reaction of *trans*-cinnamoyl chloride with imidazole in benzene solution (14). *p*-Chloro- (II), *m*-methyl- (III), and *p*-methoxy- (IV) cinnamoylimidazoles were synthesized by the method of Bernhard *et al.* (15) from the respective cinnamic acid and imidazole using dicyclohexylcarbodiimide as the catalyst. Several recrystallizations from cyclohexane gave material with the following melting points: (I) 133–134°, (II) 158–163°, (III) 119–123°, and (IV) 118–120°. Clofibric acid was prepared by the method of Jones *et al.*, mp 116–120° [lit. (16) mp 118–119°]. The ^2H content of the deuterium oxide[2] was >99.75%. All other chemicals purchased were of reagent grade.

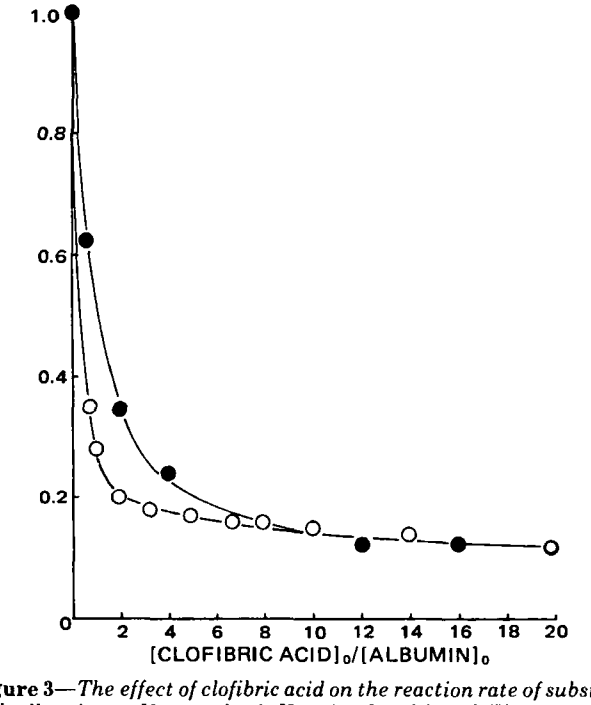

Figure 3—*The effect of clofibric acid on the reaction rate of substrate with albumin at pH 7.4 and 25°. Key: (●) I and (○) V. The initial concentrations of the substrate and albumin are 1.00 × 10^{-5} M and 5.00 × 10^{-5} M, respectively.*

[1] Sigma Chemical Co., Fraction V, lot 18c-0519.

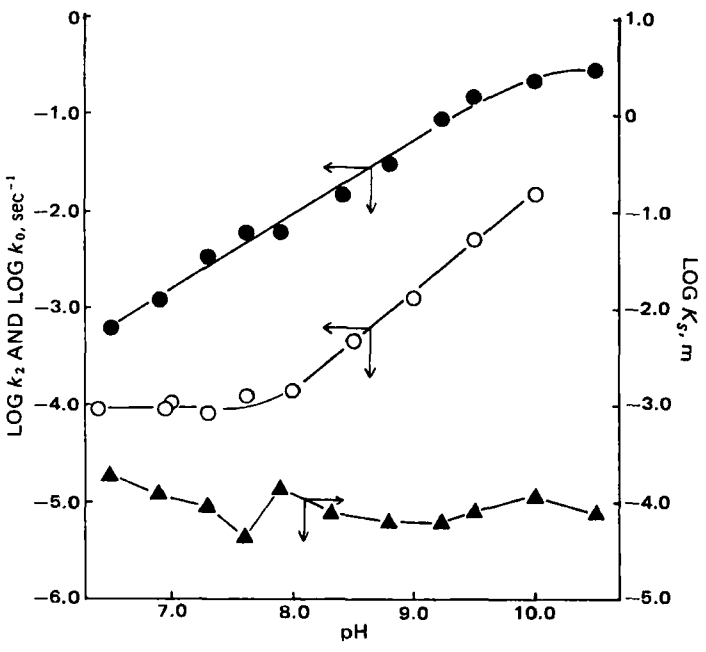

Figure 4—*Plots of log* k_2, *log* k_0, *and log* K_s *versus pH at 25°. Key: (●) log* k_2, *(○) log* k_0, *and (▲) log* K_s.

Kinetic Procedures—The reactions of the substrates with albumin were carried out in the presence of an albumin concentration more than fourfold in excess of the substrates, so that the substrates preferentially reacted with the primary reactive site (3, 4). The reactions were initiated by mixing 15 μl of the substrate in acetonitrile with 3 ml of buffered albumin solution preincubated in the spectrophotometer[3] cell kept at 25°. The acylation rate of albumin with I was followed at 330 nm to preclude interference due to the subsequent deacylation. The pseudo first-order rate constant was determined as described in a previous paper (3).

The deacylation of cinnamoyl-albumin was followed at 300 nm (Figs. 1 and 2). Sörensen buffer (0.067 *M* phosphate, pH 7.0–8.0) and Kolthoff

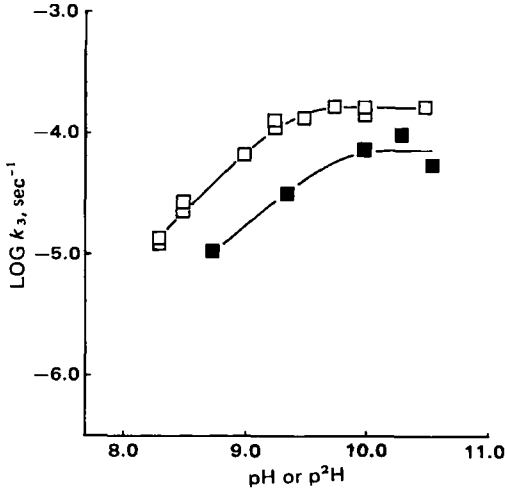

Figure 5—*Plots of log* k_3 *versus pH or* p^2H *at 25°. Key: (□) in water, and (■) in deuterium oxide.*

[2] Merck & Co., Inc.
[3] Hitachi UV-124 Spectrophotometer.

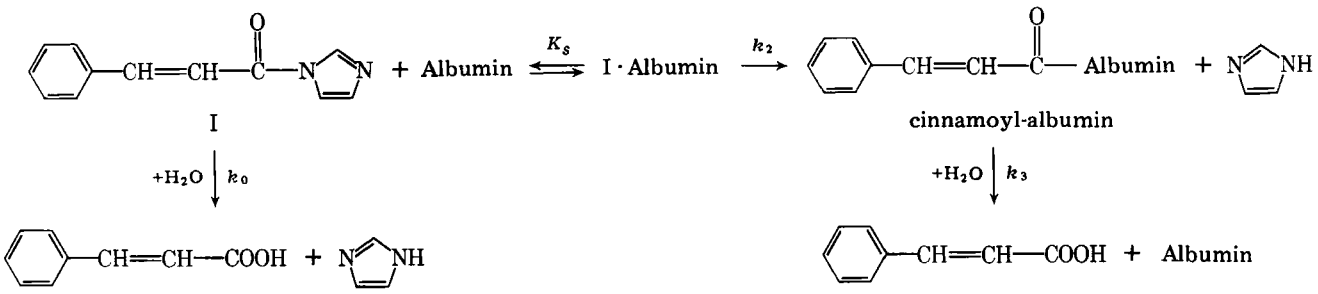

Scheme I

buffer (0.05 *M* borate, pH 8.0–10.5) were used as the reaction medium. The ionic strength was adjusted to 0.2 *M* with sodium chloride. In deuterium oxide, a p^2H value was estimated from p^2H = pH-meter reading + 0.4 (17).

RESULTS AND DISCUSSION

Reaction of *N-trans*-Cinnamoylimidazole with Albumin—The absorptivity changes noted during the reaction between albumin and I at pH 8.41 are shown in Fig. 1. Each spectrum is the difference between the reaction mixture and an equimolar albumin solution. The changes with time consist of a fast reaction followed by a slow one. The spectra eventually approach the sum of the spectra of equimolar *trans*-cinnamic acid and imidazole (represented by the dotted line). The first-order plot of the absorbance changes at 300 nm is obviously composed of the two steps (Fig. 2). The rate constant for the fast reaction obtained from the plot at 330 nm is ~300-fold larger than that obtained from the second (slow reaction) phase at 300 nm. It is probable that the fast reaction reflected by the decrease in the absorbance of I is the acylation of albumin (formation of cinnamoyl-albumin), and the subsequent slow reaction is the deacylation of the cinnamoyl-albumin.

To localize the reactive site toward I on albumin, the effect of clofibric acid on the acylation rate of albumin was examined. Clofibric acid was found previously (5–7) to bind singly at the R site on albumin and to inhibit the reaction of albumin with *p*-nitrophenyl acetate (V). The results are shown in Fig. 3. The *r* value in the ordinate of Fig. 3 represents the ratio of the rate constant in the presence of clofibric acid to that in its absence. The acylation of albumin is inhibited by clofibric acid, in a manner similar to its reaction with V. This inhibitory effect of clofibric acid indicates that both substrates I and V react with the same active site (R site, near tyrosine-411) on albumin. The tyrosine-411 residue of the R site, therefore, is considered to be acylated by I.

The overall reaction of I with albumin can be represented as in Scheme I. In this case, I·albumin is the Michaelis–Menten-type complex between I and albumin and K_s is the dissociation constant of the complex. The first-order rate constants of I and I·albumin are expressed by k_0 and k_2, respectively. The first-order rate constant for the deacylation of the cinnamoyl-albumin is given by k_3.

Acylation of Albumin with *N-trans*-Cinnamoylimidazole—The apparent first-order rate constants (k_{obs}) for the acylation of albumin were measured with several concentrations of albumin. The kinetic parameters k_2 and K_s for the acylation can be calculated from the intercept and slope of the double reciprocal plot based on the following (3):

$$\frac{1}{k_{obs} - k_0} = \frac{K_s}{(k_2 - k_0)} \frac{1}{[\text{albumin}]_0} + \frac{1}{k_2 - k_0}$$

The pH dependencies of k_2, K_s, and k_0 (for a comparison with k_2) are shown in Fig. 4. The slope of the log k_2–pH profile between pH 6.5 and 9.0 is approximately unity; at pH >9.5 k_2 becomes independent of pH. From this profile the pK_a value of the catalytic group is estimated as ~9.7. This pK_a value supports the theory that the acylation occurs at the tyrosine-411 residue of the R site, since the tyrosine-411 residue involved for the reaction with V has pK_a of ~9.5 (3, 5, 8). In addition, the absence of a deuterium oxide effect in the fast step also supports this theory for the acylation of albumin.

The value of K_s is almost independent of pH in the region examined. The spontaneous hydrolysis of I proceeds through the usual base catalysis in the alkaline region. From the comparison of k_0 with k_2, it is obvious that albumin accelerates the cleavage of amide substrate I as well as ester substrates (3, 4).

Deacylation of Cinnamoyl-Albumins—The pH dependence of k_3 for cinnamoyl-albumin is illustrated in Fig. 5. Up to pH ~9, the log k_3–pH profile shows a slope of approximately unity. However, the rate constant reaches the limiting value at higher pH. This pH dependence implies the participation of a group having pK_a of ~9.4 for the deacylation. In deuterium oxide the deacylation rate is about three–fourfold smaller than that in water, as shown in Fig. 5. This deuterium effect indicates that the water molecule also plays a role in the deacylation. Therefore, general acid or base catalysis by the group rather than nucleophilic catalysis predominates in the deacylation of cinnamoyl-albumin (18).

The substituent effect for the deacylation rate was examined to distinguish between the general acid and base catalysis. The log k_3–pH profiles for *p*-chloro-, *m*-methyl-, and *p*-methoxycinnamoyl-albumins are shown in Fig. 6. A pH variation of ~0.5 units seems to exist in the

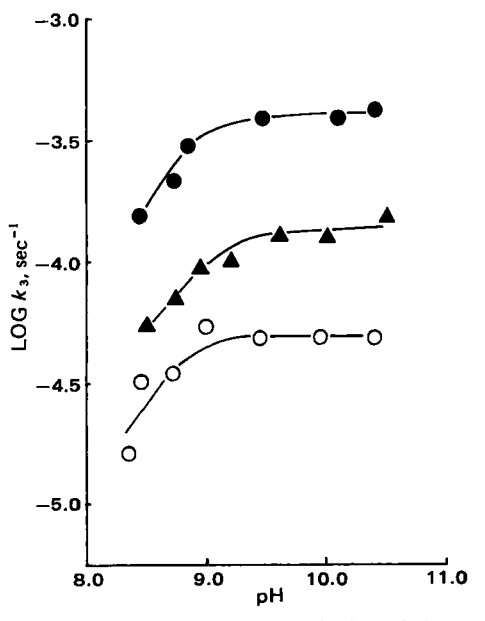

Figure 6—*pH dependence of* k_3 *for the substituted cinnamoyl-albumins at 25°. Key: (●) p-chlorocinnamoyl-albumin, (▲) m-methylcinnamoyl-albumin, and (○) p-methoxycinnamoyl-albumin.*

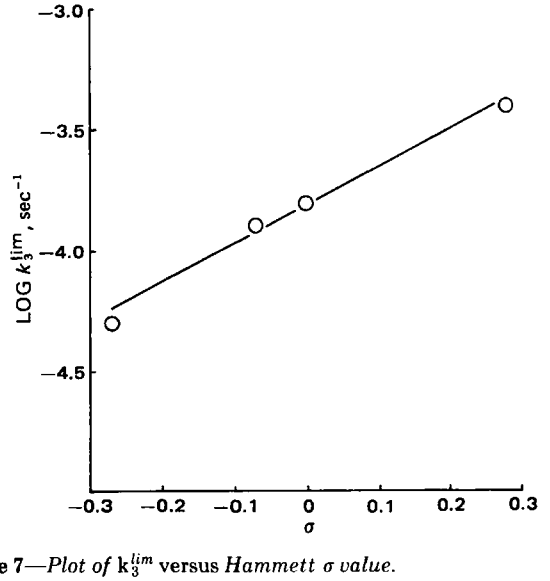

Figure 7—*Plot of* k_3^{lim} versus *Hammett σ value.*

apparent pK_a of the group participating in the deacylation. This variation may be attributable to the perturbation of the pK_a induced by the substituted cinnamoyl group (15, 19). A plot of the logarithm of the rate constants in the pH-independent region (k_3^{lim}) against the Hammett σ values gives a straight line (correlation coefficient = 0.994), as shown in Fig. 7. The electron-withdrawing substituent facilitates the reaction and the Hammett ρ value is 1.63. This ρ value suggests that the deacylation proceeds *via* general base catalysis rather than general acid catalysis, because the latter is, in general, independent of polar effects (20). The requirement of the limited conformation around the catalytic site is demonstrated by the finding that the deacylation of denatured cinnamoyl-albumin in 8 *M* urea was retarded.

Although the acylation of albumin with I (k_2) was faster than the spontaneous hydrolysis of I (k_0), as shown in Fig. 4, the deacylation of the cinnamoyl-albumin (k_3 in Fig. 5) is slower than the hydrolysis of I (k_0 in Fig. 4). The deacylation rate is related to the molecular activity (in the past the term "turn over number" has been used) which gives an indication of efficiency of an enzyme (21, 22). In this context, the esterase-like activity rather than the intrinsic esterase may be an appropriate expression for the activity of albumin toward the amide and ester substrates.

REFERENCES

(1) J. J. Vallner, *J. Pharm. Sci.*, **66**, 447 (1977).

(2) K. J. Fehske, W. E. Müller, and U. Wollert, *Biochem. Pharmacol.*, **30**, 687 (1981).

(3) Y. Kurono, T. Maki, T. Yotsuyanagi, and K. Ikeda, *Chem. Pharm. Bull.* Part I, **27**, 2781 (1979).

(4) G. E. Means and M. L. Bender, *Biochemistry*, **14**, 4989 (1975).

(5) Y. Ozeki, Y. Kurono, T. Yotsuyanagi, and K. Ikeda, *Chem. Pharm. Bull.*, **28**, 535 (1980).

(6) Y. Kurono, N. Ohta, T. Yotsuyanagi, and K. Ikeda, *ibid.*, **29**, 2345 (1981).

(7) Y. Kurono and K. Ikeda, *ibid.*, **29**, 2993 (1981).

(8) G. E. Means and H.-L. Wu, *Arch. Biochem. Biophys.*, **194**, 526 (1979).

(9) F. Sanger, *Proc. Chem. Soc.*, **1963**, 76.

(10) L. Morávek, M. A. Saber, and B. Meloun, *Collection Czechoslov. Chem. Commun.*, **44**, 1657 (1979).

(11) K. J. Fehske, W. E. Müller, and U. Wollert, *Arch. Biochem. Biophys.*, **205**, 217 (1980).

(12) V. M. Rosenoer, M. Oratz, and M. A. Rothschild, in "Albumin Structure, Function and Uses," J. R. Brown, Ed., Pergamon, Oxford, England, 1977, p. 27.

(13) R. F. Chen, *J. Biol. Chem.*, **242**, 173 (1967).

(14) G. R. Schonbaum, B. Zerner, and M. L. Bender, *ibid.*, **236**, 2930 (1961).

(15) S. A. Bernhard, E. Hershberger, and J. Keizer, *Biochemistry*, **5**, 4120 (1966).

(16) W. G. M. Jones, J. M. Thorp, and W. S. Waring, British pat., 860303 (1961).

(17) L. J. Brubacher and M. L. Bender, *J. Am. Chem. Soc.*, **88**, 5871 (1966).

(18) M. L. Bender and L. J. Brubacher, in "Catalysis and Enzyme Action," McGraw-Hill, New York, N.Y., 1973, p. 53.

(19) J. W. Amshey, S. P. Jindal, and M. L. Bender, *Arch. Biochem. Biophys.*, **169**, 1 (1975).

(20) M. Caplow and W. P. Jencks, *Biochemistry*, **1**, 883 (1962).

(21) M. L. Bender, in "Mechanisms of Homogeneous Catalysis from Protons to Proteins," Wiley, New York, N.Y., 1971, p. 397.

(22) M. Dixon and E. C. Webb, in "Enzymes," 3rd ed., Academic, New York, N.Y., 1979, p. 13.

ACKNOWLEDGMENTS

This work was supported by a grant from the Ministry of Education, Science, and Culture of Japan.

We are grateful to Miss Kinuyo Hayakawa for her excellent technical assistance.

Stability Constants for Complex Formation Between α-Cyclodextrin and Some Amines

ALBERT B. WONG, SHU-FEN LIN, and KENNETH A. CONNORS ˣ

Received March 18, 1982 from the *School of Pharmacy, University of Wisconsin, Madison, WI 53706.* Accepted for publication August 9, 1982.

Abstract □ Complex formation of α-cyclodextrin with 15 amines (including seven 4-substituted anilines) was studied by the potentiometric method, supplemented by direct UV spectrophotometry and a competitive indicator spectrophotometric method. The data were analyzed in terms of 1:1 and 1:2 complexes (amine–cyclodextrin ratios) and the stability constants K_{11a}, K_{12a}, K_{11b}, and K_{12b} were evaluated; the subscripts indicate the stoichiometry and conjugate acid–base form. For all amines K_{11b} was greater than K_{11a} and K_{12a} was 0. On the basis of the relationship of complex stability to amine structure, it was concluded that the primary binding site in anilines is the 4-substituent.

Keyphrases □ Complex formation—of α-cyclodextrin with amines, determination of the stability constants and binding sites □ α-Cyclodextrin—complex formation with amines, determination of stability constants and binding sites □ Amines—complex formation with α-cyclodextrin, determination of stability constants and binding sites

Cycloamyloses (also called cyclodextrins) are cyclic oligomers containing six or more D-glucose units linked 1 → 4; they are produced by the action of *Bacillus macerans* amylase on starch. The six- and seven-unit substances are called cyclohexaamylose (α-cyclodextrin) and cycloheptaamylose (β-cyclodextrin), respectively. These molecules are doughnut shaped, and their possession of a cavity of fixed size and shape has led to considerable interest in their chemical properties. The production, purification, and chemistry of the cycloamyloses have been reviewed (1–4).

Any molecule smaller than the cavity of a cyclodextrin can enter the cavity and there undergo noncovalent interaction with the atoms lining and rimming the cavity. The resulting association product is called an inclusion complex. The cyclodextrin is thus a host for the smaller (guest) molecule. The dimensions of the α-cyclodextrin cavity permit the inclusion of many mono- and disubstituted benzene derivatives. A 1:1 stoichiometry is commonly observed (and often assumed in experimental studies), but it has now been well established that 1:2 complexes (*i.e.*, 1 substrate:2 cyclodextrins) may exist in some systems[1] (5–9).

The present paper is one of a series that describes

[1] The substrate (S) is the guest; the cyclodextrin (ligand, L) is the host. Stoichiometric ratios are given in the form SL (1:1) and SL_2 (1:2).

0022-3549/83/0400-0388$01.00/0

apparent pK_a of the group participating in the deacylation. This variation may be attributable to the perturbation of the pK_a induced by the substituted cinnamoyl group (15, 19). A plot of the logarithm of the rate constants in the pH-independent region (k_3^{lim}) against the Hammett σ values gives a straight line (correlation coefficient = 0.994), as shown in Fig. 7. The electron-withdrawing substituent facilitates the reaction and the Hammett ρ value is 1.63. This ρ value suggests that the deacylation proceeds *via* general base catalysis rather than general acid catalysis, because the latter is, in general, independent of polar effects (20). The requirement of the limited conformation around the catalytic site is demonstrated by the finding that the deacylation of denatured cinnamoyl-albumin in 8 *M* urea was retarded.

Although the acylation of albumin with I (k_2) was faster than the spontaneous hydrolysis of I (k_0), as shown in Fig. 4, the deacylation of the cinnamoyl-albumin (k_3 in Fig. 5) is slower than the hydrolysis of I (k_0 in Fig. 4). The deacylation rate is related to the molecular activity (in the past the term "turn over number" has been used) which gives an indication of efficiency of an enzyme (21, 22). In this context, the esterase-like activity rather than the intrinsic esterase may be an appropriate expression for the activity of albumin toward the amide and ester substrates.

REFERENCES

(1) J. J. Vallner, *J. Pharm. Sci.*, **66**, 447 (1977).

(2) K. J. Fehske, W. E. Müller, and U. Wollert, *Biochem. Pharmacol.*, **30**, 687 (1981).

(3) Y. Kurono, T. Maki, T. Yotsuyanagi, and K. Ikeda, *Chem. Pharm. Bull.* Part I, **27**, 2781 (1979).

(4) G. E. Means and M. L. Bender, *Biochemistry*, **14**, 4989 (1975).

(5) Y. Ozeki, Y. Kurono, T. Yotsuyanagi, and K. Ikeda, *Chem. Pharm. Bull.*, **28**, 535 (1980).

(6) Y. Kurono, N. Ohta, T. Yotsuyanagi, and K. Ikeda, *ibid.*, **29**, 2345 (1981).

(7) Y. Kurono and K. Ikeda, *ibid.*, **29**, 2993 (1981).

(8) G. E. Means and H.-L. Wu, *Arch. Biochem. Biophys.*, **194**, 526 (1979).

(9) F. Sanger, *Proc. Chem. Soc.*, **1963**, 76.

(10) L. Morávek, M. A. Saber, and B. Meloun, *Collection Czechoslov. Chem. Commun.*, **44**, 1657 (1979).

(11) K. J. Fehske, W. E. Müller, and U. Wollert, *Arch. Biochem. Biophys.*, **205**, 217 (1980).

(12) V. M. Rosenoer, M. Oratz, and M. A. Rothschild, in "Albumin Structure, Function and Uses," J. R. Brown, Ed., Pergamon, Oxford, England, 1977, p. 27.

(13) R. F. Chen, *J. Biol. Chem.*, **242**, 173 (1967).

(14) G. R. Schonbaum, B. Zerner, and M. L. Bender, *ibid.*, **236**, 2930 (1961).

(15) S. A. Bernhard, E. Hershberger, and J. Keizer, *Biochemistry*, **5**, 4120 (1966).

(16) W. G. M. Jones, J. M. Thorp, and W. S. Waring, British pat., 860303 (1961).

(17) L. J. Brubacher and M. L. Bender, *J. Am. Chem. Soc.*, **88**, 5871 (1966).

(18) M. L. Bender and L. J. Brubacher, in "Catalysis and Enzyme Action," McGraw-Hill, New York, N.Y., 1973, p. 53.

(19) J. W. Amshey, S. P. Jindal, and M. L. Bender, *Arch. Biochem. Biophys.*, **169**, 1 (1975).

(20) M. Caplow and W. P. Jencks, *Biochemistry*, **1**, 883 (1962).

(21) M. L. Bender, in "Mechanisms of Homogeneous Catalysis from Protons to Proteins," Wiley, New York, N.Y., 1971, p. 397.

(22) M. Dixon and E. C. Webb, in "Enzymes," 3rd ed., Academic, New York, N.Y., 1979, p. 13.

ACKNOWLEDGMENTS

This work was supported by a grant from the Ministry of Education, Science, and Culture of Japan.

We are grateful to Miss Kinuyo Hayakawa for her excellent technical assistance.

Stability Constants for Complex Formation Between α-Cyclodextrin and Some Amines

ALBERT B. WONG, SHU-FEN LIN, and KENNETH A. CONNORS ˣ

Received March 18, 1982 from the *School of Pharmacy, University of Wisconsin, Madison, WI 53706.* Accepted for publication August 9, 1982.

Abstract □ Complex formation of α-cyclodextrin with 15 amines (including seven 4-substituted anilines) was studied by the potentiometric method, supplemented by direct UV spectrophotometry and a competitive indicator spectrophotometric method. The data were analyzed in terms of 1:1 and 1:2 complexes (amine–cyclodextrin ratios) and the stability constants K_{11a}, K_{12a}, K_{11b}, and K_{12b} were evaluated; the subscripts indicate the stoichiometry and conjugate acid–base form. For all amines K_{11b} was greater than K_{11a} and K_{12a} was 0. On the basis of the relationship of complex stability to amine structure, it was concluded that the primary binding site in anilines is the 4-substituent.

Keyphrases □ Complex formation—of α-cyclodextrin with amines, determination of the stability constants and binding sites □ α-Cyclodextrin—complex formation with amines, determination of stability constants and binding sites □ Amines—complex formation with α-cyclodextrin, determination of stability constants and binding sites

Cycloamyloses (also called cyclodextrins) are cyclic oligomers containing six or more D-glucose units linked 1 → 4; they are produced by the action of *Bacillus macerans* amylase on starch. The six- and seven-unit substances are called cyclohexaamylose (α-cyclodextrin) and cycloheptaamylose (β-cyclodextrin), respectively. These molecules are doughnut shaped, and their possession of a cavity of fixed size and shape has led to considerable interest in their chemical properties. The production, purification, and chemistry of the cycloamyloses have been reviewed (1–4).

Any molecule smaller than the cavity of a cyclodextrin can enter the cavity and there undergo noncovalent interaction with the atoms lining and rimming the cavity. The resulting association product is called an inclusion complex. The cyclodextrin is thus a host for the smaller (guest) molecule. The dimensions of the α-cyclodextrin cavity permit the inclusion of many mono- and disubstituted benzene derivatives. A 1:1 stoichiometry is commonly observed (and often assumed in experimental studies), but it has now been well established that 1:2 complexes (*i.e.*, 1 substrate:2 cyclodextrins) may exist in some systems[1] (5–9).

The present paper is one of a series that describes

[1] The substrate (S) is the guest; the cyclodextrin (ligand, L) is the host. Stoichiometric ratios are given in the form SL (1:1) and SL_2 (1:2).

0022-3549/83/0400-0388$01.00/0

Table I—Stability Constants for α-Cyclodextrin Complexes of 4-Substituted Anilines at 25° [a]

X[b]	K_{11b}/M^{-1}	K_{12b}/M^{-1}	K_{11a}/M^{-1}
NH_2	2.3 (0.10)	2.1 (1.0)	0
OCH_3	6.7 (0.14)	−0.5 (0.3)	0
CH_3	57.6 (0.34)	3.91 (0.09)	37.1 (1.1)
H	8.8 (0.12)	−0.39 (0.39)	0
COO^- [c]	9.0	0	—[d]
Cl	251 (10.0)	0.12 (0.16)	68.6 (3.3)
COOH[c]	1341	0	—[d]
CN	451 (33.7)	—[d]	—[d]
NO_2	635 (34.4)	—[d]	—[d]

[a] Standard deviations in parentheses. [b] X in X—C_6H_4—NH_2. [c] From Ref. 9. [d] — not determined.

measurement of stability constants for complex formation between α-cyclodextrin and many substrates in aqueous solution, with the possible presence of 1:2 complexes being taken into account. The interpretation of the results is aided and unified by a model of the complexing that describes the substrate as a species having two possible binding sites (10). Most of the substrates are 1,4-disubstituted benzenes and many of them are ionizable, so the conjugate acid and base forms constitute separate guest species. In this paper a series of amines was studied as substrates. The experimental stability constants are symbolized by K_{11a}, K_{12a}, K_{11b}, and K_{12b}, the subscripts denoting complex stoichiometry and the conjugate acid–base form of the substrate.

Since these substrates are weak bases, the potentiometric method, which has been described in detail earlier (9), was applied. This technique was supplemented by UV spectrophotometry and a competitive spectrophotometric indicator method (11).

EXPERIMENTAL

Materials—α-Cyclodextrin[2] was dried at 95° for 48 hr. The amines were from commercial sources[3]; they were purified by recrystallization or distillation, the melting and boiling points being in good agreement with literature values (12, 13).

Procedures—The potentiometric method was used as described in detail earlier (9), except that the amine substrates were half-neutralized with 0.1 *N* HCl. The method of treating the data to obtain the stability constants was explained in detail. K_{11a} for 4-toluidine was measured by the competitive spectrophotometric method, using methyl orange as the indicator. The pK_a values of 4-nitroaniline and 4-cyanoaniline are 1.00 and 1.74, respectively (14, 15)—too low for these systems to be studied potentiometrically. Their K_{11b} values were measured by UV spectrophotometry. For both systems, 1:1 stoichiometry was suggested by the observation of isosbestic points. 4-Nitroaniline yielded the same K_{11b} value from measurements at 350 and 410 nm. The 4-cyanoaniline system was studied at 260 nm. All results reported here are at 25.0° and 0.1 *M* ionic strength.

RESULTS

Seven 4-substituted anilines were studied, most of them by the potentiometric method. The stability constants found for these amines are given in Table I. For all systems K_{12a} was 0. The conjugate acid of *p*-phenylenediamine (4-aminoaniline) has $pK_{a1} = 2.89$ and $pK_{a2} = 6.16$ (16), so that measurement of pK_{a2} left the other amino group (the X in Table I) in its base form. K_{12b} is not significantly different from zero at the 95% level for X = NH_2, OCH_3, H, Cl (though for X = NH_2, K_{12b} is significant at somewhat lower confidence levels).

Eight other aromatic or heterocyclic amines were studied potentiometrically. The results are listed in Table II. For all of these systems, K_{12a} was 0. Benzylamine, 4-*tert*-butylpyridine, and isoquinoline yielded significant K_{12b} values. The K_{12b} value for *N*-methylimidazole, though small, appears to be significant; however, when this system was treated as a Case II system (9), for which $K_{12b} = 0$ by definition, it gave a correlation coefficient (R^2) of 1.00, compared with 0.03 for the Case III (finite K_{12b}) system. Therefore, it was concluded that $K_{12b} = 0$ for this system, and, evidently, for the remaining amines in Table II[4].

Table II—Stability Constants for α-Cyclodextrin Complexes of Amines at 25° [a]

Amine	K_{11b}/M^{-1}	K_{12b}/M^{-1}	K_{11a}/M^{-1}
Benzylamine	17.4 (0.35)	4.0 (0.26)	0
Phenethylamine	26.4 (0.17)	−0.44 (0.16)	0
Imidazole	16.3 (0.23)	0.05 (0.37)	0
N-Methylimidazole	13.4 (0.09)	0.81 (0.23)	0
4-Nitroimidazole	49.8 (0.81)	−0.0006 (0.16)	4.0 (0.25)
4-*tert*-Butylpyridine	84.7 (6.0)	20.1 (1.8)	0
Quinoline	28.6 (0.73)	0.63 (0.48)	0
Isoquinoline	22.7 (0.95)	10.8 (0.76)	0

[a] Standard deviations in parentheses.

DISCUSSION

Binding Site Model—Most of the substrates studied in the present investigation, as well as those in earlier studies, can be viewed as substrates possessing two potential binding sites. In 1,4-disubstituted benzenes, for example, the 1 and 4 positions are the possible sites for binding to the cyclodextrin cavity. For such a substrate, having binding sites X and Y, it was shown (9) that:

$$K_{11} = K_X + K_Y \qquad \text{(Eq. 1)}$$

and

$$K_{12} = \frac{aK_XK_Y}{K_{11}} \qquad \text{(Eq. 2)}$$

In these equations K_{11} and K_{12} are the experimental stability constants for 1:1 and 1:2 complex formation, K_X and K_Y are binding constants for 1:1 complexation of the ligand at sites X and Y, and a is a parameter that describes interaction between the two sites in a 1:2 complex. According to Eq. 1, the experimental K_{11} is the sum of binding site constants for isomeric 1:1 complexes. The 1:2 complex is formed by adding a second cyclodextrin to either of the preformed 1:1 complexes; according to Eq. 2, K_{12} can be zero only if $a = 0$ or if one of the site binding constants is zero.

If the two binding sites are identical, as in a symmetrical 1,4-disubstituted benzene, then $K_X = K_Y$, and Eqs. 1 and 2 give:

$$K_X = K_{11}/2 \qquad \text{(Eq. 3)}$$

and

$$a = 4K_{12}/K_{11} \qquad \text{(Eq. 4)}$$

For such a substrate, the binding site constant K_X and the interaction parameter a are obtainable.

The interpretation of experimental stability constants in terms of this model focuses attention on the binding sites and makes use of some chemical assumptions to assign binding constants to binding sites. It is postulated that (aside from binding site size and shape factors) the primary feature of a binding site contributing to complex stability is its electron density. Also favoring complex stability is the polarizability of the binding site, whereas complexing is weakened by high site polarity. The net effect of these factors determines the binding site constant for binding in a given solvent at constant temperature.

Anilines—The K_{11b} values in Table I show a rough trend with electron-attracting ability by the X-substituent, indicating that the X-site is the principal binding site. 4-Methylaniline appears to bind anomalously strongly. The binding of 4-aminobenzoic acid may be enhanced by hydrogen bonding. The K_{11b} values are correlated by:

$$\log K_{11b} = 1.70\sigma + 0.05R_D \qquad \text{(Eq. 5)}$$

[2] Sigma Chemical Co., Lot Nos. 20F-0507 and 29C-0425.

[3] Mallinckrodt Chemical Co.; Aldrich Chemical Co.; Eastman Organic Chemicals.

[4] Many of the constants in Tables I and II are quite small. For such systems the diagnostic plots described in Ref. 9 may be ambiguous because of the considerable relative experimental error and the limited range of the binding isotherm that is accessible to observation.

Table III—Comparison of K_{11b} for Anilines and K_{11a} for Phenols[a]

X[b]	K_{11b} (aniline)[c]	K_{11a} (phenol)[d]
OCH_3	6.7	0
CH_3	57.6	0
H	8.8	0
COO^-	9.0	16.6
Cl	251	272
COOH	1341	1130
CN	451	158
NO_2	635	245

[a] At 25°. [b] X in X—C_6H_4—NH_2 or X—C_6H_4—OH. [c] From Table I. [d] From Ref. 11.

where σ is the Hammett substituent constant of X and R_D is the molar refraction of X—C_6H_5. The standard deviation is 0.39 in log K_{11b}.

K_{11b} is larger than K_{11a} for all amines, a result that is consistent with the postulates that complex stability is enhanced by high site electron density and polarizability and decreased by high polarity.

Since 4-aminoaniline is symmetrical, Eqs. 3 and 4 are applicable, giving $K_X = 1.15$ as the binding constant for the 4-amino group in this substrate. Calculation of the a value with Eq. 4 does not seem justified, because of the large uncertainty in K_{12b}.

Since the X group in 4-aminoaniline is NH_2, the most electron-releasing group in Table I, any other X group will be even less effective in increasing electron density at the aniline NH_2 site. Thus the binding site constant for binding to the amino site should be a maximum for 4-aminoaniline (for which it is 1.15 M^{-1}). Since K_{11b} is, by Eq. 1, the sum of the binding constants at the two sites and the binding constant at the amino site has been shown to be 1.15 or smaller, the K_{11b} values in Table I can (except for X = NH_2) be essentially completely assigned to binding at the X-substituent site.

If this assignment is correct, an interesting comparison can be made between K_{11b} for anilines and K_{11a} for the corresponding phenols, for it was concluded earlier (11) that K_{11a} for phenols can be ascribed to binding at the 4-substituent site[5]. The electronic distribution of neutral anilines and phenols should be similar, as shown in Schemes I and II.

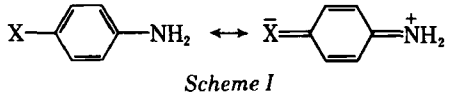

Scheme I

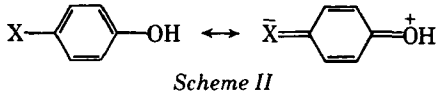

Scheme II

Therefore, it is expected that K_{11b} for anilines should be approximately equal to K_{11a} for the corresponding phenols. These quantities are compared in Table III, which shows that the agreement is reasonable in terms of this simple argument.

[5] Except for ^-OOC—C_6H_4—OH, which may bind at the hydroxy site (2).

The stability constant K_{11a} presumably describes binding at the X-site, since the positively charged protonated amine site will on all counts (reduced electron density, reduced polarizability, and increased polarity) not be expected to undergo any complexation. That K_{11a} is zero for several systems indicates that electron density at the X-site is reduced sufficiently, in the cation, that no binding occurs even at this site.

Other Amines—The data in Table II show the general pattern $K_{11b} > K_{11a}$ for amines. Many structural types are represented, so interpretations of most of the results will require more extended and systematic variation of structures to establish correlations of structure with complex stability. Some obscure points, for example, are the difference in 1:2 complex behavior for quinoline and isoquinoline and the appearance of a finite K_{12b} for benzylamine but not for aniline or phenethylamine[4]. Some results seem reasonable, however; for example, the larger K_{11b} for 4-nitroimidazole compared with imidazole suggests that the nitro group is the principal binding site. Moreover, this is the only compound in Table II that possesses a finite K_{11a}, probably because the powerfully electron-withdrawing nitro group opposes the electron withdrawal by the protonated amine, leaving sufficient electron density at the binding site to result in significant complexation.

REFERENCES

(1) D. French, *Adv. Carbohydr. Chem.*, **12**, 189 (1957).

(2) J. A. Thoma and L. Stewart, in "Starch: Chemistry and Technology," vol. I, R. L. Whistler and E. F. Paschall, Eds., Academic, New York, N.Y., 1965, p. 209.

(3) D. W. Griffiths and M. L. Bender, *Adv. Catal. Relat. Subj.*, **23**, 209 (1973).

(4) M. L. Bender and M. Komiyama, "Cyclodextrin Chemistry," Springer-Verlag, Berlin, 1978.

(5) R. I. Gelb, L. M. Schwartz, C. T. Murray, and D. A. Laufer, *J. Am. Chem. Soc.*, **100**, 3553 (1978).

(6) R. I. Gelb, L. M. Schwartz, and D. A. Laufer, *ibid.*, **100**, 5875 (1978).

(7) R. I. Gelb, L. M. Schwartz, R. F. Johnson, and D. A. Laufer, *ibid.*, **101**, 1869 (1979).

(8) K. A. Connors and T. W. Rosanske, *J. Pharm. Sci.*, **69**, 173 (1980).

(9) K. A. Connors, S.-F. Lin, and A. B. Wong, *ibid.*, **71**, 217 (1982).

(10) T. W. Rosanske and K. A. Connors, *ibid.*, **69**, 564 (1980).

(11) S.-F. Lin and K. A. Connors, *ibid.*, in press.

(12) A. B. Wong, Ph.D. Dissertation, University of Wisconsin–Madison, 1980.

(13) S.-F. Lin, Ph.D. Dissertation, University of Wisconsin–Madison, 1981.

(14) A. I. Biggs and R. A. Robinson, *J. Chem. Soc.*, **1961**, 388.

(15) M. M. Fickling, A. Fischer, B. R. Mann, J. Packer, and J. Vaughn, *J. Am. Chem. Soc.*, **81**, 4226 (1959).

(16) A. V. Willi, *Z. Physik. Chem.*, **27**, 233 (1961).

ACKNOWLEDGMENTS

This work was supported in part by a grant from The Upjohn Company.

Permeation of Skin and Eschar by Antiseptics I: Baseline Studies with Phenol

CHARANJIT R. BEHL *, EDWARD E. LINN, GORDON L. FLYNN ˣ, CARL L. PIERSON, WILLIAM I. HIGUCHI, and NORMAN F. H. HO

Received April 4, 1981 from the *College of Pharmacy and Medical School (CLP), The University of Michigan, Ann Arbor, MI 48109.* Accepted for publication July 6, 1982. *Present address: Pharmacy Research, Hoffmann-La Roche, Inc., Nutley, NJ 07110.

Abstract □ To assess how the permeability of phenol is altered by thermal injury, it was first necessary to have baselines of comparison on normal skin. Using *in vitro* diffusion cells and the skin of the hairless mouse, [^{14}C]phenol was applied to skin in an aqueous medium with a reference copermeating species, [^{3}H]methanol, and 37° permeability coefficients of the pair were evaluated as functions of animal age, skin hydration, stripping of the skin, dermis isolation, and phenol concentration. Age proved to be of little consequence to permeability over a wide age range. Prolonged aqueous soaking of the skins was also without much effect. Stripping of the skin and isolating the dermis by soaking techniques allowed assessment of individual skin strata diffusional resistances. When applied to skin in trace radiochemical concentrations, phenol behaved diffusionally as an alkanol with a chain length of six. But at concentrations >2% w/v, phenol facilitated the permeation rates of itself and methanol; the effect was markedly concentration sensitive and only fractionally reversible. Concentration studies using silicone rubber membranes proved that the effects on the skin were the results of destroyed barrier integrity. At 6% phenol concentration there was an essentially instantaneous, 10-fold increase in the phenol permeability coefficient, raising it to two-thirds that observed with fully stripped skin. Overall, the data suggest that the stratum corneum is proportionally impaired as the phenol concentration is increased.

Keyphrases □ Permeation, skin—of phenol, baseline studies with hairless mice, effects of animal age, skin hydration, skin stripping, dermis isolation, and concentration □ Phenol—effects of animal age, skin hydration, skin stripping, dermis isolation, and concentration on skin permeation, baseline studies on hairless mice

Phenol is an industrial chemical with widespread use and is so frequently a contaminant of industrial waste streams that it is designated a priority pollutant by the Environmental Protection Agency (1). It is used in topical pharmaceuticals as a microbial preservative and other medical uses include local antipruritis, an anesthetic action which requires cutaneous penetration, and antisepsis. On contact, phenol apparently diffuses through skin readily; this has caused serious injuries in the workplace (2). Phenol has been associated also with untoward systemic responses when medicinally used and fatalities have been recorded in cases where its application has been over extensive areas of barrier-impaired skin (3). Therefore, whether the skin exposure occurs accidently or in therapy, diffusive passage of phenol through skin is of some considerable concern.

It was suggested in a recent report that "the lipophilic character of solutes (phenols) and their hydrogen bonding capacity are the two main structural features determining their penetration through the human epidermis" (4). Being only mildly hydrophobic, phenol's absorption was presumed to be rate-controlled by the stratum corneum. Increased phenolic permeation rates in concentrated solution have also been recorded and speculatively attributed to protein denaturation within the skin during transport (5). Higher phenol permeability was reported for skins damaged by either simple abrasion or burning (6).

In previous investigations from these laboratories (7–10), permeabilities of normal skin as well as burn-traumatized skin (11) of the hairless mouse have been examined using water and the *n*-alkanols as test permeating species. Three basic rate-controlling mechanisms of skin permeation were evident (10): (*a*) diffusion through aqueous pores (an aqueous shunt pathway), (*b*) diffusion through lipoidal components of the stratum corneum, and (*c*) diffusion controlled by the viable strata (epidermis and dermis) lying beneath the horny layer. These studies are continued here, for the first time using a chemical with known serious local and systemic consequences in humans. The purpose of this specific study was to obtain baseline data for the assessment of thermal alterations on the permeability of phenol through skin.

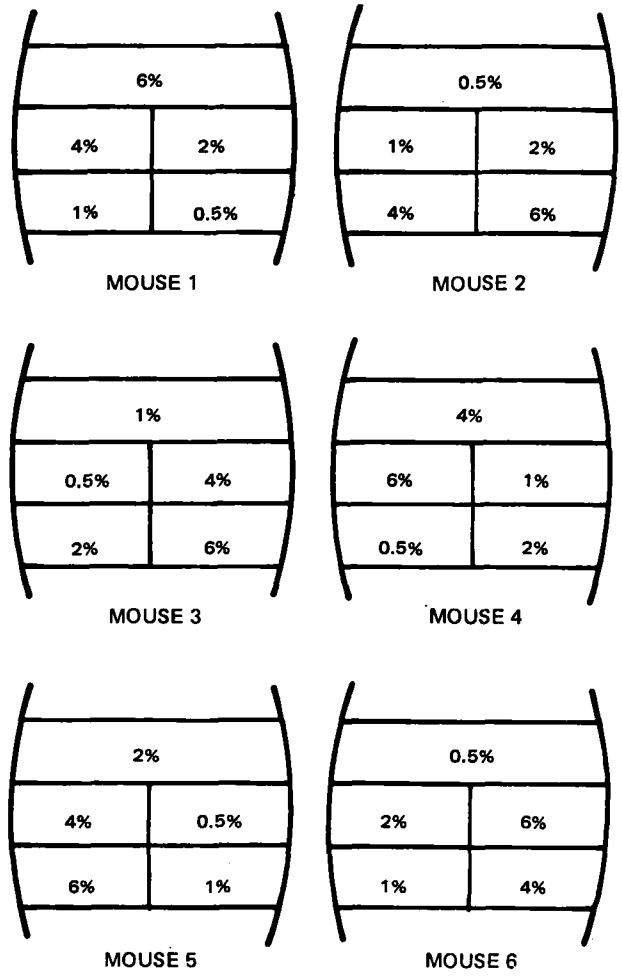

Figure 1—*Illustration of the manner of excising skin sections from the dorsal surfaces of mice for use in phenol concentration experiments. The numbers indicate the phenol concentrations; each concentration was studied six times.*

0022-3549/83/0400-0391$01.00/0

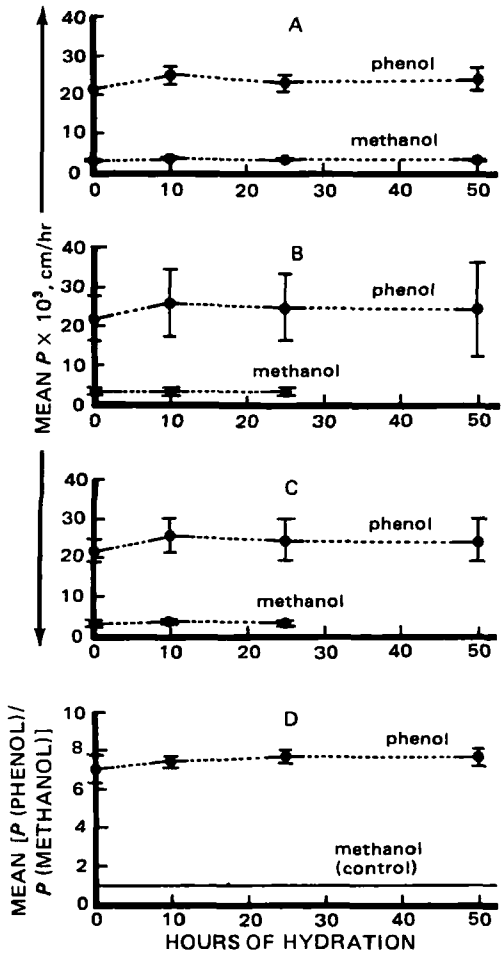

Figure 2—*Plots of average permeability coefficients of (A) the abdominal skins, (B) the dorsal skins, and (C) the average of both sites; and (D) the phenol–methanol permeability ratios as a function of hydration time. The bias represent the standard deviation for each mean value.*

EXPERIMENTAL

Chemicals—[^{3}H]methanol[1] and [^{14}C]phenol[1] were diluted with saline[2] to prepare solutions for the permeation experiments. Crystalline phenol[3] was used to prepare aqueous solutions of varying concentrations for the concentration-effect experiments. The final bulk chemical concentration of the permeating species was 10^{-4} *M* or lower except where unlabeled phenol was added to be the expressed concentrations in the concentration-effect studies.

Animals—Male hairless mice of SKh-hr^{-1} strain[4] were used. They were provided with free access to food and water. The bedding was changed at least once a week. The mice were housed individually in shoe box-type cages to prevent them from damaging one anothers skins.

Stripping and Dermis Isolation Procedures—Immediately following sacrifice by cervical dislocation, the abdominal and the dorsal surfaces of mice were stripped 5, 10, or 25 times with cellophane tape[5]. The animal was secured on a table and the skin was stripped by placing the tape on the animal surface and moving the thumb back and forth a few times, with as uniform pressure as was possible (12). A fresh piece of the tape was used for each stripping. Dermal sections were isolated by placing skin in the diffusion cell and soaking it for 24 hr (13). At this time the cell was opened and the epidermis was carefully lifted from the dermis with a pair of forceps. The cell was then reassembled for permeation experiments.

Radioisotopic Assay—Concentrations of the radiolabeled permeating species were determined using a liquid scintillation counter[6] and a commercial cocktail[7]. Permeation rates of both methanol and phenol were studied simultaneously using a technique involving dual labels.

Table I—Permeability Coefficients of Methanol as a Function of Mouse Age

Age, days	Number of Mice	$P \times 10^3 \pm SD$, cm/hr		
		Abdominal	Dorsal	Overall Average[a]
36	1	2.1	2.7	2.4
92	5	3.4 ± 0.5	2.9 ± 0.6	3.2 ± 0.6
340	6	2.2 ± 1.0	2.7 ± 0.3	2.5 ± 0.8
381	1	3.2	2.1	2.7
441	3	1.9 ± 0.8	1.6 ± 0.4	1.7 ± 0.6

[a] Average across sites.

Diffusion Cell and Permeation Procedure—A two-chamber glass diffusion cell (7–9) was employed to determine the skin permeability. The external medium of diffusion was saline, except in the concentration-effect studies where the donor compartment was filled with phenol solution of designated concentration. The half-cell contents were stirred at 150 rpm, and all permeation experiments were carried out at 37°. The half-cell facing the stratum corneum was always the donor chamber and the half-cell facing the dermis was always the receiver compartment. Therefore, the net diffusion occurred from the stratum corneum to the dermis side.

Procedure of the Hydration Effect Studies—The effect of hydration on the skin permeability to methanol (reference solute) and phenol was studied for 50 hr of skin immersion in saline, using the abdominal and the dorsal skins obtained from each of five mice. A technique of sequential experiments developed earlier (9) was employed to obtain the entire hydration profile on each of the 10 skins. This was accomplished by carrying out four permeation experiments in succession on the same piece of the skin, with rinsing between experiments.

Procedure for Studying the Concentration Effects and Reversibility Using Skin and Silicone Rubber Membranes—Permeation of methanol and phenol was studied using phenol solutions with concentrations of 0.5, 1.0, 2.0, 4.0, and 6.0% (w/v). The receiver chamber always contained saline. To minimize mouse-to-mouse and site-to-site variation, each of the five concentrations was studied in six pieces of skins excised from five different dorsal locations of six mice. The manner in which the concentrations were rotated around the sites is depicted in Fig. 1. The permeation experiment was initiated within 0.5 hr of skin exposure to the phenol solution and was completed within an additional 2 hr. At ~2.5 hr of skin contact with the phenol solutions, the donor and receiver chambers were evacuated and cleansed with saline using three triple rinsings ~0.5 hr apart. A second permeation experiment was then conducted with methanol and phenol in trace radiochemical concentrations, using saline in both compartments. This experiment [referred to as a reversibility experiment (14) in the remainder of this paper] was aimed at determining the extent to which the accelerating effects of phenol were reversible. An identical procedure was followed in assessing concentration effects and the reversibility of such effects using 0.0254-cm silicon rubber membranes[8].

Data Analysis—The data were plotted with the receiver compartment concentration (in cpm) as a function of time. The permeability coefficient was calculated from (9):

$$P = \frac{V}{A}\frac{(dC/dt)}{\Delta C} \qquad \text{(Eq. 1)}$$

where P is the permeability coefficient (cm/hr); A is the diffusional area (~0.6 cm^2); ΔC is the concentration difference across the membrane, which was taken to be equal to the donor concentration (cpm); V is the half-cell volume (1.4 ml); and dC/dt is the steady-state slope (cpm/cm^3/hr) of a counts (concentration) *versus* time plot.

RESULTS

Tables I and II contain mouse skin permeability coefficients of methanol and phenol, respectively, as a function of mouse age. The choice of the ages and the numbers of the mice per age were dependent on the availability of animals within the colony.

[1] New England Nuclear, Boston, Mass. Supplier-estimated purity >98% in each case.
[2] 0.9% Sodium chloride irrigation; Abbott Laboratories, North Chicago, Ill.
[3] Mallinckrodt, Inc., St. Louis, Mo.
[4] Skin Cancer Hospital, Temple University, Philadelphia, Pa.
[5] Scotch Brand Cellophane Tape, 3M Co., Minneapolis, Minn.
[6] Beckman LS 9000. Beckman, Irvine, Calif.
[7] Aquasol, New England Nuclear, Boston, Mass.
[8] Silastic Medical Grade Sheeting, Dow Corning, Midland, Mich.

Table II—Permeability Coefficients of Phenol as a Function of Mouse Age

Age days	Number of Mice	$P \times 10^3 \pm SD$, cm/hr		
		Abdominal	Dorsal	Overall Average[a]
36	1	19.7	21.6	20.7
92	5	28.4 ± 4.5	22.4 ± 4.3	25.4 ± 5.3
124	5	17.5 ± 5.1	23.2 ± 5.1	20.3 ± 5.7
340	6	16.0 ± 5.2	20.6 ± 2.2	18.3 ± 4.5
381	1	20.8	17.7	19.3
441	3	12.6 ± 2.6	12.4 ± 0.8	12.5 ± 1.7

[a] Average across sites.

Figure 2 illustrates the mouse skin permeability coefficients of methanol and phenol, respectively, as a function of skin hydration time. The abdominal and the dorsal skins excised from five mice were used. The permeation experiments were run at 0, 10, 25, and 50 hr of hydration on each of the skins. The animals were weighed before sacrifice and their weights were consistent with an expected weight–age relationship (1), indicating that the animals were healthy. The data are plotted to indicate the standard deviation about each point. Figures 2A, 2B, and 2C present the average abdominal, dorsal, and combined values, respectively. Figure 2D presents the data as ratios of the permeability coefficients of phenol–methanol, a data manipulation previously shown to reduce animal-to-animal variability.

Table III contains the permeability coefficients of methanol and phenol through the abdominal and the dorsal skins stripped 5, 10, or 25 times. Five mice were used for each experimental condition. The data are provided in terms of the individual and mean permeability coefficients with standard deviations. Table III also contains data for dermis isolated by the soaking procedure (13). In this case, four permeability coefficients were gathered for each permeating species, two on each skin site.

Tables IV and V contain the permeabilities of methanol and phenol as a function of phenol concentration in the donor chamber. Also summarized in these tables are data from the reversibility experiments where both compartments of the diffusion cell contained saline. At each concentration, six pieces of the skin obtained from five different sites on the dorsal surfaces of six mice were used. The vital statistics of each animal are presented and individual as well as the mean permeability coefficients, with standard deviations, are listed. From these data, a relative enhancement of the permeabilities of methanol and phenol was computed as the ratio of the mean permeability coefficient at a given phenol concentration to that at the trace radiochemical concentration of phenol. These derived data are illustrated in Figs. 3 and 4 for both the high concentration and reversibility experiments.

Table VI contains permeability coefficients of phenol and four alkanols (methanol, ethanol, butanol, and hexanol) through 0.0127-cm silicone rubber (polydimethylsiloxane) membranes. For these experiments, the concentrations of the permeating species were $\leq 10^{-4}$ *M*. Table VII contains permeability coefficients of methanol and phenol through 0.0254-cm silicone rubber membranes as a function of phenol concentration. As in the case of the skin studies, results are presented for an initial experiment at the high phenol concentrations and a second reversibility experiment. In the latter, permeability was also measured from solutions containing only trace phenol concentrations. In the initial experiments, the phenol concentrations in the donor chamber were 0.5, 1.0, 2.0, 4.0, and 6.0% w/v. At each concentration three different silicone rubber membranes were used.

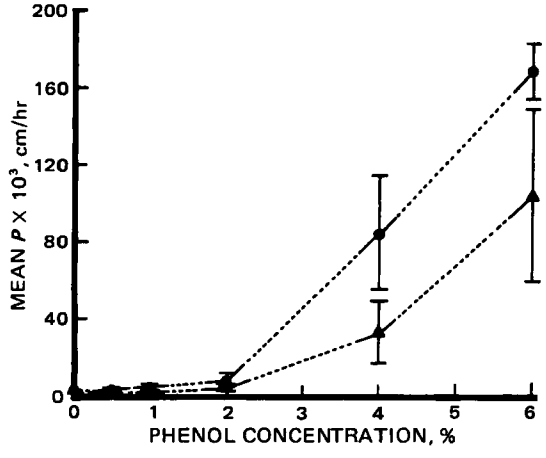

Figure 3—*Plots of the mean permeability coefficients of methanol obtained in the concentration-effect (●) and reversibility (▲) experiments. The bars represent the standard deviation for each mean value.*

Table III—Permeability Coefficients of Methanol and Phenol through Stripped Skins and the Dermis

Number of Strippings	Number of Mice[a]	$P \times 10^3 \pm SD$, cm/hr			
		Methanol		Phenol	
		Abdominal	Dorsal	Abdominal	Dorsal
0	5	3.4 ± 0.5	2.9 ± 0.6	28.4 ± 4.5	22.4 ± 4.3
5	5	154 ± 35	48.3 ± 36	210 ± 38	120 ± 44
10	5	342 ± 18	260 ± 64	354 ± 48	277 ± 49
25	5	339 ± 55	291 ± 31	318 ± 60	275 ± 25
Dermis	2	445 ± 81	395 ± 5	337 ± 101	301 ± 13

[a] All mice were 90–100 days of age.

DISCUSSION

Effect of Aging on the Permeability of Phenol—From the results of replicated experiments on mice of 36, 92, 124, and 340 days of age, the phenol permeability coefficient through hairless mouse skin underwent no appreciable change with age (Table II). A representative value for the 37° phenol permeability coefficient is 2×10^{-2} cm/hr. A 25° value for human skin (cadaver epidermis isolated using ammonia fumes) of 0.8×10^{-2} cm/hr has been reported (5), and when the temperature difference is taken into account (activation energies for structurally similar alkanols run ~15 kcal/mole), the human and mouse data are remarkably similar.

The average permeability coefficient for phenol of 1.25×10^{-2} cm/hr obtained at 441 days seems smaller than that found in younger animals. Here the value of using a copermeating-species marker with a different radiolabel becomes apparent, as the methanol average permeability coefficient at 441 days (Table I) is also of smaller magnitude than at younger ages. Extensive age-influence studies with the alkanols (10) indicate the methanol permeability coefficient to be invariant from ~90 days of age to ages exceeding 441 days. Thus it is concluded that the decline in permeability coefficients at 441 days is due more to animal variability than age. It is notable that phenol–methanol ratios of the mean permeability coefficients at 92, 340, and 441 days are 7.9, 7.3, and 7.4, respectively, showing that the relative permeability of the two chemicals remains essentially invariant even as the skins of different age groups of animals evidence variability. Permeability coefficients obtained on single sections of skin at other ages are in general accord with the values from the replicated runs. Based on these data, it was decided to use mice ~100 days old for the remainder of the study.

When the permeability coefficients for methanol and phenol are normalized to animal mass (permeability coefficient divided by body weight),

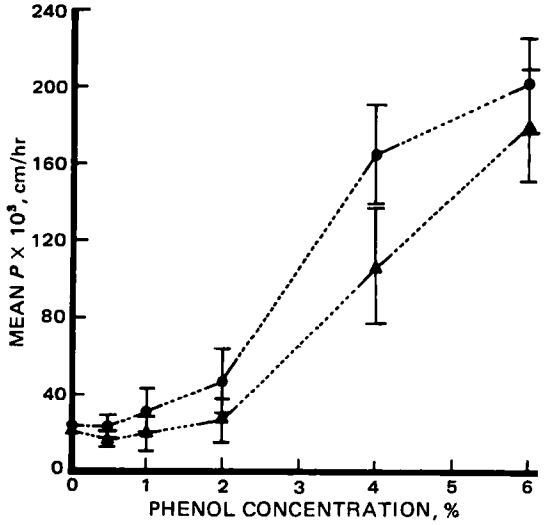

Figure 4—*Plots of mean permeability coefficients of phenol obtained in the concentration-effect (●) and reversibility (▲) experiments. The bars represent the standard deviation for each mean value.*

Table IV—Effect of Phenol Concentration on the Skin Permeability of Methanol [a]

Phenol Concentration (Donor), % w/v	$P \times 10^3$, cm/hr						
	Mouse [b]						
	1	2	3	4	5	6	Mean ± *SD*
Concentration Effect Experiment (phenol–saline):							
0.0							1.5 [c]
0.5	1.6(1)	2.4(5)	2.2(4)	5.1(2)	2.1(3)	2.4(5)	2.6 ± 1.2
1.0	4.2(2)	3.3(4)	1.1(5)	9.0(3)	3.3(1)	2.6(2)	3.9 ± 2.7
2.0	8.1(3)	5.5(3)	4.4(2)	13.0(1)	2.5(5)	7.7(4)	6.9 ± 3.7
4.0	92.5(4)	53.1(2)	81.1(3)	131.1(5)	51.7(4)	101.4(1)	85.2 ± 30.3
6.0	172.9(5)	159.6(1)	153.4(1)	193.7(4)	172.6(2)	164.0(3)	169.4 ± 14.1
Reversibility Experiment (saline–saline):							
0.0							1.5 [c]
0.5	1.1(1)	1.6(5)	1.4(4)	3.2(2)	1.4(3)	1.5(5)	1.7 ± 0.8
1.0	2.4(2)	1.8(4)	0.6(5)	5.7(3)	1.9(1)	1.9(2)	2.4 ± 1.7
2.0	4.1(3)	2.6(3)	1.9(2)	7.5(1)	0.8(5)	4.1(4)	3.5 ± 2.3
4.0	38.5(4)	19.7(2)	22.4(3)	62.1(5)	18.5(4)	37.7(1)	33.2 ± 16.7
6.0	115.8(5)	47.2(1)	70.4(1)	176.8(4)	95.3(2)	122.3(3)	104.6 ± 45.2

[a] Number in parentheses indicates the skin location at the dorsal site 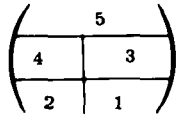

; mouse age is ~117 days. [b] Mice 1, 3, 4, and 5 each weighed 30.5 g; mice 2 and 6 weighed 31.5 and 30.0 g, respectively. [c] Data were abstracted from ref. 9.

the age patterns displayed in Fig. 5 are obtained. The mass-weighted values decline appreciably for both solutes over the initial year of age, in each case the fall in magnitude being approximately twofold. Thus, even though the skins of younger animals evidence similar mass-transfer coefficients as seen with older skins, the younger animals appear to be at greater risk to comparable area exposures of phenol and systemic accumulation of phenol would be seen to be inversely related to animal size. We believe such factors have bearing on the increased toxicity of phenol observed in infants (15, 16).

Effect of Anatomical Site on the Permeability of Phenol—Tables I and II contain permeability coefficients of methanol and phenol through the abdominal and dorsal skins. At no age is there a significant difference in values for the two sites and, moreover, for both permeating species the site of greater permeation rate changes from age to age. Therefore, it is concluded that within the age range studied there is no factorable site dependency to the permeability of these compounds. This conclusion is further supported by the hydration study data where permeability coefficients for the abdominal and dorsal skins remained unchanged during the full 50-hr hydration. The methanol data are consistent with the previous studies (10) where the permeabilities of the *n*-alkanols were shown to be site independent for animals older than ~50 days.

Influence of Hydration on the Permeability Coefficient of Phenol—Permeability coefficient values obtained for methanol and phenol as a function of hydration time are plotted in Fig. 3. There is no clear indication that the transport rate of either permeating species is altered by hydration. For methanol, this observation is fully consistent with previously published results (9). Since the phenol permeability coefficient through hairless mouse skin is, at the outset, similar to that of hexanol (Table VIII) and given the structural similarity of these two 6-carbon hydroxy compounds, it was expected there would roughly be a doubling of the permeability coefficient of phenol during hydration. Phenol permeability coefficients for fresh and extensively hydrated skins appear essentially the same, however, although the latter may be marginally larger. Exactly why there is increased facility of permeation for butanol, hexanol, and heptanol through hydration and not for the physicochemically similar phenol [the octanol–water partition coefficient of phenol is 29 (17) and lies between that of butanol, 7.6 (18) and hexanol, 76 (18)] is not understood. The aromatic compound has a larger diffusional cross-sectional area than the alkanols, which may be a factor limiting its access to presumably hydration-expanded lipoidal channels.

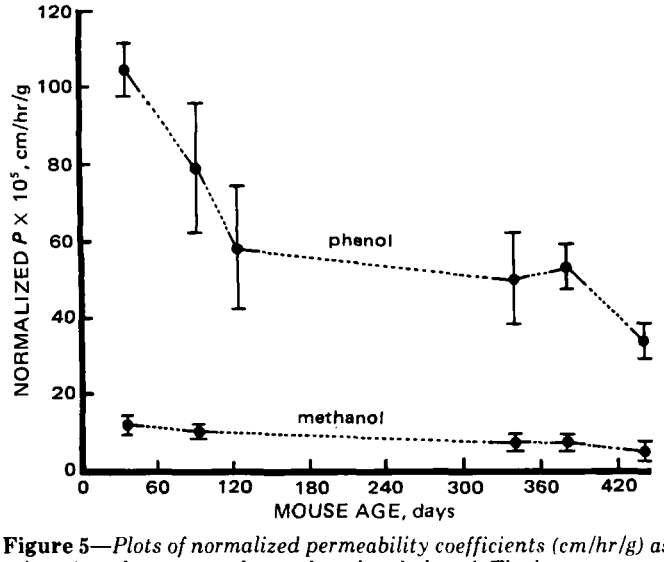

Figure 5—*Plots of normalized permeability coefficients (cm/hr/g) as a function of mouse age for methanol and phenol. The bars represent the standard deviation for each normalized value.*

Effect of Stripping and Dermis Isolation on the Permeability of Phenol—Stripping increases the permeability of both abdominal and dorsal skins to both methanol and phenol (Table III). The permeability coefficients obtained tend to level off at 10 strippings. In the earlier studies, it required more than 10 strippings to notice a comparable effect (8). The difference in observations may be due to greater care securing adhesion of the tape to the skin in the present study. The increased permeation rate on total stripping is far greater for methanol than phenol, which reflects the fact that the stratum corneum functions lipoidally to these compounds, offering higher resistance to methanol, the more polar of the two solutes. It is also evident (Table III) that abdominal permeabilities for partially and fully stripped skins invariably exceed those of the dorsal surfaces even though there is no apparent difference for the intact skins. It appears that the abdominal stratum corneum may be more easily removed and further, that the permeability of the remaining abdominal strata may be intrinsically greater than that of the dorsal skin. The latter observation is consistent with the abdominal skin being thinner than the dorsal skin (10).

The abdominal dermis isolated by the soaking technique appears to be more permeable than the dorsal dermis, although the data are too limited to draw a firm conclusion (Table III). These data, together with the stripping and whole skin data, allow quantitative assessment of the diffusional resistances of the individual strata of the skin. The following equation, derived from the previously reported physical model (8, 10), can be used to compute the individual permeabilities of the stratum corneum, the viable epidermis, and the dermis:

$$\frac{1}{P_{WS}} = \frac{1}{P_{SC}} + \frac{1}{P_{EP}} + \frac{1}{P_D} \qquad \text{(Eq. 2)}$$

where P_{WS}, P_{SC}, P_{EP}, and P_D are the permeabilities of whole skin, stratum corneum, viable epidermis, and dermis, respectively. The values of

Table V—Effect of Phenol Concentration on Skin Permeability of Phenol [a]

Phenol Concentration (Donor), % w/v	$P \times 10^3$, cm/hr Mouse[b] 1	2	3	4	5	6	Mean ± *SD*
Concentration Effect Experiment (phenol–saline):							
0.0							20.3 ± 5.7[c]
0.5	18.6(1)	19.9(5)	20.9(4)	35.7(2)	18.6(3)	22.6(5)	22.7 ± 6.5
1.0	37.7(2)	25.6(4)	15.2(5)	53.6(3)	28.8(1)	23.1(2)	30.7 ± 13.4
2.0	52.4(3)	39.9(3)	33.0(2)	76.1(1)	27.4(5)	50.9(4)	46.6 ± 17.4
4.0	169.8(4)	131.7(2)	160.7(3)	196.6(5)	141.6(4)	192.0(1)	165.4 ± 26.2
6.0	182.3(5)	239.3(1)	184.5(1)	223.8(4)	199.9(2)	186.4(3)	202.7 ± 23.7
Reversibility Experiment (saline–saline):							
0.0							20.3 ± 5.7[c]
0.5	14.3(1)	15.0(5)	14.8(4)	23.3(2)	16.3(3)	17.2(5)	16.8 ± 3.4
1.0	20.9(2)	14.6(4)	11.5(5)	37.2(3)	12.6(1)	19.5(2)	19.4 ± 9.5
2.0	29.9(3)	19.8(3)	13.6(2)	45.6(1)	17.6(5)	35.0(4)	26.9 ± 12.1
4.0	113.0(4)	75.6(2)	79.6(3)	141.7(5)	90.8(4)	142.5(1)	107.2 ± 30.0
6.0	188.0(5)	139.6(1)	151.7(1)	214.8(4)	189.9(2)	201.9(3)	181.0 ± 29.3

[a] Number in parentheses indicates the skin location at the dorsal site 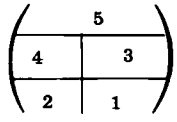

; mouse age is ~117 days. [b] Mice 1, 3, 4, and 5 each weighed 30.5 g; mice 2 and 6 weighed 31.5 and 30.0 g, respectively. [c] Data were abstracted from Table II.

P_{WS} and P_D are direct experimental values (Tables I–III). P_{EP} can be estimated from:

$$\frac{1}{P_{25\times}} = \frac{1}{P_{EP}} + \frac{1}{P_D} \qquad \text{(Eq. 3)}$$

where $P_{25\times}$ is the permeability coefficient of the skins stripped 25 times (Table III). Results of these computations are reported in Table IX. The computed P_{SC} values for methanol or phenol for either anatomical site are essentially the *same as* P_{WS} observed experimentally. This indicates that the resistance offered by the whole skin is, in fact, almost entirely due to the stratum corneum. The P_{EP} values are unrealistically large, indicating that the viable epidermis presents little resistance to the transport of methanol or phenol. In other words, insofar as can be told through estimation of difference (Eq. 3), the dermis offers the bulk of the resistance to diffusion once the stratum corneum has been removed, mostly because it is far thicker than the epidermis. But it is compositionally and structurally dissimilar as well, and these differences may also be a factor. The condition of the viable epidermis of the stripped skin is unknown; it is also possible that it is either damaged or partially removed by the repeated strippings, minimizing its apparent residual resistance.

Comparison of Phenol and Alkanol Permeabilities in Synthetic Membranes—One means of placing the phenol permeability into an overall perspective is to compare it with that of the *n*-alkanols using a membrane that, relative to the skin, is well understood in terms of its diffusional properties and mechanism. Silicone rubber sheeting provides an essentially isotropic, hydrophobic medium ideal for such purposes. In this case the permeability coefficient of phenol compares favorably with that of butanol (Table VI). But for fresh skins, data for hexanol and phénol are comparable. Moreover, as previously pointed out, the octanol–water partition coefficient for phenol of 29 (17) is bracketed by those of butanol and hexanol (18). These combined observations have an elementary significance. While phenol is structurally similar to an alkanol, its aromatic character sets it apart in terms of intermolecular interactions and, where oil–water partitioning is concerned, its affinity for different oil phases is not consistently the same as that of any particular alkanol. Nevertheless, since the differences in intermolecular associations in water immiscible phases are subtle, its distributioning behavior tends to be reasonably close to that of the alkanols of comparable size. From the standpoint of skin permeation, the lipid phase of the stratum corneum behaves as expected, "seeing" phenol more or less as it "sees" the 6-carbon alkanol, at least until the hydration effects set in.

Table VI—Comparison of Phenol and Alkanol Permeability Coefficient Through 0.0127-cm Silicone Rubber Sheeting

Compound	Number of Experiments	$P \times 10^3 \pm SD$, cm/hr
Phenol	3	175 ± 13
Ethanol[a]	3	53.5 ± 2
Butanol[a]	3	180 ± 12
Hexanol[a]	3	761 ± 54
Octanol[a]	3	1090 ± 15

[a] Abstracted from unpublished studies of G. L. Flynn, C. R. Behl, T. Kurihara, W. Smith, J. Fox, H. Dürrheim, and W. I. Higuchi, University of Michigan, College of Pharmacy.

Effect of Phenol Concentration on the Permeabilities of Methanol and Phenol Through Skin and Silicone Rubber Membranes—The hairless mouse skin permeability coefficients of methanol increased slowly up to the 2% level and then rapidly accelerated with further increases in phenol concentration (Fig. 3). The permeability coefficient of 0.17 cm/hr observed at 6% phenol concentration is >100 times that of normal skin. However, it represents only a partial compromise of the barrier function of the stratum corneum to methanol as, based on stripped-skin data, an upper limit of ~0.28 cm/hr for the methanol permeability coefficient is possible (Table III). The reversibility data indicate that there is some restoration of the barrier to methanol. Almost half of the enhancement observed at 0.5, 1.0, 2.0, 4.0, and 6.0% phenol concentrations is reversible (Fig. 3).

Phenol also accelerated its own permeability when applied in high concentration. As with methanol the effects are nominal to ~2% phenol concentration and exaggerated thereafter (Fig. 4). In this case the data suggest an upper limit on the effect is being approached at the 6% concentration. This seems reasonable as the permeability coefficient of 0.203 cm/hr at 6% phenol concentration is approaching the value of 0.275 cm/hr noted for the stripped skin. The relative enhancement in the permeability at the 6% level is 10.0 and it is reversible only to 8.9. The relative enhancement for fully stripped skin is ~13.5. All these observations are consistent with the fact that the mouse skin stratum corneum is intrinsically more permeable to phenol than to methanol; therefore, chemical

Table VII—Effect of Phenol Concentration on the Permeability of Methanol and Phenol Through 0.0254-cm Silicone Rubber

Phenol Concentration (Donor), % w/v	Mean $P \times 10^3 \pm SD$, cm/hr[a] Methanol: Concentration Effect Experiment	Methanol: Reversibility Experiment	Phenol: Concentration Effect Experiment	Phenol: Reversibility Experiment
0.5	9.5 ± 1.6	9.2 ± 1.1	90.0 ± 3.0	83.1 ± 1.4
1.0	11.7 ± 1.5	12.3 ± 2.0	107.0 ± 9.0	96.7 ± 3.0
2.0	13.0 + 2.4	10.7 + 2.1	85.8 ± 11.4	94.1 ± 14.3
4.0	12.3 ± 0.1	12.0 ± 1.2	98.5 ± 0.6	93.2 ± 20.4
6.0	11.1 ± 0.6	12.7 ± 1.5	99.9 ± 8.1	89.6 ± 4.6
Overall Mean ± *SD*	11.5 ± 1.3	11.4 ± 1.4	96.4 ± 8.2	91.3 ± 5.3

[a] All results are the average of three independent experiments.

Table VIII—Comparison of Phenol and Alkanol Permeability Coefficients Through Hairless Mouse Skin

Compound	$P \times 10^3 \pm SD$, cm/hr	
	Unhydrated Skins[b]	Hydrated Skins
Phenol	21.5 ± 3.4	24.0 ± 6.1
Methanol[a]	2.0 ± 0.4	2.0 ± 0.4
Ethanol[a]	2.1 ± 0.1	2.1 ± 0.1
Butanol[a]	5.4 ± 1.1	10.8 ± 2.2
Hexanol[a]	19.4 ± 7.8	38.8 ± 15.6
Heptanol[a]	65.9 ± 24.4	98.9 ± 36.6
Octanol[a]	73.4 ± 10.1	97.8 ± 13.5

[a] Abstracted from refs. 7, 9, and 11. Values obtained on freshly mounted skin sections.

impairment has a lesser effect on the permeability of phenol. It is notable that, at the 0.5, 1.0, 2.0, and 4.0% concentrations where enough of the stratum corneum integrity remains to essentially provide sole control of permeation, recovery of the phenol permeability coefficient on washing was roughly of the same degree as observed for methanol.

Possible Causes of the Observed Concentration Effects—In the previous section it was implied that the accelerating effect of phenol on skin permeability was due to impairment of the stratum corneum, as was also assumed by previous researchers (4, 5). The observation that the reference compound, methanol, as well as phenol experienced increased permeability in the present studies strongly supports this assumption. Moreover, the maximum enhancements for these solutes were quantitatively similar to the enhancements observed by fully stripping the stratum corneum from the skins. Nevertheless, it is possible to rationalize the data in terms of physicochemical effects such as complexation in the donor medium. It would be necessary for phenol to form complexes both with itself and methanol capable of increasing partitioning into the skin, thereby facilitating permeation, to explain the results. This implausible effect is ruled out by concentration experiments performed with silicone rubber membranes (Table VII). These membranes were assumed *a priori* to be chemically inert to phenol, which subsequently proved to be the case. When methanol and phenol permeated the synthetic membranes at concentrations used in the skin studies (0.5–6.0% w/v), no concentration-induced alterations in the permeability of either solute were noted. Since the complexes, if formed, would likely also facilitate permeation of these hydrophobic films, and since no effect was observed, complexation as the basis of enhanced permeation can be discounted. It should be noted that the complete protocol of the concentration studies was carried out using the silicone rubber and that the reversibility experiments yielded essentially the same permeability coefficients as noted at high phenol concentrations. This further strengthens the conclusion that the acceleration of skin mass-transfer rates by phenol is unrelated to external factors such as molecular association.

Significance of These Studies—Previous work (7–14) has shown that permeability of the hairless mouse skin to the *n*-alkanols to be similar quantitatively and qualitatively to that of the human epidermis. The present studies show that phenol chemically alters the mouse skin stratum corneum, leading to increased mass-transfer rates, a phenomenon also observed in isolated human epidermis (5). Moreover, the concentration reported as the threshold concentration for damage in the human skin (1.5%) is virtually the same as observed with mouse skin. And the magnitudes of phenol-induced increases in skin permeabilities at given concentrations of phenol are similar in each case. This parallelism in behavior indicates fundamental similarities in the biological compositions and the constructions of the two tissues. The implications are that the mechanisms of permeation of phenol and chemical denaturation by phenol are nearly identical in the two species. This adds to a growing body of information which suggests that hairless mouse and human skins are comparable chemical barriers and lends credibility to the use of the hairless mouse model for topical drug delivery research.

As far as the concentration effects are concerned, all signs point to phenol having a specific ability to chemically alter the stratum corneum. When it does so, the partitioning dependency of the skin permeation process is effectively lost. This action is partially reversed when the phenol is rinsed out from the diffusion cell. Relatively recent evidence proves that there is a well-defined extracellular lipid domain in the stratum corneum, comprising 10% or more of its total volume (19, 20). It is tempting to assign the lipid pathway across the tissue to this region. This would necessarily mean, for compounds like the intermediate chain-length alkanols (C_3–C_8) and phenol which are in the partitioning sensitive region, that the path of least diffusional resistance is around the cellular building blocks of the horny layer, something that could only occur if the keratinized, intracellular contents are relatively impervious.

Table IX—Individual Permeabilities of Whole Skin, Stratum Corneum, Viable Epidermis, and Dermis to Methanol and Phenol

Membrane	$P \times 10^3$, cm/hr[a]			
	Methanol		Phenol	
	Abdominal	Dorsal	Abdominal	Dorsal
Whole skin	3.2	3.2	25.4	25.4
Stratum corneum	3.2	3.2	27.5	28.0
Epidermis	1400	1100	5800	3200
Dermis	450	400	340	300

[a] Computed from eqs. 2 and 3 and from the data given in previous tables. Epidermis and dermis data are reported to the nearest 100 and 10 unit, respectively.

It is hard to believe that phenol, even at 6% w/v, would have significant effect on the lipid medium, other than perhaps just concentrating there, and inconceivable that it could all but wipe out the partitioning dependency of this postulated pathway. On the other hand, consistent with its known abilities to denature proteins, phenol may act on the keratin within the cellular building blocks and on the cell wall proteins as well, denaturing and, perhaps in the case of the semicrystalline keratin helices, uncoiling them. Such effects could be partially reversible. If the suppositions are correct that the extracellular lipids are the partitioning pathway and that the destructive activity of phenol is primarily within the intracellular space, then phenol must act to open up an alternative polar shunt route across the cells. It follows that the extent to which this occurs is proportional to the phenolic concentration. The mechanism envisioned is consistent with a threshold concentration (~2.0%) for the effects of phenol.

Phenol at ≥5% concentration is doubly dangerous since the permeability coefficient is 10-fold enhanced. The absorption rate from a 5% compared with a 1% solution is not just 5 times greater but rather 50 times. This explains many of the rapid lethal poisonings detailed by Deichmann (2). At extremely high concentrations (>75% w/v) phenol is corrosive enough locally to coagulate the epidermis, retarding its self-absorption, so that such solutions are less toxic than 5% levels (14).

REFERENCES

(1) List of Priority Pollutants—1980, Environmental Protection Agency. Cincinnati, Ohio.

(2) N. L. Sax, in "Dangerous Properties of Industrial Raw Materials," 3rd ed., Reinhold, New York, N.Y., 1968, p. 1007.

(3) T. D. Cronin and R. O. Brauer, *J. Am. Med. Assoc.*, **139,** 777 (1949).

(4) M. S. Roberts, R. A. Anderson, and J. Swarbrick, *J. Pharm. Pharmacol.*, **29,** 677 (1977).

(5) M. S. Roberts, R. A. Anderson, J. Swarbrick, and D. E. Moore, *ibid.*, **30,** 486 (1978).

(6) M. V. Freeman, E. Alvarez, and J. H. Draize, *Fed. Proc. Fed. Am. Soc. Exp. Biol.*, **9,** 273 (1950).

(7) H. Durrheim, G. L. Flynn, W. I. Higuchi, and C. R. Behl, *J. Pharm. Sci.*, **69,** 781 (1980).

(8) G. L. Flynn, H. Durrheim, and W. I. Higuchi, *ibid.*, **70,** 52 (1981).

(9) C. R. Behl, G. L. Flynn, T. Kurihara, N. Harper, W. Smith, W. I. Higuchi, N. F. H. Ho, and C. L. Pierson, *J. Invest. Dermatol.*, **75,** 346 (1980).

(10) C. R. Behl, G. L. Flynn, T. Kurihara, W. Smith, N. Harper, O. G. Gatmaitan, C. L. Pierson, W. I. Higuchi, and N. F. H. Ho, in "Abstracts," vol. 9 (1), APhA Academy of Pharmaceutical Sciences, Washington, D.C., 1979, p. 110.

(11) C. R. Behl, G. L. Flynn, T. Kurihara, W. Smith, O. G. Gatmaitan, W. I. Higuchi, N. F. H. Ho, and C. L. Pierson, *J. Invest. Dermatol.*, **75,** 340 (1980).

(12) R. Meyer, C. R. Behl, and G. L. Flynn, in "Abstracts," vol. 11 (1), APhA Academy of Pharmaceutical Sciences, Washington, D.C., 1981, p 67.

(13) C. R. Behl, G. L. Flynn, W. M. Smith, T. Kurihara, K. A. Walters, O. G. Gatmaitan, W. I. Higuchi, C. L. Pierson, and N. F. H. Ho, in "Abstracts," vol. 9 (2), APhA Academy of Pharmaceutical Sciences, Washington, D.C., 1979, p. 90.

(14) C. R. Behl, K. A. Walters, G. L. Flynn, and W. I. Higuchi, in "Abstracts," vol. 10 (1), APhA Academy of Pharmaceutical Sciences, Washington, D.C., 1980, p. 98.

(15) M. Feiwel, *Br. J. Dermatol.*, **81,** 113 (1969).

(16) R. L. Nachman and N. B. Easterly, *J. Pediatr.*, **79,** 628 (1971).

(17) F. A. Wilson and J. M. Dietschy, *Biochim. Biophys. Acta*, **363**, 112 (1974).

(18) N. F. H. Ho, J. Y. Park, W. Morozowich, and W. I. Higuchi, in "Design of Biopharmaceutical Properties and Prodrugs and Analogs," E. B. Rahe, Ed., APhA, Academy of Pharmaceutical Sciences, Washington, D.C., 1977, p. 136.

(19) P. M. Elias, J. Georke, D. S. Friend, *J. Invest. Dermatol.*, **69**, 535 (1977).

ACKNOWLEDGMENTS

This study was supported by National Institutes of Health Grant No. 5 R01 GM 24611.

Permeation of Skin and Eschar by Antiseptics II: Influence of Controlled Burns on the Permeation of Phenol

CHARANJIT RAI BEHL *, EDWARD E. LINN, GORDON L. FLYNN ˣ, NORMAN F. H. HO, WILLIAM I. HIGUCHI, and CARL L. PIERSON

Received April 6, 1981 from the *College of Pharmacy, The University of Michigan, Ann Arbor, MI 48109.* Accepted for publication July 6, 1982. * Present address: Pharmaceutical Research, Hoffmann-La Roche, Inc., Nutley, NJ 07110.

Abstract □ The safe antiseptic use of phenol over the burn-traumatized surface depends on knowledge of how the systemic accumulation of phenol is affected by burn processes. To gain insight into the underlying permeation phenomenon, the diffusion of phenol and a reference cosolute, methanol, through both scalded and branded dorsal skin sections of the hairless mouse was studied as a function of burn temperature using *in vitro* diffusion cells. Temperatures up to 100 and 150° were used for scalding and branding, respectively, using a 60-sec exposure time. Permeability coefficients of the traumatized skins were assessed at 37° and compared with control values. Coefficients of both permeating species were not increased significantly by burn temperatures up to 70° applied either by scalding or branding, however, at higher temperatures exaggerated increases in permeation rates were noted. A limiting increase of ~7 times the control value was noted for phenol irrespective of the burn method. Permeability of methanol was altered even more dramatically and at 100° by scalding and 150° by branding was over 50 times the control rate. At 80 and 100° for methanol and at 80° for phenol, scalding produced larger increases in the permeability coefficients than branding. Since contact for 1 min at 60° is capable of producing a full-thickness burn injury, it is clear that eschar permeability to phenol immediately postburn is not related to the clinical degree of burning, but is a function of the thermal intensity (hotness) of the burn stimulus. Full-thickness wounds can be expected to have highly variable rates of systemic absorption as a direct consequence of the wide-ranging permeability possible for such burns, with the risks of topical application varying accordingly.

Keyphrases □ Permeability—of phenol and methanol, through burn-traumatized skin □ Phenol—permeability through burn-traumatized skin □ Methanol—permeability through burn-traumatized skin

Survival of patients with extensive deep partial-thickness (second-degree) and full-thickness (third-degree) burns depends, in part, on limiting microbial colonization of the wound surface. Topical antiseptics are used for this purpose since eschar is nonvascularized and all but inaccessible systematically. Virtually every known antiseptic chemical has been applied to burns, all too often with serious systemic consequences due to excessive transeschar adsorption. Phenol has proven to be one of these toxic agents (1, 2).

In previous studies using model permeating species originating from these laboratories, the permeation behavior of hairless mouse skin has been shown to be altered in unique ways by both scalding (3, 4) and branding (5, 6). Skin permeation rates for water and the *n*-alkanols were maximally increased two- to fourfold when the skins were burned at 60°, irrespective of burn duration. However, when skins were burned for 60 sec at various temperatures, large increases in the permeabilities were noted beginning at ~80°; the effect was greater the more polar the permeating species. In branding experiments, it was possible to use temperatures >100° and correspondingly larger permeability increases were observed for sensitive compounds. These studies provided basic insights into the conditions for and mechanisms of thermal alteration of skin permeation.

The permeability of phenol through hairless mouse skin in its normal state and in a stripped condition was also investigated in these laboratories (7). The overall behavior of this animal tissue to phenol was found to be similar quantitatively and qualitatively to the behavior reported for the human epidermis (8, 9), including exact agreement on the concentration level where self-acceleration of permeation rates due to chemical denaturation of the stratum corneum began. Since there are reports that the percutaneous absorption of phenol through thermally damaged tissue is greatly enhanced (1, 10), the present study was undertaken to quantitate this clinically serious limitation to the topical use of phenol. Specifically, this study was aimed at investigating the influences of incrementally increased burn temperature by scalding or branding on the permeation of phenol through skin.

EXPERIMENTAL

Chemicals—[^{3}H]methanol[1] and [^{14}C]phenol[1] were diluted with 0.9% sodium chloride irrigation[2] (saline) to prepare solutions for the permeation experiments. The final chemical concentrations of the permeating species in the external diffusion medium were $\leq 10^{-4}$ *M*.

Animals—Male hairless mice of SKh-hr^{-1} strain[3] were used. Their care was as described in the preceding paper (7).

Radioisotopic Assay—Concentrations of the radiolabeled permeating species were determined using a liquid scintillation counter[4] and a suitable liquid scintillator[1]. Permeation of both methanol and phenol was studied simultaneously using a technique involving dual labels (11).

Scalding Procedure—Immediately following sacrifice, the dorsal

[1] New England Nuclear, Boston, Mass. (Supplier-estimated purity >98% in each case.)
[2] Abbott Laboratories, North Chicago, Ill.
[3] Skin Cancer Hospital, Temple University, Philadelphia, Pa.
[4] Beckman Liquid Scintillation Counter, Model LS 9000, Beckman Instruments, Inc., Fullerton, Calif.

0022-3549/83/0400-0397$01.00/0

(17) F. A. Wilson and J. M. Dietschy, *Biochim. Biophys. Acta*, **363**, 112 (1974).

(18) N. F. H. Ho, J. Y. Park, W. Morozowich, and W. I. Higuchi, in "Design of Biopharmaceutical Properties and Prodrugs and Analogs," E. B. Rahe, Ed., APhA, Academy of Pharmaceutical Sciences, Washington, D.C., 1977, p. 136.

(19) P. M. Elias, J. Georke, D. S. Friend, *J. Invest. Dermatol.*, **69**, 535 (1977).

ACKNOWLEDGMENTS

This study was supported by National Institutes of Health Grant No. 5 R01 GM 24611.

Permeation of Skin and Eschar by Antiseptics II: Influence of Controlled Burns on the Permeation of Phenol

CHARANJIT RAI BEHL *, EDWARD E. LINN, GORDON L. FLYNN ˣ, NORMAN F. H. HO, WILLIAM I. HIGUCHI, and CARL L. PIERSON

Received April 6, 1981 from the *College of Pharmacy, The University of Michigan, Ann Arbor, MI 48109.* Accepted for publication July 6, 1982. * Present address: Pharmaceutical Research, Hoffmann-La Roche, Inc., Nutley, NJ 07110.

Abstract □ The safe antiseptic use of phenol over the burn-traumatized surface depends on knowledge of how the systemic accumulation of phenol is affected by burn processes. To gain insight into the underlying permeation phenomenon, the diffusion of phenol and a reference cosolute, methanol, through both scalded and branded dorsal skin sections of the hairless mouse was studied as a function of burn temperature using *in vitro* diffusion cells. Temperatures up to 100 and 150° were used for scalding and branding, respectively, using a 60-sec exposure time. Permeability coefficients of the traumatized skins were assessed at 37° and compared with control values. Coefficients of both permeating species were not increased significantly by burn temperatures up to 70° applied either by scalding or branding, however, at higher temperatures exaggerated increases in permeation rates were noted. A limiting increase of ~7 times the control value was noted for phenol irrespective of the burn method. Permeability of methanol was altered even more dramatically and at 100° by scalding and 150° by branding was over 50 times the control rate. At 80 and 100° for methanol and at 80° for phenol, scalding produced larger increases in the permeability coefficients than branding. Since contact for 1 min at 60° is capable of producing a full-thickness burn injury, it is clear that eschar permeability to phenol immediately postburn is not related to the clinical degree of burning, but is a function of the thermal intensity (hotness) of the burn stimulus. Full-thickness wounds can be expected to have highly variable rates of systemic absorption as a direct consequence of the wide-ranging permeability possible for such burns, with the risks of topical application varying accordingly.

Keyphrases □ Permeability—of phenol and methanol, through burn-traumatized skin □ Phenol—permeability through burn-traumatized skin □ Methanol—permeability through burn-traumatized skin

Survival of patients with extensive deep partial-thickness (second-degree) and full-thickness (third-degree) burns depends, in part, on limiting microbial colonization of the wound surface. Topical antiseptics are used for this purpose since eschar is nonvascularized and all but inaccessible systematically. Virtually every known antiseptic chemical has been applied to burns, all too often with serious systemic consequences due to excessive transeschar adsorption. Phenol has proven to be one of these toxic agents (1, 2).

In previous studies using model permeating species originating from these laboratories, the permeation behavior of hairless mouse skin has been shown to be altered in unique ways by both scalding (3, 4) and branding (5, 6). Skin permeation rates for water and the *n*-alkanols were maximally increased two- to fourfold when the skins were burned at 60°, irrespective of burn duration. However, when skins were burned for 60 sec at various temperatures, large increases in the permeabilities were noted beginning at ~80°; the effect was greater the more polar the permeating species. In branding experiments, it was possible to use temperatures >100° and correspondingly larger permeability increases were observed for sensitive compounds. These studies provided basic insights into the conditions for and mechanisms of thermal alteration of skin permeation.

The permeability of phenol through hairless mouse skin in its normal state and in a stripped condition was also investigated in these laboratories (7). The overall behavior of this animal tissue to phenol was found to be similar quantitatively and qualitatively to the behavior reported for the human epidermis (8, 9), including exact agreement on the concentration level where self-acceleration of permeation rates due to chemical denaturation of the stratum corneum began. Since there are reports that the percutaneous absorption of phenol through thermally damaged tissue is greatly enhanced (1, 10), the present study was undertaken to quantitate this clinically serious limitation to the topical use of phenol. Specifically, this study was aimed at investigating the influences of incrementally increased burn temperature by scalding or branding on the permeation of phenol through skin.

EXPERIMENTAL

Chemicals—[^{3}H]methanol[1] and [^{14}C]phenol[1] were diluted with 0.9% sodium chloride irrigation[2] (saline) to prepare solutions for the permeation experiments. The final chemical concentrations of the permeating species in the external diffusion medium were $\leq 10^{-4}$ *M*.

Animals—Male hairless mice of SKh-hr^{-1} strain[3] were used. Their care was as described in the preceding paper (7).

Radioisotopic Assay—Concentrations of the radiolabeled permeating species were determined using a liquid scintillation counter[4] and a suitable liquid scintillator[1]. Permeation of both methanol and phenol was studied simultaneously using a technique involving dual labels (11).

Scalding Procedure—Immediately following sacrifice, the dorsal

[1] New England Nuclear, Boston, Mass. (Supplier-estimated purity >98% in each case.)
[2] Abbott Laboratories, North Chicago, Ill.
[3] Skin Cancer Hospital, Temple University, Philadelphia, Pa.
[4] Beckman Liquid Scintillation Counter, Model LS 9000, Beckman Instruments, Inc., Fullerton, Calif.

0022-3549/83/0400-0397$01.00/0

Table 1—Summary of the 60-Sec Scalding Data

Burn Temperature,°	Mouse Age, Days	$P \times 10^3$, cm/hr Mouse 1	2	3	4	5	Mean ± *SD*	Mean S-Values ± *SD*[a]
				Methanol				
37	—	—	—	—	—	—	—	1.0
60	110	1.7	2.6	2.3	3.4	—	2.5 ± 0.7	1.3 ± 0.3
70	110	8.8	5.9	4.6	4.7	6.8	6.2 ± 1.7	3.1 ± 0.9
80	111	52.8	52.3	48.2	70.9	49.6	54.8 ± 9.2	27.4 ± 4.6
90	111	99.6	76.9	75.7	76.4	—	82.2 ± 11.6	41.1 ± 5.8
100	115	94.9	120.6	92.5	124.6	—	108.2 ± 16.8	54.1 ± 8.4
				Phenol				
37	—	—	—	—	—	—	—	1.0
60	110	21.1	22.4	21.7	28.7	—	23.5 ± 3.5	1.0 ± 0.2
70	110	54.8	38.3	32.1	28.5	39.2	38.6 ± 10.1	1.7 ± 0.5
80	111	175.1	160.3	139.9	172.0	147.1	158.9 ± 15.3	6.9 ± 0.7
90	111	180.8	145.6	146.8	162.4	—	158.9 ± 16.5	7.0 ± 0.7
100	115	146.2	160.6	154.4	177.4	—	159.7 ± 13.2	7.0 ± 0.6

[a] Computed by using Eq. 2. The control *P*-values are: methanol, 1.9×10^{-3} cm/hr and phenol, 20.3×10^{-3} cm/hr. These values were abstracted from Refs. 7 and 8.

surface of each mouse was scalded by immersing it in water contained in a jacketed beaker (3). A desired burn temperature was achieved by perfusing water from a constant-temperature water bath through the beaker.

Branding Procedure—The dorsal sites of the mice were burned immediately following sacrifice by bringing them in contact with the upper, polished surface of a branding device (5). The desired burn temperature was achieved by perfusing the device with hot mineral oil from a constant-temperature oil bath.

Diffusion Cell and Permeation Procedure—A two-chamber glass diffusion cell (3–7, 11) was employed to determine the permeability of the skin. Mice were sacrificed by spinal cord dislocation, weighed, and visually examined for skin defects and hair distribution. The animals were selected from within a narrow age range (110–155 days) to minimize age-related effects (12). The dorsal surfaces were scalded (at temperatures ranging from 60 to 100°) or branded (at temperatures ranging from 60 to 150°) for a 60-sec duration. Each burned skin section was excised from the animal and mounted in a diffusion cell, and permeation experiments were conducted immediately, as previously described (7). Each experiment lasted for ~2 hr. This procedure ensured, insofar as possible, that the data would not be affected by the unavoidable hydrating conditions of the *diffusional system* (11). Three to five mice of about the same age were used for each compound per experimental condition. The details of the operation of the diffusion cell were as described previously (7).

Data Analysis—The data were plotted as the receiver compartment concentration (in cpm) as a function of time. The permeability coefficient was computed from the quasi steady-state slope from (3–7, 11, 12):

$$P = \frac{V}{A}\frac{(dC/dt)}{\Delta C} \qquad \text{(Eq. 1)}$$

where P is the permeability coefficient (cm/hr); A is the diffusional area (~0.6 cm^2), ΔC is the concentration difference across the membrane, which was taken to be equal to the donor concentration (cpm); V is the half-cell volume (1.4 ml); and dC/dt is the steady-state slope (cpm/cm^3/hr) from the receiver concentration *versus* time profile. The scalding coefficients (S-values) and the branding coefficients (B-values) were calculated from (3, 5):

$$\text{S-Value} = \frac{\text{dorsal (scalded) permeability coefficient}}{\text{dorsal (normal) permeability coefficient}} \qquad \text{(Eq. 2)}$$

and

$$\text{B-Value} = \frac{\text{dorsal (branded) permeability coefficient}}{\text{dorsal (normal) permeability coefficient}} \qquad \text{(Eq. 3)}$$

The normal dorsal permeability coefficients were averages for those found in previous studies (11, 12).

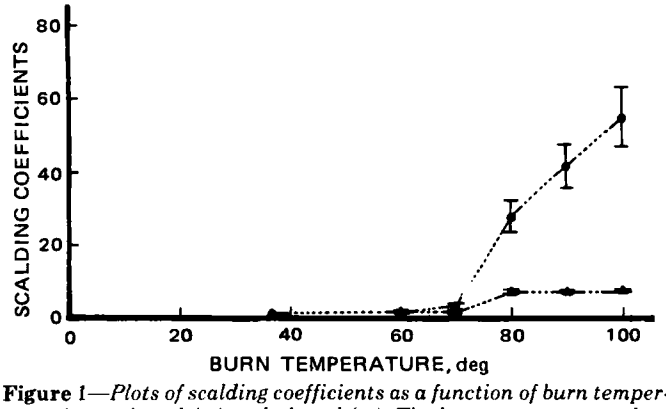

Figure 1—*Plots of scalding coefficients as a function of burn temperature for methanol (●) and phenol (▲). The bars represent standard deviations for each mean value.*

RESULTS AND DISCUSSION

Tables I and II contain summaries of data obtained in the scalding and the branding experiments, respectively. Data are tabulated separately for methanol and phenol, two solutes that diffused through the skin simultaneously. The permeability coefficients of the normal dorsal skins were abstracted from previous studies (11, 12). Figures 1 and 2 contain graphical illustrations of the burn coefficients as a function of the burn temperature for scalding and branding experiments, respectively.

Factors Influencing the Experimental Course of Action—In previous studies (3–6) two simple methods of giving graded, reproducible burns were practiced: burning at 60° for varied lengths of time and burning for 60 sec at systematically increased temperatures. Although burn wounds of third-degree depth were effected at 60° by scalding or branding for ≥1 min, the permeabilities of a spectrum of nonelectrolytes were only slightly elevated by such treatment. On the other hand, when scalding or branding was done at temperatures exceeding 70°, extraordinary augmentation of the permeabilities of some solutes was obtained. The lower the natural permeability of a species, the greater was the effect; therefore, polar solutes, held back by the effectively lipid nature of the stratum corneum, were the most affected.

The varied temperature–fixed burn duration experimental protocol yielded the optimum insight into the extent of burn enhancement of permeability, and it was therefore selectively used in these investigations. Another early observation bearing on the present study was that burns given to mice immediately postsacrifice behaved the same diffusionally as burns applied to living animals when each was studied immediately postburn. Humaneness, therefore, dictated the former procedure should be used. Since a 60-sec burn at 60° yielded a full-thickness injury, this duration was considered to be more than adequate at higher temperatures. However, retaining the duration used for the original protocol allowed direct comparison of the behavior of phenol to that of the *n*-alkanols.

Influences of Scalding on the Permeabilities of Methanol and Phenol—Scalding produced only marginal increases in the permeability coefficient for methanol up to 70° (Fig. 1). Beyond this temperature, systematic increases in the permeability coefficients are seen. At the higher temperature the scalding coefficients for methanol are quite large, reaching a value of 54 at 100°. Previously an S-value of ~31 was reported at 98° (4). The 1.7-fold difference in the quotients is more apparent than real. Previous quotients were computed with permeability coefficients of abdominal skins obtained concurrently with those of the scalded dorsum, a within-animal control method. In the present study, historical

Table II—Summary of the 60-Sec Branding Data

Burn Temperature,°	Mouse Age, Days	$P \times 10^3$, cm/hr Mouse 1	2	3	4	5	Mean ± *SD*	Mean B-Values ± *SD*
				Methanol				
37	—	—	—	—	—	—	—	1.0
60	148	2.3	1.8	2.7	2.2	1.8	2.2 ± 0.4	1.1 ± 0.2
80	148	41.4	30.0	31.3	27.4	28.7	31.8 ± 5.6	15.9 ± 2.8
100	155	79.3	81.1	77.6	92.7	52.2	76.6 ± 14.9	38.3 ± 7.4
150	155	146.0	106.5	106.6	100.6	77.6	107.5 ± 24.6	53.7 ± 12.3
				Phenol				
37	—	—	—	—	—	—	—	1.0
60	148	23.9	20.7	25.1	22.3	17.8	22.0 ± 2.9	1.1 ± 0.1
80	148	129.4	95.0	96.6	98.9	80.9	100.1 ± 17.8	5.0 ± 0.9
100	155	175.1	140.6	142.2	187.4	102.6	149.6 ± 33.3	7.4 ± 1.6
150	155	197.4	144.8	150.1	147.0	105.4	148.9 ± 32.7	7.3 ± 1.6

[a] Computed by using Eq. 3. The control P-values are: methanol, 1.9×10^{-3} cm/hr and phenol, 20.3×10^{-3} cm/hr. These values were abstracted from Refs. 7 and 8.

means for the normal dorsal skin permeability coefficients were used in lieu of running a complete set of control skins with each experiment. When the same technique of computation is used with the previous data, a 98° S-value of ~43 is obtained which is in better agreement with the present value of ~54. It is important to note that a small, absolute variation in the control permeability coefficient yields a large difference in quotients such as the S-values. To further stress this point, the absolute P-values of the burned skins can be compared. The dorsal permeability to methanol was $8.49 \pm 1.27 \times 10^{-2}$ cm/hr in the earlier experiments when the burn temperature was 98° and the mouse age was 106 days. In the present study a value of $10.8 \pm 1.68 \times 10^{-2}$ cm/hr was obtained when the burn temperature was 100° and the mouse age was 115 days. The absolute permeabilities can be considered approximately the same. Given the overall qualitative parallelism between the two studies, it can be concluded that the present results compare well with the previous results for methanol.

Like methanol, increases in the permeation rate of phenol are also marginal up to 70° (Fig. 2). Thereafter, the permeability coefficient increases to a plateau reached within the 70–80° temperature span. A limiting S-value of ~7.0 is observed (Table I). Qualitatively and quantitatively, this behavior is comparable to the data for hexanol (4) where a plateau value of 6.8 was reported for burn temperatures of 80, 90, and 98. This parallel is mechanistically interesting, especially because the two permeating species have almost identical permeability coefficients when the skin is used in its natural state of hydration (11). This is not to say that the permeation of the stratum corneum is the same for both. The permeability of hexanol through intact mouse skin doubles on long aqueous soaking (11), while the permeability of phenol is little affected (7), indicating some fundamental differences in their abilities to cross the barrier layer. Hexanol and phenol do, however, exhibit nearly the same permeation rates through highly burn-impaired skin, which is not surprising given their comparable molecular weights and the aqueous nature of the residual functioning elements of the overall skin barrier after scalding.

Permeability of Phenol and Methanol Through Branded Skins—Data for methanol indicate large branding coefficients at ≥80°. As in all previous studies, 60° branding was without pronounced effect.

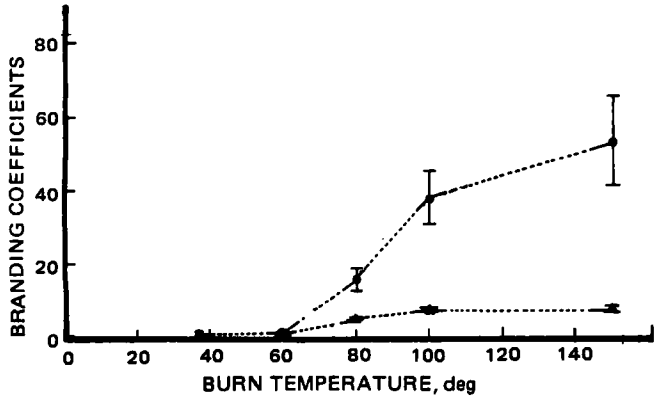

Figure 2—*Plots of branding coefficients as a function of burn temperature for methanol (●) and phenol (▲). The bars represent standard deviations for each mean value.*

While no 70° data were gathered, earlier work indicates that a transition from marginal to exaggerated burn effects took place at ~75°, which is not inconsistent with the present results. At a given temperature, branding coefficients appear consistently smaller than the scalding coefficients, suggesting that branding is an intrinsically less efficient means of damaging (presumably by denaturing the protein) the stratum corneum. At 80° for instance, the S-value is 27.4 ± 4.6, while the B-value using the same method of calculation is only 15.9 ± 2.8. At this temperature, values are significantly different ($p < 0.05$ by t test). There are several factors that might contribute to the scalding–branding disparity. In the course of scalding, the skin surface is in direct contact with the heated water; heat transfer should thus be more efficient than when there is a metal surface between the skin and the circulating thermal medium (branding). Additionally, moist heat may be more destructive than dry heat, a phenomenon that finds precedent in sterilization by autoclaving. Lastly, in the case of methanol, it appears that the closeness of the 100° S-value (54.1 and the 150° B-value (53.7) is not accidental but the consequence of the maximum possible disruption of the barrier function of the horny layer.

Branding data for phenol follow a pattern similar to that seen with scalding except that B-values again lag in magnitude behind the S-values at a given temperature. Within the limits imposed by the temperature spacing, the plateau for branding is not attained until 100° opposed to 80° for the scalding procedure. Again, the upper limit of the effects is nearly the same across burn methods: ~7 for scalding and ~7.4 for branding. The magnitude of the branding coefficients for phenol is only slightly smaller than the limiting value of ~9.5 for hexanol seen previously over the temperature range of 80–150° (6), providing another interesting parallel in the behaviors of these alkyl and aryl 6-carbon analogues.

Lastly, it has been suggested here that the barrier properties of the horny layer are destroyed at the extremes of the thermal treatments. This is true in the sense that the normal permeation selectivity is completely lost. However, permeability coefficients at their maximum for each compound are only 0.10–0.15 cm/hr, while earlier data showed stratum corneum-stripped permeability coefficients to be ~0.3 cm/hr and isolated dermis permeability coefficients to be slightly higher. It is therefore concluded that the denatured remains of the stratum corneum still offer a general diffusional resistance and are approximately as impermeable as the rest of the skin.

Clinical Relevance of the Phenol Studies—Presently, phenol is still used clinically as a local anesthetic and antipruretic, generally in whole percentage concentrations or in combination with other topical drugs (13). Its vehicles usually contain adsorptive solids and/or solvents, either of which reduces the thermodynamic activity of phenol below that of a strictly aqueous solution of the same concentration. Nevertheless, these topical preparations could be dangerous if used over burned tissue. A clinical fatality that occurred in 1949 (1) appears to be an instance where the worst possible combination of factors came together. A youth was burned by flash fire with superficial and partial-thickness burns covering 25–30% of his body. The method by which the burn was received and the clinical description of the fresh wound suggest that the burn was of short duration but very high thermal intensity: conditions which this research shows allows facile absorption through the skin. Although the phenol used for treatment was only 2% concentration in a 90% corn oil vehicle, the extensive area (fact) and highly permeable nature of the eschar (speculation) predisposed the patient to fatal systemic accumulation. Based on the work reported here, adsorption was possibly a logarithmic order

greater than it would be from the same application placed on normal skin. Given the variable but potentially high, permeability through eschar and the violent systemic toxicity (14), phenol should not be used for burn-wound antiseptics.

Another factor is that the chemical burn effected by the highest phenol concentration (6% w/v) in a preceding study (7) and the thermal burns effected here at temperatures >80° are of comparable permeability. This suggests that the chemical and thermal treatments cause the same type of destructive alteration of the stratum corneum, albeit by vastly different mechanisms, resulting in a functional impairment of the same order. We regard this as strong evidence that the stratum corneum proteins are involved and denatured by extreme treatments of either kind. It is hard to envision a means whereby these different treatments could produce like effects in purely lipid domains in the stratum corneum. By either procedure the stratum corneum loses some or all of the ability to differentiate permeating species on the basis of polarity, depending on the intensity of the burn.

REFERENCES

(1) T. D. Cronin, R. O. Brauer, *J. Am. Med. Assoc.*, **139**, 777 (1949).

(2) W. B. Deichmann, *J. Ind., Hygeine Toxicol.*, **31**, 146 (1949).

(3) C. R. Behl, G. L. Flynn, T. Kurihara, W. M. Smith, O. G. Gatmaitan, W. I. Higuchi, N. F. H. Ho, and C. L. Pierson, *J. Invest Derm.*, **75**, 340 (1980).

(4) G. L. Flynn, C. R. Behl, K. A. Walters, O. G. Gatmaitan, A. Wittkowsky, T. Kurihara, N. F. H. Ho, W. I. Higuchi, and C. L. Pierson, *Burns*, **8**, 47 (1981).

(5) C. R. Behl, G. L. Flynn, M. Barrett, K. A. Walters, E. E. Linn, Z. Mohamed, T. Kurihara, and C. L. Pierson, *ibid.*, **7**, 389 (1981).

(6) C. R. Behl, G. L. Flynn, M. Barrett, E. E. Linn, C. L. Pierson, W. I. Higuchi, and N. F. H. Ho, *ibid.*, **8**, 86 (1981).

(7) C. R. Behl, E. E. Linn, G. L. Flynn, C. L. Pierson, W. I. Higuchi, and N. F. H. Ho, *J. Pharm. Sci.*, **72**, 391 (1983).

(8) M. S. Roberts, R. A. Anderson, and J. Swarbrick, *J. Pharm. Pharmacol.*, **29**, 677 (1977).

(9) M. S. Roberts, R. A. Anderson, J. Swarbrick, and D. E. Moore, *ibid.*, **30**, 486 (1978).

(10) M. V. Freeman, E. Alvarez, J. H. Draize, *Fed. Proc. Fed. Am. Soc. Exp. Biol.*, **9**, 273 (1950).

(11) C. R. Behl, G. L. Flynn, T. Kurihara, N. Harper, W. M. Smith, W. I. Higuchi, N. F. H. Ho, and C. L. Pierson, *J. Invest. Dermatol.*, **75**, 346 (1980).

(12) C. R. Behl, G. L. Flynn, T. Kurihara, W. M. Smith, N. Harper, O. G. Gatmaitan, C. L. Pierson, W. I. Higuchi, and N. F. H. Ho, in "Abstracts," vol. 9(1), APhA Academy of Pharmaceutical Sciences, Washington, D.C., 1979, p. 110.

(13) "Handbook of Nonprescription Drugs," 5th ed., American Pharmaceutical Association, Washington, D.C., 1977, pp. 269, 277, 278, 295, 323, and 347.

(14) W. Deichmann and S. Witherup, *J. Pharmacol. Exp. Ther.*, **80**, 233 (1944).

ACKNOWLEDGMENTS

This work was presented at the 128th Annual Meeting of the American Pharmaceutical Association held in St. Louis, Missouri, March 28–April 1, 1981.

Supported by National Institutes of Health Grant GM 24611.

Low-Melting Phenytoin Prodrugs as Alternative Oral Delivery Modes for Phenytoin: A Model for Other High-Melting Sparingly Water-Soluble Drugs

YUMIKO YAMAOKA *, RICHARD D. ROBERTS, and VALENTINO J. STELLA ˣ

Received May 11, 1981, from the *Department of Pharmaceutical Chemistry, The University of Kansas, Lawrence, KS 66045.* Accepted for publication July 30, 1981. * Present address: Faculty of Pharmaceutical Sciences, Kobe Gakuin University, Kobe, Japan.

Abstract □ Phenytoin is a high-melting, weakly acidic, and sparingly water-soluble drug. Because of these physicochemical properties, phenytoin is subject to erratic bioavailability in a variety of dosage forms both in its acidic as well as sodium salt forms. A homologous series of 3-acyloxymethyl derivatives of phenytoin (acetyl through decanoyl) were synthesized and various physicochemical properties measured. The prodrugs were more readily soluble in various metabolizable glycerol esters such as tributyrin, trioctanoin, and triolein than phenytoin. The solubility of the prodrugs in the various organic vehicles studied was closely correlated to the melting point of the prodrug: the lower the melting point the greater the solubility. The cleavage rates of the prodrugs in plasma and tissue homogenates followed a parabolic relationship with chain length. The prodrug, 3-pentanoyloxymethyl-5,5-diphenylhydantoin when administered in tributyrin gave superior oral phenytoin bioavailability in rats when compared with sodium phenytoin administered as an aqueous solution.

Keyphrases □ Phenytoin—low-melting prodrugs, alternative oral delivery modes, model for high-melting sparingly water-soluble drugs □ Prodrugs—use in alternative oral delivery modes, model for high-melting sparingly water-soluble drugs, phenytoin

Phenytoin (I), a high-melting (293°) weakly acidic (1, 2) drug is sparingly soluble in water (2). Because of its physicochemical properties phenytoin is subject to erratic bioavailability in a variety of dosage forms both in the acidic as well as the sodium salt forms (3–6).

Since the problems associated with the release from the various dosage forms can be attributed to both the limited aqueous solubility and the weakly acidic nature of the phenytoin, it is likely that dissolution plays an important

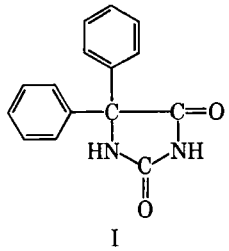

I

R	
H-	II
CH_3CO-	III
C_2H_5CO-	IV
C_3H_7CO-	V
C_4H_9CO-	VI
tert-C_4H_9CO-	VII

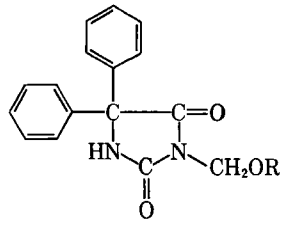

II–XII

R	
$C_5H_{11}CO$	VIII
$C_6H_{13}CO$	IX
$C_7H_{15}CO$	X
$C_8H_{17}CO$	XI
$C_9H_{19}CO$	XII

0022-3549/83/0400-0400$01.00/0

greater than it would be from the same application placed on normal skin. Given the variable but potentially high, permeability through eschar and the violent systemic toxicity (14), phenol should not be used for burn-wound antiseptics.

Another factor is that the chemical burn effected by the highest phenol concentration (6% w/v) in a preceding study (7) and the thermal burns effected here at temperatures >80° are of comparable permeability. This suggests that the chemical and thermal treatments cause the same type of destructive alteration of the stratum corneum, albeit by vastly different mechanisms, resulting in a functional impairment of the same order. We regard this as strong evidence that the stratum corneum proteins are involved and denatured by extreme treatments of either kind. It is hard to envision a means whereby these different treatments could produce like effects in purely lipid domains in the stratum corneum. By either procedure the stratum corneum loses some or all of the ability to differentiate permeating species on the basis of polarity, depending on the intensity of the burn.

REFERENCES

(1) T. D. Cronin, R. O. Brauer, *J. Am. Med. Assoc.*, **139**, 777 (1949).

(2) W. B. Deichmann, *J. Ind., Hygeine Toxicol.*, **31**, 146 (1949).

(3) C. R. Behl, G. L. Flynn, T. Kurihara, W. M. Smith, O. G. Gatmaitan, W. I. Higuchi, N. F. H. Ho, and C. L. Pierson, *J. Invest Derm.*, **75**, 340 (1980).

(4) G. L. Flynn, C. R. Behl, K. A. Walters, O. G. Gatmaitan, A. Wittkowsky, T. Kurihara, N. F. H. Ho, W. I. Higuchi, and C. L. Pierson, *Burns*, **8**, 47 (1981).

(5) C. R. Behl, G. L. Flynn, M. Barrett, K. A. Walters, E. E. Linn, Z. Mohamed, T. Kurihara, and C. L. Pierson, *ibid.*, **7**, 389 (1981).

(6) C. R. Behl, G. L. Flynn, M. Barrett, E. E. Linn, C. L. Pierson, W. I. Higuchi, and N. F. H. Ho, *ibid.*, **8**, 86 (1981).

(7) C. R. Behl, E. E. Linn, G. L. Flynn, C. L. Pierson, W. I. Higuchi, and N. F. H. Ho, *J. Pharm. Sci.*, **72**, 391 (1983).

(8) M. S. Roberts, R. A. Anderson, and J. Swarbrick, *J. Pharm. Pharmacol.*, **29**, 677 (1977).

(9) M. S. Roberts, R. A. Anderson, J. Swarbrick, and D. E. Moore, *ibid.*, **30**, 486 (1978).

(10) M. V. Freeman, E. Alvarez, J. H. Draize, *Fed. Proc. Fed. Am. Soc. Exp. Biol.*, **9**, 273 (1950).

(11) C. R. Behl, G. L. Flynn, T. Kurihara, N. Harper, W. M. Smith, W. I. Higuchi, N. F. H. Ho, and C. L. Pierson, *J. Invest. Dermatol.*, **75**, 346 (1980).

(12) C. R. Behl, G. L. Flynn, T. Kurihara, W. M. Smith, N. Harper, O. G. Gatmaitan, C. L. Pierson, W. I. Higuchi, and N. F. H. Ho, in "Abstracts," vol. 9(1), APhA Academy of Pharmaceutical Sciences, Washington, D.C., 1979, p. 110.

(13) "Handbook of Nonprescription Drugs," 5th ed., American Pharmaceutical Association, Washington, D.C., 1977, pp. 269, 277, 278, 295, 323, and 347.

(14) W. Deichmann and S. Witherup, *J. Pharmacol. Exp. Ther.*, **80**, 233 (1944).

ACKNOWLEDGMENTS

This work was presented at the 128th Annual Meeting of the American Pharmaceutical Association held in St. Louis, Missouri, March 28–April 1, 1981.

Supported by National Institutes of Health Grant GM 24611.

Low-Melting Phenytoin Prodrugs as Alternative Oral Delivery Modes for Phenytoin: A Model for Other High-Melting Sparingly Water-Soluble Drugs

YUMIKO YAMAOKA *, RICHARD D. ROBERTS, and VALENTINO J. STELLA ˣ

Received May 11, 1981, from the *Department of Pharmaceutical Chemistry, The University of Kansas, Lawrence, KS 66045.* Accepted for publication July 30, 1981. * Present address: Faculty of Pharmaceutical Sciences, Kobe Gakuin University, Kobe, Japan.

Abstract □ Phenytoin is a high-melting, weakly acidic, and sparingly water-soluble drug. Because of these physicochemical properties, phenytoin is subject to erratic bioavailability in a variety of dosage forms both in its acidic as well as sodium salt forms. A homologous series of 3-acyloxymethyl derivatives of phenytoin (acetyl through decanoyl) were synthesized and various physicochemical properties measured. The prodrugs were more readily soluble in various metabolizable glycerol esters such as tributyrin, trioctanoin, and triolein than phenytoin. The solubility of the prodrugs in the various organic vehicles studied was closely correlated to the melting point of the prodrug: the lower the melting point the greater the solubility. The cleavage rates of the prodrugs in plasma and tissue homogenates followed a parabolic relationship with chain length. The prodrug, 3-pentanoyloxymethyl-5,5-diphenylhydantoin when administered in tributyrin gave superior oral phenytoin bioavailability in rats when compared with sodium phenytoin administered as an aqueous solution.

Keyphrases □ Phenytoin—low-melting prodrugs, alternative oral delivery modes, model for high-melting sparingly water-soluble drugs □ Prodrugs—use in alternative oral delivery modes, model for high-melting sparingly water-soluble drugs, phenytoin

Phenytoin (I), a high-melting (293°) weakly acidic (1, 2) drug is sparingly soluble in water (2). Because of its physicochemical properties phenytoin is subject to erratic bioavailability in a variety of dosage forms both in the acidic as well as the sodium salt forms (3–6).

Since the problems associated with the release from the various dosage forms can be attributed to both the limited aqueous solubility and the weakly acidic nature of the phenytoin, it is likely that dissolution plays an important

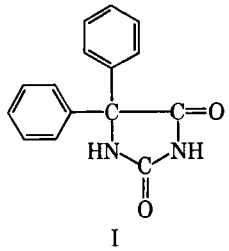

I

R	
H-	II
CH_3CO-	III
C_2H_5CO-	IV
C_3H_7CO-	V
C_4H_9CO-	VI
tert-C_4H_9CO-	VII

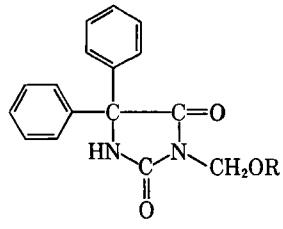

II–XII

R	
$C_5H_{11}CO$	VIII
$C_6H_{13}CO$	IX
$C_7H_{15}CO$	X
$C_8H_{17}CO$	XI
$C_9H_{19}CO$	XII

0022-3549/83/0400-0400$01.00/0

Table I—Melting Points and Elemental Analysis [a] for Various Esters of 3-Hydroxymethyl-5,5-diphenylhydantoin

Compound	mp, °	Molecular Weight, C	Calculated			Found		
			C	H	N	C	H	N
III	158–159	324.3	66.67	4.94	8.64	66.80	4.98	8.68
IV	172–174	338.4	67.47	5.33	8.28	67.90	5.38	8.30
V	134–135	352.4	68.18	5.68	7.95	68.23	5.77	8.00
VI	89–92	366.4	68.85	6.01	7.65	69.20	6.08	7.56
VII	134–135	366.4	68.85	6.01	7.65	69.31	6.20	7.58
VIII	107–108	380.4	69.47	6.32	7.37	69.68	6.39	7.33
IX	87–88	394.5	70.05	6.60	7.11	70.08	6.63	6.98
X	67.5–68.0	408.5	70.59	6.86	6.86	70.40	6.93	6.76
XI	78.5–80.0	422.5	71.09	7.11	6.64	70.93	7.28	6.54
XII	56–57	436.6	71.56	7.34	6.42	71.40	7.38	6.20

[a] Department of Medicinal Chemistry, University of Kansas.

role in the erratic *in vivo* behavior of phenytoin (3). In the case of phenytoin, strong intermolecular hydrogen bonding in the crystal lattice between the hydrogen atom on N(3) and a carbonyl oxygen of a neighboring phenytoin molecule is the probable cause of its inferior stability characteristics (7). This problem might be overcome by disrupting this hydrogen bonding in a bioreversible fashion, thereby increasing the lipid solubility of phenytoin, allowing incorporation in a dosage form such as a soft gelatin capsule or microencapsulation. In the present study, 3-hydroxymethyl-5,5-diphenylhydantoin (II) and various straight chain acyl (III–VI, VIII–XII) as well as the pivaloyl derivative of II (VII) were prepared and various physicochemical properties measured. Of particular interest was the increased solubility of compounds III–XII relative to phenytoin in cyclohexane and metabolizable lipid vehicles as well as the relationship between the structures of these prodrugs, their melting points, and lipid solubility. The ultimate objective was to see if the bioavailability of phenytoin, as a high-melting, sparingly water-soluble model compound, could be improved by the synthesis of low-melting prodrugs that could be incorporated into metabolizable vehicles suitable for formulation in soft gelatin capsules or microencapsulation.

EXPERIMENTAL

Apparatus—Ultraviolet spectral measurements[1] were performed using 1-cm cells with caps. Melting points were measured on a capillary melting point apparatus[2] and were uncorrected. A high-performance liquid chromatograph (HPLC) with an injection system[3], was used throughout the study. A gas chromatograph[4] was used for plasma and blood phenytoin analysis.

Materials and Reagents—The solvents used as a mobile phase were HPLC grade. All other chemicals were of analytical or reagent grade. 3-Hydroxy-5,5-diphenylhydantoin (II) was prepared as follows: a mixture of 45 g of phenytoin, 2.43 g of potassium carbonate, and 1620 ml of water was stirred while 180 ml of formalin was added. The stirring was continued at room temperature for 24 hr, the solution was filtered, and the solid was washed with a 3% formalin solution and then air dried for 3 days. Various esters of II were prepared by adding 10% excess of the corresponding acid chloride, dropwise with stirring, to 10 g of II dissolved in 40–50 ml of dry pyridine. For the synthesis of the 3-pentanoyloxymethyl derivative, the corresponding acid anhydride was used. The mixture was stirred until qualitative TLC showed the reaction to be complete. The pyridine solution was then poured into slightly acidic ice water with stirring. After neutralizing (or slightly acidifying) by the addition of hydrochloric acid, the solution was stirred for several hours. The acetyl and propionyl derivatives precipitated and were recrystallized from alcohol–ether. Other compounds did not solidify, but settled out as yellow oils which were purified by the following method. The water layer was removed by aspiration, and the oil was dissolved in ~150 ml of anhydrous ethyl ether (ethyl acetate was used for the butanoyl derivative). The organic layer was washed twice with 50 ml of 2% sulfuric acid, twice with 50 ml of 5% sodium carbonate, and twice with 50 ml of water. The organic layer was then dried over anhydrous magnesium sulfate for several hours. The mixture was filtered and the solvent was removed at reduced pressure to give solid material which was recrystallized from anhydrous ethyl ether. The melting point and elemental analysis of each compound are shown in Table I.

Solubilities—The solubilities of the various esters in cyclohexane were determined by placing 2–5 times excess ester and 2 ml of cyclohexane in a screw-capped vial containing a glass bead. The air was replaced by nitrogen and the vials were sealed. The mixtures were shaken for several days in a constant-temperature water bath at 25°. The mixture was filtered, an aliquot was diluted with an appropriate amount of cyclohexane, and the absorbance at 265 nm was measured. The concentration of the ester in the saturated solutions were calculated from the measured absorbances by reference to standard curves.

The solubilities in various oils were determined by suspending the compounds in oils and rotating the vials in a water bath for up to 1 month at 25°. The viscous-solutions were centrifuged for 5 min, and then the supernatant was diluted with an appropriate amount of tetrahydrofuran. The diluted solution (20 μl) was injected on an HPLC. The separation was carried out on a 25 cm × 4.6 mm (i.d.) prepacked normal-phase column[5] with use of a tetrahydrofuran–heptane (20–80 by volume) mobile

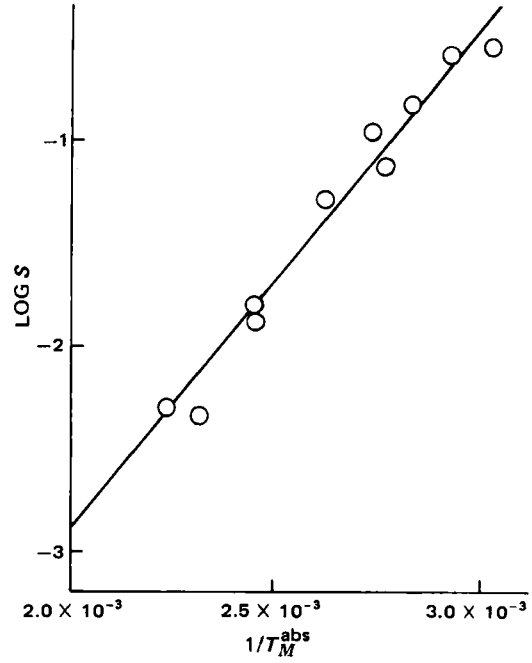

Figure 1—*Plot of the logarithm of the solubility (log S, S in units of moles/liter) of various 3-acyloxymethyl-5,5-diphenylhydantoins in ethyl oleate against the recipricol of the melting points in absolute degrees (T_M^{abs}) of the compounds. Solid line is given by the equation log S = 2404/T_M^{abs} − 7.694 (r = 0.9796).*

[1] Cary Instruments, Model 219.
[2] Uni-Melt, Thomas-Hoover.
[3] Altex Model 110A, with a Rheodyne model 7125 injector system and an Altex Model 153 detector.
[4] Varian Model 2100.
[5] Economy Column LiChrosorb Si-60-10, Chrompack.

Table II—Solubilities of Various Esters of 3-Hydroxymethyl-5,5-diphenylhydantoin at 25°

Compound	Solubilities, mg/ml					Phenytoin Equivalents
	Cyclohexane	Ethyloleate	Triolein	Trioctanoin	Tributyrin	
III	0.036	1.5	0.99	3.6	15.8	0.78
IV	0.068	1.7	0.82	3.5	15.1	0.75
V	0.11	4.6	2.4	8.2	34.4	0.72
VI	5.5	40.8	17.1	65.7	270	0.69
VII	0.44	9.5	4.9	15.5	63.0	0.69
VIII	1.9	19.9	9.5	34.2	134	0.66
IX	3.9	29.4	11.3	43.2	143	0.64
X	61.3	105	38.2	144	284	0.62
XI	20.3	54.5	20.5	75.0	196	0.60
XII	306[a]	123	81.9	224	485	0.58
Phenytoin (I)	0.039	0.36	0.28	0.92	3.9	1.00

[a] Estimated from dissolved amount.

phase at a flow rate of 2.0 ml/min. The column effluent was monitored at 254 nm at 0.08 absorbance unit full scale. The concentrations of saturated solutions were calculated from the peak height of standard solution of each compound dissolved in tetrahydrofuran.

Stabilities—The compounds with the shortest and the longest carbon chain, 3-acetyloxymethyl- and 3-decanoyloxymethyl-5,5-diphenylhydantoin, were chosen as examples for the stability studies. A solution of each ester in each solvent studied (except cyclohexane) was prepared and placed into ampules, each of which contained 200 μl of solution. The ampules were sealed under nitrogen and kept at room temperature, 40°, and 60°. After appropriate intervals, the ampules were opened and the concentrations of the prodrugs were measured by the same HPLC method as used in the solubility study.

Kinetics in Human Plasma—The stock solution of each prodrug in acetonitrile (~2 mg/ml phenytoin equivalents) was added to the human plasma[6] which was kept in a water bath at 37° so that the final concentration of phenytoin formed was 20 μg/ml. At appropriate times a 100-μl sample was removed and the concentration of phenytoin formed by hydrolysis of the prodrugs with longer carbon chains (pentanoyl to decanoyl) was measured by GLC (8). The sample was added to 100 μl of 10% *meta*-phosphoric acid to quench any enzymatic reaction, and then 500 μl of cyclohexane was added. This mixture was vortexed for 1 min and centrifuged for 5 min. The cyclohexane layer was removed by aspiration and 100 μl of the aqueous layer was analyzed as previously described (8).

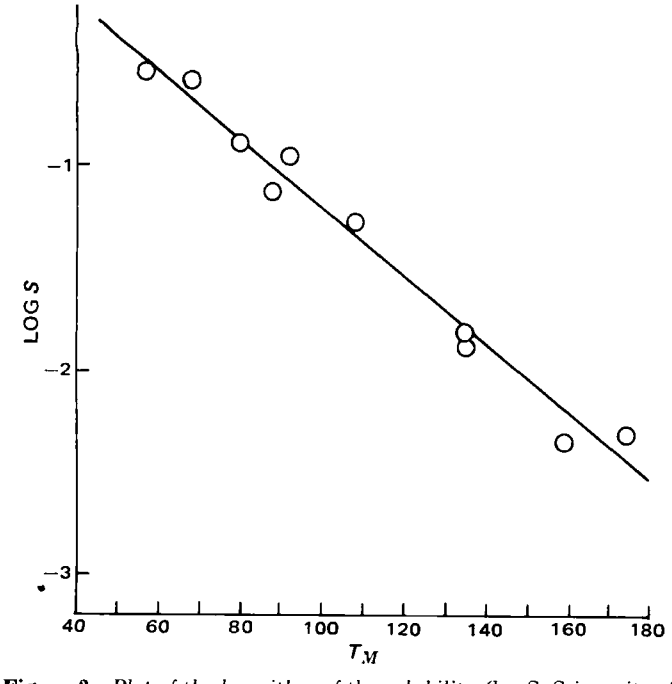

Figure 2—*Plot of the logarithm of the solubility (log* S, S *in units of moles/liter) of various 3-acyloxymethyl-5,5-diphenylhydantoins in ethyl oleate against their melting points* (T_M) *in degrees C. Solid line is given by the equation* log S = −0.0167 T_M + 0.4606 (r = 0.988).

[6] Community Blood Center of Greater Kansas City.

The concentration of phenytoin produced by the hydrolysis of prodrugs with shorter carbon chains (acetyl through to butanoyl) was determined by HPLC. The plasma samples were added to 250 μl of acetonitrile, vortexed for 5–10 sec, and then centrifuged. The supernatant was directly injected into the HPLC and was eluted with the mixture of acetonitrile and water, acidified to pH 2.5 with *meta*-phosphoric acid, at flow rate 1.3 ml/min on a 25 cm × 4.6 mm (i.d.) prepacked reverse-phase column[7]. The detector sensitivity setting was 0.005 absorbance unit full scale at 254 nm. The concentration of phenytoin was calculated from the peak height by reference to a standard curve.

The rate constants were obtained from the plots of log $(C_\infty - C_t)$ *versus* time, where C_∞ and C_t are the concentrations of phenytoin at infinity and at time t, respectively, by using the least-squares method. In all cases, the prodrugs quantitatively reverted to phenytoin and followed pseudo first-order kinetics.

Kinetics in Rat Plasma—Plasma taken from male rats were kept frozen until used. A 300-μl volume of plasma was used for each kinetic experiment. A 50-μl sample was removed at appropriate times, and the enzymatic reaction quenched by the addition of 125 μl of acetonitrile. The concentrations of phenytoin in the supernatant were measured by the HPLC method used in the kinetics in human plasma. To obtain good

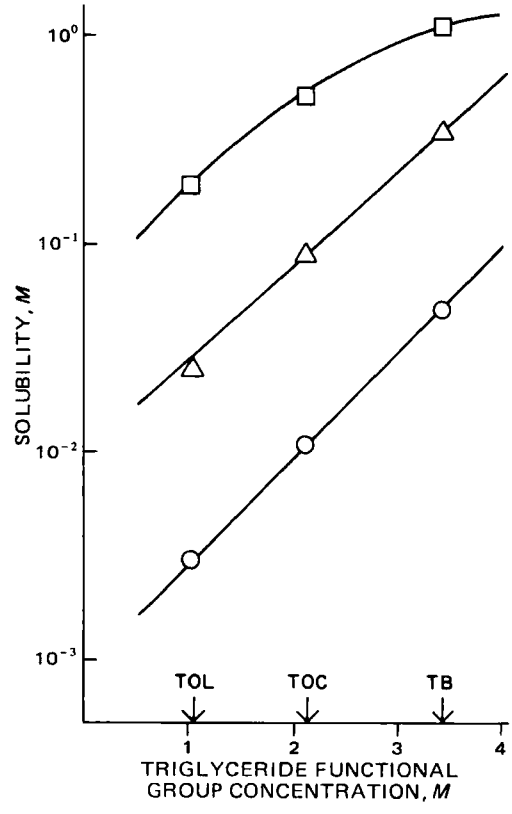

Figure 3—*Plot of log* S *for III (○), VII (△), and XII (□) versus triglyceride functional group concentration for the three solvents, tributyrin (TB), trioctanion (TOC), and triolein (TOL).*

[7] Economy Column LiChrosorb 10RP 18, Chrompack.

Table III—Half-lives for the Conversion of Various Phenytoin Prodrugs to Phenytoin at 37° in Human Plasma

Compound	$t_{1/2}$, min	k, min^{-1}
III	6.7	0.104
IV	2.3	0.306
V	1.6	0.437
VI	1.9	0.361
VII	75.6	0.00918
VIII	2.6	0.266
IX	4.7	0.148
X	12.6	0.0555
XI	14.8	0.0470
XII	33.2	0.0209

separation of the phenytoin peak from an interfering peak in rat plasma, 35% acetonitrile was used in the mobile phase instead of 40%, and the flow rate was 1.5 ml/min.

Kinetics in Rat Intestine Homogenates—A male rat (Sprague-Dawley) was sacrificed and a part of the intestine removed. After being sliced on a glass plate kept on ice, the intestine was placed in a beaker with cold Sorensen's isotonic buffer. The volume of buffer was adjusted so that the ratio of the weight of the intestine to the buffer was 1:4. The mixture was homogenized while cooling with ice, then centrifuged for 10 min at 2500 rpm, and the supernatant removed and kept cold (0°).

The kinetic studies were carried out by adding 20 μl of acetonitrile solution of the prodrug (2 mg phenytoin equivalent/ml) to 2 ml of diluted homogenate (×500) kept in a water bath (37°) for 10 min before the experiment. One hundred-microliter samples were removed at the appropriate times. The assay for phenytoin was the HPLC method used in the kinetics in human plasma except for the flow rate of mobile phase, which was 1.5 ml/min in this study.

***In Vivo* Experiment**—Adult, male Sprague-Dawley rats (225–300 g) were used in the crossover study. Six rats were randomly divided into two groups. Both groups of rats were fasted overnight as well as during the sampling time but water was allowed *ad libitum*.

Each rat was given a 100-μl sample of either sodium phenytoin in water or 3-pentanoyloxymethyl-5,5-diphenylhydantoin (VI) dissolved in tributyrin *via* gastric intubation. Approximately 30 mg/kg of phenytoin equivalents were given to each rat.

Blood sampling after drug administration was done *via* a tail clip. Two hundred microliter samples of whole blood were withdrawn at 1, 2, 4, 6, and 26 hr postdose and used for analysis. After a 2-week washout period both groups of rats received the alternate dosage form. The blood samples were analyzed for phenytoin as previously described (8).

RESULTS AND DISCUSSION

The solubilities of prodrugs III–XII in the various organic solvents are shown in Table II. For the solubility of 3-decanoyloxymethyl-5,5-diphenylhydantoin (XII) in cyclohexane only a rough estimate was made. This compound, in cyclohexane, displayed liquid crystal-like behavior, making a true solubility determination difficult. For all the prodrugs, crystals isolated from the excess solids used in the cyclohexane solubility determinations were checked for possible variations in melting behavior. In all cases the melting behavior of the excess solids was identical to the starting crystals.

There was no quantitative relationship, as expected, between the solubilities of the various esters and the length of the ester alkyl chain, but there was an obvious relationship between the melting points and solubility. Figure 1 is a plot of the logarithm of the solubility of the various esters in ethyl oleate against the reciprocal of the melting points in absolute degrees. Similar plots with correlation coefficients between 0.956 and 0.984 were seen with the other solvents.

Valvani and Yalkowsky (9) have also suggested that plots of the logarithms of solubility (as mole fraction) to the melting points may be linear for a series of structurally related molecules. Reasonable linearity of plots of the logarithm of molar solubility for our series of molecules was observed. Figure 2 shows such a plot for the esters in ethyl oleate. Neither of the plots (Figs. 1 and 2) are meant to imply anything other than the fact that crystal lattice energy differences, as indicated by melting point behavior, appear to influence the solubility of the esters in the organic solvents studied.

The low melting point of the 3-pentanoyloxymethyl derivative, VI, relative to the higher and lower homologues, V and VIII, should be noted. This unusually low melting behavior is reflected in its superior solubility in the various solvents when compared to compounds V and VIII. This

Table IV—Half-lives[a] for the Conversion of Various Phenytoin Prodrugs to Phenytoin in Different Lots of Rat Plasma at 37°

Compound	Lot I	Lot II	Lot III	Lot IV	Ratio of Rate Constant[b]
III				1.89	0.342
IV				0.85	0.753
V	1.04				0.889
VI	0.93	1.18	0.84	0.64	1.00
VII					0.442[c]
VIII		0.98			1.20
IX	0.69	0.79			1.49
X	0.52	0.71			1.67
XI			0.49		1.71
XII			0.55		1.52

[a] In minutes. [b] VI was taken as 1.0. [c] 10% rat plasma.

may represent a particularly disrupted member in the series that does not interact well with neighboring molecules in its crystal lattice.

The relative solubilities of any particular prodrug in tributyrin, trioctanoin, and triolein follow a predictable trend. The greater solubilities in tributyrin than in trioctanoin and triolein were probably due to the greater polarity of this solvent because of the higher molar concentration of the polar triglyceride functional group. For example, if the molar concentration of the triglyceride functionality is calculated from the solvent density and molecular weights of the three solvents, it can be seen in Fig. 3 that a plot of the logarithm of the solubility for compounds III, VIII, and XII in the three solvents against the molar triglyceride functional group concentration is reasonably linear. This suggested that the increased solubility of the prodrugs in going from tributyrin to triolein was largely due to specific interactions between the prodrugs and the triglyceride functional group of the solvents. In fact, if it is assumed that the triglyceride functionality acts as a single-ester function, because of steric and entropic considerations, the predicted solubility of the prodrugs in ethyl oleate can be estimated within a factor of 2–3, and the intercepts in Fig. 3 predict the solubilities in cyclohexane well within an order of magnitude.

The chemical stability of 3-acetyloxymethyl and 3-decanoyloxymethyl derivatives stored in ethyl oleate at room temperature (~25°) and at 40° and 60° was determined after 1, 3, and 5 months. No loss of the prodrugs was observed. The stabilities of these two esters in tributyrin, trioctanoin, and triolein were also evaluated after storage at 60° for 3 months. No measurable degradation was observed. Though acyl exchange reactions between the esters and solvent might have been anticipated, no such reactions could be confirmed.

Enzymatic cleavage of compounds III–XII was expected to occur *via* the following scheme (Scheme I).

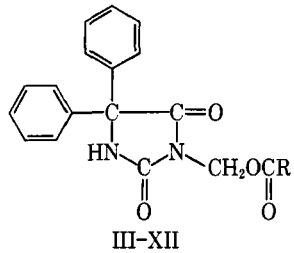

III–XII

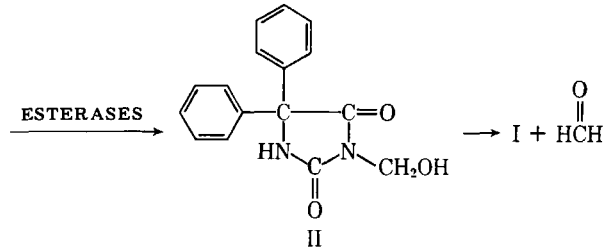

II

Scheme I

It has been shown in this laboratory[8] and by others (10) that II readily dehydroxymethylates to phenytoin at pH 7.4 and 37° with a $t_{1/2}$ of <2 sec. Therefore, phenytoin production from III–XII probably occurred *via* initial cleavage of the ester bond followed by a very rapid dehydroxymethylation step to give phenytoin without any accumulation of II. In

[8] S. Varia and V. J. Stella, unpublished results.

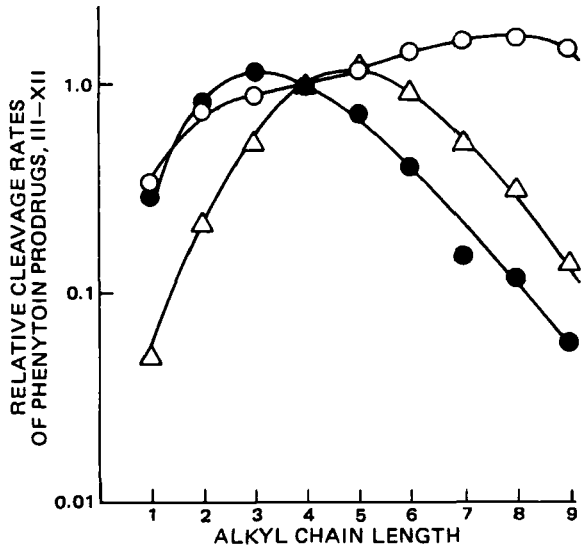

Figure 4—*Ratio of the rate constants for the cleavage of compounds III–VI, VII–XII to phenytoin in human (●) and rat (○) plasma and rat intestinal homogenates (△) at 37° to the 3-pentanoyloxymethyl derivative, VI, against alkyl chain length of the acyl function.*

all the studies with compounds III–XII quantitative cleavage to phenytoin was observed.

The rate constants and/or half-lives for the conversion of all the prodrugs to phenytoins in human and rat plasma and rat intestinal homogenates at 37° are shown in Tables III–V. In the case of rat plasma, various lots of rat plasma were studied with the cleavage rates of the prodrugs being compared with the 3-pentanoyloxymethyl derivative in each lot. The profiles for the relative cleavage rates for the prodrugs in all three tissues to the alkyl chain length are shown in Fig. 4. A parabolic relationship can be seen for each tissue, with the optimal chain length varying with the tissue and animal species.

In rat plasma all the prodrugs readily cleaved to phenytoin with half-lives of <2 min. Cleavage in human plasma was considerably slower, al-

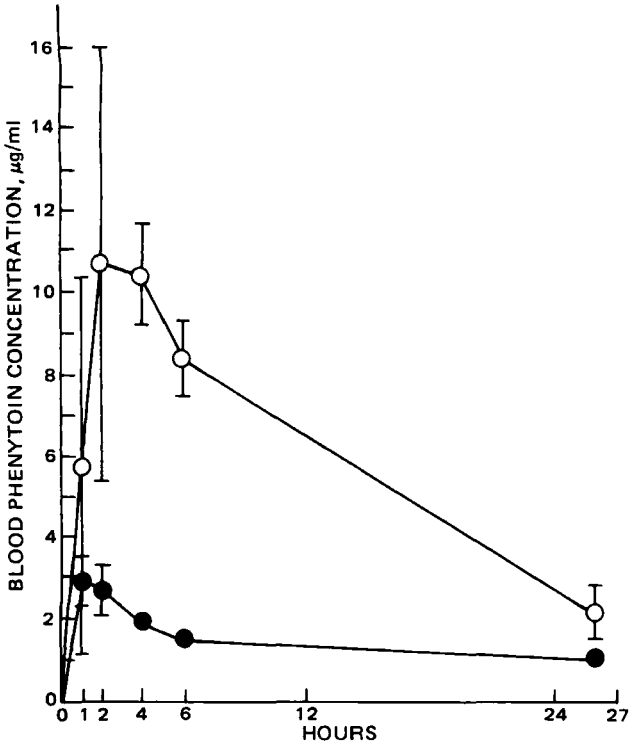

Figure 5—*Mean ± SD phenytoin whole blood concentrations in rats after oral administration of a 30-mg/kg phenytoin equivalent dose of 3-pentanoyloxymethyl-5,5-diphenylhydantoin in tributyrin (○) compared with sodium phenytoin in water (●).*

Table V—Half-lives and Rate Constants for the Conversion of Various Phenytoin Prodrugs to Phenytoin at 37° in Rat Intestine Homogenates

Compound	$t_{1/2}$, min	k, min^{-1}
III	16.4	0.0429
IV	3.78	0.184
V	1.56	0.444
VI	0.82	0.853
VII	46.7	0.0149
VIII	0.66	1.04
IX	0.87	0.796
X	1.58	0.440
XI	2.58	0.268
XII	5.86	0.118

though the 3-pentanoyloxymethyl derivative, VI, had a half-life of only 1.9 min in the human plasma used in the present study. In each tissue the cleavage rate of the 3-pivaloyloxymethyl derivative, VII, was very slow compared with the other compounds. This was presumably due to steric hindrance by the *tert*-butyl group to cleavage.

The kinetics in rat plasma diluted (to 4–20%) with isotonic Sorensen's buffer were also examined. Compounds XI and XII cleaved with half-lives of about 0.5 min in 4% plasma, while compound VI cleaved with a half-life of 3.4 min. Qualitatively, the logarithm of the rate constant *versus* alkyl chain plot did not change with the maximum cleavage still occurring with the 3-nonoyloxymethyl derivative, XI.

The cleavage rates in rat intestinal homogenate were quite rapid when the homogenate supernatant was isolated from a 2500-rpm, 10-min centrifugation of the initial homogenate. Homogenate supernatant samples prepared by ultracentrifugation at 7000×*g* for 2 hr resulted in a drop in apparent esterase activity towards the prodrugs, suggesting that both the soluble as well as microsomal-bound esterases were responsible for the observed cleavage of the esters.

Based on the melting point observations, solubilities, as well as cleavage rates, it seemed that 3-pentanoyloxymethyl-5,5-diphenylhydantoin or VI might be a viable prodrug of phenytoin. Its cleavage produces, apart from phenytoin, pentanoic or valeric acid and formaldehyde in concentrations that should not be toxic. Incorporation of this prodrug into a vehicle suitable for oral administration would depend on the dose of drug to be administered, the acceptability of the vehicle, and a reliable mechanism for drug release from the vehicle.

Studies on lipid-soluble drug release from metabolizable vehicles have suggested the following mechanism for this process. After intraluminal lipolysis of the oils by pancreatic lipases, the lipolytic products are dispersed in bile salt-mixed micelles. Calcium ions along with the fatty acids form a liquid crystal-like phase which may include monoglycerides (11). Lipid drugs are presumed to be released from the vehicle by this lipolysis. The drug along with the fatty acids and monoglycerides then become available for absorption (12).

The four vehicles chosen in the present study represented examples of short- (tributyrin), medium- (trioctanoin), and long-chain triglycerides (triolein), while ethyl oleate represented a simple long-chain fatty acid ester. The interest in these vehicles as well as others being studied, results from a long-term goal to study the mechanism of drug release from metabolizable vehicles. Long-chain triglycerides are readily attacked by the lipase–colipase–bile acid–calcium system to produce various liquid crystal and mixed micellar phases (11). The short- and medium-chain triglycerides are also cleaved (13, 14), but it is anticipated that they would tend to form a simple two-phase system of oil droplets and a true solution phase.

As an initial screen of whether the prodrug–lipid vehicle concept might

Table VI—Phenytoin Whole Blood Concentration [a] in Rats After Oral Administration of VI [b] in Tributyrin Compared with Sodium Phenytoin [b] in Aqueous Solution

Time, hr	Phenytoin Blood Concentrations	
	Sodium Phenytoin, μg/ml	VI in Tributyrin, μg/ml
1	2.91 ± 0.67	5.75 ± 4.60
2	2.69 ± 0.60	10.66 ± 5.38
4	1.93 ± 0.24	10.43 ± 1.22
6	1.52 ± 0.04	8.42 ± 0.92
26	1.03 ± 0.26	2.17 ● 0.68
$[AUC]_0^{26}$ in μg hr/ml	39.1	162.1

[a] Mean ± *SD*. [b] 30 mg/kg phenytoin equivalents.

represent a viable drug delivery mode, plasma phenytoin levels from 3-pentanoyloxymethyl-5,5-diphenylhydantoin in tributyrin, administered orally to rats at a 30 mg/kg phenytoin equivalent dose were compared with phenytoin from an aqueous solution of sodium phenytoin. Figure 5 is a plot of the mean blood levels for the two dosage forms. The superiority of the lipid vehicle–prodrug combination is obvious. Table VI summarizes the mean (and standard deviations) phenytoin blood levels at each sample time and the AUCs up to 26 hr. Presumably, the poor bioavailability of phenytoin from the sodium phenytoin solution was due to the slow redissolution of phenytoin precipitated when the sodium phenytoin was exposed to stomach acid.

In summary, the lipid solubility of high-melting, sparingly water- and lipid-soluble drugs can be altered by transient molecular modifications. Such modification may act to disrupt the major intermolecular interactions in the crystal lattice responsible for the undesired physical properties. For these poorly lipid and water soluble drugs, improved oral delivery can be effected by the synthesis of low-melting lipoidal prodrugs, which can then be incorporated into metabolizable vehicles. *In vivo* parent drug release from such a vehicle–prodrug combination is speculated to be initial lipolysis of the vehicle giving rise to prodrug release, followed by prodrug absorption and cleavage.

REFERENCES

(1) S. P. Agarwal and M. I. Blake, *J. Pharm. Sci.*, **57**, 1434 (1968).

(2) P. A. Schwartz, C. T. Rhodes, and J. W. Cooper, Jr., *ibid.*, **66**, 994 (1977).

(3) K. Arnold, N. Gerber, and G. Levy, *Can. J. Pharm. Sci.*, **5**, 89 (1970).

(4) C. M. Martin, M. Rubin, W. E. O'Malley, V. F. Garagusi, and C. E. McCauley, *Pharmacologist*, **10**, 167 (1968).

(5) L. Rail, *Med. J. Aust.*, **ii**, 339 (1968).

(6) T. Suzuki, Y. Saitoh, and K. Nishihara, *Chem. Pharm. Bull.*, **18**, 405 (1970).

(7) P. Sohor, *Acta Chim. Acad. Sci. Hung.*, **57**, 425 (1968).

(8) V. J. Stella, *J. Pharm. Sci.*, **66**, 1510 (1977).

(9) S. C. Valvani and S. H. Yalkowsky, in "Physical Chemical Properties of Drugs," S. H. Yalkowsky, A. A. Sinkula, and S. C. Valvani, Eds., Dekker, New York, N.Y., 1980, chap. 6.

(10) H. Bundgaard and M. Johansen, *Int. J. Pharmaceut.*, **5**, 67 (1980).

(11) J. S. Patton and M. C. Carey, *Science*, **204**, 145 (1979).

(12) T. Noguchi, Y. Tokunaga, H. Ichikawa, S. Muranishi, and H. Sezaki, *Chem. Pharm. Bull.*, **25**, 413 (1977).

(13) M. R. Playoust and K. Isselbacher, *J. Clin. Invest.*, **43**, 879 (1964).

(14) N. J. Greenberger, J. B. Rodgers, and K. J. Isselbacher, *ibid.*, **45**, 217 (1966).

ACKNOWLEDGMENTS

Supported by National Institutes of Health Grant GM 22357.

The assistance of Sailesh Varia with the gas chromatographic assays is gratefully acknowledged.

Computation of In-house Quality Control Limits for Pharmaceutical Dosage Forms Based on Product Variability

SANFORD BOLTON

Received December 21, 1981, from the *College of Pharmacy and Allied Health Professions, St. John's University, Jamaica, NY, 11439.* Accepted for publication December 21, 1982.

Abstract □ A method for establishing sampling plans for in-house limits that fix both the producer's and consumer's risks is presented for pharmaceutical systems in which both between-batch and within-batch variations are present. Such plans can always be constructed and require more or less sample assays depending on the variability of the process. The computations involve a numerical approximation to the bivariate normal distribution.

Keyphrases □ Product variability—pharmaceutical dosage forms, quality control limits □ Pharmaceutical dosage forms—quality control limits, product variability □ Quality control limits—pharmaceutical dosage forms, product variability

A recent article by Boudreau and Harrison (1) described a method for establishing "House Guides" that achieve "a high degree of assurance at a minimum of cost." These guides were set up in an effort to establish reasonable in-house limits, tighter than official specifications, which would give a high level of assurance that the finished product would not be out of specifications set by the NDA, FDA, official compendia, or company policy. According to Boudreau and Harrison (1), the FDA has recommended that a risk of releasing an out-of-specification product should be ≤5% based on the in-house guidelines. The establishment of in-house specifications is important because of problems that can arise when the assay of a batch of material is close to, but within, the official specifications. In these cases, the true mean potency has a good chance of being outside the official limits. Boudreau and Harrison in developing their formula, EVAL, were prompted by the difficulty of computing house limits using a single formula that would satisfy the 5% criterion and would, at the same time, consistently pass good batches which have a relatively large variation. They recommended the use of three formulas based on the relative amount of variation. It is possible to establish such in-house limits (hereafter referred to as IHLs) for any product based on its variability. If the batch-to-batch variability is so great that many batches truly fall outside the official limits, no plan will consistently pass these batches. In these situations, it is the responsibility of the manufacturer to improve the process so as to reduce the variability.

However, once the sources of variability have been identified, plans can be established with known properties. In the present case, the plans should accept out-of-specification material 5% of the time, at most. Another important criterion is that the plan should pass good material with a known probability, *e.g.*, 90% of the time.

0022-3549/83/0400-0405$01.00/0

represent a viable drug delivery mode, plasma phenytoin levels from 3-pentanoyloxymethyl-5,5-diphenylhydantoin in tributyrin, administered orally to rats at a 30 mg/kg phenytoin equivalent dose were compared with phenytoin from an aqueous solution of sodium phenytoin. Figure 5 is a plot of the mean blood levels for the two dosage forms. The superiority of the lipid vehicle–prodrug combination is obvious. Table VI summarizes the mean (and standard deviations) phenytoin blood levels at each sample time and the AUCs up to 26 hr. Presumably, the poor bioavailability of phenytoin from the sodium phenytoin solution was due to the slow redissolution of phenytoin precipitated when the sodium phenytoin was exposed to stomach acid.

In summary, the lipid solubility of high-melting, sparingly water- and lipid-soluble drugs can be altered by transient molecular modifications. Such modification may act to disrupt the major intermolecular interactions in the crystal lattice responsible for the undesired physical properties. For these poorly lipid and water soluble drugs, improved oral delivery can be effected by the synthesis of low-melting lipoidal prodrugs, which can then be incorporated into metabolizable vehicles. *In vivo* parent drug release from such a vehicle–prodrug combination is speculated to be initial lipolysis of the vehicle giving rise to prodrug release, followed by prodrug absorption and cleavage.

REFERENCES

(1) S. P. Agarwal and M. I. Blake, *J. Pharm. Sci.*, **57**, 1434 (1968).

(2) P. A. Schwartz, C. T. Rhodes, and J. W. Cooper, Jr., *ibid.*, **66**, 994 (1977).

(3) K. Arnold, N. Gerber, and G. Levy, *Can. J. Pharm. Sci.*, **5**, 89 (1970).

(4) C. M. Martin, M. Rubin, W. E. O'Malley, V. F. Garagusi, and C. E. McCauley, *Pharmacologist*, **10**, 167 (1968).

(5) L. Rail, *Med. J. Aust.*, **ii**, 339 (1968).

(6) T. Suzuki, Y. Saitoh, and K. Nishihara, *Chem. Pharm. Bull.*, **18**, 405 (1970).

(7) P. Sohor, *Acta Chim. Acad. Sci. Hung.*, **57**, 425 (1968).

(8) V. J. Stella, *J. Pharm. Sci.*, **66**, 1510 (1977).

(9) S. C. Valvani and S. H. Yalkowsky, in "Physical Chemical Properties of Drugs," S. H. Yalkowsky, A. A. Sinkula, and S. C. Valvani, Eds., Dekker, New York, N.Y., 1980, chap. 6.

(10) H. Bundgaard and M. Johansen, *Int. J. Pharmaceut.*, **5**, 67 (1980).

(11) J. S. Patton and M. C. Carey, *Science*, **204**, 145 (1979).

(12) T. Noguchi, Y. Tokunaga, H. Ichikawa, S. Muranishi, and H. Sezaki, *Chem. Pharm. Bull.*, **25**, 413 (1977).

(13) M. R. Playoust and K. Isselbacher, *J. Clin. Invest.*, **43**, 879 (1964).

(14) N. J. Greenberger, J. B. Rodgers, and K. J. Isselbacher, *ibid.*, **45**, 217 (1966).

ACKNOWLEDGMENTS

Supported by National Institutes of Health Grant GM 22357.

The assistance of Sailesh Varia with the gas chromatographic assays is gratefully acknowledged.

Computation of In-house Quality Control Limits for Pharmaceutical Dosage Forms Based on Product Variability

SANFORD BOLTON

Received December 21, 1981, from the *College of Pharmacy and Allied Health Professions, St. John's University, Jamaica, NY, 11439.* Accepted for publication December 21, 1982.

Abstract □ A method for establishing sampling plans for in-house limits that fix both the producer's and consumer's risks is presented for pharmaceutical systems in which both between-batch and within-batch variations are present. Such plans can always be constructed and require more or less sample assays depending on the variability of the process. The computations involve a numerical approximation to the bivariate normal distribution.

Keyphrases □ Product variability—pharmaceutical dosage forms, quality control limits □ Pharmaceutical dosage forms—quality control limits, product variability □ Quality control limits—pharmaceutical dosage forms, product variability

A recent article by Boudreau and Harrison (1) described a method for establishing "House Guides" that achieve "a high degree of assurance at a minimum of cost." These guides were set up in an effort to establish reasonable in-house limits, tighter than official specifications, which would give a high level of assurance that the finished product would not be out of specifications set by the NDA, FDA, official compendia, or company policy. According to Boudreau and Harrison (1), the FDA has recommended that a risk of releasing an out-of-specification product should be ≤5% based on the in-house guidelines. The establishment of in-house specifications is important because of problems that can arise when the assay of a batch of material is close to, but within, the official specifications. In these cases, the true mean potency has a good chance of being outside the official limits. Boudreau and Harrison in developing their formula, EVAL, were prompted by the difficulty of computing house limits using a single formula that would satisfy the 5% criterion and would, at the same time, consistently pass good batches which have a relatively large variation. They recommended the use of three formulas based on the relative amount of variation. It is possible to establish such in-house limits (hereafter referred to as IHLs) for any product based on its variability. If the batch-to-batch variability is so great that many batches truly fall outside the official limits, no plan will consistently pass these batches. In these situations, it is the responsibility of the manufacturer to improve the process so as to reduce the variability.

However, once the sources of variability have been identified, plans can be established with known properties. In the present case, the plans should accept out-of-specification material 5% of the time, at most. Another important criterion is that the plan should pass good material with a known probability, *e.g.*, 90% of the time.

0022-3549/83/0400-0405$01.00/0

Table I—Scheme for Nested Design to Estimate Variance

		Batch I Tablet		Batch II Tablet		Batch III Tablet	
		1	2	1	2	1	2
Replicate	1	X	X	X	X	X	X
	2	X	X	X	X	X	X

PRELIMINARY CONSIDERATIONS

If the variability in a dosage form potency is due to assay error only, then the problem of setting IHLs is relatively simple. As previously described (1), the limits for in-house specifications to maintain a 5% error rate or less are (using the authors' notation (1) and assuming that the data are normally distributed):

$$\text{UPS} - 1.65S_a, \quad \text{LPS} + 1.65S_a \qquad \text{(Eq. 1)}$$

where S_a is the assay standard deviation (SD), UPS is the upper product specification, and LPS is the lower product specification. The assay SD, S_a, can be determined from control charts or replicate assays. The IHLs can be made to be as close to the UPS and LPS as we wish by increasing the number of samples assayed. Then the IHLs are:

$$\text{UPS} - 1.65S_a/\sqrt{N}, \quad \text{LPS} + 1.65S_a/\sqrt{N} \qquad \text{(Eq. 2)}$$

where N is the number of samples assayed.

The above probability statements are correct if the product is homogeneous, such as would occur with solutions or other homogeneous mixes. In these situations, the sampling procedure and the number of samples to be assayed are unambiguously defined. If the variability is composed of both assay error and sampling error, which would occur in the case of tablets (when tablets are not identical), then the number of samples to be assayed and the procedure for setting limits require further analysis. For example, a duplicate determination could be two single-tablet assays or one tablet assayed in duplicate. If S_t, the standard deviation due to only tablet differences, is 5%, S_a is 2.5%, and the UPS is 110%, a single assay would yield IHLs of $110 - 1.65\sqrt{5^2 + 2.5^2} = 100.8\%$. Similarly if the LPS is 90%, the lower IHL would be 99.2%. These limits would probably be untenable. A duplicate assay (single assays of two tablets), for example, results in an upper IHL of $110 - 1.65\sqrt{(5^2 + 2.5^2)/2} = 103.5\%$.

The problem of setting limits based on assay variation only, as correctly pointed out (1), is that other sources of variation are not accounted for. In the above example, tablet variation is included in the error, and such a procedure would properly meet the 5% FDA recommendations. Although this takes care of the so-called consumer's risk, the producer's risk (the risk of rejecting good products) is not clearly defined. This report presents a method of constructing in-house guidelines that will define both of these risks.

STATISTICAL CONCEPTS

The problem of defining both the producer's and consumer's risks when setting acceptance/rejection in-house guidelines is more or less difficult, depending on the nature of the variability of a product. The simplest case is a homogeneous system that does not vary from batch to batch but has assay error associated with it. More common are systems that have both assay error and batch-to-batch variability as well as being nonhomogeneous, *i.e.*, having unit-to-unit variation. Thus, all of these sources of variability must be considered in setting up a suitable quality control plan.

The calculation of the aforementioned sources of error can be accomplished in several ways. Quality control records for many batches where replicate assays are performed within each batch may be sufficient to supply the necessary estimates. The use of Shewhart control charts for means and variability (range or, preferably, standard deviation) accomplish the same end. Since the discussion in this paper is based on an assumption that the process is not changing, Shewhart control charts can also help ensure that the process is in "control." An experimental design (known as a nested design) may be implemented where several units from each batch are assayed in replicate (duplicates are usually sufficient) for many batches, as shown in Table I.

Table II—Analysis of Variance for a Nested Design to Estimate Components of Variance

Source	Mean Square Estimates[a]
Batches	$rtS^2_b + rS^2_t + S^2_a$
Tablets (within batches)	$rS^2_t + S^2_a$
Assay error	S^2_a

[a] r = Number of replicate assays on each tablet; t = number of tablets; S^2_a, S^2_t, and S^2_b are the variances associated with the assay, tablets, and batches, respectively.

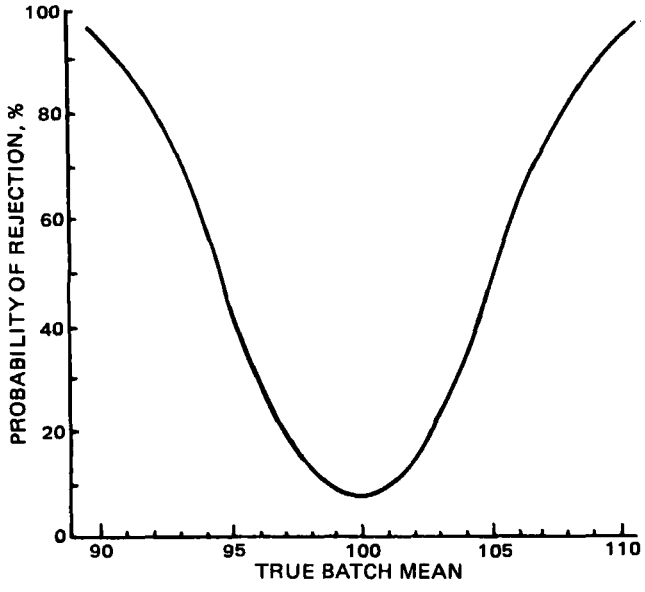

Figure 1—*OC Curve for batch with* $S^2_t + S^2_a = 25$, *true mean = 100,* N *= 3.*

This design allows the estimation of the variance due to assay, unit-to-unit, and batch-to-batch variability (components of variance) (2). The computations in this paper assume that the variances are known (typical Shewhart control charts are constructed under the same assumption). If a sufficient amount of historical data are available, this assumption will not cause problems. For a new process, specifications and/or the sampling plan should be suitably modified as data become available and variance estimates stabilize. The analysis of variance is shown in Table II.

The variance of a single tablet assay is $S^2_t + S^2_a$. If this variance is so large that an unreasonable IHL is obtained to satisfy the 5% criterion, this variability can be effectively reduced by performing replicate assays. This is usually more efficiently accomplished by assaying more than one tablet rather than performing replicate assays on the same tablet, but the optimal procedure depends on the magnitude of S^2_t, S^2_a, and time-cost estimates. For example, the variance of the average of two replicate assays of two tablets is $S^2_t/2 + S^2_a/4$. The variance of the average of four single tablet assays is $(S^2_t + S^2_a)/4$, smaller than that of two replicate assays of two tablets, but which may be more costly to run. Data derived from content uniformity tests can be useful to develop and monitor IHLs because of the relatively large amount of data (at least 20 individual tablet assays per batch) that is readily available for products

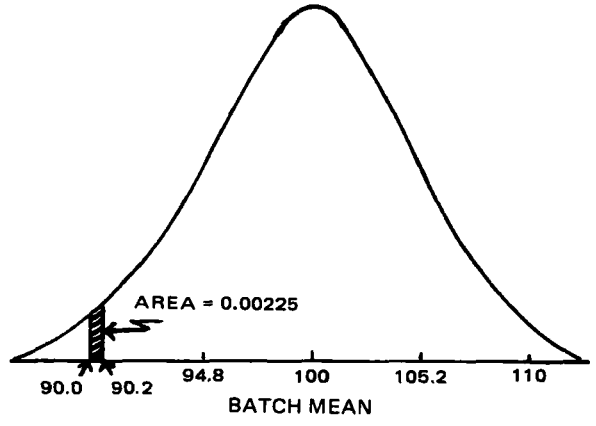

Figure 2—*The shaded area represents the probability of a batch mean falling between 90.0 and 90.2.*

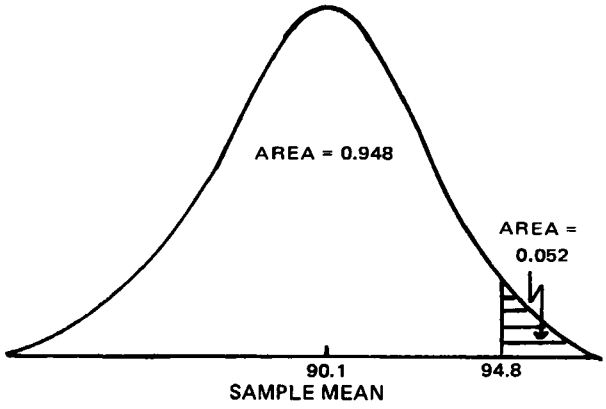

Figure 3—*Normal curve with mean equal to 90.1 showing the probability of a sample mean being below 94.8 (unshaded area, p = 0.948).*

undergoing this test. However, data may also be derived from the usual composite assays performed in replicate. Because most solid dose forms undergo content uniformity tests, and the results of these multiple single tablet (or capsule) assays provide more data for variance estimation, the remaining discussion will consider single-tablet assays. The discussion applies equally well to composite assays where sufficient data are available to precisely estimate the variance components. For composite assays, the variance of a single tablet assay, $S^2_t + S^2_a$, is replaced by $S^2_t/C^2 + S^2_a$, the variance of a single composite assay, where the composite consists of C tablets. The variance in the latter case may be reduced by performing m assays on each of n composites, where the variance of the mean result is $S^2_t/nC + S^2_a/nm$. This is analogous to the variance of the mean of t single tablet assays when $c = M = 1$.

Ignoring batch-to-batch variability for now, it is clear, based on the above discussion, that the IHLs can be made as close to the UPS and LPS as we wish by performing more assays. Consider the following example. Experience has shown that the *SD* (assay error) of a tablet with 100 mg of drug is 5% ($S^2_a + S^2_t = 25$). If single tablets are assayed and the official specifications are 90–110 mg, the IHLs are:

$$110 - 1.65 \times 5 = 101.75 \text{ and } 90 + 1.65 \times 5 = 98.25$$

a very tight specification for a 100-mg tablet. However, if three tablets are assayed, the standard error of the average is $5/\sqrt{3} = 2.89$, and the IHLs are 94.8–105.2, with the same probability (≤5%) of accepting a bad lot. Therefore, if considerable variability exists, the IHLs can be made wider (close to, but not exceeding the UPS and LPS) by performing replicate assays.

SAMPLING PLANS: MANUFACTURER'S RISK

Since there are any number of plans, depending on the number and kind of replicate assays, all of which will ensure that no more than 5% of out-of-specification product will be passed, another criterion can be used to fix the number of assays to be used for a given plan. This criterion, as previously mentioned, the manufacturer's risk, is the chance of rejecting a good batch of product based on the in-house limits. A good batch is one that is truly within the official limits, the UPS and LPS. The following discussion will present a method for establishing plans based on both the α and β risks: the chance of accepting lots of poor quality or rejecting lots of good quality, respectively. Since only one assay will be performed per tablet, the variance of a single assay is $S^2_a + S^2_t$. Also, the α error will be at most 5% for each batch.

Some practical considerations should be emphasized. When considering sampling from batches, the variance of the estimate of a mean value taken from a batch (any batch taken at random) is $S^2_b + (S^2_t + S^2_a)/t$, where t is the number of tablets assayed. Thus, it is not possible to reduce the variance of this estimate below S^2_b by increased sampling of tablets within a batch. The way to reduce batch-to-batch variation (S^2_b) is by careful and controlled manufacturing procedures, as previously noted. If the batch variation is so large that the sample averages consistently border on the official limits, it would be advantageous to the manufacturer to improve the process. Otherwise it will be difficult to pass batches using any plan.

An example will be used to illustrate the general procedure of constructing a sample plan. Consider a product whose overall average as determined from historical data or control charts over many batches is

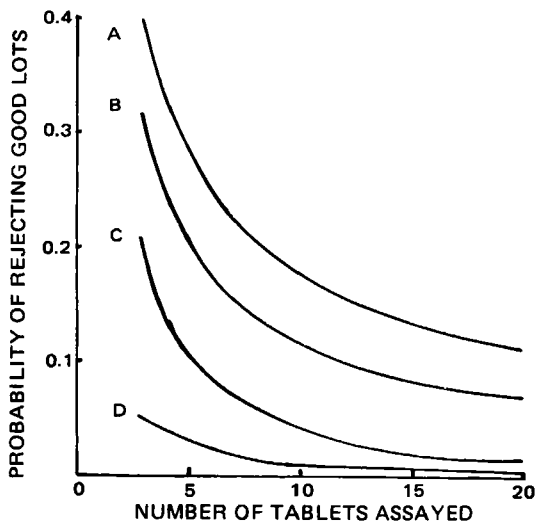

Figure 4—*Probability of rejecting good batches based on in-house limits.*
For curves A, B, and C, $S^2_t + S^2_a = 25$. For curve A, $S^2_b = 50$; for curve B, $S^2_b = 25$; for curve C, $S^2_b = 10$; for curve D, $S^2_t + S^2_a = 10$ and $S^2_b = 10$.

100% of label. The LPS and UPS are 90 and 110%, respectively, and the assay and unit-to-unit variabilities are known. The batch-to-batch variability can be obtained from historical data or by using an experimental design similar to that previously described. Suppose, in this example, that three tablets are assayed and $S^2_a + S^2_t = 25$. The IHLs are $(90 + 1.65\sqrt{25/3},\ 110 - 1.65\sqrt{25/3})$ 94.8–105.2 (Eq. 2). This fixes the consumer's risk at ≤5%. The properties of this plan for any given batch can be described by an operating characteristic (OC) curve, where the probability of rejection is plotted as a function of the true batch mean (Fig. 1). Clearly, the probability of rejection is not constant but changes depending on the true mean of the particular batch being tested. For any given batch, the true mean is not known and the probability of rejection, therefore, is also not known. (It should be again emphasized that the probability of accepting a bad batch is fixed at ≤5% for all batches by application of Eq. 2.)

The problem to be solved is to establish a sampling plan that will reject good batches using the in-house guidelines, a small but known proportion of the time over many batches. This can be accomplished if S^2_b and $S^2_t + S^2_a$ are known and if batch means and assays are normally distributed, by use of the bivariate normal distribution. The probability of rejecting a good batch (one whose true mean is between 90 and 110 mg) using the IHLs as the criteria, can be computed based on a basic probability theorem:

Probability (a sample mean falls outside the IHLs, given that the true batch mean is within the official specifications) = Probability (sample mean falls outside the IHLs and the true batch mean is within official specifications)/Probability (true batch mean is within official specifications)[1]. (Eq. 3)

The following sample calculation will give a close approximation to this probability. The example uses official limits of 90–110 with a long-term average of 100, but this process can be applied to any specified limits or any long-term mean of a product.

1. Divide the region between 90 and 110 into small intervals, *e.g.*, 100 divisions of 0.2 units each.

2. Compute the probability that the true batch mean lies in each of the 100 intervals. For example, if $S^2_b = 25$, the probability of a batch mean falling between 90.0 and 90.2 is 0.002248, as calculated from areas under the standard normal curve (Fig. 2).

3. For each of the 100 intervals, compute the probability that a sample mean from a batch in the interval will fall outside of the IHLs. This can be closely approximated by computing the probability based on a true batch mean midway in the interval. For example, to calculate the probability that the mean if a sample of size 3 will fail the in-house limits if

[1] Note that the producer's risk, the probability of rejecting a good lot, is defined here as a conditional probability, based only on the good lots manufactured. This risk may also be calculated on the basis of all lots produced, both good and bad. In this example, using the results shown in Table III, the former calculation results in a risk of 0.0664/0.955 = 0.0695; the latter calculation results in a risk of 0.0664.

Table III—Properties of a Plan with $N = 20$, $S^2_b = 25$, $S^2_t + S^2_a = 25$

	Probability that a batch is			
	Within Official Specifications (0.955) and		Outside Official Specifications (0.045) and	
Plan A[a]	Passes In-House 0.8881	Fails In-House 0.0664	Passes In-House 0.0004	Fails In-House 0.0446
Plan B[a]	Passes 0.937	Fails 0.017	Passes 0.004	Fails 0.041

[a] Plan A: Assay 20 single tablets. Pass batch if average is within IHLs.
Plan B: Assay 20 single tablets. Pass batch if average is within IHLs. Reject if average outside official specifications. If average is between IHLs and official specifications, assay 20 different tablets and average the 40 tablets. If the average of the 40 tablets is within official specifications, pass the batch. Otherwise, reject the batch.

the batch mean is between 90 and 90.2, consider μ, the true batch mean to be equal to 90.1. The problem, then, is to compute the probability that the sample mean will be <94.8 or >105.2, if the true mean of the batch is 90.1. The probability of the mean being >105.2 is virtually zero. The probability that the sample mean is less than 94.8 can be calculated knowing that the variance of the mean of three tablets is 25/3 ($S^2_t + S^2_a = 25$). Again, using areas under the standard normal curve, this area is equal to 0.948, as shown in Fig. 3.

4. Multiply the probabilities obtained from steps 2 and 3 for each of the intervals in step 1 and sum over all intervals (between 90 and 110). This result closely approximates the probability of observing a sample mean outside of the IHLs and a batch mean within official specifications. This sum is equal to 0.320 for this example.

5. Divide the probability obtained in step 4 by the probability that a batch mean will fall between 90 and 110. In this case the latter probability is equal to 0.955 (95.5% of the batches manufactured will have a true mean between 90 and 110 if $S^2_b = 25$.). This quotient is the answer to the original problem: the *probability that a good batch will fail* based on the IHLs as expressed in Eq. 3. This is equal to 0.320/0.955 = 0.335 in the present example.

There is no explicit solution to the above problem, but by selecting smaller intervals for the batch means (less than 0.2 in step 1, the approximation can be improved slightly. Although this calculation may seem complicated and tedious, it can be accomplished easily by a simple computer program[2].

Figure 4 is a plot of the probability of rejecting good batches as a function of sample size showing the effect of changing $S^2_a + S^2_t$ and S^2_b. With such information a suitable sample size can be chosen to fix the manufacturer's risk at an acceptable level. These plans always have a probability of <5% of accepting lots that are out of the official specifications.

If $S^2_t + S^2_a = 25$, a product with $S^2_b = 25$ would require more than 55 tablets to achieve an erroneous rejection rate of 5%. If $S^2_b = 10$, a sample of 8–9 tablets would suffice. If $S^2_t + S^2_a$ is reduced to 10, and $S^2_b = 10$, 3–4 tablets would give the required protection.

The complete properties of any plan can be calculated using a variation of the same computer program used to compute the probabilities of erroneously rejecting good batches as described above. The probabilities shown in Table III were derived from a plan in which 20 tablets were assayed, with $S^2_b = 25$ and $S^2_t + S^2_a = 25$, a plan that fixes the IHLs at 91.84–108.16. More than 95% of batches of this product will be within official specifications. Of these, 6.64% will fail the in-house specifications. The probability of a good batch failing the in-house specifications is 6.64/95.55 = 0.0695, the producers risk.

The consumer's risk can be defined as the probability that a bad batch will be among those passed by the producer, i.e., the probability that a batch is bad given that it is accepted by the producer. Using the data in Table III, the consumer's risk, according to this definition, is 0.0004/(0.8881 + 0.0004) = 0.00045.

If the sample mean falls between the IHLs and the official specifications, usually it would be prudent not to reject immediately the batch, but to perform further assays to zero in on the true batch average. However, such sequential sampling changes the probabilities as outlined in this paper. The probabilities resulting from sequential sampling plans depend on the nature of the sampling plan, and increase the consumer's risk and decrease the producer's risk. The probabilities resulting from a sequential plan can be closely approximated by using a procedure similar to that previously described for the single stage sampling. A reasonable sequential plan would be as follows. Assay 20 single tablets[3]. Accept the batch if the average falls within the IHLs, and reject the batch if the average is outside the official specifications. If the average falls between the IHLs and official specifications, assay 20 more single tablets and compute the average of the 40 tablets assayed. If the average of the 40 tablets falls within the official specifications, accept the batch. Otherwise, reject the batch. The probabilities of acceptance and rejection using this plan is shown in Table III, Plan B. The producer's risk is reduced to 0.018 and the consumer's risk is increased to 0.0043 as compared with the risks of 0.0695 and 0.00045 for the single-stage sampling plan.

REFERENCES

(1) C. F. Boudreau and D. J. Harrison, *Drug Dev. Ind. Pharm.*, **6**, 539 (1980).

(2) O. L. Davies (Ed.), "The Design and Analysis of Industrial Experiments," Hafner, New York, N.Y., 1963, chap. 4.

[2] The author will supply a routine for the TI 59 upon request, which will compute this probability given S^2_b, $S^2_t + S^2_a$, and the sample size for assay.

[3] Of course, a similar plan could be constructed based on composite assays.

Solubility of Hydrocortisone in Organic and Aqueous Media: Evidence for Regular Solution Behavior in Apolar Solvents

T. A. HAGEN *x and G. L. FLYNN

Received April 16, 1981 from the *College of Pharmacy, University of Michigan, Ann Arbor, MI 48109.* Accepted for publication February 22, 1982. *Present address: Pharmaceutical Research and Development, Pfizer Central Research, Groton, CT 06340.

Abstract □ The solubility of hydrocortisone was determined experimentally in a wide variety of solvents. Groups of solvents were selected to emphasize different solute–solvent interactions which can influence the solubility profile of such a large, polyfunctional solute. Regular solution theory for a crystalline solute was shown to be applicable to the solubility behavior of hydrocortisone in solvents that lack strong dipoles and the ability to hydrogen bond. A best-fit solubility parameter of 12.4 $(cal/ml)^{1/2}$ for hydrocortisone was determined from the latter solubilities and the ideal solubility of hydrocortisone. This solubility parameter estimate was significantly higher than estimates calculated from molar-attraction constants. Even though molar volume ratios between hydrocortisone and the solvents ranged from 2.25 to 3.28, the associated Flory–Huggins entropy term did not seem to be a significant solubility-determining factor. In all cases, the solubility of hydrocortisone in solvents capable of dipole–dipole interactions and hydrogen bonding was shown to be higher by logarithmic orders when compared with regular solution theory predictions. Thus, for this solute, regular solution theory was shown to be appropriate only for solvents where London dispersion forces dominate the interactions between solute and solvent molecules.

Keyphrases □ Hydrocortisone—solubility in organic and aqueous media, determination of regular solution behavior in apolar solvents □ Solubility—of hydrocortisone in apolar solvents, regular solution behavior of large polyfunctional solutes □ Regular solution theory—behavior determination for hydrocortisone solubilities in apolar solvents

The physicochemical events responsible for the solubilization of a drug in various solvent systems can be characterized rigorously on a macroscopic scale, if not a molecular scale. For a crystalline nonelectrolyte, the critical factors are the solid-phase activity of the solute and molecular interactions between solute and solvent. The ability to estimate these critical parameters for drug molecules placed in a given vehicle or solution environment has immense importance when deciphering the mechanisms of drug action and delivery. To attain such objectives, macroscopic thermodynamic functions must be coupled with phenomenological interpretations of the processes involved in solubilization. Due to the polyfunctional character of drug molecules, a wide variety of molecular interactions are often simultaneously operative. Current solubility theories are limited to specific types of intermolecular interactions. An example is regular solution theory as proposed by Scathard (1) and Hildebrand (2), which is premised on all intermolecular association being of a nonorientating variety. Although this theory has on occasion been overextended to solvent systems where this fundamental assumption is not true, valid applications have provided basic understanding of solubility behavior for various pharmaceutical systems (3–8).

The purpose of the present study was to characterize the solubility behavior of hydrocortisone in solvents that are capable of a full range of molecular interactions with this polyfunctional solute. Two reference points were employed in the analysis, the primary point being ideal behavior and the secondary point of comparison being regular solution behavior. Furthermore, the values and limitations of regular solution analysis are demonstrated for a typically complex pharmaceutical solute.

THEORETICAL

A reaction of two components, a liquid solvent and an excess of a crystalline solute, is at a state of equilibrium when the thermodynamic activity of the solute in solution (a_2) equals the thermodynamic activity of solid solute (a_2^s). In this case the activity is taken as the ratio of solute vapor pressure to the vapor pressure of pure (supercooled) liquid solute. If this activity also equals the mole fraction composition over the entire concentration range up to and including saturation, the solution is an ideal solution. This only occurs when the solute–solvent adhesiveness is exactly equal to the cohesiveness of the pure liquid components considered on a per unit volume basis. Solubility predictions for ideal solutions require only estimates of a_2^s.

Most solute–solvent mixtures do not behave ideally, and solute mole fractional concentrations often differ greatly from their activities. To establish a relationship between concentration and activity, standard states must be selected for the components. For solubility analysis a convenient selection for the solute is pure liquid solute at the temperature of interest. Unit activity is thus defined as the activity of the pure liquid at a mole fraction of 1.0. The activity of a solute in solution is defined as directly proportional to the mole fractional concentration of the solute (X_2):

$$a_2 = \gamma_2 X_2 \qquad \text{(Eq. 1)}$$

where γ_2 is the proportionality constant or mole fractional activity coefficient. As X_2 approaches unity (the standard state), the ratio a_2/X_2 (or γ_2) approaches unity. The same standard state is also convenient for the solvent. For dilute solutions, the molecular environments of both solute and solvent molecules are predominantly other solvent molecules, and consequently the activity of the solvent is proportional to its fractional composition:

$$a_1 = X_1 \qquad \text{(Eq. 2)}$$

At the same time, solute molecules essentially only interact with solvent, and γ_2 is virtually constant for small changes in solute concentration. For a poorly soluble, crystalline nonelectrolyte, the mole fractional solubility ($X_{2,sat}$) is dependent therefore on molecular interaction differences between solute and solvent, reflected by γ_2, and the activity of the crystal:

$$a_2^s = \gamma_2 X_{2,sat} \qquad \text{(Eq. 3)}$$

From a thermodynamic viewpoint, solubility prediction is possibly based on measurements or estimations of γ_2 and a_2^s.

Crystalline Phase Activity—For solutes that are crystalline at ambient temperature, the selected standard state is a hypothetical state referred to as supercooled liquid solute. The free energy change required to form supercooled liquid solute from the solid solute (ΔG^{sc}) defines the activity of the solid as:

$$a_2^s = e^{-\Delta G^{sc}/RT} \qquad \text{(Eq. 4)}$$

Associated with this process is an enthalpy change ΔH^{sc} and an entropy change (ΔS^{sc}) such that ΔG^{sc} can be expressed as:

$$\Delta G^{sc} = \Delta H^{sc} - T\Delta S^{sc} \qquad \text{(Eq. 5)}$$

It is possible to obtain an expression experimentally suited for estimating

0022-3549/83/0400-0409$01.00/0

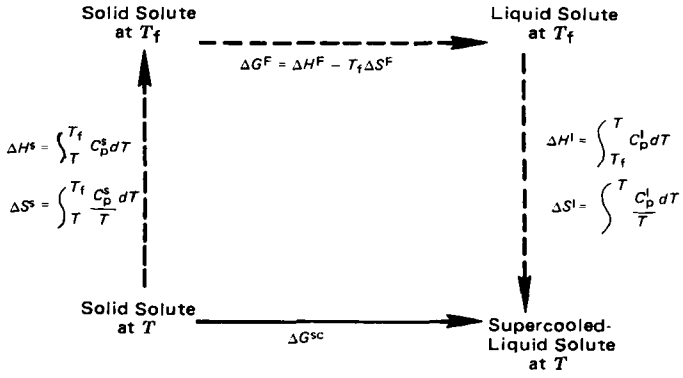

Figure 1—*Thermodynamic pathway for* ΔG^{sc} *at constant pressure.*

ΔG^{sc} at constant pressure. The thermodynamic pathway is given in Fig. 1. Here, a solid is heated to its melting temperature, melted, and the resulting melt is cooled back to the ambient temperature (T). By summing enthalpic and entropic contributions from each step, the total free energy change is obtained and, therefore, the activity of the solid can be expressed as:

$$\ln a_2^s = \frac{-\Delta H_f}{RT}\left(\frac{T_f - T}{T_f}\right) + \frac{\Delta C_p}{R}\left(\frac{T_f - T}{T}\right) - \frac{\Delta C_p}{R}\left(\ln \frac{T_f}{T}\right) \quad \text{(Eq. 6)}$$

where T_f and T are the melting and ambient temperatures, respectively, R is the gas constant, and ΔH_f is the heat of fusion for the solid at the melting point. The term ΔC_p is the difference of heat capacities between the liquid and solid. If ΔC_p and/or the temperature range T_f–T is small, the enthalpy and entropy of fusion are nearly constant, and Eq. 6 reduces to the familiar expression:

$$\ln a_2^s = \frac{-\Delta H_f}{RT}\left(\frac{T_f - T}{T_f}\right) \quad \text{(Eq. 7)}$$

The thermodynamic activity of a crystalline solute is therefore dependent on the *intrinsic properties* of the crystal lattice and can be estimated from experimental measurements of ΔH_f and T_f.

Regular Solutions—Solutions rarely conform to ideal behavior, since slight differences in molecular functionality between solvent and solute can result in large differences in their molecular interactions. Thermodynamically, the extent of deviation from the ideal case is expressed by the ratio a_2/X_2 which is the mole fractional activity coefficient γ_2. In other words, the free energy difference between ideal and nonideal behavior is defined as:

$$\Delta G_2^E = RT \ln (a_2/X_2) \quad \text{(Eq. 8)}$$

where ΔG^E is the excess free energy of mixing. Prediction of ΔG^E is difficult, since it is dependent on both the enthalpy and the entropy associated with molecular interactions for the pure components as well as their mixture. In the regular solution theory, the limiting situation is described as one in which the dominant molecular interactions between solute–solute, solvent–solvent, and solute–solvent are London forces (1, 2). This force is only dependent on the distance between atoms and their instantaneous orientation. The resulting attraction is nonorientating.

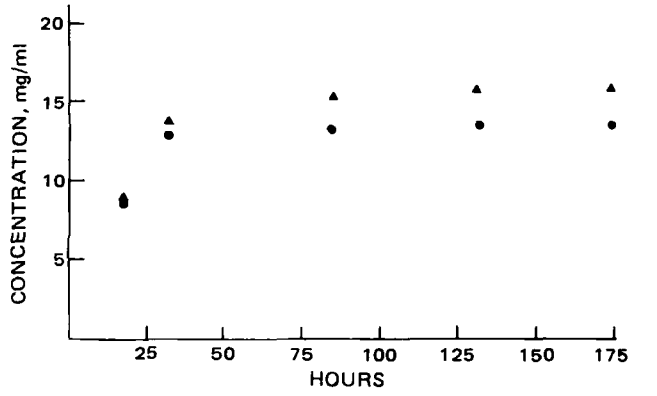

Figure 2—*Formation of saturated solution of hydrocortisone at 25°. Key: (●) 80% propylene glycol in water and (▲) 100% propylene glycol.*

Table I—Group Contributions to Molar Volume for Hydrocortisone

Functional Group or Atom	Number of Groups in Hydrocortisone	Partial Molar Volume Contribution per Group, ml/mole	Total Volume Contribution per Group[a], ml/mole
O—H	3	5.4	16.2
O=	2	5.5	11.0
CH_3	2	19.3	38.6
C	19	9.9	188.1
H	21	3.1	65.1

[a] Molar volume for hydrocortisone = 319 ml/mole.

The molecular model for regular solution behavior, therefore, allows for only an excess enthalpy of mixing arising from differences in cohesive energies between solute and solvent. Completely random mixing is assumed; thus, there is no excess entropy of mixing. The cohesive energy density of a pure liquid component is its internal energy per unit volume. Providing the vapor of a liquid is nearly ideal, the energy of vaporization per unit volume is an acceptable estimate for this internal energy.

The cohesive energy density of a mixture is much more difficult to estimate. By definition, this is the energy necessary to break all intermolecular contacts within the mixture. For these circumstances, Scathard (1) defined the cohesive energy density of a mixture as the geometric mean of the pure components' cohesive energy densities. It is this definition that limits regular solution theory to systems that predominantly interact through London forces.

Using these criteria for regular solution behavior, the energy of mixing for two components ΔE^M is as follows:

$$\Delta E^M = (X_1V_1 + X_2V_2)\left[\left(\frac{\Delta E_1^V}{V_1}\right)^{1/2} - \left(\frac{\Delta E_2^V}{V_2}\right)^{1/2}\right]^2 \phi_1\phi_2 \quad \text{(Eq. 9)}$$

where V is the molar volume, ϕ is the volume fraction, and ΔE^V is the energy of vaporization. As previously defined, the subscripts 1 and 2 designate the solvent and solute, respectively. The square root of the cohesive energy density is more often referred to as the solubility parameter δ. The partial molal energy of transferring liquid solute from pure liquid solute to solution is obtained by differentiating Eq. 9 with respect to n, *i.e.*:

$$\left(\frac{\delta \Delta E^M}{\delta n_2}\right)_{n_1} = V_2\phi_1^2(\delta_1 - \delta_2)^2 \quad \text{(Eq. 10)}$$

Assuming that there is no change in volume on mixing at constant pressure and that the entropy of transfer is ideal, it follows that:

$$\Delta G_2^E = RT \ln (a_2/X_2) = V_2\phi_1^2(\delta_1 - \delta_2)^2 \quad \text{(Eq. 11)}$$

Thus, deviation from ideality arises from the cohesive energy density difference between solvent and solute. This deviation defines the activity coefficient in terms of the excess enthalpy of mixing which, in this model, is identical to the excess free energy of mixing.

For a solid solute in equilibrium with saturated solution, the mole fractional regular solution solubility is as follows:

$$\ln X_2 = \frac{-\Delta H_f}{RT}\left(\frac{T_f - T}{T_f}\right) - \frac{V_2\phi_1^2}{RT}(\delta_1 - \delta_2)^2 \quad \text{(Eq. 12)}$$

In addition to the crystalline properties associated with fusion, application of this theory requires knowledge of the solubility parameters for solute and solvent.

EXPERIMENTAL

Materials—Hydrocortisone was obtained from The Upjohn Company and was used without further purification. For the solubility studies, double distilled water and reagent grade organic solvents[1] were used.

High-Performance Liquid Chromatographic (HPLC) Procedure—A high-performance liquid chromatograph[2], operated at ambient temperature, was equipped with a UV detector for monitoring the column effluent at 254 nm. Chromatographic systems were developed with deaerated methanol–water solvent systems and a μ-Bondapak C-18 column[3]. The flow rate was 1.0 ml/min and the detector sensitivity was

[1] Eastman or Aldrich.
[2] Waters Associates Liquid Chromatographic Systems.
[3] Waters Associates.

Table II—Physical Properties of Hydrocortisone

Molecular Structure	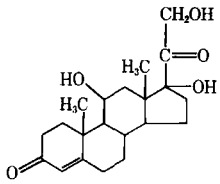
Molecular weight	362.5 g/mole
Crystalline density	1.24 g/ml
Molar volume, V_2	293 ml/mole
Melting temperature, T_f	212°
Heat of fusion, ΔH_f	8.1 Kcal/mole
Entropy of fusion, ΔS_f	16.7 cal/deg/mole
Activity of solid phase, a_2^s estimated from $\ln a_2^s = \frac{-\Delta H_f}{RT}\left(\frac{T_f - T}{T_f}\right)$	5.2×10^{-3}
Solubility parameter	12.4 $(cal/ml)^{1/2}$

adjusted as needed for each sample. Standard solutions of hydrocortisone were prepared for calibrating chromatographic peak heights. Injection volumes for standard and unknown solutions were equivalent, and internal standards were used when necessary. The sensitivity range of the chromatographic system for hydrocortisone was determined to be 10–0.01 μg/sample. Standard curves demonstrated excellent linearity over the entire concentration range.

Solubility Determination—The solubility of hydrocortisone in each solvent was obtained by equilibrating large excesses of solute with solvent in sealed glass containers. Temperature was maintained at 25° by a constant-temperature water bath and vigorous stirring was supplied by magnetic bars. An excess of solute was always present in the slurries. Solubilities in hexane and cyclohexane were determined by equilibrating large volumes of solution (300–600 ml) with excess solute for several days. Large samples were taken, filtered[4], measured, and brought to dryness; the residue was reconstituted in 3 ml of methanol with an internal standard and assayed by HPLC. The procedure was repeated three times.

The solubilities of hydrocortisone in the remaining solvents were determined in a similar manner utilizing smaller sample volumes. Samples (1 ml) were drawn from equilibrating solutions and were placed in microcentrifuge tubes. After immediate centrifugation, the supernatant was drawn through glass wool-tipped pipets and diluted in methanol. For solutions with densities greater than solid hydrocortisone, excess solute was first removed by suction. At least four samples were drawn from each solution with ~2-day intervals between samplings. Each time point (sample) was assayed by HPLC at least twice. Concentration *versus* time of equilibration plots indicated that equilibration was obtained rapidly (<24 hr) for all solutions except propylene glycol–water mixtures with high percentages of propylene glycol. Apparently due to the high viscosity of propylene glycol and its concentrated aqueous mixtures, these solutions required longer time periods to reach equilibration, as shown in Fig. 2. For all the solvent systems, once concentration plateaus were established, several values were determined at 2-day intervals to further ensure saturation. The procedure was repeated with new solutions. Dissolution profiles showed no evidence of hydrocortisone undergoing polymorphic transition or solvate formation. No decay products or impurities were detected by the HPLC assay. The specific HPLC assay ensured that only hydrocortisone was being quantified and ruled out the often troublesome complications associated with impurities.

Differential Thermal Analysis—The heat of fusion ΔH_f and the entropy of fusion ΔS_f were determined with a differential thermal analyzer[5] equipped with a standard cell attachment. A finely powdered, accurately weighed sample (1.5–2.0 mg) was spread evenly in a 40-μl aluminum crucible. A pinhole opening in the crucible lid allowed the sample to be in contact with the cell atmosphere of dry nitrogen with a regulated flow rate of 0.5 liter/min. An empty, sealed crucible served as a reference. Samples were heated at 5°/min. Heating curves were recorded at 5°/cm with a measuring range of 20 μV and recorder amplification of 100 mV. Calibration coefficients were determined with accurately weighed samples of indium. The molar heat of fusion was calculated from the area of the melting endotherm, moles of sample used, and the calibration coefficient. The entropy of fusion was obtained by dividing the heat of fusion by the absolute temperature of melting, T_f.

[4] Fluoropore, 0.22 μ, Millipore.

[5] Mettler DTA 2000.

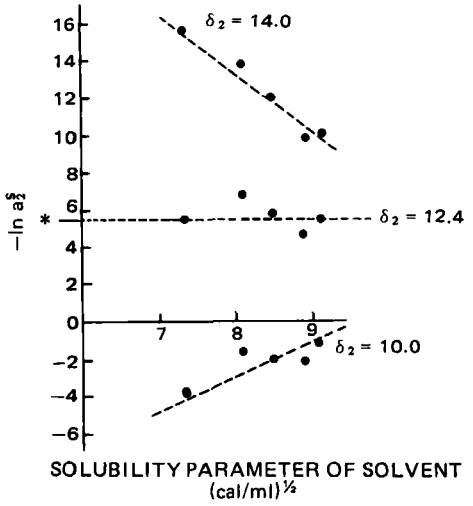

Figure 3—*Ideal solubilities of hydrocortisone (●) obtained from Eq. 14 for varying solute solubility parameters, δ_2. Key: * $-\ln a_2^s$ as calculated from crystalline properties (Table II).*

Melting Point—The melting point of hydrocortisone was determined by two methods: (*a*) controlled-heating thermal microscopy[6] and (*b*) differential thermal analysis. Heating rate for both methods was 5°/min.

RESULTS

Physical Properties—Hydrocortisone is a crystalline solid, which on heating from 25 to 220° undergoes only one thermal transition. This endothermal transition at 212° corresponds to the melting of the crystal. Hot-stage microscopy revealed no crystal morphology changes until melting. However, on cooling the melt below 212°, an amorphous glass was formed instead of the original crystalline solid. This occurrence may be, in part, the result of slight thermal decomposition within the melt. However, the sharpness and symmetrical shape of the endotherm suggest that thermal decomposition apparently is not contributing to the overall energy change during the melting phase. Moreover, melted samples assayed by HPLC showed only trace amounts of decay with essentially 100% retention of hydrocortisone. It is therefore concluded that the endotherm represents primarily energy consumed on melting. The ΔH_f for hydrocortisone is 8.1 kcal/mole and ΔS_f is 16.7 cal/deg mole. These values are averages from five determinations with $SD < \pm 5\%$. The experimental values for ΔH_f, ΔS_f, and T_f are also in good agreement with reported results (3).

A physical parameter that is necessary for solubility analysis is the molar volume of liquid solute. It has been demonstrated for several crystalline steroids that the molecular weight divided by the crystalline density can serve as a suitable molar volume estimate for the supercooled liquid solute (3). Since hydrocortisone has a crystalline density of 1.24 g/ml at 25° (9), the molar volume estimate is 293 ml/mole. An alternative means for estimating molar volume is by the summation of the partial molar volumes of a compound's functional groups (10). Applying this method to hydrocortisone (Table I), a molar volume of 319 ml/mole was obtained. This value is in reasonable agreement with the first estimate. The value of 293 ml/mole for the molar volume of supercooled liquid hydrocortisone will be used to be consistent with previously reported work (3).

The thermodynamic activity of crystalline hydrocortisone at 25° is 5.3×10^{-3}, as obtained from Eq. 7 with the experimental values for ΔH_f and T_f. The value of 5.3×10^{-3} thus represents the mole fractional ideal solubility for hydrocortisone. For a hypothetical solvent with molecular weight of 100 and density of 1.0 g/ml, the solubility of hydrocortisone would be 5.2×10^{-2} moles/liter or 18.9 mg/ml providing the two components formed an ideal mixture. These physical properties, summarized in Table II, are essential for the solubility analysis of hydrocortisone.

Solubility—The solubilities of hydrocortisone at 25°, experimentally determined in the present study, are presented in Table III along with the molar volumes and solubility parameters for the solvents. The solubility parameters for the pure solvents at 25° are taken from Hoy's tables

[6] Mettler Hot Stage with FP5 Temperature Regulator and a Zeiss Standard Microscope.

Table III—Solubilities of Hydrocortisone at 25°

Solvent	Molar Volume of Solvent[a], ml/mole	δ_1[a] (cal/ml)$^{1/2}$	Equilibrium Solubility mg/ml	Equilibrium Solubility moles/liter	Mole Fraction
Hexane	130	7.3	3.45×10^{-5}	9.53×10^{-6}	1.24×10^{-8}
2-Butyl acetate	132	8.0	1.48	4.08×10^{-3}	5.40×10^{-4}
Cyclohexane	108	8.2	8.23×10^{-4}	2.27×10^{-6}	2.24×10^{-7}
Carbon tetrachloride	97	8.6	1.00×10^{-2}	2.84×10^{-5}	2.75×10^{-6}
Isopropyl acetate	117	8.6	1.4	3.86×10^{-3}	4.53×10^{-4}
Ethyl acetate	98	8.9	2.82	7.76×10^{-3}	7.58×10^{-4}
Toluene	106	8.9	9.73×10^{-2}	2.68×10^{-4}	2.85×10^{-5}
Benzene	89	9.1	1.30×10^{-1}	3.59×10^{-4}	3.19×10^{-5}
Chloroform	80	9.2	4.08	1.12×10^{-2}	9.05×10^{-4}
Methyl acetate	79	9.5	5.88	1.62×10^{-2}	1.29×10^{-3}
Octanol	159	10.3	3.40	9.38×10^{-3}	1.49×10^{-3}
Propylene glycol	73	15.0	$1.68 \times 10^{+1}$	4.60×10^{-2}	3.38×10^{-3}
80% Propylene glycol in water	46[b]	16.5[b]	$1.32 \times 10^{+1}$	3.64×10^{-2}	1.68×10^{-3}
60% Propylene glycol in water	33[b]	18.2[b]	5.69	1.59×10^{-2}	5.20×10^{-4}
40% Propylene glycol in water	26[b]	19.8[b]	2.16	5.96×10^{-3}	1.54×10^{-4}
20% Propylene glycol in water	21[b]	21.4[b]	6.99×10^{-1}	1.93×10^{-3}	4.10×10^{-5}
Water	18	23.0	2.97×10^{-1}	8.19×10^{-4}	1.47×10^{-5}

[a] From Ref. 5 except where otherwise indicated. [b] Calculated from the method proposed in Ref. 6.

(10). Values for the cosolvent mixtures of propylene glycol and water were estimated from the expression of Smith *et al.* (11):

$$\delta_{1\text{-}3} = \frac{\phi_1\delta_1 + \phi_3\delta_3}{\phi_1 + \phi_3} \qquad \text{(Eq. 13)}$$

where the subscripts 1 and 3 denote the respective pure solvent parameters and ϕ is the corresponding volume fraction. The validity of the above expression has been demonstrated with binary solvent systems only capable of interacting through London forces (11). Use of the equation must be tentative for mixtures of propylene glycol and water as the molecular interactions of hydrogen bonding and dipole–dipole attractions for those mixtures have yet to be fully delineated.

The solubility parameter scale does provide one indication of the wide range of solvents used for these studies. The solubility parameter for propylene glycol falls roughly between that for hexane [7.3 (cal/ml)$^{1/2}$] and water [23 (cal/ml)$^{1/2}$], which represent the extremes for this solvent scale. Hydrocortisone is extremely insoluble in hexane 9.53×10^{-8} moles/liter and poorly soluble in water 8.19×10^{-4} moles/liter. The maximum molar solubility determined was with propylene glycol 4.63×10^{-2}. The solubility span for hydrocortisone in the evaluated solvents was $>10^5$. Interestingly, all solubility values are below the estimated ideal solubility and are sufficiently low to negate solute–solute interactions.

DISCUSSION

Regular Solution Analysis—It should be mentioned at the onset of this discussion that regular solution behavior, as carefully defined by Hildebrand *et al.* (12), is used as a secondary reference point for the solubility analysis of hydrocortisone. The primary reference point is ideal solution behavior. It is recognized *a priori* that the underlying theory is inapplicable where there is significant hydrogen bonding either between like or unlike species, solute or solvent. However, regular solution behavior provides a norm from which deviations from ideality, other than those derived from differential cohesiveness, can be measured.

Regular solution theory predicts a parabolic relationship between the mole fractional solubility of a given solute and the solubility parameters for solvents which span the solute's value. For a solid solute in equilibrium with its saturated solution, the regular solution solubility is given by Eq. 12. The theoretical maximum solubility is considered to be the ideal solubility where the cohesive energy differential between solute and solvent is zero. In other words, a positive excess enthalpy of mixing and a solubility less than ideal is always associated with regular solution behavior. Solvents were selected which interact within themselves and with hydrocortisone predominantly through London forces, allowing regular solution theory to be applied. Hexane, cyclohexane, carbon tetrachloride, benzene, and toluene were considered appropriate to test the hypothesis that the solubilities of a solute like hydrocortisone would conform to regular solution behavior in apolar solvents. The saturated solutions of hydrocortisone in these solvents are sufficiently dilute to preclude any appreciable solute–solute bonding. The predominant factor contributing to solution phase interaction is London forces. This is also true for cohesion of the pure liquids. The forces binding hydrocortisone in the

Table IV—Estimation of Solubility Parameter for Hydrocortisone[a]

Functional Group	$(EV)^{1/2}$, (cal/ml)$^{1/2}$	Number of Groups	Total $(EV)^{1/2}$ per Group[b], (cal/mol)$^{1/2}$
CH_3	148.3	2	296.6
CH_2	131.5	8	1052.0
—CH<	85.9	4	343.9
>C<	32.0	3	96.0
—CH=	121.5	1	121.5
>C=	84.5	3	253.5
C=O	263.0	2	526.0
OH	226.0	3	678.0
6-Membered ring	−23.4	3	−70.2
5-Membered ring	20.9	1	20.9

[a] $\delta_2 = \frac{(EV)^{1/2}}{V_2} = \frac{3318.2 \text{ (cal/ml)}^{1/2}}{293 \text{ ml}} = 11.4 \text{ (cal/ml)}^{1/2}$. [b] Total $(EV)^{1/2}$ for a mole of hydrocortisone = 3318.2 (cal/ml)$^{1/2}$.

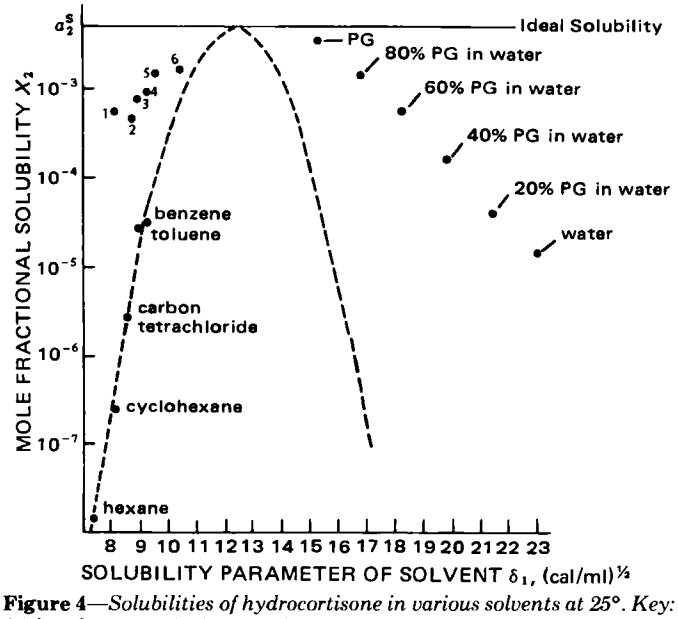

Figure 4—*Solubilities of hydrocortisone in various solvents at 25°. Key: (1) butyl acetate, (2) isopropyl acetate, (3) ethyl acetate, (4) chloroform, (5) methyl acetate, (6) octanol, and (PG) propylene glycol. The dotted line represents the regular solution parabola $\delta_2 = 12.4$ (cal/ml)$^{1/2}$.*

hypothetical supercooled liquid state are indeterminate but are presumed to have significant contributions from hydrogen and dipolar bonding.

Since the net interactions in the hydrocortisone melt include hydrogen bonding, which precludes totally random orientations of its molecules, one primary element required for regular solution behavior is missing. There is an excess entropy of mixing implicitly associated with the freeing of the hydrocortisone molecules from bonds restricting their relative motions and positions in the supercooled liquid state. However, regular solution behavior for alkyl-*p*-aminobenzoate homologues (4), which suffer the same theoretical departure, is followed closely for such polar, highly interactive solutes as long as the solvent is strictly apolar. In essence, it seems that potential sources of deviation from regular solution behavior, especially associated with disintegration of the polar solute melt structure, are insignificant against the excess free energy derived from differential cohesiveness. Thus, for the alkyl-*p*-aminobenzoates there are operative solubility parameters, likely related to the true square root cohesive energy densities, which adequately describe their solubilities in hexane. The present work is, in part, an attempt to examine the behavior of hydrocortisone, an even more complex molecular structure, in this regard. The study differs in an important way from the previous study (alkyl-*p*-aminobenzoates) in that the behavior is examined across diverse solvents and not with respect to solute structure within a fixed solvent.

To evaluate the proposed regular solution behavior for hydrocortisone, the following were assumed:

1. The crystalline properties of hydrocortisone were invariant from solvent to solvent such that the activity of the solid phase was the same in each.
2. The volume fraction for each solvent (ϕ_1) was unity.
3. The molar volume of hydrocortisone is 293 ml/mole at 25° and is independent of the solvent.

With the above assumptions and implicit simplifications, Eq. 12 is rewritten as follows:

$$\ln X_2 = \ln a_2^s - 0.5(\delta_1 - \delta_2)^2 \qquad \text{(Eq. 14)}$$

for a saturated solution of hydrocortisone at 25°. Providing the choice of solvents is satisfactory, a_2^s and the solubility parameter for hydrocortisone δ_2 can be simultaneously determined from the mole fractional solubilities of hydrocortisone in the specified solvents. The value of a_2^s, moreover, should be consistant with the value of 5.2×10^{-3} obtained from ΔH_f and T_f.

Values ranging from 7 to 23 $(cal/ml)^{1/2}$ for δ_2 were evaluated using Eq. 14 to determine δ_2 where a_2^s is most constant. Figure 3 shows $\ln a_2^s$ *versus* the solubility parameter of the solvent for three selected values for γ_2. As seen in the graphical display, a_2^s appears most constant for a δ_2 value of 12.4 $(cal/ml)^{1/2}$; however, there is scatter in the data, and based solely on this analysis, the value of δ_2, at best estimate, can be considered to lie between 12 and 13 $(cal/ml)^{1/2}$. The value of 12.4 $(cal/ml)^{1/2}$ for δ_2 predicts a_2^s to be 5.5×10^{-3} which is in excellent agreement with a_2^s as calculated from ΔH_f and T_f. Furthermore, the dashed lines in Fig. 3 show the calculated deviation in a_2^s if the solubility parameter is in fact 12.4 $(cal/ml)^{1/2}$ for hydrocortisone, but was assumed to be either 10 or 14 $(cal/ml)^{1/2}$. While each of these approaches for estimating the solubility parameter has an inherent uncertainty when considered alone, when combined they indicate a solubility parameter of hydrocortisone of 12.4 $(cal/ml)^{1/2}$. This value is consistent with minimum variability in the corresponding a_2^s values from Eq. 14 and has good agreement with a_2^s as independently predicted from crystalline properties Eq. 7.

The functional-group contribution approach provides another way of estimating the solubility parameter for hydrocortisone. In this case, the molar attraction constants for the solute functional groups are summed as originally proposed by Small (13). Using the updated molar attraction constants tabulated by Hoy (10), the solubility parameter for hydrocortisone was estimated to be 11.4 $(cal/ml)^{1/2}$, as outlined in Table IV. This estimate differs significantly from the experimental value of 12.4 $(cal/ml)^{1/2}$. The discrepancy is not unexpected, since there is little evidence that the functional-group contribution approach is suitable for such a large, polyfunctional solute, and its use for hydrocortisone likely represents an overextention of the method.

Flory–Huggins Excess Entropy of Mixing—As previously defined, regular solution theory assumes the entropy of mixing to be an ideal in which the entropy of the process arises strictly from the statistical mixing of the components. A factor not yet considered in the regular solution analysis for hydrocortisone is the inability to statistically mix molecules of unequal size. Flory (14) and Huggins (15) have considered the excess entropy associated with the mixing of molecules of unequal size. A model was designed for dilute solutions with a small molecular volume solvent and a large, polymer solute. The mixing of a liquid polymer with a solvent

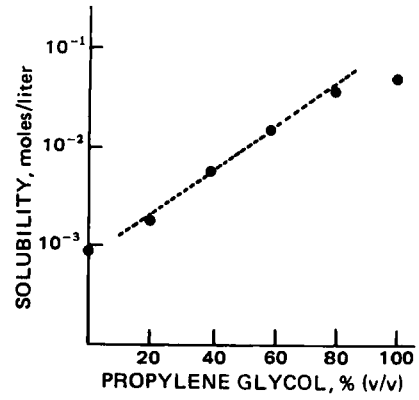

Figure 5—*Solubility of hydrocortisone in propylene glycol–water mixtures at 25°.*

to make a dilute solution with respect to the polymer leads to the total number of possible configurations for the polymer being greatly increased over what exists in the pure polymer state. This large increase in configurational entropy of mixing is expressed in the following equation for the excess free energy of mixing:

$$\Delta G^E = RT[X_1 \ln (\phi_1/X_1) + X_2 \ln (\phi_2/X_2)] \qquad \text{(Eq. 15)}$$

This expression was derived for long-chain molecules with individual segments occupying sites within a liquid lattice consisting of small solvent molecules. This factor should be an additive (independent) function. With this factor incorporated, the general regular solution solubility equation becomes:

$$\ln X_2 = \ln a_2^s - \frac{\phi_1^2 V_2}{RT}(\delta_1 - \delta_2)^2 - [\ln V_2/V_1 + 1 - V_2/V_1] \qquad \text{(Eq. 16)}$$

The validity of the Flory–Huggins model has not been established for compact molecules in a solvent composed of molecules smaller by only several multiples. It has been pointed out (16) that such an evaluation for compact molecules is difficult since possible entropy effects are often obscured by large changes in the enthalpy of mixing. The analysis of the excess entropy due to inequality of size for hydrocortisone appears to be confounded by this difficulty. The hydrocortisone–solvent molar volume ratio, V_2/V_1, is only 2.25–3.28 for those solvents considered for regular solution behavior. To evaluate the impact of the Flory–Huggins entropy correction on the regular solution analysis of hydrocortisone, the appropriate parameters were introduced into Eq. 16, and δ_2 was determined as before. The correction term did not significantly affect the estimation of δ_2, within the sensitivity of the analysis. Thus, the entropy arising from disparate molecular size does not appear to be significant as a solubility-determining factor for these hydrocortisone–solvent systems. This conclusion agrees with the observations of Shinoda and Hildebrand (16) as well as Bowen and James (8), who also noted little or no Flory–Huggins effect for mixtures of nonpolymeric substances of unequal size.

Solubility Profile—The values for the physicochemical properties of hydrocortisone utilized in the subsequent discussion are found in Table II. With appropriate substitution of the above parameters into Eq. 12, the regular solution solubility parabola was calculated for hydrocortisone about the midpoint of 12.4 $(cal/ml)^{1/2}$, where the solution is considered ideal. As expected, the solubilities of hydrocortisone in solvents essentially limited to dispersion molecular interactions conform closely to the curve Fig. 4. These solvents are hexane, cyclohexane, carbon tetrachloride, toluene, and benzene.

Regular solution theory predicts a 50-fold difference in molar solubility between hexane and cyclohexane, and this difference is observed experimentally. However, the inappropriateness of regular solution theory for solvents other than those of the London type is also demonstrated in Fig. 4. It appears inadequate for solubility estimation in all solvents capable of hydrogen bonding or other strong, orientating bonding with hydrocortisone. For example, the experimental solubility of hydrocortisone in isopropyl acetate is nearly 100 times the predicted value. There is also a 20-fold factor unaccounted for by regular solution theory between the solubilities in carbon tetrachloride, a perfectly symmetrical and apolar species, and chloroform, which has a substantial dipole. Thus, for isopropyl acetate, chloroform, and similar solvents, dipole–dipole and hydrogen bonding must contribute significantly to the solution-phase interactions.

The regular solution parabola predicts a solubility of hydrocortisone

in water, where $\gamma_1 = 23.4$ (cal/ml)$^{1/2}$, $\sim 10^{21}$ times less than the observed value. Clearly, simple differential cohesiveness is grossly inadequate to account for the specific intermolecular forces between water and hydrocortisone. Having two ketone moieties and three hydroxyl groups, hydrocortisone is capable of forming hydrogen bonds with water around these centers, which greatly favor its solubility. Contrastingly, the hydrocarbon skeleton and attached methyl groups provide surfaces for hydrophobic association with water, which is unfavorable to solubility. The net results of these additional solution-phase interactions is a large reduction in the excess free energy of transfer of a mole of supercooled liquid hydrocortisone to water. Hence, the solubility in water is orders of magnitude higher than would be expected from the noncritical use of regular solution theory, taking the solubility parameter of water at face value. It should be noted that the solubility parameter of water as a square root cohesive energy density is, in the absolute sense, a legitimate value. However, it can not be used in regular solution treatments because the general behavior of water violates the fundamental assumptions of this theory.

The incremental addition of propylene glycol to an aqueous propylene glycol solvent system is marked by an exponential increase in hydrocortisone solubility and log (solubility) increases roughly linearly with increasing volume fraction of propylene glycol (Fig. 5). This solubility pattern can be compared with the following linear free energy function:

$$\log S_f = \log S_{f=0} + \epsilon f \qquad \text{(Eq. 17)}$$

where ϵ is the incremental change in solubility per volume fraction (f) added. The actual cosolvent profile for hydrocortisone, however, has a slight sigmoidal shape which is most apparent at low and high concentration of propylene glycol. Nevertheless, an estimate for ϵ of 2.1 was obtained from regression analysis with the values for water and propylene glycol excluded because they were out of the linear region. The estimate of ϵ corresponds to an ~100-fold increase in solubility from water to pure propylene glycol, somewhat greater than actually observed.

A similar linear trend is shown in Fig. 4 for log S_f *versus* the solubility parameter estimates for the cosolvent mixtures as calculated from Eq. 12. It might appear that the cosolvent trend is a direct outcome of differential cohesiveness. This would, however, be a superficial and incorrect conclusion. Water, propylene glycol, and their mixtures are extensively hydrogen-bonded systems. Although the experimental cohesive energy densities for these solvents are meaningful as relative measures of the forces of association in the pure liquids, they are meaningless with respect to regular solution calculations. Regular solution theory requires that no significant orientating bonding can occur between solute and solvent, pure solvent, and pure liquid solute. This requirement allows the cohesive energy density of the solute–solvent mixture, C_{12}, to be approximated by $(C_{11}, C_{22})^{1/2}$. These conditions are violated as a consequence of the hydrogen bonding networks in water, propylene glycol, and their mixtures. Based on literature data which indicate that the aqueous solubility of substantially hydrophobic molecules is proportional to the low-energy molecular surface area (17) and that the sensitivity of homologue solubilities in aqueous mixtures is a function of the hydrocarbon chain length (18), it would appear that the solubility trend of hydrocortisone in propylene glycol–water mixtures is principally due to a dilution of the hydrophobically induced self-association of water.

REFERENCES

(1) G. Scathard, *Chem. Rev.*, **8**, 321 (1931).

(2) J. H. Hildebrand, *J. Am. Chem. Soc.*, **41**, 1067 (1919).

(3) A. S. Michaels, P. Wong, R. Prather, and R. Gale, *AIChE J.*, **21**, 1073 (1975).

(4) S. Yalkowsky, G. L. Flynn, and T. Slunick, *J. Pharm. Sci.*, **61**, 852 (1972).

(5) F. A. Restaino and A. Martin, *ibid.*, **53**, 636 (1964).

(6) G. A. Lewis and R. P. Enever, *Int. J. Pharm.*, **3**, 275 (1979).

(7) K. C. James and M. Roberts, *J. Pharm. Pharmacol.*, **20**, 709 (1968).

(8) D. B. Bowen and K. C. James, *ibid.*, **22**, 104 (1970).

(9) "The Merck Index," 9th ed., Merck and Co., Rahway, N.J., 1976.

(10) K. Hoy, *J. Paint Technol.*, **42**, 76 (1970).

(11) E. Smith, J. Walkley, and J. Hildebrand, *J. Phys. Chem.*, **63**, 703 (1950).

(12) J. H. Hildebrand, J. Prausnitz, and R. Scott, "Regular and Related Solutions," van Nostrand, New York, N.Y., 1970.

(13) P. A. Small, *J. Appl. Chem.*, **3**, 71 (1953).

(14) P. Flory, *J. Chem. Phys.*, **9**, 660 (1941).

(15) M. Huggins, *ibid.*, **9**, 440 (1941).

(16) K. Shinoda and J. H. Hildebrand, *J. Phys. Chem.*, **69**, 605 (1965).

(17) G. L. Amidon, S. Yalkowsky, and S. Leung, *J. Pharm. Sci.*, **63**, 1858 (1974).

(18) S. Yalkowsky, G. L. Amidon, G. Zografi, and G. L. Flynn, *ibid.*, **64**, 48 (1975).

ACKNOWLEDGMENTS

Abstracted in part from a thesis submitted by T. A. Hagen to the University of Michigan in partial fulfillment of the Doctor of Philosophy degree requirements.

Phenomenological Viscoelasticity of a Heterogeneous Pharmaceutical Semisolid

GALEN W. RADEBAUGH * AND ANTHONY P. SIMONELLI ˣ

Received April 5, 1982 from the *College of Pharmacy and Institute of Materials Science, University of Connecticut, Storrs, CT 06268.* Accepted for publication July 15, 1982. *Present address: Department of Pharmaceutics, Smith Kline and French Laboratories, Philadelphia, PA 19101.

Abstract □ This study presents the results of an investigation of the viscoelastic properties of anhydrous lanolin USP, as determined by dynamic mechanical testing. The elastic shear modulus (G'), viscous shear modulus (G''), and loss tangent ($\tan \delta$) were determined as a function of shear frequency, ν, (0.01–10.0 Hz) and temperature, T, (0–30°). These viscoelastic parameters were found to be temperature and shear frequency dependent. Up to 100-fold changes in shear moduli and $\tan \delta$ values were observed with appropriate changes in T and ν. Many of the observed properties are also characteristic of high molecular weight polymers and can be attributed to a high degree of molecular structure. It was found that dynamic mechanical testing was a sensitive tool for measuring structural changes, and was especially useful in detecting a major structural transition well below the accepted melting temperature of anhydrous lanolin.

Keyphrases □ Viscoelasticity—properties of anhydrous lanolin, determination by dynamic mechanical testing □ Lanolin, anhydrous—viscoelastic properties as determined by dynamic mechanical testing □ Dynamic mechanical testing—determination of viscoelastic properties of anhydrous lanolin

The rheology of pharmaceutical semisolids can not be understood adequately without including a discussion of viscoelastic properties. The viscoelastic properties of pharmaceutical semisolids have not been adequately investigated because pharmaceutical scientists generally lack the appropriate testing equipment. Much of the existing literature on the measurement of viscoelasticity of pharmaceutical systems, including the use of dynamic mechanical testing, has been reviewed (1). It was apparent that dynamic mechanical testing could yield unique information that could not be obtained by other available methods, and that it was important that the application of dynamic mechanical testing to measure the viscoelastic properties of pharmaceutical systems be investigated and demonstrated. For this reason this study was undertaken using anhydrous lanolin.

Dynamic mechanical testing has been used primarily by materials scientists to characterize the viscoelastic properties of polymeric systems (2, 3). For example, polymers are routinely characterized for moduli, crystallinity, plasticizer effectiveness, filler effects, creep, and stress relaxation. A knowledge of these viscoelastic properties is necessary to determine proper manufacturing techniques and end-use properties of polymeric systems.

Many rheological testing procedures used by pharmaceutical scientists are insensitive to the microcrystalline or amorphous three-dimensional networks which determine basic rheological properties. Generally, these methods use a simple shear viscometer and determine a non-Newtonian viscosity (4–6). Simple shear methods destroy the structure that one is attempting to measure and introduce the additional parameter of structural variation with time. As a result, simple shear viscometers are unable to measure fundamental viscoelastic parameters such as elastic and viscous moduli (7, 8).

This report describes the nondestructive technique, dynamic mechanical testing, and the results obtained when it was used to measure the viscoelastic properties of anhydrous lanolin. Test samples were deformed sinusoidally with respect to time and temperature, and measurements of the strain amplitude, stress amplitude, and phase angle between them were made in terms of the complex dynamic modulus. The complex dynamic modulus was then resolved into a real component (elastic or storage modulus) and an imaginary component (viscous or loss modulus.) The elastic modulus is associated with the energy stored in elastic deformation, while the viscous modulus is associated with energy dissipation effects. These moduli were used to interpret the viscoelastic behavior of anhydrous lanolin in terms of the inter- and intramolecular interactions within the semisolid.

BACKGROUND

Phenomenological Viscoelasticity—The deformation of semisolids can be divided arbitrarily into two general types: spontaneously reversible deformation (called elasticity) and irreversible deformation (called flow). Most pharmaceutical semisolids exhibit both of these phenomena and are rheologically classified as viscoelastic. Phenomenological viscoelasticity can be categorized as either linear or nonlinear, but only the former can be described theoretically with uncomplicated mathematics. The fundamental viscoelastic parameters of a linear viscoelastic system do not depend on the magnitude of the stress (or strain) and the time during which it acts; the parameters for a nonlinear viscoelastic system are dependent on stress and/or strain magnitude. Complex constitutive equations are necessary to describe nonlinear viscoelasticity (9–11).

When the input strain on a test sample is small, the strain (γ) is proportional to the stress (σ) and the sample exhibits linear viscoelasticity. Though stress and strain are proportional, they are not in phase; in addition to moduli, a phase angle or damping term is determined. The elastic modulus (G'), viscous modulus (G''), complex modulus (G^*), and phase angle (δ) are a function of shear frequency (ν) and temperature (T). For shear experiments, frequency can also be expressed in terms of radians per second (ω) where ω equals $2\pi\nu$.

Linear viscoelasticity also means that the rheology must obey the Boltzmann superposition principle (2, 12). This principle states that mechanical behavior is a function of the entire stress history of a sample. It also assumes that the effect of each deformation is independent of the others, and that the behavior of the sample can be calculated by a simple addition of the effects that would occur if the deformations took place singly.

Most theoretical treatments of dynamic mechanical testing and linear viscoelasticity use stress as the forcing function, though either stress or strain may be used. Both methods are mathematically equivalent. A theoretical treatment of the mathematics of linear viscoelasticity is given in *Appendix I*. Two important relationships are derived therein which relate G^*, G', G'', and $\tan \delta$:

$$G^* = G' + iG'' \qquad \text{(Eq. A11)}$$

and

$$\tan \delta = G''/G' \qquad \text{(Eq. A15)}$$

where $\tan \delta$ is equal to the ratio of the energy dissipated–maximum energy stored per cycle of deformation.

0022-3549/83/0400-0415$01.00/0

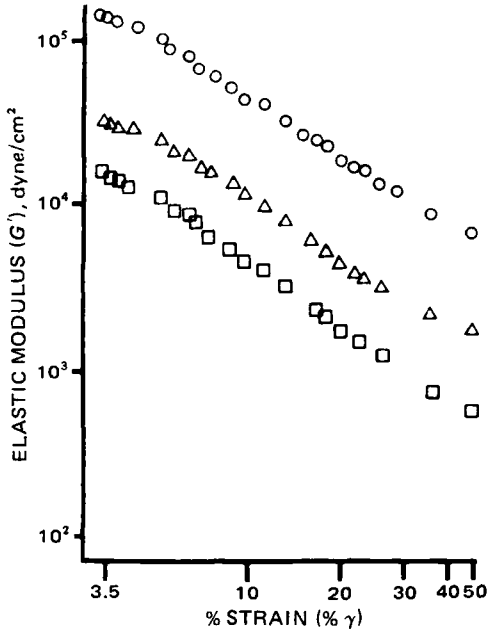

Figure 1—*Effect of shear strain on the elastic modulus of anhydrous lanolin USP, at 20°. Key: (○) 10.0 Hz, (△) 1.0 Hz and (□) 0.10 Hz.*

The relationship of tan δ and G'' to energy dissipation is fundamental to proper interpretation of dynamic mechanical data. A system with high values of tan δ exhibits high energy dissipation and is termed high damping or lossy. The significance of various transitions of a system depend on the location and intensity of the damping peaks, where tan δ or G'' is a maximum. The associated maximum in energy dissipation is interpreted in terms of an accountable increase in internal freedom, such as molecular segmental and side group motion or chain rotation. These changes can identify chemical or mechanical transitions.

Chemical Nature of Anhydrous Lanolin USP—Anhydrous lanolin, or wool fat, is designated by the USP to contain not more than 0.25% water (13). It is prepared by the purification of fatty matter (suint) obtained from the wool of sheep. The chemical composition of anhydrous lanolin is complex and can vary with the type of sheep (14). Conrad (15) and Barnett (16) have elaborated extensively on lanolin chemistry.

Anydrous lanolin is chemically a wax and not a fat. It melts between 36 and 42°. In general, it contains trace amounts of hydrocarbons and free fatty acids, 3–4% free alcohols (mostly cholesterol), and 96% wax esters. Saponification of the wax esters gives a free lanolin alcohol fraction and a free fatty acid fraction. The free alcohol fraction is composed of aliphatic, sterol, triterpene, and unclassified alcohols in approximately equal proportions. The free fatty acid fraction is composed of ~10% normal acids (n = 4–12), 4% hydroxy acids (n = 6, 7), 29% iso acids (n = 3–11), 38% anteiso acids (n = 2–13), and 19% unclassified acids.

From this information, anhydrous lanolin can be typified as a mixture of wax esters with a chemical structure much like a cholesterol molecule linked to a long-chain alcohol molecule. It can be postulated that 99% of the molecules in anydrous lanolin have a molecular weight in the range of 400–950, with an average of ~700.

EXPERIMENTAL

Materials and Apparatus—The anhydrous lanolin USP used for all experiments was from the same production lot[1]. The viscoelastic properties of anhydrous lanolin were determined with a mechanical spectrometer[2]. This rotational rheometer puts into a test sample a known deformation at a specified rate and temperature (17).

Samples of anhydrous lanolin were mounted between 50-mm diameter, hollow stainless steel cone and plate test fixtures. The cone fixture was oscillated sinusoidally at determined shear strains (γ) and frequencies (ν) by the output from a digital function generator and phase analyzer[3] (FGPA). Stresses from the sample were transmitted through the fixed plate to a multiple-stress detecting transducer. Deflections in the transducer were converted to electrical signals and relayed back to the function generator and analyzer, where they were resolved into the storage and loss components of the complex modulus. The digital outputs of the FGPA were used to calculate the dynamic moduli in terms of dyne/cm² (*Appendix II*).

Temperature control was maintained by enclosing the sample and test fixtures in an environmental chamber[4]. The chamber used high-velocity recirculated air and nichrome heating coils. A platinum resistance bulb temperature sensor, located close to the test sample, maintained temperature to ±0.5°. Temperatures below the ambient were achieved by placing solid carbon dioxide into the chamber, in the path of circulating air on the side of the sample away from the direction of flow. Excess temperature reduction was prevented by the heating coils. Chamber temperature was monitored by placing an iron–constantan thermocouple with digital readout in the path of circulating air, immediately upstream of the sample. The chamber was equipped also with a light and window for sample observation.

Differential thermal analysis[5] was used to look for structural transitions in anhydrous lanolin. This thermoanalytical technique is often useful in detecting crystallization and crystalline and glass transitions.

Sample Preparation—Anhydrous lanolin was placed in a beaker and lowered into a hot water bath at 50°. After melting, the molten lanolin was placed into a desiccator which was evacuated by a filter pump to remove entrapped air from the samples. Deaerated samples were poured onto the flat test fixture, in a manner preventing air pocket formation. After 30 min at room temperature, the plate was mounted and the cone lowered to the preset gap. Extruded lanolin was removed and the sample was allowed to equilibrate at the test temperature for 15 min.

Description of Experiments—Samples were equilibrated at 0, 5, 10, 15, 20, 25, and 30°. At each temperature, a sample was oscillated over three decades of ν, 0.01–10.0 Hz, at γ equal to 3.54%[6]. Readouts of the FGPA were used to calculate G', G'', and tan δ as a function of ν and T.

For differential thermal analysis, a sample in an aluminum pan and an empty identical reference pan were heated. A liquid nitrogen chamber was used to lower the initial temperature to −40°. The difference in T between the sample and the reference pan was recorded as function of T_r, the temperature of the reference cell.

RESULTS AND DISCUSSION

The dynamic mechanical properties of anhydrous lanolin were determined as a function of shear strain, frequency, and temperature.

Effects of Strain—The relationship between G' and γ, at 25°, is shown in Fig. 1. There is no apparent range of linear viscoelastic behavior over the entire range of γ studied (3.54–50.0%). Linear behavior would be identified as a region of constant G' with changing γ. Since linear viscoelastic behavior could not be achieved, the lowest obtainable γ (3.54%) was used in all experiments to ensure the least possible effect on molecular structure.

Because of observed nonlinear behavior, it may be said that the test samples in this study were not in their absolute rheological ground state. It has been reported that at least 24 hr were necessary for stresses produced in anhydrous lanolin by sample loading to relax prior to creep testing (18). In this study, it was not feasible to permit each sample to relax 24 hr before testing.

Even though the mechanical spectrometer was not able to reach a low enough γ to achieve linear behavior, it must be noted that the decline of G' with increasing γ is apparently a continuously smooth relationship, devoid of breaks or irregularities in the curve. Hence at any given γ, it can be assumed that there exists a small region around the corresponding point on the log G' *versus* log %γ curve where linear viscoelastic behavior can be approximated. This is particularly true at low γ where the slope has significantly decreased. Therefore, an infinitesimal increase or decrease in deformation gives a negligible change in the value of log G'. This justification for the use of linear viscoelastic theory to calculate dynamic moduli is reasonable and is commonly used in the literature.

Data Reproducibility—Since it was believed that the samples of anhydrous lanolin were not in a rheological ground state, and since reproducible data can only be obtained from reproducible structural states, it was necessary to examine data reproducibility. It was found that defined differences in sample mixing, setting time, and temperature equilibration time were found to produce differences in FGPA "a" and

[1] Ruger Chemical Co. Inc., Irvington-on-Hudson, N.Y.
[2] Model RMS-7200, Rheometrics, Inc., Union, NJ 07083.
[3] Model SA-2200, Rheometrics, Inc., Union, NJ 07083.
[4] Model EC-1000, Rheometrics, Inc., Union, NJ 07083.
[5] Dupont Model 990.
[6] Percentage shear strain is defined as 100 × amplitude of oscillation/cone angle.

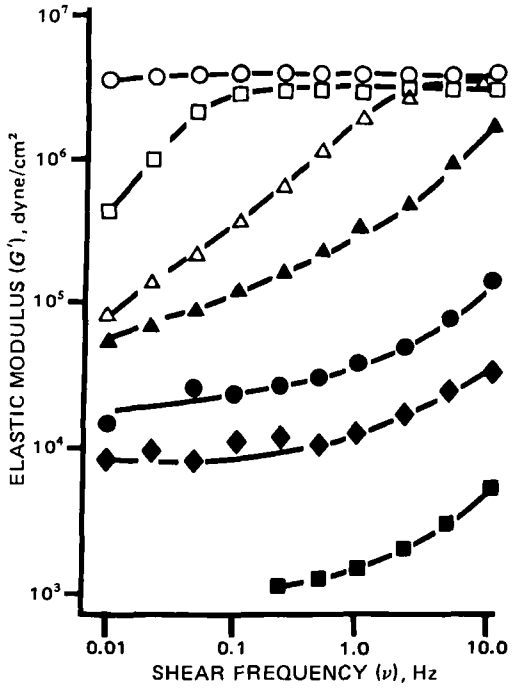

Figure 2.—*Effect of shear frequency on the elastic modulus of anhydrous lanolin USP, at 3.54% strain. Key: (○) 0°, (□) 5°, (△) 10°, (▲) 15°, (●) 20°, (◆) 25°, and (■) 30°.*

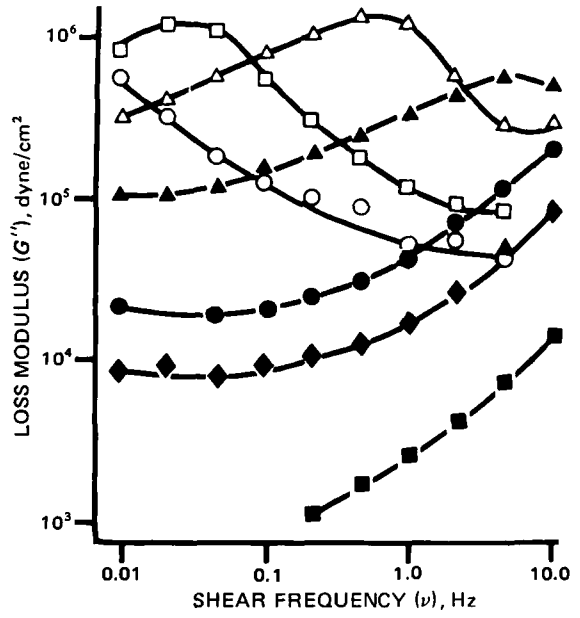

Figure 3.—*Effect of shear frequency on the viscous modulus of anhydrous lanolin USP, at 3.54% strain. Key: (○) 0°, (□) 5°, (△) 10°, (▲) 15°, (●) 20°, (◆) 25°, and (■) 30°.*

"b" outputs. Differences in observed moduli of up to 50% could be produced by exacerbated variations in sample preparation, loading, and equilibration. For that reason, care and practice were necessary to master the aforementioned sample preparation techniques before reproducible data could be obtained with confidence. It should be noted that variations of as much as ±10% in G' were tolerable as this would be small when compared with changes in G' due to temperature and shear frequency.

Effects of Temperature and Shear Frequency—From the log G' and log G'' *versus* log ν plots (Figs. 2 and 3) it is evident that ν and T are profound determinants of the viscoelastic behavior of anhydrous lanolin. In general, an increase in T causes a decrease in G', while an increase in ν causes an increase in G'. The effect of T and ν on G'' are not as simple to describe, as a maximum appears in some of the curves. If one assumes that a maximum exists in all of the curves, it can be stated that the maximum ν is increased with an increase in T. The patterns of change of G' and G'' with T and ν are characteristic and will be discussed in terms of proposed molecular changes. Figure 2 shows that an increase in ν increases G' over the temperature range of 30–25°. At 25°, this trend is modified by the formation of a plateau at the high end of the frequency spectrum. The extent of this plateau expands with decreasing T until it extends over the entire frequency spectrum at 0°.

In this plateau region, G' asymptotes to a limiting modulus, G_E. When this limiting value is attained, it can be concluded that the molecular chains are not able to rearrange themselves at all during the time of stressing. The molecules appear frozen and the only deformation is by distortion of primary and secondary bonds and bond angles. Such a limiting modulus is also observed for polymers in the glassy state (*i.e.*, at low temperatures).

Barlow and Lamb (19) gathered data of G_E for a number of organic compounds. These included glycerol, polytetrafluorethylene, 1,2,6-hexanetriol, 1,3-butanediol, and vulcanized and unvulcanized rubber. All of the G_E values for these substances were within a factor of two of 2×10^{10} dyne/cm^2, even though these compounds represent a molecular weight distribution from 90 to $>10^6$. These values can be compared with crystalline solids which generally have rigidity moduli between 10^{11} and 10^{12} dyne/cm^2. The values of G_E for the organic compounds studied by Barlow and Lamb are probably lower because they are not subject to the constraints of a crystal lattice. It was noted that the introduction of strong polar groups, hydrogen bonding, or polymerization generally caused increases in G_E, but these increases were small when compared with the magnitude of G_E. Hence it was suggested that the straining of van der Waals bonds and the flexing of main chain bonds are the origin of G_E as these phenomena are relatively independent of structure for polymers.

The value of G_E for anhydrous lanolin is $\sim 5 \times 10^6$ dyne/cm^2, a factor of 4×10^3 less than the values observed by Barlow and Lamb. This difference indicates that it may not be appropriate to refer to anhydrous lanolin as being in the glassy state. It must be noted that G_E was not reached for the listed organic compounds until T approached the vicinity of −80°. Hence, the plateau attained from 0 to 5° for anhydrous lanolin may not represent G_E, but instead a plateau in the rubbery region. Further testing at T <0° may show a rise in G' until another plateau is attained at lower T. This assumption is reasonable when one considers the fact that anhydrous lanolin is an organic mixture with an average molecular weight of ~700, which is within the range of molecular weights listed by Barlow and Lamb.

The appearance of the nonglassy state plateau between 0 and 5° can be explained on the basis that anhydrous lanolin is a complex mixture with each constituent having its own melting point. So at a given temperature, some fractions may be solid and others liquid. The solid fractions then act as a rigid matrix to give structure with the liquid fractions dispersed in its rigid matrix. Consequently, one could speculate that, from 0 to 5°, the solid matrix is sufficiently rigid to enable its elastic characteristic to mask any temperature-dependent contribution of the liquid fraction. Since the glassy state observed in the Barlow and Lamb work exhibited a considerably greater G_E at lower temperatures, it would be expected on the basis of this model that the contribution of the liquid fraction to G' would become evident as the temperature is lowered below 0° giving rise to an increase in G' until reaching the glassy state plateau.

Figure 3 shows that G'' behaves similarly to G' from 30 to 20°. At 15° however, a rounded peak appears between 2.15 and 10.0 Hz. With each successive drop in T, the location of the peak shifts horizontally to lower ν until, at 0°, the peak has apparently shifted to a ν below the range of frequency testing. The variation of G'' as opposed to G' is difficult to visualize in terms of molecular processes because it is basically a feature of a dynamic rather than a static response.

When ν is low, the molecules can rearrange themselves completely within the time scale of stressing. At maximum γ, energy is stored in the system by virtue of entropy effects. During the portion of the cycle in which σ decreases to zero, the stored strain energy is recovered elastically because the molecules rearrange faster than σ changes. Since the strain energy is almost completely elastically recoverable at low ν, the energy loss is small. Consequently G'' is small. On the other hand, G'' is small at high ν because the molecules are frozen in place and only pure elastic deformation occurs. G'' increases at intermediate ν because the molecules have time for only partial configurational rearrangement during a cycle of stressing.

At this point, it is necessary to consider the energetics responsible for the variation of dynamic moduli as a function of shear frequency and temperature. Aspects of this discussion have their foundation in the idea

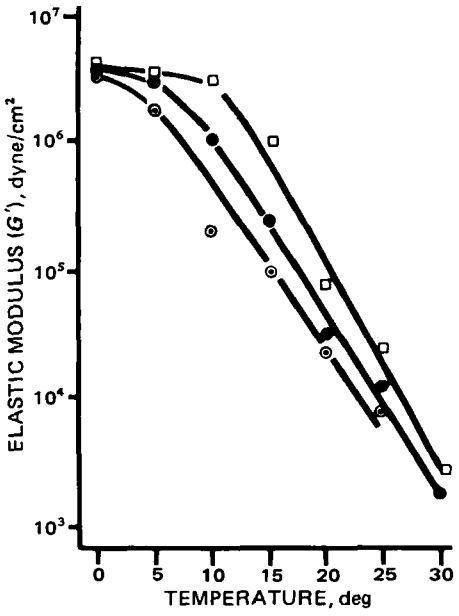

Figure 4.—*Effect of temperature on the elastic modulus of anhydrous lanolin USP, at 3.54% strain. Key: (⊙) 0.0464 Hz, (●) 0.464 Hz, and (□) 4.64 Hz.*

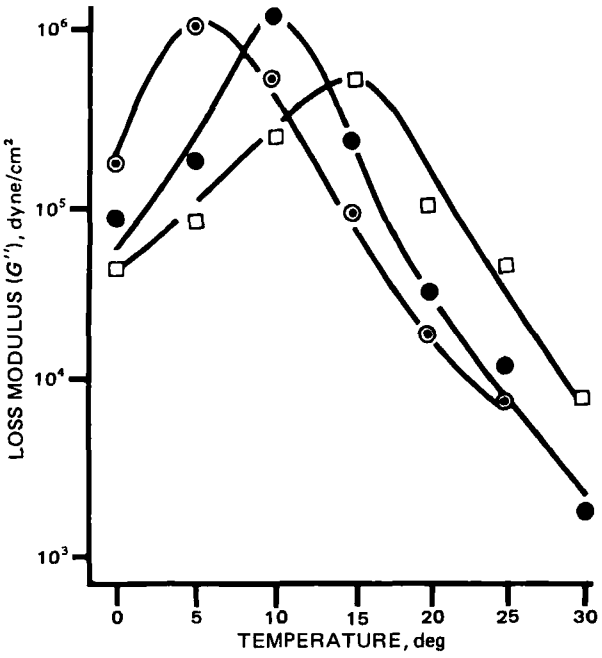

Figure 5.—*Effect of temperature on the viscous modulus of anhydrous lanolin USP, at 3.54% strain. Key: (⊙) 0.0464 Hz, (●) 0.464 Hz, and (□) 4.64 Hz.*

of a theory for rubber-like elasticity (2, 20). The idea of a network accounts for the main features of equilibrium value of rubber-like elasticity. The following account is a brief outline of the principles involved.

Consider a single molecule which possesses free rotation about all of the main chain bonds. Each C—C bond may rotate mutually provided a bond angle of ~110° is maintained. The most probable distance from the final carbon to the first carbon atom can be determined by assuming that each successive bond can fully rotate and using a probability distribution function. The most probable distance can be shown to be slightly greater than $(nl^2)^{1/2}$ where n is the total number of bonds, each of length l. For an amorphous rubber-like system, there are a large number of intertwining molecules each rapidly changing in configuration but on the average sufficiently coiled to have an end distance of approximately $(nl^2)^{1/2}$.

The state of maximum entropy (S) and minimum free energy (F)[7] occurs when the molecules are in the most probable configurational distribution. Therefore, any change in entropy is due to a change in the distribution. When the system is strained it causes the configurational distribution to change to a less probable state and the distance between the first and final atoms of a molecular chain becomes greater than the average or most probable value. While the molecule is extended, the number of different molecular configurations, w_σ, which the molecule can attain is considerably less than the maximum number, w_m, obtainable in the most probable state. The subscript σ designates the extended state, while the subscript m designates the most probable state.

Straining a system in its most probable configurational state changes the configurational distribution to a less probable state, which results in a decrease in entropy. This decrease in entropy can be described according to Boltzmann's entropy relation:

$$\Delta S_\sigma = -k \ln(w_m/w_\sigma) \qquad \text{(Eq. 1)}$$

where ΔS_σ is the decrease in entropy on the stretching of an average molecule and k is the Boltzmann constant. The greater the extension of the molecule, the greater the decrease in entropy due to the smaller number of configurations (w_σ) it can attain.

The decrease in ΔS_σ causes an increase in ΔF_σ, change in the Helmholtz free energy of the system. By definition:

$$\Delta F_\sigma = \Delta E_\sigma - T\Delta S_\sigma \qquad \text{(Eq. 2)}$$

where ΔE_σ is the change in the internal energy of the system. The symbol ΔS_σ can be replaced with $-\overline{\Delta S}_\sigma$, the average entropy decrease per molecule, from the Boltzmann relation. This value is negative because the entropy change is decreasing. It can be assumed that the internal energy is constant, *i.e.*, $\Delta E_\sigma = 0$, because the average environment of each atom in the stretched and unstretched states are identical. Consequently:

$$\Delta F_\sigma = -(-\overline{\Delta S}_\sigma)T \qquad \text{(Eq. 3)}$$

which indicates that ΔF_σ is increasingly positive as $-\overline{\Delta S}_\sigma$ becomes more negative on molecular stretching. Since every system seeks to attain the state of least free energy (unstretched state), it can be deduced that elastic behavior is due to spontaneous changes which attempt to revert the system to the state of least free energy. Rubber-like elasticity is thus explained in terms of an entropic rather than an internal energetic effect.

The almost complete absence of viscous flow must also be accounted for by entanglements or crosslinks. These interaction or junction points give rise to a structured network, which is a function of ν and T. An increase in side-chain branching increases the probability of entanglements, while functional groups generally cause greater intermolecular attraction. Each of these phenomena results in an increase in structure and a loss in degrees of freedom. Consequently, when a system is strained, the entanglements and crosslinks decrease entropy further and increase the driving force to return the system to the state of least free energy.

Figures 4 and 5 give additional insight into the effects of T and ν upon the dynamic mechanical properties of anhydrous lanolin. As evident in Fig. 4, T and ν are inversely related. An increase in T decreases G', while an increase in ν shifts the log G' *versus* T curves to higher temperatures. Similar shifting can be seen with log G'' *versus* T curves as a function of ν (Fig. 5). Such behavior commonly is observed for amorphous polymers (3).

Tan δ or damping is a dimensionless parameter, which is defined as the ratio of G''–G'. More significantly, tan δ is also proportional to the ratio of the energy lost–energy stored in a cycle of deformation. The role of tan δ is not well known. It is often the most sensitive indicator of various molecular motions within a material. All mechanical properties, and especially tan δ, are extremely sensitive to crystalline or structural transitions, relaxation processes, and the morphology of multiphase systems such as crystalline and filled polymers.

Log tan δ *versus* T curves for anhydrous lanolin are illustrated in Fig. 6. At lower ν, a maximum is evident around 10°. With an increase in ν, the height and sharpness of each successive peak decreases until it has disappeared at the highest ν. With an increase in T, the damping curves converge (possibly at one point) in the neighborhood of 17°. To the right of the convergence region, the relationship between ν and tan δ is inverse of the relationship to the left of the convergence.

[7] A good deal of confusion exists over which letter should be used to symbolize the free energy. The letter A is generally used as the Helmholtz free energy and G is used as the Gibbs free energy. A represents that part of the internal energy which is isothermally available, while G represents that portion of heat content which is isothermally available. It should be noted that $G = A + pV$, and hence $\Delta G = \Delta A + p\Delta V$. Since volume change has been assumed negligible in the anhydrous lanolin, $\Delta G \approx \Delta A$. The letter F will be used to represent free energy in this report because G is recognized in the rheological community as the shear modulus.

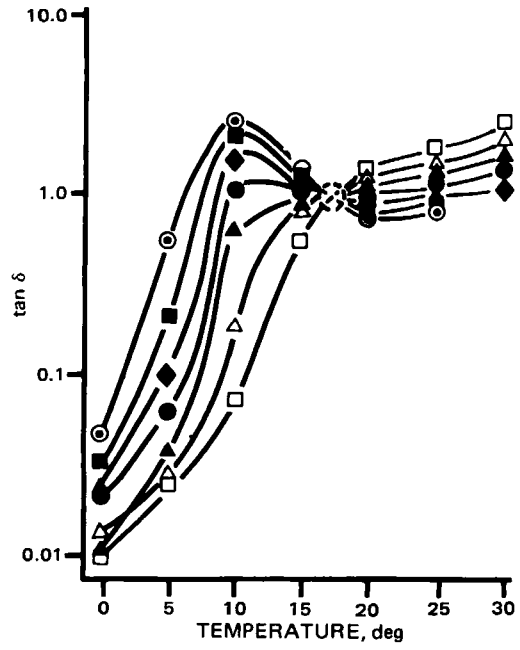

Figure 6.—*Effect of temperature on the loss tangent of anhydrous lanolin USP, at 3.54% strain. Key: (⊙) 0.0464 Hz, (■) 0.10 Hz, (◆) 0.215 Hz, (●) 0.464 Hz, (▲) 1.0 Hz, (△) 2.15 Hz, and (□) 4.64 Hz.*

At the convergence point, the damping properties of anhydrous lanolin are independent of ν, and the damping properties reverse with respect to ν at the convergence temperature. This is a very interesting phenomenon. The fact that there is a convergence point, where the material is independent of ν, suggests that this is only possible when constituent phases are in certain ratios, such that the effects of one phase cancel out the effects of another.

Evidence for a temperature-dependent transition can be found in a differential thermal analysis thermogram of anhydrous lanolin (Fig. 7). From −40 to 25°, there is a linear relationship between ΔT and T_r. A short shoulder develops at ~20°. This peak falls slightly and is followed by another linear increase until a peak is attained at 30°. This peak then rolls off and descends to 40°, where another peak rises to peak at 45°. It is evident that changes in the structure of anhydrous lanolin are occurring over the entire temperature range. But since the test temperature range for dynamic mechanical testing was 0–30°, attention will be focused on the shoulder peak that occurs around 20°.

At least two factors are operating which could move the apparent peak to a lower T. One could be the consequence of a smaller peak, at ~17°, adding onto a larger peak which occurs at ~30°. By addition, the larger peak may have pulled the smaller peak toward the larger peak by several degrees. Consequently, the smaller peak may in reality lie several degrees below 20°. The shoulder, at 20°, is probably related to the mechanical transition which was evidenced by a peak in the log tan δ *versus* T plots at 10°, from 0.0464 to 0.464 Hz. Differences are often found between the thermally indicated and the mechanically determined temperature of transition.

The second factor that can account for a thermogram shift to higher T is the thermal lag of the sample and furnace environment, which is a function of the sample heating rate and the thermal conductivity of the sample. A large difference exists between the thermal conductivities of the aluminum sample pans and anhydrous lanolin. The difference, which is of the magnitude of 10^5 in favor of aluminum, can cause the entire thermogram to shift to higher temperatures[8]. For anhydrous lanolin, it can be approximated that the thermogram shift could be as high as 5–10°. Consequently, correction for peak addition and sample thermoconductivity could place a thermogram peak in the sample temperature region where the damping maxima occur in Fig. 6.

It should be noted that this type of thermogram generally should be expected for materials composed of a large range of molecular weights and functional groups, *e.g.*, butter, lard, and cocoa butter (22). Essentially, these materials have a wide (50–100°) apparent melting range.

A better way to describe the behavior of fats, waxes, and oils is to use the concept of degrees of freedom gained as a function of T. Therefore, the thermogram for anhydrous lanolin shows that the sample is in the process of gaining degrees of freedom throughout the temperature range studied. Degrees of freedom could be gained by a decrease in the inter- and intramolecular forces. For example, a new degree of rotational freedom can allow a greater number of molecular configurations.

Heijboer (23) has presented a log tan δ *versus* T plot similar in appearance to Fig. 6. He showed that tan δ can be used to identify the composition of a composite polymer blend. The dynamic mechanical properties of a series of copolymers of cyclohexyl methacrylate and methyl methacrylate were examined as a function of weight, percentage composition, and T at constant ν. At any given T on the log tan δ *versus* T plot, tan δ maxima heights vary with percentage composition rather than ν as exhibited with anhydrous lanolin.

The composition of anhydrous lanolin as defined previously is a heterogeneous mixture of esters, alcohols, and fatty acids; therefore, a correlation between composition and ν must be considered. One could speculate that certain frequencies have orienting effects on specific fractions (entire molecules or portions thereof) of anhydrous lanolin, creating new molecular environments and consequently new molecular interactions. Shear frequency, like T, influences the degrees of freedom possessed by molecules in anhydrous lanolin. The degrees of freedom gained or lost vary for each molecular component. The effect of ν on the viscoelastic properties of anhydrous lanolin is similar to effect of composition upon Heijboer's methacrylate systems (23). It should be noted that Heijboer does not venture to describe or speculate on the nature of the convergence point.

CONCLUSIONS

Anhydrous lanolin is a thermorheologically complex material whose viscoelastic properties can be characterized with dynamic mechanical testing. Its viscoelastic properties are a function of strain, temperature, shear frequency, and shear history. Even though anhydrous lanolin is a relatively low molecular weight mixture, it has certain viscoelastic properties which are characteristic of higher molecular weight polymers. These properties include the presence of a previously undescribed structural transition and the existence of a limiting value of the elastic modulus.

The extent of data generated in this study does not permit definite conclusions to be drawn about the nature of individual inter- and intramolecular interactions of the various molecular fractions. More insight on interactions may result from studies on purified fractions of known proportion. Ultimately, these studies may enhance the ability to predict *a priori* the optimum blending of semisolid components for desired end-use properties.

APPENDIX I: MATHEMATICAL TREATMENT OF THE THEORY OF LINEAR VISCOELASTICITY

In a dynamic experiment, the stress and strain are sine or cosine functions and they can be treated as rotating vectors. The magnitudes of the vectors are equivalent to the amplitudes of the maximum stress and maximum peak strain. One revolution of the vector is equal to a full cycle of oscillation (Fig. 8).

The stress, strain, and rate of stress are complex variables which can be defined by the following equations:

$$\sigma^* = \sigma_0 \exp[i(\omega t + \delta)] \quad \text{(Eq. A1)}$$

$$\gamma^* = \gamma_0 \exp(i\omega t) \quad \text{(Eq. A2)}$$

where σ^* is the complex stress, γ^* is the complex strain, σ_0 is the maximum magnitude of the stress, γ_0 is the maximum magnitude of the strain, δ is the phase angle between strain and stress, t is time, ω is the angular frequency, and i equals $(-1)^{1/2}$. Differentiation of Eq. A2 is equivalent to a 90° counterclockwise rotation of the vector so that:

$$d\gamma^*/dt = i\omega\gamma_0 \exp(i\omega t) = \omega\gamma_0 \exp[i(\omega t + \pi/2)] \quad \text{(Eq. A3)}$$

where $\omega\gamma_0$ is the magnitude of the rate of strain vector.

The complex shear modulus, G^*, is defined as the ratio of σ^* to γ^*:

$$G^* = \sigma^*/\gamma^* \quad \text{(Eq. A4)}$$

[8] The thermal conductivity of pure aluminum, between 0 and 30°, is ~34 cal/sec cm deg. In contrast, the thermal conductivities of organic compounds similar to those found in anhydrous lanolin are of the order of $2–4 \times 10^{-4}$ cal/sec cm deg (21). For a heating rate of 10°/min and a sample thickness of 0.25 mm, a lag of ~5° could occur. A sample thickness of 0.5 mm would mean a lag of 10°.

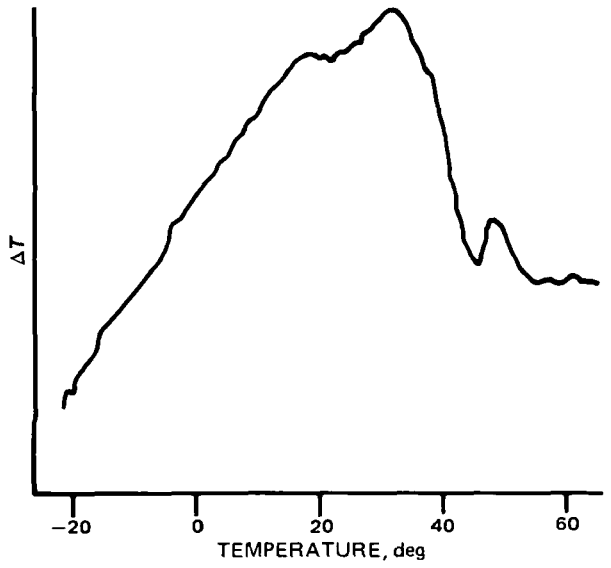

Figure 7.—*Differential thermal analysis thermogram for anhydrous lanolin USP; 10°/min, normal atmosphere.*

By substituting Eqs. A1 and A2 into Eq. A3 we obtain:

$$G^* = (\sigma_0/\gamma_0)\exp[i(\omega t + \delta)]\exp(-i\omega t) \quad \text{(Eq. A5)}$$

or

$$G^* = (\sigma_0/\gamma_0)\exp(i\delta) \quad \text{(Eq. A6)}$$

From Euler's formula, one knows that:

$$\exp(i\delta) = \cos\delta + i(\sin\delta) \quad \text{(Eq. A7)}$$

Some special values of the complex exponential are $\exp(\omega i/2) = i$ and $\exp(\pi i) = -1$. Equation A7 can then be substituted into Eq. A6 to obtain:

$$G^* = (\sigma_0/\gamma_0)\cos\delta + i(\sigma_0/\gamma_0)\sin\delta. \quad \text{(Eq. A8)}$$

But:

$$G' = (\sigma_0/\gamma_0)\cos\delta \quad \text{(Eq. A9)}$$

and

$$G'' = (\sigma_0/\gamma_0)\sin\delta \quad \text{(Eq. A10)}$$

Consequently:

$$G^* = G' + iG'' \quad \text{(Eq. A11)}$$

where G' is known as the elastic modulus, storage modulus, or the real modulus. The viscous or loss modulus, G'', is also known as the imaginary modulus.

The relationship between G', G'', and G^* can also be examined by referring to Fig. 8. One can see that the stress vector can be considered as the sum of two perpendicular components, one of which, σ' ($= \sigma_0\cos\delta$), is in phase with the strain and the other, σ'' ($= \sigma_0\sin\delta$), is out of phase. Two corresponding moduli can be defined as:

$$G' = (\sigma'/\gamma_0) = (\sigma_0/\gamma_0)\cos\delta = G^*\cos\delta \quad \text{(Eq. A12)}$$

and

$$G'' = (\sigma''/\gamma_0) = G^*\sin\delta \quad \text{(Eq. A13)}$$

Hence, G' is also referred to as the in-phase modulus, while G'' is given the out-of-phase designation. By taking the square root of the sum of the squares of Eqs. A12 and A13, one obtains:

$$G^* = [(G')^2 + (G'')^2]^{1/2} \quad \text{(Eq. A14)}$$

This relationship between G', G'', and G^* may be illustrated vectorially as in Fig. 9. The angle between G^* and G', δ, is known as the phase angle, and it is the lag between the forcing stress function and the resultant function, strain. It can also be seen from Fig. 9 that:

$$\tan\delta = G''/G' \quad \text{(Eq. A15)}$$

The physical significance of $\tan\delta$ becomes clearer when one considers

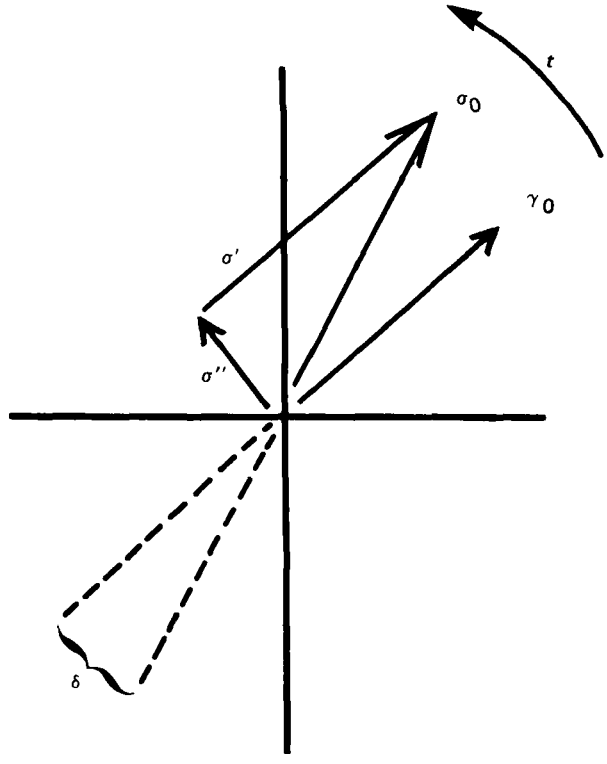

Figure 8—*Rotating vector treatment of sinusoidal deformation.*

the energy dissipated and stored per cycle of deformation for linearly viscoelastic materials. The energy dissipated per cycle is:

$$W = \oint \sigma d\gamma = \oint \sigma(d\gamma/dt)dt \quad \text{(Eq. A16)}$$

So if it is assumed that the stress is the forcing function according to:

$$\sigma(t) = \sigma_0\sin(\omega t) \quad \text{(Eq. A17)}$$

and the resultant strain can be represented by:

$$\gamma(t) = \gamma_0\sin(\omega t - \delta) \quad \text{(Eq. A18)}$$

then Eqs. A17 and A18, with the proper trigonometric identity can be used to expand Eq. A16 to:

$$\Delta W = \sigma_0\gamma_0\omega\oint \sin(\omega t)[\cos(\omega t)\cos\delta + \sin(\omega t)\cos\delta]dt \quad \text{(Eq. A19)}$$

The first term inside of the closed integral is an odd function and becomes zero upon integration. The value of the integral of the second term is $(\pi/\omega)\sin\delta$, so that the energy dissipated per cycle of deformation is given as:

$$\Delta W_{\text{cycle}} = \pi\sigma_0\gamma_0\sin\delta \quad \text{(Eq. A20)}$$

The maximum energy stored per cycle, analogous to the potential energy of a spring at the maximum displacement, is:

$$W = (1/2)G'\gamma_0^2 \quad \text{(Eq. A21)}$$

where G' is the elastic modulus of the material, equivalent to the spring constant. Since $G' = G^*\cos\delta$ and $G^*\gamma_0 = \sigma_0$, then:

$$W = (1/2)\sigma_0\gamma_0\cos\delta \quad \text{(Eq. A22)}$$

Eqs. A20 and A22 can be combined to give the ratio of energy dissipated–maximum energy stored per cycle as:

$$\Delta W/W = 2\pi\tan\delta = 2\pi(G''/G') \quad \text{(Eq. A23)}$$

APPENDIX II: CALCULATION OF DYNAMIC MODULI

During testing, digital readouts of "a" and "b" are given at each test frequency by the function generator and phase analyzer. The readout "a" is directly proportional to G' and "b" is directly proportional to G''. By neglecting inertial forces and utilizing infinitesimally small deformations, these stress–strain ratios can be related to angular displace-

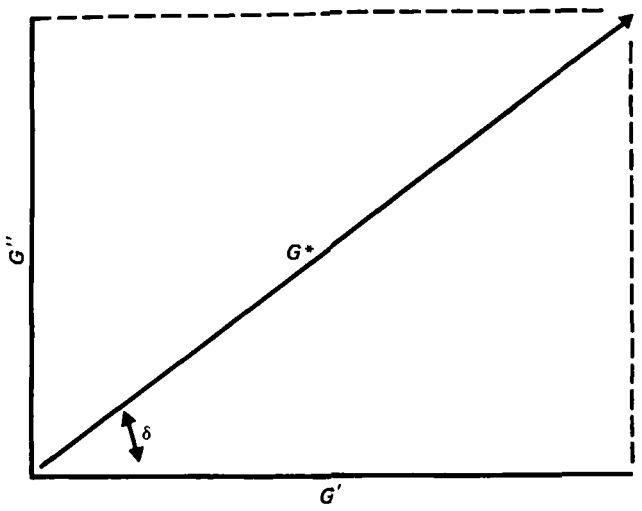

Figure 9—*Vectorial resolution of components of the complex modulus in sinusoidal deformation.*

ment–torque ratios by form factors that depend on apparatus geometry. For the viscoelastic semisolid in these experiments, the deformation corresponds to simple shear torsion between cone and plate.

The cone and plate geometry produces a strain that is nearly homogeneous throughout the sample and can provide information for the shear strain–stress ratio in small deformations. The geometrical factors for torsion between cone and plate (2) are:

$$\gamma_0/\sigma_0 = k\alpha/M_0 \qquad \text{(Eq. A24)}$$

and

$$k = 2\pi r^3/3\beta \qquad \text{(Eq. A25)}$$

where k is the form factor, γ_0 is the maximum shear strain, σ_0 is the maximum shear stress, r is the radius of sample (cm), α is the angular displacement (radians), M_0 is the torque, and β is the angle between cone and plate. If inertial and edge effects are assumed negligible, the maximum stress is expressed as:

$$\sigma_0 = 3M_0/2\pi r^3 \qquad \text{(Eq. A26)}$$

while the maximum strain is:

$$\gamma_0 = \alpha/\beta \qquad \text{(Eq. A27)}$$

The "a" and "b" outputs of the function generator and phase analyzer are equivalent to the following expressions:

$$\text{a} = \frac{M_0(\cos\delta)}{\alpha\ (980\ \text{dyne/g})(10^4\ \text{g cm})} \qquad \text{(Eq. A28)}$$

and

$$\text{b} = \frac{M_0(\sin\delta)}{\alpha\ (980\ \text{dyne/g})(10^4\ \text{g cm})} \qquad \text{(Eq. A29)}$$

The values of 980 dyne/g and 10^4 g cm are instrument constants dependent on the transducers and torque control setting used in the experiments. By substituting Eqs. A26 and A27 into Eqs. A28 and A29, respectively, one obtains:

$$\text{a} = \frac{\sigma_0 2\pi r^3(\cos\delta)}{3\beta\gamma_0(980\ \text{dyne/g})(10^4\ \text{g cm})} \qquad \text{(Eq. A30)}$$

and

$$\text{b} = \frac{\sigma_0 2\pi r^3(\sin\delta)}{3\beta\gamma_0(980\ \text{dyne/g})(10^4\ \text{g cm})} \qquad \text{(Eq. A31)}$$

Eqs. A9 and A10 are then combined with Eqs. A30 and A31, respectively, to obtain:

$$G' = \frac{3\beta(980\ \text{dyne/g})(10^4\ \text{g cm})(\text{a})}{2\pi r^3} \qquad \text{(Eq. A32)}$$

and

$$G'' = \frac{3\beta(980\ \text{dyne/g})(10^4\ \text{g cm})(\text{b})}{2\pi r^3} \qquad \text{(Eq. A33)}$$

APPENDIX III: GLOSSARY

Where applicable, the symbols in this report conform to those proposed as a uniform standard by the Society of Rheology[9] (24).

- E = internal energy of a system
- F = free energy of a system
- G' = elastic, real, or storage modulus
- G'' = viscous, imaginary, or loss modulus
- G^* = complex modulus
- G_E = limiting value of G'
- M_0 = torque
- R = gas constant
- S = entropy
- T = temperature
- ΔT = temperature difference between sample and reference pan
- T_r = temperature of reference pan
- W = energy stored per cycle of deformation
- ΔW = energy dissipated per cycle of deformation
- a = readout of FGPA directly proportional to G'
- b = readout of FGPA directly proportional to G''
- i = $(-1)^{1/2}$
- k = Boltzmann's constant
- l = bond length between atoms
- r_σ = distance between first and final atoms of a molecular chain
- t = time
- w_σ = number of obtainable molecular configurations in extended state
- w_m = maximum number of molecular configurations obtainable in the most probable state
- α = angle of oscillation
- β = cone angle
- δ = phase angle between stress and strain vectors
- γ = strain
- $\dot{\gamma}$ = rate of strain
- γ_0 = maximum strain amplitude
- γ^* = complex strain
- σ = stress
- σ' = real component of complex stress
- σ'' = imaginary component of complex stress
- σ^* = complex stress
- σ_0 = maximum stress amplitude
- ν = shear frequency (Hz)
- ω = angular shear frequency (rad/sec)

REFERENCES

(1) B. W. Barry, in "Advances in Pharmaceutical Sciences," vol. 4, H. S. Bean, A. H. Beckett, and J. E. Carless, Eds., Academic, New York, N.Y., 1974, p. 1.

(2) J. D. Ferry, "Viscoelastic Properties of Polymers," 3rd ed., Wiley, New York, N.Y., 1980.

(3) L. E. Nielsen, "Mechanical Properties of Polymers," vol. 1, Dekker, New York, N.Y., 1974.

(4) A. N. Martin, G. S. Banker, and A. H. C. Chun, in "Advances in Pharmaceutical Sciences," vol. 1, H. S. Bean, A. H. Beckett, and J. E. Carless, Eds., Academic, New York, N.Y., 1964, p. 1.

(5) H. Schott, "Remington's Pharmaceutical Sciences," Mack Publishing, Easton, Pa., 1975, chap. 24.

(6) P. Sherman, *J. Soc. Cosmet. Chem.*, **17**, 439 (1966).

(7) S. S. Davis, E. Shotton, and B. Warburton, *J. Pharm. Pharmacol., Suppl.*, **20**, 157s (1968).

(8) G. B. Thurston and A. Martin, *J. Pharm. Sci.*, **67**, 1499 (1978).

(9) D. C. Bogue, *Ind. Eng. Chem. Fundam.*, **5**, 243 (1966).

(10) *Idem.*, **5**, 253 (1966).

(11) K. Walters, "Rheometry," Halsted, New York, N.Y., 1975.

(12) H. Leaderman, "Elastic and Creep Properties of Filamentous Materials and Other High Polymers," Textile Foundation, Washington, D.C., 1943.

(13) "United States Pharmacopeia," 20th rev., U. S. Pharmacopeial Convention, Rockville, Md., 1980.

(14) E. Bertram, *Am. Perfum. Essent. Oil Rev.*, **2**, 115 (1950).

(15) L. I. Conrad, *ibid.*, **6**, 177 (1954).

(16) G. Barnett, *Drug Cosmet. Ind.*, **80**, 610 (1957).

[9] New York, N.Y.

(17) C. W. Macosko and J. Starita, *SPE J.*, **27**, 38 (1971).
(18) S. S. Davis, *J. Pharm. Sci.*, **58**, 412 (1969).
(19) A. J. Barlow and J. Lamb, *Proc. R. Soc. London Ser. A*, **253**, 52 (1959).
(20) J. J. Aklonis, W. J. MacKnight, and M. Shen, "Introduction to Polymer Viscoelasticity," Interscience, New York, N.Y., 1972.
(21) "Handbook of Chemistry and Physics," 51st ed., Chemical Rubber Co., Cleveland, Ohio, 1970.
(22) A. E. Bailey, "Melting and Solidification of Fats," Interscience, New York, N.Y., 1950, p. 291.
(23) I. J. Heijboer, *Kolloid Z.*, **171**, 7 (1960).
(24) C. L. Sieglaff, *Trans. Soc. Rheol.*, **202**, 311 (1976).

ACKNOWLEDGMENTS

Adapted in part from a dissertation submitted by Galen W. Radebaugh to the University of Connecticut in partial fulfillment of the Doctor of Philosophy degree requirements.

Partially supported with funds from the Connecticut Research Foundation.

Temperature–Frequency Equivalence of the Viscoelastic Properties of Anhydrous Lanolin USP

GALEN W. RADEBAUGH * and ANTHONY P. SIMONELLI ˣ

Received April 5 1982, from the *College of Pharmacy and Institute of Materials Science, University of Connecticut, Storrs, CT 06268.* Accepted for publication July 15, 1982. * Present address: Department of Pharmaceutics, Smith Kline and French Laboratories, Philadelphia, PA 19101.

Abstract □ Methods of data analysis novel to pharmaceutical semisolids have been applied to the dynamic mechanical data obtained for anhydrous lanolin USP. It was found that the viscoelastic parameters determined over a wide range of temperatures and shear frequencies could be superposed. Elastic moduli (G') and viscous moduli (G'') obtained at low temperatures (T) and frequencies (ν), were equivalent to moduli obtained at high T and ν. Empirical shifts of modulus *versus* shear frequency data obtained at different temperatures were used to produce G' and G'' *versus* ν master curves (complete log modulus *versus* log frequency behavior at a constant temperature). A method of reduced variables, in conjunction with an Arrhenius-type relation, proved useful in calculating the energy of activation for the structural processes involved in a major mechanical transition.

Keyphrases □ Viscoelasticity—properties of anhydrous lanolin determined by dynamic mechanical testing, temperature–frequency equivalence, superposition of parameters □ Anhydrous lanolin—viscoelastic parameter determination, temperature–frequency equivalence □ Dynamic mechanical testing—viscoelastic parameter determination for anhydrous lanolin, energy of activation for mechanical transitions

Most research which has examined the effect of temperature on viscoelastic properties has focused on rubber and nonpharmaceutical synthetic polymers (1, 2). Though the effect of temperature on viscosity has been well documented for pharmaceutical systems, little information is available on the effect of temperature on their viscoelastic properties (3, 4).

In the preceding paper, data showed that the viscoelastic properties of anhydrous lanolin USP are significantly dependent on temperature as well as shear frequency (5). Small changes in temperature caused dramatic shifts in modulus *versus* shear frequency plots. This report examines those shifts and presents a method of reduced variables, which is novel to pharmaceutical systems, to analyze the data.

THEORETICAL

The viscoelastic properties of polymeric systems have been shown to be dependent on temperature and shear frequency. According to the theory of rubber-like elasticity, the elastic moduli of ideal elastomers are proportional to absolute temperature (6). Since the deformation of a rubber-like material is an activated process in which molecular segments can only move by overcoming potential barriers, a direct relationship exists between the temperature and time dependence of viscoelastic properties.

Dynamic mechanical data taken over a range of shear frequencies (which is equivalent to reciprocal time) can be superposed in the same manner that time–temperature superposition is applied to creep and stress relaxation data (7–10). This phenomenon is extremely useful because the limitations of instrumentation or time often do not allow the measurement of a complete modulus *versus* shear frequency spectrum. In spite of this limitation, a curve-shifting procedure can be used to construct a master curve (complete log modulus *versus* log frequency spectrum at a given temperature). A change in temperature shifts the distribution of modulus curves without changing the shape of the function. The shift of a modulus curve is quantitated in terms of a_T, the shift factor.

Mathematically, the concept of temperature–shear frequency superposition can be expressed as:

$$G(T_R,\nu) = G(T,\nu/a_T) \qquad \text{(Eq. 1)}$$

where G is either the elastic or viscous modulus, ν is the shear frequency, T_R is the reference temperature of superposition, T is the test temperature, and a_T is the shift factor. The effect of a change in temperature is the same as applying a multiplicative factor to the shear frequency scale (*i.e.*, an additive factor to the log shear frequency scale). Ideally, there is often an inherent change in modulus brought about by changes in temperature. There is also a need to correct for the change in sample mass per unit volume as a function of temperature. Each of these changes are compensated for by vertical shifts during the construction of the log modulus *versus* log frequency master curve.

Consequently, these considerations lead to:

$$\frac{G(T_R,\nu)}{T_R\rho(T_R)} = \frac{G(T,\nu/a_T)}{T\rho(T)} \qquad \text{(Eq. 2)}$$

where $\rho(T_R)$ and $\rho(T)$ are the densities of the test sample at the reference temperature and test temperature, respectively (8). Division by the test temperature corrects for changes in modulus due to the inherent dependence of modulus on temperature, while division by the density corrects for volume changes. To construct a master curve, a reference temperature is arbitrarily chosen and moduli are measured at various shear frequencies and temperatures.

By rearranging Eq. 2, the modulus at any shear frequency with respect to the reference temperature can be expressed as:

$$G(T_R,\nu) = \frac{T_R\rho(T_R)}{T\rho(T)}\,G(T,\nu/a_T) \qquad \text{(Eq. 3)}$$

The shift factors are a function of temperature and are determined relative to the reference temperature. The values of the shift factors must be found empirically by matching the results of adjacent temperatures.

0022-3549/83/0400-0422$01.00/0

(17) C. W. Macosko and J. Starita, *SPE J.*, **27**, 38 (1971).
(18) S. S. Davis, *J. Pharm. Sci.*, **58**, 412 (1969).
(19) A. J. Barlow and J. Lamb, *Proc. R. Soc. London Ser. A*, **253**, 52 (1959).
(20) J. J. Aklonis, W. J. MacKnight, and M. Shen, "Introduction to Polymer Viscoelasticity," Interscience, New York, N.Y., 1972.
(21) "Handbook of Chemistry and Physics," 51st ed., Chemical Rubber Co., Cleveland, Ohio, 1970.
(22) A. E. Bailey, "Melting and Solidification of Fats," Interscience, New York, N.Y., 1950, p. 291.
(23) I. J. Heijboer, *Kolloid Z.*, **171**, 7 (1960).
(24) C. L. Sieglaff, *Trans. Soc. Rheol.*, **202**, 311 (1976).

ACKNOWLEDGMENTS

Adapted in part from a dissertation submitted by Galen W. Radebaugh to the University of Connecticut in partial fulfillment of the Doctor of Philosophy degree requirements.

Partially supported with funds from the Connecticut Research Foundation.

Temperature–Frequency Equivalence of the Viscoelastic Properties of Anhydrous Lanolin USP

GALEN W. RADEBAUGH * and ANTHONY P. SIMONELLI ˣ

Received April 5 1982, from the *College of Pharmacy and Institute of Materials Science, University of Connecticut, Storrs, CT 06268.* Accepted for publication July 15, 1982. * Present address: Department of Pharmaceutics, Smith Kline and French Laboratories, Philadelphia, PA 19101.

Abstract □ Methods of data analysis novel to pharmaceutical semisolids have been applied to the dynamic mechanical data obtained for anhydrous lanolin USP. It was found that the viscoelastic parameters determined over a wide range of temperatures and shear frequencies could be superposed. Elastic moduli (G') and viscous moduli (G'') obtained at low temperatures (T) and frequencies (ν), were equivalent to moduli obtained at high T and ν. Empirical shifts of modulus *versus* shear frequency data obtained at different temperatures were used to produce G' and G'' *versus* ν master curves (complete log modulus *versus* log frequency behavior at a constant temperature). A method of reduced variables, in conjunction with an Arrhenius-type relation, proved useful in calculating the energy of activation for the structural processes involved in a major mechanical transition.

Keyphrases □ Viscoelasticity—properties of anhydrous lanolin determined by dynamic mechanical testing, temperature–frequency equivalence, superposition of parameters □ Anhydrous lanolin—viscoelastic parameter determination, temperature–frequency equivalence □ Dynamic mechanical testing—viscoelastic parameter determination for anhydrous lanolin, energy of activation for mechanical transitions

Most research which has examined the effect of temperature on viscoelastic properties has focused on rubber and nonpharmaceutical synthetic polymers (1, 2). Though the effect of temperature on viscosity has been well documented for pharmaceutical systems, little information is available on the effect of temperature on their viscoelastic properties (3, 4).

In the preceding paper, data showed that the viscoelastic properties of anhydrous lanolin USP are significantly dependent on temperature as well as shear frequency (5). Small changes in temperature caused dramatic shifts in modulus *versus* shear frequency plots. This report examines those shifts and presents a method of reduced variables, which is novel to pharmaceutical systems, to analyze the data.

THEORETICAL

The viscoelastic properties of polymeric systems have been shown to be dependent on temperature and shear frequency. According to the theory of rubber-like elasticity, the elastic moduli of ideal elastomers are proportional to absolute temperature (6). Since the deformation of a rubber-like material is an activated process in which molecular segments can only move by overcoming potential barriers, a direct relationship exists between the temperature and time dependence of viscoelastic properties.

Dynamic mechanical data taken over a range of shear frequencies (which is equivalent to reciprocal time) can be superposed in the same manner that time–temperature superposition is applied to creep and stress relaxation data (7–10). This phenomenon is extremely useful because the limitations of instrumentation or time often do not allow the measurement of a complete modulus *versus* shear frequency spectrum. In spite of this limitation, a curve-shifting procedure can be used to construct a master curve (complete log modulus *versus* log frequency spectrum at a given temperature). A change in temperature shifts the distribution of modulus curves without changing the shape of the function. The shift of a modulus curve is quantitated in terms of a_T, the shift factor.

Mathematically, the concept of temperature–shear frequency superposition can be expressed as:

$$G(T_R,\nu) = G(T,\nu/a_T) \qquad \text{(Eq. 1)}$$

where G is either the elastic or viscous modulus, ν is the shear frequency, T_R is the reference temperature of superposition, T is the test temperature, and a_T is the shift factor. The effect of a change in temperature is the same as applying a multiplicative factor to the shear frequency scale (*i.e.*, an additive factor to the log shear frequency scale). Ideally, there is often an inherent change in modulus brought about by changes in temperature. There is also a need to correct for the change in sample mass per unit volume as a function of temperature. Each of these changes are compensated for by vertical shifts during the construction of the log modulus *versus* log frequency master curve.

Consequently, these considerations lead to:

$$\frac{G(T_R,\nu)}{T_R\rho(T_R)} = \frac{G(T,\nu/a_T)}{T\rho(T)} \qquad \text{(Eq. 2)}$$

where $\rho(T_R)$ and $\rho(T)$ are the densities of the test sample at the reference temperature and test temperature, respectively (8). Division by the test temperature corrects for changes in modulus due to the inherent dependence of modulus on temperature, while division by the density corrects for volume changes. To construct a master curve, a reference temperature is arbitrarily chosen and moduli are measured at various shear frequencies and temperatures.

By rearranging Eq. 2, the modulus at any shear frequency with respect to the reference temperature can be expressed as:

$$G(T_R,\nu) = \frac{T_R\rho(T_R)}{T\rho(T)}\,G(T,\nu/a_T) \qquad \text{(Eq. 3)}$$

The shift factors are a function of temperature and are determined relative to the reference temperature. The values of the shift factors must be found empirically by matching the results of adjacent temperatures.

0022-3549/83/0400-0422$01.00/0

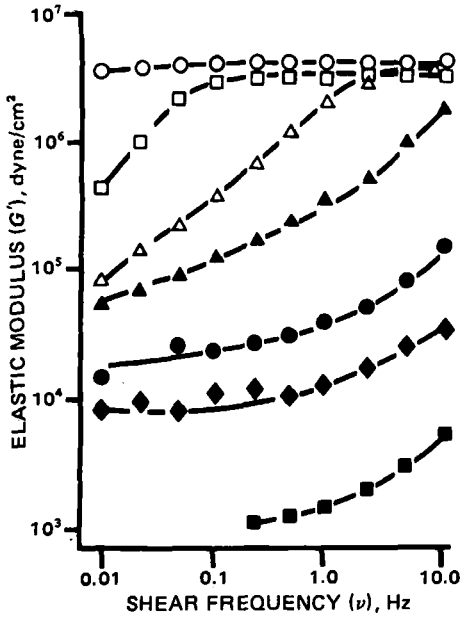

Figure 1—*Effect of shear frequency on the elastic modulus of anhydrous lanolin USP, at 3.54% strain. Key: (○) 0°, (□) 5°, (△) 10°, (▲) 15 °, (●) 20°, (◆) 25°, and (■) 30°.*

Ferry was among the first to use this technique, so the procedure is often referred to as a Ferry reduction scheme (1, 9, 11). Superposition, which is also referred to as the method of reduced variables, can reduce experimental work and extend the effective frequency range of results obtained with an instrument of limited frequency capabilities. When the temperature of testing is varied through an appropriate temperature range, a reduced frequency range of many more decades usually can be covered.

If it is theorized that the temperature dependence of the shift factors takes on the Arrhenius form, then:

$$a_T = A \exp(E_a/RT) \qquad \text{(Eq. 4)}$$

where A is the preexponential term, R is the gas constant, T is temperature, and E_a is the energy of activation (1, 12, 13). By taking the logarithm and then differentiating both sides of Eq. 4, it can be rearranged to obtain:

$$E_a = 2.303R \frac{d(\log a_T)}{d(1/T)} \qquad \text{(Eq. 5)}$$

Therefore, the shift factors of superposition can be plotted as log a_T *versus* (1/T) and the E_a for a given transition can be calculated from the slope of the plot.

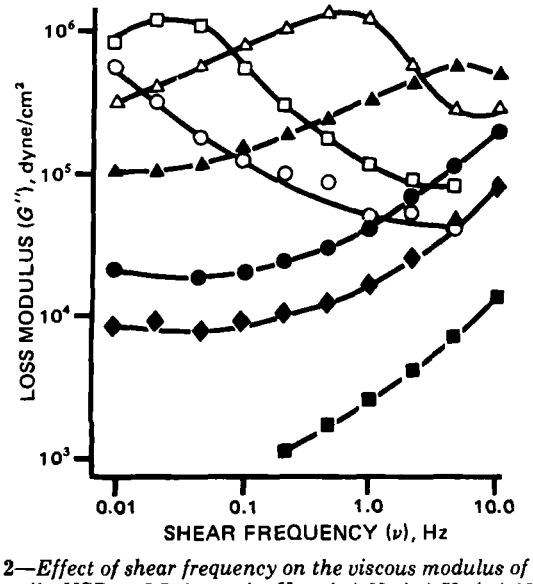

Figure 2—*Effect of shear frequency on the viscous modulus of anhydrous lanolin USP, at 3.54% strain. Key: (○) 0°, (□) 5°, (△) 10°, (▲) 15 °, (●) 20°, (◆) 25°, and (■) 30°.*

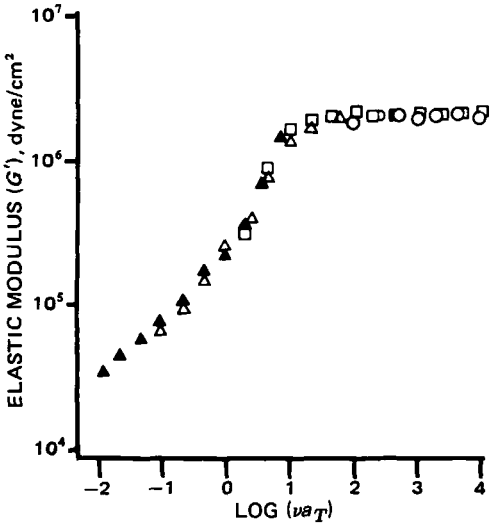

Figure 3—*Reduced frequency master curve of elastic modulus for anhydrous lanolin USP. Key: (○) 0°, (□) 5°, (△) 10°, and (▲) 15°.*

In cases of amorphous polymers where the data are taken near the glass transition, the shift factors may obey an empirical equation developed by Williams, Landel, and Ferry (14). This relationship, known as the W-L-F equation, is written as:

$$\log a_T = -C_1(T - T_g)/(C_2 + T - T_g) \qquad \text{(Eq. 6)}$$

where C_1 and C_2 are constants and T_g is the glass transition temperature. The glass transition temperature is that temperature below which the configurational rearrangements of polymer chain backbones essentially cease. The empirical constants, C_1 and C_2, were originally thought to be universal but have hence shown slight variation from polymer to polymer (6). The apparent energy of activation for a transition can also be calculated for data that fit the W-L-F relationship. By taking the derivative of Eq. 6 with respect to T, one obtains:

$$d(\log a_t)/dt = -C_1C_2/(C_2 + T - T_g)^2 \qquad \text{(Eq. 7)}$$

Equation 7 can then be combined with Eq. 5 to obtain:

$$E_a = 2.303RC_1C_2T^2/(C_2 + T - T_g)^2 \qquad \text{(Eq. 8)}$$

The magnitude of the energy of activation is an indication of the magnitude of the transition. Primary transitions usually have an energy of activation >40 kcal. Their damping peaks will shift ~7–10° for every decade change in frequency. Minor or secondary transitions with much lower energies of activation are more sensitive to frequency and show greater movement on the temperature scale with changes in frequency.

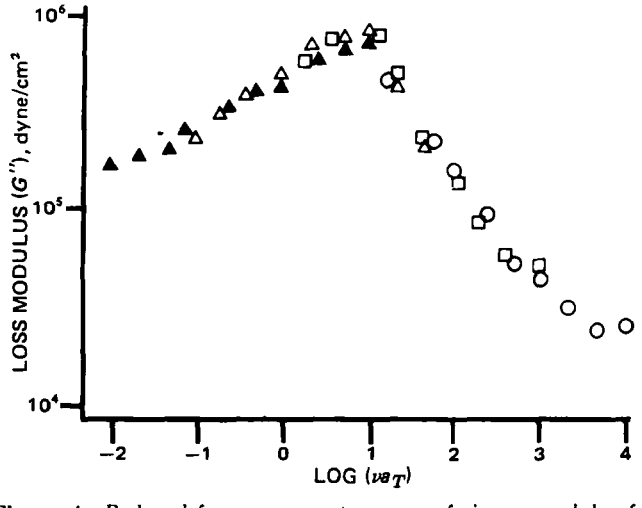

Figure 4—*Reduced frequency master curve of viscous modulus for anhydrous lanolin USP. Key: (○) 0°, (□) 5°, (△) 10°, and (▲) 15°.*

Table I—Shift Factors Determined by Superposition of Elastic Modulus *versus* Frequency Curves

$T°$	$T - T_R$	$G'(T°_R,\nu$ Hz) = $G'(T°,\nu$ Hz/a_T)	a_T	log a_T
0	−15	$G'(15,0.01) = G'(0,46.3/a_T)$	4637	3.67
5	−10	$G'(15,0.01) = G'(5,2.15/a_T)$	215	2.33
10	− 5	$G'(15,0.01) = G'(10,0.10/a_T)$	10	1.00
15	0	$G'(15,0.01) = G'(15,0.01/a_T)$	1	0

Table II—Shift Factors Determined by Superposition of Viscous Modulus *versus* Frequency Curves

$T°$	$T - T_R$	$G''(T°_R,\nu$ Hz) = $G''(T°,\nu$ Hz/a_T)	a_T	log a_T
0	−15	$G''(15,0.01) = G''(0,46.3/a_T)$	4637	3.67
5	−10	$G''(15,0.01) = G''(5,2.15/a_T)$	215	2.33
10	− 5	$G''(15,0.01) = G''(10,0.10/a_T)$	10	1.00
15	0	$G''(15,0.01) = G''(15,0.01/a_T)$	1	0

EXPERIMENTAL

The viscoelastic properties of anhydrous lanolin USP were determined with a mechanical spectrometer[1]. Complete descriptions of the materials, apparatus, method of sample preparation, and experimental procedures were given in the preceding paper (5). The procedures for calculating the elastic modulus (G') and the viscous modulus (G'') as a function of shear frequency (ν) and temperature (T) were also discussed.

RESULTS AND DISCUSSION

As previously reported, the dynamic mechanical properties of anhydrous lanolin are dependent on ν and T (5). Examination of the elastic modulus and loss modulus *versus* shear frequency curves obtained at that time (reproduced in Figs. 1 and 2, respectively) indicates that these curves lend themselves to temperature–frequency superposition. By using the superposition methods of Ferry (1) and Tobolsky (8), it was found that empirical shifts of these curves could produce the log modulus *versus* log νa_T master curves shown in Figs. 3 and 4.

The shifting procedure matched portions of adjacent curves by horizontal shifting (and minor vertical shifting as necessary) such that only one smooth composite curve resulted. The horizontal shift from the curve at the reference temperature was quantitated in terms of a_T. The reference temperature used was 15°, the highest temperature at which both the elastic modulus and viscous modulus curves fit the reduction scheme. The shift factors obtained by constructing Figs. 3 and 4 are tabulated in Tables I and II.

The shift factor calculations were made on the assumption that the density (and hence the test sample volume) was constant over the entire range of superposition (0–15°). In actuality, the density is a function of temperature and changes in sample volume may have accounted for minor vertical shifts of the modulus curves. Vertical adjustments were not uniform and were essential to produce smooth master curves.

The master curves of log modulus *versus* log νa_T can be used to represent the viscoelastic behavior of anhydrous lanolin at shear frequencies up to 10^5 Hz (628,000 radians/sec) at 15°. This exceeds the maximum shear frequency used in these tests by four decades of frequency. Consequently, the two master curves can be used to predict the dynamic moduli of anhydrous lanolin at shear frequencies which are probably unobtainable with any commercially available mechanical property tester. Knowledge of the mechanical properties of a pharmaceutical semisolid at high shear frequencies is of more than academic interest. The rates of shear of many pharmaceutical processes such as mixing, milling, filling, extrusion, and application approach the magnitude of 10^4 Hz (15).

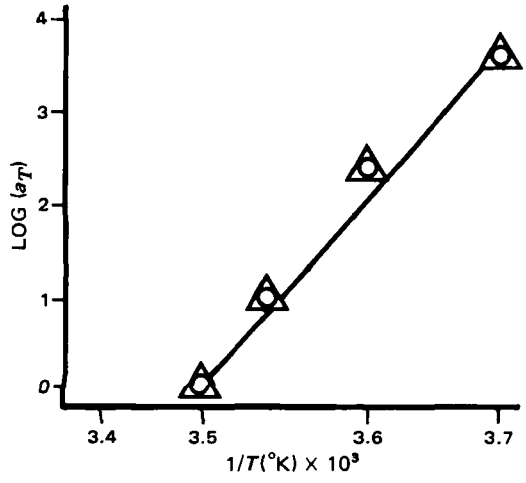

Figure 5—*Semilog plot of shift factor* versus *reciprocal temperature for anhydrous lanolin USP. Key: (○) from G' superposition and (△) from G'' superposition.*

For polymeric materials, T_R is usually taken to be the glass transition temperature T_g. The glass transition temperature is the temperature at which the polymer undergoes transition from a rubbery to a glassy state. At temperatures above T_g, the polymer is generally soft and flexible and is either an elastomer or a very viscous fluid. The glass transition temperature is important because mechanical properties change profoundly in the region of the glass transition. It is in this region of transition where a temperature–frequency reduction scheme is most applicable (11).

For anhydrous lanolin, the modulus curves are horizontally superposable only over the temperature range of 0–15°. Hence, it is reasonable to say that anhydrous lanolin undergoes a major mechanical transition in this temperature range, from a rubber-like to a nonrubber-like state. The reduction scheme does not hold at temperatures >15° due to the loss of the rubber-like structure.

Previously it was reported that the damping curves (log tan δ *versus* T) for anhydrous lanolin were at a maximum at ~15° (5). The damping maxima were suggested as being a point of significant structure change. These curves support the hypothesis that anhydrous lanolin may be in transition from a nonrubber-like to a rubber-like state.

In Fig. 5 it appears that the shift factors follow the Arrhenius relationship. The apparent energy of activation (E_a) for the molecular processes involved was calculated from the plot of log a_T *versus* $1/T$ using a least-squares fit and Eq. 5. The E_a was found to be ~90 kcal. A plot of this type can be curvilinear for polymeric materials. In such cases, E_a is temperature dependent and is approximated from the slope of the tangent line at any given point on the curve.

The significance of the value of E_a for anhydrous lanolin becomes more evident when the E_a is compared with values for polymeric systems. For main glass transitions where T_R is taken as T_g, the E_a is of the order of 10^5 cal/mole (2). Secondary transitions at cryogenic temperatures are of the order of 10^3–10^4 cal/mole. Comparison of the E_a for anhydrous lanolin with experimentally obtained E_a values for polymers would indicate that the structural transitions that occur in anhydrous lanolin at ~15° rival those of a glass transition. But this is not what would be expected by inspection of Fig. 1. The limiting value of the elastic modulus is not as large as would be expected for substances in a glassy state.

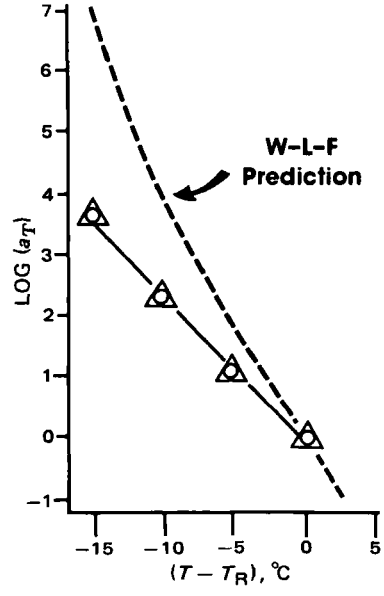

Figure 6—*Semilog plot of shift factor* versus *reduced temperature for anhydrous lanolin USP. Key: (○) from G' superposition and (△) from G'' superposition.*

[1] Model RMS-7200, Rheometrics, Inc., Union, NJ 07083.

With these thoughts in mind, the shift factors were also plotted according to the W-L-F relationship (Eq. 6) in Fig. 6. The ideal W-L-F curve generated with the "universal" constants of $C_1 = 17.4$ and $C_2 = 51.6$ is also presented in Fig. 6 for comparison. The "universal" constants do not hold for many polymers, and it is apparent that the experimentally obtained plot of $\log a_T$ *versus* $(T - T_R)$ for anhydrous lanolin does not lie where the W-L-F relationship (with "universal" constants) predicts. The lack of fit of the experimental data with the W-L-F prediction also suggests that the transition is probably not a glass transition as most polymers that undergo a glass transition obey the W-L-F prediction.

CONCLUSION

It has been demonstrated that the energy of activation for the structural changes occurring in the transition of anhydrous lanolin between 10 and 15° can be calculated by a temperature–shear frequency reduction scheme and an Arrhenius-type relationship. The E_a, which is ~90 kcal, compares favorably with the magnitude of the E_a of a high molecular weight polymer undergoing a glass transition. This comparison is significant when one considers the generally low molecular weight composition of anhydrous lanolin. The magnitude of the E_a for anhydrous lanolin suggests that the intra- and intermolecular forces are as great as those in high molecular weight polymers. Hence, the nature of the functional groups and the chain length of the molecules determine the strength of the structure of the system.

Overall, the experimental data suggest that anhydrous lanolin undergoes a major mechanical transition between 10 and 15°. Both the ability to superpose modulus *versus* shear frequency data and an E_a of 90 kcal for the transition are characteristic of a glass transition, but other observations are not. As described in the preceding paper (5), these observations are: a lower limiting value of the elastic modulus than would be expected for a glass transition, a slower rate of change of tan δ with temperature about the transition than would be expected for a glass transition, and a lack of fit of experimental data to the W-L-F relationship. Rather than a sharp transition from a rubbery to an ordered glassy state, it appears that anhydrous lanolin undergoes a mechanical transition from a rubber-like state to a structural state which is less ordered than a glassy state.

REFERENCES

(1) J. D. Ferry, "Viscoelastic Properties of Polymers," 3nd ed., Wiley, New York, N.Y., 1980.

(2) L. E. Nielsen, "Mechanical Properties of Polymers," vol. 1, Dekker, New York, N.Y., 1974.

(3) A. N. Martin, G. S. Banker, and A. H. C. Chun, "Advances in Pharmaceutical Sciences," vol. 1, H. S. Bean, A. H. Beckett, and J. E. Carless, Eds., Academic, New York, N.Y., 1964, p. 1.

(4) B. W. Barry, "Advances in Pharmaceutical Sciences," vol. 4, H. S. Bean, A. H. Beckett, and J. E. Carless, Eds., Academic, New York, N.Y., 1974, p. 1.

(5) G. W. Radebaugh and A. P. Simonelli, *J. Pharm. Sci.*, **72**, 415 (1983).

(6) J. J. Aklonis, W. J. MacKnight, and M. Shen, "Introduction to Polymer Viscoelasticity," Interscience, New York, N.Y., 1972.

(7) J. Bischoff, E. Catsiff, and A. V. Tobolsky, *J. Am. Chem. Soc.*, **74**, 3378 (1952).

(8) A. V. Tobolsky and J. R. McLoughlin, *J. Polymer Sci.*, **8**, 543 (1952).

(9) J. D. Ferry, *J. Colloid Sci.*, **10**, 474 (1955).

(10) J. R. Van Wazer, J. W. Lyons, K. Y. Kim, and R. E. Colwell, "Viscosity and Flow Measurements—A Laboratory Handbook of Rheology," Interscience, New York, N.Y., 1963.

(11) J. D. Ferry, *J. Am. Chem. Soc.*, **72**, 3746 (1950).

(12) R. C. Harper, H. Markovitz, and T. W. DeWitt, *J. Polymer Sci.*, **8**, 435 (1952).

(13) E. Catsiff and A. V. Tobolsky, *J. Colloid Sci.*, **10**, 375 (1955).

(14) M. L. Williams, R. F. Landel, and J. D. Ferry, *J. Am. Chem. Soc.*, **77**, 3701 (1955).

(15) N. L. Henderson, P. M. Meer, and H. B. Kostenbauder, *J. Pharm. Sci.*, **50**, 788 (1961).

ACKNOWLEDGMENTS

Adapted in part from a dissertation submitted by Galen W. Radebaugh to the University of Connecticut in partial fulfillment of the Doctor of Philosophy degree requirements.

Partially supported with funds from the Connecticut Research Foundation.

Reverse Permeation of Salicylate Ion Through Cellulose Membrane

FUJIO KAMETANI ˣ, SHUJI KITAGAWA, and HULKI A. GENCAY

Received December 21, 1981 from the *Faculty of Pharmaceutical Sciences, University of Tokushima, Shomachi, Tokushima 770, Japan.* Accepted for publication August 9, 1982.

Abstract □ The reverse permeation of salicylate ion and the effect of bovine serum albumin on the permeation were studied in a sodium salicylate–sodium oxalate–water system. In passive transport the permeation flux of an ion is expressed by the linear combination of the two terms which represent the concentration and electric potential gradients. Because the mobility of the sodium ion is greater than the oxalate ion, salicylate ion moves against the concentration gradient, and follows the electric potential gradient in the initial stage of permeation. The reverse permeation of salicylate ion through a cellulose membrane was accelerated with a high concentration ratio of oxalate to salicylate ions and reached a maximum value after 10 hr in the absence of bovine serum albumin. After reaching a maximum value, the salicylate ion permeated along the concentration gradient. The maximum concentration efficiency was 11.2%. In the presence of bovine serum albumin, the reverse permeation of salicylate ion reached a maximum value after 3 hr.

Keyphrases □ Reverse permeation—of salicylate ion with oxalate ion, through a cellulose membrane, protein effect on permeation flux □ Salicylate ion—permeation through a cellulose membrane, concentration by oxalate ion, protein effect on permeation flux □ Oxalate ion—permeation through a cellulose membrane with salicylate ion, protein effect on permeation flux

Most organic drugs dissociate in aqueous solutions and exist in ionic forms under biological conditions. Salicylate ion, one of the most commonly used drugs for analgesia, displaces other drugs such as the sulfonylureas (1) and sulfonamides (2), from the binding sites of the serum proteins. It has been reported that the absorption of salicylic acid is 61% in 0.1 *N* hydrochloric acid, 13% in sodium bicarbonate (pH 8) from the rat stomach (3), and 60% in physiological solution from the rat intestine (4). Effect of buffer constituents on salicylate absorption was studied with everted rat intestine and the inhibitory effect of potassium ions was reported (5–8). Since a variety of sub-

0022-3549/83/0400-0425$01.00/0

With these thoughts in mind, the shift factors were also plotted according to the W-L-F relationship (Eq. 6) in Fig. 6. The ideal W-L-F curve generated with the "universal" constants of $C_1 = 17.4$ and $C_2 = 51.6$ is also presented in Fig. 6 for comparison. The "universal" constants do not hold for many polymers, and it is apparent that the experimentally obtained plot of $\log a_T$ *versus* $(T - T_R)$ for anhydrous lanolin does not lie where the W-L-F relationship (with "universal" constants) predicts. The lack of fit of the experimental data with the W-L-F prediction also suggests that the transition is probably not a glass transition as most polymers that undergo a glass transition obey the W-L-F prediction.

CONCLUSION

It has been demonstrated that the energy of activation for the structural changes occurring in the transition of anhydrous lanolin between 10 and 15° can be calculated by a temperature–shear frequency reduction scheme and an Arrhenius-type relationship. The E_a, which is ~90 kcal, compares favorably with the magnitude of the E_a of a high molecular weight polymer undergoing a glass transition. This comparison is significant when one considers the generally low molecular weight composition of anhydrous lanolin. The magnitude of the E_a for anhydrous lanolin suggests that the intra- and intermolecular forces are as great as those in high molecular weight polymers. Hence, the nature of the functional groups and the chain length of the molecules determine the strength of the structure of the system.

Overall, the experimental data suggest that anhydrous lanolin undergoes a major mechanical transition between 10 and 15°. Both the ability to superpose modulus *versus* shear frequency data and an E_a of 90 kcal for the transition are characteristic of a glass transition, but other observations are not. As described in the preceding paper (5), these observations are: a lower limiting value of the elastic modulus than would be expected for a glass transition, a slower rate of change of tan δ with temperature about the transition than would be expected for a glass transition, and a lack of fit of experimental data to the W-L-F relationship. Rather than a sharp transition from a rubbery to an ordered glassy state, it appears that anhydrous lanolin undergoes a mechanical transition from a rubber-like state to a structural state which is less ordered than a glassy state.

REFERENCES

(1) J. D. Ferry, "Viscoelastic Properties of Polymers," 3nd ed., Wiley, New York, N.Y., 1980.

(2) L. E. Nielsen, "Mechanical Properties of Polymers," vol. 1, Dekker, New York, N.Y., 1974.

(3) A. N. Martin, G. S. Banker, and A. H. C. Chun, "Advances in Pharmaceutical Sciences," vol. 1, H. S. Bean, A. H. Beckett, and J. E. Carless, Eds., Academic, New York, N.Y., 1964, p. 1.

(4) B. W. Barry, "Advances in Pharmaceutical Sciences," vol. 4, H. S. Bean, A. H. Beckett, and J. E. Carless, Eds., Academic, New York, N.Y., 1974, p. 1.

(5) G. W. Radebaugh and A. P. Simonelli, *J. Pharm. Sci.*, **72**, 415 (1983).

(6) J. J. Aklonis, W. J. MacKnight, and M. Shen, "Introduction to Polymer Viscoelasticity," Interscience, New York, N.Y., 1972.

(7) J. Bischoff, E. Catsiff, and A. V. Tobolsky, *J. Am. Chem. Soc.*, **74**, 3378 (1952).

(8) A. V. Tobolsky and J. R. McLoughlin, *J. Polymer Sci.*, **8**, 543 (1952).

(9) J. D. Ferry, *J. Colloid Sci.*, **10**, 474 (1955).

(10) J. R. Van Wazer, J. W. Lyons, K. Y. Kim, and R. E. Colwell, "Viscosity and Flow Measurements—A Laboratory Handbook of Rheology," Interscience, New York, N.Y., 1963.

(11) J. D. Ferry, *J. Am. Chem. Soc.*, **72**, 3746 (1950).

(12) R. C. Harper, H. Markovitz, and T. W. DeWitt, *J. Polymer Sci.*, **8**, 435 (1952).

(13) E. Catsiff and A. V. Tobolsky, *J. Colloid Sci.*, **10**, 375 (1955).

(14) M. L. Williams, R. F. Landel, and J. D. Ferry, *J. Am. Chem. Soc.*, **77**, 3701 (1955).

(15) N. L. Henderson, P. M. Meer, and H. B. Kostenbauder, *J. Pharm. Sci.*, **50**, 788 (1961).

ACKNOWLEDGMENTS

Adapted in part from a dissertation submitted by Galen W. Radebaugh to the University of Connecticut in partial fulfillment of the Doctor of Philosophy degree requirements.

Partially supported with funds from the Connecticut Research Foundation.

Reverse Permeation of Salicylate Ion Through Cellulose Membrane

FUJIO KAMETANI ˣ, SHUJI KITAGAWA, and HULKI A. GENCAY

Received December 21, 1981 from the *Faculty of Pharmaceutical Sciences, University of Tokushima, Shomachi, Tokushima 770, Japan.* Accepted for publication August 9, 1982.

Abstract □ The reverse permeation of salicylate ion and the effect of bovine serum albumin on the permeation were studied in a sodium salicylate–sodium oxalate–water system. In passive transport the permeation flux of an ion is expressed by the linear combination of the two terms which represent the concentration and electric potential gradients. Because the mobility of the sodium ion is greater than the oxalate ion, salicylate ion moves against the concentration gradient, and follows the electric potential gradient in the initial stage of permeation. The reverse permeation of salicylate ion through a cellulose membrane was accelerated with a high concentration ratio of oxalate to salicylate ions and reached a maximum value after 10 hr in the absence of bovine serum albumin. After reaching a maximum value, the salicylate ion permeated along the concentration gradient. The maximum concentration efficiency was 11.2%. In the presence of bovine serum albumin, the reverse permeation of salicylate ion reached a maximum value after 3 hr.

Keyphrases □ Reverse permeation—of salicylate ion with oxalate ion, through a cellulose membrane, protein effect on permeation flux □ Salicylate ion—permeation through a cellulose membrane, concentration by oxalate ion, protein effect on permeation flux □ Oxalate ion—permeation through a cellulose membrane with salicylate ion, protein effect on permeation flux

Most organic drugs dissociate in aqueous solutions and exist in ionic forms under biological conditions. Salicylate ion, one of the most commonly used drugs for analgesia, displaces other drugs such as the sulfonylureas (1) and sulfonamides (2), from the binding sites of the serum proteins. It has been reported that the absorption of salicylic acid is 61% in 0.1 *N* hydrochloric acid, 13% in sodium bicarbonate (pH 8) from the rat stomach (3), and 60% in physiological solution from the rat intestine (4). Effect of buffer constituents on salicylate absorption was studied with everted rat intestine and the inhibitory effect of potassium ions was reported (5–8). Since a variety of sub-

0022-3549/83/0400-0425$01.00/0

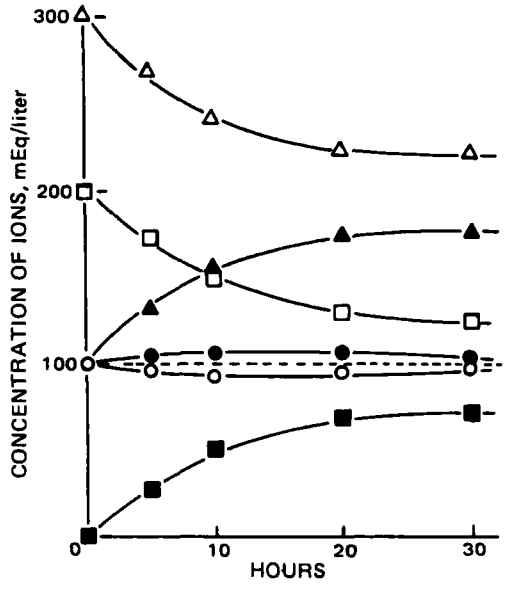

Figure 1—*Permeation of salicylate (○), oxalate (□), and sodium (△) ions. Initial concentration of sodium salicylate in compartments I and II was 100 mM; concentration of sodium oxalate in compartment I was 50 mM. Open figures represent compartment I; closed figures represent compartment II.*

stances are added to control the physical and physiological conditions of drug solutions, the absorption of drugs is affected by these multi-ionic components.

In passive transport at constant temperature, the membrane permeation flux of any ion (J_i) is given by the following equation which consists of two terms involving the concentration gradient and the electric potential gradient (9):

$$J_i = -D_i(\delta[i]/\delta x) - B_i Z_i[i](\mathrm{F/N})(\delta E/\delta x) \quad \text{(Eq. 1)}$$

where $[i]$ is the concentration of an ion i, E is the electric potential, and x is the coordinate taken in a direction of the permeation flux. D_i, B_i, F, N, and Z_i are the diffusion coefficient, the mobility, the faraday, Avogadro's number, and the valence of the ion, respectively. For the steady state of permeation, the following equation was derived from Eq. 1 (9):

$$J_i = -D_i(\delta[i]/\delta x) + \frac{B_i Z_i[i]}{\Sigma Z_j^2 B_j[j]} \Sigma Z_j D_j(\delta[j]/\delta x) \quad \text{(Eq. 2)}$$

where $[j]$ is the concentration of the coexisting ion j. Thus,

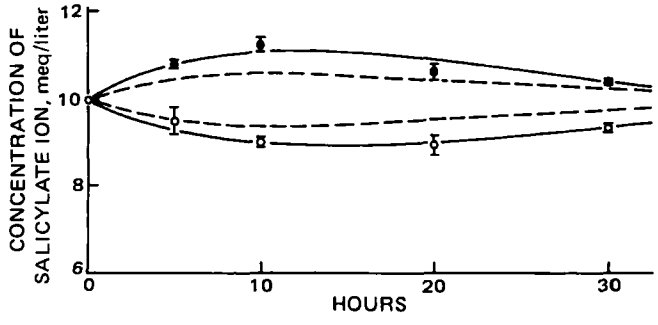

Figure 2—*Reverse permeation of salicylate ion. Initial concentration of sodium salicylate in compartments I and II was 10 mM; concentration of sodium oxalate in compartment I was 50 mM. Data points show the mean concentrations; standard deviations of four runs are indicated as bars on the data points. Key: (○) compartment I, (●) compartment II, and (- - -) values predicted from Eq. 5.*

Table I—Electric Potential Differences (ΔE)

Hours of Permeation	ΔE, mV
0	23.6
5	11.1
10	5.8
20	1.6
30	0.7

the apparent diffusion coefficient (D_i') is expressed as follows (10):

$$D_i' = kTB_i\left\{1 - \frac{Z_i[i]\Sigma Z_j B_j(\delta[j]/\delta x)}{(\Sigma Z_j^2 B_j[j])(\delta[i]/\delta x)}\right\} \quad \text{(Eq. 3)}$$

where k is the Boltzmann constant, T is the absolute temperature, and Σ means a sum of all ions. If the second term in the bracket is >1, D_i' is negative and reverse diffusion is observed in simple inorganic systems (10, 11).

In this report, the reverse permeation of salicylate ion was studied in a sodium salicylate–sodium oxalate–water system. Since oxalic acid is injected intravenously as a hemostatic agent for animals, sodium oxalate was used as a coexisting anion in this model system. The reverse permeation of salicylate ion was also studied in the presence of bovine serum albumin. Due to the reverse permeation, salicylate ion was concentrated in one compartment of the permeation cell. The concentration efficiency of salicylate ion varied with the concentration of oxalate ion.

EXPERIMENTAL

Materials and Permeation Procedures—The cellulose membrane used was 35-μm thick seamless cellulose tubing[1] purchased from a commercial source. Sodium salicylate, sodium oxalate, and sucrose were analytical grade[2]. Bovine serum albumin was purchased from a commercial source[3]. Distilled and deionized water was used for all experiments.

Permeation of salicylate ion was measured in four cells, as previously described (12). Each cell compartment was stirred by a magnet at ~900

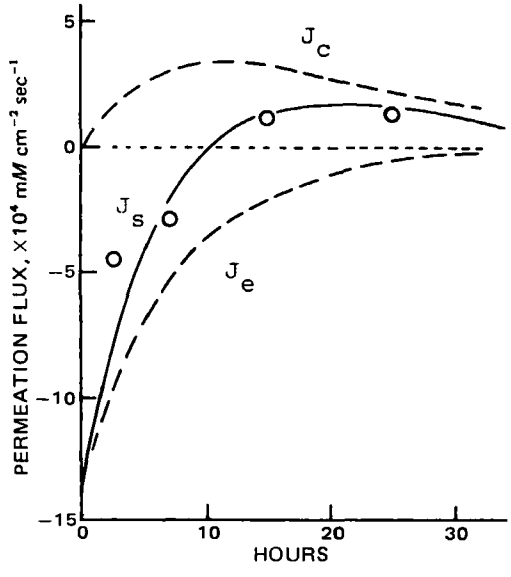

Figure 3—*Permeation flux of salicylate ion. Initial concentration of sodium salicylate and sodium oxalate are as shown in Fig. 2. Key: (J_s) total flux of salicylate ion, (J_c) flux of concentration gradient, (J_e) flux of electric potential gradient, and (○) as calculated by Eq. 4.*

[1] Union Carbide Corp., New York, N. Y.
[2] Wako Pure Chemical Industries, Osaka, Japan.
[3] Sigma Chemical Co., St. Louis, Mo.

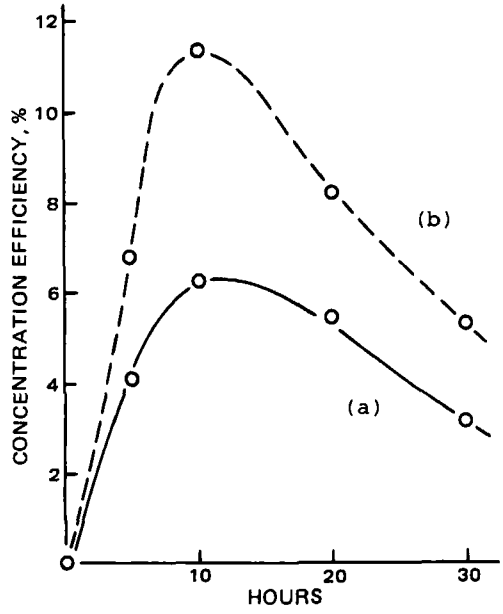

Figure 4—*Concentration efficiency of salicylate ion. Initial concentrations of sodium salicylate and sodium oxalate for (a) and (b) are as shown in Figs. 1 and 2, respectively.*

rpm at 25 ± 0.1°. In the presence of bovine serum albumin, the permeation of salicylate ion was followed in a cell where the volume of compartments I and II were 15.4 and 14.3 cm^3, respectively, and the membrane area was 3.19 cm^2. Sucrose was added to the solution without bovine serum albumin to make it isotonic. Both compartments were stirred at ~900 rpm at 10 ± 0.1°. The initial concentration of sodium salicylate was either 100 m*M* in both compartments with a 50 m*M* sodium oxalate solution in compartment I, or 10 m*M* in both compartments, with a 50 m*M* sodium oxalate solution in compartment I.

Analysis—Salicylate ion was analyzed by second differential absorption spectroscopy using a double-beam spectrophotometer[4] equipped with a derivative unit[5]. The second differential absorption spectrum ($\Delta\lambda$ = 4 nm) of the salicylate ion can be separated from that of oxalate ion. Sodium ion was analyzed with a flame photometer[6]. The concentration of oxalate ion was calculated from the difference of the concentrations of salicylate and sodium ions, on the assumption that the solution was electrically neutral. The diffusion potential through a membrane was measured with a DC-microvoltmeter[7] and calomel electrodes[8] using 3.3 *M* KCl agar bridges which contacted both cell compartments.

RESULTS AND DISCUSSION

The permeation of salicylate through a cellulose membrane in a mixed solution of sodium salicylate and sodium oxalate was measured at various times. The change in the concentration of ions where the initial concentration ratio of oxalate to salicylate in compartment I was 0.5, is shown in Fig. 1. The difference in concentration of salicylate ions in both compartments was zero at the initial stage of permeation and reached a maximum value after 10 hr. At this stage, salicylate ion was moving against the concentration gradient, *i.e.*, the salicylate ion concentration was increasing in compartment II. After the maximum reverse permeation, the concentration of salicylate ion reached the equilibrium concentration, equal to the initial concentration.

Assuming that the concentration gradient in the membrane is linear, the permeation flux can be calculated by the following equation (instead of Eq. 2):

$$J_i = -fkTB_ih_i\left\{\left(\frac{[i]_{II}-[i]_I}{L}\right)-\frac{Z_i[i]\Sigma Z_jB_jh_j([j]_{II}-[j]_I)/L}{h_i\Sigma Z_j^2B_j[j]}\right\} \quad \text{(Eq. 4)}$$

where f is the membrane constant, L is the thickness of the membrane,

[4] Model UV-180, Shimadzu Seisakusho, Kyoto, Japan.
[5] Model DES-2, Shimadzu Seisakusho, Kyoto, Japan.
[6] Type 205, Hitachi, Tokyo, Japan.
[7] Model PM-18C, Toa Electronics, Tokyo, Japan.
[8] Type 2010A, Hitachi-Horiba, Tokyo, Japan.

Table II—Initial Concentrations of Simple Permeation

Type[a]	Compartment	Sodium Salicylate, m*M*	Sodium Oxalate, m*M*
a	I	0.2	90
	II	0.4	10
b	I	0.2	10
	II	0.4	90
c	I	0.2	50
	II	0.4	50

[a] Taken from the text.

and h_i is a coefficient for the activity coefficient (γ_i) of the ion such that $h_i = 1 + \delta\ln\gamma_i/\delta\ln[i]$. Using the Güntelberg equation (13) for γ_i, the concentration of salicylate ion in compartment II was calculated by:

$$[s]_{II}^{t+\Delta t} = [s]_{II}^{t} + J_sAt/V_{II} \quad \text{(Eq. 5)}$$

In this calculation, $[s]_{II}^{t}$ and $[s]_{II}^{t+\Delta t}$ are the concentrations of salicylate ion in compartment II after t and $t + \Delta t$ hours, respectively, J_s is the permeation flux of salicylate ion, A is the membrane area, and V_{II} is the volume of compartment II. The constant (f), obtained with calcium chloride, was 0.0573. B_i values for salicylate, oxalate, and sodium ions were 2.33×10^8, 2.35×10^8, and 3.24×10^8 (cm sec^{-1} $dyne^{-1}$), respectively, which were calculated from limiting equivalent conductivities (14) according to Wendt (15). Observed and calculated values are shown in Fig. 2 when the initial concentration ratio of oxalate to salicylate ions was 5. Since the sampling time interval in the initial stage was long compared with the permeation rate, the first permeation flux of salicylate ion was sooner than estimated. Therefore, calculated concentrations are smaller values than expected because of the cumulative addition in Eq. 5.

To clarify the difference between observed and calculated values, the electric potential differences (ΔE) were measured (Table I). Assuming that the potential gradient in the membrane is linear ($\delta E/\delta x = \Delta E/L$), permeation flux due to the electric potential gradient (J_e) can be calculated using the following equation instead of the second term in Eq. 4:

$$J_e = -fB_iZ_ih_i[i](F/N)(\delta E/\delta x) \quad \text{(Eq. 6)}$$

Adding J_e to the permeation flux due to the concentration gradient (J_c) calculated by the first term in Eq. 4, the total flux of salicylate ion is obtained, as shown in Fig. 3. In this case, the calculated values are in good agreement with the observed values. The negative total flux indicates reverse permeation, which is at a maximum when the total flux is equal to zero.

To compare the reverse permeation of salicylate ion under different conditions, a mean concentration ($\overline{[s]}$) and a mean value of concentration change ($\overline{\Delta[s]}$) of the salicylate ion were calculated by:

$$\overline{[s]} = \frac{V_I([s]_I^0 + [s]_I^f) + V_{II}([s]_{II}^0 + [s]_{II}^f)}{2(V_I + V_{II})} \quad \text{(Eq. 7)}$$

and

$$\overline{\Delta[s]} = \frac{V_I([s]_I^f - [s]_I^0) + V_{II}([s]_{II}^0 - [s]_{II}^f)}{V_I + V_{II}} \quad \text{(Eq. 8)}$$

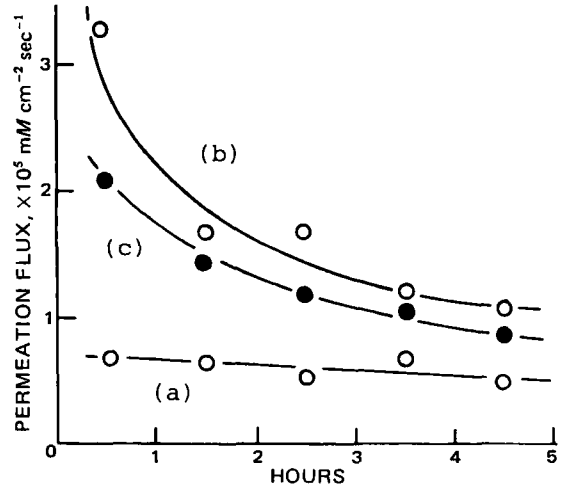

Figure 5—*Concentration gradient effect. Initial concentrations of sodium salicylate and sodium oxalate for (a), (b), and (c) are shown in Table II.*

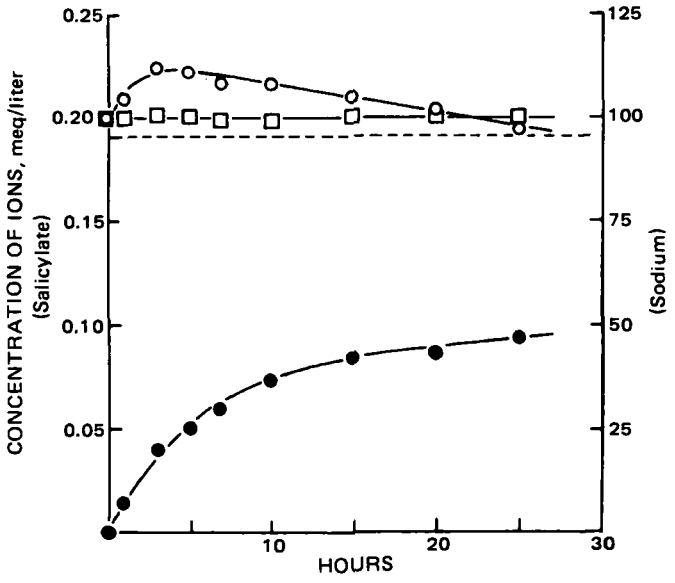

Figure 6—*Reverse permeation of salicylate ion in the presence of bovine serum albumin. Initial concentrations of sodium salicylate in compartment I and II were 0.2 and 0.4 m*M*, respectively; bovine serum albumin (0.1 m*M*) was dissolved in compartment II. Key: concentration of salicylate ion in compartment I when initial concentration of sodium oxalate in both compartments was 50 m*M *(□); concentration of salicylate (○) and sodium (●) ions in compartment I when initial concentrations of sodium oxalate in comparments I and II were 0 and 50 m*M*, respectively.*

where $[s]_I^0$ and $[s]_{II}^0$ are the initial concentrations of salicylate ion and $[s]_I^t$ and $[s]_{II}^t$ are the concentrations after time t in the indicated compartments. V_I and V_{II} are volumes of compartment I and II, respectively. In this study, the compartment of the permeation cell with a higher total concentration of salicylate ion is designated as II.

The efficiency of concentration (R) was calculated by:

$$R = -\overline{\Delta[s]}/\overline{[s]} \qquad \text{(Eq. 9)}$$

Since the numerator in Eq. 9 is negative due to the reverse permeation, a minus sign is added to the right-hand side of Eq. 9 to obtain a positive value for the efficiency of concentration. R-values at 10 hr were 6.1 and 11.2% when the initial concentration ratios of oxalate to salicylate were 0.5 and 5, respectively (Fig. 4).

To confirm the concentration gradient effect of the oxalate ion, the permeation fluxes of salicylate ion were measured under three different conditions: (*a*) the opposite direction from the concentration gradients of salicylate and oxalate ions, (*b*) the same direction as the concentration gradients, and (*c*) no concentration gradient of oxalate ion (Table II). The concentration ratio of oxalate to salicylate was greater than that used previously (Fig. 2) in order to obtain significant values for the permeation fluxes. The simple permeation of salicylate ion was accelerated most with both concentration gradients in the same direction (Fig. 5).

In the presence of bovine serum albumin, when the concentration of oxalate in both compartments was the same (*i.e.*, no concentration gradient of oxalate), a significant concentration change of salicylate was not obtained under the experimental conditions (Fig. 6). The slow permeation of the salicylate ion was due to the small membrane area and small concentration gradient. The concentration of unbound salicylate ion in compartment II would be lower than that in compartment I because of protein binding, which can be estimated by the binding parameters (16). Salicylate ion permeated from compartment II to I against the concentration gradient, with a greater concentration gradient of oxalate ion. Since it has been shown that association constants $>1 \times 10^4 M^{-1}$ affect drug distribution (17), salicylate ion bound on the secondary binding sites of bovine serum albumin can permeate with the electric potential gradient based on the oxalate concentration gradient. The reverse permeation reached a maximum value after 3 hr in the presence of bovine serum albumin. The concentration of salicylate ion in compartment I decreased after the maximum and approached the lower concentration (0.191 m*M*) which was obtained after 72 hr, as shown by the dotted line in Fig. 6. The concentration of sodium ion in compartment I showed that the solution had not equilibrated after 30 hr.

Organic drugs permeate through biomembranes mainly in their uncharged forms. If the same mechanism is applicable to biological systems, salicylate ion may be concentrated on the membrane boundary with the concentration gradient of coexisting ions. Assuming that the effective pH at the site of drug absorption is 5.3 (18), uncharged salicylic acid would be concentrated more on the membrane boundary than in the intestinal contents. When salicylate is coadministered with a weakly acidic drug, then the permeation rate of salicylate determined by dialysis techniques will vary with the concentration gradient of the coexisting drug.

REFERENCES

(1) K. F. Brown and M. J. Crooks, *Biochim. Pharmacol.*, **25,** 1175 (1976).

(2) H. Ichibagase, Y. Imamura, and H. Nakagami, *Chem. Pharm. Bull.*, **24,** 204 (1976).

(3) L. S. Schanker, P. A. Shore, B. B. Brodie, and C. A. M. Hogben, *J. Pharmacol. Exp. Ther.*, **120,** 528 (1957).

(4) L. S. Schanker, D. J. Tocco, B. B. Brodie, and C. A. M. Hogden, *ibid.*, **123,** 81 (1958).

(5) M. Mayersohn and M. Gibaldi, *J. Pharm. Sci.*, **58,** 1429 (1969).

(6) M. Mayersohn and M. Gibaldi, *Biochim. Biophys. Acta*, **196,** 296 (1970).

(7) L. Z. Benet, J. M. Orr, R. H. Turner, and H. S. Webb, *J. Pharm. Sci.*, **60,** 234 (1971).

(8) S. Kojima, T. Tenmizu, T. Shino, and M. Cho, *Chem. Pharm. Bull.*, **22,** 952 (1976).

(9) M. Nakagaki and M. Kobayashi, *Yakugaku Zasshi*, **93,** 287 (1973).

(10) M. Nakagaki and S. Kitagawa, *Bull. Chem. Soc. Jpn*, **49,** 1748 (1976).

(11) M. Nakagaki and S. Kitagawa, *Yakugaku Zasshi*, **98,** 840 (1978).

(12) F. Kametani, S. Kitagawa and K. Nishiyama, *Chem. Pharm. Bull.*, **27,** 2710 (1979).

(13) E. Güntelberg, *Z. Phys. Chem.*, **123,** 199 (1926).

(14) H. Landolt and R. Börnstein, "Zahlenwerte und Funktionen aus Astronomie, Geophysik und Technik," vol. 2, part 7, Springer-Verlag, Berlin, 1960, p. 257.

(15) R. P. Wendt, *J. Phys. Chem.*, **69,** 1227 (1965).

(16) C. A. Cruze and M. C. Meyer, *J. Pharm. Sci.*, **65,** 33 (1976).

(17) B. K. Martine, *Nature (London)*, **207,** 274 (1965).

(18) L. S. Schanker, "Fundamentals of Drug Metabolism and Drug Disposition," B. N. La Du, H. G. Mandel, and E. L. Way, Eds., Williams & Wilkins, Baltimore, Md., 1972, p. 29.

Determination of the Dissociation Constant of a Weak Acid Using a Dissolution Rate Method

JØRGEN B. HANSEN [x] **and OTTO HAFLIGER**

Received April 6, 1982, from the *Biological Pharmaceutical Research Department, Hoffmann-LaRoche & Co., Ltd., Basle, Switzerland.* Accepted for publication July 14, 1982.

Abstract □ Based on theories of diffusion-controlled mass transport for dissolution processes of weak acids in aqueous alkaline media, a method for the determination of the dissociation constant of a weak monoprotic acid is described. The method includes measurements of the initial dissolution rate as a function of pH, using the rotating-disk technique, and determination of the intrinsic solubility. The method was applied to determine the apparent dissociation constant (μ = 0.1) of 5,5-dimethyl-3-(α,α,α,4-tetrafluoro-*m*-tolyl)hydantoin, a new schistosomicide. For comparison, a spectrophotometric method for the pK_a determination was developed. Due to rapid hydrolysis of the compound in the pH range required for the determination of the pK_a, the development of the latter method turned out to be complicated and tedious. The results of both methods were in good agreement. For compounds with unfavorable properties for titrimetric or spectrophotometric determination of the pK_a value, the dissolution rate method can be a useful alternative.

Keyphrases □ Dissociation constant determinations—use of a dissolution rate method, weak acids, 5,5-dimethyl-3-(α,α,α,4-tetrafluoro-*m*-tolyl)hydantoin □ Dissolution rate method—determination of dissociation constants, weak acids, 5,5-dimethyl-3-(α,α,α,4-tetrafluoro-*m*-tolyl)hydantoin

The determination of the dissociation constant of weakly acidic or basic drugs is normally a routine matter, using one of the established techniques (1–3). However, in some cases the compound may have unfavorable properties which makes such a routine determination difficult. Such is the case when the compound undergoes a fast chemical reaction in the medium required for the measurements.

From the dissolution rate model of weak acids in alkaline media (4), and the theories of the influence of irreversible reactions on the dissolution of a solid (5), it could be expected that dissolution behavior could form the basis for a method to determine the dissociation constant of a weak acid undergoing fast degradation in the pH range around the pK_a value.

This study utilized, 5,5-dimethyl-3-(α,α,α,4-tetrafluoro-*m*-tolyl)hydantoin (I), a new schistosomicide (6).

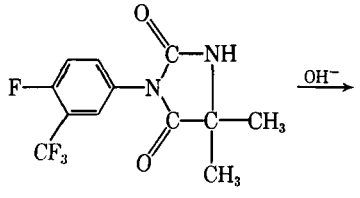

(I)

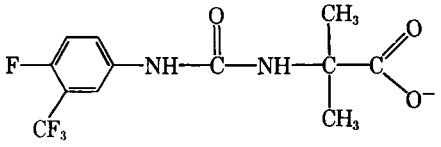

(II)

The hydantoin derivative (I) is expected to be a weak acid. The compound is stable in the acidic and neutral pH range, but undergoes a fast hydrolysis in aqueous alkaline media forming the hydantoic acid (II).

For the determination of the dissociation constant of the acid (I), two methods have been compared: the method based on the dissolution rate and a spectrometric method.

THEORETICAL

Determination of pK_a by Spectroscopy—The determination of the dissociation constant by spectroscopy is possible if un-ionized and ionized species of the molecule yield different spectra in UV-visible range (1–3). Measuring the absorbance at a particular wavelength, the K_a for acids can be obtained from the equation:

$$K_a = \frac{\epsilon_M - \epsilon}{\epsilon - \epsilon_I}[H^+] \qquad \text{(Eq. 1)}$$

where ϵ_M and ϵ_I are molar absorptivities for the un-ionized and ionized species, and ϵ is the molar absorptivity at $[H^+]$. In cases where ϵ_I is not directly obtainable, Maroni (7) has proposed a method, based on the rearrangement of Eq. 1:

$$\epsilon = \epsilon_I - \frac{(\epsilon - \epsilon_M)[H^+]}{K_a} \qquad \text{(Eq. 2)}$$

Plotting a series of ϵ values against $(\epsilon - \epsilon_M)[H^+]$ gives a straight line and K_a can be calculated from the slope. If the compound undergoes a rapid reaction, it will be impossible to measure the ϵ-values directly. However, if the reaction is of first order, the ϵ-values may be obtained from measurements of the absorbance as a function of time, using the Guggenheim method (8).

Determination of pK_a by Dissolution Rate—Based on the film theory of Nernst (9) for heterogeneous reactions, Higuchi *et al.* (4) have formulated a model for dissolution of a weak acid in a basic medium. This model postulates that the dissolution rate is controlled by a rapid, reversible chemical reaction and simultaneous diffusion of all important species taking part in the processes that occur within a boundary layer. It is assumed in this model that the diffusion layer for all solute species is equal. A schematic diagram of the Higuchi model is presented in Fig. 1, where HA is the acid, B^- is the incoming base and h is the thickness of the diffusion layer. Under sink condition, $[HA]_h$ and $[A^-]_h$ will effectively be zero.

The general equation, based on this model for the initial dissolution rate or flux J as a function of the bulk concentration of the incoming base, is relatively complicated (4). If the base happens to be the hydroxide ion, the equation will be simpler (10):

$$J = \frac{D_{HA}[HA]_0}{h} + \frac{(D_{OH})^2[OH^-]_h}{h}\left(\frac{D_A[HA]_0K_a/K_w}{(D_{OH})^2 + D_AD_{OH}[HA]_0K_a/K_w}\right) \qquad \text{Eq. 3)}$$

where D_S is the diffusion coefficient of species S in the system, $[HA]_0$ is the intrinsic solubility, *i.e.*, the solubility of the undissociated species, and K_a and K_w are dissociation constants of the acid and water, respectively.

If we assume that $D_A = D_{HA}$ and substitute $K_w/[H^+]_h$ for $[OH^-]_h$, and J_0 for $D_{HA}[HA]_0/h$, rearrangement of Eq. 3 gives:

$$J = J_0 + \frac{J_0D_{OH}K_a}{[H^+]_h(D_{OH} + D_{HA}[HA]_0K_a/K_w)} \qquad \text{(Eq. 4)}$$

Plotting a series of values of the flux against the corresponding reciprocal values of $[H^+]_h$ gives the slope:

$$a = \frac{J_0D_{OH}K_a}{D_{OH} + D_{HA}[HA]_0K_a/K_w} \qquad \text{(Eq. 5)}$$

0022-3549/83/0400-0429$01.00/0

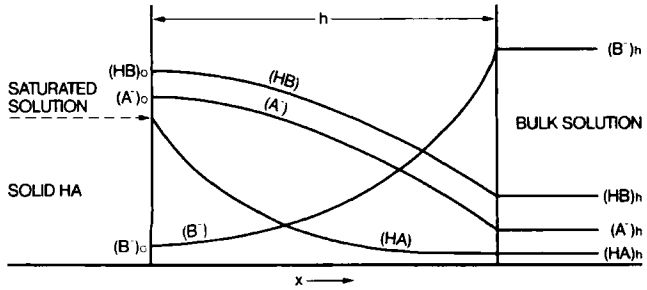

Figure 1—*Schematic diagram of the model of Higuchi* et al. *(4) for the dissolution of an acid, HA, into a reactive medium containing base* B^-.

and by rearrangement:

$$K_a = \frac{aD_{OH}K_w}{J_0D_{OH}K_w - aD_{HA}[HA]_0} \qquad \text{(Eq. 6)}$$

Studies of the dissolution rate can be performed with the rotating-disk technique, where the flux as a function of hydrodynamic conditions has been studied very extensively by Levich (11). For the rotating disk, the mass flux is given as:

$$J = 0.62D^{2/3}\nu^{-1/6}\omega^{1/2}[HA]_0 \qquad \text{(Eq. 7)}$$

where ν is the kinematic viscosity and ω is the angular velocity of rotation.

The corresponding diffusion boundary layer may be written as:

$$h = 1.612\,D^{1/3}\nu^{1/6}\omega^{-1/2} \qquad \text{(Eq. 8)}$$

Higuchi *et al.* (5) have studied the influence of an irreversible reaction on the dissolution rate of a compound undergoing a rapid hydrolytic reaction simultaneously with the dissolution. It was found that the influence depends on the diffusion time t_D, which is the average lifetime for an element to travel through the diffusion layer, and on the reaction rate of the irreversible reaction.

The diffusion time was expressed as:

$$t_D = \frac{h^2}{2D} \qquad \text{(Eq. 9)}$$

EXPERIMENTAL

Materials—5,5-Dimethyl-3-(α,α,α,4-tetrafluoro-*m*-tolyl)hydantoin was of purity >99.8%. All other chemicals were of analytical grade.

Spectrophotometric Method—A 1-ml portion of 1.7×10^{-2} *M* of the acid (I) in ethanol was added to 50 ml of 0.1 *N* NaCl or solutions of sodium hydroxide adjusted to an ionic strength of 0.1 with sodium chloride and stirred at 25.0°. The solutions were injected into a 1-cm cell of a UV-visible spectrophotometer[1], thermostated at 25.0 ± 0.1°, and the change of absorbance with time was measured at 254 nm. The pH of the solutions was measured at 25° using a combination pH microelectrode[2] with low alkaline error and a pH meter[3].

Dissolution Rate Method—The dissolution rates were determined using the rotating disk technique, with an apparatus similar to that described by Wood *et al.* (12). A disk (1.6 cm in diameter) of the compound was compressed at 3×10^3 kg for 3 min in a hydraulic press. The disk assembly was rotated by a variable-speed synchronous motor that was calibrated by a tachometer. The dissolution rates were determined at 25.0 ± 0.1° using a constant temperature water bath.

Solubility—The solubility of I was determined by shaking an excess of the compound in 0.1 *N* NaCl solution at 25.0° in a water bath for 24 hr, during which time equilibrium solubility was reached. After equilibration the solution was filtrated through a membrane filter (0.45 μm). The filtrate was diluted appropriately with water, and the assay was made spectrophotometrically at 270 nm (ϵ = 858).

Diffusion Coefficient and Boundary Layer Thickness—The dissolution rate measurements were performed using the rotating disk in 500 ml of 0.1 *N* NaCl at 25.0° with rotation speeds varying from 50 to 299 rpm. At each rotation speed the dissolution rate was determined after a rotation period of 20 min. A 1-ml solution of 1 *N* NaOH was added to 10.0 ml of the sample, and the solutions were kept at 25° for 1 hr. The solutions were diluted appropriately with 0.1 *N* sodium hydroxide and measured by UV spectrophotometry at 239 nm (ϵ = 16180).

Dissolution–pH Profile—The determination of the dissolution rate as a function of pH was performed with the same compressed disk for the whole pH profile, and the test solution was not renewed. However the different pH values were obtained by successive additions of 0.1 *N* NaOH solution to the test solution, and the dissolution was determined after each change of pH. Corrections for added volumes of 0.1 *N* NaOH and the samples withdrawn were considered.

The dissolution–pH profile was determined with a rotation speed of 100 rpm. The starting medium was 500 ml of 0.1 *N* NaCl. The disk was initially stirred in the medium for about 15 min, and the pH was then adjusted to a higher predetermined value by adding 0.1 *N* NaOH. A sample was withdrawn after equilibrating for 5 min and again after 20 min. The pH was then adjusted to the next higher pH value, and the procedure for sampling was repeated. The procedure was repeated until samples from a representative number of pH values had been collected. The assay of the samples was performed in the same way as described for determination of diffusion coefficient.

Table I—Experimental Data of the Spectrophotometric Method for the Determination of the Apparent pK_a at 25° [a]

pH	$t_{1/2}$, min	$\epsilon_{254\ nm}$	pK_a [b]
7.40		542	
11.77	9.50	787	12.12
11.89	8.21	835	12.12
11.93	7.85	861	12.10
11.99	7.43	891	12.09
12.05	6.81	915	12.10
12.11	6.41	947	12.10
12.17	6.00	950	12.14
12.28	5.56	1006	12.13
12.35	5.17	1051	12.09
12.48	4.77	1098	12.10
12.57	4.58	1131	12.10
			Average 12.11 (± 0.03)

[a] μ = 0.1. [b] The individual values were calculated from Eq. 1, where ϵ_M = 542 and ϵ_I = 1332. ϵ_I was obtained from Eq. 2.

RESULTS AND DISCUSSION

Spectrophotometric Method—The molar absorptivity of the nonionized species ϵ_M could be obtained directly from the measurement of the absorbance in the 0.1 *N* NaCl solution in which the compound is stable. In the pH range of 11.79–12.57, the absorbance at time zero had to be calculated from the absorbance–time curve. Preliminary studies have shown, that the hydrolysis of I to the corresponding hydantoic acid, as would be expected, is of first order. The Guggenheim method (8) could, therefore, be applied for the calculation of the ϵ values from the initial part of the absorbance–time curves. From these curves kinetic data of the hydrolytic reaction could also be obtained by the Guggenheim method. A reliable value for ϵ_I could not be found; therefore, K_a was calculated according to Eq. 2. This gave a slope -1.282×10^{12} (r = 0.991) corresponding to $K_a = 7.803 \times 10^{-13}$ or pK_a = 12.11.

The development of this spectrophotometric method turned out to be very tedious. Because of the fast hydrolytic reaction, it was difficult to find an optimal analytical wavelength.

Dissolution Rate Method—The intrinsic solubility $[HA]_0$ of I in 0.1 *N* NaCl was found to be 1.44×10^{-3} *M*. Rearranging Eq. 7, an expression for the diffusion coefficient can be found:

$$D_{HA} = \left(\frac{J\nu^{1/6}\omega^{-1/2}}{0.62[HA]_0}\right)^{3/2} = 4.8 \times 10^{-6}\ \text{cm}^2/\text{sec} \qquad \text{(Eq. 10)}$$

where $J\omega^{-1/2}$ determined from the slope of the linear plot J against $\omega^{1/2}$ (r = 0.996) was found to be 5.60×10^{-10} moles/cm^2/sec$^{1/2}$; $\nu = 8.93 \times 10^{-3}$ stokes is the kinematic viscosity of water at 25° (13).

From the investigations of Higuchi *et al.* (5) on the influence of irreversible chemical reactions on dissolution rate of a solid, it was found that for a diffusion time t = 3 sec, a half-life of the irreversible reaction greater than the order of 10 sec would have no influence on the dissolution rate. A rotation speed of 100 rpm of the rotating disk gives, according to Eq. 8, a diffusion layer thickness $h = 3.8 \times 10^{-3}$ cm. The diffusion time for (I) under this hydrodynamic condition will be t_D = 1.5 sec.

From the kinetic data given in Table I, it is obvious that by using the

[1] Uvikon, model 820, Kontron, Zürich, Switzerland.
[2] EA 125, Metrohm, Herisau, Switzerland.
[3] Model E 603, Metrohm, Herisau, Switzerland.

rotating disk at 100 rpm the dissolution rate will not be affected by the hydrolytic reaction in the pH range of 11.8–12.6. These hydrodynamic conditions were, therefore, used for the present pH profile study. Plotting the values of the flux J (see Table II) against the reciprocal values of the bulk hydrogen ion concentration $[H^+]_h$ a linear relationship was found. Using the least-squares method gave the slope $a = 7.530 \times 10^{-20}$ with the intercept $J_0 = 1.071 \times 10^{-7}$ moles/cm^2/min and a coefficient of correlation $r = 0.995$. Using these data, the experimental values of D_{HA} and $[HA]_0$ and assuming the diffusion coefficient of hydroxide ion in water D_{OH} to be 2.42×10^{-5} cm^2/sec (from Ref. 4), the dissociation constant was obtained from Eq. 6: $K_a = 7.178 \times 10^{-13}$ or $pK_a = 12.14$.

Equation 3 is based on the diffusion layer theory of Nernst. However, several aspects of the Nernst model have been criticized (11, 14). One drawback of the model is the erroneous assumption that the diffusion layer thickness is equal for all diffusing species under the same hydrodynamic conditions. For the rotating disk, the diffusion layer thickness of a diffusing species depends on the diffusion coefficient according to Eq. 8 (11). As D_{OH} is about 5 times greater than D_{HA}, the concentration of hydroxide ion at h_{HA}, $[OH^-]_h$ will be somewhat lower than the hydroxide ion concentration of the bulk solution $[OH^-]_{bulk}$. This could have a significant influence on the value for K_a, calculated from Eq. 6. An evaluation of $[OH^-]_h$ can be made by the following considerations.

From Eq. 8 and the numerical values of D_{HA} and D_{OH} a ratio N can be calculated:

$$N = \frac{h_{HA}}{h_{OH}} = \left(\frac{D_{HA}}{D_{OH}}\right)^{1/3} = 0.58 \qquad \text{(Eq. 11)}$$

To calculate the hydrogen ion concentration at the solid–liquid interface $[H^+]_0$ of the Higuchi model, Mooney *et al.* (15) have derived the equation:

$$-D_H[H^+]_0^2 + [H^+]_0(D_H[H^+]_h - D_{OH}[OH^-]_h) + K_w(D_{OH} + D_A[HA]_0K_a/K_w) = 0 \qquad \text{(Eq. 12)}$$

If $[H^+]_0$ and $[H^+]_h \ll [OH^-]_h$, and also assuming $D_{HA} = D_A$ and considering that $[OH^-]_0[H^+]_0 = K_w$, a rearrangement of Eq. 12 gives:

$$[OH^-]_0 = \frac{D_{OH}[OH^-]_hK_w}{D_{OH}K_w + K_aD_{HA}[HA]_0} \qquad \text{(Eq. 13)}$$

Defining the ratio R as:

$$R = \frac{[OH^-]_h - [OH^-]_0}{[OH^-]_{bulk} - [OH^-]_0} \qquad \text{(Eq. 14)}$$

and substituting Eq. 13 into Eq. 14, the following relationship between $[OH^-]_h$ and $[OH^-]_{bulk}$ is found:

$$[OH^-]_h = \frac{D_{OH}K_w + K_aD_{HA}[HA]_0}{D_{OH}K_w + K_aD_{HA}[HA]_0/R}[OH^-]_{bulk} \qquad \text{(Eq. 15)}$$

From investigations with the rotating-disk electrode, Levich (11) has derived the mathematical formula of the concentration gradient curve for a diffusing element in the diffusion layer of the rotating disk. Using this formula, the ratio R can be calculated for the value at a relative distance N from the solid–liquid interface:

$$R = \frac{\int_0^N e^{-u^3}\,du}{\int_0^\infty e^{-u^3}\,du} \qquad \text{(Eq. 16)}$$

For a value of $N = 0.58$, R was found to be 0.82. For this value of R Eq. 15 gives:

$$[OH^-]_h = 0.996\,[OH^-]_{bulk}$$

It is obvious that a factor of 0.996 will have no significant influence on the K_a value calculated on the basis of Eq. 4. For cases where the product $K_a\,[HA]_0$ is appreciably larger, a small influence may, however, be expected.

From Eq. 6 it can be estimated that the relative low value of the product $K_a[HA]_0$ also means that very high accuracy of the value for D_{OH} and D_{HA} is not required in the present case, and a simple calculation of D_{HA} using the square root method (16), for instance, may replace the experimental method used here. Equation 3 is valid only if $[OH^-]_0$ and $[OH^-]_h$ are essentially higher than $[H^+]_0$ and $[H^+]_h$. Otherwise the complete formula for the Higuchi model (4) has to be used.

The good agreement between the results of the spectrophotometric and the dissolution rate methods for determination of pK_a, shows that the theoretical approach used here may give a sound basis for the determination of the dissociation constant from the dissolution behavior.

Table II—Experimental Data of the Dissolution Method for the Determination of the Apparent pK_a at 25° [a]

pH	J, moles/cm^2/min $\times 10^7$	pK_a [b]
11.81	1.605	12.10
11.91	1.713	12.12
12.02	1.826	12.16
12.12	2.123	12.12
12.18	2.159	12.17
12.25	2.382	12.15
12.33	2.576	12.17
12.41	3.004	12.14
12.49	3.483	12.13
		Average 12.14 (± 0.04)

[a] $\mu = 0.1$. [b] The individual values were obtained from Eq. 4, where $J_0 = 1.071 \times 10^{-7}$ moles/cm^2/min.

Using the technique described here, the dissolution rate method can be applied advantageously for compounds with unfavorable properties for determination by a titrimetric or a spectrophotometric method.

In analogy to the approach used in the Higuchi model for pK_a determinations of weak acids, it may be expected that it can also be used for determinations of the pK_a values of weak bases by using, for instance, hydrochloric acid solutions as the reaction media. The dissociation constant may also be obtained from dissolution rates in buffer solutions. Simplified models for dissolution behavior in these media have been proposed (17, 18), assuming the pH of the solid–liquid interface to be equal to the pH of the bulk solution. However, as has been shown by Mooney *et al.* (19) this is generally not the case and may give erroneous results. The use of the extension of the Higuchi model for dissolution behavior in buffer solutions, as has been proposed by Mooney *et al.* (19) may, however, form a suitable basis for the determination of pK_a values in such media.

REFERENCES

(1) A. Albert and E. P. Serjeant, "The Determination of Ionization Constants," 2nd ed., Chapman and Hall, London, 1971.

(2) E. J. King, "Acid-Base Equilibria," Pergamon, Oxford, England, 1965.

(3) R. F. Cookson, *Chem. Rev.*, **74**, 5 (1974).

(4) W. I. Higuchi, E. L. Parrott, D. E. Wurster, and T. Higuchi, *J. Am. Pharm. Assoc., Sci. Ed.*, **47**, 376 (1958).

(5) T. Higuchi, H. K. Lee, and I. H. Pitman, *Farm. Notisbl.*, **80**, 55 (1971).

(6) K. Bernauer, H. Link, and H. Stohler, (Roche), Eur. Pat., 1813 (1981).

(7) P. Maroni and J. P. Calmon, *Bull. Soc. Chim. Fr.*, 519 (1964).

(8) E. A. Guggenheim, *Philos. Mag.*, **2**, 538 (1926).

(9) W. Nernst, *Z. Phys. Chem.* (Leibzig), **47**, 55 (1904).

(10) W. I. Higuchi, E. Nelson, and J. G. Wagner, *J. Pharm. Sci.*, **53**, 333 (1964).

(11) G. Levich, "Physicochemical Hydrodynamics," Prentice-Hall, Englewood Cliffs, N.J., 1962.

(12) J. H. Wood, J. E. Syarto, and H. Letterman, *J. Pharm. Sci.*, **54**, 1068 (1965).

(13) R. C. Weast, "Handbook of Chemistry and Physics," 58th ed., Chemical Rubber Publishing, Cleveland, Ohio, 1977.

(14) L. L. Bircumshaw and A. C. Riddiford, *Q. Rev. Chem. Soc.*, **6**, 157 (1952).

(15) K. G. Mooney, M. A Mintun, K. J. Himmelstein, and V. J. Stella, *J. Pharm. Sci.*, **70**, 13 (1981).

(16) T. Higuchi, S. Dayal, and I. H. Pitman, *J. Pharm. Sci.*, **61**, 695 (1972).

(17) M. Gibaldi, in "The Theory and Practice of Industrial Pharmacy," 2nd ed., L. Lachman, H. A. Lieberman, and J. Kanig, Eds., Lea & Febiger, Philadelphia, Pa., 1976, chap. 3.

(18) M. Nicklasson, A. Brodin, and H. Nyqvist, *Acta Pharm. Suec.*, **18**, 119 (1981).

(19) K. G. Mooney, M. A. Mintun, K. J. Himmelstein, and V. J. Stella, *J. Pharm. Sci.*, **70**, 22 (1981).

ACKNOWLEDGMENTS

The authors thank Ms. I. Schnyder and Ms. C. Muller for their skillful assistance in the experiments.

Kinetics of the Rapid Modification of Human Serum Albumin with Trinitrobenzenesulfonate and Localization of Its Site

YUKIHISA KURONO ˣ, KENICHI ICHIOKA, and KEN IKEDA

Received August 9, 1982, from the *Faculty of Pharmaceutical Sciences, Nagoya City University, Tanabe-dori, Mizuho-ku, Nagoya, 467, Japan.* Accepted for publication December 17, 1982.

Abstract □ The rapid reaction of human serum albumin with trinitrobenzenesulfonate (I) and the location of the reactive site were investigated to characterize the chemical modification of albumin by I. The modification proceeds through trinitrophenylation of a lysine residue of albumin and monoaddition of the byproduct, sulfite ion, to the trinitrophenylalbumin, as reported previously. The individual kinetic parameters for both reactions were determined at various pH values and 25°. The ε-amino group of the lysine residue which has a pK_a value of ~8.9 was the reactive group involved in the trinitrophenylation. The dissociation constant of the sulfite monoadduct was about 10-fold smaller than that of the monoadduct of the model compound trinitrophenyl α-acetyllysine. The modification of albumin by I reduced the fluorescence intensity of the tryptophan-214 residue in the albumin amino acid sequence. Acetylation of the lysine-199 residue with aspirin and 5-nitroaspirin decreased the trinitrophenylation rate of albumin with I. These results on the fluorescence spectroscopy and the effect of the acetylation suggest that the reactive group for I is the lysine-199 residue located near the tryptophan-214 residue.

Keyphrases □ Kinetics—of reaction of trinitrobenzenesulfonate with human serum albumin □ Albumin, human serum—kinetics of reaction with trinitrobenzenesulfonate, location of drug binding site, fluorescence spectroscopy, acetylation with aspirins □ Trinitrobenzenesulfonate—kinetics of reaction with human serum albumin □ Aspirin—acetylation of human serum albumin

Characterization of drug binding sites on human serum albumin and knowledge of drugs affecting these sites are important to predict displacement of one drug by another, when two or more drugs are administered concurrently (1). Studies on the drug binding sites of the albumin molecule have been carried out by various methods (2–5), one of which is chemical modification (4). Trinitrobenzenesulfonate (I) has been used as a reagent for amino group modification in proteins (6). Kinetic data of the reactions of human and bovine serum albumin with excess I were presented by Goldfarb (7) and Andersson *et al.* (8), respectively. Under their conditions (an excess of I over albumin), multiple reactive sites for I appear to be modified, so that it may be difficult to investigate in detail the kinetics and mechanism for the modification of a single specific site on albumin with I.

In our previous study (9), it was reported that the chemical modification of human serum albumin by I proceeds rapidly and specifically through the trinitrophenylation of a lysine residue in albumin and the sulfite monoaddition, as shown in Scheme I. Abbreviations in Scheme I are as follows: II, the Michaelis–Menten type complex of I and albumin; III, trinitrophenylalbumin; IV, sulfite ion; and V, sulfite monoadduct of III.

The present study is concerned with determination of the individual kinetic parameters in Scheme I at various pH values and with identification of the primary reactive site on albumin for I.

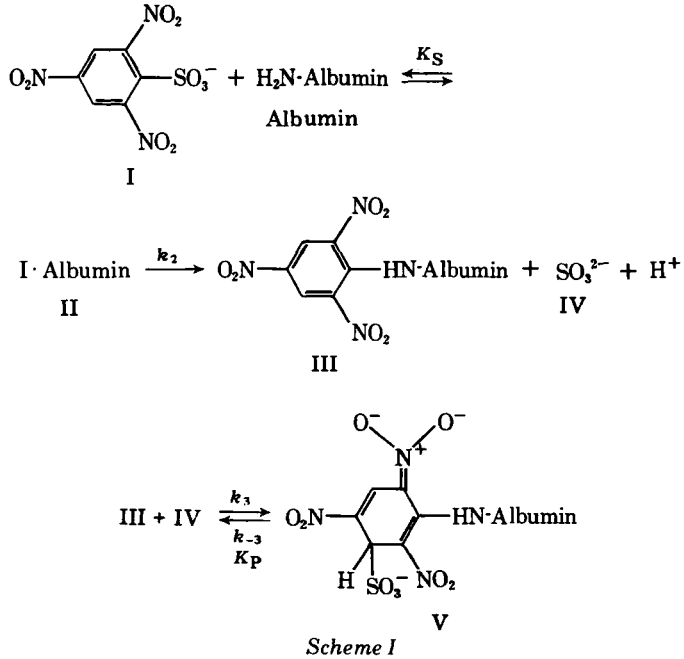

Scheme I

EXPERIMENTAL

Materials—Human serum albumin[1] was used after purification as previously described (10). The concentration of albumin was determined by use of its molar absorbance ($\epsilon_{albumin} = 3.66 \times 10^4\ M^{-1}\ cm^{-1}$) at 278 nm (11), assuming a molecular weight of 69,000. 2,4,6-Trinitrobenzenesulfonic acid sodium salt[2] and sodium bisulfite[3] were used without further purification. All other chemicals were reagent grade and were used without further purification.

Kinetic Data—The buffer systems used were: pH 6–8.3, 0.067 *M* phosphate; pH 8.3–9, 0.1 *M* phosphate and 0.05 *M* borate; pH 9–11, 0.05 *M* borate and 0.05 *M* carbonate. Ionic strength was adjusted to 0.2 *M* with sodium chloride. The temperature was kept at 25° in all experiments unless otherwise stated.

The UV spectral changes based on the reactions shown in Scheme I are presented in our previous paper (9). The trinitrophenylation rate of albumin with I was followed at a wavelength of 360 nm (showing an isosbestic point of III and V) with a stopped-flow spectrophotometer[4]. Pseudo first-order analysis was applied under the condition of excess albumin concentration relative to that of I.

For the analysis of the reversible reaction (III + IV ⇄ V) shown in Scheme I, the UV spectrum of either III or V (not of the mixture of III, IV, and V) is necessary. Since neither III nor V was isolated, each spectrum of III and V could not be measured independently, and thus the spectrum was unknown. Trinitrophenyl α-acetyllysine (VI) was chosen as a model compound for III for the following reason. The absorbance at 360 nm (isosbestic point of III and V), after completion of the spectral change due to the trinitrophenylation of albumin with I, was essentially equal to that of VI found in the literature (12), when the original absorbance based on the excess albumin over I was corrected. Therefore, the UV spectrum of III at wavelengths >360 nm could be assumed to be identical with the spectrum of VI.

[1] Sigma Chemical Co., Fraction V, lots 30F-02271 and 100F-02061.
[2] Wako Chemical Co., lot SDL 8630.
[3] Katayama-kagaku, lot 800805.
[4] Model RA-401, Union-Giken, Osaka, Japan.

0022-3549/83/0400-0432$01.00/0

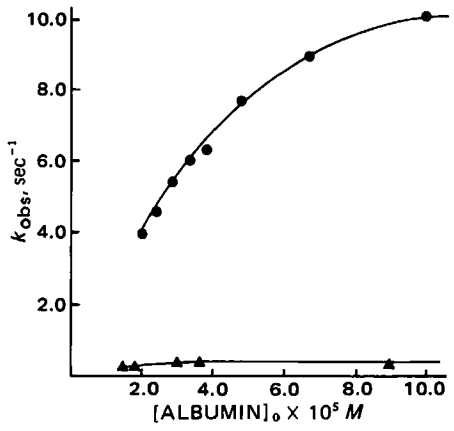

Figure 1—*Effect of albumin concentration on the rate of trinitrophenylation with I at 25°. The concentration of I was 1.0 × 10^{-5} M. Key: (●) pH 10.7; (▲) pH 7.4.*

Since it was indicated from preliminary experiments that the dissociation constant (K_P = [III][IV]/[V]) was relatively small, an elaborate method (13) was used for the determination of K_P, without employing the usual spectral method [*e.g.*, Benesi–Hildebrand method (14)]. The usual method is applicable only to the equilibrium system in which one component is much larger than the other.

Two reaction solutions were prepared (13): one was composed of an initial concentration of III ($[III]_0$) and of IV ($[IV]_{0,1}$), and the other of $[III]_0$ and a concentration $[IV]_{0,2}$. It was found that I was completely converted into III in the presence of excess albumin, and thus $[III]_0$ was equal to the initial concentration of I. The above two solutions were equilibrated together and their absorbances at 415 nm were measured. The increments of absorbances from the sum of the intact (initial) absorbances of III and IV, which are represented by ΔA_1 and ΔA_2, are proportional to the equilibrium concentrations of V, $[V]_{e,1}$ and $[V]_{e,2}$, respectively. For actual calculations of ΔA_1 and ΔA_2 the absorbance of the model compound VI was used instead of the absorbance of III, because the absorbance of III was reasonably assumed to be identical with that of VI as stated earlier. The relationship between the increment of absorbance and the equilibrium concentration is as follows: $[V]_{e,1} = \alpha\Delta A_1$ and $[V]_{e,2} = \alpha\Delta A_2$. The coefficient α is equal to $1/(\epsilon_V - \epsilon_{III} - \epsilon_{IV})$, where ϵ with subscript III, IV, or V is the molar absorbance of each species. Then, K_P can be represented as follows (13):

$$K_P = \frac{[III]_e[IV]_e}{[V]_e} \qquad \text{(Eq. 1)}$$

$$= \frac{([III]_0 - \alpha\Delta A_1)([IV]_{0,1} - \alpha\Delta A_1)}{\alpha\Delta A_1} = \frac{([III]_0 - \alpha\Delta A_2)([IV]_{0,2} - \alpha\Delta A_2)}{\alpha\Delta A_2}$$

From Eq. 1 a quadratic equation with respect to α is obtained, and the solution is (13):

$$\alpha = \frac{([IV]_{0,1} - [IV]_{0,2})\Delta A_1\Delta A_2 \pm \sqrt{\{([IV]_{0,1} - [IV]_{0,2})\Delta A_1\Delta A_2\}^2 - 4[III]_0\Delta A_1\Delta A_2(\Delta A_1 - \Delta A_2)(\Delta A_2[IV]_{0,1} - \Delta A_1[IV]_{0,2})}}{2\Delta A_1\Delta A_2(\Delta A_1 - \Delta A_2)} \qquad \text{(Eq. 2)}$$

Because α is calculated from Eq. 2, we can estimate K_P from Eq. 1. Furthermore, applying ϵ_{III} presumed from VI to the equation $\alpha = 1/(\epsilon_V -$ $\epsilon_{III} - \epsilon_{IV}$) we can obtain ϵ_V also, since ϵ_{IV} is determined independently (negligible). The K_P and α thus obtained were reproducible in other reaction solutions equilibrated from the different initial concentrations of IV.

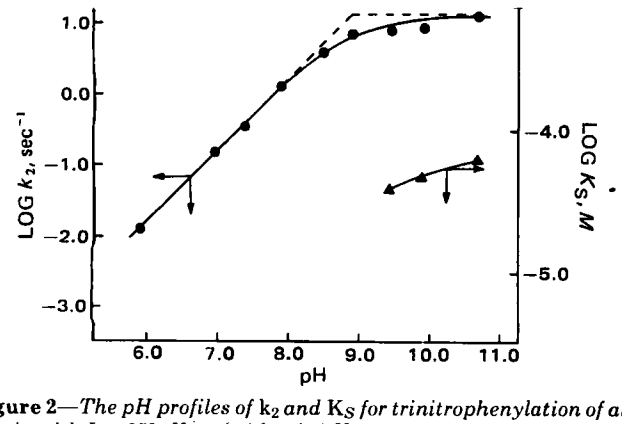

Figure 2—*The pH profiles of* k_2 *and* K_S *for trinitrophenylation of albumin with I at 25°. Key: (●)* k_2*; (▲)* K_S*.*

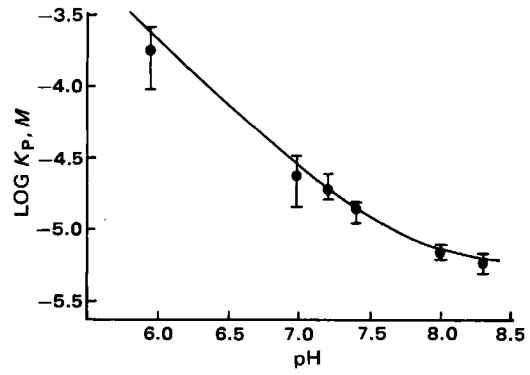

Figure 3—*The pH profile for* K_P *at 25°. The bars in this figure indicate the standard deviations. The solid curve was calculated using Eq. 6.*

The rate of the sulfite monoaddition was also followed at 415 nm. As the molar absorbance (ϵ_{III}, ϵ_{IV}, ϵ_V, and $\epsilon_{albumin}$) of each component in the reaction solution is known, the concentration of V at each time interval is calculated from the absorbance of the reaction solution. The rate constant (k_3) was determined from the slope of the plot based on Eq. (3), which is derived for the reversible reaction (15):

$$\frac{1}{E - F}\log\frac{F([V] - E)}{E([V] - F)} = \frac{k_3}{2.303}t \qquad \text{(Eq. 3)}$$

where,

$$E, F = \frac{([III]_0 + [IV]_0 + K_P) \pm \sqrt{([III]_0 + [IV]_0 + K_P)^2 - 4[III]_0[IV]_0}}{2}$$

The rate constant (k_{-3}) for the release of IV from V was calculated from K_P and k_3 already determined: $k_{-3} = K_P \cdot k_3$.

Acetylation of Albumin with Aspirin and 5-Nitroaspirin—Acetylation of albumin with aspirin (VII) was carried out by a previous method (16). A mixture of albumin (1.00 × 10^{-4} *M*) and VII (5.00 × 10^{-4} *M*) in pH 7.4 buffer was incubated at 37° for 24 hr and dialyzed at 4° for 48 hr against multiple changes of the same buffer. In the control experiment, VII was omitted and albumin was treated as above.

In the case of the acetylation by 5-nitroaspirin (VIII), the absorbance at 370 nm due to 5-nitrosalicylic acid (IX) released from the reaction of albumin (1.00 × 10^{-4} *M*) with VIII in pH 7.4 and at 25° was measured to estimate the degree of the acetylation. Three concentrations of VIII were used: 1.25 × 10^{-4} *M*, 2.50 × 10^{-4} *M*, and 3.75 × 10^{-4} *M*. When the absorbances reached corresponded to 1.0, 2.0, and 3.0 moles of IX per mole of albumin, respectively, the reaction solutions were cooled at 4° and dialyzed as described above. These albumins were denoted as monoacetyl-, diacetyl-, and triacetylalbumin, respectively.

Fluorescence Measurements—The fluorescence spectra of albumin solution (1.00 × 10^{-5} *M*) in the presence and absence of I (2.50 × 10^{-6} *M*) were measured. The excitation wavelength was 300 nm (17, 18).

RESULTS AND DISCUSSION

Kinetics on Trinitrophenylation of Albumin with I—Figure 1 shows the effect of the initial concentration of albumin ($[Albumin]_0$) on the apparent first-order rate constant (k_{obs}) for the trinitrophenylation at pH 7.4 and 10.7. At pH 10.7 the k_{obs} value increases hyperbolically with the albumin concentration, indicating saturation by trinitrophenylation (5, 19). According to Scheme I, k_{obs} can be represented as (5, 19):

$$k_{obs} = \frac{k_2[albumin]_0}{K_S + [albumin]_0} \qquad \text{(Eq. 4)}$$

where K_S and k_2 are the dissociation constant of II (= [I][albumin]/[II]) and the first-order rate constant of II for trinitrophenylation, respectively. The k_2 and K_S values were calculated from the intercept and slope of a plot based on the following, which is rearranged from Eq. 4 (5, 19):

$$\frac{1}{k_{obs}} = \frac{K_S}{k_2}\cdot\frac{1}{[albumin]_0} + \frac{1}{k_2} \qquad \text{(Eq. 5)}$$

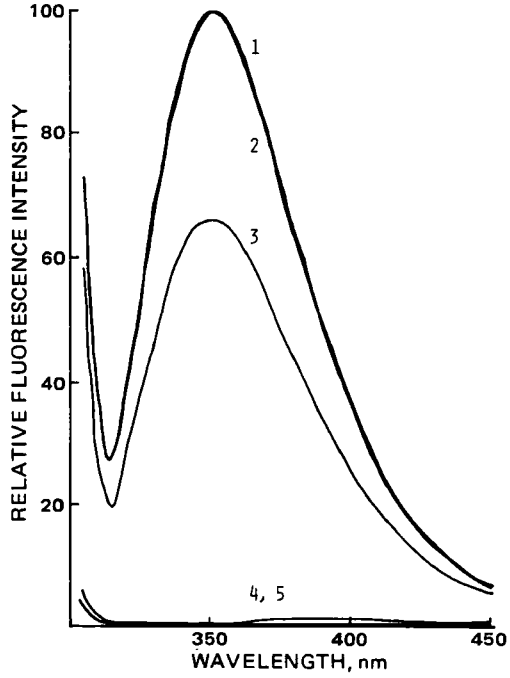

Figure 4—*Fluorescence emission spectra excited at 300 nm. Key: (1) 1.0 × 10⁻⁵ M albumin; (2) 1.0 × 10⁻⁵ M albumin and 5.0 × 10⁻⁶ M sodium bisulfite; (3) 1.0 × 10⁻⁵ M albumin and 2.5 × 10⁻⁶ M I; (4) 2.5 × 10⁻⁶ M I; and (5) 5.0 × 10⁻⁶ M sodium bisulfite.*

At pH 7.4, in contrast, the values of k_{obs} are almost independent of the albumin concentration. This independence suggests that K_S in Eq. 4 is far less than $[albumin]_0$ employed, and thus the k_{obs} value obtained under these conditions was assumed to be equal to k_2.

Figure 2 illustrates the pH dependence of k_2 and K_S thus obtained. The value of k_2 markedly depends on pH. Below pH values of about 8, the slope of the profile is 1, and above pH values of about 9.5, the k_2 value is independent of pH. From this profile the pK_a value of the ϵ-amino group of a lysine residue at the reactive site of albumin was estimated as about 8.9.

As stated earlier the data show that the K_S value at neutral pH is less than that above pH 9.5. The pH dependence of K_S may be explained qualitatively as follows. Deprotonation of basic groups (*e.g.*, ϵ-amino group of lysine and/or guanidino group of arginine) constituting the reactive site for I increases with increasing pH value, thereby decreasing positive-charge localization. Compound I is an anion, therefore, the ionic interaction (20) between I and the reactive site may decrease with increasing pH.

Sulfite Monoaddition to Trinitrophenylalbumin—Figure 3 shows a log K_P–pH profile. The K_P values decrease with increasing pH values. This pH dependence suggests that sulfite ion (IV) rather than bisulfite ion reacts with III. Then, K_P in the pH region examined can be expressed as a function of the hydrogen ion concentration $[H^+]$ by:

$$K_P = K'_P\left(\frac{[H^+] + K_2}{K_2}\right) \qquad \text{(Eq. 6)}$$

where K_2 and K'_P are the dissociation constant of bisulfite ion and the intrinsic dissociation constant of V, respectively. From a plot of K_P against $[H^+]$, K'_P and K_2 were estimated as 5.0×10^{-6} *M* and 2.2×10^{-8} *M*, respectively. The K'_P value for V is about 10-fold smaller (tight binding) than that (4.8×10^{-5} *M*) for the sulfite monoadduct of VI found in the literature (12). The difference in these K'_P values may be explained in terms of the distribution of sulfite ion between albumin and the aqueous phases. For III, the concentration of sulfite ion in the microenvironment of the trinitrophenylated group is probably higher than that in water for VI, since albumin generally has a strong affinity for anionic small ligands. The microenvironment of albumin may also affect the dissociation ($K_2 = 2.2 \times 10^{-8}$ *M*) of bisulfite ion, since in water the literature value for K_2 is about 6.2×10^{-8} *M* (21).

There was some difficulty in determining accurately the rate constant (k_3) for the sulfite monoaddition, because the absorbance changes at 415 nm due to trinitrophenylation seemed to be incomplete at the initial stage of the sulfite monoaddition; that is, the changes based on both the trinitrophenylation and the monoaddition could not be separated clearly.

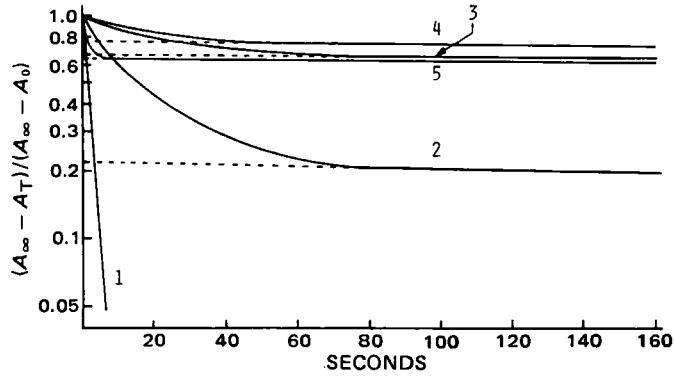

Figure 5—*Kinetics for the trinitrophenylation of albumin and acetylalbumins with I at pH 7.4 and 25° plotted as log $[(A_\infty - A_t)/(A_\infty - A_0)]$ against reaction time. Key: (1) 5.0 × 10⁻⁵ M control albumin and 1.0 × 10⁻⁵ M I; (2) 5.0 × 10⁻⁵ M monoacetylalbumin and 1.0 × 10⁻⁵ M I; (3) 5.0 × 10⁻⁵ M diacetylalbumin and 1.0 × 10⁻⁵ M I; (4) 5.0 × 10⁻⁵ M triacetylalbumin and 1.0 × 10⁻⁵ M I; (5) 3.3 × 10⁻⁵ M albumin and 8.0 × 10⁻⁵ M I.*

The approximate k_3 value at pH 7.4 and 25°, however, was estimated using Eq. 3. The value $7.0 \times 10^2\ M^{-1}\ sec^{-1}$ was obtained and compares with the literature value of $5.25 \times 10^3\ M^{-1}\ sec^{-1}$ at pH 8.0 and 25.4° for trinitrophenyl β-alanine (22). In addition, the k_{-3} value at pH 7.4 and 25° was calculated as $9.5 \times 10^{-3}\ sec^{-1}$ from the values for K_P and k_3.

Localization of Reactive Site on Albumin for I—In a series of studies on the effects of drug binding on the esterase-like activity of albumin (5, 18), it was found that albumin has some specific drug binding sites, and one of them is located near the tryptophan-214 (Trp-214) residue (23). When a drug binds to a site near Trp-214, the fluorescence intensity of Trp-214 is reduced when excited at 300 nm. To localize the reactive site for I, the fluorescence spectra of the reaction mixture of albumin with I and of each reactant solution were measured (Fig. 4). The intensity of the emission spectrum for the mixture (spectrum 3) is lower than that for the albumin solution (spectrum 1), indicating that the reactive site for I is located near the Trp-214 residue.

It has been reported that VII and VIII acetylate the ϵ-amino group of the lysine-199 (Lys-199) residue located near Trp-214 (5, 24). To examine further the reactive site for I, the effect of albumin acetylation by VII and VIII on the trinitrophenylation rate was investigated. The results are shown in Fig. 5. In this figure, $\log\{(A_\infty - A_t)/(A_\infty - A_0)\}$ is plotted against time, where A_∞, A_t, and A_0 are the absorbances at 360 nm at the completion of the reaction, at times t and zero, respectively. It is obvious that the trinitrophenylation of acetylalbumins with I (curves 2–4) is slower than that of the control albumin (curve 1). For acetylalbumins the trinitrophenylation is not a single process, but consists of an initial phase and a slower second phase. The slopes of the second phase are approximately equal to each other. Furthermore, these slopes (in curves 2–4) are almost identical with the slope (in curve 5) of the second phase obtained from the plot for the trinitrophenylation with excess I. These identities suggest that the second phase for acetylalbumins is due to the secondary reactive site(s) of albumin for I, of which the location(s) is(are) unknown at present.

For trinitrophenylation with excess I (curve 5) it is evident that a value (~0.63) on the ordinate obtained by extrapolating the line of the second phase to time zero indicates the fraction of I consumed by the secondary reactive site(s) of albumin $[(8.0 \times 10^{-5} - 3.3 \times 10^{-5})/8.0 \times 10^{-5} \approx 0.59]$. The slight discrepancy between 0.63 and 0.59 may be due to experimental error. For acetylalbumins (curves 2–4) the fractions were estimated by similar extrapolations (as expressed by dotted lines). The values obtained are ~0.22, 0.67, and 0.77 for mono-, di-, and triacetylalbumin, respectively. These values imply that $7.8 \times 10^{-6}\ M$ ($= 1.0 \times 10^{-5}\ M - 2.2 \times 10^{-6}\ M$), $3.3 \times 10^{-6}\ M$, and $2.3 \times 10^{-6}\ M$ of I were consumed by the primary reactive site, respectively. However, $5.0 \times 10^{-5}\ M$ of each acetylalbumin (fivefold excess of albumin over I) was employed for the trinitrophenylation reactions. With respect to the albumin concentration, therefore, only about 16 $[\approx(7.8 \times 10^{-6}/5.0 \times 10^{-5}) \times 100]$, 7, and 5% of the primary reactive site are unmodified (unacetylated) with VIII for mono-, di-, and triacetylalbumin, respectively. In other words, about 84, 93, and 95% of the primary reactive site for I are blocked by VIII. Since 5-nitroaspirin (VIII) primarily acetylates the ϵ-amino group of the Lys-199 residue (5, 24), these results on the effects of the acetylation suggest that the primary reactive group for I is the Lys-199 residue. The results from the experi-

ments using the albumin acetylated with aspirin (VII) also led to a similar conclusion concerning the reactive site for I.

REFERENCES

(1) K. J. Fehske, W. E. Müller, and U. Wollert, *Biochem. Pharmacol.*, **30**, 687 (1981).

(2) G. Sudlow, D. J. Birkett, and D. N. Wade, *Mol. Pharmacol.*, **12**, 1052 (1976).

(3) I. Sjöholm, E. Ekman, A. Kober, I. Ljungstedt-Påhlman, B. Seiving, and T. Sjödin, *ibid.*, **16**, 767 (1979).

(4) K. J. Fehske, W. E. Müller, and U. Wollert, *ibid.*, **16**, 778 (1979).

(5) Y. Kurono, H. Yamada, and K. Ikeda, *Chem. Pharm. Bull.*, **30**, 296 (1982).

(6) G. E. Means and R. F. Feeney, in "Chemical Modification of Proteins," Holden-Day, San Francisco, Calif., 1971.

(7) A. R. Goldfarb, *Biochemistry*, **5**, 2574 (1966).

(8) L.-O. Andersson, J. Brandt, and S. Johansson, *Arch. Biochem. Biophys.*, **146**, 428 (1971).

(9) Y. Kurono, K. Ichioka, S. Mori, and K. Ikeda, *J. Pharm. Sci.*, **70**, 1297 (1981).

(10) R. F. Chen, *J. Biol. Chem.*, **242**, 173 (1967).

(11) G. E. Means and M. L. Bender, *Biochemistry*, **14**, 4989 (1975).

(12) A. R. Goldfarb, *ibid.*, **5**, 2570 (1966).

(13) K. Ikeda, Y. Kurono, and T. Tsukamoto, *Chem. Pharm. Bull.*, **20**, 1621 (1972).

(14) H. A. Benesi and J. H. Hildebrand, *J. Am. Chem. Soc.*, **71**, 2703 (1949).

(15) A. A. Frost and R. G. Pearson, in "Kinetics and Mechanism," 2nd ed., Wiley, New York, N.Y., 1961, p. 187.

(16) D. Hawkins, R. N. Pinkard, and R. S. Farr, *Science*, **160**, 780 (1968); D. Hawkins, R. N. Pinkard, I. P. Crawford, and R. S. Farr, *J. Clin. Invest.*, **48**, 536 (1969); R. N. Pinkard, D. Hawkins, and R. S. Farr, *Ann. N.Y. Acad. Sci.*, **266**, 341 (1974).

(17) J. Steinhardt, J. Krijin, and J. G. Leidy, *Biochemistry*, **10**, 4005 (1971).

(18) Y. Ozeki, Y. Kurono, T. Yotsuyanagi, and K. Ikeda, *Chem. Pharm. Bull.*, **28**, 535 (1980).

(19) Y. Kurono, T. Maki, T. Yotsuyanagi, and K. Ikeda, *ibid.*, **27**, 2781 (1979).

(20) J. B. Swaney and I. M. Klotz, *Biochemistry*, **9**, 2570 (1970).

(21) L. C. Schroeter, in "Sulfur Dioxide," Pergamon, New York, N.Y., 1966, p. 17.

(22) G. E. Means, W. I. Congdon, and M. L. Bender, *Biochemistry*, **11**, 3564 (1972).

(23) V. M. Rosenoer, M. Oratz, and M. A. Rothschild, in "Albumin Structure, Function and Uses," J. R. Brown, Ed., Pergamon, Oxford, England, 1977, p. 27.

(24) J. E. Walker, *FEBS Lett.*, **66**, 173 (1976).

Pharmaceutical Approach to Subcutaneous Dosage Forms of Insulin

RYOHEI HORI ˣ, FUSAO KOMADA, and KATSUHIKO OKUMURA

Received January 15, 1982 from the *Department of Pharmacy, Kyoto University Hospital, Faculty of Medicine, Kyoto University, Sakyo-ku, Kyoto 606, Japan.* Accepted for publication August 12, 1982.

Abstract □ The present studies were undertaken to describe the dynamic nature of the degradation and absorption of insulin in the subcutaneous injection site and to develop agents which would stabilize this dosage form. [^{125}I]Insulin with 0.2-U/kg of unlabeled insulin in 10 μl of aqueous solution was injected subcutaneously in rats under the depilated skin of the back. At various times, radioactive skin tissue was extracted and assayed for insulin and/or its metabolites by gel filtration. Using these data, absorption and degradation rate constants of these substances were estimated according to a one-compartment model. Absorption rate constants of insulin and its metabolite of low molecular weight (monoiodotyrosine) were 0.021 min^{-1} and 0.107 min^{-1}, respectively, while the degradation rate constant for insulin to monoiodotyrosine was 0.013 min^{-1}. Thus, the bioavailability of insulin injected subcutaneously was lower than expected, suggesting the necessity of stabilizing methods. The protection of insulin from degradation at the site of injection was examined by the addition of various peptides. It was found that benzyloxycarbonyl-Gly-Pro-Leu-Gly was a good stabilizing agent, and remarkably inhibited insulin degradation. This inhibition was confirmed by the increase of immunoreactive insulin level and the decrease of the blood glucose level. We postulated that this peptide protects the injected insulin from degradation by inhibiting the peptidase present in subcutaneous tissue.

Keyphrases □ Insulin—absorption and degradation at the subcutaneous injection site, stabilizing agents for the subcutaneous dosage form □ Stabilizing agent—for insulin, subcutaneous dosage forms, use of the peptide benzyloxycarbonyl-Gly-Pro-Leu-Gly □ Subcutaneous injection—absorption and degradation of insulin, use of benzyloxycarbonyl-Gly-Pro-Leu-Gly peptide for stabilization

Endogenous peptides having specific biological effects have attracted attention as new drugs; however, effective dosage forms of these peptides for clinical usage have been difficult to assess in any but the parenteral dosage forms. Insulin, administered subcutaneously, has been the primary treatment for severe diabetes for several years, even though effective methods have been described for oral (1–3), nasal (4), aerosol (5, 6), and rectal (7, 8) administration. In previous attempts to assess the absorption of insulin from its subcutaneous depot, radioiodinated insulin preparations were injected and the disappearance of the radioactivity from the injection site was measured by an external gamma-counter (9, 10). The stability and bioavailability of insulin administered subcutaneously are not well understood since the metabolites of insulin could not be measured. The kinetics of insulin in the blood after subcutaneous injection are the result of many factors including absorption and degradation in the injection site (11).

Recently, Berger reported that aprotinin increased the absorption rate of subcutaneously injected insulin and amplified its biological effect by inhibiting the local degradation of exogenous insulin at the injection site (12). Little else has been reported about the degradation and absorption of insulin at the injection site, although the absorption characteristics of insulin and other drugs from intramuscular injection sites were investigated (13, 14). The present studies were undertaken to investigate the dynamic nature of the degradation and the absorption of insulin in the subcutaneous injection site and to develop new stabilizing agents for this dosage form.

0022-3549/83/0400-0435$01.00/0

ments using the albumin acetylated with aspirin (VII) also led to a similar conclusion concerning the reactive site for I.

REFERENCES

(1) K. J. Fehske, W. E. Müller, and U. Wollert, *Biochem. Pharmacol.*, **30**, 687 (1981).

(2) G. Sudlow, D. J. Birkett, and D. N. Wade, *Mol. Pharmacol.*, **12**, 1052 (1976).

(3) I. Sjöholm, E. Ekman, A. Kober, I. Ljungstedt-Påhlman, B. Seiving, and T. Sjödin, *ibid.*, **16**, 767 (1979).

(4) K. J. Fehske, W. E. Müller, and U. Wollert, *ibid.*, **16**, 778 (1979).

(5) Y. Kurono, H. Yamada, and K. Ikeda, *Chem. Pharm. Bull.*, **30**, 296 (1982).

(6) G. E. Means and R. F. Feeney, in "Chemical Modification of Proteins," Holden-Day, San Francisco, Calif., 1971.

(7) A. R. Goldfarb, *Biochemistry*, **5**, 2574 (1966).

(8) L.-O. Andersson, J. Brandt, and S. Johansson, *Arch. Biochem. Biophys.*, **146**, 428 (1971).

(9) Y. Kurono, K. Ichioka, S. Mori, and K. Ikeda, *J. Pharm. Sci.*, **70**, 1297 (1981).

(10) R. F. Chen, *J. Biol. Chem.*, **242**, 173 (1967).

(11) G. E. Means and M. L. Bender, *Biochemistry*, **14**, 4989 (1975).

(12) A. R. Goldfarb, *ibid.*, **5**, 2570 (1966).

(13) K. Ikeda, Y. Kurono, and T. Tsukamoto, *Chem. Pharm. Bull.*, **20**, 1621 (1972).

(14) H. A. Benesi and J. H. Hildebrand, *J. Am. Chem. Soc.*, **71**, 2703 (1949).

(15) A. A. Frost and R. G. Pearson, in "Kinetics and Mechanism," 2nd ed., Wiley, New York, N.Y., 1961, p. 187.

(16) D. Hawkins, R. N. Pinkard, and R. S. Farr, *Science*, **160**, 780 (1968); D. Hawkins, R. N. Pinkard, I. P. Crawford, and R. S. Farr, *J. Clin. Invest.*, **48**, 536 (1969); R. N. Pinkard, D. Hawkins, and R. S. Farr, *Ann. N.Y. Acad. Sci.*, **266**, 341 (1974).

(17) J. Steinhardt, J. Krijin, and J. G. Leidy, *Biochemistry*, **10**, 4005 (1971).

(18) Y. Ozeki, Y. Kurono, T. Yotsuyanagi, and K. Ikeda, *Chem. Pharm. Bull.*, **28**, 535 (1980).

(19) Y. Kurono, T. Maki, T. Yotsuyanagi, and K. Ikeda, *ibid.*, **27**, 2781 (1979).

(20) J. B. Swaney and I. M. Klotz, *Biochemistry*, **9**, 2570 (1970).

(21) L. C. Schroeter, in "Sulfur Dioxide," Pergamon, New York, N.Y., 1966, p. 17.

(22) G. E. Means, W. I. Congdon, and M. L. Bender, *Biochemistry*, **11**, 3564 (1972).

(23) V. M. Rosenoer, M. Oratz, and M. A. Rothschild, in "Albumin Structure, Function and Uses," J. R. Brown, Ed., Pergamon, Oxford, England, 1977, p. 27.

(24) J. E. Walker, *FEBS Lett.*, **66**, 173 (1976).

Pharmaceutical Approach to Subcutaneous Dosage Forms of Insulin

RYOHEI HORI ˣ, FUSAO KOMADA, and KATSUHIKO OKUMURA

Received January 15, 1982 from the *Department of Pharmacy, Kyoto University Hospital, Faculty of Medicine, Kyoto University, Sakyo-ku, Kyoto 606, Japan.* Accepted for publication August 12, 1982.

Abstract □ The present studies were undertaken to describe the dynamic nature of the degradation and absorption of insulin in the subcutaneous injection site and to develop agents which would stabilize this dosage form. [^{125}I]Insulin with 0.2-U/kg of unlabeled insulin in 10 μl of aqueous solution was injected subcutaneously in rats under the depilated skin of the back. At various times, radioactive skin tissue was extracted and assayed for insulin and/or its metabolites by gel filtration. Using these data, absorption and degradation rate constants of these substances were estimated according to a one-compartment model. Absorption rate constants of insulin and its metabolite of low molecular weight (monoiodotyrosine) were 0.021 min^{-1} and 0.107 min^{-1}, respectively, while the degradation rate constant for insulin to monoiodotyrosine was 0.013 min^{-1}. Thus, the bioavailability of insulin injected subcutaneously was lower than expected, suggesting the necessity of stabilizing methods. The protection of insulin from degradation at the site of injection was examined by the addition of various peptides. It was found that benzyloxycarbonyl-Gly-Pro-Leu-Gly was a good stabilizing agent, and remarkably inhibited insulin degradation. This inhibition was confirmed by the increase of immunoreactive insulin level and the decrease of the blood glucose level. We postulated that this peptide protects the injected insulin from degradation by inhibiting the peptidase present in subcutaneous tissue.

Keyphrases □ Insulin—absorption and degradation at the subcutaneous injection site, stabilizing agents for the subcutaneous dosage form □ Stabilizing agent—for insulin, subcutaneous dosage forms, use of the peptide benzyloxycarbonyl-Gly-Pro-Leu-Gly □ Subcutaneous injection—absorption and degradation of insulin, use of benzyloxycarbonyl-Gly-Pro-Leu-Gly peptide for stabilization

Endogenous peptides having specific biological effects have attracted attention as new drugs; however, effective dosage forms of these peptides for clinical usage have been difficult to assess in any but the parenteral dosage forms. Insulin, administered subcutaneously, has been the primary treatment for severe diabetes for several years, even though effective methods have been described for oral (1–3), nasal (4), aerosol (5, 6), and rectal (7, 8) administration. In previous attempts to assess the absorption of insulin from its subcutaneous depot, radioiodinated insulin preparations were injected and the disappearance of the radioactivity from the injection site was measured by an external gamma-counter (9, 10). The stability and bioavailability of insulin administered subcutaneously are not well understood since the metabolites of insulin could not be measured. The kinetics of insulin in the blood after subcutaneous injection are the result of many factors including absorption and degradation in the injection site (11).

Recently, Berger reported that aprotinin increased the absorption rate of subcutaneously injected insulin and amplified its biological effect by inhibiting the local degradation of exogenous insulin at the injection site (12). Little else has been reported about the degradation and absorption of insulin at the injection site, although the absorption characteristics of insulin and other drugs from intramuscular injection sites were investigated (13, 14). The present studies were undertaken to investigate the dynamic nature of the degradation and the absorption of insulin in the subcutaneous injection site and to develop new stabilizing agents for this dosage form.

0022-3549/83/0400-0435$01.00/0

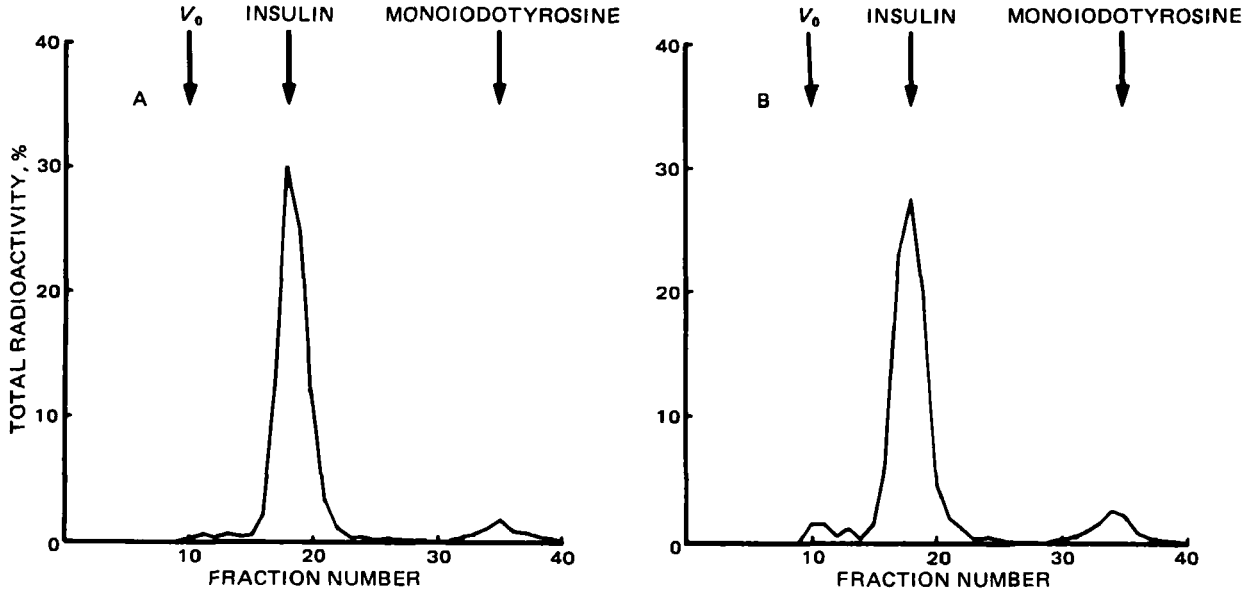

Figure 1—*Gel filtration of the radioactivity extracted from subcutaneous tissue samples 5 (A) and 10 (B) min after insulin injection of 0.2 U/kg sc.*

EXPERIMENTAL

Materials—Monocomponent porcine insulin (26.0 U/mg)[1] was used. [^{125}I]Insulin was prepared by the chloramine T method as described by Hunter and Greenwood (15). The labeled insulin was purified by gel filtration twice using a dextran gel[2]. Benzyloxycarbonyl-Gly-Pro-Leu-Gly (II)[3], benzyloxycarbonyl-Gly-Pro-Leu (III)[3], dinitrophenyl-Pro-Leu-Gly (IV)[3], benzyloxycarbonyl-Gly-Pro(V)[3], and all other chemicals were obtained from commercial sources and were analytical reagent grade.

Animals—Male Wistar rats weighing 125–150 g were used. For the experiment in diabetic rats, diabetes was induced in the rats by femoral-vein injection of streptozotocin after a 16-hr fast, as previously described (16). The streptozotocin was dissolved in acidified 0.9% NaCl (saline), pH 4.5, and given in a dose of 50 mg/kg. Control animals received no injections. The diabetic rats displayed polyuria, glycosuria, failure to gain weight, and significant hyperglycemia (mean blood sugar, 450 mg/dl) at the time of experiment (24–48 hr after the injection of streptozotocin).

Procedure—Rats were anesthetized with pentobarbital (40 mg/kg) and maintained under anesthesia during the experiment. The dorsal skin was depilated and the site for injection was demarcated. Using a thin needle (o.d. = 0.2 mm, i.d. = 0.1 mm)[4], 10 μl of drug solution containing unlabeled insulin (0.2 and 1.0 U/kg) and [^{125}I]insulin, with or without additives, were injected subcutaneously. The rectal temperature was monitored and maintained constant (36.5 ± 0.5°) by keeping the rats in a temperature-constant room. At various times, a skin sample and subcutaneous tissue around the injection site (~4 cm^2 area) was taken for analysis. To estimate the degradation rate of insulin at the injection site when its absorption would be negligible, degradation in a cardiac-arrested rat was investigated. This condition was induced by direct injection of pentobarbital (200 mg/kg) to the heart 5 sec before the experiment. For the experiment conducted to measure the immunoreactive insulin or blood glucose, unlabeled insulin with or without additives was injected.

Analytical Methods—After measurement of the residual amount of radioactivity, the sample was homogenized with 6 *M* guanidine hydrochloride in 2.4 *M* formic acid. The homogenate was centrifuged at 1500×*g* for 10 min to separate the extract. The extract then was applied to a gel filtration column (hydrophilic vinyl gel[5]) that was eluted with 3 *M* guanidine hydrochloride in 2.4 *M* formic acid at 4°. The column size was 1.5 × 48 cm and flow rate was 1 ml/min. Three-milliliter fractions were collected and the radioactivity in each fraction was counted. The column was calibrated with high molecular dextran[6] as a void volume marker (V_0) and with standard insulin and monoiodotyrosine (I). For the measure-

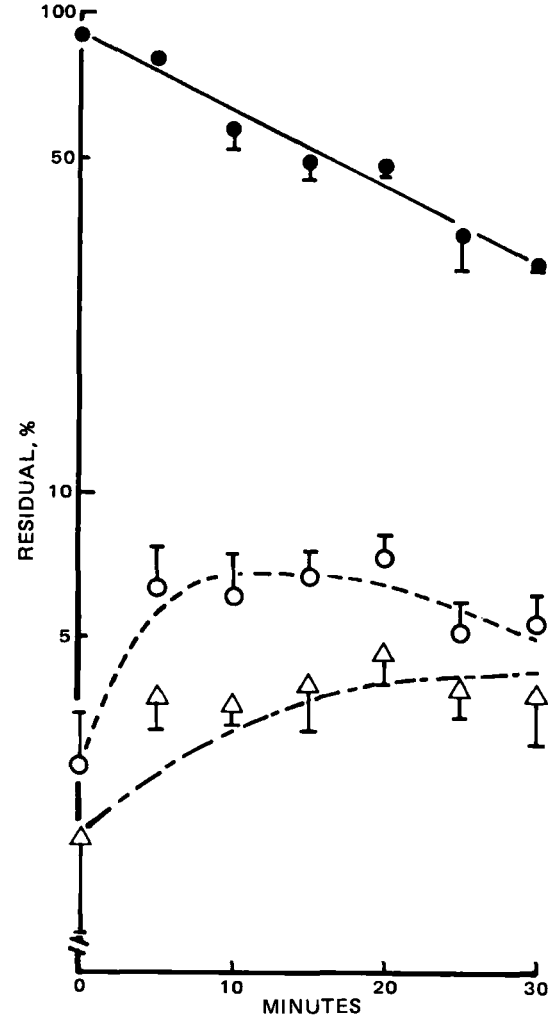

Figure 2—*Disappearance of [^{125}I]insulin from the subcutaneous injection site. Each point represents the mean value of five experiments; vertical bars indicate* SEM. *Each line represents the curve fitted with the one-compartment open model. Key: (●) intact insulin, (○) low molecular weight product (I), and (△) high molecular weight product.*

[1] Novo Industry Co., Copenhagen, Denmark.
[2] Sephadex G-25 & G-50, Pharmacia Fine Chemicals, Uppsala, Sweden.
[3] Protein Research Foundation, Osaka, Japan.
[4] N-733, Hamilton Co., Reno, Nev.
[5] Blue Dextran 2000, Pharmacia Fine Chemicals, Uppsala, Sweden.
[6] Toyopearl HW-55F, Toyo Soda Manufacturing Co., Tokyo, Japan.

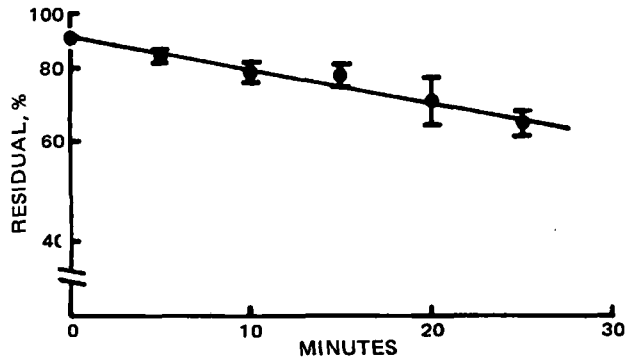

Figure 3—*Degradation of 0.2 U/kg insulin in the subcutaneous injection site of cardiac-arrested rats. The cardiac-arrested condition was induced by intracardiac injection of 200 mg/kg sodium pentobarbital 5 sec before the experiment. Each point represents the mean value of three to five experiments; vertical bars indicate* SEM.

ment of hypoglycemic effect, blood samples were collected from the jugular vein at timed intervals and glucose levels were determined in the serum by the modified method of Hyvärinen (17). Immunoreactive insulin in the plasma was determined by radioimmunoassay (18).

RESULTS AND DISCUSSION

Absorption and Degradation of Insulin in the Injection Site—The drug solution (pH 7.0) containing insulin and [^{125}I]insulin was injected subcutaneously, and the subcutaneous tissue was analyzed. Figure 1 shows the gel filtration pattern of radioactivity extracted from tissue samples obtained 5 and 10 min postinjection. Most of the radioactivity eluted at the position of intact insulin, with a small peak at the void volume (V_0) and at the position of I. The presence of a peak at V_0 indicated the production of a high molecular weight substance, as previously reported in the blood (19). It was also observed that the small peak increased gradually and the main peak (intact insulin) decreased with time.

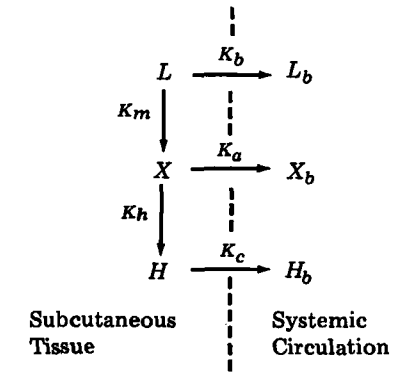

K_a = absorption rate constant of insulin, K_b = absorption rate constant of I, K_c = absorption rate constant of high molecular weight product, K_m = degradation rate constant of insulin, K_h = aggregation rate constant of insulin, X = amount of insulin in injection site, L = amount of I in injection site, H = amount of high molecular weight product in injection site, X_b = amount of insulin in the body, L_b = amount of I in the body, and H_b = amount of high molecular weight product in the body.

Scheme I

These results suggested that subcutaneously injected insulin was metabolized at the injection site before being absorbed into the systemic circulation.

To clarify this phenomenon, time courses for the clearance of insulin and the formation of its metabolites at the subcutaneous injection site were investigated. Figure 2 shows a logarithmic plot of the insulin, I, and high molecular weight product levels remaining at the injection site as a function of time over a 30-min period. Since a straight line was obtained for the intact insulin, a first-order process seems to be predominant for the clearance of the insulin from the subcutaneous injection site. As the

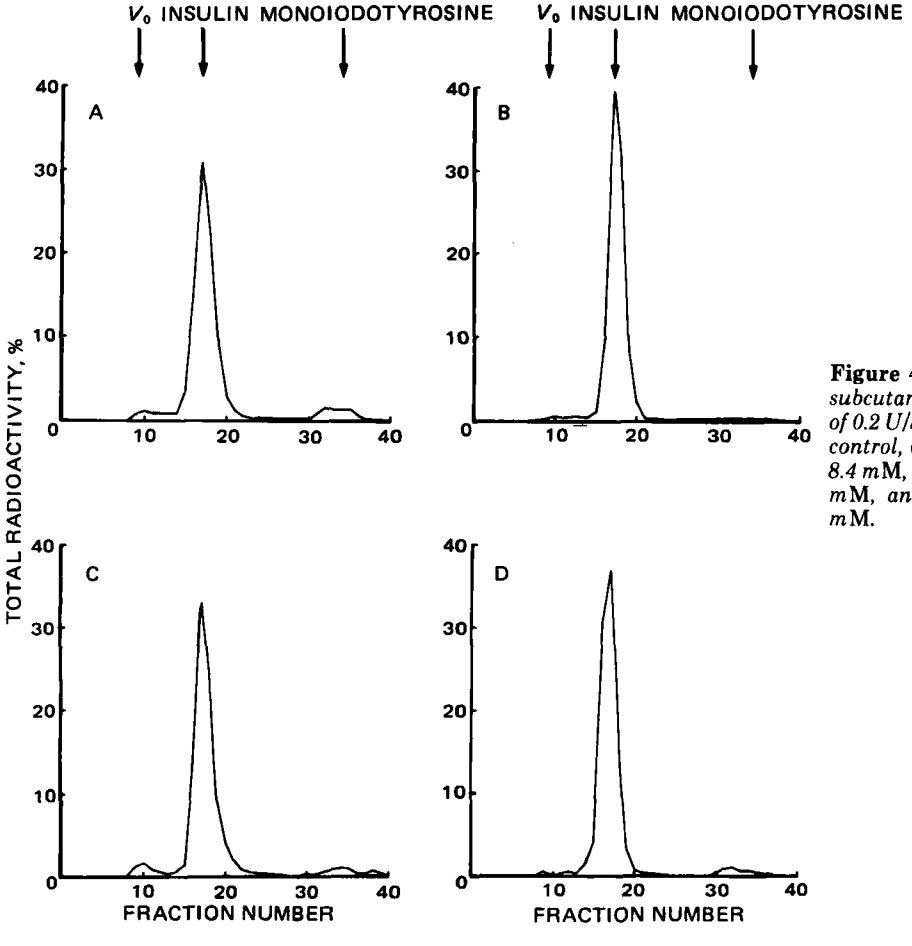

Figure 4—*Gel filtration of radioactivity extracted from subcutaneous tissue samples 5 min after insulin injection of 0.2 U/kg sc with or without stabilizing peptides. Key: (A) control, (B) with benzyloxycarbonyl-Gly-Pro-Leu-Gly(II) 8.4 m*M, *(C) with benzyloxycarbonyl-Gly-Pro-Leu(III) 8.4 m*M, *and (D) with dinitrophenyl-Pro-Leu-Gly(IV) 4.4 m*M.

Table I—Effect of Various Peptides on the Kinetic Parameters for Insulin in the Subcutaneous Injection Site

Compound Injected	Concentration	Kinetic Parameters, min^{-1}				
		K_a	K_b	K_c	K_m	K_h
Insulin	(0.2 U/kg)	0.0208	0.107	0.0113	0.0131	0.0022
Insulin + II	(0.2 U/kg + 8.4 m*M*)	0.0357	0.107	0.0113	0.0008	0.0017
Insulin + III	(0.2 U/kg + 8.4 m*M*)	0.0466	0.130	0.0113	0.0033	0.0025
Insulin + IV	(0.2 U/kg + 4.4 m*M*)	0.0229	0.109	0.0113	0.0069	0.0012
Insulin + V	(0.2 U/kg + 8.4 m*M*)	0.0324	0.201	0.0113	0.0131	0.0028

line curved for I, the main metabolite (20), a fast disappearance rate could be postulated. Meanwhile, the appearance of a high molecular weight product slowly increased. In previous papers (14, 21, 22), it was demonstrated that the rate of drug absorption from the muscle was proportional to the amount remaining in the injection site; drug absorption from the subcutaneous tissue was not demonstrated clearly to be a first-order process. From these results, the absorption mechanism for a subcutaneously injected drug would not be very different from that for an intramuscularly injected drug.

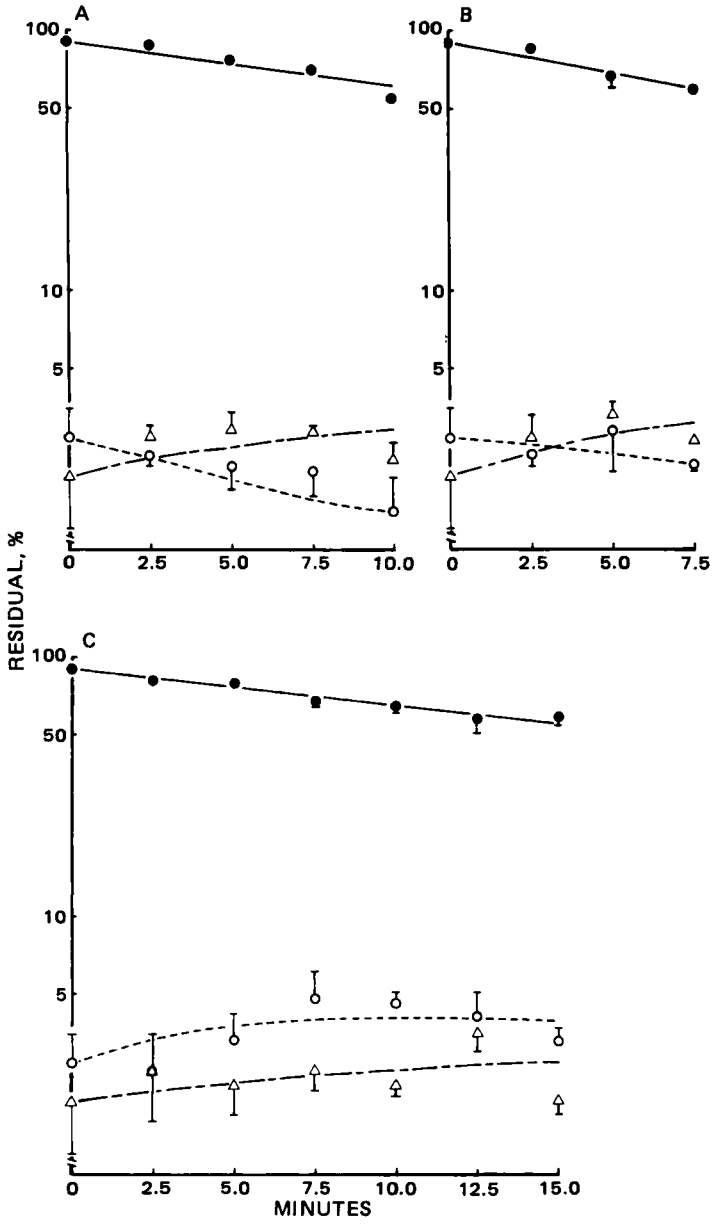

Figure 5—*Disappearance of 0.2 U/kg insulin with stabilizing peptides from the subcutaneous injection site. Each point represents the mean value of three or four experiments; vertical bars indicate* SEM. *Each line represents the curve fitted with the one-compartment open model. Key: (A) with II 8.4 m*M, *(B) with III 8.4 m*M, *and (C) with IV 4.4 m*M, *(●) intact insulin, (○) low molecular weight products (I), and (△) high molecular weight product.*

The disposition of insulin in the subcutaneous tissue was analyzed as assuming a one-compartment open model as shown in Scheme I. Insulin can be biotransformed to a low molecular weight product (I) and to a high molecular weight product, with a degradation rate constant of K_m and a formation rate constant of K_h, respectively. Compound I, insulin, and the high molecular weight product are absorbed independently with absorption rate constants of K_b, K_a, and K_c, respectively. X, L, and H were expressed by (23):

$$X = X_0 e^{-Kt} \quad \text{(Eq. 1)}$$

$$L = \frac{X_0 K_m}{K - K_b}(e^{-K_b t} - e^{-Kt}) + L_0 e^{-K_b t} \quad \text{(Eq. 2)}$$

and

$$H = \frac{X_0 K_h}{K - K_c}(e^{-K_c t} - e^{-Kt}) + H_0 e^{-K_c t} \quad \text{(Eq. 3)}$$

where X_0 is the initial amount of insulin, L_0 is the initial amount of I, H_0 is the initial amount of high molecular weight product, $K = K_a + K_m + K_h$, and t is the sampling time. Data of X, L, and H were fitted to Eqs. 1–3 by nonlinear least-squares regression (24). Refined estimates of K_a, K_b, K_m, and K_h were then obtained. K_c was determined by the subcutaneous injection of the high molecular weight product. Calculated K_a and K_h were 0.0208 and 0.0022 min^{-1}, respectively. The degradation rate constant of insulin to I (K_m) was calculated to be 0.0131 min^{-1}, a value similar to the absorption rate constant. The degradation of insulin in cardiac-arrested rats was investigated to confirm the calculated value. No absorption was observed since the systemic circulation was completely disrupted. Figure 3 shows the plot of the nondegraded insulin level at the injection site of cardiac-arrested rats as a function of time. The decrease of insulin by degradation at the injection site seems to be linear in this semilogarithmic plot. The degradation rate constant (K_m) in this experiment was 0.0137 min^{-1} which was almost the same as the calculated K_m. As K_m was close to K_a, the bioavailability of insulin injected subcutaneously could be lower than expected. The species or age variation for insulin degradation in the subcutaneous tissue will be investigated in future work, since the insulin degrading activity of muscle from rats varies with age (25).

Stabilization of Insulin Injected Subcutaneously—The results obtained in this study prompted the search for methods of stabilizing subcutaneously injected insulin to increase the bioavailability. The

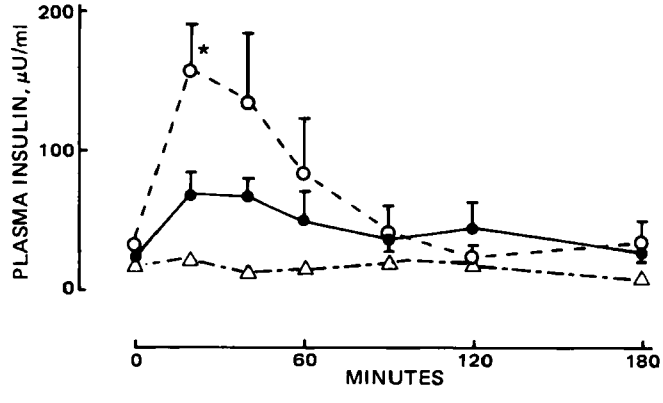

Figure 6—*Effect of II on the increase of plasma insulin levels after insulin injection of 0.2 U/kg sc in normal rats. Each point represents the mean value of four experiments. * Indicates statistical significance ($p < 0.05$), insulin* versus *insulin with II; vertical bars indicate* SEM. *Key: (●) insulin, (○) insulin with II 8.4 m*M, *and (△) II 8.4 m*M.

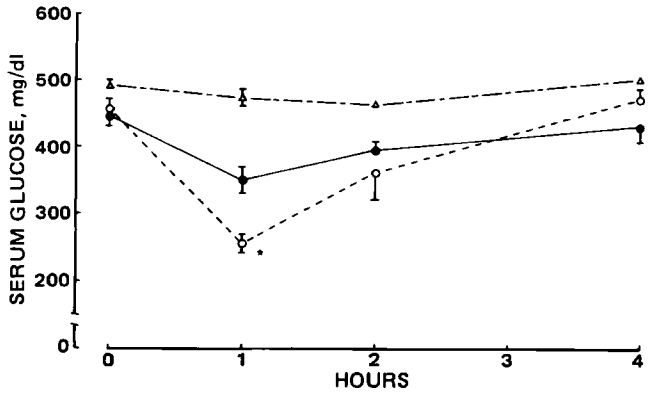

Figure 7—*Effect of II on serum glucose levels after insulin injection of 1.0 U/kg sc in diabetic rats. * Indicates statistical significance* ($p < 0.02$), *insulin* versus *insulin with II; vertical bars indicate* SE. *Key: (●) insulin, (○) insulin with II 8.4 m*M, *and (△) II 8.4 m*M.

concurrent use of peptides and amino acids as stabilizing agents of insulin degradation at the injection site was examined. Among the various peptides tested in this study, benzyloxycarbonyl-Gly-Pro-Leu-Gly (II), benzyloxycarbonyl-Gly-Pro-Leu (III), and dinitrophenyl-Pro-Leu-Gly (IV) exhibited a remarkable protection of insulin from degradation. Figure 4 demonstrates the gel filtration pattern of the radioactivity extracted from subcutaneous tissue sampled 5 min after the injection of insulin with or without these stabilizing peptides. The concentration of I at the injection site was comparatively low when these peptides were coadministered with insulin.

Many amino acids, dipeptides, and aprotinin failed to stabilize insulin at the injection site (data not shown). Aprotinin was examined as an inhibitor of peptidase. Coadministration of aprotinin with insulin led to the fast entry of insulin into the circulation and an accelerated onset of the hypoglycemic action (12). However, it appears from our studies that aprotinin does not stabilize insulin at the subcutaneous injection site; however, it could inhibit insulin degradation after entry into the systemic circulation. The stabilizing effect of these peptides was confirmed by the gel filtration pattern using cardiac-arrested rats. For kinetic analysis, the time course of insulin and its metabolites after the subcutaneous injection of insulin with or without these peptides was investigated. As shown in Fig. 5, the stabilizing effect of these peptides was clearly demonstrated. Using these data, kinetic parameters of the one-compartment model in the presence of stabilizing peptides were estimated, and are listed in Table I. The degradation rate constant of insulin (K_m) in the presence of II at the injection site was 0.0008 min^{-1}, which was less than one-sixteenth of the control. Compounds III and IV were less effective than II. Thus, it is conceivable that the degradation rate of insulin coinjected with II was negligible compared with its absorption rate. Consequently, this peptide can be regarded as a valuable stabilizing agent for insulin in a subcutaneous dosage form.

A significant increase in the absorption rate constant for intact insulin was also observed by the concurrent use of II, III, and benzyloxycarbonyl-Gly-Pro (V), but this effect was not observed using IV. It might be postulated that the amino acid sequence of V could influence this process in a variety of possible ways, such as alterations in the local circulation or possibly by changes in the permeability.

To confirm that II inhibits the degradation of insulin, plasma levels of immunoreactive insulin and serum levels of glucose were analyzed. Figure 6 reveals that the immunoreactive insulin in the plasma was significantly increased when insulin was injected with this peptide, demonstrating the inhibition of insulin degradation at the injection site. Furthermore, the hypoglycemic effect of insulin coinjected with this peptide was investigated in diabetic rats. As shown in Fig. 7, the decrease in serum glucose levels in the diabetic rats after the subcutaneous administration of insulin (1.0 U/kg) was significantly greater in the presence of this stabilizing peptide. The potent effect of II for the insulin administered subcutaneously was clearly demonstrated. We suggest that this peptide protects the injected insulin from being degraded by inhibiting the peptidase localized in subcutaneous tissue.

The study of the degradation and absorption of insulin at the subcutaneous injection site has provided a good understanding of the phenomenon involved, leading to the exploration of stabilizing agents. Further research of the insulin stabilization with other derivatives of this peptide (II) is now in progress. Although a potential effect of these peptides for insulin stabilization in the subcutaneous injection site was demonstrated, additional studies must be carried out before this methodology is useful clinically.

REFERENCES

(1) M. Shichiri, A. Okada, K. Karasaki, R. Kawamori, Y. Shigeta, and H. Abe, *Diabetes*, **21**, 203 (1972).

(2) M. Shichiri, Y. Shimizu, Y. Yoshida, R. Kawamori, M. Fukuchi, Y. Shigeta, and H. Abe, *Diabetologia*, **10**, 317 (1974).

(3) M. Schichiri, R. Kawamori, M. Yoshida, N. Etani, M. Hoshi, K. Izumi, Y. Shigeta, and H. Abe, *Diabetes*, **24**, 971 (1975).

(4) S. Hirai, T. Ikenaga, and T. Matsuzawa, *ibid.*, **27**, *296 (1978)*.

(5) F. M. Wigley, J. H. Londono, S. H. Wood, J. C. Shipp, and R. H. Waldman, *ibid.*, **20**, 552 (1971).

(6) H. Yoshida, K. Okumura, R. Hori, T. Anmo, and H. Yamaguchi, *J. Pharm. Sci.*, **68**, 670 (1979).

(7) M. Shichiri, Y. Yamasaki, R. Kawamori, M. Kikuchi, N. Hakui, and H. Abe, *J. Pharm. Pharmacol.*, **30**, 806 (1978).

(8) T. Nishihata, J. H. Rytting, T. Higuchi, and L. Caldwell, *ibid.*, **33**, 334 (1981).

(9) C. Binder, *Acta Pharmacol. Toxicol. Suppl. 2*, **27**, 1 (1969).

(10) V. A. Koivisto and P. Felig, *N. Engl. J. Med.*, **298**, 79 (1978).

(11) M. Berger, P. A. Halban, J. P. Assal, R. E. Offord, M. Vranic, and A. E. Renold, *Diabetes*, **28** (suppl. 1), 53 (1979).

(12) M. Berger, H. J. Cüppers, P. A. Halban, and R. E. Offord, *ibid.*, **29**, 81 (1980).

(13) E. Arakawa, Y. Imai, H. Kobayashi, K. Okumura, and H. Sezaki, *Chem. Pharm. Bull.*, **23**, 2218 (1975).

(14) K. Kakemi, H. Sezaki, K. Okumura, H. Kobayashi, and S. Furusawa, *ibid.*, **20**, 443 (1972).

(15) W. M. Hunter and F. C. Greenwood, *Nature (London)*, **194**, 495 (1962).

(16) A. Junod, A. E. Lambert, W. Stauffacher, and A. E. Renold, *J. Clin. Invest.*, **48**, 2129 (1969).

(17) A. Hyvärinen and E. A. Nikkilä, *Clin. Chem. Acta*, **7**, 140 (1962).

(18) C. N. Hales and P. J. Randle, *Biochem. J.*, **88**, 137 (1963).

(19) H. N. Antoniades, D. Stathakos, and J. D. Simon, *Endocrinology*, **95**, 1543 (1974).

(20) J. C. Sodoyez, F. R. Sodoyez-Goffaux, and Y. M. Moris, *Am. J. Physiol.*, **239**, E3 (1980).

(21) B. E. Ballard, *J. Pharm. Sci.*, **57**, 357 (1968).

(22) E. Secher-Hansen, H. Langgard, and J. Schou, *Acta Pharmacol. Toxicol.*, **26**, 9 (1968).

(23) M. Gibaldi and D. Perrier, in "Drugs and the Pharmaceutical Sciences, vol I, Pharmacokinetics," J. Swarbrick, Ed., Dekker, New York, N.Y., 1975, p. 17.

(24) T. Nakagawa, Y. Koyanagi, and H. Togawa, Library Program of the University of Tokyo Computer Center, Tokyo, Japan (1975).

(25) K. Runyan, W. C. Duckworth, A. E. Kitabchi, and G. Huff, *Diabetes*, **28**, 324 (1979).

Quantitative Investigation on Renal Handling of Drugs in Rabbits, Dogs, and Humans

AKIRA KAMIYA, KATSUHIKO OKUMURA, and RYOHEI HORI ˣ

Received June 18, 1982 from the *Department of Pharmacy, Kyoto University Hospital, Faculty of Medicine, Kyoto University, Sakyo-ku, Kyoto, 606, Japan.* Accepted for publication August 16, 1982.

Abstract □ A renal clearance method based on a computer analysis after administration of a single dose of drug was developed for measuring the renal handling of several drugs in rabbits, dogs, and humans. Secretion and reabsorption of sulfamethizole, sulfanilamide, cephalexin, and ampicillin in the nephron were analyzed quantitatively using the plasma concentration and the urinary excretion rate of the drugs. The validity of the proposed model was demonstrated. It appears that tubular secretion of sulfamethizole, cephalexin, and ampicillin depend on the active transport system which is described by Michaelis–Menten kinetics; the tubular reabsorption of these drugs is expressed by first-order kinetics. The maximum velocity of renal secretion per unit weight of these drugs was much higher in rabbits than in dogs or humans. Reabsorption showed similar values in dogs and humans. These findings suggest that an analysis of the renal handling of drugs in dogs might provide useful information when considering the appropriate therapeutic dose in humans.

Keyphrases □ Clearance, renal—of sulfamethizole, sulfanilamide, cephalexin, and ampicillin in the rabbit, dog, and human, determination using a computer analysis □ Sulfamethizole—determination of renal clearance using a computer analysis □ Sulfanilamide—determination of renal clearance using a computer analysis □ Cephalexin—determination of renal clearance using a computer analysis □ Ampicillin—determination of renal clearance using a computer analysis

The renal excretion of drugs is a complex phenomenon involving glomerular filtration, tubular secretion, and tubular reabsorption (1). Since the independent characterization of the transport kinetics of secretion and reabsorption is difficult, the quantitative analysis of the renal handling of drugs is not readily available, particularly in humans. Weiner *et al.* (2) described an analytical method for these processes; however, one needs a wide range of drug concentrations in plasma. Since limited plasma levels are obtained in humans, this method has little clinical applicability. Such methodology, however, is desirable when designing the drug-dosing schedule for patients with renal disease.

We have described a method that quantitatively analyzes the renal handling of drugs (3, 4). Using this method, the renal handling of sulfamethizole, sulfamethoxazole, sulfanilamide, and phenolsulfonphthalein was described in rabbits. In this study, the applicability of this method to dogs and humans was examined, and the renal handling of two widely used antibiotics (cephalexin and ampicillin) was investigated using plasma concentrations normally obtained with therapeutic doses.

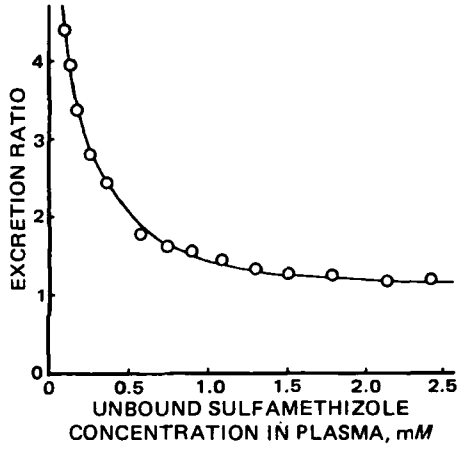

Figure 1—*Experimental renal clearance data (points) and computer-simulated curve (line) for sulfamethizole in the dog. The parameters obtained by this analysis are as follows:* V_{max} = *20 μmoles/min,* K_m = *0.16 mM, and* R = 0.13.

EXPERIMENTAL

Materials—Sulfamethizole was JP IX grade[1]; sulfanilamide was reagent grade[2]. Cephalexin monohydrate[3], sodium ampicillin[3], and iodopyracet[4] were supplied. All other chemicals were reagent grade.

Determination of Plasma Protein Binding—Plasma protein binding was determined by the ultrafiltration technique using a membrane cone[5] for sulfamethizole and sulfanilamide and cellulose tubing[6] for cephalexin and ampicillin.

Analytical Methods—Plasma and urine samples were treated with the Somogyi deproteinizing reagent (5) and then analyzed for sulfamethizole and sulfanilamide using 2-dimethylaminoethyl-1-naphthylamine as the coupling reagent (6). Inulin was determined in samples deproteinized as described above using a modification of a previously described method (7). Cephalexin and ampicillin in plasma and urine were determined fluorometrically (8, 9); creatinine was determined using picric acid (10).

Clearance Method—*Rabbits*—Male New Zealand albino rabbits, weighing 2.0–2.5 kg, were used. The determination of renal clearance using a single injection technique and the standard renal clearance and secretory inhibition using iodopyracet was described previously (4).

Dogs—Male mongrel dogs, weighing 5–11 kg, were anesthesized with pentobarbital[7] (27 mg/kg). Renal clearance was determined in the same manner as described above for the rabbit.

Humans—Sulfamethizole (4 g of an aqueous solution), sulfanilamide

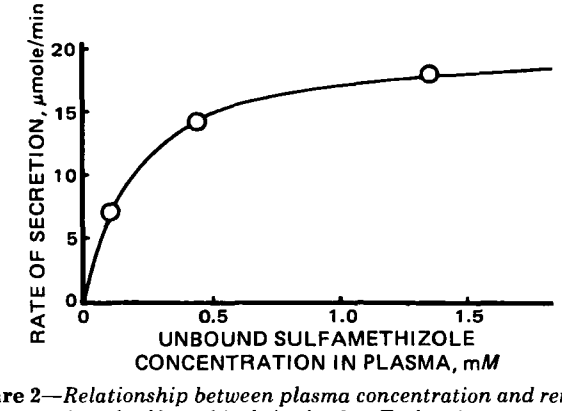

Figure 2—*Relationship between plasma concentration and renal tubular secretion of sulfamethizole in the dog. Each point represents the experimental data obtained by inhibitory experiments; the solid line represents the curve calculated using the proposed model. The parameters are as follows:* V_{max} = *20 μmoles/min and* K_m = *0.18 mM.*

[1] Eizai Co. Ltd.
[2] Nakarai Chemicals, Ltd.
[3] Toyo Jozo Co. Ltd.
[4] Daiichi Seiyaku Co. Ltd.
[5] Centriffo CF-50A, Amicon Co. Ltd.
[6] Visking Company, 8/32.
[7] Nembutal, Abbott Laboratories, North Chicago, Ill.

0022-3549/83/0400-0440$01.00/0

Table I—Renal Tubular Secretion and Reabsorption of Sulfamethizole and Sulfanilamide in Dogs

Parameter (Unit)	Sulfamethizole	Sulfanilamide
V_{max} (μmole/min)	20 ± 0.4[b]	0
K_m (mM)	0.18 ± 0.01	—
R	0.18 ± 0.01	0.37 ± 0.03
R'[a]	0.19 ± 0.01	0.40 ± 0.05

[a] Reabsorption fraction obtained by inhibitory experiments. [b] Each value represents the mean ± SE of three or four experiments.

Table II—Renal Tubular Secretion and Reabsorption of Sulfamethizole in Humans

Subject	Age	V_{max}, μmole/min	K_m, mM	R
A(M)[a]	24	91	0.09	0.10
B(M)	32	71	0.09	0.06
C(F) (1st)	23	110	0.16	0.13
C(F) (2nd)	23	110	0.16	0.33
D(M)	28	83	0.10	0.05
E(M)	46	80	0.09	0.10
F(M) (1st)	28	59	0.06	0.09
F(M) (2nd)	28	52	0.06	0.31

[a] (M) male, (F) female.

(2 g of an aqueous solution), cephalexin (500 mg of a powder), and ampicillin (500 mg of a powder) were administered orally to adult volunteers (22–46 years old, of average health and normal weight) following an overnight fast. Food was withheld for an additional 3 hr. Venous blood and urine samples were collected at intervals of 15 or 30 min up to 6 hr after drug administration. To ensure continuous flow of urine and to quantitate fluid intake, each subject received 50 ml of tap water every 30 min for the initial 4 hr postadministration. The volume and pH of each urine sample were measured and the samples were stored at 4° until analysis. The glomerular filtration rate was determined by measuring the clearance of endogenous creatinine.

Computer Analysis—As described previously (3), the excretion ratio (ER) can be expressed as:

$$ER = \left(1 + \frac{V_{max}}{(K_m + P_f)\,GFR}\right)(1 - R)$$

where P_f is the unbound drug concentration in plasma, GFR is the glomerular filtration rate, R is the reabsorption fraction, V_{max} is the maximum velocity of secretion, and K_m is the Michaelis constant. The computer analysis[8] using this equation was performed as previously described (3, 4).

RESULTS

Renal Handling of Sulfamethizole and Sulfanilamide in Dogs—The renal clearance following a single injection of sulfamethizole in the dog was analyzed using the model equation (Fig. 1). As in the case of the rabbit, a curve was obtained which fit the experimental values quite well (see Table I for a list of parameters). To ascertain the validity of the values obtained by our model, a comparison of the rate of secretion and the reabsorption fractions was made using the renal clearance method in combination with secretory inhibition by the infusion of iodopyracet.

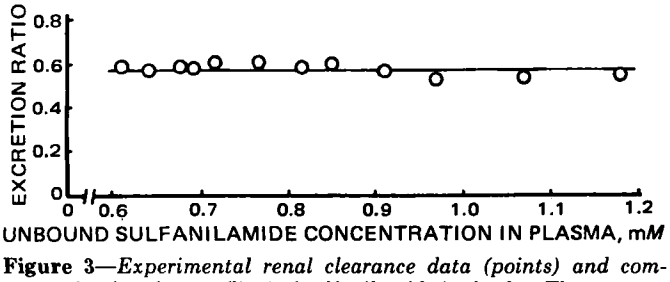

Figure 3—*Experimental renal clearance data (points) and computer-simulated curve (line) of sulfanilamide in the dog. The parameters obtained by this analysis are as follows:* V_{max} = 0 *μmole/min and* R = 0.42.

[8] HITAC 8700, Hitachi Co. Ltd.

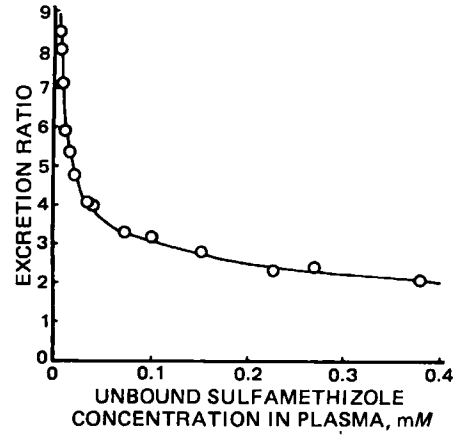

Figure 4—*Experimental renal clearance data (points) and computer-simulated curve (line) of sulfamethizole in the human. The parameters obtained by this analysis are as follows:* V_{max} = 59 *μmoles/min,* K_m = 0.06 m**M**, *and* R = 0.09.

First, a comparison was made of the rate of secretion obtained separately from inhibitory experiments and using V_{max} and K_m values obtained by our model. As shown in Fig. 2, a good agreement was achieved. Further, there was also good agreement of the reabsorption fractions: a value of 0.19 ± 0.01 was obtained from the inhibitory experiment compared with 0.18 ± 0.01 from the proposed model. Thus, it was found that the mechanism of the renal excretion of sulfamethizole in dogs was similar to that found in rabbits. That is, tubular reabsorption is dependent on passive transport, whereas tubular secretion involves active transport (which conforms to the Michaelis–Menten equation) and is dependent on the plasma concentration of unbound drug.

On the other hand, the renal clearance after a single injection of sulfanilamide is not dependent on its plasma concentration, and no active secretion process is involved (Fig. 3). Each renal clearance parameter for sulfanilamide is listed in Table I. In the inhibitory experiment for sulfanilamide, no change in renal clearance could be induced even with iodopyracet loading. As in the rabbit, there was no secretion in dogs; only reabsorption was observed. Further, the reabsorption fraction of 0.37 ± 0.03 agreed well with that obtained from the inhibitory experiment (0.40 ± 0.05). Therefore, the validity of this method has been demonstrated in dogs as well as rabbits.

Renal Handling of Sulfamethizole and Sulfanilamide in Humans—Our analytical method of renal handling of drugs was applied also to humans. The renal handling of sulfamethizole in humans is shown in Fig. 4. As in the case of rabbits and dogs, a curve was obtained which fit the experimental values quite well. This result indicates that the mechanism of sulfamethizole excretion in humans could be similar to that of other animals. The values of the parameters V_{max}, K_m, and R for all human subjects are listed in Table II. These values are quite similar to those found with dogs, although some individual variation exists. The day-to-day variation of these parameters in the same subject was also examined for subjects C and F. There was no apparent change in the secretion parameter (V_{max} and K_m), while variations were observed in the reabsorption fraction.

The results of the renal clearance of sulfanilamide in humans (Fig. 5) indicated that this drug was excreted by a mechanism similar to that found in rabbits and dogs. It is evident that there was no secretion, only reabsorption.

Renal Handling of Cephalexin and Ampicillin—Since we were

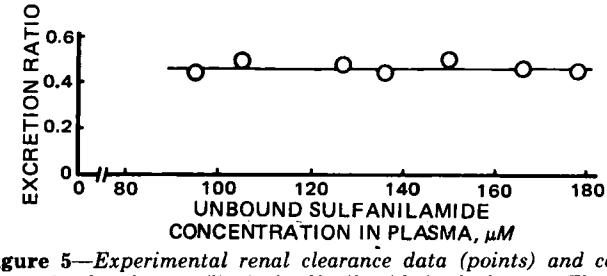

Figure 5—*Experimental renal clearance data (points) and computer-simulated curve (line) of sulfanilamide in the human. The parameters obtained by this analysis are as follows:* V_{max} = 0 *μmole/min and* R = 0.52.

Table III—Parameters for Renal Tubular Secretion and Reabsorption of Drugs in Humans, Dogs, and Rabbits [a]

Parameter (unit)	Sulfamethizole			Cephalexin			Ampicillin		
	Human	Dog	Rabbit	Human	Dog	Rabbit	Human	Dog	Rabbit
V_{max} (μmole/min/body)	82 ± 7.6	20 ± 0.4	33 ± 4	14 ± 2	0.75 ± 0.08	2.1 ± 0.2	2.6 ± 0.4	1.1 ± 0.1	0.33 ± 0.03
V_m' (μmole/min/kg)	1.4 ± 0.1	2.3 ± 0.1	15 ± 1	0.24 ± 0.03	0.14 ± 0.01	1.0 ± 0.1	0.04 ± 0.01	0.06 ± 0.01	0.14 ± 0.01
K_m (μM)	110 ± 40	180 ± 10	1700 ± 110	17 ± 3	16 ± 1	36 ± 3	10 ± 1	31 ± 5	29 ± 5
R	0.15 ± 0.04	0.18 ± 0.01	0.20 ± 0.02	0.47 ± 0.03	0.49 ± 0.02	0.33 ± 0.03	0.01 ± 0.01	0.00 ± 0.01	0.00 ± 0.01

[a] Each value represents the mean ±*SE*.

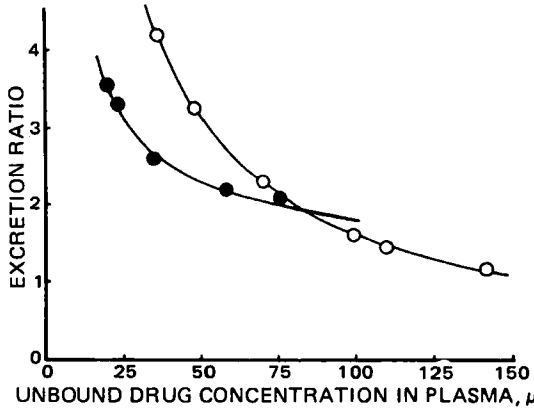

Figure 6—*Experimental renal clearance data (points) and computer-simulated curve (line) of cephalexin and ampicillin in the rabbit. Key: (○) cephalexin and (●) ampicillin.*

successful in elucidating the mechanism of the renal handling of sulfamethizole and sulfanilamide through the use of this model, we attempted to apply this methodology to other drugs using cephalexin and ampicillin. As shown in Figs. 6 (rabbit), 7 (dog), and 8 (human), good agreement was obtained between the experimental data and theoretical curves calculated using the appropriate parameters (Table III) obtained in rabbits, dogs, and humans. The data suggested that cephalexin and ampicillin were excreted from the kidney in a process similar to the excretion of sulfamethizole. Welles *et al.* described the renal handling of cephalexin in rabbits and dogs, and demonstrated that secretion and reabsorption were extensively involved in renal excretion (11). Secretion has also been reported for ampicillin (12). The results presented here support the findings that both secretion and reabsorption contribute significantly to the excretion of cephalexin, while the contribution is very small in these three species in the case of ampicillin.

Species Variation in Renal Handling of Sulfamethizole, Cephalexin, and Ampicillin—The parameters for these three drugs in rabbits, dogs, and humans are shown in Table III. The reabsorption fraction, R, in all species was almost the same, but there were differences in the secretion parameters V_{max} and K_m. Comparison of the V_{max} values per unit weight (V_m) of sulfamethizole, cephalexin, and ampicillin in the three species showed that rabbits had the highest values with all three drugs, while the values for dogs and humans were approximately the same. Petitpierre *et al.* reported that the renal function of beagle dogs resembles that of humans (13). Our data confirmed quantitatively that the two are similar. Accordingly, it is possible that the renal handling of a drug in humans can be predicted quantitatively by initially performing experiments in dogs.

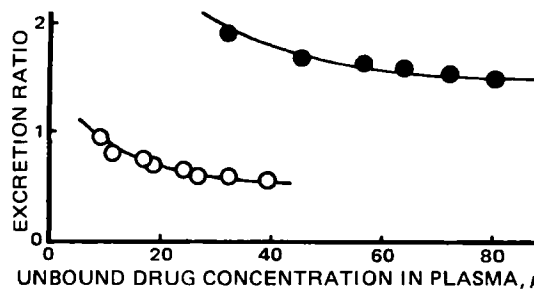

Figure 7—*Experimental renal clearance data (points) and computer-simulated curve (line) of cephalexin and ampicillin in the dog. Key: (○) cephalexin and (●) ampicillin.*

DISCUSSION

In previous reports (3, 4), we proposed a quantitative analytical method to determine the renal handling of such drugs as sulfamethizole, sulfamethoxazole, sulfanilamide, and phenolsulfonphthalein in rabbits. In this study, the methodology was applied to dogs and humans. The renal handling of two widely used antibiotics (cephalexin and ampicillin) was investigated after a single oral dose. It was demonstrated that our method can be applied to dogs and humans as well as rabbits. Some reports are available concerning the urinary excretion of such drugs as inulin (14) and phenolsulfonphthalein (15) in humans; however, few studies quantitate separately the processes of tubular secretion and reabsorption. It was also demonstrated that the tubular secretion of these drugs can be explained by an active transport process which conforms to the Michaelis–Menten equation, while tubular reabsorption can be explained by a first-order process. As our equation fit the experimental data obtained from rabbits, dogs, and humans, it can be assumed that the tubular secretion of these drugs is dependent on the unbound drug concentration in the plasma for each of these species. Levy *et al.* reported that the renal tubular secretion rate in the rat is proportional to the total concentration of sulfisoxazole in plasma rather than the free drug concentration (16, 17). Although further studies are needed, this investigation using sulfamethizole, cephalexin, and ampicillin in three different species shows that tubular secretion correlates with unbound drug concentration.

The renal handling of sulfamethizole, phenolsulfonphthalein, sulfamethoxazole, and sulfanilamide in rabbits was reported previously (4). In this study, the renal handling of cephalexin and ampicillin in rabbits, dogs, and humans was described. It was demonstrated that cephalexin belonged to the secretion and reabsorption type and ampicillin belonged to the secretion type in all three species. Although both drugs have very low lipid solubility, cephalexin showed a relatively high reabsorption. This suggests the possibility of an active-like reabsorption process for cephalexin. The renal clearance values *versus* the unbound plasma concentration curve of cephalexin in all three species did not show the

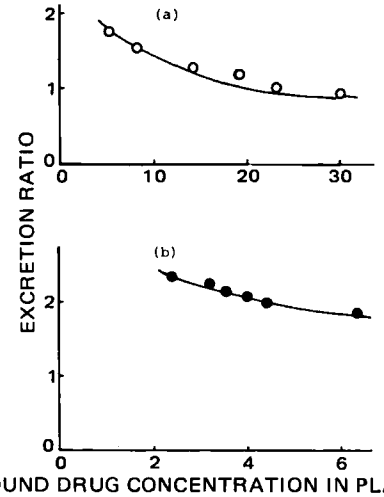

Figure 8—*Experimental renal clearance data (points) and computer-simulated curve of cephalexin (a) and ampicillin (b) in the human.*

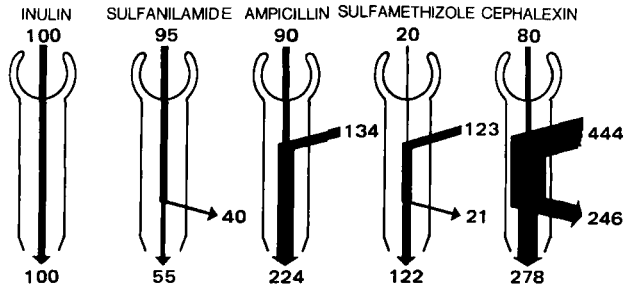

Figure 9—*Schematic representation of renal handling of drugs in the human. The parameters in Table III are used; detailed information can be found in the text.*

typical active reabsorption pattern such as that found for glucose (18). Therefore, the contribution of a nonlinear reabsorption process would not be significant under the conditions used here even if an active-like process were to be included in its reabsorption.

Figure 9 shows a schematic representation of the renal handling of these drugs in humans compared with that of inulin. The numbers given, calculated using a plasma drug concentration of 5 μM and glomerular filtration rate of 120 ml/min, represent the rate (in percent) of the designated transport process (*i.e.*, filtration, secretion, reabsorption, and urinary excretion) normalized for inulin glomerular filtration (600 nmoles/min). Plasma concentration of drugs were corrected by protein-binding percentage. Thus, for example, since sulfanilamide is 5% protein-bound in plasma, its filtration rate is 95% that of inulin (95% of 600 = 570 nmoles/min). Similarly, reabsorption of sulfanilamide occurs at a rate 40% of inulin filtration, *i.e.*, at 40% of 600 = 240 nmoles/min. It is evident that tubular secretion and reabsorption would be the most important process in regulating the urinary excretion of sulfamethizole, cephalexin, and ampicillin. If renal functions, such as renal secretion, were decreased by renal failure, the renal excretion of sulfamethizole, cephalexin, and ampicillin would be reduced greatly resulting in a high concentration in the blood and target organ. The impact of renal failure on the process of filtration, secretion, and reabsorption should be known in order to provide optimal treatment and protection from adverse reactions in patients with this disease state. We have applied the method described in this paper to the analysis of renal handling of drugs in patients with renal failure, the results of which will be discussed in an ensuing manuscript.

REFERENCES

(1) I. M. Weiner and H. Mudge, *Am. J. Med.*, **36**, 743 (1964).

(2) I. M. Weiner, K. D. Garlid, J. A. Romeo, and G. H. Mudge, *Am. J. Physiol.*, **200**, 393 (1961).

(3) R. Hori, K. Sunayashiki, and A. Kamiya, *J. Pharm. Sci.*, **65**, 463 (1976).

(4) R. Hori, K. Sunayashiki, and A. Kamiya, *Chem. Pharm. Bull.*, **26**, 740 (1978).

(5) M. Somogyi, *J. Biol. Chem.*, **128**, 655 (1930).

(6) A. C. Bratton and E. K. Marshall, Jr., *ibid.*, **128**, 537 (1939).

(7) Z. Dische and F. Borenfreund, *ibid.*, **192**, 583 (1951).

(8) K. Miyazaki, O. Ogino, and T. Arita, *Chem. Pharm. Bull.*, **27**, 2273 (1979).

(9) *Idem.*, **22**, 1910 (1974).

(10) O. Folin, *Hoppe-Seylers Z. Physiol. Chem.*, **41**, 223 (1904).

(11) J. S. Welles, R. O. Froman, W. R. Gibson, N. V. Owen, and R. C. Anderson, *Antimicrob. Agents Chemother.*, **1968**, 489.

(12) B. L. Johnson, Jr., S. Mandiola, and J. Dahlgren, *J. Infect. Dis.*, **129**, 37 (1974).

(13) B. Petitpierre, L. Perrin, M. Rudhardt, A. Herrera, and J. Fabre, *Int. J. Clin. Pharmacol. Ther. Toxicol.*, **6**, 120 (1972).

(14) J. A. Shannon, *Am. J. Physiol.*, **112**, 405 (1935).

(15) H. W. Smith, W. Goldring, and H. Chasis, *J. Clin. Invest.*, **17**, 263 (1937).

(16) A. Yacobi and G. Levy, *J. Pharm. Sci.*, **68**, 742 (1979).

(17) G. Levy, *ibid.*, **69**, 482 (1980).

(18) R. F. Pitts, "Physiology of the Kidney and Body Fluids," Year Book Medical Publishers, Chicago, Ill., 1963.

Thermodynamics of Distribution of *p*-Substituted Phenols Between Aqueous Solution and Organic Solvents and Phospholipid Vesicles

N. H. ANDERSON ‡, S. S. DAVIS *ˣ, M. JAMES*, and I. KOJIMA *§

Received December 21, 1981, from the **Department of Pharmacy, University of Nottingham, Nottingham, NG7 2RD, UK* and the ‡*Long Ashton Research Station, Long Ashton, Bristol, BS18 9AF, UK.* Accepted for publication January 14, 1983. §On leave from the Laboratory of Analytical Chemistry, Nagoya Institute of Technology, Nagoya 466, Japan.

Abstract □ The distribution of *p*-substituted phenols between 0.15 *M* NaCl and a range of organic solvents (including 1-octanol) was examined over a range of temperatures. The thermodynamic parameters of transfer, ΔG, ΔH, and ΔS, were determined and the values examined in the light of Hildebrand and Scott's solubility parameter theory, and the collision complexes between solute and organic solvent. ΔH of transfer was positive for nonpolar solvents and negative for 1-octanol; the transfer processes were entropy and enthalpy dominated, respectively. The distribution of the phenols into phospholipid vesicles was examined below the phase-transition temperature. Although ΔG of transfer for vesicle–water systems was similar to that for octanol–water systems, the full thermodynamic analysis indicated that the two systems were dissimilar. The use of vesicle distribution data in structure–activity studies is discussed.

Keyphrases □ *p*-Substituted phenols—partitioning between water and organic solvents, phospholipid vesicles, thermodynamics □ Phospholipid vesicles—partitioning of *p*-substituted phenols, water and organic solvents, thermodynamics □ Thermodynamics—*p*-substituted phenols, partitioning, water and organic solvents, phospholipid vesicles

The importance of hydrophobicity in drug absorption, drug binding, and drug-receptor site interactions is well known (1, 2). Some measure of the hydrophobicity of a solute is given by the distribution (partition) coefficient between water and a suitable organic solvent (3). Usually the choice of the organic phase has been 1-octanol; however, Rytting *et al.* (4) have argued from a thermodynamic standpoint that a nonpolar inert solvent such as isooctane or cyclohexane would be a more appropriate solvent for distribution studies.

0022-3549/83/0400-0443$01.00/0

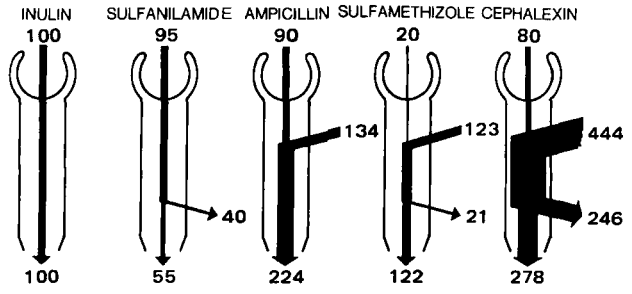

Figure 9—*Schematic representation of renal handling of drugs in the human. The parameters in Table III are used; detailed information can be found in the text.*

typical active reabsorption pattern such as that found for glucose (18). Therefore, the contribution of a nonlinear reabsorption process would not be significant under the conditions used here even if an active-like process were to be included in its reabsorption.

Figure 9 shows a schematic representation of the renal handling of these drugs in humans compared with that of inulin. The numbers given, calculated using a plasma drug concentration of 5 μM and glomerular filtration rate of 120 ml/min, represent the rate (in percent) of the designated transport process (*i.e.*, filtration, secretion, reabsorption, and urinary excretion) normalized for inulin glomerular filtration (600 nmoles/min). Plasma concentration of drugs were corrected by protein-binding percentage. Thus, for example, since sulfanilamide is 5% protein-bound in plasma, its filtration rate is 95% that of inulin (95% of 600 = 570 nmoles/min). Similarly, reabsorption of sulfanilamide occurs at a rate 40% of inulin filtration, *i.e.*, at 40% of 600 = 240 nmoles/min. It is evident that tubular secretion and reabsorption would be the most important process in regulating the urinary excretion of sulfamethizole, cephalexin, and ampicillin. If renal functions, such as renal secretion, were decreased by renal failure, the renal excretion of sulfamethizole, cephalexin, and ampicillin would be reduced greatly resulting in a high concentration in the blood and target organ. The impact of renal failure on the process of filtration, secretion, and reabsorption should be known in order to provide optimal treatment and protection from adverse reactions in patients with this disease state. We have applied the method described in this paper to the analysis of renal handling of drugs in patients with renal failure, the results of which will be discussed in an ensuing manuscript.

REFERENCES

(1) I. M. Weiner and H. Mudge, *Am. J. Med.*, **36**, 743 (1964).

(2) I. M. Weiner, K. D. Garlid, J. A. Romeo, and G. H. Mudge, *Am. J. Physiol.*, **200**, 393 (1961).

(3) R. Hori, K. Sunayashiki, and A. Kamiya, *J. Pharm. Sci.*, **65**, 463 (1976).

(4) R. Hori, K. Sunayashiki, and A. Kamiya, *Chem. Pharm. Bull.*, **26**, 740 (1978).

(5) M. Somogyi, *J. Biol. Chem.*, **128**, 655 (1930).

(6) A. C. Bratton and E. K. Marshall, Jr., *ibid.*, **128**, 537 (1939).

(7) Z. Dische and F. Borenfreund, *ibid.*, **192**, 583 (1951).

(8) K. Miyazaki, O. Ogino, and T. Arita, *Chem. Pharm. Bull.*, **27**, 2273 (1979).

(9) *Idem.*, **22**, 1910 (1974).

(10) O. Folin, *Hoppe-Seylers Z. Physiol. Chem.*, **41**, 223 (1904).

(11) J. S. Welles, R. O. Froman, W. R. Gibson, N. V. Owen, and R. C. Anderson, *Antimicrob. Agents Chemother.*, **1968**, 489.

(12) B. L. Johnson, Jr., S. Mandiola, and J. Dahlgren, *J. Infect. Dis.*, **129**, 37 (1974).

(13) B. Petitpierre, L. Perrin, M. Rudhardt, A. Herrera, and J. Fabre, *Int. J. Clin. Pharmacol. Ther. Toxicol.*, **6**, 120 (1972).

(14) J. A. Shannon, *Am. J. Physiol.*, **112**, 405 (1935).

(15) H. W. Smith, W. Goldring, and H. Chasis, *J. Clin. Invest.*, **17**, 263 (1937).

(16) A. Yacobi and G. Levy, *J. Pharm. Sci.*, **68**, 742 (1979).

(17) G. Levy, *ibid.*, **69**, 482 (1980).

(18) R. F. Pitts, "Physiology of the Kidney and Body Fluids," Year Book Medical Publishers, Chicago, Ill., 1963.

Thermodynamics of Distribution of *p*-Substituted Phenols Between Aqueous Solution and Organic Solvents and Phospholipid Vesicles

N. H. ANDERSON ‡, S. S. DAVIS *ˣ, M. JAMES*, and I. KOJIMA *§

Received December 21, 1981, from the **Department of Pharmacy, University of Nottingham, Nottingham, NG7 2RD, UK* and the ‡*Long Ashton Research Station, Long Ashton, Bristol, BS18 9AF, UK.* Accepted for publication January 14, 1983. §On leave from the Laboratory of Analytical Chemistry, Nagoya Institute of Technology, Nagoya 466, Japan.

Abstract □ The distribution of *p*-substituted phenols between 0.15 *M* NaCl and a range of organic solvents (including 1-octanol) was examined over a range of temperatures. The thermodynamic parameters of transfer, ΔG, ΔH, and ΔS, were determined and the values examined in the light of Hildebrand and Scott's solubility parameter theory, and the collision complexes between solute and organic solvent. ΔH of transfer was positive for nonpolar solvents and negative for 1-octanol; the transfer processes were entropy and enthalpy dominated, respectively. The distribution of the phenols into phospholipid vesicles was examined below the phase-transition temperature. Although ΔG of transfer for vesicle–water systems was similar to that for octanol–water systems, the full thermodynamic analysis indicated that the two systems were dissimilar. The use of vesicle distribution data in structure–activity studies is discussed.

Keyphrases □ *p*-Substituted phenols—partitioning between water and organic solvents, phospholipid vesicles, thermodynamics □ Phospholipid vesicles—partitioning of *p*-substituted phenols, water and organic solvents, thermodynamics □ Thermodynamics—*p*-substituted phenols, partitioning, water and organic solvents, phospholipid vesicles

The importance of hydrophobicity in drug absorption, drug binding, and drug-receptor site interactions is well known (1, 2). Some measure of the hydrophobicity of a solute is given by the distribution (partition) coefficient between water and a suitable organic solvent (3). Usually the choice of the organic phase has been 1-octanol; however, Rytting *et al.* (4) have argued from a thermodynamic standpoint that a nonpolar inert solvent such as isooctane or cyclohexane would be a more appropriate solvent for distribution studies.

0022-3549/83/0400-0443$01.00/0

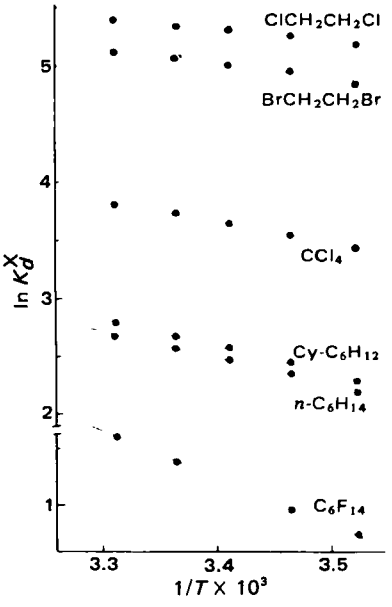

Figure 1—*van't Hoff plots for* p-*ethylphenol distributed between 0.15 M aqueous sodium chloride solution and various nonpolar organic solvents.*

In spite of the wide usage of 1-octanol–water distribution coefficients in structure–activity studies, relatively little work has been done to establish the actual basis of the relationship between distribution with octanol and biological activity (5). Martin (6) has emphasized that various absorption phenomena involving the passage of drugs across biological membranes are not well modeled by 1-octanol–water distribution coefficients. Other groups have suggested that the phospholipid vesicle (liposome) can be used as a model system to study solute distribution into membranes (7–9). Phospholipid vesicles consist of lipid bilayers in the form of multilayers arranged concentrically, or as simple bilayers encapsulating a volume of aqueous medium in the core. The vesicle can exist in liquid-crystalline or solid forms depending on the choice of the constituent phosphatidylcholine(s). Bindsley and Wright (10) have concluded that permeation rates of solutes across the toad bladder were more closely related to vesicle–water distribution data when the vesicles were below their phase-transition temperature (T_c).

The present investigation was designed to evaluate various organic solvents (including 1-octanol) as models for the distribution of solutes into membranes. The distribution of various *p*-substituted phenols between water and different organic phases as well as phospholipid vesicles were studied. The solvents were selected to give a wide range of solvent properties (solubility parameters). Data were obtained at different temperatures, allowing the calculation of the relevant thermodynamic parameters, enthalpy and entropy, which provide insight into the mechanism of solute transfer.

THEORETICAL

Organic Solvent–Water Distribution—The distribution ratio of solute between two immiscible solvents is given by:

$$D = \frac{C_{A,org}}{C_{A,aq}} \qquad \text{(Eq. 1)}$$

where $C_{A,org}$ and $C_{A,aq}$ are the total solute concentration in the organic and aqueous phases respectively. When only monomeric and un-ionized solute exist in both phases, Eq. 1 can be written as:

$$K_d = D = \frac{[\text{Solute}]_{org}}{[\text{Solute}]_{aq}} \qquad \text{(Eq. 2)}$$

The thermodynamic distribution constant K_d^X (mole fraction) (concentration units) can be written as:

$$K_d^X = K_d \left(\frac{V_{org}}{V_{aq}}\right) \qquad \text{(Eq. 3)}$$

where V_{org} and V_{aq} are the molar volumes of the organic solvent and aqueous phase. The distribution constant (K_d^X) is a free-energy (ΔG) related term:

$$\Delta G_{(transfer)} = -RT \ln K_d^X \qquad \text{(Eq. 4)}$$

As such it yields little information about the nature of the transfer process, and a more complete thermodynamic picture can be obtained by studying the change of the distribution coefficient with temperature, to provide enthalpic and entropic contributions to the free energy of transfer (11–15):

$$\ln K_d^X = -\frac{\Delta H}{R}\frac{1}{T} + \frac{\Delta S}{R} \qquad \text{(Eq. 5)}$$

where ΔG, ΔH, and ΔS are the partial molal free energy, enthalpy, and entropy change on transfer of the solute. The parameters ΔH and ΔS can be calculated from the slope and intercept of a plot of $\ln K_d^X$ *versus* $1/T$.

Phospholipid Vesicles: Water Distribution—The molal concentration scale has to be used because of the heterogeneous nature of the system under investigation (7). [A useful appraisal is the choice of concentration scale/standard state in bioenergetics and thermodynamics has been given by Jameson (16).]

The molal concentrations of solutes in the lipid (vesicle) phase (C_0^m) and the aqueous phase (C_w^m) are given by:

$$C_0^m = \frac{(C_T - C_W)w_1}{dMw_2} \qquad \text{(Eq. 6)}$$

$$C_w^m = \frac{C_W}{dM} \qquad \text{(Eq. 7)}$$

Table I—Thermodynamic Values for the Distribution of *p*-Substituted Phenol between 0.15 *M* NaCl and Organic Solvents at 25°

Organic Solvent	δ[d]	X[a]	$-\Delta G$[b]	ΔH[b]	ΔS[c]
C_6F_{14}	5.6	CH_3	−3.91	32	94
		C_2H_5	−1.46	35	111
		C_3H_7	1.07	32	111
n-C_6H_{14}	7.4	H	−0.15	21	69
		CH_3	3.18	19	74
		C_2H_5	6.39	19	85
		C_3H_7	10.00	18	95
		Cl	2.96	16	63
Cy-C_6H_{12}	8.2	H	0.03	21	70
		CH_3	3.29	21	80
		C_2H_5	6.67	20	91
		C_3H_7	10.4	19	99
		Cl	3.24	16	66
CCl_4	8.6	H	2.48	15	58
		CH_3	5.94	14	67
		C_2H_5	9.26	15	83
		C_3H_7	12.8	14	90
		Cl	6.03	13	63
$ClCH_2CH_2Cl$	9.8	H	7.39	7	50
		CH_3	10.4	9	64
		C_2H_5	13.3	8	73
		Cl	11.0	4	51
$BrCH_2CH_2Br$	10.4	H	6.42	9	51
		CH_3	9.70	10	66
		C_2H_5	12.6	10	78
		Cl	10.3	6	55
1-$C_8H_{17}OH$[e]	10.3	H	14.07	−7	23
		CH_3	16.54	−7	30
		C_2H_5	18.99	−8	36
		Cl[f]	19.05	−16	10

[a] X is the substituent of *p*-position of phenol. [b] ΔG and ΔH are given in kJ mole^{-1}. [c] ΔS is given in J mole^{-1}°K^{-1}. [d] δ-Solubility parameter in Cal$^{1/2}$cm$^{-3/2}$ from ref. 20. [e] Mean values taken from ref. 13 and F. J. C. Dearden and G. M. Bresnen, *J. Pharm. Pharmac. Suppl.* 107P (1981).

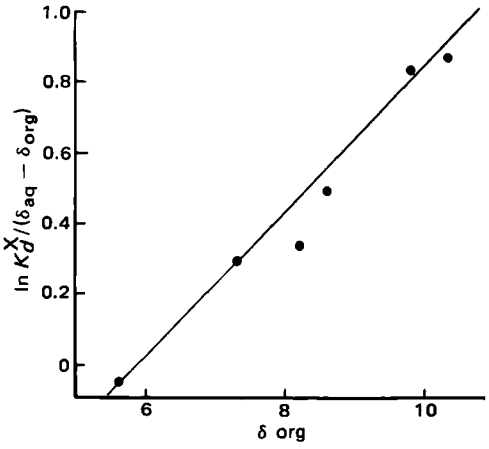

Figure 2—*The analysis of distribution data using solubility parameter theory.*

where C_T is the initial aqueous concentration before equilibrium (mg/ml), C_W is the final aqueous concentration after equilibrium (mg/ml), d is the density of the initial aqueous phase, M is the molecular weight of the solute, w_1 is the weight of aqueous phase in the sample, and w_2 is the weight of phospholipid in the sample. Thus, the molal distribution coefficient K_d^m is given by:

$$K_d^m = \frac{(C_T - C_W)w_1}{C_W w_2} \qquad \text{(Eq. 8)}$$

EXPERIMENTAL

Chemicals—Water was distilled from an all-glass still. The phenolic solutes used were as follows: phenol[1] (99.99%) was used without further purification; *p*-cresol[2], *p*-ethylphenol[2], *p*-chlorophenol[3], *p*-bromophenol[3], *p*-iodophenol[4], and *p*-fluorophenol[4] were used after recrystallization; *p*-propylphenol[4] was used after double distillation; and *p*-chloroanisole[3], resorcinol[3], *m*-methoxyphenol[2], and *m*-ethoxyphenol[2] were used as received.

Aqueous solutions of the phenols (~2 mg/100 ml) were prepared by dissolving samples in 0.15 *M* NaCl solution. The organic solvents used were perfluorohexane[1], *n*-hexane (special for spectroscopy)[3], cyclohexane (analytical grade)[3], 1,2-dichloroethane[4] (>99%) and 1,2-dibromoethane[4] (99%), carbon tetrachloride[5], and 1-octanol[4]. When necessary, they were washed successively with sodium hydroxide solution, distilled water, concentrated sulfuric acid, and finally 5 times with distilled water. L-α-Dimyristoylphosphatidylcholine[6] (DMPC) (98%) was used throughout as the sole lipid in the preparation of phospholipid vesicles.

Thin-layer chromatography of DMPC produced a single spot. Chloroform[1] was reagent grade.

Organic Solvent–Water Distribution—Oil–water distribution coefficients were obtained using the shake flask technique or a rapid mix/filter probe system (14, 17). The aqueous and organic phases were mutually saturated before use. Each experimental arrangement was thermostated at a given temperature (±0.1°), and at equilibrium the concentration of the solute in the aqueous phase was determined from the UV absorbance measured in the linear region of the Beer–Lambert plot.

Phospholipid Vesicle–Water Distribution—The vesicles were prepared using a stock solution of DMPC in chloroform containing 20-mg DMPC. This solution was placed in tared 50-ml round-bottom flasks and the chloroform removed rapidly by rotary evaporation at ~40°. The weight of the dried lipid film was measured, and multilamellar vesicles were formed at 40° by transferring 5 ml of highly dilute stock solution of phenol derivative into the flask and swirling the contents. Samples were prepared in duplicate, and the mean size and polydispersity of the vesicles were measured using a laser light scattering method (photon correlation spectroscopy)[7]. Reproducible yields of vesicles could be prepared by controlling strictly the hydration time and method of agitation.

[1] British Drug Houses.
[2] Eastman Kodak Co.
[3] Aldrich Chemical Co.
[4] Bristol Organic Ltd.
[5] Hopkins and Williams Co.
[6] Sigma Chemical Co.
[7] Malvern Instruments.

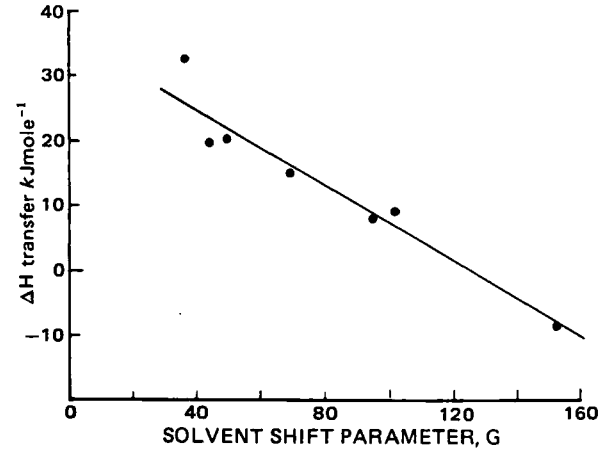

Figure 3—*The relationship between the enthalpy of transfer of* p-*substituted phenols and the solvent shift parameter* P *(Eq. 10).*

An equilibrium time for distribution of 12 hr was established from preliminary studies. The DMPC vesicles were separated from the aqueous phase by centrifugation in a thermostated centrifuge (8). The UV absorbance of the supernatant aqueous phase was measured at the λ_{max} of the phenol. After analysis the solution was returned to the phospholipid vesicle pellet and the system redispersed and re-equilibrated at the next temperature.

The processes of centrifugation, followed by resuspension did not alter significantly the mean size or polydispersity of the vesicles. Distribution studies were conducted over the temperature range 5–22° below the phase transition temperature of the phospholipid (23°) (18).

RESULTS AND DISCUSSION

Organic Solvent–Water Distribution—Preliminary studies indicated that for $C_{A,org}$ of less than 5×10^{-3} *M* the phenols existed as monomers in the organic phase. This is confirmed by literature data (19). Some typical plots of $\ln K_d^X$ *versus* $1/T$ are shown in Fig. 1. Good linearity was obtained in all cases, indicating that ΔH was independent of temperature over the range studied. Thermodynamic values obtained or calculated at 25° are summarized in Table I. The agreement with literature values (11, 13) including those obtained using microcalorimetry (15) is good in most cases, but there is some variation in ΔH (and consequently ΔS values). This is to be expected, since it is well known that the derivation of thermodynamic values from the van't Hoff isochore is dependent on good experimental data.

Examination of Fig. 1 and Table I shows clearly that the thermodynamic values of the transfer of phenols between aqueous environment and organic phases are dependent not only on the nature of the solute but also on the solvent. ΔG of transfer is positive for the lower alkyl phenols in perfluorohexane and for phenol in hexane. An increase in the distribution of the solute into the organic phase (ΔG becoming negative and increasing in magnitude) is accompanied by a decrease in ΔH and

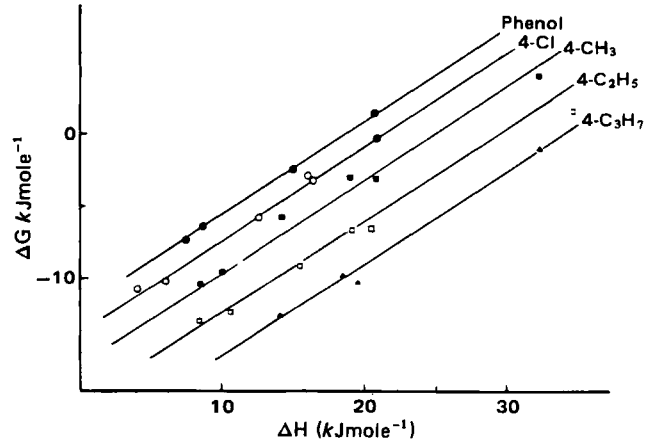

Figure 4—*Evaluation of compensation behavior. Enthalpy–free energy relationship for* p-*substituted phenols partitioned between 0.15* M *aqueous NaCl and nonpolar organic solvents.*

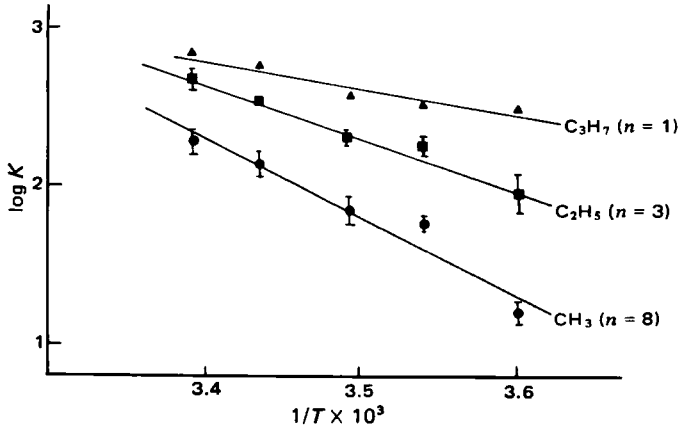

Figure 5—*The distribution of* p-*alkylphenols into DMPC vesicles—van't Hoff plots.*

a corresponding decrease in ΔS. 1-Octanol with a high extractive capacity provides large negative ΔH values and relatively small ΔS values. Such thermodynamic values reflect the important differences between the nature of the distribution process for different solvents. For inert hydrocarbon solvents, the distribution process reflects the loss of hydrogen bonding interactions between the hydroxyl group of the phenols and the aqueous phase that is compensated (in some cases) by an increase in ΔS. Any interaction between the phenolic hydroxyl group and the solvent [as well as the increased water content of the solvent and hydration of the monomeric phenol in the organic phase (21, 22)] would also be expected to lead to a decrease in the change in ΔH and a corresponding decrease in the change in ΔS. For 1-octanol, strong hydrogen bonding between the phenolic and alcohol hydroxyl groups will lead to a large and favorable ΔH (15). Consequently, control of the transfer passes from entropy domination to enthalpy domination.

When the concentration of a solute is sufficiently low in both phases, the distribution coefficient of solute distributed between water and a nonpolar organic solvent can be defined according to the theory of regular solutions (20):

$$\ln K_d^X = \frac{V_A}{RT}(\delta_{aq} - \delta_{org})(\delta_{aq} + \delta_{org} - 2\delta_A) \qquad \text{(Eq. 9)}$$

where V_A and δ_A are the molar volume and solubility parameter of solute A; δ_{aq} and δ_{org} are the solubility parameters of the aqueous solution and the organic solvent, respectively. Thus, a plot of $\ln K_d^X/(\delta_{aq} - \delta_{org})$ against δ_{org} should yield a straight line with a theoretical slope of V_A/RT. As shown in Fig. 2, using *p*-ethylphenol as an example, a linear relationship is obtained. The slope of the line is 0.206, in good agreement with the theoretical value of 0.203 calculated using $V_A = 120$ cm^3. A value of $\delta_{aq} = 16.5$ was employed rather than the usual value of 24. Davis *et al.* (23) and others (24) have shown previously that the lower value for δ_{aq} is valid for use in distribution studies involving organic solvents and aqueous phases.

Solvent effects can be considered also in terms of collision complexes between the phenolic solutes and the solvent. The aromatic carbon-hydrogen (A—H) stretching frequency in the IR is sensitive to hydrogen bond formation. Solvent shift theories and experimental studies on solvent effects have been reviewed (25). The frequency shift ΔV can be represented as the difference between the stretching frequency for the monomeric A—H in the vapor phase (V_0) and the lowered stretching frequency for A—H . . . B in the solvent in question (V_s). Badger and Bauer in 1937 (26) proposed that a linear relationship existed between the enthalpy of hydrogen bond formation and the frequency shift of the A—H stretching vibration.

In Fig. 3, the enthalpy of transfer has been plotted against the solvent shift parameter *P* (27) defined as:

$$\frac{V_0 - V_s}{V_0} = a\,P \qquad \text{(Eq. 10)}$$

The *P* values have been taken from literature sources (25, 27) on phenol in different solvents or calculated from values presented by Nakanishi *et al.* (28) for methanol and butanol systems[8]. The correlation between ΔH and *P* is good even though the *P* values refer to the anhydrous condition, and the phenols may be hydrated in the organic phase chosen for the distribution system.

[8] It should be noted that the *P* values were derived for anhydrous conditions, and the hydration of phenol in the organic phase may well alter the absolute values.

Table II—Thermodynamic Values for the Distribution of *p*-Substituted Phenols between 0.15 *M* NaCl and DMPC Vesicles at 22°

X[a]	−ΔG[b]	ΔH[b]	ΔS[c]
4-CH_3	13.3	119	448
4-C_2H_5	14.8	81	324
4-C_3H_7	15.5	31	157
4-F	12.4	37	168
4-Cl	14.6	19	112
4-Br	15.7	17	111
4-Cl anisole	17.9	102	405
3-OH	14.1	67	273
3-OCH_3	13.5	130	485
3-OC_2H_5	13.0	102	390

[a] Substituted phenol. [b] ΔG and ΔH are given in *k*J mole^{-1}. [c] ΔS is given in J mole^{-1}°K^{-1}.

Although there is no satisfactory treatment to account for solvent shifts of stretching frequencies, there is general agreement that the bulk properties of the solvent such as dielectric constant are important only for nonpolar solvents (25). Complexes between phenols and nonpolar solvents have been referred to as collision complexes to emphasize that although the interaction is very weak, it is sufficient to influence the IR spectrum (25).

Procedures for converting thermodynamic data obtained in polar solvents to those expected in an inert solvent have been proposed (25). One method is based on the assumption that the enthalpy of transfer can be written as (25):

$$-\Delta H\ (\text{nonpolar media}) = -\Delta H\ (\text{polar media}) + A \qquad \text{(Eq. 11)}$$

where *A* is a constant for the solvent pair. A free-energy related equation of similar type was proposed by Leo *et al.* (3) for the interconversion of distribution coefficient data obtained with nonpolar solvents and those obtained with octanol:

$$\log K_{d,\text{solvent}} + I_h = \log K_{d,\text{octanol}} + b \qquad \text{(Eq. 12)}$$

where I_h were additive increments to hydrogen bonding.

The use of enthalpy–entropy compensation plots has been exploited when the thermodynamic data have been evaluated. [Proportionality between ΔH and ΔS is believed to imply a single unique mechanism for a series of solutes or solvents (29).] However, when ΔH and ΔS are both derived from the van't Hoff relationship, good correlations can be obtained that arise from statistical artifacts. Krug *et al.* (30, 31) have discussed this in detail, and more recently Kinkel *et al.* (14) have shown that a so-called excellent correlation between ΔH and ΔS for the transfer of various phenols between water and 1-octanol (13) was spurious. Enthalpy–entropy compensation can be tested by plotting ΔH *versus* ΔG at the harmonic mean temperature of the experiments (31). Figure 4 shows the ΔH *versus* ΔG relationship for the various solvent systems examined. A relationship of the form:

$$\Delta G^X = 0.7\,\Delta H^X - B \qquad \text{(Eq. 13)}$$

can be obtained, where *B* is a constant that is related to the size of the phenolic solute. Similar compensation relationships have been reported by others (14, 32). (No linear relationships were observed when ΔG was plotted *versus* ΔH for a set of solutes and a given solvent.)

The linear relationship defined by Eq. 13 suggests that the various solutes are distributed between water and the various inert solvents by the same mechanism; *i.e.*, that the aqueous phase provides the major driving force for the transfer process: the hydrophobic effect. The ΔG and ΔH values for the 1-octanol system have not been shown. The values given in Table I deviate from the linear relationship. The ΔH values corresponding to measured ΔG values are much larger than would be predicted from Eq. 13.

For example:

Phenol	0.4 kJ mole^{-1}
Cresol	0.8 kJ mole^{-1}
p-Ethylphenol	1.0 kJ mole^{-1}
p-Propylphenol	1.5 kJ mole^{-1}
p-Chlorophenol	1.0 kJ mole^{-1}

These data indicate that the transfer of phenolic solutes between water and 1-octanol follows a different mechanism than that for the transfer

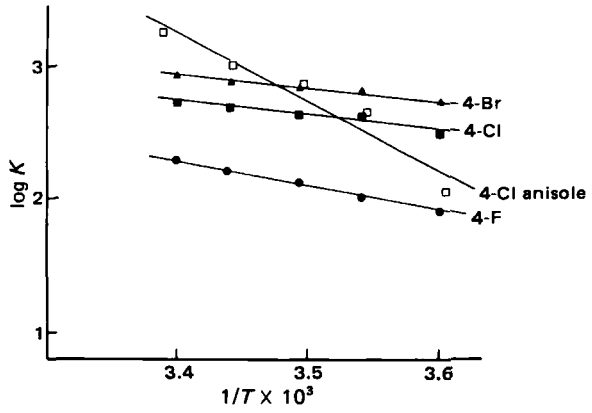

Figure 6—*The distribution of* p-*halophenols into DMPC vesicles—van't Hoff plots.*

of the same solutes between water and nonpolar solvents and, thus, ΔH–ΔS compensation is not obtained. A similar finding was reported recently by Kinkel *et al.* (14). These authors pointed out that mutually saturated 1-octanol contains a considerable quantity of dissolved water (27% on a mole fraction basis) and that water-centered aggregates (4:1 alcohol–water) have been described (5). In addition, linear aliphatic alcohols can exist in polymeric forms (33). Changes in temperature will affect these associations as well as the association between phenolic solutes and 1-octanol itself. Because of these factors, it was suggested (14) that the van't Hoff method should not be used to obtain thermodynamic quantities from the 1-octanol–water system, and microcalorimetry was proposed as an alternative. This is an attractive possibility provided the methodology can be refined to give reliable results. An alternative suggestion would be to avoid the use of 1-octanol when studying the thermodynamics of the distribution process.

Phospholipid Vesicle–Water Distribution—The temperature dependence of the molal distribution coefficient (K_d^m) for *p*-substituted phenols distributed between DMPC vesicles (below their phase transition temperatures) and 0.15 *M* NaCl is shown in Figs. 5 and 6.

The derived thermodynamic quantities are given in Table II. All values refer to initial phenol concentrations of 2×10^{-4} *M* and 20 mg of DMPC. The ΔH is large and positive for all solutes studied. The negative ΔG is the result of a large compensating increase in entropy: the process is entropy dominated. The magnitude of the absolute values is dependent on the nature of the experimental system used, and different values can result from using different phenol concentrations, phospholipid concentration, and experimental protocol. Thus, the data should be regarded as giving a qualitative rather than a precise quantitative picture (34).

In both absolute and relative terms the log K_d^m values for the alkyl and halophenols are more closely related to the distribution coefficients for the 1-octanol–water system rather than those for the so-called inert solvents such as cyclohexane. However, for the vesicles, ΔH is positive throughout which is similar to the situation for the nonpolar solvents and in direct contrast to the negative ΔH values found for the 1-octanol–water system.

Previously, Rogers and Davis (8) have reported that the thermodynamic parameters for the transfer of phenols between aqueous environment and DMPC vesicles change in sign and magnitude at the phase transition temperature. Above T_c, ΔH and ΔS are both negative. Similar changes in thermodynamic parameters at temperatures in the region of T_c have been reported by others (7, 9, 35). Diamond and Katz (7) interpreted observed enthalpy changes by proposing that in the crystalline state below T_c the hydrocarbon tails of DMPC pack closely and uniformly along their length. Thus, insertion of a solute into the membrane requires the breaking of strong intermolecular forces between the hydrocarbon tails, and entropy changes can be attributed to the disruption of the orderly crystalline array by the inserted solute. Thus, large and compensating changes in ΔH and ΔS attributable to the change in liposome structure can mask the smaller changes in ΔH and ΔS due to the actual transfer of the solute. In this respect, Lumry (36) has warned recently that ΔH and ΔS quantities each contain two parts: one (motive) that contributes to the free energy (of transfer) and one that does not (compensation) but that reflects enthalpy and entropy fluctuations. In water and most biological systems these compensation effects can dominate the motive (work-doing) contribution. Consequently, discrepancies can arise in attempts to formulate mechanistic hypotheses using ΔH and ΔS information.

The phospholipid vesicles are isotropic and will have markedly different polarity regions; consequently, the different phenolic solutes are likely to distribute into different regions. This will affect both the distribution coefficient and the thermodynamics of transfer. The high log K_d^m values obtained for the phenols with phospholipid vesicle systems indicate that the phenols could be hydrogen bonded to the phosphate group of DMPC. Comparison of the data obtained for chloroanisole with those for chlorophenol (Fig. 6) indicates that ΔH for the anisole, where there can be no hydrogen bonding, is much larger. At lower temperatures the anisole has a lower K_d^m value than the phenol, the K_d^m value being much more temperature dependent than for the phenol. The hypothesis that the phenolic hydroxyl group can (hydrogen) bond to the DMPC phosphate group was further strengthened by studies on the resorcinol monoethers. Again the hydroxy compound has a lower ΔH value than the corresponding methoxy or ethoxy compound (Table II). This suggests that the resorcinol is able to interact favorably with the phospholipid head group through both of its phenolic hydroxyl groups and that the orientation of these compounds in the lipid bilayer is quite different from that of the alkyl phenols. The ΔH values for the resorcinols were all positive (67–140 kJ mole^{-1}), whereas Beezer *et al.* (12) have shown for the 1-octanol–water system that ΔH is negative and in the range of −15 to −7 kJ mole^{-1}.

The ability of a solute-like phenol to undergo specific interactions with the bilayer membrane calls into question the use of inert hydrocarbons as model solvents for use in correlating structure with biological activity, even though inert hydrocarbons do find a role as reference states (4) and data obtained using such solvents can be converted to values more relevant to polar environments (37). A reasonable correlation can be obtained between liposome–water partition coefficients and octanol–water partition coefficients (7, 8). However, the derivation of the more complete thermodynamic picture in terms of ΔH and ΔS values indicates that the two systems are very different.

REFERENCES

(1) S. S. Davis, T. Higuchi, and J. H. Rytting, *Adv. Pharm. Sci.*, **4**, 73 (1974).

(2) C. Hansch and A. J. Leo, "Substituent Constants for Correlation Analysis in Chemistry and Biology," Wiley, New York, N.Y., 1979.

(3) A. Leo, C. Hansch, and D. Elkins, *Chem. Rev.*, **71**, 525 (1971).

(4) J. H. Rytting, S. S. Davis, and T. Higuchi, *J. Pharm. Sci.*, **61**, 816 (1972).

(5) R. N. Smith, C. Hansch, and M. M. Ames, *ibid.*, **64**, 599 (1975).

(6) Y. C. Martin, *J. Med. Chem* , **24**, 229 (1981).

(7) J. M. Diamond and Y. Katz, *J. Memb. Biol.*, **17**, 121 (1974).

(8) J. A. Rogers and S. S. Davis, *Biochim. Biophys. Acta*, **598**, 392 (1980).

(9) M. Ahmed, J. S. Burton, J. Hadgraft, and I. W. Kellaway, *J. Memb. Biol.*, **58**, 181 (1981).

(10) N. Bindsley and E. M. Wright, *ibid.*, **29**, 289 (1976).

(11) S. S. Davis, G. Elson, E. Tomlinson, G. Harrison, and J. C. Dearden, *Chem. Ind.*, **21**, 677 (1976).

(12) A. E. Beezer, W. H. Hunter, and D. E. Storey, *J. Pharm. Pharmacol.*, **32**, 815 (1980).

(13) J. A. Rogers and A. Wong, *Int. J. Pharm.*, **6**, 339 (1980).

(14) J. F. M. Kinkel, E. Tomlinson, and P. Smit, *ibid.*, **9**, 121 (1981).

(15) K. J. Breslauer, L. Witkowski, and K. Bulas, *J. Phys. Chem.*, **82**, 675 (1978).

(16) R. F. Jameson, in "Bioenergetics and Thermodynamics: Model Systems," A. Braibanti, Ed., Reidel, Amsterdam, 1980, p. 165.

(17) F. F. Cantwell and H. Y. Mohammed, *Anal. Chem.*, **51**, 218 (1979).

(18) D. Chapman, R. M. Williams, and B. D. Ladbrooke, *Chem. Phys. Lipids*, **1**, 445 (1967).

(19) J. R. Johnson, S. D. Christian, and H. E. Affsprung, *J. Chem. Soc.*, **1965**, 1.

(20) J. H. Hildebrand and R. L. Scott, "The Solubility of Non-Electrolytes," Rheinhold, New York, N.Y., 1950.

(21) J. J. Christian, A. A. Taha, and B. W. Gash, *Q. Rev.*, **24**, 20 (1970).

(22) J. R. Johnson, S. D. Christian, and H. E. Affsprung, *J. Chem. Soc.*, **1967**, 764.

(23) S. S. Davis, T. Higuchi, and J. H. Rytting, *J. Pharm. Pharmacol., Suppl.*, **24**, 30P (1972).

(24) T. Wakahayashi, S. Oki, T. Omori, and N. Suzuki, *J. Inorg. Nucl. Chem.*, **26**, 2255 (1964).

(25) M. D. Joesten and L. J. Schaad, "Hydrogen Bonding," Dekker, New York, N.Y., 1974, p. 195.
(26) R. M. Badger and S. H. Bauer, *J. Chem. Phys.*, **5**, 839 (1937).
(27) A. Allerhand and P. R. Schleyer, *J. Am. Chem. Soc.*, **85**, 371 (1963).
(28) K. Nakanishi, S. Ichinose, and H. Shirai, *Ind. Eng. Chem. Fund.*, **7**, 381 (1968).
(29) J. E. Leffler and E. Grunwald, "Rates and Equilibria of Organic Reactions," Wiley, New York, N.Y., 1963, p. 128.
(30) R. R. Krug, W. G. Hunter, and R. A. Grieger, *J. Phys. Chem.*, **80**, 2335 (1976).
(31) *Idem.*, **80**, 2341 (1976).
(32) E. Tomlinson and S. S. Davis, *J. Colloid. Inter. Sci.*, **76**, 563 (1980).
(33) B. D. Anderson, J. H. Rytting, and T. Higuchi, *Int. J. Pharm.*, **1**, 15 (1978).
(34) N. H. Anderson, M. James, and S. S. Davis, *Chem. Ind.*, **1981**, 677.
(35) S. A. Simon, W. C. Stone, and P. B. Bennett, *Biochim. Biophys. Acta*, **550**, 38 (1979).
(36) R. Lumry, in "Bioenergetics and Thermodynamics: Model Systems," A. Braibanti, Ed., Reidel, Amsterdam, 1980, p. 405.
(37) P. Seiler, *Eur. J. Med. Chem.*, **9**, 473 (1974).

ACKNOWLEGMENTS

The authors with to thank the Science Research Council, ICI Plant Protection Division, and the Japanese Ministry of Education for research grants and financial assistance.

Influence of Premicellar and Micellar Association on the Reactivity of Methylprednisolone 21-Hemiesters in Aqueous Solution

B. D. ANDERSON ˣ, R. A. CONRADI, and K. JOHNSON

Received December 11, 1980 from *The Upjohn Company, Kalamazoo, MI 49001.* Accepted for publication December 31, 1981.

Abstract □ Self-association of drug molecules at formulation concentrations can have a major impact on formulation properties. In this study a homologous series of methylprednisolone 21-hemiesters were found to undergo self-association in aqueous solution. The effect of aggregate formation on the solution degradation of these compounds was examined. To determine the nature and extent of association of these steroidal esters, partition coefficients between butyronitrile and aqueous buffer (pH 8.5) were measured as a function of ester concentration. The partitioning data were found to be consistent with dimer formation at low concentration followed by true micelle formation at higher concentration. Chain length increases favored micelle formation, but appeared to have little effect on dimerization. The first-order rate constants for ester hydrolysis and 21 → 17 acyl migration in aqueous buffer (pH 8.5) were also found to be dependent on ester concentration. The kinetic data are consistent with a model which assumes stabilization by both dimer and micelle formation, the limiting factor at high concentration being the reactivity of the ester in the micelles. The degree of stabilization due to self-association was found to increase with chain length.

Keyphrases □ Methylprednisolone—synthesis of 21-hemiester homologues, influence of premicellar and micellar association on reactivity □ Steroids—methylprednisolone, synthesis of 21-hemiester homologues, influence of premicellar and micellar association on reactivity □ Association, micellar—influence on the reactivity of methylprednisolone 21-hemiesters □ Association, premicellar—influence on the reactivity of methylprednisolone 21-hemiesters

Self-association of hydrophobic drug molecules in aqueous solution can have a profound effect on formulation properties due to the reduced effective concentration of drug at high total concentration. Specifically, molecular aggregation may result in higher drug solubility, increased or decreased solution stability, or transient masking of local biological effects.

While there is voluminous literature on the effect of micelle-forming additives on the chemical reactivity of various substrates, very few cases have been reported in which a labile substrate itself forms molecular aggregates resulting in self-stabilization. The few studies which do exist suggest that reactivity can be significantly altered either favorably or unfavorably by substrate self-aggregation into micelles (1, 2). Premicellar aggregation has also been found to dramatically alter reactivity (3–5).

Steroidal molecules, particularly bile salts, are known to undergo self-association in aqueous solution to form aggregates varying in size from dimers to much larger oligomers (6–8). Self-association has also been observed for the corticosteroid methylprednisolone 21-phosphate (9). In this case a marked acceleration in reactivity in more concentrated solutions was attributed to micelle formation.

A recent study showed that methylprednisolone 21-succinate[1] decomposes initially in aqueous solution *via* two parallel pathways (10). In addition to the well-known ester hydrolysis reaction, acyl migration from the 21- to the 17-OH occurs at a rate comparable to hydrolysis (Scheme I).

Since it was suspected that methylprednisolone 21-succinate may self-associate at formulation concentrations, a study was initiated to determine: (*a*) the nature and extent of self-association, (*b*) the effect of aggregation on the solution kinetics, and (*c*) the effect of molecular modification (increasing the hydrophobicity through increases in hemiester chain length) on both the aggregation and kinetics. To determine unambiguously the nature and extent of self-association, a partitioning method was developed enabling calculation of the monomer concentration as a function of total concentration. The initial rates of ester hydrolysis and acyl migration as a function of concentration were then combined with the partitioning data to elucidate the relative reactivities of monomeric and aggregated species.

EXPERIMENTAL

Materials—All reagents and chemicals were either analytical reagent grade or known to be of high purity. Methylprednisolone 21-hemisucci-

[1] SOLU-MEDROL (Upjohn brand of methylprednisolone sodium succinate).

0022-3549/83/0400-0448$01.00/0

(25) M. D. Joesten and L. J. Schaad, "Hydrogen Bonding," Dekker, New York, N.Y., 1974, p. 195.
(26) R. M. Badger and S. H. Bauer, *J. Chem. Phys.*, **5**, 839 (1937).
(27) A. Allerhand and P. R. Schleyer, *J. Am. Chem. Soc.*, **85**, 371 (1963).
(28) K. Nakanishi, S. Ichinose, and H. Shirai, *Ind. Eng. Chem. Fund.*, **7**, 381 (1968).
(29) J. E. Leffler and E. Grunwald, "Rates and Equilibria of Organic Reactions," Wiley, New York, N.Y., 1963, p. 128.
(30) R. R. Krug, W. G. Hunter, and R. A. Grieger, *J. Phys. Chem.*, **80**, 2335 (1976).
(31) *Idem.*, **80**, 2341 (1976).
(32) E. Tomlinson and S. S. Davis, *J. Colloid. Inter. Sci.*, **76**, 563 (1980).
(33) B. D. Anderson, J. H. Rytting, and T. Higuchi, *Int. J. Pharm.*, **1**, 15 (1978).
(34) N. H. Anderson, M. James, and S. S. Davis, *Chem. Ind.*, **1981**, 677.
(35) S. A. Simon, W. C. Stone, and P. B. Bennett, *Biochim. Biophys. Acta*, **550**, 38 (1979).
(36) R. Lumry, in "Bioenergetics and Thermodynamics: Model Systems," A. Braibanti, Ed., Reidel, Amsterdam, 1980, p. 405.
(37) P. Seiler, *Eur. J. Med. Chem.*, **9**, 473 (1974).

ACKNOWLEGMENTS

The authors with to thank the Science Research Council, ICI Plant Protection Division, and the Japanese Ministry of Education for research grants and financial assistance.

Influence of Premicellar and Micellar Association on the Reactivity of Methylprednisolone 21-Hemiesters in Aqueous Solution

B. D. ANDERSON ˣ, R. A. CONRADI, and K. JOHNSON

Received December 11, 1980 from *The Upjohn Company, Kalamazoo, MI 49001.* Accepted for publication December 31, 1981.

Abstract □ Self-association of drug molecules at formulation concentrations can have a major impact on formulation properties. In this study a homologous series of methylprednisolone 21-hemiesters were found to undergo self-association in aqueous solution. The effect of aggregate formation on the solution degradation of these compounds was examined. To determine the nature and extent of association of these steroidal esters, partition coefficients between butyronitrile and aqueous buffer (pH 8.5) were measured as a function of ester concentration. The partitioning data were found to be consistent with dimer formation at low concentration followed by true micelle formation at higher concentration. Chain length increases favored micelle formation, but appeared to have little effect on dimerization. The first-order rate constants for ester hydrolysis and 21 → 17 acyl migration in aqueous buffer (pH 8.5) were also found to be dependent on ester concentration. The kinetic data are consistent with a model which assumes stabilization by both dimer and micelle formation, the limiting factor at high concentration being the reactivity of the ester in the micelles. The degree of stabilization due to self-association was found to increase with chain length.

Keyphrases □ Methylprednisolone—synthesis of 21-hemiester homologues, influence of premicellar and micellar association on reactivity □ Steroids—methylprednisolone, synthesis of 21-hemiester homologues, influence of premicellar and micellar association on reactivity □ Association, micellar—influence on the reactivity of methylprednisolone 21-hemiesters □ Association, premicellar—influence on the reactivity of methylprednisolone 21-hemiesters

Self-association of hydrophobic drug molecules in aqueous solution can have a profound effect on formulation properties due to the reduced effective concentration of drug at high total concentration. Specifically, molecular aggregation may result in higher drug solubility, increased or decreased solution stability, or transient masking of local biological effects.

While there is voluminous literature on the effect of micelle-forming additives on the chemical reactivity of various substrates, very few cases have been reported in which a labile substrate itself forms molecular aggregates resulting in self-stabilization. The few studies which do exist suggest that reactivity can be significantly altered either favorably or unfavorably by substrate self-aggregation into micelles (1, 2). Premicellar aggregation has also been found to dramatically alter reactivity (3–5).

Steroidal molecules, particularly bile salts, are known to undergo self-association in aqueous solution to form aggregates varying in size from dimers to much larger oligomers (6–8). Self-association has also been observed for the corticosteroid methylprednisolone 21-phosphate (9). In this case a marked acceleration in reactivity in more concentrated solutions was attributed to micelle formation.

A recent study showed that methylprednisolone 21-succinate[1] decomposes initially in aqueous solution *via* two parallel pathways (10). In addition to the well-known ester hydrolysis reaction, acyl migration from the 21- to the 17-OH occurs at a rate comparable to hydrolysis (Scheme I).

Since it was suspected that methylprednisolone 21-succinate may self-associate at formulation concentrations, a study was initiated to determine: (*a*) the nature and extent of self-association, (*b*) the effect of aggregation on the solution kinetics, and (*c*) the effect of molecular modification (increasing the hydrophobicity through increases in hemiester chain length) on both the aggregation and kinetics. To determine unambiguously the nature and extent of self-association, a partitioning method was developed enabling calculation of the monomer concentration as a function of total concentration. The initial rates of ester hydrolysis and acyl migration as a function of concentration were then combined with the partitioning data to elucidate the relative reactivities of monomeric and aggregated species.

EXPERIMENTAL

Materials—All reagents and chemicals were either analytical reagent grade or known to be of high purity. Methylprednisolone 21-hemisucci-

[1] SOLU-MEDROL (Upjohn brand of methylprednisolone sodium succinate).

0022-3549/83/0400-0448$01.00/0

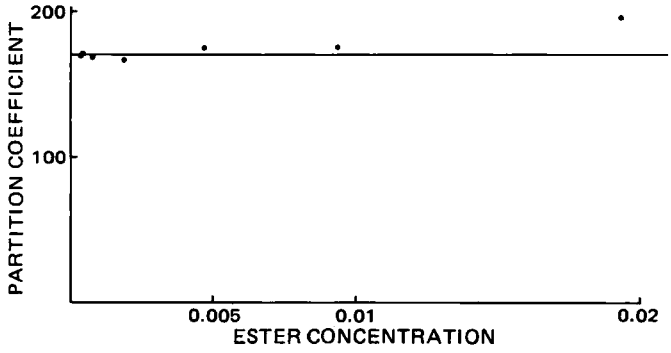

Figure 1—*Butyronitrile–0.01* N *HCl partition coefficient* versus *concentration of methylprednisolone 21-succinate in the butyronitrile phase.*

nate[2] was used as supplied without further purification. Methylprednisolone[2] for use as a high-performance liquid chromatography (HPLC) reference standard was recrystallized from tetrahydrofuran. The remaining methylprednisolone esters used in this study were synthesized as described.

Synthesis—*6α-Methylprednisolone 21-Hemiadipate*—A mixture of 5 g of 11β,17α-dihydroxy-21-iodo-6α-methylpregna-1,4-diene-3,20-dione[2], 14.6 g of adipic acid, and 34.8 ml of *N,N*-diisopropylethylamine in 45 ml of dimethylformamide and 20 ml of acetone was allowed to stand at 25° for 1 hr. The mixture was extracted with ethyl acetate (250 ml) and washed with 0.08 *M* citric acid. The organic phase was rapidly extracted (pH 10), and the resulting aqueous phase was readjusted to pH 5 and then extracted with ethyl acetate. The solvent was evaporated under reduced pressure, and the resulting solid was recrystallized twice from ethyl acetate–hexane to give an analytical specimen, mp 164.3–165.6; NMR[3a,b]: δ 7.2–7.4 (d, 1, C_1—H), 6.0–6.2 (d, 1, C_2—H), 5.9 (s, 1, C_4—H), 4.6–5.3 (m, 2, C_{21}—H_2), 4.4 (broad, 1, C_{11}—H).

Anal.—Calc. for $C_{28}H_{38}O_8$: C, 66.92; H, 7.62. Found: C, 67.01; H, 7.91.

6α-Methylprednisolone 21-Hemisuberate—The ester was prepared in the aforementioned manner using 5 g of 11β,17α-dihydroxy-21-iodo-6α-methylpregna-1,4-diene-3,20-dione, 17.4 g of octanedioic acid, 34.8 ml of *N,N*-diisopropylethylamine, 67 ml of dimethylformamide, and 20 ml of acetone to give, after recrystallization from ethyl acetate–hexane, an analytical specimen, mp 192.1–195.4; NMR[3a,b]: δ 7.2–7.4 (d, 1, C_1—H), 6.0–6.2 (d, 1, C_2—H), 5.9 (s, 1, C_4—H), 4.6–5.3 (m, 2, C_{21}—H_2), 4.4 (broad, 1, C_{11}—H).

Anal.—Calc. for $C_{30}H_{24}O_8$: C, 67.91; H, 7.98. Found: C, 67.58; H, 8.33.

6α-Methylprednisolone 17-Hemisuccinate—The synthesis and structure elucidation were reported previously (10).

6α-Methylprednisolone 17-Hemisuberate—Methylprednisolone 21-hemisuberate (4 g) was dissolved in 400 ml of water by the slow addition of 1 *N* NaOH. The pH of the final solution was maintained ≤9.5 over several hours and the 17-ester formation was monitored by HPLC. The concentration of 17-ester plateaued at ~9–10% of the total solution concentration. The reaction was stopped by acidification and products were isolated by extraction with ethyl acetate. The solvent was removed under reduced pressure and the remaining solid purified by HPLC: (*a*) reverse-phase[4] using acetonitrile–water (9:11) containing 0.05 *M* acetic acid at a flow rate of 18 ml/min[5] and (*b*) silica gel[6] using butylchloride–ethyl acetate (1:1) containing 1% acetic acid at 18 ml/min[5]. The solvent was removed to give a white amorphous solid which was reprecipitated from ethyl acetate–hexane. No methylprednisolone nor 21-suberate were detected by HPLC. UV[7]: λ_{max} = 244 nm, $\epsilon = 1.48 \times 10^4$ (methylprednisolone 17-succinate λ_{max} = 244, $\epsilon = 1.50 \times 10^4$). NMR[3] (acetone-$d_6$): δ 7.3–7.5 (d, 1, C_1—H), 6.1–6.3 (d, 1, C_2—H), 5.90–5.95 (s, 1, C_4—H), 4.55 (broad, 1, C_{11}—H), 4.2–4.25 (s, 2, C_{21}—H_2).

Sample Preparation—All sample solutions for both kinetic and partitioning studies were prepared in 0.1 *M* boric acid buffer adjusted to pH 8.47 ± 0.01 with 50% sodium hydroxide. The ionic strength of the buffer was 0.5 *M* (potassium chloride).

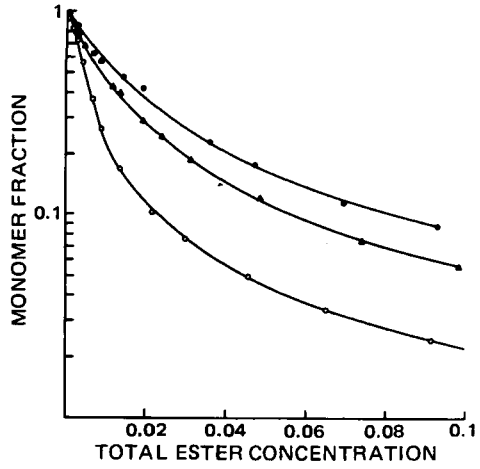

Figure 2—*Semilog plots of monomer fraction [PC/PC(O)]* versus *total concentration in ester in aqueous buffer at pH 8.47 and 25°. Key: (●) 21-succinate; (▲) 21-adipate; and (○) 21-suberate.*

Stock solutions containing ~0.1 *M* 21-ester were prepared by weighing an appropriate amount in a volumetric container and adding buffer containing the amount of excess sodium hydroxide required to neutralize the carboxylic acid. Sonication and vigorous mixing were required to rapidly dissolve the sample. The stock solutions were frozen (−20°) for later use. Aliquots of these stock solutions were diluted and pH was adjusted to 8.47 ± 0.01 if necessary. Temperature of the diluted samples was maintained at 25.0° during all studies.

Partition Coefficient Determinations—After the appropriate dilution of one of the aforementioned stock solutions, a 1–5 ml aliquot was transferred to a test tube containing 1–5 ml of butyronitrile. The biphasic mixture was brought to 25°, vortexed vigorously, centrifuged, and allowed to stand in the 25° water bath for 15–30 min. Aliquots from each layer were removed. The butyronitrile was evaporated under a nitrogen stream, and the residues from both the aqueous and butyronitrile phases were diluted with an acidified acetonitrile–water mixture. HPLC analysis was carried out as described below using standard solutions of the corresponding 21-ester in acetonitrile–water (1:3) at pH 3–3.2.

Kinetic Studies—The initial rates of product formation (up to 3%) were monitored by HPLC as a function of initial 21-ester concentration. Standards containing methylprednisolone and the corresponding 17-ester (when available) at concentrations of $\sim 1 \times 10^{-6}$–1×10^{-4} *M* were prepared in acetonitrile–water (1:3) adjusted to pH 3.2.

At suitable time intervals precise aliquots of samples prepared by

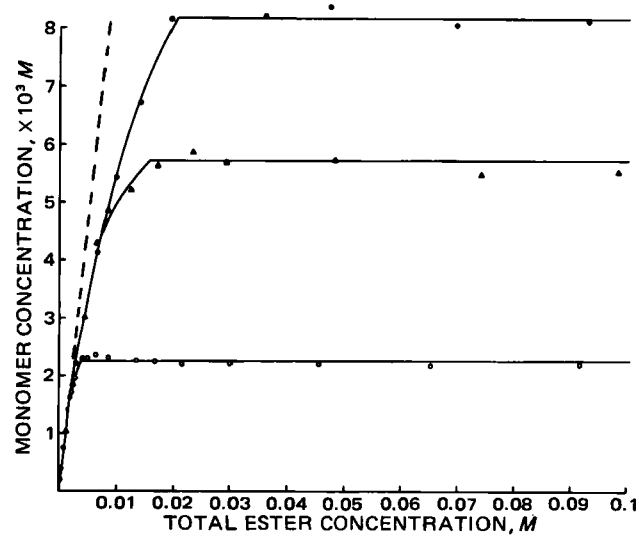

Figure 3—*Monomer concentration* versus *total ester concentration in aqueous solutions at pH 8.47 and 25°. Key: (●) 21-succinate; (▲) 21-adipate; and (○) 21-suberate. Dashed line represents the monomer concentration expected in the absence of self-association.*

[2] The Upjohn Co., Kalamazoo, Mich.

[3] (a) Model T-60 NMR Spectrometer, Varian Assoc. (b) UNISOL-d is a 4:1 mixture of $CDCl_3$–DMSO-d_6, Norell, Inc., Landisville, N.J..

[4] LOBAR—Size B RP-8 columns (2) from E. Merck, Darmstadt, Germany.

[5] Milton Roy Mini-Pump, Laboratory Data Control, Riviera Beach, Fla.

[6] LOBAR—Size B silica gel columns (3) from E. Merck, Darmstadt, Germany.

[7] Zeiss DMR-21 spectrophotometer.

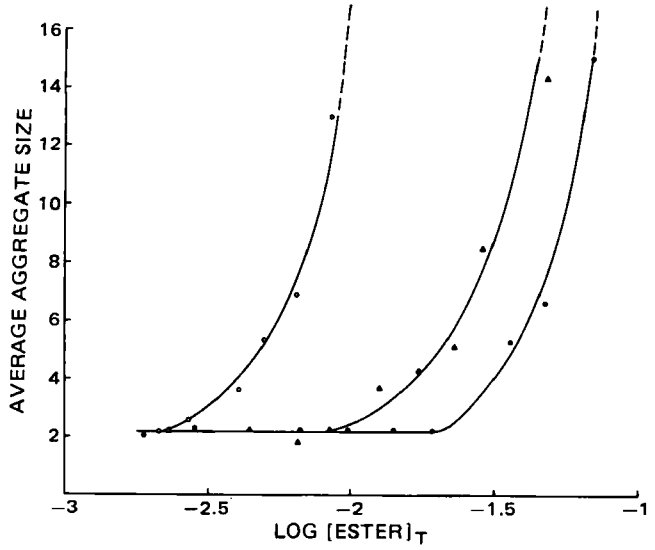

Figure 4—*Average aggregate size determined from Eq. 13* versus *log of ester concentration in aqueous buffer (pH 8.47 and 25°). Key: (●) 21-succinate; (▲) 21-adipate; and (○) 21-suberate.*

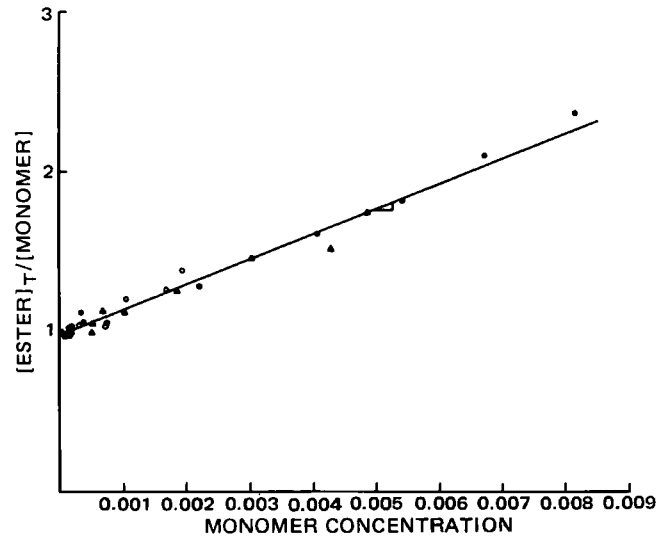

Figure 5—*Plots of* $C_T/[Mon]$ versus *monomer concentration (see Eq. 15) for estimation of dimerization equilibrium constants. Key: (●) 21-succinate; (▲) 21-adipate; and (○) 21-suberate.*

appropriately diluting the stock solutions described previously were transferred to vials containing an acetonitrile–water mixture acidified such that the final solution pH was 3–5 to immediately quench the reaction. Samples (≤100 μl) were analyzed by HPLC employing a modular chromatographic system consisting of an automated sample injector[8], a constant-flow pump[9] operated at 1.5–2.0 ml/min, a reverse-phase column[10], a variable-wavelength UV detector[11] operated at 244 nm, and a digital integrator[12].

Mobile phase compositions for the 21-succinate, 21-adipate, and 21-suberate systems were, respectively, 0.05 *M* acetic acid in acetonitrile–water (1:2) adjusted to pH 5.3 with NaOH, 0.05 *M* acetic acid in acetonitrile–water (2:3) adjusted to pH 5.0, and 0.05 *M* acetic acid in acetonitrile–water (9:11) adjusted to pH 5.2.

RESULTS AND DISCUSSION

Self-Associated Systems and Methods for Their Investigation—Although the nature of the forces in water which give rise to a hydrophobic effect are still not well understood (11–13), the tendency of hydrophobic solutes (molecules containing large regions of exposed organic groups) to self-associate in water is widely recognized (14). Typical micelle-forming surfactants, such as flexible-chain compounds with polar head groups, can form large aggregates containing ~30–120 monomers per multimer (15).

If the aggregates formed are sufficiently large, containing >20 monomers, a simple monomer–micelle model adequately represents the equilibria involved. Such systems are characterized by a distinct break point in plots of any number of properties *versus* concentration. The point at which this discontinuity occurs is termed the critical micelle concentration (CMC). Below the CMC the concentration of micelles is negligible (monomer concentration equals total concentration), while above the CMC the activity of monomer is virtually constant.

Careful studies, however, generally show curvature rather than a distinct discontinuity at the apparent CMC (14), suggesting that small aggregate formation occurs prior to true micelle formation. Even flexible long-chain fatty acid anions have been shown to dimerize in dilute aqueous solutions (16). Steroids consisting of inflexible alicylic fused-ring systems, such as the bile acid salts and the corticosteroid derivatives of interest in this study, are also quite likely to form smaller aggregates. Light scattering and solubilization studies of sodium cholate, for example, suggest that it self-associates to form dimers (6) and other small aggregates (17).

The existence of premicellar aggregates complicates the interpretation of experimental data obtained by methods that do not allow direct calculation of the monomer concentration. Most experimental methods are unsuitable, because each multimer must be described by both a formation constant and a parameter reflecting its contribution to the property being measured. Conductance methods, for example, require the estimate of an equivalent conductance for each species (18). Spectral methods require an estimate of absorptivity for each species present (19).

Partitioning Method for Monitoring the Self-Association of Methylprednisolone Hemiesters—The determination of partition equilibria has been shown to be a useful technique in monitoring self-association (16). The partition coefficient, PC(C), of an amphiphile between an organic and an aqueous solvent reflects the relative thermodynamic activity coefficients $\gamma_{H_2O}(C)$ and $\gamma_{org}(C)$, of solute in the two solvents where C is the concentration of solute in the aqueous phase.

At equilibrium, the thermodynamic activities of solute in the two phases are equal:

$$a_{H_2O} = a_{org} \qquad \text{(Eq. 1)}$$

where

$$a_{H_2O} = \gamma_{H_2O} C_{H_2O} \text{ and } a_{org} = \gamma_{org} C_{org}$$

At infinite dilution, $\gamma_{H_2O}(O)$ is defined such that:

$$\lim \gamma_{H_2O}(C) = \gamma_{H_2O}(O) = 1$$
$$C_{H_2O} \to 0 \qquad \text{(Eq. 2)}$$

Also at infinite dilution, from Eq. 1 and the definition of the partition coefficient:

$$PC(O) = \lim (C_{org}/C_{H_2O}) = \gamma_{H_2O}(O)/\gamma_{org}(O)$$
$$C_{H_2O} \to 0 \qquad \text{(Eq. 3)}$$

and, substituting the value of $\gamma_{H_2O}(O)$ from Eq. 2:

$$\gamma_{org}(O) = 1/PC(O) \qquad \text{(Eq. 4)}$$

Assuming that the activity coefficient of solute in the organic phase, γ_{org}, remains constant with changes in solute concentration:

$$\gamma_{org}(C) = \gamma_{org}(O) = 1/PC(O) \qquad \text{(Eq. 5)}$$

A further assumption is that deviations in the activity coefficient of solute in aqueous solution are due solely to self-association, so at any concentration the value of γ_{H_2O} is equal to the fraction of monomer ([Mon]) present:

$$\gamma_{H_2O}(C) = \frac{[Mon]_{H_2O}}{C_{H_2O}} \qquad \text{(Eq. 6)}$$

Two useful relationships are then obtained from Eqs. 1–6, enabling the direct calculation of monomer concentration and monomer fraction from measurements of partitioning equilibria:

$$[Mon]_{H_2O} = C_{org}/PC(O) \qquad \text{(Eq. 7)}$$

[8] Wisp Model 710A, Waters Associates, Milford, Mass.
[9] Altex Model 110A, Altex Scientific Inc, Berkeley, Calif.
[10] 10-μm LICHROSORB RP-18 column, Brownlee Labs, Berkeley, Calif.
[11] Altex/Hitachi Model 153-00, Altex Scientific.
[12] Model 3380A, Hewlett-Packard, Avondale, Mass.

and

$$[\text{Mon}] = \gamma_{H_2O}(C) = PC(C)/PC(O) \quad \text{(Eq. 8)}$$

A pH of 8.5 was selected for both the partitioning and kinetic studies, because the solutes were highly soluble at this pH and the reaction rates were in a range which could be conveniently measured in a reasonable length of time. At this pH, nonpolar solvents (isooctane, toluene, *etc.*) were unacceptable for use in partitioning studies, because partition coefficients were too low, while most polar hydrogen-donating or hydrogen-accepting solvents extracted too much solute. Butyronitrile—a polar, aprotic solvent which is immiscible with water—was found to be suitable.

The pH dependence of the partition coefficient of methylprednisolone 21-succinate suggested that only the free acid partitions into the organic phase. At pH 2 the intrinsic partition coefficient of solute, $PC_I(O)$ was found to be ~170, while the value of $PC(O)$ at pH 8.47 was 0.031. Assuming that only the free acid partitions and that the pK_a for the succinate is 4.7 (10), the predicted value of $PC(O)$ at pH 8.47 can be calculated from:

$$PC(O)_{pH\ 8.5} = \frac{PC_I(O)[H^+]}{[H^+] + K_a} = 0.029 \quad \text{(Eq. 9)}$$

which is in good agreement with the observed value.

A critical assumption on which Eqs. 7 and 8 are based is that the activity coefficient of solute in the organic phase is constant with concentration (Eq. 5). Changes in the activity coefficient of the solute due to association in the organic phase, therefore, either must be negligible or must be considered significant. Carboxylic acids are known to dimerize in nonpolar solvents (19, 20), but the equilibrium constant for dimerization in the more polar solvent butyronitrile should be substantially smaller.

To determine whether dimerization in butyronitrile is significant over the solute concentration range of interest in the pH 8.5 partitioning studies (0 to ~3.3×10^{-3} *M*), the partition coefficient of methylprednisolone 21-hemisuccinate between butyronitrile and 0.01 *N* HCl was determined as a function of concentration (Fig. 1). Since the partition coefficient is large at low pH, the aqueous concentration of solute approaches infinite dilution over the entire butyronitrile concentration range of interest. Self-association in the aqueous phase at pH 2 is, therefore, unimportant. Although there does appear to be an upward trend consistent with a very small deviation in γ_{org}, this trend is negligible over the concentration range of 0–3.3×10^{-3} *M*, indicating that self-association of solute in the organic phase can be neglected.

Partition coefficients at pH 8.47 (μ = 0.5) were determined over a concentration range of 0–0.1 *M*. Values of $PC(O)$ were estimated by linear extrapolation of the partitioning data at concentrations below 3×10^{-3} *M* to infinite dilution. The estimated values of $PC(O)$ for the succinate, adipate, and suberate are 0.031, 0.167, and 1.48, respectively. As expected, partition coefficients increase by a factor of 2.5–3 per $-CH_2-$ group increment consistent with literature values for the methylene group contribution to partitioning into polar organic solvents (21).

The monomer fraction was calculated by applying Eq. 8 to the partitioning data. Semilog plots of the monomer fraction *versus* concentration in aqueous buffer are shown in Fig. 2. Two conclusions can be drawn from the data in Fig. 2: changes in monomer fraction are observed at very low concentration (~1×10^{-3} *M*) and increased chain length results in greater association. Surface tension measurements on the succinate did not show any aggregation below ~0.02–0.03 *M*[13], while the partition coefficients clearly change at much lower concentrations. This suggests that partition coefficients are a more sensitive measure of the aggregation phenomena.

Applying Eq. 7 to the partitioning data one obtains the monomer concentration at any total ester concentration (Fig. 3). A striking observation from these plots is the existence of at least two distinct types of association—premicellar association exemplified by curvature at low concentrations and micelle formation indicated by the constancy in monomer concentration after an apparent discontinuity in each curve.

Premicellar Association—In very dilute solutions, monomer concentration very nearly equals total concentration as indicated by the dashed line in Fig. 3. The marked deviations from the extrapolated line prior to the apparent CMC suggest that premicellar association occurs. Premicellar aggregation is perhaps more noticeable in Fig. 2, since monomer fractions change markedly prior to the apparent critical micelle concentrations observed in Fig. 3.

A calculation of the average aggregate size as previously described (22) is derived in the following manner.

[13] S. L. Nail, The Upjohn Company, private communication.

Table I—Apparent Critical Micellar Concentrations, Equilibrium Constants for Dimerization, and Contribution of Each Species to Total Concentration at 0.1 *M* for Corticosteroid 21-Hemiesters Varying in Side-Chain Length

Ester	Apparent[a] CMC, *M*	$K_{1:2}$ liter mole^{-1}	Species Contribution at 0.1 *M* Monomer, *M*	Dimer, *M*	Micelle, *M*
21-Succinate	0.02	80 ± 4[b]	8.2×10^{-3}	1.1×10^{-2}	8.1×10^{-2}
21-Adipate	0.01–0.015	70 ± 7	5.7×10^{-3}	4.6×10^{-3}	9.0×10^{-2}
21-Suberate	0.003	85 ± 22	2.3×10^{-3}	8.6×10^{-4}	9.7×10^{-2}

[a] Apparent critical micelle concentration. [b] 95% Confidence limits from linear regression.

The total concentration of ester (C_T) can be expressed as,

$$C_T = [\text{Mon}] + 2K_{1:2}[\text{Mon}]^2 + 3K_{1:3}[\text{Mon}]^3 + \ldots \quad \text{(Eq. 10)}$$

where aggregated species of all sizes are allowed without any assumptions as to their tendency to form. The total species concentration (S_T) is:

$$S_T = [\text{Mon}] + K_{1:2}[\text{Mon}]^2 + K_{1:3}[\text{Mon}]^3 + \ldots \quad \text{(Eq. 11)}$$

By inspection it is clear that:

$$S_T = \int_0^{\text{Mon}} C_T/\text{Mon}\, d\text{Mon} \quad \text{(Eq. 12)}$$

The average polymer size at any concentration is defined as:

$$\text{average polymer size} = \frac{C_T - \text{Mon}}{S_T - \text{Mon}} \quad \text{(Eq. 13)}$$

The integral in Eq. 12 was evaluated by trapezoidal integration.

The results of average polymer size calculations *versus* log C_T are shown in Fig. 4. The premicellar region is indicated by the flat portion of the diagrams at an average polymer size of ~2 which is very broad for the succinate, less so for the adipate, and barely distinguishable for the suberate due to its low apparent CMC. The broad region with average polymer size of 2 is consistent with dimer formation. Since the average polymer size does not gradually increase in the premicellar region, trimers or other small oligomers do not appear to be present.

If dimerization is the major mode of association in the premicellar region, systems in this region should be adequately described by:

$$C_T = \text{Mon} + 2K_{1:2}\text{Mon}^2 \quad \text{(Eq. 14)}$$

where

$$K_{1:2} = \frac{[\text{Dimer}]}{[\text{Mon}]^2} \quad \text{(Eq. 15)}$$

Therefore, plots of C_T/Mon *versus* [Mon] should be linear with slopes of $2K_{1:2}$. These plots are shown to be approximately linear in Fig. 5. The values of $K_{1:2}$ estimated from a linear regression on the data in Fig. 5 are 80 ± 4, 70 ± 7, and 85 ± 22 liter/mole for the succinate, adipate, and suberate, respectively. $K_{1:2}$ is not affected noticeably by chain length suggesting that the C_{21} side chains are not participating in the dimerization interaction.

It is possible that dimers arise from the stacking of the steroidal portion of the molecules with the C_{21} side chains directed away from each other. Another possibility is that the side chains may be folded back in a hydrophobic interaction with the side of the steroidal nucleus not involved in dimer formation. If the latter were true, folding back of the side chain would be expected in the monomer as well. Since the infinite dilution partition coefficients increase with chain length by the magnitude predicted, this explanation does not seem likely.

Micelle Formation—The break points in Fig. 3 after which monomer concentration remains constant suggest the formation of much larger aggregates or micelles. The critical micelle concentrations for the three homologues (the concentrations at which micelles are first detectable) are listed in Table I along with the dimerization constants discussed previously. Above the CMC, the concentrations of monomer and dimer are invariant. Estimates of these concentrations are also shown in Table I. An interesting observation is that the actual monomer concentration is much lower than the apparent CMC, particularly for the succinate and adipate. In a simple monomer–micellar model, the monomer activity is generally assumed to be given by the CMC. As shown in Table I, estimates of monomer concentration from apparent critical micelle concentrations may be very misleading if premicellar association occurs.

Numerous reports in the literature cite a relationship between CMC

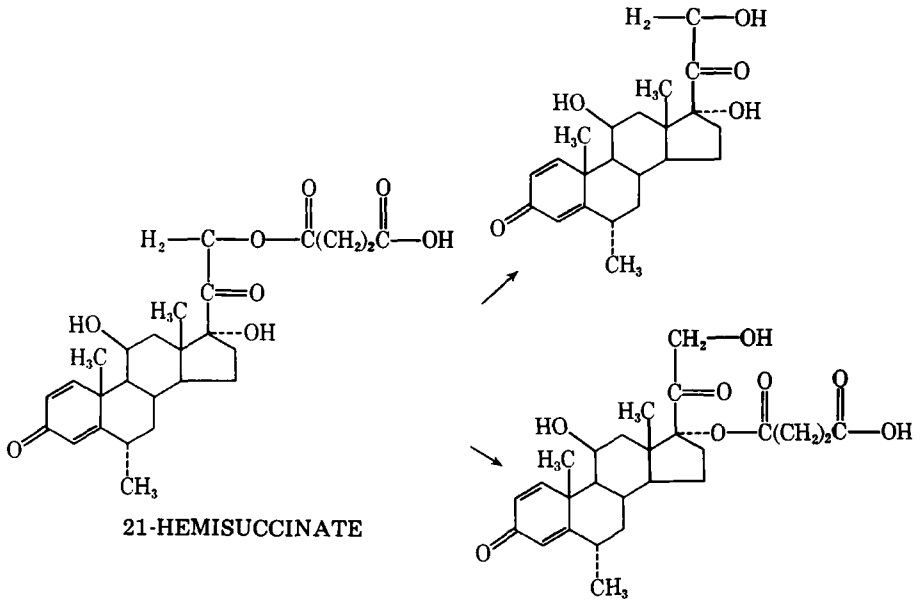

Scheme I

and the number of methylene groups in the surfactants. The relationship generally takes the form:

$$\log \text{CMC} = A - bn \qquad \text{(Eq. 16)}$$

where b is usually ~0.28–0.3 (23). A plot of log CMC *versus* chain length in the series of corticosteroid esters gave a slope of 0.24, which is close to values generally reported in the literature. The effect of chain length on monomer concentration, however, was much less (Table I) than predicted from Eq. 16 due to the importance of dimer formation.

It is difficult to speculate on the structure of these corticosteroid micelles other than to point out that they are large (average polymer size in Fig. 4 increases sharply above the CMC), and their formation is enhanced by increases in side-chain length.

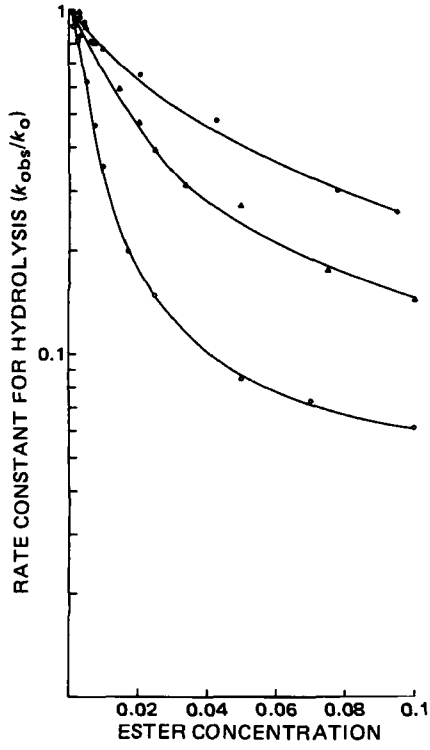

Figure 6—*Semilog plots of the ratio of the rate constant for hydrolysis at the given concentration to the infinite dilution rate constant* (k_{obs}/k_0) versus *ester concentration. Key: (●) 21-succinate; (▲) 21-adipate; and (○) 21-suberate.*

One hint as to the nature of the environment in the micelles may be obtained from UV measurements[14]. The $\pi \rightarrow \pi^*$ transition of the steroidal A-ring in the 21-esters of methylprednisolone undergoes a bathochromic shift as the polarity of the solvent is increased, due presumably to a reduction in the energy level of the excited state accompanying dipole–dipole interaction and hydrogen bonding (24). For example, λ_{max} of methylprednisolone succinate in tetrahydrofuran is 236 nm while in water it is 244 nm. A thin film of a 0.1 *M* aqueous solution of methylprednisolone succinate spread between two cuvettes exhibited a λ_{max} of ~245 nm, very similar to that observed in dilute solutions, indicating that there is no significant change in absorbance accompanying the partitioning of molecules into micelles. This observation tentatively supports the hypothesis that the environment surrounding the A-ring in the micelle is very polar or the A-ring is involved in hydrogen bonding within the micelle.

Kinetics of Hydrolysis and Acyl Migration in Aggregated Corticosteroid Systems—Catalysis and inhibition of reactions in associated systems have been the subjects of extensive research (25, 26). Of greatest interest from a pharmaceutical standpoint are those studies in which reaction rates have been markedly retarded by micelle-forming additives (27–31). Base-catalyzed hydrolysis of esters is generally inhibited by anionic surfactants (26), and since previous studies have shown (10) that both hydrolysis and 21 → 17 ester migration in methylprednisolone succinate are hydroxide ion catalyzed, it is reasonable to expect that both reactions might be slowed by self-association. The concentration of monomer in 0.1 *M* solutions of the corticosteroid homologues show a range of $2.3–8.2 \times 10^{-3}$ (Table I). If degradation were completely suppressed in the aggregates as has been shown in at least one case (27), significant stabilization should result from self-association in 0.1 *M* solutions.

As predicted, hydrolysis and 21 → 17 acyl migration (Scheme I) of the methylprednisolone 21-ester linkage is suppressed at higher concentrations. Plots of k_{obs}/k_0 *versus* concentration for hydrolysis and acyl migration, are shown in Figs. 6 and 7 respectively, where k_0 is the pseudo first-order rate constant at high dilution. From Figs. 6 and 7 the following conclusions are drawn: (*a*) significant suppression of reactivity occurs prior to the critical micelle concentrations (obtained from partitioning data) suggesting that dimerization as well as micelle formation stabilizes these esters toward hydroxide ion attack; (*b*) the overall magnitude of stabilization is much less than would be observed if monomers were the only reactive species; (*c*) increases in chain length which were earlier shown to promote micelle formation also result in larger rate suppression with increasing concentration; and (*d*) the magnitude of stabilization is about the same for both the hydrolysis reaction and 21 → 17 acyl migration.

Whereas the equilibrium constants for dimerization, critical micelle

[14] J. R. Cardinal, College of Pharmacy, University of Utah, private communication.

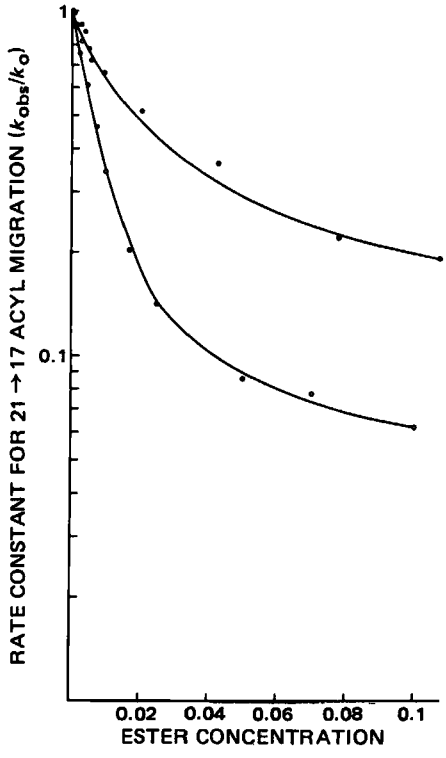

Figure 7—*Semilog plots of the ratio of the observed 21 → 17 acyl migration rate constant at the given ester concentration to the infinite dilution acyl migration rate constant* (k_{obs}/k_0) versus *ester concentration (pH 8.47 and 25°). Key: (●) 21-succinate and (○) 21-suberate.*

concentrations, *etc.* were determined in butyronitrile-saturated aqueous buffer, the kinetic data were obtained in aqueous buffer containing no butyronitrile. The use of the dimerization constants in Table I to calculate rate constants for reaction of dimers from the kinetic data is, therefore, probably not advisable. A few kinetic studies in butyronitrile-saturated buffer were done, however, and similar rate suppression *versus* concentration curves were observed even though absolute reaction rates differed. Qualitatively at least, it is apparent from Figs. 6 and 7 that reaction rates in the dimers are substantially reduced since reactivities decline with concentration even at very low concentrations.

While the percentages of monomer reported in Table I are 2–8% of the total ester at 0.1 *M*, reaction rates at 0.1 *M* are lower by a lesser amount (6–27%). Clearly, reactivity is not totally suppressed in the aggregated species. This is evident in the plots of the absolute hydrolysis rate *versus* the total ester concentration (Fig. 8). Although break points are not as sharp in the kinetic data as in the partitioning data, apparent critical micelle concentrations estimated from extrapolation of the two linear portions of each curve agree fairly well with the apparent critical micelle concentrations reported in Table I.

Reaction rates continue to increase above the critical micelle concentrations indicating that reactivity in the micelles is not totally suppressed. From the slopes above the critical micelle concentrations in Fig. 8, rate constants for hydrolysis in the micelles can be obtained. Values of pseudo first-order rate constants for monomeric and micellar species, k_{mon} and k_{mic}, are listed in Table II for both hydrolysis and acyl migration. At high concentration (0.1 *M*), the reactions occurring in the micelles are actually the major contribution to the overall degradation rate. This accounts for the fact that stabilization is less than predicted based on the monomer concentrations.

Table II—Reaction Rate Constants for Monomeric and Micellar Species of Corticosteroid 21-Esters

Ester	Hydrolysis, min^{-1}		21 → 17 Acyl Migration, min^{-1}	
	k_{mon}	k_{mic}	k_{mon}	k_{mic}
21-Succinate	4.2×10^{-4}	7.4×10^{-5}	3.2×10^{-4}	3.9×10^{-5}
21-Adipate	3.1×10^{-4}	2.1×10^{-5}	—	—
21-Suberate	2.6×10^{-4}	8.1×10^{-6}	2.8×10^{-4}	9.5×10^{-6}

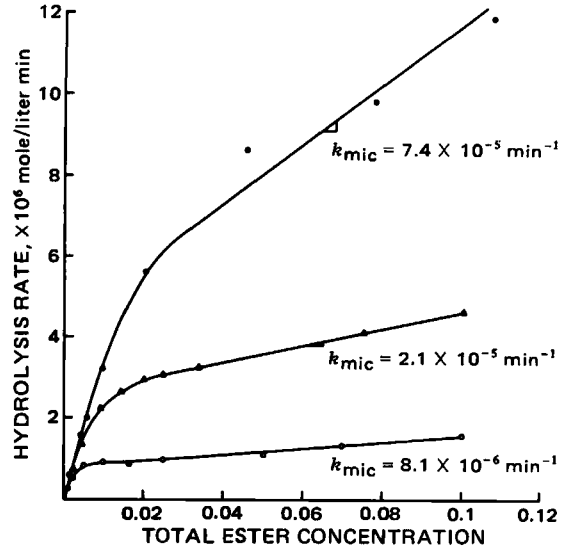

Figure 8—*Absolute hydrolysis rates* versus *total ester concentration (pH 8.5 and 25°). Key: (●) 21-succinate; (▲) 21-adipate; and (○) 21-suberate.*

The effect of chain length on stability was investigated for a similar series of hydrocortisone hemiesters by Garrett in 1962 (32). These studies were conducted in diluted alcoholic solutions, however, and it was concluded that chain length has no significant effect on corticosteroid ester stability. The results of the present study suggest that chain length does have a significant effect on stability, especially at higher concentrations. The 21-suberate of methylprednisolone is nearly an order of magnitude more stable than the 21-succinate at a 0.1 *M* concentration. This greater stability is due to a combination of factors: (*a*) a slight steric effect which increases with chain length is apparent in the reactivity of the monomeric ester; (*b*) self-association increases with chain length providing added stability to long-chain hemiesters by lowering monomer concentration; and, most important, (*c*) reactivity in the micelle apparently decreases with increasing chain length. As a result of these factors, methylprednisolone 21-suberate is >16-fold more stable at high concentration (>0.1 *M*) than in dilute solution.

By comparing Figs. 6 and 7 it is apparent that 21 → 17 acyl migration is suppressed by self-association to an extent similar to the suppression of hydrolysis. Since the approach of hydroxide ion is required for both reactions at pH 8.5, the similarity in behavior with self-association can be rationalized from simple electrostatic considerations (33). The decrease in the rate constants of both reactions with increasing chain length is not explained as readily. Since the effect is not specific for one mechanism, this must also reflect differences in the hydroxide ion activity in the immediate environment of the 21-ester linkage.

REFERENCES

(1) J. L. Kurz, *J. Phys. Chem.*, **66**, 2239 (1962).

(2) C. A. Bunton, S. Diaz, L. S. Romsted, and O. Valenzuela, *J. Org. Chem.*, **41**, 3037 (1976).

(3) C. A. Blyth and J. R. Knowles, *J. Am. Chem. Soc.*, **93**, 3017, 3021 (1971).

(4) F. M. Menger and C. E. Portnoy, *ibid.*, **90**, 1875 (1968).

(5) D. G. Oakenfull and D. E. Fenwick, *Aust. J. Chem.*, **27**, 2149 (1974).

(6) D. M. Small, *Adv. Chem. Ser.*, **84**, 31 (1968).

(7) P. Mukerjee and J. R. Cardinal, *J. Pharm. Sci.*, **65**, 882 (1976).

(8) Y. Chang and J. R. Cardinal, *ibid.*, **67**, 174 (1978).

(9) G. L. Flynn and D. J. Lamb, *ibid.*, **59**, 1433 (1970).

(10) B. D. Anderson and V. Taphouse, *ibid.*, **70**, 181 (1981).

(11) W. Kauzmann, *Adv. Protein Chem.*, **14**, 1 (1959).

(12) G. Nemethy, *Angew. Chem. Int. Ed.*, **6**, 195 (1967).

(13) C. Tanford, "The Hydrophobic Effect," Wiley-Interscience, New York, N.Y., 1973.

(14) P. Mukerjee, *J. Pharm. Sci.*, **63**, 972 (1974).

(15) K. Shinoda, T. Nakagawa, B. Tamamushi, and T. Isemura, "Colloidal Surfactants," Academic, New York, N.Y., 1963.

(16) P. Mukerjee, *J. Phys. Chem.*, **69**, 2821 (1965).

(17) J. R. Cardinal, Y. Chang, and D. D. Ivanson, *J. Pharm. Sci.*, **67**, 854 (1978).
(18) P. Mukerjee, K. J. Mysels, and C. I. Dulin, *J. Phys. Chem.*, **62**, 1390 (1958).
(19) E. Broswell, *ibid.*, **72**, 2477 (1968).
(20) D. S. Goodman, *J. Am. Chem. Soc.*, **80**, 3887 (1958).
(21) S. S. Davis, T. Higuchi, and J. H. Rytting, *J. Pharm. Pharmacol.*, **24**, 30P (1972).
(22) F. J. C. Rossotti and H. Rossotti, *J. Phys. Chem.*, **65**, 926 (1961).
(23) S. S. Davis, J. Higuchi, and J. H. Rytting, in "Advances in Pharmaceutical Sciences," vol. 4, Academic, London, 1974, p. 232.
(24) R. M. Silverstein, G. C. Bassler, and T. C. Morrill, "Spectrometric Identification of Organic Compounds," Wiley, New York, N.Y., 1974, p. 236.
(25) E. H. Cordes, Ed., "Reaction Kinetics in Micelles," Plenum, New York, N.Y., 1973.
(26) J. H. Fendler and E. J. Fendler, "Catalysis in Micellar and Macromolecular Systems," Academic, New York, N.Y., 1975.
(27) F. M. Menger and C. E. Portnoy, *J. Am. Chem. Soc.*, **80**, 4698 (1967).
(28) G. G. Smith, D. R. Kennedy, and J. G. Nairn, *J. Pharm. Sci.*, **63**, 712 (1974).
(29) S. Riegelman, *J. Am. Pharm. Assoc., Sci. Ed.*, **49**, 339 (1960).
(30) H. Tomida, T. Yotsuyanagi, and K. Ikeda, *Chem. Pharm. Bull.*, **26**, 148 (1978).
(31) M. J. Cho and M. A. Allen, *Int. J. Pharm.*, **1**, 281 (1978).
(32) E. R. Garrett, *J. Med. Pharm. Chem.*, **5**, 112 (1962).
(33) G. S. Hartley, *Trans. Faraday Soc.*, **30**, 444 (1934).

ACKNOWLEDGMENTS

The participation of K. Johnson in this study was the result of a senior independent research program jointly sponsored by The Upjohn Company and Kalamazoo College, Kalamazoo, Michigan. The authors would also like to thank J. R. Cardinal, W. Morozowich, and S. L. Nail for discussions regarding this study.

Effect of Ethyl Cellulose in a Medium-Chain Triglyceride on the Bioavailability of Ceftizoxime

IKUO UEDA ˣ, FUMIO SHIMOJO, and JUN KOZATANI

Received February 22, 1982 from the *Research Laboratories, Fujisawa Pharmaceutical Co., Ltd., Osaka 532, Japan.* Accepted for publication July 16, 1982.

Abstract □ The oral bioavailability of new formulations of ceftizoxime sodium was investigated in animals and humans. In rats, one of the formulations tested showed significant improvement, with a urinary excretion of 47.7% (0–24 hr). Good results were obtained also in dogs. In humans, the mean peak serum level was 3.6 μg/ml at 3.3 hr postadministration for formulation 10. The average ceftizoxime AUC at 0–8 hr was 17.3 μg hr/ml and urinary excretion of ceftizoxime was 9.6% (0–24 hr). The concentrations in the serum exceeded the minimum inhibitory concentrations for most of the commonly encountered bacterial pathogens.

Keyphrases □ Bioavailability—oral ceftizoxime in rats, dogs, and humans, effect of ethyl cellulose in medium-chain triglyceride □ Ceftizoxime—bioavailability of oral formulations in rats, dogs, and humans, effect of ethyl cellulose in medium-chain triglyceride □ Ethyl cellulose—effect with medium-chain triglyceride on the oral bioavailability of ceftizoxime in rats, dogs, and humans □ Triglyceride, medium-chain—effect with ethyl cellulose on the oral bioavailability of ceftizoxime in rats, dogs, and humans

Ceftizoxime (I) is a new cephalosporin antibiotic which is active against both Gram-positive and Gram-negative bacteria.

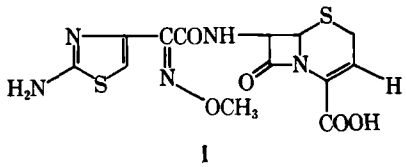

I

The activity of ceftizoxime *in vitro* has been confirmed (1), and the reports on its clinical efficiency are numerous (2). The metabolism and pharmacokinetics of this drug have also been described (3). Ceftizoxime is administered parenterally for effective systemic action since it is poorly absorbed from the GI tract[1]. The purpose of this investigation was to determine the oral bioavailability of ceftizoxime after the administration of its sodium salt to animals and humans in new formulations produced with a combination of medium-chain triglyceride and ethyl cellulose as additives.

Attempts to improve the oral bioavailability of poorly absorbed drugs by devising different pharmaceutical formulations have been reported (4–6). Similarly, our efforts have been directed to the development of new oral formulations of ceftizoxime. We have systematically studied a number of hydrophilic and hydrophobic vehicles, surfactants, and nonsurfactants as additives and found that a combination of ethyl cellulose and a medium-chain triglyceride enhanced the oral absorption of ceftizoxime in rats, dogs, and humans.

EXPERIMENTAL

Materials—Ceftizoxime sodium[2] was prepared as described in the patent (7). Commercially available ethyl cellulose[3], polyethylene glycol 400[4], a medium-chain triglyceride[5], olive oil[4], and ethyl alcohol[4] were used in the suspensions.

Formulations—Formulations containing various amounts of ethyl cellulose were tested. A medium-chain triglyceride (50 ml) and ethyl cellulose (500 mg) dissolved in 1 ml of ethyl alcohol were mixed with stirring. The ethyl alcohol was removed under reduced pressure. Ceftizoxime sodium (5 g-potency) was then dispersed in the resulting vehicle to give the formulation of ceftizoxime used. Similar formulations containing olive oil or polyethylene glycol 400 instead of the medium-chain triglyceride were also investigated.

Absorption Studies—*Rats*—Six-week-old male Sprague-Dawley rats, weighing 160–230 g, were fasted for 18 hr. The rats were given the ceftizoxime sodium formulations (Table I) using a gastric tube at a dose equivalent to 20 mg/kg. Urine was collected for 24 hr, stored at −20°, and

[1] Unpublished data.

[2] Epocelin; Fujisawa Pharmaceutical Co., Ltd. Osaka, Japan.
[3] Ethocel, 10, 45, and 100 cps; Dow Chemical Co.
[4] Hayashi Pure Chemical Industries, Ltd., Japan.
[5] Miglyol 812; Dynamit Nobel Co.

0022-3549/83/0400-0454$01.00/0

(17) J. R. Cardinal, Y. Chang, and D. D. Ivanson, *J. Pharm. Sci.*, **67**, 854 (1978).
(18) P. Mukerjee, K. J. Mysels, and C. I. Dulin, *J. Phys. Chem.*, **62**, 1390 (1958).
(19) E. Broswell, *ibid.*, **72**, 2477 (1968).
(20) D. S. Goodman, *J. Am. Chem. Soc.*, **80**, 3887 (1958).
(21) S. S. Davis, T. Higuchi, and J. H. Rytting, *J. Pharm. Pharmacol.*, **24**, 30P (1972).
(22) F. J. C. Rossotti and H. Rossotti, *J. Phys. Chem.*, **65**, 926 (1961).
(23) S. S. Davis, J. Higuchi, and J. H. Rytting, in "Advances in Pharmaceutical Sciences," vol. 4, Academic, London, 1974, p. 232.
(24) R. M. Silverstein, G. C. Bassler, and T. C. Morrill, "Spectrometric Identification of Organic Compounds," Wiley, New York, N.Y., 1974, p. 236.
(25) E. H. Cordes, Ed., "Reaction Kinetics in Micelles," Plenum, New York, N.Y., 1973.
(26) J. H. Fendler and E. J. Fendler, "Catalysis in Micellar and Macromolecular Systems," Academic, New York, N.Y., 1975.
(27) F. M. Menger and C. E. Portnoy, *J. Am. Chem. Soc.*, **80**, 4698 (1967).
(28) G. G. Smith, D. R. Kennedy, and J. G. Nairn, *J. Pharm. Sci.*, **63**, 712 (1974).
(29) S. Riegelman, *J. Am. Pharm. Assoc., Sci. Ed.*, **49**, 339 (1960).
(30) H. Tomida, T. Yotsuyanagi, and K. Ikeda, *Chem. Pharm. Bull.*, **26**, 148 (1978).
(31) M. J. Cho and M. A. Allen, *Int. J. Pharm.*, **1**, 281 (1978).
(32) E. R. Garrett, *J. Med. Pharm. Chem.*, **5**, 112 (1962).
(33) G. S. Hartley, *Trans. Faraday Soc.*, **30**, 444 (1934).

ACKNOWLEDGMENTS

The participation of K. Johnson in this study was the result of a senior independent research program jointly sponsored by The Upjohn Company and Kalamazoo College, Kalamazoo, Michigan. The authors would also like to thank J. R. Cardinal, W. Morozowich, and S. L. Nail for discussions regarding this study.

Effect of Ethyl Cellulose in a Medium-Chain Triglyceride on the Bioavailability of Ceftizoxime

IKUO UEDA ˣ, FUMIO SHIMOJO, and JUN KOZATANI

Received February 22, 1982 from the *Research Laboratories, Fujisawa Pharmaceutical Co., Ltd., Osaka 532, Japan.* Accepted for publication July 16, 1982.

Abstract □ The oral bioavailability of new formulations of ceftizoxime sodium was investigated in animals and humans. In rats, one of the formulations tested showed significant improvement, with a urinary excretion of 47.7% (0–24 hr). Good results were obtained also in dogs. In humans, the mean peak serum level was 3.6 μg/ml at 3.3 hr postadministration for formulation 10. The average ceftizoxime AUC at 0–8 hr was 17.3 μg hr/ml and urinary excretion of ceftizoxime was 9.6% (0–24 hr). The concentrations in the serum exceeded the minimum inhibitory concentrations for most of the commonly encountered bacterial pathogens.

Keyphrases □ Bioavailability—oral ceftizoxime in rats, dogs, and humans, effect of ethyl cellulose in medium-chain triglyceride □ Ceftizoxime—bioavailability of oral formulations in rats, dogs, and humans, effect of ethyl cellulose in medium-chain triglyceride □ Ethyl cellulose—effect with medium-chain triglyceride on the oral bioavailability of ceftizoxime in rats, dogs, and humans □ Triglyceride, medium-chain—effect with ethyl cellulose on the oral bioavailability of ceftizoxime in rats, dogs, and humans

Ceftizoxime (I) is a new cephalosporin antibiotic which is active against both Gram-positive and Gram-negative bacteria.

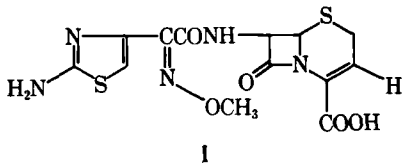

I

The activity of ceftizoxime *in vitro* has been confirmed (1), and the reports on its clinical efficiency are numerous (2). The metabolism and pharmacokinetics of this drug have also been described (3). Ceftizoxime is administered parenterally for effective systemic action since it is poorly absorbed from the GI tract[1]. The purpose of this investigation was to determine the oral bioavailability of ceftizoxime after the administration of its sodium salt to animals and humans in new formulations produced with a combination of medium-chain triglyceride and ethyl cellulose as additives.

Attempts to improve the oral bioavailability of poorly absorbed drugs by devising different pharmaceutical formulations have been reported (4–6). Similarly, our efforts have been directed to the development of new oral formulations of ceftizoxime. We have systematically studied a number of hydrophilic and hydrophobic vehicles, surfactants, and nonsurfactants as additives and found that a combination of ethyl cellulose and a medium-chain triglyceride enhanced the oral absorption of ceftizoxime in rats, dogs, and humans.

EXPERIMENTAL

Materials—Ceftizoxime sodium[2] was prepared as described in the patent (7). Commercially available ethyl cellulose[3], polyethylene glycol 400[4], a medium-chain triglyceride[5], olive oil[4], and ethyl alcohol[4] were used in the suspensions.

Formulations—Formulations containing various amounts of ethyl cellulose were tested. A medium-chain triglyceride (50 ml) and ethyl cellulose (500 mg) dissolved in 1 ml of ethyl alcohol were mixed with stirring. The ethyl alcohol was removed under reduced pressure. Ceftizoxime sodium (5 g-potency) was then dispersed in the resulting vehicle to give the formulation of ceftizoxime used. Similar formulations containing olive oil or polyethylene glycol 400 instead of the medium-chain triglyceride were also investigated.

Absorption Studies—*Rats*—Six-week-old male Sprague-Dawley rats, weighing 160–230 g, were fasted for 18 hr. The rats were given the ceftizoxime sodium formulations (Table I) using a gastric tube at a dose equivalent to 20 mg/kg. Urine was collected for 24 hr, stored at −20°, and

[1] Unpublished data.

[2] Epocelin; Fujisawa Pharmaceutical Co., Ltd. Osaka, Japan.
[3] Ethocel, 10, 45, and 100 cps; Dow Chemical Co.
[4] Hayashi Pure Chemical Industries, Ltd., Japan.
[5] Miglyol 812; Dynamit Nobel Co.

0022-3549/83/0400-0454$01.00/0

Table I—Effect of Vehicle on the Urinary Excretion of Ceftizoxime after Oral Dosing in Rats with Ceftizoxime Sodium in Different Vehicles [a]

Vehicle	Cumulative Urinary Excretion (0–24 hr), % of dose [b]	
Polyethylene glycol 400	7.1	(5)
A medium-chain triglyceride	16.2	(3)
Olive oil	9.7	(3)
A medium-chain [c] triglyceride + ethyl cellulose	37.7	(9)
Olive oil [c] + ethyl cellulose	24.6	(5)
Water	10.3	(5)

[a] At a dose of 20 mg-potency/kg. [b] Values represent the mean; sample size is in parentheses. [c] Ethyl cellulose concentration in the vehicle ~1% (w/v); viscosity of ethyl cellulose was 100 cps.

assayed within 24 hr. The amount of ceftizoxime excreted was determined by high-performance liquid chromatography (HPLC) using a standard curve.

Dogs—The formulations used in the dog experiments are shown in Table II. Male beagle dogs weighing 8.0–13.2 kg were used, with four dogs per group. The animals were fasted overnight and the drug formulations (in hard gelatin capsules) were given in doses equivalent to 40 mg ceftizoxime/kg. Urine was collected for 24 hr; 5-ml venous blood samples were drawn at 0.5, 1, 2, 4, 6, and 8 hr postadministration and centrifuged to obtain the serum. All serum and urine samples were stored at −20° and assayed within 24 hr.

Humans—Formulations 3 and 10 (Table II) were used in the human experiments. Six healthy males, 33–47 years of age and 49.5–67.5 kg, participated in the study after informed written consent was obtained. No other drugs were taken during the investigation period. Prestudy physical examinations and laboratory parameters for all subjects were normal.

Experimental Design—A two-way crossover design was used in the human studies. The two formulations (3 and 10) were given orally to the six volunteers, at an interval of 2 weeks. The volunteers drank 200 ml of water immediately after ingesting the drug. All volunteers fasted overnight before dosing and were given regular meals 2 hr after dosing. Venous blood samples (5 ml) for assay of serum concentration of ceftizoxime were drawn 0.5, 1, 2, 4, 6, 8, and 24 hr postdose. Urine samples were collected at 2-hr intervals from 0 to 8 hr and for the interval 8–24 hr postdose. All serum and urine samples were stored at −20° and assayed within 24 hr.

Assay of Ceftizoxime—The concentration of ceftizoxime in the serum and urine was determined by HPLC[6]. Samples (5 μl) were injected directly into the HPLC equipped with a 254-nm detector and a stainless steel column (30 cm × 4-mm i.d.) packed with μ-Bondapak C_{18}[7]. The mobile phase was 0.6% potassium phosphate–0.2% sodium phosphate–acetonitrile (1:1:0.22). The system was operated at 2.0 ml/min with a column pressure of 2000 psi. Sample chromatograms are shown in Fig. 1.

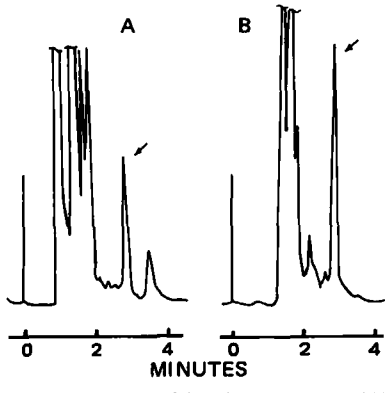

Figure 1—*Chromatogram of ceftizoxime in serum (A) and urine (B) after oral dosing with ceftizoxime sodium. The retention time of the ceftizoxime peak (indicated by the arrow) is 2.8 min in serum and 3.6 min in urine.*

[6] Model ALC/GPC 204 (model 6000A pump, U6-K, and 400 detector); Waters Associates, Milford, Mass.

[7] Waters Associates, Milford, Mass.

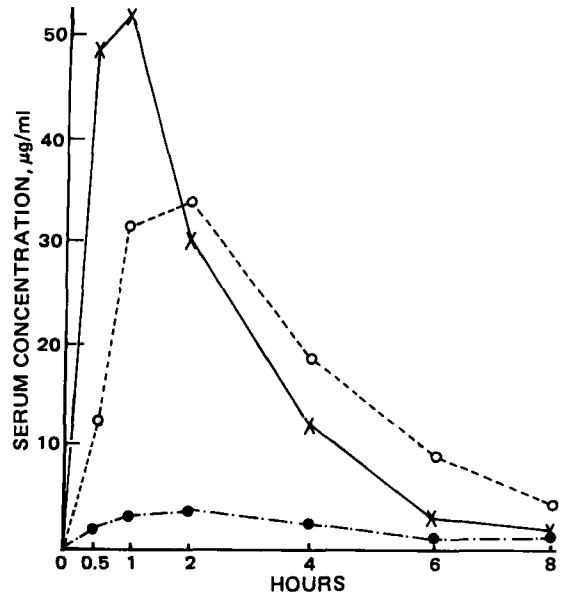

Figure 2—*Time plots of mean serum concentration of ceftizoxime in four dogs after oral dosing with formulations 3 (○) and 10 (×), and with a water vehicle (●) as the control. Dogs received ceftizoxime sodium (at a dose of 40 mg-potency/kg) in a hard gelatin capsule.*

Standard Curves—The reproducibility and linearity of standard curves generated from rat, dog, and human serum and urine containing various amounts of ceftizoxime sodium were studied. The standard curves represent triplicate analyses and were prepared over concentration ranges of 50–600 μg/ml for urine and 2–10 μg/ml for serum. In serum, the least-squares regression line had a slope of 5.324, intercept of −0.143, and correlation coefficient of 0.99996; the limit of detection is 0.2 μg/ml. In urine, the least-squares regression line had a slope of 0.152, intercept of 1.369, and correlation coefficient of 0.999969; the limit of detection is 5 μg/ml.

RESULTS AND DISCUSSION

Table I shows the urinary excretion of ceftizoxime in rats as the percentage of dose after oral administration of ceftizoxime sodium suspension in some typical vehicles. It was found that 10.3% of the dose was excreted when the drug was given in a simple water suspension (control). The urinary excretion of ceftizoxime was somewhat lower when polyethylene glycol 400 or olive oil was used; the medium-chain triglyceride slightly increased the drug bioavailability as evidenced by the urinary excretion rate of 16.2%. It was found, however, that coadministration of ethyl cellulose with ceftizoxime sodium in the medium-chain triglyceride significantly increased the drug absorption: 37.7% of the drug was excreted. The coadministration of ethyl cellulose in olive oil also produced considerably higher urinary excretion (24.6%). However, ethyl cellulose

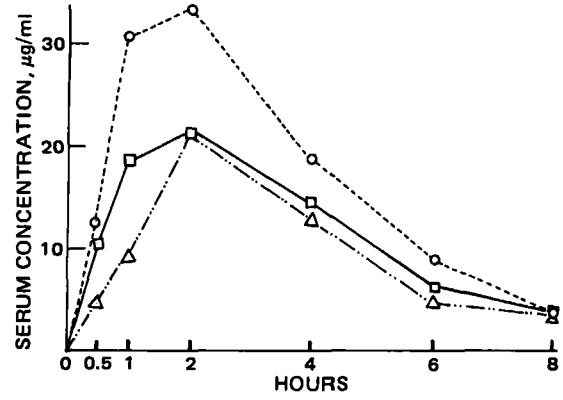

Figure 3—*Time plots of mean serum concentration of ceftizoxime in four dogs after oral dosing with formulations 3 (○), 8 (□), and 9 (△). Dogs received ceftizoxime sodium (at a dose of 40 mg-potency/kg) in a hard gelatin capsule.*

Table II—Oily Formulations for Oral Ceftizoxime Sodium

Formulation	Ceftizoxime Sodium, mg-potency	A Medium-Chain Triglyceride, ml	Ethyl Cellulose[a], mg	Ceftizoxime Sodium in Vehicle, % (w/v)	Ethyl Cellulose in a Medium-Chain Triglyceride, % (w/v)
2	500	10	100 (100 cps)	5.0	1.0
3	500	5.0	50 (100 cps)	10.0	1.0
4	500	2.5	25 (100 cps)	20.0	1.0
5	500	1.0	10 (100 cps)	50.0	1.0
8	500	5.0	50 (10 cps)	10.0	1.0
9	500	5.0	50 (45 cps)	10.0	1.0
10	500	5.0	200 (100 cps)	10.0	4.0

[a] Viscosity of ethyl cellulose in parentheses.

Table III—Effect of Ethyl Cellulose in a Medium-Chain Triglyceride on the Urinary Excretion of Ceftizoxime After Oral Dosing with Ceftizoxime Sodium in Rats[a]

Ethyl Cellulose per ml of Medium-Chain Triglyceride, mg[b]	Concentration of Ethyl Cellulose in the Vehicle, % (w/v)	Cumulative Urinary Excretion (0–24 hr), % of dose[c]
2	0.2	25.5 ± 8.9 (3)
4	0.4	36.5 ± 7.1 (3)
6	0.6	47.7 ± 3.4 (3)
8	0.8	40.7 ± 8.0 (3)
10	1.0	37.7 ± 1.9 (9)

[a] At a dose of 20 mg-potency/kg, suspended in a medium-chain triglyceride. [b] Viscosity of ethyl cellulose was 100 cps. [c] Mean ±*SE*; sample size in parentheses.

did not affect the drug absorption when given in polyethylene glycol 400.

The data in Table III indicate that the effect of ethyl cellulose in the medium-chain triglyceride on the absorption of ceftizoxime in rats was dependent on the concentration of ethyl cellulose used. Ethyl cellulose in the range of 2–10 mg/ml significantly increased the drug absorption. The maximum effect was observed at ~0.6 % (w/v) ethyl cellulose. When ceftizoxime sodium in aqueous solution was administered intravenously to rats at a dose of 20 mg-potency/kg, the urinary excretion of ceftizoxime at 0–24 hr was 79.8% of the given dose[1]. The urinary excretions of 47.7% after oral dosing indicates that ~60% of the administered drug was absorbed.

The experiments in dogs were designed on the basis of these data. The formulations used in the dog experiments are shown in Table II. Figure 2 plots the serum concentrations of ceftizoxime in dogs as a function of time postdose with formulations 3 and 10. The maximum serum concentration of ceftizoxime was significantly higher for formulation 10 than formulation 3; but when the areas under the curve (AUC), calculated by trapezoidal rule, are compared, the differences between the bioavailabilities of formulations 3 and 10 are very small.

The bioavailability studies in dogs, using ethyl cellulose of three different viscosities (10, 45, and 100 cps), demonstrate that ethyl cellulose with a viscosity of 100 cps resulted in higher serum concentrations of

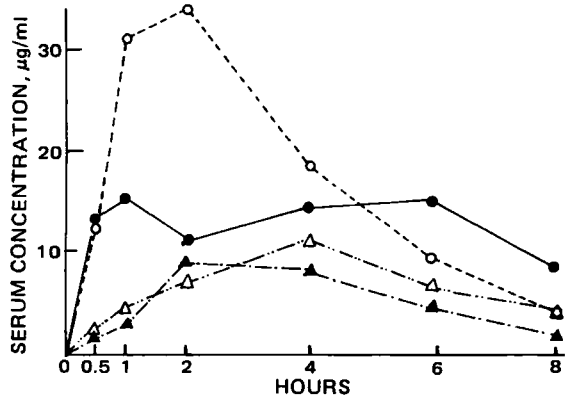

Figure 4—*Time plots of mean serum concentration of ceftizoxime in four dogs after oral dosing with formulations 2 (●), 3 (○), 4 (△), and 5 (▲). Dogs received ceftizoxime sodium (at a dose of 40 mg-potency/kg) in a hard gelatin capsule.*

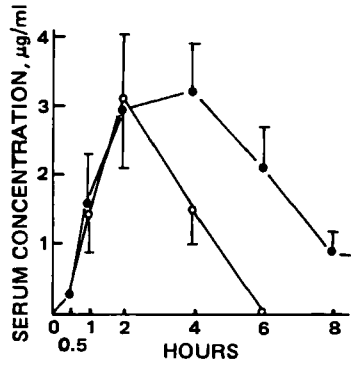

Figure 5—*Time plots of mean serum concentration of ceftizoxime in six human volunteers after oral dosing with formulations 3 (○) and 10 (●). The dose was 500 mg-potency/kg. The data points represent the mean values; standard errors are represented by the bars around each point.*

ceftizoxime than ethyl cellulose additives with viscosities of 10 and 45 cps (formulations 8 and 9) (Fig. 3).

The effect of the vehicle volume on the oral absorption of ceftizoxime was also investigated. Figure 4 shows the bioavailabilities (serum concentrations) in dogs for 5, 10, 20, and 50% (w/v) suspensions of ceftizoxime sodium in the medium-chain triglyceride containing ethyl cellulose (formulations 2, 3, 4, and 5, respectively). The oral absorption of ceftizoxime was shown to be dependent on the volume of the vehicle. The greatest absorption was observed with the 10% suspension, the next

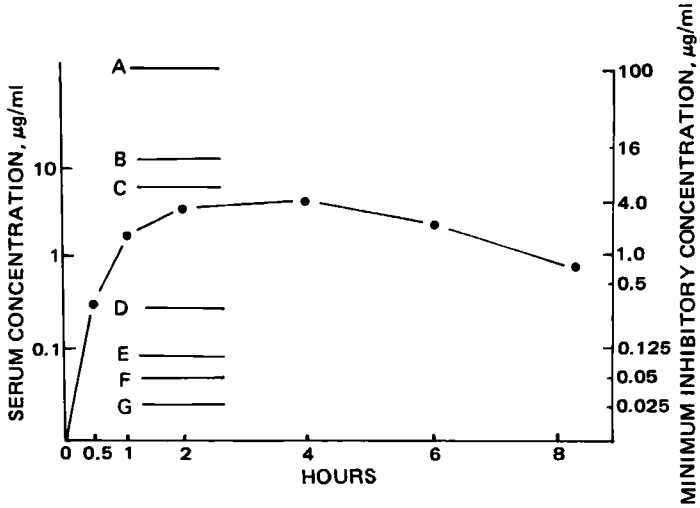

Figure 6—*Mean serum concentration of ceftizoxime (●) in six human volunteers after oral dosing with formulation 10. The lines indicate the minimum inhibitory concentrations for various bacterial pathogens. Key: (A)* Pseudomonas aeruginosa *IAM-1095; (B)* Escherichia coli *35 and* Enterobacter cloacae *1; (C)* Staphylococcus aureus *209p JC-1; (D)* E. coli *28; (E)* Proteus rettgeri *14; (F)* Proteus vulgaris *IAM-1025 and* Streptococcus pneumoniae *III; and (G)* Klebsiella pneumoniae *NCTC-418,* Shigella flexneri *la EW-8,* Proteus mirabilis *1, and* Salmonella typhi *T-287.*

Table IV—Serum Concentrations of Ceftizoxime in Human Volunteers after Oral Dosing with Formulations 3 and 10 [a]

Formulation	Subject	Age, years	Weight, kg	Serum Concentrations of Ceftizoxime, μg/ml [b] 0.5 hr	1 hr	2 hr	4 hr	6 hr	8 hr	C_{max}, μg/ml	T_{max}, hr	AUC, μg hr/ml
	A	33	66.0	0.6	2.9	3.4	2.1	0.1	—[c]	3.4	2.0	12.0
	B	46	49.5	0.1	0.2	0.3	0.2	—	—	0.3	2.0	1.1
3	C	45	66.0	—	1.0	3.7	2.1	—	—	3.7	2.0	10.5
	D	47	54.5	—	—	0.6	—	—	—	0.6	2.0	0.9
	E	38	54.5	—	2.0	6.1	3.0	—	—	6.1	2.0	16.7
	F	35	53.5	1.0	2.5	4.4	1.6	—	—	4.4	2.0	12.2
Mean				0.3	1.4	3.1	1.5			3.1	2.0	8.9
SE				±0.2	±0.5	±0.9	±0.5			±0.9	±0.0	±2.6
	A	33	67.0	—	0.9	1.7	4.9	4.2	2.2	4.9	4.0	23.6
	B	46	50.0	—	—	0.1	0.5	0.1	—	0.5	4.0	1.4
10	C	45	67.5	—	0.7	3.2	3.9	2.2	1.4	3.9	4.0	18.9
	D	47	54.5	—	0.7	3.2	2.3	1.1	0.2	3.2	2.0	12.3
	E	38	55.0	—	4.6	5.7	4.4	3.1	0.9	5.7	2.0	27.9
	F	35	54.0	1.5	2.7	3.3	3.4	2.1	0.9	3.4	4.0	19.6
Mean				0.3	1.6	2.9	3.2	2.1	0.9	3.6	3.3	17.3
SE				±0.3	±0.7	±0.8	±0.7	±0.6	±0.3	±0.7	±0.4	±3.8

[a] At a dose of 500 mg-potency/person. [b] At 24 hr no ceftizoxime could be detected. [c] — not detected.

Table V—Urinary Excretion of Ceftizoxime in Human Volunteers after Oral Dosing with Formulations 3 and 10 [a]

Formulation	Subject	Age, Years	Weight, kg	Urinary excretion at time interval in hr, % 0–2	2–4	4–6	6–8	8–24	Cumulation % (0–24 hr)
	A	33	66.0	4.4	3.1	1.3	0.2	—[b]	8.9
	B	46	49.5	0.3	0.3	0.3	0.1	—	1.0
3	C	45	66.0	0.6	2.7	0.7	—	—	4.0
	D	47	54.5	—	0.2	0.2	0.1	—	0.5
	E	38	54.5	1.2	3.6	2.1	0.2	—	7.0
	F	35	53.5	2.5	2.0	0.6	0.1	—	5.2
Mean				1.5	2.0	0.9	0.1	—	4.4
SE				±0.7	±0.6	±0.3	±0.0	—	±1.3
	A	33	67.0	2.2	6.0	4.8	3.4	1.4	17.8
	B	46	50.0	0.1	0.2	0.2	0.1	—	0.5
10	C	45	67.5	1.2	5.2	4.1	1.3	0.1	12.0
	D	47	54.5	1.3	5.7	1.2	1.3	0.2	9.6
	E	38	55.0	2.6	4.6	2.7	0.8	0.2	10.8
	F	35	54.0	3.0	2.1	1.5	0.2	—	6.8
Mean				1.7	4.0	2.4	1.2	0.3	9.6
SE				±0.4	±0.9	±0.7	±0.5	±0.2	±2.3

[a] At a dose of 500 mg-potency/person. [b] — not detected.

greatest with 5% suspension. The mean AUC of the serum concentration–time curve for the 10% suspension was a little larger than that for the 5% suspension, which resulted in a lower maximum serum concentration with a longer duration. The 20 and 50% suspensions tended to produce smaller C_{max}.

Since the animal studies described above suggest that similar effects may occur in humans, a study of the effect of the two formulations that gave the highest serum concentrations in dogs was deemed appropriate. The serum concentrations and bioavailability parameters of ceftizoxime in human volunteers after oral dosing with formulations 3 and 10 are given in Table IV. The time courses of mean serum concentrations of ceftizoxime are shown graphically in Fig. 5. After oral dosing with formulation 3, the serum concentrations of ceftizoxime peaked at 2.0 hr and then declined rather sharply up to 6 hr. The mean (±*SE*) peak concentration (C_{max}) of ceftizoxime was 3.1 ± 0.9 μg/ml (range, 0.3–6.1 μg/ml) and the mean (±*SE*) concentration was 1.5 ± 0.5 μg/ml (range, 0.2–3.0 μg/ml) at 4 hr. After oral dosing with formulation 10, the serum concentrations peaked at 3.3 hr and then declined. The mean C_{max} was 3.6 ± 0.7 μg/ml (range, 0.5–5.7 μg/ml) and the mean concentrations were 2.1 ± 0.6 (range, 0.1–4.2 μg/ml) and 0.9 ± 0.3 μg/ml (range, 0.2–2.2 μg/ml) at 6 and 8 hr, respectively. Formulation 10 gave a slightly higher C_{max} (not statistically significant) and a longer T_{max} (statistically significant at $0.01 < p < 0.05$) than formulation 3. The mean AUC (±*SE*) for the serum concentration–time curve was 8.9 ± 2.6 μg hr/ml (range, 0.9–16.7 μg hr/ml) for formulation 3 and 17.3 ± 3.8 μg hr/ml (range, 1.4–27.9 μg hr/ml) for formulation 10. Thus, formulation 10 gave an AUC double that of formulation 3 (statistically significant at $p < 0.01$).

The urinary excretion of ceftizoxime in human volunteers after dosing with formulations 3 and 10 is given in Table V. The mean (±*SE*) cumulative urinary excretions of ceftizoxime for 0–24 hr were 4.4 ± 1.3% of the dose (range, 0.5–8.9%) for formulation 3 and 9.6 ± 2.3% (range, 0.5–17.8%) for formulation 10. Formulation 10 resulted in a cumulative urinary excretion double that of formulation 3 (statistically significant at $0.01 < p < 0.05$), thus confirming the AUC values.

As shown in Fig. 6, the concentrations determined in the serum over a period of 8 hr after a single dose of 500 mg-potency of ceftizoxime sodium (formulation 10) were found to exceed the therapeutically active level (minimum inhibitory concentration *in vitro*) against many Gram-negative organisms, including strains of *Escherichia coli*, *Klebsiella*, and *Proteus* (1, 2).

In conclusion, when compared with an aqueous solution of ceftizoxime sodium, formulations containing ethyl cellulose improved oral absorption of ceftizoxime. Formulation 10, which contained the higher additive concentration gave a larger ceftizoxime AUC value and higher urinary excretion than formulation 3. The concentration in the serum exceeded the minimum inhibitory concentration for normally encountered bacterial pathogens.

REFERENCES

(1) T. Kamimura, T. Matsumoto, N. Okada, Y. Mine, M. Nishida, S. Goto, and S. Kuwabara, *Antimicrob. Agents Chemother.*, **16**, 540 (1979).

(2) *Chemotherapy (Tokyo)*, Vol **28**, Supple 5, September 1980.

(3) T. Murakawa, H. Sakamoto, S. Fukada, S. Nakamoto, T. Hirose, N. Itoh, and M. Nishida, *Antimicrob. Agents Chemother.*, **17**, 157 (1980);

K. Noda, A. Suzuki, H. Ohta, T. Furukawa, and H. Noguchi, *Arzneim.-Forsch*, **30**, 1665 (1980).

(4) V. Stella, J. Haslam, N. Yata, H. Okada, S. Lindenbaum, and T. Higuchi, *J. Pharm. Sci.*, **67**, 1375 (1978).

(5) K. Takada, H. Mikami, S. Asada, K. Tatsuo, and S. Muranishi, *Chem. Pharm. Bull.*, **26**, 19 (1978).

(6) K. Uekama, N. Matsuo, F. Hirayama, H. Ichibangase, K. Arimori, K. Tsubaki, and K. Satake, *Yakugaku Zasshi*, **100**, 903 (1980).

(7) Fujisawa Pharmaceutical Co., Ltd., Ger. Offen (1978) [*Chem. Abstr.*, **90**, 204116k (1979)].

ACKNOWLEDGMENTS

The authors are grateful to Mr. T. Oki for his valuable suggestions and to Dr. N. Bodor for constructive comments on the manuscript.

COMMUNICATIONS

Correlation Between the Psychotropic Potency of Cannabinoids and Their Effect on the ^{1}H-NMR Spectra of Model Membranes

Keyphrases □ Membranes—model, correlation between psychotropic potency of cannabinoids and their effect on the ^{1}H-NMR spectra □ Cannabinoids—correlation between psychotropic potency and their effect on the ^{1}H-NMR spectra of model membranes □ Cholesterol—model membranes, correlation between the psychotropic potency of cannabinoids and their effect on the ^{1}H-NMR spectra □ Phosphatidylcholine—model membrane, correlation between the psychotropic potency of cannabinoids and their effect on the ^{1}H-NMR spectra

To the Editor:

Little is known of the mode of psychotropic action of Δ^1-tetrahydrocannabinol (I), the major active component of hashish (1). It has been suggested that this drug, as well as other psychotropic cannabinoids, exerts its psychotropic effect through a nonspecific interaction with lipid constituents of nerve cell membranes (2). To investigate such nonspecific interactions, phospholipid vesicles (liposomes) have been used as model membranes. These models represent an oversimplification of the complex biological membranes. However, the possibility of manipulating their composition and size permits deduction of the relative importance of the various structural and compositional factors of the membrane in determining the interactions of membranes with drugs. For the effect of a drug on the physical properties of a model membrane to be regarded as relevant to the mode of action of the drug, a correlation must be established between the effect of various derivatives of the drug and their potency on the membrane.

For psychotropically active cannabinoids, electron spin resonance measurements showed that these drugs reduce the order within the bilayer (3) when introduced into vesicles composed of phosphatidylcholine and cholesterol. The disordering effect of five different cannabinoids correlated qualitatively with their psychotropic potency. The psychotropically nonactive drug, cannabidiol (VI), increased the order parameter within the bilayer (3). Since electron spin resonance, as well as several other physicochemical techniques, involve the use of external probes, which might alter the bilayer properties, we have recently studied the effect of the cannabinoids, I and VI, on the ^{1}H-NMR spectra of lipid vesicles (4). The conclusions of this research were similar to those obtained from the electron spin resonance study: addition of small amounts of I (1 mole percent) to vesicles composed of egg phosphatidylcholine and cholesterol (2:1) caused narrowing of the apparent linewidth of the phospholipid methylene groups signal, whereas the chemically similar, nonactive compound, VI, had the opposite effect.

The purpose of the present work was twofold. First, we wanted to establish a correlation between the potency of various cannabinoids[1] and the effect of small quantities (1 mole percent) of these drugs on the apparent linewidth of the NMR resonance of the phospholipid hydrocarbon chain protons in model membranes composed of egg phosphatidylcholine and cholesterol. Second, in a previous work we showed that in the absence of cholesterol in the model membranes, small amounts of I do not produce any significant change in the linewidth of the ^{1}H-NMR resonances. Therefore, we found it of interest to study the role of cholesterol in the interactions of I with the model membranes. These interactions most likely are not due to the existence of specific interactions of I with cholesterol, since there is no evidence for such interactions in the ^{1}H-NMR spectrum of a mixture of these two components in chloroform (4). One alternative explanation was that the lack of a fluidizing effect in the absence of cholesterol is due to the disrupted packing in the highly curved small unilamellar vesicles (5–7). More specifically, vesicles formed by sonification of mixtures of phosphatidylcholine and cholesterol are larger and less curved than those made of the pure phospholipid by the same method. This may cause the difference between the effect of I on vesicles with and without cholesterol. To investigate this possibility, we studied the effect of cannabinoids on the larger vesicles (~500-Å diameter) made of pure phosphatidylcholine by the French press method (8). The results of this study, in conjunction with the dependence of the fluidizing effect of I on the cholesterol content in the vesicles, indicate that cholesterol is important in the interaction of this drug with model membranes.

The model membranes were prepared as follows: solutions of phosphatidylcholine[2] and cholesterol[3] in chloro-

[1] All cannabinoids used in this study (Table I) were a gift of Professor R. Mechoulam of the Natural Products Laboratory, Hebrew University.

[2] Egg yolk phosphatidylcholine (lecithin, grade 1) was purchased from Makor Chemicals (Jerusalem). It was at least 99% pure, giving one spot on a TLC plate at a 1-μmole loading. It was used without further purification.

[3] Cholesterol (Merck) was recrystalized from ethanol.

0022-3549/83/0400-0458$01.00/0

K. Noda, A. Suzuki, H. Ohta, T. Furukawa, and H. Noguchi, *Arzneim.-Forsch*, **30**, 1665 (1980).

(4) V. Stella, J. Haslam, N. Yata, H. Okada, S. Lindenbaum, and T. Higuchi, *J. Pharm. Sci.*, **67**, 1375 (1978).

(5) K. Takada, H. Mikami, S. Asada, K. Tatsuo, and S. Muranishi, *Chem. Pharm. Bull.*, **26**, 19 (1978).

(6) K. Uekama, N. Matsuo, F. Hirayama, H. Ichibangase, K. Arimori, K. Tsubaki, and K. Satake, *Yakugaku Zasshi*, **100**, 903 (1980).

(7) Fujisawa Pharmaceutical Co., Ltd., Ger. Offen (1978) [*Chem. Abstr.*, **90**, 204116k (1979)].

ACKNOWLEDGMENTS

The authors are grateful to Mr. T. Oki for his valuable suggestions and to Dr. N. Bodor for constructive comments on the manuscript.

COMMUNICATIONS

Correlation Between the Psychotropic Potency of Cannabinoids and Their Effect on the ^{1}H-NMR Spectra of Model Membranes

Keyphrases □ Membranes—model, correlation between psychotropic potency of cannabinoids and their effect on the ^{1}H-NMR spectra □ Cannabinoids—correlation between psychotropic potency and their effect on the ^{1}H-NMR spectra of model membranes □ Cholesterol—model membranes, correlation between the psychotropic potency of cannabinoids and their effect on the ^{1}H-NMR spectra □ Phosphatidylcholine—model membrane, correlation between the psychotropic potency of cannabinoids and their effect on the ^{1}H-NMR spectra

To the Editor:

Little is known of the mode of psychotropic action of Δ^1-tetrahydrocannabinol (I), the major active component of hashish (1). It has been suggested that this drug, as well as other psychotropic cannabinoids, exerts its psychotropic effect through a nonspecific interaction with lipid constituents of nerve cell membranes (2). To investigate such nonspecific interactions, phospholipid vesicles (liposomes) have been used as model membranes. These models represent an oversimplification of the complex biological membranes. However, the possibility of manipulating their composition and size permits deduction of the relative importance of the various structural and compositional factors of the membrane in determining the interactions of membranes with drugs. For the effect of a drug on the physical properties of a model membrane to be regarded as relevant to the mode of action of the drug, a correlation must be established between the effect of various derivatives of the drug and their potency on the membrane.

For psychotropically active cannabinoids, electron spin resonance measurements showed that these drugs reduce the order within the bilayer (3) when introduced into vesicles composed of phosphatidylcholine and cholesterol. The disordering effect of five different cannabinoids correlated qualitatively with their psychotropic potency. The psychotropically nonactive drug, cannabidiol (VI), increased the order parameter within the bilayer (3). Since electron spin resonance, as well as several other physicochemical techniques, involve the use of external probes, which might alter the bilayer properties, we have recently studied the effect of the cannabinoids, I and VI, on the ^{1}H-NMR spectra of lipid vesicles (4). The conclusions of this research were similar to those obtained from the electron spin resonance study: addition of small amounts of I (1 mole percent) to vesicles composed of egg phosphatidylcholine and cholesterol (2:1) caused narrowing of the apparent linewidth of the phospholipid methylene groups signal, whereas the chemically similar, nonactive compound, VI, had the opposite effect.

The purpose of the present work was twofold. First, we wanted to establish a correlation between the potency of various cannabinoids[1] and the effect of small quantities (1 mole percent) of these drugs on the apparent linewidth of the NMR resonance of the phospholipid hydrocarbon chain protons in model membranes composed of egg phosphatidylcholine and cholesterol. Second, in a previous work we showed that in the absence of cholesterol in the model membranes, small amounts of I do not produce any significant change in the linewidth of the ^{1}H-NMR resonances. Therefore, we found it of interest to study the role of cholesterol in the interactions of I with the model membranes. These interactions most likely are not due to the existence of specific interactions of I with cholesterol, since there is no evidence for such interactions in the ^{1}H-NMR spectrum of a mixture of these two components in chloroform (4). One alternative explanation was that the lack of a fluidizing effect in the absence of cholesterol is due to the disrupted packing in the highly curved small unilamellar vesicles (5–7). More specifically, vesicles formed by sonification of mixtures of phosphatidylcholine and cholesterol are larger and less curved than those made of the pure phospholipid by the same method. This may cause the difference between the effect of I on vesicles with and without cholesterol. To investigate this possibility, we studied the effect of cannabinoids on the larger vesicles (~500-Å diameter) made of pure phosphatidylcholine by the French press method (8). The results of this study, in conjunction with the dependence of the fluidizing effect of I on the cholesterol content in the vesicles, indicate that cholesterol is important in the interaction of this drug with model membranes.

The model membranes were prepared as follows: solutions of phosphatidylcholine[2] and cholesterol[3] in chloro-

[1] All cannabinoids used in this study (Table I) were a gift of Professor R. Mechoulam of the Natural Products Laboratory, Hebrew University.

[2] Egg yolk phosphatidylcholine (lecithin, grade 1) was purchased from Makor Chemicals (Jerusalem). It was at least 99% pure, giving one spot on a TLC plate at a 1-μmole loading. It was used without further purification.

[3] Cholesterol (Merck) was recrystalized from ethanol.

0022-3549/83/0400-0458$01.00/0

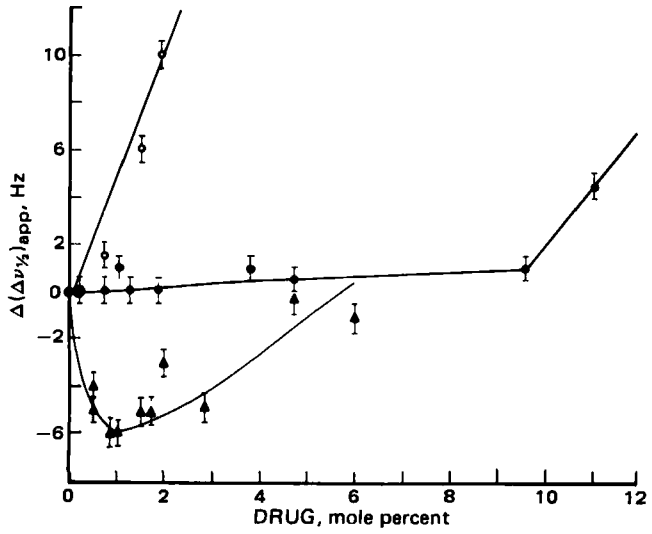

Figure 1—*The effect of I on the apparent linewidth of the phosphatidylcholine methylene signals $(\Delta\nu_{1/2})_{app}$ in vesicles made by the French press methoid (○) and by sonication with (▲) and without (●) cholesterol (33 mole percent). In the absence of cannabinoids, $(\Delta\nu_{1/2})_{app}$ was 22 Hz for the sonicated lecithin, 85 Hz for sonicated vesicles with cholesterol, and 35 Hz for the French press vesicles.*

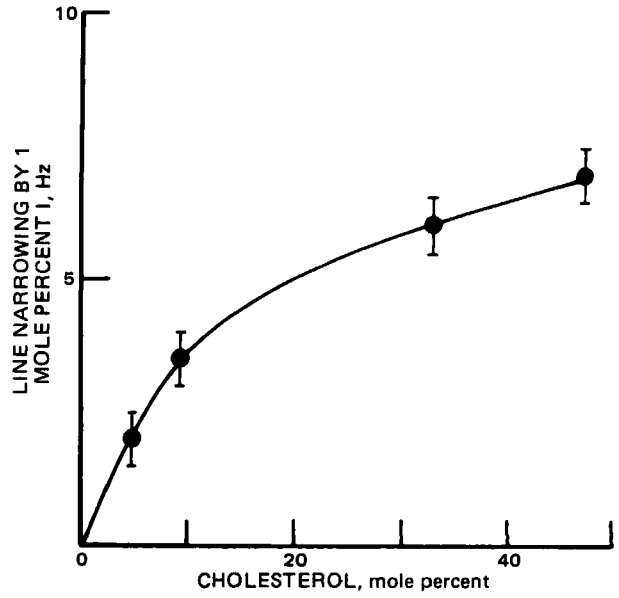

Figure 2—*The reduction in the apparent linewidth of the signal of phosphatidylcholine methylene protons introduced by 1 mole percent of I as a function of the cholesterol content of sonicated vesicles. Phosphatidylcholine concentration was 50 mg/ml.*

form were mixed at appropriate molar ratios, and the organic solutions were evaporated to dryness under nitrogen and then lyophilized. The dried mixtures were dispersed in deuterium oxide[4] to the proper concentration. Small unilamellar vesicles were prepared from these dispersions by ultrasonic irradiation[5] until clear dispersions were obtained. French press vesicles were prepared by a previous method (6)[6]. The final concentration of phosphatidylcholine for ^{1}H-NMR measurements was 50 mg/ml.

The drugs were dissolved in deuterated dimethyl sulfoxide[4], and their solutions were added to the prepared liposome dispersions to give the appropriate molar ratio of drug–phosphatidylcholine. ^{1}H-NMR spectra were recorded immediately after sonication[7]. All spectra were recorded without accumulation and under the same conditions of radio frequency (RF) and modulation. The ^{1}H linewidths ($\Delta\nu_{1/2}$) were measured using a spectral width of 10 Hz/cm and sweep rate of 1 Hz/sec and are expressed as the difference between their measured values and the width of the ^{1}H—O—^{2}H signal in the same spectrum. Each result is an average of at least four consecutive scannings under the same conditions of RF and modulation. The experimental errors, indicated in Figs. 1 and 2, represent the deviation of the results from their averages. Care was taken to ensure reproducibility in the base line determination. This was achieved by the use of the base line of the corresponding spectrum determined at a spectral width of 40 Hz/cm.

Figure 1 shows that addition of 1 mole percent of I to sonicated egg phosphatidylcholine vesicles does not change the apparent linewidth of the methylene group signal, whereas in cholesterol-containing vesicles, a small but reproducible narrowing is observed.

The effect of several other cannabinoids on the cholesterol-containing model membranes (Table I) shows a qualitative correlation between the apparent narrowing caused by the various cannabinoids and the psychotropic potency of these drugs. In spite of the difficulties in the interpretation of ^{1}H-NMR linewidths (5, 10, 11), we believe that this apparent narrowing is due to a drug-induced reduction of the restriction of the phospholipid molecular motions. However, other possibilities should also be considered. It may be thought that the signals of some protons are actually broadened by I beyond detection, which would result in an apparent narrowing of the bulk super Lorentzion methylene signal (12). This possibility can be ruled out, since the methylene signals studied are fully detected in all the spectra, as is evident from the constant ratio of intensities of the methylene–choline signals. It is also highly improbable that vesicle–vesicle interactions cause this line narrowing, as the opposite effect is expected from such interactions (5, 13). Thus, it may be concluded that in cholesterol-containing vesicles, I reduces the restriction of molecular motions of the phospholipid hydrocarbon chains. The correlation between the narrowing produced by various cannabinoids in lecithin cholesterol model membranes and the psychotropic potency of these drugs (Table I) supports the hypothesis that the reduction of molecular motion may be relevant to the psychotropic action of the cannabinoids. This is in agreement with an earlier conclusion (3), based on studies of electron spin resonance order parameters.

In an attempt to elucidate the role of cholesterol in this phenomenon, we carried out two additional experiments. First, we measured the effect of I on the apparent linewidth of pure phosphatidylcholine vesicles made by extrusion of the phospholipid through a French pressure cell (8). The latter vesicles are significantly larger than the extremely curved vesicles made by ultrasonic irradiation. Nonetheless, addition of I to the French press vesicles did not cause any narrowing of the proton signals (Fig. 1). This result is

[4] Deuterated solvents were purchased from Merck; deuterium oxide was 99.7% pure, $^2H_6$-dimethyl sulfoxide was 99% pure.
[5] Heat Systems 350W sonicator.
[6] Aminco French pressure cell, American Instrument Co.
[7] NMR measurements were done either on a Jeol JMN-100 spectrometer, operating at 100 MHz or on a Bruker WH-300 at 300 MHz.

Table I—Effects of Cannabinoid on the Apparent Linewidth of the Phosphatidylcholine Methylene Signal in Phosphatidylcholine–Cholesterol Vesicles [a] and their Psychotropic Activities [b]

		Dose, mg/kg	Activity	$\Delta\nu_{1/2}$, Hz
I (−)Δ^1-Tetrahydrocannabinol	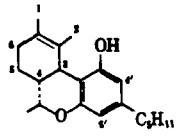	0.05 0.1 0.5	+ ++ +++	−4.8
II (−)Δ^6-Tetrahydrocannabinol	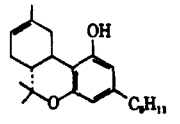	0.1 0.5–0.3 1.0–2.0	● ++ +++	−1.5
III (−)Δ^6-Tetrahydrocannabinol dimethyl heptyl	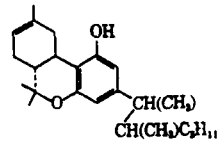	0.05 0.1 1.0	++ +++ +++	−5.5
IV (+)Δ^1-Tetrahydrocannabinol dimethyl heptyl	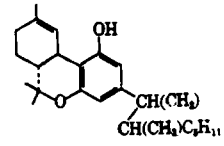	—	—	+2.0
V Nabilone	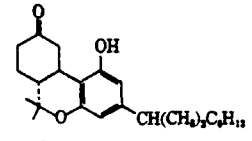			+2.1
VI Cannabidiol	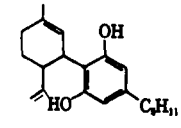	—	—	+2.3
VII Bezoxocin-4-one (2A)	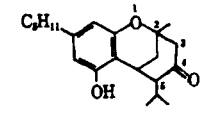	5 10	—	+4.5
VIII Bezoxocin-4-one-dimethyl heptyl(2B)	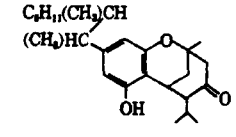	0.25 0.5 1.0	— + +	−1.5

[a] ($\Delta\nu_{1/2}$) had the value of 85 ± 1.5 Hz for phosphatidylcholine–cholesterol (molar ratio 1:2) sonicated vesicles in the absence of cannabinoids but with 0.4% (v/v) dimethyl sulfoxide. $(\Delta\nu_{1/2})_{app}$ is the change in this parameter induced by various cannabinoids. [b] The psychotropic activity of the various compounds for rhesus monkeys as defined previously (9).

similar to that observed for the small vesicles of pure phosphatidylcholine and differs significantly from the result obtained upon addition of the drug to cholesterol-containing small vesicles. In another series of experiments, we studied the dependence of the line narrowing produced by 1 mole percent of I on the cholesterol content of small (sonicated) vesicles. As seen in Fig. 2, introduction of I results in a significant narrowing of the ^{1}H-NMR resonances, provided that the model membrane contains cholesterol.

The dependence of the line narrowing, produced by 1 mole percent of I on the cholesterol content of the membranes (Fig. 2), indicates that for cholesterol contents of ≥40 mole percent, the narrowing is maximal, and the drug reduces the motional restriction of the phospholipid paraffinic chains to the extent obtained at much lower cholesterol concentrations. This is in accord with the idea that the narrowing is not caused by a strong specific interaction with a well-defined stoichiometry between I and cholesterol. It is also consistent with the high-resolution NMR studies of mixed solutions of these components in chloroform (4). Nonetheless, the lack of line narrowing, in the absence of cholesterol in vesicles of larger sizes, suggests that the narrowing in cholesterol-containing vesicles (Fig. 1) is not due only to the tighter basal packing in these vesicles (6).

The role of cholesterol in the interaction of cannabinoid with the model membranes is not clear and will have to be investigated further. Nevertheless, the present results suggest that cannabinoids probably exert their psychotropic effect by altering the physical properties of the lipid matrix of membranes through a mechanism in which cholesterol plays an important role.

(1) R. Mechoulam, A. Shani, H. Edery, and Y. Grunfeld, *Science*, **169**, 611 (1970).

(2) W. D. M. Paton, *Annu. Rev. Pharmacol.*, **15**, 191 (1975).

(3) D. K. Lawrence and E. W. Gill, *Mol. Pharmacol.*, **11**, 595 (1975).
(4) I. Tamir, D. Lichtenberg, and R. Mechoulam, in "Nuclear Magnetic Resonance Spectroscopy in Molecular Biology," B. Pullman, Ed., D. Riedel, Dordene, Holland 1978, p. 405.
(5) N. O. Petersen and S. I. Chan, *Biochemistry*, **16**, 2657 (1977).
(6) D. Lichtenberg, N. O. Petersen, J. L. Girardet, M. Kainosho, P. A. Kroon, C. H. A. Seiter, G. W. Feignenson, and S. I. Chan, *Biochim. Biophys. Acta*, **382**, 10 (1975).
(7) T. E. Thompson and C. Huang, in "Physiology of Membrane Disorders," T. E. Andreali, J. F. Hoffman, and D. D. Fanesti, Eds., Plenum, London and New York, N.Y., 1978 p. 27.
(8) Y. Barenholz, S. Amselem, and D. Lichtenberg, *FEBS Lett.*, **99**, 210 (1979).
(9) R. Mechoulam and H. Edery, in "Marijuana," R. Mechoulam, Ed., Academic, New York, N.Y. and London, 1973, p. 118.
(10) M. F. Brown, G. P. Miliganich, and E. A. Dratz, *Biochemistry*, **16**, 2640 (1977).
(11) P. L. Harris and E. R. Thornton, *J. Am. Chem. Soc.*, **100**, 6737 (1978).
(12) H. Wennerstrom, *Chem. Phys. Lett.*, **18**, 41 (1973).
(13) C. F. Schmidt, D. Lichtenberg, and T. E. Thompson, *Biochemistry*, **20**, 4732 (1981).

Ilana Tamir ˣ
Department of Natural Products
School of Pharmacy
Hebrew University
Jerusalem 91000, Israel

Dov Lichtenberg
Department of Pharmacology
School of Pharmacy
Hebrew University
Jerusalem 91000, Israel

Received March 5, 1982.
Accepted for publication October 14, 1982.
This work was supported in part by the Israel center for psychobiology (Charles E. Smith family foundation).
Professor R. Mechoulam is acknowledged for his interest and the gift of the cannabinoids.

Experimental Evidence for Concentration-Dependent Plasma Protein Binding Effects on the Apparent Half-Lives of Restrictively Cleared Drugs

Keyphrases □ Plasma protein binding—concentration dependent, effects on the apparent half-lives of restrictively cleared drugs □ Pharmacokinetics—experimental evidence for concentration-dependent plasma protein binding effects on the apparent half-lives of restrictively cleared drugs □ Disopyramide—experimental evidence for concentration-dependent plasma protein binding effects on the apparent half-lives of restrictively cleared drugs

To the Editor:

Several early publications have addressed the influence of concentration-dependent (nonlinear) plasma protein binding on the pharmacokinetics of drugs which undergo restrictive clearance (elimination is proportional to free, unbound drug in serum or plasma) (1–3). Relatively simple models which excluded the influence of tissue binding were used to simulate plasma concentrations of free drug (C_f) and of total (free plus protein bound) drug (C_t). More recently, these earlier studies were extended (4) to include models which consider tissue binding and drugs which undergo nonrestrictive clearance (elimination is proportional to total drug in plasma). It was reported that log concentration–time plots of the elimination phase of C_f and C_t for drugs which undergo restrictive clearance may be linear, concave, or convex, depending on the extent to which drugs are bound to plasma and tissue protein (4).

Experimental data verifying the results of these simulation studies in humans are difficult to obtain because of the absence of a model drug which demonstrates concentration-dependent plasma protein binding at plasma concentrations achieved following the administration of safe, therapeutic doses and the absence of an analytical method sensitive enough to accurately measure plasma concentrations for extended time periods following the administration of safe doses of the drug. This is because the behavior of the decay of plasma concentration–time plots may require a wide concentration range to be expressed fully.

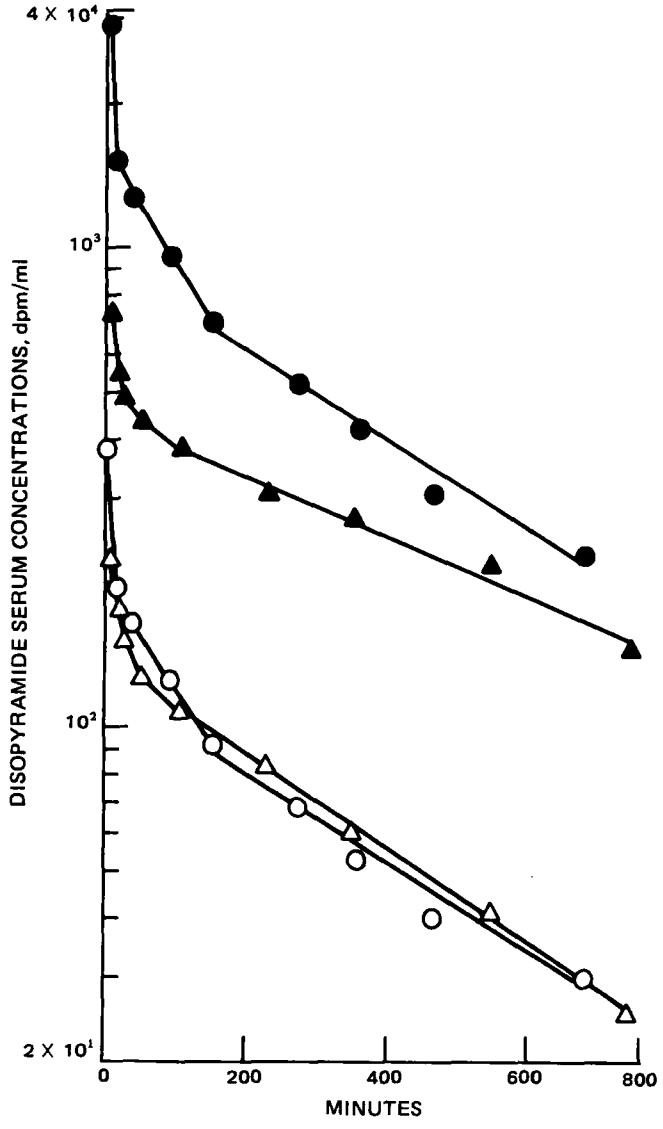

Figure 1—*Free (○,△) and total (●,▲) serum concentrations of [¹⁴C]disopyramide at various times following the administration of carbon 14 alone (○,●) and the simultaneous administration of [¹⁴C]disopyramide and the oral dose (△,▲). In each case a linear regression line was drawn through the last 5 serum concentration–time points.*

0022-3549/83/0400-0461$01.00/0

(3) D. K. Lawrence and E. W. Gill, *Mol. Pharmacol.*, **11**, 595 (1975).
(4) I. Tamir, D. Lichtenberg, and R. Mechoulam, in "Nuclear Magnetic Resonance Spectroscopy in Molecular Biology," B. Pullman, Ed., D. Riedel, Dordene, Holland 1978, p. 405.
(5) N. O. Petersen and S. I. Chan, *Biochemistry*, **16**, 2657 (1977).
(6) D. Lichtenberg, N. O. Petersen, J. L. Girardet, M. Kainosho, P. A. Kroon, C. H. A. Seiter, G. W. Feignenson, and S. I. Chan, *Biochim. Biophys. Acta*, **382**, 10 (1975).
(7) T. E. Thompson and C. Huang, in "Physiology of Membrane Disorders," T. E. Andreali, J. F. Hoffman, and D. D. Fanesti, Eds., Plenum, London and New York, N.Y., 1978 p. 27.
(8) Y. Barenholz, S. Amselem, and D. Lichtenberg, *FEBS Lett.*, **99**, 210 (1979).
(9) R. Mechoulam and H. Edery, in "Marijuana," R. Mechoulam, Ed., Academic, New York, N.Y. and London, 1973, p. 118.
(10) M. F. Brown, G. P. Miliganich, and E. A. Dratz, *Biochemistry*, **16**, 2640 (1977).
(11) P. L. Harris and E. R. Thornton, *J. Am. Chem. Soc.*, **100**, 6737 (1978).
(12) H. Wennerstrom, *Chem. Phys. Lett.*, **18**, 41 (1973).
(13) C. F. Schmidt, D. Lichtenberg, and T. E. Thompson, *Biochemistry*, **20**, 4732 (1981).

Ilana Tamir ˣ
Department of Natural Products
School of Pharmacy
Hebrew University
Jerusalem 91000, Israel

Dov Lichtenberg
Department of Pharmacology
School of Pharmacy
Hebrew University
Jerusalem 91000, Israel

Received March 5, 1982.
Accepted for publication October 14, 1982.
This work was supported in part by the Israel center for psychobiology (Charles E. Smith family foundation).
Professor R. Mechoulam is acknowledged for his interest and the gift of the cannabinoids.

Experimental Evidence for Concentration-Dependent Plasma Protein Binding Effects on the Apparent Half-Lives of Restrictively Cleared Drugs

Keyphrases □ Plasma protein binding—concentration dependent, effects on the apparent half-lives of restrictively cleared drugs □ Pharmacokinetics—experimental evidence for concentration-dependent plasma protein binding effects on the apparent half-lives of restrictively cleared drugs □ Disopyramide—experimental evidence for concentration-dependent plasma protein binding effects on the apparent half-lives of restrictively cleared drugs

To the Editor:

Several early publications have addressed the influence of concentration-dependent (nonlinear) plasma protein binding on the pharmacokinetics of drugs which undergo restrictive clearance (elimination is proportional to free, unbound drug in serum or plasma) (1–3). Relatively simple models which excluded the influence of tissue binding were used to simulate plasma concentrations of free drug (C_f) and of total (free plus protein bound) drug (C_t). More recently, these earlier studies were extended (4) to include models which consider tissue binding and drugs which undergo nonrestrictive clearance (elimination is proportional to total drug in plasma). It was reported that log concentration–time plots of the elimination phase of C_f and C_t for drugs which undergo restrictive clearance may be linear, concave, or convex, depending on the extent to which drugs are bound to plasma and tissue protein (4).

Experimental data verifying the results of these simulation studies in humans are difficult to obtain because of the absence of a model drug which demonstrates concentration-dependent plasma protein binding at plasma concentrations achieved following the administration of safe, therapeutic doses and the absence of an analytical method sensitive enough to accurately measure plasma concentrations for extended time periods following the administration of safe doses of the drug. This is because the behavior of the decay of plasma concentration–time plots may require a wide concentration range to be expressed fully.

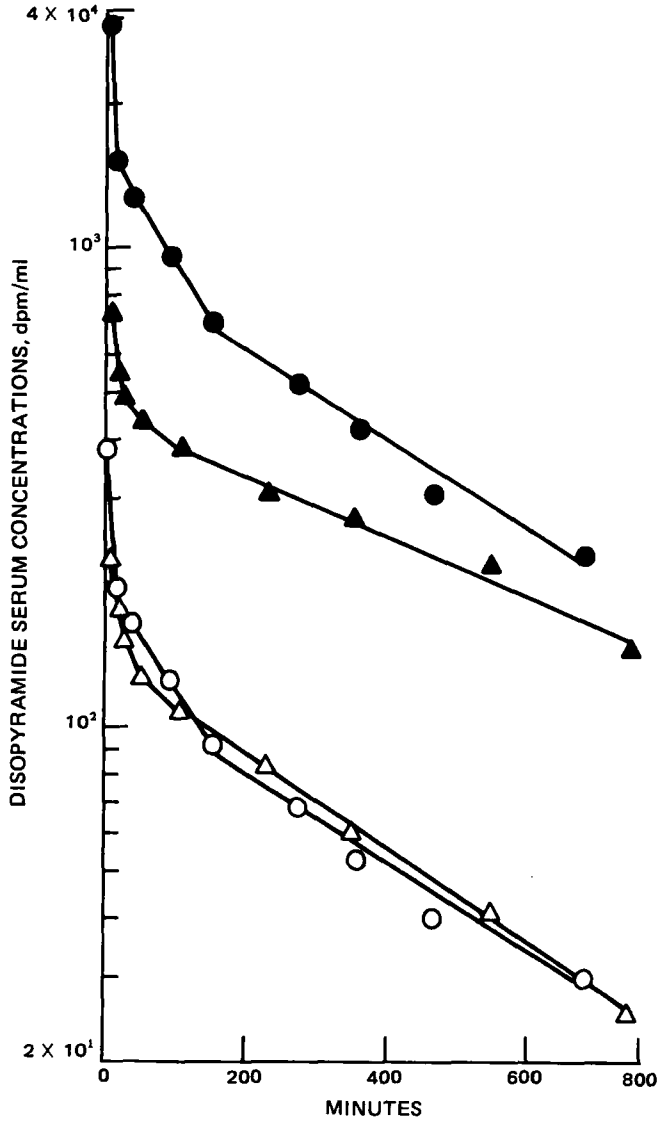

Figure 1—*Free (○,△) and total (●,▲) serum concentrations of [¹⁴C]disopyramide at various times following the administration of carbon 14 alone (○,●) and the simultaneous administration of [¹⁴C]disopyramide and the oral dose (△,▲). In each case a linear regression line was drawn through the last 5 serum concentration–time points.*

0022-3549/83/0400-0461$01.00/0

Table I—Pharmacokinetic Parameters of [^{14}C]Disopyramide

	Total (Bound + Free)				Free		
	Dose dpm	Dose[a], $AUC_{0\to\infty}$ ml/min	$t_{1/2}$[b], hr	V_{ss}[c], liters	Dose[a], $AUC_{0\to\infty}$ ml/min	$t_{1/2}$[b], hr	V_{ss}[c], liters
Tracer alone	2.09×10^7	42.7	5.3	18.0	329	5.3	138
Tracer plus oral dose	1.93×10^7	62.8	7.9	41.3	308	5.0	121

[a] *AUC* refers to the area under the [^{14}C]disopyramide concentration time curve calculated by trapezoidal rule. [b] The parameter $t_{1/2}$ refers to half-life and was calculated by: $t_{1/2} = 0.693/\lambda_z$, where λ_z is the apparent terminal slope of the serum concentration–time plot. [c] The parameter V_{ss} refers to volume of distribution at steady state.

Recent studies show that α-1-acid glycoprotein accounts for most of the plasma protein binding of disopyramide in humans (5, 6) and that plasma protein binding is concentration-dependent following the administration of therapeutic doses to patients (7) and normal subjects (6, 8). Furthermore, the clearance of disopyramide is restrictive (6–8), and pharmacodynamic activity is proportional to C_f (6). The systemic availability of disopyramide has been compared in a small group of patients and normal subjects by the administration of a 150-mg oral dose followed by an intravenous injection of 10 μCi of [^{14}C]disopyramide (specific activity = 4.259 mCi/mmole) (9) 1 hr later. At a later time, one of the normal subjects received a second tracer dose of [^{14}C]disopyramide alone. Prior to each dosing plasma was collected, and the binding of disopyramide was characterized as previously described (6).

Figure 1 compares the serum concentrations of [^{14}C]-disopyramide following the simultaneous administration of tracer and the oral dose with those following administration of just the tracer dose. Values of C_t as determined by liquid chromatography (10) following the simultaneous administration of tracer and oral disopyramide ranged between 2.47 (7.26×10^{-6} *M*) and 0.98 (2.89×10^{-6} *M*) μg/ml, respectively. The corresponding free fractions (*fu*) of the drug in plasma ranged between 0.32 and 0.18, respectively. Values of C_t, which were calculated from the specific activity, ranged between 9.4×10^{-9} and 4.0×10^{-7} *M* following administration of the tracer dose alone. The *fu* at these C_t values was 0.13 and was concentration independent. Table I compares the clearances of free ($Div/AUC^{free}_{0\to\infty}$) and total ($Div/AUC^{tot}_{0\to\infty}$) disopyramide concentrations, their respective half-lives ($t_{1/2}$), and steady-state volumes of distribution (V_{ss}). These data show that the pharmacokinetics of disopyramide calculated based on total serum concentrations are drug concentration dependent, while those based on free disopyramide are concentration independent at the concentration studied (300-fold range). The data also show that the $t_{1/2}$ of C_t is prolonged as compared with the $t_{1/2}$ calculated from C_f values when the plasma protein binding of disopyramide is drug concentration dependent. These data indicate further that as C_f and C_t decrease as a consequence of elimination following the simultaneous administration of the tracer and the oral dose, *fu* decreases to a limiting value, at which time the decay in C_f and C_t are parallel. Thus, the decay in C_t is convex over the drug concentration range achieved in this study.

It was reported (4) that in the absence of tissue binding, the decay in C_t–time data is convex when the ratio of the binding capacity of the drug-binding protein to its dissociation constant is low (low and high ratios of 9 and 100, respectively, were reported) or when tissue binding is moderate to extensive (tissue free fractions of 0.5 and 0.1, respectively, were reported). The ratio of the binding constants characterizing the interaction between disopyramide and α-1-acid glycoprotein in the serum of the subject was ~7.0, and the tissue free fraction was ~0.05 (11). Thus, the convex curvature in the terminal disopyramide C_t–time plot is consistent with previous findings (4) and provides at least some experimental support for the simulation studies described therein. Employment of tracer dose techniques provides another method (12) of examining the influence of concentration-dependent plasma protein binding on the pharmacokinetics of drugs.

(1) E. Kruger-Theimer, W. Diller, and P. Bünger, *Antimicrob. Agents Chemother.*, **5**, 183 (1965).

(2) B. K. Martin, *Nature (London)*, **1965**, 959.

(3) J. J. Coffey, F. J. Bullock, and P. T. Schoenemann, *J. Pharm. Sci.*, **60**, 1623 (1971).

(4) P. J. McNamara, G. Levy, and M. Gibaldi, *J. Pharmacokinet. Biopharm.* **7**, 195 (1979).

(5) J. J. Lima and L. B. Salzer, *Biochem. Pharmacol.*, **30**, 2633 (1981).

(6) J. J. Lima, H. Boudoulas, and M. Blanford, *J. Pharmacol. Exp. Ther.*, **219**, 741 (1981).

(7) P. J. Meffin, E. W. Roberts, R. A. Winkle, S. Harapat, F. A. Peters, and D. C. Harrison, *J. Pharmacokinet. Biopharm.*, **7**, 29 (1979).

(8) D. B. Haughey and J. J. Lima, *Biopharma Drug Disp.*, in press.

(9) D. B. Haughey, C. V. Leier, and J. J. Lima, *Clin. Pharmacol. Ther.*, **31**, 233 (1982).

(10) J. J. Lima, *Clin. Chem.*, **25**, 405 (1979).

(11) M. Gibaldi, G. Levy, and P. J. McNamara, *Clin. Pharmacol. Ther.*, **24**, I (1978).

(12) P. J. McNamara, J. T. Slattery, M. Gibaldi, and G. Levy, *J. Pharmacokinet. Biopharm.*, **7**, 397 (1979).

John J. Lima

Division of Pharmacy Practice
College of Pharmacy and
Division of Cardiology
College of Medicine
The Ohio State University
Columbus, OH 43210

Received March 1, 1982.

Accepted for publication October 28, 1982.

Supported by Grant GM-28420-01 from the National Institute of General Medical Sciences, National Institutes of Health.

1983
Volume 72

JOURNAL OF PHARMACEUTICAL SCIENCES

A publication of the American Pharmaceutical Association

The *Journal of Pharmaceutical Sciences* (ISSN 0022-3549) is published monthly by the American Pharmaceutical Association (APhA) at 2215 Constitution Ave., N.W., Washington, DC 20037. Second-class postage paid at Washington, D.C. and at additional mailing office.

All expressions of opinion and statements of supposed fact appearing in articles or editorials carried in this journal are published on the authority of the writer over whose name they appear and are not to be regarded as necessarily expressing the policies or views of APhA.

Offices—Editorial, Advertising, and Subscription: 2215 Constitution Ave., N.W., Washington, DC 20037. All Journal staff may be contacted at this address. Printing: 20th & Northampton Streets, Easton, PA 18042.

Annual Subscriptions—United States and foreign, industrial and government institutions $75; educational institutions $75; individuals *for personal use only* $40; single copies $10. APhA and SAPhA members may subscribe to *J. Pharm. Sci.* for $20.00 per year. All foreign subscriptions add $10 for postage. Subscription rates are subject to change without notice.

Claims—Missing numbers will not be supplied if dues or subscriptions are in arrears for more than 60 days or if claims are received more than 60 days after the date of the issue, or if loss was due to failure to give notice of change of address. APhA cannot accept responsibility for foreign delivery when its records indicate shipment was made.

Change of Address—Members and subscribers should notify at once both the Post Office and APhA of any change of address.

Photocopying—The code at the foot of the first page of an article indicates that APhA has granted permission for copying of the article beyond the limits permitted by Sections 107 and 108 of the U.S. Copyright Law provided that the copier sends the per copy fee stated in the code to the Copyright Clearance Center, Inc., 21 Congress St., Salem, MA 01970. Copies may be made for personal or internal use only and not for general distribution.

Microfilm—Available from University Microfilms International, 300 N. Zeeb Road, Ann Arbor, MI 48106.

The "Weak Link" in New Drug Research

No matter how critically we might examine the subject, there is no denying that the United States has a very comprehensive set of laws and regulations governing the research, testing, development, manufacture, packaging, promotion, and marketing of new drugs intended for human use. All of this did not come about overnight, nor without various triggering incidents—usually adverse—along the way that prompted Congress to enact new legislation or the Food and Drug Administration to adopt pertinent additional regulations.

The present result is that virtually each of the steps listed above now entails very elaborate, complex facilities, personnel, and equipment. No longer is the drug manufacturing business a viable activity for "the little guy." By yesterday's standards, even the smallest drug companies today are rather large, and they are only "small" in comparison to the giants and near giants that are their "friendly competitors."

For the most part, this development has been a good one because it has resulted in more highly qualified personnel, better equipment, and an overall improved standard of manufacturing performance. Long gone is the "cottage industry" dimension of the U.S. pharmaceutical industry.

At least, long gone in every area except one. And, unfortunately, that remaining area is proving to be the most serious weak link in the entire continuum that eventually leads to the successful marketing of an important new drug.

We are referring to clinical testing, and the fact is that even the largest drug companies conduct very little clinical research themselves. Traditionally, such testing is done by independent clinical investigators affiliated with universities, or teaching hospitals, or operating as very small testing laboratories.

Many disinterested observers have considered this to be a good arrangement; in fact, many of us have regarded it as the preferred one. We have thought that such independence would result in more truthful, reliable, and objective testing and test reporting.

Naturally, as with every aspect of life, we expected that there would be some flaws in this system; that some investigators would be charlatans; and that some drug firms might succeed in getting certain drugs approved that otherwise would not quite make it. Indeed, because of some abuses years ago, the FDA had found it necessary to adopt procedures designed to assure that only qualified investigators are engaged in clinical drug testing; that their facilities, record-keeping practices, and general operating procedures adhere to acceptable standards; and that there is a system for disqualifying, censuring, and permanently barring violators.

But drug testing is far from being an exact science, and despite these safeguards, certain investigators began to develop informal reputations as being far more likely to produce a test report favorable to the drug under study than if it were tested by most other investigators in the field. In turn, this induced at least some drug firms to engage in "investigator shopping." Such "shopping" would not be with the idea of being charged a lower fee for the work, but rather with the objective of benefiting from the conscious or unconscious bias of certain investigators.

But apparently, these personal propensities were equally apparent to the FDA as they were to the drug firms, and most companies quickly concluded that their drugs would fare far better in the FDA review process if they had been tested by one or more of the clinical investigators who enjoy a reputation for being tough critics in their work.

So it appeared that the system—though ever so delicately balanced—would survive and would continue to fulfill its purpose in an acceptable manner.

Sadly, however, the system was recently dealt a severe blow which causes us to reconsider our long-held belief that the independent clinical investigator system must be maintained and preserved at all costs. Specifically, there has been a rash of cases of fabricated or falsified data, and they have come from some very highly respected clinical investigators.

Indeed, the severity of the problem recently prompted *The Washington Post* to run a lead article headlined "FDA, Citing Phony Evidence, Bars Drug Tests by Researcher," and subtitled "Wave of False Medical Experiments." This March 23 article specifically reports on the chicanery of a "leading heart specialist," who is named and quoted in the article.

"The case is one of the most important in a wave of phony medical testing that is raising new concerns in federal health agencies, which rely heavily on such data to help them determine a drug's safety and effectiveness," according to the article in the *Post*.

An NIH staff official is quoted as saying that until about 1980 cases of phony medical research by NIH grantees came up rarely, "perhaps once every other year," but since then such cases "are cropping up so often, they can't be dealt with as isolated events."

The article went on to cite other facts and figures including: (*a*) seven physicians have signed a new type of "consent agreement" with FDA that they will not test future investigational drugs, (*b*) FDA's ruling of eight other physicians as ineligible to receive investigational drugs, and (*c*) several criminal prosecutions of investigators during the past year.

But the article focused on the heart specialist because it pointed out that "(his) prominence, however, makes his case stand out." He was an FDA outside advisor for six years; he was the president of a prominent society of cardiologists; he published over 200 scientific papers; he served as an advisor for 21 professional journals; and he has been a formal "consultant to numerous federal and state agencies, the American Medical Association's Department of Drugs, and the American Heart Association."

Undoubtedly, there are still many honest and reliable clinical investigators. However, these recent experiences show that the present system is no longer reliable, and therefore it is no longer acceptable. If we are misled as to whether the drug entity itself is effective, what purpose is served by elaborate good manufacturing practice requirements, extensive quality control protocols, or scrupulous adherence to rigid advertising limitations? Indeed, the clinical testing is the very heart of the entire process.

Whenever past defects at one point or another in that process have been uncovered, Congress, the FDA, or the scientific community—individually or collectively—have moved to institute corrective changes. It appears that such changes must now be made in this last of the drug-related "cottage industries," if we are to have continued confidence in the effectiveness of our new drug supply.

—EDWARD G. FELDMANN
American Pharmaceutical Association
Washington, DC 20037

0022-3549/83/0500-0463$01.00/0

JOURNAL OF PHARMACEUTICAL SCIENCES

MAY 1983
VOLUME 72 NUMBER 5

LITERATURE SURVEY

Methods for Vascular Access and Collection of Body Fluids from the Laboratory Rat

DAVID M. COCCHETTO [1] **and THORIR D. BJORNSSON** [x]

Received from the *Division of Clinical Pharmacology, Departments of Pharmacology and Medicine, Duke University Medical Center, Durham, NC 27710.*

Keyphrases □ Vascular access—in the rat, literature survey □ Body fluids—collection in the rat, literature survey □ Rat—vascular access, collection of body fluids, literature survey

CONTENTS

> When I first tried animal experimentation for the purpose of discovering the motion and functions of the heart by actual inspection and not by other people's books, I found it so truly difficult that I almost believed with Fracastorius, that the motion of the heart was to be understood by God alone.
>
> —William Harvey, M.D., 1628

INTRODUCTION

The rat has been a useful laboratory animal in virtually every area of biological and medical research since its introduction to the laboratory in adrenalectomy studies in 1856 (1). The history of the development of the rat as a laboratory animal is a fascinating story that has been well presented elsewhere (2, 3). Briggs and Oehme (4) recently provided a very useful summary of the types of pharmacokinetic and toxicological studies commonly conducted to evaluate the safety and efficacy of xenobiotics in the rat.

Pharmaceutical, pharmacological, and toxicological studies of xenobiotics in the rat often require collection of urine, feces, blood, bile, and various other body fluids. A search of the literature was conducted to locate methods for collection of these various fluids and excreta from the rat. The goal of this literature survey is to provide infor-

[1] Employed at the Wellcome Research Laboratories, Research Triangle Park, North Carolina, while part of the background literature search was completed.

0022-3549/83/0500-0465$01.00/0

Table I—Summary of Normal Parameter Values in the Adult Laboratory Rat [a]

Parameter	Normal Range or Mean
Life span	2.5–3 years
Surface area	0.03–0.06 cm^2
Water consumption	80–110 ml/kg/day
Food consumption	100 g/kg/day
Body temperature	37.5°
Gestation	21–23 days
Litter size	8–14 pups
Birth weight	5–6 g
Heart rate	330–480 beats/min
Blood pressure	
Systolic	88–184 mm Hg
Diastolic	58–145 mm Hg
Stroke volume	1.3–2.0 ml/beat
Cardiac output	10–80 ml/min (mean = 50 ml/min)
Plasma volume	36.3–45.3 ml/kg (mean = 40.4 ml/kg)
Blood volume	57.5–69.9 ml/kg (mean = 64.1 ml/kg)
RBC volume [b]	3.63 ± 0.10 ml/100g (mean ± *SEM*)
Respiration rate	66–114 per min (mean = 85.5 per min)
Tidal wave	0.60–1.25 ml (mean = 0.86 ml)
Plasma pH	7.4
Urine pH	7.3–8.5
Albumin Pools [c]	
Extravascular	365 mg/100 g body weight
Intravascular	127 mg/100 g body weight

[a] Values abstracted from Baker *et al.* (20) unless otherwise indicated. [b] Bruckner-Kardoss and Wostmann (53). [c] Sellers *et al.* (56b).

mation that will inform the experimental pharmaceutical scientist regarding available methodologies and aid the experimentalist in choosing the best method for the intended application. In addition, it is hoped that this publication will prove to be a valuable tool for introducing research trainees to the wealth of biological samples and data that can be gathered from the live animal using existing experimental methods.

Periodically, various authors have provided a review of methods in use for laboratory investigation of the rat (5–21). Such updates must be done, since scientists working with rats are constantly developing new apparatus and better techniques with special application to laboratory problems. This ongoing methodology research supports efforts to minimize animal (and scientist) stress and thereby ensure a humane research environment.

Kraus (21) has written the most recently published review of laboratory research methods for the rat. This review (including 672 references) provides a comprehensive introduction to all types of methodology including animal handling, body fluid collection, xenobiotic administration, anesthesia, and euthanasia methods. Excellent reviews of more basic information such as handling methods, laboratory personnel safety, injection procedures (volume, pH, and methods), blood collection techniques, methods for general anesthesia, and techniques for common surgical procedures have been provided by Waynforth (12) and Singh (22). A very useful introduction to basic surgical skills, from proper procedures for donning sterile gloves and gown to stages of anesthesia, has been assembled by Singh (23). The importance of aseptic techniques in rat surgery has been emphasized by Popp and Brennan (24). The reviews of previous authors were used as a gateway to the extensive literature in this area.

This review attempts to gather, for summary and comparative purposes, the literature on methods of vascular access and collection of body fluids for the rat. Papers were selected from the published literature through January 1982. Although extensive literature is summarized, some citations inadvertently may have been omitted. Nonetheless, most available methods are summarized. Since many scientists from diverse fields of study have developed methodologies for the rat, it often is difficult to attribute the origin of a particular method to a specific scientist or laboratory. Therefore, originators of most methods are not identified.

It is widely assumed that the rat is devoid of superficial blood vessels accessible to percutaneous puncture. Therefore, the novice may assume that technically complex surgical methods must be mastered to collect the blood and other biological fluids essential to whole-animal studies. Unfortunately, these assumptions have fostered, by default, a trend toward studies on isolated cells and subcellular fractions when whole-animal studies would be more appropriate. In reality, there are a multitude of surgical and percutaneous methods for acute and chronic vascular access, as well as methods for collection of other biological fluids and excreta.

In this review, summaries of these procedures are outlined in a tabular presentation. In conjunction with the tables, considerations of fundamental methodology are discussed.

GENERAL CONSIDERATIONS IN RAT EXPERIMENTATION

The purpose of this section is to guide the reader to general, but essential, information on the use of rats in laboratory science. Scher (25) has written a concise summary of some factors to be considered in designing any laboratory animal experiment. These factors include selection of the appropriate animal species, writing an experimental protocol, and procedures for data analysis.

Anatomy—Several books illustrating the anatomy of the rat are available (6, 26–31). The most recent of these anatomy texts (31) is very useful in the laboratory as it is a photographic atlas in color. A stereotaxic atlas of the rat brain has been assembled (32). The scientist seeking detailed anatomical information is referred to the atlas compiled by Greene (26). Anatomical structures in this review are referred to using the nomenclature of Greene (26).

The anatomy of specific parts of the vasculature has been summarized by several authors. Halpern (33) provided a well-illustrated, detailed manuscript on coronary circulation in the rat, while Chambers and Zweifach (34) studied the capillary beds of the visceral tissues. Several workers have reported on the collection of blood from the so-called orbital plexus (35–37) or orbital sinus (38–44). The anatomy of the orbital vasculature in the rat has been detailed by Timm (45), who demonstrated the presence of an orbital venous plexus (with no anatomical venous sinus) in the eye. Of the various veins, the caudal–dorsal anastomotic vein is defined as the major anatomical site accessible to venipuncture.

The rat differs anatomically from humans in several respects (46). Cardiac (33) and omental circulations (34) differ from their human counterparts. The rat has a relatively smaller thyroid, brain, and lungs than the human (47). The rat has no gallbladder (26), and is capable of liver regeneration following subtotal hepatectomy (48). In addition, Nairn (49) has demonstrated the presence of a di-

rect transdiaphragmatic pathway for fluid transfer between the peritoneal and pleural cavities.

Physiology—Average values in the rat for organ weights (50), hematological parameters (50–52), blood volume (53), several serum enzymes (54), physiological parameters (20), breeding characteristics (55), and interspecies comparative hematology (56a) have been enumerated and are briefly summarized in Table I. The pathophysiology of aging rats has been recently reviewed (57). A wealth of biological data on the rat were compiled by Donaldson (58). Blood flow to various organs of the rat has been detailed (59, 60). Such data, along with organ–blood flow data in humans, have been used in animal-to-human scale-up methods for physiological pharmacokinetic models (61–64).

The usual nutritional requirements of the rat (65–67) are met by a variety of commercial feeds. The rat has proven particularly useful in nutrition research because it is susceptible to dietary induction of various vitamin and amino acid deficiencies. Newberne (68) discussed the possible influence of dietary factors on pharmacological experiments.

The particular susceptibility of the rat to chronic respiratory disease has been well reviewed (69). Although contraction of human disease from laboratory rats seems to be rare, scientists should be aware of rat-borne infectious zoonotic diseases, reviewed elsewhere (70). The allergic respiratory disease commonly contracted by scientists working with various laboratory animals, including the rat, was detailed by Lutsky and Toshner (71).

Housing—Cages and rooms for housing rats must meet two essential requirements. First, the housing must facilitate maintenance of the health and comfort of the animals. Second, the cages must satisfy the requirements of the specific experiment, *e.g.*, metabolism, restraining, or exercise cages. Current space recommendations for rats are cages of 17.8 cm in height for rats of all weights, with floor surface areas of 110, 148, 187, and 258 cm^2 for rats weighing <100, 100–200, 201–300, and >300 g, respectively (72). The following equation (73) has been used in estimating the floor surface area (A, cm^2) needed for one rat of a given weight (w, g):

$$A = 0.7w + 6\sqrt{w} \qquad \text{(Eq. 1)}$$

A well-ventilated animal room should be maintained at a constant temperature within 20–25°, with relative humidity kept at 50–65% (74). Bedding for rat cages must be selected carefully since the use of softwood chips (*i.e.*, red cedar, white pine, ponderosa pine) can result in the induction of microsomal enzyme activity (75). More specific information on cages and animal rooms can be found elsewhere (6, 72, 74). Metabolism cages are discussed later in this review.

Handling—The rat can be lifted easily by the root of the tail. Since rats seem more at ease when their paws are in contact with something, one easy way to move a rat is by holding the root of the tail and resting the rat's body on the mover's hip (Fig. 1). Rats may also be picked up by slipping a hand over the shoulders to restrain its head between the thumb and first finger (Fig. 2). This procedure can be combined with restraint of a hind limb using the fifth finger of the free hand to provide a hold for intraperitoneal injection (Fig. 3). Pregnant rats should not be lifted by the tail, but either with the support of a hand under the body or with a hand over the shoulders, as described above. Gloves may be useful for momentarily restraining a rat by hand (see *Momentary Restraint*).

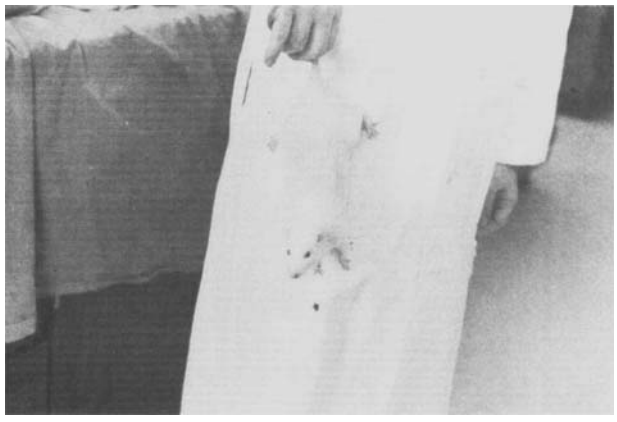

Figure 1—*Illustration of an easy method for moving a rat, without undue animal stress, around the laboratory. The rat usually remains calm while resting against the coat.*

Anesthesia—Surgical anesthesia in rats has been discussed in detail previously (21, 23, 76–82). In addition, laboratory animal scientists are advised to read an informative review of the health risks associated with chronic exposure to various gaseous anesthetics (83a).

In many laboratories, the rat is anesthetized with ether (peroxide-free, anesthetic grade) by the introduction into a large dessicator jar containing an elevated wire-mesh floor and ether, followed by maintenance of anesthesia using a 50-ml beaker containing an ether-moistened surgical sponge placed over the nose of the rat (Fig. 4). More elaborate anesthesia chambers have been described (83b). Ether anesthesia is generally administered for <5 min when brief procedures are performed immediately on the rat. If ether is administered for longer periods of time, the rat is given at least 1 day to recover to avoid experimentation during a time period in which plasma volume may be decreased due to the ether anesthesia (84). Extended (>5 min) exposure to ether vapors will irritate the eyes of the rat. This irritation is indicated in the postoperative conscious rat by increased blinking and grooming of the eyes and head with the forepaws. Topical preoperative application of one drop of an artificial tear preparation[2] to each eye prevents irritation[3].

Although ether is a widely used, reliable anesthetic, maintaining the proper depth of anesthesia requires constant, careful supervision of the rat to avoid respiratory arrest. The depth of ether anesthesia can be difficult to judge, but some useful guidelines have been presented (12). Although ether has been administered by intraperitoneal injection (85), this may cause peritoneal inflammation and adhesions, and therefore is a relatively uncommon route of administration. Several masks and other apparatus for inhalation-anesthetic delivery have been described (86–92). Of these, that described by Stark and Lipman (91) is inexpensive and can be constructed easily from a 135-ml (4.5-oz) plastic specimen jar, a 23-gauge butterfly infusion set, and a 1-ml glass syringe. Such an apparatus is useful

[2] Tears Naturale; Alcon Laboratories, Fort Worth, Tex. Tearisol; Smith, Miller, and Patch, San German, P.R.

[3] Personal communication, David Soda and Gerhard Levy, Department of Pharmaceutics, SUNY at Buffalo, Amherst, N.Y.

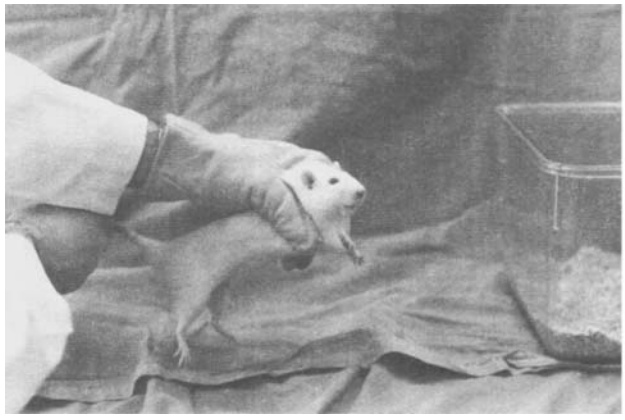

Figure 2—*An over-the-shoulder method for lifting a rat while restricting head movements by crossing the forelimbs under the chin. The leather glove is used in preventing biting by rats not conditioned to this grip.*

for administering halothane[4], ether, or methoxyflurane[5] anesthesia.

Pentobarbital[6] (30–40 mg/kg) administered intraperitoneally is a commonly used anesthetic for the rat (77, 93). Valenstein (94) has provided a table of intraperitoneal injection volumes for anesthesia *via* pentobarbital in conjunction with chloral hydrate. Pentobarbital (21 mg/kg ip) has been advantageously used in conjunction with intramuscular ketamine[7] (60 mg/kg) to induce surgical anesthesia (95). Ketamine has also been used alone (96) for acute drug-induced immobilization to facilitate cardiac puncture (22 mg/kg) and for surgical anesthesia (44 mg/kg), but its use is difficult in view of the highly variable depth of anesthesia induced by a given dose (97). Chloral hydrate (300 mg/kg ip) is still used in some laboratories, despite an ~50% incidence of adynamic ileus after a chloral hydrate administration of 400 mg/kg ip (98). A combination product[8] containing fentanyl (0.4 mg/ml) and droperidol (20 mg/ml) is available for intramuscular injection. Doses of 0.1–0.5 ml/kg have been used to induce surgical anesthesia (99–101). Alfaxalone–alfadolone combination has been used as an intravenous surgical anesthetic (102). Methohexital[9] has proven useful as an intravenous anesthetic for periodic endotracheal intubation of the rat (103).

Figure 3—*Use of the over-the-shoulder grip with the left hand to restrain the head and upper body (note the crossed forelimbs), while restraining via the fifth finger of the right hand the hind limb on the side of the peritoneum to be injected intraperitoneally. The thumb, first, and second finger of the right hand are free to administer the injection (via a syringe of appropriate volume and usually a 23-gauge, 1-in. needle).*

[4] Fluothane; Ayerst Laboratories, New York, N.Y.
[5] Penthrane; Abbott Laboratories, North Chicago, Ill.
[6] Nembutal sodium; Abbott Laboratories, North Chicago, Ill.
[7] Ketalar; Parke-Davis, Morris Plains, N.J. Ketaject; Bristol Laboratories, Syracuse, N.Y.
[8] Innovar-Vet; Pittman-Moore, Indianapolis, Ind.

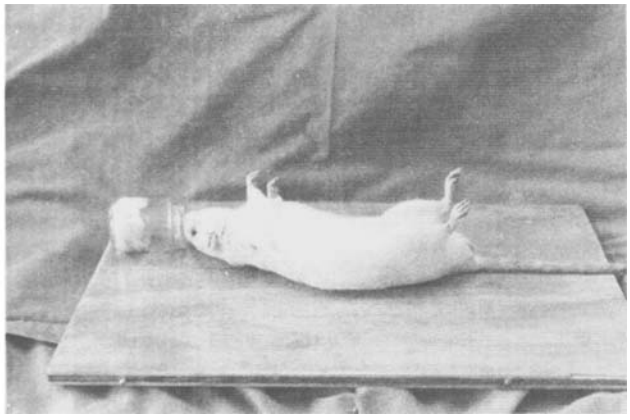

Figure 4—*The rat reclining on a home-built surgical board (41-cm long × 27-cm wide × 1-cm thick plywood painted with polyurethane varnish) while breathing some ether vaporized from an ether-moistened surgical sponge packed in the bottom of a 50-ml beaker. This procedure should be restricted to a fume hood to reduce the flammability risk of ether use.*

Parker and Adams (104) have reviewed the effects of six common anesthetics (α-chloralose, droperidol, fentanyl, halothane, ketamine, and pentobarbital) on cardiovascular function in various laboratory animals. Researchers studying the aspects of cardiovascular function in the rat should find this review helpful in choosing an anesthetic or chemical restraining agent.

Scientists placing animals under surgical anesthesia are advised to keep a resuscitation device available. Two readily constructed resuscitators have been described (105, 106). For rats with an ether overdose, some experimentalists prefer to employ the simple device described by Rassaert (106) as this can be used both to aspirate mucus from the respiratory tract and force air into the lungs. However, the simple two-bulb resuscitator described by Ingall and Hasenpusch (105) has been used successfully. In addition to these resuscitators, Shuer *et al.* (107) devised a simple mask for the artificial respiration of rats *via* a positive-pressure respirator. This procedure avoids the problematic procedures of tracheotomy (78, 108) and endotracheal intubation (103, 109, 110).

Lineberry (111) has recently provided a highly informative review of animal models used in pain research. However, we are not aware of any detailed information on either postoperative assessment or therapeutic management of pain in the laboratory rat. Brief discussions of the general aspects of postoperative care are available (23, 112). Since the majority of scientists working with laboratory rats do not have formal training in veterinary medicine, a detailed review of all aspects of postoperative care would be a valuable contribution to the literature.

Xenobiotic Administration Procedures—Procedures are described elsewhere for administration of substances to the rat *via* the oral, percutaneous, intravenous, intra-

[9] Brevital sodium; Eli Lilly and Co., Indianapolis, Ind.

Table II—Methods of Euthanasia for the Rat

Physical Methods	Chemical Methods
Cervical dislocation	Barbiturates
Decapitation[a]	Carbon dioxide gas
Decompression (oxygen lack)	Carbon monoxide gas
Electrocution	Chloral hydrate
Hemorrhage (aortic transection)[b]	Chloroform
Pneumothorax[b]	*d*-Tubocurarine chloride
Stunning (skull fracture)	Ether
	Gallamine triethiodide
	Hydrogen cyanide gas
	Magnesium sulfate
	Nitrogen gas
	Potassium cyanide
	Strychnine

[a] Rodent guillotines supplied by EDCO Scientific, Inc., Chapel Hill, N.C. and Harvard Apparatus Company, Inc., South Natick, Mass. [b] Method only for use on anesthetized rats.

muscular, intraperitoneal, subcutaneous, intra-arterial, and intracardiac routes (6, 12, 21, 113–115). Shani *et al.* (116) designed a device for the oral administration of gelatin capsule doses to rats. The use of subcutaneously implanted devices (117) and subcutaneous infusions (118) for long-term xenobiotic administration, first applied to rats by Rose and Nelson (117), has been advanced by the commercial availability of uniform osmotic pumps[10]. Novin *et al.* (119) devised an airtight injection system which minimized the need for handling unrestrained rats during injection into an indwelling cannula. Various devices have been constructed to enable intermittent intravenous self-administration of xenobiotics by rats (15, 120–122). Application of this methodology to drug addiction studies in rats has been discussed by Weeks (123).

Three invaluable compendia of drug dosages for the rat are available (124, 125a,b).

Euthanasia Methods—Euthanasia methods are procedures for the painless death of laboratory animals. Useful euthanasia procedures for the rat can be classified as physical methods, *i.e.*, severe body perturbation without administration of a toxic xenobiotic, and chemical methods, *i.e.*, administration of toxic xenobiotics, usually intraperitoneally or by inhalation. The methods outlined in Table II are discussed elsewhere in more detail (126, 127). It is difficult to evaluate the relative humaneness of these different methods. The relative humaneness of gallamine-induced asphyxia and decapitation has been studied in rats by electroencephalographic monitoring (128). Histological changes in the major organs associated with various euthanasia methods (decapitation, carbon dioxide, methoxyflurane, and pentobarbital) and the sympathoadrenal discharge induced in the rat by decapitation have also been documented (129, 130).

If tissues are to be obtained from rats for posteuthanasia study, the scientist is advised to use care in selecting the euthanasia method. For example, *in vitro* drug metabolism studies using various subcellular fractions of rat hepatic homogenates commonly are prepared from liver tissue obtained from rats sacrificed by decapitation (without prior anesthesia) or carbon dioxide asphyxiation. [A chamber for carbon dioxide euthanasia can be readily constructed from a large can (131) or plexiglass[11] (Fig. 5).] Decapitation and carbon dioxide euthanasia avoid the known alterations of microsomal enzyme activity associated with the use of ether (132–136) and other inhalation anesthetics (133, 134). This example illustrates that scientists studying various events in anesthetized rats or in tissues from sacrificed rats must verify the lack of anesthetic or euthanasia-method effect on the experimental events observed.

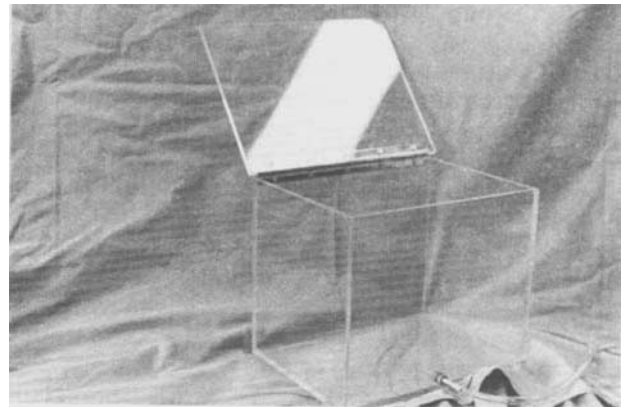

Figure 5—*Plexiglass chamber (0.6-cm thick plexiglass) used for carbon dioxide euthanasia of rats. The base of the chamber is 26-cm long and 19-cm wide, while the chamber is 21-cm high. The top serves as a hinged door and a gas inlet is placed near the bottom of the chamber. The top need not have a gasket seal.*

VASCULAR ACCESS

Methodology Overview—*Cannula Materials*—Vascular cannulas most commonly are constructed of polyethylene[12] or silicone rubber[13] (137, 138). Polypropylene, polyurethane[14], Tygon[15], polytef[16], and Micro-Line[17] tubing have had less use. All of these materials are somewhat flexible, can be molded into desired shapes (139, 140), and have various degrees of physiological inertness. These synthetic materials comprise the main substance of the cannula and are often supplemented by various other materials. Metal connectors are used to link different pieces of tubing or provide a reinforced site to facilitate ligature fixation of the cannula in the vessel (141). An alternative means of joining different pieces of polyethylene tubing consists of welding with a stream of hot air (13, 139). A short piece of flexible, heat-shrinkable polyolefin tubing[18] also can be used to provide reinforcement of the junctions between different tubing pieces or the cannula plug and tubing (13). Although a metal connector is useful for connecting two different types of tubing, such as polyethylene and silicone rubber, it has the disadvantage of promoting thrombotic occlusion of the cannula by both decreasing the cannula lumen diameter (thereby increasing turbulent blood flow distal to the metal connector) and providing a metallic intravascular thrombogenic focus. Therefore, the use of either heat welding or heat-shrinkable tubing is preferred whenever two pieces of the same type of heat-insensitive tubing (polyethylene, polypropylene, Micro-Line) are to be joined.

Methods of Inserting a Cannula in a Blood Vessel—

[10] Alza Corporation, Palo Alto, Calif.
[11] Plexiglass; Rohm and Haas Co., Philadelphia, Pa.
[12] Intramedic polyethylene tubing; Clay Adams, Parsippany, N.J.
[13] Silastic; Dow Corning Corp., Midland, Mich.
[14] Micro-Renathane, Braintree Scientific, Inc., Braintree, Mass.
[15] Tygon; Norton Co., Plastics and Synthetics Division, Akron, Ohio.
[16] Teflon; E. I. DuPont de Nemours and Co., Inc., Wilmington, Del.
[17] Micro-Line; Thermoplastic Scientific, Inc., Warren, N.J.
[18] FPS-Voltrex; Newark Electronics, Chicago, Ill.

Methods of cannula insertion in a blood vessel can be classified three ways: (*a*) two-step puncture and insertion, (*b*) cannula through a needle, and (*c*) cannula attached to a needle. The latter methods are one-step procedures, *i.e.*, puncture of the blood vessel and cannula access to the blood are both accomplished in a single step.

The most commonly used procedures for both arterial and venous cannula insertions are two-step puncture and insertion methods. Ophthalmic Castroviejo iris scissors, microdissecting scissors, or various needles are used to puncture the blood vessel. A needle (25 gauge for aorta, 23 gauge for jugular vein) with a 90° bend ~6 mm from the needle tip is particularly useful. It is inexpensive and readily available, and the tip can be used bevel up to puncture the blood vessel wall with a minimal risk of puncturing the opposite wall (13)[19]. Use of a needle for vessel puncture is often preferable to use of scissors since a needle produces a puncture hole of defined, reproducible size, which cannot be guaranteed using scissors. Using a needle with an outer diameter approximately equal to the outer diameter of the cannula tubing minimizes hemorrhagic leakage from the puncture site. Insertion of the cannula into the puncture hole can be facilitated by gently lifting the lip of the hole with a pair of fine forceps and inserting the cannula into the blood vessel with a slow, gentle rotation of the tip.

Cannula-through-a-needle methods have the advantage of combining the blood vessel puncture and cannula insertion procedures into one step. Physicians and other scientists with clinical training are usually familiar with the various devices marketed to facilitate cannula placement through a needle inserted in a blood vessel.

One device used to cannulate mesenteric veins of the rat was constructed from an ~2.5-cm segment of hollow steel tubing soldered close to the tip of a 1.5-in., 22-gauge needle (the distal third of which was bent at a right angle) (142, 143). Venipuncture with the tip of the 22-gauge needle enabled the cannula to be directed into the vein *via* the steel tubing attached below the needle. Hollow steel tubing[20] of various diameters can be used to accommodate different cannulas. The device can be stabilized to ensure a clean venipuncture by attaching the hub of the 22-gauge needle to a 1-ml syringe. The principle of this device was used in constructing a similar device which consisted of a single needle with the tip bent at a right angle to the remainder of the shaft and a semicircular tunnel in the distal portion (144). Vascular puncture is followed by insertion of the cannula in the lumen of the blood vessel *via* the semicircular tunnel. This has the advantage of facilitating easy removal of the device from the cannula tubing. The previously described device with the fully circular cannulating needle must be passed over the total length of tubing for removal. This creates the inconvenience of having to remove a fluid-containing syringe from the cannula connection to remove the device. Note that in the special case of the caudal (lateral tail) veins, a cannula may be inserted *via* a straight needle used for vessel puncture (145–148).

Cannula-attached-to-needle methods have been useful one-step procedures when placement of a needle within the blood vessel lumen was consistent with the acute nature of the experiment (149–151). The cannula-attached-to-needle method is useful for percutaneous puncture of the caudal artery (152, 153), and external jugular vein (154–156); the former effort may be aided by depilation with sodium sulfide (157). Needle-tipped cannulas have also had limited utility for chronic intermittent injections into the sagittal and transverse sinuses (158) and for chronic blood pressure–multiple blood sampling *via* the caudal artery (159). Due to the increased chance of thrombotic complications associated with the metallic needle tip in the vessel, the cannula-attached-to-needle methods are less preferred than insertion of a conventional metal-free cannula.

One novel cannula-attached-to-needle method warrants attention when the external jugular vein must be cannulated. Harms and Ojeda (160) constructed an implantation needle (20-gauge tip) to which a silicone rubber cannula is attached. The implantation needle (with attached cannula) is passed in and out of the same side of the vein. The implantation needle is disconnected from the cannula tubing, and the cannula tubing is then pulled back into the lumen for advancement to the heart. This method has the advantages of being a one-step procedure, eliminating the need to dissect the vein free from surrounding tissues, and making application of ligatures around the vein unnecessary. This method has proven a useful vascular access for pharmacokinetic studies in rats (161–163).

We are unaware of any application to the rat of the cannula-over-the-needle method used commonly in humans (164).

Methods of Fixing a Cannula in a Blood Vessel—There are four basic methods for fixing the intravascular portion of the cannula within the lumen of the blood vessel: (*a*) ligature to surrounding structures (141, 165, best illustrated in 166), (*b*) ligature around the cannula and through an occluded distal portion of the cannulated blood vessel (167, 168), (*c*) application of cyanoacrylate-type glues for the blood vessel–cannula junction (150, 169–171)[19], and (*d*) fashioning a circular shock-absorbing loop in the cannula tubing between the sites of cannula insertion and ligation to a nearby structure (165)[19]. Use of one or more of these methods should maintain the cannula within the lumen and minimize cannula-mediated abrasion of the intravascular structures. Robinson *et al.* (172) constructed a heating element device for producing a small bead on the outside of polyethylene tubing without altering the lumen. This bead served as an anchor for fixing the cannula in place.

Methods of Exteriorizing the Cannula—Intravascular and other indwelling cannulas (*e.g.*, urinary bladder, bile duct) are commonly exteriorized by subcutaneous tunneling from the vascular incision site to the back of the neck for emergence at a point midway between the clavicles or ears (13, 15, 141, 160, 165, 166, 170, 173–183)[19]. To further secure the exterior portion, the cannula may be passed through a plastic cap or steel button which is sutured to the skin of the neck (166, 177, 180). A modification of exteriorization at the neck is to subcutaneously tunnel the cannula for passage through a cranial pedestal (168, 171, 186–188).

A cannula may also be exteriorized *via* subcutaneous tunneling from the incision site to the root of the tail, where

[19] Methodology notes provided by J. R. Weeks, The Upjohn Company, Kalamazoo, Mich.

[20] Small Parts Inc., Miami, Fla.

the cannula is exteriorized and covered by some type of protective shielding (146, 148, 189–191). Cannulas have also been exteriorized *via* subcutaneous tunneling from the incision site to the side of a rat maintained in a restraining cage (192) or body harness (176).

Methods to Aid in Maintaining Cannula Patency—Various procedures have been used to minimize the incidence of thrombotic occlusion of the intravascular cannulas and to remove existing thrombotic obstructions to prolong the patent lifetime of cannulas. These procedures can be classified into three groups: (*a*) fluid-flushing procedures, (*b*) designs for the intravascular portion of cannulas, and (*c*) procedures for removal of thrombotic obstructions.

Fluid-flushing procedures consist of selection of a solution for instillation in the cannula when it is not in use and a schedule for routine cannula care, *i.e.*, withdrawal of the instilled solution, flushing the cannula to clear it of blood, and refilling the cannula with fresh solution. Six different solutions have been used to fill cannulas: heparin, heparin–povidone mixture, heparin–streptokinase solution, heparin–dextrose solution, isotonic saline, and 50% dextrose in water.

Heparin has been instilled in cannulas in concentrations of 10–1000 U/ml, usually dissolved in isotonic saline (149, 151, 159, 166, 173, 175, 181, 185, 191, 193–204). A localized anticoagulant effect can be obtained with 20 U/ml of heparin. A mixture of heparin–povidone [1 g of povidone plus 2 ml of heparin solution (500 U/ml)] has been used because of its increased viscosity to prevent diffusion of blood into the unused cannula (186). Similar mixtures of heparin–povidone were used without problem by other investigators (168, 187, 205). However, Allsop and Burke (201) found use of this heparin–povidone mixture no better than the more easily handled heparinized (10 U/ml) isotonic saline. Heparin (1000 U/ml) plus streptokinase (200 U/ml) solution was used to maintain patent aortic cannulas for blood pressure monitoring (206). This combination of an anticoagulant and plasminogen-activating agent may be more effective in maintaining patent cannulas than either agent alone. Solutions of heparin (≤500 U/ml) and dextrose (≤10%) have been used in an effort to increase the viscosity beyond that obtained with heparin alone (207, 208). For experiments in which no anticoagulant can be administered to the rat or added to the flushing solution, the two alternatives that have been used are isotonic saline (7, 13, 141, 160, 165, 170, 174, 177, 184, 209–218)[19] and 50% dextrose in water[21].

Schedules for routine cannula care have not been comparatively studied and standardized. In general, increased frequency of cannula care (withdrawal of the instilled solution, flushing the cannula to clear it of blood, and refilling the cannula with fresh solution) should ensure increased long-term cannula patency. Allsop and Burke (201) and Brown and Breckenridge (168) have provided detailed descriptions of a cannula-care schedule consisting of the following:

1. Initial aspiration of fluid from the cannula. This fluid is discarded since reinjection carries the risk of introducing aspirated thrombi.
2. Injection flushing of the cannula with a volume of solution slightly larger than the volume of the cannula as calculated by:

$$V = \pi r^2 l \qquad \text{(Eq. 2)}$$

where V is the volume, r is the radius, and l is the length of the cannula.
3. Sealing the exteriorized end of the cannula with a segment of steel stylet (13) or an epoxy-filled blunt-end needle (201).

These investigators recommended that cannula care be done once a day for the patent lifetime of the cannula. Such daily cannula servicing is useful for other types of aortic and jugular cannulas (204, 207). Based on these proven procedures, cannulas intended for chronic use should be serviced daily when not in use.

Designs for the intravascular portion of cannulas have been proposed as means of minimizing thrombotic occlusion. Simple beveled and nonbeveled cannula tips, a double-mitered cannula tip, a sealed cannula tip with laterally placed holes, and an open cannula tip with laterally placed holes have been designed. Commonly, the open end of the vascular cannula is fashioned with a 90° angle to the tubing wall (no bevel) or a 30–60° angle of the bevel.

While most investigators agree that a beveled end is more easily inserted in the blood vessel, it has been reported (*via* anecdote) that the beveled end can be occluded more readily by a flap of thrombotic material deposited over the bevel and also may rest more readily against the blood vessel wall, thereby inhibiting blood sampling (13). Scientists having difficulty maintaining cannula patency with a beveled or nonbeveled tip may consider using an alternative type of cannula tip. Nicolaidis *et al.* (187) designed a double-mitered silicone rubber cannula tip which is reported to effectively minimize local coagulation. Steffens (186) cut two 0.75-mm holes in the opposite lateral walls 0.75 mm from the tip of a silicone-rubber cannula with an open-lumen tip. Stripling (171) plugged the intravascular end of a silicone rubber cannula with hardened silicone rubber adhesive and made holes near this plugged tip by puncturing through both cannula walls six times with a 25-gauge needle. This type of cannula tip is said to comprise a one-way valve which allows drug infusion, while preventing entry of blood into the cannula (219).

Procedures for removal of thrombotic cannula obstructions can be classified in three categories: (*a*) aspiration of the obstruction, (*b*) forceful injection of the obstruction into the circulation of the rat, and (*c*) use of an obturator that fits in the cannula lumen to mobilize the obstruction. Before using any of these procedures for clearing an obstruction in a venous cannula, one can verify that the cannula is still inside the vein by injecting rapidly 3–6 mg (0.05–0.10 ml of a 60-mg/ml solution) of pentobarbital sodium (13), 1 mg (0.10 ml of a 10-mg/ml solution) of methohexital sodium[19], or thiamylal sodium[22] (15). If the cannula is out of the vein, the rat may struggle or vocalize, or the fluid may accumulate in a subcutaneous pocket with only clear fluid (no blood) aspirated (13). If the barbiturate injection is indeed intravenous, the eyes of the rat will squint closed almost immediately, the rat will lose its righting reflex, and the rat will become ataxic

[21] Personal communication, J. E. Brown, Division of Clinical Pharmacology, Duke University Medical Center, Durham, N.C.

[22] Surital; Parke-Davis, Morris Plains, N.J.

within ~10–15 sec. The rat normally recovers completely within ~5–10 min. When this procedure shows that the cannula is indeed in the vein but blood withdrawal is still difficult, flexing the head and neck of the rat or lifting it by the root of the tail so that only the forelegs touch the cage floor may aid in moving the cannula tip from against the blood vessel wall, thereby facilitating blood withdrawal. If these simple maneuvers do not work, one of the three aforementioned procedures can be tried.

Since thrombotic material can accumulate on the intravascular end of arterial and venous cannulas, it is suggested that blood be withdrawn through the cannula prior to injection to aspirate any small thrombotic obstruction (168, 201). The blood initially withdrawn should not be reinjected since it may contain small thrombi. Forceful injection of 0.10–0.15 ml of isotonic saline *via* a 0.25-ml tuberculin syringe will often break up and clear a thrombotic obstruction in a jugular venous or abdominal aortic polyethylene cannula (13, 165)[19]. The small emboli mobilized as a result of this procedure will usually be trapped in the vasculature of the lungs and legs when ejected from the external jugular vein and abdominal aorta, respectively (13)[19]. Lastly, various homemade wire or nylon obturators can be slid down the lumen of some cannulas to mobilize the obstruction. The utility of thin wire is limited by its relative inflexibility and high potential for cannula puncture. In view of this, use of wire obturators often has been limited to relatively straight cannulas implanted in the caudal vein or artery. Brown and Breckenridge (168) described a very useful and flexible obturator made from 25-pound test monofilament nylon fishing line fashioned with a ball on the end made by holding it close to a hot soldering iron. This seems relatively unlikely to puncture the cannula. Indeed, Brown and Breckenridge (168) used this obturator to clear obstructions from a curved silicone-rubber cannula implanted in the external jugular vein.

Swivel Joints—In chronic rat experiments in which xenobiotics are injected intermittently or continuously *via* the intravenous or intraventricular route, the duration of the experiment is usually limited by cannula damage (twisting and kinking) due to the physical activity of the rat. For reasons discussed elsewhere in this review, such experiments can not be executed during sustained anesthesia or restraint. Therefore, the swivel joint was introduced to prevent such motion-related cannula damage and enable chronic xenobiotic administration and blood sampling *via* indwelling cannulas in the unanesthetized, unrestrained rat. Jacobs (220) appears to be the first investigator to have devised a swivel joint for administration of a constant-rate intravenous infusion to the dog for up to 3 weeks. In principle, this and other swivel joints are fluid-tight, flow-through joints placed into the tubing near the point of emergence from the rat (back of the head or neck) so that the tubing proximal to the rat rotates within the swivel joint as the rat moves, thereby preventing cannula damage by twisting. Rhode *et al.* (221) inserted a circuit of flexible, rotatable tubing between the dog and the infusion bottle. Epstein and Teitelbaum (222) commented that such an arrangement will not work for the rat, a more active species.

Several home-built swivel joints for use with rats have been described in the literature (15, 174, 179, 186, 187, 222–233). The utility of these various devices is based on the comparative ease of construction, availability of components, cost, durability, size, force required to rotate the swivel, tendency to leak, and requirements for periodic cleaning and lubrication.

Several single-channel swivel joints are relatively inexpensive to construct with hand tools from widely available materials. These single-channel swivel joints function well (224, 225, 227, 229, 232). The single-channel swivel of Strubbe (227) was designed to minimize friction for improved utility with small-diameter tubings. While most of the single-channel swivel joints require at least one polytef component, that of Brown *et al.* (229) was constructed solely from parts of plastic syringes, disposable needles, and epoxy adhesive. Khavari (225) constructed a combined intracerebral cannula–swivel unit for use in the rat.

Double-channel swivel joints have been devised to enable either simultaneous infusion of two different fluids into the same rat, simultaneous infusion and blood pressure recording, or simultaneous infusion and blood sampling. Some double-channel swivel joints require special machining during construction (187), a motor to rotate the swivel (234), or apparent supernormal manual dexterity for assembly (233). Smith and Davis (15) described assembly of two single-channel swivel joints from commercially available parts. Blair *et al.* (231) have supplied details for construction of an inexpensive double-channel swivel joint. This construction does not require any machining of parts and uses readily available materials. Testing verified that there were no leaks between the two channels after 4 weeks of continuous use. Another easily constructed double-channel swivel joint has been described, but leak-test information was not provided (232).

Since available swivel joints can not accommodate the arterial blood back-pressure (~100 mm Hg) without leaking, Grantham *et al.* (235) designed a nonswivel spring system for use with a special cage in order to infuse drugs intra-arterially. Where the tubing emerges from the spring at the end distal to the rat, a long unencumbered loop of tubing hangs outside the cage. This absorbs the movements of the rat without kinking for ~1 day. With daily uncoiling of this tubing loop, continuous intra-arterial infusions have been done for 2 weeks.

Complications of Vascular Access—A limited amount of information is available regarding complications in the use of an indwelling vascular cannula or percutaneous vascular access in laboratory animals. Despite minimal gross indications of ocular damage, localized and reversible necrotizing inflammation of the Harderian gland develops following collection of a single blood sample from the retro-orbital venous plexus (236). The degree of thrombogenicity of some artificial (*i.e.*, nonphysiological) substances has been studied using various *ex vivo* models (237–239). Unfortunately, insufficient information is available to enable recommendation of one type of tubing over another based on inertness toward tissues.

In 22 animals (dog, cat, rabbit, and monkey) with an indwelling cannula, Hysell and Abrams (240) identified vegetative deposits on the cardiac valves, septic visceral infarcts of the kidney, spleen, and brain, and fatal hemorrhage due to a ruptured vein or artery. In all three types of cannula-related lesions, systemic bacterial infection

played an important role in the animals' deterioration. Inadequately sterilized cannulas, nonadherence to aseptic technique when injecting or withdrawing from the cannula, and infection *via* the point of exteriorization are the apparent means of bacterial access to the vasculature.

Meuleman *et al.* (241) inserted a polyethylene cannula into the abdominal aorta *via* the carotid artery to study cannula-associated platelet consumption in the rat. Platelet count and the half-life of ^{51}Cr-labeled platelets were both significantly decreased in cannulated rats compared with stressed control rats (cannula inserted, then immediately withdrawn); the degree of decrease was related to the length of the inserted cannula. Platelet turnover did not differ substantially between cannulated and control rats. These investigators have also reported aortic endothelium loss due to the presence of an indwelling cannula (241). Aortic lesions in rats having polyethylene cannulas implanted for 48 hr were also documented, and used to assess antiplatelet drug efficacy (242).

Some investigators using indwelling intravascular cannulas in the rat for various pharmacological studies have reported renal infarcts after cannulation of the carotid artery and abdominal aorta with polyethylene, polypropylene, or silicone rubber tubing (177, 201, 206). Frequency of renal infarction increased with time (177) and with injection flushing of the cannula to force thrombotic blockage into the circulation (201). Polyethylene-tipped cannulas present in the carotid artery for an average of 7.2 days were associated with renal infarcts in 11 rats (n = 15, infarction rate = 10.2% per catheter day), while silicone rubber-tipped cannulas inserted for an average of 11.5 days were associated with small, solitary renal infarcts in 10 rats (n = 25, infarction rate = 3.5% per catheter day) (201). Renal infarcts occurred in association with polyethylene-tipped cannulas even when no injection flushing was done (201). Since arterial cannulation of either the carotid artery or abdominal aorta is used commonly for serial blood sampling in pharmacokinetic studies in the rat, investigators must exercise appropriate caution (in accordance with the following five recommendations) to ensure that data is not collected from rats with impaired renal function. First, a decreased incidence of renal infarction was reported by Engberg (177) when a 12-mm intraaortic segment of polypropylene was inserted into the abdominal aorta at a point 3–4 mm above the iliac bifurcation. Second, the significantly reduced incidence of renal infarcts with silicone rubber tubing suggests that it should be preferred for carotid cannulation (201). Third, thrombi mobilized from the tip of the catheter can deposit in the kidneys. Therefore, it is suggested that blood be withdrawn through the cannula to clear such small thrombi prior to injection (168, 201). Fourth, the anchoring of a polyethylene abdominal aortic cannula alongside the aorta using a circular shock-absorbing loop in the tubing has been reported to virtually eliminate thrombotic infarctions and aortic aneurisms (165)[19]. Fifth, postexperiment necropsy of the kidneys should be done to ensure collection of pharmacokinetic data from rats with noninfarcted kidneys.

Thrombotic deposits on cannulas can also be mobilized as emboli to areas other than the kidneys. Buñag *et al.* (206) observed embolic paralysis of the hind legs of some rats having an indwelling cannula inserted in the abdominal aorta *via* the left iliac artery. Although this is apparently the only published observation, such limb paralysis has also been observed in rats following cannulation of the ipsilateral femoral vein and artery[21]. This complication should be carefully examined with respect to its ability to interfere with the experimental goals. Interestingly, limb paralysis has not been a major problem when the abdominal aorta is cannulated directly, thereby avoiding direct occlusion of the femoral or iliac arteries by a cannula[19].

Investigators using vascular cannulation methods as a means of xenobiotic administration, blood sampling, or cardiac function monitoring must remain aware of the aforementioned complications associated with indwelling intravascular cannulas. Appropriate steps must be taken both to minimize the incidence and verify the absence of such complications *post facto*.

Specific Methods for Vascular Access—To provide a more detailed summary of the numerous methods available for vascular access in the rat, methodological notes, procedural comments, and the demonstrated uses (243–294) were collected into separate tables for arterial (Table III), venous (Table IV), and miscellaneous (Table V) methods. Each table is organized by specific blood vessels, listed alphabetically according to the blood vessel nomenclature presented by Greene (26). It is hoped that scientists seeking information on access to a particular blood vessel will find these tables sufficient to enable them to limit the number of cited papers to be consulted for detail. In addition, this listing should inform scientists about published access methods for infrequently utilized blood vessels (*e.g.*, renal artery, adrenal vein) and thereby eliminate the need for an extensive noncomputerized search of the scientific literature, which is often 20–30 years old.

Although they are not presented in detail, several methods are available for cross-transfusion of blood between a pair of parabiotic rats (295–300). Such methods are useful in specialized studies investigating the association of particular effects with various blood-borne substances.

Investigators must be aware that certain parameters in the rat (plasma glucose concentration, blood coagulation parameters, plasma corticosterone concentration, plasma renin activity, serum hormone concentrations, serum enzyme activities, and drug binding to plasma proteins) may vary depending on the site and method of blood collection (301–307), the extent of rat handling (301, 308), acclimatization time (309), and the presence of another previously treated rat (310).

Vascular Access and Surgical Methods for Studying First-Pass Effect—First-pass effect is defined as the uptake and elimination of a xenobiotic during the absorption process as it passes from the lumen of the GI tract through the GI membranes and the liver for the first time, and into the circulation. Such first-pass elimination of xenobiotics can be studied in the rat by three methods: (*a*) transhepatic blood sampling, (*b*) hepatectomy, or (*c*) surgical construction of a vascular bypass to shunt blood away from the portal venous hepatic inflow (portal–systemic shunt).

Transhepatic Blood Sampling—The hepatic artery carries oxygenated blood from the aorta to the liver and supplies ~25–30% of hepatic blood flow in the cat, dog, and

Table III—Methods for Arterial Access

Arterial Site	Reference	Methodology Notes[a]	Demonstrated Uses[b]	Procedural Comments
Aorta:	Browning *et al.* (197)	PE, U, W	BP, CO	Cannula filled with heparin
	Buñag *et al.* (206)[c]	PR, TE/TY, U	BP	Cannula filled with heparin (1000 U/ml) plus streptokinase (200 U/ml)
	Carvalho *et al.* (215)[c]	PE, U, UR, W	M	Cannula filled with isotonic saline, used for 9 days
	Cocchetto & Bjornsson (unpublished)	Aortic puncture	T	Direct puncture of surgically exposed aorta just above the iliac bifurcation using a 20-ml syringe with a 20-gauge, 1.5-in. needle; anticoagulant can be in the syringe; collect up to 15 ml of blood from adult rats
	Garthoff & Towart (243)	PE, U, UR	BP	Continuous recording of BP and heart rate; data shown for 8-hr recording; requires special data collection equipment
	Kleinman *et al.* (213)	PE, U, UR	I, M	Cannula filled with isotonic saline, patent for up to ~22 days
	Laffan *et al.* (244)	PE, U, UR, W	BP	Continuous recording of BP; data gathered for 10 hr; requires special data collection equipment
	Lushbough & Moline (245)	Aortic transection	T	Reported blood yield 3% of body weight
	McIlreath *et al.* (214)	PE, U, UR, W	BP	90% surgical survival rate; cannula patent for weeks, filled with saline
	Popper *et al.* (207)	PE, TR, U, UR, W	BP, M	Cannula filled with 10% dextrose solution plus heparin (500 U/ml); used up to 10 days
	Purdy & Ashbrook (208)	PE, U, UR, W	BP	Cannula filled with 5% dextrose solution plus heparin (10 U/ml); spring attachment screwed into skull; cannula failure by 3 weeks
	Still (209); Still & Whitcomb (210, 212); Still *et al.* (211)	PE, TR, U, UR	BP, I, M	Cannula filled with isotonic saline; used up to 2 weeks
	Weeks & Jones (165)	PE, TR, U	BP, I	Cannula filled with isotonic saline, used up to 6 months; 80% surgical success rate, excellent photographs of surgical field by Stanton (501)
	Weeks (170)[19]	PE, TR, U, UR	BP, I, M	Extensive modifications of original method (165); 50 and 10 of 55 cannulas patent for 4 and 12 months, respectively; cannula fixed in vessel using cyanoacrylate glue
Carotid:	Allsop & Burke (201)	PE/SI, U, UR	M	Cannula filled with heparinized (10 U/ml) isotonic saline; 10 of 25 rats had renal infarcts after an average of 11.5 cannula-days
	Bullard (193)	PE, TR, U	BP, CO, M	Heparin given to inhibit clotting in cannula
	Buñag *et al.* (206)	PR, U	BP	Cannula failed after 7–14 days
	Burt *et al.* (204)	PE, U, UR	M	Surgery done aseptically; cannula filled with heparinized (20 U/ml) isotonic saline, patent for 3 weeks for five test rats; special swivel assembly
	D'Amour *et al.* (194)	PE		Cannula filled with heparin (1000 U/ml); excellent photographs of procedure
	Garthoff & Towart (243)	PE, U, UR	BP	Continuous recording of BP and heart rate; data shown for 8-hr recording; requires special data collection equipment
	Grantham *et al.* (235)	PE, PR, U	I	Continuous intra-arterial infusion for up to 2 weeks; cannula filled with heparinized saline
	Popovic & Popovic (173)	PE	M	Cannula filled with heparinized physiological solution; average cannula lifetime of 22 days
	Scharschmidt & Berk (246)	A, PE	M	Used a needle-three-way stopcock device for drawing blood samples up to every 30 sec
	Staub & Coutris (218)	PE, U, UR	M	Cannula filled with isotonic saline, consists of an exteriorized shunt of carotid arterial blood; 80% patent for 2–4 days, 20% patent for 5–7 days
	Waeldele & Stoclet (205)	PE/SI	BP, I, M	Cannula filled with 40% povidone plus 10% heparin; used for 10 days
Caudal:	Agrelo & Dawson (159)	N/PE, U, UR	BP, M	Cannula filled with heparinized (1000 U/ml) isotonic saline; used for up to 4 weeks
	Chiueh & Kopin (202)	PE, U, UR	BP, I, M	Cannula filled with heparinized (500 U/ml) isotonic saline; patent up to 2 weeks
	Fujita & Tedeschi (196)	PE, TR, U	BP	Cannula filled with heparinized (10 U/ml) isotonic saline; used up to 48 hr
	Hurwitz (152)	A, N, P	M	Percutaneous puncture using a clear-hub 21-gauge needle; each sample was 420 μl
Femoral:	Ekelund & Olin (247)	PE		Radiopaque cannula inserted in the aorta, superior mesenteric artery, or renal artery *via* the femoral artery; requires angiographic verification of cannula location
Hepatic:	Leivestad & Malt (248)	PE, PR, U	I	Cannula inserted with aid of magnification, exteriorized after subcutaneous tunnel to tail; rear of the animal is restrained to protect the cannula; patent up to 6 weeks
Pulmonary:	Carrillo & Aviado (249)	A, PE	BP	Cannula inserted *via* the right jugular vein
	Forrest *et al.* (250)	A, PP	BP	Cannula inserted *via* the right jugular vein; cannula is a No. 4 French gauge, balloon-tipped, Swan-Ganz flow-directed catheter; used in the rabbit and guinea pig, perhaps adaptable to the rat
	Hayes & Will (251)	A, TE	BP	Specific bends must be made in cannula; cannula inserted *via* the jugular vein in a closed-chest rat
	Herget & Paleček (252)	A, PE	BP	Cannula inserted *via* right jugular through an introducer; illustrates the use of blood pressure waves to monitor catheter tip position; cannula filled with heparinized saline
	Rabinovitch *et al.* (253)	SI, U, UR	BP	Cannula flushed with heparin (20 U/ml) and animal heparinized (150 U/kg) daily; inserted *via* a 19-gauge needle introducer
	Stinger *et al.* (254)	A	BP, CO	Cannula was a commercially available No. 3-½ French umbilical vessel catheter, inserted *via* the jugular vein in a closed-chest rat

continued

Table III—*Continued*

Arterial Site	Reference	Methodology Notes[a]	Demonstrated Uses[b]	Procedural Comments
Renal:	Beuzeville (195)	A, PE	I	Cannula filled with heparinized (10 U/ml) isotonic saline; patent up to 48 hr
	Evans & Nikitovitch (255); Evans (256)	PE, U, UR	I	Cannula exteriorized at the back of the neck *via* a plastic cap sutured to the skin

[a] Methodology key: (A) postoperative experiment on anesthetized rats; (N) needle inserted into blood vessel, with tubing attached to needle; (P) percutaneous method; (PE) polyethylene cannula; (PP) polypropylene cannula; (PR) postoperative experiment on partially restrained rats; (SI) silicone rubber cannula; (TE) polytef cannula; (TR) postoperative experiment on totally restrained rats; (TY) Tygon cannula; (U) postoperative experiment on unanesthetized rats; (UR) postoperative experiment on unrestrained rats; (W) modification of the method of Weeks and Jones (165). [b] Key for demonstrated uses and procedural comments: (BP) blood pressure determination; (CO) cardiac output determination; (I) injection; (M) multiple blood sampling with rat survival; (S) single blood sample with rat survival; (T) terminal blood sample. [c] Cannula threaded into the aorta *via* the iliac artery.

human (311). In addition to this arterial blood flow, the liver also receives blood from the visceral organ vasculature *via* the portal vein. Portal venous blood comprises 70–75% of hepatic blood flow in the cat, dog, and human (311). Blood is returned to the inferior vena cava *via* the hepatic vein. Hepatic hemodynamics and blood pressures at various locations in the inferior vena cava of the rat have been determined (312).

To study the first-pass effect with respect to a specific orally administered xenobiotic, the concentration of the xenobiotic in both portal and hepatic venous blood must be determined. Since the hepatic venous blood concentrations of a xenobiotic and associated metabolites are equivalent to that in venous blood collected from other peripheral veins (*e.g.*, external jugular, femoral, caudal) if there is no interposed organ that further metabolizes these substances, a technically easier procedure for transhepatic blood sampling is cannulation of the portal vein plus a femoral or caudal vein. Several methods (Table IV) have been described for collection of blood from each of the above vessels. An excellent example of such transhepatic blood sampling methodology is in the first-pass metabolism studies of clonazepam in the rat (313). Transhepatic blood sampling after oral xenobiotic administration is, of course, sensitive to first-pass effects due to the gut contents and GI wall as well as the liver. By infusing a xenobiotic directly into the portal vein, the first-pass effect due to the liver alone can be quantified. Several exemplary applications of this method are available for review (283, 285, 314, 315).

Hepatectomy—Hepatectomized laboratory animals have been used to construct animal models for liver disease-associated coagulopathies (316), abnormalities in amino acid transport (317), alterations in the brain uptake of glucose (318), abnormalities in drug disposition (319), and evaluation of the existence of extrahepatic drug elimination processes (320). Surgical procedures have been described for the excision of part or all of the liver (subtotal and total hepatectomy, respectively) and the production of acute functional exclusion of the liver from its normal vascular connections while leaving the nonfunctional liver in the body (exclusionary hepatectomy).

Higgins and Anderson (48) surgically excised the large median and left lateral lobes of the liver in rats, removing ~65–75% of the total liver mass (thus the name two-thirds hepatectomy) in a one-step procedure. Illustrations of this procedure are available (12). Interestingly, the remaining right lateral and caudate lobes of the liver underwent compensatory hypertrophy so that the liver essentially was restored to its preoperative weight after 10–14 days. Approximately 16 and 24% of the excised liver mass is restored within 24 and 48 hr of removal, respectively. Therefore, rats used within 48 hr after two-thirds hepatectomy can be useful in studies of drug disposition in the presence of impaired hepatic function (319). Selye and Dosne (321) extended this subtotal hepatectomy by excising the median, left lateral, and right lateral lobes in order to remove ~85% of the total liver mass. Ryan *et al.* (322) performed two-thirds hepatectomy in rats between noon and 3 pm to avoid variation in mitotic activity due to diurnal rhythm (323). Higgins and Anderson (48) calculated the ratio of total liver–whole body weight equal to 0.0358 for 30 rats weighing from 125–225 g. This number is particularly useful in estimating the number of rats in this weight range needed to supply a required amount of hepatic tissue for *in vitro* hepatic microsomal metabolism studies.

Total hepatectomy in laboratory animals can be performed using two- and three-stage surgical procedures where a portion of the total procedure is performed at each stage and the animal is allowed to partially or totally stabilize between stages. Such multiple-stage procedures allow a period of time after constriction of the portal vein and inferior vena cava for development of collateral circulation, thus minimizing engorgement of the abdominal organs during the last stage of total hepatectomy. Although the three-stage procedure (portal vein-to-inferior vena cava anastomosis, portal vein ligation proximal to the liver, and total hepatectomy) has proven useful in the dog (324), it has not been used in the rat.

Two-stage hepatectomy (portal vein and inferior vena cava constriction, then total hepatectomy) can be performed in the rat using silk ligatures as per the method of Meehan (325). Alternatively, Bollman and Van Hook (326) used a strip of cellophane in place of the silk ligature placed around the portal vein. The cellophane progressively constricts over a period of ~2 months, at which time total hepatectomy can be done. In each method, the minimum size of the portal venous constriction produced in the first stage is crucial in preventing rapid, fatal congestion of the visceral vascular bed. With an intravenous infusion of glucose following hepatectomy (150 mg/kg/hr for 8–10 hr then 250 mg/kg/hr, using a solution of glucose in isotonic saline infused at 1.25 ml/hr), ~90 and 60% of the rats survive at least 8 and 24 hr, respectively (326). Glucose can also be administered by intermittent subcutaneous injections (325). Rats treated with glucose rarely live >30 hr after hepatectomy; those not receiving glucose rarely survive >2 hr (325).

Exclusionary hepatectomy is useful for acute studies in

Table IV—Methods for Venous Access

Venous Site	Reference	Methodology Notes[a]	Demonstrated Uses[b]	Procedural Comments
Adrenal:	Schapiro & Stjarne (257)	A, PE, S	M	Uses an artificial adrenal vein–renal vein shunt, for up to 6 hr; heparin used to inhibit clotting
	Singer & Stack-Dunne (258)	A, S	T	Adrenal vein blood collected continuously for 1.5 hr; no nephrectomy; cannula construction and insertion procedure not described
Brachial:	Young & Chambers (259)	S	T	Brachial artery and vein are severed with blood collection in a pipet; developed for the mouse, probably useful for the rat
	Slusher & Browning (260)	PE, S, U, UR	M	Cannula inserted through a 19-gauge needle, exteriorized and protected in a metal button sutured to the skin; used for up to 3 weeks
Caudal:	Agrelo & Miliozzi (149)	N/PE, P, TR, U	II	Cannula filled with heparinized (100 U/ml) isotonic saline; used for 6 hr
	Born & Moller (146)	PE, PR, S, U	CI	Cannula threaded into a vein through a 20-gauge needle that is then removed; protected by electrical shielding
	Cotlove (261)	N, P, PE, TR, U	CI	A 23-gauge needle with attached tubing is inserted into the vein
	Eve & Robinson (223)	P, PE, PR	CI	Cannula threaded into the vein through a 21-gauge needle that is then removed; uses a special swivel–fluid conduit; used for >6 months continuous infusion without anticoagulants
	Kellogg *et al.* (262)	S, TR, U	C	Cannula inserted with aid of dissecting microscope
	Little *et al.* (189)	P, PE, PR, U	C	Cannula protected by plastic tubing attached to tail; 2 of 9 rats infused for 90 days
	Plum (263)	A, S	M	Blood collected with suction after cutting the distal segment of the tail
	Rhodes & Patterson (148)	P, PE, PR, U	CI, I	Cannula threaded into the vein through a 19-gauge needle that is then removed; protected by electrical shielding; 32 of 34 rats had patent cannulas for 10 days (one rat chewed through the protective shielding)
	Saarni & Viikari (147)	A, P	C	Cannula threaded into the vein through a needle that is then removed (needle gauge and cannula type not specified); heparin (40 U/kg/hr) and droperidol (0.16 mg/kg/hr) infused throughout the experiment
	Stuhlman *et al.* (264)	S, TR, U	M	Blood collected with suction after cutting the distal segment of the tail, up to 10 samples per animal; rat is restrained in a cage on a heating pad
	Videm (265)	A, P	S, SI	Used a 21-gauge needle for collection of up to 4 ml of blood or injection into the vein at the root of the tail
	Wright (266)	S, TR, U	S	Up to 3 ml of blood collected in a capillary device[c] after cutting the distal segment of the tail; rat is restrained in a cage near a heating element
Dorsal Metatarsal:	Nobunga *et al.* (267a)	P, TR, U	S, SI	Injection *via* a 27-gauge needle into the right hind leg; collection of up to 0.2 ml of blood *via* a 22- or 23-gauge needle; useful in docile rats for acute venous access without anesthesia
Dorsal Penile:	Salem *et al.* (41)	P, TR, U	SI	Injection *via* a 26–30-gauge needle; method extended to rats by Nightingale and Mouravieff (267b)
	Virolainen (268)	P, TR	II	Injection *via* a ≤20-gauge needle; each rat received up to 14 injections in 1 week; good photograph of the procedure
Femoral:	Benzman-Tarcher (269)	A, S, SI	CI	Cannula advanced into inferior vena cava, used to infuse a fatty acid emulsion for 6 hr; no anticoagulant used
	D'Amour *et al.* (194)	PE, S		Cannula filled with heparin (1000 U/ml); excellent photographs of the procedure
	Jones & Hynd (191)	NY, PR, S, U	CI, M	Cannula filled with heparinized isotonic saline; exteriorized *via* the tail and protected by a plastic sheath; up to 7 days infusion in 300 rats
	Nishihara *et al.* (270)	PE, S	SI	Cannulation of the femoral artery and vein on one side, followed after time by the same procedure on the other side to study drug interactions
Femoropopliteal[d]:	Pearce (271)	P, TR, U	SI	A 27-gauge needle is used for injection
Hepatic:	Suzuki *et al.* (272)	PE, S	M	One cannula is passed down the external jugular vein into the inferior vena cava; the blood sampling cannula is inserted in the inferior vena cava *via* an abdominal incision
	Wernze (273)	A, PE, S	II, M	Cannulation aided by a microscope; cannula filled with heparinized (10 U/ml) isotonic saline; isobutylcyanoacrylate glue used to fix the cannula in the vein
	Yokota *et al.* (150)	A, N, PE, S	M	Direct vein cannulation with the bent tip of a 25-gauge needle connected to tubing; cannula was filled with heparin and fixed to the vein using a surgical glue; 0.25 ml of blood drawn slowly over 4 min to prevent reflux; blood drawn for up to 45 min
Hypophysial portal:	Ben-Jonathan & Porter (274)	A, PE, S	M	Modified method of Porter and Smith (275) to use an embolator apparatus to enable collection of blood samples
	Porter & Smith (275)	A, PE, S	M	Collected blood is free of CSF contamination; collected continuously for up to 6 hr; requires a microscope for surgery
Inferior vena cava:	Kaufman (185)	S, SI, U, UR	II, M	Cannula filled with heparinized saline and exteriorized at the back of the neck; patent for many months
	Welch *et al.* (276)	A, S	T	Direct venipuncture of the surgically exposed vein

continued

Table IV—*Continued*

Venous Site	Reference	Methodology Notes[a]	Demonstrated Uses[b]	Procedural Comments
External jugular:	Allsop & Burke (201)	PE/SI, S, U, UR	II	Cannula filled with heparinized (10 U/ml) isotonic saline; an epoxy-filled needle used to plug the end
	Brandstaetter & Terkel (234)	DL, S, U, UR	II, M	Cannula filled with heparin (20 U/ml); rat attached to a pulley assembly for continuous vascular access; cannulas in 46 rats patent for 12–21 days
	Brown & Breckenridge (168)	S, SI, U, UR	II, M	Cannula filled with an air bubble plus heparin–povidone mixture, sutured into the vein and exteriorized *via* a cranial pedestal; aseptic surgical methods used; patent for >1 year
	Bullard (193)	A, PE, S	VBP	Rats were heparinized; acute study
	Burt *et al.* (204)	S, SI, U, UR	CI	Surgery done aseptically; cannula filled with heparinized (20 U/ml) isotonic saline; patent cannulas for 3 weeks in five test rats; special swivel assembly
	Cox & Beazley (180)	PE, S, U, UR	CI	Cannula exteriorized at the back of the neck and passed through a spring that is sutured to the rat; uses a ball swivel, requires daily catheter straightening; cannula used up to 6 weeks (gives useful technical hints concerning cannula placement)
	Dalton *et al.* (176)	H, PP, S, U	CI	Cannula threaded into the vein through a 19-gauge needle and exteriorized through a rat body harness; used for up to 3 weeks
	D'Amour *et al.* (194)	PE, S		Cannula filled with heparin (1000 U/ml)
	Edmonds & Thompson (178, 179)	PP, S, U, UR	CI	Cannula secured *via* a subcutaneous collar around the neck; used for up to 3 months; rat prevented from biting cannula by electrical-shock device
	Engberg (177)	PP, S, U, UR	CI	Cannula exteriorized *via* a plastic cap sutured to the back of the neck; filled with isotonic saline; used up to ~3 weeks
	Ensminger *et al.* (190)	PE, PR, S, U	CI, SI	Cannula exteriorized at the root of the tail and passed through a spring enclosing the tail; infusion for up to 3 days; a larger diameter cannula can be used for serial blood sampling
	Harms & Ojeda (160)	S, SI, U, UR	M	Uses an implantation needle that is passed in and out of the vessel lumen, leaving the attached cannula tubing in the lumen; anchored in place *via* an attached silicone rubber sheet; cannula filled with isotonic saline; patent for 4–8 weeks for six test rats
	Mayer *et al.* (277)	A, PE, S	II	Jugular vein shunt constructed to enable serial injections without cannula flushing; prevents undesirable blood volume expansion; used acutely for bioassay
	Nicolaidis *et al.* (187)	S, SI, U, UR	CI	Uses a double-mitered cannula tip to prevent thrombotic blockade of the cannula; exteriorized at the head *via* a cranial pedestal; cannula filled with heparin–povidone mixture; uses a special swivel assembly; cannula patent for up to 5 months
	Popovic & Popovic (173)	PE, S, U, UR	II, M	Cannula filled with heparinized isotonic saline; exteriorized at the back of the neck; average cannula lifetime of 22 days
	Popovic *et al.* (175)	PE, S, U, UR	ECG, II, M	Cannula is advanced into the right ventricle; filled with heparinized isotonic saline; exteriorized at the back of the neck; cannula patent up to 124 days (with heparin) or 50 days (without heparin flushing)
	Renaud (155)	A, P, S	II, M	Uses a 20-gauge needle for direct venipuncture of the surgically exposed vein or percutaneous rostral puncture *via* depilated skin; collected up to 2 ml of blood, up to five samples per week
	Smith & Davis (15); Davis (278)	PE/SI, S, U, UR	CI, II	Describes two cannulas for jugular vein implantation; used up to 6 months; contains a wealth of practical information on cannula construction, surgical procedures, and infusion apparatus; excellent procedural photographs
	Steffens (186)	S, SI/TE, U, UR	CI, M	Cannulation of one tributary (for infusion) or two tributaries (for simultaneous infusion and blood sampling) of the external jugular vein; cannula filled with air bubble and heparin–povidone mixture; exteriorized *via* a cranial pedestal; sampled blood may be contaminated with infused substance
	Stripling (171)	S, SI, U, UR	CI, II	Cannula has intravascular end plugged, but delivers drug *via* lateral holes that prevent blood from entering the cannula; fixed in vein using cyanoacrylate glue and exteriorized *via* a cranial pedestal; patent in 61 and 60 of 65 rats for 2–3 and 5–9 weeks, respectively
	Terkel & Urbach (166)	S, U, UR, V	M	Cannula filled with heparin (250 U/ml); anchored in vein by seven sutures and exteriorized at the back of the neck into a protective plastic cylinder sutured to the neck; cannulas in 20 rats were patent for an average of 28.5 days (maximum 88 days)
	Upton (181)	S, SI, U, UR	II, M	Cannula filled with heparinized (10 U/ml) isotonic saline; exteriorized at the back of neck; serial blood samples collected up to once per min, with up to 5 weeks usage

Continued on next page

Table IV—*Continued*

Venous Site	Reference	Methodology Notes[a]	Demonstrated Uses[b]	Procedural Comments
	Weeks (7, 13, 170)[19]; Weeks & Davis (141); Weeks & Compton (184)	PE/SI, S, U, UR	CI, II, M, SI	Cannula filled with isotonic saline; exteriorized at the back of the neck; cannula patency [injection, blood sampling] for 10 rats tested after 3 months: [8, 7], 4 months: [8, 5], 6 months: [5, 4], and 8 months: [2, 2]: methodological details are best presented in one paper (13)
Internal jugular:	Mouzas & Weiss (279)	A, N, S	M, S	Direct needle puncture of the surgically exposed vein; collects up to 5 ml of blood
Mesenteric	Rappaport *et al.* (143)	PE, PR, S, U	CI	Uses an easily constructed device to facilitate cannulation of small vessels; cannula filled with heparinized saline
	Zammit *et al.* (203)	PE/SI, S, U	II, M	Cannula filled with heparinized saline; 17 of 20 rats had patent cannulas for 3 weeks
Palpebral:	Anderson *et al.* (280)	P, TR, U	SI	Injection *via* a 30-gauge needle to the palpebral venous blood supply of the eye of newborn rats
Portal:	Cassidy & Houston (151)	A, N, S	SI	Inserted a 27-gauge butterfly infusion needle into the vein; cannula flushed with heparinized isotonic saline
	Gallo-Torres & Ludorf (282)	PE, S, TR, U	CI, M	(*a*) Splenectomy followed by threading of a cannula *via* the splenic vein into the portal vein; portal blood continuously sampled for 60 min; patent for up to 1 week; (*b*) splenectomy followed by insertion of a T-shaped cannula into the portal vein; patent for several months
		PE, S, TR, U	M	Direct cannulation of the vein followed by fixing the cannula in the vein with a piece of plastic and cyanoacrylate adhesive; patent for 3–4 days; excellent surgical field diagrams
	Hyun *et al.* (281)	A, PE, S	M	Cannula inserted in the portal vein *via* the splenic vein; filled with heparin (1000 U/ml) or distilled water
	Pelzmann & Havemeyer (198)	A, PE, S	M	A shunt of tubing was inserted in opposite directions in the portal vein; cannula filled with heparin
	Sable-Amplis & Abadie (199)	PE, S, U, UR	M	A T-shaped cannula inserted in the portal vein; cannula was siliconized, filled with heparinized (4 mg/ml) saline, and exteriorized at the back of the neck; 8 and 5 of 10 rats had patent cannulas at 1 week and 1 month, respectively
	Suzuki *et al.* (283–285)	A, PE, S	CI	Cannula threaded into the portal vein *via* the pyloric vein; methylene blue injected into the cannula after the procedure to verify location by blue staining of the liver; portal infusions given for 50 min
Retro-orbital venous plexus:	Lapeyrac (40)	A	S	Up to 0.6 ml of blood drawn into a glass pipet
	Lim *et al.* (44)	A	M	Collected up to six serial blood samples of ~0.5 ml each; diagram of ocular anatomy
	Nöller (36)	U	M	Drew up to several milliliters at once; glass capillary tube used as a collection device
	Riley (37)	U	M	Collected blood samples of ~0.2 ml each
	Salem *et al.* (41)	U	M	Collected up to 30 serial blood samples of up to 0.5 ml each; excellent description and photographs of method
	Sanders (42)	A	M	Adapted method of Riley (37) to germ-free animals
	Sorg & Buckner (43)	A/U	S, T	Up to 8 ml of blood collected into a test tube *via* the posterior canthus; claims less likelihood of nose bleeds and eye trauma
	Stone (39)	U	M	Collected up to 1 ml of blood per sample; used 2 drops of a 2% cocaine solution applied to the eye before sampling
Sagittal/Transverse Sinus:	Davis & D'Aquila (286)	N, PE, S, U, UR	II	Requires stereotaxic techniques; not used as a chronic infusion method
Saphenous:	Everett & Sawyer (287)	P, TR, U	II	Shaved the area, then dilated the vein with 70% alcohol and snapping with a finger; injection *via* a 26-gauge needle; good illustration of the injection site
	Grunt *et al.* (288)	A, N, P	II	Used an indwelling 27-gauge needle for maintenance of venous access during anesthesia
	Rusher & Birch (289)	P, U	M	Collected up to 0.2 ml of blood on each of 3–5 venipunctures per rat; used a 20-gauge needle
Sublingual:	Greene & Wade (290)	A	SI	Access to the sublingual vein is facilitated *via* a fine suture passed through the tip of the tongue; injection *via* a 26- or 27-gauge needle

[a] Methodology key: (A) postoperative experiment on anesthetized rats; (CSF) cerebrospinal fluid; (DL) double lumen cannula (1.5 mm o.d., 0.71 mm i.d.; DVE-8, Dural Plastics, Dural, NSW, Australia); (H) postoperative rat maintained in a body harness; (N) needle inserted into blood vessel, with tubing attached to needle; (NY) nylon cannula; (P) percutaneous method; (PE) polyethylene cannula; (PP) polypropylene cannula; (PR) postoperative experiment on partially restrained rats; (S) surgical method; (SI) silicone rubber cannula; (TE) polytef cannula; (TR) postoperative experiment on totally restrained rats; (TY) Tygon cannula; (U) postoperative experiment on unanesthetized rats; (UR) postoperative experiment on unrestrained rats; (V) vinyl cannula. [b] Key for demonstrated uses and procedural comments: (CI) continuous infusion; (ECG) electrocardiogram recording; (II) intermittent injections; (M) multiple blood sampling; (S) single blood sample with rat survival; (SI) single injection; (T) terminal blood sample; (VBP) venous blood pressure. [c] Unopette, Becton-Dickinson, Rutherford, N.J. [d] Lateral marginal vein.

anesthetized rats. Pang and Gillette (320) supplied evidence contrary to the hypothesis of extrahepatic elimination of acetaminophen in the rat using exclusionary hepatectomy *via* ligation of the hepatic artery and portal vein at points proximal to the liver. The absence of blue discoloration of the liver following a 0.5-ml iv injection of blue ink was used to verify the complete cessation of blood flow to the liver. Rats treated in this manner survived for ~85 min.

Portal–Systemic Shunts—A portal–systemic shunt is a surgically constructed connection between the side or end of the portal vein and a systemic vein (inferior vena cava or renal vein, a portacaval or portarenal shunt, respectively) to divert portal venous blood away from the liver.

Table V—Miscellaneous Methods for Vascular Access

Method	Reference	Demonstrated Uses[a]	Procedural Comments
Cardiac puncture:	Burhoe (5); Gupta (291); Kraus (21); Moreland (292); Waynforth (12)	M, S, T	Rats are anesthetized; generally uses a 25- or 26-gauge needle (0.5–0.75 in. long); Burhoe (5) collected up to 12 ml of blood at once without killing the rat and up to 5 ml of blood weekly for 3 months; procedure can be terminal, Stuhlman *et al.* (264) reported 12% mortality from cardiac puncture in rats; photographs and excellent procedural descriptions by Burhoe (5) and Waynforth (12); Gupta (291) used cardiac puncture for neonatal rats
Decapitation:	Bush & Bush (293); Moreland (292)	T	Particularly useful for terminal blood collection when anesthesia must be avoided; provides mixed arterial–venous blood; although aesthetically unpleasant, it is a humane procedure when done by experienced personnel using commercially available guillotines[b]
Tail amputation:	Enta *et al.* (294); Kraus (21)	M, S	Tail may be warmed before procedure; distal part (2–3 mm) of tail of unanesthetized rat is amputated to collect up to 4 ml of arterial blood (if lateral caudal veins are occluded by direct pressure) or mixed arterial–venous blood; bleeding is stopped by applying pressure or cauterization
Toe clip[c]:	Kraus (21); Moreland (292)	S	Rats are anesthetized; clipping the toe can yield up to 0.3 ml of mixed arterial–venous blood; due to postprocedural pain to the rat, this procedure is not recommended

[a] Key for demonstrated uses: (M) multiple blood samples per rat; (S) single blood sample per rat; (T) terminal procedure for blood sampling. [b] Harvard Apparatus, South Natick, Mass. and EDCO Scientific, Chapel Hill, N.C. [c] Plantar and dorsal digital arteries plus the plantar veins are clipped.

Procedures for portal–systemic shunting in the rat were introduced in 1946 by Whitaker (327) and Reinhardt and Bazell (328). Laboratory animals with a portal–systemic shunt have provided, due to conditions resulting from the shunt, useful models for the study of altered drug disposition in the dog (329, 330), altered pharmacodynamics in the cat (331), hemostatic abnormalities (thrombocytopenia, hypofibrinogenemia, impaired platelet aggregation) in the rat (332–334), hyperuricemia in the rat (335), and potentially altered blood–brain barrier permeability in the rat (336–338). A number of other shunt-caused metabolic abnormalities have yet to be exploited as animal models (339). Bircher (339) has provided a useful summary of the animal model utility of the portacaval shunt rat.

It is impractical to consider here the detailed methodologies available for portal–systemic anastomosis in the rat. Lee *et al.* (340) have presented an outstanding review of the relevant history and methodology, along with a thorough discussion of the hepatic and metabolic alterations associated with portal–systemic anastomosis. Steiner and Martinez (341) studied systematically the cytological and gross changes associated with ligation of the portal vein, hepatic artery, and bile duct. Although Bircher (339) has recently proposed routine use of the portacaval shunt rat for evaluation of first-pass effect, no study using such methodology in the rat has yet been published. The need for vascular surgical skills and an operating microscope undoubtedly hinder the widespread use of portacaval shunt methodology for studying the first-pass effect in the rat. Nonetheless, the portacaval shunt rat offers the opportunity for studies of a longer duration than can be accommodated using transhepatic blood sampling methodology. Perhaps this advantage will be exploited in the near future.

One portacaval shunt procedure requires neither an operating microscope nor vascular surgical skills, yet produces a rat useful for short-term experiments. Bernstein and Cheiker (342) completed a portacaval shunt without a vascular anastomosis by obliterating the arterial blood supply to the liver (*via* ligation of the coeliac, superior hepatic, hepatic, and gastroduodenal arteries and diverting the blood flow through a polyvinyl tube (with needle tips at both ends) connecting the portal and iliolumbar veins. Rats so prepared were used in experiments for several hours while anesthetized.

COLLECTION OF OTHER BODY FLUIDS

Urine Collection Methods—Studies of xenobiotic disposition often require sampling or total collection of excreted urine. Some investigators have developed detailed methods for renal clearance determination in the rat (343). Urinary excretion studies may often be impeded by the relatively low urine output (1.20 ± 0.24 ml/200 g/hr, mean ± *SEM*, $n = 10$) of healthy adult rats (344). Urine flow rate was increased four- to fivefold by oral gavage administration of a single volume of warm distilled water (0.05 ml/g body weight) to a maximum urine flow rate of 2.8 ± 0.2% of body weight/hr (mean ± *SEM*, $n = 4$; equal to 5.6 ml/200 g/hr) (345). Urine flow returned to the basal rate ~3 hr after the water load. Three administrations of warm distilled water at half-hour intervals (0.05 ml/g body weight each) further increased the urine flow rate to a maximum of 6.8 ± 0.4% of body weight/hr (mean ± *SEM;* equal to 13.6 ml/200 g/hr) (346, as cited in 345). Jeffers *et al.* (347) induced diuresis in the rat by oral gavage administration of a single volume (0.05 ml/g of body weight) of an aqueous ethanol solution (12% v/v of 95% ethanol in water) followed 30 min later by oral gavage administration of a volume (0.03 ml/g of body weight) of warm tap water. This regimen resulted in a stable increased urine flow rate (3.1–8.1 ml/hr) in male rats (180–220 g) achieved 90–120 min after the first gavage. However, the amount of ethanol used has a sedative effect.

Kraus (21) has classified urine collection methods as the free catch method, reflex emptying following periodic stimulation or massage, bladder puncture, cystostomy, urethral catheterization of female rats, and external drainage catheter for male rats (Table VI). For all methods, urine is collected in some type of ice-cooled receptacle. An antioxidant and a metal ion-complexing agent should be added when collecting oxidizable xenobiotics. After esti-

Table VI—Methods for Urine Collection.

Method	Advantages	Disadvantages
Free catch: Nelson *et al.* (349)	Useful in all age groups and both sexes; nonsurgical method	May not elicit complete emptying of bladder
Reflex emptying[a]: Adolph *et al.* (350)	Useful in all age groups and both sexes; nonsurgical method	Requires restraining cage; may not elicit complete emptying of bladder
Suprapubic pressure[b]: Hayashi & Sakaguchi (351)	Can collect urine in a capillary tube; useful in all age groups and both sexes; nonsurgical method	Elicits small urine volume.
Bladder centesis: Heller (352)	Useful in all age groups and both sexes; bladder can be emptied completely	Used only at necropsy
Cystostomy: Hoy & Adolph (353)	Useful in all age groups and both sexes; useful in conscious rats; provides continuous urine collection	Surgical method
Urethral catheterization: Cohen & Oliver (354)	Provides continuous urine flow; serial catheterizations are possible; nonsurgical method	Useful in adult female rats only; rats must be anesthetized
External drainage catheter: White (355)	Provides continuous urine flow; nonsurgical method	Useful in adult male rats only; rats must be anesthetized

[a] Raising and lowering the rat. [b] Applied with the fingers.

mating the volume of urine to be collected during the designated period (based on a conservative urine output of ~0.3 ml/200 g body weight/hr), an appropriate volume of stock antioxidant solution (1.0*M* α-thioglycerol plus 0.1*M* EDTA) is added to the urine to achieve final urinary concentrations of 0.01*M* α-thioglycerol and 0.001*M* EDTA (348a)[23]. Mulder *et al.* (348b) recommended addition of sodium azide to the urine receptacle to inhibit bacterial growth. For anaerobic collection and to prevent evaporation of urine, the receptacle can be partly filled with mineral (261) or paraffin oil (343).

Free Catch Method—Rats will frequently urinate when touched, picked up around the midsection, raised with their hind legs out of contact with the cage floor, or a small cotton ball moistened with diethyl ether is waved under the nose (349).

Reflex Emptying—Kraus (21) provides a description of the salient features of a restraining cage used by Adolph *et al.* (350). With a rat in this cage over a receptacle, urination was elicited by quickly raising and lowering the frame and animal. Reflex urination can also be elicited by applying digital pressure to the suprapubic region (351). A capillary tube can be used to collect urine obtained in this manner (351).

Bladder Puncture—Urine can be withdrawn *via* a needle and syringe from the bladder at the necropsy of the rat (352).

Cystostomy—Hoy and Adolph (353) surgically implanted a plastic cannula in the urinary bladder to obtain a continuous flow of urine. This cannulation method is useful in both male and female rats of all ages. Hoy and Adolph (353) observed a continuous urine flow rate of ~0.3–0.5 ml/hr in healthy, conscious adult rats.

Urethral Catheterization of Female Rats—Repeated short-term catheterization of the female rat urethra can be done using a No. 4 coude ureteral catheter (354). A continuous urinary flow for up to 4 hr while the rat was maintained under anesthesia was reported. This method apparently has not been used in conscious rats.

External Drainage Catheter for Male Rats—A modified polyethylene catheter[24] can be slipped over the tip of the penis of the anesthetized male rat, tucked under the foreskin, and secured in place by tying the foreskin around the catheter with a single silk ligature (355). Urine flow rates of 6–10 ml/hr were observed after fluid loading *via* an orogastric tube. This method cannot be used in either female or conscious rats.

Bile Collection Methods—*Introduction*—Experiments on hepatobiliary excretion of drugs often necessitate short-term, intermittent, or chronic collection of bile from the rat. Eight salient facts must be considered when collecting rat bile. First, the rat does not have a gallbladder to serve as a bile reservoir, and therefore bile flows continuously through the common bile duct into the duodenum (26). Second, the pancreatic duct empties pancreatic fluid into the common bile duct distal to the place where the bile enters. This anatomical arrangement enables the experimenter to collect either bile, pancreatic fluid, or a mixture of the two. The identity of the collected fluid must be ensured by close inspection of these anatomical features and correct placement of the ligatures. Since collection of pancreatic secretions in the rat has had limited application in the area of pharmaceutical sciences (356, 357), the interested reader is referred elsewhere for detailed methods on pancreatic secretion collection (11, 356–361). Third, electrolytes depleted by chronic bile diversion must be replenished by parenteral or oral fluid administration (362, 363). Free access to drinking water containing 2.5–5% glucose plus isotonic sodium chloride (192, 363), 0.85–1.0% sodium chloride (182, 364, 365), 5% glucose plus 0.9% sodium chloride plus 0.05% potassium chloride (366), or Ringer's solution (188) reportedly supply adequate electrolyte replacement. Intravenous saline infused at a rate of 1 ml/hr has also proven effective (367). Addition of glucose to oral fluids seems to encourage fluid intake in the rat (366). Fourth, bile flow is dependent on body temperature (368, 369). Therefore, maintenance of constant rectal temperature *via* use of a heat lamp is necessary for comparative studies of hepatobiliary excretory function (319, 369, 370). Fifth, phenobarbital (75 mg/kg/day for 4 days) can be used as an experimental tool to induce an ~50% increase in bile flow rate (371–373). Alternatively, cycloheximide reduces bile flow rate to ~33–50% of the flow rate in control rats (374). Sixth, although the rate of bile flow does not differ significantly in males compared with female rats, lactating female rats (7–10 days postpartum) and female rats at their 20th gestational day have an ~50% greater bile flow rate. On

[23] Concentrations of α-thioglycerol and EDTA specified here were modified from those stated in ref. 348a in accordance with methodology notes provided by W. D. Conway *et al.*

[24] Leur-End Intramedic polyethylene catheter; Clay Adams, Parsippany, N.J.

removal of the rat pups from the lactating female, this elevated bile flow rate decreases to that of normal female rats (370). Seventh, interruption of enterohepatic circulation by bile duct cannulation alters bile composition by lowering the ratio of cholic acid–cholesterol (375). This alteration must be considered in evaluation of the results of biliary excretion studies. Eighth, there is a circadian variation of both bile production (average nighttime production being 50 and 38% higher than daytime production in female and male rats, respectively) and bile composition which could markedly alter studies of xenobiotic disposition (376).

The physiology of bile secretion and the anatomical structures involved have been reviewed (11, 377, 378). Colwell (363) has provided a useful photograph of a bile duct injected with india ink. Mechanisms of hepatobiliary excretion and enterohepatic recycling of xenobiotics have been reviewed (379–381), as have some theoretical pharmacokinetic principles (320, 382).

Substantial research has been done to discern the general characteristics of xenobiotics undergoing hepatobiliary excretion in the rat. Sperber (383) suggested that compounds with molecular weights >400 (in the unconjugated form) are excreted efficiently in the bile. Millburn *et al.* (384) studied a group of different xenobiotics and concluded that compounds with a molecular weight of ~300 or greater containing a highly polar anionic moiety are likely to undergo significant hepatobiliary excretion. The reader interested in further details on this topic is referred to the extensive original research (192, 382, 385–390).

Concurrent with their studies of the types of compounds undergoing hepatobiliary excretion, Abou-El-Makarem *et al.* (386) compared eight species (rat, dog, hen, cat, sheep, rabbit, guinea pig, and rhesus monkey) with respect to their ability to excrete eight different xenobiotics in the bile. This excellent study revealed that the rat and dog are two of the better hepatobiliary excretors, while the rabbit, guinea pig, and rhesus monkey are poor hepatobiliary excretors. This information is valuable when evaluating interspecies differences in drug disposition characteristics.

Methods—Bile collection methods can best be considered by classifying them into three categories:

1. Intracorporeal reservoir methods, *i.e.*, cannulation of the common bile duct with total continuous diversion of bile flow into a reservoir surgically implanted in the peritoneal cavity (363, 366, 391) or abdominal wall (362).

2. Extracorporeal reservoir methods, *i.e.*, cannulation of the common bile duct with total continuous diversion of bile flow through the cannula to an extracorporeal collection reservoir (182, 188, 192, 364, 374, 376, 390, 392, 393).

3. T-cannula method, *i.e.*, implantation of a T-shaped cannula in the common bile duct to enable intermittent collection of bile (394).

In each of these three categories, various methods exist for acute sampling in anesthetized rats or chronic continuous collection in unanesthetized, unrestrained rats. Table VII provides procedural comments relevant to the advantages and disadvantages of available bile collection methods.

Continuous bile collection has been reported for up to 54 days in chronically cannulated, unrestrained rats (364).

Table VII—Methods for Bile Collection

Method	Procedural Comments[a]
Intracorporeal reservoir methods: Johnson & Rising (366)	PP-10 cannulation of the common bile duct which then drains into a 12-ml glass reservoir implanted in the peritoneum; bulb can be drained *via* an extracorporeal segment of tubing attached to the reservoir; bile collected for up to 6 days from unanesthetized, unrestrained rats
Sawyer & Lepkovsky (391)	An 18- or 19-gauge stainless steel cannula is inserted into the common bile duct and drains into a 6-ml glass bulb implanted in the peritoneum; bulb can be drained *via* an extracorporeal segment of tubing attached to the bulb; no cannulated rat survived >90 hr
Extracorporeal reservoir methods: Abou-El-Makarem *et al.* (192)	Polythene (0.4-mm i.d., 0.8-mm o.d.) cannulation of the common bile duct; cannula exteriorized *via* a subcutaneous tunnel to an extracorporeal reservoir; bile collected from unanesthetized rat in a Bollman (395) restraining cage for up to 24 hr
Balabaud *et al.* (188)	PE-50 cannulation of the common bile duct; cannula exteriorized *via* a subcutaneous tunnel to a cranial pedestal connected to an extracorporeal reservoir *via* a swivel; bile collected for up to 6 days from an unanesthetized rat in a small metabolism cage
Enderlin & Honohan (182)	PE-50 cannulation of the common bile duct; cannula exteriorized *via* a subcutaneous tunnel to an interscapular incision connected to an extracorporeal reservoir *via* a swivel; bile collected for up to 4 days from an unanesthetized rat in a small metabolism cage
Friedman *et al.* (392)	PE-10 cannulation of the common bile duct; cannula exteriorized *via* a subcutaneous tunnel exiting at the foot [see figure in Nakayama (396)]; bile collected for 24 hr from unanesthetized, restrained rats
Fisher & Vars (364)	PE-50 cannulation, of the common bile duct; cannula exteriorized *via* a subcutaneous tunnel to a midline back incision into a piggyback cylindrical collection reservoir; bile collected for up to 54 days from unanesthetized rats
Knapp *et al.* (393)	PE-50 part of the cannula is inserted into the common bile duct, then the cannula is firmly anchored in place *via* a PE-250 cannula jacket; long-term bile collection from unanesthetized rats
Lock *et al.* (374)	PE-10 cannulation of the common bile duct; cannula exteriorized *via* a subcutaneous tunnel out of the back of the head to an extracorporeal reservoir; bile collected for 14 hr from an unanesthetized rat in a small metabolism cage
Takada *et al.* (390)	PE cannulation of the common bile duct for retrograde infusion studies in anesthetized rat
Vonk *et al.* (376)	Silicone-rubber cannula inserted into the common bile duct; cannula exteriorized at the skull *via* stainless steel tubing glued to the skull
T-Cannula method: Klauda et al. (394)	Silicone-rubber T-shaped cannula inserted into the common bile duct; permits periodic sampling of bile; a rubber collar around the neck was used to prevent chewing of the cannula

[a] Key for procedural comments: (PE) polyethylene; (PP) polypropylene.

Table VIII—Methods for Lymph Collection.

Reference	Procedural Comments[a]
Bollman *et al.* (404)	0.1 ml of 0.5% Evans blue dye was injected to enable identification of the lymphatic vessels; lymph collected continuously from unanesthetized, restrained, postoperative rats; 1–1.5 mm diameter plastic cannula used for lymphatic vessels of small intestine, liver, and abdomen; lymph flow rates of 5, 20, and 25 ml/24 hr from hepatic, intestinal, and thoracic lymphatics, respectively; lymph was collected for up to 3, 10, and 10 days from hepatic, intestinal, and thoracic lymphatics, respectively
Gallo-Torres & Miller (405, 406)	PE-50 cannula inserted into the abdominal thoracic duct; common bile duct was double cannulated for bile collection and saline infusion into the intestine; used cyanoacrylate adhesive to fix the cannula in the thoracic duct; lymph flow rate was proportional to the saline infusion rate; diverted bile can be reinfused *via* the intestinal cannula
Gowans (407)	Cannulation of the abdominal thoracic duct using the method of Bollman *et al.* (404); designed a pumping apparatus to reinfuse lymph and lymphocytes *via* the femoral vein
Reinhardt (408)	0.5 ml ip of 1% trypan blue enabled identification of the lymphatic vessels; rats anesthetized throughout procedure; cannula was tapered glass with a 25–27-gauge tip; thoracic duct cannulated in the neck; lymph collected for up to 6 hr; mean flow rate was 0.45 ml/hr (range of 0.13 to 0.70 ml/hr, n = 10)
Tasker (409)	Lymph collected continuously from unanesthetized, unrestrained, postoperative rats; a plastic cannula drained an intestinal lymphatic vessel into a glass reservoir (10–20 ml) placed in the peritoneum; lymph is collected *via* an extracorporeal reservoir access tube; collection for up to 10 days; flow rates of 0.5–1.0 ml/hr in fasting rats and 2–5 ml/hr in fed rats

[a] Key for procedural comments: (PE) polyethylene.

Cannulation of the common bile duct[25] with exteriorization at an interscapular incision for flow into an extracorporeal reservoir while housing the rat in a low-ceiling metabolism cage[26] has proven a useful procedure for relatively short (≤24 hr) bile collection. For more prolonged bile collection, passage of the extracorporeal portion of the cannula through an appropriate swivel joint will facilitate maintenance of a patent, unkinked cannula.

A unique procedure for the total exclusion of bile from the GI tract of male rats was described in 1936 (362). This procedure entails construction of a fistula from the bile duct to the vas deferens so that bile is eliminated in the urine. Rats prepared by this method remained apparently healthy for 3–4 months.

Bile collection methods are currently used in drug disposition and pharmacokinetic studies (366, 367, 397–403). Johnson and Rising (366) allowed at least 16 hr for rats to recover from bile duct cannulation, then included each rat in experiments only if (a) reasonable bile flow was established, *i.e.*, ~2–3 ml/kg/hr (366, 374, 391, 392), (b) the rat seemed to defecate normally (*i.e.*, no evidence of intestinal blockage), (c) the rat appeared healthy and active, not listless or lethargic, and (d) adequate food and fluid intake was maintained. These criteria are very useful guidelines for the postoperative and periodic evaluation of the rat with a cannulated bile duct.

Lymph Collection Methods—In 1945, Reinhardt (408) reported the first method for cannulation of the thoracic duct (at its location in the neck) and collection of lymph in the anesthetized rat. A single injection (0.5 ml ip) of 1% trypan blue administered 30 min prior to cannulation facilitated identification of the main lymphatic trunks. These investigators observed a lymph flow rate of 0.13–0.70 ml/hr (mean = 0.45 ml/hr, n = 10). Methodological considerations for lymph collection (404–409) are summarized in Table VIII.

Bollman *et al.* (404) extended lymph collection methodology to unanesthetized rats by insertion of a plastic cannula in the hepatic, intestinal, and thoracic duct lymphatic vessels. Postoperative, restrained rats provided continuous collection of lymph for up to 10 days. These investigators noted development of hypoprothrombinemia within 18 hr of lymphatic cannulation (316). Subcutaneous administration of vitamin K (4-amino-2-methyl-1-naphthol) both prevented and corrected hypoprothrombinemia development.

Tasker (409) collected intestinal lymph from unanesthetized, unrestrained rats by inserting a plastic cannula into an intestinal lymphatic vessel that drained into a glass reservoir (10–20 ml volume) placed in the peritoneum. Lymph was collected periodically by emptying the peritoneal reservoir *via* rubber tubing passing from the reservoir to a point of exteriorization at the right flank. This method seems useful for continuous lymph collection when restraint is undesirable.

Gowans (407) cannulated the abdominal thoracic duct using the method of Bollman *et al.* (404) to continuously collect lymph from restrained, unanesthetized rats. The collected lymph was reinfused into the femoral vein of the same cannulated rat *via* a pump apparatus. Such continuous reinfusion of lymph and living lymphocytes prevented the marked decrease in lymphocyte output from the thoracic duct previously noted when lymph flow was diverted for >2 days (410).

Finally, Gallo-Torres and Miller (405) introduced some modifications to simplify the method of Bollman *et al.* (404). A polyethylene cannula was inserted into the abdominal thoracic duct, while two other cannulas[27] were inserted into the common bile duct to enable bile collection with simultaneous infusion of isotonic saline (1.2–4.6 ml/hr) into the intestine. In rats fed a fatty meal 1 hr prior to surgery, the thoracic duct was recognized by its white coloration. Lymph flow rate was proportional to the saline infusion rate and lymph was collected for up to 10 days (405, 406). The integrity of the hepatobiliary excretory circuit can be reestablished by connecting the bile collection cannula to the intestinal infusion cannula. These investigators used a cyanoacrylate ester adhesive[28] to fix the cannula in the thoracic duct. Several excellent diagrams of the relevant anatomical regions are provided (19, 405).

Gallo-Torres (19) has provided a well-illustrated, integrated discussion of the application of lymphatic vessel,

[25] Using a polyethylene PE-10 cannula.
[26] Maryland Plastics, Inc., Federalsburg, Md.
[27] Each of the three cannulas were polyethylene PE-50.
[28] Permabond 910 adhesive; Permabond International Corp., Englewood, N.J. Duro Super Glue; Woodhill Chemical Sales Corp., Cleveland, Ohio. Eastman 910 adhesive; Eastman Kodak Co., Rochester, N.Y.

bile duct, and portal vein cannulation in evaluation of the bioavailability of xenobiotics in the rat. Since it provides a thorough review and examples of the experimental utility of lymph collection in the setting of other cannulas, the reader contemplating use of lymph collection methods is encouraged to refer to that work.

Cerebrospinal Fluid Sampling—The development of methods for ventricular access has been a critical contribution to the effort to advance knowledge in the neuropharmacology and psychopharmacology areas. Collection of cerebrospinal fluid and intraventricular administration of xenobiotics are highly specialized, intricate procedures that usually require experience in stereotaxic methods, knowledge of the anatomy of the brain, increased attention to aseptic procedures, and a high level of manual dexterity. Stereotaxic atlases of the rat brain are available to aid efforts to gain access to specific anatomical sites (32).

The majority of methods for ventricular access were designed for administration of either a single dose, multiple intermittent doses for up to 60 days, or a continuous infusion of very small volumes of xenobiotic-containing fluids (411–419). These methods recently have been reviewed by Myers (419) and illustrated by Avery (416). An easily constructed cannula originally used for intracerebral injections into cats and rabbits has proven useful in rats as well (420, 421). Wagner and DeGroot (422) constructed a single intracerebral cannula from two hypodermic needles and a small plexiglass plate. Hayden *et al.* (423) described detailed procedures for constructing and implanting in the lateral ventricle a relatively simple, inexpensive plexiglass cannula that enabled intraventricular injection for up to 3 months. The cannula constructed by Myers *et al.* (413) has proven to have great durability through the use of vinyl tubing[29] as an external protective shield. Khavari (225) has devised a combined intracerebral cannula–swivel unit to facilitate chronic studies in unrestrained rats. Although devised to enable intraventricular injection, some of these methods undoubtedly could be modified to enable sampling of cerebrospinal fluid.

Larger laboratory animals (cat, monkey) are preferred for chronic sampling of cerebrospinal fluid. Nonetheless, serial sampling over a 2-hr period has been accomplished in the rat. Serial small-volume samples (~5 μl) of cerebrospinal fluid were collected for ~2 hr *via* cisternal–lumbar (424) and ventriculocisternal perfusions (425) in order to monitor transport of seven amino acids into the cerebrospinal fluid. The artificial cerebrospinal fluid used by Merlis (426) for perfusion of the spinal subarachnoid space of the dog was useful in these perfusion studies in the rat (424, 425).

A single sample of cerebrospinal fluid can be obtained from the carefully recovered brain of a decapitated rat by inserting a glass microcannula (0.15 mm o.d.) into the mammillary recess of the third ventricle (427). By capillary action, 0.3–0.5 μl of cerebrospinal fluid was collected. Clemens and Sawyer (428) collected *via* cisternal puncture ~0.1 ml of cerebrospinal fluid from each anesthetized rat prior to sacrifice. No details (needle size, surgical preparation, exact site of puncture) of the method were given. Chou and Levy (429) described in detail a procedure for cisternal puncture of the anesthetized rat and collection of 50–100 μl of cerebrospinal fluid. Since this procedure requires only a 25-gauge needle and a piece of silicone rubber tubing, it should prove to be a valuable technique when only a single sample is required.

Saliva Collection Methods—Saliva remains a seldom-exploited fluid for collection in studies of xenobiotic absorption, distribution, and elimination. Welch *et al.* (276) accurately determined the elimination half-life of antipyrine in rats by the serial determination of salivary antiyrine concentrations. It was necessary to administer 2.0 mg/kg sc pilocarpine to some rats to collect (by capillary tube) 5 μl of saliva per sample. DiGregorio and Kniaz (430) monitored salivary amphetamine and methamphetamine concentrations in rats receiving a constant infusion of pilocarpine (0.125 mg/min) *via* the brachial artery. Saliva was continuously collected in a piece of polyethylene tubing over discrete time intervals *via* a polyethylene cannula placed in the parotid salivary duct. This technique of saliva collection was a modification of methodology developed for the mouse (431).

Additional details, illustrations, and pharmacokinetic applications of saliva drug concentration monitoring have been presented (432, 433). A number of other methods used for collecting rat saliva have been described in the dental research literature. These methods have been reviewed by Kraus (21).

METABOLISM CAGES AND RESTRAINING DEVICES

A number of commercial and home-built cages and devices, primarily constructed of wire or plexiglass, have been designed for short-term restraint with strict spatial confinement (434–444), restriction of certain body motions without spatial confinement (10, 445–450), and housing (metabolism cages) to facilitate intravascular xenobiotic infusion, quantitative collection of urine and feces, and/or measurement of food and water intake (235, 451–464).

Cage design and selection are commonly assumed to be relatively unimportant factors in designing animal experiments. However, molybdenum toxicity is increased in rats housed in zinc-coated cages (465) and the acute toxicity of various respiratory depressants in rats is markedly affected by cage design (466). Serum creatine phosphokinase activity in rats housed in cages with large spacings in the floor grating was approximately double that observed in rats housed in cages with small spacings in the floor grating (467). The effect on physiological variables of individual as opposed to group housing of rats has been recently reviewed (468). In view of these effects of cage design and individual housing, investigators should consider carefully the experimental impact of the metabolism cages and restraining devices described in the following sections.

Restraining Devices—*Short-Term Restraint*—Short-term restraint with strict spatial confinement is provided by restraining devices. These devices are used to achieve immobilization to facilitate administration of injectable substances, application of topical medication, collection of a blood sample, artificial insemination by vaginal smear, inhibition of access to indwelling cannulas, or induction of stress in studies of stress-associated effects in rats. The old restraining method of tying the conscious rat to a board (469, 470) is clearly excessive and unneces-

[29] Biraco vinyl tubing, number 318-B, size 8 Birnbach; Terminal Radio, New York, N.Y.

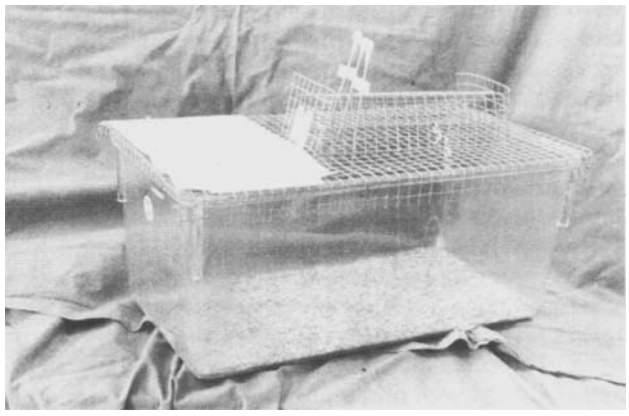

Figure 6—*A home-built restraining cage constructed from galvanized steel-wire hardware cloth. The rat fits inside the wire tunnel which has dimensions of 23-cm long, 7-cm wide, and 5.5-cm high. The size of the support wire grating can be chosen to fit on top of an available plastic animal bin.*

sary. Most commercially available restraining devices[30] resemble the Bollman-type confining tubular devices (261, 262, 395, 436–439, 471).

Each of these confining tubular devices: (a) is able to accommodate only a limited-size range of rats, (b) can accumulate feces in the rear of the cage, (c) imposes total restraint on rat movements, and (d) does not allow access to the rat for periodic oral gavage administration of xenobiotics. The novice will quickly discover that the conscious rat can not be removed effortlessly from any very confining device.

Scheline (471) modified the Bollman cage to make it adjustable to rat size and to allow urine collection. Similar characteristics are provided by a plastic stall restraining device (262). Davis and Coleman (442) used an adjustable, rectangular, plastic restraining cage for holding instrumented 200–400-g rats for up to 8 hr. Cotlove (261) used a tubular restraining cage from which the hind feet and tail protruded to collect urine during intravenous infusion into the lateral tail (caudal) vein. An adjustable cable-type restraining device was designed to restrict motion to facilitate undisturbed percutaneous absorption of substances applied topically to 200–300-g rats for $\leq$ 72 hr (115). Wilson (439) cut an opening in the top of a cardboard mailing tube to facilitate subcutaneous injection in the back of a restrained rat and access to the protruding tail for injection or blood sampling. To facilitate rapid removal of the rat from this tube, the distal end opened into a standard rectangular cage.

In designing an alternative to the Bollman cage to facilitate lymph collection, Baker *et al.* (472) placed the rat in a plexiglass rectangular cage with only the buttocks and tail restrained. This cage enabled the rat to move all but the hindquarters, allowed urine and feces to fall freely into a collecting vessel, enabled collection of lymph *via* a cannula exteriorized in the inguinal region, allowed access for oral gavage administration without removal of the rat from the cage, and accommodated rats ranging from 200 to 450 g.

As another alternative to the confining tubular devices, persons with minimal skill in the use of common hand tools (pliers and wire cutters) and a supply of inexpensive galvanized steel-wire cloth (available in most hardware stores) can readily construct the simple and durable restraining device described by Girardet (440). Figure 6 illustrates a modified version of this device, which was constructed to lie on top of a widely available plastic cage. This restraining device was constructed in ~1.5 hr and cost <$1.00 for materials (excluding plastic cage). By locating the wooden stick applicators at the buttocks of the rat, one device will accommodate rats of various body sizes. Similar characteristics are provided by a recently described restraining device which is inexpensively constructed from one small plexiglass plate (444). This device offers the advantage of enabling optional separate collection of urine and feces during restraint, but has the disadvantage of restraining the rat by greater immobilization of the limbs than used with the device illustrated in Fig. 6. Prolonged exposure to excessive restraint has been associated with increased incidence of pathological events as described in a later section.

Momentary Restraint—Momentary restraint is often essential for injection, blood sampling, collection of a vaginal smear, or artificial insemination. Such acute restraint can be accomplished by properly holding the rat in one hand (Fig. 2), using a protective glove when animal biting is a problem. Since various individuals prefer leather gloves (available in hardware stores), butcher's metal-mesh boning gloves[31] (473), or gloves made of 29 aramid[32] (474), each animal handler should try different gloves and use that which proves personally preferable.

Two alternatives to holding the rat are allowing the animal to crawl into a close-fitting restraining sack (435), polythene tube (441), or plastic cone[33], and wrapping the rat in a towel with the head, neck, and tail exposed (6). Use of these methods is restricted by the limited region of the body which remains accessible. The use of tubes into which the rat will crawl enables convenient collection of blood or injection *via* tail blood vessels by a single experimenter (441). Transillumination of the tail may also be helpful in visualizing the blood vessels (475).

Restricting Motion—Restriction of certain body motions without spatial confinement is often useful in preventing the rat from disturbing indwelling cannulas, irritating surgical wounds, or consuming fecal material (coprophagy). Graham (450) described a small box which allows the rat to hide its head for up to 1 hr, thereby facilitating investigator access to a cannula emerging from the back of the neck. Coprophagy-preventing devices and Elizabethan collars are described below.

Coprophagy and Its Prevention—The degree of coprophagy by the rat is recognized as a major variable in certain nutritional studies, particularly those involving vitamins B and K, since these are ingested by the rat following synthesis by intestinal bacteria (476–479). In fact, this behavioral drive is so strong that healthy rats consume on the average 35–65% of their total fecal output (480–482). The extent of coprophagy was most dramatically demonstrated by Greaves (483), who observed that unrestrained

[30] Model 700R rat restrainer; Braintree Scientific, Inc., Braintree, Mass. No. 56-4500 rat restrainer; Harvard Apparatus Company, Inc., South Natick, Mass. Model H2284 restraining cage; Hazelton Systems, Inc., Aberdeen, Md.

[31] Model MMG-100 metal-mesh gloves; Braintree Scientific, Inc., Braintree, Mass.

[32] Kevlar; E. I. DuPont de Nemours and Co., Inc., Wilmington, Del.

[33] Model DC-200 DecapiCones; Braintree Scientific, Inc., Braintree, Mass.

rats fed a vitamin K-free diet for 180 days remained healthy and still excreted appreciable amounts of vitamin K in their feces. Unfortunately, many scientists in areas other than the nutritional sciences are unaware that coprophagy is essential for the normal growth and development of young rats (484).

Since the rat primarily consumes feces immediately after extrusion from the anus (482), the raised wire-mesh floors in many metabolism cages are ineffective in preventing coprophagy (482). Clearly, this fecal–oral recycling may be critical to mass balance studies, quantification of drug excretion routes, and pharmacokinetic studies. Three methods have been devised to inhibit coprophagy (485): (*a*) tubular cages restricting flexion and lateral motion (481, 486), (*b*) a tight-fitting leather jacket restricting flexion (448), and (*c*) placement of a plastic cup over the tail and anus of the rat to catch fecal pellets, thus rendering them inaccessible to the rat (480, 487, 488). In addition, the Elizabethan collar may be useful in inhibiting coprophagy.

Elizabethan Collars—The Elizabethan collar is easily constructed and very useful for restricting motion to prevent the rat from disturbing indwelling cannulas, irritating surgical wounds, or consuming fecal material (Fig. 7). The collar consists of an adjustable plastic or reinforced cardboard cone which fits snugly around the neck and encloses the head in the body of the cone, thereby preventing scratching of the head, licking or biting other parts of the body, and coprophagy (10, 446, 449). The desired collar size can be calculated by:

$$\text{collar i.d.} = \frac{\text{neck circumference}}{\pi} \qquad \text{(Eq. 3)}$$

and

$$\text{collar o.d.} = \text{collar i.d.} + \text{desired depth} \qquad \text{(Eq. 4)}$$

Metabolism Cages—A metabolism cage is a unit used to house an individual rat to facilitate quantitative separate collection of urine and/or feces, measurement of food and/or water intake, quantitative collection of expired respiratory carbon dioxide, and/or containment of radiolabeled substances administered to the rat. Since most of these cages confine the animal to a relatively small defined space without immobilization, metabolism cages also provide some degree of cannula protection when housing rats with indwelling cannulas. Generally, rats will tolerate well a relatively short period in any metabolism cage. However, experiments with durations >12 hours necessitate the use of metabolism cages that enable adequate air flow to the rat, ready access to food and water, and easy retrieval of the collected urine and feces. In addition, a slightly higher room temperature (23–26°) may help prevent respiratory disease during confinement (456).

Grantham *et al.* (235) noted that rats rest easier when maintained in square, rather than circular, metabolism cages since this shape allows the rat to sleep in a corner. Lazarow (456) has provided an extensive review of the many aspects involved in designing and building metabolism cages for the rat, mouse, dog, and monkey. The basic aspects of metabolism cages have not changed much over the years (except for the availability of various polymeric construction materials such as plexiglass and Nalgene[34])

[34] Nalge Company, Rochester, N.Y.

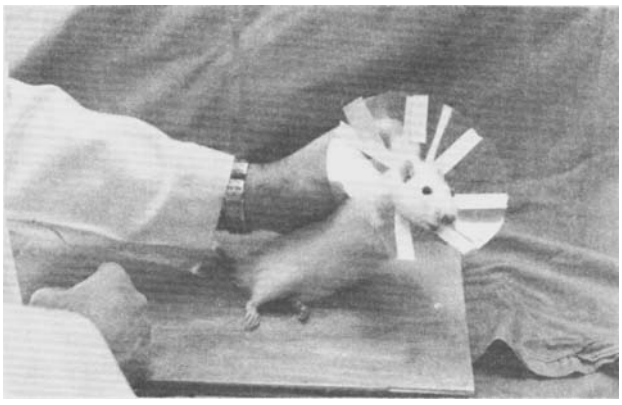

Figure 7—*An adult rat fitted with a plastic Elizabethan collar (highlighted with white tape strips for photographic clarity) around the neck. This collar (3.0-cm i.d., 16.0-cm o.d.) was cut from a rectangular plastic sheet usually used for transparencies.*

and the individual interested in home-built metabolism cages will find the detailed illustrations in this review extremely useful despite their age. A round wire-mesh cage using a funnel which contains a screen or shield for urine and feces separation, and a frame holding six such cages is described. Similar inexpensive wire cages have been described by others (452, 453, 458, 487). Suspended steel cages and a rack accommodating 36 such cages have been described (456). This unit is similar to many commercially available racks of suspended steel metabolism cages. Lazarow (456) also described cages which could be easily disassembled following studies with radioisotopes for thorough cleaning and decontamination, as well as a cage used for the quantitative collection of expired respiratory carbon dioxide.

Meticulous Urinofecal Separation—Cross contamination of urine and feces must be meticulously prevented in studies of elimination routes when the excreted substance can appear in both excretory products or when a drug excreted in the urine could be biotransformed by enzymes (such as β-glucuronidase) in the feces (348b). These situations commonly arise when studying the excretory routes of radiolabeled substances (454) and when assaying urinary activity of enzymes also present in large quantities in the feces (460a). The plastic stockade type of metabolism cage (454, 456, 460a) has been shown to meticulously prevent such cross contamination. Unlike most metabolism cages, it appears that this cage would prevent cross contamination even in the presence of diarrhea.

Leathwood and Plummer (460a) quantified the degree of fecal contamination of urine collected *via* three conventional metabolism cages, which used the following means of urinofecal separation: (*a*) a hollow, somewhat ellipsoidal glass device over which the urine flows for transfer into a collection beaker while the feces bounce off into another path (type I separator), (*b*) a urine collecting gutter, which diverts the falling urine into a collection beaker while the feces fall downward into a beaker (type II separator), and (*c*) a stockade-type metabolism cage (454, 456). Fecal contamination of the urine was most severe for the type I separator (which is used in several commercially available metabolism cages[35]). The type I

[35] Maryland Plastics, Inc., Federalsburg, Md. Model number 650-0100 metabolic cage; Nalge Company, Rochester, N.Y.

separator also failed to separately collect ~60% of the voided urine. The type II separator was fairly efficient in separating the urine and feces and in collecting urine. Efficient urinofecal separation was afforded by the stockade-type cage. However, the adverse effects (anorexia, weight loss) of strict restraint for >2 days necessitates only brief confinement of the rat to this type of cage.

Low-Temperature Urine Collection—The metabolism cage designed and illustrated by Lartigue *et al.* (463) is useful for the collection and rapid freezing of urine in cases where a voided substance is subject to temperature-sensitive degradation. This cage uses a urine collection dish immersed in propylene glycol to enable rapid freezing (−19°) of urine. Since propylene glycol is nonflammable and relatively nontoxic, it is preferred to other methods using flammable and irritating heptane and dry ice as the coolant (489, 490).

Miscellaneous Metabolism Cages—A number of metabolism cages necessitate only moderate confinement of the rat while allowing visual observation of rat behavior and providing separate collection of urine and feces, with reduced possibility of urinofecal cross contamination for the animal excreting well-formed feces (456, 457, 459, 461–463). One of these metabolism cages (459) is inexpensive to construct from widely available materials. This cage has the advantages of being easy to disassemble for cleaning and readily mountable on multi-cage racks. Lambooy (459) has provided detailed step-by-step directions for construction.

Jensh *et al.* (491) described a plexiglass cage useful for observing unrestrained pregnant rats in an anechoic, microwave-transparent chamber, which does not alter a number of potentially environment-dependent variables. Grantham *et al.* (235) built a square cage from plexiglass and wire mesh to facilitate intra-arterial infusion in relatively unrestrained, unanesthetized rats *via* a nonswivel spring attachment.

Accurate quantification of food and fluid intake is often difficult due to spillage of the food pellets and fluid into various regions of the cage. In addition, it is sometimes desirable to strictly minimize food contamination of the collected urine and feces. Guest *et al.* (455) described a metabolism cage constructed from an inverted 11.4-liter (3-gallon) narrow-necked glass bottle into which a wire-mesh floor was inserted. A fine mesh screen positioned below the floor enabled separation of urine from feces. A special detachable feeder was readily constructed from sheet metal, a 50-ml beaker, and wire mesh. This feeder minimized the amount of food dropped outside the feeder (<1% of food intake per day) and, therefore, was useful in quantifying daily food intake. In addition, this feeder minimized food contamination of the collected feces and urine. This basic type of feeder design has been incorporated into one commercially available metabolism cage[36]. To aid in accurate quantitation of fluid intake, Robbins (492) fit a modified plastic syringe with a sipper spout made of 8-mm o.d. glass tubing. Use of an appropriate size plastic syringe enables achievement of the desired degree of accuracy with respect to fluid consumption measurement.

Recently, Toon and Rowland (464) described a tubular plexiglass cage that allowed longitudinal movement by the rat, separate urine and feces collection, and access to various cannulas for up to 8 hr of confinement. Although the virtual necessity of workshop construction by skilled personnel and the relatively high cost are disadvantages, the unique features of this cage may warrant the investment by some laboratories.

Effects of Restraint—Often, observation of hyperactivity, sitting in a corner of the cage, scratching at a harness, decreased curiosity and exploratory behavior, free micturition and defecation, and/or passage of soft stools may suggest stress in a rat (460a, 493). The stress associated with various physical restraints (tying the conscious rat to a surgical board, housing in a restraining cage, application of a body cast, placement in a harness) or periodic shocks from an electrified cage has been shown in the rat to be associated with neutrophilia (approximately a sevenfold increase after 6 hr of restraint) (494), decreased whole blood clotting time (495), diminished altitude tolerance (496), occurrence of stomach lesions after as little as 48 hr of restraint with a greater frequency and severity noted in restrained rats housed in groups (497, 498), increased gastric acid concentration (499), decreased growth rate (493, 498), decreased daily food intake (493), and hyperactivity (493). Of particular interest is a study documenting the stress response associated with placement in a body harness (500) for chronic intravenous infusion (493). These stress-associated pathophysiologic events must be considered in designing experiments requiring extended restraint or harnessing of the rat.

CONCLUSIONS

The vast literature on methods of vascular access and collection of various body fluids has been reviewed. The investigator new to these methodologies is advised to gather a minimal but essential resource library consisting of papers providing highly detailed and illustrated accounts of cannula construction and implantation (13, 15, 501); aseptic surgical methods (23); rat resuscitator assembly (105, 106); a general review providing information on animal handling, anesthesia, and euthanasia (6, 10, 12, 21, 22); a well-illustrated anatomy text (31); and information on metabolism cages (456). It is hoped that this literature survey provides a useful summary of practical information and a valuable description of alternative methodologies to experimental scientists[37].

ADDENDUM

Since the submission of this manuscript, a textbook of experimental techniques for the rat has been published (C. Petty, "Research Techniques In The Rat," Charles C Thomas, Springfield, Ill., 1982). This textbook includes a broad range of experimental methods and a multitude of useful illustrations. This book is well worth its price for both the novice and experienced researcher.

Two additional publications of interest are a useful tabular compilation of LD_{50} values in several species of

[36] Model no. 650-0100 metabolic cage; Nalge Company, Rochester, N.Y.

[37] On a very limited basis, the authors will make available a photocopy of these references complete with each citation's title, all authors, and full pagination. This offer can be extended only to those scientists and information services with a serious need for such information.

newborn and adult animals [E. I. Goldenthal, *Toxicol. Appl. Pharmacol.*, **18**, 185 (1971)] and one providing a relatively simple procedure for percutaneous placement of an intravascular needle into the caudal artery for collection of serial blood samples from an anesthetized rat *via* the extravascular silicone-rubber tubing attached to the needle [L. Putcha, J. V. Bruckner, S. Muralidhara, and S. Feldman, *J. Pharmacol. Meth.*, **8**, 145 (1982)]. The latter should prove very useful for pharmacokinetic characterization of drugs in individual anesthetized rats.

REFERENCES

(1) J. M. Philipeaux, *C. R. Hebd. Seances Acad. Sci.*, **43**, 904 (1856).

(2) J. R. Lindsey, in "The Laboratory Rat. Vol. I. Biology and Diseases," H. J. Baker, J. R. Lindsey, and S. H. Weisbroth, Eds., Academic, New York, N.Y., 1979, p. 1.

(3) H. L. Foster, *Lab. Anim. Sci.*, **30**, 793 (1980).

(4) G. B. Briggs and F. W. Oehme, in "The Laboratory Rat. Vol. II. Research Applications," H. J. Baker, J. R. Lindsey, and S. H. Weisbroth, Eds., Academic, New York, N.Y., 1980, p. 103.

(5) S. O. Burhoe, *J. Hered.*, **31**, 445 (1940).

(6) E. J. Farris and J. Q. Griffith, "The Rat in Laboratory Investigation," 2nd ed., Lippincott, Philadelphia, Pa., 1949.

(7) J. R. Weeks, *Annu. Rev. Pharmacol.*, **3**, 335 (1963).

(8) H. C. Grice, *Lab. Anim. Care*, **14**, 483 (1964).

(9) M. Sandiford, *J. Anim. Tech. Assoc.*, **15–16**, 9 (1964–1965).

(10) W. I. Gay, Ed., "Methods of Animal Experimentation," Vol. I, Academic, New York, N.Y., 1965.

(11) R. Lambert, "Surgery of the Digestive System in the Rat," Charles C Thomas, Springfield, Ill., 1965.

(12) H. B. Waynforth, in "Techniques in Protein Biosynthesis," P. N. Campbell and J. R. Sargent, Eds., Academic, New York, N.Y., 1969, p. 209.

(13) J. R. Weeks, *Methods Psychobiol.*, **2**, 155 (1972).

(14) D. Singh and D. D. Avery, "Physiological Techniques In Behavioral Research," Brooks/Cole, Monterey, Calif., 1975.

(15) S. G. Smith and W. M. Davis, in "Methods in Narcotic Research," S. Ehrenpreis and A. Neidle, Eds., Dekker, New York, N.Y., 1975, p. 3.

(16) B. H. Migdalof, *Drug Metab. Rev.*, **5**, 295 (1976).

(17) B. M. Mitruka, H. M. Rawnsley, and D. V. Vadehra, Eds., "Animals for Medical Research. Models for the Study of Human Disease," Wiley, New York, N.Y., 1976.

(18) C. S. F. Williams, "Practical Guide to Laboratory Animals," C. V. Mosby, St. Louis, Mo., 1976, p. 52.

(19) H. E. Gallo-Torres, *J. Toxicol. Environ. Health*, **2**, 827 (1977).

(20) H. J. Baker, J. R. Lindsey, and S. H. Weisbroth, Eds., "The Laboratory Rat. Vol. II. Research Applications," Academic, New York, N.Y., 1980.

(21) A. L. Kraus, *ibid.*, p. 1.

(22) D. Singh, in "Physiological Techniques in Behavioral Research," D. Singh and D. D. Avery, Eds., Brooks/Cole, Monterey, Calif., 1975, p. 4.

(23) *Idem.*, p. 24.

(24) M. B. Popp and M. F. Brennan, *Am. J. Physiol.*, **241**, H606 (1981).

(25) S. Scher, *Lab Anim.*, **10**, 62 (1981).

(26) E. C. Greene, "Anatomy of the Rat," The American Philosophical Society, Philadelphia, Pa., 1935; reprint edition: Hafner, New York, N.Y., 1963.

(27) W. Zeman and J. R. M. Innes, "Craigie's Neuroanatomy of the Rat," Academic, New York, N.Y., 1963.

(28) E. M. Smith and M. L. Calhoun, "The Microscopic Anatomy of the White Rat. A Photographic Atlas," Iowa State University Press, Ames, Iowa, 1968.

(29) B. B. Chiasson, "Laboratory Anatomy of the White Rat," 3rd ed., William C. Brown, Dubuque, Iowa, 1975.

(30) R. Hebel and M. W. Stromberg, "Anatomy of the Laboratory Rat," Williams and Wilkins Co., Baltimore, Md., 1976.

(31) R. J. Olds and J. R. Olds, "A Color Atlas of the Rat—Dissection Guide," Wiley, New York, N.Y., 1979.

(32) L. J. Pellegrino and A. J. Cushman, "A Stereotaxic Atlas of the Rat Brain," Appleton-Century-Crofts, New York, N.Y., 1967.

(33) M. H. Halpern, *Am. J. Anat.*, **101**, 1 (1957).

(34) R. Chambers and B. W. Zweifach, *ibid.*, **75**, 173 (1944).

(35) B. N. Halpern and A. Pacaud, *C. R. Seances Soc. Biol. Ses. Fil.*, **145**, 1465 (1951).

(36) H. G. Nöller, *Klin. Wochenschr.*, **33**, 770 (1955).

(37) V. Riley, *Proc. Soc. Exp. Biol. Med.*, **104**, 751 (1960).

(38) A. Pettit, *C. R. Seances Soc. Biol. Ses. Fil.*, **74**, 11 (1913).

(39) S. H. Stone, *Science*, **119**, 100 (1954).

(40) F. Lapeyrac, *Rev. Fr. Etud. Clin. Biol.*, **8**, 195 (1963).

(41) H. Salem, M. H. Grossman, and D. L. J. Bilbey, *J. Pharm. Sci.*, **52**, 794 (1963).

(42) B. J. Sanders, *Am. J. Clin. Pathol.*, **40**, 46 (1963).

(43) D. A. Sorg and B. Buckner, *Proc. Soc. Exp. Biol. Med.*, **115**, 1131 (1964).

(44) J. K. Lim, W. G. Crouthamel, and J. W. Mauger, *Am. J. Pharm. Educ.*, **38**, 219 (1974).

(45) K. I. Timm, *Lab. Anim. Sci.*, **29**, 636 (1979).

(46) H. B. Allmon, *J. Public Health Dent.*, **31**, 218 (1971).

(47) H. G. Q. Rowett, "The Rat as a Small Mammal," John Murray, London, 1960.

(48) G. M. Higgins and R. M. Anderson, *Arch. Pathol.*, **12**, 186 (1931).

(49) R. C. Nairn, *Br. J. Exp. Pathol.*, **38**, 62 (1957).

(50) C. Yamauchi, S. Fujita, T. Obara, and T. Ueda, *Lab. Anim. Sci.*, **31**, 251 (1981).

(51) B. H. Doell and P. V. J. Hegarty, *Br. J. Haematol.*, **18**, 503 (1970).

(52) J. D. Caisey and D. J. King, *Clin. Chem.*, **26**, 1877 (1980).

(53) E. Bruckner-Kardoss and B. S. Wostmann, *Lab. Anim. Sci.*, **24**, 633 (1974).

(54) G. O. Korsrud and K. D. Trick, *Clin. Chim. Acta*, **48**, 311 (1973).

(55) S. K. Saksena and H. Datta, *Ind. J. Physiol. Pharmacol.*, **14**, 199 (1970).

(56a) W. Lawkowicz and P. Czerski, *Acta Hematol.*, **36**, 13 (1966).

(56b) A. L. Sellers, J. Katz, G. Bonorris, and S. Okuyama, *J. Lab. Clin. Med.*, **68**, 177 (1966).

(57) J. D. Burek, "Pathology of Aging Rats," CRC Press, West Palm Beach, Fla., 1978.

(58) H. H. Donaldson, "The Rat. Data and Reference Tables for the Albino Rat (*Mus Norvegicus albinus*) and the Norway Rat (*Mus norvegicus*)," 2nd ed., The Wistar Institute of Anatomy and Biology, Philadelphia, Pa., 1924.

(59) L. A. Sapirstein, E. H. Sapirstein, and A. Bredemeyer, *Circ. Res.*, **8**, 135 (1960).

(60) S. H. Steiner and G. C. E. Mueller, *ibid.*, **9**, 99 (1961).

(61) E. F. Adolph, *Science*, **109**, 579 (1949).

(62) R. L. Dedrick, *J. Pharmacokinet. Biopharm.*, **1**, 435 (1973).

(63) L. I. Harrison and M. Gibaldi, *J. Pharm. Sci.*, **66**, 1138 (1977).

(64) K. J. Himmelstein and R. J. Lutz, *J. Pharmacokinet. Biopharm.*, **7**, 127 (1979).

(65) M. E. Coates, P. N. O'Donaghue, P. R. Payne, and R. J. Ward, "Dietary Standards for Laboratory Rats and Mice. Laboratory Animal Handbook No. 2," Churchill Livingston, London, 1969.

(66) National Academy of Sciences, National Research Council, Agricultural Board, Committee on Animal Nutrition, "Nutrient Requirements of Laboratory Animals. No. 10. Cat, Guinea Pig, Hamster, Monkey, Mouse, Rat," 2nd rev., National Academy of Sciences, Washington, 1972.

(67) A. E. Rogers, in "The Laboratory Rat. Vol. I. Biology and Diseases," H. J. Baker, J. R. Lindsey, and S. H. Weisbroth, Eds., Academic, New York, N.Y., 1979, p. 123.

(68) P. M. Newberne, *Fed. Proc. Fed. Am. Soc. Exp. Biol.*, **34**, 209 (1975).

(69) J. R. Lindsey, H. J. Baker, R. G. Overcash, G. H. Casell, and C. E. Hunt, *Am. J. Pathol.*, **64**, 675 (1971).

(70) E. H. Geller, in "The Laboratory Rat. Vol. I. Biology and Diseases," H. J. Baker, J. R. Lindsey, and S. H. Weisbroth, Eds., Academic, New York, N.Y., 1979, p. 401.

(71) I. Lutsky and D. Toshner, *Lab. Anim. Sci.*, **28**, 751 (1978).

(72) Committee on Care and Use of Laboratory Animals of the Institute of Laboratory Animal Resources, National Research Council, National Institutes of Health, "Guide for the Care and Use of Laboratory Animals," DHEW Publication No. (NIH) 78-23, Washington, 1978.

(73) A. N. Worden and W. Lane-Petter, Eds., "The UFAW Handbook on the Care and Management of Laboratory Animals," 2nd ed., Universities Federation for Animal Welfare, London, 1957, p. 27.
(74) W. Lane-Petter, in "The UFAW Handbook on the Care and Management of Laboratory Animals," Churchill Livingstone, Edinburgh, 1976, p. 210.
(75) H. C. Ferguson, *J. Pharm. Sci.*, **55,** 1142 (1966).
(76) W. V. Lumb, "Small Animal Anesthesia," Lea & Febiger, Philadelphia, Pa., 1963.
(77) R. M. Hoar, in "Experimental Animal Anesthesiology," D. C. Sawyer, Ed., USAF School of Aerospace Medicine, Brooks Air Force Base, Texas, 1965, p. 325.
(78) A. Schaffer, in "Methods of Animal Experimentation," W. I. Gay, Ed., Academic, New York, N.Y., 1965, p. 43.
(79) S. J. Galla, *Fed. Proc. Fed. Am. Soc. Exp. Biol.*, **28,** 1404 (1969).
(80) J. W. R. McIntyre, *Lab. Anim.*, **5,** 99 (1971).
(81) A. J. C. Holland, *Can. Anaesth. Soc. J.*, **20,** 693 (1973).
(82) J. Buelke-Sam, J. F. Holson, J. J. Bazare, and J. F. Young, *Lab. Anim. Sci.*, **28,** 157 (1978).
(83a) C. J. Green, *Lab. Anim.*, **15,** 397 (1981).
(83b) *Anesthesiology*, **20,** 707 (1959).
(84) F. F. McAllister, *Am. J. Physiol.*, **124,** 391 (1938).
(85) H. D. Sanders, *J. Pharm. Pharmacol.*, **17,** 665 (1965).
(86) J. B. Mulder and R. V. Brown, *Lab. Anim. Sci.*, **22,** 422 (1972).
(87) S. Songcharoen and T. B. Hubbard, *J. Surg. Res.*, **12,** 344 (1972).
(88) D. M. Smith, K. M. Goddard, R. B. Wilson, and P. M. Newberne, *Lab. Anim. Sci.*, **23,** 869 (1973).
(89) W. R. Dudley, L. R. Soma, C. Barnes, T. C. Smith, and B. E. Marshall, *ibid.*, **25,** 481 (1975).
(90) L. M. Shuer, H. L. Vahlsing, and E. R. Feringa, *ibid.*, **28,** 433 (1978).
(91) D. M. Stark and J. M. Lipman, *Lab. Anim.*, **8,** 25 (1979).
(92) D. E. Levy, A. Zwies, and T. E. Duffy, *Lab. Anim. Sci.*, **30,** 868 (1980).
(93) S. Borodkin, L. Macy, G. Thompson, and R. Schmits, *J. Pharm. Sci.*, **66,** 693 (1977).
(94) E. S. Valenstein, *J. Exp. Anal. Behav.*, **4,** 6 (1961).
(95) R. A. Youth, S. J. Simmerman, R. Newell, and R. A. King, *Physiol. Behav.*, **10,** 633 (1973).
(96) S. H. Weisbroth and J. H. Fudens, *ibid.*, **22,** 904 (1972).
(97) P. Wilson and A. M. Wheatley, *Lab. Anim.*, **15,** 349 (1981).
(98) R. W. Fleischman, D. McCracken, and W. Forbes, *Lab. Anim. Sci.*, **27,** 238 (1977).
(99) J. B. Jones and M. L. Simmons, *Lab. Anim. Care*, **18,** 642 (1968).
(100) G. E. Lewis and P. B. Jennings, *Lab. Anim. Sci.*, **22,** 430 (1972).
(101) C. B. Thayer, S. Lowe, and W. C. Rubright, *J. Am. Vet. Med. Assoc.*, **161,** 665 (1972).
(102) C. J. Green, M. J. Halsey, S. Precious, and B. Wardley-Smith, *Lab Anim.*, **12,** *85 (1978).*
(103) R. K. Medd and R. Heywood, *ibid.*, **4,** 75 (1970).
(104) J. L. Parker and H. R. Adams, *Lab. Anim. Sci.*, **28,** 575 (1978).
(105) J. R. F. Ingall and P. H. Hasenpusch, *Lab. Anim. Care*, **16,** 82 (1966).
(106) C. L. Rassaert, *Lab. Anim. Sci.*, **21,** 420 (1971).
(107) L. M. Shuer, H. L. Vahlsing, and E. R. Feringa, *ibid.*, **28,** 433 (1978).
(108) E. R. Feringa, G. G. Gurden, W. Strodel, W. Chandler, and J. Knake, *Neurology*, **23,** 599 (1973).
(109) R. A. Jaffe and M. J. Free, *Lab. Anim. Sci.*, **23,** 266 (1973).
(110) E. Proctor and A. R. Fernando, *Br. J. Anaesth.*, **45,** 139 (1973).
(111) C. G. Lineberry, in "Methods in Animal Experimentation," W. I. Gay, Ed., Academic, New York, N.Y., 1981, p. 237.
(112) N. Bleicher, *ibid.*, 1965, p. 138.
(113) G. Woodward, *ibid.*, 1965, p. 343.
(114) G. A. Nixon and P. J. Reer, *Lab. Anim. Sci.*, **23,** 423 (1973).
(115) D. P. Rice and D. J. Ketterer, *ibid.*, **27,** 72 (1977).
(116) J. Shani, Y. Givant, and F. G. Sulman, *Lab. Anim. Care*, **20,** 1154 (1970).
(117) S. Rose and J. F. Nelson, *Aust. J. Exp. Biol.*, **33,** 415 (1955).
(118) E. Wittgenstein and K. W. Rowe, *Lab. Anim. Care*, **15,** 375 (1965).
(119) D. Novin, M. Rezek, and D. A. Vanderweele, *Physiol. Behav.*, **12,** 135 (1974).
(120) W. M. Davis and J. R. Nichols, *J. Exp. Anal. Behav.*, **6,** 233 (1963).
(121) J. R. Weeks and J. R. Collins, *Prostaglandins*, **12,** 11 (1976).
(122) J. R. Weeks, *Pharmacol. Biochem. Behav.*, **7,** 559 (1977).
(123) J. R. Weeks, *Sci. Am.*, **210,** 46 (1964).
(124) H. G. O. Holck, in "The Rat in Laboratory Investigation," 2nd ed., E. J. Farris and J. Q. Griffith, Eds., J. B. Lippincott, Philadelphia, Pa., 1949, p. 301.
(125a) C. D. Barnes and L. C. Eltherington, "Drug Dosages in Laboratory Animals: A Handbook," University of California Press, Berkeley, Calif., 1973.
(125b) S. M. Kruckenberg, in "The Laboratory Rat. Volume II. Research Applications," H. J. Baker, J. R. Lindsey, and S. H. Weisbroth, Eds., Academic, New York, N.Y., 1980, p. 259.
(126) D. C. Smith, in "Methods of Animal Experimentation," W. I. Gay, Ed., Academic, New York, N.Y., 1965, p. 167.
(127) J. E. Breazile and R. L. Kitchell, *Fed. Proc. Fed. Am. Soc. Exp. Biol.*, **28,** 1577 (1969).
(128) J. A. Mikeska and W. R. Klemm, *Lab. Anim. Sci.*, **25,** 175 (1975).
(129) D. B. Feldman and B. N. Gupta, *ibid.*, **26,** 218 (1976).
(130) M. F. Roizen, J. Moss, D. P. Henry, V. Weise, and I. J. Kopin, *J. Pharmacol. Exp. Ther.*, **204,** 11 (1978).
(131) H. S. Rudolph, *Lab. Anim. Care*, **13,** 91 (1963).
(132) N. A. Hulme and J. C. Krantz, *Anesthesiology*, **16,** 627 (1955).
(133) H. W. Linde and M. L. Berman, *Anesth. Analg.*, **50,** 656 (1971).
(134) V. Hempel, C. Von Kugelgen, and H. Remmer, *Anaesthetist*, **24,** 400 (1975).
(135) C. P. Chengelis and R. A. Neal, *Biochem. Pharmacol.*, **29,** 247 (1980).
(136) H. Aune, H. Olsen, and J. Morland, *Br. J. Anaesth.*, **53,** 621 (1981).
(137) R. D. Stewart and C. A. Sanislow, *N. Engl. J. Med.*, **265,** 1283 (1961).
(138) G. B. Bradham and N. Walsh, *J. South Carolina Med. Assoc.*, **61,** 165 (1965).
(139) N. G. Heatley and J. R. Weeks, *J. Appl. Physiol.*, **19,** 542 (1964).
(140) J. A. Herd and A. C. Barger, *ibid.*, **19,** 791 (1964).
(141) J. R. Weeks and J. D. Davis, *ibid.*, **19,** 540 (1964).
(142) P. L. E. Ross and A. M. Rappaport, *Nature (London)*, **188,** 326 (1960).
(143) A. M. Rappaport, J. W. Martyn, and P. L. E. Ross, *Angiology*, **12,** 442 (1961).
(144) M. Rezek and V. Havlicek, *Physiol. Behav.*, **15,** 623 (1975).
(145) C. Eve and S. H. Robinson, *J. Lab. Clin. Med.*, **62,** 169 (1963).
(146) C. T. Born and M. L. Moller, *Lab. Anim. Sci.*, **24,** 355 (1974).
(147) H. Saarni and J. Viikari, *Lab. Anim.*, **10,** 69 (1976).
(148) M. L. Rhodes and C. E. Patterson, *Lab. Anim. Sci.*, **29,** 82 (1979).
(149) C. E. Agrelo and J. O. Miliozzi, *J. Pharm. Pharmacol.*, **26,** 207 (1974).
(150) M. Yokota, T. Iga, S. Awazu, and M. Hanano, *J. Appl. Physiol.*, **41,** 439 (1976).
(151) M. K. Cassidy and J. B. Houston, *J. Pharm. Pharmacol.*, **32,** 57 (1980).
(152) A. Hurwitz, *J. Lab. Clin. Med.*, **78,** 172 (1971).
(153) L. B. Wingard and G. Levy, *J. Pharmacol. Exp. Ther.*, **184,** 253 (1973).
(154) R. Kassel and S. Levitan, *Science*, **118,** 563 (1953).
(155) S. Renaud, *Lab. Anim. Care*, **19,** 664 (1969).
(156) W. A. Phillips, W. W. Stafford, and J. Stuut, *Proc. Soc. Exp. Biol. Med.*, **143,** 733 (1973).
(157) P. M. Ronai, *Transplantation*, **4,** 208 (1966).
(158) M. Davis and R. D'Aquila, *Pharmacol. Biochem. Behav.*, **4,** 469 (1976).
(159) C. Agrelo and W. Dawson, *J. Pharm. Pharmacol.*, **20,** 959 (1968).
(160) P. G. Harms and S. R. Ojeda, *J. Appl. Physiol.*, **36,** 391 (1974).
(161) B. Kamath and A. Yacobi, *J. Pharm. Sci.*, **69,** 864 (1980).
(162) B. L. Kamath, C. M. Lai, S. D. Gupta, M. J. Durrani, and A.

Yacobi, *ibid.*, **70,** 299 (1981).
(163) B. L. Kamath, H. F. Stampfli, C. M. Lai, and A. Yacobi, *ibid.*, **70,** 667 (1981).
(164) P. Barr and P. Soila, *Angiology*, **11,** 168 (1960).
(165) J. R. Weeks and J. A. Jones, *Proc. Soc. Exp. Biol. Med.*, **104,** 646 (1960).
(166) J. Terkel and L. Urbach, *Horm. Behav.*, **5,** 141 (1974).
(167) C. A. Robinson, C. A. Hengeveld, and F. DeBalbian Verster, *Physiol. Behav.*, **4,** 123 (1969).
(168) R. J. Brown and C. B. Breckenridge, *Biochem. Med.*, **13,** 280 (1975).
(169) H. E. Gallo-Torres and J. Ludorf, *Proc. Soc. Exp. Biol. Med.*, **145,** 249 (1974).
(170) J. R. Weeks, *Prostaglandins*, **17,** 495 (1979).
(171) J. S. Stripling, *Pharmacol. Biochem. Behav.*, **15,** 823 (1981).
(172) C. A. Robinson, C. A. Hengeveld, and F. DeBalbian Verster, *Physiol. Behav.*, **4,** 123 (1969).
(173) V. Popovic and P. Popovic, *J. Appl. Physiol.*, **15,** 727 (1960).
(174) J. R. Weeks, *Science*, **138,** 143 (1962).
(175) V. Popovic, K. M. Kent, and P. Popovic, *Proc. Soc. Exp. Biol. Med.*, **113,** 599 (1963).
(176) R. G. Dalton, T. L. Touraine, and T. R. Wilson, *J. Lab. Clin. Med.*, **74,** 813 (1969).
(177) A. Engberg, *Acta Physiol. Scand.*, **75,** 170 (1969).
(178) C. J. Edmonds and B. D. Thompson, *J. Physiol. (London)*, **207,** 41P (1970).
(179) *Idem.*, **232,** 10P (1973).
(180) C. E. Cox and R. M. Beazley, *J. Surg. Res.*, **18,** 607 (1975).
(181) R. A. Upton, *J. Pharm. Sci.*, **64,** 112 (1975).
(182) F. E. Enderlin and T. Honohan, *Lab. Anim. Sci.*, **27,** 490 (1977).
(183) S. Lock, H. Witschi, and G. L. Plaa, *Proc. Soc. Exp. Biol. Med.*, **161,** 546 (1979).
(184) J. R. Weeks and L. D. Compton, *Prostaglandins*, **17,** 501 (1979).
(185) S. Kaufman, *Am. J. Physiol.*, **239,** R123 (1980).
(186) A. B. Steffens, *Physiol. Behav.*, **4,** 833 (1969).
(187) S. Nicolaidis, N. Rowland, M. Meile, P. Marfaing-Jallat, and A. Pesez, *Pharmacol. Biochem. Behav.*, **2,** 131 (1974).
(188) C. Balabaud, J. Saric, P. Gonzalez, and C. Delphy, *Lab. Anim. Sci.*, **31,** 273 (1981).
(189) J. R. Little, G. Brecher, T. R. Bradley, and S. Rose, *Blood*, **19,** 236 (1962).
(190) W. D. Ensminger, J. S. Greenberger, E. M. Egan, M. B. Muse, and W. C. Moloney, *J. Natl. Cancer Inst.*, **62,** 1265 (1979).
(191) P. A. Jones and J. W. Hynd, *Lab. Anim.*, **15,** 29 (1981).
(192) M. M. Abou-El-Makarem, P. Millburn, R. L. Smith, and R. T. Williams, *Biochem. J.*, **105,** 1269 (1967).
(193) R. W. Bullard, *Am. J. Physiol.*, **196,** 415 (1959).
(194) F. E. D'Amour, F. R. Blood, and D. A. Belden, "Manual for Laboratory Work in Mammalian Physiology," 3rd ed., University of Chicago Press, Chicago, Ill., 1965.
(195) C. Beuzeville, *Proc. Soc. Exp. Biol. Med.*, **129,** 932 (1968).
(196) T. Fujita and D. H. Tedeschi, *Life Sci.*, **7** (Part I), 673 (1968).
(197) C. Browning, J. M. Ledingham, and D. Pelling, *J. Physiol. (London)*, **208,** 11P (1970).
(198) K. S. Pelzmann and R. N. Havemeyer, *J. Pharm. Sci.*, **60,** 331 (1971).
(199) R. Sable-Amplis and D. Abadie, *J. Appl. Physiol.*, **38,** 358 (1975).
(200) J. Brandstaetter and J. Terkel, *Lab. Anim. Sci.*, **27,** 999 (1977).
(201) J. R. Allsop and J. F. Burke, *J. Surg. Res.*, **25,** 111 (1978).
(202) C. C. Chiueh and I. J. Kopin, *J. Pharmacol. Exp. Ther.*, **205,** 148 (1978).
(203) M. Zammit, L. H. Toledo-Pereyra, S. Malcom, and W. N. Konde, *Lab. Anim. Sci.*, **29,** 364 (1979).
(204) M. E. Burt, J. Arbeit, and M. F. Brennan, *Am. J. Physiol.*, **238,** H599 (1980).
(205) G. Waeldele and J. C. Stoclet, *J. Physiol. (London)*, **66,** 357 (1973).
(206) R. D. Buñag, J. W. McCubbin, and I. H. Page, *Cardiovasc. Res.*, **5,** 24 (1971).
(207) C. W. Popper, C. C. Chiueh, and I. J. Kopin, *J. Pharmacol. Exp. Ther.*, **202,** 144 (1977).
(208) R. E. Purdy and D. W. Ashbrook, *J. Pharm. Pharmacol.*, **30,** 436 (1978).
(209) J. W. Still, *Proc. Soc. Exp. Biol. Med.*, **81,** 579 (1952).
(210) J. W. Still and E. R. Whitcomb, *Am. J. Physiol.*, **178,** 399 (1954).
(211) J. W. Still, S. N. Pradham, and E. R. Whitcomb, *J. Appl. Physiol.*, **8,** 575 (1956).
(212) J. W. Still and E. R. Whitcomb, *J. Lab. Clin. Med.*, **48,** 152 (1956).
(213) L. I. Kleinman, E. P. Radford, and G. Torelli, *Am. J. Physiol.*, **208,** 578 (1965).
(214) F. J. McIlreath, W. DeGraw, and V. Kadar, *Arch. Int. Pharmacodyn.*, **157,** 330 (1965).
(215) J. S. Carvalho, R. Shapiro, P. Hopper, and L. B. Page, *Am. J. Physiol.*, **228,** 369 (1975).
(216) T. D. Bjornsson and G. Levy, *J. Pharmacol. Exp. Ther.*, **210,** 237 (1979).
(217) T. D. Bjornsson and G. Levy, *ibid.*, **210,** 243 (1979).
(218) J. F. Staub and G Coutris, *J. Appl. Physiol.*, **46,** 197 (1979).
(219) J. D. Davis and C. S. Campbell, in "Physiological Techniques in Behavioral Research," D. Singh, D. D. Avery, Eds., Brooks/Cole, Belmont, Calif., 1975, p. 162.
(220) H. R. D. Jacobs, *J. Lab. Clin. Med.*, **16,** 901 (1931).
(221) C. M. Rhode, W. Parkins, D. Tourtellotte, and H. M. Vars, *Am. J. Physiol.*, **159,** 409 (1949).
(222) A. N. Epstein and P. Teitelbaum, *J. Appl. Physiol.*, **17,** 171 (1962).
(223) C. Eve and S. H. Robinson, *J. Lab. Clin. Med.*, **62,** 169 (1963).
(224) D. W. Thomas and J. Mayer, *Physiol. Behav.*, **3,** 499 (1968).
(225) K. A. Khavari, *ibid.*, **5,** 1187 (1970).
(226) E. Steiger, H. M. Vars, and S. J. Dudrick, *Arch. Surg.*, **104,** 330 (1972).
(227) J. H. Strubbe, *Physiol. Behav.*, **12,** 317 (1974).
(228) J. M. Goldstein, *Pharmacol. Biochem. Behav.*, **4,** 613 (1976).
(229) Z. W. Brown, Z. Amit, and J. R. Weeks, *ibid.*, **5,** 363 (1976).
(230) J. T. Goodgame, S. F. Lowry, and M. F. Brennan, *J. Surg. Res.*, **24,** 520 (1978).
(231) R. Blair, B. Fishman, Z. Amit, and J. R. Weeks, *Pharmacol. Biochem. Behav.*, **12,** 463 (1980).
(232) C. Darracq, P. Gonzalez, and C. Balabaud, *Physiol. Behav.*, **25,** 327 (1980).
(233) P. C. Vink and F. Roelfsema, *ibid.*, **27,** 175 (1981).
(234) J. Brandstaetter and J. Terkel, *Behav. Res. Meth. Instrum.*, **7,** 11 (1975).
(235) F. H. Grantham, D. M. Hill, J. Rowland, and P. M. Gullino, *J. Natl. Cancer Inst.*, **55,** 203 (1975).
(236) M. A. McGee and R. R. Maronpot, *Lab. Anim. Sci.*, **29,** 639 (1979).
(237) A. C. Speirs and R. Blocksma, *Plast. Reconstr. Surg.*, **31,** 166 (1963).
(238) R. G. Mason, R. W. Shermer, and N. F. Rodman, *Am. J. Pathol.*, **69,** 271 (1972).
(239) S. W. Kim, S. G. Lee, H. Oster, D. Coleman, J. D. Andrade, D. J. Lentz, and D. Olsen, *Trans. Am. Soc. Artif. Intern. Organs*, **20,** 449 (1974).
(240) D. K. Hysell and G. D. Abrams, *Lab. Anim. Care*, **17,** 273 (1967).
(241) D. G. Meuleman, G. M. T. Vogel, and A. M. L. Van Delft, *Thromb. Res.*, **20,** 45 (1980).
(242) J. Vilageliu, A. Arañó, and L. Bruseghini, *Meth. Find. Exp. Clin. Pharmacol.*, **3,** 279 (1981).
(243) B. Garthoff and R. Towart, *J. Pharmacol. Meth.*, **5,** 275 (1981).
(244) R. J. Laffan, A. Peterson, S. W. Hitch, and C. Jeunelot, *Cardiovasc. Res.*, **6,** 319 (1972).
(245) C. H. Lushbough and S. W. Moline, *Proc. Anim. Care Panel*, **11,** 305 (1961).
(246) B. Scharschmidt and P. D. Berk, *Proc. Soc. Exp. Biol. Med.*, **143,** 364 (1973).
(247) L. Ekelund and T. Olin, *Invest. Radiol.*, **5,** 69 (1970).
(248) Ø. Leivestad and R. A. Malt, *Surgery*, **74,** 401 (1973).
(249) L. Carrillo and D. M. Aviado, *Lab. Invest.*, **20,** 243 (1969).
(250) J. B. Forrest, M. H. Todd, and D. J. Cragg, *Can. Anaesth. Soc. J.*, **26,** 58 (1979).
(251) B. E. Hayes and J. A. Will, *Am. J. Physiol.*, **235,** H452 (1978).
(252) J. Herget and F. Paleček, *Arch. Int. Pharmacodyn.*, **198,** 107 (1972).
(253) M. Rabinovitch, W. Gamble, A. S. Nadas, O. S. Miettinen, and L. Reid, *Am. J. Physiol.*, **236,** H818 (1979).

(254) R. B. Stinger, V. J. Iacopino, I. Alter, T. M. Fitzpatrick, J. C. Rose, and P. A. Kot, *J. Appl. Physiol.*, **51**, 1047 (1981).
(255) J. S. Evans and M. B. Nikitovitch, *Neuroendocrinology*, **4**, 83 (1969).
(256) J. S. Evans, *J. Appl. Physiol.*, **29**, 275 (1970).
(257) S. Schapiro and L. Stjarne, *Proc. Soc. Exp. Biol. Med.*, **99**, 414 (1958).
(258) B. Singer and M. P. Stack-Dunne, *J. Endocrinol.*, **12**, 130 (1955).
(259) L. Young and T. R. Chambers, *Lab. Anim. Sci.*, **23**, 428 (1973).
(260) M. A. Slusher and B. Browning, *Am. J. Physiol.*, **200**, 1032 (1961).
(261) E. Cotlove, *J. Appl. Physiol.*, **16**, 764 (1961).
(262) R. H. Kellogg, W. R. Burack, and K. J. Isselbacher, *Am. J. Physiol.*, **177**, 27 (1954).
(263) C. M. Plum, *Acta Physiol. Scand.*, **6**, 289 (1943).
(264) R. A. Stuhlman, J. T. Packer, and S. D. Rose, *Lab. Anim. Sci.*, **22**, 268 (1972).
(265) S. Videm, *Z. Versuchstierk.*, **22**, 101 (1980).
(266) B. A. Wright, *Lab. Anim. Care*, **20**, 274 (1970).
(267a) T. Nobunaga, K. Nakamura, and T. Imamichi, *ibid.*, **16**, 40 (1966).
(267b) C. H. Nightingale and M. Mouravieff, *J. Pharm. Sci.*, **62**, 860 (1973).
(268) M. Virolainen, *Transplantation*, **5**, 1530 (1967).
(269) A. Bezman-Tarcher, *J. Lipid. Res.*, **10**, 197 (1969).
(270) K. Nishihara, H. Nakamura, Y. Saitoh, and T. Suzuki, *Chem. Pharm. Bull.*, **23**, 3293 (1975).
(271) K. A. Pearce, *Nature (London)*, **180**, 709 (1957).
(272) T. Suzuki, T. Ohkuma, T. Rikihisa, and S. Isozaki, *J. Pharm. Sci.*, **64**, 895 (1975).
(273) H. Wernze, *Z. Gesamte Exp. Med.*, **153**, 234 (1970).
(274) N. Ben-Jonathan and J. C. Porter, *Endocrinology*, **94**, 864 (1974).
(275) J. C. Porter and K. R. Smith, *Endocrinology*, **81**, 1182 (1967).
(276) R. M. Welch, R. L. DeAngelis, M. Wingfield, and T. W. Farmer, *Clin. Pharmacol. Ther.*, **18**, 249 (1975).
(277) H. E. Mayer, D. R. Ballard, and F. M. Abboud, *J. Lab. Clin. Med.*, **75**, 1017 (1970).
(278) J. D. Davis, *J. Exp. Anal. Behav.*, **9**, 385 (1966).
(279) G. Mouzas and J. B. Weiss, *J. Clin. Pathol.*, **13**, 264 (1960).
(280) N. F. Anderson, E. J. Delorme, M. F. A. Woodruff, and D. C. Simpson, *Nature (London)*, **184**, 1952 (1959).
(281) S. A. Hyun, V. Vahouny, and C. R. Treadwell, *Biochim. Biophys. Acta*, **137**, 296 (1967).
(282) H. E. Gallo-Torres and J. Ludorf, *Proc. Soc. Exp. Biol. Med.*, **145**, 249 (1974).
(283) T. Suzuki, Y. Saitoh, S. Isozaki, and R. Ishida, *Chem. Pharm. Bull.*, **20**, 2731 (1972).
(284) T. Suzuki, Y. Saitoh, S. Isozaki, and R. Ishida, *J. Pharm. Sci.*, **62**, 345 (1973).
(285) T. Suzuki, S. Isozaki, R. Ishida, Y. Saitoh, and F. Nakagama, *Chem. Pharm. Bull.*, **22**, 1639 (1974).
(286) M. Davis and R. D'Aquila, *Pharmacol. Biochem. Behav.*, **4**, 469 (1976).
(287) J. W. Everett and C. H. Sawyer, *Nature (London)*, **178**, 268 (1956).
(288) J. A. Grunt, J. E. Walker, and J. T. Higgins, *Am. J. Physiol.*, **198**, 754 (1960).
(289) D. L. Rusher and R. W. Birch, *Physiol. Behav.*, **14**, 377 (1975).
(290) F. E. Greene and A. E. Wade, *Lab. Anim. Care*, **17**, 604 (1967).
(291) B. N. Gupta, *Lab. Anim. Sci.*, **23**, 559 (1973).
(292) A. F. Moreland, in "Methods of Animal Experimentation," W. I. Gay, Ed., Academic, New York, N.Y., 1965, p. 1.
(293) J. C. Bush and C. M. Bush, *Physiol. Behav.*, **7**, 647 (1971).
(294) T. Enta, S. D. Lockey, and C. E. Reed, *Proc. Soc. Exp. Biol. Med.*, **127**, 136 (1968).
(295) J. D. Davis and N. E. Miller, *J. Appl. Physiol.*, **21**, 1873 (1966).
(296) S. A. Weinstein and Z. Annau, *ibid.*, **23**, 601 (1967).
(297) J. D. Davis, R. J. Gallagher, R. F. Ladove, and A. J. Turausky, *J. Compar. Physiol. Psychol.*, **67**, 407 (1969).
(298) J. W. Pearce, H. Sonnenberg, H. T. Veness, and U. Ackerman, *Can. J. Physiol. Pharmacol.*, **47**, 377 (1969).
(299) J. Terkel, *J. Appl. Physiol.*, **33**, 519 (1972).
(300) D. E. Oken, B. Jackson, K. L. Kornetsky, and J. R. Dilley, *Kidney Int.*, **18**, 510 (1980).
(301) E. L. Besch and B. J. Chou, *Proc. Soc. Exp. Biol. Med.*, **138**, 1019 (1971).
(302) H. F. Oates and G. S. Stokes, *Clin. Exp. Pharmacol. Physiol.*, **1**, 495 (1974).
(303) A. T. Van Oosterom, W. Zuidervaart, and J. J. Veltkamp, *Haemostasis*, **3**, 296 (1974).
(304) R. Friedel, I. Trautschold, K. Gärtner, M. Helle-Feldman, and D. Gaudssuhn, *Z. Klin. Chem. Klin. Biochem.*, **13**, 499 (1975).
(305) K. D. Döhler, A. Von Zur Mühlen, K. Gärtner, and U. Döhler, *J. Endocrinol.*, **74**, 341 (1977).
(306) K. D. Döhler, C. C. Wong, D. Gaudssuhn, A. Von Zur Mühlen, K. Gärtner, and U. Döhler, *J. Endocrinol.*, **79**, 141 (1978).
(307) M. Hulse, S. Feldman, and J. V. Bruckner, *J. Pharmacol. Exp. Ther.*, **218**, 416 (1981).
(308) L. Bernstein and H. Elrick, *Metabolism*, **6**, 479 (1957).
(309) L. Grant, P. Hopkinson, G. Jennings, and F. A. Jenner, *Nature (London)*, **232**, 135 (1971).
(310) J. Dunn and L. Scheving, *J. Endocrinol.*, **49**, 347 (1971).
(311) C. V. Greenway and R. D. Stark, *Physiol. Rev.*, **51**, 23 (1971).
(312) K. Nakata, G F. Leong, and R. W. Brauer, *Am. J. Physiol.*, **199**, 1181 (1960).
(313) W. A. Colburn, I. Bekersky, B. H. Min, B. J. Hodshon, and W. A. Garland, *Res. Commun. Chem. Pathol. Pharmacol.*, **27**, 73 (1980).
(314) K. Iwamoto and C. D. Klaassen, *J. Pharmacol. Exp. Ther.*, **200**, 236 (1977).
(315) *Idem.*, **203**, 365 (1977).
(316) J. D. Mann, F. D. Mann, and J. L. Bollman, *Am. J. Physiol.*, **158**, 311 (1949).
(317) E. V. Flock and J. L. Bollman, in "Amino Acid Pools: Distribution, Formation and Function of Free Amino Acids," J. T. Holden, Ed., Elsevier, Amsterdam, 1962, p. 449.
(318) E. V. Flock, G. M. Tyce, and C. A. Owen, *J. Neurochem.*, **13**, 1389 (1966).
(319) C. D. Klaassen, *J. Pharmacol. Exp. Ther.*, **191**, 25 (1974).
(320) K. S. Pang and J. R. Gillette, *J. Pharmacokinet. Biopharm.*, **6**, 355 (1978).
(321) H. Selye and C. Dosne, *Am. J. Physiol.*, **128**, 729 (1939–1940).
(322) C. J. Ryan, J. Guest, A. M. Harper, and L. H. Blumgart, *Br. J. Exp. Pathol.*, **59**, 111 (1978).
(323) J. J. Jaffe, *Anatom. Rec.*, **120**, 935 (1954).
(324) F. D. Mann, E. S. Shonyo, and F. C. Mann, *Am. J. Physiol.*, **164**, 111 (1951).
(325) F. P. Meehan, *ibid.*, **179**, 282 (1954).
(326) J. L. Bollman, E. Van Hook, *J. Appl. Physiol.*, **24**, 722 (1968).
(327) W. L. Whitaker, *Proc. Soc. Exp. Biol. Med.*, **61**, 420 (1946).
(328) W. O. Reinhardt and A. H. Bazell, *ibid.*, **62**, 270 (1946).
(329) R. Gugler, P. Lain, and D. L. Azarnoff, *J. Pharmacol. Exp. Ther.*, **195**, 416 (1975).
(330) K. M. Giacomini, S. M. Nakeeb, and G. Levy, *J. Pharm. Sci.*, **69**, 786 (1980).
(331) S. Agoston, M. C. Houwertjes, and P. J. Salt, *Br. J. Pharmacol.*, **68**, 637 (1980).
(332) M. G. Doni, R. Aragno, and P. Vassanelli, *Thromb. Res.*, **10**, 539 (1977).
(333) M. G. Doni, P. Vassanelli, L. Bonadiman, and G. L. Avventi, *Hemostasis*, **7**, 19 (1978).
(334) M. G. Doni, P. Vassanelli, G. L. Avventi, L. Bonadiman, and F. Meduri, *ibid.*, **9**, 36 (1980).
(335) V. R. Olgiati, U. Fox, C. Netti, and A. Pecile, *Pharmacol. Res. Commun.*, **10**, 195 (1978).
(336) A. J. Zamora, J. B. Cavanagh, and M. H. Kyu, *J. Neurol. Sci.*, **18**, 25 (1973).
(337) H. Laursen and E. Westergaard, *Neuropathol. Appl. Neurobiol.*, **3**, 29 (1977).
(338) C. S. Sarna, M. W. B. Bradbury, and J. Cavanagh, *Brain. Res.*, **138**, 550 (1977).
(339) J. Bircher, *Pharmacol. Ther.*, **5**, 219 (1979).
(340) S. Lee, J. G. Chandler, C. E. Broelsch, Y. M. Flamant, and M. J. Orloff, *J. Surg. Res.*, **17**, 53 (1974).
(341) P. E. Steiner and J. B. Martinez, *Am. J. Pathol.*, **39**, 257 (1961).
(342) D. E. Bernstein and S. Cheiker, *J. Appl. Physiol.*, **14**, 469 (1959).
(343) S. O. Stitzer and M. Martinez-Maldonado, *Methods Pharmacol.*,

4B, 23 (1978).
(344) J. A. Kittelson, *Anatom. Rec.*, **13,** 385 (1917).
(345) G. Falk, *Am. J. Physiol.*, **181,** 157 (1955).
(346) E. F. Adolph and J. P. Northrop, *ibid.*, **168,** 320 (1952).
(347) W. A. Jeffers, M. M. Livezey, and J. H. Austin, *Proc. Soc. Exp. Biol. Med.*, **50,** 184 (1942).
(348a) W. D. Conway, H. Minatoya, A. M. Lands, and J. M. Shekosky, *J. Pharm. Sci.*, **57,** 1135 (1968).
(348b) G. J. Mulder, E. Scholtens, and D. K. F. Meijer, *Methods Enzymol.*, **77,** 21 (1981).
(349) E. Nelson, M. Hanano, and G. Levy, *J. Pharmacol. Exp. Ther.*, **153,** 159 (1966).
(350) E. F. Adolph, J. P. Barker, and P. A. Hoy, *Am. J. Physiol.*, **178,** 538 (1955).
(351) S. Hayashi and T. Sakaguchi, *Lab. Anim. Sci.*, **25,** 781 (1975).
(352) H. Heller, *J. Physiol. (London)*, **106,** 245 (1947).
(353) P. A. Hoy and E. F. Adolph, *Am. J. Physiol.*, **187,** 32 (1956).
(354) A. E. Cohen and H. M. Oliver, *Lab. Anim. Care*, **14,** 471 (1964).
(355) W. A. White, *Lab. Anim. Sci.*, **21,** 401 (1971).
(356) P. Alm, R. Ekholm, and L. Ericson, *Acta Pharm. Suec.*, **9,** 401 (1972).
(357) R. P. Maickel and D. P. McFadden, *J. Pharmacol. Methods*, **2,** 323 (1979).
(358) A. R. Colwell, *Am. J. Physiol.*, **164,** 812 (1951).
(359) L. C. U. Junqueira, G. C. Hirsch, and H. A. Rothschild, *Biochem. J.*, **61,** 275 (1955).
(360) J. W. Love, *Q. J. Exp. Physiol.*, **42,** 279 (1957).
(361) R. Lambert, *C. R. Seances Soc. Biol. Ses. Fil.* **156,** 1421 (1962).
(362) F. G. Harrington, J. D. Greaves, and C. L. A. Schmidt, *Proc. Soc. Exp. Biol. Med.*, **34,** 611 (1936).
(363) A. R. Colwell, *Am. J. Dig. Dis.*, **17,** 270 (1950).
(364) B. Fisher and H. M. Vars, *Am. J. Med. Sci.*, **222,** 116 (1951).
(365) S. Eriksson, *Proc. Soc. Exp. Biol. Med.*, **94,** 578 (1957).
(366) P. Johnson and P. A. Rising, *Xenobiotica*, **8,** 27 (1978).
(367) M. Vore, E. Soliven, and M. Blunden, *J. Pharmacol. Exp. Ther.*, **208,** 257 (1979).
(368) R. J. Roberts and G. L. Plaa, *Gastroenterology*, **50,** 768 (1966).
(369) R. J. Roberts, C. D. Klaassen, and G. L. Plaa, *Proc. Soc. Exp. Biol. Med.*, **125,** 313 (1967).
(370) C. D. Klaassen and S. C. Strom, *Drug Metab. Dispos.*, **6,** 120 (1978).
(371) C. D. Klaassen, *J. Pharmacol. Exp. Ther.*, **175,** 289 (1970).
(372) *Idem.*, **176,** 743 (1971).
(373) L. Manzo, C. Gregotti, P. Richelmi, A. DiNucci, and F. Berté, *Chemotherapy*, **26,** 164 (1980).
(374) S. Lock, H. Witschi, and G. L. Plaa, *Proc. Soc. Exp. Biol. Med.*, **161,** 546 (1979).
(375) H. G. Light, C. Witmer, and H. M. Vars, *Am. J. Physiol.*, **197,** 1330 (1959).
(376) R. J. Vonk, A. B. D. Van Doorn, and J. H. Strubbe, *Clin. Sci. Mol. Med.*, **55,** 253 (1978).
(377) K. G. Wakim, *Am. J. Med.*, **16,** 256 (1954).
(378) P. H. Jordan, *Am. J. Surg.*, **107,** 367 (1964).
(379) R. T. Williams, P. Millburn, and R. L. Smith, *Ann. N.Y. Acad. Sci.*, **123,** 110 (1965).
(380) C. D. Klaassen, *CRC Crit. Rev. Toxicol.*, **4,** 1 (1975).
(381) D. E. Rollins and C. D. Klaassen, *Clin. Pharmacokinet.*, **4,** 368 (1979).
(382) G. Segre, in "Liver and Drugs," F. Orlandi and A. M. Jezequel, Eds., Academic, New York, N.Y., 1972.
(383) I. Sperber, in "Proceeding of the First International Pharmacological Meeting. Drugs and Membranes," vol. 4, C. A. M. Hogben, Ed., Pergamon, New York, N.Y., 1963, p. 137.
(384) P. Millburn, R. L. Smith, and R. T. Williams, *Biochem. J.*, **105,** 1275 (1967).
(385) *Idem.*, **105,** 1283 (1967).
(386) M. M. Abou-El-Makarem, P. Millburn, R. L. Smith, and R. T. Williams, *Biochem. J.*, **105,** 1289 (1967).
(387) M. M. Abou-El-Makarem, P. Millburn, and R. L. Smith, *ibid.*, **105,** 1295 (1967).
(388) K. Takada, Y. Mizobuchi, and S. Muranishi, *Chem. Pharm. Bull.*, **22,** 922 (1974).
(389) H. Nakae, R. Sakata, and S. Muranishi, *ibid.*, **24,** 886 (1976).
(390) K. Takada, Y. Tokunaga, and S. Muranishi, *ibid.*, **24,** 871 (1976).
(391) L. Sawyer and S. Lepkovsky, *J. Lab. Clin. Med.*, **20,** 958 (1935).
(392) M. Friedman, S. O. Byers, and F. Michaelis, *Am. J. Physiol.*, **162,** 575 (1950).
(393) W. C. Knapp, G. A. Leeson, and G. J. Wright, *Lab. Anim. Sci.*, **21,** 403 (1971).
(394) H. C. Klauda, R. F. McGovern, and F. W. Quackenbush, *Lipids*, **8,** 459 (1973).
(395) J. L. Bollman, *J. Lab. Clin. Med.*, **33,** 1348 (1948).
(396) F. Nakayama, *Am. J. Physiol.*, **196,** 319 (1959).
(397) P. M. Harrison and G. T. Stewart, *Br. J. Pharmacol.*, **17,** 420 (1961).
(398) *Idem.*, **17,** 414 (1961).
(399) J. Adir, *J. Pharm. Sci.*, **64,** 1847 (1975).
(400) A. G. Clark and R. Cooke, *J. Pharm. Pharmacol.*, **30,** 382 (1978).
(401) H. G. Dammann, *ibid.*, **30,** 381 (1978).
(402) M. Israel, P. M. Wilkinson, W. J. Pegg, and E. Frei, *Cancer Res.*, **38,** 365 (1978).
(403) W. A. Colburn, P. C. Hirom, R. J. Parker, and P. Milburn, *Drug Metab. Dispos.*, **7,** 100 (1979).
(404) J. L. Bollman, J. C. Cain, and J. H. Grindlay, *J. Lab. Clin. Med.*, **33,** 1349 (1948).
(405) H. E. Gallo-Torres and O. N. Miller, *Proc. Soc. Exp. Biol. Med.*, **130,** 552 (1969).
(406) *Idem.*, **132,** 1 (1969).
(407) J. L. Gowans, *Br. J. Exp. Pathol.*, **38,** 67 (1957).
(408) W. O. Reinhardt, *Proc. Soc. Exp. Biol. Med.*, **58,** 123 (1945).
(409) R. R. Tasker, *J. Physiol. (London)*, **115,** 292 (1951).
(410) J. D. Mann and G. M. Higgins, *Blood*, **5,** 177 (1950).
(411) R. D. Myers, *J. Appl. Physiol.*, **18,** 221 (1963).
(412) J. Olds, A. Yuwiler, M. E. Olds, and C. Yun, *Am. J. Physiol.*, **207,** 242 (1964).
(413) R. D. Myers, G. Casaday, and R. B. Holman, *Physiol. Behav.*, **2,** 87 (1967).
(414) E. P. Noble, R. J. Wurtman, and J. Axelrod, *Life Sci.*, **6,** 281 (1967).
(415) F. DeBalbian Verster, C. A. Robinson, C. A. Hengeveld, and E. S. Bush, *ibid.*, **10,** (Part I), 1395 (1971).
(416) D. D. Avery, in "Physiological Techniques in Behavioral Research," D. Singh and D. D. Avery, Eds., Brooks/Cole, Monterey, Calif. 1975, p. 68.
(417) R. D. Myers, in "Handbook of Psychopharmacology," vol. 2, L. L. Iversen, S. D. Iversen, and S. H. Snyder, Eds., Plenum, New York, N.Y., 1975, p. 1.
(418) F. R. Popick, *Life Sci.*, **18,** 197 (1976).
(419) R. D. Myers, *Meth. Psychobiol.*, **3,** 281 (1977).
(420) E. Decima and R. George, *Electroenceph. Clin. Neurophysiol.*, **17,** 438 (1964).
(421) V. J. Lotti, P. Lomax, and R. George, *Int. J. Neuropharmacol.*, **5,** 35 (1966).
(422) J. W. Wagner and J. DeGroot, *Electroenceph. Clin. Neurophysiol.*, **15,** 125 (1963).
(423) J. F. Hayden, L. R. Johnson, and R. P. Maickel, *Life Sci.*, **5,** 1509 (1966).
(424) D. S. Dudzinski and R. W. P. Cutler, *J. Neurochem.*, **22,** 355 (1974).
(425) G. M. Franklin, D. S. Dudzinski, and R. W. P. Cutler, *ibid.*, **24,** 367 (1975).
(426) J. K. Merlis, *Am. J. Physiol.*, **131,** 67 (1940–1941).
(427) K. M. Knigge and S. A. Joseph, *Acta Endocrinol.*, **76,** 209 (1974).
(428) J. A. Clemens and B. D. Sawyer, *Exp. Brain Res.*, **21,** 399 (1974).
(429) R. C. Chou and G. Levy, *J. Pharmacol. Exp. Ther.*, **219,** 42 (1981).
(430) G. J. DiGregorio and E. K. Kniaz, *Drug Alcohol Depend.*, **1,** 377 (1975/76).
(431) W. S. Chernick, E. Bobyock, and G. J. DiGregorio, *J. Dent. Res.*, **50,** 165 (1971).
(432) G. J. DiGregorio, A. J. Piraino, and E. Ruch, *J. Pharm. Sci.*, **68,** 1192 (1979).
(433) A. J. Piraino, G. J. DiGregorio, and R. K. Ruch, *J. Pharmacol. Meth.*, **3,** 1 (1980).
(434) R. R. Scheline, *J. Pharm. Pharmacol.*, **17,** 52 (1965).
(435) R. L. Lawson, S. Barranco, and A. M. Sorenson, *Lab. Anim.*

Care, **16**, 72 (1966).
(436) J. H. Thompson, *ibid.*, **16**, 520 (1966).
(437) D. Kissil, R. C. Robichaud, and I. W. Hillyard, *J. Appl. Physiol.*, **23**, 769 (1967).
(438) K. H. Lee, *Lab. Anim. Care*, **18**, 650 (1968).
(439) J. T. Wilson, *ibid.*, **19**, 533 (1969).
(440) R. Girardet, *J. Surg. Res.*, **17**, 131 (1974).
(441) L. Davies, *Lab. Pract.*, **25**, 234 (1976).
(442) M. H. Davis and T. G. Coleman, *Lab. Anim. Sci.*, **29**, 499 (1979).
(443) J. B. Mulder, *ibid.*, **29**, 507 (1979).
(444) D. L. Roerig, A. T. Hasegawa, and R. I. H. Wang, *ibid.*, **30**, 549 (1980).
(445) L. Najar and A. M. Rappaport, *Proc. Soc. Exp. Biol. Med.*, **95**, 65 (1957).
(446) M. Barnett, *J. Anim. Tech. Assoc.*, **9**, 50 (1958).
(447) R. D. Baker, G. C. Guillet, and C. C. Maynes, *J. Appl. Physiol.*, **17**, 1020 (1962).
(448) B. K. Armstrong and A. Softly, *Br. J. Nutr.*, **20**, 595 (1966).
(449) A. Einheber, R. E. Wren, D. Carter, and L. R. Rose, *Lab. Anim. Care*, **17**, 345 (1967).
(450) M. M. Graham, *J. Appl. Physiol.*, **30**, 772 (1971).
(451) V. Henriques and C. Hansen, *Hoppe-Seyler's Z. Physiol. Chem.*, **43**, 418 (1904–1905).
(452) S. E. Owen, *J. Lab. Clin. Med.*, **19**, 1135 (1934).
(453) B. K. Harned, R. W. Cunningham, and E. R. Gill, *Science*, **109**, 489 (1949).
(454) A. C. Peacock and R. S. Harris, *Arch. Biochem.*, **27**, 198 (1950).
(455) G. M. Guest, W. A. Brodsky, and N. Nelson, *Metabolism*, **1**, 89 (1952).
(456) A. Lazarow, in "Methods in Medical Research," vol. 6, section IV, J. M. Steele, Ed., Year Book Publishers, Chicago, Ill., 1954, p. 216.
(457) H. H. Draper and A. F. Robbins, *Proc. Soc. Exp. Biol. Med.*, **91**, 174 (1956).
(458) G. E. Folk and M. A. Folk, *J. Anim. Tech. Assoc.*, **9**, 53 (1958).
(459) J. P. Lambooy, *Lab. Anim. Care*, **17**, 351 (1967).
(460) (a)P. D. Leathwood and D. T. Plummer, *Enzymologia*, **37**, 240 (1969). (b) D. T. Plummer and P. J. Wright, *J. Physiol. (London)*, **209**, 16P (1970).
(461) L. Hansen, and H. Holm, *Lab. Anim.*, **5**, 221 (1971).
(462) E. M. Blass, *Physiol. Behav.*, **9**, 681 (1972).
(463) C. W. Lartigue, T. B. Driscoll, and P. C. Johnson, *Lab. Anim. Sci.*, **28**, 594 (1978).
(464) S. Toon and M. Rowland, *J. Pharmacol. Meth.*, **5**, 321 (1981).
(465) G. L. Brinkman and R. F. Miller, *Science*, **134**, 1531 (1961).
(466) C. A. Winter and L. Flataker, *Toxicol. Appl. Pharmacol.*, **4**, 650 (1962).
(467) M. Fröhlich, S. T. Walma, and J. H. M. Souverijn, *Lab. Anim. Sci.*, **31**, 510 (1981).
(468) P. Brain and D. Benton, *Life Sci.*, **24**, 99 (1979).
(469) J. V. Scott and P. J. Dzink, *Anat. Rec.*, **133**, 655 (1959).
(470) D. Birnbaum and T. Hall, *ibid.*, **140**, 49 (1961).
(471) R. R. Scheline, *Acta Pharmacol. Toxicol.*, **24**, 275 (1966).
(472) R. D. Baker, G. C. Guillet, and C. C. Maynes, *J. Appl. Physiol.*, **17**, 1020 (1962).
(473) C. F. Cisar, *Lab. Anim.*, **7**, 139 (1973).
(474) C. E. Cover, *Lab. Anim. Sci.*, **27**, 1033 (1977).
(475) G. Keighley, *Lab. Anim. Care*, **16**, 185 (1966).
(476) H. Steenbock, M. T. Sell, and E. M. Nelson, *J. Biol. Chem.*, **55**, 399 (1923).
(477) S. Orla-Jensen, A. D. Orla-Jensen, H. Dam, and J. Glavind, *Zentralbe Bakteriol, Parasitenk Infectionskr.*, **104**, (Abt. II), 202 (1941).
(478) R. H. Barnes and G. Fiala, *J. Nutr.*, **68**, 603 (1959).
(479) M. S. Mameesh and B. C. Johnson, *Proc. Soc. Exp. Biol. Med.*, **101**, 467 (1959).
(480) R. H. Barnes, G. Fiala, B. McGehee, and A. Brown, *J. Nutr.*, **63**, 489 (1957).
(481) V. C. Metta, L. Nash, and B. C. Johnson, *ibid.*, **74**, 473 (1961).
(482) R. H. Barnes, *Nutr. Rev.*, **20**, 289 (1962).
(483) J. D. Greaves, *Am. J. Physiol.*, **125**, 429 (1939).
(484) K. Schwartzer, *Z. Gestante Exp. Med.*, **101**, 502 (1937).
(485) Anonymous, *Nutr. Rev.*, **25**, 192 (1967).
(486) R. P. Geyer, B. R. Geyer, P. H. Derse, T. Zinkin, C. A. Elvehjem, and E. B. Hart, *J. Nutrit.*, **33**, 129 (1947).
(487) D. L. Frape, J. Wilkinson, and L. G. Chubb, *Lab. Anim.*, **4**, 67 (1970).
(488) F. H. Ryer and D. W. Walker, *Lab. Anim. Sci.*, **21**, 942 (1971).
(489) W. D. Denckla, *J. Lab. Clin. Med.*, **68**, 173 (1966).
(490) W. D. Denckla, *J. Appl. Physiol.*, **26**, 393 (1969).
(491) R. P. Jensh, I. Weinberg, W. H. Vogel, and R. L. Brent, *Lab Anim.*, **9**, 45 (1980).
(492) R. J. Robbins, *Lab. Anim. Sci.*, **27**, 1038 (1977).
(493) R. H. Birkhahn, L. L. Bellinger, L. Bernardis, and J. R. Border, *J. Surg. Res.*, **21**, 185 (1976).
(494) J. S. Latta and W. W. Nelson, *Am. J. Anat.*, **82**, 321 (1948).
(495) E. DeLong, H. N. Uhley, and M. Friedman, *Am. J. Physiol.*, **196**, 429 (1959).
(496) R. G. Bartlett and P. D. Altland, *J. Appl. Physiol.*, **14**, 395 (1959).
(497) J. A. Stern, G. Winokur, A. Eisenstein, R. Taylor, and M. Sly, *J. Psychosomatic Res.*, **4**, 185 (1960).
(498) C. J. Pfeiffer, *Exp. Med. Surg.*, **25**, 201 (1967).
(499) D. A. Brodie, R. W. Marshall, and O. M. Moreno, *Am. J. Physiol.*, **202**, 812 (1962).
(500) E. Steiger, H. M. Vars, and S. J. Dudrick, *Arch. Surg.*, **104**, 330 (1972).
(501) H. C. Stanton, *Meth. Pharmacol.*, **1**, 125 (1971).

ACKNOWLEDGMENTS

This work was supported in part by NIH Grant HL-24343. T. D. Bjornsson is a recipient of a Pharmaceutical Manufacturers Association Foundation Faculty Development Award in Clinical Pharmacology.

The authors are grateful to Ms. Coyla McCullough (Wellcome Research Laboratories) for her invaluable assistance in searching this large body of scientific literature. Valuable comments on an initial draft of this manuscript were provided by Dr. James E. Brown and Ms. Linda F. Cook, the latter of whom also graciously did the photography for all figures. Informative conversations with Dr. James R. Weeks (The Upjohn Company) are gratefully acknowledged. The authors thank Dr. Gerhard Levy, Mr. David Soda, Dr. Beresford Stock, and Dr. Chii-Ming Lai for introducing them to experimentation with the laboratory rat. Finally, the patience and skilled typing assistance of Ms. Wanda Seymour are gratefully acknowledged.

Pharmacokinetic Relationships Between Cinromide and Its Metabolites in the Rhesus Monkey I: 3-Bromocinnamamide, an Active Metabolite

ELIZABETH A. LANE * **and RENÉ H. LEVY** ˣ

Received February 8, 1982 from the *Department of Pharmaceutics, BG-20, University of Washington, Seattle, WA 98195.* Accepted for publication May 25, 1982. *Present address: Laboratory of Chemical Pharmacology, NHLBI, National Institutes of Health, Bethesda, MD 20205.

Abstract □ Fifty percent of a cinromide dose was metabolized to an active metabolite in the rhesus monkey. The steady-state concentration of this metabolite was 3–6 times that of the parent drug, depending on the route of administration. Cinromide is a medium-extraction ratio drug with a short half-life (0.92 ± 0.23 hr) when compared with the active metabolite, which has a low extraction ratio and a longer half-life (4.43 ± 0.76 hr). Incomplete oral bioavailability of cinromide is a result of first-pass metabolism rather than incomplete absorption.

Keyphrases □ Cinromide—pharmacokinetics, 3-bromocinnamamide metabolite, bioavailability, first-pass effect □ 3-Bromocinnamamide—active metabolite of cinromide, pharmacokinetics, bioavailability □ Pharmacokinetics—cinromide, 3-bromocinnamamide, primate model □ Bioavailability—cinromide, 3-bromocinnamamide, primate model

Whenever a drug yields a metabolite known to have similar pharmacological activity, speculation arises regarding the extent to which the metabolite is responsible for the apparent effect of the parent drug. Therefore, it becomes important to understand the relative disposition characteristics of the parent drug and active metabolite. Cinromide (3-bromo-*N*-ethylcinnamamide) is a new anticonvulsant drug which has reached Phase II of pharmacological evaluation (1–7). Cinromide is known to have an active metabolite resulting from *N*-deethylation (3-bromocinnamamide) which accumulates in humans (8). This investigation addressed two questions pertaining to the relative importance of the parent drug and metabolite: (*a*) the prediction of the steady-state metabolite–parent drug concentration ratio (9) and (*b*) the fraction of cinromide metabolized to the active metabolite. Prior to testing cinromide efficacy for epilepsy in the chronic primate model (6), it was necessary to define the pharmacokinetic characteristics (in particular, the dose dependency and bioavailability) of both of these compounds in this animal model.

EXPERIMENTAL

Animal Studies—Five male rhesus monkeys (*Macaca mulatta*), weighing 4–6 kg and adapted to primate restraining chairs, were each equipped with a jugular catheter for blood withdrawal and a femoral catheter for intravenous drug administration. These studies included the following treatments: (*a*) three intravenous infusions of cinromide[1], (*b*) two intravenous bolus doses of metabolite[1], (*c*) and one oral dose each of cinromide and metabolite.

The three cinromide infusions and the two bolus doses of metabolite were administered according to a randomized Latin-square design. The poor solubility of cinromide (0.09 mg/ml of water) even in 60% polyethylene glycol 400 (29 mg/ml), and its toxicity after large doses, precluded administration of intravenous bolus doses >25 mg/kg. Therefore, to test for dose dependency, cinromide was administered by intravenous infusion (25 mg/ml in 60% polyethylene glycol 400) at rates of 1, 2, and 4 ml/hr for 5 hr. A total of 30 plasma samples (0.5 ml) were collected during the infusion and 30 hr into the postinfusion phase. Urine was collected from the beginning of the infusion until 30 hr postinfusion. Doses of the amide metabolite (10 and 20 mg/kg) were injected over 1–2 min, and 20–25 plasma samples were collected over 30 hr. Urine samples were collected every 12 hr for a 24-hr period after each dose. Oral doses of 125 mg/kg of cinromide and 20 mg/kg of 3-bromocinnamamide were administered to each monkey by nasogastric intubation. Plasma samples were collected for 30 hr after each dose.

The ratios of blood–plasma concentration (λ) for cinromide and the metabolite were estimated from two samples taken from each of four monkeys after a single dose of cinromide. The fraction of cinromide and metabolite bound to plasma proteins was measured after equilibrium dialysis of spiked monkey plasma against isotonic phosphate buffer (pH 7.4). Ten to fifteen replicate determinations of the binding of cinromide at 25, 50, and 101 μmoles/liter and metabolite at 28, 60, and 133 μmoles/liter were made. The samples were dialyzed at 37° for 6 hr (the time required to reach equilibrium).

Analytical Procedure—Plasma samples were analyzed simultaneously for cinromide and the amide metabolite by high-performance liquid chromatography (HPLC). A 0.2-ml sample of plasma was extracted with 5 ml of benzene. The solvent was removed under a nitrogen stream at 50° and reconstituted with 100 μl of the mobile phase (methanol–water, 70:30). Two internal standards (3-bromo-*N*-butylcinnamamide[2] and 3-iodo-*N*-cyclopentylcinnamamide[2]), cinromide, and the metabolite were separated on a C_{18} μ Bondapak column[3] and measured by absorbance at 280 nm. Specificity of this assay was verified by comparison with another method (10).

Accuracy and precision of this assay were monitored by analysis of six control samples (duplicates of three different concentrations of cinromide and amide metabolite) with each set of unknowns. The difference between the known and assayed concentrations, divided by the known concentration, measured the accuracy of the assay. The difference between duplicates, divided by the average, measured the precision of the assay.

Urine (0.5 ml) was analyzed for cinromide in a similar manner. For the metabolite, a sample of urine was extracted and the benzene extract was washed with 2 ml of 0.2 *N* HCl before evaporation.

Pharmacokinetic Analysis—The area under the plasma concentration *versus* time curve (AUC) for each compound was measured by the trapezoidal rule with the terminal area estimated by C/β, where C is the concentration of the last sample and β is the rate constant for the slowest log-linear phase. Clearance (CL) was calculated from dose/AUC and steady-state volume of distribution by a previous method (11). Fitting of concentration time data was performed with the BMD-07R program (12).

[1] Supplied by Burroughs Wellcome Co., Research Triangle Park, N.C.

[2] Supplied by Dr. R. Welch, Wellcome Research Laboratories. Research Triangle Park, N.C.

[3] Waters Associates, Milford, Mass.

0022-3549/83/0500-0493$01.00/0

Table I—Pharmacokinetic Parameters of Cinromide in the Rhesus Monkey

Monkey	Clearance liter/hr Infusion 1[a]	Clearance liter/hr Infusion 2[b]	Clearance liter/hr Infusion 3[c]	Volume of Distribution, liter/kg Infusion 1	Volume of Distribution, liter/kg Infusion 2	Volume of Distribution, liter/kg Infusion 3	Elimination Half-Life, hr Infusion 1	Elimination Half-Life, hr Infusion 2	Elimination Half-Life, hr Infusion 3
336	9.6	4.6	6.6	7.2	3.3	5.3	0.87	0.77	1.28
326	10.1	8.9	—	8.3	6.5	—	0.69	0.90	—
316	4.6	8.3	3.4	3.1	6.8	7.1	0.40	1.08	1.08
184	6.3	6.7	7.8	4.9	5.1	6.9	0.80	0.72	1.08
266	3.9	3.4	3.7	3.9	3.1	3.3	1.05	0.96	1.17
Mean	6.9	6.4	5.4	5.5	5.0	5.6	0.76	0.89	1.15[d]
SD	2.8	2.4	2.2	2.2	1.7	1.7	0.24	0.15	0.10

[a] Infusion 1 rate is 25 mg/hr. [b] Infusion 2 rate is 50 mg/hr. [c] Infusion 3 rate is 100 mg/hr. [d] Statistically significant ($p < 0.05$) compared with infusions 1 and 2.

RESULTS AND DISCUSSION

Assay—The recovery of cinromide and metabolite averaged 98 ± 11% and 93 ± 9%, respectively ($n = 27$: nine replicates at three concentrations, 0.4–12.8 μg/ml for both compounds). Over 13 months, >300 control samples were analyzed yielding accuracy values of 8.2 ± 6.7% and 7.5 ± 6.0% for cinromide and the metabolite, respectively. The precision was 3.4 ± 3.5% and 4.0 ± 4.0% for cinromide and the metabolite, respectively. Within the ranges examined, no concentration dependence for accuracy or precision was apparent.

Cinromide Pharmacokinetics—The postinfusion decay of cinromide was fitted to a monoexponential equation. The average half-life (0.92 ± 0.23 hr) is consistent with achievement of steady state during the 5-hr infusion in most monkeys (Fig. 1). The half-life, clearance, and volume of distribution of cinromide measured from the infusion data are reported in Table I. The volume of distribution was constant in the dose range examined [one-way analysis of variance (ANOVA) on repeated measures, BMDP2V (13)]. Although there was a trend for the lowest clearance at the highest dose, there was no significant difference. However, the postinfusion half-life after 100 mg/hr was significantly longer than the postinfusion half-lives after 25 and 50 mg/hr ($p < 0.05$).

It was found that cinromide had a blood clearance (CL_{plasma}/λ) of 7.5 ± 2.9 liter/hr ($\lambda = 0.82$), about one-half of liver blood flow in the monkey (14). Less than 1% of a dose of cinromide was excreted unchanged in the urine and, assuming all metabolism occurs in the liver, this blood clearance may be regarded as the systemic hepatic clearance (CL_{sys}) of cinromide. CL_{sys} is a nonlinear function of liver blood flow and intrinsic hepatic clearance (CL_{int}) (15, 16), and therefore, it is not a sensitive index of dose dependency of intrinsic clearance. In addition, measurement of clearance as dose/AUC is a time-averaged value and less sensitive to dose-dependent nonlinearities than measurements of clearance at steady state. At the lower two infusion rates, cinromide reached steady state in all monkeys; at the highest infusion rate, steady state did not appear to have been reached in three of the five monkeys. This observation indicates that cinromide may be cleared in a dose-dependent fashion not detected through measurements of average intravenous clearances (dose/AUC).

Metabolite Pharmacokinetics—The amide metabolite could be adequately described by a one-compartment model in three of the five monkeys and a two-compartment model in the other two. The metabolite half-life (4.43 ± 0.76 hr; Table II) was 3–8 times longer than the parent drug half-life (0.92 ± 0.23 hr). Because of the long half-life, the amide metabolite did not reach steady state during the 5-hr cinromide infusion (Fig. 1). The difference in the time course of the two compounds was highlighted in the postinfusion phase. Cinromide could not be measured in the plasma 4 hr after the infusion was stopped, whereas the metabolite was present for >30 hr.

Table II—Pharmacokinetic Parameters for 3-Bromocinnamamide in the Rhesus Monkey Following Intravenous Bolus Doses

Monkey	Plasma Clearance, liters/hr 10-mg/kg Dose	Plasma Clearance, liters/hr 20-mg/kg Dose	Volume of Distribution, liter/kg 10-mg/kg Dose	Volume of Distribution, liter/kg 20-mg/kg Dose	Half-Life, hr 10-mg/kg Dose	Half-Life, hr 20-mg/kg Dose
336	0.78	0.49	0.92	0.65	4.2	5.0
326	1.02	0.78	1.03	0.78	3.7	3.2
316	0.88	0.70	1.06	0.69	4.8	3.5
184	0.84	0.57	1.09	0.85	4.5	5.0
266	0.52	0.63	0.98	0.91	5.6	4.8
Mean	0.81	0.63	1.02	0.78[a]	4.6	4.3
SD	0.18	0.11	0.07	0.11	0.71	0.88

[a] Statistically significant, $p < 0.05$ compared with the 10-mg/kg dose.

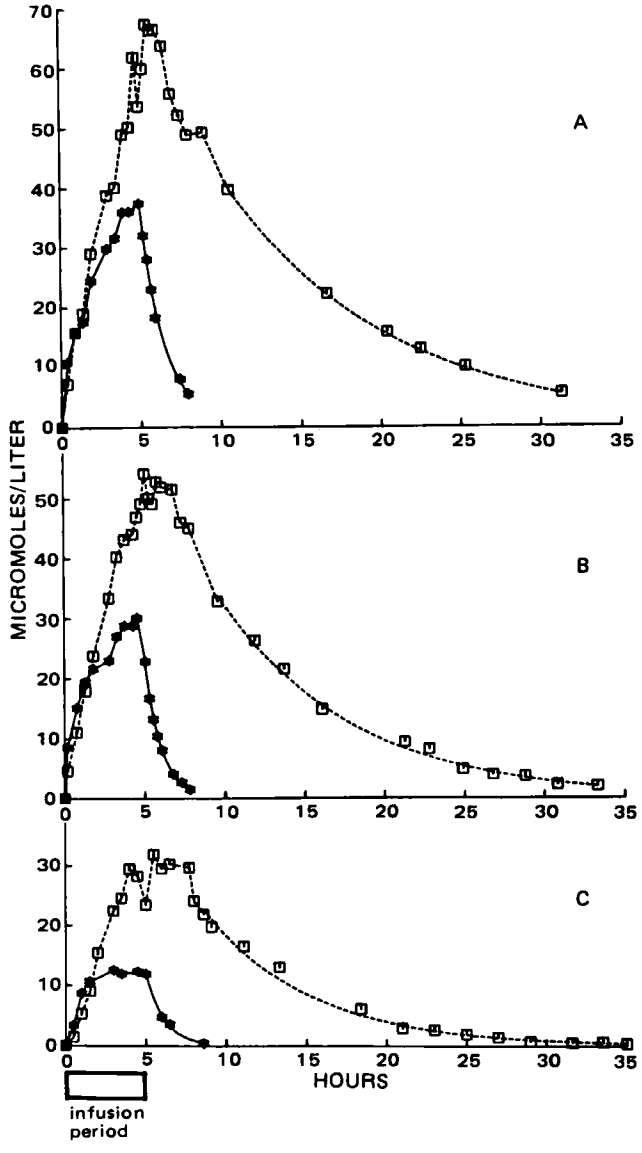

Figure 1—*Cinromide and 3-bromocinnamamide plasma levels during and following three separate cinromide infusions to monkey 184. Infusion concentrations were: (A) 291, (B) 189, and (C) 83 μmoles/hr. Key: (★) cinromide data, (□) 3-bromocinnamamide data, (—) least-squares fit to a monoexponential equation for cinromide (end of infusion to not detectable), and (---) least-squares fit to a monoexponential equation for 3-bromocinnamamide (from the time cinromide is no longer detectable).*

The average plasma clearance of 3-bromocinnamamide decreased from 0.80 ± 0.18 liter/hr to 0.63 ± 0.11 liter/hr when the dose was increased from 10 to 20 mg/kg (Table II). This apparent dose dependency was not significant at the 5% level ($p = 0.077$, paired t test). The volume of distribution of 3-bromocinnamamide decreased significantly ($p < 0.05$) when the dose was increased through this range. Administration of the amide metabolite suggested nonlinear behavior, both in clearance and distribution. However, these two nonlinearities affect half-life in opposite directions. This situation may explain the lack of dose effect on half-life.

The overall average amide metabolite half-life was significantly longer after administration of the parent drug than after administration of the

Table III—Variation in the Half-Life of the Amide Metabolite at Different Doses of Cinromide

Monkey	Cinromide Dose, mg/hr 25	50	100
336	4.6	4.9	8.3
326	6.6	6.3	6.8
316	3.9	4.1	6.6
184	4.6	5.8	7.3
266	6.2	5.4	5.7
Mean	5.2	5.3	6.9[a]
SD	1.2	0.9	0.9

[a] Statistically significant ($p < 0.05$) compared with infusion of 50 or 25 mg/hr.

metabolite. Also, the half-life of this amide metabolite (Table III) increased with increasing doses of cinromide [$p < 0.05$, one-way ANOVA on repeated measures, BMDP2V (13)].

The larger metabolite half-life observed after administration of the parent drug could be due to a type of nonlinearity different from saturation, *e.g.*, inhibition of metabolism by the parent drug or any of its metabolites. Such a phenomenon could also explain the dose-dependent half-life of the metabolite generated *in vivo*.

Fraction Metabolized and Steady-State Metabolite–Parent Drug Concentration Ratio—The fraction of a dose of cinromide metabolized to the amide metabolite (fm) was calculated in a model-independent manner (17):

$$fm = \frac{(AUC_m)_p}{D_p} \times \frac{D_m}{(AUC_m)_m} \qquad \text{(Eq. 1)}$$

where $(AUC_m)_p$ and $(AUC_m)_m$ are the AUC values of the metabolite following a dose of the parent drug and metabolite, respectively, D_p is the dose of the parent drug, and D_m is the dose of the metabolite. The areas under the curve and doses are expressed in molar units.

Since 3-bromocinnamamide is a low-extraction ratio drug, intravenous administration provided an appropriate estimate of intrinsic metabolite clearance for calculation of the fraction metabolized (18). This equation assumes a dose-independent metabolite clearance which measures the clearance of metabolite formed *in situ*. The preceding analysis implies that this is not the case. Therefore, the clearance of a 3-bromocinnamamide dose that was associated with approximately the same plasma concentrations of 3-bromocinnamamide as observed after cinromide, was used in calculation of the fraction metabolized. This matching of 3-bromocinnamamide concentrations would be appropriate if the apparent nonlinearity in metabolite clearance is due to a saturation phenomenon of the Michaelis–Menten type.

The fraction of cinromide metabolized to 3-bromocinnamamide in five monkeys after 14 doses of cinromide averaged 0.47 ± 0.12 (Table IV). This fraction of cinromide metabolized by *N*-deethylation showed no apparent dose dependence. Although theoretically the fraction metabolized is independent of metabolite clearance, it is not when calculated by this method. Therefore, the intra- or interanimal variability in the fraction metabolized may reflect a true variability in the fraction metabolized, as well as variability in the metabolite clearance.

From measurements of the total AUC of the metabolite and the parent drug after a single dose of cinromide, the steady-state metabolite–parent drug concentration ratio during intravenous infusion was predicted at 3.2 ± 0.9 (9). The fraction of free cinromide in monkey plasma (0.17 ± 0.04) was constant over the range examined (25–101 μmoles/liter). The binding of the amide metabolite was similar to the binding of the parent drug, *i.e.*, the free fraction was 0.18 ± 0.04 in the 28–133-μmoles/liter range. Therefore, the ratio of unbound metabolite to parent drug in plasma was predicted to be ~3.

Oral Bioavailability of the Parent Drug and the Metabolite—

Table IV—Fraction of a Cinromide Dose Metabolized by *N*-Deethylation in the Rhesus Monkey

Monkey	Cinromide Dose, mg/hr 25	50	100
336	0.32	0.44	0.39
326	0.43	0.47	0.40
316	0.61	0.28	0.44
184	0.71	0.60	0.35
266	0.48	0.36	0.50
Mean	0.52	0.43	0.42
SD	0.16	0.12	0.06

Table V—Bioavailability of Cinromide and 3-Bromocinnamamide

Monkey	Parent Drug Bioavailability	Metabolite Bioavailability After Administration of Parent Drug	After Administration of Metabolite
336	0.72	0.90	0.99
326	0.35	1.17	0.95
184	0.39	0.82	1.97
266	0.40	0.98	1.03
183	0.79	1.20	1.07
Mean	0.53	1.01	1.20
SD	0.21	0.17	0.43
CV, %	39	16	36

Since the systemic clearance of cinromide was a significant fraction of the hepatic blood flow, an appreciable first-pass effect was expected. The maximum bioavailability of an oral dose (F) can be predicted from the systemic clearance and hepatic blood flow (19, 20):

$$F = 1 - \frac{\text{Hepatic blood clearance}}{\text{Hepatic blood flow}} \qquad \text{(Eq. 2)}$$

This calculation assumes: (*a*) complete absorption from the GI tract; (*b*) metabolism only in the liver; and (*c*) an average hepatic blood flow of 3.18 liters/hr/kg (14). The maximum predicted bioavailability of cinromide was 0.57 ± 0.12, while the observed bioavailability was 0.52 ± 0.12 (Table V). There was no significant difference between the two values. Thus, the incomplete oral bioavailability of cinromide is probably not a result of a dosage form effect or incomplete absorption from the GI tract. Confirmation of the fact that the incomplete availability of oral cinromide is a result of a presystemic first-pass effect, rather than incomplete absorption, was obtained from the metabolite data. The AUC ratio of oral–intravenous metabolite (corrected for dose) averaged 1.01 ± 0.17 (Table V). The equal availability of the active metabolite by both routes of parent drug administration decreases the therapeutic consequences of the first-pass effect of the parent drug.

In view of the low extraction ratio of 3-bromocinnamamide, no reduction in oral bioavailability by a first-pass effect was predicted. The observed bioavailability (median = 1.05) confirmed this prediction (Table V).

In the rhesus monkey, cinromide is a medium-extraction ratio drug with a relatively short half-life. One-half of a cinromide dose is converted to 3-bromocinnamamide by *N*-deethylation. This metabolite has a low extraction ratio and a longer half-life than its precursor. The predicted high metabolite–parent drug steady-state concentration ratio suggests that this metabolite may contribute significantly to the anticonvulsant activity observed after administration of the parent drug. These findings led to the independent evaluation of the efficacy of the amide metabolite, 3-bromocinnamamide, for epilepsy in the primate model (7).

REFERENCES

(1) G. Cloutier, M. Gabriel, E. Geiger, L. Cook, J. Rogers, W. Cummings, and A. Cato, in "Advances in Epileptology: Xth Epilepsy International Symposium," J. A. Wada and J. K. Penry, Eds., Raven, New York, N.Y., 1980, p. 351.

(2) R. M. Welch, S. Hsu, E. Grivsky, and F. E. Soroko, Eleventh Collegium Internationale Neuro-Psychopharmacologicum, Vienna, Austria (1978).

(3) F. E. Soroko, E. M. Grivsky, B. T. Kenney, R. E. Bache, and R. A. Maxwell, *Fed. Proc.*, **38**, 753 (1979).

(4) L. A. Lockman, A. D. Rothner, G. Erenberg, F. W. Wright, G. Cloutier, and E. H. Geiger, American Epilepsy Society Meeting, San Diego, Calif. (1980).

(5) A. J. Wilensky, E. A. Lane, R. H. Levy, L. M. Ojemann, and P. N. Friel, *Eur. J. Clin. Pharmacol.*, **21**, 149 (1981).

(6) J. S. Lockard, R. H. Levy, L. L. DuCharme, and W. C. Congdon, *Epilepsia*, **20**, 339 (1979).

(7) *Idem.*, **21**, 177 (1980).

(8) J. A. Cramer and R. H. Mattson, American Epilepsy Society Meeting, San Diego, Calif., 1980.

(9) E. A. Lane and R. H. Levy, *J. Pharm. Sci.*, **69**, 610 (1980).

(10) R. L. D'Angelis, N. M. Robertson, A. R. Brown, T. E. Johnson, and R. M. Welch, *J. Chromatogr.*, **221**, 353 (1980).

(11) L. Z. Benet and R. L. Galeazzi, *J. Pharm. Sci.*, **68**, 1071 (1979).

(12) "Biomedical Computer Programs," 3rd ed., W. J. Dickson, Ed., University of California Press, Berkeley, Calif., 1973, p. 387.
(13) "Biomedical Computer Programs—P Series," W. J. Dickson and M. B. Brown, Eds., University of California Press, Berkeley, Calif., 1977, p. 540, 601.
(14) R. P. Forsyth, A. S. Nies, F. Wyler, J. Neutze, and K. L. Melmon, *J. Appl. Physiol.*, **25**, 736 (1968).
(15) M. Rowland, L. Z. Benet, and G. G. Graham, *J. Pharmacokinet. Biopharm.*, **1**, 123 (1973).
(16) G. R. Wilkinson and D. G. Shand, *Clin. Pharmacol. Ther.*, **18**, 377 (1975).
(17) S. A. Kaplan, M. L. Jack, S. Cotler, and K. Anderson, *J. Pharmacokinet. Biopharm.*, **1**, 201 (1973).
(18) K. S. Pang and J. R. Gillette, *ibid.*, **7**, 275 (1979).
(19) M. Rowland, *J. Pharm. Sci.*, **61**, 70 (1972).
(20) M. Gibaldi, R. N. Boyes, and S. Feldman, *ibid.*, **60**, 1338 (1971).

ACKNOWLEDGMENTS

This study was supported in part by NINCDS Research Contract NO1-NS-1-2282.

The authors acknowledge the analytical assistance of Ms. Jennifer Andrews and the editorial assistance of Ms. Colleen Montoya.

Use of Isosorbide Dinitrate Saliva Concentrations for Biopharmaceutical Investigations

H. LAUFEN ˣ, M. SCHMID, and M. LEITOLD

Received December 17, 1981, from the *Department of Pharmacology, Heinrich Mack Nachf., 7918 Illertissen/Bayern, West Germany.* Accepted for publication May 18, 1982.

Abstract □ The concentration of isosorbide dinitrate in paired samples of plasma and mixed saliva was monitored for up to 24 hr after oral administration of 60 mg of sustained-release isosorbide dinitrate to eight healthy volunteers. Measured isosorbide dinitrate plasma concentrations were mainly in the range of 0.1–10 ng/ml. Isosorbide dinitrate was excreted into saliva resulting in a mean (±*SD*) saliva–plasma concentration ratio of 0.68 ± 0.37. A significant correlation between concentrations of isosorbide dinitrate in saliva and plasma was found ($p < 0.01$). The sustained-release properties of the administered formulation were confirmed from the concentrations of isosorbide dinitrate found in both saliva and plasma. Saliva–plasma ratios were independent of the absolute concentrations of isosorbide dinitrate but showed a slight tendency to decrease with time. The principal factor relating saliva and plasma isosorbide dinitrate concentrations appeared to be the degree of plasma protein binding of the drug.

Keyphrases □ Isosorbide dinitrate—saliva–plasma ratios following oral administration of a sustained-release preparation □ Sustained-release formulations—saliva–plasma ratios of isosorbide dinitrate following oral administration □ Excretion, salivary—use of isosorbide dinitrate saliva concentrations for biopharmaceutical investigations □ Pharmacokinetics—use of isosorbide dinitrate saliva concentrations for biopharmaceutical investigations

In recent years many investigations have been made on the salivary excretion of drugs in humans. For a number of drugs, it has been demonstrated that the measurement of their concentrations in saliva can be a convenient substitute for plasma analyses, both in monitoring therapeutic drug concentrations and in pharmacokinetic and biopharmaceutical studies. The advantage offered by the measurement of drug concentrations in saliva as well as the limitations of this procedure have been the subject of recent reviews (1–8).

Whether salivary concentration measurements are of value in monitoring pharmacokinetic properties of drugs or not depends on how closely saliva and plasma levels are related. Variations in the saliva–plasma ratio are produced by a number of factors, including variation of the pH of plasma and saliva, the extent of the drug's plasma protein binding, salivary flow rate, active secretion processes, buccal reabsorption, delayed appearance of the drug in saliva, and the technique of saliva sampling (9).

Isosorbide dinitrate is used in the treatment of coronary disease. The plasma pharmacokinetics of this drug are characterized by its rapid excretion (10). This is a disadvantage in long-term therapy with isosorbide dinitrate, and a sustained-release oral formulation of the drug has been used in an attempt to overcome this problem (11–17). During the development of a sustained-release preparation of isosorbide dinitrate, the usefulness of salivary concentration monitoring by multiple paired measurement of isosorbide dinitrate in saliva and plasma was tested.

The present report describes the saliva–plasma ratios of isosorbide dinitrate in eight healthy humans following oral administration of 60 mg of a sustained-release preparation.

EXPERIMENTAL

Eight healthy, fasted, volunteers (3 females and 5 males; 18–38 year; 42–75 kg) were each given one capsule of a slow-release formulation of isosorbide dinitrate[1] (60 mg) with 100 ml of water. Three hours after drug ingestion, a normal breakfast was taken. Blood samples were collected by venipuncture at 0, 0.25, 0.5, 1, 2, 3, 4, 5, 6, 7, 8, 9, 10, 12, 15, and 24 hr after drug administration. At each time the volunteers expectorated 1 ml of mixed saliva into a glass vial. When necessary, to enhance the spontaneous saliva flow, a small crystal of citric acid was applied to the volunteer's tongue. Saliva and plasma (separated from whole blood by centrifugation) were stored at −30° until analysis. Concentrations of isosorbide dinitrate in plasma and saliva were determined by an identical GC procedure with an internal standard (18). The lower limit of isosorbide dinitrate detection was 0.05 ng/ml. All analyses were performed in duplicate.

Statistical calculations on the concentration data obtained were performed with a desk-top computer[2]. The correlation of saliva and plasma levels was determined by linear regression. The coefficient of regression was tested for significant difference from zero, the 95% confidence limits of the coefficient of regression were calculated, and an analysis of variance of the regression was performed (19). Using the same procedures, possible correlations of the saliva–plasma ratio with the absolute plasma concentrations of isosorbide dinitrate as well as with sampling time were tested. The areas under the saliva and plasma level curves were calculated using the trapezoidal rule. An approximate estimation of the apparent

[1] Iso Mack Retard 60 mg, batch No. Ph 2009.
[2] Hewlett-Packard 9815.

0022-3549/83/0500-0496$01.00/0

(12) "Biomedical Computer Programs," 3rd ed., W. J. Dickson, Ed., University of California Press, Berkeley, Calif., 1973, p. 387.
(13) "Biomedical Computer Programs—P Series," W. J. Dickson and M. B. Brown, Eds., University of California Press, Berkeley, Calif., 1977, p. 540, 601.
(14) R. P. Forsyth, A. S. Nies, F. Wyler, J. Neutze, and K. L. Melmon, *J. Appl. Physiol.*, **25**, 736 (1968).
(15) M. Rowland, L. Z. Benet, and G. G. Graham, *J. Pharmacokinet. Biopharm.*, **1**, 123 (1973).
(16) G. R. Wilkinson and D. G. Shand, *Clin. Pharmacol. Ther.*, **18**, 377 (1975).
(17) S. A. Kaplan, M. L. Jack, S. Cotler, and K. Anderson, *J. Pharmacokinet. Biopharm.*, **1**, 201 (1973).
(18) K. S. Pang and J. R. Gillette, *ibid.*, **7**, 275 (1979).
(19) M. Rowland, *J. Pharm. Sci.*, **61**, 70 (1972).
(20) M. Gibaldi, R. N. Boyes, and S. Feldman, *ibid.*, **60**, 1338 (1971).

ACKNOWLEDGMENTS

This study was supported in part by NINCDS Research Contract NO1-NS-1-2282.

The authors acknowledge the analytical assistance of Ms. Jennifer Andrews and the editorial assistance of Ms. Colleen Montoya.

Use of Isosorbide Dinitrate Saliva Concentrations for Biopharmaceutical Investigations

H. LAUFEN ˣ, M. SCHMID, and M. LEITOLD

Received December 17, 1981, from the *Department of Pharmacology, Heinrich Mack Nachf., 7918 Illertissen/Bayern, West Germany.* Accepted for publication May 18, 1982.

Abstract □ The concentration of isosorbide dinitrate in paired samples of plasma and mixed saliva was monitored for up to 24 hr after oral administration of 60 mg of sustained-release isosorbide dinitrate to eight healthy volunteers. Measured isosorbide dinitrate plasma concentrations were mainly in the range of 0.1–10 ng/ml. Isosorbide dinitrate was excreted into saliva resulting in a mean (±*SD*) saliva–plasma concentration ratio of 0.68 ± 0.37. A significant correlation between concentrations of isosorbide dinitrate in saliva and plasma was found ($p < 0.01$). The sustained-release properties of the administered formulation were confirmed from the concentrations of isosorbide dinitrate found in both saliva and plasma. Saliva–plasma ratios were independent of the absolute concentrations of isosorbide dinitrate but showed a slight tendency to decrease with time. The principal factor relating saliva and plasma isosorbide dinitrate concentrations appeared to be the degree of plasma protein binding of the drug.

Keyphrases □ Isosorbide dinitrate—saliva–plasma ratios following oral administration of a sustained-release preparation □ Sustained-release formulations—saliva–plasma ratios of isosorbide dinitrate following oral administration □ Excretion, salivary—use of isosorbide dinitrate saliva concentrations for biopharmaceutical investigations □ Pharmacokinetics—use of isosorbide dinitrate saliva concentrations for biopharmaceutical investigations

In recent years many investigations have been made on the salivary excretion of drugs in humans. For a number of drugs, it has been demonstrated that the measurement of their concentrations in saliva can be a convenient substitute for plasma analyses, both in monitoring therapeutic drug concentrations and in pharmacokinetic and biopharmaceutical studies. The advantage offered by the measurement of drug concentrations in saliva as well as the limitations of this procedure have been the subject of recent reviews (1–8).

Whether salivary concentration measurements are of value in monitoring pharmacokinetic properties of drugs or not depends on how closely saliva and plasma levels are related. Variations in the saliva–plasma ratio are produced by a number of factors, including variation of the pH of plasma and saliva, the extent of the drug's plasma protein binding, salivary flow rate, active secretion processes, buccal reabsorption, delayed appearance of the drug in saliva, and the technique of saliva sampling (9).

Isosorbide dinitrate is used in the treatment of coronary disease. The plasma pharmacokinetics of this drug are characterized by its rapid excretion (10). This is a disadvantage in long-term therapy with isosorbide dinitrate, and a sustained-release oral formulation of the drug has been used in an attempt to overcome this problem (11–17). During the development of a sustained-release preparation of isosorbide dinitrate, the usefulness of salivary concentration monitoring by multiple paired measurement of isosorbide dinitrate in saliva and plasma was tested.

The present report describes the saliva–plasma ratios of isosorbide dinitrate in eight healthy humans following oral administration of 60 mg of a sustained-release preparation.

EXPERIMENTAL

Eight healthy, fasted, volunteers (3 females and 5 males; 18–38 year; 42–75 kg) were each given one capsule of a slow-release formulation of isosorbide dinitrate[1] (60 mg) with 100 ml of water. Three hours after drug ingestion, a normal breakfast was taken. Blood samples were collected by venipuncture at 0, 0.25, 0.5, 1, 2, 3, 4, 5, 6, 7, 8, 9, 10, 12, 15, and 24 hr after drug administration. At each time the volunteers expectorated 1 ml of mixed saliva into a glass vial. When necessary, to enhance the spontaneous saliva flow, a small crystal of citric acid was applied to the volunteer's tongue. Saliva and plasma (separated from whole blood by centrifugation) were stored at −30° until analysis. Concentrations of isosorbide dinitrate in plasma and saliva were determined by an identical GC procedure with an internal standard (18). The lower limit of isosorbide dinitrate detection was 0.05 ng/ml. All analyses were performed in duplicate.

Statistical calculations on the concentration data obtained were performed with a desk-top computer[2]. The correlation of saliva and plasma levels was determined by linear regression. The coefficient of regression was tested for significant difference from zero, the 95% confidence limits of the coefficient of regression were calculated, and an analysis of variance of the regression was performed (19). Using the same procedures, possible correlations of the saliva–plasma ratio with the absolute plasma concentrations of isosorbide dinitrate as well as with sampling time were tested. The areas under the saliva and plasma level curves were calculated using the trapezoidal rule. An approximate estimation of the apparent

[1] Iso Mack Retard 60 mg, batch No. Ph 2009.
[2] Hewlett-Packard 9815.

0022-3549/83/0500-0496$01.00/0

Table 1—Individual and Mean Saliva–Plasma Ratios of Isosorbide Dinitrate Concentrations [a]

Time, hr	Volunteer 1	2	3	4	5	6	7	8	Mean	*SD*
0.25	1.73	0.44	0.77	—	2.25	—	0.00	0.50	0.95	0.86
0.5	1.67	0.66	1.13	0.41	1.23	1.11	0.28	0.67	0.90	0.47
1	1.16	0.59	0.61	0.66	1.20	0.88	0.64	0.55	0.79	0.26
2	0.59	0.81	1.06	0.48	0.87	0.83	1.06	0.48	0.77	0.23
3	0.55	0.55	0.67	—	0.85	0.80	0.53	0.48	0.63	0.14
4	0.88	0.27	0.74	0.89	0.82	0.96	0.72	0.63	0.74	0.22
5	0.26	0.70	0.61	—	0.79	0.63	0.73	0.67	0.63	0.17
6	0.97	0.59	0.55	0.90	0.42	1.14	—	0.65	0.75	0.26
7	0.95	0.59	0.49	0.52	0.42	0.53	0.53	0.52	0.27	0.16
8	0.87	0.36	0.51	0.89	0.41	0.71	0.48	—	0.60	0.22
9	0.98	0.66	1.33	0.58	0.49	1.00	0.93	0.67	0.83	0.28
10	0.50	0.15	0.67	0.63	0.29	0.40	0.56	0.25	0.43	0.19
12	0.34	0.04	—	1.50	0.43	1.00	0.33	0.33	0.57	0.50
15	0.21	0.28	—	1.09	1.67	0.00	0.09	1.00	0.62	0.63
24	0.00	0.29	—	0.5	0.75	—	—	—	0.39	0.32
Individual Mean	0.78	0.47	0.76	0.75	0.86	0.77	0.53	0.57		
SD	0.50	0.22	0.27	0.32	0.54	0.32	0.30	0.18		
CV, %	64	47	36	43	63	42	57	32		

[a] After administration of a 60-mg isosorbide dinitrate sustained-release formulation.

terminal half-lives was obtained by exponential regression analysis. Possible differences in the terminal half-lives and the times to peak saliva and plasma concentration were analyzed by paired Student's *t* test. The mean course of absorption of isosorbide dinitrate into saliva and plasma was determined by a previously described method (20).

RESULTS

Isosorbide dinitrate concentrations were measured in 111 saliva–plasma paired samples. The calculated saliva–plasma concentration ratios are listed in Table I. In 15 of the sample pairs, the measured saliva concentrations exceeded the plasma concentrations; in 92 cases the plasma levels of isosorbide dinitrate were higher than the corresponding saliva levels. The overall arithmetic mean of the saliva–plasma ratio was 0.68 ± 0.37 (*SD*). The correlation between plasma and salivary concentrations of isosorbide dinitrate for all individual values is shown in Fig. 1. The proportionality factor relating plasma to saliva concentrations was 0.60 and the correlation coefficient was 0.83. The analysis of variance of the regression revealed that 68.57% of the variation was explained by linear regression and that this was significant at the 1% level ($p < 0.01$). The 95% confidence interval for the coefficient of regression ranged between 0.52 and 0.68. The overall geometric mean for the saliva–plasma ratios was 0.61. This value corresponds well with the mean saliva–plasma ratio obtained from the regression analysis.

The individual means for the saliva–plasma ratios (Table I) ranged from 0.47 to 0.86. The corresponding coefficients of variation indicate that the extent of correlation varied between the eight volunteers. Examples of both poor and good correlations between saliva and plasma concentrations are shown in Fig. 2. The arithmetic means and standard deviations of the saliva–plasma ratio for each sample time are also given in Table I. A tendency for a decrease in the ratio with time occurred; however, the regression analysis of saliva–plasma ratios *versus* time did not show a significant correlation ($p > 0.05$). Furthermore, the correlation between the saliva–plasma ratio and absolute plasma concentration was not significant ($p > 0.05$).

Mean saliva and plasma concentrations of isosorbide dinitrate and the corresponding coefficients of variation are given in Table II. Variances between individuals in isosorbide dinitrate levels were similar in both plasma and saliva specimens. Up to 9 hr after drug intake, the coefficient of variation was 50% and, thereafter, increased to >100%.

At all sampling times, the mean concentration of drug in the plasma exceeded that found in the saliva. The saliva and plasma concentration–time curves were approximately parallel. Due to the relatively high variances both in saliva and in plasma concentrations, the observed mean saliva and plasma levels are significantly different only at the 2, 3, 5, 7, and 8 hr time intervals (paired Student's *t* test, $p < 0.05$).

The mean area under the concentration–time curve was 44.7 ± 20.4 (*SD*) hr ng/ml in saliva and 71.4 ± 39.0 hr ng/ml in plasma, corresponding to a saliva–plasma ratio of 0.63. Mean time to peak and mean apparent terminal half-life were estimated as the average of the individual calculated values. In saliva a mean peak time of 2.6 ± 2.2 hr and in plasma a mean peak time of 3.5 ± 1.4 hr were obtained. The terminal half-life was 3.0 ± 1.2 hr in saliva and 3.7 ± 1.9 hr in plasma. For both parameters, the mean difference between saliva and plasma was not significant (Student's *t* test, $p > 0.05$).

To assess the absorption characteristics of isosorbide dinitrate fol-

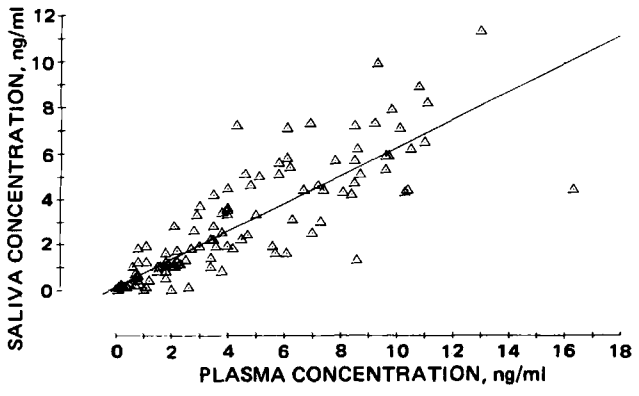

Figure 1—*Regression line for the correlation between saliva and plasma isosorbide dinitrate concentrations observed after administration of a 60-mg isosorbide dinitrate sustained-release formulation: c(saliva) = 0.60 × c(plasma) + 0.28;* r = *0.83.*

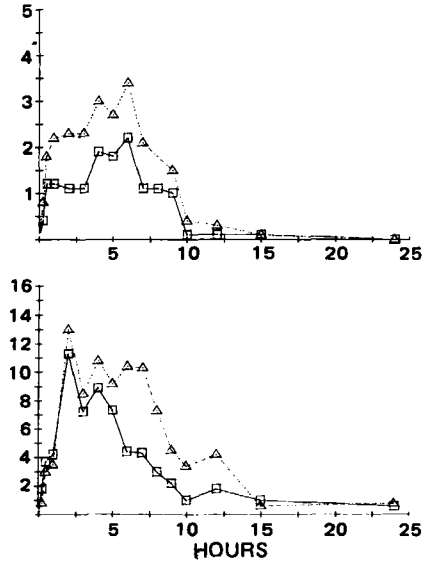

Figure 2—*Examples of different degrees of correlation between saliva (□) and plasma (△) isosorbide dinitrate concentrations in two subjects after administration of a 60-mg isosorbide dinitrate sustained-release formulation.*

Table II—Mean Isosorbide Dinitrate Concentrations in Saliva and Plasma[a]

Time, hr	Saliva Concentrations, ng/ml			Plasma Concentrations, ng/ml		
	Mean	CV, %	n	Mean	CV, %	n
0.25	1.1	73.6	6	1.3	38.4	8
0.50	3.6	58.1	8	4.2	36.7	8
1.00	4.3	44.0	8	5.6	47.5	8
2.00	6.1	60.8	8	7.5	50.5	8
3.00	4.4	44.9	7	6.5	45.5	8
4.00	5.3	44.0	8	8.0	56.6	8
5.00	4.3	56.7	8	7.0	42.7	7
6.00	4.4	33.8	7	6.7	48.9	8
7.00	2.8	65.0	8	5.0	61.5	8
8.00	2.2	71.0	8	4.3	63.7	7
9.00	2.3	61.2	8	3.0	57.6	8
10.00	1.3	101.7	8	3.3	100.6	8
12.00	0.9	87.2	8	2.1	98.3	7
15.00	0.5	85.0	8	1.2	104.6	7
24.00	0.1	186.7	8	0.5	138.5	7

[a] After administration of a 60-mg isosorbide dinitrate sustained-release formulation.

lowing ingestion of the administered slow-release formulation, absorption curves were constructed from both the experimental mean saliva curve and the mean plasma curve. For the calculation a mean elimination rate constant of 0.071 min^{-1} was employed, which was observed in plasma of human volunteers after intravenous administration of isosorbide dinitrate (10). The Wagner–Nelson curves (20) are given in Fig. 3. For comparison, in the same figure absorption curves of two standard formulations of isosorbide dinitrate are shown. These curves are reproduced from mean plasma levels obtained in other pharmacokinetic trials in which 5 and 20 mg isosorbide dinitrate were administered as plain tablet formulations to healthy human volunteers (this report will be published separately). During the first 6 hr after administration of the sustained-release formulation, the mean absorption curve calculated from isosorbide dinitrate saliva concentrations increased slightly more rapidly than the plasma absorption curve. This specimen-related difference is only marginal compared with the formulation-related differences: in contrast to the slow absorption of isosorbide dinitrate from the sustained-release preparation, the Wagner–Nelson curves (20) of the plain tablets show a steep initial increase.

DISCUSSION

The saliva–plasma ratio of drugs is influenced by many factors relating to the physicochemical characteristics of the drug and the mechanism of its salivary excretion, as well as to variable conditions such as salivary pH and flow. When a drug enters the saliva through the membranes by a simple diffusion process without the contribution of active secretion, saliva could be regarded as a plasmatic ultrafiltrate. Indeed, it has been shown for a large number of drugs that the concentration in the salivary fluid reflects the fraction of free or protein-unbound drug in plasma (1–8). As free diffusion is confined to the uncharged drug molecule, corrections should be made for pH differences on both sides of the membrane for weak acids and bases (21, 22). As isosorbide dinitrate is a lipid soluble molecule that remains uncharged within the physiological pH range, a pH-dependent effect on its membrane permeation is excluded.

Following equilibrium dialysis experiments, it was concluded that isosorbide dinitrate was not extensively bound to human plasma proteins *in vitro* (23). Within a concentration range of 1–100 ng/ml, the free fraction was found to be 0.72 ± 0.12 (mean ± *SD*). This value corresponds well with both the mean saliva–plasma ratio of isosorbide dinitrate obtained by linear regression, which was 0.60 ± 0.08 (coefficient of regression ±95% confidence limits), and the arithmetic mean of the individual saliva–plasma ratios of 0.68 ± 0.37 (mean ± *SD*). Therefore, it was suggested that the principal factor relating isosorbide dinitrate saliva to isosorbide dinitrate plasma concentrations is the degree of plasma protein binding of the drug.

Since the standard deviation of the isosorbide dinitrate protein binding (±0.12) reported previously (23) reflects the variation between different subjects, the degree of isosorbide dinitrate plasma binding determined *in vitro* is less variable between individuals than the saliva–plasma ratio found in this trial (*SD* = ±0.37). Therefore, it seems unlikely that the high variabilities of isosorbide dinitrate saliva–plasma ratios could be attributed mainly to variations in the degree of plasma binding.

In 15 of the analyses, saliva levels of isosorbide dinitrate exceeded those

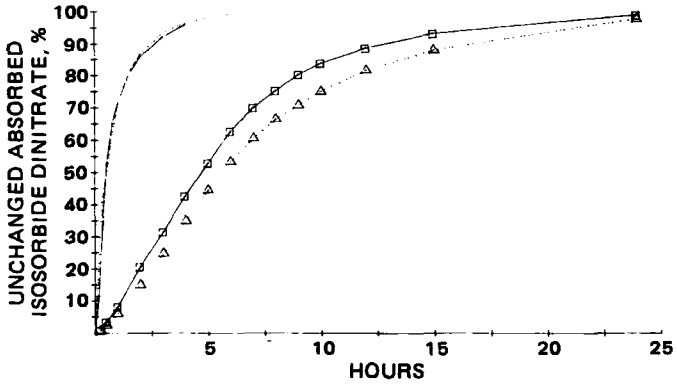

Figure 3—*Wagner–Nelson absorption curves of isosorbide dinitrate, calculated from mean isosorbide dinitrate plasma (△) and saliva (□) curves obtained after the administration of a 60-mg isosorbide dinitrate sustained-release formulation as well as after oral ingestion of a 5-mg tablet (——) and a 20-mg tablet (- - - -).*

in plasma. For some drugs [lithium is the best known example (24, 25)] saliva–plasma ratios >1 have been discussed as an indication of active transport mechanisms. It was suggested (7) that active secretion into saliva might explain the discrepancies in the saliva–plasma ratio often observed in single-dose studies, particularly when the saliva–plasma ratio appears to be time dependent. As an example, bioavailability studies for theophylline (26, 27) are reported where the saliva–plasma ratio was higher in the absorption phase than in the elimination phase and where saliva concentrations sometimes exceeded the plasma concentrations. Both phenomena were also observed for isosorbide dinitrate in the present study, so that active secretion processes should be considered as one source of the observed variation in the saliva–plasma ratios of isosorbide dinitrate.

An alternative explanation for the inconsistent ratio could be that saliva levels are influenced by isosorbide dinitrate partition into and/or absorption through the oral mucosa. As has been shown (18), the buccal absorption of isosorbide dinitrate is very rapid. Therefore, it may be possible that changes in the extent and the speed of buccal reabsorption of isosorbide dinitrate from saliva contribute considerably to the deviations in saliva–plasma ratios.

Due to the high variability of the observed saliva–plasma ratios, the prediction intervals of single plasma concentrations on the basis of corresponding saliva concentrations are considerable: the 95% confidence interval of the plasma level predicted for a saliva concentration of 5 ng/ml is 7.7 ● 3.9 ng/ml. In comparison, the mean plasma concentration of a sufficient number of subjects can be predicted with narrower confidence intervals: for eight subjects the 95% confidence interval of the mean plasma level is 7.7 ± 1.5 ng/ml. This corresponds to the observation that the mean saliva curve of isosorbide dinitrate mimics the shape of the mean plasma curve, although this does not always hold for the individual curves. Consequently, the characteristic slow-release properties of the administered formulation could be inferred from the mean saliva curve as well as from the mean plasma curve. This was particularly evident when the corresponding Wagner–Nelson absorption curves (20) were compared with the absorption curves of standard formulations of isosorbide dinitrate.

Provided these results can be confirmed for other isosorbide dinitrate preparations, it is suggested that mean saliva concentrations of a sufficient number of subjects ($n \geq 8$) can serve as a substitute for mean plasma levels in biopharmaceutical investigations of isosorbide dinitrate.

REFERENCES

(1) M. M. Joselow, R. Riuz, and L. J. Goldwater, *Am. Ind. Hyg. Assoc. J.*, **30**, 77 (1969).

(2) P. Simon and E. Singlas, *J. Pharmacol. Clin.*, **3**, 177 (1975).

(3) C. F. Speirs, *Br. J. Clin. Pharmacol.*, **4**, 97 (1977).

(4) K. Keller and G. le Petit, *Int. J. Clin. Pharmacol.*, **15**, 468 (1977).

(5) M. G. Horning, L. Brown, J. Nowlin, K. Lertratanangkoon, P. Kellaway, and T. E. Zion, *Clin. Chem.*, **23**, 157 (1977).

(6) J. G. Van Dam and A. C. Van Loenen, *Pharm. Weekbl.*, **113**, 65 (1978).

(7) M. Danhof and D. D. Breimer, *Clin. Pharmacokinet.*, **3**, 39

(1978).
(8) J. W. Paxton, *Meth. Findings Expl. Clin. Pharmacol.*, **1**, 11 (1979).
(9) K. W. Stephen and C. F. Speirs, *Br. J. Clin. Pharmacol.*, **3**, 315 (1976).
(10) T. Taylor, L. F. Chasseaud, and E. Doyle, *Biopharm. Drug Dispos.*, **1**, 149 (1980).
(11) D. F. Assinder, L. F. Chasseaud, J. O. Hunter, R. J. Jung, and T. Taylor, *Arzneim.-Forsch.*, **27**, 156 (1977).
(12) D. F. Assinder, L. F. Chasseaud, and T. Taylor, *J. Pharm. Sci.*, **66**, 775 (1977).
(13) T. Taylor, D. A. O'Kelly, R. M. Major, A. Darragh, and L. F. Chasseaud, *Arzneim.-Forsch.*, **28**, 1426 (1978).
(14) R. Kato, Y. Yamazoe, T. Nara, T. Kimura, and S. Chida, *Rinsho Yakuri*, **10**, 509 (1979).
(15) M. G. Bogaert and M. T. Rosseel, *Nouv. Presse Med.*, **9**, 2424 (1980).
(16) V. Gladigau, G. Neurath, M. Dünger, K. Schnelle, and K. I. Johnson, *Arzneim.-Forsch.*, **31**, 835 (1981).
(17) K. Schnelle, E. Fenzl, K. I. Johnson, V. Gladigau, and A. Schinz, *ibid.*, **31**, 840 (1981).
(18) H. Laufen, F. Scharpf, and G. Bartsch, *J. Chromatogr.*, **146**, 457 (1978).
(19) E. Weber, "Grundriss der Biologischen Statistik," Gustav Fischer Verlag, Stuttgart, West Germany, 1972, p. 344.
(20) J. Wagner and E. Nelson, *J. Pharm. Sci.*, **52**, 610 (1963).
(21) S. B. Matin, S. H. Wan, and J. H. Karam, *Clin. Pharmacol. Ther.*, **16**, 1052 (1974).
(22) B. H. Dvorchik and E. S. Vesell, *Clin. Chem.*, **22**, 868 (1976).
(23) H.-L. Fung, E. F. McNiff, D. Ruggirello, A. Darke, U. Thadani, and J. O. Parker, *Br. J. Clin. Pharmacol.*, **11**, 579 (1981).
(24) U. Groth, W. Prellwitz, and E. Jähnchen, *Clin. Pharmacol. Ther.*, **16**, 490 (1974).
(25) M. Shimizu and D. F. Smith, *ibid.*, **21**, 212 (1977).
(26) C. J. De Blaey and A. G. De Boer, *Pharm. Weekbl.*, **111**, 1216 (1976).
(27) H. J. Knop, T. Kalafusz, A. J. F. Knols, and E. Van der Kleijn, *ibid.*, **110**, 1297 (1975).

Densitometric Determination of the Solubility Parameter and Molal Volume of Compounds of Medicinal Relevance

ZVI LIRON and SASSON COHEN ˣ

Received May 18, 1981, from the *Department of Physiology and Pharmacology, Sackler School of Medicine, Tel-Aviv University*, and the *Institute for Biological Research, Ness-Ziona, Israel.* Accepted for publication April 30, 1982.

Abstract □ A procedure is described for the simultaneous determination of molal volumes (v_2^0) and solubility parameters (δ) of compounds of medicinal interest. These include alkanoic acids of various chain length and branching (some solid at room temperature), cholesterol, and cholesteryl esters. The procedure is based on the determination of partial molal volumes ($\bar{v}_2$) from high-precision density measurements of dilute solutions of these compounds in reference solvents, which range in polarity from carbon tetrachloride (δ = 8.6) to nitrobenzene (δ = 10.0). In some cases, the present results do not agree with values of δ published in the literature. Values calculated from group contributions proposed by other authors are prone to error particularly in the case of branched acids and cholesteryl esters.

Keyphrases □ Densitometric determination—solubility parameter and molal volume of compounds of medicinal relevance □ Solubility—densitometric determination of parameters, molal volume of compounds of medicinal relevance □ Molal volume—densitometric determination of solubility parameter of compounds of medicinal relevance

In a series of studies with structurally nonspecific ethers, it was found that the pharmacological profile of a given member could be a consequence of its solubility parameter (1–3). This finding led to the proposition that such molecules associate with a particular membrane subregion, such as an ionic channel or boundary lipid, in accordance with regular solution theory (4). That is, a given substrate will partition between two phases that differ in solubility parameter at a ratio that can be predicted from the solubility parameters of the interacting species and their partial molal volumes (5). Further exploration of this concept in pharmacology and its possible application in medicinal chemistry required knowledge of reliable data pertaining to these parameters or a suitable experimental procedure for their determination. The main sources on this subject are the works of Hildebrand *et al.* (6) and reviews by Barton (7) and Burrell and Immergut (8). Although helpful, they did not meet the need because they made no reference to compounds of medicinal relevance and lack data on molal volumes, especially for solids. Therefore, this study explores the simultaneous determination of partial molal volumes and solubility parameters from high-precision density measurements of dilute regular solutions. Alkanoic acids, cholesterol, and cholesteryl esters were the compounds of choice for this exploratory study.

BACKGROUND

Definitions—The solubility parameter (δ) of a pure liquid is the square root of the cohesive energy density, and is usually given by:

$$\delta = \left(\frac{-E}{v}\right)^{1/2} = \left(\frac{\Delta H^v - RT}{v}\right)^{1/2} \text{cal}^{1/2}\,\text{cm}^{-3/2} \qquad \text{(Eq. 1)}$$

where E is the energy of the liquid expressing the molal heat of vaporization to the gas state at zero pressure, v is the molal volume of the liquid, and ΔH^v is the heat of vaporization at low vapor pressure. Under conditions of high vapor pressure, the gas law correction should be applied and ZRT should replace RT (1), Z being the compressibility factor.

If no calorimetric data are available, the Clausius–Clapeyron equation may be applied to derive the apparent heat of vaporization from pressure–temperature data:

$$\frac{d\ln P}{dT} = \frac{\Delta H^v}{RT\Delta v^v} = \frac{\Delta H^v_{app}}{RT^2} \qquad \text{(Eq. 2)}$$

where Δv^v is the change in volume on vaporization, $v^g - v^l$. The apparent heat of vaporization is equal to the true one only if the vapor is ideal. Otherwise, the compressibility factor must be used, and Eq. 1 then assumes the form:

$$\delta = \left\{\frac{(\Delta H^v_{app} - RT)Z}{v}\right\}^{1/2} \qquad \text{(Eq. 3)}$$

In the case of solid substances, application of the above relationships is not straightforward. First, many of these are nonvolatile or poorly

0022-3549/83/0500-0499$01.00/0

(1978).
(8) J. W. Paxton, *Meth. Findings Expl. Clin. Pharmacol.*, **1**, 11 (1979).
(9) K. W. Stephen and C. F. Speirs, *Br. J. Clin. Pharmacol.*, **3**, 315 (1976).
(10) T. Taylor, L. F. Chasseaud, and E. Doyle, *Biopharm. Drug Dispos.*, **1**, 149 (1980).
(11) D. F. Assinder, L. F. Chasseaud, J. O. Hunter, R. J. Jung, and T. Taylor, *Arzneim.-Forsch.*, **27**, 156 (1977).
(12) D. F. Assinder, L. F. Chasseaud, and T. Taylor, *J. Pharm. Sci.*, **66**, 775 (1977).
(13) T. Taylor, D. A. O'Kelly, R. M. Major, A. Darragh, and L. F. Chasseaud, *Arzneim.-Forsch.*, **28**, 1426 (1978).
(14) R. Kato, Y. Yamazoe, T. Nara, T. Kimura, and S. Chida, *Rinsho Yakuri*, **10**, 509 (1979).
(15) M. G. Bogaert and M. T. Rosseel, *Nouv. Presse Med.*, **9**, 2424 (1980).
(16) V. Gladigau, G. Neurath, M. Dünger, K. Schnelle, and K. I. Johnson, *Arzneim.-Forsch.*, **31**, 835 (1981).
(17) K. Schnelle, E. Fenzl, K. I. Johnson, V. Gladigau, and A. Schinz, *ibid.*, **31**, 840 (1981).
(18) H. Laufen, F. Scharpf, and G. Bartsch, *J. Chromatogr.*, **146**, 457 (1978).
(19) E. Weber, "Grundriss der Biologischen Statistik," Gustav Fischer Verlag, Stuttgart, West Germany, 1972, p. 344.
(20) J. Wagner and E. Nelson, *J. Pharm. Sci.*, **52**, 610 (1963).
(21) S. B. Matin, S. H. Wan, and J. H. Karam, *Clin. Pharmacol. Ther.*, **16**, 1052 (1974).
(22) B. H. Dvorchik and E. S. Vesell, *Clin. Chem.*, **22**, 868 (1976).
(23) H.-L. Fung, E. F. McNiff, D. Ruggirello, A. Darke, U. Thadani, and J. O. Parker, *Br. J. Clin. Pharmacol.*, **11**, 579 (1981).
(24) U. Groth, W. Prellwitz, and E. Jähnchen, *Clin. Pharmacol. Ther.*, **16**, 490 (1974).
(25) M. Shimizu and D. F. Smith, *ibid.*, **21**, 212 (1977).
(26) C. J. De Blaey and A. G. De Boer, *Pharm. Weekbl.*, **111**, 1216 (1976).
(27) H. J. Knop, T. Kalafusz, A. J. F. Knols, and E. Van der Kleijn, *ibid.*, **110**, 1297 (1975).

Densitometric Determination of the Solubility Parameter and Molal Volume of Compounds of Medicinal Relevance

ZVI LIRON and SASSON COHEN ˣ

Received May 18, 1981, from the *Department of Physiology and Pharmacology, Sackler School of Medicine, Tel-Aviv University*, and the *Institute for Biological Research, Ness-Ziona, Israel.* Accepted for publication April 30, 1982.

Abstract □ A procedure is described for the simultaneous determination of molal volumes (v_2^0) and solubility parameters (δ) of compounds of medicinal interest. These include alkanoic acids of various chain length and branching (some solid at room temperature), cholesterol, and cholesteryl esters. The procedure is based on the determination of partial molal volumes ($\bar{v}_2$) from high-precision density measurements of dilute solutions of these compounds in reference solvents, which range in polarity from carbon tetrachloride (δ = 8.6) to nitrobenzene (δ = 10.0). In some cases, the present results do not agree with values of δ published in the literature. Values calculated from group contributions proposed by other authors are prone to error particularly in the case of branched acids and cholesteryl esters.

Keyphrases □ Densitometric determination—solubility parameter and molal volume of compounds of medicinal relevance □ Solubility—densitometric determination of parameters, molal volume of compounds of medicinal relevance □ Molal volume—densitometric determination of solubility parameter of compounds of medicinal relevance

In a series of studies with structurally nonspecific ethers, it was found that the pharmacological profile of a given member could be a consequence of its solubility parameter (1–3). This finding led to the proposition that such molecules associate with a particular membrane subregion, such as an ionic channel or boundary lipid, in accordance with regular solution theory (4). That is, a given substrate will partition between two phases that differ in solubility parameter at a ratio that can be predicted from the solubility parameters of the interacting species and their partial molal volumes (5). Further exploration of this concept in pharmacology and its possible application in medicinal chemistry required knowledge of reliable data pertaining to these parameters or a suitable experimental procedure for their determination. The main sources on this subject are the works of Hildebrand *et al.* (6) and reviews by Barton (7) and Burrell and Immergut (8). Although helpful, they did not meet the need because they made no reference to compounds of medicinal relevance and lack data on molal volumes, especially for solids. Therefore, this study explores the simultaneous determination of partial molal volumes and solubility parameters from high-precision density measurements of dilute regular solutions. Alkanoic acids, cholesterol, and cholesteryl esters were the compounds of choice for this exploratory study.

BACKGROUND

Definitions—The solubility parameter (δ) of a pure liquid is the square root of the cohesive energy density, and is usually given by:

$$\delta = \left(\frac{-E}{v}\right)^{1/2} = \left(\frac{\Delta H^v - RT}{v}\right)^{1/2} \text{cal}^{1/2}\,\text{cm}^{-3/2} \qquad \text{(Eq. 1)}$$

where E is the energy of the liquid expressing the molal heat of vaporization to the gas state at zero pressure, v is the molal volume of the liquid, and ΔH^v is the heat of vaporization at low vapor pressure. Under conditions of high vapor pressure, the gas law correction should be applied and ZRT should replace RT (1), Z being the compressibility factor.

If no calorimetric data are available, the Clausius–Clapeyron equation may be applied to derive the apparent heat of vaporization from pressure–temperature data:

$$\frac{d\ln P}{dT} = \frac{\Delta H^v}{RT\Delta v^v} = \frac{\Delta H^v_{app}}{RT^2} \qquad \text{(Eq. 2)}$$

where Δv^v is the change in volume on vaporization, $v^g - v^l$. The apparent heat of vaporization is equal to the true one only if the vapor is ideal. Otherwise, the compressibility factor must be used, and Eq. 1 then assumes the form:

$$\delta = \left\{\frac{(\Delta H^v_{app} - RT)Z}{v}\right\}^{1/2} \qquad \text{(Eq. 3)}$$

In the case of solid substances, application of the above relationships is not straightforward. First, many of these are nonvolatile or poorly

0022-3549/83/0500-0499$01.00/0

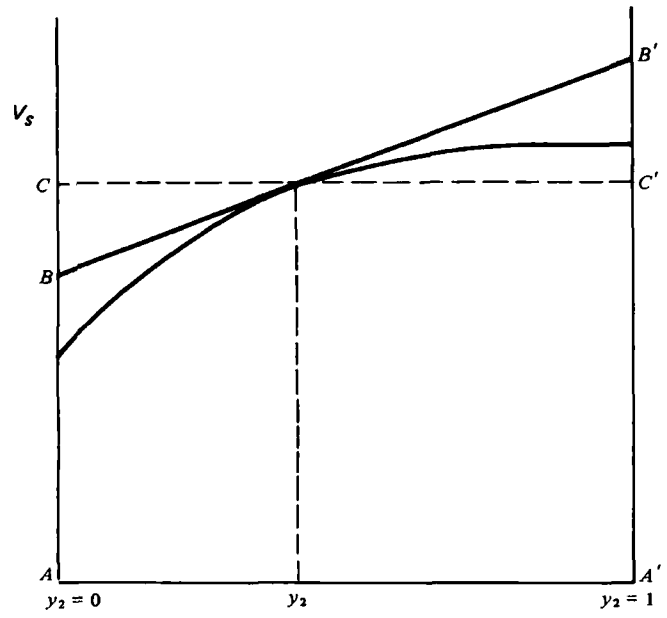

Figure 1—*The relation between the specific volume* V_s *and the mass fraction* y_2 *in a mixture of two components.* AB = $\overline{V}_{s1}$; A'B' = $\overline{V}_{s2}$ *at mass fraction = 0 of the second component.*

volatile. Second, there is an uncertainty in the value of v which must be approximated by extrapolating from the fused substance to the supercooled liquid. In this case, δ is calculated from experimental solubility data, as in the following relationship offered previously (9):

$$RT \ln\left(\frac{a_2^s}{X_2}\right) = v_2\phi_1^2(\delta_2 - \delta_1)^2 \qquad \text{(Eq. 4)}$$

where the subscripts 1 and 2 refer to solvent and solute, respectively, X_2 is the solubility at saturation in mole fraction, v_2 is the molal volume of solute as supercooled liquid, ϕ_1 is the solvent volume fraction, and a_2^s is the activity of the solute as a solid. Calculation of the latter term is an intricate operation which requires knowledge of the heat of fusion at the temperature of fusion and also of the difference between the heat capacity of the liquid and solid states. In a more empirical approach (10), the solubility at saturation of a substance was determined in each of a series of solvents or solvent mixtures of known solubility parameter. The solubility parameter of the solute was then approximated with that of the best solvent. This method has many limitations, especially the need to use high solute concentrations which must inevitably alter the solubility parameter of the reference solvents, since:

$$\delta_{app} = \sum \delta_i \phi_i \qquad \text{(Eq. 5)}$$

where ϕ is the volume fraction. It is particularly doubtful when water is one of the solvent components, because its solubility parameter is still uncertain (11). A previous review gives other empirical procedures (12).

Table I—Determination of the Densities of Various Solutions of Cholesterol in Toluene at 25° [a]

Sample	Mass fraction, $y_2\ 10^3$	Densitometer T value	d Calc, gcm^{-3}	V_{s2}, $cm^3\ g^{-1}$
Toluene	0	1781331	0.86216	1.15987
1	1.129	1781391	0.86229	1.15970
2	2.685	1781473	0.86247	1.15946
3	3.901	1781536	0.86260	1.15928
4	5.233	1781607	0.86276	1.15908
5	6.313	1781662	0.86287	1.15892
6	7.947	1781746	0.86306	1.15868
7	9.910	1781848	0.86327	1.15838
8	11.598	1781935	0.86346	1.15813

[a] From $d_{sample} = d_{air} + 6.03449 \times 10^{-13}(T^2_{sample} - T^2_{air})$; T value for air, 1321506; density of air, 0.001185 gcm^{-3}; T value for water, 1843002; density of water, 0.997043. In this particular example, the relationship between V_{s2} and y_2 is given by: $V_{s2} = 1.15987 - 0.14987y$ ($r^2 = 0.99995$). At $y_2 = 1$, $\overline{V}_{s2} = 1.01000$ which is the partial specific volume of cholesterol in toluene. Multiplication by 386.66 gives $\overline{v}_2 = 390.53$ which is the partial molal volume of cholesterol in toluene at a concentration approaching zero.

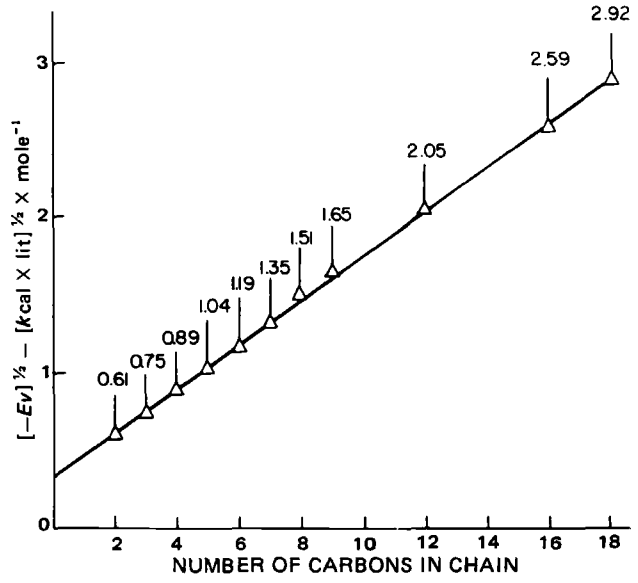

Figure 2—*Alkanoic acids: square root of volume cohesive energy product as a function of acid carbon number (n).*

In a more recent extension of Eq. 4 (13), the geometric mean $\delta_1\delta_2$ of the Hildebrand approach has been replaced by $K\delta_1\delta_2$, which is the solute–solvent interaction energy.

An experimental method of general applicability is now described for the determination of the solubility parameter from partial molal volumes. The method dwells on the same theoretical principles as the dilatometric method described previously (14) and applied earlier (1), but is based on a measurement of density rather than volume change, and does not require prior knowledge of the molal volume of the pure solute.

THEORETICAL

The partial molal volume of a solute, $\overline{v}_2$, is the rate of change of volume of its solution, V, referred to the rate of change of the mole number of solute, n_2:

$$\overline{v}_2 = \frac{\partial v}{\partial n_2} \qquad \text{(Eq. 6)}$$

Now, consider a solution of two components, 1 and 2. A plot of the specific volume, V_s, which is the reciprocal of density, d, against the mass fraction of component 2, y_2, yields a curve as shown in Fig. 1. A tangent to this curve at any point must intercept the ordinate at $y_2 = 0$ at a point B, so that $AB = \overline{V}_{s1}$, the partial specific volume of component 1, and at $y_2 = 1$ at a point B', so that $A'B' = \overline{V}_{s2}$, the partial specific volume of component 2. It can be shown (15) that:

$$\overline{V}_{s1} = V_s - y_2\frac{dV_s}{dy_2} \qquad \text{(Eq. 7)}$$

$$\overline{V}_{s2} = V_s + y_1\frac{dV_s}{dy_2} \qquad \text{(Eq. 8)}$$

The partial molal volume, $\overline{v}_2$, is given by:

$$\overline{v}_2 = M_2\overline{V}_{s2} \qquad \text{(Eq. 9)}$$

where M_2 is the molecular weight of component 2.

An experimental curve as shown in Fig. 1 can be constructed from density measurements of solutions having a predetermined mass fraction of component 2 in the mixture. However, we are interested in the partial molal volume of the solute at a vanishingly small mass fraction, corresponding to a point on the curve at $y_2 = 0$. Hence, a tangent to the curve must be drawn at $y_2 = 0$. In practice, this tangent has the function of a straight line drawn through a series of points having y_2 values $<10^{-2}$. The desired value:

$$\overline{v}_2 \underset{y_2 \to 0}{}$$

is calculated by multiplying the intercept of this tangent at the ordinate $y_2 = 1$ by the molecular weight (see Table I).

Table II—Specific Volumes (V_{s2}^0) and Partial Specific Volumes ($\bar{V}_{s2}$) of Straight-Chain Alkanoic Acids in Two Reference Solvents, at 25°

Number of Carbons in Molecule	V_{s2}^0, $cm^3\ g^{-1}$	$\bar{V}_{s2}$ in Carbon Tetrachloride			$\bar{V}_{s2}$ in Toluene		
		$cm^3\ g^{-1}$	r^2 [a]	SE [b]	$cm^3\ g^{-1}$	r^2 [a]	SE [b]
2	0.95768	1.00075	0.99898	1	0.99706	0.99985	1
3	1.01200	1.03706	0.99968	1	1.02327	0.99968	1
4	1.04960	1.06063	0.99947	1	1.05565	0.99972	1
5	1.07008	1.08048	0.99932	1	1.07396	0.99985	0
6	1.08294	1.09267	0.99994	1	1.08529	0.99704	2
7	1.09436	1.10612	0.99980	1	1.09822	0.99987	1
8	1.10313	1.11254	0.99946	1	1.10758	0.99961	1
9	1.11005	1.11768	0.99885	1	1.11423	0.99903	1
12	S [c]	1.13334	0.99997	0	1.13063	0.99995	0
16	S	1.14462	0.99992	1	1.14391	0.99954	0
18	S	1.15010	0.99972	1	1.14877	0.99969	1

[a] r^2 = Coefficient of determination. [b] SE = standard error × 10^5 for a sample of 8. [c] Solid at room temperature.

According to Hildebrand (14) the partial molal volume of a solute is related to its solubility parameter, as follows:

$$\frac{\bar{v}_2 - v_2^0}{v_2^0} = \frac{(\delta_1 - \delta_2)^2}{(\partial E/\partial v)_T} \qquad \text{(Eq. 10)}$$

Now, if $(\bar{v}_2 - v_2^0)$ and v_2^0 are divided by M_2, the molecular weight of the solute, a form is obtained in which δ could be related directly to specific volume:

$$\frac{\bar{V}_{s2} - V_{s2}^0}{V_{s2}^0} = \frac{(\delta_1 - \delta_2)^2}{(\partial E/\partial v)_T} \qquad \text{(Eq. 11)}$$

For liquids, V_s^0 can be determined by direct measurement of density; hence, δ_2 can be calculated by measurement of $\bar{V}_{s2}$ in a reference solvent for which δ_1 and $(\partial E/\partial v)_T$ must be known. For solids, V_{s2}^0 is not usually readily accessible; in this case, measurements of $\bar{V}_{s2}$ in two reference solvents yield a set of two simultaneous equations from which the two unknowns, V_{s2}^0 and δ_2, may be calculated (*Appendix*).

EXPERIMENTAL

Apparatus—The high-precision, density-measuring assembly used consisted of a measuring cell unit and density meter with digital display[1]. The assembly was placed in a room in which the temperature was thermostatically controlled at 23 ± 1°. The measuring cell unit contained a U-shaped sample tube which was rigidly supported at its open ends. The sample tube was electromagnetically excited to vibrate at its natural frequency. The period of oscillation, T, of the sample tube was related to the density, d, of the sample contained within by the following relationship:

$$d = A(T^2 - B) \qquad \text{(Eq. 12)}$$

where A and B were apparatus constants that had been predetermined by calibration with two fluids of known densities. The sample, ~0.7 ml, was injected into the sample tube with a hypodermic syringe. Excess fluid was allowed to overflow past the vibrating segment. After 2–3 min, thermal equilibration was reached and the period of oscillation was directly read on the digital display. The sample was removed and the tube flushed with solvent and dried with a stream of air until it reached the oscillation period of the empty tube; then a new sample was introduced. The thermostatic system consisted of a main thermostat—a circulator with suction and pressure pumps. The instrument had a digital temperature setting, an antidrift control, a heater capacity of 1000 W, and a cooling coil through which cold water could be run when necessary. The circulator was immersed in a glass cylindrical bath which contained 50 liters of water. The temperature in the bath was measured with a calibrated and tested glass thermometer[2] with a scale division of 0.1°. The temperature deviations in the bath and in the effluent line of the density-measuring cell were measured with thermometers[3] with a 0.01° scale division. Measurements at 25° required the use of a cooler system, which was coupled to the circulator of the main thermostat and which consisted of a control unit and a circulator. The cooler was immersed in 50 liters of water at 20 ± 0.5°. Altogether, the accuracy achieved inside the density-measuring cell that contained the sample was ±0.005°.

Materials—Straight-chain (>99% pure) and branched-chain (>98%) alkanoic acids, cyclopropane carboxylic acid (97%), cholesterol (>98%), and cholesteryl esters (97–98%) were purchased from commercial sources. The solvents were carbon tetrachloride, chlorobenzene, and toluene (>99.5%); chloroform (99.8%); and nitrobenzene (>99%). Chloroform was pretreated with molecular sieves and redistilled before use.

Procedure—For each solute tested, at least eight different samples were weighed, each in a calibrated volumetric flask. The desired weight of solvent was then added. The solute mass fraction (y_2), which was usually in the range of 10^{-4} to 10^{-3}, was determined for each solution to the nearest hundred thousandth. The density meter was calibrated by measuring the oscillatory periods for air and distilled water. The solutions were introduced into the sample tube in order of increasing mass fraction, the oscillatory periods were determined, and the densities calculated. The actual data from these measurements is too voluminous for inclusion in this report; one example is reproduced to illustrate the operation involved (Table I). Thus, for each solution a set of data points was obtained giving the specific volume as a function of mass fraction. Curve fitting was made by a linear least-squares regression analysis program using a desk calculator. The coefficient of determination r^2, the value of $\bar{V}_{s2}$ at $y_2 = 1$, and the standard error, SE, in the estimate of $\bar{V}_{s2}$ on y_2 were derived through the same operation.

RESULTS AND DISCUSSION

Straight-Chain Alkanoic Acids—The partial specific volumes of straight-chain alkanoic acids, in each of two solvents, are given in Table II. The accuracy of measurement can be ascertained from the value of r^2, the coefficient of determination. The precision of data can be checked in each case from the intercept of the regression line with the ordinate at a mass fraction of solute $y_2 = 0$ (Fig. 1). Whenever the assumption of the working hypothesis was satisfied (*i.e.*, there should occur no detectable change in the specific volume of the solvent under working conditions), then the value of this intercept agreed with the specific volume of the solvent which could be determined independently. If this was not the case, then it could be inferred that there occurred an appreciable change in the slope of $\bar{V}_{s2}$ *versus* mass fraction y_2 over the range of concentrations tested. Usually, deviation from linearity became detectable in the mass fraction range $>10^{-2}$.

From the data of Table II the partial molal volumes were derived by application of Eq. 9 and solubility parameters by application of Eq. 11 for liquids (C_2–C_9) and solids (C_{12}–C_{18}) alike, the latter as supercooled liquids at room temperature (Table III). One sees a gradual decrease in δ as the contribution of the polar head becomes less important with the increasing length of the hydrocarbon chain. For a comparison of results with values of δ reported in the literature, some authors have made a distinction between a single solubility parameter, which is usually calculated from the heat of vaporization, and the total solubility parameter, which is the calculated sum total of dispersion, polar, and hydrogen-bond forces (16). The reported single solubility parameters for the acids, propionic (9.9) and valeric (9.8), are in fair agreement with the values presently reported; but that of butyric acid (10.5) is higher than the value found in this study (9.7). The opposite is true for acetic acid for which the total solubility parameter (10.5) (16) is closer to the present value (10.6) than its single parameter (10.1). The calculated value of the total solubility parameter of stearic acid (8.6) is significantly lower than found here (8.9). With the exception of this last example, no records of the solubility parameters of alkanoic acids that exist in solid form at room temperature were found.

The group contributions to v_2^0 and δ, derived from the present data, do not agree in all cases with values published previously (17). The mean

[1] DMA 602 and DMA-60, Anton-Paar, Gretz, Austria.
[2] Brand.
[3] Beckman.

Table III—Molal Volumes (v_2^0), Partial Molal Volumes ($\bar{v}_2$), and Solubility Parameters (δ) of Straight-Chain Alkanoic Acids at 25° [a]

Number of Carbons in Molecule	v_2^0, cm³ mole⁻¹	$\bar{v}_2$, cm³ mole⁻¹		Increment per CH_2			δ, cal$^{1/2}$ cm$^{-3/2}$	
		Carbon Tetrachloride	Toluene	Pure	Carbon Tetrachloride	Toluene	Carbon Tetrachloride	Toluene
2	57.51	60.09	59.87				10.5	10.7
				17.46	16.74	16.00		
3	74.96	76.83	75.80				10.0	9.9
				17.51	16.89	17.14		
4	92.47	93.72	93.01				9.7	9.6
				16.92	16.64	16.68		
5	109.29	110.36	109.69				9.5	9.5
				16.50	16.56	16.45		
6	125.80	126.92	126.14				9.5	9.4
				16.67	17.09	16.65		
7	142.47	144.01	142.79				9.5	9.3
				16.62	16.44	17.08		
8	159.09	160.45	159.87				9.4	9.5
				16.56	16.41	16.45		
9	175.65	176.86	176.32				9.3	9.5
				16.92	16.72	16.72		
12	226.41 [b]	227.03	226.49				9.1	
				16.72	16.62	16.71		
16	293.28 [b]	293.52	293.33				8.8	
				16.76	16.84	16.69		
18	326.81 [b]	327.19	326.72				8.9	

[a] Derived from the data in Table II, by application of Eqs. 9 and 11; δ and $(\partial E/\partial V)_T$ for carbon tetrachloride, 8.6 and 81.0; for toluene, 8.9 and 83.0. [b] As supercooled liquid.

Table IV—Specific Volumes (V_{s2}^0), Partial Specific Volumes ($\bar{V}_{s2}$), Molal Volumes (v_2^0), and Solubility Parameters (δ) of Branched and Other Congeners of Butyric Acid [a]

Acid	V_{s2}^0, cm³ g⁻¹	$\bar{V}_{s2}$ in Carbon Tetrachloride, $n = 8$			v_2^0, cm³ mole⁻¹	δ, cal$^{1/2}$ cm$^{-3/2}$
		cm³ g⁻¹	r^2	$SE \times 10^5$		
2-Methylbutyric	1.07352	1.08074	0.99996	0	109.65	9.3
3-Methylbutyric	1.08512	1.09830	0.99936	1	110.83	9.6
2-Ethylbutyric	1.08836	1.09961	0.99988	1	126.42	9.5
3,3-Dimethylbutyric	1.10194	1.10909	0.99992	1	128.00	9.3
Pivalic	S [b]	1.11104	0.99987	1	109.71	10.3
2-Phenylbutyric	S [b]	0.93129	0.99982	1	150.83	7.8
Cyclopropane carboxylic	0.92362	0.93187	0.99982	1	79.51	9.5

[a] At 25°; solvent data as in Table III. [b] Solids at room temperature; v_2^0 and δ were calculated by use of Eq. 11 and the following additional parameters: $\bar{V}_{s2(\text{toluene})}$ for pivalic acid, 1.09819 ($r^2 = 0.99918$), for phenylbutyric acid, 0.93004 ($r^2 = 0.99972$).

incremental molal volume per CH_2 group for all compounds tested is 16.86 ± 0.60 (pure), 16.72 ± 0.45 (carbon tetrachloride), and 16.66 ± 0.57 (toluene) cm³ mole⁻¹. However, the inclusion of the lower alkanoic acids in the sample is questionable, in view of the observation that the incremental volume of propionic acid over acetic acid is larger in the pure state (17.46) than in solution in either carbon tetrachloride (16.74) or toluene (16.00), implying considerable contraction in these solvents. The significance of this observation is that a CH_2 group adjacent to a COOH group occupies relatively more space in the pure state than in solution in either solvent; *i.e.*, its contribution to the partial molal volume in these states is reduced, even though $\bar{v}_2 > v_2^0$ for the molecule as a whole in almost all cases. In fact, the mean incremental molal volume for the series exclusive of propionic acid, 16.71 ± 0.15 (pure) or 16.68 ± 0.19 (toluene), is significantly different from the corresponding value in propionic acid ($p < 0.001$). The group contribution of a CH_2 group is listed (17) as 16.1 cm³ mole⁻¹ which, obviously, does not apply in the case of a CH_2 adjacent to COOH.

A more generalized presentation of data, inclusive of that of the lower alkanoic acids, may be made according to a previous study (18) where a linear relationship was found between the number of carbon atoms in a given homologous series and the square root of volume-cohesive energy product, $(-Ev)^{1/2}$, which is numerically equal to δv. A plot of δv of straight-chain alkanoic acids against the number of carbons in the chain is shown in Fig. 2. The fit to a straight line is excellent ($r^2 = 1.00$). The slope has a value of 0.14 (kcal liter)$^{1/2}$ mole⁻¹ per carbon atom, as compared with 0.13 for hydrocarbons and ethers. A higher slope value is usually taken to mean a greater interaction energy between the CH_2 groups and the polar end groups (18).

Table V—Partial Specific Volume ($\bar{V}_{s2}$) of Cholesterol in Five Different Solvents [a]

Solvent	$\bar{V}_{s2}$, cm³ g⁻¹	r^2	SE 10^5
Carbon tetrachloride	1.01094	0.99981	1
Toluene	1.01000	0.99995	0
Chloroform	1.01300	0.99981	1
Chlorobenzene	1.01334	0.99981	0
Nitrobenzene	1.01764	0.99977	1

[a] At 25°, $n = 8$.

Branched-Chain Alkanoic Acids—Table IV shows that branching has little effect on v_2^0 and δ, but with the notable exception of pivalic acid and cyclopropane carboxylic acid. Pivalic acid and 2-methylbutyric acid have practically identical molal volumes, but δ in the former is one unit larger than in its isomer. Also, the incremental molal volume in 3,3-dimethylbutyric acid over pivalic acid is 18.29 cm³ mole⁻¹ in the pure state, and which undergoes apparent contraction to 15.33 cm³ mole⁻¹ in carbon tetrachloride. Again, the relative contribution of α-methylene to molal volume is larger in the pure state (0.142) than in solution (0.119). The reason for the difference in δ between pivalic acid and its isomers is not clear at present. Obviously, it does not arise from a difference in v_2^0 of the respective compounds. Group contributions found previously (17) correctly predict the experimental values of v_2^0 for 2-methylbutyric acid (110.60) and pivalic acid (109.8), but not their δ values (9.6 and 9.9, respectively). The same calculations applied to cyclopropane carboxylic acid yield values that disagree with the experimental ones: v_2^0, 77.70 (calc.) against 79.51 (found); δ, 11.6 (calc.) against 9.5 (found).

The function relating δv to the number of carbon atoms in the straight chain alkanoic acids (Fig. 2) applies also to the branched-chain acids, but again with the exception of pivalic and cyclopropane carboxylic acids. Inclusion of 2-methyl-, 3-methyl-, 3,3-dimethyl-, and 2-ethylbutyric acids in the graph does not alter the correlation coefficient ($r^2 = 1.00$); but pivalic acid deviates by +0.1000 from the predicted value and cyclopropane carboxylic acid by −0.1350 (kcal liter)$^{1/2}$ mole⁻¹. This may be taken as an indication that there is more interaction with the polar head in the former and less in the latter, relative to the corresponding straight-chain member.

Cholesterol—The partial specific volumes of cholesterol in five dif-

Table VI—Solubility Parameter (δ) and Molal Volume (v_2^0) of Cholesterol [a]

Solvent	Toluene		Carbon Tetrachloride		Chlorobenzene		Chloroform		Nitrobenzene	
	δ	v_2^0	δ	v_2^0	δ	v_2^0	δ	v_2^0	δ	v_2^0
Toluene			8.9	390.89	8.9	390.52	8.8	390.46	9.0	390.43
Carbon tetrachloride	8.9	390.89			8.9	390.17	8.8	390.65	9.0	390.13
Chlorobenzene	8.9	390.52	8.9	390.17			9.3	391.68	9.2	391.52
Chloroform	8.8	390.46	8.8	390.65	9.3	391.68			9.3	391.68
Nitrobenzene	9.0	390.43	9.0	390.13	9.2	391.52	9.3	391.68		
Mean	8.9	390.58	8.9	390.46	9.1	390.97	9.1	391.12	9.1	390.94
SD	0.1	0.21	0.1	0.37	0.2	0.74	0.3	0.65	0.2	0.77

[a] Derived from the data in Table V by application of Eq. 11 for solvent pairs; δ and $(\partial E/\partial V)_T$ of reference solvents: chlorobenzene, 9.5 and 93.2; chloroform, 9.3 and 86.6; nitrobenzene, 10.0 and 117.1; others as in Table III.

ferent solvents are given in Table V. These data were used to derive the two unknowns, solubility parameter and molal volume of cholesterol, by application of simultaneous equations (11) for solvent pair (Table VI). For each reference solvent, the mean value is listed at the end of the column. The relatively high δ derived from the more polar solvents is significant and needs explanation. In view of the accuracy and precision achieved in the measurement of densities in these solvents (Table V), we assume that the deviation of the experimental system from the theoretical model is minimal and cannot account for the differences among the reference solvents. There remains to be considered the reliability of the published values of δ and $(\partial E/\partial v)_T$ of the reference solvents. Solubility parameter data derived from ΔH^v are usually fairly reliable, but the energy–volume coefficient or internal pressure term, $(\partial E/\partial v)_T$, is a more problematic entity. Internal pressure values can be obtained through direct measurements of $(\partial P/\partial T)_V$, or indirectly by measuring the coefficient of expansion and isothermal compressibility. For most liquids, including some of those used in this study, the indirect and less reliable methods were used to derive the internal pressure values (19–21). Thus, the data derived from carbon tetrachloride and toluene are considered more precise than from the other solvents; the internal pressure of these two solvents had been measured directly.

The mean solubility parameter of cholesterol in the less polar solvents is 8.9, whereas the mean in the more polar ones is 9.1. The mean of means is 9.0 ± 0.1 cal$^{1/2}$ cm$^{-3/2}$ and v_2^0 is 390.81 ± 0.28 cm^3 mole^{-1}, as compared with a previous estimate (17) of 8.0 and 382.20, respectively.

The results for these compounds, all solid at room temperature, are summarized in Tables VII and VIII. The cholesteryl esters of straight-chain alkanoic acids deserve special consideration. If they are treated as a homologous series, a gradual decrease in δ with increasing length of the alkanoyl group, in analogy with the corresponding parent acids would be expected. But this is not the case. An attempt to relate $(-Ev)^{1/2}$ to the number of carbon atoms in the parent acid gave a poor correlation, $(-Ev)^{1/2} = 3.20 \pm 0.15\,n$, $r^2 = 0.94$. The heptanoate ester has the highest δ value in the series, which then declines with either increasing or decreasing chain length. In this context, it should be recalled that compounds possessing liquid crystal properties exhibit unusual dependencies of their physical properties on chain length. The mesomorphic thermal transition of cholesteryl esters from cholesteryl formate to decanoate shows a similar, perhaps related dependency on chain length: the lower six members of the series exhibit only cholesteric mesophases, while the remaining members exhibit both smectic and cholesteric mesophases (22). Another example is offered by previous researchers (23) who observed a definite break at the butyl ester in the melting point and solubility profiles of a series of normal alkyl *p*-aminobenzoates. However, it has been noted (24) that the point of break in properties depends on the loading group, cholesteryl in the present case. In general, larger loading groups require more methylene units to offset their effect on crystal packing. While this generalization may explain the gradual decrease in cohesive energy density in the cholesteryl esters of longer chain than the heptanoate, it does not apply in the case of the lower esters, especially the butyrate which has an unusually low δ value. The emerging profile of δ with respect to chain length in this series may parallel the pattern of mesophase transitions mentioned earlier. In this respect, one must assume that some property of liquid crystal compounds persists into the isotropic phase. This is because the solubility parameter is an intensive property of matter, which, by definition, exists in the form of an isotropic liquid.

There remains to be considered the level of significance at which δ could be determined. This is an important issue in the context of drug distribution, because it can be shown that a hypothetical substrate (i.e., $\delta = 9.0$; $v_2^0 = 100$) will distribute at room temperature between two phases *A* and *B* (δ, 10.0 and 10.5, respectively) in a ratio of 0.81; the corresponding ratios for *B* having δ values of 10.6, 10.7, 10.8, are 0.77, 0.72, 0.68, etc. From the preceding work, δ is calculated from values of partial molal volume that are significant to the second decimal point, and from solubility parameter and internal pressure data of the reference solvents, as published in the literature. Thus, the precision of the calculated δ values must reflect that of the published data.

In any case, a set of such values, generated by reference to a common set of solvents, must remain accurate enough to justify comparison between members, as given for the cholesteryl esters. In the present report, the values of δ for all reference solvents used were taken from a previous study (7). Data on $(\partial E/\partial V)_T$ were used as given for carbon tetrachloride, toluene (25); for chlorobenzene, nitrobenzene (Ref. 20) (given in kilobars (kbar), then transformed into cal$^{1/2}$ cm$^{-3/2}$ by multiplication by 1000/41.84); for chloroform (21), given at 20°, the data were transformed to 25° (19).

As a final check on the validity of the present procedure, the densitometric method was further applied to two reference compounds, as shown in Table IX. The values of the solubility parameter by the present method come very close to the values calculated from the heat of vaporization.

APPENDIX

For solids the solubility parameter of the solute, δ_2, and its molal volume, v_2^0, are derived by solving a set of two simultaneous equations:

$$\frac{\overline{V}_{s21} - V_{s2}^0}{V_{s2}^0} = \frac{(\delta_1 - \delta_2)^2}{P_{i1}} \qquad \text{(Eq. 13)}$$

$$\frac{\overline{V}_{s23} - V_{s2}^0}{V_{s2}^0} = \frac{(\delta_3 - \delta_2)^2}{P_{i3}} \qquad \text{(Eq. 14)}$$

where P_i stands for $(\partial E/\partial V)_T$, the internal pressure of two solvents 1 and 3, and the subscript 2 refers to the solute.

After rearrangement, the following quadratic equation is obtained:

$$a\delta_2^2 + b\delta_2 + c = 0 \qquad \text{(Eq. 15)}$$

where

$$a \equiv \frac{P_{i3}\overline{V}_{s23}}{P_{i1}\overline{V}_{s21}} - 1 \qquad \text{(Eq. 16)}$$

$$b \equiv 2\left(\delta_3 - \delta_1 \frac{P_{i3}\overline{V}_{s23}}{P_{i1}\overline{V}_{s21}}\right) \qquad \text{(Eq. 17)}$$

$$c \equiv \frac{P_{i3}\overline{V}_{s23}}{P_{i1}\overline{V}_{s21}}(\delta_1^2 + P_{i1}) - P_{i3} - \delta_3^2 \qquad \text{(Eq. 18)}$$

Table VII—Partial Specific Volumes ($\overline{V}_{s2}$) of Cholesteryl Esters in Two Reference Solvents, at 25°

Cholesteryl Esters	$\overline{V}_{s2}$ Carbon Tetrachloride			$\overline{V}_{s2}$ Toluene		
	cm^3 g^{-1}	r^2	*SE* × 10^5	cm^3 g^{-1}	r^2	*SE* × 10^5
Acetate	0.99845	0.99996	0	1.00172	0.99988	1
Propionate	0.99740	0.99981	1	1.00243	0.99982	1
Butyrate	1.00554	0.99984	1	1.01240	0.99991	1
Hexanoate	1.02041	0.99994	0	1.02433	0.99997	0
Heptanoate	1.03220	0.99972	1	1.02918	0.99976	1
Laurate	1.05050	0.99977	1	1.04948	0.99974	1
Myristate	1.05130	0.99960	1	1.05501	0.99956	1
Palmitate	1.06078	0.99936	1	1.06201	0.99984	0
Stearate	1.06264	0.99968	1	1.06665	0.99974	1
Oleate	1.04773	0.99980	1	1.05717	0.99965	1
Chloride	0.98712	0.99970	1	0.99226	0.99998	0

[a] $n = 8$.

Table VIII—Molal Volumes (v_2^0), Partial Molal Volumes ($\bar{v}_2$), and Solubility Parameters (δ) of Cholesteryl Esters at 25° [a]

Cholesteryl Esters	v_2^0, cm³ mole⁻¹	$\bar{v}_2$, cm³ mole⁻¹ Carbon Tetrachloride	$\bar{v}_2$, cm³ mole⁻¹ Toluene	δ, cal$^{1/2}$ cm$^{-3/2}$
Acetate	427.54	428.04	429.49	8.3
Propionate	439.83	441.55	443.78	8.0
Butyrate	455.46	459.33	462.46	7.8
Hexanoate	493.77	494.69	496.60	8.2
Heptanoate	513.02	514.90	513.40	9.1
Laurate	597.12	597.72	597.12	8.9
Myristate	627.49	627.66	629.87	8.7
Palmitate	663.07	663.07	663.84	8.6
Stearate	692.81	694.04	696.66	8.2
Oleate	670.79	682.20	688.34	7.4
Chloride	398.19	397.02	401.98	8.0

[a] Derived from the data in Table VII by application of Eq. 11 for solvent pairs; solvent data as in Table III.

Table IX—Comparison Among Values of Solubility Parameter Determined by Various Procedures

Parameter	Method	Reference Compound: Carbon Disulfide	Reference Compound: Carbon Tetrachloride
v_2^0, cm³ mole⁻¹	Present	60.63	97.10
	Ref. 6	60.7	97.1
$\bar{v}_2$, cm³ mole⁻¹ in carbon tetrachloride at 25°	present	62.36[a]	
	dilatometry (6)	62.0	
In cyclohexane at 25°	present		97.46[b]
	dilatometry (6)		97.7
Solubility parameter, cal$^{1/2}$ cm$^{-3/2}$, calculated from $(\bar{v}_2 - v_2^0)/\bar{v}_2$	present	10.1	8.7
	dilatometry (6)	10.1	8.9
From ΔH^v	Ref. 6	10.0	8.6

[a] $r^2 = 0.99890$. [b] $r^2 = 0.99980$.

The molal volume of the solute is given by:

$$v_2^0 = \frac{P_{i1}\bar{V}_{s21}M_2}{\delta_2^2 - 2\delta_2\delta_1 + \delta_1^2 + P_{i1}} \qquad \text{(Eq. 19)}$$

As an example, the above was used to calculate values for δ_2 and v_2^0 for cholesterol by application to the data shown in Table V for the solvent pair nitrobenzene–toluene:

$$a = \frac{117.1 \times 1.01764}{83.0 \times 1.0100} - 1 = 0.42152$$

$$b = 2(10.0 - 8.9 \times 1.42152) = -5.30298$$

$$c = 1.42152\,(8.9^2 + 83.0) - 117.1 - 10.0^2 = 13.48403$$

$$\delta_2 = 9.04335 \rightarrow 9.0$$

$$v_2^0 = \frac{83.0 \times 1.01000 \times 386.66}{9.04335^2 - 2 \times 9.04335 \times 8.9 + 8.9^2 + 83.0} = 390.43$$

REFERENCES

(1) S. Cohen, A. Goldschmid, G. Shtacher, S. Srebrenik, and S. Gitter, *Mol. Pharmacol.*, **11**, 379 (1975).

(2) J. Richter, E. M. Landau, and S. Cohen, *ibid.*, **13**, 548 (1977).

(3) E. M. Landau, J. Richter, and S. Cohen, *J. Med. Chem.*, **22**, 325 (1979).

(4) J. H. Hildebrand and R. L. Scott, "Solubility of Nonelectrolytes," 3rd ed., Reinhold, New York, N.Y., 1950.

(5) S. Srebrenik and S. Cohen, *J. Phys. Chem.*, **80**, 996 (1976).

(6) J. H. Hildebrand, J. M. Prausnitz, and R. L. Scott, "Regular and Related Solutions," Van Nostrand-Reinhold, New York, N.Y., 1970.

(7) A. F. M. Barton, *Chem. Rev.*, **75**, 731 (1975).

(8) H. Burrell and B. Immergut, in "Polymer Handbook," J. Brandrup and B. Immergut, Eds., Interscience, New York, N.Y., 1966.

(9) J. H. Hildebrand, J. M. Prausnitz, and R. L. Scott, "Regular and Related Solutions," Van Nostrand-Reinhold, New York, N.Y., 1970, p. 147.

(10) M. J. Chertkoff and A. N. Martin, *J. Am. Pharm. Assoc., Sci. Ed.*, **49**, 444 (1960).

(11) S. S. Davis, *Experientia*, **26**, 671 (1970).

(12) A. Martin, J. Newburger, and A. Adjei, *J. Pharm. Sci.*, **69**, 487 (1980).

(13) A. Martin and J. Carstensen, *ibid.*, **70**, 170 (1981).

(14) J. H. Hildebrand, J. M. Prausnitz, and R. L. Scott, "Regular and Related Solutions," Van Nostrand-Reinhold, New York, N.Y., 1970, pp. 184–186.

(15) I. Klotz and R. Rosenberg, "Chemical Thermodynamics," Benjamin, Menlo Park, Calif., 1972, pp. 268–270.

(16) C. M. Hansen and H. Beerbower, in "Encyclopedia of Chemical Technology," suppl. vol., 2nd ed., A. Standen, Ed., Wiley, New York, N.Y., 1971.

(17) R. F. Fedors, *Polym. Eng. Sci.*, **14**, 147 (1974).

(18) G. Scatchard, *Chem. Rev.*, **44**, 7 (1949).

(19) S. Chen and E. B. Bagley, *Chem. Eng. Sci.*, **33**, 153 (1978).

(20) R. E. Gibson and O. H. Loeffler, *J. Am. Chem. Soc.*, **61**, 2515 (1939).

(21) G. Allen, G. Gee and G. J. Wilson, *Polymer*, **1**, 456 (1960).

(22) G. W. Gray, *J. Chem. Soc.*, 3733 (1956).

(23) S. H. Yalkowsky, G. L. Flynn, and T. G. Slunik, *J. Pharm. Sci.*, **61**, 852 (1972).

(24) F. L. Breusch, *Fortsch. Chem. Forsch.*, **12**, 119 (1969).

(25) J. H. Hildebrand, J. M. Prausnitz, and R. L. Scott, "Regular and Related Solutions," Van Nostrand-Reinhold, New York, N.Y., 1970, p. 216.

ACKNOWLEDGMENTS

This work was supported by the Recanati Fund for Medical Research.

The authors wish to thank Dr. A. Goldschmid for helpful discussion.

Comparison of High-Performance Liquid Chromatography and Radioimmunoassay in the Determination of Content Uniformity of Digoxin Tablets

MARTIN W. BEASLEY, PAUL SKIERKOWSKI *, ROBERT W. CLEARY ˣ, ALAN B. JONES, and ARTHUR H. KIBBE

Received February 1, 1982, from the *Department of Pharmaceutics, School of Pharmacy, The University of Mississippi, University, MS 38677.* Accepted for publication May 14, 1982. *Present address: Department of Radiation Safety, University of Oklahoma, Norman, OK 73019.

Abstract □ Digoxin 0.25-mg tablets were dissolved and assayed by the standard high-performance liquid chromatography (HPLC) method specified in USP XX and by a radioimmunoassay (RIA) method modified for the assay of tablet solutions. For the RIA method, the filtrate was diluted to a theoretical concentration of 5 ng/ml. Aliquots of this dilution were then assayed for digoxin content using a commercial digoxin ^{125}I RIA kit. Results from both methods were extrapolated to total tablet content and compared with the labeled amount for 20 individual tablets. All tablet assay results were within the USP standards for content uniformity of individual tablets. The individual tablet deviations from labeled amount by the RIA method were smaller when compared with the USP XX-specified HPLC method. Comparison of individual tablet assays show the RIA method to be both as precise and as accurate as the USP XX-specified HPLC method.

Keyphrases □ Digoxin—determination of content uniformity, comparison of high-performance liquid chromatography and radioimmunoassay, tablets □ Radioimmunoassay—comparison with high-performance liquid chromatography in determination of content uniformity of digoxin tablets □ High-performance liquid chromatography—comparison with radioimmunoassay in determination of content uniformity of digoxin tablets

Digoxin is the most predominant digitalis cardiac glycoside prescribed for clinical use. It is a potent drug used to increase the efficiency of the circulation in the treatment of congestive heart failure and to delay the ventricular rate in the treatment of atrial fibrillation and flutter (1).

BACKGROUND

The United States Pharmacopeia (USP) established the content uniformity test for tablets of certain potent drugs in 1965 with USP XVII (2). Due to the small dose (*i.e.*, 0.25 mg) utilized to elicit pharmacological response, digoxin must be assayed on a tablet-to-tablet basis. The USP XX potency definition for digoxin tablets states that the tablets must contain not <90% or not >105% of the labeled amount (3). A representative sample of 30 tablets was selected, and 10 of these tablets were assayed individually according to the drug monograph. The limits of the test state that not more than one tablet can be outside 85–115% of the average of the potency definition, and none of the tablets can be outside 75–125% of the average of the potency definition. The remaining 20 tablets must be assayed if any tablet exceeds the limits as stated. Requirements for content uniformity are met if these 20 tablets fall within the 85–115% average of the potency definition limit (4).

The digoxin content in single tablets has been determined by various methods, including colorimetric, fluorometric, polarographic, and GLC procedures (5–8). Although these methods were adequate in sensitivity, they were relatively cumbersome—either requiring formation of derivatives or complicated extractions or were limited to quantitation of millimolar concentrations. High-performance liquid chromatography (HPLC), a versatile separation technique, is the official assay method for the determination of digoxin tablet content uniformity in USP XX (3).

A number of radioimmunoassay (RIA) procedures for the measurement of biological and drug molecules in body fluids are available. Sensitive assay systems are capable of measuring antigen in the range of femtomole concentrations (9). RIA has been employed in bioavailability studies of digoxin (10–12), and is a highly sensitive method that is able to detect digoxin in human serum at the ng/ml level. The USP does not recognize it as an official test for tablet content uniformity at the present time. Since digoxin can be measured at such dilute levels in blood, it may be possible to utilize this method to determine drug levels in a dilute solution prepared from a single tablet.

EXPERIMENTAL

Materials—Digoxin 0.25-mg tablets[1] and digoxin reference standard powder[2] were used. Acetonitrile[3] was HPLC grade, and the dilute alcohol was USP grade. A [^{125}I]digoxin kit[4] was used in the RIA of the tablets.

Apparatus—A HPLC[5] equipped with a reverse-phase column[6] was connected to a variable-wavelength detector[7] and an automatic integrator[8]. The detector was operated at 218 nm and was attenuated at 0.04 AUFS for digoxin. A single-channel analyzer and amplifier[9] were connected to a counter timer[10] and a NaI(Tl) well crystal[11] for the RIA.

A 250 × 4.6-mm i.d. column, packed with 10-μm hydrocarbon (C18) bonded to silica gel[12], was used at ambient temperature with a mobile phase flow rate of 1.17 ml/min.

The mobile phase consisted of a mixture of acetonitrile–distilled water in a 1:2 ratio. The mixture was allowed to equilibrate 30 min before transfer to the solvent reservoir.

External standard—The digoxin reference standard power was dried for 1 hr at 105° and stored under vacuum in a glass desiccator before preparation. A standard solution (39.8 μg/ml) was prepared in dilute alcohol USP and stored at ambient temperature.

Digoxin 0.25-mg Tablet Assay Solutions—Samples of 10 tablets from two lots of digoxin 0.25-mg tablets were selected at random. Each individual tablet was placed in the center of a single sheet of weighing paper. The paper was tightly folded lengthwise around the tablet to form a cylinder and a 1-cm fold was made at each end of the paper. The tablet was crushed lightly, but completely, into powder with a glass pestle. One end of the paper was opened and inserted well into a clean, dry 10-ml volumetric flask to allow the powdered tablet to slide from the paper to the bottom of the flask. The other end of the paper was opened for the addition of dilute alcohol USP. Six milliliters of dilute alcohol was added through the paper cylinder, washing the residual tablet into the flask. The flask was covered and mixed for 15 sec by a mechanical shaker[13] and then sonicated[14] for 30 min. After sonication, the flask was removed from the sonicator and allowed to cool for 15 min. The solution was brought to volume with dilute alcohol USP and mixed for 15 sec on the mechanical shaker. Immediately after mixing, the entire solution was filtered through a medium-porosity sintered glass funnel. The first five drops of filtrate were discarded, and the remaining filtrate was collected in a clean, dry 10-ml volumetric flask and covered tightly with laboratory film. Based on the labeled quantity of digoxin in the tablets (0.25 mg), theoretical concentrations of the tablet test solution were in the range of 25 μg/ml.

[1] Lanoxin, 0.25-mg tablets, lots 9L2297 and 0J2236; Burroughs Wellcome Co., Research Triangle Park, N.C.
[2] Digoxin Reference Standard, lot 48C 0239; Sigma Chemical Co., St. Louis, Mo.
[3] Burdick & Jackson Laboratories, Inc., Muskegon, Mich.
[4] RIANEN, New England Nuclear Corp., Billerica, Mass.
[5] Model 4200, Varian, Varian Aerograph, Walnut Creek, Calif.
[6] HIBAR-II, MCB Manufacturing Chemists, Inc., Cincinnati, Ohio.
[7] Model 970, Tracor, Tracor Instruments, Austin, Tex.
[8] Model 3380A, Hewlett-Packard, Avondale, Pa.
[9] Model TL 200, Tennelec, Oak Ridge, Tenn.
[10] Model TL 400, Tennelec, Oak Ridge, Tenn.
[11] Model 51SP51, Quartz and Silice, Scintibloc, Paris, France.
[12] Lichrosorb RP-18, MCB Manufacturing Chemists, Cincinnati, Ohio.
[13] Mini-Shaker, Model 58, Fisher Scientific, Pittsburgh, Pa.
[14] Sonicor, Model SC-101th, Sonicor Instrument Corp., Copiague, N.Y.

0022-3549/83/0500-0505$01.00/0

Table I—HPLC Assay Results of Digoxin 0.25-mg Tablets

Sample	AUC	μg of Digoxin, Calculated	Average Recovery, %	Sample	AUC	μg of Digoxin, Calculated	Average Recovery, %
Digoxin, RS	2.56 2.50 (Avg. 2.53)	—	—	Digoxin, RS	3.43 3.59 (Avg. 3.51)	—	—
A1	1.53	241		B1	1.91	217	
	1.65	260	100.4		2.16	245	92.4
A2	1.50	236		B2	2.01	228	
	1.47	231	93.6		2.17	246	94.8
A3	1.50	236		B3	2.36	268	
	1.53	241	95.6		2.35	267	107.0
A4	1.50	236		B4	2.18	247	
	1.56	246	96.4		2.11	239	97.2
A5	1.29	203		B5	2.02	229	
	1.50	236	88.0		2.15	244	94.6
A6	1.43	225		B6	2.09	237	
	1.43	225	90.0		2.07	235	94.4
A7	1.56	246		B7	2.07	235	
	1.45	228	94.8		2.04	231	93.2
A8	1.48	233		B8	2.09	237	
	1.48	233	93.2		1.88	213	90.0
A9	1.61	253		B9	1.99	226	
	1.53	241	98.8		1.94	220	89.2
A10	2.02	229		B10	2.20	250	
	2.02	229	91.6		2.18	247	99.4

The solutions of the 20 individual tablets were designated A1–A10 and B1–B10.

Linearity Test of External Standard—A stock solution (100 μg/ml) was prepared with the digoxin reference standard powder in dilute alcohol USP. Dilutions of 10, 20, 30, 40, 50, 60, 70, and 80 μg/ml were prepared from the stock solution with dilute alcohol USP. Duplicate aliquots of 35-μl injections of the stock solution and each dilution were chromatographed. The average retention time was 5.52 min. Linearity ($r = 0.99708$) was observed.

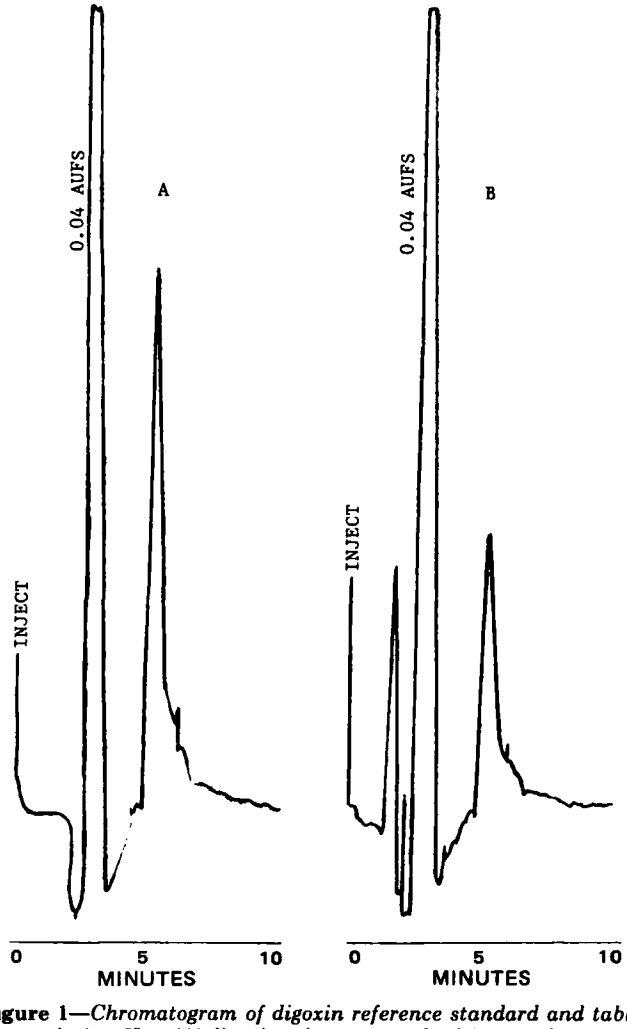

Figure 1—*Chromatogram of digoxin reference standard and tablet assay solution. Key: (A) digoxin reference standard (external standard, 39.8 μg/ml); (B) digoxin tablet assay solution (theoretical concentration of 25 μg/ml).*

HPLC Assay of Digoxin Tablet Solutions—Duplicate 35-μl aliquots of each digoxin tablet solution were chromatographed. Prior to injection of the digoxin tablet assay solutions, between the different sample lots, and after the chromatographs of all the digoxin tablet assay solutions, duplicate 35-μl aliquots of each digoxin reference standard solution (external standard, 39.8 μg/ml) were chromatographed.

Quantitation—The areas under the curve (AUC) generated by duplicate assays of each tablet solution were averaged and compared with the average of the initial duplicate digoxin reference standard solution injections by the formula specified in the USP (3): μg of digoxin = $10C(H_u/H_s)$, where 10 is the dilution volume of each tablet assay solution, C is the concentration of digoxin reference standard in μg/ml, H_u is the average AUC of the tablet assay solution, and H_s is the average AUC of the digoxin reference standard solution.

Preparation of RIA Kit—The [^{125}I]digoxin kit was prepared at room temperature as required by the manufacturer's instructions. The range of the standards for the kit was 0–8.0 ng/ml.

Dilution of Digoxin Reference Standard Solution and Digoxin 0.25-mg Tablet Assay Solutions—An exact volume (1.4 ml) of the digoxin reference standard solution (39.8 μg/ml) was pipeted into a clean, dry 100-ml volumetric flask with a 2-ml glass pipet (0.2-ml graduations). The solution was brought to volume with dilute alcohol USP and allowed to equilibrate overnight. A 1-ml glass pipet was used to transfer 1.0 ml of the equilibrated solution into another clean, dry 100-ml volumetric flask. The solution was brought to volume with dilute alcohol USP to a final concentration of 5.57 ng/ml.

Two milliliters of each tablet solution was pipeted into separate clean, dry 100-ml volumetric flasks with 2-ml glass pipets. The solutions were then brought to volume with dilute alcohol USP and allowed to equilibrate overnight. A 1-ml glass pipet was used to transfer 1.0 ml of each equilibrated solution into another 100-ml volumetric flask. Each solution was brought to volume with dilute alcohol USP. Based on the labeled

Table II—RIA Results of Digoxin 0.25-mg Tablets

Sample	Average Net cpm	μg of Digoxin in Tablet	Sample	Average Net cpm	μg of Digoxin in Tablet
A1	2305	251	B1	2370	247
A2	2323	250	B2	2216	256
A3	2237	255	B3	2383	246
A4	2325	250	B4	2245	254
A5	2266	253	B5	2229	255
A6	2353	248	B6	2312	250
A7	2220	256	B7	2154	260
A8	2137	261	B8	2547	237
A9	2318	250	B9	2240	255
A10	2284	252	B10	2356	248

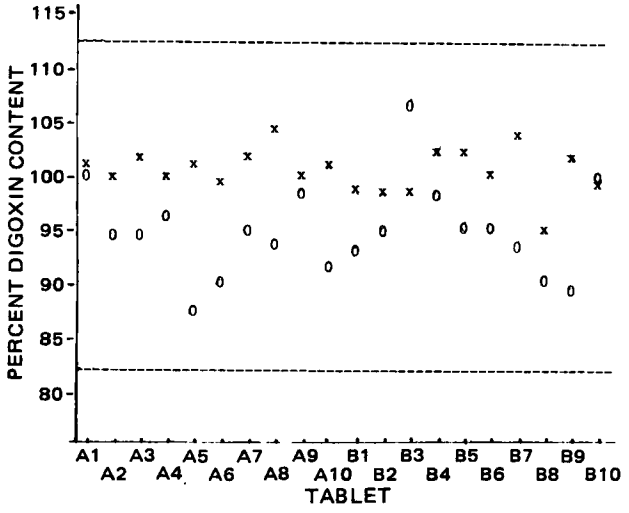

Figure 2—*Comparison of content uniformity test results of single digoxin tablets by HPLC and RIA. Key: (O) percent digoxin recovery by HPLC assay method; (X) percent digoxin recovery by RIA method; (---) limits of digoxin content uniformity.*

quantity of digoxin in the tablets (0.25 mg), theoretical concentrations of the tablet test solutions were in the range of 5 ng/ml.

Gamma Counter Calibration—A simulated iodine-125 source (iodine-129, 0.108 μCi) was utilized to calibrate the single-channel gamma analyzer. The sample[2]–background ratio for the energy peak in the differential mode was utilized to determine the optimum window setting, baseline, and high-voltage potential.

RIA of the Digoxin 0.25-mg Tablet Assay Solutions—All solutions assayed were done in duplicate. The assay consisted of a series of known digoxin standards from the kit (16 tubes), digoxin tablet solution (5 ng/ml) samples (40 tubes), and digoxin reference standard solution (5.57 ng/ml) samples (two tubes). Samples were pipeted into polystyrene 12 × 75-mm tubes[15] with an adjustable microliter pipet[16]. Known digoxin standards consisted of the following duplicate tubes: blank solution (0.02 *M* phosphate buffer, pH 7.4, with 0.5% bovine serum albumin); 0, 0.5, 1.0, 2.0, 4.0, and 8.0 ng/ml standards of digoxin in human serum; and control serum (human serum containing a digoxin concentration of 3 ± 0.3 ng/ml). The duplicate blank solution tubes contained 200 μl of 0.02 *M* phosphate buffer in place of antiserum and 50 μl of 0-ng/ml standard. Each of the remaining digoxin standard duplicate tubes consisted of 50 μl of the respective tablet solution and 200 μl of antiserum (digoxin rabbit serum albumin). The duplicate control serum tubes contained 50 μl of control serum and 200 μl of antiserum. The duplicate digoxin tablet solution samples consisted of 50 μl of the respective tablet solution and 200 μl of antiserum. The duplicate digoxin reference standard solution tubes consisted of 50 μl of digoxin reference standard solution (5.57 ng/ml) and 200 μl of antiserum. After adding 200 μl of radioactive tracer (histamine–digoxin conjugate labeled with iodine-125) to all tubes, the solutions were mixed and incubated at room temperature for 30 min. Following incubation, 1000 μl of concentrated charcoal suspension was added to each tube. The tubes were mixed and incubated again for 10 min. The unbound antigen was adsorbed on the charcoal and separated from the bound antigen by centrifugation[17] at 1200×*g* for 10 min. The supernatant solutions containing the antigen–antibody complexes from each tube were decanted into clean, dry polystyrene tubes, and the radioactivity was determined in the gamma counter.

Quantitation—The counts were averaged for each set of duplicate samples. Average net counts were calculated for all standards and samples by subtracting from each the average blank counts. The average net counts for each standard and sample were expressed as a percentage of the average net counts for the 0-ng/ml standard (normalized percent bound or percent of B/B_0) (13):

$$\text{percent of } B/B_0 = \frac{\text{Average net counts of standard or sample}}{\text{Average net counts of zero standard}}$$

Determinations of digoxin in the control and tablet solutions were made by preparing an exponential least-squares plot of percent of B/B_0 for each standard against the corresponding log concentration of digoxin in ng/ml and calculating the concentration of digoxin in ng/ml from the formula for the line of best fit. Samples were calculated as ng/ml since identical volumes were used for all standards and samples.

[15] Disposable polystyrene culture tubes, Curtin Matheson Scientific, Inc., Houston, Tex.
[16] Pipetman, Model P200D, Rainin Instrument Co., Inc., Woburn, Mass.
[17] Model K size 2, International Equipment Co., Boston, Mass.

Table III—Comparison of Digoxin Tablet Content Assayed by HPLC and RIA

Sample	High-Performance Liquid Chromatography: μg Digoxin in Tablet	HPLC: Recovery, %	Radioimmunoassay: μg of Digoxin in Tablet	RIA: Recovery, %
A1	251	100.4	251	100.4
A2	234	93.6	250	100.0
A3	239	95.6	255	102.0
A4	241	96.4	250	100.0
A5	220	88.0	253	101.2
A6	225	90.0	248	99.2
A7	237	94.8	256	102.4
A8	233	93.2	261	104.4
A9	247	98.8	250	100.0
A10	229	91.6	252	100.8
	avg. 235.6 ± 9.5	avg. 94.2 ± 3.8	avg. 252.6 ± 3.8	avg. 101.0 ± 1.5
B1	231	92.4	247	98.8
B2	237	94.8	256	102.4
B3	268	107.0	246	98.4
B4	243	97.2	254	101.6
B5	237	94.8	255	102.0
B6	236	94.4	250	100.0
B7	233	93.2	260	104.0
B8	225	90.0	237	94.8
B9	223	89.2	255	102.0
B10	249	99.4	248	99.2
	avg. 238.2 ± 13.0	avg. 95.3 ± 5.2	avg. 250.8 ± 6.6	avg. 100.3 ± 2.6

RESULTS AND DISCUSSION

A typical chromatogram of the digoxin reference standard solution and a tablet assay solution is shown in Fig. 1. The area under the curve unexpectedly increased by ~40% on sample A10. Two aliquots of digoxin reference standard solution (39.8 μg/ml) were injected and the AUC had increased almost twofold. The AUC from the nearly twofold increase of digoxin reference standard solution was utilized to calculate the amount of digoxin in tablet assay solutions A10–B10.

There was a considerable degree of tailing from each peak on all reference standard and tablet assay solutions. Amounts of digoxin calculated by the USP formula appeared to be 10–15% lower than expected due to the tailing. Adjustment of the slope sensitivity setting in the integrator did not provide any remedy. The decision was made to calculate the AUC manually by the triangle formula $A = H(W_{1/2})$. The width at mid-height is used instead of the width at baseline to reduce errors. A baseline was drawn, mid-height was determined, and height and width at mid-height were measured in centimeters (14). The assay results of the digoxin tablet solutions are shown in Table I.

The results of the RIA of the digoxin tablet solutions are shown in Table II. A comparison of each individual tablet from the two lots by the two assay methods is shown in Table III. The assay results by both methods are compared with the limits of the USP content uniformity test for digoxin tablets in Fig. 2. Statistical analysis by the paired *t* test is shown in Table IV.

The results in Tables III and IV show that the assay amounts for both methods for each digoxin tablet solution differed by significant amounts at the 95% confidence level. Assay results by HPLC were slightly higher for tablet solutions B3 and B10. RIA results were equal or higher for the remaining tablet solutions. The HPLC assay results for digoxin content ranged from 220 μg (88.0% recovery) to 268 μg (107.2% recovery). Assay results from digoxin content by RIA ranged from 237 μg (94.8% recovery) to 261 μg (104.4% recovery). Assay results of lot A indicated an average digoxin content recovery of 94.2% by HPLC as compared with an average digoxin content recovery of 101.0% by RIA. Results from lot B indicated an average digoxin content recovery of 95.3% by HPLC and an average digoxin content recovery of 100.3% by RIA. The average digoxin content recovery by RIA was 6.8 and 5.0% higher for both lots of digoxin tablets than the average digoxin content recovery by HPLC.

The RIA results for the digoxin tablet solutions were expected to be close to the results provided by the HPLC assay, because it was assumed

Table IV—Statistical Analysis of Digoxin 0.25-mg Tablet Content by HPLC and RIA with Paired t Test at 95% Confidence Level

Lot[a]	Method	Average Digoxin Content, μg	p
A	HPLC	235.6 ± 9.5	<0.05
A	RIA	252.6 ± 3.8	
B	HPLC	238.2 ± 13.0	<0.05
B	RIA	250.8 ± 6.6	

[a] $n = 10$.

that the digoxin would inhibit the radiolabeled antigen from binding with the antiserum in the same manner as if the digoxin was present in human serum. Since the drug was dissolved in USP dilute alcohol, there were no other steroid molecules present in the solutions which might cross-react with the antiserum. The filtering step prior to the assay procedure eliminates most of the excipient ingredients in the tablet dosage form.

As mentioned previously, the content uniformity test for tablets in USP XX required that each tablet must contain not <85% or not >115% of the average of the limits specified in the drug monograph. Digoxin tablets must contain <90% or not >105% of the label claim. Thus, a conforming tablet must fall within 82.9 and 112.1% of the average of the digoxin monograph limits[18].

All digoxin tablets assayed by both HPLC and RIA met the requirements of the content uniformity test.

This study showed that RIA is an accurate alternative to HPLC for content uniformity of digoxin tablets. The data showed the range of digoxin content determined by RIA was narrower than the range of digoxin content determined by HPLC. The significant difference at the 95% confidence level with the paired t test between the assay results of both methods showed that the RIA method appeared to be more precise and closer to the labeled amount than HPLC in the determination of digoxin content in the two lots of digoxin tablets.

[18] "The United States Pharmacopeia," personal communication.

REFERENCES

(1) B. F. Hoffman and J. T. Bigger, Jr., in "Goodman and Gilman's The Pharmacological Basis of Therapeutics," A. G. Gilman, L. S. Goodman, and A. Gilman, Eds., 6th ed., Macmillan, New York, N.Y., 1980, p. 730.

(2) "The United States Pharmacopeia," 17th rev., United States Pharmacopeial Convention, Inc., Rockville, Md., 1965, pp. 905, 906.

(3) "The United States Pharmacopeia," 20th rev., First Supplement USP-NF, United States Pharmacopeial Convention, Inc., Rockville, Md., 1980, p. 30.

(4) "The United States Pharmacopeia," 20th rev., United States Pharmacopeial Convention, Inc., Rockville, Md., 1980, p. 957.

(5) D. Scruffam, *Proc. Soc. Anal. Chem.*, **10**, 208 (1973).

(6) L. F. Cullen, D. L. Packman, and G. J. Papariello, *J. Pharm. Sci.*, **59**, 697 (1970).

(7) K. M. Kadish and V. R. Spiehler, *Anal. Chem.*, **47**, 1714, (1975).

(8) A. H. Kibbe and O. E. Araujo, *J. Pharm. Sci.*, **62**, 1703, (1973).

(9) C. W. Parker, *Annu. Rev. Pharmacol. Toxicol.*, **21**, 114, (1981).

(10) J. Lindenbaum, M. H. Mellow, M. O. Blackstone, and V. P. Butler, *N. Engl. J. Med.*, **285**, 1344, (1971).

(11) P. F. Binnion, *Clin. Pharmacol. Ther.*, **16**, 807, (1974).

(12) P. F. Binnion, M. McDermott, and D. LeSher, *Lancet*, **1**, 1118, (1973).

(13) RIANEN Brand Digoxin (^{125}I) Radioimmunoassay Kit Instruction Manual, New England Nuclear, Billerica, Mass., July 1979, p. 18.

(14) F. Bauman, in "Basic Liquid Chromatography," N. Hadden and F. Bauman, Eds., Varian Aerograph, Walnut Creek, Calif., 1971, pp. 8–5.

ACKNOWLEDGMENTS

Supported by the School of Pharmacy and the Research Institute of Pharmaceutical Sciences, University of Mississippi.

In-Beam Electron Ionization Mass Spectra of Penicillins

MAMORU OHASHI, ROBERT P. BARRON ˣ, and WALTER R. BENSON

Received March 4, 1982, from the *Division of Drug Chemistry, Food and Drug Administration, Washington, DC 20204.* Accepted for publication May 21, 1982.

Abstract □ The characteristics of in-beam electron ionization mass spectra of 6-aminopenicillanic acid and several penicillins, which yield no detectable molecular ion peaks using a conventional direct-insertion probe, have been established. The spectra of all compounds studied, with the exception of amoxicillin, exhibited molecular ion or (M+1) peaks with spectral features similar to the reported methyl ester or amide derivatives of the compounds. The fragmentation of penicillin G on electron impact under in-beam conditions can be described on the basis of data from mass analyzed ion kinetic energy spectrometry. A desorption technique utilizing polyethylene glycol 4000 was used as a means of obtaining satisfactory spectra of ampicillin and amoxicillin.

Keyphrases □ Penicillin—in-beam ionization mass spectra β-lactam antibiotics, amoxicillin, ampicillin □ Electron ionization mass spectra, in-beam—penicillin, β-lactam antibiotics, amoxicillin, ampicillin □ Amoxicillin—in-beam electron ionization mass spectra of penicillins, β-lactam antibiotics □ Ampicillin—in-beam electron ionization mass spectra of penicillins, β-lactam antibiotics

Because of their low vapor pressure and thermal instability, penicillins, a class of β-lactam antibiotics, have generally required chemical pretreatment with formation of their esters or amides prior to mass spectrometric investigations (1, 2). Recently, isobutane and ammonia chemical ionization (CI) mass spectrometric data were published on the free acids of penicillins G and V (3), and the ammonia CI mass spectrum of the potassium salt of penicillin G was reported (4). Pyrolysis mass spectrometry was investigated (5) as a means of characterizing the compounds. The use of in-beam or extended-probe techniques to study apparently nonvolatile and thermally unstable compounds is now commonplace and well documented in the literature (6–14). Using this technique, ammonia-positive and methane-negative ion desorption CI of penicillins was reported (15); however, this report did not include any electron ionization (EI) data. Other researchers[1] have developed a technique using a mixture of the respective potassium salt and ammonium chloride to obtain the EI mass spectra of several penicillins. Accordingly, results obtained in this laboratory are presented on in-beam EI mass spectra of several penicillins, as their free acids, and their fragmentation processes based on mass analyzed ion kinetic energy spectrometric studies (16).

[1] A. K. Bose and B. N. Pramanik, private communication; Stevens Institute of Technology, Hoboken, N.J.

0022-3549/83/0500-0508$01.00/0

Table IV—Statistical Analysis of Digoxin 0.25-mg Tablet Content by HPLC and RIA with Paired t Test at 95% Confidence Level

Lot[a]	Method	Average Digoxin Content, μg	p
A	HPLC	235.6 ± 9.5	<0.05
A	RIA	252.6 ± 3.8	
B	HPLC	238.2 ± 13.0	<0.05
B	RIA	250.8 ± 6.6	

[a] $n = 10$.

that the digoxin would inhibit the radiolabeled antigen from binding with the antiserum in the same manner as if the digoxin was present in human serum. Since the drug was dissolved in USP dilute alcohol, there were no other steroid molecules present in the solutions which might cross-react with the antiserum. The filtering step prior to the assay procedure eliminates most of the excipient ingredients in the tablet dosage form.

As mentioned previously, the content uniformity test for tablets in USP XX required that each tablet must contain not <85% or not >115% of the average of the limits specified in the drug monograph. Digoxin tablets must contain <90% or not >105% of the label claim. Thus, a conforming tablet must fall within 82.9 and 112.1% of the average of the digoxin monograph limits[18].

All digoxin tablets assayed by both HPLC and RIA met the requirements of the content uniformity test.

This study showed that RIA is an accurate alternative to HPLC for content uniformity of digoxin tablets. The data showed the range of digoxin content determined by RIA was narrower than the range of digoxin content determined by HPLC. The significant difference at the 95% confidence level with the paired t test between the assay results of both methods showed that the RIA method appeared to be more precise and closer to the labeled amount than HPLC in the determination of digoxin content in the two lots of digoxin tablets.

[18] "The United States Pharmacopeia," personal communication.

REFERENCES

(1) B. F. Hoffman and J. T. Bigger, Jr., in "Goodman and Gilman's The Pharmacological Basis of Therapeutics," A. G. Gilman, L. S. Goodman, and A. Gilman, Eds., 6th ed., Macmillan, New York, N.Y., 1980, p. 730.

(2) "The United States Pharmacopeia," 17th rev., United States Pharmacopeial Convention, Inc., Rockville, Md., 1965, pp. 905, 906.

(3) "The United States Pharmacopeia," 20th rev., First Supplement USP-NF, United States Pharmacopeial Convention, Inc., Rockville, Md., 1980, p. 30.

(4) "The United States Pharmacopeia," 20th rev., United States Pharmacopeial Convention, Inc., Rockville, Md., 1980, p. 957.

(5) D. Scruffam, *Proc. Soc. Anal. Chem.*, **10**, 208 (1973).

(6) L. F. Cullen, D. L. Packman, and G. J. Papariello, *J. Pharm. Sci.*, **59**, 697 (1970).

(7) K. M. Kadish and V. R. Spiehler, *Anal. Chem.*, **47**, 1714, (1975).

(8) A. H. Kibbe and O. E. Araujo, *J. Pharm. Sci.*, **62**, 1703, (1973).

(9) C. W. Parker, *Annu. Rev. Pharmacol. Toxicol.*, **21**, 114, (1981).

(10) J. Lindenbaum, M. H. Mellow, M. O. Blackstone, and V. P. Butler, *N. Engl. J. Med.*, **285**, 1344, (1971).

(11) P. F. Binnion, *Clin. Pharmacol. Ther.*, **16**, 807, (1974).

(12) P. F. Binnion, M. McDermott, and D. LeSher, *Lancet*, **1**, 1118, (1973).

(13) RIANEN Brand Digoxin (^{125}I) Radioimmunoassay Kit Instruction Manual, New England Nuclear, Billerica, Mass., July 1979, p. 18.

(14) F. Bauman, in "Basic Liquid Chromatography," N. Hadden and F. Bauman, Eds., Varian Aerograph, Walnut Creek, Calif., 1971, pp. 8–5.

ACKNOWLEDGMENTS

Supported by the School of Pharmacy and the Research Institute of Pharmaceutical Sciences, University of Mississippi.

In-Beam Electron Ionization Mass Spectra of Penicillins

MAMORU OHASHI, ROBERT P. BARRON ˣ, and WALTER R. BENSON

Received March 4, 1982, from the *Division of Drug Chemistry, Food and Drug Administration, Washington, DC 20204.* Accepted for publication May 21, 1982.

Abstract □ The characteristics of in-beam electron ionization mass spectra of 6-aminopenicillanic acid and several penicillins, which yield no detectable molecular ion peaks using a conventional direct-insertion probe, have been established. The spectra of all compounds studied, with the exception of amoxicillin, exhibited molecular ion or (M+1) peaks with spectral features similar to the reported methyl ester or amide derivatives of the compounds. The fragmentation of penicillin G on electron impact under in-beam conditions can be described on the basis of data from mass analyzed ion kinetic energy spectrometry. A desorption technique utilizing polyethylene glycol 4000 was used as a means of obtaining satisfactory spectra of ampicillin and amoxicillin.

Keyphrases □ Penicillin—in-beam ionization mass spectra β-lactam antibiotics, amoxicillin, ampicillin □ Electron ionization mass spectra, in-beam—penicillin, β-lactam antibiotics, amoxicillin, ampicillin □ Amoxicillin—in-beam electron ionization mass spectra of penicillins, β-lactam antibiotics □ Ampicillin—in-beam electron ionization mass spectra of penicillins, β-lactam antibiotics

Because of their low vapor pressure and thermal instability, penicillins, a class of β-lactam antibiotics, have generally required chemical pretreatment with formation of their esters or amides prior to mass spectrometric investigations (1, 2). Recently, isobutane and ammonia chemical ionization (CI) mass spectrometric data were published on the free acids of penicillins G and V (3), and the ammonia CI mass spectrum of the potassium salt of penicillin G was reported (4). Pyrolysis mass spectrometry was investigated (5) as a means of characterizing the compounds. The use of in-beam or extended-probe techniques to study apparently nonvolatile and thermally unstable compounds is now commonplace and well documented in the literature (6–14). Using this technique, ammonia-positive and methane-negative ion desorption CI of penicillins was reported (15); however, this report did not include any electron ionization (EI) data. Other researchers[1] have developed a technique using a mixture of the respective potassium salt and ammonium chloride to obtain the EI mass spectra of several penicillins. Accordingly, results obtained in this laboratory are presented on in-beam EI mass spectra of several penicillins, as their free acids, and their fragmentation processes based on mass analyzed ion kinetic energy spectrometric studies (16).

[1] A. K. Bose and B. N. Pramanik, private communication; Stevens Institute of Technology, Hoboken, N.J.

0022-3549/83/0500-0508$01.00/0

Table I—In-beam EI Spectra [a] of Penicillins (Based on Cleavages in Scheme I)

Compound	$M^{+\cdot}$	a	b	c	d	e 160	f 115	g 100	h 114	i 75	Others [b]		
6-Amino-penicill-anic acid	216(9)	57(31)	(−)	(−)	116(40)	(91)	(9)	(17)	(69)	(100)			
I	334(2)	175(14)	119(18)	91(100)	234(−)	(20)	(16)	(40)	(32)	(44)	141(16)	118(47)	
II	350(2)	191(14)	135(20)	107(85)	250(3)	(68)	(13)	(42)	(55)	(66)	77(100)	94(85)	179(25)
											209(33)	211(48)	
III	402(1) (M + 1)	242(18)	186(8)	158(−)	301(−)	(12)	(14)	(31)	(19)	(36)	187(55)	144(100)	77(62)
											103(22)	217(18)	
IV	414(1)	255(25)	199(100)	171(98)	314(−)	(10)	(84)	(80)	(60)	(44)	69(68)	170(67)	
V	378(1)	220(−)	164(−)	136(9)	278(−)	(24)	(6)	(14)	(7)	(45)	91(100)	92(52)	102(24)
											135(10)	217(5)	
VI	349(0.3)	190(5)	134(−)	106(48)	249(−)	(53)	(12)	(30)	(37)	(100)	91(58)	104(49)	147(31)
											332(5)		
VII	365(−)	206(−)	150(−)	122(36)	265(−)	(67)	(24)	(60)	(80)	(100)	107(64)	120(41)	122(36)
	348(3) [c]										134(32)	163(24)	

[a] Unless otherwise noted, the numbers in parentheses represent percent relative intensity with (−) indicating not observed; all other numbers represent m/z values above m/z 50. [b] All spectra exhibit an intense peak at m/z 44. [c] No molecular ion was observed; the highest ion observed was M—OH at m/z 348.

EXPERIMENTAL

Apparatus—All spectra were recorded on a double-focusing mass spectrometer[2] equipped with a modified field-desorption (FD)/EI source. The emitter heating current contact of the FD source was modified for in-beam purposes similar to that reported previously (17). An unactivated tungsten wire (10-μm diameter) or stainless-steel wire (125-μm diameter) was substituted for an activated emitter, and no high voltage was applied to the source except the usual 3K accelerating voltage. The sample on the FD wire was placed at a distance <3 mm from the ionizing electron beam and quickly heated by a maximum of 50 mA of the heating current (17–19) supplied by a standard heating current supply unit. The spectra were recorded under the following conditions: ionizing energy, 80 eV; source temperature, 280–300°; sample heater, 50 mA; emission current, 500 mA; accelerating voltage, 3 kV. Mass analyzed ion kinetic energy spectra, using identical parameters, were recorded by electric sector scanning.

Reagents—The following commercially available penicillins or precursors were used without additional purification: 6-aminopenicillanic acid[3] (*a*) and the penicillins (*b*), penicillin G potassium (I)[4], penicillin V potassium (II)[4], sodium oxacillin (III)[3], sodium nafcillin (IV)[5], disodium carbenicillin (V)[6], ampicillin (VI)[5], amoxicillin trihydrate (VII)[6] (Fig. 1). The metallic salts of the particular penicillins (~1 mg) were dissolved in 0.5 ml of water and acidified by addition of a drop of 88% aqueous formic acid solution. Immediately after formation of the precipitated free acid, 0.5 ml of ethanol was added to make a clear solution. Then 1–2 μl of the solution was deposited on the tungsten wire from a microsyringe[7].

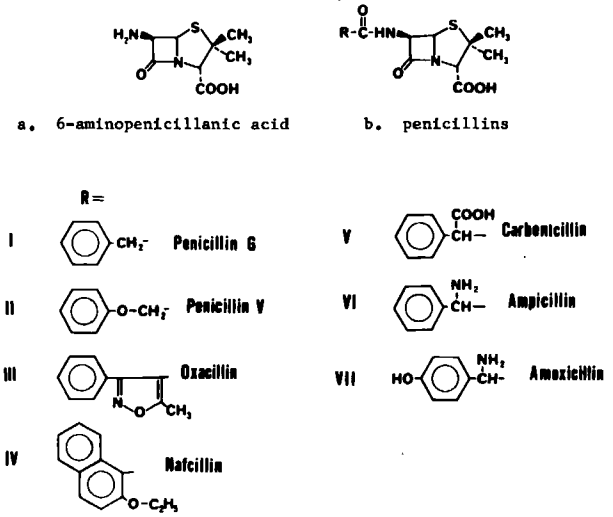

Figure 1—*Structures of pencillin analogues.*

[2] Varian MAT 311A, Varian Associates, Palo Alto, CA 94303.
[3] Bristol Lab., Syracuse, NY 13201.
[4] Pfizer Inc., Groton, CT 06340.
[5] Wyeth Lab., Philadelphia, PA 19101.
[6] Beecham Lab., Piscataway, NJ 08854.
[7] Unimetrics Corp., Anaheim, CA 92801.

The solvent was evaporated in the mass spectrometer before final insertion of the sample into the ion source.

To obtain more reproducible results with the free acids of ampicillin and amoxicillin, ~5 mg of polyethylene glycol 4000 was added to the aqueous solution of the sample and stirred until dissolved. An aliquot of the solution was deposited on the wire, and spectra were obtained as previously described. The addition of low levels of polyethylene glycol to the sample did not contribute markedly to the sample spectrum and could easily be subtracted from the spectrum by computer techniques. One explanation for this lack of contribution of the polyethylene glycol is the greatly varying vaporization temperatures between the desorption enhancer and the sample, similar to the best emitter temperature effect observed in field desorption mass spectrometry.

RESULTS AND DISCUSSION

Previous studies (1, 2) reported the electron ionization-induced fragmentation of penicillins G and V as the methyl ester or amide. An adaptation of these findings is summarized in Scheme I. Based on the ions in the spectrum, the nature of the R substituents could easily be assigned. In this work, the in-beam EI spectra of 6-aminopenicillanic acid, I, II, IV, V, and VI exhibit molecular ions, or MH ions in the case of III; VII, however, did not give $(M^{+\cdot})$ but gave instead $(M—OH)^+$ or $(MH—H_2O)^+$. The general fragmentation patterns of these compounds are similar to those reported for penicillin methyl esters or amides (1, 2) (Scheme I). The results are summarized in Table I in a format similar to that of previous work (2, 20).

The simplest compound, 6-aminopenicillanic acid, is an amino acid thought to be difficult to vaporize without decomposition, but the in-beam EI technique routinely gave useful spectra, including the molecular ion at m/z 216. The abundant peaks are explained on the basis of fragmentation of the methyl esters presented previously (1). The electron ionization-induced fragmentation by the in-beam technique of the β-lactam ring system having the free acid moiety is shown below.

An important rearrangement ion at m/z 160 containing the thiazoline moiety is commonly observed in all spectra studied to date (Scheme I, *e*).

The fragmentation processes originating from the molecular ion of I have been examined by the mass analyzed ion kinetic energy spectrometric technique and are shown in Fig. 2A and 2B. The first spectrum (Fig. 2A) was recorded immediately after insertion of the sample into the ion source; the second spectrum (Fig. 2B) was recorded after a few min-

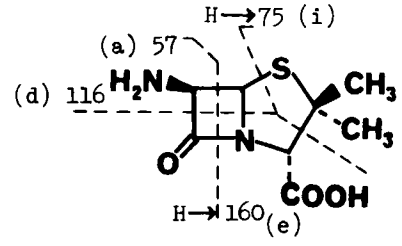

6-Aminopenicillanic Acid
$M^{+\cdot}$ 216

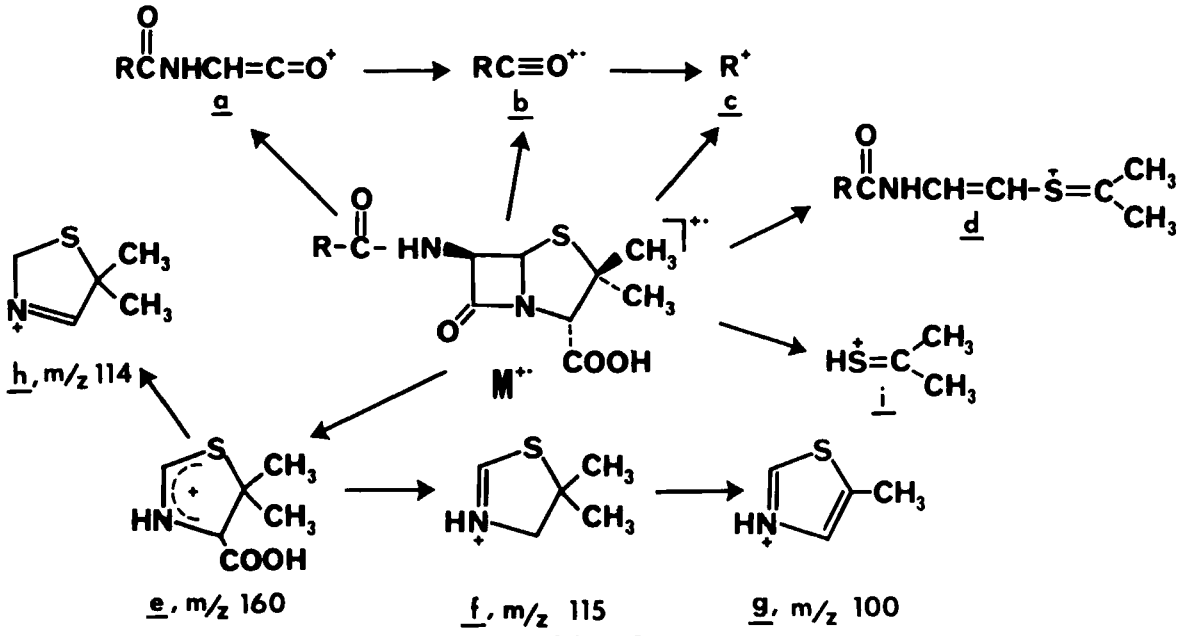

Scheme I

utes. This change in mass analyzed ion kinetic energy spectrometric spectral features suggests that the structures of the molecular ions undergo isomerization with time, *i.e.*, thermal alterations of the compound prior to electron ionization in the mass spectrometer. The major cleavages and metastable transitions from the molecular ion of I are summarized in Scheme II:

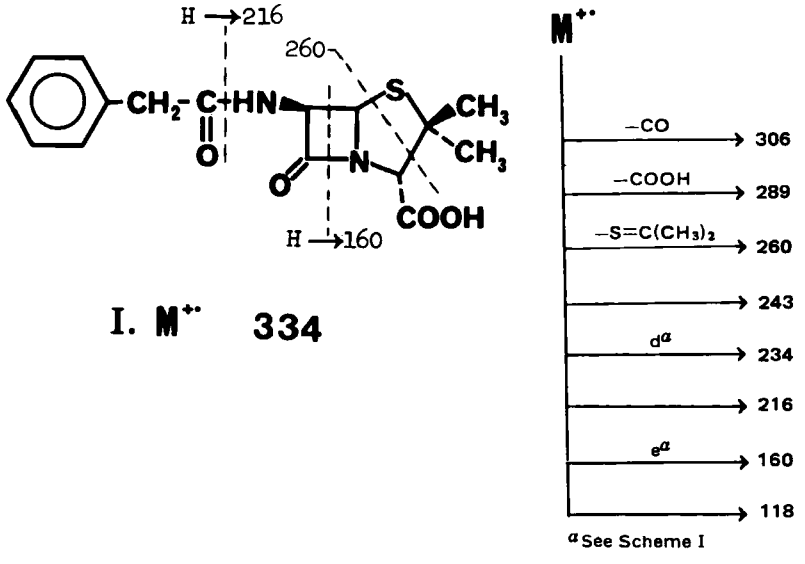

Scheme II

Eight transitions were clearly recognized. The transitions leading to the ions at *m/z* 289, 260, 234, 216, 160, and 118 have been suggested by previous investigators (1, 2) on the basis of accurate mass measurements and are confirmed by the mass analyzed ion kinetic energy studies. The transitions leading to the ions at *m/z* 234 and 160 correspond to processes d and e in Scheme I, respectively. In the mass analyzed ion kinetic energy spectra (Fig. 2A and 2B), one of the most abundant transitions is the rearrangement process with cleavage leading to the ion at *m/z* 216, corresponding to the molecular ion of 6-aminopenicillanic acid. Alternatively, the loss of carbon dioxide from the ion at *m/z* 260 could also conceivably yield *m/z* 216. However, since the methyl ester of I exhibits the same rearrangement ion with the empirical formula of 6-aminopenicillanic acid methyl ester confirmed by accurate mass measurement, the former process would be more probable. Additionally, transitions leading to the ion at *m/z* 293 corresponding to the loss of benzyl from the molecular ion and the ion at *m/z* 118 were observed. Since the contribution of the fragment ions to the in-beam spectra is negligibly small, successive transitions from these ions could not be investigated to further clarify the fragmentation scheme.

The in-beam EI spectrum of II exhibits a base peak at *m/z* 77 and abundant ions at *m/z* 94 and 107. These ions are commonly observed in the spectra of the methyl esters of I and II and are derived from the phenoxymethyl group based on accurate mass measurements (1). The mass analyzed ion kinetic energy spectrum of II (Fig. 2C) exhibits features suggesting that many isomerized forms of the molecular ion exist before and/or after electron ionization. The most intense transition in the spectrum at *m/z* 256 arises by the loss of phenol. The transitions leading to ions at *m/z* 216 and 160 (Scheme III) represent the rearrangement ions involving the β-lactam ring system; the fragment ions at *m/z* 276 and 250 are the phenoxy analogues of the ions at *m/z* 260 and 234, respectively. The other transitions are difficult to analyze because of the extensive thermal alterations of the molecule suggested earlier (Scheme III).

In the case of III, the $(M + 1)^+$ peak was observed at *m/z* 402 instead of $(M^{+\cdot})$. A series of peaks corresponding to $(MH—H_2O)^+$, $(MH—H_2O—CO)^+$, and $(MH—H_2O—CO_2)^+$ were detected at *m/z* 384, 356, and 340, respectively. The base peak at *m/z* 144, shown below, is believed to be derived from the *m/z* 187 ion, based on data of the well-known electron-impact fragmentation of the isoxazole moiety (21–25).

The in-beam EI spectrum of IV exhibits very intense peaks due to the naphthalene moiety at *m/z* 199 (base peak), 171, and 170 as well as the

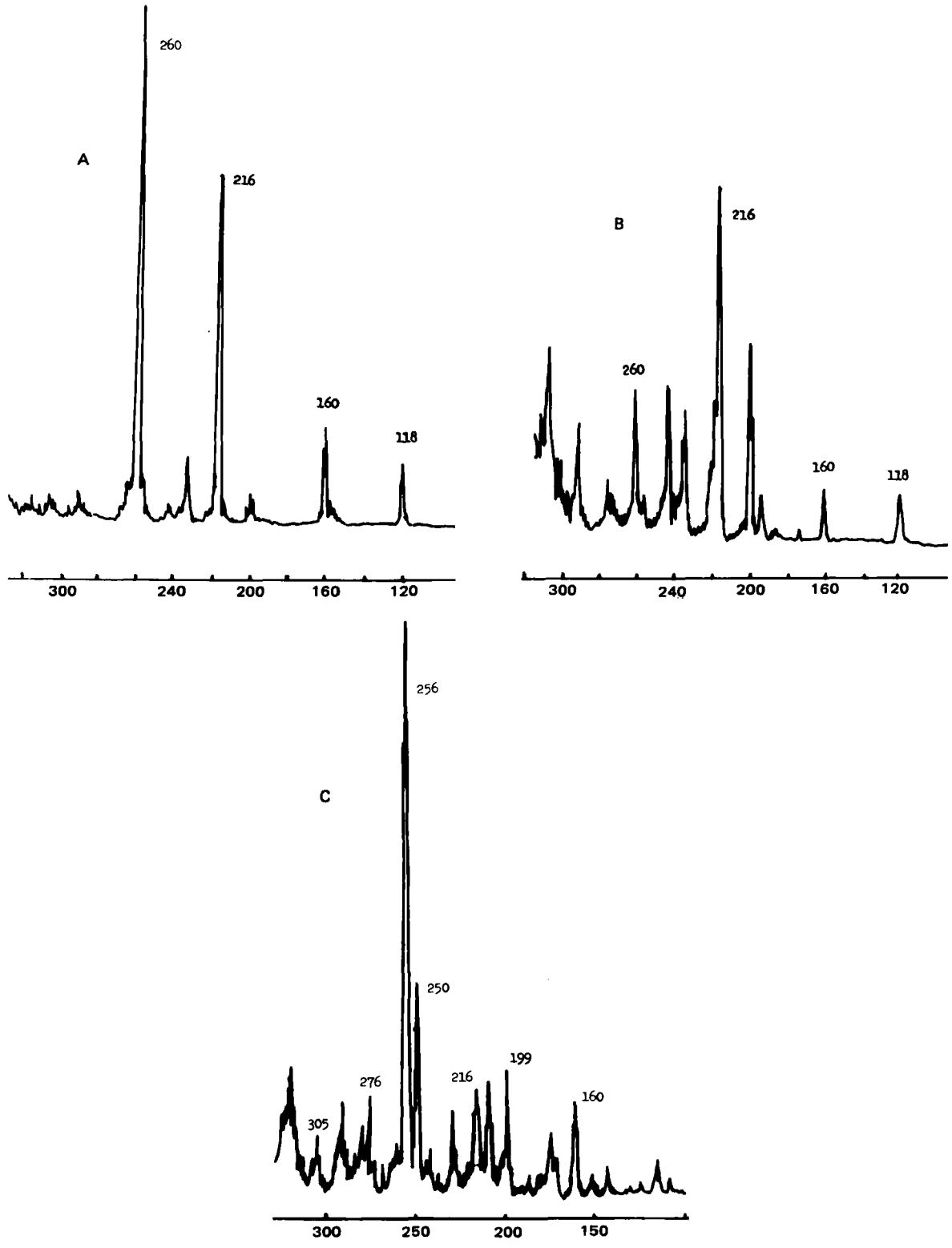

Figure 2—*Mass analyzed ion kinetic energy spectra. Key: from penicillin G molecular ion (m/z 334): (A) immediately after insertion, (B) after elapsed time, (C) from penicillin V molecular ion (m/z 350).*

peaks due to the general fragmentation at *m/z* 115(*f*), 114(*h*), and 100(*g*) as delineated in Scheme I. The abundance of fragment *e*, Scheme I, becomes rather weak.

Since V has a β-carbonyl carboxylic acid moiety, electron-impact or thermal-induced decarboxylation must take place easily, producing the abundant ions at *m/z* 91 and 92 in its spectrum. The peak corresponding to ion *c*, Scheme I, which is diagnostic of the R substituent, was also observed. Additionally, the spectrum exhibited peaks similar to those observed in the spectrum of I (*m/z* 334, 316, 288, 272, 160, 118, 114, 100, 92, and 91).

Ampicillin (VI) is an amino acid and as such is rather difficult to vaporize. Nevertheless, satisfactory in-beam EI spectra were obtained that exhibited $(M + 1)^+$, $(M^{+\cdot})$, and $(M - 17)^+$ at *m/z* 350, 349, and 332, respectively, when the compound was mixed with polyethylene glycol and examined under in-beam EI conditions (Fig. 3). Without polyethylene glycol, the in-beam spectral features were variable and were lacking characteristic peaks in the molecular weight region. The mechanism by which polyethylene glycol acts is not clear, but it appears to absorb the sample, and under quick-heating conditions, the sample was efficiently desorbed intact from its surface as in the case of polyimide- (26),

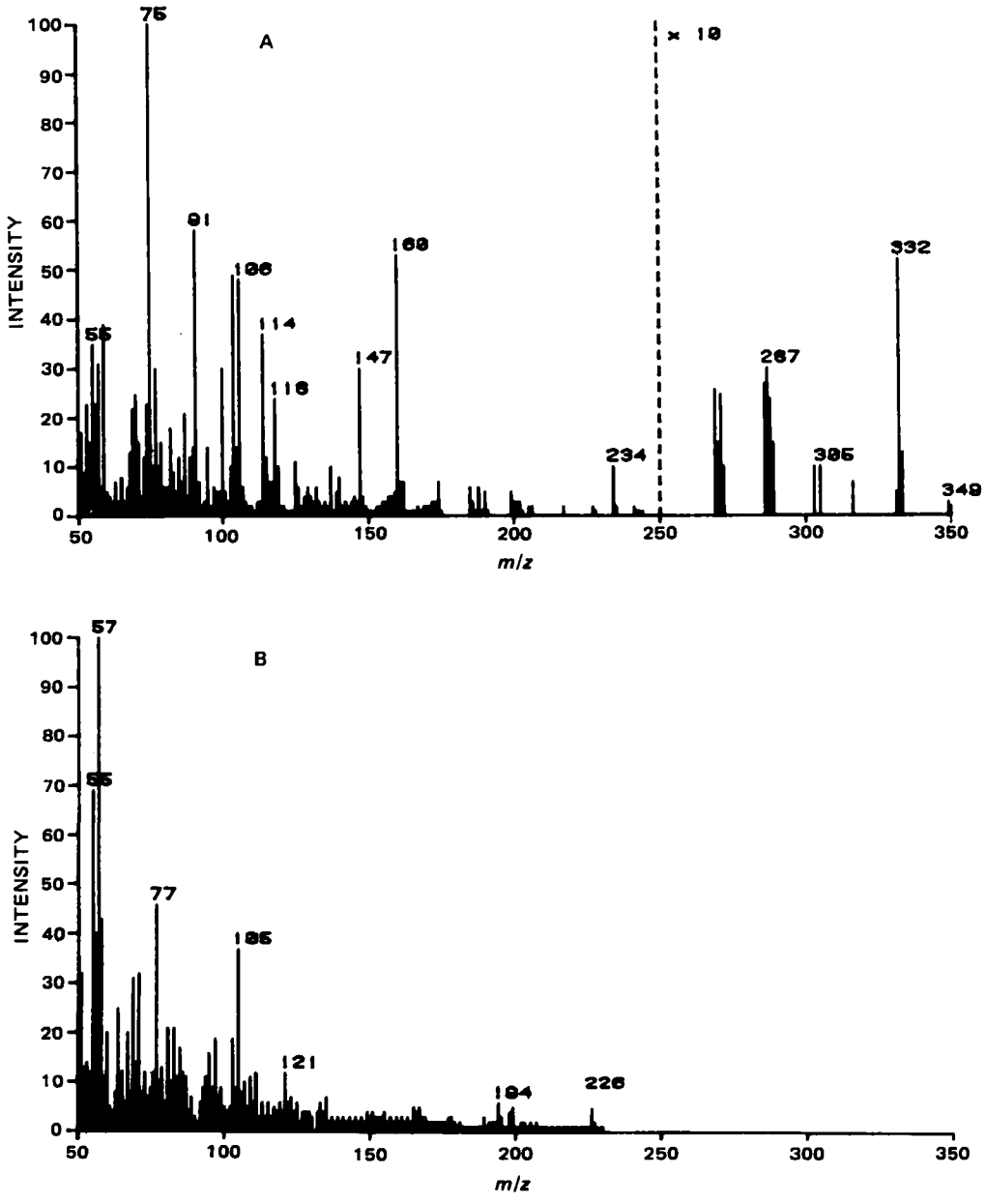

Figure 3—*Mass spectra of (A) ampicillin with polyethylene glycol 4000; (B) polyethylene glycol.*

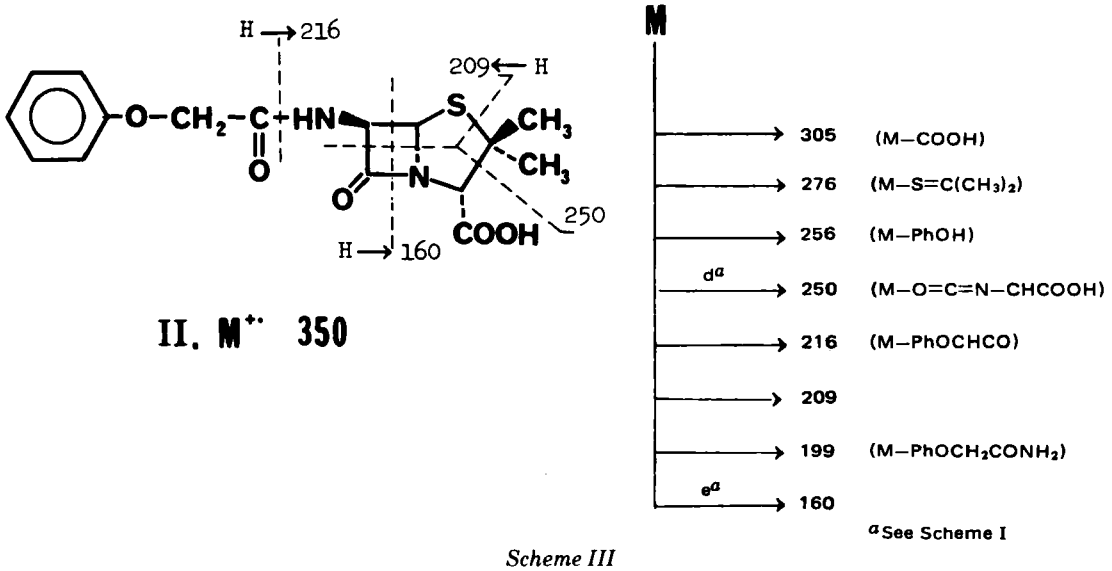

Scheme III

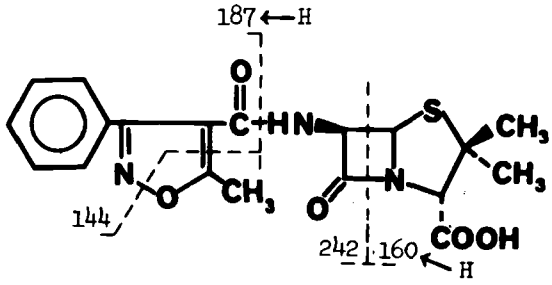

III. MH^+ 402

polytetrafluoroethylene- (27), or silicone- (28) coated tips. It should be noted that previous researchers have demonstrated the utility of polyethylene glycol in negative ion FD mass spectrometry (29, 30). Figure 3A shows the in-beam EI spectrum of VI mixed with polyethylene glycol and Fig. 3B shows the spectrum of polyethylene glycol. A comparison of these spectra indicates that polyethylene glycol contributes negligibly to the spectra of VI.

Amoxicillin trihydrate (VII) has a similar structure to VI. Mass spectra of this compound can be interpreted by the classical mass shift technique (31). Peaks at *m/z* 75, 100, 114, and 160 were commonly observed in the spectra of both compounds; the peaks at *m/z* 91, 104, 106, 118, and 147 in the spectrum of VI shift to *m/z* 107, 120, 122, 134, and 163, respectively, in the spectrum of VII[8]. It is clear that the common peaks are derived from the penicillanic acid moiety and the shifted peaks involve the aromatic moiety. The major fragmentation ions of these compounds are summarized below.

In conclusion, it has been demonstrated that EI mass spectra of intact, unmodified penicillins can be obtained by the in-beam EI technique. Although the contributions to spectra of thermal degradation products formed during sample heating cannot be excluded, the spectral features proved more than satisfactory for obtaining structural information on the samples. When the sample was difficult to vaporize, as in the case of VI, the desorption technique from polyethylene glycol 4000 was useful to obtain the spectra. The general fragmentation of free acid forms of penicillins under in-beam conditions were in accord with those reported for methyl esters and amides, further indicating the usefulness of the in-beam electron-impact technique.

REFERENCES

(1) W. Richter and K. Biemann, *Monatsh. Chem.*, **95**, 766 (1964).

(2) V. Bochkarev, N. Ovchinnikova, N. S. Vulfson, E. M. Kleiner, and A. S. Khokhlov, *Dokl. Akad. Nauk. SSSR*, **172**, 1079 (1967).

(3) L. A. Mitscher, H. D. H. Showalter, K. Shirahata, and R. L. Faltz, *J. Antibiot.*, **28**, 668 (1975).

(4) A. K. Bose, H. Fujiwara, B. N. Pramanik, E. Lazaro, and C. R. Spillert, *Anal. Biochem.*, **89**, 284 (1978).

(5) M. D. Muller, J. Seibl, and W. Simon, *Anal. Chim. Acta*, **100**, 263 (1978).

(6) A. Dell, D. H. Williams, H. R. Horris, G. A. Smith, J. Feeney, and G. C. K. Robert, *J. Am. Chem. Soc.*, **97**, 2497 (1975).

(7) M. Ohashi, K. Tsujimoto, and A. Yasuda, *Chem. Lett. Jpn.*, 439 (1976).

(8) M. Ohashi, S. Yamada, H. Kudo, and N. Nakayama, *Biomed. Mass Spectrom.*, **5**, 578 (1978).

[8] When the in-beam EI spectrum of VII was obtained by use of a Finnigan 4023 mass spectrometer (Finnigan Corp., Sunnyvale, CA 94086) equipped with a direct insertion probe tip coated (32) with Pyre M.L. (DuPont) under the in-beam conditions (6–12), a simpler and clearer spectrum was obtained than described in the text: *m/z* 75(11), 79(16), 106(100), 1145(9), 118(8), 160(20), 271(0.8), 332(0.1), 350(0.01).

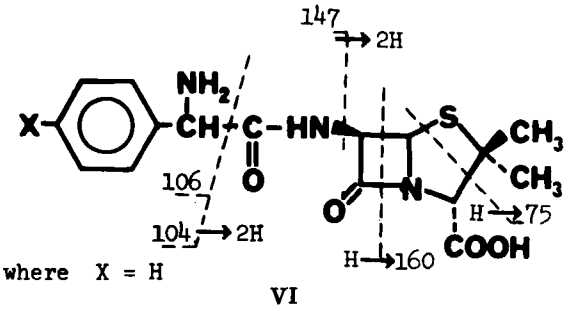

VI

(9) M. Ohashi, K. Tsujimoto, S. Tamura, N. Nakayama, Y. Okumura, and A. Sakurai, *ibid.*, **7**, 153 (1980).

(10) M. Ohashi, and N. Nakayama, *Org. Mass Spectrom.*, **13**, 642 (1978).

(11) M. Ohashi, N. Nakayama, H. Kudo, and S. Yamada, *Mass Spectrosc. (Tokyo)*, **24**, 265 (1976).

(12) M. Ohashi, R. Barron, and W. Benson, *J. Am. Chem. Soc.*, **103**, 3943 (1981).

(13) R. J. Cotter, *Anal. Chem.*, **52**, 1589A (1980).

(14) G. D. Daves, Jr., *Acc. Chem. Res.*, **12**, 359 (1979).

(15) J. L. Gower, C. Beaugrand, and C. Sallot, *Biomed. Mass Spectrom.*, **8**, 36 (1981).

(16) R. G. Cooks, J. H. Beynon, R. M. Caprioli, and G. R. Lester, "Metastable Ions," Elsevier, Amsterdam, 1973, p. 42.

(17) B. Soltmann, C. C. Sweeley, and J. F. Holland, *Anal. Chem.*, **49**, 1164 (1977).

(18) D. Kummler and H. R. Schulten, *Org. Mass Spectrom.*, **10**, 813 (1975).

(19) H. U. Winkler and B. Linden, *ibid.*, **11**, 329 (1976).

(20) K. L. Rinehart, Jr. and G. E. Van Lear, in "Biomedical Application of Mass Spectrometry," G. R. Waller, Ed., Wiley Interscience, New York, N.Y., 1972, p. 48.

(21) M. Ohashi, H. Kamachi, H. Kakisawa, A. Tatematsu, H. Yoshizumi, and H. Nakata, *Tetrahedron Lett.*, 379 (1968).

(22) M. Ohashi, H. Kamachi, H. Kakisawa, A. Tatematsu, H. Yoshizumi, H. Kano, and H. Nakata, *Org. Mass Spectrom.*, **2**, 195 (1969).

(23) H. Nakata, H. Sakurai, H. Yoshizumi, and A. Tatematsu, *ibid.*, **1**, 199 (1968).

(24) J. H. Bowie, R. K. M. R. Kallury, and R. G. Cooks, *Aust. J. Chem.*, **22**, 563 (1969).

(25) T. Nishiwaki, *Tetrahedron*, **25**, 747 (1969).

(26) R. J. Cotter, *Anal. Chem.*, **51**, 317 (1979).

(27) G. Hansen and B. Munson, *ibid.*, **50**, 1130 (1978); **52**, 245 (1980).

(28) J. P. Thenot, J. Nowlin, D. I. Carroll, F. E. Montgomery, and E. C. Horning, *ibid.*, **51**, 1101 (1979).

(29) K. H. Ott, F. W. Rollgen, J. J. Zwinselman, R. H. Fokkens, and N. M. M. Nibbering, *Org. Mass Spectrom.*, **15**, 419 (1980).

(30) H. J. Heinen, U. Giessmann, and F. W. Rollgen, *ibid.*, **12**, 710 (1977).

(31) K. Biemann, "Mass Spectrometry, Organic Chemical Applications," McGraw-Hill, New York, N.Y., 1962, p. 305.

(32) V. N. Reinhold and S. A. Carr, Abstract Papers, 29th Annual Conference on Mass Spectrometry and Allied Topics, May 1981, Minneapolis, Minn., Paper RPA 14.

ACKNOWLEDGMENTS

The authors thank Michel Margosis of the National Center for Antibiotics Analysis, FDA, for a generous supply of samples and R. Venable of the Division of Drug Chemistry, FDA, for assistance in the computer drawing of Fig. 3.

Mamoru Ohashi is a Visiting Scientist on leave from the University of Electro-Communications, Chofu, Tokyo 182, Japan.

Direct Preparation of Solid Particulates of Aminopyrine–Barbital Complex (Pyrabital) from Droplets by a Spray-Drying Technique

YOSHIAKI KAWASHIMA *x, SHAN-YANG LIN *, MASUMI UEDA *, HIDEO TAKENAKA *, and YUTAKA ANDO ‡

Received January 4, 1982, from the *Gifu College of Pharmacy, Mitahora, Gifu 502, Japan and ‡Ichimaru Co. Ltd., Matsuhora, Takatomi, Gifu 502-21, Japan. Accepted for publication May 14, 1982.

Abstract □ Aqueous slurries of aminopyrine and barbital (molecular ratio 2:1) containing various excipients such as colloidal silica, synthetic aluminum silicate, montmorillonite clay, corn starch, microcrystalline cellulose, hydroxypropylcellulose, methylcellulose, gelatin, and chitosan were spray-dried by a centrifugal wheel atomizer with various rotation speeds (10,000–40,000 rpm) at various temperatures (85–145 ± 5°). The spray-dried products were a mixture of aminopyrine–barbital complex (molecular ratio 1:1), aminopyrine, and the excipient used. The flowability and the packing property of the products were improved by compounding colloidal silica into the formulation used for spray-drying. The products with montmorillonite clay, chitosan, and a corn starch–colloidal silica mixture were compressed directly into tablets. It was found that aminopyrine in the products was oxidized during spray-drying. The oxidation products were assumed to be a trace mixture of 5-oxo-2-methyl-4-dimethylamino-1-phenyl-3-pyrazoline carboxyaldehyde and miscellaneous oxidation products. Montmorillonite clay compounded in the formulation considerably prevented the oxidation of aminopyrine during spray-drying. The present study proposes an improved method for the preparation of solid particulates of aminopyrine–barbital complex for tableting, which combines the synthesis, drying, and agglomeration processes into a single process.

Keyphrases □ Aminopyrine—complex with barbital (pyrabital), direct preparation of solid particulates from droplets by a spray-drying technique □ Barbital—complex with aminopyrine (pyrabital), direct preparation of solid particulates from droplets by a spray-drying technique □ Pyrabital—direct preparation of solid particulates of aminopyrine–barbital complex from droplets by a spray-drying technique □ Solid particulate—direct preparation of aminopyrine–barbital complex (pyrabital) from droplets by spray-drying technique

A spray-drying technique has been used widely as a preferable drying method for heat-sensitive materials (foods, drugs, *etc.*). One advantage claimed for this technique is that both drying and agglomeration or microencapsulation of the drugs can be accomplished simultaneously. Microcapsules of barbituric acid and phenobarbital were prepared (1, 2) with a tensioactive precondensate of hexamethylolmelamine type. Enteric-coated microcapsules of sulfamethoxazole for tableting also were prepared (3).

Direct preparation of solid particulates from liquid droplets by a chemical reaction is one of the recent advances in spray-drying techniques. Ammonium sulfate spheres were produced (4) by the reaction of liquid droplets of orthophosphoric acid with gaseous ammonia. Solid particulates of theophylline–ethylenediamine complex were prepared (5) directly from liquid droplets.

The objective of the present study was to prepare solid particulates of a mixture of aminopyrine–barbital complex and aminopyrine, termed pyrabital in the Japanese Pharmacopeia (JP) IX (6), employing a spray-drying technique. Several methods of preparation of the analgesic,

Table I—Formulation for Spray Drying

Excipient		Dispersing medium	
Colloidal silica	10, 20 g	Water	600 ml
Synthetic aluminum silicate	20 g	Water	600 ml
Montmorillonite clay	20 g	Water	600 ml
Microcrystalline cellulose	20 g	Water	600 ml
Colloidal silica	10 g	Water	600 ml
Corn starch	20 g		
Colloidal silica	10 g	Aqueous hydroxypropylcellulose solution (0.42%)	600 ml
Hydroxypropylcellulose	2.5 g		
Colloidal silica	10 g	Aqueous methylcellulose solution (0.83%)	600 ml
Methylcellulose	5 g		
Colloidal silica	10 g	Acetic acid solution (0.48%)	600 ml
Chitosan	2 g		
Colloidal silica	10 g	Aqueous gelatin solution (2%)	1000 ml
Gelatin	20 g		

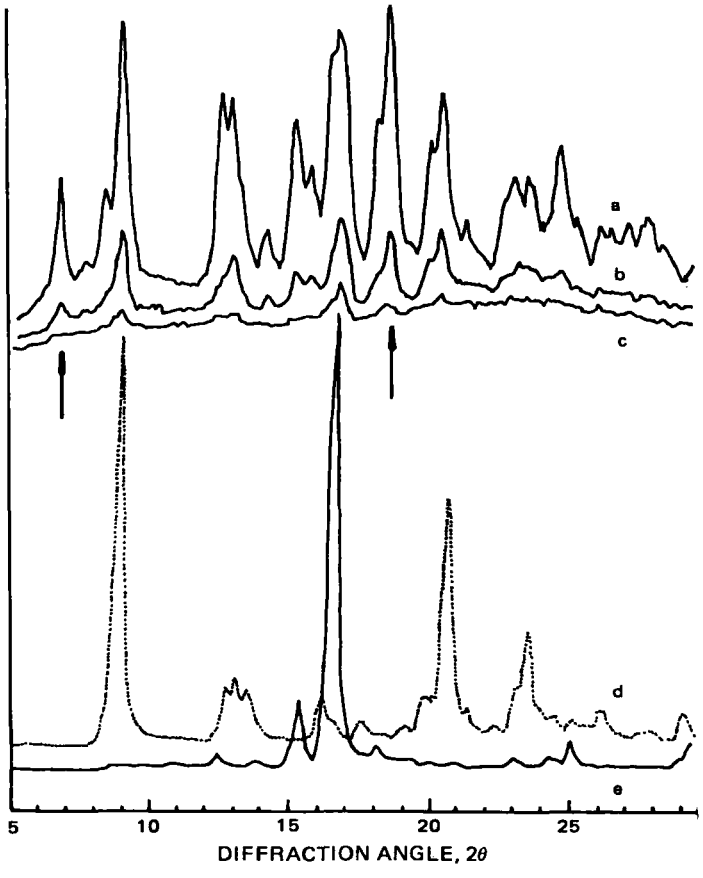

Figure 1—*X-ray diffraction patterns of the spray-dried products, pyrabital, aminopyrine, and barbital. Key: (a) pyrabital; (b) spray-dried products prepared at 85°; (c) spray-dried products prepared at 145°; (d) aminopyrine; (e) barbital.*

0022-3549/83/0500-0514$01.00/0

Table II—Effects of Excipient Used on the Drug Contents and the Micromeritic Properties of the Spray-Dried Products [a]

Excipient	Aminopyrine content, %	Barbital content, %	Molecular content ratio of aminopyrine to barbital	Geometric mean diameter, μm	Angle of repose	Parameters in Kawakita and Ludde's (10) equation a	b
Colloidal silica (20 g)	35.45	13.30	2.1:1	12.0	45	0.22	0.082
Synthetic aluminum silicate	34.00	11.15	2.4:1	—	51	0.33	0.023
Montmorillonite clay	23.10	7.90	2.3:1	11.0	52	0.24	0.050
Microcrystalline cellulose	31.20	11.40	2.2:1	—	55	0.39	0.063
Colloidal silica + corn starch	32.60	12.70	2.0:1	11.0	47	0.23	0.062
Colloidal silica + hydroxypropylcellulose	35.35	14.80	1.9:1	16.5	54	0.27	0.044
Colloidal silica + methylcellulose	22.53	7.23	2.5:1	13.0	45	0.27	0.040
Colloidal silica + gelatin	16.53	9.20	1.4:1	8.0	47	0.33	0.032
Colloidal silica + chitosan	24.70	11.58	1.7:1	11.0	42	0.23	0.058

[a] Spray-drying conditions: drying temperature 130°; atomizer speed, 40,000 rpm.

Table III—Effects of Rotation Speed of Atomizer on the Drug Contents and the Micromeritic Properties of the Spray-Dried Products [a]

Rotation speed of atomizer, rpm	Aminopyrine content, %	Barbital content, %	Molecular content ratio of aminopyrine to barbital	Geometric mean diameter, μm	Angle of repose	Parameters in Kawakita and Ludde's (10) equation a	b
10,000	36.35	11.90	2.4:1	15.0	45	0.29	0.047
20,000	39.35	12.65	2.2:1	14.0	47	0.31	0.056
30,000	40.90	14.60	2.5:1	12.5	46	0.26	0.057
40,000	45.34	14.15	2.2:1	10.0	47	0.28	0.050

[a] Spray-drying conditions: drying temperature 130°; excipient, colloidal silica.

pyrabital, have been developed as described elsewhere (6). These methods involve several processes, such as reaction, filtration, drying, *etc.* Furthermore, the agglomeration process subsequently is required for compounding the synthesized drug into a suitable dosage form. However, the present method combines these multiple processes into one step. In addition, the resultant products are compressed directly into tablets. Also examined were the parameters affecting the micromeritic properties of the product and the autoxidation of aminopyrine in the product during spray-drying.

EXPERIMENTAL

Materials—Aminopyrine and barbital were JP grade. Pyrabital produced by the fusion method (7) was used as a reference compound for identifying the spray-dried products. The mixture of aminopyrine (0.0173 mole) and barbital (0.00865 mole) was gradually heated in a beaker until a yellow melt was obtained. The melt was cooled to room temperature resulting in a yellow compound. The physicochemical characteristics of the resultant product, such as IR spectrum and melting point (96–103°), coincided with those specified in the JP.

Spray-Drying Technique—Aminopyrine (34 g), barbital (13.5 g), and excipients such as colloidal silica[1], synthetic aluminum silicate (JP grade), montmorillonite clay[2], corn starch (JP grade), microcrystalline cellulose[3], hydroxypropylcellulose[4], methylcellulose[5], gelatin[6], and chitosan[7] were dispersed in 600 ml of distilled water by a jet-type homogenizer. The system was held for 20 min and was heated at 60° when necessary. The resultant uniform aqueous slurry was atomized into a drying chamber. The detailed formulations are in Table I. Preliminary examination showed that no products were recovered from the formulation without excipient. Therefore, the excipient contained in the formulation was necessary to obtain the products. The feeding rate of the aqueous slurry was 20–33 ml/min. The atomization of the slurry was carried out by employing a centrifugal wheel atomizer (diameter, 4 cm)[8] rotated at 10,000, 20,000, 30,000, or 40,000 rpm. The drying chamber was maintained at 85, 100, 115, 130, or 145 ± 5°. Spray-dried aminopyrine with colloidal silica was also produced at 40,000 rpm and 130°.

Measurement of Micromeritic Properties—The sizes of the spray-dried products were measured by a photographic counting method using a particle size analyzer[9]. The packing and the flow properties were

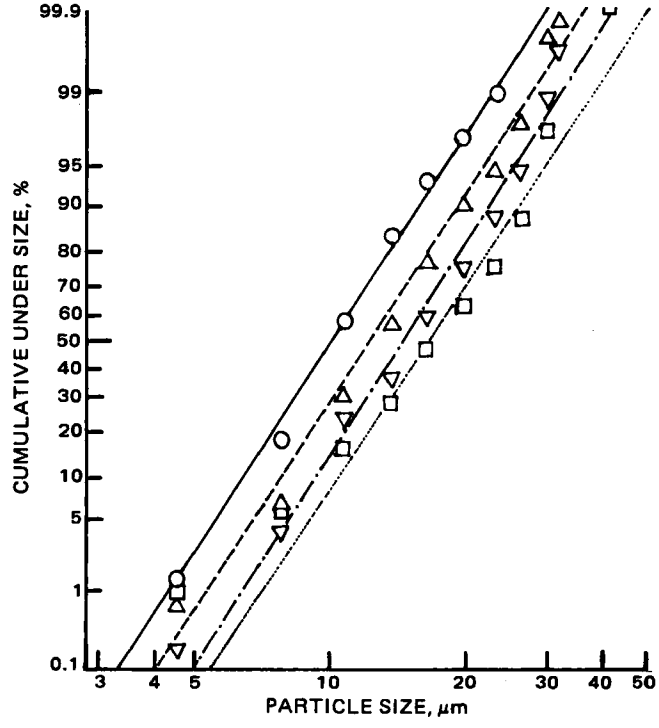

Figure 2—*Size distributions of the spray-dried products rotation speed of atomizer (rpm). Key: (▽) 10,000; (△) 30,000; (○) 40,000; (□) the products containing hydroxypropylcellulose (40,000).*

[1] Aerosil, Japan Aerosil Co. Ltd., Japan.
[2] Veegum-K, R. T. Vanderbilt Co.
[3] Avicel, Asahi Kasei Kogyo Co. Ltd., Japan.
[4] HPC-L, Shinetsu Kagaku Co. Ltd., Japan.
[5] MC (4000 cps), Wako Pure Chemical Co. Ltd., Japan.
[6] Koso Chemical Co. Ltd., Japan.
[7] Flonac, Kyowa Yushi Ind. Co. Ltd., Japan.
[8] Type 1051, Iwai Kikai Co. Ltd., Japan.
[9] TGZ-3, Karl Zeiss Co. Ltd., West Germany.

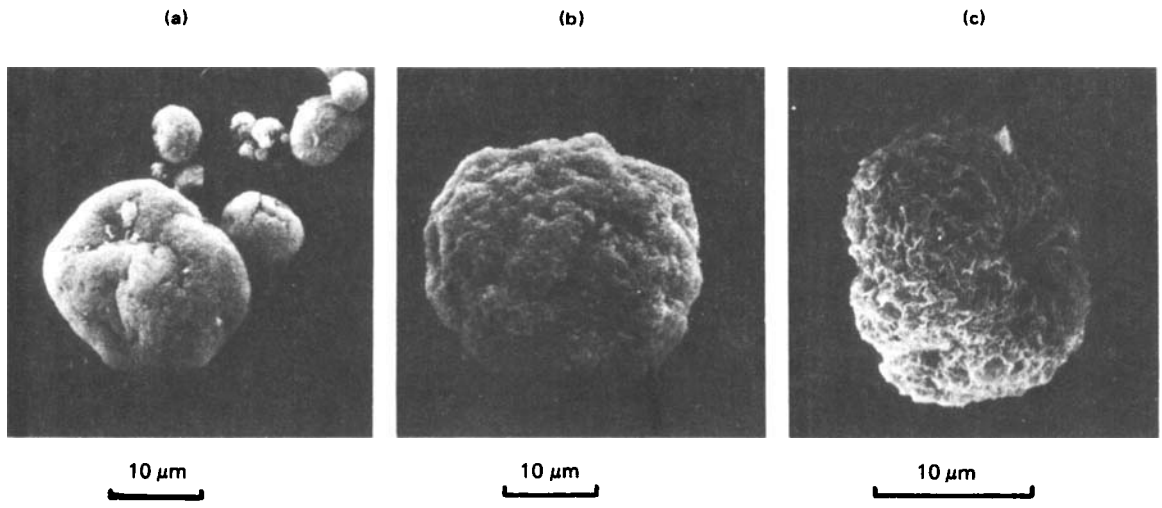

Figure 3—*Scanning electron microscopic photographs of the spray-dried products. Key: Spray-dried products containing (a) colloidal silica; (b) colloidal silica and hydroxypropylcellulose; (c) montmorillonite clay.*

investigated by using a tapping machine[10] generating a uniform force with each tap and by pouring powder on a plate (diameter, 3 cm), respectively. The direct compressibility of the spray-dried products was examined by employing a single-punch tableting machine[11]. The internal diameter of the die was 10 mm. The surface topography of the products coated with gold were investigated by a scanning electron microscope[12].

Measurement of Physicochemical Properties—The contents of aminopyrine and barbital in the products were measured with a double-beam spectrophotometer[13]: aminopyrine in acidic solution at pH 1.2[14] at 270 nm and barbital in alkaline solution at pH 9.6[15] at 250 and 269 nm. Identification of the spray-dried products was carried out by IR spectroscopy[16] and X-ray analysis[17]. Degradation of aminopyrine in the products during spray-drying was investigated by TLC on silica gel[18] using chloroform–methanol (14:1), and isopropyl alcohol–chloroform–ammonium hydroxide (28%) (9:4.5:2) as solvents and by UV spectroscopy[13]. As a reference, autoxidation of aminopyrine was carried out in an acetic acid (160 ml) and ethanol (40 ml) mixture by introducing air.

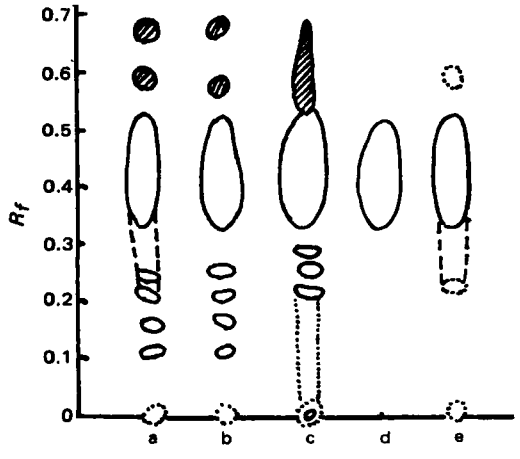

Figure 4—*Thin-layer chromatogram of the spray-dried products and the reference compounds developed with chloroform and methanol (14:1). Key: (a) spray-dried products with colloidal silica; (b) spray-dried aminopyrine; (c) oxidized aminopyrine; (d) aminopyrine; (e) pyrabital. Dotted drawing illustrates a trace spot or tailing. Shaded area indicates yellow spot or band.*

[10] Apparent specific volume meter PHK type, Konishi Manufactory Co. Ltd., Japan.
[11] Type KUI, Erweka GmbH, West Germany.
[12] JMS-SI, Nihon Denshi Co. Ltd., Japan.
[13] Model 556, Hitachi Manufactory Co. Ltd., Japan.
[14] Sodium chloride (2.0 g) and dilute hydrochloric acid (24.0 ml) made up to 1 liter with distilled water.
[15] 0.05 mole borax (44.5 ml) and 0.05 mole sodium carbonate (55.5 ml).
[16] A-102, Nihon Bunko Co. Ltd., Japan.
[17] JDX, Nihon Denshi Co. Ltd., Japan.
[18] DC-Fertig platten Kiesel 60 F_{254}, Merck Co.

RESULTS AND DISCUSSION

Identification of the Spray-Dried Products—It was found that the contents of aminopyrine and barbital in the products depended on the formulation for spray-drying and on the operating conditions as seen in Tables II–IV. The drug contents varied with the type of excipients used. The drug content in the product containing colloidal silica and gelatin was the lowest compared with the other excipients used in the present study (Table II). For the spray-drying condition, the drying temperature and the rotation speed of the atomizer were the main factors affecting the drug content in the products (Tables III and IV). With increasing rotation speed or decreasing drying temperature, the drug content increased. The inertia force exerted on the excipient was stronger than on the drugs in the droplet due to the fact that the density of the excipient was greater than that of the drug. Therefore, the excipient was separated more easily from the droplet than the drugs by increasing the rotation speed of the atomizer, which resulted in increasing the drug content in the spray-dried products. The effect of temperature on decreasing the drug content in the product was more significant than that of the rotation speed of the atomizer. An explanation for this finding is not clear at present. Although the percentage of drug content in the products varied widely, the molecular ratio of aminopyrine to barbital was fairly constant (2.2 ± 0.2 as shown in Tables II–IV).

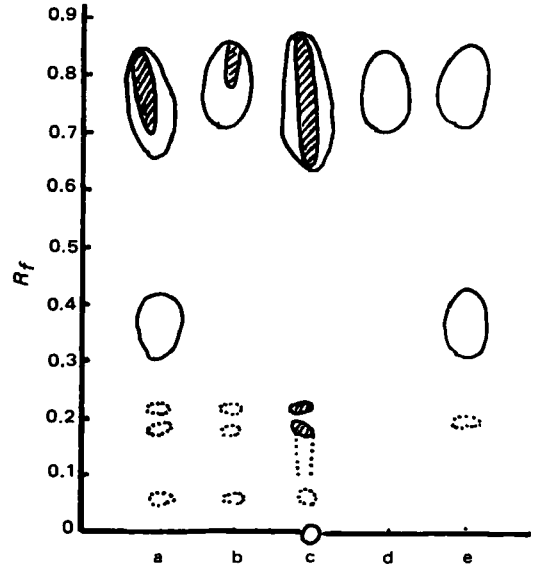

Figure 5—*TLC of the spray-dried products and the reference compounds developed with isopropyl alcohol–chloroform–ammonium hydroxide (9:4.5:2). Key: (a) spray-dried products with colloidal silica; (b) spray-dried aminopyrine; (c) oxidized aminopyrine; (d) aminopyrine; (e) pyrabital.*

Table IV—Effects of Drying Temperature of the Chamber on the Drug Contents and the Micromeritic Properties of the Spray-Dried Products [a]

Drying temperature of chamber	Aminopyrine content, %	Barbital content, %	Molecular content ratio of aminopyrine to barbital	Geometric mean diameter, μm	Angle of repose	Parameters on Kawakita and Ludde's (10) equation	
						a	*b*
85 ± 5	56.00	18.20	2.4:1	12.0	51	0.35	0.053
100 ± 5	54.75	18.20	2.4:1	8.9	55	0.29	0.068
115 ± 5	46.45	15.15	2.5:1	9.2	46	0.28	0.080
130 ± 5	45.34	14.15	2.2:1	10.0	47	0.28	0.050
145 ± 5	36.20	11.75	2.4:1	9.5	46	0.28	0.051

[a] Spray-drying conditions: atomizer speed, 40,000 rpm; excipient, colloidal silica.

IR spectra of the spray-dried products, pyrabital, and the mixture of aminopyrine and barbital (2:1) showed a broad peak of colloidal silica contained in the product at 1000–1200 cm^{-1} that partly impaired the identification of the spray-dried products. The characteristic bands of pyrabital appeared at 1703, 1656, and 1584 cm^{-1}, strongly suggesting the existence of pyrabital in the products. None of these characteristic peaks appeared in the IR spectra of aminopyrine, barbital, and a mixture of the two.

X-ray diffraction patterns of the spray-dried products, pyrabital, aminopyrine, and barbital are seen in Fig. 1. Although the intensities of the diffraction peaks of the products were weaker than those of pyrabital, aminopyrine, and barbital, the characteristic peaks of pyrabital at a diffraction angle of 6.6 and 18.5° were detected. The reduced intensities of the product peaks indicated that some crystals in the product converted to a disordered form due to rapid crystallization during spray-drying. The more reduced intensities of the products prepared at 145° instead of 85° also indicated that the amorphism occurred because of the rapid crystallization.

It was reported (8) that pyrabital was a mixture consisting of a molecular compound of aminopyrine and barbital (molecular ratio 1:1) and an additional molecule of aminopyrine. Recalling that the molecular ratio of aminopyrine to barbital contained in the products was >2 (Tables II–IV), it appears that the present product was a mixture of pyrabital, aminopyrine, and the excipient used.

Micromeritic Properties of the Spray-Dried Products—The spray-dried products were observed to be fairly spherical particles under an optical microscope. Their sizes varied from 4 to 40 μm, and their distributions were described by a logarithmic plot shown in Fig. 2. As suggested from a previous study (9), the geometric mean diameter of the products increased with a decrease in the rotational speed of the atomizer.

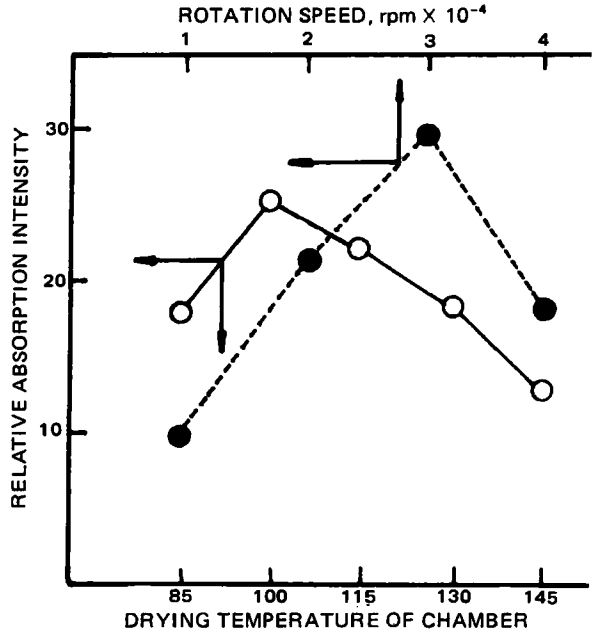

Figure 6—*The relative absorption intensities at 385 nm of the spray-dried products to pyrabital as a function of atomizer speed and drying temperature of the chamber.*

Hydroxypropylcellulose contained in the formulation also acted to increase the product size as seen in Fig. 2 and Table II.

Surface topography of the products depended mainly on the type of the excipient used. The products with colloidal silica and binder (hydroxypropylcellulose) revealed a fairly smooth surface, whereas the surface of the products with montmorillonite clay were pitted as shown in Fig. 3.

The angle of repose of the products with colloidal silica and chitosan was fairly low compared with the other products, as shown in Table II. The packing property of the products was evaluated by the parameter *a* from a previously described equation (10), which describes the packing process of powders by tapping into a measuring cylinder:

$$\frac{N}{C} = \frac{N}{a} + \frac{1}{ab} \quad \text{(Eq. 1)}$$

$$C = (V_0 - V_N)/V_N \quad \text{(Eq. 2)}$$

where *b* is a constant, *C* is the compaction ratio, *N* is the number of taps, V_0 is the volume of powder in a measuring cylinder at the loosest packing, and V_N is the volume after the *N*th tapping. The parameter *a* corresponds to the proportion of consolidation at the closest packing attained; therefore, the smaller *a* indicates easier packing. The parameter *a* of the products with colloidal silica was the smallest among the products, indicating that they were the most easily packed.

It was found that the products with chitosan, montmorillonite clay, and a mixture of corn starch and colloidal silica were directly compressible

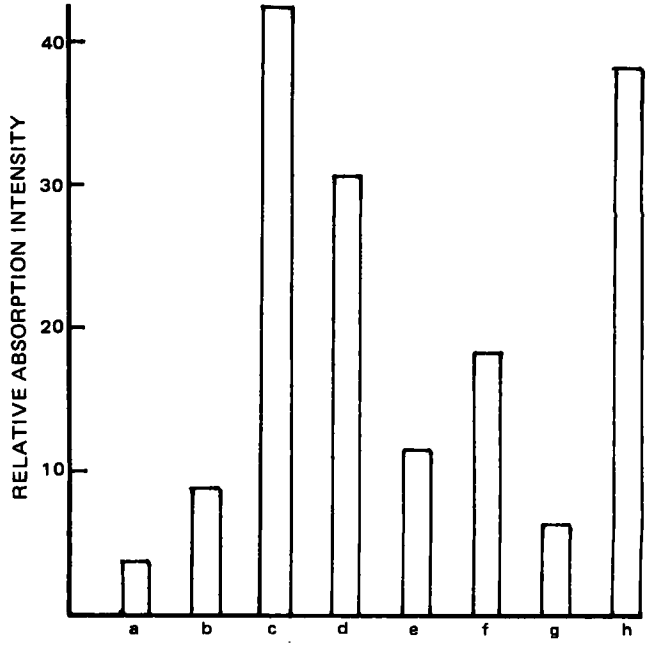

Figure 7—*The effects of excipient used on the relative absorption intensities at 385 nm of the spray-dried products to pyrabital. Excipient contained in the spray-dried products: (a) montmorillonite clay; (b) colloidal silica and gelatin; (c) microcrystalline cellulose; (d) colloidal silica and methylcellulose; (e) colloidal silica and chitosan; (f) colloidal silica and corn starch; (g) synthetic aluminum silicate; (h) colloidal silica and hydroxypropylcellulose.*

into tablets. The hardness[19] values of the resultant tablets were 4–4.5 kg. The weight variation tests of the tablets with <324 mg average weight were within the tolerances specified in the USP and the JP. For the other products, it was necessary to compound some microcrystalline cellulose (>50% w/w) in the formulations for tableting to obtain satisfactory tablets.

Degradation of Aminopyrine During Spray-Drying—Extracts of the spray-dried products exhibited absorbance at 385 nm, where aminopyrine does not absorb. The intensity of the peak depended on the excipient used and on the operating conditions (drying temperature and the rotation speed of the atomizer).

Thin-layer chromatograms of the spray-dried products containing colloidal silica developed with chloroform–methanol (14:1) coincided with that of spray-dried aminopyrine as seen in Fig. 4. As a reference, TLC of the autoxidized aminopyrine in the acetic acid–ethanol solution was also conducted as shown in Fig. 4. No separated yellow spots appeared at R_f 0.60 and 0.68, but a long yellow band appeared in the chromatogram of the autoxidized aminopyrine (Fig. 4c). The main spot at R_f 0.44 in the chromatograms was identified as aminopyrine (Fig. 4). The chromatograms developed with isopropyl alcohol–chloroform–ammonium hydroxide (9:4.5:2) are shown in Fig. 5. Two major spots at R_f 0.36 and 0.75 appeared in the spray-dried products. The spot at R_f 0.36 was identified as barbital by referring to the chromatograms of barbital and pyrabital in Fig. 5. The yellow band appearing at R_f 0.75 is characteristic of spray-dried products and oxidized and spray-dried aminopyrine.

The findings from spectrophotometric and TLC analysis (Figs. 4 and 5) suggested that the absorbance peak at 385 nm and the yellow spots on the chromatograms of the spray-dried products were attributed to the oxidation products of aminopyrine produced during spray-drying. The yellow substance in the spray-dried products detected by TLC in Figs. 4 and 5 could not be separated because of its low yield. A yellow substance was obtained previously (7) as an oxidation byproduct in the preparation by fusion of a molecular compound of aminopyrine and barbital. It was found that this substance was 5-oxo-2-methyl-4-dimethylamino-1-phenyl-3-pyrazoline carboxyaldehyde (I), which exhibits a strong absorbance band at 389 nm. The coexistence of other miscellaneous oxidation products of aminopyrine that caused shifting of the band at 389 nm from I toward the shorter wavelength region was reported (11), and it was suggested that the yellow substance in the spray-dried products might be a mixture of I and miscellaneous oxidation products.

The relative absorbance intensities at 385 nm of the spray-dried products to that of pyrabital (A_s/A_p) are plotted in Fig. 6, as a function of the operating conditions (the rotation speed of the atomizer and the drying temperature). The relative absorbance intensities increased with increasing atomizer speed up to a maximum at 30,000 rpm. Above this point, the relative intensity decreased as shown for 40,000 rpm in Fig. 6. With increasing rotation speed of the atomizer, the diameters of atomized droplets may decrease resulting in an increase in the total air-exposed surface area of the droplets. Therefore, autoxidation of aminopyrine in the droplets could be enhanced with increasing rotation speed of the atomizer up to 30,000 rpm. The increased rotation speed of the atomizer also accelerates the drying speed of the resultant smaller droplets. Once the droplets are solidified, the oxidation of aminopyrine in the solid state may be reduced compared with that in the liquid state. At a 40,000-rpm rotation speed of the atomizer, the rapid solidification of droplets might prevent further oxidation of aminopyrine that appears above 20,000 rpm (Fig. 6).

By increasing the drying temperature, the oxidation rate of aminopyrine in the droplets increases. At the same time, the evaporation rate of droplets increases. The rapid solidification of the droplets by increasing the drying temperature may reduce the oxidation of aminopyrine which is similar to that found at the 40,000-rpm rotation speed of the atomizer. The relative absorbance intensity was the highest at 100°. At temperatures >100°, aminopyrine autoxidation was reduced with increasing temperature because of the more rapid solidification of aminopyrine. The oxidation of aminopyrine during spray-drying also depended on the excipient contained in the products, as seen in Fig. 7. The absorbances of the product with hydroxypropylcellulose and microcrystalline cellulose are distinguishable from the other products. The products with montmorillonite clay exhibited the lowest absorbances, indicating that the oxidation of aminopyrine during spray-drying largely was prevented. The products with synthetic aluminum silicate, similar to montmorillonite clay, showed the next lowest absorbance at 385 nm. At present, no physicochemical explanation for this finding is apparent.

[19] A moving platen-type hardness tester, Kyowa Seiko Co. Ltd., Japan.

REFERENCES

(1) P. Speiser, H. P. Merkle, and L. Schibler, *Ger. Offen.*, **2**, 233, 428 (1973).

(2) C. Voellmy, P. Speiser, and M. Soliva, *J. Pharm. Sci.*, **66**, 631 (1977).

(3) H. Takenaka, Y. Kawashima, and Shan-Yang Lin, *ibid.*, **69**, 1387 (1980).

(4) Y. A. K. Abdul-Rahman and E. J. Crosby, *Chem. Eng. Sci.*, **28**, 1273 (1973).

(5) H. Takenaka, Y. Kawashima, S.-Y. Lin, and Y. Ando, *J. Pharm. Sci.*, **71**, 914 (1982).

(6) Instruction of JP IX, Hirokawa Shoten, Tokyo, 1976, pp. C-1112.

(7) T. Kametani, K. Kigasawa, N. Ikari, T. Iwata, M. Saito, and H. Yagi, *Chem. Pharm. Bull.*, **15**, 1305 (1967).

(8) P. Pfeiffer and R. Seydel, *Z. Physiol. Chem.*, **176**, 1 (1928).

(9) H. Takenaka, Y. Kawashima, T. Yoneyama, and K. Matsuda, *Chem. Pharm. Bull.*, **19**, 1234 (1971).

(10) K. Kawakita and K. H. Ludde, *Powder Technol.*, **4**, 61 (1970/71).

(11) K. Kigasawa, N. Ikari, M. Saito, T. Iwata, and R. Shoji, *YAKUZAIGAKU*, **33**, 31 (1973).

ACKNOWLEDGMENTS

This paper is Part XIII of a series on spray-drying agglomeration.

The authors thank Prof. A. Otsuka, Meijo University, Nagoya, Japan for use of the X-ray diffractometer.

GLC Determination of Phendimetrazine in Human Plasma, Serum, or Urine

G. R. RUDOLPH, J. R. MIKSIC ˣ, and M. J. LEVITT

Received February 5, 1982, from the *Biodecision Laboratories, Pittsburgh, PA 15213.* Accepted for publication May 19, 1982.

Abstract □ A sensitive, specific, and quantitative GLC method is described for the determination of phendimetrazine in plasma, serum, or urine. An internal standard was used, which was extracted along with the drug. This mixture then was acetylated to improve the chromatographic separation. A concentration as low as 2 ng/ml of phendimetrazine could be measured from 2 ml of sample using a nitrogen-phosphorous detector. Linearity extended from 2 to 500 ng/ml, and the coefficient of variation was 7%. The method was shown to be applicable to a single-dose bioavailability study.

Keyphrases □ GLC—determination of phendimetrazine in human plasma, serum, or urine □ Phendimetrazine—GLC determination in human plasma, serum, or urine □ Bioavailability—GLC determination of phendimetrazine in human plasma, serum, or urine

Phendimetrazine (I) is a sympathomimetic amine with anorectic activity used in nonprescription products for appetite suppression (1). As a condition of marketing phendimetrazine tartrate drug products in the United States, the Food and Drug Administration (FDA) has required bioavailability testing since 1973. To measure serum or plasma concentrations following a single dose of 105 mg in a bioavailability study, an analytical method with a sensitivity of ~5 ng/ml was required.

Phendimetrazine has been measured by TLC (2) and GLC (3, 4). These methods lack sufficient sensitivity to be useful for pharmacokinetic studies after a single 105-mg dose of drug. One GLC assay procedure does have adequate sensitivity (5), but only if 5 ml of serum is analyzed. Moreover, it was confirmed that the internal standard employed in this procedure was unstable, as previously reported (6).

The assay procedure described in this paper uses GLC with nitrogen-phosphorous detection to measure as little as 2 ng/ml of I in a 2-ml sample. Phentermine (II) is added to the samples to serve as an internal standard. Acetic anhydride is used to form an *N*-acetyl derivative of II which is suitable for GLC. Phenmetrazine (III), a metabolite of phendimetrazine (7), is also acetylated providing a derivative which does not interfere with the analysis of I.

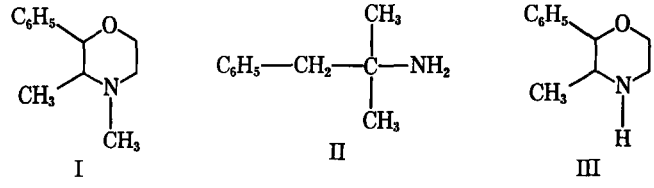

I II III

EXPERIMENTAL

Reagents and Chemicals—All chemicals were used as supplied. Phendimetrazine tartrate[1], phentermine hydrochloride[2], and phenmetrazine[3] were pharmaceutical grade. Sodium chloride, potassium hydroxide, anhydrous ethyl ether, and acetic anhydride were ACS certified reagent grade[4]. HPLC grade toluene[4] was used. Phentermine hydrochloride was dissolved in deionized water (450 ng/ml) for use as the internal standard. Standards and controls were prepared by diluting aqueous solutions of phendimetrazine tartrate with pooled plasma, serum, or urine previously checked for interfering peaks. Concentrations of I at 0, 2, 5, 10, 25, 50, 80, and 150 ng/ml in serum or plasma and 0, 10, 25, 50, 80, 150, 200, 300, and 400 ng/ml in urine were analyzed. Standards stored at −15° were stable for at least 3 months.

Instrumentation—Analyses were performed on a gas chromatograph[5] equipped with a nitrogen-phosphorous detector, an auto injector[6], a recording integrator, and a 1.5-m × 2.0-mm i.d. glass column containing 3% SP-2100 on 80–100 mesh Supelcoport[7]. The column temperature was 140° during each analysis and was raised to 200° for 5 min following elution of the internal standard. The injection port and detector temperatures were 210 and 290°, respectively. Prepurified nitrogen[8] was used as a carrier gas at 30 ml/min. Samples were mechanically vortexed and shaken. Two-milliliter glass autoinjector vials with polytef-lined, red rubber caps and aluminum seals were used[9].

Analytical Procedure—Internal standard solution (700 μl, equivalent to 315 ng of phentermine hydrochloride) and sodium chloride (1 ± 0.2 g) were added to 2.0 ml of plasma, serum, or urine in a 16 × 125-mm screw-cap tube. The sample was made basic by the addition of 2 *N* KOH (300 μl). After brief mixing, I and II were extracted into ethyl ether (3 ml)

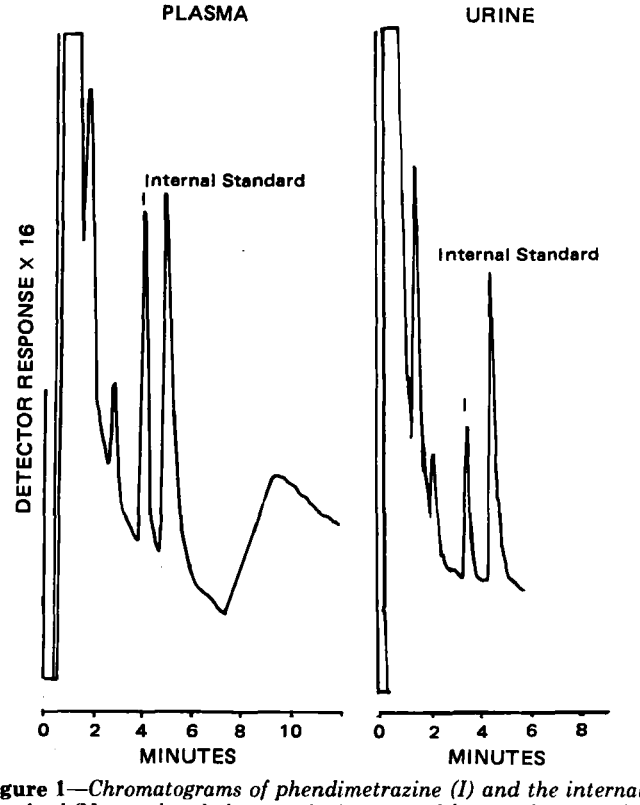

Figure 1—*Chromatograms of phendimetrazine (I) and the internal standard (N-acetylated phentermine) extracted from a plasma and a urine sample. The phendimetrazine concentrations were 39 ng/ml in plasma and 1621 ng/ml in urine (diluted 40-fold).*

[1] KV Pharmaceuticals, St. Louis, Mo.
[2] Beecham Laboratories, Bristol, Tenn.
[3] Preludin tablets, Boehringer Ingelheim, Elmsford, N.Y.
[4] J.T. Baker Chemical Co., Phillipsburg, N.J.
[5] Model 5840 A, Hewlett-Packard, Avondale, Pa.
[6] Model 7672 A, Hewlett-Packard, Avondale, Pa.
[7] Supelco, Bellefonte, Pa.
[8] Air Reduction Co., Pittsburgh, Pa.
[9] Models 5080-8712 and -8713, Hewlett-Packard, Avondale, Pa.

0022-3549/83/0500-0519$01.00/0

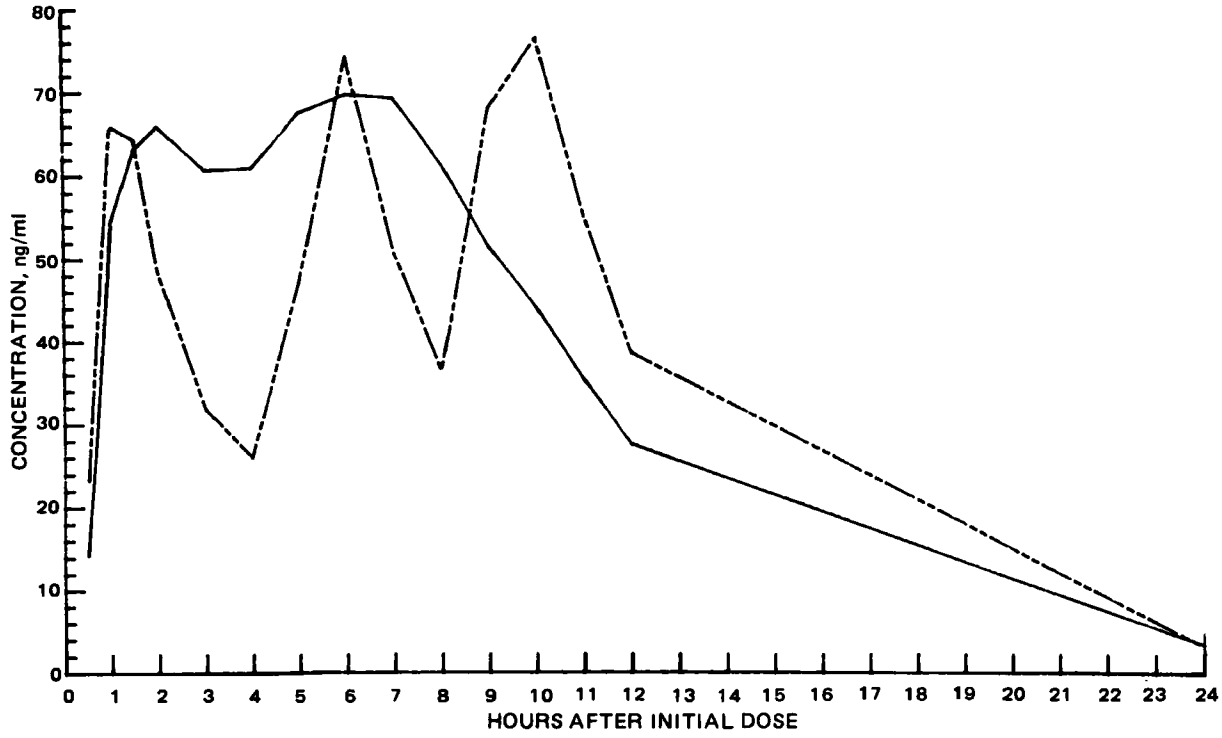

Figure 2—*Average plasma levels of phendimetrazine in 20 males who received a 105-mg controlled-release product at 0 hr or a 35-mg immediate-release product at 0, 4, and 8 hr. Key: (- - -) immediate release; (——) controlled release.*

by shaking for 10 min, and then the ether layer was transferred to another 16 × 125-mm tube. The drug and internal standard were then extracted from the ether into 0.1 *N* HCl (1.0 ml) by vortexing for 2 min. After centrifuging at 2800×*g* for 5 min, the ether layer was aspirated and discarded. Toluene (300 μl) and 10 *N* KOH (100 μl) were added to the remaining aqueous layer. After vortexing for 2 min and centrifuging at 2800×*g* for 5 min, the toluene layer was transferred to an injector vial. Acetic anhydride (50 μl) was added, the vial was capped, mixed briefly, and allowed to stand for at least 5 min. An aliquot (4 μl) then was injected into the gas chromatograph.

Human Bioavailability Study—A two-way crossover study was performed in 20 males (age, 18–37 years; weight, 60–89 kg). All of the subjects had hematology, blood chemistry, and urinalysis values within the normal range. The subjects received no medication for 7 days prior to the study and only the prescribed medications during the study. All the subjects were administered oral doses of enteric-coated ammonium chloride starting two days before dosing in order to maintain urine pH <7. They were fasted overnight at least 10 hr predose and for 2 hr postdose. A light breakfast was eaten 2 hr after initial dosing.

In each phase of the study, half of the subjects were administered a single 105-mg controlled-release phendimetrazine tartrate capsule[10] at 0 hr. The remaining subjects were administered one 35-mg immediate-release phendimetrazine tartrate tablet[11] at 0, 4, and 8 hr. Each dose was administered with 177 ml of water.

Blood samples (10 ml) were drawn from an antecubital vein into heparinized evacuated blood collection tubes[12] at intervals from 0 to 48 hr after initial dosing. The blood samples were centrifuged at 2000×*g* for 10 min within 10 min of collection. The plasma samples were transferred to polystyrene culture tubes[13] and stored at −15° until analyzed. Urine samples were collected at 12-hr intervals for 48 hr after initial dosing and were stored at −15° until analyzed.

Calculations—Peak height ratios were calculated by dividing the height of the phendimetrazine peak by the height of the acetylated internal standard peak. A best-fit line was determined by linear regression for standards ranging from 0 to 150 ng/ml (to 400 ng/ml for urine) that were processed along with the samples. The peak height ratio for each sample was used to calculate its concentration from the best-fit line. Comparable results were obtained when peak area ratios were used instead of peak height ratios. Control samples consisting of phendimetrazine added to plasma at 20 and 75 ng/ml and to urine at 20 and 158 ng/ml were also analyzed with each set of samples, and day-to-day coefficients of variation were determined from these controls.

[10] Rexar Pharmaceutical Corp., Valley Stream, N.Y.
[11] Plegine, Ayerst Laboratories, New York, N.Y.
[12] Model 6480, Becton-Dickinson, Rutherford, N.J.
[13] Model 2054, Falcon, Oxnard, Calif.

RESULTS AND DISCUSSION

Chromatography—The retention times of phendimetrazine and *N*-acetyl phentermine were 4.1 and 4.8 min, respectively (Fig. 1). Because some serum and plasma samples had a late-eluting peak at ~10 min, the column temperature was programmed to increase to 200° for 5 min after the internal standard peak was completely eluted.

Acetic anhydride was added to improve the chromatographic separation and eliminate a metabolic interference. In the absence of acetic anhydride, phentermine was poorly resolved from the solvent front as a tailing peak (retention time of 1.4 min), and phenmetrazine (a metabolite of phendimetrazine) was incompletely resolved from the phendimetrazine peak. Injection of acetic anhydride remaining from the acetylation reaction had no perceptible effect on column performance and, therefore, was left in the reaction mixture.

Extraction and Derivatization—The total recovery of phendimetrazine from plasma or serum was 73% ($n = 5$, $CV = 4\%$) of that obtained with a single extraction from aqueous solutions. Gel formation was encountered during the initial extraction with ethyl ether but was eliminated by the addition of salt and gentle shaking.

The reaction of acetic anhydride with phentermine was complete within 5 min at room temperature. Acetic anhydride obtained from one other alternate source produced a large peak at the retention time of phendimetrazine. Redistillation of this anhydride did not prevent the appearance of the interfering peak. Alternate bottles from the manufacturer listed in this paper had no interfering peaks.

Internal Standard—Biogenic amines such as pseudoephedrine, phenylpropanolamine, phentermine (underivatized), and diethylpropion were unsuitable as internal standards, because they were unstable, produced tailed chromatographic peaks, or had undesirable retention times. The internal standard used in this procedure, phentermine, was extracted with phendimetrazine and the mixture treated with acetic anhydride. Phentermine formed a stable *N*-acetyl compound which afforded a suitable retention time and peak shape.

Assay Sensitivity, Linearity, and Precision—Phendimetrazine standards in plasma and serum produced linear responses over the range of 2 to at least 200 ng/ml. Urine standards gave linear responses to at least 500 ng/ml. The standard curves typically had regression coefficients >0.99. The lower limit of quantitation of the analysis was 2 ng/ml from

an initial 2-ml sample. The day-to-day coefficients of variation (n = 24) of the procedure over a 3-week period, during which ~1000 plasma samples were analyzed, were 7% at 20 ng/ml and 6% at 75 ng/ml. The day-to-day coefficients of variation (n = 5) for the urine analyses were 6% at 20 ng/ml and 4% at 158 ng/ml. Within-day reproducibility for the plasma assay with n = 5 at concentrations of 2 and 50 ng/ml was CV = 8.7 and 1.3%, respectively.

Bioavailability Study Results—The assay procedure was used to measure the plasma and urine concentrations of phendimetrazine in 20 subjects in a two-way crossover bioavailability study (Fig. 2). The peak concentration of 70 ng/ml observed after one 35-mg dose of phendimetrazine tartrate and the elimination half-life of 2 hr observed for the immediate-release product were similar to those previously reported (5, 7). The average total recovery in urine over 48 hr after a 105-mg dose amounted to 5.72 ± 3.01 mg for the controlled-release formulation and 4.72 ± 2.89 mg for the immediate-release formulation. The assay procedure had adequate sensitivity to measure phendimetrazine in plasma at 24 hr, even for the subjects who received the immediate-release formulation. No predose plasma or urine samples had interferences at the phendimetrazine or internal standard retention times.

REFERENCES

(1) *Fed. Reg.*, **44**, 47618 (1979).

(2) R. T. Macnab, *Can. J. Med. Technol.*, **25**, 43 (1965).

(3) A. H. Beckett, *J. Pharm. Pharmacol.*, **19**, 273 (1967).

(4) D. V. Canfield, P. Lorimer, and R. L. Epstein, *J. Forensic Sci.*, **22**, 429 (1977).

(5) H. D. L. Hundt, E. C. Clark, and F. O. Muller, *J. Pharm. Sci.*, **64**, 1041 (1975).

(6) S. M. Walters, *ibid.*, **69**, 1206 (1980).

(7) A. H. Beckett and A. Raisi, *J. Pharm. Pharmacol.*, **28**, Suppl: 40P (1976).

ACKNOWLEDGMENTS

The authors thank Charles Bon and Mimi Passarello for the bioavailability analyses and statistics.

Determination of Benzalkonium Chloride in the Presence of Interfering Alkaloids and Polymeric Substrates by Reverse-Phase High-Performance Liquid Chromatography

DENNIS F. MARSH ˣ **and LLOYD T. TAKAHASHI**

Received October 9, 1981, from *Allergan Pharmaceuticals, Inc., Irvine, CA 92713.* Accepted for publication May 24, 1982.

Abstract □ A specific assay for the analysis of benzalkonium chloride in the presence of interfering substances was conducted. The approach involved complexing benzalkonium chloride in an ophthalmic system with methyl orange, extraction of the complex into 1,2-dichloroethane, and subsequent analysis by reverse-phase high-performance liquid chromatography. Since the method separates each homologue of benz*alkonium chloride*, homologues not resident in the ophthalmic system were added as internal standards to improve both recovery and precision in the method.

Keyphrases □ High-performance liquid chromatography—determination of benzalkonium chloride, ophthalmic systems, complex with methyl orange □ Benzalkonium chloride—high-performance liquid chromatography, ophthalmic systems, complex with methyl orange

Various nonspecific dye extraction methods (1–3) have been developed for the determination of benzalkonium chloride. Recently, a specific analysis for benzalkonium chloride in aqueous solution by high-performance liquid chromatography (HPLC) was developed (4). This method involves direct injection of the aqueous formulation onto the chromatographic column. However, this method of analysis proved unsatisfactory for ophthalmic systems containing polymeric material. Polyvinyl alcohol, for example, precipitates under assay conditions, thus plugging the HPLC column. Suspended particulate matter in the formulation, such as steroid suspensions, also precludes the use of the method for the same reason.

Another difficulty encountered with the direct injection procedure is the interference of active alkaloids with the benzalkonium chloride during chromatography. Benzalkonium chloride is generally present in ophthalmic systems at the antimicrobial level of 0.004%, while active ingredients are present in considerably greater concentration. Also, active ingredients have considerably higher extinction coefficients in the UV than does the benzalkonium chloride preservative. These factors make benzalkonium chloride difficult to detect by HPLC if its retention time and that of the active ingredients are at all similar.

The purpose of this paper is to describe an extraction procedure to determine benzalkonium chloride in problem systems which preclude direct injection of the samples.

EXPERIMENTAL

Apparatus—The HPLC consisted of a pump[1], an automatic sampler[2], a reverse-phase microcyano column[3], a 254-nm detector[4], and a recorder[5]. Peak integrations were performed with a laboratory data system[6].

Reagents and Solvents—The mobile phase was 58% acetonitrile[7] (UV grade) and 42% 0.161 *M* sodium propionate at pH 5.35. Sodium carbonate[8] (7.5 g) was mixed with distilled water in a 2000-ml volumetric flask. Propionic acid[9] (12 ml) was added, and the solution was brought to volume (2000 ml) with distilled, deionized water. This solution was mixed with 2800 ml of acetonitrile.

Preparation of the C_{10} and C_{18} Homologues of Benzalkonium Chloride (as the Methyl Orange Complex)—In a 1000-ml round-bottom flask 22.1 g (0.1 mole) of 1 bromodecane[10], 13.5 g (0.1 mole) of *N,N*-dimethylbenzylamine[9], 500 ml of acetonitrile, and 30 ml of dimethylformamide[9] were added. This solution was allowed to reflux (86°)

[1] Model 6000A, Waters Associates, Milford, Mass.
[2] Wisp 710B, Waters Associates, Milford, Mass.
[3] μBondapak CN (10-μm particle size, 30-cm long × 4-mm i.d. column), Waters Associates, Milford, Mass.
[4] Model 440, Waters Associates, Milford, Mass.
[5] Omniscribe, Houston Instruments, Austin, Tex.
[6] Model 3352B, Hewlett-Packard, Fullerton, Calif.
[7] Burdick & Jackson Laboratories, Muskegon, Mich.
[8] Mallinckrodt, Inc., St. Louis, Mo.
[9] J. T. Baker Chemical Co., Phillipsburg, N.J.

0022-3549/83/0500-0521$01.00/0

an initial 2-ml sample. The day-to-day coefficients of variation (n = 24) of the procedure over a 3-week period, during which ~1000 plasma samples were analyzed, were 7% at 20 ng/ml and 6% at 75 ng/ml. The day-to-day coefficients of variation (n = 5) for the urine analyses were 6% at 20 ng/ml and 4% at 158 ng/ml. Within-day reproducibility for the plasma assay with n = 5 at concentrations of 2 and 50 ng/ml was CV = 8.7 and 1.3%, respectively.

Bioavailability Study Results—The assay procedure was used to measure the plasma and urine concentrations of phendimetrazine in 20 subjects in a two-way crossover bioavailability study (Fig. 2). The peak concentration of 70 ng/ml observed after one 35-mg dose of phendimetrazine tartrate and the elimination half-life of 2 hr observed for the immediate-release product were similar to those previously reported (5, 7). The average total recovery in urine over 48 hr after a 105-mg dose amounted to 5.72 ± 3.01 mg for the controlled-release formulation and 4.72 ± 2.89 mg for the immediate-release formulation. The assay procedure had adequate sensitivity to measure phendimetrazine in plasma at 24 hr, even for the subjects who received the immediate-release formulation. No predose plasma or urine samples had interferences at the phendimetrazine or internal standard retention times.

REFERENCES

(1) *Fed. Reg.*, **44**, 47618 (1979).

(2) R. T. Macnab, *Can. J. Med. Technol.*, **25**, 43 (1965).

(3) A. H. Beckett, *J. Pharm. Pharmacol.*, **19**, 273 (1967).

(4) D. V. Canfield, P. Lorimer, and R. L. Epstein, *J. Forensic Sci.*, **22**, 429 (1977).

(5) H. D. L. Hundt, E. C. Clark, and F. O. Muller, *J. Pharm. Sci.*, **64**, 1041 (1975).

(6) S. M. Walters, *ibid.*, **69**, 1206 (1980).

(7) A. H. Beckett and A. Raisi, *J. Pharm. Pharmacol.*, **28**, Suppl: 40P (1976).

ACKNOWLEDGMENTS

The authors thank Charles Bon and Mimi Passarello for the bioavailability analyses and statistics.

Determination of Benzalkonium Chloride in the Presence of Interfering Alkaloids and Polymeric Substrates by Reverse-Phase High-Performance Liquid Chromatography

DENNIS F. MARSH ˣ **and LLOYD T. TAKAHASHI**

Received October 9, 1981, from *Allergan Pharmaceuticals, Inc., Irvine, CA 92713.* Accepted for publication May 24, 1982.

Abstract □ A specific assay for the analysis of benzalkonium chloride in the presence of interfering substances was conducted. The approach involved complexing benzalkonium chloride in an ophthalmic system with methyl orange, extraction of the complex into 1,2-dichloroethane, and subsequent analysis by reverse-phase high-performance liquid chromatography. Since the method separates each homologue of benz*alkonium chloride*, homologues not resident in the ophthalmic system were added as internal standards to improve both recovery and precision in the method.

Keyphrases □ High-performance liquid chromatography—determination of benzalkonium chloride, ophthalmic systems, complex with methyl orange □ Benzalkonium chloride—high-performance liquid chromatography, ophthalmic systems, complex with methyl orange

Various nonspecific dye extraction methods (1–3) have been developed for the determination of benzalkonium chloride. Recently, a specific analysis for benzalkonium chloride in aqueous solution by high-performance liquid chromatography (HPLC) was developed (4). This method involves direct injection of the aqueous formulation onto the chromatographic column. However, this method of analysis proved unsatisfactory for ophthalmic systems containing polymeric material. Polyvinyl alcohol, for example, precipitates under assay conditions, thus plugging the HPLC column. Suspended particulate matter in the formulation, such as steroid suspensions, also precludes the use of the method for the same reason.

Another difficulty encountered with the direct injection procedure is the interference of active alkaloids with the benzalkonium chloride during chromatography. Benzalkonium chloride is generally present in ophthalmic systems at the antimicrobial level of 0.004%, while active ingredients are present in considerably greater concentration. Also, active ingredients have considerably higher extinction coefficients in the UV than does the benzalkonium chloride preservative. These factors make benzalkonium chloride difficult to detect by HPLC if its retention time and that of the active ingredients are at all similar.

The purpose of this paper is to describe an extraction procedure to determine benzalkonium chloride in problem systems which preclude direct injection of the samples.

EXPERIMENTAL

Apparatus—The HPLC consisted of a pump[1], an automatic sampler[2], a reverse-phase microcyano column[3], a 254-nm detector[4], and a recorder[5]. Peak integrations were performed with a laboratory data system[6].

Reagents and Solvents—The mobile phase was 58% acetonitrile[7] (UV grade) and 42% 0.161 *M* sodium propionate at pH 5.35. Sodium carbonate[8] (7.5 g) was mixed with distilled water in a 2000-ml volumetric flask. Propionic acid[9] (12 ml) was added, and the solution was brought to volume (2000 ml) with distilled, deionized water. This solution was mixed with 2800 ml of acetonitrile.

Preparation of the C_{10} and C_{18} Homologues of Benzalkonium Chloride (as the Methyl Orange Complex)—In a 1000-ml round-bottom flask 22.1 g (0.1 mole) of 1 bromodecane[10], 13.5 g (0.1 mole) of *N,N*-dimethylbenzylamine[9], 500 ml of acetonitrile, and 30 ml of dimethylformamide[9] were added. This solution was allowed to reflux (86°)

[1] Model 6000A, Waters Associates, Milford, Mass.
[2] Wisp 710B, Waters Associates, Milford, Mass.
[3] μBondapak CN (10-μm particle size, 30-cm long × 4-mm i.d. column), Waters Associates, Milford, Mass.
[4] Model 440, Waters Associates, Milford, Mass.
[5] Omniscribe, Houston Instruments, Austin, Tex.
[6] Model 3352B, Hewlett-Packard, Fullerton, Calif.
[7] Burdick & Jackson Laboratories, Muskegon, Mich.
[8] Mallinckrodt, Inc., St. Louis, Mo.
[9] J. T. Baker Chemical Co., Phillipsburg, N.J.

0022-3549/83/0500-0521$01.00/0

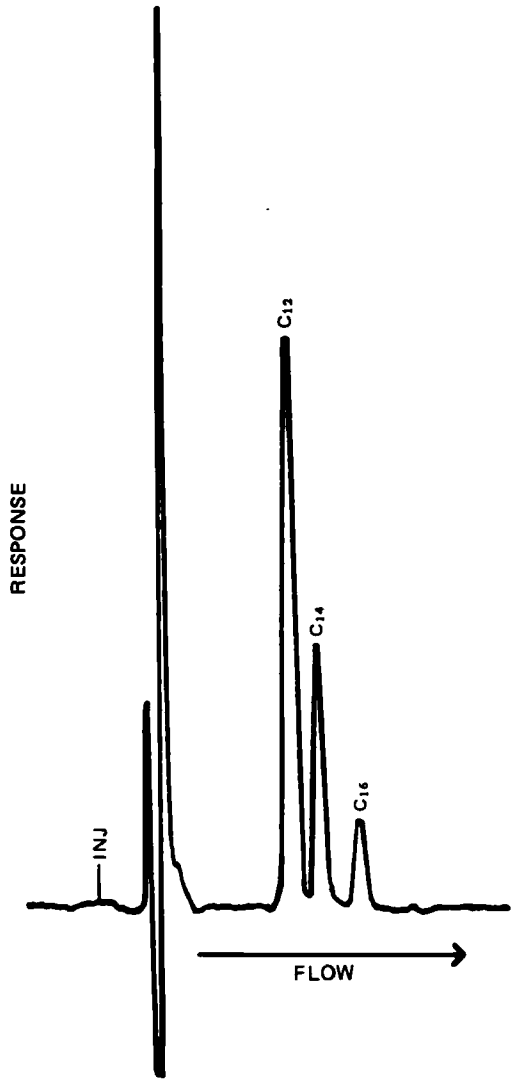

Figure 1—*Chromatogram of benzalkonium chloride without internal standards.*

for 3 days. To the hot, well-stirred solution was added 20 g of methyl orange[9]. The resulting solution was filtered hot. After cooling, the filtrate was refiltered. The orange crystalline needles thus obtained were analyzed by HPLC. The C_{10} homologue was the only peak observed. This peak had the same retention time as a USP standard benzalkonium chloride sample containing the C_{10} homologue. The C_{18} homologue was prepared in an analogous manner from 0.1 mole each of 1-chlorooctadecane[10] and *N,N*-dimethylbenzylamine in 500 ml of acetonitrile and 200 ml of dimethylformamide (heated at reflux for 5 days).

Preparation of the Internal Standard Mixture—Three grams of the C_{10} homologue of benzalkonium chloride was combined with 2 g of the C_{18} homologue. This mixture was finely ground with a mortar and pestle. A 0.06-g portion of this mixture was placed in a 1000-ml volumetric flask and 250 ml of dimethylformamide was added. A 0.250-g sample of methyl orange was dissolved in 500 ml of water. The aqueous solution of methyl orange was combined with the dimethylformamide solution of the benzalkonium chloride complex and 25 ml of acetic acid[9] was added. The solution was brought to volume with dimethylformamide.

Procedure—Samples and standards can be prepared and analyzed by HPLC both with and without the use of internal standards (Methods 1 and 2, respectively). Samples containing suspended steroids have been assayed by either method.

Standard Preparation—Raw material (50% w/v)[11] to be used as a secondary reference standard was diluted to 0.1% with water and assayed using a USP primary reference standard (10% w/v)[12] diluted to 0.100%.

[10] Matheson Coleman & Bell, Norwood, Ohio.
[11] Ruger Chemical Co., Inc. Irvington, N.J.
[12] U.S. Pharmacopeial Convention, Inc., Rockville, Md.

Table I—Recoveries of Benzalkonium Chloride in Nonextracted *versus* Extracted Samples

	UV Detector Responses of Homologues, mV/min			
	C_{12}	C_{14}	C_{16}	Total
	(A) Standard—Direct Injection			
	693	304	112	1,109
	673	302	119	1,094
	679	294	112	1,085
	687	319	119	1,117
	660	321	119	1,127
	660	309	112	1,081
	666	301	116	1,083
Mean	673.9	307.1	115.6	1,099
SD	14.6	9.9	3.5	18.3
RSD (±%)	2.2	3.2	3.0	1.7
	(B) Standard—Extraction Procedure			
	662	277	100	1,039
	659	285	121	1,065
	669	262	105	1,066
	660	283	117	1,060
	639	291	109	1,000
	670	280	109	1,069
Mean	659.8	280.4	109.0	1,049
SD	11.2	9.1	7.7	26.3
RSD, ± %	1.7	3.2	7.0	2.5
	(C) In Spiked Placebo—Extraction Procedure			
	639	280	102	1,021
	652	282	99	1,033
	670	290	99	1,059
	644	278	81	1,003
	649	266	84	1,000
	669	249	98	1,016
Mean	653.8	274	93.8	1,022
SD	12.9	14.6	8.9	21.8
RSD, ± %	2.0	5.3	9.5	2.1

Since no interfering substances are present in these aqueous solutions, these standards were not extracted and were injected directly without use of internal standards. For the assay of benzalkonium chloride in samples, the secondary reference standard was further diluted to the same concentration as the samples, usually 0.004% w/v.

Method 1 (Using Both Internal Standards)—The solution of sample or working standard (1.00 ml) was placed into a 12 ml plastic centrifuge tube[13], and 2.00 ml of the working internal standard solution was added. The solution was agitated briefly and allowed to equilibrate for 10 min. Then, 1.00 ml of 1,2-dichloroethane[9] was added, the mixture was vortexed for 1 min, allowed to stand for a few moments, and vortexed for an additional minute. The mixture was then centrifuged for 20 min at 8000 rpm. The phases were separated, and the organic phase was dried (anhydrous sodium sulfate) to give a yellow solution which was assayed by HPLC.

Method 2 (Using No Internal Standard)—The solution (1.00 ml) was added to a 10 ml plastic centrifuge tube, and 1.00 ml of a 0.05% aqueous solution of methyl orange, followed by 1.00 ml of a 10% aqueous solution of acetic acid were added. The solution was agitated briefly and allowed to equilibrate for 10 min. 1,2-Dichloroethane (1.0 ml) was added and the procedure in Method 1 was followed.

Assay—The mobile phase was filtered (1 μm) and deaerated. The system had the following parameters: a flow rate of 2.0 ml/min, giving a pressure of 1000–1500 psi, a 180-μl injector volume, an analysis time of 13 min, 254 nm detection at 0.01 AUFS, and a chart speed of 0.25 cm/min. After a stable baseline was achieved, replicate standards were run to ensure reproducibility, followed by the samples. A standard was run after every third sample.

The laboratory data system[6] was used to monitor the internal standard and the benzalkonium chloride peak areas. Since the concentration of the homologues other than C_{12}, C_{14}, and C_{16} in a benzalkonium chloride sample typically comprised <2% of the total, only the C_{12}, C_{14}, and C_{16} peaks were monitored. Chromatograms of benzalkonium chloride with and without internal standards are shown in Figs. 1 and 2.

Calculations for samples run without the use of internal standards are straightforward, relating the peak areas of the sample to the standard and adjusting this ratio for the standard concentration. When both in-

[13] Nalge Co., Division of Sybron Co., Rochester, N.Y.

Table II—Recovery and Precision of Benzalkonium Chloride in Spiked Placebo Containing Naphazoline Hydrochloride, Polyvinyl Alcohol, and Disodium Edetate [a]

	Weight/Volume, %		
	Operator 1—Day 1	Operator 1—Day 2	Operator 2
	0.00419	0.00421	0.00435
	0.00417	0.00423	0.00434
	0.00418	0.00417	0.00430
	0.00410	0.00421	0.00424
	0.00422	0.00420	0.00432
Mean	0.00417	0.00420	0.00431
SD	0.000044	0.000022	0.000044
RSD, ± %	1.1	0.52	1.0
Recovery, %	99.8	100.5	103.1

[a] No internal standard used; Method 2; theoretical value 0.00418% (w/v).

Table III—Recovery and Precision of Benzalkonium Chloride in Spiked Placebo Containing Phenylephrine Hydrochloride, Disodium Edetate, Pyrilamine Maleate, and Polyvinyl Alcohol [a]

	Weight/Volume, %		
	Operator 1—Day 1	Operator 1—Day 2	Operator 2
	0.00397	0.00404	0.00389
	0.00414	0.00409	0.00403
	0.00404	0.00404	0.00389
	0.00406	0.00405	0.00420
	0.00417	0.00404	0.00401
Mean	0.00408	0.00405	0.00400
SD	0.000080	0.000022	0.00013
RSD, ± %	2.0	0.54	3.2
Recovery, %	97.6	95.7	95.7

[a] No internal standard used; Method 2; theoretical value 0.00418% (w/v).

Table IV—Recovery and Precision of Benzalkonium Chloride in Spiked Placebo Containing Fluorometholone (as Suspension) and Polyvinyl Alcohol [a]

	Weight/Volume, %		
	Operator 1—Day 1	Operator 1—Day 2	Operator 2
	0.00404	0.00402	0.00401
	0.00398	0.00408	0.00400
	0.00408	0.00407	0.00389
	0.00401	0.00405	0.00406
	0.00406	0.00405	0.00402
Mean	0.00403	0.00405	0.00400
SD	0.000040	0.000023	0.000064
RSD, ± %	0.99	0.57	1.6
Recovery, %	96.5	97.0	95.8

[a] No internal standard used; Method 1; theoretical value 0.00418% (w/v).

ternal standards are used (Method 1), the calculations are more involved.

The weighting system described below is used to adjust for the varying partition coefficients of each homologue of benzalkonium chloride in the systems studied.

In many formulations, the extractability of each homologue follows the chain length. Recoveries of the individual homologues diminish as the chain length increases (see Table IB and C). For this reason, two internal standards, the C_{10}–C_{18} homologues are used to bracket the C_{12}–C_{16} benzalkonium chloride homologue resident in the formulation. If the C_{10} homologue alone is used as the internal standard, recoveries of total benzalkonium chloride are low due to the disproportionately high percentage of longer length homologues retained by the polymeric formulations. Conversely, inordinately high recoveries are obtained if the C_{18} homologue is used as the internal standard.

Thus, it is necessary to use both internal standards in such a way as to correct for the retention of each individual homologue. While both internal standards are used in these corrections, the internal standard with a chain length nearest the homologue in question is given the heaviest weight. All weighting factors (Method 1) in the equations that follow are a function of the chain-length differences of the homologues involved.

$$\% \text{ Benzalkonium Chloride} = \frac{C^*[F_1{}^*P_2 + F_2{}^*P_3 + F_3{}^*P_4]}{[PS_2 + PS_3 + PS_4]}$$

Table V—Recovery and Precision of Benzalkonium Chloride in Spiked Placebo Containing Polyvinyl Alcohol and Prednisolone Acetate (as Suspension) [a]

	Weight/Volume, %		
	Operator 1—Day 1	Operator 1—Day 2	Operator 2
	0.00420		0.00395
	0.00412	0.00415	0.00417
	0.00409	0.00440	0.00413
	0.00425	0.00419	0.00408
	0.00428	0.00420	0.00404
Mean	0.00419	0.00423	0.00407
SD	0.000082	0.00011	0.000085
RSD, ± %	1.9	2.6	2.1
Recovery, %	100.3	101.4	97.5

[a] No internal standard used; Method 2; theoretical value 0.00418% (w/v).

Table VI—Effectiveness of the Internal Standard in the Recovery of Benzalkonium Chloride [a]

	% Recovery Without Internal Standards	% Recovery With Internal Standards
	82.9	99.9
	93.4	97.4
	88.5	99.7
	88.0	101.9
	90.2	102.9
	87.8	95.5
		96.9
		102.4
Mean	88.5	99.6
SD	3.4	2.7
RSD, ± %	3.9	2.8

[a] Sample contains polyvinyl alcohol and prednisolone acetate.

Table VII—Recovery and Precision of Benzalkonium Chloride in Spiked Placebo Containing Polyvinyl Alcohol and Disodium Edetate [a]

	Weight/Volume, %		
	Operator 1—Day 1	Operator 1—Day 2	Operator 2
	0.00395	0.00378	0.00404
	0.00385	0.00383	0.00396
	0.00394	0.00385	0.00400
	0.00391	0.00379	0.00412
	0.00393	0.00384	0.00415
	0.00395	0.00380	0.00392
Mean	0.00392	0.00381	0.00403
SD	0.00004	0.00003	0.00009
RSD, ± %	0.97	0.76	2.2
Recovery, %	99.5	96.8	102.4

[a] Using both internal standards; Method 1; theoretical value 0.00394% (w/v).

where,

C = Concentration of benzalkonium chloride standard in % (w/v)

$F_1 = [3^*R_1 + R_2]/4$

$F_2 = [R_1 + R_2]/2$

$F_3 = [R_1 + 3^*R_2]/4$

and,

$R_1 = PS_1/P_1$

$R_2 = PS_5/P_5$

and,

P_1 = Peak area of the C_{10} homologue in the sample

P_2 = Peak area of the C_{12} homologue in the sample

P_3 = Peak area of the C_{14} homologue in the sample

P_4 = Peak area of the C_{16} homologue in the sample

P_5 = Peak area of the C_{18} homologue in the sample

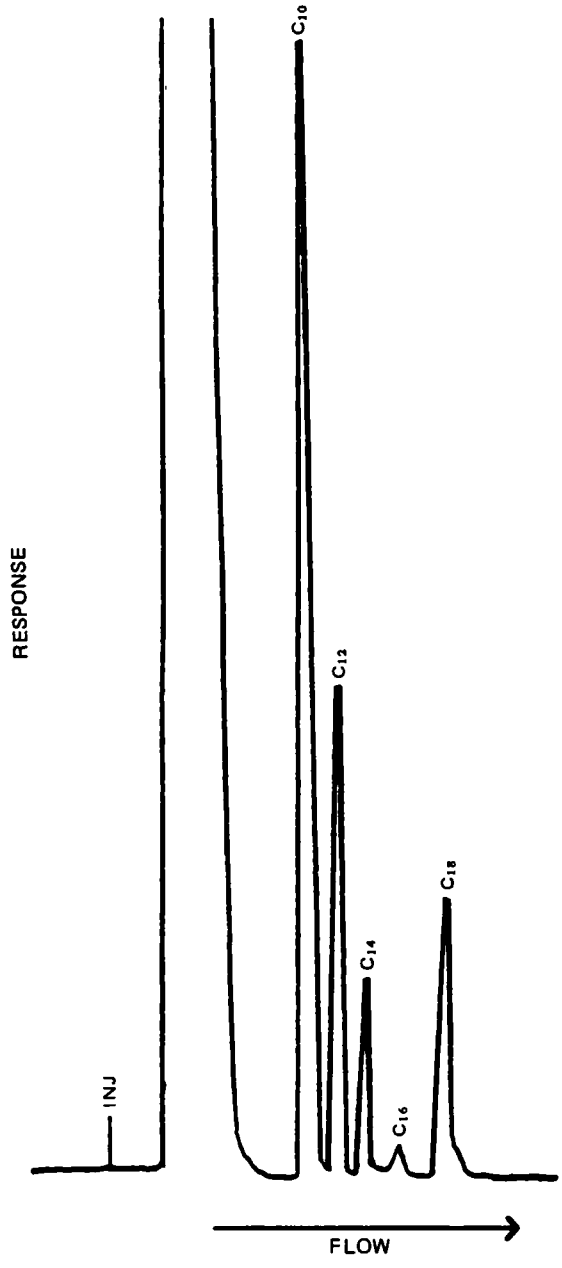

Figure 2—*Chromatogram of benzalkonium chloride with internal standards.*

and,

PS_1 = Average peak area of the C_{10} homologue in the standard

PS_2 = Average peak area of the C_{12} homologue in the standard

PS_3 = Average peak area of the C_{14} homologue in the standard

PS_4 = Average peak area of the C_{16} homologue in the standard

PS_5 = Average peak area of the C_{18} homologue in the standard

The PS_{1-5} values represent an average of the standard peaks that precede and follow the sample being calculated.

RESULTS AND DISCUSSION

Since benzalkonium chloride is now widely used in a variety of ophthalmic formulations, several problems have surfaced which have made direct sample injection impossible. These problems, which have been mentioned earlier, have been circumvented by preliminary treatment of the benzalkonium chloride with methyl orange. This procedure takes advantage of the lipophilic properties of the benzalkonium chloride–methyl orange ion pair. The dye complex is removed from interfering polymers and alkaloids by extraction into 1,2-dichloroethane. It is this isolated dye complex and the subsequent chromatography that gives the assay procedure its specificity. Experiments in validating this procedure are described.

Table VIII—Recovery and Precision of Benzalkonium Chloride in Spiked Placebo Containing Fluorometholone, Gentamicin, and Polyvinyl Alcohol [a]

	Weight/Volume, %		
	Operator 1—Day 1	Operator 1—Day 2	Operator 2
	0.00429	0.00430	
	0.00431	0.00424	0.00410
	0.00390	0.00430	0.00422
	0.00425	0.00428	0.00418
	0.00422	0.00426	0.00434
	0.00435	0.00437	0.00424
	0.00422	0.00441	0.00401
	0.00425	0.00425	0.00415
	0.00416	0.00426	0.00376
Mean	0.00422	0.00430	0.00413
SD	0.00013	0.00006	0.00018
RSD, ± %	3.1	1.3	4.3
Recovery, %	100.9	102.8	98.7

[a] Using both internal standards; Method 1; theoretical value 0.004176% (w/v).

An aqueous benzalkonium chloride standard (0.004%) was injected several times onto the chromatograph. The results, shown in UV-detector response for the three major homologues and the total, are shown in Table IA. This same aqueous standard was extracted into an equal volume of 1,2-dichloroethane as the methyl orange complex. The results are shown in Table IB. Also, a typical ophthalmic formulation containing polyvinyl alcohol was spiked to give 0.004% benzalkonium chloride and extracted in the same manner as the standard into an equal volume of 1,2-dichloroethane. The results are shown in Table IC. Analysis of the mean values for total response in the three experiments indicates that, while benzalkonium chloride is readily extractable into dichloroethane as the methyl orange complex, the extraction is not complete. The Student's *t* values obtained by comparing the mean total response value in Table IA *versus* those in Table IB and C demonstrate that significant differences exist between the mean values involved. Comparison of the mean values for total response for the extracted aqueous standard in Table IB and the extracted spiked formulation in Table IC show equivalence of means and variances using Student's *t* and F tests. The mean total response for the extracted placebo in Table IC represents a 97.4% recovery when compared with the mean total response for the extracted standard in Table IB. If standards and samples are treated in the same manner, recoveries of 95–100% are found for most ophthalmic systems. Shown in Tables II–V are the results obtained in four representative studies.

While in the majority of cases acceptable recoveries are obtained by the simple extraction method (Method 2), low recovery values are sometimes observed. To improve the recovery, two benzalkonium chloride homologues not present in the ophthalmic formulation were added as internal standards (Method 1). Observations of the data shown in Table IA, B, and C demonstrate that not only does the extractability of benzalkonium chloride vary in ophthalmic systems but also within the homologous series itself. The longer length homologues are clearly more

Table IX—Recovery and Precision of Benzalkonium Chloride in Spiked Placebo Containing Polyvinyl Alcohol (3%) and Disodium Edetate [a]

	Weight/Volume, %		
	Operator 1—Day 1	Operator 1—Day 2	Operator 2
	0.00414	0.00429	0.00420
	0.00447	0.00433	0.00423
	0.00423	0.00444	0.00405
	0.00430	0.00417	0.00449
	0.00438	0.00444	0.00456
	0.00450	0.00430	0.00456
	0.00408	0.00410	0.00456
	0.00389	0.00407	0.00439
	0.00400	0.00405	0.00435
Mean	0.00422	0.00424	0.00438
SD	0.00021	0.00015	0.00019
RSD, ± %	5.0	3.6	4.3
Recovery, %	101.0	101.5	104.8

[a] Using both internal standards; Method 1; theoretical value 0.004176% (w/v).

Table X—Recovery and Precision of Benzalkonium Chloride in Spiked Placebo Containing Oxymetazoline and Polyvinyl Alcohol [a]

	Weight/Volume, %		
	Operator 1—Day 1	Operator 1—Day 2	Operator 2
	0.00434	0.00409	0.00410
	0.00402	0.00419	0.00446
	0.00418	0.00389	0.00414
	0.00419	0.00399	0.00452
	0.00418	0.00410	0.00429
	0.00415	0.00424	0.00425
	0.00431	0.00426	0.00434
	0.00421	0.00434	0.00426
	0.00446	0.00409	0.00423
Mean	0.00423	0.00413	0.00430
SD	0.00013	0.00014	0.00014
RSD, ± %	3.0	3.4	3.2
Recovery, %	101.1	98.9	102.8

[a] Using both internal standards; Method 1; theoretical value 0.004176% (w/v).

difficult to extract from aqueous solutions containing polymers. Therefore, both internal standards must be used to achieve consistently good recoveries for benzalkonium chloride in the many different types of ophthalmic solutions. For instance, shown in Table VI is an example of a formulation containing polyvinyl alcohol and prednisolone acetate in which poor recoveries were obtained without internal standards, but recoveries were acceptable with the internal standards. In Tables VII–X are four representative studies using Method 1 to determine benzalkonium chloride.

The methyl orange-benzalkonium chloride complex proves surprisingly stable in both acid and basic environments. Several aliquots of the 1,2-dichloroethane solution of the methyl orange-benzalkonium chloride complex were washed with 1*N* sodium hydroxide and analyzed. Several aliquots of the complex were washed with 10% acetic acid and analyzed. No significant differences were observed (Student's *t*) when the two studies were compared. This permits an acid or base wash of the extracted methyl orange-benzalkonium chloride complex in further clean-up of the sample.

Table XI shows the assay results obtained by a modification of Method 1 and Method 2 on a formulation containing a 1000:1 ratio of antazoline phosphate to benzalkonium chloride. The dichloroethane solution of methyl orange–benzalkonium chloride complex, obtained by the extraction of the aqueous formulation, also contains significant amounts of antazoline. The presence of the antazoline makes analysis of benzalkonium chloride impossible, as retention times for each substance are similar. The antazoline can be removed, however, by two extractions with 10% acetic acid. As the results in Table XI clearly indicate, internal standards must be used when additional extractions are necessary.

Table XI—Recoveries After Double-Acid Wash of Extracted Sample (% w/v)

Method 2—No Internal Standard [a]	Method 1 with Internal Standard [b]
0.00300	0.00387
0.00325	0.00392
0.00303	0.00399
0.00303	0.00388
0.00305	0.00398
	0.00420
	0.00402
	0.00415
Mean 0.00307	0.00400
SD 0.000101	0.00012
RSD, ± % 3.3	3.0
Recovery, % 72.7	98.9

[a] Theoretical value 0.00418% (w/v). [b] Theoretical value 0.00404% (w/v).

System suitability requirements for multiple standard injections are that the relative standard deviation be <±3%. A column should have at least 2000 plates per column for the C_{12} homologue calculated by $N = 16\text{-}(w/v)^2$.

The versatility of this method has been shown in its ability to be used for various types of formulations including suspensions of steroids, polymeric compounds, and other ingredients which would interfere without prior sample workup. Because of the capability of using either (or both) acid and base washing of the extracted benzalkonium–dye complex, the method is very flexible in removing these interferences. Whatever modifications to the assay are required, it is essential that the standards and samples be treated in exactly the same way throughout the assay.

REFERENCES

(1) C. W. Ballard, J. Isaacs, and P. G. W. Scott, *J. Pharm. Pharmacol.*, **6**, 971 (1954).

(2) E. L. Colichman, *Anal. Chem.*, **19**, 430 (1947).

(3) L. G. Chatten and K. O. Okamura, *J. Pharm. Sci.*, **62**, 1328 (1973).

(4) R. C. Meyer, *ibid.*, **69**, 1148 (1980).

ACKNOWLEDGMENTS

The authors wish to thank H. Wierzba for editorial assistance and K. Lee, M. Pollay, and C. Martin for valuable assistance in testing the procedures and collection of data for validation.

Gas Chromatographic–Mass Spectrometric Quantitation of Theophylline and Its Metabolites in Biological Fluids

KOU-YI TSERNG

Received September 18, 1981, from the *Division of Pediatric Metabolism, Department of Pediatrics, Case Western Reserve University at Cleveland Metropolitan General Hospital, Cleveland, OH 44109.* Accepted for publication May 24, 1982.

Abstract □ In premature infants, theophylline is converted to caffeine, and the biological half-life is prolonged. To assess the metabolic alterations of theophylline during development of premature infants, a sensitive and simple method was developed which quantitated all theophylline metabolites in plasma, urine, and red blood cells. Theophylline and its metabolites in the sample were converted to the *N*-propyl derivative using *n*-propyl iodide in dimethylformamide with potassium carbonate catalysis and were analyzed under isothermal conditions on a gas chromatograph–mass spectrometer with a 3% methylsilicone–phenylsilicone column. Deuterated caffeine (caffeine-d_3) was used as the internal standard. A selected ion-monitoring technique, together with 70-eV electron impact ionization mode, was used. The ion current ratios between caffeine-d_3 (*m/z* 197) and caffeine (*m/z* 194), theophylline (*m/z* 222), 3-methylxanthine (*m/z* 250), 1,3-dimethyluric acid (*m/z* 280), and 1-methyluric acid (*m/z* 308) were monitored. The total analysis time was 12 min with a detection limit ranging from 500 pg to 10 ng, depending on the metabolites. With this sensitivity, sample sizes of 50–100 μl of plasma and 0.5 ml of urine were sufficient for the analysis of all theophylline metabolites. The coefficient of variation of this method was <5% for the analysis of biological samples.

Keyphrases □ GC–mass spectrometry—quantitation of theophylline and its metabolites in biological fluids, infants □ Theophylline—GC–mass spectrometric quantitation in biological fluids, infants □ Biological fluids—GC–mass spectrometric quantitation of theophylline and its metabolites, infants □ Caffeine—metabolite of theophylline in infants, GC–mass spectrometric quantitation in biological fluids

Theophylline has been used widely for the treatment of apnea in premature infants (1). Due to the narrow margin between effective and toxic doses, the plasma level of this drug during treatment is usually monitored to ensure safety. Over the past several years, a number of analytical methods have been developed specifically for this purpose (2). These include GC methods (3) and the newer high-performance liquid chromatographic (HPLC) methods (2). However, none of these methods are capable of measuring theophylline and metabolites in a microsample from a pediatric population.

The metabolism of drugs in premature infants is different from that of adults. The differences generally are limited to the pharmacokinetic parameters, such as elimination half-life, volume of distribution, and renal clearance. A recent report stating that in premature infants theophylline is methylated to caffeine (4) points out an important change in the concept of drug metabolism in premature infants. Not only the kinetic aspect of drug metabolism must be compared between premature infants and adults, but the quantitation of metabolic pathways also must be studied.

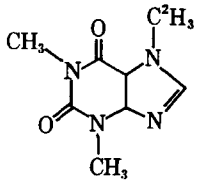

I

To investigate the metabolism of theophylline in premature infants, a simple and sensitive GC–MS method was developed. This method is capable of measuring theophylline, theobromine, caffeine, 3-methylxanthine, 1,3-dimethyluric acid, and 1-methyluric acid in as little as 50 μl of plasma and 0.5 ml of urine.

EXPERIMENTAL

Reagents—Caffeine[1], theophylline[1], theobromine (3,7-dimethylxanthine)[2], 3-methylxanthine[2], 1,3-dimethyluric acid[2], and 1-methyluric acid[3] were used as standards. Anhydrous potassium carbonate was of commercial reagent grade. Dimethylformamide[4] and 1-iodopropane[5] were purified by distillation.

7-[$^2H_3$]Methyl-1,3-dimethylxanthine (Caffeine-d_3) (I)—Powdered anhydrous potassium carbonate (20 mg) and 5 drops of iodomethane-d_3 (99 + atom % D)[4] were added to a solution of theophylline (15.8 mg) in 0.25 ml of dimethylformamide. The mixture was heated with occasional swirling at 70° for 15 min. Additional iodomethane-d_3 (1 drop) was then added to the mixture and the reaction was continued for an additional 15 min. After cooling, the reaction mixture was diluted with 4 ml of water and then extracted with methylene chloride (1 ml × 2). The methylene chloride extract was evaporated to dryness to obtain caffeine-d_3 (5.4 mg). GC analysis of this product showed a single peak with no side products. The 70-eV mass spectrum had the following fragments: *m/z* (percent of base peak), 197(100), 112(45), 85(20), 70(14), 67(11), and 58(17). The isotopic purity of this compound was: d_0, 0.09%; d_1, 5.51%; d_2, 6.99%; and d_3, 87.41%.

Internal Standard Solution—The caffeine-d_3 internal standard was dissolved in water to a final concentration of 2.14 μg/20 μl (for urine analysis) and 0.215 μg/20 μl (for plasma analysis).

Standard Solution of Theophylline and Its Metabolites—Caffeine (4.22 mg), theophylline (33.35 mg), 3-methylxanthine (4.40 mg), 1,3-dimethyluric acid (7.98 mg), and 1-methyluric acid (4.43 mg) were suspended in 3 ml of water. To this stirred mixture, a solution of 0.5 *N* NaOH was added drop-wise to convert the turbid suspension into a clear solution. Enough water then was added to make a final volume of 5 ml.

This stock solution then was diluted with water to a final concentration of caffeine in the following order: 1.68 μg/20 μl, 168 ng/20 μl, 16.8 ng/20 μl, and 1.68 ng/20 μl.

Standard Curve—In a glass disposable tube (12 × 75 mm), the standard metabolite solutions (20 μl, containing caffeine and other metabolites in the range of 1.68 μg to 1.68 ng) and 20 μl of internal standard solution (containing caffeine-d_3, 2.14 μg) were evaporated to dryness in a stream of air. Powdered potassium carbonate (0.5 mg), dimethylformamide (0.25 ml), and 1-iodopropane (50 μl) were then added to the dried residue. The mixture was heated at 70° in an evaporator[6] for 15 min. Vacuum was then applied to this unit to evaporate all the solvent and reagents (~15 min). The dried tube was then capped and kept at −20° until ready for analysis.

Similarly, standard curves in urine, plasma, and red blood cells were constructed by spiking blank samples with standard solutions. The spiked samples were then analyzed as described for each individual biological fluid, except in the case of red blood cells. For the standard curve in red blood cells, the spiked cells were not washed with normal saline. The standard curves in biological samples were identical to those in water,

[1] Calbiochem, San Diego, Calif.
[2] Sigma Chemical Co., St. Louis, Mo.
[3] Adams Chemical Co., Round Lake, Ill.
[4] Aldrich Chemical Co., Milwaukee, Wis.
[5] Eastman Kodak Co., Rochester, N.Y.
[6] Vortex-Evaporator, Buchler Instruments, Fort Lee, N.J.

0022-3549/83/0500-0526$01.00/0

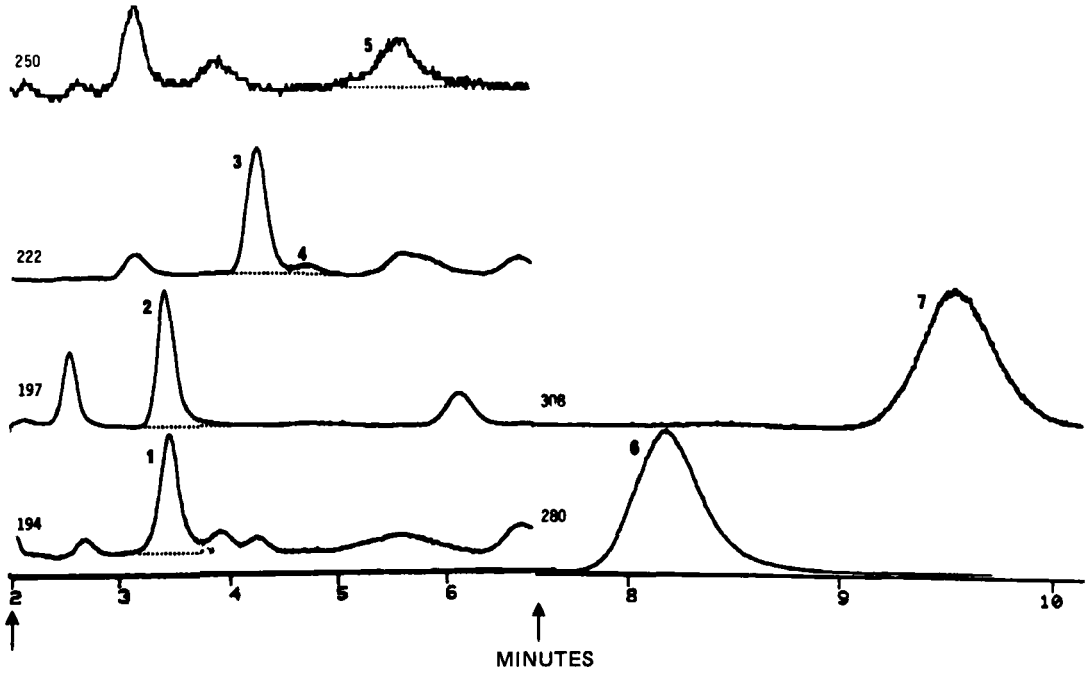

Figure 1—*A representative selected ion-monitoring chromatogram of theophylline metabolites in the urine of premature infants. The metabolites are: (1) caffeine; (2) caffeine-d_3; (3) theophylline; (4) theobromine; (5) 3-methylxanthine; (6) 1,3-dimethyluric acid; (7) 1-methyluric acid. The number in the beginning of each chromatogram indicates the ion (m/z) monitored. The arrows indicate the switching of ion sets monitored.*

with the exception of 3-methylxanthine in urine, in which the slope was lower than that in water.

Analysis of Urine Samples—In a disposable tube (12 × 75 mm), urine (0.5 ml) was mixed with 20 μl of the internal standard solution (2.14 μg of caffeine-d_3). It was then evaporated to dryness at 40° under vacuum in an evaporator (~15 min). Powdered potassium carbonate (5 mg), dimethylformamide (0.25 ml), and 1-iodopropane (50 μl) were added to the residue. The procedure for the standard curve was then followed.

Analysis of Plasma Samples—Plasma (50–100 μl) was mixed with 20 μl of internal standard solution (0.214 μg of caffeine-d_3). The plasma proteins were then precipitated by the addition of methanol (1 ml). After mixing and keeping in an ice bath for 10 min, the mixture was centrifuged and the supernatant was decanted into another disposable tube. It was evaporated in a stream of air, then to dryness at 40° in vacuum in an evaporator. The dried residue was then mixed with powdered potassium carbonate (5 mg), dimethylformamide (0.25 ml), and 1-iodopropane (50 μl). The procedure for the standard curve was then followed.

Analysis of Red Blood Cells—After separating the plasma, the red blood cells were washed twice with normal saline. An aliquot (100 μl) of this cell sample was then mixed with the internal standard solution (0.214 μg of caffeine-d_3 in 20 μl of water), and methanol was added (1 ml) to hemolize the blood cells and to precipitate the proteins. After centrifuging, the supernatant was transferred to another tube and the plasma procedure commenced.

Gas Chromatography—A conventional gas chromatograph[7] was used. It was equipped with a flame ionization detector. The glass column (0.3 cm × 1.83 m) was packed with 50% phenyl silicone and 50% methyl silicone on treated white diatomaceous earth[8]. Nitrogen was used as a carrier gas at 30 ml/min. The column was maintained at 200°. The injection port temperature was 250° and the detector was 350°.

Gas Chromatography–Mass Spectrometry—A computerized GC–MS[9] was used. The GC condition was the same as described in the previous section except that helium was used as carrier gas instead of nitrogen. A glass jet separator, maintained at 250° was used between the GC and the MS ion source, which was maintained at 200°. The analyzer region was kept at 200°. Electron-impact ionization at 70 eV was used for the study. The derivatized sample was dissolved in 50 μl of methylene chloride. After mixing well, the mixture was allowed to stand until the undissolved solid settled at the bottom. An aliquot (1–3 μl) of the supernatant was injected onto the GS–MS. The selected ion-monitoring software provided by the instrument manufacturer was used for the analysis. From 2.5 to 7.5 min, the instrument was focused alternately on *m/z* 194, 197, 222, and 250 with a dwelling time of 100 msec on each. After 7.5 min, the ion fragments *m/z* 280 and 308 were monitored with a dwelling time of 100 msec on each. The total analysis time was 12 min. The standard curves were constructed by plotting the area ratio of each individual ion (caffeine-194, theophylline-222, 3-methylxanthine-250, 1,3-dimethyluric acid-280, and 1-methyluric acid-308) with internal standard (caffeine-d_3-197), against the amounts of each individual metabolite. Regression analysis of the standard curve and data reduction of samples were done with a calculator[10].

Table I—Theophylline and Metabolites in Urine, Plasma, and Red Blood Cells of a Premature Infant

Samples	Metabolites[a], μg/ml					
	I	II	III	IV	V	VI
Urine	2.20 (8.7%)[b]	12.10 (51.5%)	1.70 (7.2%)	0.38 (1.8%)	5.58 (21.8%)	2.14 (9.0%)
Plasma	2.41 (25.5%)	5.70 (64.8%)	0.4 (4.6%)	0.08 (1.0%)	0.3 (3.1%)	0.1 (1.1%)
Red Blood Cells	0.54 (28.7%)	1.00 (57.4%)	0.1 (5.7%)	0.08 (5.0%)	0.05 (2.6%)	0.01 (2.6%)

[a] Metabolites: I, caffeine; II, theophylline; III, theobromine; IV, 3-methylxanthine; V, 1,3-dimethyluric acid; VI, 1-methyluric acid. [b] Values in parentheses are the percentage of total metabolites.

RESULTS AND DISCUSSION

Theophylline is metabolized extensively to 3-methylxanthine, 1,3-dimethyluric acid, and 1-methyluric acid in human adults (5, 6). The current observation that theophylline is also methylated to another pharmacologically active xanthine, caffeine, in premature infants (4, 7, 8) makes it necessary to study the metabolism of theophylline in this population.

There are several published methods capable of measuring theophylline and its metabolites (3, 6, 9). The older method of column chromatography and UV spectrophotometry is too tedious to be useful in the assay of large numbers of samples. The HPLC method described previously (5) lacks the sensitivity required in the analysis of pediatric samples. The preliminary report of another HPLC method (9) has the required sensitivity and simplicity. However, no specificity and reproducibility of the method was reported. To achieve the specificity and sensitivity

[7] Model 5840A, Hewlett-Packard Co., Avondale, Pa.
[8] 3% OV-17 on gas chrom Q, 100/120 #, Applied Science, State College, Pa.
[9] Model 5985A gas chromatograph-mass spectrometer with a Model-7906 disc drive, Hewlett-Packard Co., Palo Alto, Calif.
[10] Model 9830A calculator, Hewlett-Packard Co., Loveland, Col.

Table II—Precision of GC–MS Analysis of Theophylline and Metabolites [a]

Analysis	Metabolites,[b] μg/ml				
	I	II	IV	V	VI
1	0.91	2.97	0.011	1.15	0.60
2	0.91	2.81	0.017	1.14	0.57
3	0.93	2.87	0.014	1.15	0.61
4	0.94	2.83	0.011	1.17	0.61
5	0.91	2.80	0.011	1.23	0.66
Mean ± *SD*	0.92 ± 0.01	2.86 ± 0.07	0.013 ± 0.003	1.17 ± 0.04	0.61 ± 0.03
CV,[c] %	1.1	2.4	23.1	3.4	4.9

[a] Urine sample from a premature infant maintained on aminophylline. [b] Metabolites: See Table I. [c] Coefficient of variation.

required in the analysis of pediatric samples, a GC–MS method with selected ion monitoring technique was chosen. The high specificity obtained by this technique can also reduce the time required for sample purification and, thus, facilitate the analysis of large numbers of samples.

Extraction of Theophylline and Metabolites from Biological Fluids—A number of solvent systems have been used to extract theophylline or its metabolites from biological fluids (3, 9, 10). The extracted metabolites are then analyzed with GC, HPLC, or GC–MS. For less specific quantitative methods, solvent extraction is a necessary step in the procedure to eliminate the possible interfering substances. These solvent-extraction procedures can be grouped into three categories. The most primitive one is the simple solvent extraction with methylene chloride or chloroform (3, 11). A second approach has been the use of a more polar solvent mixture in conjunction with the saturation of biological fluids with salt (9). The third approach is the extractive alkylation procedure with alkyl iodide and hydrophobic quaternary ammonium ion (10). For the analysis of the true composition of metabolites in a sample, the extraction steps should not discriminate among different compounds and distort the results. Caffeine, theophylline, methylxanthines, and methyluric acids are compounds with widely varying polarity and solvent solubility. The simple solvent extraction procedure is not expected to extract any significant amounts of methylxanthines and methyluric acids. In numerous attempts in this laboratory, extractive alkylation with a high concentration of tetrabutylammonium ion in aqueous solution and iodopropane in chloroform failed to recover polar metabolites such as 3-methylxanthine and monomethyluric acids. The recovery experiments using a modified procedure (9) which involved saturating the aqueous standard solution with ammonium sulfate and extracting with a chloroform–isopropyl alcohol mixture, gave the following results (compared with direct derivatization): caffeine, 104 ± 1%; theophylline, 23 ± 3%; 3-methylxanthine, 6 ± 3%; 1,3-dimethyluric acid, 9 ± 3%; and 1-methyluric acid, 5 ± 2% (mean ± *SD*, $N = 3$). The lower recovery obtained in these experiments compared with those reported previously (9) probably resulted from the smaller amount of extraction solvent used (20% of the original solvent volume but extracted twice). Nevertheless, these data did indicate a differential extraction of metabolites, even with the most strenuous extraction procedure, *i.e.*, salt saturation and polar solvents. To overcome the difficulty of low and variable recovery of different metabolites, no solvent extraction was used in the procedure described in this report. The urine samples were dried directly and then derivatized, while the plasma samples were deproteinized with methanol and prepared as the urine samples.

Derivatization with Iodopropane and Sodium Carbonate in Dimethylformamide—For GC analysis, theophylline and metabolites are usually derivatized into *N*-alkylated derivatives such as butyl or pentyl derivatives. The advantage of using the *N*-propyl derivative over other alkylated derivatives has been discussed previously (12). The fastest and most convenient derivatization procedure was found to be the use of iodopropane in a polar solvent, such as dimethylformamide, and a basic catalyst, such as potassium carbonate. This reaction was rapid and was completed within 5 min at 70°. When the reaction mixture was analyzed at different reaction times, the intensity of all the derivatized metabolites did not change with heating from 5 min to 1 hr. This indicated not only that the derivatization procedure was completed within 5 min, but also that the derivatives were stable in the reaction mixture for at least 1 hr. After the reaction, the reagents were evaporated in vacuum. The residue was extracted with methylene chloride (50 μl) before analysis with GC–MS. For lower concentration determinations, larger volumes of methylene chloride can be used to extract the solid residue. The combined extract is then evaporated and reconstituted with a smaller volume of solvent. Water cannot be used to wash the methylene chloride solution of the derivatized sample, since this procedure results in differential extraction. Caffeine has higher water solubility than any other *N*-propylated xanthines and uric acids. Because caffeine-d_3 was used as the internal standard in the procedure, the disproportional removal of caffeine from methylene chloride extract resulted in a falsely higher result for theophylline, 3-methylxanthine, 1,3-dimethyluric acid, and 1-methyluric acid.

Gas Chromatography–Mass Spectrometry—The ideal internal standards for the GC–MS method are the stable isotope-labeled analogues of each metabolite. However, such a task would be impractical for extensively metabolized drugs such as theophylline. Therefore, caffeine-d_3 (I) was chosen as an internal standard for all metabolites. Caffeine-d_3, can be synthesized easily from theophylline and iodomethane-d_3 in 1 hr. It is obtained in high isotopic purity ($do = 0.09\%$).

The *N*-propyl derivatives of theophylline metabolites were well resolved on a 3% mixed phase of phenyl silicone and methyl silicone column in a period of 12 min. Furthermore, their 70-eV electron-impact mass spectra showed prominent molecular ions (12). Therefore, the molecular ions were monitored using a selected ion-monitoring technique. The ion current ratio of the metabolite's molecular ion with that of internal standard (m/z 197) was plotted against the amount of metabolites. The standard curves obtained were linear over a range of 1 ng to 2 μg. However, the detection limit can be lowered further to 500 pg for caffeine and theophylline. The detection limit of other metabolites (3-methylxanthine, 1,3-dimethyluric acid, and 1-methyluric acid) were in the range of 1–20 ng. The lower sensitivity of this procedure toward monomethylxanthine and uric acid metabolites was due to the fact that the derivatives of these metabolites gave molecular ions with lower abundances as a result of more extensive fragmentation.

A typical selected ion chromatogram of urinary theophylline metabolites of premature infants is shown in Fig. 1. The metabolite patterns of theophylline in plasma, urine, and red blood cells taken at the same

Table III—Recovery of GC–MS Procedure for Theophylline and Metabolites in Urine

Samples	Metabolites, μg[a]				
	I	II	IV	V	VI
Urine[b]	0.93	3.50	0.05	1.86	1.48
Urine + Standard 1[c]	1.12	5.30	0.19	2.11	1.54
	(102%)	(110%)	(86%)	(97%)	(93%)
Urine + Standard 2[d]	2.65	16.65	0.98	4.78	3.24
	(102%)	(101%)	(55%)	(95%)	(100%)
Urine + Standard 2[d]	2.65	16.65	0.95	4.78	3.28
	(102%)	(101%)	(54%)	(95%)	(101%)
Recovery Mean ± *SD*	102 ± 0%	104 ± 5%	65 ± 18%	96 ± 1%	98 ± 4%

[a] Metabolite designations (see Table I). [b] Urine (0.5 ml) of a premature infant on theophylline treatment. [c] Standard 1 = caffeine (0.17 μg), theophylline (1.33 μg), 3-methylxanthine (0.17 μg), 1,3-dimethyluric acid (0.32 μg), 1-methyluric acid (0.18 μg). [d] Standard 2 = caffeine (1.68 μg), theophylline (13.34 μg), 3-methylxanthine (1.72 μg), 1,3-dimethyluric acid (3.19 μg), 1-methyluric acid (1.77 μg).

Table IV—Recovery of GC–MS Procedure for Theophylline and Metabolites in Plasma and Red Blood Cells

Samples	Metabolites, μg[a]				
	I	II	IV	V	VI
Plasma Blank[b]	0	0	0.02	0.01	0.01
Plasma + Standard 1[c]	0.35	2.16	0.38	0.60	0.37
	(95%)	(97%)	(103%)	(102%)	(100%)
Plasma + Standard 1[c]	0.36	2.21	0.38	0.57	0.37
	(97%)	(99%)	(103%)	(97%)	(100%)
Plasma + Standard 2[d]	1.74	11.26	1.74	2.77	1.67
	(94%)	(101%)	(98%)	(95%)	(92%)
Cell Blank[e]	0	0	0	0	0
Cells + Standard 1[c]	0.40	2.06	0.30	0.60	0.32
	(108%)	(92%)	(86%)	(103%)	(89%)
Cells + Standard 3[f]	0.07	0.44	0.06	0.11	0.07
	(100%)	(98%)	(86%)	(92%)	(100%)
Average Recovery: Mean ± *SD*	99 ± 6%	97 ± 3%	95 ± 9%	98 ± 5%	96 ± 5%

[a] Metabolite designations (see Table I). [b] Plasma (100 μl) of an adult man without coffee or tea intake. [c] Standard 1 = caffeine (0.37 μg), theophylline (2.23 μg), 3-methylxanthine (0.35 μg), 1,3-dimethyluric acid (0.58 μg), 1-methyluric acid (0.36 μg). [d] Standard 2 = caffeine (1.85 μg), theophylline (11.15 μg), 3-methylxanthine (1.75 μg), 1,3-dimethyluric acid (2.91 μg), 1-methyluric acid (1.80 μg). [e] Washed red blood cells (100 μl). [f] Standard 3 = caffeine (0.07 μg), theophylline (0.45 μg), 3-methylxanthine (0.07 μg), 1,3-dimethyluric acid (0.12 μ), 1-methyluric acid (0.07 μg).

time interval are shown in Table I. The details of this study have been reported elsewhere (12, 13).

Using this sensitive and specific method, it was shown for the first time that some of the 3-methylxanthine and 1-methyluric acid had a possible endogenous origin. In addition, the oxidation pathways of theophylline were quantified and shown to be important. Substantial amounts of theophylline are converted to 1,3-dimethyluric acid in premature infants, while the metabolic capability of converting theophylline to 3-methylxanthine and 1-methyluric acid is relatively undeveloped. The unusual metabolic conversion of theophylline to caffeine in premature infants is also confirmed.

Precision and Recovery of the Method—The precision of this method in analyzing theophylline metabolites is shown in Table II. The analysis of caffeine had the lowest coefficient of variation (*CV*) partly due to the fact that the stable isotope-labeled internal standard of caffeine was used in the procedure. This internal standard compensated for the variation due to incomplete recovery and instrumental instability. With the exception of 3-methylxanthine, the coefficients of variation of analyses are all within 5%. The high variation on 3-methylxanthine analysis was due to the fact that its concentration in the urine of premature infants was low as compared with other metabolites.

The recovery of theophylline metabolites was studied by spiking urine, plasma, and red blood cell samples with solutions of known amounts of metabolites. The samples were analyzed before and after spiking. The results are shown in Tables III and IV. With the exception of 3-methylxanthine, the recovery of all metabolites was essentially quantitative. The lower urinary recovery of 3-methylxanthine at a higher concentration is probably due to incomplete alkylation under experimental conditions. As discussed before, all theophylline metabolites from aqueous solutions were alkylated quantitatively within 5 min of the reaction time. The slower reaction time of 3-methylxanthine in urine is unclear at the present time. It could be partly due to the buffer action of urinary electrolytes, which reduce the effectiveness of catalysis by potassium carbonate. This hypothesis was supported by the fact that recovery of 3-methylxanthine was reduced further without affecting the recovery of all other metabolites when the amount of potassium carbonate was lowered.

Attempts were made to improve the recovery of 3-methylxanthine by increasing the amount of potassium carbonate and *n*-propyl iodide or by increasing the reaction time. The recovery of urinary 3-methylxanthine did improve with these experiments. However, quantitative recovery was never obtained. Because increasing the reagents and the reaction time increases the possibility of interfering peaks without correcting the problem of incomplete recovery of 3-methylxanthine, this modification of the procedure was abandoned.

REFERENCES

(1) J. V. Aranda and T. Turman, *Clin. Perinat.*, **6**, 87 (1979).

(2) G. P. Butrimovitz and V. A. Raisys, *Clin. Chem.*, **25**, 1461 (1979).

(3) B. Vinet and L. Zizian, *ibid.*, **25**, 156 (1979).

(4) M. J. Boutroy, P. Vert, R. H. Royer, P. Monin, and M. J. Royer-Morrot, *J. Pediatr.*, **94**, 996 (1979).

(5) R. D. Thompson, H. T. Nagasawa, and M. W. Jenne, *J. Lab. Clin. Med.*, **84**, 581 (1974).

(6) H. H. Cornish and A. A. Christman, *J. Biol. Chem.*, **228**, 315 (1957).

(7) C. Bory, P. Baltassat, M. Dorthault, M. Bethenod, A. Frederich, and J. V. Aranda, *J. Pediatr.*, **94**, 988 (1979).

(8) H. S. Bada, N. N. Khanna, and S. J. Somani, *ibid.*, **94**, 993 (1979).

(9) A. Aldrige, J. V. Aranda, and A. H. Neims, *Clin. Pharmacol. Ther.*, **25**, 447 (1979).

(10) W. A. Joern, *Clin. Chem.*, **24**, 1458 (1978).

(11) G. F. Johnson, W. A. Dechtiarruck, and H. M. Solomon, *ibid.*, **21**, 144 (1975).

(12) K.-Y. Tserng, K. C. King, and F. N. Takieddine, *Clin. Pharmacol. Ther.*, **29**, 594 (1981).

(13) F. N. Takieddine, K.-Y. Tserng, K. C. King, and S. C. Kalhan, *Semin. Perinatol.*, **5**, 351 (1981).

ACKNOWLEDGMENTS

This investigation was supported in part by Grant HD 11089 from the National Institute of Child Health and Human Development.

The author thanks Dr. Katherine C. King of the Newborn Intensive Care Unit for providing the samples. The secretarial assistance of Ms. Debbie Johnson and Ms. Sandee Riedrich are acknowledged.

Comparison of Granule Strength and Tablet Tensile Strength

PAUL J. JAROSZ * and EUGENE L. PARROTT ˣ

Received March 29, 1982, from the *Division of Pharmaceutics, College of Pharmacy, University of Iowa, Iowa City, IA 52242.* *Present address: Ortho Pharmaceutical Corporation, Raritan, NJ 08869. Accepted for publication May 28, 1982.

Abstract □ The granule strength (crushing load) of lactose granulated with 1–9% povidone was measured initially and at intervals during a 1-year period. The granule strengths of dibasic calcium phosphate dihydrate granulated with various concentrations of starch and povidone were measured. The axial and radial tensile strengths of tablets compressed from these granules were determined and related to concentration of binder and granule strength. The effect of compressional force on the integrity of granules in a tablet matrix is shown in scanning electron photomicrographs of the fractured tablets which had undergone a diametral compression test. It appears that the compressional force and the concentration of binder contribute more than granule strength to tablet tensile strength.

Keyphrases □ Tablet compression—comparison of granule and tensile strength, lactose, povidone □ Granule strength—tablet compression, comparison with tensile strength, lactose, povidone □ Tensile strength—tablet compression, comparison with granule strength, lactose, povidone

Most materials require pretreatment to ensure tablet formation and free flow in the tablet machine. Granulation is the process by which fine powders are converted to granules with these properties to ensure a uniform fill of the die cavity, formation of a tablet, and easy ejection of the finished tablet. Granulation also facilitates handling, prevents segregation in the formulation blend, and minimizes dust. Granule strength and friability are important as they affect changes in particle size distribution of granulations and, consequently, compressibility into cohesive tablets, and also unit dose precision in some tablet formulations. They may be useful as quality control parameters so that reproducible granulations can be manufactured (1). Granule strength is usually greater as the concentration of binder is increased (2–7). For a given lot, the larger granules have a greater strength than the smaller granules (5, 8, 9).

The compression process of particulate material into a tablet and the fate of the granule in the tablet have been studied (6, 10–12). Most investigations have considered the external dimensions of the tablet, although these may not reflect the situation within the tablet matrix (13). It seems that granular integrity is progressively lost during compression.

The present study was conducted to compare the granule strength with the axial and radial tensile strengths of tablets compressed from the granules. Scanning electron microscopy was used in an attempt to visualize the granule within the tablet matrix.

Table I—Effect of Humidity on the Crushing Load of 16/20-Mesh Granules of Lactose Monohydrate Granulated with 5.0% Povidone

	Relative Humidity, %				
	0	20	45	70	90
Exposure, days	14	5	6	4	11
Loss on drying, %	5.2	5.4	6.4	5.9	7.5
Crushing load, g	773.4	873.8	496.7	796.6	241.6
	678.3	667.7	274.4	523.9	712.1
	386.1	241.2	491.8	575.3	367.0
	568.5	830.6	458.4	438.3	143.7
	425.3	842.3	590.7	411.2	466.8
	655.4	422.4	472.7	418.5	583.6
	496.4	214.4	418.5	378.6	489.7
	352.9	190.3	184.1	640.1	778.4
	374.9	373.4	512.7	726.0	540.2
	465.6	326.3	120.4	396.3	207.9
Average crushing load, g	513.7	498.3	402.0	530.5	453.1
SD, g	137.5	277.1	155.1	148.9	212.7

EXPERIMENTAL

Preparation of Granules and Measurement of Crushing Strength—All materials were USP or NF grade. A 60/80-mesh size fraction of all materials was used. An appropriate quantity of aqueous granulating liquid was added to the powder in a planetary mixer[1] and blended for 5 min. The wet mass was then passed through an appropriate screen in an oscillating granulator[2] operating at slow speed and collected on drying trays. The granulation was dried overnight in a forced-air oven at ambient temperature. Size classification of the dried granules was carried out by shaking for 5 min with a sieve shaker[3].

The technique used to measure the crushing strength of a granule was essentially that from a previous study (14) using 50- and 100-ml glass

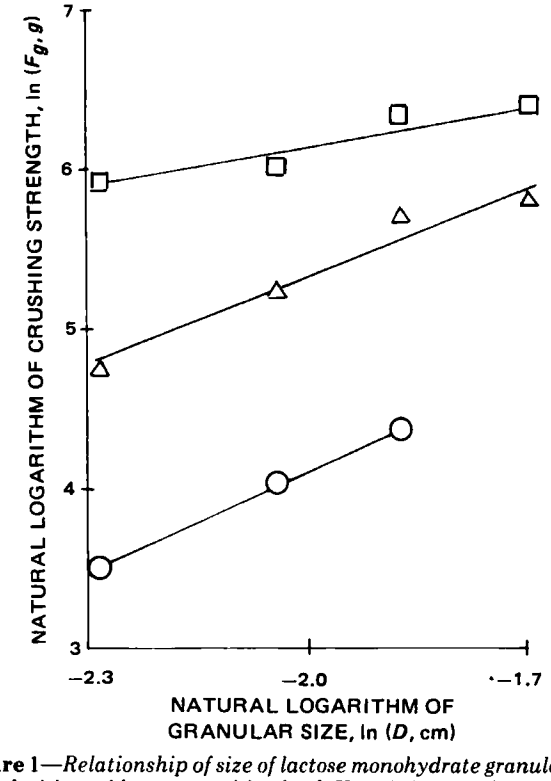

Figure 1—*Relationship of size of lactose monohydrate granules granulated with povidone to crushing load. Key: (○) 1.0%; (△) 3.0%; and (□) 7.0% povidone.*

[1] KitchenAid, Hobart, Troy, Ohio.
[2] Type FGS, Erweka-Apparatebau, GmbH., Heusenstamm Kr., Offenbach/Main.
[3] Cenco-Meinzer, Central Scientific Co., Chicago, Ill.

0022-3549/83/0500-0530$01.00/0

Table II—Crushing Strength of Several Size Fractions of Granules of Lactose Monohydrate Granulated with Various Concentrations of Povidone

Fraction Size	D, cm	Crushing Strength, g, Percent Povidone 1	3	5	7	9
10/12	0.184	39.0	333.0	383.4	600.6	904.7
12/14	0.154	79.6	305.4	672.5	571.7	529.5
14/16	0.130	56.9	189.0	436.6	409.7	877.4
16/20	0.102	33.9	116.0	358.8	376.6	726.7

hypodermic syringes[4]. The modification included the removal of the tip of the syringe barrel and the top end of the plunger. The barrel was then used as a hollow support and guide tube with close-fitting tolerances to the plunger. The hollow plunger with one open end served as a load cell to which mercury could be added. A window was cut into the barrel to facilitate placement of the granule on the base platen. The plunger acted as the movable platen and was set directly on the granule positioned on the lower platen. As the rate of loading may effect crushing load (9), mercury was introduced from a reservoir into the upper chamber at the rate of 10 g/sec until the single granule failed. Loading time was <3 min. The total weight of the plunger and the mercury required to fracture a granule was the crushing load. A minimum of 10 granules were tested, and the average load in grams was taken as the crushing strength, F_g. In the figures only the upper standard deviation bar for granule strength is shown.

The sensitivity of crushing strength to humidity was considered for hydrous lactose granulated with 5% povidone. The granules were stored in humidity chambers at 0, 20, 45, 70, and 90% relative humidity (15) for various lengths of time as shown in Table I. The percent loss on drying was determined by a moisture balance[5] after 20 min of IR exposure at

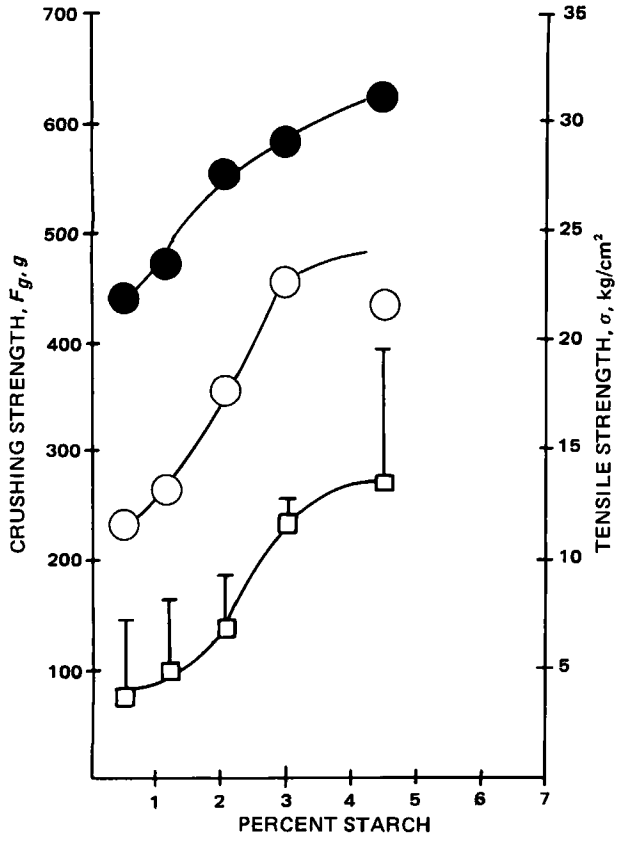

Figure 2—*Relationship of binder concentration to granule strength and tensile strengths of tablets compressed at 2268 kg from granules of dibasic calcium phosphate dihydrate granulated with starch. Key: (□) granule strength; (○) axial tensile strength; and (●) radial tensile strength.*

[4] Yale Luer-Lok, Becton Dickenson and Co., Rutherford, N.J.
[5] Ohaus Scale Corp., Florham Park, N.J.

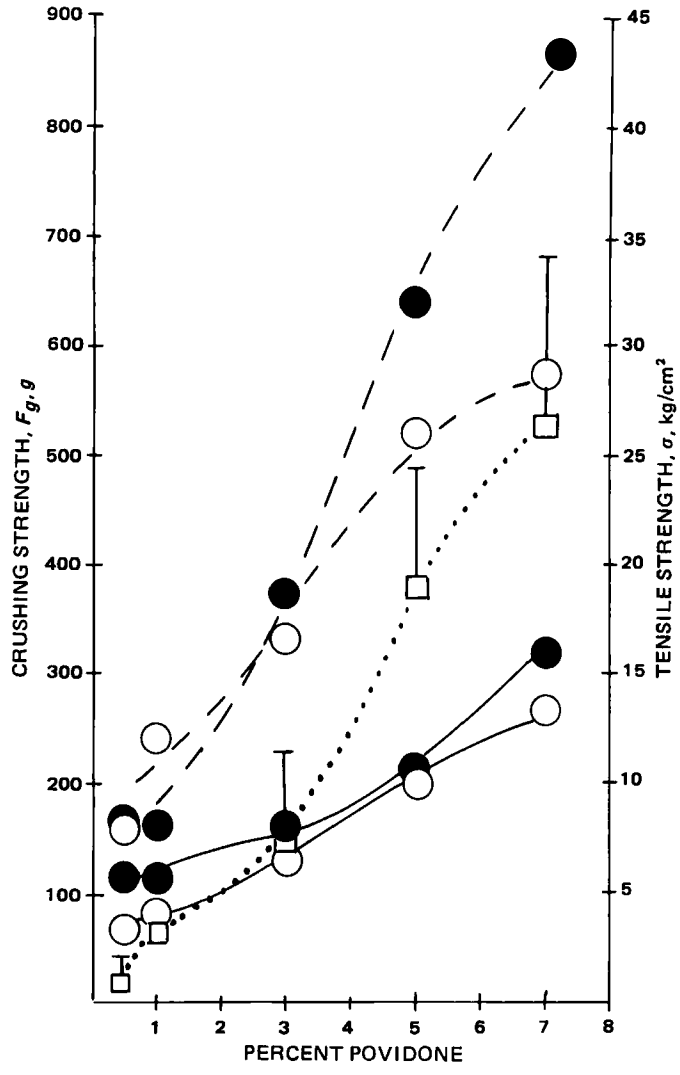

Figure 3—*Relationship of binder concentration to granule strength and tensile strengths of tablets compressed at 2268 (—) and 4536 (- - -) kg from granules of dibasic calcium phosphate dihydrate granulated with povidone. Key: (□) granule strength; (○) axial tensile strength; (●) radial tensile strength.*

an input of 12 W. The load at which a granule failure occurs may be difficult to experimentally observe, since a granule may deform plastically or a high point on its surface may fracture without failure of the entire granule. Thus, there is considerable variance in the crushing loads, as shown in Table I and as previously reported (5). Within the precision of the apparatus used, it does not appear that humidity significantly affected the strength of the granule. Although the relative humidity ranged from 0 to 90%, the moisture content of the granules was from 5.2 to 7.5%.

Preparation of Tablets and Measurement of Tensile Strength—An appropriate weight of 16/20-mesh size fraction of granules was compressed for 5 sec at the desired force by 1.275 cm diameter punches and die-fitted to a hydraulic press[6]. At least 72 hr elapsed between tableting and tablet evaluation to allow for any stress relaxation within the tablet. The weight and thickness of a minimum of 10 tablets were determined. The method of measurement of the axial tensile strength (σ_z) and the radial tensile strength (σ_x) of tablets by a tensiometer has been described (16). The mean force of tensile failure of 10 tablets was used to calculate the tensile strength.

RESULTS AND DISCUSSION

Mechanical Strength of Granules—The crushing strength of granules of lactose monohydrate granulated with povidone solution is

[6] Carver model C, Monomonee Falls, Wis.

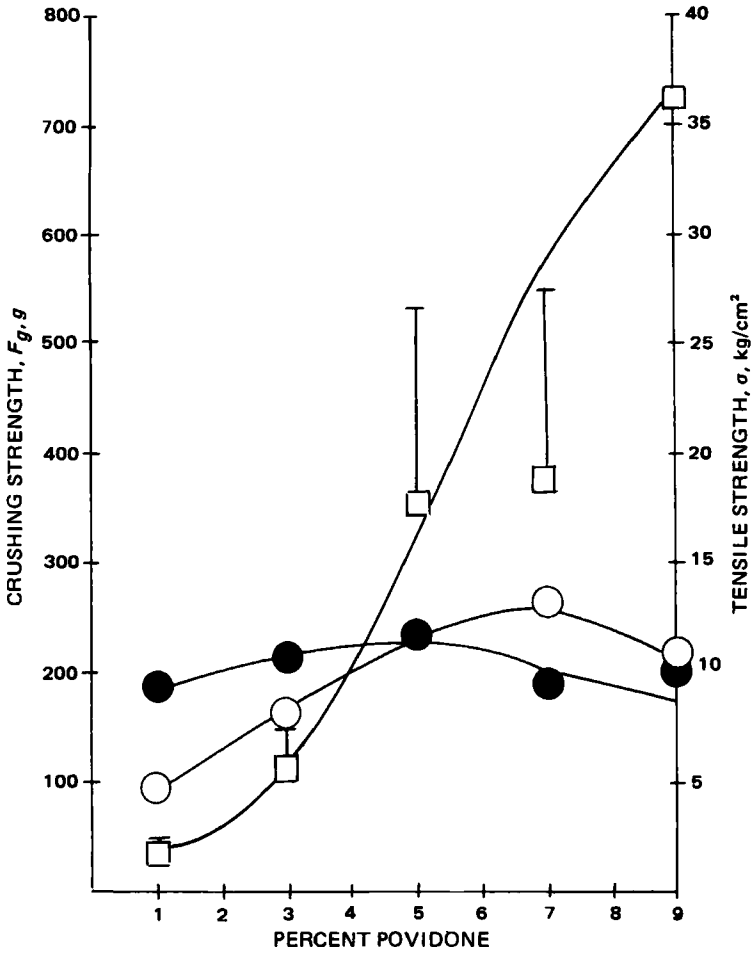

Figure 4—*Relationship of binder concentration to granule strength to tensile strengths of tablets compressed at 1134 kg from lactose monohydrate granules granulated with povidone. Key: (□) granule strength; (○) axial tensile strength; and (●) radial tensile strength.*

shown in Table II. For a given concentration of povidone the strength of a granule is a function of its size. It was suggested previously that (17):

$$F_g = q\,D^n \qquad \text{(Eq. 1)}$$

where D is the diameter of the granule and q and n are constants for a material. Using the natural logarithmic form of Eq. 1:

$$\ln F_g = q' + n \ln D \qquad \text{(Eq. 2)}$$

the constants may be evaluated by plotting as shown in Fig. 1. The slopes are 2.10, 1.90, and 0.88 for 1.0, 3.0, and 7.0% povidone, respectively. The decrease of the slope as the concentration of binder is increased suggested that particle size influences the granule resistance to crushing to a lesser extent than the concentration of the binder (18–21).

The strength of dibasic calcium phosphate dihydrate[7] granules containing 0.6–4.5% starch is shown in Fig. 2. At low concentrations of starch, the granule resistance to crushing is weak. As the concentration of binder is increased (2–3%), there is a considerable increase in the granule strength, and further increases in the concentration of binder only slightly increase the granule strength. The inflection in Fig. 2 may represent the binder concentration just sufficient to encase the granule surface under the conditions of preparation. A further increase of binder will fill in the porous openings of the granule, continuing, but to a lesser extent, to increase the granule resistance to crushing (18).

The effect of concentration of povidone on the strength of granules of dibasic calcium phosphate dihydrate[8] is shown in Fig. 3. The relationship is similar to that obtained with starch, and in the range of 3–6% povidone in the granules there is the greatest increase in strength.

The effect of concentration of povidone on the strength of granules of lactose monohydrate is shown in Fig. 4. Again the range of 3–6% povidone in the granules provides the greatest increase in strength of the granule.

[7] Encompress, Edward Mendell Co., Carmel, N.Y.
[8] USP, Ruger Chemical Corp., Irvington, N.J.

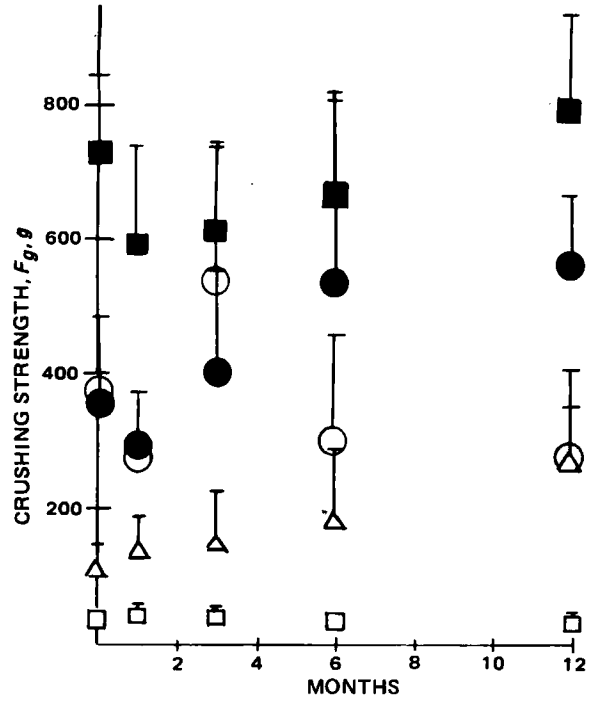

Figure 5—*Effect of time on the granule strength of 16/20-mesh granules of lactose monohydrate granulated with various concentrations of povidone. Key: (□) 1%; (△) 3%; (●) 5%; (○) 7%; and (■) 9% povidone.*

Aging has been reported to affect the mechanical properties of compressed tablets (22). Lactose granules containing 1–9% povidone were stored at 40–45% relative humidity and at ambient temperature, and the crushing load was measured initially and at 1, 3, 6, and 12 months. The data are plotted in Fig. 5. Within the variance of the experimental apparatus aging does not appear to markedly affect the crushing strength of the granule.

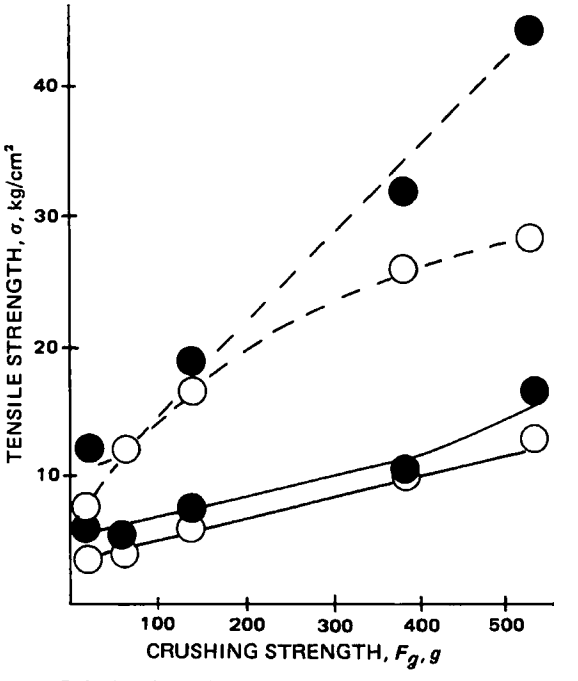

Figure 6—*Relationship of granule strength to tensile strengths of tablets compressed at 2268 and 4536 kg from dibasic calcium phosphate dihydrate granulated with povidone. Key: (○) axial and (●) radial tensile strengths; (—) 2268 kg; and (- - -) 4536 kg.*

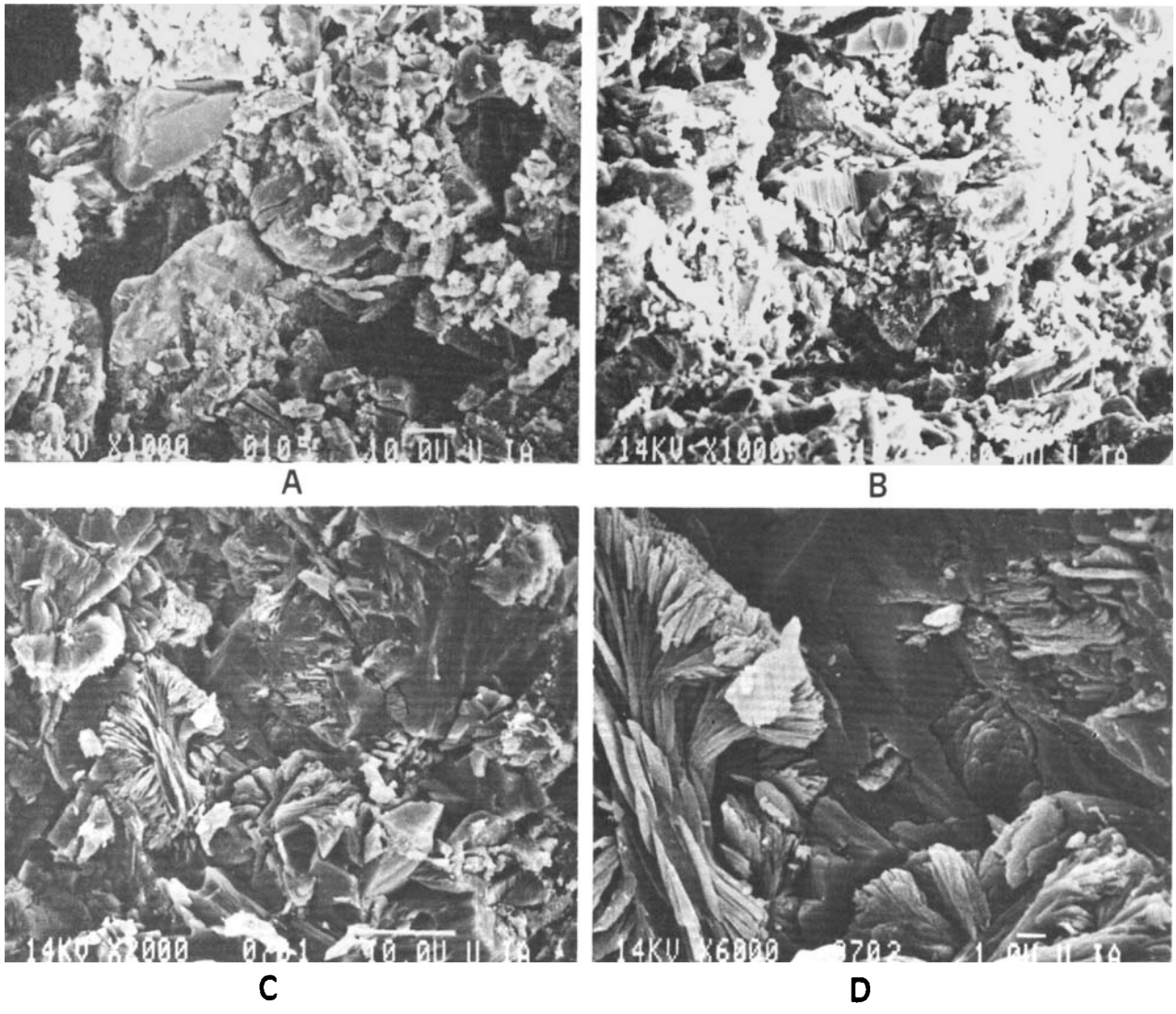

Figure 7—*Scanning electron photomicrographs of tablets of dibasic calcium phosphate dihydrate and starch. Key: (A) location above center of tablet, compressional force 454 kg, starch 1.2%, original magnification 1000×; (B) location near axial and radial tablet surface, same tablet as (A); (C) location near center of tablet, compressional force 1134 kg, starch 4.5%, original magnification 2000×; and (D) same as (C) but original magnification 6000×.*

Relationship of Granule Strength to Tablet Tensile Strength—A 16/20-mesh size fraction of granule was selected for investigation, since this is a tablet granulation size often used in commercial production. The relationship of the axial and radial tensile strengths of tablets compressed at 2268 and 4536 kg of force to the crushing strength of granules of dibasic calcium phosphate dihydrate[8] granulated with povidone is shown in Fig. 6. For the various granules compressed at a given force, the tensile strength of the tablet is increased as the resistance to crushing is increased. The granule strength is increased as the concentration of binder is increased; therefore, the effect of granule strength on tensile strength is probably inseparable from the effect of concentration. The form of a plot of tensile strength against concentration of binder is similar to that of the granule strength against concentration, as shown in Fig. 3.

The relationship of concentration of binder to granule strength and to tensile strengths of dibasic calcium phosphate dihydrate tablets granulated with starch and compressed at 2268 kg is shown in Fig. 2. The plot of granule strength against concentration of binder is similar to that of the plot of tablet tensile strength against concentration.

The relationship of concentration of binder to granule strength and to tensile strengths of lactose monohydrate tablets granulated with povidone and compressed at 1134 kg is shown in Fig. 4. Again, the form of the granule strength–concentration curve and the tensile strength–concentration curve is similar.

Visualization of Granule Fate—The fate of a granule in the tableting process has been followed by several investigators (10, 13, 23). It has been reported (11) that within a given range of compression the integrity of an individual granule in a compact may be demonstrated. Another report (12) showed that at low compressional force there was no apparent change in volume because interparticulate slippage shortens the granule, but its diameter increased as it was flattened. At intermediate forces, plastic deformation and consolidation continued to flatten the granule, but solid bridges were formed without the diameter of the granule increasing, so that a reduction of volume occurred. Finally, at high compressional force, a structure was formed that could support the applied force without further consolidation.

The effect of compressional force on the deformation of granules within a tablet may be visualized by scanning electron microscopy of the surface produced by fracture of the tablet in the diametral compression test. Differences in porosity within a compact have been reported (13). In Fig. 7A the photomicrograph is of a porous region immediately above the less porous center of a dibasic calcium phosphate dihydrate tablet compressed at 454 kg from granules containing 1.2% starch. In Fig. 7B the photomicrograph is of a denser region near the surface of the same tablet.

The structure of a dibasic calcium phosphate dihydrate tablet compressed at 1134 kg from granules containing 4.5% starch is shown in Fig. 7C and D. Two pockets of starch may be seen within the matrix of the tablet. It may be that the pockets occur because the amount of starch is greater than that amount required to just encase the granule (18). At higher compressional forces these starch structures become indistinguishable.

The porosity of a compressed tablet is decreased as compressional force is increased (24, 25). Photomicrographs of the center of tablets of dibasic

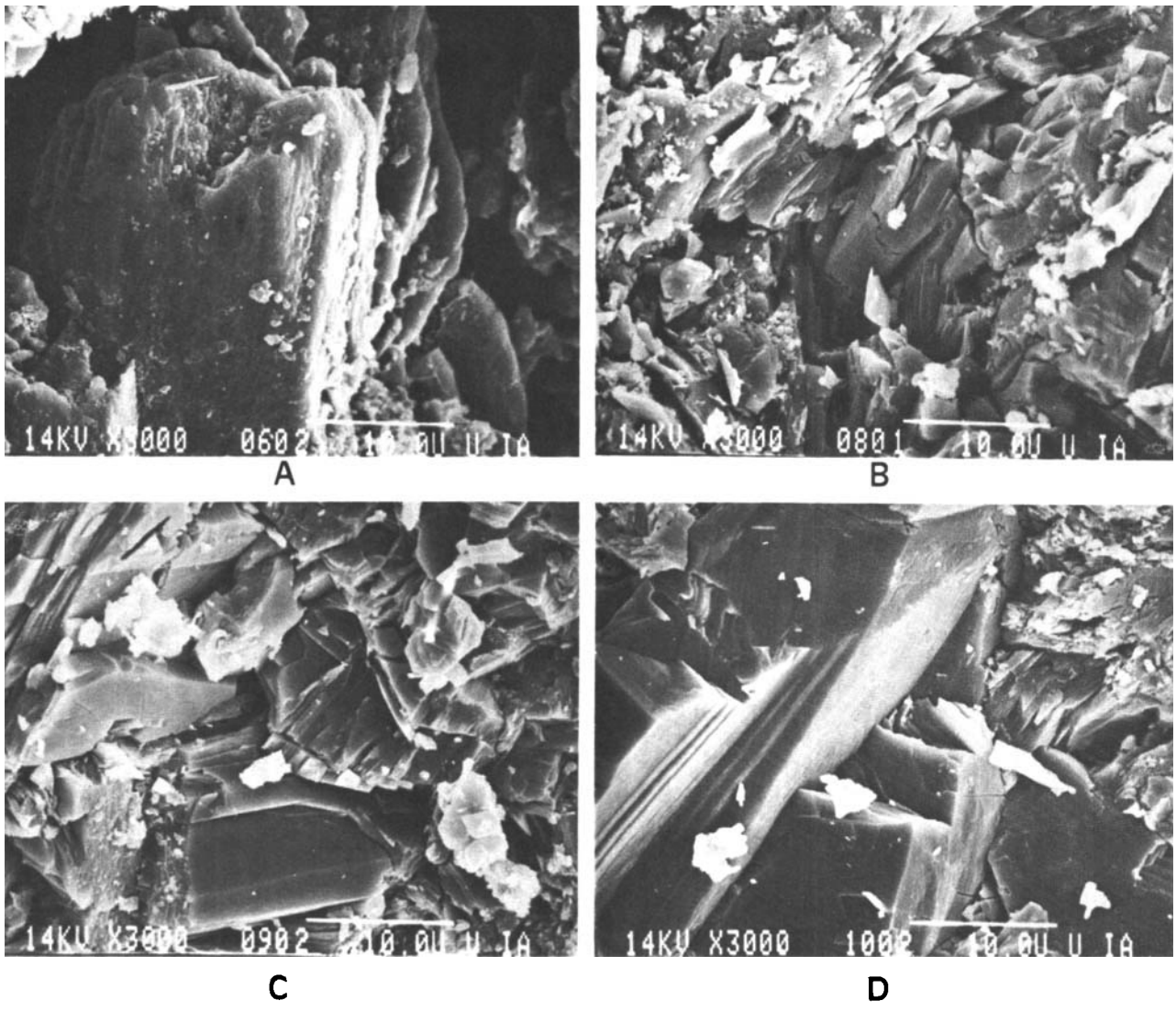

Figure 8—*Scanning electron photomicrographs of center of tablet of dibasic calcium phosphate[7] and 4.5% starch. Original magnification 3000×. Key: compressional force (A) 454; (B) 2268; (C) 4536; and (D) 9402 kg.*

calcium phosphate dihydrate compressed at 454, 2268, 4536, and 9402 kg from granules containing 4.5% starch are shown in Fig. 8. In Fig. 8A, at a low compressional force of 454 kg, the original granule may be distinguished. As the compressional force is increased, the granule is fractured, and no original granules can be seen because consolidation has occurred (Fig. 8B–D). This agrees with the general thought that they should break down on compaction in the die (26).

As shown in Fig. 6, as the compressional force is increased from 2268 to 4536 kg, the tablet tensile strength is increased. Although the crushing strength of granules is important in the handling of the granulation in the tablet process and in tablet reproducibility, the compressional force and the concentration of binder appear to be more basically related to the tablet tensile strength.

REFERENCES

(1) D. E. Fonner, N. R. Anderson, and G. S. Banker, in "Pharmaceutical Dosage Forms: Tablets, Volume 2," H. A. Lieberman and L. Lachman, Eds., Dekker, New York, N.Y., 1981, p. 216.

(2) B. M. Hunter and D. Ganderton, *J. Pharm. Pharmacol.*, **25**, 71P (1973).

(3) W. L. Davis and W. T. Gloor, *J. Pharm. Sci.*, **61**, 618 (1972).

(4) N. A. Armstrong and G. A. March, *ibid.*, **65**, 198 (1976).

(5) C. F. Harwood and N. Pilpel, *ibid.*, **57**, 478 (1968).

(6) D. Ganderton and A. A. Selkirk, *J. Pharm. Pharmacol.*, **22**, 345 (1970).

(7) K. T. Jaiyeoba and M. S. Spring, *ibid.*, **31**, 192 (1978).

(8) A. M. Marks and J. H. Sciarra, *J. Pharm. Sci.*, **57**, 497 (1968).

(9) G. Gold, R. N. Duvall, B. T. Palermo, and R. L. Hurtle, *ibid.*, **60**, 922 (1971).

(10) W. A. Strickland, Jr., E. Nelson, L. W. Busse, and T. Higuchi, *J. Am. Pharm. Assoc., Sci. Ed.*, **45**, 51 (1956).

(11) E. Shotton and D. Ganderton, *J. Pharm. Pharmacol.*, **12**, 93T (1960).

(12) M. H. Rubinstein, *J. Pharm. Sci.*, **65**, 376 (1976).

(13) D. Train, *J. Pharm. Pharmacol.*, **8**, T45 (1956).

(14) W. Erni and W. A. Ritschel, *Pharm. Ind.*, **39**, 82 (1977).

(15) "Handbook of Chemistry and Physics," R. C. Weast, Ed., 55th ed., CRC Press, Cleveland, Ohio, 1974, p. E-46.

(16) P. J. Jarosz and E. L. Parrott, *J. Pharm. Sci.*, **71**, 607 (1982).

(17) C. E. Capes, in "Proceedings of Powtech '71," A. S. Goldberg, Ed., Powder Advisory Centre, London, England, 1971, p. 151.

(18) K. Nishimura, N. Ikeda, and T. Fukazawa, *Yakuzaigaku*, **38**, 190 (1978).

(19) W. O. Opakunle and M. S. Spring, *J. Pharm. Pharmacol.*, **28**, 508 (1976).

(20) W. O. Opakunle and M. S. Spring, *J. Pharm. Pharmacol.*, **28**, 806 (1976).

(21) W. O. Opakunle and M. S. Spring, *J. Pharm. Pharmacol.*, **28**, 915 (1976).

(22) A. S. Alam and E. L. Parrott, *J. Pharm. Sci.*, **60**, 263 (1971).

(23) R. J. Rue, H. Seager, J. Ryder, and I. Burt, *Int. J. Pharm. Tech. Prod. Mfr.*, **1**, 2 (1980).

(24) T. Higuchi, A. N. Rao, L. W. Busse, and J. V. Swintosky, *J. Am. Pharm. Assoc., Sci. Ed.*, **42**, 194 (1953).

(25) S. A. Shah and E. L. Parrott, *J. Pharm. Sci.*, **65**, 1784 (1976).
(26) E. Shotton, J. A. Hershey, and P. E. Wray, in "The Theory and Practice of Industrial Pharmacy," 2nd ed., L. Lachman, H. A. Lieberman, and J. L. Kanig, Eds., Lea & Febiger, Philadelphia, Pa., 1976, p. 309.

ACKNOWLEDGMENTS

Abstracted in part from a dissertation submitted by Paul J. Jarosz to the Graduate College, University of Iowa, in partial fulfillment of the Doctor of Philosophy degree requirements.

High-Performance Liquid Chromatographic Determination of Vincristine Sulfate in Preformulation Studies

J. E. BODNAR, J. R. CHEN *, W. H. JOHNS, E. P. MARIANI ˣ, and E. C. SHINAL ‡

Received February 19, 1982 from the *Science and Technology Division, Pharmaceutical Research and Development Division, Product Development Research Department, Bristol-Myers, Inc., Syracuse, NY 13201.* Accepted for publication May 26, 1982. Present address: *Boots Pharmaceutical, Inc., Shreveport, LA 71106. ‡American Cyanamid, Medical Research Division, Lederle Laboratories, Pearl River, NY 10965.

Abstract □ A fast and simple procedure was developed for the quantitative determination of vincristine sulfate for use in preformulation studies. The procedure involves the use of high-performance liquid chromatography with a reverse-phase column and a mobile phase containing the sodium salt of 1-pentanesulfonic acid for ion-pairing. The procedure has been shown to be specific for vincristine sulfate in the presence of forced degradation products of this substance, vinblastine (a structurally similar *Vinca* alkaloid), and several possible formula excipients. The procedure is linear from 10–200% of the normal injection concentration, and has an assay precision (relative 2σ) of ±1.6%. Recovery of known samples averaged 99.7%.

Keyphrases □ Vincristine sulfate—high-performance liquid chromatography, preformulation studies, degradation □ High-performance liquid chromatography—vincristine sulfate, degradation products □ Preformulation studies—vincristine sulfate, degradation products, high-performance liquid chromatography

Vincristine sulfate (I), an antineoplastic agent originally obtained from extracts of *Vinca rosea*, is structurally related to vinblastine. An analytical procedure was required for the determination of vincristine sulfate in samples resulting from preformulation studies. The procedure had to be capable of accurate and precise quantitation, specific in the presence of a number of possible excipients, and stability indicating. Because a large number of samples were to be examined, it was also necessary that the procedure be rapid and simple.

A number of assay procedures have been reported for vincristine sulfate (1); however, some are not stability indicating (direct spectrophotometric analysis), others are time consuming and complex (colorimetric analysis), and some are not sufficiently accurate and precise (TLC analysis). Several high-performance liquid chromatographic (HPLC) methods have been reported. One procedure (2) requires a 40-min gradient with a vincristine retention time of ~25 min. This was deemed too lengthy for the proposed purpose.

Another procedure (3) required the use of ammonium carbonate in the mobile phase. Since the column life might be shortened appreciably by the presence of ammonium carbonate[1], this procedure was not used. This paper reports the development of a simple and rapid HPLC procedure for the determination of vincristine sulfate stability.

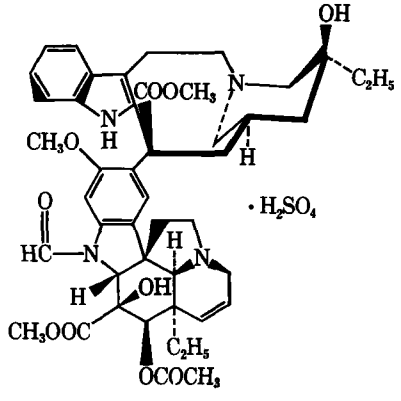

EXPERIMENTAL

Reagent and Chemicals—Acetonitrile and methanol were HPLC grade[2], and were used without further purification. Water was distilled and filtered[3] prior to use. Vincristine sulfate was used as received[4]. All other reagents were ACS grade or better and used without further purification.

Equipment—A liquid chromatograph[5] was connected to an injection valve[6], a variable-wavelength detector[7], a recorder[8], and an integrator[9].

A column[10] consisting of a monomolecular layer of a phenylorganosilicone permanently bonded to polar, porous silica particles was used.

The mobile phase consisted of 30% acetonitrile and 70% aqueous solution which contained 0.02 *M* ammonium acetate and 0.005 *M* of the sodium salt of 1-pentanesulfonic acid adjusted to pH 2.0 with 10% v/v nitric acid[11]. The flow rate was 2.5 ml/min (pressure was ~2000 psi). The detector sensitivity was 0.1 AUFS at 254 nm. Chart speed was 60 cm/hr.

Internal Standard Preparation—Propyl *p*-hydroxybenzoate (~30 mg) was accurately weighed and transferred to a 100-ml volumetric flask.

[1] μ-Bondapak and μ-Porasil Liquid Chromatography Columns Care and Use Manual, Waters Associates, Milford, Mass.
[2] Burdick and Jackson Laboratories, Inc., Muskegon, Mich.
[3] Type HA, 0.45μ filter, Millipore Corp., Bedford, Mass.
[4] Gedeon Nichter Ltd., Budapest, Hungary.
[5] Model 5000 Varian Associates, Walnut Creek, Calif.
[6] Valco injection valve with pneumatic actuator, Valco Instruments, Houston, Tx.
[7] Model UV-50 Varichrom, Varian Associates, Walnut Creek, Calif.
[8] Model 9176, Varian Associates, Walnut Creek, Calif.
[9] Model CDS-111L, Varian Associates, Walnut Creek, Calif.
[10] μ-Bondapak Phenyl, Catalog No. 17198 (30 cm × 3.9-mm i.d.), Waters Associates, Milford, Mass.
[11] Beckman Model Zeromatic II, Beckman Instruments, Fullerton, Calif.

0022-3549/83/0500-0535$01.00/0

(25) S. A. Shah and E. L. Parrott, *J. Pharm. Sci.*, **65**, 1784 (1976).
(26) E. Shotton, J. A. Hershey, and P. E. Wray, in "The Theory and Practice of Industrial Pharmacy," 2nd ed., L. Lachman, H. A. Lieberman, and J. L. Kanig, Eds., Lea & Febiger, Philadelphia, Pa., 1976, p. 309.

ACKNOWLEDGMENTS

Abstracted in part from a dissertation submitted by Paul J. Jarosz to the Graduate College, University of Iowa, in partial fulfillment of the Doctor of Philosophy degree requirements.

High-Performance Liquid Chromatographic Determination of Vincristine Sulfate in Preformulation Studies

J. E. BODNAR, J. R. CHEN *, W. H. JOHNS, E. P. MARIANI ˣ, and E. C. SHINAL ‡

Received February 19, 1982 from the *Science and Technology Division, Pharmaceutical Research and Development Division, Product Development Research Department, Bristol-Myers, Inc., Syracuse, NY 13201.* Accepted for publication May 26, 1982. Present address: *Boots Pharmaceutical, Inc., Shreveport, LA 71106. ‡American Cyanamid, Medical Research Division, Lederle Laboratories, Pearl River, NY 10965.

Abstract □ A fast and simple procedure was developed for the quantitative determination of vincristine sulfate for use in preformulation studies. The procedure involves the use of high-performance liquid chromatography with a reverse-phase column and a mobile phase containing the sodium salt of 1-pentanesulfonic acid for ion-pairing. The procedure has been shown to be specific for vincristine sulfate in the presence of forced degradation products of this substance, vinblastine (a structurally similar *Vinca* alkaloid), and several possible formula excipients. The procedure is linear from 10–200% of the normal injection concentration, and has an assay precision (relative 2σ) of ±1.6%. Recovery of known samples averaged 99.7%.

Keyphrases □ Vincristine sulfate—high-performance liquid chromatography, preformulation studies, degradation □ High-performance liquid chromatography—vincristine sulfate, degradation products □ Preformulation studies—vincristine sulfate, degradation products, high-performance liquid chromatography

Vincristine sulfate (I), an antineoplastic agent originally obtained from extracts of *Vinca rosea*, is structurally related to vinblastine. An analytical procedure was required for the determination of vincristine sulfate in samples resulting from preformulation studies. The procedure had to be capable of accurate and precise quantitation, specific in the presence of a number of possible excipients, and stability indicating. Because a large number of samples were to be examined, it was also necessary that the procedure be rapid and simple.

A number of assay procedures have been reported for vincristine sulfate (1); however, some are not stability indicating (direct spectrophotometric analysis), others are time consuming and complex (colorimetric analysis), and some are not sufficiently accurate and precise (TLC analysis). Several high-performance liquid chromatographic (HPLC) methods have been reported. One procedure (2) requires a 40-min gradient with a vincristine retention time of ~25 min. This was deemed too lengthy for the proposed purpose.

Another procedure (3) required the use of ammonium carbonate in the mobile phase. Since the column life might be shortened appreciably by the presence of ammonium carbonate[1], this procedure was not used. This paper reports the development of a simple and rapid HPLC procedure for the determination of vincristine sulfate stability.

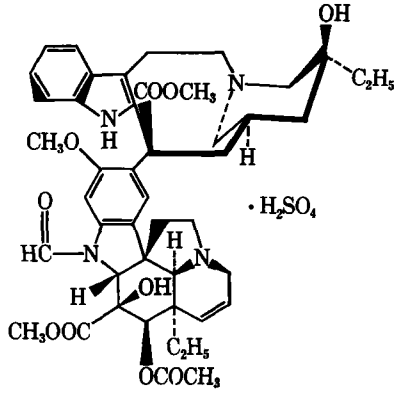

EXPERIMENTAL

Reagent and Chemicals—Acetonitrile and methanol were HPLC grade[2], and were used without further purification. Water was distilled and filtered[3] prior to use. Vincristine sulfate was used as received[4]. All other reagents were ACS grade or better and used without further purification.

Equipment—A liquid chromatograph[5] was connected to an injection valve[6], a variable-wavelength detector[7], a recorder[8], and an integrator[9].

A column[10] consisting of a monomolecular layer of a phenylorganosilicone permanently bonded to polar, porous silica particles was used.

The mobile phase consisted of 30% acetonitrile and 70% aqueous solution which contained 0.02 *M* ammonium acetate and 0.005 *M* of the sodium salt of 1-pentanesulfonic acid adjusted to pH 2.0 with 10% v/v nitric acid[11]. The flow rate was 2.5 ml/min (pressure was ~2000 psi). The detector sensitivity was 0.1 AUFS at 254 nm. Chart speed was 60 cm/hr.

Internal Standard Preparation—Propyl *p*-hydroxybenzoate (~30 mg) was accurately weighed and transferred to a 100-ml volumetric flask.

[1] μ-Bondapak and μ-Porasil Liquid Chromatography Columns Care and Use Manual, Waters Associates, Milford, Mass.
[2] Burdick and Jackson Laboratories, Inc., Muskegon, Mich.
[3] Type HA, 0.45μ filter, Millipore Corp., Bedford, Mass.
[4] Gedeon Nichter Ltd., Budapest, Hungary.
[5] Model 5000 Varian Associates, Walnut Creek, Calif.
[6] Valco injection valve with pneumatic actuator, Valco Instruments, Houston, Tx.
[7] Model UV-50 Varichrom, Varian Associates, Walnut Creek, Calif.
[8] Model 9176, Varian Associates, Walnut Creek, Calif.
[9] Model CDS-111L, Varian Associates, Walnut Creek, Calif.
[10] μ-Bondapak Phenyl, Catalog No. 17198 (30 cm × 3.9-mm i.d.), Waters Associates, Milford, Mass.
[11] Beckman Model Zeromatic II, Beckman Instruments, Fullerton, Calif.

0022-3549/83/0500-0535$01.00/0

Table I—Forced Degraded Specificity

Product	Amount Degraded, %	295 nm/ 254 nm	Error[a], %	275 nm/ 254 nm	Error[a], %
Intact	—	0.974	—	0.776	—
Acid degradation	65	0.963	−1.1	0.755	−2.7
Base degradation	81	0.964	−1.0	0.770	−0.8
Aqueous degradation	24	0.933	−4.2	0.783	+0.9
Dry powder degradation	27	0.984	+1.0	0.801	+3.2
Light degradation	28	0.969	−0.5	0.801	+3.2

[a] $\text{Error} = \frac{\text{test ratio} - \text{intact ratio}}{\text{intact ratio}} \times 100\%$.

The material was dissolved in 25 ml of methanol and diluted to volume with water.

Standard and Sample Preparation—Approximately 25 mg of vincristine sulfate standard or sample was accurately weighed (or an accurate volume of a sample solution containing ~25 mg of vincristine sulfate was pipeted) and transferred to a 100-ml volumetric flask. Exactly 10 ml of internal standard solution was added and the resulting solution was diluted to volume with water.

Assay Method—A 20-μl aliquot of the standard and of each sample was injected under the chromatographic conditions described. Standards were injected at the beginning, the middle, and the end of each run. Each sample was injected once. Samples and standards were not allowed to remain in solution more than 8 hr and were protected from light. Samples were calculated using a factor derived from the average of all standards injected. A typical chromatogram is shown in Fig. 1.

Calculations—Results were calculated as vincristine sulfate.

$$\text{Standard Factor} = \frac{\text{Standard Wt (mg)} \times \text{\% Purity} \times \text{Internal Standard Area}}{\text{Standard Area} \times \text{Internal Standard Wt (mg)} \times 100\%}$$

$$\text{Vincristine Sulfate (mg)} = \frac{\text{Standard Factor} \times \text{Sample Area} \times \text{Internal Standard Wt (mg)}}{\text{Internal Standard Area}}$$

$$\text{Vincristine Sulfate (mg/ml)} = \frac{\text{Standard Factor} \times \text{Sample Area} \times \text{Internal Standard Wt (mg)}}{\text{Internal Standard Area} \times \text{Volume Sample Taken (ml)}}$$

Degradation Procedure—Vincristine sulfate was degraded under the following conditions to test the procedure for specificity in the presence of vincristine degradation products:

1. A weighed portion of dry material was held at 85° for 80 hr in an open vial.
2. A portion of dry material was placed in an open quartz vessel and subjected to 2437-Å light[12] (~16,000 μW/cm²) for 80 hr.
3. An aqueous solution of the material at a concentration of 0.25 mg/ml was titrated to pH 2.0 with 2 *N* HCl and held for 2 hr at 85°.
4. An aqueous solution of the material at a concentration of 0.25 mg/ml was titrated to pH 11.5 with 2 *N* NaOH and held at room temperature (25°) for 1.5 hr. This solution was neutralized before injection.
5. An aqueous solution of the material at a concentration of 0.25 mg/ml was held unchanged (pH 7.5) at 85° for 4 hr.

In each case, degradation was allowed to proceed until ~25–75% of the vincristine sulfate had been degraded. Thus, some intact vincristine sulfate remained at the end of each time interval. Dry materials were dissolved in water at a concentration of 0.25 mg/ml. Separate injections were made of each of the degradation solutions with detection at 254 nm (vincristine sulfate maximum at 255 nm), 296 nm (maximum), and 275 nm (minimum) (1). Area ratios were then calculated for the peak assumed to be pure vincristine sulfate and these were compared with area ratios obtained from a freshly prepared solution of pure vincristine sulfate at the same wavelengths.

RESULTS AND DISCUSSION

The method originally used an eluant consisting of 50% methyl alcohol and 50% 0.01 *M* ammonium acetate adjusted to pH 4.0, and an octadecylsilane reverse-phase column[13]. However, peak shape was rather poor. It was found that the peak shape could be improved by lowering the pH to 2.0 with 10% v/v nitric acid. Preliminary examination of this method with a partially degraded vincristine sulfate solution indicated a lack of resolution between vincristine sulfate and an unknown degradation product. Addition of a 0.005 *M* solution of the sodium salt of heptanesulfonic acid and increasing the ammonium acetate concentration to 0.02 *M* improved the resolution, but not sufficiently. Switching from methyl alcohol to acetonitrile (which required an adjustment in the aqueous–organic ratio from 50:50 to 70:30 for adequate retention) greatly increased resolution. The resolution between vincristine sulfate and the unknown degradation product at this point was ~1.0. Although this may have been adequate, it was found that by changing from an octadecylsilane to a phenyl column, baseline separation could be achieved between these two compounds.

Table II—Relative Retention Times of Some Compounds of Interest

Compound	Relative Retention[a]
Vincristine sulfate	1.00
Vinblastine sulfate	1.57
Major acid degradation product	1.32
Major base degradation product	0.40, 0.51
Light degradation product	1.34
Benzyl alcohol	0.27
Parabens	
Methyl	0.40
Ethyl	0.55
Propyl	0.78
Butyl	1.20

[a] $\text{Relative retention} = \frac{\text{retention time of compound (min)}}{\text{retention time of vincristine sulfate (min)}}$

In the subsequent use of this system, it was found that minor changes in the acetonitrile concentration of the eluant produced major changes in the retention time of vincristine sulfate. To reduce this tendency, and also to shorten the retention time and further improve peak shape, the ion-pairing reagent was changed from a 0.005 *M* solution of the sodium salt of heptanesulfonic acid to a 0.005 *M* solution of the sodium salt of pentanesulfonic acid. This produced the system described above (*Experimental*), which was tested for specificity, linearity, precision, and accuracy.

Specificity—The forced degradation products of vincristine sulfate, which were produced as described above, were examined using the HPLC procedure to ensure that none would interfere with intact vincristine. The results (Table I) indicate that the forced degradation products do not interfere with the vincristine sulfate. A few of the results have 3–4% errors. If the three wavelengths had been monitored simultaneously for each injection, this might have been significant. However, each of these ratios is the result of two separate injections each of which has a precision of ~ ±2%.

Vincristine sulfate is isolated from extracts of the periwinkle plant; thus, isolated precursors probably are nonexistent. However, other *Vinca* alkaloids are possible interferences. One of these, vinblastine sulfate, was found to have a retention time of 12.1 min. Vinblastine sulfate differs structurally from vincristine sulfate only by the presence of a methyl group instead of an aldehyde moiety at the anilino-nitrogen in the vindoline portion of the molecule (1).

A number of possible formulation excipients were examined for interference with vincristine sulfate in this system:

1. Buffers: citrate–citric acid, acetate–acetic acid, and phosphate buffers at 0.1 *M* and 0.2 *M* did not interfere.
2. Sugars: lactose and mannitol at 1 mg/ml showed no interference.
3. Sodium chloride: sodium chloride did not interfere.
4. Benzyl alcohol: benzyl alcohol had a retention time of 2.2 min.
5. Parabens: none of the parabens (methyl, ethyl, propyl, or butyl) interfered with vincristine sulfate using this system. Table II shows the relative retention times of some compounds of interest using this system.

Linearity—Vincristine sulfate showed a linear response from 10–200% of the normal injection concentration. The linear correlation coefficient was found to be +0.99990, and the intercept was −0.06% of the response of the normal injection concentration. Thus single-point standardization was deemed to be adequate.

[12] Rayonet Photochemical Reactor, The South New England Ultraviolet Co., Middletown, Conn.

[13] Internal communication from J. T. Woolever, Analytical Research and Development Department, Bristol Laboratories, Syracuse, NY 13201.

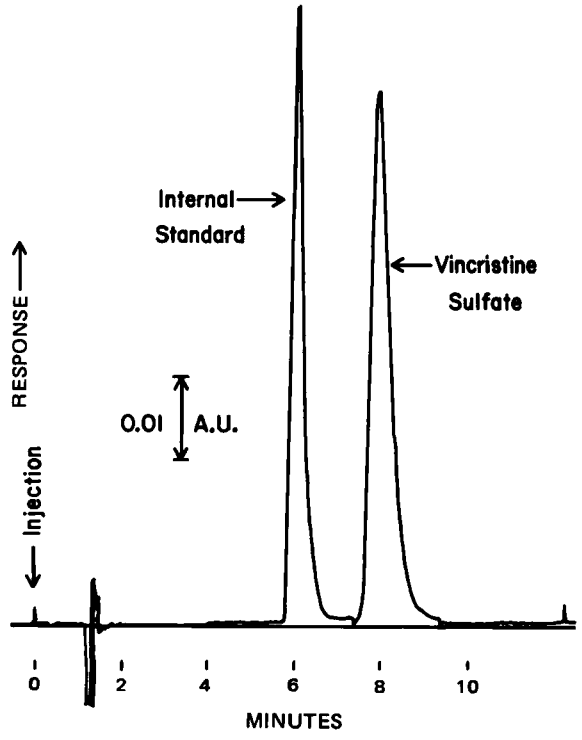

Figure 1—*Typical vincristine sulfate chromatogram with retention times.*

Chromatographic Precision—The chromatographic precision was determined by making six injections from a single freshly prepared solution of vincristine sulfate in water (0.25 mg/ml) on each of 3 days. The precision was calculated each day as two standard deviation units (95% confidence interval) relative to the mean expressed as a percentage. The chromatographic precision was taken to be the root mean square of the three relative 2σs, and was found to be ±2.3%.

Accuracy and Assay Precision—An estimate of the procedural accuracy was obtained by assaying six replicate weighings of vincristine sulfate *versus* a seventh weighing used as a standard. The reproducibility of the recoveries was used as an estimate of assay precision. Table III lists the results.

Stability in Diluent—The six solutions used for accuracy determination were held for 24 hr in the dark at room temperature (25°). They were then reassayed *versus* a fresh standard solution as an estimate of stability in diluent. As shown in Table IV, the average loss over 24 hr was ~5%. Therefore automated runs are feasible as long as vincristine sulfate is not held in solution for >8 hr and is protected from light.

In the routine use of this procedure, several precautions need to be taken. The mobile phase should be prepared with care, since small changes in the acetonitrile percentage produce large retention-time changes. However, as the column ages, small changes in the acetonitrile concentration may be necessary to maintain vincristine–internal standard resolution. Prior to beginning a run, the column should be conditioned with eluant for at least 30 min and several standard injections should be made until retention times are constant (usually ~3–5 injections). After use, the column should be rinsed with 30–50 ml of 1:1 v/v acetonitrile–water. Vincristine sulfate is extremely toxic and possibly carcinogenic; therefore, it should be handled with caution. Protective apparel should be worn, and all solutions (including spent HPLC eluant) should be disposed of properly.

Table III—Accuracy and Assay Precision

Sample	Calc. Wt, mg	Actual Wt, mg	Recovery[a], %
1	24.71	25.09	98.5
2	26.36	26.49	99.5
3	25.26	25.03	100.9
4	24.40	24.44	99.8
5	25.85	25.85	100.0
6	25.17	25.29	99.5

[a] Average is 99.7% with a relative 2σ value of ±1.57%.

Table IV—Stability in Diluent

Sample	Calc. Wt, mg	Actual Wt, mg	Recovery[a], %
1	23.88	25.09	95.2
2	24.81	26.49	93.6
3	24.26	25.03	96.9
4	23.28	24.44	95.2
5	24.81	25.85	96.0
6	23.89	25.29	94.5

[a] Average is 95.2%.

As a measure of system suitability, typical chromatographic parameters are shown below:

	Vincristine Sulfate	Propylparaben
Efficiency (plates/column)	1700	3500
HEPT[14]	0.018	0.008
Asymmetry	1.2	1.05
k'	7	5

The minimum acceptable values for vincristine sulfate are an efficiency of 1000 plates/column and a k' value of 6–10. In addition, there should be baseline separation between vincristine sulfate and propylparaben, the internal standard.

REFERENCES

(1) K. Florey, Ed., "Analytical Profiles of Drug Substances," Vol. 1, Academic, New York, N.Y., 1972, pp. 464–480.

(2) M. C. Castle and J. A. M. Mead, *Biochem. Pharmacol.*, **27**, 37 (1978).

(3) S. Gorog, B. Herenyi, and K. Jovanovics, *J. Chromatogr.*, **139**, 203 (1977).

ACKNOWLEDGMENTS

The authors wish to thank Ms. K. Green for technical help during the course of this work, and Ms. F. Ferraro and Ms. P. White for manuscript preparation.

[14] Height equivalent of a theoretical plate.

Enzyme Inhibition VI: Inhibition of Reverse Transcriptase Activity by Protoberberine Alkaloids and Structure–Activity Relationships

MANOHAR L. SETHI

Received November 30, 1981, from the *Department of Medicinal Chemistry, College of Pharmacy and Pharmacal Sciences, Howard University, Washington DC 20059.* Accepted for publication May 27, 1982.

Abstract □ Protoberberine alkaloids such as palmatine (I), 13-methylpalmatine iodide (II), 2,3-methylenedioxy-10,11-dimethoxy-13-methylprotoberberine iodide (III), 2,3-methylenedioxy-9,10-dimethoxy-13-methylprotoberberine chloride (IV), and berberine (V) showed inhibition of reverse transcriptase activity of RNA tumor viruses in the presence of polyriboadenylic acid·oligodeoxythymidylic acid (VI), polydeoxyadenylic acid·oligodeoxythymidylic acid (VII), activated calf thymus deoxyribonucleic acid (IX), and 70S ribonucleic acid (X), but not in the presence of polyribocytidylic acid·oligodeoxyguanylic acid (VIII). These results indicated that the alkaloids caused inhibition of the enzyme activity by interacting with the template primer, particularly of the adenine–thymine base pair. Furthermore, the alkaloids competed with the template primer-binding site of the enzyme. The time course inhibition indicated that the alkaloids stopped the DNA synthesis instantly when added after the initiation of polymerization processes. Inhibition of reverse transcriptase activity was correlated with the structure and antileukemic activity of the protoberberine alkaloids.

Keyphrases □ Protoberberine alkaloids—inhibition of reverse transcriptase activity, reaction kinetics, structure–activity relationships □ Reverse transcriptase—effect of protoberberine alkaloids, reaction kinetics, structure–activity relationships □ Enzyme inhibition—effect of protoberberine alkaloids on viral DNA polymerase, reaction kinetics, structure–activity relationships □ Structure–activity relationships—protoberberine alkaloids, *in vitro* inhibition of reverse transcriptase activity

Protoberberine alkaloids are a class of isoquinoline alkaloids that possess a wide variety of biological properties (1) [*i.e.*, antimicrobial (2–4), uterine contracting or stimulating (5, 6), and anticancer (7–9)]. Berberine chloride, one of the protoberberine alkaloids has been extensively studied, and exhibits antibacterial, antifungal, and antiprotozoal properties (10, 11). It also antagonizes cholera toxin (12, 13) and possesses intercalating (14–16) and mutagenic properties (17). Recently, berberine (V), 13-methylpalmatine (II), and 2,3-methylenedioxy-10,11-dimethoxy-13-methylprotoberberine (III) were reported to possess antitumor activity against experimental tumors (18), but lacked antileukemic activity against P-388 murine lymphocyte leukemia (19).

In view of the observation that some benzophenanthridine alkaloids are potential inhibitors of reverse transcriptase activity (20–22), the structurally related protoberberine alkaloids were examined for their effect on reverse transcriptase activity of RNA tumor viruses. It was considered worthwhile to screen these alkaloids for their antireverse transcriptase activity and correlate this activity with their structures and their antileukemic activity.

Reverse transcriptase (RNA-directed DNA polymerase) enzyme was discovered in RNA tumor viruses (retroviruses) by Baltimore (23) and Temin and Mizutani (24) in 1970. Since this discovery and association of the retroviruses with leukemia, lymphoma, and sarcoma of several vertebrates including primates (25), massive literature on the isolation, characterization, cell transformation, inhibitors, *etc.*, has accumulated over the past decade (26, 27). Recent findings of retroviral information in human leukemia (28, 29) and human cutaneous T-cell lymphoma cell line (30, 31) suggests a link between the RNA tumor viruses and human cancer. Consequently, the inhibitors of viral reverse transcriptase may contribute to approaches made toward the prevention of cancer.

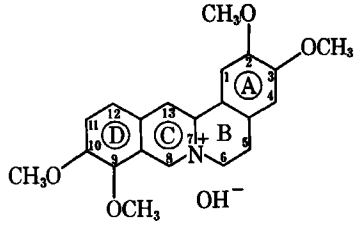

I

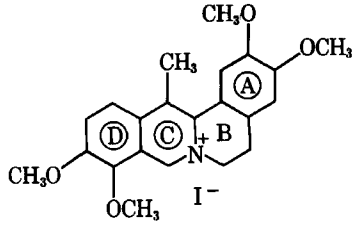

II

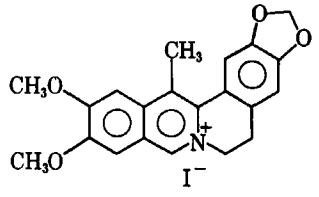

III

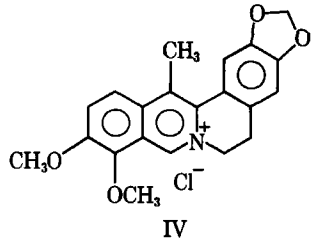

IV

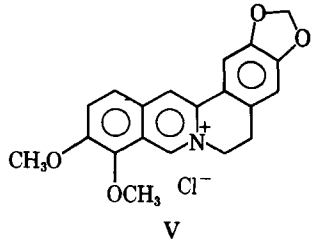

V

0022-3549/83/0500-0538$01.00/0

Table I—Effect of Different Template Primers on Inhibition of AMV Reverse Transcriptase Activity by Protoberberine Alkaloid [a]

Alkaloid	Template Primer [b]	Inhibition, %
I	VI	100
	VII	99
	VIII	1
	IX	98
	X	98
II	VI	98
	VII	97
	VIII	2
	IX	97
	X	96
III	VI	95
	VII	95
	VIII	3
	IX	94
	X	94
IV	VI	97
	VII	96
	VIII	4
	IX	96
	X	95
V	VI	90
	VII	85
	VIII	5
	IX	84
	X	80

[a] Alkaloid used for each inhibition was 12 μg/assay and the standard assay conditions as published previously (21) were followed. DNA and RNA polymerases of *E. Coli* under the standard assay conditions were less sensitive than viral polymerases to alkaloid inhibition. [b] Standard assay conditions were followed using thymidine triphosphate radioactive substrate except where otherwise specified under *Experimental*. The names of template primers and templates used are given in *Materials and Methods*.

EXPERIMENTAL

Materials and Methods—Purified reverse transcriptase from avian myeloblastosis virus[1] (AMV) contained specific activity of 92,472 U/mg of protein. The enzyme preparation contained 10,072 U/ml of reverse transcriptase activity and a protein content of 0.11 mg/ml. One unit of enzyme activity was expressed as the incorporation of 1 nmole of deoxythymidine monophosphate into an acid-insoluble product in 10 min at 37°. The purity of the enzyme preparation was determined by an established procedure (32). Reverse transcriptase from Rauscher murine virus[2] (MuLV), propagated from JLS-V9 cell line had an activity of 4.00 nmoles of thymidine monophosphate incorporation/30 min/ml. DNA polymerase from simian sarcoma virus type 1[3] (SSV) was derived from tissue culture fluids of the SSV-I-NC-37 cell line and purified by a previous method (20). It had an activity of 6.00 nmoles of thymidine monophosphate incorporation/30 min/ml. The 70S RNA[4] from MuLV was purified by a published method (33). Reverse transcriptase assay and enzyme inhibition were carried out by a method previously reported (21). Appropriate concentrations of the protoberberine alkaloids[5,6] were dissolved in dimethyl sulfoxide. Control assays were performed without the alkaloids but contained an equivalent volume of dimethyl sulfoxide. The results were expressed as the percent of control activity.

The protoberberine alkaloids tested were palmatine[5] (I,NSC 209407), 13-methylpalmatine iodide[6] (II), 2,3-methylenedioxy-10,11-dimethoxy-13-methylprotoberberine iodide[5] (III,NSC 276348), 2,3-methylenedioxy-9,10-dimethoxy-13-methylprotoberberine chloride[6] (IV), and berberine chloride[5] (V,NSC 163088).

The template primers or templates used were polyriboadenylic acid·oligodeoxythymidylic acid (VI), polydeoxyadenylic acid·oligodeoxythymidylic acid (VII); polyribocytidylic acid·oligodeoxyguanylic acid (VIII) (2.00 nmoles of [^{3}H]deoxyguanosine triphosphate, 380 cpm/mole substrate), activated calf thymus DNA (IX) (2.20 μg activated deoxyribonucleic acid, 10 nmoles each of deoxyadenosine, deoxycytidine, and deoxyguanosine triphosphates and 2.50 nmoles of [^{3}H]thymidine triphosphate substrates); 70S ribonucleic acid (X) (MuLV) of 0.05 optical density units (260 nm).

[1] Life Science Research Labs., St. Petersburg, Fla., through the courtesy of Dr. J. Beard.
[2] Bionetics Laboratory Products, Kensington, Md.
[3] Pfizer, Inc., Maywood, N.J.
[4] Gift from Dr. M. Reitz, Litton Bionetics, Bethesda, Md.
[5] Drug Synthesis and Chemistry, Division of Cancer Treatment, NCI, Bethesda, Md.
[6] Dr. Mark Cushman, Purdue University, West Lafayette, IN 47907.

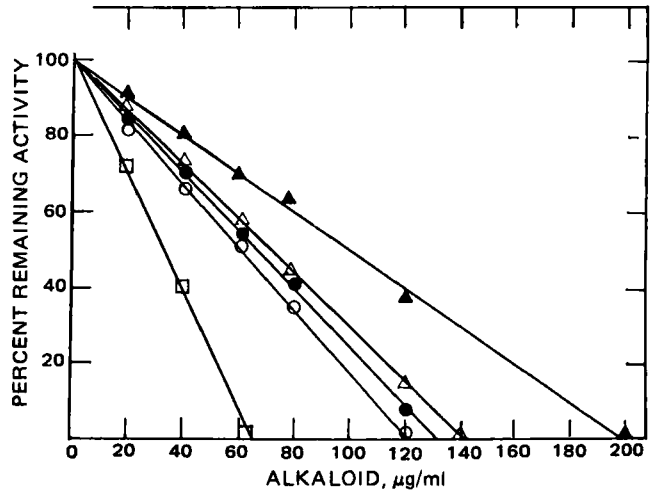

Figure 1—*Effect of protoberberine alkaloids on AMV reverse transcriptase activity. In a standard assay mixture (0.10 ml) containing 5 μl of enzyme, different concentrations of alkaloids I (□), II (○), III (●), IV (△), and V (▲) were used for enzyme inhibition.*

RESULTS AND DISCUSSION

The *in vitro* inhibition of AMV reverse transcriptase activity by protoberberine alkaloids I–V in the presence of template primer (VI) is shown in Fig. 1. Fifty percent enzyme inhibition by alkaloids I–V was in the range of 30–35 μg/ml (I), 60–65 μg/ml (II), 65–70 μg/ml (III), 70–75 μg/ml (IV), and 100–105 μg/ml (V). Similar results were obtained on MuLV and SSV reverse transcriptase activity (data not shown). Based on the nature of inhibitory curves and 50% inhibition of enzyme activity, alkaloids I, II–IV, and V were classified as potent, moderate, and very weak inhibitors of reverse transcriptase activity, respectively. Purified AMV, MuLV, and SSV reverse transcriptase activities were also inhibited by these protoberberine alkaloids in the presence of VII, IX, and X template primers, but a very low degree of inhibition of enzyme activity was observed when VIII template primer was used (Table I). The different percentage of inhibition of enzyme activity observed in the presence of these template primers indicated that the inhibition of the enzyme activity was due to the interaction of alkaloids with template primers and not with the enzyme protein; otherwise the same percentage of inhibition of enzyme activity would have been observed regardless of the different template primers used. A very low degree of inhibition of enzyme activity in the presence of VIII as compared with VI, VII, IX, and X was indicative of the strong binding affinity of alkaloids with the adenine–thymine base

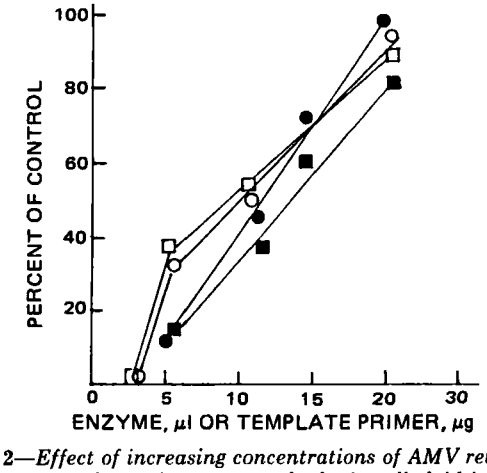

Figure 2—*Effect of increasing concentrations of AMV reverse transcriptase or template primer on protoberberine alkaloid-inhibited reaction mixture. The standard assay mixture (0.10 ml) contained 5 μl of AMV reverse transcriptase and 6 μg of I (●) or 12 μg of III (■) or 2.5 μg of VI template primer and 6 μg of I (○) or 12 μg of III (□).*

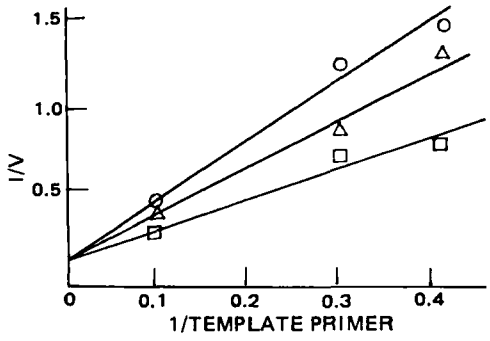

Figure 3—*Double-reciprocal plot (Lineweaver–Burk plot) of 1/velocity versus 1/template primer shown by alkaloid I. Units of velocity (V) are expressed as counts per min × 10^{-4} of methyl-[^{3}H]thymidine monophosphate incorporated into DNA synthesis. Concentrations of template primer (VI) are expressed in μg/ml. Alkaloid I concentrations were 0 (□); 0.3 μg/ml (△); 0.9 μg/(○) in the standard assay mixture.*

pair template primers. The interaction or competition of alkaloids with manganese chloride was ruled out, because the increasing concentration of this metal ion in the assay mixture did not change the enzyme activity *(data not shown)*. The possibility of interaction of alkaloids with potassium chloride or substrate ([^{3}H]thymidine or guanosine triphosphate) was not considered, since the latter was present in the reaction mixture in 8- or 25-fold, respectively, in excess of the ID_{50} of the alkaloid concentration.

To explain further the mode of action of alkaloids I and III, the effect of increasing the concentrations of AMV reverse transcriptase enzyme or template primer (VI) on the alkaloid-inhibited reaction mixture was observed, as shown in Fig. 2. The increasing concentration of the enzyme from 5 to 20 μl or template primer from 3 to 20 μg in the assay mixture resulted in the full restoration of enzyme activity of the alkaloid-inhibited reaction mixture. Similar results were shown by alkaloids II, IV, and V (data not shown). These results could be due to the dissociation of the enzyme–template–alkaloid ternary complex in the reaction mixture in the presence of excess template primer or enzyme. The data support the previous observation that the alkaloids interacted with the template primer. The Lineweaver–Burk plot (Fig. 3) obtained by alkaloid I was of a competitive type indicating interaction of the alkaloid with the template primer binding site of the enzyme. Similar plots were obtained in the case of alkaloids II–IV (data not shown). The time course of inhibition of reverse transcriptase activity by alkaloids I and III is shown in

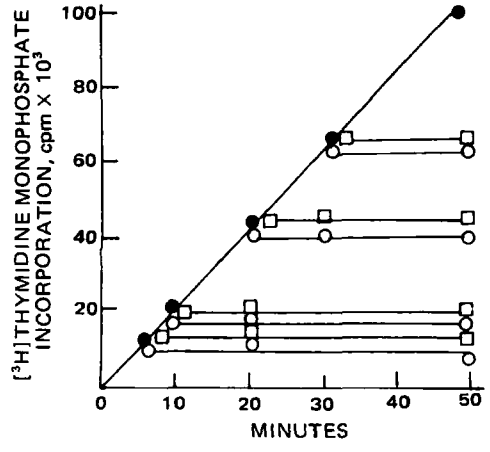

Figure 4—*Effect of addition of protoberberine alkaloids during AMV reverse transcriptase kinetic reaction. For each assay, 2 ml of standard assay mixture containing 100 μl of enzyme was divided into four parts: A(0.60 ml), B(0.50 ml), C(0.50 ml), D(0.40 ml). From A, a 0.10-sample was withdrawn at zero min, and the remaining quantity was incubated at 37°. One-tenth-milliliter samples from A(control, ●) were withdrawn at 5, 10, 20, 30, and 50 min after incubation. Parts B, C, and D were also incubated at 37°, and 60 μg/ml or 120 μg/ml solutions of alkaloid I (○) or III (□), respectively, were added at 5, 10, 20, and 30 min after incubation. One minute after addition of the alkaloid, 0.10-ml samples were withdrawn from B, C, and D at 5-min intervals. Radioactivity of each sample was determined.*

Table II—Effect of Functional Groups of Protoberberine Alkaloids on Inhibition of Reverse Transcriptase Activity

Alkaloid	50% Inhibition, μg/ml	Functional Group[a]
I	32	Maximum inhibition due to methoxyl groups at positions 2, 3, 9, and 10
II	62	Decrease of inhibition due to methyl group at position 13
III	67[b]	Increase of inhibition due to methoxyl groups at positions 10 and 11 as compared with positions 9 and 10
IV	72	Decrease of inhibition due to methyl group at position 13
V	102	Decrease of inhibition due to methylenedioxy group at positions 2 and 3

[a] For functional groups refer to the individual structure of the alkaloids. [b] This increase in 50% inhibition is relative to the inhibition exhibited by alkaloid IV. Other 50% inhibitions are compared with the maximum inhibition displayed by alkaloid I.

Fig. 4. The controlled activity of the reaction mixture was determined without the alkaloids. During the time course of the reaction, the alkaloids were added at 10, 20, 30, and 50 min after initiation of DNA synthesis. As soon as the alkaloids were added, the enzyme activity was abruptly changed, as indicated by the [^{3}H]thymidine monophosphate incorporation. Further incubation of the reaction mixture did not change the kinetics of DNA synthesis or degrade the product. The immediate cessation of the polymerization reaction by the alkaloids may be due to the interaction of the alkaloids with the template primer. Similar results were obtained with alkaloids II, IV, and V (data not shown).

The individual members of the protoberberine alkaloids showed different degrees of inhibition of reverse transcriptase activity, although the mode of action was similar in each case. Therefore, variation in 50% inhibition of enzyme activity by the protoberberine alkaloids could be attributed to the structure of the alkaloids. A maximum of 50% inhibition of enzyme activity (32 μg/ml) was observed in alkaloid I (base or iodide), which has two methoxyl groups at positions 2 and 3 of ring A and two methoxyl groups at positions 9 and 10 of ring D (Table II). In the structure of alkaloid I, when an additional methyl group was present at position 13 of ring C, 50% enzyme inhibition by alkaloid II was decreased considerably (62 μg/ml) indicating the influence of a methyl group. On the other hand, with substitution of a methylenedioxy group at positions 2 and 3 of ring A in place of methoxyl groups at these positions of alkaloid I, 50% inhibition of enzyme activity by alkaloid V was almost lost (102 μg/ml). However, the presence of a methyl group at position 13 of ring C resulted in an increase of 50% enzyme inhibition (72 μg/ml) by alkaloid IV (Table II). Alkaloid III showed slightly more enzyme inhibition (67 μg/ml) than alkaloid IV, although two methoxyl groups in alkaloid III were present at positions 10 and 11 of ring D. Whether the presence of methoxyl groups at positions 9 and 10 or positions 10 and 11 of ring D play an important role in the inhibition of enzyme activity is not yet conclusively determined. However, previous results in structurally related benzophenanthridine alkaloids (22) indicated that the presence of substituent groups at positions analogous to 10 and 11 of ring D were important to exhibit increased inhibition of reverse transcriptase activity. In fact, alkaloid III was a better inhibitor of reverse transcriptase activity than alkaloid IV, which indicated that the presence of methoxyl groups at positions 10 and 11 of ring D (alkaloid III) increased the inhibition of enzyme activity. In any case, the present investigation reveals that the placing of methoxyl groups at positions 2 and 3 of ring A, regardless of such groups at positions 9 and 10 or 10 and 11 of ring D, was an essential requirement in possessing the inhibitory effect of the alkaloids.

The cytotoxic alkaloids I–V displayed an effective antitumor activity against experimental tumors (18) but did not show antileukemic activity against P-388 lymphocytic leukemia in mice (19). Earlier studies have indicated that the inhibition of reverse transcriptase activity by benzophenanthridine alkaloids corresponded well with their antileukemic activity (22). Surprisingly, except alkaloid V, protoberberine alkaloids failed to exhibit such a correlation. The lack of antileukemic activity of alkaloid V was, thus, in agreement with the observation that this alkaloid exhibited very weak inhibition of reverse transcriptase activity. However, lack of antileukemic activity of alkaloids I–IV, but possession of inhibition of reverse transcriptase activity by these alkaloids, could not be explained at the present time. Further work is in progress to establish the relationship of enzyme inhibition and antileukemic or antitumor activity.

Alkaloids I–V showed less inhibition of reverse transcriptase activity compared with the analogous benzophenanthridine alkaloids. Such a difference in reverse transcriptase inhibition by the protoberberines and benzophenanthridines could be due to the stereochemistry, presence of *N*-methyl (—N—CH_3) group in ring C and/or influence of counterions of different salts of benzophenanthridine alkaloids. A previous report related an antileukemic activity of certain cytotoxic protoberberine alkaloids with the conformations and DNA binding properties of the alkaloids (19). Other studies reported that the biological activity of alkaloid V (34) (and a few protoberberines) was due to their binding to double-helical DNA by intercalation (35, 36). Furthermore, protoberberine alkaloids were reported to inhibit a number of enzymes such as NADH oxidase (37), horse liver alcohol dehydrogenase (38, 39), and xanthine oxidase (40) by different mechanisms. The present study reports inhibitory effect of protoberberine alkaloids on another enzyme (reverse transcriptase) for the first time. It would be worthwhile to investigate the exact mechanism of action of protoberberine alkaloids in order to justify the cytotoxicity and diverse biological activities of the alkaloids.

REFERENCES

(1) Y. Kondo, *Heterocycles*, **4**, 197 (1976).

(2) S. A. Gharbo, J. L. Beal, R. W. Doskotch, and L. A. Mitscher, *Lloydia*, **36**, 349 (1973).

(3) E. A. Steck, in "Progress in Drug Research," vol. 18, E. Jucker, Ed., Birkhäuser Verlag, Basel, Switzerland, 1974, p. 289.

(4) F. E. Hahn and J. Ciak, "Antibiotics," vol. 3, D. Gottliele, P. D. Shaw, and J. W. Cocoran, Eds., Springer-Verlag, New York, N.Y., 1975, p. 577.

(5) Y. Kitabatake, K. Ito, and M. Tajima, *J. Pharm. Soc. Jpn.*, **84**, 73 (1964).

(6) N. R. Farnsworth, A. S. Bingel, G. A. Cordell, F. A. Crane, and H. H. S. Fong, *J. Pharm. Sci.*, **64**, 535 (1975).

(7) G. A. Cordell and N. R. Farnsworth, *Heterocycles*, **4**, 393 (1976).

(8) Y. Sawa, Kanebo Co., Ltd., Japan. Pat.; through *Chem. Abstr.*, **84**, 90384g (1975).

(9) V. Preiniger, in "The Alkaloids," vol. 15, R. H. F. Manske, Ed., Academic, New York, N.Y., 1975 p. 231.

(10) A. H. Amin, T. V. Subbaiah, and K. M. Abbasi, *Can. J. Microbiol.*, **15**, 1067 (1969).

(11) T. V. Subbaiah, and A. H. Amin, *Nature (London)*, **215**, 527 (1967).

(12) M. Sabir, M. H. Akhter, and N. K. Bhide, *Indian J. Med. Res.*, **65**, 305 (1977).

(13) M. Sabir, M. H. Akhter, and N. K. Bhide, *Indian J. Med. Res.*, **65**, 133 (1977).

(14) F. E. Hahn and J. Ciak, *Ann. N.Y. Acad. Sci.*, **182**, 295 (1971).

(15) F. E. Hahn, *Antibiot. Chemother. (Basel)*, **20**, 196 (1976).

(16) F. E. Hahn and J. Ciak, "Drug Inactivating Enzymes and Antibiotic Resistance," S. Mitsuhashi, L. Rosival, and V. Krčměry, Eds., Springer-Verlag, New York, N.Y., 1975, p. 235.

(17) M. N. Meisel and T. S. Sokolova, *Dokl. Akad. Nauk. USSR*, **131**, 436 (1959).

(18) T. Y. Owen, S. Y. Wang, S. Y. Chang, F. L. Lu, C. L. Yang, and B. Hsu, *K'O Hsueh Tung Pao*, **21**, 285 (1976); through *Chem. Abstr.*, **86**, 5660a (1976).

(19) M. Cushman, F. W. Dekow, and L. B. Jacobsen, *J. Med. Chem.*, **22**, 331 (1979).

(20) V. S. Sethi and M. L. Sethi, *Biochem. Biophys. Res. Commun.*, **63**, 1070 (1975).

(21) M. L. Sethi, *J. Natl. Prod. (Lloydia)*, **42**, 187 (1979).

(22) M. L. Sethi, *Can. J. Pharm Sci.*, **16**, 29 (1981).

(23) D. Baltimore, *Nature (London)*, **226**, 1209 (1970).

(24) H. M. Temin and S. Mizutani, *Nature (London)*, **226**, 1211 (1970).

(25) R. C. Gallo and F. Wong-Staal, in "Viral Oncology," G. Klein, Ed., Raven, New York, N.Y., 1980, pp. 399–431.

(26) A. M. Wu, in "Recent Advances in Cancer Research Cell Biology, Molecular Biology and Tumor Virology," vol. II, R. C. Gallo, Ed., CRC Press, Cleveland, Ohio, 1977, pp. 1–36.

(27) I. M. Verma, *Biochim. Biophys, Acta.*, **473**, 1 (1977).

(28) R. C. Gallo, W. C. Saxinger, R. E. Gallagher, D. H. Gillespie, G. S. Aulakh, F. Wong-Staal, F. W. Ruscetti, and M. S. Reitz, in "Origin of Human Cancer," H. H. Hiatt, J. D. Watson, and J. A. Winsten, Eds., Cold Spring Harbor Laboratory, Cold Spring Harbor, N.Y., 1977, Book B, pp. 1253–1285.

(29) E. Pimetel, *Biochim. Biophys. Acta*, **560**, 169 (1979).

(30) B. J. Poiesz, F. W. Ruscetti, A. F. Gazdar, P. A. Bunn, J. D. Minna, and R. C. Gallo, *Proc. Natl. Acad. Sci. USA*, **77**, 7415 (1980).

(31) H. M. Rho, B. Poiesz, F. W. Ruscetti, and R. C. Gallo, *Virology*, **112**, 355 (1981).

(32) D. L. Kacian and S. Speegelman, in "Methods in Enzymology," vol. 29, E. Grossman and K. Moldave, Eds., Academic, New York, N.Y., 1973, pp. 150–173.

(33) J. Battacharyya, M. Xuma, M. Reitz, P. S. Sarin, and R. C. Gallo, *Biochem. Biophys. Res. Commun.*, **54**, 324 (1973).

(34) A. K. Krey and F. E. Hahn, *Science*, **166**, 755 (1969).

(35) K. Y. Zee-Cheng and C. C. Cheng, *J. Pharm. Sci.*, **62**, 1572 (1973).

(36) W. D. Wilson, A. N. Gough, J. J. Doyle, and M. W. Davidson, *J. Med. Chem.*, **19**, 1261 (1976).

(37) T. Schewe and W. Meuller, *Acta. Biol. Med. Ger.*, **35**, 1019 (1976); through *Chem. Abstr.*, 171590b (1976).

(38) J. Kovar and S. Pavelka, *Collect Czech. Chem. Commun.*, **41**, 1081 (1976).

(39) J. Kovar and S. Panelka, *Collect Czech. Chem. Commun.*, **40**, 753 (1975).

(40) T. Shimada, T. Ikegawa, S. Daibo, Y. Okazaki, K. Tachibana, T. Endo, T. Kono, H. Kuroda, and Y. Ikeda, Kanebo Co., Ltd., Japan. Pat.; through *Chem. Abstr.*, **83**, 114716g (1975).

ACKNOWLEDGMENTS

The author is grateful to Dr. Mark Cushman, Purdue University and Drug Synthesis and Chemistry Division of Cancer Treatment, NCI, Bethesda, Maryland for the supply of alkaloid samples.

Other publications in this series are: *Biochem. Biophys. Res. Commun.*, **63**, 1070 (1975); *Can. J. Pharm. Sci.*, **12**, 7 (1977); *J. Pharm. Sci.*, **66**, 130 (1977); *J. Nat. Prod. (Lloydia)*, **42**, 187 (1979); *Can. J. Pharm. Sci.*, **16**, 29 (1981).

Furosemide Binding by Human Albumin: Comparison of Two Methods of Fluorescence Quenching Analysis

D. L. PARSONS

Received December 28, 1981, from the *Department of Pharmaceutical Sciences, College of Pharmacy, The University of Arizona, Tucson, AZ 85721.* Accepted for publication May 27, 1982. Present address: Department of Pharmacal Sciences, School of Pharmacy, Auburn University, Auburn, AL 36849.

Abstract □ Disagreement exists over the primary-site binding constant for the interaction of furosemide with human albumin. Disagreement also exists over which experimental methods are accurate in this particular interaction. Therefore, furosemide binding by human albumin was examined using albumin fluorescence quenching by both the method of Levine and the method of Steiner *et al.* The binding constants obtained by each method differed greatly, with the results of the latter method being similar to those of other experimental methods. It was concluded that the method of Levine overestimates the binding constant for this drug–protein interaction.

Keyphrases □ Furosemide—binding by human albumin, comparison of two methods of fluorescence quenching analysis □ Binding—furosemide by human albumin, comparison of two methods of fluorescence quenching, analysis □ Human albumin—furosemide binding, comparison of two methods of fluorescence quenching analysis

The binding of a drug by blood proteins can influence the therapeutic, pharmacodynamic, and toxicological actions of the drug (1). Studies of drug binding by albumin are important since this is the major plasma protein responsible for the nonspecific binding of drugs (2). Most drugs that are extensively bound by plasma proteins are anions that bind to albumin (3), and these ligands can undergo competition for the limited number of albumin binding sites (4).

At low concentrations in plasma, furosemide is extensively bound exclusively or almost exclusively to albumin (5). However, there has been disagreement over the magnitude of the binding constant for the interaction of furosemide with its primary binding site on human albumin. Using the method of intrinsic protein fluorescence quenching and a new method of data analysis, a primary-site binding constant of $1.3 \times 10^7\ M^{-1}$ has been obtained for the interaction of furosemide with human albumin (6). As shown in Table I, this value considerably exceeds other reported values obtained using various experimental methods and conditions. It was suggested that the reason for the large affinity constant obtained using the new method of data analysis is that other experimental methods, such as equilibrium dialysis, give erroneously low binding constant values for strongly bound ligands (6). Previous work (13) has provided a theoretical alternative for this large binding constant obtained for the interaction of furosemide with human albumin; *i.e.*, the new method of data analysis employed overestimates the binding constant for certain interactants.

As discussed previously (13), the method of Levine is based on assumptions that are not strictly valid when the protein contains more than one binding site for the ligand. When this is the case, and with a low value of n_1k_1/n_2k_2, where n_i is the number of binding sites of class i and k_i is the site binding (affinity) constant for binding sites of class i, the method of Levine will, theoretically, overestimate the value of k_1 (13).

A third possible explanation for the large value of k_1 obtained using the new method of data analysis (6) is that different experimental conditions were employed. Factors such as the pH, temperature, and buffer system used, the method of albumin isolation, and presence of fatty acids can affect both the number and the affinity of binding sites (14).

Since the binding of a drug by albumin may greatly affect the *in vivo* actions of the drug, it is important that large discrepancies in reported binding constants be resolved. It is also important that possible limitations of new methods of data analysis be examined both theoretically and experimentally, since many investigators may eventually employ the new method. Theoretical limitations of the method of Levine were discussed previously (13). To evaluate experimentally the limitations of this method, the binding of furosemide by human albumin was re-examined using the quenching of intrinsic protein fluorescence by both the Levine (6) and Steiner *et al.* (15) methods. The method of Steiner *et al.* is theoretically sound and applicable when the protein contains more than one binding site for the ligand.

EXPERIMENTAL

Materials and Methods—Fatty acid free human albumin[1] and furosemide[2] as a pure powder were used as received. All protein solutions were prepared using 0.125 *M* phosphate buffer at pH 7.4. The buffer was prepared immediately prior to the experiment using analytical grade monosodium and disodium phosphates and water purified by reverse osmosis followed by distillation.

Fluorescence measurements were made with a spectrofluorometer[3], and spectrophotometric measurements were made with a spectrophotometer[4]. Rectangular quartz fluorescence cells with a path length of 10 mm were used for both fluorescence and spectrophotometric measurements.

Albumin solutions of 1.9, 6.0, 10, 50, and 100 μmoles/liter were utilized in this study. All albumin solutions were corrected for moisture content and purity and were ~2-hr old at the start of each experiment. Furosemide solutions (0.3–1.2 mmoles/liter) were prepared immediately prior to use and were protected from light. Furosemide solutions were prepared using a portion of the albumin solutions under investigation to avoid dilution of the albumin solution upon addition of drug.

The decrease in the magnitude of intrinsic albumin fluorescence upon the addition of microliter volumes of furosemide solution to 2 ml of protein solution was measured at ambient temperature (24.5 ± 0.8°). Excitation and emission wavelengths of 292 and 370 nm, respectively, were used to minimize the absorption of light by furosemide. Excitation and emission slit widths of 2 and 12 nm, respectively, were used, except at the higher protein concentration (100 μmoles/liter) where an emission slit width of 10 nm was utilized. The fluorescence intensity of cells containing buffer only and albumin only, at the same concentration as the sample cell, was measured prior to each measurement of sample cell fluorescence intensity. These reference solutions were used to correct the

[1] Miles Laboratories, Inc., Elkhart, IN 46514.
[2] Hoechst-Roussel Pharmaceuticals, Inc., Somerville, NJ 08876.
[3] Model 650-10M, Perkin-Elmer Corp., Norwalk, CT 06856.
[4] DU-8, Beckman Instruments, Inc., Irvine, CA 92713.

0022-3549/83/0500-0542$01.00/0

Table I—Binding Constants for the Interaction of Furosemide with Human Albumin Previously Reported Using a Variety of Experimental Methods and Conditions

n_1	k_1, kl/mole	n_2	k_2, kl/mole	Reference
1	13,000	—	—	(6)
1	27	—	—	(7)
1.42	50.7	3.4	15.8	(8)
—	237[a]	—	31[a]	(9)
0.90	168	4.56	9.6	(10)
1.3	26.8	2.2	0.59	(11)
1	120	3	3	(12)

[a] Rough approximation.

sample fluorescence for background fluorescence and any variations in instrument response or protein fluorescence. The solutions were only exposed to the excitation light for the few seconds required for each measurement.

Four fluorescence quench titrations were performed at each albumin concentration investigated except 100 μmoles/liter, where six titrations were conducted. For a given albumin concentration, the fluorescence quench titrations were identical in that fluorescence measurements were always made at the same total molar drug concentration to total molar protein concentration ratio, D/P. Each sample fluorescence measurement was corrected for the inner filter effect based on the absorbance of the solution at the wavelengths of excitation and emission (16). Three absorbance titrations were performed at each albumin concentration investigated. The absorbance titrations at any given protein concentration were identical to the fluorescence quench titrations at the same protein concentration, in that fluorescence and absorbance measurements were obtained at the same values of D/P. The mean absorbance of the sample solutions at both 292 and 370 nm at each D/P value was used to correct the corresponding fluorescence measurements at the same protein concentration and D/P value.

After correcting for the inner filter effect, each fluorescence measurement was converted to percent initial fluorescence. The mean percent initial fluorescence at each value of D/P at each protein concentration was calculated and plotted as a function of D/P. These quench curves were used to calculate values of r, the ratio of molar concentration of bound ligand to total molar protein concentration, and $[L]$, the molar concentration of free ligand at each protein concentration using both the method of Levine (6) and the method of Steiner *et al.* (15). The values of r and $[L]$ were then used to construct a Scatchard plot (17) based on the following equation:

$$r = \sum_{i=1}^{m} \frac{n_i k_i [L]}{1 + k_i [L]} \qquad \text{(Eq. 1)}$$

Binding constants were obtained by a computer fit (18) of the binding data obtained using the method of Steiner *et al.* (15). Since the method of Levine (6) assumes that essentially no ligand is bound to secondary albumin binding sites until the primary binding site is saturated, the data obtained by this method are treated on the assumption that albumin contains a single binding site for ligand. In this case, a Scatchard plot (17) and linear regression can be used to obtain values of n_1 and k_1 or Eq. 2 (6) can be used to calculate k_1 directly from the quench curve:

$$k_1 = \frac{Q}{(1 - Q)P[(D/P) - Q]} \qquad \text{(Eq. 2)}$$

where: $Q = (F_0 - F)/m$, F_0 = fluorescence at $D/P = 0$, F = fluorescence at a given value of D/P, m = slope of the initial portion of the quench curve, *i.e.*, at low values of D/P, and P = total molar albumin concentration.

Using Eq. 2, a value of k_1 can be calculated for each experimental point on the quench curve that lies above the straight line fitted to the initial portion of the quench curve. Equation 2 assumes that $n_1 = 1$ and that $Q = r$.

RESULTS

The quench curves obtained at each albumin concentration investigated are presented in Fig. 1. For clarity, a few experimental points obtained at the lower albumin concentrations and D/P values >7, and at the higher albumin concentrations and D/P values <1, are not presented in this figure. As expected, the mean percent initial fluorescence at any given D/P value decreases as the albumin concentration increases. The coefficient of variation for the individual values of mean percent initial

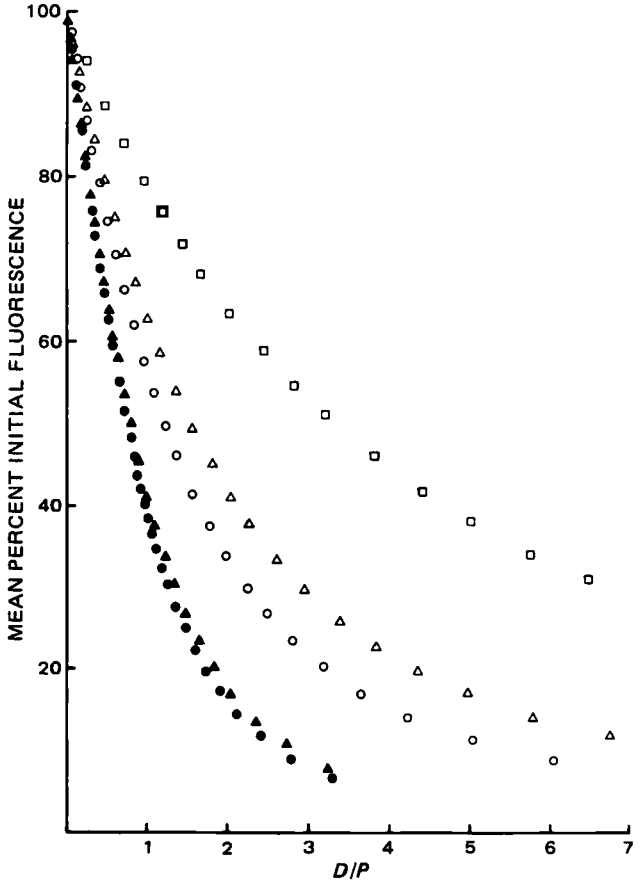

Figure 1—*Fluorescence quench curves obtained for the interaction of furosemide with 1.9 (□), 6.0 (△), 10 (○), 50 (▲), and 100 (●) μmoles/liter of human albumin.*

fluorescence ranged from 0.001 to 0.043 and the standard deviation for these individual values ranged from 0.1 to 0.9 for all but the largest albumin concentration. At an albumin concentration of 100 μmoles/liter, the coefficient of variation for the individual values of mean percent initial fluorescence ranged from 0.001 to 0.104 and the standard deviation for these individual values ranged from 0.1 to 2.5. As a result of the larger data variability observed at an albumin concentration of 100 μmoles/liter, six, rather than four, fluorescence quench titrations were performed at this protein concentration. The larger variability observed at the highest albumin concentration may be due to the larger inner filter effect and/or the smaller decrease in observed fluorescence between additions of furosemide solution. Data could not be obtained at higher protein concentrations due to the large sample absorbance encountered at relatively low D/P values.

Figure 1 shows that the quench curves obtained at the two largest albumin concentrations investigated (50 and 100 μmoles/liter) are identical at low D/P values and are very similar throughout the D/P range investigated. The portion of these curves that is identical represents the percent of initial fluorescence observed when all of the added ligand is bound (19), *i.e.*, a plot of percent initial fluorescence as a function of r. The fact that these two quench curves are very similar at higher D/P values suggests that a larger portion of the quench curve obtained at an albumin concentration of 100 μmoles/liter represents a plot of percent initial fluorescence as a function of r. Therefore, the quench curve obtained at an albumin concentration of 100 μmoles/liter and the method of Steiner *et al.* (15) were used to construct a Scatchard plot (17) of the data obtained at albumin concentrations of 1.9, 6.0, and 10 μmoles/liter. The quench curve obtained at an albumin concentration of 50 μmoles/liter could not be used due to its similarity to the quench curve obtained at an albumin concentration of 100 μmoles/liter.

The Scatchard plot obtained using the method of Steiner *et al.* (15) is presented in Fig. 2. This plot becomes unusual in appearance at values of $r > \sim 1.5$, in that the data obtained at different protein concentrations no longer represent a single curve, and the instantaneous slope of each curve becomes increasingly negative. This shows that the quench curve obtained at an albumin concentration of 100 μmoles/liter does not rep-

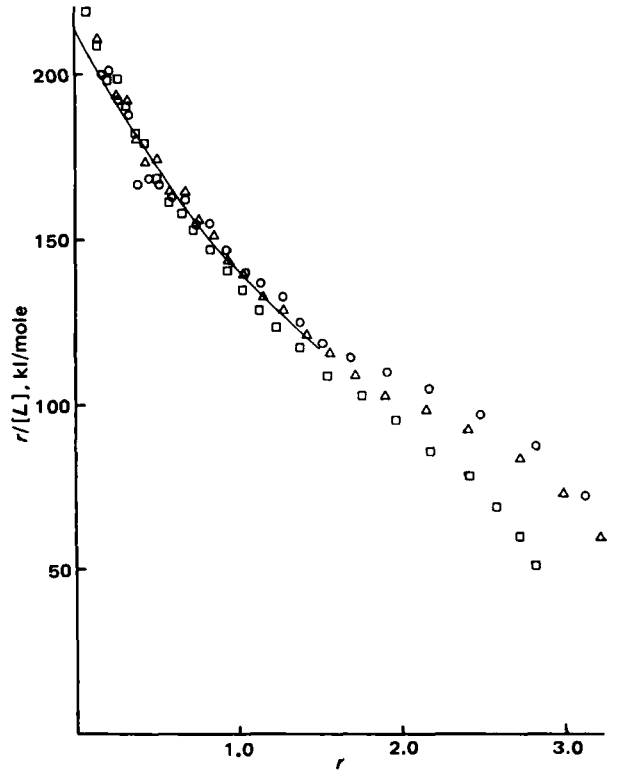

Figure 2—*Scatchard plot obtained for the binding of furosemide by 1.9 (□), 6.0 (△), and 10 (○) μmoles/liter of human albumin using the method of Steiner* et al. *(15).*

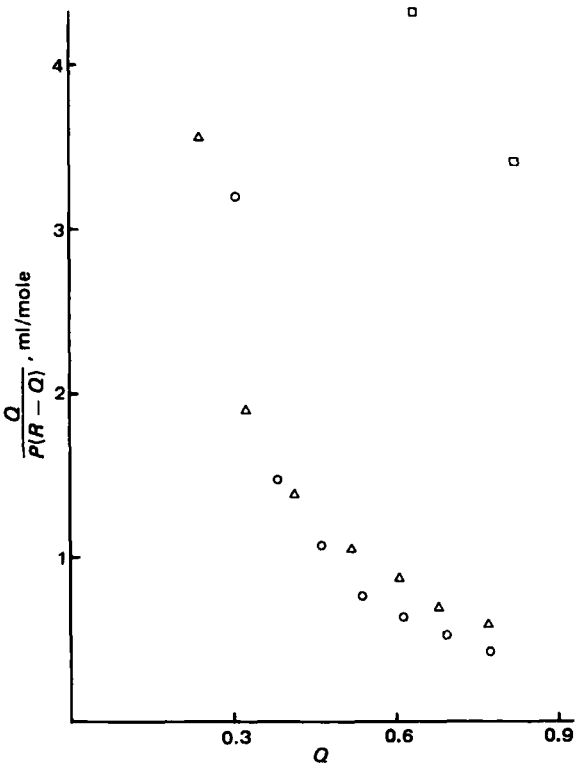

Figure 3—*Scatchard plot obtained for the binding of furosemide by 1.9 (□), 6.0 (△),and 10 (○) μmoles/liter of human albumin using the method of Levine (6).*

resent the stoichiometric binding of ligand at D/P values >1.5. Use of this quench curve at these values results in an overestimate of the affinity of albumin for ligand at higher r values and this results in an increase in the slope of the Scatchard plot at r >1.5. Assuming two classes of binding sites, a fit of the data of r <1.5 presented in Fig. 2 to Eq. 1 yields $n_1 = 0.70$, $k_1 = 166$ kl/mole, $n_2 = 5.5$, and $k_2 = 17.7$ kl/mole. These constants were used to compute the solid line in Fig. 2. The deviation of this line at lower r values results from the computer fit of the data to Eq. 1, rather than to $r/[L]$ as a function of r.

The method of Levine (6) also was used to interpret the quench curves obtained at albumin concentrations of 1.9, 6.0, and 10 μmoles/liter. Using Eq. 2, a value of k_1 was calculated for each experimental point on the quench curve of D/P <1 that lies above the straight line fitted to the initial portion of the quench curve. The results are presented in Table II.

The method of Levine (6) was also used to construct a Scatchard plot (17) of the data obtained at albumin concentrations of 1.9, 6.0, and 10 μmoles/liter. This Scatchard plot is presented in Fig. 3. As discussed, linear regression analysis of the Scatchard plot (17) is used in the method of Levine (6) to obtain values of n_1 and k_1. Values of n_1 and k_1 were not obtained for the data of Fig. 3 due to the nonlinearity of this plot.

Table II—Affinity Constant (k_1) Values Obtained for the Binding of Furosemide by its Primary Site on Human Albumin Using the Method of Levine (6) and Eq. 2

1.9 μmole/liter[a] (m = 25.2)		6.0 μmole/liter[a] (m = 48.4)		10 μmole/liter[a] (m = 55.1)	
D/P	k_1, Ml/mole	D/P	k_1, Ml/mole	D/P	k_1, Ml/mole
0.47	18.8	0.25	4.68	0.31	4.60
0.71	11.8	0.35	2.81	0.40	2.37
0.95	19.0	0.47	2.40	0.51	2.00
		0.60	2.18	0.61	1.64
		0.72	2.21	0.71	1.66
		0.84	2.16	0.82	1.69
		0.99	2.56	0.95	1.86
Mean	16.5		2.72		2.26
SD	4.08		0.898		1.06
CV	0.247		0.330		0.469

[a] Albumin concentration.

DISCUSSION

The quenching of the intrinsic fluorescence of human albumin upon the binding of furosemide was used to study this drug–protein interaction. The quench curves obtained (Fig. 1) show that at the lower albumin concentrations examined, only a few, if any, of the experimental points lie on the quench curve obtained at the largest albumin concentration. This shows that only a small section, if any, of the initial portion of the quench curves obtained at the lowest three albumin concentrations represents the fluorescence observed when all of the added furosemide is bound. Thus, the initial apparently linear portion of the quench curves obtained at albumin concentrations of 1.9, 6.0, and 10 μmoles/liter do not represent the stoichiometric binding of furosemide as is assumed by the method of Levine.

Binding constants for both the primary and secondary binding sites on human albumin for furosemide were determined from the quench curves using the method of Steiner *et al.* (15). The quench curve obtained at an albumin concentration of 100 μmoles/liter through a D/P value of 1.5 was used as the stoichiometric curve. If any portion of this curve does not represent the stoichiometric binding of furosemide, the binding constants obtained will be too high rather than too low. The values of the binding constants obtained in this study using the method of Steiner *et al.* (15) are similar to the values obtained previously (Table I) with the exception of the k_1 value obtained using the method of Levine (6). The lower value of n_1 and the higher value of n_2 obtained in the present study is at least partially due to the limited range of r values that could be obtained.

The quench curves obtained at albumin concentrations of 1.9, 6.0, and 10 μmoles/liter (Fig. 1) were also analyzed by the method of Levine (6) using both Eq. 2 and a Scatchard plot (17) (Fig. 3). The quench curves obtained at albumin concentrations of 50 and 100 μmoles/liter were not analyzed by this method, since they represent the stoichiometric binding of furosemide. The values of k_1 obtained using Eq. 2 are presented in Table II. For each albumin concentration examined, the k_1 value obtained appears to be dependent on the experimental point (D/P) used in the calculation of k_1. As the D/P value increases, the value of k_1 appears to decrease to some minimum value and then increase. The value of k_1 does not vary in the random fashion expected due to experimental error. This apparent dependence of k_1 on D/P implies that one or more of the assumptions of this method of data analysis is invalid for this particular drug–protein interaction. The coefficient of variation values for the mean

values of k_1 are very high relative to the coefficient of variation values obtained for the individual experimental points of the quench curve. The nonlinearity of the Scatchard plot obtained using this method of data analysis (Fig. 3) also implies that one or more of the assumptions of this method is invalid for this particular drug–protein interaction.

The Scatchard plot previously obtained by this method for the binding of furosemide by human albumin was not published (6). Thus, the experimental data suggest that one or more of the assumptions on which the method of Levine is based is invalid as was previously suggested (13) based on theoretical considerations.

The mean value of k_1 ($1.65 \times 10^7\ M^{-1}$) obtained using Eq. 2 and an albumin concentration of 1.9 μmoles/liter is very similar to the value of $1.3 \times 10^7\ M^{-1}$ previously obtained (6) using the same albumin concentration, experimental conditions, and method of data analysis. As shown in Table II, the mean value of k_1 decreased and the value of m increased as the albumin concentration increased. This is to be expected, since the initial apparently linear portion of the quench curve obtained at each protein concentration does not represent the stoichiometric binding of the ligand. This shows how difficult it is to determine the stoichiometric region of a quench curve when data are collected at a single protein concentration. The method of Levine assumes that this stoichiometric region can be determined using a single protein concentration.

Based on these results, the reason for the large value of k_1 previously obtained (6) for the binding of furosemide by human albumin using the new method of data analysis is not that other experimental methods, such as equilibrium dialysis, resulted in erroneously low values of this constant. Since the same set of data was analyzed by two different methods in the present investigation, the large difference in the values of k_1 obtained cannot be attributed to a difference in experimental conditions. Instead, the results of this study show that the new method of data analysis (6) overestimates the value of k_1 in this particular drug–protein interaction. As discussed previously (13), the method of Levine will, theoretically, overestimate the value of k_1 when the protein contains more than one binding site and has a low value of n_1k_1/n_2k_2. The experimental results of the present work support these theoretical findings. This overestimation of k_1 also results from the inaccurate determination of the stoichiometric region of the fluorescence quench curve obtained at a single albumin concentration.

As discussed previously (13), the method of Levine (6) has several advantages over the method of Steiner *et al.* (15) and results in accurate estimates of k_1 for certain ligand–protein interactions, such as the binding of bilirubin by human albumin. However, the method of Levine will overestimate the value of k_1 when the protein contains more than one binding site for the ligand and the value of n_1k_1/n_2k_2 for the interaction is low. The binding of furosemide by human albumin is an example of such an interaction. For this reason, the binding constant obtained using this new method of data analysis (6) should always be verified by an additional experimental method. When a drug–protein interaction is being investigated for the first time, and the method of intrinsic protein fluorescence quenching is the only experimental method used, the data should always be analyzed by the method of Steiner *et al.* (15).

REFERENCES

(1) J. J. Vallner, *J. Pharm. Sci.*, **66**, 447 (1977).

(2) W. J. Jusko and M. Gretch, *Drug Metab. Rev.*, **5**, 43 (1976).

(3) D. N. Wade, *Adv. Pharmacol. Ther.*, **7**, 101 (1979).

(4) J. Koch-Weser and E. M. Sellers, *N. Engl. J. Med.*, **294**, 526 (1976).

(5) R. E. Cutler and A. D. Blair, *Clin. Pharmacokinet.*, **4**, 279 (1979).

(6) R. L. Levine, *Clin. Chem.*, **23**, 2292 (1977).

(7) L. F. Rasmussen and R. Wennberg, *Pediatr. Res.*, **10**, 334 (1976).

(8) J. Prandota and A. W. Pruitt, *Clin. Pharmacol. Ther.*, **17**, 159 (1975).

(9) F. Andreasen and P. Jakobsen, *Acta Pharmacol. Toxicol.*, **35**, 49 (1974).

(10) B. Sebille, N. Thuaud, and J. P. Tillement, *J. Chromatogr.*, **167**, 159 (1978).

(11) M. Nakano, K. Fujii, and S. Goto, *Chem. Pharm. Bull.*, **27**, 101 (1979).

(12) M. Bordeaux-Pontier, M. Chauvet-Deroudihle, M. Sarrazin, and E. Briand, *J. Chim. Phys.*, **75**, 973 (1978).

(13) D. L. Parsons, *Clin. Chem.*, **26**, 1869 (1980).

(14) G. Sudlow, *Adv. Pharmacol. Ther.*, **7**, 113 (1979).

(15) R. F. Steiner, J. Roth, and J. Robbins, *J. Biol. Chem.*, **241**, 560 (1966).

(16) C. F. Chignell, *Methods Pharmacol.*, **2**, 33 (1972).

(17) G. Scatchard, *Ann. N.Y. Acad. Sci.*, **51**, 660 (1949).

(18) C. M. Metzler, Technical Report 7296/69/7292/005, The Upjohn Co., Kalamazoo, Mich. (1969).

(19) R. F. Chen, in "Fluorescence Techniques in Cell Biology," A. A. Thaer and M. Sernetz, Eds., Springer-Verlag, New York, N.Y., 1973, pp. 273–282.

ACKNOWLEDGMENTS

The author wishes to thank Fredrich Harding and Charles Steiner for their technical assistance in the collection of preliminary data. The author also wishes to thank Hoechst-Roussel Pharmaceuticals, Inc. for the gift of furosemide.

Thermal and Photolytic Degradation Studies of Promethazine Hydrochloride: A Stability-Indicating Assay

S. STAVCHANSKY *x, J. E. WALLACE ‡, and P. WU *

Received February 11, 1982, from the *University of Texas at Austin, College of Pharmacy, Division of Pharmaceutics, Drug Dynamics Institute, Austin, TX 78712, and the ‡University of Texas Health Science Center, Department of Pathology, San Antonio, TX 78284. Accepted for publication May 25, 1982.

Abstract □ A stability-indicating GLC method for the analysis of promethazine hydrochloride in polyethylene glycol delivery systems is reported. This method is capable of distinguishing the intact drug from its thermal and photodegradation products. A linear relationship between peak height ratio (promethazine–promazine) and promethazine concentration is found up to a concentration of 600 μg/ml. Kinetic studies were performed to determine the photolytic and thermal degradation rates of promethazine hydrochloride as a function of pH. The activation energies at pH 2.98, 3.94, and 5.12 were obtained from linear Arrhenius plots and were found to be 6601, 5888, 5570 cal/mole, respectively. The first-order rate constant increased with increasing pH. The photolytic degradation of promethazine hydrochloride does not follow simple first-order kinetics.

Keyphrases □ Promethazine hydrochloride—thermal and photolytic degradation studies, stability-indicating GLC assay □ Thermal degradation—promethazine hydrochloride, photolytic degradation, stability-indicating GLC assay □ Photolytic degradation—promethazine hydrochloride, thermal degradation, stability-indicating GLC assay

Evaluation of the stability of promethazine hydrochloride in rectal delivery systems containing polyethylene glycols requires an assay method that is specific for the drug in the presence of degraded products and vehicles. There have been several spectrophotometric methods developed (1–3), but none of them has adequate specificity for stability testing. A direct GLC method without prior extraction has been used (4), but in the presence of polyethylene glycol, the flame ionization detectors are adversely affected. In addition, the injection of water and ethanol into the gas chromatographic system causes a rapid column deterioration. In the present investigation, a GLC method with a simple organic phase extraction was developed to specifically determine promethazine hydrochloride in polyethylene glycol suppositories undergoing stability testing.

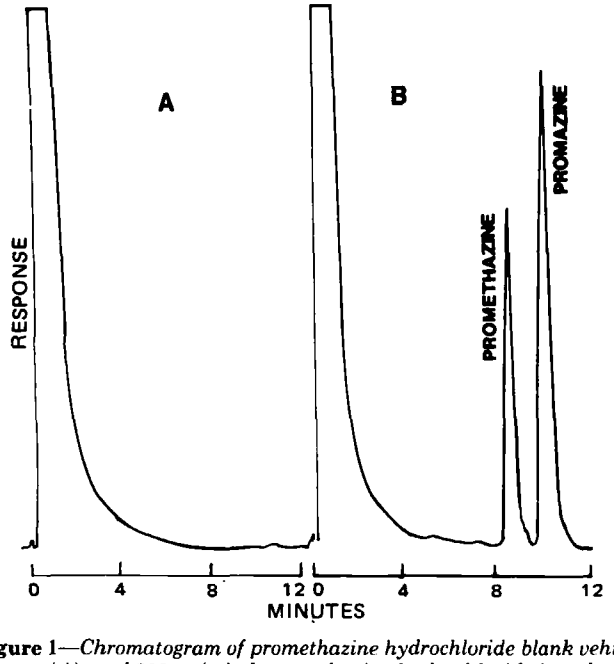

Figure 1—*Chromatogram of promethazine hydrochloride blank vehicle extract (A), and 300 μg/ml of promethazine hydrochloride in polyethylene glycol aqueous solution in the presence of promazine as internal standard, (B).*

EXPERIMENTAL

Materials—Promethazine hydrochloride[1] and promazine hydrochloride[2] were used as received. All solvents and chemicals were commercial analytical grade[3]. Precoated silica gel plates[4] were used.

Chromatographic Conditions—A dual-column GC[5] with a flame ionization detector was used. A silylated, coiled glass column, 183 cm in length, 0.6-cm o.d., 0.4-cm i.d., was packed with 3% OV-17 on 100–120 mesh Gas Chrom Q[6]. The column was conditioned for 36 hr at 280° and was treated with a silylating agent, *N,O*-bis(trimethylsilyl)acetamide[7]. Nitrogen carrier gas flow, hydrogen flow, and air flow were 37, 37, and 350 ml/min, respectively. The column, detector, and sample injection port temperatures were 250, 300, and 260°, respectively.

Polyethylene Glycol Vehicle Solution—A stock solution was prepared using the excipients and preservatives employed in the manufacture of the suppositories. Appropriate dilutions were made with deionized water. The resulting solutions reflect the actual amount of each of the ingredients in the formulation.

Internal Standard Solution—Fifty milligrams of promazine hydrochloride[2] was placed in a 100-ml volumetric flask and appropriately diluted with deionized water.

Standard Solutions—Sixty milligrams of promethazine hydrochloride was placed in a 100-ml volumetric flask and diluted with deionized water. Two, 4, 6, 8, and 10 ml of the above solution were placed in five 10-ml volumetric flasks and diluted with deionized water. The concentration of promethazine hydrochloride was 120, 240, 360, 480, and 600 μg/ml, respectively.

Standard Curve of Promethazine Hydrochloride in Water—One milliliter of each standard solution was placed in a 12-ml centrifuge tube and to each tube was added 1.0 ml of the internal standard and 0.3 ml of 5 *N* NaOH. The centrifuge tube was mixed thoroughly with a vortex mixer for 30 sec. Then 4.0 ml of *n*-hexane was added to the tube and the tube placed on the vortex mixer for 1 min. The mixture was centrifuged at 2000 rpm for 2 min. Three microliters of the hexane layer was injected directly into the GC.

Standard Curve of Promethazine Hydrochloride in Polyethylene Glycol Vehicle—The procedures were the same as for the determination of promethazine hydrochloride in water, except for the addition of 0.1 ml of the polyethylene glycol vehicle solution to each centrifuge tube prior to extraction. This volume of solution represents the amount of each of the excipients in each polyethylene glycol suppository after the suppository has been dissolved for analytical purposes. This procedure compares with the extraction of promethazine hydrochloride from a suppository.

[1] Napp Chemicals, Inc., Ladi, N.J.
[2] Wyeth Labs, Inc., Philadelphia, Pa.
[3] Fisher Scientific Co., Fair Lawn, N.J.
[4] Analabs, Inc., North Haven, Conn.
[5] Tracor Instruments Inc., Austin, Tex.
[6] Supelco, Inc., Bellefonte, Pa.
[7] Pierce Chemical Co., Rockford, Ill.

0022-3549/83/0500-0546$01.00/0

Table I—Standard Curve of Promethazine Hydrochloride in Water and in Polyethylene Glycol Vehicle

Concentration, μg/ml	n	Water		Polyethylene Glycol Vehicle	
		Mean Peak Height Ratio	CV, %	Mean Peak Height Ratio	CV, %
120	3	0.290	4.30	0.280	3.37
240	3	0.580	1.40	0.580	0.81
360	3	0.860	0.97	0.850	1.11
480	3	1.13	0.42	1.17	3.04
600	2	1.38	3.62	—	—

Thermal Degradation of Promethazine Hydrochloride—To test the validity of the assay for promethazine in the presence of its degradation products, the thermal degradation of promethazine hydrochloride in aqueous solution was performed. Promethazine hydrochloride, 5 g, was dissolved in 100 ml of water; oxygen was then bubbled through the solution for 30 min. The solution was placed in a screw-capped light-proof amber bottle saturated with oxygen and kept at 65° for 5 days. The mixture was cooled, made alkaline with 1 *N* NaOH, and extracted with methylene chloride. The aqueous layer was acidified with 1 *N* H_2SO_4 and extracted with methylene chloride (5).

Both organic phases were evaporated to dryness in the dark under a nitrogen stream to afford a solid residue. Approximately 100 mg of the residue was dissolved in 2 ml of dichloromethane. A total of 9 μl was applied to a silica gel G.F. TLC plate[4], (0.25 mm, 5 × 20 cm) and chromatographed in the dark (acetone–6*N* ammonia; 100:2).

The solvent was evaporated and the plate was placed under a short-wavelength UV light for visualization. The spots were scraped individually and placed in a conical centrifuge tube with a glass stopper. One milliliter of dichloromethane was added to each tube and the mixture was agitated with a vortex mixer for ~1 min. The tube was centrifuged and the supernatant was transferred to a small test tube and evaporated to dryness under a nitrogen stream. The residue was dissolved with 1 ml of methanol. One microliter of this solution was injected into the GC.

To investigate the influence of pH, 40 ml of 0.05% promethazine hydrochloride in Sörensen citrate buffer solutions (pH 2.98, 3.94, and 5.12) was placed in 100-ml light-proof amber volumetric flasks and kept at temperatures of 60, 70, 80, and 90°, accurate to within ±0.2°, in a thermostatically controlled oil bath. A solution containing 0.1% of EDTA [tetrasodium(ethylenedinitrilo)tetraacetate] was added to the promethazine buffer solutions before heating. The solutions were adjusted to the same ionic strength ($\mu = 0.2$) with potassium chloride. The pH of the solutions was measured at the beginning and at the end of the heating periods. Then 1 ml of the test solution was withdrawn from the flasks, immediately cooled, and analyzed as previously described. These samples were not chromatographed by TLC. Immedately after the sample was withdrawn from the volumetric flask, the flask was recharged with a stream of oxygen in order to maintain excess oxygen tension.

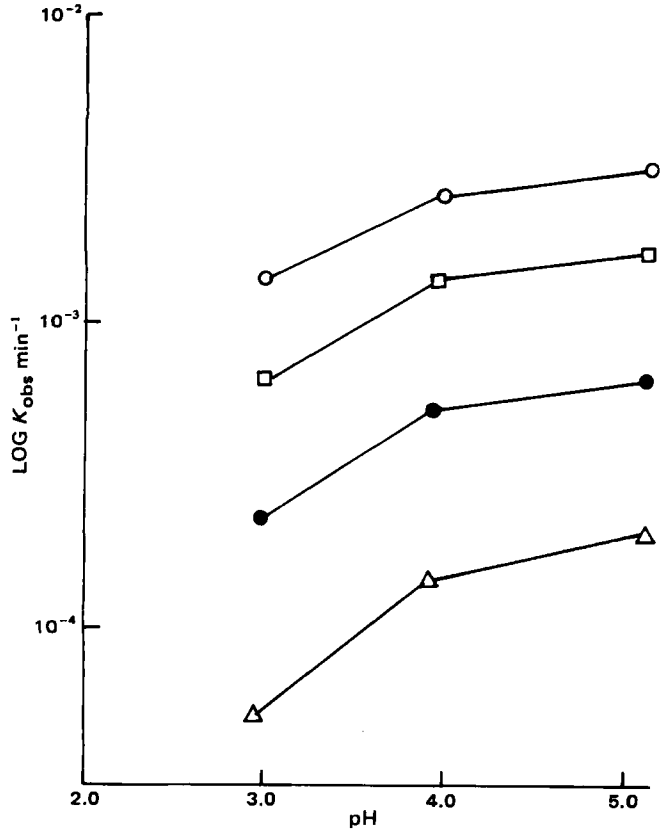

Figure 2—*Influence of pH on the thermal degradation rates of promethazine hydrochloride. Key:* (△) *60°*, (●) *70°*, (□) *80°, and* (○) *90°.*

Table II—Regression Coefficients for Promethazine Hydrochloride Standard in Water

Regression Coefficients	With Polyethylene Glycol	Without Polyethylene Glycol
n	14	12
a (y-intercept)	0.0256	0.0133
b (slope)	0.0022	0.0025
R	0.998	0.998

Photolytic Degradation of Promethazine Hydrochloride—Promethazine hydrochloride (0.3% w/v) was dissolved in water. The solution was placed in a quartz reactor tube[9], length 43 cm, 2.6-cm o.d. and 2.4-cm i.d., which was equipped with a water cooling tube, 1.2-cm o.d. and exposed to UV light (300 nm) by means of a photolytic reactor[8] at 10° for 74 hr.

Following the exposure time, 70 ml of the solution was freeze-dried. The residue was dissolved in 7 ml of methanol. Fifty microliters of the solution was applied to a silica gel G.F. TLC plate (0.25 mm, 10 × 20 cm^2) and chromatographed using acetone–methanol–6 *N* NH_3 (140:60:1) as the mobile phase.

The solvent was evaporated and the plate was placed under a short wavelength UV light for visualization. The GC specimen was prepared

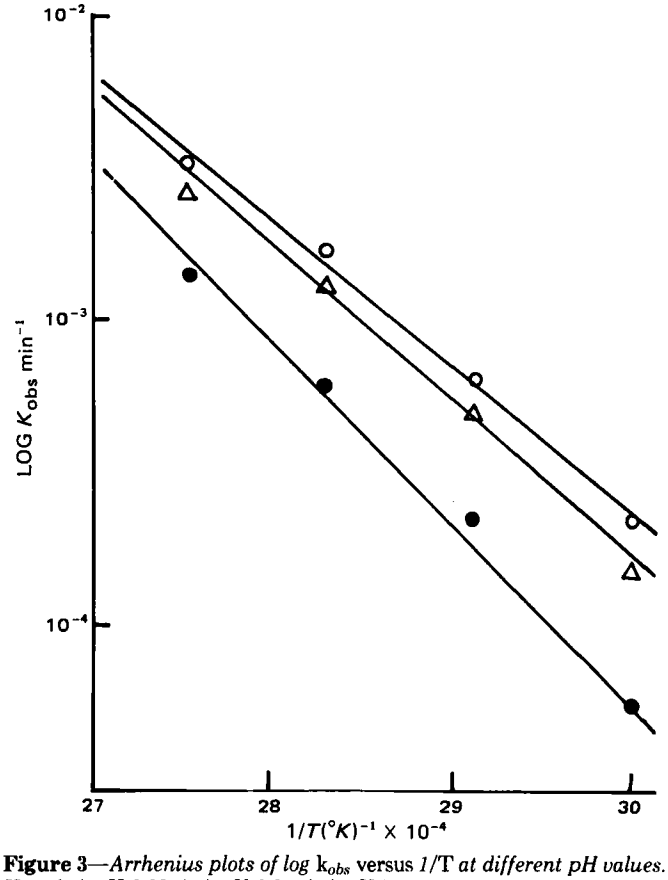

Figure 3—*Arrhenius plots of log* k_{obs} versus *1/T at different pH values. Key:* (●) *pH 2.98*, (△) *pH 3.94*, (○) *pH 5.12.*

[8] The South New England Ultraviolet Co.

Table III—The Apparent Pseudo First-Order Rate Constants of Thermal Degradation of Promethazine Hydrochloride at Different pH and Temperatures

Temperature	pH	Rate Constants[a], $min^{-1} \times 10^5$	Half-Life, hr
60°	2.98	5.38 (0.41)[b]	214.7
	3.94	14.8 (0.66)	78.3
	5.12	21.1 (0.49)	54.7
70°	2.98	22.6 (0.67)	51.1
	3.94	52.9 (2.4)	21.8
	5.12	65.4 (4.1)	17.7
80°	2.98	63.1 (1.7)	18.3
	3.94	142.9 (3.8)	8.1
	5.12	172.7 (3.5)	6.7
90°	2.98	140.6 (5.1)	8.2
	3.94	263.8 (4.9)	4.4
	5.12	320.9 (23.7)	3.6

[a] k_{obs}. [b] Data in the parentheses represent the standard deviations.

as described under *Thermal Degradation of Promethazine HCl.* One microliter of solution was injected into the GC.

One hundred milliliters of 0.05% promethazine hydrochloride–Sörensen buffer solutions (pH 2.93, 3.94, and 5.12) was placed in quartz reactor tubes as described above and exposed to UV light (330 nm) by means of a photolytic reactor at 30 ± 5°. EDTA 0.1% was added to the promethazine–buffer solutions and the ionic strength adjusted to μ = 0.2 with potassium chloride. The pH of the solutions was measured at the beginning and at the end of the exposure periods. Periodically, 1 ml of test solution was withdrawn from the flasks, immediately cooled, and analyzed as previously described.

RESULTS AND DISCUSSION

Promethazine and promazine gave retention times of 8.5 and 10.0 min, respectively (see Fig. 1). Blank vehicle extracts yielded no interferences as illustrated in the same figure.

Quantitation of promethazine hydrochloride in water was obtained from a standard curve in which the peak height ratio (promethazine hydrochloride–promazine hydrochloride) was plotted against the promethazine hydrochloride concentration. The results are shown in Table I. There is a linear relationship between peak height ratio of promethazine hydrochloride to promazine hydrochloride and the concentration of promethazine hydrochloride in water over the range of 120–600 μg/ml. The least-squares regression equation for the curve is $y = 0.0023x + 0.0256$ and the correlation coefficient is 0.998. The results of nine replicate assays carried out over several days indicate that the assay method has adequate precision. The coefficients of variation of the assays are 1.4 and 1.1% in the presence and absence of polyethylene glycol vehicle.

The results of the quantitation of promethazine hydrochloride in water in the presence of polyethylene glycol vehicles are shown in Table I. There is a linear relationship between peak height ratio of promethazine hydrochloride to promazine hydrochloride and the concentration of promethazine hydrochloride with polyethylene glycol vehicle over the range of 120–480 μg/ml. The least-squares regression equation is $y = 0.0025x - 0.0133$, and the correlation coefficient is 0.998.

The regression fits of promethazine hydrochloride standard in water with and without polyethylene glycol vehicles are shown in Table II. The slope and intercept of the standard curves with and without polyethylene glycol vehicles were not significantly different (F test, $p > 0.05$).

The thermally degraded promethazine hydrochloride solution was separated with the TLC system previously described. Seven spots with R_f values of 0.0, 0.10, 0.16, 0.41, 0.57, 0.64, and 0.73, visualized under UV light, were obtained. The R_f value of promethazine was 0.4 which was confirmed with pure promethazine applied on the same TLC plate. The extracts of each spot were injected into the GC. None of the spots present in the TLC system interfered with the GLC procedure for promethazine and promazine. Only spots with R_f values of 0.73 and 0.41 showed significant peaks in the GC with retention times of 5.99 and 7.39 min, respectively.

Table IV—Photolytic Degradation of Promethazine Hydrochloride at Different pH, at 30°

Degradation, hr	% of Promethazine Hydrochloride Remaining					
	pH 2.98		pH 3.94		pH 5.12	
0	100.0	100.0	100.0	100.0	100.0	100.0
0.5	82.4	84.3	85.0	—	85.9	87.5
1.0	81.1	81.2	83.7	—	81.4	85.0
2.0	78.2	79.2	—	—	79.5	81.8
3.0	—	—	74.9	69.8	—	—
4.0	72.7	75.5	—	—	73.8	74.5
7.0	63.8	66.4	67.3	54.8	65.2	63.5
12.0	51.7	54.2	53.8	42.4	55.3	53.3
24.0	27.7	32.7	30.7	27.9	36.1	31.8
36.0	10.7	15.2	13.0	6.4	20.2	14.6
48.0	1.6	4.0	3.1	0.73	8.8	4.1

The degradation of promethazine hydrochloride from pH 2.98 to 5.12 followed pseudo first-order kinetics at constant pH, temperature, and ionic strength. Linear semilogarithmic plots of percent of promethazine hydrochloride remaining *versus* time in three different pH-value buffer solutions at 60, 70, 80, and 90° were obtained. The pseudo first-order rate constants, k_{obs}, for each pH value at four different temperatures are given in Table III.

Arrhenius plots were constructed and found to be straight lines as illustrated in Fig. 2. From the slopes of the lines, the apparent activation energies of the thermal degradation reactions at pH 2.98, 3.94, and 5.12 were calculated to be 6601, 5888, 5570 cal/mole, respectively.

The influence of pH on degradation rate of promethazine hydrochloride is shown in Fig. 3. The rate constant increased with increasing pH in this experimental range.

The photolytically degraded promethazine hydrochloride was separated by the TLC system previously described. Five spots, R_f 0.81, 0.58, 0.52, 0.44, and 0.00, were obtained. Only the spot with R_f 0.44, which represents promethazine, gave a good response by GC. None of the other spots interfered with the GLC procedure for promethazine and promazine.

The photolytic degradation rate of promethazine hydrochloride was studied in three buffer solutions (pH 2.98, 3.94, *and* 5.12). The results are shown in Table IV. No linear relationship could be found from the logarithmic percent of promethazine remaining *versus* time plots at three different pH values at 30°. The photolytic degradation of promethazine hydrochloride under intense UV light did not follow simple kinetics. These results are in agreement with a previous report (6).

In summary, a GLC method with an organic phase extraction was developed and is being used to specifically determine promethazine hydrochloride in polyethylene glycol suppositories undergoing stability testing.

REFERENCES

(1) A. Felemeister and C. A. Discher, *J. Pharm. Sci.*, **53**, 756 (1964).

(2) A. Felemeister, R. Schaubman, and H. Howe, *ibid.*, **54**, 1589 (1965).

(3) J. A. Ryan, *J. Am. Pharm. Assoc., Sci. Ed.*, **48**, 240 (1959).

(4) B. J. Meakin, D. J. G. Davies, N. Cox, and J. Stevens, *Analyst (London)*, **101**, 720 (1976).

(5) W. J. M. Underberg, *J. Pharm. Sci.*, **67**, 1128 (1978).

(6) N. Cox, B. J. Meakin, and D. J. G. Davies, *J. Pharm. Pharmacol.*, 28, suppl. 45 (1976).

ACKNOWLEDGMENTS

Supported by a grant from Alcon Laboratories, Inc., Fort Worth, Texas.

Aspects of the Chemical Stability of Mitomycin and Porfiromycin in Acidic Solution

W. J. M. UNDERBERG * **and H. LINGEMAN**

Received August 11, 1981 from the *Pharmaceutical Laboratory, Department of Analytical Pharmacy, State University of Utrecht, Catharijnesingel 60, 3511 GH Utrecht, The Netherlands.* Accepted for publication May 28, 1982.

Abstract □ Aspects of the degradations of mitomycin and porfiromycin were studied. The initial degradation processes of the compounds in an acidic medium were investigated. Influences of pH, buffers, and other additives such as halogenides and dioctyl sodium sulfosuccinate [sodium 1,4-bis(2-ethylhexyl)sulfosuccinate] were studied. The hydrogen ion catalyzes the degradation of both the uncharged and the protonated species. Anions also promote the degradation of the compounds in an acidic medium. Rate constants for all of the catalytic reactions could be determined. From the pH profiles, after correction for buffer influences, accurate pK_a values for the aziridine nitrogens could be obtained. The protective influence of the dioctyl sulfosuccinate ion could be explained. From the data obtained a plausible mechanism for the initial acidic degradation reactions was developed.

Keyphrases □ Degradation—in acidic solution, mitomycin, porfiromycin, pK_a determination □ Mitomycin—degradation in acidic solution, rate constant determination □ Porfiromycin—degradation in acidic solution, rate constant determination □ pK_a determination—aziridine nitrogens, mitomycin, porfiromycin

Mitomycin (I), an important antitumor antibiotic originating from *Streptomyces caespitosus* (1), appears to be unstable in solution. Several investigators studied aspects of the degradation of I and of porfiromycin (II), which differs from I only in the methyl substituent on the aziridine nitrogen. The structure of I was determined by studying the products resulting from acid hydrolysis (2). Knowledge of the physicochemical properties of I was expanded by synthesizing derivatives and studying the acid hydrolysis (3). From these studies it became obvious that the degradations of I and II follow very complex patterns. Suggestions that the aziridine ring opens prior to the rapid solvolytic cleavage of the 9α-methoxyl group in acidic media have been reported previously (2). The degradation of II was studied using spectrophotometric techniques and the appearance of 12 different products during acidic and alkaline hydrolysis were reported (4, 5), in general agreement with other sources (2, 3). Kinetic data of the degradative transformation of II were also presented (4, 5). Most degradation processes followed pseudo first-order kinetics.

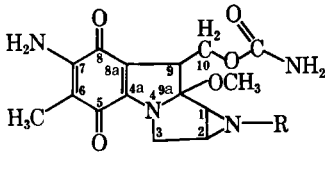

I: R = H
II: R = CH_3

The acid catalysis of the degradation of protonated II has a smaller specific rate constant than that of the nonprotonated species. This results in an estimated pK_a of the protonated group in II of ~1.5. Furthermore, a study of the influence of buffers on the degradation led to the conclusion that buffer components such as $H_2PO_4^-$ and CH_3COOH have catalytic effects on certain steps in the degradation process. Indications were found for both general acid and specific acid–base catalysis on the solvolysis. The primary degradation mechanism is the hydrolysis of the fused aziridine ring, while mild alkaline conditions lead to substitution of the amino group attached to the quinoid ring by a hydroxyl group (5). Although data on the degradation of I and II appear in the literature, no systematic study is available which includes the influences of external factors (ionic strength, buffer components, *etc.*). The present study was undertaken to elucidate the mechanism of the primary degradation of I and II in acidic solution and to establish the influence of a number of external factors on the process.

During previous work on the physicochemical properties of I and II, pK_a values of several groups in the molecules were determined (6). To complete the prototropic characterization of the compounds, more accurate pK_a values of the aziridine nitrogen in I and II will be presented as a result of a closer look at the kinetics of the initial acidic degradation.

EXPERIMENTAL

Materials—Mitomycin[1] and porfiromycin[2] were used as supplied. All other materials were reagent grade, and deionized water was used throughout.

Methods—*Kinetic Studies of I and II Degradation*—The appropriate compound was dissolved in methanol to a concentration of 3×10^{-3} *M*. This was used as the stock solution. For stability tests the stock solution was diluted with buffer solutions at the appropriate pH (after addition of any other additive) to a concentration of 3×10^{-5} *M*. The degradation of the compound was observed by monitoring the absorbance at 363 nm (4, 5) using an absorption spectrophotometer with an automatic cell positioner[3]. All measurements were performed at 40 ± 1°. The pH was measured with a glass-reference electrode using an appropriate pH meter[4]. Absorption spectra were taken with a recording spectrophotometer[5]. Calculation of the first-order rate constants were done using plots of log (percent undegraded compound) *versus* time.

Assay of I and II—The percentage of remaining I and II during the degradation, in general, can be calculated from the relationship:

$$\% \text{ undegraded I or II} = \frac{A_t}{A_0} \times 100 \qquad \text{(Eq. 1)}$$

in which A_t is the absorbance at 363 nm at time t and A_0 is the absorbance at time zero. Equation 1 is valid when the resulting absorbance (A_∞) after completion of the degradation approaches zero.

In the case of the degradation of the mitosanes, however, the primary degradation product in acidic medium has an absorbance that is not negligible. Exact measurements of this absorbance revealed A_∞ to be 0.18

[1] Supplied by Bristol Myers B. V., Bussum, The Netherlands.
[2] Supplied by Cyanamid, Pearl River, N.Y.
[3] Shimadzu UV-140 Double Beam Spectrophotometer with ACP-140 Cell Positioner.
[4] Metrohm Herisau E516 Titriskop pH meter.
[5] Shimadzu UV-200 Double Beam Spectrophotometer with Kipp BD 40 Recorder.

0022-3549/83/0500-0549$01.00/0

Table I—Determination of k_{obs} of the Degradation of I at Different Acidities and Total Phosphate Concentrations at 40° [a]

H_0/pH	Total Phosphate Concentration			
	10^{-2} M	5×10^{-2} M	10^{-1} M	5×10^{-1} M
−1.02	7.1×10^{-2}(−1.15)	7.2×10^{-2}(−1.14)	8.0×10^{-2}(−1.09)	7.4×10^{-2}(−1.13)
0.37	1.5×10^{-2}(−1.81)	1.5×10^{-2}(−1.81)	1.4×10^{-2}(−1.84)	1.4×10^{-2}(−1.84)
2.16	8.2×10^{-3}(−2.08)	8.3×10^{-3}(−2.08)	8.5×10^{-3}(−2.07)	9.6×10^{-3}(−2.02)
3.16	2.4×10^{-3}(−2.62)	3.1×10^{-3}(−2.50)	3.8×10^{-3}(−2.42)	5.5×10^{-3}(−2.26)
4.64	6.0×10^{-5}(−4.22)	1.1×10^{-4}(−3.95)	1.4×10^{-4}(−3.85)	3.4×10^{-4}(−3.47)

[a] Table values expressed as k_{obs} in sec^{-1} (log k_{obs}).

A_0. A first approximation of the exact percentage of the undegraded compound was made by modifying Eq. 1 to:

$$\% \text{ undegraded I or II} = \frac{A_t - \left(\frac{A_0 - A_t}{A_0}\right) A_\infty}{A_0} \times 100 \qquad \text{(Eq. 2)}$$

Four repetitions of this approximation led to a refinement of Eq. 2 to:

$$\% \text{ undegraded I or II} = \frac{A_0^3(A_t - A_\infty)(A_0 + A_\infty) + A_0(A_0 + A_\infty)(A_t - A_\infty)A_\infty^2 + A_t(A_\infty^4)}{A_0^5} \times 100 \qquad \text{(Eq. 3)}$$

which has been used to calculate the percent undegraded compound as a function of time.

RESULTS

Degradation Kinetics of I and II in Acidic Solution—Studies on the stability of II in both acidic and alkaline solutions have been published (4, 5). The structures of a number of degradation products were determined, the pK_a of the aziridine nitrogen was estimated, rate constants for the degradation in acidic as well as in alkaline solution were determined, and an overall mechanism for the degradation of II was described. The influence of several buffer components on the degradation was also studied. Some data on the kinetics of the degradation of I have been published (7). So far no data are available on the mechanism of the initial degradation steps of I and II nor the nature of the buffer influences on the degradation. Determination of the exact pH profiles for the degradation of both compounds should lead to more accurate pK_a values for the aziridine nitrogen.

Standard Deviation in k_{obs}—The standard deviation in the overall rate constant, k_{obs}, for degradation of I in an acid solution was determined at pH 3.0 and buffer concentration 10^{-2} M total phosphate. At 40 ± 1° all experiments showed linearity between log [I] and time, indicating the process as pseudo first-order, which is in agreement with the literature data (2, 4, 5, 7). The value of k_{obs} (and log k_{obs}) and the standard deviation, calculated from 16 observations, is $2.3 \pm 0.1 \times 10^{-3}$ sec^{-1} (and −2.64 ± 0.03).

pH Profiles for the I and II Degradations—In unbuffered solutions pH values of partially degraded solutions of I will differ from the starting value due to the disappearance of a compound with pK_a ~1.5 and the appearance of a compound with pK_a ~7. Starting at pH 5.0, for instance, a solution with [I] = 3.0×10^{-5} M, after being kept at 40° for 4 hr, has a pH of 5.6. This pH shift results in a change in k_{obs}.

To keep the pH constant during the process, buffer solutions of various compositions and concentrations were used. Since the influences of buffer components were already recognized (4), accurate pH profiles for the degradation processes have to be corrected for these influences. For these corrections k_{obs} was determined at several H_0/pH values. In the H_0/pH region <3.0, the pH was adjusted with perchloric acid and various concentrations of sodium biphosphate were added. At pH values >3.0, the pH was adjusted using various concentrations of sodium biphosphate and dropwise addition of either dilute perchloric acid or sodium hydroxide. At each pH value and each phosphate concentration, k_{obs} was determined (Table I). From Table I it becomes clear that at pH <2 the influence of phosphate or phosphoric acid on k_{obs} becomes negligible. At pH >3 this influence is very important.

Considering the reported value for the pK_a of I of ~1.5 (4) at pH >3.5, the compound should be exclusively in the unprotonated form. In that case k_{obs} can be expressed as:

$$k_{obs} = k_0^I + k_H^I[H^+] + k_{buffer}^I[\text{buffer}] \qquad \text{(Eq. 4)}$$

Table II—Rate Constants for Catalyzed Degradation Reactions of I and II at 40°

Rate Constant	I	II
k_0^I	~1×10^{-6} sec^{-1}	~6×10^{-6} sec^{-1}
$k_{H^+}^{IH^+}$	1.0×10^{-2} $mole^{-1}$ sec^{-1}	5.7×10^{-3} $mole^{-1}$ sec^{-1}
$k_{H_3PO_4}^{IH^+}$	0	0
$k_{H_2PO_4^-}^{IH^+}$	5.7×10^{-1} $mole^{-1}$ sec^{-1}	9.6×10^{-1} $mole^{-1}$ sec^{-1}
k_H^I	4.07 $mole^{-1}$ sec^{-1}	2.89 $mole^{-1}$ sec^{-1}
$k_{acetic\ acid}^I$	0	0
$k_{acetate^-}^I$	8.7×10^{-4} $mole^{-1}$ sec^{-1}	
$k_{H_3PO_4}^I$	0	0
$k_{H_2PO_4^-}^I$	5.4×10^{-4} $mole^{-1}$ sec^{-1}	4.7×10^{-4} $mole^{-1}$ sec^{-1}
$k_{citric\ acid}^I$	0	0
$k_{H_2\text{-}citrate^-}^I$	~8×10^{-3} $mole^{-1}$ sec^{-1}	~9×10^{-3} $mole^{-1}$ sec^{-1}
$k_{Cl^-}^I$	3.8×10^{-4} $mole^{-1}$ sec^{-1}	5.9×10^{-3} $mole^{-1}$ sec^{-1}
$k_{Br^-}^I$	5.1×10^{-4} $mole^{-1}$ sec^{-1}	
$k_{I^-}^I$	6.4×10^{-4} $mole^{-1}$ sec^{-1}	
$k_{SO_4^{2-}}^I$	3.2×10^{-4} $mole^{-1}$ sec^{-1}	

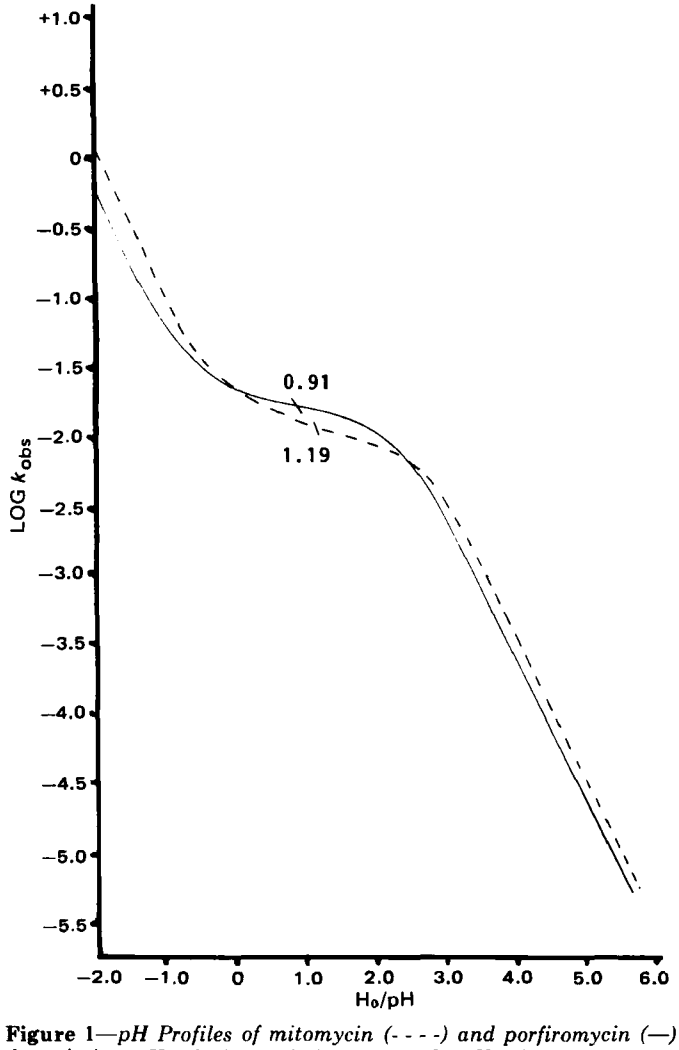

Figure 1—*pH Profiles of mitomycin (- - - -) and porfiromycin (—) degradation; pK_a of mitomycin is 1.19 and the pK_a of porfiromycin is 0.91.*

Table III—Influence of Dioctyl Sodium Sulfosuccinate on k_{obs} for Degradation of I and II in an Acidic Solution at 40° [a]

pH	k_{obs}(log k_{obs}), sec^{-1} [b]		k_{obs}(log k_{obs}), sec^{-1} [c]		Δlog k_{obs}
	I	II	I	II	
1.97	$8.3 \times 10^{-3}(-2.08)$		$6.3 \times 10^{-3}(-2.20)$		−0.12
2.10		$1.04 \times 10^{-2}(-1.98)$		$7.9 \times 10^{-3}(-2.10)$	−0.12
2.49	$5.5 \times 10^{-3}(-2.26)$		$3.2 \times 10^{-3}(-2.49)$		−0.23
2.91	$3.0 \times 10^{-3}(-2.55)$		$1.7 \times 10^{-3}(-2.77)$		−0.22
3.08		$2.3 \times 10^{-3}(-2.63)$		$8.8 \times 10^{-4}(-3.05)$	−0.42
3.47	$7.8 \times 10^{-4}(-3.11)$		$5.0 \times 10^{-4}(-3.30)$		−0.19
3.84		$4.0 \times 10^{-4}(-3.40)$		$1.5 \times 10^{-4}(-3.81)$	−0.41
4.23	$2.5 \times 10^{-4}(-3.89)$		$1.2 \times 10^{-4}(-3.93)$		−0.04

[a] The [I] and [II] was 3×10^{-5} *M*; the dioctyl sodium sulfosuccinate concentration was 1.25×10^{-3} *M*. [b] In the presence of dioctyl sodium sulfosuccinate. [c] In the absence of dioctyl sodium sulfosuccinate.

where k_0^I is the first-order rate constant for degradation in water only, k_H^I is the second-order rate constant for proton-catalyzed degradation of the unprotonated compound, and $[H^+]$ is the hydrogen ion concentration. The third term of Eq. 4 is the sum of several terms representing the products of the second-order rate constants for the degradation catalyzed by each of the buffer components and the concentrations of these buffer components. For each pH this sum can be written as the product of an overall second-order rate constant (k'_{buffer}) and the total buffer concentration ([buffer]), expressed in terms of total phosphate concentration. For each pH the pseudo first-order rate constant for [buffer] = 0, $k' = k_0^I + k_H^I[H^+]$, can be calculated as the intercept from a plot of k_{obs} *versus* [buffer]. The corrected pH profiles for the degradation of I and II are obtained by plotting log k' *versus* pH. These pH profiles are given in Fig. 1. The curves show log k' *versus* pH to have a slope of negative unity both in the regions $H_0 < -0.8$ and pH >3.2 indicating that there is specific proton catalysis on the degradation of the protonated as well as the unprotonated forms of I and II, while, in agreement with other findings (4), the rate constants for the proton-catalyzed degradation of the protonated species are smaller than those for the uncharged forms. This phenomenon permits the calculation of the pK_a for the aziridine nitrogen in I and II from the curves of Fig. 1. For I this pK_a turns out to be 1.19, while for II the pK_a is 0.91. The latter pK_a value is substantially different from a previously determined value (4), probably due to the corrections made for the buffer influence.

The difference between the pK_a values for I and II are in agreement with the usual differences in pK_a between secondary and tertiary amines (8). It is also possible to calculate the second-order rate constants $k_H^{IH^+}$ and k_H^I of the proton-catalyzed degradation of the protonated and unprotonated species. $k_H^{IH^+}$ can be determined from:

$$k_{obs} = k_0^{IH^+} + k_H^{IH^+}[H^+] \quad \text{(Eq. 5)}$$

which is valid at $H_0 < -0.8$. At these high acidities $k_0^{IH^+} \ll k_H^{IH^+}[H^+]$ so that Eq. 5 simplifies to:

$$k_{obs} = k_H^{IH^+}[H^+] \quad \text{(Eq. 6)}$$

from which $k_H^{IH^+}$ can be calculated.

The rate constants k_H^I for the proton-catalyzed degradation of uncharged I, and k_0^I for the degradation in water only, can be determined from the expression:

$$k' = k_0^I + k_H^I[H^+] \quad \text{(Eq. 7)}$$

obtained from Eq. 4 after correction for buffer influences. Equation 7 is valid at pH > 3.2, where $[IH^+]$ becomes extremely small. A plot of k' *versus* $[H^+]$ yields a straight line with slope k_H^I and intercept k_0^I. The values of $k_H^{IH^+}$, $k_H^{IIH^+}$, k_H^I, k_H^{II}, k_0^I and k_0^{II} are listed in Table II.

Influence of Buffer Components—From the previous experiments it is obvious that biphosphate ions have a positive influence on the degradation of I and II. Other sources (4, 5) also indicate positive catalytic effects of buffer components on the degradation rate of II in an acid solution. A catalytic effect of undissociated acetic acid has been suggested (5), although the experimental conditions also permit the conclusion that acetate ions produced the catalytic effect. Even though the aziridine ring is not attacked by the strong nucleophilic hydroxyl ion (4), it is known that other nucleophiles, such as chloride, promote the opening of the aziridine ring in an acidic medium (9–11) with the formation of chlorinated degradation products. Therefore, it appears that the acetate ion, rather than acetic acid, promotes the cleavage of the aziridine group. The influence of uncharged acetic acid on the degradation of I is studied at pH 2.77, where acetic acid exists almost completely in the uncharged form while $[IH^+] \ll [I]$. All other conditions kept constant, variation of the [acetic acid] is the only factor influencing k_{obs}, according to Eq. 4. However, no significant changes in k_{obs} occur on changing the [acetic acid] from 10^{-2} *M* to 5×10^{-1} *M*. The term k'_{buffer}[buffer] in that case must be zero and, consequently, $k^I_{acetic\ acid}$ must be zero.

Influences of the phosphate buffer components of pH 1–5 can be determined as follows. Phosphoric acid has pK_{a1} 2.16 and pK_{a2} 7.21. In the region of 4.2 < pH < 5.2, phosphate buffers almost exclusively consist of $H_2PO_4^-$ ions, so that this ion can be considered the only potential catalytic species. In this case, Eq. 4 can be rewritten as:

$$k_{obs} = k_0^I + k_H^I[H^+] + k^I_{H_2PO_4^-}[H_2PO_4^-] \quad \text{(Eq. 8)}$$

and a plot of k_{obs} *versus* $[H_2PO_4^-]$ yields a straight line with slope $k^I_{H_2PO_4^-}$.

The influence of molecular H_3PO_4 on the degradation of both the protonated and the unprotonated species as well as the influence of $H_2PO_4^-$ on the degradation of the protonated species also can be established. To achieve this, solutions of pH 3.2–3.6 were prepared using different concentrations of total phosphate. At a given pH $[H_3PO_4] = (f)$ [total phosphate], and $[H_2PO_4^-] = (1 - f)$ [total phosphate], where f is the fraction remaining. For each pH, f can be calculated using the Henderson–Hasselbach equation.

In the chosen pH region, $[IH^+]$ approaches zero and $[I] \approx [I_{total}]$. In this case Eq. 4 is valid with one adjustment. The value of $k^{IH^+}_{H_2PO_4^-}$ can be expected to be large due to the electrostatic attraction between ions of opposite charge. The term $k^{IH^+}_{H_2PO_4^-}[H_2PO_4^-][IH^+]$ cannot be neglected *a priori*, but has to be included in Eq. 4, which then must be written as:

$$k_{obs} = k_0^I + k_H^I[H^+] + k^I_{H_3PO_4}[H_3PO_4] + k^I_{H_2PO_4^-}[H_2PO_4^-] + k^{IH^+}_{H_2PO_4^-}[H_2PO_4^-]\frac{[IH^+]}{[I_{total}]} \quad \text{(Eq. 9)}$$

or, after rearrangement:

$$k_{obs} = k_0^I + k_H^I[H^+] + [\text{total phosphate}]\left(f\,k^I_{H_3PO_4} + (1-f)k^I_{H_2PO_4^-} + \frac{[IH^+]}{[I_{total}]}(1-f)k^{IH^+}_{H_2PO_4^-}\right) \quad \text{(Eq. 10)}$$

Graphical treatment of Eq. 10 by plotting k_{obs} *versus* [total phosphate] yields a straight line with slope:

$$\left(f\,k^I_{H_3PO_4} + (1-f)k^I_{H_2PO_4^-} + \frac{[IH^+]}{[I_{total}]}(1-f)k^{IH^+}_{H_2PO_4^-}\right)$$

Knowing the value of $k^I_{H_2PO_4^-}$, combination of the slopes of plots at two different pH values in the region 3.2–3.6 yields both the values of $k^I_{H_3PO_4}$ and $k^{IH^+}_{H_2PO_4^-}$. These values, and the corresponding rate constants for II, are listed in Table II.

Influence of Other Additives—The influence of halide ions has been established by adding various concentrations of the appropriate sodium salts to solutions of I at pH 4.2, while $[H_2PO_4^-]$ is kept constant at 10^{-2}

Table IV—Enthalpy of Activation (ΔH) for the Initial Degradation of I at Various pH Values in the Acidic Region

H_0/pH	ΔH, kJ/mole
−1.02	78
1.34	77
2.06	77
2.80	76
3.66	73
4.74	76
5.02	68
5.20	68

M. In this case one extra term involving the influence of the halide ion has to be included in Eq. 8, yielding (in the case of chloride):

$$k_{obs} = k_0^I + k_H^I[H^+] + k_{H_2PO_4^-}^I[H_2PO_4^-] + k_{Cl^-}^I[Cl^-] \quad \text{(Eq. 11)}$$

From Eq. 11 $k_{Cl^-}^I$ can be obtained either by plotting k_{obs} *versus* $[Cl^-]$, yielding a straight line with slope $k_{Cl^-}^I$, or by calculating the rate constant using various concentrations of Cl^- and the data in Table II. The specific rate constants for the halide ions and sulfate are also listed in this table.

The influence of ion-pairing compounds like dioctyl sodium sulfosuccinate [sodium 1,4-bis(2-ethylhexyl)sulfosuccinate] on the degradation was also studied. At various pH, using phosphate buffers with [total phosphate] = 10^{-2} M, dioctyl sodium sulfosuccinate was added to a concentration of 1.25×10^{-3} M while [I] and [II] both were adjusted to 3×10^{-5} M. In Table III the pseudo first-order rate constants, k_{obs}, for degradation in the presence as well as in the absence of dioctyl sulfosuccinate anion at various pH are listed. The data illustrate clearly the decrease in k_{obs} on addition of dioctyl sodium sulfosuccinate in the pH range of 1.5 to 4.0. The decrease for II is even more dramatic than for I, probably due to the more lipophilic properties of II and, hence, the increased lipophilic character of the ion pair. At pH > 5 the inhibition of the degradation disappears, probably because the compounds are virtually not in the protonated form at these acidities. At pH < 1.5 the inhibition also vanishes due to protonation of the sulfonic acid group and subsequent loss of the ion-pairing properties of the additive.

Influence of Temperature—The temperature influence on the degradation rate is determined using an Arrhenius plot from:

$$\ln k_{obs} = \ln A + \frac{\Delta H}{RT} \quad \text{(Eq. 12)}$$

in which A represents the frequency factor, ΔH the enthalpy of activation, R the gas constant, and T the temperature in °Kelvin. The ΔH values for the initial degradation of I at various pH values in the acidic region, using buffers with [total phosphate] = 10^{-2} M, are listed in Table IV. ΔH appears to be constant in the region pH < 5 and the values are in good agreement with those previously obtained (7). In the region pH > 5 ΔH tends to lower somewhat. This may be an indication that other degradation processes occur in this pH region.

DISCUSSION

Although an overall scheme for the degradation of II (4) and mechanisms for the aziridine ring to open in deuteroacetic acid (2) and in water (12) have been published, no explanation for the very fast opening of the aziridine ring in I and II in comparison with other aziridines (13) has been given. The first degradation products of I and II isolated after degradation in an acidic solution appear to be compounds III and IV, respectively, where the 9-methoxyl group is cleaved, the 9=9a double bond is formed, and the aziridine ring is opened to form a 2-amino-1-hydroxy compound. The C-9 carbon carries two hetero atoms, N-4 and the methoxy oxygen, and this configuration can be considered as an amino–acetal. It is most likely that, as in acetal hydrolysis, cleavage of the methoxyl group starts with protonation of the oxygen, followed by the formation of methanol and a 9a-carbenium ion (14). Protonation of the aziridine nitrogen destabilizes this carbenium ion, which explains the shape of the pH profiles of the degradation. Subsequent deprotonation of C-9 results in the formation of the 9=9a double bond. It has been indicated that compound IV exists in one isomer, always with the hydroxyl group at C-1 and the amino group at C-2 (15). The positions of the groups at C-1 and C-2 are mainly *cis*-orientated. Thus the cleavage of the aziridine ring starts with protonation of the nitrogen followed by opening of the ring and formation of a carbenium ion at C-1.

The stability of this carbenium ion is enhanced by the presence of the 9=9a double bond. This serves as an explanation for the stereospecificity of the reaction with respect to the positions of the hydroxyl and amino groups. Attack of a water molecule on the carbenium ion is the final step in the reaction. The major compound formed is *cis*-2,7-diamino-1-hydroxymitosene (15) which indicates that this attack must have some stereospecificity. An explanation for the predominant existence of the *cis*-isomer might be the possibility of the existence of weak hydrogen bonds between the attacking water molecule and the ester oxygen of the

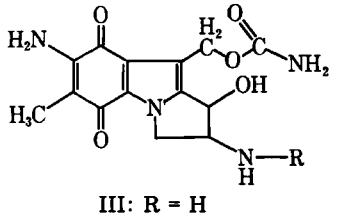

III: R = H
IV: R = CH_3

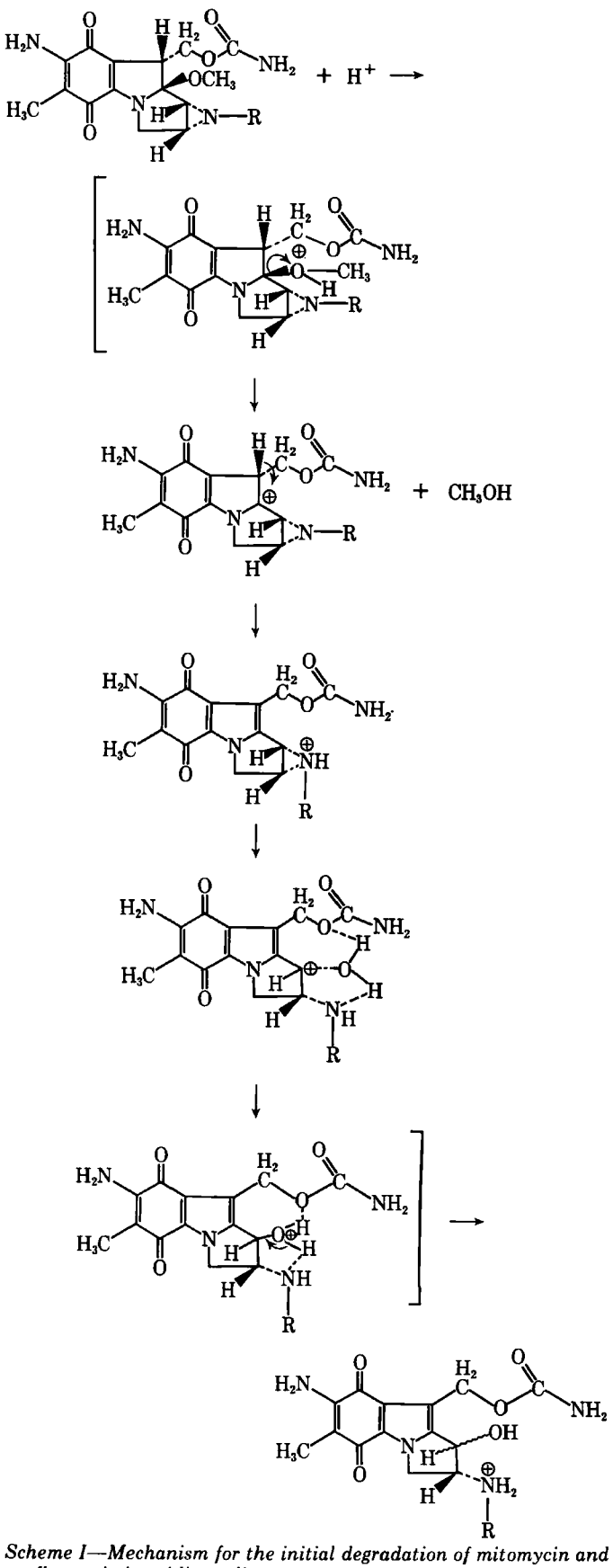

Scheme I—Mechanism for the initial degradation of mitomycin and profiromycin in acidic medium.

9-methylcarbamoyl and 2-amino groups. In the entire process the formation of the 9a-carbenium ion is the rate-determining step (16). The mechanism for acid degradation is presented in Scheme I.

The decrease in k_{obs} on addition of dioctyl sodium sulfosuccinate in the pH region 1.5–4 can be explained by the formation of an ion pair between the dioctyl sulfosuccinate anion and the protonated species. The octyl groups of the anion sterically hinder the protonation and subsequent cleavage of the 9a-methoxyl group. At pH > 5 the degree of protonation of the aziridine group, with pK_a 1.19 and 0.91 for I and II, respectively, becomes so small that the ion pair is virtually nonexistent and, hence, the protective influence of the additive disappears.

All buffer components and other additives with a negative charge had positive influences on the rate constants. Uncharged buffer species, such as phosphoric acid, acetic acid, and citric acid did not have a catalytic influence on the degradation processes, which differs from previous findings (4). The influences of the anions on the degradation can be associated with influences on the aziridine ring opening. In general, nucleophiles have negative effects on the stability of the aziridine moiety (9–11, 14). Degradation products containing chlorine, for instance, were isolated (9, 10). Analogues of these products in the degradation of mitosanes like I and II, however, could not be isolated. All rate constants for catalysis by singly charged anions are of the same order of magnitude (Table II) with the exception of dihydrogen citrate (H_2-citrate$^-$). This suggests a general ionic strength effect rather than more specific anionic catalysis on the degradation. In the case of H_2-citrate$^-$ the rate constant is determined at pH 3.06, being the pK_{a1} of citric acid. Although the pK_{a2} of this acid is 4.74, the [H-citrate^{2-}] was considered to be negligible for the calculation of $k_{H_2\text{-citrate}^-}$ of I and II. This is of course very approximate and makes the reported values of $k_{H_2\text{-citrate}^-}$ only a rough estimate which most likely includes an influence of H-citrate^{2-}. The rate constants for the $H_2PO_4^-$-catalyzed degradation of the protonated species are several orders of magnitude bigger than the other constants. This must be due to the fact that as a result of the opposite charges of the reacting species, electrostatic attraction causes a much greater possibility of encounter and, therefore, reaction.

REFERENCES

(1) S. Wakaki, H. Marumo, K. Tomioka, G. Shimizu, E. Kato, H. Kamada, S. Kudo, and Y. Fujimoto, *Antibiot. Chemother.*, **8**, 228 (1958).

(2) C. L. Stevens, K. G. Taylor, M. E. Munk, W. S. Marshall, K. Noll, G. D. Shah, L. G. Shah, and K. Uzu, *J. Med. Chem.*, **8**, 1 (1964).

(3) K. Uzu, Y. Harada, and S. Wakaki, *Agr. Biol. Chem.*, **28**, 338 (1964).

(4) E. Garrett, *J. Med. Chem.*, **6**, 488 (1963).

(5) E. Garrett and W. Schroeder, *J. Pharm. Sci.*, **53**, 917 (1964).

(6) W. J. M. Underberg and H. Lingeman, *J. Pharm. Sci.*, **72**, 553 (1983).

(7) D. Edwards, A. B. Selkirk, and R. B. Taylor, *Int. J. Pharm.*, **4**, 21 (1979).

(8) G. B. Barlin and D. D. Perrin, in "Elucidation of Organic Structures by Physical and Chemical Methods," K. W. Bently and G. W. Kirby, Eds., Wiley-Interscience, New York-London-Sydney-Toronto, 1972, part I, 2nd ed., p. 611.

(9) J. E. Early, C. E. O'Rourke, L. B. Clapp, J. O. Edwards, and B. C. Lawes, *J. Am. Chem. Soc.*, **80**, 3458 (1958).

(10) G. Berti, G. Camici, B. Macchia, F. Macchia, and C. Monti, *Tetrahedron Lett.*, **25**, 2591 (1972).

(11) G. K. Poochikian and J. A. Kelly, *J. Pharm. Sci.*, **70**, 162 (1981).

(12) L. Cheng and W. A. Remers, *J. Med. Chem.*, **20**, 767 (1977).

(13) G. K. Poochikian and J. C. Craddock, *J. Pharm. Sci.*, **70**, 159 (1981).

(14) E. Schmitz and I. Eichhorn, in "The Chemistry of The Ether Linkage," S. Patai, Ed., Wiley-Interscience, London-New York-Sidney, 1967, p. 332.

(15) W. G. Taylor and W. A. Remers, *J. Med. Chem.*, **18**, 307 (1975).

(16) M. M. Kreevoy, C. R. Morgan, and R. W. Taft, Jr., *J. Am. Chem. Soc.*, **82**, 3064 (1960).

ACKNOWLEDGMENTS

The authors wish to express their gratitude to Dr. J. Wilting, Dr. W. F. van der Giesen, and Prof. Dr. H. J. T. Bos for helpful discussions, and to Mr. G. Wiese for drawing the figures.

Determination of pK_a Values of Some Prototropic Functions in Mitomycin and Porfiromycin

W. J. M. UNDERBERG ˣ and H. LINGEMAN

Received August 11, 1981 from the *Pharmaceutical Laboratory, Department of Analytical Pharmacy, State University of Utrecht, Catharijnesingel 60, 3511 GH Utrecht, The Netherlands.* Accepted for publication May 28, 1982.

Abstract □ The prototropic properties of mitomycin and porfiromycin were studied. pK_a values for two potentially basic groups and one acidic function could be established by titration. The kinetics of the tautomerization preceding the prototropic reaction in an alkaline medium were investigated.

Keyphrases □ Prototropic properties—mitomycin, porfiromycin, alkaline medium, kinetics of tautomerization □ Mitomycin—prototropic properties, pK_a determinations, tautomerization kinetics □ Porfiromycin—prototropic properties, pK_a determinations, tautomerization kinetics □ Kinetics—tautomerization, mitomycin, porfiromycin

Mitomycin (I), originating from *Streptomyces caespitosus* (1), is an important antitumor antibiotic. The compound is unstable in solution and aspects of the degradation of I and porfiromycin (II), which differs from I only in the methyl substituent on the aziridine nitrogen, have been studied by several investigators (2–6). For a systematic study of the chemistry of these compounds, including the stability, it is necessary to characterize the prototropic properties of I and II.

From the structures it can be seen that the compounds have several basic groups, including the aziridine nitrogen, the N-4 nitrogen, and the 7-amino function. In the literature data are available only on the protonation of one basic function; these data are either unreliable or are approximations. The pK_a of a basic group in I has been deter-

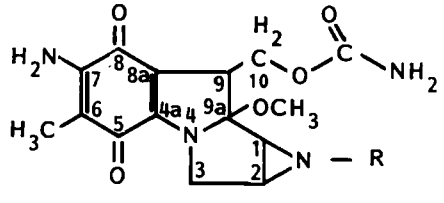

I: R = H
II: R = CH_3

0022-3549/83/0500-0553$01.00/0

9-methylcarbamoyl and 2-amino groups. In the entire process the formation of the 9a-carbenium ion is the rate-determining step (16). The mechanism for acid degradation is presented in Scheme I.

The decrease in k_{obs} on addition of dioctyl sodium sulfosuccinate in the pH region 1.5–4 can be explained by the formation of an ion pair between the dioctyl sulfosuccinate anion and the protonated species. The octyl groups of the anion sterically hinder the protonation and subsequent cleavage of the 9a-methoxyl group. At pH > 5 the degree of protonation of the aziridine group, with pK_a 1.19 and 0.91 for I and II, respectively, becomes so small that the ion pair is virtually nonexistent and, hence, the protective influence of the additive disappears.

All buffer components and other additives with a negative charge had positive influences on the rate constants. Uncharged buffer species, such as phosphoric acid, acetic acid, and citric acid did not have a catalytic influence on the degradation processes, which differs from previous findings (4). The influences of the anions on the degradation can be associated with influences on the aziridine ring opening. In general, nucleophiles have negative effects on the stability of the aziridine moiety (9–11, 14). Degradation products containing chlorine, for instance, were isolated (9, 10). Analogues of these products in the degradation of mitosanes like I and II, however, could not be isolated. All rate constants for catalysis by singly charged anions are of the same order of magnitude (Table II) with the exception of dihydrogen citrate (H_2-citrate$^-$). This suggests a general ionic strength effect rather than more specific anionic catalysis on the degradation. In the case of H_2-citrate$^-$ the rate constant is determined at pH 3.06, being the pK_{a1} of citric acid. Although the pK_{a2} of this acid is 4.74, the [H-citrate^{2-}] was considered to be negligible for the calculation of $k_{H_2\text{-citrate}^-}$ of I and II. This is of course very approximate and makes the reported values of $k_{H_2\text{-citrate}^-}$ only a rough estimate which most likely includes an influence of H-citrate^{2-}. The rate constants for the $H_2PO_4^-$-catalyzed degradation of the protonated species are several orders of magnitude bigger than the other constants. This must be due to the fact that as a result of the opposite charges of the reacting species, electrostatic attraction causes a much greater possibility of encounter and, therefore, reaction.

REFERENCES

(1) S. Wakaki, H. Marumo, K. Tomioka, G. Shimizu, E. Kato, H. Kamada, S. Kudo, and Y. Fujimoto, *Antibiot. Chemother.*, **8**, 228 (1958).

(2) C. L. Stevens, K. G. Taylor, M. E. Munk, W. S. Marshall, K. Noll, G. D. Shah, L. G. Shah, and K. Uzu, *J. Med. Chem.*, **8**, 1 (1964).

(3) K. Uzu, Y. Harada, and S. Wakaki, *Agr. Biol. Chem.*, **28**, 338 (1964).

(4) E. Garrett, *J. Med. Chem.*, **6**, 488 (1963).

(5) E. Garrett and W. Schroeder, *J. Pharm. Sci.*, **53**, 917 (1964).

(6) W. J. M. Underberg and H. Lingeman, *J. Pharm. Sci.*, **72**, 553 (1983).

(7) D. Edwards, A. B. Selkirk, and R. B. Taylor, *Int. J. Pharm.*, **4**, 21 (1979).

(8) G. B. Barlin and D. D. Perrin, in "Elucidation of Organic Structures by Physical and Chemical Methods," K. W. Bently and G. W. Kirby, Eds., Wiley-Interscience, New York-London-Sydney-Toronto, 1972, part I, 2nd ed., p. 611.

(9) J. E. Early, C. E. O'Rourke, L. B. Clapp, J. O. Edwards, and B. C. Lawes, *J. Am. Chem. Soc.*, **80**, 3458 (1958).

(10) G. Berti, G. Camici, B. Macchia, F. Macchia, and C. Monti, *Tetrahedron Lett.*, **25**, 2591 (1972).

(11) G. K. Poochikian and J. A. Kelly, *J. Pharm. Sci.*, **70**, 162 (1981).

(12) L. Cheng and W. A. Remers, *J. Med. Chem.*, **20**, 767 (1977).

(13) G. K. Poochikian and J. C. Craddock, *J. Pharm. Sci.*, **70**, 159 (1981).

(14) E. Schmitz and I. Eichhorn, in "The Chemistry of The Ether Linkage," S. Patai, Ed., Wiley-Interscience, London-New York-Sidney, 1967, p. 332.

(15) W. G. Taylor and W. A. Remers, *J. Med. Chem.*, **18**, 307 (1975).

(16) M. M. Kreevoy, C. R. Morgan, and R. W. Taft, Jr., *J. Am. Chem. Soc.*, **82**, 3064 (1960).

ACKNOWLEDGMENTS

The authors wish to express their gratitude to Dr. J. Wilting, Dr. W. F. van der Giesen, and Prof. Dr. H. J. T. Bos for helpful discussions, and to Mr. G. Wiese for drawing the figures.

Determination of pK_a Values of Some Prototropic Functions in Mitomycin and Porfiromycin

W. J. M. UNDERBERG ˣ and H. LINGEMAN

Received August 11, 1981 from the *Pharmaceutical Laboratory, Department of Analytical Pharmacy, State University of Utrecht, Catharijnesingel 60, 3511 GH Utrecht, The Netherlands.* Accepted for publication May 28, 1982.

Abstract □ The prototropic properties of mitomycin and porfiromycin were studied. pK_a values for two potentially basic groups and one acidic function could be established by titration. The kinetics of the tautomerization preceding the prototropic reaction in an alkaline medium were investigated.

Keyphrases □ Prototropic properties—mitomycin, porfiromycin, alkaline medium, kinetics of tautomerization □ Mitomycin—prototropic properties, pK_a determinations, tautomerization kinetics □ Porfiromycin—prototropic properties, pK_a determinations, tautomerization kinetics □ Kinetics—tautomerization, mitomycin, porfiromycin

Mitomycin (I), originating from *Streptomyces caespitosus* (1), is an important antitumor antibiotic. The compound is unstable in solution and aspects of the degradation of I and porfiromycin (II), which differs from I only in the methyl substituent on the aziridine nitrogen, have been studied by several investigators (2–6). For a systematic study of the chemistry of these compounds, including the stability, it is necessary to characterize the prototropic properties of I and II.

From the structures it can be seen that the compounds have several basic groups, including the aziridine nitrogen, the N-4 nitrogen, and the 7-amino function. In the literature data are available only on the protonation of one basic function; these data are either unreliable or are approximations. The pK_a of a basic group in I has been deter-

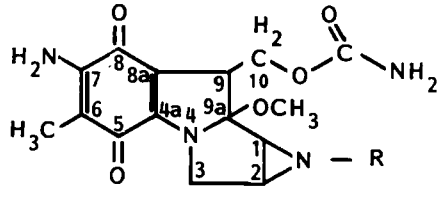

I: R = H
II: R = CH_3

0022-3549/83/0500-0553$01.00/0

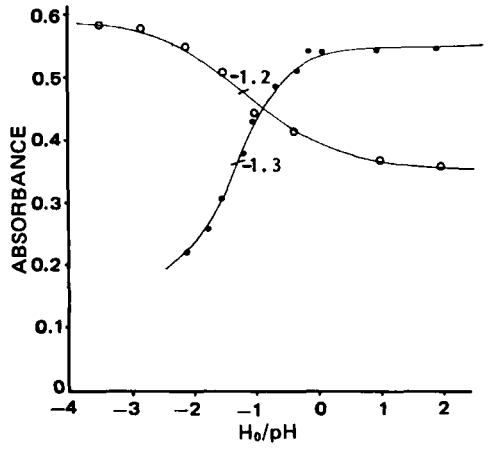

Figure 1—*Relation between absorbance and acidity; determination of pK_a (at room temperature) of the 7-amino group and N-4 nitrogen. Key: (●) mitomycin degradation product (IV), absorbance monitored at 310 nm, pK_{a2} −1.3; and (○) mitomycin analogue (III), absorbance monitored at 268 nm, pK_{a2} −1.2.*

mined by titration with acid to be 3.2 (2), but I in acid medium is very unstable. By a kinetic model, the pK_a of the protonated group in II was estimated to be ~1.5, and it was suggested that this pK_a could be assigned to the aziridine nitrogen in II (4). The present study was undertaken to determine the pK_a values of the other prototropic groups in I and II in an attempt to complete the prototropic characterization of the compounds.

EXPERIMENTAL

Materials—Mitomycin[1] and porfiromycin[2] were used as supplied. All other materials were reagent grade, and deionized water was used throughout.

Methods—*Measurement of pK_a Values*—For the measurement of pK_a values of III and IV, the compounds were titrated with perchloric acid while the absorbances at 268 and 310 nm, respectively, were monitored as a function of acidity (pH or H_0). The pK_a values of the basic groups were calculated from these relationships. For the determination of the pK_a of the acidic function in I, a titration of the compound with sodium hydroxide was performed while monitoring the absorbance at 363 nm. Up to pH 13 the degradation was too slow to interfere with the

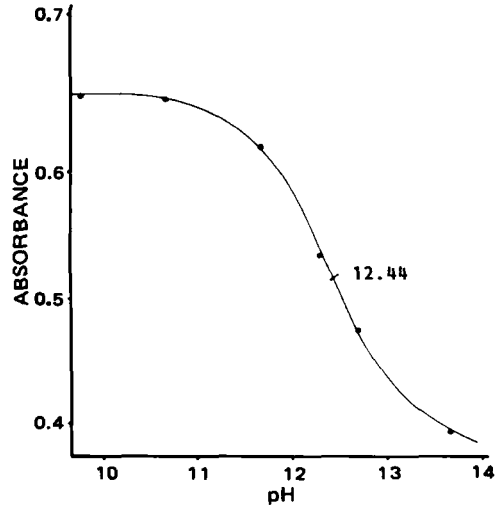

Figure 2—*Relation between absorbance at 363 nm and pH; determination of pK_a of the acidic function of mitomycin at room temperature, pK_{a4} 12.44.*

[1] Supplied by Bristol Myers B. V., Bussum, The Netherlands.
[2] Supplied by Cyanamid, Pearl River, N.Y.

Table I—First-Order Rate Constants for Deprotonation (k_{dep}) and half-lives ($t_{1/2}$) of I at Various pH Values at 40°

pH	k_{dep}, sec^{-1}	$t_{1/2}$, sec
12.0	$8.2 \pm 0.5 \times 10^{-2}$	8.5 ± 0.6
12.7	$5.5 \pm 0.6 \times 10^{-2}$	13 ± 1
13.0	$3.4 \pm 0.4 \times 10^{-2}$	20 ± 1
13.4	$2.8 \pm 0.2 \times 10^{-2}$	25 ± 1

change in absorbance due to deprotonation. At pH values >13 a continuous decrease in absorbance at 363 nm was observed, which was due to degradation of the compound in a strong alkaline solution (5). Consequently, the absorbance–pH relationship could only be obtained incompletely and A_{I^-}, the absorbance of the deprotonated species, was not measurable. In terms of absorbance, the acidity constant K_a can be expressed as

$$K_a = \frac{(A_I - A)[H^+]}{(A - A_{I^-})} \qquad \text{(Eq. 1)}$$

where A_I is the absorbance of uncharged I, A_{I^-} is the absorbance of deprotonated I, and A is the absorbance of the solution at a given pH. Equation 1 can be rearranged to:

$$(A_I - A)[H^+] = K_a(A - K_a)(A_{I^-}) \qquad \text{(Eq. 2)}$$

A plot of A *versus* $(A_I - A)[H^+]$ yields a straight line with slope K_a and intercept $(-K_a)(A_{I^-})$, thus leading to the values of K_a, pK_a, and A_{I^-}.

Kinetic Study of I Deprotonation—For the study of the kinetics of I deprotonation, several solutions in water with concentrations varying from 1.5×10^{-6} *M* to 1.8×10^{-4} *M* were prepared. After mixing equal volumes of sodium hydroxide solutions at various pH with the aforementioned solutions of I, the decrease in absorbance at 363 nm was monitored using stopped-flow equipment[3]. Measurements of pH were done with a glass-reference electrode using an appropriate pH meter[4]. Rate constants and half-lives were calculated using plots of log (percent uncharged I) *versus* time.

RESULTS

The basic groups of I and II, apart from the aziridine function, are the N-4 nitrogen and the 7-amino group. The pK_a of the N-4 nitrogen can be established by titration of an analogue of I (III) with perchloric acid. The absorption spectrum of uncharged III has a maximum at 280 nm. During protonation this maximum shifts to 268 nm, with an increase in absorptivity. Thus it is possible to follow the degree of protonation by monitoring the absorption at 268 nm, provided that no degradation occurs during the process. A solution of III in 1 *M* perchloric acid (H_0 −0.3) does not show changes in absorptivity at 268 nm when kept at 40° for 1 hr. The relation between the absorbance at 268 nm and the acidity, expressed in terms of the Hammett acidity scale, is shown in Fig. 1. The pK_a of the nitrogen in III calculated from this relationship is −1.2 and almost certainly this value can also be assigned to the N-4 nitrogen in I and II.

The spectra of I and II quickly change in acidic solution due to cleavage of the 9a-methoxyl group and opening of the aziridine ring, thus producing degradation products IV and V, respectively. Compound IV in acidic solution also undergoes degradative processes but at a much slower rate (4, 5). The pK_a of the 2-amino group in the compound is ~7 (5) so that degradations of I and II at pH 5 result in the formation of protonated IV and V, respectively. These compounds are sufficiently stable to be titrated with perchloric acid to establish the pK_a of the other basic functions. The absorption maximum of IV in the neutral form is 310 nm; on acidification this maximum disappears.

The absorption band at ~250 nm changes in shape while the absorp-

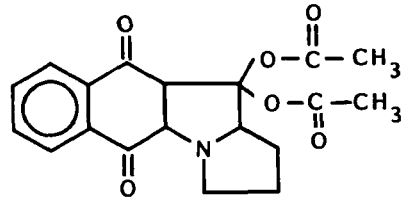

III

[3] Durrum 110 with Durrum 13000 Spectrophotometer.
[4] Metrohm Herisau E516 Titriskop pH meter.

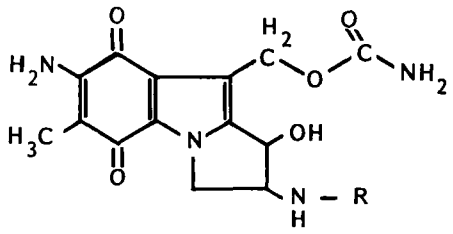

IV: R = H
V: R = CH_3

tivity increases. The pK_a can be established from the relation between the absorbance at 310 nm and the acidity (Fig. 1). The more acidic part of the curve is unreliable because degradation of IV in that acidity region cannot be neglected. The pH of the protonated group, determined using Eq. 2 after rearrangement, appears to be −1.3. The N-4 nitrogen in IV is much less basic than in I due to the introduction of the 9=9a double bond, as can be seen from indole (pK_a −2.5) (7). Therefore, the pK_a of IV can be assigned to the 7-amino group. From the similarity in the structures of I, II, and IV, it becomes clear that this pK_a value also can be assigned to the 7-amino groups in I and II.

The absorption spectrum of I does not change between pH 6 and 10. At pH < 6 a gradual shift in spectrum with time takes place due to degradation, while at pH > 10.5 a sudden change in the absorption spectrum occurs. The maximum at 363 nm (pH 10.5) shifts to 295 nm (pH 13.0) with a sharp decrease in absorptivity. This shift could be due to a configurative change in the molecule, stabilized by deprotonation of I at the higher pH. The pK_a of the acidic function can be determined from the relation between the absorbance at 363 nm and the pH, provided no degradation occurs. Although alkaline degradation of II takes place at rates comparable to those in acidic medium (4), the stability of I in the region pH < 13 is sufficiently high to permit the determination of the pK_a using Eq. 2. The curve cannot be completed because the degradation of I cannot be neglected at pH > 13. The relation between the absorbance at 363 nm and pH, represented in Fig. 2, leads to the calculation of a pK_a of 12.44.

Although the change in absorptivity with change in pH at 363 nm in the region of pH > 10.4 is very rapid, it is not instrumentally instantaneous. The kinetic process involved can be monitored using stopped-flow equipment. These experiments indicate that the reaction follows (pseudo) first-order kinetics. The relation between the apparent rate constant for deprotonation, k_{dep}, and the pH is presented in Table I. The influence of the initial [I] at a pH > pK_a and at a pH < pK_a is listed in Table II. The data of Table I show that k_{dep} decreases with increasing pH.

At pH 13.0, k_{dep} is independent of [I] in the chosen concentration range but at pH 12.0 an increase of [I] causes a decrease in k_{dep} as presented in Table II. The data obtained at pH > pK_a indicate that the process follows first-order kinetics, but the data at pH < pK_a contradict such a conclusion. A plausible explanation for the results is that aggregation occurs between the molecules at higher concentrations of uncharged I. At pH < pK_a the majority of the molecules appears in the protonated neutral form so that in this pH region the possibility of aggregation will be relatively high. Other properties, such as the absorptivity, may change also with an increase in the concentration. In Fig. 3 the relation between the absorbance at 290 nm and [I] at pH 10 is presented. The curve shows linearity between absorbance and concentration up to 1.5×10^{-5} *M* I. At concentrations over 2.0×10^{-5} *M* the absorbance is no longer linear with [I], which means that the chromophore is influenced by interaction with other molecules.

Table II—Rate Constants (k_{dep}) and Half-Lives ($t_{1/2}$) of I at Various Concentrations at Two Different pH Values at 40°

pH	[I] × 10^5 *M*	k_{dep}, sec^{-1}	$t_{1/2}$, sec
12.0	1.5	8.9×10^{-2}	7.7
	3.0	8.7×10^{-2}	8.0
	6.0	6.8×10^{-2}	10.2
	9.0	4.7×10^{-2}	15.0
13.0	3.0	3.5×10^{-2}	20.0
	6.0	3.3×10^{-2}	21.0
	9.0	3.4×10^{-2}	20.5

DISCUSSION

The data presented above lead to the following conclusions on the prototropic nature of I and II. Both compounds have three basic functions:

1. The 7-amino group, with pK_{a1} − 1.3 at room temperature.
2. The N-4 nitrogen, with pK_{a2} −1.2 at room temperature. It is possible that pK_{a2} is a little higher, due to mesomeric effects of the 7-amino group.
3. The aziridine nitrogen, with pK_{a3} ~1.5 (4).

The compounds also have an acidic function, with pK_{a4} 12.44 at room temperature. This pK_a must be assigned to the 7-amino–quinoid moiety in the compounds, as is shown in Scheme I. The keto–enol tautomerism in this structure is responsible for the spectral changes, while the absorbance value marks the position of the equilibrium. The tautomeric reaction has a finite rate.

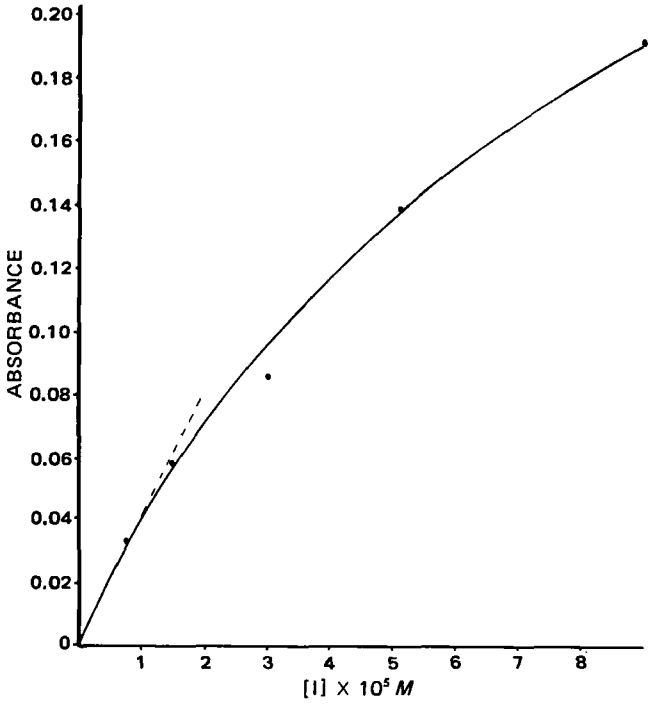

Figure 3—*Relation between absorbance at 290 nm and mitomycin concentration at pH 10 at room temperature.*

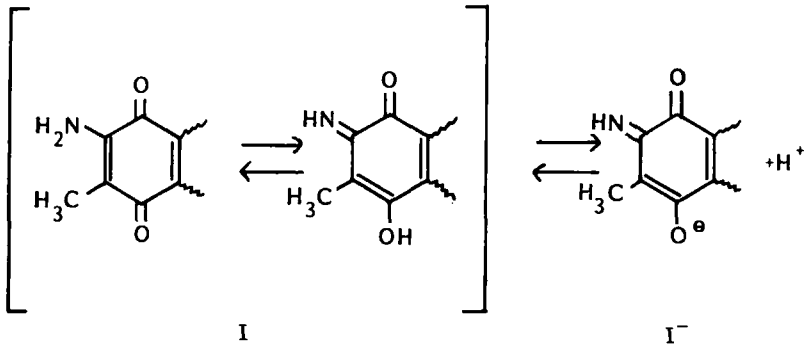

I I⁻

Scheme I—Deprotonation of mitomycin, Key: I, uncharged mitomycin; I⁻, deprotonated mitomycin.

The degree of protonation (α) of the reaction can be written as:

$$\alpha = \frac{[I^-]}{[I + I^-]} = \frac{K_a}{K_a + [H^+]} \quad \text{(Eq. 3)}$$

The overall rate constant k_{dep} consists of:

$$k_{dep} = k_t^{I}[I] + k_t^{I^-}[I^-] = k_t^{I}(1 - \alpha) + k_t^{I^-}(\alpha) \quad \text{(Eq. 4)}$$

where k_t^{I} is the rate constant for tautomerization of uncharged I and $k_t^{I^-}$ the same constant for I^- (deprotonated I). Combination of Eqs. 3 and 4 yields:

$$k_{dep} = (k_t^{I})\frac{[H^+]}{K_a + [H^+]} + (k_t^{I^-})\frac{K_a}{K_a + [H^+]} \quad \text{(Eq. 5)}$$

Assuming that, with respect to tautomerization, I is much more active than I^- or that $k_t^{I} \gg k_t^{I^-}$, it is obvious that on increasing the pH, the term $k_t^{I}([H^+]/K_a + [H^+])$ will decrease more rapidly than the term $k_t^{I^-}([H^+]/K_a + [H^+])$ increases which will result in a lower value of k_{dep}. Under the assumption that $k_t^{I^-}$ is so small that the term $k_t^{I^-}(K_a/K_a + [H^+])$ can be neglected, Eq. 5 permits the estimation of k_t^{I}, using pK_a 12.44 of the acidic group and the values for k_{dep} listed in Table I. The calculation results in a k_t^{I} of $1.4 \pm 0.4 \times 10^{-1}$ sec^{-1} and a half-life ($t_{1/2}$) of the process of 5.0 sec. The explanation of the concentration dependence of k_{dep} at $pH < pK_a$ lies in the aforementioned possibility of interaction between the 7-amino–quinoid moieties on increasing [I]. The occurrence of these interactions is shown by the changes in absorptivity at higher [I] at pH 10, where the compound is present almost completely in the uncharged form. The decrease in the molar absorptivity must be due to interaction of the 7-amino–quinoid chromophores. Since the tautomerization occurs in the same functional group in the molecule, this interaction most likely also causes a decrease in the overall rate constant k_{dep} at higher [I] at pH 12.0, as the concentration of the unaffected 7-amino–quinoidal function decreases due to this interaction. Equation 4 shows that on decreasing [I] and $[I^-]$, k_{dep} will decrease. At pH 13.0, where $[I] = 0.2\ [I + I^-]$, the concentration of uncharged I in the range studied is too low for aggregation to occur.

REFERENCES

(1) S. Wakaki, H. Marumo, K. Tomioka, G. Shimizu, E. Kato, H. Kamada, S. Kudo, and Y. Fujimoto, *Antibiot. Chemother.*, **8**, 228 (1958).

(2) C. L. Stevens, K. G. Taylor, M. E. Munk, W. S. Marshall, K. Noll, G. D. Shah, L. G. Shah, and K. Uzu, *J. Med. Chem.*, **8**, 1 (1964).

(3) K. Uzu, Y. Harada, and S. Wakaki, *Agr. Biol. Chem.*, **28**, 338 (1964).

(4) E. Garrett, *J. Med. Chem.*, **6**, 488 (1963).

(5) E. Garrett and W. Schroeder, *J. Pharm. Sci.*, **53**, 917 (1964).

(6) D. Edwards, A. B. Selkirk, and R. B. Taylor, *Int. J. Pharm.*, **4**, 21 (1979).

(7) C. G. Greig and C. D. Johnson, *J. Am. Chem. Soc.*, **90**, 6453 (1968).

ACKNOWLEDGMENTS

The authors wish to express their gratitude to Dr. J. M. H. Terbeek-Kremer for assistance with the stopped-flow experiments, Dr. J. Wilting and Dr. W. F. van der Giesen for helpful discussions, and Mr. G. Wiese for drawing the figures.

NOTES

Tissue Distribution of [^{14}C]Bretylium Tosylate in Rats

AVRAHAM YACOBI ˣ, BURDE L. KAMATH *, CHII-MING LAI, and HERMAN F. STAMPFLI

Received March 2, 1982, from the *Department of Pharmaceutical Development, Research and Development Department, American Critical Care, McGaw Park, IL 60085.* Accepted for publication April 21, 1982. *Present address: Xavier University, New Orleans, LA 70125.

Abstract □ The distribution of [^{14}C]bretylium tosylate in the body and the relationship between tissue and plasma concentrations was determined following intravenous administration of the drug to Charles River rats. The renal excretion of bretylium was rapid in rats and follows an active process. On the average, 50% of the administered dose was excreted in the urine within 1 hr. In the postequilibrium phase, the plasma concentration declined with a half-life of 5 hr. Bretylium concentrations in all tissues, except the heart, declined rapidly according to a triexponential equation. The liver and kidney bretylium concentrations declined in parallel to the plasma concentration with mean tissue–plasma concentration ratios of 6.04 and 12.3, respectively, in the β phase. However, the concentration of bretylium in the heart increased gradually and peaked at 2 hr, with a tissue–plasma concentration ratio of 121, which, in turn, declined to a value of >60 after 8 hr. The data indicated that (*a*) bretylium is rapidly distributed into the liver and kidney immediately after reaching the systemic circulation; (*b*) the distribution into the heart occurs at a slower rate compared with the other organs, and the drug has a high affinity to the myocardium; and (*c*) since the heart is the site of action and there is no direct correlation between the concentrations in myocardium and plasma, the antiarrhythmic effect of bretylium may not be related to the plasma concentration.

Keyphrases □ Bretylium tosylate—^{14}C-labeled, tissue distribution, rats, plasma, renal excretion □ Distribution—tissue, [^{14}C]bretylium tosylate in the rat, plasma, renal excretion □ Excretion, renal—tissue distribution of [^{14}C]bretylium tosylate in rats, plasma

Bretylium tosylate is a quaternary ammonium salt given in the treatment of cardiac arrhythmia. It suppresses *ventricular* fibrillation within minutes of intravenous infusion (1). The suppression of ventricular tachycardia, however, developed more slowly, usually 20–120 min after intramuscular administration of 4 mg/kg of bretylium tosylate in humans (2). The effect of bretylium in the intact heart was shown to be biphasic, with an initial transient increase in blood pressure and heart rate followed by an opposite and more prolonged depression of these same

0022-3549/83/0500-0556$01.00/0

The degree of protonation (α) of the reaction can be written as:

$$\alpha = \frac{[I^-]}{[I + I^-]} = \frac{K_a}{K_a + [H^+]} \quad \text{(Eq. 3)}$$

The overall rate constant k_{dep} consists of:

$$k_{dep} = k_t^{I}[I] + k_t^{I^-}[I^-] = k_t^{I}(1 - \alpha) + k_t^{I^-}(\alpha) \quad \text{(Eq. 4)}$$

where k_t^{I} is the rate constant for tautomerization of uncharged I and $k_t^{I^-}$ the same constant for I^- (deprotonated I). Combination of Eqs. 3 and 4 yields:

$$k_{dep} = (k_t^{I})\frac{[H^+]}{K_a + [H^+]} + (k_t^{I^-})\frac{K_a}{K_a + [H^+]} \quad \text{(Eq. 5)}$$

Assuming that, with respect to tautomerization, I is much more active than I^- or that $k_t^{I} \gg k_t^{I^-}$, it is obvious that on increasing the pH, the term $k_t^{I}([H^+]/K_a + [H^+])$ will decrease more rapidly than the term $k_t^{I^-}([H^+]/K_a + [H^+])$ increases which will result in a lower value of k_{dep}. Under the assumption that $k_t^{I^-}$ is so small that the term $k_t^{I^-}(K_a/K_a + [H^+])$ can be neglected, Eq. 5 permits the estimation of k_t^{I}, using pK_a 12.44 of the acidic group and the values for k_{dep} listed in Table I. The calculation results in a k_t^{I} of $1.4 \pm 0.4 \times 10^{-1}$ sec^{-1} and a half-life ($t_{1/2}$) of the process of 5.0 sec. The explanation of the concentration dependence of k_{dep} at $pH < pK_a$ lies in the aforementioned possibility of interaction between the 7-amino–quinoid moieties on increasing [I]. The occurrence of these interactions is shown by the changes in absorptivity at higher [I] at pH 10, where the compound is present almost completely in the uncharged form. The decrease in the molar absorptivity must be due to interaction of the 7-amino–quinoid chromophores. Since the tautomerization occurs in the same functional group in the molecule, this interaction most likely also causes a decrease in the overall rate constant k_{dep} at higher [I] at pH 12.0, as the concentration of the unaffected 7-amino–quinoidal function decreases due to this interaction. Equation 4 shows that on decreasing [I] and $[I^-]$, k_{dep} will decrease. At pH 13.0, where $[I] = 0.2\ [I + I^-]$, the concentration of uncharged I in the range studied is too low for aggregation to occur.

REFERENCES

(1) S. Wakaki, H. Marumo, K. Tomioka, G. Shimizu, E. Kato, H. Kamada, S. Kudo, and Y. Fujimoto, *Antibiot. Chemother.*, **8**, 228 (1958).

(2) C. L. Stevens, K. G. Taylor, M. E. Munk, W. S. Marshall, K. Noll, G. D. Shah, L. G. Shah, and K. Uzu, *J. Med. Chem.*, **8**, 1 (1964).

(3) K. Uzu, Y. Harada, and S. Wakaki, *Agr. Biol. Chem.*, **28**, 338 (1964).

(4) E. Garrett, *J. Med. Chem.*, **6**, 488 (1963).

(5) E. Garrett and W. Schroeder, *J. Pharm. Sci.*, **53**, 917 (1964).

(6) D. Edwards, A. B. Selkirk, and R. B. Taylor, *Int. J. Pharm.*, **4**, 21 (1979).

(7) C. G. Greig and C. D. Johnson, *J. Am. Chem. Soc.*, **90**, 6453 (1968).

ACKNOWLEDGMENTS

The authors wish to express their gratitude to Dr. J. M. H. Terbeek-Kremer for assistance with the stopped-flow experiments, Dr. J. Wilting and Dr. W. F. van der Giesen for helpful discussions, and Mr. G. Wiese for drawing the figures.

NOTES

Tissue Distribution of [^{14}C]Bretylium Tosylate in Rats

AVRAHAM YACOBI ˣ, BURDE L. KAMATH *, CHII-MING LAI, and HERMAN F. STAMPFLI

Received March 2, 1982, from the *Department of Pharmaceutical Development, Research and Development Department, American Critical Care, McGaw Park, IL 60085.* Accepted for publication April 21, 1982. *Present address: Xavier University, New Orleans, LA 70125.

Abstract □ The distribution of [^{14}C]bretylium tosylate in the body and the relationship between tissue and plasma concentrations was determined following intravenous administration of the drug to Charles River rats. The renal excretion of bretylium was rapid in rats and follows an active process. On the average, 50% of the administered dose was excreted in the urine within 1 hr. In the postequilibrium phase, the plasma concentration declined with a half-life of 5 hr. Bretylium concentrations in all tissues, except the heart, declined rapidly according to a triexponential equation. The liver and kidney bretylium concentrations declined in parallel to the plasma concentration with mean tissue–plasma concentration ratios of 6.04 and 12.3, respectively, in the β phase. However, the concentration of bretylium in the heart increased gradually and peaked at 2 hr, with a tissue–plasma concentration ratio of 121, which, in turn, declined to a value of >60 after 8 hr. The data indicated that (*a*) bretylium is rapidly distributed into the liver and kidney immediately after reaching the systemic circulation; (*b*) the distribution into the heart occurs at a slower rate compared with the other organs, and the drug has a high affinity to the myocardium; and (*c*) since the heart is the site of action and there is no direct correlation between the concentrations in myocardium and plasma, the antiarrhythmic effect of bretylium may not be related to the plasma concentration.

Keyphrases □ Bretylium tosylate—^{14}C-labeled, tissue distribution, rats, plasma, renal excretion □ Distribution—tissue, [^{14}C]bretylium tosylate in the rat, plasma, renal excretion □ Excretion, renal—tissue distribution of [^{14}C]bretylium tosylate in rats, plasma

Bretylium tosylate is a quaternary ammonium salt given in the treatment of cardiac arrhythmia. It suppresses *ventricular* fibrillation within minutes of intravenous infusion (1). The suppression of ventricular tachycardia, however, developed more slowly, usually 20–120 min after intramuscular administration of 4 mg/kg of bretylium tosylate in humans (2). The effect of bretylium in the intact heart was shown to be biphasic, with an initial transient increase in blood pressure and heart rate followed by an opposite and more prolonged depression of these same

0022-3549/83/0500-0556$01.00/0

Table I—Tissue to Plasma Concentration Ratios of [^{14}C]Bretylium Tosylate During 8 hr After Drug Administration

Hours	Tissue–Plasma Concentration Ratio						
	Serum	Red Blood Cells[a]	Liver	Kidney	Heart	Lung	Spleen
0.1[b]	1.13	1.23	14.1	25.8	3.23	3.23	3.19
0.5	1.30	1.41	19.2	27.0	16.1	—	—
1.0[b]	1.69	1.82	16.2	19.3	57.9	16.4	6.86
2.0	1.80	2.05	11.6	17.3	121	—	—
4.0[b]	2.19	2.56	6.69	14.6	94.1	9.78	11.6
6.0[b]	1.86	1.89	4.69	9.48	60.0	7.93	8.07
8.0	2.16	2.48	6.74	12.8	69.5	—	—
Mean[c] β-Phase Ratio	2.07	2.31	6.04	12.3	74.5	8.86	9.84

[a] Amount of drug in red blood cells was determined by amount in whole blood minus amount in plasma, where amount in plasma was determined by plasma concentration [volume of whole blood (1-hematocrit)] and red blood cell concentration was determined by amount/(volume of whole blood × hematocrit). [b] Average ratios from eight rats for red blood cells, liver, kidney, and heart. Lung and spleen values and all other values are average ratios from four animals. [c] The β-phase ratio was calculated from the linear portion of each curve, *i.e.*, 4–8 hr for each tissue.

parameters (3). These effects probably can be related to the time course of bretylium in the heart following administration.

In dogs, the myocardial drug concentrations were shown to increase gradually with a peak occurring at 1.5–6.0 hr after intravenous administrations of 2 and 6 mg/kg of bretylium tosylate (4). The myocardial tissue–serum concentration ratio increased progressively to 6.4–12.6 after 12 hr. In the same study, the antifibrillatory effect was correlated with the myocardial levels of bretylium but not with serum concentrations.

Pharmacokinetic studies in humans and animals showed that bretylium has a very large volume of distribution (5–7), indicating a high affinity to tissues. Over 80% of a 5-mg/kg bretylium tosylate dose is excreted unchanged in urine by active renal excretion processes (5, 8). The average biologic half-life of bretylium is 8 hr in four normal subjects (5) and becomes longer in patients with impaired renal function (9).

In rats, the biologic half-life of bretylium is ~5 hr (7). An average of 94–95% of a 10-mg/kg [^{14}C]bretylium tosylate dose was recovered in 72 hr, of which 63–65% was excreted unchanged in urine and 30–31% was eliminated unchanged in feces following intravenous administration, indicating a pronounced biliary excretion (7, 8). The purpose of the present investigation was to examine the distribution pattern of bretylium in well-perfused organs, heart, kidney, and liver, which are the sites of pharmacological action, urinary excretion, and possible metabolism of the drug, respectively, in rats.

EXPERIMENTAL

This investigation was carried out in two separate studies and on two different occasions. For this purpose, male Charles River rats[1] weighing 300–400 g were used. Custom synthesized [^{14}C]bretylium tosylate labeled on the benzylic carbons (specific activity 27.3 μCi/mg, 99% purity) was purchased[2]. The labeled compound was mixed with cold bretylium tosylate[3] and dissolved in saline to produce the injection solution (5 mg/ml, specific activity 3.4 μCi/mg).

In study I, 28 animals were divided into seven groups of four rats each. Each animal received an intravenous injection of 10 mg/kg of [^{14}C]-bretylium tosylate, and each group was then sacrificed by portal vein bleeding under ether anesthesia at the following times postdose: 0.1, 0.5, 1, 2, 4, 6, and 8 hr. A portion of the blood sample was centrifuged in a tube containing dry heparin to separate plasma, and the other was allowed to coagulate and then centrifuged to collect serum. An aliquot of the heparinized blood was dispensed into a combustion cup for total radioactivity determination in whole blood. The kidneys, liver, and heart were removed.

Study II was performed approximately 1 year later. Sixteen animals were divided into four groups of four rats each. Each animal received an intravenous dose of 10 mg/kg of [^{14}C]bretylium tosylate, and each group was sacrificed at 0.1, 1, 4, and 6 hr after drug administration, in the same manner as described in study I. Again plasma and serum were collected. In addition, the kidneys, liver, heart, lung, spleen, and carcass were separated. All urine and feces were quantitatively collected.

Immediately after removal, the organs were sliced, blotted in tissue paper to remove excess blood, and weighed. To the organs, the carcass, and the feces, a saline solution 3–5 times the weight of the organ was added. The mixture was then homogenized[4] in an ice bath. An aliquot of each homogenate was frozen and stored until assay.

The total radioactivity in plasma was determined on an aliquot of the samples in a liquid scintillation counter[5]. The total radioactivity in blood, tissue, and feces samples was measured after combustion[6] of an aliquot of the homogenate and by counting the processed samples in the liquid scintillation counter.

Mean concentrations (n = 4) in the plasma, serum, red blood cells, liver, and kidney were fitted to a triexponential equation, describing a typical three-compartment open model (7). The concentration in the heart did not follow the same model. The terminal disposition half-life in myocardium was calculated using nonlinear regression analysis of a concentration–time profile. The data from study II served for comparative purposes and allowed the estimation of the percentage of the dose remaining in various tissues at different times.

RESULTS AND DISCUSSION

Figure 1 depicts the time course of bretylium concentration in various tissues and plasma following intravenous administration. The data from study II, which was conducted 1 year later, were included. There was good agreement between the two sets of data showing an excellent reproducibility of bretylium pharmacokinetics in rats. The concentrations in plasma, liver, and kidney declined in parallel following intravenous administration. In general, there was a good fit of these data to a triexponential equation describing a three-compartment open model. The elimination half-life was 5 hr, which is in agreement with the previously reported value (7).

The accumulation and decline of bretylium concentration in the heart resembled the simulated time course of the drug in a deep peripheral compartment. There was a gradual accumulation of bretylium in the heart with a peak occurring between 1–2 hr. This was also in agreement with reported data of a gradual increase in myocardium levels in dogs (4). The postdistribution decline in bretylium heart concentration, however, was more rapid, showing a biological half-life of 2 hr. It is possible that this decline is part of a redistribution process and that concentration in the heart will eventually reach an equilibrium with that in plasma and other tissues. Since the heart is the site of action, it will be expected that antiarrhythmic action will be associated with the concentration of bretylium in myocardium. Such a situation has been demonstrated in

[1] Charles River Breeding Laboratories, Wilmington, Mass.
[2] New England Nuclear, Boston, Mass.
[3] American Critical Care, McGaw Park, Ill.
[4] Polytron Homogenizer, Brinkman Instruments, Inc., Westbury, N.Y.
[5] Models 425 and 460C, Packard Instruments, Inc., Downers Grove, Ill.
[6] Sample Oxidizer Model B306, Packard Instruments, Inc., Downers Grove, Ill.

Table II—Percent of Dose Excreted in Urine and Feces and Remaining in Selected Organs Following Intravenous Administration of Bretylium Tosylate to Rats

Hours	Percent of Dose[a]							
	Blood	Kidney	Liver	Heart	Spleen	Lung	Urine	Feces
0.1	4.49	12.0	29.6	0.972	0.364	0.786	—	—
	(0.327)	(3.68)	(1.87)	(0.029)	(0.053)	(0.084)		
1.0	0.916	1.14	5.69	1.43	0.156	0.653	49.2	1.29
	(0.120)	(0.187)	(1.04)	(0.104)	(0.006)	(0.042)	(3.30)	(1.25)
4.0	0.339	0.375	0.694	0.579	0.069	0.099	55.9	0.733
	(0.011)	(0.208)	(0.123)	(0.209)	(0.004)	(0.020)	(6.12)	(1.465)
6.0	0.215	0.143	0.388	0.288	0.038	0.061	61.1	3.48
	(0.066)	(0.016)	(0.097)	(0.101)	(0.015)	(0.010)	(1.66)	(1.04)

[a] Mean of four rats, standard deviation in parentheses.

dogs (4). Thus, until an equilibrium between myocardium and plasma levels is attained, it is reasonable to presume that there will be no correlation between antiarrhythmic action and plasma concentration.

Table I summarizes the tissue–plasma concentration ratios of serum, red blood cells, liver, kidney, heart, lung, and spleen tissues. Table II summarizes the tissue content of bretylium and amounts excreted in urine and feces at various times after intravenous administration of the drug. For both liver and kidney, which are well-perfused organs, the tissue–plasma concentration ratios were generally higher in the distribution phase than in the β-phase during which average equilibrium ratios of 6.0 and 12.3, respectively, were attained. At 0.1 hr, the uptake of bretylium in liver and kidney accounted for 30 and 12% of the dose, respectively. The high bretylium levels in the liver and kidney are consistent with rapid elimination of the drug: ~50% of the dose is excreted in urine within 1 hr (Table II). Also, it was demonstrated that about one-third of the dose is eliminated by biliary excretion (7).

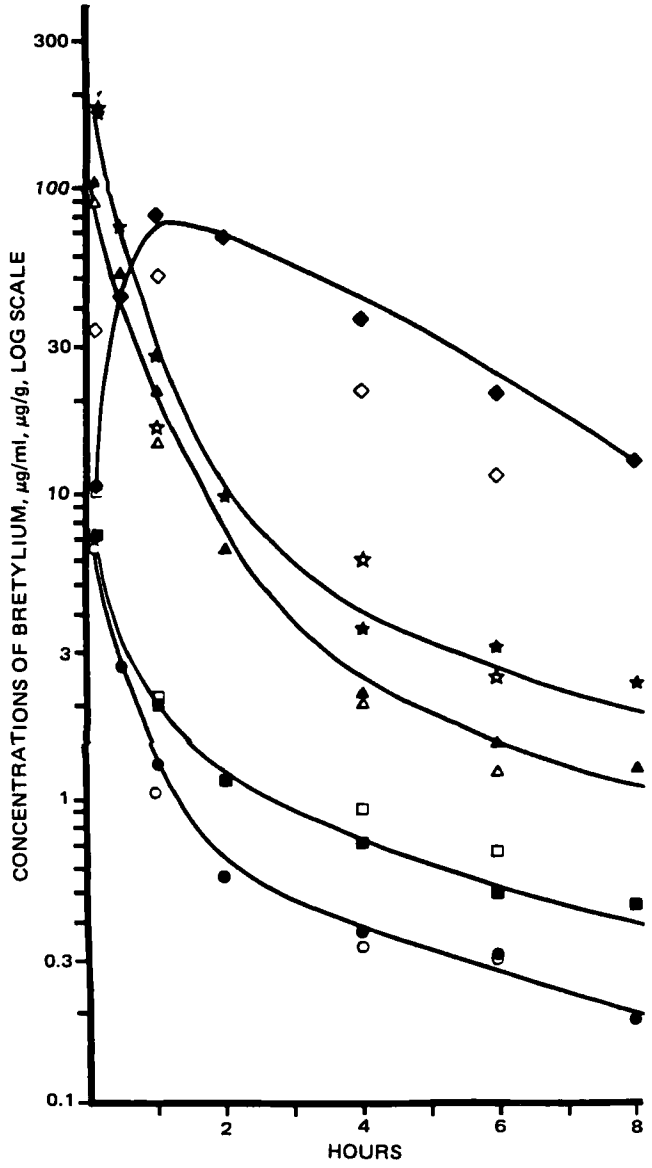

Figure 1—*Mean concentration of bretylium in plasma (●), red blood cells (■), liver (▲), kidney (★), and heart (◆) following intravenous administration of 10 mg/kg of bretylium tosylate in rats in study I. The respective open symbols represent data from study II. Observations from study I were used to fit the curves. Each data point is the mean of four animals. The concentrations in plasma are given by micrograms per milliliter and in the tissues by micrograms per gram.*

The heart–plasma concentration ratio increased gradually from 3.2 after 6 min to 121 after 2 hr. The peak ratio was much higher than that observed in dogs, 12.6 (4), which may indicate species differences in bretylium distribution in the body. There was a sharp decrease in the heart–plasma concentration ratio to ~70 after 8 hr. The continuous change in this concentration ratio is consistent with delayed onset of action followed by a more prolonged effect reported in the literature (3, 4).

For red blood cells, there was also a gradual increase in the tissue–plasma concentration ratios, reaching an apparent equilibrium within 2 hr. This gradual change in the ratios may be due to either a rapid distribution in the cells followed by a slower rate of redistribution in the plasma or a gradual uptake of the drug by red blood cells against a concentration gradient, presumably by an active mechanism. The lung and spleen uptake also appears to be similar to that in the red blood cells. An active tissue uptake has been suggested for another quaternary ammonium compound, tetraethylammonium, in rats (10).

One hr after drug administration, on the average, 49 and 1.3% of the dose were found in the urine and feces, respectively. The initial rapid elimination of bretylium in urine was proportional to the initial high plasma concentration (8 μg/ml). When the plasma level declined to <1 μg/ml (1 hr postdose), the urinary excretion accounted for ~12% over the next 5 hr. Of the remaining 50% at 1 hr, 10% of the dose could be accounted for in blood, kidney, liver, heart, spleen, and lung tissues. This amount decreased significantly to ~2% at 6 hr following administration.

The data suggest that at 1 hr, 39% of the dose should be accounted for in the carcass. The overall radioactivity determined in the carcass, however, was equivalent to 50% of the dose. Unfortunately, the homogenization of the carcass was later found to be incomplete, and it is possible that this caused the overestimation of body content by nearly 10%. Previously, it was shown that about one-third of the bretylium dose was eliminated in the feces through biliary excretion (7). Therefore, the intestines might contain most of the radioactivity which was found in the carcass.

In summary, bretylium is rapidly distributed in the body, particularly in the liver and kidneys, immediately after reaching systemic circulation. While there was a parallel decline in liver, kidney, and plasma concentrations of bretylium, there was no correlation between plasma and heart concentrations of the drug. The heart showed high affinity to bretylium with its concentration reaching 120 times plasma levels within 2 hr. These data suggest that the antiarrhythmic effect of bretylium will not be associated with its plasma concentrations until an equilibrium between heart and plasma concentrations is attained.

REFERENCES

(1) G. Sanna and R. Arcidiacono, *Am. J. Cardiol.*, **32**, 982 (1973).

(2) D. W. Romhilt, S. S. Bloomfield, and R. J. Lipicky, *Circulation*, **45**, 800 (1972).

(3) K. Chattergee, W. J. Mandel, J. K. Vyden, W. W. Parmley, and J. S. Forrester, *J. Am. Med. Assoc.*, **223**, 757 (1973).

(4) J. L. Anderson, E. Patterson, M. Conlon, S. Pasyk, B. Pitt, and B. Lucchesi, *Am. J. Cardiol.*, **46**, 583 (1980).
(5) P. K. Narang, J. Adir, J. Josselson, A. Yacobi, and J. Sadler, *J. Pharmacokinet Biopharm.*, **8**, 365 (1980).
(6) J. L. Anderson, E. Patterson, J. G. Wagner, J. K. Stewart, H. L. Behm, and B. R. Lucchesi, *Clin. Pharmacol. Ther.*, **28**, 468 (1980).
(7) B. L. Kamath, H. F. Stampfli, C. M. Lai, and A. Yacobi, *J. Pharm. Sci.*, **70**, 667 (1981).
(8) R. Kuntzman, I. Tsai, R. Chang, and A. H. Conney, *Clin. Pharmacol. Ther.*, **11**, 829 (1970).
(9) J. Adir, P. K. Narang, J. Josselson, and J. H. Sadler, *N. Engl. J. Med.*, **300**, 1390 (1979).
(10) M. Mintun, K. J. Himmelstein, R. L. Schroder, M. Gibaldi, and D. D. Shen, *J. Pharmacokinet Biopharm.*, **8**, 373 (1980).

Room Temperature Phosphorescence Determination of Propranolol in Pharmaceutical Formulations

RICKY P. BATEH and J. D. WINEFORDNER ˣ

Received March 19, 1982, from the *University of Florida, Department of Chemistry, Gainesville, FL 32611.* Accepted for publication May 14, 1982.

Abstract □ A simple, rapid, and specific procedure was used for the analysis of propranolol in pharmaceutical formulations. The procedure consisted of dissolving (diluting) appropriate quantities of preparations and standards in (with) a 2 *M* potassium iodide–ethanol–water solution, spotting 5 μl of each resultant solution onto filter paper disks, determining the phosphorescence intensities at room temperature, and comparing sample signal levels with those of standards. The results indicated that room temperature phosphorescence can be easily applied to the analysis of pharmaceutical formulations where active ingredients are generally contained in a wide variety of matrices.

Keyphrases □ Propranolol—room temperature phosphorescence determination in tablets and injections □ Phosphorescence—determination of propranolol in tablets and injections □ β-adrenergic agents—propranolol, room temperature phosphorescence determination, tablets and injections

Propranolol hydrochloride, a β-adrenergic blocker, is commonly used for the treatment of nonacute hypertension, angina pectoris, and cardiac arrhythmias. With the patent on the only marketed product nearing its expiration, generic brands of propranolol will soon become available. Because generic manufacturers often use a variety of materials (diluents, binders, *etc.*) in their formulations, a specific procedure is needed for the quantitation of the active ingredient in the formulation.

The current USP procedure (1) for propranolol is cumbersome, and as a result, many pharmaceutical manufacturers are currently investigating fluorometry and high-performance liquid chromatography (HPLC) for quality control.

The present report describes a simple and rapid room temperature phosphorescence procedure applicable to the determination of propranolol in several pharmaceutical preparations. While room temperature phosphorescence has been shown to be analytically useful, real sample applications have been limited (2, 3). Overall, room temperature phosphorescence offers good selectivity with moderate sensitivity and detection power.

EXPERIMENTAL

Reagents—Propranolol hydrochloride[1] (I) and hydrochlorothiazide[2] (II) were used as received. All pharmaceutical preparations were purchased through a local hospital pharmacy[3]. All other materials were of analytical reagent grade.

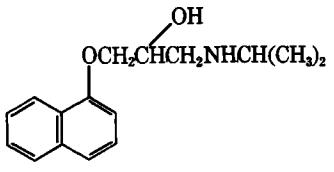

I

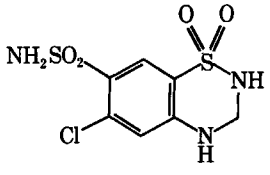

II

Apparatus—All room temperature phosphorescence measurements were made with a spectrophotofluorometer[4] fitted with a 150-W xenon arc lamp[5], a laboratory-constructed phosphoroscope (4) for bar, room temperature phosphorescence (5), and a potted photomultiplier tube[6]. A ratio photometer[7] supplied high voltage to the photomultiplier tube in addition to serving as a DC amplifier. All line voltages were regulated with an AC regulator[8].

Standard and Sample Preparation—A standard stock solution (400 μg/ml) was prepared by dissolving an accurately weighed portion of propranolol hydrochloride in a 2 *M* potassium iodide solution (ethanol–water, 50:50). Standard solutions (5, 10, 20, 50, 100, 200, and 300 μg/ml) were prepared daily by mixing appropriate volumes of the stock solution with the ethanolic solution. Samples were prepared for assay by dissolution–dilution in/with the ethanolic solution. For analysis of representative samples, 20 tablets were weighed and powdered with a mortar and pestle, and four portions (equivalent to 100 μg/ml of active ingredient in a total volume of 10 ml) were dissolved in the ethanolic solution. This procedure was repeated for each solid sample. For the analysis of liquid preparations, appropriate volumes (same equivalence as tablets) of the samples were diluted with the ethanolic solution. Four different test solutions were prepared for each pharmaceutical formulation; each test solution contained 100 μg/ml of active ingredient.

Procedure—Bar, room temperature phosphorescence analysis consisted of an aluminum bar, a cover plate with four holes (each ~0.64-cm diameter) and filter paper disks[9]. The filter paper disks were placed under the cover plate and the cover plate was tightened into place on the bar with four screws. Samples were spotted onto the paper disks in 5-μl vol-

[1] Ayerst Laboratories, New York, N.Y.: Inderal, propranolol hydrochloride; Inderide, propranolol hydrochloride with hydrochlorothiazide.
[2] Ciba Pharmaceutical Co., Summit, N.J.
[3] Pharmacy Stores, Shands Teaching Hospital, Gainesville, Fla.
[4] Aminco-Bowman SPF, American Instrument Co., Jessup, Md.
[5] Canrad-Hanovia, Newark, N.J.
[6] 1P21, Hamamatsu, Middlesex, N.J.
[7] American Instrument Co.
[8] Sorenson 1001, Norwalk, Conn.
[9] Grade 903, Schleicher & Schuell, Keene, N.H.

0022-3549/83/0500-0559$01.00/0

(4) J. L. Anderson, E. Patterson, M. Conlon, S. Pasyk, B. Pitt, and B. Lucchesi, *Am. J. Cardiol.*, **46**, 583 (1980).
(5) P. K. Narang, J. Adir, J. Josselson, A. Yacobi, and J. Sadler, *J. Pharmacokinet Biopharm.*, **8**, 365 (1980).
(6) J. L. Anderson, E. Patterson, J. G. Wagner, J. K. Stewart, H. L. Behm, and B. R. Lucchesi, *Clin. Pharmacol. Ther.*, **28**, 468 (1980).
(7) B. L. Kamath, H. F. Stampfli, C. M. Lai, and A. Yacobi, *J. Pharm. Sci.*, **70**, 667 (1981).
(8) R. Kuntzman, I. Tsai, R. Chang, and A. H. Conney, *Clin. Pharmacol. Ther.*, **11**, 829 (1970).
(9) J. Adir, P. K. Narang, J. Josselson, and J. H. Sadler, *N. Engl. J. Med.*, **300**, 1390 (1979).
(10) M. Mintun, K. J. Himmelstein, R. L. Schroder, M. Gibaldi, and D. D. Shen, *J. Pharmacokinet Biopharm.*, **8**, 373 (1980).

Room Temperature Phosphorescence Determination of Propranolol in Pharmaceutical Formulations

RICKY P. BATEH and J. D. WINEFORDNER ˣ

Received March 19, 1982, from the *University of Florida, Department of Chemistry, Gainesville, FL 32611.* Accepted for publication May 14, 1982.

Abstract □ A simple, rapid, and specific procedure was used for the analysis of propranolol in pharmaceutical formulations. The procedure consisted of dissolving (diluting) appropriate quantities of preparations and standards in (with) a 2 *M* potassium iodide–ethanol–water solution, spotting 5 μl of each resultant solution onto filter paper disks, determining the phosphorescence intensities at room temperature, and comparing sample signal levels with those of standards. The results indicated that room temperature phosphorescence can be easily applied to the analysis of pharmaceutical formulations where active ingredients are generally contained in a wide variety of matrices.

Keyphrases □ Propranolol—room temperature phosphorescence determination in tablets and injections □ Phosphorescence—determination of propranolol in tablets and injections □ β-adrenergic agents—propranolol, room temperature phosphorescence determination, tablets and injections

Propranolol hydrochloride, a β-adrenergic blocker, is commonly used for the treatment of nonacute hypertension, angina pectoris, and cardiac arrhythmias. With the patent on the only marketed product nearing its expiration, generic brands of propranolol will soon become available. Because generic manufacturers often use a variety of materials (diluents, binders, *etc.*) in their formulations, a specific procedure is needed for the quantitation of the active ingredient in the formulation.

The current USP procedure (1) for propranolol is cumbersome, and as a result, many pharmaceutical manufacturers are currently investigating fluorometry and high-performance liquid chromatography (HPLC) for quality control.

The present report describes a simple and rapid room temperature phosphorescence procedure applicable to the determination of propranolol in several pharmaceutical preparations. While room temperature phosphorescence has been shown to be analytically useful, real sample applications have been limited (2, 3). Overall, room temperature phosphorescence offers good selectivity with moderate sensitivity and detection power.

EXPERIMENTAL

Reagents—Propranolol hydrochloride[1] (I) and hydrochlorothiazide[2] (II) were used as received. All pharmaceutical preparations were purchased through a local hospital pharmacy[3]. All other materials were of analytical reagent grade.

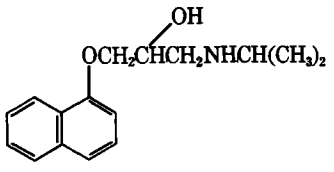

I

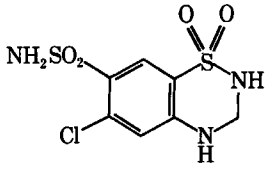

II

Apparatus—All room temperature phosphorescence measurements were made with a spectrophotofluorometer[4] fitted with a 150-W xenon arc lamp[5], a laboratory-constructed phosphoroscope (4) for bar, room temperature phosphorescence (5), and a potted photomultiplier tube[6]. A ratio photometer[7] supplied high voltage to the photomultiplier tube in addition to serving as a DC amplifier. All line voltages were regulated with an AC regulator[8].

Standard and Sample Preparation—A standard stock solution (400 μg/ml) was prepared by dissolving an accurately weighed portion of propranolol hydrochloride in a 2 *M* potassium iodide solution (ethanol–water, 50:50). Standard solutions (5, 10, 20, 50, 100, 200, and 300 μg/ml) were prepared daily by mixing appropriate volumes of the stock solution with the ethanolic solution. Samples were prepared for assay by dissolution–dilution in/with the ethanolic solution. For analysis of representative samples, 20 tablets were weighed and powdered with a mortar and pestle, and four portions (equivalent to 100 μg/ml of active ingredient in a total volume of 10 ml) were dissolved in the ethanolic solution. This procedure was repeated for each solid sample. For the analysis of liquid preparations, appropriate volumes (same equivalence as tablets) of the samples were diluted with the ethanolic solution. Four different test solutions were prepared for each pharmaceutical formulation; each test solution contained 100 μg/ml of active ingredient.

Procedure—Bar, room temperature phosphorescence analysis consisted of an aluminum bar, a cover plate with four holes (each ~0.64-cm diameter) and filter paper disks[9]. The filter paper disks were placed under the cover plate and the cover plate was tightened into place on the bar with four screws. Samples were spotted onto the paper disks in 5-μl vol-

[1] Ayerst Laboratories, New York, N.Y.: Inderal, propranolol hydrochloride; Inderide, propranolol hydrochloride with hydrochlorothiazide.
[2] Ciba Pharmaceutical Co., Summit, N.J.
[3] Pharmacy Stores, Shands Teaching Hospital, Gainesville, Fla.
[4] Aminco-Bowman SPF, American Instrument Co., Jessup, Md.
[5] Canrad-Hanovia, Newark, N.J.
[6] 1P21, Hamamatsu, Middlesex, N.J.
[7] American Instrument Co.
[8] Sorenson 1001, Norwalk, Conn.
[9] Grade 903, Schleicher & Schuell, Keene, N.H.

0022-3549/83/0500-0559$01.00/0

Table 1—Results for the Determination of Active Ingredients in Pharmaceutical Formulations [a]

Formulation, mg Active Ingredient/ Dosage Form	Concentration Found Experimental, μg/ml[b]		Coefficient of Variation, %	Experimental Amount (mg) of Active Ingredient/ Dosage Form[c]
Propranolol	Mean	Range		
20	98	90–108	5.2	20
40	97	88–108	7.2	39
80	102	94–108	4.0	82
1 (injection 1-ml ampule)	103	94–111	4.4	1
Propranolol/Hydrochlorothiazide				
40/25	102	94–110	5.0	41
80/25	101	94–110	4.5	81

[a] All test samples were 100 μg/ml of active ingredient. [b] Calculated from 16 measurements of each of four samples. [c] Mean value calculated from 16 determinations of active ingredients in each of four weighed portions.

umes with a micropipet[10]. After spotting, the bar was slipped into the sample compartment (equipped with a phosphoroscope can with a chopping rate of 200 Hz) and the samples were allowed to dry for 7 min under a flow of dehumidified nitrogen gas (~20 liters/min). During the drying process, signals increased over a period of ~6 min at which time a plateau was reached for ~2 min. Measurements were made on this plateau. This procedure was repeated 16 times for each sample and standard. The excitation and emission wavelengths used in the analyses were 306 and 492 nm, respectively.

Quantitation—Quantitation was achieved by comparing the relative phosphorescence intensities of the samples with those of the standards. For the analyses, the linear range of the propranolol standard solutions extended from 20 to 300 μg/ml. Linear regression analysis gave the line $y = 0.725x - 7.34$ with a correlation coefficient of +0.999.

RESULTS AND DISCUSSION

The results in Table I indicate that room temperature phosphorescence can be successfully applied to the determination of propranolol in pharmaceutical preparations. Precision studies with 16 determinations of each sample and standard gave coefficients of variation between 4 and 8%. While room temperature phosphorescence is well established as a method of analysis with great selectivity, its sensitivity generally lags behind that of other techniques.

Both propranolol and hydrochlorothiazide phosphoresce when 2 *M* NaOH is added to the ethanolic solution. However, because of the weaker phosphorescence signal of hydrochlorothiazide, it was not possible for it to be quantitatively determined in the prepared mixtures. Only propranolol appeared to phosphoresce when present in the ethanolic solution, and this component was analyzed in the prepared mixtures. Figures 1 and 2 illustrate what is spectrally observed without and with the addition of 2 *M* NaOH to the ethanolic solutions.

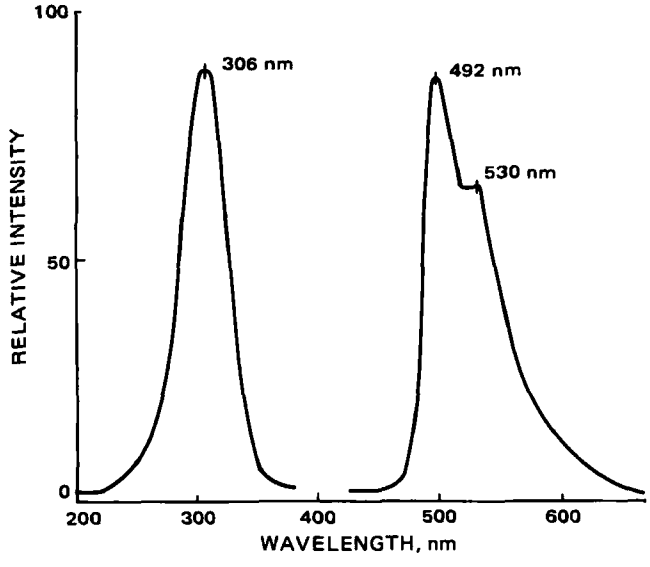

Figure 1—*Room temperature phosphorescence obtained from 100-μg/ml propranolol hydrochloride in an ethanolic solution and from a mixture of 100-μg/ml propranolol hydrochloride and 50-μg/ml hydrochlorothiazide.*

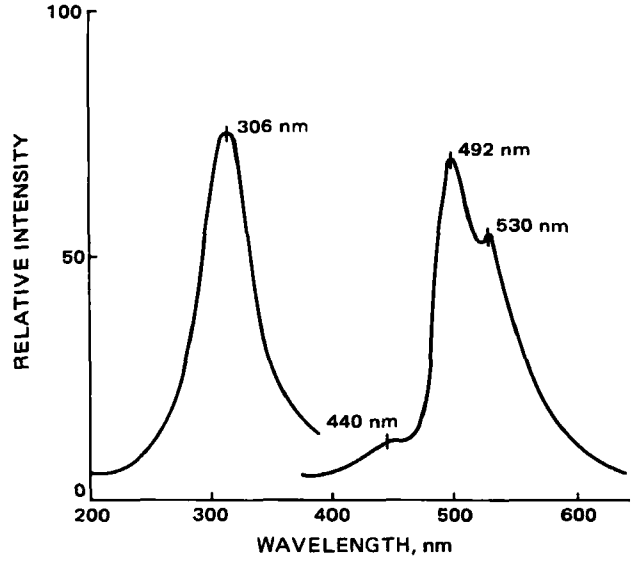

Figure 2—*Room temperature phosphorescence obtained from a mixture of 100-μg/ml propranolol hydrochloride and 50-μg/ml hydrochlorothiazide with 2 M NaOH in an ethanolic solution.*

The selectivity factor in room temperature phosphorescence was advantageous in that no compound other than propranolol appeared to phosphoresce. Because pharmaceuticals are proprietary in nature, no absolute assurance of any other species contributing to the phosphorescence of the sample can be given. It would be expected that those species in the formulations that may phosphoresce are minor constituents and are subsequently diluted when the sample is prepared for analysis. Thus, this procedure is reported to be quite simple and specific for the determination of propranolol in pharmaceutical formulations.

[10] SMI micro/pettor, Scientific Manufacturing Industries, Emeryville, Calif.

REFERENCES

(1) "United States Pharmacopeia XX/National Formulary XV," United States Pharmacopeial Convention, Rockville, Md., 1980, p. 684.

(2) R. J. Hurtubise, "Solid Surface Luminescence Analysis: Theory, Instrumentation, Applications," Dekker, New York, N.Y., 1982.

(3) R. P. Bateh and J. D. Winefordner, *Anal. Lett.*, **15**, 373 (1982).

(4) J. L. Ward, Ph.D. Thesis, University of Florida, 1980.

(5) J. L. Ward, R. P. Bateh, and J. D. Winefordner, *Analyst*, **107**, 335 (1982).

ACKNOWLEDGMENTS

This research was supported by NIH grant GM-11373-19. Partial support for this research was received through a University of Florida Biomedical Grant. The authors would like to thank Ayerst Laboratories for their samples of propranolol hydrochloride. Hydrochlorothiazide was kindly provided by the Ciba Pharmaceutical Company.

Convenient Method of Simultaneously Analyzing Aluminum and Magnesium in Pharmaceutical Dosage Forms Using Californium-252 Thermal Neutron Activation

ROBERT R. LANDOLT *x **and STANLEY L. HEM** ‡

Received June 19, 1981, from the *Departments of *Bionucleonics and ‡Industrial and Physical Pharmacy, School of Pharmacy and Pharmacal Sciences, Purdue University, West Lafayette, IN 47907.* Accepted for publication May 6, 1982.

Abstract □ A commercial antacid suspension containing aluminum hydroxide and magnesium hydroxide products was used as a model sample to study the use of a californium-252 thermal neutron activation as a method for quantifying aluminum content as well as for the simultaneous assay of aluminum and magnesium. A 3.5-μg californium-252 source was used for the activation, and the induced aluminum-28 and magnesium-27 activity was simultaneously measured by sodium iodide crystal gamma-ray spectrometry using dual single-channel analyzers and scalers. The antacid suspension was contained in a chamber designed with the unique capability of serving as the container for counting the induced radioactivity in addition to being the irradiation chamber itself. Ten replicate irradiations were performed, and the precision was compared with 10 replicate analyses of the antacid suspension using the official ethylenediaminetetraacetic acid titration method. For aluminum the precision was 1.4 *versus* 0.62% for the titration method. For the magnesium the precision was 5.3 *versus* 0.79% for the titration method. This pilot study demonstrated that use of more intense californium-252 sources, which are commonly available, would provide a method that is competitive with the ethylenediaminetetraacetic acid titration method in precision and in other aspects as well.

Keyphrases □ Californium-252—thermal neutron activation, method of simultaneously analyzing aluminum and magnesium in pharmaceutical dosage forms □ Dosage forms—method of simultaneously analyzing aluminum and magnesium using californium-252 thermal neutron activation □ Aluminum—method of anlaysis in pharmaceutical dosage forms using californium-252 thermal neutron activation □ Magnesium—method of analysis in pharmaceutical dosage forms using californium-252 thermal neutron activation

Analysis of aluminum in pharmaceutical formulations by thermal neutron activation in a reactor has been proposed (1) as an alternative to the official but somewhat cumbersome ethylenediaminetetraacetic acid titration method (2). However, limited access to reactors often makes neutron activation an uneconomical and inconvenient analysis technique. The recent availability of high intensity, relatively inexpensive, californium-252 neutron sources provides another means of analyzing pharmaceuticals for certain activable constituents. This report is a study of the feasibility of using californium-252 neutron activation analysis for aluminum quantification as well as for the simultaneous assay of aluminum and magnesium. A commercial antacid suspension containing aluminum hydroxide and magnesium hydroxide products was chosen as a typical sample for this study. However, the technique should apply to other products containing one or both of these minerals such as aluminum hydroxychloride or sterile penicillin G procaine suspension, which often is formulated with aluminum stearate.

EXPERIMENTAL

The californium-252 neutron source was in the form of a needle 5-cm long and 0.5-cm in diameter. The californium-252 content at the time of irradiation was 3.5 μg, which gave an emission rate of 8.1×10^6 neutrons/sec.

The chamber (Fig. 1) in which the suspension was contained during irradiation also had the unique capability of serving as the chamber for counting the induced radioactivity following irradiation. During irradiation the chamber was placed upright in a tank of water moderator, such that the level of the water was the same height as the level of solution in the chamber. After irradiation the californium-252 source and its surrounding plexiglass moderator sleeve were removed from the chamber. The chamber was then simply inverted and placed over a sodium iodide crystal for counting, thereby resembling a Marinelli-type counting chamber. All irradiations were for exactly 36 min, followed by a 90-sec delay, and then a 36-min count. The predominant activation reactions of aluminum and magnesium (Table I) are caused by neutrons thermalized by the water moderator and by water present in the antacid suspension.

The instrumentation required for analysis of the gamma rays emitted from the magnesium-27 and aluminum-28 can be economically assembled by using dual single-channel analyzers and scalers. One analyzer–scaler was used to count the 0.83-MeV full-energy peak of magnesium-27 and the other analyzer–scaler simultaneously counted the 1.78-MeV peak of aluminum-28. The magnesium-27 analyzer was calibrated with a manganese-54 (0.835 MeV) standard source, and the aluminum-28 analyzer was calibrated with an aluminum-26 (1.81 MeV) standard. Figure 2 is a gamma-ray spectrum obtained using a multichannel analyzer to count the antacid sample showing the two full energy peak bands used to measure the magnesium-27 and aluminum-28 with the dual single-channel analyzers.

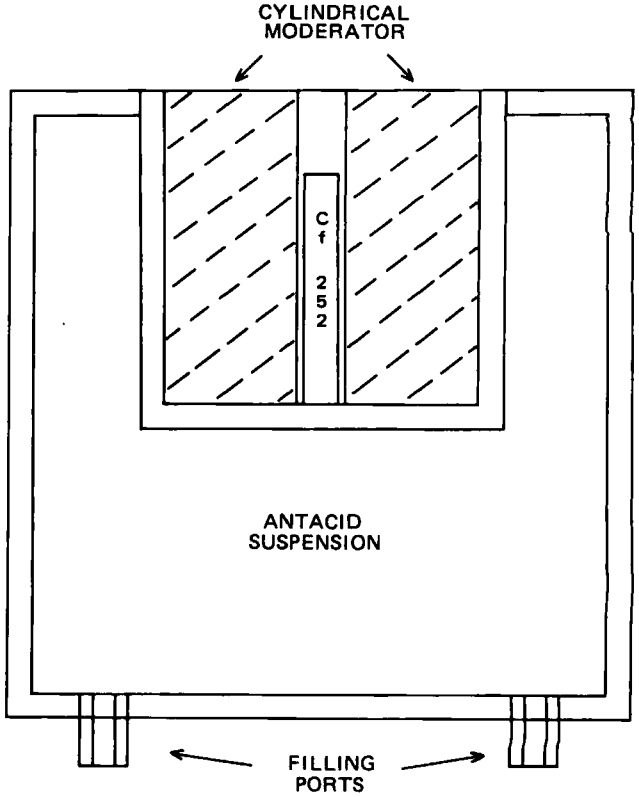

Figure 1—*Cross-section of cylindrical irradiation–counting chamber showing the californium-252 (Cf 252) source position. Diameter = 14.5 cm; height = 14.5 cm; volume = 2.1 liters.*

0022-3549/83/0500-0561$01.00/0

Table I—Magnesium and Aluminum Reaction Parameters (3)

Parameter	Magnesium	Aluminum
Reaction	$^{26}Mg(n,\gamma)^{27}Mg$	$^{27}Al(n,\gamma)^{28}Al$
Isotope abundance	11.2%	100%
Cross section (thermal)	27 mb[a]	210 mb
Half-life	9.5 min	2.3 min
Gamma-ray energy	0.83, 0.01 MeV	1.78 MeV
Interferences	None	$^{27}Al(n,p)^{27}Mg$
Cross section	—	3 mb

[a] Millibarns.

Table II—Aluminum and Magnesium Analysis of Commercial Antacid Suspension by Californium-252 Neutron Activation Analysis and by the Official Ethylenediaminetetraacetic Acid Titration Method

Neutron Activation, net counts[a]		USP Method, %	
Aluminum 28	Magnesium 27	Equivalent Aluminum Oxide	Magnesium Hydroxide
5218	1221	2.20	4.04
5384	1147	2.21	4.00
5333	1102	2.19	3.98
5243	1244	2.18	3.96
5333	1180	2.20	3.97
5165	1127	2.17	3.99
5347	1080	2.20	4.03
5285	1121	2.20	3.97
5224	1187	2.18	4.05
5154	1146	2.21	4.01
Mean 5229	1166	2.19	4.00
SD 75.6	61.2	0.0135	0.0316
(1.4%)	(5.3%)	(0.62%)	(0.79%)

[a] Aluminum-28 background = 252 counts; magnesium-27 background = 1282 counts.

Ten replicate irradiations of the commercial antacid suspension were performed over a 16-day period. The counts of all replicates were normalized to the time of the first irradiation in order to correct for the decay of the californium-252 during the course of the experiment. A separate irradiation of only aluminum, in the form of a commercial aluminum hydroxide gel containing 9% equivalent aluminum oxide, was used to determine the Compton contribution of the aluminum-28 activity to the 0.830-MeV peak of magnesium-27. This constant ratio of the aluminum-28 peak counts to the counts in the magnesium-27 peak from aluminum-28 was used to remove the aluminum-28 contribution to the total magnesium-27 counts for each of the 10 irradiations.

Because of its low cross-section, the $^{27}Al(n,p)^{27}Mg$-interference reaction should not contribute significantly to the magnesium-27 peak. However, any contribution from that reaction would be eliminated when the Compton contribution to the magnesium-27 peak from aluminum-28 was subtracted.

To compare the precision of the californium-252 neutron activation analysis method with that of the official method, replicate analyses of the commercial antacid suspension were performed on 10 different days over a 2-week period by the official ethylenediaminetetraacetic acid titration method (2).

RESULTS AND DISCUSSION

The gross counting rates for the magnesium-27 and aluminum-28 peak channels were corrected for background, and in the case of the magnesium-27, for the aluminum-28 contribution to the 0.83-MeV magnesium-27 peak. The results are given in Table II along with the results of the ethylenediaminetetraacetic acid titration analysis.

It can be seen from Table II that the californium-252 method provides a precision for aluminum-28 that is considerably better than for magnesium-27. This is expected because of the higher thermal neutron activation cross section (Table I) for the $^{27}Al(n,\gamma)^{28}Al$-reaction. The precision for both aluminum and magnesium can be improved considerably by using a more intense californium-252 source than the relatively weak one which was used for this pilot study. Because of the large volumes used and the minimum amount of sample manipulation required, it can be assumed that the overall error in this technique is due entirely to the counting error. In this case the precision, expressed as the counting error, decreases inversely as the ratio of the square root of the total counts. Consequently, for example, if a californium-252 source 30 times the strength of the source utilized in this experiment were used, the magnesium-27 precision would be improved to $(\sqrt{1166}/\sqrt{1166 \times 30})$ (5.3%) = 0.97%, and the aluminum-28 precision would be improved by the same factor to a value of 0.26%.

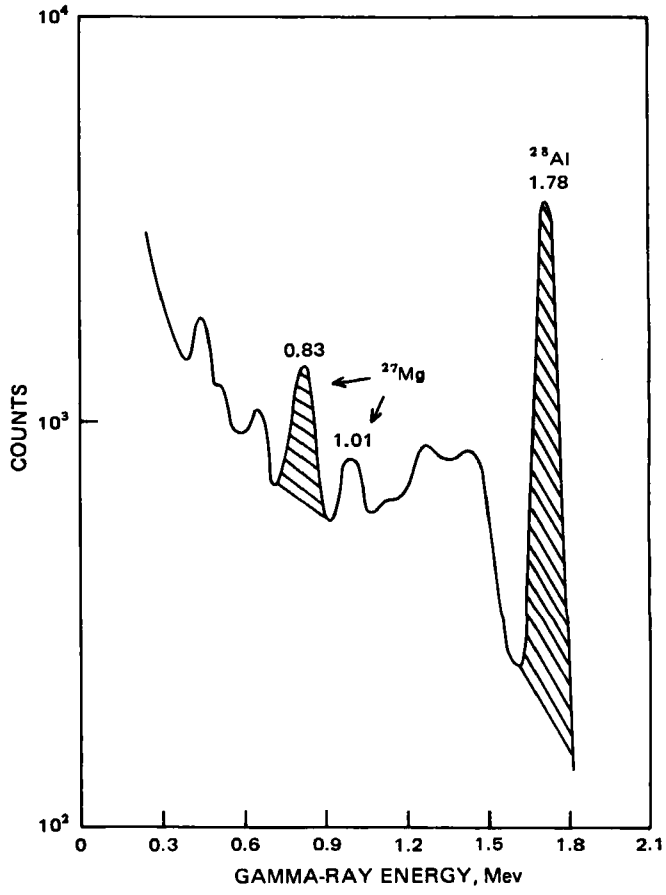

Figure 2—*Gamma-ray spectrum of neutron irradiated antacid suspension containing magnesium and aluminum showing the magnesium-27 and aluminum-28 peaks.*

This improved magnesium-27 value is competitive with the precision for the USP magnesium hydroxide method shown in Table II, and the aluminum-28 determination is more precise than the USP method for aluminum. Sources of californium-252 of this intensity, ~100 μg, are commonly available, relatively inexpensive, and the amount of shielding required is not restrictive. This technique, when used with an appropriate companion standard, should have potential application as an accurate, in-house quality control technique for products containing aluminum and magnesium.

REFERENCES

(1) J. P. F. Lambert and M. Margosis, *J. Pharm. Sci.*, **59**, 1005 (1970).

(2) "The United States Pharmacopeia," 20th rev., U.S. Pharmacopeial Convention, Inc., Rockville, Md., 1980, p. 23.

(3) A. I. Aliev, V. I. Drynkin, D. I. Leipunskaya, and V. A. Kasatkin, "Handbook of Nuclear Data for Neutron Activation Analysis" (trans. Russian by B. Benny), Keter Press, Jerusalem, 1970.

ACKNOWLEDGMENTS

The authors thank Mr. T. L. McDaniel for constructing the irradiation-counting chamber.

(−)-α-Isosparteine from *Lupinus argenteus* var. *stenophyllus*

WILLIAM J. KELLER ˣ, BRIAN N. MEYER *, and JERRY L. McLAUGHLIN*

Received March 19, 1982, from the *School of Pharmacy, Northeast Louisiana University, Monroe, LA 71209.* Accepted for publication May 12, 1982. *Present address: Department of Medicinal Chemistry and Pharmacognosy, School of Pharmacy and Pharmacal Sciences, Purdue University, West Lafayette, IN 47907.

Abstract □ Combined GLC–mass spectrometry revealed that an unidentified sparteine isomer was the major component of an alkaloid extract of the aboveground portions of *Lupinus argenteus* Pursh. var. *stenophyllus* (Rydb.) Davis (Leguminosae). After isolation, this alkaloid was characterized as the least common of the known sparteine isomers, (−)-α-isosparteine. A preliminary pharmacological study showed (−)-α-isosparteine to have a more rapid onset and a shorter duration of action when compared with (−)-sparteine on rat myocardium.

Keyphrases ◻ *Lupinus argenteus* var. *stenophyllus*—(−)-α-isosparteine, GLC-mass spectrometry, sparteine isomer ◻ (−)-α-Isosparteine—*Lupinus argenteus* var. *stenophyllus*, GLC-mass spectrometry, sparteine isomer ◻ GLC-mass spectrometry—(−)-α-isosparteine from *Lupinus argenteus* var. *stenophyllus*, sparteine isomer

The legume genus *Lupinus* is a rich source of a wide variety of quinolizidine alkaloids. Due to high concentrations of these quinolizidine bases, lupines have been implicated in acute toxicoses and death in grazing livestock (1–3). Additionally, certain lupines have been shown to cause crooked calf disease (4), and the quinolizidine alkaloid anagyrine appears to be the teratogen responsible for congenital deformities (5).

The silvery lupine, *L. argenteus* Pursh., has long been considered to be highly toxic to grazing sheep (6, 7). Recently this species has been found to exhibit marked toxicity in cattle as well (4). A chemical study of the previously uninvestigated *stenophyllus* variety of the silvery lupine revealed the presence of α-isolupanine (0.60% of dry weight), thermopsine (0.36%), sparteine (0.05%), Δ^5-dehydrolupanine (0.04%), anagyrine (0.01%), lupanine (0.01%), and β-isosparteine (0.005%) (8). The concentrations of these quinolizidine alkaloids provided an explanation for the acute toxicity associated with this plant and suggested that it may be teratogenic.

The present study was directed at characterizing the major component of the alkaloid fraction from the aboveground portions of mature, flowering *L. argenteus* Pursh. var. *stenophyllus* (Rydb.) Davis. At the time of the initial investigation (8), the most abundant alkaloid in this plant was thought to be an unknown sparteine isomer. However, the data presented here show that this compound is (−)-α-isosparteine.

Sparteine was originally isolated in 1851 from *Cytisus scoparius* (L.) Link. (9) and has since been found to occur in many other members of the Leguminosae as well as in species belonging to the Monimiaceae, Papaveraceae, and Scrophulariaceae (10). The known isomers of sparteine, α-isosparteine and β-isosparteine, have a much more restricted distribution and were isolated at a later date (11). Genisteine, for instance, was first isolated in 1918 from *C. scoparius* (12), and its identity as (−)-α-isosparteine was confirmed in 1951 (13). Since that time (−)-α-isosparteine has been isolated from only two other legumes, *Lupinus caudatus* Kell. (14) and *Genista tinctoria* L. (15).

EXPERIMENTAL[1]

Plant Material—The flowering aboveground portions of *Lupinus argenteus* Pursh. var. *stenophyllus* (Rydb.) Davis (Leguminosae) were used[2].

Extraction and Fractionation—The air-dried powdered plant material (500 g) was homogenized with ethanol in a blender[3]. After filtration, the ethanolic extract was concentrated to 30 ml *in vacuo*, acidified with 10% aqueous acetic acid, and extracted with two successive 200-ml portions of ether, ethyl acetate, and chloroform. The acidic aqueous solution was made basic with 58% ammonium hydroxide and extracted with four 200-ml portions of chloroform. The combined chloroform extracts were filtered through anhydrous magnesium sulfate and evaporated to give a brown syrup (6 g), which solidified on standing.

Chromatographic Systems—The following TLC systems utilized 0.25-mm silica gel G layers: system A, chloroform–methanol–58% ammonium hydroxide (100:10:1); system B, cyclohexane–diethylamine (9:1). Alkaloids were detected using Dragendorff's reagent, and both systems provided a good separation of the major alkaloid from the available sparteine isomers and the other components of the extract.

The GLC system consisted of 3% OV-17 on Gas Chrom Q(2-m × 2 mm-i.d. glass column) and a program of 4°/min from 140 to 265°. This system produced a good resolution of the alkaloid mixture with the major component being eluted first.

Mass Spectral Analysis—The major component of the alkaloid fraction was analyzed using combined GLC-MS. The effluent from the 3% OV-17 GLC column entered the mass spectrometer through a glass jet separator maintained at 220°. The ion source temperature was 220° with an ionizing voltage of 70 eV. The mass spectrum of the major alkaloid component in the extract was basically the same as that recorded for the available sparteine isomers (8).

Isolation of the Major Alkaloid—A portion (2.5 g) of the alkaloid fraction was dissolved in ethanol–chloroform (1:1) and chromatographed (preparative TLC, 36 silica gel PF 254 plates, 1 mm thickness, TLC system B). The large band at R_f 0.61 was scraped from the plates, and the alkaloid material was eluted from the silica gel scrapings with three 100-ml portions of methanol. The eluates were combined and processed in the usual fashion (16) to give a light-brown oil which crystallized immediately upon exposure to air. Recrystallization of the free base from dry acetone gave 745 mg of colorless needles, mp 60–62°. The melting point remained constant after sublimation. Portions of the isolated free base were converted to the following derivatives using standard procedures: bisulfate, mp 244–245°; picrate, mp 205–207°; perchlorate, mp 302–304°; methiodide, mp 217–218°. The free base was used to determine the specific rotation, $[\alpha]_D^{26} = -48.1°$ (c = 0.006 g/ml in methanol).

Quantitation of the Major Alkaloid—Using a previously described GLC method (17), the major alkaloid was found to be present in the dry plant material at a level of 0.72%. This represents 40% of the total alkaloid content in the plant.

Synthesis of α-Isosparteine—Starting with sparteine sulfate[4], the method of Leonard and Beyler (18) was used to produce α-didehydros-

[1] IR spectra were determined neat using a Beckman IR-33 spectrophotometer. ^{1}H-NMR spectra were recorded on a Perkin-Elmer model R-24 spectrometer. ^{13}C-NMR spectra were obtained on a Varian XL-200 spectrometer. GLC was conducted using a Hewlett-Packard model 5720A gas chromatograph. Combined GLC–mass spectrometry was carried out with a Du Pont 321 Dimaspec low-resolution mass spectrometer interfaced with a 320 data reduction system. Melting points were determined on a Fisher-Johns melting point apparatus and are uncorrected. Optical rotations were measured with a Perkin-Elmer model 241 polarimeter.

[2] Collected in Boulder Basin, Blaine County, Idaho, on August 19, 1977 and identified by Dr. Karl Holte, Department of Botany, Idaho State University. A voucher specimen (No. 51553) is on deposit at the Idaho State University Herbarium, Pocatello, ID 83201.

[3] Waring.

[4] Merck and Co., lot. no. 52421.

0022-3549/83/0500-0563$01.00/0

parteinium bisulfate. A portion of this compound (122 mg) was converted to the free base and hydrogenated over palladium-on-carbon catalyst for 15 hr at room temperature and 45 lbs of pressure. This reaction mixture was filtered, concentrated *in vacuo* to 1 ml, and chromatographed over a small (4 g) silica gel column. The free base (26 mg) was eluted with ether containing 10% of a mixture of methanol–58% ammonium hydroxide (7:3) and was found to have mp 59–60° [lit. (19) mp 60–62°] after sublimation.

RESULTS AND DISCUSSION

During the course of a chemical investigation of *L. argenteus* var. *stenophyllus*, large quantities of the major alkaloid were isolated in chromatographically pure form. Spectral data (IR, ^{1}H-NMR, and MS) suggested the isolate to be an isomer of sparteine. Initially, the alkaloid was thought to be (−)-α-isosparteine, since the two known isomers of this compound, sparteine and β-isosparteine, were shown to be present in the plant (8). However, chromatographic (TLC and GLC) comparisons with a commercial sample[5] of (−)-α-isosparteine refuted this original postulate. Differences in observed and literature melting points for both the free base and numerous derivatives also supported the view that the major alkaloid from *L. argenteus* var. *stenophyllus* was an unknown sparteine isomer.

An X-ray crystallographic study was performed on the perchlorate salt of the isolated alkaloid in an effort to establish its molecular structure. Data from this investigation revealed the compound to be α-isosparteine perchlorate[6] and corresponded very closely with a previous X-ray diffraction study of α-isosparteine (20). Synthesis of α-isosparteine supported the information from the X-ray diffraction study with the synthetic material corresponding in all respects (TLC, GLC, IR, ^{1}H-NMR, ^{13}C-NMR, MS, and mp of the free base) with the isolated alkaloid. This evidence together with an observed $[\alpha]_D^{26} = -48.1°$ [lit. (14) $[\alpha]_D^{22} = -51.3°$] established the major alkaloid from *L. argenteus* var. *stenophyllus* as (−)-α-isosparteine. A reference sample of 1-α-isosparteine, purchased from a second commercial supplier[7], was also identical with the isolated and synthesized products.

The initial anomalous observations involving chromatographic differences between isolated and reference materials were resolved by determining that the initial commercial sample, labeled α-isosparteine, was misbranded. The mislabeled commercial sample[5] is, from TLC and ^{13}C-NMR evidence, actually a mixture of sparteine: (−)-α-isosparteine, 4:1. Further, there have been confusing discrepancies in the literature regarding the melting points of α-isosparteine and some of its derivatives. For example, the degree of crystal hydration greatly affects the melting point of the free base α-isosparteine. A previous study (14) reported the monohydrate as mp 108–110°, while another study (19) found the anhydrous free base to be mp 60–62°. The α-isosparteine isolated in this study apparently crystallized in the anhydrous form. The same situation probably exists with the picrate, mp 205–207° [lit. (21) mp 221–222°] and the perchlorate, mp 302–304° [lit. (14) mp 262–263°]. The bisulfate mp 244–245° [lit. (22) mp 244–245°] and the methiodide, mp 217–218° [lit. (19) mp 217–218°] correlated well with literature values.

The present study establishes *L. argenteus* var. *stenophyllus* as the richest source of (−)-α-isosparteine yet reported. For example, less than 0.01% of (−)-α-isosparteine was found (14) in *L. caudatus* while this work demonstrated a concentration of 0.72% in the title plant. Additionally, *L. argenteus* var. *stenophyllus* is now the only plant known to produce and accumulate all three sparteine isomers.

Sparteine has been used for many years in the management of various cardiac arrhythmias (23). In isolated atria, sparteine exhibits a positive inotropic action and prolongs the refractory period (24). Preliminary pharmacologic studies in this laboratory have revealed that (−)-α-isosparteine exhibits basically the same action as does (−)-sparteine but possesses a more rapid onset and a shorter duration when compared using rat myocardial tissue[8]. A more complete pharmacologic characterization of (−)-α-isosparteine is presently in progress.

REFERENCES

(1) J. M. Kingsbury, "Poisonous Plants of the United States and Canada," Prentice-Hall, Englewood Cliffs, N.J., 1964, pp. 333–341.

(2) J. F. Couch, *J. Chem. Educ.*, **14**, 16 (1937).

(3) R. F. Keeler, *Lloydia*, **38**, 56 (1975).

(4) J. L. Shupe, W. Binns, L. F. James, and R. F. Keeler, *J. Am. Vet. Med. Assoc.*, **151**, 198 (1967).

(5) R. F. Keeler, *Teratology*, **7**, 31 (1973).

(6) O. A. Beath, *Wyo. Agr. Exp. Sta. Bull.*, **1920**, 125.

(7) C. D. Marsh, A. B. Clawson, and H. Marsh, *USDA Bull.*, **1916**, 405.

(8) W. J. Keller and S. G. Zelenski, *J. Pharm. Sci.*, **67**, 430 (1978).

(9) J. Stenhouse, *Ann.*, **78**, 1 (1851).

(10) J. J. Willaman and H.-L. Li, *Lloydia*, **33**, 99–117, 137, 158, 201 (1970).

(11) J. A. Mears and T. J. Mabry, in "Chemotoxonomy of the Leguminosae," J. B. Harbourne, D. Boulter, and B. L. Turner, Eds., Academic, New York, N.Y., 1971, pp. 100–105.

(12) A. Valeur, *Compt. Rend.*, **167**, 163 (1918).

(13) L. Marion and N. J. Leonard, *Can. J. Chem.*, **29**, 297 (1951).

(14) L. Marion, F. Turcotte, and J. Ouellet, *ibid.*, **29**, 22 (1951).

(15) M. Przyborowska, E. Soczewinski, A. Waksmundzki, and W. Golkiewicz, *Diss. Pharm. Pharmacol.*, **19**, 289 (1967).

(16) W. J. Keller, J. L. McLaughlin, and L. R. Brady, *J. Pharm. Sci.*, **62**, 408 (1973).

(17) G. M. Hatfield, L. J. J. Valdez, W. J. Keller, W. L. Merrill, and V. H. Jones, *Lloydia*, **40**, 374 (1977).

(18) N. J. Leonard and R. E. Beyler, *J. Am. Chem. Soc.*, **72**, 1316 (1950).

(19) D. Kettelhack, M. Rink, and K. Winterfeld, *Arch. Pharm.*, **287**, 1 (1954).

(20) M. Przyblyska and W. H. Barnes, *Acta Crystallogr.*, **6**, 377 (1953).

(21) M. Rink, *Ann.*, **588**, 131 (1954).

(22) K. Winterfeld and C. Rauch, *Arch. Pharm.*, **272**, 273 (1934).

(23) H. J. Dengler, N. Eichelbaum, J. Hengstmann, and J. Wieber, *Pharmacol. Clin.*, **2**, 189 (1970).

(24) G. Zetler and O. Strubelt, *Naunyn-Schmiedeberg's Arch. Pharmacol.*, **271**, 335 (1971).

ACKNOWLEDGMENTS

This research was supported, in part, by a grant from the Northeast Louisiana University Faculty Research Fund and by NIH BRSG RRO-5586 at Purdue University.

The authors thank Mr. Hatch Buttram for his assistance in overcoming the difficulties associated with collecting the plant material in the Boulder Basin area of Idaho. The authors also wish to thank Dr. William Watson for his interpretation of the X-ray crystallographic data which he generated and Dr. Terry Martinez for conducting the preliminary pharmacologic investigations.

[5] K & K Laboratories [ICN Pharmaceuticals, 1-α-isosparteine (genisteine), lot no. 70956].

[6] W. H. Watson, personal communications, December 12, 1979 and June 2, 1980.

[7] Pfaltz and Bauer Inc., genisteine, no. G00900.

[8] T. Martinez, personal communication, November 1, 1979.

Antidiabetic Behavior of Biguanides

F. VICENTE-PEDRÓS ˣ, J. TREJUEQUE MONGE, and F. TOMÁS VERT

Received February 12, 1981, from the *Department of Physical Chemistry, Faculty of Chemistry, University of Valencia, Burjasot (Valencia), Spain.* Accepted for publication May 19, 1982.

Abstract □ The existence of active electron pairs on some nitrogen atoms in phenformin hydrochloride is inferred from the presence of a hydrogen catalytic polarographic wave. This finding emphasizes the ability of biguanides to form hydrogen bridges with other molecular species such as amino acids and proteins, as well as to form coordination complexes with zinc and other metallic cations by means of these electron pairs. The antidiabetic action of phenformin and other related biguanides can be explained in terms of competition between these molecules and insulin to coordinate cationic oligoelements together with their ability to form hydrogen bonds between the biguanide moiety and insulin itself.

Keyphrases □ Insulin—complexation with zinc *in vivo*, effect of phenformin determination by polarography □ Phenformin—effect on insulin-zinc complexes, determination by polarography □ Polarography—determination of effect of phenformin on insulin-zinc complexes.

Some aspects of the biological behavior of biguanides such as the blood sugar-lowering effect and metabolic interactions have been widely studied (1, 2). Biguanides form stable coordination complexes with divalent cations of oligoelements existing in living organisms. Phenformin [*N*-(2-phenylethyl)imidodicarbonimidic diamide] and other related oral antidiabetic biguanides form very strong complexes with Zn^{2+} and other divalent cations (3). This finding suggests that biguanides produce alterations in the distribution and ratios of divalent cations in biological media (4). It was shown (5, 6) that phenformin administered *in vivo* produced consistent and significant effects on hepatic mitochondrial divalent metal ion content through a more complex mechanism than competitive binding. All of these facts point to the use of biguanides as regulators of oligoelement proportions in living organisms.

Structures for this type of complex have been suggested, but the one reported by Rây and Saha (7) (I) is the most widely accepted.

The antidiabetic action of biguanides (phenformin as an example) can be derived from this complexation phenomenon. This action must be consistent with the following sequence of events:

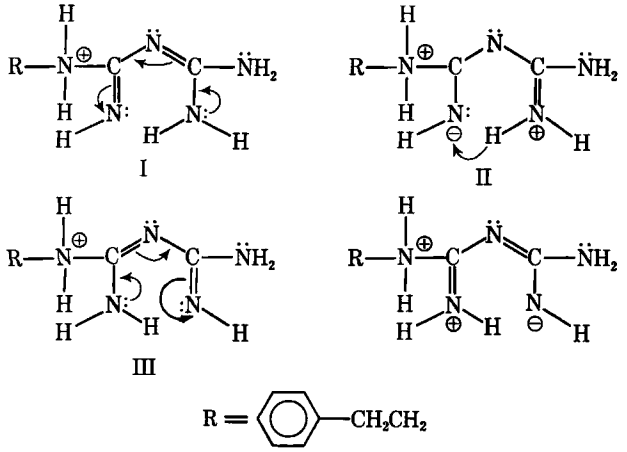

I II III

R = —CH_2CH_2—

1. Natural insulin is stored in the β-cells of the pancreas in the form of insoluble insulin–zinc granules (8).

2. Biguanides form stronger complexes than insulin does with Zn^{2+}. Formation of such complexes releases insulin from the granules allowing it to go through cellular membranes and enter the systemic circulation.

This scheme is consistent with the physicochemical properties of biguanides and phenformin in particular:

1. These molecules are soluble in biological hydroorganic media, which explains their widely observed, fast conveyance and action (9).

2. At pH values close to human physiological pH, the stable form of biguanides is the cationic monoprotonated form, BH^+ (10). These cations retain the delocalized π-electronic structure of the biguanide group of the free base, as can be seen from the persistence of the 232-nm band of the UV spectra of bases, at pH values less than the pK_{a_2} of biguanides, and in any case at pH values <7. According to a previous report (11), the protonated biguanide group can be formulated in several resonant forms (Fig. 1), all of them with nitrogen atoms exhibiting localized electron pairs, which accounts for the ability of monoprotonated biguanides to form hydrogen bonds and coordination compounds with metallic cations.

These structural features call for the solubilization of the insulin–zinc granules in the pancreatic β-cells, which involve the accessibility of insulin–zinc complexes to biguanides at a molecular level. Such accessibility requires the breaking of the hydrogen bonds that link insulin polyamino acid chains in the building of granules. This breaking process should be enhanced, because of the strong ability of biguanides themselves to form hydrogen bonds. Both the ability to form hydrogen bonds and to chelate with zinc are located at the electron pairs of nitrogen.

This work was directed to characterize this structural feature by using direct current (DC) and superimposed alternating current of first harmonic (AC_1) polarographic techniques on phenformin as a representative of oral antidiabetic biguanides.

EXPERIMENTAL

A polarograph[1] was used and pH measurements were carried out by means of a pH meter[2]. Polarographic parameters were fixed (unless their

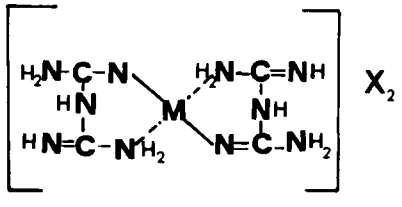

Figure 1—*Resonant forms for biguanide monoprotonated group.*

[1] Metrohm E-506 Polarograph.
[2] Radiometer pH M-62.

0022-3549/83/0500-0565$01.00/0

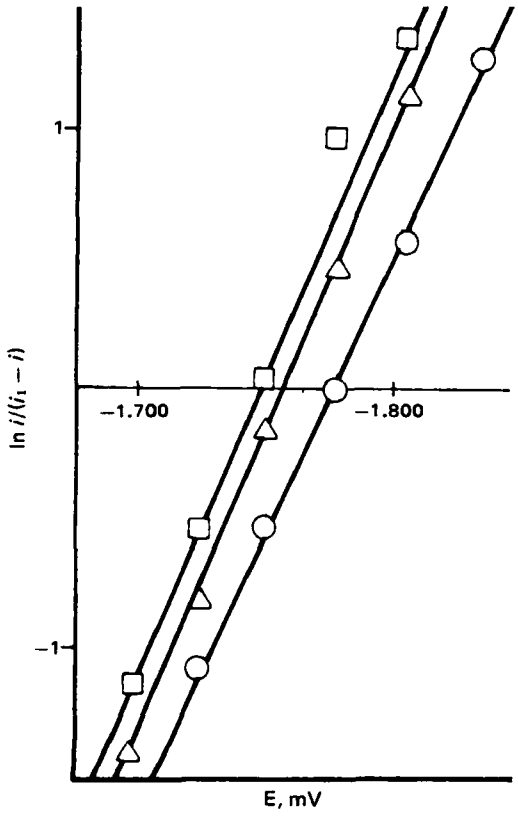

Figure 2—*Tomes representations;* i_1, *limit current; 1, DC current; E, potential* versus *Ag/AgCl, saturated lithium chloride. Key: (□) pH 6.87; (△) pH 6.79; (○) pH 6.13.*

influence was considered) as follows: dropping time, τ, 0.6 sec; height of the mercury-containing vessel, h, 54 cm; temperature, T, 25°; phenformin hydrochloride concentration, c, 3.8×10^{-4} M; the ionic strength was adjusted to μ 0.5 with 1:1 inert electrolyte; mercury flow, m, 0.88 mg/sec (at the referred height h).

A sample volume of 25 ml of freshly prepared solution was used in all of the polarographic experiments. Gelatin was used as a suppressor in a proportion of 0.01% by weight, in the polarographic recordings of phenformin only. Auxiliary and reference silver/silver chloride electrodes together with a 1:1 electrolyte-saturated salt bridge were used.

The polarographic result found by means of the DC technique agreed well with the ones found using the AC_1 technique.

Phenformin hydrochloride was used as supplied[3], and the melting point (175 ± 1°) and IR spectra were tested. Two aqueous suspensions of insulin–zinc complexes both of 40 IU/ml were used[4]: a mixture of 70% crystalline and 30% amorphous porcine and bovine and a 100% amorphous porcine insulin–zinc suspension, respectively.

RESULTS AND DISCUSSION

An irreversible cathodic polarographic wave is detected in buffered lithium–phosphate–chloride–gelatin aqueous solutions of phenformin in the pH range 4–7. This wave involves a one-electron transfer according to the slopes of Tomes representations obtained from DC data (Fig. 2). This wave does not appear in the same media in the absence of phenformin.

The peak potential, E_p, depends slightly on phenformin concentration (Fig. 3), but the height of the wave is independent of that concentration at pH values >5.5.

Such polarographic behavior implies the presence of active catalytic centers for the reduction of hydrogen ions, and more precisely it points to the existence of localized electron pairs over nitrogen on phenformin, since such active centers occur in other related substances (12).

The formation of Zn^{2+}–phenformin complexes (MF_j) has been studied by DC polarography in Britton–Robinson buffered media. Provided that the detected polarographic wave results are quasi-reversible, the procedure

[3] Funk Laboratories S. A., Barcelona, Spain.
[4] Novo Laboratories, Copenhagen, Denmark.

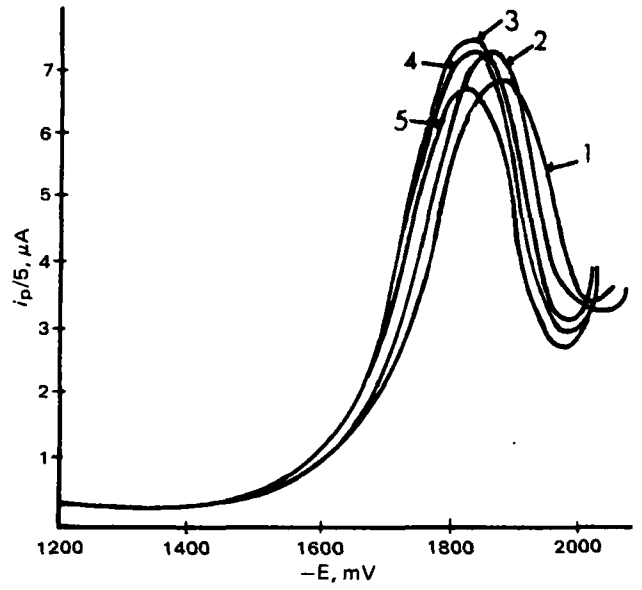

Figure 3—*Effect of phenformin concentration on AC_1 waves. Key: (1) c = 3.8 × 10⁻⁴ M; (2) c = 4.6 × 10⁻⁴ M; (3) c = 5.3 × 10⁻⁴ M; (4) c = 6.1 × 10⁻⁴ M; (5) c = 6.8 × 10⁻⁴ M. E, potential* versus *Ag/AgCl, saturate lithium chloride; ΔE = 30 mV, pH 5.40.*

developed by Lingane (13) to express the variation of half-wave potential on complexation has been used:

$$\Delta E_{1/2} = j\frac{0.0591}{n\alpha}\log c_F + \frac{0.0591}{n\alpha}\log \beta_{(MF_j)} \qquad \text{(Eq. 1)}$$

where $\Delta E_{1/2} = E^f_{1/2} - E^c_{1/2}$ expresses the difference between half-wave potentials of free and complexed zinc cation, respectively, and c_F is the ligand concentration.

The dependence of $\Delta E_{1/2}$ measured values with $\log c_F$ adjusts well to a linear equation for a concentration range of $4 \times 10^{-4} < c_F < 7 \times 10^{-4}$ M, and $[Zn^{2+}] = 2 \times 10^{-4}$ M (T = 25°; pH 4.97). From this linear dependence, a ligand number of $j = 2$ is found, and the adjusted stability constant is $\beta_{(MF_2)} \simeq 2 \times 10^{11}$ M^{-2}. [Despite the fact that the stability constant value found indicates that the phenformin–Zn^{2+} complex is a quite stable complex, it must be noted that biguanides form stronger complexes with some other metallic cations (14)].

The stoichiometry of zinc–insulin complexes is less clear. As reported previously (15), zinc ions appear to combine preferentially with imidazole groups. Several Zn^{2+}–imidazole relationships have been noted: from 1:1 complexes to 1:3 and 1:4. There is strong binding between two metal ions and three imidazole dimers, especially in crystalline metal–insulin complexes (16). These authors suggest that the first zinc ion is bound by three coordination bonds, being the association constant of the order of the ones normally found for zinc–imidazole interactions ($\simeq 10^9$), and the bonding of the second Zn^{2+} appears to be 10^4 times stronger.

Insulin binds strongly with zinc cations in both amorphous and crystalline complexes, impeding the polarographic reduction of Zn^{2+} (15). The polarographic reductions observed in the study of amorphous insulin–zinc suspensions (curve A, Fig. 4) and crystalline–amorphous mixture suspensions (curve C, Fig. 4C) are due to free zinc cations whose concentrations polarographically derived are: $[Zn^{2+}]_A = 1.64 \times 10^{-5}$ M, and $[Zn^{2+}]_C = 2.24 \times 10^{-5}$ M.

The addition of phenformin to insulin–zinc complex suspensions modifies the polarographic recordings (curves B and D, Fig. 4). In the case of the addition to amorphous complex suspension (curve B) a shift to more negative values of half-wave potential is observed, indicating that phenformin has complexed zinc cations. The increasing curve height (curve B from A) indicates that the phenformin complexed Zn^{2+} concentration (recorded in B) $[Zn^{2+}]_B = 2.1 \times 10^{-5}$ M, is greater that the previous free Zn^{2+} concentration $[Zn^{2+}]_A$. This increase in the reducible phenformin complexed Zn^{2+} concentration can only be explained if some insulin–zinc complexes have been broken by the action of phenformin.

In the case of the amorphous and crystalline insulin–zinc mixture (curves C and D, Fig. 4) a quite different behavior is observed. Also the half-wave potential is shifted to more negative values, indicating the complexation of Zn^{2+} with phenformin, but the increase in reducible Zn^{2+} concentration $[Zn^{2+}]_D = 2.36 \times 10^{-5}$ M is less than in the previous case of pure amorphous insulin–zinc suspensions. This small increase corre-

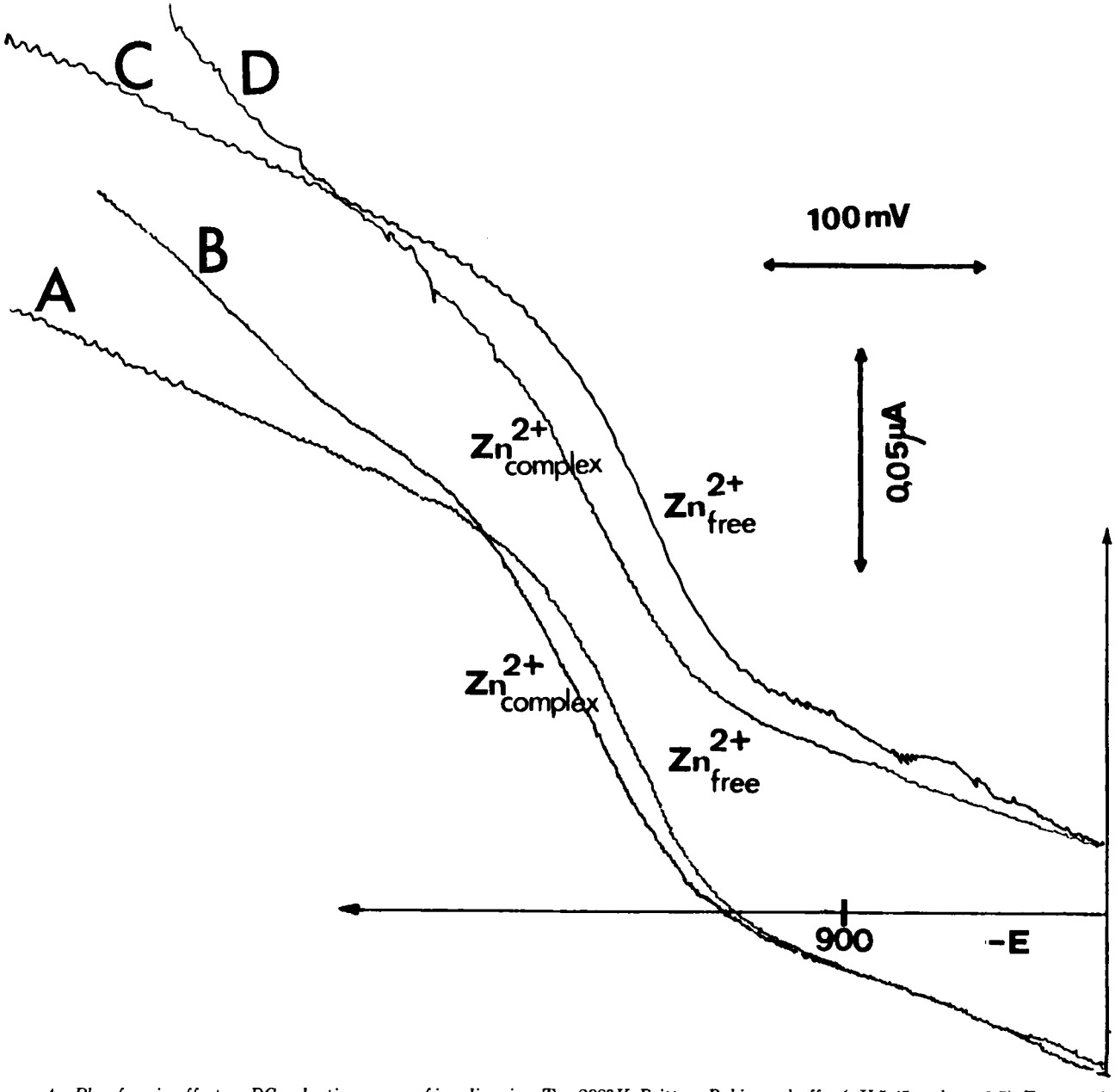

Figure 4—*Phenformin effect on DC reduction waves of insulin–zinc.* T = 298°K; *Britton–Robinson buffer (pH 5,45 and* μ = 0.5); *E* versus *Ag/AgCl, saturated potassium chloride; [Zn^{2+}] measured by DC polarography. (A) 8.366 g/liter amorphous insulin–zinc; (B) 8.366 g/liter amorphous insulin–zinc with phenformin (4 × 10^{-4} M); (C) 8.366 g/liter crystalline (70%) and amorphous (30%) insulin–zinc; (D) 8.366 g/liter crystalline (70%) and amorphous (30%) insulin–zinc with phenformin (4 × 10^{-4} M).*

sponds only to the amorphous part of the mixture as can be derived from the increase detected in the first case, indicating that the crystalline insulin–zinc complex remains stable despite the presence of phenformin.

The polarographic experiments showed that there is a competition between phenformin and insulin toward zinc cations. The antidiabetic behavior of phenformin can be related to this competition. This competition is not restricted to β-cells environment, rather it will work in any part of the living organism where these molecules meet and also can explain the protection of insulin against biochemical degradation (17).

REFERENCES

(1) R. Beckman, in "Handbook of Experimental Pharmacology" (New Series) Vol. 29, H. Maske, Ed., Springer-Verlag, Berlin, Heidelberg, New York 1971, pp. 439–596.

(2) G. Schäfer, *Biochem. Pharmacol.*, **25**, 2015 (1976).

(3) P. Rây, *Chem. Rev.*, **61**, 319 (1961).

(4) J. Trijueque, F. Vicente, and F. Tomás, "IV Reunión de Química (Sanitaria)," ANQUE, Madrid, 1981.

(5) D. Haas and F. Davidoff, *Biochem. Pharmacol.*, **27**, 2263 (1978).

(6) F. Davidoff and D. Haas, *Biochem. Pharmacol*, **28**, 3457 (1979).

(7) P. Rây and H. Saha, *J. Indian Chem. Soc.*, **14**, 670 (1937).

(8) P. E. Lacy, *Diabetes*, **19**, 985 (1970).

(9) H. Förster, *Pharm. Ztg. Nachr.*, **18**, 721 (1977).

(10) F. Kurzer and E. D. Pitchfork, *Fortschr. Chem. Forsch.* **1968**, 381.

(11) L. Seymour, V. Shapiro, A. Parrino, and L. Freedman, *J. Org. Chem.*, **81**, 2220 (1959).

(12) S. G. Mairanovskii, "Catalytic and Kinetic Waves in Polarography;" Plenum, New York, N.Y., 1960, p. 285.

(13) J. Lingane, *J. Chem. Rev.*, **29**, 1 (1941).

(14) G. Schwarzenbach and G. Anderegg, *Pharm. Acta Helv.*, **38**, 547 (1963).

(15) C. Tanford, *J. Am. Chem. Soc.*, **74**, 211 (1952).

(16) A. S. Brill and J. H. Venable, Jr., *ibid.*, **89**, 3622 (1967).

(17) F. Pretes, C. Eduardo, L. Yuquico, C. R. Pinheiro, and B. Leo, *Metabolism*, **29**, 270 (1980).

Synthesis of Isopromethazine Hydrochloride

FRED S. FRY, JR.[x], MILLARD MAIENTHAL, and WALTER R. BENSON

Received January 4, 1982, from the *Division of Drug Chemistry, Food and Drug Administration, Washington, DC 20204.* Accepted for publication May 19, 1982.

Abstract □ Isopromethazine hydrochloride was synthesized in gram quantities by using a method which ensures that the isopromethazine is not contaminated with promethazine hydrochloride.

Keyphrases □ Isopromethazine hydrochloride—synthesis □ Promethazine hydrochloride—synthesis of isopromethazine □ Promethazine isomer—synthesis □ Antihistamine—isopromethazine synthesis

Promethazine (*N,N,α*-trimethyl-10*H*-phenothiazine-10-ethanamine, I) is an antihistamine that is usually synthesized by the reaction of either 2-chloro-1-dimethylaminopropane (1–7) or 1-chloro-2-dimethylaminopropane (2) with phenothiazine in the presence of bases such as sodium hydroxide, sodium amide, or phenyllithium (1), or with the Grignard derivative of phenothiazine (7). When *β*-haloamines are treated with bases, aziridinium salts are frequently formed (8, 9), and the three-membered ring can be opened by a nucleophile at either ring carbon to produce isomeric alkylation products (10) (Scheme I). Thus, in the alkylation of phenothiazine with 2-chloro-1-dimethylaminopropane, *N,N,β*-trimethyl-10*H*-phenothiazine-10-ethanamine (isopromethazine, II) is obtained in addition to the desired I[1]. These isomeric compounds can be separated by fractional crystallization (6), but small amounts of II usually remain in the purified samples of I. Therefore, a sample of pure II was needed as a reference standard for the analysis of I (13–17)[2,3].

EXPERIMENTAL

Phenothiazine[4] was recrystallized from 95% ethanol. Butyllithium[4] (1.6 *M* in hexane) and 2-chloropropionyl chloride[4] were used without further purification. Previously unopened anhydrous ethyl ether and tetrahydrofuran were used without further drying. NMR[5], MS[6], and IR spectra[7] were obtained. Melting points were uncorrected.

***N,N,β*-Trimethyl-10*H*-phenothiazine-10 - *α* - oxoethanamine** (V)—To a solution of phenothiazine (15.9 g, 0.08 mole) in 500 ml of dry ether under a nitrogen atmosphere and cooled to −20 to −30°, 50 ml of 1.6 *M* *n*-butyllithium in hexane was added with stirring. The resulting bright-yellow solution was stirred for 30 min, then *N,N*-dimethyl-2-chloropropionamide (18) (IV, 10.9 g, 0.08 mole) in 25 ml of ethyl ether was added over 1 hr. The solution was warmed to room temperature, the unreacted 10-lithiophenothiazine was hydrolyzed with water, the organic layer was dried over sodium sulfate, and the solvent was removed under reduced pressure to yield 21.7 g of residue, which was dissolved in toluene and transferred to a silica gel (60–200-mesh) column. Elution with toluene removed unreacted phenothiazine (6 g) and traces of highly colored impurities. Subsequent elution with toluene–ethyl acetate (85:15) afforded 11.4 g of nearly colorless amide (V, mp 161–163° [lit. (19) mp 165–167°] 76% based on unrecovered phenothiazine). ^{1}H-NMR ($CDCl_3$, 60 MHz): 1.9 (C—CH_3, 3H, d, J = 8 Hz), 2.9, 3.1 (N—CH_3, 6H, two s), 4.8 (CH, 1H, q, J = 8 Hz), 7.1 ppm (ArH, 8H, m); ^{13}C-NMR ($CDCl_3$): 15.97, 36.23, 37.37, 56.93, 116.27, 123.03, 124.35, 127.15, 127.79, 143.64, 169.84 ppm; IR: 1645 cm^{-1} (ν C=O, s); mass spectrum (80 eV, 300°): m/z 298 (M^+), 226 (M − C_3H_6NO), 198 (M − $C_5H_{10}NO$), 194 (M − C_3H_6NO − S), 154 (M − $C_5H_{10}NO$ − CS), 72 (C_3H_6NO, 100%).

Anal.—Calc. for $C_{17}H_{18}N_2OS$: C, 68.42; H, 6.08; N, 9.39; S, 10.75. Found: C, 68.41; H, 5.91; N, 9.42; S, 10.46.

***N,N,β*-Trimethyl-10*H*-phenothiazine-10-ethanamine Hydrochloride**—To a solution of lithium aluminum hydride (2 g, 0.053 mole) in 500 ml of dry tetrahydrofuran, V (5.0 g, 0.0167 mole) in 50 ml of tetrahydrofuran was added. The reaction mixture was stirred for 2 hr, then the excess hydride was destroyed with ethyl acetate and dilute sodium hydroxide solution. The reaction mixture was filtered and the solvent removed under reduced pressure. The residue was dissolved in ether and treated with hydrogen chloride gas to yield the crude hydrochloride of II. This material was recrystallized from acetonitrile to yield 3.9 g of nearly colorless prisms (72%, mp 196–198° [lit. (5) mp 193–194°]). ^{1}H-NMR ($CDCl_3$, 200 MHz): 1.84 (C—CH_3, 3H, d, J = 8 Hz), 2.72 (N—CH_3, 6H, s), 3.2–3.8 (CH_2, 2H, m), 4.78 (CH, 1H, m), 6.9–7.2 ppm (ArH, 8H, m); ^{13}C-NMR ($CDCl_3$): 21.72, ~42 (broad), 52.53, 57.79, 117.14, 123.73, 126.40, 127.73, 127.95, 143.52 ppm; IR: 2300 cm^{-1} (ν N^+H, broad); mass spectrum (80 eV, 300°): m/z 284 (M − HCl), 226 (M − HCl − C_3H_8N), 198 (M − HCl − $C_5H_{12}N$), 194 (M − HCl − C_3H_8M − S), 58 (C_3H_8N, 100%), 36,38 (HCl).

Anal.—Calc. for $C_{17}H_{21}ClN_2S$: C, 63.62; H, 6.59; Cl, 11.05; N, 8.73. Found: C, 63.78; H, 6.83; Cl, 10.97; N, 9.02.

***N*-(2-Hydroxy-1-propyl)phthalimide**—A solution of 1-amino-2-propanol (5 g, 0.066 mole) and *N*-carboethoxyphthalimide (10 g, 0.05 mole) in 200 ml of 1,2-dichloroethane was stirred 2 hr at room temperature. An aqueous solution of potassium carbonate was added, and after stirring 15 min, the organic phase was separated, washed with water, and dried. The solvent was removed under reduced pressure, and the oily residue was recrystallized from ether–hexane to yield 1.7 g of the phthalimide, mp 86–87°.

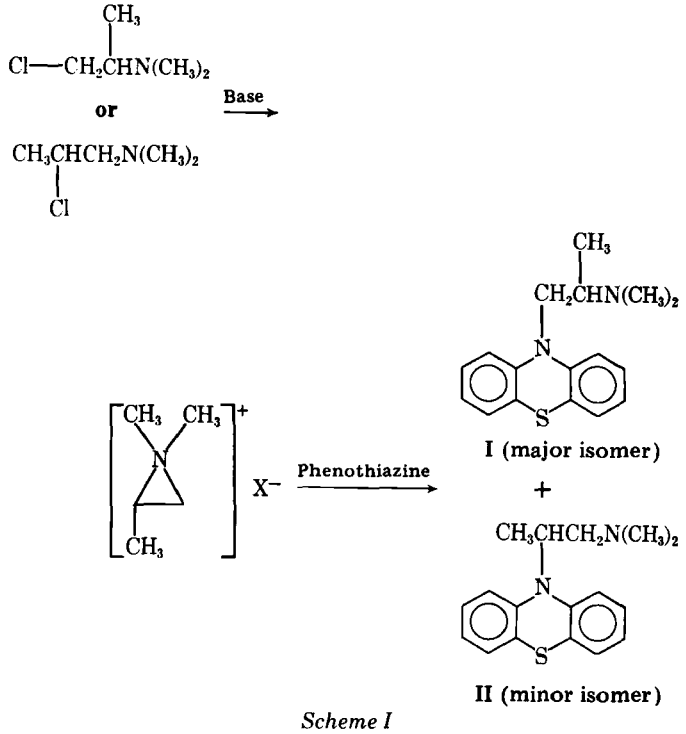

Scheme I

[1] Under certain conditions, II has been reported as the predominant isomer (11, 12).

[2] A small sample of II (Chemical Reference Substance) may be obtained from the European Pharmacopoeia Commission, 67006 Strasbourg, Strasbourg, France.

[3] The USP (17) does not mention II in its monograph on promethazine hydrochloride.

[4] Aldrich Chemical Co.

[5] Perkin-Elmer R12B or Varian XL-200 spectrometer.

[6] Varian MAT-311A spectrometer.

[7] Perkin-Elmer 621 spectrophotometer.

0022-3549/83/0500-0568$01.00/0

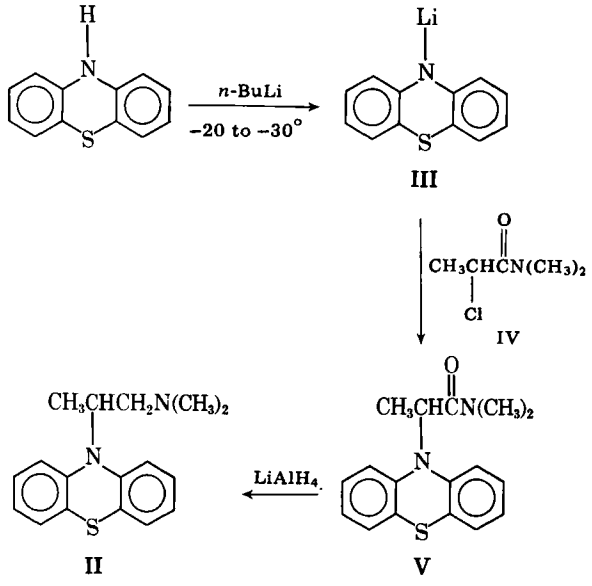

Scheme II

Anal.—Calc. for $C_{11}H_{11}NO_3$: C, 64.37; H, 5.40; N, 6.83. Found: C, 64.39; H, 5.22; N, 6.71.

The reaction of this material with phosphorus tribromide in pyridine yielded a white crystalline compound (mp 162–164°) that contained no bromine by elemental analysis; the compound was not identified.

RESULTS AND DISCUSSION

Due to the rearrangements noted with β-haloamines (8, 9), it was necessary to use an alkylating agent, which precluded the formation of isomeric products. This involved selecting a 2-halopropylamine with the amino group protected to prevent aziridine formation. The approach utilized (Scheme II) is similar to that reported previously (20). Compound III was prepared from phenothiazine and *n*-butyllithium by the procedure of Gilman and Diehl (21), and IV was prepared from dimethylamine and 2-chloropropionyl chloride by the procedure of Weaver and Whalen (18). When III was prepared at −20 to −30° and allowed to react with IV, a 76% yield of V resulted. This material was separated from unreacted phenothiazine by chromatography on silica gel. The reaction of V with lithium aluminum hydride in tetrahydrofuran afforded a 72% yield of II, which was isolated as the hydrochloride salt. The nearly colorless prisms (mp 196–198°) exhibited no loss of weight when heated in a thermal balance, indicating no solvent of crystallization.

The isopromethazine hydrochloride was shown to be identical to a European Pharmacopoeia Reference Standard[2] by UV and IR spectroscopy and by GLC on a 3% OV-101 on Chromosorb W column at 230° (retention time, 6.69 min). The GLC analyses of both prepared and standard isopromethazine hydrochloride indicated traces of phenothiazine (retention time, 3.73 min) and an unidentified compound (retention time, 3.24 min), which may have been formed by degradation on the column. The analyses indicated that no promethazine hydrochloride (retention time, 7.72 min; detection limit, ~0.1%) was present[8].

When III was prepared at room temperature and allowed to react with IV, a mixture of products including phenothiazine and V was obtained. One of the products appeared to be one of the dimers of phenothiazine (22, 23) (mass spectrum: *m/z* 396).

Another approach to the preparation of II involved the protection of the side-chain amine as a phthalimide. The reaction of 2-hydroxy-aminopropane with *N*-carboethoxyphthalimide (24) produced *N*-(2-hydroxy-1-propyl)phthalimide (mp 87–88°; elemental analysis and ^{1}H-NMR spectrum were satisfactory for this compound). However, attempts to replace the hydroxyl group with a halogen using either phosphorus tribromide in pyridine or triphenylphosphine and carbon tetrachloride were unsuccessful.

The use of a haloamide as a alkylating agent for III produced II in good yield. This method should prove useful as a general route to phenothiazine-containing compounds.

[8] Mr. Bobby R. Rader, Food and Drug Administration, Los Angeles, Calif., personal communication.

REFERENCES

(1) C. M. Shearer and S. M. Miller, in "Analytical Profiles of Drug Substances," vol. 5, K. Florey, Ed., Academic, New York, N.Y., 1976, pp. 429–466.

(2) D. Barton and W. D. Ollis, "Comprehensive Organic Chemistry," vol. 4, Pergamon, New York, N.Y., 1979, pp. 1102–1107.

(3) C. Bodea and I. Silberg, in "Advances in Heterocyclic Chemistry," vol. 9, A. R. Katritzky and A. J. Boulton, Eds., Academic, New York, N.Y., 1968, pp. 321–460.

(4) S. P. Massie, *Chem. Rev.*, **54**, 797 (1954).

(5) N. D. Edge and W. R. Wragg, *J. Pharm. Pharmacol.*, **5**, 279 (1953).

(6) M. P. Charpentier, *C. R. Acad. Sci.*, **225**, 306 (1947).

(7) S. S. Berg and J. N. Ashley, U.S. pat. 2,607,773 (Aug. 19, 1952); through *Chem. Abstr.*, **47**, 6989h (1953).

(8) D. R. Crist and N. J. Leonard, *Angew. Chem. Int. Ed. Engl.*, **8**, 962 (1969).

(9) D. Barton and W. D. Ollis, "Comprehensive Organic Chemistry," vol. 2, Pergamon, New York, N.Y., 1979, pp. 52–55.

(10) W. A. Szabo, R. H. Chung, C. C. Tam, and M. Tischler, *J. Org. Chem.*, **45**, 744 (1980).

(11) H. Wunderlich, East German pat. 48,397 (Sept. 15, 1966); through *Chem. Abstr.*, **66**, 28790u (1967).

(12) H. Wunderlich, East German pat. 31,884 (July 15, 1965); through *Chem. Abstr.*, **64**, 2102b (1966).

(13) N. J. Pound and R. W. Sears, *Can. J. Pharm. Sci.*, **8**, 84 (1973).

(14) W. N. French, F. Matsui, D. L. Robertson, and S. J. Smith, *ibid.*, **10**, 27 (1975).

(15) "British Pharmacopoeia," vol. I, Rittenhouse, Philadelphia, Pa., 1980, p. 372.

(16) "European Pharmacopoeia," vol. 3, Rittenhouse, Philadelphia, Pa., 1976, pp. 332–334.

(17) "The United States Pharmacopeia," 20th rev., U.S. Pharmacopeial Convention, Rockville, Md., 1980, p. 669.

(18) W. E. Weaver and W. M. Whalen, *J. Am. Chem. Soc.*, **69**, 515 (1947).

(19) Rhone Poulenc, British pat. 732,488 (June 22, 1955); through *Chem. Abstr.*, **50**, 7881b (1956).

(20) P. Gailliot, J. Robert, and J. Gaudechon, British pat. 773,403 (April 24, 1957); through *Chem. Abstr.*, **52**, 1283i (1958).

(21) H. Gilman and J. W. Diehl, *J. Org. Chem.*, **26**, 2938 (1961).

(22) H. Roseboom and J. H. Perrin, *J. Pharm. Sci.*, **66**, 1392, 1395 (1977).

(23) Y. Tsujino, *Tetrahedron Lett.*, **11**, 763 (1969).

(24) L. Fieser and M. Fieser, "Reagents for Organic Synthesis," vol. 1, Wiley, New York, N.Y., 1967, p. 111.

ACKNOWLEDGMENTS

The authors thank Dr. Mamoru Ohashi, Visiting Foreign Scientist, and Wilson Brannon, Division of Drug Chemistry, Food and Drug Administration for the mass and IR spectra, respectively; and Byron Baer and Alice Wong of the Section on Microanalytical Services and Instrumentation, National Institute of Arthritis, Metabolism, and Digestive Diseases for the elemental analyses. We thank Dr. Shu-Yen Jan (deceased) and Dr. J. D. Weber for their suggestions on this work. We also acknowledge Mr. Bobby R. Rader, FDA, Los Angeles District Laboratory, Los Angeles, Calif. for his work on the analysis of impurities in promethazine samples.

Determination of Serum Tulobuterol Concentrations by Mass Fragmentography: Comparison with an Electron-Capture Gas Chromatographic Method

KUGAKO MATSUMURA *x, OSAMU KUBO *, TOSHIKO SAKASHITA *, HIDEO KATO *, KEIZO WATANABE ‡, and MASAAKI HIROBE ‡

Received November 3, 1981, from the *Research Laboratories, Hokuriku Seiyaku Co., Ltd., Inokuchi, Katsuyama-shi, Fukui 911, Japan, and the ‡Faculty of Pharmaceutical Sciences, University of Tokyo, Hongo, Bunkyo-ku, Tokyo 133, Japan. Accepted for publication May 26, 1982.

Abstract □ A simple and sensitive method is reported for the quantitative determination of the bronchodilator tulobuterol in human serum. Tulobuterol and an internal standard were extracted from alkalinized serum with ether and then back-extracted into dilute hydrochloric acid. After alkalinization and extraction of the aqueous solution, the extract was evaporated to dryness. The residue was silylated and subjected to mass fragmentography.

Keyphrases □ Tulobuterol—serum, extraction, derivatization, mass fragmentography □ Bronchodilator—tulobuterol, serum analysis, mass fragmentography □ Mass fragmentography—analysis, tulobuterol, serum

Tulobuterol (I) is a newly synthesized bronchodilator having a potent and long-lasting effect (1, 2). An electron-capture GLC determination of this drug in human serum was reported previously (3). This method was specific and sensitive, but the procedure was tedious and time consuming. Application of mass fragmentography to the detection of plasma albuterol and terbutaline, which possess similar chemical structures to tulobuterol, has been reported (4–6). This paper describes a sensitive and rapid analytical method for determining tulobuterol in human serum by mass fragmentography. The analytical results are compared with those obtained by electron-capture GLC.

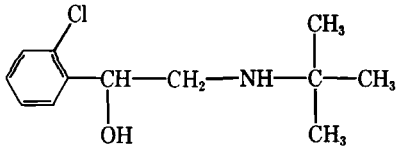

I

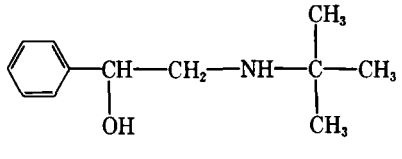

II

EXPERIMENTAL

Materials—Tulobuterol hydrochloride was synthesized previously (7). The internal standard, α-[(*tert*-butylamino)methyl]benzyl alcohol (II), was synthesized using a previously described method (8). *N,O*-Bis(trimethylsilyl)acetamide[1] (III) was employed as the derivatization reagent. Other reagents and solvents were of analytical grade and were used without further purification.

Drug Administration and Sample Collection—Four healthy, male volunteers each received a 2-mg oral dose of tolubuterol hydrochloride in the form of a syrup solution[2] or tablets. Blood samples of ~8 ml were withdrawn before the administration and at 0.5, 1, 1.5, 2, 3, 4, and 6 hr.

[1] Nakarai Chemical, Ltd., Kyoto, Japan.
[2] Prepared by dissolving the granulated drug in 20 ml of water.

Table I—Typical Tulobuterol Calibration Curve

Drug Concentration, ng/ml	Peak Area Ratio[a]	Ratio[b]
1	0.096	0.096
2	0.141	0.071
4	0.295	0.074
7	0.573	0.082
10	0.766	0.077

[a] Ratio of drug–internal standard. [b] Peak area ratio divided by drug concentration.

After standing for ~30–60 min, the serum was separated by centrifugation (2000×*g*, 10 min) and stored frozen until analysis.

Apparatus—GLC[3]-MS[4,5] determinations were performed using a glass column of 2-m length and 2-mm i.d., packed with 2% OV-1 on 100–120 mesh chromosorb G (HP)[6], operating at 165°. The injector, separator, and ion source were held at 210, 290, and 150°, respectively. The ionization energy and trap current were 70 eV and 30Q μA, respectively. Measurements were performed by single-ion monitoring at *m/z* 86.

Extraction Procedure and Sample Preparation—A solution of internal standard (1 ml of an 8-ng/ml solution in methanol) was evaporated to dryness under reduced pressure in a 15-ml glass centrifuge tube, and 1 ml of serum and 0.5 ml of 1 *N* NaOH were added. The tube was stoppered and extracted with 6 ml of ether by a reciprocating shaker at 160 strokes/min for 5 min. After centrifugation (2000×*g*, 5 min), the ether layer was transferred to a second tube containing 5 ml of 0.1 *N* HCl. The tube was shaken, centrifuged, and the ether layer removed.

Four milliliters of the aqueous layer was transferred to a third tube and alkalinized with 1 ml of 1 *N* NaOH. After extraction with 6 ml of ether, the tube was shaken and centrifuged. Five milliliters of the ether phase was transferred to a fourth tube and evaporated to dryness in a water bath at 50°. The residue was dissolved in 100 μl of III (1:4 solution in ethyl acetate), and 1 μl was chromatographed.

RESULTS AND DISCUSSION

Figure 1 shows a mass fragmentogram obtained from a serum sample to which a known amount of tulobuterol hydrochloride had been added, together with those obtained from a serum blank and from a volunteer receiving tulobuterol hydrochloride by the oral route. The peaks of tulobuterol and internal standard were well resolved and no interfering peaks from endogenous materials were present.

The mean percent recovery and standard deviation of tulobuterol hydrochloride were 65.02% and ±3.45, respectively. The corresponding values for the internal standard were 63.82% and ±2.52. Results were obtained from six determinations using serum with 5 ng/ml of tulobuterol hydrochloride and 8 ng/ml of the internal standard added. Although the recoveries of tulobuterol hydrochloride and internal standard in the present assay are low, they are reproducible. Attempts to improve the drug recovery led to either added complexities or irreproducibility.

The ratio of the peak area of tulobuterol to that of the internal standard was calculated. Statistical analysis indicated excellent linearity in the range of 1–10 ng/ml serum with a correlation coefficient of 0.998, a slope of 0.0775, and an intercept of 0.002 (Table I).

[3] JGC-20K, JEOL, Tokyo, Japan.
[4] JMS D-300, JEOL, Tokyo, Japan.
[5] JMA-2000, JEOL, Tokyo, Japan.
[6] Wako Pure Chemical Industries, Ltd., Osaka, Japan.

0022-3549/83/0500-0570$01.00/0

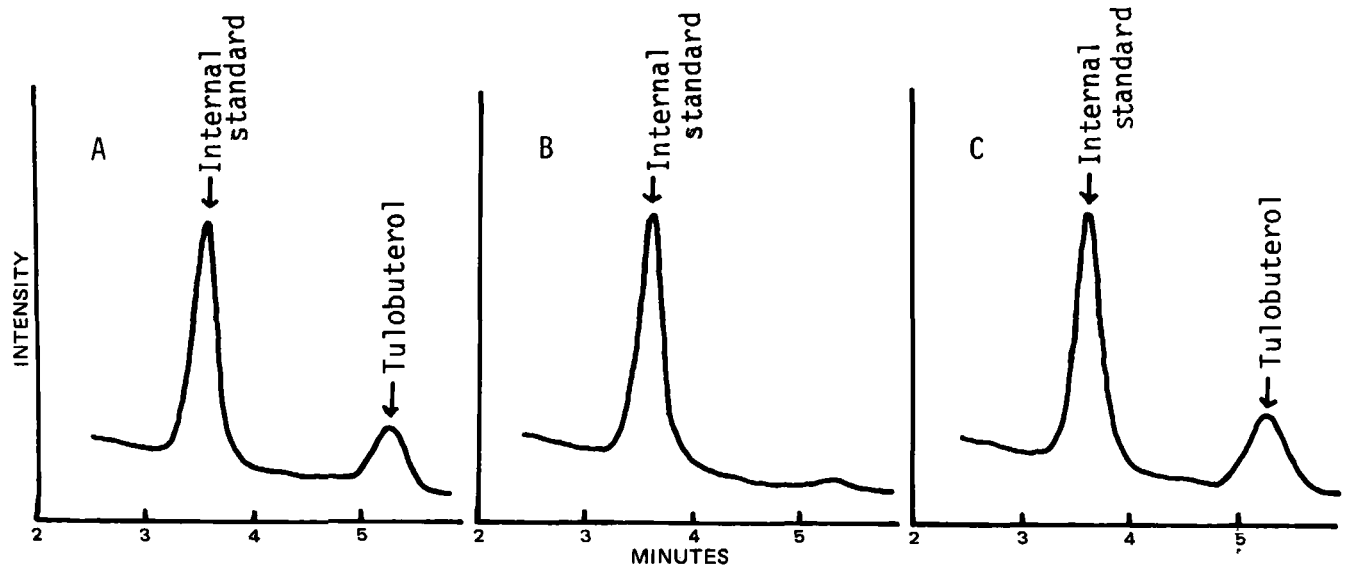

Figure 1—*Mass fragmentograms of serum extracts. Key: (A) serum to which known amounts of tulobuterol hydrochloride (4 ng) and internal standard (8 ng) were added; (B) serum free from drug; and (C) serum of volunteer who took 2 mg of tulobuterol hydrochloride orally (Subject 1, 3 hr).*

Although a previous assay (3) has been used extensively to determine serum levels of tulobuterol <10 ng/ml in humans, the present assay was found to be linear up to 50 ng/ml. When six replicate 1-ml samples of serum each containing 7 ng of tulobuterol hydrochloride/ml were analyzed, the mean value was 7.03 ng of tulobuterol hydrochloride/ml with a standard deviation of ±0.17 and a coefficient of variation of 2.42%. When serum samples containing 2 ng of tulobuterol hydrochloride/ml were analyzed, the mean value was 2.03 ng of tulobuterol hydrochloride with a standard deviation of ±0.10 ng/ml and a coefficient of variation of 4.93%.

To show the applicability of the method described, a serum concentration–time profile of tulobuterol was established from four volunteers following an oral dose of tulobuterol hydrochloride (Fig. 2). The among-subject variability was estimated by examination of the differences in the peak concentration and time to reach the peak.

Tulobuterol and some urinary metabolites can be determined simultaneously by mass fragmentography (9). Two major modifications were made in the present assay, compared with the single-extraction procedure used previously for tulobuterol in urine, *viz.*, ethyl acetate–acetone (3:1, v/v) extraction from a solution made alkaline with ammonium hydroxide. The extraction solvent was changed to ether, and back-extraction into the aqueous layer (pH ~1.0) and reextraction into the ether layer were added. Interference from endogenous materials in the serum was avoided with the improved cleanup procedure, although this was time consuming and lowered the overall recovery of tulobuterol. This method was inapplicable for determinations in human serum due to the low serum levels (<10 ng/ml) at a therapeutic dose (1–2 mg).

Albuterol and terbutaline were quantitated at low plasma levels using the relatively high mass ion $[M - 86]^+$ after forming the *tert*-butyldimethylsilyl derivatives (4, 5). In the case of tulobuterol, however, the relative intensity of $[M - 86]^+$ was <0.1%, which does not ensure adequate sensitivity.

To validate the present mass fragmentographic method, serum specimens were assayed by both mass fragmentography and electron-capture GLC. The analytical data obtained by both methods were correlated by linear regression analysis, yielding a correlation coefficient of 0.905 and a slope of 0.987 (Fig. 3).

In the latter method, an additional step was needed for the removal of excess derivatizing reagent (trifluoroacetic anhydride). Moreover,

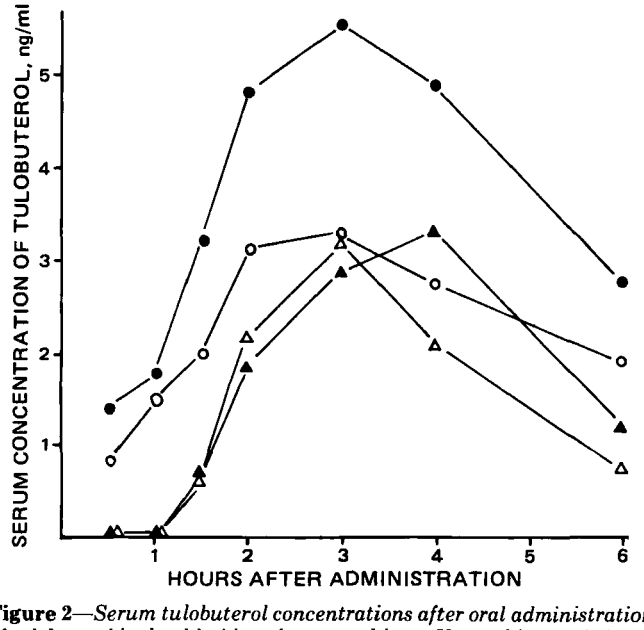

Figure 2—*Serum tulobuterol concentrations after oral administration of tulobuterol hydrochloride to human subjects. Key: subjects 1 (●) and 2 (○), administered in the form of a syrup solution; subjects 3 (▲) and 4 (△), administered in the form of tablets.*

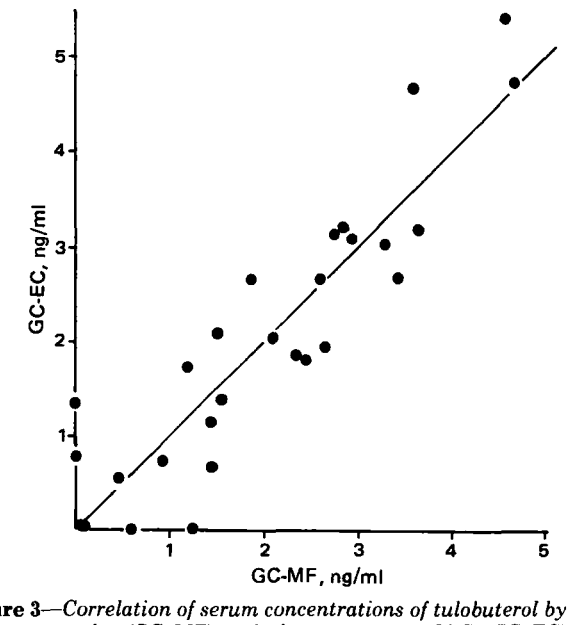

Figure 3—*Correlation of serum concentrations of tulobuterol by mass fragmentography (GC–MF) and electron-capture GLC (GC–EC). The line was calculated by least-squares linear regression analysis; y = 0.987x ± 0.060 and r = 0.905.*

measurement time of one sample in the electron-capture GLC (~15 min) is longer than that in the mass fragmentography. The mass fragmentography appears to be more readily adaptable to large numbers of samples.

REFERENCES

(1) S. Kubo, Y. Kase, T. Miyata, and I. Uesaka, *Arzneim.-Forsch.*, **25,** 1028 (1975).

(2) S. Kubo, I. Uesaka, I. Matsubara, I. Ishihara, and Y. Kase, *ibid.*, **27,** 1433 (1977).

(3) K. Matsumura, O. Kubo, T. Tsukada, K. Nishide, and H. Kato, *J. Chromatogr.*, **230,** 148 (1982).

(4) L. E. Martin, I. Oxford, R. J. N. Tanner, and M. J. Hetheridge, *Biomed. Mass Spectrom.*, **6,** 460 (1979).

(5) L. E. Martin, J. Rees, and R. J. N. Tanner, *ibid.*, **3,** 184 (1976).

(6) J. G. Leferink, I. Wagemaker-Engles, and R. A. A. Meaes, *J. Chromatogr.*, **143,** 299 (1977).

(7) E. Koshinaka, S. Kurata, K. Yamagishi, S. Kubo, and H. Kato, *Yakugaku Zasshi*, **98,** 1198 (1978).

(8) J. A. Deyrup and C. L. Moyer, *J. Org. Chem.*, **34,** 175, (1969).

(9) K. Matsumura, O. Kubo, T. Sakashita, Y. Adachi, H. Kato, K. Watanabe, and M. Hirobe, *J. Chromatogr.*, **222,** 53 (1981).

ACKNOWLEDGMENTS

The authors would like to thank Dr. N. Ogawa and Mr. S. Kurata for supplying the reference sample of tulobuterol hydrochloride and the internal standard.

COMMUNICATIONS

Pharmacokinetics of Drugs in Blood III: Metabolism of Procainamide and Storage Effect of Blood Samples

Keyphrases □ Pharmacokinetics—procainamide metabolism, storage effect of blood samples, *N*-acetylprocainamide □ Procainamide metabolism—pharmacokinetics, storage effect of blood samples, *N*-acetylprocainamide

To the Editor:

The distribution kinetics and metabolism of drugs in blood are of importance in pharmacokinetic studies. For instance, if a drug equilibrates slowly between plasma and blood cells, the time elapsed between collection and centrifugation of a blood sample could have a significant effect on the plasma concentration measured, which might differ considerably from the true *in vivo* concentration. This has been recently shown with gentamicin and furosemide (1, 2). A similar problem might also be anticipated if a drug undergoes *in vitro* metabolism in the blood. The above phenomenon has been referred to as the storage effect of blood (1, 2). This communication reports our preliminary studies on the metabolism of procainamide in blood and the storage effect of blood samples for procainamide and its metabolites.

Freshly withdrawn[1], heparinized control blood from five healthy subjects, aged 25–41 years, was used. None of the subjects received any medication for at least 1 month prior to the study. The whole blood (10 ml) in test tubes[2] from each subject was spiked with procainamide[3] stock solution (2 mg/ml of free base) to yield a concentration of 20 μg/ml. After manually mixing for 30 sec, each blood sample was quickly divided (1.0 ml) into 10 vials. The sealed vials were then stored (time zero) in a refrigerator (5°). To prevent any interaction between the drug and the stopper, the screw caps of the test tubes and vials used were all lined with aluminum foil. Similar preparations were carried out with blood samples kept at ambient temperature (25 ± 1.0°). These temperatures were chosen in order to simulate common procedures for handling blood samples. The vials were removed and centrifuged immediately at various times up to 48 hr. All the plasma samples were frozen until analyzed for procainamide and its metabolite, *N*-acetylprocainamide, using a modified high-performance liquid chromatographic (HPLC) method which was developed earlier in this laboratory (3).

Briefly, the assay involved the addition of 0.25 ml acetonitrile to 0.1 ml of plasma sample in a test tube[2]. After vortex-mixing and centrifugation, 20 μl of the supernatant solution was injected directly onto the column. The instrumentation consisted of a solvent delivery pump[4], a syringe-loading sample injector[5], a cation exchange column[6], and a fixed-wavelength detector[7] with 254-nm filter. The mobile phase was made of 75% (v/v) 0.12 *M* ammonium phosphate acidified with phosphoric acid (0.2%) and 25% acetonitrile; the flow rate was 2.5 ml/min. By this method, the detection limit was 0.2 μg/ml for both procainamide and *N*-acetylprocainamide in plasma.

Figure 1 shows the typical plasma concentration profiles of procainamide from the above studies in three subjects. Assuming that procainamide initially was only confined to plasma, based on the individually determined hematocrits, one could estimate its concentrations from the three subjects to be 40, 40, and 35 μg/ml, respectively. However, the results (Fig. 1) show much lower concentrations (15.6–18.7 μg/ml) obtained immediately after spiking and brief mixing, indicating an initial rapid and extensive distribution of the drug to blood cells. Adsorption of the drug onto the glass tube could be ruled out, since there was no initial loss of procainamide from the whole blood in subsequent studies.

The plasma concentrations, in general, decreased with time (Fig. 1). However, fluctuations in the measured concentration were usually found during the initial 12 hr of

[1] Vacutainer, Division of Becton, Dickinson and Co., Rutherford, N.J.
[2] Fisher Scientific Co., Pittsburgh, Pa.
[3] Hydrochloride salt, E. R. Squibb & Sons, Inc., Princeton, N.J.
[4] Model 6000A, Waters Associates, Milford, Mass.
[5] Model 7125, Rheodyne, Berkeley, Calif.
[6] Partisil PXS 10/25 SCX, Whatman, Clifton, N.J.
[7] Model 440, Waters Associates, Milford, Mass.

0022-3549/83/0500-0572$01.00/0

measurement time of one sample in the electron-capture GLC (~15 min) is longer than that in the mass fragmentography. The mass fragmentography appears to be more readily adaptable to large numbers of samples.

REFERENCES

(1) S. Kubo, Y. Kase, T. Miyata, and I. Uesaka, *Arzneim.-Forsch.*, **25,** 1028 (1975).

(2) S. Kubo, I. Uesaka, I. Matsubara, I. Ishihara, and Y. Kase, *ibid.*, **27,** 1433 (1977).

(3) K. Matsumura, O. Kubo, T. Tsukada, K. Nishide, and H. Kato, *J. Chromatogr.*, **230,** 148 (1982).

(4) L. E. Martin, I. Oxford, R. J. N. Tanner, and M. J. Hetheridge, *Biomed. Mass Spectrom.*, **6,** 460 (1979).

(5) L. E. Martin, J. Rees, and R. J. N. Tanner, *ibid.*, **3,** 184 (1976).

(6) J. G. Leferink, I. Wagemaker-Engles, and R. A. A. Meaes, *J. Chromatogr.*, **143,** 299 (1977).

(7) E. Koshinaka, S. Kurata, K. Yamagishi, S. Kubo, and H. Kato, *Yakugaku Zasshi*, **98,** 1198 (1978).

(8) J. A. Deyrup and C. L. Moyer, *J. Org. Chem.*, **34,** 175, (1969).

(9) K. Matsumura, O. Kubo, T. Sakashita, Y. Adachi, H. Kato, K. Watanabe, and M. Hirobe, *J. Chromatogr.*, **222,** 53 (1981).

ACKNOWLEDGMENTS

The authors would like to thank Dr. N. Ogawa and Mr. S. Kurata for supplying the reference sample of tulobuterol hydrochloride and the internal standard.

COMMUNICATIONS

Pharmacokinetics of Drugs in Blood III: Metabolism of Procainamide and Storage Effect of Blood Samples

Keyphrases □ Pharmacokinetics—procainamide metabolism, storage effect of blood samples, *N*-acetylprocainamide □ Procainamide metabolism—pharmacokinetics, storage effect of blood samples, *N*-acetylprocainamide

To the Editor:

The distribution kinetics and metabolism of drugs in blood are of importance in pharmacokinetic studies. For instance, if a drug equilibrates slowly between plasma and blood cells, the time elapsed between collection and centrifugation of a blood sample could have a significant effect on the plasma concentration measured, which might differ considerably from the true *in vivo* concentration. This has been recently shown with gentamicin and furosemide (1, 2). A similar problem might also be anticipated if a drug undergoes *in vitro* metabolism in the blood. The above phenomenon has been referred to as the storage effect of blood (1, 2). This communication reports our preliminary studies on the metabolism of procainamide in blood and the storage effect of blood samples for procainamide and its metabolites.

Freshly withdrawn[1], heparinized control blood from five healthy subjects, aged 25–41 years, was used. None of the subjects received any medication for at least 1 month prior to the study. The whole blood (10 ml) in test tubes[2] from each subject was spiked with procainamide[3] stock solution (2 mg/ml of free base) to yield a concentration of 20 μg/ml. After manually mixing for 30 sec, each blood sample was quickly divided (1.0 ml) into 10 vials. The sealed vials were then stored (time zero) in a refrigerator (5°). To prevent any interaction between the drug and the stopper, the screw caps of the test tubes and vials used were all lined with aluminum foil. Similar preparations were carried out with blood samples kept at ambient temperature (25 ± 1.0°). These temperatures were chosen in order to simulate common procedures for handling blood samples. The vials were removed and centrifuged immediately at various times up to 48 hr. All the plasma samples were frozen until analyzed for procainamide and its metabolite, *N*-acetylprocainamide, using a modified high-performance liquid chromatographic (HPLC) method which was developed earlier in this laboratory (3).

Briefly, the assay involved the addition of 0.25 ml acetonitrile to 0.1 ml of plasma sample in a test tube[2]. After vortex-mixing and centrifugation, 20 μl of the supernatant solution was injected directly onto the column. The instrumentation consisted of a solvent delivery pump[4], a syringe-loading sample injector[5], a cation exchange column[6], and a fixed-wavelength detector[7] with 254-nm filter. The mobile phase was made of 75% (v/v) 0.12 *M* ammonium phosphate acidified with phosphoric acid (0.2%) and 25% acetonitrile; the flow rate was 2.5 ml/min. By this method, the detection limit was 0.2 μg/ml for both procainamide and *N*-acetylprocainamide in plasma.

Figure 1 shows the typical plasma concentration profiles of procainamide from the above studies in three subjects. Assuming that procainamide initially was only confined to plasma, based on the individually determined hematocrits, one could estimate its concentrations from the three subjects to be 40, 40, and 35 μg/ml, respectively. However, the results (Fig. 1) show much lower concentrations (15.6–18.7 μg/ml) obtained immediately after spiking and brief mixing, indicating an initial rapid and extensive distribution of the drug to blood cells. Adsorption of the drug onto the glass tube could be ruled out, since there was no initial loss of procainamide from the whole blood in subsequent studies.

The plasma concentrations, in general, decreased with time (Fig. 1). However, fluctuations in the measured concentration were usually found during the initial 12 hr of

[1] Vacutainer, Division of Becton, Dickinson and Co., Rutherford, N.J.
[2] Fisher Scientific Co., Pittsburgh, Pa.
[3] Hydrochloride salt, E. R. Squibb & Sons, Inc., Princeton, N.J.
[4] Model 6000A, Waters Associates, Milford, Mass.
[5] Model 7125, Rheodyne, Berkeley, Calif.
[6] Partisil PXS 10/25 SCX, Whatman, Clifton, N.J.
[7] Model 440, Waters Associates, Milford, Mass.

0022-3549/83/0500-0572$01.00/0

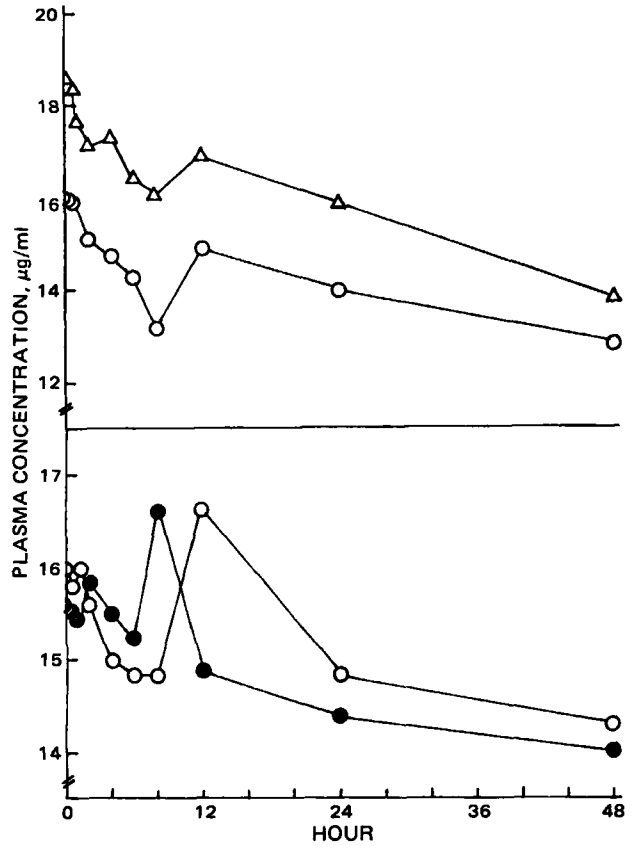

Figure 1—*Procainamide plasma concentration–time profiles from blood spiked with 20 μg/ml, and kept at ambient temperature (upper panel) or 5° (lower panel). Key: (○) subject 1; (●) subject 2; (△) subject 3.*

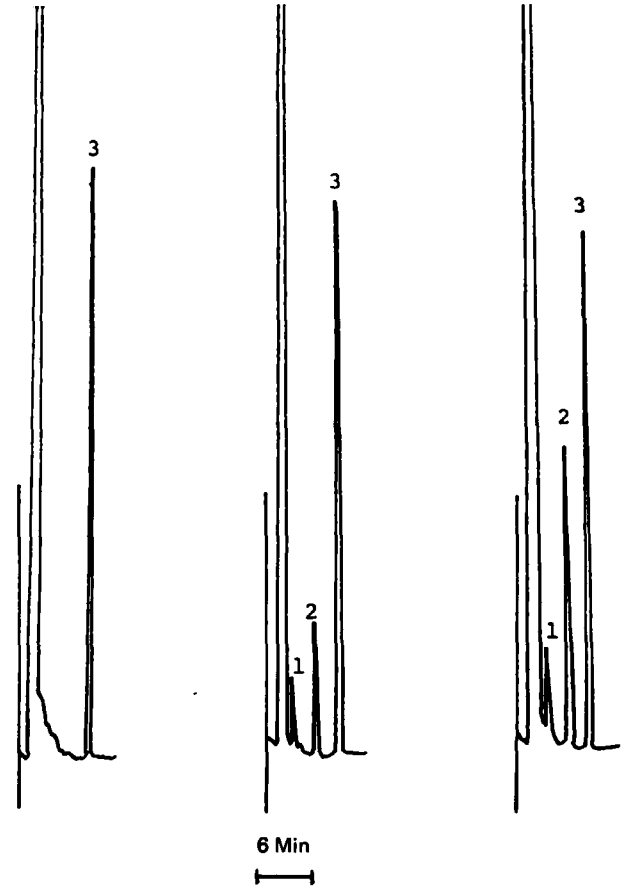

Figure 2—*Typical HPLC chromatograms from the blood of the first subject spiked with 20 μg/ml of procainamide and kept at ambient temperature for various periods of time: left, immediately after spiking (time zero); middle, 12 hr; right, 24 hr. Key: (1) unknown metabolite; (2) N-acetylprocainamide; (3) procainamide.*

study. Similar results were obtained when blood samples were spiked with 6 μg/ml of procainamide. These unusual distribution kinetics were observed in most of our studies either at 25 or 5°. It is felt that the above findings, especially those showing larger fluctuations, could not be an artifact, since the assays were conducted in duplicate and their coefficients of variation were <3.5%. In addition, simultaneous analysis of blood procainamide concentration in separate studies showed essentially a declining pattern, presumably due to metabolism of the drug in blood. At present, the cause or exact mechanism is unclear. Nevertheless, a possible reason might be the formation of Schiff bases between the drug and free fatty aldehydes on cell membranes, as proposed for gentamicin (1).

The formation of *N*-acetylprocainamide occurred in all the *in vitro* studies. This was shown by the appearance of peaks in the chromatograms (Fig. 2), with their retention time identical to that from the authentic samples. Typical time profiles of *N*-acetylprocainamide from subject 2 are depicted in Fig. 3. The *in vitro* formation of this metabolite in the present study appeared to be temperature dependent and to follow approximately a zero-order process, which could last up to 24 hr in some subjects. Based on the apparent linear portion of the curves (Fig. 3), the mean appearance rates of *N*-acetylprocainamide in plasma at 5 and 25° were calculated to be ~0.05 and 0.10 μg/ml/hr, respectively. It should be noted that although *N*-acetylation of procainamide has been found to take place in whole blood (4), the distribution kinetics and its implication were not reported.

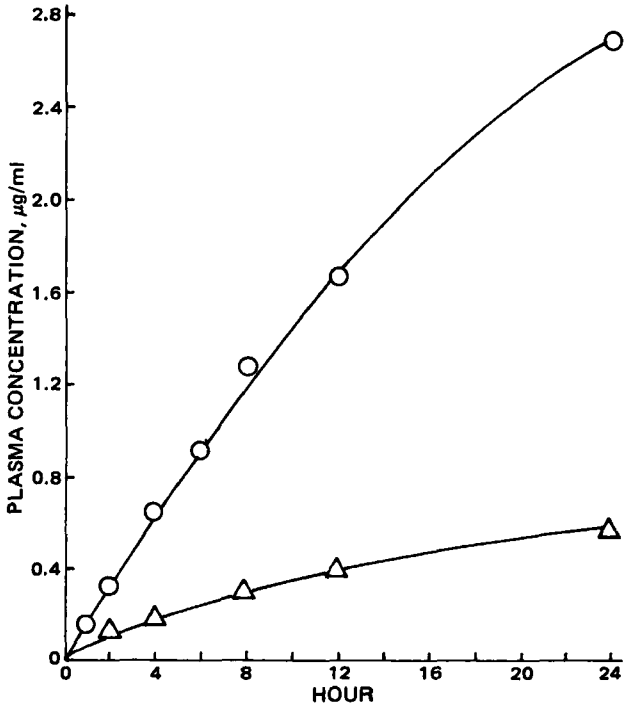

Figure 3—N-*Acetylprocainamide plasma concentration–time profiles from the blood of the second subject spiked with 20 μg/ml of procainamide and kept at 5° (△) and 25° (○).*

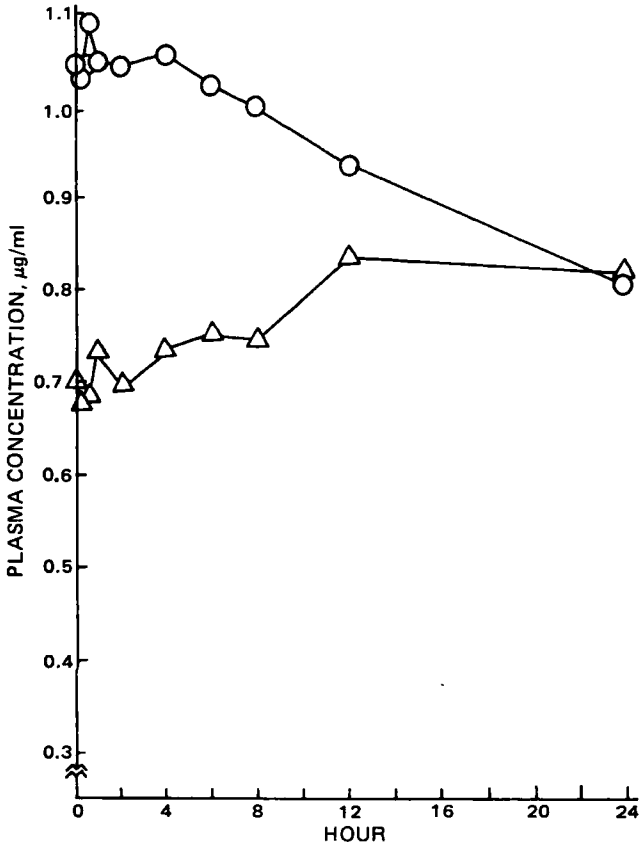

Figure 4—*Procainamide (○) and N-acetylprocainamide (△) plasma concentration–time profiles in a blood sample kept at ambient temperature.*

A second metabolite with shorter retention than *N*-acetylprocainamide (Fig. 2) was found in all chromatograms except those from samples obtained at earlier times. This unidentified metabolite was also found in many cases after the administration of procainamide to rabbits (5) and humans (6). Recent studies (7) have shown that desethyl procainamide and desethyl *N*-acetylprocainamide might be two additional metabolites of procainamide. However, identification of the unknown product was not made due to the lack of authentic samples. According to the relative peak heights, the appearance rate of this unidentified metabolite in plasma also followed a zero-order process in the first 12 hr of study.

To ascertain whether metabolism took place in plasma or blood cells, pooled plasma was spiked with procainamide to yield an initial concentration of 20 μg/ml and kept at ambient temperature for various periods of time. No metabolite formation could be found up to 48 hr, indicating that blood cells are the sole site of metabolism in whole blood. Since the plasma concentrations of procainamide were essentially identical during the study, no degradation of plasma samples could be assumed.

The results of the above *in vitro* studies suggest that the time between collection and centrifugation of a blood sample may have a considerable influence on the measured plasma levels of procainamide and its metabolites. This was supported by another experiment in which ~10 ml of blood was collected shortly before the next scheduled dose from an adult male patient on chronic oral procainamide therapy (Fig. 4). During the 24 hr of storage, the difference between the minimum and maximum plasma concentrations measured for procainamide was ~ 35% and that for *N*-acetylprocainamide was 24%. Similar effects also were observed from two rabbits, whose blood was collected in syringes[8] after intravenous dosing of procainamide.

In light of the results of this study, it appears that a prudent approach is to separate plasma as soon as the blood sample is collected; this might minimize the difference between the true *in vivo* plasma concentration and the measured *in vitro* concentration. More work is required in order to fully assess the potential significance of the present findings in the pharmacokinetic studies.

(1) M. G. Lee, M.-L. Chen, S.-M. Huang, and W. L. Chiou, *Biopharm. Drug. Disp.*, **2**, 89 (1981).

(2) M. G. Lee, M.-L. Chen, and W. L. Chiou, *Res. Commun. Chem. Pathol. Pharmacol.*, **34**, 17 (1981).

(3) M. A. F. Gadalla, G. W. Peng, and W. L. Chiou, *J. Pharm. Sci.*, **67**, 869 (1978).

(4) D. E. Drayer, J. M. Strong, B. Jones, A. Sandler, and M. M. Reidenberg, *Metab. Disp.*, **2**, 499 (1974).

(5) G. Lam, Ph.D. thesis, University of Illinois at the Medical Center, Chicago, Ill. 1981.

(6) R. L. Nation, M. G. Lee, S.-M. Huang, and W. L. Chiou, *J. Pharm. Sci.*, **68**, 532 (1979).

(7) T. I. Ruo, Y. Morita, A. J. Atkinson, Jr., T. Henthorn, and J.-P. Thenot, *J. Pharmacol. Exp. Ther.*, **216**, 357 (1981).

Mei-Ling Chen
Myung G. Lee
Win L. Chiou ˣ
Department of Pharmacodynamics
College of Pharmacy
University of Illinois
Chicago, IL 60612

Received August 31, 1982
Accepted for publication December 1, 1982

[8] Plastipak syringe, Division of Becton, Dickinson and Co., Rutherford, N.J.

Nonlinear Regression Approach for Determining Whether Absorption and Elimination Rate Constants are Equal in the One-Compartment Open Model with First-Order Processes

Keyphrases □ Pharmacokinetics—one-compartment open model, nonlinear regression analysis, absorption rate constants, elimination rate constants

To the Editor:

Recently Bialer reported a simple method for determining whether absorption and elimination rate constants are equal in the one-compartment open model with first-order processes (1). The basis for this method is that whenever the product of time of peak drug concentration (t_{max}) is equal to total area under curve (AUC) divided by the base of natural logarithm (e), the absorption rate constant (k_a) must be equal to the elimination rate con-

0022-3549/83/0500-0574$01.00/0

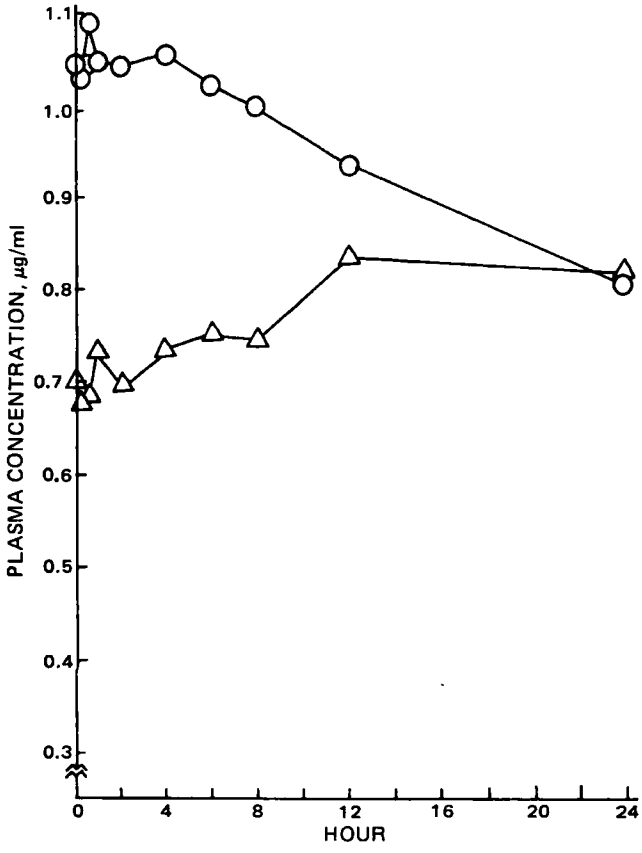

Figure 4—*Procainamide (○) and N-acetylprocainamide (△) plasma concentration–time profiles in a blood sample kept at ambient temperature.*

A second metabolite with shorter retention than *N*-acetylprocainamide (Fig. 2) was found in all chromatograms except those from samples obtained at earlier times. This unidentified metabolite was also found in many cases after the administration of procainamide to rabbits (5) and humans (6). Recent studies (7) have shown that desethyl procainamide and desethyl *N*-acetylprocainamide might be two additional metabolites of procainamide. However, identification of the unknown product was not made due to the lack of authentic samples. According to the relative peak heights, the appearance rate of this unidentified metabolite in plasma also followed a zero-order process in the first 12 hr of study.

To ascertain whether metabolism took place in plasma or blood cells, pooled plasma was spiked with procainamide to yield an initial concentration of 20 μg/ml and kept at ambient temperature for various periods of time. No metabolite formation could be found up to 48 hr, indicating that blood cells are the sole site of metabolism in whole blood. Since the plasma concentrations of procainamide were essentially identical during the study, no degradation of plasma samples could be assumed.

The results of the above *in vitro* studies suggest that the time between collection and centrifugation of a blood sample may have a considerable influence on the measured plasma levels of procainamide and its metabolites. This was supported by another experiment in which ~10 ml of blood was collected shortly before the next scheduled dose from an adult male patient on chronic oral procainamide therapy (Fig. 4). During the 24 hr of storage, the difference between the minimum and maximum plasma concentrations measured for procainamide was ~ 35% and that for *N*-acetylprocainamide was 24%. Similar effects also were observed from two rabbits, whose blood was collected in syringes[8] after intravenous dosing of procainamide.

In light of the results of this study, it appears that a prudent approach is to separate plasma as soon as the blood sample is collected; this might minimize the difference between the true *in vivo* plasma concentration and the measured *in vitro* concentration. More work is required in order to fully assess the potential significance of the present findings in the pharmacokinetic studies.

(1) M. G. Lee, M.-L. Chen, S.-M. Huang, and W. L. Chiou, *Biopharm. Drug. Disp.*, **2**, 89 (1981).

(2) M. G. Lee, M.-L. Chen, and W. L. Chiou, *Res. Commun. Chem. Pathol. Pharmacol.*, **34**, 17 (1981).

(3) M. A. F. Gadalla, G. W. Peng, and W. L. Chiou, *J. Pharm. Sci.*, **67**, 869 (1978).

(4) D. E. Drayer, J. M. Strong, B. Jones, A. Sandler, and M. M. Reidenberg, *Metab. Disp.*, **2**, 499 (1974).

(5) G. Lam, Ph.D. thesis, University of Illinois at the Medical Center, Chicago, Ill. 1981.

(6) R. L. Nation, M. G. Lee, S.-M. Huang, and W. L. Chiou, *J. Pharm. Sci.*, **68**, 532 (1979).

(7) T. I. Ruo, Y. Morita, A. J. Atkinson, Jr., T. Henthorn, and J.-P. Thenot, *J. Pharmacol. Exp. Ther.*, **216**, 357 (1981).

Mei-Ling Chen
Myung G. Lee
Win L. Chiou ˣ
Department of Pharmacodynamics
College of Pharmacy
University of Illinois
Chicago, IL 60612

Received August 31, 1982
Accepted for publication December 1, 1982

[8] Plastipak syringe, Division of Becton, Dickinson and Co., Rutherford, N.J.

Nonlinear Regression Approach for Determining Whether Absorption and Elimination Rate Constants are Equal in the One-Compartment Open Model with First-Order Processes

Keyphrases □ Pharmacokinetics—one-compartment open model, nonlinear regression analysis, absorption rate constants, elimination rate constants

To the Editor:

Recently Bialer reported a simple method for determining whether absorption and elimination rate constants are equal in the one-compartment open model with first-order processes (1). The basis for this method is that whenever the product of time of peak drug concentration (t_{max}) is equal to total area under curve (AUC) divided by the base of natural logarithm (e), the absorption rate constant (k_a) must be equal to the elimination rate con-

0022-3549/83/0500-0574$01.00/0

stant (k_e). This method is mathematically sound, but when applied to clinical study data, t_{max} and C_{max} are difficult to determine with sufficient accuracy, and the true t_{max} and C_{max} may be missed with routine sampling protocol. Additionally, the calculation of the AUC requires an accurate estimate of the half-life of the terminal portion of the concentration–time curve to estimate the residual area remaining after the last measured concentration. The terminal half-life estimation requires fitting the terminal portion concentration–time of the curve or, preferentially, the entire profile by some standard fitting procedure to an *a priori* model. Thus, satisfaction of the criterion stated above may not be obvious. It is, therefore, of interest to see if there is an alternate method which can achieve the same result.

In a one-compartment open model with first-order absorption and elimination the plasma–drug concentration (C_b) is defined generally by:

$$C_b = \frac{FDk_a}{V_d(k_a - k_e)}(e^{-k_e t} - e^{-k_a t}) \qquad \text{(Eq. 1)}$$

The relevance of this equation and the relationship between k_a and k_e have been discussed extensively in standard texts (2, 3). Generally speaking, when k_a is larger than k_e, the terminal phase reflects the process of elimination. The other case is the flip-flop model where k_a is smaller than k_e, and the terminal phase reflects the process of absorption. In the special case where k_a is equal to k_e Eq. 1 becomes mathematically irrelevant, since the derivation of Eq. 1 requires that $k_a \neq k_e$. In this case, the general equation describing the plasma–drug concentration has to be derived from the basic model setting $k = k_a = k_e$. By employing a standard technique such as Laplace transform, Eq. 2 can be obtained (1, 2):

$$C_b = \frac{FD}{V_d} kte^{-kt} \qquad \text{(Eq. 2)}$$

There are a number of techniques commonly used to obtain values for the rate constants of absorption and elimination. These include the manual method of residuals (feathering) and computer-based nonlinear regression techniques using least-squares criteria. The Wagner–Nelson method makes no specific compartmental model assumption and can also be used to estimate k_a. However, when $k_a = k_e$, absorption occurs throughout the whole process. Therefore, any technique that involves assuming the terminal phase reflects solely an absorption or elimination process will fail to reveal the true rate constants. This is not the case for nonlinear least-squares regression analysis. Provided that there is some minute difference between k_a and k_e, nonlinear regression may be applied to the data. To test this alternative, data with only rounding error were generated using Eq. 2 with FD/V_d = 10, $k = k_a = k_e = 0.5$ (Table I). Concentrations with 5% random noise are also listed in Table I.

Table I—Simulated Concentration Data Using Eq. 2 with $FD/V_d = 10$ and $k = k_a = k_e = 0.5$

Time	Concentration	Concentration with 5% Noise
0.25	1.10	1.10
0.5	1.95	1.95
1.0	3.03	3.18
2.0	3.68	3.68
3.0	3.35	3.52
4.0	2.71	2.85
5.0	2.05	2.05
6.0	1.49	1.42
8.0	0.73	0.69
10.0	0.34	0.36
12.0	0.15	0.14

With no *a priori* knowledge of the values of k_a and k_e, the two rate constants were estimated by using the method of residuals, the Wagner–Nelson method (4), the decision-making program AUTOAN (5), and the nonlinear regression program NONLIN (6). The results are listed in Table II.

Application of the graphical method of residuals revealed no problems except that the residual line seemed to show some curvature. The values for k_a and k_e obtained by this method were 0.87 and 0.39, respectively. The Wagner–Nelson method also revealed no problems and the values for k_a and k_e obtained by this method were 0.67 and 0.40, respectively. The same data were fitted by the decision-making program AUTOAN. Curve stripping, the first part of the AUTOAN output, indicated that the best number of exponential is 3 and the data are best described by a one-compartment open model with two first-order input steps, k_1 and k_2. The second part of the AUTOAN output using the 1969 version of NONLIN to fit the data according to this model yielded values for k_1, k_2, k_e, and R^2 of 0.707, 2.634, 0.450, and 0.855, respectively. Finally, using rate constants obtained from the method of residuals as initial estimates, and assuming the model described by Eq. 1, the 1974 version of NONLIN successfully converged to the real values. The goodness of fit was exemplified by the R^2 value and the small standard deviation of the parameters estimates (Table II).

The method of residuals, the Wagner–Nelson method, curve stripping, and nonlinear regression are probably the

Table II—Comparison of Real and Estimated Values Obtained by the Method of Residuals, the Wagner–Nelson Method, AUTOAN, and NONLIN [a]

	FD/V_d	k_e	k_a	k_1	k_2	R^2
Real Values	10	0.500	0.500	—	—	—
Method of Residuals[b]	7.4	0.39	0.87	—	—	—
Wagner–Nelson Method[b]	7.7	0.40	0.67	—	—	—
AUTOAN[b]	5.79	0.450	—	0.707	2.634	0.855
	(23.01)	(1.937)	—	(3.937)	(8.343)	
AUTOAN[c]	6.64	0.695	—	0.771	1.030	0.718
	(67.17)	(6.86)	—	(13.05)	(11.85)	
NONLIN[b]	9.98	0.499	0.501	—	—	1.000
	(0.06)	(0.003)	(0.003)			
NONLIN[c]	10.31	0.506	0.501	—	—	0.997
	(0.89)	(0.042)	(0.049)			

[a] Standard deviation of the parameter estimates in parentheses. [b] Using data with only rounding error. [c] Using data with 5% noise.

most routine procedures for determining model rate constants. The first three methods are obviously bad choices when $k_a = k_e$. A nonlinear regression analysis program such as NONLIN, with the simplest model, successfully revealed the real values of k_a and k_e. Bialer's criteria (1) can serve as additional proof of the NONLIN output.

It should be emphasized that although nonlinear regression techniques successfully converged to the real rate constants used to generate the data in the example, this does not imply that Eq. 1 is the only model which can be fitted to the data. The problems associated with obtaining a reliable value for a pharmacokinetic parameter, such as absorption rate constants after oral administration, have been previously identified. For example, a multiple-compartment open model may also be collapsed to a one-compartment open model under certain conditions (7). In reality, the true model is rarely known, and in most cases one can not distinguish one model from another. However, this study demonstrated that if Eq. 1 represents a true model, nonlinear regression analysis separates the rate constants where other methods can not.

(1) M. Bialer, *J. Pharmacokinet. Biopharm.*, **8**, 111 (1980).
(2) M. Gibaldi and D. Perrier, "Pharmacokinetics," Dekker, New York, N.Y., 1975, pp. 33–39.
(3) J. G. Wagner, "Fundamentals of Clinical Pharmacokinetics," Drug Intelligence Publications, Hamilton, Ill., 1975, pp. 74–82.
(4) J. G. Wagner and E. Nelson, *J. Pharm. Sci.*, **53**, 1392 (1964).
(5) A. J. Sedman and J. G. Wagner, "AUTOAN: A Decision-Making Pharmacokinetic Computer Program," Publication Distribution Service, Ann Arbor Mich., 1974.
(6) C. M. Metzler, G. L. Elfring, and A. J. McEwen. (Abstract), *Biometrics*, **30**, 562 (1974).
(7) R. A. Ronfeld and L. Z. Benet, *J. Pharm. Sci.*, **66**, 178 (1977).

Keith K. H. Chan ˣ
Research and Development Department
Pharmaceuticals Division
Ciba-Geigy Corporation
Ardsley, New York 10502

Kenneth W. Miller
Department of Pharmaceutics
College of Pharmacy
University of Minnesota
Minneapolis, Minnesota 55455

Received May 5, 1982
Accepted for publication November 29, 1982.

Kinetic Interpretation of the Microparameters in Compartmental Modeling When Adjoining Compartments are Sampled

Keyphrases □ Pharmacokinetic analysis—compartmental modeling □ Compartmental modeling—kinetic interpretation of microparameters □ Diffusional transport hypothesis—compartmental modeling

To The Editor:

In linear compartmental modeling, the rate of mass transfer of drug from compartment i to compartment j is $k_{ij}x_i$, and for the reverse transfer $k_{ji}x_j$, where the k's are constant microparameters and the x's stand for the amounts in the compartments (1). It appears tempting to justify compartmental pharmacokinetic analysis by attaching special kinetic significance to the microparameters. However, it is well recognized that this type of modeling is merely an abstract mathematical way of accounting for the combined effect of many complex disposition processes, which are too difficult or impossible to consider individually, in order to explain the concentration profile in a sampled compartment; typically the blood. It is also recognized that in pharmacokinetic practice when dealing with prediction and adjustment of blood levels, in the calculation of dosage regimens and in the evaluation of drug input, there is no need for compartmental modeling. It would be irrational to do so, because the required calculations can (at least for dose-linear systems) be done simply on the basis of the principles of superposition, convolution, or deconvolution. However, there are cases in pharmacokinetics where more than one tissue compartment is sampled for the drug. A compartmental type of kinetic analysis is then definitely justified. The blood–brain barrier (BBB) transfer kinetics of theophylline in dogs has recently been investigated. In the analysis, the classical linear compartmental approach was avoided because it appears completely irrational to assume that the transfer across a membrane is proportional to amounts and not to a concentration differential. A model-independent approach combined with a more rational compartmental transport mechanism was applied instead. In analyzing the equations resulting from this approach an interesting relationship was discovered between the diffusion and binding parameters and the microparameters in a classical compartmental approach. It is of interest to communicate these findings which bring the classical compartmental modeling into a different perspective.

The Diffusion Approach: The diffusion rate of the drug across the BBB is proportional to the difference between the free drug concentrations on the two sides of the barrier:

$$\frac{d}{dt}[V_cC_c(t)] = K_1[F_sC_s(t) - F_cC_c(t)] \quad \text{(Eq. 1)}$$

Subscripts c and s denote cerebrospinal fluid (CSF) and serum, respectively; V, C, and F stand for volume, total drug concentration, and free (unbound) fraction, respectively; while K_1 is a positive diffusion constant. Equation 1 assumes that the drug is not metabolized in the CSF, which is consistent with our current knowledge about the metabolic systems present on the CNS side of the BBB (2). The equation can readily be solved by Laplace transforms to give the following expression relating the total concentration of the drug in the CSF to the total concentration in the serum:

$$C_c(t) = \left(\frac{F_cK_1}{V_c}\frac{F_s}{F_c}\right) C_s(t) * e^{(F_cK_1/V_c)t} \quad \text{(Eq. 2)}$$

where * denotes convolution.

The derivation of Eq. 2 assumes that F_c and F_s do not depend significantly on the drug concentration. The free fractions depend on the unbound protein concentration as well as on the affinity of the protein for the drug. Usually only a small fraction of the available binding sites is occupied at therapeutic drug concentrations; therefore, the

0022-3549/83/0500-0576$01.00/0

most routine procedures for determining model rate constants. The first three methods are obviously bad choices when $k_a = k_e$. A nonlinear regression analysis program such as NONLIN, with the simplest model, successfully revealed the real values of k_a and k_e. Bialer's criteria (1) can serve as additional proof of the NONLIN output.

It should be emphasized that although nonlinear regression techniques successfully converged to the real rate constants used to generate the data in the example, this does not imply that Eq. 1 is the only model which can be fitted to the data. The problems associated with obtaining a reliable value for a pharmacokinetic parameter, such as absorption rate constants after oral administration, have been previously identified. For example, a multiple-compartment open model may also be collapsed to a one-compartment open model under certain conditions (7). In reality, the true model is rarely known, and in most cases one can not distinguish one model from another. However, this study demonstrated that if Eq. 1 represents a true model, nonlinear regression analysis separates the rate constants where other methods can not.

(1) M. Bialer, *J. Pharmacokinet. Biopharm.*, **8**, 111 (1980).
(2) M. Gibaldi and D. Perrier, "Pharmacokinetics," Dekker, New York, N.Y., 1975, pp. 33–39.
(3) J. G. Wagner, "Fundamentals of Clinical Pharmacokinetics," Drug Intelligence Publications, Hamilton, Ill., 1975, pp. 74–82.
(4) J. G. Wagner and E. Nelson, *J. Pharm. Sci.*, **53**, 1392 (1964).
(5) A. J. Sedman and J. G. Wagner, "AUTOAN: A Decision-Making Pharmacokinetic Computer Program," Publication Distribution Service, Ann Arbor Mich., 1974.
(6) C. M. Metzler, G. L. Elfring, and A. J. McEwen. (Abstract), *Biometrics*, **30**, 562 (1974).
(7) R. A. Ronfeld and L. Z. Benet, *J. Pharm. Sci.*, **66**, 178 (1977).

Keith K. H. Chan ˣ
Research and Development Department
Pharmaceuticals Division
Ciba-Geigy Corporation
Ardsley, New York 10502

Kenneth W. Miller
Department of Pharmaceutics
College of Pharmacy
University of Minnesota
Minneapolis, Minnesota 55455

Received May 5, 1982
Accepted for publication November 29, 1982.

Kinetic Interpretation of the Microparameters in Compartmental Modeling When Adjoining Compartments are Sampled

Keyphrases □ Pharmacokinetic analysis—compartmental modeling □ Compartmental modeling—kinetic interpretation of microparameters □ Diffusional transport hypothesis—compartmental modeling

To The Editor:

In linear compartmental modeling, the rate of mass transfer of drug from compartment i to compartment j is $k_{ij}x_i$, and for the reverse transfer $k_{ji}x_j$, where the k's are constant microparameters and the x's stand for the amounts in the compartments (1). It appears tempting to justify compartmental pharmacokinetic analysis by attaching special kinetic significance to the microparameters. However, it is well recognized that this type of modeling is merely an abstract mathematical way of accounting for the combined effect of many complex disposition processes, which are too difficult or impossible to consider individually, in order to explain the concentration profile in a sampled compartment; typically the blood. It is also recognized that in pharmacokinetic practice when dealing with prediction and adjustment of blood levels, in the calculation of dosage regimens and in the evaluation of drug input, there is no need for compartmental modeling. It would be irrational to do so, because the required calculations can (at least for dose-linear systems) be done simply on the basis of the principles of superposition, convolution, or deconvolution. However, there are cases in pharmacokinetics where more than one tissue compartment is sampled for the drug. A compartmental type of kinetic analysis is then definitely justified. The blood–brain barrier (BBB) transfer kinetics of theophylline in dogs has recently been investigated. In the analysis, the classical linear compartmental approach was avoided because it appears completely irrational to assume that the transfer across a membrane is proportional to amounts and not to a concentration differential. A model-independent approach combined with a more rational compartmental transport mechanism was applied instead. In analyzing the equations resulting from this approach an interesting relationship was discovered between the diffusion and binding parameters and the microparameters in a classical compartmental approach. It is of interest to communicate these findings which bring the classical compartmental modeling into a different perspective.

The Diffusion Approach: The diffusion rate of the drug across the BBB is proportional to the difference between the free drug concentrations on the two sides of the barrier:

$$\frac{d}{dt}[V_cC_c(t)] = K_1[F_sC_s(t) - F_cC_c(t)] \quad \text{(Eq. 1)}$$

Subscripts c and s denote cerebrospinal fluid (CSF) and serum, respectively; V, C, and F stand for volume, total drug concentration, and free (unbound) fraction, respectively; while K_1 is a positive diffusion constant. Equation 1 assumes that the drug is not metabolized in the CSF, which is consistent with our current knowledge about the metabolic systems present on the CNS side of the BBB (2). The equation can readily be solved by Laplace transforms to give the following expression relating the total concentration of the drug in the CSF to the total concentration in the serum:

$$C_c(t) = \left(\frac{F_cK_1}{V_c}\frac{F_s}{F_c}\right) C_s(t) * e^{(F_cK_1/V_c)t} \quad \text{(Eq. 2)}$$

where * denotes convolution.

The derivation of Eq. 2 assumes that F_c and F_s do not depend significantly on the drug concentration. The free fractions depend on the unbound protein concentration as well as on the affinity of the protein for the drug. Usually only a small fraction of the available binding sites is occupied at therapeutic drug concentrations; therefore, the

0022-3549/83/0500-0576$01.00/0

free fraction is relatively constant and independent of the drug concentration (3).

The diffusional transport hypothesis (Eq. 1) was verified kinetically in the following manner according to Eq. 2: A suitable arbitrary function was chosen to approximate the $C_s(t)$ response. (The fitting of a two-exponential expression to the C_s, t data appeared to give an excellent approximation.) The fitting of the arbitrary function to the serum data was done simultaneously with the fitting to the CSF data of a second function resulting from convoluting the first function according to Eq. 2. Good correlations to the CSF and serum data were observed.

The Classical Compartmental Approach: The rate of change of the amount, x_c, of drug in the CSF is

$$\frac{dx_c}{dt} = k_{sc}x_s - k_{cs}x_c \qquad \text{(Eq. 3)}$$

where k_{sc} and k_{cs} are the first-order rate constants for the transfer of drug from serum to CSF and reverse, respectively. Solving Eq. 3 through Laplace transforms gives:

$$x_c(t) = k_{sc}x_s(t)*e^{-k_{cs}t} \qquad \text{(Eq. 4)}$$

so that

$$C_c(t) = k_{sc}\left(\frac{V_s}{V_c}\right)C_s(t)*e^{-k_{cs}t} \qquad \text{(Eq. 5)}$$

By comparing Eqs. 5 and 2 the following relations are obtained:

$$V_c k_{cs} = F_c K_1 \qquad \text{(Eq. 6)}$$

$$V_s k_{sc} = F_s K_1 \qquad \text{(Eq. 7)}$$

One can, therefore, in this case of compartmental analysis with data available from adjoining compartments, relate the microparameters of the abstract mass transfer of classical compartmental modeling to the more meaningful parameters of a rational, diffusional-based transport mechanism (Eq. 1).

The relationships (Eqs. 6 and 7) may be stated simply as follows: The intercompartmental clearances are equal to the intercompartmental diffusion rate constant multiplied by the free fraction of the drug in the respective compartment.

The above analysis is valid for any complexity of the compartmental system as long as one of the two sampled, adjoining compartments is not connected to other compartments.

(1) P. Veng-Pedersen, *J. Pharm. Sci.*, **67**, 187 (1978).

(2) W. H. Oldendorf, *Exp. Eye Res. Suppl.*, **25**, 177 (1977).

(3) M. Rowland and T. N. Tozer, in "Clinical Pharmacokinetics: Concepts and Applications," Lea & Febiger, Philadelphia, Pa., 1980, p. 42.

P. Veng-Pedersen ˣ

Division of Pharmacokinetics
School of Pharmacy
Purdue University
West Lafayette, IN 47907

R. Brashear

School of Medicine
Department of Medicine
University Hospital N559
Indianapolis, IN 46223

Received September 1, 1982.
Accepted for publication November 24, 1982.

Predicting the Dose-Dependent Bioavailability of Hydrocortisone and Chlorothiazide in Humans

Keyphrases □ Bioavailability—dose dependency, hydrocortisone, chlorothiazide □ Hydrocortisone—dose-dependent bioavailability, saturable absorption kinetics □ Chlorothiazide—dose-dependent bioavailability, saturable absorption kinetics

To the Editor:

A recent report (1) described the occurrence and mechanisms of dose-dependent saturable absorption kinetics for several commonly used drugs. Equations were also derived, on the basis of the classical Michaelis–Menten approach, to predict such dose-dependent absorption kinetics (1). In the present communication, these equations are applied, in an effort to predict the recently reported, nonproportional dose bioavailability data on hydrocortisone (2) and chlorothiazide (3).

Predicted values for hydrocortisone plasma levels (C_{max}), area under the curve (AUC) and AUC corrected for variance in the first-order rate constant for drug elimination (AUC_{kel}) as well as chlorothiazide urine recovery were calculated using the parameters obtained from the derived equations reported earlier (1). Tables I and II list these calculated parameters and compare the observed values with the predicted values for each dose of hydrocortisone and chlorothiazide, respectively. The excellent correlations between the observed and predicted values attest to the validity of the saturable absorption predictive model for those two drugs. It should be noted that the dose-dependent hydrocortisone tablet data (4) also can be treated in a similar manner with good predictability.

The saturable absorption of chlorothiazide is probably related to the existence of an absorption window (1), inasmuch as the average urinary recovery of chlorothiazide is increased in humans in the presence of food (5) and in dogs following propantheline bromide administration (6).

Table I—Comparison of Observed and Predicted Values for Hydrocortisone

Dose, mg	C_{max}[a], ng/ml		AUC[b], ng·hr/ml		$AUC_{\cdot k_{el}}$[c], ng/ml	
	Obs[d]	Pred[e]	Obs	Pred	Obs	Pred
5	119	114	293	278	171	162
10	175	188	447	502	248	267
20	263	278	835	838	377	396
40	389	366	1340	1259	553	521
r value	0.990		0.996		0.991	

[a] C_{max} = 533 ng/ml when the Michaelis constant (K_m) is 18.2 mg. [b] AUC_{max} = 2531 ng·hr/ml when K_m = 40.4 mg. [c] $(AUC \cdot k_{el})_{max}$ = 763 ng/ml when K_m = 18.5 mg. [d] Observed values (Obs) from previously published work (2). [e] Predicted values (Pred) calculated using previously derived equations (1).

Table II—Comparison of Observed and Predicted Urine Recovery for Chlorothiazide

Dose, mg	Recovery, mg[a]	
	Obs[b]	Pred[c]
50	28.3	28.0
100	47.0	47.8
250	83.3	82.7
r value	0.999	

[a] $Recovery_{max}$ = 161.6 mg when K_m = 238.2 mg. [b] Observed values (Obs) from previously published work (3). [c] Predicted values (Pred) calculated using previously derived equations (1).

0022-3549/83/0500-0577$01.00/0

free fraction is relatively constant and independent of the drug concentration (3).

The diffusional transport hypothesis (Eq. 1) was verified kinetically in the following manner according to Eq. 2: A suitable arbitrary function was chosen to approximate the $C_s(t)$ response. (The fitting of a two-exponential expression to the C_s, t data appeared to give an excellent approximation.) The fitting of the arbitrary function to the serum data was done simultaneously with the fitting to the CSF data of a second function resulting from convoluting the first function according to Eq. 2. Good correlations to the CSF and serum data were observed.

The Classical Compartmental Approach: The rate of change of the amount, x_c, of drug in the CSF is

$$\frac{dx_c}{dt} = k_{sc}x_s - k_{cs}x_c \qquad \text{(Eq. 3)}$$

where k_{sc} and k_{cs} are the first-order rate constants for the transfer of drug from serum to CSF and reverse, respectively. Solving Eq. 3 through Laplace transforms gives:

$$x_c(t) = k_{sc}x_s(t)*e^{-k_{cs}t} \qquad \text{(Eq. 4)}$$

so that

$$C_c(t) = k_{sc}\left(\frac{V_s}{V_c}\right)C_s(t)*e^{-k_{cs}t} \qquad \text{(Eq. 5)}$$

By comparing Eqs. 5 and 2 the following relations are obtained:

$$V_c k_{cs} = F_c K_1 \qquad \text{(Eq. 6)}$$

$$V_s k_{sc} = F_s K_1 \qquad \text{(Eq. 7)}$$

One can, therefore, in this case of compartmental analysis with data available from adjoining compartments, relate the microparameters of the abstract mass transfer of classical compartmental modeling to the more meaningful parameters of a rational, diffusional-based transport mechanism (Eq. 1).

The relationships (Eqs. 6 and 7) may be stated simply as follows: The intercompartmental clearances are equal to the intercompartmental diffusion rate constant multiplied by the free fraction of the drug in the respective compartment.

The above analysis is valid for any complexity of the compartmental system as long as one of the two sampled, adjoining compartments is not connected to other compartments.

(1) P. Veng-Pedersen, *J. Pharm. Sci.*, **67**, 187 (1978).

(2) W. H. Oldendorf, *Exp. Eye Res. Suppl.*, **25**, 177 (1977).

(3) M. Rowland and T. N. Tozer, in "Clinical Pharmacokinetics: Concepts and Applications," Lea & Febiger, Philadelphia, Pa., 1980, p. 42.

P. Veng-Pedersen ˣ

Division of Pharmacokinetics
School of Pharmacy
Purdue University
West Lafayette, IN 47907

R. Brashear

School of Medicine
Department of Medicine
University Hospital N559
Indianapolis, IN 46223

Received September 1, 1982.
Accepted for publication November 24, 1982.

Predicting the Dose-Dependent Bioavailability of Hydrocortisone and Chlorothiazide in Humans

Keyphrases □ Bioavailability—dose dependency, hydrocortisone, chlorothiazide □ Hydrocortisone—dose-dependent bioavailability, saturable absorption kinetics □ Chlorothiazide—dose-dependent bioavailability, saturable absorption kinetics

To the Editor:

A recent report (1) described the occurrence and mechanisms of dose-dependent saturable absorption kinetics for several commonly used drugs. Equations were also derived, on the basis of the classical Michaelis–Menten approach, to predict such dose-dependent absorption kinetics (1). In the present communication, these equations are applied, in an effort to predict the recently reported, nonproportional dose bioavailability data on hydrocortisone (2) and chlorothiazide (3).

Predicted values for hydrocortisone plasma levels (C_{max}), area under the curve (AUC) and AUC corrected for variance in the first-order rate constant for drug elimination (AUC_{kel}) as well as chlorothiazide urine recovery were calculated using the parameters obtained from the derived equations reported earlier (1). Tables I and II list these calculated parameters and compare the observed values with the predicted values for each dose of hydrocortisone and chlorothiazide, respectively. The excellent correlations between the observed and predicted values attest to the validity of the saturable absorption predictive model for those two drugs. It should be noted that the dose-dependent hydrocortisone tablet data (4) also can be treated in a similar manner with good predictability.

The saturable absorption of chlorothiazide is probably related to the existence of an absorption window (1), inasmuch as the average urinary recovery of chlorothiazide is increased in humans in the presence of food (5) and in dogs following propantheline bromide administration (6).

Table I—Comparison of Observed and Predicted Values for Hydrocortisone

Dose, mg	C_{max}[a], ng/ml		AUC[b], ng·hr/ml		$AUC_{\cdot k_{el}}$[c], ng/ml	
	Obs[d]	Pred[e]	Obs	Pred	Obs	Pred
5	119	114	293	278	171	162
10	175	188	447	502	248	267
20	263	278	835	838	377	396
40	389	366	1340	1259	553	521
r value	0.990		0.996		0.991	

[a] C_{max} = 533 ng/ml when the Michaelis constant (K_m) is 18.2 mg. [b] AUC_{max} = 2531 ng·hr/ml when K_m = 40.4 mg. [c] $(AUC \cdot k_{el})_{max}$ = 763 ng/ml when K_m = 18.5 mg. [d] Observed values (Obs) from previously published work (2). [e] Predicted values (Pred) calculated using previously derived equations (1).

Table II—Comparison of Observed and Predicted Urine Recovery for Chlorothiazide

Dose, mg	Recovery, mg[a]	
	Obs[b]	Pred[c]
50	28.3	28.0
100	47.0	47.8
250	83.3	82.7
r value	0.999	

[a] $Recovery_{max}$ = 161.6 mg when K_m = 238.2 mg. [b] Observed values (Obs) from previously published work (3). [c] Predicted values (Pred) calculated using previously derived equations (1).

0022-3549/83/0500-0577$01.00/0

Additional evidence for such site-specific absorption of chlorothiazide is presented by way of similar observations for the related drug hydrochlorothiazide in humans (7, 8).

The mechanism for the dose-dependency of hydrocortisone has been suggested to be an increased first-pass metabolism (2). By means of carefully planned studies, saturable binding and formulation factors were ruled out as determinants of the nonproportional dose–concentration relationship for hydrocortisone. Ease of absorption and linear absorption at the higher dosages used in previous studies (9, 10) were cited as the reasons for excluding saturable absorption as a contributing factor.

However, critical analysis of the two cited references (9, 10) on hydrocortisone absorption revealed the following information. First, a limited zone for absorption of hydrocortisone and hydrocortisone acetate existed in the small intestine of humans, inasmuch as the absorption from the proximal zone was nearly twice that from the distal zone. Absorption within the zones was linear. Second, the acetate ester was more efficiently absorbed than hydrocortisone. Third, both rate and extent of absorption was decreased in a malnourished patient in relapse with severe malabsorption. Last, absorption was higher when the gut was perfused under comparable conditions, using 1–5% glucose–Ringer's rather than Ringer's solution. This was probably due to the increased viscosity of the glucose–Ringer's solution and/or its energy-supplying potential as theorized previously (11). It should be mentioned that both the suspension and tablet studies (2, 4) administered the hydrocortisone dose with 180 ml of fluid, probably causing the drug to be washed past the zone of maximal absorption. The parallels between these observations for hydrocortisone and those aforementioned for chlorothiazide and hydrochlorothiazide absorption are all too obvious.

Further proof of a dose-dependent absorption phenomenon being operative for hydrocortisone is obtained by comparing the systemic availability, calculated by dividing mean AUC values after the suspension and tablet doses by those obtained after equivalent intravenous doses (2, 4, 12). The average systemic availability (F/V) of hydrocortisone was 71, 58, 56, 52, and 54% from the 5-, 10-, 20-, 30-, and 50-mg doses. In other words, there was a decrease in F, the fraction absorbed, with increasing dose, which contributed to the decrease in F/V with increasing dose seen in the tablet study (4). If, as suggested (2), there was a dose-dependent increase in the metabolism of an increased free fraction during the first pass, the systemic availability should increase, not decrease, with increasing dose. The latter would occur because of saturation of the hepatic enzymes by the increasing drug fraction. Increased systemic availability with increasing dose has been observed in the literature for propoxyphene (13) and several other drugs (14) known to undergo first-pass metabolism in humans. Additional factors that could possibly contribute to the dose-dependent bioavailability of hydrocortisone in humans include micromeritic and polymorphic effects with attendant stability and dissolution problems, as were observed with other corticosteroids (15).

In conclusion, hydrocortisone and chlorothiazide absorption after increasing, single, oral doses in humans, can be described by site-specific saturable absorption kinetics in the therapeutic dose range. The consequent dose-dependent bioavailability of these two drugs can be effectively predicted by use of the appropriate equations reported earlier (1). Use of these equations in the clinical setting should aid in the development of efficacious dosing protocols for any drug whose oral absorption is limited by the magnitude of the administered dose.

(1) J. H. Wood and K. M. Thakker, *Eur. J. Clin. Pharmacol.*, **23,** 183 (1982).

(2) R. D. Toothaker, W. A. Craig, and P. G. Welling, *J. Pharm. Sci.*, **71,** 1182 (1982).

(3) M. A. Osman, R. B. Patel, D. S. Irwin, W. A. Craig, and P. G. Welling, *Biopharm. Drug Dispos.*, **3,** 89 (1982).

(4) R. D. Toothaker, G. M. Sundaresan, J. P. Hunt, T. J. Goehl, K. S. Rotenberg, V. K. Prasad, W. A. Craig, and P. G. Welling, *J. Pharm. Sci.*, **71,** 573 (1982).

(5) P. G. Welling and R. H. Bharbhaiya, *ibid.*, **71,** 32 (1982).

(6) D. E. Resetarits and T. R. Bates, *J. Pharmacokinet. Biopharm.*, **7,** 463 (1979).

(7) B. Berrmann and M. Groschinky-Grind, *Eur. J. Clin. Pharmacol.*, **13,** 125 (1978).

(8) B. Berrmann and M. Groschinky-Grind, *ibid.*, **13,** 385 (1978).

(9) H. P. Schedl, J. A. Clifton, and G. Nokes, *J. Clin. Endocrinol.*, **24,** 224 (1964).

(10) H. P. Schedl, *ibid.*, **25,** 1309 (1965).

(11) H. P. Schedl and J. A. Clifton, *Gastroenterology*, **44,** 134 (1963).

(12) R. D. Toothaker and P. G. Welling, *J. Pharmacokinet. Biopharm.*, **10,** 147 (1982).

(13) M. Gibaldi and D. Perrier, "Pharmacokinetics," Dekker, New York, N.Y., 1975, p. 240.

(14) M. Rowland, in "Current Concepts in the Pharmaceutical Sciences: Dosage Form Design and Bioavailability," J. Swarbrick, Ed., Lea & Febiger, Philadelphia, Pa., 1973, p. 196.

(15) M. Gibaldi, in "The Theory and Practice of Industrial Pharmacy," L. Lachman, H. A. Lieberman, and J. L. Kanig, Eds., Lea & Febiger, Philadelphia, Pa. 1970, p. 253.

Kamlesh M. Thakker
Department of Pharmaceutics
and Division of Clinical Pharmacokinetics
College of Pharmacy
University of Florida
Gainesville, FL 32610

Received November 1, 1982.
Accepted for publication, December 17, 1982.

Modified Wagner–Nelson Absorption Equations for Multiple-Dose Regimens

Keyphrases □ Absorption—Wagner–Nelson equations, multiple-dose regimens, one-compartment open model □ Wagner–Nelson equations—modification, multiple-dose regimens, one-compartment model □ Kinetics—absorption, Wagner–Nelson equations

To the Editor:

Equations to calculate the amount of drug absorbed per milliliter of the volume of distribution and the percent absorbed as functions of time for the one-compartment open model (1) are commonly referred to as Wagner–Nelson equations. The nature of such plots when the equations are applied to data obeying the two-compartment open model with first-order absorption was discussed by Wagner (2). In this communication modified equations

0022-3549/83/0500-0578$01.00/0

Additional evidence for such site-specific absorption of chlorothiazide is presented by way of similar observations for the related drug hydrochlorothiazide in humans (7, 8).

The mechanism for the dose-dependency of hydrocortisone has been suggested to be an increased first-pass metabolism (2). By means of carefully planned studies, saturable binding and formulation factors were ruled out as determinants of the nonproportional dose–concentration relationship for hydrocortisone. Ease of absorption and linear absorption at the higher dosages used in previous studies (9, 10) were cited as the reasons for excluding saturable absorption as a contributing factor.

However, critical analysis of the two cited references (9, 10) on hydrocortisone absorption revealed the following information. First, a limited zone for absorption of hydrocortisone and hydrocortisone acetate existed in the small intestine of humans, inasmuch as the absorption from the proximal zone was nearly twice that from the distal zone. Absorption within the zones was linear. Second, the acetate ester was more efficiently absorbed than hydrocortisone. Third, both rate and extent of absorption was decreased in a malnourished patient in relapse with severe malabsorption. Last, absorption was higher when the gut was perfused under comparable conditions, using 1–5% glucose–Ringer's rather than Ringer's solution. This was probably due to the increased viscosity of the glucose–Ringer's solution and/or its energy-supplying potential as theorized previously (11). It should be mentioned that both the suspension and tablet studies (2, 4) administered the hydrocortisone dose with 180 ml of fluid, probably causing the drug to be washed past the zone of maximal absorption. The parallels between these observations for hydrocortisone and those aforementioned for chlorothiazide and hydrochlorothiazide absorption are all too obvious.

Further proof of a dose-dependent absorption phenomenon being operative for hydrocortisone is obtained by comparing the systemic availability, calculated by dividing mean AUC values after the suspension and tablet doses by those obtained after equivalent intravenous doses (2, 4, 12). The average systemic availability (F/V) of hydrocortisone was 71, 58, 56, 52, and 54% from the 5-, 10-, 20-, 30-, and 50-mg doses. In other words, there was a decrease in F, the fraction absorbed, with increasing dose, which contributed to the decrease in F/V with increasing dose seen in the tablet study (4). If, as suggested (2), there was a dose-dependent increase in the metabolism of an increased free fraction during the first pass, the systemic availability should increase, not decrease, with increasing dose. The latter would occur because of saturation of the hepatic enzymes by the increasing drug fraction. Increased systemic availability with increasing dose has been observed in the literature for propoxyphene (13) and several other drugs (14) known to undergo first-pass metabolism in humans. Additional factors that could possibly contribute to the dose-dependent bioavailability of hydrocortisone in humans include micromeritic and polymorphic effects with attendant stability and dissolution problems, as were observed with other corticosteroids (15).

In conclusion, hydrocortisone and chlorothiazide absorption after increasing, single, oral doses in humans, can be described by site-specific saturable absorption kinetics in the therapeutic dose range. The consequent dose-dependent bioavailability of these two drugs can be effectively predicted by use of the appropriate equations reported earlier (1). Use of these equations in the clinical setting should aid in the development of efficacious dosing protocols for any drug whose oral absorption is limited by the magnitude of the administered dose.

(1) J. H. Wood and K. M. Thakker, *Eur. J. Clin. Pharmacol.*, **23,** 183 (1982).

(2) R. D. Toothaker, W. A. Craig, and P. G. Welling, *J. Pharm. Sci.*, **71,** 1182 (1982).

(3) M. A. Osman, R. B. Patel, D. S. Irwin, W. A. Craig, and P. G. Welling, *Biopharm. Drug Dispos.*, **3,** 89 (1982).

(4) R. D. Toothaker, G. M. Sundaresan, J. P. Hunt, T. J. Goehl, K. S. Rotenberg, V. K. Prasad, W. A. Craig, and P. G. Welling, *J. Pharm. Sci.*, **71,** 573 (1982).

(5) P. G. Welling and R. H. Bharbhaiya, *ibid.*, **71,** 32 (1982).

(6) D. E. Resetarits and T. R. Bates, *J. Pharmacokinet. Biopharm.*, **7,** 463 (1979).

(7) B. Berrmann and M. Groschinky-Grind, *Eur. J. Clin. Pharmacol.*, **13,** 125 (1978).

(8) B. Berrmann and M. Groschinky-Grind, *ibid.*, **13,** 385 (1978).

(9) H. P. Schedl, J. A. Clifton, and G. Nokes, *J. Clin. Endocrinol.*, **24,** 224 (1964).

(10) H. P. Schedl, *ibid.*, **25,** 1309 (1965).

(11) H. P. Schedl and J. A. Clifton, *Gastroenterology*, **44,** 134 (1963).

(12) R. D. Toothaker and P. G. Welling, *J. Pharmacokinet. Biopharm.*, **10,** 147 (1982).

(13) M. Gibaldi and D. Perrier, "Pharmacokinetics," Dekker, New York, N.Y., 1975, p. 240.

(14) M. Rowland, in "Current Concepts in the Pharmaceutical Sciences: Dosage Form Design and Bioavailability," J. Swarbrick, Ed., Lea & Febiger, Philadelphia, Pa., 1973, p. 196.

(15) M. Gibaldi, in "The Theory and Practice of Industrial Pharmacy," L. Lachman, H. A. Lieberman, and J. L. Kanig, Eds., Lea & Febiger, Philadelphia, Pa. 1970, p. 253.

Kamlesh M. Thakker
Department of Pharmaceutics
and Division of Clinical Pharmacokinetics
College of Pharmacy
University of Florida
Gainesville, FL 32610

Received November 1, 1982.
Accepted for publication, December 17, 1982.

Modified Wagner–Nelson Absorption Equations for Multiple-Dose Regimens

Keyphrases □ Absorption—Wagner–Nelson equations, multiple-dose regimens, one-compartment open model □ Wagner–Nelson equations—modification, multiple-dose regimens, one-compartment model □ Kinetics—absorption, Wagner–Nelson equations

To the Editor:

Equations to calculate the amount of drug absorbed per milliliter of the volume of distribution and the percent absorbed as functions of time for the one-compartment open model (1) are commonly referred to as Wagner–Nelson equations. The nature of such plots when the equations are applied to data obeying the two-compartment open model with first-order absorption was discussed by Wagner (2). In this communication modified equations

0022-3549/83/0500-0578$01.00/0

are derived which apply to plasma, serum, or whole blood concentrations of unchanged drug during a dosage interval of any multiple-dose regimen including the steady state. As before (1) the derivation assumes applicability of the one-compartment open-disposition model but no particular kinetics of absorption need be assumed.

Let A_T represent the amount of drug which is absorbed from time zero (beginning of the dosage interval concerned) to some time T in the dosage interval (*i.e.*, $0 \leq T \leq \tau$ where τ is the time at the end of the dosage interval); A_b represent the total amount of drug remaining in the body at time T; A_b^0 be the amount of drug in the body at time zero, resulting from administration of doses previous to the one of interest; A_m be the total amount of drug metabolized between time zero and time T; A_e be the total amount of drug excreted in the urine between time zero and time T; V be the volume of distribution; C_n be the drug concentration in the interval $0 \leq T \leq \tau$; C_n^0 be the drug concentration at time zero as above; and k_e represent the elimination rate constant of the simple one-compartment open model. Then mass balance gives:

$$A_T = A_b - A_b^0 + A_m + A_e \qquad \text{(Eq. 1)}$$

Taking the derivative of Eq. 1 with respect to time gives:

$$\frac{dA}{dt} = \frac{dA_b}{dt} - \frac{dA_b^0}{dt} + \frac{d(A_m + A_e)}{dt} \qquad \text{(Eq. 2)}$$

but,

$$A_b = VC_n \qquad \text{(Eq. 3)}$$

and,

$$A_b^0 = VC_n^0 \qquad \text{(Eq. 4)}$$

and,

$$\frac{d(A_m + A_e)}{dt} = Vk_eC_n \qquad \text{(Eq. 5)}$$

Substituting from Eqs. 3–5 into Eq. 2 gives:

$$\frac{dA}{dt} = V\frac{dC_n}{dt} - V\frac{dC_n^0}{dt} + Vk_eC_n \qquad \text{(Eq. 6)}$$

Integrating Eq. 6 by term between the limits $t = 0$ and $t = T$ gives:

$$A_T = VC_n - VC_n^0 + Vk_e\int_0^T C_n dt \qquad \text{(Eq. 7)}$$

Division of both sides of Eq. 7 by V gives:

$$\frac{A_T}{V} = C_n + k_e\int_0^T C_n dt - C_n^0 \qquad \text{(Eq. 8)}$$

Equation 8 is the same as the single-dose Wagner–Nelson equation (1) except that C_n replaces C and there is the additional term $-C_n^0$ on the right-hand side. This indicates that for multiple-dose data the usual Wagner–Nelson calculation is performed, namely $C_n + k_e \int_0^T C_n dt$, then the value C_n^0 is subtracted from each value calculated. It should be noted that an incorrect set of A_T/V values would be obtained if C_n^0 was subtracted from each C_n value first, followed by the usual Wagner–Nelson calculation.

The total amount of drug absorbed per milliliter of the volume of distribution from the dose of interest A_τ/V is given by:

$$\frac{A_\tau}{V} = k_e\int_0^\tau C_n dt \qquad \text{(Eq. 9)}$$

Equation 9 gives the correct asymptotic value of A_T/V_p when the dose of interest is given at steady state and when absorption of the dose of interest is complete between the time zero and τ. If one or both of these conditions are not met and absorption is not zero order, then it is very difficult to obtain an accurate asymptotic value of the function.

The fraction absorbed (based on the amount of drug absorbed, not the dose) to time T is given by:

$$\text{Fraction absorbed} = \frac{A_T/V}{A_\tau/V} = \frac{A_T}{A\tau} \qquad \text{(Eq. 10)}$$

To appropriately apply Eqs. 8–10 the protocol for most routine multiple-dose pharmacokinetic studies will have to be modified. Modifications should include: (*a*) the dose of interest should be the last of a series of doses and preferably steady state should have been reached; (*b*) there should be intensive sampling of blood during the absorption phase; (*c*) the blood concentrations should be followed down well beyond the end of the dosage interval at τ hr to allow an estimation of k_e which is not biased by continuing absorption; and (*d*) in evaluating the integrals of Eqs. 8 and 9 it is best to use a combination such that the ordinary trapezoidal rule is used when the concentration is increasing or constant and the logarithmic trapezoidal rule when the concentration is decreasing.

Greater accuracy will be attained by determining the kinetics of absorption (if feasible at all) by resolving fraction absorbed values (Eq. 10) rather than A_T/V values (Eq. 8). If absorption is zero order then the slope of the straight line when the fraction absorbed is plotted *versus* time on reactilinear graph paper will be the correct zero-order constant even when the drug obeys two-compartment kinetics as well as one-compartment kinetics. This has been supported by simulations, and details will be published elsewhere. When absorption is first order and the one-compartment open model holds the ratio of the fraction absorbed values given by the method to the actual fraction absorbed, values will be equal to $1/(1 - e^{-k_a\tau})$ where k_a is the first-order absorption rate constant and τ is the uniform dosing interval. In almost all cases this ratio will have a numerical value between 1.001 and 1.100. An exception will be a very long half-life drug which is dosed too frequently.

(1) J. G. Wagner and E. Nelson, *J. Pharm. Sci.*, **52**, 610 (1963).
(2) J. G. Wagner, *J. Pharmacokinet. Biopharm.*, **2**, 469 (1974).

John G. Wagner
College of Pharmacy and
Upjohn Center for Clinical Pharmacology,
Medical School,
The University of Michigan
Ann Arbor, MI 48109

Received September 24, 1982.
Accepted for publication December 17, 1982.

External Scintigraphy in Evaluating Delivery Techniques of Sodium Cromolyn–[^{99m}Tc] Diethylenetriaminepentacetic Acid Aerosol in the Lungs of the Horse

Keyphrases □ Scintigraphy—noninvasive method of study, aerosol dispersion, horse respiratory tract □ Nebulization—^{99m}Tc-labeled sodium cromolyn, device comparison □ Sodium cromolyn—technectium-99m labeling, nebulization, scintigraphy in the horse

To the Editor:

Aerosol delivery of drugs has been used in the prophylaxis and therapy of acute and chronic conditions of the lower respiratory tract. The aerosol methods for drug delivery allow targeting of the drug in the lungs, thereby eliminating the need for systemic administration. This in turn may reduce the level and frequency of dosing as well as the incidence and severity of adverse drug effects, thereby improving the therapeutic effect–toxicity ratio (1, 2). Administration of the same dose of nebulized drug using different nebulization devices and modes may conceivably give rise to the same blood levels if the drug is systemically absorbed; however, this does not imply uniform distribution of the drug throughout the lung mass.

External scintigraphy may provide a good opportunity for noninvasive study of the distribution of aerosols labeled with gamma ray-emitting nuclides in the lungs. In this investigation, external scintigraphy was used to explore two different modes of administering nebulized sodium cromolyn to the horse. Four male and two female horses ranging in age from 2 to 6 years and in weight from 338 to 540 kg were used in this study. These animals were free from clinical signs of respiratory disease.

Two different devices were used to nebulize a solution of sodium cromolyn[1] (7 ml, 2% w/v) in separate nebulizer studies on the same six animals. The first device was an air compressor assembly[2], connected to a nebulizer chamber[3]. A corrugated delivery tube (105-cm length, 3.2-cm diameter) was connected to the outlet of the nebulizer and to the face mask[4] which completely covered the nostrils and muzzle of the horse. The diameter of 63.1% of the droplets produced from this nebulizer was <6.5 μm[5]. The second device consisted of a noncollapsible nylon tube (100-cm length, 0.5-cm diameter) which bore a sintered glass disk at one end and was connected with a hand-operated nebulizer at the other end. The tube was inserted through the nostril and placed in the pharynx of the horse. The diameter of 99.6% of the droplets produced by this nebulizer was >8.5 μm[5].

The sodium cromolyn solution (7 ml) was mixed with 1 ml of [^{99m}Tc] diethylenetriaminepentacetic acid (I[6], 40 mCi/ml) in the nebulizer to form a homogeneous solution. In both techniques, the delivery of the nebulized sodium cromolyn–[^{99m}Tc]I solution to the lung required multiple inhalations by the animal. Blood samples (5 ml) taken immediately after the aerosol administration was completed showed that the radioactivity levels were <2000 dpm/ml, implying that only a small amount of [^{99m}Tc]I had diffused into the circulation at that point.

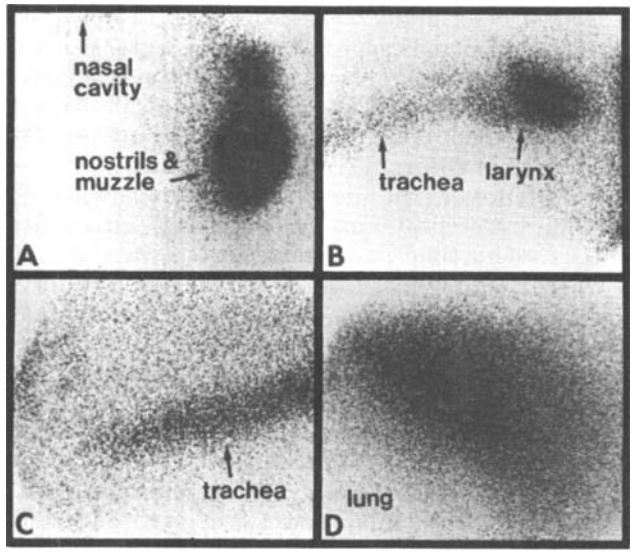

Figure 1—*Scintigraphic images of the distribution of sodium cromolyn–[^{99m}Tc]I aerosol in the respiratory tract of a horse administered through an air compressor–nebulizer–face mask. Radioactivity in the (A) nostrils and muzzle, (B) larynx, and (C) trachea; and (D) homogeneous spread of activity in the lung.*

Each horse was lightly sedated with 100 mg iv of xylazine[7], before administration of the nebulized sodium cromolyn solution. Each horse was then placed parallel to the front of the detector of a gamma camera[8] fitted with a high-resolution parallel-hole collimator. Scintigraphic images in the right lateral plane were obtained of the head, neck, and thorax. A maximum of 100,000 counts were collected for each image. Areas of high activity, such as the nostrils and thorax, required 2–3 min to yield 100,000 counts, while areas of low activity, such as the trachea, yielded only 20,000–60,000 counts in the same period.

Similar distribution patterns were present in all six animals that were administered the nebulized sodium cromolyn solution using the nebulizer connected to the air compressor. A large amount of radioactivity was evident around the nostrils and muzzle, but there was relatively little in the nasal cavity (Fig. 1A). A distinct localized area of radioactivity was detected in the larynx (Fig. 1B). There was very little radioactivity in the trachea, but a homogeneous spread of radioactivity was evident in the lung (Fig. 1C and D).

The distribution pattern of sodium cromolyn solution was different when the hand-operated nebulizer was used. A large amount of radioactivity was present in the posterior pharynx, corresponding to the position of the fritted glass disk (Fig. 2A). Radioactivity extended down the trachea, reaching a peak at the thoracic inlet, suggesting that pooling may have occurred at this level (Fig. 2B). The ^{99m}Tc-labeled sodium cromolyn solution was very poorly

[1] Cromovet, Fisons Animal Health, Fisons Limited, Pharmaceutical Division, Leicestershire, England.
[2] De Vilbiss Pulmo-Aide series 561 Portable Compressor.
[3] Cromovet Nebuliser, Fisons Animal Health, Fisons Limited, Pharmaceutical Division, Leicestershire, England.
[4] Cromovet Face Mask Kit, Fisons Animal Health, Fisons Limited, Pharmaceutical Division, Leicestershire, England.
[5] Droplet size estimates were provided by Fison Limited, Pharmaceutical Division.
[6] Mallinckrodt Diagnostics, Mallinckrodt, St. Louis, Mo.
[7] Rompun (xylazine), Bagvet, Division of Cutter Laboratories, Shawnee, Kans.
[8] Siemens Gammasonics, Pho/Gamma HP (formerly Searle Diagnostics), Des Plaines, Ill.

0022-3549/83/0500-0580$01.00/0

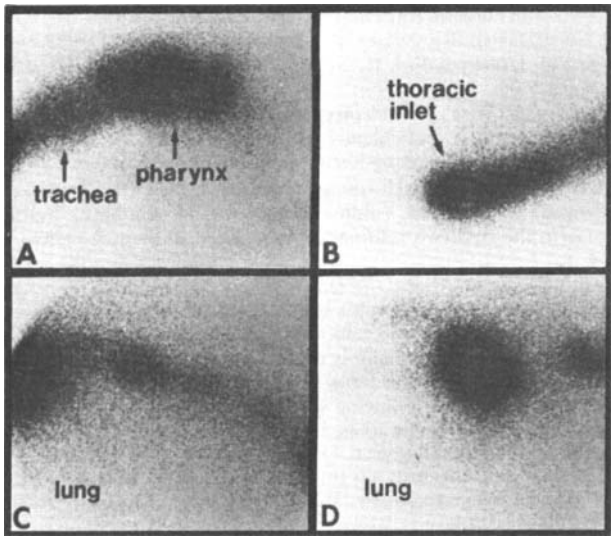

Figure 2—*Scintigraphic images of the distribution of sodium cromolyn-[^{99m}Tc]I aerosol in the respiratory tract of a horse administered through a hand-operated nebulizer. Radioactivity in the (A) posterior pharynx and trachea, (B) thoracic inlet, and (C) and (D) caudodorsal region of the lung.*

distributed in the lungs using this method of administration, detectable radioactivity being largely confined to the caudodorsal region (Fig. 2C and D).

A simple visual comparison of images showed that satisfactory pulmonary distribution of sodium cromolyn aerosol in normal horses occurred following administration by the combination air compressor–nebulizer–face mask. Preliminary analysis of the distribution data of the radioactivity in the respiratory tract indicated that 7.5% of the initial dose remained in the nebulizer, while 30–40% remained in the tubing and face mask. It is estimated that 40–50% of the radioactivity was confined to the nostrils and muzzle, while 10–15% of the radioactivity was distributed in the lungs.

In conclusion, external scintigraphy may provide a convenient noninvasive method for evaluating the different techniques and modes of aerosol administration and visualizing their distribution in the lungs of the horse. Further research is in progress to assess the effect of the droplet size on the resolution of the technique and the distribution of the aerosol in the lungs. In addition, an effort is being made to develop a model in which the count rates taken from the lung area are weighted for tissue attenuation and variable geometry so that more accurate estimates can be obtained.

(1) A. Pines, H. Raafat, G. M. Siddiqui, and J. S. B. Greenfield, *Br. Med. J.*, 1, 663 (1970).

(2) R. E. Wood, J. D. Klinger, M. J. Thomassen, and H. A. Cash, in "Proceedings of the 8th International Cystic Fibrosis Congress," J. Sturgess, Ed., Canadian Cystic Fibrosis Foundation, Toronto, Canada, 1980, p. 365.

*Michael C. Theodorakis**‡x*
Christopher J. Hillidge§
*Roger A. Allhands**
Section of Nuclear Medicine*
and Equine Section§
College of Veterinary Medicine
and Department of Bioengineering*
College of Engineering
University of Illinois at Urbana-Champaign
Urbana, IL 61801

Received March 9, 1982.
Accepted for publication December 21, 1982.
Supported in part by Illinois Thoroughbred Breeder's Fund, STILAGHORSE 06-39333 and 06-39330.

‡ Present address: VA Medical Center, Nuclear Medicine Service, Philadelphia, PA 19104.

BOOKS

REVIEWS

Recent Advances in the Biology of Alcoholism. Edited by C. S. LIEBER and B. STIMMEL. (Advances in Alcoholism and Substance Abuse, Vol. 1 No. 2). The Haworth Press, 28 East 22nd Street, New York, N.Y. 10010. 1982. Hardcover.

This book contains several authoritative and timely review articles about the effects of ethanol on the liver and the endocrine system. The coverage is much narrower than indicated by the title: effects of the drug on the brain are not included. The chapters are papers delivered in a 1980 symposium at the Alcohol Research and Treatment Center at the Bronx VA Hospital; several of the papers are by Dr. Lieber and his group at the Center. The authors are recognized experts in their fields, which vary from pure biochemistry to clinical gastroenterology.

J.-P. Von Wartburg provides a lucid review of alcohol metabolism by alcohol and aldehyde dehydrogenases, including recent genetic information about racial differences in responses to alcohol. S. Orrenius writes a concise description of metabolic drug interactions from a biochemist's point of view, and Lieber and Pirola follow with a detailed clinically oriented review of the same topic, with many specific examples. Both reviews of drug interaction emphasize and explain the role of MEOS, the hepatic microsomal ethanol-oxidizing system. Lieber also contributes a general chapter on the effects of ethanol on the liver, largely from his own extensive work. The final chapter by T. J. Cicero covers recent important advances in our understanding of effects of ethanol on the endocrine system, with emphasis on the factors that affect testosterone levels. This is a logical and sensible essay which minimizes controversy and brings scattered data together into a reasonably coherent picture.

Technical details such as typographical errors, poor quality paper, and inadequate reproduction of some figures detract slightly from the otherwise admirable text. More important is the lack of an index, which will greatly reduce the usefulness of this book.

Reviewed by Dora B. Goldstein
Department of Pharmacology
Stanford University School of Medicine
Stanford, CA 94305

Handbook of Dissolution Testing. By WILLIAM A. HANSON. Pharmaceutical Technology Book Division, 320 N. A St., P.O. Box 50, Springfield, OR 97477. 1982. 163 pp. 13 × 22 cm. Price $26.50.

This book describes in detail the two official USP-NF dissolution test methods and the nonofficial flow-through method. The author views dissolution testing solely as a quality control test whether or not the test

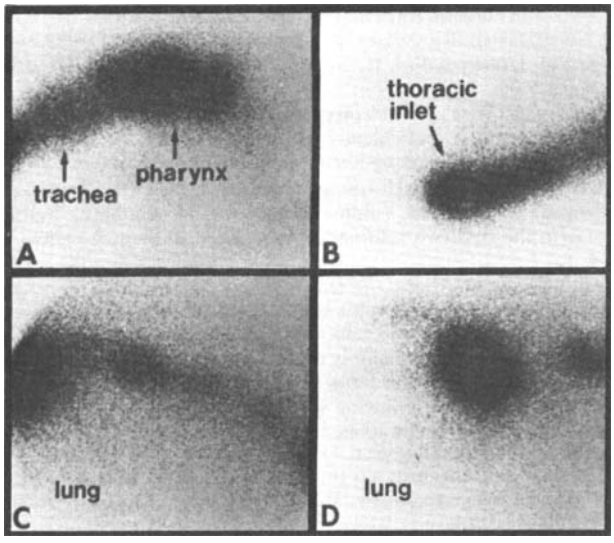

Figure 2—*Scintigraphic images of the distribution of sodium cromolyn-[^{99m}Tc]I aerosol in the respiratory tract of a horse administered through a hand-operated nebulizer. Radioactivity in the (A) posterior pharynx and trachea, (B) thoracic inlet, and (C) and (D) caudodorsal region of the lung.*

distributed in the lungs using this method of administration, detectable radioactivity being largely confined to the caudodorsal region (Fig. 2C and D).

A simple visual comparison of images showed that satisfactory pulmonary distribution of sodium cromolyn aerosol in normal horses occurred following administration by the combination air compressor–nebulizer–face mask. Preliminary analysis of the distribution data of the radioactivity in the respiratory tract indicated that 7.5% of the initial dose remained in the nebulizer, while 30–40% remained in the tubing and face mask. It is estimated that 40–50% of the radioactivity was confined to the nostrils and muzzle, while 10–15% of the radioactivity was distributed in the lungs.

In conclusion, external scintigraphy may provide a convenient noninvasive method for evaluating the different techniques and modes of aerosol administration and visualizing their distribution in the lungs of the horse. Further research is in progress to assess the effect of the droplet size on the resolution of the technique and the distribution of the aerosol in the lungs. In addition, an effort is being made to develop a model in which the count rates taken from the lung area are weighted for tissue attenuation and variable geometry so that more accurate estimates can be obtained.

(1) A. Pines, H. Raafat, G. M. Siddiqui, and J. S. B. Greenfield, *Br. Med. J.*, 1, 663 (1970).

(2) R. E. Wood, J. D. Klinger, M. J. Thomassen, and H. A. Cash, in "Proceedings of the 8th International Cystic Fibrosis Congress," J. Sturgess, Ed., Canadian Cystic Fibrosis Foundation, Toronto, Canada, 1980, p. 365.

*Michael C. Theodorakis**‡x*
Christopher J. Hillidge§
*Roger A. Allhands**
Section of Nuclear Medicine*
and Equine Section§
College of Veterinary Medicine
and Department of Bioengineering*
College of Engineering
University of Illinois at Urbana-Champaign
Urbana, IL 61801

Received March 9, 1982.
Accepted for publication December 21, 1982.
Supported in part by Illinois Thoroughbred Breeder's Fund, STILAGHORSE 06-39333 and 06-39330.

‡ Present address: VA Medical Center, Nuclear Medicine Service, Philadelphia, PA 19104.

BOOKS

REVIEWS

Recent Advances in the Biology of Alcoholism. Edited by C. S. LIEBER and B. STIMMEL. (Advances in Alcoholism and Substance Abuse, Vol. 1 No. 2). The Haworth Press, 28 East 22nd Street, New York, N.Y. 10010. 1982. Hardcover.

This book contains several authoritative and timely review articles about the effects of ethanol on the liver and the endocrine system. The coverage is much narrower than indicated by the title: effects of the drug on the brain are not included. The chapters are papers delivered in a 1980 symposium at the Alcohol Research and Treatment Center at the Bronx VA Hospital; several of the papers are by Dr. Lieber and his group at the Center. The authors are recognized experts in their fields, which vary from pure biochemistry to clinical gastroenterology.

J.-P. Von Wartburg provides a lucid review of alcohol metabolism by alcohol and aldehyde dehydrogenases, including recent genetic information about racial differences in responses to alcohol. S. Orrenius writes a concise description of metabolic drug interactions from a biochemist's point of view, and Lieber and Pirola follow with a detailed clinically oriented review of the same topic, with many specific examples. Both reviews of drug interaction emphasize and explain the role of MEOS, the hepatic microsomal ethanol-oxidizing system. Lieber also contributes a general chapter on the effects of ethanol on the liver, largely from his own extensive work. The final chapter by T. J. Cicero covers recent important advances in our understanding of effects of ethanol on the endocrine system, with emphasis on the factors that affect testosterone levels. This is a logical and sensible essay which minimizes controversy and brings scattered data together into a reasonably coherent picture.

Technical details such as typographical errors, poor quality paper, and inadequate reproduction of some figures detract slightly from the otherwise admirable text. More important is the lack of an index, which will greatly reduce the usefulness of this book.

Reviewed by Dora B. Goldstein
Department of Pharmacology
Stanford University School of Medicine
Stanford, CA 94305

Handbook of Dissolution Testing. By WILLIAM A. HANSON. Pharmaceutical Technology Book Division, 320 N. A St., P.O. Box 50, Springfield, OR 97477. 1982. 163 pp. 13 × 22 cm. Price $26.50.

This book describes in detail the two official USP-NF dissolution test methods and the nonofficial flow-through method. The author views dissolution testing solely as a quality control test whether or not the test

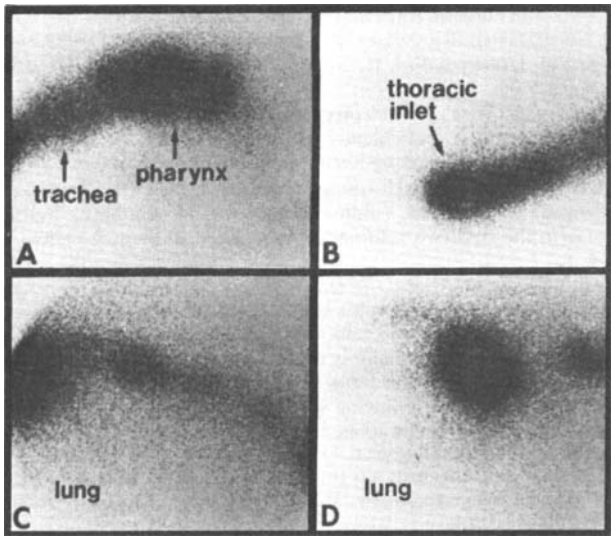

Figure 2—*Scintigraphic images of the distribution of sodium cromolyn-[^{99m}Tc]I aerosol in the respiratory tract of a horse administered through a hand-operated nebulizer. Radioactivity in the (A) posterior pharynx and trachea, (B) thoracic inlet, and (C) and (D) caudodorsal region of the lung.*

distributed in the lungs using this method of administration, detectable radioactivity being largely confined to the caudodorsal region (Fig. 2C and D).

A simple visual comparison of images showed that satisfactory pulmonary distribution of sodium cromolyn aerosol in normal horses occurred following administration by the combination air compressor–nebulizer–face mask. Preliminary analysis of the distribution data of the radioactivity in the respiratory tract indicated that 7.5% of the initial dose remained in the nebulizer, while 30–40% remained in the tubing and face mask. It is estimated that 40–50% of the radioactivity was confined to the nostrils and muzzle, while 10–15% of the radioactivity was distributed in the lungs.

In conclusion, external scintigraphy may provide a convenient noninvasive method for evaluating the different techniques and modes of aerosol administration and visualizing their distribution in the lungs of the horse. Further research is in progress to assess the effect of the droplet size on the resolution of the technique and the distribution of the aerosol in the lungs. In addition, an effort is being made to develop a model in which the count rates taken from the lung area are weighted for tissue attenuation and variable geometry so that more accurate estimates can be obtained.

(1) A. Pines, H. Raafat, G. M. Siddiqui, and J. S. B. Greenfield, *Br. Med. J.*, 1, 663 (1970).

(2) R. E. Wood, J. D. Klinger, M. J. Thomassen, and H. A. Cash, in "Proceedings of the 8th International Cystic Fibrosis Congress," J. Sturgess, Ed., Canadian Cystic Fibrosis Foundation, Toronto, Canada, 1980, p. 365.

*Michael C. Theodorakis**‡x*
Christopher J. Hillidge§
*Roger A. Allhands**
Section of Nuclear Medicine*
and Equine Section§
College of Veterinary Medicine
and Department of Bioengineering*
College of Engineering
University of Illinois at Urbana-Champaign
Urbana, IL 61801

Received March 9, 1982.
Accepted for publication December 21, 1982.
Supported in part by Illinois Thoroughbred Breeder's Fund, STILAGHORSE 06-39333 and 06-39330.

‡ Present address: VA Medical Center, Nuclear Medicine Service, Philadelphia, PA 19104.

BOOKS

REVIEWS

Recent Advances in the Biology of Alcoholism. Edited by C. S. LIEBER and B. STIMMEL. (Advances in Alcoholism and Substance Abuse, Vol. 1 No. 2). The Haworth Press, 28 East 22nd Street, New York, N.Y. 10010. 1982. Hardcover.

This book contains several authoritative and timely review articles about the effects of ethanol on the liver and the endocrine system. The coverage is much narrower than indicated by the title: effects of the drug on the brain are not included. The chapters are papers delivered in a 1980 symposium at the Alcohol Research and Treatment Center at the Bronx VA Hospital; several of the papers are by Dr. Lieber and his group at the Center. The authors are recognized experts in their fields, which vary from pure biochemistry to clinical gastroenterology.

J.-P. Von Wartburg provides a lucid review of alcohol metabolism by alcohol and aldehyde dehydrogenases, including recent genetic information about racial differences in responses to alcohol. S. Orrenius writes a concise description of metabolic drug interactions from a biochemist's point of view, and Lieber and Pirola follow with a detailed clinically oriented review of the same topic, with many specific examples. Both reviews of drug interaction emphasize and explain the role of MEOS, the hepatic microsomal ethanol-oxidizing system. Lieber also contributes a general chapter on the effects of ethanol on the liver, largely from his own extensive work. The final chapter by T. J. Cicero covers recent important advances in our understanding of effects of ethanol on the endocrine system, with emphasis on the factors that affect testosterone levels. This is a logical and sensible essay which minimizes controversy and brings scattered data together into a reasonably coherent picture.

Technical details such as typographical errors, poor quality paper, and inadequate reproduction of some figures detract slightly from the otherwise admirable text. More important is the lack of an index, which will greatly reduce the usefulness of this book.

Reviewed by Dora B. Goldstein
Department of Pharmacology
Stanford University School of Medicine
Stanford, CA 94305

Handbook of Dissolution Testing. By WILLIAM A. HANSON. Pharmaceutical Technology Book Division, 320 N. A St., P.O. Box 50, Springfield, OR 97477. 1982. 163 pp. 13 × 22 cm. Price $26.50.

This book describes in detail the two official USP-NF dissolution test methods and the nonofficial flow-through method. The author views dissolution testing solely as a quality control test whether or not the test

results correlate with the drug bioavailability. Hence, throughout the book, major emphasis is given to the procedural details and the regulatory requirements of the test, but little on its importance as predictor of drug bioavailability.

Overall consideration for dissolution testing, presented in Chapter 1, gives a brief historical perspective of the dissolution test development. Only the contributions made by the author and the individuals associated with the USP Drug Standards Laboratories were credited with the early developments in this field. It is unfortunate that the author failed to recognize the contributions made by industry, government, and academia. Instead, the author wrongly criticized them for suggesting test methods because they all had "a private axe to grind."

Chapter 2 deals with the discussion of the classical Noyes-Whitney equation with respect to the dissolution test conditions. The necessity of having laminar, nonturbulent fluid dynamics recommended by the author is unwarranted. Some degree of turbulence is actually desirable for achieving homogeneous mixing of the dissolved drug. A detailed description of the official USP-NF methods including allowable design variables and compendial constraints set for those methods is described in Chapter 3. The following chapter gives a description of the flow-through apparatus and a few other nonofficial methods. Here, as well as in Chapter 8, the author advocates the use of only the official methods. It is doubtful that such a view will be shared by the scientific community, simply because it can stifle future progress in the field. Chapters 5 and 6 deal with the various test variables and provide guidelines for setting-up the official test methods. The last chapter deals with the methods employed for the automated monitoring of dissolution rates. Overall, the book gives practical guidance for the routine analysis of dissolution rates by the current official methods.

Reviewed by Ashok C. Shah
Pharmacy Research Unit
The Upjohn Company
Kalamazoo, Michigan 49001

Analytical Profiles of Drug Substances, Vol. 11. Edited by KLAUS FLOREY, Academic Press, 111 Fifth Avenue, New York, NY 10003. 1982. 665 pp. 15 × 23 cm. Price $39.00.

In continuation of the yearly volumes of this series, this collection gives (in about 550 pages) analytical profiles of 16 drug substances: aminophylline, ascorbic acid, captopril, cefotaxime, cefoxitin sodium, clofibrate, clotrimazole, dopamine hydrochloride, ergonovine maleate, flufenamic acid, hexestrol, mestranol, noscapine, penicillin G benzathine, phenylbutazone, and sulfadiazine.

A new feature has been introduced in this volume: profile supplements. These profiles are intended to be a regular part of future volumes. The profile supplements, occupying about 110 pages, are for five substances that originally appeared in Volume 1: levarterenol bitartrate, meprobamate, triamcinolone, triamcinolone acetonide, triamcinolone diacetate. The supplements are not a republishing of the original monographs, they are only additions and/or changes. The paragraph numbering of the original profile has been retained, so that the new or altered data can easily be correlated with the original. This volume does not contain the 'Addendum' section which was a feature of several previous volumes.

The profiles in this hard-bound book contain the following nine major sections: description, physical properties, methods of preparation, stability-degradation, methods of analysis, metabolism, biopharmaceutics and pharmacokinetics, toxicity, and references. There are numerous figures of structures and spectra, and tables of properties and chromatographic systems. Since each profile is by a different author, this basic outline may be expanded to other topics or somewhat curtailed, depending upon the information available from the extensive review of the literature and unpublished works. The difference in authorship causes a difference in type size and face style from profile to profile. A cumulative index gives the volume and page number of each substance that is the subject of a particular profile.

This volume, like others in the series, is a valuable reference for those interested in pharmaceutical formulation and pharmaceutical quality assurance and should be available as a reference for those requiring information on drug metabolism, biopharmaceutics, and pharmacokinetics.

Reviewed by Murray M. Tuckerman
School of Pharmacy
Temple University
Philadelphia, PA 19130

Modern Methods of Pharmaceutical Analysis. Edited by ROGER E. SCHIRMER. CRC Press Inc., Boca Raton, FL 33431. 1982. 18 × 25 cm. **Vol. I,** 304 pp. **Vol. II,** 264 pp. Price $81.00 ea. **Vol. III,** 244 pp. Price $72.00.

Modern Methods of Pharmaceutical Analysis is a three-volume set mostly written by R. E. Schirmer. Of the 13 chapters, Dr. Schirmer has written eight. The remaining five have been authored by three scientists from Eli Lilly and Co. Each volume is self-contained with identical Forwards and Introductions. Volume III contains the cumulative index; the indexes in the first two volumes are restricted to their respective contents.

It is not completely clear to this reviewer the rationale for assigning specific chapters to each volume unless it was to restrict each of the "guest" authors to only one volume per author or to keep the number of pages per volume approximately equal. Volume I contains five chapters starting with Separation of Drugs from Excipients. The remaining four chapters describe the following spectroscopic methodologies: UV and Visible Absorption Techniques, IR Methods of Analysis, Fluorometric Analysis, and Optical Rotation. Other methods of separation and purity analysis are not encountered until Volume III. Its five chapters are Gas-Liquid Chromatography, High-Performance Liquid Chromatography, Thermal Analysis, Phase-Solubility Analysis, and The Determination of Isomeric Purity. Situated in the middle is Volume II with Nuclear Magnetic Resonance Spectroscopy, Polarography, and Coulometry.

A better title might have been "Industrial Methods of Pharmaceutical Analysis." The selection of chapters is based on the analytical problems defined by the editor as those commonly encountered in the pharmaceutical industry. These include analysis of the raw materials, synthetic intermediates, the final drug entity, and the formulated product. The analytical methodology must detect types and levels of impurities and degradation products. Lacking is a chapter on mass spectrometry, although there is a brief mention of its use as a detector in chromatography and determination of isomeric purity. Also there is no chapter on immunoassay methodology.

In general each subject is well covered. There is a detailed topic outline for each chapter. The typical format is to begin with a discussion of the principles of the analytical technique followed by a description of the specific instrumentation. Then, depending on the analytical method, there may be an overview of the sample preparation. Each chapter concludes with pharmaceutical applications and a reasonable number of examples. For the most part, the individual chapters should not be considered exhaustive reviews of the pharmaceutical analysis literature. Nevertheless, good bibliographies accompany each chapter. There is good consistency, which probably is due to the majority of the chapters being written by one person.

This is an expensive set of volumes for individual purchase, considering the fact that the basic information of theory, instrumentation, and sample preparation already will be adequately covered in one or more advanced undergraduate or graduate level analytical chemistry textbooks. The cost of the latter is generally lower due to their volume of sales. The on-line searches of the *Chemical Abstracts* data bases permit the analytical chemist to rapidly obtain the most current applications. A few years ago this reviewer probably would have ended with the usual recommendation for library purchase. This is not true in today's economic times. Libraries and individuals should first determine if their collections are adequate and current before making such a major purchase.

Reviewed by John H. Block
School of Pharmacy
Oregon State University
Corvallis, OR 97331

Dictionary of Organic Compounds, 5th Ed. Edited by J. BUCKINGHAM, J. D. G. CADOGAN, R. A. RAPHAEL, C. W. REES, and an INTERNATIONAL ADVISORY BOARD. Chapman and Hall, 733 Third Avenue, New York, NY 10017. 1982. 7766 pp. 28 × 20.5 cm. Price $1950.00 (Canada $2350.00).

The fifth edition of Heilbron's *Dictionary of Organic Compounds*, now in five volumes with two additional volumes of indexes, includes about 50,000 entries listing more than 150,000 compounds. The intent of the *Dictionary* is to describe structural, chemical, and physical properties of common organic compounds of importance to chemists, biochemists, pharmacologists, and biologists. The present edition includes some types of information not listed previously. Leading literature references are included, and annual supplements (including about 2000 entries each)

results correlate with the drug bioavailability. Hence, throughout the book, major emphasis is given to the procedural details and the regulatory requirements of the test, but little on its importance as predictor of drug bioavailability.

Overall consideration for dissolution testing, presented in Chapter 1, gives a brief historical perspective of the dissolution test development. Only the contributions made by the author and the individuals associated with the USP Drug Standards Laboratories were credited with the early developments in this field. It is unfortunate that the author failed to recognize the contributions made by industry, government, and academia. Instead, the author wrongly criticized them for suggesting test methods because they all had "a private axe to grind."

Chapter 2 deals with the discussion of the classical Noyes-Whitney equation with respect to the dissolution test conditions. The necessity of having laminar, nonturbulent fluid dynamics recommended by the author is unwarranted. Some degree of turbulence is actually desirable for achieving homogeneous mixing of the dissolved drug. A detailed description of the official USP-NF methods including allowable design variables and compendial constraints set for those methods is described in Chapter 3. The following chapter gives a description of the flow-through apparatus and a few other nonofficial methods. Here, as well as in Chapter 8, the author advocates the use of only the official methods. It is doubtful that such a view will be shared by the scientific community, simply because it can stifle future progress in the field. Chapters 5 and 6 deal with the various test variables and provide guidelines for setting-up the official test methods. The last chapter deals with the methods employed for the automated monitoring of dissolution rates. Overall, the book gives practical guidance for the routine analysis of dissolution rates by the current official methods.

Reviewed by Ashok C. Shah
Pharmacy Research Unit
The Upjohn Company
Kalamazoo, Michigan 49001

Analytical Profiles of Drug Substances, Vol. 11. Edited by KLAUS FLOREY, Academic Press, 111 Fifth Avenue, New York, NY 10003. 1982. 665 pp. 15 × 23 cm. Price $39.00.

In continuation of the yearly volumes of this series, this collection gives (in about 550 pages) analytical profiles of 16 drug substances: aminophylline, ascorbic acid, captopril, cefotaxime, cefoxitin sodium, clofibrate, clotrimazole, dopamine hydrochloride, ergonovine maleate, flufenamic acid, hexestrol, mestranol, noscapine, penicillin G benzathine, phenylbutazone, and sulfadiazine.

A new feature has been introduced in this volume: profile supplements. These profiles are intended to be a regular part of future volumes. The profile supplements, occupying about 110 pages, are for five substances that originally appeared in Volume 1: levarterenol bitartrate, meprobamate, triamcinolone, triamcinolone acetonide, triamcinolone diacetate. The supplements are not a republishing of the original monographs, they are only additions and/or changes. The paragraph numbering of the original profile has been retained, so that the new or altered data can easily be correlated with the original. This volume does not contain the 'Addendum' section which was a feature of several previous volumes.

The profiles in this hard-bound book contain the following nine major sections: description, physical properties, methods of preparation, stability-degradation, methods of analysis, metabolism, biopharmaceutics and pharmacokinetics, toxicity, and references. There are numerous figures of structures and spectra, and tables of properties and chromatographic systems. Since each profile is by a different author, this basic outline may be expanded to other topics or somewhat curtailed, depending upon the information available from the extensive review of the literature and unpublished works. The difference in authorship causes a difference in type size and face style from profile to profile. A cumulative index gives the volume and page number of each substance that is the subject of a particular profile.

This volume, like others in the series, is a valuable reference for those interested in pharmaceutical formulation and pharmaceutical quality assurance and should be available as a reference for those requiring information on drug metabolism, biopharmaceutics, and pharmacokinetics.

Reviewed by Murray M. Tuckerman
School of Pharmacy
Temple University
Philadelphia, PA 19130

Modern Methods of Pharmaceutical Analysis. Edited by ROGER E. SCHIRMER. CRC Press Inc., Boca Raton, FL 33431. 1982. 18 × 25 cm. **Vol. I,** 304 pp. **Vol. II,** 264 pp. Price $81.00 ea. **Vol. III,** 244 pp. Price $72.00.

Modern Methods of Pharmaceutical Analysis is a three-volume set mostly written by R. E. Schirmer. Of the 13 chapters, Dr. Schirmer has written eight. The remaining five have been authored by three scientists from Eli Lilly and Co. Each volume is self-contained with identical Forwards and Introductions. Volume III contains the cumulative index; the indexes in the first two volumes are restricted to their respective contents.

It is not completely clear to this reviewer the rationale for assigning specific chapters to each volume unless it was to restrict each of the "guest" authors to only one volume per author or to keep the number of pages per volume approximately equal. Volume I contains five chapters starting with Separation of Drugs from Excipients. The remaining four chapters describe the following spectroscopic methodologies: UV and Visible Absorption Techniques, IR Methods of Analysis, Fluorometric Analysis, and Optical Rotation. Other methods of separation and purity analysis are not encountered until Volume III. Its five chapters are Gas-Liquid Chromatography, High-Performance Liquid Chromatography, Thermal Analysis, Phase-Solubility Analysis, and The Determination of Isomeric Purity. Situated in the middle is Volume II with Nuclear Magnetic Resonance Spectroscopy, Polarography, and Coulometry.

A better title might have been "Industrial Methods of Pharmaceutical Analysis." The selection of chapters is based on the analytical problems defined by the editor as those commonly encountered in the pharmaceutical industry. These include analysis of the raw materials, synthetic intermediates, the final drug entity, and the formulated product. The analytical methodology must detect types and levels of impurities and degradation products. Lacking is a chapter on mass spectrometry, although there is a brief mention of its use as a detector in chromatography and determination of isomeric purity. Also there is no chapter on immunoassay methodology.

In general each subject is well covered. There is a detailed topic outline for each chapter. The typical format is to begin with a discussion of the principles of the analytical technique followed by a description of the specific instrumentation. Then, depending on the analytical method, there may be an overview of the sample preparation. Each chapter concludes with pharmaceutical applications and a reasonable number of examples. For the most part, the individual chapters should not be considered exhaustive reviews of the pharmaceutical analysis literature. Nevertheless, good bibliographies accompany each chapter. There is good consistency, which probably is due to the majority of the chapters being written by one person.

This is an expensive set of volumes for individual purchase, considering the fact that the basic information of theory, instrumentation, and sample preparation already will be adequately covered in one or more advanced undergraduate or graduate level analytical chemistry textbooks. The cost of the latter is generally lower due to their volume of sales. The on-line searches of the *Chemical Abstracts* data bases permit the analytical chemist to rapidly obtain the most current applications. A few years ago this reviewer probably would have ended with the usual recommendation for library purchase. This is not true in today's economic times. Libraries and individuals should first determine if their collections are adequate and current before making such a major purchase.

Reviewed by John H. Block
School of Pharmacy
Oregon State University
Corvallis, OR 97331

Dictionary of Organic Compounds, 5th Ed. Edited by J. BUCKINGHAM, J. D. G. CADOGAN, R. A. RAPHAEL, C. W. REES, and an INTERNATIONAL ADVISORY BOARD. Chapman and Hall, 733 Third Avenue, New York, NY 10017. 1982. 7766 pp. 28 × 20.5 cm. Price $1950.00 (Canada $2350.00).

The fifth edition of Heilbron's *Dictionary of Organic Compounds*, now in five volumes with two additional volumes of indexes, includes about 50,000 entries listing more than 150,000 compounds. The intent of the *Dictionary* is to describe structural, chemical, and physical properties of common organic compounds of importance to chemists, biochemists, pharmacologists, and biologists. The present edition includes some types of information not listed previously. Leading literature references are included, and annual supplements (including about 2000 entries each)

results correlate with the drug bioavailability. Hence, throughout the book, major emphasis is given to the procedural details and the regulatory requirements of the test, but little on its importance as predictor of drug bioavailability.

Overall consideration for dissolution testing, presented in Chapter 1, gives a brief historical perspective of the dissolution test development. Only the contributions made by the author and the individuals associated with the USP Drug Standards Laboratories were credited with the early developments in this field. It is unfortunate that the author failed to recognize the contributions made by industry, government, and academia. Instead, the author wrongly criticized them for suggesting test methods because they all had "a private axe to grind."

Chapter 2 deals with the discussion of the classical Noyes-Whitney equation with respect to the dissolution test conditions. The necessity of having laminar, nonturbulent fluid dynamics recommended by the author is unwarranted. Some degree of turbulence is actually desirable for achieving homogeneous mixing of the dissolved drug. A detailed description of the official USP-NF methods including allowable design variables and compendial constraints set for those methods is described in Chapter 3. The following chapter gives a description of the flow-through apparatus and a few other nonofficial methods. Here, as well as in Chapter 8, the author advocates the use of only the official methods. It is doubtful that such a view will be shared by the scientific community, simply because it can stifle future progress in the field. Chapters 5 and 6 deal with the various test variables and provide guidelines for setting-up the official test methods. The last chapter deals with the methods employed for the automated monitoring of dissolution rates. Overall, the book gives practical guidance for the routine analysis of dissolution rates by the current official methods.

Reviewed by Ashok C. Shah
Pharmacy Research Unit
The Upjohn Company
Kalamazoo, Michigan 49001

Analytical Profiles of Drug Substances, Vol. 11. Edited by KLAUS FLOREY, Academic Press, 111 Fifth Avenue, New York, NY 10003. 1982. 665 pp. 15 × 23 cm. Price $39.00.

In continuation of the yearly volumes of this series, this collection gives (in about 550 pages) analytical profiles of 16 drug substances: aminophylline, ascorbic acid, captopril, cefotaxime, cefoxitin sodium, clofibrate, clotrimazole, dopamine hydrochloride, ergonovine maleate, flufenamic acid, hexestrol, mestranol, noscapine, penicillin G benzathine, phenylbutazone, and sulfadiazine.

A new feature has been introduced in this volume: profile supplements. These profiles are intended to be a regular part of future volumes. The profile supplements, occupying about 110 pages, are for five substances that originally appeared in Volume 1: levarterenol bitartrate, meprobamate, triamcinolone, triamcinolone acetonide, triamcinolone diacetate. The supplements are not a republishing of the original monographs, they are only additions and/or changes. The paragraph numbering of the original profile has been retained, so that the new or altered data can easily be correlated with the original. This volume does not contain the 'Addendum' section which was a feature of several previous volumes.

The profiles in this hard-bound book contain the following nine major sections: description, physical properties, methods of preparation, stability-degradation, methods of analysis, metabolism, biopharmaceutics and pharmacokinetics, toxicity, and references. There are numerous figures of structures and spectra, and tables of properties and chromatographic systems. Since each profile is by a different author, this basic outline may be expanded to other topics or somewhat curtailed, depending upon the information available from the extensive review of the literature and unpublished works. The difference in authorship causes a difference in type size and face style from profile to profile. A cumulative index gives the volume and page number of each substance that is the subject of a particular profile.

This volume, like others in the series, is a valuable reference for those interested in pharmaceutical formulation and pharmaceutical quality assurance and should be available as a reference for those requiring information on drug metabolism, biopharmaceutics, and pharmacokinetics.

Reviewed by Murray M. Tuckerman
School of Pharmacy
Temple University
Philadelphia, PA 19130

Modern Methods of Pharmaceutical Analysis. Edited by ROGER E. SCHIRMER. CRC Press Inc., Boca Raton, FL 33431. 1982. 18 × 25 cm. **Vol. I,** 304 pp. **Vol. II,** 264 pp. Price $81.00 ea. **Vol. III,** 244 pp. Price $72.00.

Modern Methods of Pharmaceutical Analysis is a three-volume set mostly written by R. E. Schirmer. Of the 13 chapters, Dr. Schirmer has written eight. The remaining five have been authored by three scientists from Eli Lilly and Co. Each volume is self-contained with identical Forwards and Introductions. Volume III contains the cumulative index; the indexes in the first two volumes are restricted to their respective contents.

It is not completely clear to this reviewer the rationale for assigning specific chapters to each volume unless it was to restrict each of the "guest" authors to only one volume per author or to keep the number of pages per volume approximately equal. Volume I contains five chapters starting with Separation of Drugs from Excipients. The remaining four chapters describe the following spectroscopic methodologies: UV and Visible Absorption Techniques, IR Methods of Analysis, Fluorometric Analysis, and Optical Rotation. Other methods of separation and purity analysis are not encountered until Volume III. Its five chapters are Gas-Liquid Chromatography, High-Performance Liquid Chromatography, Thermal Analysis, Phase-Solubility Analysis, and The Determination of Isomeric Purity. Situated in the middle is Volume II with Nuclear Magnetic Resonance Spectroscopy, Polarography, and Coulometry.

A better title might have been "Industrial Methods of Pharmaceutical Analysis." The selection of chapters is based on the analytical problems defined by the editor as those commonly encountered in the pharmaceutical industry. These include analysis of the raw materials, synthetic intermediates, the final drug entity, and the formulated product. The analytical methodology must detect types and levels of impurities and degradation products. Lacking is a chapter on mass spectrometry, although there is a brief mention of its use as a detector in chromatography and determination of isomeric purity. Also there is no chapter on immunoassay methodology.

In general each subject is well covered. There is a detailed topic outline for each chapter. The typical format is to begin with a discussion of the principles of the analytical technique followed by a description of the specific instrumentation. Then, depending on the analytical method, there may be an overview of the sample preparation. Each chapter concludes with pharmaceutical applications and a reasonable number of examples. For the most part, the individual chapters should not be considered exhaustive reviews of the pharmaceutical analysis literature. Nevertheless, good bibliographies accompany each chapter. There is good consistency, which probably is due to the majority of the chapters being written by one person.

This is an expensive set of volumes for individual purchase, considering the fact that the basic information of theory, instrumentation, and sample preparation already will be adequately covered in one or more advanced undergraduate or graduate level analytical chemistry textbooks. The cost of the latter is generally lower due to their volume of sales. The on-line searches of the *Chemical Abstracts* data bases permit the analytical chemist to rapidly obtain the most current applications. A few years ago this reviewer probably would have ended with the usual recommendation for library purchase. This is not true in today's economic times. Libraries and individuals should first determine if their collections are adequate and current before making such a major purchase.

Reviewed by John H. Block
School of Pharmacy
Oregon State University
Corvallis, OR 97331

Dictionary of Organic Compounds, 5th Ed. Edited by J. BUCKINGHAM, J. D. G. CADOGAN, R. A. RAPHAEL, C. W. REES, and an INTERNATIONAL ADVISORY BOARD. Chapman and Hall, 733 Third Avenue, New York, NY 10017. 1982. 7766 pp. 28 × 20.5 cm. Price $1950.00 (Canada $2350.00).

The fifth edition of Heilbron's *Dictionary of Organic Compounds*, now in five volumes with two additional volumes of indexes, includes about 50,000 entries listing more than 150,000 compounds. The intent of the *Dictionary* is to describe structural, chemical, and physical properties of common organic compounds of importance to chemists, biochemists, pharmacologists, and biologists. The present edition includes some types of information not listed previously. Leading literature references are included, and annual supplements (including about 2000 entries each)

results correlate with the drug bioavailability. Hence, throughout the book, major emphasis is given to the procedural details and the regulatory requirements of the test, but little on its importance as predictor of drug bioavailability.

Overall consideration for dissolution testing, presented in Chapter 1, gives a brief historical perspective of the dissolution test development. Only the contributions made by the author and the individuals associated with the USP Drug Standards Laboratories were credited with the early developments in this field. It is unfortunate that the author failed to recognize the contributions made by industry, government, and academia. Instead, the author wrongly criticized them for suggesting test methods because they all had "a private axe to grind."

Chapter 2 deals with the discussion of the classical Noyes-Whitney equation with respect to the dissolution test conditions. The necessity of having laminar, nonturbulent fluid dynamics recommended by the author is unwarranted. Some degree of turbulence is actually desirable for achieving homogeneous mixing of the dissolved drug. A detailed description of the official USP-NF methods including allowable design variables and compendial constraints set for those methods is described in Chapter 3. The following chapter gives a description of the flow-through apparatus and a few other nonofficial methods. Here, as well as in Chapter 8, the author advocates the use of only the official methods. It is doubtful that such a view will be shared by the scientific community, simply because it can stifle future progress in the field. Chapters 5 and 6 deal with the various test variables and provide guidelines for setting-up the official test methods. The last chapter deals with the methods employed for the automated monitoring of dissolution rates. Overall, the book gives practical guidance for the routine analysis of dissolution rates by the current official methods.

Reviewed by Ashok C. Shah
Pharmacy Research Unit
The Upjohn Company
Kalamazoo, Michigan 49001

Analytical Profiles of Drug Substances, Vol. 11. Edited by KLAUS FLOREY, Academic Press, 111 Fifth Avenue, New York, NY 10003. 1982. 665 pp. 15 × 23 cm. Price $39.00.

In continuation of the yearly volumes of this series, this collection gives (in about 550 pages) analytical profiles of 16 drug substances: aminophylline, ascorbic acid, captopril, cefotaxime, cefoxitin sodium, clofibrate, clotrimazole, dopamine hydrochloride, ergonovine maleate, flufenamic acid, hexestrol, mestranol, noscapine, penicillin G benzathine, phenylbutazone, and sulfadiazine.

A new feature has been introduced in this volume: profile supplements. These profiles are intended to be a regular part of future volumes. The profile supplements, occupying about 110 pages, are for five substances that originally appeared in Volume 1: levarterenol bitartrate, meprobamate, triamcinolone, triamcinolone acetonide, triamcinolone diacetate. The supplements are not a republishing of the original monographs, they are only additions and/or changes. The paragraph numbering of the original profile has been retained, so that the new or altered data can easily be correlated with the original. This volume does not contain the 'Addendum' section which was a feature of several previous volumes.

The profiles in this hard-bound book contain the following nine major sections: description, physical properties, methods of preparation, stability-degradation, methods of analysis, metabolism, biopharmaceutics and pharmacokinetics, toxicity, and references. There are numerous figures of structures and spectra, and tables of properties and chromatographic systems. Since each profile is by a different author, this basic outline may be expanded to other topics or somewhat curtailed, depending upon the information available from the extensive review of the literature and unpublished works. The difference in authorship causes a difference in type size and face style from profile to profile. A cumulative index gives the volume and page number of each substance that is the subject of a particular profile.

This volume, like others in the series, is a valuable reference for those interested in pharmaceutical formulation and pharmaceutical quality assurance and should be available as a reference for those requiring information on drug metabolism, biopharmaceutics, and pharmacokinetics.

Reviewed by Murray M. Tuckerman
School of Pharmacy
Temple University
Philadelphia, PA 19130

Modern Methods of Pharmaceutical Analysis. Edited by ROGER E. SCHIRMER. CRC Press Inc., Boca Raton, FL 33431. 1982. 18 × 25 cm. **Vol. I,** 304 pp. **Vol. II,** 264 pp. Price $81.00 ea. **Vol. III,** 244 pp. Price $72.00.

Modern Methods of Pharmaceutical Analysis is a three-volume set mostly written by R. E. Schirmer. Of the 13 chapters, Dr. Schirmer has written eight. The remaining five have been authored by three scientists from Eli Lilly and Co. Each volume is self-contained with identical Forwards and Introductions. Volume III contains the cumulative index; the indexes in the first two volumes are restricted to their respective contents.

It is not completely clear to this reviewer the rationale for assigning specific chapters to each volume unless it was to restrict each of the "guest" authors to only one volume per author or to keep the number of pages per volume approximately equal. Volume I contains five chapters starting with Separation of Drugs from Excipients. The remaining four chapters describe the following spectroscopic methodologies: UV and Visible Absorption Techniques, IR Methods of Analysis, Fluorometric Analysis, and Optical Rotation. Other methods of separation and purity analysis are not encountered until Volume III. Its five chapters are Gas-Liquid Chromatography, High-Performance Liquid Chromatography, Thermal Analysis, Phase-Solubility Analysis, and The Determination of Isomeric Purity. Situated in the middle is Volume II with Nuclear Magnetic Resonance Spectroscopy, Polarography, and Coulometry.

A better title might have been "Industrial Methods of Pharmaceutical Analysis." The selection of chapters is based on the analytical problems defined by the editor as those commonly encountered in the pharmaceutical industry. These include analysis of the raw materials, synthetic intermediates, the final drug entity, and the formulated product. The analytical methodology must detect types and levels of impurities and degradation products. Lacking is a chapter on mass spectrometry, although there is a brief mention of its use as a detector in chromatography and determination of isomeric purity. Also there is no chapter on immunoassay methodology.

In general each subject is well covered. There is a detailed topic outline for each chapter. The typical format is to begin with a discussion of the principles of the analytical technique followed by a description of the specific instrumentation. Then, depending on the analytical method, there may be an overview of the sample preparation. Each chapter concludes with pharmaceutical applications and a reasonable number of examples. For the most part, the individual chapters should not be considered exhaustive reviews of the pharmaceutical analysis literature. Nevertheless, good bibliographies accompany each chapter. There is good consistency, which probably is due to the majority of the chapters being written by one person.

This is an expensive set of volumes for individual purchase, considering the fact that the basic information of theory, instrumentation, and sample preparation already will be adequately covered in one or more advanced undergraduate or graduate level analytical chemistry textbooks. The cost of the latter is generally lower due to their volume of sales. The on-line searches of the *Chemical Abstracts* data bases permit the analytical chemist to rapidly obtain the most current applications. A few years ago this reviewer probably would have ended with the usual recommendation for library purchase. This is not true in today's economic times. Libraries and individuals should first determine if their collections are adequate and current before making such a major purchase.

Reviewed by John H. Block
School of Pharmacy
Oregon State University
Corvallis, OR 97331

Dictionary of Organic Compounds, 5th Ed. Edited by J. BUCKINGHAM, J. D. G. CADOGAN, R. A. RAPHAEL, C. W. REES, and an INTERNATIONAL ADVISORY BOARD. Chapman and Hall, 733 Third Avenue, New York, NY 10017. 1982. 7766 pp. 28 × 20.5 cm. Price $1950.00 (Canada $2350.00).

The fifth edition of Heilbron's *Dictionary of Organic Compounds*, now in five volumes with two additional volumes of indexes, includes about 50,000 entries listing more than 150,000 compounds. The intent of the *Dictionary* is to describe structural, chemical, and physical properties of common organic compounds of importance to chemists, biochemists, pharmacologists, and biologists. The present edition includes some types of information not listed previously. Leading literature references are included, and annual supplements (including about 2000 entries each)

are planned. Obviously, the selection of compounds is of paramount importance for a work of this type: the fifth edition has maintained the careful and useful selection that has characterized the previous editions.

Compounds are listed by the most commonly used name, with other names included. The structural formula is included with the entry, which shows the stereochemical configuration where required. The R,S and E,Z systems have replaced the older D,L and *cis-trans* stereochemical conventions. Other information provided in each entry includes the molecular formula and weight, source, physical data for stereoisomeric forms, melting points of both compound and derivatives, spectral data, and use. Hazard and toxicity information is included in this edition, along with a Registry of Toxic Effects of Chemical Substances number. Bibliographic references include both old and new references (up to 1981), and many indicate the type of information included. Physical constants such as pK_a and optical rotations are often listed in the entry; specific references generally indicate synthetic methods, reviews, and some spectroscopic data. Crystallization solvents are also frequently mentioned.

The selection of compounds for inclusion followed these criteria: fundamental organic compounds of simple structure, most compounds of widespread industrial or commercial use, all important natural products, and other compounds of particular chemical or biological interest. More than 12,000 natural products have been entered, and this may well be the most current and extensive compilation of natural products available. Also, more than 10,000 heterocyclics and 1,500 organometallics are recorded. In regard to compounds of pharmaceutical interest, about 450 drug substances are listed under *C* alone, which compares with 118 substances listed under this letter in the *USP XX*.

Page layouts and the typographic plan for each entry have been improved over those of previous editions, and the pages have a distinctly uncluttered appearance. The structural formulae also reflect a new standard. A greater clarity, and consequent ease of use, has been achieved.

Changes over previous editions include a much greater amount of stereochemical data, the inclusion of hazard warnings and toxicity data, greater use of *Chemical Abstracts Service* names, as well as *USAN* and *BAN* names and *CAS Registry* numbers. Also, the annotation of the bibliography is a marked improvement.

Multiple indexes are also included for the first time. Four indexes are provided: a *Name* index, which includes alternative names; a *Molecular Formula* index; a *Heteroatom* index; and a *CAS Registry Number* index. The latter provides a link to computer-based information services which incorporate these numbers.

Heilbron's *Dictionary of Organic Compounds* has been valued by organic chemists for practically 50 years; the fifth edition should be as valuable to biochemists, biologists, and pharmacologists. It is recommended for every library serving these disciplines as a most time-saving and convenient source of information on the more useful organic compounds.

Reviewed by William O. Foye
Massachusetts College of Pharmacy and Allied Health Sciences
Boston, MA 02115

NOTICES

Advances in Thyroid Neoplasia 1981. Editors: MARIO ANDREOLI, FABRIZIO MONACO, and JACOB ROBBINS. Field Educational Italia, Piazza Montegrappa, 4, Rome, Italy. 1981. 361 pp. 16 × 23 cm. Price Lire 10,000.

The Alkaloids, Vol. 11. (A Specialist Periodical Report). A Review of the Literature Published Between 7/79–6/80. Senior Reporter: M. F. GRUNDON. Royal Society of Chemistry, Burlington House, London, WIV OBN, England. 1982. 259 pp. 13 × 22 cm. Price $111.00 (£50.00).

Analyzing Experimental Data by Regression. By DAVID M. ALLEN and FOSTER B. CADY. Lifetime Learning Publications, Ten Davis Drive, Beltmont, CA 94002. 1982. 394 pp. 16 × 24 cm. Price $28.95.

Annual Report 1981. International Agency for Research on Cancer. 150, cours Albert-Thomas, 69372 Lyons Cedex 2, France. Health & Biomedical Information Programme, World Health Organization, 1211 Geneva 27, Switzerland. 166 pp. 18 × 24 cm.

Antacids in the Eighties. Edited by F. HALTER. Urban & Schwarzenberg, 7 E. Redwood St., Baltimore, MD 21202. 1982. 153 pp. 15 × 23 cm. Price $22.00.

Applications of Mass Spectrometry to Trace Analysis. (Lectures of a course held at the Joint Research Centre, Ispra, Italy, 29 Sept.–3 Oct. 1980). Edited by S. FACCHETTI. Elsevier Scientific Publishing Co., P. O. Box 330, Amsterdam, The Netherlands. 1982. 321 pp. 16 × 14 cm. Price $78.75 (Dfl. 185.00).

Atricular Synovium: Anatomy, Physiology, Pathology, Pharmacology, and Therapy. Edited by P. FRANCHIMONT LIEGE. S. Karger AG, Basel, P. O. Box Postfach, CH-4009 Basel, Switzerland. 1982. 183 pp. 15 × 23 cm. Price $68.50 (Sw Fr. 114/DM 137).

Biological Substances: International Standards Reference Preparations and Reference Reagents. Geneva, World Health Organization, 1211 Geneva 27, Switzerland. 1982. 87 pp. 15 × 24 cm. Price: Sw Fr. 11.

Chemotherapy of Malaria. 2nd Ed. Edited by L. J. BRUCE CHWATT. Health & Biomedical Information Programme, World Health Organization, 1211 Geneva 27, Switzerland. 1981. 259 pp. 15 × 24 cm. Price: Sw Fr. 30.

Clinical and Experimental Hypertension: Part B: Hypertension in Pregnancy. Edited by FREDERICK P. ZUSPAN and E. MALCOLM SYMONDS. Dekker, 270 Madison Ave., New York, NY 10016. 1982. 141 pp. 17 × 25 cm. Price $346.00 (for Parts A and B).

Clinical Pharmacy and Hospital Drug Management. By DAVID H. LAWSON and R. MICHAEL E. RICHARDS. Chapman and Hall (In Association with Methuen, Inc.), 733 Third Ave., New York, NY 10017. 1982. 383 pp. 15 × 23 cm. Price $39.95.

Compendium of Current Source Materials for Drugs. By EUTYCHIA G. LONDOS. Scarecrow Press, Inc., 52 Libert St., P. O. Box 656, Metuchen, NJ 08840. 1982. 140 pp. 21 × 28 cm. Price $12.50.

Compendium of Pharmaceuticals and Specialties. 7th Ed. Edited by CARMEN M. E. KROGH, Dekker, 270 Madison Ave., New York, NY 10016. 1982. 824 pp. 20 × 28 cm. Price $65.00 (20% higher outside the U.S.).

Comprehensive Analytical Chemistry (Edited by G. SVEHLA) *Vol. XII—Thermal Analysis: Part B: Biochemical and Clinical Applications of Thermometric and Thermal Analysis.* Edited by NEIL D. JESPERSEN. Elsevier Scientific Publishing Co., P. O. Box 330, Amsterdam, The Netherlands. 254 pp. 15 × 22 cm. Price $69.75 (Dfl 150).

Covalent Catalysis by Enzymes. By LEONARD B. SPECTOR. Springer-Verlag New York Inc., 44 Hartz Way, Secaucus, NJ 07094. 1982. 276 pp. 15 × 23 cm. Price $32.90.

Disposition of Toxic Drugs and Chemicals in Man. 2nd Ed. By RANDALL C. BASELT. Biomedical Publications, P. O. Box 495, Davis, CA 95617. 1982. 795 pp. Price $49.50.

The Enchanted Ring (The Untold Story of Penicillin). By JOHN C. SHEEHAN. The MIT Press, 28 Carleton St., Cambridge, MA 02142. 1982. 224 pp. 13 × 20 cm. Price $15.00.

Endorphins: Chemistry, Physiology, Pharmacology and Clinical Relevance. (Modern Pharmacology—Toxicology Series. Vol. 20). Edited by JEFFREY B. MALICK and ROBERT M. S. BELL. Dekker, 270 Madison Ave., New York, NY 10016. 1982. 296 pp. 15 × 23 cm. Price $37.50 (20% higher outside the U.S. and Canada).

Environmental Carcinogens—Selected Methods of Analysis. Vol. 4. (Some Aromatic Amines and Azo Dyes in the General and Industrial Environment). IARC Scientific Publications No. 40. Edited by H. EGAN, L. FISHBEIN, M. M. CASTEGNARO, I. K. O'NEILL, and H. BARTSCH. Lyons, France. International Agency for Research on Cancer. (Distributed for IARC by the World Health Organization.) 1981. 347 pp. 18 × 24 cm. Price $30 (Sw Fr. 60).

Environmental Health Criteria 17: Manganese. Published under the joint sponsorship of the United Nations Environment Programme, the International Labour Organization, and the World Health Organization, 1211 Geneva 27, Switzerland. 1981. 110 pp. 14 × 21 cm.

The Essential Guide to Prescription Drugs. 3rd Ed. By JAMES W. LONG. Harper & Row. 10 E. 53rd St., New York, NY 10022. 1982. 935 pp. 15 × 23 cm. Price: cloth $32.95, paper $9.95.

Family Formation Patterns and Health: An International Collaborative Study Colombia, Egypt, Pakistan, and the Syrian Arab Republic. Study Coordinators and Editors: A. R. OMRAN and C. C. STANDLEY. World Health Organization, Geneva, Switzerland. 1981. 464 pp. 15 × 24 cm. Price Sw Fr. 44.

Frequently Prescribed and Abused Drugs. Reference Edition (Their Indications, Efficacy, Rational Prescribing). Edited by SIDNEY COHEN, CHARLES BUCHWALD, JOEL SOLOMON, JAMES CALLAHAN, and DANIEL KATZ. The Haworth Press, Inc., 28 E

are planned. Obviously, the selection of compounds is of paramount importance for a work of this type: the fifth edition has maintained the careful and useful selection that has characterized the previous editions.

Compounds are listed by the most commonly used name, with other names included. The structural formula is included with the entry, which shows the stereochemical configuration where required. The R,S and E,Z systems have replaced the older D,L and *cis-trans* stereochemical conventions. Other information provided in each entry includes the molecular formula and weight, source, physical data for stereoisomeric forms, melting points of both compound and derivatives, spectral data, and use. Hazard and toxicity information is included in this edition, along with a Registry of Toxic Effects of Chemical Substances number. Bibliographic references include both old and new references (up to 1981), and many indicate the type of information included. Physical constants such as pK_a and optical rotations are often listed in the entry; specific references generally indicate synthetic methods, reviews, and some spectroscopic data. Crystallization solvents are also frequently mentioned.

The selection of compounds for inclusion followed these criteria: fundamental organic compounds of simple structure, most compounds of widespread industrial or commercial use, all important natural products, and other compounds of particular chemical or biological interest. More than 12,000 natural products have been entered, and this may well be the most current and extensive compilation of natural products available. Also, more than 10,000 heterocyclics and 1,500 organometallics are recorded. In regard to compounds of pharmaceutical interest, about 450 drug substances are listed under *C* alone, which compares with 118 substances listed under this letter in the *USP XX*.

Page layouts and the typographic plan for each entry have been improved over those of previous editions, and the pages have a distinctly uncluttered appearance. The structural formulae also reflect a new standard. A greater clarity, and consequent ease of use, has been achieved.

Changes over previous editions include a much greater amount of stereochemical data, the inclusion of hazard warnings and toxicity data, greater use of *Chemical Abstracts Service* names, as well as *USAN* and *BAN* names and *CAS Registry* numbers. Also, the annotation of the bibliography is a marked improvement.

Multiple indexes are also included for the first time. Four indexes are provided: a *Name* index, which includes alternative names; a *Molecular Formula* index; a *Heteroatom* index; and a *CAS Registry Number* index. The latter provides a link to computer-based information services which incorporate these numbers.

Heilbron's *Dictionary of Organic Compounds* has been valued by organic chemists for practically 50 years; the fifth edition should be as valuable to biochemists, biologists, and pharmacologists. It is recommended for every library serving these disciplines as a most time-saving and convenient source of information on the more useful organic compounds.

Reviewed by William O. Foye
Massachusetts College of Pharmacy and Allied Health Sciences
Boston, MA 02115

NOTICES

Advances in Thyroid Neoplasia 1981. Editors: MARIO ANDREOLI, FABRIZIO MONACO, and JACOB ROBBINS. Field Educational Italia, Piazza Montegrappa, 4, Rome, Italy. 1981. 361 pp. 16 × 23 cm. Price Lire 10,000.

The Alkaloids, Vol. 11. (A Specialist Periodical Report). A Review of the Literature Published Between 7/79–6/80. Senior Reporter: M. F. GRUNDON. Royal Society of Chemistry, Burlington House, London, WIV OBN, England. 1982. 259 pp. 13 × 22 cm. Price $111.00 (£50.00).

Analyzing Experimental Data by Regression. By DAVID M. ALLEN and FOSTER B. CADY. Lifetime Learning Publications, Ten Davis Drive, Beltmont, CA 94002. 1982. 394 pp. 16 × 24 cm. Price $28.95.

Annual Report 1981. International Agency for Research on Cancer. 150, cours Albert-Thomas, 69372 Lyons Cedex 2, France. Health & Biomedical Information Programme, World Health Organization, 1211 Geneva 27, Switzerland. 166 pp. 18 × 24 cm.

Antacids in the Eighties. Edited by F. HALTER. Urban & Schwarzenberg, 7 E. Redwood St., Baltimore, MD 21202. 1982. 153 pp. 15 × 23 cm. Price $22.00.

Applications of Mass Spectrometry to Trace Analysis. (Lectures of a course held at the Joint Research Centre, Ispra, Italy, 29 Sept.–3 Oct. 1980). Edited by S. FACCHETTI. Elsevier Scientific Publishing Co., P. O. Box 330, Amsterdam, The Netherlands. 1982. 321 pp. 16 × 14 cm. Price $78.75 (Dfl. 185.00).

Atricular Synovium: Anatomy, Physiology, Pathology, Pharmacology, and Therapy. Edited by P. FRANCHIMONT LIEGE. S. Karger AG, Basel, P. O. Box Postfach, CH-4009 Basel, Switzerland. 1982. 183 pp. 15 × 23 cm. Price $68.50 (Sw Fr. 114/DM 137).

Biological Substances: International Standards Reference Preparations and Reference Reagents. Geneva, World Health Organization, 1211 Geneva 27, Switzerland. 1982. 87 pp. 15 × 24 cm. Price: Sw Fr. 11.

Chemotherapy of Malaria. 2nd Ed. Edited by L. J. BRUCE CHWATT. Health & Biomedical Information Programme, World Health Organization, 1211 Geneva 27, Switzerland. 1981. 259 pp. 15 × 24 cm. Price: Sw Fr. 30.

Clinical and Experimental Hypertension: Part B: Hypertension in Pregnancy. Edited by FREDERICK P. ZUSPAN and E. MALCOLM SYMONDS. Dekker, 270 Madison Ave., New York, NY 10016. 1982. 141 pp. 17 × 25 cm. Price $346.00 (for Parts A and B).

Clinical Pharmacy and Hospital Drug Management. By DAVID H. LAWSON and R. MICHAEL E. RICHARDS. Chapman and Hall (In Association with Methuen, Inc.), 733 Third Ave., New York, NY 10017. 1982. 383 pp. 15 × 23 cm. Price $39.95.

Compendium of Current Source Materials for Drugs. By EUTYCHIA G. LONDOS. Scarecrow Press, Inc., 52 Libert St., P. O. Box 656, Metuchen, NJ 08840. 1982. 140 pp. 21 × 28 cm. Price $12.50.

Compendium of Pharmaceuticals and Specialties. 7th Ed. Edited by CARMEN M. E. KROGH, Dekker, 270 Madison Ave., New York, NY 10016. 1982. 824 pp. 20 × 28 cm. Price $65.00 (20% higher outside the U.S.).

Comprehensive Analytical Chemistry (Edited by G. SVEHLA) *Vol. XII—Thermal Analysis: Part B: Biochemical and Clinical Applications of Thermometric and Thermal Analysis.* Edited by NEIL D. JESPERSEN. Elsevier Scientific Publishing Co., P. O. Box 330, Amsterdam, The Netherlands. 254 pp. 15 × 22 cm. Price $69.75 (Dfl 150).

Covalent Catalysis by Enzymes. By LEONARD B. SPECTOR. Springer-Verlag New York Inc., 44 Hartz Way, Secaucus, NJ 07094. 1982. 276 pp. 15 × 23 cm. Price $32.90.

Disposition of Toxic Drugs and Chemicals in Man. 2nd Ed. By RANDALL C. BASELT. Biomedical Publications, P. O. Box 495, Davis, CA 95617. 1982. 795 pp. Price $49.50.

The Enchanted Ring (The Untold Story of Penicillin). By JOHN C. SHEEHAN. The MIT Press, 28 Carleton St., Cambridge, MA 02142. 1982. 224 pp. 13 × 20 cm. Price $15.00.

Endorphins: Chemistry, Physiology, Pharmacology and Clinical Relevance. (Modern Pharmacology—Toxicology Series. Vol. 20). Edited by JEFFREY B. MALICK and ROBERT M. S. BELL. Dekker, 270 Madison Ave., New York, NY 10016. 1982. 296 pp. 15 × 23 cm. Price $37.50 (20% higher outside the U.S. and Canada).

Environmental Carcinogens—Selected Methods of Analysis. Vol. 4. (Some Aromatic Amines and Azo Dyes in the General and Industrial Environment). IARC Scientific Publications No. 40. Edited by H. EGAN, L. FISHBEIN, M. M. CASTEGNARO, I. K. O'NEILL, and H. BARTSCH. Lyons, France. International Agency for Research on Cancer. (Distributed for IARC by the World Health Organization.) 1981. 347 pp. 18 × 24 cm. Price $30 (Sw Fr. 60).

Environmental Health Criteria 17: Manganese. Published under the joint sponsorship of the United Nations Environment Programme, the International Labour Organization, and the World Health Organization, 1211 Geneva 27, Switzerland. 1981. 110 pp. 14 × 21 cm.

The Essential Guide to Prescription Drugs. 3rd Ed. By JAMES W. LONG. Harper & Row. 10 E. 53rd St., New York, NY 10022. 1982. 935 pp. 15 × 23 cm. Price: cloth $32.95, paper $9.95.

Family Formation Patterns and Health: An International Collaborative Study Colombia, Egypt, Pakistan, and the Syrian Arab Republic. Study Coordinators and Editors: A. R. OMRAN and C. C. STANDLEY. World Health Organization, Geneva, Switzerland. 1981. 464 pp. 15 × 24 cm. Price Sw Fr. 44.

Frequently Prescribed and Abused Drugs. Reference Edition (Their Indications, Efficacy, Rational Prescribing). Edited by SIDNEY COHEN, CHARLES BUCHWALD, JOEL SOLOMON, JAMES CALLAHAN, and DANIEL KATZ. The Haworth Press, Inc., 28 E

22nd St., New York, NY 10010. 1982. 80 pp. 22 × 28 cm. Price $20.00.

Glial–Neurone Interactions. Vol. 95. Edited by J. E. TREHERNE. Cambridge University Press, 32 E. 57th St., New York, NY 10022. 1981. 240 pp. 17 × 25 cm. Price $60.00.

Halogenated Hydrocarbons: Solubility–Miscibility with Water. By A. L. HORVATH. Dekker, 270 Madison Ave., New York, NY 10016. 1982. 889 pp. 17 × 25 cm. Price $125.00 (20% higher outside the U.S. and Canada).

Handbook of Enzyme Inhibitors (1965–1966). By MAHENDRA KUMAR JAIN. Wiley, One Wiley Drive, Somerset, NJ 08873. 1982. 447 pp. 21 × 28 cm. Price $100.00.

Heterocyclic Chemistry: Vol. 2. (A Specialist Periodical Report). A Review of the Literature Abstracted Between 7/79–6/80. Senior Reporters: H. SUSCHITZKY and O. METH-COHN. Royal Society of Chemistry, Burlington House, London WIV OBN, England. 1981. 441 pp. 13 × 23 cm. Price $155.00.

Hormone Receptors: Horizons in Biochemistry and Biophysics: Vol. 6. Edited by L. D. KOHN. Wiley, One Wiley Drive, Somerset, NJ 08875. 1982. 392 pp. 15 × 23 cm. Price $67.95.

Human Cancer Markers. Edited by STEWART SELL and BRITTA WAHREN. The Humana Press, P. O. Box 2148, Clifton, NJ 07015. 1982. 450 pp. 15 × 23 cm. Price $59.50 ($69.50 outside the U.S.).

The Human Side of Statistical Consulting. By JAMES R. BOEN and DOUGLAS A. ZAHN. Lifetime Learning Publications, Ten Davis Drive, Belmont, CA 94002. 1982. 196 pp. 15 × 23 cm.

Immunological Approaches to Cancer Therapeutics. Edited by ENRICO MIHICH. Wiley, 605 Third Ave., New York, NY 10157. 1982. 587 pp. 15 × 23 cm. Price $75.00.

Inflammatory Diseases and Copper. Edited by JOHN R. J. SORENSON. The Humana Press Inc., P. O. Box 2148, Clifton, NJ 07015. 1982. 622 pp. 15 × 23 cm. Price $69.50. ($79.50 outside the U.S.).

Ion-Selective Electrodes, 3. Analytical Chemistry Symposia Series—Vol. 8. 3rd Symposium held at Matrafured, Hungary, 13–15 Oct. 1980. Edited by E. PUNGOR. Elsevier Scientific Pub. Co., P. O. Box 330, Amsterdam, The Netherlands. 1981. 427 pp. 15 × 24 cm. Price $100.00 (Dfl. 215.00).

Laboratory Decontamination and Destruction of Aflatoxins B_1, B_2, G_1, G_2 In Laboratory Wastes. Edited by M. CASTEGNARO *et al.* International Agency for Research and Cancer. Health & Biomedical Information Programme, World Health Organization, 1211 Geneva 27, Switzerland. 1980. 59 pp. 17 × 24 cm. Price $10.00 (Sw Fr. 18).

Marihuana: An Annotated Bibliography, Vol. II. By COY W. WALLER, RASHMI S. NAIR, ANN F. McALLISTER, BEVERLY S. URBANEK, CARLTON E. TURNER. Macmillan, 866 3rd Ave., New York, NY 10022. 1982. 620 pp. 18 × 26 cm. Price $29.95.

Mutagenicity: New Horizons in Genetic Toxicology. Edited by JOHN A. HEDDLE. Academic Press Inc., 111 Fifth Ave., New York, NY 10003. 1982. 471 pp. 15 × 23 cm. Price $55.00.

Neurotransmission, Neurotransmitters, and Neuromodulators: Vol. 89. Edited by E. A. KRAVITZ & J. E. TREHERNE. Cambridge University Press, 32 E. 57th St., New York, NY 10022. 1981. 286 pp. 17 × 25 cm. Price $41.50.

New Zealand Medicinal Plants. By S. G. BROOKER, R. C. CAMBIE, and R. C. COOPER. Heinemann Publishers, Corner College Rd. and Kilham Ave., Auckland, New Zealand. 1981. 117 pp. 22 × 28 cm. Price $36.95.

Organic Pharmaceutical Chemistry. By HARKISHAN SINGH and V. K. KAPOOR. Vallabh Prakashan, B-27 Ashok Vihar, Phase I, Delhi, 110 052, India. 1982. 316 pp. 13 × 22 cm.

Patenting in the Biological Sciences. By R. S. CRESPI. Wiley, One Wiley Drive, Somerset, NJ 08873. 1982. 211 pp. 15 × 23 cm. Price $38.00.

Pharmacy Practice: Social and Behavioral Aspects. 2nd Ed. Edited by ALBERT I. WERTHEIMER and MICKEY C. SMITH. University Park Press, 300 N. Charles St., Baltimore, MD 21201. 1981. 444 pp. 15 × 23 cm. Price $25.50.

Photochemistry Vol. 12. A Review of the Literature Published Between 7/79–6/80. Senior Reporter: D. BRYCE-SMITH. Royal Society of Chemistry, Burlington House, London WIV OBN, England. 1982. 587 pp 14 × 22 cm. Price $145.00 (£70.00).

Prescriptions for Death: The Drugging of the Third World. By MILTON SILVERMAN, PHILIP R. LEE, and MIA LYDECKER. University of California Press, 2223 Fulton St., Berkeley, CA 94720. 1982. 186 pp. 15 × 23 cm. Price $16.95.

Principles of Biochemical Toxicology. By JOHN A. TIMBRELL. Taylor & Francis Ltd., 4 John St., London, WC1N 2ET, England. 1982. 249 pp. 15 × 23 cm.

Propädeutische Arzneiformenlehre: Einfuhrung in die Arzneiformenlehre und Laboratoriums Praxis. By ENGELBERT GRAF and HAROLD HAMACHER. Wissenschaftliche Verlagsgesellschaft mbH, Postfach 40, D-7000 Stuttgart 1, Germany. 1982. 151 pp. 17 × 24 cm. Price DM 38.

Prostaglandins: Organ- and Tissue-Specific Actions. (Modern Pharmacology and Toxicology Series: Vol. 21.) Edited by STAN GREENBERG, PHILIP J. KADOWITZ, and THOMAS F. BURKS. Dekker, 270 Madison Ave., New York, NY 10016. 1982. 454 pp. 15 × 23 cm. Price $59.50 (20% higher outside the U.S. and Canada).

Psychopharmacology of Anticonvulsants. (A British Association for Psychopharmacology Monograph No. 2). Edited by MERTON SANDLER. Oxford University Press, 200 Madison Ave., New York, NY 10016. 1982. 163 pp. 15 × 23 cm. Price $29.50.

Rattlesnake Venoms: Their Actions of Treatment. Edited by ANTHONY T. TU. Dekker, 270 Madison Ave., New York, NY 10016. 1982. 393 pp 15 × 23 cm. Price $75.00 (20% higher outside the U.S. and Canada).

Shunts and Problems in Shunts. (Symposium on Shunts and Problems in Shunts, Marselle, June 24–25, 1980). Volume Editor: M. CHOUX. S. Karger, AG, P. O. Box Postfach CH-4009, Basel, Switzerland. 1982. 230 pp. 16 × 25 cm. Price $69.00 (Sw Fr. 115/DM 138).

Terpenoids and Steroids: Vol. 11. A Review of the Literature Published Between 9/79–8/80. (A Specialist Periodical Report). Senior Reporter: J. R. HANSON. Royal Society of Chemistry, Burlington House, London, WIV OBN, England. 1982. 241 pp. 14 × 22 cm. Price $94.00 (£45.00).

Textbook of Pharmaceutical Formulation. By B. M. MITHAL. Vallabh Prakashan, B-27 Ashok Vihar, Phase 1, Delhi, 110 052, India. 1980. 264 pp. 13 × 22 cm. Price $20.00.

The Treatment and Management of Severe Protein-Energy Malnutrition. World Health Organization. Health & Biomedical Information Programme, World Health Organization, 1211 Geneva 27, Switzerland. 1981. 47 pp. 16 × 24 cm. Price Sw. Fr. 8. (French & Spanish editions in preparation).

Trends in Autonomic Pharmacology. Vol. 2. Edited by STANLEY KALSNER. Urban & Schwarzenberg, Inc., 7 E. Redwood St., Baltimore, MD 21202. 1982. 563 pp. 15 × 23 cm. Price $45.00.

USP XX NF XV Addendum a to Supplement #3. The United States Pharmacopeial Convention, Inc., 12501 Twinbrook Parkway, Rockville, MD 20852. 653 pp. 20 × 27 cm. Includes: 102 new dissolution tests and 89 new monographs.

USP XX NF XV Supplement 3. Cumulative with First Two Supplements. The United States Pharmacopeial Convention, Inc., 12601 Twinbrook Parkway, Rockville, MD 20852. 1982. 440 pp. 20 × 29 cm. Includes 95 new dissolution tests, 44 new monographs, new DEA regulations governing prescription transfers, and child-safety packaging regulations.

Veterinary Drug Index. By BENJAMIN P. LEWIS, Jr. and LEON O. WILKEN, W. B. Saunders, West Washington Square, Philadelphia, PA 19105. 1982. 387 pp. 19 × 27 cm. Price $35.00.

The World of WHO: 1980–1981. (Biennial Report of the Director-General to the World Health Assembly and to the United Nations. Health & Biomedical Information Programme, World Health Organization, 1211 Geneva 27, Switzerland. 291 pp. 18 × 24 cm. Price Sw Fr. 18.

NEW JOURNALS

International Journal of Quantum Chemistry. Quantum Biology Symposium No. 8. Proceedings of the International Symposium on Quantum Biology and Quantum Pharmacology. Held at Palm Beach, Fla. March 5–7, 1981. Editor in Chief: PER OLOV LOWDIN. Wiley, One Wiley Drive, Somerset, NJ 08873. 1982. 464 pp. 15 × 23 cm. Price $50.00.

Journal of Bioelectricity. Editor: ANDREW A. MARINO. Dekker, 270 Madison Ave., New York, NY 10016. 1982. 159 pp. 15 × 23 cm. (3 issues per volume). Price $75.00 per volume (institutional rate); $37.50 per volume (individual rate).

22nd St., New York, NY 10010. 1982. 80 pp. 22 × 28 cm. Price $20.00.

Glial–Neurone Interactions. Vol. 95. Edited by J. E. TREHERNE. Cambridge University Press, 32 E. 57th St., New York, NY 10022. 1981. 240 pp. 17 × 25 cm. Price $60.00.

Halogenated Hydrocarbons: Solubility–Miscibility with Water. By A. L. HORVATH. Dekker, 270 Madison Ave., New York, NY 10016. 1982. 889 pp. 17 × 25 cm. Price $125.00 (20% higher outside the U.S. and Canada).

Handbook of Enzyme Inhibitors (1965–1966). By MAHENDRA KUMAR JAIN. Wiley, One Wiley Drive, Somerset, NJ 08873. 1982. 447 pp. 21 × 28 cm. Price $100.00.

Heterocyclic Chemistry: Vol. 2. (A Specialist Periodical Report). A Review of the Literature Abstracted Between 7/79–6/80. Senior Reporters: H. SUSCHITZKY and O. METH-COHN. Royal Society of Chemistry, Burlington House, London WIV OBN, England. 1981. 441 pp. 13 × 23 cm. Price $155.00.

Hormone Receptors: Horizons in Biochemistry and Biophysics: Vol. 6. Edited by L. D. KOHN. Wiley, One Wiley Drive, Somerset, NJ 08875. 1982. 392 pp. 15 × 23 cm. Price $67.95.

Human Cancer Markers. Edited by STEWART SELL and BRITTA WAHREN. The Humana Press, P. O. Box 2148, Clifton, NJ 07015. 1982. 450 pp. 15 × 23 cm. Price $59.50 ($69.50 outside the U.S.).

The Human Side of Statistical Consulting. By JAMES R. BOEN and DOUGLAS A. ZAHN. Lifetime Learning Publications, Ten Davis Drive, Belmont, CA 94002. 1982. 196 pp. 15 × 23 cm.

Immunological Approaches to Cancer Therapeutics. Edited by ENRICO MIHICH. Wiley, 605 Third Ave., New York, NY 10157. 1982. 587 pp. 15 × 23 cm. Price $75.00.

Inflammatory Diseases and Copper. Edited by JOHN R. J. SORENSON. The Humana Press Inc., P. O. Box 2148, Clifton, NJ 07015. 1982. 622 pp. 15 × 23 cm. Price $69.50. ($79.50 outside the U.S.).

Ion-Selective Electrodes, 3. Analytical Chemistry Symposia Series—Vol. 8. 3rd Symposium held at Matrafured, Hungary, 13–15 Oct. 1980. Edited by E. PUNGOR. Elsevier Scientific Pub. Co., P. O. Box 330, Amsterdam, The Netherlands. 1981. 427 pp. 15 × 24 cm. Price $100.00 (Dfl. 215.00).

Laboratory Decontamination and Destruction of Aflatoxins B_1, B_2, G_1, G_2 In Laboratory Wastes. Edited by M. CASTEGNARO *et al.* International Agency for Research and Cancer. Health & Biomedical Information Programme, World Health Organization, 1211 Geneva 27, Switzerland. 1980. 59 pp. 17 × 24 cm. Price $10.00 (Sw Fr. 18).

Marihuana: An Annotated Bibliography, Vol. II. By COY W. WALLER, RASHMI S. NAIR, ANN F. McALLISTER, BEVERLY S. URBANEK, CARLTON E. TURNER. Macmillan, 866 3rd Ave., New York, NY 10022. 1982. 620 pp. 18 × 26 cm. Price $29.95.

Mutagenicity: New Horizons in Genetic Toxicology. Edited by JOHN A. HEDDLE. Academic Press Inc., 111 Fifth Ave., New York, NY 10003. 1982. 471 pp. 15 × 23 cm. Price $55.00.

Neurotransmission, Neurotransmitters, and Neuromodulators: Vol. 89. Edited by E. A. KRAVITZ & J. E. TREHERNE. Cambridge University Press, 32 E. 57th St., New York, NY 10022. 1981. 286 pp. 17 × 25 cm. Price $41.50.

New Zealand Medicinal Plants. By S. G. BROOKER, R. C. CAMBIE, and R. C. COOPER. Heinemann Publishers, Corner College Rd. and Kilham Ave., Auckland, New Zealand. 1981. 117 pp. 22 × 28 cm. Price $36.95.

Organic Pharmaceutical Chemistry. By HARKISHAN SINGH and V. K. KAPOOR. Vallabh Prakashan, B-27 Ashok Vihar, Phase I, Delhi, 110 052, India. 1982. 316 pp. 13 × 22 cm.

Patenting in the Biological Sciences. By R. S. CRESPI. Wiley, One Wiley Drive, Somerset, NJ 08873. 1982. 211 pp. 15 × 23 cm. Price $38.00.

Pharmacy Practice: Social and Behavioral Aspects. 2nd Ed. Edited by ALBERT I. WERTHEIMER and MICKEY C. SMITH. University Park Press, 300 N. Charles St., Baltimore, MD 21201. 1981. 444 pp. 15 × 23 cm. Price $25.50.

Photochemistry Vol. 12. A Review of the Literature Published Between 7/79–6/80. Senior Reporter: D. BRYCE-SMITH. Royal Society of Chemistry, Burlington House, London WIV OBN, England. 1982. 587 pp 14 × 22 cm. Price $145.00 (£70.00).

Prescriptions for Death: The Drugging of the Third World. By MILTON SILVERMAN, PHILIP R. LEE, and MIA LYDECKER. University of California Press, 2223 Fulton St., Berkeley, CA 94720. 1982. 186 pp. 15 × 23 cm. Price $16.95.

Principles of Biochemical Toxicology. By JOHN A. TIMBRELL. Taylor & Francis Ltd., 4 John St., London, WC1N 2ET, England. 1982. 249 pp. 15 × 23 cm.

Propädeutische Arzneiformenlehre: Einfuhrung in die Arzneiformenlehre und Laboratoriums Praxis. By ENGELBERT GRAF and HAROLD HAMACHER. Wissenschaftliche Verlagsgesellschaft mbH, Postfach 40, D-7000 Stuttgart 1, Germany. 1982. 151 pp. 17 × 24 cm. Price DM 38.

Prostaglandins: Organ- and Tissue-Specific Actions. (Modern Pharmacology and Toxicology Series: Vol. 21.) Edited by STAN GREENBERG, PHILIP J. KADOWITZ, and THOMAS F. BURKS. Dekker, 270 Madison Ave., New York, NY 10016. 1982. 454 pp. 15 × 23 cm. Price $59.50 (20% higher outside the U.S. and Canada).

Psychopharmacology of Anticonvulsants. (A British Association for Psychopharmacology Monograph No. 2). Edited by MERTON SANDLER. Oxford University Press, 200 Madison Ave., New York, NY 10016. 1982. 163 pp. 15 × 23 cm. Price $29.50.

Rattlesnake Venoms: Their Actions of Treatment. Edited by ANTHONY T. TU. Dekker, 270 Madison Ave., New York, NY 10016. 1982. 393 pp 15 × 23 cm. Price $75.00 (20% higher outside the U.S. and Canada).

Shunts and Problems in Shunts. (Symposium on Shunts and Problems in Shunts, Marselle, June 24–25, 1980). Volume Editor: M. CHOUX. S. Karger, AG, P. O. Box Postfach CH-4009, Basel, Switzerland. 1982. 230 pp. 16 × 25 cm. Price $69.00 (Sw Fr. 115/DM 138).

Terpenoids and Steroids: Vol. 11. A Review of the Literature Published Between 9/79–8/80. (A Specialist Periodical Report). Senior Reporter: J. R. HANSON. Royal Society of Chemistry, Burlington House, London, WIV OBN, England. 1982. 241 pp. 14 × 22 cm. Price $94.00 (£45.00).

Textbook of Pharmaceutical Formulation. By B. M. MITHAL. Vallabh Prakashan, B-27 Ashok Vihar, Phase 1, Delhi, 110 052, India. 1980. 264 pp. 13 × 22 cm. Price $20.00.

The Treatment and Management of Severe Protein-Energy Malnutrition. World Health Organization. Health & Biomedical Information Programme, World Health Organization, 1211 Geneva 27, Switzerland. 1981. 47 pp. 16 × 24 cm. Price Sw. Fr. 8. (French & Spanish editions in preparation).

Trends in Autonomic Pharmacology. Vol. 2. Edited by STANLEY KALSNER. Urban & Schwarzenberg, Inc., 7 E. Redwood St., Baltimore, MD 21202. 1982. 563 pp. 15 × 23 cm. Price $45.00.

USP XX NF XV Addendum a to Supplement #3. The United States Pharmacopeial Convention, Inc., 12501 Twinbrook Parkway, Rockville, MD 20852. 653 pp. 20 × 27 cm. Includes: 102 new dissolution tests and 89 new monographs.

USP XX NF XV Supplement 3. Cumulative with First Two Supplements. The United States Pharmacopeial Convention, Inc., 12601 Twinbrook Parkway, Rockville, MD 20852. 1982. 440 pp. 20 × 29 cm. Includes 95 new dissolution tests, 44 new monographs, new DEA regulations governing prescription transfers, and child-safety packaging regulations.

Veterinary Drug Index. By BENJAMIN P. LEWIS, Jr. and LEON O. WILKEN, W. B. Saunders, West Washington Square, Philadelphia, PA 19105. 1982. 387 pp. 19 × 27 cm. Price $35.00.

The World of WHO: 1980–1981. (Biennial Report of the Director-General to the World Health Assembly and to the United Nations. Health & Biomedical Information Programme, World Health Organization, 1211 Geneva 27, Switzerland. 291 pp. 18 × 24 cm. Price Sw Fr. 18.

NEW JOURNALS

International Journal of Quantum Chemistry. Quantum Biology Symposium No. 8. Proceedings of the International Symposium on Quantum Biology and Quantum Pharmacology. Held at Palm Beach, Fla. March 5–7, 1981. Editor in Chief: PER OLOV LOWDIN. Wiley, One Wiley Drive, Somerset, NJ 08873. 1982. 464 pp. 15 × 23 cm. Price $50.00.

Journal of Bioelectricity. Editor: ANDREW A. MARINO. Dekker, 270 Madison Ave., New York, NY 10016. 1982. 159 pp. 15 × 23 cm. (3 issues per volume). Price $75.00 per volume (institutional rate); $37.50 per volume (individual rate).

1983
Volume 72

JOURNAL OF PHARMACEUTICAL SCIENCES

A publication of the American Pharmaceutical Association

The *Journal of Pharmaceutical Sciences* (ISSN 0022-3549) is published monthly by the American Pharmaceutical Association (APhA) at 2215 Constitution Ave., N.W., Washington, DC 20037. Second-class postage paid at Washington, D.C. and at additional mailing office.

All expressions of opinion and statements of supposed fact appearing in articles or editorials carried in this journal are published on the authority of the writer over whose name they appear and are not to be regarded as necessarily expressing the policies or views of APhA.

Offices—Editorial, Advertising, and Subscription: 2215 Constitution Ave., N.W., Washington, DC 20037. All Journal staff may be contacted at this address. Printing: 20th & Northampton Streets, Easton, PA 18042.

Annual Subscriptions—United States and foreign, industrial and government institutions $75; educational institutions $75; individuals *for personal use only* $40; single copies $10. APhA and SAPhA members may subscribe to *J. Pharm. Sci.* for $20.00 per year. All foreign subscriptions add $10 for postage. Subscription rates are subject to change without notice.

Claims—Missing numbers will not be supplied if dues or subscriptions are in arrears for more than 60 days or if claims are received more than 60 days after the date of the issue, or if loss was due to failure to give notice of change of address. APhA cannot accept responsibility for foreign delivery when its records indicate shipment was made.

Change of Address—Members and subscribers should notify at once both the Post Office and APhA of any change of address.

Photocopying—The code at the foot of the first page of an article indicates that APhA has granted permission for copying of the article beyond the limits permitted by Sections 107 and 108 of the U.S. Copyright Law provided that the copier sends the per copy fee stated in the code to the Copyright Clearance Center, Inc., 21 Congress St., Salem, MA 01970. Copies may be made for personal or internal use only and not for general distribution.

Microfilm—Available from University Microfilms International, 300 N. Zeeb Road, Ann Arbor, MI 48106.

Adverse Drug Reactions—A Continuing Problem

During the past year, there have been several major drug recalls and withdrawals from the market. We are referring here to those cases involving toxicity and adverse reactions associated with the active ingredient itself, rather than recalls resulting from product tampering, faulty manufacturing of dosage forms, or other considerations relating to the quality of the drug product.

Two of the more publicized such recalls were for benoxaprofen (Oraflex) and zomepirac (Zomax).

Various interested observers of the national pharmaceutical scene have drawn a variety of conclusions from this rash of recalls. The conclusions have been diverse and, in many cases, filled with conjecture and hypothesis. As such, they have ranged from "look how poorly the new drug approval system is working to allow all these unsuitable drugs to be placed on the market" to the other extreme, namely, "look how well the new drug approval system is working since these adverse reactions were identified and the drugs pulled off the market." But in any event, everyone seems agreed that there are, and will continue to be, instances where significant drug toxicity does not become evident until the product involved goes into general distribution and thereby experiences widespread use in patients.

Given that situation, a problem with a drug will only come to light if a sufficient number of physicians, pharmacists, or other health care practitioners in a position to monitor patient reaction to therapy (*a*) note that a patient has suffered an untoward effect, (*b*) make the critical mental connection between drug and untoward reaction, and (*c*) duly report it to the manufacturer and/or the Food and Drug Administration.

Unfortunately, however, this sequence often does not occur. In fact, the usual pattern is that—*after* the first such clinical experiences are reported in the letters columns of medical journals—there is then a flurry of similar reports from practitioners who had previously failed to make the mental association in patients they had treated earlier. But aside from efforts to make practitioners more alert, to sharpen their association skills, and to urge them to be conscientious in reporting adverse reactions, there seems to be little that can be done to improve the reporting system from the field.

Moving on, then, after adverse reaction reports have been filed with FDA, what happens next?

The apparent general supposition on the part of the public, members of Congress, and many members of the health care professions is that an alarm is immediately triggered, the FDA springs into action, and the drug is immediately whisked off the market. In essence, a reaction is assumed that would be comparable in speed and effectiveness to that expected from our national military defense in the event of a nuclear attack.

Obviously, however, even under the best of circumstances and even under ideal operating conditions, no adverse reaction system will work that well.

So, how well is the present FDA system working?

The answer appears to be: Not very well. In fact, rather poorly, indeed.

A little over a year ago, on March 8, 1982, the watch-dog agency in the federal government—the General Accounting Office, or GAO—released a report on 21 selected prescription drugs and found that it took an average of five months for adverse drug reaction (ADR) reports just to be entered into the computer files of the FDA's Division of Drug Experience.

In summarizing their findings, the GAO said: *"Based on a sample of almost 2,000 adverse reaction reports submitted by manufacturers, (1) 42% of these reports never reached the Drug Experience Division, (2) an additional 14% had been received but either had not been evaluated or were in a backlog waiting to be entered into the system, and (3) reports that had been entered into the system [were entered] an average of five months [after they were received at FDA]."*

This was not the first time the GAO had delved into FDA's ADR reporting system. In fact, it was a follow-up to a 1974 report that had pointed out many qualitatively similar deficiencies. In its current 1982 report, the GAO concluded that the new review *"of FDA's monitoring of prescription drugs showed that many of the problems found in 1974 still exist."*

Now in the spring of 1983, the efficiency and effectiveness of the FDA's system has again come into question.

As part of the "fallout" from the Zomax recall, the U.S. House of Representatives Subcommittee on Intergovernmental Relations held oversight hearings on April 26–27 specifically targeted at reviewing (*a*) the decision to approve the marketing of Zomax, (*b*) the ADR reports that followed its approval, and (*c*) the decision to remove it—at least temporarily—from the market. And from those specific considerations, questions and concerns gradually broadened to the more general subject of the agency's ADR reporting system in overall.

Press reports summarizing the two-day congressional hearing cryptically concluded that even FDA officials admit significant flaws still exist in the system. For example, *The Wall Street Journal* reported:

"The FDA's system for tracking reports of adverse drug reactions is significantly flawed, agency officials suggested in congressional testimony.

"One official told a House subcommittee that he had been surprised to learn from Johnson & Johnson that the company knew of nearly twice as many instances of adverse reactions (1,100) from its prescription pain reliever Zomax than the agency had known about (500 to 600)."

Our purpose here is not to point an accusing finger at FDA or anyone else. The FDA has long recognized its weakness in this area and explains that limitations of personnel and resources are the root cause of such weakness in this as well as several other areas of its responsibility. This prompts many agency observers to wonder whether some readjustment of its priorities and budgetary allocations might not significantly relieve the situation.

But, for purposes of our present consideration, let us accept the FDA's explanation at face value. Doing so suggests to us that the broad issue of postmarketing drug surveillance, that was such a dominant health care concern 3 to 5 years ago—if not *the* dominant concern—is still very much alive. It has not been resolved. It has not gone away. It has simply been pushed aside. And it has been pushed aside not only by FDA but also by other relevant groups—the drug industry, health care practitioners, their professional societies, and pertinent trade and consumerist organizations.

Although practically studied to death by various groups and organizations in the mid- to late-1970s, followed by the usual pattern of reports and recommendations, no clear-cut simple solution to the problem was identified. About the most that interested analysts seemed to be able to agree upon was that efforts should be directed at expanding and upgrading the existing system and fostering a greater awareness among practitioners for their need to participate as an on-going practice.

It is human nature that old, chronic problems spark little interest, and correspondingly little attention is usually devoted to them. In this instance, the potential major health hazards are clearly evident. Hence, they dictate that we cannot allow disinterest or "boredom" to divert us from devoting the needed efforts and resources toward improving this "significantly flawed" system.

—EDWARD G. FELDMANN
American Pharmaceutical Association
Washington, DC 20037

0022-3549/83/0600-0585$01.00/0

JOURNAL OF PHARMACEUTICAL SCIENCES

JUNE 1983
VOLUME 72 NUMBER 6

RESEARCH ARTICLES

Extended Hildebrand Solubility Approach: *p*-Hydroxybenzoic Acid in Mixtures of Dioxane and Water

P. L. WU * and A. MARTIN ˣ

Received April 5, 1982, from the *Drug Dynamics Institute, College of Pharmacy, University of Texas, Austin, TX 78712.* Accepted for publication June 2, 1982. *Present address: China Chemical & Pharmaceutical Company, Shu-Lin, Taipei, Taiwan 00238, ROC.

Abstract □ The extended Hildebrand solubility approach was used to reproduce the solubilities of *p*-hydroxybenzoic acid in a dioxane–water system. The solubility parameter of *p*-hydroxybenzoic acid was determined and found to be ~15 $(cal/cm^3)^{1/2}$. Residual plots (scattergrams) were used in conjunction with R^2, F, and standard deviation values to determine whether a quadratic, cubic, quartic, or higher degree polynomial was required in the calculations. The earlier iteration method for back-calculations of solubilities was replaced by the more reliable root-finder method[1]. The solubility profile of *p*-hydroxybenzoic acid in dioxane–water mixtures did not follow a log linear relationship even in the ranges where the solubility parameters of the water–cosolvent mixture might be expected to produce a straight-line function, as observed in other studies.

Keyphrases □ Dioxane—extended Hildebrand solubility approach, *p*-hydroxybenzoic acid, water □ *p*-Hydroxybenzoic acid—extended Hildebrand solubility approach, water □ Hildebrand solubility approach, extended—*p*-hydroxybenzoic acid in mixtures of dioxane and water □ Solubility parameters—*p*-hydroxybenzoic acid in mixtures of dioxane and water

The theory of solutions is one of the most challenging and least understood branches of physical chemistry. The Hildebrand–Scatchard theory of regular solution (1–3) is the pioneer approach in this field. In recent years the solubility parameter concept has been extended to the practical realm of industrial and commercial paints, inks, polymers, plastics, insecticides, and pharmaceuticals. Recently, the Hildebrand–Scatchard equation has been successfully modified and the solubilities of methylxanthines estimated in binary solvents within an error of ≤10% values approximating those of experimentally determined solubilities (4, 5). The original Hildebrand–Scatchard equation has been discussed in a number of papers (4–6) in this series and need not be repeated here.

[1] International Mathematical and Statistical Library.

BACKGROUND

The Hildebrand–Scatchard approach may be used to estimate solubility only for relatively nonpolar drugs in nonpolar solvents according to regular solution theory (1). The solubility parameter, δ, is the square root of cohesive energy density (1), with subscripts 1 and 2 for solvent and solute, respectively. In pharmaceutical solutions, the geometric mean (1) of δ_1^2 and δ_2^2, that is, $\delta_1\delta_2 = (\delta_1^2\delta_2^2)^{1/2}$, is too restrictive and ordinarily provides a poor fit to experimental data in irregular solutions. Instead, $\delta_1\delta_2$ can be replaced by W, which is allowed to take on values as required to yield correct mole fraction solubilities, X_2:

$$-\log X_2 = -\log X_2^i + A(\delta_1^2 + \delta_2^2 - 2W) \qquad \text{(Eq. 1)}$$

where

$$\log X_2^i \cong \frac{\Delta H_m^f}{2.303R}\left(\frac{1}{T_m} - \frac{1}{T}\right) \qquad \text{(Eq. 2)}$$

and

$$A = \frac{V_2\phi_1^2}{2.303RT} \qquad \text{(Eq. 3)}$$

ΔH_m^f is the heat of fusion of the solute and R is the gas constant. T_m is the melting point of the solute, T is the temperature of interest, and both are in °K. The volume fraction of the solvent (ϕ_1) is expressed as:

$$\phi = \frac{V_1(1 - X_2)}{V_1(1 - X_2) + V_2X_2} \qquad \text{(Eq. 4)}$$

V_1 and V_2 are the molar volumes of solvent and supercooled solute, respectively. For drugs in binary solvent mixtures, it has been found (4–6) that the W values may be regressed in a power series on the solvent solubility parameters:

$$W = C_0 + C_1\delta_1 + C_2\delta_1^2 + \ldots\ldots + C_n\delta_1^n \qquad \text{(Eq. 5)}$$

One obtains a reasonable estimate, W_{calc}, by this procedure. W_{calc} is then substituted in Eq. 1 for W to obtain mole fraction solubilities in polar binary solvents which are usually within <10% of the experimental results.

According to well-known thermodynamic principles, the relationship of mole fraction solubility to ideal mole fraction solubility and activity coefficient may be expressed as:

$$-\log X_2 = -\log X_2^i + \log \alpha_2 \qquad \text{(Eq. 6)}$$

0022-3549/83/0600-0587$01.00/0

Table I—Solubility of *p*-Hydroxybenzoic Acid in Dioxane–Water Mixtures at 25 [a]

Volume Fraction of Dioxane, f	Solubility parameter, δ_1	Molar Volume, V_1	Mole Fraction Solubility, X_2	Solubility, S_2, moles/liter	A [b]	K [c]	δ_{app} [d]	Equation 18 $\log \alpha_2/A$ (obs)	Equation 18 $\log \alpha_2/A$ (calc)	Equation 18 $X_{2\,calc}$	Equation 18 Residual	Equation 18 Percent Error
0.0	23.45	18.08	0.00060	0.0335	0.0687	1.070	23.42	15.96	16.02	0.00059	0.00001	1.7
0.20	20.76	21.22	0.0072	0.330	0.0649	1.047	20.59	0.25	−0.01	0.0075	−0.0003	−4.2
0.45	18.07	25.88	0.0302	1.06	0.0558	1.034	17.79	−10.87	−10.50	0.0291	0.0011	3.6
0.50	16.73	29.20	0.0478	1.45	0.0512	1.034	16.53	−15.75	−15.59	0.0472	0.0006	1.3
0.55	16.06	31.25	0.0585	1.64	0.0490	1.038	15.94	−18.23	−18.13	0.0581	0.0004	0.7
0.60	15.39	33.65	0.0710	1.83	0.0469	1.044	15.37	−20.86	−20.58	0.0699	0.0011	1.5
0.65	14.71	36.33	0.0820	1.95	0.0456	1.052	14.82	−22.84	−22.90	0.0823	−0.0003	−0.4
0.70	14.04	39.64	0.0939	2.05	0.0445	1.061	14.29	−24.70	−24.88	0.0947	−0.0008	−0.9
0.80	12.70	48.32	0.115	2.10	0.0439	1.087	13.23	−27.05	−27.24	0.116	−0.001	−0.9
0.85	12.03	54.27	0.121	2.02	0.0450	1.102	12.67	−28.93	−27.22	0.123	−0.002	−1.7
0.90	11.33	61.84	0.127	1.89	0.0463	1.122	12.05	−26.60	−25.98	0.123	0.004	3.1
0.95	10.68	71.84	0.122	1.62	0.0494	1.141	11.42	−24.59	−23.44	0.114	0.008	6.6
1.00	10.01	85.71	0.0844	0.968	0.0570	1.152	10.52	−18.47	−19.09	0.0890	−0.0046	−5.5

[a] V_2 = 94.35 cm³/mole, δ_2 = 15.3 (cal/cm³)$^{1/2}$, $X_2{}^i$ = 0.00747, log $X_2{}^i$ = −2.1267. [b] Eqs. 3 and 4. [c] $K = W/\delta_1\delta_2$, a proportionality factor (13). [d] Eq. 15.

where α_2 is the activity coefficient of the solute in the solution. Equation 1 may be written, in light of Eq. 6, as:

$$\log\left(\frac{X_2{}^i}{X_2}\right) = \log \alpha_2 = A(\delta_1{}^2 + \delta_2{}^2 - 2W) \qquad \text{(Eq. 7)}$$

and

$$(\log \alpha_2)/A = \delta_1{}^2 + \delta_2{}^2 - 2W \qquad \text{(Eq. 8)}$$

Log α_2/A may be regressed directly against δ_1, bypassing W, and obviating the need for δ_2 as described in earlier work (6). The estimated solubility, $X_{2\,calc}$, is identical to that obtained with W_{calc} except for rounding-off errors. The entire procedure, referred to as the Extended Hildebrand Solubility Approach (4), is conducted by a computer program, the regression subroutine of which is found in SPSS (7). The program allows a stepwise addition of independent variables, analysis of variance, and examination of the residuals, $X_2 - X_{2\,calc}$, by means of scatter plots. These plots are useful in indicating when the proper degree of the polynomial has been reached.

EXPERIMENTAL

Materials—*p*-Hydroxybenzoic acid[2] was recrystallized from aqueous ethanol (8) then dried at 105° overnight. The heat of fusion, 7510 cal/mole, of *p*-hydroxybenzoic acid was determined by differential scanning calorimetry[3]. The melting point obtained from this method is 485.9°K which is consistent with the value from a hot-stage method[4]. A pure grade of dioxane[5] was used as received. Since *p*-hydroxybenzoic acid is a weak acid with pK_a equal to 4.54 ($K_a = 2.9 \times 10^{-5}$) at 25° (9), the pH of water affects its solubility. Furthermore, the dissociation constant, K_a, decreases in organic aqueous mixtures (9, 10). To ensure that the *p*-hydroxybenzoic acid was in undissociated form, the pH of the water was adjusted to 2.0 using hydrochloric acid. The pH 2 hydrochloric acid–aqueous solution was used alone or mixed with dioxane as the binary solvent for this study.

Solubility Analysis—The solubility of *p*-hydroxybenzoic acid was determined in binary solvent mixtures of dioxane and water. A suitable amount of dioxane, water, or binary solvent was introduced into screw-capped vials containing an excess amount of solute. After being sealed with several turns of electrical tape, the vials were submerged in water at 25 ± 0.1° and were shaken at 100 cpm for 24 hr in a constant-temperature bath[6]. Preliminary studies showed that this time period was sufficient to ensure saturation at 25°.

After equilibrium had been attained, each vial was removed and analyzed. The solutions were transferred to a syringe and filtered using a filter[7] of pore size <1 μm. After suitable dilution, the solutions were assayed using a spectrophotometer[8] set at the wavelength of maximum absorption of the solute. The solubility of the solute was determined at least six times for each solvent, and the average value was taken. The experimental variation in solubility was <3% in replicate samples and was consistent with a titrimetric assay method used with a number of samples. The densities of the saturated solutions were determined with calibrated pycnometers at 25° and the variation was <0.03% for six determinations.

Stability of Solute—The stability of the solute was tested by subjecting the saturated solutions to TLC[9] using 2-propanol–ammonia–water (8:1:1) (11) as a developing system, then observing the developed TLC plate under a long wavelength UV-lamp[10]. There was no evidence of decomposition within 36 hr.

Ideal Solubility—The ideal solubility of *p*-hydroxybenzoic acid may be calculated from the heat of fusion of the solid and the melting temperature:

$$\log X_2{}^i \cong \frac{\Delta H_m{}^f}{2.303R}\left(\frac{1}{T_m} - \frac{1}{T}\right) \qquad \text{(Eq. 9)}$$

$$\log X_2{}^i = \frac{7510}{(2.303)(1.987)}\left(\frac{1}{485.9} - \frac{1}{298.15}\right)$$

giving:

$$\log X_2{}^i = -2.127 \qquad X_2 = 0.00747$$

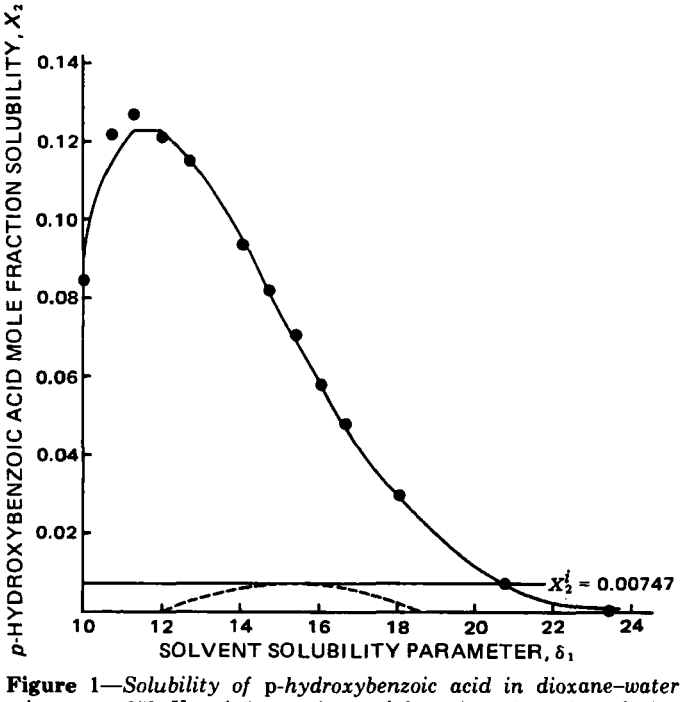

Figure 1—*Solubility of* p-*hydroxybenzoic acid in dioxane–water mixtures at 25°. Key: (●) experimental data; (- - - -) regular solution curve; (——) back calculation using regression equation, Eq. 18.*

[2] Matheson Coleman Bell, Norwood, OH 45212.
[3] Perkin-Elmer DSC Model 1 B, Norwalk, Conn.
[4] Digital Melting Point Analyzer Model 335, Fisher Scientific Co., Fair Lawn, NJ 07410.
[5] Mallinckrodt Chemical Works, St. Louis, MO 63160.
[6] Blue-M Electric Co., Blue Island, Ill.
[7] Filter Paper, Glass Fiber, Whatman Grade FG/F.
[8] Beckman Model 25 Spectrophotometer.
[9] Polygram SILG/UV 254, Brinkman Instruments, Inc., Westbury, NY 11590.
[10] Chromato-VUE Cabinet Model CC-20, Ultra-Violet Products, Inc., San Gabriel, Calif.

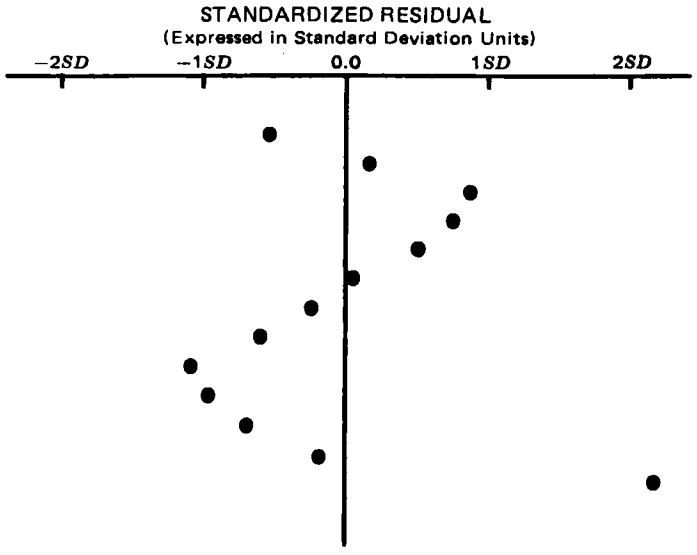

No.	log α / A (calc)	Residual	SD units
1	17.2444	-1.2875	-0.56
2	-0.1179	0.3633	0.16
3	-12.8684	2.0037	0.87
4	-17.4991	1.7514	0.76
5	-19.3853	1.1607	0.50
6	-20.9854	0.1226	0.05
7	-22.3169	-0.5243	-0.23
8	-23.3405	-1.3574	-0.59
9	-24.5295	-2.5171	-1.09
10	-24.6949	-2.2385	-0.97
11	-24.5620	-2.0389	-0.89
12	-24.1590	-0.4257	-0.19
13	-23.4618	4.9874	2.17

Figure 2—*Plot of residuals obtained from quadratic regression equation, Eq. 16, for p-hydroxybenzoic acid in dioxane–water mixtures at 25°. (Log α_2)/A_{calc} is plotted along the vertical axis and residuals along the horizontal axis as described in this report. The residual in Table I is the difference between the observed x_2 and x_{2calc}, whereas the residuals in Figs. 2, 3, and 4 are [(logα_2)/A(obs)] − [(logα_2)/ A(calc)].*

RESULTS AND DISCUSSION

The solubility of *p*-hydroxybenzoic acid in dioxane–water at 25° is found in Table I, and the solubility profile is shown in Fig. 1 where X_2 is plotted against δ_1.

Estimating the Solubility Parameter of *p*-Hydroxybenzoic Acid from its Solubility Profile—It has been shown (12) that the solubility parameter of a solid can be estimated from the point of maximum solubility in a binary solvent, such as ethyl acetate and ethanol. When a solvent mixture is found that yields a peak in the solubility profile for a regular solution, δ_1 is assumed to equal δ_2.

In an irregular solution, these relations do not obtain exactly as in a regular solution, and the geometric mean, $W_{12} = (\delta_1^2\delta_2^2)^{1/2}$, seldom can be assumed to apply. W_{12} and $\delta_1\delta_2$ may be related by introducing a proportionality factor, K (13)[11]:

$$W_{12} = K\delta_1\delta_2 \qquad \text{(Eq. 10)}$$

Equation 8 then becomes:

$$\frac{\log \alpha_2}{A} = \delta_1^2 + \delta_2^2 - 2K\delta_1\delta_2 \qquad \text{(Eq. 11)}$$

The partial derivative of (log α_2)/A is taken with respect to δ_1 and the result is set equal to zero to obtain the value of δ_2 at the peak in the solubility profile:

$$\left(\frac{\partial(\log \alpha_2/A)}{\partial(\delta_1)}\right)_{\delta_2} = 2\delta_1 - 2K\delta_2 = 0 \qquad \text{(Eq. 12)}$$

and

$$\delta_1 = K\delta_2 \qquad \text{(Eq. 13)}$$

Thus, in irregular solutions, δ_1 is not equal to δ_2 at the maximum in the solubility profile, but is equal to $K\delta_2$ (13). As can be seen in Table I and Fig. 1, the maximum solubility of *p*-hydroxybenzoic acid in dioxane–water is at a solvent solubility parameter of 11.33 (*i.e.*, dioxane–water 90:10%, v/v) and K = 1.122. Therefore, the solubility parameter of *p*-hydroxybenzoic acid is 10.10 as obtained from:

$$\delta_2 = \frac{\delta_1}{K} = \frac{11.33}{1.122} = 10.10 \text{ (cal/cm}^3)^{1/2} \qquad \text{(Eq. 14)}$$

Solubility parameters of solid drugs can also be obtained by a group contribution method developed by Fedors (15). The δ value of *p*-hydroxybenzoic acid obtained from Fedors' method[12] is 15.3. A method for obtaining the solubility parameter of a drug molecule using internal pressure values and accurately measured solution densities was also previously suggested (16).

It has been shown that the solubility parameter of the solute obtained from the peak of the solubility profile may vary depending on the mixed solvent used (6). If the cosolvent has the tendency to form a complex with the solute, the maximum solubility may be shifted to the δ_1 value of a mixed solvent which contains a high percentage of this solvating cosolvent. Dioxane is a Lewis base and *p*-hydroxybenzoic acid a Lewis acid; these molecules have a tendency to form a complex, which may account for the shift of maximum solubility to the lower δ_1 value of the dioxane–water mixture. It is not necessary to know δ_2 to calculate the solubility in mixed solvents, for it has been found (4–6) that the estimated solubility can be obtained from a regression of (log α_2)/A against δ_1, obviating the need of δ_2. The back calculation of *p*-hydroxybenzoic acid solubility in dioxane–water is discussed later.

Effect of Solute on the Solubility Parameter of the Solution—The amount of solute in a saturated solution may alter the solubility parameter of the reference solvent (17) when in high concentration, since:

$$\delta_{app} = \Sigma\delta_i\phi_i \qquad \text{(Eq. 15)}$$

where ϕ_i is the volume fraction of component i in the solution. The solubility parameters of the saturated solutions, δ_{app}, are listed in Table I. The two solubility parameters, δ_1 and δ_{app}, are almost identical when the mole fraction solubility is <0.1 (volume fraction of dioxane is <70%). The solubility parameter of the saturated solution is a little higher (less than one unit) than that of the reference solvent when the solvent mixture contains >80% of dioxane. In the extended Hildebrand approach, (log α_2)/A is regressed on the solubility parameter of the solvent in a polynomial equation. A similar approach can be taken by regressing (log α_2)/A against δ_{app}, the solubility parameter of the solution. These two solubility

Table II—Demonstration of Trial-and-Error Process for the Back-Calculation of *p*-Hydroxybenzoic Acid in Water Using Eqs. 18 and 19

Step	X_2	$f(X_2)$
1	0.001	−100323
2	0.0001	342188
3	0.0005	32358
4	0.0006	−2594
5	0.00055	14082
6	0.00058	3902
7	0.00059	626
8	0.000595	−990
9	0.000592	−21
10	0.0005917	75
11	0.0005919	10
12	0.00059195	−5
13	0.00059193	0

[11] It should be noted that K as defined by Walker (13) and used here does not have the same meaning as K employed in another previous paper (14). In Ref. 14, K is a constant for a solute over the entire composition of a binary solvent. Here, and in other papers of this series, K varies across the solvent composition. The constant in Ref. 14 should probably be designated by another symbol, such as κ (kappa) to prevent confusion.

[12] [83.94 (Phenylene) + 72.61 (CO_2H) + 78.33 (OH)]$^{1/2}$ = (234.88)$^{1/2}$ = 15.3 (cal/cm^3)$^{1/2}$.

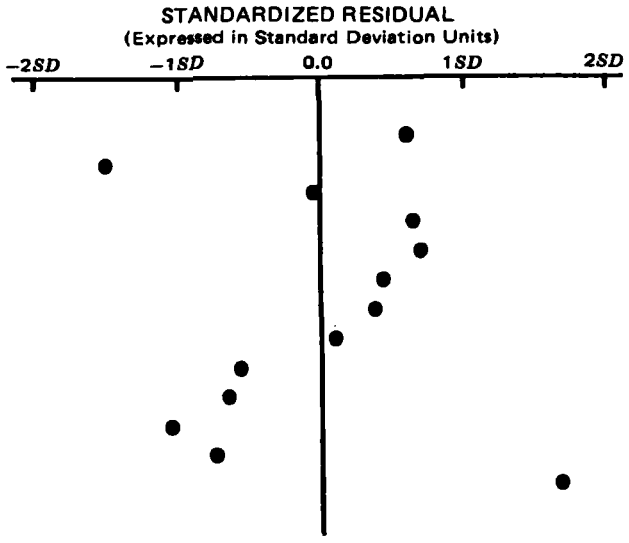

No.	$\frac{\log \alpha_2}{A}$ (calc)	Residual	SD units
1	15.0454	0.9115	0.59
2	2.5640	-2.3186	-1.50
3	-10.8254	-0.0393	-0.03
4	-16.7334	0.9857	0.64
5	-19.3055	1.0808	0.70
6	-21.5499	0.6871	0.44
7	-23.4366	0.5954	0.38
8	-24.8546	0.1567	0.10
9	-26.1580	-0.8886	-0.57
10	-25.9339	-0.9994	-0.65
11	-24.9973	-1.6036	-1.04
12	-23.4310	-1.1537	-0.75
13	-21.0603	2.5860	1.67

Figure 3—*Plot of residuals obtained from cubic regression equation, Eq. 17, for* p*-hydroxybenzoic acid in dioxane–water mixtures at 25°.*

parameter systems yield the same results except for rounding-off error.

Extended Hildebrand Approach Using Polynomial Regression and Scattergrams—The $(\log \alpha_2)/A$ for *p*-hydroxybenzoic acid was regressed against δ_1 values of dioxane–water mixtures at 25°. Three polynomial equations and associated statistical parameters[13] are quadratic:

$$\frac{\log \alpha_2}{A} = 21.02\ (\pm 10.36) - 7.6338\ (\pm 1.3152)\delta_1 + 0.31866\ (\pm 0.03984)\delta_1^2 \quad \text{(Eq. 16)}$$

$n = 13, s = 2.30, r^2 = 0.972, F = 173, F(2, 10, 0.01) = 7.56$

cubic:

$$\frac{\log \alpha_2}{A} = 142.51\ (\pm 34.32) - 31.582\ (\pm 6.683)\delta_1 + 1.82625\ (\pm 0.41788)\delta_1^2 - 0.0303307\ (\pm 0.0083899)\delta_1^3 \quad \text{(Eq. 17)}$$

$n = 13, s = 1.55, r^2 = 0.989, F = 259, F(3, 9, 0.01) = 6.99$

and quartic:

$$\frac{\log \alpha_2}{A} = 564.07\ (\pm 54.45) - 142.18\ (\pm 14.12)\delta_1 + 12.396\ (\pm 1.339)\delta_1^2 - 0.46689\ (\pm 0.05504)\delta_1^3 + 0.0065807\ (\pm 0.0008284)\delta_1^4 \quad \text{(Eq. 18)}$$

$n = 13, s = 0.55, r^2 = 0.999, F = 1550, F(4, 8, 0.01) = 7.01$

The residual plots (scattergrams) (7) of these equations are shown in Figs. 2–4 for quadratic, cubic, and quartic, respectively. In the figures, the horizontal axis represents the residuals standardized by dividing each by its standard deviation, while the vertical axis represents $(\log \alpha_2)/A_{calc}$ against which the residuals are plotted. The residual, or deviation of an estimated value, $(\log \alpha_2)/A_{calc}$, from the observed value, $(\log \alpha_2)/A_{obs}$, indicates which regression equation is the most suitable. As can be seen in Fig. 2, the residuals are not randomly scattered along the vertical axis. Therefore, the quadratic equation is not satisfactory, although R^2 is very high. In Fig. 3 the ordered arrangement of the points of Fig. 2 has mostly disappeared, and in Fig. 4 the residuals are scattered randomly along the vertical axis. None of the points in Fig. 4 is outside of a range of 2 σ. By comparing the statistics of the quadratic, cubic, and quartic equations (Eqs. 16, 17, and 18), it is observed that the quartic equation is the best choice due to its high r^2 and F values, and its small s value. The random scattering of points in the scattergram also shows Eq. 18 to be superior.

[13] The statistical quantities associated with each equation are: r^2 is the squared correlation coefficient (index of determination); s is the standard deviation or average of deviations about the arithmetic mean; F is the Fisher F ratio; n is the number of cases; and $F(k, n-k-1, 0.01)$ is the table value of F with k-independent variables; and k and $(n-k-1)$ degrees of freedom at the 99% confidence level. The ± values in parentheses associated with each regression coefficient, B, is the standard error of B.

In the back calculation, $(\log \alpha_2)/A_{calc}$ obtained from Eq. 18 was multiplied by A and the antilog was taken to obtain the activity coefficient, α_{2calc}. The estimated solubility was obtained from $X_{2\ calc} = X_2^i/\alpha_{2\ calc}$.

The values of A as listed in Table I are calculated (see Eqs. 3 and 4) from experimental solubilities and molar volumes. The back-calculated solubilities may be obtained using Eqs. 3 and 4 and an iteration procedure (18) beginning with a value of 1.0 for ϕ_1 and iterating until X_2 or ϕ_1 no longer changes by more than some desired small value. However, a simple iteration procedure does not always behave in a well-conditioned manner. Assuming that the quartic equation (Eq. 18) is a function of δ_1, *i.e.*, $f(\delta_1)$, and combining it with Eqs. 3 and 4, one obtains:

$$f(X_2) = (\log X_2{}^i - \log X_2)(2.303RT)[V_1(1-X_2) + V_2X_2]^2 - V_2[V_1(1-X_2)]^2 f(\delta_1) = 0 \quad \text{(Eq. 19)}$$

X_2 can now be solved by a trial-and-error root finding method. For example, in pure water, $f_D = 0$, $\delta_1 = 23.45$, $\delta_2 = 15.3$ (cal/cm^3)$^{1/2}$, $V_1 = 18.08$, $V_2 = 94.35$ and $\log X_2{}^i = -2.1267$, and substituting 23.45 for δ_1 in Eq. 18 one obtains $f(\delta_1) = (\log \alpha_2)/A_{calc} = 16.020$. Table II lists the steps during the trial-and-error procedure. This computation can be carried out easily by use of a programmable hand calculator. The root finder subroutine, ZBRENT, found in IMSL (19) can also be used for the computation; the earlier iteration procedure of the extended Hildebrand solubility approach has been replaced in this study by the root finder method (19). The back-calculated solubilities from Eq. 18 are listed in Table I and also plotted in Fig. 1. The results compare well with the observed solubilities, having errors <7%.

Log Solubility and Volume Fraction of the Cosolvent—A log linear relationship between moles/liter or mole fraction solubility and volume fraction of the cosolvent has been proposed (20, 21). The log solubility of *p*-hydroxybenzoic acid in units of moles/liter and mole fraction were plotted against the volume fraction of the cosolvent, dioxane, in Fig. 5 to test whether this relationship holds for *p*-hydroxybenzoic acid solutions. Also marked along the horizontal axis (top of the figure) is the solubility parameter of the mixed solvents. It is evident from Fig. 5 that a log linear relation is not observed in the binary solvent mixture, dioxane and water, as the curves are quite nonlinear. They can, however, be reproduced by use of the following quadratic expressions:

$$\log S_2 = -1.430(\pm 0.050) + 4.874(\pm 0.192)f - 3.374(\pm 0.175)f^2$$
$$r^2 = 0.990, s = 0.056, F = 474, F(2, 10, 0.01) = 7.56 \quad \text{(Eq. 20)}$$

and

$$\log X_2 = -3.178(\pm 0.051) + 5.226(\pm 0.194)f - 3.047(\pm 0.176)f^2$$
$$r^2 = 0.994, s = 0.057, F = 806, F(2, 10, 0.01) = 7.56 \quad \text{(Eq. 21)}$$

where S_2 is the molar and X_2 the mole fraction solubility of *p*-hydroxybenzoic acid in dioxane–water mixtures with various volume fractions f of dioxane at 25°.

In another study (22) it was shown that the log linear rule often holds for drugs in binary solvents of water combined with an organic cosolvent particularly when the cosolvent interacts strongly with the solute and when the solubility parameter of the cosolvent is several units above that

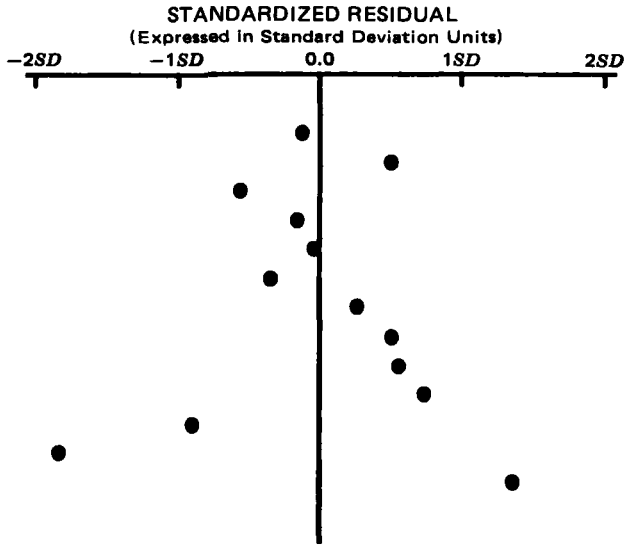

No.	$\frac{\log \alpha_2}{A}$ (calc)	Residual	SD units
1	16.0248	-0.0679	-0.12
2	-0.0327	0.2781	0.50
3	-10.5570	-0.3077	-0.56
4	-15.6597	-0.0880	-0.16
5	-18.2040	-0.0206	-0.04
6	-20.6693	-0.1935	-0.35
7	-22.9922	0.1510	0.27
8	-24.9750	0.2771	0.50
9	-27.3573	0.3107	0.56
10	-27.3418	0.4085	0.74
11	-26.1098	-0.4911	-0.89
12	-23.5708	-0.0139	-1.84
13	-19.2316	0.7572	1.39

Figure 4—*Plot of residuals obtained from quartic regression equation, Eq. 18, for* p*-hydroxybenzoic acid in dioxane–water mixtures at 25°. The almost complete scatter here indicates that Eq. 18 is superior to Eqs. 16 and 17 (Figs. 2 and 3).*

of the solute. Although dioxane appears to interact with *p*-hydroxybenzoic acid and elevates the solubility of the drug above the ideal solubility line, X_2^i, dioxane does not solvate or complex the solute sufficiently to yield a straight line relationship. Furthermore, the solubility parameter of *p*-hydroxybenzoic acid lies between the solubility parameters of water and dioxane and this militates against a log linear relationship. Instead, these conditions create a peak value on a plot of log solubility *versus* volume fraction of cosolvent or *versus* solubility parameter of mixed solvent.

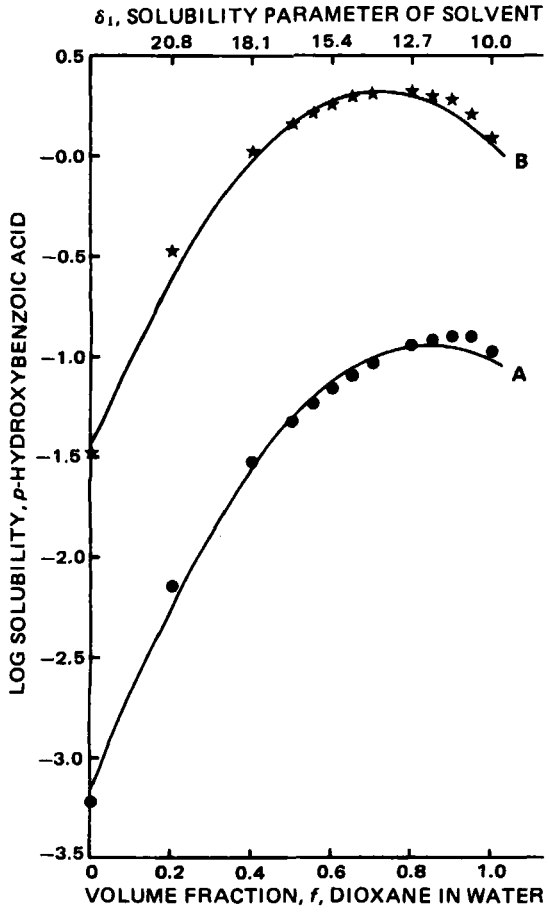

Figure 5—*Log solubility of* p*-hydroxybenzoic acid in dioxane–water mixtures at 25°. Curves A and B are back-calculated from Eqs. 21 and 20, respectively. Key: (★) moles/liter; (●) mole fraction.*

CONCLUSIONS

The solubility parameter of *p*-hydroxybenzoic acid was estimated by determining the peak in the solubility profile, Fig. 1, and by a group-contribution method (15). Interaction of the solute with the cosolvent, dioxane, may have unduly lowered the δ_2 value obtained by the peak solubility technique. The two methods do not yield values that agree closely; the δ_2 value was taken as ~15 $(cal/cm^3)^{1/2}$, a reasonable value for this highly polar compound.

The effect of a saturated solution of the solute on the solubility parameter of the mixed solvent was tested in this system and was found not to influence δ_1 markedly. In predicting solubilities using the extended Hildebrand solubility approach, the slight effect on δ_1 does not change the back-calculated solubility values.

To estimate solubilities of *p*-hydroxybenzoic acid in mixtures of dioxane and water, $(\log \alpha_2)/A$ was regressed in a polynomial on δ_1 of the solvent mixtures according to the extended Hildebrand solubility approach. The residual plots (scattergrams) for the quadratic, cubic, and quartic equations serve together with the standard deviation, r^2 and F values to indicate whether a quadratic equation is satisfactory or whether a cubic, quartic, or higher-order polynomial is required to fit the data. From an analysis of r^2, F, and the scattergram, it was observed that the quartic equation was required to reproduce the solubility data of *p*-hydroxybenzoic acid.

The iteration procedure for the back-calculation of solubilities was studied in detail in this paper, because it was found to be a problem in earlier works, causing an oscillation between two values or a divergence rather than convergence to the proper mole fraction solubility. A root finder method, involving trial-and-error, or better, use of an IMSL subroutine [ZBRENT (19)] proved to be the solution to this problem.

The solubility of *p*-hydroxybenzoic acid in dioxane–water mixtures was observed not to follow a log linear relationship: a regularity earlier observed for some drugs in water combined with nonaqueous cosolvents. The failure of the log linear relationship is expected (22) in this case, however, since the solubility parameter of *p*-hydroxybenzoic acid ($\delta_2 \simeq 15$) lies between that of water ($\delta_1 = 23.4$) and the cosolvent, dioxane ($\delta_1 = 10$).

REFERENCES

(1) J. H. Hildebrand and R. L. Scott, "Regular Solution," Prentice-Hall, Englewood Cliffs, N.J., 1962.

(2) J. H. Hildebrand and R. L. Scott, "The Solubility of Nonelectrolytes," 3rd ed., Dover, New York, N.Y., 1964.

(3) G. Scatchard, *Chem. Rev.*, **8**, 321 (1931).

(4) A. Martin, J. Newburger, and A. Adjei, *J. Pharm. Sci.*, **69**, 487 (1980).

(5) A. Martin, J. Newburger, and A. Adjei, *J. Pharm. Sci.*, **69**, 659 (1980).

(6) A. Martin, A. N. Paruta, and A. Adjei, *ibid.*, **70**, 1115 (1981).

(7) N. H. Nie, C. H. Hull, J. G. Jenkins, K. Steinbrenner, and D. H.

Bent, "SPSS, Statistical Package for the Social Sciences," 2nd ed., McGraw-Hill, New York, N.Y., 1975, Chap. 20.
(8) C. K. Hancock, J. N. Pawloski, and J. P. Indoux, *J. Org. Chem.*, **31**, 3801 (1966).
(9) G. E. K. Branch and D. L. Yabroft, *J. Am. Chem. Soc.*, **56**, 2568 (1934).
(10) W. L. Bright and H. T. Briscoe, *J. Phys. Chem.*, **37**, 787 (1933).
(11) H. Seligson, B. Kramer, D. Seligson, and H. Baltrush, *Anal. Biochem.*, **6**, 362 (1963).
(12) M. J. Chertkoff and A. Martin, *J. Am. Pharm. Assoc. Sci. Ed.*, **49**, 444 (1960).
(13) E. E. Walker, *J. Appl. Chem.*, **2**, 470 (1952).
(14) A. Martin and J. Carstensen, *J. Pharm. Sci.*, **70**, 170 (1981).
(15) R. F. Fedors, *Polym. Eng. Sci.*, **14**, 147 (1974).
(16) S. Cohen, A. Goldschmid, G. Shtacher, S. Srebrenik, and S. Gitter, *Mol. Pharmacol.*, **11**, 379 (1975).
(17) S. A. Khalil and A. Martin, *J. Pharm. Sci.*, **56**, 1225 (1967).
(18) A. Martin, J. Swarbrick, and A. Cammarata, "Physical Pharmacy," 2nd ed., Lea & Febiger, Philadelphia, Pa., 1969, p. 303.
(19) "IMSL Reference Manual," International Mathematical and Statistical Libraries, Houston, Texas, 1979.
(20) S. H. Yalkowsky, G. L. Flynn, and G. L. Amidon, *J. Pharm. Sci.*, **61**, 983 (1972).
(21) S. H. Yalkowsky, S. C. Valvani, and G. L. Amidon, *ibid.*, **65**, 1488 (1976).
(22) A. Martin, P. L. Wu, A. Adjei, R. Lindstrom, and P. Elworthy, *ibid.*, **71**, 849 (1982).

ACKNOWLEDGMENTS

Support was obtained in part from the professorship provided to A. Martin by Coulter R. Sublett.

The authors thank Alan Burbower, Energy Center, University of California at San Diego for advice and assistance.

Molecular Interaction Between Riboflavin and Salicylic Acid Derivatives in Nonpolar Solvents

BYUNG SUL YU ˣ, SANG JONG LEE, SEUNG JIN LEE, and HYUN HO CHUNG

Received November 23, 1981, from the *Department of Physical Pharmacy, College of Pharmacy, Seoul National University, San 56-1, Shinrim-Dong, Kwanak-Ku, Seoul 151, Korea.* Accepted for publication June 2, 1982.

Abstract □ The interaction of riboflavin-2′,3′,4′,5′-tetrabutyrate (I) with salicylic acid (II), aspirin (acetylsalicylic acid, III), and salicylamide (IV) has been spectroscopically investigated to determine the binding mechanism. NMR and absorption spectra were measured in nonpolar solvents. The association constant K of the formation of complex was calculated from the absorption spectra. Compounds I and II form a 1:1 cyclic hydrogen-bonded dimer through the N-3 proton and the C-2 carbonyl oxygen of the isoalloxazine ring, and the carboxylic hydroxyl proton and carbonyl oxygen of II. Compounds I and III form a 1:1 cyclic hydrogen-bonded dimer by the same mode. Compound IV forms a 1:1 cyclic hydrogen-bonded dimer with I through the N-3 proton and the C-2 carbonyl oxygen of the isoalloxazine ring, and the amino proton and the carbonyl oxygen of IV. Salicylates produce marked changes in the absorption spectra of I. These spectral changes are attributed to the formation of the hydrogen-bonded dimer. It appeared that the strongest complex was formed with salicylic acid, a weaker one with aspirin, and an even weaker one with salicylamide.

Keyphrases □ Riboflavin—molecular interactions with salicylic acid derivatives, NMR and absorption spectroscopy in nonpolar solvents, association constant determinations for hydrogen-bonded dimers □ Salicylates—molecular interactions with riboflavin, NMR and absorption spectroscopy in nonpolar solvents, association constant determinations for hydrogen-bonded dimers

Salicylate, one of the oldest synthetic drugs, remains the most widely used analgesic and antipyretic agent. It is known that the hydrogen bonding of salicylates in biological systems is related to their drug action (1). It has been determined experimentally that higher concentrations of salicylates result in marked stimulation of respiration while low concentrations depress this function (2–7). Salicylic acid derivatives act as uncoupling agents on the isolated mitochondrial respiration and lower the respiration rate of dinitrophenol-uncoupled mitochondria; inhibition of state 3 mitochondrial respiration by salicylic acid derivatives is accompanied by an increase in the oxidized state of all electron transport systems (8).

The electron-transfer from nicotinamide adenine dinucleotide (NADH) to flavoprotein, or the charge-transfer complex thus formed, was studied by a number of authors to give an account of the function of the respiratory chain (9–13). It has been determined that reduced NAD-coupling enzyme[1] complex converts spontaneously to the hypothetical intermediate as oxidized NAD-coupling enzyme[2], which is considered indispensable to the formation of adenosine triphosphate (ATP) in the respiratory chain (14). Simultaneously, the electrons in $(NADox)^{-2}$ can be transferred to flavoprotein. It is generally agreed that salicylates, which act as uncoupling agents, cause the breakdown of some high-energy intermediate involved in the phosphorylation process. However, the mechanism of such a breakdown has not previously been determined. The mechanism of action of salicylate could be described as: (*a*) salicylate associates with the adenine moiety of flavin adenine dinucleotide (FAD) or NAD, (*b*) salicylate inhibits the interaction of the flavin moiety with the adenine moiety of FAD or NAD, (*c*) salicylate affects the electronic environment due to an association with flavin, or (*d*) salicylate inhibits the interactions of FAD and the flavin mononucleotide (FMN) with apoprotein. Therefore, it seems worthwhile to examine the molecular interaction between salicylate and riboflavin. In this paper a detailed analysis of the NMR and absorption spectra of the complex will be presented and a structure of the complex will

[1] Enzyme-coupled reduced nicotinamide adenine dinucleotide.
[2] Enzyme-coupled oxidized nicotinamide adenine dinucleotide.

0022-3549/83/0600-0592$01.00/0

Bent, "SPSS, Statistical Package for the Social Sciences," 2nd ed., McGraw-Hill, New York, N.Y., 1975, Chap. 20.
(8) C. K. Hancock, J. N. Pawloski, and J. P. Indoux, *J. Org. Chem.*, **31**, 3801 (1966).
(9) G. E. K. Branch and D. L. Yabroft, *J. Am. Chem. Soc.*, **56**, 2568 (1934).
(10) W. L. Bright and H. T. Briscoe, *J. Phys. Chem.*, **37**, 787 (1933).
(11) H. Seligson, B. Kramer, D. Seligson, and H. Baltrush, *Anal. Biochem.*, **6**, 362 (1963).
(12) M. J. Chertkoff and A. Martin, *J. Am. Pharm. Assoc. Sci. Ed.*, **49**, 444 (1960).
(13) E. E. Walker, *J. Appl. Chem.*, **2**, 470 (1952).
(14) A. Martin and J. Carstensen, *J. Pharm. Sci.*, **70**, 170 (1981).
(15) R. F. Fedors, *Polym. Eng. Sci.*, **14**, 147 (1974).
(16) S. Cohen, A. Goldschmid, G. Shtacher, S. Srebrenik, and S. Gitter, *Mol. Pharmacol.*, **11**, 379 (1975).
(17) S. A. Khalil and A. Martin, *J. Pharm. Sci.*, **56**, 1225 (1967).
(18) A. Martin, J. Swarbrick, and A. Cammarata, "Physical Pharmacy," 2nd ed., Lea & Febiger, Philadelphia, Pa., 1969, p. 303.
(19) "IMSL Reference Manual," International Mathematical and Statistical Libraries, Houston, Texas, 1979.
(20) S. H. Yalkowsky, G. L. Flynn, and G. L. Amidon, *J. Pharm. Sci.*, **61**, 983 (1972).
(21) S. H. Yalkowsky, S. C. Valvani, and G. L. Amidon, *ibid.*, **65**, 1488 (1976).
(22) A. Martin, P. L. Wu, A. Adjei, R. Lindstrom, and P. Elworthy, *ibid.*, **71**, 849 (1982).

ACKNOWLEDGMENTS

Support was obtained in part from the professorship provided to A. Martin by Coulter R. Sublett.

The authors thank Alan Burbower, Energy Center, University of California at San Diego for advice and assistance.

Molecular Interaction Between Riboflavin and Salicylic Acid Derivatives in Nonpolar Solvents

BYUNG SUL YU ˣ, SANG JONG LEE, SEUNG JIN LEE, and HYUN HO CHUNG

Received November 23, 1981, from the *Department of Physical Pharmacy, College of Pharmacy, Seoul National University, San 56-1, Shinrim-Dong, Kwanak-Ku, Seoul 151, Korea.* Accepted for publication June 2, 1982.

Abstract □ The interaction of riboflavin-2′,3′,4′,5′-tetrabutyrate (I) with salicylic acid (II), aspirin (acetylsalicylic acid, III), and salicylamide (IV) has been spectroscopically investigated to determine the binding mechanism. NMR and absorption spectra were measured in nonpolar solvents. The association constant K of the formation of complex was calculated from the absorption spectra. Compounds I and II form a 1:1 cyclic hydrogen-bonded dimer through the N-3 proton and the C-2 carbonyl oxygen of the isoalloxazine ring, and the carboxylic hydroxyl proton and carbonyl oxygen of II. Compounds I and III form a 1:1 cyclic hydrogen-bonded dimer by the same mode. Compound IV forms a 1:1 cyclic hydrogen-bonded dimer with I through the N-3 proton and the C-2 carbonyl oxygen of the isoalloxazine ring, and the amino proton and the carbonyl oxygen of IV. Salicylates produce marked changes in the absorption spectra of I. These spectral changes are attributed to the formation of the hydrogen-bonded dimer. It appeared that the strongest complex was formed with salicylic acid, a weaker one with aspirin, and an even weaker one with salicylamide.

Keyphrases □ Riboflavin—molecular interactions with salicylic acid derivatives, NMR and absorption spectroscopy in nonpolar solvents, association constant determinations for hydrogen-bonded dimers □ Salicylates—molecular interactions with riboflavin, NMR and absorption spectroscopy in nonpolar solvents, association constant determinations for hydrogen-bonded dimers

Salicylate, one of the oldest synthetic drugs, remains the most widely used analgesic and antipyretic agent. It is known that the hydrogen bonding of salicylates in biological systems is related to their drug action (1). It has been determined experimentally that higher concentrations of salicylates result in marked stimulation of respiration while low concentrations depress this function (2–7). Salicylic acid derivatives act as uncoupling agents on the isolated mitochondrial respiration and lower the respiration rate of dinitrophenol-uncoupled mitochondria; inhibition of state 3 mitochondrial respiration by salicylic acid derivatives is accompanied by an increase in the oxidized state of all electron transport systems (8).

The electron-transfer from nicotinamide adenine dinucleotide (NADH) to flavoprotein, or the charge-transfer complex thus formed, was studied by a number of authors to give an account of the function of the respiratory chain (9–13). It has been determined that reduced NAD-coupling enzyme[1] complex converts spontaneously to the hypothetical intermediate as oxidized NAD-coupling enzyme[2], which is considered indispensable to the formation of adenosine triphosphate (ATP) in the respiratory chain (14). Simultaneously, the electrons in $(NADox)^{-2}$ can be transferred to flavoprotein. It is generally agreed that salicylates, which act as uncoupling agents, cause the breakdown of some high-energy intermediate involved in the phosphorylation process. However, the mechanism of such a breakdown has not previously been determined. The mechanism of action of salicylate could be described as: (*a*) salicylate associates with the adenine moiety of flavin adenine dinucleotide (FAD) or NAD, (*b*) salicylate inhibits the interaction of the flavin moiety with the adenine moiety of FAD or NAD, (*c*) salicylate affects the electronic environment due to an association with flavin, or (*d*) salicylate inhibits the interactions of FAD and the flavin mononucleotide (FMN) with apoprotein. Therefore, it seems worthwhile to examine the molecular interaction between salicylate and riboflavin. In this paper a detailed analysis of the NMR and absorption spectra of the complex will be presented and a structure of the complex will

[1] Enzyme-coupled reduced nicotinamide adenine dinucleotide.
[2] Enzyme-coupled oxidized nicotinamide adenine dinucleotide.

0022-3549/83/0600-0592$01.00/0

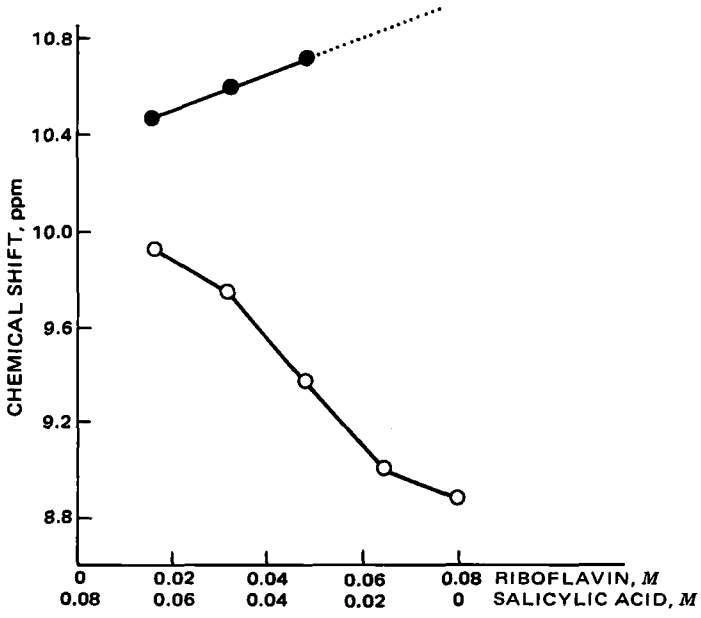

Figure 1—*Stoichiometric pairing of I and II: dependence of the chemical shifts of the riboflavin N-3 (○) and salicylic acid carboxyl (●) protons in a mixing experiment of I and II. Total concentration was constant at 0.08* M.

be proposed. These results may provide a basis for interpreting the mode of action of salicylic acid derivatives.

EXPERIMENTAL

Materials—Riboflavin-2′,3′,4′,5′-tetrabutyrate[3] (I) was obtained commercially. It was recrystallized from chloroform and the purity was confirmed by TLC. Salicylic acid[4] (II), aspirin[5] (III), and salicylamide[5] (IV) were used after recrystallization from chloroform. Deuterochloroform was purified by filtration through an alumina gel column, 5 cm in length. Carbon tetrachloride was treated with methanolic potassium hydroxide solution, washed with water several times, dried over calcium chloride overnight, and fractionally distilled from phosphorus pentoxide through a 120-cm column packed with glass helices. The distillate was refluxed and again fractionally distilled. Benzene was treated with concentrated sulfuric acid several times. After repeated washing with potassium hydroxide solution, it was dried over calcium chloride overnight, fractionally distilled from phosphorus pentoxide through a 120-cm column packed with glass helices, and crystallized twice. It was refluxed and again fractionally distilled.

Methods—^{1}H-NMR spectra were recorded on a 90-MHz spectrometer equipped with a temperature-control unit[6]. For the measurement of NMR spectra, the samples of I and salicylate at various molar ratios were dissolved in deuterochloroform. Sample volumes of 5 ml in 5-mm diameter tubes with polytef caps were used. Tetramethylsilane (0.3%) was added to the deuterochloroform to provide the field lock signal; chemical shifts were measured from the signals. The probe temperature was 35°. Absorption spectra were measured in a UV visible spectrophotometer[7] connected to a linear recorder[8]. Fused quartz cells of 10-mm light path were used, each of which was fitted with a polytef stopper. The slit width was chosen so that the effective band width of the exit beam was sufficiently narrow compared with the width of absorption bands.

To determine the association constant of complex of the absorption spectra as precisely as possible, ternary solutions which contained small amounts of I and II (or III) in nonpolar solvents, such as carbon tetrachloride and benzene, were used. For each set of I and II (or III), several solutions containing equal quantities of I and different amounts of II (or III) were prepared. The actual concentration of I was of the order of 10^{-5} M (3×10^{-5}, 5×10^{-5}, and 8×10^{-5} M), while that of II (or III) ranged from 0 to 10^{-2} M (or 2×10^{-2} M). The concentration of I was small enough to allow the effect of self-association of I molecules to be ignored. The absorbance changes of I were measured at 436 and 446 nm, the association constants were calculated, and the experimental data were treated statistically.

[3] Dae Woong Pharm. Co. Ltd., Seoul, Korea.
[4] E. Merck, Darmstadt, West Germany.
[5] Il Sung Corp., Seoul, Korea.
[6] Perkin-Elmer R 32 NMR Spectrometer.
[7] Unicam SP 1750 Ultraviolet Spectrophotometer.
[8] Unicam AR 25 Linear Recorder.

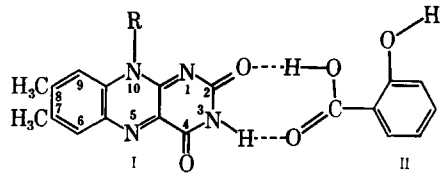

V

RESULTS

NMR Spectra—The ^{1}H-HMR spectra of riboflavin and salicylic acid derivatives in deuterochloroform are relatively simple in the downfield region. In the spectrum of II, the absorption of the carboxyl proton is observed below 10 ppm, the phenol proton is not evident at low concentrations but is weakly observed at high concentrations, and the aromatic protons appear at 6.9–8.1-ppm. The carboxyl proton of III is not evident. In the spectrum of IV, absorption of the amino proton was observed at ~6 ppm and that of the hydroxyl proton below 12 ppm. As the concentration of IV increased, the signal for the hydroxyl proton moved only slightly, but the signal for the amino proton shifted downfield.

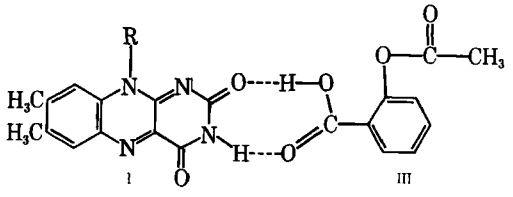

VI

The N-3 proton of I is the most deshielded proton in the molecule and occurs farther downfield than all the other resonances. The C-6 and C-9 protons of I are both downfield from the residual nondeuterated chloroform peak. These two protons are concentration independent. When these protons take part in hydrogen bonding to form cyclic self-association dimers or I–salicylate pairs or triplets, they become less shielded and their resonances shift downfield. The exact positions of the hydroxyl, amino, and imino resonances depend on the degree of association and hydrogen-bond formation; therefore, both vary with temperature and concentration.

To obtain information on the characteristics of complex in deuterochloroform, experiments were performed at constant total concentration. Unlike the results obtained from optical methods, these curves do not show a maximum (or minimum) at the relative concentrations indicative of the stoichiometry of the reaction (15). Figure 1 shows the dependence of the chemical shifts for the N-3 proton of I and the carboxyl proton of II when I was mixed with II. The N-3 proton signal of I shifted downfield as the relative concentration of II increased. The carboxyl proton signal of II also moved downfield as the concentration of I increased. From these observations it can be inferred that the association between I and II is stronger than the self-association of either compound. When I was mixed with III, the dependence of the chemical shifts on the N-3 proton of I was similar to that of II (Fig. 2). In the case of IV, the N-3 proton signal of I changed slightly and the amino proton signal of IV moved downfield slightly as the concentration of I increased and that of IV decreased (Fig. 3). This implies that the association between I and IV is stronger than the self-association of IV and approximately the same as the self-association of I. It may be assumed by the shape of the slope of all three curves that 1:1 complexes are formed in each case (15, 16).

The chemical shifts of the N-3 proton of I were plotted against the

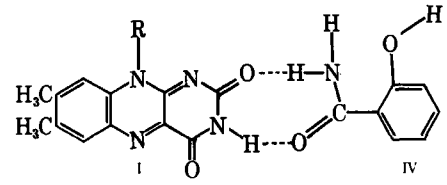

VII

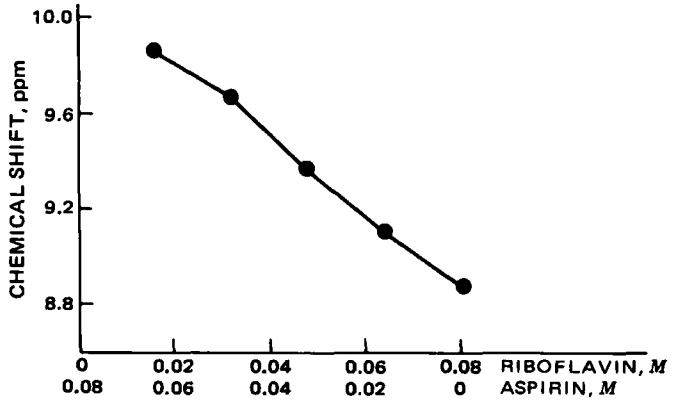

Figure 2—*Stoichiometric pairing of I and III: dependence of the chemical shifts of the riboflavin N-3 proton in a mixing experiment of I and III. Total concentration was constant at 0.08* M.

concentration of the three salicylic acid derivatives at 35°, keeping the concentration of I constant at 0.04 *M* (Fig. 4). The slopes of the N-3 proton curves of I for II and III are much greater than that of the chemical shift due to the self-association of I, while that for IV is slightly greater. These data can be interpreted to indicate that I associates somewhat more strongly with II or III than with IV, which is consistent with the other data obtained. The carboxyl proton signal of II was more upfield as the concentration of II was increased while keeping the concentration of I constant (not shown). From this fact alone, it can be inferred that the association between I and II is stronger than the self-association of II and the mole ratio of complex is the 1:1 type.

Figure 5 shows the chemical shift of the carboxyl and phenol protons of II plotted against the concentration of I, while keeping the concentration of II constant at 0.1 *M*. The curve of the carboxyl proton of II is convex upward, while the curve of the phenol proton is concave upward. As the concentration of I increased, the carboxyl proton signal appeared to broaden whereas the phenol proton signal sharpened. The downfield shift and broadening effect of the carboxyl proton are presumably because this proton takes part in the hydrogen bonding to form a I–II complex. The upfield shift and sharpening effect of the phenol proton indicate the possibility of a stacked configuration or two components of the complex not being in one plane. The N-3 proton signal of I was more upfield as the concentration of I was increased while keeping the concentration of II constant (not shown). From this fact, it can be suggested that the association between I and II is stronger than the self-association of I and the mole ratio of the complex is the 1:1 type. A similar phenomenon was observed with III on addition of I while keeping the concentration of III constant at 0.06 *M* (not shown). In the case of IV, the curve of the amino proton is straight upward (Fig. 6). The phenol proton signal decreased in intensity and then disappeared without a shielding effect as the concentration of I was increased (not shown). This implies that only the amino proton takes part in hydrogen bonding to form a I–IV complex.

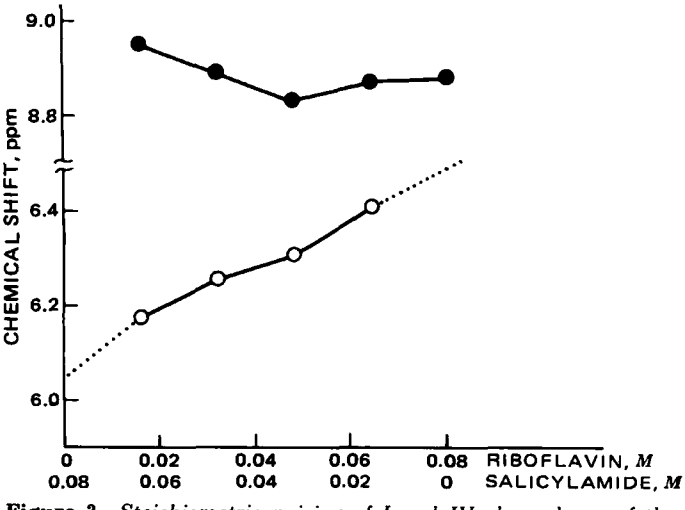

Figure 3—*Stoichiometric pairing of I and IV: dependence of the chemical shifts of the riboflavin N-3 (●) and salicylamide amino (○) protons in a mixing experiment of I and IV. Total concentration was constant at 0.08* M.

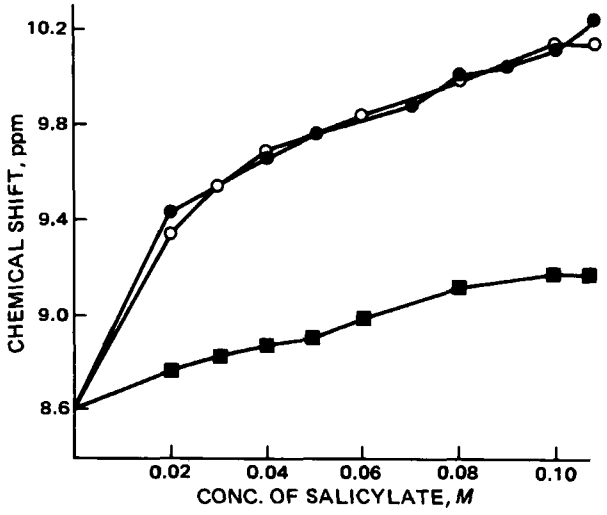

Figure 4—*Effects of the concentrations of salicylates on the chemical shifts of the riboflavin N-3 proton in deuterochloroform, keeping the concentration of I constant at 0.04* M. *Key: (●) salicylic acid, (○) aspirin, and (■) salicylamide.*

Besides the observation of complex formation in the downfield shift of the protons directly involved, a secondary effect also may be noted which is due to a change in the electron density at sites where several bonds are altered in the donor or acceptor atoms during hydrogen-bond formation. Small changes may be produced in the ring currents and the electron densities in the acceptor molecules, resulting in shifts in the resonances of the other protons. It is also possible to produce small changes in the ring resonance positions due to neighboring unsaturated ring systems. The resonances of the C-6 and C-9 protons of I are not shielded. But small upfield shifts were observed in all of the ring protons of II and III. In the case of IV, some of the ring protons moved downfield slightly and others shifted upfield.

Absorption Spectra—As shown in Fig. 7, a marked spectral change was produced on adding II to I in a nonpolar solvent, carbon tetrachloride. It may be assumed that this spectral change is due solely to the formation of a hydrogen bond between I and II. This view is further substantiated by the existence of several isosbestic points in each set of spectra. The shorter wavelength band shifted to the red, the longer band shifted to the blue, and hyperchromism of the longer band was observed. Frequency shifts due to hydrogen bonding were determined from the spectra of the

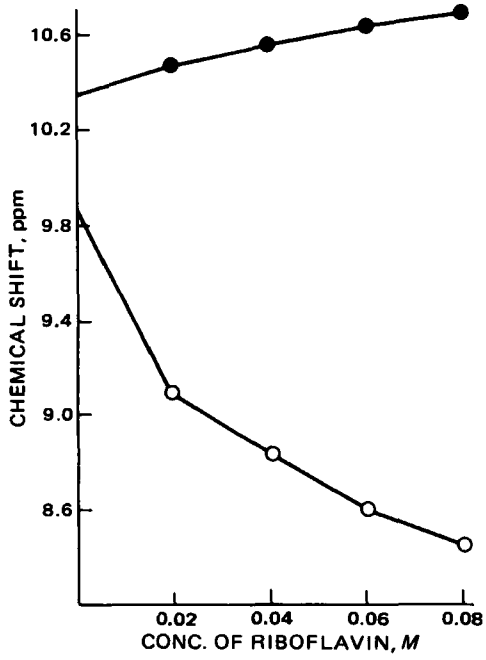

Figure 5—*Effects of the concentration of I on the chemical shifts of the carboxyl (●) and the phenol (○) protons of II in deuterochloroform, keeping the concentration of II constant at 0.1* M.

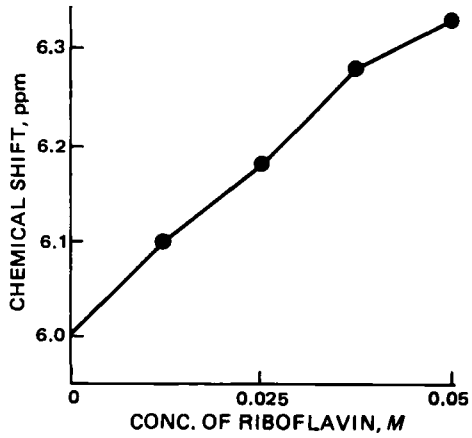

Figure 6—*Effects of the concentration of I on the chemical shifts of the salicylamide amino protons in deuterochloroform, keeping the concentration of IV constant at 0.05* M.

free and hydrogen-bonded species (resulting from the difference between the energy of the hydrogen bond in the excited and ground states). These phenomena were observed with III or IV in carbon tetrachloride. In the other nonpolar solvent, benzene, similar phenomena also were observed.

Determination of the association constant of the complex is possible from spectral data if the complex shows a significantly different spectrum from that of its components. The association constant of the hydrogen-bonding complex was obtained using the following:

$$\frac{1}{\Delta\epsilon_{obs}} = \frac{1}{K(\epsilon_c - \epsilon_a)}\frac{1}{C_b} + \frac{1}{\epsilon_c - \epsilon_a}$$

where $\Delta\epsilon_{obs} = \epsilon_{obs} - \epsilon_a$, ϵ_a and ϵ_c are the molar absorptivities at a given frequency of I in uncomplexed form and in pure complex, respectively, ϵ_{obs} is the observed absorptivity at a given frequency of I in complexed media, C_b is the concentration of salicylates (on some scale defined in the *Experimental* section), and K is the association constant of the complex (17). This can be easily derived with the assumption that the concentration of I is negligibly small compared with that of salicylate; such is actually the case in the present study. From this equation, a plot of $I/\Delta\epsilon_{obs}$ *versus* $1/C_b$ is expected to give a straight line. When both the concentration of I and the cell length are kept constant throughout a set of spectra, the absorptivities (ϵ) in the equation may be replaced by the corresponding absorbances (A). Thus $1/\Delta A_{obs}$ was plotted against $1/C_b$ for various frequencies. These plots gave straight lines, and the extrapolation of the lines for each of the salicylates led to K values which were

Table I—Measured and Calculated Properties of I and Salicylates on Absorption Spectra

Salicylate	Range of Salicylate Concentration, M	Solvent	Association constant (K), M^{-1}
II	1×10^{-3}–1×10^{-2}	Benzene	450
III	1×10^{-3}–1×10^{-2}	Benzene	370
II	1×10^{-3}–1×10^{-2}	Carbon tetrachloride	435
III	2×10^{-4}–1×10^{-3}	Carbon tetrachloride	350

equal to one another within experimental error. One example of such plots is shown in Fig. 8. The K values were calculated from the plots and are summarized in Table I. These association constants were obtained by averaging the values from three different concentrations of I (3×10^{-5}, 5×10^{-5}, and 8×10^{-5} M).

DISCUSSION

High-resolution ^{1}H-NMR techniques provide a direct observation of the hydrogen bonding in solution. As shown in the NMR spectra, the N-3 proton of I, the carboxyl protons of II and III, and the amino protons of IV seem to participate in the bonding. The NMR method utilized here measures the chemical shifts of the donor proton in hydrogen-bond formation. The acceptor atoms do not have protons and therefore do not give rise to resonances. Hence, no direct information can be gained on the identity of these acceptors. Using IR spectra, it was determined which carbonyl group of riboflavin was involved (18). In the 6-μm region of the spectra, the association through the C-2 carbonyl group of the isoalloxazine ring predominates. This is consistent with the suggestion that, in the hydrogen bonding on the isoalloxazine ring, the C-2 carbonyl group is preferred to the one at C-4 (19). This can be illustrated by the fact that the proton affinities of the heteroatoms in the isoalloxazine ring are actually different from one another (14, 19–21). As determined previously (14), the charge density of the C-2 carbonyl oxygen atom in the isoalloxazine ring is greater than that of the C-4 carbonyl oxygen atom; the N-3 proton is extremely labile and a good electron acceptor since the charge density of N-3 nitrogen atom is higher than any of the other heteroatoms. The change of the absorption spectra supports hydrogen-bond formation at the aforementioned binding sites (22).

Thus, the most probable hydrogen bonding is represented in the following manner. Compounds I and II form the 1:1 cyclic hydrogen-bonded dimer (V) through the N-3 proton and the C-2 carbonyl oxygen of the isoalloxazine ring, and the carboxylic hydroxyl proton and carbonyl oxygen of II. Compounds I and III form the 1:1 cyclic hydrogen-bonded dimer (VI) in the same manner. Compound IV forms the 1:1 cyclic hydrogen-bonded dimer (VII) with I through the N-3 proton and the C-2

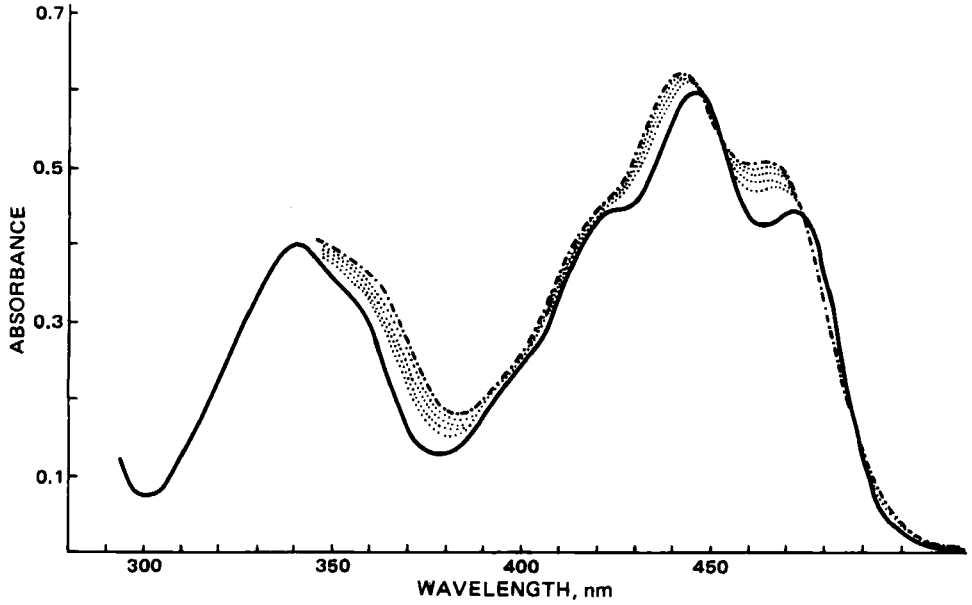

Figure 7—*Effects of II on the absorbance spectrum of I (5×10^{-5} M) in carbon tetrachloride. Salicylic acid was added from 0 to 1×10^{-2} M. Key: (—) free molecule, (· · ·) spectra in the presence of II in order of increasing concentration of II, (· - · - ·) spectra in the presence of 1×10^{-2} M II.*

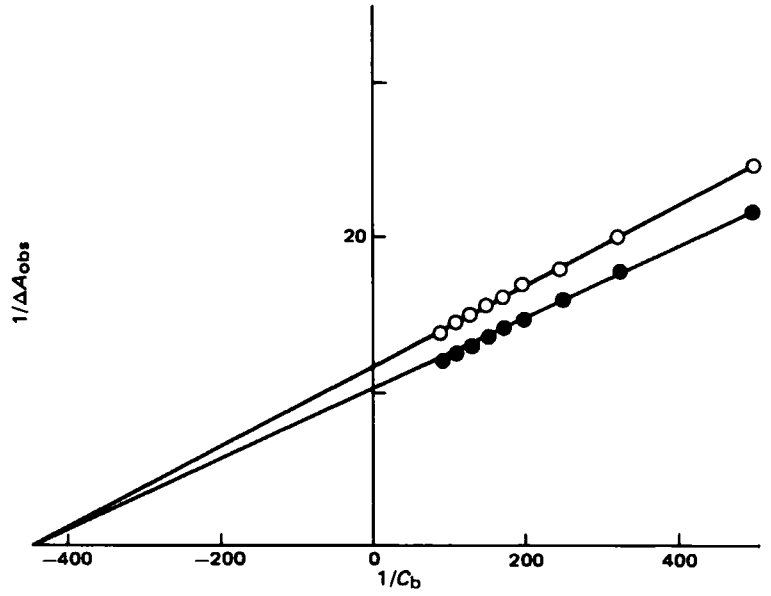

Figure 8—*Relationship between $1/A_{obs}$ and $1/C_b$ values of the I–II system in benzene obtained according to the association constant equation. Key: (○) 436 nm, (●) 446 nm.*

carbonyl oxygen of the isoalloxazine ring, and the amino proton and carbonyl oxygen of IV. The frontier orbital density of N-5 is the greatest of all the atoms in the isoalloxazine ring (20). Therefore, N-5 seems to be the entrance of electrons. The formation of various types of hydrogen bonding affects the frontier orbital density of N-5 of the isoalloxazine ring (22). Considering that salicylates interact with riboflavin at the aforementioned sites, the electron affinity of the isoalloxazine ring and the frontier electron density of N-5 increase, which accelerates the electron flow from the substrate to the coenzyme (19–26). The hydrogen bonding involved in flavoproteins may be considered to be significant with respect to their catalytic activity.

In nonpolar solvents (carbon tetrachloride and benzene) marked absorption spectral changes due to hydrogen bonding were produced when salicylates were added to I. Frequency shifts were observed. It is known that the energy of the hydrogen bond in the excited state is differentiated from that in the ground state. The association constants of I with II or III in nonpolar solvents are large, however, with IV it is too small to be calculated from the absorption spectral data. The NMR data produced similar results. On the other hand, in chloroform solution the absorption spectral change due to hydrogen bonding was weak (not shown). This could be attributed to the solute–solvent interaction.

Although II, III, and IV are very similar structurally, their effects on the body may be quite diverse. Sodium salicylate and III effectively depress oxidative phosphorylation while IV is a weak or ineffective uncoupling agent. Compound III is more potent than sodium salicylate as an analgesic and antipyretic, and IV is much less effective than either (27, 28). These facts are consistent with the experimental results obtained in this study. The use of deuterochloroform, carbon tetrachloride, and benzene as solvents in these experiments enabled observation of these interactions free of strong solute–solvent association effects. This environment may mimic in some ways the inside of the enzyme–substrate complex from which water may be excluded. It has been suggested that FAD in the enzyme is surrounded by a hydrophobic environment even in the aqueous phase (29, 30). If one considers that the oxidation–reduction process in these systems occurs in a lipophilic rather than an aqueous environment, it may be worthwhile to research the direct interaction between salicylates and the riboflavin moiety in a nonpolar system. Further quantitative analysis of these data should lead to a more precise fundamental understanding of the riboflavin–salicylate complex formation.

REFERENCES

(1) C. O. Wilson, O. Gisvold, and R. F. Doerge, "Textbook of Organic Medicinal and Pharmaceutical Chemistry," Lippincott, Philadelphia, Pa., 1977, p. 47.

(2) T. M. Brody, *J. Pharmacol. Exp. Ther.*, **117**, 39 (1956).

(3) D. H. Sproull, *Br. J. Pharmacol.*, **9**, 262 (1954).

(4) J. G. Spenny and M. Brown, *Gastroenterology*, **73**, 995 (1977).

(5) J. T. Fishgold, J. Field, and V. E. Hall, *Am. J. Physiol.*, **164**, 727 (1951).

(6) J. Levy, *Bull. Soc. Chim. Biol.*, **28**, 338 (1946).

(7) J. D. P. Graham and W. A. Parker, *Q. J. Med.*, **17**, 153 (1948).

(8) F. X. Galen, R. Truchot, and R. Michel, *Biochem. Pharmacol.*, **23**, 1379 (1974).

(9) B. Pullman and A. Pullman, *Proc. Natl. Acad. Sci. USA*, **45**, 136 (1959).

(10) B. Grabe, *Biochim. Biophys. Acta*, **30**, 560 (1958).

(11) S. Shifrin, *ibid.*, **81**, 205 (1964).

(12) S. Yomasa, *Progr. Theor. Phys. Suppl.*, **40**, 249 (1967).

(13) T. Sakurai and H. Hosoya, *Biochim. Biophys. Acta*, **112**, 459 (1966).

(14) M. Honda, *J. Phys. Soc. Japan.*, **31**, 1196 (1971).

(15) L. Katz, *J. Mol. Biol.*, **44**, 279 (1969).

(16) L. Katz and S. Penman, *ibid.*, **15**, 220 (1966).

(17) H. Baba and S. Suzuki, *J. Chem. Phys.*, **35**, 1118 (1961).

(18) J. W. Huh and B. S. Yu, *J. Pharm. Soc. Korea*, **20**, 130 (1976).

(19) K. Yagi, N. Ohishi, K. Nishimoto, J. D. Choi, and P-S. Song, *Biochemistry*, **19**, 1553 (1980).

(20) P.-S. Song, J. D. Choi, R. D. Fugate, and K. Yagi, "Flavins and Flavoproteins," T. P. Singer, Ed., Elsevier, Amsterdam, 1976, p. 381.

(21) M. Sun and P.-S. Song, *Biochemistry*, **12**, 4663 (1973).

(22) K. Nishimoto, Y. Watanabe, and K. Yagi, *Biochim. Biophys. Acta*, **526**, 34 (1978).

(23) P. Hemmerich, *Fortschr. Chem. Org. Naturst.*, **33**, 451 (1976).

(24) T. C. Bruice, *Prog. Bioorg. Chem.*, **4**, 2 (1976).

(25) P.-S. Song and M. Sun, "Chemical and Biochemical Reactivity," B. Pullman and E. Bergmann, Eds., Israel Academy of Sciences, Jerusalem, 1974, p. 407.

(26) D. E. Edmonson, B. Barman, and G. Tollin, *Biochemistry*, **11**, 1133 (1972).

(27) A. Goth, "Medical Pharmacology," C. V. Mosby, Saint Louis, Mo., 1976, p. 328.

(28) A. G. Gilman, L. S. Goodman, and A. Gilman (Eds.), "The Pharmacological Basis of Therapeutics," Macmillan, New York, N.Y., 1980, p. 668.

(29) F. Muller, S. G. Mayhew, and V. Massey, *Biochemistry*, **12**, 4654 (1973).

(30) V. Massey and H. Gather, *ibid.*, **4**, 1161 (1965).

ACKNOWLEDGMENTS

This research was supported by the 1981 grant from the Korea Science and Engineering Foundation.

5-Fluorouracil Concentrations in Rat Plasma, Parotid Saliva, and Bile and Protein Binding in Rat Plasma

LEE A. CELIO, G. JOHN DiGREGORIO ˣ, EILEEN RUCH
JOSEPH N. PACE, and ANTHONY J. PIRAINO

Received November 23, 1981, from the *Department of Pharmacology, Hahnemann Medical College, Philadelphia, PA 19102.* Accepted for publication May 7, 1982.

Abstract □ The pharmacokinetics of 5-fluorouracil were studied over a 60-min period in rats that received 12.5, 25.0, and 50.0 mg/kg iv. The plasma concentration–time relationship and the detectability in bile and parotid saliva (a route of elimination heretofore given little or no attention) were examined. Protein binding of 5-fluorouracil at concentrations chosen to approximate those found in plasma was determined by equilibrium dialysis. Bile–plasma and parotid saliva–plasma concentration ratios were calculated. 5-Fluorouracil concentrations were quantitated by high-performance liquid chromatography. Plasma concentrations at all doses studied appeared to rapidly decline. The half-life, however, at the 50.0-mg/kg dose (27 min) was significantly longer ($p < 0.025$) than the corresponding half-life at the 25.0-mg/kg dose (22 min). This may be attributed to an easily saturable hepatic degradation. Although an observed decline in bile–plasma and parotid saliva–plasma concentration ratios at higher doses may represent saturation of these excretary routes, the small amounts of 5-fluorouracil detected in bile and parotid saliva probably contribute negligibly to the elimination of the total drug equivalents administered. Parotid saliva–plasma concentration ratios were not useful in predicting plasma protein binding as determined by equilibrium dialysis. Excretion of intravenously administered 5-fluorouracil in saliva, however, exposes the upper GI tract to this agent and may play a part in causing stomatitis in patients receiving the drug by this route.

Keyphrases □ 5-Fluorouracil—concentrations in rat plasma, bile, and parotid saliva as determined by high-performance liquid chromatography, protein binding, pharmacokinetics □ Chemotherapeutic agents—5-fluorouracil, concentration in rat plasma, bile, and parotid saliva, protein binding, pharmacokinetics *in vivo* □ Pharmacokinetics—of the chemotherapeutic agent 5-fluorouracil in rats, concentrations in plasma, bile, and parotid saliva

5-Fluorouracil, an antineoplastic agent which inhibits the synthesis of DNA (1), is extensively used in the treatment of neoplasms of the breast and GI tract (2), with a trend toward utilizing it in combination with several chemotherapeutic agents in complex schedules for disseminated disease (3–5). Information concerning the concentration–time course in plasma and body excretions may be helpful in establishing dose schedules with a pharmacological rationale. In this work a simple, sensitive, and specific method, high-performance liquid chromatography (HPLC), was used to study the decline of 5-fluorouracil concentration in plasma and its excretion in bile and parotid saliva, a route of excretion heretofore given little or no attention. Bile–plasma and parotid saliva–plasma concentration ratios were calculated and the significance of biliary and parotid saliva excretion as routes of elimination were evaluated. The extent to which 5-fluorouracil is bound to rat plasma proteins, at a concentration chosen to approximate amounts detected in rat plasma, was measured by equilibrium dialysis. The calculated percentage of free drug in plasma was determined from the parotid saliva–plasma concentration ratios and compared with the calculated percentage of free drug determined by equilibrium dialysis.

Table I—Concentration of 5-Fluorouracil in Rat Plasma Following Intravenous Administration

Minutes Postdose	Concentration in Plasma, μg/ml[a]		
	12.5-mg/kg Dose[b]	25.0-mg/kg Dose[b]	50.0-mg/kg Dose[c]
5	9.9 ± 0.9	33.6 ± 1.7	52.8 ± 3.8
10	8.2 ± 1.2	21.6 ± 2.1	45.5 ± 4.7
15	6.0 ± 0.6	15.1 ± 1.3	34.2 ± 3.7
30	3.5 ± 0.8	9.0 ± 1.7	23.0 ± 1.9
60	1.6 ± 0.2	5.9 ± 1.4	11.7 ± 1.0

[a] Data expressed as mean ± *SE*. [b] $n = 5$. [c] $n = 6$.

EXPERIMENTAL

Material—All solvents and reagents were analytical grade. A commercial preparation of 5-fluorouracil[1] (injectable form) and 5-fluorocytosine[1] (powder form) were utilized.

Apparatus—The liquid chromatograph[2] was fitted with a loop injector and fixed-wavelength UV detector (254 nm). A 1-mV recorder[3] was utilized and the detector was attenuated at 0.20 AUFS. A prepacked, 300 × 3.9-mm (i.d.) reverse-phase μ-Bondapak C_{18} analytical column[4] was run at ambient temperature. One liter of 5% glacial acetic acid was added to 27 mg of heptane sulfonic acid for the mobile phase. The mixture was pumped isocratically through the column at a flow rate of 1.5 ml/min.

Animal Experiment—Male Wistar rats, 220–270 g, were anesthetized and prepared for drug administration and parotid saliva collection by the method described by Piraino, DiGregorio, and Ruch (6). In addition, the bile duct was surgically exposed and cannulated with polyethylene tubing[5]. Blood samples (0.5 ml) were collected in heparinized tubes at 0, 5, 10, 15, 30, and 60 min after the administration of 5-fluorouracil through the femoral vein. Parotid saliva and bile were collected over 0–15, 15–30, and 30–60 min postdose.

Equilibrium Dialysis—One-milliliter samples of rat plasma containing 60.0 or 12.5 μg of 5-fluorouracil were placed into bags formed from standard dialysis tubing[6]. The bags were tied and put in 50-ml culture tubes containing 10 ml of 0.067 *M* phosphate buffer and spiked to yield a solution of 100% of the 5-fluorouracil concentration that was placed in the plasma compartment. The tubes were sealed tightly and agitated in a shaker-water bath maintained at 37° for 4–12 hr.

Extractions—Extractions were done using a modified method of Christophides *et al.* (7). Plasma (200 μl), bile (100 μl), parotid saliva (50–100 μl), or dialysis tubing was added to 0.5 ml of saturated sodium sulfate solution and 50 μl of sodium acetate (200 g/liter). 5-Fluorocytosine, the internal standard, was dissolved in distilled water to yield a solution of 1.00 μg/ml, and 100 μl was added to the sample before extraction. The sample was then shaken with 5 ml of a solution of ether and *n*-propyl alcohol (4:1 v/v) for 5 min. After centrifugation the aqueous phase was removed and discarded. The organic phase was evaporated under a steady stream of air in a water bath maintained at 55°. The residue was redissolved in 20–50 μl of distilled water, and a 5–10 μl aliquot was injected into the liquid chromatograph. Quantitation was performed using the method of internal standards.

Calculations—Linear regression analysis of the serum level data from each animal after logarithmic transformation of the serum concentration data was used to calculate half-lives, volumes of distribution, and total body clearances. Statistical significance was determined at $p < 0.05$ using two-sided variance analysis to determine the significance of differences between the groups studied.

[1] Roche Laboratories, Nutley, N.J.
[2] Mode 200; Waters Associates, Milford, Mass.
[3] Perkin-Elmer Corp., Norwalk, Conn.
[4] Waters Associates, Milford, Mass.
[5] PE 50; Clay Adams, Parsippany, N.J.
[6] Fisher Chemical Co., King of Prussia, Pa.

0022-3549/83/0600-0597$01.00/0

Table II—Concentration of 5-Fluorouracil in Rat Bile Following Intravenous Administration

Minutes Postdose	Concentration in Bile, μg/ml[a]		
	12.5-mg/kg Dose[b]	25.0-mg/kg Dose[b]	50.0-mg/kg Dose[c]
15	6.1 ± 0.9	17.3 ± 2.2	28.5 ± 2.9
30	3.8 ± 0.3	8.2 ± 1.5	11.6 ± 2.1
60	2.9 ± 0.4	4.4 ± 0.7	7.3 ± 1.1

[a] Data expressed as mean ± *SE*. [b] $n = 5$. [c] $n = 6$.

RESULTS AND DISCUSSION

The separation and identification of 5-fluorouracil was suitable for monitoring plasma, bile, and parotid saliva concentrations of the drug. The retention time for 5-fluorouracil was 2.0 min; the internal standard, 5-fluorocytosine, had a retention time of 4 min. The separation was reproducible and sensitive for extracted plasma, bile, and parotid saliva. Calibration curves for spiked plasma, bile, and parotid saliva were linear when the injected sample contained 0.05–5.0 μg of 5-fluorouracil, corresponding to concentrations over a range of 0.25–25 μg/ml. Extraction recoveries were 65% for 5-fluorouracil.

Following surgery, parotid saliva and bile flow rates did not differ among experimental groups over the range of doses administered. The mean (±*SE*) plasma, bile, and parotid saliva 5-fluorouracil concentrations in rats receiving 12.5, 25.0, and 50.0 mg/kg iv are presented in Tables I–III. The plasma half-lives (±*SE*) for the 12.5-, 25.0-, and 50.0-mg/kg doses were 22 ± 2, 25 ± 5, and 27 ± 3 min, respectively. The half-life at the 50.0-mg/kg dose was significantly longer ($p < 0.025$) than the corresponding half-life at the 12.5-mg/kg dose. Total body clearances (±*SE*) were 2.4 ± 0.2, 1.6 ± 0.2, and 1.4 ± 0.1 liters/kg/hr in rats receiving 12.5, 25.0, and 50.0 mg/kg iv of 5-fluorouracil, respectively. Volumes of distribution (±*SE*) were 1.23 ± 0.11, 0.89 ± 0.10, and 0.94 ± 0.10 liters/kg. While volumes of distribution did not change significantly over the range of doses studied, the total body clearance of 5-fluorouracil decreased significantly ($p < 0.001$) in animals that received 50.0 mg/kg compared with the group which received 12.5 mg/kg. The mean (±*SE*) bile–plasma and parotid saliva–plasma concentration ratios were calculated and are presented in Tables IV and V. Compared with bile–plasma concentration ratios at 60 min for a dose of 50.0 mg/kg, bile–plasma concentration ratios were approximately two times higher with the administration of 25.0 mg/kg and four times higher with the administration of 12.5 mg/kg (Table IV). The parotid saliva–plasma concentration ratios also tended to decrease at higher doses (Table V). The free plasma 5-fluorouracil concentrations predicted using the parotid saliva–plasma concentration ratios 60 min following the intravenous administration of 5-fluorouracil were 49, 36, and 24% for the 12.5-, 25.0-, and 50.0-mg/kg doses, respectively.

When determined by equilibrium dialysis, however, the extent to which 5-fluorouracil is bound to rat plasma at 18.7 ± 2.0 and 65.7 ± 0.9 μg/ml, was <10%. The percentage of drug calculated to be free from protein binding was >90% for the aforementioned concentrations. The percent protein-bound drug did not vary significantly between 0.40 and 12-hr incubation when the drug was added to both sides of the system. Ninety-eight percent of the measured concentration of 5-fluorouracil added to the dialysis system was accounted for by drug assayed from both sides of the dialysis system after equilibrium. No 5-fluorouracil binding to the dialysis membrane was detected.

5-Fluorouracil, an antimetabolite, is an antineoplastic agent extensively used for a variety of solid neoplasms and has toxicities that include bone marrow suppression and damage to the GI tract (8). Stomatitis and esophagopharyngitis are common side effects. In the past, pharmacokinetic studies using rats have shown saturation of degradative metabolism at high doses, which is presumed to correlate with the clinical observation that increasing doses of 5-fluorouracil results in unproportional increases in toxicity (9, 10). This investigation examined the plasma concentration–time relationship and the detectability and excretion in parotid saliva and bile of intravenously administered 5-fluorouracil in rats. The excretion of 5-fluorouracil in body fluids, in addition to the plasma–concentration time course, may be useful in predicting the mechanisms of clinically encountered toxicities.

In this work 5-fluorouracil plasma concentrations dropped rapidly after intravenous administration. This is consistent with the hypothesis that only a small amount of pharmacologically active drug remains in the tissues, while most of the dose administered is rapidly eliminated from the body (11). As reported previously, the plasma half-life of 5-fluorouracil was found to increase at higher doses (9). While differences in plasma half-life were not striking, the half-life at the 50.0-mg/kg dose appeared significantly ($p < 0.05$) prolonged compared with the corresponding half-life at the 12.5-mg/kg dose.

5-Fluorouracil is metabolized primarily via the liver by an easily saturable pathway (9, 10). Although bile flow rates were unchanged, the proportion of 5-fluorouracil excreted in bile, as reflected by the bile–plasma concentration ratio at a dose of 50.0 mg/kg, was approximately one-fourth and one-half of that at the 12.5- and 25.0-mg/kg doses, respectively. A decline in the bile–plasma concentration ratio at higher doses is consistent with a saturable hepatic excretory process. The relative decrease in biliary excretion probably does not contribute greatly to a longer plasma half-life at higher doses, since 5-fluorouracil is mainly eliminated by urinary excretion (12). In general, low molecular weight compounds are not eliminated primarily *via* bile even in rats with ligated renal pedicles (13). A longer half-life at higher doses remains best explained by saturation of the degradative metabolism. The dependency of half-life on dose can not be attributed to changes in the volumes of distribution since these tended to decrease at higher doses. Total body clearances, however, of 5-fluorouracil decreased at higher doses consistent with a saturable elimination. Ongoing clinical investigations are assessing how alterations in urinary excretion of 5-fluorouracil and its metabolites can account for some of the variation observed in response to therapeutic doses (14).

Although urinary and biliary excretion have been previously studied, heretofore little or no information has been available concerning the detectability and excretion of 5-fluorouracil in saliva. This work demonstrates that this chemotherapeutic agent is excreted in detectable amounts in rat parotid saliva after intravenous administration. The concentration of 5-fluorouracil in parotid saliva is low and probably contributes negligibly to the total drug equivalents eliminated from the body. The calculated percentage of free 5-fluorouracil in plasma predicted by the parotid saliva–plasma concentration ratios consistently yielded values too low to reflect the percentage of free drug in plasma as determined by equilibrium dialysis. Parotid salivary excretions of 5-fluorouracil may be affected by back-diffusion, ion trapping, alterations in blood supply, and damage of the parenchyma of the gland. It is hypothesized that cytological changes in the salivary glands of mice following sublethal doses of 5-fluorouracil may impair the discharge of secretory materials (15). Furthermore, excretion in the saliva exposes the mucosa of the upper GI tract to 5-fluorouracil after intravenous administration. This may correlate with the clinical observation that intravenously administered 5-fluorouracil has been found to cause stomatitis (11). Structural changes similar to those found in the parotid glands of mice have been described in the pancreas (16) of Brunner's glands (17) of rats. 5-Fluorouracil may affect these metabolically active organs by incorpo-

Table III—Concentration of 5-Fluorouracil in Rat Parotid Saliva Following Intravenous Administration

Minutes Postdose	Concentration in Parotid Saliva, μg/ml[a]		
	12.5-mg/kg Dose[b]	25.0-mg/kg Dose[b]	50.0-mg/kg Dose[c]
15	3.0 ± 0.7	7.3 ± 0.3	7.6 ± 0.6
30	1.6 ± 0.1	3.9 ± 0.4	5.9 ± 0.5
60	0.7 ± 0.1	1.7 ± 0.4	2.8 ± 0.7

[a] Data expressed as mean ± *SE*. [b] $n = 5$. [c] $n = 6$.

Table IV—Bile–Plasma Concentration Ratios Following Intravenous Adminstration of 5-Fluorouracil to Rats

Minutes Postdose	Concentration Ratio[a]		
	12.5-mg/kg Dose[b]	25.0-mg/kg Dose[b]	50.0-mg/kg Dose[c]
15	1.03 ± 0.12	1.18 ± 0.18	0.84 ± 0.04
30	1.28 ± 0.24	0.95 ± 0.17	0.54 ± 0.12
60	1.80 ± 0.22	1.00 ± 0.39	0.64 ± 0.09

[a] Data expressed as mean ± *SE*. [b] $n = 5$. [c] $n = 6$.

Table V—Saliva–Plasma Concentration Ratios Following Intravenous Administration of 5-Fluorouracil to Rats

Minutes Postdose	Concentration Ratios[a]		
	12.5-mg/kg Dose[b]	25.0-mg/kg Dose[b]	50.0-mg/kg Dose[c]
15	0.50 ± 0.10	0.50 ± 0.05	0.24 ± 0.04
30	0.56 ± 0.13	0.49 ± 0.10	0.27 ± 0.04
60	0.49 ± 0.08	0.36 ± 0.05	0.24 ± 0.04

[a] Data expressed as mean ± *SE*. [b] $n = 5$. [c] $n = 6$.

rating into RNA, since it has been reported to inhibit protein synthesis in mammals by this mechanism (16).

In the past rat studies have been used to develop optimal scheduling programs and predict mechanisms of toxicity of 5-fluorouracil (9, 18). Findings of these investigations are presumed to correlate with clinical observations. In this work, concentrations of 5-fluorouracil in the excreted fluids of rats were used to supplement information derived from the plasma concentration time course. This work has demonstrated that unmetabolized 5-fluorouracil is excreted in detectable amounts in rat bile and parotid saliva. Biliary excretion appears to occur *via* a saturable process. Excretion of 5-fluorouracil in parotid saliva exposes the upper GI tract to this agent, even when administered intravenously. These routes of excretion appear to contribute negligibly to the total drug equivalents eliminated from the body.

REFERENCES

(1) C. Heidelberger, *Prog. Nucleic Acid Res.*, **4**, 1 (1965).

(2) C. Heidelberger and F. J. Ansfield, *Cancer Res.*, **23**, 1226 (1963).

(3) B. A. Chabner, C. E. Myers, N. Coleman, and D. G. John, *N. Engl. J. Med.*, **292**, 1107 (1975).

(4) V. T. DeVita, R. C. Young, and G. P. Canellos, *Cancer*, **35**, 98 (1975).

(5) B. J. Kennedy and A. Theologides, *Ann. Int. Med.*, **55**, 719 (1961).

(6) A. J. Piraino, G. J. DiGregorio, and E. K. Ruch, *J. Pharmacol. Meth.*, **3**, 1 (1980).

(7) N. Christophides, G. Mihaly, F. Vajda, and W. Louis, *Clin. Chem.*, **25**, 83 (1979).

(8) B. L. Hillcoat, B. P. McCulloch, A. T. Figuerdo, M. H. Ehsom, and J. M. Rosenfield, *Br. J. Cancer*, **38**, 719 (1978).

(9) C. Finn and W. Sadée, *Cancer Chemother. Rep.*, **59**, 279 (1975).

(10) J. J. Ambre and L. J. Fischer, *J. Lab. Clin. Med.*, **78**, 343 (1971).

(11) R. J. Fraile, L. H. Baker, T. R. Buroker, J. Horwitz, and V. K. Vailkevicius, *Cancer Res.*, **40**, 2223 (1980).

(12) M. J. Meeks, W. V. Kessler, and J. N. Arvesen, *Radiat. Res.*, **52**, 82 (1972).

(13) P. C. Hirom, P. Millburn, and R. L. Smith, *Xenobiotica*, **6**, 55 (1966).

(14) D. S. Sitar, D. H. Shaw, Jr., M. P. Thirlwell, and J. R. Ruedy, *Cancer Res.*, **37**, 3981 (1977).

(15) M. K. Kim and S. S. Han, *Proc. Soc. Exp. Biol. Med.*, **139**, 1246 (1972).

(16) J. Y. Kuo, H. Y. Shen, P. Wolfson, and D. A. Direling, *Am. J. Gastroenterol.*, **70**, 89 (1978).

(17) C. Anand and S. S. Han, *J. Anat.*, **119**, 1 (1975).

(18) J. H. Mulder, T. Smink, T. Ossewaarde, and L. M. Van Putten, *Eur. J. Cancer*, **16**, 699 (1980).

Liquid Membrane Phenomenon in Reserpine Action

S. B. BHISE, P. R. MARWADI, S. S. MATHUR, and R. C. SRIVASTAVA ˣ

Received March 2, 1982, from the *Birla Institute of Technology and Science, Pilani-333031, Rajasthan, India.* Accepted for publication May 26, 1982.

Abstract □ Reserpine was shown to generate a liquid membrane. Transport of adrenaline, noradrenaline, dopamine, 5-hydroxytryptamine, glutamic acid, and γ-aminobutyric acid in the presence of the reserpine liquid membrane was studied. The data indicate that the phenomenon of liquid membrane formation is likely to play a role in the mechanism of reserpine action.

Keyphrases □ Reserpine—liquid membrane phenomenon, biogenic amines, neurotransmitter amino acids, surface activity □ Liquid membrane phenomenon—reserpine action, biogenic amines, neurotransmitter amino acids, surface activity

Surface activity is exhibited by a wide variety of biologically active agents (1). The fact that surface activity may play a role in the mechanism of action of some drugs is evident from the correlations obtained (2) between surface activity and biological effects. Previous researchers (3) have concluded that in the case of psychotropic drugs, surface activity is the primary factor which determines their potency and not the specific chemical structure.

According to a previous hypothesis (4), surface-active agents, when added to water or aqueous solutions, generate liquid membranes which completely cover the interface at concentrations equal to the critical micelle concentration of the surfactant. It is, therefore, logical to expect that the liquid membranes generated by surface-active drugs may play a role in the mechanism of their action. Studies on haloperidol, a surface-active neuroleptic drug, were recently undertaken (5), and it was shown that the liquid membrane generated by haloperidol contributes significantly to the mechanism of its action.

To establish the role of liquid membrane phenomena in the mechanism of action of surface-active drugs, it is necessary to conduct studies, on structurally dissimilar drugs. Reserpine, a drug structurally different from haloperidol, is discussed in the present report. Existence of a liquid membrane generated by reserpine was demonstrated and data on the transport of biogenic amines and relevant neurotransmitter amino acids, through the liquid membrane generated by reserpine, were obtained.

EXPERIMENTAL

Materials—Reserpine[1], dopamine chlorhydrate[2], adrenaline hydrogen tartrate[2], L-noradrenaline[3], 5-hydroxytryptamine creatinine sulfate[4], L-glutamic acid[5], γ-aminobutyric acid[5], and distilled water (glass-distilled once from potassium permanganate) were used.

Methods—The critical micelle concentration (CMC) of aqueous reserpine was determined from the variation of surface tension with concentration. The surface tensions were measured using a tensiometer[6]. To prepare aqueous solutions of reserpine, the necessary volume of an ethanolic solution of known concentration of the drug was added to the aqueous phase with constant stirring. Since the aqueous solution of reserpine always contained some alcohol, in no case >1%, the blanks used also contained the same amount of alcohol in water. The CMC value of aqueous reserpine was found to be 1.6×10^{-6} *M*.

The all-glass cell described earlier (5, 6) was used for transport studies. A cellulose nitrate millipore filter[7], which acted as a support for the liquid

[1] BP-USP Roussel UCLAF, Paris.
[2] Loba Chemie.
[3] Fluka A.G.
[4] Koch-Light Laboratories Ltd.
[5] BDH.
[6] Fisher Surface Tensiomat Model 21.
[7] Sortorious Cat. No. 11307 of thickness 1×10^{-4} m and area 5.373×10^{-5} m^2.

0022-3549/83/0600-0599$01.00/0

rating into RNA, since it has been reported to inhibit protein synthesis in mammals by this mechanism (16).

In the past rat studies have been used to develop optimal scheduling programs and predict mechanisms of toxicity of 5-fluorouracil (9, 18). Findings of these investigations are presumed to correlate with clinical observations. In this work, concentrations of 5-fluorouracil in the excreted fluids of rats were used to supplement information derived from the plasma concentration time course. This work has demonstrated that unmetabolized 5-fluorouracil is excreted in detectable amounts in rat bile and parotid saliva. Biliary excretion appears to occur *via* a saturable process. Excretion of 5-fluorouracil in parotid saliva exposes the upper GI tract to this agent, even when administered intravenously. These routes of excretion appear to contribute negligibly to the total drug equivalents eliminated from the body.

REFERENCES

(1) C. Heidelberger, *Prog. Nucleic Acid Res.*, **4**, 1 (1965).

(2) C. Heidelberger and F. J. Ansfield, *Cancer Res.*, **23**, 1226 (1963).

(3) B. A. Chabner, C. E. Myers, N. Coleman, and D. G. John, *N. Engl. J. Med.*, **292**, 1107 (1975).

(4) V. T. DeVita, R. C. Young, and G. P. Canellos, *Cancer*, **35**, 98 (1975).

(5) B. J. Kennedy and A. Theologides, *Ann. Int. Med.*, **55**, 719 (1961).

(6) A. J. Piraino, G. J. DiGregorio, and E. K. Ruch, *J. Pharmacol. Meth.*, **3**, 1 (1980).

(7) N. Christophides, G. Mihaly, F. Vajda, and W. Louis, *Clin. Chem.*, **25**, 83 (1979).

(8) B. L. Hillcoat, B. P. McCulloch, A. T. Figuerdo, M. H. Ehsom, and J. M. Rosenfield, *Br. J. Cancer*, **38**, 719 (1978).

(9) C. Finn and W. Sadée, *Cancer Chemother. Rep.*, **59**, 279 (1975).

(10) J. J. Ambre and L. J. Fischer, *J. Lab. Clin. Med.*, **78**, 343 (1971).

(11) R. J. Fraile, L. H. Baker, T. R. Buroker, J. Horwitz, and V. K. Vailkevicius, *Cancer Res.*, **40**, 2223 (1980).

(12) M. J. Meeks, W. V. Kessler, and J. N. Arvesen, *Radiat. Res.*, **52**, 82 (1972).

(13) P. C. Hirom, P. Millburn, and R. L. Smith, *Xenobiotica*, **6**, 55 (1966).

(14) D. S. Sitar, D. H. Shaw, Jr., M. P. Thirlwell, and J. R. Ruedy, *Cancer Res.*, **37**, 3981 (1977).

(15) M. K. Kim and S. S. Han, *Proc. Soc. Exp. Biol. Med.*, **139**, 1246 (1972).

(16) J. Y. Kuo, H. Y. Shen, P. Wolfson, and D. A. Direling, *Am. J. Gastroenterol.*, **70**, 89 (1978).

(17) C. Anand and S. S. Han, *J. Anat.*, **119**, 1 (1975).

(18) J. H. Mulder, T. Smink, T. Ossewaarde, and L. M. Van Putten, *Eur. J. Cancer*, **16**, 699 (1980).

Liquid Membrane Phenomenon in Reserpine Action

S. B. BHISE, P. R. MARWADI, S. S. MATHUR, and R. C. SRIVASTAVA ˣ

Received March 2, 1982, from the *Birla Institute of Technology and Science, Pilani-333031, Rajasthan, India.* Accepted for publication May 26, 1982.

Abstract □ Reserpine was shown to generate a liquid membrane. Transport of adrenaline, noradrenaline, dopamine, 5-hydroxytryptamine, glutamic acid, and γ-aminobutyric acid in the presence of the reserpine liquid membrane was studied. The data indicate that the phenomenon of liquid membrane formation is likely to play a role in the mechanism of reserpine action.

Keyphrases □ Reserpine—liquid membrane phenomenon, biogenic amines, neurotransmitter amino acids, surface activity □ Liquid membrane phenomenon—reserpine action, biogenic amines, neurotransmitter amino acids, surface activity

Surface activity is exhibited by a wide variety of biologically active agents (1). The fact that surface activity may play a role in the mechanism of action of some drugs is evident from the correlations obtained (2) between surface activity and biological effects. Previous researchers (3) have concluded that in the case of psychotropic drugs, surface activity is the primary factor which determines their potency and not the specific chemical structure.

According to a previous hypothesis (4), surface-active agents, when added to water or aqueous solutions, generate liquid membranes which completely cover the interface at concentrations equal to the critical micelle concentration of the surfactant. It is, therefore, logical to expect that the liquid membranes generated by surface-active drugs may play a role in the mechanism of their action. Studies on haloperidol, a surface-active neuroleptic drug, were recently undertaken (5), and it was shown that the liquid membrane generated by haloperidol contributes significantly to the mechanism of its action.

To establish the role of liquid membrane phenomena in the mechanism of action of surface-active drugs, it is necessary to conduct studies, on structurally dissimilar drugs. Reserpine, a drug structurally different from haloperidol, is discussed in the present report. Existence of a liquid membrane generated by reserpine was demonstrated and data on the transport of biogenic amines and relevant neurotransmitter amino acids, through the liquid membrane generated by reserpine, were obtained.

EXPERIMENTAL

Materials—Reserpine[1], dopamine chlorhydrate[2], adrenaline hydrogen tartrate[2], L-noradrenaline[3], 5-hydroxytryptamine creatinine sulfate[4], L-glutamic acid[5], γ-aminobutyric acid[5], and distilled water (glass-distilled once from potassium permanganate) were used.

Methods—The critical micelle concentration (CMC) of aqueous reserpine was determined from the variation of surface tension with concentration. The surface tensions were measured using a tensiometer[6]. To prepare aqueous solutions of reserpine, the necessary volume of an ethanolic solution of known concentration of the drug was added to the aqueous phase with constant stirring. Since the aqueous solution of reserpine always contained some alcohol, in no case >1%, the blanks used also contained the same amount of alcohol in water. The CMC value of aqueous reserpine was found to be 1.6×10^{-6} *M*.

The all-glass cell described earlier (5, 6) was used for transport studies. A cellulose nitrate millipore filter[7], which acted as a support for the liquid

[1] BP-USP Roussel UCLAF, Paris.
[2] Loba Chemie.
[3] Fluka A.G.
[4] Koch-Light Laboratories Ltd.
[5] BDH.
[6] Fisher Surface Tensiomat Model 21.
[7] Sortorious Cat. No. 11307 of thickness 1×10^{-4} m and area 5.373×10^{-5} m^2.

0022-3549/83/0600-0599$01.00/0

Table I—Values of L at Various Concentrations of Reserpine

Concentration of Reserpine $\times 10^6$ M	0	0.800 (0.5 CMC)	1.200 (0.75 CMC)	1.600 (1 CMC)	6.400 (4 CMC)
$L^a \times 10^8$ ($m^3 s^{-1} N^{-1}$)	2.482 ± 0.086	2.191 ± 0.055	1.918 ± 0.090	1.848 ± 0.057	1.431 ± 0.031
$L^b \times 10^8$ ($m^3 s^{-1} N^{-1}$)	—	2.165 ± 0.071	2.006 ± 0.064	—	—

[a] Experimental values. [b] Calculated values on the basis of mosaic model.

membrane, separated the transport cell into two compartments, C and D (Fig. 1) (5, 6).

Measurements of hydraulic permeability were carried out using the method described earlier (5, 6) at various concentrations of reserpine, ranging from 0 to 6.4×10^{-6} M. The concentration range was selected to get data from both the lower and the higher sides of the reserpine CMC.

For solute permeability of biogenic amines and amino acids, two sets of experiments were performed. In the first set, compartment C of the transport cell (Fig. 1) (5, 6) was filled with the solution of the respective permeable solutes prepared in 6.4×10^{-6} M aqueous solutions of reserpine, and compartment D was filled with distilled water. In the second set of experiments, compartment C was filled with the aqueous solution of the permeable solutes, and compartment D was filled with the aqueous solution of reserpine of 6.4×10^{-6} M concentration. In the control experiments no reserpine was used. The concentration of reserpine of 6.4×10^{-6} M, well above its CMC, was deliberately chosen for solute permeability measurements to ensure formation of a complete layer of liquid membrane on the supporting membrane. The values of the solute permeabilities (ω) were estimated using (7, 8):

$$\left(\frac{J_s}{\Delta\pi}\right)_{J_v=0} = \omega \qquad \text{(Eq. 1)}$$

where $\Delta\pi$ is the osmotic pressure difference, J_s is the solute flux per unit area of the membrane, and J_v is the volume flux. The method of measurement was described earlier (5).

Since reserpine is known to be photosensitive (9), in all the permeability experiments, the part of the transport cell containing reserpine solution was covered with black paper. All measurements including CMC determinations were carried out at 37 ± 0.1°.

Estimation of Biogenic Amines—Transport of adrenaline, noradrenaline, dopamine, and 5-hydroxytryptamine was estimated in the presence of reserpine. Reserpine was observed to interfere with fluorometric estimation of biogenic amines; therefore, the estimations were carried out using a spectrophotometer[8] by measuring absorbance at 282.4 nm (λ_{max}). Calibration curves were constructed by noting the absorbance of the solutions of varying concentrations of biogenic amines; prepared in a solution of a fixed concentration of reserpine, which was equal to its concentration in solute permeability experiments. The calibration curves thus constructed were found to be linear in accordance with Beer's law.

Estimation of Amino Acids—The amounts of glutamic acid and γ-aminobutyric acid were estimated from the amount of their reaction products with ninhydrin[5], measured spectrophotometrically[9] at 570 nm.

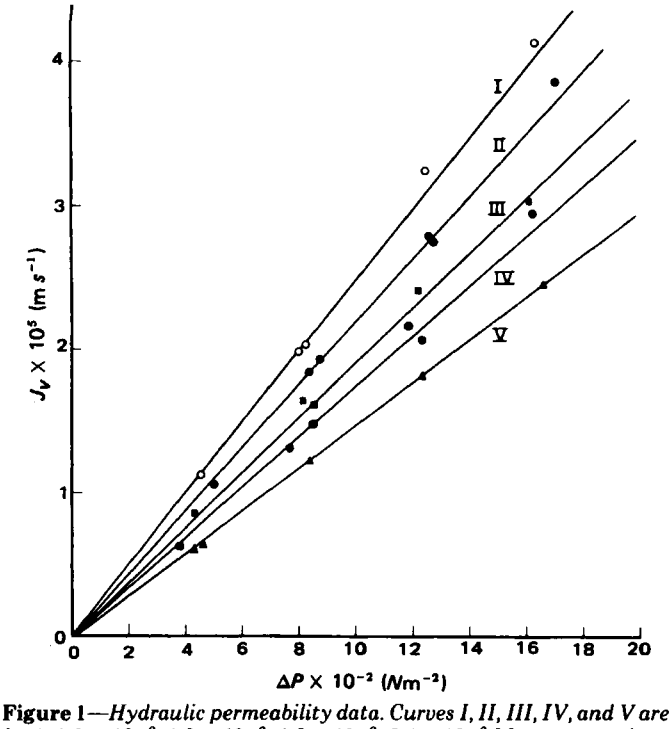

Figure 1—*Hydraulic permeability data. Curves I, II, III, IV, and V are for 0; 0.8×10^{-6}; 1.2×10^{-6}; 1.6×10^{-6}; 6.4×10^{-6} M, concentrations of reserpine, respectively.*

RESULTS AND DISCUSSION

From the hydraulic permeability data at various concentrations of reserpine (Fig. 1), it is observed that the linear relationship:

$$J_v = L\Delta P \qquad \text{(Eq. 2)}$$

where J_v represents volume flux per unit area of the membrane, ΔP the applied pressure difference, and L the hydraulic conductivity coefficient, holds good in all cases. The values of L (Table I) show a progressive decrease with an increase in concentration of reserpine up to its CMC, beyond which the decrease is only nominal. This trend is indicative of progressive coverage of the supporting membrane with the reserpine liquid membrane in accordance with a previous hypothesis (4). The decrease in the values of L beyond the CMC of reserpine possibly is due to an increase in density of the liquid membrane as postulated previously (4).

Analysis of the flow data (Fig. 1, Table I) in relation to a mosaic membrane model (10, 11) further supports the existence of the liquid membrane in series with the supporting membrane. Following the arguments given earlier (5, 6) it can be shown that if the concentration of the surfactant is n times its CMC, with $n \leq 1$, the values of L would be equal to $[(1-n)L^c + nL^s]$ where L^c and L^s represent the values of L at 0 and CMC of the surfactant, respectively.

The values of L, computed at various concentrations of reserpine, lower than its CMC value, match favorably with the values obtained experimentally (Table I).

The values of ω for the biogenic amines and amino acids recorded in Table II indicate that the maximum reduction in the permeability values is observed in the second set of experiments where compartment D was filled with reserpine and compartment C with permeable solute. When reserpine is present in compartment D (Fig. 1) (5, 6) the liquid membrane generated will present the hydrophobic surface to the permeable solute that is present in compartment C. Since reserpine is known to act by reduction in the uptake of biogenic amines (12), it appears that this specific orientation of reserpine with the hydrophobic ends facing the various solutes may be necessary even in biological cells.

Reserpine is known to inhibit intraneuronal storage of catecholamines (12). Although inhibition of the ATP-Mg^{2+}-dependent uptake mechanism in isolated chromaffin granules has been considered to be a factor governing this mechanism (13), effects on other subcellular particles is also believed to occur by a common, nonspecific mechanism (3). The results of the present experiments indicate that the liquid membrane phenomenon is such a nonspecific mechanism. The phenomenon appears to be of special significance because the liquid membrane is formed at micromolar concentrations of the drug.

While some of the wide-ranging actions of reserpine can be explained on the basis of blocking of catecholamine uptake (12), it is difficult to find a common mechanism for other effects such as inhibition of experimentally provoked thrombus formation in rats (14), decreased oxygen utilization in the brain (15) and liver (16), antitumor effects (17), extrapyramidal symptoms (18), and reduction of thyroid secretion (19). Im-

[8] Varian Cary 17-D Spectrophotometer.
[9] Bausch and Lomb Spectronic—20.

Table II—Solute Permeability (ω) of Biogenic Amines and Amino Acids in The Presence of 6.4×10^{-6} *M* Reserpine

	ω_1[a] $\times 10^{12}$ moles $s^{-1} N^{-1}$	ω_2[b] $\times 10^{12}$ moles $s^{-1} N^{-1}$	ω_3[c] $\times 10^{12}$ moles $s^{-1} N^{-1}$
Dopamine[d]	1137.0	738.2	883.6
Noradrenaline[d]	1155.0	67.8	658.3
Adrenaline[d]	1165.0	567.3	880.2
5-Hydroxy-tryptamine[d]	1063.0	311.6	518.9
Glutamic acid[e]	403.6	217.5	491.7
γ-aminobutyric acid[f]	695.1	407.1	1115.0

[a] Control value, when no reserpine was used. [b] Reserpine in compartment D of the transport cell. [c] Reserpine in compartment C of the transport cell. [d] Initial concentration used, 10 μg/ml. [e] Initial concentration used, 500 μg/ml. [f] Initial concentration used, 200 μg/ml.

pairment of catecholamine release by reserpine has also been reported (20), for which no explanation has been given at a molecular level. The liquid membrane phenomenon seems to offer a common mechanism for all such effects. Alteration in transport of biologically relevant molecules by the reserpine liquid membrane could be a plausible explanation.

Reserpine is also known to reduce the permeability of biological cells to 5-hydroxytryptamine (20), which may contribute to its sedative effect. The present set of experiments also shows reduction in permeability of 5-hydroxytryptamine because of reserpine liquid membrane. Reserpine is known to lower electroshock threshold in rats (21), which is related to depletion of γ-aminobutyric acid in the brain. Since reserpine liquid membrane reduces the permeability of this amino acid (Table II), the above effect can be at least partially assigned to the formation of a liquid membrane by reserpine *in situ*.

Although reduction in the permeabilities of biogenic amines and amino acids (Table II), due to the liquid membrane generated by reserpine, is passive in nature, it is also likely to be accompanied by a subsequent reduction in their active transport. Access of the permeable solutes to the active site located on the biological membrane is likely to be effectively reduced due to the resistance offered by the reserpine liquid membrane.

REFERENCES

(1) A. Felmeister, *J. Pharm. Sci.*, **61**, 151 (1972).

(2) P. Seeman and H. S. Bialy, *Biochem. Pharmacol.*, **12**, 1181 (1963).

(3) D. Palm, H. Grobecker, and I. J. Bak, in Bayer Symposium-II "New Aspects of Storage and Release Mechanisms of Catecholamines" H. J. Shumann and G. Kroneberg, Eds., Springer-Verlag, Berlin, 1970, pp. 188–198.

(4) R. E. Kesting, W. J. Subcasky, and J. D. Paton, *J. Colloid Interface Sci.*, **28**, 156 (1968).

(5) S. B. Bhise, P. R. Marwadi, S. S. Mathur, and R. C. Srivastava, *J. Pharm. Sci.*, **71**, 526 (1982).

(6) R. C. Srivastava and R. P. S. Jakhar, *J. Phys. Chem.*, **85**, 1457 (1981).

(7) A. Katchalsky and P. F. Curran, "Nonequilibrium Thermodynamics in Biophysics," Harvard University Press, Cambridge, Mass. 1967, pp. 113–116.

(8) A. Katchalsky and O. Kedem, *Biophys. J.*, **2**, 53 (1962).

(9) R. H. Hammer, in "Principles of Medicinal Chemistry," William A. Foye, Ed., Lea & Febiger, Philadelphia, Pa., 1976, p. 383.

(10) K. S. Speigler and O. Kedem, *Desalination*, **1**, 311 (1966).

(11) T. K. Sherwood, P. L. T. Brian, and R. E. Fischer, *Ind. Eng. Chem. Fundam.*, **6**, 2 (1957).

(12) Norman Weiner, in "Pharmacological Basis of Therapeutics," 6th ed., A. Goodman Gilman, L. S. Goodman, and A. Gilman, Eds., Macmillan, New York, N.Y., 1980, pp. 202.

(13) J. Haggendal and A. Dahlshrom, *J. Pharm. Pharmacol.*, **24**, 565 (1972).

(14) J. G. Ashwin and L. B. Jacques, *Thromb. Diath. Haemorrh.*, **5**, 543 (1961).

(15) B. C. Bose and R. Vijayavargirja, *Arch. Int. Pharmacodyn.*, **127**, 27 (1960).

(16) S. M. Kirpekar and J. J. Lewis, *Anesthesia*, **15**, 175 (1960).

(17) A. Soulairac and M. L. Soulairac, *Soc. Biol.*, **154**, 510 (1960).

(18) D. R. Laurence, "Clinical Pharmacology," 4th ed., E. L. B. S. & Churchill Livingstone, Edinburgh, 1973, p. 18.15.

(19) B. N. Premchandra and C. W. Turner, *Proc. Soc. Exp. Biol. Med.*, **104**, 306 (1960).

(20) W. C. Bowman and M. J. Rand, "Textbook of Pharmacology," 2nd ed., Blackwell Scientific, Oxford, 1980, pp. 11.13, 12.19.

(21) J. Knoll, *Arch. Exp. Pathol. Pharmakol.*, **238**, 114 (1960).

ACKNOWLEDGMENT

The authors wish to thank the Department of Science and Technology, Government of India for supporting the investigation.

Studies on the Absorption of Practically Water-Insoluble Drugs Following Injection VII: Plasma Concentration after Different Subcutaneous Doses of a Drug in Aqueous Suspension in Rats

KOICHIRO HIRANO ˣ and HIDEO YAMADA

Received June 30, 1981, from the *Shionogi Research Laboratories, Shionogi & Co., Ltd., Fukushima-ku, Osaka 553, Japan.* Accepted for publication April 30, 1982.

Abstract □ The response patterns of the time profile of plasma drug level to dose elevation after subcutaneous administration of a practically water-insoluble drug in aqueous suspension were investigated. Equations to predict the plasma drug concentration at any time and the time T_{max} at which it reaches the maximum (C_{max}) at different doses were derived using empirical equations describing the subcutaneous absorption kinetic process as an input function of one- and two-compartment models. Computer simulation for the one-compartment model showed that C_{max} tended to increase curvilinearly with dose elevation accompanied by the retardation of T_{max}. It also showed that this tendency was noticeable in dose elevation at fixed injection volume and became more significant for drugs with a smaller absorption rate and/or a larger elimination rate. This suggested that a more effective means of raising the drug plasma level for such drugs would be improvement of the formulation. The validity of the information obtained from the simulation was confirmed by various subcutaneous administration experiments of N^1-acetylsulfamethoxazole aqueous suspensions in rats. Further, the multiple-point injection method was ascertained to be useful for avoiding the nonlinear increase in plasma drug concentration with dose elevation appearing in the subcutaneous administration of aqueous suspensions.

Keyphrases □ Absorption—studies on practically water-insoluble drugs following injection, plasma concentration after different subcutaneous doses of a drug in aqueous suspensions in rats □ Aqueous suspensions—studies on absorption of practically water-insoluble drugs following injection, plasma concentration after different subcutaneous doses in rats

Aqueous suspensions are extensively used as a parenteral dosage form for practically water-insoluble drugs. Despite their usefulness for early screening and preclinical testing of newly developed drugs in laboratory animals, little is known about the patterns of plasma drug level change with time and dose after subcutaneous, intramuscular, or intraperitoneal administration. This is undoubtedly due to insufficient information on the absorption kinetics for aqueous suspensions when using such administration routes.

Drug administration *via* the subcutaneous route is convenient for early animal experiments because it allows injections of a larger volume than possible with the intramuscular route and does not involve the first-pass effect sometimes observed when the intraperitoneal route is used (1). Previous studies on the subcutaneous absorption kinetics of practically water-insoluble drugs in aqueous suspension using the local clearance method in rats (2) gave a kinetic equation which was not of the first order and which differed from that for oily (3) or surfactant micellar solutions[1]. The rate constant, which was empirically derived from the experimental results, was a complex function of the initial drug concentration and injection volume, *i.e.*, the dose (2).

[1] K. Hirano and H. Yamada, unpublished results.

The purpose of the present study was to examine plasma drug levels after different subcutaneous doses of a practically water-insoluble drug in aqueous suspension. First, pharmacokinetic approaches were made using the previously obtained kinetic equation for absorption as an input function of one- and two-compartment models to generate equations describing the time course of the plasma drug level. Next, computer simulations were undertaken to clarify the response patterns of the plasma drug concentration–time curve for the change in dose or absorption rate constant. Then the validity of the information obtained from the simulation was checked experimentally in rats with aqueous suspensions of N^1-acetylsulfamethoxazole. In addition, the usefulness of multiple-point injections for drugs having an exceedingly slow absorption rate was examined experimentally.

THEORETICAL

Previous investigations have shown that the drug absorption process from aqueous suspensions injected subcutaneously (2) or intramuscularly (4) can be represented, if the injected particles loosely agglomerate and if dissolution (or release) of the drug from the surface of the particle agglomerate is the rate-limiting step for overall drug absorption, by:

$$W = W_0(1 - jt)^3 \qquad (0 \le t \le 1/j) \qquad \text{(Eq. 1)}$$

where W_0 and W are the dose and the amount of the drug remaining at the injection site at any time t, respectively, and j is defined as an apparent absorption rate constant[2]. This constant could be related to the initial drug concentration C_0 and the injection volume V_0 by the following empirical equation:

$$j = fC_0^g V_0^h \qquad \text{(Eq. 2)}$$

where the term f is a constant that depends on the drug, preparation

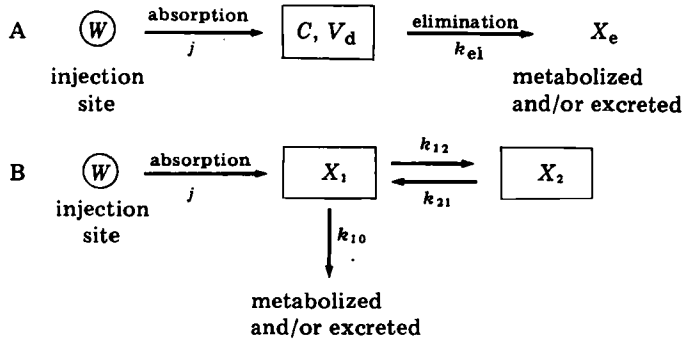

Figure 1—*(A) One- and (B) two-compartment models with nonlinear subcutaneous absorption.*

[2] The term "apparent" is used, since the assumption that Eq. 1 reflects the true absorption of the drug into the systemic circulation was not checked directly by experiments [although its validity was indirectly confirmed by the local clearance method (2, 4)]. The validity will be verified in the latter half of this paper.

0022-3549/83/0600-0602$01.00/0

conditions (particle size, *etc.*), injection site, and physiological state of the subject. The exponents g and h in this equation are constants determined experimentally. For the subcutaneous route in rats, the experimental values for g and h are −0.66 and −0.32, respectively (2).

Applying the above kinetic equations as an input function of a one- or two-compartment model, the following pharmacokinetic approaches can be made to derive equations which give the plasma drug concentration as a function of time.

One-Compartment Model—For the one-compartment model (Fig. 1A), the elimination rate of the drug (dX_e/dt) can be defined as:

$$dX_e/dt = k_{el}CV_d \qquad \text{(Eq. 3)}$$

where X_e is the amount of the drug eliminated from time 0 to t and C represents the plasma concentration of the drug. The parameters k_{el} and V_d are the apparent first-order elimination rate constant and the apparent volume of distribution, respectively. Differentiation of Eq. 1 with respect to time gives the rate of absorption of the drug from the injection site:

$$dW/dt = -3W_0j(1 - jt)^2 \qquad \text{(Eq. 4)}$$

And from mass balance:

$$\frac{dCV_d}{dt} = -\frac{dW}{dt} - \frac{dX_e}{dt} \qquad \text{(Eq. 5)}$$

Combining Eqs. 3–5 results in:

$$\frac{dC}{dt} + k_{el}C = \frac{3W_{0j}}{V_d}(1 - jt)^2 \qquad \text{(Eq. 6)}$$

Solving for C gives two relationships between the plasma drug concentration and time.

For $0 \le t \le t^*$:

$$C = P[Q(1 - e^{-k_{el}t}) + Rt + St^2] \qquad \text{(Eq. 7)}$$

and for $t > t^*$:

$$C = C^*e^{-k_{el}(t-t^*)} \qquad \text{(Eq. 8)}$$

The terms t^*, P, Q, R, S, and C^* are written by setting $\gamma = j/k_{el}$ as follows:

$$\left.\begin{aligned} t^* = 1/j, \quad P = 3W_0/V_d, \quad Q = \gamma(1 + 2\gamma + 2\gamma^2) \\ R = -2j\gamma(1 + \gamma), \quad S = j^2\gamma, \\ C^* = P[Q(1 - e^{-k_{el}t^*}) + Rt^* + St^{*2}] \end{aligned}\right\} \qquad \text{(Eq. 9)}$$

When the plasma concentration reaches maximum (C_{max}) at time T_{max} ($0 < T_{max} < t^*$), then $dC/dt = 0$. Therefore:

$$Qk_{el}e^{-k_{el}T_{max}} + R + 2ST_{max} = 0 \qquad \text{(Eq. 10)}$$

T_{max} is given as one of the real solutions of this transcendental equation. (Numerical analysis may be useful for solving this equation.) C_{max} is obtained by substituting T_{max} for t in Eq. 7.

Two-Compartment Model—Analytical treatment for a multicompartment model with a complex input function not having a simple Laplace transform, is not as simple as a one-compartment model. Also, a previous general treatment for linear mamillary models (5, 6) may not be applicable for such a model.

Recently, a valuable partial transformation approach was reported (7), which avoids Laplace transformation of the input function and the use of convolution integrals, and can be used for treatment of a linear multicompartment model with complex input functions in one or more compartments. According to this approach:

$$X = \Phi(t)[X(0) + \int_0^t \Phi(-t)f(t)dt] \qquad \text{(Eq. 11)}$$

where the ith component of vector X or f is the amount X_i at time t or the input function $f_i(t)$ in the ith compartment, respectively, and $X(0)$ is the vector X at time $t = 0$. The ijth component Φ_{ij} of matrix Φ is given by:

$$\Phi_{ij} = L^{-1}(|S_{ij}|/|S|) \qquad \text{(Eq. 12)}$$

where L^{-1} is the inverse Laplace transform operator, $|S|$ is the determinant of the matrix S, and S_{ij} is the cofactor corresponding to the ijth element. Here, the matrix S is defined as:

$$S = -K + \text{diag}(s + E_1, s + E_2, \ldots, s + E_n) \qquad \text{(Eq. 13)}$$

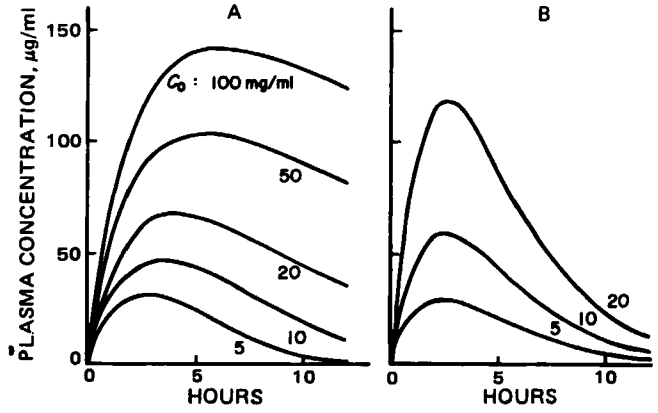

Figure 2—*Computer-predicted plasma levels after different subcutaneous doses of a drug in aqueous suspension (A) and oily solution (B) at fixed injection volume (0.5 ml). Plasma concentrations were calculated from hypothetical parameters:* k_{el}, *0.5 hr*$^{-1}$; V_d, *25 ml*; j*(1) (at* C_0 *= 5 mg/ml and* V_0 *= 0.5 ml), 0.10 hr*$^{-1}$ *(*$t_{1/2}$, *2.06 hr);* k, *0.336 hr*$^{-1}$ *(*$t_{1/2}$, *2.06 hr).*

where the ijth element k_{ij} of the matrix K is the first-order intercompartmental transfer rate constant between the ith and jth compartments, and E_i is the sum of the exit rate constants of the ith compartment. The symbol s represents the Laplace operator and $s + E_i$ is the ith diagonal element of the diagonal matrix, diag$(s + E_1, s + E_2, \ldots, s + E_n)$.

Using Eq. 11 for analytical treatment of the two-compartment model with an input function of Eq. 4 (Fig. 1B) yields the following equations which describe the drug amounts in the central and peripheral compartments (X_1 and X_2, respectively) as a function of time. Thus, for $0 \le t \le t^*$:

$$X_1 = \frac{3(\alpha - k_{21})W_0}{\alpha - \beta}[Q_1(1 - e^{-\alpha t}) + R_1t + S_1t^2] + \frac{3(k_{21} - \beta)W_0}{\alpha - \beta}[Q_2(1 - e^{-\beta t}) + R_2t + S_2t^2] \qquad \text{(Eq. 14)}$$

and:

$$X_2 = \frac{3k_{12}W_0}{\beta - \alpha}[Q_1(1 - e^{-\alpha t}) + R_1t + S_1t^2 - Q_2(1 - e^{-\beta t}) - R_2t - S_2t^2] \qquad \text{(Eq. 15)}$$

For $t > t^*$ (setting t' equal to $t - t^*$):

$$X_1 = \frac{3W_0}{(\alpha - \beta)^2}[\{(\alpha - k_{21})^2 + k_{12}k_{21}\}U_1e^{-\alpha t'} + \{(k_{21} - \beta)^2 + k_{12}k_{21}\}U_2e^{-\beta t'}] \qquad \text{(Eq. 16)}$$

and:

$$X_2 = \frac{3k_{12}W_0}{\beta - \alpha}(U_1e^{-\alpha t'} - U_2e^{-\beta t'}) \qquad \text{(Eq. 17)}$$

where α and β are the real solutions ($\alpha > \beta$) of the equation $y^2 - (k_{10} + k_{12} + k_{21})y + k_{21}k_{10} = 0$. The terms Q_1, Q_2, R_1, R_2, S_1, S_2, U_1, and U_2 are written, using $\gamma_1 = j/\alpha$ and $\gamma_2 = j/\beta$, as follows:

$$\left.\begin{aligned} Q_1 = \gamma_1(1 + 2\gamma_1 + 2\gamma_1^2), \quad Q_2 = \gamma_2(1 + 2\gamma_2 + 2\gamma_2^2) \\ R_1 = -2\gamma_1j(1 + \gamma_1), \quad R_2 = -2\gamma_2j(1 + \gamma_2), \quad S_1 = j^2\gamma_1 \\ S_2 = j^2\gamma_2, \quad U_1 = \frac{2S_1}{\alpha^2} - Q_1e^{-\alpha t^*}, \quad U_2 = \frac{2S_2}{\beta^2} - Q_2e^{-\beta t^*} \end{aligned}\right\} \qquad \text{(Eq. 18)}$$

By introducing the apparent volume (V_c) of the central compartment, the plasma drug concentration (C) is given as:

$$C = X_1/V_c \qquad \text{(Eq. 19)}$$

In addition, T_{max} ($0 < T_{max} \le t^*$) is also given as one of the real solutions of the following transcendental equation:

$$(\alpha - k_{21})(Q_1\alpha e^{-\alpha T_{max}} + R_1 + 2S_1T_{max}) + (k_{21} - \beta)(Q_2\beta e^{-\beta T_{max}} + R_2 + 2S_2T_{max}) = 0 \qquad \text{(Eq. 20)}$$

Thus, plasma concentration C at any time t, T_{max}, and C_{max} can be readily calculated for different doses of a drug when only one absorption rate constant (under certain administration conditions) and other

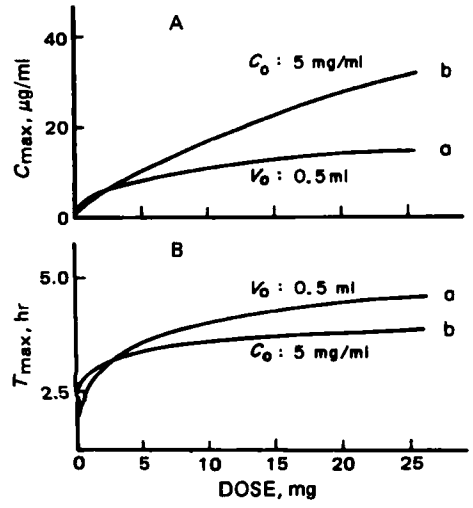

Figure 3—*Relationship between C_{max} (A) or T_{max} (B) and subcutaneous dose of aqueous suspension at fixed injection volume (a) or fixed drug concentration (b). These curves were obtained using hypothetical parameters:* k_{el}, *1.0 hr*$^{-1}$; V_d, *25 ml; j(1) (at* C_0 = *5 mg/ml and* V_0 = *0.5 ml), 0.0238 hr*$^{-1}$.

pharmacokinetic parameters are known; this confers one- or two-compartment characteristics on the body. In the present study, using the one-compartment model as an example, the response pattern of the plasma drug concentration–time curve to a change in dose or absorption rate constant was examined through some simulations and experiments.

EXPERIMENTAL

Calculation of Plasma Concentration—The apparent absorption rate constant j at any drug concentration (C_0) and at any injection volume (V_0), *i.e.*, at any dose, was calculated from one set of known data [$j(1)$ at $C_0(1)$ and $V_0(1)$], assuming the same injection site and an aqueous suspension of the same prescription, using the following equation derived readily from Eq. 2:

$$j = j(1)[C_0/C_0(1)]^g[V_0/V_0(1)]^h \qquad \text{(Eq. 21)}$$

In this study, the experimentally determined values of −0.66 and −0.32 were used for g and h, respectively (2). Drug plasma concentration C at any time t was calculated from Eq. 7 or 8 using values of j obtained from Eq. 21, pharmacokinetic parameters (k_{el} and V_d), and dose W_0. T_{max} was obtained by solving Eq. 10 with the aid of numerical analysis (Newton–Raphson method). For calculation of the sulfamethoxazole plasma concentration after subcutaneous doses of N^1-acetylsulfamethoxazole in aqueous suspension, the experimental value of 0.17 hr^{-1} (C_0 = 5 mg/ml; V_0 = 0.5 ml of N^1-acetylsulfamethoxazole), which was reported in a previous paper (2), was used as $j(1)$. All of the above calculations were carried out with a FACOM 270-20/30 computer.

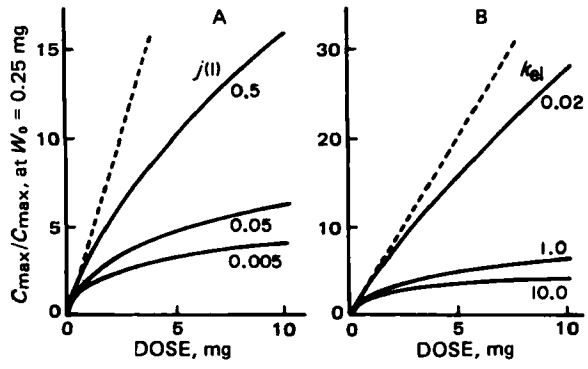

Figure 4—*Curvilinear increase in C_{max} with dose elevation at different j(1) (section A) or k_{el} values (section B) under fixed injection volume (0.5 ml). These curves were calculated from hypothetical parameters:* V_d, *25 ml;* k_{el} *in section A, 1.0 hr*$^{-1}$; *j(1) in section B, 0.05 hr*$^{-1}$. *j(1) shows the* j *value at* C_0 = *5 mg/ml and* V_0 = *0.5 ml.*

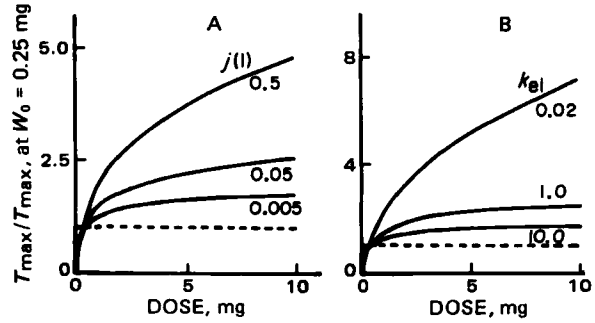

Figure 5—*Retardation of T_{max} with dose elevation at different j(1) (section A) or k_{el} values (section B) under fixed injection volume (0.5 ml). These curves were calculated from the same hypothetical parameters:* V_d, *25 ml;* k_{el} *in section A, 1.0 hr*$^{-1}$; *j(1) in section B, 0.05 hr*$^{-1}$.

Materials and Test Suspensions—N^1-Acetylsulfamethoxazole[3] was selected as a model of a practically water-insoluble drug and aqueous suspensions of the different concentrations (5, 10, 20, 50, and 100 mg/ml), prepared according to the controlled preparation method described in a previous report (4), were used as test suspensions for the subcutaneous administration experiments. N^1-Acetylsulfamethoxazole[3] and a dispersion medium[4] used for these preparations were the same as those reported in the previous paper (2). The mean particle diameter, distribution constant, and sedimentation volume of the test suspensions were 3.7–4.2 μm, 2.4–2.6, and 1.7–1.8 cm^3/g, respectively. These colloidal properties were similar to those reported in the previous paper (2). In addition, sulfamethoxazole solutions (concentration: 1.25, 2.50, and 5.0 mg/ml; medium: saline) were also used for the intravenous administration experiments. These solutions were prepared using the sodium salt[3] of sulfamethoxazole; pH values were adjusted to 8.0 with 1 *N* HCl.

Animal Experiments—Male Wistar albino rats weighing 250–292 g were used in all animal experiments. All test suspensions were administered into the dorsal subcutaneous region of the rats according to the manner described in a previous paper (3). Blood samples were withdrawn periodically through a tail vein. The rats were placed in a conventional cage with free access to water and food, except for a short period during drug administration and blood sampling when they were placed under light anesthesia with ether. One hundred microliters of plasma was collected for the following assay. A group of three to six rats was used in each experiment.

In vitro incubation of N^1-acetylsulfamethoxazole (I) at 37° [concentration of I in medium, 76 μg/ml (below solubility level of I)] with fresh rat plasma or saline shaken with subcutaneous connective tissues and interstitial materials[5], caused >90% of I to be transformed into sulfamethoxazole (II) within a 30-sec period. A similar conversion has been reported (8) for N^1-acetylsulfisoxazole using human plasma. It is inferred from these findings that N^1-deacetylation of I occurs immediately after dissolution in the injection site medium and that II is actually the compound being absorbed. In practice, I could not be detected in blood samples taken at 10 and 20 min and 1, 2, and 5 hr after subcutaneous administration of an aqueous suspension of I (dose: 5 mg/0.5 ml/rat) even in carefully conducted experiments[6].

Although I, when dissolved in the injection site medium, is deacetylated to II, the resultant II disappeared much more rapidly[7] than the dissolution of I. Thus, no significant accumulation of II at the injection site was

[3] Shionogi Research Laboratories, Shionogi & Co., Ltd., Fukushima-ku, Osaka 553, Japan.

[4] 0.5% (w/v) Methylcellulose (Metolose SM-15) + 0.005% (w/v) polysorbate 80 + 0.9% (w/v) NaCl.

[5] This incubation medium was obtained as follows: The rat was injected at four different points with 0.5 sc ml of saline. Immediately after the injections, the connective tissues containing saline depot were excised, minced, shaken with 2 ml of saline for 30 min, and centrifuged at 3000 rpm for 10 min. The resultant supernatant was used as the medium.

[6] Immediately after blood sampling, 0.2 ml of blood was mixed vigorously with 2 ml of 0.03 *N* HCl kept at 0° and 2 ml of 6% (w/v) $HClO_4$ was added. The mixture was shaken well and centrifuged at 5°. A portion of the clear, deproteinized solution was injected into the high-performance liquid chromatographic (HPLC) system as follows: Shimadzu LC-3A; column, Nucleosil 10C_{18} (4-mm i.d. × 300 mm); mobile phase, pH 6.3 phosphate buffer (50 m*M*)–acetonitrile (3:1, v/v); flow rate, 2 ml/min; detection, UV (290 nm); retention time, 14.1 min for I; detection limit for I (determined using blood samples inactivated with HCl then added with I), 1–2 μg/ml of blood.

[7] For example, the half-life of II in aqueous solution in the injection site was ~8.3 min (dose, 260.4 μg/0.5 ml/rat), while that of I in aqueous suspension was ~70 min (dose, 2.5 mg/0.5 ml/rat).

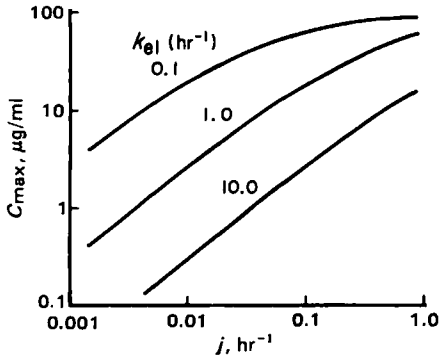

Figure 6—*Relationship between maximum plasma concentration (C_{max}) and absorption rate constant (j) at different k_{el} values under a fixed dose. These curves were obtained using hypothetical parameters: V_d, 25 ml; W_0, 2.5 mg.*

observed under the present administration conditions[8]. Therefore, postabsorptive pharmacokinetic parameters of I were estimated from plasma concentration–time profiles after intravenous administration of II. All test solutions of II were injected into a tail vein, and blood samples were periodically taken from the vein in the other side of the tail.

Analytical Method—Sulfamethoxazole in rat plasma was measured according to the fluorometric method with fluorescamine reported previously (9). To 100 μl of plasma were added 2 ml of pH 4.7 buffer (1 *N* HCl–1 *N* CH_3COONa, 3:7, v/v) and 6 ml of 1,2-dichloroethane. This was shaken well and then centrifuged. Three milliliters was withdrawn from the 1,2-dichloroethane layer, 3 ml of pH 10.6 buffer (0.1 *N* $NaHCO_3$–0.1 *N* Na_2CO_3, 1:9, v/v) was added, and the mixture was shaken and centrifuged. To 2 ml of the buffer layer (after dilution with the same buffer as necessary) were added 5 ml of pH 2.6 buffer (1 *N* HCl–1 *N* CH_3COONa, 1:1, v/v) and 1 ml of fluorescamine[9] reagent (0.2 mg/ml in acetone), and the mixture was shaken vigorously for several seconds. After this had been left standing for ~40 min, its fluorescent intensity was measured with a spectrophotometer[10] at excitation and emission wavelengths of 405 and 490 nm (uncorrected), respectively.

RESULTS AND DISCUSSION

Simulation Study—*Plasma Levels after Different Subcutaneous Doses of a Drug in Aqueous Suspension*—General patterns in the response of plasma concentration to the change in the subcutaneous dose of a drug in aqueous suspension were examined under various administration conditions, using computer simulation with hypothetical data in a one-compartment model. Figure 2A shows computer-simulated time courses of the plasma level after different subcutaneous doses of a drug in aqueous suspension at a fixed injection volume (plasma concentration shown here was calculated from Eq. 7 or 8 using j values generated from Eq. 21). The values of the absorption rate constant $j(1)$ and other pharmacokinetic parameters k_{el} and V_d used for these computations are shown in the legend. For comparison, plasma concentration–time curves for oily solutions are also shown in Fig. 2B as an example of first-order absorption (rate constant, k). Figure 2A shows the typical features of the subcutaneous administration of aqueous suspension, *i.e.*, the curvilinear increase of the maximum plasma concentration and the retardation of T_{max} with dose elevation. It should be noted that these tendencies differ from those of the preparations with first-order absorption characteristics such as oily (3) and surfactant micellar solutions[1] as shown in Fig. 2B. The above two features were more evident in dose elevation with fixed injection volume than with fixed drug concentration, as can be seen from Fig. 3.

Figure 4 compares the degree of deviation from the linear response of the maximum plasma concentration C_{max} to dose elevation among different $j(1)$ values (A) or k_{el} values (B). In this figure, the ratio of C_{max} at any dose to the C_{max} where C_0 = 0.5 mg/ml and V_0 = 0.5 ml was taken as a measure representing such a degree and is plotted against the dose. The downward deviation of this plot from the broken line, which showed

[8] The percentages of the dose disappearing from the injection site at 40, 90, and 180 min after administration of I in aqueous suspension (dose, 2.5 mg/0.5 ml/rat) were ~31, 63, and 75%, respectively, while those for II appearing at the site were ~5, 6, and 4%, respectively (each value was the mean of two experimental determinations).

[9] F. Hoffmann-La Roche Co., A. G., Basel, Switzerland.

[10] Hitachi Model 203, Hitachi, Ltd., Japan.

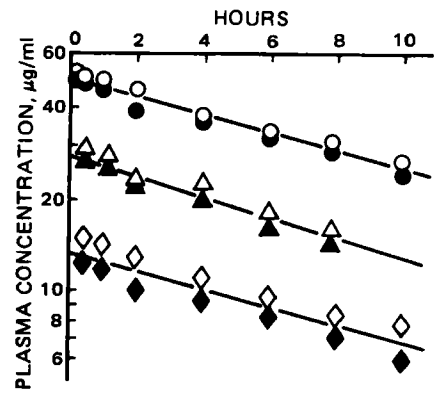

Figure 7—*Plasma concentration–time curves following three intravenous doses of sulfamethoxazole in rats. The data points in the same symbol show the plasma concentrations for each rat. Key (dose per rat): (○, ●) 2.50 mg; (△, ▲) 1.25 mg; (◇, ◆) 0.625 mg.*

a proportional relationship between C_{max} and the dose, demonstrates the phenomenon of deviation from the linear response. The deviation became larger for drugs with smaller absorption rate constants, $j(1)$, and those with larger elimination rate constants, k_{el}. Figure 5 shows the retardation of T_{max} with dose elevation at various $j(1)$ values (A) or k_{el} values (B). Similarly, the ratio of T_{max} at any dose to the T_{max} at C_0 = 0.5 mg/ml and V_0 = 0.5 ml was used as an index for this retardation. This figure indicated that the retardation of T_{max} with dose elevation became more marked the larger the $j(1)$ value and the smaller the k_{el} value.

For the subcutaneous administration of a drug in aqueous suspension, these simulations indicated that the rate of systemic drug availability decreases with increasing dose and that this decrease becomes more significant for drugs having a smaller $j(1)$ and a larger k_{el}.

Relationship Between Peak Plasma Level and Absorption Rate Constant—The parenteral drug absorption rate from an aqueous suspension can be altered by modifying not only preparation conditions such as particle size but also administration conditions such as drug concentration and injection volume (2, 4). The relationship between the absorption rate constant j and the maximum plasma concentration C_{max} at a fixed dose was examined by computer simulation. Figure 6 shows this relationship at various values of the elimination rate constant k_{el} on a log–log scale. This figure demonstrates that the curve representing such a relationship becomes closer to a straight line having a slope of unity with smaller j and larger k_{el}, while it tends to level off with larger j and smaller k_{el}. This also suggests that an attempt to elevate the drug plasma level by particle size reduction is more effective for drugs with a smaller j value [for example, due to a lower water solubility (2)] and a larger k_{el} value.

Comparison of the Results from Simulation Analyses with Experiments—Equation 1 was derived from a model in which injected particles loosely agglomerate and dissolution (or release) of the drug from the surface of the particle agglomerate is the rate-limiting process for overall drug absorption. Equation 2 was derived from the experimental

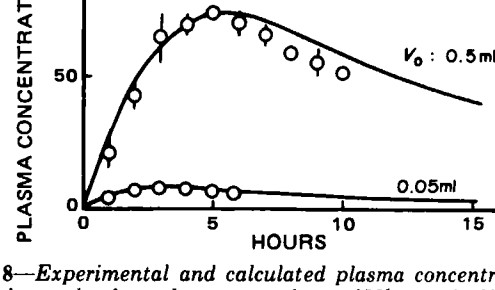

Figure 8—*Experimental and calculated plasma concentrations of sulfamethoxazole after subcutaneous doses of N^1-acetylsulfamethoxazole aqueous suspension at fixed initial drug concentration (10 mg/ml) in rats (mean body weight, 286 g). Each experimental value was given by the mean (open circle) and standard deviation (vertical bar) of three or four rats. Calculated values (solid line) were obtained with the following parameters: k_{el}, 0.072 hr^{-1}; V_d, 49.5 ml; $j(1)$, 0.17 hr^{-1}.*

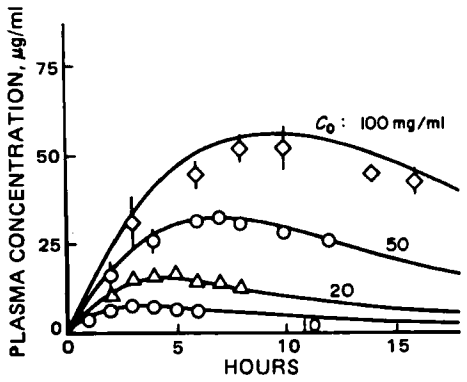

Figure 9—*Experimental and calculated plasma concentrations of sulfamethoxazole after different subcutaneous doses of* N^1*-acetylsulfamethoxazole aqueous suspensions at fixed injection volume (0.048 ml) in rats (mean body weight, 277 g). Each experimental value was given by the mean and standard deviation of four to six rats. Calculated values (solid line) were obtained with the following parameters:* k_{el}, *0.072* hr^{-1}; V_d, *48.0 ml;* $j(1)$, *0.17* hr^{-1}.

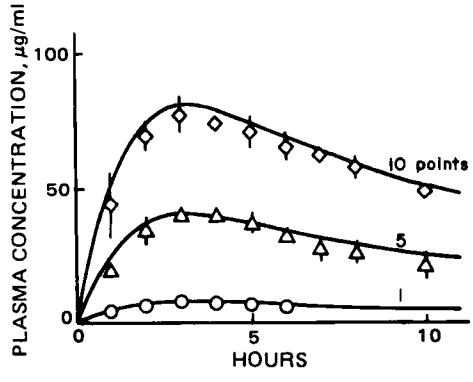

Figure 10—*Experimental and calculated plasma concentrations of sulfamethoxazole after subcutaneous doses of* N^1*-acetylsulfamethoxazole aqueous suspension by the multiple-point injection method in rats (mean body weight, 284 g).* C_0 *and* V_0 *for each injection point were 10 mg/ml and 0.048 ml, respectively. Each experimental value was given by the mean and standard deviation of four to six rats. Calculated values (solid line) were obtained with the following parameters:* k_{el}, *0.072* hr^{-1}; V_d, *49.1 ml;* $j(1)$, *0.17* hr^{-1}.

results by the local clearance method in rats (2, 4). Based on the assumption that these equations reflect the true overall absorption of the drug (or active metabolites) into the systemic circulation, the results obtained by computer simulation should be valid. However, until now the validity of this assumption had not been checked directly by experimentation. To check the feasibility of the above simulation results, plasma drug levels after subcutaneous doses using aqueous suspensions of N^1-acetylsulfamethoxazole (I) were followed in rats and compared with the calculated levels.

As mentioned in *Experimental*, I is very rapidly deacetylated to sulfamethoxazole (II) immediately after dissolution in the injection site medium, inferring absorption as II. However, absorption of II formed at the injection site occurred more rapidly than dissolution of I, and, thus, no significant accumulation of II at the injection site was observed under these injection conditions. This indicates that the rate-limiting process in overall absorption of I from aqueous suspension is the dissolution step and that the disappearance rate of I estimated by the local clearance method can be regarded as approximately equivalent to the overall absorption rate of I.

In this case, the absorption behavior for I is summarized in Scheme I:

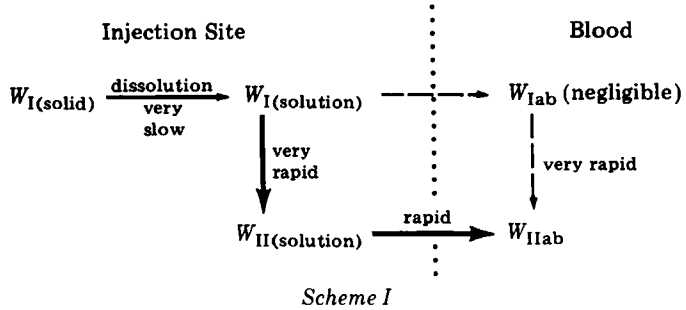

Scheme I

The amount of I (W_{ab}) absorbed *via* II (W_{IIab}) can be represented as:

$$\left.\begin{aligned} W_{ab} &= W_{IIab} \\ &= W_0 - [W_{I(solid)} + W_{I(solution)} + W_{II(solution)}] \\ &= W_0 - [W_I + W_{II(solution)}] \end{aligned}\right\} \quad \text{(Eq. 22)}$$

where W_0 is the amount injected. Since $W_I = W_{I(solid)} + W_{I(solution)} \gg W_{II(solution)}$, therefore:

$$W_{ab} \simeq W_0 - W_I \quad \text{(Eq. 23)}$$

By differentiation of this equation with respect to time (t), the following equation was obtained:

$$dW_{ab}/dt \simeq -dW_I/dt \quad \text{(Eq. 24)}$$

Accordingly, the disappearance rate of I (dW_I/dt) is approximately equal to the overall absorption rate of I (dW_{ab}/dt).

The equation for the absorption kinetics (Eq. 1) is based on the premise that dissolution (or release) is the rate-limiting step for overall drug absorption. Compound I satisfies this premise and is adequate as a model compound for this study, although it undergoes site metabolism to II.

First, plasma concentrations of sulfamethoxazole (II) after different intravenous doses were measured to examine the postabsorptive pharmacokinetic characteristics of N^1-acetylsulfamethoxazole (I) in rats. The reason for the use of II instead of I is explained in detail in *Experimental* and in the previous paragraphs. Figure 7 shows semilogarithmic plots of plasma concentrations of II as a function of time for each dose in a rat. From the nearly linear relationship of these curves, with a similar slope and linear response of the plasma levels to the intravenous dose, the pharmacokinetic characteristics of II could be explained approximately by a one-compartment model under the described experimental conditions.

From each plot in this figure, the apparent elimination rate constant k_{el} and distribution volume V_d were estimated by the least-squares method. The mean (standard deviation, *SD*) values of k_{el} and V_d' (equal to V_d per body weight) for these six experiments were 0.072 (0.008) hr^{-1} and 0.173 (0.006) ml/g, respectively. These parameters are used below together with the absorption rate constant $j(1)$, described in *Experimental*, to calculate plasma concentrations of II after different subcutaneous doses of aqueous suspensions of I *in rats*.

Single-Point Injection—Plasma concentrations of II after different subcutaneous doses of I in aqueous suspension were determined in rats and compared with calculated plasma concentrations. Figures 8 and 9 show the results of these comparisons for different doses at fixed drug concentration and fixed injection volume, respectively. These comparisons indicated that the observed plasma concentrations for all the doses

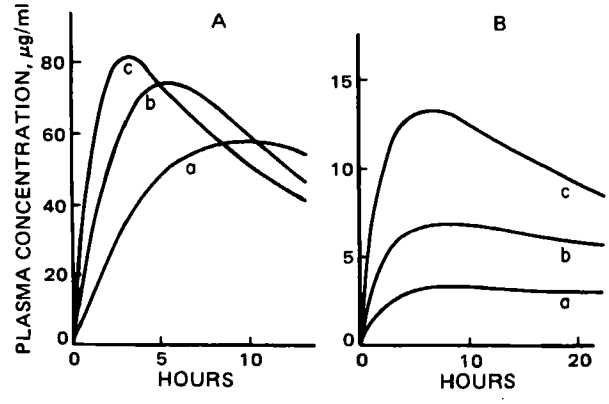

Figure 11—*Comparison of predicted plasma levels after subcutaneous administrations of aqueous suspensions among three injection methods at a fixed dose. The curves in section A were calculated from the parameters of* N^1*-acetylsulfamethoxazole (the same as shown in Fig. 10), and those in section B from hypothetical parameters as follows:* k_{el}, *0.5* hr^{-1}; V_d, *48 ml;* $j(1)$, *0.01* hr^{-1}. *Key:* a, *100 mg/ml–0.05 ml;* b, *10 mg/ml–0.5 ml;* c, *10 mg/ml–0.05 ml (10-point injection).*

examined corresponded with the calculated curves. Also, it should be noted that the curves in Figs. 8 and 9 showed the typical characteristics of subcutaneous administration of aqueous suspensions, *i.e.*, the nonlinear increase in C_{max} and retardation in T_{max} with dose elevation.

These findings appear to support the validity of the aforementioned assumption that Eqs. 1 and 2 reflect the true overall absorption of a drug in aqueous suspension into the systemic circulation.

Multiple-Point Injection—As mentioned above, dose elevation by a single subcutaneous injection of aqueous suspension may result more or less, in a nonlinear increase in plasma drug concentration. In most screening tests or preclinical testing of new drugs in laboratory animals, this phenomenon may be undesirable. It can be overcome by increasing the number of injection points in the neighboring subcutaneous area for dose elevation while keeping the drug concentration and injection volume fixed. In this multiple-point injection method, the drug absorption from each point can be expected to occur independently at nearly equal rates, and, therefore, the plasma drug level would increase in proportion to the number of injection points, *i.e.*, the dose, if the postabsorptive disposition of the drug in the body occurs in a linear manner.

To confirm this expectation, plasma sulfamethoxazole concentrations after 1-, 5-, and 10-point subcutaneous injections of N^1-acetylsulfamethoxazole aqueous suspension (C_0, 10 mg/ml; V_0, 0.048 ml) were followed in rats and compared with calculated plasma concentrations. Figure 10 shows a good agreement between the experimental and calculated values. Therefore, this multiple-point injection method seems to be a simple and convenient way to obtain a high plasma drug level without retardation of T_{max} after subcutaneous administration of a suspension.

Figure 11A compares the predicted plasma concentration–time curves following subcutaneous doses of N^1-acetylsulfamethoxazole aqueous suspension among the three injection methods at a fixed dose: C_0–V_0, (a) 100 mg/ml–0.05 ml; (b) 10 mg/ml–0.5 ml; (c) 10 mg/ml–0.05 ml, 10-point injection. This figure shows that the multiple-point injection is useful for obtaining a higher plasma drug level at a fixed dose. Figure 11B shows similar computer-simulated curves for another drug which has $j(1)$ and k_{el} values one order of magnitude below and above those in Fig. 11A, respectively. The comparison of the two figures suggests that multiple-point injection is especially effective for drugs with a small absorption rate constant and a large elimination rate constant.

The good agreement between the observed and calculated plasma concentrations presented in Figs. 8 and 9 support the validity of the assumption that Eqs. 1 and 2, derived from the experimental results by the local clearance method (2), reflect the true pattern of drug absorption into the systemic circulation. From this finding, it can be predicted that with multiple-point injection, C_{max} should be proportional to the dose without a change in T_{max}, unlike the case of single-point injection; this prediction was verified by the results shown in Fig. 10. In addition, it is indicated that the plasma concentration–time curve should differ considerably even at a fixed dose depending on the administration conditions (Fig. 11). All results of this study confirm the suitability of the analytical treatment chosen for subcutaneous drug absorption from aqueous suspensions.

Information from the simulation study presented here should be useful for predicting the dose-response pattern of plasma concentration–time curves after subcutaneous administrations in aqueous suspensions of other practically water-insoluble drugs with similar pharmacokinetic characteristics. It should also be applicable to intramuscular administrations and to drugs with two- or multicompartmental characteristics in the body.

REFERENCES

(1) G. Lukas, S. D. Brindle, and P. Greengard, *J. Pharmacol. Exp. Ther.*, **178**, 562 (1971).

(2) K. Hirano and H. Yamada, *J. Pharm. Sci.*, **71**, 500 (1982).

(3) K. Hirano, T. Ichihashi, and H. Yamada, *ibid.*, **71**, 495 (1982).

(4) K. Hirano, T. Ichihashi, and H. Yamada, *Chem. Pharm. Bull.*, **29**, 817 (1981).

(5) L. Z. Benet, *J. Pharm. Sci.*, **61**, 536 (1972).

(6) M. Gibaldi and D. Perrier, "Pharmacokinetics," Dekkar, New York, N.Y., 1975, p. 273.

(7) P. Veng-Pedersen, *J. Pharm. Sci.*, **67**, 187 (1978).

(8) L. O. Randall, R. Engelberg, V. Iliev, M. Roe, H. Haar, and T. H. Mcgavack, *Antibiot.Chemother.*, **4**, 877 (1954).

(9) T. Sakano, M. Masuda, A. Yamaji, T. Amano, and H. Oikawa, *Yakugaku Zasshi (Tokyo)*, **97**, 464 (1977).

ACKNOWLEDGMENTS

The authors acknowledge with thanks the skillful, technical assistance of Mrs. J. Kagawa and thank Prof. M. Nakagaki, Kyoto University, for his valuable comments on the manuscript.

Studies on the Absorption of Practically Water-Insoluble Drugs following Injection VIII: Comparison of the Subcutaneous Absorption Rates from Aqueous Suspensions in the Mouse, Rat, and Rabbit

KOICHIRO HIRANO ˣ **and HIDEO YAMADA**

Received August 3, 1981, from the *Shionogi Research Laboratories, Shionogi & Co., Ltd., Fukushima-ku, Osaka 553, Japan.* Accepted for publication September 14, 1981.

Abstract □ Subcutaneous drug absorption rates from aqueous suspensions were measured in the mouse and the rabbit by a local clearance method and compared with those in the rat. A plot of the cube root of the residual fraction (W/W_0) of the drug at the injection site *versus* time (t) gave a good linear relationship for the former two species. This implied that the kinetic equation for the absorption process in the rat, $(W/W_0)^{1/3} = 1 - jt$, could be applied to them. In addition, the absorption rate constants (j) of the mouse and rabbit were close to that of the rat when the drug concentration (C_0) in the suspension and the injection volume (V_0) were fixed. These results led to the presumption that the correlation between j and C_0 or V_0 in the mouse and rabbit might be similar to that in the rat, and therefore, drug plasma levels for the former two at any dose might be roughly predictable even from one j value of the rat. The validity of this assumption was confirmed by comparison of the observed and predicted plasma concentrations after different subcutaneous doses of aqueous suspensions of N^1-acetylsulfamethoxazole in the mouse and rabbit. These findings strongly supported the idea that for the subcutaneous administration of the drug in aqueous suspension under fixed dose per body weight, the rate of bioavailability should decrease with animal size, and therefore, the plasma drug level in larger species is not likely to be as high as that expected, from the data obtained for smaller species.

Keyphrases □ Absorption—studies of practically water-insoluble drugs following injection, comparison of subcutaneous absorption rates from aqueous suspensions, mouse, rat, rabbit □ Aqueous suspensions—studies on the absorption of practically water-insoluble drugs following injection, comparison of subcutaneous absorption rates, mouse, rat, rabbit

Previous reports (1, 2) showed that the absorption rate process after intramuscular or subcutaneous administration of practically water-insoluble drugs in aqueous suspensions was not linear and had a complicated dose dependency. Therefore, single administration of such drug preparations led to nonlinear response of the plasma–drug concentration, that is, a curvilinear increase of its peak and retardation of the time at which the peak occurred with increasing dose (3).

In earlier testings of pharmacological activities and dispositions of new drugs under development in laboratory animals, the dose elevation experiment is often done, not only when examining the dose response in one animal species, but also when maintaining the same or a similar dose per body weight for scale-up in various animal species. Accordingly, the problem arises that the rate of bioavailability at the same dose per body weight may vary for different species; that is, the rate of bioavailability for larger animals given a comparatively large amount of the drug may be lower compared with that for smaller animals. Since such a phenomenon, in some cases, may result in significant species differences in the drug potency, clarification of this problem is important.

In the present report, three laboratory animals, having different body weights, the mouse, rat, and rabbit, were selected as representatives to examine this problem. First, subcutaneous absorption time courses were compared among the three species using the local clearance method to determine whether a significant species difference existed in the absorption rate. Next, plasma concentrations after subcutaneous doses were followed to confirm the validity of the above comparison using N^1-acetylsulfamethoxazole in aqueous suspension. It is indicated that there is a "pitfall of dose per kilogram" in interpreting the results obtained from subcutaneous administration experiments of aqueous suspensions in various animal species.

EXPERIMENTAL

Materials—Suspensions of *p*-aminoazobenzene, *p*-hydroxyazobenzene, *o*-aminoazotoluene, and N^1-acetylsulfamethoxazole were used as models for practically water-insoluble drugs as reported previously (2). The sodium salt of sulfamethoxazole was used for the intravenous injection preparation as reported previously (3). For the fluorometry of sulfamethoxazole in plasma, fluorescamine[1] was used. All other chemicals were of reagent or analytical grade.

Preparation of Test Suspensions and Solutions—The same vehicle[2] described in the previous paper (3) was used to prepare the test aqueous suspensions. All suspensions were prepared according to the controlled preparation method reported previously (1). Their colloidal properties[3]

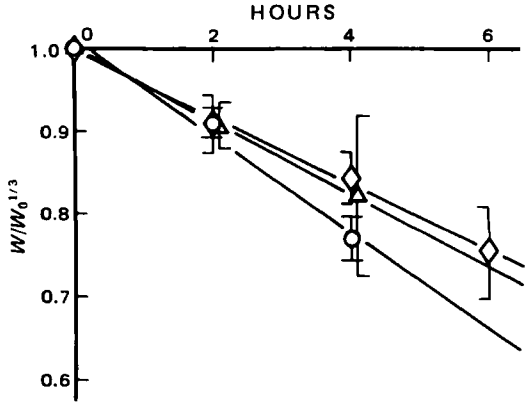

Figure 1—*Comparison of absorption rates following subcutaneous injections of* p-*aminoazobenzene aqueous suspension among three animal species. Each plot represents the mean and standard deviation of three or four animals.* C_0, *5 mg/ml;* V_0, *0.5 ml. Key:* ⊟ *mouse;* ⊕ *rat;* ⊟ *rabbit.*

[1] F. Hoffmann-La Roche and Co., A. G. Diagnostica, Basel, Switzerland.
[2] 0.5% (w/v) Methylcellulose (Metolose SM-15) + 0.005% (w/v) polysorbate 80 + 0.9% (w/v) NaCl.
[3] Mean particle diameter, 3.6–4.2 μm; distribution constant, 2.6–2.7; sedimentation volume, 1.7–2.8 cm^3/g.

0022-3549/83/0600-0608$01.00/0

Table I—Comparison of Subcutaneous Absorption Rate Constants (j) from Various Aqueous Suspensions among Three Animal Species

Compound	C_0, mg/ml	V_0, ml	j, hr^{-1} Mouse[a]	Rat[a]	Rabbit[a]
p-Hydroxyazobenzene	50	0.05	0.022 (0.004)	0.018 (0.002)	0.026 (0.005)
			NS	NS	
			NS		
p-Hydroxyazobenzene	5	0.5	0.048 (0.004)	0.043 (0.002)	0.042 (0.004)
			NS	NS	
			NS		
p-Aminoazobenzene	5	0.5	0.043 (0.009)	0.057 (0.004)	0.040 (0.004)
			NS	$p < 0.05$	
			NS		

[a] Each j value was obtained from the data shown in Figs. 1 and 2 by the least-squares method and is given with the standard error in parentheses. A t test was performed between j values of two animals each. NS = not significant ($p > 0.1$).

were similar to those reported previously (2). In addition, sulfamethoxazole solutions were prepared by the same method described in the previous paper (3) and used for the intravenous administration experiments.

Animal Experiments—*Animals*—ICR Jcl strain mice (male, 26–34 g), Wistar albino rats (male, 250–305 g), and mongrel rabbits (male, 2.6–4.0 kg) were used. During the experiments, they were kept in cages with free access to water and food.

Absorption Experiment Procedure—All the test suspensions were administered into the subcutaneous region near the center of the shorn dorsum of the animals, and their absorption rates were measured by the local clearance method described previously (4). In the mouse and rat experiments, each animal received a single injection. In the rabbit experiments, three successive injections were given at designated time intervals into different sites sufficiently apart from each other but within the dorsum of each animal; the amount of the drug remaining at each injection site was measured separately. When the experimental period ended, the mice and rats were sacrificed by exsanguination, and the rabbits were killed by intravenous administration of sodium pentobarbital[4]. The drug remaining in the injection site was recovered from the excised tissues including the depot by extraction with ethyl acetate, and its amount was determined. A group of three to six animals was used in each experiment.

Plasma Drug Level—All the aqueous suspensions of N^1-acetylsulfamethoxazole were administered subcutaneously to mice or rabbits in the manner described above. Blood samples from the mice were withdrawn from the heart at set time intervals and from the rabbits, from an ear vein periodically (serial sampling). One-hundred microliters of plasma was collected for the following analysis. *In vitro* incubation of N^1-acetylsulfamethoxazole with fresh plasma at 37° showed that this compound was very quickly transformed into sulfamethoxazole. The following intravenous administration experiments using sulfamethoxazole instead of N^1-acetylsulfamethoxazole were done in mice and rabbits to examine postabsorptive pharmacokinetic characteristics of N^1-acetylsulfamethoxazole subcutaneously administered. Test solutions of sulfamethoxazole were administered *via* a tail vein for mice (0.05 ml) and an ear vein for rabbits (2.5 ml), then blood samples were taken from the heart for the former and from another ear vein for the latter. For each rabbit, the above subcutaneous and intravenous administration experiments were performed alternately every 7–10 days for a 2-month period.

Analytical Method—The remaining amounts of *p*-aminoazobenzene, *p*-hydroxyazobenzene, and *o*-aminoazotoluene from the injection site were analyzed colorimetrically after extraction, as described previously (2). The plasma concentrations of sulfamethoxazole after subcutaneous injections of N^1-acetylsulfamethoxazole and intravenous injections of sulfamethoxazole in mice or rabbits were determined according to a fluorometric method with fluorescamine as described in the previous report (3).

Prediction of Plasma Drug Concentration—Sulfamethoxazole-plasma concentrations after different subcutaneous doses of the controlled suspension of N^1-acetylsulfamethoxazole in mice or rabbits were predicted from their postabsorptive pharmacokinetic parameters (elimination rate constant and volume of distribution) and one basic absorption rate constant $j(1)$ in rats using the equations[5] presented in the previous report (3). The postabsorptive pharmacokinetic parameters were estimated from the plasma concentration–time curves after different intravenous doses of sulfamethoxazole in mice and rabbits. The experimental value of 0.17 hr^{-1} (N^1-acetylsulfamethoxazole concentration in the test suspension, 5 mg/ml; injection volume, 0.5 ml) from a previous report (2) was used as $j(1)$.

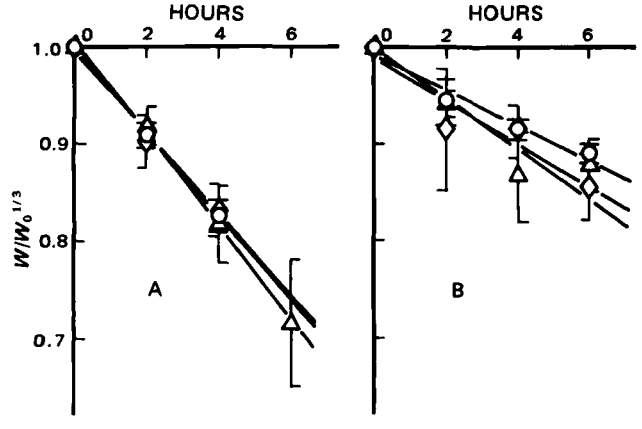

Figure 2—*Comparison of absorption rates following subcutaneous injections of* p-*hydroxyazobenzene aqueous suspensions among three animal species. Each result is given as the mean and standard deviation of three or four animals. (A):* C_0, *5 mg/ml;* V_0, *0.5 ml. (B):* C_0, *50 mg/ml;* V_0, *0.05 ml. Key:* mouse; rat; rabbit.

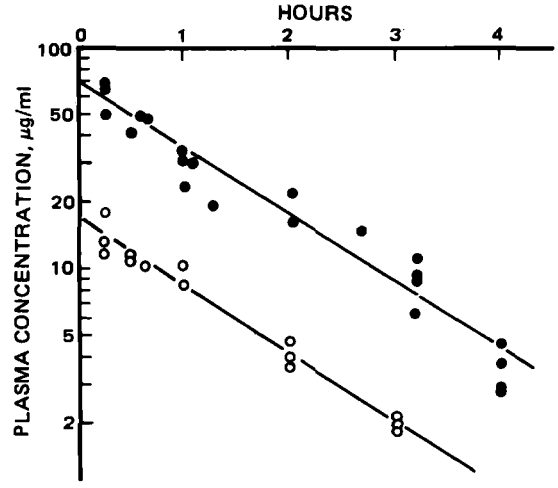

Figure 3—*Plasma concentration of sulfamethoxazole after intravenous doses in mice (26–34 g). Key: (●) 0.502 mg/mouse; (○) 0.103 mg/mouse.*

[4] Pitman-Moore, Inc., N.J.

[5] Equation 7 or 8 and Eq. 21 in the previous report (3).

Table II—An Example for Comparison of Subcutaneous Absorption Rate Constants (j) at Fixed Dose per Body Weight among Three Animal Species

Animal	Body Weight kg	C_0, mg/ml	V_0, ml	Dose, mg/kg	j/j(rat)[a]
Mouse	0.03	5	0.05	8.3	2.1
Rat	0.3	5	0.5	8.3	1.0
Rabbit	3	50	0.5	8.3	0.29

[a] Estimated from Eq. 2 (using $g = -0.66$ and $h = -0.32$).

RESULTS AND DISCUSSION

Comparison of Subcutaneous Absorption Rates among Three Animals—Previous studies (5, 6) have reported the species difference in the absorption rates of solid drugs implanted subcutaneously. However, few detailed investigations have been done on the species difference in subcutaneous absorptions from aqueous suspensions as well as from other conventional dosage forms. Therefore, the difference in the rate of bioavailability among various animal species has been discussed little until now. The subcutaneous absorption rates of practically water-insoluble drugs in aqueous suspension were compared directly among three popular laboratory animal species, the mouse, rat, and rabbit, using a local clearance method. For this comparison, the dorsal subcutaneous region of each animal was selected as the model injection site.

Figure 1 shows the results for subcutaneous administrations of the controlled aqueous suspension of p-aminoazobenzene. In this comparison, the initial concentration (C_0) of p-aminoazobenzene in the suspension and the injection volume (V_0) were fixed as given in the legend. The cube root of the residual function (W/W_0) at the injection site for each animal species was plotted against time. A previous report (2) indicated that such a plot gave a good linear relationship for rats. This appeared to be also true for mice and rabbits, as indicated in Fig. 1. It was surprising that the slopes of these absorption time curves were close to each other. These tendencies were further examined by similar experiments using other test suspensions of p-hydroxyazobenzene. Figure 2 shows the results. The comparisons under the two conditions of different C_0 and V_0 also showed tendencies similar to those shown in Fig. 1. These results suggested that the kinetic equation for rats should also be applicable for describing the subcutaneous absorption process from aqueous suspensions in other animals such as mice and rabbits; that is:

$$(W/W_0)^{1/3} = 1 - jt \qquad \text{(Eq. 1)}$$

where j was defined as an absorption rate constant (2).

Table I summarizes the absorption rate constants with their standard errors estimated from the data in Figs. 1 and 2 by the least-squares method. This table shows that the difference in j among these three species is not very significant and this tendency may be true for other suspensions with variable drug concentrations and injection volumes. This also implies that the following relationship derived from the rat

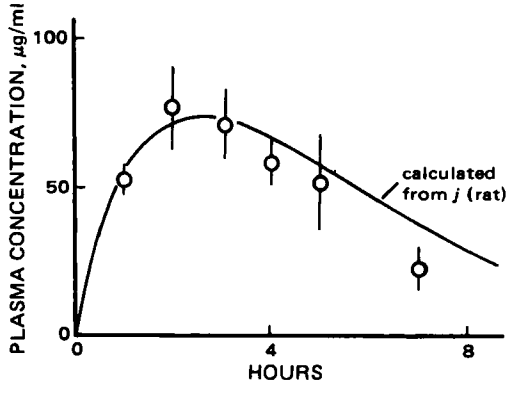

Figure 4—*Observed and predicted plasma concentrations of sulfamethoxazole after subcutaneous administration of* N^1*-acetylsulfamethoxazole aqueous suspension in mice (30.6 ± 1.6 g). Each observed value represents the mean and standard deviation of three mice.* C_0 = *51.6 mg/ml,* V_0 = *0.05 ml. The predicted value (solid line) was obtained using the following parameters:* k_{el}, *0.711 hr*$^{-1}$; V_d, *7.19 ml; j(1) (at* C_0 = *5 mg/ml and* V_0 = *0.5 ml in rats), 0.17 hr*$^{-1}$.

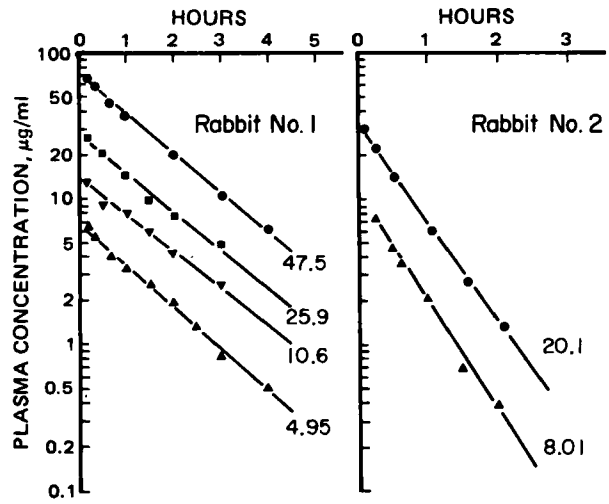

Figure 5—*Plasma concentration after different intravenous doses of sulfamethoxazole in rabbits. The value next to each curve shows the dose of sulfamethoxazole (mg/rabbit). Mean body weights of the rabbits during the experiments: No. 1, 3.96 kg; No. 2, 2.70 kg.*

experiments may also be applied to the subcutaneous absorption in mice and rabbits:

$$j = fC_0^g V_0^h \qquad \text{(Eq. 2)}$$

where g and h are the constants determined empirically [for rats, the experimental values of g and h were -0.66 and -0.32, respectively (2)]. The term f represents a constant that depends on such biological factors as the injection site and its physiological or histological state when the drug and suspension are the same. Such factors would influence the *in vivo* dispersion and dissolution of the injected particles and, hence, the absorption rate. Accordingly, the above results seem to show that the difference in the apparent *in vivo* dissolution rates of the drug among the three species may not be very large.

Comparison of Predicted and Observed Plasma Drug Concentrations in Mouse and Rabbit—It has been shown (3) that Eqs. 1 and 2, which had been derived empirically based on the results obtained from the local clearance method, reflected the true absorption of a drug into the systemic circulation in rats. The check, from the same point of view, was also performed in mice and rabbits, as described below.

The results shown above indicate that the absorption rate did not vary considerably for the mouse, the rat, and the rabbit when the drug concentration and injection volume were fixed, and that Eqs. 1 and 2 might be applicable for animals other than rats. These results also presented a possibility that the absorption rate constant j for the rat can be used, in rough approximation, as a substitute for that used for the mouse and rabbit. To confirm the validity of this presumptive evidence from the absorption experiments by the local clearance method, plasma drug concentration after different doses of the controlled aqueous suspension of N^1-acetylsulfamethoxazole were followed in the mouse and the rabbit, then compared with those predicted from their individual postabsorptive pharmacokinetic parameters and the absorption rate constant of the rat.

Mouse—Prior to subcutaneous administration experiments of N^1-acetylsulfamethoxazole (I) aqueous suspension, intravenous administration experiments of sulfamethoxazole (II) aqueous solution were undertaken to examine the postabsorptive pharmacokinetic characteristics of I. The reason for use of II instead of I was explained in detail in *Experimental*. Figure 3 shows semilogarithmic plots of plasma concentrations of II *versus* time after two intravenous doses (0.103 and 0.502 mg/mouse) of II in mice. Although the experimental values were slightly scattered, the plasma concentration–time curve for each dose could be approximated as a straight line. The plasma level appeared to be in proportion with the dose. These results suggested that the analytical treatment by a one-compartment model should be approximately possible for II in mice under the present experimental conditions. From the data in Fig. 3, the estimates (standard error, SE) of the apparent elimination rate constant (k_{el}) and volume of distribution per body weight (V_d') were calculated by the least-squares method to be 0.711 (0.020) hr^{-1} and 0.235 (0.047) ml/g, respectively. These parameters were used to predict plasma concentrations of II after the subcutaneous administration of I in aqueous suspension.

Table III—Predicted and Observed Percent Absorbed of *o*-Aminoazotoluene at 7.5 hr after Subcutaneous Administration of Its Aqueous Suspension under Fixed Dose per Body Weight in Three Animal Species

Animal	Percent Absorbed[a]		
	Known	Predicted	Observed[b]
Mouse[c]	—	65.7	60.9 ± 12.5
Rat[d]	36.9[e]		
Rabbit[f]	—	9.2	12.2 ± 4.0

[a] At the same C_0 and V_0 as shown in Table II. [b] Mean ± *SD* of three to six animals. [c] Body weight, 29–32 g. [d] Body weight, 290–305 g. [e] Reported previously (2). [f] Body weight, 2.85–3.20 kg.

Figure 4 compares the observed plasma level of II with the predicted level after the subcutaneous dose of I in aqueous suspension in mice (concentration of I in the suspension, 51.6 mg/ml; injection volume, 0.05 ml). The predicted plasma concentrations were calculated from the above estimated k_{el} and V_d (V_d' × mean body weight) in mice and one subcutaneous absorption rate constant in rats, $j(1)$, which had been reported in a previous paper (2), according to the procedure[5] described in the previous report (3). As is evident from Fig. 4, the observed plasma concentrations were in fair agreement with the predicted plasma-concentration curve. These results suggest the applicability of the above rough approximation in which the subcutaneous absorption rate constant of a drug from aqueous suspension in rats can be used as a substitute for that in mice.

Rabbit—Similar examinations were also performed with rabbits. Figure 5 shows time courses of the sulfamethoxazole (II) plasma concentration on a semilogarithmic scale after different intravenous doses of II in two rabbits (Nos. 1 and 2). The plasma concentration of II appeared to be nearly proportional to the dose for each rabbit. Within a short period after injection (0–20 min), some curvatures showing the distribution phase were observed in the plasma drug concentration–time curves and this was similar to results reported previously (7). However, these curvatures were minute under the present experimental conditions, so each time profile was regarded as a straight line. This allowed use of the one-compartment model for treatment of the data in Fig. 5. The apparent elimination rate constant, k_{el} and volume of distribution per body weight, V_d', were estimated for each rabbit. Their estimated values (*SE*) were 0.584 (0.042) hr^{-1} and 0.199 (0.007) ml/g for rabbit 1 and 1.50 (0.09) hr^{-1} and 0.285 (0.057) ml/g for rabbit 2. Since differences in the parameters k_{el} and V_d' were very large between these two rabbits, individual data for these parameters were used below to predict the plasma drug concentration in each rabbit.

Figure 6 compares the observed and predicted plasma concentrations of II after different subcutaneous doses of N^1-acetylsulfamethoxazole (I) in aqueous suspension in each rabbit. In rabbit 1, the plasma concentrations after three doses with a fixed injection volume (1.0 ml) were followed and in rabbit 2, those after two doses with a fixed concentration of I (50 mg/ml) were examined. The predicted plasma concentrations were obtained using one absorption rate constant $j(1)$, which was the same as that used in the mouse experiments, and k_{el} and V_d values for each rabbit are represented by the solid line in Fig. 6. The experimental plasma concentrations, on the whole, appeared to be close to the predicted curves for both rabbits, although slight deviations were occasionally seen. These results suggest that the rough approximation, in which the subcutaneous absorption rate constant in rats is used as a substitute for that in rabbits, is possible.

The above findings in mice and rabbits support the prediction obtained from the local clearance method, that the subcutaneous absorption rate of a drug in aqueous suspension may not vary considerably among the mouse, rat, and rabbit under the same administration conditions and that Eq. 2 may be approximately applicable for the mouse and rabbit as well as the rat.

Problem in Animal Scale-up: The Pitfall of Dose per Kilogram—The action, metabolism, and disposition of new drugs under development are usually examined in various animal species under similar dose per kilogram schedules and species differences are often discussed. This may be adequate in most cases. However, for the case of subcutaneous administration of drugs in aqueous suspension, such discussions should be handled with caution.

The results mentioned above suggest that Eq. 2 originally derived in the rat might be approximately applicable for different animal species (at least for mice and rabbits). This implies that an unexpected phenomenon for early screening tests may occur in animal scale-up: we call

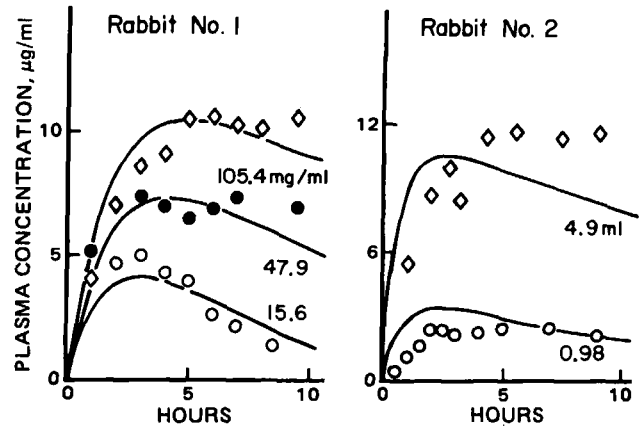

Figure 6—*Observed and predicted plasma concentrations of sulfamethoxazole after subcutaneous administrations of* N^1*-acetylsulfamethoxazole aqueous suspensions in rabbits. The predicted value (solid line) was obtained using the following parameters:* k_{el} *and* V_d, *0.584* hr^{-1} *and 789 ml (Rabbit No. 1,* V_0 *= 1.0 ml), 1.50* hr^{-1} *and 770 ml (Rabbit No. 2,* C_0 *= 50 mg/ml); j(1) (at* C_0 *= 5 mg/ml and* V_0 *= 0.5 ml in rats), 0.17* hr^{-1}.

this the pitfall of dose per kilogram. This pitfall is concretely demonstrated by the following example. Let us consider a case in which the same dose per kilogram of a drug in aqueous suspension is administered subcutaneously to three animal species with different body weights: the mouse, rat, and rabbit. In this case, the amount of drug administered (W_0) must differ among these animal species. Table II shows an example of such an administration schedule. Here, the drug concentration C_0 in the suspension or the injection volume V_0 for each animal is appropriately modified to fix the dose per kilogram. As estimated from Eq. 2, the subcutaneous absorption rate constants in these three animal species under given administration conditions differ from each other. The ratio of the rate constant in the mouse or rabbit to that in the rat, j/j(rat), which can be estimated from Eq. 2 using $g = -0.66$ and $h = -0.32$, are also listed in Table II. Comparisons of these ratios show that the j value in the mouse is about sevenfold as large as that in the rabbit.

The validity of the above predictions was confirmed experimentally using the controlled aqueous suspension of another compound *o*-aminoazotoluene, which has a measured subcutaneous absorption rate constant for rats (2). The absorption rate constants (j) in the mouse and the rabbit after subcutaneous administration of this test suspension under the conditions (C_0 and V_0) shown in Table II can be readily predicted from the j/j(rat) ratios. Then the absorbed fractions (W_{ab}/W_0) of *o*-aminoazotoluene in the mouse and the rabbit at any time (t) are calculated from their individual j values using the equation $W_{ab}/W_0 = 1 - (1 - jt)^3$. The calculation showed that 60–70% of the dose is absorbed at 7.5 hr after administration in the mouse but only ~10% in the rabbit (Table III). Experimental results for the mouse and the rabbit agreed well with the calculated values, as shown in Table III. This ascertains the validity of the predictions in Table II.

The results mentioned above strongly suggest that the absorbed amount of the drug per kilogram for a period after the subcutaneous administration of the drug in aqueous suspension differs considerably among animal species when the same dose per kilogram is given to them: the rate of bioavailability decreases with animal scale-up. This means that the plasma drug level in large animal species may not be as high as expected from the data in small animal species if the elimination rate constant and the apparent volume of distribution per kilogram for the former species are not much smaller than those for the latter. Such a phenomenon may emerge more significantly and seriously for drugs with a slower absorption rate, due to a lower water solubility, for example. This can be understood from the simulation study in our previous report (3).

Accordingly, in the case where species-specific differences in the drug action and disposition are discussed based on the data generated by subcutaneous administration of a drug in aqueous suspension, attention should be paid to the difference in the rate of bioavailability among the species. And it should be noted that the phenomenon called the "pitfall of dose per kilogram" may occur not only for the system presented here but also for drug administration in other heterogeneous dosage forms or for injections into tissues other than the subcutis (e.g., intramuscular administrations). In addition, caution should be exercised against this

pitfall when extrapolating the data from small animal species to humans.

REFERENCES

(1) K. Hirano, T. Ichihashi, and H. Yamada, *Chem. Pharm. Bull. (Tokyo)*, **29**, 817 (1981).

(2) K. Hirano and H. Yamada, *J. Pharm. Sci.*, **71**, 500 (1982).

(3) K. Hirano and H. Yamada, *J. Pharm. Sci.*, **72**, 602 (1983).

(4) K. Hirano, T. Ichihashi, and H. Yamada, *J. Pharm. Sci.*, **71**, 495 (1982).

(5) P. H. F. Bishop and S. J. Folley, "Ciba Foundation Colloquia on Endocrinology," vol. 3, J. and A. Churchill, Ltd., London, 1952, p. 265.

(6) E. S. Horning, *Br. J. Cancer*, **10**, 678 (1956).

(7) T. Nishihata, N. Yata, and A. Kamada, *Chem. Pharm. Bull. (Tokyo)*, **26**, 2058 (1978).

ACKNOWLEDGMENTS

The authors thank Prof. M. Nakagaki, Kyoto University, for his valuable suggestions on the manuscript.

Determination of Salicylamide and Five Metabolites in Biological Fluids by High-Performance Liquid Chromatography

MARILYN E. MORRIS and GERHARD LEVY ˣ

Received April 16, 1982 from the *Department of Pharmaceutics, School of Pharmacy, State University of New York at Buffalo, Amherst, NY 14260.* Accepted for publication June 4, 1982.

Abstract □ Two high-performance liquid chromatographic (HPLC) assay procedures were developed for the determination of salicylamide and its metabolites in serum, urine, and saliva. One method involves reverse-phase ion-pair chromatography and UV detection, and is used to determine salicylamide, salicylamide glucuronide, and salicylamide sulfate. The other method, with a different mobile phase and without the *ion-pairing reagent, is used to* determine gentisamide (the hydroxylated metabolite of salicylamide), gentisamide glucuronide, and gentisamide sulfate. The assays are performed by direct injection of the sample after protein precipitation with ethanol containing the internal standard. Increased sensitivity for the determination of low concentrations of salicylamide is obtained by organic extraction of this drug from serum or saliva. Calibration curves for the conjugates of salicylamide and gentisamide were obtained, in the absence of authentic standards, by partial enzymatic hydrolysis, using the decrease of the conjugate peaks and the concomitant increase of free salicylamide or gentisamide concentrations to determine peak area ratio–concentration relationships. Application of the HPLC assay procedures to the determination of salicylamide excretion products in the urine of three normal human subjects resulted in 98.6% (range: 97.1–100.1%) recovery of a 1-g oral dose of the drug. All five metabolites of salicylamide were found in urine, but only salicylamide glucuronide, salicylamide sulfate, and gentisamide glucuronide were found consistently and in appreciable quantities. Salicylamide and all of its metabolites except gentisamide sulfate were found in human and rat serum, and unconjugated salicylamide as well as gentisamide were found in human saliva.

Keyphrases □ High-performance liquid chromatography—assay for salicylamide and metabolites in biological fluids, drug conjugate calibration curves in the absence of authentic standards □ Salicylamide—determination in biological fluids, high-performance liquid chromatography □ Metabolites—salicylamide, determination in biological fluids, high-performance liquid chromatography

Salicylamide has analgesic, antipyretic, and hypnotic activities (1–3) but its clinical effectiveness is limited (4–6) due to extensive presystemic biotransformation after oral administration (7, 8). The drug is, however, a valuable research tool for the exploration of drug conjugation reactions (9, 10), drug absorption (11–14) and metabolism interactions (15, 16), route of administration effects on drug disposition (17, 18), effects of disease on drug disposition (19–21), drug concentration–effect relationships (22), product inhibition (23), fetal development (24), and the clinical assessment of metabolic immaturity and disorders (25–27).

Salicylamide is eliminated almost entirely by biotransformation (Scheme I). Many assay methods are available for the determination of this drug in biological fluids (9, 14, 22, 28–36), but none of these provide for the direct determinations (*i.e.*, without prior hydrolysis) of salicylamide conjugates. Apparently only an indirect colorimetric method (9) and a qualitative TLC method (37) have been used for the determination of gentisamide, the hydroxylated metabolite of salicylamide. To facilitate future pharmacokinetic studies with salicylamide, we have developed high-performance liquid chromatographic (HPLC) procedures for the direct determination of salicylamide, gentisamide, and their glucuronide and sulfate

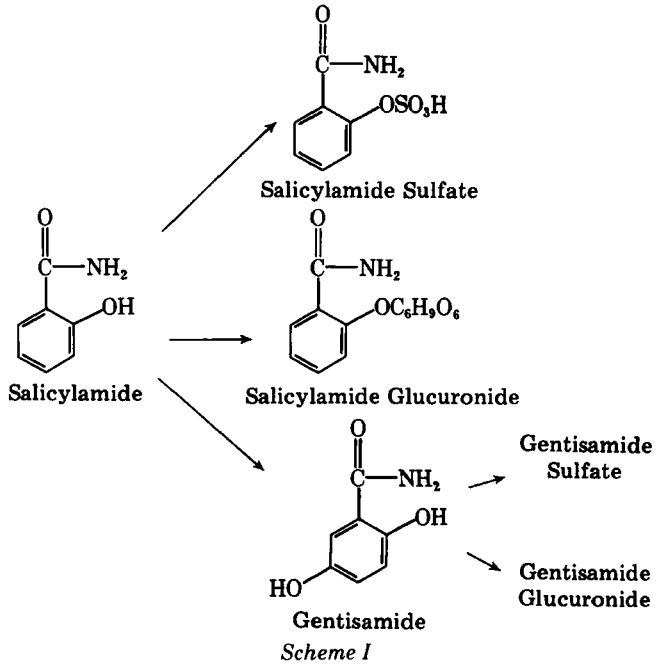

Scheme I

0022-3549/83/0600-0612$01.00/0

pitfall when extrapolating the data from small animal species to humans.

REFERENCES

(1) K. Hirano, T. Ichihashi, and H. Yamada, *Chem. Pharm. Bull. (Tokyo)*, **29**, 817 (1981).

(2) K. Hirano and H. Yamada, *J. Pharm. Sci.*, **71**, 500 (1982).

(3) K. Hirano and H. Yamada, *J. Pharm. Sci.*, **72**, 602 (1983).

(4) K. Hirano, T. Ichihashi, and H. Yamada, *J. Pharm. Sci.*, **71**, 495 (1982).

(5) P. H. F. Bishop and S. J. Folley, "Ciba Foundation Colloquia on Endocrinology," vol. 3, J. and A. Churchill, Ltd., London, 1952, p. 265.

(6) E. S. Horning, *Br. J. Cancer*, **10**, 678 (1956).

(7) T. Nishihata, N. Yata, and A. Kamada, *Chem. Pharm. Bull. (Tokyo)*, **26**, 2058 (1978).

ACKNOWLEDGMENTS

The authors thank Prof. M. Nakagaki, Kyoto University, for his valuable suggestions on the manuscript.

Determination of Salicylamide and Five Metabolites in Biological Fluids by High-Performance Liquid Chromatography

MARILYN E. MORRIS and GERHARD LEVY ˣ

Received April 16, 1982 from the *Department of Pharmaceutics, School of Pharmacy, State University of New York at Buffalo, Amherst, NY 14260.* Accepted for publication June 4, 1982.

Abstract □ Two high-performance liquid chromatographic (HPLC) assay procedures were developed for the determination of salicylamide and its metabolites in serum, urine, and saliva. One method involves reverse-phase ion-pair chromatography and UV detection, and is used to determine salicylamide, salicylamide glucuronide, and salicylamide sulfate. The other method, with a different mobile phase and without the *ion-pairing reagent, is used to* determine gentisamide (the hydroxylated metabolite of salicylamide), gentisamide glucuronide, and gentisamide sulfate. The assays are performed by direct injection of the sample after protein precipitation with ethanol containing the internal standard. Increased sensitivity for the determination of low concentrations of salicylamide is obtained by organic extraction of this drug from serum or saliva. Calibration curves for the conjugates of salicylamide and gentisamide were obtained, in the absence of authentic standards, by partial enzymatic hydrolysis, using the decrease of the conjugate peaks and the concomitant increase of free salicylamide or gentisamide concentrations to determine peak area ratio–concentration relationships. Application of the HPLC assay procedures to the determination of salicylamide excretion products in the urine of three normal human subjects resulted in 98.6% (range: 97.1–100.1%) recovery of a 1-g oral dose of the drug. All five metabolites of salicylamide were found in urine, but only salicylamide glucuronide, salicylamide sulfate, and gentisamide glucuronide were found consistently and in appreciable quantities. Salicylamide and all of its metabolites except gentisamide sulfate were found in human and rat serum, and unconjugated salicylamide as well as gentisamide were found in human saliva.

Keyphrases □ High-performance liquid chromatography—assay for salicylamide and metabolites in biological fluids, drug conjugate calibration curves in the absence of authentic standards □ Salicylamide—determination in biological fluids, high-performance liquid chromatography □ Metabolites—salicylamide, determination in biological fluids, high-performance liquid chromatography

Salicylamide has analgesic, antipyretic, and hypnotic activities (1–3) but its clinical effectiveness is limited (4–6) due to extensive presystemic biotransformation after oral administration (7, 8). The drug is, however, a valuable research tool for the exploration of drug conjugation reactions (9, 10), drug absorption (11–14) and metabolism interactions (15, 16), route of administration effects on drug disposition (17, 18), effects of disease on drug disposition (19–21), drug concentration–effect relationships (22), product inhibition (23), fetal development (24), and the clinical assessment of metabolic immaturity and disorders (25–27).

Salicylamide is eliminated almost entirely by biotransformation (Scheme I). Many assay methods are available for the determination of this drug in biological fluids (9, 14, 22, 28–36), but none of these provide for the direct determinations (*i.e.*, without prior hydrolysis) of salicylamide conjugates. Apparently only an indirect colorimetric method (9) and a qualitative TLC method (37) have been used for the determination of gentisamide, the hydroxylated metabolite of salicylamide. To facilitate future pharmacokinetic studies with salicylamide, we have developed high-performance liquid chromatographic (HPLC) procedures for the direct determination of salicylamide, gentisamide, and their glucuronide and sulfate

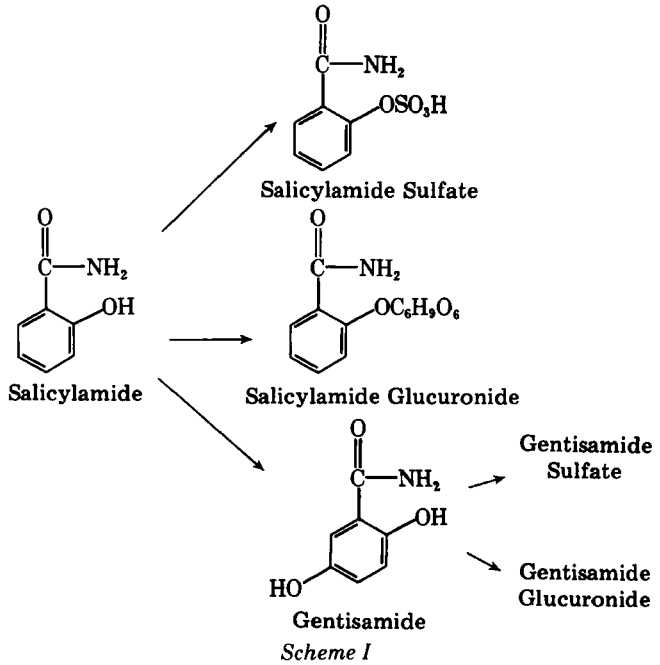

Scheme I

0022-3549/83/0600-0612$01.00/0

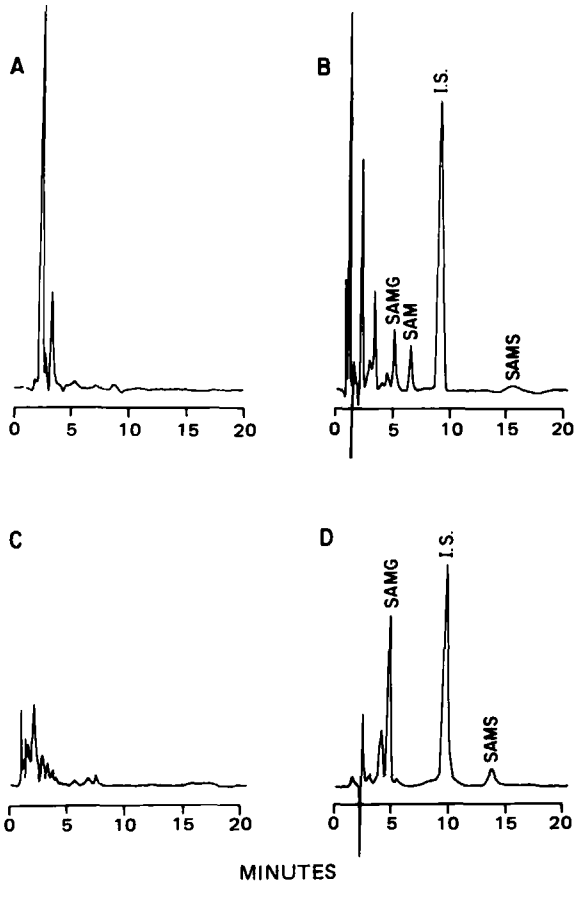

Figure 1—*Chromatograms of human serum and urine samples obtained before and after ingestion of 1 g of salicylamide by a healthy human subject. Key: (A) serum before drug ingestion; (B) serum obtained 1 hr after drug ingestion; (C) control urine diluted 1:25 with water; (D) urine obtained between 1.5 and 2.5 hr after drug ingestion and diluted 1:25 with water. Abbreviations: (SAM) salicylamide, (SAMS) salicylamide sulfate, (SAMG) salicylamide glucuronide, (I.S.) internal standard.*

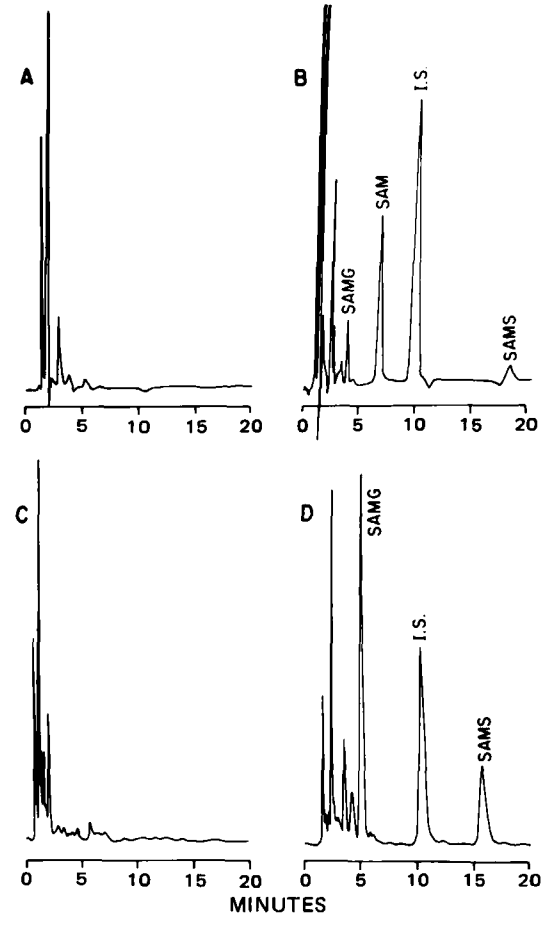

Figure 2—*Chromatograms of rat serum and urine samples obtained before and after intravenous administration of salicylamide. Key: (A) serum before drug administration; (B) serum obtained 30 min after administration of salicylamide, 62.5 mg/kg; (C) control urine diluted 1:25 with water; (D) urine collected ~4 hr after administration of salicylamide, 125 mg/kg, and diluted 1:25 with water. Abbreviations: (SAM) salicylamide, (SAMS) salicylamide sulfate, (SAMG) salicylamide glucuronide, (I.S.) internal standard.*

conjugates in human and rat serum and urine, and human saliva. The assay development for the conjugated metabolites was carried out without authentic standards and exemplifies a general approach that can be used when conjugated drug metabolites are not available in pure form.

EXPERIMENTAL

A high-performance liquid chromatograph[1] equipped with a UV detector[2], automatic injector[3], integrator[4], and an octadecyltrichlorosilane-bonded column[5] was used in this investigation. The column temperature was ambient and the flow rate of the mobile phase varied between 1.6 and 2.0 ml/min in the different assays. The injection volume was 25 μl.

Urine samples were assayed after dilution with distilled water and filtration through a membrane filter[6]. One milliliter of the diluted sample was added to 0.5 ml of a 100-μg/ml aqueous solution of the internal standard, *o*-methoxybenzoic acid[7]. Serum samples were assayed after protein precipitation. One part by volume of serum was added to 2 parts absolute ethanol containing the internal standard (concentration ~40 μg/ml).

An extraction procedure was developed to increase the sensitivity of the assay for unconjugated salicylamide in human serum or saliva. One milliliter of sodium acetate buffer (2 *M*, pH 5.0) plus 1 g of sodium chloride were added to 1 ml of saliva or serum. This mixture was shaken with 6 ml of ether for 10 min and centrifuged. A 4-ml aliquot of the ether phase was removed and the extraction procedure was repeated. The two 4-ml aliquots (one from each extraction) were combined, evaporated to dryness under nitrogen, and redissolved in 0.2 ml of methanol containing the internal standard, *o*-methoxybenzoic acid (concentration ~25 μg/ml).

Salicylamide and its conjugated metabolites were assayed by reverse-phase ion-pair chromatography with UV detection at 254 nm. The mobile phase consisted of 3 m*M* tetrabutylammonium hydroxide[8] in a mixture of 8 parts methanol and 92 parts (v/v) acetic acid 7%.

Low concentrations of unconjugated salicylamide, such as found in human serum or saliva, were assayed after extraction with UV detection at 313 nm. The mobile phase consisted of 1% acetic acid in 25% (v/v) methanol–water solution. Gentisamide and its conjugates were assayed by a separate procedure. The sample preparation and internal standard were the same as described for salicylamide and its conjugates; only one sample preparation was necessary. UV detection was at 313 nm and the mobile phase consisted of 1% acetic acid in 15% (v/v) methanol–water solution. Unconjugated salicylamide is also separated and detected by this procedure.

The intraday reproducibility of the serum salicylamide and gentisamide assay procedures at various concentrations was determined using blank human serum with added salicylamide or gentisamide or pooled rat serum samples obtained after administration of salicylamide.

Gentisamide was synthesized by a previously described procedure (38).

[1] Model M6000A, Waters Associates, Milford, Mass.
[2] Model 440, Waters Associates, Milford, Mass.
[3] WISP 710B, Waters Associates, Milford, Mass.
[4] Data Module, Waters Associates, Milford, Mass.
[5] μBondapak C_{18}, Waters Associates, Milford, Mass.
[6] Metricel, Lot 3056031, Gelman Sciences Inc., Ann Arbor, Mich.
[7] Lot 95C-0165, Sigma Chemical Co., St. Louis, Mo.
[8] Lot 081797, Aldrich Chemical Co., Milwaukee, Wis.

Table I—Reproducibility of Calibration Curves for the Conjugates of Salicylamide and Gentisamide

Metabolite	Number of Samples[a]	Slope Ratio[b]	r^{2c}
Salicylamide	14	0.772	0.982
glucuronide	6	0.772	0.998
Salicylamide	12	0.497	0.984
sulfate	6	0.505	0.992
Gentisamide	13	1.17	0.998
glucuronide	29	1.17	0.992
Gentisamide	5	0.754	0.994
sulfate	3	0.744	0.994
	9	0.750	0.974

[a] Samples assayed in duplicate. [b] Ratio of the slope of the calibration curve for the metabolite to the slope of the calibration curve for the parent compound (salicylamide or gentisamide). Concentration of the metabolites are expressed in terms of the parent compound. [c] Coefficient of determination for the linear regression of the peak area ratio of the metabolite and the concentration of the metabolite (expressed in terms of salicylamide or gentisamide).

It was characterized by NMR, mass spectroscopy, melting point, TLC, HPLC, and elemental analysis[9].

For assay development, the conjugates of salicylamide and gentisamide were quantitated after partial or complete enzymatic hydrolysis of biological samples or sample fractions collected from the HPLC which contain these conjugates. HPLC fractions containing the individual conjugates were lyophilized and reconstituted to various volumes; these solutions were analyzed before and after enzymatic hydrolysis.

Hydrolysis of the glucuronide conjugates was carried out with a β-glucuronidase[10] preparation which, in preliminary studies, produced negligible hydrolysis of the sulfate conjugates. Equal volumes of sample, β-glucuronidase (typically 1250 Fishman U/ml) dissolved in sodium acetate buffer (pH 4.5), and 2.0 or 0.1 *M* sodium acetate buffer pH 4.5

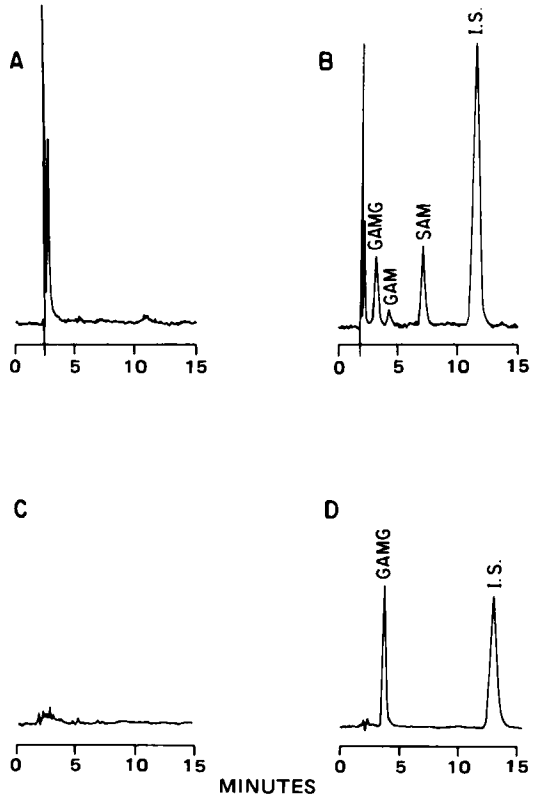

Figure 3—*Chromatograms of human serum and urine samples obtained before and after ingestion of 1 g of salicylamide by a healthy human subject. Key: (A) serum before drug ingestion; (B) serum obtained 1 hr after drug ingestion; (C) control urine diluted 1:25 with water; (D) urine obtained between 1.5 and 2.5 hr after drug ingestion and diluted 1:25 with water. Abbreviations: (GAM) gentisamide, (SAM) salicylamide, (GAMG) gentisamide glucuronide, (I.S.) internal standard.*

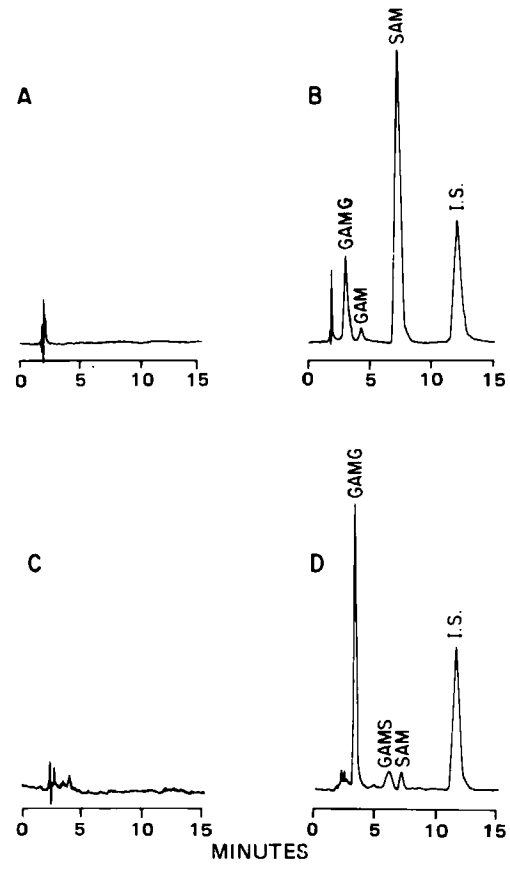

Figure 4—*Chromatograms of rat serum and urine obtained before and after intravenous administration of salicylamide. Key: (A) serum before drug administration; (B) serum obtained 30 min after administration of salicylamide, 125 mg/kg; (C) control urine diluted 1:10 with water; (D) urine collected ~5 hr after administration of salicylamide, 62.5 mg/kg, and diluted 1:10 with water. Abbreviations: (GAMS) gentisamide sulfate, (GAM) gentisamide, (SAM) salicylamide, (GAMG) gentisamide glucuronide, (I.S.) internal standard.*

were mixed and incubated at 37° for varying periods of time. Since only partial hydrolysis of the conjugates was desired, the hydrolysis times were kept short (0.5–4 hr). The sulfate conjugates were hydrolyzed with a β-glucuronidase–sulfatase[11] mixture, with and without the addition of the β-glucuronidase inhibitor, saccharo-1,4-lactone[12], at a final concentration of 0.33 mg/ml. Hydrolysis was carried out similarly to that described for the glucuronide conjugates except that a 2.0 or 0.1 *M* sodium acetate buffer (pH 5.2) was used with the β-glucuronidase–sulfatase preparation (which was usually diluted six- to tenfold with buffer). A limpet sulfatase preparation[13] with low β-glucuronidase activity was tried for the quantitation of salicylamide sulfate, but was found to be unsuitable due to assay interference.

The enzymatic hydrolyses of the gentisamide conjugates were carried out with 0.1 *M* buffer solutions, since there was some loss of gentisamide when added to the 2.0 *M* acetate buffer. No such problem was noted with salicylamide, and, therefore, most hydrolysis experiments with salicylamide conjugates were carried out using the 2.0 *M* buffer.

Assay calibration curves were obtained from the results of the hydrolysis of biological samples or HPLC fractions containing the conjugates. The peak area ratio of the conjugate (ratio of the area of the conjugate peak–area of the internal standard peak) was plotted against the concentration of the conjugate, measured and expressed in terms of the parent compound salicylamide or gentisamide. The slope of this plot, calculated by linear regression, and the slope of the plot of the parent compound were determined on the same day. The ratio of the two slopes was calculated. The hydrolysis experiments and slope value determinations for each conjugate were repeated several times within a 6-month period to check the reproducibility of the slope ratios.

The serum, saliva, and urine samples used in the assay development

[9] M. E. Morris and G. Levy, manuscript in preparation.

[10] Lot 76C-7370, Sigma Chemical Co., St. Louis, Mo.

[11] Glusulase, Lot 00550A, Endo Laboratories, Garden City, N.Y.

[12] Lot 410104, Calbiochem-Behring Corp., LaJolla, Calif.

[13] Lot 47C-9540, S-8629, Sigma Chemical Co., St. Louis, Mo.

Table II—Recovery of Salicylamide and Metabolites in Urine of Normal Human Subjects Determined by HPLC and Colorimetric Methods [a]

Subject	HPLC			Colorimetric [b]		
	Total Salicylamide, mg	Total Gentisamide [c], mg	Recovery, % of dose	Total Salicylamide, mg	Total Gentisamide [c], mg	Recovery, % of dose
A-1 (M, 86) [d]	821	150	97.1	820	156	97.6
A-2	792	181	97.3	796	185	98.1
B (F, 46)	867	140	100.1	872	140	101.2
C (M, 57)	852	147	99.9	824	151	97.5

[a] Volunteers ingested 1 g of salicylamide in aqueous solution and urine was collected for 24 hr. [b] Total salicylamide and total gentisamide were determined using previous methods (refs. 9 and 37, respectively). [c] Expressed in terms of salicylamide. [d] Gender and body weight in kilograms in parentheses.

Table III—Composition of Salicylamide Metabolites in Urine of Human Subjects Determined by HPLC Assay [a]

Subject	Salicylamide Glucuronide	Salicylamide Sulfate	Salicylamide	Gentisamide Glucuronide	Gentisamide Sulfate	Gentisamide
A-1	47.8	34.3	ND [b]	14.9	ND	0.39
A-2	45.5	33.1	0.68	16.3	1.76	ND
B	59.5	26.3	0.88	13.1	0.79	ND
C	51.5	33.7	0.39	14.7	ND	ND

[a] Salicylamide (1 g) in aqueous solution was ingested and urine collected for 24 hr. Results are expressed as percent of dose. [b] Not detected.

were obtained from healthy human volunteers who ingested salicylamide orally (1 g in aqueous solution), or from rats following intravenous administration of salicylamide or gentisamide (62.5–125 mg/kg) *via* a right jugular cannula.

The results of the HPLC assay were compared with results obtained by colorimetric techniques in terms of urinary recovery of metabolites from healthy volunteers and rats. Three volunteers (one on two occasions) ingested 1 g of salicylamide in aqueous solution and collected urine over a 24-hr period. Urinary recovery of total salicylamide (free and conjugates) determined by HPLC was compared with that determined by the colorimetric method of Levy and Matsuzawa (9). Total gentisamide was determined by HPLC and colorimetrically by the method of Becher *et al.* (37). This method involves the acid hydrolysis of gentisamide and its conjugates to gentisic acid and determination using Folin–Ciocalteu reagent[14]. Two rats were administered gentisamide (100 mg/kg iv) *via* a right jugular cannula and urine was collected for 48 hr. All samples were stored at −20° until analyzed. They were assayed by HPLC and colorimetrically (37).

RESULTS AND DISCUSSION

Salicylamide and its glucuronide and sulfate conjugates in human or rat serum and urine are readily separated and detected by HPLC (Figs. 1 and 2). There are no interferences by endogenous substances. Use of the ion-pairing reagent tetrabutylammonium hydroxide and the low pH of the mobile phase (~2.6) cause a selective increase in the retention time of salicylamide sulfate with only a small effect on the retention time of the glucuronide. Gentisamide and its conjugates are also detected by this assay, but their retention times are inconvenient: gentisamide and its glucuronide are eluted before salicylamide glucuronide, while gentisamide sulfate elutes after salicylamide sulfate.

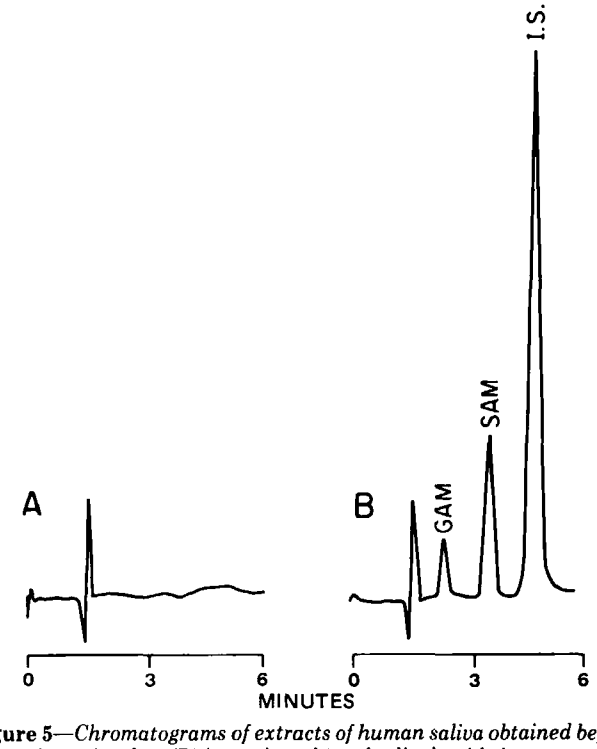

Figure 5—*Chromatograms of extracts of human saliva obtained before (A) and 45 min after (B) ingestion of 1 g of salicylamide in aqueous solution by a healthy human subject. Abbreviations: (SAM) salicylamide, (GAM) gentisamide, (I.S.) internal standard.*

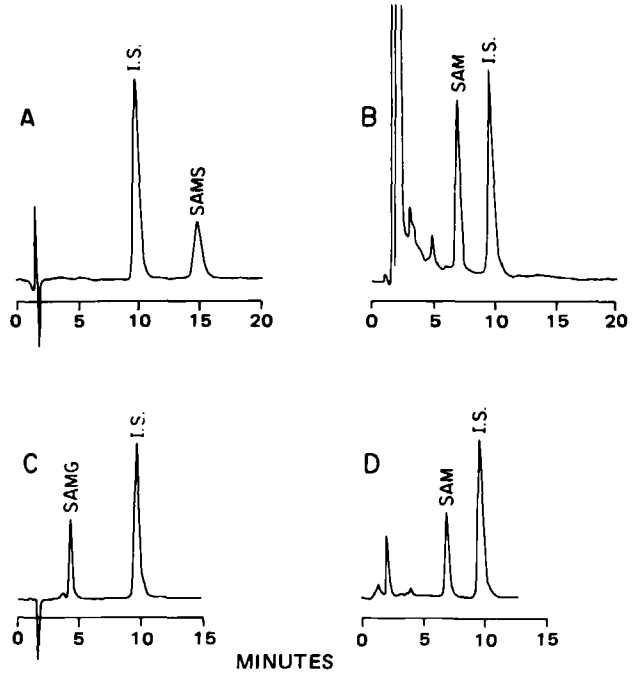

Figure 6—*Chromatograms of chromatographic fractions of human urine containing either salicylamide sulfate (SAMS) or salicylamide glucuronide (SAMG), before and after enzymatic hydrolysis. Key: (A) fraction containing salicylamide sulfate (diluted 1:2 with water); (B) salicylamide sulfate fraction after enzymatic hydrolysis with β-glucuronidase–sulfatase mixture (diluted 1:2 with water); (C) fraction containing salicylamide glucuronide (diluted 1:10 with water); (D) salicylamide glucuronide fraction after enzymatic hydrolysis with β-glucuronidase (diluted 1:10 with water); (I.S.) internal standard; (SAM) salicylamide.*

[14] Lot 707013, Fisher Scientific Co., Fair Lawn, N.J.

Table IV—Urinary Excretion Products of Gentisamide in Rats After Administration of Gentisamide [a]

Rat	HPLC				Colorimetric
	Gentisamide Glucuronide[b], mg	Gentisamide Sulfate[b], mg	Free Gentisamide, mg	Total Gentisamide, mg	Total Gentisamide, mg
N	16.5	14.7	1.98	33.2	32.2
O	17.6	16.7	1.51	35.9	33.9

[a] Dose of gentisamide was 100 mg/kg iv; N and O received 40.1 and 43.7 mg, respectively. Urine was collected for 48 hr. [b] Expressed in terms of gentisamide.

A separate HPLC assay procedure was developed for gentisamide and its glucuronide and sulfate conjugates. The internal standard used in this procedure, *o*-methoxybenzoic acid, is the same as that used in the assay of salicylamide and its metabolites. This affords the convenience of only one sample preparation for both assays. The gentisamide assay involves use of a mobile phase without an ion-pairing reagent and UV detection at 313 nm rather than at 254 nm. At this wavelength, gentisamide and its conjugates and salicylamide absorb more strongly, thereby increasing the sensitivity of the assay. On the other hand, the conjugates of salicylamide have little absorptivity at 313 nm and do not appear in the chromatograms. Gentisamide and its glucuronide and sulfate conjugates are well separated and detected in serum and urine (Figs. 3 and 4). Gentisamide sulfate has not been reported previously as a metabolite of salicylamide. In these experiments, it was found regularly in rat urine but only in some human urine samples after salicylamide administration. It is a quantitatively minor metabolite.

Gentisamide sulfate is relatively stable, showing negligible hydrolysis in rat urine at room temperature over 24 hr. Gentisamide glucuronide is less stable; rat urine samples containing this metabolite should not be keep at room temperature for >4 hr. The glucuronide is more stable in human urine and serum.

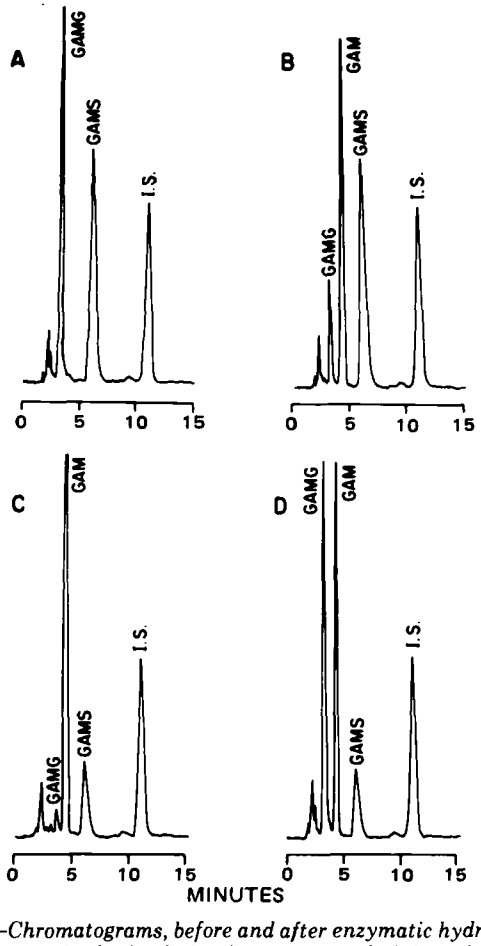

Figure 7—*Chromatograms, before and after enzymatic hydrolysis, of a rat urine sample obtained after intravenous administration of gentisamide (GAM), 100 mg/kg. Key: (A) before hydrolysis; (B) after partial hydrolysis with β-glucuronidase. [There was no hydrolysis of gentisamide sulfate (GAMS) since the peak height ratio of this metabolite to the internal standard is the same as that in A.] (C) after partial hydrolysis with β-glucuronidase–sulfatase mixture; (D) after partial hydrolysis with β-glucuronidase–sulfatase mixture plus saccharo-1,4-lactone, 0.33 mg/ml. [There was no hydrolysis of gentisamide glucuronide (GAMG) in D since the peak height ratio of this metabolite to the internal standard is the same as that in A.] (I.S.) internal standard.*

The relationship between detector response (peak area ratio relative to the internal standard) and concentration of salicylamide and gentisamide is linear over a wide range (at least 4–200 μg/ml for salicylamide and 2–100 μg/ml for gentisamide). The intraday variability of the assay for serum salicylamide in the 10–200 μg/ml concentration range was independent of concentration (n = 5–10 at each of six concentrations), with a coefficient of variation from 1.7 to 3.4%. The coefficient increased to 5.5% at a serum salicylamide concentration of 4 μg/ml. The coefficient of variation for gentisamide in serum (n = 10 per concentration) ranged from 7.0 to 3.3% at concentrations from 2 to 28 μg/ml. The lowest of these concentrations is approximately twice the minimum detectable concentration in these assays.

To increase the sensitivity of the assay for salicylamide, particularly for determinations in serum and saliva, an organic extraction procedure was used and the wavelength for detection was changed from 254 to 313 nm. Use of sodium chloride in the extraction procedure increased extraction efficiency from ~75 to 95%. The coefficient of variation of this more sensitive assay at concentrations of 1–3 μg/ml is <3%. Using the extraction procedure, a chromatogram of saliva obtained from a human subject 45 min after an oral dose of salicylamide indicated the presence of both salicylamide and gentisamide (Fig. 5).

During the assay development for gentisamide conjugates, some loss of gentisamide was observed at high (1–2 M) acetate buffer concentrations. This was not a function of the pH or ionic strength and was not accompanied by formation of gentisic acid. Use of 0.1 M acetate (but not citrate) buffer prevented the loss of gentisamide which may have been due, at least in part, to precipitation.

Calibration (reference) curves for the HPLC assay of salicylamide and gentisamide conjugates were obtained by partial selective hydrolysis of urine samples containing these metabolites (Figs. 6 and 7). The decrease in peak area ratio of a conjugate and the corresponding increase in peak area ratio of the unconjugated compound provided the necessary data for the construction of the calibration curves. The curves were linear over the concentration range examined (~2–60 μg/ml in terms of the parent compound). The slope values of these curves were calculated as a ratio relative to the slope for the unconjugated compound, which was determined on the same day under the same conditions. The slope ratio values for the conjugated metabolites of salicylamide were determined on several occasions over 6 months and were found to be highly reproducible (Table I). Peak area rather than height ratios were used for the calibration curves, since peak height ratios are sensitive to changing column conditions (retention times). This was found to be a problem particularly with salicylamide sulfate, the metabolite with the longest retention time.

The suitability of the HPLC procedures and calibration curves for metabolic studies was tested and confirmed by determining the excretion products of salicylamide in the urine of three human subjects by the HPLC method and by a previously used colorimetric method which requires hydrolysis of the conjugated metabolites. The recovery of salicylamide excretion products was excellent and the results obtained by the two methods were in good agreement (Table II). The HPLC assay revealed the presence of salicylamide and five of its metabolites in human urine, including gentisamide sulfate, a metabolite not previously reported (Table III). The amounts of salicylamide glucuronide, salicylamide sulfate, and total gentisamide recovered are similar to those found in other studies (9, 16, 21).

The results for total gentisamide determined by colorimetry are slightly higher than those obtained by HPLC (Table II). This may be because the colorimetric analysis requires correction for a relatively high (~1 mg/hr) blank value for excretion rate. The colorimetric method detects 2,3,4-trihydroxybenzamide and 2,3-dihydroxybenzoic acid as gentisic acid (the form in which gentisamide is assayed by colorimetry) and may therefore be affected by as yet unidentified minor metabolites of salicylamide and gentisamide.

A limited study of the disposition of gentisamide in rats revealed extensive biotransformation of this compound, including substantial for-

mation of gentisamide sulfate (Table IV). The good agreement between the HPLC and colorimetric assay results for total gentisamide demonstrate the suitability of the HPLC assay for gentisamide and its metabolites.

In conclusion, a combination of two HPLC procedures with the same sample preparation (deproteinization and addition of internal standard) were developed for the direct determination of salicylamide and its metabolites in biological fluids. One of these metabolites, gentisamide sulfate, is reported for the first time. The excretion products of salicylamide in human urine can account for essentially the total amount of administered drug. The HPLC assays for the conjugated metabolites were developed without synthetic or isolated pure standards by a procedure that should be useful also for conjugates of other drugs.

REFERENCES

(1) E. M. Bavin, F. J. MacRae, D. E. Seymour, and P. D. Waterhouse, *J. Pharm. Pharmacol.*, **4**, 872 (1952).

(2) E. L. Way, A. E. Takemori, G. E. Smith, H. H. Anderson, and D. C. Brodie, *J. Pharmacol. Exp. Ther.*, **108**, 450 (1953).

(3) F. M. Berger, *Proc. Soc. Biol. Exp. Med.*, **87**, 449 (1954).

(4) M. P. Borovsky, *Am. J. Dis. Child.*, **100**, 23 (1960).

(5) S. L. Wallenstein and R. W. Houde, *Fed. Proc. Fed. Am. Soc. Exp. Biol.*, **13**, 414 (1954).

(6) R. C. Batterman and A. J. Grossman, *J. Am. Med. Assoc.*, **159**, 1619 (1955).

(7) W. H. Barr, *Drug Inform. Bull.*, **3**, 27 (1969).

(8) L. Fleckenstein, G. R. Mundy, R. A. Horovitz, and J. M. Mazzullo, *Clin. Pharmacol. Ther.*, **19**, 451 (1976).

(9) G. Levy and T. Matsuzawa, *J. Pharmacol. Exp. Ther.*, **156**, 285 (1967).

(10) M. Koike, K. Sugeno, and M. Hirata, *J. Pharm. Sci.*, **70**, 308 (1981).

(11) J. B. Houston and G. Levy, *ibid.*, **64**, 1504 (1975).

(12) R. H. Reuning and G. Levy, *ibid.*, **57**, 1342 (1968).

(13) R. H. Reuning and G. Levy, *ibid.*, **58**, 79 (1969).

(14) W. H. Barr and S. Riegelman, *J. Pharm. Sci.*, **59**, 154 (1970).

(15) G. Levy and J. A. Procknal, *ibid.*, **57**, 1330 (1968).

(16) G. Levy and H. Yamada, *ibid.*, **60**, 215 (1971).

(17) J. B. Houston and G. Levy, *J. Pharmacol. Exp. Ther.*, **198**, 284 (1976).

(18) J. Shibasaki, R. Konishi, M. Koike, A. Imamura, and M. Sueyasu, *J. Pharm. Dyn.*, **4**, 91 (1981).

(19) E. A. Neal, P. J. Meffin, P. B. Gregory, and T. F. Blaschke, *Gastroenterology*, **77**, 96 (1979).

(20) R. Gugler, P. Lain, and D. L. Azarnoff, *J. Pharmacol. Exp. Ther.*, **195**, 416 (1975).

(21) C. S. Song, N. A. Gelb, and S. M. Wolff, *J. Clin. Invest.*, **51**, 2959 (1972).

(22) M. Kakemi, T. Kobayashi, C. Mamuro, M. Ueda, and T. Koizumi, *Chem. Pharm. Bull.*, **24**, 2254 (1976).

(23) G. Levy and J. J. Ashley, *J. Pharm. Sci.*, **62**, 161 (1973).

(24) P. K. Halstead and D. A. Roe, *Drug-Nutr. Interac.*, **1**, 75 (1981).

(25) S. J. Yaffe, G. Levy, T. Matsuzawa, and T. Baliah, *N. Engl. J. Med.*, **275**, 1461 (1966).

(26) L. Stern, N. N. Khanna, G. Levy, and S. J. Yaffe, *Am. J. Dis. Child.*, **120**, 26 (1970).

(27) G. Levy and I. J. Ertel, *Pediatrics*, **47**, 811 (1971).

(28) J. Crampton and E. Vass, *J. Am. Pharm. Assoc., Sci. Ed.*, **43**, 470 (1954).

(29) T. Shibazaki, *Chem. Pharm. Bull.*, **26**, 1985 (1978).

(30) S. A. Veresh, F. S. Hom, and J. J. Miskel, *J. Pharm. Sci.*, **60**, 1092 (1971).

(31) W. E. Lange, D. G. Floriddia, and F. J. Pruyn, *ibid.*, **58**, 771 (1969).

(32) A. G. DeBoer, J. M. Gubbens-Stibbe, F. H. DeKoning, A. Bosma, and D. D. Breimer, *J. Chromatogr.*, **162**, 457 (1979).

(33) M. J. Rance, B. J. Jordan, and J. D. Nickols, *J. Pharm. Pharmacol.*, **27**, 425 (1975).

(34) S. R. Gautam, V. Chungi, A. Hussain, S. Babhair, and D. Papadimitrou, *Anal. Lett.*, **14**, 577 (1981).

(35) D. Blair, B. H. Rumack, and R. G. Peterson, *Clin. Chem.*, **24**, 1543 (1978).

(36) S. Ebel, R. Liedtke, and B. Miszler, *Arch. Pharm.*, **313**, 674 (1980).

(37) A. Becher, J. Miksch, P. Rambacher, and A. Schäfer, *Klin. Wochenschr.*, **30**, 913 (1952).

(38) J. A. Faust, L. H. Jules, and M. Sahyun, *J. Am. Pharm. Assoc., Sci. Ed.*, **45**, 514 (1956).

ACKNOWLEDGMENTS

Supported in part by Grant GM 19568 from the National Institute of General Medical Sciences, National Institutes of Health, by Biomedical Research Support Grant 2S077RR05454-19, and by a fellowship for M. E. Morris from the Graduate School of the State University of New York at Buffalo.

Synthesis, Isolation, and Characterization of Two Stereoisomeric Ring Sulfoxides of Thioridazine

ERIC C. JUENGE *x, CLYDE E. WELLS *, DONALD E. GREEN ‡, IRENE S. FORREST ‡, and JAMES N. SHOOLERY §

Received February 12, 1982, from the **National Center for Drug Analysis, Food and Drug Administration, St. Louis, MO 63101*, the ‡*Veterans Administration Hospital, Palo Alto, CA 94304*, and §*Varian Associates, Palo Alto, CA 94303.* Accepted for publication June 3, 1982.

Abstract □ A selective oxidation of thioridazine to give exclusively its ring sulfoxides and a separation of the resulting products as diastereoisomeric pairs of enantiomers (DL, LD and DD, LL) are reported. These pairs were characterized by TLC, high-performance liquid chromatographic, IR, UV, ^{1}H-NMR, ^{13}C-NMR, GC–MS, and elemental analyses, and by reduction to thioridazine by lithium aluminum hydride. Structural data for the separated diastereoisomeric pairs or their nitric acid salts were obtained from NMR and IR studies. Gram quantities of each of the two diastereoisomeric pairs of enantiomers were isolated in better than 99% purity.

Keyphrases □ Thioridazine—oxidation to ring sulfoxides, separation of the diastereoisomeric pairs of the ring sulfoxides by crystallization of the nitric acid salts, ^{13}C-NMR analysis of thioridazine ring sulfoxides

A single ring sulfoxide of thioridazine has been detected by TLC (1–5), high-performance liquid chromatography (HPLC) (6, 7), and GC (8–10). Also, EKG abnormalities have been attributed "to a single ring sulfoxide" in plasma (8). Recently "two very similar ring sulfoxides" of thioridazine were identified (11) as urinary metabolites and prepared (with other products) by chemical oxidation.

Evidence is presented here that these ring sulfoxides are

0022-3549/83/0600-0617$01.00/0

mation of gentisamide sulfate (Table IV). The good agreement between the HPLC and colorimetric assay results for total gentisamide demonstrate the suitability of the HPLC assay for gentisamide and its metabolites.

In conclusion, a combination of two HPLC procedures with the same sample preparation (deproteinization and addition of internal standard) were developed for the direct determination of salicylamide and its metabolites in biological fluids. One of these metabolites, gentisamide sulfate, is reported for the first time. The excretion products of salicylamide in human urine can account for essentially the total amount of administered drug. The HPLC assays for the conjugated metabolites were developed without synthetic or isolated pure standards by a procedure that should be useful also for conjugates of other drugs.

REFERENCES

(1) E. M. Bavin, F. J. MacRae, D. E. Seymour, and P. D. Waterhouse, *J. Pharm. Pharmacol.*, **4**, 872 (1952).

(2) E. L. Way, A. E. Takemori, G. E. Smith, H. H. Anderson, and D. C. Brodie, *J. Pharmacol. Exp. Ther.*, **108**, 450 (1953).

(3) F. M. Berger, *Proc. Soc. Biol. Exp. Med.*, **87**, 449 (1954).

(4) M. P. Borovsky, *Am. J. Dis. Child.*, **100**, 23 (1960).

(5) S. L. Wallenstein and R. W. Houde, *Fed. Proc. Fed. Am. Soc. Exp. Biol.*, **13**, 414 (1954).

(6) R. C. Batterman and A. J. Grossman, *J. Am. Med. Assoc.*, **159**, 1619 (1955).

(7) W. H. Barr, *Drug Inform. Bull.*, **3**, 27 (1969).

(8) L. Fleckenstein, G. R. Mundy, R. A. Horovitz, and J. M. Mazzullo, *Clin. Pharmacol. Ther.*, **19**, 451 (1976).

(9) G. Levy and T. Matsuzawa, *J. Pharmacol. Exp. Ther.*, **156**, 285 (1967).

(10) M. Koike, K. Sugeno, and M. Hirata, *J. Pharm. Sci.*, **70**, 308 (1981).

(11) J. B. Houston and G. Levy, *ibid.*, **64**, 1504 (1975).

(12) R. H. Reuning and G. Levy, *ibid.*, **57**, 1342 (1968).

(13) R. H. Reuning and G. Levy, *ibid.*, **58**, 79 (1969).

(14) W. H. Barr and S. Riegelman, *J. Pharm. Sci.*, **59**, 154 (1970).

(15) G. Levy and J. A. Procknal, *ibid.*, **57**, 1330 (1968).

(16) G. Levy and H. Yamada, *ibid.*, **60**, 215 (1971).

(17) J. B. Houston and G. Levy, *J. Pharmacol. Exp. Ther.*, **198**, 284 (1976).

(18) J. Shibasaki, R. Konishi, M. Koike, A. Imamura, and M. Sueyasu, *J. Pharm. Dyn.*, **4**, 91 (1981).

(19) E. A. Neal, P. J. Meffin, P. B. Gregory, and T. F. Blaschke, *Gastroenterology*, **77**, 96 (1979).

(20) R. Gugler, P. Lain, and D. L. Azarnoff, *J. Pharmacol. Exp. Ther.*, **195**, 416 (1975).

(21) C. S. Song, N. A. Gelb, and S. M. Wolff, *J. Clin. Invest.*, **51**, 2959 (1972).

(22) M. Kakemi, T. Kobayashi, C. Mamuro, M. Ueda, and T. Koizumi, *Chem. Pharm. Bull.*, **24**, 2254 (1976).

(23) G. Levy and J. J. Ashley, *J. Pharm. Sci.*, **62**, 161 (1973).

(24) P. K. Halstead and D. A. Roe, *Drug-Nutr. Interac.*, **1**, 75 (1981).

(25) S. J. Yaffe, G. Levy, T. Matsuzawa, and T. Baliah, *N. Engl. J. Med.*, **275**, 1461 (1966).

(26) L. Stern, N. N. Khanna, G. Levy, and S. J. Yaffe, *Am. J. Dis. Child.*, **120**, 26 (1970).

(27) G. Levy and I. J. Ertel, *Pediatrics*, **47**, 811 (1971).

(28) J. Crampton and E. Vass, *J. Am. Pharm. Assoc., Sci. Ed.*, **43**, 470 (1954).

(29) T. Shibazaki, *Chem. Pharm. Bull.*, **26**, 1985 (1978).

(30) S. A. Veresh, F. S. Hom, and J. J. Miskel, *J. Pharm. Sci.*, **60**, 1092 (1971).

(31) W. E. Lange, D. G. Floriddia, and F. J. Pruyn, *ibid.*, **58**, 771 (1969).

(32) A. G. DeBoer, J. M. Gubbens-Stibbe, F. H. DeKoning, A. Bosma, and D. D. Breimer, *J. Chromatogr.*, **162**, 457 (1979).

(33) M. J. Rance, B. J. Jordan, and J. D. Nickols, *J. Pharm. Pharmacol.*, **27**, 425 (1975).

(34) S. R. Gautam, V. Chungi, A. Hussain, S. Babhair, and D. Papadimitrou, *Anal. Lett.*, **14**, 577 (1981).

(35) D. Blair, B. H. Rumack, and R. G. Peterson, *Clin. Chem.*, **24**, 1543 (1978).

(36) S. Ebel, R. Liedtke, and B. Miszler, *Arch. Pharm.*, **313**, 674 (1980).

(37) A. Becher, J. Miksch, P. Rambacher, and A. Schäfer, *Klin. Wochenschr.*, **30**, 913 (1952).

(38) J. A. Faust, L. H. Jules, and M. Sahyun, *J. Am. Pharm. Assoc., Sci. Ed.*, **45**, 514 (1956).

ACKNOWLEDGMENTS

Supported in part by Grant GM 19568 from the National Institute of General Medical Sciences, National Institutes of Health, by Biomedical Research Support Grant 2S077RR05454-19, and by a fellowship for M. E. Morris from the Graduate School of the State University of New York at Buffalo.

Synthesis, Isolation, and Characterization of Two Stereoisomeric Ring Sulfoxides of Thioridazine

ERIC C. JUENGE *x, CLYDE E. WELLS *, DONALD E. GREEN ‡, IRENE S. FORREST ‡, and JAMES N. SHOOLERY §

Received February 12, 1982, from the **National Center for Drug Analysis, Food and Drug Administration, St. Louis, MO 63101*, the ‡*Veterans Administration Hospital, Palo Alto, CA 94304*, and §*Varian Associates, Palo Alto, CA 94303.* Accepted for publication June 3, 1982.

Abstract □ A selective oxidation of thioridazine to give exclusively its ring sulfoxides and a separation of the resulting products as diastereoisomeric pairs of enantiomers (DL, LD and DD, LL) are reported. These pairs were characterized by TLC, high-performance liquid chromatographic, IR, UV, ^{1}H-NMR, ^{13}C-NMR, GC–MS, and elemental analyses, and by reduction to thioridazine by lithium aluminum hydride. Structural data for the separated diastereoisomeric pairs or their nitric acid salts were obtained from NMR and IR studies. Gram quantities of each of the two diastereoisomeric pairs of enantiomers were isolated in better than 99% purity.

Keyphrases □ Thioridazine—oxidation to ring sulfoxides, separation of the diastereoisomeric pairs of the ring sulfoxides by crystallization of the nitric acid salts, ^{13}C-NMR analysis of thioridazine ring sulfoxides

A single ring sulfoxide of thioridazine has been detected by TLC (1–5), high-performance liquid chromatography (HPLC) (6, 7), and GC (8–10). Also, EKG abnormalities have been attributed "to a single ring sulfoxide" in plasma (8). Recently "two very similar ring sulfoxides" of thioridazine were identified (11) as urinary metabolites and prepared (with other products) by chemical oxidation.

Evidence is presented here that these ring sulfoxides are

0022-3549/83/0600-0617$01.00/0

Table I—Chromatographic Detection of Oxidation Products of Thioridazine (I) and Mesoridazine (III) as TLC Spots or HPLC Peaks

Sample[a]	Compound I	IIF[b]	IIS[b]	III	IV[c]	System[d]
A	x	x	x	x		I, II, V[e], VI
B	x	x	x	x	x	I, II, V[f], VI
C				x	x	I, V[g]
D	x	x	x	x	x	I, II, VI
E	x	x	x	x	x	I, V[e]
F	x	x	x	x	x	I, V
G		x	x			I, III[h], IV[h,i], V[e]

[a] Sample A is a synthetic mixture. B–F are oxidation mixtures from hydrogen peroxide treatment and G from nitrous acid treatment. C involves the oxidation of mesoridazine. [b] IIS and IIF were found in about equal amounts in all samples of oxidized I. [c] Further identified by its intense blue fluorescence under long-wavelength UV irradiation. [d] Various solvent systems, I–IV and VI, on silica gel TLC, and an HPLC method, V, were used. [e] Chromatograms are presented in Fig. 1. [f] Approximate compound ratios 2.8:12.5:14.4:37.7:29.9, respectively. [g] Percent of IV (peak area) = 90.1. [h] Failed to separate IIF and IIS. [i] Gave R_f 0.45, close to the literature report of R_f 0.46 (13–15).

actually diastereoisomeric pairs of enantiomers (DL, LD and DD, LL). TLC and HPLC methods used to detect and distinguish these diastereoisomeric pairs and a crystallization method that yields gram amounts of each pair with better than 99% purity are described. These pure materials have been used to develop an HPLC assay of thioridazine and its metabolites in plasma (12).

RESULTS AND DISCUSSION

TLC—Literature methods (1, 2, 13–15) were used. Thioridazine (I), the pairs of enantiomeric ring sulfoxides (IIF and IIS, fast and slow migrators on silica gel, respectively), the side-chain sulfoxide of thioridazine [mesoridazine (III)], and thioridazine disulfoxide (IV) were detected (Table I) in the reaction products from hydrogen peroxide oxidation of thioridazine. Many minor products were also produced. On silica gel, the ring sulfoxides generally tend to elute between thioridazine and mesoridazine. The more polar disulfoxide elutes after mesoridazine, and the less polar sulfone, sulforidazine, elutes just after thioridazine. Both the disulfoxide and sulfone are readily distinguished by their pronounced fluorescence under long-wavelength UV irradiation. Although sulforidazine may occur in relatively high concentrations in thioridazine metabolism (16), it was not found as a product in the chemical oxidations performed in this study. Sulfoxidation occurs before any appreciable *N*-oxidation is observed.

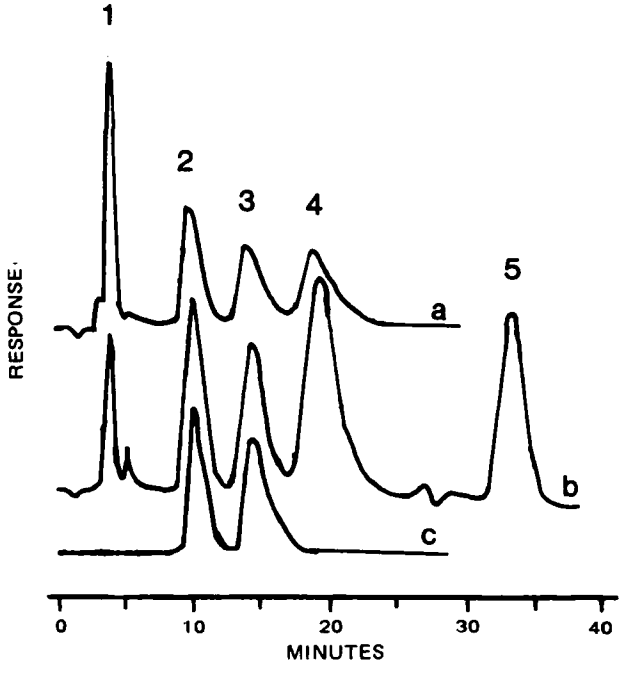

Figure 1—*High-performance liquid chromatograms. Key: a, reference mixture; b, product of reaction of thioridazine and hydrogen peroxide in refluxing alcohol, as previously described (1); and c, product of reaction of thioridazine hydrochloride and nitrous acid. (1) Thioridazine; (2 and 3) thioridazine ring sulfoxides; (4) mesoridazine; and (5) thioridazine disulfoxide. In curve b, the polarity of the mobile phase was increased after peak 4 to achieve elution of the disulfoxide.*

Table II—R_f Values and Color Detection for the Oxidation Products of Thioridazine Formed by Hydrogen Peroxide (in Acetic Acid and Aqueous Solvent) and by Nitrous Acid[a]

Compound	R_f, System I[d]	System VI, Reagents[b] Folin	H_2SO_4	100°	R_f, System II[c] Found	Reported[e]
I	0.71	B–G	—	—	0.75	0.83
IIF	0.62	—	B–V[f]	—	0.55	0.54
IIS	0.54	—	B–V[f]	—	0.50	0.54
III	0.39	P	—	—	0.43	0.45
IV	0.23	—	—	P	0.28	0.29

[a] Nitrous acid oxidation products gave only two spots for the ring sulfoxides (IIF and IIS). [b] Sprays or operations (2) done in sequence to produce the colors shown; B = blue, G = green, P = pink, V = violet. [c] Acetone–12 *N* ammonium hydroxide (100:7) (2). [d] Chloroform–95% ethanol–12 *N* ammonium hydroxide (80:20:1). [e] R_f values from the literature (2), including value for a single ring sulfoxide. [f] Initial B–G spots turned B–V after several hours.

HPLC—A highly sensitive assay method (12), which employs a silica gel column, was used to provide qualitative and semiquantitative data on the distribution of products in some of the oxidation mixtures. Figure 1 (curve a) illustrates a typical chromatogram, obtained from a mixture of ring sulfoxides (IIF and IIS) and reference standards of I and III. Products from the hydrogen peroxide oxidations (*Experimental, Methods* I–III) included both ring sulfoxides, which eluted with the same retention times as shown in Fig. 1 (curve a).

Literature Reports of a Single Ring Sulfoxide—The approach taken in this study was to show that ordinary oxidations of thioridazine, including some published methods (1, 17), gave two enantiomeric pairs (IIF and IIS) of the ring sulfoxides (two TLC spots and not one) and to examine TLC systems, including some reported in the literature (1, 2, 13–15), for their effectiveness in separating IIF and IIS. Next, the isolation of larger amounts of each ring sulfoxide (IIF and IIS) was undertaken to provide samples for identification, particularly by instrumental techniques.

Both ring sulfoxides (IIF and IIS) were found in about equal amounts in all the samples of oxidized thioridazine (Table I; samples and detection systems are described in detail in the *Experimental* section). TLC systems I and II, as well as HPLC system V, separated IIS and IIF, but TLC systems III and IV failed to give a separation. Samples A, B, and D were used to evaluate a reported TLC system (2); solvent system II and spray system VI produced the R_f values and colors presented in Table II. Although this report (2) described a single spot for thioridazine ring sulfoxide, a small but clear separation was obtained in the present work. All materials gave colors that matched those described (2).

Under conditions of more extensive oxidation, more thioridazine disulfoxide (IV) formed at the expense of the ring sulfoxides (II) and mesoridazine (III). After a reaction time of 24 hr, concentrated aqueous hydrogen peroxide gave primarily the disulfoxide (IV) and a small amount of mesoridazine (III), whereas dilute aqueous hydrogen peroxide generated the usual major products, I, IIF, IIS, III, and IV, with some minor products appearing as very faint spots on the TLC plates.

Analysis of Commercial Samples of Thioridazine Ring Sulfoxide—Two samples were assayed by HPLC system V (12). The first contained ~ 98% of IIS and 2% of IIF, and the second ~ 85% of IIS and 15% of IIF. TLC (system I) gave a rough confirmation of these results. The IR spectrum of the first commercial sample matched that of analytically pure IIS.

Study of the Reaction of Zehnder *et al.* (1)—To determine whether ring sulfoxides IIF and IIS were produced under these reaction conditions, the solution of the crude reaction product (sample E) was examined by TLC (Table I) and by HPLC (Fig. 1, curve b). Thioridazine (I), the two ring sulfoxides (IIF and IIS), mesoridazine (III), and the disulfoxide (IV) appeared at essentially the same R_f values and retention times observed for products of the hydrogen peroxide oxidations. The two ring sulfoxides were found in about equal amounts. Retention times in Fig. 1, curve b, matched those of the reference mixture (sample A) in Fig. 1, curve a. The area percentages for substances in curve b are: I, 4.4; IIF, 15.6; IIS, 17.3; III, 34.4; and IV, 23.3.

Effect of pH—Zehnder *et al.* (1) refluxed thioridazine hydrochloride with hydrogen peroxide in ethanol, mildly acidic conditions. Sample E,

Table III—Physical and Analytical Data for Thioridazine Ring Sulfoxides

Compound	Melting Point		Analyses Calc.	Found	Purity, %[a]
		Nitric Acid Salts			
VF	254.5–255.0°	C	56.10	55.87	99.9
		H	6.05	6.03	
		N	9.35	9.21	
VS	226.2–227.0°	C	56.10	56.09	99.3
		H	6.05	6.05	
		N	9.35	9.16	
V[b]	204.0–224.0°		—	—	—
		Free Bases[c]			
IIF	119.0–120.0°	C	65.25	65.00	—
		H	6.78	6.81	
IIS	141.0–142.0°	C	65.25	65.32	—
		H	6.78	6.90	
II	113.5–128.5°	C	65.25	65.06	—
		H	6.78	6.77	

[a] Based on HPLC analyses of nitric acid salts neutralized with 12 *N* ammonium hydroxide. [b] Mixture of both salts (VF and VS) obtained as the reaction product. [c] The free bases, IIF, IIS, and II, were obtained from the corresponding salts, VF, VS, and V.

obtained in this way, gave an amount of mesoridazine roughly equal to the total amount of the ring sulfoxides. By substitution of the free base of thioridazine in the refluxing medium, sample F was obtained under mildly basic conditions and was found to contain about three times as much mesoridazine as the amount of total ring sulfoxides. Thus, oxidation under mildly basic conditions favors side-chain sulfoxidation. A previous report (16) found that the rates of formation of mesoridazine and sulforidazine (side-chain sulfoxidation) in plasma are greater than that of ring sulfoxidation. One might speculate that oxidation of thioridazine under acidic conditions in the stomach could favor formation of ring sulfoxides and contribute to toxic side reactions (8).

Disadvantages of Hydrogen Peroxide Oxidations—Complex product mixtures are obtained, and intricate, inefficient separations must be used to isolate the pure ring sulfoxides from the hydrogen peroxide oxidations. Thus, a new method for the oxidation of thioridazine exclusively to its ring sulfoxides and a technique for their separation as two pairs of enantiomers should be useful for analytical studies of thioridazine metabolites and perhaps for toxicological studies.

Nitrous Acid Oxidation of Thioridazine Hydrochloride—The nitric acid salts of the ring sulfoxides (VF and VS) are generated exclusively when thioridazine hydrochloride is oxidized with nitrous oxide (sample G, Table I). The freshly prepared reaction mixture was immediately examined by HPLC system V; the product was > 99% thioridazine ring sulfoxides (Fig. 1, curve c), which eluted at the same retention times as the analytically pure sulfoxides (Fig. 1, curve a, peaks 2 and 3). TLC (Table I, system I) also showed essentially only the ring sulfoxides.

Formation of the nitric acid salts can be described by these equations (18) (T = thioridazine).

$$2HNO_2 + T(I) \rightarrow TO(II) + 2NO + H_2O \quad \text{(Eq. 1)}$$

$$4HNO_2 \rightarrow 4NO + O_2 + 2H_2O \quad \text{(Eq. 2)}$$

$$3HNO_2 \rightleftarrows HNO_3 + 2NO + H_2O \quad \text{(Eq. 3)}$$

$$2NO + O_2 \rightarrow 2NO_2 \quad \text{(Eq. 4)}$$

$$2NO_2 + H_2O \rightleftarrows HNO_3 + HNO_2 \quad \text{(Eq. 5)}$$

$$TO(II) + HNO_3 \rightarrow TO \cdot HNO_3(V) \quad \text{(Eq. 6)}$$

Nitrous acid can be an effective oxidizing agent (Eqs. 1 and 2). The nitric acid salt V (Eq. 6) is readily generated from nitrous acid, which is unstable and decomposes to nitric acid (Eq. 3), and also through other reactions (Eqs. 4 and 5). The observed oxidation with nitrous acid is not due to nitric acid. Substitution of sodium nitrate for sodium nitrite in the reaction procedure failed to give any oxidation of thioridazine.

Separation of Ring Sulfoxides as Free Bases—Attempts to isolate the ring sulfoxides (IIF and IIS) by HPLC followed by crystallization yielded only small amounts of material of ~ 95% purity, as determined by HPLC analyses. The UV spectra (λ_{max} = 279 nm, weak peak at 342 nm) of the collected fractions were identical. The free bases crystallized well from hexane or heptane, but such recrystallization failed to purify them. Vacuum sublimation (175°, 1 mm) of the mixed free bases yielded no isomeric enrichment.

Table IV—^{13}C-NMR Data (ppm) for Thioridazine Ring Sulfoxides in Deuterochloroform[a]

Peak Number	Compound IIF	IIS
1	145.50	145.50
2	138.51[b]	138.61[b]
3	138.23[b]	138.07[b]
4	132.85	132.79
5	131.98[b]	131.89[b]
6	131.65[b]	131.72[b]
7	124.60	124.69
8	121.93	121.85
9	121.06	120.96
10	118.98	119.00
11	115.73	115.61
12	112.20	112.23
13	78.73[c]	78.74[c]
14	77.33[c]	77.34[c]
15	77.14[c]	77.14[c]
16	75.53	75.54
17	62.01	61.92
18	56.78	56.80
19	44.92	44.86
20	43.25	43.18
21	30.66	30.68
22	29.23	29.28
23	25.42	25.45
24	24.08	24.13
25	15.40	15.35

[a] TMS added as an internal standard. [b] Four aromatic carbons nearest the ring sulfur. [c] Deuterochloroform lines in spectrum of IIF and IIS demonstrate instrument reproducibility to 0.01 ppm.

Separation of Ring Sulfoxides as Nitric Acid Salts—A mixture of the nitric acid salts of the ring sulfoxides (V) was separated by fractional crystallization (19) from 95% ethanol. After six recrystallizations, all cuts contained essentially one isomer and some were fairly pure, *e.g.*, 99.9% VF and 96.8% VS, as determined by peak ratios from HPLC analyses. After two more recrystallizations from fresh solvent, VS was 99.3% pure (Table III).

These high-purity samples gave TLC R_f values that matched those of the original reaction mixture (Table II). The elemental analyses of the materials were consistent for the nitric acid salts of the ring sulfoxide isomers of thioridazine, and their melting points were sharp (Table III).

Characterization of the Ring Sulfoxides as Free Bases (IIF and IIS)—The free bases were obtained from the purified nitric acid salts and gave material with sharp melting points. Elemental analyses were consistent for the isomeric ring sulfoxides of thioridazine (Table III).

NMR Studies of Thioridazine Ring Sulfoxides as Free Bases—The ^{13}C-NMR spectra of IIF and IIS are tabulated (Table IV). The fact that most of the signals in the spectra of the two compounds agreed to within 0.1 ppm shows that the two types of ring sulfoxides (IIF and IIS) are very similar. Nevertheless, a difference in stereochemistry of the sulfoxide groups of IIS and IIF is suggested by the differences in the signals from the four aromatic carbons nearest the ring sulfur.

NMR Studies of Thioridazine Ring Sulfoxides as Nitric Acid Salts—The ^{13}C-NMR spectra of VF and VS (Table V), taken at 30° in deuterium oxide, are also clearly different for the nonprotonated aromatic carbons located next to the sulfoxide group. The broadening of peaks for aliphatic carbons can be explained if the protonated piperidine coordinates with the sulfoxide group. If the change in the precession frequencies of the aliphatic carbons resulting from the formation of a complex is comparable to the rate of forming and breaking the complex, line broadening will occur.

At 90° (Table V) either the complex is forming and breaking rapidly enough to average the chemical shifts, or it is broken up and the chemical shifts are characteristic of the freely rotating side chain resulting in sharp aliphatic peaks. Merging of aromatic signals at 90° is attributed to conformational mobility of the molecules which leads to some averaging of the aromatic carbon-13 chemical shifts.

Chemical Shifts of *S*- and *N*-Methyl Proton Signals of Thioridazine and Related Compounds—As side-chain sulfoxidation increases, only the *S*-methyl signal is shifted to lower field, but ring sulfoxidation causes a shift of both the *S*- and *N*-methyl proton signals to lower field relative to thioridazine (Table VI).

The *N*-methyl proton singlets from the ring sulfoxide free bases (IIF and IIS) did not show different chemical shifts. The differences in

Table V—^{13}C-NMR Data (ppm) for the Nitric Acid Salts of the Thioridazine Ring Sulfoxides in Deuterium Oxide

Peak Number	Compound VF	VS
	At 30°[a]	
1	146.59	146.75
2	138.49[b]	138.85[b]
3	137.53[b]	137.19[b]
4	134.16	134.04
5	131.24	131.16
6	131.00	130.96
7	123.08	123.14
8	119.14	119.05
9	118.66	118.24
10	117.04	117.26
11	112.39	112.09
12	41.99	42.13
13	14.02	26.82
14	—	20.68
15	—	14.00
	At 90°[c]	
1	134.07	134.01
2	131.35	131.42
3	130.95	131.01
4	123.14	123.26
5	119.99	120.10
6	117.02	117.22
7	113.19	113.19
8	61.94	61.98
9	55.41	55.44
10	42.57	42.77
11	27.11	38.97
12	26.80	27.25
13	21.49	26.86
14	20.33	21.50
15	14.53	20.39
16	—	14.63

[a] Twelve aromatic peaks were tabulated in both VF and VS. Many of the peaks from aliphatic carbons appeared as broad areas at the baseline and were not tabulated by the spectrometer. [b] Nonprotonated aromatic carbons located next to the sulfoxide group, 0.96 ppm apart for VF and 1.66 ppm apart for VS. [c] Nine sharp aliphatic peaks were observed and tabulated. Some of the aromatic signals are merged at the higher temperature.

chemical shifts of the *N*-methyl protons in VF and VS may be due to differences in the ring sulfoxide stereochemistry, which influences their coordination with the protonated *N*-methylpiperidinyl moiety. An analogous coordination occurs between the sulfoxide group in dimethyl sulfoxide and the hydroxyl groups in alcohols (20). The lack of dissociation of the protonated amine in the rather nonpolar deuterochloroform is suggested as the cause of *N*-methyl proton splitting in these compounds. Ratios of the salts (VF and VS) in mixtures can be determined by deuterium exchange and by integration of the piperidyl *N*-methyl peaks. Such mixtures are usually soluble enough to permit accurate estimation of the ratios of VF to VS to within 2–5% with a conventional NMR spectrometer.

Reductions with Lithium Aluminum Hydride—In anhydrous ether, lithium aluminum hydride reduced a mixture of the ring sulfoxides (IIF and IIS) to a single product, thioridazine. The reduction product matched reference standard thioridazine in TLC (system I), IR spectra, and GC–MS data. Mesoridazine was also reduced under similar conditions and gave the same TLC, IR, and GLC–MS characteristics for the reaction product, thioridazine.

Mass Spectra of Ring Sulfoxides—Essentially identical spectra were obtained when IIF and IIS were passed through the GC–MS. Programmed-temperature GC of IIF and IIS gave identical retention times; the peaks of these polar compounds were broad and appeared after the thioridazine peak. Upon direct injection, postcolumn with a heated vaporizer, both materials produced spectra showing the molecular ion. The spectra of both IIF and IIS had many peaks in common with thioridazine, including the molecular-ion peak for thioridazine and the base peak for the *N*-methylpiperidyl fragment.

The ring sulfoxides theoretically exist as two diastereoisomeric pairs, and these pairs are separable by physical means such as chromatography or fractional recrystallization. These compounds are of interest because of the known metabolic conversion of thioridazine to such oxidation products. Methods for syntheses of the materials in pure form are described. Elemental analyses and IR data are consistent with the *S*-oxide structure. ^{1}H-NMR clearly rules out the *N*-oxide in favor of the *S*-oxide structure because of the chemical shift of the *N*-methyl group. ^{13}C-NMR gives the unambiguous determination of the site of this oxidation as the ring sulfur atom.

Table VI—Chemical Shifts (ppm) [a] of *S*- and *N*-Methyl Proton Signals of Thioridazine and Related Compounds

Compound (Side-Chain Group)	*S*-Methyl	*N*-Methyl
Shifts Observed After Progressive Side-Chain Sulfoxidation		
I (CH_3S)	2.40	2.20
III (CH_3SO)	2.70	2.20
VI (CH_3SO_2)	3.00	2.20
VII (CH_3SO_2)[b]	3.00	—
Shifts Caused by Ring Sulfoxidation and Splitting Generated by Subsequent Protonation[c]		
IIF (CH_3S)	2.59	2.40
IIS (CH_3S)	2.59	2.40
VF (CH_3S)[d]	2.59	2.38, 2.44[e]
VS (CH_3S)	2.59	2.30, 2.36[e]

[a] In deuterochloroform; compared to thioridazine (I). [b] Methylsulfonylphenothiazine (VII) for comparison as parent structure of sulforidazine (VI). [c] Protons were retained on the more basic piperidine nitrogens. [d] A sensitive Fourier-transform NMR instrument was needed since VF was rather insoluble in deuterochloroform. [e] J_{NH-CH_3} = 5 Hz. Centers of these doublets are chemically shifted by 0.08 ppm. Both doublets collapsed to singlets on treatment with deuterium oxide. Deuterochloroform (100%) must be used to observe sharp peaks.

EXPERIMENTAL

Materials—All chemicals were official or reagent grade. Thioridazine hydrochloride, thioridazine free base, and two samples of ring sulfoxide were obtained commercially[1]. 3-Methylsulfonylphenothiazine (21) and sulforidazine (22) were synthesized.

Instruments—A grating IR spectrophotometer[2], a UV-visible spectrophotometer with recorder[3], a 60-MHz NMR spectrometer[4], and a Fourier-transform 80-MHz NMR spectrometer[4] were used. The 60-MHz instrument was used only for ^{1}H-NMR studies of free bases. The 80-MHz instrument was operated at 79.542 MHz for ^{1}H-NMR and at 20 MHz for ^{13}C-NMR. An electron-impact (70 eV) GLC–MS[5], operated with an 88-cm × 2-mm i.d. glass column[6], was used for the lithium aluminum hydride reduction studies. A GLC–MS[7] equipped with a 61-cm × 2-mm i.d. glass column[8] was used for analysis of the ring sulfoxides; alternatively, these compounds were directly inserted into a postcolumn vaporizer operated at 270°. All UV spectra were obtained with methanol solutions. All melting points were taken on a melting-point stage[9]. All IR frequencies are reported as corrected values. A molecular model set[10] was used for structural analyses. The HPLC system is reported elsewhere (12).

TLC—All chromatograms were performed with fluorescent, precoated silica gel sheets[11], cut to 50 × 75 mm, by ascending development under equilibrated conditions in a tank lined with filter paper[12]. Spots were located by irradiation with short- or long-wavelength UV or by this sequential treatment: spray with Folin reagent[13], spray with 50% H_2SO_4, and heat at 100° for a few minutes (2).

Reactions of Thioridazine and Mesoridazine with Hydrogen Peroxide—*Method I, Oxidation in Acetic Acid*—Thioridazine and mesoridazine bases were oxidized with hydrogen peroxide in glacial acetic acid at 45° as described previously (17). The reaction product was examined by TLC with a solvent system composed of chloroform–95% ethanol–12 *N* ammonium hydroxide (80:20:1). The sample was spotted

[1] Sandoz Pharmaceuticals, Hanover, NJ 07936.
[2] Model 3-200, Pye Unicam Ltd., Cambridge, England.
[3] Spektralphotometer DM 4 and linear recorder Model 300, Carl Zeiss, Oberkochen, West Germany.
[4] Models T60-A and FT-80A, Varian Associates, Palo Alto, CA 94303.
[5] Model 5992A, Hewlett-Packard, Palo Alto, CA 94304.
[6] OV-101 (2%) and 0.2% carbowax 20M on 100/200 mesh Chromosorb W-HP, Hewlett-Packard.
[7] Olfax IIA, Vitek Systems, Inc., McDonnell Douglas Corp., Hazelwood, MO 63042.
[8] OV-225 (1.5%) on Chromosorb G, Applied Science Laboratories, State College, PA 16801.
[9] Fisher Scientific Co., Pittsburgh, PA 15219.
[10] Dreiding stereomodels, Fisher Scientific Co.
[11] Silica gel 60 F-254, 0.20-mm thick, on aluminum, E. Merck, Darmstadt, Germany.
[12] Whatman No. 1, Whatman, Inc., Clifton, NJ 07014.
[13] Phenol Reagent Solution, 2 *N*, Folin-Ciocalteau, Fisher Scientific Co.

beside reference standards of thioridazine (I) and mesoridazine (III) and synthetic samples of the thioridazine ring sulfoxides (IIF and IIS). The chromatograms were inspected by short- and long-wavelength UV irradiation and by a detection system used for locating and identifying the spots by color (1). An HPLC system (12) was also used to identify the reaction products and to obtain approximate product ratios.

Method II—Thioridazine hydrochloride (40.7 mg) was treated in four different reactions with increasing concentrations of aqueous hydrogen peroxide. The drug was dissolved in the following amounts of water, and the following amounts of hydrogen peroxide were added to the solutions over about a 2-min period: 5 ml of water, 0.1 ml of 15% H_2O_2; 15 ml of water, 0.1 ml of 15% H_2O_2; 5 ml of water, 25 μl of 15% H_2O_2; and 15 ml of water, 25 μl of H_2O_2. The studies examined whether more strenuous oxidation conditions would favor formation of the dioxide over that of the ring sulfoxides (IIF and IIS). Products from these reactions were examined by TLC as in Method I.

Method III—Thioridazine hydrochloride and 40% hydrogen peroxide were refluxed 4 hr in ethanol, as described previously (1). The crude reaction product was examined by TLC and HPLC. This oxidation process was also conducted on thioridazine free base to determine whether there was a difference in the distribution of reaction products under mildly basic conditions.

Samples Prepared for Oxidation Studies—Sample A consisted of a mixture of reference standards of I and III with synthetic IIF and IIS, prepared as described below. The rest of the samples were reaction products formed by the following oxidations: B, I with hydrogen peroxide in glacial acetic acid (17); C, III with hydrogen peroxide in glacial acetic acid; D, the hydrochloride of I with hydrogen peroxide in aqueous solution; E, the hydrochloride of I with hydrogen peroxide in refluxing ethanol (1); F, I with hydrogen peroxide in refluxing ethanol; G, I with nitrous acid.

Chromatography Systems Used to Study Oxidation Products—Systems I–IV and VI were used with silica gel TLC: I, chloroform–95% ethanol–12 *N* ammonium hydroxide (80:20:1); II, acetone–12 *N* ammonium hydroxide (100:7) (2); III, ethyl acetate–glacial acetic acid–water (5:2:2) (1); IV, a solution of 1.5 g of ammonium acetate in 10 ml of water mixed with 50 ml of methanol (13–15). System V was an HPLC method (12); identification was made by observation of an increase of peak response without appearance of new peaks after the samples were spiked with appropriate individual components of sample A. System VI: TLC plates were sprayed with Folin reagent, then with 50% sulfuric acid, and were heated at 100° for a few minutes. TLC identifications were made by observing R_f values which were identical to those of the components of sample A.

Specific Oxidation of Thioridazine to Generate Only the Ring Sulfoxides of Thioridazine and Isolation as Nitric Acid Salts (VF and VS)—To a solution of 1.521 g of thioridazine hydrochloride in 100 ml of deionized water was added 10 drops of concentrated hydrochloric acid. To this mixture a sodium nitrite solution (1 g/10 ml) was added dropwise with stirring until the solution turned from blue to yellow-brown or started to turn orange. A small portion of this reaction mixture was analyzed immediately by HPLC; the ring sulfoxides had been formed exclusively. The mixture was extracted with two 30-ml portions of chloroform. The chloroform was removed by evaporation (steam bath) and then heptane (50 ml) was added to the glassy residue, and the solvent was again removed (steam bath) to give a yellow-orange powder. Residual heptane was removed by decantation. A small amount of this decanted heptane was boiled to dryness and contained no dissolved substances. The hard granular solid (VF and VS) after air drying weighed 1.07 g. The reaction was repeated with 3- and 6-g portions of thioridazine hydrochloride to yield 2.18 and 5.02 g, respectively. Melting points are given in Table III.

The nitric acid salts of the thioridazine ring sulfoxides (5.7 g) were fractionally crystallized (19) from 95% ethanol to give 290 mg of 99.9% VF and 360 mg of 99.3% VS. Purity was determined by HPLC (12). Melting points are given in Table III.

Conversion of the Nitric Acid Salts to Free Bases—The salt (VF or VS), 140 mg, was dissolved in 10 ml of warm deionized water. Concentrated ammonium hydroxide (60 μl) was added and an oil separated. The mixture was extracted with two 5-ml portions of chloroform, and the combined extracts were passed through filter paper[9], to remove water. The chloroform was removed (steam bath, nitrogen flush), and then methanol (5 ml) was added and removed in the same manner. The product was recrystallized from hexane or heptane to give a mixture of IIF and IIS (from VF and VS). When VF and VS were treated individually, analytically pure IIF and IIS were obtained. Melting points and analyses are given in Table III. IR (Nujol mull or KBr disk): IIF, 1019 (s) and 1050 (s) cm^{-1}; IIS, 1028 (s) and 1050 (s) cm^{-1}; (cast films): both IIF and IIS, 1028 (s) and 1050 (s) cm^{-1} and superimposable from 4000 to 6000 cm^{-1}. IR sulfoxide bands: II, 1020 and 1045 cm^{-1} (S=O) (1). IR (KBr) commercial sample of ring sulfoxide (IIS–IIF = 85:15): 1028 (s) and 1050 (s) cm^{-1} and superimposable from 4000 to 6000 cm^{-1} with a spectrum of IIS; mass spectrum: *m/z* (relative abundance, percent), IIF, 386 (0.5) (M^+); 370 (M − 16), 98; IIS, 386 (2.0) (M^+); 370 (M − 16), 98.

Reduction of Thioridazine Ring Sulfoxides to Thioridazine with Lithium Aluminum Hydride—The mixed nitric acid salts VF and VS (0.1 g) were converted to the thioridazine sulfoxide free bases IIS and IIF as described directly above. A solution of the free bases in 1.3 ml of anhydrous ether was stirred under a nitrogen atmosphere, and then a slurry of 0.1 g of lithium aluminum hydride in 1.3 ml of anhydrous ether was slowly added. A vigorous reaction occurred, and the solution turned orange and then yellow. After the reaction subsided, the mixture was refluxed for 24 hr. Water was added and the mixture was extracted three times with heptane–toluene (4:1). The solvent was removed to give 35 mg of thioridazine. Mesoridazine was reduced to thioridazine in the same manner. The products were compared with thioridazine by TLC, IR spectrophotometer, and GC–MS (identical retention times with thioridazine): *m/z* 370 (M^+), 98 (base peak, *N*-methyl piperidinyl fragment); instrument correlation index for thioridazine, 0.911.

REFERENCES

(1) K. Zehnder, F. Kalberer, W. Kreis, and J. Rutschmann, *Biochem. Pharmacol.*, **11**, 535 (1962).

(2) I. A. Zingales, *J. Chromatogr.*, **44**, 547 (1969).

(3) R. G. Muusze and J. F. K. Huber, *ibid.*, **83**, 405 (1973).

(4) F. A. J. Vanderheeren and R. G. Muusze, *Eur. J. Clin. Pharmacol.*, **11**, 135 (1977).

(5) R. G. Muusze and F. A. J. Vanderheeren, *ibid.*, **11**, 141 (1977).

(6) R. G. Muusze and J. F. K. Huber, *J. Chromatogr. Sci.*, **12**, 779 (1974).

(7) W. Lindner, R. W. Frei, and W. Santi, *J. Chromatogr.*, **111**, 365 (1975).

(8) L. Gottschalk, E. Dinovo, R. Biener, and B. R. Nandi, *J. Pharm. Sci.*, **67**, 155 (1978).

(9) E. C. Dinovo, L. A. Gottschalk, B. R. Nandi, and P. G. Geddes, *ibid.*, **65**, 667 (1976).

(10) E. C. Dinovo, L. A. Gottschalk, E. P. Noble, and R. Biener, *Res. Commun. Chem. Pathol. Pharmacol.*, **7**, 489 (1974).

(11) L. C. Brookes, F. C. Chao, I. S. Forrest, D. E. Green, K. O. Loeffler, and M. T. Serra, *Clin. Chem.*, **24**, 1031 (1978).

(12) C. E. Wells, E. C. Juenge, and W. B. Furman, *J. Pharm. Sci.*, **72**, 622 (1983).

(13) E. G. C. Clarke, "Isolation and Identification of Drugs," Pharmaceutical Press, London, England, 1969, reprinted 1974, p. 49.

(14) C. Korczak-Fabierkiewicz, J. Kofoed, and G. H. W. Lucas, *J. Forensic Sci.*, **10**, 308 (1965).

(15) C. Korczak-Fabierkiewicz, J. Kofoed, and G. H. W. Lucas, *Nature (London)*, **211**, 147 (1966).

(16) E. C. Dinovo and L. A. Gottschalk, *Clin. Chem.*, **21**, 1033 (1975).

(17) L. K. Turner, *J. Forensic Sci.*, **4**, 39 (1963).

(18) J. R. Partington, "A Text-book of Organic Chemistry," 6th ed., Macmillian, London, England, 1950, pp. 532, 537, 550.

(19) R. S. Tipson, in "Technique of Organic Chemistry," vol. III, pt. I, A. Weissberger, Ed., Interscience, New York, N.Y., 1956, p. 490.

(20) O. L. Chapman and R. W. King, *J. Am. Chem. Soc.*, **86**, 1256 (1964).

(21) *Societe des usines chimiques Rhone-Poulenc*, Brit. pat. 799,919 (1958); through *Chem. Abstr.*, **53**, 4312a (1959).

(22) J. Renz, J. P. Bourquin, H. Winkler, P. Gagnaux, L. Ruesch, and G. Schwarb, Fr. addn. pat. 90,868 (1968); through *Chem. Abstr.*, **70**, 96806m (1969).

ACKNOWLEDGMENTS

The authors thank Dr. Neal Castagnoli, Jr., and Dr. Edward Biehl for their helpful suggestions, Dr. Shirley S. Chu for insight regarding structural features of phenothiazines, and Miss Brenda Stringer for assistance in the preparation of the figures.

Simultaneous Assay of Thioridazine and Its Major Metabolites in Plasma at Single Dosage Levels with a Novel Report of Two Ring Sulfoxides of Thioridazine

CLYDE E. WELLS ˣ, ERIC C. JUENGE, and WILLIAM B. FURMAN

Received February 12, 1982, from the *National Center for Drug Analysis, Food and Drug Administration, St. Louis, MO 63101.* Accepted for publication June 3, 1982.

Abstract □ A highly sensitive and selective method of analysis of plasma for thioridazine and its major metabolites, including two isomers of the ring sulfoxide, is presented. It is suitable for following the metabolism of thioridazine for 24 hr after a single dose. The method involves extraction of the materials from plasma, high-performance liquid chromatographic separation, and postcolumn oxidation and fluorometric detection. The sensitivity of the method to thioridazine and its metabolites is 2 ng/ml. Recoveries ranged from 87.8 to 100.6% at levels between 20 and 400 ng/ml.

Keyphrases □ Thioridazine—isomeric ring sulfoxides, metabolism, high-performance liquid chromatography with fluorometric detection, determination in plasma □ High-performance liquid chromatography—thioridazine metabolism, formation of two isomeric ring sulfoxides, determination in plasma

In preparation for a clinical study designed to compare the bioavailability of various brands of thioridazine tablets, it was necessary to develop a sensitive, specific method for the determination of thioridazine and its major metabolites in plasma. The metabolites of interest were sulforidazine (thioridazine 2-sulfone), mesoridazine (thioridazine 2-sulfoxide), and the two isomers of thioridazine ring sulfoxide (thioridazine 5-sulfoxide) for which analyses have not been reported in the literature.

The concentrations of thioridazine and its metabolites in biological fluids have been measured by fluorometric (1, 2), TLC (2–5), GLC (2, 6–14), and high-performance liquid chromatographic (HPLC) (15–17) methods. Most of these methods were developed to measure thioridazine and its metabolites in the blood of patients who were placed on a therapeutic regimen of thioridazine. For the study of the metabolism of thioridazine arising from a single dose, a method capable of detecting these compounds in the range of 10–500 ng/ml of plasma was needed. None of the methods reported in the literature provide both the sensitivity and specificity necessary.

Although the fluorometric methods provide the required sensitivity, they are not specific and do not differentiate among the metabolites. The GLC methods are not suitable at levels <50 ng/ml because of the instability of the metabolites on the chromatographic columns. The TLC procedures lack the necessary sensitivity.

The method of Muusze and Huber (15), which employs an HPLC separation of thioridazine and its metabolites followed by postcolumn oxidation and fluorescence, showed the most promise. However, at a sensitivity that would allow the detection of the eluted compounds at levels <50 ng/ml, the baseline signal from the fluorometer became excessively noisy. To eliminate the noisy baseline and allow the detection of lower levels of the metabolites, the detection system was modified to extract the eluted products into a phosphoric acid solution of potassium permanganate for oxidation.

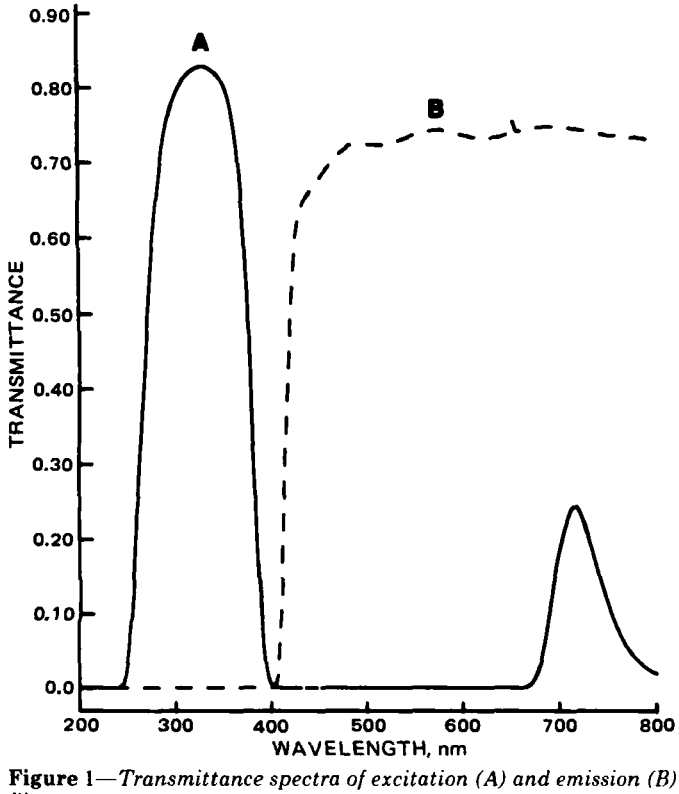

Figure 1—*Transmittance spectra of excitation (A) and emission (B) filters.*

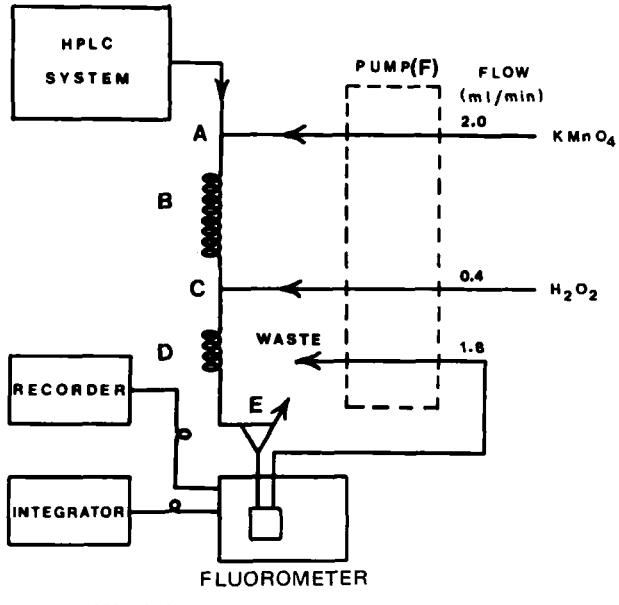

Figure 2—*HPLC detection system. Key: A, PT18; B, 14-turn phasing coil, 2.4-mm i.d.; C, A6; D, 1X mixing coil, 1-mm i.d.; E, B0; and F, Pump I*[6].

0022-3549/83/0600-0622$01.00/0

Table I—Linearity Data for Thioridazine and Metabolites (Spiked Plasma)

Concentration[b]	Ratio[a] I C[c]	I I[d]	II C[c]	II I[d]	III C[c]	III I[d]	IV C[c]	IV I[d]
Blank[e]	0.089	0.090	—	—	—	—	—	—
10	0.346	0.347	0.131	—[f]	0.079	0.068	0.050	—[f]
20	0.755	0.741	0.287	0.278	0.170	0.163	0.117	0.107
50	1.45	1.42	0.572	0.569	0.343	0.332	0.241	0.230
100	—[g]	2.76	1.09	1.10	0.673	0.672	0.480	0.486
250	—[g]	6.42	—[g]	2.70	—[g]	1.58	—[g]	1.16
400	—[g]	10.49	—[g]	4.30	—[g]	2.45	—[g]	1.78
500	—[g]	12.62	—[g]	5.48	—[g]	3.15	—[g]	2.26
Slope	36.2	39.6	95.7	92.6	154.2	161.7	213.2	224.2
Intercept	−3.9	−6.3	−4.8	−2.7	−3.8	−4.4	−2.3	−5.1
Correlation Coefficient	0.9942	0.9997	0.9987	0.9998	0.9991	0.9997	0.9989	0.9998

[a] Standard peak height to internal standard peak height. I = thioridazine; II = thioridazine ring sulfoxide (fast eluter); III = thioridazine ring sulfoxide (slow eluter); IV = mesoridazine. [b] ng/ml of plasma. [c] Peak height taken from recorder chart. Recorder set at 20 mV full scale. [d] Peak height reported by integrator. [e] No II, III, or IV detected in blank. [f] Integrator failed to detect peak. [g] Peaks were off-scale on the recorder.

Although that study (15) reported only a single thioridazine ring sulfoxide, another study (18) reported the presence of two isomers. The mobile phase used in the HPLC system was modifed to permit the separation of all the metabolites of interest, including the two ring sulfoxide isomers, and to allow the use of an internal standard.

EXPERIMENTAL

Apparatus—The HPLC system consisted of a pump[1], a syringe injector[1], a recorder[2], an integrator[3], a 3.2- × 250-mm column packed with 10-μm spherical particle silica[4], a 2- × 50-mm precolumn of solid-core silica[5], a peristaltic pump[6], mixing coils and connecting tees[6], and a fluorometer[7] equipped with excitation[8] and emission[9] filters. The transmittance spectra of these filters are shown in Fig. 1. Samples were stored in a freezer[10] at −40°. A vortex mixer[11] and a centrifuge[12] were used in the extraction of the plasma samples. The detection system was assembled as shown in Fig. 2.

Reagents—Potassium permanganate, sodium nitrite, diethylamine, hydrogen peroxide, and phosphoric acid were reagent grade. Ethyl acetate, heptane, 1-chlorobutane, methylene chloride, and 2-propanol were HPLC grade. The water was deionized. Thioridazine hydrochloride[13], mesoridazine besylate[13], thioridazine ring sulfoxide nitric acid salts[14] (18), sulforidazine[14], and triflupromazine hydrochloride[15] were used as standards. Plasma was obtained from the Red Cross blood bank.

The potassium permanganate solution was prepared by dissolving 100 mg of potassium permanganate in 1 liter of 5% aqueous phosphoric acid. The hydrogen peroxide solution was prepared by diluting 1 ml of 30% hydrogen peroxide to 250 ml with water.

HPLC Operating Conditions—The mobile phase was 1-chlorobutane–2-propanol–water–diethylamine (92:7.9:0.08:0.016). The flow rate was 1.5 ml/min at 25°. The potassium permanganate solution flow rate was 2.0 ml/min, and the hydrogen peroxide solution flow rate was 0.4 ml/min. The flow rate through the fluorometer flowcell was 1.8 ml/min. The recorder sensitivity was set at 20 mV full scale (the output of the fluorometer was 100 mV full scale). The fluorometer sensitivity was adjusted so that the internal standard peak height was ~ 80% of full scale on the recorder when 100 μl of sample extract was injected. The integrator was set to measure peak heights. Instrument operating conditions were maintained for 0.5 hr before injection of the first sample or standard solution.

Preparation of the Internal Standard Solution—An aqueous solution of triflupromazine hydrochloride (10 mg/25 ml) was transferred to a separatory funnel. A 1-ml portion of 0.1 *N* hydrochloric acid and a 1-ml portion of sodium nitrite solution (10 g/100 ml) were added, and the funnel was shaken for 2 min. The solution was made alkaline with concentrated ammonium hydroxide, the oxidized triflupromazine was extracted with one 50-ml portion of methylene chloride, and the extract was diluted to 100.0 ml with methylene chloride. A 3.0-ml aliquot of the

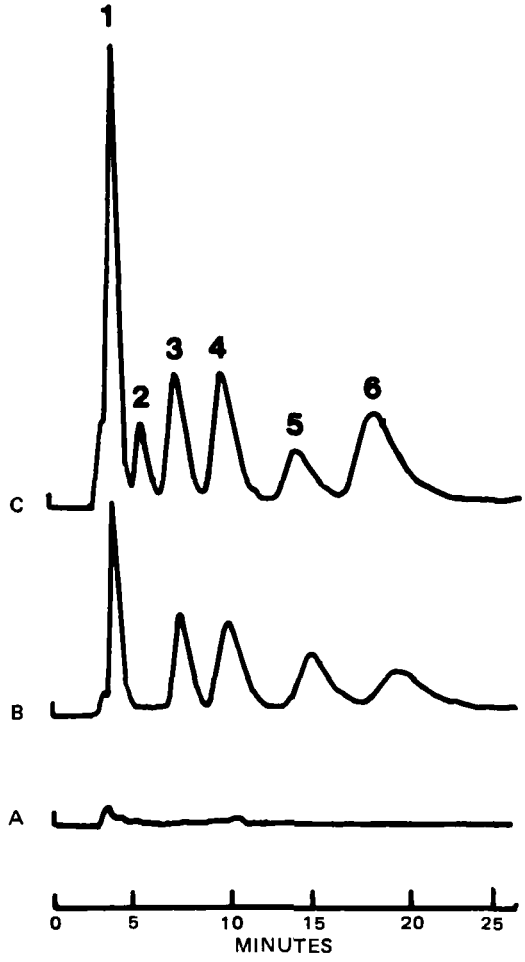

Figure 3—*HPLC chromatograms. Key: A, extract of blank plasma; B, standards added to plasma at a level of ~100 ng/ml each; C, extract from whole blood of patient on thioridazine therapy; (1) thioridazine; (2) sulforidazine; (3) internal standard; (4 and 5) thioridazine ring sulfoxides; and (6) mesoridazine.*

[1] Model 6000A pump and model U6K injector, Waters Associates, Milford, MA 01757.
[2] Model PS01W6A, Texas Instruments, Inc., Houston, TX 77001.
[3] Model 3390A, Hewlett-Packard, Palo Alto, CA 94304.
[4] 10-μm LiChrosphere Si-500, Alltech Associates, Inc., Deerfield, IL 60015.
[5] Corasil, 30–50 μm, Waters Associates.
[6] Technicon Instruments Corp., Tarrytown, NY 10591. See Fig. 2 for part numbers.
[7] Ratio Fluorometer 2, Farrand Optical Co., Inc., Valhalla, NY 10595.
[8] Schott UG-11.
[9] Wratten 2B.
[10] Model ULT 1535-A-J-6, Rheem Manufacturing Co., West Columbia, SC 29169.
[11] Model M-16715, Thermolyne Corp., Dubuque, IA 52001.
[12] Spinette, International Equipment Co., Damon Corp., Needham Heights, MA 02194.
[13] Sandoz Pharmaceuticals, Hanover, NJ 07936.
[14] Prepared in our laboratory.
[15] USP reference standard.

Table II—Recovery Data for Thioridazine (ng/ml of Plasma) from Four Spiked Samples of Plasma

Sample	Sample[a] 1	2	3	4
1	377.1	147.3	75.3	17.7
2	373.1	149.7	75.2	19.2
3	376.9	150.8	73.1	18.4
4	393.7	141.6	71.5	18.3
Mean	380.2	147.3	73.8	18.4
SD	9.19	4.10	1.82	0.62
CV, %	2.42	2.78	2.47	3.35
Added	407.8	163.0	81.5	20.4
Percent recovery	93.2	90.4	90.5	90.2

[a] For concentrations of other components in these samples, see Tables III–V.

methylene chloride solution was diluted to 250 ml with heptane–ethyl acetate–diethylamine (100:100:1). The internal standard solution gave an HPLC peak with a retention time identical to that of triflupromazine sulfoxide prepared from a previous procedure (19). The latter material was crystallized from ethyl acetate and dried (55°, 3 mm, 3 hr) to give a product, mp 94–96°, which was submitted for carbon and hydrogen elemental analysis.

Anal.—Calc. for $C_{18}H_{19}F_3N_2OS$: C, 58.68; H, 5.20. Found: C, 58.43; H, 5.33.

Preparation of Sample Solutions—A 2.0-ml aliquot of plasma was transferred to a 16- × 100-cm screw-capped test tube containing 2.0 ml of the internal standard solution and 3 ml of heptane–ethyl acetate (1:1). The tube was capped, mixed on a vortex mixer for 2 min, centrifuged for 5 min, and placed in the freezer until the plasma was frozen. The organic layer was decanted into a second tube. The frozen plasma was allowed to thaw and was re-extracted with 3 ml of heptane–ethyl acetate (1:1). The organic layers were combined and evaporated to dryness (steam bath, nitrogen stream). The residue was dissolved in 0.5 ml of the HPLC mobile phase.

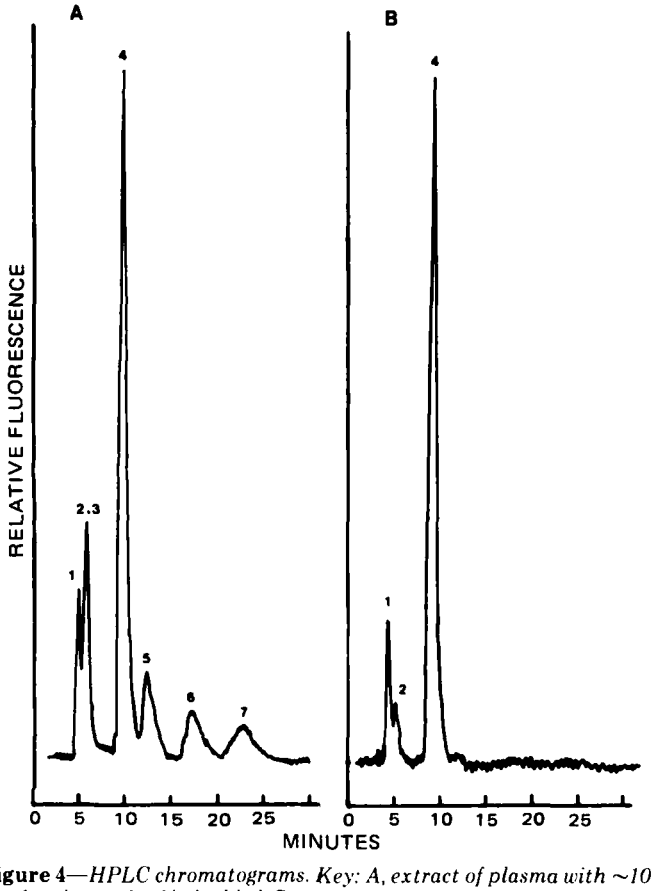

Figure 4—*HPLC chromatograms. Key: A, extract of plasma with ~10 ng of each standard/ml added; B, extract of blank plasma with internal standard added; (1 and 2) plasma blanks; (3) thioridazine; (4) internal standard; (5 and 6) thioridazine ring sulfoxides; and (7) mesoridazine.*

Table III—Recovery Data for Thioridazine Ring Sulfoxide (Fast Eluter) (ng/ml of Plasma) from Four Spiked Samples of Plasma

Sample	Sample[a] 1	2	3	4
1	42.9[b]	38.9	207.7	393.2
2	18.7	35.9	201.2	388.7
3	16.6	35.5	188.1	394.6
4	16.6	40.8	193.7	390.9
Mean	17.3	37.8	197.7	391.8
SD	1.21	2.52	8.57	2.60
CV, %	7.00	6.68	4.34	0.66
Added	19.7	39.3	196.8	393.6
Percent recovery	87.8	96.2	100.4	99.5

[a] For concentrations of other components in these samples, see Tables II, IV, and V. [b] Sample contaminated; not used in calculation of mean, *SD*, and *CV*.

Preparation of Standard Solutions—Portions of the salts of thioridazine, mesoridazine, and the ring sulfoxides equivalent to 20 mg of the corresponding free bases were each dissolved in 95% ethanol and diluted to 100.0 ml. These solutions were diluted with 95% ethanol to give mixed standard solutions containing 0.8, 1.6, 4, 8, 20, 32, and 40 μg of each standard/ml. A 25-μl aliquot of each solution was added to 2 ml of plasma. At this low level, the ethanol neither denaturated the plasma nor influenced the partition coefficients in the extractions. The sample-preparation procedure was used for the extraction of the standard solutions.

Recovery of Thioridazine and Metabolites from Plasma—Four plasma samples containing thioridazine and each of its metabolites at levels of 20 to 400 ng/ml were prepared. Aqueous solutions of the ethanolic standard solutions were added to the plasma to avoid denaturing of the plasma and to avoid changes in the partition coefficients in the extraction steps. Four aliquots of each prepared plasma sample and four aliquots of blank plasma were extracted.

Stability of Thioridazine and Its Metabolites in Plasma—Aliquots of one of the plasma samples used in the recovery experiment were transferred to test tubes and stored in the freezer. At intervals over a 3-week period, the samples were removed from the freezer and extracted. The dried extracts were stored in the freezer until the end of the 3-week period; all extracts were then injected into the HPLC system on the same day. In a second experiment, samples were removed from the freezer and stored at room temperature for 0, 1, 2, 5, and 24 hr before extraction; all five of these extracts were injected on the same day.

HPLC Separation and Analysis—A 100-μl aliquot of the extract of each standard and sample was injected into the liquid chromatograph. The ratios of each peak height to the peak height of the internal standard were calculated from the integrator output and from the recorder chart for those peaks that remained on scale. Linear regression calculations were performed on the standards, and the slope and intercept so obtained were used to calculate the concentration of the sample solutions.

RESULTS AND DISCUSSION

Preliminary tests showed that, at levels < 50 ng of metabolite per ml of plasma, the peak height measurement by the integrator was more reliable than the area measurement. Integration would sometimes stop before the baseline was reached at the end of the peak, causing relatively large errors in the calculations based on peak area.

The peak height ratios of the plasma standards were subjected to a

Table IV—Recovery Data for Thioridazine Ring Sulfoxide (Slow Eluter) (ng/ml of Plasma) from Four Spiked Samples of Plasma

Sample	Sample[a] 1	2	3	4
1	28.8[b]	39.2	206.3	378.2
2	20.2	37.2	206.1	396.6
3	18.0	40.0	199.7	410.0
4	19.0	36.6	197.9	400.2
Mean	19.1	38.2	202.5	396.2
SD	1.10	1.61	4.33	13.33
CV, %	5.77	4.21	2.14	3.36
Added	20.7	41.4	206.9	413.8
Percent recovery	92.2	92.3	97.9	95.7

[a] For concentrations of other components in these samples, see Tables II, III, and V. [b] Sample contaminated; not used in calculation of mean, *SD*, and *CV*.

Table V—Recovery Data for Mesoridazine (ng/ml of Plasma) from Spiked Samples of Plasma

Sample	Sample[a] 1	2	3	4[b]
1	81.0	379.6	198.5	—
2	81.4	355.7	197.3	—
3	79.2	384.9	195.7	—
4	78.1	362.0	197.6	—
Mean	79.9	370.6	197.3	—
SD	1.55	13.9	1.17	—
CV, %	1.94	3.76	0.59	—
Added	79.5	397.4	198.7	20.0
Percent recovery	100.5	93.3	99.3	—

[a] For concentrations of other components in these samples, see Tables II–IV. [b] Level of mesoridazine in sample 4 not detectable in the presence of 400 ng of the ring sulfoxide/ml of plasma.

linear regression analysis (Table I). Each of the four compounds tested showed a linear response in the 10- to 500-ng/ml range. The peak height ratios calculated from the recorder chart could be used interchangeably with those calculated by the integrator. Occasionally the integrator failed to detect peaks at levels of 10–20 ng/ml. The recorder chart then provided a convenient backup for measurement of the peak height ratio.

Recoveries (Tables II–V) ranged from 87.8 to 100.5%, and coefficients of variation ranged from 0.6 to 7.0%. The largest variations were found for the ring sulfoxides in the 20- to 40-ng/ml range. The recovery of sulforidazine was not studied due to lack of sufficient material.

The results of the stability tests (Tables VI and VII) show that thioridazine and its metabolites are stable in frozen plasma for at least 3 weeks and are stable in plasma at room temperature for at least 24 hr.

Figure 3 shows the integrator curves for blank plasma, plasma with each standard added at the 100-ng/ml level, and a whole blood sample from a patient on thioridazine therapy. Figure 4 shows the recorder tracing of a plasma sample with each standard added at the 10-ng/ml level and that of a plasma blank with the internal standard added. The estimated detection limit for each standard in plasma is 2 ng/ml.

The HPLC system gives good resolution of thioridazine and its major metabolites. When used with the new sample extraction procedure and the new procedures for postcolumn extraction, oxidation, and fluorometric detection reported here, the system provides a highly sensitive and specific method of analysis with minimum interferences.

A modification of the procedure has been used to measure thioridazine and its metabolites in postmortem whole blood samples. Thioridazine,

Table VI—Stability of Compounds[a] in Frozen Plasma Samples (Sample 3)

Days in Freezer	Peak Height Ratios[b] I	II	III	IV
1	1.761	1.839	1.200	0.912
2	2.062	2.132	1.362	1.035
2	1.957	1.969	1.282	0.955
5	2.096	2.032	1.339	1.012
14	1.870	2.034	1.274	0.955
14	2.067	1.993	1.304	0.963
21	1.997	2.162	1.372	1.031
21	2.048	2.005	1.289	0.958
Mean	1.982	2.021	1.303	0.978
SD	0.1154	0.1000	0.0556	0.0435
CV, %	5.82	4.92	4.27	4.45

[a] I = thioridazine; II = thioridazine ring sulfoxide (fast eluter); III = thioridazine ring sulfoxide (slow eluter); IV = mesoridazine. [b] Standard peak height–internal standard peak height.

Table VII—Stability of Compounds[a] in Plasma Samples at Room Temperature

Hours	Peak Height Ratios[b] I	II	III	IV
0	1.951	1.805	1.223	0.911
1	1.870	1.744	1.142	0.862
2	1.971	1.818	1.216	0.922
5	2.073	1.844	1.228	0.919
24	1.963	1.842	1.195	0.920
Mean	1.966	1.811	1.201	0.907
SD	0.0723	0.0411	0.0350	0.0253
CV, %	3.66	2.25	2.95	2.80

[a] I = thioridazine; II = thioridazine ring sulfoxide (fast eluter); III = thioridazine ring sulfoxide (slow eluter); IV = mesoridazine. [b] Standard peak height–internal standard peak height.

sulforidazine, the two ring sulfoxides, and mesoridazine were detected at levels that ranged from 20 ng to 20 μg/ml[16].

REFERENCES

(1) N. R. West, M. P. Rosenblum, H. Sprince, S. Gold, D. H. Boehme, and W. H. Vogel, *J. Pharm. Sci.*, **63**, 417 (1974).

(2) E. C. Dinovo, L. A. Gottschalk, E. P. Noble, and R. Biener, *Res. Commun. Chem. Pathol. Pharmacol.*, **7**, 489 (1974).

(3) F. A. J. Vanderheeren and R. G. Muusze, *Eur. J. Clin. Pharmacol.*, **11**, 135 (1977).

(4) R. G. Muusze and F. A. J. Vanderheeren, *ibid.*, **11**, 141 (1977).

(5) G. Sakalis, L. J. Traficante, and S. Gershon, *Curr. Ther. Res.*, **21**, 720 (1977).

(6) S. H. Curry and G. P. Mould, *J. Pharm. Pharmacol.*, **21**, 674 (1969).

(7) E. Martensson and B. E. Roos, *Eur. J. Clin. Pharmacol.*, **6**, 181 (1973).

(8) E. C. Dinovo and L. A. Gottschalk, *Clin. Chem.*, **21**, 1033 (1975).

(9) E. C. Dinovo, L. A. Gottschalk, B. R. Nandi, and P. G. Geddes, *J. Pharm. Sci.*, **65**, 667 (1976).

(10) F. A. J. Vanderheeren and D. J. C. J. Theunis, *J. Chromatogr.*, **120**, 123 (1976).

(11) R. Axelsson, *Curr. Ther. Res.*, **21**, 587 (1977).

(12) C. H. Ng and J. L. Crammer, *Br. J. Clin. Pharmacol.*, **4**, 173 (1977).

(13) L. A. Gottschalk, E. C. Dinovo, R. Biener, and B. R. Nandi, *J. Pharm. Sci.*, **67**, 155 (1978).

(14) E. C. Dinovo, R. O. Bost, I. Sunshine, and L. A. Gottschalk, *Clin. Chem.*, **24**, 1828 (1978).

(15) R. G. Muusze and J. F. K. Huber, *J. Chromatogr. Sci.*, **12**, 779 (1974).

(16) D. C. Williams, III and R. W. Burnett, *Clin. Chem.*, **23**, 1139 (1977).

(17) L. C. Brookes, F. C. Chao, I. S. Forrest, D. E. Green, K. O. Loeffler, and M. T. Serra, *ibid.*, **24**, 1031 (1978).

(18) E. C. Juenge, C. E. Wells, D. E. Green, I. S. Forrest, and J. N. Shoolery, *J. Pharm. Sci.*, **72**, 617 (1983).

(19) L. K. Turner, *J. Forensic Sci.*, **4**, 39 (1963).

ACKNOWLEDGMENTS

The authors wish to express their appreciation to Alphonse Poklis for supplying the whole blood samples, to James W. Myrick for preparing the plasma samples for the recovery experiment, and to John C. Black for preparing the drawings.

[16] Manuscript in preparation.

Antitumor Agents LIX: Effects of Quassinoids on Protein Synthesis of a Number of Murine Tumors and Normal Cells

I. H. HALL *x, Y. F. LIOU *, K. H. LEE *, S. G. CHANEY ‡, and W. WILLINGHAM, JR. ‡

Received February 8, 1982, from the *Division of Medicinal Chemistry, School of Pharmacy and ‡Department of Biochemistry, School of Medicine, University of North Carolina at Chapel Hill, Chapel Hill, NC 27514. Accepted for publication June 2, 1982.

Abstract □ The quassinoids (brusatol, bruceantin, bisbrusatolyl esters, and bisbruceantinyl esters of succinic and malonic acids) were observed not to be universal protein synthesis inhibitors. Rather, they were selective for both the types of cancers, *e.g.*, P-388 lymphocytic leukemia, Ehrlich and hepatoma carcinoma and L-1210 lymphoid leukemia, as well as types of normal tissues (*e.g.*, lymphocytes), in which they demonstrated protein synthesis inhibition. The data suggest that the observed difference in the magnitude of protein synthesis inhibition of two P-388 lymphocytic leukemia cell lines by the quassinoids was at the ribosomal levels, whereas the observed difference in normal livers from various strains of mice involve differences in cell membrane transport of the quassinoids into the various tissues. Detailed studies indicated that the mode of action of the quassinoids as protein synthesis inhibitors was identical in all of the cells where inhibition was observed; *i.e.*, the elongation step of protein synthesis was blocked by the quassinoids. The data derived from assays for polyuridine-directed polyphenylalanine synthesis of isolated ribosomes demonstrated that the ID_{50} values obtained were consistent with the observed inhibition of whole cell protein synthesis inhibition for P-388 cells, as well as for BDF_1 and DBA/2 liver cells. The ID_{50} values obtained from various cells, *e.g.*, P-388 cells and normal liver, were all in the μM range and are consistent with previously published values for the quassinoids in the rabbit reticulocyte and yeast systems.

Keyphrases □ Brusatol—effects on protein synthesis of murine tumors □ Bruceantin—effects on protein synthesis of murine tumors □ Bisbrusatolyl esters—effects on protein synthesis of murine tumors □ Protein synthesis—inhibition by quassinoids, P-388 lymphocytic leukemia cells

Recently a number of quassinoids including brusatol (I), bruceantin (II), bisbrusatolyl malonate (III), bisbrusatolyl succinate (IV), bisbruceantinyl malonate (V), and bisbruceantinyl succinate (VI) were observed to inhibit *in vitro* protein synthesis of P-388 lymphocytic leukemia cells (1). The inhibition of protein synthesis correlated positively with P-388 tumor cell growth inhibition (2), and further work demonstrated that the elongation step of protein synthesis was being inhibited by the quassinoids (1–3). In earlier studies, this laboratory observed that different lines of P-388 lymphocytic cells, P-388-UNC and P-388-NIH, metabolically responded quantitatively differently to the quassinoids; *i.e.*, in the two cell lines different magnitudes of protein synthesis inhibition were observed. Thus, the objectives of the present study were to examine (*a*) the effects of time of incubation to determine how rapidly the agents act on protein synthesis, (*b*) the effects of quassinoids on protein synthesis in two lines of P-388 cells as well as other murine tumor lines, (*c*) the effects of quassinoids on normal tissue protein synthesis to determine if they are ubiquitous mammalian protein synthesis inhibitors, and (*d*) the effects of the quassinoids on *in vivo* protein synthesis using multiple doses and different concentrations (mg/kg) of drugs.

EXPERIMENTAL

Sources of Compounds—The sources of the quassinoids as well as their physical and chemical characteristics have previously been reported

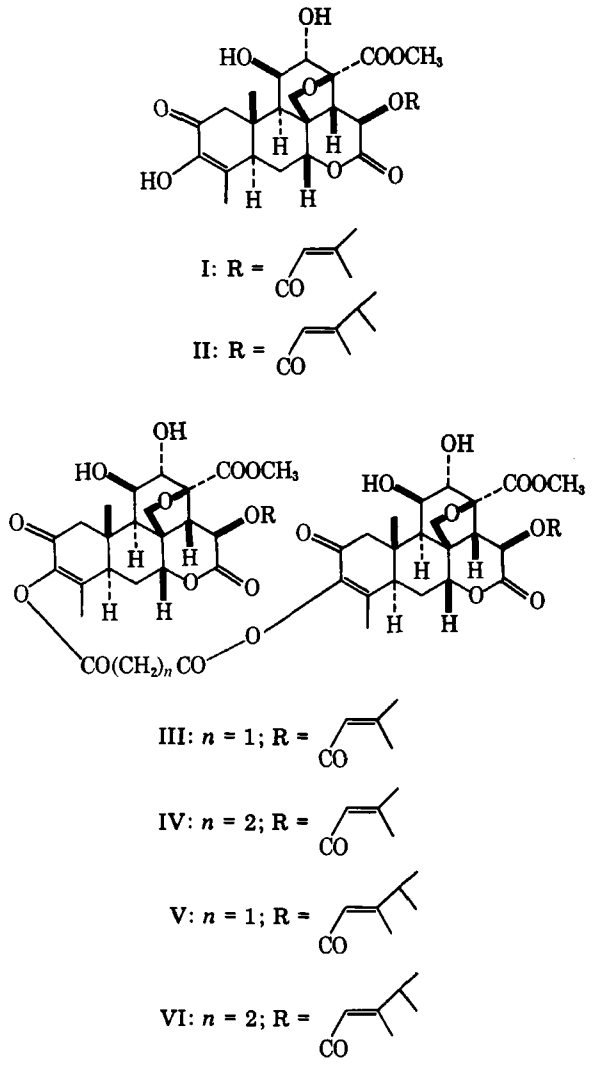

Structures of Quassinoids

(4, 5). All of the agents were homogenized in 0.05% polysorbate-80–water for use in the *in vivo* and *in vitro* studies.

Sources of Tumor and Normal Cells—P-388 lymphocytic leukemia cells were obtained through the National Cancer Institute. The P-388-UNC tumor line was obtained in June 1978 and the P-388-NCI was obtained in December 1980. Both P-388 lymphocytic leukemia lines were maintained in DBA/2 or BDF_1 male mice (~18 g). On day zero, 10^6 P-388 cells were implanted intraperitoneally, and on day 9 the cells were harvested for the *in vitro* studies. Antineoplastic activity was determined for P-388 screen by the NCI protocol (6). The L-1210 lymphoid leukemia line was maintained in DBA/2 male mice (~20 g). On day zero, 10^5 cells were implanted intraperitoneally, and the cells were harvested on day 8 for *in vitro* studies. The hepatoma 129 line was maintained similarly to the P-388 line except the host species was male C_3H mice (~18 g). Cells for the *in vitro* study were removed on day 8. The renal cell carcinoma (RCO_2) was maintained in CDF male mice (~20 g). On day zero, 0.1 ml of ascites fluid was implanted into new donor mice. Three weeks later, cells were harvested for *in vitro* studies.

0022-3549/83/0600-0626$01.00/0

Table I—The Effect of Quassinoid Esters on Protein Synthesis of Two Strains of P-388 Lymphocytic Leukemia Cells for 90-min Incubation

	Control, %									
	P-388-UNC					P-388-NCI				
	5 μM	10 μM	15 μM	25 μM	50 μM	5 μM	10 μM	15 μM	25 μM	50 μM
0.05% Polysorbate 80	100 ± 7	100 ± 7	100 ± 7	100 ± 7	100 ± 7	100 ± 8	100 ± 8	100 ± 8	100 ± 8	100 ± 8
Brusatol	23 ± 6	22 ± 4	19 ± 4	18 ± 3	16 ± 3	24 ± 7	23 ± 5	20 ± 6	18 ± 5	13 ± 3
Bruceantin	75 ± 7	57 ± 6	49 ± 7	38 ± 6	32 ± 4	28 ± 4	19 ± 4	18 ± 6	17 ± 3	19 ± 3
Bisbrusatolyl malonate	54 ± 5	17 ± 4	14 ± 3	5 ± 2	5 ± 2	85 ± 7	70 ± 6	55 ± 5	50 ± 7	50 ± 7
Bisbrusatolyl succinate	58 ± 4	28 ± 4	23 ± 3	—	—	87 ± 9	75 ± 5	63 ± 6	—	—
Bisbruceantinyl malonate	72 ± 5	60 ± 6	45 ± 4	—	—	81 ± 7	76 ± 6	68 ± 6	—	—
Bisbruceantinyl succinate	78 ± 6	68 ± 5	50 ± 4	—	—	90 ± 8	78 ± 6	70 ± 7	—	—

All of the solid tumors were maintained in male $C_{57}B1/6$ mice (~22 g). On day zero a fragment (~30 mg) was implanted into the mice. For the B-16 melanotic melanoma, brain glioma 261 and the ependymoblastoma, the fragment was implanted into the inguinal region of the hind leg. For the Lewis lung, the tumor was implanted intramuscularly into the hind leg. Cells were harvested on day 14 and homogenized with a loose pestle to obtain individual cells in 0.25 *M* sucrose and 0.001 *M* EDTA (ethylenediaminetetraacetic acid), pH 7.4.

The Ehrlich ascites tumor line was maintained in CF_1 male mice (~20 g) by implanting 2×10^6 cells on day zero. Cells were collected on day 8. The sarcoma 180 ascites tumor line was maintained in Swiss Webster male mice (~20 g). Cells were harvested on day 8. The KB human epidermoid carcinoma of the mouth was maintained as a tissue culture in *minimum essential medium and 10% fetal calf serum containing the* antibiotics, penicillin and streptomycin (7).

Normal tissues were selected from the strain of mice that acted as host for the tumor transplant. Normal kidneys were obtained from CDF_1 male mice; normal brain tissue was obtained from $C_{56}B1/6$ male mice; normal liver was obtained from C_3H male mice, and spleen lymphocytes were obtained from DBA/2 male mice.

***In Vitro* Whole Cell Leucine Incorporation into Protein**—These studies were conducted with 10^6 cells (homogenized and whole cell) from tumor or normal tissues, 1 μCi of L-leucine [4,5-^{3}H, 56.5 Ci/mmole] with minimum essential medium in a total volume of 1 ml, which was incubated 60 min at 37°. The time of incubation was varied in the P-388, L-1210, hepatoma, and Ehrlich ascites studies from 30–120 min. The reaction was stopped with 10% trichloroacetic acid, and the insoluble protein was collected on filters[1] by vacuum suction and the filters counted[2] (8, 9). The results are expressed as dpm/10^6 cells.

Polyuridine-Directed Polyphenylalanine Synthesis—Tumor lysates were prepared by a previous method (10). The following were isolated from tumor lysates by literature techniques: runoff ribosomes (11), pH 5 enzymes (10), and uncharged tRNA (12). The reaction medium (13) contained 50 m*M* *tris*(hydroxymethyl)aminomethane, pH 7.6, 12.5 m*M* magnesium acetate, 80 m*M* KCl, 5 m*M* creatine phosphate, 0.05 mg/ml creatine phosphokinase, 0.36 mg/ml polyuridine [poly(U)]-(A_{280}/A_{260} = 0.34), 0.5 μCi [^{3}H]phenylalanine (536 mCi/mmole), 75 μg uncharged tumor cell tRNA, 70 μg of tumor pH 5.0 enzyme preparation, and 0.9 A_{260} of P-388 tumor cell or liver runoff ribosomes. Test drugs were present in 0–30 μ*M* concentration. Incubation was for 20 min at 30° after which a 35-μl aliquot was spotted on filter papers[3] which were treated for 10 min in boiling 5% trichloroacetic acid and washed with cold 5% trichloroacetic acid, ether–ethanol (1:1), and ether. The filter papers were dried and counted in scintillation fluid[2].

***In Vivo* Studies of Protein Synthesis Inhibition**—In order to determine the effects of quassinoids on normal *in vivo* protein synthesis, CF_1 male mice (~22 g) were injected with brusatol, bruceantin, or bisbrusatolyl malonate at a dose of 0.6 mg/kg ip for 3 days. On the 4th day, 1 hr prior to sacrifice, 10 μCi of [^{3}H]leucine was injected intraperitoneally. The liver, kidney, spleen, and lung were excised, and the protein was extracted by a previous method (14) and counted. Protein content was determined by another method (15). *In vivo* P-388 tumor cell studies were conducted to determine the dose response effect on protein synthesis by implanting 10^6 cells on day zero into BDF_1 mice. On days 7, 8, and 9, brusatol, bruceantin, or bisbrusatolyl malonate was injected intraperitoneally from 0.10 to 0.60 mg/kg/day. On day 10, the cells were harvested and extracted as described above. In other studies, brusatol and bruceantin were injected as a single dose on day 7, as two doses on days 7 and 8, and three doses on days 7, 8, and 9 at 0.3 mg/kg/day. Cells were harvested 6 hr after the last dose. Protein was extracted (14), counted, and protein content (15) determined. Results are expressed as dpm/mg of isolated protein.

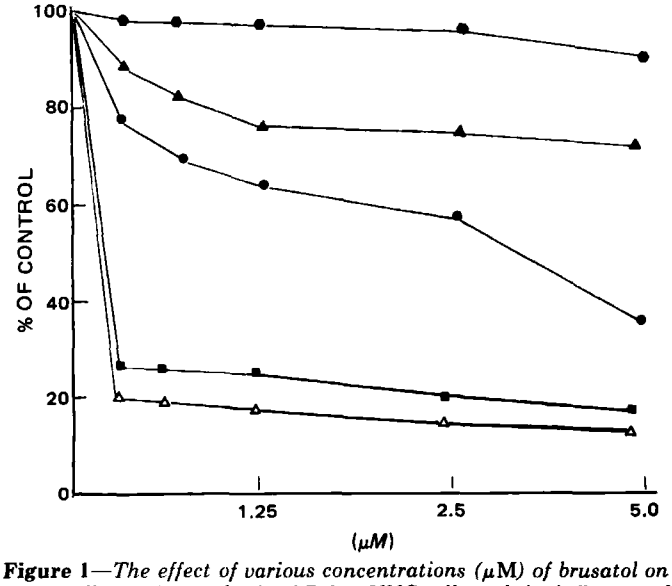

Figure 1—*The effect of various concentrations (μM) of brusatol on whole cell protein synthesis of P-388-UNC cells and the influence of time of incubation. Key: (●) 30 min; (▲) 45 min; (●) 60 min; (■) 90 min; (△) 120 min.*

RESULTS

In initial studies, brusatol (I), bruceantin (II), and bisbrusatolyl malonate (III) were incubated with P-388-UNC lymphocytic leukemia cells between 30–120 min. Brusatol required more than 60 min incubation to obtain maximal inhibition (Fig. 1). Little difference was observed in the extent of inhibition after 90- or 120-min incubations. Similar data were obtained with bruceantin and bisbrusatolyl malonate. Thus, 90-min incubations were used routinely in subsequent experiments. Under these conditions, brusatol was the most effective inhibitor causing an inhibition of 75–80% at concentrations between 1.25 and 5 μ*M* (Fig. 1). The quassinoid esters, III and IV, caused the same magnitude of protein synthesis inhibition but required concentrations of 10–15 μ*M* (Table I). Compound II was not that active as a protein synthesis inhibitor at this concentration range in P-388 cells (Table I). Concentrations above 10 μ*M* were required for II to afford more than 50% inhibition of protein synthesis.

Comparison between two P-388 lymphocytic leukemia lines of tumor (P-388-UNC and P-388-NCI) shows that the quassinoids have a differential effect on tumor growth suppression as well as protein synthesis inhibition (Table I). Compounds I and II at 0.6 mg/kg/day were slightly more active against the growth of the P-388 NCI tumor line compared with the P-388-UNC line (Table II). Compound III was less active against the growth of the P-388-NCI tumor line compared with the P-388-UNC tumor line. Protein synthesis was inhibited (Table II) in a similar manner; *e.g.*, I and II were slightly better inhibitors in the P-388-NCI tumor cell system, whereas III had less effect on protein synthesis in the P-388-NCI tumor line. Approximately the same degree of inhibition of protein

[1] Millipore nitrocellulose.

[2] Fisher Scintiverse in a Packard Counter.

[3] Whatman No. 3.

Table II—The Effects of Quassinoids on *In Vivo* P-388 Lymphocytic Leukemia Tumor Growth

		T/C% at 0.6 mg/kg/day	
		P-388 UNC	P-388 NCI
I	Brusatol	149	156
II	Bruceantin	146	162
III	Bisbrusatolyl malonate	212	135
IV	Bisbrusatolyl succinate	217	161
V	Bisbruceantinyl malonate	139	139
VI	Bisbruceantinyl succinate	153	151
	5 Fluorouracil (12.5 mg/kg)	186	209

synthesis was observed for homogenized cell preparations from both P-388 lines (data not shown). Since III is a dimer connected through an ester group, the question arose whether the difference in response in both antineoplastic activity and inhibition of protein synthesis could be the property of the ester linkage. Thus, three other esters were examined: bisbrusatolyl succinate (IV), bisbruceantinyl malonate (V), and bisbruceantinyl succinate (VI). As can be seen in Table II, all three of these esters demonstrated less antineoplastic activity in the P-388-NCI tumor line compared with the P-388-UNC tumor line. The same analogy can be observed with respect to protein synthesis inhibition; i.e., the esters had less activity as protein synthesis inhibitors in the P-388-NCI tumor cell line (Table II).

In vivo protein synthesis studies in BDF_1 mice inoculated with tumor P-388-NCI lymphocytic leukemia cells demonstrated that after a 3-day administration of the quassinoids from 0.10 to 0.60 mg/kg, brusatol had the strongest effect on protein synthesis inhibition causing greater than 80% inhibition at 0.10 mg/kg/day (Fig. 2). Compound II required a dose of 0.30 mg/kg to produce greater than 80% inhibition, whereas bisbrusatolyl malonate only caused 70% inhibition at 0.60 mg/kg for 3 days. Examination of single and multiple dosing of I, II, and III at 0.3 mg/kg shows that 6 hr after the first dose I caused >90% inhibition of *in vivo* protein synthesis (Fig. 3). Bruceantin, on the other hand, only caused 25% inhibition of protein synthesis 6 hr after a single dose, two doses caused 77% inhibition, and three doses were required to cause >90% inhibition of protein synthesis. Three doses of bisbrusatolyl malonate were required to cause greater than 50% inhibition of protein synthesis. Thus, the *in vivo* studies on the effects of quassinoids on P-388-NCI leukemia cell protein synthesis afforded consistent results with *in vitro* studies.

The quassinoids are potent inhibitors of the polyuridine-directed polyphenylalanine synthesis reaction of P-388 ribosomes. The ID_{50} values obtained for I, II, and III were for the P-388-UNC ribosomes 6.4, 11.5, and 1.9, respectively, and for the P-388-NCI ribosomes 0.4, 0.6, and 25 μM, respectively.

Since the specificity of the quassinoids as protein synthesis inhibitors varied so strikingly between the two P-388 cell lines, the effects of these compounds on the inhibition of *in vitro* protein synthesis of a series of unrelated murine tumors were also examined. As can be seen in Table III, compounds I, II, and III were found to be potent protein synthesis inhibitors in both Ehrlich and hepatoma 129 carcinomas at various concentrations. Again, 90-min incubations resulted in the maximum degree of protein synthesis by the quassinoids for inhibition in Ehrlich and hepatoma cells (data not shown). A moderate protein synthesis inhibition was observed by the quassinoids in the L-1210 lymphoid leukemia, B-16 melanotic melanoma, and ependymoblastoma tumor cells. Compounds I and II at the high concentrations (50 μM) produced mild inhibition of protein synthesis in the brain glioma 261 tumor cells. The quassinoids actually stimulated whole cell protein synthesis in the Lewis lung carcinoma, renal cell carcinoma, and human KB tissue culture system.

As can be observed from Table III, normal lungs from C_3H mice and normal kidneys from CDF mice demonstrated the same pattern of protein synthesis as the Lewis lung carcinoma and renal cell carcinoma of that tissue, *i.e.*, an increase in protein synthesis after 90-min incubation with the quassinoids. The quassinoids inhibited both normal spleen lymphocytic and lymphoid leukemia cells in DBA/2 mice. However, the quassinoids did not cause protein synthesis inhibition of normal liver from C_3H mice but did cause inhibition of the hepatoma from this same strain of mice.

As can be noted in Table III, only protein synthesis from noncancerous livers of BDF_1 and DBA/2 mice was inhibited by the quassinoids at 50-μM concentrations. All other whole cell liver studies from different strains of mice, CF_1, CDF, and $C_{56}B1/6$, demonstrated no inhibition of protein synthesis by the quassinoids. Since liver cells from most strains of mice seemed to be relatively resistant to inhibition by the quassinoids, the effect of these compounds on polyuridine-directed polyphenylalanine synthesis *in vitro* for two of these cell types was determined. In BDF_1 liver, compounds I, II, and III afforded ID_{50} values of 0.3, 0.6, and 25 μM, whereas the DBA/2 liver ribosomes, the ID_{50} values were 0.4, 0.7, and >50 μM, respectively. Bruceantin afforded an ID_{50} of >50 μM with CF_1 liver ribosomes.

DISCUSSION

The quassinoids do not appear to be universal protein synthesis inhibitors. Instead, they are selective for the tissue type as well as noncancerous and cancerous tissue cell types. In some cases this selectivity appears to be due to inherent differences at the ribosome level, while in other cases it seems to be a result of differences in tissue cell permeability to the quassinoids. In whole cell studies the quassinoids require an interval of time before they effectively bring about protein synthesis inhibition. This phenomenon may be due to delayed transport of the quassinoid into the cell, to a time lag necessary for binding of the quassinoids to their intracellular target, or to metabolism of the quassinoids to an active species which inhibits protein synthesis.

The quassinoids did appear to exhibit a quantitative difference in blocking protein synthesis of the P-388-NCI and P-388-UNC lymphocytic leukemia lines. The bis-quassinoid esters were not as active in the P-388-NCI tumor line compared with the P-388-UNC leukemia line. In the *in vivo* studies, the inhibition of protein by compounds I, II, and III after 3 days administration was dose related. Brusatol was more active than bruceantin, and bisbrusatolyl malonate was the least active in the

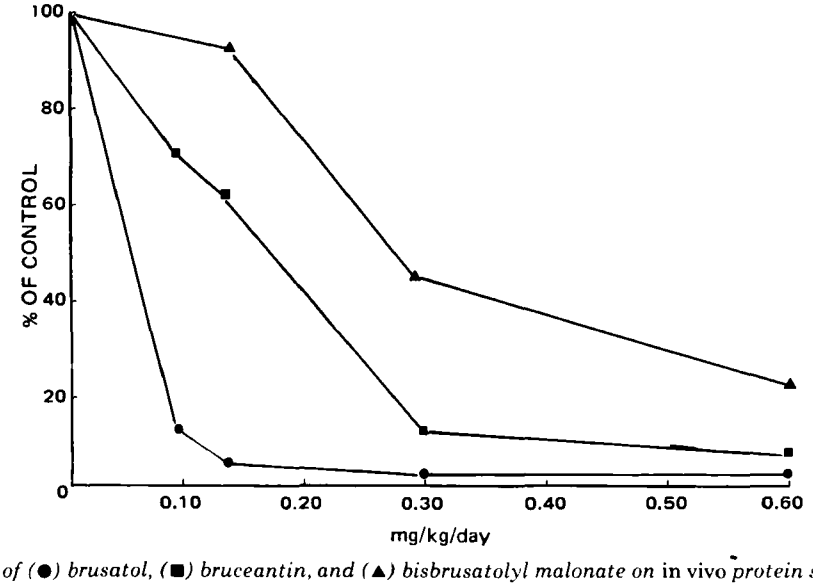

Figure 2—*The effect of dose of (●) brusatol, (■) bruceantin, and (▲) bisbrusatolyl malonate on* in vivo *protein synthesis of P-388-NCI cells.*

Table III—The Effects of Brusatol, Bruceantin, and Bisbrusatolyl Malonate on *In Vitro* Protein Synthesis on Normal and Carcinoma Tissues From the Same Species of Mice [a]

Cancerous Tissues	Control	Control, % Brusatol 10	Brusatol 25	Brusatol 50	Bruceantin 10	Bruceantin 25	Bruceantin 50	Bisbrusatolyl Malonate 10	Bisbrusatolyl Malonate 25	Bisbrusatolyl Malonate 50
Ehrlich Ascites Carcinoma in CF_1	100 ± 5	19 ± 3	23 ± 4	23 ± 3	15 ± 2	22 ± 3	20 ± 3	25 ± 4	27 ± 3	28 ± 3
Hepatoma from C_3H	100 ± 8	74 ± 6	76 ± 6	66 ± 4	78 ± 7	79 ± 6	76 ± 5	72 ± 6	78 ± 7	79 ± 7
L-1210 Lymphoid Leukemia in DBA/2	100 ± 10	72 ± 5	69 ± 4	71 ± 6	78 ± 7	79 ± 8	76 ± 5	72 ± 6	78 ± 7	79 ± 6
B-16 Melanotic Melanoma in $C_{57}B1/6$	100 ± 9	71 ± 6	64 ± 6	60 ± 7	79 ± 5	58 ± 4	52 ± 3	85 ± 6	78 ± 7	76 ± 7
Ependymoblastoma in $C_{57}B1/6$	100 ± 8	89 ± 8	79 ± 9	60 ± 6	84 ± 6	81 ± 5	76 ± 6	130 ± 9	81 ± 8	78 ± 8
Glioma 261 in $C_{57}B1/6$	100 ± 5	104 ± 7	62 ± 6	58 ± 7	112 ± 7	100 ± 6	76 ± 5	102 ± 6	103 ± 7	110 ± 8
Sarcoma 180	100 ± 6	102 ± 8	64 ± 7	50 ± 6	110 ± 7	88 ± 4	66 ± 7	122 ± 8	107 ± 8	81 ± 9
Lewis Lung Carcinoma from $C_{57}B1/6$	100 ± 7	137 ± 8	105 ± 6	123 ± 7	133 ± 8	132 ± 9	108 ± 7	111 ± 6	106 ± 5	134 ± 16
Renal Cell Carcinoma from CDF	100 ± 8	92 ± 7	387 ± 40	499 ± 35	94 ± 6	130 ± 7	208 ± 13	131 ± 10	243 ± 15	380 ± 16
Normal Tissue		12	25	50	12	25	50	12	25	50
Liver from C_3H	100 ± 9	133 ± 12	139 ± 13	142 ± 15	76 ± 6	94 ± 9	165 ± 12	122 ± 10	122 ± 12	129 ± 9
Liver from DBA/2	100 ± 7	92 ± 6	84 ± 6	44 ± 5	94 ± 6	75 ± 3	49 ± 4	79 ± 7	74 ± 5	79 ± 8
Liver from BDF	100 ± 6	83 ± 7	43 ± 5	22 ± 4	82 ± 4	61 ± 5	31 ± 4	72 ± 6	71 ± 7	59 ± 6
Lung from $C_{57}B1/6$	100 ± 7	137 ± 8	105 ± 6	123 ± 7	133 ± 8	132 ± 9	108 ± 7	111 ± 6	106 ± 5	134 ± 16
Kidney from CDF	100 ± 7	116 ± 8	110 ± 9	122 ± 11	106 ± 6	127 ± 12	127 ± 8	107 ± 6	129 ± 12	145 ± 20
Spleen Lymphocytes from DBA/2	100 ± 6	94 ± 6	96 ± 7	92 ± 5	80 ± 6	74 ± 6	63 ± 5	83 ± 5	76 ± 6	65 ± 4

[a] μM Concentrations.

P-388-NCI tumor line. The same relationship can also be observed among the quassinoids with respect to the time after administration of the agents to obtain significant protein synthesis inhibition. These quantitative differences were positively correlated with the antineoplastic activity of the quassinoids obtained in the individual P-388 tumor lines. However, in both P-388 tumor lines, the quassinoids acted identically as elongation inhibitors in polyuridine-directed polyphenylalanine synthesis in the fractionated system. Previous studies have shown that inhibition of the polyuridine-directed polyphenylalanine synthesis is a measure of their effectiveness as antineoplastic agents (2). This system does not require initiation or termination factors. Thus, an inhibitor of this reaction can be considered to be an elongation inhibitor of protein synthesis. Detailed studies have previously demonstrated that the peptidyl transferase reaction is blocked by the quassinoids (1–3). The ID_{50} values obtained for each of the quassinoids in the two P-388 cell lines were consistent with the observed whole cell protein synthesis inhibition; *i.e.*, I and II produced ID_{50} values of lower magnitude in the P-388-NCI line, whereas III afforded an ID_{50} value of lower magnitude in the P-388-UNC line. The fact that these quassinoids were equally effective in whole cell suspensions and in homogenates as well as fractionated protein-synthesizing systems derived from P-388 cells rules out differences in transport or metabolism of these drugs by the two different cell lines. In this case the quantitative differences between the sensitivities of these two cell lines appear to reside at the ribosome level.

The quassinoids were potent protein synthesis inhibitors of some murine tumors: Ehrlich ascites and hepatoma carcinoma were significantly inhibited, whereas L-1210 lymphoid leukemia, B-16 melanotic melanoma, and brain ependymoblastoma were moderately inhibited. However, the quassinoids had no effect on other tumors including human KB cells. A reason for this observation is not obvious, but may involve the transport or metabolism of the quassinoids at different rates or manners by the individual tumors or intrinsic differences in ribosome sensitivity to the drugs. In those tumors where whole cell protein synthesis was inhibited (Ehrlich ascites, hepatoma, and L-1210 lymphoid leukemia), similar times were required to observe maximum protein synthesis inhibition (90 min) as were observed for P-388 cells. There did not appear to be a selectivity of protein synthesis inhibition between normal and cancer cells in the same mouse species. Except for hepatoma in C_3H mice, the quassinoids were not specific inhibitors in cancer cells exclusively, but inhibited protein synthesis of some normal tissues such as spleen lymphocytes, which were proliferating regularly, and DBA/2 and BDF_1 liver cells. Interestingly, the ID_{50} values obtained in the polyuridine-directed polyphenylalanine system of ribosomes isolated from different strains of mice again shows that in those livers where good inhibition by the quassinoids of whole cell protein synthesis was observed, the ID_{50} values were of a low magnitude (0.4 and 0.6 μM), whereas when the whole cell inhibition was not significant, the ID_{50} values were high (>50 μM in CF_1 liver). The ID_{50} value for inhibition of polyphenylalanine synthesis in fractionated systems appeared to be in the same concentration range for both DBA/2 and BDF_1 liver cells and P-388 tumor cells. The poor inhibition of protein synthesis in some tumors and normal liver cells, may be due to inability of the quassinoids to enter the cell, particularly in view of the fact that no inhibition was observed in whole cells of CF_1 liver, yet in the ribosomal fractionated system an ID_{50} of ~50 μM was observed. The observation that the quassinoids do not inhibit protein synthesis of all tumors may explain why bruceantin has not been observed in clinical trials to be effective against certain solid tumors. Perhaps it may be necessary to ascertain if the quassinoids are potent *in vitro* protein synthesis inhibitors of human solid tumors obtained by biopsy prior to administering the drug *in vivo*.

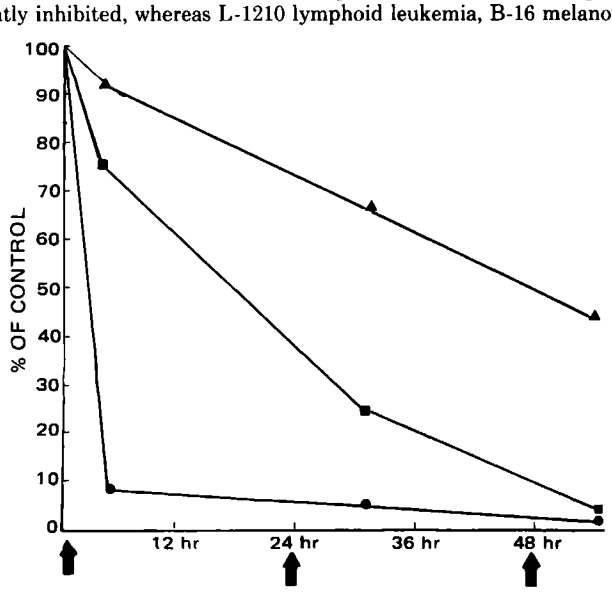

Figure 3—*The effect of (●) brusatol, (■) bruceantin, and (▲) bisbrusatolyl malonate on* in vivo *protein synthesis of P-388-NCI 6 hr after 1, 2, and 3 doses at 0.3 mg/kg ip.*

REFERENCES

(1) I. H. Hall, Y. F. Liou, K. H. Lee, M. Okano, and S. G. Chaney, *J. Pharm. Sci.*, **71**, 257 (1982).

(2) Y. F. Liou, I. H. Hall, M. Okano, K. H. Lee, and S. G. Chaney, *ibid.*, **71**, 430 (1982).

(3) W. Willingham, E. A. Stafford, S. H. Reynolds, S. G. Chaney, K. H. Lee, M. Okano, and I. H. Hall, *Biochim. Biophy. Acta*, **654**, 169 (1981).

(4) K. H. Lee, Y. Imakura, Y. Sumida, R. Y. Wu, I. H. Hall, H. C. Huang, *J. Org. Chem.*, **44**, 2180 (1979).

(5) K. H. Lee, M. Okano, I. H. Hall, D. A. Brent, and B. Soltmann, *J. Pharm. Sci.*, **71**, 338 (1982).

(6) R. I. Geran, N. H. Greenberg, M. M. MacDonald, A. M. Schumacher, and B. J. Abbott, *Cancer Chemother. Rep.*, **3**, 9 (1972).

(7) E. S. Huang, K. H. Lee, C. Piantadosi, T. A. Geissman, and J. S. Pagano, *J. Pharm. Sci.*, **61**, 1960 (1972).

(8) I. H. Hall, K. H. Lee, M. Okano, D. Sims, T. Ibuka, Y. F. Liou, and Y. Imakura, *ibid.*, **70**, 1147 (1981).

(9) L. L. Liao, S. M. Kupchan, and S. B. Horwitz, *Mol. Pharmacol.*, **12**, 167 (1976).
(10) J. Kruh, L. Grossman, and K. Moldave, *Methods Enzymol.*, **12**, 732 (1968).
(11) M. H. Schreier and T. Staehelin, *J. Mol. Biol.*, **73**, 329 (1973).
(12) A. Kaji, *Methods Enzymol.*, **12**, 692 (1968).
(13) A. Jimenez, L. Sanchez, and D. Vazquez, *Biochim. Biophy. Acta*, **383**, 427 (1975).
(14) A. C. Sartorelli, *Biochem. Biophys. Res. Commun.*, **27**, 26 (1967).
(15) O. H. Lowry, N. J. Rosebrough, A. L. Farr, and R. J. Randall, *J. Biol. Chem.*, **193**, 265 (1951).

ACKNOWLEDGMENTS

Supported by National Cancer Institute Grants CA 17625 (in part) (K. H. Lee) and CA 26466 (S. G. Chaney, I. H. Hall, and K. H. Lee).
For part LVIII in this series, see N. Hayashi, K. H. Lee, I. H. Hall, A. T. McPhail, and H. C. Huang, *Phytochemistry*, **21**, 2371 (1982).

High-Performance Liquid Chromatographic Assay of Methadone, Phencyclidine, and Metabolites by Postcolumn Ion-Pair Extraction and On-Line Fluorescent Detection of the Counterion with Applications

HARTMUT DERENDORF and EDWARD R. GARRETT ˣ

Received February 2, 1982, from *The Beehive, College of Pharmacy, J. H. Miller Health Center, University of Florida, Gainesville, FL 32610.* Accepted for publication June 11, 1982.

Abstract □ Methadone, phencyclidine, and their metabolites were extracted from plasma and separated on a high-performance liquid chromatographic (HPLC) column using the fluorescent 9,10-dimethoxyanthracene-2-sulfonic acid as a counterion. The chromatographed mobile phase was subsequently extracted on-line with chloroform. The separated organic phase, containing the fluorescent ion-pairs of the investigated amines, was analyzed in the flow cell of a fluorometer (excitation 380 nm, emission 445 nm). The phase separator volume was as small as possible to avoid dead volume. The method was also applied to the bioassay of cocaine with a sensitivity of 1–6 ng/ml of plasma. Application of these assays gave a red blood cell–plasma water partition coefficient for methadone of 3.39 ± 0.26 (*SD*) in a concentration range up to 20 μg/ml, and demonstrated a time-dependent partition with a diffusion half-life of 1.44 min ± 0.26 min (*SD*). The protein binding of methadone determined by ultracentrifugation was concentration dependent and varied between 75–62% at the highest concentration studied (9 μg/ml). The presence of the major metabolite did not have any influence on the protein binding. The results were confirmed by using the red blood cell-partitioning method to determine the protein binding.

Keyphrases □ Phencyclidine—high-performance liquid chromatographic assay of methadone and metabolites by postcolumn ion-pair extraction, on-line fluorescent detection of counterion with applications □ Methadone—high-performance liquid chromatographic assay of phencyclidine and metabolites by postcolumn ion-pair extraction, on-line fluorescent detection of counterion with applications □ High-performance liquid chromatography—assay of methadone, phencyclidine ion-pair extraction of counterion with applications

Classical high-performance liquid chromatography (HPLC) detection of drugs and their metabolites in biological fluids is by spectrophotometry and fluorescence. These methods were expanded by application of electrochemical detectors (1) and derivatization reactions (2) to get high sensitivities. Unfortunately, these direct detection methods are inadequate for some pharmacokinetic studies of drugs that are given in low doses and show low levels in biological fluids. Sensitive HPLC methods have not yet been developed (3) for methadone (I) and its major metabolite, 2-ethylidene-3,3-diphenyl-1,5-dimethylpyrrolidine (II) (Scheme I), nor for phencyclidine (III) and its hydroxylated metabolites (V, VI). These drugs have insufficient UV-absorbance, no fluorescence, and cannot be readily derivatized. Classical carbonyl reactions are not possible with methadone due to the steric effects of the two phenyl rings. Although cocaine (IV) can be spectrophotometrically detected in HPLC, greater sensitivity than the 15 ng/ml reported (4) would be advantageous in forensic and pharmacokinetic studies.

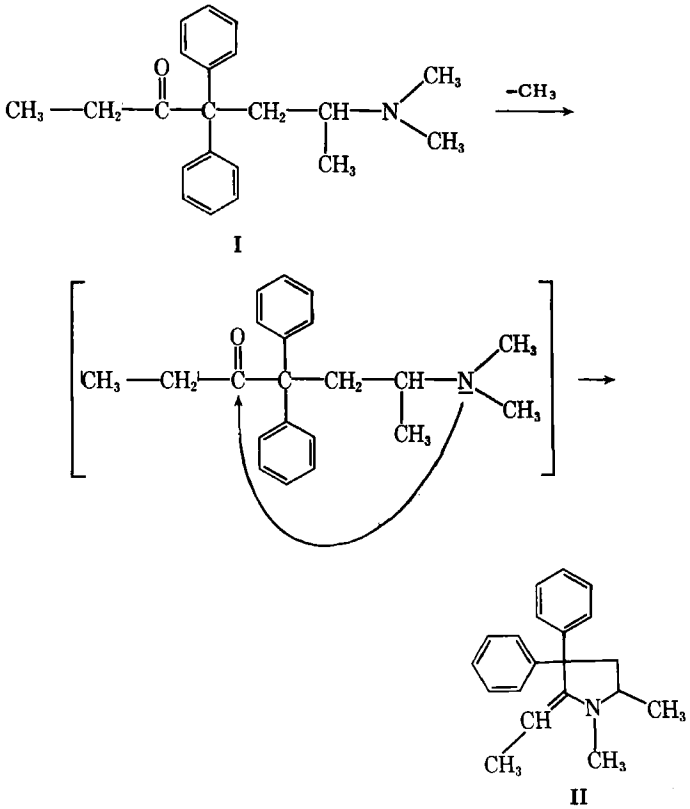

Scheme I—Major pathway of methadone metabolism.

All of these substances are tertiary amines which are readily protonated. They can be extracted into organic

0022-3549/83/0600-0630$01.00/0

(9) L. L. Liao, S. M. Kupchan, and S. B. Horwitz, *Mol. Pharmacol.*, **12**, 167 (1976).
(10) J. Kruh, L. Grossman, and K. Moldave, *Methods Enzymol.*, **12**, 732 (1968).
(11) M. H. Schreier and T. Staehelin, *J. Mol. Biol.*, **73**, 329 (1973).
(12) A. Kaji, *Methods Enzymol.*, **12**, 692 (1968).
(13) A. Jimenez, L. Sanchez, and D. Vazquez, *Biochim. Biophy. Acta*, **383**, 427 (1975).
(14) A. C. Sartorelli, *Biochem. Biophys. Res. Commun.*, **27**, 26 (1967).
(15) O. H. Lowry, N. J. Rosebrough, A. L. Farr, and R. J. Randall, *J. Biol. Chem.*, **193**, 265 (1951).

ACKNOWLEDGMENTS

Supported by National Cancer Institute Grants CA 17625 (in part) (K. H. Lee) and CA 26466 (S. G. Chaney, I. H. Hall, and K. H. Lee).
For part LVIII in this series, see N. Hayashi, K. H. Lee, I. H. Hall, A. T. McPhail, and H. C. Huang, *Phytochemistry*, **21**, 2371 (1982).

High-Performance Liquid Chromatographic Assay of Methadone, Phencyclidine, and Metabolites by Postcolumn Ion-Pair Extraction and On-Line Fluorescent Detection of the Counterion with Applications

HARTMUT DERENDORF and EDWARD R. GARRETT ˣ

Received February 2, 1982, from *The Beehive, College of Pharmacy, J. H. Miller Health Center, University of Florida, Gainesville, FL 32610.* Accepted for publication June 11, 1982.

Abstract □ Methadone, phencyclidine, and their metabolites were extracted from plasma and separated on a high-performance liquid chromatographic (HPLC) column using the fluorescent 9,10-dimethoxyanthracene-2-sulfonic acid as a counterion. The chromatographed mobile phase was subsequently extracted on-line with chloroform. The separated organic phase, containing the fluorescent ion-pairs of the investigated amines, was analyzed in the flow cell of a fluorometer (excitation 380 nm, emission 445 nm). The phase separator volume was as small as possible to avoid dead volume. The method was also applied to the bioassay of cocaine with a sensitivity of 1–6 ng/ml of plasma. Application of these assays gave a red blood cell–plasma water partition coefficient for methadone of 3.39 ± 0.26 (*SD*) in a concentration range up to 20 μg/ml, and demonstrated a time-dependent partition with a diffusion half-life of 1.44 min ± 0.26 min (*SD*). The protein binding of methadone determined by ultracentrifugation was concentration dependent and varied between 75–62% at the highest concentration studied (9 μg/ml). The presence of the major metabolite did not have any influence on the protein binding. The results were confirmed by using the red blood cell-partitioning method to determine the protein binding.

Keyphrases □ Phencyclidine—high-performance liquid chromatographic assay of methadone and metabolites by postcolumn ion-pair extraction, on-line fluorescent detection of counterion with applications □ Methadone—high-performance liquid chromatographic assay of phencyclidine and metabolites by postcolumn ion-pair extraction, on-line fluorescent detection of counterion with applications □ High-performance liquid chromatography—assay of methadone, phencyclidine ion-pair extraction of counterion with applications

Classical high-performance liquid chromatography (HPLC) detection of drugs and their metabolites in biological fluids is by spectrophotometry and fluorescence. These methods were expanded by application of electrochemical detectors (1) and derivatization reactions (2) to get high sensitivities. Unfortunately, these direct detection methods are inadequate for some pharmacokinetic studies of drugs that are given in low doses and show low levels in biological fluids. Sensitive HPLC methods have not yet been developed (3) for methadone (I) and its major metabolite, 2-ethylidene-3,3-diphenyl-1,5-dimethylpyrrolidine (II) (Scheme I), nor for phencyclidine (III) and its hydroxylated metabolites (V, VI). These drugs have insufficient UV-absorbance, no fluorescence, and cannot be readily derivatized. Classical carbonyl reactions are not possible with methadone due to the steric effects of the two phenyl rings. Although cocaine (IV) can be spectrophotometrically detected in HPLC, greater sensitivity than the 15 ng/ml reported (4) would be advantageous in forensic and pharmacokinetic studies.

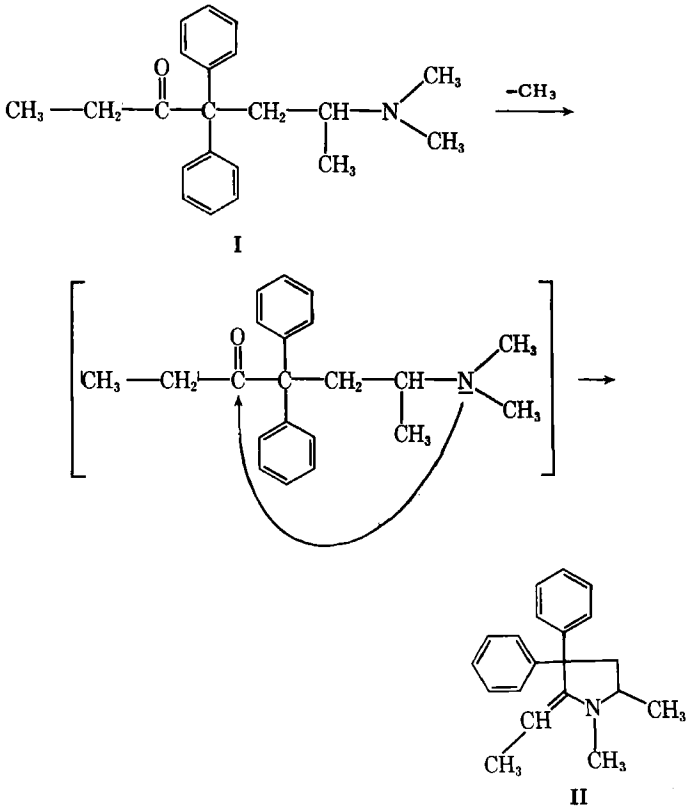

Scheme I—Major pathway of methadone metabolism.

All of these substances are tertiary amines which are readily protonated. They can be extracted into organic

0022-3549/83/0600-0630$01.00/0

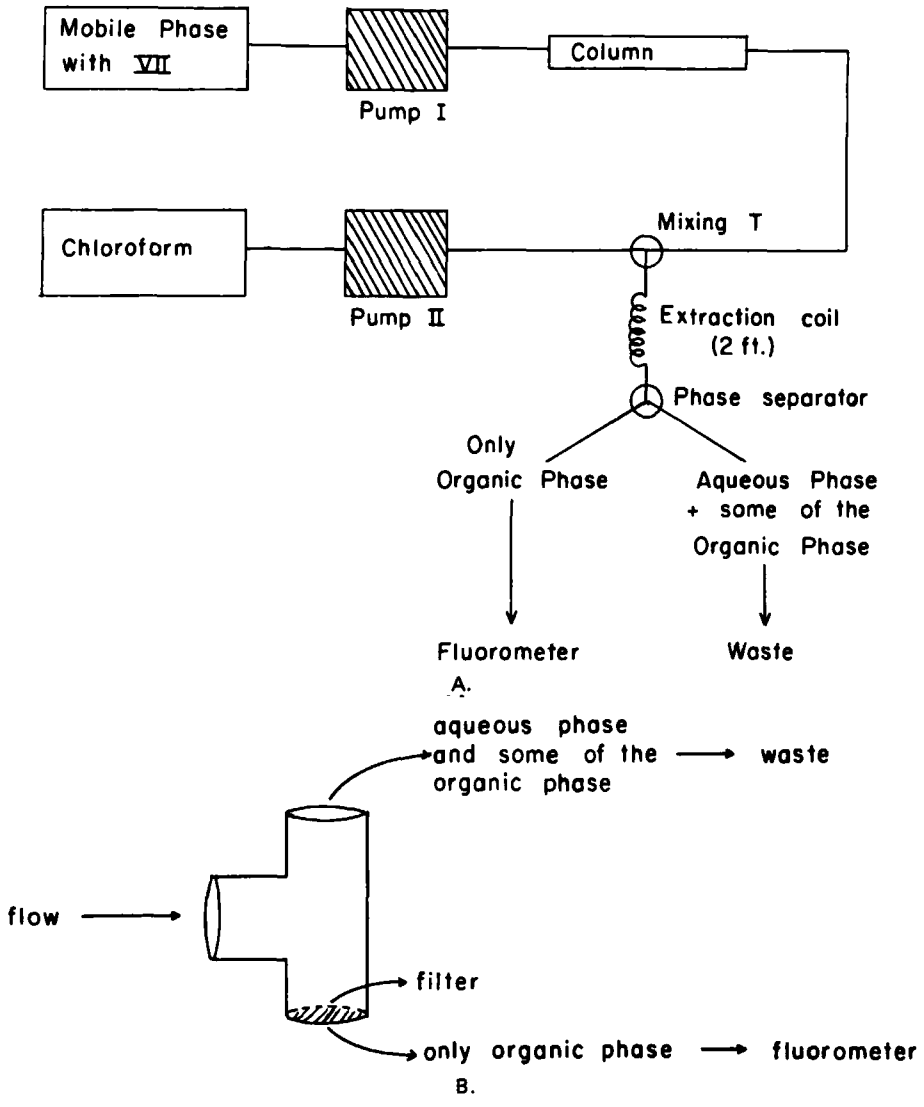

Figure 1—*(A) Schematic representation of HPLC system with postcolumn extraction; (B) phase separator.*

solvents as ion-pairs with aromatic sulfonic acids such as 9,10-dimethoxyanthracene-2-sulfonic acid, (VII). This counterion is highly effective in ion-pair extraction and has a strong fluorescence which can be used for indirect detection of amines with high sensitivity (5–8).

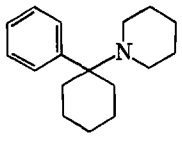

III

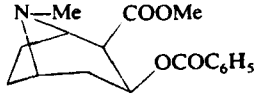

IV

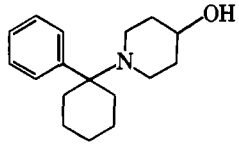

V

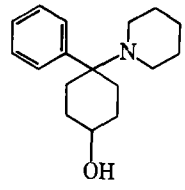

VI

These properties can be utilized after HPLC separation by postcolumn ion-pair extraction and fluorescent detection of the ion-pair. This was described previously (5, 8) where a system was applied to both normal-phase and reverse-phase chromatography. However, a proper phase separator is critical in such systems to provide only one phase for the detector. Commercially available phase separators frequently show significant peak broadening and lessened specificity and sensitivity due to relatively large dead volumes (7). Thus a new phase separator was constructed with a polytef filter and the developed assay systems applied to the determination of the protein binding and red blood cell partitioning of methadone. The plasma protein binding of radiolabeled methadone, reported in the literature, varies widely between 40 and 90% (9–12) with a possible concentration dependence (12).

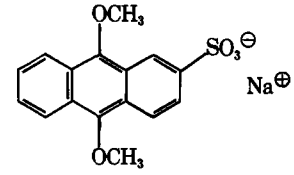

VII

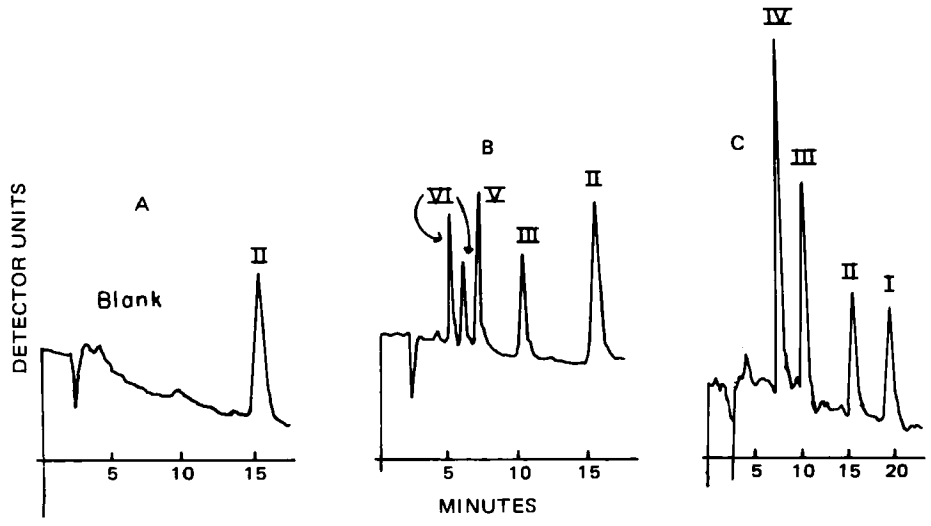

Figure 2—*Chromatograms of 1 ml of plasma alkalinized, extracted with hexane, evaporated to dryness under nitrogen, and reconstituted in 250 μl of 0.025* M *acetate buffer, pH 3.6 with 100 μl injected into the chromatograph. (A) The initial plasma contained 100 ng/ml of internal standard II. (B) The initial plasma contained 50 ng/ml phencyclidine (III), phencyclidine metabolite (V), the* cis- *and* trans-*isomers of phencyclidine metabolite VI, and 100 ng/ml of II as internal standard. (C) The initial plasma contained 60 ng/ml of cocaine (IV), II, methadone (I), and 100 ng/ml of phencyclidine (III) as internal standard.*

EXPERIMENTAL

Materials—The following analytical grade materials were used: sodium acetate[1], acetic acid[1], dibasic and monobasic sodium phosphates[1], sodium chloride[1], and volumetric concentrates of sodium hydroxide[2]. Acetonitrile[3] and chloroform[3] were HPLC-grade; hexane[4] was UV-grade. Methadone[5] (I), 2-ethylidene-3,3-diphenyl-1,5-dimethylpyrrolidine[5] (II), phencyclidine[5] (III), 1-(1-phencyclohexyl)-4-hydroxypiperidine[5] (V) 4-phenyl-4-piperidinocyclohexanol[5] (VI), cocaine[5] (IV), and the sodium salt of 9,10-dimethoxyanthracene-2-sulfonic acid[6] (VII) were used as received. Sodium chloride injection USP[7], sodium heparin injection USP[8], and disposable syringes[9] were used in the preparation of red blood cell suspensions.

Apparatus—For the HPLC assay, the following were used: two pumps[10], an automatic injector[11], a cyano column[12], a fluorescence detector[13], a phase separator constructed from a purchased mixing tee[14] and equipped with a filter made of polytef[15], and a data station[16]. Plasma protein binding was determined with an ultracentrifuge[17]. A laboratory centrifuge[18] was used in the separation of organic extract from plasma and aqueous phases.

HPLC Systems—A postcolumn extraction procedure was used in all HPLC assays (Fig. 1). The mobile phase was a mixture of 0.025 *M* acetate buffer, adjusted to a measured pH of 3.6, and acetonitrile (80:20). It contained 30 mg/liters of 9,10-dimethoxyanthracene-2-sulfonic acid. The flow rate was 2 ml/min with a back pressure of 10 MPa. Immediately after passing the 50°-heated column, the chromatographed mobile phase was mixed with chloroform from another pump at a flow rate of 2 ml/min. The extraction of the ion-pairs into the chloroform was performed in a 0.61-m extraction coil, followed by separation in the constructed phase separator (Fig. 1B).

The phase separator used a mixing tee[14] with upper and lower outlets. It was maintained at a perpendicular angle. Its lower outlet was fitted with a hydrophobic filter made of polytef to increase the efficiency of the phase separation by repelling droplets of the aqueous phase. The back pressures of the two outlets were adjusted so that a constant fraction of the organic phase ran through the lower outlet of the phase separator into the fluorometer with 90% of the extraction mixture going to waste. The excitation wavelength was 380 nm (slit 10 nm), emission 445 nm (slit 5 nm).

Extraction Procedure from Plasma—Freshly prepared dog plasma (1.00 ml) samples were spiked with an appropriate amount of drug and an internal standard. Cocaine, phencyclidine, or its metabolite 1-(1-phenylcyclohexyl)-4-hydroxypiperidine (V) were used as internal standards in the methadone assay. The methadone metabolite (II) was used as an internal standard for the assay of phencyclidine and its metabolites. The plasma was alkalinized with 200 μl of 1 *N* sodium hydroxide and extracted with 6 ml of hexane for 10 min with slow shaking.

The tubes were centrifuged at 2000 rpm for 10 min, and 5 ml of the organic phase was evaporated to dryness under a nitrogen stream. The residue was reconstituted in 250 μl of 0.025 *M* acetate buffer at pH 3.6, and 100 μl was injected into the HPLC system.

Plasma Protein Binding by Ultracentrifugation—Fresh heparinized dog blood was centrifuged for 15 min at 3000 rpm. Plasma aliquots (5 ml) were spiked with different amounts of methadone, and 1 ml was taken for analysis. After ultracentrifugation at 35,000 rpm for 18 hr, 1 ml of the supernatant plasma water was analyzed for methadone.

The influence of the presence of the major metabolite of methadone (II) on the protein binding of methadone was studied in ratios of 1:10, 1:2, 2:1, and 10:1 of II:I.

Red Blood Cell–Buffer Partition Studies of Methadone and its Metabolite (II)—Fresh heparinized dog blood was centrifuged for 15 min at 3000 rpm. The plasma was removed and isoosmotic phosphate buffer pH 7.4, was added to the erythrocytes. Red blood cells were gently suspended and centrifuged for 10 min at 2000 rpm. This washing procedure was repeated three times. Red blood cell suspensions in phosphate buffer were spiked with methadone and its metabolite (II) to yield total drug concentrations in the range of 1–20 μg/ml. The hemocrit was determined routinely using a microcentrifuge with capillary tubes. The spiked suspensions were allowed to equilibrate for 60 min and then centrifuged for 10 min at 2000 rpm. An aliquot of the supernatant solution was analyzed and the red blood cell–buffer partition coefficient was calculated.

Determination of the Protein Binding by Red Blood Cell Partition Method (13)—Fresh heparinized dog blood was spiked with different amounts of methadone, shaken carefully, and centrifuged for 30 min. The plasma concentrations were determined as described previously.

[1] Mallinckrodt Inc., Paris, KY 40361.
[2] Ricca Chemical Co., Arlington, TX 76012.
[3] Fisher Scientific Co., Fair Lawn, NJ 07410.
[4] Burdick & Jackson Laboratories Inc., Muskegon, MI 49442.
[5] National Institute on Drug Abuse, Research Technology Branch, Rockville, MD 20852.
[6] Fluka AG, CH-9470, Buchs, Switzerland.
[7] McGaw Laboratories, Irvine, CA 92714.
[8] The Upjohn Co., Kalamazoo, MI 49001.
[9] Monoject, Division of Sherwood Medical, A. Brunswick Co., St. Louis, MO 63103.
[10] Series 3B Microcomputer Controlled Pump Module, Perkin-Elmer, Norwalk, CT 06856.
[11] Model 420B Auto Sampler, Perkin-Elmer, Norwalk, CT 06856.
[12] CN-μBondapak column, Waters Associates, Milford, MA 01751.
[13] Model 650 Fluorescence Spectrophotometer, Perkin-Elmer, Norwalk, CT 06856.
[14] Tee for 0.8-mm bore tubing, Rainin Instrument Co. Inc., Woburn, MA 01801.
[15] 75-XF pure TFE filter membrane, Laboratory Supplies Co., Chemware Inc., Hicksville, NY 11801.
[16] Model Sigma 15 Data Station, Perkin-Elmer, Norwalk, CT 06856.
[17] Beckman Ultracentrifuge Model LS-50 with rotor Ti 50, Beckman Instruments, Norcross, GA 30092.
[18] Lab centrifuge, International Centrifuge Equipment Co., Needham Hts., MA 02194.

Table I—Statistics of Calibration Curves[a] After Extraction from Plasma (1.00 ml)

Compound	Internal Standard	c_{IS}[b]	m[c]	b[d]	$s_{x,y}$[e]
Methadone	phencyclidine	50.0	131.8	−3.2	3.0
Methadone metabolite (II)	phencyclidine	50.0	109.1	−3.2	3.6
Cocaine	phencyclidine	50.0	36.8	−0.3	0.6
Phencyclidine	II	100.0	83.1	−0.4	3.3
Phencyclidine metabolite (V)	II	100.0	54.6	−2.3	1.8
Phencyclidine metabolite (VIa)	II	100.0	70.7	−7.0	2.9
Phencyclidine metabolite (VIb)	II	100.0	97.3	−1.1	1.1

[a] Concentrations in ng/ml of plasma *versus* peak height ratio relative to internal standard. [b] Concentration of the internal standard in ng/ml. [c] Slope of the calibration curve. [d] Intercept of the calibration curve. [e] Standard error of estimate y on x, concentration in ng/ml plasma on peak height ratio.

Table II—Red Blood Cell–Plasma Partition Coefficients for Methadone at Different Concentrations of Drug

A_{tot}, μg[a]	c_{PW}[b]	V_B[c]	V_{PW}[d]	H[e]	D[f]
45	1.20	18.0	10.80	0.40	3.71
10	1.67	3.5	2.415	0.31	3.29
90	2.66	18.0	11.88	0.34	3.59
20	3.14	3.5	2.415	0.31	3.64
100	4.48	14.0	9.66	0.31	2.92
30	5.01	3.5	2.415	0.31	3.29
180	5.69	18.0	12.06	0.33	3.30
40	6.22	3.5	2.415	0.31	3.70
300	12.71	14.0	9.66	0.31	3.21
500	20.37	14.0	9.66	0.31	3.28
				mean	3.39
				SD	0.26

[a] Total amount of drug added to a red blood cell suspension. [b] Drug concentration (μg/ml) in plasma water. [c] Volume (ml) of the red blood cell suspension. [d] Volume (ml) of the plasma water. [e] Hematocrit. [f] Red blood cell–plasma water partition coefficient.

RESULTS AND DISCUSSION

HPLC System with a Postcolumn Extraction—This HPLC system (Fig. 1) can determine amine concentrations indirectly. Substances are chromatographed as ion-pairs on the column with the ion-pairing VII in the mobile phase used for the detection after coextraction into chloroform in stoichiometric ratios with an organic amine. Stoichiometric highly fluorescent dimethoxyanthracene sulfonic acid of the ion-pairs can be detected with high sensitivity in the flow cell of a fluorometer.

A general and highly sensitive method was developed with the system to analyze methadone, phencyclidine and its metabolites, and cocaine. The designed phase separator (Fig. 1B) has a small inner volume and a hydrophobic filter made of polytef to repel water droplets in the separated organic layer. Such droplets would contain the counterion (VII), which would give irregular and interfering background in the fluorescent detection.

Mobile phase was limited to <20% acetonitrile to maintain a reasonable extractability into the chloroform. However, this lengthened the retention times for methadone and its metabolite (II), on the cyano column, the most polar reverse-phase column available. Column heating to 50° lessened the retention times. The described system and conditions were applicable for all the studied compounds with retention times: methadone (I), 17 min; methadone metabolite (II), 14 min; phencyclidine (III), 10 min; phencyclidine metabolite (V), 7 min; phencyclidine metabolite (VI), 5 and 6 min (*cis* and *trans* forms); cocaine (IV), 6 min.

In the chromatogram the background from biological fluids was satisfactory when hexane was used for extraction (Fig. 2A); however, it was unsatisfactory when chloroform was used for extraction. Typical chromatograms of substances at 50–60 ng/ml in plasma are shown in Figs. 2B and 2C. Calibration curves were set up to determine the sensitivity of the method. Statistics for calibration curves of the substances are given in Table I. The limit of sensitivity for all compounds was in the range 1.0–6.0 ng/ml of plasma ($2 \times s_{xy}$).

Determination of the Red Blood Cell–Plasma Water Partition Coefficient—The red blood cell partition coefficient of a drug can be defined as:

$$D = \frac{C_{RBC}}{C_{PW}} = \frac{A_{RBC}}{A_{PW}} \times \frac{V_{PW}}{(V_B - V_{PW})} = \frac{(A_{tot} - A_{PW})V_{PW}}{A_{PW}(V_B - V_{PW})} = \frac{A_{tot} - A_{PW}}{C_{PW}(V_B - V_{PW})} = \frac{A_{tot} - C_{PW}V_{PW}}{C_{PW}(V_B - V_{PW})} \quad \text{(Eq. 1)}$$

where D is the red blood cell partition coefficient, C_{RBC} is the concentration of the drug in the erythrocytes, C_{PW} is the concentration in plasma water, A_{RBC} is the amount of drug in the erythrocytes, A_{PW} is the amount in plasma water, A_{tot} is the total amount of drug added to the red blood cell suspension, V_B is the volume of the red blood cell suspension, and V_{PW} is the volume of plasma water.

Red blood cell–plasma water partition coefficients were determined for 10 different concentrations of methadone (Table II) and averaged D = 3.39 ± 0.26 (*SD*). There was no concentration dependence for partitioning in the studied concentration range up to 20 μg/ml.

The partitioning was time dependent. Diffusion half-life into the red blood cells was determined for three different concentrations and the average was 1.44 ± 0.26 (*SD*) min (Fig. 3).

Protein Binding of Methadone by Ultracentrifugation—The ultrafiltration method for the determination of the protein binding of

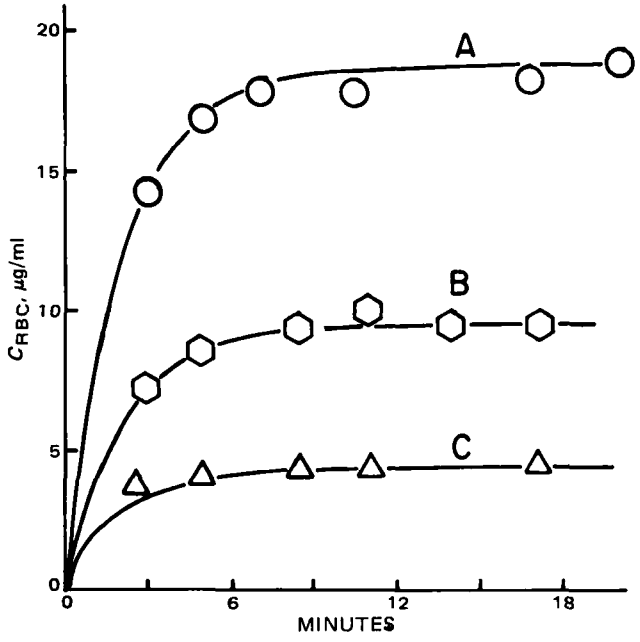

Figure 3—*Time dependence of the red blood cell partitioning in three different concentrations of methadone. The curves through the experimental values, concentrations of drug in red blood cells (C_{RBC}) over time, were fitted for a diffusion half-life of 1.44 min. The concentrations of methadone in plasma water were: (A) 5.7 μg/ml; (B) 2.7 μg/ml; (C) 1.2 μg/ml.*

Table III—Percent Protein Binding of Methadone by the Ultracentrifugation Method

c_{pre}[a]	c_{post}[b]	r[c]	V_{dil}[d]	m[e]	$f_b \times 100$, %[f]
99.9	27.2	0.272	0.005	1.001	72.8
199.6	59.1	0.296	0.010	1.002	70.4
497.5	124.1	0.249	0.025	1.005	75.2
990.1	342.6	0.346	0.050	1.010	65.6
1960.0	677.5	0.346	0.100	1.020	65.8
4760.0	1870.0	0.393	0.250	1.050	61.9
9090.0	3636.0	0.400	0.500	1.100	62.3

[a] Concentration of methadone in plasma before ultracentrifugation in ng/ml. [b] Concentration of methadone in plasma water after ultracentrifugation in ng/ml. [c] Ratio between the concentrations after and before ultracentrifugation. [d] Volume in ml of spiked solution that was added to 5 ml of plasma. [e] Dilution factor $(5 + V_{dil})/5$. [f] Percentage of methadone bound to plasma proteins.

Table IV—Protein Binding of Methadone in Presence of its Major Metabolite (II) at Different Drug–Metabolite Ratios

R[a]	c_{pre}[b]	c_{post}[c]	r[d]	V_{dil}[e]	m[f]	$f_b \times 100$, %[g]
10.5	1.996	0.679	0.340	0.11	1.022	66.9
10.5	1.996	0.717	0.359	0.11	1.022	65.0
2.0	1.942	0.743	0.383	0.15	1.030	62.9
2.0	1.942	0.623	0.321	0.15	1.030	69.0
0.5	1.887	0.511	0.271	0.30	1.060	74.4
0.5	1.887	0.684	0.362	0.30	1.060	65.5
0.1	1.640	0.656	0.400	1.10	1.220	64.7
0.1	1.640	0.622	0.379	0.10	1.220	66.7

[a] Drug–metabolite ratio for 2 μg of methadone/ml of plasma. [b] Concentration of methadone in plasma before ultracentrifugation in μg/ml. [c] Concentration of methadone in plasma water after ultracentrifugation in μg/ml. [d] Ratio between the concentrations after and before ultracentrifugation. [e] Volume of ml of spiked solution that was added to 5 ml of plasma. [f] Dilution factor $(5 + V_{dil})/5$. [g] Percentage of methadone bound to plasma proteins.

methadone was not useful because of high binding to the ultrafilters. Therefore, the protein binding was determined by the ultracentrifugation method, where methadone-spiked plasma was separated into plasma proteins and plasma water and the plasma water was assayed. The calculation of the fraction of drug bound to the plasma proteins was based on the following principles.

The equilibrium constant between protein-bound methadone and methadone in the plasma water can be defined as:

$$K = \frac{c_b}{c_f} = \frac{A_b}{A_f} \times \frac{V_{PW}}{A_{Pr}} = \frac{A_b}{A_f} \times \frac{V_{PW}}{c_{Pr} V_{PW}} = \frac{A_b}{A_f c_{Pr}} \qquad \text{(Eq. 2)}$$

where c_b is the concentration of protein-bound methadone, c_f is the concentration of the free methadone in the plasma water, c_{Pr} is the protein concentration of the plasma, A_b is the amount of methadone bound to the protein, A_f is the amount of methadone free in the plasma water, A_{Pr} is the amount of protein in the plasma water, and V_{PW} the volume of the plasma water. If the protein concentration in plasma is constant:

$$K_s = K c_{Pr} \qquad \text{(Eq. 3)}$$

then,

$$K_s = \frac{A_b}{A_f} \qquad \text{(Eq. 4)}$$

Since the plasma is slightly diluted by a volume V_{dil} of the spiking solution, the dilution factor is:

$$m = \frac{V_{PW} + V_{dil}}{V_{PW}} \qquad \text{(Eq. 5)}$$

and the protein concentration after spiking is:

$$c'_{Pr} = \frac{C_{Pr}}{m} \qquad \text{(Eq. 6)}$$

Thus, the equilibrium in the diluted plasma is:

$$K = \frac{c'_b}{c'_f} = \frac{A'_b}{A'_f c'_{Pr}} = \frac{A'_b m}{A'_f C_{Pr}} \qquad \text{(Eq. 7)}$$

Table V—Plasma Protein Binding of Methadone by the Red Blood Cell–Plasma Partition Method[a]

A_{tot}[b]	V_B[c]	H[d]	c_{Pl}[e]	$f_b \times 100$, %[f]
10.0	4.5	0.49	1.90	63.1
20.0	4.5	0.49	4.05	67.2
30.0	4.5	0.49	5.79	64.1

[a] The red blood cell–plasma water partition coefficient used was 3.39. [b] Total amount of methadone added to the blood in mg. [c] Volume of blood in ml. [d] Hematocrit. [e] Concentration of methadone in plasma in μg/ml. [f] Percentage of methadone bound to plasma proteins.

and

$$K_s = m \frac{A'_b}{A'_f} \qquad \text{(Eq. 8)}$$

where the primed values are the amounts in the diluted sample studies.

Methadone concentrations were assayed before (c_{pre} in plasma) and after ultracentrifugation (c_{post} in plasma water). The ratios of these two concentrations are:

$$r = \frac{c_{post}}{c_{pre}} = \frac{A'_f}{A'_f + A'_b} \qquad \text{(Eq. 9)}$$

Thus, from Eqs. 8 and 9:

$$K_s = m \frac{1 - r}{r} \qquad \text{(Eq. 10)}$$

The fraction of methadone bound to the plasma proteins, f_b, is

$$f_b = \frac{A_b}{A_b + A_f} \text{ or } \frac{1}{f_b} = 1 + \frac{A_f}{A_b} \qquad \text{(Eq. 11)}$$

so that on realization of Eqs. 4, 10, and 11, the fraction bound is

$$f_b = \frac{m(1 - r)}{r + m(1 - r)} \qquad \text{(Eq. 12)}$$

and can be calculated from the ratio of the methadone concentrations before and after ultracentrifugation. The results are summarized in Table III. Protein binding of methadone was concentration dependent in agreement with the previous studies by equilibrium dialysis (12) of 100–10,000 ng/ml of plasma. Protein binding varied 75–62% to give the low value at the highest 9 μg/ml of plasma studied.

The determination of the protein binding of methadone was repeated in the presence of different amounts of its major metabolite (II). Ratios, R, between parent drug and metabolite were 10:1, 2:1, 1:2, and 1:10 for a methadone concentration of 2 μg/ml of plasma. The results in Table IV indicate no significant effect of a 10-fold greater concentration of metabolite on the protein binding of methadone.

Protein Binding of Methadone by Red Blood Cell–Plasma Partitioning—Protein binding of a drug can be calculated from the known or assayed concentrations in blood and plasma after equilibration on the premise that only free drug can partition into the erythrocytes. The fraction of the drug bound to the plasma proteins can be calculated (13) from:

$$f_b = 1 - \frac{A_{tot} - c_{Pl} V_b (1 - H)}{D c_{Pl} V_b (1 - H)} \left(\frac{1}{H} - 1 \right) \qquad \text{(Eq. 13)}$$

where A_{tot} is the total amount of drug added to the volume V_b of the blood, D is the red blood cell–plasma water partition coefficient, H the hematocrit, and C_{pl} the concentration of the drug in the plasma. The

results in Table V agree with the results that were obtained by the ultracentrifugation method. Significant amounts of methadone are bound to the plasma proteins in the therapeutic range. The results confirm previous data (12), but disagree markedly from the results of other investigators (9, 10).

REFERENCES

(1) P. Kissinger, *Anal. Chem.*, **46**, 15R (1974).

(2) K. Bean and G. S. King, "Handbook of Derivatives for Chromatography," Heyden and Sons Ltd., London, England, 1978.

(3) W. Sadee and G. C. M. Beelen, "Drug Level Monitoring," Wiley, New York, N.Y., 1980, p. 28.

(4) E. R. Garrett and K. Seyda, *J. Pharm. Sci.*, **72**, 258 (1983).

(5) J. L. Gfeller, G. Frey, J. M. Huen, and J. P. Thevenin, *J. Chromatogr.*, **172**, 141 (1979).

(6) C. Van Buuren, J. F. Lawrence, U. A. Th. Brinkman, I. L. Honigberg, and R. W. Frei, *Anal. Chem.*, **52**, 700 (1980).

(7) J. F. Lawrence, U. A. Th. Brinkman, and R. W. Frei, *J. Chromatogr.*, **185**, 473 (1979).

(8) J. F. Lawrence, U. A. Th. Brinkman, and R. W. Frei, *ibid.*, **171**, 73 (1979).

(9) J. Judis, *J. Pharm. Sci.*, **66**, 802 (1977).

(10) G. D. Olsen, *Clin. Pharm. Ther.*, **14**, 338 (1973).

(11) M. K. Romach, K. M. Piafsky, J. G. Abel, V. Khouw, and E. M. Sellers, *Clin. Pharm. Ther.*, **29**, 211 (1981).

(12) W. H. Horns, M. Rado, and A. Goldstein, *ibid.*, **17**, 636 (1975).

(13) E. R. Garrett and C. A. Hunt, *J. Pharm. Sci.*, **63**, 1056 (1974).

Physical Chemistry of Freeze-drying: Measurement of Sublimation Rates for Frozen Aqueous Solutions by a Microbalance Technique

M. J. PIKAL ˣ, S. SHAH, D. SENIOR, and J. E. LANG

Received October 14, 1981, from *Eli Lilly and Company, Indianapolis, IN 46285.* Accepted for publication April 30, 1982.

Abstract □ The sublimation rate of frozen solutions was studied as a function of freezing rate, thickness of dried product (l), temperature, residual air pressure, and solute concentration. Data are presented for pure water, aqueous potassium chloride, aqueous povidone, and aqueous dobutamine hydrochloride–mannitol (System I). The resistance of the dried product to water vapor flow ($\hat{R}_p$) was evaluated from the sublimation rate and the sample temperature. The primary experimental technique was based on freeze-drying a cylindrical microsample isothermally, with the sample suspended from one arm of a vacuum microbalance. Methodology to evaluate resistance data from vial freeze-drying experiments is also described. In separate experiments, samples in the form of a thin (15-μm) film were visually observed through a microscope during freeze-drying. Freeze-drying of most samples appeared to occur by water vapor escaping through open channels created by prior sublimation of ice. Contrary to the usual theoretical model, $\hat{R}_p$ is neither independent of temperature nor directly proportional to l. Rather, $\hat{R}_p$ decreases with increasing temperature and the l dependence is normally of the form $\hat{R}_p = (A_0 + A_1 l)/(1 + A_2 l)$, where A_i ($i = 0, 1, 2$) are constants. In several cases, $\hat{R}_p$ is very large near $l = 0$, decreases sharply at $l \simeq 0.1$ cm, and obeys the above equation where $l > 0.2$ cm, a result suggesting an amorphous surface skin which cracks on desorption of water. The temperature dependence of $\hat{R}_p$ suggests that, as the sample temperature approaches the eutectic (or collapse) temperature, hydrodynamic surface flow of adsorbed water is an important flow mechanism.

Keyphrases □ Sublimation rate—measurement for frozen aqueous solutions, microbalance technique, as a function of process variables □ Freeze-drying—methodology of rate measurements for aqueous solutions, influence of process variables, mechanisms of mass transfer in the dried solid □ Dosage forms—freeze-drying of aqueous solutions, effect of process variables on sublimation rate, mechanisms for mass transfer through the dried solid

As sublimation of ice proceeds during freeze-drying, a dried product layer above the ice is produced which acts as a barrier, or resistance, for transport of water vapor. The dried product resistance is generally regarded as the most important factor in determining the drying rate at fixed sample temperature and therefore has a major impact on the process economics. However, published experimental data are confined to food products or biological tissue samples, and the effects of major process or formulation variables on the dried product resistance have not been studied.

This report describes the direct experimental determination of the resistance of the dried product as a function of freezing rate, thickness of dried product, temperature, residual air pressure, and solute concentration. Data are presented for aqueous potassium chloride, aqueous povidone, and aqueous dobutamine hydrochloride–mannitol in a 1.12:1 weight ratio (System I)[1]. Sublimation rate data for pure water are also presented. To aid in the interpretation of the resistance data, the freeze-drying process was also observed microscopically using thin (~15-μm) samples confined between two glass coverslips. Procedures for determining the dried product resistance from vial freeze-drying studies are also described. Comparison of resistance data determined from vial freeze-drying with corresponding data determined by the microbalance procedure confirms that microbalance data are indeed predictive of the dried product resistance encountered in vial freeze-drying.

BACKGROUND

Freeze-drying, or lyophilization, is a process where a solvent (normally water) is removed from a frozen solution by sublimation. Freeze-drying has several advantages over competing processes for production of pharmaceuticals. First, as freeze-drying is a low temperature process, chemical decomposition is minimized. Second, since the solution may be sterile filtered immediately before introduction into a vial and no powder-handling steps are involved in the subsequent processing of a parenteral product, particulate levels may be reduced to a minimum. Due to the high capital equipment costs and typically long processing times, freeze-drying is frequently regarded as an expensive process. However, due to a lack of fundamental understanding of freeze-drying, a given process is often not optimized for the maximum production rate consistent with product quality. Consequently, freeze-drying, in practice, often is much more expensive than necessary.

[1] DOBUTREX, Eli Lilly and Co., Indianapolis, Ind.

0022-3549/83/0600-0635$01.00/0

results in Table V agree with the results that were obtained by the ultracentrifugation method. Significant amounts of methadone are bound to the plasma proteins in the therapeutic range. The results confirm previous data (12), but disagree markedly from the results of other investigators (9, 10).

REFERENCES

(1) P. Kissinger, *Anal. Chem.*, **46**, 15R (1974).

(2) K. Bean and G. S. King, "Handbook of Derivatives for Chromatography," Heyden and Sons Ltd., London, England, 1978.

(3) W. Sadee and G. C. M. Beelen, "Drug Level Monitoring," Wiley, New York, N.Y., 1980, p. 28.

(4) E. R. Garrett and K. Seyda, *J. Pharm. Sci.*, **72**, 258 (1983).

(5) J. L. Gfeller, G. Frey, J. M. Huen, and J. P. Thevenin, *J. Chromatogr.*, **172**, 141 (1979).

(6) C. Van Buuren, J. F. Lawrence, U. A. Th. Brinkman, I. L. Honigberg, and R. W. Frei, *Anal. Chem.*, **52**, 700 (1980).

(7) J. F. Lawrence, U. A. Th. Brinkman, and R. W. Frei, *J. Chromatogr.*, **185**, 473 (1979).

(8) J. F. Lawrence, U. A. Th. Brinkman, and R. W. Frei, *ibid.*, **171**, 73 (1979).

(9) J. Judis, *J. Pharm. Sci.*, **66**, 802 (1977).

(10) G. D. Olsen, *Clin. Pharm. Ther.*, **14**, 338 (1973).

(11) M. K. Romach, K. M. Piafsky, J. G. Abel, V. Khouw, and E. M. Sellers, *Clin. Pharm. Ther.*, **29**, 211 (1981).

(12) W. H. Horns, M. Rado, and A. Goldstein, *ibid.*, **17**, 636 (1975).

(13) E. R. Garrett and C. A. Hunt, *J. Pharm. Sci.*, **63**, 1056 (1974).

Physical Chemistry of Freeze-drying: Measurement of Sublimation Rates for Frozen Aqueous Solutions by a Microbalance Technique

M. J. PIKAL ˣ, S. SHAH, D. SENIOR, and J. E. LANG

Received October 14, 1981, from *Eli Lilly and Company, Indianapolis, IN 46285.* Accepted for publication April 30, 1982.

Abstract □ The sublimation rate of frozen solutions was studied as a function of freezing rate, thickness of dried product (l), temperature, residual air pressure, and solute concentration. Data are presented for pure water, aqueous potassium chloride, aqueous povidone, and aqueous dobutamine hydrochloride–mannitol (System I). The resistance of the dried product to water vapor flow ($\hat{R}_p$) was evaluated from the sublimation rate and the sample temperature. The primary experimental technique was based on freeze-drying a cylindrical microsample isothermally, with the sample suspended from one arm of a vacuum microbalance. Methodology to evaluate resistance data from vial freeze-drying experiments is also described. In separate experiments, samples in the form of a thin (15-μm) film were visually observed through a microscope during freeze-drying. Freeze-drying of most samples appeared to occur by water vapor escaping through open channels created by prior sublimation of ice. Contrary to the usual theoretical model, $\hat{R}_p$ is neither independent of temperature nor directly proportional to l. Rather, $\hat{R}_p$ decreases with increasing temperature and the l dependence is normally of the form $\hat{R}_p = (A_0 + A_1 l)/(1 + A_2 l)$, where A_i ($i = 0, 1, 2$) are constants. In several cases, $\hat{R}_p$ is very large near $l = 0$, decreases sharply at $l \simeq 0.1$ cm, and obeys the above equation where $l > 0.2$ cm, a result suggesting an amorphous surface skin which cracks on desorption of water. The temperature dependence of $\hat{R}_p$ suggests that, as the sample temperature approaches the eutectic (or collapse) temperature, hydrodynamic surface flow of adsorbed water is an important flow mechanism.

Keyphrases □ Sublimation rate—measurement for frozen aqueous solutions, microbalance technique, as a function of process variables □ Freeze-drying—methodology of rate measurements for aqueous solutions, influence of process variables, mechanisms of mass transfer in the dried solid □ Dosage forms—freeze-drying of aqueous solutions, effect of process variables on sublimation rate, mechanisms for mass transfer through the dried solid

As sublimation of ice proceeds during freeze-drying, a dried product layer above the ice is produced which acts as a barrier, or resistance, for transport of water vapor. The dried product resistance is generally regarded as the most important factor in determining the drying rate at fixed sample temperature and therefore has a major impact on the process economics. However, published experimental data are confined to food products or biological tissue samples, and the effects of major process or formulation variables on the dried product resistance have not been studied.

This report describes the direct experimental determination of the resistance of the dried product as a function of freezing rate, thickness of dried product, temperature, residual air pressure, and solute concentration. Data are presented for aqueous potassium chloride, aqueous povidone, and aqueous dobutamine hydrochloride–mannitol in a 1.12:1 weight ratio (System I)[1]. Sublimation rate data for pure water are also presented. To aid in the interpretation of the resistance data, the freeze-drying process was also observed microscopically using thin (~15-μm) samples confined between two glass coverslips. Procedures for determining the dried product resistance from vial freeze-drying studies are also described. Comparison of resistance data determined from vial freeze-drying with corresponding data determined by the microbalance procedure confirms that microbalance data are indeed predictive of the dried product resistance encountered in vial freeze-drying.

BACKGROUND

Freeze-drying, or lyophilization, is a process where a solvent (normally water) is removed from a frozen solution by sublimation. Freeze-drying has several advantages over competing processes for production of pharmaceuticals. First, as freeze-drying is a low temperature process, chemical decomposition is minimized. Second, since the solution may be sterile filtered immediately before introduction into a vial and no powder-handling steps are involved in the subsequent processing of a parenteral product, particulate levels may be reduced to a minimum. Due to the high capital equipment costs and typically long processing times, freeze-drying is frequently regarded as an expensive process. However, due to a lack of fundamental understanding of freeze-drying, a given process is often not optimized for the maximum production rate consistent with product quality. Consequently, freeze-drying, in practice, often is much more expensive than necessary.

[1] DOBUTREX, Eli Lilly and Co., Indianapolis, Ind.

0022-3549/83/0600-0635$01.00/0

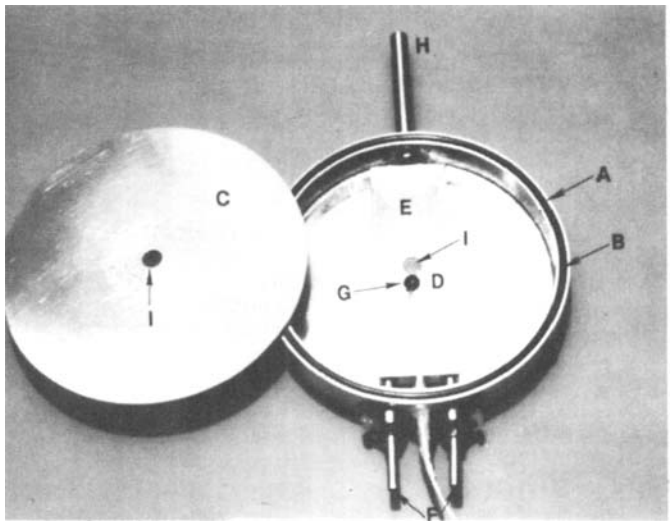

Figure 1—*High-vacuum microscope cold stage. Key: (A) vacuum chamber, (B) rubber seal, (C) lid, (D) sample, (E) temperature-controlled plate, (F) entrance and exit ports (tubes), (G) thermistor surface probe, (H) tube connected to the vacuum line, (I) observation holes.*

The freeze-drying process may be divided into three stages: freezing, primary drying, and secondary drying. For pharmaceutical products, the solution is normally filled into vials to a depth of ~1 cm, and the vials are placed on refrigerated shelves in the freeze-drying chamber. The specific freezing process influences the size and shape of the ice crystals formed and, therefore, affects the structure of the porous solid product remaining after drying (1–3). Thus, the freezing stage may influence strongly the time required to complete the next two steps of the process as well as influence the properties of the final product. After the solutions are frozen the chamber is evacuated, and the shelf temperature is increased to provide energy for the sublimation of ice during primary drying. A frozen solution dries from the top, thereby producing a dried product layer above the ice which increases in thickness as sublimation proceeds. Secondary drying begins locally when all ice has been removed from that region. Thus, in general, secondary drying proceeds simultaneous with primary drying in different regions of the same sample. Normally, secondary drying continues for some time after all ice has been removed from the sample. During secondary drying, the water removed from the solid phase is either bound as a crystalline hydrate or dissolved in an amorphous solid.

The objective of freeze-drying process development is to minimize the process time within the constraints imposed by product quality specifications. Excessive chemical decomposition must be avoided, residual water content often must be low for acceptable stability (4), and the product appearance must conform to standards. To avoid the foaming or puffing that develops during solution vacuum-drying, freeze-drying must be carried out below the eutectic temperature for a crystalline solute or below the collapse temperature for an amorphous solute (2, 3, 5–8). Selection of the shelf temperature and chamber pressure required to maintain the ice temperature just below the eutectic or collapse temperature in all vials during primary drying is a problem in coupled heat and mass transfer. Heat must be transferred from the shelf to the vial bottom and through the frozen solution to the sublimation interface to compensate for the heat removed by sublimation. The rate of heat transfer increases with increased shelf temperature and chamber pressure (9). Therefore, in principle the ice temperature may be maintained constant by adjustment of shelf temperature and chamber pressure.

Assuming that heat is supplied to maintain constant ice temperature, the sublimation rate, and therefore, the total time required for primary drying, will depend on the total resistance to transport of water vapor from the ice–vapor interface to the condenser. The total resistance has three contributors: resistance of the dried product (a porous solid), resistance of the semistoppered vial, and resistance in transfer from the chamber to the condenser. Mass transfer is discussed in terms of resistance, which is defined as the ratio of the difference in water partial pressure to the water flow rate. Resistance is used rather than permeability (the reciprocal of resistance) since the total resistance is additive for component resistances in series. That the dried product resistance is dominant in most freeze-drying applications (10, 11) is supported by theoretical calculations. Using mass flow equations developed for the flow of rarified gases through tubes and orifices (11, 12) and assuming the dried product equivalent to a bundle of capillary tubes, the resistance may be calculated from the dimensions of the vial, stopper, and freeze-dryer and estimates of the pore size of the dried product. Due to the small dimensions of the pores in a typical dried product, flow in the dried product is Knudsen or free molecular flow (11, 12) and contributes ~90% of the total resistance. Clearly, the dried product resistance is an important parameter which may dominate the economics of the freeze-drying process. It is this property with which we are concerned in this study.

The most common procedure used to estimate the dried product resistance is an indirect method which involves measurement of gas flow rate and corresponding pressure difference across a previously freeze-dried specimen of known area and thickness (11). A theoretical model is used to evaluate pore-size parameters for the porous solid which, in turn, are used to calculate the resistance to water vapor flow during ice sublimation from the sample. However, the validity of the model (in particular the assumption that the resistance is directly proportional to the thickness of the dried layer) may be questioned when the dried product is produced from a frozen solution. Microscopic data (2, 3, 13, 14) suggest that the dried product is not necessarily homogeneous, and the mass transfer rate is not always limited by flow in capillary channels. Given the complexity of freeze-drying from frozen solutions, it would seem prudent to avoid the use of theoretical models and evaluate resistances directly from the sublimation rate data.

Quantitative sublimation rate data are available for several frozen systems (15–18), but [with the exception of one study on guinea pig liver (18)] either the vapor pressure difference across the dried product is not available (16–17) or the sample geometry does not allow resistance data to be evaluated for dried product thicknesses of practical interest. A recording high-vacuum microbalance apparatus designed to determine sublimation rates of frozen solutions at controlled temperatures has been described (19). The sample form is a thin (~1-mm) disk of known area. Since the temperature of subliming ice is known and the partial pressure of water at the dried product–vacuum chamber interface is maintained near zero, the water vapor pressure gradient across the dried product is determined and the dried product resistance may be evaluated. The sample holder design limits studies to relatively low sublimation rates (*i.e.*, temperatures <−30°), and the effect of dried product thicknesses characteristic of those encountered in vial freeze-drying (~1 cm) cannot be studied.

The methodology chosen for this research is based on determination of the sublimation rate of a frozen sample with a recording high-vacuum microbalance and, in this respect, is similar to the methodology used by MacKenzie and Luyet (19). However, the sample cell design is more convenient and permits resistance data to be obtained at higher temperatures (~−10°) for dried product thicknesses up to 1 cm. The sample is contained in a 1.3-mm diameter glass tube which is embedded in an aluminum heat exchanger, allowing isothermal operation at the thermostat temperature for most systems of interest.

EXPERIMENTAL

Materials—The potassium chloride used was recrystallized reagent grade material; the mannitol (USP) and povidone (USP, viscosity average molecular weight of 35,000) were used as received. The dobutamine hydrochloride was commercial material[2] used without further purification. Solutions were prepared by weighing the appropriate quantities of distilled water and solute. System I was aqueous dobutamine hydrochloride–mannitol in a 1.12:1 weight ratio with total solids being 53 mg/ml. Conversion of concentration from weight percent to volume percent was accomplished assuming the solute specific volume in solution is the same as that in the solid[3].

Freeze-Drying Microscope—The high-vacuum cold stage (Fig. 1) used in conjunction with an optical microscope[4] for visual observation of freeze-drying is similar to the designs suggested by Flink and Geil-Hansen (20). A nickel-plated brass vacuum chamber (A) ~10 cm in diameter and 1.5 cm in height was sealed using a rubber "O" ring (B) and a stainless steel lid (C). The sample (D) was a thin (~15-μm) film constrained between two glass coverslips. Thermal contact between the bottom coverslip and the temperature-controlled plate (E) was achieved by glueing the coverslip to the plate with silicone stopcock grease. The plate (E) was nickel-plated brass. The distance from the sample to the

[2] Eli Lilly and Co.

[3] Densities used were 1.98 g/ml (potassium chloride), 1.10 g/ml (povidone), and 1.50 g/ml (System I).

[4] Carl Zeiss, Inc.

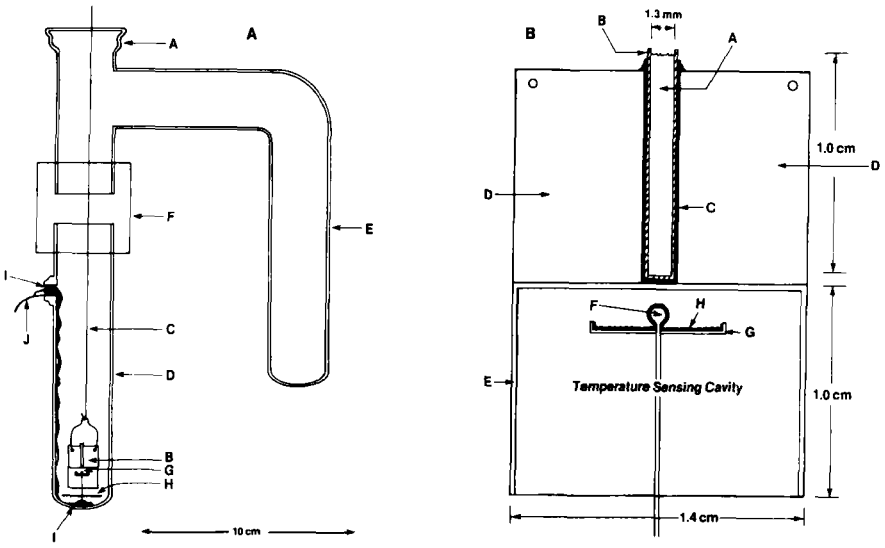

Figure 2—*Microbalance sublimation apparatus. (A) balance tube–condensor assembly, Key: (A) connecting "0" ring joint, (B) sublimation cell (enlarged as Fig. 2B), (C) suspension wire, (D) glass balance tube, (E) glass side arm tube, (F) high-vacuum union, (G) thermocouple probe, (H) heat shield, (I) high-vacuum wax seal, (J) thermocouple wires; (B) sublimation cell, Key: (A) sample, (B) glass capillary tube, (C) high-vacuum wax film, (D and E) top and bottom of the heat exchanger, respectively, (F) thermocouple junction, (G) aluminum disk, (H) thin coat of high-vacuum wax.*

top of the lid was 4–5 mm, allowing the vacuum cold stage to be used with any microscope system having a working distance >5 mm. Temperature control was achieved by passing cold nitrogen gas through channels in the plate. Tubes (F) served as entrance and exit ports for gas flow. The plate was fixed in position ~2 mm from the bottom of the chamber by a plastic spacer (not shown) on the underside of the plate. Temperature of the sample was measured by a thermistor surface probe[5] (G), which was fixed to the top coverslip with silicone stopcock grease. Low pressures (0.02–0.05 torr) were achieved by a tube (H) connected to a vacuum line. Holes (I) cut in the lid and vacuum chamber bottom to allow observation of the sample were covered with glass coverslips sealed to the metal with silicone rubber glue. Rubber supports insulated the cold stage assembly from the microscope stage.

In operation, 5 λ of solution was placed on a 24 × 24-mm coverslip and an 18 × 18-mm coverslip was placed on the droplet, causing the solution to spread evenly over the area of the smaller coverslip. The sample was mounted on the plate (E), the temperature probe (G) was attached, and the lid (C) was placed on the chamber. Nitrogen from a pressurized tank was passed through a 3-Å molecular sieve drying tower and then through copper heat-exchanger coils immersed in liquid nitrogen. Temperature control in the plate was achieved by manual control of the gas flow rate (0–5 liter/min, for ambient to −50°); with periodic adjustment of the nitrogen pressure, temperature control of ±0.5° may be achieved. Accuracy of the temperature measuring system within ±0.5° was established by eutectic and melting point determinations on selected materials spanning the temperature range of interest. The sample was frozen by cooling at a rate of ~1°/min. The samples studied supercooled ~10° below the equilibrium freezing point and froze completely within a few seconds.

Freeze-Drying Microbalance—*Design*—The sample was suspended from one arm of an electronic vacuum microbalance[6] which in turn was connected to a high-vacuum line. For operation at zero pressure, an oil diffusion pump backed by a mechanical pump reduced the air pressure above the sample to ~5×10^{-6} torr. For operation at high residual air pressure, a controlled leak was located ~115 cm downstream from the sample through 2.5-cm diameter tubing. The controlled leak was simply a manually adjusted needle valve. During controlled-leak experiments, only the mechanical pump was operated. Pressure measurements in the range of 0.001–10 torr were made with a capacitance manometer[7] located near the leak site. Residual air pressures <0.001 torr were monitored with a cold cathode ionization gauge[8] ~175 cm downstream from the sample after the vapor stream had passed through a liquid nitrogen cold trap[9].

The sublimation cell, or sample holder, was enclosed by a balance tube–condenser assembly (Fig. 2A) which was connected to the balance using an "0" ring joint (A). The sublimation cell (B) was suspended from the balance beam by a 0.25-mm diameter nichrome wire (C). During operation, the glass balance tube (D) was immersed in a thermostat and the glass side arm tube (E) was immersed in dry ice–acetone to serve as the condenser. A high-vacuum union (F)[10] allowed rapid connection of the balance tube to the rest of the assembly. A copper–constantan thermocouple probe (G) was fitted inside a cylindrical cavity formed by the bottom portion of the sublimation cell. A circular aluminum foil heat shield (H) isolated the thermocouple probe from thermal radiation coming from the sample tube bottom so that the thermocouple probe more accurately sensed the temperature of the sample when the sample and thermostat temperatures differed. High-vacuum wax[11] (I) was used to seal the thermocouple wires (J) to the sample tube (forming a vacuum seal at the point where the wires left the tube) and to support the thermocouple probe in a fixed position at the bottom of the balance tube.

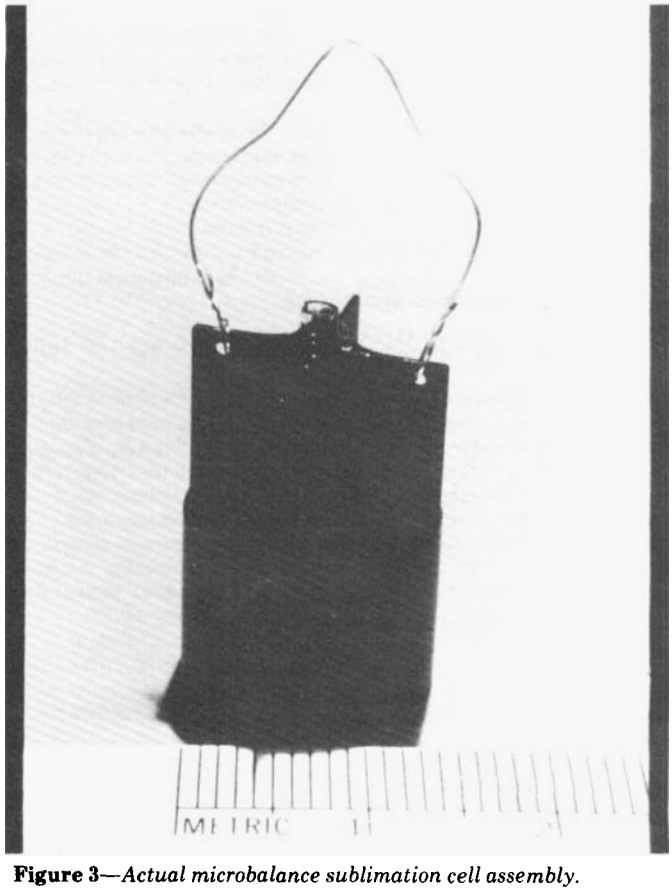

Figure 3—*Actual microbalance sublimation cell assembly.*

[5] Temperature measured with YSI model 42SL telethermometer, Yellow Springs Instrument Co.

[6] Sartorius Model 4102, Brinkmann Instruments, Westbury, NY 11590.

[7] MKS Model 220 Baratron, MKS Instruments, Inc., Burlington, MA 01803.

[8] Kontes/Martin, Evanston, Ill.

[9] Separate experiments indicates that the air pressure measured 175 cm downstream from the sample is a factor of ~5 lower than that above the sample.

[10] CAJON Ultra Torr Union, Cajon Co., Solon, OH 44139.

[11] Apiezon Type W.

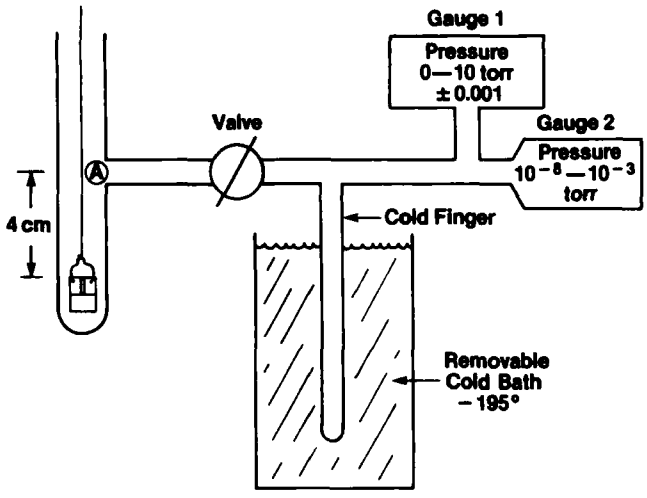

Figure 4—*Balance tube assembly for vapor composition measurements.*

A critical aspect of the sublimation rate measurement is the ability to control and measure the sample temperature. The sublimation cell (Figs. 2B, 3) is essentially a glass capillary tube in good thermal contact with an efficient radiative heat exchanger. This design allows the heat required for sublimation to be transferred from the thermostat to the sample with minimal temperature gradients. The sample (A) was in a glass capillary tube (B) which was fixed into a cylindrical hole in the aluminum heat exchanger by a thin film of high-vacuum wax[11] (C). To maximize radiative heat transfer, the aluminum was given a black anodized finish. The total weight of the sublimation cell was 1.17 g. The top portion of the heat exchanger had four fins (D) at 90° with respect to each other (Fig. 3), while the bottom portion (E) was a cylindrical cavity termed the temperature sensing cavity. The thermocouple probe protruded into this cavity without touching the sublimation cell. To increase the efficiency of heat exchange between the thermocouple probe and the sublimation cell, the effective area of the probe was increased by glueing the thermocouple junction (F) to an aluminum disk (G) with a thin coat of high-vacuum wax (H).

Temperature Measurement—Ideally, the probe measures the cell temperature, which is identical to the sample temperature. In practice, the probe temperature does not exactly measure the cell temperature and, at high sublimation rates, the sample temperature is lower than the cell temperature. A theoretical analysis of heat transfer in the apparatus and a series of calibration experiments (Appendix I) yielded the following relationship between the probe temperature (T_p), the sample temperature (T_s), and ambient temperature (T_a).

$$T_s = T_p - K_p \frac{(1 + 68.1\,P)}{(1 + 87.0\,P)} \dot{m} - K_a(T_a - T_p) \qquad \text{(Eq. 1)}$$

where P is the pressure in the balance tube in torr and $\dot{m}$ is the sublimation rate in mg/min. The parameters K_p and K_a were evaluated by fitting the theoretical model to calibration data, yielding a K_p of 10.2 and K_a of 0.010 at $P = 0$ and K_a of 0.006 for P between 0.05–1 torr, respectively[12]. The probe temperature measured with the system at ambient pressure was identical to the thermostat temperature as measured by the probe thermocouple. Thus, the temperature data for each experiment were corrected for thermocouple inaccuracy by comparing the probe temperature at ambient pressure with the thermostat temperature measured with a glass mercury thermometer (accuracy ±0.1°).

With the above procedures, the magnitude of the uncertainty in T_s was estimated to be 0.5° (due mostly to the uncertainty in K_a) plus 15% of the correction term (Eq. 1) proportional to $\dot{m}$[12]. Thus, the temperature uncertainty was ±0.5° for most of the sublimation experiments but increased to ±1.5° for the experiments with pure water at high temperature and zero pressure.

Background Mass Loss Correction—The rate of mass loss, computed by numerical differentiation from the recorder *versus* time curve[13], contains a background contribution, *i.e.*, mass loss other than sublimation of ice from the sample. The background mass loss arises from loss of adsorbed water from the balance system and the sublimation cell surface; it was determined experimentally by blank runs. No temperature effects were noted between −15 and −25°, and the background effect was assumed to be independent of temperature. The background contribution to the rate of mass loss ($\dot{m}_B$) decreased with time according to the empirical equation:

$$\dot{m}_B = \frac{A}{1 + kt^n} \qquad \text{(Eq. 2)}$$

where t is the time expired after sublimation begins and A, k, and n are constants. With $\dot{m}_B$ in mg/min, the values of A, k, and n, determined by regression analysis of several blank runs, are 0.01252, 0.10836, and 1.0554, respectively. The background correction is significant only for small values of t.

Chamber Pressure and Composition Measurements—Routinely, the pressure in the balance tube and the composition of vapor are not measured. However, such data were determined during representative sublimation experiments. For this series of experiments, a modified balance tube assembly was used (Fig. 4). With the liquid nitrogen cold bath removed, the total pressure at point A was measured using either gauge 1[7] or 2[8], depending on the pressure range studied. The valve was then closed and the cold bath was placed over the cold finger, condensing all water vapor. The residual pressure (due to air) was then measured. This residual pressure was slightly lower than the air pressure in the original vapor since the air remaining in the cold finger was at a lower temperature. The original air pressure was obtained from the measured residual pressure using an empirically determined correction factor (1.10_3 for the apparatus used). The correction factor was determined by measuring the pressure reduction induced by placing the cold bath on the cold finger at high pressure when the vapor was almost entirely air. With the air and total pressures in the sample determined, the water vapor pressure in the sample was obtained by difference[14].

In high-vacuum operation, the mole fraction of water vapor in the sample tube is unity (within experimental error) and the partial pressure of water vapor is <0.01 torr, even for sublimation of pure ice at high temperature. Thus, the partial pressure of water vapor above the sample was negligible compared with the vapor pressure of ice in all experiments carried out at high vacuum. When sublimation was carried out with a controlled air leak into the vacuum system to investigate the effect of air pressure on the sublimation rate, the mole fraction of air in the sample tube (X_2) is found to obey the empirical expression:

$$X_2 = \exp(-0.602\,\dot{m}), \qquad \text{(Eq. 3)}$$

where $\dot{m}$ is the sublimation rate in mg/min. The equation is valid for sublimation from pure ice and frozen solutions over the range in total pressures studied (0.04–0.8 torr). With the frozen solutions studied, $\dot{m}$

[12] Due to a small probe area and significant heat transfer from the ambient through the 30-gauge thermocouple wires (0.023-cm diameter), the thermocouple probe assembly shown here is only partially successful in directly measuring the cell temperature. The design has recently been improved by using smaller thermocouple wire (0.0076-cm diameter) and allowing the wire to equilibrate to the thermostat temperature before entry into the balance tube through the bottom. Also, the probe area is increased by press fitting the thermocouple junction into a finned heat exchanger similar in design to the top portion of the sublimation cell. The area is 1.7 cm², as compared with 0.7 cm² for the probe used to generate the data reported here. With the new finned probe, the value of K_a (Eq. 1) is 0.000 and K_p is 7.1. With the finned probe, the uncertainty in T_s is estimated at ±0.2° with $\dot{m} = 0$.

[13] The balance measures the sum of the gravitational force on the sample and the momentum force resulting from subliming water molecules. As long as the sublimation rate is independent of time, the momentum force is independent of time and the rate of mass loss is correctly computed from the balance readout. However, when the sublimation rate is time dependent, the momentum force is time dependent and contributes to the apparent rate of mass loss (computed from the balance readout). A maximum value for this effect may be estimated by assuming all subliming water molecules leave the sample at right angles to the sample surface. Taking the momentum as the product of the root mean square velocity and the mass of the water molecule, imposing conservation of momentum leads to:

$$\dot{m}_a/\dot{m} = 1 + \frac{1}{g}\left(\frac{3RT}{M_1}\right)^{1/2} \frac{d\ln\dot{m}}{dt}$$

where $\dot{m}_a$ is the apparent (or measured) sublimation rate, $\dot{m}$ is the true sublimation rate, $d\dot{m}/dt$ is the time derivative of the sublimation rate, R is the gas constant, M_1 is the molecular weight of water, T is the absolute temperature, and g is the gravitational constant. Evaluation of the fundamental constants yields:

$$\dot{m}_a/\dot{m} = 1 + 1.0\frac{d\ln\dot{m}}{dt}$$

where time is in min. The correction term $d\ln\dot{m}/dt$ is largest for experiments with pure water at high temperature; but even for this case, the correction is only ~4%.

[14] The cold cathode gauge (gauge 2, Fig. 4) readout was calibrated for air. A calibration curve giving water vapor pressure as a function of gauge reading was obtained by determining the gauge response, while ice in the cold finger slowly sublimed at known temperature and essentially zero air pressure. The water vapor pressure was taken as the equilibrium vapor pressure of ice at the measured temperature corrected for thermal transpiration effects (21).

was small enough that X_2 equaled 1.00 and, even for the studies with pure water, the vapor in the sample tube was mostly air. In experiments with a controlled leak, the total pressure in the balance tube was the same as the total pressure measured at the normal pressure measurement position (located 115 cm downstream from the sample).

Vial Freeze-Drying—*Apparatus*—Vial freeze-drying was carried out in a commercial laboratory freeze-dryer[15] which was modified by inclusion of a temperature-controlled shelf (530 cm^2 area), thermocouple (copper–constantan, 30-gauge) measurement of shelf and product temperature, and pressure measurement[5] in the sample chamber and inside one of the vials.

Pressure inside a vial was measured by connecting a glass tube to the interior of the vial at a location between the vial neck and the top surface of the product. This tube was joined to another tube leading out of the vacuum chamber to the vial pressure sensor. Vial pressure, chamber pressure, and all thermocouple outputs were displayed as a function of time by a 24-channel recorder[16].

Calculation of Sublimation Rate—Calculation of the resistance of the dried product requires the following data: the vapor pressure of ice (evaluated from the product temperature[17]), the pressure in the vial[18], the area of the product (calculated from the vial dimensions), and the sublimation rate. Since the apparatus did not allow the mass of a vial to be monitored continuously, the sublimation rate was evaluated by an alternate procedure.

Phenomenologically the sublimation rate, $\dot{m}$ (in g/hr), is given by:

$$\dot{m} = R_s^{-1}(P_v - P_c) \qquad \text{(Eq. 4)}$$

where R_s is the stopper (or closure) resistance and P_v and P_c are the pressures in the vial and chamber, respectively. Theoretical considerations suggest that the stopper resistance as defined by Eq. 4 should be pressure dependent (12) and may depend slightly on the sublimation rate (22). Empirically for the stoppers used in this research[19], the stopper resistance was found to be essentially independent of sublimation rate and varied with pressure as:

$$R_s = \overline{R}_s/\overline{P} \qquad \text{(Eq. 5)}$$

where $\overline{P}$ is the mean pressure across the stopper [$\overline{P} = (P_v + P_c)/2$)] and, as a first approximation, $\overline{R}_s$ is a constant[20]. Combining Eqs. 4 and 5 yields:

$$\dot{m} = \overline{R}_s^{-1}(P_v^2 - P_c^2)/2 \qquad \text{(Eq. 6)}$$

Since the total mass of water removed during drying (Δm) is known from the solution concentration and fill volume, the value of $\overline{R}_s$ for a given experiment may be evaluated by integration of Eq. 6 over the time period τ_D, where $P_v > P_c$, giving:

$$\overline{R}_s = \frac{1}{2\Delta m}\int_0^{\tau_D}(P_v^2 - P_c^2)dt \qquad \text{(Eq. 7)}$$

where the integration is performed numerically. Since slight variations in stopper placement causes variations in $\overline{R}_s$, a value of $\overline{R}_s$ was determined for each experiment. Once $\overline{R}_s$ was determined using Eq. 7, the sublimation rate at any time during primary drying was evaluated using Eq. 6.

Freezing Procedures—Frozen solutions for microbalance studies were prepared by loading the capillary with 13 λ of solution using a syringe, taking care not to introduce air bubbles. The sublimation cell was suspended from the balance and the balance tube was put into place. The balance tube was then immersed in 2-propanol at −40° (contained in a Dewar flask). When the sample froze, the probe temperature *versus* time plot showed a small change in slope, thereby allowing the freezing temperature to be determined. The studied solutions supercooled 20–25° below the equilibrium freezing point before freezing began. After the probe temperature decreased to <−35°, the 2-propanol bath was removed and the balance tube was immersed in a thermostat at the temperature desired for freeze-drying.

With pure water, 10% v/v potassium chloride, and 22.8% v/v povidone, the temperature history of the sample during freezing was studied by placing two thermocouple junctions (0.0076-cm diameter wire) in the capillary tube. One junction was placed near the tube bottom while the other was placed in the solution at the top of the capillary tube.

NORMALIZED DRIED PRODUCT RESISTANCE

The normalized dried product resistance ($\hat{R}_p$) is defined by:

$$\hat{R}_p = \frac{A_p(P_0 - P_1^D)}{\dot{m}} \qquad \text{(Eq. 8)}$$

where A_p is the geometric cross-sectional area of the product normal to the direction of water vapor flow, P_0 is the equilibrium vapor pressure of ice at the temperature of the subliming ice, P_1^D is the vapor pressure of water above the dried product, and $\dot{m}$ is the sublimation rate. Thus, the normalized dried product resistance is a per-unit-area (or area-normalized) dried product resistance which is a function of the thickness of the dried product layer.

In a vial freeze-drying experiment, P_1^D is the pressure of water vapor in the vial. Since the vapor in the vial during primary drying is essentially all water vapor[18], P_1^D is taken as the measured vial pressure. In a microbalance experiment, P_1^D is essentially zero during high-vacuum operation. During operation with a controlled leak, P_1^D is calculated from the total pressure and the vapor composition given by Eq. 3. Under all conditions studied in this research, P_1^D was small compared to P_0 and was normally negligible. With area in cm^2, pressure in torr, and $\dot{m}$ in g hr^{-1}, the units of $\hat{R}_p$ are cm^2 torr hr g^{-1} and numerically represents the approximate time (in hours) to freeze-dry a solution 1 cm thick at a temperature of −20°.

The thickness of the dried product (l) is evaluated from:

$$l = \frac{m_0 - m_t}{\rho_I A_p \epsilon} \qquad \text{(Eq. 9)}$$

where m_0 is the initial sample mass, m_t is the mass remaining at time t, ρ_I is the density of ice, and ϵ is the porosity or volume fraction of ice. In the microbalance experiment the masses were evaluated directly from the recorder output. In a vial freeze-drying experiment the mass difference, $m_0 - m_t$, was calculated by numerical integration of the sublimation rate over the relevant time interval.

Equation 9 assumes that the ice–vapor boundary remains planar and normal to the axis of the cylindrical container during sublimation. Sublimation of ice from pure ice and frozen aqueous potassium chloride contained in a 1.3-mm diameter capillary tube was examined microscopically by glueing the capillary tube to a glass coverslip and using the aforementioned microscopic observation techniques. The observations demonstrated that this assumption is justified for microbalance experiments. During vial freeze-drying the assumption is valid as a first approximation until near the end of primary drying.

RESULTS AND DISCUSSION

Freezing Rates—Representative data for potassium chloride and povidone are shown in Fig. 5. Onset of freezing is indicated by the sharp increase in temperature, while completion of the freezing process is indicated by a return to the cooling rate characteristic of the sample before

---

[15] Virtis Unitrap.

[16] Esterline Angus Speed Servo II.

[17] Product temperature was routinely measured in the center of the vial at the bottom, in the center about 8 mm up from the bottom, and at the bottom edge. Normally, temperature differences within the vial were small (<1°) and the thermocouple nearest the sublimation surface was used to evaluate the temperature of the subliming ice. If the temperature gradient was significant, the temperature of the ice was calculated using the measured temperature gradient and the estimated distance between the ice interface and the nearest thermocouple.

[18] The partial pressure of water vapor was required but both theoretical calculations and experimental data (23) indicated that the vapor in the vial was essentially 100% water.

[19] In the semistoppered position used during freeze-drying, the 20-mm finish closure has two openings of ~0.4-cm diameter. The 13-mm finish closure, used only for the −15° experiments with System I, has two openings of ~0.2-cm diameter, West Co.

[20] Application of the theories describing flow of rarified gases (12, 22) to the problem of water vapor flow through the closure opening, indicates $\overline{R}_s$ varies with pressure and sublimation rate according to the form:

$$\overline{R}_s^{-1} = a + b\dot{m} + c/[\overline{P}]$$

where a, b and c are constants and the bracket symbols, [ ], indicate the mean for a given experiment. The term in a represents a transport coefficient for viscous flow according to Poiseuille's law, the term in b is a correction of Poiseuille's law for short tubes, and the term in c represents the contribution of free molecular or Knudsen flow. As the pressure decreases and water–stopper collisions become much more frequent than water–water collisions, the term in c dominates and R_s (Eq. 4) becomes independent of pressure.

Regression analysis of $\overline{R}_s$ data for the 20-mm closure determined from Eq. 7 for runs where [P] varied between 0.08 and 0.35 mm and $\dot{m}$ varied between 0.25 and 0.6 g/hr resulted in a = 183, b = −8.0, and c = 3.7. For the pressures and sublimation rates encountered in this research, the term in a dominated, indicating the flow mechanism as mostly viscous. Moreover, during any given experiment designed to measure dried product resistance, variations in $\dot{m}$ and P during primary drying are modest, causing only slight variation in $\overline{R}_s$. Typically, $\overline{R}_s$ deviates from its mean value by no more than ~ ±5% during the portion of primary drying where product resistance data is evaluated, and $\overline{R}_s$ may be regarded as a constant without introducing significant error. For experiments with the 13-mm closure, P was nearly constant so $\overline{R}_s$ also was considered constant.

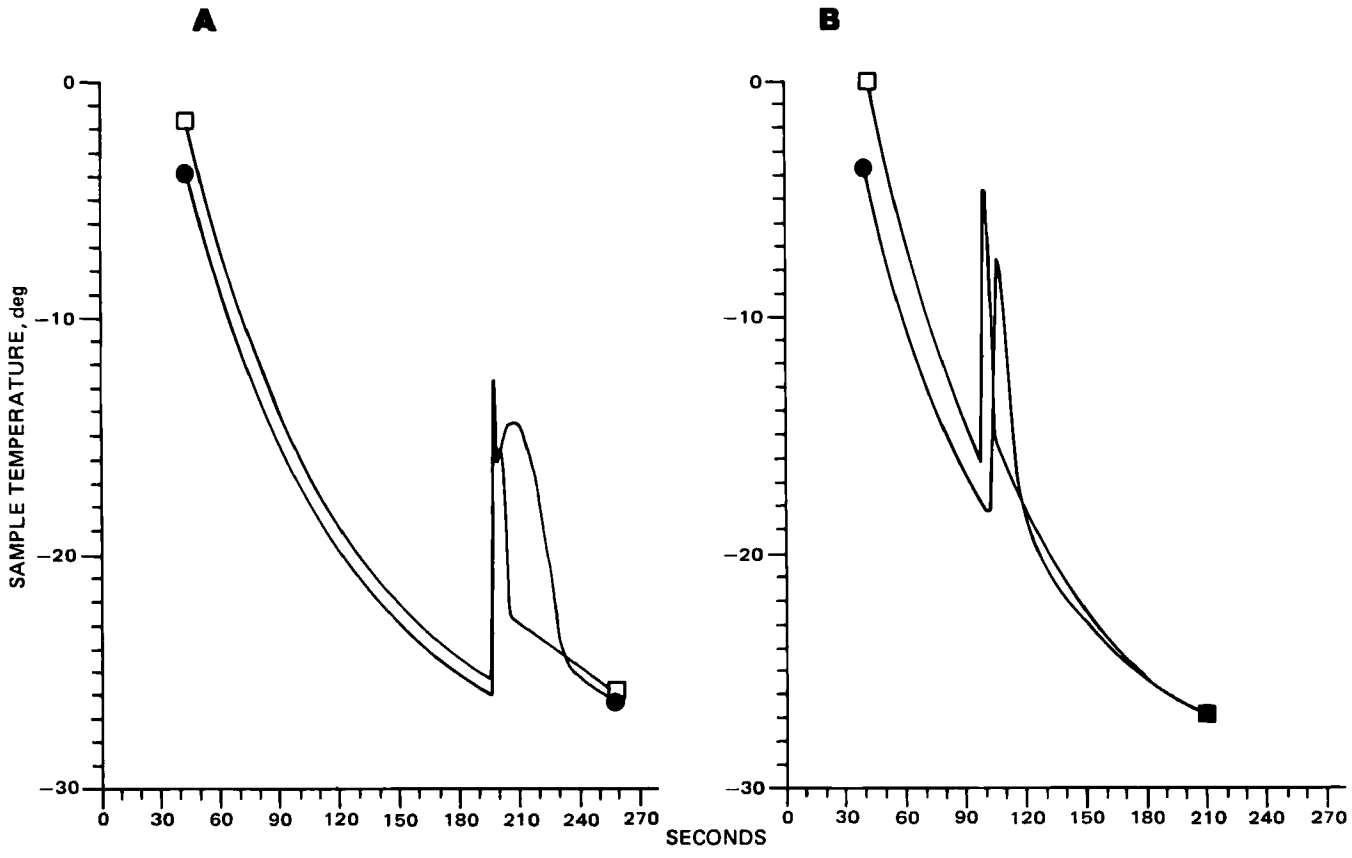

Figure 5—*Freezing curves for microbalance samples of potassium chloride 10% v/v (A) and 22.8% v/v povidone (B). Key: (●) top and (□) bottom of each sample.*

freezing. For both water and potassium chloride, freezing began simultaneously at the top and bottom; for povidone freezing began at the bottom ~4 sec before the top started to freeze. In all cases, freezing was complete at the bottom before the top was completely frozen. The time elapsed between onset and completion of freezing was 13.8 ± 4.2 sec for pure water, 10.2 ± 0.3 sec for povidone, and 31.2 ± 6.0 sec for potassium chloride (mean ± *SD* calculated from replicate experiments).

Cooling curves for the samples frozen in vials qualitatively show the same features exhibited for the microbalance samples (Fig. 5). The samples supercooled, some ice formed throughout the solution quickly, and there was a delay in freezing the remainder of the water, with the top being the last to completely freeze. However, potentially significant quantitative differences exist between the microbalance and vial-freezing behavior. The degree of supercooling for vial-frozen solutions was <50% of that found for the corresponding microbalance solutions, and the time elapsed between onset and completion of freezing was ~30 min for vial-frozen samples. Thus, a vial-frozen sample is subjected to a much slower freezing rate, which may allow ice crystals to anneal or grow in size during freezing.

In both the freeze-drying microscope and microbalance studies, freezing was completed very quickly after the first ice crystals formed; a slow-freezing process which accurately imitates vial freezing was not possible. However, as a first approximation to a vial-freezing process, a sample quick-frozen normally in the microscope or microbalance apparatus was annealed at ~ −8° for 0.5 hr, after which the temperature was reduced to the desired freeze-drying temperature at a rate of ~0.4°/min. This procedure was intended to allow ice crystal growth similar to that which occurs during slow-freezing in a vial.

Microscopic Observation of Freeze-Drying—Photomicrographs (Fig. 6) illustrate the change in structure of a given material on annealing for 0.5 hr at −8°. The darker region at the left of the photograph is the dried sample, while the lighter region on the right still contains ice. Photographs in the left column are quick-frozen samples where the entire sample freezes within seconds, while the right column contains the corresponding annealed samples. Local regions which contain only ice or void are transparent and appear light. The solute is concentrated between the ice crystals and also appears to deposit in a very thin film on the surfaces of the glass coverslips used to contain the sample. The solute concentrated between ice crystals appears dark in both dried and undried regions. The solute deposited on the coverslips is normally semitransparent in the region still containing ice but, at least for crystalline solutes (*i.e.*, potassium chloride), appears dark after the ice has sublimed.

Annealing increased the size of the ice crystals and therefore also increased the size of the voids or pores left after sublimation of the ice. The effect was modest for System I but was marked for both potassium chloride and povidone, where qualitative changes in structure accompanied the growth of ice crystals. The dendrite (1) pattern of ice crystals formed when the aqueous potassium chloride solution froze (Fig. 6A) was lost on annealing (Fig. 6B). The pattern in aqueous povidone (Fig. 6C), which might be classified as irregular dendrite (1, 2), was transformed by annealing to an ice structure largely composed of large globular ice crystals completely surrounded by solute (Fig. 6D). This globular ice structure (Fig. 6C) is qualitatively similar to the ice structure in concentrated (50% solute) aqueous povidone (13).

All nonannealed samples appeared to freeze-dry predominantly by a MacKenzie type I mechanism (13), where water vapor escaped *via* open channels or pores created by prior sublimation of ice until the boundary between dried solute and vacuum chamber (edge of sample) was reached. Both amorphous samples (System I and povidone) showed a glassy region (without ice crystals) at this boundary which developed cracks during drying. This region was presumably a film of solute containing absorbed water which, on partial dehydration, decreased in volume sufficiently to form cracks. Annealed povidone freeze-dried largely by a MacKenzie type II mechanism (13). Here, the water vapor dissolved in and diffused through the solute wall surrounding the ice crystal before leaving the globular cavity. The arrow in the lower center of Fig. 6D indicates the ice–vapor interface in the interior of one partially dried cavity. Thus, the rate of freeze-drying for a type II mechanism potentially is determined by solid-state diffusion of water in the amorphous solute, while the rate for a type I mechanism is determined by flow of water vapor in the porous matrix created by the solute pore structure.

The annealing temperature (−8°) was higher than the eutectic temperature of aqueous potassium chloride (−11°) (24) and the collapse temperature of the povidone used (−17°), but was lower than the collapse temperature of System I[21]. Thus, both potassium chloride and povidone were present in a fluid state during annealing, but the solute in System I was a nonflowable amorphous solid during annealing. The observation that ice crystal growth was rapid in the potassium chloride and povidone

Table I—Microbalance Sublimation Rate Data for Pure Water [a]

n[b]	$t°(l=0)$[c]	$\langle t° \rangle$[d]	P_2^D, torr	A_0	A_1	$\langle \hat{R}_p \rangle$
2	−24	−21.6	0	0.100 ± 0.035[e]	0.175 ± 0.045	0.19 ± 0.02
5	−30	−27.2	0	0.067 ± 0.013	0.153 ± 0.024	0.143 ± 0.005
2	−43	−42.5	0	0.0418 ± 0.0021	0.075 ± 0.003	0.079 ± 0.003
3	−29	−28.4	0.176	0.126 ± 0.038	0.226 ± 0.036	0.24 ± 0.03
2	−29	−28.1	0.309	0.152 ± 0.016	0.313 ± 0.025	0.31 ± 0.02

[a] Parameters for the normalized product resistance equation $\hat{R}_p = A_0 + A_1 l$; units of $\hat{R}_p$ are cm² torr hr g⁻¹. [b] Number of replicate experiments. [c] Temperature of subliming ice at $l = 0$. [d] Mean temperature of subliming ice over the entire experiment. [e] Mean ± *SE*; intended only to provide information on reproducibility between replicate experiments.

systems but slow in System I during annealing suggests that the rate of ice crystal growth is determined, in part, by the fluidity of the solute phase.

Sublimation of Pure Ice—Resistance data calculated from Eq. 8 for pure ice are summarized in Table I. When pure ice is sublimed, $\hat{R}_p$ reflects the resistance in transforming water from the solid state to the vapor state (*i.e.*, the phase change) plus the resistance in transport of water vapor from the ice–vapor interface to the top of the capillary tube. The value of l, as calculated from Eq. 9, is the distance from the ice–vapor interface to the location of this interface at time zero. Since the interface is 0.1 cm below the top of the capillary tube at time zero, the total tube length above the interface (l_T) is given by: $l_T = 0.1 + l$. The $\hat{R}_p$ data were found to increase linearly with increasing l:

$$\hat{R}_p = A_0 + A_1 l \qquad \text{(Eq. 10)}$$

where A_0 and A_1 are constants for a particular temperature. Since the sublimation rates are high and decrease as l increases, the sample temperature increases slightly during an experiment. Thus, both the initial temperature, $t(l = 0)$, and the mean sample temperature during the experiment, $\langle t \rangle$, are reported. The mean normalized product resistance, $\langle \hat{R}_p \rangle$, defined by:

$$\langle \hat{R}_p \rangle = \int_0^1 \hat{R}_p dl \qquad \text{(Eq. 11)}$$

is also tabulated.

The evaporation coefficient (α_v) where $0 < \alpha_v < l$, represents the ratio of the actual sublimation rate to the sublimation rate calculated from simple kinetic theory under conditions of zero resistance offered by the sample container (*i.e.*, the capillary tube). The evaporation coefficient is defined by:

$$\dot{m}(l_T = 0) = \alpha_v A_p \left(\frac{M_1}{2RT}\right)^{1/2} (P_0 - P_1^D) \qquad \text{(Eq. 12)}$$

where $\dot{m}(l_T = 0)$ is the sublimation rate extrapolated to $l_T = 0$, M_1 is the molecular weight of water, R is the gas constant, and T is the absolute temperature (25). All quantities are in CGS units. Combination of Eqs. 8, 10, and 12, evaluation of constants, and conversion to consistent units give:

$$\alpha_v = (1.122)10^{-3}\sqrt{T}/(A_0 - 0.1A_1) \qquad \text{(Eq. 13)}$$

Evaporation coefficients calculated from Eq. 13 and the data in Table I where $P_2^D = 0$ compare favorably with literature data (25–27) (Fig. 7). Since potential errors in sample temperature measurement are much higher for pure ice than for frozen solutions, the agreement shown in Fig. 7 provides strong evidence for the validity of the temperature measurement procedures used in this research.

An increase in residual air pressure (*i.e.*, $P_2^D > 0$) increases both the resistance of the phase change, measured by A_0, and the resistance of the capillary tube, measured by A_1. Both effects presumably originate from collisions between water molecules and air. However, even when P_2^D is approximately equal to the equilibrium vapor pressure of ice (0.350 torr), the sublimation rate remains high, decreasing by a factor of ~2 from the rate at zero pressure.

Dried Product Resistance—*Representation of Data by Empirical Equations*—The variation of normalized product resistance ($\hat{R}_p$) with thickness of dried product (l) is represented by the empirical equation:

$$\hat{R}_p = (A_0 + A_1 l)/(1 + A_2 l), \qquad l' \le l \le 1 \text{ cm} \qquad \text{(Eq. 14)}$$

where $l' = 0$ for most systems studied (*i.e.*, Eq. 14 is valid over the interval $0 \le l \le 1$ cm).

[21] System I does not exhibit a collapse temperature up to −6.5°, where partial melting of the ice crystals (melt-back) occurs.

The parameters A_0, A_1, and A_2 are determined by regression analysis of the raw data. The data are summarized in Table II where the first column provides a curve identification number for each set of experimental conditions, and the corresponding, the A_i ($i = 0, 1, 2$) parameters, mean normalized product resistance ($\langle \hat{R}_p \rangle$), and value of the normalized product resistance at $l = 0$ [$\hat{R}_p(0)$], which are reported in each row. The value of n gives the number of independent replicate experiments. The A_i ($i = 0, 1, 2$) and resistance data tabulated are mean values with the corresponding uncertainty being the standard deviation of the mean. The uncertainty figures are given only to indicate the reproducibility between replicate experiments. Reproducibility of $\hat{R}_p$ data (approximately given by the reproducibility of the corresponding $\langle \hat{R}_p \rangle$ data) was frequently much poorer than one might predict from the scatter in $\hat{R}_p$ *versus* l data from a single experiment, a result perhaps attributable to real differences between samples caused by the inability to precisely control the freezing process. Even for the same chemical system, reproducibility of the raw data (Fig. 8) varies from excellent (curve 16) to poor (curve 15).

In general, Eq. 14 is a valid representation of the raw data even as $l \to 0$, and $\hat{R}_p(0) = A_0$. However, for curves 13, 14, 16, and 17, Eq. 14 is valid only for $l > 0.2$ cm [$\hat{R}_p(0) > A_0$]. In the following discussion all $\hat{R}_p$ *versus* l data were calculated from Eq. 14 where this equation was a valid representation of the raw data. In those cases where Eq. 14 was not valid, mean values of the raw data are used.

Dependence of $\hat{R}_p$ on l—Theoretical models in common use (11, 28) assume the equivalent of $\hat{R}_p \propto l$, which results in the quantity of ice sublimed being directly proportional to the square root of time. Essen-

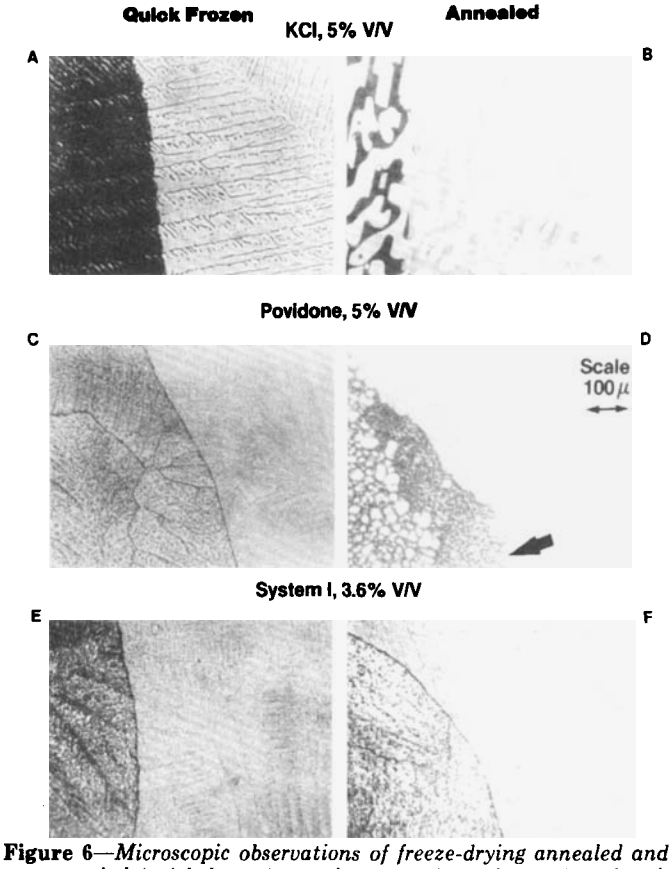

Figure 6—*Microscopic observations of freeze-drying annealed and nonannealed (quick-frozen) samples at −25°. Darker region of each photograph is the dried sample, lighter region still contains ice. The arrow indicates the ice–vapor interface.*

Table II—Microbalance Sublimation Rate Data for Selected Frozen Aqueous Solutions [a]

Curve ID No.	n	Annealed ?	Solute, % (v/v)	$t°$	P_2^Dtorr	A_0	A_1	A_2	$\langle\hat{R}_p\rangle$	$\hat{R}_p(0)$
					Potassium Chloride					
1	2	No	5.0	−13.9	0	1.5 ± 0.6	41.2 ± 4.4	7.7 ± 0.2	4.27 ± 0.16	1.5 ± 0.6
2	6	No	5.0	−20.9	0	2.98 ± 0.29	37.5 ± 4.8	2.90 ± 0.48	8.3 ± 0.6	2.98 ± 0.29
3	2	No	5.0	−29.8	0	2.29 ± 0.25	27.3 ± 0.2	0.93 ± 0.04	10.2 ± 0.1	2.29 ± 0.25
4	4	Yes	5.0	−22.0	0	1.22 ± 0.24	7.1 ± 0.5	0.20 ± 0.08	4.25 ± 0.16	1.22 ± 0.24
5	2	No	5.0	−21.3	0.102	4.7 ± 0.8	30.7 ± 4.7	1.45 ± 0.34	11.0 ± 0.6	4.7 ± 0.8
6	2	No	5.0	−19.6	0.696	3.83 ± 0.37	22.6 ± 3.4	1.57 ± 0.24	8.0 ± 0.1	3.83 ± 0.37
7	2	No	2.5	−21.6	0	1.22 ± 0.18	10.1 ± 1.9	1.05 ± 0.28	3.88 ± 0.07	1.22 ± 0.18
8	2	No	10.0	−19.4	0	0.1 ± 1.7	113 ± 27	4.5 ± 1.3	15.6 ± 0.7	0.1 ± 1.7
					Povidone					
9	3	No	5.0	−26.0	0	1.7 ± 0.3	3.8 ± 1.3	0.00	3.6 ± 0.3	1.7 ± 0.3
10	4	No	5.0	−31.2	0	1.2 ± 0.2	5.2 ± 0.9	0.00	3.8 ± 0.3	1.2 ± 0.3
11	2	Yes	5.0	−26.3	0	0.84 ± 0.16	5.1 ± 1.0	0.50 ± 0.27	2.61 ± 0.06	0.84 ± 0.16
12	2	No	5.0	−31.2	0.186	0.54 ± 0.14	11.5 ± 0.4	0.00	6.3 ± 0.1	0.54 ± 0.14
13	2	No	10.0	−26.2	0	2.9 ± 0.4[b]	3.6 ± 0.2[b]	0.00	4.7 ± 0.5	6.1 ± 0.9[b]
14	2	No	22.8	−25.8	0	3.6 ± 0.6[b]	3.6 ± 0.8[b]	0.00	5.4 ± 0.2	13.3 ± 0.9[b]
					Dobutamine Hydrochloride–Mannitol (System I)					
15	2	No	3.6	−14.0	0	3.3 ± 0.7	50.5 ± 24.3	6.0 ± 3.2	6.8 ± 0.5	3.3 ± 0.7
16	2	No	3.6	−21.2	0	4.0 ± 0.4[b]	24.8 ± 0.6[b]	0.00	18.7 ± 0.1	13.8 ± 1.3
17	2	No	3.6	−21.4	0.190	3.3 ± 1.1[b]	25.6 ± 1.6[b]	0.28 ± .28[b]	16.6 ± 1.4	7.3 ± 4.0

[a] Parameters for the normalized product resistance equation $\hat{R}_p(l) = (A_0 + A_1 l)/(1 + A_2 l)$. [b] Normalized product resistance equation represents data for only $l > 0.2$ cm. As $l \to 0$, the resistance increases to $\hat{R}_p(0)$. Only one of the duplicate experiments on System I at $P_2^D = 0.190$ showed this phenomenon, resulting in the unusually high uncertainty in $\hat{R}_p(0)$.

tially four classes of $\hat{R}_p$ dependence on l have been observed in this research (Fig. 9), none of which correspond to a simple proportionality to l. With the possible exception of curve 8 (Table II), all data show a nonzero intercept at $l = 0$ and the dependence of $\hat{R}_p$ on l is frequently nonlinear. Type I curves show a linear dependence of $\hat{R}_p$ on l throughout the range $0 \leq l \leq 1$. A type II curve exhibits a sharp decrease in $\hat{R}_p$ at low l, followed by a linear increase in $\hat{R}_p$ with increasing l for $l > 0.2$ cm. Type III and type IV curves are concave toward the l axis, the curvature being slight for type III curves but severe for type IV.

The observation that $\hat{R}_p(0)$ is significantly larger than zero suggests the presence of a surface barrier resulting from a different structure for the dried product near the surface, a conclusion consistent with scanning electron microscopic observations (14). A large resistance accompanying the phase change at the ice–vapor interface would give the same result. However, the $\hat{R}_p(0)$ data for solution systems (Table II) are generally one to two orders of magnitude greater than $\hat{R}_p(0)$ for pure ice (Table I), and it does not appear reasonable that the phase change resistance for ice crystallized from a solution would be that much higher than the corresponding resistance for ice crystallized from pure water. As suggested by the microscopic observations discussed earlier, the surface barrier for type II curves appears to be a relatively high-resistance amorphous skin which, after some water desorption, cracks and decreases in effective resistance.

The nonlinearity of the type III and type IV curves may be related, in part, to a gradual variation in dried product structure as l increases. However, the observation that the curvature is temperature dependent (*i.e.*, compare curves 1–3, 15, and 16) indicate that product heterogeneity is not the only factor.

Effect of Solute Concentration on $\hat{R}_p$—An increase in concentration changed the $\hat{R}_p$ *versus* l curve for potassium chloride from a type III to a type IV curve (Fig. 10). The resistance curves for povidone (Fig. 11) show a transition from type I at low concentration to type II at high concentration, where the resistance at $l = 0$ increased sharply at high

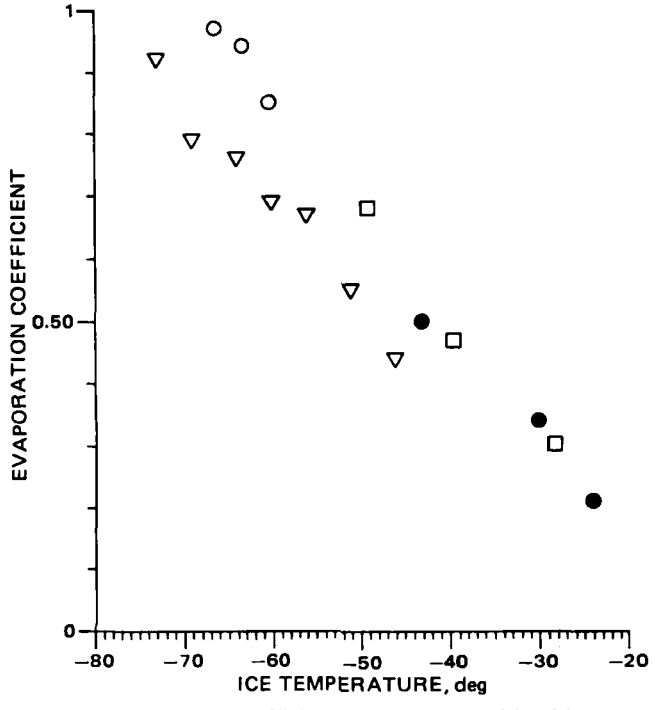

Figure 7—*Evaporation coefficients for ice obtained by this research (●), and (for comparison) taken from Refs. 25 (□), 26 (○), and 27 (▽).*

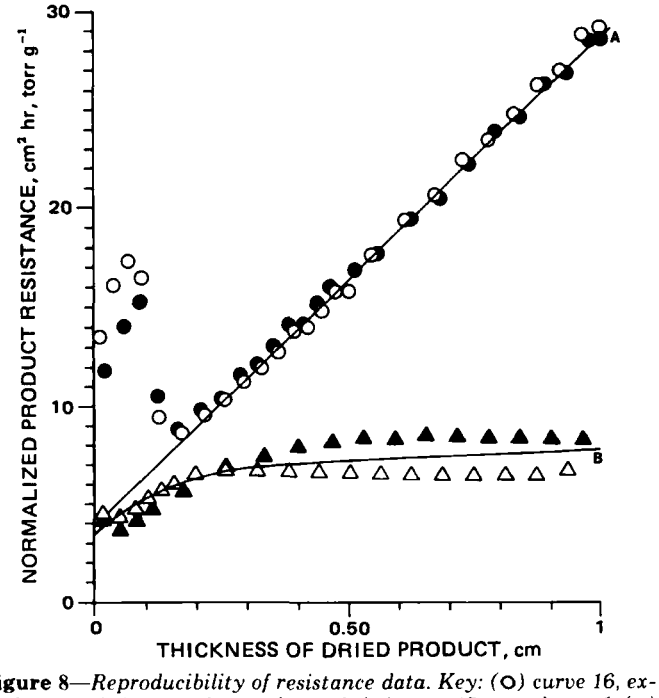

Figure 8—*Reproducibility of resistance data. Key: (○) curve 16, experiment 1; (●) curve 16, experiment 2; (△) curve 15, experiment 1; (▲) curve 15, experiment 2. The lines represent predictions of curves 16 (A) and 15 (B) calculated using Eq. 29.*

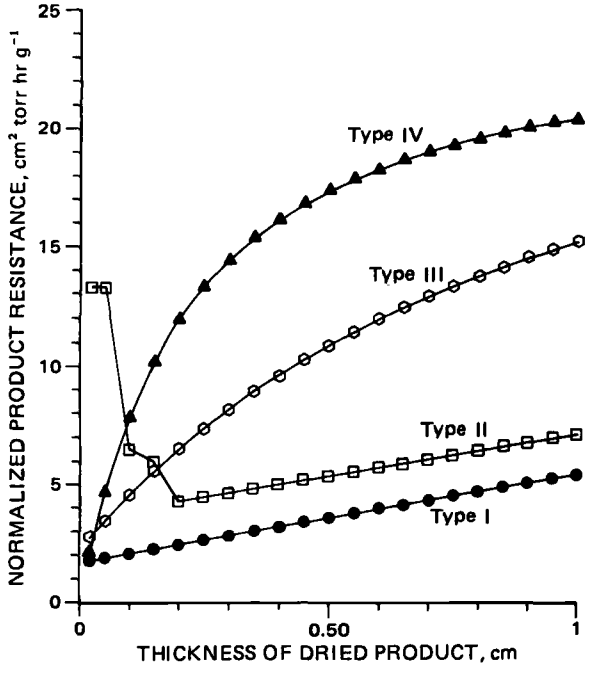

Figure 9—*Curves for $\hat{R}_p$ dependence on dried product thickness. Key: (●) 5% povidone at −26°, type I; (□) 22.8% povidone at −26°, type II; (○) 5% potassium chloride at −30°, type III; (▲) 10% potassium chloride at −20°, type IV.*

concentration. Evidently, the postulated amorphous skin phenomenon increases in significance as the concentration increases.

The mean normalized product resistance ($\langle \hat{R}_p \rangle$) increased as the concentration increased (Fig. 12). For potassium chloride, the increase was essentially linear in volume percent solid, while in the case of povidone, $\langle \hat{R}_p \rangle$ increased sharply with increasing concentration only at low concentration. Above ~10% solute (v/v), $\langle \hat{R}_p \rangle$ for povidone is nearly independent of concentration. Therefore, the drying time for a 1-cm deep potassium chloride solution will be twice as long for a 10% as for a 5% solution[22]. As a first approximation, the drying time for a 1-cm deep povidone solution is independent of concentration between 10% and at least 23% solute.

Effect of Annealing—The microscopic studies (Fig. 6) indicate that annealing resulted in larger ice crystals with correspondingly larger voids or pores in the dried solid. For potassium chloride, both quick-frozen and annealed samples appeared to freeze-dry by a type I mechanism, but annealing a povidone system caused a change from a type I to a type II freeze-drying mechanism. Assuming resistance decreases as pore size increases, one would expect that annealing the potassium chloride system would result in a lower product resistance. Since annealing a povidone system changes the freeze-drying mechanism, the net effect of annealing on the product resistance is not obvious.

Comparison of quick-frozen with annealed samples shows a significant decrease in $\hat{R}_p$ at all l values on annealing. This effect is very pronounced for potassium chloride (Fig. 13) and smaller, though still significant, for povidone (Fig. 14). Annealing potassium chloride resulted in a transition from a type III curve (nonlinear) to a curve which is nearly type I (linear). Intuitively, one would expect variations in product structure with l to be reduced by annealing. Thus, the observed effect of annealing on the resistance curve type appears consistent with the postulate that curvature in a resistance curve is related to structural heterogeneity.

[22] The reviewer suggested that the concentration dependence of $\langle \hat{R}_p \rangle$ for potassium chloride may be related to the increase in the ratio of eutectic–pre-eutectic ice as the solute concentration increases. Eutectic ice refers to ice which crystallizes with simultaneous crystallization of solute while pre-eutectic ice denotes ice formed prior to the crystallization of solute. Assuming equilibrium data (24) may be used to calculate the relative amount of eutectic ice formed in a nonequilibrium freezing process, the fraction of ice crystallizing as eutectic ice varies from 0.21 for 2.5% (v/v) to 0.90 for 10% (v/v) potassium chloride. Thus, at 2.5% potassium chloride, $\langle \hat{R}_p \rangle$ should be dominated by the pore structure created by pre-eutectic ice while at 10% potassium chloride the eutectic ice structure should largely determine the resistance behavior. Microscopic observations indicate that eutectic ice is much more finely divided than pre-eutectic ice, and water vapor originating from sublimation of eutectic ice must pass through a network of relatively small pores. Since theory (11) indicates that resistance to vapor flow through pores increases as the pore size decreases, one would expect a higher $\langle \hat{R}_p \rangle$ at higher solute concentration, as observed.

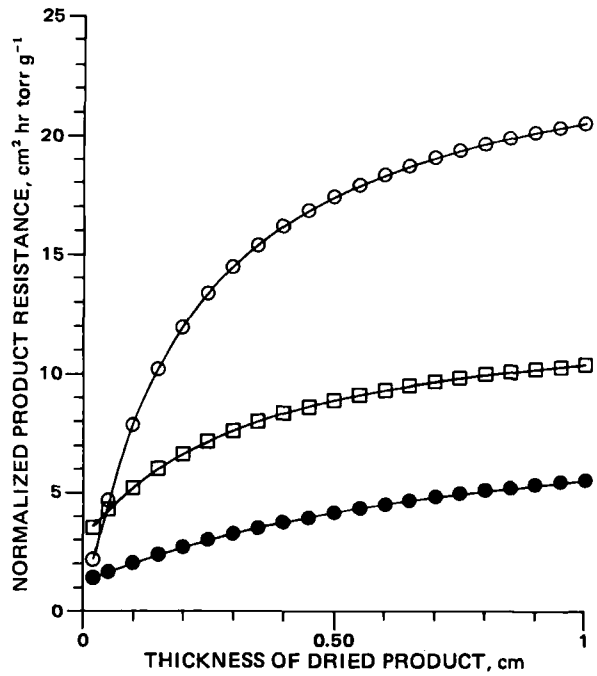

Figure 10—*Effect of solute concentration on $\hat{R}_p$ for potassium chloride at −21°, $P_1^D = 0$. Key: (●) 2.5% v/v; (□) 5.0% v/v; (○) 10.0% v/v.*

Effect of Residual Air Pressure—The data (Table II) indicate a significant increase in $\hat{R}_p$ with increasing air pressure (P_2^D) for 5% povidone at −31° and essentially no pressure effect for System I. The effect of pressure on $\hat{R}_p$ for 5% potassium chloride is small and erratic, probably reflecting sample-to-sample freezing variation more than the effect of pressure. To eliminate the effects of sample variation, the effect of air pressure was studied for a given sample by determining the sublimation rate as a function of pressure at constant l; *i.e.*, during the experiment the pressure was increased stepwise and then decreased stepwise. The mean of the $\hat{R}_p$ values (at corresponding pressures) for the increasing and decreasing parts of the experiment generate a set of $\hat{R}_p$ values at constant l as a function of air pressure. The results (Fig. 15) indicate $\hat{R}_p$ increased with increasing air pressure, the effect being very small for 5% potassium chloride at −21°, but quite significant for 5% povidone at −31°.

One would expect that increasing air pressure would yield an increasing probability of gas phase molecular collisions between water and air. When the frequency of water vapor–air collisions in the dried product becomes comparable in magnitude to the frequency of water vapor collisions with

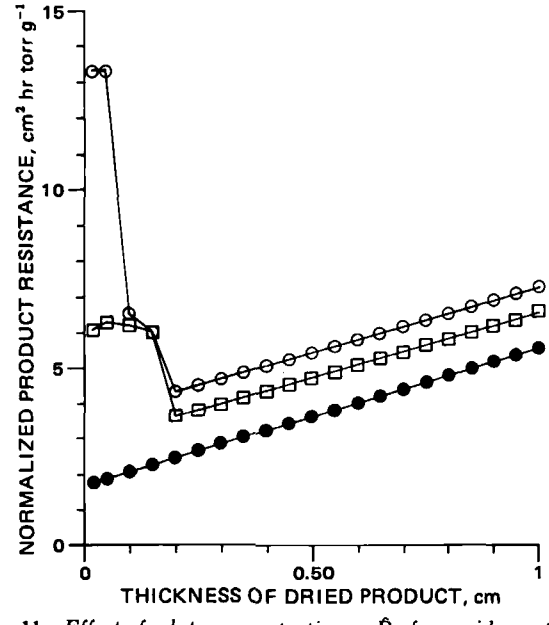

Figure 11—*Effect of solute concentration on $\hat{R}_p$ for povidone at −26°, $P_1^D = 0$. Key: (●) 5.0% v/v; (□) 10.0% v/v; (○) 22.8% v/v.*

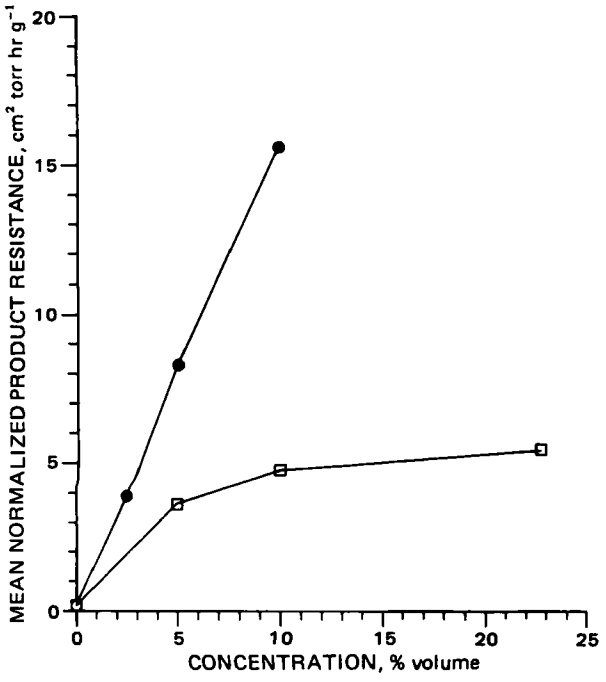

Figure 12—*Mean normalized product resistance ($\langle \hat{R}_p \rangle$) versus solute concentration for (●) potassium chloride at −21°; (□) povidone at −26°.*

the dried product matrix, the resistance due to water–air collisions should become a measurable fraction of the resistance originating from water–matrix collisions. Thus, increasing the air pressure above the sample should increase the product resistance, as observed. As the pore size decreases, the frequency of water–matrix collisions increases and the air pressure at which water–air collisions become comparable to water–matrix collisions will increase. Thus, the product resistance should be less sensitive to air pressure as the pore size decreases. The product resistance of potassium chloride at zero air pressure was much greater than the corresponding resistance for povidone, suggesting that the pore size in freeze-dried potassium chloride is much smaller. Consequently, the slope of the resistance *versus* air pressure curve should be less for potassium chloride than for povidone. The difference in pore size between potassium chloride and povidone is probably a result of the formation

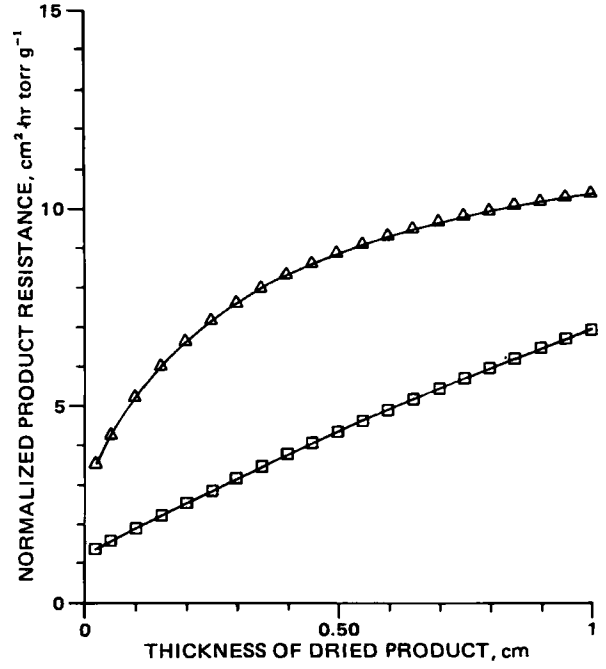

Figure 13—*Effect of annealing on $\hat{R}_p$ for potassium chloride 5% v/v at −21°, P_1^D = 0. Key: (△) not annealed; (□) annealed.*

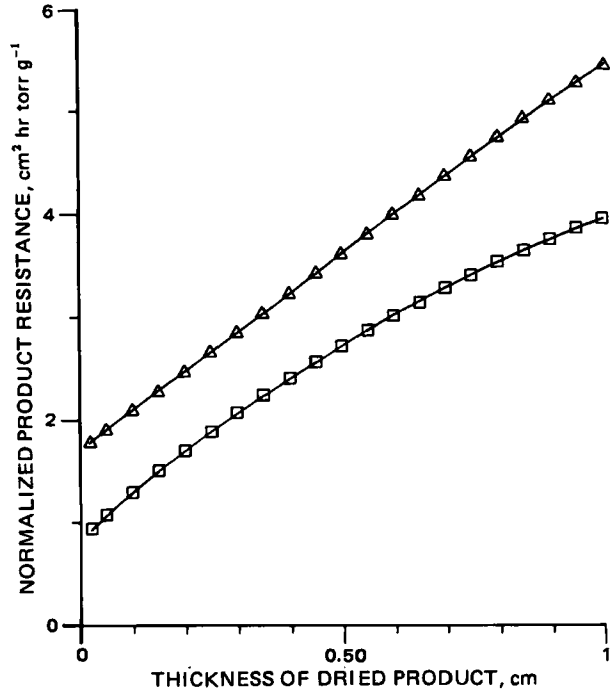

Figure 14—*Effect of annealing on $\hat{R}_p$ for 5% v/v povidone at −26°, P_1^D = 0. Key: (△) not annealed; (□) annealed.*

of eutectic ice in the potassium chloride system. Being amorphous, povidone does not form a eutectic.

The arrows in Fig. 15 indicate the values of the vapor pressure of ice at the corresponding product temperatures (−21.2° for potassium chloride and −31° for povidone). The normalized product resistance increased smoothly as the residual air pressure approached and exceeded the vapor pressure of ice. Thus, the common observation that the sublimation rate decreases sharply as the chamber pressure approaches the vapor pressure of ice (29) is not a result of increasing product resistance. Indeed, sublimation proceeded rapidly even when the residual air pressure was well above the vapor pressure of ice. This apparent anomaly may be resolved by reference to Eq. 8, where the driving force for sublimation is taken as the difference in pressure of water vapor between the ice–vapor

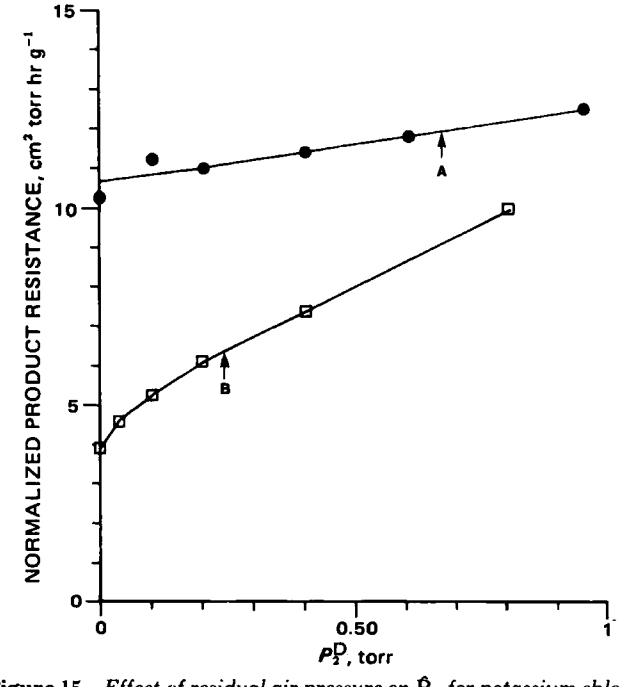

Figure 15—*Effect of residual air pressure on $\hat{R}_p$ for potassium chloride 5% v/v at −21.2°, l = 0.52 cm (●) and 5% v/v povidone at −31.0°, l = 0.70 cm (□). The arrows indicate the vapor pressure of ice (P_0) at −21.2° (A) and −31.0° (B).*

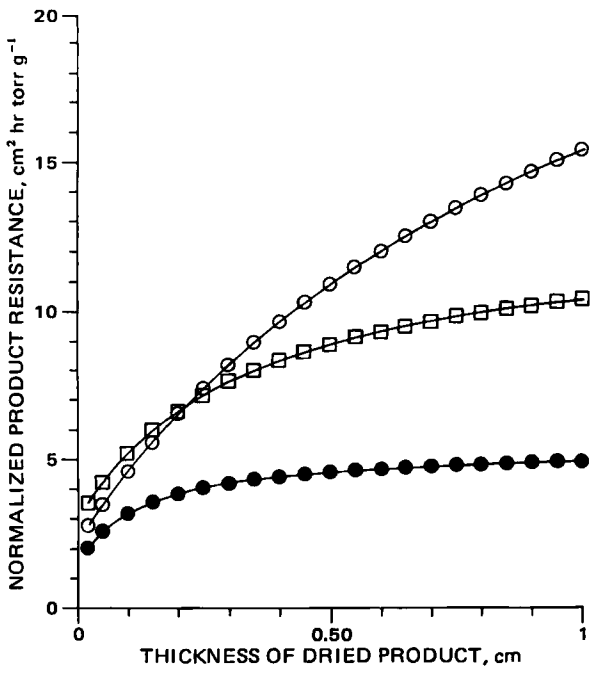

Figure 16—*Effect of temperature on* $\hat{R}_p$ *for potassium chloride 5% v/v,* $P_1^D = 0$. *Key: (●) −13.9°; (□) −20.9°; (○) −29.8°.*

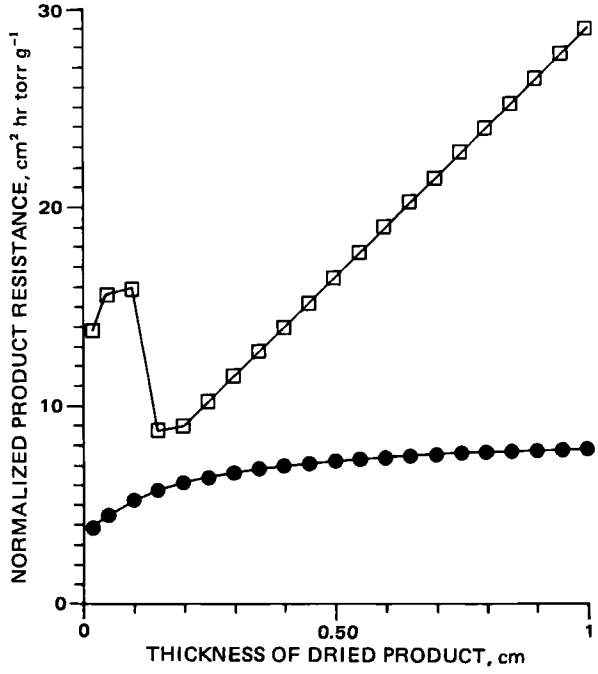

Figure 17—*Effect of temperature on* $\hat{R}_p$ *for System I,* $P_1^D = 0$. *Key: (●) −14.0°; (□) −21.2°.*

interface (P_0) and the region above the dried product (P_1^D). With the microbalance apparatus, P_1^D is essentially zero even when the chamber pressure is well above the vapor pressure of ice. However, in an apparatus designed for vial freeze-drying, an increase in chamber pressure by means of a controlled air leak increases the value of P_1^D. Indeed, as a first approximation, P_1^D is equal to the chamber pressure. If the shelf temperature is adjusted to maintain constant product temperature, P_0 is constant, and the driving force for sublimation decreases sharply as the chamber pressure approaches P_0, thereby sharply decreasing the sublimation rate.

Effect of Temperature—The effect of temperature (Figs. 16–18) on $\hat{R}_p$ is quite dramatic for potassium chloride and System I, but is barely significant for povidone (between −26 and −31°). An increase in temperature resulted in a transition from a type III (potassium chloride) or a type II (System I) curve to a type IV curve with a significant reduction in $(\hat{R}_p)$ (Fig. 19).

It might be postulated that the observed temperature effect is really a pressure effect. That is, the higher temperature produces a higher mean pressure in the porous medium which, in turn, changes the gas flow mechanism from a free molecular (Knudsen) flow to a viscous flow mechanism. For viscous flow, the dried product resistance is inversely proportional to the mean pressure in the dried product (11, 12), which is one-half the vapor pressure of ice for the data in Figs. 16–18. Thus, if the mean pressure were high enough to result in viscous flow of water vapor, an increase in temperature would decrease the dried product resistance. However, based on the usual theories for flow of rarified gases in channels (11, 12), the mean pressure was far too low for viscous flow of water vapor in the dried product.

For the usual capillary-tube model describing gas flow in a porous system (11, 12, 30), the normalized product resistance is given by:

$$\hat{R}_p = \hat{R}_k[1 - (1 - 35\pi/128)X/(1 + X) + (3\pi/128)X^2/(1 + X)]^{-1} \quad \text{(Eq. 15)}$$

where X is the ratio of the capillary pore diameter (D) to the mean free path (λ): $X = D/\lambda$. The low pressure limit for $\hat{R}_p$ is the Knudsen flow resistance ($\hat{R}_k$) which, in CGS units of dynes sec g^{-1}, is given by:

$$\hat{R}_k = l\frac{\tau^2}{\epsilon}\frac{3}{2}\sqrt{\frac{\pi RT}{2M_1}}\frac{(f)}{(2-f)}\frac{1}{D} \quad \text{(Eq. 16)}$$

where τ is the tortuosity (or ratio of the actual length of a capillary tube to the thickness of the dried product) and f denotes a momentum accommodation coefficient representing the fraction of gas molecule–tube collisions which result in diffuse reflectance upon collision (*i.e.*, for diffuse reflectance the velocity of a molecule after collision is independent of its incident velocity). Normally, f is assumed to be unity.

Since the mean free path is inversely proportional to pressure, X approaches zero at low pressure and $\hat{R}_p \to \hat{R}_k$. At high pressure, $X \gg 1$ and transport of water vapor is by a viscous flow mechanism yielding $\hat{R}_p = \hat{R}_k(128/3\pi)/X$. For a freeze-drying experiment where the mean pressure in the dried product is one-half of the vapor pressure of ice, numerical evaluation yields $X = P_0D$ (μm)/146. Thus, the condition $X \gg 1$ implies $D \gg 100$ μm for the highest pressure studied in this research. However, the pore diameters determined either from the sample surface area[23] (30) or microscopic examination (Fig. 6) are $\ll 100$ μm, indicating $X \ll 1$. Thus, the vapor flow mechanism in freeze-drying closely approximates Knudsen flow, not viscous flow.

The pore diameter for freeze-dried potassium chloride evaluated from the surface area is ~10 μm, while the microscopic data (Fig. 6) indicate that the larger pores or channels have a diameter of ~30 μm. Assuming that f is independent of temperature and vapor pressure, and taking D = 30 μm, the calculated change in $\hat{R}_p$ on increasing the temperature from −30 to −14° is an increase of 5%, obviously not consistent with the data which show a decrease in resistance of ~60%.

If the momentum accommodation coefficient (f) were assumed to decrease as the freeze-drying temperature increases, the data could be reconciled with Eqs. 15 and 16. Accommodation coefficients are extremely sensitive to the nature of the surface and, particularly for very clean solid surfaces, may be much less than unity (12, 21, 31). However, as surface impurities are introduced or the vapor is adsorbed on the surface, accommodation coefficients generally increase, and at a surface coverage of one or more monolayers, diffuse scattering (*i.e.*, $f = 1$) is observed (31). This result is consistent with the observation that the energy accommodation coefficient is unity for liquids and their own vapors (31) and the conclusion that under conditions where the energy accommodation coefficient is unity, the momentum accommodation coefficient is also unity (32). Thus, if the surface coverage would decrease below monolayer coverage as the freeze-drying temperature increased, there would be justification for assuming the temperature dependence of $\hat{R}_p$ is due to a decrease in f.

As the temperature increases at constant water activity, the surface coverage will decrease slightly (33), at least in the submonolayer region. However, in the freeze-drying system, an increase in temperature also increases the thermodynamic activity of water, which increases the surface coverage. The net effect of increasing the temperature will depend on the nature of the adsorption isotherm. Extrapolation of adsorption data for water–alkali halide systems (34–36) to the temperature range of interest in freeze-drying indicates that the mean surface coverage in the dried product at −30° is considerably in excess of monolayer, and the

[23] The specific surface areas for vial freeze-dried samples, determined by BET (Brunauer-Emmett-Teller) treatment of gas adsorption, are: potassium chloride (4 m^2/g), povidone (0.7 m^2/g), and System I (3 m^2/g).

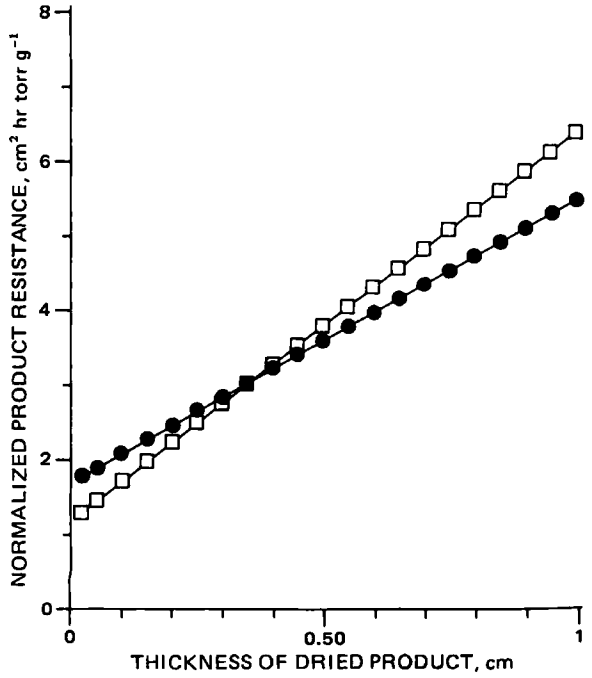

Figure 18—*Effect of temperature on* $\hat{R}_p$ *for 5% v/v povidone,* $P_1^p = 0$. *Key: (●) −26.0; (□) −31.2°.*

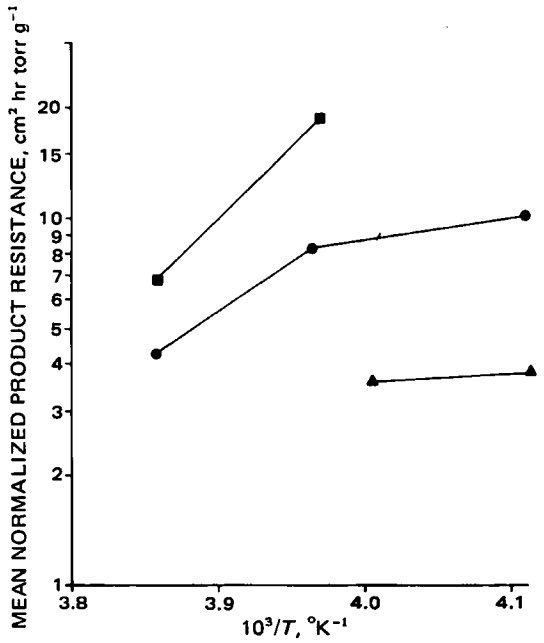

Figure 19—*Mean normalized product resistance* ($\langle \hat{R}_p \rangle$) *versus reciprocal absolute temperature. Key: (▲) povidone, 5% v/v; (●) potassium chloride 5% v/v; (■) System I.*

surface coverage increases with increasing temperature. Thus, the mean momentum accommodation coefficient should be close to unity at all temperatures; if there is a small change in f with increasing temperature, this change should be an increase toward a limiting value of unity. Thus, the observed decrease in resistance as the freeze-drying temperature increases cannot be attributed to changes in f. Rather it appears that there exists some flow mechanism other than that described by Eq. 16.

Equation 16 describes only the flow of water vapor in the open channels of the porous system. However, experimental and theoretical studies of the flow of condensable gases in porous media indicate that surface flow of the adsorbed gas can be the dominant flow mechanism when the mass of the adsorbed phase in the sample greatly exceeds the mass of the vapor phase (30, 37–39). Since the mass of the adsorbed phase is proportional to the product of the specific surface area (S) and the fraction of surface coverage (θ), surface flow may be important even below monolayer coverage (*i.e.*, $\theta < 1$) provided the specific surface area is large. Alternately, surface flow may be important with samples of moderate surface area provided the pressure is high enough to result in multilayer coverage (*i.e.*, $\theta > 1$). In the submonolayer case, surface flow proceeds by a diffusion mechanism involving activated translational motion from an occupied adsorption site to an unoccupied site. In the multilayer case, particularly when $\theta \gg 1$, surface flow is more properly described as hydrodynamic flow of the adsorbed gas analogous to either flow of a thin liquid film along a surface (large pores) or capillary flow of a liquid (micropores).

We therefore postulate that, at least at high temperature where surface coverage is high, mass transfer in freeze-drying may be dominated by hydrodynamic surface flow of the adsorbed water. As the freeze-drying temperature increases, the surface coverage (θ) and the fluidity of the adsorbed phase increase, both effects increasing the rate of surface flow. Adsorption data (34, 40) for potassium chloride indicate that θ increased very rapidly as the thermodynamic activity of water approached the water activity of the saturated solution, and the adsorbed film reached a thickness of 0.1–1 μm before the solid dissolved. Similarly one would expect that, as the temperature of a freeze-drying system approaches the eutectic temperature (or collapse temperature for an amorphous solute), θ would increase rapidly. Indeed, microscopic observations of a potassium chloride–water system freeze-drying near the eutectic temperature (13) of −11° appear consistent with an adsorbed film of liquid ~1 μm in thickness near −13° which decreased sharply in thickness as the temperature decreased. Since the evidence suggests that θ increases dramatically as the eutectic temperature is approached, one might also expect the ratio of surface flow–gas flow to increase as the temperature increases, resulting in surface flow being dominant near the eutectic (or collapse) temperature where θ is very large. Thus, we propose that the observed decrease in dried product resistance resulting from an increase in temperature is a consequence of the emergence of surface flow as an additional flow mechanism for transport of water.

Comparison of Microbalance and Vial Results—The question of how closely a microsample freeze-drying in a capillary tube represents a macrosample freeze-drying in a vial remains. In principle, since the diameter of the capillary tube is much greater than the pore diameter of the dried product, the normalized resistance should be independent of the sample geometry. However, differences in pore structure caused by differences in thermal history are potentially quite important. Moreover, the effect of a nonzero partial pressure of water vapor above the surface of the dried product (0.1 torr for vial studies *versus* 0.00 torr for microbalance studies) may be significant, at least for an amorphous product where the resistance is determined partially by permeability and cracking of the amorphous skin covering the surface.

Since the thermal history of an annealed microbalance sample more closely resembles the thermal history of a vial-frozen sample, one expects better agreement of the vial data with the annealed microbalance samples than with the quick-frozen microbalance samples. Indeed, for potassium chloride the agreement between vial and annealed microbalance results is nearly quantitative (Table III), whereas the quick-frozen microbalance resistance data are higher by nearly a factor of 2. The data for System I (Table III) demonstrate that the effect of temperature is qualitatively the same for both vial- and quick-frozen microbalance results. In both cases, the resistance increased linearly with l for the −21° data, but when the temperature was increased to ~ −15°, the resistance became independent of l over the range of l values studied and the value of $\langle \hat{R}_p \rangle$ decreased. In the case of povidone, the vial resistance data are in much better agreement with the *quick-frozen* microbalance data. This observation may suggest that annealing is a poor approximation for a slow-freeze when the product changes its freeze-drying mechanism on annealing, as is the case with povidone (Fig. 6). In any case, it may be concluded that agreement between vial and microbalance data is at least qualitative and may be quantitative for some materials if the thermal histories of the samples are similar.

CONCLUSIONS

The effect of the potential process variables on the resistance of the dried product layer have been studied by direct determination of sublimation rate under isothermal conditions using a microbalance technique. The results have at least qualitative validity for vial freeze-drying. Contrary to popular theoretical models, the resistance of the dried product layer is not directly proportional to its thickness (a result attributed to heterogeneity in solute structure) and is not independent of temperature. Current theoretical models assume mass transfer is exclusively *via* the gas phase. This study suggests that, at least at higher

temperatures, hydrodynamic surface flow of adsorbed water is an important flow mechanism which may account for the observed temperature dependence of the dried product resistance.

APPENDIX I: HEAT TRANSFER THEORY AND TEMPERATURE MEASUREMENTS

Although the sublimation cell is designed to maximize heat transfer, numerical estimates suggest that, at least for the high sublimation rates expected for pure water, the temperature difference between thermostat and the subliming ice could be significant. In this section, a theoretical model is developed which, on experimental evaluation of heat transfer parameters, allows the ice temperature to be determined from measurement of probe (or thermostat) temperature, sublimation rate, and residual air pressure in the chamber. The heat transfer coefficients were evaluated with a series of sublimation experiments where the sample temperature was measured by a thermocouple (denoted J) embedded in the sample 1 mm from the bottom of the capillary tube.

Assuming steady state:

$$\dot{m}\Delta\overline{H}_s = \dot{Q}_s = \dot{q}_{bc} + \dot{q}_{pc} + \dot{q}_{aJ} + \dot{q}_{ac} \qquad \text{(Eq. A17)}$$

where $\dot{m}$ is the sublimation rate (g/sec), $\Delta\overline{H}_s$ is the heat of sublimation (cal/g), $\dot{Q}_s$ is the rate of heat removal by sublimation, $\dot{q}_{bc}$ is the heat transfer rate from thermostat (bath) to the sublimation cell by radiation and conduction, $\dot{q}_{pc}$ is the heat transfer rate from the probe to the cell by radiation and conduction, $\dot{q}_{aJ}$ is the heat transfer rate from ambient to the J thermocouple junction in the sample through the 30-gauge (0.23-mm diameter) thermocouple wires, and $\dot{q}_{ac}$ is the heat conducted from the balance at ambient temperature to the cell *via* radiation and conduction through the hang-down wire. Numerical estimates indicate $\dot{q}_{bc} \gg \dot{q}_{pc}$. Since heat transferred to the cell is then transferred to the subliming ice (sample), the rate of heat transfer from cell to sample ($\dot{q}_{cs}$) is:

$$\dot{q}_{cs} = \dot{q}_{bc} + \dot{q}_{pc} + \dot{q}_{ac} \qquad \text{(Eq. A18)}$$

The heat transfer rates, $\dot{q}_{ij}$ (i = a, b, c, p; j = c, s, J) are assumed to be of the form:

$$\dot{q}_{ij} = k_{ij}(T_i - T_j) \qquad \text{(Eq. A19)}$$

where k_{ij} are heat transfer parameters and T_i and T_j are the absolute temperatures of apparatus components i and j, respectively. While Eq. A19 is rigorous for heat transfer *via* conduction, the form of Eq. A19 is only an approximation for heat transferred *via* radiation[24].

The probe thermocouple wire makes thermal contact at three points: with the surroundings at ambient temperature (T_a), with the bath at temperature T_b, and with the cell at temperature T_c. The thermal resistance of the wire between the ambient contact and the bath contact is denoted R_{w1}, the thermal resistance of the bath–wire contact (through the apiezon wax) is denoted R_{wb}, and the thermal resistance of the wire from the bath–wire contact to the probe junction is denoted R_{w2}. With these definitions, analysis of the steady-state heat flow in the probe wire yields:

$$\dot{q}_{pc} = k_{pc}(T_p - T_c) = k_{ap}(T_a - T_p) + k_{bp}(T_b - T_p) \qquad \text{(Eq. A20)}$$

where T_p is the probe temperature and k_{ap} and k_{bp} are composite heat transfer coefficients given by:

$$k_{ap} = \frac{R_{wb}}{R_{wb}(R_{w1} + R_{w2}) + R_{w1}R_{w2}} \qquad \text{(Eq. A21)}$$

[24] For radiative heat transfer between two bodies (22):

$$\dot{q}_{ij} = a_{ij}(T_i^4 - T_j^4)$$

where T_i and T_j are the absolute temperatures of bodies i and j, respectively, and a_{ij} depends on system geometry and emissivities of the bodies. When the temperature difference ($T_i - T_j$) is significantly less than the mean temperature ($\overline{T}_{ij}$):

$$\dot{q}_{ij} = 4\,\overline{T}_{ij}^3 a_{ij}(T_i - T_j) = k_{ij}(T_i - T_j)$$

which is of the same form as Eq. A19. However, the k_{ij} parameter for radiative heat transfer is temperature dependent, whereas the corresponding parameter describing conductivity is essentially independent of temperature. As a first approximation, valid for modest temperature ranges, the temperature dependence of k_{ij} for radiative heat transfer can be ignored. Also, for purposes of numerical estimates, the approximation, $a_{ij} = e\sigma A_{ij}$, will be used, where e is the emissivity (1 for the bodies of interest in this research), A_{ij} is the area common to both bodies, and σ is the Stefan-Boltzmann constant.

Table III—Comparison of Microbalance and Vial Resistance Data

l, cm	Normalized Product Resistance ($\hat{R}_p$), cm² hr torr g⁻¹: Vial[a]	Microbalance, Annealed	Microbalance, Quick-Frozen
	5% Potassium Chloride, −21°		
0.27	3.8 ± 0.5[b]	3.0 ± 0.1[b]	7.4 ± 0.5[b]
0.41	4.9 ± 0.6	3.8 ± 0.1	8.4 ± 0.6
0.53	4.9 ± 0.7	4.5 ± 0.2	9.0 ± 0.6
0.70	5.4 ± 0.6	5.4 ± 0.2	9.6 ± 0.7
	5% Povidone, −26°		
0.31	2.4 ± 0.8	2.10 ± 0.05	2.9 ± 0.2
0.48	3.8 ± 0.2	2.65 ± 0.06	3.5 ± 0.3
0.58	4.1 ± 0.1	2.94 ± 0.07	3.9 ± 0.3
0.71	5.0 ± 1.0	3.19 ± 0.08	4.4 ± 0.4
0.92	5.5 ± 0.6	3.79 ± 0.09	5.2 ± 0.4
	System I[c], −21°		
0.17	4.8 ± 0.5		8.5 ± 0.1
0.28	6.0 ± 0.5		10.9 ± 0.1
0.38	7.0 ± 0.4		13.4 ± 0.1
0.48	8.0 ± 0.7		15.9 ± 0.1
	System I[c], −14° (Microbalance), −15° (Vial)		
0.30	6.5 ± 1.8		6.6 ± 0.5
0.48	6.1 ± 1.7		7.1 ± 0.5
0.74	5.8 ± 1.0		7.5 ± 0.6
1.03	6.0 ± 0.8		7.7 ± 0.6

[a] The resistance data represent the mean of four replicate experiments for potassium chloride, two replicate experiments for povidone, and two replicate experiments for System I. [b] Uncertainties are estimated standard errors as calculated from reproducibility of replicate experiments. [c] The microbalance samples are amorphous but the vial samples contain some poorly crystallized mannitol (X-ray and microscopic observations).

and

$$k_{bp} = \frac{R_{w1}}{R_{wb}(R_{w1} + R_{w2}) + R_{w1}R_{w2}} \qquad \text{(Eq. A22)}$$

With perfect thermal contact of the probe wire with the bath ($R_{wb} = 0$), $k_{bp} = R_{w2}^{-1}$, and $k_{ap} = 0$.

Combination of Eqs. A17–A20 and use of the approximations[25] $k_{pc}/k_{bc} \ll 1$, $k_{ac}/k_{bc} \ll 1$, $(T_a - T_i)/(T_a - T_s) = 1$ (i = p, J), yields:

$$T_p - T_s = (1 + r_p\alpha k_{cs}^{-1})(1 + r_p)^{-1}\alpha^{-1}\Delta\overline{H}_s\dot{m} + (1 + r_p)^{-1}[k_{ap}/k_{bp} - k_{aJ}\alpha^{-1}(1 + r_p\alpha k_{cs}^{-1}) - k_{ac}/k_{bc}](T_a - T_s) \qquad \text{(Eq. A23)}$$

$$T_b - T_p = r_p(1 + r_p)^{-1}k_{bc}^{-1}\Delta\overline{H}_s\dot{m} - (1 + r_p)^{-1}(k_{ap}/k_{bp} + k_{aJ}r_pk_{bc}^{-1} + r_pk_{ac}/k_{bc})(T_a - T_s) \qquad \text{(Eq. A24)}$$

and

$$T_b - T_s = \alpha^{-1}\Delta\overline{H}_s\dot{m} - (\alpha^{-1}k_{aJ} + k_{ac}/k_{bc})(T_a - T_s) \qquad \text{(Eq. A25)}$$

with α and r_p defined by:

$$\alpha = k_{bc}k_{cs}(k_{bc} + k_{cs})^{-1} \qquad \text{(Eq. A26)}$$

and

$$r_p = k_{pc}/k_{bp} \qquad \text{(Eq. A27)}$$

The temperature of the subliming ice is denoted T_s.

Since both the bath–cell and probe–cell heat transfer coefficients, k_{bc} and k_{pc}, respectively, include contributions from vapor phase heat conduction, both coefficients are pressure dependent. Using the Smoluchowski theory (12) to relate the thermal conductivity of a gas to pressure, the heat transfer coefficients (k_{ic}, i = p,b) are of the form:

$$k_{ic} = k_{ic}^0\left[1 + \frac{(\bar{a}\Lambda_0/k_r)P}{1 + \bar{a}(\Lambda_0/\lambda)d_iP}\right] \qquad \text{(Eq. A28)}$$

where

$$\bar{a} = \frac{a_c}{2 - a_c}\sqrt{\frac{273.2}{T}} \qquad \text{(Eq. A29)}$$

The energy accommodation coefficient (a_c) is a numerical constant near

[25] As a first approximation, the ratio k_{pc}/k_{bc} is equal to the ratio of the probe area–cell area, which is ~0.06.

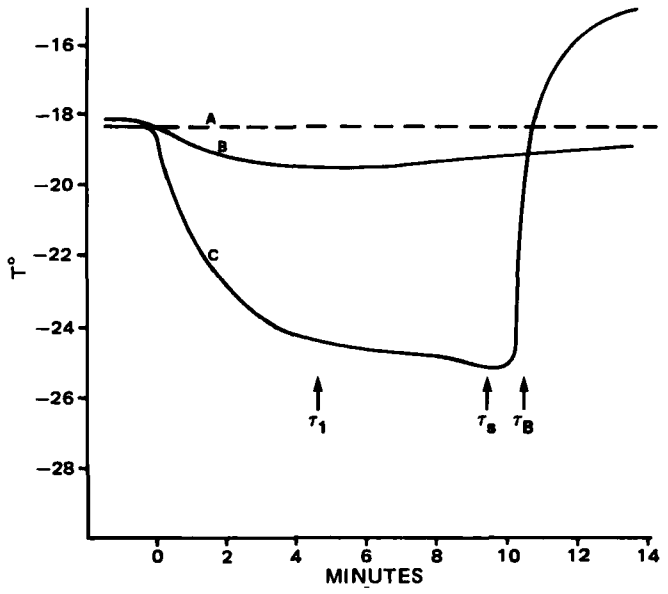

Figure 20—*Temperature* versus *time curve for a calibration experiment at zero pressure using a 10-mg sample of pure water. Key for lines: (A) thermostat; (B) probe; (C) J thermocouple.*

unity (3); k_{ic}^0 represents the radiative heat transfer coefficient; k_r is defined by $k_{ic}^0 = A_i k_r$, where A_i is the area of the probe or cell; Λ_0 is the free-molecule heat conductivity of the gas at 0° (12); λ is the heat conductivity of the gas at ambient pressure (~1 atm); d_i is the separation distance of the hot and cold surfaces, where $d_p = 0.3$ cm and $d_c = 0.6$ cm; P and T are the pressure and absolute temperature, respectively[26].

Preliminary calculations indicate that, as a first approximation, the term $(1 + r_p \alpha k_{cs}^{-1})(1 + r_p)^{-1}$ is essentially independent of pressure. Thus, the pressure dependence in the coefficients of $\dot{m}$ in both Eqs. A23 and A25 is due to the pressure dependence of α, which (from Eqs. A26 and A28) may be written in the form:

$$\alpha^{-1} = (\alpha^0)^{-1} \frac{[1 + (\Lambda_0/\lambda)(d_c + (\lambda/k_r)(1 + k_{cs}/k_{bc}^0)^{-1}P]}{[1 + (\Lambda_0/\lambda)(d_c + \lambda/k_r)P]} \quad \text{(Eq. A30)}$$

where the approximation $\bar{a} = 1$ has been used and the superscript zero on a parameter represents the value of that parameter at zero pressure.

When the sample temperature is not measured directly by a thermocouple embedded in the sample (*i.e.*, as in a normal sublimation experiment), $k_{aJ} = 0$ by definition. A theoretical estimate indicates that k_{ac} is $< 1 \times 10^{-5}$. With this estimate and the experimental value found for k_{bc}, the approximation $k_{ac} = 0$ results in a temperature error of <0.2°. Thus, with $k_{ac} = 0$, combination of Eqs. A23 and A24 gives:

$$T_s = T_p - (1 + r_p^0 \alpha^0 k_{cs}^{-1})(1 + r_p^0)^{-1}\alpha^{-1}\Lambda \bar{H}_s \dot{m} - (1 + r_p)^{-1}(k_{ap}/k_{bp})(T_a - T_p) \quad \text{(Eq. A31)}$$

The parameter k_{cs} in Eq. A31 now refers to the value of the cell–sample heat transfer coefficient in the absence of the J thermocouple wire.

In a temperature calibration experiment the sublimation cell is supported by copper–constantan thermocouple wires (0.23-mm diameter) where the measuring junction (J) is located ~1 mm from the bottom of the capillary tube. This configuration allows the sample temperature to be measured but also prevents the sample mass from being determined. After equilibration of the sample (10.0 mg of pure water) with the thermostat, the chamber was evacuated to the desired pressure and sublimation started. Thermostat, probe, and J thermocouple (T_J) temperatures were monitored as a function of time. When the pressure decreases below ~1 mm and sublimation started (time zero), T_J sharply decreased (Fig. 20) until a steady state was reached at approximately time τ_1. The T_J reading abruptly increased at time τ_B when the ice–vapor interface moved below the bottom of the J thermocouple and thermal contact was broken. When the sublimation rate was high, T_J passed through a minimum at time τ_s, where $\tau_s = 0.9\,\tau_B$. Interpreting τ_s as the time when the ice–vapor interface just covers the measuring junction J, $T_J(\tau_s) = T_s$, where T_s is the temperature of the subliming ice.

In a calibration experiment, the sublimation rate in mg/min at time $\tau_i (i = 1,s)$ is calculated from $\dot{m}_i = (8.8/\tau_B)f_i$, where 8.8 is the difference between the total sample mass of 10.0 mg and the mass remaining at τ_B, the latter calculated assuming the J thermocouple is exactly 1 mm from the bottom of the capillary tube. The factor f_i is the ratio of the sublimation rate at τ_i to the average rate over the time interval $0 \le t \le \tau_B$. This factor, which is near unity, is determined from sublimation experiments where mass is monitored (*i.e.*, no J wire).

A total of 16 calibration experiments were conducted over the bath temperature and chamber pressure ranges $-39° < T_b < -15°$ and $0 < P < 0.6$ mm, respectively, generating the data set (T_b, T_p, T_s, τ_1, τ_s, τ_B, P) for each experiment. These data were used to evaluate the heat transfer parameters appearing in Eqs. A23–A27 *via* regression analysis.

The parameters k_{cs} and k_{aJ} were evaluated by an iterative procedure. First k_{cs} was evaluated from the time dependence of T_J and a preliminary estimate of k_{aJ}, using only data where the sublimation rate was high (Appendix II). Next, k_{bc} and k_{aJ} were evaluated by regression analysis using Eqs. A25 and A30[26]. The resulting value of k_{aJ} was then used to obtain a second approximation of k_{cs}, *etc.* Convergence was obtained after two iterations. Finally, the ratios r_p^0 and k_{ap}/k_{bp} were evaluated from the data by regression analysis using Eqs. A23, A27, and A28. The resulting parameters with their corresponding standard errors are listed in Table IV. Agreement between data and the theoretical model is within the anticipated experimental error. Due to the difficulty in placing the J thermocouple always at the same level in the sample, measurement of the average sublimation rate is subject to sizable random error.

With the evaluated parameters (Table IV), Eq. A31 becomes Eq. 1 (text):

$$T_s = T_p - K_p \frac{(1 + 68.1P)}{(1 + 87.0P)}\dot{m} - K_a(T_a - T_p)$$

where K_p is 10.2 and K_a is 0.010 and 0.006 at $P = 0$ and $P = 0.05$–1.0 torr, respectively. The sublimation rate $\dot{m}$ is in mg/min. In principle, K_a is a smooth function of pressure through r_p. However, the step function representation given above is a simpler yet adequate representation of the data. With the improved probe design described earlier[12], $k_{ap} = 0$ and $r_p \gg 1$ experimentally ($r_p \simeq 14$ in theory). In this case, $K_a = 0$ and $K_p = 7.1$.

Table IV—Values of Heat Transfer Parameters Evaluated from Temperature Calibration Data [a]

Parameter	Value
k_{cs}	$1.55 \times 10^{-3} \pm 0.07 \times 10^{-3}$ cal sec^{-1} °K^{-1}
k_{bc}^0	$2.2 \times 10^{-3} \pm 0.04 \times 10^{-3}$ cal sec^{-1} °K^{-1}
r_p^0	0.61 ± 0.28
k_{ap}/k_{bp}	0.016 ± 0.012

[a] Parameters refer to experiment without a thermocouple embedded in the sample.

APPENDIX II: THEORY OF CELL–SAMPLE HEAT TRANSFER COEFFICIENT

Heat is transferred from the aluminum cell to the sample through the wall and bottom of the glass capillary tube. Since the area available for heat transfer decreases as the length of the ice column decreases during sublimation, the parameter characterizing this heat transfer (k_{cs}) may not be constant. Moreover, in a calibration experiment, the presence of the thermocouple wire in the capillary tube changes the thermal conductivity of the system and, consequently, k_{cs}. The purpose of this section is to present a semiquantitative theoretical argument which indicates that k_{cs} is indeed a constant during sublimation of all but the last traces of ice, and to provide a theoretical basis for the evaluation of k_{cs} under conditions of a sublimation rate experiment (no thermocouple in the sample) using calibration data obtained where a thermocouple is in the sample. The length of the ice column at time zero is denoted L.

A simple steady-state model for heat transfer in the cell–sample system is illustrated by Fig. 21. Heat conducted from ambient to the sample *via* the J thermocouple ($\dot{q}_{aJ}$), assumed to dissipate at the ice–vapor interface, is not shown. The temperature in the aluminum cell (T_c) is assumed independent of the distance variable, x. The ice at the ice–vapor interface ($x = l$) is at a mean temperature T_s, while the average temperature of the

[26] The parameter k_r is calculated from theory (22) with unit emissivity for a temperature of 253°K. For air, literature data (12) for Λ_0 and λ then yield: $\Lambda_0/\lambda = 68.9$ cm^{-1} torr^{-1}, $\lambda/k_r = 0.662$ cm. The distance parameters d_c and d_p are approximately measured as 0.6 and 0.3 cm, respectively. The calculations are not sensitive to small variations in d_c and d_p. The enthalpy of sublimation $\Delta \bar{H}_s$ is 660 cal/g (41).

sample in any volume element of thickness (dx) is T, where T is a function of x.

In any volume element bounded by planes at $x - dx/2$ and $x + dx/2$, the heat flow out of the volume element through the plane at $x - dx/2$ ($\delta\dot{q}_3$) is the sum of the radial heat flow through the container wall ($\delta\dot{q}_1$) and the vertical heat flow into the volume element at the plane $x + dx/2$ ($\delta\dot{q}_2$). The radial heat flow, $\delta\dot{q}_1$, is proportional to the length of the volume element, dx, and the temperature difference $T_c - T$:

$$\delta\dot{q}_1 = k_w dx(T_c - T) \qquad \text{(Eq. A32)}$$

where k_w is a heat transfer coefficient for heat flow through the apiezon wax and the capillary tube wall, and reflects the heat-flow rate for a tube of unit length with a temperature difference of 1° applied. The vertical heat transfer rate is of the form:

$$\delta\dot{q}_i = k_I \frac{(dT)}{(dx)_{x_i}}, \quad i = 2, 3 \qquad \text{(Eq. A33)}$$

where for $i = 2, x_i = x + dx/2$ and for $i = 3, x_i = x - dx/2$. The parameter k_I is the product of the cross-sectional area and the thermal conductivity of the material present in the capillary tube[27]. During a calibration experiment both ice and the J thermocouple wires contribute to k_I. From Eqs. A33 and A32 and the steady-state requirement $\delta\dot{q}_3 = \delta\dot{q}_1 + \delta\dot{q}_2$, we find:

$$\frac{d^2T}{dx^2} = -\frac{k_w}{k_I}(T_c - T) \qquad \text{(Eq. A34)}$$

With the transformation of variables:

$$y = T_c - T \qquad \text{(Eq. A35)}$$

and

$$z = (x - l)/(L - l) \qquad \text{(Eq. A36)}$$

Eq. A34 becomes:

$$\frac{d^2y}{dz^2} - a^2y = 0, \qquad \text{(Eq. A37)}$$

where:

$$a = (L - l)\sqrt{\frac{k_w}{k_I}} \qquad \text{(Eq. A38)}$$

One boundary condition follows from the requirement that the vertical heat flow at the ice–vapor interface ($z = 0$) is equal to the total heat flow from cell to sample ($\dot{q}_{cs}$):

$$\dot{q}_{cs} = -\frac{k_I}{(L - l)}\left(\frac{dy}{dz}\right), \quad z = 0 \qquad \text{(Eq. A39)}$$

where, denoting $\dot{Q}_s$ as the heat removed by sublimation, $\dot{q}_{cs} = \dot{Q}_s - \dot{q}_{aJ}$. This relationship assumes $\dot{q}_{aJ}$ is dissipated at the $z = 0$ surface. $\dot{Q}_s$ is the product of the sublimation rate and the heat of sublimation per gram: $\dot{Q}_s = \dot{m}\Delta\bar{H}_s$. The second boundary condition is obtained from the requirement that $\dot{q}_{cs}$ is given by the sum of the heat flow through the bottom ($\delta\dot{q}_B$) and the integral of $\delta\dot{q}_1$ over the length of the ice column, $0 \leq z \leq 1$. Since $\delta\dot{q}_B = k_B y(1)$, the boundary condition becomes:

$$\dot{q}_{cs} = k_w(L - l)\int_0^1 y(z)dz + k_B y(l), \qquad \text{(Eq. A40)}$$

[27] The parameter k_I is given by:

$$k_I = \pi r^2 \kappa_I$$

where r is the radius of the capillary tube (0.0648 cm) and κ_I is the thermal conductivity of the material within the capillary tube (ice and, in a calibration experiment, the J thermocouple wires of diameter 0.23 mm):

$$\kappa_I = \frac{1}{A_T}\sum_i A_i\kappa_i$$

where, A_T is the total tube cross-sectional area, while A_i and κ_i are the cross-sectional area and thermal conductivity for the ith material (i = ice, copper, constantan).

Based on handbook data for thermal conductivities, k_I (cal cm sec^{-1} °K^{-1}) is calculated as 6.9×10^{-5} for a normal sublimation experiment (without a thermocouple junction in the sample) and 5.0×10^{-4} for a calibration experiment. The parameters k_w and k_B may be estimated from the relationships:

$$k_w = 2\pi r(l_{wx}/\kappa_{wx} + lg/\kappa_g)^{-1},$$

$$k_B = \pi r^2(l_{wx}/\kappa_{wx} + lg/\kappa_g)^{-1}$$

where l_{wx} and κ_{wx} are the thickness and thermal conductivity of the wax, respectively, and l_g and κ_g are the corresponding parameters for the glass tube. By measurement, $l_{wx} = 10^{-2}$ cm, $l_g = 0.037$ cm. Assuming the apiezon wax has the same thermal conductivity as paraffin, $\kappa_{wx} = 6 \times 10^{-4}$ cal cm^{-1} sec^{-1} °K^{-1}. Since $\kappa_g = 2.6 \times 10^{-3}$ cal cm^{-1} sec^{-1} °K^{-1}, $k_w = 1.3 \times 10^{-2}$ cal cm^{-1} sec^{-1} °K^{-1} and $k_B = 4 \times 10^{-4}$ cal sec^{-1} °K^{-1}.

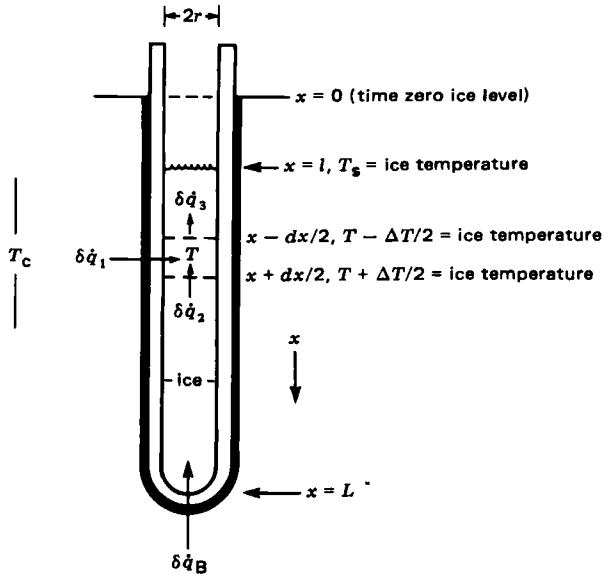

Figure 21—*Schematic of heat flow in the sublimation cell.*

with k_B representing the heat transfer coefficient through the bottom of the capillary tube. Solution of the differential equation (Eq. A37) subject to the boundary conditions (Eqs. A39 and A40) yields:

$$y(z) = b\dot{q}_{cs}\left\{e^{-az} + \frac{e^{-a}(1 - bk_B)\cosh(az)}{\cosh(a)[\tanh(a) + bk_B]}\right\} \qquad \text{(Eq. A41)}$$

where:

$$b^{-1} = \sqrt{k_w k_I} \qquad \text{(Eq. A42)}$$

The constant k_{cs}, defined by $\dot{q}_{cs} = k_{cs}(T_c - T_s)$ where $(T_c - T_s) = y(z = 0)$, is then:

$$k_{cs} = b^{-1}\frac{[\tanh(a) + bk_B]}{[1 + bk_B\tanh(a)]} \qquad \text{(Eq. A43)}$$

The parameter k_I (cal cm sec^{-1} °K^{-1}) is 6.9×10^{-5} with only ice in the capillary tube and is 5.0×10^{-4} in a calibration experiment where thermocouple wires are present[27]. Rough estimates[27] yield, $k_w = 1.3 \times 10^{-2}$ cal cm^{-1} sec^{-1} °K^{-1} and $k_B = 4 \times 10^{-4}$ cal sec^{-1} °K^{-1}. Therefore, in a sublimation rate experiment (no J wire) $\sqrt{k_w/k_I} = 14$ and for $L - l > 0.1$ cm (through ~90% of the sublimation experiment), $a > 1.4$ and Eqs. A41 and A43 simplify to give:

$$y(z) = b\dot{Q}_s e^{-az}, \quad L - l > 0.1 \text{ cm} \qquad \text{(Eq. A44)}$$

and

$$k_{cs} = \sqrt{k_w k_I}, \quad L - l > 0.1 \text{ cm} \qquad \text{(Eq. A45)}$$

As the last traces of ice are sublimed, $l \approx L$ and $k_{cs} = k_B$. Since the estimates indicate $k_B \ll \sqrt{k_w k_I}$, the theory suggests that as $l \to L$, the value of k_{cs} should decrease sharply causing a decrease in ice temperature and a corresponding decrease in the sublimation rate in those cases where the sublimation rate is high. This qualitative prediction is verified in experiments with pure water at high temperature (*i.e.*, −20°) where the sublimation rate is found to sharply decrease when $L - l$ is ~0.1 or less.

Equation A41 may be used to evaluate k_w from the time dependence of T_J determined in a calibration experiment. The resulting value of k_w may then be used with the calculated value of k_I to evaluate k_{cs} using Eq. A43. Denoting T_J as the temperature measured by the thermocouple junction in the sample at location x_J, $T_c - T_J = y(z_J)$, where z_J is given by Eq. A36 with $x = x_J = 0.72$ cm[28]. Equation A41 and the relationship $T_b - T_c = k_{bc}^{-1}\dot{q}_{cs}$ then results in:

$$\left(\frac{T_b - T_J}{\dot{q}_{cs}}\right) = k_{bc}^{-1} + b \cdot G(k_w, l) \qquad \text{(Eq. A46)}$$

where the function $G(k_w, l)$ denotes the terms enclosed in brackets on

[28] At time τ_s, the J thermocouple measures the surface temperature of the ice, the surface located at x_J. From the interpretation given earlier, x_J represents the value of x at the top of the thermocouple measuring junction. Since the junction head is ~0.5 mm in diameter and the bottom of the junction is at $x = 0.77$ cm, $x_J = 0.72$ cm. Since $l = x_J$ at time τ_s and $L = 0.87$ cm, $L - l = 0.15$ cm at τ_s.

the right-hand side of Eq. A41. As indicated, G depends on k_w and the position of the ice–vapor interface, which in turn depends on time. The time when the ice–vapor interface is at the same location as the thermocouple (*i.e.*, $az_J = 0$) is denoted τ_s. The time τ_1 represents a time large enough to establish steady-state heat flow but small enough so that the ice–vapor interface is still several millimeters above the thermocouple. With the above definitions for τ_s and τ_1:

$$\left(\frac{T_b - T_J}{\dot{q}_{cs}}\right)_{\tau_s} - \left(\frac{T_b - T_J}{\dot{q}_{cs}}\right)_{\tau_1} = H(k_w) \qquad \text{(Eq. A47)}$$

where for fixed τ_s and τ_1, H is a function of k_w only, given by:

$$H(k_w) = (k_w k_I)^{-1/2}\left\{\exp(-a_1 z_1) + \frac{\exp(-a_s)(1 - bk_B)}{\cosh(a_s)[\tanh(a_s) + bk_B]} - \frac{\exp(-a_1)(1 - bk_B)\cosh(a_1 z_1)}{\cosh(a_1)[\tanh(a_1) + bk_B]}\right\} \qquad \text{(Eq. A48)}$$

where a_s and a_1 are values of the parameter a (Eq. A38) at times τ_s and τ_1, respectively, and z_1 is the value of z_J (Eq. A36 with $x = x_J$) corresponding to time τ_1. Equation A48 is not sensitive to the precise choice of τ_1. For convenience, τ_1 is always taken as $\tau_1 = 0.4\,\tau_B$, where τ_B is the time for the ice–vapor interface to move below the bottom of the J thermocouple. Sublimation rate experiments (no J wire) indicate that with a sample of 10.0 mg of water ($L = 0.87$ cm), $L - l = 0.53$ cm at τ_1 (= $0.4\tau_B$). Thus, from Eq. A36, $z_1 = 0.72$[28]. The parameter k_B is related to k_w by $k_B = (r/2)k_w$[27] with r representing the radius of the capillary tube (0.0648 cm.). Since k_I may be calculated from theory[27], a_1, a_s, and k_B depend only on k_w and $H(k_w)$ is easily tabulated as a function of k_w.

With $\dot{q}_{cs} = \dot{Q}_s - k_{aJ}(T_a - T_J)$, and $\dot{Q}_s = \Delta\overline{H}_s\dot{m}$, values of $\dot{q}_{cs}$ at times τ_1 and τ_s are evaluated from the sublimation rates ($\dot{m}$) at these times and a value of k_{aJ} is estimated from the calibration data. Sublimation rates are evaluated from τ_B data as outlined in Appendix I. Using only data where the sublimation rate is high, the value of k_{cs} is relatively insensitive to the choice of k_{aJ}.

Thus, with T_b, T_J, and $\dot{q}_{cs}$ determined at τ_s and τ_1, $H(k_w)$ is determined from the data, which then determines an experimental value for k_w. The iterative procedure outlined in Appendix I determines both k_{aJ} and k_w, yielding the result $k_w = 0.035 \pm 0.003$. For a sublimation rate experiment (no J wire), $k_I = 6.9 \times 10^{-5}$ cal cm sec^{-1} °K^{-1} [27], which then gives (Eq. A45) $k_{cs} = 1.55 \times 10^{-3}$ cal sec^{-1} °K^{-1}. The value of k_w obtained is larger than the theoretically estimated value[27]. A strict interpretation of the theory would imply that the wax sealing the capillary tube in the aluminum cell offers essentially zero thermal resistance. However, the difference between the experimental and theoretical k_w values probably reflects, in large part, the theory's neglect of vertical heat transfer in the walls of the glass capillary tube. In any case, use of the experimental k_w should yield a reliable value of k_{cs} for experimental use.

REFERENCES

(1) B. J. Luyet, *Ann. N.Y. Acad. Sci.*, **125,** 502 (1965).

(2) A. P. MacKenzie, *Transplant. Proc.*, 8 (Suppl. 1), 181 (1976).

(3) A. P. MacKenzie, *Bull. Parenter. Drug Assoc.*, **20,** 101 (1966).

(4) M. J. Pikal, A. L. Lukes, and J. E. Lang, *J. Pharm. Sci.*, **66,** 1312 (1977).

(5) K. Ito, *Chem. Pharm. Bull.*, **18,** 1509 (1970).

(6) K. Ito, *Chem. Pharm. Bull.*, **18,** 1519 (1970).

(7) K. Ito, *Chem. Pharm. Bull.*, **19,** 1095 (1971).

(8) R. Patel and A. Hurwitz, *J. Pharm. Sci.*, **61,** 1806 (1972).

(9) S. L. Nail, *J. Parenter. Drug Assoc.*, **34,** 358 (1980).

(10) D. Saravacus, *Food Technol.*, **19,** 193 (1965).

(11) J. D. Mellor, "Fundamentals of Freeze-Drying," Academic, New York, N.Y., 1978.

(12) S. Dushman and J. M. Lafferty, "Scientific Foundations of Vacuum Technique," 2nd. ed., Wiley, New York, 1962.

(13) A. P. MacKenzie, *Ann. N.Y. Acad. Sci.*, **125,** 522 (1965).

(14) H. Seager, *Manuf. Chem. Aerosol News*, **Feb.,** 41 (1979).

(15) L. F. Ginette, R. P. Graham, and A. I. Morgan, Jr., *Trans. 5th. Natl. Vac. Symp.*, 268 (1958).

(16) G. D. Saravacos, *Food Technol.*, **19,** 193 (1965).

(17) T. Nei, H. Souzu, and N. Hanafusa, *Low Temp. Sci., Ser. B*, **21,** 71 (1963).

(18) J. L. Stephenson, *Bull. Math. Biophys.*, **15,** 411 (1953).

(19) A. P. MacKenzie and B. J. Luyet, *Biodynamica*, **9,** 193 (1964).

(20) J. Flink and F. Geyl-Hansen, *Rev. Sci. Instrum.*, **49,** 269 (1978).

(21) J. R. Partington, "An Advanced Treatise on Physical Chemistry," Vol. 1, Wiley, New York, N.Y., 1949.

(22) J. H. Perry, "Chemical Engineer's Handbook," 4th ed., McGraw-Hill, New York, N.Y., 1963.

(23) J. Amoignon, "Freeze-Drying and Advanced Food Technology," Academic, London, 1975, p. 445.

(24) "International Critical Tables," vol. 4, McGraw-Hill, New York, N.Y., 1978, p. 259.

(25) R. Toei, M. Okazaki, and M. Asaeda, *J. Chem. Eng.*, 8, 277 (1977).

(26) K. Tschudin, *Helv. Phys. Acta*, **19,** 91 (1946).

(27) J. G. Davy, Ph.D. Dissertation, Univ. of California, Berkeley, 1970.

(28) N. F. Ho and T. J. Roseman, *J. Pharm. Sci.*, **68,** 1170 (1979).

(29) B. Couriel, *Bull. Parenter. Drug Assoc.*, **31,** 227 (1977).

(30) R. M. Barrer, *Appl. Mater. Res.*, **2,** 129 (1963).

(31) F. O. Goodman and H. Y. Wachman, "Dynamics of Gas-Surface Scattering," Academic, New York, N.Y. 1976.

(32) E. A. Flood, R. H. Tomlinson, and A. E. Leger, *Can. J. Chem.*, **30,** 348 (1952).

(33) A. W. Adamson, "Physical Chemistry of Surfaces," Interscience, New York, N.Y., 1960.

(34) M. Kaiho, M. Chikazawa, and T. Kanazawa, *Nippon Kagaku Kaishi*, **1972,** 1386.

(35) H. Walter, *Z. Phys. Chem. (Frankfurt/Main)*, **75,** 287 (1971).

(36) T. Kanazawa, M. Chikazawa, M. Kaiho, and T. Fujimaki, *Nippon Kagaku Kaishi*, **1973,** 1669.

(37) J. R. Dacey, "Solid Surfaces and the Gas-Solid Interface," Advances in Chemistry Series, No. 33, American Chemical Society, Washington, D.C., 1961.

(38) J. R. Dacey, *Ind. Eng. Chem.*, **57,** 27 (1965).

(39) E. A. Flood, R. H. Tomlinson, and A. E. Leger, *Can. J. Chem.*, **30,** 389 (1952).

(40) O. Knacke and D. Neuschutz, *Z. Phys. Chem. (N.F.)* **71,** 247 (1970).

(41) G. Janesco, J. Pupezin, and W. A. Van Hook, *J. Phys. Chem.*, **74,** 2984 (1970).

Effects of Surfactants on the GI Absorption of β-Lactam Antibiotics in Rats

ETSUKO MIYAMOTO *, AKIRA TSUJI ‡ ˣ, and TSUKINAKA YAMANA §

Received January 13, 1982, from the **School of Pharmacy, Hokuriku University, Kanagawa-machi, Kanazawa 920-11, Japan*, and the ‡*Faculty of Pharmaceutical Sciences* and §*Hospital Pharmacy, Kanazawa University, Takara-machi, Kanazawa 920, Japan.* Accepted for publication June 4, 1982.

Abstract □ The effects of various nonionic and ionic surfactants and two bile salts (sodium cholate and sodium taurocholate) on the GI absorption of β-lactam antibiotics were investigated using the *in situ* rat GI perfusion technique. Addition of 10 m*M* polyoxyethylene-23-lauryl ether in the perfusion solution reduced the absorption of propicillin by the stomach and markedly increased the absorption of propicillin and cefazolin by the small intestine. Ester-type nonionic surfactants and bile salts exerted no significant influence on the intestinal absorption of these antibiotics.

Keyphrases □ Surfactants—effects on GI absorption of β-lactam antibiotics in rats □ Propicillin—effects of surfactants on GI absorption □ Cefazolin—effects of surfactants on GI absorption □ Absorption, GI—effects of surfactants, β-lactam antibiotics

Nonionic surfactants have often been employed in pharmaceutical preparations to formulate dispersed and solubilized systems, since they are less toxic to biological systems (1). It is known that drug–surfactant interactions modify the rate of intestinal absorption of drugs (2); some tend to enhance drug absorption and others tend to retard it.

GI absorption of nonabsorbed or poorly absorbed classes of β-lactam antibiotics can be promoted in rats and dogs by nonionic, anionic, and cationic surface-active agents. It was suggested that this promotion of antibiotic absorption was attributable to alteration of the membrane permeability of surfactants (3, 4). In previous studies (5, 6), nonionic and cationic surfactants were found to entrap penicillin molecules under pH conditions found in the stomach, resulting in remarkable stabilization and solubilization of penicillins. On the other hand, anionic surfactant micelles facilitated β-lactam cleavage. These results (3–6) indicated that acid-labile penicillins coated with relatively nontoxic nonionic surfactant micelles may increase the bioavailability after oral administration. The present study was undertaken to determine the effects of anionic, cationic, and nonionic surfactants, as well as bile salts on the GI absorption of β-lactam antibiotics using the *in situ* rat GI perfusion technique.

EXPERIMENTAL

Materials—Propicillin potassium[1] (993 μg/mg) and cefazolin sodium[2] (966 μg/mg) were used as received. Most surfactants employed were supplied by a commercial source[3]. Polyoxyethylene-23-lauryl ether (I), cetyltrimethylammonium bromide (II), and sodium lauryl sulfate (III) were the same as used in a previous study (6). Sodium taurocholate and sodium cholate were obtained commercially[4]. All other chemicals were of reagent grade and used without further purification.

***In Situ* GI Absorption Procedures**—Male albino rats of the Wistar strain, weighing ~200 g, were fasted overnight (20 hr) prior to the experiments, with water freely available. The rats were anesthetized 1 hr prior to surgery with urethan (1.3 g/kg ip). The procedures for rat surgery and absorption experiments using the GI recirculating method were those reported previously (7–9). The small intestine employed was a 30-cm length from the pylorus. The stomach or small intestine was washed with 50 ml of isotonic buffer solution of the desired pH, and then with 10 ml of the same buffer solution containing an appropriate concentration of surfactant. The drug solution was prepared using the buffer–surfactant solution maintained at 37° and perfused in a recirculating fashion with a pump at a rate of 10 ml/min for the stomach and 2 ml/min for the intestine. Unless otherwise stated, the antibiotic concentrations were 1 and 5 mg/ml for the stomach and intestinal experiments, respectively. The perfusion was maintained at the desired pH with a pH-stat[5] during the absorption experiments. The perfusion periods were 3 and 2 hr for the stomach and intestinal experiments, respectively.

At the end of the absorption experiments, the recirculating drug solution and the isotonic buffer solution perfused to wash the GI tract were collected into an appropriate volumetric flask, and the required amount of the same buffer solution was added to achieve the desired volume. To obtain the final sample, the solution was filtered through a 0.45-μm membrane filter[6]. The initial sample was prepared by dilution of un-

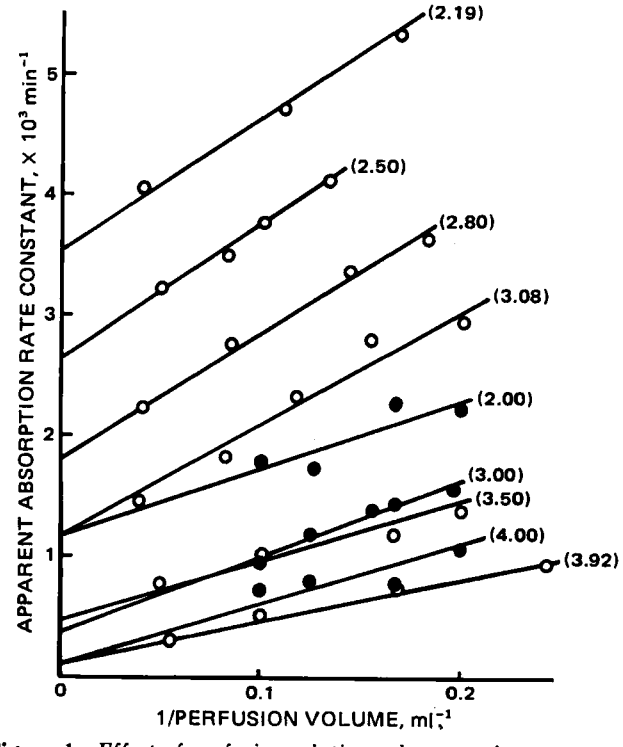

Figure 1—*Effect of perfusion solution volume on the apparent absorption rate constants (k_{app}) of propicillin from* in situ *rat stomach at various pHs (in parentheses) and 37°. The drug solution was perfused at a flow rate of 10 ml/min and the pH of the solution was maintained constant with a pH-stat. The points indicate experimental values: (●) in the presence of 10 mM I and (○) in the absence of I redrawn from Ref. 8.*

[1] Takeda Chemical Industries, Osaka, Japan.
[2] Fujisawa Pharmaceutical Co., Osaka, Japan.
[3] Nikko Chemicals Co., Tokyo, Japan.
[4] Wako Pure Chemical Industries, Osaka, Japan.
[5] pH-Stat titrator assembly consisting of a TTT2 titrator and ABU12b autoburette, Radiometer, Copenhagen, Denmark.
[6] Sartorius-membranfilter, GmbH, 34 Göttingen, West Germany.

0022-3549/83/0600-0651$01.00/0

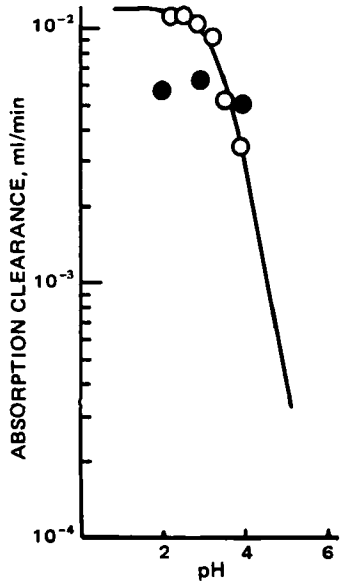

Figure 2—*Plots of the* in situ *rat stomach absorption clearance* CL_a *of propicillin* versus *the pH of the perfusion solution. The points indicate experimental values: (●) in the presence of 10 mM I and (○) in the absence of I redrawn from Ref. 8.*

perfused drug solution with isotonic buffer solution to the same volume.

The apparent first-order rate constants for the drug disappearance from the perfusate, k_{app}, were calculated as follows:

$$k_{app} = -\frac{1}{t}\ln\frac{C_t}{C_0} \qquad \text{(Eq. 1)}$$

where t represents the perfusion period and C_t and C_0 represent the drug concentrations in the final and initial samples, respectively.

Analytical Procedures—Propicillin and cefazolin in samples from the *in situ* absorption experiments were determined by reverse-phase high-performance liquid chromatography (HPLC) under the following conditions. The liquid chromatograph[7] was equipped with a UV detector[8] set at 254 nm. The stationary phase, made by chemically bonding a octadecylsilanol group to totally porous silica gel, was prepacked into a stainless steel column[9,10]. The mobile phases were 10 and 30% (v/v) acetonitrile–0.01 *M* ammonium acetate for cefazolin and propicillin, respectively. The instrument was operated at ambient temperature and at a flow rate of 1 ml/min. Samples were injected *via* a 100-μl loop injector[11] on flow. Peak heights were used for quantification.

During the *in situ* intestinal absorption experiments, 0.2-ml aliquots of blood were taken periodically from the jugular vein and assayed by the microbiological paper disk method employing *Salutina lutea*[12] as a test organism, after being hemolyzed with an equivalent volume of distilled water. The standard was established by employing pooled fresh blood from control rats.

The lower limit of sensitivity was 10 μg/ml for the HPLC assay and 1 μg/ml for the microbiological assay. The coefficients of variation ($SD \times 100$/mean) of the HPLC and microbiological assays throughout the analytical experiments were 3 and 5%, respectively, from many trials using standard solutions of each antibiotic.

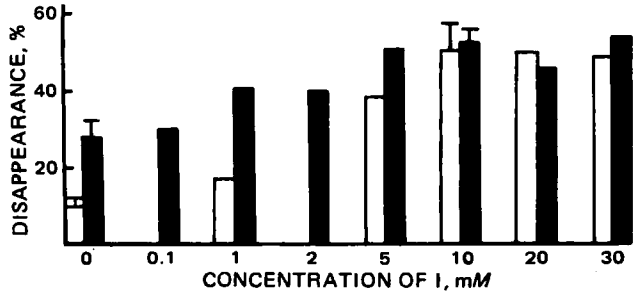

Figure 3—*Percentage disappearance of propicillin (■) and cefazolin (□) from the rat intestinal lumen as a function of the concentration of I. The perfusion solution was recirculated at a rate of 2 ml/min at pH 7.4, maintained constant with a pH-stat.*

[7] Model FLC-A700, Japan Spectroscopic Co., Ltd., Tokyo, Japan.
[8] Model UVIDEC-100, Japan Spectroscopic Co., Ltd., Tokyo, Japan.
[9] SC-01 (12.5 cm long × 4.6-mm i.d. column), Japan Spectroscopic Co., Ltd., Tokyo, Japan.
[10] μ-Bondapak C_{18} (30 cm long × 3.9-mm i.d. column), Waters Associates, Milford, Mass.
[11] Model LP1-350, Japan Spectroscopic Co., Ltd., Tokyo, Japan.

Table I—Percentage Disappearance of Cefazolin and Propicillin from *In Situ* Rat Small Intestine in the Presence of Various Surfactants and Bile Salts at pH 7.4 and 37°

Surfactant	HLB[a]	Concentration	Disappearance of Drugs, % (±*SD*)	n[b]
Cefazolin[c]				
None			9.7(1.8)[d]	3
Polyoxyethylene-10-oleyl ether	14.0	10 m*M*	52.8(12.1)	3
Polyoxyethylene-15-oleyl ether	16.0	10 m*M*	88.6	1
Polyoxyethylene-20-oleyl ether	17.0	10 m*M*	79.8	1
Polyoxyethylene-10-polyoxypropylene-4-cetyl ether	10.5	2% (w/v)	45.5(21.7)	3
Polyoxyethylene-20-polyoxypropylene-4-cetyl ether	16.5	2% (w/v)	65.4(11.7)	3
Polyoxyethylene-60-hydrogenated castor oil	14.0	1 m*M*	5.9	1
		5 m*M*	19.0(1.4)	3
		10 m*M*	14.4(3.3)	3
Polyoxyethylene-20-sorbitan monooleate	15.0	1% (w/v)	29.4	1
		2% (w/v)	4.9	1
Glyceryl monostearate	4.5	10 m*M*	22.7	1
Polyoxyethylene-20-glycerin vegetable oil fatty acid ester	15.5	2% (w/v)	16.1	1
Polyoxyethylene-15-glyceryl monostearate	13.5	10 m*M*	16.2	1
Polyoxyethylene-10-monooleate	11.0	5 m*M*	3.8	1
		10 m*M*	2.8	1
Polyoxyethylene-10-monolaurate	12.5	10 m*M*	19.2(10.1)	3
Polyoxyethylene-20-sorbitan monolaurate	16.9	10 m*M*	14.3	1
III		1 m*M*	5.0	1
		5 m*M*	48.2	1
		10 m*M*	52.1(6.9)	3
		20 m*M*	64.1	1
		30 m*M*	70.8	1
Sodium cetyl sulfate		1 m*M*	11.6	1
		2.5 m*M*	12.5	1
Sodium di-2-ethylhexyl sulfosuccinate		10 m*M*	28.2	1
Sodium taurocholate		10 m*M*	12.0(5.7)	5
Sodium cholate		10 m*M*	14.1(4.4)	5
Propicillin[c]				
None			28.4(4.1)[d]	3
II		10 m*M*	28.0(4.4)	5

[a] Hydrophilic–lipophilic balance. [b] Number of experiments. [c] The initial antibiotic concentration was 5000 μg/ml. [d] The data were taken from Ref. 8.

RESULTS

Effects of I on Stomach Absorption—The total disappearance of propicillin from the stomach perfusion solution has been reported to follow first-order kinetics (8). In this case, the apparent first-order rate constant undoubtedly includes the rate constants for both acid-catalyzed degradation and absorption, which proceed competitively during the absorption experiments.

As verified previously (7, 8), the apparent first-order rate constant, k_{app}, can be expressed as:

$$k_{app} = CL_a\frac{1}{V} + k_d \qquad \text{(Eq. 2)}$$

where CL_a is the absorption clearance in milliliters/time, k_d is the first-order rate constant for chemical degradation, and V is the volume of re-

[12] IFO 12708, Institute for Fermentation, Osaka, Japan; the strain was derived from ATCC 9341.

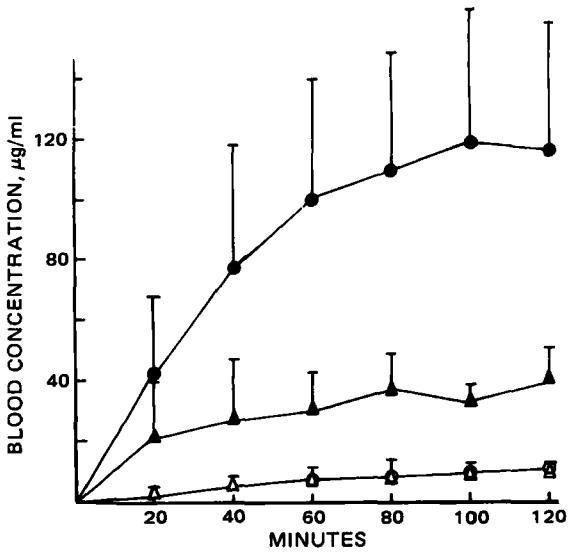

Figure 4—*Mean blood concentrations of propicillin (▲) and cefazolin (●) during* in situ *intestinal perfusion at pH 7.4 in the presence of 10 mM I. Open symbols indicate the blood concentrations in the absence of I. The vertical bars represent* SD *from three or more experiments.*

circulating drug solution. As shown in Fig. 1, plots of k_{app} obtained from absorption experiments with propicillin containing 10 m*M* I in the perfusion solution *versus* $1/V$ yielded a straight line similar to those obtained previously (8) for control experiments in the absence of I. The intercepts of these lines provided k_d values (in min^{-1}), which were evaluated to be 1.06×10^{-3}, 0.40×10^{-3}, and 0.30×10^{-3} at pH 2.00, 3.00, and 4.00, respectively.

It was found that the degradation of propicillin was much slower in the presence of the nonionic surfactant, which is consistent with the previous observations (5, 6). The CL_a of propicillin calculated from the slopes in Fig. 1 is plotted in Fig. 2 as a function of the perfusion solution pH. In this figure, the log CL_a–pH profile for propicillin determined under the same conditions in the absence of I was redrawn from our previous study (8). The absorption of propicillin below pH 3 was inhibited twofold in the presence of 10 m*M* I.

Effect of Surfactants on Intestinal Absorption—*Dependency on Concentration of I*—The effect of I on the intestinal absorption of two β-lactam antibiotics possessing different physicochemical characteristics was investigated. Propicillin was chosen since it has a high lipophilicity (10) and shows some incorporation (5, 6) of its ionized species into micelles of I; cefazolin has a low lipophilicity and exhibits negligible interaction with the surfactant micelles (5, 6).

Since the values of pK_a for the carboxylic acid groups of propicillin and cefazolin are 2.76 (10) and 2.54 (11), respectively, both antibiotics were largely in the form of anion at pH 7.4 in the present absorption experiments. Figure 3 shows the percentage disappearance of both antibiotics after recirculation through the small intestine for 2 hr as a function of the concentration of I. The total percentage disappearance for propicillin and cefazolin were determined previously (9) to be 28.4 ± 4.1 and 9.7 ± 1.8%, respectively. It was also found (9) that the greater disappearance of propicillin could be attributed mostly to intestinal degradation rather than absorption, and that the first-order rate constant ($\times 10^3$ min^{-1}) for the intestinal absorption was 1.29 ± 0.34 for propicillin and 0.85 ± 0.16 for cefazolin.

The relationship between the surfactant concentration and rate of antibiotic absorption represented one important aspect of the action of the surfactants. In the presence of I, the percentage disappearance of both antibiotics first increased markedly with increasing surfactant concentration ≤10 m*M* and then approached a constant value of ~50% >10 m*M*, which is much higher than the critical micellar concentration of 0.092 m*M* under comparative conditions (5, 6). For both antibiotics, no acceleration of the *in vitro* degradation in the presence of I was observed under the present experimental conditions, suggesting that the enhanced disappearance was a result of the absorption.

During the recirculating absorption experiments, the blood concentrations of propicillin and cefazolin were determined in the presence or absence of 10 m*M* I. The results are shown in Fig. 4 and clearly indicate that the presence of I remarkably increased the blood levels of both antibiotics. The accumulation of cefazolin in the gut tissue was only 0.2% after 2 hr. These findings strongly suggest that the amount of antibiotic disappearing from the intestinal perfusate in the presence of I was largely transferred to the serosal site.

Table II—Influence of Perfusion Solution pH on the Percentage Disappearance of Cefazolin from Rat Small Intestine in the Presence of 10 m*M* I Surfactant at 37°

pH	Disappearance, % (±*SD*)	*n*[a]
4.0	63.4(11.5)	3
4.7	50.4(5.8)	3
6.4	52.9(15.3)	3
7.4	50.7(6.6)	5

[a] Number of experiments.

Effect of Various Surfactants and Bile Salts—The promotional effect of surfactants on the intestinal absorption was investigated using concentrations of various surfactants and bile salts. The results are summarized in Table I. Promoted absorption by the surfactants was observed for both the anionic surfactant and the ether-type class of nonionic surfactants. Bile salts revealed no significant promotional effect. For nonionic surfactants used in this study, the ester groups showed a reduced or insignificant effect on cefazolin absorption.

Dependency on Intestinal Solution pH and the Initial Concentration of Drug—Absorption of cefazolin from the rat small intestine was examined in the presence of 10 m*M* I as a function of the perfusion solution pH. The results are shown in Table II. Between pH 4 and 7.4, there was no significant difference in the absorption behavior. Figure 5 gives logarithmic plots of the residual cefazolin concentration in the perfusate containing 10 m*M* I *versus* time for three different initial concentrations (1, 10, and 50 m*M*) at pH 7.4. The observed pseudo first-order rate constants were almost identical and independent of the initial drug concentration.

DISCUSSION

Davis *et al.* (3, 4) described the effects of surfactants on the GI absorption of poorly absorbed β-lactam antibiotics in dogs or rats, and attributed the promoted absorption by surfactants to alteration of the membrane permeability. In the present study, it was found that the absorption of propicillin from the rat stomach was reduced in the presence

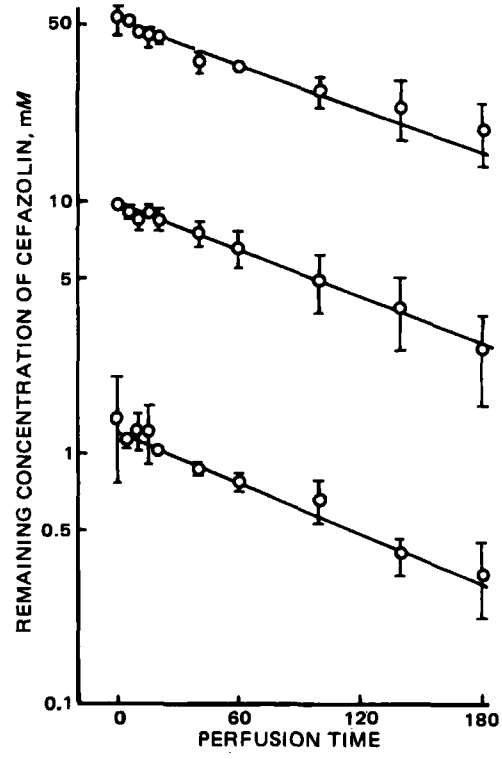

Figure 5—*Plots of the remaining cefazolin concentration in the perfusate* versus *the recirculating time at 37° and pH 7.4, maintained constant with a pH-stat. The perfusion solution was recirculated at a rate of 2 ml/min.*

of 10 m*M* I. Such reduction was interpreted as the result of entrapment of propicillin molecules into micelles of I. A similar phenomenon has been reported in absorption experiments with other drugs (12, 13). While the absorption of antibiotics by the small intestine increased in the presence of surfactants, such promoted absorption depended on the nature of the surfactants rather than the physicochemical properties of the antibiotics. Interestingly, the existence of a significant interaction between antibiotics and surfactants appeared not to influence the absorption by the small intestine. Despite the entrapment of 90% of the anionic propicillin into micelles of II (5, 6), no reduced absorption was observed (Table I). In the presence of 10 m*M* I, absorption of the antibiotic was promoted with 30% of the anionic species incorporated into the micelles. These results suggest that alteration of the membrane permeability by nonionic and cationic surfactants induced the promoted absorption in the small intestine, concurring with the findings made by other laboratories (3, 4).

Walters and Dugard (14) demonstrated that the hydrophilic–lipophilic balance (HLB) of a surfactant represents an important property in determining the promoted absorption. However, our results from the intestinal experiments indicated that significant absorption enhancement was observed only with ether-type surfactants, suggesting that HLB cannot be the sole cause for the observed promotional effect in the intestinal absorption of β-lactam antibiotics. Alteration of the permeability sometimes can be a result of disruption of the membrane structure by surfactants (15–17). In the present study, however, no significant disruption of the membrane was detected by light microscopy. The change in membrane permeability with the surfactant, therefore, may reflect a reversible alteration of the diffusion barrier to lipid soluble, poorly ionized drugs as claimed by Davis *et al.* (3, 4).

REFERENCES

(1) B. A. Mulley, in "Advances in Pharmaceutical Sciences," vol. 1, H. S. Bean, A. H. Beckett, and J. E. Carless, Eds., Academic, London, 1964, p. 164.

(2) M. Gibaldi and S. Feldman, *J. Pharm. Sci.*, **59**, 579 (1970).

(3) W. W. Davis, R. R. Pfeiffer, and J. F. Quay, *ibid.*, **59**, 960 (1970).

(4) C. J. Kreutler and W. W. Davis, *ibid.*, **60**, 1835 (1971).

(5) A. Tsuji, M. Matsuda, E. Miyamoto, and T. Yamana, *J. Pharm. Pharmacol.*, **30**, 442 (1978).

(6) A. Tsuji, E. Miyamoto, M. Matsuda, K. Nishimura, and T. Yamana, *J. Pharm. Sci.*, **71**, 1313 (1982).

(7) A. Tsuji, E. Miyamoto, I. Kagami, H. Sakaguchi, and T. Yamana, *ibid.*, **67**, 1701 (1978).

(8) A. Tsuji, E. Miyamoto, N. Hashimoto, and T. Yamana, *ibid.*, **67**, 1705 (1978).

(9) A. Tsuji, E. Miyamoto, O. Kubo, and T. Yamana, *ibid.*, **68**, 812 (1979).

(10) A. Tsuji, O. Kubo, E. Miyamoto, and T. Yamana, *ibid.*, **66**, 1675 (1977).

(11) T. Yamana and A. Tsuji, *ibid.*, **65**, 1563 (1976).

(12) K. Kakemi, T. Arita, and S. Muranishi, *Chem. Pharm. Bull.*, **13**, 969 (1965).

(13) K. Kakemi, T. Arita, and S. Muranishi, *ibid.*, **13**, 976 (1965).

(14) K. A. Walters and P. H. Dugard, *J. Pharm. Pharmacol.*, **30**, Suppl. 23p (1978).

(15) T. Nadai, R. Kondo, A. Tatematsu, and H. Sezaki, *Chem. Pharm. Bull.*, **20**, 1139 (1972).

(16) T. Nadai, M. Kume, A. Tatematsu, and H. Sezaki, *ibid.*, **23**, 543 (1975).

(17) A. J. Bryan, R. Kaur, G. Robinson, N. W. Thomas, and C. G. Wilson, *Int. J. Pharm.*, **7**, 145 (1980).

ACKNOWLEDGMENTS

Presented in part at the APhA Academy of Pharmaceutical Sciences meeting held in San Antonio, Texas, November 1980.

The authors express their appreciation to Professor S. Odashima, Department of Pathology, Kanazawa Medical University for his help regarding the light microscopic aspects of the intestinal membrane and his invaluable discussions. They also thank Miss S. Unno for her excellent technical assistance. They are grateful to Takeda Chemical Industries and Fujisawa Pharmaceutical Co. for the gifts of β-lactam antibiotics and to Nikko Chemicals Co. for the gift of surfactants.

Acrylic Microspheres *In Vivo* VI: Antitumor Effect of Microparticles with Immobilized L-Asparaginase Against 6C3HED Lymphoma

PETER EDMAN * and INGVAR SJÖHOLM *x

Received October 13, 1981, from the *Department of Pharmaceutical Biochemistry, Biomedical Center, University of Uppsala, S-751 23 Uppsala, Sweden.* Accepted for publication June 7, 1982.

*Present address: Department of Drugs, National Board of Health and Welfare, Division of Pharmacy, 751 25 Uppsala, Sweden.

Abstract □ The antitumor effect of immobilized L-asparaginase was tested against lymphoid leukemia in mice with concomitant scanning of the L-asparagine level in serum. L-Asparaginase was immobilized in microspheres of polyacrylamide or polyacryldextran. These particles were used in C3H mice bearing the L-asparagine-dependent lymphoma (6C3HED). The tumor was maintained as an ascites tumor, 1×10^6 cells were injected intraperitoneally and on day 4 after inoculation, L-asparaginase was injected intramuscularly or intraperitoneally in microparticles. After injection of 5.0 IU ip of L-asparaginase in microparticles, partial remission was induced, generally, however, the cancer relapsed and killed the mice within 2–3 weeks. To obtain complete regression, it was necessary to inject 20 IU of L-asparaginase in microparticles intraperitoneally. The best therapeutic effect was obtained when the particles were administered intramuscularly. After injection of 5 IU the survival time was prolonged, but complete regression was not achieved. The best effect was obtained when the particles were given intramuscularly in two small doses (2.5 IU) at a 3-day interval. Such treatment induced complete regression; 10 out of 12 treated mice were completely cured and lived for several months. It is concluded that the L-asparagine level in serum has to be depressed to <20% of the normal level for at least 6–7 days to obtain complete regression of the tumor.

Keyphrases □ Acrylic microspheres—*in vivo*, antitumor effect of microparticles with immobilized L-asparaginase against lymphoma □ L-asparaginase—acrylic microspheres, *in vivo*, antitumor effect of microparticles with immobilized L-asparaginase against lymphoma □ Antitumor effect—acrylic microspheres, *in vivo*, microparticles with immobilized L-asparaginase against lymphoma

L-Asparaginase of bacterial origin has been used extensively during the last 10 years in the treatment of lymphatic leukemia (1–3) as either a complement to or in combination with chemotherapy. The remission of the tumors is dose dependent (3) and considered to be due primarily to the deprivation of the cells of L-asparagine

0022-3549/83/0600-0654$01.00/0

of 10 m*M* I. Such reduction was interpreted as the result of entrapment of propicillin molecules into micelles of I. A similar phenomenon has been reported in absorption experiments with other drugs (12, 13). While the absorption of antibiotics by the small intestine increased in the presence of surfactants, such promoted absorption depended on the nature of the surfactants rather than the physicochemical properties of the antibiotics. Interestingly, the existence of a significant interaction between antibiotics and surfactants appeared not to influence the absorption by the small intestine. Despite the entrapment of 90% of the anionic propicillin into micelles of II (5, 6), no reduced absorption was observed (Table I). In the presence of 10 m*M* I, absorption of the antibiotic was promoted with 30% of the anionic species incorporated into the micelles. These results suggest that alteration of the membrane permeability by nonionic and cationic surfactants induced the promoted absorption in the small intestine, concurring with the findings made by other laboratories (3, 4).

Walters and Dugard (14) demonstrated that the hydrophilic–lipophilic balance (HLB) of a surfactant represents an important property in determining the promoted absorption. However, our results from the intestinal experiments indicated that significant absorption enhancement was observed only with ether-type surfactants, suggesting that HLB cannot be the sole cause for the observed promotional effect in the intestinal absorption of β-lactam antibiotics. Alteration of the permeability sometimes can be a result of disruption of the membrane structure by surfactants (15–17). In the present study, however, no significant disruption of the membrane was detected by light microscopy. The change in membrane permeability with the surfactant, therefore, may reflect a reversible alteration of the diffusion barrier to lipid soluble, poorly ionized drugs as claimed by Davis *et al.* (3, 4).

REFERENCES

(1) B. A. Mulley, in "Advances in Pharmaceutical Sciences," vol. 1, H. S. Bean, A. H. Beckett, and J. E. Carless, Eds., Academic, London, 1964, p. 164.

(2) M. Gibaldi and S. Feldman, *J. Pharm. Sci.*, **59**, 579 (1970).

(3) W. W. Davis, R. R. Pfeiffer, and J. F. Quay, *ibid.*, **59**, 960 (1970).

(4) C. J. Kreutler and W. W. Davis, *ibid.*, **60**, 1835 (1971).

(5) A. Tsuji, M. Matsuda, E. Miyamoto, and T. Yamana, *J. Pharm. Pharmacol.*, **30**, 442 (1978).

(6) A. Tsuji, E. Miyamoto, M. Matsuda, K. Nishimura, and T. Yamana, *J. Pharm. Sci.*, **71**, 1313 (1982).

(7) A. Tsuji, E. Miyamoto, I. Kagami, H. Sakaguchi, and T. Yamana, *ibid.*, **67**, 1701 (1978).

(8) A. Tsuji, E. Miyamoto, N. Hashimoto, and T. Yamana, *ibid.*, **67**, 1705 (1978).

(9) A. Tsuji, E. Miyamoto, O. Kubo, and T. Yamana, *ibid.*, **68**, 812 (1979).

(10) A. Tsuji, O. Kubo, E. Miyamoto, and T. Yamana, *ibid.*, **66**, 1675 (1977).

(11) T. Yamana and A. Tsuji, *ibid.*, **65**, 1563 (1976).

(12) K. Kakemi, T. Arita, and S. Muranishi, *Chem. Pharm. Bull.*, **13**, 969 (1965).

(13) K. Kakemi, T. Arita, and S. Muranishi, *ibid.*, **13**, 976 (1965).

(14) K. A. Walters and P. H. Dugard, *J. Pharm. Pharmacol.*, **30**, Suppl. 23p (1978).

(15) T. Nadai, R. Kondo, A. Tatematsu, and H. Sezaki, *Chem. Pharm. Bull.*, **20**, 1139 (1972).

(16) T. Nadai, M. Kume, A. Tatematsu, and H. Sezaki, *ibid.*, **23**, 543 (1975).

(17) A. J. Bryan, R. Kaur, G. Robinson, N. W. Thomas, and C. G. Wilson, *Int. J. Pharm.*, **7**, 145 (1980).

ACKNOWLEDGMENTS

Presented in part at the APhA Academy of Pharmaceutical Sciences meeting held in San Antonio, Texas, November 1980.

The authors express their appreciation to Professor S. Odashima, Department of Pathology, Kanazawa Medical University for his help regarding the light microscopic aspects of the intestinal membrane and his invaluable discussions. They also thank Miss S. Unno for her excellent technical assistance. They are grateful to Takeda Chemical Industries and Fujisawa Pharmaceutical Co. for the gifts of β-lactam antibiotics and to Nikko Chemicals Co. for the gift of surfactants.

Acrylic Microspheres *In Vivo* VI: Antitumor Effect of Microparticles with Immobilized L-Asparaginase Against 6C3HED Lymphoma

PETER EDMAN * and INGVAR SJÖHOLM *x

Received October 13, 1981, from the *Department of Pharmaceutical Biochemistry, Biomedical Center, University of Uppsala, S-751 23 Uppsala, Sweden.* Accepted for publication June 7, 1982.

*Present address: Department of Drugs, National Board of Health and Welfare, Division of Pharmacy, 751 25 Uppsala, Sweden.

Abstract □ The antitumor effect of immobilized L-asparaginase was tested against lymphoid leukemia in mice with concomitant scanning of the L-asparagine level in serum. L-Asparaginase was immobilized in microspheres of polyacrylamide or polyacryldextran. These particles were used in C3H mice bearing the L-asparagine-dependent lymphoma (6C3HED). The tumor was maintained as an ascites tumor, 1×10^6 cells were injected intraperitoneally and on day 4 after inoculation, L-asparaginase was injected intramuscularly or intraperitoneally in microparticles. After injection of 5.0 IU ip of L-asparaginase in microparticles, partial remission was induced, generally, however, the cancer relapsed and killed the mice within 2–3 weeks. To obtain complete regression, it was necessary to inject 20 IU of L-asparaginase in microparticles intraperitoneally. The best therapeutic effect was obtained when the particles were administered intramuscularly. After injection of 5 IU the survival time was prolonged, but complete regression was not achieved. The best effect was obtained when the particles were given intramuscularly in two small doses (2.5 IU) at a 3-day interval. Such treatment induced complete regression; 10 out of 12 treated mice were completely cured and lived for several months. It is concluded that the L-asparagine level in serum has to be depressed to <20% of the normal level for at least 6–7 days to obtain complete regression of the tumor.

Keyphrases □ Acrylic microspheres—*in vivo*, antitumor effect of microparticles with immobilized L-asparaginase against lymphoma □ L-asparaginase—acrylic microspheres, *in vivo*, antitumor effect of microparticles with immobilized L-asparaginase against lymphoma □ Antitumor effect—acrylic microspheres, *in vivo*, microparticles with immobilized L-asparaginase against lymphoma

L-Asparaginase of bacterial origin has been used extensively during the last 10 years in the treatment of lymphatic leukemia (1–3) as either a complement to or in combination with chemotherapy. The remission of the tumors is dose dependent (3) and considered to be due primarily to the deprivation of the cells of L-asparagine

0022-3549/83/0600-0654$01.00/0

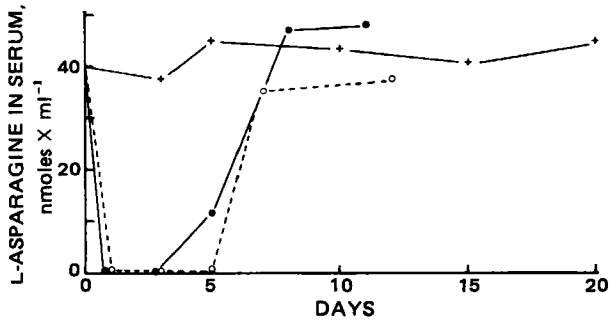

Figure 1—*L-Asparagine concentration in serum of healthy mice after a single intraperitoneal injection of L-asparaginase (5 IU/animal) in free solution (○) or in microparticles (●). Pooled serum from 4 to 6 mice was used for each time interval. The normal L-asparagine concentration (+) was obtained from a control group given physiological saline.*

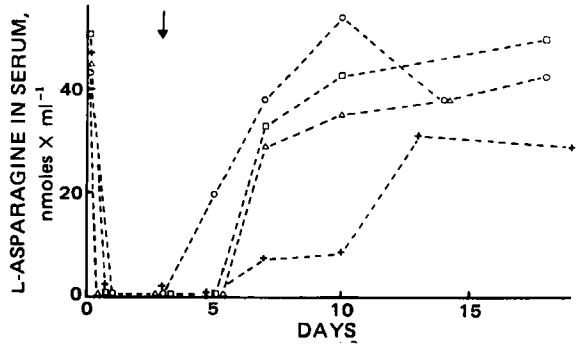

Figure 2—*L-Asparagine concentration in serum after intramuscular injection of L-asparaginase in free form, 5 IU/animal (○), 20 IU/animal (△), 2 × 2.5 IU/animal (□) and 2 × 2.5 IU/tumor-bearing animal (+). In the infected animals, 6C3HED cells (1 × 10⁶) were injected 4 days prior to the first injection on day 0. The arrow shows the time for the second injection of 2.5 IU of L-asparaginase in free form. Pooled serum from five mice was used for each time interval.*

and to some extent of L-glutamine (4). However, the short biological half-life of the enzyme necessitates frequent administration, which often leads to antibody production and hypersensitivity (5). This and other side reactions prevent the prolonged use of L-asparaginase with a subsequent relapse of the tumor and the development of L-asparaginase-resistant tumors.

The stability of enzymes against thermal denaturation and proteolytic degradation is generally improved when they are immobilized or polymerized. L-Asparaginase has been used successfully in immobilized form *in vivo* to prolong the duration of action in monkeys (6), rats (7), rabbits (8), and mice (9–11). When the enzyme is immobilized in porous microparticles of polyacrylamide with a mean diameter of 0.2–0.5 μm, the enzymic characteristics are essentially retained and the effects on the L-asparagine level in plasma is prolonged after intraperitoneal administration in rats (12). When the L-asparaginase microparticles are embedded in a polyacrylic gel the duration of action was prolonged up to ~25 days after implantation in the rat (13).

The present study was undertaken to correlate the L-asparagine-depressing activity of immobilized L-asparaginase in microparticles with the inhibition of tumor growth in mice, as well as to ascertain the optimal route of administration and the minimal dose of the immobilized L-asparaginase, to keep the serum L-asparagine concentration at a low enough level to prevent tumor growth in mice.

EXPERIMENTAL

Materials—L-Asparaginase[1] (E.C. 3.5.1.1), aspartate aminotransferase[2] (E.C. 2.6.1.1) (83 U/mg) isolated from porcine heart, and malic dehydrogenase[2] (E.C. 1.1.1.37) (2000 U/ml) from pigeon breast muscle were used without further purification. Acrylamide[3], *N,N'*-methylenebisacrylamide[3], *N,N,N',N'*-tetramethylethylenediamine[2], α-ketoglutaric acid[2], nicotinamide adenine dinucleotide[2] (NADH, reduced form) L-asparagine monohydrate[4], dextran[5], Nessler's reagent[2] (ammonia color reagent), and other chemicals were of analytical grade. Male mice[6] weighing 20–25 g were used throughout. The cell line used was the Gardner lymphosarcoma 6C3HED. It was grown in ascites form and was propagated every 7th day in C3H mice with 1 × 10⁶ cells suspended in a balanced salt solution ($CaCl_2$ 0.14 g, NaCl 8 g, KCl 0.4 g, $MgSO_4 \times 7 H_2O$ 0.2 g, KH_2PO_4 0.06 g, and water to 1000 g, pH 6.9).

Preparation of Microparticles Containing L-Asparaginase—Microparticles[7] of polyacrylamide (TC = 8-25)[8] or polyacryldextran (DTC = 11-1-75)[8] containing L-asparaginase were prepared according to a reported method (12, 14). L-Asparaginase, corresponding to 10,000 IU, was dissolved with the acrylic monomers (acrylamide, *N,N'*-methylenebisacrylamide or acryldextran) in 5 ml of 0.005 *M* sodium phosphate buffer, pH 7.4. After addition of the catalyst, ammonium peroxydisulphate (100 μl of a solution of 0.5 g/ml), the solution was poured into 200 ml of a mixture consisting of toluene and chloroform (4:1) and 0.5 g of a detergent[9].

The mixture was homogenized to produce a water–oil emulsion. The homogenizer was removed and the emulsion slowly stirred with a magnetic stirrer. The polymerization was started by adding 1 ml of the accelerator *N,N,N',N'*-tetramethylethylenediamine to the emulsion. During the whole procedure, oxygen was excluded from the system by bubbling nitrogen gas through the emulsion.

The microparticles were isolated by centrifugation, washed several times with buffer, and suspended in physiological saline after the last washing. Under the conditions used, the polyacrylamide particles (TC = 8-25) had a mean diameter of 0.1–0.4 μm, and polyacryldextran particles (DTC = 11-1-75) were 0.2–1.2 μm in diameter.

Preparation of Polyacrylamide Gel for Implantation—Microparticles of polyacrylamide (TC = 8–25) containing L-asparaginase (10 or 20 IU) were embedded in 200–300 μl of a polyacrylamide gel (TC = 16-25) prepared in the usual way in a small perspex box (1 × 1 × 0.7 cm). The gel tablet formed was washed with buffer and physiological saline,

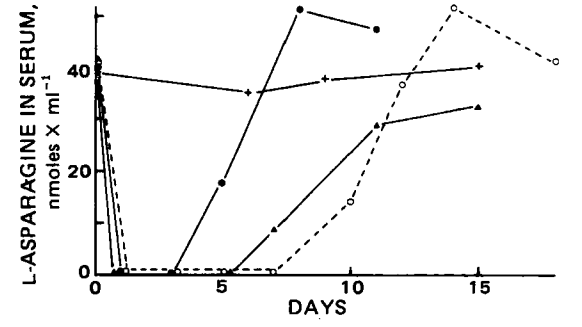

Figure 3—*L-Asparagine concentration in mice bearing the lymphosarcoma 6C3HED, administered intraperitoneally (1 × 10⁶ cells) 4 days prior to the start of the experiment. L-Asparaginase was injected intraperitoneally in free form (5 IU/mouse, ○) or in microparticles (5 IU/mouse, ●, 20 IU/mouse, ▲). A control group was given physiological saline (+). Each point is obtained from the pooled blood from 4 to 6 mice.*

[1] Asparaginase (Crasnitin) was obtained as a gift from Bayer (Sverige) AB, Stockholm.
[2] Sigma Chemical Co.
[3] Eastman Kodak Co.
[4] Merck Co.
[5] Dextran T40 (molecular weight: 40,000) was purchased from Pharmacia Fine Chemicals, Uppsala, Sweden.
[6] C3H mice, Bomholtsgård, Denmark.
[7] U.S. Pat. 4,061,466.
[8] The nomenclature is explained in a previous study (14).
[9] Pluronics F-68 (polyoxyethylene-derived polyoxypropylene) from Ugine Kuhlmann, Paris, France.

Table I—Antitumor Activity of L-Asparaginase Against 6C3HED Lymphoma [a]

Enzyme Preparation	Route of Administration	Survival Time, days	Mean Survival Time (± *SD*) or Median Survival Time (lower and upper quartile)	Treated 50-day Survivors
Control, particles	ip	10, 10, 10, 11	10.3 ± 0.5	0/4
Control, saline	ip	10, 10, 11, 11, 11, 11, 11, 12, 12, 13, 13, 13	11.5 ± 1.1	0/12
Microparticles, 5 IU	ip	14, 14, 15, 15, 15, 16, 16, 16, 16, 17, 18, 34	17.2 ± 5.4	0/12
Enzyme solution, 5 IU	ip	48, >50, >50, >50, >50, >50, >50, >50, >50, >50, >50,	>50	11/12
Microparticles, 20 IU	ip	16, 22, 44, 45, 50, 50, 50, >50, >50, >50, >50, >50	50 (44, >50)	5/12
Microparticles, (DTC = 11-1-75) 5 IU	ip	15, 15, 16, 17, 19, 35, 37, 47, 48, >50, >50, >50	37 (16, 48)	3/12
Microparticles[b], 5 IU + 6C3HED cells	ip	12, 13, 14, 16, 16, 16, 16, 16, 17, 17	15.3 ± 1.7	0/10
Enzyme solution[b], 5 IU + 6C3HED cells	ip	14, 15, 18, 18, 18, 32, 35, 42, 42	26.0 ± 11.7	0/9
Microparticles, 5 IU	im	11, 12, 14, 14, 14, >50, >50, >50	14 (12, >50)	3/8
Microparticles, 20 IU	im	31, 35, 38, 38, >50, >50, >50, >50, >50, >50, >50, >50	>50	8/12
Microparticles, 2 × 2.5 IU	im	31, 46, >50, >50, >50, >50, >50, >50, >50, >50, >50, >50	>50	10/12
Implant, 10 IU	sc	11, 11, 11, 12, 12, 12, 12, 13, 13, 13, 13, >50	12 (11, 13)	1/12
Implant, 20 IU	sc	10, 10, 10, 11, 11, 11, 12, 13, 14, 14, 14, 43	11.8 ± 1.7	0/12

[a] The mice were given 1 × 10^6 6C3HED cells ip, and on the 4th (or 4th and 7th) day after inoculation the mice were treated with different enzyme preparations by different routes. The survival time given is calculated from the day of inoculation. When not otherwise stated, the microparticles used in these experiments had the composition TC = 8–25. [b] The enzyme in free form or in microparticles was administered on the day of inoculation.

as earlier described (13), in order to free it from the remaining catalyst.

Assay of Native and Immobilized L-Asparaginase—L-Asparaginase activity was determined from the amount of ammonia produced by its reaction with the substrate L-asparagine at 37° (15). After the addition of Nessler's reagent, the absorbance was determined at 500 nm. Appropriate enzyme and substrate blanks were included in all assays. A standard curve was prepared with known amounts of ammonium sulphate.

Determination of blood L-asparagine was performed according to a fluorometric method (16). Blood was drawn each time from the tail vein or the orbital plexus from four to six mice. The blood samples were pooled and centrifuged. If not analyzed immediately the serum was frozen and stored at −18° until the analysis.

RESULTS

Serum L-Asparagine after L-Asparaginase Administration in Healthy and Tumor-Bearing Mice—After injection of 5 IU, ip of either immobilized or native L-asparaginase into the mice, serum L-asparagine dropped from a normal level of ~40–45 nmoles/ml to an undetectable level after 1 day and remained so for 4–5 days. Serum L-asparagine became normalized after days 6–7 as seen in Fig. 1.

Figure 2 illustrates the effects on the serum L-asparagine of native *L-asparaginase (2 × 2.5, 5, and 20 IU)* administered intramuscularly to healthy mice. A single injection of 5 IU im of the free enzyme lowered the serum L-asparagine level to zero and maintained it at zero for 3 days.

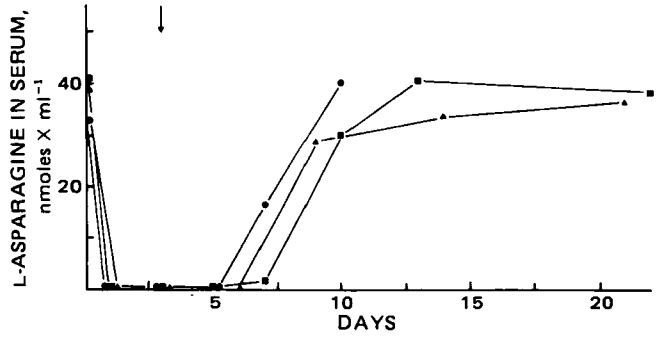

Figure 4—*Blood levels of L-asparagine in mice bearing 6C3HED cells (1 × 10^6 inoculated intraperitoneally 4 days in advance) after intramuscular injection of L-asparaginase in microparticles, 5 IU/animal (●), 20 IU/animal (▲), and 2 × 2.5 IU/animal (■). The arrow indicates the time for the second injection of 2.5 IU of L-asparaginase in microparticles.*

Injection of 2 × 2.5 IU and 20 IU of the free enzyme retained a zero L-asparagine level for up to 5 days. The effect on the serum L-asparagine of free L-asparaginase (2 × 2.5 IU) administered intramuscularly into mice bearing 6C3HED lymphoma is also shown in Fig. 2. The 6C3HED cells (1 × 10^6) were inoculated intraperitoneally 4 days prior to the first injection on day 0. The serum L-asparagine level was depressed to <10 nmoles/ml for 10 days due to the $t_{1/2}$-prolonging effect from the LDH-virus (lactate dehydrogenase-elevating virus) contamination of the cell line.

Figure 3 illustrates the effects on the serum L-asparagine of L-asparaginase (5 or 20 IU) administered intraperitoneally to mice bearing 6C3HED lymphoma. The 6C3HED cells (1 × 10^6) were inoculated intraperitoneally, and at day 4 after inoculation, native or immobilized L-asparaginase was injected intraperitoneally. After injection of the free enzyme, the L-asparagine level dropped from the normal value, was undetectable within 1 day, and remained so for 7 days. The serum L-asparagine level became normal after day 12, which means that the enzymic effect was significantly prolonged in the tumor-bearing mice, when compared with the effect seen in the healthy mice (Fig. 1). The same was seen after injection of 2 × 2.5 IU im as shown in Fig. 2. The prolonged effect is the result of the increased half-life of soluble L-asparaginase, which is caused by the LDH-virus contaminating the 6C3HED and other mouse lymphoma cell lines (4, 17). The increased $t_{1/2}$ of L-asparaginase is a secondary effect of the virus infection, and it is not seen when the 6C3HED cells are inoculated 1 hr after intraperitoneal injection of L-asparaginase (5 IU). In these animals the L-asparagine level followed the same time course as in noninfected mice, as shown in Fig. 1. Thus, the L-asparagine level was maintained at zero for only 5 days.

The therapeutic effect of L-asparaginase in tumor-infected mice is directly related to the duration of the enzymic effect—as will be discussed later—and thus to the $t_{1/2}$ value of the enzyme. In the mice infected with the 6C3HED cells on the same day, administration of L-asparaginase suppressed the growth rate of the lymphoma, but complete regression was not achieved. All the mice died after 14–50 days with grossly enlarged lymph nodes. However, when L-asparaginase was administered on day 4 after infection, 11 out of 12 mice were cured and survived 50 days as a result of the prolonged $t_{1/2}$ value of the enzyme. The results are summarized in Table I.

Immobilized L-asparaginase in microparticles administered intraperitoneally had the same effect on the L-asparagine level in mice bearing the 6C3HED lymphoma as in healthy mice (Figs. 1 and 3). Obviously, the LDH-virus contaminating the 6C3HED cells has no effect on the $t_{1/2}$ of immobilized L-asparaginase. Injection of physiological saline or microparticles without enzyme had no effect on the L-asparagine level.

Figure 4 illustrates the effects of microparticles with L-asparaginase administered intramuscularly in the scapular area of C3H mice bearing the lymphoma 6C3HED. L-Asparaginase (2 × 2.5, 5, and 20 IU) was in-

jected into 8–12 mice in three groups. After injection of 5 IU of immobilized L-asparaginase, normal serum values were obtained on days 8–9, whereas the normal level was reached on days 12–13 when 20 or 2 × 2.5 IU was administered. The results were the same in tumor-bearing and healthy mice. It is obvious that a prolonged effect on the plasma L-asparagine level is obtained by giving L-asparaginase in immobilized form intramuscularly, especially when the effects of 2 × 2.5 IU are compared in infected (Fig. 4) and healthy mice given free enzyme (Fig. 2).

The Growth-Inhibiting Effect of L-Asparaginase on Ascites Tumor—When studied in the ascites form, the tumor cells (1×10^6 cells) were generally given to groups of 12 C3H mice. After 4 days (or after 4 and 7 days), the mice were treated with different doses of L-asparaginase given by different routes or with saline or microparticles not containing any enzyme. Table I summarizes the survival times of differently treated groups. In untreated animals, the tumor grew rapidly and killed the hosts after 10–12 days. Immobilized L-asparaginase (5 IU ip given in microparticles) generally prolonged the survival time to 15–16 days. In a large dose (20 IU) or in polyacryldextran particles (from which enzyme can leak out) immobilized L-asparaginase had a longer effect and was able to cure five and three animals in respective groups.

As mentioned, the effect of native L-asparaginase is prolonged in infected animals and most of the mice (11 out of 12) were cured by 5 IU ip administered as shown in Table I for comparison. As expected and already discussed, the same dose did not cure the animals when the tumor was inoculated concomitantly with the administration of native L-asparaginase. These results are in complete accordance with the effect on the serum L-asparagine level shown in Figs. 1 and 3.

The tumor growth-inhibiting effect of immobilized L-asparaginase is improved when administered intramuscularly. The survival time of the different groups is shown in Table I. Three mice out of eight were cured when 5 IU of immobilized L-asparaginase was given intramuscularly. When 20 IU or 2 × 2.5 IU was administered, 8 and 10 animals, respectively, out of 12 survived for several weeks and were considered to be cured.

Intraperitoneal injection of acryldextran particles (DTC = 11-1-75) with L-asparaginase (5 IU) to C3H mice with 6C3HED cells, prolonged the survival time significantly compared with controls. Figure 5 and Table I summarize the results. After injection of particles with enzyme, normal serum values were obtained on days 9–10.

The Effect on Ascites Tumor by Implantation of L-Asparaginase in Polyacrylamide—L-Asparaginase in microparticles (TC = 8-25) was incorporated into a polyacrylamide gel (TC = 16-25). This gel, containing 10 or 20 IU of L-asparaginase, was then implanted subcutaneously on the backs of the mice.

The effect on the L-asparagine level is shown in Fig. 5. The serum concentration of L-asparagine fell from normal (40 nmoles/ml) to 18 nmoles/ml after 1 day and remained at this level during the rest of the experiment. On days 10–14 after inoculation of the cells (6–10 days after the implantation), all the animals died with one exception. This animal survived for several months and was considered to be cured. Table I summarizes the results. There were no significant differences between implants with 10 or 20 IU of L-asparaginase. These results indicate that it is necessary to depress the L-asparagine concentration at least to <10 nmoles/ml to obtain regression of the lymphoma.

DISCUSSION

It was shown earlier that immobilization of L-asparaginase significantly prolongs the depressive effect on the L-asparagine level in blood (6, 7, 9, 12). Potentially, an immobilized system would be of value to decrease the side effects seen when native L-asparaginase is used in high doses. The purpose of the present work was to correlate the effect on the L-asparagine level and the effect on an L-asparagine-glutamine-dependent lymphoma cell line. In addition, the purpose was to ascertain the optimal route of administration of the immobilized enzyme in microparticles and the minimal dose required to cure infected animals. The 6C3HED ascites tumor growing in C3H mice has been used, but it suffers from the disadvantage shared with other transplantable tumors growing in mice of contamination by the benign LDH-virus (14, 17). Unfortunately, this virus will, by some unknown mechanism, significantly increase the $t_{1/2}$ of native L-asparaginase. The duration of 5 IU L-asparaginase given intraperitoneally (measured by the period during which serum concentration of L-asparagine was undetectable) was increased from 5 to 7 days. However, the virus will have no effect on the duration of L-asparaginase in microparticles, which in essence is determined by the endocytic activity of the reticuloendothelial system (12). In an attempt to simulate the clinical situation, the effect of the enzyme was tested from day 4 after

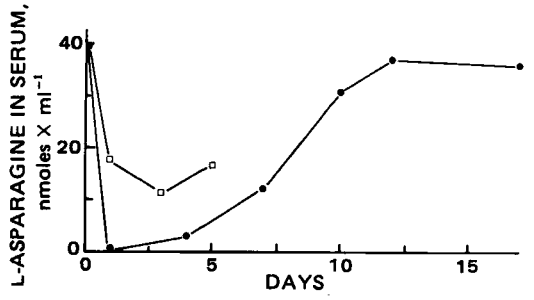

Figure 5—*L-Asparagine concentration in serum after a single intraperitoneal injection of L-asparaginase (5 IU/animal) in microparticles of polyacryldextran (●) or after implantation of 10 IU/animal sc on the backs of the mice (□). The mice were infected by the 6C3HED lymphoma, inoculated 4 days prior to the treatment. Pooled blood from 4 to 6 animals was used for each point.*

inoculation, when the virus already was sufficiently active and the number of tumor cells had significantly increased. This means that evaluation of the effect of the immobilized L-asparaginase unfortunately must be based on the comparison with the effect on the L-asparagine level obtained by giving the native enzyme on the inoculation day (before the cancer has proliferated in the host or in healthy mice).

When administered intraperitoneally, the efficiency of L-asparaginase immobilized in microparticles is equivalent to that of free enzyme, as depicted in Fig. 1. However, intramuscular administration clearly shows that the enzyme in immobilized form had longer L-asparagine-depressing activity than in free form (compare Figs. 2 and 4).

Within some limits the therapeutic effects of L-asparaginase in humans are dose related (3). The primary parameter of this effect, is the L-asparagine serum concentration, which has to be depressed to very low levels in order to prevent the growth of the tumor. We found that this level has to be <10 nmoles/ml in the C3H mice, while the normal value is ~40–45 nmoles/ml. Moreover, it is important that the L-asparagine concentration be kept at this very low level for at least 6–7 days to obtain complete regression of the tumor in the mice (measured as the survival time of 50 days). When the L-asparagine concentration was depressed to 0 values for only 5 days, the cancer growth generally recurred and the mice died within 2–3 weeks.

L-Asparaginase is very stably bound in the porous polyacrylamide microparticles and can therefore not interact directly with the tumor cells. It is obvious that the therapeutic effect of L-asparaginase is mediated *via* its L-asparagine-depressing activity.

In this study, the best L-asparagine-depressing effects were obtained with L-asparaginase in microparticles given intramuscularly. Table I, shows that the groups treated with immobilized enzyme contain more 50-day survivors than those treated with the same doses intraperitoneally. Particles administered intraperitoneally are rapidly cleared by the reticuloendothelial system and stored in the lysosomal vacuomes (18). The enzyme is thus secluded from the systemic circulation and cannot affect the L-asparagine level. The same will happen with microparticles injected intravenously (18), and to date no intravenous studies have been performed. When larger polyacryldextran particles were used intraperitoneally, the systemic effect lasted a little longer than with small polyacrylamide particles, which probably was due to enzyme leaking out from the polyacryldextran particles prior to their phagocytosis. It was shown earlier (14) that proteins immobilized in biodegradable polyacryldextran are not stably bound in such particles.

Microparticles given intramuscularly are eventually taken up by invading macrophages and/or encapsulated by fibroblasts, which will prevent further effects on the systemic L-asparagine level of the immobilized enzyme. In the present case a small dose (2.5 IU im) was administered. Although such a small dose was effective, the duration was limited by the phagocytosis of particles; this was circumvented by giving a second small dose after an interval of 3 days. Such a regimen was shown to be significantly more effective than one single dose of the same amount of L-asparaginase. Ten out of 12 treated mice were completely cured and lived for several months.

In an evaluation of the optimal route of administration, the immunological properties of the immobilized enzyme should be considered. Preliminary results (19) indicate that L-asparaginase in microparticles given intramuscularly is less immunogenic than the native form of the enzyme as manifested by a lower antibody production in mice. In addition, no toxic effects have been detected after injection of moderate doses of microparticles in mice (20).

In summary, all the results indicate that the optimal effect of L-asparaginase is obtained when the enzyme is injected intramuscularly in immobilized form in small doses.

REFERENCES

(1) H. F. Oettgen, L. J. Old, E. A. Boyse, H. A. Campbell, F. S. Philips, B. D. Clarkson, L. Tallal, R. D. Leeper, M. K. Schwartz, and J. H. Kim, *Cancer Res.*, **27**, 2619 (1967).

(2) T. Ohnuma, J. F. Holland, A. Freeman, and L. F. Sinks, *ibid.*, **30**, 2297 (1970).

(3) I. J. Ertel, M. E. Nesbit, D. Hammond, J. Weiner, and H. Sather, *ibid.*, **39**, 3893 (1979).

(4) V. Riley, D. H. Spackman, and M. A. Fitzmaurice, in "La L-Asparaginase," M. Boiron, Ed., Colloques Internationaux C.N.R.S., Paris, 1971, p. 139.

(5) D. Killander *et al.*, *Cancer*, **37**, 220 (1976).

(6) S. J. Updike, R. T. Wakamiya, and E. N. Lightfoot, Jr., *Science*, **193**, 681 (1976).

(7) S. Updike, C. Prieve, and J. Magnuson, *Birth Defects. Orig. Artic. Ser.*, **9**, 77 (1973).

(8) J. E. Benbough, C. N. Wiblin, T. N. A. Rafter, and J. Lee, *Biochem. Pharmacol.*, **28**, 833 (1979).

(9) T. M. S. Chang, *Nature (London)*, **229**, 117 (1971).

(10) E. D. Neerunjun and G. Gregoriadis, *Biochem. Soc. Trans.*, **4**, 133 (1976).

(11) K. F. O'Driscoll, R. A. Korus, T. Ohnuma, and I. M. Walczack, *J. Pharmacol Exp. Ther.*, **195**, 382 (1975).

(12) P. Edman and I. Sjöholm, *ibid.*, **211**, 663 (1979).

(13) P. Edman and I. Sjöholm, *J Pharm. Sci.*, **70**, 684 (1981).

(14) P. Edman, B. Ekman, and I. Sjöholm, *ibid.*, **69**, 838 (1980).

(15) T. O. Yellin and J. C. Wriston, Jr., *Biochemistry*, **5**, 1605 (1966).

(16) D. A. Cooney, R. L. Capizzi, and R. E. Handschumacher, *Cancer Res.*, **30**, 929 (1970).

(17) V. Riley, D. Spackman, M. A. Fitzmaurice, J. Roberts, J. S. Holcenberg, and W. C. Dolowy, *ibid.*, **34**, 429 (1974).

(18) I. Sjöholm and P. Edman, *J. Pharmacol. Exp. Ther.*, **211**, 656 (1979).

(19) P. Edman and I. Sjöholm, *J. Pharm. Sci.*, **71**, 576 (1982).

(20) P. Edman, I. Sjöholm, and U. Brunk, *J. Pharm. Sci.*, **72**, 658 (1982).

ACKNOWLEDGMENTS

The Swedish Board for Technical Development (project no 78-3614) and the I. F. Foundation for Pharmaceutical Research have financially supported the work.

The authors thank Miss Siv Larsson and Mrs. Linnéa Wallsten for technical assistance, Professor G. Klein, Department of Tumor Biology, Karolinska Institutet, Stockholm for placing the tumor cells at our disposal and Bayer (Sverige) AB, for the L-asparaginase.

Acrylic Microspheres *In Vivo* VII: Morphological Studies on Mice and Cultured Macrophages

PETER EDMAN *, INGVAR SJÖHOLM *x, and ULF BRUNK

Received October 13, 1981, from the *Departments of Pharmaceutical Biochemistry and Pathology, University of Uppsala, S-751 23 Uppsala, Sweden.* Accepted for publication June 7, 1982.

* Present address: Department of Drugs, National Board of Health and Welfare, Division of Pharmacy, S-751 25 Uppsala, Sweden.

Abstract □ Intravenously injected microparticles of polyacrylamide were cleared from the circulatory system in mice predominantly in liver, spleen, and bone marrow in mice by macrophages belonging to the reticuloendothelial system. In these cells, particles were found in dilated secondary lysosomes. The lysosomotropic character of the particles was further demonstrated using cultured peritoneal mouse macrophages. Histological changes of the liver, spleen, and bone marrow detectable by light and electron microscopy could only be seen after administration of massive doses of microparticles corresponding to 160 mg/kg body weight. In such cases, a medium-coarse vacuolization of liver parenchymal cells could be seen 1–2 days after particle administration. After 3–5 days, degeneration and necrotic cellular alteration occurred in the liver, spleen, and bone marrow. One week after particle administration, regeneration started under formation of granulomas which replaced the necrotic areas. The tissues later became normalized (after 2–3 weeks), but small granulomas remained for several weeks. The damage was parallelled by changes in the liver and spleen weights. Electron microscopy of the liver revealed that the initiated vacuolization of the parenchymal cells was due to mitochondrial swelling with rupture of the mitochondrial cristae.

Keyphrases □ Acrylic microspheres—*in vivo*, morphological studies on mice and cultured macrophages, polyacrylamide, liver, spleen, marrow □ Macrophages, cultured—acrylic microspheres, *in vivo*, morphological studies on mice, polyacrylamide, liver, spleen, marrow □ Polyacrylamide—acrylic microspheres, *in vivo*, morphological studies on mice and cultured macrophages, liver, spleen, marrow

Microparticles of highly cross-linked polyacrylamide, or derivatives, have recently been introduced as a slowly degradable carrier system for immobilized enzymes *in vivo* (1). Such particles have a pronounced porous structure allowing substrates to freely penetrate the particles and interact with the immobilized enzymes. They are small enough (mean diameter 0.1–0.4 μm) to be injected intravenously without causing respiratory complications. After intravenous or intraperitoneal injection, the microparticles are taken up by cells of the reticuloendothelial system, essentially in the liver and spleen, where they are probably localized in the lysosomal vacuome, although no direct evidence has yet been presented. Microparticles with immobilized L-asparaginase have been used to depress the level of circulating L-asparagine with resulting growth inhibition of the ascites tumor 6C3HED in mice (2). In addition, particles containing dextranase have successfully been used to treat an artificial storage disease in mice, which is produced by polyacryldextran (3).

In all studies performed to date, no signs of acute toxicity have been detected. Thus, the growth rate and survival time have been unaffected, and no tissue incompatibility has been noticed, besides the normal encapsulation of implants or intramuscularly injected microparticles. Very large doses of microparticles (100–200 mg/kg of body weight), however, have produced a transient hepatosplenomegaly in mice, lasting 4–8 weeks, resulting from the localization of the spheres in the liver and spleen. The purpose of the present work was to study microscopically the possible morphological alterations of several organs following the administration of such provocative doses of

0022-3549/83/0600-0658$01.00/0

In summary, all the results indicate that the optimal effect of L-asparaginase is obtained when the enzyme is injected intramuscularly in immobilized form in small doses.

REFERENCES

(1) H. F. Oettgen, L. J. Old, E. A. Boyse, H. A. Campbell, F. S. Philips, B. D. Clarkson, L. Tallal, R. D. Leeper, M. K. Schwartz, and J. H. Kim, *Cancer Res.*, **27**, 2619 (1967).

(2) T. Ohnuma, J. F. Holland, A. Freeman, and L. F. Sinks, *ibid.*, **30**, 2297 (1970).

(3) I. J. Ertel, M. E. Nesbit, D. Hammond, J. Weiner, and H. Sather, *ibid.*, **39**, 3893 (1979).

(4) V. Riley, D. H. Spackman, and M. A. Fitzmaurice, in "La L-Asparaginase," M. Boiron, Ed., Colloques Internationaux C.N.R.S., Paris, 1971, p. 139.

(5) D. Killander *et al.*, *Cancer*, **37**, 220 (1976).

(6) S. J. Updike, R. T. Wakamiya, and E. N. Lightfoot, Jr., *Science*, **193**, 681 (1976).

(7) S. Updike, C. Prieve, and J. Magnuson, *Birth Defects. Orig. Artic. Ser.*, **9**, 77 (1973).

(8) J. E. Benbough, C. N. Wiblin, T. N. A. Rafter, and J. Lee, *Biochem. Pharmacol.*, **28**, 833 (1979).

(9) T. M. S. Chang, *Nature (London)*, **229**, 117 (1971).

(10) E. D. Neerunjun and G. Gregoriadis, *Biochem. Soc. Trans.*, **4**, 133 (1976).

(11) K. F. O'Driscoll, R. A. Korus, T. Ohnuma, and I. M. Walczack, *J. Pharmacol Exp. Ther.*, **195**, 382 (1975).

(12) P. Edman and I. Sjöholm, *ibid.*, **211**, 663 (1979).

(13) P. Edman and I. Sjöholm, *J Pharm. Sci.*, **70**, 684 (1981).

(14) P. Edman, B. Ekman, and I. Sjöholm, *ibid.*, **69**, 838 (1980).

(15) T. O. Yellin and J. C. Wriston, Jr., *Biochemistry*, **5**, 1605 (1966).

(16) D. A. Cooney, R. L. Capizzi, and R. E. Handschumacher, *Cancer Res.*, **30**, 929 (1970).

(17) V. Riley, D. Spackman, M. A. Fitzmaurice, J. Roberts, J. S. Holcenberg, and W. C. Dolowy, *ibid.*, **34**, 429 (1974).

(18) I. Sjöholm and P. Edman, *J. Pharmacol. Exp. Ther.*, **211**, 656 (1979).

(19) P. Edman and I. Sjöholm, *J. Pharm. Sci.*, **71**, 576 (1982).

(20) P. Edman, I. Sjöholm, and U. Brunk, *J. Pharm. Sci.*, **72**, 658 (1982).

ACKNOWLEDGMENTS

The Swedish Board for Technical Development (project no 78-3614) and the I. F. Foundation for Pharmaceutical Research have financially supported the work.

The authors thank Miss Siv Larsson and Mrs. Linnéa Wallsten for technical assistance, Professor G. Klein, Department of Tumor Biology, Karolinska Institutet, Stockholm for placing the tumor cells at our disposal and Bayer (Sverige) AB, for the L-asparaginase.

Acrylic Microspheres *In Vivo* VII: Morphological Studies on Mice and Cultured Macrophages

PETER EDMAN *, INGVAR SJÖHOLM *x, and ULF BRUNK

Received October 13, 1981, from the *Departments of Pharmaceutical Biochemistry and Pathology, University of Uppsala, S-751 23 Uppsala, Sweden.* Accepted for publication June 7, 1982.

* Present address: Department of Drugs, National Board of Health and Welfare, Division of Pharmacy, S-751 25 Uppsala, Sweden.

Abstract □ Intravenously injected microparticles of polyacrylamide were cleared from the circulatory system in mice predominantly in liver, spleen, and bone marrow in mice by macrophages belonging to the reticuloendothelial system. In these cells, particles were found in dilated secondary lysosomes. The lysosomotropic character of the particles was further demonstrated using cultured peritoneal mouse macrophages. Histological changes of the liver, spleen, and bone marrow detectable by light and electron microscopy could only be seen after administration of massive doses of microparticles corresponding to 160 mg/kg body weight. In such cases, a medium-coarse vacuolization of liver parenchymal cells could be seen 1–2 days after particle administration. After 3–5 days, degeneration and necrotic cellular alteration occurred in the liver, spleen, and bone marrow. One week after particle administration, regeneration started under formation of granulomas which replaced the necrotic areas. The tissues later became normalized (after 2–3 weeks), but small granulomas remained for several weeks. The damage was parallelled by changes in the liver and spleen weights. Electron microscopy of the liver revealed that the initiated vacuolization of the parenchymal cells was due to mitochondrial swelling with rupture of the mitochondrial cristae.

Keyphrases □ Acrylic microspheres—*in vivo*, morphological studies on mice and cultured macrophages, polyacrylamide, liver, spleen, marrow □ Macrophages, cultured—acrylic microspheres, *in vivo*, morphological studies on mice, polyacrylamide, liver, spleen, marrow □ Polyacrylamide—acrylic microspheres, *in vivo*, morphological studies on mice and cultured macrophages, liver, spleen, marrow

Microparticles of highly cross-linked polyacrylamide, or derivatives, have recently been introduced as a slowly degradable carrier system for immobilized enzymes *in vivo* (1). Such particles have a pronounced porous structure allowing substrates to freely penetrate the particles and interact with the immobilized enzymes. They are small enough (mean diameter 0.1–0.4 μm) to be injected intravenously without causing respiratory complications. After intravenous or intraperitoneal injection, the microparticles are taken up by cells of the reticuloendothelial system, essentially in the liver and spleen, where they are probably localized in the lysosomal vacuome, although no direct evidence has yet been presented. Microparticles with immobilized L-asparaginase have been used to depress the level of circulating L-asparagine with resulting growth inhibition of the ascites tumor 6C3HED in mice (2). In addition, particles containing dextranase have successfully been used to treat an artificial storage disease in mice, which is produced by polyacryldextran (3).

In all studies performed to date, no signs of acute toxicity have been detected. Thus, the growth rate and survival time have been unaffected, and no tissue incompatibility has been noticed, besides the normal encapsulation of implants or intramuscularly injected microparticles. Very large doses of microparticles (100–200 mg/kg of body weight), however, have produced a transient hepatosplenomegaly in mice, lasting 4–8 weeks, resulting from the localization of the spheres in the liver and spleen. The purpose of the present work was to study microscopically the possible morphological alterations of several organs following the administration of such provocative doses of

0022-3549/83/0600-0658$01.00/0

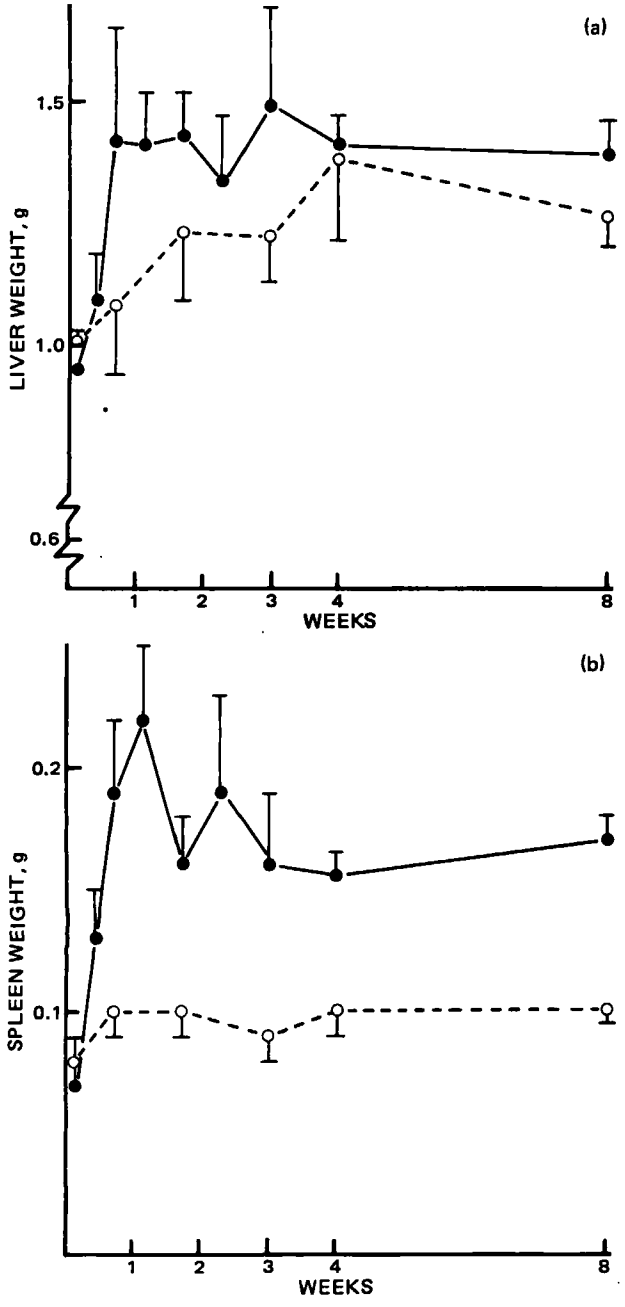

Figure 1—*(a) Weight of the liver after injection of 4 mg of polyacrylamide microparticles iv (●) or physiological saline (○) in mice. Each point shows the mean ±SD from the five animals. (b) Weight of the spleen after injection of 4 mg of polyacrylamide microparticles iv (●) or physiological saline (○) in mice. Each point represents mean ±SD from five animals.*

microparticles to mice. Concomitantly, the lysosomotropic character of the particles has been established using cultured mouse peritoneal macrophages.

EXPERIMENTAL

Chemicals—Acrylamide[1], *N,N'*-methylenebisacrylamide[1], cationized ferritin[2], *N,N,N',N'*-tetramethylethylenediamine[2], and dextran[3] were of analytical grade. Acrylic acid–glycidyl ester[4] and catalase[4] (E.C. 1.11.1.6) were used without further purification.

[1] Eastman Kodak Co.
[2] Sigma Chemical Co.
[3] Dextran T40 (mol.wt. 40,000), Pharmacia Fine Chemicals, Uppsala, Sweden.
[4] Fluka AG.

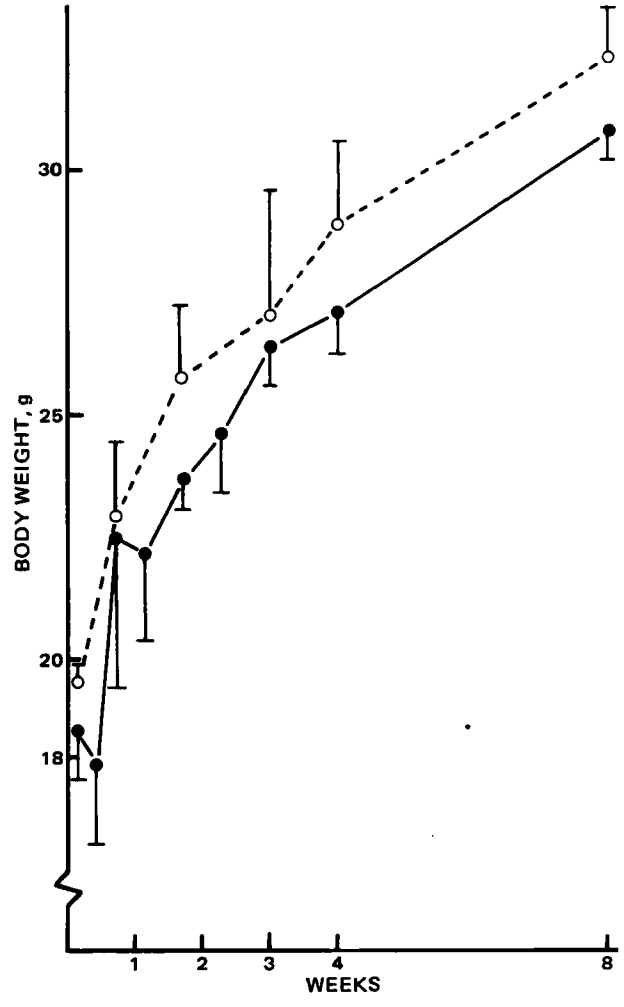

Figure 2—*Body weight of mice given 4 mg of polyacrylamide particles (●) or physiological saline (○) intravenously. Each point represents mean ±SD from five animals.*

Preparation and Administration of Microparticles—Microparticles[5] of polyacrylamide (TC = 8-25)[6] or polyacryldextran (DTC = 11-1-75)[6] were prepared according to a reported method (4, 5). Acrylamide or acryldextran and *N,N'*-methylenebisacrylamide were dissolved in sodium phosphate buffer, pH 7.4. Oxygen was eliminated from this solution with nitrogen gas. The toluene–chloroform mixture (4 + 1) containing a detergent[7] was treated in the same manner. After addition of the catalyst, ammonium peroxydisulfate (dissolved in water), the mixture was homogenized to produce a water-in-oil emulsion. The polymerization of the emulsion was initiated by adding *N,N,N',N'*-tetramethylethylenediamine.

The suspension was stirred for 20 min and the phases were separated by centrifugation. The microparticles located at the bottom of the water phase were washed at least five times, and after the last washing the particles were suspended in physiological saline.

When microparticles with immobilized ferritin or immobilized catalase were prepared, ferritin (52 mg) or catalase (20 mg) was dissolved in 2.5 ml of the acrylic monomer solution. After polymerization, the particles were washed as described above.

The microparticles were resuspended carefully in physiological saline prior to administration. The size of the particles was measured from photographs taken by scanning electron microscopy, which was done as described earlier (4). With the method used, 92.6% of the polyacrylamide particles (TC = 8-25) had a diameter of 0.1–0.4 μm, 2.2% were <0.1 μm, and 5.2% had a diameter of 0.4–0.5 μm. The polyacryldextran particles (DTC = 11-1-75) had essentially a diameter of 0.2–1.2 μm; 72.8% of the particles had a diameter within this range, and 8.9% were <0.2 μm and 5.8% were >2.1 μm.

[5] U.S. Patent 4,061,466.
[6] The nomenclature is explained in Refs. 4 and 5.
[7] Pluronics F-68, Trebac AB Stockholm, Sweden.

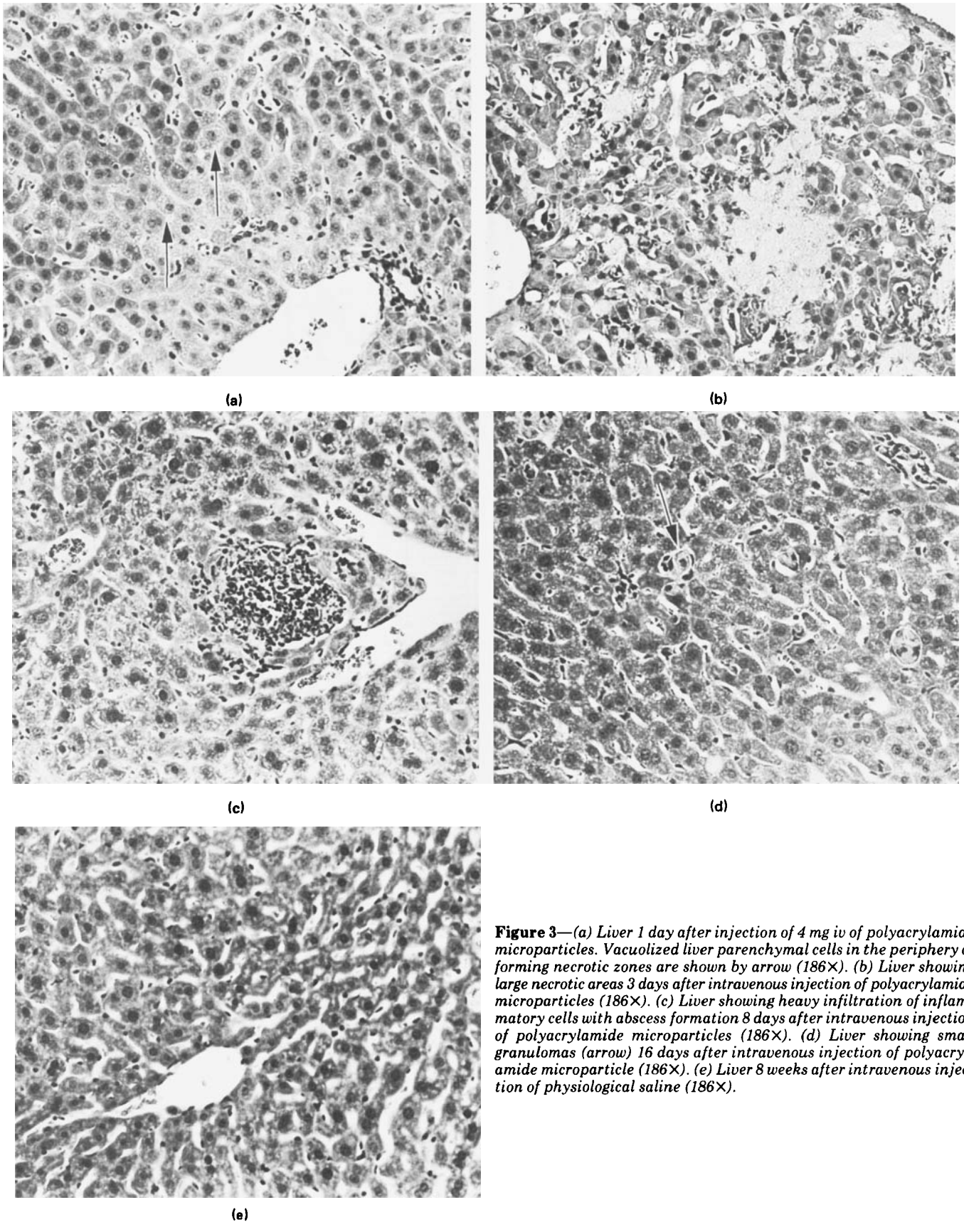

Figure 3—*(a) Liver 1 day after injection of 4 mg iv of polyacrylamide microparticles. Vacuolized liver parenchymal cells in the periphery of forming necrotic zones are shown by arrow (186×). (b) Liver showing large necrotic areas 3 days after intravenous injection of polyacrylamide microparticles (186×). (c) Liver showing heavy infiltration of inflammatory cells with abscess formation 8 days after intravenous injection of polyacrylamide microparticles (186×). (d) Liver showing small granulomas (arrow) 16 days after intravenous injection of polyacrylamide microparticle (186×). (e) Liver 8 weeks after intravenous injection of physiological saline (186×).*

Male mice[8] weighing 20–25 g were used throughout. Microparticles of polyacrylamide or polyacryldextran were suspended in physiological saline (0.1 or 0.2 ml) and injected intravenously. The doses corresponded to 1–4 mg of lyophilized microparticles.

[8] NMRI-mice, Anticimex, Stockholm, Sweden.

Preparation of Tissue Samples for Light and Transmission Electron Microscopy—At various time intervals (1–56 days) after exposure to the microparticles, five animals from each group were sacrificed by cervical dislocation, and the liver, spleen, heart, lungs, kidneys, brain, and bone marrow from the spine were collected. At each time interval, three mice from an untreated group were sacrificed and their organs used

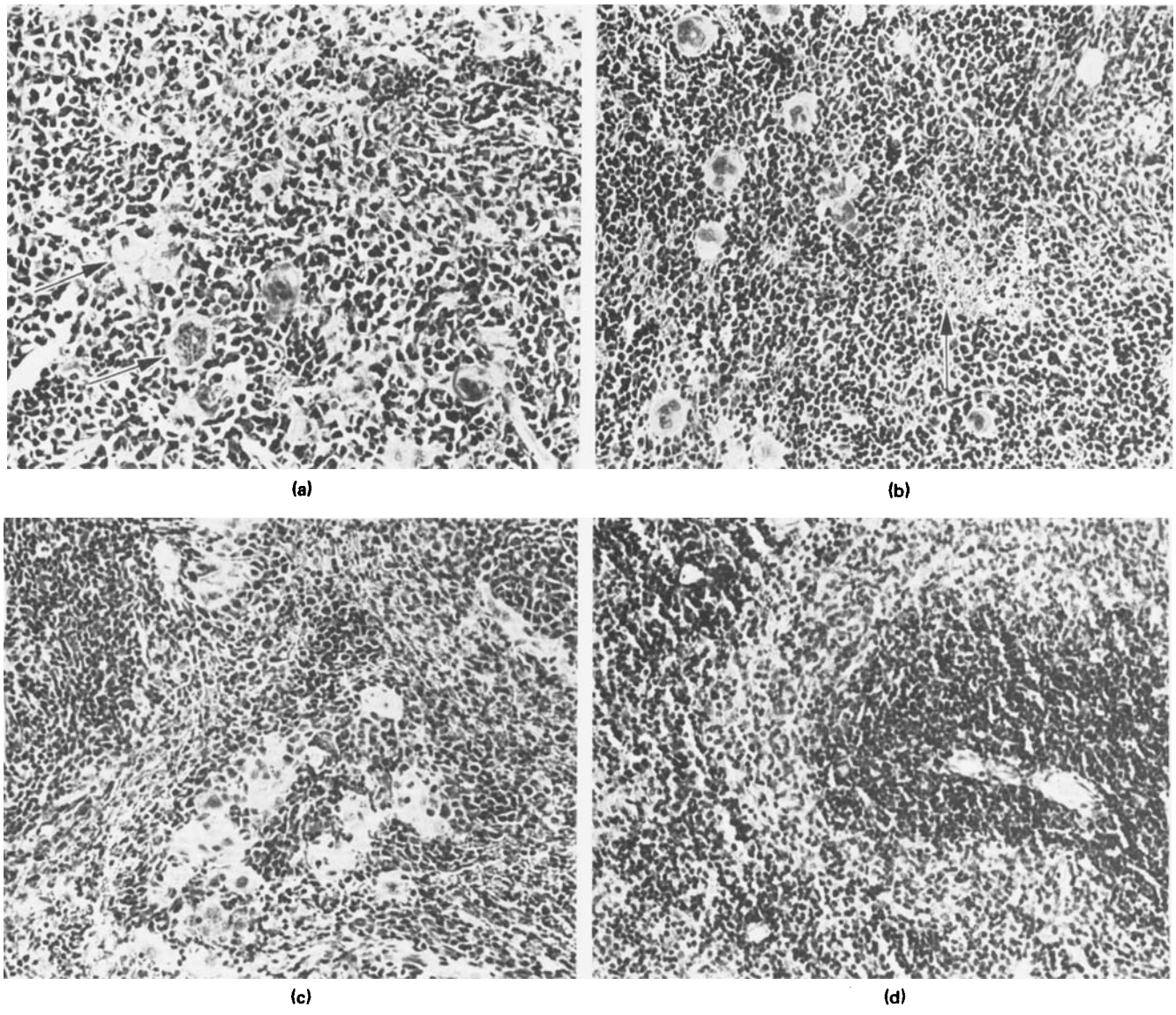

Figure 4—*(a) Spleen 3 days after intravenous injection of polyacrylamide microparticles. The architecture is much altered, with no demarcation between the red and white pulp and heavy infiltration of inflammatory cells. Small abscesses are shown by arrow (186×). (b) Spleen with forming granulomas (arrow) 8 days after intravenous injection of polyacrylamide microparticles (186×). (c) Spleen 21 days after intravenous injection of polyacrylamide microparticles; reconstitution of red and white pulps but remaining granulomas (186×). (d) Spleen 8 weeks after intravenous injection of physiological saline (186×).*

as the control group. The liver, spleen, heart, lungs, brain, and kidneys were weighed, and thin (2 mm) tissue specimens were cut from the organs immediately, and immersed in chilled 5% formaldehyde in 0.15 *M* phosphate buffer, pH 7.2. The specimens were subsequently embedded in paraffin, cut at 2–3 μm, stained with hematoxylin and eosin, and studied under the light microscope.

For transmission electron microscopy, small samples (<1 mm thick) were removed from the liver immediately after the animals were sacrificed. The specimens were immersed in ice-cold 2% glutaraldehyde in 0.1 *M* sodium cacodylate buffer with 0.1 *M* sucrose (pH 7.2; total osmotic pressure 510 mOsm, effective osmotic pressure 300 mOsm) (6, 7). After glutaraldehyde fixation for 24 hr, the specimens were rinsed in 0.15 *M* sodium cacodylate buffer, pH 7.2, and cut into small pieces which were postfixed in 1% OsO_4 in 0.15 *M* sodium cacodylate buffer for 90 min at room temperature. The specimens were dehydrated in an ethanol series, stained *en masse* with 2% uranyl acetate in 50% ethanol for 12 hr, and embedded in expoxy[9]. Thin sections were cut with diamond knives, stained with lead (8), and examined at 60 kV with an electron microscope[10].

Transmission Electron Microscopy of Negatively Stained Microparticles—A suspension of ferritin-labeled microparticles was placed as a tiny drop on formvar coated 300-mesh copper electron microscopy grids and most of the fluid was immediately removed with a piece of filter paper. A drop of a 0.2% water solution of uranyl acetate was applied for 30 sec and removed with filter paper. After drying, the grids were examined at 80 kV with the electron microscope[10], using a 50-μm objective aperture.

Cultures of Mice Peritoneal Macrophages—Mouse macrophages were collected by washing the unstimulated peritoneum of adult male animals[8] with 3 ml of warm (37°) phosphate-buffered saline. The cells were further suspended in 10 ml of cold (0°) phosphate buffer and mildly spun down at 180×*g* for 10 min. The pellet was resuspended in F-10 medium (9) with 20% newborn calf serum and 15 m*M* *N*-2-hydroxyethylpiperazine-*N*-2-ethanesulfonic acid buffer, supplemented with 10 μg/ml of streptomycin and 100 U/ml of penicillin. The cells were seeded into 50-mm plastic petri dishes at 5×10^5 cells/dish and cultured at 37° in 5% carbon dioxide in air at 85% humidity. The dishes were carefully rinsed with new, complete medium 24 hr after the initial seeding, to eliminate red blood cells, lymphocytes, and macrophages that had not attached to the solid support. During the ensuing cultivation period the medium was changed every 48 hr.

Cultures were exposed to 0.1 mg/ml of microspheres containing ferritin as a marker 24 hr after seeding (immediately after being rinsed). The cells were exposed to these particles for 48 and 72 hr and then fixed in 2% glutaraldehyde in 0.1 *M* sodium cacodylate buffer with 0.1 *M* sucrose (pH

[9] Epon 812.
[10] JEOL 100-C microscope.

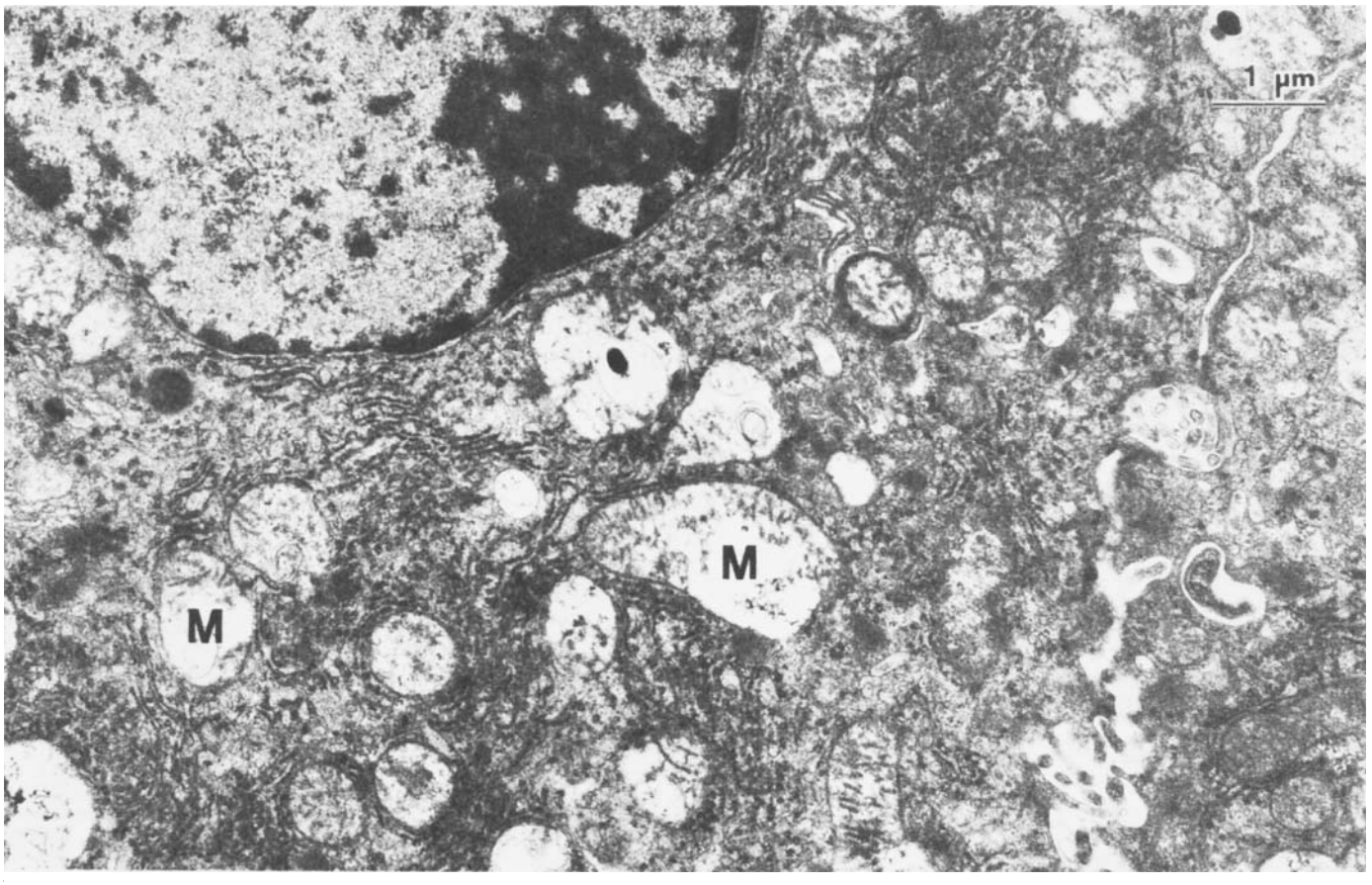

Figure 5—*Liver parenchymal cells 2 days after injection of 4 mg iv polyacrylamide microparticles containing catalase. Several swollen mitochondria (M) with ruptured cristae can be seen.*

7.2, total osmotic pressure 510 mOsm, effective osmotic pressure 300 mOsm (6, 7) for 60 min at 0°, rapidly rinsed in 0.15 *M* sodium cacodylate buffer and postfixed in 1% OsO_4 in 0.15 *M* sodium cacodylate buffer for 90 min at room temperature. The cells were then dehydrated *in situ* in an ethanol series, counter-stained *en masse* for 12 hr in 2% uranyl acetate in 50% ethanol, and embedded in small capsules in epoxy as described earlier (10). Untreated control cells were harvested at the same time intervals. Thin sections were cut with diamond knives, stained with lead citrate (8), and examined at 60 kV with the electron microscope[10].

RESULTS

Gross Distribution of Microparticles After Intravenous Injection—It was shown in an earlier study (11) that the distribution of large doses of microparticles to the reticuloendothelial system in mice after intravenous injections results in a transient hepatosplenomegaly. To correlate the megaly with the microscopic findings, the weight changes were studied in some detail.

Figures 1a and 1b show the variations in weight of the liver and the spleen, respectively, with time after 4-mg iv injections of microparticles. The liver weight reached its maximum after 5–8 days and was essentially normalized after 4–8 weeks. The effects of the microparticles on the growth of the spleen were relatively greater than on the liver (Fig. 1b). One week after the injection, the weight was ~220% of that of the controls. The megaly was successively retracted, but the organ weight was not normalized within the 8-week study period. In the earlier work (11), the weight of the spleen was normalized after 16–24 weeks. With smaller doses of polyacrylamide (1 mg) or of polyacryldextran (2 mg) enlargement of the liver and spleen was not as great. This weight increase was strictly dose dependent.

The variation in body weight after intravenous injection of 4-mg polyacrylamide microparticles is shown in Fig. 2. As is apparent from the figure, there were no significant differences between the control and test groups. Although the overall weight of the test group was lower at the time of injection, the increase in weight with time was the same. Consequently, the administration of large doses of microparticles to the mice did not affect growth.

Light Microscopy of Mouse Tissue—*Following* the administration of 1 mg of particles, no changes were detected by light microscopy in any of the studied organs. No demonstrable changes were noted in the brain, heart, kidneys, or the lungs, while the liver, spleen, and the bone marrow showed pronounced alterations after injection of 4 mg of particles.

As early as 1 day after particle administration, the parenchymal cells of the liver showed a medium coarse vacuolization, which had a patchy distribution (Fig. 3a). After a few more days, necrotic areas of various sizes had developed corresponding to the areas of initial vacuolization, as well as unicellular necrosis (Fig. 3b). There was a diffuse, sparse infiltration of inflammatory cells (Figs. 3c and d). Later, regeneration started with mitotic activity within the parenchymal liver cell population. After 7–10 days, granulomas composed of macrophages, epithelioid cells, lymphocytes, and polymorphonuclear cells formed and replaced the necrotic cells and areas (Fig. 3d). These granulomas remained for several weeks. The number of Kupffer cells was found to have increased at later time intervals. The normal ultrastructural appearance of the liver 8 weeks after intravenous injection of physiological saline is shown in (Fig. 3e).

In the bone marrow there was an early (after 1 day) and massive infiltration of mature, irregularly distributed polymorphonuclear cells and macrophages with the formation of granulomas. After 7–10 days, the bone marrow had regained an apparently normal appearance.

The spleen showed early and pronounced changes. After 1–3 days, the limits between the white and the red pulps were blurred, the sinusoids were dilated and lined with prominent endothelial cells, and the number of megakaryocytes was increased (Fig. 4a). Later (4–10 days) there was a heavy infiltration of various inflammatory cells under formation of small abscesses and granulomas (Fig. 4b). The tissue became normalized later, but small granulomas, composed of histiocytes, remained for many weeks (Fig. 4c). The normal appearance of the spleen is shown in (Fig. 4d).

Transmission Electron Microscopy of Liver Tissue—The vacuoles of the liver cells, which were so strikingly observed 1 or 2 days after the administration of large amounts of particles, were found to be due to mitochondrial swelling with rupture of the mitochondrial cristae (Fig. 5). There was no obvious alteration of the lysosomal vacuome of the parenchymal cells. The Kupffer cells showed many dilated lysosomes filled with an amorphous material.

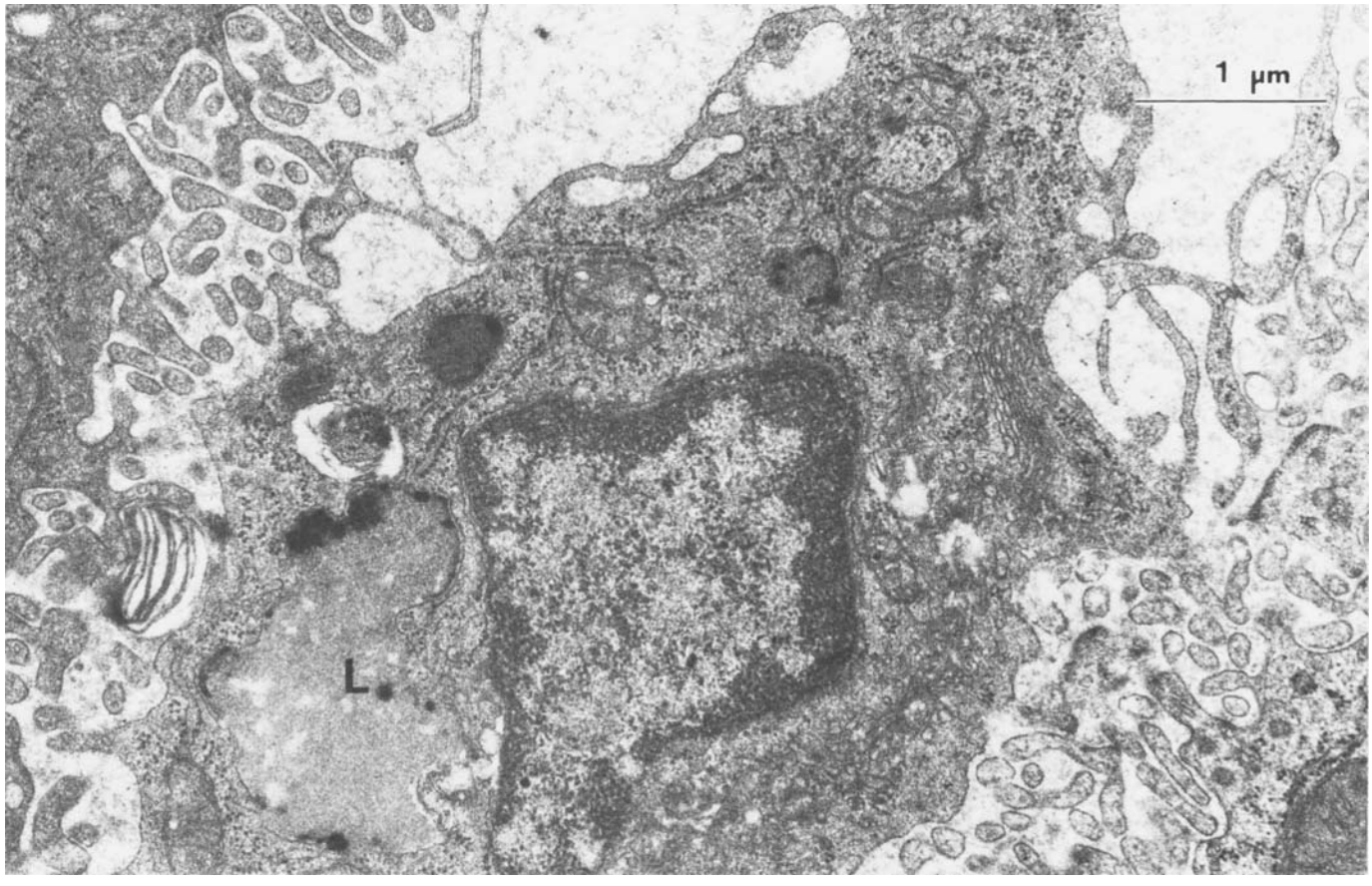

Figure 6—*Kupffer cell 2 months after injection of 4 mg iv polyacrylamide microparticles loaded with catalase. Note large vacuoles (L, secondary lysosomes) filled with an amorphous material.*

At later time intervals, the tissue degeneration prevented detailed studies on cellular alterations until the acute inflammatory response had declined. In the specimens studied ~2 months after the administration of the catalase-loaded particles, these lysosomes were still frequently observed (Fig. 6). It was, however, not possible to discern individual particles either in liver parenchymal or in Kupffer cells. Obviously, the particles have an electron density about equal to that of the embedding resin and do not bind osmium, uranyl, or lead.

Transmission Electron Microscopy of Negatively Stained Microparticles—Transmission electron microscopy of the ferritin-loaded microparticles indirectly confirmed (12) that the polyacrylamide particles were spherical and had a diameter between 0.1 and 0.4 μm. Ferritin gave the particles a dotted appearance.

Transmission Electron Microscopy of Cultured Macrophages—Macrophages exposed to 0.1 mg of microparticles with ferritin per milliliter of medium for 72 hr showed a high increased rate of autophagocytosis and an increased number of secondary lysosomes containing an amorphous material with tiny electron dense particles corresponding to the ferritin of the labeled microspheres. In most lysosomes the electron dense particles were concentrated toward the periphery of the organelles (Figs. 7a and b).

DISCUSSION

As mentioned earlier, no signs of acute toxicity were detected when microparticles of acrylic polymers were used as carriers for enzymes in various experiments on mice and rats (1). When the distribution of such small particles was studied in mice (11) only a transient hepatosplenomegaly was noticed. The present work has, moreover, demonstrated that a large number of spheres must be administered in order to produce any pathological morphological alterations in the liver, spleen, and bone marrow, which constitute the tissues where the microparticles are localized *in vivo* (11). The effects described in the present study are generally obtained after treatment with doses corresponding to 160 mg of dried material per kg of body weight. Such a very large dose is necessary to produce the adverse reactions, which are important to know, since the microparticles are an attractive alternative as enzyme carriers for future human applications.

It is important to stress that when dose levels of 40 mg/kg were used (corresponding to the administration of 1 mg of particles to the mice), only insignificant, hardly detectable morphological reactions could be seen in the liver, spleen, and bone marrow.

The first general reaction in the liver tissue, detected by light microscopy and transmission electron microscopy, on exposure to the high doses of microparticles, was the swelling of the mitochondria of the parenchymal cells, which were eventually ruptured as part of cellular degeneration. Necrosis of the tissues followed, and inflammatory cells migrated into the area, with a megaly as a consequence. The weight changes of the liver and spleen followed very closely the morphological changes seen with the light and electron microscopes and reached maxima at the same time as the maximum of the tissue damage. Thus, the megaly was probably essentially due to the increased number of cells in the liver and spleen, and only to a minor extent a result of cellular edema.

The reason for the initial hepatocellular degeneration is not obvious, and the interpretation of our results is hampered by the fact that the microparticles could not be seen directly with the electron microscope. The spherical form of the ferritin-loaded microparticles was confirmed by negative staining, and ferritin could be used as a marker in the *in vitro* experiments with cultured macrophages to trace the microparticles.

In these studies it was quite evident that the microparticles had been taken up by the cells and introduced into the lysosomal vacuome, as seen both indirectly by the markedly increased number of lysosomes and their swelling, and directly by the localization of large amounts of electron dense material in the lysosomes (Fig. 7b), which was not seen in the control (Fig. 7a). Consequently, it might be suggested that the degenerative cellular alterations, *e.g.*, the swelling and rupture of the mitochondria, giving rise to the vacuolization of the liver parenchymal cells, are due to an altered function of the lysosomal apparatus. It was thus not possible to directly detect the particles in the hepatocytes in the tissue samples. The indirect evidence, however, suggests an uptake both in the Kupffer and the parenchymal cells. Most probably the small size of the particles allows their passage into the space of Dissé through the existing gaps in the sinusoidal endothelium exposing the microparticles to the liver parenchymal cells which could bring about their endocytosis.

The present work is only semiquantitative, in the sense that the toxic

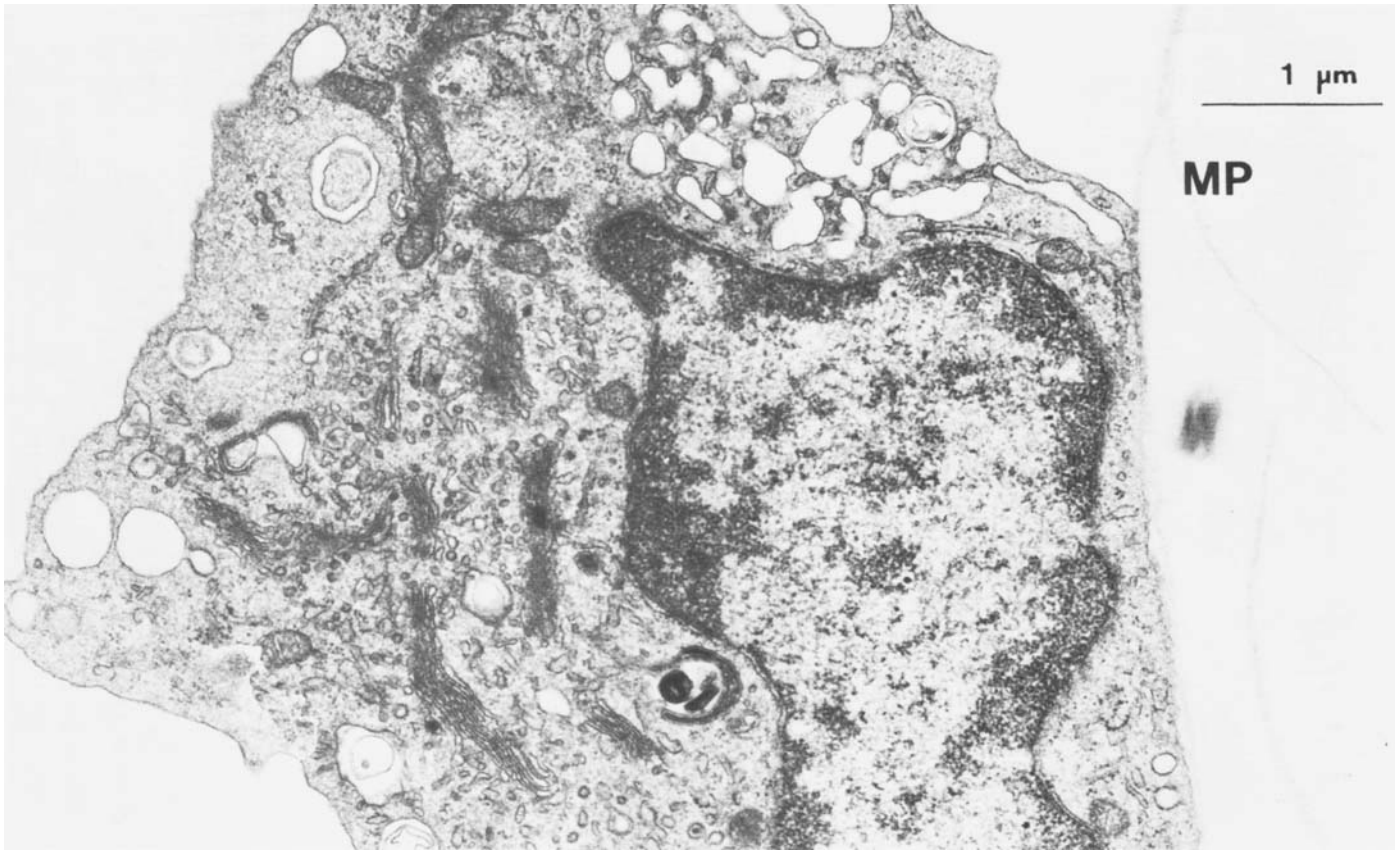

(a)

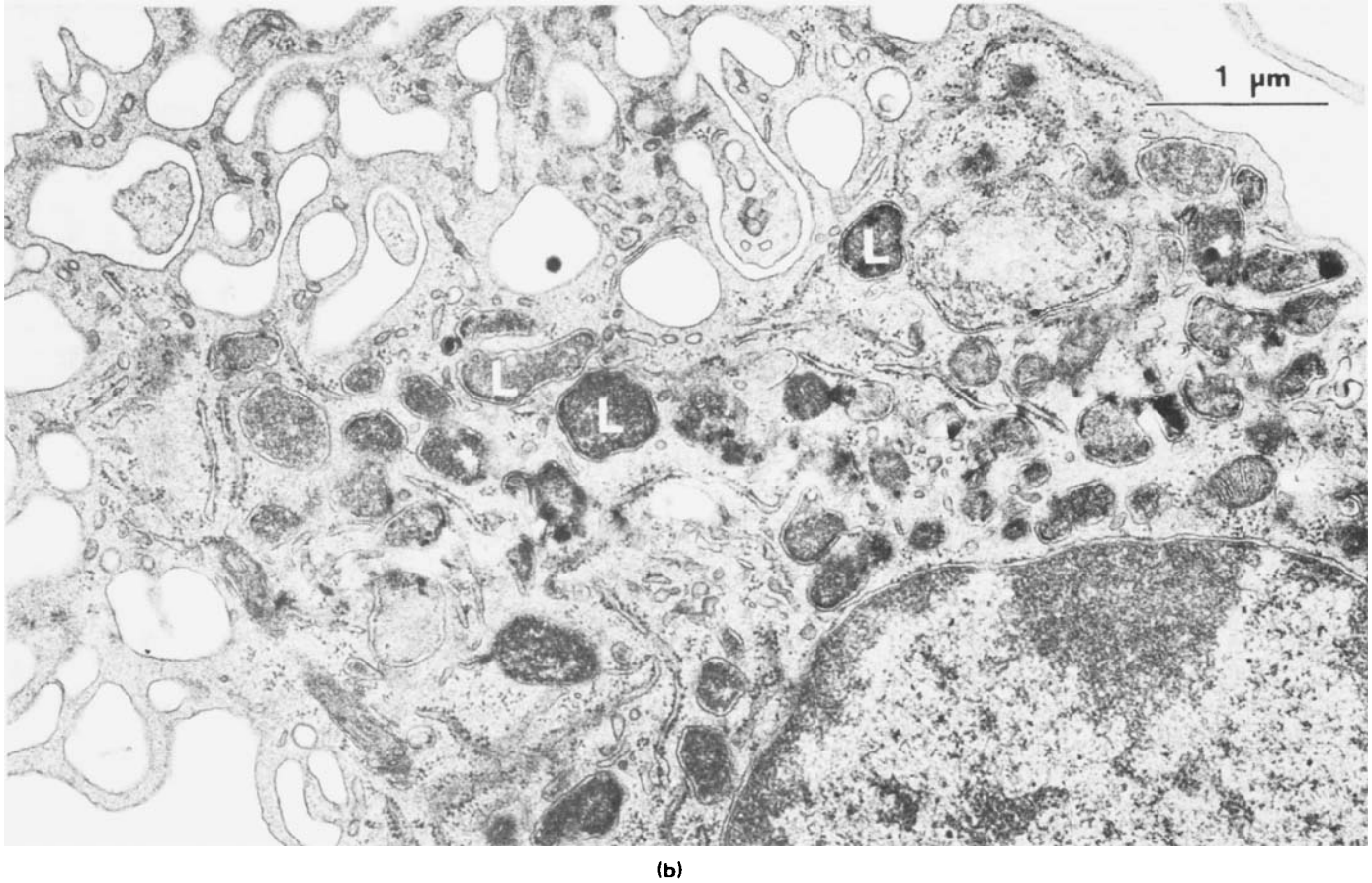

(b)

Figure 7—*(a) Normal mouse peritoneal macrophage cultured* in vitro. *MP denotes the microprecipitate to which the cells have attached. (b) Macrophage 72 hr after exposure to ferritin-labeled polyacrylamide microparticles (0.1 mg/ml of medium). Note the large number of lysosomes (L) containing microparticles with ferritin.*

reactions seen in the mice are proportional to the doses given, and only detectable when the mice are exposed to very high doses exceeding 40 mg/kg of body weight. Quantitative studies are not possible *in vivo*, when the relationship between the number of particles taken up per cell cannot be satisfactorily controlled. For such studies, it is necessary to use suitable *in vitro* systems, *e.g.*, cultured peritoneal macrophages, where the relationship between the number of particles and cells can be carefully controlled. Such studies will be presented separately, showing when exposure of cultured macrophages to microspheres will lead to changed intracellular function and cellular degeneration. Subsequent *in vivo* applications with acrylic microspheres must be based on such studies.

REFERENCES

(1) P. Edman and I. Sjöholm, *J. Pharmacol. Exp. Ther.*, **211**, 663 (1979).

(2) P. Edmon and I. Sjöholm, *J. Pharm. Sci.*, **72**, 654 (1982).

(3) P. Edmon and I. Sjöholm, *Life Sci.*, **30**, 327 (1982).

(4) B. Ekman, C. Lofter, and I. Sjöholm, *Biochemistry*, **15**, 5115 (1975).

(5) P. Edman, B. Ekman, and I. Sjöholm, *J. Pharm. Sci.*, **69**, 838 (1980).

(6) B. Arborgh, P. Bell, U. Brunk, and V. P. Collins, *J. Ultrastruct. Res.*, **56**, 339 (1976).

(7) V. P. Collins, B. Arborgh, and U. Brunk, *Acta Pathol. Microbiol. Scand. Sect. A*, **85**, 157 (1977).

(8) E. S. Reynolds, *J. Cell Biol.*, **17**, 208 (1963).

(9) R. G. Ham, *Exp. Cell Res.*, **29**, 515 (1963).

(10) U. Brunk, J. L. E. Ericsson, J. Pontén, and B. Westermark, *Exp. Cell. Res.*, **67**, 407 (1971).

(11) I. Sjöholm and P. Edman, *J. Pharmacol. Exp. Ther.*, **211**, 656 (1979).

(12) B. Ekman and I. Sjöholm, *Nature (London)*, **257**, 825 (1975).

ACKNOWLEDGMENTS

Supported by the Swedish Medical Research Council and the Swedish Board for Technical Development (project 75-4415).

Poly-L-methionine Sulfoxide: A Biologically Inert Analogue of Dimethyl Sulfoxide with Solubilizing Potency

JOSEF PITHA *x, LAJOS SZENTE *, and JUDITH GREENBERG ‡

Received January 18, 1982, from the **National Institutes of Health, National Institute on Aging-GRC, Baltimore, Maryland 21224* and the ‡*National Institute of Dental Research-NIH, Bethesda, Maryland 20205.* Accepted for publication June 8, 1982.

Abstract □ Poly-L-methionine sulfoxide is a water-soluble polymer containing the sulfoxide moiety. The preparation and radiolabeling of this polymer is described and its bioeffects are compared with those of dimethyl sulfoxide. Poly-L-methionine sulfoxide is similar to dimethyl sulfoxide in that it is a potent solubilizer of lipophilic compounds in water. Although the partition coefficient of poly-L-methionine sulfoxide in 1-octanol–water is only 20 times lower than that of dimethyl sulfoxide, it was found not to penetrate into intracellular spaces. In contrast to dimethyl sulfoxide, poly-L-methionine sulfoxide and L-methionine sulfoxide were found to be ineffective in inducing differentiation in murine erythroleukemia cells and inhibiting differentiation of avian neural crest cells, suggesting that compounds effective in these processes must have the ability to penetrate into cells or membrane proteins. Overall lack of bioactivity of poly-L-methionine sulfoxide, combined with low toxicity (2 g/kg, iv, in the mouse with no effect), makes this compound a suitable inert solubilizer and carrier for lipophilic drugs.

Keyphrases □ Dimethyl sulfoxide—poly-L-methionine sulfoxide, biologically inert analogue with solubilizing potency □ Poly-L-methionine sulfoxide—biologically inert analogue of dimethyl sulfoxide with solubilizing potency □ Solubilization potency—poly-L-sulfoxide, biologically inert analogue of dimethyl sulfoxide

A majority of the applications of polymers in pharmacy are based on their mechanical properties and inertness. Also, polymers are able to form complexes with pharmaceuticals; this property has been used relatively rarely, *e.g.*, in decreasing the aggressive properties of iodine by complexation with povidone. Furthermore, polymers possessing complexing power can be used, instead of organic

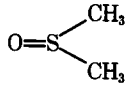

Dimethyl Sulfoxide

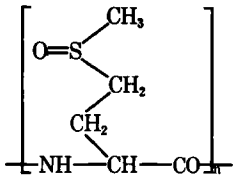

Polymethionine Sulfoxide

solvents, to dissolve nonpolar drugs in aqueous media and to promote sorption of pharmaceuticals. Dimethyl sulfoxide (I), one of the solvents often used for this purpose (1, 2), is relatively nontoxic to cells, yet easily penetrates cellular membranes and, in some cases, triggers very complex biological responses, *e.g.*, induction (3–8) and inhibition (9–12) of cellular differentiation.

It may be advantageous, for both practical applications and for studies of the induction mechanism, to supress some of its bioeffects, *i.e.*, to make a new selective agent by chemical modifications from a pluripotent compound. This may be possible by preparing a macromolecule that contains structural elements of dimethyl sulfoxide. A

Table I—Solubility (μg/ml) of Lipophilic Compounds in Phosphate-Buffered Isotonic Saline in the Presence (5%) or Absence of Poly-L-methionine Sulfoxide

Compound	Saline	Saline and Poly-L-methionine Sulfoxide
β-Ionone, $C_{13}H_{20}O$	7.3	1400
Retinol, $C_{20}H_{30}O$	<4.6	12
β-Carotene, $C_{40}H_{56}$	Nondetectable	6
Lycopene, $C_{40}H_{56}$	Nondetectable	4
Vitamin D_3, $C_{27}H_{44}O$	<0.18	138

0022-3549/83/0600-0665$01.00/0

reactions seen in the mice are proportional to the doses given, and only detectable when the mice are exposed to very high doses exceeding 40 mg/kg of body weight. Quantitative studies are not possible *in vivo*, when the relationship between the number of particles taken up per cell cannot be satisfactorily controlled. For such studies, it is necessary to use suitable *in vitro* systems, *e.g.*, cultured peritoneal macrophages, where the relationship between the number of particles and cells can be carefully controlled. Such studies will be presented separately, showing when exposure of cultured macrophages to microspheres will lead to changed intracellular function and cellular degeneration. Subsequent *in vivo* applications with acrylic microspheres must be based on such studies.

REFERENCES

(1) P. Edman and I. Sjöholm, *J. Pharmacol. Exp. Ther.*, **211**, 663 (1979).

(2) P. Edmon and I. Sjöholm, *J. Pharm. Sci.*, **72**, 654 (1982).

(3) P. Edmon and I. Sjöholm, *Life Sci.*, **30**, 327 (1982).

(4) B. Ekman, C. Lofter, and I. Sjöholm, *Biochemistry*, **15**, 5115 (1975).

(5) P. Edman, B. Ekman, and I. Sjöholm, *J. Pharm. Sci.*, **69**, 838 (1980).

(6) B. Arborgh, P. Bell, U. Brunk, and V. P. Collins, *J. Ultrastruct. Res.*, **56**, 339 (1976).

(7) V. P. Collins, B. Arborgh, and U. Brunk, *Acta Pathol. Microbiol. Scand. Sect. A*, **85**, 157 (1977).

(8) E. S. Reynolds, *J. Cell Biol.*, **17**, 208 (1963).

(9) R. G. Ham, *Exp. Cell Res.*, **29**, 515 (1963).

(10) U. Brunk, J. L. E. Ericsson, J. Pontén, and B. Westermark, *Exp. Cell. Res.*, **67**, 407 (1971).

(11) I. Sjöholm and P. Edman, *J. Pharmacol. Exp. Ther.*, **211**, 656 (1979).

(12) B. Ekman and I. Sjöholm, *Nature (London)*, **257**, 825 (1975).

ACKNOWLEDGMENTS

Supported by the Swedish Medical Research Council and the Swedish Board for Technical Development (project 75-4415).

Poly-L-methionine Sulfoxide: A Biologically Inert Analogue of Dimethyl Sulfoxide with Solubilizing Potency

JOSEF PITHA *x, LAJOS SZENTE *, and JUDITH GREENBERG ‡

Received January 18, 1982, from the **National Institutes of Health, National Institute on Aging-GRC, Baltimore, Maryland 21224* and the ‡*National Institute of Dental Research-NIH, Bethesda, Maryland 20205.* Accepted for publication June 8, 1982.

Abstract □ Poly-L-methionine sulfoxide is a water-soluble polymer containing the sulfoxide moiety. The preparation and radiolabeling of this polymer is described and its bioeffects are compared with those of dimethyl sulfoxide. Poly-L-methionine sulfoxide is similar to dimethyl sulfoxide in that it is a potent solubilizer of lipophilic compounds in water. Although the partition coefficient of poly-L-methionine sulfoxide in 1-octanol–water is only 20 times lower than that of dimethyl sulfoxide, it was found not to penetrate into intracellular spaces. In contrast to dimethyl sulfoxide, poly-L-methionine sulfoxide and L-methionine sulfoxide were found to be ineffective in inducing differentiation in murine erythroleukemia cells and inhibiting differentiation of avian neural crest cells, suggesting that compounds effective in these processes must have the ability to penetrate into cells or membrane proteins. Overall lack of bioactivity of poly-L-methionine sulfoxide, combined with low toxicity (2 g/kg, iv, in the mouse with no effect), makes this compound a suitable inert solubilizer and carrier for lipophilic drugs.

Keyphrases □ Dimethyl sulfoxide—poly-L-methionine sulfoxide, biologically inert analogue with solubilizing potency □ Poly-L-methionine sulfoxide—biologically inert analogue of dimethyl sulfoxide with solubilizing potency □ Solubilization potency—poly-L-sulfoxide, biologically inert analogue of dimethyl sulfoxide

A majority of the applications of polymers in pharmacy are based on their mechanical properties and inertness. Also, polymers are able to form complexes with pharmaceuticals; this property has been used relatively rarely, *e.g.*, in decreasing the aggressive properties of iodine by complexation with povidone. Furthermore, polymers possessing complexing power can be used, instead of organic

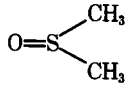

Dimethyl Sulfoxide

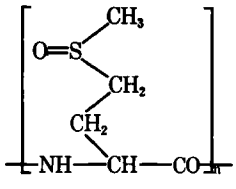

Polymethionine Sulfoxide

solvents, to dissolve nonpolar drugs in aqueous media and to promote sorption of pharmaceuticals. Dimethyl sulfoxide (I), one of the solvents often used for this purpose (1, 2), is relatively nontoxic to cells, yet easily penetrates cellular membranes and, in some cases, triggers very complex biological responses, *e.g.*, induction (3–8) and inhibition (9–12) of cellular differentiation.

It may be advantageous, for both practical applications and for studies of the induction mechanism, to supress some of its bioeffects, *i.e.*, to make a new selective agent by chemical modifications from a pluripotent compound. This may be possible by preparing a macromolecule that contains structural elements of dimethyl sulfoxide. A

Table I—Solubility (μg/ml) of Lipophilic Compounds in Phosphate-Buffered Isotonic Saline in the Presence (5%) or Absence of Poly-L-methionine Sulfoxide

Compound	Saline	Saline and Poly-L-methionine Sulfoxide
β-Ionone, $C_{13}H_{20}O$	7.3	1400
Retinol, $C_{20}H_{30}O$	<4.6	12
β-Carotene, $C_{40}H_{56}$	Nondetectable	6
Lycopene, $C_{40}H_{56}$	Nondetectable	4
Vitamin D_3, $C_{27}H_{44}O$	<0.18	138

0022-3549/83/0600-0665$01.00/0

Table II—Distribution of the Studied Compounds between Murine Erythroleukemia Cells and Serum-Free Medium

Compound	cpm Added	cpm in Cell Pellet	cpm Recovered in Pellet and Supernatant, %	cpm in Non-Cellular Component of Pellet[a]	cpm per 10^8 Cells	Compound per Cell, fg[b]
Inulin	50,000	4367	91	4367	0	—
	25,000	2986	96	2986	0	—
	25,000	2520	99	2520	0	—
Poly-L-methionine sulfoxide	50,000	4723	102	5126	(−403)	—
	50,000	4674	102	5126	(−452)	—
	25,000	2668	95	2563	105	—
	25,000	2748	101	2563	185	—
Dimethyl sulfoxide	52,000	7831	99	5331	2,500	1.1
	52,000	7670	103	5331	2,339	1.0
	26,000	4192	106	2666	1,526	0.6
	26,000	4448	106	2666	1,782	0.8

[a] Calculated on the assumption that inulin does not absorb or penetrate cells. [b] Femtograms.

nondegradable polymer containing the structural elements of dimethyl sulfoxide was prepared previously by a multi-step synthesis (13). In contrast to that study, this study describes a facile synthesis of a degradable polymer: poly-L-methionine sulfoxide.

EXPERIMENTAL

Preparation of Poly-L-methionine Sulfoxide—A saturated aqueous solution of sodium periodate (321 mg) was added slowly to a stirred solution of 224 mg of poly-L-methionine[1] (average molecular weight 30,000) in 7 ml of acetic acid at room temperature. Stirring was continued for 12 hr. Water (14 ml) was then added to the reaction mixture, the solution was dialyzed against water, clarified by centrifugation (10,000 rpm for 10 min), and freeze-dried. This procedure yielded 120 mg of colorless polymer. To quantitate the extent of oxidation, the polymer was dissolved in deuterium oxide and its NMR spectrum measured on a 60-MHz spectrometer[2]. Resonance of the methyl group of sulfoxide residues occurs at 2.75 ppm and that of sulfone residues occurs at 3.15 ppm; no signal attributable to methylthio groups could be detected. From the integration of the spectrum it was calculated that the sulfoxide methyl group predominates over the sulfone methyl group by a ratio of 5:1.

Tritiation of Poly-L-methionine Sulfoxide—Poly-L-methionine sulfoxide (4 mg) was added to a solution of 3.5 ml of benzene containing [^{3}H]ethyl methanesulfonate (225 μCi, 0.4 mg)[3]. The mixture was stirred for 15 min, frozen, kept at −20° overnight, and then kept at 80° for 1 week; the solvent was then evaporated. The residue was dissolved in water and dialyzed against water. The residue contained 1 μCi of radioactive polymer (3 mg).

All other compounds used were obtained commercially.

Solubilization of Lipophilic Compounds by Poly-L-methionine Sulfoxide—Excess lipophilic compound (5–10 mg) was enclosed in a test tube (polyethylene, volume 1.2 ml) with phosphate-buffered isotonic saline (1 ml) lacking or containing poly-L-methionine sulfoxide (50 mg). The suspension was stirred by rotating the test tube for 1 day in the dark at 20–22°. Thereafter the suspension was centrifuged and the concentration of lipophilic compound in the clear supernatant was determined spectrophotometrically.

Measurement of Distribution of Compounds Between 1-Octanol and Water—Compounds were equilibrated with the above solvents for 6–24 hr at 20–22° and their concentration determined by liquid scintillation counting (dimethyl sulfoxide) or spectrophotometrically (poly-L-methionine sulfoxide, 210-nm wavelength).

Measurement of Distribution of Compounds Between the Cells in Culture and the Medium—The assay contained a 0.2-ml pellet of murine erythroleukemia cells[4] (14) (1×10^8 cells) and the medium[5] in addition to the radioactive compound studied, in a total volume of 1 ml. The equilibrium distribution of the compound studied was established by incubation for 2 hr at 37°. The cells and medium were separated by centrifugation and the concentration of the compound was calculated from the results of liquid scintillation counting.

Induction and Inhibition of Cell Differentiation—Murine erythroleukemia cells were grown in suspension cultures in medium[5] supplemented with 10% calf serum and antibiotics. The cells were exposed to a potential inducer for 5 days, and their differentiation was assayed by calculating the percentage of cells that were stained by benzidine (14).

Cultures of avian neural crest cells were initiated as described previously (12). Cells were subcultured in replicate plates (10,000–15,000 cells/plate) 2 days after explantation (day 2) and grown in a 1:1 mixture of medium[6] and broth[7] supplemented with 2% chick embryo extract and 5% calf serum.

The assay on neural crest cells was run as follows. Cells were grown in the presence or absence of the test compound from day 2 to 7 of culture. On day 7 fresh medium containing the test compound was added. Cells were then labeled for 5 hr with 5 μCi/ml of [^{14}C]tyrosine[8]. Incorporation of radioactivity into the trichloroacetic acid-insoluble fraction of the cells and melanin-specific incorporation was determined as described previously (12). All values given represent means of duplicates that differed by <10%.

RESULTS

The easiest procedure for preparing poly-L-methionine sulfoxide is the one involving the mild oxidation of poly-L-methionine. Various agents oxidize sulfides to sulfoxides (15, 16). *m*-Chloroperbenzoic acid, iodine, and sodium periodate were tested as oxidizing agents. When sodium periodate was used, no detectable methylthio residues remained, and the overoxidation of the sulfoxide group to the sulfone moiety was only ~16% of the total. Radioactive labeling of poly-L-methionine sulfoxide was performed by an exchange of some of the methyl groups in the polymer for [^{3}H]ethyl groups; since only ~0.05% of these groups were exchanged, the effects of such an introduced structural change on the polymer properties may be disregarded. This labeling occurred using only small amounts of radioactive [^{3}H]ethyl methanesulfonate (0.4%); however, good yields of ^{3}H-polymer (75%) were readily obtained in this manner.

Poly-L-methionine was found to be a potent solubilizer of organic compounds. A series of terpenoid-like lipophilic compounds containing up to 40 carbon atoms was evaluated (Table I).

Next, the partition coefficients (1-octanol–water) of dimethyl sulfoxide and poly-L-methionine sulfoxide were measured. The partition coefficient of dimethyl sulfoxide was found to be 0.038 ($\sigma = 0.007$, $N = 10$). This value compares with 0.01 and 0.04 reported previously (17, 18). The partition coefficient of poly-L-methionine sulfoxide was found to be 0.002 ($\sigma = 5 \times 10^{-5}$, $N = 3$).

The partition of a compound between the cultured cells and surrounding medium is a good indicator of the ability of that compound to be adsorbed by and penetrate cells, the latter process being the important one in equilibrium. For calculation of such distribution from the directly measurable concentrations of the compound in the medium and in the cell pellet, it is necessary to estimate the amount of medium that is retained in the cell pellet. Inulin, an electroneutral polysaccharide which does not penetrate into cells and is only slightly adsorbed by cells, was used for this estimate. The results (Table II) show that poly-L-methionine sulfoxide is excluded from cells to the same extent as inulin. On the other

[1] Sigma Chemical Co., St. Louis, Mo.
[2] Varian Instrument Co., Cheverly, Md.
[3] New England Nuclear, Boston, Mass.
[4] Obtained from the laboratory of Dr. Philip Leder, Bethesda, Md.
[5] Minimum Essential Medium (Eagle, without serum).
[6] Minimum Essential Medium, Delbecco.
[7] Ham's F-12.
[8] New England Nuclear, Boston, Mass.; sp. act. 512 mCi/mmole.

Table III—Induction of Differentiation of Murine Erythroleukemia Cells by Studied Compounds

Compound	Concentration, %	Benzidine-Positive Cells; 5th Day of Induction, %
—	—	1.6
Dimethyl sulfoxide	1	28.0
	1.5	39.0
	2.0	76.0
Poly-L-methionine sulfoxide	0.2	0.2
	0.5	2.5
	1.5	0.0[a]
L-Methionine sulfoxide	1.0	0.0
	1.5	0.0[a]

[a] No cell growth.

hand, 0.6–1.1 fg of dimethyl sulfoxide were taken up per cell. The partition coefficient (concentration in cells/concentration in medium) of dimethyl sulfoxide, when calculated from these measurements, is 0.52 ($\sigma = 0.1, N = 4$).

The ability of the test compounds to induce differentiation of erythroleukemia cells was assessed by calculating the percentage of hemoglobin-synthesizing cells (*i.e.*, benzidine positive) on the 5th day of exposure to the agent. Dimethyl sulfoxide increased the percentage of benzidine-positive cells up to 40 times over that of the untreated controls (Table III). In contrast, poly-L-methionine sulfoxide was completely inactive. For further comparison L-methionine sulfoxide was also included in the test and found inactive (Table III). Concentrations up to the toxic range were tested (Table III), and additional measurements at longer exposure times were also performed to confirm the above conclusions (results not given).

Dimethyl sulfoxide is known to inhibit differentiation of neural crest cells (melanin synthesis) (12). The effects of dimethyl sulfoxide, poly-L-methionine sulfoxide, and L-methionine sulfoxide on the incorporation of [^{14}C]tyrosine into melanin were compared (Table IV). Dimethyl sulfoxide, as expected, inhibited incorporation, whether it was added to the cells only during the labeling period or was present throughout the culture period. In contrast, poly-L-methionine sulfoxide and L-methionine sulfoxide were inactive at 0.05%.

Toxic effects of poly-L-methionine *in vitro* in culture were relatively insignificant. To measure the toxicity of poly-L-methionine *in vivo* doses of 500, 1000, and 2000 mg/kg were injected intravenously into mice (strain C57B1/6J, 9 weeks old, females) using a peristaltic pump system described previously (19). No toxic effects or weight losses were observed when compared with controls, even with the highest dose.

DISCUSSION

Poly-L-methionine sulfoxide, in contrast to poly-L-methionine, is very water soluble. This solubility, its one-step preparation, and its ease of radiolabeling, make it suitable for biological studies.

Preparation of a macromolecular analogue of a pharmacon often leads to the elimination of some of its effects. Of the various bioeffects of dimethyl sulfoxide, conversion to the macromolecular poly-L-methionine sulfoxide, resulted in the retention of only the solubilization effects. Compounds used in solubilization tests (Table I) are structurally related. β-Ionone, a monocyclic terpene with a short side chain, was efficiently solubilized, whereas retinol, which contains the same monocyclic structure but has a longer side chain, was only moderately solubilized. β-Carotene and lycopene were solubilized to a moderate extent. These data suggest that poly-L-methionine sulfoxide preferentially solubilizes compounds which have a compact structure, *i.e.*, without long hydrocarbon chains. Vitamin D_3, which has such a compact structure, was indeed efficiently solubilized.

Partition coefficients of drugs and other organic compounds between 1-octanol and water have been used extensively in the correlation of their bioeffects. This coefficient is a measure of the ability of the drugs to interact and penetrate the lipid bilayer of cellular membranes, which is thought to be well approximated by 1-octanol. Using this established comparison system it was found that poly-L-methionine sulfoxide distributes less uniformly (0.002) than dimethyl sulfoxide (0.04). The value of the distribution coefficient of poly-L-methionine sulfoxide *per se* is not low enough to lead to the assumption that no penetration into cells or bioeffects may be achieved by this compound (18). Probably, the macromolecular character of poly-L-methionine sulfoxide is another

Table IV—Effect of Compounds on Pigmentation of Neural Crest Cells

Compound	Concentration, %	[^{14}C]Tyrosine Incorporation into Melanin, cpm/cell	
		Day 7	Days 2–7
—	—	0.008	0.004
Dimethyl sulfoxide	1	0	0
Poly-L-methionine sulfoxide	0.5	Not determined	Toxic
	0.05	0.007	0.006
L-Methionine sulfoxide	0.05	Not determined	0.006

contributing factor leading to the observed inertness. Poly-L-methionine sulfoxide was found, as described in the *Results* section, not to penetrate into the cellular spaces and, thus, may only interact with the external surface of cellular membranes.

In the context of the study on the mechanism of changes in cell differentiation induced by dimethyl sulfoxide it is important to note that its nonpenetrating analogue, poly-L-methionine sulfoxide, failed to affect cell differentiation in either of the systems tested. These findings suggest that the mechanism of action of dimethyl sulfoxide requires its entry into cells or into the hydrophobic interior of some protein on the cell surface, a process that can change the structure and function of the protein. The lack of penetration of poly-L-methionine sulfoxide into cells was proven experimentally; entry of a compound into the hydrophobic sections of proteins is possible only for small molecular weight hydrophobic or amphophilic molecules and, thus, poly-L-methionine sulfoxide is automatically excluded (20). A low molecular weight, highly polar analogue of dimethyl sulfoxide, L-methionine sulfoxide, also lacked any inducing ability (Tables III and IV).

In addition to the lack of cell-inducing activity, poly-L-methionine sulfoxide has low acute toxicity, even when given intravenously.

Thus, the most promising application of poly-L-methionine sulfoxide seems to be in the complexing of bioactive lipophilic compounds. This complexing converts the lipophilic compounds into water soluble ones; thus, to an extent poly-L-methionine sulfoxide may functionally imitate carrier serum proteins. Such complexing of drugs has often led to a decrease in their toxicity, as shown, for example, in the case of retinoids (21). Complexing of drugs with poly-L-methionine may possibly have the same consequences.

REFERENCES

(1) D. Martin, A. Weise, and H. J. Niclas, *Angew. Chem.*, **79**, 340 (1967).

(2) W. A. Ritschel, *Angew. Chem., Int. Ed.*, **8**, 699 (1969).

(3) C. Friend, W. Scher, J. G. Holland, and T. Sato, *Proc. Natl. Acad. Sci. USA*, **68**, 378 (1971).

(4) P. A. Marks and R. A. Rifkind, *Annu. Rev. Biochem.*, **47**, 419 (1978).

(5) C. Li, L. S. Rittmann, A. S. Tsiftsoglou, K. K. Bhargava, and A. C. Sartorelli, *J. Med. Chem.*, **21**, 874 (1978).

(6) E. Fibach, R. Gambari, P. A. Shaw, G. Maniatis, R. C. Reuben, S. Sassa, R. A. Rifkind, and P. A. Marks, *Proc. Natl. Acad. Sci. USA*, **76**, 1906 (1979).

(7) C. Palfrey, Y. Kimhi, and U. Z. Littauer, *Biochem. Biophys. Res. Commun.*, **76**, 937 (1977).

(8) J. F. Tallman, C. C. Smith, and R. C. Henneberry, *Proc. Natl. Acad. Sci. USA*, **74**, 873 (1977).

(9) A. F. Miranda, E. G. Nette, S. Khan, K. Brockbank, and M. Schonberg, *Proc. Natl. Acad. Sci. USA*, **75**, 3826 (1978).

(10) H. M. Blau and C. J. Epstein, *Cell*, **17**, 95 (1979).

(11) K. H. Stenzel, R. Schwartz, A. L. Rubin, and A. Novogrodsky, *Nature (London)*, **285**, 106 (1980).

(12) J. H. Greenberg and C. Oliver, *Arch. Biochem. Biophys.*, **204**, 1 (1980).

(13) H. G. Batz, V. Hofmann, and H. Ringsdorf, *Makromol. Chem.*, **169**, 323 (1973).

(14) A. Leder and P. Leder, *Cell*, **5**, 319 (1975).

(15) G. Hilgetag and A. Martin, "Weygand's Preparative Organic Chemistry," Wiley, New York, N.Y., 1972.

(16) R. Jost, E. Bramlilla, J. C. Monti, and P. L. Luisi, *Helv. Chim. Acta*, **63**, 375 (1980).

(17) A. Bernstein, A. S. Boyd, V. Crichley, and V. Lamb, in "Induction and Inhibition of Friend Leukemic Cell Differentiation: The Role of

Membrane-Active Compounds in Biogenesis and Turnover of Membrane Macromolecules," J. S. Cook, Ed., Raven, New York, N.Y., 1976, p. 145.

(18) C. Hansch and A. Leo, in "Substituent Constants for Correlation Analysis in Chemistry and Biology," Wiley, New York, N.Y., 1979.

(19) E. L. Schneider, J. R. Chaillet, and R. R. Tice, *Exp. Cell Res.*, **100**, 396 (1976).

(20) C. Tanford, "The Hydrophobic Effect: Formating of Micelles and Biological Membranes," Wiley, New York, N.Y., 1973.

(21) J. Pitha, S. Zawadzki, F. Chytil, D. Lotan, and R. Lotan, *J. Natl. Cancer Inst.*, **65**, 1011 (1980).

ACKNOWLEDGMENTS

The authors wish to thank Mrs. B. A. Hughes for measurements of hemoglobin, Dr. S. Zawadzki and Dr. J. W. Kusiak for preparation of some materials used in this study, and Mrs. D. A. Lamartin for help with the manuscript.

Nonisothermal Kinetics Using a Microcomputer: A Derivative Approach to the Prediction of the Stability of Penicillin Formulations

J. M. HEMPENSTALL *, W. J. IRWIN *x, A. LI WAN PO*, and A. H. ANDREWS ‡

Received March 2, 1982, from the **Department of Pharmacy, University of Aston in Birmingham, Gosta Green, Birmingham, B4 7ET, UK,* and the ‡ *Beecham Pharmaceuticals, Research Division, Worthing, West Sussex, BN14 8QH, UK.* Accepted for publication June 9, 1982.

Abstract □ A procedure is described for the determination of the shelf-life of pharmaceutical preparations using nonisothermal kinetics. A BASIC computer program, which enables the data analysis to be undertaken rapidly and automatically on a microcomputer, is presented.

Keyphrases □ Kinetics, nonisothermal—derivative approach to the prediction of the stability of penicillin formulations using a microcomputer □ Stability—nonisothermal kinetics using a microcomputer, a derivative approach to the prediction, penicillin formulations □ Penicillin—nonisothermal kinetics using a microcomputer, a derivative approach to the prediction of stability in formulations □ Formulations—penicillin, nonisothermal kinetics using a microcomputer, a derivative approach to the prediction of stability

Nonisothermal methods for the prediction of the shelf-life of pharmaceutical preparations are an attractive alternative to traditional isothermal accelerated storage tests. A nonisothermal study involves a temperature change throughout the reaction and enables a full stability–temperature profile to be determined from one experiment. This procedure offers a considerable reduction in effort for the estimation of shelf-life and has received much attention. Early methods (1, 2) were extended to pharmaceuticals by Rogers (3) who used a defined temperature rise profile to simplify data handling. The validity of this approach, using various heating programs, has been confirmed (4–8), but theoretical and practical limitations have been discussed (9, 10). Greater freedom in experimental design is available if a predetermined temperature–time profile is not demanded. Methodology has therefore been extended to allow the rate of temperature increase to be determined by experimental, rather than theoretical, expedience (11, 12). Nonisothermal–isothermal methods have also been reported (13, 14), and many important applications of nonisothermal kinetics to solid-state degradations have appeared (15, 16). The estimation of the errors involved in these procedures has also received attention (12, 17).

Despite the success of these methods, few applications to formulated products have appeared (18). In this study a general method for the determination of nonisothermal kinetic profiles is described, and a BASIC computer program (NONISO) is presented, which can be implemented on a microcomputer, to undertake the calculations automatically. The procedures are shown to be comparable to methods requiring large computing facilities (12) and prove satisfactory for formulated products.

THEORETICAL

Degradation Rates—The rate of degradation of a drug can be represented by:

$$\frac{-dC_t}{dt} = k_T C_t^n \qquad \text{(Eq. 1)}$$

where C_t is the concentration at time t, k_T is the specific rate constant at temperature T, and n is the order of reaction. For a first order reaction ($n = 1$) this can be written as:

$$C_t = C_0 e^{-k_T t} \qquad \text{(Eq. 2)}$$

In logarithmic form this is:

$$\ln C_t = \ln C_0 - k_T t \qquad \text{(Eq. 3)}$$

and the negative slope of the plot k *versus* $\ln C_t$ yields the rate constant.

When the temperature is continually increased throughout the reaction, the degradation rate progressively increases. The isothermal rate constant is now approximated by:

$$k_T = -\left[\frac{\ln C_t - ln C_{t-\delta t}}{\delta t}\right] \qquad \text{(Eq. 4)}$$

where δt is a small increment of time, over which period the temperature may be considered constant. For an infinitesimal increase in time and temperature, the specific rate constant is given by:

$$k_T = -\frac{d(\ln C_t)}{dt} \qquad \text{(Eq. 5)}$$

The slope of the tangent at a point for the plot of t *versus* $\ln C_t$ for nonisothermal data yields the specific rate constant at the temperature observed.

If other orders of reaction are followed the appropriate equations are:

$$\text{zero order:} \quad k_T = -d(C_t)/dt \qquad \text{(Eq. 6)}$$

$$\text{2nd order (a = b):} \quad k_T = d(1/C_t)/dt \qquad \text{(Eq. 7)}$$

0022-3549/83/0600-0668$01.00/0

Membrane-Active Compounds in Biogenesis and Turnover of Membrane Macromolecules," J. S. Cook, Ed., Raven, New York, N.Y., 1976, p. 145.

(18) C. Hansch and A. Leo, in "Substituent Constants for Correlation Analysis in Chemistry and Biology," Wiley, New York, N.Y., 1979.

(19) E. L. Schneider, J. R. Chaillet, and R. R. Tice, *Exp. Cell Res.*, **100**, 396 (1976).

(20) C. Tanford, "The Hydrophobic Effect: Formating of Micelles and Biological Membranes," Wiley, New York, N.Y., 1973.

(21) J. Pitha, S. Zawadzki, F. Chytil, D. Lotan, and R. Lotan, *J. Natl. Cancer Inst.*, **65**, 1011 (1980).

ACKNOWLEDGMENTS

The authors wish to thank Mrs. B. A. Hughes for measurements of hemoglobin, Dr. S. Zawadzki and Dr. J. W. Kusiak for preparation of some materials used in this study, and Mrs. D. A. Lamartin for help with the manuscript.

Nonisothermal Kinetics Using a Microcomputer: A Derivative Approach to the Prediction of the Stability of Penicillin Formulations

J. M. HEMPENSTALL *, W. J. IRWIN *x, A. LI WAN PO*, and A. H. ANDREWS ‡

Received March 2, 1982, from the **Department of Pharmacy, University of Aston in Birmingham, Gosta Green, Birmingham, B4 7ET, UK,* and the ‡ *Beecham Pharmaceuticals, Research Division, Worthing, West Sussex, BN14 8QH, UK.* Accepted for publication June 9, 1982.

Abstract □ A procedure is described for the determination of the shelf-life of pharmaceutical preparations using nonisothermal kinetics. A BASIC computer program, which enables the data analysis to be undertaken rapidly and automatically on a microcomputer, is presented.

Keyphrases □ Kinetics, nonisothermal—derivative approach to the prediction of the stability of penicillin formulations using a microcomputer □ Stability—nonisothermal kinetics using a microcomputer, a derivative approach to the prediction, penicillin formulations □ Penicillin—nonisothermal kinetics using a microcomputer, a derivative approach to the prediction of stability in formulations □ Formulations—penicillin, nonisothermal kinetics using a microcomputer, a derivative approach to the prediction of stability

Nonisothermal methods for the prediction of the shelf-life of pharmaceutical preparations are an attractive alternative to traditional isothermal accelerated storage tests. A nonisothermal study involves a temperature change throughout the reaction and enables a full stability–temperature profile to be determined from one experiment. This procedure offers a considerable reduction in effort for the estimation of shelf-life and has received much attention. Early methods (1, 2) were extended to pharmaceuticals by Rogers (3) who used a defined temperature rise profile to simplify data handling. The validity of this approach, using various heating programs, has been confirmed (4–8), but theoretical and practical limitations have been discussed (9, 10). Greater freedom in experimental design is available if a predetermined temperature–time profile is not demanded. Methodology has therefore been extended to allow the rate of temperature increase to be determined by experimental, rather than theoretical, expedience (11, 12). Nonisothermal–isothermal methods have also been reported (13, 14), and many important applications of nonisothermal kinetics to solid-state degradations have appeared (15, 16). The estimation of the errors involved in these procedures has also received attention (12, 17).

Despite the success of these methods, few applications to formulated products have appeared (18). In this study a general method for the determination of nonisothermal kinetic profiles is described, and a BASIC computer program (NONISO) is presented, which can be implemented on a microcomputer, to undertake the calculations automatically. The procedures are shown to be comparable to methods requiring large computing facilities (12) and prove satisfactory for formulated products.

THEORETICAL

Degradation Rates—The rate of degradation of a drug can be represented by:

$$\frac{-dC_t}{dt} = k_T C_t^n \qquad \text{(Eq. 1)}$$

where C_t is the concentration at time t, k_T is the specific rate constant at temperature T, and n is the order of reaction. For a first order reaction ($n = 1$) this can be written as:

$$C_t = C_0 e^{-k_T t} \qquad \text{(Eq. 2)}$$

In logarithmic form this is:

$$\ln C_t = \ln C_0 - k_T t \qquad \text{(Eq. 3)}$$

and the negative slope of the plot k *versus* $\ln C_t$ yields the rate constant.

When the temperature is continually increased throughout the reaction, the degradation rate progressively increases. The isothermal rate constant is now approximated by:

$$k_T = -\left[\frac{\ln C_t - ln C_{t-\delta t}}{\delta t}\right] \qquad \text{(Eq. 4)}$$

where δt is a small increment of time, over which period the temperature may be considered constant. For an infinitesimal increase in time and temperature, the specific rate constant is given by:

$$k_T = -\frac{d(\ln C_t)}{dt} \qquad \text{(Eq. 5)}$$

The slope of the tangent at a point for the plot of t *versus* $\ln C_t$ for nonisothermal data yields the specific rate constant at the temperature observed.

If other orders of reaction are followed the appropriate equations are:

$$\text{zero order:} \quad k_T = -d(C_t)/dt \qquad \text{(Eq. 6)}$$

$$\text{2nd order (a = b):} \quad k_T = d(1/C_t)/dt \qquad \text{(Eq. 7)}$$

0022-3549/83/0600-0668$01.00/0

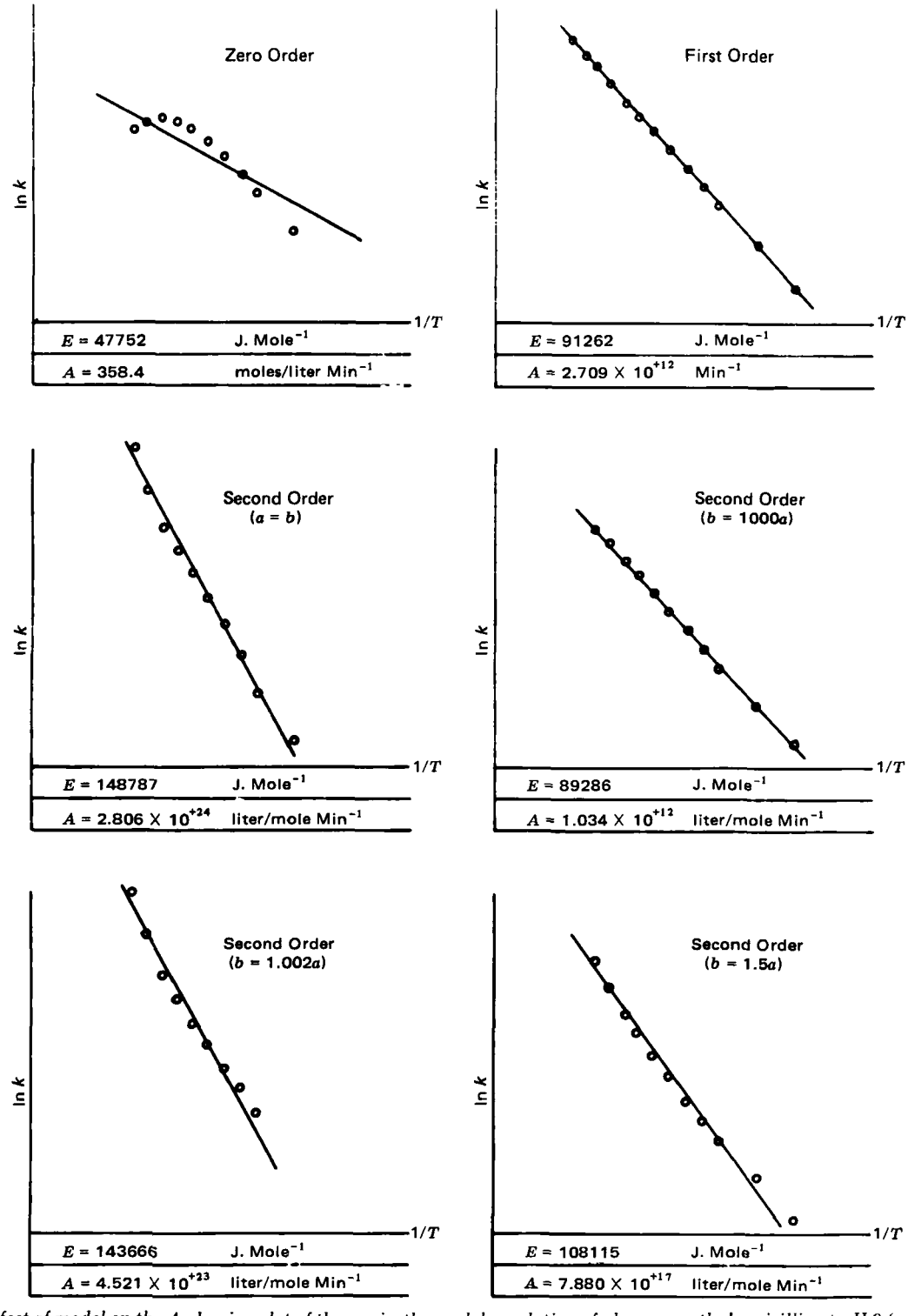

Figure 1—*The effect of model on the Arrhenius plot of the nonisothermal degradation of phenoxymethylpenicillin at pH 9* (a *and* b *refer to the initial concentrations of penicillin and hydroxide in second-order reactions).*

$$\text{2nd order (a} \neq \text{ b):} \quad k_T = \frac{d\left[\left(\frac{1}{B_0 - C_0}\right) \ln \frac{(B_0 - C_0 + C_t)C_0}{C_t B_0}\right]}{dt} \qquad \text{(Eq. 8)}$$

where C_t is the concentration (moles/liter), at time t, of the monitored drug of initial concentration C_0. B_0 is the initial concentration (moles/liter) of the excess reagent in a second-order reaction when the initial concentrations of the two reactants (a,b) are not identical.

The values of k_T are calculated by fitting a polynomial to the transformed data as a function of time. For the first-order case this is:

$$\ln C_t = a_0 + a_1 t + a_2 t^2 \ldots a_n t^n \qquad \text{(Eq. 9)}$$

Differentiation at the experimental points yields the corresponding rate constants:

$$\frac{d(\ln C_t)}{dt} = -k_T = a_1 + 2a_2 t + 3a_3 t^2 \ldots n a_n t^{n-1} \qquad \text{(Eq. 10)}$$

The rate constants at the experimentally measured temperatures are then used to compute the activation energy (E) and pre-exponential factor (A) in the Arrhenius Equation:

$$k_T = Ae^{-E/RT}$$

These data enable the calculation of rate constants at storage temperatures and the prediction of shelf-life ($t_{90\%}$) and half-life ($t_{1/2}$) to be made.

Table I—Input Data and Isothermal Rate Constants[a] for the Degradation of Phenoxymethylpenicillin at pH 9

Minutes	Concentration, %	Temperature, °	Rate Constant, 1/min
0	100.00	28.3	6.75997 E-05
9	99.60	32.8	7.16944 E-04
19	98.50	39.4	1.55624 E-03
29	96.40	45.8	3.07291 E-03
39	92.10	52.0	5.83865 E-03
44	89.10	54.8	7.85191 E-03
49	85.20	57.5	1.03574 E-02
52	82.50	59.0	1.21146 E-02
55	79.40	60.6	1.40709 E-02
58	75.90	62.1	1.62312 E-02
61	71.80	63.6	1.85985 E-02
64	67.90	64.9	2.11736 E-02
67	63.40	66.2	2.39550 E-02
70	58.40	67.5	2.69387 E-02
73	53.90	68.6	3.01181 E-02
76	48.80	69.8	3.34838 E-02
79	43.80	70.8	3.70232 E-02
82	39.00	71.8	4.07210 E-02
85	34.40	72.7	4.45581 E-02
88	30.00	73.6	4.85123 E-02
91	26.00	74.5	5.25574 E-02
94	22.00	75.3	5.66638 E-02
97	18.40	76.0	6.07977 E-02
100	15.10	76.7	6.49210 E-02
103	12.50	77.4	6.89917 E-02
106	10.00	78.0	7.29629 E-02
109	7.90	78.5	7.67834 E-02
112	6.40	79.0	8.03970 E-02

[a] Polynomial coefficients are: 4.60496, -6.75179×10^{-5}, -4.09094×10^{-5}, 6.03266×10^{-7}, -1.93521×10^{-8}, -1.08408×10^{-10}, and 9.47380×10^{-13} (a_0 term first).

EXPERIMENTAL

Nonisothermal Kinetics—*At pH 9*—A borate buffer (500 ml) containing boric acid (5.17 g), sodium hydroxide (1.67 g), and hydrochloric acid (5 *M*, 1.9 ml) was placed in a three-necked round-bottomed flask suspended in a thermostated water-bath (20-liter capacity, 1 kW). A thermometer, graduated to 0.1°, was placed into the buffer solution through one neck, a polytef sampling-tube was fitted through the second neck, and a stirrer rotated at 200 rpm was positioned through the third neck. When the buffer had reached thermal equilibrium, potassium phenoxymethylpenicillin [potassium (2*s*, 5*R*, 6*R*)-3-3-dimethyl-7-oxo-6-(2-phenoxyacetamido)-4-thia-1-azabicyclo[3.2.0]heptane-2-carboxylate] (250 mg) was rapidly added to the buffer. When solution was complete (2 min), the water-bath heater was set at 100° (providing a temperature increase to 80° in 2 hr). A sample (5 ml) was immediately withdrawn and two 2-ml volumes were accurately measured. To each was added a solution of phenol (2 ml, 0.02% w/v in a phosphate buffer containing 0.9073% KH_2PO_4 adjusted to pH 5) as internal standard. This gave a final solution pH of 7: a more stable value for the penicillin (19). The initial penicillin concentration was determined in duplicate by high-performance liquid chromatographic (HPLC) analysis through interpolation onto a calibration curve prepared similarly over a penicillin concentration range of 0–50 mg/100 ml ($r = 0.999$). At frequent intervals throughout the run, samples (3 ml) were removed and a 2-ml aliquot was assayed. Time and precise temperature were also noted.

Table II—Arrhenius Parameter Estimates for the Nonisothermal Degradation of Phenoxymethylpenicillin at pH 9

All Data Points[a]

Parameter	Value	Range	Units
E	103044	95431–110657	J/Mole
A	1.7066 E + 14	1.1225 *E* + 13–2.5945 *E* + 15	/Min

Omission of 28.3° Point[b]

Parameter	Value	Range	Units
E	91262	90862–91663	J/mole
A	2.7090 *E* + 12	2.3491 *E* + 12–3.1241 *E* + 12	/Min

[a] Slope −12393.6 ± 915.7 (p = 95%), intercept 32.771 ± 2.722 (p = 95%), r = 0.98367. [b] Slope −10976.6 ± 48.2 (p = 95%), intercept 28.628 ± 0.143 (p = 95%), r = 0.99994.

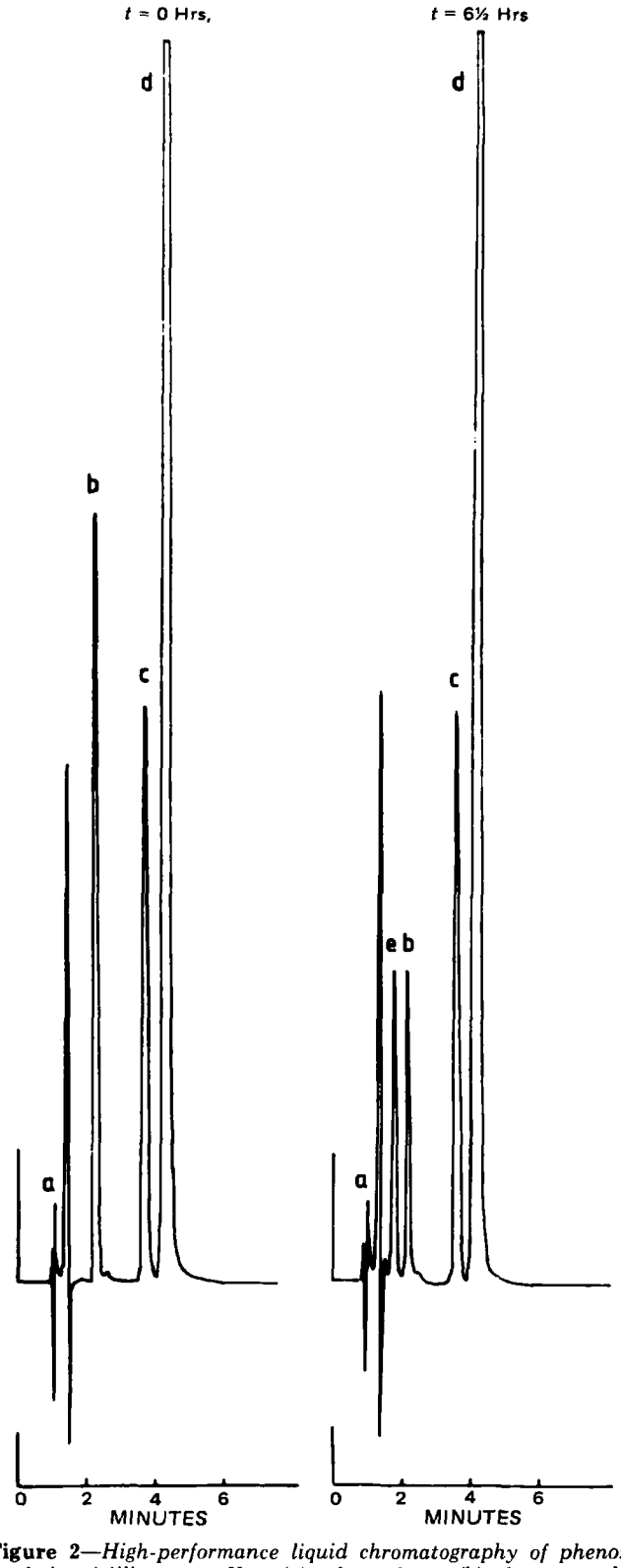

Figure 2—*High-performance liquid chromatography of phenoxymethylpenicillin syrup. Key: (a) solvent front; (b) phenoxymethylpenicillin; (c) phenol (internal standard); (d) methyl paraben; (e) degradation product.*

At pH 6—A citrate buffer (140 ml) containing citric acid (1.76 g) and sodium hydroxide (0.90 g) were placed in a medicine bottle fitted with a thermometer and sampling port. When temperature equilibrium was reached potassium phenoxymethylpenicillin (70 mg) was added, samples were removed, and the temperature program was initiated.

In these experiments the water-bath was programmed to rise from 60 to 95° over a 6-hr period. This was achieved by using a motorized syringe-drive unit to continuously adjust the thermostat. At frequent in-

tervals through the run, samples (3 ml) were removed and a phenol solution (2 ml, 0.02% w/v in water) as internal standard was added to an aliquot (2 ml). HPLC analysis was undertaken through interpolation onto a calibration curve prepared similarly over a penicillin concentration range of 0–50 mg/100 ml (r = 0.999). Time and precise temperatures were noted for each assay point.

Formulated Products—Syrups were reconstituted as directed by the manufacturer. Typically, this involved addition of 70 ml of water to the product (in the case of Syrup 1) and shaking vigorously to facilitate dissolving granules. The reconstituted product of nominal concentration (62.5 mg/5 ml and pH 5.8) was then transferred to a 150-ml clear bottle fitted with a sampling tube and a thermometer.

The stability of the syrups was monitored from 60 to 95° for the pH 6 samples. The HPLC assay was undertaken by adding phenol solution (2 ml, 0.25% w/v in water) to aliquots (1 ml), which were then diluted to 50 ml with water.

Isothermal Kinetics—Isothermal degradation was undertaken as described for the nonisothermal runs except that the selected temperature was held constant throughout the experiment. A series of temperatures within the range of those in the corresponding nonisothermal program was used.

HPLC—The stationary phase[1] was 5 μm in a 10-cm column with a 4.6 mm i.d. The mobile phase was acetonitrile (28% v/v) in phosphate buffer (0.132% $Na_2HPO_4 \cdot 2H_2O$, 0.807% KH_2PO_4; pH 6) pumped[2] at 1 ml min^{-1} under a pressure of ~600 psi. The UV detector[3] was operated at 271 nm with a sensitivity of 0.16 AUFS. Samples (20 μl) were injected onto the column by means of a loop injector[4]. Under these conditions phenoxymethylpenicillin had a retention time of 2.2 min and phenol 3.6 min.

Calculations were undertaken on a computer[5] using a BASIC version (see *Appendix*) of NONISO or by means of a FORTRAN integral nonisothermal kinetics program (12) implemented on a main frame system[6].

RESULTS AND DISCUSSION

Typical results for the nonisothermal degradation of phenoxymethylpenicillin (penicillin V) are shown in Table I. The transformed concentration–time polynomial coefficients for a first-order model and the isothermal rate constants attained by differentiation at the experimental points are also shown. The Arrhenius parameter estimates for these data are presented in Table II. The limits of error about the estimates are rather wide and the poor nature of the fit is further revealed by the correlation coefficient (r = 0.984), the coefficient of variation (CV = 10.52%), and the chi-squared statistic (6.37×10^{-3}; 26 degrees of freedom). Examination of the plotted data reveals that almost all of the variation arises from the first point (28.3°). This is due to the small amount of degradation that occurs over this initial temperature range. The true polynomial gradient is small, and the estimated rate constant is significantly affected by experimental error. The removal of this one point from the data set has a dramatic effect on the quality of the fit (Table II). The activation energy is now estimated to $<\pm 0.5\%$ (p = 95%). The rate constants calculated from these estimates are available for scrutiny and the predicted shelf-lives are shown in Table III. The output from the plotting routine is depicted in Fig. 1, which shows the effect of the chosen model on the Arrhenius plot. This rapid visualization of the data immediately reveals problems in the fit. When the reaction order is unknown, each model can be examined sequentially, and the best-fitting data (low χ^2, CV; high r) can be used for the shelf-life estimates.

To establish the validity of the NONISO approach a series of experiments were undertaken to establish the reproducibility of the method. The results were calculated using NONISO and the FORTRAN program described in an earlier study (12). These data, and those from a traditional isothermal study, are recorded in Table IV. Also included are the results reported previously (12) for riboflavin which have been recalculated using NONISO. Data taken from a graphical presentation in a previous report (8) on the nonisothermal degradation of p-acetamidophenol and procainamide have also been recalculated using NONISO and the integral approach. Parameter estimates from these calculations are also reported in Table IV. The agreement between these various estimates confirms the validity of the NONISO approach reported here.

[1] Hypersil ODS Shandon Scientific.
[2] Model 100A, Altex Corp.
[3] LC3, Pye Unichem Ltd.
[4] Rheodyne 7120.
[5] North Star Horizon.
[6] ICL 1904S.

Table III—Shelf-life Predictions for Phenoxymethylpenicillin at pH 9

Temperature, °	Shelf-life Predictions $t_{1/2}$	First Order Model $t_{90\%}$
5	24.44 days	3.72 days
10	12.18 days	1.85 days
15	149.12 hr	22.67 hr
20	77.87 hr	11.84 hr
25	41.56 hr	6.31 hr
30	22.64 hr	3.44 hr

When all experimental points are used in the computation (typically 25–30) the major source of error occurs in the calculation of rate constants at the temperature range extremes. Inspection of the graphical presentation reveals any deviation, and recalculation with the omission of ill-fitting data dramatically increases the validity of the parameter estimates. For this reason, points that correspond to degradation in excess of 95% for a first-order process or in excess of 80% for the zero- or second-order models are automatically eliminated from the data set. The elimination of points determined in the initial stages of the degradation is left to the operator's discretion. Usually few points require attention so that, providing a reasonably complete data set has been collected, sufficient points remain to establish a valid analysis. In the case of phenoxymethylpenicillin (pH 9) 33 points were collected, 28 were used in the initial calculation (Table I), and the final parameter estimates were derived from 27 observations (Tables II and III). The reduced data set may be recalculated in part, *via* the Arrhenius subroutines, or in total, through the generation of a new polynomial expression. The first option is satisfactory if analytical error is small and has been adopted in all calculations reported here. However, if less precise assay results are available it is more effective to generate a new polynomial equation. The two approaches are compared in Table V. This records the effect of a ±2% random error incorporated into the concentration values and reveals that polynomial regeneration is more effective in providing an acceptable solution with this degree of error. To reduce the effect of analytical error it is advisable to design the nonisothermal temperature program to cover a range not less than 25° and to monitor the degradation over a period of at least one half-life.

Figure 2 is a typical chromatogram from a phenoxymethylpenicillin syrup and shows that excipients and degradation products are detectable but do not interfere with the analysis. The results of the nonisothermal

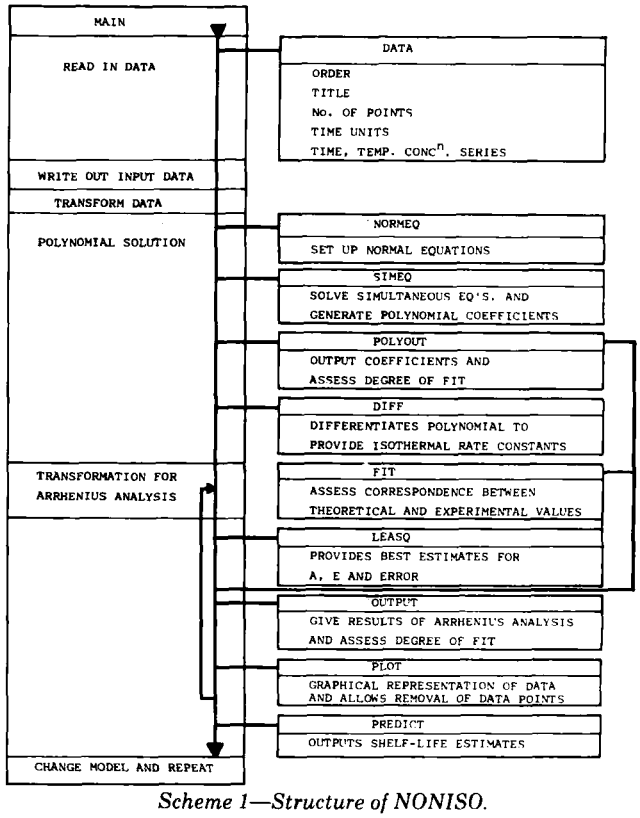

Scheme 1—Structure of NONISO.

Table IV—Comparison of Differential and Integral Calculations of Nonisothermal Degradation Data [a]

Run	Temperature Range	Differential (NONISO) E (J/mole)	A ($\times 10^{-14}$ hr^{-1})	Predicted K ($\times 10^2$ hr^{-1}) 25°	50°	Integral (Anderson) E (J/mole)	A ($\times 10^{-14}$ hr^{-1})	Predicted K ($\times 10^2$ hr^{-1}) 25°	50°
Nonisothermal (Phenoxymethylpenicillin pH 9)									
1	28°–81°	91024 (413)[a]	1.496 (0.205)[a]	1.697	29.07	91209 (43)[b]	1.588 (0.024)[b]	1.673	28.81
2	31°–78°	90966 (1125)[a]	1.345 (0.444)[a]	1.562	26.71	90076 (71)[b]	0.977 (0.025)[b]	1.625	27.02
3	31°–60°	89496 (2305)[a]	0.809 (0.464)[a]	1.700	27.76	94494 (157)[b]	5.045 (0.028)[b]	1.412	26.95
Isothermal (Phenoxymethylpenicillin pH 9)	3°–72°	86485 (2282)[a]	0.261 (0.152)[a]	1.848	27.46				
Nonisothermal Riboflavin (12)	21°–70.5°	82552 (2420)[a]	0.1075 (0.064)[a]	3.718	48.89	84888 (242)[b]	0.2558 (0.0221)[b]	3.448	48.77
p-Acetamidophenol (8) (Nonisothermal)	34.9°–83°	67245 (4632)[a] 71128(8)[c]	5.282×10^{-7} (4.244×10^{-7})	8.745×10^{-3}	7.131×10^{-2}	68810 (3284)[b]	9.2316×10^{-7} (9.606×10^{-7})	8.129×10^{-3}	6.961×10^{-2}
Procainamide HCl (8) (Nonisothermal)	34.9°–82.6°	129513 (9232)[a] 121336(8)[c]	4.57×10^3 (4.39×10^3)	9.328×10^{-4}	5.311×10^{-2}	120967 (3396)[b]	2.3383×10^2 (2.363×10^2)	1.500×10^{-3}	6.539×10^{-2}

[a] Confidence interval 95%. [b] Standard deviation units. [c] Literature values.

Table V—Effect of ±2% Random Error in Concentration on E from Nonisothermal Degradation of Phenoxymethylpenicillin (pH = 9)

Source	Run 1	2	3	4	5	Result Mean	CV, %
Arrhenius Recalculated	111674	94420	90161	93714	85814	95157	10.3
Polynomial Regenerated	91655	86647	90850	88772	88662	89317	2.2

degradation of formulated products are illustrated in Table VI. A high degree of similarity is observed between shelf-life estimates from NONISO and those obtained using the integral method of Anderson *et al.* (12). The estimates compare well with those predicted from isothermal accelerated tests and with shelf-lives measured at the storage temperature. The advantages of this approach include the availability of a full kinetic profile with no more effort than is required by a single isothermal rate determination. Zero-, first-, and second-order (a = b; a ≠ b) and first-order equilibrium reactions may be handled. A set temperature program is not required and the heating rate can be adjusted readily to suit the stability of the formulation. Only simple apparatus is required, and degradation in the final dispensing container is easily monitored. In addition, the use of an analytical rather than an iterative solution to the kinetic equations requires a relatively short processing time. This allows effective use of a BASIC program, which can be run on inexpensive microcomputers rather than requiring main-frame computing facilities. The use of this approach should enable nonisothermal kinetic procedures to be available on a routine basis.

APPENDIX

NONISO, a BASIC computer program, has been written for implementation on a Z80-based microcomputer with 64K RAM[5] and requires ~22K for the fully labeled version. A listing of the program is available on request, from the authors. Scheme I illustrates the structure of this program. Individual operations have, as far as possible, been incorporated into separate subroutines to allow modification or extension to be easily achieved. Although BASIC does not allow subroutine names, these are used in the discussion for purposes of clarity. DATA (lines 3940–4300) are written into the program before computation. This records the proposed order of reaction, an identifying label for the experiment, the number of data points, and the time units used. This is followed by time, temperature, and residual concentration measurements for each experimental point beginning with time zero.

The segment MAIN (lines 470–1080) sets dimensions, reads in the input data, and transforms the concentration values (compare Eqs. 4–7) so that differentiation of the polynomial yields k_T values. Subsequent calls to the major subroutines follow.

The NORMEQ (lines 1150–1270) routine sets up the normal equations for the solution of the transformed concentration data in terms of a time polynomial. The normal equations take the form:

$$\sum_{i=1}^{N} (\ln C_{t_i}) = a_0 N + a_1 \Sigma t_i + a_2 \Sigma t_i^2 + \ldots + a_n \Sigma t_i^n$$

$$\sum_{i=1}^{N} t_i (\ln C_{t_i}) = a_0 \Sigma t_i + a_1 \Sigma t_i^2 + a_2 \Sigma t_i^3 + \ldots + a_n \Sigma t_i^{n+1} \quad \text{(Eq. 11)}$$

$$\sum_{i=1}^{N} t_i^2 (\ln C_{t_i}) = a_0 \Sigma t_i^2 + a_1 \Sigma t_i^3 + a_2 \Sigma t_i^4 + \ldots a_n \Sigma t_i^{n+2}$$

$$\sum_{i=1}^{N} t_i^n (\ln C_{t_i}) = a_0 \Sigma t_i^n + a_1 \Sigma t_i^{n+1} + a_2 \Sigma t_i^{n+2} + \ldots a_n \Sigma t_i^{2n}$$

where n is the order of the polynomial and N is the number of data points; the program is able to generate polynomials up to the tenth order. The maximum available order, however, is dictated by the word length of the computer used. Values in excess of Σt_i^{2n} are generated and overflow errors may occur. In practice, a sixth-order polynomial was found satisfactory, with higher orders giving no improvement.

The subroutine SIMEQ (lines 1280–1700) solves up to 10 simultaneous equations by the Gauss Elimination Method (20). A typical execution time for 30 points is 90 sec.

POLYOUT (lines 1710–1930) presents the coefficients for the polynomial and the calculated values are compared with the observed transformations. Subroutine FIT (lines 1940–2100) is also called to calculate a determination coefficient, the coefficient of variation, and the chi-squared value.

DIFF (lines 2110–2330) differentiates the polynomial expression and the result is solved for the experimental points to yield the isothermal rate constants throughout the run. The experimental data are modeled well but extrapolation beyond this range rapidly introduces unacceptable error. Transformation for the Arrhenius analysis ($k_T \rightarrow \ln k_T$; $T \rightarrow 1/T$) is thus undertaken, and the parameters (A,E) are estimated by LEASQ (lines 2340–2540), which undertakes a linear least-squares analysis of the data.

The parameter estimates and correlation coefficients are printed by OUTPUT (lines 2550–2780) which also provides 95% error limits for the estimates. The isothermal rate constants predicted by the model are compared with the experimental values, and the degree of correspondence is again assessed by subroutine FIT.

PLOT (lines 3000–3750) is a subroutine that displays the theoretical regression line together with the experimental points, thus allowing a visual assessment of the significance of the fit. Options are available to remove wildly deviating points: in practice, if this is necessary, these are

Table VI—Parameter Estimates for Formulated Products [a]

Run	Temperature Range	Differential (NONISO) E (J/mole)	A ($\times 10^{-12}$ hr^{-1})	Predicted $t_{90\%}$ 25° (days)	50° (hr)	Integral (Anderson) E (J/mole)	A ($\times 10^{-2}$ hr^{-1})	Predicted $t_{90\%}$ 25° (days)	50° (hr)
Syrup 1									
Nonisothermal	60°–94°	82717 (967)[a]	0.251 (0.070)[a]	5.4	9.8	86951 (789)[b]	1.040 (0.263)[b]	7.2	11.5
Isothermal	25°–50°	80250	0.1067	4.70	9.2				
Syrup 2		83945	0.557	4.0	7.0	83992	0.560	4.0	8.9
Nonisothermal	61–95°	(±1788)[a]	(±0.254)[a]			(356)[b]	(0.066)[b]		
		85840 (2169)[a]	1.115 (0.579)[a]	4.3	7.1	87091 (254)[b]	1.684 (0.142)[b]	4.7	7.5
Solution (pH 6)									
Nonisothermal	60°–95°	92610 (6804)[a]	2.639 (2.37)[a]	27.9	37.2	92169 (5470)[b]	2.251 (3.719)[b]	27.4	37.0

[a] Confidence interval. [b] Standard deviation units.

the initial data points when the concentration is changing slowly and is thus subject to more error. The regression calculations are then repeated on the reduced data set.

When a satisfactory model is obtained, the subroutine PREDICT (2790–2990) calculates the $t_{90\%}$ and $t_{1/2}$ values at typical storage temperatures to assess the shelf-life of the formulation. The model can then be changed by the use of the appropriate code [line 3940; 0—zero-order, 1—first-order, 2—second-order ($a = b$), 3—second-order ($a \neq b$)] and the calculations are repeated.

REFERENCES

(1) H. J. Borchardt and F. Daniels, *J. Am. Chem. Soc.*, **79**, 41 (1957).

(2) R. E. Davis, *J. Phys. Chem.*, **63**, 307 (1959).

(3) A. R. Rogers, *J. Pharm. Pharmacol.*, **15**, 101T (1963).

(4) S. P. Ericksen and H. J. Stelmach, *J. Pharm. Sci.*, **54**, 1029 (1965).

(5) B. Göber, U. Timm, and S. Pfeifer, *Pharmazie*, **34**, 161 (1979).

(6) B. Göber, U. Timm, S. Pfeifer, and S. Hübel, *ibid.*, **34**, 237 (1979).

(7) A. I. Kay and T. H. Simon, *J. Pharm. Sci.*, **60**, 205 (1971).

(8) M. A. Zoglio, J. J. Windheuser, R. Vatti, H. V. Maulding, S. S. Kornblum, A. Jacobs, and H. Hamot, *ibid.*, **57**, 2080 (1968).

(9) B. R. Cole and L. Leadbeater, *J. Pharm. Pharmacol.*, **18**, 101 (1966).

(10) J. T. Carstensen, A. Koff, and S. H. Rubin, *J. Pharm. Pharmacol.*, **20**, 485 (1968).

(11) H. V. Maulding and M. A. Zoglio, *J. Pharm. Sci.*, **59**, 333 (1970).

(12) B. W. Masen, R. A. Anderson, D. Herbison-Evans, and W. Sneddon, *ibid.*, **63**, 777 (1974).

(13) M. A. Zoglio, H. V. Maulding, W. H. Streng, and W. C. Vincek, *ibid.*, **64**, 1381 (1975).

(14) B. Edel and M. O. Baltzer, *ibid.*, **69**, 287 (1980).

(15) M. E. Brown and C. A. R. Phillpotts, *J. Chem. Ed.*, **55**, 556 (1978).

(16) W. E. Brown, D. Dollinore, and A. K. Galvey, "Comprehensive Chemical Kinetics," vol. 22. C. H. Banford and C. F. H. Tipper, Eds., Elsevier, Oxford, N.Y. 1980.

(17) O. C. Davies and D. A. Budgett, *J. Pharm. Pharmacol.*, **32**, 155 (1980).

(18) W. Yang, *Drug Dev. Indust. Pharm.*, **7**, 539 (1981).

(19) G. de la Pena and M. Jose, *Rev. Fac. Cienc.*, **2**, 3 (1970).

(20) G. Flegg and R. Meetham, "An Introduction to Calculus and Algebra," vol. 3., Algebra, Open University Press, 1972. pp. 238 and 287.

ACKNOWLEDGMENTS

The authors thank the SRC and Beecham Pharmaceuticals for the award of a CASE studentship to J. M. Hempenstall.

Topical Vaginal Drug Delivery I: Effect of the Estrous Cycle on Vaginal Membrane Permeability and Diffusivity of Vidarabine in Mice

C. C. HSU, J. Y. PARK, N. F. H. HO, W. I. HIGUCHI ˣ, and J. L. FOX

Received July 13, 1981, from the *College of Pharmacy, The University of Michigan, Ann Arbor, MI 48109.* Accepted for publication June 11, 1982.

Abstract □ Preliminary studies showed that the vaginal membrane permeability coefficients for vidarabine (9-β-D-arabinofuranosyladenine) varied widely within a group of mice of the same species and age. This finding prompted an investigation of the influence of the female mouse sexual cycle on the vidarabine permeability. By means of a vaginal smear technique, the sexual cycle, which was ~5 days in duration, was divided into five phases. The vaginal membrane permeability of vidarabine was determined during each phase. The results revealed that the permeability coefficients for vidarabine during the diestrus phase (3×10^{-6}–4×10^{-5} cm/sec) were 10–100 times higher than those obtained at the early estrus or estrus phases ($1–3 \times 10^{-7}$ cm/sec). Further permeation studies on membranes at early estrus and estrus were performed by separating the cornified layer from the noncornified portion of the membrane. The low permeability coefficient of vidarabine across the cornified layer (4×10^{-7} cm/sec) suggests that this layer may be the major diffusion barrier for vidarabine when the drug is topically applied. Collectively, the data also suggest that during estrus a three-layer diffusion model is appropriate, that during early diestrus a single-layer diffusion model may apply, and that during proestrus and postestrus the situations are intermediate and more complicated.

Keyphrases □ Vidarabine—vaginal membrane permeability in mice, diffusion barriers, effect of the estrous cycle □ Permeability—vaginal membrane to vidarabine, determination of coefficients, effect of the estrous cycle □ Estrous cycle—effect of vaginal membrane permeability to vidarabine in mice

A physical model of simultaneous transport and bioconversion of vidarabine (9-β-D-arabinofuranosyladenine, I) in the hairless mouse skin has been reported, (1, 2). It was concluded that the low efficacy of I in topical therapy involving skin may be due to the extremely low permeability of I through the stratum corneum and the rapid enzymatic decomposition of I to 9-β-D-arabinofuranosylhypoxanthine (II). In more recent reports (3, 4), the model was explored in detail, and a prodrug of I, vidarabine-5′-valerate (III), was investigated for its ability to overcome both the low permeability and enzymatic decomposition problems.

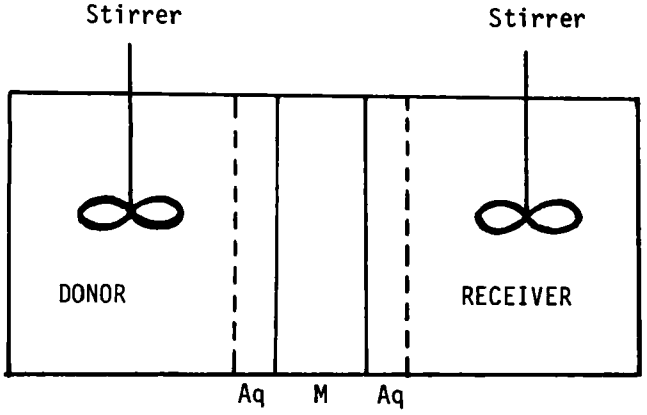

Figure 1—*Diffusion cell for the membrane permeability coefficient determinations. Key: (M) membrane; (Aq) aqueous diffusion layer.*

Since infections of the human genital tract with Herpes simplex virus (HSV types 1 and 2) have become increasingly important (5–7), it is desirable to investigate the deliverability of I, an antiviral drug, in the genital tract using an animal model. In the present report the permeability and diffusivity parameters of I were studied on excised vaginal membranes of the female mouse, with particular emphasis on how the estrous cycle may affect these transport parameters.

THEORETICAL

Aqueous Diffusion Layer Permeability Coefficient—Often the aqueous diffusion layer is unimportant in influencing overall transport in membrane diffusion experiments. However, in instances where the aqueous diffusion layer thickness is relatively large, its influences on both the steady-state transport and the lag time may be appreciable. The aqueous diffusion layer permeability (P_{aq}) of I may be calculated from:

$$P_{aq} = \frac{D_a}{h_{aq}} \qquad \text{(Eq. 1)}$$

where D_a is the aqueous diffusivity of I and h_{aq} is the aqueous diffusion layer thickness. The aqueous diffusion layer thickness has been determined (4) from initial dissolution rate data obtained using benzoic acid disks placed in the same configuration as the membrane in the diffusion cell by means of:

$$\frac{R}{A} = \left(\frac{D}{h_{aq}}\right)(C_s) \qquad \text{(Eq. 2)}$$

where R is the initial dissolution rate of benzoic acid, A is the effective diffusional area, C_s is the aqueous solubility of benzoic acid, and D is the aqueous diffusivity of benzoic acid. The initial dissolution rate of benzoic acid is the initial linear slope obtained by plotting the amount of benzoic acid dissolved in the diffusion cell against time. The aqueous diffusivity of I can be estimated from:

$$D_a = \left(\frac{M}{M_a}\right)^{1/3} D \qquad \text{(Eq. 3)}$$

where M_a is the molecular weight of I and M is the molecular weight of benzoic acid.

Vaginal Membrane Permeability Coefficient—The vaginal membrane permeability coefficient (P) of I can be determined by conducting a permeation experiment in a diffusion cell (Fig. 1). In such an experiment the steady-state flux of I across the membrane is equated to the product of the apparent permeability coefficient and the concentration gradient:

$$\left(\frac{dC_t}{dt}\right)\left(\frac{V}{A}\right) = \frac{1}{\frac{1}{P} + \frac{1}{2P_{aq}}}(C_t^d - C_t) \qquad \text{(Eq. 4)}$$

Where V is the volume of solution in the receiver cell, C_t^d is the donor side concentration of I at time t, and C_t is the concentration of I in the receiver cell at time t. When only initial steady-state flux is used, C_t is much smaller than C_t^d, and $C_t^d - C_t \approx C_0$, where C_0 is the initial donor side concentration of I. Equation 4 may be simplified and solved to give:

$$C_t = \left(\frac{A}{V}\right) C_0 \left(\frac{1}{\frac{1}{P} + \frac{1}{2P_{aq}}}\right)(t - L) \qquad \text{(Eq. 5)}$$

0022-3549/83/0600-0674$01.00/0

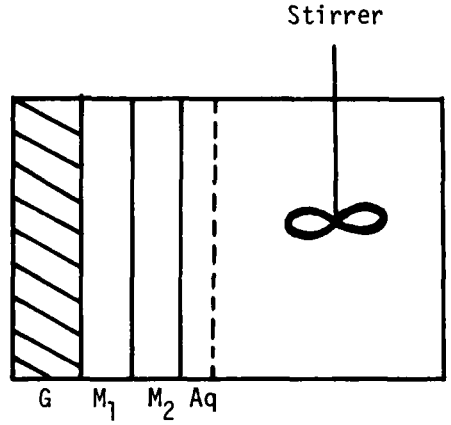

Figure 2—*Diffusion chamber modified for a bilayer membrane desorption experiment. Key: (M_1) membrane sublayer 1; (M_2) membrane sublayer 2; (G) glass block; (Aq) aqueous diffusion layer.*

where L is the lag time and may be obtained from experimental data as the intercept on the time-axis when the steady-state C_t values are plotted against time. The membrane permeability coefficient of I can thus be calculated from the initial linear slope of the concentration–time plot.

Calculation of the Membrane Thickness from the Lag Time—If the vaginal membrane can be viewed as mono- or multi-ply laminate-like skin, it is possible to calculate the theoretical membrane thickness from the permeation lag time. The general relationship between the lag time and the layer thickness for an n-layer laminate (8) is:

$$L = \left[\sum_{i=1}^{n}\left(\frac{h_i}{D_i}\prod_{j=0}^{i-1}k_j\right)\right]^{-1}\left[\sum_{i=1}^{n}\left\{\frac{h_i^2}{2D_i}\sum_{i=i}^{n}\left(\frac{h_i}{D_i}\prod_{j=0}^{i-1}k_j\right)-\frac{h_i^3}{3D_i}\prod_{j=0}^{i-1}k_j\right\}\right.$$

$$\left.+\sum_{i=1}^{n}\left\{\frac{h_i}{D_i}\left(\prod_{j=0}^{i-1}k_j\right)\sum_{\beta=i+1}^{n}\left[\frac{h_\beta}{\prod_{j=0}^{\beta-1}k_j}\sum_{\beta=\beta}^{n}\left(\frac{h_\beta}{D_\beta}\prod_{j=0}^{\beta-1}k_j\right)-\frac{h_\beta^2}{2D_\beta}\right]\right\}\right] \quad \text{(Eq. 6)}$$

where L is the lag time, k_i is the partition coefficient between ith and (i + 1)th layers, D_i is the diffusivity of ith layer, and h_i is the thickness of ith layer.

In the case of a homogeneous membrane, the total number of layers in Eq. 6 is 3 (n = 3), because there exist two identical aqueous diffusion layers, one on each side of the membrane. Also, if it is assumed that the partition coefficient of I between viable tissue and water is unity [which is a good assumption for the solute in this study (4)], then:

$$P_i = \frac{D_i}{h_i} \quad \text{(Eq. 7)}$$

where P_i is the permeability coefficient of the ith layer. Equation 6 can be rewritten as:

$$L = \left(\frac{2}{P_{aq}}+\frac{1}{P}\right)^{-1}\left[\frac{h_{aq}}{P_{aq}}\left(\frac{4}{3P_{aq}}+\frac{1}{P}\right)+\frac{h}{P}\left(\frac{1}{P_{aq}}+\frac{1}{6P}\right)+\frac{h}{P_{aq}^2}\right] \quad \text{(Eq. 8)}$$

where p is the permeability of homogeneous membrane and h is the membrane thickness.

Membrane Diffusivity from a Desorption Experiment—To confirm the diffusivity values obtained from the permeation experiments, an alternative experiment, called the desorption experiment, may be conducted which gives a direct estimate of the membrane diffusivity. In this method, the initial desorption rate of a membrane that has been loaded with a known concentration of drug is measured. The membrane diffusivity is then determined from:

$$\frac{dC_t}{dt}\frac{V}{A} = C_0\sqrt{\frac{D}{\pi t}} \quad \text{(Eq. 9)}$$

and

$$C_t = \left(\sqrt{\frac{4C_0^2A^2D}{V^2\pi}}\right)\sqrt{t} \quad \text{(Eq. 10)}$$

where C_t is the solution concentration at time t, V is the volume of the diffusion cell solution, A is the effective diffusional area, C_0 is the initial drug concentration in the membrane, and D is the diffusivity of the membrane. Equation 9 is solved to give Eq. 10. By plotting the C_t *versus* $\sqrt{t}$, the diffusivity of the membrane can be calculated easily from the initial slope.

If the membrane is effectively multilayered, only the diffusivity of the sublayer facing the diffusion chamber is determined from the initial desorption rate. In the simplest case of a bilayer membrane, the diffusivity of each layer may be measured independently with this method (Fig. 2).

Table I—Microscopic Characteristics of the Vaginal Smear as a Function of the Sexual Cycle

Phase	Duration, days	Microscopic Characteristics of Vaginal Smears
Diestrus	1–3	Exclusively leukocytes
Proestrus	~1	Leukocytes and nucleated epithelial cells
Early estrus	0.5–1	Epithelial cells, may have some cornified cells
Estrus	0.5–1	Exclusively cornified cells
Postestrus	~1	Leukocytes and cornified cells

Table II—Aqueous Diffusion Layer Permeability Coefficients of I

Experiment	$h_{aq} \times 10^2$, cm	$P_{aq} \times 10^3$, cm/sec
1	1.07	1.01
2	1.00	1.08
3	1.02	1.06
Average	1.03	1.05

EXPERIMENTAL

Materials—[^{3}H]-2-I[1] was used after being purified by high-performance liquid chromatography (HPLC), and the purity was further checked by TLC before experiments were started. [^{3}H]-2-II was prepared from [^{3}H]-2-I by treating the latter with adenosine deaminase[2] and TLC purification. Female Swiss Webster mice[3], 10–14 weeks old, were used for the experiments. Liquid scintillation counter cocktail[4], normal saline solution[5], 1% methylene blue in methanol solution, cellulose membrane[6], sulfuric acid[7], and sodium sulfite[7] were also used in the experiments.

Diffusion Cells—Because of the small available area of the mouse vaginal membrane (~0.8 cm × 1.0 cm), specially designed diffusion cells were used in these experiments. The outside dimensions of the glass diffusion cell are shown in Fig. 3. It has two ports, one for the stirrer and the other for sampling access. The stirrer port was 2.2 cm in length and the sampling port was 1.0 cm in length. The diameter of the cell opening was 0.6 cm, which provides an effective diffusional area of 0.28 cm^2 for a cell volume of 1 ml. The stirrer was made of polytetrafluoroethylene[8] and was operated by a constant-speed motor[9].

Vaginal Membrane Preparation—The female mouse was sacrificed by snapping the spinal cord at the neck. The lower abdomen was cut open, and the fat tissue was removed to reveal the Y-shaped reproductive system. A pair of hemostatic forceps were clamped on the uterus ~0.5 cm above the cervix to fix the position while the pubic bone was cut open, and the connection between the system and the surrounding tissue was carefully removed. The vagina, which is located between the cervix and the orifice, was then separated from the uterus. The tube-shaped vagina was carefully checked to free any tissue debris from the surface prior to cutting it open and using it for the experiment.

In cases where only the noncornified part of the membrane was to be used for an experiment, the vagina of the mouse at estrus was obtained by the aforementioned method. After cutting open the membrane, the cornified layer, which is on the mucosal side, was completely removed from the rest of the membrane with a pair of tweezers.

[1] Courtesy of Dr. T. H. Haskell, Warner-Lambert Labs., Ann Arbor, MI 48105.
[2] Sigma Chemical Co., St. Louis, MO 63178.
[3] Charles River Breeding Labs., Inc., Wilmington, Mass.
[4] Amersham Corp., Arlington Hts., IL 60005.
[5] 0.9% NaCl irrigation USP, Abbott Labs., N. Chicago, IL 60060.
[6] Spectrapor #1, Spectrum Medical Industries, Inc., Los Angeles, CA 90054.
[7] Fisher Scientific Co., Fair Lawn, NJ 07410.
[8] Teflon; registered trademark of E.I. du Pont de Nemours & Co., Inc., Wilmington, Del.
[9] Hurst Mfg. Co., Princeton, Ind.

Table III—Vaginal Membrane Stability with Respect to the Permeability of I

Cycle Phase	Mouse	Permeability Coefficient × 10^6, cm/sec					
		Fresh	t = 4 hr	t = 8 hr	t = 16 hr	t = 20 hr	t = 27 hr
Diestrus	79013	30.8	29.6	30.7	74.0	—[b]	97.1
	79016	41.1	35.2	39.5	50.5	—	63.4
	79018	35.1	33.8	34.4	56.5	—	71.2
	79023	30.3	38.9	26.6	50.4	—	71.5
	79051	16.2	14.5	21.1	56.4	67.7	—
	79030	08.5	07.8	—	—	—	—
	79020	03.4	03.2	—	—	—	—
	79045	06.5	02.7	01.8	—	—	—
	79044	05.9	03.9	03.8	12.6	16.5	—
	79052	04.7	01.1	01.8	04.9	06.3	—
	79053	05.1	05.6	16.9	53.5	58.6	—
Estrus[a]	79043	0.98	0.65	0.55	—	—	—
	79009	0.93	0.74	—	—	—	—
	79067	1.25	—	0.90	—	—	—

[a] Only the noncornified part of the estrus membrane was used in this experiment. [b] — Not determined.

Vaginal Membrane Thickness Measurement—A micrometer[10] was used to obtain the membrane thickness. The vaginal membrane, after being removed from the body and cut open, was sandwiched between two microscope cover glasses. The total thickness was then measured with the micrometer. The membrane thickness was obtained by subtracting the thicknesses of the cover glasses from the total thickness.

Mouse Estrous Cycle Determination—The female mouse estrous cycle could be determined easily by microscopic examination of the vaginal smears (9). The vaginal smears were obtained by means of an ordinary pipet, the tip of which had been flamed to a smooth, reduced aperture. A few drops of normal saline solution were drawn into the pipet, introduced into the vagina, and then retracted into the pipet. The fluid was transferred to a microscope slide and stained with a drop of methylene blue to add contrast and bring out the nuclei. Examination for cell type was carried out under low- and high-power magnification. Three major types of cells were found in the vaginal smears: leukocytes, epithelial cells, and cornified epithelial cells. The estrous cycle phase was determined by the types of cells present in the vaginal smears (Table I).

Aqueous Permeability Coefficient Determination—Benzoic acid pellets were made by directly compressing 100 mg of the material in a die (1.3-cm i.d.) under a force of 1362 kg (3000 lb) using a laboratory press[11]. The pellet was mounted between one chamber of a diffusion cell and a same-size glass plate. The whole setup was coated with wax and immersed in a 37° water bath. One milliliter of 0.01 *N* HCl, pre-equilibrated at 37°, was introduced into the cell at time zero. The benzoic acid concentration in the solution was determined by UV absorption at 227 nm against a standard curve.

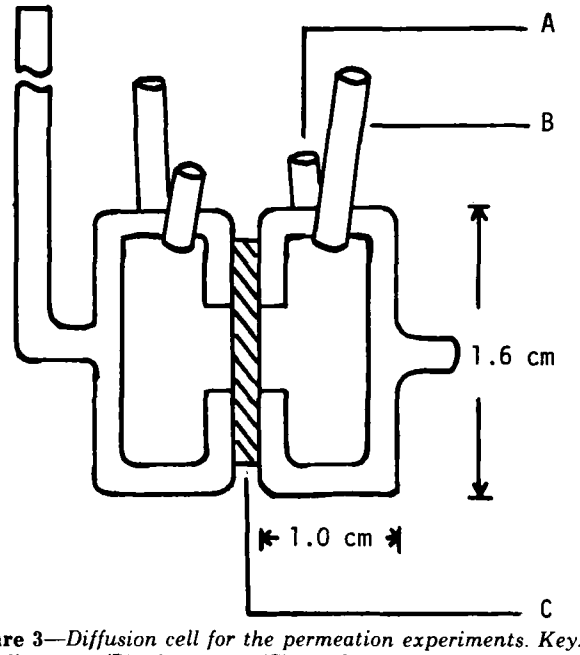

Figure 3—*Diffusion cell for the permeation experiments. Key: (A) sampling port; (B) stirrer port; (C) membrane.*

Vaginal Membrane Permeability Coefficient Determination—As soon as the vaginal membrane was sandwiched between two diffusion cells, 0.9 ml of the normal saline solution, pre-equilibrated at 37°, was introduced into each chamber. The diffusion cell setup was then immersed in a 37° water bath and was allowed to stand for 5 min to reach thermal equilibrium. Normal saline solution (100 μl) was added to the receiver chamber at the end of this 5-min period, and [^{3}H]-2-I or [^{3}H]-2-II in 100 μl of normal saline solution was added to the donor chamber by pipet to start the experiment. Aliquots (100 μl) from the receiver solution were drawn with a micropipet at given time intervals and were transferred immediately into a scintillation vial containing 10 ml of scintillation counter cocktail. An equal volume of normal saline solution was added to the receiver chamber after each draw to replace the removed aliquot. The donor solution concentrations at the first half-minute and at the end of the experiment also were determined in the same way to obtain the initial concentration and to check the mass balance.

Preparation of Cellulose Membrane—The cellulose membrane was cut to a suitable size before it was soaked in running water for 3–4 hr to remove the glycerol. The membrane was then treated with 0.3% sodium sulfite solution, preheated to 80°, for 1 min followed by washing with 60° distilled water for 2 min. The washed membrane was acidified with 0.2% sulfuric acid and then cleaned with distilled water. The purpose of this procedure was to remove sulfides on the membrane.

Cellulose Membrane Permeability Coefficients—Experiments to determine the cellulose membrane permeability coefficients were performed in the same manner as the determination of vaginal membrane permeability coefficients, except that the cellulose membrane was mounted in the diffusion cell.

Stability of the Vaginal Membrane—The vaginal membrane stability under the experimental conditions was studied by performing consecutive permeation experiments on the same membrane. The membrane was washed several times with normal saline solution for 2 hr between the two experiments. The washing solution from both chambers was checked to make certain that the membrane was free of any residue from the previous run. When the cellulose membrane was used to increase the vaginal membrane stability, the excised vaginal membrane was sandwiched between two pieces of cellulose membrane

Table IV—Stability of Cellulose Membrane-Protected Vaginal Membrane with Respect to the Permeability of I[a]

Cycle Phase	Mouse	Permeability Coefficient × 10^6, cm/sec				
		Fresh	t = 2 hr	t = 4 hr	t = 8 hr	t = 24 hr
Diestrus	80113	4.6	5.0	5.2	4.5	7.8
	80139	3.8	3.6	3.2	3.6	3.5
Estrus[b]	80146	1.10	—[d]	1.02	1.08	—
	80160	1.17	—	1.21	1.15	—
Cellulose membrane[c]	—	90.0	—	91.0	—	89.5

[a] The membrane was sandwiched between two pieces of cellulose membrane before being mounted in the diffusion cells. Each permeability measurement was conducted for 2 hr. The membrane was washed with normal saline between runs. [b] Noncornified part of the membrane. [c] The reported values have been corrected for the presence of aqueous diffusion layers. [d] — Not determined.

[10] L. S. Starrett Co., Athol, MA 01331.
[11] Model B, Fred Carver, Inc., Summit, N.J.

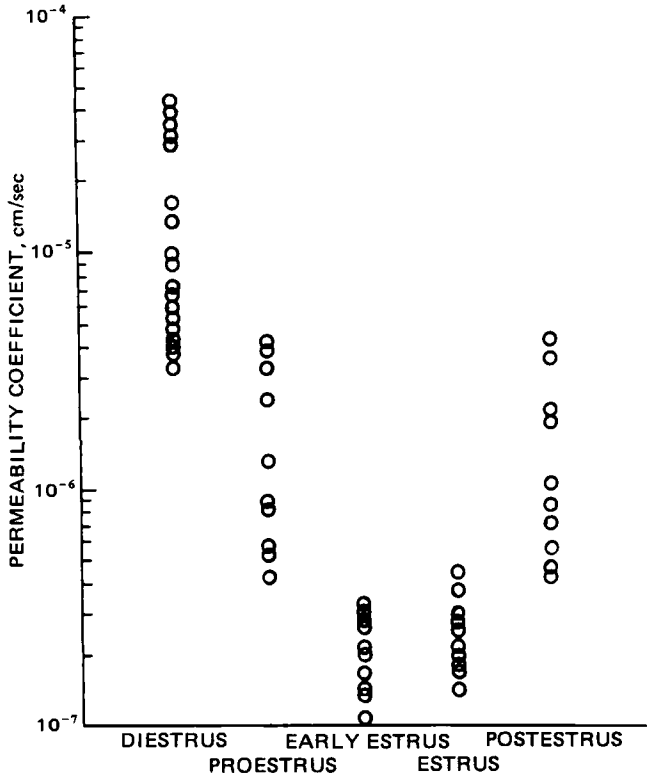

Figure 4—*Vaginal membrane permeability coefficients of I during different estrous cycle phases.*

before being mounted in the diffusion cell. This procedure was carried out very carefully to prevent any air bubbles from being trapped between the vaginal and cellulose membranes.

Desorption Experiment—The prepared vaginal membrane was soaked for 3 hr in 0.5 ml of normal saline with a known amount of compound I in the solution. It was then mounted between a diffusion cell and a glass block. One milliliter of normal saline, pre-equilibrated at 37°, was added to the diffusion chamber at time zero. The concentration in the diffusion cell was determined in the same manner used in the membrane permeability experiment.

RESULTS AND DISCUSSION

Aqueous Diffusion Layer Permeability—Three benzoic acid dissolution experiments were conducted which gave an average aqueous

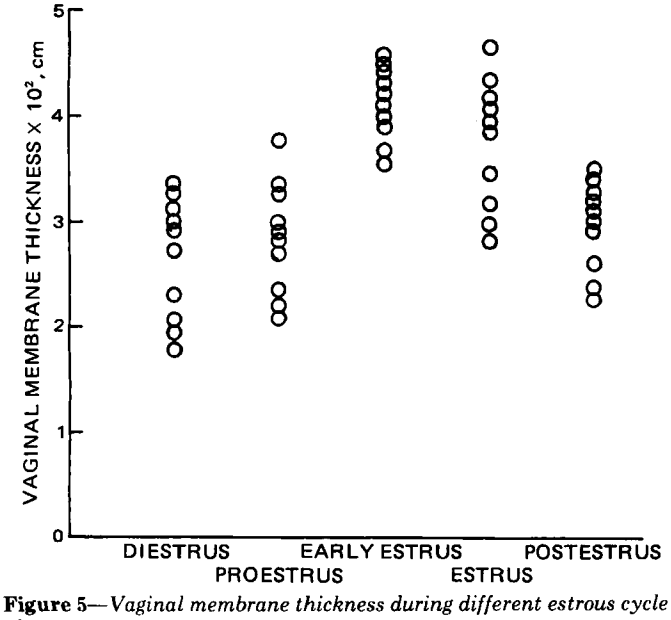

Figure 5—*Vaginal membrane thickness during different estrous cycle phases.*

Table V—Comparison of Vaginal Membrane Permeability Coefficients of I and II[a]

Cycle Phase	Mouse	Permeability Coefficient[b] × 10^6, cm/sec I	II
Diestrus	80157	9.24 (1)[c]	9.37 (2)
	80233	5.28 (2)	5.40 (1)
Estrus[d]	80229	1.34 (1)	1.21 (2)
	80228	1.01 (2)	1.08 (1)

[a] Membranes were protected with cellulose membrane to increase stability. [b] Covidarabine, an adenosine deaminase inhibitor, was used in the permeability coefficient measurement of I to inhibit the conversion of I to II. [c] The number in the parentheses indicates the run order. [d] Noncornified part of the membrane.

Table VI—Statistical Comparison of Vaginal Membrane Permeability Coefficients of I During Different Cycle Phases[a]

	Significance[b]				
	Diestrus	Proestrus	Early estrus	Estrus	Postestrus
Diestrus	—	0.0000	0.0000	0.0000	0.0000
Proestrus	0.0000	—	0.0002	0.0002	0.6501
Early estrus	0.0000	0.0002	—	0.5706	0.0002
Estrus	0.0000	0.0002	0.5706	—	0.0002
Postestrus	0.0000	0.6501	0.0002	0.0002	—

[a] Nonparametric Mann-Whitney method was used in this statistical comparison. [b] Significance value smaller than 0.05 was considered as an indication of significant difference between phases.

Table VII—Statistical Comparison of Vaginal Membrane Thicknesses During Different Cycle Phases[a]

	Significance[b]				
	Diestrus	Proestrus	Early estrus	Estrus	Postestrus
Diestrus	—	0.5437	0.0002	0.0035	0.2879
Proestrus	0.5437	—	0.0003	0.0040	0.6493
Early estrus	0.0002	0.0003	—	0.3047	0.0002
Estrus	0.0035	0.0040	0.3047	—	0.0100
Postestrus	0.2879	0.6493	0.0002	0.0100	—

[a] Nonparametric Mann-Whitney method was used in this statistical comparison. [b] Significance value smaller than 0.05 was considered as an indication of significant difference between phases.

Table VIII—Permeability Coefficients of I in the Noncornified Part of the Vaginal Membrane at the Estrus Phase

Mouse	Permeability Coefficient × 10^6, cm/sec
79009	0.93
79043	0.98
79067	1.25
80109	1.32
80122	1.32
80127	1.00
Average	1.13 ± 0.07

diffusion layer thickness of 1.03×10^{-2} cm. The aqueous diffusivity of I was estimated from Eq. 3 using a reported value (10) of 1.4×10^{-5} cm^2/sec for the aqueous diffusivity of benzoic acid. The aqueous diffusion layer permeability coefficient was then calculated from Eq. 1 (Table II).

Stability of the Vaginal Membrane—The vaginal membrane stability was checked at two different cycle phases (Table III). The membranes obtained during the diestrus phase could be divided roughly into two groups. Those with lower permeability coefficients ($4–9 \times 10^{-6}$ cm/sec) showed different degrees of drop in the P-values for the first 4–8 hr followed by a slow increase in P afterward. On the other hand, the membranes with high P-valves ($3–5 \times 10^{-5}$ cm/sec) were fairly stable up to 8 hr. The membranes obtained at estrus failed to show good stability.

It was found that membranes protected with the cellulose membrane had increased stability (Table IV). The permeability coefficients were essentially constant up to 8 hr for the protected vaginal membranes. This technique was of great value for those situations in which a direct comparison of P-values was desired using the same vaginal membrane. The

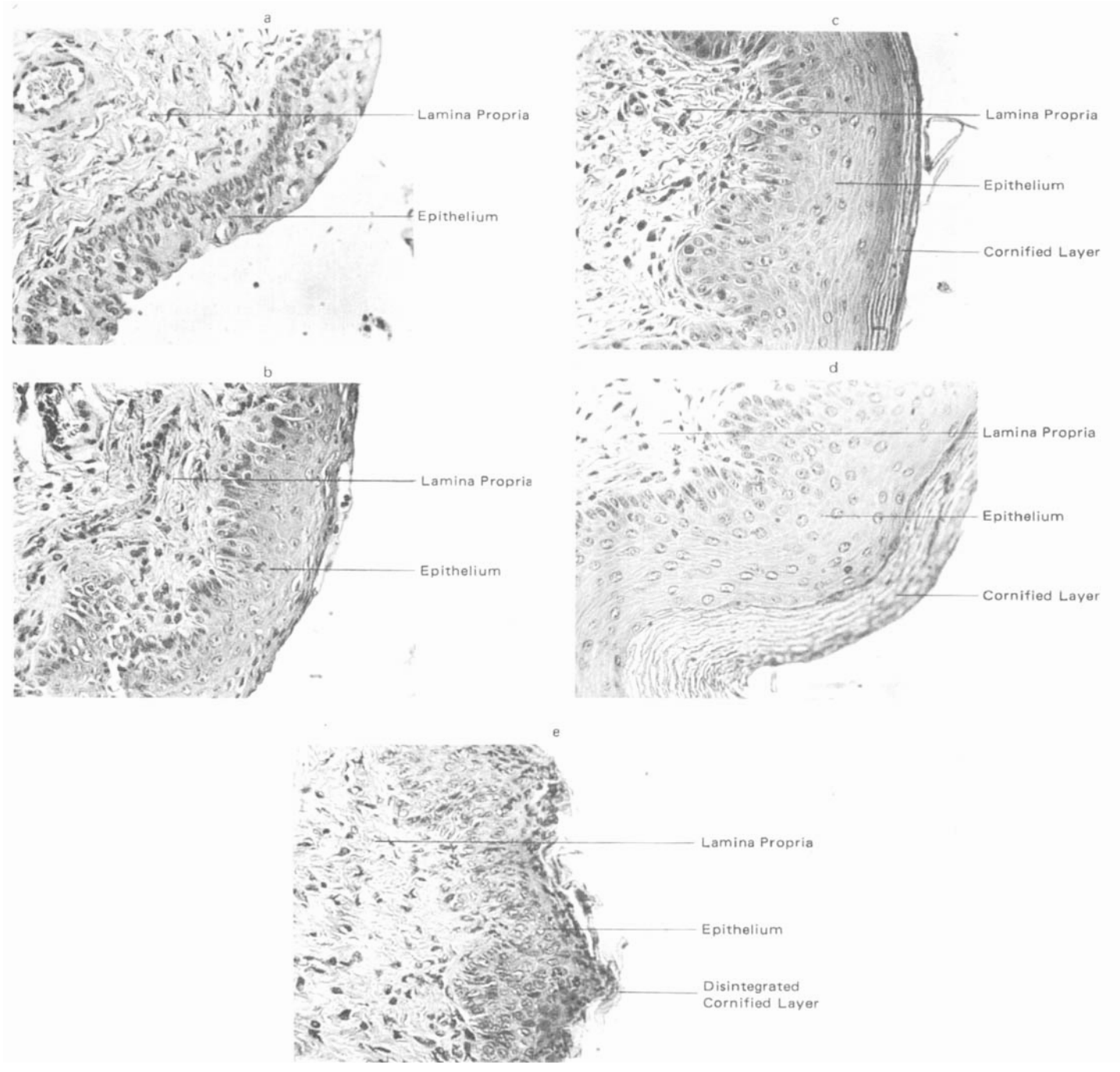

Figure 6—*Cross sections of mice vaginal membrane during different estrus cycle phases. Key: (a) diestrus phase; (b) proestrus phase; (c) early estrus phase; (d) estrus phase; (e) postestrus phase.*

cellulose membrane permeability coefficients of I are also listed in Table IV.

Permeability Coefficients of I and II—Since an adenosine deaminase inhibitor was not used in the experiments, it was necessary to prove that I and its metabolite, II, possessed the same permeability coefficient in the vaginal membrane. The permeability coefficients for both I and II were obtained on the same piece of vaginal membrane using the aforementioned membrane protection technique. As expected, the vaginal membrane permeability coefficients of I and II were essentially identical regardless of the cycle phase (Table V).

Table IX—Permeability Coefficient of Cornified, Noncornified, and Full-Thickness Membrane During the Estrus Phase

Membrane Preparation	Thickness[a] × 10^4, cm	Permeability Coefficient × 10^7, cm/sec
Cornified layer	40	2.98[b]
Noncornified layer	320	11.3 ± 0.07[c]
Full-thickness membrane	410	2.36 ± 0.07

[a] An estimate from direct measurement of the separated cornified layer and from microscopic measurement of the membrane cross section. [b] Calculated from permeability coefficients of the noncornified layer and full-thickness membrane using Eq. 12. [c] Average value from Table VIII.

Effect of the Estrous Cycle on the Vaginal Membrane Thickness and Permeability Coefficient—The permeability coefficient data collected from 58 permeability experiments were grouped according to the different phases of the cycle (Fig. 4). Statistical comparison of these five groups of data was done with the nonparametric Mann-Whitney method[12] and the results are reported in Table VI. It was clear that the differences between the permeability coefficients at the diestrus phase and those at any other phase were highly significant. On the other hand, no significant difference in the permeability coefficients between the early estrus and estrus phases was shown, although these two phases were

[12] MIDAS program; Michigan Terminal System, University of Michigan, Ann Arbor, Mich.

Table X—Calculation of Theoretical Membrane Thickness from Permeation Lag Time

Cycle Phase	Mouse	Permeability Coefficient × 10^6, cm/sec	Membrane Thickness × 10^4, cm		Diffusivity[b] × 10^6, cm^2/sec
			Calculated[a]	Measured	
	65799	0.93	63	290	
Estrus[c]	47943	0.98	71	320	
	79067	1.25	66	310	
	80109	1.35	66	300	
	80122	1.32	70	330	
	80127	1.00	74	330	
Average		1.13 ± 0.07	68.3 ± 3.7	313 ± 7	
	79015	30.8	284	300	0.88
	79016	41.1	310	270	1.27
Diestrus[d]	79018	35.1	317	340	1.11
	79023	30.3	368	280	1.12
	79060	37.8	305	320	1.15
Average		35.0 ± 2.0	317 ± 14	302 ± 13	1.10 ± 0.06

[a] Calculated from the permeation lag time using Eq. 8, when $P_{aq} = 1.05 \times 10^{-3}$ cm/sec and $haq = 1.03 \times 10^{-2}$ cm. [b] Calculated (for diestrus only) from the permeability coefficient and measured membrane thickness using Eq. 13. [c] Noncornified part of the membrane only. [d] Early stage of the diestrous phase.

distinguishable with the vaginal smear technique. Since the permeability coefficient was also a function of membrane thickness, the estrous cycle effect on vaginal membrane thickness was estimated; such data are shown in Fig. 5. Although statistical treatment of the data (Table VII) indicated that the membrane thickness at the diestrus phase was different from the thickness at the early estrus or estrus phase, the difference was only about twofold. In contrast, the permeability coefficients of I at estrus or early estrus were at least 10 and up to 100 times lower than those at diestrus. This suggested that the change of the permeability coefficients for I during the estrous cycle probably was due mainly to the physiological changes in the membrane cells rather than simply the increase of membrane thickness. A cross section of the membrane at each phase was examined under a microscope (Fig. 6). It showed that the membrane consisted of either two or three layers, *i.e.*, a loose cornified epithelial layer, a regular epithelial layer, and a combined lamina propria and muscular layer. The cornified epithelial layer, which appeared only at estrus and early estrus, was suspected as the major barrier for the penetration of I into the membrane. The permeability data also showed, however, that the mean permeability coefficient of I for the membrane at proestrus (for which there is not a cornified layer) already was reduced to 1.8×10^{-6} cm/sec. This value was about 10-fold lower than the corresponding value at diestrus. Another point is the relatively wide variation in permeability coefficients of I observed during diestrus. All these suggest that although the cornified epithelial layer could be a primary barrier for the transport of I through the membrane, it was not the sole barrier. A decrease in permeability could be caused also by the changes in the cell properties during proestrus.

Further permeation studies on vaginal membrane at estrus were performed by separating the cornified epithelial layer from the noncornified part of the membrane, the latter consisting of an epithelial layer and the combined lamina propria and muscular layer. Since it was very difficult to obtain intact cornified epithelial layers, only the permeability coefficient of the noncornified part of the membrane was measured (Table VIII). The permeability coefficient of the cornified epithelial layer (P_1) could then be estimated indirectly from:

$$\frac{1}{P_1} = \frac{1}{P_{1+2}} - \frac{1}{P_2} \qquad \text{(Eq. 11)}$$

where the permeability coefficients for the full-thickness membrane at estrus (P_{1+2}) and the permeability coefficients of the noncornified part of the membrane (P_2) were determined experimentally. The results are reported in Table IX. Statistical comparison showed that the permeability coefficients of the noncornified part of the membrane at estrus were significantly lower than those values obtained for the membrane at diestrus. They were, in fact, comparable to the permeability coefficients of the membrane at proestrus. These findings support the previous suggestion that there is a cycle-related low permeability layer in the vaginal membrane in addition to the cornified layer.

Estimation of the Permeability Coefficients of Membrane Sublayers—To investigate the homogeneity of the membranes with respect to diffusivity, theoretical membrane thickness was calculated from permeation lag times using Eq. 8. Two special cases are discussed here. The first is the results obtained using the noncornified part of the membrane obtained at estrus. These results show that the calculated membrane thicknesses are much smaller than those obtained from direct measurement (Table X). The second case involves membranes obtained during the early stage of the diestrus phase. These were the membranes with very large P-values for I. The calculated membrane thicknesses in this case showed no statistically significant differences from measured membrane thickness (Table X). The results from the second case suggest that, although there were two distinct physiological layers in the membrane at this stage in the estrous cycle, the differences between the diffusivities of I in these two layers must be either small or negligible. Therefore, a homogeneous membrane model should be a proper approximation for the membrane at this stage as far as diffusivity is concerned. The diffusivity for I for this homogeneous membrane may be calculated (assuming $k_P = 1$) from:

$$D = P \cdot h \qquad \text{(Eq. 12)}$$

The calculated diffusivity is shown in Table X.

The inconsistency of the calculated and measured membrane thickness in the first case strongly indicates that the noncornified part of the membrane at the estrus phase was not homogeneous. Since it is believed that membrane changes during the estrous cycle involve mainly the epithelial cells (9), the diffusivity of I in the combined lamina propria and muscular layer may be viewed as essentially constant throughout the cycle. Accordingly, the average diffusivity of I in membrane during the early stage of the diestrus phase (Table X) could be used as the diffusivity in the combined lamina propria and muscular layer at estrus. By microscopic estimation, of the thickness of this layer was $\sim 2.5 \times 10^{-2}$ cm; therefore, the estimated permeability coefficient was 4.4×10^{-5} cm/sec. This high permeability coefficient value shows that the combined lamina propria and muscular layer has little influence on the total permeability of I at estrus. As a result, the average permeability coefficient of 1.13×10^{-6} cm/sec obtained from the noncornified part of the membrane at estrus could be treated as the permeability coefficient of the epithelial layer at this phase without causing any serious error.

Direct Measurement of Membrane Diffusivity from Desorption Experiment—The diffusivity data obtained from desorption experiments for both layers of the membrane during the early stage of the diestrus phase of the estrous cycle are given in Table XI. Although the diffusivity of I in the epithelial layer was lower than that of the combined

Table XI—Direct Measurement of the Diffusivity of I on Mouse Vaginal Membrane from the Desorption Experiments

Cycle Phase	Mouse	Diffusivity[a] × 10^7, cm^2/sec	
		Epithelial Layer	Combined Lamina Propria and Muscular Layer
	80099	8.91	09.6
Diestrus[b]	80111	8.50	13.0
	80102	8.63	08.3
	80126	9.41	12.6
Average		8.9 ± 0.2	10.9 ± 1.2
	80110	0.080	15.6
Estrus[c]	80149	0.108	17.1
	80136	0.089	14.2
	80141	0.097	17.5
Average		0.094 ± 0.006	16.1 ± 0.8

[a] Calculated from Eq. 10, where $k_P = 1$, $A = 0.28$ cm^2, and $V = 1$ cm^3. [b] Early stage of the diestrus phase. [c] Noncornified part of the membrane.

Table XII—Estimation of the Epithelial Layer Thickness from Permeability and Desorption Experiments[a]

Mouse	Measured Membrane Thickness $\times 10^4$, cm	Permeability Coefficient[a] $\times 10^6$, cm/sec	Diffusivity of Epithelial Layer[b] $\times 10^9$, cm^2/sec	Diffusivity of Combined Lamina Propria and Muscular Layer[b] $\times 10^6$, cm^2/sec	Epithelial Layer Thickness[c] $\times 10^4$, cm
80127	330	1.00	8.49	1.60	87.7
80122	320	1.32	9.53	1.74	70.8
80109	300	1.35	11.4	1.46	83.0
Average:					78.8

[a] Noncornified part of the membrane during the estrus phase. [b] Determined from the permeability experiments. [c] Determined from the desorption experiments. [d] Calculated from Eq. 13.

lamina propria and muscular layer, the differences were small. Thus, the homogeneous membrane model still could be considered a good approximation for the membrane at the early stage of diestrus; this is in agreement with the previous discussion. The average diffusivities (as listed in the last row of Table XI) also were comparable to the diffusivity data calculated from the permeability coefficient (Table X).

In the case of the noncornified part of the membrane obtained at estrus, the results showed a great difference between the diffusivities of I in the two layers (Table XI). The average diffusivity value in the combined lamina propria and muscular layer, 1.61×10^{-6} cm^2/sec, was only slightly higher than the corresponding value, 1.09×10^{-6} cm^2/sec, obtained during diestrus. These results support the concept that the cycle effect is confined to the epithelial layer, as mentioned previously.

Calculation of Epithelial Layer Thickness—By performing the permeability and desorption experiments on the same piece of membrane, the thickness of the epithelial layer for the membrane during estrus could be calculated with better accuracy, using:

$$\frac{1}{P_2} = \frac{h_1}{D_1} + \frac{h_2 - h_1}{D_L} \qquad \text{(Eq. 13)}$$

where P_2 is the permeability coefficient of the noncornified part of the membrane, h_1 is the thickness of the epithelial layer, h_2 is the thickness of the noncornified part of the membrane, D_1 is the diffusivity of I in the epithelial layer, and D_L is the diffusivity of I in combined lamina propria and muscular layer. P_2 could be obtained from the permeability experiment; D_1 and D_L could be obtained from the desorption experiment; h_2 is estimated from direct measurement. The only unknown left is h_1, which then could be calculated easily. The results are listed in Table XII. The average thickness of the epithelial layer, 78.8×10^{-4} cm, is in good agreement with the thickness estimated from the microscopic membrane cross section ($70–90 \times 10^{-4}$ cm).

REFERENCES

(1) H. Y. Ando, N. F. H. Ho, and W. I. Higuchi, *J. Pharm. Sci.*, **66,** 1525 (1977).

(2) H. Y. Ando, N. F. H. Ho, and W. I. Higuchi, *J. Pharm Sci.*, **66,** 755 (1977).

(3) C. D. Yu, J. L. Fox, N. F. H. Ho, and W. I. Higuchi, *J. Pharm. Sci.*, **68,** 1341 (1979).

(4) C. D. Yu, J. L. Fox, N. F. H. Ho, and W. I. Higuchi, *J. Pharm Sci.*, **68,** 1347 (1979).

(5) T. W. Chang, N. J. Fiumara, and L. Weinstein, *J. Am. Med. Assoc.*, **229,** 544 (1974).

(6) A. J. Nahmias and B. Roizman, *N. Engl. J. Med.*, **289,** 719 (1973).

(7) A. J. Nahmias and B. Roizman, *N. Engl. J. Med.*, **289,** 781 (1973).

(8) R. Ash, R. M. Barrer, and D. G. Palmer, *Br. J. Appl. Phys.*, **16,** 873 (1965).

(9) R. Rugh, in "The Mouse, Its Reproduction and Development," Burgess, Minneapolis, Minn., 1968.

(10) W. I. Higuchi, S. Prakongpan, and F. Young, *J. Pharm. Sci.*, **62,** 945 (1973).

ACKNOWLEDGMENTS

This work was supported by Grant AI14987 from the National Institutes of Health.

In Vivo–In Vitro Correlations with a Commercial Dissolution Simulator II: Papaverine, Phenytoin, and Sulfisoxazole

MARTIN K. T. YAU and MARVIN C. MEYER ˣ

Received February 19, 1982, from the *Division of Biopharmaceutics and Pharmacokinetics, Department of Pharmaceutics, College of Pharmacy, University of Tennessee, Center for the Health Sciences, Memphis, TN 38163.* Accepted for publication June 15, 1982.

Abstract □ The dissolution profiles of 11 commercially available papaverine, phenytoin, and sulfisoxazole dosage forms were determined using a dissolution simulator. The products had been the subject of earlier *in vivo* bioavailability studies with human subjects. The use of an absorption simulator, which is designed to provide an estimate of the optimum sampling scheme for the dissolution simulator, did not provide useful data for this purpose. Good *in vivo–in vitro* correlations were found for the papaverine dosage forms, which included nine controlled-release products. Less satisfactory correlations were obtained for the phenytoin capsules and the sulfisoxazole tablet products.

Keyphrases □ *In vivo–in vitro* correlations—papaverine, phenytoin, and sulfisoxazole using a commercial dissolution simulator □ Papaverine—*in vivo–in vitro* correlations using a commercial dissolution simulator □ Phenytoin—*in vivo–in vitro* correlations using a commercial dissolution simulator □ Sulfisoxazole—*in vivo–in vitro* correlations using a commercial dissolution simulator

An earlier paper (1) described attempts to correlate the *in vitro* dissolution and *in vivo* bioavailability of several solid dosage forms, using commercial absorption[1] and dissolution[2] simulators. That study involved the testing of marketed methenamine, nitrofurantoin, and chlorothiazide dosage forms, which had been the subject of human urinary excretion bioavailability studies. Marketed dosage forms of papaverine, phenytoin, and sulfisoxazole, which were previously evaluated in human bioavailability studies (2–4) using plasma concentration measurements, are the subject of the present study.

EXPERIMENTAL

Absorption Simulator Studies—The design and application of the absorption simulator were described previously (1); the experimental conditions were essentially identical to the earlier study. The initial drug concentrations employed in the absorption studies were as follows: papaverine, 100 and 200 μg/ml; phenytoin, 30 μg/ml; and sulfisoxazole, 200 μg/ml. The surface areas of the artificial lipid barriers[3] were as follows: papaverine, 80 cm^2 and 12 cm^2 for the gastric phase; phenytoin, 40 cm^2 for the gastric phase, 80 cm^2 for the intestinal phase; and sulfisoxazole, 40 cm^2 for both the gastric and intestinal phase studies.

Dissolution Simulator Studies—The experimental approach and the design of the dissolution simulator were discussed previously (1). The following sampling rates were utilized: papaverine, 2.5 ml every 4 min for 56 min in the gastric phase and every 6 min for 123 min in the intestinal phase; sulfisoxazole, 2.5 ml every 2.5 min for 32 min in the gastric phase and 188 min in the intestinal phase; phenytoin, 7.5 ml every 0.5 min for 46 min (gastric phase), using distilled water as the dissolution medium.

The 11 papaverine hydrochloride dosage forms, previously identified (2), consisted of one elixir (150 mg/22.5 ml), eight 150-mg sustained-release capsules, one 200-mg sustained-release tablet, and one 30-mg compressed tablet (with a five-tablet dosage). The 11 phenytoin dosage forms were each 100-mg capsules of sodium phenytoin (3), and the 11 sulfisoxazole tablets each contained 500 mg of drug (4).

Analytical Methods—All drug solutions obtained from the absorption and dissolution studies were assayed spectrophotometrically at a wavelength appropriate for the drug and solvent. Papaverine solutions were diluted with 0.06 *N* hydrochloric acid and measured at 252 nm. Sulfisoxazole solutions, diluted when necessary with the buffer solutions employed in the absorption and dissolution studies, were measured at 253 and 267 nm for the pH 6.5 and 1.3 buffer solutions, respectively. In preliminary studies it was determined that constituents of the phenytoin capsules appeared to interfere in the direct spectrophotometric analysis of dissolution samples. Therefore, dissolution samples were acidified with 3 drops of hydrochloric acid, extracted into 20 ml of chloroform–ethanol (20:1, v/v), and back-extracted into 5 ml of 0.1 *N* sodium hydroxide. The aqueous solution was then measured spectrophotometrically at 230 nm. Phenytoin samples obtained with the absorption simulator were diluted with 0.1 *N* sodium hydroxide and measured directly at 230 nm.

Treatment of Dissolution Data—Two approaches were employed in the analysis of the dissolution rate data: simulated absorption data and general correlations. These procedures were described in detail previously (1), using urinary excretion data.

According to the manufacturer of the dissolution simulator (5, 6), the cumulative amount of drug withdrawn from the dissolution vessel (*Mi*) is related to the cumulative amount of drug absorbed *in vivo*. Using the

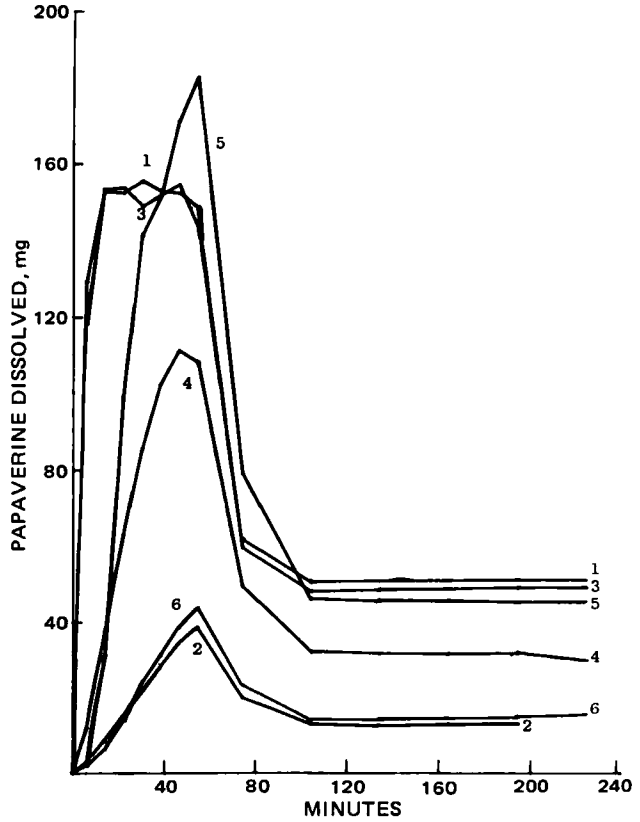

Figure 1—*Dissolution profiles for six papaverine formulations in study group 1. Each data point is the mean of two determinations. The simulated intestinal phase began after 56 min.*

[1] Sartorius Absorption Simulator SM 16753, Sartorius Filters, Inc., San Francisco, Calif.

[2] Sartorius Dissolution Simulator SM 16752, Sartorius Filters, Inc., San Francisco, Calif.

[3] Artificial Gastric Lipid Barrier SM 15701 and Artificial Intestinal Lipid Barrier SM 15702, Sartorius Filters, Inc., San Francisco, Calif.

0022-3549/83/0600-0681$01.00/0

Table I—Diffusion Characteristics and Sampling Rates Determined with the Absorption Simulator

Drug	$K_d \times 10^3$, cm/min^{-1} [a]		Time Between Samples, min			
			Calculated [b]		Actual	
	Gastric Phase	Intestinal Phase	Gastric Phase	Intestinal Phase	Gastric Phase	Intestinal Phase
Papaverine	—	—	—	—	4.0	6.0
Phenytoin	12.99	26.60	1.90	0.94	0.5	—
Sulfisoxazole [c]	9.62	10.02	2.6	2.5	2.6	2.5

[a] Diffusion rate constant, calculated according to Stricker (5). [b] Theoretical sampling rates for the dissolution simulator, calculated from absorption simulator diffusion rate according to the method of Stricker (5). [c] Values represent the mean of two determinations.

previously obtained plasma concentration data for each drug, the amount of drug absorbed (A_t) was calculated from:

$$\frac{A_t}{V_d} = C_t + K(\mathrm{AUC})_{0-t}$$

based on the Wagner–Nelson method (7). In this equation, V_d is the apparent volume of distribution; C_t is the plasma concentration at time t; K is the apparent first-order elimination rate constant, assuming a one-compartment model involving first-order absorption and elimination; and $(\mathrm{AUC})_{0-t}$ is the area under the plasma concentration–time curve over the time period 0–t, estimated with the trapezoidal rule. A direct comparison could not be made of the amount of dissolved drug withdrawn from the dissolution fluid (*Mi*) and the amount of drug absorbed *in vivo* (A_t) because the V_d term could not be estimated accurately from the *in vivo* data. To relate the amount dissolved *in vitro* to the *in vivo* plasma drug concentrations, plots were constructed of A_t/V_d *versus Mi*. The slope of the least-squares line forced through the origin was then used to adjust the A_t/V_d data.

A wide variety of correlations were also attempted to relate the *in vitro* and *in vivo* data. Initially, the dissolution rate profiles were examined systematically to determine dissolution rate parameters which exhibited a reasonable rank-order relationship to a given *in vivo* parameter. The correlation was then evaluated further from the statistical analyses of plots of *in vivo versus in vitro* data. The various *in vivo* values considered included the maximum plasma drug concentration, the time of maximum plasma concentration, the total area under the plasma concentration–time curve (AUC) at specific times, the time to achieve a given percent of the total AUC, and the percent of total AUC achieved at a given time. The *in vitro* values tested included the time for a given percentage of drug to be dissolved, the area under the dissolution–time profile at a given time, and the percentage of drug dissolved at a given time.

RESULTS AND DISCUSSION

Analytical Methods—The spectrophotometric methods employed for the analysis of samples obtained with the absorption and dissolution simulator were all relatively simple, and the linearity and reproducibility of the standard curves were excellent. The correlation coefficients describing the various standard curves were all >0.999. The slopes of these curves were reproducible on a daily basis and exhibited relative standard deviations of <3% for three to six determinations.

Absorption Simulator—According to Stricker (5), the diffusion rate constants obtained with the absorption simulator may be employed to determine the optimal sampling rates for the dissolution apparatus. The apparent first-order diffusion rate constants obtained with the absorption simulator are given in Table I, along with the theoretical optimal sampling rates and the sampling rates which were actually employed.

Attempts to study the diffusion of papaverine across the lipid barriers were not successful. The limited solubility of the drug in the receptor fluid (pH 7.5) and the apparent retention of the drug within the membrane resulted in negligible diffusion. Attempts to increase the rate of diffusion with a membrane of smaller surface area (12 cm^2) and a higher papaverine concentration (200 ng/ml) failed to provide adequate diffusion. Thus, the selection of sampling intervals of 4 min (gastric phase) and 6 min (intestinal phase) was based on preliminary trials with the dissolution simulator.

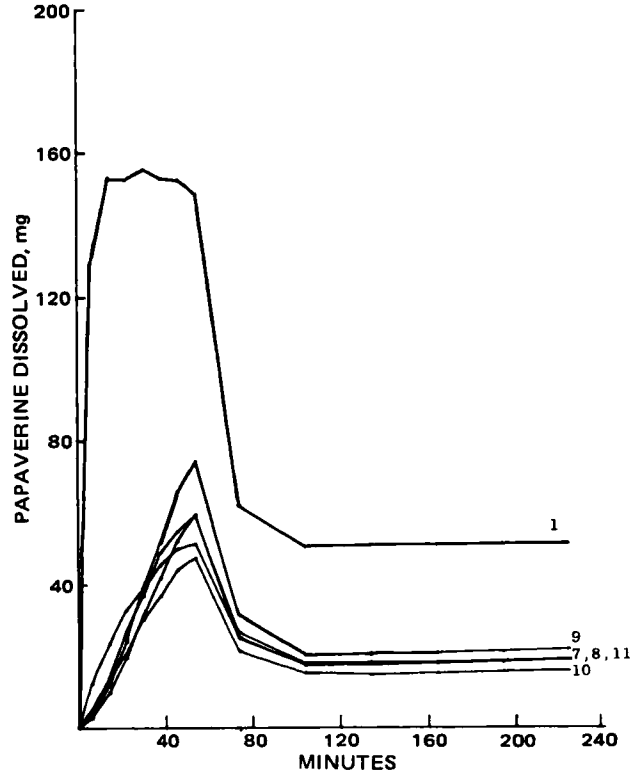

Figure 2—*Dissolution profiles for six papaverine formulations in study group 2. Each data point is the mean of two determinations. The simulated intestinal phase began after 56 min.*

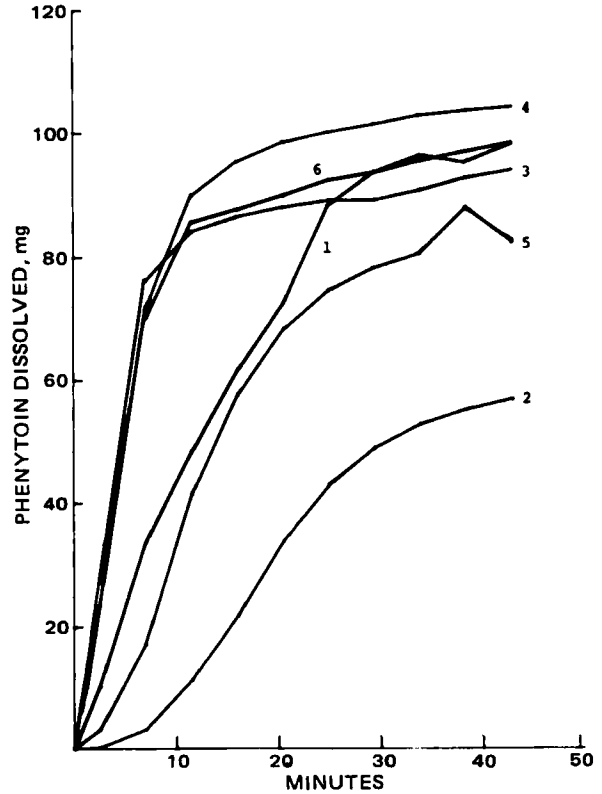

Figure 3—*Dissolution profiles for six phenytoin formulations in study group 1. Each data point is the mean of two determinations.*

Table II—Reproducibility of the Dissolution Simulator [a]

Sample Time, min	Total Amount of Dissolved Drug, mg											
	Sulfisoxazole (Group 1)				Phenytoin (Group 1)				Papaverine (Group 1)			
	Product 2		Product 5		Product 2		Product 4		Product 2		Product 3	
	A	B	A	B	A	B	A	B	A	B	A	B
6	—	—	—	—	—	—	—	—	5	1	120	116
7	49	40	3	3	1	5	61	83	—	—	—	—
14	—	—	—	—	—	—	—	—	11	6	115	150
16	—	—	—	—	16	28	91	101	—	—	—	—
18	63	58	26	18	—	—	—	—	—	—	—	—
29	70	64	45	46	—	—	—	—	—	—	—	—
30	—	—	—	—	46	53	99	105	27	16	151	147
43	—	—	—	—	57	58	103	107	—	—	—	—
46	—	—	—	—	—	—	—	—	40	29	158	151
64	396	432	268	290	—	—	—	—	—	—	—	—
74	—	—	—	—	—	—	—	—	19	21	61	59
134	—	—	—	—	—	—	—	—	13	12	49	49
139	539	539	377	375	—	—	—	—	—	—	—	—

[a] A and B represent duplicate determinations.

The diffusion of the phenytoin across the lipid barriers was quite rapid from both gastric and intestinal media. The theoretical sampling intervals were 1.9 and 0.9 min for dissolution in the simulated gastric and intestinal fluids, respectively, based on the diffusion data. However, phenytoin was poorly soluble in the gastric and intestinal fluids of the dissolution apparatus, and the dissolution fluid was rapidly saturated as the 100-mg dosage form dissolved in 100 ml of the fluid. As a result, the sampling rate was changed to the maximum rate possible with the apparatus: 7.5 ml every 30 sec, for 45 min. In addition, distilled water was employed as the dissolution medium, as currently used in the USP XX dissolution procedure.

In preliminary trials with the dissolution of the sulfisoxazole tablets, it was determined that the theoretical sampling rates suggested by the absorption simulator were satisfactory for the study of these dosage forms. Duplicate determinations were made for sulfisoxazole, and the mean values are given in Table I.

Individual diffusion rate constants differed from the mean by < 3% for both the gastric and intestinal phase studies. Only single determinations were made for phenytoin and papaverine because of the limited value of the absorption simulator for these drugs. As noted in the previous study (1), data obtained with the absorption simulator generally was not applicable to the selection of appropriate conditions for the dissolution tests.

Dissolution Profiles—The dissolution rate profiles of the various formulations of the three drugs are shown in Figs. 1–6. Each data point represents the mean of two dosage forms, except for the papaverine elixir (product 1). Too little of the elixir remained from the earlier studies to permit duplicate dissolution studies. The reference to groups 1 and 2 in each of the dissolution study profiles relates to the fact that each *in vivo* bioavailability study involved two groups of subjects, with a reference (product 1) being common to both groups; e.g., six subjects received each of five papaverine dosage forms and the elixir, and an additional six

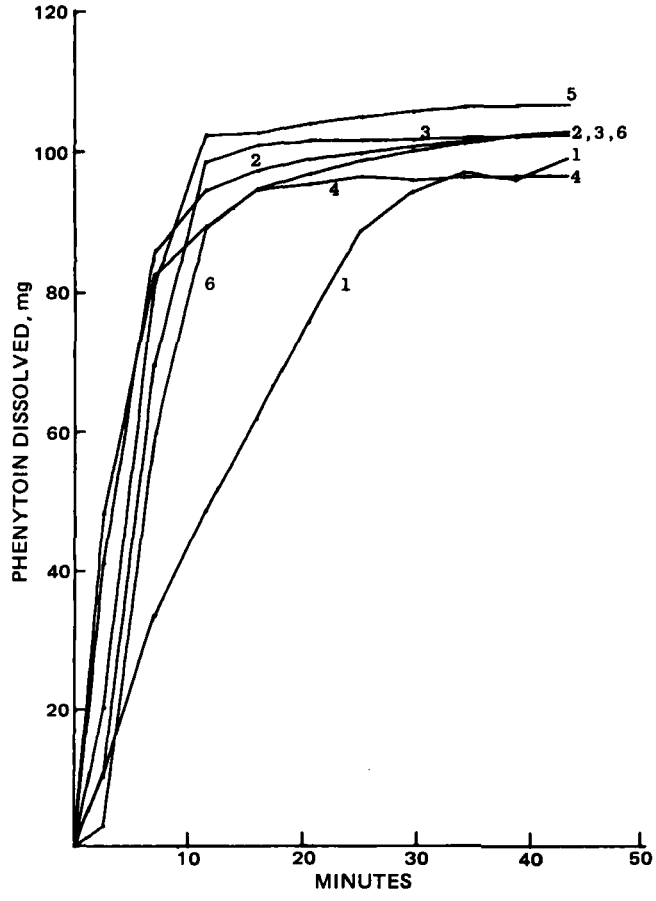

Figure 4—*Dissolution profiles for six phenytoin formulations in study group 2. Each data point is the mean of two determinations.*

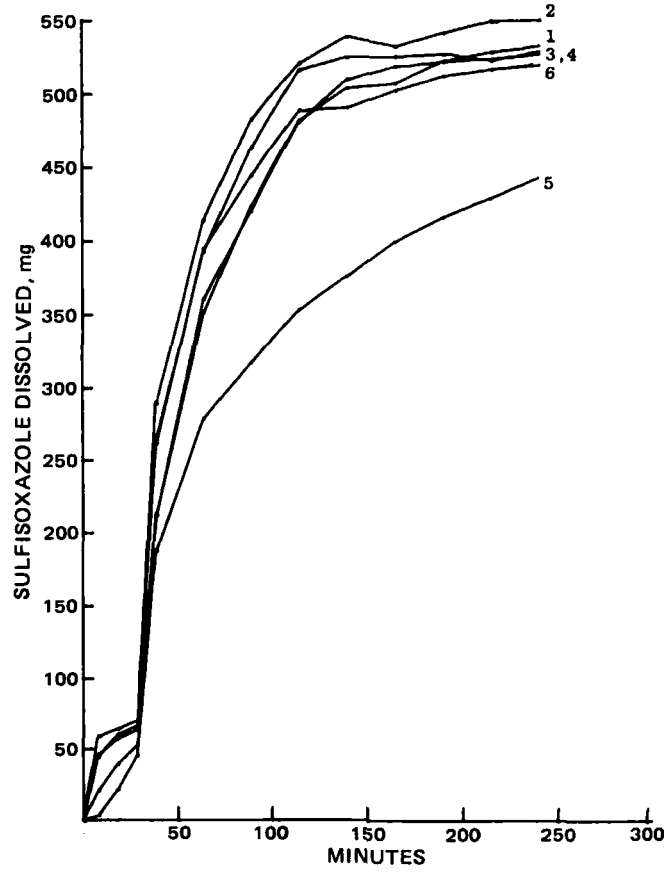

Figure 5—*Dissolution profiles for six sulfisoxazole formulations in study group 1. Each data point is the mean of two determinations. The simulated intestinal phase began after 32 min.*

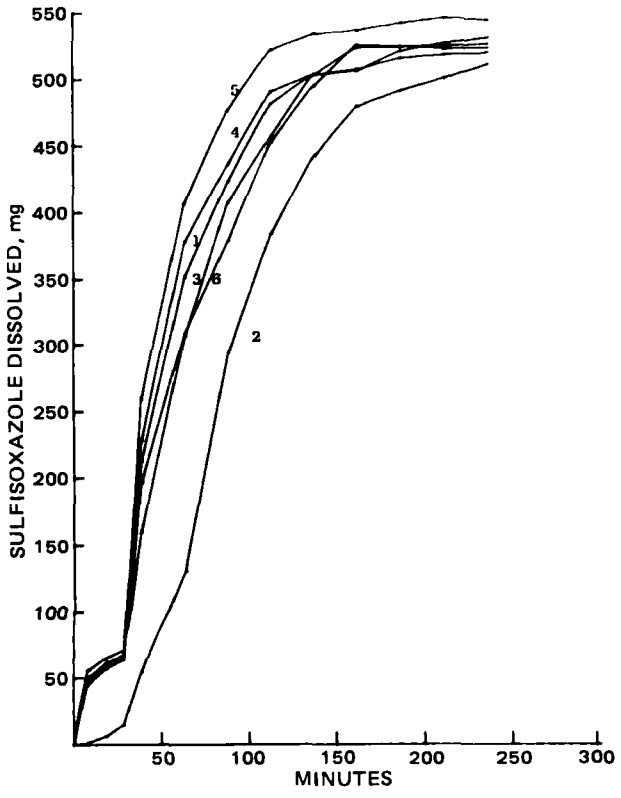

Figure 6—*Dissolution profiles for six sulfisoxazole formulations in study group 2. Each data point is the mean of two determinations. The simulated intestinal phase began after 32 min.*

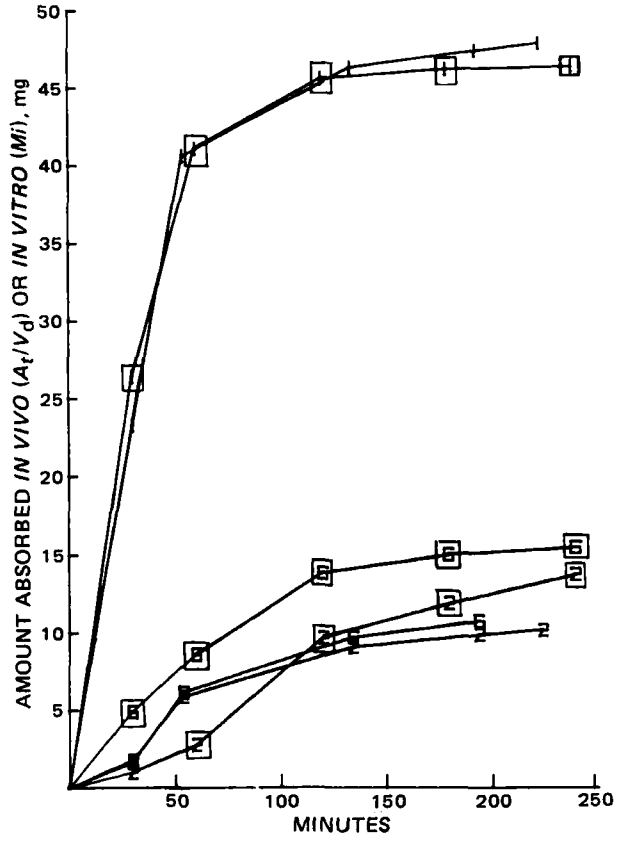

Figure 7—*Comparison of the total amount of papaverine withdrawn from the* in vitro *dissolution system (*Mi*) and the adjusted* in vivo *absorption profiles (A_t/V_d) for three papaverine formulations in study group 1. Each* in vitro *data point is the mean of two determinations for products 2 and 6 and a single determination for product 1. Each* in vivo *data point (□) is the mean of six subjects.*

subjects received the other five papaverine dosage forms and the elixir (2).

The data for the papaverine formulations (Figs. 1–2) demonstrated rapid dissolution for both the elixir (product 1) and the compressed tablets (product 3). Each of the sustained-release dosage forms dissolved more slowly, including product 5 which was a 200-mg tablet. The amount of drug dissolved for each product decreased when the pH of the dissolution medium was increased to 6.5 after 56 min, suggesting precipitation of the papaverine under these conditions.

The dissolution of the majority of the phenytoin capsules was quite rapid, with all but 3 of the 11 products being at least 85% dissolved within 10 min. Product 2 in group 1 was slowly and incompletely dissolved even after 45 min, and this product also exhibited the poorest *in vivo* bioavailability (3).

The dissolution of each of the sulfisoxazole tablet products (Figs. 5 and 6) proceeded more rapidly after 32 min when the pH of the dissolution fluid was increased to 6.5. The two products which dissolved the slowest, product 5 (group 1) and product 2 (group 2), also failed the USP XVIII dissolution specifications (applicable at the time the *in vivo* studies were conducted).

In general, the reproducibility of the duplicate determinations was reasonably good. Table II summarizes individual dosage form values for the fastest and slowest dissolving formulation of each of the three drugs. By comparison, relative standard deviations for 12 replicate determinations of the dissolution of the phenytoin capsules, using the USP XX method (8), were <5% at each sampling time[4]. At the time of the sulfisoxazole bioavailability study, the various tablets were also subjected to the USP XVIII dissolution test, using six replicates. Samples were obtained only at 30 min. The dissolution values obtained for products 2 and 5 (Table II) were 475–511 mg and 90–125 mg, respectively. There is no official dissolution test for controlled-release papaverine dosage forms; therefore, these products were only studied with the dissolution simulator.

Simulated Absorption Profiles—Using the approach described earlier, attempts were made to relate the amount of drug dissolved *in vitro* and the amount in the body during the *in vivo* studies. This approach was not successful with data from either the phenytoin or the sulfisoxazole studies. Since the dissolution rate determinations for the phenytoin capsules were terminated after only 45 min, comparisons of the *in vitro* and *in vivo* absorption profiles were not meaningful. With the sulfisoxazole tablets, it was determined that the amount dissolved *in vitro*, in general, greatly underestimated the amount of drug absorbed *in vivo* for all products. Thus, no useful relationships could be discerned. However, there was a reasonably good correlation between the *in vitro* and *in vivo* data for the papaverine products, except for products 4 and 5 of group 1. Representative data are shown in Figs. 7 and 8. Since the two *in vivo* study groups differed significantly in the plasma papaverine concentrations obtained with the reference elixir, the data were analyzed separately for the two groups. Plots of A_t/V_d *versus Mi* yielded slopes of 1.77×10^{-5} and 1.15×10^{-5} ml^{-1} for groups 1 and 2, respectively. The slope value can be considered as a correction factor incorporating the V_d term and other *in vivo* variables not present in the *in vitro* system.

General Correlations—This data treatment represents a more classical approach which attempts to relate an *in vitro* parameter, such as percent dissolved at a given time, to an *in vivo* parameter, such as area under the plasma concentration–time curve (AUC), maximum plasma concentration (C_{max}), or time of maximum plasma concentration (t_{max}). Although a wide variety of potential correlations were tested, only those resulting in the best correlation are presented herein.

Papaverine—Good correlations were observed for plots of C_{max} *versus* percent dissolved in 30 min *in vitro*, $r = 0.917$ ($p < 0.01$), and the 0–10 hr AUC, $r = 0.899$ ($p < 0.01$), or C_{max}, $r = 0.869$ ($p < 0.01$), *versus* area under the dissolution–time curve for 3.2 hr. The best correlation (Fig. 9) related the 0–10 hr AUC to the percent dissolved in 30 min, $r = 0.922$ ($p < 0.01$). The group 1 and group 2 data were plotted together by normalizing the group 2 AUC values by the ratio of the AUC values for the reference elixir which was common to both study groups.

Phenytoin—The best correlations resulted when *in vivo* t_{max} values were plotted *versus* the time for 50% dissolution *in vitro* ($t_{50\%}$), $r = 0.909$ ($p < 0.01$), or the percent dissolved in 7 min, $r = 0.827$ ($p < 0.01$). The t_{max} values for the group 2 subjects were normalized by the ratio of the t_{max} values for reference (product 1), which was common to both groups.

[4] Personal communication from V. P. Shah, Division of Biopharmaceutics, Food and Drug Administration, Rockville, MD 20857, on April 14, 1982.

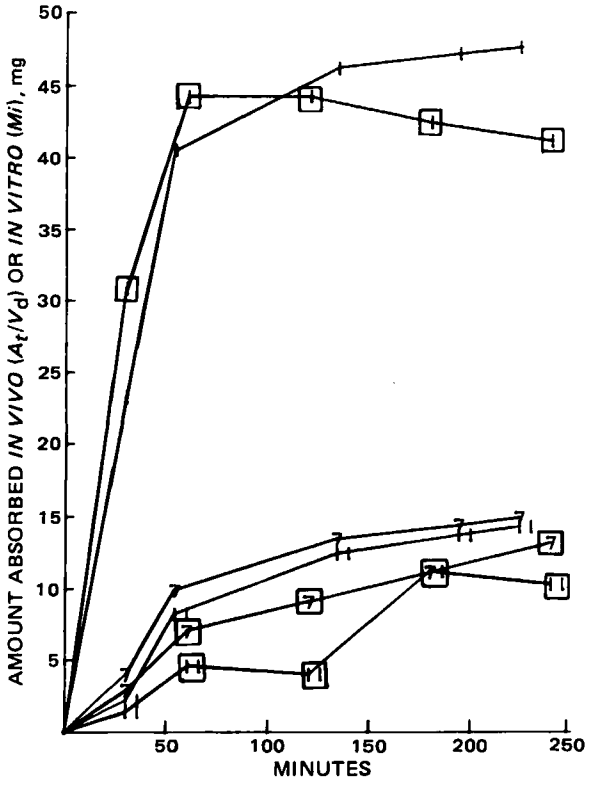

Figure 8—*Comparison of the total amount of papaverine withdrawn from the* in vitro *dissolution system* (Mi) *and the adjusted* in vivo *absorption profiles* (A_t/V_d) *for three papaverine formulations in study group 2. Each* in vitro *data point is the mean of two determinations for products 7 and 11 and a single determination for product 1. Each* in vivo *data point* (□) *is the mean of six subjects.*

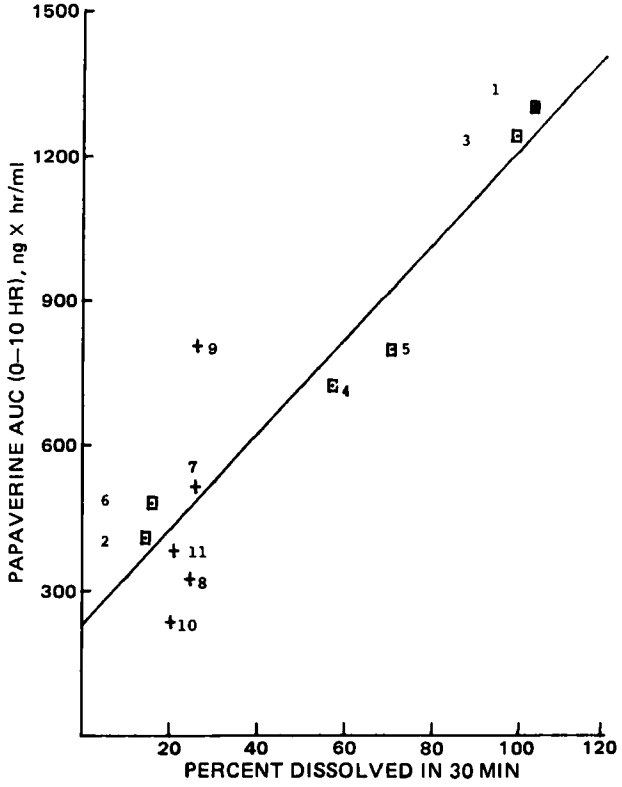

Figure 9—In vivo–in vitro *correlation for 11 papaverine formulations,* r = *0.922* (p < *0.01*). *Each data point represents the mean of two* in vitro *and six* in vivo *values, except the* in vitro *value of product 1 which is the result of a single dissolution study. Key:* (⊡) *data from group 1;* (+) *data from group 2* (⊞) *product 1.*

As shown in Fig. 10, products 2 and 5 of group 1 did not fit the correlation employed to describe the other nine dosage forms.

Since the completion of these studies, new USP dissolution specifications have been published for phenytoin capsules (9). These dosage forms have been divided into two types, based on dissolution characteristics. "Prompt" capsules must dissolve ≥85% within 30 min, using 900 ml of water and the USP Apparatus I at 50 rpm. "Extended" capsules must dissolve ≤35% in 30 min, 30–70% at 60 min, and ≥80% in 120 min, using the same dissolution system. As shown in Fig. 3, only products 2 and 5 of group 1 failed to dissolve at least 85% in 30 min using the dissolution simulator. However, both products were >35% dissolved at 30 min. Thus, these two products dissolved too slowly to be considered "prompt" and too fast to be considered "extended" using the USP XX criteria. Product 1, which is a formulation that meets the USP XX specifications of "extended," also dissolved ~90% in 30 min using the dissolution simulator. With the exception of product 5 (group 1), the relationship illustrated in Fig. 10 could be employed. This suggests that if the time for 50% dissolution exceeded 5 min, the t_{max} value *in vivo* would exceed 4.5 hr. On the basis of dissolution testing, as well as *in vivo* bioavailability studies, current phenytoin products may be employed in different dosage regimens, depending on whether they are labeled "prompt" or "extended." The "prompt" formulations are recommended for three times a day (TID) administration, while the "extended" capsules may be given once a day after an initial period to reach the optimal titer.

Thus if the data from the dissolution simulator were to be employed to establish such specifications, products 1, 2, and 5 (group 1) and 6 (group 2) each would be considered "extended." However, the t_{max} for product 5, which exhibited the second longest dissolution time, was not appreciably different from that for the majority of the other products. The *in vitro* studies carried out with some of these products using the USP XX method (8) found products 1 and 2 (group 1) and 6 (group 2) to be the slowest dissolving, which is consistent with the present data. However, product 5 (group 1) was one of the more rapidly dissolving products. Thus the USP XX method provided dissolution data which were more consistent with the *in vivo* observations than that obtained with the dissolution simulator employed in the present study.

Sulfisoxazole—As part of the previous *in vivo* studies, all of the tablets

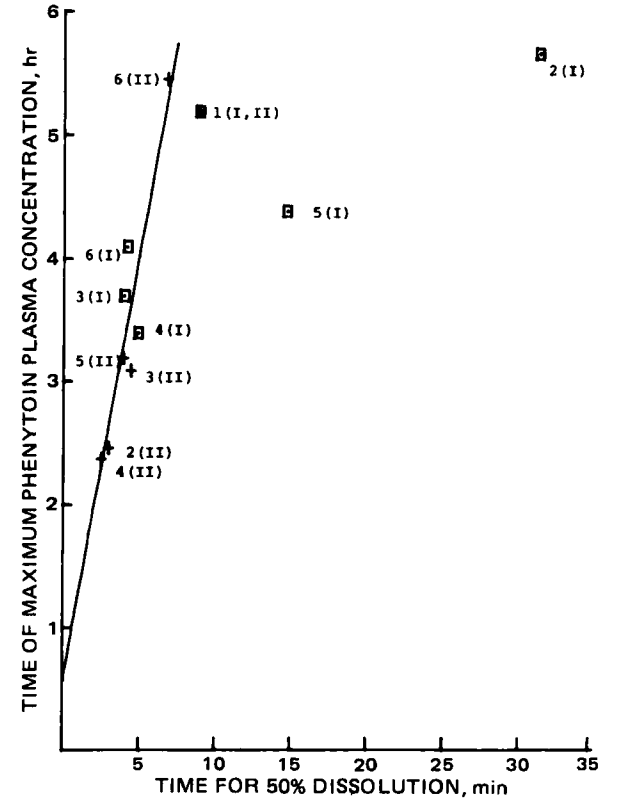

Figure 10—In vivo–in vitro *correlation for 11 phenytoin formulations,* r = *0.909* (p < *0.01*). *Each data point represents the mean of two* in vitro *and six* in vivo *values. Products 2 and 5 (group 1) were omitted from the correlation. Key: (I) group 1; (II) group 2.*

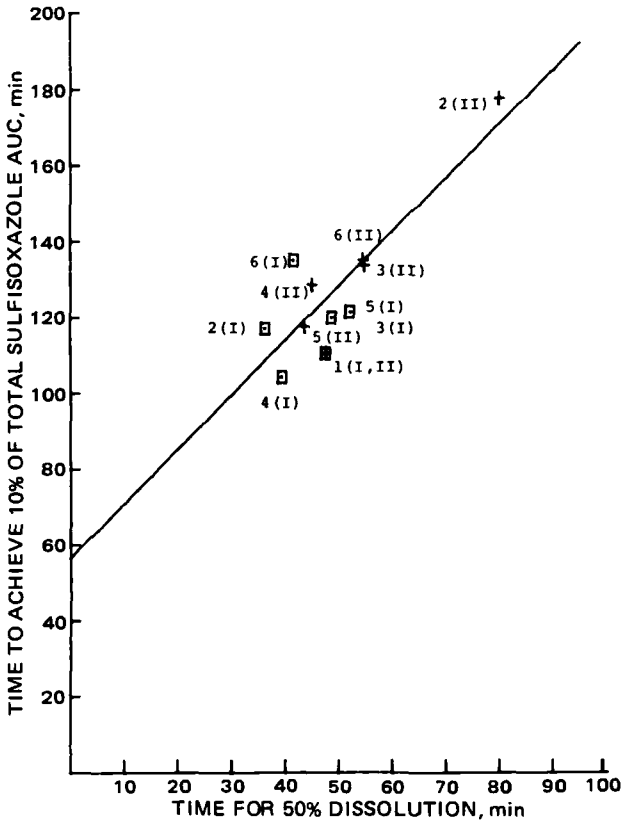

Figure 11—In vivo–in vitro *correlation for 11 sulfisoxazole formulations,* r = *0.870 (*p < *0.01). Each data point represents the mean of two* in vitro *and six* in vivo *values. Key: (I) group 1; (II) group 2.*

were evaluated using the USP XVIII dissolution method. Products 3 and 5 of group 1 and product 2 of group 2 failed the USP requirement of ≥60% dissolution in 30 min. The extent of dissolution was 12.6, 21.4, and 49% after 30 min for products 2, 5, and 3, respectively. Figure 11 illustrates the best correlation obtained in the present study, $r = 0.87$ ($p < 0.01$), relating time for 50% dissolution to the time to achieve 10% of the total AUC. Attempts to relate more conventional parameters such as total AUC, t_{max}, or C_{max} did not result in meaningful correlations, due in part to the relatively narrow range of *in vivo* bioavailability characteristics. The data of the *in vivo* studies resulted in a conclusion that the 11 dosage forms did not differ significantly in terms of any of the usual bioavailability parameters. Since product 5 (group 1) and product 2 (group 2) were the slowest dissolving tablets with both the USP method and the dissolution simulator, and yet did not differ significantly *in vivo*, there did not appear to be any advantage to the use of the dissolution simulator.

Study Limitations—As with the previous study (1), the expiration dates for several of the products had passed prior to the completion of the dissolution studies. Furthermore, too few dosage units remained to permit a determination of content uniformity. However, 90–100% of the labeled product content was dissolved during the period of the dissolution test for the papaverine elixir and compressed tablets, the majority of the phenytoin capsules, and the sulfisoxazole tablets, indicating no significant degradation had occurred during storage of these products. In addition, the slow dissolution of two of the sulfisoxazole tablets and three of the phenytoin capsules was consistent with other results obtained using USP methodology.

CONCLUSIONS

As was determined in the previous study (1), the use of the absorption simulator did not always provide useful information for establishing the optimum sampling rates for the dissolution simulator. Of the three drugs studied with the dissolution simulator, only the papaverine dosage forms resulted in a reasonable correlation between the *in vivo* bioavailability and the *in vitro* dissolution data. For the phenytoin capsules a reasonable correlation was obtained between the *in vitro* t_{max} and dissolution, except for two slowly dissolving capsules, thus limiting the general applicability of the relationship. Furthermore, other studies of these phenytoin capsules have indicated the present USP XX dissolution method provides better *in vivo–in vitro* correlations. The lack of suitable correlations was probably due, in part, to the limited fluid volume of the dissolution chamber, which was rapidly saturated with phenytoin. Finally, studies involving the sulfisoxazole tablets also failed to provide any significant *in vivo–in vitro* correlations, due in part to the similar *in vivo* characteristics of the 11 products. As with most, if not all *in vitro* dissolution systems, it is not possible to assume *a priori* that data obtained with the dissolution simulator will relate to the *in vivo* performance of a given dosage form.

REFERENCES

(1) M. K. T. Yau and M. C. Meyer, *J. Pharm. Sci.*, **70**, 1017 (1981).

(2) M. C. Meyer, R. Gollamudi, and A. B. Straughn, *J. Clin. Pharmacol.*, **19**, 435 (1979).

(3) A. P. Melikian, A. B. Straughn, G. W. A. Slywka, P. L. Whyatt, and M. C. Meyer, *J. Pharmacokinet. Biopharm.*, **5**, 133 (1977).

(4) G. W. A. Slywka, A. P. Melikian, A. B. Straughn, P. L. Whyatt, and M. C. Meyer, *J. Pharm. Sci.*, **65**, 1497 (1976).

(5) H. Stricker, *Drugs Made Ger.*, **16**, 80 (1973).

(6) H. Stricker, "On the Relationship between Drug Absorption and Dissolution in the Gastro-Intestinal Tract (I)," C. H. Boehringer Sohn. Ingelheim; distributed by Beckman Instruments, Inc., Anaheim, Calif.

(7) J. G. Wagner, "Fundamentals of Clinical Pharmacokinetics," Drug Intelligence Publications, Hamilton, Ill., 1975, p. 174.

(8) V. P. Shah, V. K. Prasad, R. Alston, B. E. Cabana, R. P. Gural, and M. C. Meyer, *J. Pharm. Sci.*, **72**, 306 (1983).

(9) "The United States Pharmacopeia XX," U.S. Pharmacopeial Convention, Inc., Rockville, Md., 1980.

ACKNOWLEDGMENTS

This work was adapted in part from a thesis submitted by M. K. T. Yau to the University of Tennessee Center for the Health Sciences, in partial fulfillment of the MS degree requirements, and was supported in part by contracts from the Food and Drug Administration (FDA No. 223-74-3097 and FDA No. 223-77-3011) and the Tennessee Department of Public Health.

The use of the Sartorius Absorption and Dissolution Simulators, provided by Sartorius Filters, Inc., is gratefully acknowledged.

Synthesis and Evaluation of 3-Halocyclophosphamides and Analogous Compounds as Novel Anticancer "Pro-Prodrugs"

GERALD ZON *x, SUSAN MARIE LUDEMAN *, GÜNAY ÖZKAN *, SRINIVASAN CHANDRASEGARAN ‡, CHARLES F. HAMMER ‡, RUTH DICKERSON §, KAZUTAKA MIZUTA ¶, and WILLIAM EGAN **

Received March 19, 1982, from the *Department of Chemistry, The Catholic University of America, Washington, DC 20064, ‡Department of Chemistry, Georgetown University, Washington, DC 20057, §The Johns Hopkins Oncology Center, Baltimore, Maryland 21205, ¶Otsuka Pharmaceutical Co., Ltd., Osaka, Japan, and **Division of Biochemistry and Biophysics, Bureau of Biologics, Food and Drug Administration, Bethesda, Maryland 20205. Accepted for publication June 11, 1982.

Abstract □ 3-Fluoro-, 3-chloro-, and 3-bromocyclophosphamide were prepared from the reaction of trifluoromethylhypofluorite, sodium hypochlorite, and bromine with the anticancer drug cyclophosphamide. Treatment of *cis*- and *trans*-4-phenylcyclophosphamide and 5,6-benzocyclophosphamide with sodium hypochlorite afforded *cis*- and *trans*-3-chloro-4-phenylcyclophosphamide and 3-chloro-5,6-benzocyclophosphamide, respectively. ^{31}P-NMR spectroscopy was used to study the reactivity of these compounds: the fluoro derivative was reduced to cyclophosphamide on incubation with mouse liver slices, and the reactivity order for sulfhydryl-induced reduction of the 3-halocyclophosphamides was Br ≅ Cl ≫ F. Compared with the therapeutic efficacy of cyclophosphamide against L-1210 and P-388 cancers in mice, 3-fluoro- and 3-chlorocyclophosphamide were less active, although the fluoro derivative was more efficacious than the 3-chloro compound. The individual *R* and *S* enantiomers of 3-chlorocyclophosphamide, prepared from (*S*)- and (*R*)-cyclophosphamide, respectively, showed no significant difference in therapeutic activity in the P-388 test system.

Keyphrases □ Cyclophosphamide—synthesis of *N*-halogenated derivatives, NMR spectroscopic characterization, therapeutic efficacy in mouse cancers □ Synthesis—of *N*-halogenated derivatives of cyclophosphamide, NMR spectroscopic characterizations, therapeutic efficacy in mouse cancers □ Antineoplastic agents—cyclophosphamide and *N*-halogented derivatives, synthesis and NMR characterization, therapeutic efficacy in mouse cancers

The *N*,*N*-bis(2-chloroethyl)amino functionality has been used frequently in the design of antineoplastic agents (1) and prodrugs (1, 2). Studies of such prodrugs by Zon *et al.* (3–8) have included labile precursors of the well-known anticancer agent cyclophosphamide (I) (9). Since I functions as a prodrug (2, 9), these *in vivo* precursors of cyclophosphamide may be viewed as "pro-prodrugs." For example, 3-(*tert*-butyldimethylsilyl)cyclophosphamide (II) can release I by spontaneous hydrolysis (5), and 3-hydroxycyclophosphamide (III) can afford I by reductive cleavage of the N—O bond (6). While II proved to be inactive against L-1210 leukemia in mice (5), the *in vivo* conversion of III to I was evidenced by comparable antileukemic activities for III and I in the L-1210 system and by the rapid formation of I on incubation of III with liver microsomes (6).

A variety of other biologically reducible linkages (10–14) may be incorporated at the N-3 position of the cyclophosphamide ring system; however, the nitrogen–halogen bond is particularly interesting, since it apparently represents a new moiety for the reversible modification of N—H groups in drugs (11–15). In addition, the N—F modification, exemplified by 3-fluorocyclophosphamide (IV), could allow metabolic studies by ^{19}F-NMR spectroscopy, as with fluorine-labeled amino acids (16). Reports dealing with other types of halogenated cyclophosphamides [*e.g.*, *cis*- and *trans*-5-fluoro- (17, 18), 5-chloro- (17), and 5-bromocyclophosphamide (19)] have been published; however, unlike the *N*-halo series, the drug-design concepts were predicated on the *in vivo* stability of carbon–halogen bonds. 3-Fluoro- (IV) and 3-bromocyclophosphamide (VI) have not, to our knowledge, been previously synthesized; 3-chlorocyclophosphamide (V) has been mentioned only briefly in the literature (20). The present report describes the preparation of IV–VI and several 3-chloro analogues of I (X–XII). Data are also presented regarding the chemical charactristics and anticancer activity of these intended "pro-prodrugs."

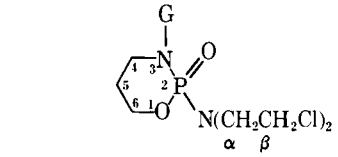

G

I: H
II: $Si(CH_3)_2C(CH_3)_3$
III: OH
IV: F
V: Cl
VI: Br

I → (CF_3OF, NaOCl, Br_2)

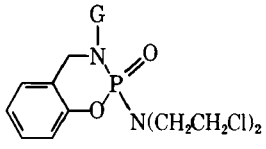

G

VII: H
X: Cl

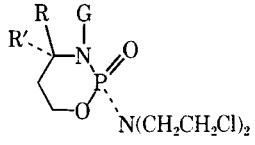

	R	R′	G
VIII:	C_6H_5	H	H
XI:	C_6H_5	H	Cl
IX:	H	C_6H_5	H
XII:	H	C_6H_5	Cl

EXPERIMENTAL

Commercially available racemic[1] cyclophosphamide monohydrate (I·H_2O) was used as received; however, when necessary, I·H_2O was converted to anhydrous I as previously described (21). Enantiomerically pure

[1] Unless specified otherwise, all chiral compounds were used as their racemates.

0022-3549/83/0600-0687$01.00/0

Table I—^{13}C-NMR Parameters for Cyclophosphamide (I) and Its Analogues (III–XII) [a]

Compound	C-4	C-5	C-6	C-α	C-β
I	41.44(3.7)	25.75(4.9)	67.66(6.1)	48.78(4.9)	42.28
III	52.68	27.20	67.47(6.1)	49.40(4.9)	42.23
IV	54.14(3.7)[b]	27.63[c]	68.73(6.1)	49.54(2.5)	42.59
V	56.90	28.61	67.54(6.1)	49.44(4.9)	41.79
VI	58.62(3.7)	29.53	67.61(6.1)	49.62(3.7)	41.93
VII[d]	43.25	118.8(7.3)	172.0(10)	49.10(3.7)	42.22
X[e]	49.32	119.0(5.5)	172.0(10)	49.06(3.0)	41.84
VIII[f]	56.93	33.61(7.9)	65.41(6.7)	48.78(4.2)	42.11
XI[g]	70.00	35.50(3.7)	62.91(6.1)	50.02(4.3)	41.95
IX[h]	57.15	34.78	66.36	48.87	42.36
XII[i]	69.7	37.9	65.8	49.8	41.9

[a] The tabulated chemical shifts (δ) refer to internal tetramethylsilane in deuterochloroform solvent, except for III and IV, which were dissolved in deuterium oxide and acetone-d_6, respectively. The values in parentheses are ^{13}C—^{31}P coupling constants in Hz-units. The carbon positions are as shown in the structure for I. [b] J_{CF} = 11.6 Hz. [c] J_{CF} = 9.8 Hz. [d] Other aromatic carbons at δ123.8, 126.5, and 128.8. [e] Other aromatic carbons at δ124.2, 130.6, and 135.9. [f] Other aromatic carbons at δ126.2, 127.8, and 128.7. [g] Other aromatic carbons at δ127.0, 128.0, and 128.8. [h] Other aromatic carbons at δ126.1, 128.3, 129.0, and 146.9. [i] Dilute sample; δ values are approximate and coupling constants were not measured, due to added line broadening.

samples of (+)-(*R*)- and (−)-(*S*)-I·H_2O were used as received[2]. The syntheses of 5,6-benzocyclophosphamide (VII), *cis*-4-phenylcyclophosphamide (VIII), and *trans*-4-phenylcyclophosphamide (IX) were reported elsewhere (22, 23), as were the details of the 40.25-MHz ^{31}P-NMR[3] and 25-MHz ^{13}C-NMR[3] measurements (6). Analogous procedures for data acquisition and processing were employed for obtaining 36.23-MHz[4] and 121.5-MHz[5] ^{31}P-NMR, 22.49-MHz[4] and 75.47-MHz[5] ^{13}C-NMR, 89.55-MHz ^{1}H-NMR[4] and 93.65-MHz ^{19}F-NMR[3] spectra. Chemical shift (δ, ppm) references were as follows: phosphorus-31, 25% (v/v) H_3PO_4 in deuterium oxide (external); carbon-13, tetramethylsilane (internal); fluorine-19, hexafluorobenzene (internal). Electron-impact (70 eV) mass spectra[6] (MS) were recorded with samples introduced *via* a solids' inlet probe, which was heated from ambient temperature to 100°. TLC plates had 0.25-mm coatings of silica gel and were developed by exposure to iodine vapor, which led to either absorptive (brown) or repellent (white) spots.

3-Fluorocyclophosphamide (IV)—A magnetically stirred and dry nitrogen-purged solution of anhydrous I (3.64 g, 13.9 mmoles) in dry methylene chloride (50 ml) was cooled to −78°. Trifluoromethylhypofluorite gas[7] (4.65 mmoles) was slowly introduced over a period of 3 hr into the nitrogen flush line *via* a Y-tube connected with tubing[8] to a cylinder, using a series of valves and a metering gauge that are described elsewhere (24). The nitrogen from the reaction flask was passed into a bubble cylinder containing an alkaline solution of potassium iodide to remove all by-products[9] and unreacted trifluoromethylhypofluorite. After the addition of the hypofluorite, the solution was allowed to gradually warm to room temperature (overnight) using a very slow nitrogen flush. The reaction mixture was filtered, and an aliquot (0.2 ml) of the filtrate was diluted with deuterochloroform (1.8 ml) prior to ^{31}P-NMR analysis. The remaining solution was concentrated on a rotary evaporator, without heating[10], and the resultant oil was chromatographed on a column (2.2 cm × 25 cm) of silica gel using ethyl acetate as the eluent. Compound IV (R_f 0.5, ethyl acetate) was eluted with 85–135 ml of solvent and was obtained as a pale-yellow oil (252 mg, 20% yield); ^{31}P-NMR (deuterium oxide): δ 16.17, J_{PF} = 22 Hz; ^{19}F-NMR (deuterochloroform): δ 83.27, J_{FP} = 22 Hz; ^{13}C-NMR, *cf.* Table I; MS, *m/z* 278, 280, and 282 (M^+, 2 Cl), 229 and 231 (base-peak cluster, $M-CH_2Cl$).

3-Chlorocyclophosphamide (V)—A magnetically stirred solution of I·H_2O (270 mg, 0.97 mmole) in chloroform (15 ml) was cooled with an ice-water bath, and an aqueous solution of sodium hypochlorite[11] [15 ml, 5.25% (w/w) NaOCl, 10.6 mmoles] was added; after 4 hr, the water bath was removed. Aliquots (1 ml) of the chloroform layer were periodically removed, diluted with deuterochloroform (1 ml), and the relative signal intensities for I (δ12.10) and the only detectable product (δ15.95) were measured by ^{31}P-NMR: 50:50, 2 hr; 25:75, 4 hr; 0:100, 18 hr. After 18 hr of stirring, TLC (ethyl acetate) of the chloroform layer confirmed the absence of I (R_f 0.1) and a single spot was evident (R_f 0.5). The 18-hr NMR sample and the remainder of the chloroform layer (13 ml) were combined, washed with water (15 ml) twice, dried with sodium sulfate, and then concentrated *in vacuo* without heating. Based on elemental composition, the resultant oil (280 mg, 87% yield) was identified as V·HCl, which was converted to V (^{13}C-NMR, Table I) by dissolving in chloroform and stirring with solid potassium carbonate.

Anal.—Calc. for $C_7H_{15}Cl_4N_2O_2P$: C, 25.32; H, 4.55; N, 8.44; Cl, 42.71. Found: C, 26.74; H, 4.71; N, 8.55; Cl, 43.12.

Application of the above procedure to (*R*)- and (*S*)-I·H_2O (2-g scale) gave (*S*)- and (*R*)-V, respectively[12], which were identified and checked for purity by TLC.

3-Bromocyclophosphamide (VI)—Bromine (0.135 ml, 2.6 mmoles) was added in one portion to a magnetically stirred, cold (5°) mixture of I·H_2O (0.70 g, 2.5 mmoles) and potassium carbonate (0.34 g, 2.5 mmoles) in methylene chloride (10 ml). After being stirred for 2 hr, the mixture was filtered and the solvent was removed on a rotary evaporator, without heating, and the residue was then placed under a high vacuum. The resultant orange-colored oil was free of TLC-detectable I (R_f 0.1, ethyl acetate), and gave rise to a single spot (R_f 0.4, ethyl acetate) which was identified by ^{13}C-NMR (Table I) as VI (0.88 g, 100% yield).

3-Chloro-5,6-benzocyclophosphamide (X)—Compound VII (31 mg, 0.1 mmole) in chloroform (3 ml) was treated with aqueous sodium hypochlorite (3 ml) as described above for the preparation of V. After stirring at room temperature overnight, the separated chloroform layer was washed with water (6 ml) twice, dried with magnesium sulfate, and then concentrated *in vacuo* to give X as an unstable oil (26 mg, 80% yield): TLC (ethyl acetate): R_f 0.8 for X *versus* R_f 0.4 for VII; see Table I for ^{13}C-NMR data for X *versus* VII. After 24 hr at room temperature, the two sets of protonated aromatic carbon signals for X and VII had relative intensities of ~67% and ~33%, respectively, indicating spontaneous decomposition.

***cis*- and *trans*-3-Chloro-4-phenylcyclophosphamide (XI) and (XII)**—A solution of VIII (28 mg, 0.08 mmole) in chloroform (3 ml) was stirred with aqueous sodium hypochlorite (6 ml) at room temperature for 7 days. Workup, as described above for X, afforded XI as an oil (17.4 mg, 59% yield) that was free of TLC-detectable VIII (R_f 0.5, ethyl acetate) and was seen as a single, faster eluting spot (R_f 0.9, ethyl acetate). A scaled-down version of this reaction using IX (3.5 mg, 0.01 mmole) gave XII (3.5 mg, 94% yield), which showed one spot on TLC (ethyl acetate), R_f 0.8 *versus* R_f 0.3 for IX. Compounds XI and XII were identified by ^{13}C-NMR comparisons with VIII and IX, respectively (Table I).

Incubation Studies—Female Balb/C mice (~25 g) were sacrificed by cervical dislocation. The livers were immediately removed for manual slicing, and the slices were stored temporarily in saline at 5°. Separate saline (10 ml) solutions of III (10 mg, 0.036 mmole) and IV (10 mg, 0.036 mmole), obtained by sonication, were equilibrated at 37° using open 50-ml Erlenmeyer flasks and a shaker incubator, and ~1- and 3-g portions of the liver slices were then added. After 10 min, each of the incubation mixtures was vigorously stirred with chloroform (25 ml) for 20 min; the separated organic layers were then dried with magnesium sulfate, filtered, and concentrated on a rotary evaporator. Both samples derived from III weighed ~10 mg, whereas the 1-g and 3-g incubations with IV afforded ~4 and 2 mg of recovered material, respectively. Each of the extracts was

[2] Otsuka Pharmaceutical Co., Ltd. For (*R*)-I·H_2O (mp 68°), $[\alpha]_D^{25}$ = 2.40 (c = 10, methanol); for (*S*)-I·H_2O (mp 68°), $[\alpha]_D^{25}$ = −2.47 (c = 10, methanol).

[3] FX-100 spectrometer, *JEOL U.S.A.*, Inc.

[4] FX-90Q spectrometer, JEOL U.S.A., Inc.

[5] WM-300 spectrometer, Bruker Instruments, Inc.

[6] Model JMS-01SG-2 spectrometer, JEOL U.S.A., Inc.

[7] PCR Research Chemicals, Inc.

[8] Teflon.

[9] Carbonyl difluoride and hydrofluoric acid.

[10] Above ~50°, product IV underwent relatively rapid decomposition. Pure IV was obtained from partially decomposed samples by extraction into methylene chloride.

[11] *Commercially available bleach.*

[12] On conversion of I to V, the *R* and *S* descriptors for the absolute configuration of I respectively change to *S* and *R* for V, although the stereochemistry about phosphorus is preserved.

Table II—Anticancer Screening Data for Analogues of Cyclophosphamide Against Mouse L-1210 Lymphoid Leukemia

Compound[a]	Mouse Type	Injection Data	Dose, mg/kg	ILS[b], %	T/C[b], %
(*R*,*S*)-IV[c] (in Vehicle 1)	BDF_1 (*n* = 7)	10^5 cells/mouse on day 2	200	30.6	
			100	8.0	
			50	9.6	
(*R*,*S*)-I·H_2O[c] (concurrent positive control)			100	62.5	
(*R*,*S*)-IV[d] (in vehicle 2)	BD_2F_1 (*n* = 4)	10^6 cells/mouse on day 5	250	—[g]	
			200	—	
			150	86	
			100	35	
			50	14	
(*R*,*S*)-I·H_2O[d] (concurrent positive control)			250	All cured	
			200	175 ± 25	
			100	87 ± 12	
(*R*,*S*)-V[e] (in vehicle 3)	C57BL/6 (*n* = 6)	10^6 cells/mouse on day 1	500		129
			250		109
			125		96
			63		96
			31		93
(R,S)-I·H_2O[e] (concurrent positive control)			500		112[h]
			250		282
			125		173
			63		124
(*R*)-V[c] (in vehicle 4)	BDF_1 (*n* = 7–8)	10^5 cells/mouse on day 2	339	15.9	
			226	9.5	
			113	8.1	
(*S*)-V[c] (in vehicle 4)			339	25.0	
			226	17.7	
			113	5.6	
(*R*,*S*)-I·H_2O[c] (concurrent positive control)			300	81.6	
			200	76.5	
			100	49.3	
XI–XII (~1:1 in vehicle, 3)[e]	CD_2F_1 (*n* = 6)	10^6 cells/mouse on day 1	350		110
			175		106
			88		103
			44		106
VIII–IX (~1:1 in vehicle 3)[e,f]	CD_2F_1 (*n* = 6)	10^6 cells/mouse on day 1	500		204
			250		122
			125		120
			63		105

[a] Vehicle key: (1) corn oil; (2) ethanol–propylene glycol–water (30:30:40 v/v/v); (3) aqueous ethanol with polyoxyethylene sorbitan *monooleate*; (4) 1% (v/v) carboxymethylcellulose in water. [b] (ILS) increased life span; (T/C) test/control. [c] Conducted at Otsuka Pharmaceutical Co. Ltd., Osaka, Japan. [d] Conducted at Johns Hopkins Oncology Center, Baltimore, Md. [e] Conducted at the Division of Cancer Treatment, National Cancer Institute, Bethesda, Md. [f] Taken from Ref. 23. [g] — Unacceptable level of toxicity. [h] Four of six toxicity-day survivors.

analyzed by 40.25-MHz ^{31}P-NMR using deuterochloroform solvent (1.8 ml), a $\pi/2$ pulse, 2-sec pulse-repetition time, and nuclear Overhauser enhancement. The presence of I was established by TLC (ethyl acetate) and addition of authentic I·H_2O (^{31}P-NMR). Integrated signal intensities were measured by the "cut-and-weigh" method.

Partition Coefficients—The ^{31}P-NMR spectrum of 27.9 m*M* I in water [5% (v/v) ^2H_2O] was obtained using a standard set of acquisition parameters [80 pulses ($\pi/2$), no nuclear Overhauser enhancement, and a 10-sec pulse-repetition time] and a standard set of display parameters. Comparison of the resultant signal intensity [(peak height) × (width at half-height) = 283 units] with the signal intensity (153 units) similarly obtained with a saturated solution of V in water gave an initial value of 15.1 m*M* V. A 2-ml aliquot of 27.9 m*M* I was vigorously stirred (25°, 5 min) with 1 ml of 1-octanol, and a 2-ml aliquot of 15.1 m*M* V was extracted with 0.1 ml of 1-octanol in exactly the same manner. The ^{31}P-NMR spectrum for each of the separated aqueous layers was recorded as described above, and the signal intensities (61.2 units for I, 28.5 units for V) were used to compute the concentration of I and V in the water and octanol layers: $[I]_{water}$ = 6.02 m*M*, $[I]_{octanol}$ = 43.71 m*M*, $[V]_{water}$ = 2.81 m*M*, and $[V]_{octanol}$ = 245.6 m*M*. The partition coefficients (P = $[compound]_{octanol}/[compound]_{water}$) for I and V were 7.26 and 87.6, respectively.

Anticancer Screening—On day 0, groups of 4–8 male and/or female mice (~25 g) were inoculated with cancerous cells (either L-1210 or P-388) at a level of either 10^5 or 10^6 cells/mouse. On the specified day (see Tables II and III), the test groups received single intraperitoneal injections of the test compound using a suitable vehicle and various doses; untreated control groups were injected with vehicle only. Each test compound was studied in parallel with I·H_2O, which served as a positive control for the screening protocol. Evaluations using mean survival times for test groups *versus* untreated control groups were scored as either increased life-span or test/control percentages. Pertinent experimental details and results are summarized in Tables II and III.

RESULTS AND DISCUSSION

Syntheses and Structure Determinations—Very little is known (25) about the *N*-fluorination of phosphoramides. The reaction of fluorine with the secondary phosphoramidic moiety, P(O)NHR, results in *N*-fluorination followed by P—N bond cleavage to give *N*-fluoroamines (25), whereas the secondary sulfonamide moiety SO_2NHR, reacts cleanly with trifluoromethylhypofluorite to give the corresponding *N*-fluorosulfonamide (26). Thus, it appeared that IV might be obtained directly from I using this hypofluorite reagent. Consideration of reported reaction mechanisms (26), in addition, suggested that subsequent P—N bond cleavage in IV might be minimized by using a fairly large molar excess of I, relative to the fluorinating reagent. Accordingly, the anhydrous reaction of I with 0.3 equivalents of the fluorinating agent led to ^1H-decoupled ^{31}P-NMR spectra at 40.25 and 121.5 MHz showing a singlet due to residual I (δ10.76) and a 1:1 doublet (J_{PF} = 22 Hz), which was shifted to lower field (δ12.64) and indicated the presence of IV. Following column chromatography, the structure of IV (20% yield) was unambiguously established by MS, ^{19}F-NMR, and ^{13}C-NMR. Comparison of ^{13}C-NMR parameters (Table I) for I, III, and IV showed that the electronegative OH and F substituents caused relatively large downfield shifts ($\Delta\delta$11–13) of the C-4 resonance absorption. This effect, although smaller ($\Delta\delta$1–2),

Table III—Anticancer Screening Data for 3-Chlorocyclophosphamide (V) Enantiomers and Racemic Cyclophosphamide Against P-388 Tumor Cells in Mice [a]

Compound [b]	Mouse Type	Injection Data [c]	Dose, mg/kg	ILS [b], %
(*R*)-V	BDF_1	10^6 cells/	113 [d]	31.6
(in vehicle 4)	(n = 8)	mouse	56	17.4
		on day 0	28	6.3
(*S*)-V			113 [d]	31.6
(in vehicle 4)			56	22.5
			28	9.3
(*R,S*)-I·H_2O			100 [d]	113.2 [e]
(concurrent positive			50	87.3
control)			25	47.8

[a] Conducted at Otsuka Pharmaceutical Co. Ltd., Osaka, Japan. The control groups (n = 23) received 5 ml/kg of the vehicle. [b] Vehicle 4 and ILS as defined on Table II. [c] Injected intraperitoneally; test compounds were given orally on day 2. [d] Doses of 113 mg/kg of (*R*)- or (*S*)-V and 100 mg/kg (*R,S*)-I·H_2O represent equimolar doses. [e] One 30-day survivor.

was evidenced also by the C-5 signal positions, whereas the more remote carbons (C-6, C-α, and C-β) in I, III, and IV were not significantly influenced by the nature of the N-3 substituent. The long-range $^{13}C—^{19}F$ couplings observed for C-4 (J = 11.6 Hz) and C-5 (J = 9.8 Hz) were also indicative of the location of the fluorine substituent in IV[13].

^{31}P-NMR was used to monitor the reaction of I·H_2O with 10 equivalents of sodium hypochlorite in 1:1 (v/v) chloroform–water, and it was found that I (δ12.10) underwent a gradual conversion ($t_{1/2} \cong$ 2 hr) to a single product having a downfield-shifted resonance signal (δ15.95). The ^{13}C-NMR parameters (Table I) measured for the isolated reaction product were in accord with V (87% yield), which gave rise to downfield-shifted absorptions for C-4 ($\Delta\delta$15) and C-5 ($\Delta\delta$3), in comparison with I[14]. Analogous reactions of sodium hypochlorite with 5,6-benzocyclophosphamide (VII) and *cis*- and *trans*-4-phenylcyclophosphamide (VIII and IX) gave 80, 59, and 94% yields, respectively, of the corresponding 3-chloro derivatives, X–XII. The substantial downfield shift of each compound's C-4 signal ($\Delta\delta$6 for X, $\Delta\delta$13 for XI and XII), relative to its precursor, was again characteristic of the assigned structure[15].

The conversion of the 4-phenyl analogues of I to XI and XII were ~5–10-times slower than chlorination of either I or VII. This rate difference was attributed to steric hindrance of the N-3 position by the adjacent 4-phenyl substituent, which is evident in the crystal structure of VIII (23).

Reaction of a methylene chloride solution of I·H_2O with 1.04 equivalents of bromine in the presence of potassium carbonate gave a quantitative yield of VI. As with IV and V, introduction of the 3-bromo substituent resulted in characteristic downfield shifts of the C-4 ($\Delta\delta$17) and C-5 ($\Delta\delta$4) ^{13}C-NMR signals, compared with I (Table I).

Reactivity Studies—Fluoro-derivative IV was indefinitely stable in chloroform solution at −80° and failed to undergo reductive dehalogenation to give I on contact with thiophenol in chloroform (15 hr, 25°). Compound IV was also stable for 4 hr at 25° in a 10:1 (v/v) mixture of 2,6-lutidine (pH 7.2) and *p*-dioxane. On the other hand, ^{31}P-NMR spectra in unbuffered water showed the gradual disappearance of IV (δ16.17) with concomitant formation of decomposition products giving rise to singlets at δ12.78, 12.53, and 1.30. The characteristic doublet for IV was no longer detectable after 16 hr, and the three product signals in the now acidic solution (pH 3) had relative intensities of 33, 50, and 17%, respectively. The absence of resolvable $^{19}F—^{31}P$ couplings in the products indicated the absence of P(O)NF moieties; the addition of potassium dihydrogenphosphate established that the signal at δ1.30 was due to inorganic phosphate, which most likely resulted from proton-catalyzed P—N bond hydrolysis (27, 28). Since the P—N bonds in I are known to be sensitive to acid-catalyzed hydrolysis (27), the aforementioned results were consistent with the decomposition of IV to I and hydrofluoric acid, which then afforded hydrolytic products of the type previously found with I (27). Solutions of IV or IV–bovine serum albumin (20:1) in 0.1*M* NaCl gave results similar to those obtained in unbuffered water.

Surprisingly, ^{31}P-NMR studies of the chloro derivative (V) revealed reactivity patterns opposite to those of IV: V was instantaneously (<3 min) reduced to I by 20-fold molar excesses of either thiophenol (in chloroform) or mercaptoethanol (in water) at 25°, but there was only 8% conversion of V to I in unbuffered water after 7 days at 25°. Analogous results were obtained with the bromo compound (VI) which was somewhat more reactive than V in water, *i.e.*, 8% hydrolysis after 16 hr at room temperature.

The marked susceptibility of V and VI to reductive generation of I *via* reaction with sulfhydryl-containing compounds led to the use of the fluoro derivative (IV) to assess the possibility of an enzyme-mediated reduction process formally analogous to that found for III and mouse liver microsomes (6). Due to the hydrolytic instability of IV, incubations were terminated after 10 min, during which time there was negligible hydrolysis to I. The 37° incubations of IV in saline were performed in parallel with III, which served as a control for establishing the reducing capability of the whole-liver slices. Chloroform extraction of the incubation mixtures containing 3.6 m*M* substrate and 1-g portions of liver slices afforded samples having ^{31}P-NMR spectra which showed 96:4 and 79:21 relative ratios of III–I and IV–I, respectively; however, sample weights and absolute signal intensities for III and IV revealed that, unlike III, ~60% of IV had not been extracted. Thus, the corrected yield of I from IV was ~8%, roughly twice the yield of I from III. Use of 3-g portions of sliced liver failed to significantly increase the yield of I from either III or IV; the recovery of unreacted IV was only ~20%, whereas unreacted III was again quantitatively recovered.

Anticancer Screening—The comparatively stable compounds, *i.e.*, IV, V, and XI, were screened for anticancer activity using established protocols for analogues of I. Unfortunately, however, it was not possible to use a single methodology for the evaluations, as three independent laboratories were involved in these tests. From the data summary given in Table II, it was evident that while IV was the most active analogue in the mouse L-1210 leukemia system, it was less effective than the parent prodrug, I.

The individual enantiomers of V had statistically identical therapeutic efficacy in both the L-1210 (Table II) and P-388 (Table III) screens. The absence of significant therapeutic differences between (*R*)- and (*S*)-V thus paralleled findings reported for the enantiomers of I (29). As found for I and V, the introduction of a 3-chloro substituent (XI) into the 4-phenylcyclophosphamide analogue (VIII) had a negative impact on the anticancer activity.

Partition Coefficients—Conversion of the N—H moiety in I to either N—F or N—Cl moieties must alter solubility characteristics which are related, in part, to the aforementioned anticancer screening results. The magnitude of the solubility change resulting from the *N*-chlorination of I was therefore quantified using ^{31}P-NMR to measure partition coefficients (P) in octanol–water, where $P = [\text{compound}]_{\text{octanol}}/[\text{compound}]_{\text{water}}$. By this method, log P = 0.86 for I[16] and 1.94 for the chloro-derivative V, revealing a 12-fold greater partitioning of V into octanol. The increased lipophilicity resulting from this introduction of chlorine [$\pi_{Cl} \equiv \log P_V - \log P_I = 1.08$] was comparable in magnitude to the influence of introducing a *para* chlorine substituent in phenol [π_{Cl} = 0.93 (31, 32)]. This correlation allowed the calculation of log P for IV, which was not studied by the ^{31}P-NMR method because of possible complications due to solvolysis. The *p*-fluorophenol π_F value of 0.31 (31) thus gave log $P \cong$ 1.22 for IV, indicating only an approximately twofold increase in lipophilicity, relative to I.

CONCLUSIONS

3-Chlorocyclophosphamide (V) was rapidly converted to cyclophosphamide (I) on contact with sulfhydryl-containing compounds and could thus afford the same level of anticancer activity as I, if the unmasking of V were fast, relative to the metabolic oxidative activation (2) of either V or I. On the other hand, the 12-fold increase in the lipophilicity of V, relative to I, might decrease its accessibility to sulfhydryl moieties and thereby account for the lower therapeutic efficacy found for V *versus* I. Sulfhydryl-mediated chemical reduction of the *N*-fluoro analogue IV was a very slow process, by comparison with V; however, IV was calculated to be considerably less lipophilic than V and, moreover, the possibility for *in vivo* enzymatic conversion of IV to I was supported by incubation experiments with mouse liver slices. Consequently, the anticancer activity of IV, although lower than that of I, was tentatively ascribed to its func-

[13] For directly bonded carbon-13 and fluorine-19 in analogous structures, $J \cong$ 175 Hz (17).

[14] The alternative 4-chlorocyclophosphamide structure was ruled out by obtaining the ^{13}C-NMR spectrum with off-resonance hydrogen decoupling, which demonstrated that C-4 was bonded to two protons.

[15] The possibility of benzylic chlorination of VIII to give its 4-chloro derivative was excluded by ^1H-NMR homonuclear decoupling, *i.e.*, simultaneous irradiation of the axial and equatorial C-5 hydrogens (δ2.0–2.3) in product XI led to the observation of the C-4 hydrogen (δ4.7) as a 1:1 doublet with $^3J_{HP}$ = 19 Hz.

[16] Hansch and Leo (30) have cited an unpublished log P value of 0.63 for I in octanol–water.

tioning as an enzyme-activated "pro-prodrug," which reductively released prodrug I for subsequent oxidative conversion of I to a known array of oncostatic metabolites (2). Alternatively, and by analogy to the metabolism of I (2), oxidation of the C-4 position in IV could afford the *N*-fluoro derivative of phosphoramide mustard as the ultimate lethal cytotoxic agent. However, the highly electronegative fluorine substituent would, as in *N*-hydroxyphosphoramide mustard (6), diminish the phosphoramide mustard's alkylating activity by several orders of magnitude, which argues against a mechanism of action for IV wherein the N—F bond remains intact.

For the extensions of the presently reported *N*-fluorination of I, candidate structures having secondary phosphoramide groups include the anticancer drug isophosphamide (8, 9) and various cytotoxic phosphoramidic nitrogen mustards (2). Moreover, there are numerous drugs of various types which contain secondary sulfonamide and, especially, carboxamide groups that offer the possibility for *N*-fluorination by trifluoromethylhypofluorite. It is hoped that the studies reported herein will stimulate an interest in *N*-fluorinated amido groups as a new approach for investigating prodrugs, "pro-prodrugs," and congeners.

REFERENCES

(1) R. F. Struck, in "Annual Reports in Medicinal Chemistry," vol. 16, H.-J. Hess, Ed., Academic, New York, N.Y., 1981, p. 137.

(2) O. M. Friedman, A. Myles, and M. Colvin, in "Advances in Cancer Chemotherapy," vol. 1, A. Rosowsky, Ed., Dekker, New York, N.Y., 1979, p. 143.

(3) F.-T. Chiu, F.-P. Tsui, and G. Zon, *J. Med. Chem.*, **22,** 802 (1979).

(4) G. Zon, in "Magnetic Resonance in Biology," vol. 1, J. S. Cohen, Ed., Wiley-Interscience, New York, N.Y., 1980, p. 127.

(5) F.-T. Chiu, Y. H. Chang, G. Özkan, G. Zon, K. C. Fichter, and L. R. Phillips, *J. Pharm. Sci.*, **71,** 542 (1982).

(6) J. A. Brandt, S. M. Ludeman, G. Zon, J. A. Todhunter, W. Egan, and R. Dickerson, *J. Med. Chem.*, **24,** 1404 (1981).

(7) G. Zon, S. M. Ludeman, E. M. Sweet, W. Egan, and L. R. Phillips, *J. Pharm. Sci.*, **71,** 443 (1982).

(8) G. Zon, *Progr. Med. Chem.*, **19,** 205 (1982).

(9) D. L. Hill, "A Review of Cyclophosphamide," Charles C Thomas, Springfield, Ill., 1975, p. 3.

(10) B. Testa and P. Jenner, "Drug Metabolism: Chemical and Biochemical Aspects," Dekker, New York, N.Y., 1976, p. 116.

(11) A. A. Sinkula and S. H. Yalkowsky, *J. Pharm. Sci.*, **64,** 181 (1975).

(12) A. A. Sinkula, in "Annual Reports in Medicinal Chemistry," vol. 10, R. V. Heinzelman, Ed., Academic, New York, N.Y., 1975, p. 306.

(13) S. D. Nelson, in "Design of Biopharmaceutical Properties through Prodrugs and Analogs," E. B. Roche, Ed., American Pharmaceutical Association, Washington, D.C., 1977, p. 316.

(14) I. H. Pitman, *Med. Res. Rev.*, **1,** 189 (1981).

(15) P. C. Bansal, I. H. Pitman, J. N. S. Tam, M. Mertes, and J. J. Kaminski, *J. Pharm. Sci.*, **70,** 850 (1981).

(16) B. D. Sykes and J. H. Weiner, in "Magnetic Resonance in Biology," vol. 1, J. S. Cohen, Ed., Wiley-Interscience, New York, N.Y., 1980, p. 171.

(17) A. B. Foster, M. Jarman, R. W. Kinas, J. M. S. van Maanen, G. N. Taylor, J. L. Gaston, A. Parkin, and A. C. Richardson, *J. Med. Chem.*, **24,** 1399 (1981).

(18) S. D. Cutbush, S. Neidle, G. N. Taylor, and J. L. Gaston, *J. Chem. Soc., Perkin Trans.*, **2,** 980 (1981).

(19) S. M. Ludeman, G. Zon, and W. Egan, *J. Med. Chem.*, **22,** 151 (1979).

(20) A. Takamizawa, S. Matsumoto, T. Iwata, and I. Makino, *Heterocycles*, **7,** 1091 (1977).

(21) T. Kawashima, R. D. Kroshefsky, R. A. Kok, and J. G. Verkade, *J. Org. Chem.*, **43,** 1111 (1978).

(22) S. M. Ludeman and G. Zon, *J. Med. Chem.*, **18,** 1251 (1975).

(23) V. L. Boyd, G. Zon, V. L. Himes, J. K. Stalick, A. D. Mighell, and H. V. Secor, *ibid.*, **23,** 372 (1980).

(24) S. Chandrasegaran, Ph.D. Thesis, Georgetown University, 1981.

(25) J. Bensoam and F. Mathey, *C. R. Acad. Sci., Ser. C*, **278,** 1313 (1974).

(26) D. H. R. Barton, R. H. Hesse, M. M. Pechet, and H. T. Toh, *J. Chem. Soc., Perkin Trans.*, **1,** 732 (1974).

(27) G. Zon, S. M. Ludeman, and W. Egan, *J. Am. Chem. Soc.*, **99,** 5785 (1977).

(28) T. W. Engle, G. Zon, and W. Egan, *J. Med. Chem.*, **22,** 897 (1979).

(29) M. Jarman, P. J. Cox, P. B. Farmer, A. B. Foster, R. A. V. Milsted, R. W. Kinas, and W. J. Stec, in "Stable Isotopes, Proceedings of the Third International Conference," E. R. Klein and P. D. Klein, Eds., Academic, New York, N.Y., 1979, p. 363.

(30) C. Hansch and A. Leo, "Substituent Constants for Correlation Analysis in Chemistry and Biology," Wiley-Interscience, New York, N.Y., p. 223.

(31) T. Fujita, J. Iwasa, and C. Hansch, *J. Am. Chem. Soc.*, **86,** 5175 (1964).

(32) A. Leo, C. Hansch, and D. Elkins, *Chem. Rev.*, **71,** 525 (1971).

ACKNOWLEDGMENTS

This investigation was supported in part by Research Grant CA-21345 from the National Institutes of Health (to Gerald Zon).

The 100-MHz and 300-MHz NMR spectrometers were made available to Gerald Zon, as a Visiting Scientist, at the Food and Drug Administration, Bureau of Biologics. The authors thank Drs. Peter Roller and Richard Miller of the National Cancer Institute for obtaining the mass spectra.

Comparative Study of Immunoactivity and Bioactivity of Sodium Insulin

C. R. KOWARSKI *x, B. BADO *, S. SHAH *, D. KOWARSKI§, and A. A. KOWARSKI ‡

Received February 19, 1982, from *Temple University School of Pharmacy, Philadelphia, PA 19140 and the ‡University of Maryland School of Medicine, Baltimore, MD 21201. Accepted for publication May 21, 1982. §Present address: University of Pennsylvania School of Medicine, Philadelphia, PA 19104.

Abstract □ The bioactivity of equal doses (by radioimmunoassay) of regular insulin and sodium insulin were measured in six preconditioned female mongrel hound dogs by a previously described bioassay. The hypoglycemic nadir of blood glucose induced by intravenous injection of the drugs was compared with the nadirs induced by a known amount of the international standard insulin. The level of blood glucose was monitored instantaneously and continuously using a nonthrombogenic continuous glucose-monitoring system. The hypoglycemic effect of subcutaneously injected sodium insulin was compared with the effect of subcutaneously injected regular insulin. The two drugs were injected at 1–2-week intervals to seven dogs. While the bioactivity of intravenously administered sodium insulin was equal to the bioactivity of intravenously administered *regular insulin*, the hypoglycemic effect of subcutaneously injected sodium insulin differed from the effect of subcutaneously injected regular insulin. The blood glucose nadir after subcutaneous injection of regular insulin occurred 101 ± 21 min after the injection. The nadir after subcutaneous injection of sodium insulin occurred 163 ± 33 min after the injection.

Keyphrases □ Sodium insulin—comparative study of immunoactivity and bioactivity □ Immunoactivity–comparative study of bioactivity of sodium insulin □ Bioactivity—comparative study of immunoactivity of sodium insulin

Sodium insulin is a new semisynthetic dosage form of insulin. Sodium insulin, like insulin, can be measured by an immunoassay, since both contain the same immunospecific binding site to the antibodies to insulin. However, equal doses of the two types of insulin, as measured by the immunoassay, are not necessarily equal in their biological activity. Also, equal biological activity after intravenous administration does not necessarily mean that the two types of insulin are of equal biological activity when injected subcutaneously.

An improved bioassay for insulin (1) was reported and is based on a previously described nonthrombogenic continuous glucose-monitoring device (2, 3). The bioassay was used to compare the intravenous biological activity of equal doses of sodium insulin and insulin standard (USP reference standard) measured by immunoassay. The hypoglycemic effect of subcutaneously administered sodium insulin was also compared with the effect of an equal dose of regular insulin.

EXPERIMENTAL

Immunoassay of Sodium Insulin—The immunoactivity of sodium insulin was measured six times, using a previously described immunoassay (4). The average of the six immunoassays was used to prepare the solution of sodium insulin used in the bioassay.

Bioassay of Sodium Insulin—*Instrument and Dogs*—Six preconditioned female mongrel hound dogs (16–17 kg) were used. The dogs were fasted overnight and anesthetized in the morning using sodium pentobarbital. Continuous glucose monitoring was initiated using a previously described nonthrombogenic system (2, 3). The instrument consisted of systems for nonthrombogenic blood withdrawal and for blood glucose measurement. The blood withdrawal system included a disposable sterile intravenous needle and tubing, coated with a nonthrombogenic substance connected to a peristaltic pump. The glucose-measuring system used a glucose oxidase sensor generating a continuous record of the level of blood glucose.

Priming Procedure—The bioassay was preceded by a priming procedure consisting of an intravenous administration of insulin followed by glucose.

The blood level of glucose was monitored for at least 30 min in order to establish the baseline level of glucose. Each dog was then given an injection of 0.4 U iv of USP reference standard insulin prepared in accordance with the USP procedure (5). The level of blood glucose fell rapidly reaching the initial priming nadir (N_0) within 30–35 min. After recording N_0, the level of glucose was raised by intravenous administration of 15–20 ml of a 25% solution of glucose. An additional 10 ml of glucose solution was given when necessary, until the blood glucose level stabilized within 10% of the baseline (~45–55 min).

Bioassay Procedure—After ascertaining maintenance of the glucose level at a consistent level for 10 min, the first dose of the USP standard insulin (0.4 U) was administered intravenously in one rapid bolus. The first nadir (N_1) was recorded by the glucose monitor within 35 min after the injection of insulin. As soon as an upturn in the level of blood glucose was established, the level of blood glucose was raised using a 25% intravenous glucose solution administered in 3 to 4 increments as previously described.

After ascertaining the reestablishment of a constant glucose level within 10% of baseline, the procedure was repeated twice: using 0.8 U of USP standard insulin, recording the second nadir (N_2) of blood glucose, and subsequently, using 0.6 U of sodium insulin as measured by immunoassay (4) and measuring the third nadir (N_3).

The bioactivity of the assayed sodium insulin was calculated using a least-squares linear regression of the logarithm of the two standard doses and the three nadirs.

Hypoglycemic Effect of Subcutaneous Sodium Insulin and Regular Insulin—Seven preconditioned female mongrel hound dogs (16–17 kg) were fasted and anesthetized as described previously. A nonthrombogenic catheter was inserted in one of the major veins of the front leg. The catheter was connected to the continuous glucose-monitoring device (2, 3). After a steady glucose level was observed for 10 min, 1 U of sodium insulin dissolved in sterile insulin diluent USP was injected

Table I—Six Repeated Bioassays of 0.6 U Sodium Insulin

Assay No.	Nadirs of Blood Glucose Levels, mg/dl: N_1 (0.4 U of Reference Standard)	N_2 (0.8 U of Reference Standard)	N_3 (0.6 U of Sodium Insulin)	Bioactivity of 0.6 U of Sodium Insulin
(1)	59	25	41	0.59
(2)	50	22	32	0.63
(3)	38	20	29	0.60
(4)	49	38	42	0.63
(5)	44	25	34	0.58
(6)	40	21	29	0.60
Mean	46.7	25.2	34.5	0.60
±1 *SD*	7.0	6.0	5.3	0.02

0022-3549/83/0600-0692$01.00/0

Table II—Hypoglycemic Effects of 1 U of Subcutaneously Administered Regular Insulin and Sodium Insulin

Assay No.	Nadirs of Blood Glucose Levels, mg/dl		Time of Nadir, min	
	Regular Insulin	Sodium Insulin	Regular Insulin	Sodium Insulin
(1)	32	47	100	148
(2)	46	40	90	190
(3)	27	43	130	195
(4)	24	42	130	195
(5)	50	48	100	145
(6)	45	32	80	105
(7)	38	41	80	162
Mean	37.4	41.8	101.4	162.9
±1 *SD*	10.1	5.3	21.2	33.4
p	*NS*		<0.001	

subcutaneously. The site of injection was always 2.54 cm from the center of the third nipple from the head. The glucose monitor measured the lowering of the blood glucose level. The nadir blood glucose level and the time of its occurrence were noted.

This procedure was repeated in each dog, after a rest period of 1 or 2 weeks, using 1 U of regular insulin instead of 1 U of sodium insulin.

RESULTS AND DISCUSSION

The results of the six repeated bioassays of a solution containing 0.6 U of sodium insulin as measured by immunoassay are shown in Table I. The mean biological activity of sodium insulin was equal to its immunoactivity. The coefficient of variation of the six consecutive immunoassays of sodium insulin was 3%.

The hypoglycemic effects of subcutaneously administered sodium insulin and regular insulin are compared in Table II. There was no significant difference between the nadirs of blood glucose following the two forms of insulin, but the nadir induced by sodium insulin occurred significantly later than the nadir induced by regular insulin.

Chemical manipulation of a biologically active molecule can have a significant effect on its biological as well as its immunological activity. The two effects may differ, leading to a new relationship between the two activities.

We have found that sodium insulin, a new dosage form of insulin, has the same ratio of biological *versus* immunological activity as the USP reference standard insulin.

Even though the biological effect of intravenously injected sodium insulin was equal to the effect of regular insulin, there was a significant difference between the effects of the two dosage forms of insulin when administered subcutaneously. The difference between the activity of subcutaneously administered sodium insulin and regular insulin, therefore, should be attributed only to the difference in the rate at which they are absorbed into the bloodstream.

REFERENCES

(1) C. R. Kowarski, D. Kowarski, B. D. Bick, H. Stein, D. Rudzavich, and A. A. Kowarski, *J. Clin. Endocrinol. Metab.*, **53**, 1145 (1981).

(2) M. I. Schmidt, A. Hadji-Georgopoulos, M. Rendell, S. Margolis, D. Kowarski, and A. A. Kowarski, *Diabetes Care*, **2**, 457 (1979).

(3) A. Hadji-Georgopoulos, M. I. Schmidt, S. Margolis, and A. A. Kowarski, *J. Clin. Endocrinol. Metab.*, **50**, 371 (1980).

(4) C. R. Morgan and A. Lazatow, *Diabetes*, **12**, 115 (1963).

(5) "The United States Pharmacopeia," 20th rev., United States Pharmacopeial Convention, Inc., Rockville, Md., 1980, p. 900.

ACKNOWLEDGMENTS

Supported by Grant HD-16077 of the National Institutes of Health, United States Public Health Service. Sodium insulin and sterile insulin diluent, USP, were a gift from Dr. W. D. Storvick, Manager of Insulin Operation, Eli Lilly and Company. The regular insulin used was Illetin 100 U/ml from Eli Lilly and Company. The sodium insulin was batch 674-91GP-1-2.

Determination of Hydralazine in Human Whole Blood

T. M. LUDDEN *‡x, L. K. LUDDEN ‡, K. E. WADE ‡, and S. R. B. ALLERHEILIGEN *‡

Received January 18, 1982, from the **College of Pharmacy, University of Texas-Austin* and the ‡*Department of Pharmacology, University of Texas Health Science Center, San Antonio, TX 78284.* Accepted for publication June 2, 1982.

Abstract □ The time required for the separation of plasma from the cellular components of blood can permit the *in vitro* loss of hydralazine. Thus, a high-performance liquid chromatographic (HPLC) procedure for the measurement of hydralazine in blood has been developed. 4-Methylhydralazine was used as an internal standard. The addition of *p*-anisaldehyde led to the formation of the *p*-anisaldehyde hydrazones of hydralazine and the internal standard. HPLC on a reverse-phase cyano column provided an analytical procedure in which the average relative standard deviation over the concentration range of 1–160 ng/ml was 8.3%. Hydralazine pyruvic acid hydrazone, a known circulating metabolite of hydralazine, yielded only 0.05 mole % hydralazine when submitted to this assay procedure.

Keyphrases □ Hydralazine—whole blood, derivatization, *p*-anisaldehyde hydrazones of hydralazine, analysis, high-performance liquid chromatography □ Whole blood—analysis, hydralazine, high-performance liquid chromatography □ High-performance liquid chromatography—hydralazine, whole blood analysis, *p*-anisaldehyde hydrazone of hydralazine

Selective assays for the measurement of hydralazine in plasma have been recently described (1–3). A major disadvantage of these procedures is the time required for separation of plasma from the cellular components of blood. Hydralazine disappears rapidly from plasma or blood *in vitro* (2, 4–6). Rapid sample processing at reduced temperature has been used to slow the loss prior to derivatization (7–9). The measurement of hydralazine in whole blood would circumvent this problem. In addition, because the clearance of hydralazine is high (7, 8), blood hydralazine concentrations are extremely useful for pharmacokinetic studies. However, attempts to measure hydralazine in whole blood using previously published techniques for plasma (1, 3) resulted in fouling of the chromatographic column after only a few sample injections. This paper describes a high-performance liquid chromatographic (HPLC) assay for the determination of hydralazine in whole blood using a different chromatographic column and a less polar extraction solvent.

EXPERIMENTAL

Reagents and Chemicals—Hexane, methanol, and acetonitrile were purchased as glass-distilled solvents. The acetonitrile was filtered before

0022-3549/83/0600-0693$01.00/0

Table II—Hypoglycemic Effects of 1 U of Subcutaneously Administered Regular Insulin and Sodium Insulin

Assay No.	Nadirs of Blood Glucose Levels, mg/dl		Time of Nadir, min	
	Regular Insulin	Sodium Insulin	Regular Insulin	Sodium Insulin
(1)	32	47	100	148
(2)	46	40	90	190
(3)	27	43	130	195
(4)	24	42	130	195
(5)	50	48	100	145
(6)	45	32	80	105
(7)	38	41	80	162
Mean	37.4	41.8	101.4	162.9
±1 *SD*	10.1	5.3	21.2	33.4
p	*NS*		<0.001	

subcutaneously. The site of injection was always 2.54 cm from the center of the third nipple from the head. The glucose monitor measured the lowering of the blood glucose level. The nadir blood glucose level and the time of its occurrence were noted.

This procedure was repeated in each dog, after a rest period of 1 or 2 weeks, using 1 U of regular insulin instead of 1 U of sodium insulin.

RESULTS AND DISCUSSION

The results of the six repeated bioassays of a solution containing 0.6 U of sodium insulin as measured by immunoassay are shown in Table I. The mean biological activity of sodium insulin was equal to its immunoactivity. The coefficient of variation of the six consecutive immunoassays of sodium insulin was 3%.

The hypoglycemic effects of subcutaneously administered sodium insulin and regular insulin are compared in Table II. There was no significant difference between the nadirs of blood glucose following the two forms of insulin, but the nadir induced by sodium insulin occurred significantly later than the nadir induced by regular insulin.

Chemical manipulation of a biologically active molecule can have a significant effect on its biological as well as its immunological activity. The two effects may differ, leading to a new relationship between the two activities.

We have found that sodium insulin, a new dosage form of insulin, has the same ratio of biological *versus* immunological activity as the USP reference standard insulin.

Even though the biological effect of intravenously injected sodium insulin was equal to the effect of regular insulin, there was a significant difference between the effects of the two dosage forms of insulin when administered subcutaneously. The difference between the activity of subcutaneously administered sodium insulin and regular insulin, therefore, should be attributed only to the difference in the rate at which they are absorbed into the bloodstream.

REFERENCES

(1) C. R. Kowarski, D. Kowarski, B. D. Bick, H. Stein, D. Rudzavich, and A. A. Kowarski, *J. Clin. Endocrinol. Metab.*, **53**, 1145 (1981).

(2) M. I. Schmidt, A. Hadji-Georgopoulos, M. Rendell, S. Margolis, D. Kowarski, and A. A. Kowarski, *Diabetes Care*, **2**, 457 (1979).

(3) A. Hadji-Georgopoulos, M. I. Schmidt, S. Margolis, and A. A. Kowarski, *J. Clin. Endocrinol. Metab.*, **50**, 371 (1980).

(4) C. R. Morgan and A. Lazatow, *Diabetes*, **12**, 115 (1963).

(5) "The United States Pharmacopeia," 20th rev., United States Pharmacopeial Convention, Inc., Rockville, Md., 1980, p. 900.

ACKNOWLEDGMENTS

Supported by Grant HD-16077 of the National Institutes of Health, United States Public Health Service. Sodium insulin and sterile insulin diluent, USP, were a gift from Dr. W. D. Storvick, Manager of Insulin Operation, Eli Lilly and Company. The regular insulin used was Illetin 100 U/ml from Eli Lilly and Company. The sodium insulin was batch 674-91GP-1-2.

Determination of Hydralazine in Human Whole Blood

T. M. LUDDEN *‡x, L. K. LUDDEN ‡, K. E. WADE ‡, and S. R. B. ALLERHEILIGEN *‡

Received January 18, 1982, from the **College of Pharmacy, University of Texas-Austin* and the ‡*Department of Pharmacology, University of Texas Health Science Center, San Antonio, TX 78284.* Accepted for publication June 2, 1982.

Abstract □ The time required for the separation of plasma from the cellular components of blood can permit the *in vitro* loss of hydralazine. Thus, a high-performance liquid chromatographic (HPLC) procedure for the measurement of hydralazine in blood has been developed. 4-Methylhydralazine was used as an internal standard. The addition of *p*-anisaldehyde led to the formation of the *p*-anisaldehyde hydrazones of hydralazine and the internal standard. HPLC on a reverse-phase cyano column provided an analytical procedure in which the average relative standard deviation over the concentration range of 1–160 ng/ml was 8.3%. Hydralazine pyruvic acid hydrazone, a known circulating metabolite of hydralazine, yielded only 0.05 mole % hydralazine when submitted to this assay procedure.

Keyphrases □ Hydralazine—whole blood, derivatization, *p*-anisaldehyde hydrazones of hydralazine, analysis, high-performance liquid chromatography □ Whole blood—analysis, hydralazine, high-performance liquid chromatography □ High-performance liquid chromatography—hydralazine, whole blood analysis, *p*-anisaldehyde hydrazone of hydralazine

Selective assays for the measurement of hydralazine in plasma have been recently described (1–3). A major disadvantage of these procedures is the time required for separation of plasma from the cellular components of blood. Hydralazine disappears rapidly from plasma or blood *in vitro* (2, 4–6). Rapid sample processing at reduced temperature has been used to slow the loss prior to derivatization (7–9). The measurement of hydralazine in whole blood would circumvent this problem. In addition, because the clearance of hydralazine is high (7, 8), blood hydralazine concentrations are extremely useful for pharmacokinetic studies. However, attempts to measure hydralazine in whole blood using previously published techniques for plasma (1, 3) resulted in fouling of the chromatographic column after only a few sample injections. This paper describes a high-performance liquid chromatographic (HPLC) assay for the determination of hydralazine in whole blood using a different chromatographic column and a less polar extraction solvent.

EXPERIMENTAL

Reagents and Chemicals—Hexane, methanol, and acetonitrile were purchased as glass-distilled solvents. The acetonitrile was filtered before

0022-3549/83/0600-0693$01.00/0

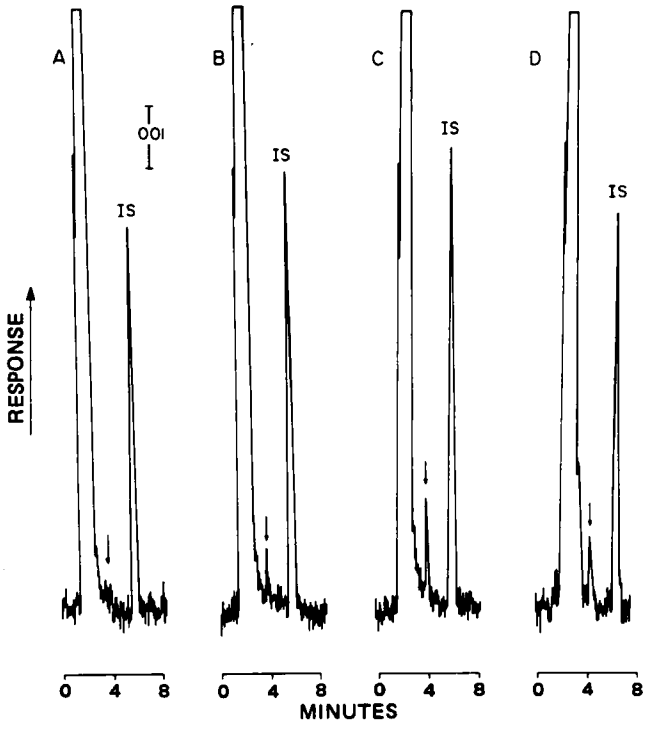

Figure 1—*Chromatograms of derivatized 3-ml blood samples containing 40 ng/ml of internal standard and (A) 0, (B) 1, (C) 2 ng/ml of hydralazine; (D) a sample obtained 150 min after administration of a 1-mg/kg oral dose of hydralazine hydrochloride to a hypertensive patient.*

being used. Hexane, hydralazine hydrochloride[1], 4-methylhydralazine[2], 4-(2-acetylhydrazino)phthalazin-1-one[3], and *p*-anisaldehyde[4] were used as received. Reference samples (3-methyl-*s*-triazolophthalazine, 4-hydrazinophthalazin-1-one) and hydralazine hydrazones of pyruvic acid, α-ketoglutaric acid, acetaldehyde, acetone, and *p*-anisaldehyde were prepared, and their identity and purity verified by gas chromatography–mass spectrometry as previously described (1, 10).

Standard Solutions—No pretreatment of the glassware was used. Hydralazine hydrochloride (61.4 mg) equivalent to 50 mg of the free base, was diluted to 50 ml with normal saline to give a concentration of 1 mg/ml. This stock solution was prepared daily. Standard A was prepared by diluting 0.6 ml of the stock solution to 10 ml with normal saline to yield a concentration of 60 ng/μl. Standard B was prepared by diluting 0.5 ml of Standard A to 10 ml with normal saline resulting in a concentration of 3 ng/μl. The internal standard solution was prepared by dissolving 50 μg of 4-methylhydralazine in 10 ml of 0.01 *N* HCl.

Standard Curve Samples—Three milliliters of whole blood containing EDTA (ethylenediaminetetraacetic acid) as an anticoagulant was placed in a 35-ml centrifuge tube fitted with a polytef-lined screw cap. After addition of 20 μl of *p*-anisaldehyde, appropriate volumes of either standard A or B were added along with 8 μl (40 ng) of the internal standard solution. The tube was capped immediately and mixed for 15 sec on a vortex mixer. Each sample was prepared individually to minimize the intervals between additions. Samples were allowed to stand at room temperature for 10 min. Preliminary studies indicated that 10 min is optimal for the formation of the *p*-anisaldehyde hydrazones of hydralazine and the internal standard. After derivatization, 10 ml of hexane was added and the sample was placed immediately on a reciprocal shaker[5] (180 strokes/min) for 10 min.

Phases were separated by centrifugation at 1000×*g* for 10 min. The organic phase was transferred to a 15-ml conical centrifuge tube and the solvent removed under a nitrogen stream. The remaining aqueous phase was processed as previously described (3) in order to measure the hydralazine pyruvic acid hydrazone concentration.

Chromatography—Each extraction residue was diluted with 100 μl of methanol and the entire volume was injected onto a reverse-phase column (3.9-mm i.d. × 30 cm)[6]. The mobile phase was 70% (v/v) acetonitrile in 0.15 *M* sodium acetate buffer, pH 3.0, pumped[7] at a flow rate of 2 ml/min. Detection[8] was at 365 nm.

Table I—Conversion of Hydralazine Hydrazones to Derivatized Hydralazine During the Analytical Process

Hydrazone	Initial Hydrazone Concentration, μg/ml	Hydralazine *p*-Anisaldehyde Hydrazone Found, mole %[a]
Pyruvic Acid	5	0.05
α-Ketoglutaric Acid	1	0.15
Acetone	1	4.2
Acetaldehyde	1	27.1

[a] Mean of two determinations.

Assay Evaluation—The efficiencies of derivatization and extraction were determined as previously described for plasma (1, 3) using fresh, whole human blood. Selectivity was evaluated by adding known or potential metabolites to whole blood and immediately assaying for hydralazine. Intraassay precision was determined by assaying multiple standard samples containing hydralazine concentrations of 1, 2, 8, 20, 40, 80, and 160 ng/ml.

Patient Samples—Blood, 3 ml, was drawn rapidly and placed in a 35-ml centrifuge tube containing EDTA. The internal standard and 20 μl of *p*-anisaldehyde were added immediately. The time between blood drawing and the addition of derivatizing reagent was <30 sec. After derivatization, samples were immediately extracted and prepared for chromatography as described for standard curve samples.

RESULTS

The retention times for hydralazine *p*-anisaldehyde hydrazone and 4-methylhydralazine *p*-anisaldehyde hydrazone were 3.5 and 6 min, respectively. Typical chromatograms are shown in Fig. 1. Maximum sensitivity for purposes of quantitation was ~1 ng/ml using a 3-ml blood sample. Derivatization efficiency for hydralazine was 103 ± 9% (mean ± *SD*) and extraction recovery was 70.5 ± 1.9%. The 3-methyl-*s*-triazolophthalazine, 4-hydrazinophthalazin-1-one, and 4-(2-acetylhydrazino)phthalazin-1-one yielded no chromatographic peaks when assayed with this procedure.

The acetaldehyde and acetone hydrazones yielded peaks at 4.1 and 2.9 min, respectively, which correspond to the retention times for standards of these materials. These hydrazones, as well as the hydrazones of α-ketoglutaric acid and pyruvic acid, yielded various quantities of derivatized hydralazine (Table I). The pyruvic acid hydrazone, the only one of the four hydrazones known to be present in the circulation (2–4), yields the least amount of apparent hydralazine. The acetaldehyde hydrazone is particularly labile. No significant quantities of this hydrazone or the hydrazones of α-ketoglutaric acid or acetone have been found in humans (2). These four hydrazones have similar stabilities in plasma (Table I).

The results of the intra-assay precision study are shown in Table II. The mean relative standard deviation was 8.3%. Precision is somewhat decreased at the lower concentrations, particularly at 1 ng/ml. This assay has been applied to blood from several patients receiving various drugs, including propranolol, furosemide, hydrochlorthiazide, digoxin, and nitroglycerin, without evidence of interference.

DISCUSSION

The assay described here has two advantages over other recently published techniques for the determination of hydralazine (1–3). First, it can be used to measure hydralazine concentrations in whole blood. This eliminates the time required to separate plasma, during which a significant fraction of hydralazine can continue to react with pyruvic acid to form the corresponding hydrazone. The use of whole blood also decreases the total blood volume required per determination. Second, the sensitivity of the assay has been extended to 1 ng/ml of blood when a 3-ml blood sample is used.

Hydralazine pyruvic acid hydrazone yields only 0.05 mole % hydrala-

[1] Sigma Chemical Co., St. Louis, Mo.
[2] Ciba-Geigy Co., Summit, N.J.
[3] Ciba-Geigy, Ltd., Basel, Switzerland.
[4] Eastman Kodak Co., Rochester, N.Y.
[5] Eberbach Horizontal Shaker.
[6] μBondapak CN, Waters Associates, Milford, Mass.
[7] Model 6000, Waters Associates, Milford, Mass.
[8] Model 970, Tracor, Austin, Tex.
[9] Unpublished results.

Table II—Intraassay Precision of Hydralazine Assay

Hydralazine Added ng/ml	Peak Height Ratio[a]	Hydralazine Found, ng/ml[b]
1	0.120 ± 0.022	1.14
2	0.210 ± 0.027	1.91
8	0.827 ± 0.031	7.22
20	2.24 ± 0.186	19.4
40	4.57 ± 0.245	39.4
80	9.54 ± 0.440	82.2
160	18.6 ± 0.875	160.

[a] Mean ± *SD*, $n = 4$. [b] Based on regression analysis of peak height ratio *versus* added hydralazine concentration weighted by the reciprocal of the peak height ratio.

zine when assayed in this manner. Thus, a plasma concentration of 12.5 μM (2.9 μg/ml) of this hydrazone would be required to yield 1 ng/ml of hydralazine. After multiple 1-mg/kg doses of oral hydralazine, peak hydralazine pyruvic acid hydrazone concentrations averaged only ~2.5 μM, range: 0.9–6.0 μM (9).

Steady-state predose apparent hydralazine concentrations up to 17 μM have been reported for patients with low creatinine clearances who received ≤200 mg of hydralazine hydrochloride daily (11), using a nonselective GLC assay (12) which converts both hydralazine pyruvic acid hydrazone and hydralazine to tetrazolophthalazine (4, 5). However, even this high concentration of acid-labile hydrazones, if composed primarily of hydralazine pyruvic acid hydrazone, would yield less than 2 ng/ml of hydralazine when the current assay is used. Other hydralazine adducts, such as the acetone, α-ketoglutaric acid, and acetaldehyde hydrazones, are less stable, but have not been detected in significant concentrations in plasma (2) or whole blood[9].

Approximately 10% of the α-ketoglutaric acid hydrazone adduct has been reported to be converted to apparent hydralazine in a selective assay procedure (2), while the pyruvic acid and acetone hydrazones did not yield apparent hydralazine. The lowest detectable hydralazine concentration and the stability of the acetaldehyde hydrazone using this procedure were not reported.

The assay procedure described here, as well as other recently published methods applicable to plasma (1–3), are much more selective than older procedures. However, the lability of the various known and potential circulating metabolites of hydralazine makes it difficult to believe that any procedure will be completely selective for unchanged hydralazine. The procedure for measuring hydralazine in whole blood is being evaluated in hypertensive patients with renal failure and in patients with congestive heart failure since these individuals are likely to have the highest concentrations of circulating metabolites.

REFERENCES

(1) T. M. Ludden, L. K. Goggin, J. L. McNay, Jr., K. D. Haegele, and A. M. M. Shepherd, *J. Pharm. Sci.*, **68**, 1423 (1979).

(2) P. A. Reece, I. Cozamanis, and R. Zacest, *J. Chromatogr.*, **181**, 427 (1980).

(3) T. M. Ludden, L. K. Ludden, J. L. McNay, Jr., H. B. Skrdlant, P. J. Swaggerty, and A. M. M. Shepherd, *Anal. Chim. Acta*, **120**, 297 (1980).

(4) P. A. Reece, C. E. Stanley, and R. Zacest, *J. Pharm. Sci.*, **67**, 1150 (1978).

(5) P. A. Reece and R. Zacest, *Clin. Exp. Pharmacol. Physicol.*, **6**, 207 (1979).

(6) T. M. Ludden, A. M. M. Shepherd, and J. L. McNay, Jr., "Abstracts," The 29th National Meeting of the APhA Academy of Pharmaceutical Sciences, **10**, 96 (1980).

(7) T. M. Ludden, A. M. M. Shepherd, J. L. McNay, Jr., and M.-S. Lin, *Clin. Pharmacol. Ther.*, **28**, 736 (1980).

(8) P. A. Reece, I. Cozamanis, and R. Zacest, *ibid.*, **28**, 769 (1980).

(9) A. M. M. Shepherd, T. M. Ludden, J. L. McNay, Jr., and M.-S. Lin, *ibid.*, **28**, 804 (1980).

(10) K. D. Haegele, H. B. Skrdlant, N. W. Robie, D. Lalka, and J. L. McNay, Jr., *J. Chromatogr.*, **126**, 517 (1976).

(11) T. Talseth, *Eur. J. Clin. Pharmacol.*, **10**, 311 (1976).

(12) D. B. Jack, S. Brechbühler, P. G. Degen, P. Zbinden, and W. Riess, *J. Chromatogr.*, **115**, 87 (1975).

ACKNOWLEDGMENTS

This work was supported in part by grants from the Texas Affiliate, Inc. of the American Heart Association, and by NIH Grant GM24092.

The authors thank Ms. Leslie Burks for her assistance with the preparation of this manuscript, Drs. W. Riess and K. Schmid (Ciba-Geigy, Ltd, Basal, Switzerland) for their gift of authentic 4-(2-acetylhydrazino)phthalazin-1-one, and Dr. M. F. Bartlett (Ciba-Geigy, Inc., Ardsley, N.Y.) for providing 4-methylhydralazine.

Quantitation of Meperidine Hydrochloride in Pharmaceutical Dosage Forms by High-Performance Liquid Chromatography

V. DAS GUPTA

Received January 22, 1982, from the *College of Pharmacy, University of Houston, Houston, TX 77030.* Accepted for publication June 2, 1982.

Abstract □ A high-performance liquid chromatographic (HPLC) method for the quantitative determination of meperidine hydrochloride in pharmaceutical dosage forms was developed. The method is reproducible and precise with relative standard deviations (based on six readings) of 1.2% with hydroxyzine and 0.93% with hydroxyprogesterone caproate as the internal standards. A variety of other active and inactive ingredients which were mixed with meperidine hydrochloride did not interfere with the assay procedure. Among the ingredients tested were acetaminophen, atropine sulfate, disodium edetate, metacresol, phenol, promethazine, and sodium metabisulfite. This method appears to be stability-indicating since a hydrolyzed sample of meperidine showed zero potency and a new peak with a different retention time.

Keyphrases □ Meperidine hydrochloride—quantitation in pharmaceutical dosage forms by high-performance liquid chromatography □ Pharmaceutical dosage forms—quantitation of meperidine hydrochloride by high-performance liquid chromatography □ High-performance liquid chromatography—quantitation of meperidine hydrochloride in pharmaceutical dosage forms

Meperidine hydrochloride (ethyl 1-methyl-4-phenylisonipecotate hydrochloride) is widely used as a narcotic analgesic. In addition to single ingredient dosage forms, meperidine is also mixed with acetaminophen, atropine sulfate, and promethazine hydrochloride in commercial dosage forms.

0022-3549/83/0600-0695$01.00/0

Table II—Intraassay Precision of Hydralazine Assay

Hydralazine Added ng/ml	Peak Height Ratio[a]	Hydralazine Found, ng/ml[b]
1	0.120 ± 0.022	1.14
2	0.210 ± 0.027	1.91
8	0.827 ± 0.031	7.22
20	2.24 ± 0.186	19.4
40	4.57 ± 0.245	39.4
80	9.54 ± 0.440	82.2
160	18.6 ± 0.875	160.

[a] Mean ± *SD*, $n = 4$. [b] Based on regression analysis of peak height ratio *versus* added hydralazine concentration weighted by the reciprocal of the peak height ratio.

zine when assayed in this manner. Thus, a plasma concentration of 12.5 μM (2.9 μg/ml) of this hydrazone would be required to yield 1 ng/ml of hydralazine. After multiple 1-mg/kg doses of oral hydralazine, peak hydralazine pyruvic acid hydrazone concentrations averaged only ~2.5 μM, range: 0.9–6.0 μM (9).

Steady-state predose apparent hydralazine concentrations up to 17 μM have been reported for patients with low creatinine clearances who received ≤200 mg of hydralazine hydrochloride daily (11), using a nonselective GLC assay (12) which converts both hydralazine pyruvic acid hydrazone and hydralazine to tetrazolophthalazine (4, 5). However, even this high concentration of acid-labile hydrazones, if composed primarily of hydralazine pyruvic acid hydrazone, would yield less than 2 ng/ml of hydralazine when the current assay is used. Other hydralazine adducts, such as the acetone, α-ketoglutaric acid, and acetaldehyde hydrazones, are less stable, but have not been detected in significant concentrations in plasma (2) or whole blood[9].

Approximately 10% of the α-ketoglutaric acid hydrazone adduct has been reported to be converted to apparent hydralazine in a selective assay procedure (2), while the pyruvic acid and acetone hydrazones did not yield apparent hydralazine. The lowest detectable hydralazine concentration and the stability of the acetaldehyde hydrazone using this procedure were not reported.

The assay procedure described here, as well as other recently published methods applicable to plasma (1–3), are much more selective than older procedures. However, the lability of the various known and potential circulating metabolites of hydralazine makes it difficult to believe that any procedure will be completely selective for unchanged hydralazine. The procedure for measuring hydralazine in whole blood is being evaluated in hypertensive patients with renal failure and in patients with congestive heart failure since these individuals are likely to have the highest concentrations of circulating metabolites.

REFERENCES

(1) T. M. Ludden, L. K. Goggin, J. L. McNay, Jr., K. D. Haegele, and A. M. M. Shepherd, *J. Pharm. Sci.*, **68**, 1423 (1979).

(2) P. A. Reece, I. Cozamanis, and R. Zacest, *J. Chromatogr.*, **181**, 427 (1980).

(3) T. M. Ludden, L. K. Ludden, J. L. McNay, Jr., H. B. Skrdlant, P. J. Swaggerty, and A. M. M. Shepherd, *Anal. Chim. Acta*, **120**, 297 (1980).

(4) P. A. Reece, C. E. Stanley, and R. Zacest, *J. Pharm. Sci.*, **67**, 1150 (1978).

(5) P. A. Reece and R. Zacest, *Clin. Exp. Pharmacol. Physicol.*, **6**, 207 (1979).

(6) T. M. Ludden, A. M. M. Shepherd, and J. L. McNay, Jr., "Abstracts," The 29th National Meeting of the APhA Academy of Pharmaceutical Sciences, **10**, 96 (1980).

(7) T. M. Ludden, A. M. M. Shepherd, J. L. McNay, Jr., and M.-S. Lin, *Clin. Pharmacol. Ther.*, **28**, 736 (1980).

(8) P. A. Reece, I. Cozamanis, and R. Zacest, *ibid.*, **28**, 769 (1980).

(9) A. M. M. Shepherd, T. M. Ludden, J. L. McNay, Jr., and M.-S. Lin, *ibid.*, **28**, 804 (1980).

(10) K. D. Haegele, H. B. Skrdlant, N. W. Robie, D. Lalka, and J. L. McNay, Jr., *J. Chromatogr.*, **126**, 517 (1976).

(11) T. Talseth, *Eur. J. Clin. Pharmacol.*, **10**, 311 (1976).

(12) D. B. Jack, S. Brechbühler, P. G. Degen, P. Zbinden, and W. Riess, *J. Chromatogr.*, **115**, 87 (1975).

ACKNOWLEDGMENTS

This work was supported in part by grants from the Texas Affiliate, Inc. of the American Heart Association, and by NIH Grant GM24092.

The authors thank Ms. Leslie Burks for her assistance with the preparation of this manuscript, Drs. W. Riess and K. Schmid (Ciba-Geigy, Ltd, Basal, Switzerland) for their gift of authentic 4-(2-acetylhydrazino)phthalazin-1-one, and Dr. M. F. Bartlett (Ciba-Geigy, Inc., Ardsley, N.Y.) for providing 4-methylhydralazine.

Quantitation of Meperidine Hydrochloride in Pharmaceutical Dosage Forms by High-Performance Liquid Chromatography

V. DAS GUPTA

Received January 22, 1982, from the *College of Pharmacy, University of Houston, Houston, TX 77030.* Accepted for publication June 2, 1982.

Abstract □ A high-performance liquid chromatographic (HPLC) method for the quantitative determination of meperidine hydrochloride in pharmaceutical dosage forms was developed. The method is reproducible and precise with relative standard deviations (based on six readings) of 1.2% with hydroxyzine and 0.93% with hydroxyprogesterone caproate as the internal standards. A variety of other active and inactive ingredients which were mixed with meperidine hydrochloride did not interfere with the assay procedure. Among the ingredients tested were acetaminophen, atropine sulfate, disodium edetate, metacresol, phenol, promethazine, and sodium metabisulfite. This method appears to be stability-indicating since a hydrolyzed sample of meperidine showed zero potency and a new peak with a different retention time.

Keyphrases □ Meperidine hydrochloride—quantitation in pharmaceutical dosage forms by high-performance liquid chromatography □ Pharmaceutical dosage forms—quantitation of meperidine hydrochloride by high-performance liquid chromatography □ High-performance liquid chromatography—quantitation of meperidine hydrochloride in pharmaceutical dosage forms

Meperidine hydrochloride (ethyl 1-methyl-4-phenylisonipecotate hydrochloride) is widely used as a narcotic analgesic. In addition to single ingredient dosage forms, meperidine is also mixed with acetaminophen, atropine sulfate, and promethazine hydrochloride in commercial dosage forms.

0022-3549/83/0600-0695$01.00/0

Table I—Assay Results of Various Commercial Dosage Forms and Synthetic Mixtures

Dosage Form	Conc. of Meperidine HCl, mg/ml or per Tablet	Other Ingredients, mg/ml	Percent[a] of the Label Claim	
			Hydroxyzine	Hydroxyprogesterone Caproate
Ampule	25.0	—	99.2	100.1
Ampule	50.0	—	99.9	100.1
Ampule	75.0	—	98.4	99.6
Ampule	100.0	—	100.3	99.2
Syrup	10.0	[b]	98.8	99.1
Tablet	50.0	[b]	99.5	100.0
Vial	50.0	Metacresol 1	99.1	98.7
Synthetic Mixture 1	50.0	Promethazine hydrochloride 50	100.8[c]	100.3
Synthetic Mixture 2	50.0	Atropine sulfate 0.4	100.7	100.6
Synthetic Mixture 3	50.0	Phenol 20, Disodium edetate 3, $CaCl_2$ 1 and sodium metabisulfite 5	99.1	99.4
Synthetic Mixture 4	50.0	Metacresol 1	99.2	99.0
Synthetic Mixture 5	50.0	Acetaminophen 300	99.8	99.2

[a] The percent relative standard deviations based on six readings were 1.2 and 0.93 with hydroxyzine and hydroxyprogesterone caproate as the internal standards, respectively. [b] The excipients were not disclosed on the label. [c] The concentration of promethazine hydrochloride was determined to be 99.1% of the label claim. It was determined by comparing the peak heights of assay and the standard mixtures.

The USP-NF method (1) for the quantitation of meperidine hydrochloride is based on the nonaqueous titration with perchloric acid. Promethazine which is mixed with meperidine in a commercial dosage form[1] is also assayed (2) using the nonaqueous titration with perchloric acid. The method is nonspecific and cannot make a distinction between meperidine and promethazine or other weak bases.

A GLC (3) method for the quantitation of meperidine in plasma has been reported with a relative standard deviation of 9.9%. A suitable high-performance liquid chromatographic (HPLC) method for the analysis of meperidine has not been described.

The purpose of these investigations was to develop an HPLC method for the quantitation of meperidine hydrochloride in pharmaceutical dosage forms which would be useful in the presence of other ingredients.

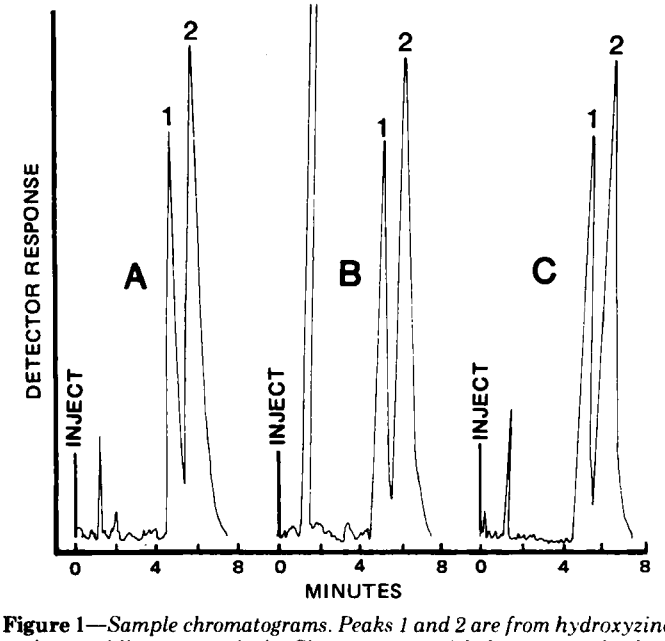

Figure 1—*Sample chromatograms. Peaks 1 and 2 are from hydroxyzine and meperidine, respectively. Chromatogram A is from a standard solution; B from a hydrolyzed sample of meperidine (see* Experimental*) and C from an ampule (number 3 in Table I). For chromatographic conditions, see text.*

EXPERIMENTAL

Chemicals and Reagents—All chemicals and reagents were either USP, NF, or ACS quality and used without further purification. Hydroxyprogesterone caproate[2], hydroxyzine hydrochloride[3], meperidine hydrochloride[4], and promethazine hydrochloride[5] were used as received.

An HPLC[6] equipped with a multiple wavelength detector[7], a recorder[8], and an integrator[9], was used. A μ-Bondapak-C_{18} column[10] (30 cm × 4 mm i.d.) was used at ambient temperature.

Chromatographic Conditions—The mobile phase contained 60% by volume of acetonitrile in 0.02 *M* aqueous solution of ammonium acetate. The flow rate was 2.0 ml/min (3.0 ml/min when hydroxyprogesterone caproate was the internal standard), the sensitivity was 0.04 AUFS at 232 nm, and the chart speed was 30.5 cm/hr.

Preparation of Stock and Standard Solutions—The stock solutions of hydroxyzine hydrochloride, meperidine hydrochloride, and promethazine hydrochloride were prepared by dissolving 100.0 mg of the powder in enough water to make 100.0 ml. The stock solutions were diluted further with water as needed. The standard solution contained 500.0 μg/ml of meperidine hydrochloride and 28 μg/ml of hydroxyzine hydrochloride. A standard mixture containing 250.0 μg/ml each of meperidine hydrochloride and promethazine hydrochloride and 14.0 μg/ml of hydroxyzine hydrochloride was also prepared.

The solutions of acetaminophen (~3 mg/ml), atropine sulfate (20 μg/ml), calcium chloride (10 μg/ml), disodium edetate (30 μg/ml), metacresol (10 μg/ml), phenol (200 μg/ml), and sodium metabisulfite (50 μg/ml) in water were also prepared to determine the possible interference from these ingredients, since they are added to commercial dosage forms.

Preparation of Assay Solutions, Injections (Ampules or Vials)—To an appropriate quantity of the injection containing 50.0 mg of meperidine hydrochloride, 2.8 ml of hydroxyzine hydrochloride stock solution was added and the mixture was diluted to 100.0 ml with water.

Assay solutions were made from syrup (10 mg/ml) by mixing 2.5 ml of the mixture with 1.4 ml of the stock solution of hydroxyzine hydrochloride and diluting to 50.0 ml with water, and from 50-mg tablets by weighing 20 tablets accurately and grinding them to a fine powder. An appropriate quantity of the powder containing 50.0 mg of meperidine hydrochloride was mixed with 50 ml of water and 2.8 ml of the stock solution of hydroxyzine hydrochloride. The mixture was brought to a volume (100.0

[1] Mepergan by Wyeth Laboratories, Philadelphia, Pa.
[2] E. R. Squibb Research Institute, Princeton, N.J.
[3] Pfizer Laboratories, New York, N.Y.
[4] Winthrop Laboratories, New York, N.Y.
[5] Wyeth Laboratories, Philadelphia, Pa.
[6] ALC 202 equipped with U6K universal injector, Waters Associates, Milford, Mass.
[7] Spectroflow monitor SF770, Schoeffel Instruments, Westwood, N.J.
[8] Omniscribe 5213-12, Houston Instruments, Austin, Tex.
[9] Autolab Minigrator, Spectra-Physics, Santa Clara, Calif.
[10] Waters Associates, Milford, Mass.

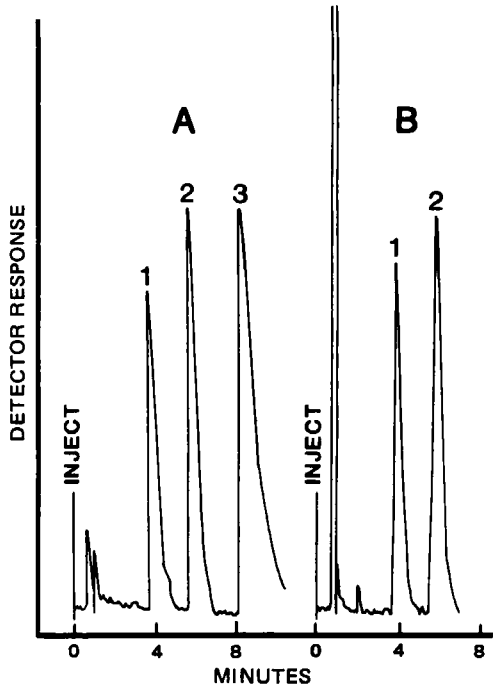

Figure 2—*Sample chromatograms. Peaks 1–3 are from meperidine, hydroxyprogesterone caproate, and promethazine, respectively. Chromatogram A is from a standard mixture containing (in μg per ml): meperidine hydrochloride (310), hydroxyprogesterone caproate (30), and promethazine hydrochloride (50). Chromatogram B is from a syrup with 350 μg/ml of meperidine hydrochloride and 30 μg/ml of hydroxyprogesterone caproate. For chromatographic conditions, see text. Flow rate was 3.0 ml/min.*

ml) with water and then filtered. The first 20 ml of the filtrate was discarded and the remainder collected for the assay.

Modifications with Hydroxyprogesterone Caproate as the Internal Standard—A stock solution of hydroxyprogesterone caproate was prepared by dissolving 100.0 mg of the powder in enough ethanol to make 100.0 ml. The standard solutions were prepared by mixing 3.0 ml of the stock solution with 60 ml of acetonitrile, an appropriate quantity of the meperidine hydrochloride stock solution concentrated (2.0 mg/ml), and enough water to make 100.0 ml. A similar procedure was used to prepare the assay solutions. In the case of tablets, only 30 ml of water was used instead of 50 ml in the extraction procedure. The assay solutions were filtered if necessary.

Assay Procedure—A 20 μl aliquot of the sample was injected into the chromatograph using the described conditions. For purpose of comparison, an identical volume of the standard solution–mixture was injected after the assay material was eluted.

Because preliminary investigations indicated that the ratio of peak heights (meperidine–hydroxyzine or meperidine–hydroxyprogesterone caproate) were directly related to the concentrations (5–13-μg range tested), the results were calculated using a standard curve or the following equation:

$$\frac{(R_{ph})_a}{(R_{ph})_s} \times 100 = \text{percent of the label claim}$$

where $(R_{ph})_a$ is the ratio of the peak heights of the assay solution and $(R_{ph})_s$ is that of the standard solution. The results are presented in Table I and Figs. 1 and 2.

In other experiments a 6.25-ml solution of meperidine hydrochloride (2 mg/ml) was mixed with 1 ml of ~1 *N* NaOH in a 25-ml volumetric flask. The flask (with lid on) was stored in an electric oven at 50° (±1°) for 48 hr. After cooling the mixture, 1 ml of ~1 *N* HCl and 0.7 ml of the stock solution of hydroxyzine hydrochloride were added. The mixture was brought to volume with water and assayed using the procedure described above. The results are presented in Fig. 1B.

RESULTS AND DISCUSSION

The results indicate (Table I, Figs. 1 and 2) that this HPLC method can be used for the quantitative determination of meperidine hydrochloride in pharmaceutical dosage forms. The results on different days were highly reproducible and precise. The relative standard deviations based on six readings were 1.2% with meperidine hydrochloride and 0.93% with hydroxyprogesterone caproate, as the internal standard, respectively. The ratio of the peak heights was directly related to the concentrations of meperidine hydrochloride (5–13-μg range tested).

A variety of other active and inactive ingredients, which are usually mixed with meperidine in commercial dosage forms, did not interfere with the assay procedure. The concentrations (in μg) tested (with 10 μg of meperidine hydrochloride) were: acetaminophen, 60; atropine sulfate, 0.4; calcium chloride, 0.2; disodium edetate, 0.6; metacresol, 0.2; phenol, 4; promethazine hydrochloride, 10; and sodium metabisulfite, 1. In addition to these ingredients, the excipients in syrup such as flavors and preservative(s) eluted immediately after the solvent peak (Fig. 2B) and did not interfere with the assay procedure. The exact nature of the excipients added was not disclosed on the label.

Since meperidine did not separate completely from hydroxyzine (Fig. 1), another internal standard (hydroxyprogesterone caproate) was developed later in these investigations. The results obtained with this internal standard were similar (Table I) to those with hydroxyzine as the internal standard. Hydroxyprogesterone caproate separated completely from meperidine and promethazine (Fig. 2) and is recommended as the internal standard. The relative standard deviations based on six readings were 0.93 *versus* 1.2% with hydroxyzine hydrochloride (an alternative internal standard). To keep hydroxyprogesterone caproate in solution, it was necessary to add 60% (v/v) of acetonitrile (same concentration as in the mobile phase) to the standard/assay solutions. The flow rate was increased to 3.0 ml/min to hasten the assay procedure.

It was possible to determine the concentration of promethazine hydrochloride (Table I, footnote *c* and Fig. 2A) present in the synthetic mixture similar to a commercial dosage form[1]. The promethazine eluted ~4.5 min later (peak 3 in Fig. 2A) than meperidine (peak 1 in Fig. 2A).

The developed method appears to be stability-indicating, since a sample of meperidine which was hydrolyzed to the free acid (see *Experimental*) showed almost zero potency (Fig. 1B), and the product(s) of decomposition eluted immediately after the solvent. The *N*-oxide, another possible degradation product, was not chromatographed.

REFERENCES

(1) "The United States Pharmacopeia," 20th ed.; "The National Formulary," 15th ed., U.S. Pharmacopeial Convention, Inc., Rockville, Md., 1980, pp. 477–478.

(2) *Idem.*, p. 669.

(3) T. J. Goehl and C. Davison, *J. Pharm. Sci.*, **62**, 907 (1973).

Involvement of Active Sodium Transport in the Rectal Absorption of Gentamicin Sulfate in the Presence and Absence of Absorption-Promoting Adjuvants

JOSEPH A. FIX ˣ, PATRICIA A. PORTER, and PAULA S. LEPPERT

Received January 13, 1982, from the *INTERx Research Corporation, Subsidiary of Merck & Co., Inc., Lawrence, KS 66045.* Accepted for publication June 4, 1982.

Abstract □ The involvement of active sodium transport in the rectal absorption of gentamicin sulfate was examined in rats, employing aqueous microenemas of known total ionic strength (μ) in the presence or absence of absorption-promoting adjuvants. Rectal gentamicin bioavailability, which is negligible (1 ± 1.2%) at an ionic strength of 0.15 without adjuvants, is significantly ($p < 0.01$) increased by including adjuvants in the formulation (sodium salicylate, 12 ± 4.0%; sodium-5-bromosalicylate, 59 ± 15.1%; disodium ethylene(dinitrilo)tetraacetate, 24 ± 9.3%). Pretreating the rectal mucosa cells with ouabain, a specific inhibitor of active sodium transport, significantly ($p < 0.01$) reduced gentamicin absorption in response to all three adjuvants. In contrast to previous findings with sodium chloride, high ionic strength choline chloride (μ = 1.056) did not promote gentamicin absorption. The data indicate that active sodium transport is an integral component of rectal absorption of water-soluble compounds and may be involved in the mechanism of action of absorption-promoting adjuvants.

Keyphrases □ Gentamicin sulfate—rectal absorption, effect of choline chloride and ouabain □ Choline chloride—effect on rectal absorption of gentamicin sulfate adjuvant enhancement □ Ouabain—effect on the rectal absorption of gentamicin sulfate □ Rectal absorption—gentamicin sulfate, effect of choline chloride and ouabain.

Normal rectal mucosa is capable of transporting sodium chloride and water from the luminal to the serosal side of the epithelial barrier (1). The bidirectional movement of sodium ions is regulated by both passive and active components, and has been shown to be directly correlated with the rectal transluminal potential difference (2). Previous work in this laboratory has shown that increasing the ionic strength in a microenema containing gentamicin, a water-soluble antibiotic, significantly enhanced the rectal absorption of the drug (3). The enhancing effect due to high ionic strength appeared to be additive to the enhanced rectal absorption effected by sodium salicylate, a proven absorption adjuvant (4, 5).

Two factors in a previous study on ionic strength (3) suggested that there was a possible specific involvement of sodium transport in rectal gentamicin delivery, including delivery which was adjuvant (sodium salicylate) assisted. In the absence of sodium salicylate, gentamicin absorption (at ionic strength of μ = 1.054) was twofold greater when sodium chloride, rather than potassium chloride, was the major contributor to total ionic strength. The addition of sodium salicylate to both sodium chloride and potassium chloride microenemas significantly increased rectal gentamicin absorption, but the same twofold difference in efficacy between sodium chloride and potassium chloride was still observed.

In the current study, the possible involvement of active sodium transport was further investigated by employing two agents, ouabain and choline chloride, which alter electrogenic sodium transport. Ouabain is a metabolic inhibitor which specifically blocks the membrane sodium–potassium pump. Choline chloride is used as a sodium chloride substitute since equivalent ionic strength can be established; but choline itself is not transported by the sodium–potassium pump. The use of these agents has provided data suggesting a direct involvement of active sodium transport in the rectal absorption of gentamicin. The results obtained here may also be of general applicability to other water-soluble compounds whose rectal absorption is enhanced by salicylate-type adjuvants (5–7).

EXPERIMENTAL

Adult male Sprague-Dawley rats (200–250 g) were fasted, with free access to water, for 18–24 hr prior to the experiment. Animals were anesthetized with intramuscular injections of urethane (0.5 ml of 43% ethylcarbamate[1] in distilled water per 100 g of body weight).

Aqueous microenemas (250 μl, pH 5) containing 2.5 mg of gentamicin sulfate[1] were administered with a 1-ml syringe at an intrarectal depth of 2.5 cm. Ionic species (sodium chloride, potassium chloride, or choline chloride) and/or absorption adjuvant were included in the microenemas as indicated in the text and legends. In one set of experiments, sodium-free microenemas were prepared by dissolving gentamicin sulfate and salicylic acid in 50-m*M* tromethamine hydrochloric acid (Tris-HCl) buffer. In experiments employing ouabain, animals received a 250-μl microenema of 25 m*M* ouabain either 15 or 30 min prior to administration of the gentamicin formulation. The gentamicin formulation also contained 25-m*M* ouabain in these experiments. Total ionic strength and percent bioavailability were calculated as described previously (3).

RESULTS

Rectal absorption of gentamicin is negligible (1 ± 1.2%, $n = 3$) when the drug is administered in an aqueous microenema at μ = 0.15 and without an adjuvant. Gentamicin absorption was significantly increased by the addition of 20 mg/kg of sodium salicylate (12 ± 4.0%, $n = 6$, $p < 0.01$), disodium ethylene(dinitrilo)tetraacetate (24 ± 9.3%, $n = 3$, $p < 0.01$), or sodium-5-bromosalicylate (59 ± 15.1%, $n = 3$, $p < 0.01$).

Increasing the microenema ionic strength by the addition of sodium chloride or potassium chloride was previously shown to significantly increase rectal gentamicin absorption (3). Data for choline chloride are shown in Fig. 1. Gentamicin bioavailability in the presence of 1.0 *M* choline chloride (μ = 1.054) was 6 ± 1.0% ($n = 3$) with no significant differences at other choline chloride concentrations (μ = 0.304–0.754). Compared with previous data on increasing ionic strength, the relative order of effectiveness in promoting gentamicin absorption was sodium chloride > potassium chloride > choline chloride (Fig. 1A). The incorporation of sodium salicylate into the choline chloride microenema resulted in gentamicin bioavailability greater than that seen with choline chloride alone (Fig. 1B). When the ionic contributions of sodium salicylate were included in calculations of total ionic strength and the results presented as bioavailability *versus* total ionic strength (3) (Fig. 1B), the profiles with salicylate demonstrated higher bioavailabilities and were approximately parallel to the ionic profiles with the salts alone.

Ouabain pretreatment significantly ($p < 0.01$) decreased gentamicin bioavailability in response to sodium salicylate, sodium-5-bromosalicylate, and disodium ethylene(dinitrilo)tetraacetate (Fig. 2). The effect was more pronounced following the 30-min pretreatment. Even though 30-min ouabain pretreatment significantly reduced bioavailabilities, the

[1] Sigma Chemical Co., St. Louis, Mo.

0022-3549/83/0600-0698$01.00/0

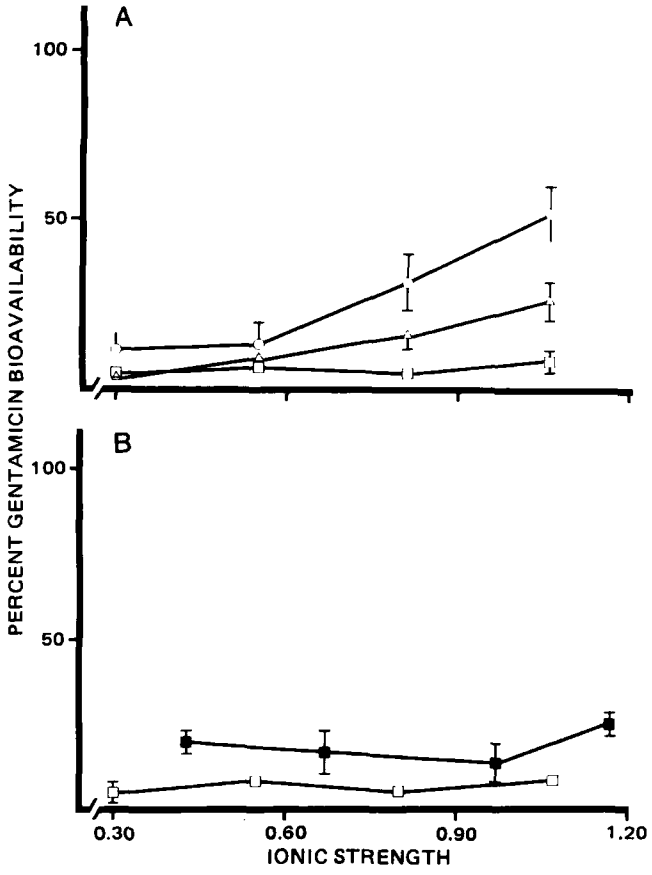

Figure 1—*Gentamicin bioavailability in the presence of various ionic strengths (μ) of sodium chloride (○), potassium chloride (△), and choline chloride (□), choline chloride–sodium salicylate (■). Panel A shows ionic strength profiles for each of the three salts in the absence of sodium salicylate. Panel B shows results of ionic strength profiles with choline chloride in the presence and absence of sodium salicylate. Error bars represent the standard deviation for* n = *3–6 experiments. Where error bars are not shown, the standard deviation is within the dimensions of the symbol.*

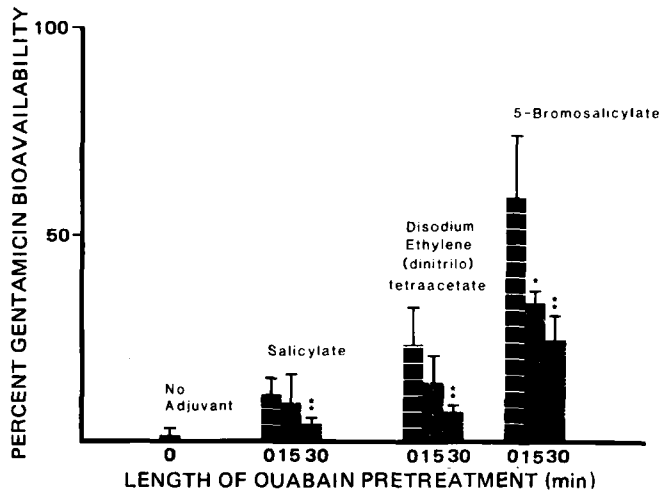

Figure 2—*Effect of ouabain pretreatment on gentamicin bioavailability in response to sodium salicylate, disodium ethylene(dinitrilo)tetraacetate, and sodium-5-bromosalicylate. Gentamicin bioavailability achieved with 20 mg of adjuvant/kg of body weight is represented as 0-min ouabain pretreatment. Histogram bars designated 15 and 30 represent gentamicin bioavailability observed in response to adjuvant activity following a 15 or 30-min exposure of the rectal tissue to 25 m*M *ouabain. Error bars represent the standard deviation for* n = *3–6 experiments. Key: (*)* $p < 0.025$, *(**)* $p < 0.01$.

levels of drug absorption were still greater ($p < 0.05$) than those observed with control microenemas (no adjuvant).

The effect of ouabain pretreatment on salicylate-assisted, high ionic strength rectal gentamicin absorption was examined using microenemas containing 0.5 *M* NaCl. Without ouabain pretreatment, gentamicin bioavailability in the presence of sodium chloride and 20 mg of sodium salicylate/kg body weight ($\mu = 0.574$) was 47 ± 7.1% ($n = 3$). Following a 30-min ouabain pretreatment, bioavailability was reduced to 22 ± 4.4% ($n = 3$, $p < 0.001$).

Sodium-free microenemas, prepared using salicylic acid and nonsodium buffering salts, resulted in gentamicin bioavailability of 9 ± 0.3% ($n = 3$), which was significantly ($p < 0.001$) greater than adjuvant-free control microenemas (1 ± 1.2%, $n = 3$).

DISCUSSION

Previous work in this laboratory suggested the possible involvement of monovalent cation specificity in the rectal delivery of gentamicin, a water-soluble antibiotic (3). Ionic strength profiles demonstrated that sodium chloride afforded higher levels of gentamicin absorption than potassium chloride. The absorption-promoting activity of sodium salicylate appeared to be additive to the enhancing effects of ionic strength.

The possible involvement of active sodium transport was further investigated in this study. Choline chloride, a nontransported ionic equivalent of sodium chloride, and ouabain, a specific inhibitor of the membrane sodium-potassium pump, were tested for effects on rectal gentamicin absorption.

Increasing the microenema ionic strength by the addition of sodium chloride, potassium chloride, or choline chloride demonstrated a preferential response in bioavailability to sodium ions. The inability of high ionic strength choline chloride ($\mu = 1.054$) to promote gentamicin absorption indicated that ionic strength alone was not a major modulator of rectal absorption.

Involvement of the membrane sodium-potassium transport system was further verified in experiments employing ouabain pretreatment of the rectal mucosal cells. The ability of ouabain to significantly reduce gentamicin bioavailability in response to all three adjuvants [salicylate, disodium ethylene(dinitrilo)tetraacetate, 5-bromosalicylate], at normal and elevated sodium chloride ionic strengths, indicates an important influence of active sodium transport in rectal absorption. After 30-min ouabain pretreatment, the level of gentamicin absorption was still significantly greater than the bioavailability observed in experiments with untreated animals given microenemas without adjuvant. One possible explanation for this is that at least a fraction of the adjuvant-enhanced absorption is independent of active sodium transport, assuming that a total inhibition of sodium transport would occur in response to 25 m*M* ouabain pretreatment (not verified by measurements of sodium transport). An alternative explanation is that the ouabain concentration or time of membrane exposure to ouabain may have been insufficient to totally suppress membrane sodium transport. In either case, the definite involvement of active sodium transport in rectal gentamicin absorption has been demonstrated.

The ability of salicylic acid to promote rectal gentamicin absorption when administered as a sodium-free microenema suggests that sodium may not be absolutely required for this delivery system. However, sufficient sodium may normally be present in the fluids of the rectal compartment to permit salicylate-enhanced gentamicin absorption.

The mechanism(s) by which active sodium transport affects rectal absorption of water-soluble compounds is unknown, although the direction and magnitude of fluid movement is significantly affected by the sodium gradient. Regardless of the exact mechanism(s) involved, it is clear that active sodium transport is intimately related to rectal absorption systems. The applicability of these findings to the further development of traditional dosage forms (*e.g.*, suppositories) remains to be demonstrated. However, the regulation of sodium transport may provide a means to predictably alter the permeability of the rectal mucosal cell barrier and to more carefully control adjuvant-enhanced absorption of water-soluble compounds.

REFERENCES

(1) C. J. Edmonds, *Gut*, **12**, 356 (1971).

(2) J. Rask-Madsen, *Scand. J. Gastroenterol.*, **8**, 327 (1973).

(3) J. A. Fix, P. S. Leppert, P. A. Porter, and L. J. Caldwell, *J. Pharm. Sci.*, in press.

(4) T. Nishihata, J. H. Rytting, and T. Higuchi, *ibid.*, **69**, 744 (1980).
(5) H. Yaginuma, T. Nakata, H. Toya, T. Murakami, M. Yamazaki, and A. Kamada, *Chem. Pharm. Bull.*, **29**, 2974 (1981).
(6) T. Nishihata, J. H. Rytting, T. Higuchi, and L. Caldwell, *J. Pharm. Pharmacol.*, **33**, 334 (1980).
(7) T. Nishihata, J. H. Rytting, and T. Higuchi, *J. Pharm. Sci.*, **70**, 71 (1981).

Synthesis and Anticonvulsant Screening of 3,3-Diphenyl-2-pyrrolidone Derivatives

GEORGE A. BRINE ˣ **and KARL G. BOLDT**

Received March 3, 1982, from the *Chemistry and Life Sciences Group, Research Triangle Institute, Research Triangle Park, NC 27709.* Accepted for publication June 7, 1982.

Abstract □ Six derivatives of 3,3-diphenyl-2-pyrrolidone were synthesized and screened for anticonvulsant activity. The synthetic route involved a mono-*N*-demethylation of an intermediate *N*,*N*-dimethylaminonitrile with methyl chloroformate followed by cleavage of the carbamate group. Of the six derivatives, (±)-2-imino-1,5-dimethyl-3,3-diphenylpyrrolidine hydrochloride was effective in protecting mice against maximal electroshock (MES) -induced seizures at a 30-mg/kg dose level.

Keyphrases □ Anticonvulsant screening—synthesis of 3,3-diphenyl-2-pyrrolidone derivatives, maximal electroshock-induced seizures, mice □ 3,3-Diphenyl-2-pyrrolidone—synthesis and anticonvulsant screening, derivatives, maximal electroshock-induced seizures, mice

The reported (1) anticonvulsant activity of 2-pyrrolidone (I), the lactam of γ-aminobutyric acid, stimulated interest in 2-pyrrolidone derivatives as potential anticonvulsants. As it incorporated several features of the anticonvulsant diphenylhydantoin (II), the 3,3-diphenyl-2-pyrrolidone (III) system seemed a promising one for the study. When tested in rats, 3,3-diphenyl-2-pyrrolidone (III) itself was less effective than (±)-3-ethyl-3-phenyl-2-pyrrolidone against both pentylenetetrazol[1] and electrically-induced convulsions (2). Somewhat earlier, it was observed (3) that the structurally related α,α-diphenylsuccinimide (IVa) and its *N*-methyl derivative (IVb) ranked first and eighth in a series of 39 succinimides in protecting mice against electrically induced convulsions.

The work on 3,3-disubstituted-2-pyrrolidones (2) and α-phenylsuccinimides (3) showed that the presence of an asymmetric center at the 3-position often enhanced anticonvulsant activity. The present study was undertaken to determine if the introduction of an asymmetric center at the 4- or 5-position of the 3,3-diphenyl-2-pyrrolidone (III) system would have a similar beneficial effect. Accordingly, (±)-1,4-dimethyl-3,3-diphenyl-2-pyrrolidone (Va) and (±)-1,5-dimethyl-3,3-diphenyl-2-pyrrolidone (VIa) were synthesized and evaluated for anticonvulsant activity. The corresponding amidines, Vb and VIb, were also prepared to compare them with the neutral lactams. Moreover, the amidine functionality was expected to provide a handle for further structural modification as exemplified by the acyl derivatives, VIc and VId. The test compounds were prepared using modifications of previously reported (4–6) procedures.

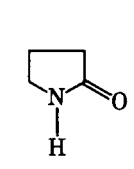

I

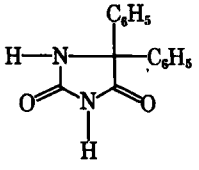

II

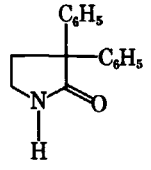

III

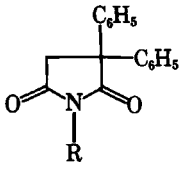

IVa: R = H
IVb: R = CH_3

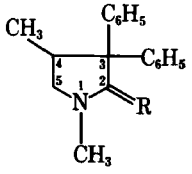

Va: R = O
Vb: R = NH

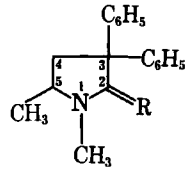

VIa: R = O
VIb: R = NH
VIc: R = $NCOCH_3$
VId: R = NCO_2CH_3

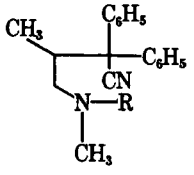

VIIa: R = CH_3
VIIb: R = CO_2CH_3

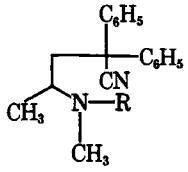

VIIIa: R = CH_3
VIIIb: R = CO_2CH_3

RESULTS AND DISCUSSION

Because of the interest in amidines Vb and VIb, the synthetic route (4–6) involving them as intermediates was preferred to other procedures (7, 8) for preparing (±)-1,4-dimethyl-3,3-diphenyl-2-pyrrolidone (Va) and (±)-1,5-dimethyl-3,3-diphenyl-2-pyrrolidone (VIa). The mono-*N*-demethylation of the *N*,*N*-dimethylaminonitriles VIIa and VIIIa was readily effected using excess methyl chloroformate. The subsequent conversion of carbamate VIIIb to VIb hydrochloride was carried out in refluxing hydrochloric acid. In contrast, carbamate VIIb failed to either dissolve or react in hydrochloric acid. Moreover, the compound was recovered essentially unchanged after 17 days of reflux in ethanol–hydrochloric acid (2:1). Ultimately, the transformation of VIIb to Vb was

[1] Metrazol.

0022-3549/83/0600-0700$01.00/0

(4) T. Nishihata, J. H. Rytting, and T. Higuchi, *ibid.*, **69**, 744 (1980).
(5) H. Yaginuma, T. Nakata, H. Toya, T. Murakami, M. Yamazaki, and A. Kamada, *Chem. Pharm. Bull.*, **29**, 2974 (1981).
(6) T. Nishihata, J. H. Rytting, T. Higuchi, and L. Caldwell, *J. Pharm. Pharmacol.*, **33**, 334 (1980).
(7) T. Nishihata, J. H. Rytting, and T. Higuchi, *J. Pharm. Sci.*, **70**, 71 (1981).

Synthesis and Anticonvulsant Screening of 3,3-Diphenyl-2-pyrrolidone Derivatives

GEORGE A. BRINE ˣ **and KARL G. BOLDT**

Received March 3, 1982, from the *Chemistry and Life Sciences Group, Research Triangle Institute, Research Triangle Park, NC 27709.* Accepted for publication June 7, 1982.

Abstract □ Six derivatives of 3,3-diphenyl-2-pyrrolidone were synthesized and screened for anticonvulsant activity. The synthetic route involved a mono-*N*-demethylation of an intermediate *N*,*N*-dimethylaminonitrile with methyl chloroformate followed by cleavage of the carbamate group. Of the six derivatives, (±)-2-imino-1,5-dimethyl-3,3-diphenylpyrrolidine hydrochloride was effective in protecting mice against maximal electroshock (MES) -induced seizures at a 30-mg/kg dose level.

Keyphrases □ Anticonvulsant screening—synthesis of 3,3-diphenyl-2-pyrrolidone derivatives, maximal electroshock-induced seizures, mice □ 3,3-Diphenyl-2-pyrrolidone—synthesis and anticonvulsant screening, derivatives, maximal electroshock-induced seizures, mice

The reported (1) anticonvulsant activity of 2-pyrrolidone (I), the lactam of γ-aminobutyric acid, stimulated interest in 2-pyrrolidone derivatives as potential anticonvulsants. As it incorporated several features of the anticonvulsant diphenylhydantoin (II), the 3,3-diphenyl-2-pyrrolidone (III) system seemed a promising one for the study. When tested in rats, 3,3-diphenyl-2-pyrrolidone (III) itself was less effective than (±)-3-ethyl-3-phenyl-2-pyrrolidone against both pentylenetetrazol[1] and electrically-induced convulsions (2). Somewhat earlier, it was observed (3) that the structurally related α,α-diphenylsuccinimide (IVa) and its *N*-methyl derivative (IVb) ranked first and eighth in a series of 39 succinimides in protecting mice against electrically induced convulsions.

The work on 3,3-disubstituted-2-pyrrolidones (2) and α-phenylsuccinimides (3) showed that the presence of an asymmetric center at the 3-position often enhanced anticonvulsant activity. The present study was undertaken to determine if the introduction of an asymmetric center at the 4- or 5-position of the 3,3-diphenyl-2-pyrrolidone (III) system would have a similar beneficial effect. Accordingly, (±)-1,4-dimethyl-3,3-diphenyl-2-pyrrolidone (Va) and (±)-1,5-dimethyl-3,3-diphenyl-2-pyrrolidone (VIa) were synthesized and evaluated for anticonvulsant activity. The corresponding amidines, Vb and VIb, were also prepared to compare them with the neutral lactams. Moreover, the amidine functionality was expected to provide a handle for further structural modification as exemplified by the acyl derivatives, VIc and VId. The test compounds were prepared using modifications of previously reported (4–6) procedures.

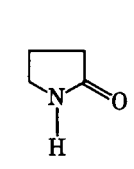

I

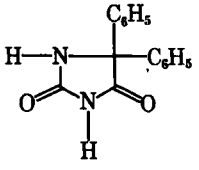

II

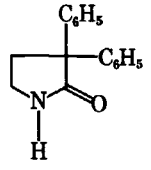

III

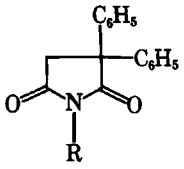

IVa: R = H
IVb: R = CH_3

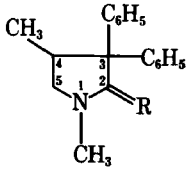

Va: R = O
Vb: R = NH

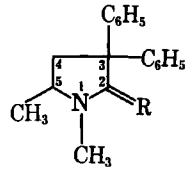

VIa: R = O
VIb: R = NH
VIc: R = $NCOCH_3$
VId: R = NCO_2CH_3

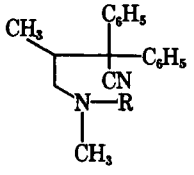

VIIa: R = CH_3
VIIb: R = CO_2CH_3

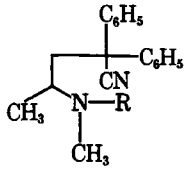

VIIIa: R = CH_3
VIIIb: R = CO_2CH_3

RESULTS AND DISCUSSION

Because of the interest in amidines Vb and VIb, the synthetic route (4–6) involving them as intermediates was preferred to other procedures (7, 8) for preparing (±)-1,4-dimethyl-3,3-diphenyl-2-pyrrolidone (Va) and (±)-1,5-dimethyl-3,3-diphenyl-2-pyrrolidone (VIa). The mono-*N*-demethylation of the *N*,*N*-dimethylaminonitriles VIIa and VIIIa was readily effected using excess methyl chloroformate. The subsequent conversion of carbamate VIIIb to VIb hydrochloride was carried out in refluxing hydrochloric acid. In contrast, carbamate VIIb failed to either dissolve or react in hydrochloric acid. Moreover, the compound was recovered essentially unchanged after 17 days of reflux in ethanol–hydrochloric acid (2:1). Ultimately, the transformation of VIIb to Vb was

[1] Metrazol.

0022-3549/83/0600-0700$01.00/0

achieved using hydrogen bromide in glacial acetic acid. In addition, the nitrous acid reaction (4) was found to require a large excess of reagent added in portions in order to effect complete conversion of starting material to product. Throughout the synthesis, the geometric isomers were easily distinguished from each other by the ^{1}H-NMR chemical shifts of the various methyl groups.

The lactams Va and VIa were inactive in all tests at all dose levels. In contrast, amidine VIb was effective in protecting mice against maximal electroshock (MES)-induced seizures at a 30-mg/kg dose level, although it afforded no protection at lower dose levels (3, 10, and 20 mg/kg). Amidine Vb was inactive in all tests at 30 mg/kg. Both Vb and VIb were too toxic to be administered at dose levels >30 mg/kg. Of the acyl compounds derived from VIb, the carbomethoxyimino derivative VId was inactive at all dose levels. The acetimido derivative VIc, on the other hand, appeared to exacerbate the effects of MES and subcutaneous pentylenetetrazol treatment, thereby causing death. Furthermore, at dose levels of 300 and 600 mg/kg, compound VIc caused death through CNS depression.

Since the presence of an *N*-methyl group was shown to decrease the effectiveness of α-phenylsuccinimides against electrically induced convulsions (3), it was reasonable that *N*-demethylation of VIb might yield a compound with improved activity in the MES screen. However, compounds VIb and VIa were both unaffected by refluxing with 47% hydriodic acid. Treatment of compound VIc with excess methyl chloroformate also failed to effect an *N*-demethylation. Moreover, two attempts to further functionalize lactam VIa by nitration of an aromatic ring were unsuccessful.

In summary, the combination of *N*-methylation and the generation of an asymmetric center by introduction of a methyl group at the 4- or 5-position of the 3,3-diphenyl-2-pyrrolidone (III) system had no apparent beneficial effect on anticonvulsant activity. Although the amidine VIb was active in the MES screen at a low dose level, this activity was offset by the neurotoxicity of the compound at higher dose levels. Finally, the preparation of simple acyl derivatives failed to improve the activity, and the chemical inertness of the system made further structural modifications difficult.

EXPERIMENTAL[2]

(±)-4-Dimethylamino-2,2-diphenyl-3-methylbutyronitrile (VIIa) and (±)-4-Dimethylamino-2,2-diphenylvaleronitrile (VIIIa)—The isomeric nitriles were prepared by condensation of diphenylacetonitrile and 2-chloro-1-dimethylaminopropane in the presence of potassium *tert*-butoxide (7). The less soluble valeronitrile (VIIIa) was obtained in isomerically pure form by hexane trituration followed by recrystallization from absolute ethanol. Vacuum distillation of the hexane-soluble fraction afforded a 7:3 mixture of VIIa–VIIIa; bp 131–137° (0.15–0.20 mm). The total yield of nitriles was 58%.

(±) -4- (*N* - Carbomethoxy -*N*- methylamino)-2,2-diphenyl-3-butyronitrile (VIIb)—The 7:3 nitrile mixture (36 g, 0.13 mole), sodium bicarbonate (126 g, 1.5 moles), and methyl chloroformate (208 g, 2.2 moles) were refluxed for 26 hr in chloroform (1.4 liters). The reaction mixture was filtered and the filtrate washed with 3 *N* hydrochloric acid, 5% sodium bicarbonate, and water. Evaporation of the organic layer afforded a 7:3 mixture of VIIb–VIIIb (^{1}H-NMR analysis). Ether trituration removed the more soluble valeronitrile carbonate, VIIIb. Recrystallization of the residual solid from ethyl acetate–petroleum ether gave 19 g (45%) of VIIb as a white solid; mp 145–147°; IR 1697 cm^{-1} (C=O); ^{1}H-NMR δ 1.04 (d, 3, CHCH_3), 2.88 (s, 3, NCH_3), 3.70 ppm (s, 3, OCH_3). There was no detectable amount of the isomeric carbamate by ^{1}H-NMR.

(±) -4- (*N* - Carbomethoxy -*N*- methylamino)-2,2-diphenylvaleronitrile (VIIIb)—A mixture of VIIIa (5.0 g, 0.018 mole), sodium bicarbonate (10.0 g, 0.12 mole), and methyl chloroformate (36 g, 0.38 mole) in chloroform (260 ml) was refluxed for 48 hr with half of the methyl chloroformate being added after 24 hr. Workup as described above afforded 5.8 g (100%) of VIIIb as viscous oil; IR 1695 cm^{-1} (C=O); ^{1}H-NMR δ 1.16 (d, 3, CHCH_3), 2.28 (s, 3, NCH_3), 3.53 ppm (s, 3, OCH_3).

(±)-2-Imino-1,4-dimethyl-3,3-diphenylpyrrolidine (Vb) Hydrochloride—Hydrogen bromide gas was bubbled through a solution of VIIb (7.0 g, 0.022 mole) in glacial acetic acid (250 ml) for 30 min. The resultant mixture was stirred at room temperature for 4 days. Then it was diluted with water, basified with concentrated ammonium hydroxide, and extracted with methylene chloride. The residue obtained from evaporation of the organic extracts was partitioned between ether and 6 *N* hydrochloric acid. The resultant aqueous layer was extracted with chloroform and the extracts evaporated to obtain 5.8 g of crude product as a white foam. Crystallization from methanol–ethyl acetate gave 1.8 g (28%) of Vb hydrochloride as a white solid; mp 241–245° (hot stage) after *in vacuo* drying at 100° overnight [lit (4): mp 239°]; IR 3420, 1690 (C=N) cm^{-1}; ^{1}H-NMR δ 0.87 (d, 3, CHCH_3), 3.67 ppm (s, 3, NCH_3).

Anal.—Calc. for $C_{18}H_{21}ClN_2 \cdot \frac{1}{2} H_2O$: C, 69.75; H, 7.16; N, 9.04. Found: C, 69.69; H, 7.15; N, 8.98.

A subsequent preparation yielded material that had mp 239.5–242° (hot stage) and analyzed for $C_{18}H_{21}ClN_2 \cdot \frac{3}{4} H_2O$. Attempts to prepare Vb hydrochloride by refluxing VIIb in concentrated hydrochloric acid or in ethanol saturated with hydrogen chloride gas were unsuccessful.

(±)-1,4-Dimethyl-3,3-diphenyl-2-pyrrolidone (Va)—Compound Vb (1.5 g, 0.005 mole) was converted to Va using excess nitrous acid (4). Recrystallization of the crude product from 95% ethanol afforded 0.86 g (65%) of Va as clear crystals; mp 122–122.5° [lit. (8): mp 122–123°]; IR 1689 cm^{-1} (C=O); ^{1}H-NMR δ 0.80 (d, 3, CHCH_3), 2.98 ppm (s, 3, NCH_3).

(±)-2-Imino-1,5-dimethyl-3,3-diphenylpyrrolidine (VIb) Hydrochloride—A solution of VIIIb (5.8 g, 0.018 mole) in concentrated hydrochloric acid (150 ml) was refluxed for 43.5 hr under nitrogen. The mixture was cooled, diluted with water (300 ml), and extracted with chloroform. Evaporation of the organic extracts afforded the crude product as a white foam. Crystallization from 2-propanol–ether gave 4.6 g (85%) of VIb hydrochloride as a white solid; mp 281–283° [lit. (5): mp 279–281°]; IR 3420, 1690 (C=N) cm^{-1}; ^{1}H-NMR δ 1.30 (d, 3, CHCH_3), 3.45 ppm (s, 3, NCH_3).

(±)-1,5-Dimethyl-3,3-diphenyl-2-pyrrolidone (VIa)—Compound VIb (4.2 g, 0.015 mole) was converted to VIa using excess nitrous acid (4). Recrystallization from ethanol afforded 2.7 g (73%) of VIa as a white solid; mp 121–123° [lit. (8): mp 121–122°]; IR 1682 cm^{-1} (C=O); ^{1}H-NMR δ 1.25 (d, 3, CHCH_3), 2.88 ppm (s, 3, NCH_3).

(±)-2-Acetimido-1,5-dimethyl-3,3-diphenylpyrrolidine (VIc)—A solution of VIb hydrochloride (3.0 g, 0.01 mole) in pyridine (30 ml) and acetic anhydride (3 ml) was stirred at room temperature overnight. The solvents were removed *in vacuo* and the residue dissolved in chloroform. After washing with water, 10% sodium hydroxide, and saturated sodium chloride, the chloroform layer was evaporated to give an off-white solid. Recrystallization from cyclohexane–ethyl acetate provided 2.3 g (75%) of VIc as a white solid; mp 127–128° [lit. (4): mp 126.5–127.5°]; IR 1630, 1600 (sh) cm^{-1}; ^{1}H-NMR δ 1.27 (d, 3H, CHCH_3), 1.67 (s, 3H, COCH_3), 2.88 ppm (s, 3H, NCH_3).

Anal.—Calc. for $C_{20}H_{22}N_2O$: C, 78.40; H, 7.24; N, 9.14. Found: C, 78.37; H, 7.29; N, 9.08.

(±)-2-Carbomethoxyimino-1,5-dimethyl-3,3-diphenylpyrrolidine (VId)—A mixture of VIb (5.7 g, 0.022 mole), sodium bicarbonate (20 g, 0.24 mole), and methyl chloroformate (12 g, 0.13 mole) in chloroform was refluxed for 24 hr. The reaction mixture was filtered and the filtrate washed with 10% hydrochloric acid and saturated sodium chloride. Evaporation of the organic layer afforded a white solid which was recrystallized from ethyl acetate–petroleum ether to give 5.0 g (71%) of VId as a white solid; mp 166–167°; IR 1690, 1630 cm^{-1}; ^{1}H-NMR δ 1.22 (d, 3, CHCH_3); 2.88 (s, 3, NCH_3), 3.10 (s, 3, OCH_3).

Anal.—Calc. for $C_{20}H_{22}H_2O_2$: C, 74.51; H, 6.88; N, 8.69. Found: C, 74.46; H, 6.89; N, 8.67.

Screening Procedures—The test compounds underwent an anticonvulsant screening[3]. The compounds were screened at 30, 100, 300, and 600-mg/kg dose levels in adult male CF 1 mice (intraperitoneal injection). Compounds Vb hydrochloride and VIb hydrochloride were administered in 0.9% saline solution, other test compounds as suspensions in 30% aqueous polyethylene glycol 400. Each compound was screened in an MES test, a subcutaneous pentylenetetrazol seizure threshold test, and a rotorod test for neurotoxicity. Screening procedures, protocols, and data interpretation have been published (9).

REFERENCES

(1) J. E. Hawkins, Jr. and L. H. Sarett, *Clin. Chim. Acta*, **2**, 481 (1957).

(2) F. J. Marshall, *J. Org. Chem.*, **23**, 503 (1958).

[2] Melting points were determined on either a Thomas-Hoover capillary tube apparatus or a Kofler hot stage apparatus and are uncorrected. IR spectra were obtained in methylene chloride solution on a Perkin-Elmer 467 spectrophotometer. ^{1}H-NMR spectra were obtained in deuteriochloroform solution on a Varian HA-100 spectrometer. Chemical shifts are reported in parts per million downfield from tetramethylsilane. Analyses were performed by Micro-Tech Laboratories, Inc., Skokie, Ill. Organic extracts and solutions were routinely dried over sodium sulfate prior to evaporation.

[3] Epilepsy Branch, NINCDS, National Institutes of Health.

(3) C. A. Miller and L. M. Long, *J. Am. Chem. Soc.*, **73**, 4895 (1955).
(4) W. Wilson, *J. Chem. Soc.*, **1952**, 3524.
(5) J. Cymerman and W. S. Gilbert, *ibid.*, **1952**, 3529.
(6) N. J. Harper, D. Jones, and A. B. Simmonds, *ibid.*, (*C*), **1966**, 438.
(7) E. M. Schultz, C. M. Robb, and J. M. Sprague, *J. Am. Chem. Soc.*, **69**, 2454 (1947).
(8) J. H. Gardner, N. R. Easton, and J. R. Stevens, *ibid.*, **70**, 2906 (1948).
(9) R. L. Krall, J. K. Penry, B. G. White, H. L. Kupferberg, and E. A. Swinyard, *Epilepsia*, **19**, 400 (1978).

ACKNOWLEDGMENTS

The assistance of the Epilepsy Branch, National Institute of Neurological and Communicative Disorders and Stroke, National Institutes of Health, is gratefully acknowledged.

Synthesis of Deuterium-Labeled Prochlorperazine

EDWARD M. HAWES, TREVOR S. GURNSEY, H. UMESHA SHETTY, and KAMAL K. MIDHA ˣ

Received February 18, 1982, from the *College of Pharmacy, University of Saskatchewan, Saskatoon, Saskatchewan, Canada, S7N OWO.* Accepted for publication June 8, 1982.

Abstract □ The propylpiperazine side chain of prochlorperazine was labeled with two, four, or six deuterium atoms by lithium aluminum deuteride reduction of the appropriate amide. The isotopic purity of the products after correcting for chlorine isotopes was >95.7%.

Keyphrases □ Prochlorperazine—deuterium-labeled synthesis □ Deuterium label—prochlorperazine synthesis

Prochlorperazine (V*a*), a piperazine-type phenothiazine, is primarily used as an antiemetic or antipsychotic. There are no literature reports that describe the usual plasma levels of this drug in patients under treatment, and, in fact, no suitable analytical methods have been described. The development of suitable analytical methods for the determination of the plasma concentrations of all piperazine-type phenothiazines has been slow, due to their instability in all stages of sample handling, as well as the extremely low plasma levels observed in the few studies involving humans.

BACKGROUND

The analytical procedures which have met the stringent sensitivity requirements of subnanogram determinations of these piperazine-type phenothiazines are either radioimmunoassay (RIA) or GLC–MS procedures (1, 2). In the case of prochlorperazine, an RIA method, which is capable of quantitating 0.125 ng/ml using 200-μl plasma aliquots, has been developed recently[1]. Following single 5-mg oral doses of prochlorperazine mesylate in healthy volunteers, the peak plasma concentrations were determined by RIA to be between 1–2 ng/ml. To verify the specificity of this sensitive biological procedure, a specific and sensitive chemical method such as GLC–MS is required. A stable isotope analogue of prochlorperazine was needed as a true internal standard for obtaining the required sensitivity by the chemical procedure. In addition, the availability of two other deuterium-labeled prochlorperazine standards will allow reliable pharmacokinetic studies to be carried out with fewer volunteers and animals, by administering these analogues by one or two routes and analyzing the plasma concentrations by GLC–MS using selected ion monitoring. Such studies will allow definitive pharmacokinetics of prochlorperazine to be obtained with far fewer administrations in volunteers.

The propylpiperazine side chain was chosen as the most suitable labeling site, since normally only the *N*-methyl group is lost during metabolism. It also offers adequate variation in the number of labeled atoms. Recently, the synthesis of labeled trifluoperazine, the 2-trifluoromethyl analogue of prochlorperazine, with two, four, or six deuterium atoms in the propylpiperazine side chain was successfully achieved (3). Similarly, this paper describes the synthesis of prochlorperazine with two, four, or six deuterium atoms.

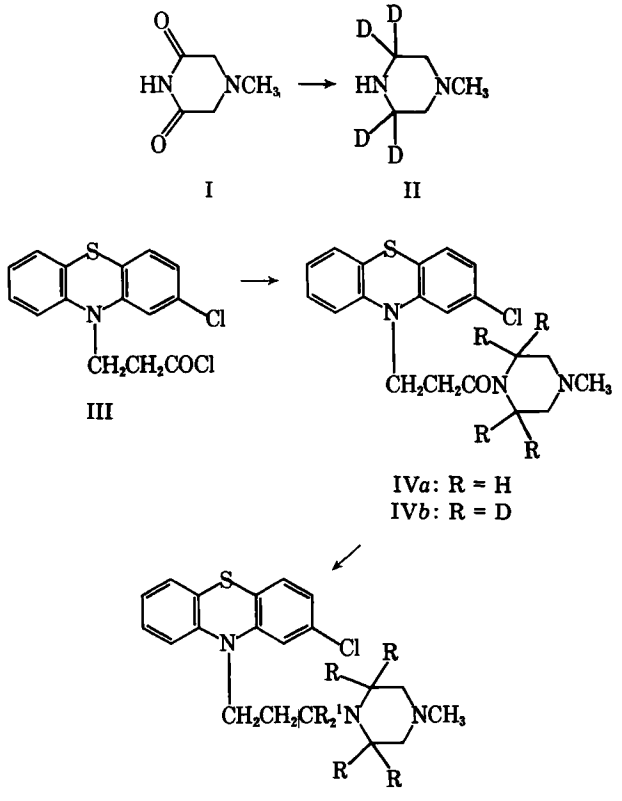

Scheme I

RESULTS AND DISCUSSION

The synthesis (Scheme I) of the key tetradeuterated intermediate, 1-methyl(3,3,5,5-$^2H_4$)piperazine (II), from the lithium aluminum deuteride reduction of 1-methyl-3,5-piperazinedione (I) was previously described (3). Subsequent treatment of the unlabeled or labeled *N*-methylpiperazine in dry benzene with 3-[10-(2-chlorophenothiazinyl)]-

[1] K. K. Midha, E. M. Hawes, G. Rauw, J. McVittie, G. McKay, J. K. Cooper, and H. U. Shetty, unpublished work.

0022-3549/83/0600-0702$01.00/0

(3) C. A. Miller and L. M. Long, *J. Am. Chem. Soc.*, **73**, 4895 (1955).
(4) W. Wilson, *J. Chem. Soc.*, **1952**, 3524.
(5) J. Cymerman and W. S. Gilbert, *ibid.*, **1952**, 3529.
(6) N. J. Harper, D. Jones, and A. B. Simmonds, *ibid.*, (*C*), **1966**, 438.
(7) E. M. Schultz, C. M. Robb, and J. M. Sprague, *J. Am. Chem. Soc.*, **69**, 2454 (1947).
(8) J. H. Gardner, N. R. Easton, and J. R. Stevens, *ibid.*, **70**, 2906 (1948).
(9) R. L. Krall, J. K. Penry, B. G. White, H. L. Kupferberg, and E. A. Swinyard, *Epilepsia*, **19**, 400 (1978).

ACKNOWLEDGMENTS

The assistance of the Epilepsy Branch, National Institute of Neurological and Communicative Disorders and Stroke, National Institutes of Health, is gratefully acknowledged.

Synthesis of Deuterium-Labeled Prochlorperazine

EDWARD M. HAWES, TREVOR S. GURNSEY, H. UMESHA SHETTY, and KAMAL K. MIDHA ˣ

Received February 18, 1982, from the *College of Pharmacy, University of Saskatchewan, Saskatoon, Saskatchewan, Canada, S7N OWO.* Accepted for publication June 8, 1982.

Abstract □ The propylpiperazine side chain of prochlorperazine was labeled with two, four, or six deuterium atoms by lithium aluminum deuteride reduction of the appropriate amide. The isotopic purity of the products after correcting for chlorine isotopes was >95.7%.

Keyphrases □ Prochlorperazine—deuterium-labeled synthesis □ Deuterium label—prochlorperazine synthesis

Prochlorperazine (V*a*), a piperazine-type phenothiazine, is primarily used as an antiemetic or antipsychotic. There are no literature reports that describe the usual plasma levels of this drug in patients under treatment, and, in fact, no suitable analytical methods have been described. The development of suitable analytical methods for the determination of the plasma concentrations of all piperazine-type phenothiazines has been slow, due to their instability in all stages of sample handling, as well as the extremely low plasma levels observed in the few studies involving humans.

BACKGROUND

The analytical procedures which have met the stringent sensitivity requirements of subnanogram determinations of these piperazine-type phenothiazines are either radioimmunoassay (RIA) or GLC–MS procedures (1, 2). In the case of prochlorperazine, an RIA method, which is capable of quantitating 0.125 ng/ml using 200-μl plasma aliquots, has been developed recently[1]. Following single 5-mg oral doses of prochlorperazine mesylate in healthy volunteers, the peak plasma concentrations were determined by RIA to be between 1–2 ng/ml. To verify the specificity of this sensitive biological procedure, a specific and sensitive chemical method such as GLC–MS is required. A stable isotope analogue of prochlorperazine was needed as a true internal standard for obtaining the required sensitivity by the chemical procedure. In addition, the availability of two other deuterium-labeled prochlorperazine standards will allow reliable pharmacokinetic studies to be carried out with fewer volunteers and animals, by administering these analogues by one or two routes and analyzing the plasma concentrations by GLC–MS using selected ion monitoring. Such studies will allow definitive pharmacokinetics of prochlorperazine to be obtained with far fewer administrations in volunteers.

The propylpiperazine side chain was chosen as the most suitable labeling site, since normally only the *N*-methyl group is lost during metabolism. It also offers adequate variation in the number of labeled atoms. Recently, the synthesis of labeled trifluoperazine, the 2-trifluoromethyl analogue of prochlorperazine, with two, four, or six deuterium atoms in the propylpiperazine side chain was successfully achieved (3). Similarly, this paper describes the synthesis of prochlorperazine with two, four, or six deuterium atoms.

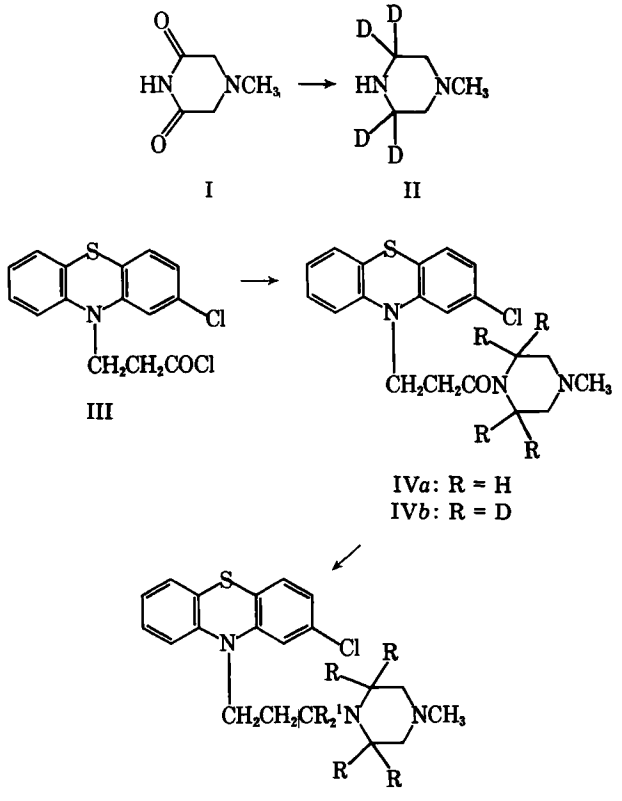

Scheme I

RESULTS AND DISCUSSION

The synthesis (Scheme I) of the key tetradeuterated intermediate, 1-methyl(3,3,5,5-$^2H_4$)piperazine (II), from the lithium aluminum deuteride reduction of 1-methyl-3,5-piperazinedione (I) was previously described (3). Subsequent treatment of the unlabeled or labeled *N*-methylpiperazine in dry benzene with 3-[10-(2-chlorophenothiazinyl)]-

[1] K. K. Midha, E. M. Hawes, G. Rauw, J. McVittie, G. McKay, J. K. Cooper, and H. U. Shetty, unpublished work.

0022-3549/83/0600-0702$01.00/0

propionyl chloride (III) gave the desired amides (IVa and b). In the case of the labeled *N*-methylpiperazine, the free base could not be obtained in a dry condition, necessitating the use of the hydrochloride in this reaction accompanied by the addition of sodium carbonate. This choice of route, involving an amide intermediate, allowed for the possibility of introducing two additional deuterium atoms. Reduction of the amides with lithium aluminum hydride or deuteride gave the desired prochlorperazine (V) with two, four, or six deuterium atoms in ~55% yield. The isotopic purity of the labeled, purified products was determined by MS spectrometry using a single-ion monitoring technique. The ratio for the molecular ions (^{35}Cl) $^2H_0/^2H_n$ was determined to be 0.43, 0.78, and 0.30% for the di-(n = 2), tetra-(n = 4), and hexa-(n = 6)deuterated prochlorperazine, respectively. The isotopic purities (after correcting for chlorine isotopes) for $^2H_2$, $^2H_4$, and $^2H_6$ were 98.11, 95.77, and 96.16%, respectively. The $^2H_1$ contaminant in the $^2H_2$ isomer was 1.89%, $^2H_2$ and $^2H_3$ contaminants collectively represented 4.23% in $^2H_4$, and $^2H_5$ contaminant in the $^2H_6$ isomer was 3.84%. It is evident that this purity is sufficient for use in GLC–MS and pharmacokinetic studies. These results will be reported elsewhere.

EXPERIMENTAL[2]

2-Chloro-10*H*-phenothiazine-10-propionyl Chloride (III)—A solution of phosphorus pentachloride (1.66 g, 8 mmoles) in 10 ml of dry benzene was added with stirring over 1.5 hr to a stirred suspension of 2-chloro-10-(2-carboxyethyl)-10*H*-phenothiazine (2.14 g, 7 mmoles) (4) in 25 ml of dry benzene at 5°. The reaction was allowed to proceed for 1 hr at room temperature during which time the pink mixture became colorless. Removal of the solvent *in vacuo* at 30° gave an oily residue which, on treatment with petroleum ether (40–60°), gave the acid chloride (III) in a 90% yield, mp 115–116° [lit. (4) mp 114–116°]. The product was unstable at room temperature and was immediately used in the next stage of the synthesis.

2 - Chloro - 10 - [[3-[4-methyl-1-(2,2,6,6-$^2H_4$)piperazinyl]-3-oxopropyl]]-10*H*-phenothiazine (IV*b*)—A mixture of 1-methyl(3,3,5,5-$^2H_4$)piperazine dihydrochloride (II) (3) (0.78 g, 4.4 mmoles) sodium carbonate (1.0 g), and dry benzene (20 ml) was refluxed until the evolution of carbon dioxide ceased. The mixture was then cooled to 0° and a solution of the acid chloride (III) (1.3 g, 4 mmoles) in 10 ml of dry benzene was added with stirring. When the addition was complete, the cooling bath was removed, and the mixture was allowed to warm to room temperature with continued stirring. After 3 hr, water (10 ml) was added, and vigorous stirring continued for 15 min. The organic layer was separated and washed successively with 10% aqueous sodium hydroxide (3 × 5 ml) and water (10 ml). The benzene layer was dried ($MgSO_4$) and evaporated to leave a yellow oil, which was purified by elution from a neutral alumina oxide column using benzene to give IV*b* as a colorless viscous oil in an 80% yield. TLC: R_f 0.44 (benzene–methanol, 95:5); IR (film) 1640 (C=O) cm^{-1}; NMR ($CDCl_3$): δ 2.34 (m, 7H, piperazine-3,5-methylene and NCH_3), 2.85 (t, 2H, CH_2CO, J = 7 Hz), 4.23 (t, 2H, phenothiazine-CH_2, J = 7 Hz), and 6.8–7.4 (m, 7H, aromatic); MS: m/z 391(M^+, 100%), 248(31), 246(83), 234(33), 232(78), 214(27), and 159(77).

[2] *Melting points* were determined with a Gallenkamp melting point apparatus and are uncorrected. All TLCs were performed using Eastman Chromatogram sheets, type 13254 (silica gel with fluorescent indicator); spots were observed under shortwave UV light. IR spectra were taken on a Perkin-Elmer 297 spectrophotometer. NMR spectra were determined on a Varian T-60 instrument with tetramethylsilane as internal reference. Low resolution electron impact mass spectra were recorded on a VG Micromass MM16F instrument at 70 eV. Lithium aluminum deuteride (>99% deuterium) was obtained from Merck Sharp and Dohme, Dorval, Quebec and all other chemicals from Aldrich Chemical Co., Montreal, Quebec.

2-Chloro-10-[3-(4-methyl-1-piperazinyl)(3,3-$^2H_2$)propyl]-10*H*-phenothiazine Dihydrochloride (V*b*)—A solution of 2-chloro-10-[3-(4-methyl-1-piperazinyl)-3-oxopropyl]-10*H*-phenothiazine (IV*a*) (0.39 g, 1 mmole), a previously reported (5) compound prepared in a manner similar to IV*b*, in 5 ml of dry ether was added dropwise over 1 hr to a stirred suspension of lithium aluminum deuteride (0.042 g, 1 mmole) in 5 ml of dry ether at 0°. The mixture was stirred for an additional 15 min, and after treatment with water (0.5 ml) and 20% aqueous sodium hydroxide (1 ml) the ether layer was decanted off. The inorganic material was mixed with sodium chloride (0.25 g), placed in the thimble of a Soxhlet apparatus, and extracted for 3 hr with ether. The combined ether fractions were extracted with 10% HCl (4 × 5 ml). The combined aqueous extracts were then washed with ether (3 × 5 ml) and the pH adjusted to 8.0 with saturated sodium carbonate solution. The product was then extracted with ether (4 × 10 ml), and the combined ether extracts dried ($MgSO_4$) and filtered. Dry hydrogen chloride in ether was added to the filtrate and the separated solid crystallized from ethanol to afford ($^2H_2$)-prochlorperazine (V*b*) as the dihydrochloride salt (0.25 g, 55%), mp 242–243°. Mixed melting points with the authentic nondeuterated samples (V*a*), prepared by the same route with lithium aluminum hydride or prepared from a commercial sample of prochlorperazine free base, were not depressed. TLC: R_f 0.55 (methanol–water–ammonium acetate, 100:20:3); NMR (free base, $CDCl_3$): δ 1.85 (t, 2H, CH_2CD_2, J = 6.5 Hz), 2.24 (s, 3H, NCH_3), 2.40 (s, 8H, piperazine methylene), 3.84 (t, 2H, phenothiazine-CH_2, J = 6.5 Hz), and 6.72–7.20 (m, 7H, aromatic); MS: m/z 375(M^+, 47%), 274(7), 246(8), 232(16), 143(33), and 115(100).

2-Chloro-10-[[3-[4-methyl-1-(2,2,6,6-$^2H_4$)piperazinyl]-propyl]]-10*H*-phenothiazine Dihydrochloride (V*c*)—($^2H_4$)-Prochlorperazine (V*c*) was prepared (55%) from IV*b* and lithium aluminum hydride using the method described above for V*b*: mp and TLC as for V*b*. NMR (free base, $CDCl_3$): δ 1.94 (m, 2H, propyl central CH_2), 2.30–2.66 (m, 9H, CH_2-piperazine, piperazine-3,5-methylene, and NCH_3), 3.88 (t, 2H, phenothiazine-CH_2, J = 6.5 Hz), and 6.60–7.18 (m, 7H, aromatic); MS: m/z 377(M^+, 69%), 273(14), 246(11), 232(13), 145(40), and 117(100).

2-Chloro-10-[[3-[4-methyl-1-(2,2,6,6-$^2H_4$)piperazinyl](3,3-$^2H_2$)propyl]]-10*H*-phenothiazine Dihydrochloride (V*d*)—($^2H_6$)-Prochlorperazine (V*d*) was prepared (55% yield) from IV*b* and lithium aluminum deuteride using the method described above for V*b*: mp and TLC as for V*b*. NMR (free base, $CDCl_3$): δ 1.85 (t, 2H, CH_2CD_2, J = 6.5 Hz), 2.20 (s, 3H, NCH_3), 2.37 (s, 4H, piperazine-3,5-methylene), 3.85 (t, 2H, phenothiazine-CH_2, J = 6.5 Hz), and 6.62–7.15 (m, 7H, aromatic); MS: m/z 379(M^+, 49%), 276(10), 274(10), 246(8), 232(14), 214(8), 147(48), and 119(100).

REFERENCES

(1) K. K. Midha, J. W. Hubbard, J. K. Cooper, E. M. Hawes, S. Fournier, and P. Yeung, *Br. J. Clin. Pharmacol.*, **12**, 189 (1981).

(2) K. K. Midha, R. M. H. Roscoe, K. Hall, E. M. Hawes, J. K. Cooper, G. McKay, and H. U. Shetty, *Biomed. Mass Spectrom.*, **9**, 186 (1982).

(3) H. U. Shetty, E. M. Hawes, and K. K. Midha, *J. Labeled Comp. Radiopharm.*, **18**, 1633 (1981).

(4) E. F. Godefroi and E. L. Wittle, *J. Org. Chem.*, **21**, 1163 (1956).

(5) E. L. Anderson, *et al.*, *Arzneim.-Forsch.*, **12**, 937 (1962).

ACKNOWLEDGMENTS

The authors gratefully acknowledge the Medical Research Council of Canada (Grant MA-6767) for financial support for this research and thank Mr. K. Hall for the mass spectra.

Spectrophotometric Promethazine Hydrochloride Determination Using Bromcresol Green

ABDOL-ALI M. EMAMI KHOI

Received May 17, 1978, from the *Department of Pharmaceutical Chemistry, Faculty of Pharmacy, Tehran University, Tehran, Iran.* Accepted for publication October 30, 1978.

Abstract □ A spectrophotometric method was developed for determining promethazine hydrochloride (I) complexed with bromcresol green and then extracted with chloroform. The complex in chloroform showed maximum absorption at 415 nm and obeyed Beer's law over 1.2–8.5 μg/ml. The complex molar absorptivity was 1.93×10^4 *M*. Complex formation and extraction were complete and quantitative over pH 2.7–2.8. The promethazine hydrochloride–bromcresol green molar ratio was 1:1. Excipients, coloring matter, flavoring agents, and other substances likely to be present in promethazine preparations did not interfere in the determination. Direct determination in tablet, syrup, and injection preparations were carried out satisfactorily.

Keyphrases □ Promethazine hydrochloride—spectrophotometric analysis, color complex with bromcresol green, various pharmaceutical formulations □ Bromcresol green—promethazine hydrochloride spectrophotometric analysis, various pharmaceutical formations □ Spectrophotometry—analysis, promethazine hydrochloride, various pharmaceutical formulations □ Antihistaminic agents—promethazine hydrochloride, spectrophotometric analysis, various pharmaceutical formulations

Various methods have been described for promethazine hydrochloride (I) determination. The official nonaqueous USP titration method (1) is not applicable to microgram I determinations. Volumetric (2), ion-exchange (3), chromatographic (4), polarographic (5), gravimetric (6), complexometric (7), and luminescence (8) methods all lack simplicity and sensitivity.

Spectrophotometric methods also have been used for the analysis of the base. Eriochrome black T (9), perchloric acid–nitromethane (10), sodium 1,2-naphthoquinone-4-sulfonate in 50% H_2SO_4 (11), and ferric chloride (12) were employed to create a colored product that could be determined spectrophotometrically. Some of these methods are not simple; others are not sensitive.

This report describes a direct, simple, and sensitive spectrophotometric determination for I. This method is applicable to powder, syrup, injection, and tablet forms. The procedure depends on complex formation between I and bromcresol green (II) which is extractable by chloroform at pH 2.7–2.8. This method can be carried out successfully in the presence of caffeine and many other substances.

Bromcresol green has been used for determining small amounts of long-chain tertiary alkylamines and quaternary ammonium salts (13). It was recently used for the direct determination of thebaine in *Papaver bracteatum* Lindl Arya II papulation capsules (14) and to determine diphenhydramine hydrochloride (15).

Table I—Effect of Other Compounds on the Determination of Promethazine Hydrochloride

Substance	Amount Ratio[a]	Recovery %[b]
Ascorbic acid	50	100.0
Sodium saccharin	250	100.9
Cinnamon oil	10	100.0
Orange oil	60	100.5
Clove oil	70	100.0
Amaranth	120	100.2

[a] The ratio of the amount of substances to promethazine hydrochloride in the determination. [b] Promethazine hydrochloride concentration = 3.2×10^{-4} *M*.

EXPERIMENTAL[1]

Apparatus and Reagents.—All glassware was washed with 0.1 *N* HCl followed by distilled water. All reagents were analytical grade.

Bromcresol Green (10^{-4} M)—Accurately weighed bromcresol green powder was dissolved in 2 ml of 0.1 *N* NaOH, and the volume was brought to 1 liter with citric acid-sodium hydrogen phosphate buffer, pH 2.7–2.8. The resulting solution was adjusted to pH 2.7–2.8.

Promethazine Hydrochloride (10^{-4} M) *Standard*—Accurately weighed, dry, pure promethazine hydrochloride powder USP (32.09 mg) was dissolved in water and diluted to 1 liter.

Buffer Solution—A citric acid–sodium hydrogen phosphate buffer (pH 2.2–2.8) was used (16).

Determination—A solution containing 12–80 μg of I was pipetted into a 100-ml separatory funnel followed by 20 ml of 10^{-4} *M* II, and the two solutions were mixed. The yellow complex that formed was extracted with 5-, 3-, and 2-ml portions of chloroform by vigorous shaking. The extracts were collected in a 10-ml volumetric flask. The volume was adjusted with chloroform, and the absorbance was measured within 0.5 hr against chloroform at 415 nm. The amount of I was calculated by comparison with a standard curve.

RESULTS AND DISCUSSION

The yellow I–II complex in chloroform showed maximum absorption at 415 nm. Complex formation and extraction were complete and quantitative over the pH 2.7–2.8 range citric acid-sodium hydrogen phosphate buffer solution. The complex composition was studied by the molar ratio method (17). The ratio of I to II was 1:1, but the required ratio for complete complexation and quantitative extraction was 1:3.

Eight standard series of six samples, 1.0–9.0 μg I/ml, were analyzed. The optimum concentration range for the measurements at 415 nm and 1.00-cm optical path length was 1.2–8.5 μg of promethazine hydrochloride/ml. The complex solution molar absorptivity in chloroform at 415 nm was 1.93×10^4. The relative standard deviation of the calculated absorptivities in the optimum concentration range was ±1%.

To determine the effect of compounds commonly present with I in pharmaceutical preparations, known volumes of standard solutions containing caffeine (23 mg), sodium gentisate (20 mg), ammonium chloride (20 mg), menthol (90 mg), sodium citrate (20 mg), acetaminophen (200 mg), and alcohol (1 ml) were studied at different concentrations. There was no interference in the determinations. Ascorbic acid, sodium saccharin, cinnamon oil, orange oil, clove oil, and amaranth (Table I) also did not interfere and produced slight deviation in the determination only at high concentrations.

Under acid conditions, most substances with a tertiary amine group or quaternary ammonium salts form yellow complexes with II that are extractable with chloroform. Pharmaceutical I preparation from different manufacturers were free of such substances, so a confirmatory test was not needed.

To test the method validity, I was added to pharmaceutical preparations[2] and determined by the proposed procedure. The recovery (99–100.25%) (Table II) proved the selectivity and specificity of the method for direct I determination in pharmaceutical preparations.

[1] A Beckman DB-GT spectrophotometer with 1.00-cm glass cells, a Bausch & Lomb Spectronic 21, and a Beckman H_3 pH meter were used.

[2] Phenergan tablets, syrup, and injection, France.

0022-3549/83/0600-0704$01.00/0

Table II—Determination and Recovery of Promethazine Hydrochloride (Micrograms) in Pharmaceutical Preparations

Preparation	Present	Added	Determined	Recovery, %
Tablet	37.97	41.76	41.30	99.00
Syrup	30.00	23.64	23.70	100.25
Injection	35.00	32.65	32.70	100.15

ACKNOWLEDGMENT

The author thanks Mr. Rostam H. Maghssoudi for support and encouragement in the preparation of this manuscript.

REFERENCES

(1) "The United States Pharmacopeia," 19th rev. U.S. Pharmacopeial Convention, Rockville, Md., 1975, p. 412.

(2) Z. Kurzawa, L. Balcerkiewicz, and A. Kryzminska, *Chem. Anal. (Warsaw)*, **1974**, 333.

(3) J. Jarzebinski, Z. Zakrezewski, and M. J. Szatynska, *Farm. Pol.* **9**, 335 (1973).

(4) S. Ebel, B. Dobmeier, M. Fick, H. Kussmaul, *Arch. Pharm. (Weinheim, Germany)*, **307**, 878 (1974).

(5) E. Pungor, K. Toth, and M. Papay, *Chem. Anal. (Warsaw)*, **17**, 947 (1972).

(6) J. Blazek and M. Travnickova, *Cesk. Farm.*, **22**, 207 (1973).

(7) B. Dembinski and K. Nowakowski, *Farm. Pol.*, **30**, 423 (1974).

(8) N. Kosta and S. Leposava, *Tehnika (Belgrade)*, **22**, 693 (1967).

(9) F. Pellerin, J. A. Gautier, O. Barat, and D. Demay, *Chim. Anal. (Paris)*, **45**, 395 (1963).

(10) L. G. Chatten and F. D. Semaka, *Can. J. Pharm. Sci.*, **5**, 4 (1970).

(11) H. T. Fawzy, I. A. Saad, and L. N. Gadel-Rub, *Pharmazie*, **28**, 322 (1973).

(12) M. K. Youssef and I. A. Attia, *Indian J. Pharm.*, **37**, 121 (1975).

(13) H. M. N. H. Irving and J. J. Markham, *Anal. Chim. Acta*, **39**, 7 (1967).

(14) R. H. Maghssoudi and A. B. Fawzi, *J. Pharm. Sci.*, **67**, 32 (1978).

(15) R. H. Maghssoudi, A. B. Fawzi, and M. A. N. Moosavi Meerkalaie, *J. Assoc. Off. Anal. Chem.*, **60**, 926 (1977).

(16) A. I. Vogel, "A Text-Book of Macro and Semimicro Qualitative Inorganic Analysis," 4th ed., Longmans, London, England, 1964, p. 644.

(17) J. H. Yoe and A. L. Jones, *Ind. Eng. Chem. Anal. Ed.*, **16**, 111 (1944).

NMR Studies and GC Analysis of the Antibacterial Agent Taurolidine

B. I. KNIGHT *, G. G. SKELLERN *, G. A. SMAIL *, M. K. BROWNE ‡, and R. W. PFIRRMANN§ ˣ

Received December 9, 1981, from the **Department of Pharmacy, University of Strathclyde, Glasgow G1 1XW, U.K.*; ‡*Monklands District General Hospital, Airdrie ML6 0JS, U.K.*; and §*Geistlich-Pharma, 6110 Wolhusen, Switzerland.* Accepted for publication June 10, 1982.

Abstract □ The NMR spectrum of taurolidine in deuterium oxide was compared with spectra obtained from model experiments with amines and formaldehyde. Head-space analysis combined with capillary GC showed that there was <0.004% free formaldehyde present in 2% solutions of taurolidine. This value is comparable to the concentration of formaldehyde found when the taurolidine solutions were injected directly onto GC columns.

Keyphrases □ Taurolidine—NMR spectral analysis, head-space analysis–GC methods for the determination of formaldehyde □ NMR spectroscopy—analysis of taurolidine □ GC analysis—direct or combined with head-space analysis, quantitation of formaldehyde concentration in taurolidine □ Head-space analysis—with capillary GC, quantitation of formaldehyde concentration in taurolidine

Taurolidine [4,4′-methylenebis(tetrahydro-1,2,4-thiadiazine 1,1-dioxide), I] is a broad spectrum bactericide and antiendotoxin (1–3) which is being used widely in clinical trials to counteract bacterial infections following GI surgery and to treat peritonitis (4–6). It is administered intraperitoneally *via* a catheter inserted when the abdomen is closed, as a 2% aqueous solution[1] containing 5% povidone[2] (added to increase the solubility of taurolidine).

As a result of NMR studies (7) of aqueous solutions of taurolidine, equilibria are considered to exist between taurolidine, 4-hydroxymethyltetrahydro-2*H*-1,2,4-thiadiazine 1,1-dioxide (II), tetrahydro-2*H*-1,2,4-thiadiazine 1,1-dioxide (III)[3], and formaldehyde.

The existence of such equilibria was studied with the aid of solutions of morpholine–formaldehyde and III–formaldehyde as models. Also, because of the concern regarding toxicity, the determination of the formaldehyde concentration in solutions of taurolidine (which have been used in large volumes for the treatment of septicemia) is of considerable interest. Thus, this paper also describes the quantitative determination of formaldehyde using combined head-space analysis–capillary GC and direct GC.

EXPERIMENTAL

NMR—The NMR spectra of taurolidine were determined in deuterium oxide and deuterodimethylsulfoxide. Taurolidine (20 mg/ml) together with 1-vinyl-2-pyrrolidinone polymer (50 mg/ml) in deuterium oxide, and morpholine and III in deuterium oxide (before and after gaseous formaldehyde had been passed through the solution), were also determined[4]. The reference standard was sodium 3-trimethylsilylpropionate-2,2,3,3-$^2H_4$.

GC Analysis of Formaldehyde—*Head-Space Analysis*—Aqueous solutions (10 ml) of formaldehyde (0.005–0.01%) containing sodium chloride (5 g) were added to 100-ml injection vials which were tightly stoppered. The vials were incubated at 20, 40, or 60° for 1 hr to allow the

[1] Taurolin.
[2] Polyvinylpyrrolidone-17, mol. wt. 11,000, BASF (Germany).
[3] Taurultam.
[4] Perkin-Elmer R32 90-MHz NMR spectrometer.

0022-3549/83/0600-0705$01.00/0

Table II—Determination and Recovery of Promethazine Hydrochloride (Micrograms) in Pharmaceutical Preparations

Preparation	Present	Added	Determined	Recovery, %
Tablet	37.97	41.76	41.30	99.00
Syrup	30.00	23.64	23.70	100.25
Injection	35.00	32.65	32.70	100.15

ACKNOWLEDGMENT

The author thanks Mr. Rostam H. Maghssoudi for support and encouragement in the preparation of this manuscript.

REFERENCES

(1) "The United States Pharmacopeia," 19th rev. U.S. Pharmacopeial Convention, Rockville, Md., 1975, p. 412.

(2) Z. Kurzawa, L. Balcerkiewicz, and A. Kryzminska, *Chem. Anal. (Warsaw)*, **1974**, 333.

(3) J. Jarzebinski, Z. Zakrezewski, and M. J. Szatynska, *Farm. Pol.* **9**, 335 (1973).

(4) S. Ebel, B. Dobmeier, M. Fick, H. Kussmaul, *Arch. Pharm. (Weinheim, Germany)*, **307**, 878 (1974).

(5) E. Pungor, K. Toth, and M. Papay, *Chem. Anal. (Warsaw)*, **17**, 947 (1972).

(6) J. Blazek and M. Travnickova, *Cesk. Farm.*, **22**, 207 (1973).

(7) B. Dembinski and K. Nowakowski, *Farm. Pol.*, **30**, 423 (1974).

(8) N. Kosta and S. Leposava, *Tehnika (Belgrade)*, **22**, 693 (1967).

(9) F. Pellerin, J. A. Gautier, O. Barat, and D. Demay, *Chim. Anal. (Paris)*, **45**, 395 (1963).

(10) L. G. Chatten and F. D. Semaka, *Can. J. Pharm. Sci.*, **5**, 4 (1970).

(11) H. T. Fawzy, I. A. Saad, and L. N. Gadel-Rub, *Pharmazie*, **28**, 322 (1973).

(12) M. K. Youssef and I. A. Attia, *Indian J. Pharm.*, **37**, 121 (1975).

(13) H. M. N. H. Irving and J. J. Markham, *Anal. Chim. Acta*, **39**, 7 (1967).

(14) R. H. Maghssoudi and A. B. Fawzi, *J. Pharm. Sci.*, **67**, 32 (1978).

(15) R. H. Maghssoudi, A. B. Fawzi, and M. A. N. Moosavi Meerkalaie, *J. Assoc. Off. Anal. Chem.*, **60**, 926 (1977).

(16) A. I. Vogel, "A Text-Book of Macro and Semimicro Qualitative Inorganic Analysis," 4th ed., Longmans, London, England, 1964, p. 644.

(17) J. H. Yoe and A. L. Jones, *Ind. Eng. Chem. Anal. Ed.*, **16**, 111 (1944).

NMR Studies and GC Analysis of the Antibacterial Agent Taurolidine

B. I. KNIGHT *, G. G. SKELLERN *, G. A. SMAIL *, M. K. BROWNE ‡, and R. W. PFIRRMANN§ ˣ

Received December 9, 1981, from the **Department of Pharmacy, University of Strathclyde, Glasgow G1 1XW, U.K.*; ‡*Monklands District General Hospital, Airdrie ML6 0JS, U.K.*; and §*Geistlich-Pharma, 6110 Wolhusen, Switzerland.* Accepted for publication June 10, 1982.

Abstract □ The NMR spectrum of taurolidine in deuterium oxide was compared with spectra obtained from model experiments with amines and formaldehyde. Head-space analysis combined with capillary GC showed that there was <0.004% free formaldehyde present in 2% solutions of taurolidine. This value is comparable to the concentration of formaldehyde found when the taurolidine solutions were injected directly onto GC columns.

Keyphrases □ Taurolidine—NMR spectral analysis, head-space analysis–GC methods for the determination of formaldehyde □ NMR spectroscopy—analysis of taurolidine □ GC analysis—direct or combined with head-space analysis, quantitation of formaldehyde concentration in taurolidine □ Head-space analysis—with capillary GC, quantitation of formaldehyde concentration in taurolidine

Taurolidine [4,4′-methylenebis(tetrahydro-1,2,4-thiadiazine 1,1-dioxide), I] is a broad spectrum bactericide and antiendotoxin (1–3) which is being used widely in clinical trials to counteract bacterial infections following GI surgery and to treat peritonitis (4–6). It is administered intraperitoneally *via* a catheter inserted when the abdomen is closed, as a 2% aqueous solution[1] containing 5% povidone[2] (added to increase the solubility of taurolidine).

As a result of NMR studies (7) of aqueous solutions of taurolidine, equilibria are considered to exist between taurolidine, 4-hydroxymethyltetrahydro-2*H*-1,2,4-thiadiazine 1,1-dioxide (II), tetrahydro-2*H*-1,2,4-thiadiazine 1,1-dioxide (III)[3], and formaldehyde.

The existence of such equilibria was studied with the aid of solutions of morpholine–formaldehyde and III–formaldehyde as models. Also, because of the concern regarding toxicity, the determination of the formaldehyde concentration in solutions of taurolidine (which have been used in large volumes for the treatment of septicemia) is of considerable interest. Thus, this paper also describes the quantitative determination of formaldehyde using combined head-space analysis–capillary GC and direct GC.

EXPERIMENTAL

NMR—The NMR spectra of taurolidine were determined in deuterium oxide and deuterodimethylsulfoxide. Taurolidine (20 mg/ml) together with 1-vinyl-2-pyrrolidinone polymer (50 mg/ml) in deuterium oxide, and morpholine and III in deuterium oxide (before and after gaseous formaldehyde had been passed through the solution), were also determined[4]. The reference standard was sodium 3-trimethylsilylpropionate-2,2,3,3-$^2H_4$.

GC Analysis of Formaldehyde—*Head-Space Analysis*—Aqueous solutions (10 ml) of formaldehyde (0.005–0.01%) containing sodium chloride (5 g) were added to 100-ml injection vials which were tightly stoppered. The vials were incubated at 20, 40, or 60° for 1 hr to allow the

[1] Taurolin.
[2] Polyvinylpyrrolidone-17, mol. wt. 11,000, BASF (Germany).
[3] Taurultam.
[4] Perkin-Elmer R32 90-MHz NMR spectrometer.

0022-3549/83/0600-0705$01.00/0

Table I—Proton NMR Structural Assignments of Taurolidine

Solvent	Chemical Shift (δ)[a]				
	>NH	HN—CH_2—N		>N—CH_2—N<	SO_2CH_2—CH_2—N<
Deuterodimethylsulfoxide	7.25(t)	4.14(d)		3.59(s)	3.17(m)
	CH_2O	>N—CH_2OH	HN—CH_2—N	>N—CH_2—N<	SO_2CH_2—CH_2—N<
Deuterium oxide	4.82(s)	4.47(s)	4.27(s)	3.65(s)	3.30(m)

[a] Key: (s) singlet; (d) doublet; (t) triplet; (m) multiplet.

Table II—Proton NMR Structural Assignments of Morpholine and III Solutions in the Absence or Presence of Formaldehyde

	Chemical Shift (δ)[a]				
Morpholine			—CH_2—O—CH_2— 3.5(t)		—CH_2NHCH_2— 2.58(t)
Morpholine + formaldehyde	CH_2O 4.88(s)	>N—CH_2OH 4.44(s)	—CH_2—O—CH_2- 3.93(t)	>N—CH_2—N< 3.25(s)	—CH_2NHCH_2- 2.77(t)
Compound III			HN—CH_2—N— 4.25(s)		SO_2CH_2—CH_2—N< 3.30(m)
Compound III + formaldehyde	CH_2O 4.82(s)	>N—CH_2OH 4.47(s)	HN—CH_2—N— 4.27(s)	>N—CH_2—N< 3.65(s)	SO_2CH_2—CH_2—N< 3.30(m)

[a] Key: (s) singlet; (d) doublet; (t) triplet; (m) multiplet.

system to equilibrate. A 200-μl sample of the gaseous phase was removed from the vial with a microliter syringe and injected into a gas chromatograph[5] fitted with a 15 m × 0.47-mm capillary column[6] (column A). The temperatures of the injection port, column, and detector were 175, 65, and 150°, respectively. The carrier gas was helium at a pressure of 0.2 bar. Aqueous solutions of taurolidine and taurolidine with 5% 1-vinyl-2-pyrrolidinone polymer were analyzed in a similar manner.

Direct Analysis—Formaldehyde concentrations were also determined by injecting aliquots (1 μl) of taurolidine solution into the gas chromatograph fitted with a glass column (2.1 m × 4 mm) packed with 5% polyoxyethylene glycol stearate[7] on 80–100 mesh chromosorb W-AW (column B). The temperatures of the injection port, column, and detector were 125, 95, and 200°, respectively. The carrier gas was helium at a flow rate of 40 ml/min.

Aqueous solutions of formaldehyde (0.0025–0.01%) were prepared as calibration standards. Formaldehyde (0.0025–0.01%) was added to the taurolidine and taurolidine plus 1-vinyl-2-pyrrolidinone polymer solutions. Formaldehyde concentrations were also determined by injecting aliquots (0.5 μl) of taurolidine solution onto the capillary column (column A) used for head-space analysis.

RESULTS AND DISCUSSION

The singlet at δ3.59 in the NMR spectrum of taurolidine in deuterodimethylsulfoxide (Table I) was assigned to the protons of the methylene group joining the two molecules of II (Scheme I). However in deuterium oxide the signal (δ3.65) due to these protons is reduced to <10% of the intensity observed in deuterodimethylsulfoxide. In deuterium oxide the signals at δ4.47 and δ4.82 have been assigned to the hydroxymethyl group of II and formaldehyde, respectively. That the signal at δ4.47 arises from the hydroxymethyl group has been shown in model experiments with morpholine and formaldehyde, which behave in a manner analogous to solutions of III and formaldehyde (Table II). Thus, the NMR spectrum of a solution of morpholine in deuterium oxide is modified by treatment with formaldehyde gas, the additional peaks observed at δ4.44, δ3.25, and δ4.88 being ascribed to a hydroxymethyl group on the morpholine nitrogen, the methylene bridge of the *N,N'*-methylenediamine, and formaldehyde, respectively. The addition of sodium carbonate eliminated the signal ascribed to the hydroxymethyl group (δ4.44); these derivatives are known to undergo hydrolysis at alkaline pH (8). Solutions of III and

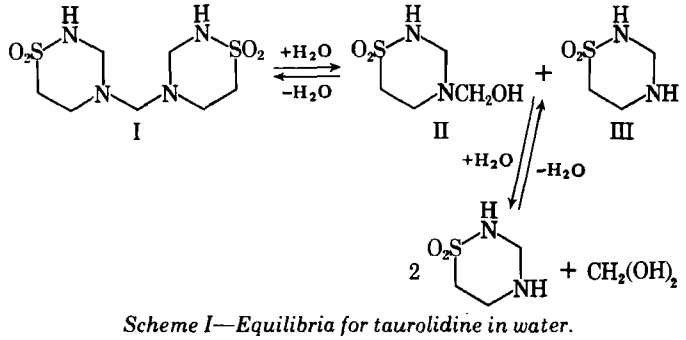

Scheme I—Equilibria for taurolidine in water.

formaldehyde, in turn, mimic the behavior of taurolidine in deuterium oxide: III plus formaldehyde gives an NMR spectrum identical to that of taurolidine in deuterium oxide (Table II).

The equilibria existing between amines and aldehydes in aqueous solutions are not simple (8, 9). There is also evidence[8] to suggest that the equilibria shown in Scheme I only partially represent those that exist in solutions of taurolidine. With saturated solutions of taurolidine in deuterium oxide, the intensity of the signal due to the bridging methylene group (δ3.65) increased and the peak height ratio of the signals ascribed to formaldehyde and the hydroxymethyl group of II decreased in comparison with the ratio of these peaks in the spectrum of the 1% taurolidine solution. Moreover the NMR spectrum of taurolidine (2%) in deuterium oxide containing 5% 1-vinyl-2-pyrrolidinone polymer was comparable to the spectrum of a saturated solution of taurolidine, with respect to the signal intensities due to the bridging methylene protons and formaldehyde, suggesting this substance may influence the equilibria.

Semiquantification of the amount of free formaldehyde present in aqueous solutions of taurolidine has been attempted using NMR spectroscopy (7). Measurement of the area of the signal due to the bridging methylene protons presents problems, since there is not a complete conversion of taurolidine to its hydrolysis products. Theoretically, this means comparing the taurolidine spectrum in deuterodimethylsulfoxide (where no such equilibria exist) with that in deuterium oxide with the assumption that the methylene bridge proton signals are comparable in both solvents. Although NMR spectroscopy would be the method of choice since it is a noninvasive technique and does not disturb the proposed equilibria, integration of this minor peak is unsatisfactory, espe-

[5] Pye Unicam Model 204.
[6] Silar-5CP (Silicone).
[7] Ethofat 60/25.

[8] Unpublished results.

Table III—Percentage of Free Formaldehyde Present in Aqueous Solutions of Taurolidine and Taurolidine Plus 1-Vinyl-2-pyrrolidinone Polymer [a]

Method	Taurolidine 1%	Taurolidine 2%	Taurolidine (2%) plus 1-vinyl-2-pyrrolidinone polymer (5%)
Head-space with capillary column A	0.0036 ± 0.0004	0.0037 ± 0.0004	Not measurable due to the presence of isopropyl alcohol
Direct analysis			
Column A	0.0022 ± 0.0006	0.0038 ± 0.0003	Not measurable due to the presence of isopropyl alcohol
Column B	0.0013 ± 0.0001	0.0027 ± 0.0001	0.0032 ± 0.0006

[a] Mean ± *SD*.

cially in the presence of 1-vinyl-2-pyrrolidinone polymer, where signals in this molecule interfere with the signal assigned to the bridging methylene protons.

GC combined with head-space analysis can also be regarded as a noninvasive technique, the amount of gaseous formaldehyde in the head-space being proportional to the concentration of formaldehyde present in the aqueous phase. The assay was carried out at different temperatures to determine whether the equilibria changed. At all temperatures the formaldehyde calibration curves were linear. The equations for the plots at 20, 40, and 60° were $y = 0.032 + 40.93x$, $y = 120x$, and $y = 0.036 + 266.2x$, respectively. The correlation coefficients (r) were 0.99, 1, and 0.99 respectively. The precision of the method was ±3% for a 0.01% formaldehyde solution at 40°. At the three assay temperatures, there was <0.004% free formaldehyde present in the taurolidine solutions (Table III).

Rectilinear relationships between detector response and formaldehyde concentrations for the direct GC method were also observed when known amounts of formaldehyde were added to water or taurolidine solutions, or taurolidine solutions containing 1-vinyl-2-pyrrolidinone polymer ($y = 0.165 + 1407x$, $r = 0.99$). That the slope and intercept were the same in all cases, would indicate that the equilibria did not change, especially in the presence of the polymer. Unfortunately, 1-vinyl-2-pyrrolidinone polymer contains a small amount (60–100 ppm) of isopropyl alcohol (1-vinyl-2-pyrrolidinone is polymerized in this solvent). Since isopropyl alcohol has the same retention time as formaldehyde (1.25 min) on column B, it was necessary to subtract the height of the peak observed when an aliquot of a 5% 1-vinyl-2-pyrrolidinone polymer solution was injected on this column from the height of the peak from the formaldehyde–isopropyl alcohol in the taurolidine–1-vinyl-2-pyrrolidinone polymer solution. Comparable amounts of free formaldehyde were found when solutions of taurolidine were injected directly onto either column A or B, indicating that the direct method could be regarded as a noninvasive technique and was suitable for the determination of formaldehyde.

That the equilibria may be sensitive to the concentrations of the molecular species present but not to the presence of 1-vinyl-2-pyrrolidinone polymer is shown by direct GC analysis (Table III) but head-space analysis GC does not support this contention. The concentration of free formaldehyde is not clinically important since no formaldehyde toxicity has been observed with solutions of taurolidine containing 1-vinyl-2-pyrrolidinone polymer either in humans or experimental animals. Moreover, the formaldehyde concentration is considerably lower than the amount of formaldehyde produced in the body after administration of certain antibiotic prodrugs (10).

Compound III has also been shown to possess antibacterial and antiendotoxin activity similar to taurolidine, although higher concentrations are required[8]. This activity also is not related to the presence of free formaldehyde, since solutions of III have been shown to be stable by NMR and GC, liberating no measurable amounts of formaldehyde.

REFERENCES

(1) M. K. Browne, G. B. Leslie, and R. W. Pfirrmann, *J. Appl. Bacteriol.*, **41**, 363 (1976).

(2) R. W. Pfirrmann and G. B. Leslie, *ibid.*, **46**, 97 (1979).

(3) M. K. Browne, G. B. Leslie, R. W. Pfirrmann, and H. Brodhage, *Surg. Gynecol. Obstet.*, **145**, 842 (1977).

(4) M. K. Browne, M. Mackenzie, and P. J. Doyle, *ibid.*, **146**, 721 (1978).

(5) C. H. Ruegsegger and R. Mosimann, *Helv. Chir Acta*, **45**, 743 (1978).

(6) B. I. Knight, G. G. Skellern, M. K. Browne, and R. W. Pfirrmann, *Br. J. Clin. Pharmacol.*, **12**, 695 (1981).

(7) E. Myers, M. C. Allwood, M. J. Gidley, and J. K. M. Sanders, *J. Appl. Bacteriol.*, **48**, 89 (1980).

(8) R. G. Kallen and W. P. Jencks, *J. Biol. Chem.*, **241**, 5864 (1966).

(9) R. G. Kallen, R. O. Viale, and L. K. Smith, *J. Am. Chem. Soc.*, **94**, 576 (1972).

(10) P. C. Bansal, I. H. Pitman, J. N. S. Tam, M. Mertes, and J. J. Kaminski, *J. Pharm. Sci.*, **70**, 850 (1981).

ACKNOWLEDGMENTS

The authors thank I. Baumeler (Geistlich Söhne AG, Wolhusen, Switzerland) for the GC analyses.

The Perkin-Elmer ^1H NMR spectrometer used in this study was purchased on Grant A, 80754 from the Science Research Council.

Solid Dispersions of Testosterone with Reduced Presystemic Inactivation

ALMAS BABAR and C. I. JAROWSKI ×

Received April 1, 1982, from *St. John's University, College of Pharmacy & Allied Professions, Jamaica, NY, 11439.* Accepted for publication June 10, 1982.

Abstract □ Dissolution rates of solid dispersions of testosterone in various lipids or polyethylene glycol 6000 with and without surfactants were determined. In a limited study, selected dispersions were evaluated for oral absorption efficiency in a 32-year-old male. Significant reductions in urinary testosterone metabolites to testosterone ratios were observed with a 1:4 weight ratio of testosterone–polyethylene glycol 6000 and a 1:4:0.25 weight ratio of testosterone–cholesteryl stearate–sorbitan monolaurate.

Keyphrases □ Testosterone—solid dispersions with reduced presystemic inactivation, dissolution, absorption efficiency □ Dissolution—solid dispersions of testosterone with reduced presystemic inactivation, absorption efficiency □ Presystemic inactivation—reduced, solid dispersions of testosterone, absorption efficiency □ Absorption—efficiency, solid dispersions of testosterone with reduced presystemic inactivation

Solid dispersions and eutectic mixtures of drugs with inert carriers such as urea and succinic acid have been used to enhance the rate of dissolution and oral absorption of therapeutic agents poorly soluble in water (1). Previous work (2, 3) has dealt with the *in vitro* dissolution characteristics of such systems. In *in vivo* studies griseofulvin dispersions in polyethylene glycol 6000 were found (4) to be completely and rapidly absorbed after oral administration to humans, and a morphine–tristearin dispersion in a weight ratio of 1:1 exhibited reduced presystemic inactivation in rats (5).

When testosterone therapy is indicated, parenteral administration is preferred, since oral administration is inefficient due to presystemic inactivation (6). Hepatic enzymes were predominantly responsible for the chemical modification of testosterone. It has been reported that twice as much testosterone (I) was required to match the androgenic effect of methyl testosterone when administered sublingually (7). It was recently demonstrated (8) that clinical efficacy upon oral administration required 400-mg doses of I.

The purpose of this investigation was to study the oral absorption efficiency of I from various solid dispersions. The dissolution rates of the dispersions were evaluated *in vitro*, and selected dispersions were chosen for evaluation *in vivo*. The urinary recovery of I and its principal metabolites was used as a measure of oral absorption efficiency in a 32-year-old male.

EXPERIMENTAL

Materials—The following were obtained from commercial sources: I (NF grade)[1], polyoxyethylene (20) sorbitan monooleate (II)[2], sorbitan monolaurate (III)[2], sodium cholate (IV)[3], sodium deoxycholate (V)[3], β-sitosterol (VI)[3], cholesteryl stearate (VII)[3], lactose (VIII)[3], cholesterol (IX)[4], polyethylene glycol 6000 (X)[5], chloroform[6], hydrochloric acid[6], β-glucuronidase (beef liver)[7], androsterone (XI)[8], etiocholanolone (XII)[8], and tripalmitin (XIII)[8].

Equipment—The following equipment was used: spectrophotometer[9], thermal analyzer with differential scanning colorimeter[10], USP dissolution apparatus with basket assembly[11], and a GC equipped with an electronic integrator[12].

Preparation of Solid Dispersions—Micronized I and various surfactants were weighed in ratios of 1:0.05. The mixtures were dissolved in 50 ml of chloroform. The solvent was evaporated in a stream of air while the solution was stirred with a magnetic stirrer. The residue was dried in a vacuum oven at 40°, ground in a mortar, and then passed through an 80-mesh screen. After blending to ensure homogeneity, aliquots were assayed. Only samples assaying 100 ± 5% of I were used in the dissolution and absorption studies. Dispersions containing I–lipid in weight ratios of 1:4, 1:6, and 1:8 as well as I–lipid–surfactants in weight ratios of 1:4:0.05 were prepared in a similar fashion. Polyethylene glycol 6000 dispersions also used chloroform. The I–lipid–lactose dispersions in weight ratios of 1:4:4 were prepared by evaporating the chloroform in the presence of lactose.

Dissolution Studies—The dissolution rates of I and its dispersions were conducted in simulated gastric fluid, without pepsin, by the procedure described in the USP (9). Simulated gastric fluid (900 ml) was placed in a 1-liter beaker and maintained at 37 ±0.5° in a constant-temperature bath. A sintered-glass immersion filter (medium porosity) was placed in a medium for aliquot withdrawals. The basket was lowered to 1 cm above the bottom of the beaker and rotated at 300 rpm. Accurately weighed samples equivalent to 20 mg of I were spread over the surface of the medium. Any aggregates that formed at this stage were submerged by a microspatula within 10 sec after sample addition. Five-milliliter aliquots were removed at intervals of 15, 30, 45, 60, 90, and 120 min using a 5-ml pipet. A constant volume of dissolution medium was maintained by additions of preheated medium. The filtered aliquots were passed through a micropore filter (0.45-μm) and read directly for their absorbance at 248 nm. A cumulative correction was made for the previously removed samples to determine the total quantity of I that had dissolved (10). Sink conditions were maintained, since the solubility of I was determined to be 44 mg/900 ml.

Assay Procedure for Testosterone—Plots of absorbance *versus* wavelength for solutions of I in water, simulated gastric fluid, and methanol were developed. The maximum absorbance values observed were 248 nm for water and simulated gastric fluid and 244 for methanolic solutions of I. Beer's law was followed for 1–20-μg/ml concentrations. The stability of I in simulated gastric fluid was determined. After 24 hr at 37° no potency change was noted.

Assay of Urinary Testosterone and its Metabolites—Selected test samples were evaluated in a healthy, adult male, 32 years of age. Each sample was tested on at least three occasions. The subject was administered an equivalent of 50 mg of I in a hard gelatin capsule after an overnight fast, with 240 ml of water. Food was avoided for at least 2 hr. Urine samples were collected for 24 hr, pooled, and frozen until assayed. One week or more was allowed to elapse between oral dosings. Free I and XI and XII were determined by a modification of published procedures (11, 12). Essentially, the derivatization step was eliminated since adequate quantities of I, XI, and XII were present. In addition, the GC procedure was altered to afford more efficient separation of the components. Details of the assay procedure will be presented in a separate publication.

RESULTS AND DISCUSSION

Dissolution Rate Studies—Only 54.6% of I had dissolved after 2 hr

[1] Roussel Corporation, New York, N.Y.
[2] ICI, Atlas Chemical Corp., Wilmington, Del.
[3] Aldrich Chemical Co., Milwaukee, Wis.
[4] Croda Inc., New York, N.Y.
[5] Union Carbide, Tarrytown, N.Y.
[6] Fisher Scientific Co., Springfield, N.J.
[7] Worthington Biochemicals Inc., Freehold, N.J.
[8] Pfaltz and Bauer, Inc., Stamford, Conn.
[9] Model 25, Beckman Instruments Inc., Mountainside, N.J.
[10] Model 990, E.I. DuPont, Instrument Division, Wilmington, Del.
[11] Hanson Research Corp., Northridge, Calif.
[12] Model 5840-A, Hewlett-Packard Co., Avondale, Pa.

0022-3549/83/0600-0708$01.00/0

Table I—Dissolution Rate of Testosterone Dispersions in Simulated Gastric Fluid at 37°

Sample	Weight Ratio	Percent Dissolved (Min) 15	30	45	60	90	120
I		4.3	11.3	25.3	37.7	45.6	54.6
I-II	1:0.05	4.0	24.6	36.0	54.3	56.3	66.7
I-III	1:0.05	5.0	27.0	42.6	50.6	58.7	67.0
I-IV	1:0.05	4.3	14.6	23.3	34.3	44.6	50.3
I-V	1:0.05	2.0	8.3	16.0	26.0	34.6	44.3
I-IX	1:4	3.0	8.7	14.3	19.6	24.0	30.6
I-IX	1:6	3.3	7.0	8.6	10.6	16.3	21.6
I-IX	1:8	2.3	6.3	13.0	16.0	20.6	25.6
I-VI	1:4	1.0	6.6	13.6	17.0	20.0	21.6
I-VI	1:6	2.6	4.3	4.6	6.3	7.0	7.3
I-VI	1:8	0.3	2.0	3.6	5.0	5.6	6.3
I-VII	1:4	1.0	14.0	17.6	21.0	24.6	31.0
I-VII	1:6	2.6	8.6	17.3	23.6	31.3	39.0
I-VII	1:8	1.3	9.6	21.6	26.0	20.6	35.0
I-XIII	1:4	3.6	8.6	11.3	15.3	19.0	24.3
I-XIII	1:6	3.0	6.0	8.6	10.0	12.0	16.0
I-XIII	1:8	2.3	6.0	7.3	12.0	15.6	18.3
I-IX-II	1:4:0.25	8.0	25.6	38.3	45.0	49.0	58.6
I-IX-III	1:4:0.25	3.3	14.0	22.0	28.0	31.3	38.6
I-IX-IV	1:4:0.25	6.3	13.0	19.0	25.3	27.3	36.0
I-IX-V	1:4:0.25	3.6	15.0	20.6	21.6	26.3	31.3
I-VI-II	1:4:0.25	2.0	29.0	38.0	42.0	43.0	48.6
I-VI-III	1:4:0.25	4.0	9.6	11.6	16.0	19.0	22.3
I-VI-IV	1:4:0.25	0.6	9.0	17.3	25.6	34.6	43.3
I-VI-V	1:4:0.25	4.6	12.3	19.6	26.0	29.3	39.0
I-VII-II	1:4:0.25	5.3	21.6	35.6	43.3	49.0	58.0
I-VII-III	1:4:0.25	10.3	30.6	47.0	61.3	69.6	79.3
I-VII-IV	1:4:0.25	3.3	21.6	37.0	48.0	57.6	67.3
I-VII-V	1:4:0.25	9.6	19.3	27.0	35.6	39.6	48.3
I-XIII-II	1:4:0.25	4.6	33.0	55.0	65.0	71.0	77.0
I-XIII-III	1:4:0.25	6.6	33.6	49.3	56.3	62.0	73.6
I-XIII-IV	1:4:0.25	4.3	21.6	31.0	41.6	49.0	60.0
I-XIII-V	1:4:0.25	4.6	19.0	34.0	46.0	53.6	64.3
I-IX-VIII	1:4:4	2.3	17.6	29.3	34.6	43.6	49.0
I-VI-VIII	1:4:4	7.0	15.6	20.3	23.6	24.6	27.6
I-VII-VIII	1:4:4	4.0	15.3	26.0	36.3	46.3	57.3
I-XIII-VIII	1:4:4	1.7	11.6	22.0	31.0	37.6	44.3
I-X	1:4	9.0	58.3	84.6	96.0	97.6	99.3

Table II—Urinary Recovery of Testosterone and its Principal Metabolites after Oral Administration of Selected Dispersions (50-mg equivalent) to a Male Subject

Sample	Experiment No.	Recovered, % XI plus XII	I	Ratio of Metabolites-I
I	1	27.4	1.6	17:1
	2	27.3	1.3	21:1
	3	17.4	0.7	25:1
	Average	24.1	1.2	21:1
I-VII[a]	1	24.5	1.4	17:1
	2	28.6	1.6	18:1
	3	31.7	2.8	11:1
	Average	28.3	1.9	15:1
I-VII-III	1	27.4	3.1	9:1
	2	37.4	1.6	23:1
	3	41.6	4.7	9:1
	Average	35.5	3.1	13:1
I-X	1	37.2	8.2	4.5:1
	2	32.1	2.2	14.6:1
	3	39.9	7.3	5.5:1
	4	46.4	10.6	4.4:1
	Average	38.9	7.1	7:1

[a] Weight ratio 1:4.

(Table I). A slight increase was observed when synthetic surfactants were added(I-II, I-III); however, the two bile salts were ineffective (I-IV, I-V). The lipid dispersions of I with 1:4–1:8 weight ratios released the hormone more slowly (I-IX, I-VI, I-VII, and I-XIII). The addition of the various surfactants increased the release rate. The most rapid dissolution rate for the lipid–surfactant dispersions was exhibited by I-VII-III (79.3%). Solvent dispersion of I on lactose with the various lipids resulted in an improvement in the dissolution rates: whereas I-IX released 30.6% of I after 2hr, I-IX-VIII released 49%. The sample exhibiting the fastest rate of dissolution was I-X (99.3%).

The rapid dissolution of I-X is likely due to the release of microcrystalline I as the water-soluble X dissolves. The lipid dispersions without surfactants were dissolution-rate retarding. However, inclusion of surfactants would again ensure the release of microcrystalline particles. The lipids in such preparations would be readily dispersed because of the presence of the surfactants. The beneficial effect of lactose with the solvent-deposited lipid dispersions is most likely the result of greater surface exposure to the aqueous dissolution medium.

Oral Absorption Studies—On the basis of the dissolution data in Table I three dispersions were selected for the oral absorption studies. The urinary excretion data are presented in Table II. The recovery of I ranged from 0.7 to 1.6% following a 50-mg dose of micronized particles. The lipid dispersion plus surfactant produced levels of I ranging from 1.6 to 4.7%. The best recovery of I, as anticipated from the *in vitro* data, was shown by I-X (range: 2.2–10.6%). Metabolite recovery followed a similar progressive increase. The ratios of metabolites-I showed significant decreases with the more efficiently absorbed samples. Thus, the ratio was 21:1 for I alone, whereas for I-X the ratio was reduced to 7:1.

The results of the very limited oral absorption studies correlate very well with the dissolution data. The data suggest that rapid oral absorption of I is a desirable goal, since metabolite formation was reduced. Although a clear advantage was shown by using X as the excipient, a combination of VII and III may be indicated when acid-labile drugs are used. The latter would be expected to release the drugs more slowly in acidic media as compared with the former.

REFERENCES

(1) K. Sekiguchi and N. Obi, *Chem. Pharm. Bull.*, **9**, 866 (1961).

(2) A. H. Goldberg, M. Gibaldi, and J. L. Kanig, *J. Pharm. Sci.*, **55**, 482 (1966).

(3) A. H. Goldberg, M. Gibaldi, J. L. Kanig, and M. Mayersohn, *ibid.*, **55**, 581 (1966).

(4) W. L. Chiou and S. Riegelman, *ibid.*, **59**, 973 (1970).

(5) K. S. Chang and C. I. Jarowski, *ibid.*, **69**, 466 (1980).

(6) E. B. Estwood, "Pharmacological Basis of Therapeutics," Goodman and Gilman, 4th ed., Macmillan, New York, N.Y., 1970, p. 1571.

(7) G. L. Foss, *Lancet*, 502 (March, 1939).

(8) S. G. Johnsen, *ibid.*, 1473 (1974).
(9) "The United States Pharmacopeia," 18th rev., U.S. Pharmacopeial Convention, Rockville, Md., p. 934.
(10) D. Wurster and P. Taylor, *J. Pharm. Sci.*, **54**, 670 (1965).
(11) H. Ibayashi, M. Nakamura, and K. Nakao, *Steroids*, **2**, 559 (1964).
(12) W. Futterweit, N. L. McNiven, and R. I. Dorfman, *ibid.*, **1**, 628 (1963).

COMMUNICATIONS

Esmolol: A Pharmacokinetic Profile of a New Cardioselective β-Blocking Agent

Keyphrases □ β-Adrenergic blocking agents—esmolol hydrochloride, pharmacokinetic profile, metabolism □ Pharmacokinetic profile—cardioselective β-adrenergic blocking agent, methyl 3-[4-(2-hydroxy-3-(isopropylamino)propoxy]phenylpropionate hydrochloride □ Esmolol—cardioselective β-adrenergic blocking agent, pharmacokinetic profile

To the Editor:

β-Adrenergic receptor blocking drugs exert their effects by competitively inhibiting the binding of catecholamines to β-adrenergic receptors. To attain therapeutic levels rapidly, intravenous bolus or infusions of β-blockers are usually instituted. However, since these agents have cardiac depressant properties, they are initially used at low doses, and slowly increased until the desired effects are obtained. Because currently available β-adrenergic blocking agents are long acting, the emergence of side effects, especially acute cardiac failure, poses a significant problem in their use because their action cannot be readily terminated. Therefore, there is a need for a β-adrenergic blocking drug with a short onset of action which can be rapidly terminated if side effects develop.

Esmolol (ASL-8052, Scheme I) is a new cardioselective intravenous β-receptor blocking agent with a very short duration of action in humans (unpublished data) and dogs (1). It is extensively metabolized in blood and liver by hydrolysis of the methyl ester functionality to form its major metabolites, ASL-8123 and methanol.

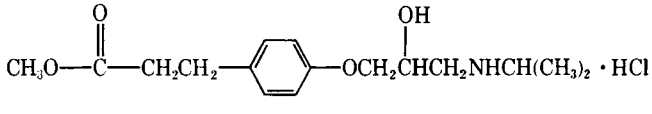

Esmolol (ASL-8052)

Methyl 3-[4-(2-Hydroxy-3-(isopropylamino)propoxy]phenylpropionate hydrochloride

Scheme I

To study the pharmacokinetics of esmolol, eight healthy male subjects (21–27 years old) weighing 62.4–76.2 kg received constant intravenous infusions of 50, 150, and 400 μg/kg/min for 2 hr on three different days. Each subject received an intravenous dose of isoproterenol, which had previously been determined to produce a 50% increase in heart rate. The suppression of the isoproterenol-induced increase in heart rate and blood pressure was determined on several occasions during and up to 60 min after the cessation of the esmolol infusion. At each dose level, blood samples were collected for determinations of esmolol and ASL-8123 by gas chromatography–mass spectrometry and high performance liquid chromatography, respectively (2). Esmolol and ASL-8123 concentrations, as a function of time during and after the infusion, were fitted to equations describing a two-compartment open model (3, 4) and modified one-compartment open model, respectively, by nonlinear least-squares regression analysis.

Esmolol infusion significantly blocked the isoproterenol effects with its action being most evident at the 400-μg/kg/min dose. The duration of action of esmolol was, however, very short with no significant effect evident 30 min after cessation of the infusion at all three doses. There was a significant correlation between the reduction of the isoproterenol-induced increase in heart rate and blood pressure and the logarithm of esmolol blood concentrations. Blood levels of 0.3 and 1 μg/ml esmolol were associated with 50 and 80%, respectively, reduction in heart rate and 30 and 50%, respectively, reduction in blood pressure.

The steady-state concentrations of esmolol increased proportionally with the dose ($r = 0.866$, $p < 0.001$, $n = 24$). The mean concentrations (±*SD*) were 0.164 ± 0.068, 0.569 ± 0.204, and 1.59 ± 0.605 μg/ml, respectively, after 2-hr infusions of 50, 150, and 400 μg/kg/min. The respective values for the total clearance were 363 ± 184, 298 ± 112, and 285 ± 104 ml/min/kg, which were not correlated with dose ($r = 0.210$, $p > 0.3$, $n = 24$). These findings suggest that the elimination of esmolol is linear within the 50–400 μg/kg/min dosing range given for 2 hr.

Table I summarizes several of the key pharmacokinetic parameters for esmolol and ASL-8123 after the 400

Table I—Summary of Some Pharmacokinetic Parameters of Esmolol and its Metabolite after Administration of 400 μg/kg/min infusion of the Drug for 2 hr in Normal Subjects

Pharmacokinetic Parameters	Esmolol	ASL-8123
Steady-state concentration, μg/ml	1.59 ± 0.605[a]	—
Peak concentration, μg/ml	—	77.9 ± 3.93
Peak time, min	—	146 ± 11.1
Terminal half-life, min	9.19 ± 3.51	223 ± 14.0
Half-life of formation of metabolite(s), min	—	2.82 ± 0.592
Total clearance, ml/min/kg	285 ± 104	1.28 ± 0.19
Volume of distribution, liters/kg	3.43 ± 1.42	0.411 ± 0.057
Calculated fraction of metabolite formed[b]	—	0.829

[a] Mean ± *SD*; $N = 8$. [b] Ratio of formation and elimination rate constants (k_f/k_{10}).

0022-3549/83/0600-0710$01.00/0

(8) S. G. Johnsen, *ibid.*, 1473 (1974).
(9) "The United States Pharmacopeia," 18th rev., U.S. Pharmacopeial Convention, Rockville, Md., p. 934.
(10) D. Wurster and P. Taylor, *J. Pharm. Sci.*, **54**, 670 (1965).
(11) H. Ibayashi, M. Nakamura, and K. Nakao, *Steroids*, **2**, 559 (1964).
(12) W. Futterweit, N. L. McNiven, and R. I. Dorfman, *ibid.*, **1**, 628 (1963).

COMMUNICATIONS

Esmolol: A Pharmacokinetic Profile of a New Cardioselective β-Blocking Agent

Keyphrases □ β-Adrenergic blocking agents—esmolol hydrochloride, pharmacokinetic profile, metabolism □ Pharmacokinetic profile—cardioselective β-adrenergic blocking agent, methyl 3-[4-(2-hydroxy-3-(isopropylamino)propoxy]phenylpropionate hydrochloride □ Esmolol—cardioselective β-adrenergic blocking agent, pharmacokinetic profile

To the Editor:

β-Adrenergic receptor blocking drugs exert their effects by competitively inhibiting the binding of catecholamines to β-adrenergic receptors. To attain therapeutic levels rapidly, intravenous bolus or infusions of β-blockers are usually instituted. However, since these agents have cardiac depressant properties, they are initially used at low doses, and slowly increased until the desired effects are obtained. Because currently available β-adrenergic blocking agents are long acting, the emergence of side effects, especially acute cardiac failure, poses a significant problem in their use because their action cannot be readily terminated. Therefore, there is a need for a β-adrenergic blocking drug with a short onset of action which can be rapidly terminated if side effects develop.

Esmolol (ASL-8052, Scheme I) is a new cardioselective intravenous β-receptor blocking agent with a very short duration of action in humans (unpublished data) and dogs (1). It is extensively metabolized in blood and liver by hydrolysis of the methyl ester functionality to form its major metabolites, ASL-8123 and methanol.

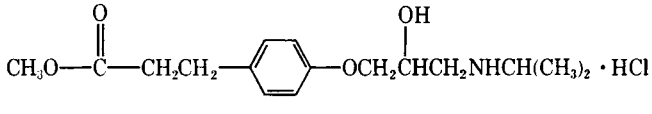

Esmolol (ASL-8052)

Methyl 3-[4-(2-Hydroxy-3-(isopropylamino)propoxy]phenylpropionate hydrochloride

Scheme I

To study the pharmacokinetics of esmolol, eight healthy male subjects (21–27 years old) weighing 62.4–76.2 kg received constant intravenous infusions of 50, 150, and 400 μg/kg/min for 2 hr on three different days. Each subject received an intravenous dose of isoproterenol, which had previously been determined to produce a 50% increase in heart rate. The suppression of the isoproterenol-induced increase in heart rate and blood pressure was determined on several occasions during and up to 60 min after the cessation of the esmolol infusion. At each dose level, blood samples were collected for determinations of esmolol and ASL-8123 by gas chromatography–mass spectrometry and high performance liquid chromatography, respectively (2). Esmolol and ASL-8123 concentrations, as a function of time during and after the infusion, were fitted to equations describing a two-compartment open model (3, 4) and modified one-compartment open model, respectively, by nonlinear least-squares regression analysis.

Esmolol infusion significantly blocked the isoproterenol effects with its action being most evident at the 400-μg/kg/min dose. The duration of action of esmolol was, however, very short with no significant effect evident 30 min after cessation of the infusion at all three doses. There was a significant correlation between the reduction of the isoproterenol-induced increase in heart rate and blood pressure and the logarithm of esmolol blood concentrations. Blood levels of 0.3 and 1 μg/ml esmolol were associated with 50 and 80%, respectively, reduction in heart rate and 30 and 50%, respectively, reduction in blood pressure.

The steady-state concentrations of esmolol increased proportionally with the dose ($r = 0.866$, $p < 0.001$, $n = 24$). The mean concentrations (±*SD*) were 0.164 ± 0.068, 0.569 ± 0.204, and 1.59 ± 0.605 μg/ml, respectively, after 2-hr infusions of 50, 150, and 400 μg/kg/min. The respective values for the total clearance were 363 ± 184, 298 ± 112, and 285 ± 104 ml/min/kg, which were not correlated with dose ($r = 0.210$, $p > 0.3$, $n = 24$). These findings suggest that the elimination of esmolol is linear within the 50–400 μg/kg/min dosing range given for 2 hr.

Table I summarizes several of the key pharmacokinetic parameters for esmolol and ASL-8123 after the 400

Table I—Summary of Some Pharmacokinetic Parameters of Esmolol and its Metabolite after Administration of 400 μg/kg/min infusion of the Drug for 2 hr in Normal Subjects

Pharmacokinetic Parameters	Esmolol	ASL-8123
Steady-state concentration, μg/ml	1.59 ± 0.605[a]	—
Peak concentration, μg/ml	—	77.9 ± 3.93
Peak time, min	—	146 ± 11.1
Terminal half-life, min	9.19 ± 3.51	223 ± 14.0
Half-life of formation of metabolite(s), min	—	2.82 ± 0.592
Total clearance, ml/min/kg	285 ± 104	1.28 ± 0.19
Volume of distribution, liters/kg	3.43 ± 1.42	0.411 ± 0.057
Calculated fraction of metabolite formed[b]	—	0.829

[a] Mean ± *SD*; $N = 8$. [b] Ratio of formation and elimination rate constants (k_f/k_{10}).

0022-3549/83/0600-0710$01.00/0

μg/kg/min infusion. The half-life of the formation of ASL-8123 averaged 2.82 min, and the calculated fraction of the overall metabolite generated was 82.9%. The elimination half-lives of esmolol and ASL-8123 averaged 9.19 and 223 min, respectively, suggesting accumulation and relatively slow elimination of the metabolite in humans. The peak concentration of ASL-8123 averaged 77.9 μg/ml and occurred 26 min after the cessation of the esmolol infusion. This peak concentration was ~50 times larger than the steady-state concentration of esmolol at which maximum β-blockade was observed.

The total clearance of esmolol was 4 times greater than the total cardiac output (70 ml/min/kg) and 14 times greater than hepatic blood flow (5), suggesting that the high clearance was primarily due to metabolism by esterases in the blood. The rapid metabolism of ASL-8052 results in a very short duration of action. The fact that there was no noticeable β-blockade 30 min after cessation of the infusion (which is the time of peak concentration of the metabolite) also suggests that ASL-8123 does not possess β-blocking activity at the concentrations generated in these subjects.

(1) J. Zaroslinski, R. J. Borgman, J. P. O'Donnell, W. G. Anderson, P. W. Erhardt, S. T. Kam, R. D. Reynolds, R. J. Lee, and R. J. Gorczynski, *Life Sci.*, **31**, 899 (1982).

(2) C. Y. Sum and A. Yacobi, "Proceedings of the 33rd National Meeting of the Academy of Pharmaceutical Sciences," 1982.

(3) M. Gibaldi, and D. Perrier, "Drugs and The Pharmaceutical Sciences, vol. 1, Pharmacokinetics," Dekker, New York, N.Y., 1975, p. 69.

(4) J. G. Wagner, "Fundamentals of Clinical Pharmacokinetics," 1st ed., Drug Intelligence Publication, Hamilton, Ill., 1975, p. 90.

(5) A. C. Clayton, "Textbook of Medical Physiology," 4th ed., W. B. Saunders, 1971, p. 369.

*Avraham Yacobi**x
Ronald Kartzinel
Chii-Ming Lai
Check Y. Sum,
Research and Development
American Critical Care
McGaw Park, IL 60085

Received November 26, 1982.
Accepted for publication January 20, 1983.

* Present address:
Medical Research Div.
American Cyanamid Co.
Pearl River, NY 10965

First-Pass, Formation-Rate-Limiting Metabolism

Keyphrases □ First-pass metabolism—impact on pharmacokinetic parameters, use of simulation techniques, formation-rate-limited metabolism □ Formation-rate-limited metabolism—pharmacokinetic parameters, use of simulation techniques □ Pharmacokinetic parameters—use of simulation techniques for first-pass and formation-rate-limited metabolism studies

To the Editor:

It has become increasingly apparent that there is a general misunderstanding of the driving forces that control first-pass and formation-rate-limited metabolism. In fact, a single metabolite can be the result of both first-pass and formation-rate-limited metabolism. To clarify this issue, simulation techniques were used to delineate the causative factors that determine both first-pass and formation-rate-limited metabolism.

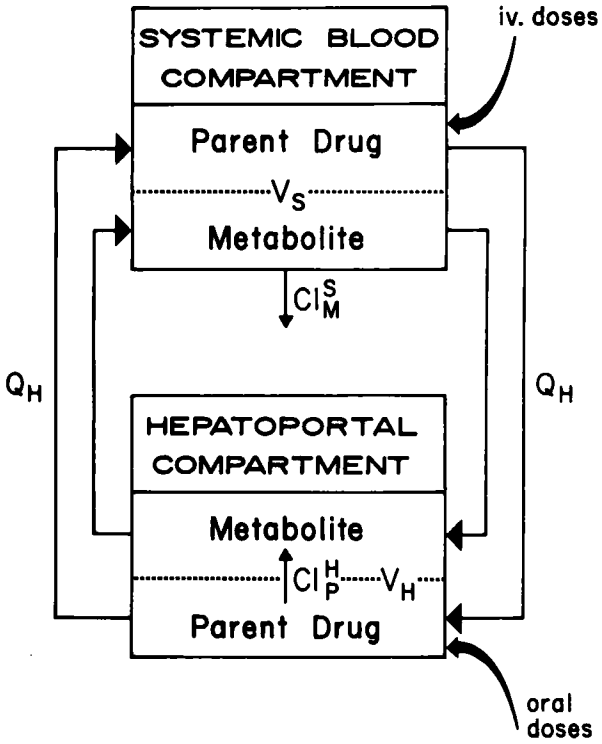

Scheme I—First pass metabolism model used to simulate both parent drug and metabolite plasma concentrations under various conditions. Q_H is the hepatic blood flow, CL_M^S is the systemic clearance of the metabolite, CL_P^H is the hepatoportal clearance of parent drug to metabolite, V_P^S, V_P^H, V_M^S, and V_M^H are the systemic and hepatoportal volumes of parent and metabolite, respectively. The volume of distribution for the metabolite ($V_M^S + V_M^H$) is assumed to be equivalent to the systemic volume of distribution (V_P^S) of the parent drug and V_M^H is set equal to 1; e.g., the metabolite is not retained in the liver after formation (60 mg administered). Oral doses (60 mg) are absorbed into the hepatoportal compartment with the rate constant k_a, and intravenous doses (60 mg) are administered instantly into the systemic blood compartment.

The differential equations (see *Appendix*) needed to describe the first-pass metabolism model shown in Scheme I were used for the simulation of plasma concentration–time data for both parent drug and a single metabolite following oral and intravenous doses. The differential equations required to describe the model were used in conjunction with the nonlinear regression program NONLIN (1), to simulate parent drug and metabolite concentration–time data for drugs with varied pharmacokinetic characteristics. A 60-mg dose was used for each simulation. Several biopharmaceutic and pharmacokinetic parameters such as the time (t_{max}) of the maximum observed concentration (C_{max}) following oral doses, the areas under the plasma concentration–time curve (AUC) for parent drug and metabolite following oral (AUC_P^O and AUC_M^O) and intravenous (AUC_P^{IV} and AUC_M^{IV}) doses, the terminal elimination half-lives for parent drugs ($t_{1/2P}$) and metabolite ($t_{1/2M}$), the ratio of oral to intravenous area of parent (F_P) and metabolite (F_M), and the ratio of metabolite–parent drug following oral (R_O) and intravenous (R_{IV}) doses were calculated from the simulated plasma concentration–time data. The constants used for

0022-3549/83/0600-0711$01.00/0

μg/kg/min infusion. The half-life of the formation of ASL-8123 averaged 2.82 min, and the calculated fraction of the overall metabolite generated was 82.9%. The elimination half-lives of esmolol and ASL-8123 averaged 9.19 and 223 min, respectively, suggesting accumulation and relatively slow elimination of the metabolite in humans. The peak concentration of ASL-8123 averaged 77.9 μg/ml and occurred 26 min after the cessation of the esmolol infusion. This peak concentration was ~50 times larger than the steady-state concentration of esmolol at which maximum β-blockade was observed.

The total clearance of esmolol was 4 times greater than the total cardiac output (70 ml/min/kg) and 14 times greater than hepatic blood flow (5), suggesting that the high clearance was primarily due to metabolism by esterases in the blood. The rapid metabolism of ASL-8052 results in a very short duration of action. The fact that there was no noticeable β-blockade 30 min after cessation of the infusion (which is the time of peak concentration of the metabolite) also suggests that ASL-8123 does not possess β-blocking activity at the concentrations generated in these subjects.

(1) J. Zaroslinski, R. J. Borgman, J. P. O'Donnell, W. G. Anderson, P. W. Erhardt, S. T. Kam, R. D. Reynolds, R. J. Lee, and R. J. Gorczynski, *Life Sci.*, **31**, 899 (1982).

(2) C. Y. Sum and A. Yacobi, "Proceedings of the 33rd National Meeting of the Academy of Pharmaceutical Sciences," 1982.

(3) M. Gibaldi, and D. Perrier, "Drugs and The Pharmaceutical Sciences, vol. 1, Pharmacokinetics," Dekker, New York, N.Y., 1975, p. 69.

(4) J. G. Wagner, "Fundamentals of Clinical Pharmacokinetics," 1st ed., Drug Intelligence Publication, Hamilton, Ill., 1975, p. 90.

(5) A. C. Clayton, "Textbook of Medical Physiology," 4th ed., W. B. Saunders, 1971, p. 369.

*Avraham Yacobi**x
Ronald Kartzinel
Chii-Ming Lai
Check Y. Sum,
Research and Development
American Critical Care
McGaw Park, IL 60085

Received November 26, 1982.
Accepted for publication January 20, 1983.

* Present address:
Medical Research Div.
American Cyanamid Co.
Pearl River, NY 10965

First-Pass, Formation-Rate-Limiting Metabolism

Keyphrases □ First-pass metabolism—impact on pharmacokinetic parameters, use of simulation techniques, formation-rate-limited metabolism □ Formation-rate-limited metabolism—pharmacokinetic parameters, use of simulation techniques □ Pharmacokinetic parameters—use of simulation techniques for first-pass and formation-rate-limited metabolism studies

To the Editor:

It has become increasingly apparent that there is a general misunderstanding of the driving forces that control first-pass and formation-rate-limited metabolism. In fact, a single metabolite can be the result of both first-pass and formation-rate-limited metabolism. To clarify this issue, simulation techniques were used to delineate the causative factors that determine both first-pass and formation-rate-limited metabolism.

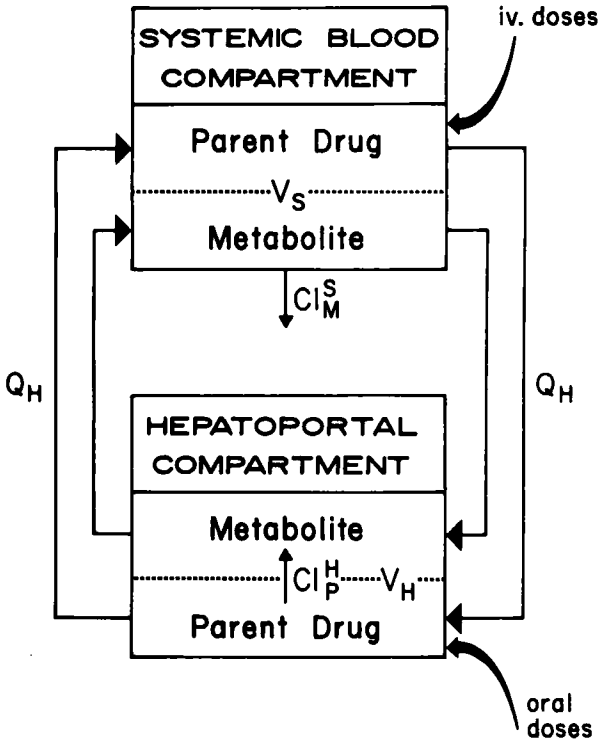

Scheme I—First pass metabolism model used to simulate both parent drug and metabolite plasma concentrations under various conditions. Q_H is the hepatic blood flow, CL_M^S is the systemic clearance of the metabolite, CL_P^H is the hepatoportal clearance of parent drug to metabolite, V_P^S, V_P^H, V_M^S, and V_M^H are the systemic and hepatoportal volumes of parent and metabolite, respectively. The volume of distribution for the metabolite ($V_M^S + V_M^H$) is assumed to be equivalent to the systemic volume of distribution (V_P^S) of the parent drug and V_M^H is set equal to 1; e.g., the metabolite is not retained in the liver after formation (60 mg administered). Oral doses (60 mg) are absorbed into the hepatoportal compartment with the rate constant k_a, and intravenous doses (60 mg) are administered instantly into the systemic blood compartment.

The differential equations (see *Appendix*) needed to describe the first-pass metabolism model shown in Scheme I were used for the simulation of plasma concentration–time data for both parent drug and a single metabolite following oral and intravenous doses. The differential equations required to describe the model were used in conjunction with the nonlinear regression program NONLIN (1), to simulate parent drug and metabolite concentration–time data for drugs with varied pharmacokinetic characteristics. A 60-mg dose was used for each simulation. Several biopharmaceutic and pharmacokinetic parameters such as the time (t_{max}) of the maximum observed concentration (C_{max}) following oral doses, the areas under the plasma concentration–time curve (AUC) for parent drug and metabolite following oral (AUC_P^O and AUC_M^O) and intravenous (AUC_P^{IV} and AUC_M^{IV}) doses, the terminal elimination half-lives for parent drugs ($t_{1/2P}$) and metabolite ($t_{1/2M}$), the ratio of oral to intravenous area of parent (F_P) and metabolite (F_M), and the ratio of metabolite–parent drug following oral (R_O) and intravenous (R_{IV}) doses were calculated from the simulated plasma concentration–time data. The constants used for

0022-3549/83/0600-0711$01.00/0

Table I—Effect of First-Pass, Formation-Rate-Limited Metabolism on Various Pharmacokinetic Parameters [a]

Simulation Constants	Case I A	I B	I C	II A	II B	II C	III A	III B	III C	IV A	IV B	IV C
k_a, hr^{-1}	1.0	1.0	1.0	1.0	1.0	1.0	1.0	1.0	1.0	1.0	1.0	1.0
Q_H, liter/hr	90	90	90	90	90	90	90	90	90	90	90	90
CL_P^H, liter/hr	450	450	450	4,500	4,500	4,500	450	450	450	4,500	4,500	4,500
CL_M^S, liter/hr	600	6,000	60,000	600	6,000	60,000	18	180	1,800	18	180	1,800
V_P^S, liter	60	600	6,000	60	6,000	60,000	60	600	6,000	60	600	6,000
V_P^H, liter	60	60	60	600	600	600	60	60	60	600	600	600
V_M^S, liter	59	599	5,999	59	599	5,999	59	599	5,999	59	599	5,999
V_M^H, liter	1	1	1	1	1	1	1	1	1	1	1	1
Biopharmaceutic Parameters												
t_{maxP}, hr	1.0	2.5	4.5	1.0	2.5	4.5	1.0	2.5	4.5	1.0	2.5	4.5
C_{maxP}, μg/ml	53.3	12.2	2.57	5.80	1.39	0.184	53.3	12.2	1.57	5.80	1.39	0.184
t_{maxM}, hr	0.5	0.5	0.5	0.5	0.5	0.5	2.0	2.0	2.0	2.0	2.0	2.0
C_{maxM}, μg/ml	61.4	5.87	0.584	68.3	6.80	0.679	571	50.9	4.98	591	58.4	5.82
$t_{1/2P}$, hr	0.57	5.6	55.4	0.47	4.7	47.1	0.57	5.6	55.4	0.47	4.7	47.1
$t_{1/2M}$, hr	0.57	5.6	55.4	0.47	4.7	47.1	2.3	5.6	55.4	2.3	4.7	47.1
Pharmacokinetic Parameters												
AUC_P^0, μg hr/ml	133	133	133	12.5	13.3	13.3	133	133	133	12.5	13.3	13.3
AUC_M^0, μg hr/ml	797	800	800	680	680	680	797	800	800	680	680	680
AUC_M^O, μg hr/ml	99	9.91	1.00	100	10	1.0	3290	329	32.9	3,290	329	32.9
AUC_M^{IV}, μg hr/ml	100	10.0	1.00	100	10	1.0	3290	329	32.9	3,290	329	32.9
F_P	0.17	0.17	0.17	0.02	0.02	0.02	0.17	0.17	0.17	0.02	0.02	0.02
F_M	1.0	1.0	1.0	1.0	1.0	1.0	1.0	1.0	1.0	1.0	1.0	1.0
R_O	0.74	0.074	0.0075	8.0	0.75	0.075	24.7	2.47	0.25	263	24.7	2.47
R_{IV}	0.13	0.013	0.0013	0.15	0.015	0.0015	4.13	0.411	0.041	4.83	0.483	0.048
$CL_{B,P}$ liter/hr	75	75	75	88	88	88	75	75	75	88	88	88
$C_{B,M}$ liter/hr	600	6,000	60,000	600	6,000	60,000	600	6,000	60,000	600	6,000	60,000

[a] Parameters defined in text.

the simulations as well as the calculated pharmacokinetic and biopharmaceutic parameters are presented in Table I.

Substantial first-pass metabolism occurs in all cases, because the metabolic organ clearance (CL_P^H) exceeds hepatic blood flow (Q_H). t_{maxP} is earlier than t_{maxM} when the metabolite is not formation-rate limited, (Table I, Cases IIIA and IVA); *i.e.*, the half-life of the metabolite exceeds the half-life of the parent drug. Therefore, it is apparent that t_{maxM} occurs earlier than t_{maxP} only when the metabolite is the result of first-pass metabolism and the elimination of the metabolite is limited by the parent half-life. In addition, it is apparent that the volume of distribution of the parent drug is the controlling factor in determining whether a first-pass metabolite will ultimately be formation-rate limited. Although the clearance of parent drug does not change as the volume of distribution for the parent drug increases, the half-life of the parent drug ($t_{1/2P}$) will ultimately limit the *apparent* rate of elimination of the metabolite ($t_{1/2M}$) as the metabolite formation rather than its elimination becomes rate determining (Table I, Case IIIA–C and Case IVA–C).

The effective hepatic volume of distribution for the parent drug is important to the extent of first-pass metabolism (2). Although the half-life does not change (Table I, Case IA–C *versus* Case IIA–C and Case IIIA–C *versus* Case IVA–C), the extent of first-pass metabolism increases as the hepatic organ clearance (CL_P^H) increases as a function of increasing effective hepatic volume (2), such that the data reflect a decrease in the bioavailability parameter (F_P). The relative bioavailability of the metabolite (F_M) does not change, since all of the administered drug is ultimately converted to metabolite in the simplistic model used for these simulations. If an alternative route of elimination exists for the parent drug, then relative metabolite bioavailability would change as well. The ratios of the metabolite AUC to the parent AUC following oral (R_O) and intravenous (R_{IV}) doses increase as the effective hepatic volume increases (Table I, Case I *versus* Case II). However, due to first-pass metabolism, the increase in R_O is much higher than the increase in R_{IV}.

Additional observations became apparent as a result of the simulation procedures. The concentration–time data simulated from Case IVB are presented in Fig. 1 to illustrate various phenomena that were observed. First, under the conditions of this simulation, metabolite concentrations following oral doses decrease with an apparent half-life shorter than that of the parent drug for an interval of 48 hr before becoming formation-rate limited. If the analytical sensitivity is limiting or its sampling is restricted to 24 hr or less, it would appear that the metabolite was being eliminated more quickly than the parent drug.

In conclusion, it has been demonstrated that first-pass and formation-rate metabolism are not mutually exclusive. In fact, even first-pass metabolites with reasonably long elimination half-lives can be formation-rate limited if the volume of distribution of the parent drug is sufficiently large. This results because the driving force for first-pass metabolism is a high extraction ratio for the parent compound, *i.e.*, high organ clearance, whereas the driving force for formation-rate limited metabolism is a shorter half-life for the metabolite than that of the parent compound. This can occur easily if the volume of distribution of the parent compound is extremely large. Finally, the impact of first-

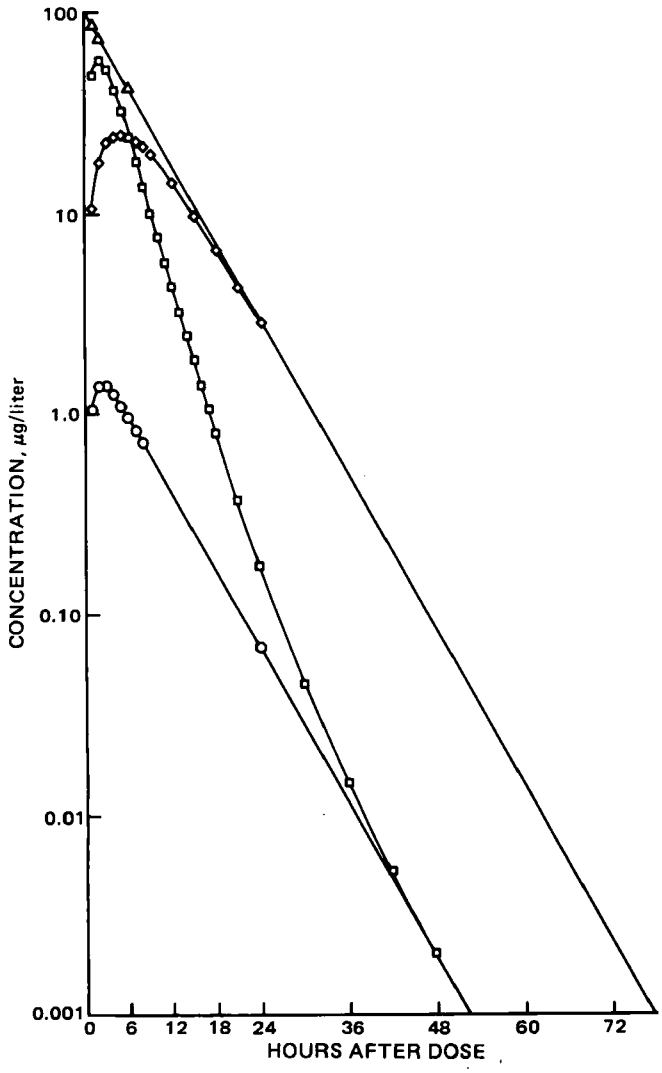

Figure 1—*Blood concentrations of drug and metabolite following oral (○ and □) and intravenous (△ and ◇) doses, respectively, simulated according to Case IVB.*

pass metabolism on various pharmacokinetic parameters has been delineated using simulation techniques.

APPENDIX

The following differential equations were used to simulate the plasma concentration–time data presented in this report.

$$\frac{dC_P^S}{dt} = Q_H \cdot (C_P^H - C_P^S)/V_P^S \qquad \text{(Eq. A-1)}$$

$$\frac{dC_M^S}{dt} = [Q_H \cdot C_M^H - (Q_H + CL_M^S) \cdot C_M^S]/V_M^S \qquad \text{(Eq. A-2)}$$

$$\frac{dC_P^H}{dt} = [k_a De^{-k_{at}} + Q_H \cdot C_P^S - (Q_H + CL_P^H) \cdot C_P^H]/V_P^H \qquad \text{(Eq. A-3)}$$

$$\frac{dC_M^H}{dt} = [Q_H \cdot C_M^S + CL_P^H C_P^H - Q_H C_M^H]/V_M^H \qquad \text{(Eq. A-4)}$$

Where D is the oral dose and the remaining terms have been identified in the text and legend to Scheme I. The $k_a De^{-k_{at}}$ term is the source of drug input for the oral dose. This source is not used for the IV dose, whereas the initial condition for C_P^S is set equal to D/V_P^S for the IV dose.

(1) C. M. Metzler, G. L. Elfring, and A. J. McEwen, *Biometrics*, **30**, 562 (1974).

(2) W. A. Colburn, *J. Pharm. Sci.*, **70**, 969 (1981).

Wayne A. Colburn
Department of Pharmacokinetics and Biopharmaceutics
Hoffmann-La Roche Inc.
Nutley, NJ 07110

Received March 10, 1982.
Accepted for Publication January 5, 1983.

Factors Affecting the Accuracy of Estimated Mean Absorption Times and Mean Dissolution Times

Keyphrases □ Statistical moment analysis—estimation of absorption and dissolution rates, effects of the sampling schedule, importance of the estimate of the terminal elimination rate constant (β)

To the Editor:

Recent discussions in the literature concerning the application of the concept of statistical moments to pharmacokinetic analysis has stimulated interest in the method and its potential utility in the evaluation of pharmacokinetic and bioavailability data. The most appealing aspect of statistical moment analysis is the potential for model-independent estimates of *in vivo* dissolution and absorption rates. A thorough discussion of this method and its potential applications was presented by Riegelman and Collier (1) and Yamaoka *et al* (2).

Using simulation techniques, the present study evaluates the ability of statistical moment analysis to provide accurate estimates of absorption and dissolution rates and the effects of sampling schedule, random error, and the estimate of the terminal elimination rate constant (β) on the accuracy of these estimates.

Simulations of drug concentration–time data corresponding to administration of an intravenous bolus, oral solution, and tablet dosage forms were generated by the CSSL-IV simulation program (3) based on the pharmacokinetic models presented in Scheme I. Unless otherwise specified, the parameter values presented in Table

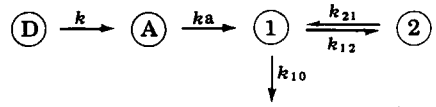

Scheme I—Two-compartment pharmacokinetic model with sequential first-order dissolution and absorption, where k = *first-order dissolution rate constant and* k_a = *first-order absorption rate constant. To simulate intravenous data, the dose was entered into compartment 1; for oral solution data, the dose was entered into the absorption compartment (A); and for solid oral dosage form data, the dose was entered into the dissolution compartment (D).*

0022-3549/83/0600-0713$01.00/0

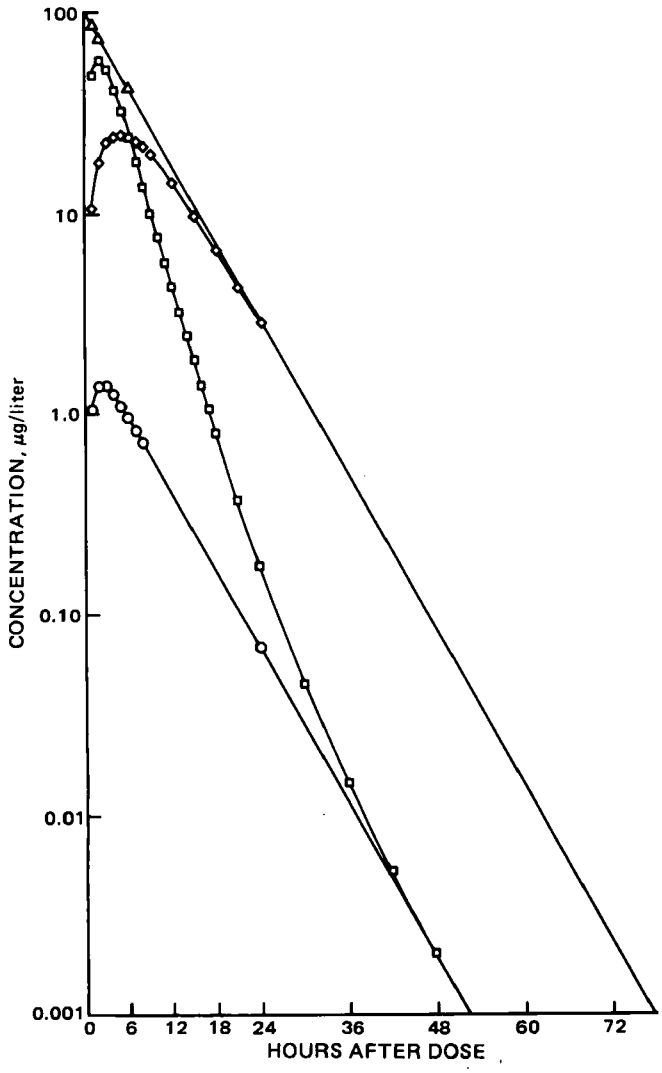

Figure 1—*Blood concentrations of drug and metabolite following oral (○ and □) and intravenous (△ and ◇) doses, respectively, simulated according to Case IVB.*

pass metabolism on various pharmacokinetic parameters has been delineated using simulation techniques.

APPENDIX

The following differential equations were used to simulate the plasma concentration–time data presented in this report.

$$\frac{dC_P^S}{dt} = Q_H \cdot (C_P^H - C_P^S)/V_P^S \qquad \text{(Eq. A-1)}$$

$$\frac{dC_M^S}{dt} = [Q_H \cdot C_M^H - (Q_H + CL_M^S) \cdot C_M^S]/V_M^S \qquad \text{(Eq. A-2)}$$

$$\frac{dC_P^H}{dt} = [k_a De^{-k_{at}} + Q_H \cdot C_P^S - (Q_H + CL_P^H) \cdot C_P^H]/V_P^H \qquad \text{(Eq. A-3)}$$

$$\frac{dC_M^H}{dt} = [Q_H \cdot C_M^S + CL_P^H C_P^H - Q_H C_M^H]/V_M^H \qquad \text{(Eq. A-4)}$$

Where D is the oral dose and the remaining terms have been identified in the text and legend to Scheme I. The $k_a De^{-k_{at}}$ term is the source of drug input for the oral dose. This source is not used for the IV dose, whereas the initial condition for C_P^S is set equal to D/V_P^S for the IV dose.

(1) C. M. Metzler, G. L. Elfring, and A. J. McEwen, *Biometrics*, **30**, 562 (1974).

(2) W. A. Colburn, *J. Pharm. Sci.*, **70**, 969 (1981).

Wayne A. Colburn
Department of Pharmacokinetics and Biopharmaceutics
Hoffmann-La Roche Inc.
Nutley, NJ 07110

Received March 10, 1982.
Accepted for Publication January 5, 1983.

Factors Affecting the Accuracy of Estimated Mean Absorption Times and Mean Dissolution Times

Keyphrases □ Statistical moment analysis—estimation of absorption and dissolution rates, effects of the sampling schedule, importance of the estimate of the terminal elimination rate constant (β)

To the Editor:

Recent discussions in the literature concerning the application of the concept of statistical moments to pharmacokinetic analysis has stimulated interest in the method and its potential utility in the evaluation of pharmacokinetic and bioavailability data. The most appealing aspect of statistical moment analysis is the potential for model-independent estimates of *in vivo* dissolution and absorption rates. A thorough discussion of this method and its potential applications was presented by Riegelman and Collier (1) and Yamaoka *et al* (2).

Using simulation techniques, the present study evaluates the ability of statistical moment analysis to provide accurate estimates of absorption and dissolution rates and the effects of sampling schedule, random error, and the estimate of the terminal elimination rate constant (β) on the accuracy of these estimates.

Simulations of drug concentration–time data corresponding to administration of an intravenous bolus, oral solution, and tablet dosage forms were generated by the CSSL-IV simulation program (3) based on the pharmacokinetic models presented in Scheme I. Unless otherwise specified, the parameter values presented in Table

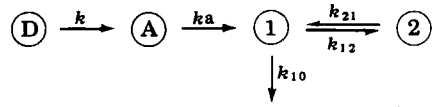

Scheme I—Two-compartment pharmacokinetic model with sequential first-order dissolution and absorption, where k = *first-order dissolution rate constant and* k_a = *first-order absorption rate constant. To simulate intravenous data, the dose was entered into compartment 1; for oral solution data, the dose was entered into the absorption compartment (A); and for solid oral dosage form data, the dose was entered into the dissolution compartment (D).*

0022-3549/83/0600-0713$01.00/0

Table I—Parameter Values Used in the Simulations

Simulation	Dose, mg	V_1, liters	k, hr^{-1}	k_a, hr^{-1}	k_{10}, hr^{-1}	k_{21}, hr^{-1}	k_{12}, hr^{-1}
Intravenous	100	1.0	—	—	0.20	0.60	0.50
Liquid	100	1.0	—	3.0	0.20	0.60	0.50
Tablet	100	1.0	0.78	3.0	0.20	0.60	0.50

Table II—Sampling Schedules Used for Calculation of Parameters

Schedule	Sampling Times, hr
A	Every 0.05 hr for 36 hr
B	0, 0.25, 0.5, 0.75, 1, 1.5, 2, 2.5, 3, 4, 6, 8, 10, 12, 18, 24, 36
C	0, 0.5, 1, 1.5, 2, 3, 4, 6, 8, 10, 12, 24
D	0, 0.5, 1, 1.5, 2, 3, 4, 6, 8, 10, 12, 24, 48, 72, 96

I were used for all simulations. Four sampling schedules were evaluated (Table II) with schedule A providing parameter estimates corresponding to the theoretical values.

Areas under the concentration–time curves (AUC_0^{24}) and areas under the moment curve ($AUMC_0^{24}$) to 24 hr were calculated using the linear trapezoidal method. Extrapolations to infinity and calculations of mean residence time (MRT), mean absorption time (MAT), and mean dissolution time (MDT) were performed as described previously (1).

For those simulations in which random error was added to the concentration data, data corresponding to sampling schedule C were simulated and normally distributed random error with a coefficient of variation of ±10% was added to each concentration value. This was done for 18 data sets per group. Extrapolations of AUC_0^{24} and $AUMC_0^{24}$ to infinity were performed using the theoretical value of β (*i.e.*, 0.1 hr^{-1}) and the β value generated by linear regression of the transformed data from 8 to 24 hr. Two MDT values were then calculated, one using AUC_0^∞ and $AUMC_0^\infty$ extrapolated with the theoretical β (Footnote *b*, Table III) and one using AUC_0^∞ and $AUMC_0^\infty$ extrapolated with the β value corresponding to the transformed data (Footnote *c*, Table III).

The effect of sampling schedule on the accuracy of the calculated estimates of MAT and MDT is presented in Table IV. As expected, the values of MAT and MDT calculated from sampling schedule A correspond to the theoretical values; *i.e.*, the reciprocal values of MAT and MDT are equivalent to the values of k_a and k used to generate the theoretical data. Comparing the results from sampling schedules B and C with those from schedule A gives an indication of the accuracy of the estimates of MAT and MDT when these reduced sampling schedules are utilized.

In general, sampling schedule B provided reasonably good estimates of the theoretical values of MAT and MDT (Table IV). In many cases, however, the parameters calculated with schedule C (typical for many protocols) were relatively poor estimates of the theoretical values. The accuracy of MAT and MDT tended to decrease as the rate constants k_a and k increased and as the two-compartment characteristics of the concentration–time curve became more pronounced (as k_{21} varied from 0.6 to 0.1 hr^{-1}). Increased sampling during the absorptive phase (schedule B) improved the accuracy of MAT and MDT (compared with schedule C), and the improvement was most pronounced when a k_{21} value of 0.1 hr^{-1} was utilized and when k and k_a were large. It is obvious from these data that the sampling schedule is critical for obtaining accurate and meaningful estimates of mean absorption times and mean dissolution times.

The importance of an accurate estimate of β when calculating various statistical moment parameters has been discussed previously (1, 2) and is demonstrated in our results. Using sampling schedule C and a k_{21} value of 0.2 hr^{-1}, 27% of AUC_0^∞ and 69% of $AUMC_0^\infty$ are due to extrapolation from the last data point to infinity using β. A ±10% error in β yields MDT estimates of −0.15 and 2.60 hr, respectively, compared with 1.07 hr when the correct β value is used. Utilizing sampling schedule D, only 1% of AUC_0^∞ and 6% of $AUMC_0^\infty$ are due to extrapolation, and the same ±10% error in β results in MDT estimates of 0.91 and 1.14 hr, respectively, compared with 1.01 hr when the

Table III—Mean Parameter Values Determined from Data Generated with Normally Distributed Random Error (CV ± 10%)

k, hr^{-1}	$1/k$,[a] hr	MDT[b], hr			β, hr^{-1}		MDT[c], hr		
		Mean	*SD*	*CV*	Mean	*SD*	Mean	*SD*	*CV*
0.60	1.67	1.56	0.39	25%	0.100	0.010	1.53	0.72	47%
0.72	1.39	1.27	0.42	32%	0.099	0.007	1.34	0.68	51%
0.78	1.28	1.26	0.33	26%	0.098	0.006	1.33	0.84	63%
0.90	1.11	1.05	0.24	23%	0.100	0.008	1.06	0.86	81%

[a] Theoretical value of MDT. [b] Calculated from AUC_0^∞ and $AUMC_0^\infty$ values in which extrapolation from 24 hr to infinity was performed using β = 0.1 hr^{-1}. [c] Calculated from AUC_0^∞ and $AUMC_0^\infty$ values in which extrapolation from 24 hr to infinity was performed using β determined by linear regression of the transformed data from 8 to 24 hr.

Table IV—Estimated Values of MAT and MDT from Data Generated for Sampling Schedules A, B, and C

Parameter Value, hr^{-1}	k_{21} = 0.1 hr^{-1}						k_{21} = 0.6 hr^{-1}					
	MAT, hr			MDT, hr			MAT, hr			MDT, hr		
	A	B	C	A	B	C	A	B	C	A	B	C
k = 0.4				2.50	2.45	2.11				2.50	2.46	2.26
0.7				1.43	1.36	1.05				1.43	1.39	1.25
1.0				1.00	0.91	0.62				1.00	0.96	0.84
k_a = 1	1.00	1.08	1.17	1.28	1.28	1.19	1.00	1.00	1.01	1.28	1.26	1.19
3	0.33	0.42	0.76	1.28	1.20	0.90	0.33	0.36	0.45	1.28	1.24	1.11
5	0.20	0.42	0.84	1.28	1.15	0.71	0.20	0.26	0.39	1.28	1.21	1.06
k_{10} = 0.1	0.33	0.40	0.69	1.28	1.23	1.00	0.33	0.29	0.42	1.28	1.30	1.24
0.3	0.33	0.41	0.77	1.28	1.18	0.90	0.33	0.36	0.49	1.28	1.25	1.14
0.5	0.33	0.44	0.81	1.28	1.15	0.88	0.33	0.37	0.54	1.28	1.19	1.14

correct value is used. Errors in the estimate of β are inherent due to biological and analytical variability, but their impact can be reduced drastically by expanding the sampling schedule to longer times. Since this is not always possible because of analytical and practical limitations, the use of statistical moments may not be appropriate if there is insufficient sampling to provide accurate and consistent estimates of β.

Routine analytical error in drug concentration data can affect estimates of MAT and MDT in two ways: first, by its effects on the calculation of $AUMC_0^t$ and AUC_0^t, which should be rather insignificant, and second, by its effects on the estimate of β, which in turn may affect the calculation of $AUMC_0^\infty$ and AUC_0^∞ significantly. The first case is illustrated in Table III by the values of MDT^b generated using the theoretical value of β (i.e. 0.1 hr^{-1}) for all extrapolations. The average ($n = 18$) estimated MDT values were good estimates of the theoretical values with coefficients of variation ranging from 23 to 32%. The effect of variations in β caused by random error and the subsequent impact on MDT^c is also shown in Table III. The average MDT^c values were again good estimates of the theoretical values but the coefficients of variation were quite large, ranging from 47 to 81%. With this sampling schedule ~8% of AUC_0^∞ and 31% of $AUMC_0^\infty$ were due to extrapolation, and this would not be uncommon for a typical bioavailability study. The large variability in these MDT values could affect the ability to statistically detect small differences in MDT values under such conditions.

Overall, the results of these studies suggest that the statistical moment approach to the analysis of bioavailability data may offer an attractive alternative to C_{max} and t_{max} or to the model-dependent methods for assessing the rate of drug absorption. However, accurate results and meaningful conclusions using this method are very much dependent on the experimental design of the studies from which the data are generated. To obtain optimal information, frequent sampling during the absorption phase is necessary. In addition, sufficient sampling during the terminal elimination phase is needed to minimize the impact of extrapolation error and to provide an accurate estimate of β. MAT and MDT values calculated from data generated *via* a less than rigorous experimental design may yield poor estimates of the actual values and can result in misleading conclusions. Therefore, an understanding of the influence of the various factors affecting the accuracy of the calculated MAT and MDT values, along with a well-defined pharmacokinetic profile of the drug, are essential to achieve an experimental design which will allow for the determination of meaningful estimates of mean absorption and dissolution times.

(1) S. Riegelman and P. Collier, *J. Pharmacokinet. Biopharm.*, **8**, 509 (1980).

(2) K. Yamaoka, T. Nakagana, and T. Uno, *ibid.*, **6**, 547 (1978).

(3) "CSSL IV Users Guide and Reference Manual," Nielsen Associates, 1976.

Romulus K. Brazzell ˣ
Stanley A. Kaplan
Department of Pharmacokinetics and Biopharmaceutics
Hoffmann-La Roche Inc.
Nutley, N.J. 07110

Received July 28, 1982
Accepted for Publication January 27, 1983

Plasma Inorganic Sulfate Concentrations in Pregnant Women

Keyphrases □ Sulfate concentration—effect of pregnancy in humans □ Plasma sulfate concentrations—effect of pregnancy in humans

To the Editor:

The physiological process of sulfation has important biosynthetic and detoxification functions. It is necessary in the developing fetus for the formation of glycosaminoglycans, a structural component of cartilage and other tissues, and cerebroside sulfate, a constituent of the brain (1, 2). The sulfated glycosaminoglycans may also be involved in cell differentiation (2).

The biotransformation of certain phenolic drugs to sulfate conjugates is limited by the availability of inorganic sulfate (3, 4); the formation of such drug conjugates can cause depletion of endogenous inorganic (free) sulfate in animals and humans (4–6). Decreased sulfate availability in pregnant rats, due to administration of salicylamide, which produces sulfate depletion concomitant with salicylamide sulfate formation (3, 5), has been associated with decreased availability and decreased tissue incorporation of sulfate in the fetuses and may be the cause of teratogenic effects (7, 8). Depletion of endogenous sulfate can decrease the rate of sulfation of phenolic drugs, such as acetaminophen, and thereby decrease their clearance (4), while hypersulfatemia, such as occurs in renal dysfunction, can facilitate drug sulfate conjugate formation and thereby increase drug clearance (9). The maternal level of endogenous inorganic sulfate may, therefore, affect fetal development and fetal exposure to certain drugs and other xenobiotics.

The plasma or serum concentrations of most electrolytes tend to decrease slightly during pregnancy (10). We have found only one report concerning the effect of pregnancy on serum sulfate concentrations: Tallgren observed concentrations of 0.592 ± 0.275 mmole/liter (mean ± *SD*) in 118 Scandinavian women during their third trimester and 0.263 ± 0.091 mmole/liter in 42 age-matched nonpregnant controls (11). On the other hand, Lin and Levy recently determined serum sulfate concentrations in 20-day pregnant rats and nonpregnant controls and found no apparent difference between the two groups[1]. The effect of pregnancy on endogenous sulfate concentrations in women was, therefore, reexamined.

Seven Caucasian women in their third trimester of pregnancy and nine Caucasian nonpregnant women of similar age were the subjects in this study. They were medication-free for at least 1 week before the study and were in apparent good health. None of the controls were taking an oral contraceptive. Nine-milliliter blood samples were drawn from an antecubital vein into 10-ml capacity plastic disposable syringes containing 1 ml of trisodium citrate solution each. The citrated blood was centrifuged in plastic tubes at 12,000×*g* for 15 min at 25°, and the plasma was frozen pending assay. Inorganic sulfate concentration was determined by a modification (12) of the turbidimetric method of Berglund and Sörbo (13), using

[1] Results to be published.

0022-3549/83/0600-0715$01.00/0

correct value is used. Errors in the estimate of β are inherent due to biological and analytical variability, but their impact can be reduced drastically by expanding the sampling schedule to longer times. Since this is not always possible because of analytical and practical limitations, the use of statistical moments may not be appropriate if there is insufficient sampling to provide accurate and consistent estimates of β.

Routine analytical error in drug concentration data can affect estimates of MAT and MDT in two ways: first, by its effects on the calculation of $AUMC_0^t$ and AUC_0^t, which should be rather insignificant, and second, by its effects on the estimate of β, which in turn may affect the calculation of $AUMC_0^\infty$ and AUC_0^∞ significantly. The first case is illustrated in Table III by the values of MDT^b generated using the theoretical value of β (i.e. 0.1 hr^{-1}) for all extrapolations. The average ($n = 18$) estimated MDT values were good estimates of the theoretical values with coefficients of variation ranging from 23 to 32%. The effect of variations in β caused by random error and the subsequent impact on MDT^c is also shown in Table III. The average MDT^c values were again good estimates of the theoretical values but the coefficients of variation were quite large, ranging from 47 to 81%. With this sampling schedule ~8% of AUC_0^∞ and 31% of $AUMC_0^\infty$ were due to extrapolation, and this would not be uncommon for a typical bioavailability study. The large variability in these MDT values could affect the ability to statistically detect small differences in MDT values under such conditions.

Overall, the results of these studies suggest that the statistical moment approach to the analysis of bioavailability data may offer an attractive alternative to C_{max} and t_{max} or to the model-dependent methods for assessing the rate of drug absorption. However, accurate results and meaningful conclusions using this method are very much dependent on the experimental design of the studies from which the data are generated. To obtain optimal information, frequent sampling during the absorption phase is necessary. In addition, sufficient sampling during the terminal elimination phase is needed to minimize the impact of extrapolation error and to provide an accurate estimate of β. MAT and MDT values calculated from data generated *via* a less than rigorous experimental design may yield poor estimates of the actual values and can result in misleading conclusions. Therefore, an understanding of the influence of the various factors affecting the accuracy of the calculated MAT and MDT values, along with a well-defined pharmacokinetic profile of the drug, are essential to achieve an experimental design which will allow for the determination of meaningful estimates of mean absorption and dissolution times.

(1) S. Riegelman and P. Collier, *J. Pharmacokinet. Biopharm.*, **8**, 509 (1980).

(2) K. Yamaoka, T. Nakagana, and T. Uno, *ibid.*, **6**, 547 (1978).

(3) "CSSL IV Users Guide and Reference Manual," Nielsen Associates, 1976.

Romulus K. Brazzell ˣ
Stanley A. Kaplan
Department of Pharmacokinetics and Biopharmaceutics
Hoffmann-La Roche Inc.
Nutley, N.J. 07110

Received July 28, 1982
Accepted for Publication January 27, 1983

Plasma Inorganic Sulfate Concentrations in Pregnant Women

Keyphrases □ Sulfate concentration—effect of pregnancy in humans □ Plasma sulfate concentrations—effect of pregnancy in humans

To the Editor:

The physiological process of sulfation has important biosynthetic and detoxification functions. It is necessary in the developing fetus for the formation of glycosaminoglycans, a structural component of cartilage and other tissues, and cerebroside sulfate, a constituent of the brain (1, 2). The sulfated glycosaminoglycans may also be involved in cell differentiation (2).

The biotransformation of certain phenolic drugs to sulfate conjugates is limited by the availability of inorganic sulfate (3, 4); the formation of such drug conjugates can cause depletion of endogenous inorganic (free) sulfate in animals and humans (4–6). Decreased sulfate availability in pregnant rats, due to administration of salicylamide, which produces sulfate depletion concomitant with salicylamide sulfate formation (3, 5), has been associated with decreased availability and decreased tissue incorporation of sulfate in the fetuses and may be the cause of teratogenic effects (7, 8). Depletion of endogenous sulfate can decrease the rate of sulfation of phenolic drugs, such as acetaminophen, and thereby decrease their clearance (4), while hypersulfatemia, such as occurs in renal dysfunction, can facilitate drug sulfate conjugate formation and thereby increase drug clearance (9). The maternal level of endogenous inorganic sulfate may, therefore, affect fetal development and fetal exposure to certain drugs and other xenobiotics.

The plasma or serum concentrations of most electrolytes tend to decrease slightly during pregnancy (10). We have found only one report concerning the effect of pregnancy on serum sulfate concentrations: Tallgren observed concentrations of 0.592 ± 0.275 mmole/liter (mean ± *SD*) in 118 Scandinavian women during their third trimester and 0.263 ± 0.091 mmole/liter in 42 age-matched nonpregnant controls (11). On the other hand, Lin and Levy recently determined serum sulfate concentrations in 20-day pregnant rats and nonpregnant controls and found no apparent difference between the two groups[1]. The effect of pregnancy on endogenous sulfate concentrations in women was, therefore, reexamined.

Seven Caucasian women in their third trimester of pregnancy and nine Caucasian nonpregnant women of similar age were the subjects in this study. They were medication-free for at least 1 week before the study and were in apparent good health. None of the controls were taking an oral contraceptive. Nine-milliliter blood samples were drawn from an antecubital vein into 10-ml capacity plastic disposable syringes containing 1 ml of trisodium citrate solution each. The citrated blood was centrifuged in plastic tubes at 12,000×*g* for 15 min at 25°, and the plasma was frozen pending assay. Inorganic sulfate concentration was determined by a modification (12) of the turbidimetric method of Berglund and Sörbo (13), using

[1] Results to be published.

0022-3549/83/0600-0715$01.00/0

Table I—Effect of Pregnancy on Sulfate Concentrations in Plasma of Caucasian Women [a]

	Pregnant (n = 7)	Nonpregnant (n = 9)	Significance
Plasma sulfate, mM	0.410 ± 0.035	0.333 ± 0.038	$p < 0.005$
Age, yr	24.4 ± 4.2	27.2 ± 5.5	NS
Gestation age, wk	35.8 ± 3.8		
Total protein, g/dl	6.08 ± 0.29	6.43 ± 0.35	NS
Albumin, g/dl	3.28 ± 0.19	4.14 ± 0.20	$p < 0.001$

[a] Results expressed as mean ± SD.

pooled citrated plasma from nonpregnant women with known concentrations of added sodium sulfate for preparation of a standard curve. All samples were assayed on the same day, and the results were corrected for sample dilution with citrate anticoagulant solution. Total plasma protein concentrations (14) and albumin fraction[2] were also determined. Results were examined by one-way ANOVA, and possible associations between sulfate concentration and other variables were determined by correlation analysis[3].

The results of this study are summarized in Table I. Plasma sulfate concentrations were significantly higher in the pregnant women, but the quantitative difference between the pregnant and nonpregnant women was relatively small. Plasma albumin concentrations were significantly decreased in late pregnancy, consistent with previous observations (15). The difference in sulfate concentration between pregnant and nonpregnant subjects remained when smokers were eliminated (0.427 ± 0.039 mmole/liter in four pregnant women and 0.328 ± 0.036 in eight nonpregnant women, $p < 0.005$). Eight Black women (including two smokers) in their third trimester of pregnancy were also studied; their plasma sulfate concentration (0.360 ± 0.072 mmole/liter) is not significantly different from those of the Caucasian pregnant and nonpregnant women, respectively. There is a significant negative correlation between the plasma sulfate concentration of the 15 pregnant women (Black and Caucasian combined) and their plasma albumin concentration ($r = -0.548$, $p < 0.05$). No other significant correlations were found.

The results of this investigation are in qualitative agreement with those of Tallgren (11) with respect to Caucasian women, but the quantitative difference between pregnant and nonpregnant women is considerably smaller in our study. Our results for nonpregnant females are similar to those described (11), but the inorganic sulfate concentrations in pregnant women are appreciably lower in our study. The intake of proteins rich in sulfur-containing amino acids is an important determinant of endogenous inorganic sulfate levels (11, 16), but it appears unlikely that the difference between the two groups of pregnant women is due to diet, since the two nonpregnant control groups had similar sulfate concentrations. Tallgren's analytical procedure (11) requires incubation of the serum sample for 4 hr at 37° and pH <1, which may favor hydrolysis of endogenous steroid sulfates, while the procedure used by us requires no such incubation. However, the plasma concentrations of these conjugates in pregnancy (17, 18) are much too low to account for the observed differences.

(1) C. P. Dietrich, L. O. Sampaio, O. M. S. Toledo, and C. M. F. Cassaro, *Biochem. Biophys. Res. Commun.*, **75**, 329 (1977).

(2) R. H. DeMeio, in "Metabolic Pathways," 3rd ed., D. M. Greenberg, Ed., Academic, New York, N.Y., 1975, pp. 287–357.

(3) G. Levy and T. Matsuzawa, *J. Pharmacol. Exp. Ther.*, **156**, 285 (1967).

(4) R. E. Galinsky and G. Levy, *ibid.*, **219**, 14 (1981).

(5) J. H. Lin and G. Levy, *Biochem. Pharmacol.*, **30**, 2723 (1981).

(6) M. E. Morris and G. Levy, "Abstracts," American Pharmaceutical Assoc. Academy of Pharmaceutical Sciences national meeting, **12**, 88 (1982).

(7) E. Knight, J. VanWart and D. A. Roe, *J. Nutr.*, **108**, 216 (1978).

(8) P. K. Halstead and D. A. Roe, *Drug-Nutr. Interac.*, **1**, 75 (1981).

(9) J. H. Lin and G. Levy, *J. Pharmacol. Exp. Ther.*, **221**, 80 (1982).

(10) T. Lind, in "Advances in Clinical Chemistry," Vol. 21, Academic, New York, N.Y., 1980, pp. 1–24.

(11) L. G. Tallgren, *Acta Med. Scand., Suppl.*, **640**, 1 (1980).

(12) K. R. Krijgsheld, H. Frankena, E. Scholtens, J. Zweens, and G. J. Mulder, *Biochim. Biophys. Acta*, **586**, 492 (1979).

(13) F. Berglund and B. Sörbo, *Scand. J. Clin. Invest.*, **12**, 147 (1960).

(14) A. G. Gornall, C. J. Bardawill, and M. M. David, *J. Biol. Chem.*, **177**, 751 (1948).

(15) M. Dean, B. Stock, R. J. Patterson, and G. Levy, *Clin. Pharmacol. Ther.*, **28**, 253 (1980).

(16) Z. I. Sabry, S. B. Shadarevian, J. W. Cowan, and J. A. Campbell, *Nature (London)*, **206**, 931 (1965).

(17) K. Sjövall, *Ann. Clin. Res.*, **2**, 393 (1970).

(18) D. L. Loriaux, H. J. Ruder, D. R. Knab, and M. B. Lipsett, *J. Clin. Endocrinol. Metab.*, **35**, 887 (1972).

Marilyn E. Morris
Gerhard Levy[x]

Department of Pharmaceutics
School of Pharmacy
State University of New York at Buffalo
Amherst, NY 14260

Received October 12, 1982.

Accepted for publication January 10, 1983.

Supported in part by Grant GM 19568 from the National Institutes of Health.

Changes in Plasma Protein Binding of Drugs after Blood Collection from Pregnant Women

Keyphrases □ Protein binding—plasma, changes after blood collection from pregnant women □ Unesterified fatty acids—plasma, changes after blood collection from pregnant women

To the Editor:

Drug-protein binding in plasma obtained from 20-day pregnant rats can decrease rapidly *in vitro* after blood collection (1) due to lipolysis and the consequent increase in the concentrations of unesterified fatty acids[1]. These

[2] By Gilman Sepratek Electrophoresis System.
[3] BMPD-79 statistical package.

[1] Results to be published.

0022-3549/83/0600-0716$01.00/0

Table I—Effect of Pregnancy on Sulfate Concentrations in Plasma of Caucasian Women [a]

	Pregnant (n = 7)	Nonpregnant (n = 9)	Significance
Plasma sulfate, mM	0.410 ± 0.035	0.333 ± 0.038	$p < 0.005$
Age, yr	24.4 ± 4.2	27.2 ± 5.5	NS
Gestation age, wk	35.8 ± 3.8		
Total protein, g/dl	6.08 ± 0.29	6.43 ± 0.35	NS
Albumin, g/dl	3.28 ± 0.19	4.14 ± 0.20	$p < 0.001$

[a] Results expressed as mean ± SD.

pooled citrated plasma from nonpregnant women with known concentrations of added sodium sulfate for preparation of a standard curve. All samples were assayed on the same day, and the results were corrected for sample dilution with citrate anticoagulant solution. Total plasma protein concentrations (14) and albumin fraction[2] were also determined. Results were examined by one-way ANOVA, and possible associations between sulfate concentration and other variables were determined by correlation analysis[3].

The results of this study are summarized in Table I. Plasma sulfate concentrations were significantly higher in the pregnant women, but the quantitative difference between the pregnant and nonpregnant women was relatively small. Plasma albumin concentrations were significantly decreased in late pregnancy, consistent with previous observations (15). The difference in sulfate concentration between pregnant and nonpregnant subjects remained when smokers were eliminated (0.427 ± 0.039 mmole/liter in four pregnant women and 0.328 ± 0.036 in eight nonpregnant women, $p < 0.005$). Eight Black women (including two smokers) in their third trimester of pregnancy were also studied; their plasma sulfate concentration (0.360 ± 0.072 mmole/liter) is not significantly different from those of the Caucasian pregnant and nonpregnant women, respectively. There is a significant negative correlation between the plasma sulfate concentration of the 15 pregnant women (Black and Caucasian combined) and their plasma albumin concentration ($r = -0.548$, $p < 0.05$). No other significant correlations were found.

The results of this investigation are in qualitative agreement with those of Tallgren (11) with respect to Caucasian women, but the quantitative difference between pregnant and nonpregnant women is considerably smaller in our study. Our results for nonpregnant females are similar to those described (11), but the inorganic sulfate concentrations in pregnant women are appreciably lower in our study. The intake of proteins rich in sulfur-containing amino acids is an important determinant of endogenous inorganic sulfate levels (11, 16), but it appears unlikely that the difference between the two groups of pregnant women is due to diet, since the two nonpregnant control groups had similar sulfate concentrations. Tallgren's analytical procedure (11) requires incubation of the serum sample for 4 hr at 37° and pH <1, which may favor hydrolysis of endogenous steroid sulfates, while the procedure used by us requires no such incubation. However, the plasma concentrations of these conjugates in pregnancy (17, 18) are much too low to account for the observed differences.

(1) C. P. Dietrich, L. O. Sampaio, O. M. S. Toledo, and C. M. F. Cassaro, *Biochem. Biophys. Res. Commun.*, **75**, 329 (1977).

(2) R. H. DeMeio, in "Metabolic Pathways," 3rd ed., D. M. Greenberg, Ed., Academic, New York, N.Y., 1975, pp. 287–357.

(3) G. Levy and T. Matsuzawa, *J. Pharmacol. Exp. Ther.*, **156**, 285 (1967).

(4) R. E. Galinsky and G. Levy, *ibid.*, **219**, 14 (1981).

(5) J. H. Lin and G. Levy, *Biochem. Pharmacol.*, **30**, 2723 (1981).

(6) M. E. Morris and G. Levy, "Abstracts," American Pharmaceutical Assoc. Academy of Pharmaceutical Sciences national meeting, **12**, 88 (1982).

(7) E. Knight, J. VanWart and D. A. Roe, *J. Nutr.*, **108**, 216 (1978).

(8) P. K. Halstead and D. A. Roe, *Drug-Nutr. Interac.*, **1**, 75 (1981).

(9) J. H. Lin and G. Levy, *J. Pharmacol. Exp. Ther.*, **221**, 80 (1982).

(10) T. Lind, in "Advances in Clinical Chemistry," Vol. 21, Academic, New York, N.Y., 1980, pp. 1–24.

(11) L. G. Tallgren, *Acta Med. Scand., Suppl.*, **640**, 1 (1980).

(12) K. R. Krijgsheld, H. Frankena, E. Scholtens, J. Zweens, and G. J. Mulder, *Biochim. Biophys. Acta*, **586**, 492 (1979).

(13) F. Berglund and B. Sörbo, *Scand. J. Clin. Invest.*, **12**, 147 (1960).

(14) A. G. Gornall, C. J. Bardawill, and M. M. David, *J. Biol. Chem.*, **177**, 751 (1948).

(15) M. Dean, B. Stock, R. J. Patterson, and G. Levy, *Clin. Pharmacol. Ther.*, **28**, 253 (1980).

(16) Z. I. Sabry, S. B. Shadarevian, J. W. Cowan, and J. A. Campbell, *Nature (London)*, **206**, 931 (1965).

(17) K. Sjövall, *Ann. Clin. Res.*, **2**, 393 (1970).

(18) D. L. Loriaux, H. J. Ruder, D. R. Knab, and M. B. Lipsett, *J. Clin. Endocrinol. Metab.*, **35**, 887 (1972).

Marilyn E. Morris
Gerhard Levy[x]

Department of Pharmaceutics
School of Pharmacy
State University of New York at Buffalo
Amherst, NY 14260

Received October 12, 1982.

Accepted for publication January 10, 1983.

Supported in part by Grant GM 19568 from the National Institutes of Health.

Changes in Plasma Protein Binding of Drugs after Blood Collection from Pregnant Women

Keyphrases □ Protein binding—plasma, changes after blood collection from pregnant women □ Unesterified fatty acids—plasma, changes after blood collection from pregnant women

To the Editor:

Drug-protein binding in plasma obtained from 20-day pregnant rats can decrease rapidly *in vitro* after blood collection (1) due to lipolysis and the consequent increase in the concentrations of unesterified fatty acids[1]. These

[2] By Gilman Sepratek Electrophoresis System.
[3] BMPD-79 statistical package.

[1] Results to be published.

0022-3549/83/0600-0716$01.00/0

changes are much less pronounced in plasma of nonpregnant rats (1). Since there are pronounced differences in the drug-protein binding characteristics of rat and human plasma and serum (2, 3), this investigation was designed to determine if the rapid and pronounced decrease in drug-protein binding and increase in fatty acid concentrations observed in plasma of pregnant rats occur also in plasma of pregnant women.

Blood samples were obtained from 15 healthy women, 18 to 29 years old, who were in the third trimester of pregnancy and who were not taking any medications. The blood was drawn from an antecubital vein into a heparinized plastic syringe, and plasma was separated immediately by 1-min centrifugation. A 0.1-ml aliquot of the plasma was immediately extracted into hexane for determination of fatty acid concentrations by gas chromatography (4). Fifty microliters of an aqueous solution of either sodium phenytoin or sodium salicylate was added to another 5- to 6-ml aliquot of plasma to yield final concentrations of ~20 and 200 μg/ml (in terms of the acid), respectively. Two milliliters of this plasma was immediately ultrafiltered (35 min) through a cellophane membrane (Visking, molecular weight cut-off 12,000–14,000), another 2 ml was maintained at 37° for 6 hr and then ultrafiltered after removal of 0.1 ml for determination of fatty acid concentrations, and 0.4 ml was placed in a dialysis cell for equilibrium dialysis (6 hr) against an equal volume of 0.13 *M* sodium–potassium phosphate buffer, pH 7.4, at 37°. A 0.1-ml portion of the plasma phase was collected after dialysis for fatty acid assays. Phenytoin and salicylic acid concentrations in ultrafiltrate, dialysate, and plasma phases were determined by high-performance liquid chromatography, as previously described (5), except that *o*-methoxybenzoic acid was used as the internal standard for the salicylate assay. The equilibrium dialysis procedures were repeated ~1 week later, but at 25°. In view of the concentration dependence of salicylate protein binding, sodium salicylate in a concentration approximately equal to that found previously in the ultrafiltrates was added to the buffer solution. No such precaution was required with respect to phenytoin because of the relative concentration independence of its plasma-free fraction value in the therapeutic concentration range. The plasma for the repeat dialysis procedure had been stored frozen at −20°.

The results of the protein binding determinations are summarized in Table I. Neither incubation of the plasma at 37° nor the 6-hr incubation at 25° associated with equilibrium dialysis had any significant effect on the plasma protein binding of phenytoin. These same procedures caused a pronounced decrease of phenytoin protein binding in plasma of pregnant rats (1). Technical difficulties related to the need for immediate ultrafiltration in the clinic prevented measurements at 37°, except for equilibrium dialysis. The phenytoin free-fraction value at 37° (0.175 ± 0.016) is considerably higher than the corresponding value in nonpregnant individuals (≃0.1) and is in good agreement with previous determinations of phenytoin free fraction in pregnant women (6, 7).

Table I—Changes in Plasma Protein Binding of Phenytoin and Salicylate after Blood Collection from Pregnant Women in the Third Trimester of Pregnancy

Procedure	Free Fraction in Plasma × 100, mean ± *SD*	
	Phenytoin[a]	Salicylate[b]
Immediate ultrafiltration at 25°	9.29 ± 2.32	28.2 ± 6.9
Ultrafiltration at 25° after 6 hr at 37°	9.89 ± 2.41	34.9 ± 7.8[c]
Dialysis for 6 hr at 25°	10.9 ± 1.5	28.7 ± 3.7
Dialysis for 6 h at 37°	17.5 ± 1.6	

[a] Concentration, 22.8 ± 1.8 μg/ml; $n = 8$. [b] Concentration, 203 ± 15 μg/ml; $n = 7$. [c] Significantly different from value after immediate ultrafiltration ($p < 0.05$). The ratio of free-fraction values, 6 hr/immediate, is 1.27 ± 0.26.

Table II—Changes in Concentrations of Unesterified Fatty Acids in Plasma after Blood Collection from Pregnant Women in the Third Trimester of Pregnancy

Fatty Acid	Fatty Acid Concentration, μM[a]			Concentration Ratio, 6 hr/immediate
	Immediately after Plasma Separation	6 hr at 37° after Plasma Separation	After 6-hr Dialysis at 37°	
Linoleic	46.4 ± 30.2	63.2 ± 30.5	60.0 ± 25.2	1.67 ± 0.60
Oleic	123 ± 109	143 ± 102	136 ± 102	1.32 ± 0.23
Palmitic	118 ± 63	157 ± 65	146 ± 64	1.46 ± 0.34
Stearic	61.3 ± 25.6	67.3 ± 21.6	58.6 ± 19.0	1.17 ± 0.26
Total	348 ± 218	430 ± 213	401 ± 205	1.36 ± 0.27

[a] Mean ± *SD*, $n = 15$.

The process of equilibrium dialysis at 25° had no apparent effect on the plasma protein binding of salicylate, but incubation of the plasma for 6 hr at 37° decreased protein binding slightly (Table I). Results of equilibrium dialysis at 37° are not listed in the table, because the buffer phase was not spiked with salicylate to prevent a decrease in drug concentration in the plasma phase. However, the free-fraction values (0.242 ±0.035) are in good agreement with those of an earlier study under similar experimental conditions (8).

The results of fatty acid concentration determinations are summarized in Table II. Some lipolysis occurred in plasma during 6 hr of incubation at 37°, but the fatty acid concentrations increased only by 17–67% on average during incubation and somewhat less during equilibrium dialysis. Under similar conditions, total fatty acid concentrations in plasma from pregnant rats increase by ~500% when heparin is used as the *in vitro* anticoagulant and by 200% when EDTA is used as the anticoagulant[1]. Heparin added *in vitro* to plasma from nonpregnant humans has no apparent effect on the protein binding of phenytoin and salicylic acid (3).

In summary, it has been found that the drug-protein binding characteristics of plasma from healthy women in the third trimester of pregnancy are relatively stable, at least with respect to the drugs tested. These observations are consistent with the relatively small increase of fatty acid concentrations due to *in vitro* lipolysis in plasma during incubation or dialysis at 37° for 6 hr after blood collection. While all plasma samples should be processed to minimize *in vitro* lipolysis, this precaution applies much more to pregnant rats (and perhaps other species) than to pregnant women.

(1) R. C. Chou and G. Levy, *J. Pharm. Sci.*, 71, 471 (1982).
(2) U. W. Wiegand, J. T. Slattery, K. L. Hintze, and G. Levy, *Life Sci.*, 25, 471 (1979).
(3) U. W. Wiegand, K. L. Hintze, J. T. Slattery, and G. Levy, *Clin. Pharmacol. Ther.*, 27, 297 (1980).
(4) S. D. Brunk and J. R. Swanson, *Clin. Chem.*, 27, 924 (1981).
(5) R. C. Chou and G. Levy, *J. Pharmacol. Exp. Ther.*, 219, 42 (1981).
(6) C. Hamar and G. Levy, *Clin. Pharmacol. Ther.*, 28, 58 (1980).

(7) M. Dean, B. Stock, R. J. Patterson, and G. Levy, *ibid.*, **28**, 253 (1980).
(8) C. Hamar and G. Levy, *Pediatr. Pharmacol.*, **1**, 31 (1980).

Ruby C. Chou
Ulf W. Wiegand
Amol S. Lele
Gerhard Levy[x]
Departments of Pharmaceutics and Gynecology and Obstetrics
State University of New York at Buffalo
Amherst, NY 14260

Received October 13, 1982.
Accepted for publication January 10, 1983.
Supported in part by Grant GM 20852 from the National Institute of General Medical Sciences, National Institutes of Health.

Drug Kinetics in Low-Flux (Small) Anatomic Compartments

Keyphrases □ Pharmacokinetics—low-flux peripheral compartment □ Cochlear perilymph—aminoglycoside kinetics

To the Editor:

Small anatomic compartments may be the site of action or toxicity of drugs. Because the kinetics in the anatomic compartment may differ significantly from those in the sampled compartment, pharmacokinetic modeling of such drugs requires the development of explicit expressions for the time course of drug concentrations in the anatomic compartment. Classical compartmental analysis is based on large (kinetic) compartments, which exchange enough drug that measurable alterations in the concentration of drug in the sampled compartment result. A small (anatomic) compartment may not give rise to a detectable alteration in drug concentration in the sampled compartment, because its drug flux is small. In such a case, the anatomic compartment can not be represented by a peripheral kinetic compartment. This communication describes the derivation of an equation for the time course of drug concentrations in such small compartments based on a modified compartmental analysis.

Consider an n-compartment linear mammillary system with first-order rate constants and elimination from the central compartment (denoted by subscript 1) only. Let there be an $(n + 1)$th compartment that exchanges drug with the central compartment but for which the flux of drug into and out of the compartment is so minute that it does not measurably alter levels of the drug in the central compartment. This compartment will be called the low-flux peripheral compartment and will be labeled LF.

The differential equations governing this model are:

$$\frac{dC_1}{dt} = \sum_{j=2}^{n}\left(k_{j1}\frac{V_j}{V_1}C_j - k_{1j}C_1\right) - k_{10}C_1 \quad \text{(Eq. 1)}$$

$$\frac{dC_j}{dt} = k_{1j}\frac{V_1}{V_j}C_1 - k_{j1}C_j,\ n \geq j > 1 \quad \text{(Eq. 2)}$$

$$\frac{dC_{LF}}{dt} = k_{1LF}\frac{V_1}{V_{LF}}C_1 - k_{LF1}C_{LF} \quad \text{(Eq. 3)}$$

where

C_j = concentration of drug in the jth compartment;
V_j = pharmacokinetic volume of distribution of drug in the jth compartment;
k_{ab} = first-order transfer rate constant from the ith to the jth compartment;
k_{10} = first-order elimination rate constant from the central compartment;
C_{LF} = concentration of drug in the low-flux compartment;
k_{1LF}, k_{LF1} = first-order transfer rate constants into and out of the low-flux compartment.

If the drug enters the central compartment as a result of bolus injection, the drug concentration in that compartment, as a function of time, will be a sum of exponentials (1):

$$C_1(t) = \sum_{i=1}^{n} a_i e^{-\lambda_i t} \quad \text{(Eq. 4)}$$

where a_i = coefficient of ith exponential term and λ_i = exponent of the ith exponential term. The general equation for the drug concentration in the jth peripheral compartment is found by the use of Laplace transforms (2):

$$C_j(t) = \frac{V_1}{V_j}\sum_{i=1}^{n}\frac{k_{1j}}{(k_{j1} - \lambda_i)}a_i(e^{-\lambda_i t} - e^{-k_{j1}t}) \quad \text{(Eq. 5)}$$

The equation for the drug concentration in the low flux compartment is:

$$C_{LF}(t) = \frac{V_1}{V_{LF}}\sum_{i=1}^{n}\frac{k_{1LF}}{(k_{LF1} - \lambda_i)}a_i(e^{-\lambda_i t} - e^{-k_{LF1}t}) \quad \text{(Eq. 6)}$$

By similar means, expressions can be found for the drug concentration in the low-flux compartment following entry of the drug into the central compartment by first-order absorption or continuous infusion.

As an example of the application of this model, Eq. 6 is used to describe the kinetics of amikacin, an aminoglycoside antibiotic, in cochlear perilymph, presumably a low-flux compartment. The data are taken from a study performed in guinea pigs, as reported by Brummett *et al.* (3). The concentrations of amikacin were determined in serum and in cochlear perilymph over time following a single subcutaneous injection of the drug (as detailed in Ref. 3). The subcutaneous absorption of amikacin was very rapid, resulting in a monoexponential serum drug concentration *versus* time curve. Therefore, Eq. 4, and consequently Eq. 6, can be used in this case even though the injection was not intravenous.

The equation for the serum drug concentration *versus* time curve is:

$$C_{serum}(t) = 489e^{-0.6992t\,(\text{in hr})} \text{ in micrograms per milliliter}$$

The experimental data and corresponding predicted values are presented in Table I. The perilymph drug concentration *versus* time curve is fitted to a biexponential

0022-3549/83/0600-0718$01.00/0

(7) M. Dean, B. Stock, R. J. Patterson, and G. Levy, *ibid.*, **28**, 253 (1980).
(8) C. Hamar and G. Levy, *Pediatr. Pharmacol.*, **1**, 31 (1980).

Ruby C. Chou
Ulf W. Wiegand
Amol S. Lele
Gerhard Levy[x]
Departments of Pharmaceutics and Gynecology and Obstetrics
State University of New York at Buffalo
Amherst, NY 14260

Received October 13, 1982.
Accepted for publication January 10, 1983.
Supported in part by Grant GM 20852 from the National Institute of General Medical Sciences, National Institutes of Health.

Drug Kinetics in Low-Flux (Small) Anatomic Compartments

Keyphrases □ Pharmacokinetics—low-flux peripheral compartment □ Cochlear perilymph—aminoglycoside kinetics

To the Editor:

Small anatomic compartments may be the site of action or toxicity of drugs. Because the kinetics in the anatomic compartment may differ significantly from those in the sampled compartment, pharmacokinetic modeling of such drugs requires the development of explicit expressions for the time course of drug concentrations in the anatomic compartment. Classical compartmental analysis is based on large (kinetic) compartments, which exchange enough drug that measurable alterations in the concentration of drug in the sampled compartment result. A small (anatomic) compartment may not give rise to a detectable alteration in drug concentration in the sampled compartment, because its drug flux is small. In such a case, the anatomic compartment can not be represented by a peripheral kinetic compartment. This communication describes the derivation of an equation for the time course of drug concentrations in such small compartments based on a modified compartmental analysis.

Consider an n-compartment linear mammillary system with first-order rate constants and elimination from the central compartment (denoted by subscript 1) only. Let there be an $(n + 1)$th compartment that exchanges drug with the central compartment but for which the flux of drug into and out of the compartment is so minute that it does not measurably alter levels of the drug in the central compartment. This compartment will be called the low-flux peripheral compartment and will be labeled LF.

The differential equations governing this model are:

$$\frac{dC_1}{dt} = \sum_{j=2}^{n}\left(k_{j1}\frac{V_j}{V_1}C_j - k_{1j}C_1\right) - k_{10}C_1 \quad \text{(Eq. 1)}$$

$$\frac{dC_j}{dt} = k_{1j}\frac{V_1}{V_j}C_1 - k_{j1}C_j,\ n \geq j > 1 \quad \text{(Eq. 2)}$$

$$\frac{dC_{LF}}{dt} = k_{1LF}\frac{V_1}{V_{LF}}C_1 - k_{LF1}C_{LF} \quad \text{(Eq. 3)}$$

where

C_j = concentration of drug in the jth compartment;
V_j = pharmacokinetic volume of distribution of drug in the jth compartment;
k_{ab} = first-order transfer rate constant from the ith to the jth compartment;
k_{10} = first-order elimination rate constant from the central compartment;
C_{LF} = concentration of drug in the low-flux compartment;
k_{1LF}, k_{LF1} = first-order transfer rate constants into and out of the low-flux compartment.

If the drug enters the central compartment as a result of bolus injection, the drug concentration in that compartment, as a function of time, will be a sum of exponentials (1):

$$C_1(t) = \sum_{i=1}^{n} a_i e^{-\lambda_i t} \quad \text{(Eq. 4)}$$

where a_i = coefficient of ith exponential term and λ_i = exponent of the ith exponential term. The general equation for the drug concentration in the jth peripheral compartment is found by the use of Laplace transforms (2):

$$C_j(t) = \frac{V_1}{V_j}\sum_{i=1}^{n}\frac{k_{1j}}{(k_{j1} - \lambda_i)}a_i(e^{-\lambda_i t} - e^{-k_{j1}t}) \quad \text{(Eq. 5)}$$

The equation for the drug concentration in the low flux compartment is:

$$C_{LF}(t) = \frac{V_1}{V_{LF}}\sum_{i=1}^{n}\frac{k_{1LF}}{(k_{LF1} - \lambda_i)}a_i(e^{-\lambda_i t} - e^{-k_{LF1}t}) \quad \text{(Eq. 6)}$$

By similar means, expressions can be found for the drug concentration in the low-flux compartment following entry of the drug into the central compartment by first-order absorption or continuous infusion.

As an example of the application of this model, Eq. 6 is used to describe the kinetics of amikacin, an aminoglycoside antibiotic, in cochlear perilymph, presumably a low-flux compartment. The data are taken from a study performed in guinea pigs, as reported by Brummett *et al.* (3). The concentrations of amikacin were determined in serum and in cochlear perilymph over time following a single subcutaneous injection of the drug (as detailed in Ref. 3). The subcutaneous absorption of amikacin was very rapid, resulting in a monoexponential serum drug concentration *versus* time curve. Therefore, Eq. 4, and consequently Eq. 6, can be used in this case even though the injection was not intravenous.

The equation for the serum drug concentration *versus* time curve is:

$$C_{serum}(t) = 489e^{-0.6992t\,(\text{in hr})} \text{ in micrograms per milliliter}$$

The experimental data and corresponding predicted values are presented in Table I. The perilymph drug concentration *versus* time curve is fitted to a biexponential

0022-3549/83/0600-0718$01.00/0

Table I—Concentration of Amikacin in Serum Following a Bolus Subcutaneous Injection

Time, hr	Amikacin Concentration, μg/ml Experimental	Predicted Value
0.5	315	345
1.0	270	244
2.0	132	121
4.0	25	29
6.0	8	7

Table II—Concentration of Amikacin in Cochlear Perilymph Following a Bolus Subcutaneous Injection

Time, hr	Amikacin Concentration, μg/ml Experimental	Predicted Value
0.5	2.0	2.2
1.0	6	5.7
2.0	9	9.1
4.0	10	9.2
6.0	7	7.0
12.0	2.5	2.1

equation, which is the form prescribed by Eq. 6 and is also as many exponential terms as can confidently be generated for six data points:

$$C_{\text{perilymph}}(t) = 29e^{-0.2169t(\text{in hr})} - 32e^{-0.6019t(\text{in hr})}$$

in micrograms per milliliter

The experimental data and corresponding predicted values are listed in Table II. For both the serum and perilymph, the equations fit the data well.

If the model is appropriate, the values of k_{10} estimated from each of these two equations should be equal. The estimate of k_{10} from the serum drug concentration *versus* time equation is the exponent of the single exponential term, 0.6992 hr^{-1}. The estimate of k_{10} from the perilymph drug concentration *versus* time equation is the exponent for the exponential term with a negative coefficient, 0.6019 hr^{-1}. These estimates show a 16% difference. Such a small difference is within the limits of accuracy expected in such an experimental setting. The close agreement provides evidence of the validity of the model. This model might be found useful in describing other small anatomic compartments of pharmacological interest.

(1) G. Segre, *Pharmacol. Ther.*, **17**, 111 (1982).
(2) L. Z. Benet, *J. Pharm. Sci.*, **61**, 536 (1972).
(3) R. E. Brummett, K. E. Fox, T. H. Bendrick, and D. L. Hines, *J. Antimicro. Chemother.*, 4 (Suppl. A), 73 (1978).

Dennis A. Noe *
Karen M. Kumor ‡x
Department of Pathology and Laboratory Medicine
University of Texas Medical School
Houston, TX 77025

Received December 27, 1982.
Accepted for publication January 21, 1983.

Present address:
* Department of Medicine
Johns Hopkins Hospital
Baltimore, MD 21205
‡ Addiction Research Center
National Institute on Drug Abuse
Baltimore, MD 21224

BOOKS

REVIEWS

Encyclopedia of Emulsion Technology, Vol. 1: Basic Theory. Edited by PAUL BECHER. Marcel Dekker, Inc., New York, NY 10016. 1983. 744 pp. 17 × 25 cm. Price $95.00 (20% higher outside the U.S. and Canada).

This book is the first in a series of volumes devoted to various aspects of emulsion science and technology. It contains one of the most comprehensive and authoritative reviews of the basic principles underlying emulsification and emulsion properties now available. Each chapter has been prepared by individuals actively involved in the area about which they have written. The editor, himself widely recognized for his work with emulsions, has done an excellent job in bringing this work together in a well-edited volume.

The book contains nine chapters, all developed at a fairly fundamental level. In Chapter 1, the authors provide an excellent review of basic interfacial chemistry and physics using the oil–water interface as the main focus. The next two chapters address the fundamentals of emulsion formation and stabilization. The former is an extremely unique and in-depth treatment of droplet formation and coalescence and the underlying fluid dynamics involved, while the latter represents the most complete and up-to-date fundamental discussion of emulsion stability that this reviewer has seen.

The remaining chapters provide excellent in-depth coverage of such topics as: microemulsions, phase equilibria and phase inversion temperatures, particle size evaluation, rheology, optical properties, and dielectric properties. The chapter on rheology, written by P. Sherman, presents material which should be read by anyone seriously concerned with the complex problems of evaluating emulsion product stability. The material on the viscoelastic properties of emulsions is particularly relevant for this purpose. The very long chapter on the fundamental dielectric properties of emulsions (over 200 pages) is a unique resource of information which offers interesting possibilities for evaluating emulsion behavior in a new way. The proportion of the book devoted to this chapter, however, is much too large, relative to the importance of the other subjects presented. As in this latter chapter, all of the material in this volume is treated at a fairly fundamental level with the assumption that the reader has a reasonably good basic background in the physical chemistry of surfaces and disperse systems. Consequently, this book should be thought of as primarily suitable for a graduate-level course dealing with emulsions or for the pharmaceutical scientist seriously prepared to approach this subject at a very fundamental level.

Reviewed by George Zografi
School of Pharmacy
University of Wisconsin–Madison
Madison, WI 53706

0022-3549/83/0600-0719$01.00/0

Table I—Concentration of Amikacin in Serum Following a Bolus Subcutaneous Injection

Time, hr	Amikacin Concentration, μg/ml Experimental	Predicted Value
0.5	315	345
1.0	270	244
2.0	132	121
4.0	25	29
6.0	8	7

Table II—Concentration of Amikacin in Cochlear Perilymph Following a Bolus Subcutaneous Injection

Time, hr	Amikacin Concentration, μg/ml Experimental	Predicted Value
0.5	2.0	2.2
1.0	6	5.7
2.0	9	9.1
4.0	10	9.2
6.0	7	7.0
12.0	2.5	2.1

equation, which is the form prescribed by Eq. 6 and is also as many exponential terms as can confidently be generated for six data points:

$$C_{\text{perilymph}}(t) = 29e^{-0.2169t(\text{in hr})} - 32e^{-0.6019t(\text{in hr})}$$

in micrograms per milliliter

The experimental data and corresponding predicted values are listed in Table II. For both the serum and perilymph, the equations fit the data well.

If the model is appropriate, the values of k_{10} estimated from each of these two equations should be equal. The estimate of k_{10} from the serum drug concentration *versus* time equation is the exponent of the single exponential term, 0.6992 hr^{-1}. The estimate of k_{10} from the perilymph drug concentration *versus* time equation is the exponent for the exponential term with a negative coefficient, 0.6019 hr^{-1}. These estimates show a 16% difference. Such a small difference is within the limits of accuracy expected in such an experimental setting. The close agreement provides evidence of the validity of the model. This model might be found useful in describing other small anatomic compartments of pharmacological interest.

(1) G. Segre, *Pharmacol. Ther.*, **17**, 111 (1982).
(2) L. Z. Benet, *J. Pharm. Sci.*, **61**, 536 (1972).
(3) R. E. Brummett, K. E. Fox, T. H. Bendrick, and D. L. Hines, *J. Antimicro. Chemother.*, 4 (Suppl. A), 73 (1978).

Dennis A. Noe *
Karen M. Kumor ‡x
Department of Pathology and Laboratory Medicine
University of Texas Medical School
Houston, TX 77025

Received December 27, 1982.
Accepted for publication January 21, 1983.

Present address:
* Department of Medicine
Johns Hopkins Hospital
Baltimore, MD 21205
‡ Addiction Research Center
National Institute on Drug Abuse
Baltimore, MD 21224

BOOKS

REVIEWS

Encyclopedia of Emulsion Technology, Vol. 1: Basic Theory. Edited by PAUL BECHER. Marcel Dekker, Inc., New York, NY 10016. 1983. 744 pp. 17 × 25 cm. Price $95.00 (20% higher outside the U.S. and Canada).

This book is the first in a series of volumes devoted to various aspects of emulsion science and technology. It contains one of the most comprehensive and authoritative reviews of the basic principles underlying emulsification and emulsion properties now available. Each chapter has been prepared by individuals actively involved in the area about which they have written. The editor, himself widely recognized for his work with emulsions, has done an excellent job in bringing this work together in a well-edited volume.

The book contains nine chapters, all developed at a fairly fundamental level. In Chapter 1, the authors provide an excellent review of basic interfacial chemistry and physics using the oil–water interface as the main focus. The next two chapters address the fundamentals of emulsion formation and stabilization. The former is an extremely unique and in-depth treatment of droplet formation and coalescence and the underlying fluid dynamics involved, while the latter represents the most complete and up-to-date fundamental discussion of emulsion stability that this reviewer has seen.

The remaining chapters provide excellent in-depth coverage of such topics as: microemulsions, phase equilibria and phase inversion temperatures, particle size evaluation, rheology, optical properties, and dielectric properties. The chapter on rheology, written by P. Sherman, presents material which should be read by anyone seriously concerned with the complex problems of evaluating emulsion product stability. The material on the viscoelastic properties of emulsions is particularly relevant for this purpose. The very long chapter on the fundamental dielectric properties of emulsions (over 200 pages) is a unique resource of information which offers interesting possibilities for evaluating emulsion behavior in a new way. The proportion of the book devoted to this chapter, however, is much too large, relative to the importance of the other subjects presented. As in this latter chapter, all of the material in this volume is treated at a fairly fundamental level with the assumption that the reader has a reasonably good basic background in the physical chemistry of surfaces and disperse systems. Consequently, this book should be thought of as primarily suitable for a graduate-level course dealing with emulsions or for the pharmaceutical scientist seriously prepared to approach this subject at a very fundamental level.

Reviewed by George Zografi
School of Pharmacy
University of Wisconsin–Madison
Madison, WI 53706

0022-3549/83/0600-0719$01.00/0

Polyether Antibiotics, Vol. 1: Naturally Occurring Acid Ionophores. Edited by JOHN W. WESTLEY. Dekker, New York, N.Y. 1982. 565 pp. 15 × 23 cm. Price $65.00 (20% higher outside the U.S. and Canada).

This is the first volume of a two-volume work on the naturally occurring ionophore antibiotics. These antibiotics bind monovalent or divalent cations. The best known and commercially produced ones are the anticoccidia agents lasalocid and monensin.

The book starts with a classification scheme for the 76 polyether antibiotics known by 1982. There are 10 chapters. Chapter 1 is on notation and classification. Structural formulas are used in large number as they should be in such a book. Chapter 2 is on taxonomy of the organisms that produce the antibiotics. One half of the antibiotics are produced by different strains of two species of *Streptomyces.* Chapter 3 discusses biosynthesis, production, and assay. Chapter 4 is on the complexes formed by the antibiotics and cations, and transport of the cations by the complexes. Chapter 5 "provides a broad overview of the many, diverse effects of the carboxylic acid ionophores on biological systems." There is a chapter on veterinary applications, one on the effect of lasalocid and monensin in chickens, one on the pharmacology of lasalocid (cardiovascular action), one on cardiovascular and renal effects of an ionophore, and the final chapter on bromolasalocid as an antihypertensive ionophore. Those with an interest in monensin will find the coverage as complete as published literature permits.

This book has some interesting statistics. Ten of the authors were from Hoffmann-LaRoche, Inc.; the other eight were from medical schools, USDA, *etc.* Of the 465 pages, 200 were text and figures, 135 were tables, 95 were bibliography, 30 were an author index, and 6 were a subject index. The subject index is skimpy for a book of this size and importance. References are collected at the end of each chapter. A very unusual feature is giving of the complete title of each publication cited.

The publisher is to be commended for departing from the current norm of bookmaking by printing the title in large blue letters on a white spine thus enabling the title to be read from a distance greater than 2 feet. This book illustrates one advantage of having a domestic company with close ties to Europe with its concept of scholarly works.

All who work with polyether antibiotics should have a copy of this book.

Reviewed by Frederick Kavanagh
Corvallis, OR 97330

Trends in Inflammation Research 2. (Agents and Actions Supplements, Vol. 10). Edited by H. BEKEMEIER AND R. HIRSCHELMANN. Birkhäuser Boston, Inc., Cambridge, MA 02139. 1982. 315 pp. 16.5 × 23.5 cm. Price $37.95.

All of the papers in this book were presented at the 4th Summer Colloquium on Pharmacology, Biochemistry, and Immunology of Inflammation held at the Martin Luther University in Germany during July 1981. The title of the book, together with the description of the contents on the outside back cover, suggests that this collection of papers should be a valuable source of information on recent anti-inflammatory research carried out in West Germany.

On closer reading, however, the book proved disappointing. The authors are drawn mainly from just a few research centers so that the book covers only limited aspects of inflammation research. Of the 52 contributors to the volume, no less than 20 come from the Martin Luther University; 40 of the 52 contributors are from just four German universities. Furthermore, of the 23 chapters in the book, 10 are co-authored by H. Bekemeier and 7 are co-authored by R. Hirschelmann.

Other aspects of the book can be criticized. The sentence structure is often very awkward, evidently arising from an inadequate translation from the original German. This makes it difficult for the English-speaking reader to understand the material. It appears as though every paper submitted for publication was accepted without modification. A number of chapters are not written in a proper scientific journal format nor do they appear to have been critically reviewed prior to publication. The book serves as a vehicle for reporting many negative laboratory results that would not be publishable elsewhere. As a result, the quality of the papers in this book is below that found in an average journal.

I cannot recommend this book. It is not of general utility to scientists in the field of anti-inflammatory drug research. The book is difficult to read and too diffuse in subject matter. A few of the papers may be worthy of publication in a scientific journal, but only after appropriate impartial review and editorial revision.

Reviewed by Joseph G. Lombardino
Central Research Division
Pfizer, Inc.
Groton, CT 06340

Hormone Drugs. Workshop Organizers, JOHN L. GUERIGUIAN, EDWIN D. BRANSOME, JR., and AUDREY S. OUTSCHOORN. U.S. Pharmacopeial Convention, Inc., 12601 Twinbrook Parkway, Rockville, MD 20852. 1982. 584 pp. 15 × 23 cm. Price $49.00 (plus postage).

This book contains the proceedings of the FDA–USP Workshop on Drug and Reference Standards for Insulins, Somatropins, and Thyroid-axis Hormones, which was held in Bethesda, Maryland, in May 1982.

The volume contains over 50 papers presented at the meeting by experts in the field from Europe, New Zealand, and the United States. The subjects covered are timely from the clinical, scientific, and commercial standpoints, since they concern problems relating to standardization of these substances. Representative examples of papers presented at the Workshop are: "Production of Human Monocomponent Insulin," "Radioimmunological Determinations of Contaminants in Insulins," "Desired Characteristics of Insulins to be used in Insulin Pumps," "Structure and Function of Growth Hormones," "The Human Growth Hormone Gene Family," "Non-Isotopic Methods for Determination of Oral Thyroxine Absorption," and "Hypothalamic Peptide Hormones for Clinical Use."

For each of the three groups of hormone drugs, the proceedings include a summary presentation of current viewpoints regarding standardization with an eventual aim of precise dosage efficacy and safety. Also included is a general overview which describes potential developments in newer forms and formulations for better patient treatment.

This series of well-written papers clearly provides comprehensive information on drug and reference standards for insulins, somatropins, and thyroid-axis hormones and problems relating to the standardization of these substances. It is a valuable resource for scientists with interests in these aforementioned areas.

Reviewed by Jack M. Rosenberg
International Drug Information Center
Arnold & Marie Schwartz College of Pharmacy and Health Sciences
Long Island University
Brooklyn, NY 11201

NOTICES

Advanced Interpretation of Clinical Laboratory Data. (Clinical and Biochemical Analysis Series, Vol. 13). Edited by CAMILLE HEUSGHEM, ADELIN ALBERT, and ELLIS S. BENSON. Dekker, 270 Madison Ave., New York, NY 10016. 1982. 420 pp. 15 × 24 cm. Price $55.00 (20% higher outside the U.S. and Canada).

Advances in Chromatography. Vol. 20. Edited by J. CALVIN GIDDINGS, ELI GRUSHKA, JACK CAZES, and PHYLLIS R. BROWN. Dekker, 270 Madison Ave., New York, NY 10016. 1982. 286 pp. 15 × 23 cm. Price $45.00 (20% higher outside the U.S. and Canada).

Analysis of Drugs and Metabolites By Gas Chromatography–Mass Spectrometry. Vol. 7. By BENJAMIN J. GUDZINOWICZ and MICHAEL J. GUDZINOWICZ. Dekker, 270 Madison Ave., New York, NY 10016. 1980. 557 pp. 15 × 23 cm. Price $69.50.

Antibiotics in Laboratory Medicine. By VICTOR LORIAN. Williams & Wilkins, P.O. Box 64024, Baltimore, MD 21264. 1980. 737 pp. 17 × 25 cm. Price $65.00.

Polyether Antibiotics, Vol. 1: Naturally Occurring Acid Ionophores. Edited by JOHN W. WESTLEY. Dekker, New York, N.Y. 1982. 565 pp. 15 × 23 cm. Price $65.00 (20% higher outside the U.S. and Canada).

This is the first volume of a two-volume work on the naturally occurring ionophore antibiotics. These antibiotics bind monovalent or divalent cations. The best known and commercially produced ones are the anticoccidia agents lasalocid and monensin.

The book starts with a classification scheme for the 76 polyether antibiotics known by 1982. There are 10 chapters. Chapter 1 is on notation and classification. Structural formulas are used in large number as they should be in such a book. Chapter 2 is on taxonomy of the organisms that produce the antibiotics. One half of the antibiotics are produced by different strains of two species of *Streptomyces.* Chapter 3 discusses biosynthesis, production, and assay. Chapter 4 is on the complexes formed by the antibiotics and cations, and transport of the cations by the complexes. Chapter 5 "provides a broad overview of the many, diverse effects of the carboxylic acid ionophores on biological systems." There is a chapter on veterinary applications, one on the effect of lasalocid and monensin in chickens, one on the pharmacology of lasalocid (cardiovascular action), one on cardiovascular and renal effects of an ionophore, and the final chapter on bromolasalocid as an antihypertensive ionophore. Those with an interest in monensin will find the coverage as complete as published literature permits.

This book has some interesting statistics. Ten of the authors were from Hoffmann-LaRoche, Inc.; the other eight were from medical schools, USDA, *etc.* Of the 465 pages, 200 were text and figures, 135 were tables, 95 were bibliography, 30 were an author index, and 6 were a subject index. The subject index is skimpy for a book of this size and importance. References are collected at the end of each chapter. A very unusual feature is giving of the complete title of each publication cited.

The publisher is to be commended for departing from the current norm of bookmaking by printing the title in large blue letters on a white spine thus enabling the title to be read from a distance greater than 2 feet. This book illustrates one advantage of having a domestic company with close ties to Europe with its concept of scholarly works.

All who work with polyether antibiotics should have a copy of this book.

Reviewed by Frederick Kavanagh
Corvallis, OR 97330

Trends in Inflammation Research 2. (Agents and Actions Supplements, Vol. 10). Edited by H. BEKEMEIER AND R. HIRSCHELMANN. Birkhäuser Boston, Inc., Cambridge, MA 02139. 1982. 315 pp. 16.5 × 23.5 cm. Price $37.95.

All of the papers in this book were presented at the 4th Summer Colloquium on Pharmacology, Biochemistry, and Immunology of Inflammation held at the Martin Luther University in Germany during July 1981. The title of the book, together with the description of the contents on the outside back cover, suggests that this collection of papers should be a valuable source of information on recent anti-inflammatory research carried out in West Germany.

On closer reading, however, the book proved disappointing. The authors are drawn mainly from just a few research centers so that the book covers only limited aspects of inflammation research. Of the 52 contributors to the volume, no less than 20 come from the Martin Luther University; 40 of the 52 contributors are from just four German universities. Furthermore, of the 23 chapters in the book, 10 are co-authored by H. Bekemeier and 7 are co-authored by R. Hirschelmann.

Other aspects of the book can be criticized. The sentence structure is often very awkward, evidently arising from an inadequate translation from the original German. This makes it difficult for the English-speaking reader to understand the material. It appears as though every paper submitted for publication was accepted without modification. A number of chapters are not written in a proper scientific journal format nor do they appear to have been critically reviewed prior to publication. The book serves as a vehicle for reporting many negative laboratory results that would not be publishable elsewhere. As a result, the quality of the papers in this book is below that found in an average journal.

I cannot recommend this book. It is not of general utility to scientists in the field of anti-inflammatory drug research. The book is difficult to read and too diffuse in subject matter. A few of the papers may be worthy of publication in a scientific journal, but only after appropriate impartial review and editorial revision.

Reviewed by Joseph G. Lombardino
Central Research Division
Pfizer, Inc.
Groton, CT 06340

Hormone Drugs. Workshop Organizers, JOHN L. GUERIGUIAN, EDWIN D. BRANSOME, JR., and AUDREY S. OUTSCHOORN. U.S. Pharmacopeial Convention, Inc., 12601 Twinbrook Parkway, Rockville, MD 20852. 1982. 584 pp. 15 × 23 cm. Price $49.00 (plus postage).

This book contains the proceedings of the FDA–USP Workshop on Drug and Reference Standards for Insulins, Somatropins, and Thyroid-axis Hormones, which was held in Bethesda, Maryland, in May 1982.

The volume contains over 50 papers presented at the meeting by experts in the field from Europe, New Zealand, and the United States. The subjects covered are timely from the clinical, scientific, and commercial standpoints, since they concern problems relating to standardization of these substances. Representative examples of papers presented at the Workshop are: "Production of Human Monocomponent Insulin," "Radioimmunological Determinations of Contaminants in Insulins," "Desired Characteristics of Insulins to be used in Insulin Pumps," "Structure and Function of Growth Hormones," "The Human Growth Hormone Gene Family," "Non-Isotopic Methods for Determination of Oral Thyroxine Absorption," and "Hypothalamic Peptide Hormones for Clinical Use."

For each of the three groups of hormone drugs, the proceedings include a summary presentation of current viewpoints regarding standardization with an eventual aim of precise dosage efficacy and safety. Also included is a general overview which describes potential developments in newer forms and formulations for better patient treatment.

This series of well-written papers clearly provides comprehensive information on drug and reference standards for insulins, somatropins, and thyroid-axis hormones and problems relating to the standardization of these substances. It is a valuable resource for scientists with interests in these aforementioned areas.

Reviewed by Jack M. Rosenberg
International Drug Information Center
Arnold & Marie Schwartz College of Pharmacy and Health Sciences
Long Island University
Brooklyn, NY 11201

NOTICES

Advanced Interpretation of Clinical Laboratory Data. (Clinical and Biochemical Analysis Series, Vol. 13). Edited by CAMILLE HEUSGHEM, ADELIN ALBERT, and ELLIS S. BENSON. Dekker, 270 Madison Ave., New York, NY 10016. 1982. 420 pp. 15 × 24 cm. Price $55.00 (20% higher outside the U.S. and Canada).

Advances in Chromatography. Vol. 20. Edited by J. CALVIN GIDDINGS, ELI GRUSHKA, JACK CAZES, and PHYLLIS R. BROWN. Dekker, 270 Madison Ave., New York, NY 10016. 1982. 286 pp. 15 × 23 cm. Price $45.00 (20% higher outside the U.S. and Canada).

Analysis of Drugs and Metabolites By Gas Chromatography–Mass Spectrometry. Vol. 7. By BENJAMIN J. GUDZINOWICZ and MICHAEL J. GUDZINOWICZ. Dekker, 270 Madison Ave., New York, NY 10016. 1980. 557 pp. 15 × 23 cm. Price $69.50.

Antibiotics in Laboratory Medicine. By VICTOR LORIAN. Williams & Wilkins, P.O. Box 64024, Baltimore, MD 21264. 1980. 737 pp. 17 × 25 cm. Price $65.00.

Polyether Antibiotics, Vol. 1: Naturally Occurring Acid Ionophores. Edited by JOHN W. WESTLEY. Dekker, New York, N.Y. 1982. 565 pp. 15 × 23 cm. Price $65.00 (20% higher outside the U.S. and Canada).

This is the first volume of a two-volume work on the naturally occurring ionophore antibiotics. These antibiotics bind monovalent or divalent cations. The best known and commercially produced ones are the anticoccidia agents lasalocid and monensin.

The book starts with a classification scheme for the 76 polyether antibiotics known by 1982. There are 10 chapters. Chapter 1 is on notation and classification. Structural formulas are used in large number as they should be in such a book. Chapter 2 is on taxonomy of the organisms that produce the antibiotics. One half of the antibiotics are produced by different strains of two species of *Streptomyces.* Chapter 3 discusses biosynthesis, production, and assay. Chapter 4 is on the complexes formed by the antibiotics and cations, and transport of the cations by the complexes. Chapter 5 "provides a broad overview of the many, diverse effects of the carboxylic acid ionophores on biological systems." There is a chapter on veterinary applications, one on the effect of lasalocid and monensin in chickens, one on the pharmacology of lasalocid (cardiovascular action), one on cardiovascular and renal effects of an ionophore, and the final chapter on bromolasalocid as an antihypertensive ionophore. Those with an interest in monensin will find the coverage as complete as published literature permits.

This book has some interesting statistics. Ten of the authors were from Hoffmann-LaRoche, Inc.; the other eight were from medical schools, USDA, *etc.* Of the 465 pages, 200 were text and figures, 135 were tables, 95 were bibliography, 30 were an author index, and 6 were a subject index. The subject index is skimpy for a book of this size and importance. References are collected at the end of each chapter. A very unusual feature is giving of the complete title of each publication cited.

The publisher is to be commended for departing from the current norm of bookmaking by printing the title in large blue letters on a white spine thus enabling the title to be read from a distance greater than 2 feet. This book illustrates one advantage of having a domestic company with close ties to Europe with its concept of scholarly works.

All who work with polyether antibiotics should have a copy of this book.

Reviewed by Frederick Kavanagh
Corvallis, OR 97330

Trends in Inflammation Research 2. (Agents and Actions Supplements, Vol. 10). Edited by H. BEKEMEIER AND R. HIRSCHELMANN. Birkhäuser Boston, Inc., Cambridge, MA 02139. 1982. 315 pp. 16.5 × 23.5 cm. Price $37.95.

All of the papers in this book were presented at the 4th Summer Colloquium on Pharmacology, Biochemistry, and Immunology of Inflammation held at the Martin Luther University in Germany during July 1981. The title of the book, together with the description of the contents on the outside back cover, suggests that this collection of papers should be a valuable source of information on recent anti-inflammatory research carried out in West Germany.

On closer reading, however, the book proved disappointing. The authors are drawn mainly from just a few research centers so that the book covers only limited aspects of inflammation research. Of the 52 contributors to the volume, no less than 20 come from the Martin Luther University; 40 of the 52 contributors are from just four German universities. Furthermore, of the 23 chapters in the book, 10 are co-authored by H. Bekemeier and 7 are co-authored by R. Hirschelmann.

Other aspects of the book can be criticized. The sentence structure is often very awkward, evidently arising from an inadequate translation from the original German. This makes it difficult for the English-speaking reader to understand the material. It appears as though every paper submitted for publication was accepted without modification. A number of chapters are not written in a proper scientific journal format nor do they appear to have been critically reviewed prior to publication. The book serves as a vehicle for reporting many negative laboratory results that would not be publishable elsewhere. As a result, the quality of the papers in this book is below that found in an average journal.

I cannot recommend this book. It is not of general utility to scientists in the field of anti-inflammatory drug research. The book is difficult to read and too diffuse in subject matter. A few of the papers may be worthy of publication in a scientific journal, but only after appropriate impartial review and editorial revision.

Reviewed by Joseph G. Lombardino
Central Research Division
Pfizer, Inc.
Groton, CT 06340

Hormone Drugs. Workshop Organizers, JOHN L. GUERIGUIAN, EDWIN D. BRANSOME, JR., and AUDREY S. OUTSCHOORN. U.S. Pharmacopeial Convention, Inc., 12601 Twinbrook Parkway, Rockville, MD 20852. 1982. 584 pp. 15 × 23 cm. Price $49.00 (plus postage).

This book contains the proceedings of the FDA–USP Workshop on Drug and Reference Standards for Insulins, Somatropins, and Thyroid-axis Hormones, which was held in Bethesda, Maryland, in May 1982.

The volume contains over 50 papers presented at the meeting by experts in the field from Europe, New Zealand, and the United States. The subjects covered are timely from the clinical, scientific, and commercial standpoints, since they concern problems relating to standardization of these substances. Representative examples of papers presented at the Workshop are: "Production of Human Monocomponent Insulin," "Radioimmunological Determinations of Contaminants in Insulins," "Desired Characteristics of Insulins to be used in Insulin Pumps," "Structure and Function of Growth Hormones," "The Human Growth Hormone Gene Family," "Non-Isotopic Methods for Determination of Oral Thyroxine Absorption," and "Hypothalamic Peptide Hormones for Clinical Use."

For each of the three groups of hormone drugs, the proceedings include a summary presentation of current viewpoints regarding standardization with an eventual aim of precise dosage efficacy and safety. Also included is a general overview which describes potential developments in newer forms and formulations for better patient treatment.

This series of well-written papers clearly provides comprehensive information on drug and reference standards for insulins, somatropins, and thyroid-axis hormones and problems relating to the standardization of these substances. It is a valuable resource for scientists with interests in these aforementioned areas.

Reviewed by Jack M. Rosenberg
International Drug Information Center
Arnold & Marie Schwartz College of Pharmacy and Health Sciences
Long Island University
Brooklyn, NY 11201

NOTICES

Advanced Interpretation of Clinical Laboratory Data. (Clinical and Biochemical Analysis Series, Vol. 13). Edited by CAMILLE HEUSGHEM, ADELIN ALBERT, and ELLIS S. BENSON. Dekker, 270 Madison Ave., New York, NY 10016. 1982. 420 pp. 15 × 24 cm. Price $55.00 (20% higher outside the U.S. and Canada).

Advances in Chromatography. Vol. 20. Edited by J. CALVIN GIDDINGS, ELI GRUSHKA, JACK CAZES, and PHYLLIS R. BROWN. Dekker, 270 Madison Ave., New York, NY 10016. 1982. 286 pp. 15 × 23 cm. Price $45.00 (20% higher outside the U.S. and Canada).

Analysis of Drugs and Metabolites By Gas Chromatography–Mass Spectrometry. Vol. 7. By BENJAMIN J. GUDZINOWICZ and MICHAEL J. GUDZINOWICZ. Dekker, 270 Madison Ave., New York, NY 10016. 1980. 557 pp. 15 × 23 cm. Price $69.50.

Antibiotics in Laboratory Medicine. By VICTOR LORIAN. Williams & Wilkins, P.O. Box 64024, Baltimore, MD 21264. 1980. 737 pp. 17 × 25 cm. Price $65.00.

Polyether Antibiotics, Vol. 1: Naturally Occurring Acid Ionophores. Edited by JOHN W. WESTLEY. Dekker, New York, N.Y. 1982. 565 pp. 15 × 23 cm. Price $65.00 (20% higher outside the U.S. and Canada).

This is the first volume of a two-volume work on the naturally occurring ionophore antibiotics. These antibiotics bind monovalent or divalent cations. The best known and commercially produced ones are the anticoccidia agents lasalocid and monensin.

The book starts with a classification scheme for the 76 polyether antibiotics known by 1982. There are 10 chapters. Chapter 1 is on notation and classification. Structural formulas are used in large number as they should be in such a book. Chapter 2 is on taxonomy of the organisms that produce the antibiotics. One half of the antibiotics are produced by different strains of two species of *Streptomyces.* Chapter 3 discusses biosynthesis, production, and assay. Chapter 4 is on the complexes formed by the antibiotics and cations, and transport of the cations by the complexes. Chapter 5 "provides a broad overview of the many, diverse effects of the carboxylic acid ionophores on biological systems." There is a chapter on veterinary applications, one on the effect of lasalocid and monensin in chickens, one on the pharmacology of lasalocid (cardiovascular action), one on cardiovascular and renal effects of an ionophore, and the final chapter on bromolasalocid as an antihypertensive ionophore. Those with an interest in monensin will find the coverage as complete as published literature permits.

This book has some interesting statistics. Ten of the authors were from Hoffmann-LaRoche, Inc.; the other eight were from medical schools, USDA, *etc.* Of the 465 pages, 200 were text and figures, 135 were tables, 95 were bibliography, 30 were an author index, and 6 were a subject index. The subject index is skimpy for a book of this size and importance. References are collected at the end of each chapter. A very unusual feature is giving of the complete title of each publication cited.

The publisher is to be commended for departing from the current norm of bookmaking by printing the title in large blue letters on a white spine thus enabling the title to be read from a distance greater than 2 feet. This book illustrates one advantage of having a domestic company with close ties to Europe with its concept of scholarly works.

All who work with polyether antibiotics should have a copy of this book.

Reviewed by Frederick Kavanagh
Corvallis, OR 97330

Trends in Inflammation Research 2. (Agents and Actions Supplements, Vol. 10). Edited by H. BEKEMEIER AND R. HIRSCHELMANN. Birkhäuser Boston, Inc., Cambridge, MA 02139. 1982. 315 pp. 16.5 × 23.5 cm. Price $37.95.

All of the papers in this book were presented at the 4th Summer Colloquium on Pharmacology, Biochemistry, and Immunology of Inflammation held at the Martin Luther University in Germany during July 1981. The title of the book, together with the description of the contents on the outside back cover, suggests that this collection of papers should be a valuable source of information on recent anti-inflammatory research carried out in West Germany.

On closer reading, however, the book proved disappointing. The authors are drawn mainly from just a few research centers so that the book covers only limited aspects of inflammation research. Of the 52 contributors to the volume, no less than 20 come from the Martin Luther University; 40 of the 52 contributors are from just four German universities. Furthermore, of the 23 chapters in the book, 10 are co-authored by H. Bekemeier and 7 are co-authored by R. Hirschelmann.

Other aspects of the book can be criticized. The sentence structure is often very awkward, evidently arising from an inadequate translation from the original German. This makes it difficult for the English-speaking reader to understand the material. It appears as though every paper submitted for publication was accepted without modification. A number of chapters are not written in a proper scientific journal format nor do they appear to have been critically reviewed prior to publication. The book serves as a vehicle for reporting many negative laboratory results that would not be publishable elsewhere. As a result, the quality of the papers in this book is below that found in an average journal.

I cannot recommend this book. It is not of general utility to scientists in the field of anti-inflammatory drug research. The book is difficult to read and too diffuse in subject matter. A few of the papers may be worthy of publication in a scientific journal, but only after appropriate impartial review and editorial revision.

Reviewed by Joseph G. Lombardino
Central Research Division
Pfizer, Inc.
Groton, CT 06340

Hormone Drugs. Workshop Organizers, JOHN L. GUERIGUIAN, EDWIN D. BRANSOME, JR., and AUDREY S. OUTSCHOORN. U.S. Pharmacopeial Convention, Inc., 12601 Twinbrook Parkway, Rockville, MD 20852. 1982. 584 pp. 15 × 23 cm. Price $49.00 (plus postage).

This book contains the proceedings of the FDA–USP Workshop on Drug and Reference Standards for Insulins, Somatropins, and Thyroid-axis Hormones, which was held in Bethesda, Maryland, in May 1982.

The volume contains over 50 papers presented at the meeting by experts in the field from Europe, New Zealand, and the United States. The subjects covered are timely from the clinical, scientific, and commercial standpoints, since they concern problems relating to standardization of these substances. Representative examples of papers presented at the Workshop are: "Production of Human Monocomponent Insulin," "Radioimmunological Determinations of Contaminants in Insulins," "Desired Characteristics of Insulins to be used in Insulin Pumps," "Structure and Function of Growth Hormones," "The Human Growth Hormone Gene Family," "Non-Isotopic Methods for Determination of Oral Thyroxine Absorption," and "Hypothalamic Peptide Hormones for Clinical Use."

For each of the three groups of hormone drugs, the proceedings include a summary presentation of current viewpoints regarding standardization with an eventual aim of precise dosage efficacy and safety. Also included is a general overview which describes potential developments in newer forms and formulations for better patient treatment.

This series of well-written papers clearly provides comprehensive information on drug and reference standards for insulins, somatropins, and thyroid-axis hormones and problems relating to the standardization of these substances. It is a valuable resource for scientists with interests in these aforementioned areas.

Reviewed by Jack M. Rosenberg
International Drug Information Center
Arnold & Marie Schwartz College of Pharmacy and Health Sciences
Long Island University
Brooklyn, NY 11201

NOTICES

Advanced Interpretation of Clinical Laboratory Data. (Clinical and Biochemical Analysis Series, Vol. 13). Edited by CAMILLE HEUSGHEM, ADELIN ALBERT, and ELLIS S. BENSON. Dekker, 270 Madison Ave., New York, NY 10016. 1982. 420 pp. 15 × 24 cm. Price $55.00 (20% higher outside the U.S. and Canada).

Advances in Chromatography. Vol. 20. Edited by J. CALVIN GIDDINGS, ELI GRUSHKA, JACK CAZES, and PHYLLIS R. BROWN. Dekker, 270 Madison Ave., New York, NY 10016. 1982. 286 pp. 15 × 23 cm. Price $45.00 (20% higher outside the U.S. and Canada).

Analysis of Drugs and Metabolites By Gas Chromatography–Mass Spectrometry. Vol. 7. By BENJAMIN J. GUDZINOWICZ and MICHAEL J. GUDZINOWICZ. Dekker, 270 Madison Ave., New York, NY 10016. 1980. 557 pp. 15 × 23 cm. Price $69.50.

Antibiotics in Laboratory Medicine. By VICTOR LORIAN. Williams & Wilkins, P.O. Box 64024, Baltimore, MD 21264. 1980. 737 pp. 17 × 25 cm. Price $65.00.

Antibiotics in the Management of Infections: Outlook for the 1980s. (Merck Sharp & Dohme International Medical Advisory Council; Paris, France—June 14–15, 1982). Edited by ALEXANDER G. BEARN. Raven, 1140 Avenue of the Americas, New York, NY 10036. 1983. 258 pp. 15 × 23 cm. Price $27.50.

Arsenic: Industrial, Biomedical, Environmental Perspectives. Edited by WILLIAM H. LEDERER and ROBERT J. FENSTERHEIM. Van Nostrand Reinhold, 135 W. 56th St., New York, NY 10020. 1982. 464 pp. 17 × 24 cm. Price $42.00.

Azospirillum: Genetics, Physiology, Ecology. (Experientia Supplementum Vol. 42). Edited by W. KLINGMÜLLER. Birkhäuser Boston, 380 Green St., Cambridge, MA 02139. 1982. 149 pp. 16 × 24 cm. Price $24.95 (softcover).

Behavioral Models and the Analysis of Drug Action. Edited by MICHAEL Y. SPIEGELSTEIN and AHARON LEVY. Elsevier Scientific Publishing, 52 Vanderbilt Ave., New York, NY 10017. 1982. 498 pp. 16 × 25 cm. Price $139.50 (Dfl. 300.00).

The Botany and Chemistry of Hallucinogens. 2nd Ed. By RICHARD EVANS SCHULTES and ALBERT HOFMANN. Charles C. Thomas, 301–327 E. Lawrence Ave., Springfield, Ill. 1980. 437 pp. 15 × 23 cm. Price $28.75.

Cardiovascular Survey Methods. 2nd Ed. By G. A. ROSE, H. BLACKBURN, R. F. GILLUM, and R. J. PRINEAS, Geneva, World Health Organization. (Monographs Series No. 56). 178 pp. 15 × 24 cm. Price Sw Fr. 22. (Also available in Spanish; French edition in preparation).

Clinical and Biochemical Luminescence. (Clinical and Biochemical Analysis Series, Vol. 12). Edited by LARRY J. KRICKA and TIMOTHY J. N. CARTER. Dekker, 270 Madison Ave., New York, NY 10016. 1982. 289 pp. 15 × 23 cm. Price $45.00 (20% higher outside the U.S. and Canada).

Contemporary Heterocyclic Chemistry: Synthesis Reactions, and Applications. By GEORGE R. NEWKOME and WILLIAM W. PAUDLER. Wiley, 605 Third Ave., New York, NY 10016. 1982. 422 pp. 15 × 24 cm.

Development and Management of Research Groups. By ROBERT V. SMITH. The University of Texas Press, Austin, TX 78712. 1980. 91 pp. 15 × 23 cm. Price $10.95 (cloth); $7.95 (paper).

Directory of On-going Research in Cancer Epidemiology. Edited by C. S. MUIR and C. WAGNER. Lyons, International Agency for Research on Cancer. (IARC Scientific Publications No. 46). Health & Biomedical Information Programme, World Health Organization, 1211 Geneva 27, Switzerland. 1982. 722 pp. 16 × 24 cm. Price SW Fr. 40.

Electrophoresis. A Survey of Techniques and Applications Part B: Applications. Edited by Z. DEYL. Co-Editors: A. CHRAMBACH, F. M. EVERAERTS, and Z. PRUSIK. Elsvier Scientific Publishing, Amsterdam, The Netherlands. 1983. 462 pp. 16 × 24 cm. Price $104.75 (Dfl. 225).

Ethics and Regulation of Clinical Research. By ROBERT J. LEVINE. Uraban & Schwarzenberg, 7 East Redwood St., Baltimore, MD 21202. 1981. 299 pp. 15 × 23 cm. Price $35.00.

Genetic Engineering Applications for Industry. Edited by J. K. PAUL. Noyes Data Corp., Mill Rd. at Grand Ave., Park Ridge, NJ 07656. 1981. 580 pp. 15 × 23 cm.

Handbook of Clinical Drug Data. 5th Ed. Edited by JAMES E. KNOBEN and Phillip O. ANDERSON. Drug Intelligence Publications, 1241 Broadway, Hamilton, IL 62341. 1983. 669 pp. 10 × 19 cm. Price $29.50.

Handbook: Interactions of Selected Drugs and Nutrients in Patients. 3rd Ed. By DAPHNE A. ROE. The American Dietetic Assn. 430 N. Michigan Ave., Chicago, IL 60611. 139 pp. 21 × 26 cm. Price $17.50.

IARC Monographs on the Evaluation of the Carcinogenic Risk of Chemicals to Humans, Vol. 29: Some Industrial Chemicals and Dyestuffs, Lyons, International Agency for Research on Cancer. Health & Biomedical Information Programme, World Health Organizations, 1211 Geneva 27, Switzerland. 1982. 416 pp. 17 × 24 cm. Price $30.00 (Sw Fr. 60).

IARC Monographs on the Evaluation of the Carcinogenic Risk of Chemicals to Humans, Supplement 3: Cross Index of Synonyms and Trade Names in Vols. 1 to 26, Lyon, International Agency for Research on Cancer. Health & Biomedical Information Programme, World Health Organization, 1211 Geneva 27, Switzerland. 1982. 199 pp. 17 × 24 cm. Price $30.00. (Sw. Fr. 60).

IARC Monographs on the Evaluation of the Carcinogenic Risk of Chemicals to Humans, Supplement 4: Chemicals, Industrial Processes and Industries Associated with Cancer in Humans—IARC Monographs Vols. 1–29. Lyons, International Agency for Research on Cancer. World Health Organization, 1211, Geneva 27, Switzerland. 1982. 292 pp. 18 × 24 cm. Price $30.00 (Sw Fr. 60).

International Drinking Water Supply and Sanitation Decade. National Decade Plans: Eight Questions They Answer. World Health Organization, Geneva, Switzerland. 1982. 18 pp. 16 × 24 cm.

Molecular Electronic Devices. Edited by FORREST L. CARTER. Dekker, 270 Madison Ave., New York, NY 10016. 1982. 386 pp. 17 × 26 cm. Price $65.00 (20% higher outside the U.S. and Canada).

Multivariate Data Analysis in Industrial Practice. By PAUL J. LEWI. Wiley, One Wiley Drive, Somerset, NJ 08873. 1982. 244 pp. 15 × 23 cm. Price $31.95.

Narcotic Antagonists: Naltrexone Pharmacochemistry and Sustained-Release Preparations. NIDA Research Monograph 28. Edited by ROBERT E. WILLETTE and GENE BARNETT. 1981. 276 pp. 15 × 23 cm.

Neurobiology. By GORDON M. SHEPHERD. Oxford University Press, 200 Madison Ave., New York, NY 10016. 1983. 611 pp. 17 × 25 cm. Price $49.50 (clothbound); $24.95 (paperback).

New Approaches to Treatment of Chronic Pain: (A Review of Multidisciplinary Pain Clinics and Pain Centers. Research Monograph Series No. 36, 5/81. National Institute on Drug Abuse, Division of Research, 5600 Fishers Lane, Rockville, MD 20857. 198 pp. 14 × 23 cm.

Nonionizing Radiation Protection. Edited by MICHAEL J. SUESS. WHO Regional Office for Europe, Scherfgsvej 8, DK-2100, Copenhagen, Denmark. 1982. 267 pp. 16 × 24 cm.

Nuclear Power: Health Implications of Transuranium Elements. WHO Regional Publications European Series No. 11. (Report on a Working Group Brussels, 6–9 November 1979). World Health Organization, Regional Office for Europe, Copenhagen, Denmark. 1982.

Pediatric Nutrition: Infant Feedings–Deficiencies–Diseases. (Clinical Disorders in Pediatric Nutrition Series, Vol. 2). Edited by FIMA LIFSCHITZ. Dekker, 270 Madison Ave., New York, NY 10016. 1982. 648 pp. 15 × 23 cm. Price $55.00 (20% higher outside the U.S. and Canada).

Pesticides. Theory and Application. By GEORGE W. WARE. W. H. Freeman, 660 Market St., San Francisco, CA 94104. 1982. 308 pp. 21 × 28 cm. Price $19.95 (paper).

Pharmacological Basis of Nursing Practice. By JULIA B. CLARK, SHERRY F. QUEENER, and VIRGINIA BURKE KARB. C. V. Mosby, 11830 Westline Industrial Drive, St. Louis, MO 63141. 1982. 692 pp. 21 × 28 cm. Price $24.95.

Pharmacology and Biochemistry of Psychiatric Disorders. By A. RICHARD GREEN and DAVID W. COSTAIN. Wiley, One Wiley Drive, Somerset, NJ 08873. 1981. 217 pp. 15 × 23 cm.

Pharmacology of Hydroxyethyl Starch: Use in Therapy and Blood Banking. By JOHN MILTON MISHLER IV. Oxford University Press, 200 Madison Ave., New York, NY 10016. 1982. 207 pp. 15 × 24 cm. Price $39.50.

Pharmacology and Pharmacologists. An International Directory. Oxford University Press, 200 Madison Ave., New York, NY 10016. 1981. 387 pp. 16 × 25 cm. Price $110.00.

Plan of Action for Implementing the Global Strategy for Health for All and Index to the "Health for All" Series No. 1–7. World Health Organization, 1211 Geneva 27, Switzerland 1982. 55 pp. 18 × 24 cm.

Presynaptic Receptors: Mechanism and Function. Edited by J. de BELLEROCHE. Wiley, One Wiley Drive, Somerset, NJ 08873. 1982. 223 pp. 15 × 23 cm. Price $64.95.

Principles of Pharmaceutical Marketing. 3rd Ed. By MICKEY C. SMITH. Lea & Febiger, 600 S. Washington Square, Philadelphia, PA 19106. 1983. 529 pp. 15 × 23 cm. Price $29.75. ($37.25 in Canada).

Psychopharmacology of Affective Disorders. (A British Association for Psychopharmacology Monograph). Edited by E. S. PAYKEL and A. COPPEN. Oxford University Press, 200 Madison Ave., New York, NY 10016. 1981. 261 pp. 15 × 23 cm. Price $27.50.

Psychopharmacology of Old Age. British Association for Psychopharmacology Monograph No. 3. Edited by DAVID WHEATLEY. Oxford University Press, 200 Madison Ave., New York, NY 10016. 1982. 194 pp. 15 × 23 cm. Price $29.50.

Quality Assurance in Nuclear Medicine. Geneva, World Health Organization. Health & Biomedical Information Programme, World Health Organization, 1211 Geneva 27, Switzerland. 1982. 72 pp. 15 × 24 cm. Price $11.00. (French edition in preparation.)

Reactive Intermediates. Vol. 2. Edited by R. A. ABRAMOVITCH. Plenum, 233 Spring St., New York, NY 10013. 1982. 15 × 23 cm. Price $59.50.

Recent Progress on Kinins. Agents and Actions Supplements, Vol. 9. (International Conference "Kinin 81 Munich," Munich, November 2–5, 1981.) Edited by H. FRITZ, G. DIETZE, F. FIELDER, and G. L. HABERLAND. Birkhäuser Boston, 380 Green St., Cambridge, MA 02139. 1982. 707 pp. 16 × 24 cm. Price $74.00.

The Rights of Doctors, Nurses and Allied Health Professionals: A Health Law Primer. By GEORGE J. ANNAS, LEONARD H. GLANTZ, and BARBARA F. KATZ. An American Civil Liberties Union Handbook. 1981. 382 pp. 10 × 18 cm.

Selected Petroleum Products: Environmental Health Criteria 20. World Health Organization. 1211 Geneva 27, Switzerland. 1982. 137 pp. 14 × 21 cm.

Selective Toxicity. The Physico-Chemical Basis of Therapy. 6th Ed. By ADRIEN ALBERT. Methuen, 733 Third Ave., New York, NY 10017. 1981. 662 pp. 15 × 23 cm. Price $39.95.

Seventh General Programme of Work Covering the Period 1984–1989. World Health Organization, 1211 Geneva 27, Switzerland. 1982. 153 pp. 18 × 24 cm.

Single Dose Therapy of Urinary Tract Infection. By ROSS R. BAILEY. John Wright–PSG, 545 Great Rd., Littleton, MA 01460. 1983. 125 pp. 16 × 24 cm.

Species-Specific Potential of Invertebrates for Toxicological Research. By HANS E. KAISER. University Park Press, 233 E. Redwood St., Baltimore, MD 21202. 1980. 223 pp. 21 × 28 cm. Price $29.50.

The Tao of Medicine: Ginseng, Oriental Remedies and the Pharmacology of Harmony. By STEPHEN FULDER. Inner Tradisions International Ltd. 377 Park Ave. South, New York, NY 10016. 1982. 328 pp. 13 × 22 cm.

NEW JOURNALS

Cancer Investigation. Edited by YASHAR HIRSHAUT. (Vol. 1, No. 1: 1983—6 issues). Dekker, 270 Madison Ave., New York, NY 10016. 109 pp. 21 × 28 cm. Price $65.00 (Institutional); $45.00 (Individual).

Clinical Research Practices and Drug Regulatory Affairs. Edited by GARY MORTON MATOREN, et al. (Vol. 1, No. 1: 1983). Dekker, 270 Madison Ave., New York, NY 10016. 107 pp. 18 × 26 cm. Price $75.00 (Institutional); $37.50 (Individual).

International Journal of Quantum Chemistry. Quantum Biology Symposium No. 9. Proceedings of the International Symposium on Quantum Biology and Quantum Pharmacology held at Palm Coast, Fla. March 4–6, 1982. Editor in Chief: PER-OLOV LÖWDIN. Assistant Editor: JOHN R. SABIN. Wiley, One Wiley Drive, Somerset, NJ 08873. 1982. 630 pp. 15 × 23 cm. Price $64.95.

Journal of Toxicology: Toxin Reviews. Editor W. T. SHIER. (Vol. 1: 1982–2 issues). Dekker, 270 Madison Ave., New York, NY 10016. 203 pp. 15 × 23 cm. $55.00 (Institutional); $27.75 (Individual). Add postage ($4.20, surface; $5.60, airmail) outside the U.S.

Psychopharmacology of Old Age. British Association for Psychopharmacology Monograph No. 3. Edited by DAVID WHEATLEY. Oxford University Press, 200 Madison Ave., New York, NY 10016. 1982. 194 pp. 15 × 23 cm. Price $29.50.

Quality Assurance in Nuclear Medicine. Geneva, World Health Organization. Health & Biomedical Information Programme, World Health Organization, 1211 Geneva 27, Switzerland. 1982. 72 pp. 15 × 24 cm. Price $11.00. (French edition in preparation.)

Reactive Intermediates. Vol. 2. Edited by R. A. ABRAMOVITCH. Plenum, 233 Spring St., New York, NY 10013. 1982. 15 × 23 cm. Price $59.50.

Recent Progress on Kinins. Agents and Actions Supplements, Vol. 9. (International Conference "Kinin 81 Munich," Munich, November 2–5, 1981.) Edited by H. FRITZ, G. DIETZE, F. FIELDER, and G. L. HABERLAND. Birkhäuser Boston, 380 Green St., Cambridge, MA 02139. 1982. 707 pp. 16 × 24 cm. Price $74.00.

The Rights of Doctors, Nurses and Allied Health Professionals: A Health Law Primer. By GEORGE J. ANNAS, LEONARD H. GLANTZ, and BARBARA F. KATZ. An American Civil Liberties Union Handbook. 1981. 382 pp. 10 × 18 cm.

Selected Petroleum Products: Environmental Health Criteria 20. World Health Organization. 1211 Geneva 27, Switzerland. 1982. 137 pp. 14 × 21 cm.

Selective Toxicity. The Physico-Chemical Basis of Therapy. 6th Ed. By ADRIEN ALBERT. Methuen, 733 Third Ave., New York, NY 10017. 1981. 662 pp. 15 × 23 cm. Price $39.95.

Seventh General Programme of Work Covering the Period 1984–1989. World Health Organization, 1211 Geneva 27, Switzerland. 1982. 153 pp. 18 × 24 cm.

Single Dose Therapy of Urinary Tract Infection. By ROSS R. BAILEY. John Wright–PSG, 545 Great Rd., Littleton, MA 01460. 1983. 125 pp. 16 × 24 cm.

Species-Specific Potential of Invertebrates for Toxicological Research. By HANS E. KAISER. University Park Press, 233 E. Redwood St., Baltimore, MD 21202. 1980. 223 pp. 21 × 28 cm. Price $29.50.

The Tao of Medicine: Ginseng, Oriental Remedies and the Pharmacology of Harmony. By STEPHEN FULDER. Inner Tradisions International Ltd. 377 Park Ave. South, New York, NY 10016. 1982. 328 pp. 13 × 22 cm.

NEW JOURNALS

Cancer Investigation. Edited by YASHAR HIRSHAUT. (Vol. 1, No. 1: 1983—6 issues). Dekker, 270 Madison Ave., New York, NY 10016. 109 pp. 21 × 28 cm. Price $65.00 (Institutional); $45.00 (Individual).

Clinical Research Practices and Drug Regulatory Affairs. Edited by GARY MORTON MATOREN, et al. (Vol. 1, No. 1: 1983). Dekker, 270 Madison Ave., New York, NY 10016. 107 pp. 18 × 26 cm. Price $75.00 (Institutional); $37.50 (Individual).

International Journal of Quantum Chemistry. Quantum Biology Symposium No. 9. Proceedings of the International Symposium on Quantum Biology and Quantum Pharmacology held at Palm Coast, Fla. March 4–6, 1982. Editor in Chief: PER-OLOV LÖWDIN. Assistant Editor: JOHN R. SABIN. Wiley, One Wiley Drive, Somerset, NJ 08873. 1982. 630 pp. 15 × 23 cm. Price $64.95.

Journal of Toxicology: Toxin Reviews. Editor W. T. SHIER. (Vol. 1: 1982–2 issues). Dekker, 270 Madison Ave., New York, NY 10016. 203 pp. 15 × 23 cm. $55.00 (Institutional); $27.75 (Individual). Add postage ($4.20, surface; $5.60, airmail) outside the U.S.

1983
Volume 72

JOURNAL OF PHARMACEUTICAL SCIENCES

A publication of the American Pharmaceutical Association

The *Journal of Pharmaceutical Sciences* (ISSN 0022-3549) is published monthly by the American Pharmaceutical Association (APhA) at 2215 Constitution Ave., N.W., Washington, DC 20037. Second-class postage paid at Washington, D.C. and at additional mailing office.

All expressions of opinion and statements of supposed fact appearing in articles or editorials carried in this journal are published on the authority of the writer over whose name they appear and are not to be regarded as necessarily expressing the policies or views of APhA.

Offices—Editorial, Advertising, and Subscription: 2215 Constitution Ave., N.W., Washington, DC 20037. All Journal staff may be contacted at this address. Printing: 20th & Northampton Streets, Easton, PA 18042.

Annual Subscriptions—United States and foreign, industrial and government institutions $75; educational institutions $75; individuals *for personal use only* $40; single copies $10. APhA and SAPhA members may subscribe to *J. Pharm. Sci.* for $20.00 per year. All foreign subscriptions add $10 for postage. Subscription rates are subject to change without notice.

Claims—Missing numbers will not be supplied if dues or subscriptions are in arrears for more than 60 days or if claims are received more than 60 days after the date of the issue, or if loss was due to failure to give notice of change of address. APhA cannot accept responsibility for foreign delivery when its records indicate shipment was made.

Change of Address—Members and subscribers should notify at once both the Post Office and APhA of any change of address.

Photocopying—The code at the foot of the first page of an article indicates that APhA has granted permission for copying of the article beyond the limits permitted by Sections 107 and 108 of the U.S. Copyright Law provided that the copier sends the per copy fee stated in the code to the Copyright Clearance Center, Inc., 21 Congress St., Salem, MA 01970. Copies may be made for personal or internal use only and not for general distribution.

Microfilm—Available from University Microfilms International, 300 N. Zeeb Road, Ann Arbor, MI 48106.

Food and Pharmacy—A Close Relationship

Ever since late 1959, when Senator Estes Kefauver launched his epochal hearings on drugs, their prices, and competition within the pharmaceutical industry, we have witnessed an ongoing Congressional fascination with the subject of drug regulation and legislation. This has been most manifest in the form of a variety of highly publicized Congressional committee hearings, chaired at various times by Senators Kefauver, Nelson, or Kennedy, and Congressmen Cellers, Harris, Rogers, or Fountain, among others.

The hearings themselves have covered the full spectrum of drug-related matters from the so-called "drug lag" to bioequivalency, from their relative prices to the adequacy of their existing test standards.

But little—in fact, *very little* congressional attention has been given to food matters, including safety and quality, during this same time period.

As a consequence, we noted with interest that the U.S. Senate Committee on Labor and Human Resources was launching a series of hearings "on the nation's food safety laws and regulations," beginning June 8, 1983.

Interestingly, with a bipartisan touch, the announcement was issued jointly by the Committee Chairman, Orrin Hatch (R-Utah), and the Ranking Minority Member, Edward M. Kennedy (D-Massachusetts). Specifically, they stated their intended thrust as follows: "The hearings will focus on two central issues: (*1*) how recent scientific and technological developments have affected food safety regulation, and (*2*) whether existing law should be revised in order to accommodate advances in science and technology."

They went on to state, "We hope to accumulate a hearing record that addresses advances in food science and toxicological testing, as well as advances in our ability to identify toxicological substances and to estimate or extrapolate the risk to humans posed by such substances."

The balance of the announcement contained strongly expressed intentions to solicit testimony from appropriately qualified scientific experts in the field, to seek the views of former Commissioners of the Food and Drug Administration as to their experiences in enforcing the existing food safety laws, and to explore the question of introducing risk–benefit judgments—based on scientific data and information—in arriving at food safety decisions.

On the surface, food-related issues might appear to be remote to pharmacy, the pharmaceutical sciences, and pharmaceutical scientists. Upon reflection, however, we quickly see that there are many factors that result in a close linkage between foods and drugs.

Historically, the preponderance of drugs and nostrums had a food origin. And certainly, the entire subject of modern-day vitamins and essential minerals is continually a gray area; are they foods or are they drugs? However we may regard them today—*i.e.*, as foods or as drugs or as both, depending on their form and potency—their initial origin was from foods and foodstuffs. And for most people, food constitutes their principal or sole source of vitamins and minerals except when deficiencies arise.

Out of Congressional recognition of the close association between the two subject areas, the first federal law was entitled the "Pure Food and Drugs Act" of 1906; subsequent legislation, including the current "Federal Food, Drug, and Cosmetic Act," as well as virtually all state laws, continue this joint legislative approach.

Similarly, the federal agency charged with administering these laws is known as the "Food and Drug Administration," and it is headed by an official with the title of "Commissioner of Foods and Drugs."

In addition to vitamins and minerals, there are numerous substances that may be regarded as either foods or drugs, depending upon intent, use, or labeling. Classic examples would include sodium chloride and sucrose; but there are many others such as FD&C coloring agents, artificial sweeteners, suspending agents, thickeners, preservatives, solvents, starch, and so on.

The celebrated controversy over the use and safety of saccharin was raised in terms of its food aspects rather than its drug aspects—although both areas were affected in actual practice. This was because the legislation under which it would have been banned is the so-called Delaney Amendment, and this amendment specifically pertains to the potential carcinogenecity of foods and food ingredients.

And there are also pharmacy-related clinical implications involving substances that are clearly foods, *per se*. For example, certain food–drug interactions may be every bit as important and critical to the patient as drug–drug interactions.

Finally, in recent years, APhA has addressed, from a scientific standpoint, the policy implications of several health care related issues directly involving foods. One of these occurred in 1979–1980, when the APhA Policy Committee on Scientific Affairs recommended a policy position on the subject of food labeling as to qualitative and quantitative information about ingredients. A second occurred in 1980–1981, when the Scientific Affairs Committee focussed more specifically on dietary salt and recommended a policy position on the establishment of federal regulations on the inclusion of salt in processed foods. Both of these recommended policy statements were subsequently adopted as formal APhA positions by the APhA House of Delegates.

Consequently, it is evident that there is far more than a casual tie between foods and pharmacy or between foods and the pharmaceutical sciences. As such, we will want to follow with appropriate interest the upcoming Congressional hearings on food safety, its regulations, and its legislation. We earnestly hope they will prove to be productive in meeting their announced objectives.

—EDWARD G. FELDMANN
American Pharmaceutical Association
Washington, DC 20037

0022-3549/83/0700-0723$01.00/0

JOURNAL OF PHARMACEUTICAL SCIENCES

JULY 1983
VOLUME 72 NUMBER 7

RESEARCH ARTICLES

Dose-Dependent Elimination of Propranolol and its Major Metabolites in Humans

BERNIE M. SILBER *x, NICHOLAS H. G. HOLFORD, and SIDNEY RIEGELMAN †

Received January 15, 1982, from the *Departments of Pharmaceutical Chemistry and Pharmacy, School of Pharmacy and Division of Clinical Pharmacology, Department of Medicine, School of Medicine, University of California, San Francisco, CA 94143.* Accepted for publication July 1, 1982. *Present address: Department of Pharmaceutics, BG-20, School of Pharmacy, University of Washington, Seattle, WA 98195. †Deceased.

Abstract □ The disposition of propranolol and the formation of its major metabolites, propranolol glucuronide (I), 4-hydroxypropranolol glucuronide (II), and α-naphthoxylactic acid (III), were examined at steady state in four healthy volunteers given oral doses of 40–320 mg/day. The blood to plasma ratio of propranolol was 0.85 ± 0.11 (*SD*). In all subjects, the average steady-state concentration ($\bar{C}_{ss}$) of propranolol in plasma increased disproportionately with dose. There was a 1.8- to 2.6-fold difference in the $\bar{C}_{ss}$ between subjects, a 56 ± 20% reduction in the intrinsic clearance, and a 175% increase in the half-life of propranolol over the range of doses administered. The renal clearance was 75.4 ± 17.5 ml/min for I, 130.6 ± 28.3 ml/min for II, and 56.8 ± 13.3 ml/min for III. The formation of I was saturable in three subjects; the V_{max} and K_m were 103 ± 43 mg/day and 124 ± 46 ng/ml, respectively. In the remaining subject the nonrenal clearance of I was 496 ml/min. The formation of II and III was saturable in all subjects. The V_{max} and K_m were 71 ± 25 mg/day and 46 ± 22 ng/ml, respectively, for II and 92 ± 35 mg/day and 35 ± 24 ng/ml, respectively, for III. In each subject, the formation clearance associated with the unidentified metabolic pathway(s) (accounting for ~45% of the dose) was best described by a saturable process. The V_{max} and K_m estimated for this pathway were 212 ± 34 mg/day and 40 ± 12 ng/ml, respectively. These results suggest that the elimination of propranolol is saturable in the human at doses from 40 to 320 mg/day and can be explained only partly by saturability in the metabolic pathways resulting in the formation of I, II, and III.

Keyphrases □ Propranolol—formation of metabolites, dose-dependent elimination in humans, metabolic pathways □ Metabolites—of propranolol in humans, dose-dependent elimination, metabolic pathways □ Metabolism—of propranolol in the human, elimination, metabolic pathways

Propranolol is used extensively in the treatment of angina pectoris, hypertension, cardiac arrhythmia, and other disease states in which β-adrenergic blockade is desirable. The β-blocking activity of propranolol approaches a maximal therapeutic effect at a plasma concentration of ~80–100 ng/ml (1).

The absorption of propranolol following its oral administration is complete in the human (2); gut-wall metabolism has not been found in the dog (3). The drug has a high extraction ratio and is metabolized virtually completely in the liver (4, 5): <1% of the intact drug is found in the urine (6).

The disposition of propranolol can be affected by age (7, 8); cigarette smoking (6, 7); concomitant drug administration (9); and renal (10), hepatic (11), or thyroid disease (12–14). Pharmacokinetic studies in healthy adults and in patients with various disease states have demonstrated as much as 10- to 20-fold variation in the plasma concentrations of propranolol between individuals after oral, but not intravenous, doses of the drug (15–21). However, Walle *et al.* (22) reported only a threefold intersubject variability in peak concentrations of propranolol with doses of 40–320 mg/day and suggested that their findings resulted from careful study design, control of factors such as concomitant drug intake, and use of specific analytical procedures.

The metabolism of propranolol is complex. More than 18 metabolites have been identified (22–24), with at least four of these having pharmacological activity (25–27). Walle *et al.* (28–30) reported that at steady state, ~60% of an oral dose can be accounted for by metabolites detectable in both plasma and urine. The major metabolites are propranolol glucuronide (I), 4-hydroxypropranolol glucuronide (II), and α-naphthoxylactic acid (III). To our knowledge, no one has investigated whether the formation of these metabolites occurs by first-order or saturable processes.

Kornhauser *et al.* (31) reported an average intrinsic clearance (CL_{int}) of 2.71 liters/min for propranolol (based

0022-3549/83/0700-0725$01.00/0

Table I—Blood to Plasma Ratio (B/P) of Propranolol

Subject	Concentration of Propranolol in Blood, ng/ml 4.9	9.8	24.6	49.1	73.7	98.2	280.4	Mean ± SD
A	1.17	0.82	0.83	0.78	0.82	0.78	0.80	0.86 ± 0.14
B	0.75	0.84	0.83	0.88	0.80	0.76	—[a]	0.81 ± 0.05
C	0.91	0.75	0.77	1.09	0.82	0.87	—	0.87 ± 0.12
D	0.96	0.99	0.69	0.90	0.76	0.88	—	0.86 ± 0.12
							Mean ± SD	0.85 ± 0.11

[a] — Not determined.

Table II—Relationship Between the Intrinsic Clearance and the Rate of Propranolol Dosing

Subject	Age, year	Weight, kg	Intrinsic Clearance (CL_{int})[a] liter/min Week 1	Week 2	Week 3	Week 4	Week 5	Change[b], %
A	26	64	4.59	4.93	4.64	2.43	1.03	−78
B	28	75	6.62	6.08	6.93	4.16	2.57	−61
C	24	68	4.51	3.82	3.78	3.44	2.01	−55
D	25	82	3.85	3.65	4.51	3.42	2.69	−30
							Mean ± SD	−56 ± 20

[a] The intrinsic clearance (CL_{int}) was calculated according to Eq. 4 as described in *Theoretical*. The dosage of propranolol given was 40, 80, 160, 240, and 320 mg/day during weeks 1, 2, 3, 4, and 5, respectively. [b] Percentage difference between weeks 1 and 5.

on whole blood concentrations) at a dose of 240 mg/day. Because urinary recovery of I, II, and III accounts for about one-half of the oral dose at steady state, the CL_{int} accounted for by these metabolites is ~1.36 liters/min. The renal clearance (CL_r) is 57 ml/min for I (30), 60 ml/min for II (29), and 37 ml/min for III (28). Therefore, the CL_{int} for each of these metabolites is much greater than their CL_r. Because the apparent volume of distribution of these metabolites is unknown, the rate constant of formation (k_f) and elimination (k_{el}) for each cannot be determined from administration of propranolol alone. However, if $k_f \gg k_{el}$ for each metabolite, the formation clearances can be determined from steady-state experiments only.

The results of several investigations suggest that an increase in the rate of propranolol dosing results in a disproportionate increase in the observed concentrations of the drug (4, 5, 22, 32). However, these results have been obtained from single-dose studies, steady-state studies spanning a narrow range of doses in a given individual, or steady-state studies employing analytical techniques having questionable specificity. No studies have examined the relationship between the average steady-state concentrations ($\bar{C}_{ss}$) of propranolol over a wide range of doses in the same individual, the variability between individuals under these conditions, or the mechanisms responsible for the nonlinear relationship between the dosing rate and $\bar{C}_{ss}$. This study was designed to examine these points in healthy adult volunteers. Urinary excretion rates of I, II, and III were measured simultaneously to identify the metabolic pathways responsible for differences between individuals.

THEORETICAL

After a sufficient number of oral doses of a drug have been given to reach steady state, the average steady-state concentration of a drug ($\bar{C}_{ss}$) can be related to the dose (D_0) by:

$$\frac{D_0}{\tau} = \frac{CL}{F} \cdot \bar{C}_{ss} \qquad \text{(Eq. 1)}$$

where CL is the systemic clearance of the drug, F is the fraction of the dose reaching the systemic circulation (bioavailability), and τ is the dosing interval. The $\bar{C}_{ss}$ can be defined by:

$$\bar{C}_{ss} = \frac{\int_{t_1}^{t_2} C(t)dt}{\tau} = \frac{AUC_0}{\tau} \qquad \text{(Eq. 2)}$$

where $C(t)$ is an expression describing concentration as a function of time (t) and AUC_0 is the area under the blood or plasma concentration time curve during one dosing interval. Therefore, $\bar{C}_{ss}$ can be estimated from the AUC_0 at steady state and τ; this does not require explicit knowledge of F even though F may change with a change in the dose.

Based on the venous equilibration model described by Rowland *et al.* (33), the intrinsic clearance (CL_{int}), which estimates the activity of the drug metabolizing enzymes in the liver, may be defined. Wilkinson and Shand (34) have shown that the apparent oral clearance (CL_o) of a drug is equivalent to CL_{int} and is defined by:

$$CL_{int} = \frac{D_0}{AUC_0} = \frac{CL}{F} \qquad \text{(Eq. 3)}$$

This relationship assumes that the drug is totally absorbed from the GI tract, that all blood containing the drug passes through the liver before reaching the systemic circulation, and that the liver accounts for all loss processes. Therefore, a change in F results from a change in the hepatic extraction of propranolol by the liver.

A basic presumption in the derivation of CL_{int} (33) is that the drug is undergoing metabolism by a first-order process. If, however, metabolism involves capacity-limited kinetics in the concentration range involved, then the CL_{int} calculated by Eq. 3 will be an average of the values over the concentration range. Substituting CL_{int} for CL/F in Eq. 1 yields:

$$\frac{D_0}{\tau} = CL_{int} \cdot \bar{C}_{ss} \qquad \text{(Eq. 4)}$$

The relationship between the dose rate and C_{ss} may be defined by a series of potential models for propranolol elimination processes symbolized by CL_{int} in Eq. 4:

$$\frac{D_0}{\tau} = f_x \cdot \sum_{i=1}^{n} dAe_{M_i}/dt \qquad \text{(Model 1)}$$

Model 1 assumes that the measured pathways (forming I, II, and III) account for all of the dose. Based on urinary recovery, these major metabolites of propranolol account for <100% of the parent drug. The term $\Sigma_{i=1}^{n} dAe_{M_i}/dt$ is the sum of metabolite formation only accounted for by urinary excretion of I, II, and III. It is possible that these metabolites are also eliminated by extrarenal routes (*e.g.*, biliary). In this model, the term f_x is a unitless number >1.0 which attempts to correct for these extrarenal losses.

$$\frac{D_0}{\tau} = CL_x \cdot \bar{C}_{ss} + \sum_{i=1}^{n} dAe_{M_i}/dt \qquad \text{(Model 2)}$$

In Model 2, the term Cl_x identifies the sum of all first-order metabolic pathways of propranolol to unknown or unidentified metabolites.

Table III—Time[a] to Peak Concentration (t_{peak}) and the Terminal Half-Life ($t_{1/2}$) at Increasing Dosing Levels of Propranolol

	Daily Dose of Propranolol, mg/day									
	40		80		160		240		320	
Subject	t_{peak}	$t_{1/2}$	t_{peak}	$t_{1/2}$	t_{peak}	$t_{1/2}$	t_{peak}	$t_{1/2}$	t_{peak}	$t_{1/2}$
A	4.0	2.6	3.3	3.6	3.5	3.5	3.5	4.7	4.0	8.3
B	2.2	1.6	2.0	2.8	2.0	3.5	2.5	3.8	3.0	4.7
C	2.0	2.0	2.0	3.0	2.0	3.0	3.0	3.5	2.0	4.8
D	2.0	1.8	1.8	2.0	3.2	2.7	2.0	3.7	2.0	4.3
Mean	2.5	2.0	2.3	2.9	2.7	3.2	2.8	3.9[b]	2.8	5.5[b,c]
(SD)	(1.0)	(0.4)	(0.7)	(0.6)	(0.8)	(0.4)	(0.6)	(0.5)	(1.0)	(1.9)

[a] In hours. [b] Significantly different at $p < 0.05$ when compared with the value obtained at the 40-mg/day dose. [c] Significantly different at $p < 0.05$ when compared with the value obtained at the 240-mg/day dose.

Table IV—Akaike Information Criterion (AIC) Calculated for Each Model Describing the Elimination Rate of Propranolol[a]

Subject	Model 1	Model 2	Model 3	Model 4	Model 5
A	187.5	177.7	174.6[b]	181.9	275.9
B	174.2[b]	177.4	176.4	177.4	230.3
C	197.9	191.6	189.6[b]	200.2	200.2
D	214.0	213.9	211.8[b]	215.6	228.2

[a] See *Data Analysis* for a description of the AIC calculation procedure. [b] Model with minimum AIC.

$$\frac{D_0}{\tau} = \frac{V_{max_x} \cdot \bar{C}_{ss}}{K_{m_x} + \bar{C}_{ss}} + \sum_{i=1}^{n} dAe_{M_i}/dt \qquad \text{(Model 3)}$$

In Model 3, the first term represents a saturable clearance pathway for unidentified metabolites with parameters V_{max_x} and K_{m_x}; added to these unidentified metabolites is the sum of the elimination accounted for by known metabolites.

$$\frac{D_0}{\tau} = CL_x \cdot \bar{C}_{ss} + f_x \cdot \sum_{i=1}^{n} dAe_{M_i}/dt \qquad \text{(Model 4)}$$

Model 4 is a combination of Models 1 and 2.

$$\frac{D_0}{\tau} = CL_x \cdot \bar{C}_{ss} + \frac{V_{max_x} \cdot \bar{C}_{ss}}{K_{m_x} + \bar{C}_{ss}} + \sum_{i=1}^{n} dAe_{M_i}/dt \qquad \text{(Model 5)}$$

Model 5 is a combination of Models 2 and 3.

The known (or measured) excretion rate for each metabolite in these models may be calculated from:

$$dAe_{M_i}/dt = \frac{V_{max,M_i} \cdot \bar{C}_{ss}}{K_{m,M_i} + \bar{C}_{ss}} \qquad \text{(Eq. 5)}$$

where V_{max,M_i} and K_{m,M_i} are parameters for each known metabolite formation pathway for propranolol. At steady state, dAe_{M_i}/dt is equal to the formation rate for that particular metabolite.

When the apparent $K_m \gg \bar{C}_{ss}$, the relationship between dAe_{M_i}/dt and $\bar{C}_{ss}$ is linear. The slope of this line is equal to the metabolic clearance for this pathway.

EXPERIMENTAL

Subjects—The subjects were four healthy adult volunteers. Informed consent was obtained, and the protocol approved by the University of California, San Francisco, Committee on Human Research. A medical history, physical examination, electrocardiogram (ECG), complete blood count with differential, urinalysis, and selected blood chemistries were completed for all subjects. There was no evidence of renal or hepatic disease in the medical history, and values of blood urea nitrogen, serum creatinine, urinalysis and urine culture, serum glutamic oxaloacetic transaminase, lactic dehydrogenase, alkaline phosphatase, bilirubin, prothrombin time, and total serum proteins were normal. All were nonsmokers and abstained from alcohol, marijuana, and other medications until completion of the study. On each of the four days per week that propranolol was taken, the subjects had their pulse and blood pressure measured, underwent a 1-min ECG, and were interviewed to determine side effects.

Propranolol Administration—All subjects were given 40, 80, 160, 240, and 320 mg/day of propranolol in divided doses over a 5-week period. Each subject took one-fourth of the daily dose every 6 hr for a total of 13 doses at each dosing rate. No dietary restrictions were imposed, but food was withheld for at least 9 hr before and 3 hr after the 13th dose.

Blood Sampling—Blood samples were obtained at the end of the 8th, 9th, and 12th dosing intervals (trough concentrations) and at 0, 15, 30, 45, 60, and 90 min and 2, 3, 4, 5, 6, 8, 10, and 12 hr following the 13th dose. Venous blood samples were obtained using an indwelling catheter[1]; patency was maintained by flushing with 1 ml of heparinized saline (10 U/ml) after obtaining each blood sample (35). It was shown that these small doses of heparin do not affect the plasma protein binding or disposition of propranolol (36). After discarding 0.5 ml of blood, a 7-ml blood sample was transferred immediately to a 16 × 150-mm polytef-lined[2] screw-cap test tube to which had been added 100 U of aqueous sodium heparin. After gentle mixing, blood samples were centrifuged at 2000 rpm (500×*g*) for 10 min. Plasma was transferred with a disposable pasteur pipet to glass screw-cap vials and stored at −20° until assay.

Urine Sampling—Urine samples were collected during the 5th, 9th, and 12th dosing intervals and at frequent times for up to 12 hr after the 13th dose each week. Urine volumes were recorded and 10 mg of (−)-ascorbic acid was added to prevent oxidation of phenolic metabolites (27); aliquots were stored at −20° until assayed.

Assay Procedures—Propranolol and 4-hydroxypropranolol concentrations were measured in plasma before and after enzymatic hydrolysis of the glucuronide conjugate[3] and in urine after enzymatic hydrolysis (37). The limits of sensitivity are 0.4 and 1.0 ng/ml, respectively. α-Naphthoxylactic acid concentration in plasma and urine were measured directly after protein precipitation by a method previously described (38).

Blood to Plasma Ratio of Propranolol—The equilibrium time for propranolol between human erythrocytes and plasma was reported to be ~5 min (39). The blood to plasma ratio (B/P) was determined over the range of measured concentrations by adding propranolol to test tubes containing 2 ml of fresh blood obtained from each individual and 100 U of heparin (to prevent clotting). After allowing each sample to stand for 2 hr (with gentle agitation every 15 min), the test tubes were centrifuged, and the plasma was measured. These measurements were compared with 2 ml of plasma containing the same amount of drug, to account for possible *in vitro* degradation of propranolol by plasma.

Data Analysis—The CL_{int} of propranolol at each C_{ss} was calculated according to Eq. 4. The AUC of propranolol, I, II, and III during the 13th dosing interval were calculated by the trapezoidal rule. The half-life of propranolol was calculated as 0.693/terminal elimination rate constant (determined by least-squares regression utilizing at least four plasma concentration time points in the log-linear region). The renal clearance (CL_r) of each metabolite was calculated as the slope of the line determined by least-squares regression of the rate of urinary excretion *versus* C_{ss} for each metabolite in plasma. The C_{ss} of propranolol and its metabolites at each dosing rate was calculated from the data obtained during the 13th dosing interval using Eq. 2.

The elimination rate models described in *Theoretical* were specified using MKMODEL (40). The predicted value for C_{ss} was calculated for each rate model using the ROOT function in MLAB (41). This function determines the value of C_{ss} that satisfies the rate model equation. The

[1] Butterfly Catheter, Abbott Laboratories, North Chicago, IL 60064.
[2] Teflon.
[3] Glusulase, Cat. No. GD 751, Sigma Chemical Co., St. Louis, MO 63178.

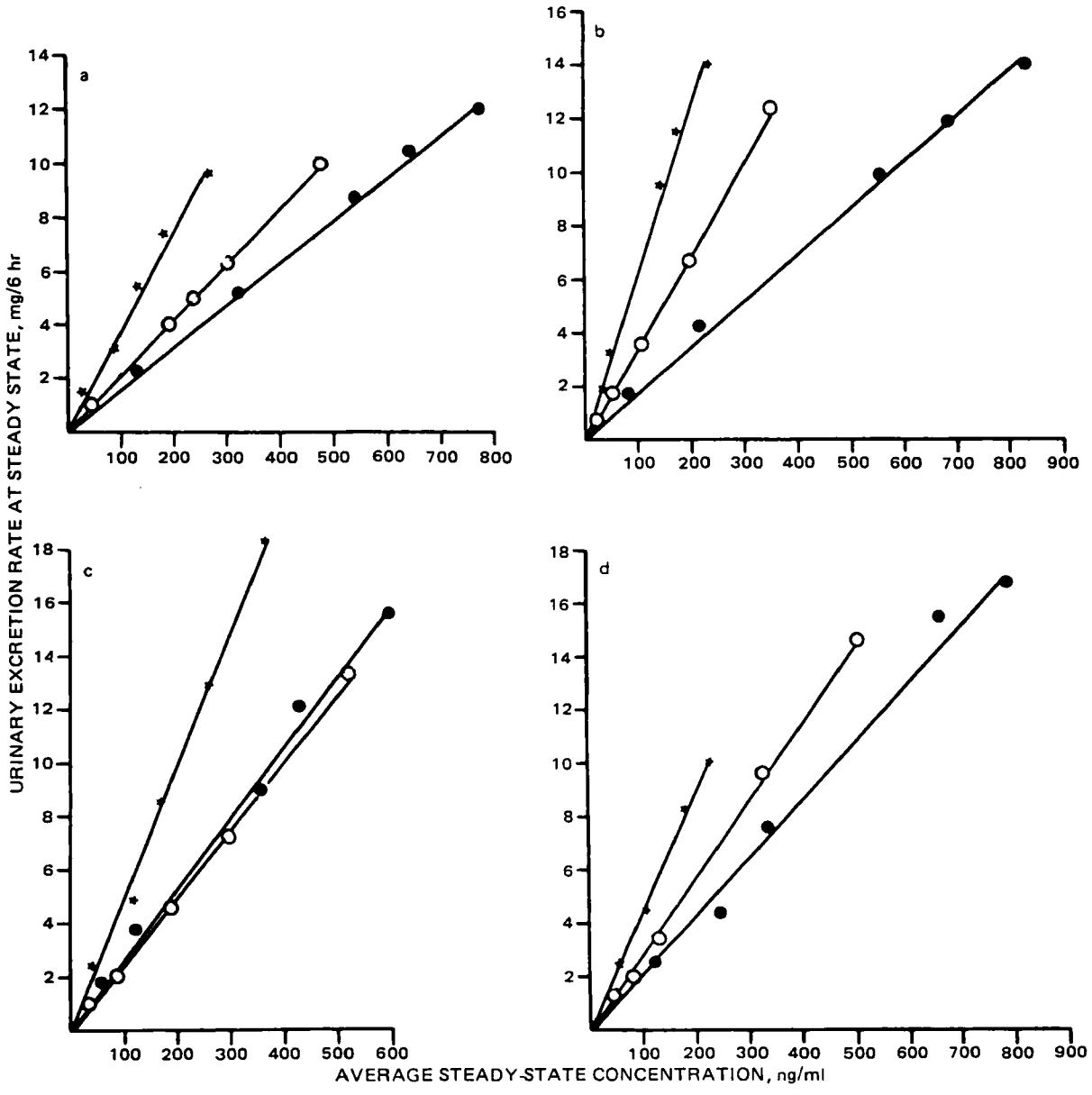

Figure 1—*Urinary excretion rate of each measured metabolite for each subject (a–d) as a function of the average steady-state concentration of the corresponding metabolite in plasma. Key: (○) propranolol glucuronide; (★) 4-hydroxypropranolol glucuronide; (●) α-naphthoxylactic acid.*

parameters of the models were estimated by simultaneous unweighted nonlinear least-squares regression (41) of the dose rate *versus* the measured C_{ss} and metabolite excretion rates.

Discrimination between the models was made with the Akaike information criterion (AIC) (42–44):

$$\text{AIC} = N \ln \text{RSQ} + 2p \qquad \text{(Eq. 6)}$$

where N is the number of observations, p is the number of parameters, and RSQ is the residual sums of squares of the observed points. The model yielding the lowest AIC value was considered to be the best representation of the experimental data for each subject.

Mean values are reported with standard deviations; differences between means were evaluated by one-way analysis of variance and the Newman-Keuls multiple-range test (45). Data anlaysis and graphical examination of the results were performed with the PROPHET (46) computer system[4].

RESULTS

Side Effects—No major adverse effects resulted from the administration of propranolol. The only side effect noted was in subject A while receiving 320 mg/day. Five hours after the 13th dose, he developed weakness and dizziness. After resting supine for 1 hr, he was able to resume his usual activities.

Validation of Steady-State Conditions—In each subject, steady-state trough concentrations were attained by the ninth dose (or less) and, once achieved, were associated with only slight interday variation.

Quantitation of 4-Hydroxypropranolol in Plasma—Because 4-hydroxypropranolol concentrations in plasma were <20 ng/ml and were ~25- to 30-fold greater after enzymatic hydrolysis, 4-hydroxypropranolol glucuronide concentrations were considered to be equivalent to the total 4-hydroxypropranolol concentration posthydrolysis.

Blood to Plasma Ratio of Propranolol—The blood to plasma ratio (B/P) of propranolol measured over the observed concentration range is shown in Table I. The B/P was independent of concentration, and only slight interindividual variability in the B/P was observed. In our subjects, the B/P was 0.85 ± 0.11.

Relationship Between the Intrinsic Clearance and the Dosing Rate of Propranolol—The CL_{int} of propranolol was determined at each of five dosing rates using Eq. 4. There was a 56 ± 20% reduction in CL_{int} on average over the eightfold range in doses (Table II).

Disposition of Propranolol During the 13th Dosing Interval—The time to peak concentration of propranolol during the 13th dosing interval ranged from 2.5 ± 1.0 to 2.8 ± 1.0 hr at doses from 40 to 320 mg/day. As

[4] A specialized resource developed by the Chemical Biological Information Handling Program of the National Institutes of Health.

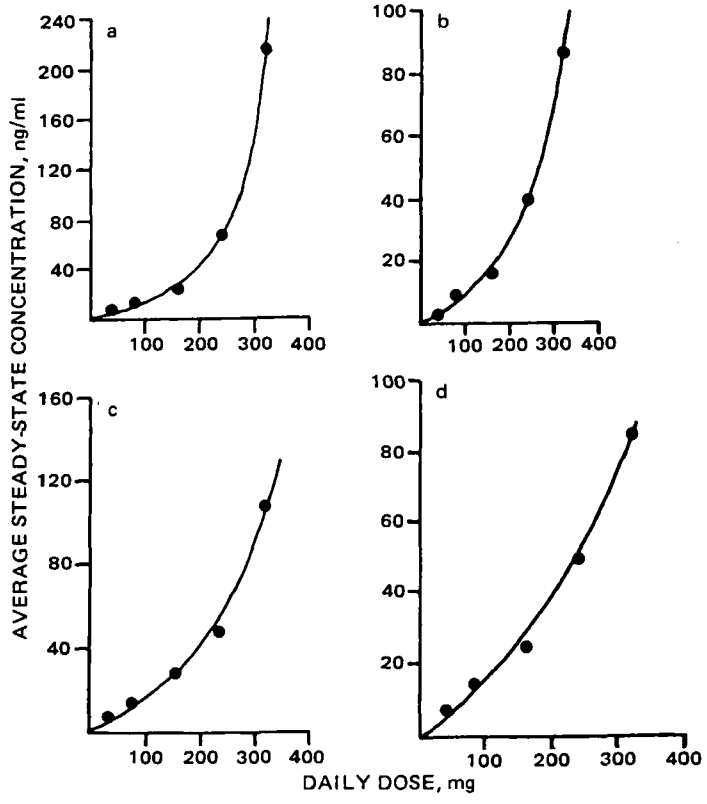

Figure 2—*Average steady-state concentration of propranolol in plasma during the 13th dosing interval at dosing rates from 40 to 320 mg/day. The line is the concentration predicted by the best elimination-rate model for each subject (a–d).*

shown in Table III, the terminal half-life of propranolol increased significantly, from 2.0 ± 0.4 to 5.5 ± 1.9 ($p < 0.05$), as the dose was increased from 40 to 320 mg/day.

Renal Clearance of Propranolol Metabolites—Less than 2% of propranolol was recovered in urine as free propranolol or 4-hydroxypropranol (unconjugated); no α-naphthoxylactic acid glucuronide was detected in the urine. There was a linear relationship between the urinary excretion rate of propranolol glucuronide (I), 4-hydroxypropranolol glucuronide (II), and α-naphthoxylactic acid (III) *versus* $\bar{C}_{ss}$ of each metabolite in plasma over the entire range of observed concentrations. The CL_r was 75.4 ± 17.5 ml/min for I, 130.6 ± 28.3 ml/min for II, and 56.8 ± 13.3 ml/min for III (Fig. 1).

Fraction of Propranolol Excreted in Urine as Propranolol Metabolites—The percentage of propranolol (on a molar basis) excreted in urine increased from 9.6 ± 2.5 to 16.2 ± 2.0 (significant at $p < 0.05$) for I, decreased from 17.7 ± 2.7 to 14.7 ± 3.3 for II, and decreased from 25.1

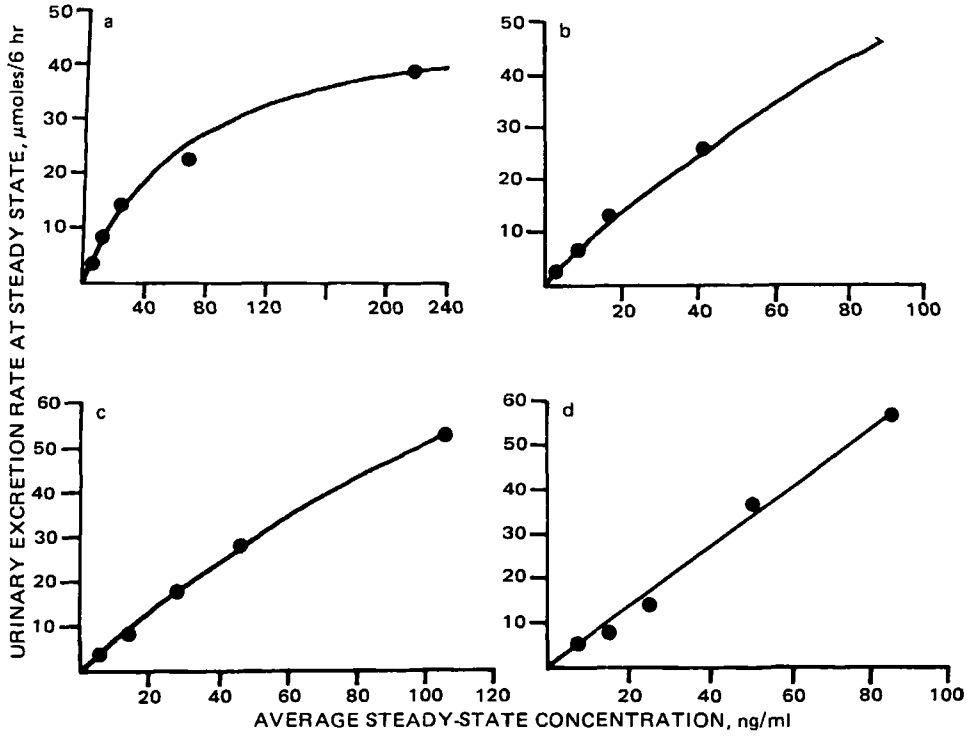

Figure 3—*Urinary excretion rate of propranolol glucuronide during the 13th dosing interval as a function of the average steady-state concentration of propranolol in plasma for each subject (a–d).*

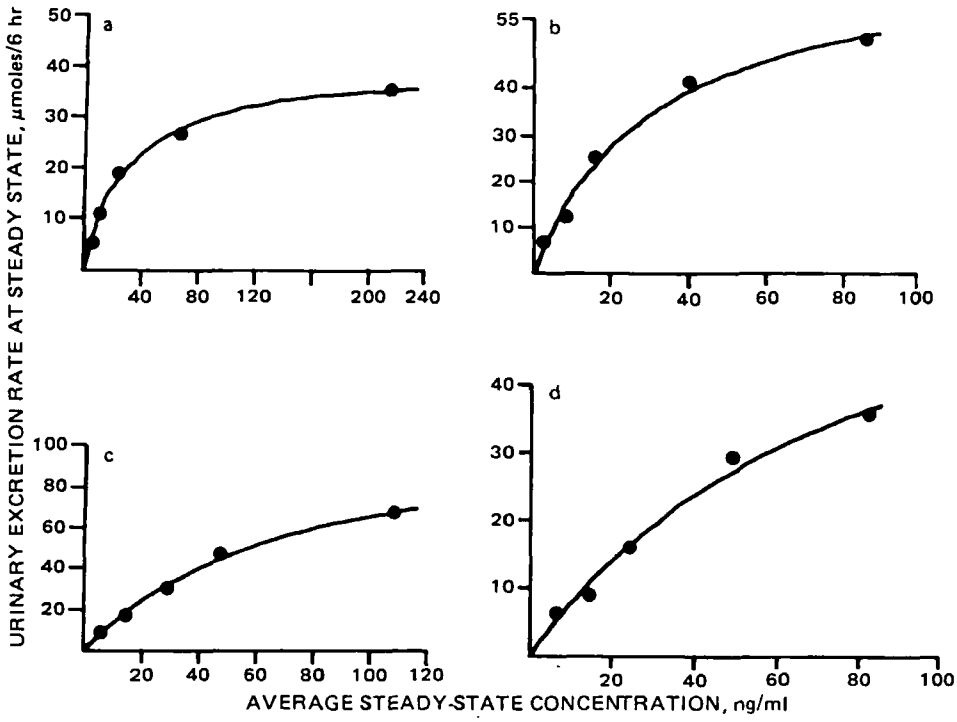

Figure 4—*Urinary excretion rate of 4-hydroxypropranolol glucuronide during the 13th dosing interval as a function of the average steady-state concentration of propranolol in plasma for each subject (a–d).*

± 3.7 to 18.6 ± 3.3 (significant at $p < 0.05$) for III as the dosing rate of propranolol was increased from 40 to 320 mg/day.

Relationship Between the $\bar{C}_{ss}$ of Propranolol and the Daily Dose—There was a disproportionate increase in the $\bar{C}_{ss}$ of propranolol as the daily dose was increased in each subject. There was a 1.8–2.6-fold difference in the $\bar{C}_{ss}$ of propranolol between subjects as the dose was increased from 40 to 320 mg/day (Fig. 2). The clearance associated with the unidentified metabolic pathway(s) was best described by a saturable (Models 1 and 3) rather than a first-order (Model 2) process (Table IV). In three subjects, the parameters of this saturable process were clearly different from those of the measured metabolites (Model 3), but in the remaining subject (B) they were indistinguishable (Model 1). These models were superior to either combination model (Models 4 and 5). The f_x-values estimated from Model 1 were 2.4, 2.0, 1.7, and 1.9 in subjects A, B, C, and D, respectively.

Formation Clearance Estimates for Known and Unknown Metabolic Pathway(s)—The formation of I was best described by a saturable process in three of four subjects (A, B, C) (Fig. 3). Using the estimates from Model 3 for all subjects, the V_{max} for propranolol glucuronide was 114 ± 51 mg/day and the K_m was 140 ± 55 ng/ml. In subject D, the apparent K_m for I was much greater than the C_{ss} of propranolol. The corresponding first-order metabolic clearance estimated from the slope of *dAe/dt versus* C_{ss} of propranolol was 496 ml/min. The formation of II and III was saturable in all four subjects over the dosing range studied (Figs. 4 and 5). The V_{max} for II was 72 ± 25 mg/day, and the K_m was 46 ± 21 ng/ml; the V_{max} for III was 92 ± 35 mg/day, and the K_m was 35 ± 234 ng/ml. The V_{max} for the unidentified metabolic pathway(s) was 212 ± 34 mg/day, and the K_m was 40 ± 12 ng/ml. These results are summarized in Table V.

DISCUSSION

The results from the present investigation demonstrate that the elimination of propranolol is nonlinear with doses of 40–320 mg/day and can be explained by capacity limitation in the major metabolic pathways that result in the formation of propranolol glucuronide (I), 4-hydroxypropranolol glucuronide (II), α-naphthoxylactic acid (III), and unidentified metabolite(s).

The 4-hydroxy metabolite of propranolol (4-hydroxypropranolol, IV) has similar β-blocking activity to the parent drug (25). Free (unconjugated) concentrations of IV reported by other workers following oral doses of propranolol have varied greatly. The ratio of IV to propranolol reported by others has ranged from 0.03 to 1.07, but was generally ~0.2 (29, 47, 48). By employing an analytical technique having a sensitivity limit for IV of ~1.0 ng/ml (37), it was found that concentrations of this metabolite were <20 ng/ml even at propranolol doses of 320 mg/day; the ratio of IV to propranolol was ~0.08. The lower ratio of IV-propranolol observed in this study relative to those by other workers may be due to differences between patients and healthy volunteers. Virtually all (>97%) of IV in the plasma was present as the glucuronide conjugate (II). Therefore, concentrations of II were estimated as the total IV concentration following enzymatic hydrolysis. Unlike propranolol, which is known to undergo conjugation at the secondary hydroxyl group on the side chain yielding an ether linkage, the specific location of the glucuronide on IV in the human is unknown; the conjugate may involve an ether or phenolic linkage, or may be a mixture of both. Fenseleau and Johnson have previously stressed that enzymatic hydrolytic techniques cannot discriminate between potential glucuronide conjugates when multiple sites of glucuronidation are possible (49).

The blood to plasma ratio (B/P) of propranolol was determined for each subject, and, in contrast to previous results (39), it was found that the B/P was unchanged over the 20–50-fold range of observed concentrations (Table I).

In the present study, the intrinsic clearance (CL_{int}) of propranolol varied from 1.8- to 2.6-fold between subjects at doses of 40 and 320 mg/day, respectively (Table II). On average, there was a 56% reduction in the CL_{int} over the eightfold range in daily doses of the drug. Makichan *et al.* (32) reported a 44% decrease in CL_{int} after doses from 10 to 80 mg, and Schneck *et al.* (4) reported a 53% decrease in CL_{int} after 160- and 320-mg doses. These results, however, were obtained from single-dose rather than steady-state experiments. Because CL_{int} is concentration dependent, estimates of its value are best obtained at steady state.

The time to peak concentration was similar, whereas the half-life of propranolol increased approximately threefold as the dose was increased from 40 to 320 mg/day (Table III). If it is assumed that the apparent volume of distribution of propranolol remains unchanged throughout the study, then the observed increase in the half-life must be due to a change in the systemic clearance.

The renal clearance (CL_r) of I, II, and III was linear over the range of observed metabolite concentrations (Fig. 1). The CL_r of II in the present study was about twice that previously reported [130 *versus* 60 ml/min (29)]; the CL_r of I and III were closer to those in previous reports [75 *versus* 57 ml/min (30), and 57 *versus* 37 ml/min (28), respectively]. Stone and Walle recently reported that the plasma concentrations of I, II, and III were ~20-fold greater in uremic patients when compared with patients having normal renal function (50). However, because the pharmacological and toxicological activities of these compounds are unknown, the clinical significance of these findings is uncertain.

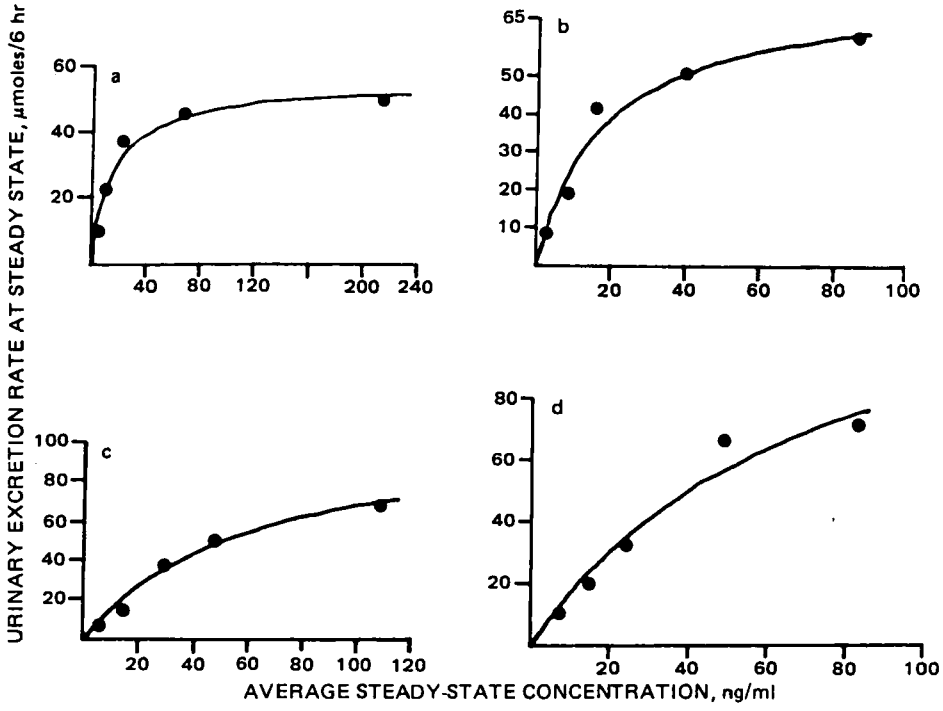

Figure 5—*Urinary excretion rate of α-naphthoxylactic acid during the 13th dosing interval as a function of the average steady-state concentration of propranolol in plasma for each subject (a–d).*

The formation of I from propranolol appeared to be saturable in three of four subjects (Fig. 3). In subject D, the metabolic clearance of I (496 ml/min) was ~6.4 times greater than its renal clearance (77.3 ml/min). Saturable glucuronidation has been reported previously for salicylamide and salicylic acid (51–53).

The V_{max} and K_m for II rather than for IV were estimated (Table V); there was essentially no free IV excreted in the urine. Therefore, saturability in the formation of II could be due either to saturation in the formation of IV from propranolol or in the formation of II from IV. If formation of IV from propranolol was a first-order process and formation of II from IV was saturable, one would expect to see disproportionate increases in IV concentrations (because it would accumulate) as the dose of propranolol was increased. That this was not observed suggests that saturability in the formation of II results from saturation in the formation of IV from propranolol.

In contrast to previous findings (28, 47), it was observed that the formation of III from propranolol was saturable (Fig. 5). However, this contention is predicated on several assumptions, because propranolol is not converted directly to this metabolite. Side-chain oxidation of propranolol first results in the formation of *N*-desisopropylpropranolol (V). Further oxidation of V yields a reactive aldehyde intermediate that can undergo either reduction to propranolol glycol or oxidation to III. In addition, III can be further oxidized to α-naphthoxyacetic acid (VI). Measurable concentrations of V, propranolol glycol (mainly as the glucuronide), and VI were detected in the urine of our subjects. As in previous studies (47), these metabolites accounted for <2% of the dose. Lo observed a similar urinary excretion profile for propranolol metabolism in the dog, but found significant concentrations of propranolol glycol (as the glucuronide) in the bile (3). Because only trace amounts of V, propranolol glycol (glucuronide), and VI are excreted in the urine at steady state (whereas up to 25% of propranolol can be accounted for as III), saturability in the formation of III is probably a reflection of the primary metabolic step in the *N*-dealkylation of propranolol to V. However, the value of V_{max} estimated for III is probably an underestimate of the total V_{max} for this metabolic pathway, since it is likely that other unidentified metabolism *via* this pathway is occurring and not being detected in the urine.

Elimination Models 1 and 3 adequately described the urinary excretion of the three measured metabolites in all individuals (Table IV). There was, however, a consistent underestimation of C_{ss} at the 40- and 80-mg dose rates in each individual (Fig. 2). This error was small (5% of C_{ss}) and does not detract from the overall ability of these models to describe C_{ss}

Table V—Estimated Michaelis–Menten Parameters for Propranolol Metabolism [a]

Subject	Propranolol Metabolite			
	Propranolol Glucuronide	4-Hydroxy-propranolol Glucuronide	α-Naphthoxylactic Acid	Unidentified Metabolic/ Pathway(s)
	V_{max}, mg/day			
A	55	41	56	230
B	142	72	77	205
C	146	101	99	167
D	4,577	72	137	244
Mean	114[b]	72	92	212
(*SD*)	(51)	(25)	(35)	(34)
	K_m, ng/ml			
A	76	29	14	45
B	175	31	18	28
C	168	51	43	33
D	6,297	74	63	55
Mean	140[b]	46	35	40
(*SD*)	(55)	(21)	(23)	(12)

[a] All values of V_{max} and K_m were estimated from Model 3. [b] Excludes values from subject D. Since the apparent K_m for propranolol glucuronide for subject D was much greater than C_{ss}, a metabolic clearance for this pathway of 496 ml/min was estimated from the slope of dAe/dt *versus* C_{ss}.

and metabolite excretion over a wide range of doses. However, it does suggest the existence of some time-related change in one or more clearance pathways. There was no evidence of a first-order elimination process for propranolol distinguishable from the saturable pathways.

To obtain a relationship between the C_{ss} of propranolol and the dosing rate (D_0/τ) using Eq. 4, the fraction of the dose not explained by measurement of I, II, and III had to be accounted for. The metabolic pathway(s) responsible for the formation of these unidentified metabolites was best described by a saturable rather than a first-order process. This may reflect either elimination of I, II, and III by routes other than in urine or in the formation of metabolites not measured (*e.g.*, propranolol glycol glucuronide in bile). The improved fit of Model 3 compared with Model 1 in three of four subjects supports the latter explanation.

The finding of saturable propranolol elimination in each individual studied suggests that clinicians should not presume linear pharmacokinetics when dosing patients with propranolol. It should be anticipated, therefore, that dosage increases may result in disproportionate increases in the plasma concentration of the drug. Although a 2.6-fold variation in the C_{ss} of propranolol between individuals was observed (Fig. 2), there was up to a fourfold difference in K_m for the various metabolic pathways (Table V). This latter finding may be of particular importance if one or more metabolites arising from the various metabolic pathways contribute to the clinical effects of propranolol.

REFERENCES

(1) A. S. Nies and D. G. Shand, *Circulation*, **52**, 6 (1975).

(2) J. W. Paterson, M. E. Conolly, C. T. Dollery, A. Hayes, and R. G. Cooper, *Pharmacol. Clin.*, **2**, 127 (1970).

(3) M. Lo, PhD thesis, University of California at San Francisco, 1981.

(4) D. G. Shand, E. M. Nuckolls, and J. A. Oates, *Clin. Pharmacol. Ther.*, **11**, 112 (1970).

(5) D. G. Shand and R. E. Ragno, *Pharmacology*, **7**, 159 (1972).

(6) R. E. Vestal, A. J. J. Wood, R. A. Branch, D. G. Shand, and G. R. Wilkinson, *Clin. Pharmacol. Ther.*, **26**, 8 (1979).

(7) C. M. Castleden, C. M. Kay, and R. L. Parsons, *Br. J. Clin. Pharmacol.*, **2**, 303 (1975).

(8) C. M. Castleden and C. F. George, *Br. J. Clin. Pharmacol.*, **7**, 49 (1979).

(9) R. E. Vestal, D. M. Kornhauser, J. W. Hollifield, and D. G. Shand, *Clin. Pharmacol. Ther.*, **25**, 19 (1979).

(10) G. Bianchetti, G. Grazini, and D. Branacaccio, *Clin. Pharmacokinet.*, **1**, 373 (1976).

(11) R. A. Branch and D. G. Shand, *Clin. Pharmacokinet.*, **17**, 264 (1976).

(12) J. Feely and I. H. Stevenson, *Br. J. Clin. Pharmacol.*, **6**, 446 (1978).

(13) J. Feely, I. H. Stevenson, and J. Crooks, *Clin. Pharmacol. Ther.*, **28**, 40 (1980).

(14) J. G. Riddell, J. D. Neill, J. G. Kelly, and D. G. McDevitt, *Clin. Pharmacol. Ther.*, **28**, 565 (1980).

(15) W. A. Briggs, D. T. Lowenthal, W. J. Cirksena, W. E. Price, T. P. Gibson, and W. Flamenbaum, *Clin. Pharmacol. Ther.*, **18**, 606 (1975).

(16) C. A. Chidsey, P. Morselli, G. Bianchetti, A. Morganti, G. Lenonetti, and A. Zanchetti, *Circulation*, **52**, 313 (1975).

(17) M. Esler, A. Zweifler, O. Randall, and V. DeQuattro, *Clin. Pharmacol. Ther.*, **22**, 299 (1977).

(18) A. Lehtonen, J. Kanto, and T. Kleimola, *Eur. J. Clin. Pharmacol.*, **11**, 155 (1977).

(19) M. Pine, L. Favrot, S. Smith, V. McDonald, and C. A. Chidsey, *Circulation*, **52**, 886 (1975).

(20) D. G. Shand, *Med. Clin. North Am.*, **58**, 1063 (1974).

(21) E. Vervolet, B. C. M. J. Takx-Kohlen, B. F. M. Pluym, and F. W. H. M. Merkus, *Clin. Pharmacol. Ther.*, **23**, 133 (1978).

(22) T. Walle, E. C. Conradi, U. K. Walle, T. C. Fagan, and T. E. Gaffney, *Clin. Pharmacol. Ther.*, **24**, 668 (1978).

(23) T. Walle and T. E. Gaffney, *J. Pharmacol. Exp. Ther.*, **182**, 83 (1972).

(24) T. Walle, J. I. Morrison, and G. L. Tindell, *Res. Commun. Chem. Pathol. Pharmacol.*, **9**, 1 (1974).

(25) J. D. Fitzgerald and S. R. O'Donnell, *Br. J. Pharmacol.*, **45**, 207 (1972).

(26) T. Ishizaki, P. J. Privitera, T. Walle, and T. E. Gaffney, *J. Pharmacol. Exp. Ther.*, **189**, 626 (1974).

(27) D. A. Saelens, T. Walle, T. E. Gaffney, and P. J. Privitera, *Eur. J. Pharmacol.*, **42**, 39 (1977).

(28) T. Walle, E. C. Conradi, U. K. Walle, T. C. Fagan, and T. E. Gaffney, *Clin. Pharmacol. Ther.*, **26**, 548 (1979).

(29) T. Walle, E. C. Conradi, U. K. Walle, T. C. Fagan, and T. E. Gaffney, *Clin. Pharmacol. Ther.*, **27**, 22 (1980).

(30) T. Walle, T. C. Fagan, E. C. Conradi, U. K. Walle, and T. E. Gaffney, *Clin. Pharmacol. Ther.*, **26**, 167 (1979).

(31) D. M. Kornhauser, A. J. J. Wood, R. E. Vestal, G. R. Wilkinson, R. A. Branch, and D. G. Shand, *Clin. Pharmacol. Ther.*, **23**, 165 (1978).

(32) J. J. Makichan, D. R. Pyzcznski, and W. J. Jusko, *Biopharm. Drug Dispos.*, **1**, 159 (1980).

(33) M. Rowland, L. Z. Benet, and G. G. Graham, *J. Pharmacokinet. Biopharm.*, **1**, 123 (1973).

(34) G. R. Wilkinson and D. G. Shand, *Clin. Pharmacol. Ther.*, **18**, 377 (1975).

(35) N. H. G. Holford, S. Vozeh, P. Coates, J. R. Powell, J. F. Thiercelin, and R. Upton, *N. Engl. J. Med.*, **296**, 1300 (1977).

(36) B. Silber, M. Lo, and S. Riegelman, *Res. Commun. Chem. Pathol. Pharmacol.*, **27**, 419 (1980).

(37) M. Lo, B. Silber, and S. Riegelman, *J. Chromatogr. Sci.*, **20**, 126 (1982).

(38) M. Lo and S. Riegelman, *J. Chromatogr.*, **183**, 213 (1980).

(39) G. Sager and S. Jacobsen, *Acta Pharmaceut. Suec.*, **17**, 86 (1980).

(40) N. H. G. Holford, "MKMODEL—A Mathematical Modeling Tool, PROPHET Public Procedures Notebook," Bolt Beranek and Newman, Cambridge, Mass., 1980.

(41) A. G. Knott, *Comp. Progr. Biomed.*, **10**, 271 (1979).

(42) H. Akaike, *I.E.E.E. Tr. Automat. Contr.*, **19**, 716 (1973).

(43) H. Akaike, *Biometrika*, **66**, 237 (1979).

(44) A. C. Atkinson, *Biometrika*, **67**, 413 (1980).

(45) J. H. Zar, "Biostatistical Analysis," Prentice-Hall, Englewood Cliffs, N.J., 1974, p. 130.

(46) W. F. Raub, *Fed. Proc.*, **33**, 2390 (1974).

(47) D. W. Schneck, J. F. Pritchard, T. P. Gibson, J. E. Vary, and A. H. Hayes, *Clin. Pharmacol. Ther.*, **27**, 744 (1980).

(48) A. M. Taburet, A. A. Taylor, J. R. Mitchell, D. E. Rollins, and J. L. Pool, *Life Sci.*, **24**, 209 (1979).

(49) C. Fenseleau and L. P. Johnson, *Drug. Metab. Dispos.*, **8**, 274 (1980).

(50) W. J. Stone and T. Walle, *Clin. Pharmacol. Ther.*, **28**, 449 (1980).

(51) W. H. Barr and S. Riegelman, *J. Pharm. Sci.*, **59**, 164 (1970).

(52) G. Levy and J. A. Procknal, *J. Pharm. Sci.*, **57**, 1330 (1968).

(53) G. Levy, *Chem. Biol. Interact.*, **3**, 291 (1971).

ACKNOWLEDGMENTS

This work was supported in part by Grant GM-26556 from the National Institute of General Medical Sciences, National Institutes of Health.

The authors wish to thank Ms. Danielle M. Dols and Ms. Deborah J. Johnson for expert technical assistance during the course of this study.

Microbial Transformations of Pergolide to Pergolide Sulfoxide and Pergolide Sulfone

ROBERT V. SMITH *x, PATRICK J. DAVIS ‡, and KATHLEEN M. KERR ‡

Received February 22, 1982, from the *Drug Dynamics Institute and ‡Division of Medicinal and Natural Products Chemistry, College of Pharmacy, University of Texas at Austin, Austin, TX 78712. Accepted for publication June 22, 1982.

Abstract □ Fifty-eight microorganisms were investigated for their ability to effect the biotransformation of the ergoline alkaloid pergolide. A majority of these organisms formed pergolide sulfoxide, and a *Helminthosporium* species was investigated in greater detail since it yielded significant amounts of pergolide sulfoxide. A preparative-scale transformation afforded material which was identified as the sulfoxide based on melting point, spectral, and chromatographic comparison with authentic material as well as its conversion to pergolide by reduction with triphenylphosphine. An analytical high-performance liquid chromatographic determination of the enzymatic *versus* spontaneous air-oxidation of pergolide in growing cultures and controls showed negligible air-oxidation and an ~40% enzymatic conversion of pergolide to the sulfoxide. Several organisms, including *Aspergillus alliaceus* formed a second metabolite, pergolide sulfone, which was identified on the basis of cochromatographic data.

Keyphrases □ Pergolide—sulfoxide and sulfone metabolites, biotransformation in 58 microorganisms, identification by preparative-scale TLC and high-performance liquid chromatography □ TLC, preparative-scale—of pergolide and its sulfoxide and sulfone metabolites, following microbial transformation □ High-performance liquid chromatography—of pergolide and its sulfoxide and sulfone metabolites, following microbial transformation

The dopaminergic properties of ergoline alkaloids are responsible for their use in the treatment of prolactin-dependent disorders such as galactorrhea and amenorrhea, hyperprolactinemic anovulation, prolactin-dependent breast cancers, and other dopaminergic disorders such as acromegaly and Parkinson's disease (1–8). Ergoline derivatives such as bromocriptine and lergotrile are potential inhibitors of prolactin secretion (9, 10), and bromocriptine also may be useful therapeutically in combination with levodopa for the management of "on–off" reactions in parkinsonism (11). At dose levels needed to treat this disease, however, heptatotoxicity has been observed with lergotrile (11), which has led to the disruption of clinical trials.

As a result of studies undertaken to define the structural requirements necessary for prolactin inhibition and to develop more selective dopaminergic agents for the treatment of hyperprolactinemic states and Parkinson's disease (12–14), a semisynthetic ergoline, pergolide (I), was investigated and found to be one of the most potent dopamine agonists *in vitro* and *in vivo* (15–17). Clinical investigations of I in the treatment of galactorrhea and amenorrhea (18) indicated that I was a more potent prolactin inhibitor than previously studied ergolines, and that it had a longer duration of action with more tolerable side effects. Pergolide also has shown marked advantages compared with bromocriptine and lergotrile, either alone or in combination with levodopa, in the treatment of Parkinson's disease (19).

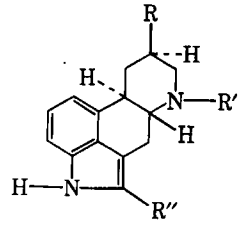

I: R = CH_2SCH_3, R′ = $CH_2CH_2CH_3$, R″ = H

II: R = $CH_2S(O)CH_3$, R′ = $CH_2CH_2CH_3$, R″ = H

III: R = $CH_2S(O_2)CH_3$, R′ = $CH_2CH_2CH_3$, R″ = H

IV: R = $CH_2C{\equiv}N$, R′ = CH_3, R″ = Cl

Two metabolites of I, pergolide sulfoxide (II) and pergolide sulfone (III), have been reported in mammalian systems[1]. Using the rationale of "microbial models of mammalian metabolism" (20, 21), a study was undertaken to identify microorganisms which form the two metabolites found in mammalian species. The present report describes the investigation of 58 microorganisms for their ability to effect the biotransformation of I, the preparative-scale conversion and identification of the metabolite pergolide sulfoxide (II) from *Helminthosporium* species NRRL 4671 cultures, the identification of pergolide sulfone (III) in *Aspergillus alliaceus* UI 315 cultures, and the high-performance liquid chromatographic (HPLC) determination of the enzymatic *versus* spontaneous air-oxidation of I to II from growing cultures and controls.

EXPERIMENTAL

Materials—Pergolide mesylate[2], pergolide sulfoxide[2], and lergotrile mesylate[2] (internal standard) were used without further purification. Water for use in the HPLC was deionized and double-distilled in glass; acetonitrile[3] was HPLC grade. The mobile phase was prepared by the filtration of individual components[4], mixing, and deaerating prior to use. All other solvents and reagents were analytical reagent quality or better. All extraction tubes, vials, and stage-2 Erlenmeyer flasks used in the analytical studies were silylated using 2% trimethylchlorosilane[5] in toluene and were rinsed prior to use.

Analytical Methods—Analytical TLC was performed with silica gel plates[6] or aluminum oxide plates[7] in the following TLC systems: (*a*) silica gel developed in chloroform–methanol–acetone–28% ammonium hydroxide (63:7:27:2), (*b*) silica gel developed in chloroform–methanol–glacial acetic acid (13:6:1), (*c*) aluminum oxide developed in acetone, and (*d*) aluminum oxide developed in toluene–morpholine (18:2). Under these conditions, the following R_f values were observed: I (*a*) 0.81, (*b*) 0.91, (*c*) 0.95, and (*d*) 0.63; II (*a*) 0.54, (*b*) 0.44, (*c*) 0.52, and (*d*) 0.20; and III (*a*)

[1] Personal communications, E. C. Kornfeld, Eli Lilly Research Laboratories, 1978.
[2] Eli Lilly Co., Indianapolis, Ind.
[3] OmniSolv, M.C.B. Reagents, Cincinnati, Ohio.
[4] G/F grade glass fiber filter, Whatman, Clifton, N.J.
[5] Aldrich, Milwaukee, Wis.
[6] Polygram Sil G/UV 254, 0.25 mm, Brinkmann, Westbury, N.Y.
[7] Polygram Alox N/UV 254, 0.20 mm, Brinkmann, Westbury, N.Y.

0022-3549/83/0700-0733$01.00/0

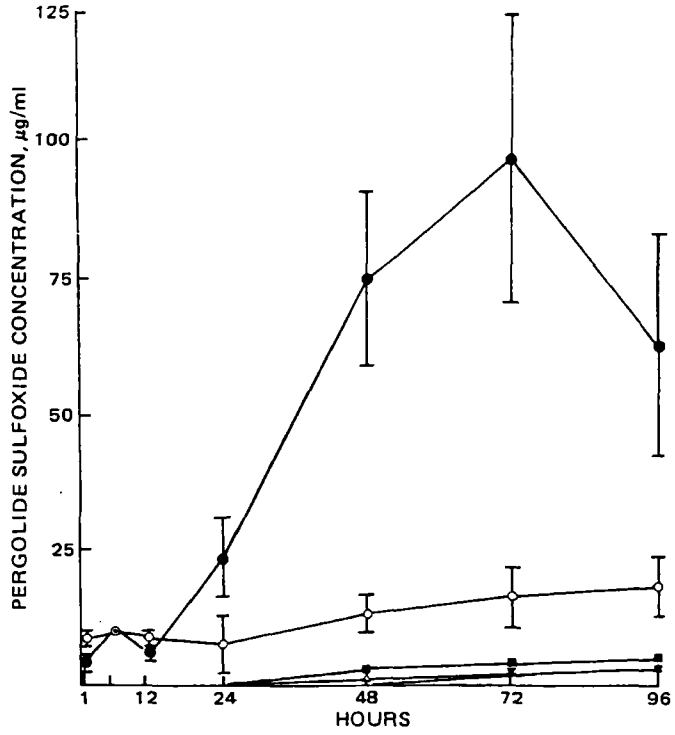

Figure 1—*Enzymatic* versus *spontaneous air-oxidation of pergolide measured by HPLC in live* Helminthosporium *species NRRL 4671 cultures (●) and in controls consisting of autoclaved* Helminthosporium *species culture (○) and phosphate buffers at pH 4 (■), pH 7 (△), and pH 11 (▼). Determinations were made in triplicate; bars represent the* SD *of each mean value.*

0.70, (*b*) 0.71, (*c*) 0.92, and (*d*) 0.39. Plates were visualized under UV light (254 nm) and sprayed with either Van Urks–Salkowski (modified) reagent for indoles (22), or Gibb's (23) and Pauly's (20) reagents in anticipation of hydroxylated metabolites (24). Screening experiments were monitored with TLC system *a*, and co-chromatography of the metabolites II and III with the standard materials was performed using all four TLC systems.

All analytical HPLC analyses were conducted as described previously (25) using an octadecyl reverse-phase 10-μm 3.9 × 300-mm column[8]. The mobile phase consisted of acetonitrile–0.01 *M* ammonium carbonate buffer pH 8.4 (3.75:2); the flow rate was 2 ml/min. Under these conditions, retention times were as follows: I, 6.74 min, II, 3.22 min, III, 2.31 min, and lergotrile (internal standard), 2.42 min. Preparative HPLC was run using an octadecyl reverse-phase, 10-μm, 8 × 500-mm column[9]. The mobile phase was the same as above but used at 3 ml/min. Under these conditions, retention times were as follows: II, 11.98 min and III, 9.49 min.

Mass spectra[10] (MS) gave the following results: I, *m/z* (% relative abundance), 314 (100), 299 (20), 285 (65), 267 (30); II (synthetic material and metabolite), *m/z* (% relative abundance), 330 (25), 315 (15), 313 (100), 301 (10), 267 (35); and III (synthetic material only), *m/z* (% relative abundance), 346 (100), 330 (3), 317 (89), 267 (22). ^{1}H-NMR spectra were recorded on a 100-MHz[11], or a 200-MHz spectrometer[12] using tetramethylsilane as the internal standard: I, δ(ppm) (deuterochloroform), 2.16 [3, s, $-SCH_3$], 6.80–7.22 [4, aromatic protons], 7.95 [1, broad s, NH]; II (synthetic material and metabolite), δ(ppm) (deuterochloroform), 2.64 and 2.63 [3, 2s, $-SOCH_3$], 6.80–7.22 [4, aromatic protons], 8.16 [1, broad s, NH]; and III (synthetic), δ(ppm) (deuterochloroform), 3.00 [3, s, $-SO_2CH_3$], 6.8–7.2 [4, aromatic protons], 7.91 [1, broad s, NH]. Melting points for I (212.7–216.8°) and II (174.0–177.0°) were determined with a Fisher digital melting point analyzer[13] at a rate of 2°/min and are uncorrected.

General Fermentation Conditions—All microorganisms were maintained on refrigerated (4°) slants of either Sabouraud-maltose agar[14], mycophyl agar[15], or ATCC medium 5 sporulation agar[14] and were transferred every 6 months to maintain viability. Incubations were performed in a two-stage fermentation procedure with soybean–dextrose medium (26). Appropriate substrates (I or II) were added to 24-hr stage-2 flasks. Portions (2 ml) were removed at 1, 2, 3, 6, and 10 days and extracted as described previously (26).

Preparative-Scale Production of Pergolide Sulfoxide (II) with *Helminthosporium* Species NRRL 4671—Six milliliters of stage-1 growth was used to inoculate each of six 250-ml stage-2 Erlenmeyer flasks containing 50 ml of soybean–dextrose medium (300 ml total), which were incubated at 27°, 250 rpm, for 24 hr. A total of 75 mg of pergolide mesylate was dissolved in 6 ml of sterile water and aseptically distributed among the flasks (0.25 mg/ml). After 5 days, the cultures were combined and homogenized, adjusted to pH 8.5 with an equal volume of 0.1 *M* sodium carbonate–sodium bicarbonate buffer (pH 8.5), and exhaustively extracted with ethyl acetate in a separatory funnel. The ethyl acetate extracts were combined, concentrated *in vacuo*, and partitioned against 0.05 *N* HCl. The acidic, aqueous extract was adjusted to pH 9 with 1 *N* NaOH and partitioned against ethyl acetate. The final ethyl acetate extracts were combined, concentrated *in vacuo* (520 mg), and chromatographed using preparative-scale TLC plates[16]. After development in TLC system *a* (*Analytical Methods*), the band representing II was scraped from the plate and eluted in a glass column with ethanol to remove the metabolite (46.2 mg). Compound II was recrystallized from ethanol (16.7 mg).

Triphenylphosphine Reduction of Pergolide Sulfoxide (II)—Following the procedure of Castrillon and Szmant (27), 1 mg of II was dissolved in 5.0 ml of carbon tetrachloride in a 1-ml conically tipped and capped vial[17]. Two equivalents of triphenylphosphine (1.66 mg) were added to the vial and the mixture was heated (90°) for 3 hr in a metal heating mantle[18]. After being concentrated under a nitrogen stream, the reaction mixture was analyzed by TLC and HPLC.

Peracid Oxidation of Pergolide (I) to Pergolide Sulfoxide (II)—Following the procedure of Curci and Modena (28), 5 mg of I was dissolved in 10 ml of 0.01 *N* HCl–ethanol (50:50); 2.7 mg of *m*-chloroperbenzoic acid (1 equivalent) was added and the reaction was allowed to proceed at room temperature. After a perioid of 4 hr, the ethanol was removed under a nitrogen stream, the mixture was adjusted to pH 9 with 1 *N* NaOH, and then extracted with ethyl acetate. The ethyl acetate extract was concentrated *in vacuo* to yield an oil which was analyzed by TLC and HPLC.

Peracid Oxidation of Pergolide (I) to Pergolide Sulfone (III)—Compound I (50 mg) and *m*-chloroperbenzoic acid (27 mg) were dissolved in 25 ml of 0.01 *N* HCl–methanol (50:50). After 24 hr, additional peracid (29.7 mg, 1 equivalent plus 10%) was added to the flask, and the reaction was allowed to proceed at 27° for 4 days. The products were extracted as described above and concentrated under a nitrogen stream. The resulting syrup was dissolved in 2 ml of mobile phase, and III was isolated by preparative HPLC, concentrated *in vacuo*, and purified by preparative-scale TLC (8.1 mg, oil) as described above for II.

Determination of the Enzymatic *versus* Spontaneous Air-Oxidation of Pergolide (I) by *Helminthosporium* species NRRL 4671—A 2-ml portion of a stage-1 culture of *Helminthosporium* species NRRL 4671 was used to inoculate each of seven stage-2 cultures which were generated in silylated 125-ml culture flasks[19] containing 22 ml of medium. After incubating at 27° for 24 hr using a gyrorotary shaker[20] at 250 rpm, three of the cultures were autoclaved. Compound I (6.25 mg) in 1 ml of sterile water–ethanol (95:5) was added to each of the autoclaved and three of the live cultures. No substrate was added to the seventh flask to serve as a control for HPLC analyses. Triplicate control incubations were also conducted for I in 25 ml of autoclaved 0.1 *M* potassium phosphate buffer at pH 3, pH 7, and pH 11. A stock solution of the internal standard, lergotrile (IV) (1 mg/ml of methanol), was prepared; a 100-μl portion was placed in all extraction tubes, and the solvent was removed under a nitrogen stream. Two-milliliter portions of incubation samples were removed at 1, 6, 12, 24, 48, 72, and 96 hr; these were extracted and analyzed by HPLC as described previously (25). Results were expressed as amount of II produced (Fig. 1).

[8] μ-Bondapak C-18, Waters Associates, Milford, Mass.
[9] Lichrosorb RP-18, Whatman, Clifton, N.J.
[10] Dupont Model 21491, Dupont Instruments Products Division, Wilmington, Del.
[11] Varian HA-100, Varian Associates, Palo Alto, Calif.
[12] Nicolet Model NT-200 Wide Bore, Nicolet Magnetics, Mountain View, Calif.
[13] Fisher Scientific, Pittsburgh, Pa.
[14] Difco Laboratories, Detroit, Mich.
[15] B.B.L. Microbiological Systems, Cockeysville, Md.
[16] Silica gel G, 1.0 mm, Analtech, Newark, N.J.
[17] Reacti-Vial, Pierce Chemical Co., Rockford, Ill.
[18] Reacti-Therm, Pierce Chemical Co., Rockford, Ill.
[19] Bellco Delong culture flasks, Bellco Glass, Inc., Vineland, N.J.
[20] NBS Model G25-R Environmental Shaker, New Brunswick Scientific, Edison, N.J.

Table I—Microorganisms *Examined for* Their Ability to Effect the Biotransformation of Pergolide.

Microorganism	Source and Reference Number[a]
Aspergillus alliaceus[b]	UI 315
A. foetidus	NRRL 337
A. niger	UI-X-172
A. niger[b]	ATCC 16888
A. niger	ATCC 10581
A. niger	ATCC 10548
A. oryzae	NRRL 447
Beauvaria bassiana	ATCC 13144
B. sulfurescens	ATCC 7159
Calonectria decora[b]	ATCC 14767
Cryptococcus mascerans	Ziffer
Cunninghamella bainieri	UI 3065
C. bertholletiae	NRRL 3644
C. bertholletiae	ATCC 11064
C. blakesleeana	NRRL 1369
C. blakesleeana	ATCC 8688a
C. blakesleeana	UI Sih-2138
C. echinulata[b]	ATCC 9244
C. echinulata[b]	UI Sih-1387
C. echinulata[b]	UI 3655
C. echinulata[b]	UI Sih-1386
C. echinulata[b]	ATCC 11585a
C. echinulata[b]	ATCC 11585b
C. elegans	ATCC 9245
C. elegans	UI Sih-1393
Curvularia lunata	ATCC 13633
Gliocladium deliquescens	UI 1086
Helicostylum piriforme	UI-2-QM 6945
H. piriforme (+)	UI-QM 6945
H. piriforme (−)	UI-QM 6944
Helminthosporium species	NRRL 4671
Microsporum gypseum	ATCC 11395
Mortierella isabellina	Abushanab
Mucor mucedo	UI 4605
Saccharomyces cerevisiae	NRRL Y-2034
Schizosaccharomyces pombe	ATCC 2476
S. pombe	ATCC 20130
Sepedonium chrysospermum	ATCC 13378
Sporobolomyces pararoseus	ATCC 11386
Streptomyces albogriseolus	NRRL B-1305
S. aureofaciens	ATCC 13304
S. flocculus	ATCC 25453
S. griseus	ATCC 10137
S. griseus	NRRL B-599
S. griseus	NRRL 3242
S. griseus	UI 1158W
S. lavendulae	NRRL B-2036
S. lavendulae	UI Sih L-105
S. lincolnensis	ATCC 25466
S. lincolnensis	NRRL 2936
S. paucisporogenes	ATCC 12596
S. platensis	NRRL 2364
S. punipaulis	NRRL 3529
S. purpurascens	ATCC 21326
S. rimosus	ATCC 23955
S. rimosus	NRRL 2234
S. rutgersensis	NRRL B-1256
S. scabies	UI Sih-1627
Streptomyces species	UI MR-127

[a] Key: (ATCC) American Type Culture Collection, Rockville, Md.; (NRRL) Northern Regional Research Laboratories, Peoria, Ill.; (QM) Quartermaster Collection, Mycological Services, Amherst, Mass.; (UI) College of Pharmacy, University of Iowa, Iowa City, Iowa; (Abushanab) received from Dr. E. Abushanab, University of Rhode Island, Kingston, R.I.; (Ziffer) received from Dr. H. Ziffer, National Institute of Arthritis, Metabolism and Digestive Diseases, Bethesda, Md. [b] These microorganisms formed both pergolide sulfoxide (II) and pergolide sulfone (III).

Determination of the Enzymatic *versus* Spontaneous Air-Oxidation of Pergolide Sulfoxide (II) to Pergolide Sulfone (III) by *Aspergillus alliaceus* UI 315—A 2-ml portion of the stage-1 culture of *Aspergillus alliaceus* UI 315 was used to inoculate each of three stage-2 culture flasks containing 25 ml of medium. After incubating at 27° for 24 hr using a gyrorotary shaker at 250 rpm, one of the cultures was autoclaved. Compound II (6.25 mg) in 1 ml of sterile water–ethanol (95:5) was added to the autoclaved and live cultures and to sterile media used as a control. A fourth culture (without added substrate) served as a control in the TLC analyses. Two-milliliter portions of incubation samples were removed at 1, 2, 3, 6, and 10 days, extracted, and analyzed by TLC system *a*.

RESULTS AND DISCUSSION

The metabolism of many xenobiotics by microorganisms parallels their metabolism in mammalian systems. The observation that xenobiotics are modified chemically in a highly selective way by microorganisms (29) has formed the basis for studies of microbial models of mammalian metabolism (20, 21). A desire to produce sufficient quantities of metabolites of the ergoline pergolide (I) for biological evaluation prompted us to examine 58 microorganisms for their ability to effect the biotransformation of I (Table I). These microorganisms were chosen based on their reported ability to catalyze oxidations of sulfur or affect indole hydroxylations (30–34). A majority of the microorganisms investigated formed pergolide sulfoxide (II), a known mammalian metabolite; several (*A. alliaceus* UI 315, *Aspergillus niger* ATCC 16888, *Calonectria decora* ATCC 14767, and all *Cunninghamella echinulata* strains) formed another known metabolite, pergolide sulfone (III), in addition to II. Additional studies were performed with *Helminthosporium* species NNRL 4671, since it yielded significant amounts of II from I. *A. alliaceus* UI 315 was employed to study the formation of III.

A preparative-scale incubation of I with the *Helminthosporium* species allowed the identification of the major metabolite, II, based on the MS and ^{1}H-NMR spectral data. The melting point of the metabolite was identical to authentic sulfoxide and did not change during mixed melting point determinations. The products of the triphenylphosphine reduction of II and the peracid oxidation of I were cochromatographed with I and II, respectively, in TLC system *a* and by HPLC. Cochromatography of the metabolite with authentic sulfoxide in four TLC systems provided additional evidence of its identity. Characterization of III was based on cochromatography of this metabolite obtained from *A. alliaceus* microbial extracts with synthetic III in all four TLC systems and by its HPLC retention time.

Verification that III was formed enzymatically was accomplished through an analytical experiment in which II was incubated with *A. alliaceus* cultures. The formation of III and I in active cultures, as determined by TLC, indicated that III formed from I *via* the sulfoxide. The fact that sulfide oxidation was reversible and that III did not form in control incubations supports enzyme-mediated reactions.

The problem of the air-oxidation of I to II necessitated a study of the enzymatic *versus* spontaneous air-oxidation of I. HPLC was chosen as the method of analysis based on its demonstrated utility in the rapid analysis of microbial extracts (35). This experiment (Fig. 1) illustrated the large difference between the enzymatic (40%) oxidation of I by *Helminthosporium* species and the maximum spontaneous air-oxidation (6%) of the drug. The substrate, I, was converted maximally after 48 hr, and there were no significant differences (*F* test) in product formation during subsequent time periods.

The utility of the microbial production of pergolide metabolites for biological evaluation was varied. The apparently low yield in the transformation of I to III by *A. alliaceus* makes the chemical preparation of this compound a more viable procedure. There are many examples of the stereoselective formation of sulfoxides by microorganisms (36). However, only minor (if any) stereoselectivity in the formation of one pergolide sulfoxide diastereomer by *Helminthosporium* species was suggested from ^{1}H-NMR data (diastereomeric thiomethyl signals). Other organisms producing the sulfoxide might be examined for a higher degree of stereoselectivity.

In summary, an investigation of 58 microorganisms for their ability to effect the biotransformation of the semisynthetic ergoline alkaloid, pergolide, indicated that a majority produced the known mammalian metabolite pergolide sulfoxide (II), and that several microorganisms formed a second mammalian metabolite, pergolide sulfone (III), in addition to II. These results further support the concept of microbial models of mammalian metabolism.

REFERENCES

(1) H. G. Floss, J. M. Cassady, and J. E. Robbers, *J. Pharm. Sci.*, **62**, 699 (1973).

(2) J. A. Clemens, C. J. Shaar, E. B. Smalstig, N. J. Bach, and E. C. Kornfeld, *Endocrinology*, **94**, 1171 (1974).

(3) M. Goldstein, J. Y. Lew, A. F. Battista, A. Lieberman, and K. Fuxe, *Fed. Proc. Fed. Am. Soc. Exp. Biol.*, **37**, 2202 (1978).

(4) D. L. Kleinberg, M. Shaaf, and A. G. Frantz, *ibid.*, **37**, 2198 (1978).

(5) K. Fuxe, B. B. Fredholm, S. O. Ogren, L. F. Agnati, T. Hokfelt, and J. A. Gustafsson, *ibid.*, **37**, 2181 (1978).

(6) A. G. Frantz and D. L. Kleinberg, *ibid.*, **37**, 2192 (1978).
(7) L. Lemberger, *ibid.*, **37**, 2176 (1978).
(8) H. H. Keller and M. DaPrada, *Life Sci.*, **24**, 1211 (1979).
(9) D. L. Kleinberg, G. L. Noel, and A. G. Frantz, *N. Engl. J. Med.*, **296**, 589 (1977).
(10) S. J. Judd, *Drugs*, **16**, 167 (1978).
(11) D. B. Calne, *Fed. Proc. Fed. Am. Soc. Exp. Biol.*, **37**, 2207 (1978).
(12) J. M. Cassady, G. S. Li, E. B. Spitzner, and H. G. Floss, *J. Med. Chem.*, **17**, 300 (1974).
(13) G. S. Li, M. Robinson, H. G. Floss, J. M. Cassady, and J. A. Clemens, *ibid.*, **18**, 892 (1975).
(14) P. L. Stutz, P. A. Stadler, J. M. Vigouret, and A. Jaton, *ibid.*, **21**, 754 (1978).
(15) G. DeLitala, T. Yeo, A. Grossman, N. R. Hathaway, and G. M. Besser, *J. Endocrinol.*, **87**, 95 (1980).
(16) R. W. Fuller, J. A. Clemens, E. C. Kornfeld, H. D. Snoddy, E. B. Smalstig, and N. J. Bach, *Life Sci.*, **24**, 375 (1979).
(17) J. G. Cannon, B. J. Demopoulos, J. P. Long, J. R. Flynn, and F. M. Sharabi, *J. Med. Chem.*, **24**, 238 (1981).
(18) J. T. Callaghan, R. E. Cleary, R. Crabtree, and L. Lemberger, *Life Sci.*, **28**, 95 (1981).
(19) E. R. Gonzalez, *J. Am. Med. Assoc.*, **246**, 11 (1981).
(20) R. V. Smith and J. P. Rosazza, *Arch. Biochem. Biophys.*, **161**, 551 (1974).
(21) J. P. Rosazza and R. V. Smith, *Adv. Appl. Microbiol.*, **25**, 169 (1979).
(22) A. Ehman, *J. Chromatogr.*, **132**, 267 (1977).
(23) P. J. Davis, L. K. Jamieson, and R. V. Smith, *Anal. Chem.*, **50**, 736 (1978).
(24) C. J. Parli, B. Schmidt, and C. J. Shaar, *Biochem. Pharmacol.*, **27**, 1405 (1978).
(25) K. M. Kerr, R. V. Smith, and P. J. Davis, *J. Chromatogr.*, **219**, 317 (1981).
(26) P. J. Davis, J. E. Glade, A. M. Clark, and R. V. Smith, *Appl. Environ. Microbiol.*, **38**, 891 (1979).
(27) J. P. A. Castrillon and H. H. Szmant, *J. Org. Chem.*, **30**, 1338 (1965).
(28) R. Curci and G. Modena, *Tetrahedron*, **22**, 1227 (1966).
(29) K. Kieslich, "Microbial Transformations of Non-steroid Cyclic Compounds," Wiley, New York, N.Y. 1976.
(30) C. E. Holmund, K. J. Sax, B. E. Nielsen, R. E. Hartman, R. H. Evans, and R. H. Blank, *J. Org. Chem.*, **27**, 1468 (1962).
(31) B. J. Auret, D. R. Boyd, and H. B. Henbest, *J. Chem. Soc. (C)*, **1968**, 2374.
(32) B. J. Auret, D. R. Boyd, H. B. Henbest, and C. G. Watson, *Phytochemistry*, **13**, 65 (1964).
(33) R. V. Smith and J. P. Rosazza, *J. Pharm. Sci.*, **64**, 1737 (1975).
(34) E. Abushanab, D. Reed, F. Suzuki, and C. J. Sih, *Tetrahedron Lett.*, 3415 (1978).
(35) P. J. Davis, *J. Chromatogr.*, **193**, 170 (1980).
(36) B. J. Auret, D. R. Boyd, F. Breen, and R. M. E. Greene, *J. Chem. Soc. Perkin Trans. I*, **1981**, 930.

ACKNOWLEDGMENTS

This research was supported, in part, by the Eli Lilly Research Foundation.

Stereospecific Radioimmunoassays for *l*-Ephedrine and *d*-Ephedrine in Human Plasma

K. K. MIDHA ˣ, J. W. HUBBARD, J. K. COOPER, and C. MACKONKA

Received December 28, 1981, from the *College of Pharmacy, University of Saskatchewan, Saskatoon, Saskatchewan, Canada, S7N 0W0.* Accepted for publication June 10, 1982.

Abstract □ Haptens were prepared by the reaction of *d*-ephedrine or *l*-ephedrine with methyl acrylate and subsequent alkaline hydrolysis of the methyl ester groups. The haptens were coupled to bovine serum albumin by a mixed anhydride method, and the resulting drug–protein conjugates were used to immunize rabbits. Antiserum raised to these conjugates were highly stereospecific. Neither antiserum cross-reacted with the optical antipode of its substrate nor with racemic pseudoephedrine. Separate radioimmunoassays (RIAs), developed for *d*-ephedrine and *l*-ephedrine, were used to measure the concentrations of the enantiomers of ephedrine in the blood of two volunteers dosed with racemic ephedrine. The RIAs were validated by comparing the sum of the concentrations of the enantiomers, determined by RIA, with total ephedrine concentrations determined by a nonstereoselective GLC–ECD method.

Keyphrases □ Ephedrine—stereospecific radioimmunoassay using (*d*) and (*l*) antisera □ Radioimmunoassay—for *d*- and *l*-ephedrine, stereospecific □ Antisera—for *d*- and *l*-ephedrine, cross-reactivity, use in stereospecific radioimmunoassays

2-Methylamino-1-phenylpropanol has two chiral centers which give rise to four optical isomers. Racemic ephedrine is a mixture of the erythro pair of diastereomers (*l*), (1*R*,2*S*) and (*d*), (1*S*,2*R*), while the threo pair of diastereomers, (*l*), (1*S*,2*S*) and (*d*), (1*R*,2*R*) is called pseudoephedrine (1, 2). The four optical isomers differ from each other in their pharmacological activities (3–7) and rates of metabolism (8–13).

Preparations containing *l*- or *dl*-ephedrine are used for a wide variety of therapeutic applications, such as the treatment of nasal congestion in colds and allergic rhinitis, the treatment of orthostatic hypotension, as mydriatics, and as prophylactics against asthma attacks, urinary incontinence, and motion sickness (14). Of the published analytical methods for ephedrine (15–21), only GLC–ECD (22, 23) and GLC–MS (24) are applicable to the measurement of therapeutic concentrations in plasma; none of the methods distinguish between the enantiomers of ephedrine. Recently however, Findlay *et al.* (25) developed a stereospecific radioimmunoassay (RIA) for *d*-pseudoephedrine. This paper describes the development of separate RIAs for *l*-ephedrine and *d*-ephedrine and their validation by comparison with a GLC–ECD method.

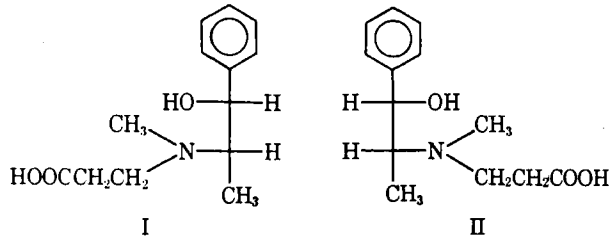

I II

Figure 1—*Haptens for* l-*ephedrine (I) and* d-*ephedrine (II).*

0022-3549/83/0700-0736$01.00/0

(6) A. G. Frantz and D. L. Kleinberg, *ibid.*, **37**, 2192 (1978).
(7) L. Lemberger, *ibid.*, **37**, 2176 (1978).
(8) H. H. Keller and M. DaPrada, *Life Sci.*, **24**, 1211 (1979).
(9) D. L. Kleinberg, G. L. Noel, and A. G. Frantz, *N. Engl. J. Med.*, **296**, 589 (1977).
(10) S. J. Judd, *Drugs*, **16**, 167 (1978).
(11) D. B. Calne, *Fed. Proc. Fed. Am. Soc. Exp. Biol.*, **37**, 2207 (1978).
(12) J. M. Cassady, G. S. Li, E. B. Spitzner, and H. G. Floss, *J. Med. Chem.*, **17**, 300 (1974).
(13) G. S. Li, M. Robinson, H. G. Floss, J. M. Cassady, and J. A. Clemens, *ibid.*, **18**, 892 (1975).
(14) P. L. Stutz, P. A. Stadler, J. M. Vigouret, and A. Jaton, *ibid.*, **21**, 754 (1978).
(15) G. DeLitala, T. Yeo, A. Grossman, N. R. Hathaway, and G. M. Besser, *J. Endocrinol.*, **87**, 95 (1980).
(16) R. W. Fuller, J. A. Clemens, E. C. Kornfeld, H. D. Snoddy, E. B. Smalstig, and N. J. Bach, *Life Sci.*, **24**, 375 (1979).
(17) J. G. Cannon, B. J. Demopoulos, J. P. Long, J. R. Flynn, and F. M. Sharabi, *J. Med. Chem.*, **24**, 238 (1981).
(18) J. T. Callaghan, R. E. Cleary, R. Crabtree, and L. Lemberger, *Life Sci.*, **28**, 95 (1981).
(19) E. R. Gonzalez, *J. Am. Med. Assoc.*, **246**, 11 (1981).
(20) R. V. Smith and J. P. Rosazza, *Arch. Biochem. Biophys.*, **161**, 551 (1974).
(21) J. P. Rosazza and R. V. Smith, *Adv. Appl. Microbiol.*, **25**, 169 (1979).
(22) A. Ehman, *J. Chromatogr.*, **132**, 267 (1977).
(23) P. J. Davis, L. K. Jamieson, and R. V. Smith, *Anal. Chem.*, **50**, 736 (1978).
(24) C. J. Parli, B. Schmidt, and C. J. Shaar, *Biochem. Pharmacol.*, **27**, 1405 (1978).
(25) K. M. Kerr, R. V. Smith, and P. J. Davis, *J. Chromatogr.*, **219**, 317 (1981).
(26) P. J. Davis, J. E. Glade, A. M. Clark, and R. V. Smith, *Appl. Environ. Microbiol.*, **38**, 891 (1979).
(27) J. P. A. Castrillon and H. H. Szmant, *J. Org. Chem.*, **30**, 1338 (1965).
(28) R. Curci and G. Modena, *Tetrahedron*, **22**, 1227 (1966).
(29) K. Kieslich, "Microbial Transformations of Non-steroid Cyclic Compounds," Wiley, New York, N.Y. 1976.
(30) C. E. Holmund, K. J. Sax, B. E. Nielsen, R. E. Hartman, R. H. Evans, and R. H. Blank, *J. Org. Chem.*, **27**, 1468 (1962).
(31) B. J. Auret, D. R. Boyd, and H. B. Henbest, *J. Chem. Soc. (C)*, **1968**, 2374.
(32) B. J. Auret, D. R. Boyd, H. B. Henbest, and C. G. Watson, *Phytochemistry*, **13**, 65 (1964).
(33) R. V. Smith and J. P. Rosazza, *J. Pharm. Sci.*, **64**, 1737 (1975).
(34) E. Abushanab, D. Reed, F. Suzuki, and C. J. Sih, *Tetrahedron Lett.*, 3415 (1978).
(35) P. J. Davis, *J. Chromatogr.*, **193**, 170 (1980).
(36) B. J. Auret, D. R. Boyd, F. Breen, and R. M. E. Greene, *J. Chem. Soc. Perkin Trans. I*, **1981**, 930.

ACKNOWLEDGMENTS

This research was supported, in part, by the Eli Lilly Research Foundation.

Stereospecific Radioimmunoassays for *l*-Ephedrine and *d*-Ephedrine in Human Plasma

K. K. MIDHA ˣ, J. W. HUBBARD, J. K. COOPER, and C. MACKONKA

Received December 28, 1981, from the *College of Pharmacy, University of Saskatchewan, Saskatoon, Saskatchewan, Canada, S7N 0W0.* Accepted for publication June 10, 1982.

Abstract □ Haptens were prepared by the reaction of *d*-ephedrine or *l*-ephedrine with methyl acrylate and subsequent alkaline hydrolysis of the methyl ester groups. The haptens were coupled to bovine serum albumin by a mixed anhydride method, and the resulting drug–protein conjugates were used to immunize rabbits. Antiserum raised to these conjugates were highly stereospecific. Neither antiserum cross-reacted with the optical antipode of its substrate nor with racemic pseudoephedrine. Separate radioimmunoassays (RIAs), developed for *d*-ephedrine and *l*-ephedrine, were used to measure the concentrations of the enantiomers of ephedrine in the blood of two volunteers dosed with racemic ephedrine. The RIAs were validated by comparing the sum of the concentrations of the enantiomers, determined by RIA, with total ephedrine concentrations determined by a nonstereoselective GLC–ECD method.

Keyphrases □ Ephedrine—stereospecific radioimmunoassay using (*d*) and (*l*) antisera □ Radioimmunoassay—for *d*- and *l*-ephedrine, stereospecific □ Antisera—for *d*- and *l*-ephedrine, cross-reactivity, use in stereospecific radioimmunoassays

2-Methylamino-1-phenylpropanol has two chiral centers which give rise to four optical isomers. Racemic ephedrine is a mixture of the erythro pair of diastereomers (*l*), (1*R*,2*S*) and (*d*), (1*S*,2*R*), while the threo pair of diastereomers, (*l*), (1*S*,2*S*) and (*d*), (1*R*,2*R*) is called pseudoephedrine (1, 2). The four optical isomers differ from each other in their pharmacological activities (3–7) and rates of metabolism (8–13).

Preparations containing *l*- or *dl*-ephedrine are used for a wide variety of therapeutic applications, such as the treatment of nasal congestion in colds and allergic rhinitis, the treatment of orthostatic hypotension, as mydriatics, and as prophylactics against asthma attacks, urinary incontinence, and motion sickness (14). Of the published analytical methods for ephedrine (15–21), only GLC–ECD (22, 23) and GLC–MS (24) are applicable to the measurement of therapeutic concentrations in plasma; none of the methods distinguish between the enantiomers of ephedrine. Recently however, Findlay *et al.* (25) developed a stereospecific radioimmunoassay (RIA) for *d*-pseudoephedrine. This paper describes the development of separate RIAs for *l*-ephedrine and *d*-ephedrine and their validation by comparison with a GLC–ECD method.

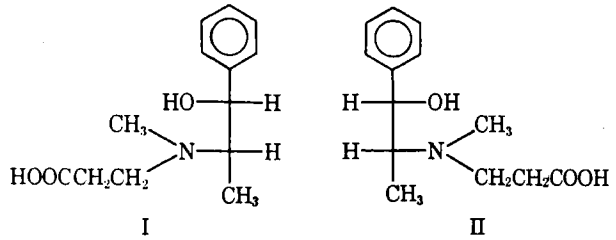

I II

Figure 1—*Haptens for* l-*ephedrine (I) and* d-*ephedrine (II).*

0022-3549/83/0700-0736$01.00/0

Table I—Cross-Reactions of Ephedrine Antisera

Compound	Cross-Reaction, % *d*-Ephedrine Antiserum	*l*-Ephedrine Antiserum
l-Ephedrine	<2	100
d-Ephedrine	100	<2
dl-Pseudoephedrine	<1	<1
dl-Norephedrine	0	<1
dl-*p*-Hydroxyephedrine	0	0

EXPERIMENTAL

Preparation of Drug–Protein Conjugates—*N*-(2-carboxyethyl) derivatives of both *d*- and *l*-ephedrine[1] were prepared by the treatment of *d*- and *l*-ephedrine with methyl acrylate[2], followed by the subsequent mild alkaline hydrolysis of the resulting methyl esters as described previously (26, 27). The purity of the haptens was established by GLC–FID[3] examination of the appropriate methyl esters prepared by reaction of the carboxylic acids with diazomethane[4]. Each chromatogram contained a single peak which had the same retention time (3.2 min) as the methyl esters obtained directly by the reaction of the ephedrine enantiomers with methyl acrylate. Thus, it was concluded that the haptens were free from reaction side products or other extraneous materials which might couple to carrier-antigen and subsequently compromise the specificity of the antisera. The chemical structures of the haptens (Fig. 1) were confirmed by direct probe mass spectrometry[5].

The haptens were coupled to bovine serum albumin by a modified mixed anhydride method (26). The solutions were dialyzed[6] against bicarbonate buffer (0.042 *M*, pH 8.0, 6 × 500 ml) and then against acetate buffer (0.012 *M*, pH 4.0, 6 × 500 ml). Both buffer systems contained 0.2% sodium azide[2]. After lyophilization[7], the *d*- and *l*-ephedrine–protein conjugates were obtained as white crystalline solids. The numbers of hapten residues per mole of bovine serum albumin, calculated by the isotope dilution technique, were 17 for *d*-ephedrine–protein conjugate and 21 for *l*-ephedrine–protein conjugate.

Immunization—The hapten–protein conjugates (1 mg) were dissolved in 0.25 ml of normal saline and emulsified with 0.25 ml of Freund's complete adjuvant[8]. The emulsion was administered by intradermal injection (0.5 ml) to eight, 4-month-old, female New Zealand White rabbits. At 2-week intervals thereafter, the injections (0.5 ml) were repeated with a similar emulsion prepared with Freund's incomplete adjuvant. Serum samples were obtained from the marginal ear vein at weekly intervals after the third injection. Titers of the antisera were checked by evaluating the binding characteristics of tritiated *dl*-ephedrine[9]. The procedure was essentially as described in *Radioimmunoassay Procedures*, except that various dilutions of the antisera in distilled water were evaluated. Selectivities of the antisera were checked periodically by measuring the ability of *d*- or *l*-ephedrine to displace the radiotracer from its binding sites on the antibodies. The antisera were harvested by cardiac puncture when their selectivities were optimal, lyophilized[7], and stored at −70° until required.

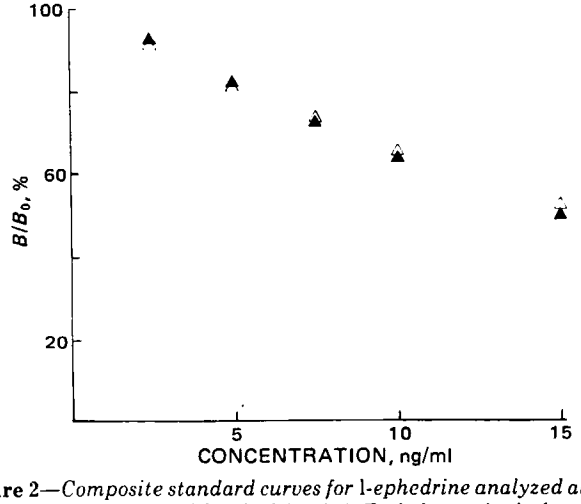

Figure 2—*Composite standard curves for* l-*ephedrine analyzed alone (△) and in the presence of* d-*ephedrine (▲). Each data point is the mean of five determinations.*

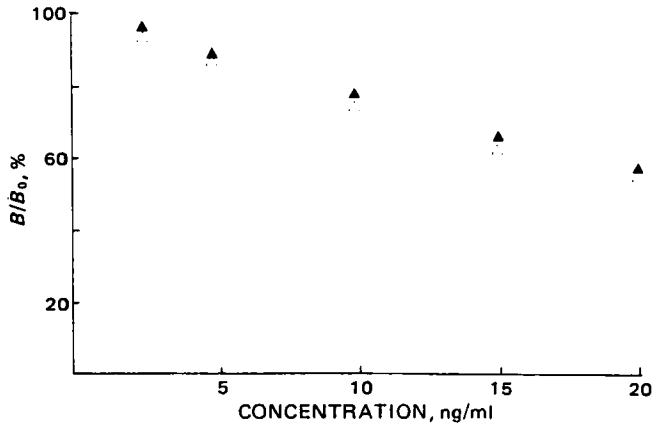

Figure 3—*Composite standard curves for* d-*ephedrine analyzed alone (△) and in the presence of* l-*ephedrine (▲). Each data point is the mean of five determinations.*

Radioimmunoassay Procedures—A 50–200-μl aliquot of plasma, spiked or from volunteers dosed with *dl*-ephedrine, was transferred to the bottom of a 2 × 75-mm tube[10]. [^{3}H]*dl*-Ephedrine (~2000 cpm) in 300 μl of phosphate buffer (0.2 *M*, pH 6.5) was added, and the solutions were mixed[11]. Antiserum (200 μl of a 10% dilution in distilled water) was added, and the solutions were mixed[11] again and incubated at 4° for 30 min. A suspension (1.0 ml) of dextran-coated charcoal[12], previously chilled to 4°, was added and, after mixing[11], each tube was incubated at 4° for an additional 10 min. The resulting suspension was then centrifuged[13] (1720 × *g*) at 4° for 10 min. The supernatant solution was decanted into a scintillation vial containing 18.0 ml of scintillation cocktail[14] and counted[15].

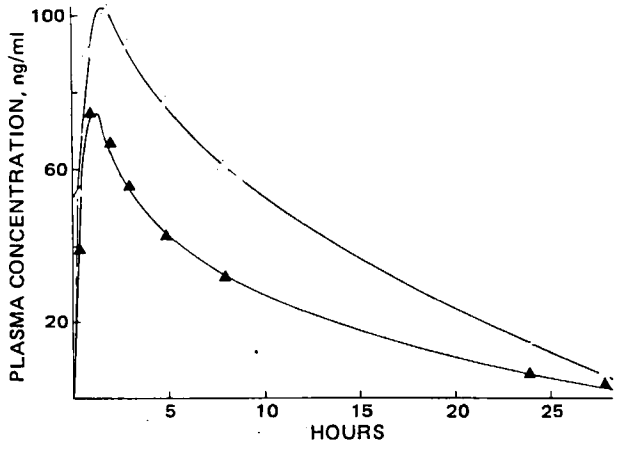

Figure 4—d-*Ephedrine (△) and* l-*ephedrine (▲) concentrations in the plasma of a healthy human volunteer following a single 50-mg oral dose of* dl-*ephedrine hydrochloride.*

[1] Aldrich Chemical Co., Milwaukee, Wis.
[2] British Drug Houses, Toronto, Canada.
[3] Model 3920, Perkin-Elmer Co., Montreal, Quebec, Canada. 5% OV-7 (Chromatographic Specialties, Brockville, Ontario, Canada) on acid-washed dimethylchlorosilane-treated high-performance chromosorb W. Operating temperatures: injection port and detector 300°, column oven 275°. Nitrogen flow rate: 60 ml/min. Hydrogen and compressed air flow rates were adjusted to give maximum detector response.
[4] Prepared from Diazald, Aldrich Chemical Co., Milwaukee, Wis.
[5] V. G. Micromass MM 16F.
[6] Fisher dialyzer tubing (size C), Fisher Scientific Co., Pittsburgh, Pa.
[7] Bench top freeze-dryer Model 75034, Labconco Corp., Kansas City, Mo.
[8] Grand Island Biological Co., Grand Island, N.Y.
[9] Generally labeled; specific activity 1.7 Ci/mmole; Nuclear Research Centre, Negev, Israel. Radiochemical purity was checked by TLC and HPLC.
[10] Falcon, Calif.
[11] Vortex Genie, Fisher Scientific Co., Canada.
[12] Bio-RIA, Montreal, Canada; used without modification.
[13] Model TJ-6 refrigerated centrifuge, Beckman Instruments Inc., Fullerton, Calif.
[14] PCS II TM, Amersham Corp., Arlington Heights, Colo.
[15] LKB Rackbeta Liquid Scintillation Counter, Model 1215 equipped with automatic quench compensation, Fisher Scientific Co., Canada.

Table II—Concentrations of Ephedrine as Determined by GLC and as Calculated from the Sum of Enantiomer Concentrations Determined by RIA

Hours	Analysis by RIA		Total Concentration, ng/ml	
	l-Ephedrine, ng/ml	*d*-Ephedrine, ng/ml	RIA	GLC
0.5	77	80	157	164
1	103	125	228	256
1.5	100	119	219	223
2	95	106	201	210
3	82	93	175	190
5	61	68	129	117
7.5	43	42	85	82
24	3.7	3.4	7.1	7.4

Tracer Solutions—Appropriate aliquots of the methanolic solution of tritiated *dl*-ephedrine were diluted daily with phosphate buffer (0.2 *M*, pH 6.5) so that 300 μl of the diluted tracer solution gave ~8000 cpm.

Calibration Curves—*l*-Ephedrine hydrochloride (5 mg) was dissolved in 400 ml of distilled water. Serial dilutions in plasma were made to provide working standards of 2.5, 5.0, 7.5, 10, and 15 ng/ml. Similarly, serial dilutions of *d*-ephedrine in plasma were made to provide working standards of 2.5, 5.0, 10, 15, and 20 ng/ml. Calibration curves for *l*-ephedrine, both with and without the presence of *d*-ephedrine, were obtained by using the spiked plasma samples in the aforementioned RIA procedure (antiserum for *l*-ephedrine). The calibration curves for *l*-ephedrine in the presence of *d*-ephedrine were constructed by pairing a specified concentration of *l*-ephedrine with *d*-ephedrine. The paired *l*-ephedrine–*d*-ephedrine concentrations were 2.5:20.0, 5.0:15.0, 7.5:10.0, 10.0:5.0, and 15.0:2.5 ng/ml of plasma.

Calibration curves for *d*-ephedrine, both with and without the presence of *l*-ephedrine, were obtained in a similar manner except that the antiserum for *d*-ephedrine was used in the RIA. All calibration curves were constructed by plotting percent bound/percent bound at zero concentration (B/B_0) *versus* concentration (in ng/ml) of substrate in the sample.

Specificities—Cross-reactivities of the optical isomers and metabolites of ephedrine were determined according to the criteria of Abraham (28).

Human Studies—Single doses of *dl*-ephedrine hydrochloride (50 mg) were administered to each of two healthy male volunteers. Blood samples were collected in evacuated heparinized collection tubes[16], without allowing the blood to contact the rubber stopper. Samples collected over a 24-hr period were centrifuged, and separated plasma was stored at −15° until analyzed.

Validation Studies—The aforementioned plasma samples were each analyzed by the RIA for *d*-ephedrine, the RIA for *l*-ephedrine, and a published GLC–ECD method (23) for *dl*-ephedrine. Plasma concentration *versus* time plots were constructed for *dl*-ephedrine from the GLC–ECD data and compared with similar plots obtained by adding together the concentrations of the individual enantiomers determined by the RIA procedures.

RESULTS AND DISCUSSION

The cross-reactivities of the antisera for *d*- and *l*-ephedrine are shown in Table I. Both antisera were highly stereospecific. Neither antiserum cross-reacted with the optical antipode of its substrate, nor with racemic pseudoephedrine. Neither antiserum recognized the ring-modified metabolite *dl*-*p*-hydroxyephedrine nor the side chain-modified metabolite *dl*-norephedrine. The latter is particularly significant because many antisera cross-react with compounds that differ in structure from the substrate only at the point of haptenic modification. For example, similar *N*-substituted haptens were used in the development of antisera for chlorpromazine, imipramine, amitriptyline, and *trans*-doxepin. Each antiserum cross-reacted (100%) with the *N*-desmethyl metabolite of its appropriate substrate (29, 30). In the present case, however, the antisera for the enantiomers of ephedrine appear to be specific for both ring system and side chain.

Standard curves for *l*-ephedrine (Fig. 2) and *d*-ephedrine (Fig. 3) were constructed after analysis of spiked plasma which contained the substrate alone or the substrate plus varying quantities of its enantiomer. The concentrations of the contaminating enantiomer were varied from 16.7 to 800% of the substrate concentration. This allowed for the possibility that plasma concentration ratios of the enantiomers differed from unity after dosing with the racemic drug.

The standard curve obtained using the *l*-ephedrine antisera in the presence of only *l*-ephedrine fit the equation $y = -3.18x + 98.31$, with a correlation coefficient of 0.9956 (Fig. 2). When the standard curve for *l*-ephedrine was analyzed in the presence of *d*-ephedrine the resultant standard curve fit the equation $y = -3.42x + 99.57$, with a correlation coefficient of 0.9974. These two curves are virtually superimposable, indicating that the *l*-ephedrine antisera was not sensitive to the presence of *d*-ephedrine (Fig. 2).

When the *d*-ephedrine antiserum was used to construct a standard curve in the presence of only *d*-ephedrine a straight line was obtained which fit the equation $y = -2.30x + 98.58$ and had a correlation coefficient of 0.9952. The standard curve of *d*-ephedrine analyzed in the presence of *l*-ephedrine was also a straight line with the equation $y = -2.35x + 102.22$ and a correlation coefficient of 0.9983 (Fig. 3).

These experiments demonstrated that the presence of the optical antipode has little effect on the standard curves and that the RIA procedures can be used to measure the concentration of *d*-ephedrine or *l*-ephedrine in the plasma of a patient dosed with *dl*-ephedrine.

Figure 4 shows the plasma concentration–time curves obtained for *d*- and *l*-ephedrine after a single 50-mg oral dose of racemic ephedrine hydrochloride was administered to a healthy male volunteer. *d*-Ephedrine reached significantly higher plasma concentrations and was eliminated more slowly than *l*-ephedrine. Similar results (Table II) were obtained when the study was repeated in a second volunteer. Both enantiomers reached higher concentrations in the plasma of the second individual, although the peak concentration of the more active *l*-ephedrine was again significantly lower than that of *d*-ephedrine.

The intraassay variances (31) of the RIA procedures, *i.e.*, the overall coefficients of variation for five replicates each at five concentrations were: *l*-ephedrine antiserum with *l*-ephedrine alone, 1.63 (2.67); *l*-ephedrine antiserum with *l*-ephedrine in the presence of *d*-ephedrine, 2.45 (3.30); *d*-ephedrine antiserum with *d*-ephedrine alone 2.90 (4.20); and *d*-ephedrine antiserum with *d*-ephedrine in the presence of *l*-ephedrine 3.76 (5.73). The value in parentheses is the highest coefficient of variation for each case. Interassay variances were of the same order. In each assay, the detection limit was <0.5 ng of the appropriate ephedrine enantiomer in a 200-μl sample.

To validate the RIA procedures, aliquots of the plasma samples from the two volunteers were examined also by a nonstereoselective, though sensitive, GLC–ECD method (23). This procedure was used to measure the total plasma concentration of ephedrine which was compared with the sum of the concentrations of the individual enantiomers determined by RIA (Table II). The results yielded a straight line when total plasma ephedrine as determined by GLC–ECD was plotted against the sum of *d*-ephedrine and *l*-ephedrine as determined by RIA. The slope of this line was 1.1, with a correlation coefficient of 0.99. These results show the plasma concentration–time curves generated by RIA and by GLC–ECD to be comparable. This indicates that the RIA procedures are not subject to interference from the metabolites of ephedrine or from endogenous plasma constituents.

[16] Vacutainer tubes, Beckton, Dickenson and Co., Toronto, Canada.

REFERENCES

(1) N. Witkop and C. M. Foltz, *J. Am. Chem. Soc.*, **79**, 197 (1957).

(2) H. Pfang and G. Kirchner, *Ann. Chim.*, **614**, 149 (1958).

(3) J. B. LaPidus, A. Tye, P. N. Patil, and B. A. Modi, *J. Med. Chem.*, **6**, 76 (1963).

(4) P. N. Patil, A. Tye, and J. B. LaPidus, *J. Pharmacol. Exp. Ther.*, **148**, 158 (1964).

(5) A. H. Abdallah, A. Tye, J. B. LaPidus, and P. N. Patil, *Life Sci.*, **6**, 39 (1967).

(6) P. N. Patil, J. B. LaPidus, and A. Tye, *J. Pharmacol. Exp. Ther.*, **155**, 1 (1967).

(7) P. N. Patil, J. B. LaPidus, and A. Tye, *J. Pharm. Sci.*, **59**, 1205 (1970).

(8) J. Axelrod, *J. Pharmacol. Exp. Ther.*, **114**, 430 (1955).

(9) R. E. McMahon, *Life Sci.*, **3**, 235 (1964).

(10) S. Baba, A. Matsuda, Y. Nagase, and K. Kawai, *Yakugaku Zasshi*, **91**, 584 (1971).

(11) D. R. Feller and L. Malspeis, *Fed. Proc. Fed. Am. Soc. Exp. Biol.*, **30**, 225 (1971).

(12) R. E. Rann, D. R. Feller, and J. F. Snell, *Eur. J. Pharmacol.*, **16**, 233 (1971).

(13) D. R. Feller, P. Basu, W. Mellon, J. Curott, and L. Malspeis, *Arch. Int. Pharmacodyn.*, **203**, 187 (1973).
(14) N. Weiner, in "The Pharmacological Basis of Therapeutics," A. Goodman Gilman, L. S. Goodman, and A. Gilman, Eds., Macmillan, New York, N.Y., 6th ed., 1980, p. 168.
(15) "The Assay of Ephedrine," a report prepared by a joint committee of the Pharmaceutical Society of Great Britain and the Society for Analytical Chemistry, *Analyst*, **100**, 136 (1975).
(16) V. Das Gupta and Ana J. L. de Lara, *J. Pharm. Sci.*, **64**, 2001 (1975).
(17) C. Bye, H. M. Hill, D. T. D. Hughes, and A. W. Peck *Eur. J. Clin. Pharmacol.*, 8, 47 (1975).
(18) M. E. Pickup and J. W. Paterson, *J. Pharm. Pharmacol.*, **26**, 561 (1974).
(19) G. R. Wilkinson and A. H. Beckett, *J. Pharmacol. Exp. Ther.*, **162**, 139 (1968).
(20) T. R. Koziol, J. R. Jacob, and R. G. Achari, *J. Pharm. Sci.*, **68**, 1135 (1979).
(21) R. Bottler and Th. Knur, *Fresenius Z. Anal. Chem.*, **302**, 286 (1980).
(22) L. M. Cummins and M. J. Fourier, *Anal. Lett.*, **2**, 403 (1969).
(23) K. K. Midha, J. K. Cooper, and I. J. McGilveray, *J. Pharm. Sci.*, 68, 557 (1979).
(24) T. Nagata, K. Hara, M. Kageura, K. Totoki, and M. Takomoto, *Nippon Hoigaku Zasshi*, **31**, 146 (1977).
(25) J. W. A. Findlay, J. T. Warren, J. A. Hill, and R. M. Welch, *J. Pharm. Sci.*, **70**, 624 (1981).
(26) J. W. Hubbard, K. K. Midha, I. J. McGilveray, and J. K. Cooper, *ibid.*, **67**, 1563 (1978).
(27) J. W. Hubbard, K. K. Midha, J. K. Cooper, and C. Charette, *ibid.*, **67**, 1571 (1978).
(28) G. E. Abraham, *J. Clin. Endocrinol. Metab.*, **29**, 866 (1969).
(29) K. K. Midha, J. C. K. Loo, J. W. Hubbard, M. L. Rowe, and I. J. McGilveray, *Clin. Chem.*, **25**, 166 (1979).
(30) K. K. Midha, J. C. K. Loo, C. Charette, M. L. Rowe, J. W. Hubbard, and I. J. McGilveray, *J. Anal. Toxicol.*, **2**, 185 (1978).
(31) D. Rodbard, *Clin. Chem.*, **20**, 1255 (1974).

ACKNOWLEDGMENTS

This work was presented in part at the APhA Academy of Pharmaceutical Sciences meeting at Orlando in November 1981.

The authors gratefully acknowledge Drs. G. McKay and E. M. Hawes of the College of Pharmacy, University of Saskatchewan, for their helpful comments and advice.

A Highly Sensitive Pyrogen Test for Antibiotics I: Detection of Trace Amounts of Endotoxin in Injectable Sodium Ampicillin Preparations

S. TAKAHASHI *, S. YANO *, Y. NAGAOKA *, K. KAWAMURA ‡x, and S. MINAMI ‡

Received August 24, 1981, from the **Department of Antibiotics, National Institute of Health, Kamiosaki 2-chome, Shinagawa-ku, Tokyo 141, Japan* and the ‡*Department of Quality Control, Takeda Chemical Industries, Ltd., Doshomachi, Osaka 541, Japan.* Accepted for publication June 17, 1982.

Abstract □ The rabbit pyrogen test (specified in the pharmacopeia) and the Limulus amebocyte lysate (LAL) test are influenced by high concentrations of certain antibiotics. Therefore, it has not been possible to detect trace amounts of endotoxin which may contaminate these antibiotics. To detect trace amounts of endotoxin in injectable sodium ampicillin, an ultrafiltration technique was utilized which removed the antibiotic and left a solution which contained predominantly the endotoxin. After ultrafiltration, a trace amount of pyrogen (which otherwise could not be detected) was found using both the rabbit pyrogen and the LAL tests. The endotoxin was also determined quantitatively using a chromogenic endotoxin reagent which is made by combining the Limulus amebocyte lysate and a synthetic substrate with a suitable chromophore.

Keyphrases □ Ampicillin—detection of trace amounts of endotoxin using ultrafiltration with pyrogen tests, chromogenic assay □ Ultrafiltration—of ampicillin solutions, use with pyrogen tests to detect trace amounts of endotoxin in antibiotics □ Chromogenic assay—of ampicillin solution, detection of trace amounts of endotoxin in antibiotics

It is important to develop highly sensitive methods for detecting trace amounts of pyrogen to ensure that pharmaceutical preparations are completely pyrogen free. Several cases of fever have been reported after the injection of β-lactam antibiotics such as methicillin and cloxacillin (1–6). However, in only one case (methicillin) was the presence of a pyrogen detected (6). Fever is caused in most cases by lipopolysaccharide from the outer layer of the cell walls of Gram-negative bacteria. Pyrogens, a type of endotoxin, are often complex, high molecular weight substances containing lipid A (7).

Endotoxins are usually detected by the pyrogen test using rabbits, or by the Limulus amebocyte lysate (LAL) test. The former method is specified in the pharmaceutical compendia of both the U.S. (8) and Japan (9). The latter method is specified in the United States Pharmacopeia XX (10). In the pyrogen test, the rise in the body temperature of rabbits caused by the endotoxin is sometimes inhibited by the pharmacological activity of the coexistent drugs. The sensitivity of the LAL test also is affected by the presence of certain drugs (11). In such cases, it would be desirable to separate the endotoxin from the drug and concentrate the endotoxin.

Minami *et al.* used an ultrafiltration method to separate endotoxins from antipyretics (12). Sullivan *et al.* showed that β-lactam antibiotics such as sodium penicillin G do not combine with endotoxin using ultrafiltration (13).

It was reported that gel formation in the LAL test was induced by the amidase activity of a clotting enzyme in the lysate, which is activated by a bacterial endotoxin (14). Harada *et al.* applied this principle to the colorimetric determination of endotoxins using a synthetic substrate which activates the amidase activity of the enzyme and releases a chromophore (15).

This study reports the detection of trace amounts of

0022-3549/83/0700-0739$01.00/0

(13) D. R. Feller, P. Basu, W. Mellon, J. Curott, and L. Malspeis, *Arch. Int. Pharmacodyn.*, **203**, 187 (1973).
(14) N. Weiner, in "The Pharmacological Basis of Therapeutics," A. Goodman Gilman, L. S. Goodman, and A. Gilman, Eds., Macmillan, New York, N.Y., 6th ed., 1980, p. 168.
(15) "The Assay of Ephedrine," a report prepared by a joint committee of the Pharmaceutical Society of Great Britain and the Society for Analytical Chemistry, *Analyst*, **100**, 136 (1975).
(16) V. Das Gupta and Ana J. L. de Lara, *J. Pharm. Sci.*, **64**, 2001 (1975).
(17) C. Bye, H. M. Hill, D. T. D. Hughes, and A. W. Peck *Eur. J. Clin. Pharmacol.*, 8, 47 (1975).
(18) M. E. Pickup and J. W. Paterson, *J. Pharm. Pharmacol.*, **26**, 561 (1974).
(19) G. R. Wilkinson and A. H. Beckett, *J. Pharmacol. Exp. Ther.*, **162**, 139 (1968).
(20) T. R. Koziol, J. R. Jacob, and R. G. Achari, *J. Pharm. Sci.*, **68**, 1135 (1979).
(21) R. Bottler and Th. Knur, *Fresenius Z. Anal. Chem.*, **302**, 286 (1980).
(22) L. M. Cummins and M. J. Fourier, *Anal. Lett.*, **2**, 403 (1969).
(23) K. K. Midha, J. K. Cooper, and I. J. McGilveray, *J. Pharm. Sci.*, 68, 557 (1979).
(24) T. Nagata, K. Hara, M. Kageura, K. Totoki, and M. Takomoto, *Nippon Hoigaku Zasshi*, **31**, 146 (1977).
(25) J. W. A. Findlay, J. T. Warren, J. A. Hill, and R. M. Welch, *J. Pharm. Sci.*, **70**, 624 (1981).
(26) J. W. Hubbard, K. K. Midha, I. J. McGilveray, and J. K. Cooper, *ibid.*, **67**, 1563 (1978).
(27) J. W. Hubbard, K. K. Midha, J. K. Cooper, and C. Charette, *ibid.*, **67**, 1571 (1978).
(28) G. E. Abraham, *J. Clin. Endocrinol. Metab.*, **29**, 866 (1969).
(29) K. K. Midha, J. C. K. Loo, J. W. Hubbard, M. L. Rowe, and I. J. McGilveray, *Clin. Chem.*, **25**, 166 (1979).
(30) K. K. Midha, J. C. K. Loo, C. Charette, M. L. Rowe, J. W. Hubbard, and I. J. McGilveray, *J. Anal. Toxicol.*, **2**, 185 (1978).
(31) D. Rodbard, *Clin. Chem.*, **20**, 1255 (1974).

ACKNOWLEDGMENTS

This work was presented in part at the APhA Academy of Pharmaceutical Sciences meeting at Orlando in November 1981.

The authors gratefully acknowledge Drs. G. McKay and E. M. Hawes of the College of Pharmacy, University of Saskatchewan, for their helpful comments and advice.

A Highly Sensitive Pyrogen Test for Antibiotics I: Detection of Trace Amounts of Endotoxin in Injectable Sodium Ampicillin Preparations

S. TAKAHASHI *, S. YANO *, Y. NAGAOKA *, K. KAWAMURA ‡x, and S. MINAMI ‡

Received August 24, 1981, from the **Department of Antibiotics, National Institute of Health, Kamiosaki 2-chome, Shinagawa-ku, Tokyo 141, Japan* and the ‡*Department of Quality Control, Takeda Chemical Industries, Ltd., Doshomachi, Osaka 541, Japan.* Accepted for publication June 17, 1982.

Abstract □ The rabbit pyrogen test (specified in the pharmacopeia) and the Limulus amebocyte lysate (LAL) test are influenced by high concentrations of certain antibiotics. Therefore, it has not been possible to detect trace amounts of endotoxin which may contaminate these antibiotics. To detect trace amounts of endotoxin in injectable sodium ampicillin, an ultrafiltration technique was utilized which removed the antibiotic and left a solution which contained predominantly the endotoxin. After ultrafiltration, a trace amount of pyrogen (which otherwise could not be detected) was found using both the rabbit pyrogen and the LAL tests. The endotoxin was also determined quantitatively using a chromogenic endotoxin reagent which is made by combining the Limulus amebocyte lysate and a synthetic substrate with a suitable chromophore.

Keyphrases □ Ampicillin—detection of trace amounts of endotoxin using ultrafiltration with pyrogen tests, chromogenic assay □ Ultrafiltration—of ampicillin solutions, use with pyrogen tests to detect trace amounts of endotoxin in antibiotics □ Chromogenic assay—of ampicillin solution, detection of trace amounts of endotoxin in antibiotics

It is important to develop highly sensitive methods for detecting trace amounts of pyrogen to ensure that pharmaceutical preparations are completely pyrogen free. Several cases of fever have been reported after the injection of β-lactam antibiotics such as methicillin and cloxacillin (1–6). However, in only one case (methicillin) was the presence of a pyrogen detected (6). Fever is caused in most cases by lipopolysaccharide from the outer layer of the cell walls of Gram-negative bacteria. Pyrogens, a type of endotoxin, are often complex, high molecular weight substances containing lipid A (7).

Endotoxins are usually detected by the pyrogen test using rabbits, or by the Limulus amebocyte lysate (LAL) test. The former method is specified in the pharmaceutical compendia of both the U.S. (8) and Japan (9). The latter method is specified in the United States Pharmacopeia XX (10). In the pyrogen test, the rise in the body temperature of rabbits caused by the endotoxin is sometimes inhibited by the pharmacological activity of the coexistent drugs. The sensitivity of the LAL test also is affected by the presence of certain drugs (11). In such cases, it would be desirable to separate the endotoxin from the drug and concentrate the endotoxin.

Minami *et al.* used an ultrafiltration method to separate endotoxins from antipyretics (12). Sullivan *et al.* showed that β-lactam antibiotics such as sodium penicillin G do not combine with endotoxin using ultrafiltration (13).

It was reported that gel formation in the LAL test was induced by the amidase activity of a clotting enzyme in the lysate, which is activated by a bacterial endotoxin (14). Harada *et al.* applied this principle to the colorimetric determination of endotoxins using a synthetic substrate which activates the amidase activity of the enzyme and releases a chromophore (15).

This study reports the detection of trace amounts of

0022-3549/83/0700-0739$01.00/0

Table I—Temperature Increase in Rabbits for the Pyrogen Test [a]

Sample	Dose	Rise in Temperature °			Mean ± SE[b]
Test sample	25 mg(potency)/kg	0	0.2	0.3	0.25 ± 0.06
		0.3	0.3	0.4	
	20 mg(potency)/kg	0	0.1	0.2	0.22 ± 0.07
		0.2	0.4	0.4	
Control	25 mg(potency)/kg	0	0.2	0.3	0.25 ± 0.06
		0.3	0.3	0.4	

[a] According to the method specified in the Compendia. [b] $n = 6$.

pyrogen contaminants in injectable sodium ampicillin preparations using ultrafiltration followed by rabbit pyrogen and LAL tests. The quantitative determination of endotoxin by a chromogenic assay method using a reagent made from the Limulus amebocyte lysate and a synthetic substrate is also reported in this paper.

EXPERIMENTAL

Materials—*Samples and Reagents*—An injectable sodium ampicillin preparation in vials of 1 g(potency), suspected to be contaminated with pyrogen, was used as the test sample. A sodium ampicillin preparation for injection manufactured prior to the test sample was used as the control. Commercially available endotoxin from *Escherichia coli* (0111-B4)[1] was dissolved in physiological saline solution immediately before use and diluted to the required concentration, to provide a standard endotoxin. The Limulus amebocyte lysate[2] and chromogenic endotoxin assay[3] reagents were obtained commercially. The chromogenic endotoxin assay reagent is made from Limulus amebocyte lysate and the *p*-nitroaniline derivative of a synthetic oligopeptide as the substrate. Tromethamine hydrochloride[1] (0.1 *M*, pH 8.0) was used as a buffer. The blue dextran solution (2 μg/ml of dye-combined dextran, average molecular weight 2,000,000)[4] was used after it was confirmed to be pyrogen free.

Ultrafiltration Apparatus—The ultrafiltration apparatus[5] (stirring type) was used after washing with pyrogen-free distilled water and drying at 60° for 1 hr. The ultrafiltration membrane[6] had a fraction molecular weight of 10,000 and a diameter of 76 mm. It was used after soaking overnight in 0.1 *N* NaOH solution; the surface of the membrane was washed with distilled water for injection prior to use.

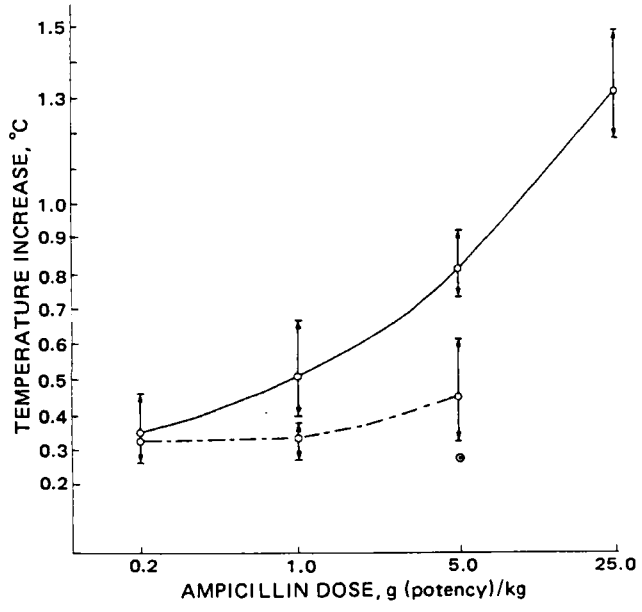

Figure 1—*Dose-response curve of sodium ampicillin in the rabbit pyrogen test. Key: (—) ultrafiltrated sample, n = 10–26; (- · -) without ultrafiltration, n = 9–10; (⊙) control sodium ampicillin, n = 9.*

[1] Seikagaku Kogyo Co. Ltd., Tokyo.
[2] Pregel, Seikagaku Kogyo Co. Ltd., Tokyo.
[3] ETC, Seikagaku Kogyo Co. Ltd., Tokyo.
[4] Blue Dextran 2000, Pharmacia Fine Chemical Co. Ltd., Uppsala, Sweden.
[5] Diaflowcell Model 402, Amicon Corp., Lexington, Mass.
[6] Diaflowmembrane PM10, Amicon Corp., Lexington, Mass.

Table II—Recovery of *E. Coli* 0111-B4 Endotoxin after Ultrafiltration (LAL Test) [a]

Sample	Dilution of Endotoxin Stock Solution[b]				
	× 1	× 2	× 4	× 8	× 16
Untreated solution (I)	++	+	+	±	−
Ultrafiltrated solution (II)	++	++	++ ~ +	±	−

[a] After the mixture was incubated at 37° for 1 hr and then allowed to stand for 5 min. [b] The original concentration of the solution was 5 ng/ml. The key is as listed in the text.

Rabbits—Japanese white, male rabbits weighing 2.0–2.7 kg were bred and maintained in a room kept at 25 ± 2° with a relative humidity of 50 ± 10%. They were fed daily (~100 g of solid food[7]) with an automatic rabbit feeding apparatus. Water was supplied *ad libitum* using an automatic water-supplying system. Only those rabbits that maintained their weight for at least 1 week were used in the experiments. They were conditioned for 1–3 days prior to the pyrogen test by conducting sham tests (*i.e.*, without injection).

Methods—*Ultrafiltration*—All glass apparatus were depyrogenized by heating at 250° for 2 hr. After the ultrafiltration membrane was attached to the apparatus, the apparatus was washed three times with pyrogen-free distilled water and once with 0.01 *N* NaOH solution. The surface of the membrane was coated with 100 ml of dye-combined dextran (average molecular weight 2,000,000) solution to prevent adsorption of the pyrogen. The inside of the apparatus was rinsed with 30 ml of physiological saline solution using manual stirring; the washings were confirmed to be pyrogen free by the LAL and rabbit pyrogen tests (dose: 10 ml/kg).

The samples of sodium ampicillin were dissolved in physiological saline, placed in the ultrafiltration apparatus, and filtered under pressure using nitrogen gas (3.5 kg/cm^2) until the volume of the residual solution was reduced to one-tenth the original volume. If the concentration of sodium ampicillin in the residual solution exceeded 10 mg (potency)/ml, the dilution and filtration were repeated until the concentration of sodium ampicillin became ≤10 mg(potency)/ml. The membrane filter was changed between treatments.

Determination of Endotoxin—For the rabbit pyrogen test, rabbit rectal temperatures were measured using a thermoelectric couple-type thermometer[8]. Temperatures were measured three times at 45-min intervals prior to administration; the third measurement was regarded as the control. Immediately thereafter, the sample solutions (10 ml/kg) were

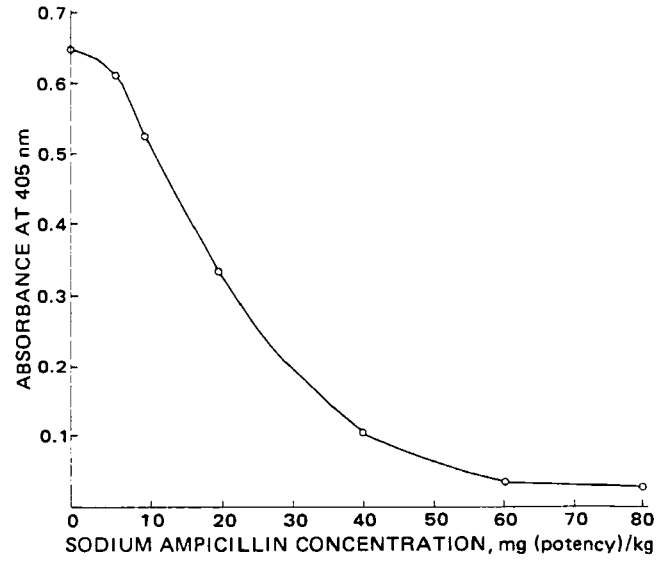

Figure 2—*Influence of the concentration of sodium ampicillin on the determination of endotoxin by the chromogenic assay method. The sample solution was* E. coli *endotoxin at 0.4 ng/ml; the incubation time was 50 min.*

[7] Oriental Solid Feed (ORC-5), Oriental Kobo, Co. Ltd., Tokyo.
[8] Ellab TE3 Type, Ellab Instruments, Copenhagen, Denmark.

Table III—Influence of the Ampicillin Concentration on the LAL Test

Concentration of Endotoxin[a], ng/ml	Concentration of Ampicillin[b], mg(potency)/ml							
	100	60	40	20	10	5	1	0
10	−	−	+	++	++	++	++	++
1	−	−	±	+~±	+	+	+	+

[a] *E. coli* 0111-B4. [b] Key is as given in the text.

administered intravenously through the auricular vein. Rectal temperatures were taken at 1, 1.5, 2, and 3 hr postadministration. The difference between the highest temperature recorded after injection and the control temperature was regarded as the rise in temperature.

For the LAL test, the limulus amebocyte lysate reagent was dissolved in 0.1 ml of pyrogen-free distilled water in an ampule. The sample solutions (0.1 ml) were added to the reagent and the ampules were allowed to stand in an incubator at 37° for 1 hr. After incubation, the ampules were allowed to stand an additional 5 min at room temperature, then were slanted at 45°. Each ampule was judged using the following four grades: (++) a solid gel was formed and it did not move when the ampule was slanted; (+) although a gel was formed, it moved when the ampule was slanted; (±) a coarse granular gel was formed and the viscosity was increased; and (−) the media remained in the liquid state without any change.

For the chromogenic assay method, the contents of each vial of the chromogenic assay reagent were dissolved in 0.1 ml of 0.1 *M* tromethamine buffer (pH 8.0) while being cooled in an ice-water bath. Aliquots (0.1 ml) of the test solution were added to the vials, and the mixtures were incubated for 40 or 50 min in a water bath at 37°. After incubation, the reaction mixture was cooled rapidly in an ice-water bath and then was quenched by adding 1.0 ml of a 12.5% acetic acid solution. The absorbance was measured at 405 nm using a spectrophotometer.

RESULTS

Rabbit Pyrogen Test—Temperature rises in rabbits for samples of sodium ampicillin were measured according to the method in the Japanese Minimum Requirements for Antibiotics [25 mg(potency)/kg] and Code of Federal Regulation (20 mg/kg). No differences in the temperature rise were noted between the test and control samples in the dose range of 20–25 mg(potency)/kg.

After being concentrated by ultrafiltration, the ampicillin solution test samples were administered to rabbits, and the temperature rise was monitored. When the test samples of 0.2–5 g(potency)/kg were administered without ultrafiltration, no significant temperature differences were observed between the test and control samples (Fig. 1). However, when the test samples corresponding to 0.2–25 g(potency)/kg of the original samples were administered after ultrafiltration, temperature rises were clearly observed and were found to be dose dependent. The difference in the temperature rise was highly significant between the test and control samples at 5 g(potency)/kg.

Recovery of Endotoxin After Ultrafiltration—An endotoxin solution was prepared by diluting 200 ng of standard endotoxin (*E. coli* 0111-B4) with 40 ml of physiological saline solution (solution I). This solution was diluted by 400 ml and concentrated again to 40 ml by ultrafiltration (solution II). Solutions I and II were diluted stepwise and tested by the LAL test. As shown in Table II, almost complete recovery of endotoxin was obtained. These results were consistent with the results of Minami *et al.* (12) and Sullivan (13).

Effect of Sodium Ampicillin on the LAL Test—The effect of various amounts of the control sample of sodium ampicillin on the LAL test was studied. As shown in Table III, the gel reaction by 10 ng/ml of endotoxin was inhibited by >40 mg(potency)/ml of sodium ampicillin, and 1 ng/ml of endotoxin was inhibited by >20 mg(potency)/ml of sodium ampicillin. These results indicate that the gel reaction by the LAL test is inhibited by certain concentrations of sodium ampicillin, in agreement with Newsome's data (11).

LAL Test of Samples After Ultrafiltration—Four groups of 60 vials each of injectable sodium ampicillin preparations (1 g of test sample/vial) were treated by ultrafiltration to separate and concentrate the suspected pyrogen contaminant, and then were tested by the LAL test. The results are shown in Table IV. Although the data for the test samples showed some variation, they clearly exhibited a stronger gel reaction than that shown by the control sample. The control sample also showed a slightly positive reaction, possibly due to the sensitivity of this method. Trace amounts of pyrogen were detected in the distilled water used as the blank.

Table IV—LAL Test of Ampicillin After Ultrafiltration

Sample	Test Run	Equivalent[a]/Residual[b] Amount of Ampicillin, mg(potency)/ml: 250[a]/5[b] (×2)	125[a]/2.5[b] (×4)	62.5[a]/1.25[b] (×8)	Endotoxin Reference[c]
Test sample	1	++	++	+	
	2	++	+	±	±
	3	++	+	±	±
	4	++	++	+	+
Blank	1	+	±	−	+
	2	±	−	−	±
	3	+	−	−	±
	4	−	−	−	+
Control		+	±	−	+
Blank		±	−	−	+

[a] The equivalent amount of ampicillin is the initial concentration before ultrafiltration. [b] The residual amount of ampicillin is determined after ultrafiltration. The number in parentheses is the dilution. The key is as in the text. [c] *E. coli* 0111-B4, 1 ng/ml.

Chromogenic Assay Method—This assay is possibly more sensitive and leads to better quantitation than the LAL test. It was used to detect endotoxin in the injectable sodium ampicillin preparations with and without prior ultrafiltration. The effect of sodium ampicillin on this assay method was examined. To 0.4 ng/ml of the standard endotoxin was added 6, 10, 20, 40, 60, and 80 mg(potency)/ml of control sodium ampicillin, and the mixtures were incubated at 37° for 50 min. As shown in Fig. 2, when the concentration of sodium ampicillin was increased, the absorbance decreased depending on the drug dose. It has been reported that the minimal detectable amount of endotoxin varies and depends on the incubation time (15). Therefore, calibration curves were obtained for 0.1–0.6 ng of endotoxin in the presence of the control sodium ampicillin [20 mg(potency)/ml] for incubation periods of 40 and 50 min (Fig. 3). The curves indicated that the absorbance at 405 nm varied depending on the incubation time. The absorbance observed was ~0.3 for 0.6 ng/ml of en-

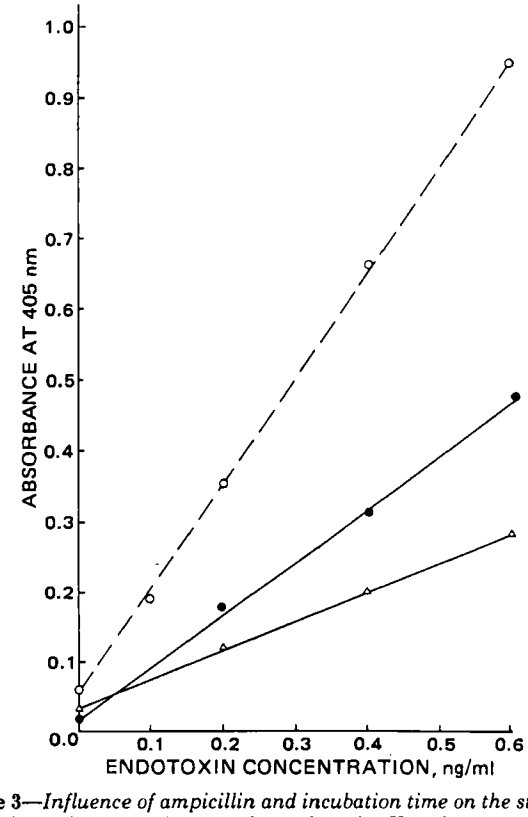

Figure 3—*Influence of ampicillin and incubation time on the standard curve of the chromogenic assay for endotoxin. Key: (○) 50-min incubation without ampicillin; (●) 50-min incubation with 20 mg of ampicillin/ml; (△) 40-min incubation with 20 mg of ampicillin/ml.*

dotoxin after a 40-min incubation and ~0.5 after 50 min. However, for the reaction mixture without ampicillin, the observed absorbance was ~0.95 for 0.6 ng/ml of endotoxin after 50 min.

From the calibration curve obtained in the presence of sodium ampicillin, the amount of endotoxin in the concentrated sample which was used in the rabbit pyrogen LAL tests was determined. It was revealed that 1 g (potency) of sodium ampicillin was contaminated with 6.4 ng of endotoxin (*E. coli* 0111-B4 endotoxin). Furthermore, the endotoxin in each vial was determined quantitatively without ultrafiltration by this chromogenic assay method using 40 vials (1 g/vial) of test samples. The results showed that the sodium ampicillin test samples were contaminated with an average of 4.73 ng of endotoxin (expressed as *E. coli* 0111-B4 endotoxin activity) per vial (gram) with a standard deviation (*SD*) of 1.75 ng/vial.

DISCUSSION

In the injectable sodium ampicillin test sample suspected of contamination, a trace amount of pyrogen (endotoxin) was detected by three methods. For each method, experiments were performed using a pyrogen-free sodium ampicillin preparation and as a control endotoxin derived from *E. coli*. The data indicate the following:

1. The presence of sodium ampicillin interferes with the detection of endotoxin, but sodium ampicillin could be separated from the endotoxin by ultrafiltration. Using ultrafiltration. it is possible not only to eliminate the coexistent drugs but also to concentrate the endotoxin. This makes it possible to detect the endotoxin in minute amounts.
2. The results obtained by the rabbit pyrogen test, LAL test, and chromogenic assay method indicated that the test samples of sodium ampicillin were contaminated with small amounts of endotoxin.
3. The endotoxin could be determined quantitatively in the presence of <20 mg/ml of sodium ampicillin. This study showed that the LAL test and the rabbit pyrogen test gave consistent results, suggesting that the *in vitro* method may become a useful method for the detection of pyrogens in drug preparations.

REFERENCES

(1) R. F. Spengler, V. B. Melvin, P. S. Lietman, and W. B. Greenough, *Lancet*, **i**, 168 (1974).

(2) R. F. Spengler, V. B. Melvin, P. S. Lietman, and W. B. Greenough, *Johns Hopkins Med. J.*, **134**(1), 28 (1974).

(3) J. K. Mann and W. A. Mahon, *Can. Med. Assoc. J.*, **111**, 23 (1974).

(4) J. Portnoy, A. Torchinsky, J. Mendelson, and E. Kagan, *ibid.*, **112**, 280 (1975).

(5) J. A. Smith, *ibid.*, **112**, 1044 (1975).

(6) R. F. Spengler and W. B. Greenough, *Lancet*, **i**, 865 (1975).

(7) O. Westphal, O. Luenderitz, and F. Z. Bester, *Z. Naturforsh.*, **76**, 148 (1952).

(8) "U.S. Pharmacopeia," 20th Rev., U.S. Pharmacopeial Convention, Inc. Rockville, Md., 1979, p. 902.

(9) "Japanese Pharmacopeia," vol. X, Nippon Koteisho Kyokai, Tokyo, 1981, p. 721.

(10) "U.S. Pharmacopeia," 20th Rev., U.S. Pharmacopeial Convention, Inc. Rockville, Md., 1979, p. 888.

(11) P. M. Newsome, *J. Pharm. Pharmacol.*, **29**, 704 (1977).

(12) S. Minami, N. Sakaguchi, and S. Shintani, *J. Takeda Res. Lab.*, **33**(3), 213 (1974).

(13) J. D. Sullivan, F. W. Valvis, and W. Watson, "Mechanisms in Bacterial Toxicology," A. W. Bernheimer, Ed., Wiley, New York, N.Y., 1976, p. 217.

(14) E. H. Mueller, J. Levin, and R. Holme, *J. Cell Physiol.*, **86**, 533 (1975).

(15) T. Harada, T. Morita, and S. Iwanaga, *J. Med. Enzymol.*, **3**, 43 (1978).

ACKNOWLEDGMENTS

The authors thank Drs. S. Okamoto and S. Mizuno in the National Institute of Health and Messrs. A. Ueki, H. Kubota, and S. Matsumoto in the Ministry of Health and Welfare for their helpful advice and encouragement throughout the course of this work.

Evaluation of the Teratogenicity of Morphine Sulfate Administered *Via* a Miniature Implantable Pump

ARTHUR A. CIOCIOLA and RONALD F. GAUTIERI ˣ

Received May 14, 1982, from the *Temple University, School of Pharmacy, Department of Pharmacology, Philadelphia, PA 19140.* Accepted for publication June 29, 1982.

Abstract □ A technique has been developed for the implantation of miniature infusion pumps in pregnant mice with minimal teratogenic and toxic side effects. In 7- to 10-day pregnant CF-1 mice receiving constant low doses of morphine sulfate *via* the infusion pump, the results, including fetal weight reduction and various skeletal and soft tissue abnormalities, were similar to those reported in previous investigations using single injections.

Keyphrases □ Delivery systems—implantable infusion pump, teratology studies □ Morphine sulfate—use of implantable infusion pumps for teratology studies, comparison with conventional techniques □ Infusion pump—delivery of test drug in teratology studies, comparison to conventional techniques

Teratology studies have often shown that drugs can affect the developing fetus, thereby dispelling the myth of a fully protective placental barrier. Many of these drugs have been administered to the pregnant animal in a single dose on a specific day of gestation allowing investigators to observe their teratogenic effects at different times of fetal development (1–3). However, with the introduction of a new type of drug dosing, the miniature infusion pump[1], a distinctly different approach can be used to study the possible teratogenic influence of drugs. This instrument is a constant-flow delivery system which allows the long-term steady-state effects of a drug on the developing fetus to be ascertained. Because there has been no reported use of this constant-flow delivery system for teratology studies, the feasibility of using the miniature infusion pump in such a study was investigated.

To determine if the use of the miniature infusion pump was a reasonable alternative to other types of drug dosing, a pilot study was undertaken comparing the fetal effects of saline administered *via* the pump and by hypodermic injection. The pump implantation procedure and the presence of the pump during pregnancy was observed to have a minimal effect on the fetus, thereby providing the

[1] Alzet mini-osmotic pump, Model 2001, Lot No. 07885, Alza Corp., Palo Alto, CA 94304.

0022-3549/83/0700-0742$01.00/0

dotoxin after a 40-min incubation and ~0.5 after 50 min. However, for the reaction mixture without ampicillin, the observed absorbance was ~0.95 for 0.6 ng/ml of endotoxin after 50 min.

From the calibration curve obtained in the presence of sodium ampicillin, the amount of endotoxin in the concentrated sample which was used in the rabbit pyrogen LAL tests was determined. It was revealed that 1 g (potency) of sodium ampicillin was contaminated with 6.4 ng of endotoxin (*E. coli* 0111-B4 endotoxin). Furthermore, the endotoxin in each vial was determined quantitatively without ultrafiltration by this chromogenic assay method using 40 vials (1 g/vial) of test samples. The results showed that the sodium ampicillin test samples were contaminated with an average of 4.73 ng of endotoxin (expressed as *E. coli* 0111-B4 endotoxin activity) per vial (gram) with a standard deviation (*SD*) of 1.75 ng/vial.

DISCUSSION

In the injectable sodium ampicillin test sample suspected of contamination, a trace amount of pyrogen (endotoxin) was detected by three methods. For each method, experiments were performed using a pyrogen-free sodium ampicillin preparation and as a control endotoxin derived from *E. coli*. The data indicate the following:

1. The presence of sodium ampicillin interferes with the detection of endotoxin, but sodium ampicillin could be separated from the endotoxin by ultrafiltration. Using ultrafiltration. it is possible not only to eliminate the coexistent drugs but also to concentrate the endotoxin. This makes it possible to detect the endotoxin in minute amounts.
2. The results obtained by the rabbit pyrogen test, LAL test, and chromogenic assay method indicated that the test samples of sodium ampicillin were contaminated with small amounts of endotoxin.
3. The endotoxin could be determined quantitatively in the presence of <20 mg/ml of sodium ampicillin. This study showed that the LAL test and the rabbit pyrogen test gave consistent results, suggesting that the *in vitro* method may become a useful method for the detection of pyrogens in drug preparations.

REFERENCES

(1) R. F. Spengler, V. B. Melvin, P. S. Lietman, and W. B. Greenough, *Lancet*, **i**, 168 (1974).

(2) R. F. Spengler, V. B. Melvin, P. S. Lietman, and W. B. Greenough, *Johns Hopkins Med. J.*, **134**(1), 28 (1974).

(3) J. K. Mann and W. A. Mahon, *Can. Med. Assoc. J.*, **111**, 23 (1974).

(4) J. Portnoy, A. Torchinsky, J. Mendelson, and E. Kagan, *ibid.*, **112**, 280 (1975).

(5) J. A. Smith, *ibid.*, **112**, 1044 (1975).

(6) R. F. Spengler and W. B. Greenough, *Lancet*, **i**, 865 (1975).

(7) O. Westphal, O. Luenderitz, and F. Z. Bester, *Z. Naturforsh.*, **76**, 148 (1952).

(8) "U.S. Pharmacopeia," 20th Rev., U.S. Pharmacopeial Convention, Inc. Rockville, Md., 1979, p. 902.

(9) "Japanese Pharmacopeia," vol. X, Nippon Koteisho Kyokai, Tokyo, 1981, p. 721.

(10) "U.S. Pharmacopeia," 20th Rev., U.S. Pharmacopeial Convention, Inc. Rockville, Md., 1979, p. 888.

(11) P. M. Newsome, *J. Pharm. Pharmacol.*, **29**, 704 (1977).

(12) S. Minami, N. Sakaguchi, and S. Shintani, *J. Takeda Res. Lab.*, **33**(3), 213 (1974).

(13) J. D. Sullivan, F. W. Valvis, and W. Watson, "Mechanisms in Bacterial Toxicology," A. W. Bernheimer, Ed., Wiley, New York, N.Y., 1976, p. 217.

(14) E. H. Mueller, J. Levin, and R. Holme, *J. Cell Physiol.*, **86**, 533 (1975).

(15) T. Harada, T. Morita, and S. Iwanaga, *J. Med. Enzymol.*, **3**, 43 (1978).

ACKNOWLEDGMENTS

The authors thank Drs. S. Okamoto and S. Mizuno in the National Institute of Health and Messrs. A. Ueki, H. Kubota, and S. Matsumoto in the Ministry of Health and Welfare for their helpful advice and encouragement throughout the course of this work.

Evaluation of the Teratogenicity of Morphine Sulfate Administered *Via* a Miniature Implantable Pump

ARTHUR A. CIOCIOLA and RONALD F. GAUTIERI ˣ

Received May 14, 1982, from the *Temple University, School of Pharmacy, Department of Pharmacology, Philadelphia, PA 19140.* Accepted for publication June 29, 1982.

Abstract □ A technique has been developed for the implantation of miniature infusion pumps in pregnant mice with minimal teratogenic and toxic side effects. In 7- to 10-day pregnant CF-1 mice receiving constant low doses of morphine sulfate *via* the infusion pump, the results, including fetal weight reduction and various skeletal and soft tissue abnormalities, were similar to those reported in previous investigations using single injections.

Keyphrases □ Delivery systems—implantable infusion pump, teratology studies □ Morphine sulfate—use of implantable infusion pumps for teratology studies, comparison with conventional techniques □ Infusion pump—delivery of test drug in teratology studies, comparison to conventional techniques

Teratology studies have often shown that drugs can affect the developing fetus, thereby dispelling the myth of a fully protective placental barrier. Many of these drugs have been administered to the pregnant animal in a single dose on a specific day of gestation allowing investigators to observe their teratogenic effects at different times of fetal development (1–3). However, with the introduction of a new type of drug dosing, the miniature infusion pump[1], a distinctly different approach can be used to study the possible teratogenic influence of drugs. This instrument is a constant-flow delivery system which allows the long-term steady-state effects of a drug on the developing fetus to be ascertained. Because there has been no reported use of this constant-flow delivery system for teratology studies, the feasibility of using the miniature infusion pump in such a study was investigated.

To determine if the use of the miniature infusion pump was a reasonable alternative to other types of drug dosing, a pilot study was undertaken comparing the fetal effects of saline administered *via* the pump and by hypodermic injection. The pump implantation procedure and the presence of the pump during pregnancy was observed to have a minimal effect on the fetus, thereby providing the

[1] Alzet mini-osmotic pump, Model 2001, Lot No. 07885, Alza Corp., Palo Alto, CA 94304.

0022-3549/83/0700-0742$01.00/0

Table I—Mean Values of Treatment Groups

Treatment Group[a]	Maternal Weight Gain, g	Fetal Ratio[b]	Resorption Ratio[b]	Fetal Weight, g	Sex Ratio M/F	Abnormalities[c] Soft Tissue	Abnormalities[c] Skeletal
Untreated	23.2	5.8/3.3	0.3/0.8	1.34	5.5/3.6	0.6	1.6
Injection-saline-7	26.9	5.0/6.5[d]	0.8/0.3	1.17[d]	6.0/5.5[d]	0.5	4.3
Injection-saline-8	20.2	2.6[d]/5.1	1.1/1.6	1.18[d]	3.3[d]/4.5	0.6	5.0[d]
Injection-saline-9	25.3	6.1/4.0	0.1/1.0	1.21	5.5/4.6	0.6	3.0
Injection-saline-10	23.9	4.5/5.6	0.3/1.0	1.12[d]	5.6/4.8	0.5	5.5[d]
Pump-saline-7	25.4	5.5/3.6[e]	0.8/0.6	1.30[e]	4.6/4.5	0.3	2.8
Pump-saline-8	20.7	4.0/4.6	0.3/0.6	1.17	4.0/4.6	0.3	4.8
Pump-saline-9	17.6	4.6/4.0	0.5/0.8	1.11	4.3/4.3	1.6	4.6
Pump-saline-10	19.4[e]	4.8/4.8	0.6/0.3	1.14	4.8/5.0	0.6	4.3
Pump-4.0% morphine sulfate-7	21.2	4.6/5.5	0.8/0.5	1.15[f]	5.8/4.3	1.3	5.6
Pump-4.0% morphine sulfate-8	21.5	6.1[f]/4.3	0.5/0.6	1.24	5.6/4.8	2.0[f]	2.8
Pump-4.0% morphine sulfate-9	21.8	4.3/6.6[f]	0.3/0.5	1.20	5.3/5.6	2.1	4.3
Pump-4.0% morphine sulfate-10	19.6	5.0/4.1	0.5/0.8	1.21	5.3/3.8	1.8	3.5
Pump-0.4% morphine sulfate-7	23.6	5.8/4.5	0.3/0.1	1.24	5.6/4.6	1.3	4.5
Pump-0.4% morphine sulfate-8	19.7	3.5/5.3	0.5/1.1	1.17	4.5/4.3	0.8	6.0
Pump-0.4% morphine sulfate-9	22.3	7.1/4.6	0.5/0.3	1.08	6.1/5.6	0.6	10.1
Pump-0.4% morphine sulfate-10	22.5	5.3/5.1	0.5/0.6	1.14	5.1/5.3	1.0	7.5[l]
Pump-0.04% morphine sulfate-7	16.2[f]	4.0/4.6	0.8/0.6	0.96[f,g]	4.0/4.6	2.0	12.1[f,g]
Pump-0.04% morphine sulfate-8	21.6	5.1/5.8	0.5/1.0	1.15	5.0/6.0	2.6	9.8[h]
Pump-0.04% morphine sulfate-9	17.8	4.5/5.1	0.1/0.3	1.04[i]	4.8/4.8	3.6[k]	9.8[i]
Pump-0.04% morphine sulfate-10	17.8	5.5/4.0	0.1/0.6	1.04	4.5/5.0	3.0	14.3[f,j]

[a] Designated as method of delivery-solution administered-gestation day of dosing. The saline dosage was 0.3 ml sc; the volume released by the infusion pump was 0.17 ml. [b] Right horn/left horn of the uterus. [c] Average per litter. [d] Significantly different ($p < 0.05$) compared with the untreated control. [e] Significantly different ($p < 0.05$) compared with the subcutaneously delivered saline control. [f] Significantly different ($p < 0.05$) compared with the pump-delivered saline control. [g] Significantly different ($p < 0.05$) compared with the pump-4.0% morphine sulfate-7 and pump-0.4% morphine sulfate-7 groups. [h] Significantly different ($p < 0.05$) compared with the pump-4.0% morphine sulfate-8 group. [i] Significantly different ($p < 0.05$) compared with the pump-4.0% morphine sulfate-9 group. [j] Significantly different ($p < 0.05$) compared with the pump-4.0% morphine sulfate-10 group. [k] Significantly different ($p < 0.05$) compared with the pump-0.4% morphine sulfate-9 group. [l] Significantly different ($p < 0.05$) compared with the pump-4.0% morphine sulfate-10 group.

rationale for a full investigation of the long-term steady-state effects of a drug on the developing fetus. Because this laboratory has conducted several studies with morphine sulfate and elucidated its teratogenic effects, this drug was selected for the test system. The reproductive effects of low constant doses of morphine sulfate administered *via* the miniature infusion pump throughout specific critical days of gestation are reported herein.

EXPERIMENTAL

Animals—CF-1 albino mice[2], weighing at least 25 g, were used in all of the procedures. All females were placed in aggregate cages, each containing 10 animals. They were allowed to acclimatize for 2 weeks. Following this period, those females weighing at least 25 g were allowed to mate. The male mice were housed in individual cages measuring 12.5 × 15 × 10 cm, each with a wire mesh front and floor[3]. Food[4] and tap water were offered *ad libitum;* artificial light was supplied with a 12-hr light/dark cycle.

Drugs and Solutions—Normal saline[5] was used as the vehicle for the morphine sulfate[6] solutions (40, 4.0, and 0.4 mg/ml); fresh solutions were prepared weekly. In addition, normal saline was administered to all vehicle controls including subcutaneous injection and infusion pump groups. All injections were given subcutaneously with a 1-ml glass syringe equipped with a 0.5-cm 26-gauge needle. All pumps were filled with filtered solutions[7] using a specially designed blunt-tipped 26-gauge steel needle[8]. The injection volume was 0.3 ml; the pump release was 0.17 ml of solution.

The bone-staining solution and decalcifying Bouin's solution were prepared according to previously published reports (2).

Breeding, Group Selection, and Treatment—The breeding procedure has been described previously (4). Gravid females were randomly assigned to the 21 experimental groups. The controls consisted of one untreated group and four groups given single subcutaneous saline injections on day 7, 8, 9, or 10 of gestation. There were 16 treatment groups; infusion pumps containing either saline or a 4.0% (40 mg/ml), 0.4% (4.0 mg/ml), or 0.04% (0.4 mg/ml) solution of morphine sulfate were implanted in each mouse on day 7, 8, 9 or 10 of gestation.

Surgical Procedure—On the day of treatment, the body hair of the animals in the dorsal-scapular area was sheared with scissors, and the mice were anesthetized with ether[9]. A small skin incision (1–1.5 cm) was made perpendicular to the backbone in the dorsal-scapular area. The infusion pump was inserted into a subcutaneous pouch made by separating the skin from the underlying muscle and secured by the closure of the incision with three or more interrupted sutures. The anesthesia duration was ~3 min, and an antiseptic solution[10] was used as a postoperative wound dressing. All animals, regardless of the treatment, were allowed to recover undisturbed.

Examination of Fetuses—On day 18 (1 day prior to full term), each mouse was weighed; the terminal maternal weight was adjusted for pump weight if necessary. Each mouse was then sacrificed by cervical dislocation, at which time the number and position of the fetuses and resorption sites (metrial glands) were recorded. The fetuses were blotted dry and checked for viability by reflex movement on stimulation with a blunt probe. Further examination consisted of the observation of each fetus under a dissecting microscope[11] for gross defects and sex; the weight of each fetus was recorded to the nearest hundredth of a gram on a torsion balance[12]. One-half of the fetuses were then randomly selected for preparation in a bone-staining solution for skeletal examination by the method of Staples and Schnell (5). The remaining fetuses were prepared in Bouin's solution for soft tissue examination by the method of Wilson (6). The statistical significance of the observations was determined using Student's t test and the uncorrected chi-square test for a binomial population.

RESULTS AND DISCUSSION

Effects of Pumps Implantation—*Maternal Effects*—Two deaths occurred during the pump implantation procedures; both were attributed to an overdose of the ether anesthesia and not to surgical trauma. There were no maternal deaths due to drug toxicity or postsurgical complications observed in any treatment group.

Most animals became fully conscious within minutes following the pump implantation procedure, although spontaneous activity was suppressed for several hours. This was judged to be the result of the proce-

[2] Charles River Breeding Laboratories, Wilmington, Mass.
[3] Norwich Wire Works, Norwich, N.Y.
[4] Purina Laboratory Chow, Ralston-Purina Co., St. Louis, Mo.
[5] 0.9% Sodium Chloride Injection USP, Lot No. 92-166-DE-7 exp. 9/1/82, Abbott Laboratories, North Chicago, IL 60064.
[6] Morphine Sulfate, Lot No. 4455, Merck & Co., Rahway, N.J.
[7] Millex H-A Filters, 45 μm, Lot No. SLHA02505, Millipore Corp., Bedford, MA 01730.
[8] Alza Corp., Palo Alto, CA 94304.
[9] Ether, ethyl ether, Lot No. 413759, J. T. Baker Chemical Co., Phillipsburg, NJ 08865.
[10] Betadine solution, Purdue Frederick Co., Norwalk, CT 06856.
[11] Binocular dissecting microscope, Bausch & Lomb, Lot. ASZ3012.
[12] Torsion Balance Co., Model PL-800, 500820, Ireland.

Table II—Fetal Anomalies Occurring in Significant Numbers in the Pump-Administered Morphine Sulfate Groups

Anomaly	Group[a] 4.0% Morphine Sulfate 7 8 9 10	0.4% Morphine Sulfate 7 8 9 10	0.04% Morphine Sulfate 7 8 9 10
Exencephaly	— — — —	— — — —	L — — —
Hydronephrosis	— B — F	— — — —	B B — F
Intestinal hemorrhage	— — — —	— — — —	— B B B
Split supraoccipital	— — — —	— — B —	B — — F
Malformed sternebrae	L L B —	— — B F	B — L F
Malformed xiphoid	— — — —	— — — —	B — B B

[a] Based on six litters per group. Key: significantly different ($p < 0.05$) from the pump saline control on a litter basis (L), a fetal basis (F), or both (B).

dure and not a drug effect, because similar observations were noted for the saline groups and, also, several hours are needed for the pump to reach full capacity. Observation of the spontaneous activity of the animals on subsequent days showed little difference between the treatment (pump-implanted) groups and the untreated controls. On sacrifice of the animals, the pumps were excised and the pouch area examined. In no case was there any evidence of gross infection or any type of inflammation present in or around the pouch area.

The only maternal variable measured during this experiment was the maternal weight gain. There were no significant differences between the untreated controls and any treatment group. However, when the pump-saline-10[13] group was compared with the injection-saline-10 group (Table I), there was a significant decrease in maternal weight gain observed, obviously a direct consequence of the pump implantation procedure.

Fetal Effects—A crucial point in this study was to determine the feasibility of the pump implantation procedure for use in a teratology study. The fetal effects resulting from the pump implantation procedure were determined by the statistical comparison of saline administered *via* the infusion pump *versus* subcutaneous injection. Only one group (pump-saline-7) showed any significant differences: an increase in mean fetal weight and a reduction in the number of fetuses in the left uterine horn. Because the number of fetal resorptions was not significantly different, these effects are possibly due to an increased uterine blood supply and not the pump implantation procedure (which is performed after uterine implantation of the ova). Therefore, there does not appear to be any major difference in the fetal effects of saline administered *via* subcutaneous injection or the pump implantation procedure.

Effects of Morphine Sulfate—The doses used in this study were only a fraction of the morphine sulfate doses administered in previous studies (7–9). The exact dose administered is a function of the animal body weight as the drug concentration and release rate is the same in all cases.

Maternal Effects—Observation of the animals implanted with a pump containing morphine sulfate showed the discernable effects of the drug to be quite minimal. The maternal weight gain significantly decreased in only one group (pump-0.04% morphine sulfate-7), which is in general agreement with previous reports (7–9).

Fetal Effects—A significant reduction in mean fetal weight was noted which agreed with previous data (7–9). Significant fetal resorptions, which were noted in one of the previous studies (7), did not occur in the present investigation.

Three groups (pump-4.0% morphine sulfate-8, pump-0.04% morphine sulfate-7, and pump-0.04% morphine sulfate-10) showed significant increases in the total number of soft tissue and/or skeletal defects when compared with the pump saline controls. A trend in the mean values of the total number of soft tissue/skeletal abnormalities and fetal weights is evident. With the exception of the soft tissue anomalies of the pump-morphine sulfate-8 groups, the lowest doses of morphine sulfate (0.04%) have nearly twice the number of abnormalities and much lower mean fetal weights compared with the corresponding gestation day for the highest doses (4.0%). This trend is supported statistically, as significance was noted for dose comparisons involving the mean fetal weight and total number of soft tissue and/or skeletal abnormalities (Table I), with the greatest difference appearing between the highest (4.0%) and lowest doses (0.04%) of morphine sulfate.

In view of the type of dosing and since it is well known that constant morphine administration induces tolerance to many of its physiological effects, a logical explanation for these trends might be the induction of microsomal liver enzymes. However, the induction of microsomal liver enzymes does not explain the increase in fetal defects at the lowest dose of morphine as compared with the high dose; the enzymatic *N*-demethylation of morphine is reduced with chronic administration (10–12). This reduction of the *N*-demethylation of morphine can be partially reversed by nalorphine (10). Because of the similar substrate stereospecificity between the liver enzymes and the opiate receptors, Axelrod (10) suggested that the depression of enzymatic activity may be related to a similar depression of receptor activity, seen physiologically as the development of tolerance. To further elucidate the similarity of the stereospecificity between the enzyme, *N*-demethylase, and the opiate receptor, Mannering and Takemori (11) used the steric isomers of 3-hydroxy-*N*-methylmorphinan (dextrorphan and levorphan) in chronic doses and measured the *N*-demethylase enzyme activity in response to a test dose of morphine. Dextrorphan is known to lack most morphine-like properties, while levorphan produces many morphine-like effects. Mannering and Takemori (11) reported that the rate of enzymatic *N*-demethylation of morphine was inhibited with chronic administration of levorphan, while dextrorphan was observed to be relatively noneffective.

If the teratogenic effects of morphine are expressed through the opiate receptor activity, the inhibition of the receptor by chronic administration of morphine may result in a lower incidence of fetal anomalies at higher doses (4.0%). There is a possibility that constant administration at the lowest dose of morphine (0.04%) may not be sufficient to inhibit the receptor but is large enough to cause fetal abnormalities. With morphine *N*-demethylation inhibited at higher doses, the production of the end product (formaldehyde) is also inhibited; with constant administration of low doses of morphine, tissue levels of formaldehyde, a secondary teratogenic agent, may build up. However, the development of tolerance and the induction of fetal defects by morphine are probably not due to a single cause, but to multiple and presently unknown factors.

The fetal abnormalities produced in significant numbers as a result of morphine sulfate administration *via* the infusion pump have been listed in Table II. Specifically, those malformations include exencephaly, hydronephrosis, intestinal hemorrhage, split supraoccipital bone, (malformed, crankshaft, fused, poly, and split) sternebrae, and malformed (butterfly and split) xiphoid bone. In addition, various soft tissue anomalies were also observed in this study, although their incidence was not significant. These defects included: cleft palate, cryptorchidism, ectopic ovary or testis, hydrocephaly, microphthalmia, missing lens, skin bumps, abnormal tail, and polydactyly. There were also numerous skeletal defects observed in significant numbers, including: brachygnathia; delayed ossification of the ribs, skull, sternebrae, and xiphoid; split ribs; malformed basiphenoid, xiphoid, and centrum; and missing sternebrae and supraoccipital bone.

It is known that the specific fetal malformation is related to the fetal organs most susceptible to injury at the time of drug challenge (7–9). Therefore, one would expect that litters from dams with the morphine-containing pump implanted on day 7 of gestation should show all the defects observed in the litters from dams implanted on subsequent days because of the continually present drug levels. However, the data does not show such a trend. Possibly, the teratogenic insult is greatest on the first day of drug administration (and on the organs developing at that time) and lessens thereafter.

In conclusion, this study has proven that the infusion pump is a feasible dosage form in teratology studies. The methodology necessary for future studies of this type has been developed. In administering morphine sulfate *via* the implantable pump, this study has shown fetal abnormalities similar to those observed in previous (injection) studies.

[13] Each group was designated by method of delivery—solution administered-gestation day of dosing.

REFERENCES

(1) J. E. Zellers and R. F. Gautieri, *J. Pharm. Sci.*, **66**, 1727 (1977).

(2) J. M. McDevitt, R. F. Gautieri, and D. E. Mann, Jr., *J. Pharm. Sci.*, **70**, 631 (1981).

(3) M. P. Mahalik, R. F. Gautieri, and D. E. Mann, Jr., *J. Pharm. Sci.*, **69**, 703 (1980).

(4) R. S. Thompson and R. F. Gautieri, *J. Pharm. Sci.*, **58**, 406 (1969).

(5) R. E. Staples and V. L. Schnell, *Stain Technol.*, **39**, 61 (1964).

(6) J. G. Wilson, in "Teratology Principles and Techniques," J. G. Wilson and J. Warkany, Eds., University of Chicago Press, Chicago, Ill., 1965, p. 267.

(7) H. S. Harpel and R. F. Gautieri, *J. Pharm. Sci.*, **57**, 1590

(1968).
(8) J. D. Iuluicci and R. F. Gautieri, *J. Pharm. Sci.*, **60**, 420 (1971).
(9) P. A. Arcuri and R. F. Gautieri, *J. Pharm. Sci.*, **62**, 1626 (1973).
(10) J. Axelrod, *Science*, **124**, 263 (1956).
(11) G. L. Mannering and A. E. Takemori, *J. Pharmacol. Exp. Ther.*, **127**, 187 (1959).
(12) J. Cochin and S. Economan, *Fed. Proc.*, **18**, 377 (1959).

ACKNOWLEDGMENTS

Abstracted in part from a thesis submitted by Arthur A. Ciociola to Temple University in partial fulfillment of the Master of Science degree requirements.

Pharmacokinetics and Bioavailability of Intravenous and Topical Nitroglycerin in the Rhesus Monkey: Estimate of Percutaneous First-Pass Metabolism

RONALD C. WESTER *x, PATRICK K. NOONAN ‡, STEPHEN SMEACH, and LARRY KOSOBUD

Received April 1, 1982, from *Searle Research and Development, G. D. Searle & Co., Skokie, IL 60076.* Accepted for publication June 28, 1982. Present address: *Department of Dermatology and ‡School of Pharmacy, University of California, San Francisco, CA 94143.

Abstract □ [^{14}C]Nitroglycerin was administered intravenously and topically to three rhesus monkeys and the pharmacokinetics were determined. The rhesus monkey is an animal model for which percutaneous absorption is similar to that in the human. After intravenous administration the decline in plasma nitroglycerin concentration was biexponential with an initial half-life of 0.8 min (2–5 min postadministration) and a terminal half-life of 18 min (5–60 min postadministration). After topical application in an ointment, plasma concentrations of unchanged nitroglycerin were first detectable at 0.25 hr postapplication. Peak plasma nitroglycerin concentrations occurred between 4–6 hr, and nitroglycerin was still detectable at 24 hr postapplication. Plasma levels fit a biexponential curve with an α-phase half-life of 3.0 hr, a β-phase half-life of 4.3 hr, and a lag time of 0.5 hr. The absolute bioavailability of topical nitroglycerin was 56.6 ± 5.8%. The differences in bioavailability estimates between unchanged nitroglycerin and total carbon-14 is considered to be the amount of nitroglycerin which is metabolized as it is absorbed through the skin (percutaneous first-pass effect). This value for topical nitroglycerin was quite small, only 16–21% depending on the method of comparison.

Keyphrases □ Nitroglycerin—percutaneous absorption pharmacokinetics in the rhesus monkey, comparison of intravenous and topical administration bioavailability □ Pharmacokinetics—nitroglycerin in the rhesus monkey, comparison of intravenous and topical administration bioavailability □ Bioavailability—topical nitroglycerin in the rhesus monkey, comparison with intravenous administration, pharmacokinetics □ Percutaneous absorption—topical nitroglycerin, determination of first-pass effect

Nitroglycerin is a drug shown to be effective in angina pectoris (1–4) which may be effective in other cardiac diseases (5). The usual dosage form is a sublingual tablet, which has the disadvantage of a short duration of action. Nitroglycerin is also administered orally; however, first-pass metabolism during absorption is estimated to be large (6, 7). A third route of administration is transdermal delivery. Transdermal administration results in a longer duration of action than sublingual administration and may bypass the first-pass metabolism seen with oral administration. The result is a dosage form that delivers nitroglycerin over an extended time period. Recent publications attest to the clinical effectiveness of topically applied nitroglycerin (4, 5). Thus, it is important to determine the pharmacokinetic parameters of nitroglycerin after topical administration. This information can help in understanding the effectiveness of the drug and perhaps can be used to improve nitroglycerin therapy.

The animal model chosen for the study of the transdermal delivery of nitroglycerin was the rhesus monkey. Percutaneous absorption of several compounds in the rhesus monkey have been shown to be similar to that in the human (8–11).

EXPERIMENTAL

Female rhesus monkeys weighing ~4–6 kg were used. The monkeys were lightly anesthetized with 50–100 mg ketamine[1] for placement in the metabolism chairs. The monkeys were restrained in the metabolism chairs for 24 hr after drug administration (length of topical application) and then returned to metabolism cages for continued blood and urine collection. The monkeys had free access to food and water in the metabolism cages; they were hand fed and watered while confined to the metabolism chairs. In the topical application studies, the wrists of the monkey were taped to the sides of the chair to prevent the monkey from removing the applied dose. Each animal had an indwelling catheter in the saphenous vein for blood collection; a saline drip was connected to the cathether while blood samples were not being collected.

[^{14}C]Nitroglycerin was prepared from uniformly labeled glycerol and had a specific activity of 128 μCi/mg. The synthetic material was purified by chromatography on silica gel (toluene) followed by further purification using high-performance liquid chromatography (HPLC) on a μ-Bondapack C-18 column (water–methanol, 60:40) at a flow rate of 2 ml/min. The chemical and radiochemical purity, as determined by HPLC and TLC, was 99%.

The intravenous dosage form was 1.92 mg of labeled nitroglycerin with a specific activity of 250 μCi in 0.5 ml of ethanol. Administration was by bolus injection in the saphenous vein of the noncatheterized leg. The topical dosage form was 2% nitroglycerin ointment[2] containing 19.0 mg of labeled nitroglycerin (specific activity 210 μCi) spread over a 50-cm^2 area of skin. [^{14}C]Nitroglycerin was added to the ointment using the procedure of Lindsay *et al.* (12). Topical administration was to the inner upper arm. The area was lightly clipper shaved, which does not affect percutaneous absorption in the rhesus monkey (8). [The application site also has been determined not to affect the percutaneous absorption of nitroglycerin in the rhesus monkey (13).] The topical application was occluded with aluminum foil and adhesive tape. The ointment was left in place for 24 hr, and then the site was washed with soap and water. There was a 1-week period between drug administrations.

At each sampling time, ~3 ml of blood was drawn and placed in a

[1] Ketaset; Bristol Laboratories, Syracuse, N.Y.
[2] Nitro-BID; Marion Laboratories, Kansas City, Mo.

0022-3549/83/0700-0745$01.00/0

(1968).
(8) J. D. Iuluicci and R. F. Gautieri, *J. Pharm. Sci.*, **60**, 420 (1971).
(9) P. A. Arcuri and R. F. Gautieri, *J. Pharm. Sci.*, **62**, 1626 (1973).
(10) J. Axelrod, *Science*, **124**, 263 (1956).
(11) G. L. Mannering and A. E. Takemori, *J. Pharmacol. Exp. Ther.*, **127**, 187 (1959).
(12) J. Cochin and S. Economan, *Fed. Proc.*, **18**, 377 (1959).

ACKNOWLEDGMENTS

Abstracted in part from a thesis submitted by Arthur A. Ciociola to Temple University in partial fulfillment of the Master of Science degree requirements.

Pharmacokinetics and Bioavailability of Intravenous and Topical Nitroglycerin in the Rhesus Monkey: Estimate of Percutaneous First-Pass Metabolism

RONALD C. WESTER *x, PATRICK K. NOONAN ‡, STEPHEN SMEACH, and LARRY KOSOBUD

Received April 1, 1982, from *Searle Research and Development, G. D. Searle & Co., Skokie, IL 60076.* Accepted for publication June 28, 1982. Present address: *Department of Dermatology and ‡School of Pharmacy, University of California, San Francisco, CA 94143.

Abstract □ [^{14}C]Nitroglycerin was administered intravenously and topically to three rhesus monkeys and the pharmacokinetics were determined. The rhesus monkey is an animal model for which percutaneous absorption is similar to that in the human. After intravenous administration the decline in plasma nitroglycerin concentration was biexponential with an initial half-life of 0.8 min (2–5 min postadministration) and a terminal half-life of 18 min (5–60 min postadministration). After topical application in an ointment, plasma concentrations of unchanged nitroglycerin were first detectable at 0.25 hr postapplication. Peak plasma nitroglycerin concentrations occurred between 4–6 hr, and nitroglycerin was still detectable at 24 hr postapplication. Plasma levels fit a biexponential curve with an α-phase half-life of 3.0 hr, a β-phase half-life of 4.3 hr, and a lag time of 0.5 hr. The absolute bioavailability of topical nitroglycerin was 56.6 ± 5.8%. The differences in bioavailability estimates between unchanged nitroglycerin and total carbon-14 is considered to be the amount of nitroglycerin which is metabolized as it is absorbed through the skin (percutaneous first-pass effect). This value for topical nitroglycerin was quite small, only 16–21% depending on the method of comparison.

Keyphrases □ Nitroglycerin—percutaneous absorption pharmacokinetics in the rhesus monkey, comparison of intravenous and topical administration bioavailability □ Pharmacokinetics—nitroglycerin in the rhesus monkey, comparison of intravenous and topical administration bioavailability □ Bioavailability—topical nitroglycerin in the rhesus monkey, comparison with intravenous administration, pharmacokinetics □ Percutaneous absorption—topical nitroglycerin, determination of first-pass effect

Nitroglycerin is a drug shown to be effective in angina pectoris (1–4) which may be effective in other cardiac diseases (5). The usual dosage form is a sublingual tablet, which has the disadvantage of a short duration of action. Nitroglycerin is also administered orally; however, first-pass metabolism during absorption is estimated to be large (6, 7). A third route of administration is transdermal delivery. Transdermal administration results in a longer duration of action than sublingual administration and may bypass the first-pass metabolism seen with oral administration. The result is a dosage form that delivers nitroglycerin over an extended time period. Recent publications attest to the clinical effectiveness of topically applied nitroglycerin (4, 5). Thus, it is important to determine the pharmacokinetic parameters of nitroglycerin after topical administration. This information can help in understanding the effectiveness of the drug and perhaps can be used to improve nitroglycerin therapy.

The animal model chosen for the study of the transdermal delivery of nitroglycerin was the rhesus monkey. Percutaneous absorption of several compounds in the rhesus monkey have been shown to be similar to that in the human (8–11).

EXPERIMENTAL

Female rhesus monkeys weighing ~4–6 kg were used. The monkeys were lightly anesthetized with 50–100 mg ketamine[1] for placement in the metabolism chairs. The monkeys were restrained in the metabolism chairs for 24 hr after drug administration (length of topical application) and then returned to metabolism cages for continued blood and urine collection. The monkeys had free access to food and water in the metabolism cages; they were hand fed and watered while confined to the metabolism chairs. In the topical application studies, the wrists of the monkey were taped to the sides of the chair to prevent the monkey from removing the applied dose. Each animal had an indwelling catheter in the saphenous vein for blood collection; a saline drip was connected to the cathether while blood samples were not being collected.

[^{14}C]Nitroglycerin was prepared from uniformly labeled glycerol and had a specific activity of 128 μCi/mg. The synthetic material was purified by chromatography on silica gel (toluene) followed by further purification using high-performance liquid chromatography (HPLC) on a μ-Bondapack C-18 column (water–methanol, 60:40) at a flow rate of 2 ml/min. The chemical and radiochemical purity, as determined by HPLC and TLC, was 99%.

The intravenous dosage form was 1.92 mg of labeled nitroglycerin with a specific activity of 250 μCi in 0.5 ml of ethanol. Administration was by bolus injection in the saphenous vein of the noncatheterized leg. The topical dosage form was 2% nitroglycerin ointment[2] containing 19.0 mg of labeled nitroglycerin (specific activity 210 μCi) spread over a 50-cm^2 area of skin. [^{14}C]Nitroglycerin was added to the ointment using the procedure of Lindsay *et al.* (12). Topical administration was to the inner upper arm. The area was lightly clipper shaved, which does not affect percutaneous absorption in the rhesus monkey (8). [The application site also has been determined not to affect the percutaneous absorption of nitroglycerin in the rhesus monkey (13).] The topical application was occluded with aluminum foil and adhesive tape. The ointment was left in place for 24 hr, and then the site was washed with soap and water. There was a 1-week period between drug administrations.

At each sampling time, ~3 ml of blood was drawn and placed in a

[1] Ketaset; Bristol Laboratories, Syracuse, N.Y.
[2] Nitro-BID; Marion Laboratories, Kansas City, Mo.

0022-3549/83/0700-0745$01.00/0

Table I—Plasma Levels of Nitroglycerin Following Intravenous and Topical Administration

Time, hr	Nitroglycerin Concentration, ng/ml[a]	
	Intravenous	Topical
0.0	<0.1	<0.1
0.02	80.7 ± 5.5	—[b]
0.03	200.7 ± 31.0	—
0.05	90.3 ± 9.9	—
0.08	35.1 ± 5.7	—
0.25	17.6 ± 2.8	0.3 ± 0.03
0.5	9.0 ± 0.8	0.7 ± 0.3
0.75	3.5 ± 0.6	1.0 ± 0.4
1.0	1.8 ± 1.0	1.9 ± 0.5
2.0	<0.1	2.9 ± 0.4
3.0	<0.1	4.6 ± 1.1
4.0	—	6.8 ± 0.3
6.0	<0.1	6.7 ± 0.4
8.0	—	5.4 ± 0.3
12.0	—	3.6 ± 0.4
24.0	<0.1	0.7 ± 0.2
48.0	<0.1	<0.1
72.0	<0.1	<0.1

[a] Mean ± *SEM* for three monkeys. [b] — Plasma samples not drawn.

Table II—Plasma Levels of Carbon-14 Following Intravenous and Topical Administration

Time, hr	Concentration, ng equivalents/ml[a]	
	Intravenous	Topical
0.0	0	0
0.02	386 ± 54	—[b]
0.03	289 ± 48	—
0.05	292 ± 15	—
0.08	259 ± 3	—
0.25	338 ± 27	8 ± 4
0.5	353 ± 6	24 ± 12
0.75	340 ± 7	34 ± 17
1.0	333 ± 10	57 ± 25
2.0	314 ± 13	177 ± 41
3.0	295 ± 13	315 ± 69
4.0	—	426 ± 64
6.0	220 ± 24	616 ± 69
8.0	—	762 ± 46
12.0	—	917 ± 45
24.0	62 ± 7	754 ± 54
48.0	37 ± 2	374 ± 25
72.0	28 ± 2	249 ± 28

[a] Mean ± *SEM* for three monkeys. [b] — Plasma samples not drawn.

heparinized tube. The tube was centrifuged immediately (5 min from start-up to finish); the plasma was removed, placed in a vial containing 50 μl of 1.0 *M* silver nitrate for protein precipitation, and mixed. The samples were then frozen in a mixture of isopropyl alcohol and solid carbon dioxide. The majority of each plasma sample (1.0 ml) was utilized for nitroglycerin assay; a small aliquot (0.1 ml) was utilized for carbon-14 assay.

Blood sampling times following intravenous administration were 0, 1, 2, 3, 5, 15, 30, and 45 min and 1, 2, 3, 6, 24, 48, and 72 hr. Blood was withdrawn following topical administration at 0, 15, 30, and 45 min and 1, 2, 3, 4, 6, 8, 12, 24, 48, and 72 hr. Urine samples for carbon-14 analysis were collected at 0–24, 24–48, and 48–72 hr.

A GC method modified from Yap *et al.* (14) was used to analyze the nitroglycerin content in the monkey plasma. Nitroglycerin and the internal standard, isosorbide dinitrate, were extracted from plasma with hexane. The extract was then evaporated, reconstituted with ethyl acetate, and analyzed by GC[3] using an electron-capture detector. A glass column (1.2 m × 2 mm) was packed with 3% OV-1 liquid phase on Chromosorb W-HP, 100–200 mesh[4]. The injection port, column, and detector temperatures were 200°, 110°, and 200°, respectively. The carrier gas was 5% methane–argon and had a flow rate of 25 ml/min. The retention times for nitroglycerin and isosorbide dinitrate were 1.8 and 6.0 min, respectively.

Bioavailability of nitroglycerin was determined by the ratios of the areas under the concentration–time curves (AUC $0 \rightarrow \infty$) for intravenous and topical plasma nitroglycerin and plasma carbon-14. The trapezoidal area was measured to the last data point, and the remaining area was determined using the terminal slope of the concentration–time curve. The ratio of the topical AUC to the intravenous AUC is the absolute bioavailability of nitroglycerin following topical administration. Bio-

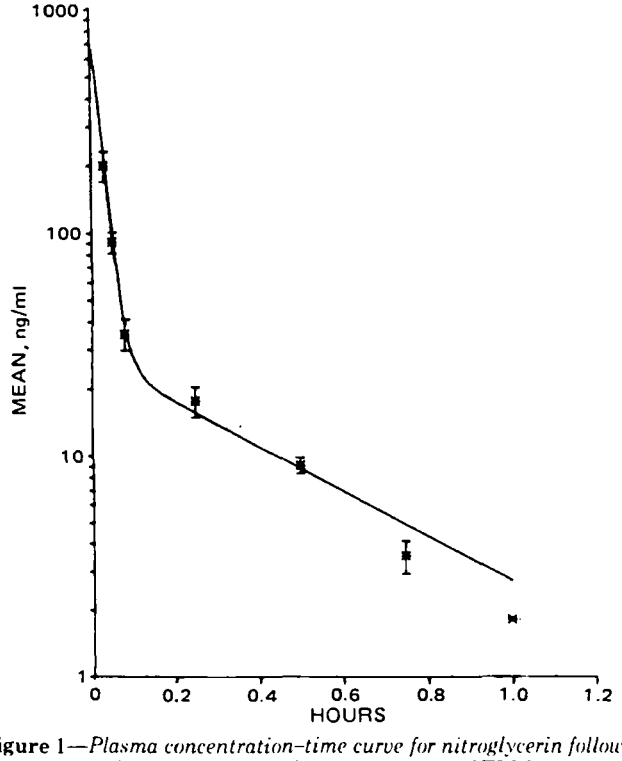

Figure 1—*Plasma concentration–time curve for nitroglycerin following intravenous administration. The bars represent the* SEM *for each mean value.*

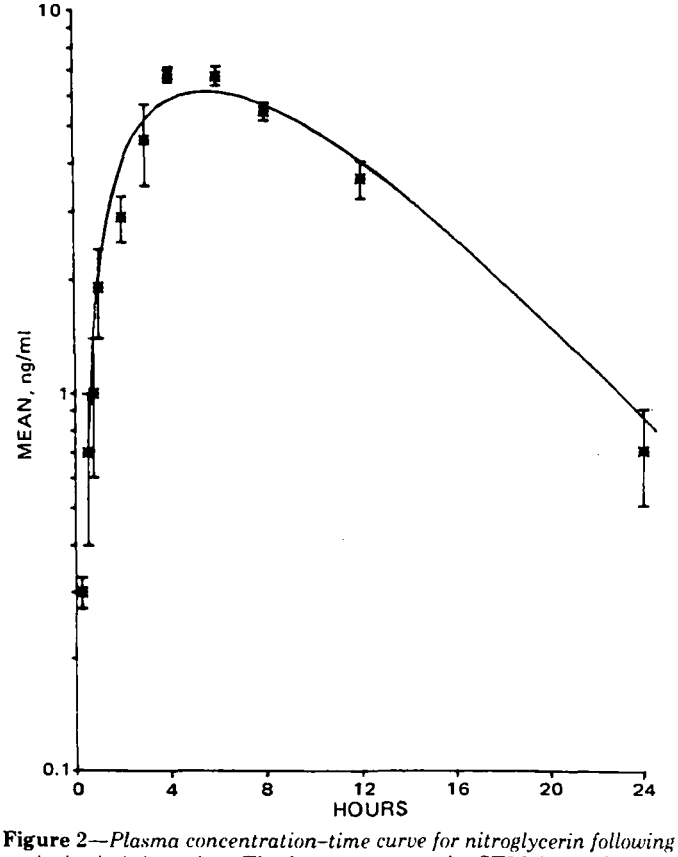

Figure 2—*Plasma concentration–time curve for nitroglycerin following topical administration. The bars represent the* SEM *for each mean value.*

[3] Hewlett-Packard Model 5710A; Avondale, Pa.

[4] Ohio Valley Specialty Chemical Inc., Marietta, Ohio.

Table III—Urinary Excretion of Carbon-14 Following Intravenous and Topical Administration of [^{14}C]Nitroglycerin

Time, hr	Excretion, % of dose[a]	
	Intravenous	Topical
0–24	50.9 ± 4.2	30.9 ± 3.9
24–48	2.4 ± 0.3	7.0 ± 0.2
48–72	0.3 ± 0.2	0.9 ± 0.03
0–72	53.7 ± 3.9	38.8 ± 3.7

[a] Mean ± *SEM* for three monkeys.

availability of nitroglycerin was also determined from the urinary excretion of carbon-14 following topical and intravenous administration. Blood levels were fit to the appropriate pharmacokinetic model using NONLIN (15).

The absolute bioavailability of nitroglycerin and carbon-14 was estimated by:

$$\text{percentage} = \frac{\text{AUC topical/topical dose}}{\text{AUC intravenous/intravenous dose}} \times 100 \quad \text{(Eq. 1)}$$

where the AUC is expressed as ng hr ml^{-1}. Bioavailability was estimated from urinary excretion using:

$$\text{percentage} = \frac{\text{total [}^{14}\text{C] excretion topical administration}}{\text{total [}^{14}\text{C] excretion intravenous administration}} \times 100 \quad \text{(Eq. 2)}$$

RESULTS

Table I and Fig. 1 show the plasma concentrations of unchanged nitroglycerin following intravenous administration. The decline in plasma nitroglycerin concentration was biexponential with an initial half-life of 0.8 min (2- to 5-min interval) and a terminal half-life of 18 min (5- to 60-min interval). The first data point (0.02 min) was not used in the NONLIN analysis.

Table I and Fig. 2 show the plasma concentrations of unchanged nitroglycerin following topical administration of the ointment. Nitroglycerin was first detected at 0.25 hr postapplication. Peak plasma nitroglycerin concentration occurred between 4 and 6 hr and nitroglycerin was still detectable at 24 hr postapplication. The NONLIN analysis best fit a biexponential curve with an α-phase half-life of 3.0 hr, a β-phase half-life of 4.3 hr, and a lag time of 0.5 hr.

Table II gives the plasma concentrations of carbon-14 following intravenous and topical administration of [^{14}C]nitroglycerin. After intravenous administration, plasma concentrations of carbon-14 fluctuated for the first 3 hr, probably due to metabolite formation. Levels then declined and by 72 hr had decreased 10-fold. After topical administration, plasma carbon-14 concentrations did not peak until 12 hr postadministration. Urinary excretion of carbon-14 was also determined (Table III). Within 72 hr 53.7 ± 3.9 (*SEM*) % of the intravenous dose and 38.8 ± 3.7% of the topical dose were excreted. Most of the radioactivity was excreted in the first 24 hr. Radioactivity not accounted for in urinary excretion probably was excreted by some other route (*e.g.*, feces).

Based on the data given in Tables I–III, the topical bioavailability of nitroglycerin was estimated by three methods; these are summarized in Table IV. The absolute bioavailability of topical nitroglycerin, determined from the ratio of the nitroglycerin AUC values following intravenous and topical administrations, was 56.6 ± 2.5% for the three monkeys. Bioavailability determined from the ratio of the plasma carbon-14 AUC values was 77.2 ± 6.7%, and the estimate from the urinary excretion of carbon-14 was 72.7 ± 5.8%.

The difference in bioavailability estimates between unchanged nitroglycerin and total carbon-14 is the amount of nitroglycerin which is metabolized as it is absorbed through the skin (percutaneous first-pass effect). By comparison of the plasma nitroglycerin AUC with the plasma carbon-14 AUC, the estimate of first-pass percutaneous metabolism is 20.6%; by comparison to urine carbon-14 excretion, the estimate is 16%. Therefore, we can conclude that the percutaneous first-pass effect is quite small, only 16–21% depending on the method of comparison.

DISCUSSION

Yap and Fung (16) studied the pharmacokinetics of nitroglycerin in rats after intracardiac, oral, and topical administrations. Nitroglycerin had a half-life of ~4 min after intracardiac administration and showed "flip-flop" kinetics after oral administration. The oral bioavailability was

Table IV—Bioavailability of Topical Nitroglycerin[a]

Pharmacokinetic Parameter	Monkey			Mean Bioavailability[b]
	1	2	3	
Dose, mg				
Intravenous	1.92	1.92	1.93	
Topical	18.0	19.7	19.4	
Plasma nitroglycerin AUC, ng hr ml^{-1}				
Intravenous	22.35	18.48	16.60	
Topical	127.98	99.75	93.82	
Bioavailability, %	61.1	52.5	56.2	56.6 ± 2.5
Plasma total radioactivity AUC, μg hr ml^{-1}				
Intravenous	6.77	6.92	8.22	
Topical	48.65	63.32	54.44	
Bioavailability, %	76.6	89.2	65.9	77.2 ± 6.7
Urinary total radioactivity				
Intravenous, % dose excreted	60.2	46.6	53.6	
Topical, % dose excreted	39.1	32.2	45.1	
Bioavailability, %	65.0	69.1	84.1	72.7 ± 5.8

[a] Determined from the plasma nitroglycerin AUC, plasma carbon-14 AUC, and urinary excretion of carbon-14. [b] Mean ± *SEM*.

1.6%, supporting the concept of extensive first-pass metabolism (17). No detectable levels of nitroglycerin after topical administration were found (16). However, it was suggested later (18) that this may have been due to site-dependent absorption. Site-dependent absorption also occurs in the rhesus monkey and the human (19); however, this does not occur with the topical administration of nitroglycerin in the rhesus monkey (13).

In the human, information on the topical administration of nitroglycerin is limited. In one subject, nitroglycerin was not detected until 20 min after topical application (20). When the study was stopped (60 min) nitroglycerin was still detected. This suggested a sustained delivery of nitroglycerin since administration of a sublingual tablet afforded measurable plasma nitroglycerin levels at 3 min and no detectable amounts at 16 min. Maier-Lenz *et al.* (21) similarly reported that the half-life of nitroglycerin with sublingual administration was 8 min, but with topical administration a lag time of 14 min existed and measurable levels of nitroglycerin were present through a 3-hr period. Clinically, the effectiveness of topical nitroglycerin in patients with angina has been demonstrated for up to 8 hr after administration (22).

The data in this study agree with the literature reports on sublingual and topical nitroglycerin administration. Intravenously administered nitroglycerin disappeared from the blood very rapidly with a terminal half-life of 18 min. With topical administration there was a lag time of 0.5 hr with detectable levels of nitroglycerin occurring through a 24-hr period with peak levels at 4–6 hr postapplication. Topical nitroglycerin ointment can be considered a sustained-release dosage form, especially when compared with a sublingual tablet.

The pharmacokinetics of topical nitroglycerin administration are of interest since the short half-life seen with intravenous administration was not present. Instead, the plasma concentration–time curve was a broad curve with an α-phase half-life of 3 hr and a β-phase half-life of 4.3 hr. It seems reasonable that these phases of the curve are part of the complex absorption process and that any true elimination phase for nitroglycerin is lost among the absorption kinetics. It should be stated also that the AUC values following topical administration may be overestimated due to the inability to accurately calculate β. The degree of error for the total is dependent on the degree of error in β and the fraction of the total AUC composed of the fraction from 24 hr. However, this degree of error probably is small since the extrapolated area fraction involves only ~5% of the total AUC.

The absolute bioavailability of nitroglycerin following topical administration was 56.6%. There are no literature values for comparison. The mean bioavailability in male volunteers of isosorbide dinitrate from an ointment was ~30% of the bioavailability from the sublingual tablet (23). Plasma levels of isosorbide dinitrate were present up to 120 min following sublingual administration and up to 32 hr following topical administration. These estimates of 30–60% are certainly greater than the very low bioavailability estimates for oral preparations.

Nitroglycerin bioavailability measurements using the plasma AUC (total carbon-14) method were similar to those obtained by total urinary excretion of the radioactive label. Estimates from carbon-14 analysis were only 16–21% above the absolute bioavailability, a difference probably due to percutaneous first-pass effect. Use of plasma carbon-14 AUC and total urinary carbon-14 excretion to estimate percutaneous absorption has

been reported previously (24). The methods seem appropriate for estimates of transdermal absorption if a specific analytical procedure is not available and percutaneous first-pass metabolism is not extensive.

REFERENCES

(1) N. V. Kaverina and V. B. Chumburidze, *Pharmacol. Ther.*, **4**, 109 (1979).
(2) H. Ikram, *Drugs*, **18**, 130 (1979).
(3) J. R. Parratt, *Pharm. Pharmacol.*, **31**, 801 (1979).
(4) N. Reicheck, R. E. Goldstein, and S. E. Epstein, *Circulation*, **50**, (1974).
(5) R. M. Moskowitz, E. L. Kinney, and R. F. Zelis, *Chest*, **76**, 640 (1979).
(6) R. Needleman, *Ann. Intern. Med.*, **78**, 458 (1973).
(7) J. C. Krantz, and C. D. Leake, *Am. J. Cardiol.*, **36**, 407 (1975).
(8) R. C. Wester and H. I. Maibach, *Toxicol. Appl. Pharmacol.*, **32**, 394 (1975).
(9) R. C. Wester and H. I. Maibach, *J. Invest. Dermatol.*, **67**, 518 (1976).
(10) R. C. Wester, P. K. Noonan, and H. I. Maibach, *J. Soc. Cosmet. Chem.*, **30**, 297 (1979).
(11) R. C. Wester and P. K. Noonan, *Int. J. Pharmacol.*, **7**, 99 (1980).
(12) C. Lindsay, R. Feldmann, and H. I. Maibach, *Arch. Dermatol. Res.*, **257**, 89 (1976).
(13) P. I. Noonan and R. C. Wester, *J. Pharm. Sci.*, **69**, 365 (1980).
(14) P. S. K. Yap, E. F. McNiff, and H.-L. Fung, *ibid.*, **67**, 582 (1978).
(15) C. M. Metzler, G. L. Elfring, and A. J. McEwen, *Biometrics*, **30**, 562 (1974).
(16) P. S. K. Yap and H.-L. Fung, *J. Pharm. Sci.*, **67**, 584 (1978).
(17) P. Needleman, S. Lang, and E. M. Johnson, Jr., *J. Pharmacol. Exp. Ther.*, **181**, 489 (1972).
(18) S. T. Horhota and H.-L. Fung, *J. Pharm. Sci.*, **67**, 1345 (1978).
(19) R. C. Wester, P. K. Noonan, and H. I. Maibach, *Arch. Dermatol. Res.*, **267**, 229 (1980).
(20) H. P. Blumenthal, H.-L. Fung, and E. F. McNiff, *Br. J. Clin. Pharmacol.*, **4**, 241 (1977).
(21) V. H. Maier-Lenz, L. Ringwelski, and A. Windorfer, *Arzneim-Forsch. Drug Res.*, **30**, 320 (1980).
(22) M. E. Davidov and W.J. Mroczek, *Clin. Res.*, **25**, 545A (1977).
(23) D. Mansel-Jones, T. Taylor, E. Doyle, L. F. Chasseuad, A. Darrogh, D. A. O'Kelly, and H. Over, *J. Clin. Pharmacol.*, **18**, 544 (1978).
(24) R. C. Wester and P. K. Noonan, *J. Invest. Dermatol.*, **70**, 92 (1978).

ACKNOWLEDGMENTS

The authors thank Mr. Christopher Gresk for the radiolabeled nitroglycerin and Dr. Biliana Nicolova, Ms. Katherine Pilipauskas, and Ms. Mary Dal Corobbo for assistance with the animal studies.

N-Acetyl-D-Mannosamine Analogues as Potential Inhibitors of Sialic Acid Biosynthesis

ANTHONY F. HADFIELD ˣ, SHARON L. MELLA, and ALAN C. SARTORELLI

Received March 29, 1982, from the *Department of Pharmacology and Developmental Therapeutics Program, Comprehensive Cancer Center, Yale University School of Medicine, New Haven, CT 06510.* Accepted for publication June 22, 1982.

Abstract □ The 1,3,6-tri-*O*-acetyl and 1,3,6-tri-*O*-acetyl-4-*O*-mesyl analogues of *N*-acetyl-D-mannosamine and the corresponding *N*-trifluoroacetyl derivative have been synthesized, and their effects on the proliferation of Friend erythroleukemia cells in culture have been evaluated. The acetamido series showed a dependency on the 4-substituent for optimum cytotoxicity while the trifluoroacetamido series did not. Thus, the 1,3,4,6-tetra-*O*-acetyl and 1,3,6-tri-*O*-acetyl-4-*O*-mesyl analogues of *N*-acetyl-D-mannosamine were 10-fold and 42-fold more active, respectively, than 2-acetamido-1,3,6-tri-*O*-acetyl-2-deoxy-α-D-mannopyranose as inhibitors of cellular replication. The corresponding trifluoroacetamido analogues were essentially equiactive and had a potency equivalent to that of the 4-*O*-mesyl derivative in the acetamido series.

Keyphrases □ *N*-Acetyl-D-mannosamine—synthesis of acetamido and trifluoroacetamido analogues, effects on the proliferation of Friend leukemia cells □ Analogues—of *N*-acetyl-D-mannosamine, acetamido and trifluoroacetamido series, synthesis, effects on the proliferation of Friend leukemia cells □ Antileukemic agents—potential, acetamido and trifluoroacetamido analogues of *N*-acetyl-D-mannosamine, tested against Friend leukemia cells

2 - Acetamido - 1,3,4,6 - tetra - *O* - acetyl - 2 - deoxy - β-D-mannopyranose (I), the peracetylated analogue of *N*-acetyl-D-mannosamine, a metabolic precursor in the biosynthetic pathway for sialic acid (1) (Fig. 1), and the corresponding trifluoroacetamido analogue (V) were recently reported to be inhibitors of the growth of Friend erythroleukemia cells in culture (2). Both analogues were equipotent inhibitors of the incorporation of [^{3}H]*N*-acetyl-D-mannosamine into the glycoprotein-bound sialic acid of Friend erythroleukemia cells (2); however, different enzymatic sites appeared to be involved. Compound I caused an accumulation of radioactivity from [^{3}H]*N*-acetyl-D-mannosamine in *N*-acetylneuraminic acid and a decrease in cytidine monophosphate-*N*-acetylneuraminic acid in the ethanol-soluble metabolites of cells, while V caused an accumulation of [^{3}H]cytidine monophosphate-*N*-acetylneuraminic acid. In addition, both I and V produced an increase in the amount of neuraminidase-hydrolyzable sialic acid-like material on the surface of treated cells, presumably as a result of their metabolic utilization and incorporation into cellular macromolecules (3).

Since intracellular deacetylation must precede metabolism of these analogues along the sialic acid biosynthetic pathway, we presumed that I would ultimately give the noncytotoxic metabolite, *N*-acetyl-D-mannosamine; it was therefore surprising to find that I was relatively active as an inhibitor of cellular replication. Consideration of the hydroxyl groups which are required for the conversion of *N*-acetyl-D-mannosamine to *N*-acetylneuraminic acid-9-phosphate (1) (Fig. 1), reveals that such metabolic conversion only necessitates the removal of acetyl groups from the 1, 3, and 6 positions of I, thereby suggesting that the 4-*O*-acetyl group remains intact and is responsible for the

0022-3549/83/0700-0748$01.00/0

been reported previously (24). The methods seem appropriate for estimates of transdermal absorption if a specific analytical procedure is not available and percutaneous first-pass metabolism is not extensive.

REFERENCES

(1) N. V. Kaverina and V. B. Chumburidze, *Pharmacol. Ther.*, **4**, 109 (1979).
(2) H. Ikram, *Drugs*, **18**, 130 (1979).
(3) J. R. Parratt, *Pharm. Pharmacol.*, **31**, 801 (1979).
(4) N. Reicheck, R. E. Goldstein, and S. E. Epstein, *Circulation*, **50**, (1974).
(5) R. M. Moskowitz, E. L. Kinney, and R. F. Zelis, *Chest*, **76**, 640 (1979).
(6) R. Needleman, *Ann. Intern. Med.*, **78**, 458 (1973).
(7) J. C. Krantz, and C. D. Leake, *Am. J. Cardiol.*, **36**, 407 (1975).
(8) R. C. Wester and H. I. Maibach, *Toxicol. Appl. Pharmacol.*, **32**, 394 (1975).
(9) R. C. Wester and H. I. Maibach, *J. Invest. Dermatol.*, **67**, 518 (1976).
(10) R. C. Wester, P. K. Noonan, and H. I. Maibach, *J. Soc. Cosmet. Chem.*, **30**, 297 (1979).
(11) R. C. Wester and P. K. Noonan, *Int. J. Pharmacol.*, **7**, 99 (1980).
(12) C. Lindsay, R. Feldmann, and H. I. Maibach, *Arch. Dermatol. Res.*, **257**, 89 (1976).
(13) P. I. Noonan and R. C. Wester, *J. Pharm. Sci.*, **69**, 365 (1980).
(14) P. S. K. Yap, E. F. McNiff, and H.-L. Fung, *ibid.*, **67**, 582 (1978).
(15) C. M. Metzler, G. L. Elfring, and A. J. McEwen, *Biometrics*, **30**, 562 (1974).
(16) P. S. K. Yap and H.-L. Fung, *J. Pharm. Sci.*, **67**, 584 (1978).
(17) P. Needleman, S. Lang, and E. M. Johnson, Jr., *J. Pharmacol. Exp. Ther.*, **181**, 489 (1972).
(18) S. T. Horhota and H.-L. Fung, *J. Pharm. Sci.*, **67**, 1345 (1978).
(19) R. C. Wester, P. K. Noonan, and H. I. Maibach, *Arch. Dermatol. Res.*, **267**, 229 (1980).
(20) H. P. Blumenthal, H.-L. Fung, and E. F. McNiff, *Br. J. Clin. Pharmacol.*, **4**, 241 (1977).
(21) V. H. Maier-Lenz, L. Ringwelski, and A. Windorfer, *Arzneim-Forsch. Drug Res.*, **30**, 320 (1980).
(22) M. E. Davidov and W.J. Mroczek, *Clin. Res.*, **25**, 545A (1977).
(23) D. Mansel-Jones, T. Taylor, E. Doyle, L. F. Chasseuad, A. Darrogh, D. A. O'Kelly, and H. Over, *J. Clin. Pharmacol.*, **18**, 544 (1978).
(24) R. C. Wester and P. K. Noonan, *J. Invest. Dermatol.*, **70**, 92 (1978).

ACKNOWLEDGMENTS

The authors thank Mr. Christopher Gresk for the radiolabeled nitroglycerin and Dr. Biliana Nicolova, Ms. Katherine Pilipauskas, and Ms. Mary Dal Corobbo for assistance with the animal studies.

N-Acetyl-D-Mannosamine Analogues as Potential Inhibitors of Sialic Acid Biosynthesis

ANTHONY F. HADFIELD ˣ, SHARON L. MELLA, and ALAN C. SARTORELLI

Received March 29, 1982, from the *Department of Pharmacology and Developmental Therapeutics Program, Comprehensive Cancer Center, Yale University School of Medicine, New Haven, CT 06510.* Accepted for publication June 22, 1982.

Abstract □ The 1,3,6-tri-*O*-acetyl and 1,3,6-tri-*O*-acetyl-4-*O*-mesyl analogues of *N*-acetyl-D-mannosamine and the corresponding *N*-trifluoroacetyl derivative have been synthesized, and their effects on the proliferation of Friend erythroleukemia cells in culture have been evaluated. The acetamido series showed a dependency on the 4-substituent for optimum cytotoxicity while the trifluoroacetamido series did not. Thus, the 1,3,4,6-tetra-*O*-acetyl and 1,3,6-tri-*O*-acetyl-4-*O*-mesyl analogues of *N*-acetyl-D-mannosamine were 10-fold and 42-fold more active, respectively, than 2-acetamido-1,3,6-tri-*O*-acetyl-2-deoxy-α-D-mannopyranose as inhibitors of cellular replication. The corresponding trifluoroacetamido analogues were essentially equiactive and had a potency equivalent to that of the 4-*O*-mesyl derivative in the acetamido series.

Keyphrases □ *N*-Acetyl-D-mannosamine—synthesis of acetamido and trifluoroacetamido analogues, effects on the proliferation of Friend leukemia cells □ Analogues—of *N*-acetyl-D-mannosamine, acetamido and trifluoroacetamido series, synthesis, effects on the proliferation of Friend leukemia cells □ Antileukemic agents—potential, acetamido and trifluoroacetamido analogues of *N*-acetyl-D-mannosamine, tested against Friend leukemia cells

2 - Acetamido - 1,3,4,6 - tetra - *O* - acetyl - 2 - deoxy - β-D-mannopyranose (I), the peracetylated analogue of *N*-acetyl-D-mannosamine, a metabolic precursor in the biosynthetic pathway for sialic acid (1) (Fig. 1), and the corresponding trifluoroacetamido analogue (V) were recently reported to be inhibitors of the growth of Friend erythroleukemia cells in culture (2). Both analogues were equipotent inhibitors of the incorporation of [^{3}H]*N*-acetyl-D-mannosamine into the glycoprotein-bound sialic acid of Friend erythroleukemia cells (2); however, different enzymatic sites appeared to be involved. Compound I caused an accumulation of radioactivity from [^{3}H]*N*-acetyl-D-mannosamine in *N*-acetylneuraminic acid and a decrease in cytidine monophosphate-*N*-acetylneuraminic acid in the ethanol-soluble metabolites of cells, while V caused an accumulation of [^{3}H]cytidine monophosphate-*N*-acetylneuraminic acid. In addition, both I and V produced an increase in the amount of neuraminidase-hydrolyzable sialic acid-like material on the surface of treated cells, presumably as a result of their metabolic utilization and incorporation into cellular macromolecules (3).

Since intracellular deacetylation must precede metabolism of these analogues along the sialic acid biosynthetic pathway, we presumed that I would ultimately give the noncytotoxic metabolite, *N*-acetyl-D-mannosamine; it was therefore surprising to find that I was relatively active as an inhibitor of cellular replication. Consideration of the hydroxyl groups which are required for the conversion of *N*-acetyl-D-mannosamine to *N*-acetylneuraminic acid-9-phosphate (1) (Fig. 1), reveals that such metabolic conversion only necessitates the removal of acetyl groups from the 1, 3, and 6 positions of I, thereby suggesting that the 4-*O*-acetyl group remains intact and is responsible for the

0022-3549/83/0700-0748$01.00/0

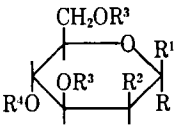

I: R = H, R^1 = $OCOCH_3$, R^2 = $NHCOCH_3$, R^3 = R^4 = $COCH_3$
II: R = $OCOCH_3$, R^1 = H, R^2 = $NHCOCH_3$, R^3 = $COCH_3$, R^4 = H
III: R = $OCOCH_3$, R^1 = H, R^2 = $NHCOCH_3$, R^3 = $COCH_3$, R^4 = SO_2CH_3
VI: R = $OCOCH_3$, R^1 = H, R^2 = CF_3CONH, R^3 = $COCH_3$, R^4 = H
VII: R = $OCOCH_3$, R^1 = H, R^2 = CF_3CONH, R^3 = $COCH_3$, R^4 = SO_2CH_3

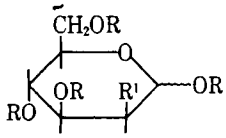

IV: R = H, R^1 = CF_3CONH
V: R = $COCH_3$, R^1 = CF_3CONH

biological and biochemical effects of this agent in erythroleukemia cells. In an effort to gain evidence to support these conclusions, the preparation and evaluation of the cytotoxicity in Friend erythroleukemia cells of 2-acetamido-1,3,6-tri-*O*-acetyl-2-deoxy-α-D-mannopyranose (II), 1,3,6-tri-*O*-acetyl-2-deoxy-2-trifluoroacetamido-α-D-mannopyranose (VI), and their corresponding 4-*O*-mesylates (III and VII) was undertaken.

BACKGROUND

The carbohydrates present on mammalian cell surfaces exist as components of glycolipid, glycoprotein, and glycosaminoglycan macromolecules, which collectively participate in functional properties such as adhesion, cellular interactions, and immunological phenomena (4). In recent years, studies directed at the surface properties of neoplastic cells have highlighted many structural and functional differences between tumor cells and their normal counterparts (5). Although no universal property characteristic of malignancy has resulted from such studies, they have stimulated drug design targeted at the neoplastic cell membrane (6). Of the various cell-surface components, sialic acid (7) is of special interest, since it appears to be involved in fundamental properties of neoplastic cells such as the capacity to metastasize (8–10).

Elevated levels of sialyltransferase activity (11, 12) and cell surface-bound sialic acid (13, 14) have been reported in some transformed cell lines in culture. Although such changes have not been observed uniformly, elevated levels of sialic acid and sialyltransferase activity have been reported in the serum of animals (15–17) and humans (16, 18–20) bearing malignant neoplasms, and a variety of human lung carcinomas also have been shown to contain higher levels of protein-bound sialic acid than corresponding normal tissue (21). Since drugs that are capable of altering the synthesis, and thereby the content, of cell surface sialic acid-containing macromolecules may have utility as therapeutic agents, analogues of *N*-acetyl-D-mannosamine (a biosynthetic precursor of sialic acid) have been prepared.

EXPERIMENTAL[1]

Methods—All evaporations were performed under reduced pressure, and melting points[2] were uncorrected. Column chromatography[3] and TLC[4] were performed on silica gel, the latter being developed by heating after the application of an ethanol–5% sulfuric acid spray. ^{1}H-NMR spectra[5] were run in deuterochloroform. Petroleum ether refers to a fraction having a bp of 35–60°.

2-Acetamido-1,3,6-tri-O-acetyl-2-deoxy-α-D-mannopyranose (II)—Aliquots of acetyl chloride were added to a solution of *N*-acetyl-β-D-mannosamine·H_2O (1 g, 4.5 mmoles) in pyridine (15 ml) at room temperature. The reaction was monitored by TLC (chloroform–methanol, 9:1, v/v) until optimal conversion to an anomeric mixture of tri-*O*-acetyl derivatives was obtained. Toluene was added and the mixture was evaporated under reduced pressure. The residue was chromatographed on silica gel (chloroform–methanol, 97.5:2.5) to give a mixture of tri-*O*-acetyl derivatives (0.51 g, 33%) which showed as three major spots on TLC. This material was crystallized from acetone–petroleum ether to give II (0.19 g, 12%), mp 216–217° (dec), $[\alpha]_D^{23}$ − 63° (*c* 1, methanol); ^{1}H-NMR[6]: δ 5.84 (d, 1, $J_{1,2}$ 1.5 Hz, H-1), 5.76 (d, 1, $J_{2,NH}$ 9.1 Hz, NH), 4.90 (dd, 1, $J_{2,3}$ 4.0, $J_{3,4}$ 9.5 Hz, H-3), 4.73 (m, 1, H-2), 4.52 (dd, 1, $J_{5,6}$ 4.1, $J_{6,6'}$ −12.2 Hz, H-6), 4.30 (dd, 1, $J_{5,6'}$ 1.6 Hz, H-6'), 3.76–3.63 (m, 2, H-4, H-5), 2.80 (d, 1, $J_{4,OH}$ 3.7 Hz, OH), 2.14 (3, $NHCOCH_3$), 2.10, 2.08, 2.07 (9H, $OCOCH_3$).

Anal.—Calc. for $C_{14}H_{21}NO_9$: C, 48.41; H, 6.05; N, 4.03. Found: C, 48.29; H, 6.22; N, 4.25.

2-Acetamido-1,3,6-tri-O-acetyl-2-deoxy-4-O-mesyl-α-D-mannopyranose (III)—Methanesulfonyl chloride (0.05 g, 0.44 mmole) was added to a solution of II (0.1 g, 0.29 mmole) in pyridine (5 ml) cooled to −10°. The mixture was allowed to stand at room temperature overnight, after which time TLC (chloroform–methanol, 9:1, v/v) indicated a new product. Toluene was added and the mixture was then evaporated under reduced pressure. The residue was chromatographed on silica gel to afford the 4-mesylate III, (chloroform–methanol, 49:1) as a syrup (0.1 g, 82%), $[\alpha]_D^{23}$ − 18.9° (c 1, chloroform); ^{1}H-NMR[6]: δ 5.86 (d, 1, $J_{1,2}$ 1.8 Hz, H-1), 5.81 (d, 1, $J_{2,NH}$ 8.8 Hz, NH), 5.14 (dd, 1, $J_{2,3}$ 4.1, $J_{3,4}$ 9.9 Hz, H-3), 4.82–4.75 (m, 2, H-2, H-4), 4.45 (dd, 1, $J_{5,6}$ 4.4, $J_{6,6'}$ −12.4 Hz, H-6), 4.25 (dd, 1, $J_{5,6'}$ 2.2 Hz, H-6'), 3.86 (m, 1, $J_{4,5}$ 9.5 Hz, H-5), 3.07 (OSO_2CH_3), 2.11, 2.10, 2.05 (12, $NHCOCH_3$, $OCOCH_3$).

Anal.—Calc. for $C_{15}H_{23}NO_{11}S$: C, 42.35; H, 5.41; N, 3.29; S, 7.53. Found: C, 42.10; H, 5.68; N, 3.02; S, 7.74.

2-Deoxy-2-trifluoroacetamido-D-mannopyranose (IV)—A solution of methanol (5 ml) and ethyl trifluoroacetate (1 ml) was added to a mixture of D-mannosamine hydrochloride[7] (0.5 g, 2.3 mmoles) and sodium carbonate (0.25 g). The reaction was shown by TLC (ethyl acetate–methanol, 4:1, v/v) to be essentially complete after 2–3 hr. The mixture was evaporated with silica gel and applied to a dry-packed column of silica gel. Elution with chloroform–methanol (9:1, v/v) afforded IV (0.44 g, 69%) as an immobile syrup, $[\alpha]_D^{23}$ + 19° (c 1, methanol).

Anal.—Calc. for $C_8H_{12}F_3NO_6$: C, 34.91; H, 4.36; N, 5.09; F, 18.54. Found: C, 35.13; H, 4.67; N, 4.89; F, 18.16.

1,3,6-Tri-O-acetyl-2-deoxy-2-trifluoroacetamido-α-D-mannopyranose (VI)—Acetyl chloride was added to a solution of IV (2.83 g, 7.1 mmoles) in pyridine (180 ml) at room temperature. The reaction was conducted and processed as described for the preparation of II. Chromatography of the mixture of products on silica gel (chloroform), afforded the anomeric mixture of tri-*O*-acetyl derivatives (0.88 g, 21.2%) from which VI (0.22 g, 5.3%) was obtained on crystallization from ether, mp

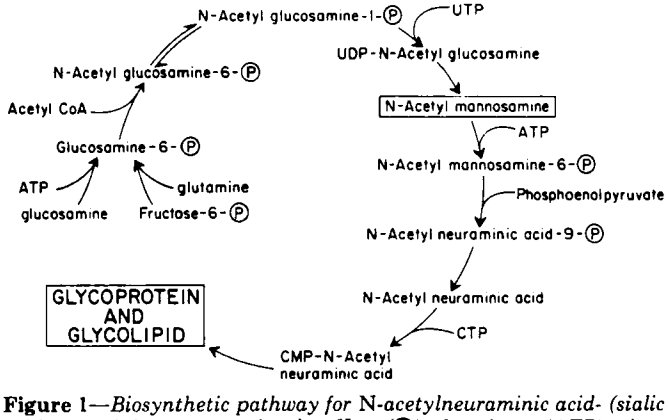

Figure 1—*Biosynthetic pathway for* N-*acetylneuraminic acid- (sialic acid) containing macromolecules. Key: (Ⓟ) phosphate; (ATP) adenosine triphosphate; (UTP) uridine triphosphate; (UDP) uridine diphosphate; (CTP) cytidine triphosphate; (CMP) cytidine monophosphate.*

[1] Elemental analyses and optical rotations were performed by Baron Consulting Co., Orange, Conn.
[2] Thomas-Hoover capillary melting point apparatus.
[3] Silica gel 60 (70–230 mesh), EM Laboratories, Inc., Elmsford, NY 10523.
[4] Silica gel GF, 250-μm layer prescored 10 × 20-cm plates, Analtech, Inc., Newark, DE 19711.
[5] 270-MHz Bruker HX-270 spectrometer.
[6] The proton at C-6 giving a higher field signal is designated H-6'.
[7] Sigma Chemical Co., St. Louis, MO 63178.

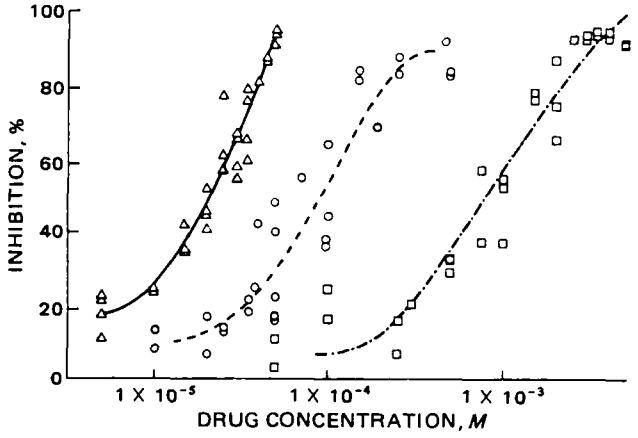

Figure 2—*Effects of* N-*acetyl-*D-*mannosamine analogues on the proliferation of Friend erythroleukemia cells. Key: (---) I, ID_{50} ~9 × 10^{-5} M; (-·-) II, ID_{50} ~8.5 × 10^{-4} M; (—) III, ID_{50} ~2 × 10^{-5} M.

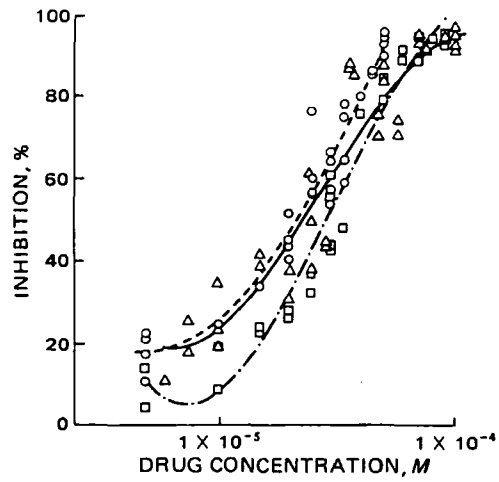

Figure 3—*Effects of* N-*trifluoroacetamido-*D-*mannosamine analogues on the proliferation of Friend erythroleukemia cells. Key: (---) VII, ID_{50} ~2 × 10^{-5} M; (—) V, ID_{50} ~2 × 10^{-5} M; (-·-) VI, ID_{50} ~3 × 10^{-5} M.

148–150°, $[\alpha]_D^{23}$ + 36° (c 1, methanol); ^{1}H-NMR[6]: δ 6.49 (d, 1, $J_{2,NH}$ 8.8 Hz, NH), 6.07 (d, 1, $J_{1,2}$ 1.8 Hz, H-1), 5.24 (dd, 1, $J_{2,3}$ 4.4, $J_{3,4}$ 9.9 Hz, H-3), 4.62 (m, 1, H-2), 4.55 (dd, 1, $J_{5,6}$ 4.0, $J_{6,6}$ −12.4 Hz, H-6), 4.25 (dd, 1, $J_{5,6'}$ 2.4 Hz, H-6'), 3.97 (m, 1, H-5), 3.74 (td, 1, $J_{4,5}$ 9.9 Hz, H-4), 2.86 (d, 1, $J_{4,OH}$ 4.4 Hz, OH), 2.20, 2.14, 2.08 (9, $OCOCH_3$).

Anal.—Calc. for $C_{14}H_{18}F_3NO_9$: C, 41.90; H, 4.49; N, 3.49; F, 14.21. Found: C, 41.78; H, 4.68; N, 3.37; F, 13.92.

*1,3,6-Tri-*O*-acetyl-2-deoxy-2-trifluoroacetamido-4-*O*-mesyl-α-*D*-mannopyranose (VII)*—Methanesulfonyl chloride (0.22 g) was added to a solution of VI (0.25 g, 0.52 mmole) in pyridine (2.5 ml) cooled to −10°. The mixture was allowed to stand at room temperature overnight, when TLC (chloroform) indicated completion. The mixture was processed as described for III; the product was chromatographed on silica gel (chloroform–petroleum ether 3:1, v/v) to afford VII as a syrup (0.275 g, 93%), $[\alpha]_D^{23}$ + 68.3 (c 1, chloroform); ^{1}H-NMR[6]: δ 6.79 (d, 1, $J_{2,NH}$ 8.8 Hz, NH), 6.12 (d, 1, $J_{1,2}$ 2.2 Hz, H-1), 5.48 (dd, 1, $J_{2,3}$ 4.4, $J_{3,4}$ 10.3 Hz, H-3), 4.88 (t, 1, $J_{4,5}$ 9.9 Hz, H-4), 4.67 (m, 1, H-2), 4.47 (dd, 1, $J_{5,6}$ 4.0, $J_{6,6'}$ −12.4 Hz, H-6), 4.23 (dd, 1, $J_{5,6'}$ 2.2 Hz, H-6'), 4.14 (m, 1, H-5), 3.08 (3H, OSO_2CH_3), 2.18, 2.13, 2.09 (9H, $OCOCH_3$).

Anal.—Calc. for $C_{15}H_{20}F_3NO_{11}S$: C, 37.58; H, 4.80; N, 2.92; S, 6.68; F, 11.90. Found: C, 37.79; H, 4.38; N, 3.30; S, 6.38; F, 11.89.

Assay of Cytotoxic Activity in Cell Culture—Friend erythroleukemia cells were grown at 37° in a suspension culture of Dulbecco's modified Eagle's medium containing 15% fetal calf serum and 0.02 m*M* glutamine. Exponentially growing Friend cells were seeded in 25-cm² plastic culture flasks at 1 × 10^5 cells/ml in 5 ml of medium. The test substance at various concentrations in phosphate-buffered saline was added at time zero, and the cells were incubated for 48 hr. The total number of cells in each of duplicate flasks was determined for the three separate experiments with a particle counter[8].

RESULTS AND DISCUSSION

In an effort to determine whether the biological properties of 2-acetamido-1,3,4,6-tetra-*O*-acetyl-2-deoxy-β-D-mannopyranose (I) were related to the presence of a more stable 4-*O*-acetyl group relative to the other acetyl groups and, in addition, to ascertain whether this substituent is also involved in the cytotoxic action of the trifluoroacetamido analogue (V), 2-acetamido-1,3,6-tri-*O*-acetyl-2-deoxy-α-D-mannopyranose (II), 1,3,6-tri-*O*-acetyl-2-deoxy-2-trifluoroacetamido-α-D-mannopyranose (VI), and their corresponding 4-*O*-mesylates (III) and (VII) were prepared and evaluated for their cytotoxicity in culture. It was speculated that removal of the 4-*O*-acetyl group from I to give II would result in a significant reduction in the cytotoxic properties in culture, while substitution of the 4-*O*-mesyl group, which is structurally similar and might be expected to be relatively more resistant to enzymatic hydrolysis, would result in greater activity than I.

The synthesis of trifluoroacetamido derivatives has been reported utilizing a variety of reagents, including ethyl trifluoroacetate (22, 23), trifluoroacetyl triflate (24), and trichlorotrifluoroacetone (25). *S*-Ethyl trifluorothioacetate (26) and trifluoroacetic anhydride (27–30) have been used previously in the synthesis of amino sugar nucleosides, in which the trifluoroacetyl moiety served as an *N*-blocking group. Accordingly, treatment of D-mannosamine hydrochloride with ethyl trifluoroacetate in methanol in the presence of sodium carbonate afforded 2-deoxy-2-trifluoroacetamido-D-mannopyranose (IV) as an immobile syrup in 69% yield. Compounds II and VII were prepared by a selective reaction involving treatment of *N*-acetyl-β-D-mannosamine and IV in pyridine with acetyl chloride until an optimum conversion to a triacetylated mixture was apparent. These products were purified by silica gel column chromatography, to afford anomeric mixtures of triacetylated derivatives from which the appropriate α-anomers II and VII were crystallized in 12% and 5.3% yields, respectively.

The structures of the analogues were confirmed by ^{1}H-NMR spectroscopy. The $J_{1,2}$ coupling constants for II and VI were 1.5 and 1.8 Hz, respectively, indicating the α-configuration (31). The signals due to H-4 coincided with H-5 (δ 3.76–3.63) in II and appeared at 3.74 in VI, essentially resonating at a higher field when compared with the other ring protons (as would be expected). Doublets at δ 2.80 in II and δ 2.86 in VI were assigned to the OH groups at H-4, since addition of deuterium oxide caused the signals to collapse while the triplet of doublets due to H-4 in VI reverted to a triplet. Further treatment of II and VII with methanesulfonyl chloride in pyridine afforded mesylates (III) and (VII) as syrupy products. The ^{1}H-NMR spectra of III and VII both showed shifts of their H-4 resonance signals to lower field in comparison with II and VI, respectively, while three proton singlets at δ 3.07 in II and δ 3.08 in VII were assigned to the mesyl groups.

Compounds I–III and V–VII were tested for their ability to inhibit the growth of Friend erythroleukemia cells in culture. The tetraacetate (I) had an ID_{50}[9] of ~9 × 10^{-5} *M*, while that of II and III were ~8.5 × 10^{-4} *M* and 2 × 10^{-5} *M*, respectively (Fig. 2). In contrast, the trifluoroacetamido analogues V, VI, and VII all gave similar ID_{50} values of 2–3 × 10^{-5} *M* (Fig. 3)[10]. The triacetate (II) is, therefore, 10-fold less active than I, while the 4-*O*-mesylate (III) is at least fourfold more active. These findings support the conclusion that the 4-*O*-acetyl and 4-*O*-mesyl groups play an important role in the cytotoxic properties of these compounds. The finding of similar activity for analogues in the trifluoroacetamido series (V–VII) implies that the biological properties of these compounds are due predominantly to the trifluoroacetamido moiety and are independent of substituents at the 4-position.

REFERENCES

(1) E. J. McGuire, "Biological Roles of Sialic Acid," A. Rosenberg and C. L. Schengrund, Eds., Plenum, New York, N.Y., 1976, Chap. 4, p. 123.

(2) E. L. Schwartz, A. F. Hadfield, A. E. Brown, and A. C. Sartorelli, *Fed. Proc. Fed. Am. Soc. Exp. Biol.*, **39**, 2003 (1980).

(3) A. F. Hadfield, E. L. Schwartz, S. L. Mella, and A. C. Sartorelli, CARB 26, 180th ACS Meeting, Las Vegas, Nevada (1980).

[8] Model ZBI particle counter, Coulter Electronics, Hialeah, Fla.

[9] The ID_{50} is the concentration necessary to inhibit cell replication by 50%.

[10] Compound IV was inactive up to a concentration of 10^{-3} *M*.

(4) K. W. Talmadge and M. M. Burger, *MTP Int. Rev. Sci.: Biochem., Ser. One*, **5**, 43 (1975).
(5) G. L. Nicolson, *Biochim. Biophys. Acta*, **458**, 1 (1976).
(6) R. Bernacki, C. Porter, W. Korytnyk, and E. Mihich, *Adv. Enzyme Reg.*, **16**, 215 (1978).
(7) C. W. Lloyd, *Biol. Rev.*, **50**, 325 (1975).
(8) H. B. Bosmann, G. F. Bieber, A. E. Brown, K. R. Case, D. M. Gersten, T. W. Kimmerer, and A. Lione, *Nature (London)*, **246**, 487 (1973).
(9) G. Yogeeswaran, B. S. Stein, and H. Sebastian, *Cancer Res.*, **38**, 1336 (1978).
(10) G. Yogeeswaran and T.-W. Tao, *Biochem. Biophys. Res. Commun.*, **95**, 1452 (1980).
(11) L. Warren, J. P. Fuhrer, and C. A. Buck, *Proc. Natl. Acad. Sci. USA*, **69**, 1838 (1972).
(12) L. Warren, J. P. Fuhrer, and C. A. Buck, *Fed. Proc. Fed. Am. Soc. Exp. Biol.*, **32**, 80 (1973).
(13) W. P. van Beek, L. A. Smets, and P. Emmelot, *Cancer Res.*, **33**, 2913 (1973).
(14) L. Warren, C. A. Buck, and G. P. Tuszynski, *Biochim. Biophys. Acta*, **516**, 97 (1978).
(15) H. B. Bosmann, A. C. Spataro, M. W. Myers, R. J. Bernacki, M. J. Hillman, and S. E. Caputi, *Res. Commun. Chem. Pathol. Pharmacol.*, **12**, 499 (1975).
(16) T. M. Kloppel, T. W. Keenan, M. J. Freeman, and D. J. Morre, *Proc. Natl. Acad. Sci. USA*, **74**, 3011 (1977).
(17) R. J. Bernacki and U. Kim, *Science*, **195**, 577 (1977).
(18) T. P. Waalkes, J. E. Mrochek, S. R. Dinsmore, and D. C. Tormey, *J. Natl. Cancer Inst.*, **61**, 703 (1978).
(19) H. K. B. Silver, D. M. Rangel, and D. L. Morton, *Cancer*, **41**, 1497 (1978).
(20) A. Lipton, H. A. Harvey, S. Delong, J. Allegra, D. While, M. Allegra, and E. A. Davidson, *ibid.*, **43**, 1766 (1979).
(21) M. L. Bryant, G. D. Stoner, and R. P. Metzger, *Biochim. Biophys. Acta*, **343**, 226 (1974).
(22) M. M. Joullie, *J. Am. Chem. Soc.*, **77**, 6662 (1955).
(23) A. C. Pierce and M. M. Joullie, *J. Org. Chem.*, **28**, 658 (1963).
(24) T. R. Forbus, Jr. and J. C. Martin, *ibid.*, **44**, 313 (1979).
(25) C. A. Panetta and T. G. Casanova, *ibid.*, **35**, 4275 (1970).
(26) M. L. Wolfrom and P. J. Conigliaro, *Carbohydr. Res.*, **11**, 63 (1969).
(27) M. L. Wolfrom and H. B. Bhat, *J. Chem. Soc. Chem. Commun.*, **1966**, 146.
(28) M. L. Wolfrom and H. B. Bhat, *J. Org. Chem.*, **32**, 1821 (1967).
(29) M. L. Wolfrom, H. B. Bhat, and P. J. Conigliaro, *Carbohydr. Res.*, **20**, 375 (1971).
(30) H. G. Garg and R. W. Jeanloz, *ibid.*, **62**, 185 (1978).
(31) A. DeBruyn and M. Anteunis, *Org. Magn. Reson.*, **8**, 228 (1976).

ACKNOWLEDGMENTS

This research was supported in part by U.S. Public Health Service Grants CA-02817 and CA-16357 from the National Cancer Institute.

High-Performance Liquid Chromatographic Determination of Pralidoxime Chloride and Its Major Decomposition Products in Injectable Solutions

DAVID G. PRUE ˣ, RAYMOND N. JOHNSON, and BOEN T. KHO

Received April 23, 1982, from *Ayerst Laboratories, Inc., Rouses Point, NY 12979.* Accepted for publication June 22, 1982.

Abstract □ A high-performance liquid chromatographic (HPLC) method for the simultaneous determination of pralidoxime chloride (I) and its major decomposition products in an injectable formulation is described. I and its decomposition products were detected and quantitated by their UV absorbances at 270 nm, after being separated from related compounds and formulation excipients on a reverse-phase C-18 column using a mobile phase consisting of 52% acetonitrile and 48% of an aqueous solution containing 0.005 *M* phosphoric acid and 0.001 *M* tetraethylammonium chloride. The major decomposition products of I in the injectable formulation were identified by their retention times and stop-flow spectroscopy as 2-carboxy-*N*-methylpyridinium chloride, *N*-methyl-2-pyridone, 2-carbamoyl-*N*-methylpyridinium chloride, 2-hydroxymethyl-*N*-methylpyridinium chloride, and 2-cyano-*N*-methylpyridinium chloride. A substance of unknown identity also was detected in degraded solutions of I. Stop-flow spectroscopy, employing the spectral discrimination technique, showed that the method is specific for I. Recovery of I from a spiked placebo formulation averaged 99.9%. The accuracy of the method was also demonstrated for the decomposition products over a range of concentrations representing 1–50% decomposition. Replicate determinations of I in degraded solutions gave coefficients of variation of 1.0 and 1.5%, while the precision of determining the decomposition products range from 1.3 to 6.5%. Regression lines with correlation coefficients >0.9999 were obtained for I and its decomposition products, and solutions of these compounds were shown to be stable in the mobile phase for several days. Results for I by the HPLC and USP procedures are compared.

Keyphrases □ Pralidoxime chloride—decomposition products in aqueous solutions, concurrent high-performance liquid chromatographic determination □ High-performance liquid chromatography—concurrent determination of pralidoxime chloride and its decomposition products in aqueous solutions, comparison to USP procedure □ Degradation products—of pralidoxime chloride, concurrent high-performance liquid chromatographic determination

Pralidoxime chloride, 2-[(hydroxyimino)methyl]-1-methylpyridinium chloride (I), is a reactivator of organophosphate-inhibited cholinesterase. It has therapeutic value as an antidote to poisoning by organophosphate agricultural chemicals, chemical warfare agents, and drugs acting as cholinesterase inhibitors. Compound I is typically formulated as an aqueous injectable solution which is administered intramuscularly immediately after the onset of anticholinesterase poisoning.

Unfortunately, aqueous solutions of the various salts of pralidoxime have been shown to be unstable. The instability of pralidoxime in both acidic and basic media was first described in a series of reports (1–4) which proposed the existence of several decomposition products of pralidoxime iodide: the iodide salts of the 2-carboxy-, 2-formyl-, 2-carbamoyl-, and 2-cyano-*N*-methylpyridinium ions and *N*-methyl-2-pyridone. In addition, two major decomposition products were detected in solutions of pralidoxime

0022-3549/83/0700-0751$01.00/0

(4) K. W. Talmadge and M. M. Burger, *MTP Int. Rev. Sci.: Biochem., Ser. One*, **5**, 43 (1975).
(5) G. L. Nicolson, *Biochim. Biophys. Acta*, **458**, 1 (1976).
(6) R. Bernacki, C. Porter, W. Korytnyk, and E. Mihich, *Adv. Enzyme Reg.*, **16**, 215 (1978).
(7) C. W. Lloyd, *Biol. Rev.*, **50**, 325 (1975).
(8) H. B. Bosmann, G. F. Bieber, A. E. Brown, K. R. Case, D. M. Gersten, T. W. Kimmerer, and A. Lione, *Nature (London)*, **246**, 487 (1973).
(9) G. Yogeeswaran, B. S. Stein, and H. Sebastian, *Cancer Res.*, **38**, 1336 (1978).
(10) G. Yogeeswaran and T.-W. Tao, *Biochem. Biophys. Res. Commun.*, **95**, 1452 (1980).
(11) L. Warren, J. P. Fuhrer, and C. A. Buck, *Proc. Natl. Acad. Sci. USA*, **69**, 1838 (1972).
(12) L. Warren, J. P. Fuhrer, and C. A. Buck, *Fed. Proc. Fed. Am. Soc. Exp. Biol.*, **32**, 80 (1973).
(13) W. P. van Beek, L. A. Smets, and P. Emmelot, *Cancer Res.*, **33**, 2913 (1973).
(14) L. Warren, C. A. Buck, and G. P. Tuszynski, *Biochim. Biophys. Acta*, **516**, 97 (1978).
(15) H. B. Bosmann, A. C. Spataro, M. W. Myers, R. J. Bernacki, M. J. Hillman, and S. E. Caputi, *Res. Commun. Chem. Pathol. Pharmacol.*, **12**, 499 (1975).
(16) T. M. Kloppel, T. W. Keenan, M. J. Freeman, and D. J. Morre, *Proc. Natl. Acad. Sci. USA*, **74**, 3011 (1977).
(17) R. J. Bernacki and U. Kim, *Science*, **195**, 577 (1977).
(18) T. P. Waalkes, J. E. Mrochek, S. R. Dinsmore, and D. C. Tormey, *J. Natl. Cancer Inst.*, **61**, 703 (1978).
(19) H. K. B. Silver, D. M. Rangel, and D. L. Morton, *Cancer*, **41**, 1497 (1978).
(20) A. Lipton, H. A. Harvey, S. Delong, J. Allegra, D. While, M. Allegra, and E. A. Davidson, *ibid.*, **43**, 1766 (1979).
(21) M. L. Bryant, G. D. Stoner, and R. P. Metzger, *Biochim. Biophys. Acta*, **343**, 226 (1974).
(22) M. M. Joullie, *J. Am. Chem. Soc.*, **77**, 6662 (1955).
(23) A. C. Pierce and M. M. Joullie, *J. Org. Chem.*, **28**, 658 (1963).
(24) T. R. Forbus, Jr. and J. C. Martin, *ibid.*, **44**, 313 (1979).
(25) C. A. Panetta and T. G. Casanova, *ibid.*, **35**, 4275 (1970).
(26) M. L. Wolfrom and P. J. Conigliaro, *Carbohydr. Res.*, **11**, 63 (1969).
(27) M. L. Wolfrom and H. B. Bhat, *J. Chem. Soc. Chem. Commun.*, **1966**, 146.
(28) M. L. Wolfrom and H. B. Bhat, *J. Org. Chem.*, **32**, 1821 (1967).
(29) M. L. Wolfrom, H. B. Bhat, and P. J. Conigliaro, *Carbohydr. Res.*, **20**, 375 (1971).
(30) H. G. Garg and R. W. Jeanloz, *ibid.*, **62**, 185 (1978).
(31) A. DeBruyn and M. Anteunis, *Org. Magn. Reson.*, **8**, 228 (1976).

ACKNOWLEDGMENTS

This research was supported in part by U.S. Public Health Service Grants CA-02817 and CA-16357 from the National Cancer Institute.

High-Performance Liquid Chromatographic Determination of Pralidoxime Chloride and Its Major Decomposition Products in Injectable Solutions

DAVID G. PRUE ˣ, RAYMOND N. JOHNSON, and BOEN T. KHO

Received April 23, 1982, from *Ayerst Laboratories, Inc., Rouses Point, NY 12979.* Accepted for publication June 22, 1982.

Abstract □ A high-performance liquid chromatographic (HPLC) method for the simultaneous determination of pralidoxime chloride (I) and its major decomposition products in an injectable formulation is described. I and its decomposition products were detected and quantitated by their UV absorbances at 270 nm, after being separated from related compounds and formulation excipients on a reverse-phase C-18 column using a mobile phase consisting of 52% acetonitrile and 48% of an aqueous solution containing 0.005 *M* phosphoric acid and 0.001 *M* tetraethylammonium chloride. The major decomposition products of I in the injectable formulation were identified by their retention times and stop-flow spectroscopy as 2-carboxy-*N*-methylpyridinium chloride, *N*-methyl-2-pyridone, 2-carbamoyl-*N*-methylpyridinium chloride, 2-hydroxymethyl-*N*-methylpyridinium chloride, and 2-cyano-*N*-methylpyridinium chloride. A substance of unknown identity also was detected in degraded solutions of I. Stop-flow spectroscopy, employing the spectral discrimination technique, showed that the method is specific for I. Recovery of I from a spiked placebo formulation averaged 99.9%. The accuracy of the method was also demonstrated for the decomposition products over a range of concentrations representing 1–50% decomposition. Replicate determinations of I in degraded solutions gave coefficients of variation of 1.0 and 1.5%, while the precision of determining the decomposition products range from 1.3 to 6.5%. Regression lines with correlation coefficients >0.9999 were obtained for I and its decomposition products, and solutions of these compounds were shown to be stable in the mobile phase for several days. Results for I by the HPLC and USP procedures are compared.

Keyphrases □ Pralidoxime chloride—decomposition products in aqueous solutions, concurrent high-performance liquid chromatographic determination □ High-performance liquid chromatography—concurrent determination of pralidoxime chloride and its decomposition products in aqueous solutions, comparison to USP procedure □ Degradation products—of pralidoxime chloride, concurrent high-performance liquid chromatographic determination

Pralidoxime chloride, 2-[(hydroxyimino)methyl]-1-methylpyridinium chloride (I), is a reactivator of organophosphate-inhibited cholinesterase. It has therapeutic value as an antidote to poisoning by organophosphate agricultural chemicals, chemical warfare agents, and drugs acting as cholinesterase inhibitors. Compound I is typically formulated as an aqueous injectable solution which is administered intramuscularly immediately after the onset of anticholinesterase poisoning.

Unfortunately, aqueous solutions of the various salts of pralidoxime have been shown to be unstable. The instability of pralidoxime in both acidic and basic media was first described in a series of reports (1–4) which proposed the existence of several decomposition products of pralidoxime iodide: the iodide salts of the 2-carboxy-, 2-formyl-, 2-carbamoyl-, and 2-cyano-*N*-methylpyridinium ions and *N*-methyl-2-pyridone. In addition, two major decomposition products were detected in solutions of pralidoxime

0022-3549/83/0700-0751$01.00/0

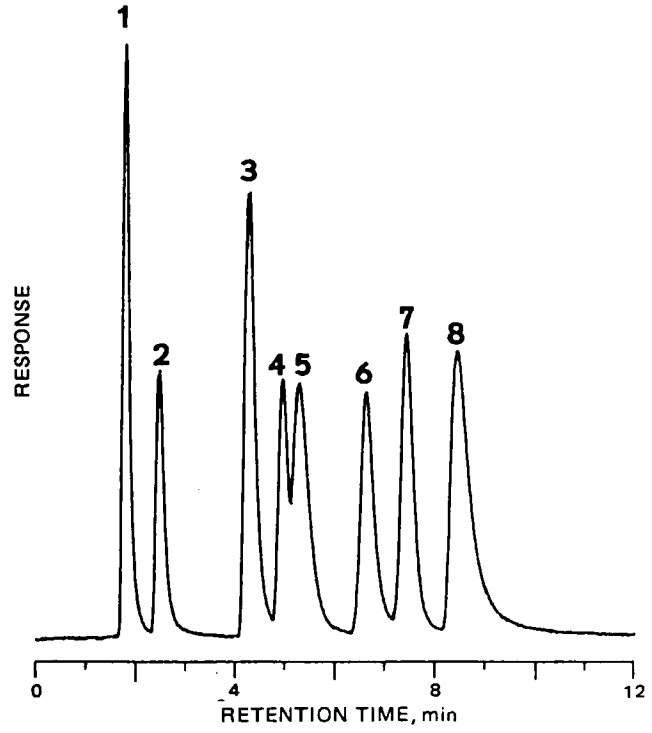

Figure 1—*Chromatogram of a synthetic mixture of I–XII. Key: (1) II, (2) III and IV, (3) V, (4) VI and VII, (5) VIII, (6) IX and X, (7) I, and (8) XI. Compound XII is not shown (retention time = 27.4 min).*

methanesulfonate (5), which were identified as the methanesulfonate salts of the 2-carbamoyl- and 2-cyano-*N*-methylpyridinium ions. The kinetics of the hydrolysis of the cyano-pyridinium ions were studied (6), and it was shown that 99.1% of the material from the alkaline hydrolysis of the 2-cyano-*N*-methylpyridinium ion could be accounted for as 2-carbamoyl-*N*-methylpyridinium ion and *N*-methyl-2-pyridone. A fluorescent product was isolated from the alkaline hydrolysis of I (7). On the basis of physical and physicochemical properties, it was concluded that this product was 2-cyano-1-methyl-4-pyridone.

Although a complete decomposition profile of I has not been described in the literature, it was anticipated that the decomposition of I would lead to the same decomposition products as reported for the corresponding iodide and methanesulfonate salts. The procedure in the USP XX (8) for determining I does not adequately separate and isolate these decomposition products before analysis. I is quantitated in the presence of its decomposition products at the UV wavelength of 336 nm, which is sensitive for I but has only minimal sensitivity for the decomposition products. A number of high-performance liquid chromatographic (HPLC) procedures (9–11) for determining pyridinium aldoximes have been reported; however, not one is suitable for studying the stability of I.

In this present study, a specific HPLC method has been developed which separates and simultaneously quantitates I and its major decomposition products. In addition, this chromatographic system separates I from its primary synthetic precursor, pyridine-2-aldoxime, and a number of other structurally related compounds. This method was used to study the stability of an injectable formulation of I and two previously unreported decomposition products were detected.

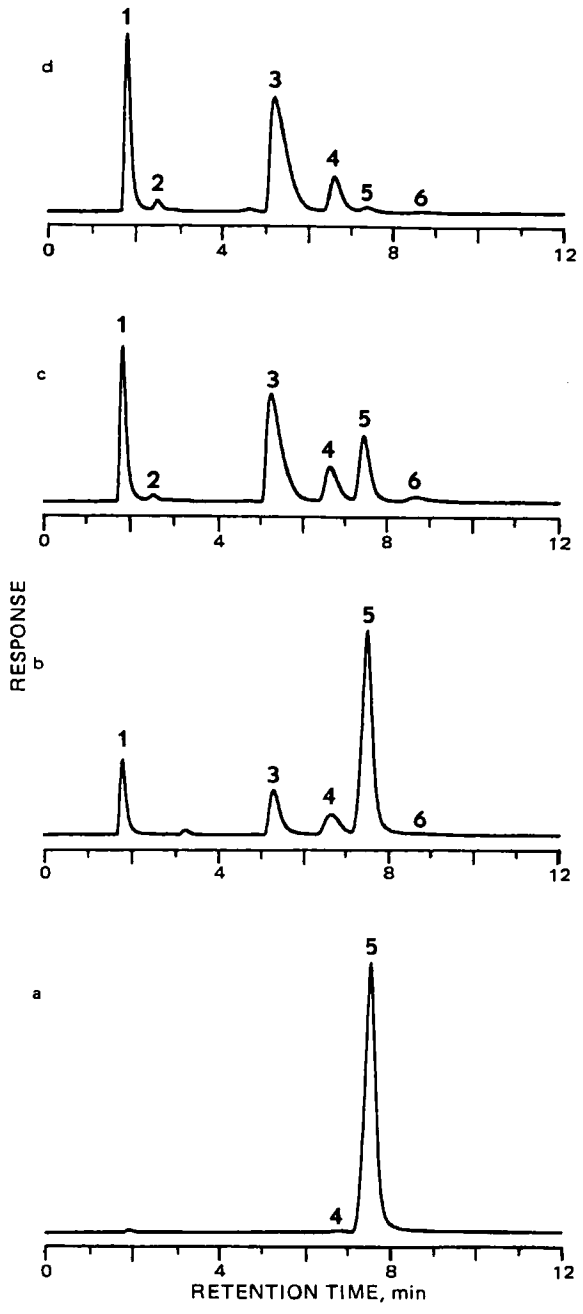

Figure 2—*Chromatograms of the injectable formulation at day zero (a) and after being stored at 80° for 2 (b), 4 (c), and 8 (d) weeks. Key: (1) II, (2) III, (3) VIII, (4) X and the unknown compound, (5) I, and (6) XI.*

EXPERIMENTAL

Reagents—Phosphoric acid[1] was reagent grade; tetraethylammonium chloride[2] was used without further purification; acetonitrile[3] was UV grade, distilled in glass. The following reference compounds were used: pralidoxime chloride[4] (I), 2-carboxy-*N*-methylpyridinium chloride[5] (II), *N*-methyl-2-pyridone[5] (III), 2-cyano-1-methyl-4-pyridone[6] (IV), pyridine-2-aldoxime[5] (V), *syn*-pralidoxime chloride[7] (VI), 2-formyl-*N*-methylpyridinium chloride[8] (VII), 2-carbamoyl-*N*-methylpyridinium

[1] Mallinckrodt Inc., Paris, Ky.
[2] Eastman Kodak Co., Rochester, N.Y.
[3] Burdick and Jackson Laboratories, Muskegon, Mich.
[4] House reference standard strength *versus* USP reference standard is 100.3%.
[5] Aldrich Chemical Co., Milwaukee, Wis.; used without further purification.
[6] Synthesized by the procedure of Spoljarić *et al.* (7).
[7] Synthesized by the procedure of Ginsburg and Wilson (12).
[8] Synthesized by the procedure of Ellin and Kondritzer (2).

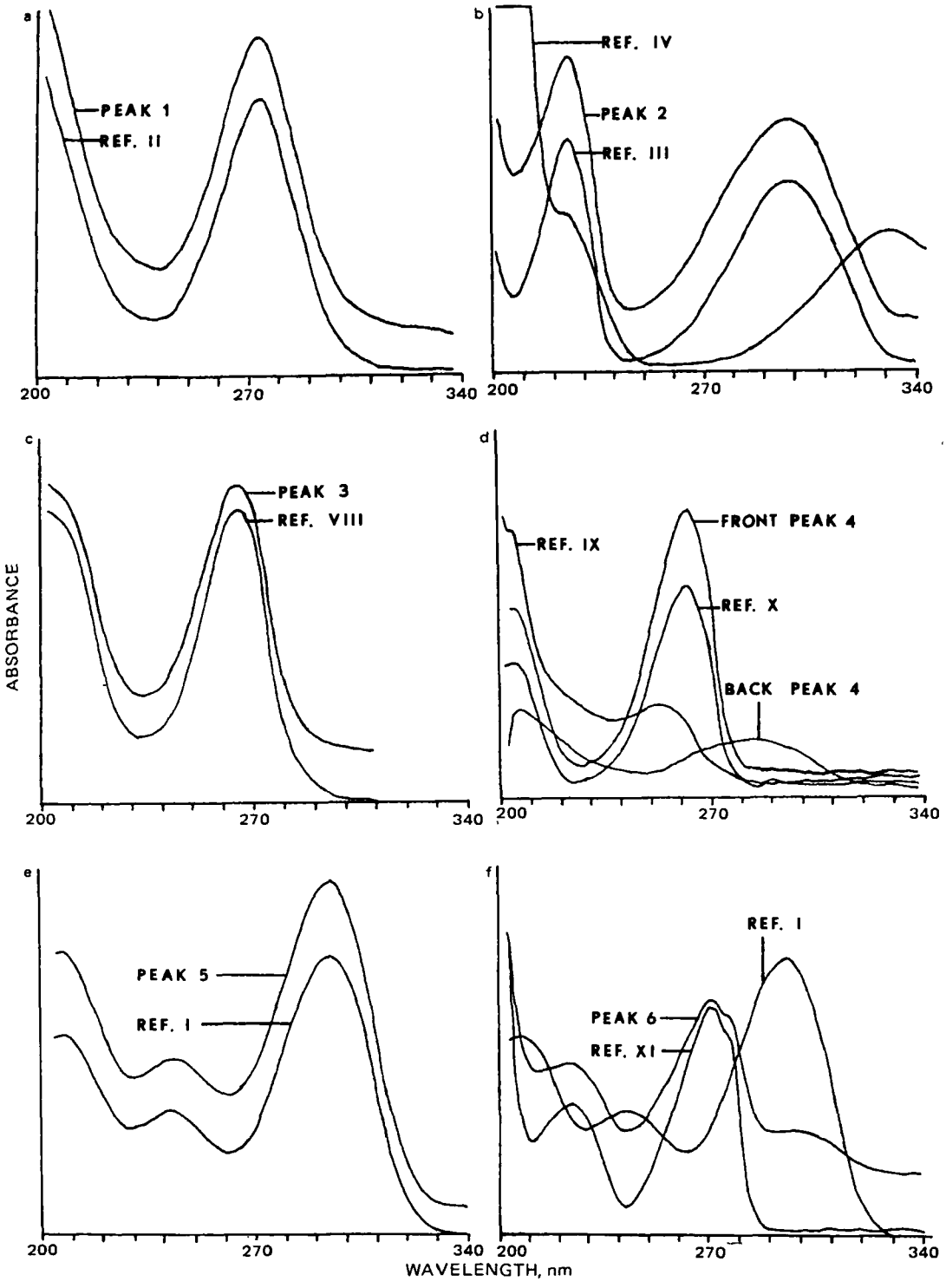

Figure 3—*Stop-flow UV absorption spectra of peaks 1–6 in Fig. 2c (injectable formulation stored at 80° for 4 weeks) and reference compounds of corresponding retention time.*

chloride[9] (VIII), 2-aminomethyl-*N*-methylpyridinium chloride[9] (IX), 2-hydroxymethyl-*N*-methylpyridinium chloride[9] (X), 2-cyano-*N*-methylpyridinium chloride[10] (XI), and *N*-methylpyridinium chloride[9] (XII).

Chromatographic System—The high-performance liquid chromatograph consisted of a mobile-phase pump[11] operated at 0.8 ml/min (1600 psi), a sample injector[12] set for a 15-μl injection volume, a variable-wavelength UV detector[13] at 270 nm (0.08 AUFS), a precolumn[14] positioned between the pump and the injector, and an analytical reverse-phase C-18 column[15]. Areas under the chromatographic peaks were measured by electronic integration[16]. The mobile phase consisted of 52% acetonitrile and 48% of an aqueous solution of 0.005 *M* phosphoric acid and 0.001 *M* tetraethylammonium chloride. Chromatographic data were acquired at ambient temperature.

Analytical Procedure—*Preparation of Sample and Standard Solutions*—A volume equivalent to 330 mg of I was transferred to a 250-ml volumetric flask and diluted to volume with water. A 1.0-ml aliquot of this solution was pipetted into a 50-ml volumetric flask and diluted to volume with the mobile phase.

Stock solutions were prepared by accurately weighing ~25, 50, and 75

[9] Synthesized by C. E. Orzech and F. Q. Gemmill, Jr., Ayerst Laboratories, Inc., Rouses Point, N.Y.

[10] Synthesized by the procedure of Ellin (1).

[11] Model 740-P, Spectra Physics, Santa Clara, Calif.

[12] WISP 710B, Waters Associates, Milford, Mass.

[13] Model LC-75 with autocontrol, Perkin-Elmer Corp., Norwalk, Conn.

[14] 250 × 4.6-mm i.d. column packed with LiChrosorb Si-60 (10 μm), MC/B Manufacturing Chemist Inc., Cincinnati, Ohio.

[15] 250 × 3.2-mm i.d., column packed with Spherisorb-ODS (5 μm), Phase Separations, Hauppauge, N.Y.

[16] Model 3354B, Hewlett-Packard, Avondale, Pa.

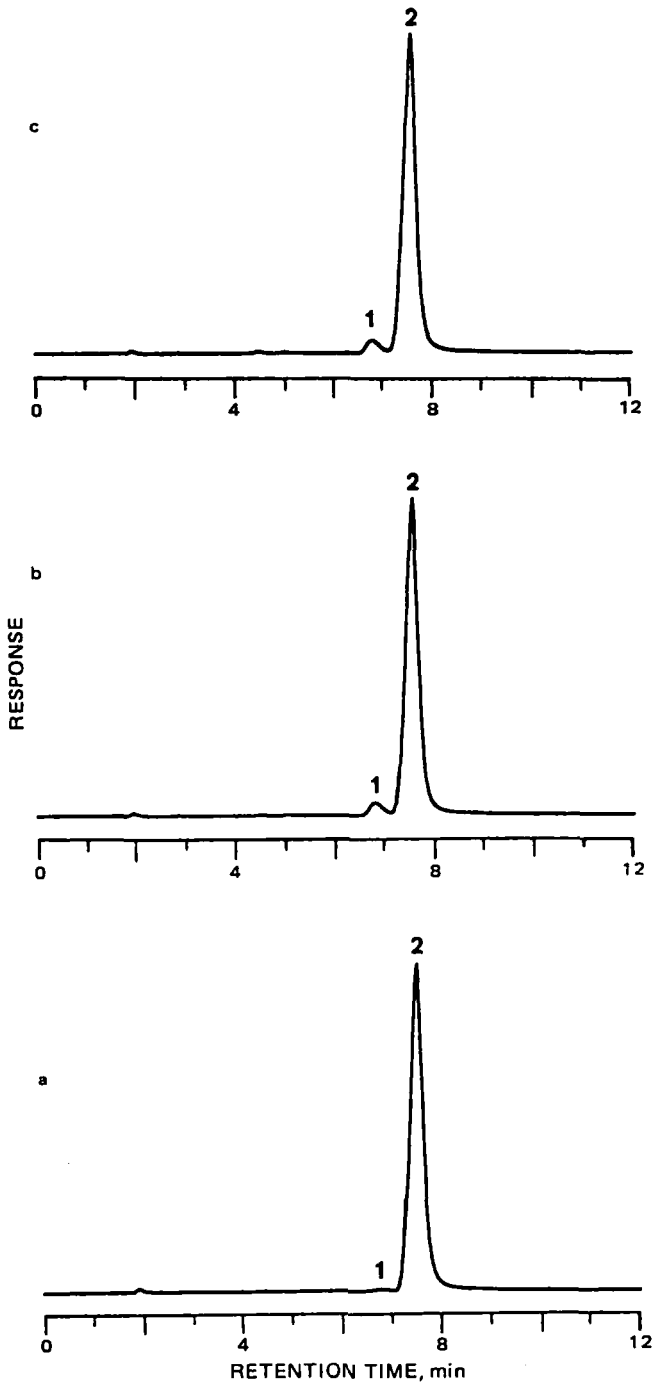

Figure 4—*Chromatograms of the injectable formulation at day zero (a) and after storage at room temperature for 8 (b) and 48 (c) weeks. Key: (1) unknown compound; (2) I.*

mg of I, transferring these amounts to separate 50-ml volumetric flasks, and dissolving them in water. A 1.0-ml aliquot of each stock solution was diluted separately to 50 ml with mobile phase. A standard solution containing II, III, VIII, and XI was prepared by accurately weighing ~33 mg of each compound, transferring these amounts to a single 50-ml volumetric flask, and dissolving and diluting them to volume with water. A 10.0-ml aliquot of this solution was diluted to 50 ml with water. A 1.0-ml aliquot of this diluted solution was pipetted into a 50-ml volumetric flask, which contained 1.0 ml of the stock solution containing 50 mg of I. The mixture was diluted to volume with the mobile phase.

System Suitability Test—The detector wavelength was set to 270 nm, 15 μl of the middle (50 mg) standard preparation was injected, and the flow rate of the mobile phase and sensitivity of the detector were adjusted so that the I peak eluted in ~7.5 min (~0.8 ml/min) and was at least 50% of full scale (~0.08 AUFS). After the chromatographic conditions stabilized, 15 μl of the middle (50 mg) standard preparation and 15 μl of the

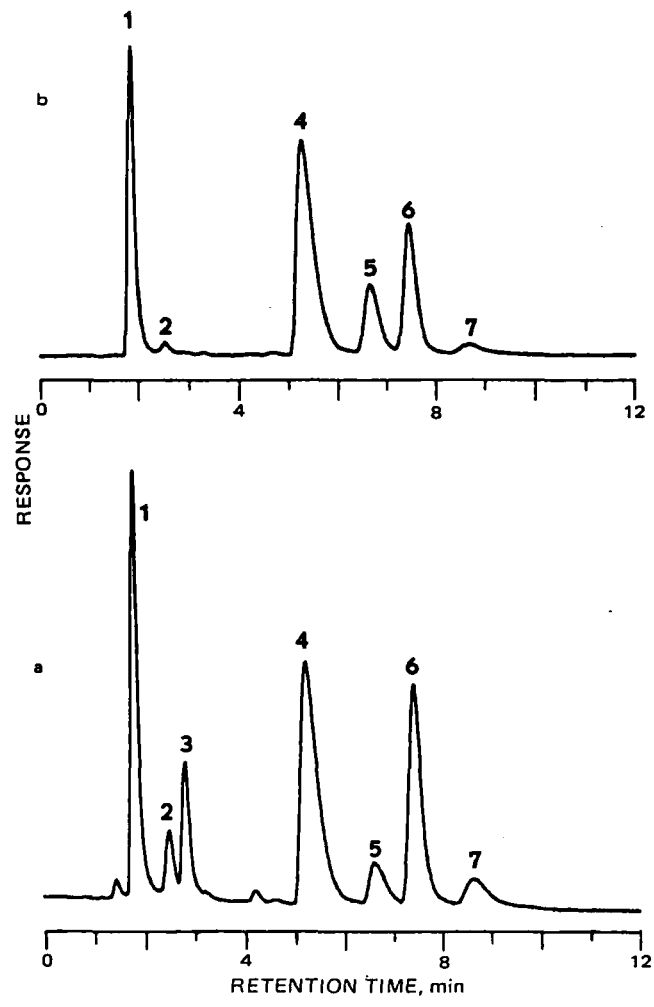

Figure 5—*Chromatograms of the injectable formulation stored at 80° for 4 weeks, using a detector wavelength of 200 nm (a) or 270 nm (b). Key: (1) II, (2) III, (3) benzyl alcohol, (4) VIII, (5) X and the unknown compound, (6) I, and (7) XI.*

standard preparation containing II, III, VIII, and XI were injected. The areas of the I peak in each chromatogram were obtained and compared; the chromatographic system was considered suitable for use if the areas were within 2%.

Injection Procedure—A 15-μl aliquot of each standard preparation was injected and the areas of the peaks for I, II, III, VIII, and XI were obtained. The same volume of each sample preparation was injected and the corresponding peak areas were determined.

Calculations—A least-squares linear regression line of the peak area *versus* weight of I (W_p) was obtained. The weight (W) corresponding to the peak area of I in the sample preparation was obtained from the regression line. The concentration of I in the sample was calculated from:

$$[\text{mg/ml}] = (W)(5)(P)(1/V) \qquad \text{(Eq. 1)}$$

where W is the weight of I corresponding to the area of I in the sample preparation chromatogram, P is the strength of the I reference standard (decimal), V is the volume (ml) of sample solution assayed, and 5 is the dilution factor (250/50). The concentration of each decomposition product detected in the sample was calculated from:

$$[\text{mg/ml}] = (A_2/A_1)(W_d)(P)(1/V) \qquad \text{(Eq. 2)}$$

where A_1 and A_2 are the areas of the appropriate decomposition product peaks (II, III, VIII, or XI) in the standard and sample preparations, respectively; W_d is the weight (mg) of the decomposition product; and P is the strength of the decomposition product standard (decimal). If a peak(s) was observed eluting between that of VIII and I (~6.7 min), a response equal to the latter was assumed and the concentration was calculated accordingly.

Table I—Wavelength Absorbance Ratios for Reference I and Injectable Formulation Stored for 2 Weeks at 80° [a]

Wavelength (λ), nm	Absorbance Ratios (Q) Peak Identity Reference/Sample	Peak Homogeneity Middle/Front	Middle/Back	Front/Back
210	0.74	3.10 (min)	3.70	1.20 (max)
220	0.75 (max)	3.24	3.51 (min)	1.09
240	0.75	3.47	3.81	1.10
250	0.75	3.54	3.82	1.08
270	0.74	3.87 (max)	4.30 (max)	1.11
280	0.74	3.56	3.68	1.04
290	0.75	3.40	3.53	1.04
300	0.74	3.48	3.59	1.03
310	0.72 (min)	3.85	3.85	1.00 (min)
$D = Q_{max}/Q_{min}$ =	1.04	1.25	1.23	1.20

[a] Front, middle, and back of peak 5 in Fig. 2b.

RESULTS AND DISCUSSION

Specificity and Identification of Decomposition Products—Previous reports (1–7) have indicated that the degradation of I can proceed *via* hydrolysis or dehydration to form a number of decomposition products. Among those decomposition products previously reported are II, III, IV, VII, VIII, and XI. Since pyridinium compounds readily form decomposition products, some of which may not have been described in these original studies, additional compounds including V (the primary synthetic precursor of I), VI (the *syn*-isomer of I), IX, X, and XII were also studied.

To accurately monitor the stability of I in the injectable formulation, it is mandatory that the chromatographic system be capable of separating I from all its possible decomposition products. Because of the quaternary structure of the pyridinium aldoximes, ion-pair HPLC was expected to provide the required separation. However, various mobile phase combinations employing classical ion-pairing reagents of opposite charge, *e.g.*, *N*-heptanesulfonic acid and sodium dodecanesulfonate, produced only partial separations and tailing of some peaks. Mobile phases employing tetraethylammonium chloride, a modifier with the same charge as the pyridine aldoximes, produced superior separations and more symmetrical peaks. Control of retention and peak shape by a modifier of the same charge as the sample is not considered to be the classical ion-pairing phenomenon, but is better explained by the broader-scoped concept of ion interaction (13).

The separation of I from II–XII using the aforementioned HPLC system is shown in Fig. 1. Compound XII is not shown in the chromatogram due to its excessively long retention time of 27.4 min. Experience with this chromatographic system has shown that different batches of Spherisorb-ODS have slightly different separation characteristics. These differences are attributed to variations in the amounts of free silanols present on the bonded silica. These differences can be minimized by modifying the composition of the mobile phase. The retention time of I can be shortened or lengthened by increasing or decreasing, respectively, the concentrations of tetraethylammonium chloride. Modifiers such as tetraethylammonium chloride minimize the interactions of the sample with residual silanols on the surface because the modifier can cover, or mask, these silanol groups. This coverage of accessible silanols is the basis of the competing base concept (14).

Table II—Wavelength Absorbance Ratios for Reference I and the Injectable Formulation Stored for 4 Weeks at 80° [a]

Wavelength (λ), nm	Absorbance Ratios (Q) Peak Identity Reference/Sample	Peak Homogeneity Middle/Front	Middle/Back	Front/Back
210	0.83 (min)	1.90 (min)	3.04 (min)	1.60
220	0.85	1.98	3.21	1.62
240	0.86 (max)	2.15	3.80	1.77
250	0.86	2.24 (max)	4.3 (max)	1.94 (max)
270	0.85	2.21	4.22	1.90
280	0.86	2.02	3.24	1.60
290	0.86	2.01	3.10	1.54
300	0.86	2.00	3.06	1.53 (min)
310	0.85	2.10	3.52	1.68
$D = Q_{max}/Q_{min}$ =	1.04	1.18	1.43	1.27

[a] Front, middle, and back of peak 5 in Fig. 2c.

Table III—Recovery of II, III, VIII, and XI from the Injectable Formulation

Spike Level[a], %	Recovery, % II	III	VIII	XI
1	114.7	115.4	100.0	114.7
2	105.9	109.1	92.6	106.0
5	99.4	98.8	97.6	95.8
10	100.9	101.2	99.1	100.3
20	99.4	100.0	101.0	102.2
50	96.8	97.6	100.0	100.8

[a] Concentration (in mg/ml) of II, III, VIII, or XI divided by 330 mg/ml, expressed as percent.

Table IV—Precision of the Concentrations of I and Its Major Decomposition Products Found in the Injectable Formulation Stored at 80° for 7 and 26 Days

Compound	7 Days @ 80° Average Concentration[a], mg/ml	*CV*	26 Days @ 80° Average Concentration[a], mg/ml	*CV*
I	276	1.0	93.3	1.5
II	15.7	3.9	83.7	1.3
III	—[b]	—	3.0	3.5
VIII	17.9	3.9	103	2.2
XI	—	—	4.3	6.5
Other[c]	15.5	5.4	22.3	3.0

[a] n = 10, five determinations on each of 2 days. [b] — None detected. [c] Composite of X and an unknown compound; assumes a response equal to I.

Figure 2 depicts the loss of I and the formation of its decomposition products in the injectable formulation which was stored at 80°. After 2, 4, and 8 weeks at 80°, the amounts of I remaining were 65, 20, and 3% of the initial concentration, respectively. Use of another mobile phase, which shortened the retention time of XII to 8 min, indicated that XII was not formed in measurable quantities in any of the degraded samples of the formulation.

The peaks corresponding to the decomposition products in Fig. 2 were tentatively identified by comparison of their respective retention times with those of reference compounds I–XII. Confirmation of the identity of each peak was made by comparison of its stop-flow UV absorption spectra with the stop-flow spectra of the reference compound of corresponding retention time. Stop-flow UV spectra of peaks 1–6 in Fig. 2c (injectable formulation stored for 4 weeks at 80°) are given in Fig. 3.

Other investigators (11) have recently studied the degradation of I under both acidic and basic conditions using ion-pair HPLC. Unfortunately, in the chromatographic system they employed, VII and VIII have the same retention time. Nevertheless, based on retention time data, it was reported that the only hydrolytic byproduct of I in acid solution (0.1 *N* HCl) was VII. Under basic conditions (0.1 *N* NaOH) it was reported that II, III, and VIII were formed. Although acid hydrolysis was the expected mode of decomposition in the injectable formulation (which is buffered at pH 2.5), it is evident from Fig. 2 that primarily products usually associated with base hydrolysis are formed. It is readily seen that the major decomposition products of I in the injectable formulation are II and VIII; III and XI are also formed, but in relatively small amounts. Compound VII, which is separated from VIII in Fig. 1, is not observed in any of the chromatograms in Fig. 2.

In addition to peaks corresponding to decomposition products previously reported, another peak (peak 4) with a retention time of 6.7 min was observed in the chromatograms in Fig. 2. The retention time of this peak corresponds exactly to X, since compound IX has a retention time of 6.5 min. As shown in Fig. 3d, the frontside of peak 4 has a stop-flow UV spectra consistent with the reference spectra of X, but the backside of

Table V—Stability of I, II, III, VIII, and XI in Mobile Phase

Compound	Days at Room Temperature[a] 2	5	6	8	12
I	99.1	100.5	—	—	100.2
II	102.5	—	104.2	102.2	101.4
III	99.1	—	98.1	100.6	99.9
VIII	100.8	—	101.1	103.8	104.5
XI	99.0	—	100.1	100.9	108.8

[a] Results are expressed as percent of initial input.

Table VI—Comparison of HPLC and USP Results For I in the Injectable Formulation

Storage Conditions	Concentration of I, mg/ml HPLC	USP
Initial	324	328
2 Days, 80°	309	316
6 Days, 80°	285	294
9 Days, 80°	272	281
13 Days, 80°	249	255
21 Days, 80°	156	160
28 Days, 80°	62.6	66.6

the peak has a spectra which does not match any of the reference compounds. These differing spectra suggest that peak 4 is a composite of X and another substance. This was later confirmed when peak 4 was resolved into two components using a different mobile phase. The first component was identified as X. The identity of the second component is unknown, but is of major interest because it has been detected in solutions of I when no other decomposition peaks are observed (Fig. 4). This substance seems to be formed soon after the dissolution of I in aqueous media, then gradually increases to an equilibrium concentration of ~3% (area percent relative to I). Similar observations have been made by other investigators[17] using a method based on ion-pairing HPLC. As of this writing, the presence of X and the unknown compound in degraded solutions of I has not been reported in the literature.

The formulation that was decomposed at 80° for 4 weeks (Fig. 2c) was chromatographed at the nonspecific wavelength of 200 nm to observe any other peaks that might appear and are not detected at 270 nm. Figure 5 demonstrates that no other decomposition peaks of significant intensity were detected at 200 nm, and that the analytical wavelength of 270 nm provides adequate sensitivity for I and the corresponding decomposition products. However, a formulation excipient, benzyl alcohol, was detected at 200 nm (Fig. 5a).

Stop-flow spectroscopy, employing the spectral discrimination technique (15), was performed on the peaks corresponding to I in the injectable formulations that were decomposed at 80° for 2 (Fig. 2b) and 4 weeks (Fig. 2c). These storage conditions produced 35 and 80% decomposition of I, respectively. Absorbance readings at nine discrete wavelengths across the UV spectrum were obtained on the front, middle, and back of each I peak. Similarly, absorbances at each wavelength were obtained on a reference peak of I from a separation injection. If the ratio (Q) of absorbance values at each wavelength between the reference and sample peaks remains constant ($D = Q_{max}/Q_{min} \leq 1.5$), evidence is strong that the sample peak has the same identity as the reference peak. Likewise, if the ratio of absorbances taken from different portions of a single peak are constant, then the peak is considered homogeneous and is, therefore, the response of a single molecular species. For all cases, the test for peak identity and peak homogeneity was positive, *i.e.*, the values of the spectral discriminator (D) were between 1 and 1.5 (Tables I and II). These data strongly suggest that the chromatographic system separates I from all UV-absorbing components in the degraded formulation.

Accuracy—Known amounts of I corresponding to 80, 100, and 120% of the label claim (330 mg/ml) were added to a placebo of the injectable formulation and assayed. The recoveries of I from the spiked formulations were 100.2, 99.9, and 99.6%, respectively.

The accuracy of determining various concentrations of the decomposition products (those actually detected in the decomposed formulation) was determined by adding known amounts of II, III, VIII, and XI to the formulation at levels corresponding to 1, 2, 5, 10, 20, and 50% decomposition. Therefore, the spiked formulation representing 1% decomposition contained ~3.3 mg/ml of each decomposition product, the spiked formulation representing 10% decomposition contained ~33 mg/ml of each decomposition product, *etc.* Recoveries of II, III, VIII, and XI were calculated from a single chromatogram that represented each spike level. The results are given in Table III. The accuracy of determining the concentration of X was not evaluated because its peak, being a composite of two substances in the degraded formulation, precludes such a determination.

Precision—Replicate assays were performed on the injectable formulation which was stored for 7 and 26 days at 80° to promote decomposition. Assays were performed 10 times over a period of 2 days using freshly prepared standards on each day of analysis. Between determinations the solutions were stored at 4°. The results are given in Table IV and indicate that the method has acceptable precision for determining all compounds of interest.

Linearity—The UV absorbance of I at 270 nm increased linearly (r = 0.9999874, y-intercept = −338) with concentration in the range corresponding to 125–375 mg/ml in the injectable formulation. Although the analytical method does not require that a calibration curve be prepared for each decomposition product, the responses of II, III, VIII, and XI at 270 nm are linear over the range 3.3 (limit of detection) to 165 mg/ml in the injectable formulation. The correlation coefficients for curves in this range were: II, r = 0.9999504, y-intercept = 452; III, r = 0.9999574, y-intercept = 243; VIII, r = 0.9999806, y-intercept = −73; and XI, r = 0.9999516, y-intercept = 62. An evaluation of the y-intercepts of each curve indicated that they were not statistically different from zero at $p < 0.05$.

Stability of I and Decomposition Products in Mobile Phase—The stability of I and its decomposition products during the time required to perform the analytical procedure is an important consideration. During the determination, I and its decomposition products should not be subjected to conditions of acid or base hydrolysis other than that which has actually occurred in the formulation. The high pH requirements of the UV procedure in USP XX for determining I in the presence of its decomposition products promotes base hydrolysis and requires that the analytical measurements be performed as rapidly as possible. The UV method does not easily lend itself to unattended operation because of this requirement.

The stability of I and its decomposition products during the time required to perform the HPLC procedure was assessed by preparing solutions of I, II, III, VIII, and XI in accordance with the analytical procedure, and assaying them at various intervals after storage at ambient laboratory conditions. The results (Table V) indicate that solutions of these compounds are stable in the mobile phase not only for the time required to perform the procedure, but for extended times up to several days. Consequently, with the use of an autoinjector, unattended chromatographic separation and measurement may be performed.

Comparison of HPLC and USP Procedures on Degraded Formulations—A comparison of the concentrations of I in degraded formulations found by the HPLC and USP procedures is given in Table VI. Although good agreement is observed, there is a consistent bias of ~2–3% between the two procedures. The higher values obtained by the USP procedure may be the result of interference, since the USP procedure requires that the measurement of I be made in the presence of its decomposition products. To its advantage, the HPLC procedure separates the decomposition product prior to the determination of I.

REFERENCES

(1) R. I. Ellin, *J. Am. Chem. Soc.*, **80**, 6588 (1958).

(2) R. I. Ellin and A. A. Kondritzer, *Anal. Chem.*, **31**, 200 (1959).

(3) R. I. Ellin and D. E. Easterday, *J. Pharm. Pharmacol.*, **13**, 370 (1961).

(4) R. I. Ellin, J. S. Carlese, and A. A. Kondritzer, *J. Pharm. Sci.*, **51**, 141 (1962).

(5) B. Barkman, B. Edgren, and A. Sunderwall, *J. Pharm. Pharmacol.*, **15**, 671 (1963).

(6) E. M. Kosower and J. W. Patton, *Tetrahedron*, **22**, 2081 (1966).

(7) G. Špoljarić, Z. Lozanović, and R. Bonevski, *Arh. Hig. Rada Toksikol.*, **30**, 333 (1979).

(8) "U.S. Pharmacopeia," 20th rev., U.S. Pharmacopeial Convention, Inc., Rockville, Md., 1980.

(9) N. D. Brown, L. L. Hall, H. K. Sleeman, B. P. Doctor, and G. E. Demarce, *J. Chromatogr.*, **148**, 453 (1978).

(10) H. P. Benschop, K. A. G. Konings, S. P. Kossen, and D. A. Ligtenstein, *ibid.*, **225**, 107 (1981).

(11) N. D. Brown, M. P. Strichler, H. K. Sleeman, and B. P. Doctor, *ibid.*, **212**, 361 (1981).

(12) S. Ginsburg and I. B. Wilson, *J. Am. Chem. Soc.*, **79**, 481 (1957).

(13) B. A. Bidlingmeyer, S. N. Deming, W. P. Price, Jr., B. Sachok, and M. Petrusek, *J. Chromatogr.*, **186**, 419 (1979).

(14) N. Cooke and K. Olsen, *Am. Lab.*, **11**, 45 (1979).

(15) A. F. Poile and R. D. Conlon, *J. Chromatogr.*, **204**, 149 (1981).

ACKNOWLEDGMENTS

The authors thank Dr. C. E. Orzech and F. Q. Gemmill, Jr. for preparation of the reference compounds, F. P. DiBernardo for providing UV/USP data, and Dr. E. Nordbrock for statistical support.

[17] L. Ernerot, Astra Lakemedal AB, S-151 85 Sodertalje, Sweden, personal communication.

Dissolution Kinetics of a Three-Component Solid I: Ethylparaben, Phenacetin, and Salicylamide

MICHAEL SIMPSON and EUGENE L. PARROTT ˣ

Received March 12, 1982, from the *Division of Pharmaceutics, College of Pharmacy, University of Iowa, Iowa City, IA 52242.* Accepted for publication June 29, 1982.

Abstract □ The dissolution rates of each component in compressed spheres consisting of three components were measured under sink conditions. A film diffusion model is discussed and presented diagrammatically to illustrate the 13 possible dissolution behaviors of a three-component solid. Experimental dissolution rates compare favorably to dissolution rates calculated according to the model at mass fractions representative of the 13 dissolution behaviors

Keyphrases □ Ethylparaben—dissolution kinetics of a three-component solid, phenacetin, salicylamide □ Phenacetin—dissolution kinetics of a three-component solid, ethylparaben, salicylamide □ Salicylamide—dissolution kinetics of a three-component solid, ethylparaben, phenacetin

A limited number of reports on dissolution rates have been concerned with multicomponent solids. Recently, a general model for the dissolution rates of a nondisintegrating sphere composed of any number of components was presented (1). The purpose of this study was to develop a dissolution model for a three-component solid (ethylparaben, phenacetin, and salicylamide). The model suggests 13 possible dissolution behaviors, which are dependent on composition. A further purpose was to compare the experimental dissolution rates of each of the components with the dissolution rates predicted by the model.

EXPERIMENTAL

Preparation of Spheres—Twenty grams of each composition were prepared by blending the appropriate amounts of 60/80-mesh size fraction of ethylparaben[1], phenacetin[2], and salicylamide[3] for 15 min in a V-blender[4]. By means of a hydraulic press[5] fitted with a spherical punch and die set, each composition was compressed at a force of 2268 kg into spheres having a diameter of 1.273 ± 0.005 cm. The compositions (represented by solid circles) were selected according to the scheme shown in Fig. 1. Each corner of the triangle represents a compressed sphere composed of a single component. The three straight lines joining the corners of the triangle represent two-component compositions. Thus, the lines AB, BC, and AC represent two-component mixtures of A and B, B and C, and A and C, respectively. Each side of the triangle was divided into 10 equal segments. For example, a point on line AC midway between A and C represents a composition of 50% A and 50% C with no component B. The area within the triangle represents all mass fraction compositions of A, B, and C in a three-component system. The intercept of any three lines parallel to one of the lines AB, BC, and AC represents the composition of a particular three-component mixture. With high percentages of phenacetin the spheres were not readily formed, and heat was used to facilitate formation. With compositions containing ethylparaben the die was at 110°, and the force of compression was exerted for 3 min. In the absence of ethylparaben a temperature of 134° was used. Comparison of the dissolution rates of compacts made at room temperature to those made with heat showed that the difference did not exceed 2.7%, which was considered to be within experimental error.

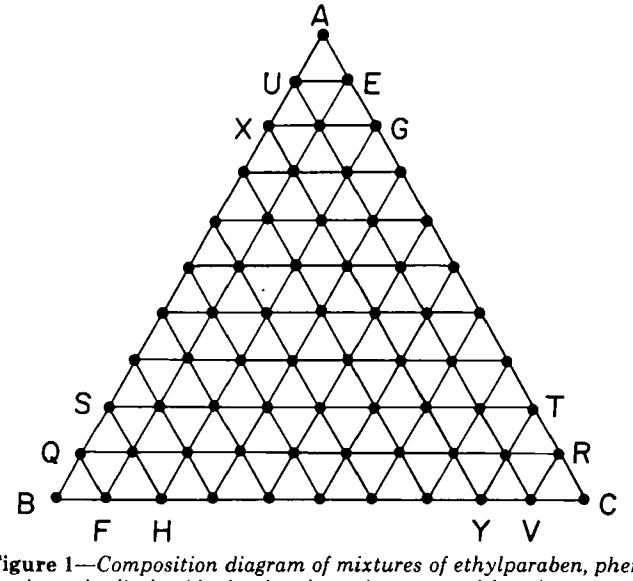

Figure 1—*Composition diagram of mixtures of ethylparaben, phenacetin, and salicylamide showing the various compositions (represented by solid circles) selected for investigation.*

Dissolution Rate—The dissolution rate was determined in distilled water at 25 ± 0.1°, as described previously (2, 3), under conditions where the concentration of the solutes did not exceed 5% of solubility. The dissolution apparatus and method were described previously (3, 4).

Solubility—Solubility measurements were made at 25°, as reported earlier (5). The solubilities of ethylparaben, phenacetin, and salicylamide are 0.939 ± 0.010, 0.842 ± 0.016, and 2.511 ± 0.018 mg/ml, respectively.

Analytical Procedure—The UV spectrum for each component was determined in a solution of that component containing 1.0 ml of 1.0 *N* sodium hydroxide in 25.0 ml of solution. The wavelengths of 296, 244, and 329 nm were selected. The standard curve of each component at each wavelength exhibited a Beer's law relationship. From these plots the nine

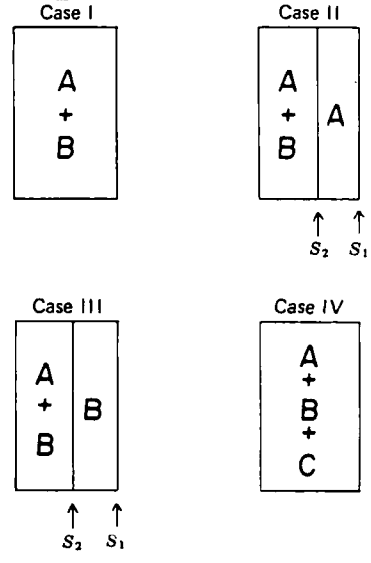

Figure 2—*Dissolution behaviors of two-component solids of components A and B and dissolution behavior of a three-component solid at its critical composition.*

[1] Sigma Chemical Co., Lot 117C-0156.
[2] Eastman, Lot A44.
[3] Sigma Chemical Co., Lot 107C-0409.
[4] Patterson-Kelly.
[5] Carver press, model C.

0022-3549/83/0700-0757$01.00/0

Table I—Molar Absorptivities of Ethylparaben, Phenacetin, and Salicylamide

Wavelength, nm	Molar Absorptivity		
	Ethylparaben	Phenacetin	Salicylamide
244	1,227	11,328	6,733
296	23,268	492	1,419
329	510	0	5,632

molar absorptivities were calculated (Table I). For a three-compartment system since absorbancies are additive:

$$A_1 = a_{11}C_A + a_{12}C_B + a_{13}C_C \quad \text{(Eq. 1)}$$

$$A_2 = a_{21}C_A + a_{22}C_B + a_{23}C_C \quad \text{(Eq. 2)}$$

$$A_3 = a_{31}C_A + a_{32}C_B + a_{33}C_C \quad \text{(Eq. 3)}$$

in which a_{ij} is the molar absorptivity of the species i at wavelength j, and A_j is the absorbance of the mixture at wavelength j. When the values of A_j and a_{ij} are substituted into Eqs. 1–3, and the equations are solved simultaneously, the concentrations C_A, C_B, and C_C are determined. Thus, the concentration of each component was obtained by UV absorbance at three selected wavelengths. The method was tested with seven solutions containing known concentrations of the three components. The percent determined by the analytical procedure ranged from 98.9 to 102.8% of the known concentration. The concentration was converted to amount dissolved in order to express a dissolution rate.

THEORY

With the dissolution of three-component solids if one assumes a Noyes–Whitney film theory, there are 13 dissolution behaviors possible. In Case IV dissolution behavior as shown in Fig. 2, the three components coexist at the solid–liquid interface, because as dissolution proceeds their boundaries recede at the same rate. This dissolution behavior occurs at a unique composition (critical composition) of the components at which:

$$\frac{N_A}{N_B} = \frac{D_A C_A}{D_B C_B} \quad \text{(Eq. 4)}$$

$$\frac{N_A}{N_C} = \frac{D_A C_A}{D_C C_C} \quad \text{(Eq. 5)}$$

and

$$\frac{N_B}{N_C} = \frac{D_B C_B}{D_C C_C} \quad \text{(Eq. 6)}$$

where N_A, N_B, and N_C are the mass fractions of components designated in general as A, B, and C; C_A, C_B, and C_C are their solubilities; and D_A, D_B, and D_C are their diffusion coefficients, respectively.

In Case V component C dissolves faster than components A and B, and

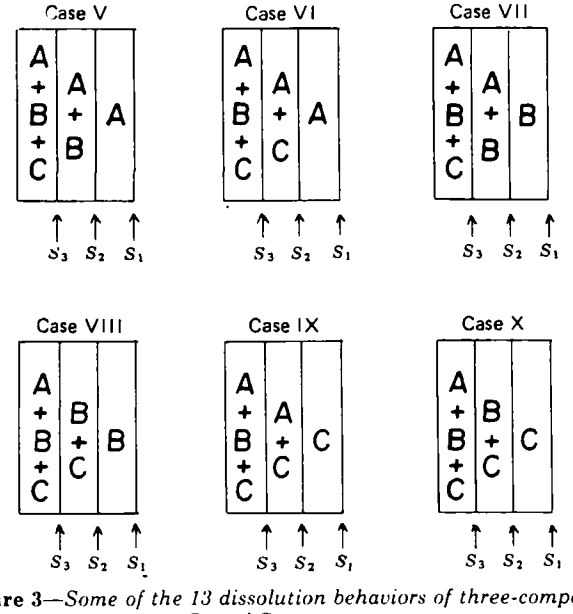

Figure 3—*Some of the 13 dissolution behaviors of three-component solids of components A, B, and C.*

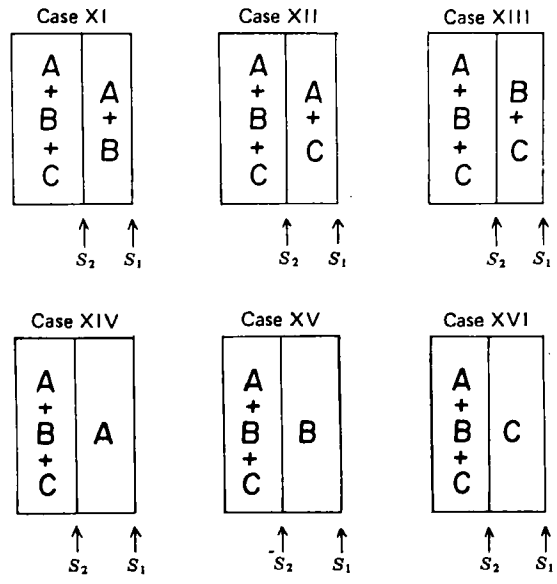

Figure 4—*Other possible dissolution behaviors of three-component solids of components A, B, and C.*

the dissolving boundary of component C recedes into the solid, as shown in Fig. 3. Component B dissolves faster from the solid surface than component A, so that the dissolving boundary of component B recedes within the solid leaving a surface layer of component A. Case V dissolution behavior occurs under the condition that:

$$\frac{N_A}{N_B} > \frac{D_A C_A}{D_B C_B} \quad \text{(Eq. 7)}$$

$$\frac{N_A}{N_C} > \frac{D_A C_A}{D_C C_C} \quad \text{(Eq. 8)}$$

and

$$\frac{N_B}{N_C} > \frac{D_B C_B}{D_C C_C} \quad \text{(Eq. 9)}$$

Cases VI, VII, VIII, IX, and X in Fig. 3 describe dissolution behaviors similar to Case V; however, the order of dissolving and the receding of the boundaries are different with different mass fractions of components A, B, and C.

In Case XI component C dissolves faster than the other two components and as dissolution proceeds the boundary of component C recedes within the solid leaving a layer of components A and B, which coexists

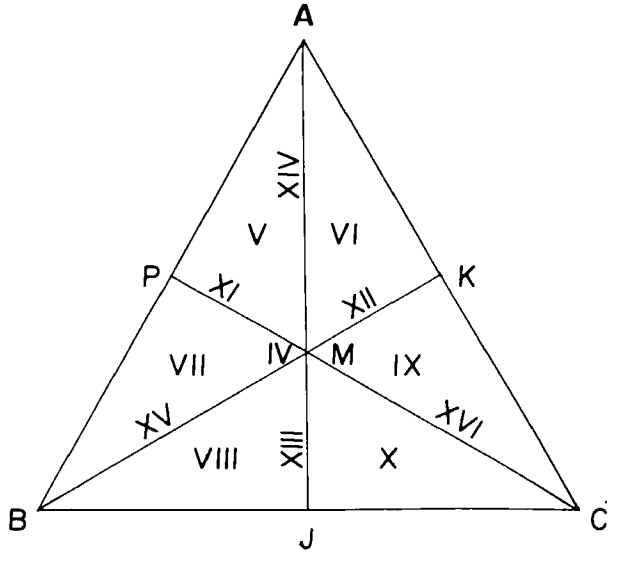

Figure 5—*Composition diagram for a three-component mixture of components having equal solubilities and diffusion coefficients showing the regions corresponding to the 13 dissolution behaviors. Roman numerals refer to the use of dissolution behavior described in the text.*

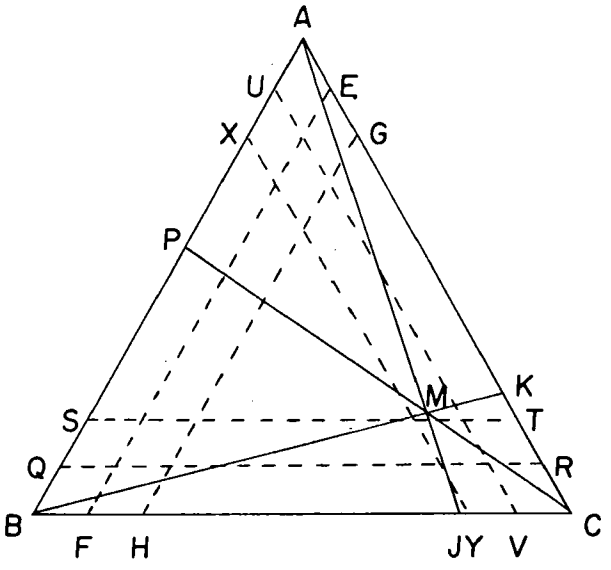

Figure 6—*Composition diagram for mixtures of ethylparaben, phenacetin, and salicylamide showing the regions corresponding to the 13 dissolution behaviors and their relationship to the compositions selected for investigation according to Fig. 1.*

at the surface, as shown in Fig. 4. Case XI dissolution behavior occurs under the conditions that:

$$\frac{N_A}{N_C} > \frac{D_A C_A}{D_C C_C} \quad \text{(Eq. 10)}$$

$$\frac{N_B}{N_C} > \frac{D_B C_B}{D_C C_C} \quad \text{(Eq. 11)}$$

and

$$\frac{N_A}{N_B} = \frac{D_A C_A}{D_B C_B} \quad \text{(Eq. 12)}$$

Cases XII and XIII in Fig. 4 describe dissolution behaviors similar to Case XI; however, the order of dissolving and the receding of the boundaries are different with different mass fractions of components A, B, and C.

In Case XIV both components B and C dissolve faster than component A and at the same rate, so that the boundaries of components B and C recede at the same rate and both coexist at the same boundary leaving a surface layer of component A. Case XIV dissolution behavior occurs under the conditions that:

$$\frac{N_A}{N_B} > \frac{D_A C_A}{D_B C_B} \quad \text{(Eq. 13)}$$

$$\frac{N_A}{N_C} > \frac{D_A C_A}{D_C C_C} \quad \text{(Eq. 14)}$$

and

$$\frac{N_B}{N_C} = \frac{D_B C_B}{D_C C_C} \quad \text{(Eq. 15)}$$

Cases XV and XVI in Fig. 4 describe dissolution behaviors similar to Case XIV; however, the order of dissolving and the receding of the boundaries are different with different mass fractions of components A, B, and C.

Using any two combinations of Eqs. 4, 5, or 6 and Eq. 16,

$$N_A + N_B + N_C = 1 \quad \text{(Eq. 16)}$$

the critical composition of components A, B, and C may be calculated. Similarly, for two-component mixtures of components A and B, components A and C, and components B and C, the critical composition may be calculated by use of the appropriate relationships. Dissolution behaviors of two-component solids have been previously described (6) and are presented as Cases I, II, and III in Fig. 2. Using these critical compositions a composition diagram can be drawn for a three-component system. Figure 5 shows the compositions corresponding to the 13 dissolution behaviors cited for three hypothetical components, which have equal solubilities and diffusion coefficients. Case IV dissolution behavior

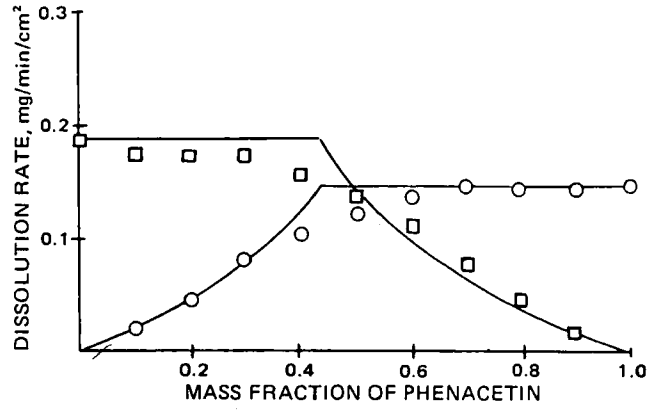

Figure 7—*Comparison of experimental dissolution rates of the components of ethylparaben and phenacetin mixtures corresponding to line AB of Fig. 1 and the smooth curves representing the theoretical rates. Key: (□) ethylparaben; (○) phenacetin.*

at the critical composition of the three-component mixture is represented by point M. Points P, J, and K represent the critical compositions of two-component mixtures of components A and B, components B and C, and components A and C, respectively. The line AMJ represents a three-component mixture, which contains components B and C (both in a mass fraction the same as the critical mass fraction for a two-component mixture of components B and C) with component A. From A to J the mass fraction of component A decreases while the mass fractions of components B and C increase.

The region APMK represents the condition in which components B and C have their boundaries within the solid coexisting, or following one another, depending on which portion is being considered. If the compositions of the three-component mixtures are on the line AM, there is a Case XIV dissolution behavior in which both components B and C coexist and have dissolving and receding boundaries within the solid, and component A is at the surface of the solid. Compositions within the region APM represent Case V dissolution behavior in which the dissolving boundary is deeper for component C than for component B, which in turn is deeper than that of component A, the surface component. Compositions within the region AMK represent Case VI dissolution behavior in which the dissolving boundary is deeper for component B than for component C, which in turn is deeper than that of component A, the surface component. Similarly, Case XI is represented by line PM; Case XII is represented by line MK; Case XIII is represented by line MJ; Case XIV is represented by line AM; Case XV is represented by line BM; and Case XVI is represented by line CM. Case VII is represented by the region BMP; Case VIII is represented by the region BMJ; Case X is represented by the region CMJ; and Case IX is represented by the region CMK.

The derivation of equations to describe dissolution of a three-component solid is illustrated for Case V dissolution behavior. Let S_1, S_2, and S_3 be the coordinate values representing the component A–solution boundary, component A–components A and B boundary, and compo-

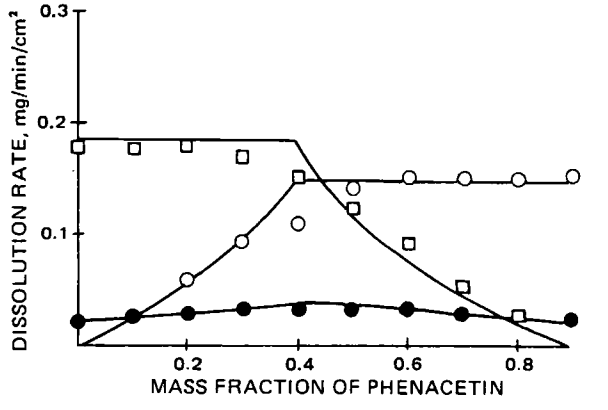

Figure 8—*Comparison of experimental dissolution rates of the components of ethylparaben, phenacetin, and salicylamide mixtures with a constant mass fraction of 0.1 salicylamide corresponding to line EF of Fig. 1 and the curves representing the theoretical rates. Key: (□) ethylparaben; (○) phenacetin; (●) salicylamide.*

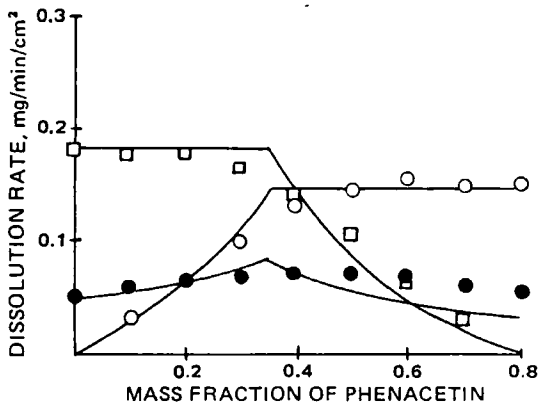

Figure 9—*Comparison of experimental dissolution rates of the components of ethylparaben, phenacetin, and salicylamide mixtures with a constant mass fraction of 0.2 salicylamide corresponding to line GH of Fig. 1 and the curves representing the theoretical rates. Key: (□) ethylparaben; (○) phenacetin; (●) salicylamide.*

nents A, B, and C–components A and B boundary, respectively. These are defined so that at a time $t = 0, S_3 = S_2 = S_1 = 0$. At $t > 0, S_2 - S_1$ is the thickness of the layer of component A, and $S_3 - S_2$ is the thickness of the layer of components A and B. Since component A is always on the surface, the dissolution rate (R_A) of component A is:

$$R_A = \frac{D_A C_A}{h} \qquad \text{(Eq. 17)}$$

where h is the effective diffusion layer thickness.

Component B must diffuse through the layer of component A of thickness $S_2 - S_1$, porosity ϵ_1, and tortuosity τ_1, and the liquid diffusion layer. The dissolution rate (R_B) of component B is:

$$R_B = \frac{D_B C_B}{h + (\tau_1/\epsilon_1)(S_2 - S_1)} \qquad \text{(Eq. 18)}$$

Component C must diffuse not only through the liquid diffusion layer but also through the interstitial space between the undissolved components A and B of thickness, $S_3 - S_2$, porosity, ϵ_2, and tortuosity, τ_2, and through the layer of component A of thickness $S_2 - S_1$, porosity ϵ_1, and tortuosity τ_1. The dissolution rate (R_C) of component C is:

$$R_C = \frac{D_C C_C}{h + (\tau_1/\epsilon_1)(S_2 - S_1) + (\tau_2/\epsilon_2)(S_3 - S_2)} \qquad \text{(Eq. 19)}$$

The dissolution rates may also be expressed:

$$R_A = A_A \frac{dS_1}{dt} \qquad \text{(Eq. 20)}$$

$$R_B = A_B \frac{dS_2}{dt} \qquad \text{(Eq. 21)}$$

$$R_C = A_C \frac{dS_3}{dt} \qquad \text{(Eq. 22)}$$

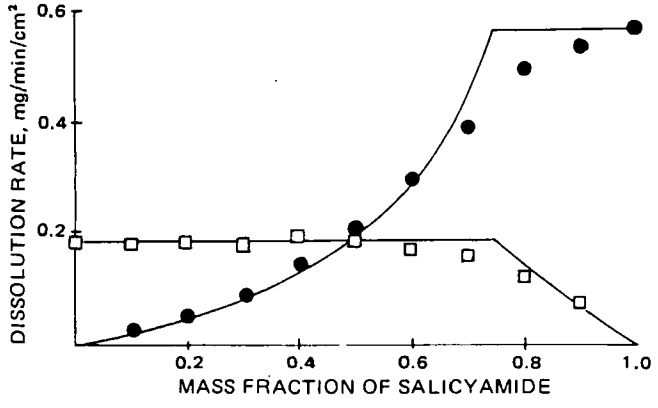

Figure 10—*Comparison of experimental dissolution rates of the components of ethylparaben and salicylamide mixtures corresponding to line AC of Fig. 1 and the smooth curves representing the theoretical dissolution rates. Key: (□) ethylparaben; (●) salicylamide.*

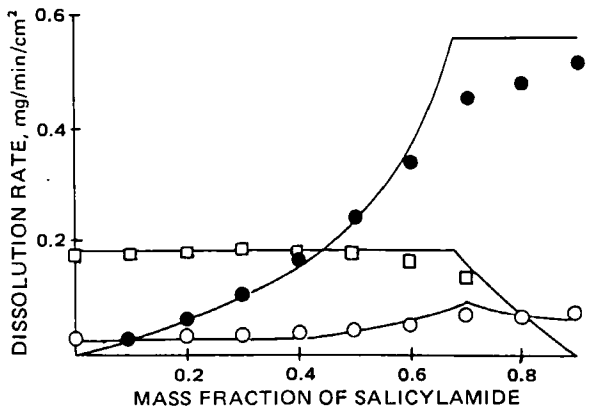

Figure 11—*Comparison of experimental dissolution rates of the components of ethylparaben, phenacetin, and salicylamide mixtures with a constant mass fraction of 0.1 phenacetin corresponding to line UV of Fig. 1 and the curves representing the theoretical rates. Key: (□) ethylparaben; (○) phenacetin; (●) salicylamide.*

where A_A, A_B, and A_C are the amounts per unit volume of component A, B, and C in the mixture. These equations state that the dissolution rate of a component is the product of the rate of movement of its boundary and the concentration in that layer. The amount of components B and C remaining in solution in the pores have not been considered. As the dissolution rate of component A is represented by Eqs. 17 and 20, it follows that:

$$A_A \frac{dS_1}{dt} = \frac{D_A C_A}{h} \qquad \text{(Eq. 23)}$$

$$\frac{dS_1}{dt} = \frac{D_A C_A}{A_A h} \qquad \text{(Eq. 24)}$$

When $S_1 = 0$ at $t = 0$, the solution to Eq. 24 is:

$$S_1 = \frac{D_A C_A t}{A_A h} \qquad \text{(Eq. 25)}$$

Substituting Eq. 25 into Eq. 18 and combining it with Eq. 22 yields:

$$\frac{dS_2}{dt} = \frac{D_B C_B}{A_B[h + (\tau_1/\epsilon_1)(S_2 - D_A C_A t/h)]} \qquad \text{(Eq. 26)}$$

$$= \frac{K_2}{h + (\tau_1/\epsilon_1)(S_2 - K_1 t)} \qquad \text{(Eq. 27)}$$

where $K_1 = D_A C_A / A_A h$ and $K_2 = D_B C_B / A_B$.

Using Laplace transforms (7) if $S_2 = 0$ at $t = 0$, the solution to Eq. 27 is:

$$t = 1/K_1[S_2 - (\epsilon_1/\tau_1)(K_2/K_1 - h)(1 - \exp -(K_1\tau_1/K_2\epsilon_1)S_2)] \qquad \text{(Eq. 28)}$$

If $S_2 \gg \epsilon_1 K_2/\tau_1 K_1 = \epsilon_1 D_B C_B A_A h/\tau_1 D_A C_A A_B$, Eq. 28 is approximately:

$$t = 1/K_1[S_2 - (\epsilon_1/\tau_1)(K_2/K_1 - h)] \qquad \text{(Eq. 29)}$$

which may be rearranged to:

$$S_2 = K_1 t + (\epsilon_1/\tau_1)(K_2/K_1 - h) \qquad \text{(Eq. 30)}$$

Differentiation of Eq. 30 yields:

$$\frac{dS_2}{dt} = K_1 = \frac{D_A C_A}{A_A h} \qquad \text{(Eq. 31)}$$

Substitution of Eq. 31 into Eq. 21 yields:

$$R_B = \frac{A_B D_A C_A}{A_A h} \qquad \text{(Eq. 32)}$$

$$R_B = \frac{N_B}{N_A} R_A \qquad \text{(Eq. 33)}$$

where N_A and N_B are the mass fractions of component A and B, respectively.

To derive the equation for the dissolution rate of component C, Eqs. 25 and 30 are substituted into Eq. 19 to yield:

$$R_C = \frac{D_C C_C}{h + (\tau_1/\epsilon_1)(K_1 t + Y - K_1 t) + (\tau_2/\epsilon_2)[S_3 - (K_1 t + Y)]} \qquad \text{(Eq. 34)}$$

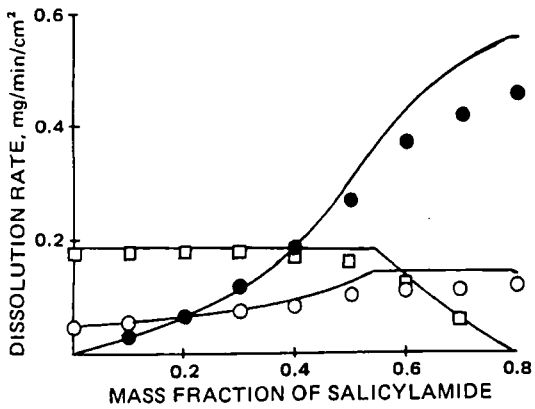

Figure 12—*Comparison of experimental dissolution rates of the components of ethylparaben, phenacetin, and salicylamide mixtures with a constant mass fraction of 0.2 phenacetin corresponding to line XY of Fig. 1 and the curves representing the theoretical rates. Key: (□) ethylparaben; (○) phenacetin; (●) salicylamide.*

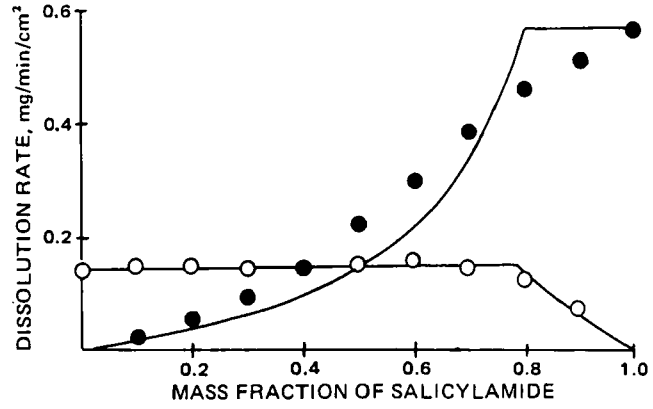

Figure 13—*Comparison of experimental dissolution rates of the components of phenacetin and salicylamide mixtures corresponding to line BC of Fig. 1 and the curves representing the theoretical rates. Key: (○) phenacetin; (●) salicylamide.*

where $Y = (\epsilon_1/\tau_1)(K_2/K_1 - h)$. Combining of Eqs. 22 and 34:

$$\frac{dS_3}{dt} = \frac{K_3}{h + (\tau_1/\epsilon_1)(Y) + (\tau_2/\epsilon_2)[S_3 - (K_1t + Y)]} \quad \text{(Eq. 35)}$$

and $K_3 = D_C C_C / A_C$.

Using Laplace transforms, the solution to Eq. 35 is:

$$t = 1/K_1[S_3 + (\epsilon_2/\tau_2)(K_3K_4 - K_3/K_1) \times (1 - \exp -(\tau_2K_1/\epsilon_2K_3)S_3)] \quad \text{(Eq. 36)}$$

where $K_4 = 1/K_3[h + Y([\tau_1/\epsilon_1] - [\tau_2/\epsilon_2])]$ and $Y = (\epsilon_1/\tau_1)(K_2/K_1 - h)$. If $S_3 \gg \epsilon_2K_3/\iota_2K_1 = \epsilon_2D_CC_CA_Ah/\tau_2D_AC_AA_C$, Eq. 36 simplifies to:

$$t = 1/K_1[S_3 + (\epsilon_2/\tau_2)(K_3K_4 - K_3/K_1)] \quad \text{(Eq. 37)}$$

Differentiating Eq. 37:

$$\frac{dS_3}{dt} = K_1 \quad \text{(Eq. 38)}$$

where $K_1 = D_AC_A/A_Ah$. Substituting Eq. 37 into Eq. 22:

$$R_C = \frac{A_CD_AC_A}{A_Ah} \quad \text{(Eq. 39)}$$

$$R_C = \frac{N_C}{N_A}R_A \quad \text{(Eq. 40)}$$

Equations 17, 33, and 40 may be used to calculate the theoretical dissolution rates of each of the components in a three-component mixture with the dissolution behaviors represented by Cases VI, VII, VIII, IX, and X.

By differential equations similar to those employed in the discussion of Case V dissolution behavior, the theoretical dissolution rate equations for Case XI dissolution behavior are:

$$R_A = \frac{D_AC_A}{h} \quad \text{(Eq. 41)}$$

$$R_B = \frac{D_BC_B}{h} \quad \text{(Eq. 42)}$$

$$R_C = \frac{N_C}{N_A}R_A = \frac{N_C}{N_B}R_B \quad \text{(Eq. 43)}$$

The dissolution rate equations for Case XII and XIII dissolution behavior are similar to those of Case XI.

The dissolution rate equations for Case XIV dissolution behavior are:

$$R_A = \frac{D_AC_A}{h} \quad \text{(Eq. 44)}$$

$$R_B = \frac{N_B}{N_A}R_A \quad \text{(Eq. 45)}$$

$$R_C = \frac{N_C}{N_A}R_A \quad \text{(Eq. 46)}$$

The dissolution rate equations for Case XV and XVI dissolution behavior are similar to those of Case XIV.

The dissolution rate equations for Case IV dissolution behavior are

$$R_A = \frac{D_AC_A}{h} \quad \text{(Eq. 47)}$$

$$R_B = \frac{D_CC_B}{h} \quad \text{(Eq. 48)}$$

$$R_C = \frac{D_CC_C}{h} \quad \text{(Eq. 49)}$$

as the three components coexist at the solid–liquid interface.

RESULTS AND DISCUSSION

Dissolution rates were measured at 25° under sink conditions at the various compositions shown as solid circles in Fig. 1 on lines AB, EF, GH, AC, UV, XY, BC, QR, and ST. For the system investigated A represents ethylparaben, B represents phenacetin, and C represents salicylamide. Lines AB, EF, and GH correspond to varying compositions of ethylparaben and phenacetin with a constant mass fraction of salicylamide of 0, 0.1, and 0.2, respectively. A similar interpretation is given to the other axes of the ternary diagram.

Dissolution rates were measured under identical experimental conditions used previously (3) to determine the effective diffusion layer thickness to be 3×10^{-3} cm. The solubility was experimentally measured. When the dissolution of a nondisintegrating pure solid occurring in a nonreactive medium at sink conditions is diffusion controlled, the dissolution rate may be expressed as (5):

$$R = \frac{DC_s}{h} \quad \text{(Eq. 50)}$$

The only unknown term in Eq. 50 is the diffusion coefficient. Rearranging Eq. 50 and substituting the experimental values for ethylparaben gives:

$$D = \frac{0.0031 \times 3 \times 10^{-3}}{0.939} = 1.00 \times 10^{-5} \text{ cm}^2/\text{sec} \quad \text{(Eq. 51)}$$

In a similar manner the diffusion coefficients of phenacetin and salicylamide were found to be 0.86×10^{-5} and 1.124×10^{-5} cm²/sec, respectively.

To determine the critical composition at which each of the components coexist at the solid–liquid interface with their dissolving boundaries receding at the same rate, the values of the diffusion coefficient and the solubility of the components were substituted into any two combinations of Eqs. 4, 5, or 6 with Eq. 16. By simultaneous solution the critical mass fractions are 0.209 ethylparaben, 0.163 phenacetin, and 0.628 salicylamide.

Similarly, by using the values of solubility and diffusion coefficient and appropriate equations (6), the critical mass fractions for two-component mixtures were calculated. The critical mass fractions are 0.562 ethylparaben and 0.438 phenacetin, 0.25 ethylparaben and 0.75 salicylamide, and 0.794 phenacetin and 0.206 salicylamide.

With these critical compositions for two- and three-component mixtures, Fig. 6 was constructed to show the regions that represent 13 dissolution behaviors and the lines of Fig. 1 from which the various com-

positions were chosen for investigation. By consideration of Fig. 6 and by then employing appropriate equations, the theoretical dissolution rates were calculated from dissolution behavior in the various regions of the diagram.

For Case IV dissolution behavior at the critical composition of the three components, the boundaries recede at the same rate, and the dissolution rates according to Eqs. 47–49 are:

$$R_A = \frac{1.00 \times 10^{-5} \times 0.939}{3 \times 10^{-3}} = 0.0031 \text{ mg/sec/cm}^2 \ (0.188 \text{ mg/min/cm}^2) \quad \text{(Eq. 52)}$$

$$R_B = \frac{0.86 \times 10^{-5} \times 0.842}{3 \times 10^{-3}} = 0.0024 \text{ mg/sec/cm}^2 \ (0.145 \text{ mg/min/cm}^2) \quad \text{(Eq. 53)}$$

$$R_C = \frac{1.124 \times 10^{-5} \times 2.511}{3 \times 10^{-3}} = 0.0094 \text{ mg/sec/cm}^2 \ (0.565 \text{ mg/min/cm}^2) \quad \text{(Eq. 54)}$$

To illustrate other calculations, consider the line QR passing through the regions BMP, BJM, CMJ, and CKM of Fig. 6. In the BMP region the dissolution behavior described as Case VII exists. A composition of 0.75 phenacetin, 0.10 ethylparaben, and 0.15 salicylamide on line QR lies in this regions in which:

$$\frac{N_B}{N_A} > \frac{D_B C_B}{D_A C_A} \quad \text{(Eq. 55)}$$

and

$$\frac{N_B}{N_C} > \frac{D_B C_B}{D_C C_C} \quad \text{(Eq. 56)}$$

Thus, phenacetin exists in a layer at the solid surface while the boundaries of ethylparaben and salicylamide have receded into the solid. At this composition:

$$\frac{N_A}{N_C} > \frac{D_A C_A}{D_C C_C} \quad \text{(Eq. 57)}$$

so that the dissolving and receding boundary of salicylamide recedes further than that of ethylparaben.

The dissolution rate of phenacetin according to Eq. 50 is:

$$R_B = \frac{0.86 \times 10^{-5} \times 0.842}{3 \times 10^{-3}} = 0.0024 \text{ mg/sec/cm}^2 \ (0.145 \text{ mg/min/cm}^2) \quad \text{(Eq. 58)}$$

The dissolution rates of ethylparaben and salicylamide are:

$$R_A = \frac{0.1}{0.75} \times 0.145 = 0.019 \text{ mg/min/cm}^2 \quad \text{(Eq. 59)}$$

and

$$R_C = \frac{0.15}{0.75} \times 0.145 = 0.029 \text{ mg/min/cm}^2 \quad \text{(Eq. 60)}$$

according to Eqs. 33 and 40.

For a solid composition of three components with mass fractions of 0.1 ethylparaben, 0.6 phenacetin, and 0.3 salicylamide on lines QR and BM separating regions BMP and BJM of Fig. 6:

$$\frac{N_B}{N_A} > \frac{D_B C_B}{D_A C_A} \quad \text{(Eq. 61)}$$

$$\frac{N_B}{N_C} > \frac{D_B C_B}{D_C C_C} \quad \text{(Eq. 62)}$$

and

$$\frac{N_A}{N_C} = \frac{D_C C_A}{D_C C_C} \quad \text{(Eq. 63)}$$

This composition is described as Case XV dissolution behavior in which both ethylparaben and salicylamide have their dissolving and receding boundaries at the same rate within the solid leaving phenacetin at the solid surface.

The dissolution rate of phenacetin according to Eq. 50 is 0.145 mg/min/cm^2. The dissolution rates of ethylparaben and salicylamide are:

$$R_A = \frac{0.1}{0.6} \times 0.145 = 0.023 \text{ mg/min/cm}^2 \quad \text{(Eq. 64)}$$

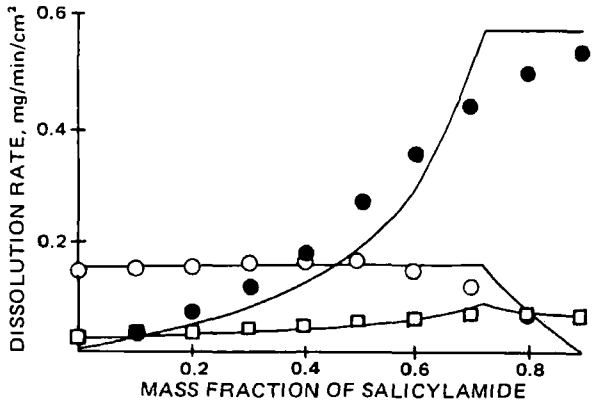

Figure 14—*Comparison of experimental dissolution rates of the components of ethylparaben, phenacetin, and salicylamide mixtures with a constant mass fraction of 0.1 ethylparaben corresponding to line QR of Fig. 1 and the curves representing the theoretical rates. Key: (□) ethylparaben; (○) phenacetin; (●) salicylamide.*

and

$$R_C = \frac{0.3}{0.6} \times 0.145 = 0.073 \text{ mg/min/cm}^2 \quad \text{(Eq. 65)}$$

according to Eqs. 45 and 46.

A solid composition of 0.1 ethylparaben, 0.4 phenacetin, and 0.5 salicylamide is described by Case VIII dissolution behavior in region BJM in which:

$$\frac{N_B}{N_A} > \frac{D_B C_B}{D_A C_A} \quad \text{(Eq. 66)}$$

$$\frac{N_B}{N_C} > \frac{D_B C_B}{D_C C_C} \quad \text{(Eq. 67)}$$

and

$$\frac{N_C}{N_A} > \frac{D_C C_C}{D_A C_A} \quad \text{(Eq. 68)}$$

The dissolution rate of phenacetin according to Eq. 50 is 0.145 mg/min/cm^2. The dissolution rates of salicylamide and ethylparaben are:

$$R_C = \frac{0.5}{0.4} \times 0.145 = 0.181 \text{ mg/min/cm}^2 \quad \text{(Eq. 69)}$$

and

$$R_A = \frac{0.1}{0.4} \times 0.145 = 0.036 \text{ mg/min/cm}^2 \quad \text{(Eq. 70)}$$

A solid composition of three components with mass fractions of 0.1 ethylparaben, 0.184 phenacetin, and 0.716 salicylamide on line QR is described by Case XIII dissolution behavior on line JM (which separates regions BJM and CMJ) on which:

$$\frac{N_A}{N_B} < \frac{D_A C_A}{D_B C_B} \quad \text{(Eq. 71)}$$

$$\frac{N_A}{N_C} < \frac{D_A C_A}{D_C C_C} \quad \text{(Eq. 72)}$$

and

$$\frac{N_B}{N_C} = \frac{D_B C_B}{D_C C_C} \quad \text{(Eq. 73)}$$

The dissolution rates of phenacetin and salicylamide according to Eqs. 41 and 42 are 0.145 and 0.565 mg/min/cm^2. The dissolution rate of ethylparaben according to Eq. 43 is:

$$R_A = \frac{0.1}{0.184} \times 0.145 = 0.079 \text{ mg/min/cm}^2 \quad \text{(Eq. 74)}$$

A solid with a mass fraction of 0.1 ethylparaben, 0.13 phenacetin, and

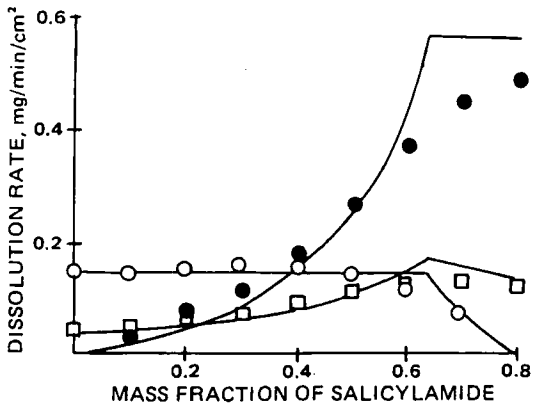

Figure 15—*Comparison of experimental dissolution rates of the components of ethylparaben, phenacetin, and salicylamide mixtures with a constant mass fraction of 0.2 ethylparaben corresponding to line ST of Fig. 1 and the curves representing the theoretical rates. Key: (□) ethylparaben; (○) phenacetin; (●) salicylamide.*

0.77 salicylamide on line QR has a Case X dissolution behavior in the region CMJ in which:

$$\frac{N_C}{N_A} > \frac{D_C C_C}{D_A C_A} \quad \text{(Eq. 75)}$$

$$\frac{N_C}{N_B} > \frac{D_C C_C}{D_B C_B} \quad \text{(Eq. 76)}$$

and

$$\frac{N_B}{N_A} > \frac{D_B C_B}{D_A C_A} \quad \text{(Eq. 77)}$$

In Case X dissolution behavior the dissolving and receding boundary of ethylparaben is deepest within the solid, the boundary of salicylamide is at the surface, and the boundary of phenacetin is between the two boundaries. The dissolution rate of salicylamide according to Eq. 50 is 0.565 mg/min/cm². The dissolution rate of phenacetin is:

$$R_B = \frac{0.13}{0.77} \times 0.565 = 0.095 \text{ mg/min/cm}^2 \quad \text{(Eq. 78)}$$

The dissolution rate of ethylparaben is:

$$R_A = \frac{0.1}{0.77} \times 0.565 = 0.073 \text{ mg/min/cm}^2 \quad \text{(Eq. 79)}$$

A solid composition with mass fractions of 0.1 ethylparaben, 0.075 phenacetin, and 0.825 salicylamide on line QR is described by Case XVI dissolution behavior on line CM (which separates regions CMJ and CKM) on which:

$$\frac{N_C}{N_A} > \frac{D_C C_C}{D_A C_A} \quad \text{(Eq. 80)}$$

$$\frac{N_C}{N_B} > \frac{D_C C_C}{D_B C_B} \quad \text{(Eq. 81)}$$

and

$$\frac{N_A}{N_B} = \frac{D_A C_A}{D_B C_B} \quad \text{(Eq. 82)}$$

At this composition salicylamide forms the surface layer, and the dissolving and receding boundaries of ethylparaben and phenacetin recede at the same rate within the solid. The dissolution rate of salicylamide according to Eq. 50 is 0.565 mg/min/cm². The dissolution rate of ethylparaben is:

$$R_A = \frac{0.1}{0.825} \times 0.565 = 0.068 \text{ mg/min/cm}^2 \quad \text{(Eq. 83)}$$

The dissolution rate of phenacetin is:

$$R_B = \frac{0.075}{0.825} \times 0.565 = 0.051 \text{ mg/min/cm}^2 \quad \text{(Eq. 84)}$$

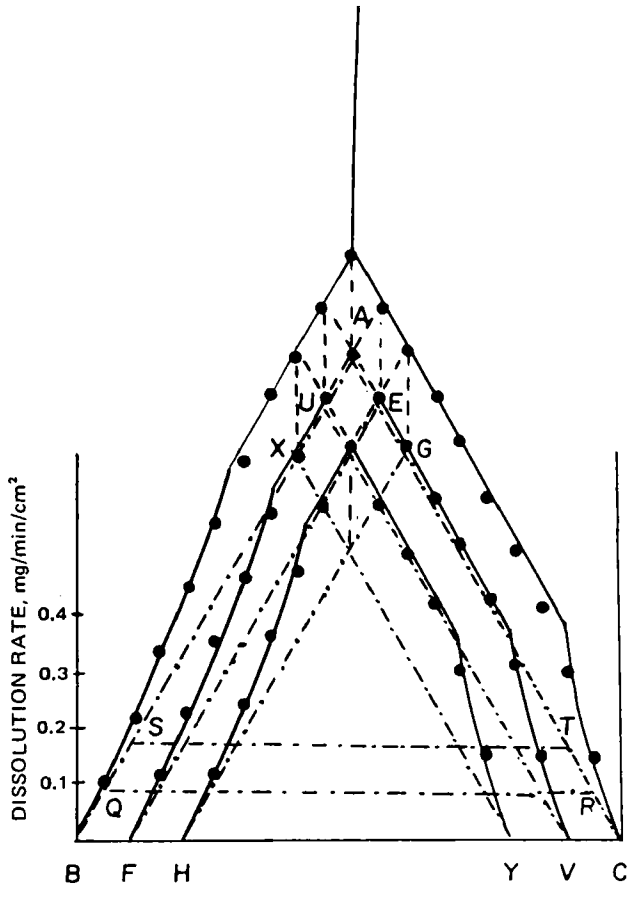

Figure 16—*Comparison of experimental dissolution rates of ethylparaben in solids of various compositions of ethylparaben, phenacetin, and salicylamide with theoretical dissolution rates represented by the solid lines in a three-dimensional perspective. Key: (A) ethylparaben; (B) phenacetin; (C) salicylamide.*

A solid composition with mass fractions of 0.1 ethylparaben, 0.05 phenacetin, and 0.85 salicylamide is described by Case IX dissolution behavior in region CKM in which the dissolving and receding boundary of phenacetin is deepest within the solid, the boundary of salicylamide is the surface layer, and the boundary of ethylparaben is between the two boundaries. The dissolution rate of salicylamide according to Eq. 50 is 0.565 mg/min/cm². The dissolution rate of ethylparaben is:

$$R_A = \frac{0.10}{0.85} \times 0.565 = 0.066 \text{ mg/min/cm}^2 \quad \text{(Eq. 85)}$$

The dissolution rate of phenacetin is:

$$R_B = \frac{0.05}{0.85} \times 0.565 = 0.033 \text{ mg/min/cm}^2 \quad \text{(Eq. 86)}$$

For two-component mixtures the dissolution rates were calculated according to the equations presented previously (6) for Cases I, II, and III. For example, a mixture of ethylparaben and phenacetin has a critical composition of 0.562 ethylparaben and 0.438 phenacetin at which:

$$\frac{N_A}{N_B} = \frac{D_A C_A}{D_B C_B} \quad \text{(Eq. 87)}$$

At the critical composition as represented by point P on line AB in Fig. 6, the dissolution rates of ethylparaben and phenacetin according to Eq. 50 are 0.188 and 0.145 mg/min/cm², respectively. A two-component solid composed of mass fractions of 0.3 ethylparaben and 0.7 phenacetin is represented by line BP on which:

$$\frac{N_A}{N_B} < \frac{D_A C_A}{D_B C_B} \quad \text{(Eq. 88)}$$

Phenacetin exists as the surface layer with the dissolving and receding boundary of ethylparaben within the solid. The dissolution rate of

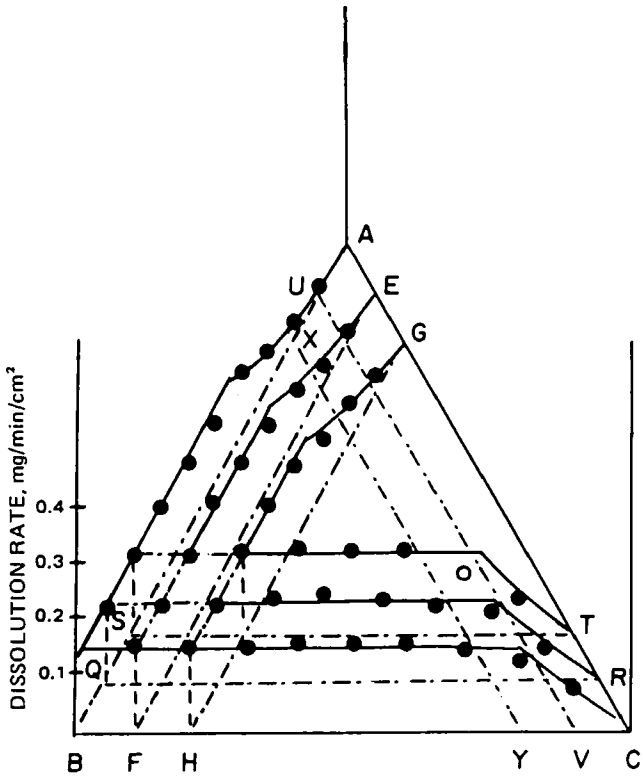

Figure 17—*Comparison of experimental dissolution rates of phenacetin in solids of various compositions of ethylparaben, phenacetin, and salicylamide with theoretical dissolution rates represented by solid lines in a three dimensional perspective. Key: (A) ethylparaben; (B) phenacetin; (C) salicylamide.*

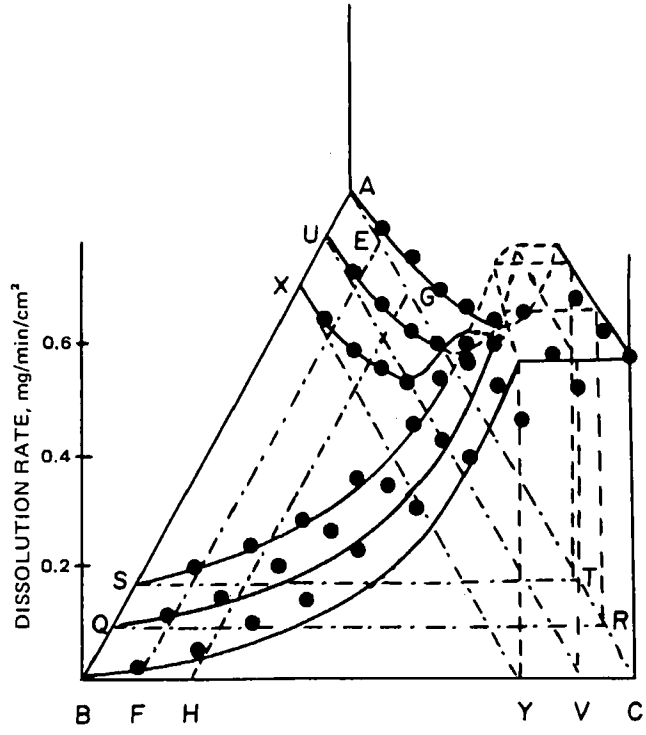

Figure 18—*Comparison of experimental dissolution rates of salicylamide in solids of various compositions of ethylparaben, phenacetin, and salicylamide with theoretical dissolution rates represented by the solid lines in a three dimensional perspective. Key: (A) ethylparaben; (B) phenacetin; (C) salicylamide.*

phenacetin according to Eq. 50 is 0.145 mg/min/cm^2. The dissolution rate of ethylparaben is:

$$R_A = \frac{0.3}{0.7} \times 0.145 = 0.062 \text{ mg/min/cm}^2 \quad \text{(Eq. 89)}$$

In a similar manner the predicted dissolution rates of each component were calculated and compared in Figs. 7–15 to the experimental dissolution rates at corresponding compositions. In Figs. 7, 10, and 13 the experimental dissolution rates of two-component mixtures of ethylparaben and phenacetin, ethylparaben and salicylamide, and phenacetin and salicyamide correspond in Fig. 6 to lines AB, AC, and BC, respectively. The experimental dissolution rates approximate the predicted dissolution rates for the ethylparaben and phenacetin mixture and for the ethylparaben and salicylamide mixture. As it has been observed previously (4, 6), the greatest difference between the predicted and experimental values occurs about the critical composition. This may result because the model ignores the amount of components in solution in the pores of the layers. In Fig. 13 for the phenacetin and salicylamide mixture, the experimental dissolution rates of salicylamide are faster than the predicted dissolution rates at mass fractions of 0.1–0.7 salicylamide. These faster dissolution rates may be attributed to the greater solubility of salicylamide, which dissolves faster leaving a surface layer of phenacetin. The mechanically weak surface of phenacetin, which possesses poor bonding characteristics, erodes slightly, and the increase in the effective surface area because of flaking results in a greater quantity dissolving per unit time.

In Figs. 8, 9, 11, 12, 14, and 15 the theoretical and experimental dissolution rates are compared for compositions in which the mass fraction of one component is constant and the mass fractions of the other components are varied. Figures 8 and 9 show the comparison of the predicted and experimental dissolution rates of ethylparaben, phenacetin, and salicylamide with a constant mass fraction of salicylamide of 0.1 and 0.2 corresponding to lines EF and GH, respectively, and varying mass fractions of ethylparaben and phenacetin. The predicted and experimental dissolution rates vary only about the critical composition. In Fig. 9 the experimental dissolution rates are faster than the predicted dissolution rates at mass fractions >0.5 phenacetin for solids with a constant mass fraction of 0.2 salicylamide. Again this may be attributed to the weak mechanical strength and consequential flaking due to the weak bonding of phenacetin.

The dissolution rates of ethylparaben, phenacetin, and salicylamide are shown in Figs. 11 and 12 with a constant mass fraction of phenacetin of 0.1 and 0.2 corresponding to lines UV and XY of Fig. 6. The dissolution rates of ethylparaben, phenacetin, and salicylamide are shown in Figs. 14 and 15 with a constant mass fraction of ethylparaben corresponding to lines QR and ST in Fig. 6.

A diagram of three-dimensional perspective is shown in Fig. 16 for the experimental and predicted dissolution rates of ethylparaben from three-component mixtures. Similarly, the experimental and predicted dissolution rates of phenacetin and salicylamide from three-component mixtures are presented in Figs. 17 and 18, respectively.

The experimental dissolution rates of the components of various compositions of ethylparaben, phenacetin, and salicylamide from compressed spheres essentially substantiates the suggested model for the dissolution kinetics of a three-component, nondisintegrating solid.

REFERENCES

(1) G. R. Carmichael, S. A. Shah, and E. L. Parrott, *J. Pharm. Sci.*, **70**, 1331 (1981).

(2) E. L. Parrott, D. E. Wurster, and T. Higuchi, *J. Am. Pharm. Assoc., Sci. Ed.*, **44**, 269 (1955).

(3) R. J. Braun and E. L. Parrott, *J. Pharm. Sci.*, **61**, 175 (1972).

(4) S. A. Shah and E. L. Parrott, *ibid.*, **65**, 1874 (1976).

(5) E. L. Parrott and V. K. Sharma, *ibid.*, **56**, 1341 (1967).

(6) W. I. Higuchi, N. A. Mir, and S. J. Desai, *ibid.*, **54**, 1405 (1965).

(7) E. D. Rainville, "The Laplace Transforms, An Introduction," Macmillan, New York, N.Y., 1963.

ACKNOWLEDGMENTS

Abstracted in part from a dissertation submitted by Michael Simpson to the Graduate College, University of Iowa in partial fulfillment of the Doctor of Philosophy degree requirements.

Dissolution Kinetics of a Three-Component Solid II: Benzoic Acid, Salicylic Acid, and Salicylamide

E. L. PARROTT ˣ, M. SIMPSON, and D. R. FLANAGAN

Received March 22, 1982, from the *Division of Pharmaceutics, College of Pharmacy, University of Iowa, Iowa City, IA 52242.* Accepted for publication May 24, 1982.

Abstract □ The dissolution rates of each component in compressed spheres consisting of three components were measured under sink conditions. The observed dissolution rates of benzoic acid, salicylic acid, and salicylamide compare favorably to the predicted dissolution rates according to a previously presented kinetic model.

Keyphrases □ Benzoic acid—dissolution kinetics of a three-component solid, salicylic acid, salicylamide □ Salicylic acid—dissolution kinetics of a three-component solid, benzoic acid, salicylamide □ Salicylamide—dissolution kinetics of a three-component solid, benzoic acid, salicylic acid

A dissolution model has been presented to describe the 13 dissolution behaviors of three-component, nondisintegrating solids (1). In continuing the study of dissolution phenomena the dissolution rates of benzoic acid, salicylic acid, and salicylamide from compressed spheres were determined and compared to calculated dissolution rates in order to examine the suitability of the suggested dissolution model.

EXPERIMENTAL

Preparation of Spheres—Twenty grams of each composition was prepared by blending the appropriate amounts of 60/80-mesh size fraction of benzoic acid[1], salicylic acid[2], and salicylamide[3] for 15 min in a V-blender[4]. By means of a hydraulic press[5] fitted with a spherical punch and die set, each composition was compressed at a force of 2268 kg into spheres having a diameter of 1.273 ± 0.005 cm. The compositions were selected according to a scheme previously described (1).

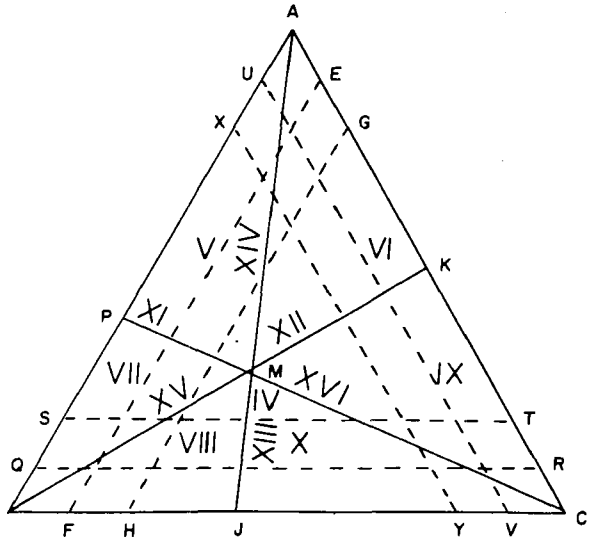

Figure 1—*Composition diagram for mixtures of benzoic acid, salicylic acid, and salicylamide showing the regions corresponding to the 13 dissolution behaviors and their relation to the compositions selected for investigation according to the scheme in Fig. 1 of Ref. 1.*

[1] ACS, Fisher, lot no. 783313.
[2] USP, J. T. Baker, lot no. 43397.
[3] Sigma, lot no. 106C-0409.
[4] Patterson-Kelly.
[5] Carver press, model C.

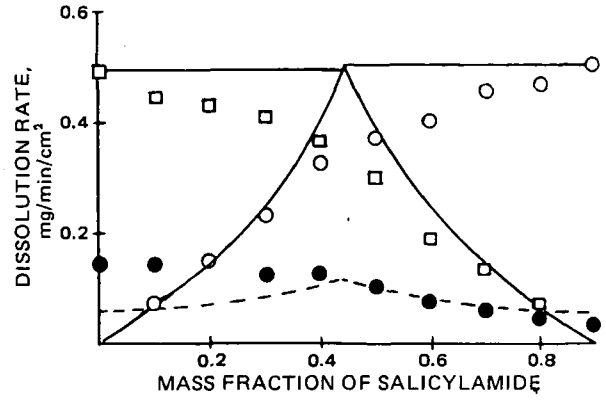

Figure 2—*Comparison of experimental dissolution rates of the components of benzoic acid, salicylic acid, and salicylamide mixtures with a constant mass fraction of 0.1 benzoic acid corresponding to line UV of Fig. 1 and the smooth curves representing the theoretical rates. Key: (●) benzoic acid; (□) salicylic acid; and (○) salicylamide.*

Dissolution Rate—The dissolution rate was determined in distilled water at 25 ± 0.1° at 300 rpm, as described previously (2, 3), under conditions where the concentration of the solutes did not exceed 5% of solubility.

Solubility—Solubility measurements were made at 25 ± 0.1° as reported earlier (4). The solubilities of benzoic acid, salicylic acid, and salicylamide are 3.428 ± 0.064, 2.239 ± 0.027, and 2.511 ± 0.018 mg/ml, respectively.

Analytical Procedure—The absorbance of each sample was measured at 269.5, 298, and 329 nm. The standard curve of each component at each wavelength exhibited a Beer's law relationship. From these plots the nine molar absorptivities were calculated (Table I). As previously described (1) the concentration of each component in solution was obtained by the solution of simultaneous equations. The method was tested with seven solutions containing known concentrations of the three components. The percent determined by the analytical procedure ranged from 98.9 to 101.8% of the known concentration. The concentration was converted to amount dissolved in order to express a dissolution rate.

RESULTS AND DISCUSSION

A detailed discussion of a model for dissolution of a three-component solid has been presented (1). The 13 dissolution behaviors at various compositions are identified by the Roman numerals in Fig. 1. For the system investigated, A represents salicylic acid, B represents benzoic acid, and C represents salicylamide.

Dissolution rates (R) were measured at 25° under sink conditions at various compositions. The solubilities (C_s) were experimentally measured. When the dissolution of a nondisintegrating pure solid occurring in a nonreactive medium at sink conditions is diffusion controlled, the dissolution rate may be expressed (2):

$$R = \frac{DC_s}{h} \qquad \text{(Eq. 1)}$$

Table I—Molar Absorptivities of Benzoic Acid, Salicylic Acid, and Salicylamide

Wavelength, nm	Molar Absorptivity		
	Benzoic Acid	Salicylic Acid	Salicylamide
269.5	578	680	195
298	0	3,522	1,477
329	0	256	5,632

0022-3549/83/0700-0765$01.00/0

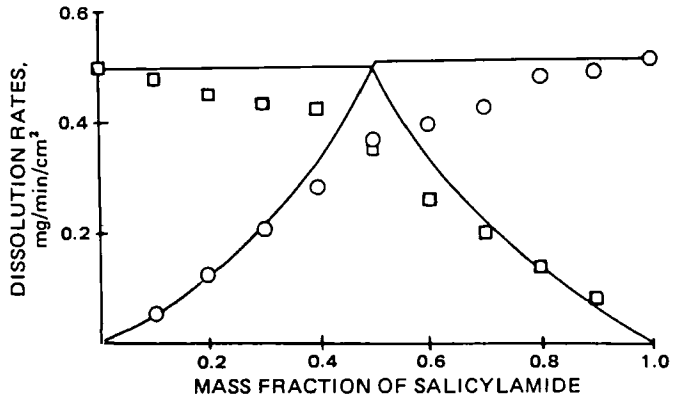

Figure 3—*Comparison of experimental dissolution rates of the components of salicylic acid and salicylamide mixtures corresponding to line AC of Fig. 1 and the smooth curves representing the theoretical rates. Key: (□) salicylic acid; and (○) salicylamide.*

where h is the effective diffusion layer thickness. The diffusion coefficient of salicylamide was reported (1) to be 1.12×10^{-5} cm²/sec. The only unknown term in the equation is h, which may be calculated by rearrangement and substitution of experimental values for salicylamide:

$$h = \frac{1.12 \times 10^{-5} \times 2.51}{0.505/60} = 0.0033 \text{ cm} \quad \text{(Eq. 2)}$$

Using this value of h, the diffusion coefficients of benzoic acid and salicylic acid were calculated to be 1.19×10^{-5} and 1.21×10^{-5} cm²/sec, respectively.

The critical composition (Case IV at point M of Fig. 1) at which the three components coexist at the solid–liquid interface may be expressed:

$$\frac{N_A}{N_B} = \frac{D_A C_A}{D_B C_B} \quad \text{(Eq. 3)}$$

$$\frac{N_A}{N_C} = \frac{D_A C_A}{D_C C_C} \quad \text{(Eq. 4)}$$

and

$$\frac{N_B}{N_C} = \frac{D_B C_B}{D_C C_C} \quad \text{(Eq. 5)}$$

where N is the mass fraction of a component, and C is the solubility of that component. Since:

$$N_A + N_B + N_C = 1 \quad \text{(Eq. 6)}$$

substitution of the values of diffusion coefficient and solubility of the components into any two combinations of Eqs. 3, 4, or 5 with Eq. 6 and solution of the simultaneous equations permit the calculation of the mass fraction of each component. The critical mass fractions are 0.425 benzoic acid, 0.293 salicylamide, and 0.282 salicylic acid.

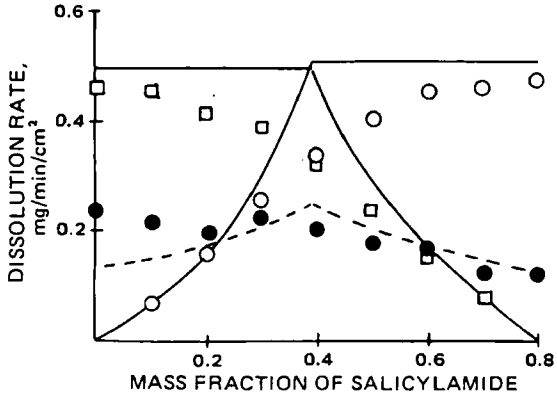

Figure 4—*Comparison of experimental dissolution rates of the components of benzoic acid, salicylic acid, and salicylamide mixtures with a constant mass fraction of 0.2 benzoic acid corresponding to line XY of Fig. 1 and the smooth curves representing the theoretical rates. Key: (●) benzoic acid; (□) salicylic acid; and (○) salicylamide.*

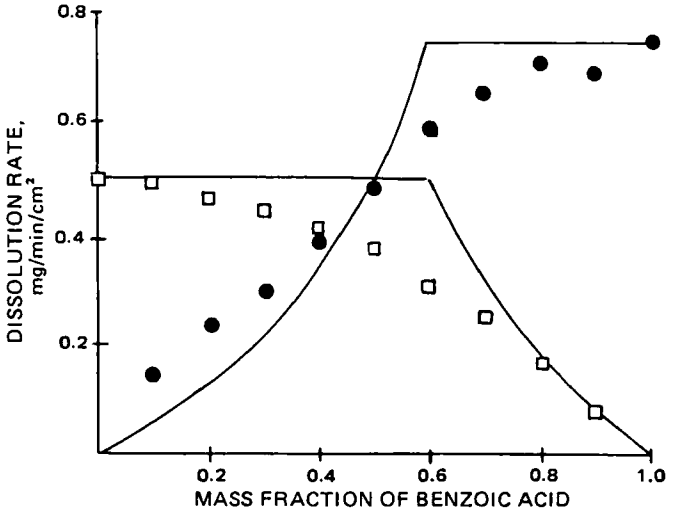

Figure 5—*Comparison of experimental dissolution rates of the components of salicylic acid and benzoic acid mixtures corresponding to line AB of Fig. 1 and the smooth curve representing the theoretical rates. Key: (□) salicylic acid; and (●) benzoic acid.*

Similarly, by use of the values of solubility and diffusion coefficient and appropriate equations (5), the critical mass fractions for two-component mixtures were calculated. The critical mass fractions are 0.40 salicylic acid and 0.60 benzoic acid, 0.59 benzoic acid and 0.41 salicylamide, and 0.49 salicylic acid and 0.51 salicylamide.

Using these critical compositions for two- and three-component mixtures, Fig. 1 was constructed to show the regions that represent the 13 dissolution behaviors. By considering Fig. 1 and by then using appropriate equations, the theoretical dissolution rates were calculated for dissolution behavior in the various regions of the diagram.

For Case IV dissolution behavior at the critical composition of the three components and boundaries recede at the same rate, and the dissolution rates may be calculated by Eq. 1. The dissolution rates of benzoic acid, salicylic acid, and salicylamide are 0.742, 0.493, and 0.505 mg/min/cm², respectively.

A constant mass fraction of 0, 0.1, and 0.2 benzoic acid and varying mass fractions of salicylic acid and salicylamide are represented by lines AC, UV, and XY, respectively, in Fig. 1. In considering line UV at point U there is a two-component solid for which salicylic acid is the surface layer, and the dissolution behavior is expressed by Case II behavior in which:

$$\frac{N_A}{N_B} > \frac{D_A C_A}{D_B C_B} \quad \text{(Eq. 7)}$$

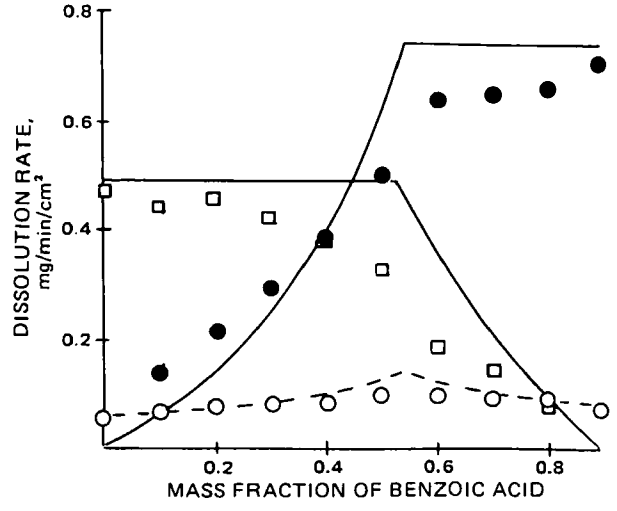

Figure 6—*Comparison of experimental dissolution rates of the components of benzoic acid, salicylic acid, and salicylamide mixtures with a constant mass fraction of 0.1 salicylamide corresponding to line EF of Fig. 1 and the smooth curves representing the theoretical rates. Key: (●) benzoic acid; (□) salicylic acid; and (○) salicylamide.*

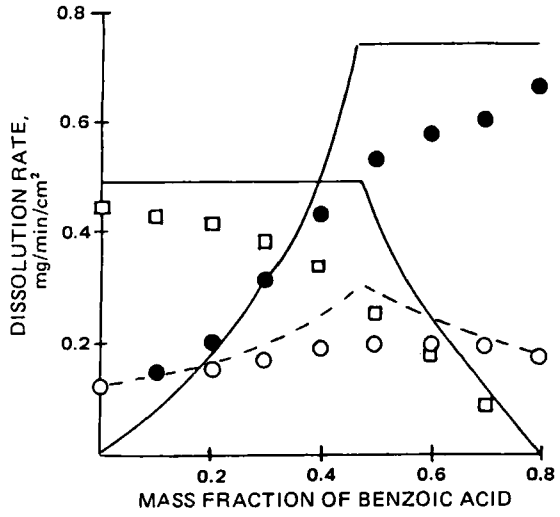

Figure 7—*Comparison of experimental dissolution rates of the components of benzoic acid, salicylic acid, and salicylamide mixtures with a constant mass fraction of 0.2 salicylamide corresponding to line GH of Fig. 1 and the smooth curves representing the theoretical rates. Key: (●) benzoic acid; (□) salicylic acid; and (○) salicylamide.*

and the dissolution rate of salicylic acid according to Eq. 1 is 0.493 mg/min/cm², and the dissolution rate of benzoic acid is:

$$R_B = \frac{N_B}{N_A} R_A \qquad \text{(Eq. 8)}$$

$$R_B = \frac{0.1}{0.9} \times 0.493 \qquad \text{(Eq. 9)}$$

$$= 0.055 \text{ mg/min/cm}^2$$

Since the mass fraction of salicylamide is progressively increased along line UV, the dissolution behaviors are expressed by Case V in region APM, Case XIV on line AM, Case VI in region AMK, Case XII on line MK, Case IX in region KMC, Case XVI on line MC, and Case X in region MCJ. At point V there is a two-component solid for which:

$$\frac{N_C}{N_B} > \frac{D_C C_C}{D_B C_B} \qquad \text{(Eq. 10)}$$

and the dissolution rate of salicylamide according to Eq. 1 is 0.511 mg/min/cm², and the dissolution rate of benzoic acid is:

$$R_B = \frac{N_B}{N_C} R_C \qquad \text{(Eq. 11)}$$

$$R_B = \frac{0.1}{0.9} \times 0.511 \qquad \text{(Eq. 12)}$$

$$= 0.057 \text{ mg/min/cm}^2$$

In Case V dissolution behavior, salicylamide dissolves faster than benzoic acid and salicylic acid, and the boundary of salicylamide recedes into the solid. Benzoic acid dissolves faster from the solid surface than salicylic acid, so that the dissolving boundary of benzoic acid recedes within the solid leaving a surface layer of salicylic acid. This dissolution behavior occurs under the conditions that:

$$\frac{N_A}{N_B} > \frac{D_A C_A}{D_B C_B} \qquad \text{(Eq. 13)}$$

$$\frac{N_A}{N_C} > \frac{D_A C_A}{D_C C_C} \qquad \text{(Eq. 14)}$$

and

$$\frac{N_B}{N_C} > \frac{D_B C_B}{D_C C_C} \qquad \text{(Eq. 15)}$$

Since salicylic acid is always on the surface at compositions represented by Eqs. 13–15, its dissolution rate (R_A) is calculated by Eq. 1 is 0.493 mg/min/cm². The benzoic acid must diffuse through the layer of salicylic acid and the liquid diffusion layer, and its dissolution rate (R_B) is:

$$R_B = \frac{N_B}{N_A} R_A \qquad \text{(Eq. 16)}$$

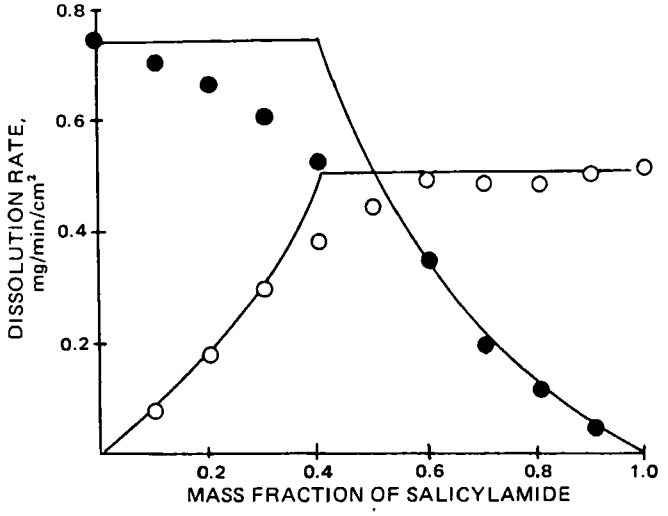

Figure 8—*Comparison of experimental dissolution rates of the components of benzoic acid and salicylamide mixtures corresponding to line BC of Fig. 1 and the smooth curves representing the theoretical rates. Key: (●) benzoic acid; and (○) salicylamide.*

For example, at mass fractions of 0.1 benzoic acid, 0.88 salicylic acid, and 0.02 salicylamide, the dissolution rate of benzoic acid (R_B) is:

$$R_B = \frac{0.1}{0.88} \times 0.493$$

$$= 0.056 \text{ mg/min/cm}^2 \qquad \text{(Eq. 17)}$$

The salicylamide must diffuse through the layer of benzoic acid and salicylic acid, the layer of salicylic acid, and the liquid diffusion layer, and its dissolution rate (R_C) is:

$$R_C = \frac{N_C}{N_A} R_A \qquad \text{(Eq. 18)}$$

At mass fractions of 0.1 benzoic acid, 0.88 salicylic acid, and 0.02 salicylamide, the dissolution rate of salicylamide (R_C) is:

$$R_C = \frac{0.22}{0.88} \times 0.493$$

$$= 0.011 \text{ mg/min/cm}^2 \qquad \text{(Eq. 19)}$$

Case VI, IX, and X in Fig. 1 describe dissolution behaviors similar to Case V; however, the order of dissolving and the receding of the boundaries are different with different mass fractions of salicylic acid and salicylamide along line UV. The dissolution rates may be calculated by the same reasoning used for Case V dissolution behavior.

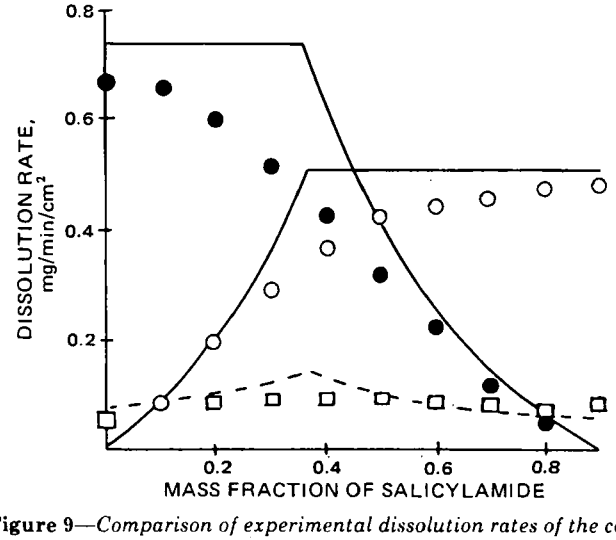

Figure 9—*Comparison of experimental dissolution rates of the components of benzoic acid, salicylic acid, and salicylamide mixtures with a constant mass fraction of 0.1 salicylic acid corresponding to line QR of Fig. 1 and the smooth curves representing the theoretical rates. Key: (●) benzoic acid; (□) salicylic acid; and (○) salicylamide.*

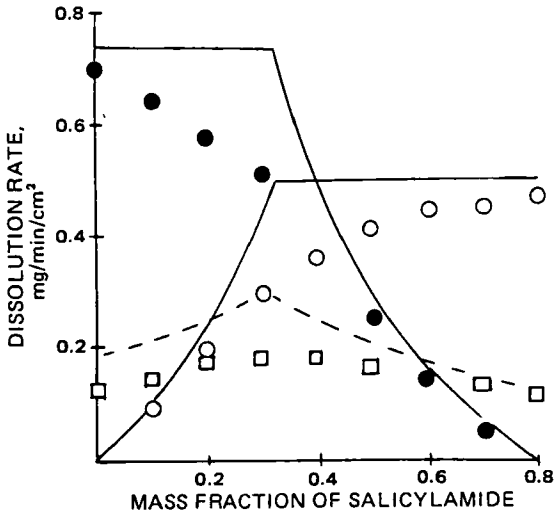

Figure 10—*Comparison of experimental dissolution rates of the components of benzoic acid, salicylic acid, and salicylamide mixtures with a constant mass fraction of 0.2 salicylic acid corresponding to line ST of Fig. 1 and the smooth curves representing the theoretical rates. Key: (●) benzoic acid; (□) salicylic acid; and (○) salicylamide.*

In Case XIV dissolution behavior on line AM, both benzoic acid and salicylamide dissolve faster than salicylic acid so that the boundaries of benzoic acid and salicylamide recede at the same rate and coexist at the same boundary leaving a surface layer of salicylic acid. Case XIV dissolution behavior occurs under the condition that:

$$\frac{N_A}{N_B} > \frac{D_A C_A}{D_B C_B} \quad \text{(Eq. 20)}$$

$$\frac{N_A}{N_C} > \frac{D_A C_A}{D_C C_C} \quad \text{(Eq. 21)}$$

and

$$\frac{N_B}{N_C} = \frac{D_B C_B}{D_C C_C} \quad \text{(Eq. 22)}$$

The dissolution rate equations for Case XIV dissolution behavior are:

$$R_A = \frac{D_A C_A}{h} \quad \text{(Eq. 23)}$$

$$R_C = \frac{N_B}{N_A} R_A \quad \text{(Eq. 24)}$$

and

$$R_C = \frac{N_C}{N_A} R_A \quad \text{(Eq. 25)}$$

At mass fractions of 0.831 salicylic acid, 0.1 benzoic acid, and 0.069 salicylamide, the dissolution rate of salicylic acid as calculated by Eq. 23 is 0.493 mg/min/cm². The dissolution rate of benzoic acid according to Eq. 24 is:

$$R = \frac{0.1}{0.831} \times 0.493 = 0.056 \text{ mg/min/cm}^2 \quad \text{(Eq. 26)}$$

and the dissolution rate of salicylamide according to Eq. 25 is:

$$R = \frac{0.069}{0.831} \times 0.493 = 0.041 \text{ mg/min/cm}^2 \quad \text{(Eq. 27)}$$

Case XVI dissolution behavior is similar to Case XIV except that the order of dissolving and the receding of the boundaries are different with their respective mass fractions of salicylic acid and salicylamide. The dissolution rates may be calculated by the same reasoning used for Case XIV dissolution behavior.

In Case XII dissolution behavior benzoic acid dissolves leaving a surface layer of salicylic acid and salicylamide under the conditions that:

$$\frac{N_B}{N_A} < \frac{D_B C_B}{D_A C_A} \quad \text{(Eq. 28)}$$

$$\frac{N_B}{N_C} < \frac{D_B C_B}{D_C C_C} \quad \text{(Eq. 29)}$$

and

$$\frac{N_A}{N_C} = \frac{D_A C_A}{D_C C_C} \quad \text{(Eq. 30)}$$

The dissolution rates as calculated by use of Eq. 1 are 0.493 and 0.511 mg/min/cm² for salicylic acid and salicylamide, respectively. The dissolution rate of benzoic acid is:

$$R_B 2 = \frac{N_B}{N_A} R_A \quad \text{(Eq. 31)}$$

$$R_B = \frac{0.1}{0.46} \times 0.493 = 0.107 \text{ mg/min/cm}^2 \quad \text{(Eq. 32)}$$

Thus, along line UV from point U to point V the nine dissolution behaviors and the calculation of the dissolution rates of the components at each composition have been considered as shown in Fig. 2. Similarly, the dissolution rates of benzoic acid, salicylic acid, and salicylamide are shown at various compositions with a constant mass fraction of 0 and 0.2 benzoic acid along lines AC and XY in Figs. 3 and 4, respectively.

The dissolution rates of benzoic acid and salicylic acid at various compositions along line AB are shown in Fig. 5. The dissolution rates of benzoic acid, salicylic acid, and salicylamide are shown at various compositions with a constant mass fraction of 0.1 and 0.2 salicylamide along lines EF and GH in Figs. 6 and 7, respectively.

The dissolution rates of benzoic acid and salicylamide at various compositions along line BC are shown in Fig. 8. The dissolution rates of benzoic acid, salicylic acid, and salicylamide are shown at various compositions with a constant mass fraction of 0.1 and 0.2 salicylic acid along lines QR and ST in Figs. 9 and 10, respectively.

The agreement of the theoretical dissolution rates with the experimental data is satisfactory. The greatest variance occurs in the vicinity of the critical composition at which the experimental dissolution rates are slower. The model neglects the amount of the components that remained as solutions in the pores of the layers. This may contribute to the variance. Variance may also be caused by lack of uniformity of the blend and the limits of the analytical method at small mass fractions of a component.

CONCLUSION

The dissolution rates of each component of benzoic acid, salicylic acid, and salicylamide compacts were measured and compared to theoretical dissolution rates based on a previously described model. On initially presenting the model a similar comparison was made for ethylparaben, phenacetin, and salicylamide compacts (1). The agreement between the experimental and calculated dissolution rates for both systems support the suitability of the model.

REFERENCES

(1) M. Simpson and E. L. Parrott, *J. Pharm. Sci.*, **72**, 757 (1983).

(2) E. L. Parrott, D. E. Wurster, and T. Higuchi, *J. Am. Pharm. Assoc., Sci. Ed.*, **44**, 269 (1955).

(3) R. J. Braun and E. L. Parrott, *J. Pharm. Sci.*, **61**, 175 (1972).

(4) E. L. Parrott and V. K. Sharma, *ibid.*, **56**, 1341 (1967).

(5) W. I. Higuchi, N. A. Mir, and S. J. Desai, *ibid.*, **54**, 1405 (1965).

ACKNOWLEDGMENTS

Abstracted in part from a dissertation submitted by Michael Simpson to the Graduate College, University of Iowa in partial fulfillment of the Doctor of Philosophy degree requirements.

Stabilization of Aluminum Hydroxide Gel by Specifically Adsorbed Carbonate

CARLOS J. SERNA ‡, JILL C. LYONS *, JOE L. WHITE ‡, and STANLEY L. HEM *x

Received April 26, 1982, from the *Department of Industrial and Physical Pharmacy and the ‡Department of Agronomy, Purdue University, West Lafayette, IN 47907. Accepted for publication July 1, 1982.

Abstract □ Ion-free aluminum hydroxide gel, prepared by the hydrolysis of aluminum tri-*sec*-butoxide, was observed by IR, X-ray analysis, and pH-stat titration to undergo rapid structural changes leading to the formation of pseudoboehmite and bayerite. The rate of development of order was directly related to the water–aluminum molar ratio. The Al—O bands at 625 and 470 cm^{-1} were the most sensitive indicators of the development of order in the gel structure. Direct evidence for the stabilizing effect of specifically adsorbed carbonate was obtained when carbon dioxide was introduced during the hydrolysis of aluminum tri-*sec*-butoxide. The resulting aluminum hydroxycarbonate gel possessed excellent antacid properties, retained its amorphous nature upon aging, and contained no cations other than aluminum. Hydrolysis of aluminum tri-*sec*-butoxide in the presence of stoichiometric amounts of sodium bicarbonate resulted in the immediate formation of crystalline sodium aluminum hydroxycarbonate (dawsonite).

Keyphrases □ Hydrolysis of aluminum tri-*sec*-butoxide—use of carbon dioxide-saturated water, formation of amorphous aluminum hydroxycarbonate gel, excellent properties, free of sodium and potassium □ Aluminum hydroxide gel—stabilization by specifically adsorbed carbonate □ Ion-free aluminum hydroxide gel—ordered structure, as an antacid

Aluminum hydroxide gel is an effective antacid largely due to its high rate of acid neutralization and its ability to react with acid at a pH of 3.5–4.0 (1). The chemical name implies a compound consisting of three hydroxyl groups per aluminum atom. This formula describes the crystalline forms of aluminum hydroxide known as gibbsite, bayerite, or norstrandite. These polymorphs have a very low rate of acid neutralization and are, therefore, not useful as antacids. However, a number of reports have suggested that the aluminum hydroxide gel used as an antacid contains specifically adsorbed anions and that these anions act to stabilize the gel structure (2–7) and facilitate the acid neutralization reaction (8).

The anions that are incorporated in the gel structure are usually supplied by the reactants used in the precipitation, such as carbonate from sodium carbonate or sodium bicarbonate or sulfate from aluminum sulfate (3). Aluminum hydroxide gel may also be prepared by the controlled hydrolysis of aluminum tri-*sec*-butoxide, I (9–14). This method permits precipitation under ion-free conditions as well as in the presence of selected ions. This system was used to study the structure and acid reactivity of ion-free aluminum hydroxide gel as well as the stabilizing effect of specifically adsorbed carbonate on the gel structure.

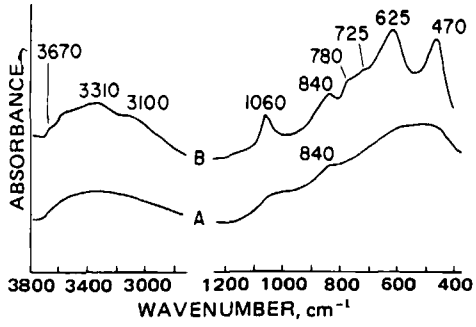

Figure 1—*IR spectra of ion-free aluminum hydroxide gel precipitated with water–aluminum ratio of 3. Key: (A) initial; (B) after 1 week at 25°.*

EXPERIMENTAL

Ion-free aluminum hydroxide gel was prepared by dissolving 6.15 g of I in 40 ml of anhydrous isopropyl alcohol and adding the required quantity of water with agitation. For example, 1.35 ml of water was used to hydrolyze I at a water–aluminum molar ratio of 3.

Aluminum hydroxycarbonate gel was prepared by hydrolyzing I with 3 moles of water/mole of I. The water was saturated with carbon dioxide prior to its addition to I. In addition, carbon dioxide was vigorously bubbled into the I solution during the hydrolysis reaction.

Compound I was hydrolyzed in the presence of 1 mole of sodium bicarbonate/mole of I. Because of the limited solubility of sodium bicarbonate, a water–aluminum molar ratio of 41 was needed to dissolve the sodium bicarbonate.

The hydrolysis products were analyzed for equivalent aluminum oxide content (15). Acid reactivity was determined by pH-stat titration of a sample containing 38 meq aluminum oxide at pH 3, 25° (16).

For X-ray analysis, the samples were dried at room temperature and ground to a fine powder. The diffraction patterns were recorded from 4 to 60° 2θ using CuK_α radiation. The same powder samples were diluted in potassium bromide (2 mg/300 mg) and examined by IR spectroscopy.

RESULTS AND DISCUSSION

Ion-Free Aluminum Hydroxide Gel—Ion-free aluminum hydroxide gel, precipitated with 3 moles of water/mole of I, undergoes very rapid structural changes which were observed by IR and X-ray analysis. The development, within a week, of absorption bands at 3670, 3310, and 3100 cm^{-1} (Fig. 1), indicates that the initial random structure changed rapidly and that the hydroxyl groups became part of a more uniform environment as the gel aged (17).

The most striking changes are observed in the IR region between 1200 and 400 cm^{-1}. The two strong absorption bands at 625 and 470 cm^{-1} are in a similar position as the Al—O vibrations observed in boehmite (18). The environment around the Al—O bonds became ordered more rapidly during aging than the environment of the hydroxyl groups. Thus, this IR region is more useful for detecting the earliest stages of crystallization. The vibrations in the hydroxyl region have been useful for monitoring long-term aging (17–19).

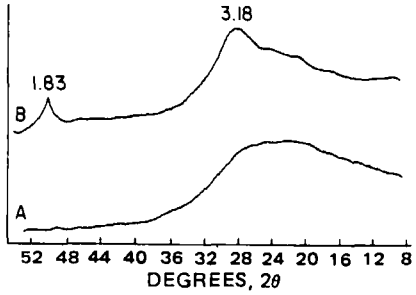

Figure 2—*X-ray diffractograms of ion-free aluminum hydroxide gel precipitated with water–aluminum ratio of 3. Key: (A) initial; (B) after 1 week at 25°.*

0022-3549/83/0700-0769$01.00/0

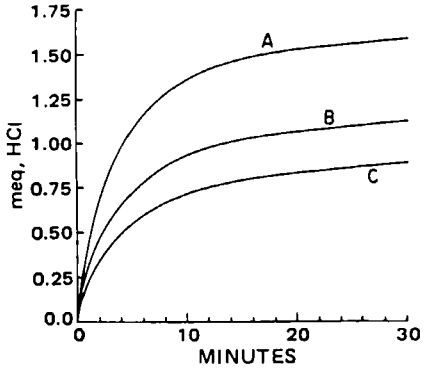

Figure 3—*pH Stat titrigraphs at pH 3, 25° of ion-free aluminum hydroxide gel aged at 25°. Key: (A) initial; (B) after 2 days; (C) after 4 days.*

The similarity in the IR spectrum of the hydroxyl vibrations at 3310, 3100 (stretching), and 1060 cm^{-1} (bending) to the spectrum of boehmite suggests that the developing crystalline phase was a disordered boehmite (pseudoboehmite) (13). This conclusion is supported by the X-ray diffractogram (Fig. 2). Initially an amorphous material was formed. At 1 week, the presence of pseudoboehmite was indicated by reflection peaks at 3.18, 1.83, and 1.44 Å (20).

The rate of reaction with acid decreased rapidly as the gel aged. As seen in Fig. 3, the development of an ordered structure in the gel was accompanied by an increase in the fraction of slowly reacting material present in the gel. Theoretically, the 38-meq aluminum oxide sample will neutralize 2.235 meq-HCl. Thus, the ion-free aluminum hydroxide gel would not be effective as an antacid, since only a small fraction of the ion-free aluminum hydroxide will react during the estimated gastric residence time for antacids of 15 min (21).

The rate of development of order was directly related to the amount of water used to hydrolyze I (13). The IR spectra of the aluminum hydroxide gels prepared using 3, 6, 12, and 24 moles of water/mole of I and aged for 24 hr at 25° are shown in Fig. 4. At lower water-aluminum ratios, amorphous aluminum hydroxide was observed, as indicated by the broad absorption bands.

As noted previously, the Al—O vibration gives the earliest indication of the development of order. At a water-aluminum ratio of 6, a featureless absorption band for the hydroxyl groups was observed between 3700 and 2600 cm^{-1}, while the presence of more ordered Al—O bonds was observed at 620 and 480 cm^{-1}. This absorption, together with the band at 1055 cm^{-1}, indicates that pseudoboehmite, $AlOOH{\cdot}H_2O$, is forming.

IR spectroscopy (Fig. 4) is a more sensitive technique to follow the development of order than X-ray diffraction, because the X-ray diffractograms of the aluminum hydroxide gels prepared with water-aluminum ratios of 3 and 6 were amorphous. However, in the presence of a large excess of water, a mixture of pseudoboehmite and bayerite was produced. Characteristic bands of pseudoboehmite were observed at 3300,

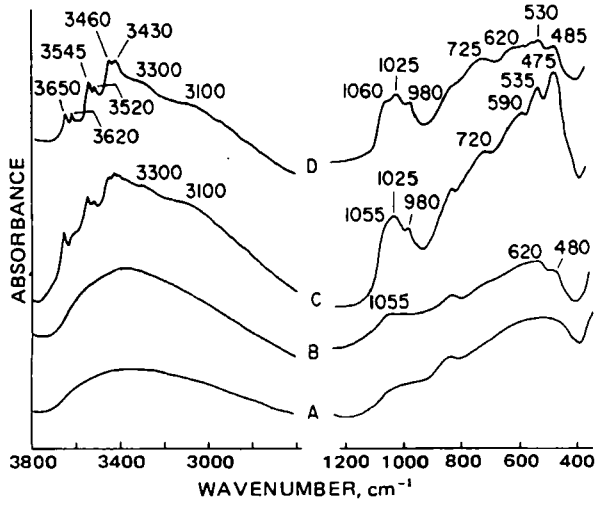

Figure 4—*IR spectra after 1 day at 25° of ion-free aluminum hydroxide gel hydrolyzed with various water-aluminum ratios. Key: (A) 3; (B) 6; (C) 12; (D) 24.*

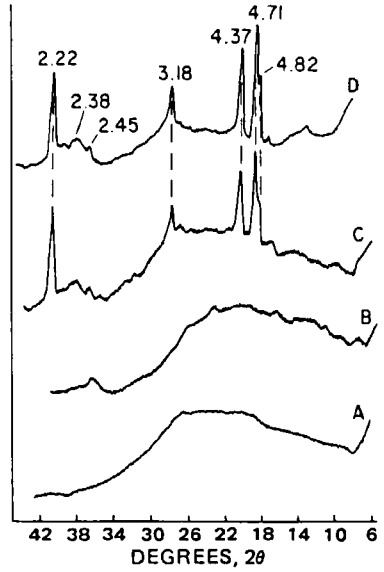

Figure 5—*X-ray diffractograms after 1 day at 25° of ion-free aluminum hydroxide gel hydrolyzed with various water-aluminum ratios. Key: (A) 3; (B) 6; (C) 12; (D) 24.*

3100, and 1055 cm^{-1} for the hydroxyl stretching and bending vibrations. Bayerite, $Al(OH)_3$, was observed at a water-aluminum ratio of 12 and predominated at higher water content. The more defined environment of the hydroxyl groups in the bayerite structure was indicated by the sharpness of the absorption bands at 3650, 3545, and 3430 cm^{-1}. The low IR region was not useful in detecting the mixture of pseudoboehmite and bayerite, since the Al—O vibrations are similar in both compounds.

The X-ray diffractograms (Fig. 5) support the conclusions drawn from IR analysis. At a water-aluminum ratio of 12, bayerite was indicated by the peaks at 4.71, 4.37, 3.18, and 2.22 Å. The transformation of pseudoboehmite to bayerite at higher water content was indicated by the loss of the broad background reflection between 30 and 22° 2θ that corresponds to the broad reflection peak at 3.18 Å for pseudoboehmite.

Small amounts of gibbsite were present in the aluminum hydroxide gel precipitated at a water-aluminum ratio of 24 as indicated by the IR bands at 3620 and 3520 cm^{-1} and by the diffraction peak at 4.82 Å (Figs. 4 and 5).

Stabilization of Aluminum Hydroxide Gel—The stabilizing effect of anions present at the time of precipitation has been hypothesized based on indirect evidence such as the relationship between anion content and the rate of loss of acid reactivity (2, 6), the effect of washing (5), and the dependence of the rate of crystallization on the nature of the anion (2, 3). The hydrolysis of I provides an excellent system to demonstrate directly the stabilizing action of anions. The interaction of carbonate anion with aluminum hydroxide was achieved by saturating the water used for hydrolysis with carbon dioxide and by bubbling carbon dioxide into the reaction medium during hydrolysis. X-ray diffraction patterns of the product were amorphous both initially and after aging for 1 month at 25°. This result agrees with Torkar's earlier observation that the reaction product of aluminum ethoxide and water saturated with carbon dioxide remained amorphous for 20 days at 22° (22).

The IR spectrum of the precipitate formed in the presence of carbon dioxide-saturated water (Fig. 6) indicates an amorphous aluminum hydroxycarbonate gel. The broad hydroxyl stretching band at 3460 cm^{-1}

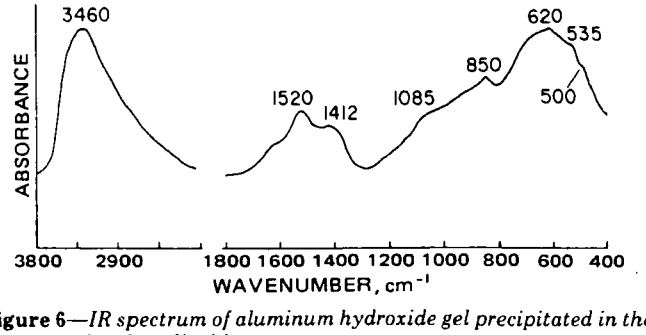

Figure 6—*IR spectrum of aluminum hydroxide gel precipitated in the presence of carbon dioxide.*

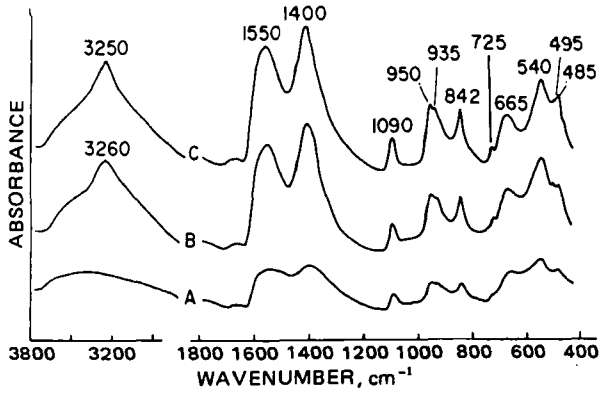

Figure 7—*IR spectra of the precipitate obtained by the hydrolysis of I in the presence of sodium bicarbonate aged at 25°. Key: (A) initial; (B) 30 min; (C) 1 day.*

indicates that the hydroxyl groups are disordered, while the ν_3 carbonate bands at 1520 and 1412 cm^{-1} indicate that carbonate is directly coordinated to aluminum in the gel structure (4, 6, 23–25). The absorption band at 1085 cm^{-1} (ν_1) also supports the direct coordination of carbonate to aluminum since this absorption is only active in the Raman when the carbonate anion has full symmetry.

The amorphous aluminum hydroxycarbonate gel reacted completely with acid and exhibited a T_{50} of 3 min by pH-stat titration. The rate of acid neutralization was virtually unchanged during the 1-month evaluation period.

Compound I was also hydrolyzed in the presence of carbonate ion using 1 mole of sodium bicarbonate per mole of I. The sodium bicarbonate was dissolved in the water for hydrolysis. This reaction resulted in the immediate formation of sodium aluminum hydroxycarbonate which is known mineralogically as dawsonite (13) and is contained in the USP as dihydroxyaluminum sodium carbonate (26). As can be seen in Fig. 7, the initial IR spectrum showed the split carbonate band, ν_3, at 1550 and 1400 cm^{-1}, which is characteristic of the distortion of carbonate in dawsonite (13). Rapid structural development occurred during the first 30 min as evidenced by the appearance of a hydroxyl stretching band at 3260 cm^{-1} and the general sharpening of the bands observed in the initial spectrum. Little indication of further structural development is observed in the 24-hr spectrum.

The IR spectrum of the 1-day sample was identical to the spectrum of dawsonite (27), except that the bands are broader suggesting a more poorly ordered structure of a smaller particle size than the mineralogical sample.

The rapid structural development of dawsonite was also observed in the X-ray diffractograms (Fig. 8), which exhibit the major peaks of

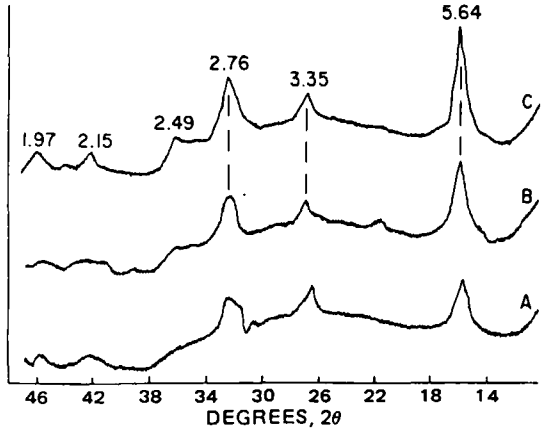

Figure 8—*X-ray diffractograms of the precipitate obtained by the hydrolysis of I in the presence of sodium bicarbonate aged at 25°. Key: (A) initial; (B) 30 min; (C) 1 day.*

dawsonite immediately after precipitation and show some refinement in the structure upon aging.

The synthetic dawsonite exhibited a rapid rate of acid neutralization as evidenced by its T_{50} of 3 min. The rate of neutralization was virtually unchanged during the 1-month observation period. The presence of a stoichiometric amount of sodium bicarbonate at the time of precipitation produced a highly reactive, crystalline hydroxycarbonate which contains 158 mg of sodium per gram of sodium aluminum hydroxycarbonate.

Summary—Aluminum hydroxide gel produced under ion-free conditions rapidly developed an ordered structure which reacts too slowly with acid to be effective as an antacid. The use of carbon dioxide-saturated hydrolysis water as the source of carbonate ion produced an amorphous aluminum hydroxycarbonate gel which exhibited excellent antacid properties and was totally free of foreign cations such as sodium or potassium. The use of a stoichiometric amount of sodium bicarbonate as the source of carbonate resulted in the formation of crystalline sodium aluminum hydroxycarbonate which possesses excellent antacid properties but which has a high sodium content.

REFERENCES

(1) S. L. Hem, *J. Chem. Ed.*, **52**, 383 (1975).

(2) P. H. Hsu and T. F. Bates, *Mineral Mag.*, **33**, 749 (1964).

(3) S. L. Hem, E. J. Russo, S. M. Bahal, and R. S. Levi, *J. Pharm. Sci.*, **59**, 317 (1970).

(4) J. L. White and S. L. Hem, *J. Pharm. Sci.*, **64**, 468 (1975).

(5) S. L. Nail, J. L. White, and S. L. Hem, *J. Pharm. Sci.*, **65**, 1192 (1976).

(6) C. J. Serna, J. L. White, and S. L. Hem. *Soil Sci. Soc. Am. Proc.*, **41**, 1009 (1977).

(7) C. J. Serna, J. L. White, and S. L. Hem, *J. Pharm. Sci.*, **67**, 1144 (1978).

(8) N. J. Kerkhof, J. L. White, and S. L. Hem, *J. Pharm. Sci.*, **66**, 1533 (1977).

(9) M. R. Harris and K. S. W. Sing, *J. Appl. Chem.*, **8**, 586 (1958).

(10) G. C. Bye and J. G. Robinson, *Chem. Ind.*, **1961**, 433.

(11) D. Aldcroft, G. C. Bye, and C. A. Hughes, *J. Appl. Chem.*, **19**, 167 (1969).

(12) D. L. Catone and E. Matijevic, *J. Colloid Interface Sci.*, **48**, 291 (1974).

(13) C. J. Serna, J. L. White, and S. L. Hem, *Clays Clay Miner.*, **25**, 384 (1977).

(14) P. Pascoe, F. Josten, W. Haferkamp, and W. Lucker, U.S. Pat. 3,698,861, October 17, 1972.

(15) "The United States Pharmacopeia," 20th rev. United States Pharmacopeial Convention, Rockville, Md., 1980, p. 25.

(16) N. J. Kerkhof, R. K. Vanderlaan, J. L. White, and S. L. Hem, *J. Pharm. Sci.*, **66**, 1528 (1977).

(17) S. L. Nail, J. L. White, and S. L. Hem, *J. Pharm. Sci.*, **64**, 1166 (1975).

(18) J. J. Frippiat, H. Bosmans, and P. G. Rouxhet, *J. Phys. Chem.*, **71**, 1097 (1967).

(19) S. L. Nail, J. L. White, and S. L. Hem, *J. Pharm. Sci.*, **65**, 231 (1976).

(20) D. Papee, R. Tertian, and R. Biais, *Bull. Soc. Chim.*, **1958**, 1301.

(21) *Fed. Reg.*, **38** (65), April 5, 1973, p. 8717.

(22) K. Torkar, *Mh. Chem.*, **92**, 755 (1961).

(23) K. Nakamoto, "Infrared Spectra of Inorganic and Coordination Compounds," Wiley, New York, N.Y., 1963, p. 159.

(24) P. C. Healy and A. H. White, *J. Chem. Soc.*, **1972**, 1913.

(25) P. C. Healy and A. H. White, *Spectrochim. Acta*, **29A**, 1191 (1973).

(26) "The United States Pharmacopeia," 20th rev., United States Pharmacopeial Convention, Rockville, Md., 1980, p. 246.

(27) C. J. Serna, J. L. White, and S. L. Hem, *J. Pharm. Sci.*, **67**, 324 (1978).

ACKNOWLEDGMENTS

The report is Journal Paper 9020, Purdue University Agricultural Experiment Station, West Lafayette, IN 47907.

Membrane-Coated Tablets: A System for the Controlled Release of Drugs

GÖRAN KÄLLSTRAND and BO EKMAN ˣ

Received May 18, 1981, from the *Pharmaceutical Research and Development, AB Ferrosan, S-201 80 Malmö, Sweden.* Accepted for publication June 28, 1982

Abstract □ Membrane-coated tablets were developed to provide a dosage form which exhibits zero-order kinetics. The delivery system consisted of a soluble tablet core surrounded by a porous membrane which controls the diffusion rate. In the system studied, the diffusion rate of potassium chloride was found to be more constant than with other controlled-release products and independent of pH changes within the physiological range. The release profile of a drug can be varied by changing the composition of the membrane. Substantial amounts of the active substance can be loaded into membrane-coated tablets. The membrane protects the gastric mucosa from direct contact with the undissolved active substance. This delivery system has a potential for use with all water-soluble agents where a controlled release is desirable.

Keyphrases □ Controlled release of drugs—membrane-coated tablets, zero-order delivery, potassium chloride, potential use for all water-soluble drugs □ Delivery systems—membrane-coated tablets, controlled release, potassium chloride

The concept of the slow release of drugs has attracted much interest, and numerous delivery systems are commercially available. The purpose of these preparations is to release the drug continuously during its passage through the GI tract, thereby giving a constant plasma concentration over a long period of time and possibly reducing side effects. Slow-release delivery would be suitable for drugs with a rapid clearance from plasma or drugs that cause adverse effects locally or systemically. An ideal slow-release preparation depends only on the dissolution rate of the active substance. Factors such as mechanical influence, enzymes, viscosity, surface tension, pH, and salt concentration should not affect the release of the active substance. However, the absorption phase must be completed within 8–10 hr for most drugs to achieve good biological availability (1). Drug dissolution from tablets prepared by a technique called membrane coating, using potassium chloride as a model drug, is described.

Uncoated and enteric-coated potassium chloride tablets cause side effects in the GI tract with a high degree of frequency (2). The only difference between the standard tablets and the enteric-coated ones has been the localization of the ulceration in the gut. Several cases of duodenal ulceration resulting in stenosis of the intestine have been caused by enteric-coated potassium chloride tablets (3, 4).

If potassium chloride is delivered at a constant rate for a longer period of time while in the GI tract, the side effects can be minimized. Newer controlled-release potassium chloride tablets have a slow dissolution rate, which gives

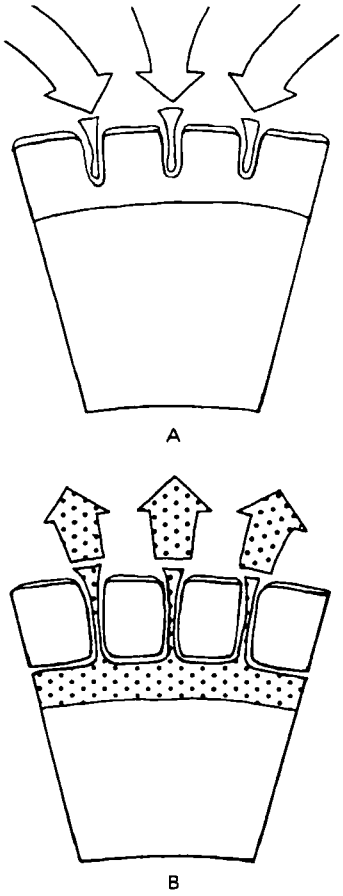

Figure 1—*Segment of membrane-coated tablet (A) liquid penetrating into the membrane, dissolving the sucrose particles and (B) drug solution diffusing through the membrane.*

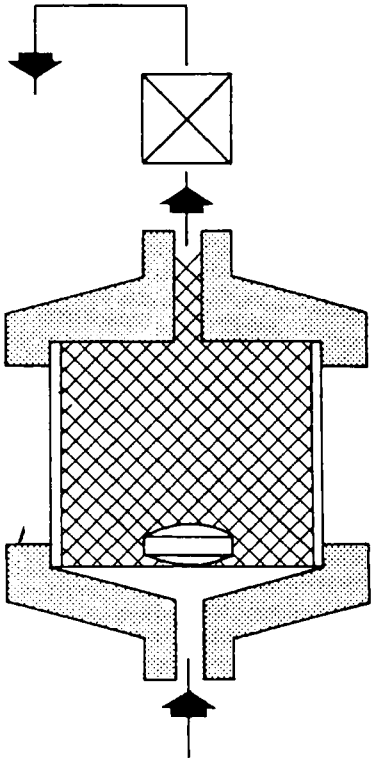

Figure 2—*Sketch of the flow-through cell.*

0022-3549/83/0700-0772$01.00/0

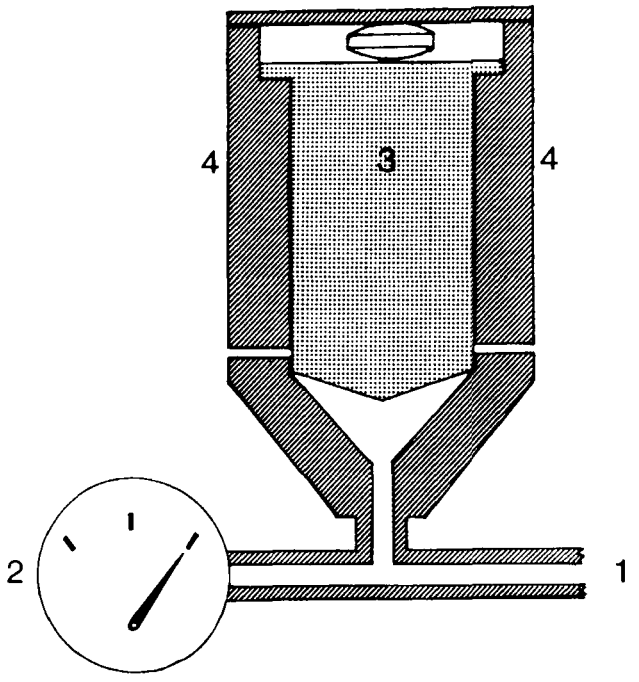

Figure 3—*Sketch of the equipment for testing mechanical resistance of coating shells. Key: (1) air inlet; (2) manometer; (3) plunger; (4) cylinder.*

a considerably lower concentration of the drug in the GI tract and, consequently, a lower frequency of adverse reactions (5, 6). The principle of delivering drugs by solution diffusion through a rate-controlling microporous membrane has been shown earlier to be dependable (7). This report describes a practical way to utilize this technique.

Membrane coating involves coating a tablet with a porous, water-permeable membrane, which is insoluble in the GI tract. The gastric juices penetrate the tablet through the pores and dissolve the drug (Fig. 1).

The following quality controls must be met when choosing a water-insoluble polymer. It must have low toxicity and be unaffected by the GI fluids and by the motility of the intestinal system. It should have good solubility in a nontoxic solvent, appropriate for tablet coating, and give films of good mechanical stability. After testing several different polymers (cellulose derivatives, nylon, and various acrylic polymers) we decided to investigate a polyvinyl chloride plastic. This polymer combines the favorable properties of good mechanical resistance and satisfactory adhesion to the potassium chloride surface of the tablet core.

EXPERIMENTAL

Preparation of Tablet Core—Potassium chloride was granulated with a 50% solution of polyvinyl pyrrolidone in ethanol–acetone (1:1). A 32-g volume of the solution was mixed with 1000 g of KCl. The wet granulation was screened through a 0.5–0.7-mm aperture and dried in a forced-air oven at 40° for 2 hr. Circular, biconvex tablets with a 12-mm diameter were compressed to a hardness of 8 kp[1]. The disintegration time in water at 37° was 8 min[2]. The tablet weight was 1016 mg, of which 1000 mg was potassium chloride.

Preparation of Membrane-Coated Tablets—The polymeric film coatings were applied to the tablets in batch sizes of 5000 in a conven-

[1] Tablet hardness tester, Schleuniger & Co., Zürich, Switzerland.
[2] Measured by equipment from Manesty Machines Ltd., Liverpool, England.

A

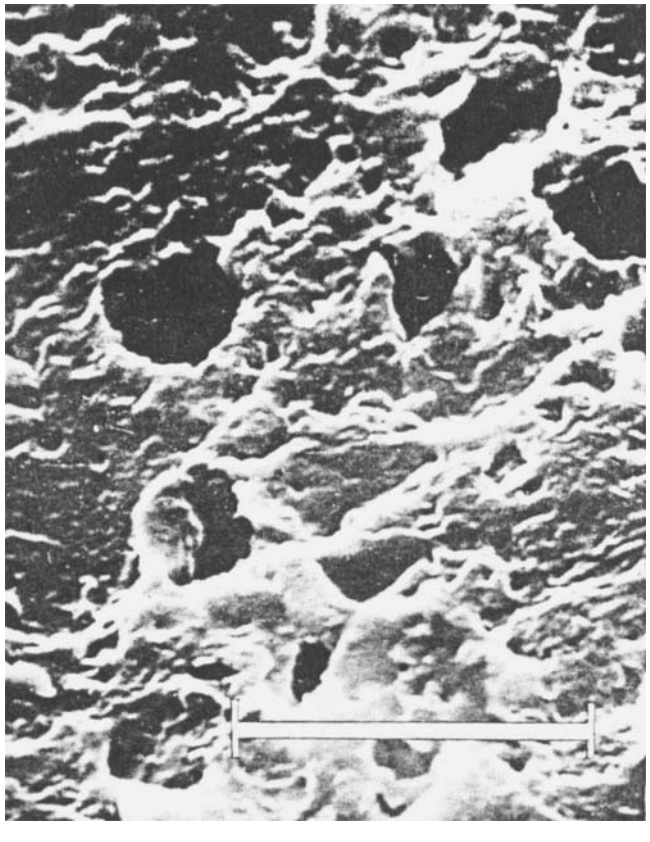

B

Figure 4—*Scanning electron microphotographs of the membrane coat of potassium chloride tablets: (A) membrane with suspended sucrose crystals and (B) the membrane after dissolution of the crystals. The bar indicates 10 μm.*

Table I—Reproducibility of the Membrane-Coating Process [a]

Batch	Potassium Chloride Released During 1st hr, %	Time for 90% release of Potassium Chloride, hr
A	16.9	5.9 ± 0.6 0.4
B	15.9	5.8 ± 0.8 0.6
C	16.7	5.8 ± 0.6 0.5
D	17.0	6.1 ± 0.8 0.5

[a] Six tablets were analyzed out of each of the four batches, using the rotating-basket method. The values for 90% release also show the two most extreme values obtained in the analysis.

tional 50-cm diameter coating pan without baffles. Coating consisted of 13% w/v polymer[3] in acetone. Because of their high viscosity, it was not possible to use more concentrated solutions. Different amounts of micronized sucrose (particle size <10 μm) was suspended in the polymer solutions. Coating was achieved by spraying the various suspensions on the moving bed of tablets with an airless sprayer[4], using a 0.1-mm nozzle. Spray rate was 30 ml/min. Coating was continued until the weight of the coat on each tablet was 50 mg.

Drug Diffusion Studies—Potassium chloride diffusion from tablets was followed by using the modified beaker method (8, 9), the ascending-column method (10, 11), and the rotating-basket method (USP/NF). Diffusion studies according to the beaker method were performed using 1000 ml of dissolution medium at 37° and a paddle stirrer rotating at 60 rpm. Studies with the rotating-basket method were carried out in a 1000-ml cylindrical vessel at 37° with the tablet held in a 40-mesh stainless steel basket. Rotating speed was 100 rpm. The ascending-column method utilized a flow-through cell 25-mm high with a 14-mm diameter. The tablet was placed on a net at the bottom of the cell (Fig. 2). Fresh dissolution medium (37°) was pumped through the cell at a rate of 40 ml/min, and the concentration of potassium chloride was measured at the outlet every 3rd min. Results obtained by the three methods for determining drug diffusion from membrane-coated tablets showed excellent agreement.

Deionized water was used as the dissolution medium, except in the pH influence studies. In these experiments, artificial gastric juice without pepsin was used according to USP XIII, pH 1.2. Artificial intestinal juice was prepared according to USP XIII, without pancreatin, and potassium

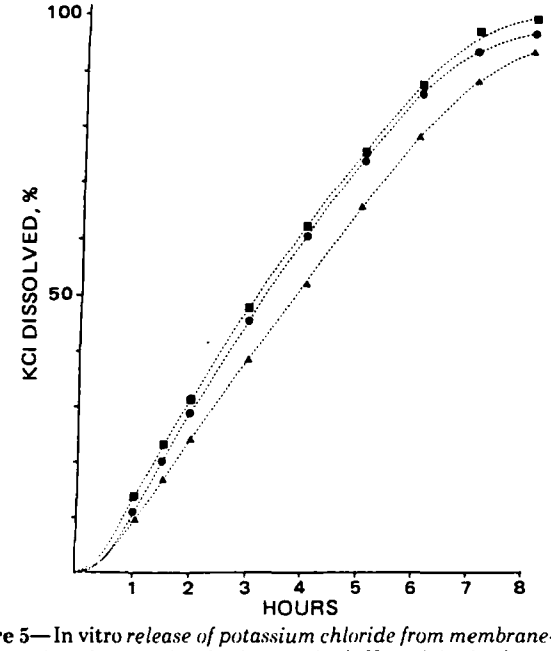

Figure 5—In vitro *release of potassium chloride from membrane-coated tablets using the rotating-basket method. Key: deionized water (●), artificial gastric juice (▲), and artificial intestinal juice (■).*

[3] High purity polyvinyl chloride, Chemoswed Co., Malmö, Sweden.
[4] Nordson Corp., Amherst, Ohio.

Table II—Influence by Membrane Coating Composition on the Release of Potassium Chloride (Rotating-Basket, 37°)

Batch	1	2	3	4
Ratio soluble–insoluble components (w/w)	1.81	2.12	2.57	2.82
Time for 50% dissolution (min)	121	88	64	48

dihydrogen phosphate substituted with sodium dihydrogen phosphate, pH 7.5. Potassium chloride concentrations were determined by conductometry in most experiments. In the pH influence studies, however, atomic absorption spectrometry was used for potassium. Slow-release potassium chloride preparations[5] used in the comparison studies were purchased commercially.

Measurement of Membrane Strength—The mechanical resistance of the membrane coat was measured on empty coating shells after the complete release of potassium chloride. Empty coating shells were obtained by placing membrane-coated potassium chloride tablets in a large volume of distilled water for 24 hr. When the drug was diffused from the tablets and the solid core was replaced with liquid the shells floated and became layered beneath the liquid surface. The visible appearance of the tablets did not change. A tool was developed for checking the mechanical resistance of the membrane-coated shell (Fig. 3). The empty coating shell was compressed in a cylinder by a piston which was regulated by compressed air. The resistance of the coating shell against the movement of the piston was registered by a manometer. Compressed air (8 kg/cm^2) reached the throttle valve and penetrated the cylinder. The piston moved upward and pressed the coating shell against the lid of the cylinder. When the coating shell was compressed or burst, the channels were free and the air escaped. This procedure was recorded by a manometer which showed the pressure of the air in kp/cm^2 at the moment the coating shell burst. The maximal air pressure at the compression represents a measure of the mechanical resistance of the membrane.

RESULTS AND DISCUSSION

Characteristics of the Membrane Coating—The coating consists of a water-insoluble polymer and a dispersed water-soluble pore-creating substance. When a membrane-coated tablet is swallowed, the gastric juice dissolves the pore forming substance (Fig. 1). The structure of the membrane can be seen in Fig. 4, as observed by scanning electron microscopy before and after removal of the water-soluble material.

The amount of residual monomer (vinyl chloride) was determined by GC. The accuracy of the method is ~1 ppm, and our results show that the content of monomer is <1 ppm. The pore-forming substance consists of micronized sucrose, which proved to be ideally suited with regard to toxicity and solubility.

Drug Diffusion Studies—The diffusion of dissolved substances from the tablet through the pores can be calculated by using Fick's first law of diffusion.

$$q = D\,(C_s - C_u)\,\frac{A}{h} \qquad \text{(Eq. 1)}$$

where q is the rate of diffusion, D the diffusion constant, A the surface area, and h the thickness of the diffusion layer.

As long as the membrane coating contains a saturated solution together with solid drug substance the concentration inside the coating shell, C_s, is much higher than the concentration outside the coating shell, C_u. For potassium chloride C_s is ~25%, while C_u in our *in vitro* studies has reached maximally 0.1%. Thus, the diffusion has taken place during sink conditions (which means C_u is negligible compared with C_s) and Eq. 1 is reduced to:

$$q = D\,\frac{C_s}{h}\,A \qquad \text{(Eq. 2)}$$

This implies that the diffusion should proceed at a constant rate (zero-order reaction). At the point where no solid substance is left within the membrane coating, the rate of diffusion declines with decreasing concentration (first-order reaction).

The release pattern of active substance from a membrane-coated tablet is shown in Fig. 5. When the release of potassium chloride begins, the sucrose particles in the membrane are dissolved. The rate increases sharply to a maximum in a few minutes.

Theoretically, 70–80% of the potassium chloride should be released

[5] Kalium-Duretter, 0.75 g, Hässle Sweden (formulation A); Slow-K, 0.6 g, Ciba (formulation B).

Table III—Diffusion of Potassium Chloride During 6 hr from Three Different Formulation Principles

Hours	Percent Released from Tablets[a]		
	Membrane-Coated Tablets	Formulation A	Formulation B
1st	16.7	39.6	32.4
2nd	19.8	17.2	25.5
3rd	17.4	11.3	16.0
4th	15.6	8.7	11.2
5th	13.7	6.7	7.8
6th	10.7	4.9	5.3
Total	93.9	88.4	98.2

[a] The figures given are mean values of six single tablet analyses. Released potassium chloride is expressed as percentage of the total content of the different products. The amounts of potassium chloride were: membrane-coated tablets, 1 g; formulation A, 0.75 g; and formulation B, 0.6 g.

at a constant rate. In practical situations, however, the rate decreases slowly and linearly until ~80% of the content is released. At this point there is no solid potassium chloride left in the shell and the rate accordingly decreases rapidly.

The effect of the dissolution medium pH on the potassium chloride diffusion was studied. Figure 5 shows the release pattern in deionized water, artificial intestinal juice (pH 7.5), and artificial gastric juice (pH 1.2). The three media, which represent the physiological pH range, did not influence the diffusion significantly. As can be seen from Fig. 5, the amount of potassium chloride dissolved in 6 hr varies between 80 and 90%.

The reproducibility of the coating process is high. Table I shows release characteristics of four consecutive batches of membrane-coated potassium chloride tablets. The ratio of soluble components to insoluble polymer in the coating material influences the release rate. The importance of this ratio is evident from the data in Table II. A high ratio of soluble/insoluble components gives a high-porosity coating. This ratio is used to produce tablets with a desired release pattern.

Studies on the Membrane Strength—The main factor influencing shell hardness was found to be the thickness of the membrane. Minor changes from the composition of the membrane given in the *Experimental* section do not significantly alter the mechanical strength of the membrane. The compression resistance of membrane-coated tablets measured according to the method described in the *Experimental* section is ~7 kp. To investigate if this is sufficient for the *in vivo* conditions, a study was performed on the empty shells after passage through the GI tract. One membrane-coated tablet/day was given to ten volunteers during 2 days. The stools were collected and the empty shells were examined for ruptures. No ruptures of the membrane were found. (Tablets of different membrane-coat thickness were prepared for this study and checked for membrane strength, which ranged between 5.2 and 7.2 kp.) This proves that the mechanical stability is sufficient to withstand passage through the human GI tract.

Comparison with Other Controlled-Release Principles Used for Potassium Chloride—The membrane-coated potassium chloride tablet was compared with two commercially available slow-release formulations of potassium chloride. These formulations utilize the so-called embedment principle, which means that potassium chloride is embedded in a carrier substance that either forms an insoluble matrix (formulation A) from which the potassium chloride diffuses (12), or a wax matrix (formulation B) which releases the potassium chloride by a combination of diffusion and erosion. Determinations of potassium chloride have been performed according to the method described in the *Experimental* section (rotating basket, 37°).

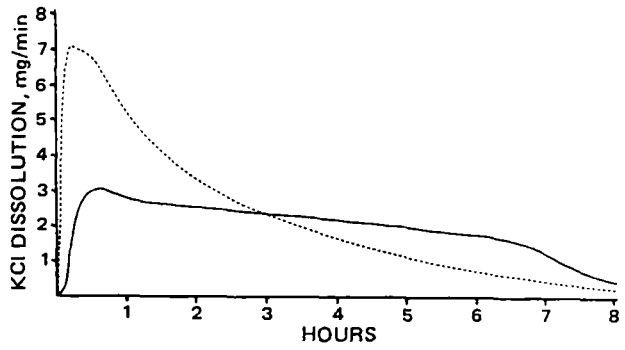

Figure 6—In vitro *release rate of potassium chloride from membrane-coated tablets [1 g (—)] and formulation B [0.6 g (- - - -)]. Data for formulation B have been recalculated in relation to 1 g of KCl.*

As can be seen from Table III, the two commercially available preparations initially released large amounts of active substances. The rate of release then gradually decreased. Membrane-coated tablets, however, gave a slower and more uniform release during the 6-hr period. Figure 6 shows a comparison between membrane-coated tablets and formulation B. An ideal formulation would show a constant diffusion rate, thereby releasing constant amounts of active substance each hour until no more substance remained in the tablet. In the study the membrane-coated tablets have a release pattern that is closer to the ideal situation.

REFERENCES

(1) J. R. Robinson, Ed., "Sustained and Controlled Release Drug Delivery Systems," Dekker, New York, N.Y., 1978, p. 130.

(2) "AMA Drug Evaluations," 2nd ed., AMA Department of Drugs, American Medical Association, Chicago, Ill., 1973, p. 183.

(3) L. Gee, B. Berg, T. G. Tong, and C. Becker, *J. Am. Med. Assoc.*, **228**, 975 (1974).

(4) J. M. Jefferson and P. Aukland, *Br. Med. J.*, **1**, 456 (1974).

(5) E. L. Tarpley, *Curr. Ther. Res.*, **16**, 734 (1974).

(6) C. Graffner and J. Sjögren, *Acta Pharm. Suec.*, **8**, 13 (1971).

(7) R. W. Baker and H. K. Lonsdale, in "Controlled Release of Biologically Active Agents, Advances in Experimental Medicine and Biology," vol. 47, A. C. Tanquary and R. E. Lacely, Eds., Plenum, New York, N.Y., 1974, p. 15.

(8) G. Levy and B. A. Hayes, *N. Engl. J. Med.*, **262**, 1053 (1960).

(9) R. V. Bathe, O. Häftiger, F. Langenbucher, and D. Schönleber, *Pharm. Acta Helv.*, **50**(12), 3 (1975).

(10) F. Langenbucher, *J. Pharm. Sci.*, **58**, 1265 (1969).

(11) J. E. Tingstad and S. Riegelman, *J. Pharm. Sci.*, **59**, 692 (1970).

(12) J. Sjögren, *Dan. Tidsskr. Farm.*, **34**, 189 (1960).

Kinetics of Decomposition and Formulation of Hydrocortisone Butyrate in Semiaqueous and Gel Systems

Y. W. YIP, A. LI WAN PO ˣ, and W. J. IRWIN

Received February 3, 1982, from the *Department of Pharmacy, University of Aston, Gosta Green, Birmingham, UK.* Accepted for publication June 29, 1982.

Abstract □ The stability of hydrocortisone butyrate in semiaqueous and formulated gel systems has been investigated. It was shown that hydrocortisone butyrate underwent reversible isomerization to the C-21 ester of butyric acid. This ester then hydrolyzed to hydrocortisone, which in turn degraded to a complex mixture of compounds. This step is metal catalyzed and can be inhibited by the addition of EDTA [disodium(ethylenedinitrilo)tetraacetate]. The kinetics of decomposition is modeled using nonlinear regression analysis, and the rate constants for the various decomposition pathways are quantified.

Keyphrases □ Hydrocortisone butyrate—decomposition in semiaqueous and gel systems, kinetics □ Kinetics—decomposition of hydrocortisone butyrate in semiaqueous and gel systems □ Decomposition—hydrocortisone butyrate in semiaqueous and gel systems, kinetics □ Dosage forms, topical—hydrocortisone butyrate, decomposition in semiaqueous and gel systems, kinetics

Hydrocortisone butyrate (I) is available in various formulations for topical application. Studies *in vivo* have shown that the ester is many times more active than the parent alcohol, hydrocortisone (1). The presence of the ester function appears to improve delivery of corticosteroids to the site of action as well as increase steroidal activity by imparting resistance to the cutaneous metabolic enzymes involved in the disposition of the steroids from the site of action (2, 3).

Steroid-17-esters, however, readily rearrange to the thermodynamically more stable but topically less active (1) 21-esters under nonideal conditions (4). It was shown that in some extemporaneously diluted ointments, the half-life of betamethasone valerate may be <1 hr at room temperature (5). Previous studies (6, 7) showed that hydrocortisone butyrate (I) underwent acyl migration to the 21-ester (II) followed by hydrolysis of this ester to hydrocortisone (III). This paper reports the formulation and stability of the steroid in semiaqueous and gel systems.

EXPERIMENTAL

Steroid Analysis—High-performance liquid chromatography (HPLC) analyses were performed on an apparatus constructed from a constant-flow solvent pump[1], an injector[2] fitted with a 20-μl loop, and a variable-wavelength monitor[3] equipped with an 8-μl flow-cell. Aqueous acetonitrile[4] mixtures were used as the mobile phase, and hydrocortisone acetate (0.08 mg/ml) was the internal standard for reverse-phase chromatography on a 10-cm, 5-μm ODS column[5]. Normal-phase chromatography was performed as previously described (7) using caffeine (0.1 mg/ml) as the internal standard.

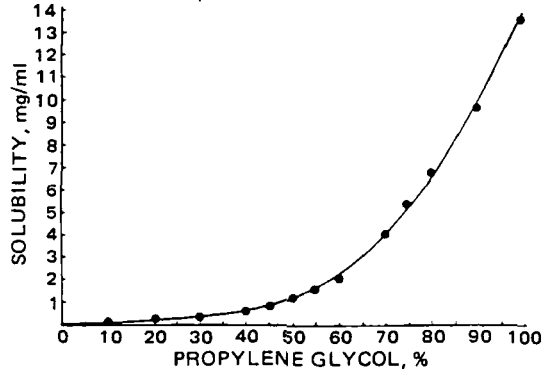

Figure 1—*Solubility profile of hydrocortisone butyrate (I) in aqueous propylene glycol mixtures at 25°.*

HPLC-grade solvents[4], propylene glycol BP[6], hydrocortisone[7], and the buffer salts[8] were purchased from various manufacturers. The hydrocortisone butyrate[9] and the gelling agents[10] were gifts and were used as supplied.

Preparation of Gels—To prepare a carboxypolymethylene polymer gel, 0.8 g of the polymer was dissolved in 30 g of propylene glycol and ~45 g of water. The product was neutralized with 2.5 ml of 2.5 *N* NaOH, and 0.1 g of the steroid was incorporated into the resultant gel using the remaining 20 g of propylene glycol. The gel was adjusted to 100 g with water to produce a 0.1% w/w hydrocortisone butyrate gel for subsequent studies. Entrapped air was removed by vacuum suction in a desiccator.

The other gel systems were prepared as recommended by the manufacturers. Initial experiments with these systems showed that, following topical application, unacceptable films were formed on the skin. All subsequent formulations, therefore, were carried out with the carboxypolymethylene polymers.

Preparation of Aqueous Propylene Glycol–Steroid Solutions—Both nonbuffered and buffered aqueous propylene glycol solutions were used in the kinetic experiments. Aqueous propylene glycol solutions (50% v/v) were adjusted to the required pH by addition of sodium hydroxide. These are referred to as nonbuffered solutions although such solutions should possess some buffer capacity. The buffered aqueous propylene glycol solutions were prepared by mixing equal volumes of propylene glycol and McIlvaine's citrate buffer adjusted to a constant ionic strength of 0.5 *M* with potassium chloride (8). As expected, addition of propylene glycol to an aqueous buffer produced large changes in the pH. Typically, a buffer with an initial pH of 6.91 was altered to pH 7.60 on dilution with an equal volume of propylene glycol. The pH quoted in the stability studies are all final values in the aqueous propylene glycol systems.

Solubility of Hydrocortisone Butyrate—The solubility of hydrocortisone butyrate (I) in aqueous propylene glycol or propylene glycol was determined by adding excess steroid to 10 ml of the appropriate propylene glycol solution preheated to 80°. The suspension was then placed in an ultrasonic bath for 15 min and transferred to a shaking water bath, maintained at 25°. The solution was filtered after overnight storage at this temperature, and an aliquot of the filtrate was assayed by HPLC. Initial estimates were obtained using normal-phase chromatography (6) and confirmed by reverse-phase chromatography. No decomposition was observed during the storage under the conditions described.

Storage and Assay of Gel—The hydrocortisone butyrate gels were stored at 60° in a water bath. Samples of ~1.2 g were withdrawn at appropriate intervals, and 5 ml of 0.5% w/v hydrochloric acid was added to quench the reaction. The tubes were shaken until homogeneous, and 10 ml of chloroform was added. The chloroform extracts were assayed by HPLC (6). Recovery studies showed a mean value of 99.17 ± 0.52% on six replicate determinations.

Storage and Assay of Aqueous Propylene Glycol–Steroid Solutions—The solutions (1 mg/ml) were stored in water baths maintained

[1] Altex 100A model.
[2] Rheodyne 7120.
[3] Pye LC3.
[4] Fisons Ltd (UK).
[5] Hypersil-ODS.
[6] McCarthys Ltd.
[7] Sigma Chemical Co. (UK).
[8] British Drug Houses.
[9] Brocades Ltd UK.
[10] Carbopol 940 (carboxypolymethylene polymers), Goodrich Chemical Co.; Klucel HF (hydroxypropylcellulose), Natrosal (hydroxyethylcellulose), and sodium carboxymethylcellulose, Hercules Ltd.

0022-3549/83/0700-0776$01.00/0

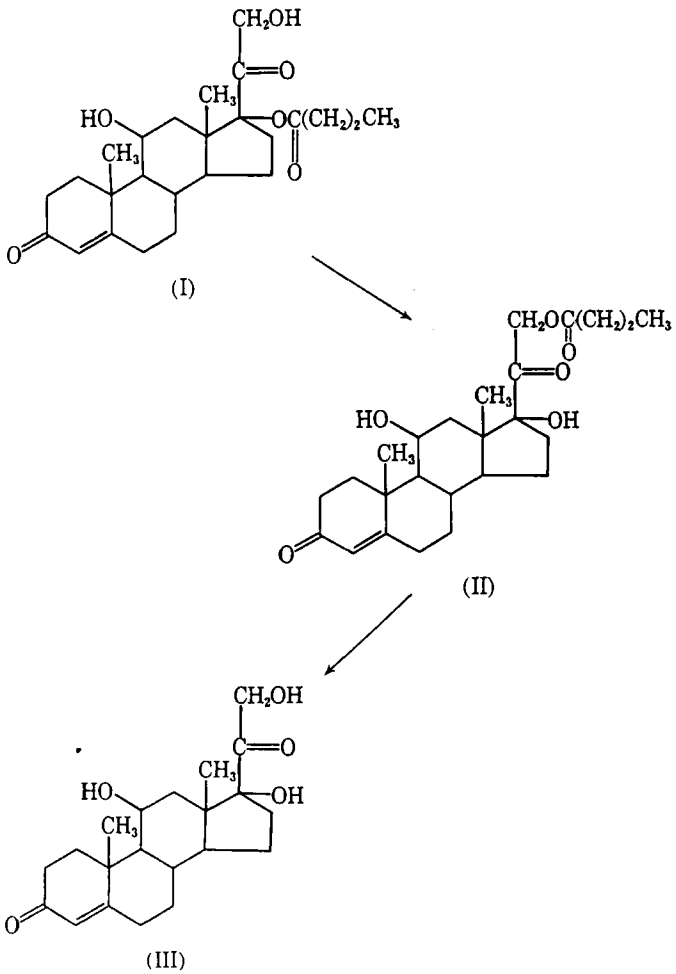

Scheme I: Decomposition pathway of hydrocortisone butyrate.

at 60°, and 1-ml aliquots were withdrawn at appropriate intervals for assay by reverse-phase HPLC. The reaction was halted by the addition of 4 ml of 0.024 *M* hydrochloric acid in 50% aqueous acetonitrile. Such diluted samples could be stored at 4° for at least a week without measurable decomposition. The samples were diluted with an additional 5 ml of the acetonitrile–hydrochloric acid mixture which contained 0.16 mg/ml of hydrocortisone acetate as an internal standard. When hydrocortisone was studied alone, an internal standard concentration of 0.32 mg/ml was used to obtain more precise data. EDTA [disodium(ethylenedinitrilo)tetraacetate] (0.05% w/v) was added when indicated.

RESULTS AND DISCUSSION

Products commercially available indicate that a 0.1% w/w hydrocortisone butyrate concentration would be a useful starting point when formulating a topical preparation of the steroid. To enhance percutaneous absorption of the steroid from the gel system, it was necessary to optimize the thermodynamic activity of the steroid in the formulation. Since a solution system was considered desirable, the continuous phase vehicle ideally should be chosen in such a way that the concentration of steroid is as close as possible to the saturation concentration. To do this quantitatively, a solubility profile of hydrocortisone butyrate in aqueous propylene glycol, the chosen continuous phase, was constructed (Fig. 1). On the basis of the data obtained, a 48% w/w propylene glycol in water solution was chosen for formulating the 0.1% w/w hydrocortisone butyrate gel.

Analysis of the steroids by HPLC and by reference to authentic specimens showed that, like betamethasone valerate, hydrocortisone butyrate (I) isomerizes to the corresponding C-21 ester of butyric acid (II), which then hydrolyzes to hydrocortisone (III) as shown in Scheme I.

To obtain adequate HPLC resolution of the steroids, three aqueous acetonitrile mixtures were necessary. Quantitation of I and II was carried out using a 50% v/v acetonitrile–water mixture. Under these conditions, hydrocortisone showed significant overlap with other minor decomposition products (Fig. 2*a*). Decreasing the acetonitrile concentration prolonged the retention times of all the steroids. The quantitative assay of hydrocortisone was possible with a mobile phase consisting of 35% v/v acetonitrile–water (Fig. 2*b*). Although I and II were resolved from the other steroids using this weaker solvent, the quantitation was not satisfactory because of peak broadening. In the initial stages of decomposition, a 40% v/v acetonitrile–water mixture was adequate in resolving hydrocortisone for quantitative assay (Fig. 2*c*). Considerable time could be saved using this system instead of the 35% v/v aqueous acetonitrile mixture. Whenever possible, therefore, the 40% mixture was chosen for assaying hydrocortisone in the presence of the other steroids.

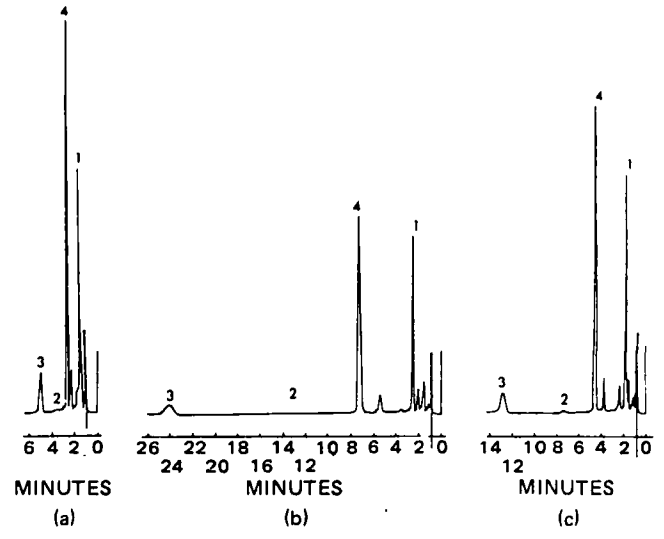

Figure 2—*HPLC separation of I from its decomposition products using an aqueous acetonitrile mobile phase at concentrations of 50% (a), 35% (b), and 40% v/v (c). Key: (1) hydrocortisone; (2) I, (3) II; (4) internal standard.*

Where the assay solutions were diluted prior to injection, care was taken to ensure that the final solvent composition was identical to that used for the standard solution. This was necessary because, as previously reported (9), peak height ratios can show considerable variation, depending on the solvent used.

Kinetic analysis of the gel data (Fig. 3) showed that disappearance of I followed first-order kinetics. Unlike betamethasone valerate (5, 6), however, the overall decomposition did not follow a sequential first-order pattern. Monitoring the decomposition at various pH values showed that the isomerization of I to the C-21 ester (II) was base catalyzed, and pH dependent (Table I). Such base catalysis has been shown in semisolid systems (7, 9, 10). The changes in pH do not appear to be the only factor of importance, since dilution of a betamethasone valerate ointment with a different ointment base significantly altered the decomposition rate even though the pH was near that of the stable undiluted product (7).

To dissociate any effects produced by the gelling agent from other effects, the kinetics of decomposition of I was followed in the absence of the vinyl polymer. The data obtained showed that the decomposition was again pH dependent (Table II); but, unlike the gel system, even the disappearance rate of I in this nonbuffered system did not follow first-order kinetics. The profile for the three steroids in a 50% v/v aqueous propylene glycol system adjusted to pH 7.9 with sodium hydroxide is illustrated in Fig. 4. At this stage it was postulated that base was consumed during at least one of the reactions involved in the overall degradation of I since there was a pH change of ~2 units. To test this, the decomposition was

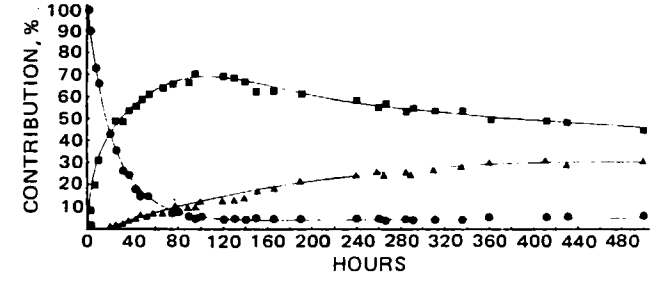

Figure 3—*Profile for I (●), II (■), and hydrocortisone (▲) during the decomposition at 60° of I in a gel system (initial pH 6.78).*

Table I—Effect of pH on the Isomerization of Hydrocortisone Butyrate[a] in a Gel System at 60°

pH	Observed Rate Constant,[b] $hr^{-1} \times 10^4$
6.78	412
5.07	11.5
4.42	6.6

[a] To C-21 ester of butyric acid. [b] Rate constant refers to the overall disappearance of the 17-butyrate.

Table II—Effect of pH on the Decomposition of Hydrocortisone Butyrate[a] in the Aqueous Propylene Glycol Mixture[b] at 60°

pH	Hydrocortisone-butyrate, %	Hydrocortisone-21-butyrate, %	Hydrocortisone, %
7.89	87	8	0
9.95	4	57	37
11.17	0	0	77

[a] Steroid composition at 30 min. [b] 50% v/v.

followed in buffered aqueous propylene glycol systems. Under such conditions one would expect linearization of the data if the reaction sequence was indeed a sequential, irreversible, first-order pathway (Table III, model 1). In fact, the data obtained gave a reasonable fit when subjected to nonlinear regression analysis (11). For most stability prediction studies, such a fit would be adequate, and the confidence limits of the data support this (Table IV). For precise modeling, however, the computerized plot of the experimental data against the predicted data using model 1 shows that discrepancies are present (Fig. 5).

The integrated form of the rate equations were used in the computation. These (Eqs. A1–A4) and equations relevant to the other kinetic models used in this study are listed in *Appendix I*. The kinetic parameters are listed in Tables IV–VIII.

Both previous (12) and the present data show that other products besides II and the free alcohol are produced during the decomposition at 60°. HPLC of a decomposed sample (Fig. 2) clearly demonstrates the complexity of the pathways. Hansen and Bundgaard (12) have reported that at least seven products are formed during the decomposition of hydrocortisone. If the decomposition of hydrocortisone to other products were all first-order parallel processes, the sequential first-order model would hold because the rate constant for the decomposition (K_3) would then equal the sum of the individual rate constants.

The possibility that experimental error accounted for the results was discounted by repeating the experiment: similar deviations were noted in both sets of data. There was good agreement between the estimates for the rate constants (Table IV). Two alternative models to account for the discrepancies are possible. The first is that the isomerization of I to II is reversible, and that the reverse rate constant is not negligible (Table III, model 2). An analogous situation has been previously reported in studies on tricyclic antidepressants (13, 14). In a recent study, Anderson and Taphouse showed that acyl migration from the C-21 to the C-17 position was also possible with methylprednisolone hemisuccinate (15). The second alternative is that I hydrolyzes to hydrocortisone directly and not solely *via* the formation of II (Table III, model 3). To test these possibilities, the hydrolysis of II was followed in samples initially free of I (Table VI, $|B|_0 = 100\%$). Formation of I would show any reversibility. This was the case, and the kinetic parameters for this system under identical conditions are shown in Table V. The improved fit to the model can be seen in Fig. 6. Since K_1 is ~14 times greater than K_4, these rate

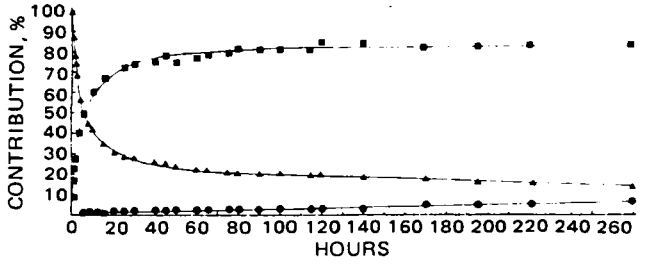

Figure 4—*Profile of I (▲), II (■), and hydrocortisone (●) during the decomposition at 60° of the steroid-17-ester in an aqueous propylene glycol solution (initial pH 7.9).*

Table III—Kinetic Models for the Decomposition of Hydrocortisone Butyrate

Model	Decomposition Scheme
1	$I \xrightarrow{K_1} II \xrightarrow{K_2} III \xrightarrow{K_3} IV$
2	$I \underset{K_4}{\overset{K_1}{\rightleftharpoons}} II \xrightarrow{K_2} III \xrightarrow{K_3} IV$
3	$I \underset{K_4}{\overset{K_1}{\rightleftharpoons}} II \xrightarrow{K_2} III \xrightarrow{K_3} IV$, $II \xrightarrow{K_5} III$

constants are expected to be imprecise when derived from experiments where the initial concentration of I is zero. This is reflected in the wide confidence limits (Table VI).

It is interesting to note that the reverse rate constant for betamethasone valerate isomerization to the C-21 ester was negligible (6), while the ratio of the forward and reverse rate constants for methylprednisolone hemisuccinate was 3–5 (15). The diacidic nature of succinic acid and the C-16 methyl group in betamethasone may explain the observed differences. The free acid function of prednisolone is able to interact freely with the C-17 hydroxyl group without ester function cleavage. In betamethasone, the C-17 hydroxyl group is sterically hindered to a greater extent than in the other two steroids. Its interaction with the C-21 ester function, therefore, is associated with a higher energy barrier and hence a lower reverse rate constant. The experiment does not exclude reversibility in the hydrolysis of I. Therefore, the decomposition of hydrocortisone was studied in the presence of an equimolar amount of sodium butyrate and in the absence of the esters. A control was carried out without the sodium butyrate: no hydrocortisone ester was detected throughout the run, and the rate constants in the control and test systems (0.0096 and 0.0102 hr^{-1}, respectively) were equal within experimental error. Having confirmed that the isomerization, but not the hydrolysis, of I was reversible, the fit to models 2 and 3 were compared to exclude

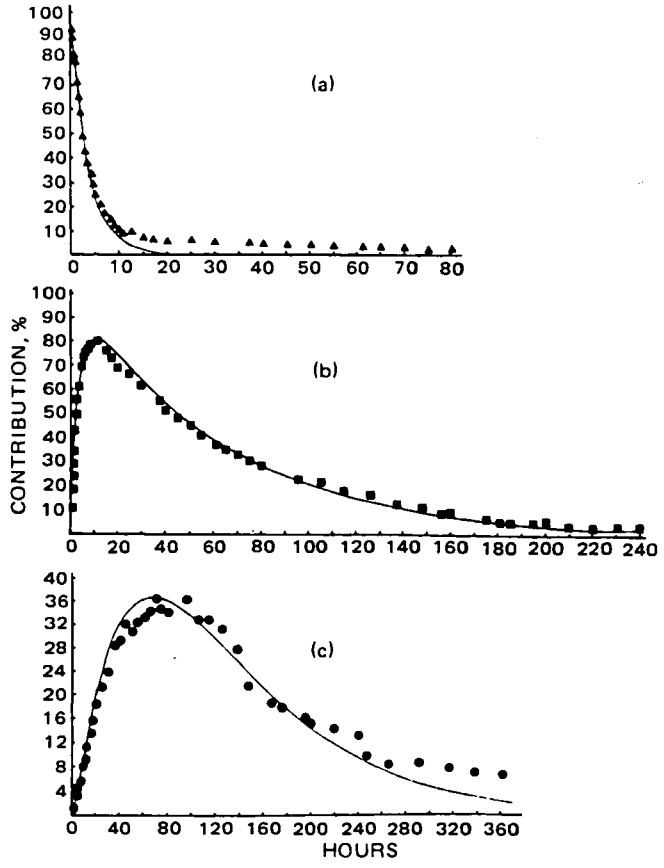

Figure 5—*Profiles for I (a), II (b), and hydrocortisone (c) during the decomposition at 60° of the steroid-17-ester in a buffered aqueous propylene glycol solution (50% v/v, pH 7.6). The lines represent the theoretical predictions according to model 1.*

Table IV—Rate Constants for the Decomposition of Hydrocortisone Butyrate According to Model 1 [a]

Data Set	Calculated Rate Constants[b], hr^{-1}	95% Confidence Limits	Correlation Coefficient[c]
1	$K_1 = 0.290 \pm 0.005$	0.281–0.300	0.999 (A)
	$K_2 = 0.016 \pm 0.0003$	0.016–0.017	0.995 (B)
	$K_3 = 0.0173 \pm 0.001$	0.016–0.019	0.979 (C)
2	$K_1 = 0.288 \pm 0.004$	0.260–0.277	0.998 (A)
	$K_2 = 0.016 \pm 0.0003$	0.015–0.016	0.995 (B)
	$K_3 = 0.015 \pm 0.0004$	0.014–0.016	0.987 (C)

[a] As defined in Table III with initial conditions: $|A|_0 = 100\%$ and $|B|_0 = |C|_0 = 0$. [b] Reactions in buffered (pH 7.6) aqueous propylene glycol (50% v/v) at 60°. [c] Function designation in parentheses.

Table V—Rate Constants for the Isomerization and Decomposition of Hydrocortisone Butyrate According to Model 2 [a]

Data Set	Calculated Rate Constants[b], hr^{-1}	95% Confidence Limits	Correlation Coefficient[c]
1	$K_1 = 0.308 \pm 0.00485$	0.299–0.318	1.000 (A)
	$K_2 = 0.016 \pm 0.00026$	0.016–0.017	0.997 (B)
	$K_3 = 0.017 \pm 0.00057$	0.016–0.018	0.983 (C)
	$K_4 = 0.020 \pm 0.00253$	0.015–0.025	
2	$K_1 = 0.292 \pm 0.00321$	0.285–0.298	0.999 (A)
	$K_2 = 0.016 \pm 0.00015$	0.0157–0.0164	0.999 (B)
	$K_3 = 0.015 \pm 0.00024$	0.015–0.016	0.989 (C)
	$K_4 = 0.025 \pm 0.00163$	0.021–0.028	

[a] As defined in Table III with initial conditions: $|A|_0 = 100\%$ and $|B|_0 = |C|_0 = 0$. [b] Reactions in buffered (pH 7.6) aqueous propylene glycol (50% v/v) at 60°. [c] Function designation in parentheses.

Table VI—Rate Constants for the Isomerization and Decomposition of Hydrocortisone Butyrate According to Model 2 [a]

Calculated Rate Constants[b], hr^{-1}	95% Confidence Limits	Correlation Coefficients[c]
$K_1 = 0.348 \pm 0.195$	(−) 0.041–0.737	0.983 (A)
$K_2 = 0.015 \pm 0.00019$	(−) 0.258–0.051	0.999 (B)
$K_3 = 0.019 \pm 0.00038$	0.150–0.016	0.983 (C)
$K_4 = 0.024 \pm 0.0135$	0.018–0.020	

[a] As defined in Table III with initial conditions: $|A|_0 = 0$, $|B|_0 = 100\%$, and $|C|_0 = 0$. [b] Reactions in buffered (pH 7.6) aqueous propylene glycol (50% v/v) at 60°. [c] Function designation in parentheses.

the possibility that I is converted directly to hydrocortisone. The statistical data and the plots (Figs. 6 and 7) show that direct conversion was likely. Because of the small magnitude of the rate constant for the direct conversion of the I to hydrocortisone (K_5) relative to the other routes, the estimate for its value is imprecise, as is evident in the wide span of 95% confidence limits (Table VII).

Preliminary work on the effect of buffers on the decomposition indicated that the decomposition rates of I to II and of the latter to III were not significantly affected by doubling the buffer concentration. However, the rate of hydrocortisone disappearance was increased (Tables VII and VIII). Recent work has shown that the decomposition of III was metal catalyzed and that EDTA significantly decreased the rate of decomposition (12). Indeed, buffer effects were rationalized on the basis of trace metal contaminants both for hydrocortisone (12) and prednisolone (16). In the present system, the isomerization and hydrolysis steps were unaffected; these steps were not expected to be metal catalyzed. Using different batches of the same grade[11] of buffer salts, the same rate constants for the decomposition of III were obtained (Table IX). However, this does not exclude metal catalysis.

The effect of EDTA on the decomposition therefore was investigated. In addition to explaining in part the mechanism of decomposition, the data was expected to aid in selecting suitable methods for stabilizing the hydrocortisone formulations. Additionally, it had been suggested that some of the decomposition products were potentially immunogenic (17). When compared with control systems (free from the chelating agent),

[11] Analar.

Table VII—Rate Constants for the Isomerization and Decomposition of Hydrocortisone Butyrate According to Model 3 [a]

Data Set	Calculated Rate Constants[b], hr^{-1}	95% Confidence Limits	Correlation Coefficient[c]
1	$K_1 = 0.310 \pm 0.0077$	0.295–0.325	1.000 (A)
	$K_2 = 0.018 \pm 0.00079$	0.0163–0.019	0.998 (B)
	$K_3 = 0.015 \pm 0.00076$	0.0138–0.017	0.975 (C)
	$K_4 = 0.022 \pm 0.0042$	0.0134–0.030	
	$K_5 = 0.0001 \pm 0.0045$	(−) 0.009–0.009	
2	$K_1 = 0.292 \pm 0.0033$	0.286–0.299	0.999 (A)
	$K_2 = 0.016 \pm 0.00031$	0.215–0.280	0.999 (B)
	$K_3 = 0.015 \pm 0.00024$	0.0155–0.017	0.989 (C)
	$K_4 = 0.025 \pm 0.0017$	0.0146–0.0155	
	$K_5 = 0.0001 \pm 0.0018$	(−) 0.003–0.004	

[a] As defined in Table III with initial conditions: $|A|_0 = 100\%$ and $|B|_0 = |C|_0 = 0$. [b] Reactions in buffered (pH 7.6) aqueous propylene glycol (50% v/v) at 60°. [c] Function designation in parentheses.

a stabilizing effect on hydrocortisone was observed when EDTA was added. As expected, the isomerization and hydrolysis rate constants were not significantly altered (Table X). Comparison of the chromatograms (Fig. 8) for the decomposed solutions shows that the profiles for hydrocortisone and the minor decomposition products were markedly different when the system with added EDTA was compared with a control. At 105 hr, the residual steroid concentrations in the control system were 1.2% for I, 21% for II, and 32.6% for III; the respective concentrations for the system with added EDTA were 1.8, 24, and 52%. No attempt was made to identify the minor decomposition products, but published work suggests that oxidation of the side chain of hydrocortisone (leading to the formation of steroid glyoxals, 17-oxo-steroids, and glycolic acids) was likely (12).

The rate constants for the loss of hydrocortisone were lower for solutions initially containing only hydrocortisone compared with solutions

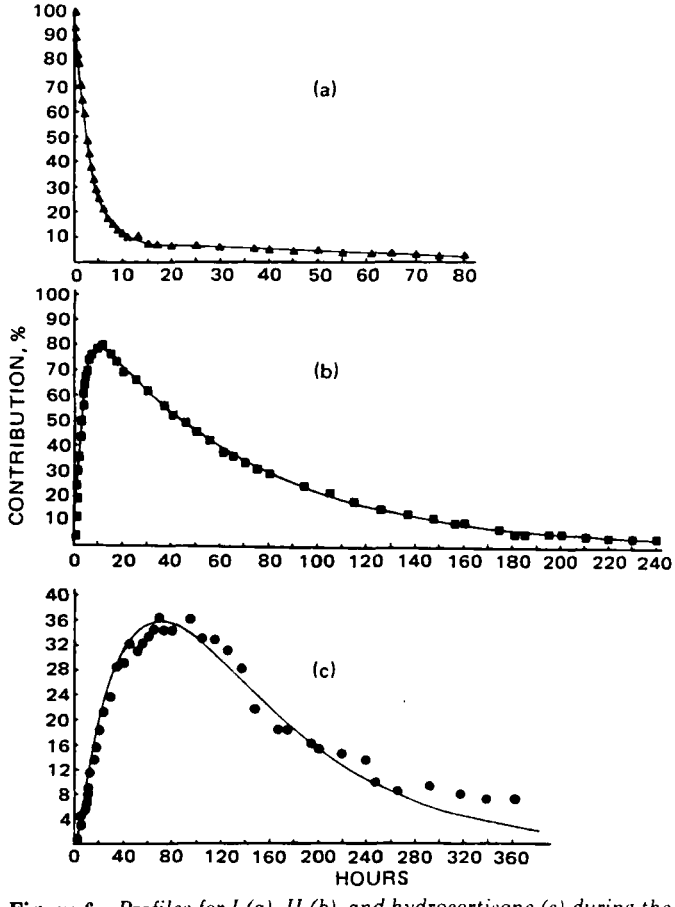

Figure 6—*Profiles for I (a), II (b), and hydrocortisone (c) during the decomposition at 60° of the steroid-17-ester in a buffered aqueous propylene glycol solution (50% v/v, pH 7.6). The lines represent the theoretical predictions according to model 2.*

Table VIII—Rate Constants for the Isomerization and Decomposition of Hydrocortisone Butyrate According to Model 3[a]

Calculated Rate Constants[b], hr^{-1}	95% Confidence Limits	Correlation Coefficient[c]
$K_1 = 0.289 \pm 0.0052$	0.278–0.299	0.999 (A)
$K_2 = 0.016 \pm 0.00034$	0.016–0.017	0.998 (B)
$K_3 = 0.032 \pm 0.0014$	0.029–0.035	0.947 (C)
$K_4 = 0.025 \pm 0.0027$	0.020–0.031	

[a] As defined in Table III with initial conditions: $|A|_0 = 100\%$ and $|B|_0 = |C|_0 = 0$. [b] Reactions in aqueous propylene glycol (50% v/v) at 60°, with twice the added buffer than in the system for Table V. [c] Function designation in parentheses.

initially composed of only I (Tables IV and IX). The rate constant in the latter system had to be obtained by curve-fitting, and, as expected, the value of the rate constant for the loss of hydrocortisone was less accurate than that for the simpler system with hydrocortisone alone. This discrepancy in the rate constants for hydrocortisone disappearance also accounts for the deviation between the predicted and actual hydrocortisone profiles at longer time intervals (Figs. 5–7).

CONCLUSIONS

It has been shown that, in the systems studied, hydrocortisone butyrate (I) underwent reversible isomerization to hydrocortisone butyrate (II). Compound II was then hydrolyzed to hydrocortisone (III) which in turn degraded to a complex mixture of oxidation products. Although the decomposition pathways are complex, they can satisfactorily be modeled by a series of first-order equations. Nonlinear regression analysis of the data indicated that both models 2 and 3 (Table III) satisfactorily described the decomposition, and that model 3 appeared to be a marginally better fit. Direct hydrolysis of I to III and the reverse rate constant for its isomerization to II were so small relative to the hydrolysis rate of II

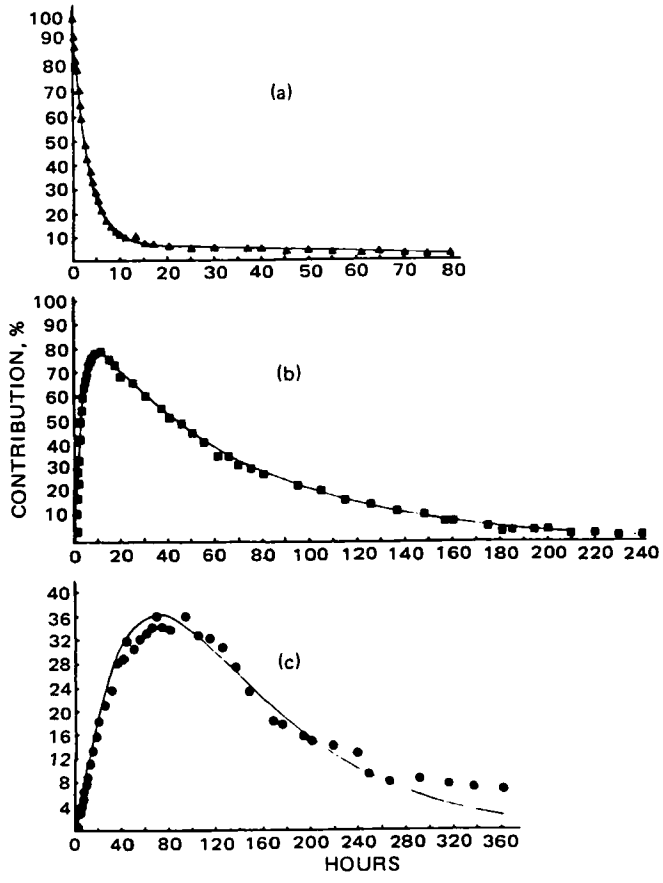

Figure 7—*Profiles for I (a), II (b), and hydrocortisone (c) during the decomposition at 60° of the steroid-17-ester in a buffered aqueous propylene glycol solution (50% v/v, pH 7.6). The lines represent the theoretical predictions according to model 3.*

Table IX—Rate Constants for the Decomposition of Hydrocortisone in Buffered Solutions Using Different Batches of Buffer Salts

Batch	Rate Constant, hr^{-1}
2	0.00964
2	0.01114
1	0.00926
3	0.0107

and the forward rate constant of isomerization that, for most shelf-life predictions, estimates using model 1 (Table III) should be adequate. While the decomposition of III is slow when compared with that of the esters, the suggestion (16) that some of the products may be immunogenic indicates that these slow rates may need to be taken into consideration for the expiration dating of hydrocortisone esters. This requires confirmation; but if such is the case, the more complex models described in this paper should be adequate for this purpose.

APPENDIX

Integrated Rate Equations for Table IV—

$$|A|_t = |A|_0 e^{-K_1 t} \quad \text{(Eq. A1)}$$

$$|B|_t = \frac{|A|_0 K_1}{K_2 - K_1}(e^{-K_1 t} - e^{-K_2 t}) \quad \text{(Eq. A2)}$$

$$|C|_t = |A|_0 \left[\left[\frac{K_1K_2}{(K_2 - K_1)(K_3 - K_1)}\right] e^{-K_1 t} + \left[\frac{K_1K_2}{(K_1 - K_2)(K_3 - K_2)}\right] e^{-K_2 t} + \left[\frac{K_1K_2}{(K_1 - K_3)(K_2 - K_3)}\right] e^{-K_3 t}\right] \quad \text{(Eq. A3)}$$

$$|D|_t = |A|_0 \left[1 - \left[\frac{K_2K_3}{(K_2 - K_1)(K_3 - K_1)}\right] e^{-K_1 t} - \left[\frac{K_1K_3}{(K_1 - K_2)(K_3 - K_2)}\right] e^{-K_2 t} - \left[\frac{K_1K_2}{(K_1 - K_3)(K_2 - K_3)}\right] e^{-K_3 t}\right] \quad \text{(Eq. A4)}$$

Integrated Rate Equations for Table V—

$$|A|_t = |A|_0 \left(\frac{K_2 + K_4 - \gamma_1}{\gamma_2 - \gamma_1} e^{-\gamma_2 t} + \frac{K_4 + K_2 - \gamma_2}{\gamma_1 - \gamma_2} e^{-\gamma_2 t}\right) \quad \text{(Eq. A5)}$$

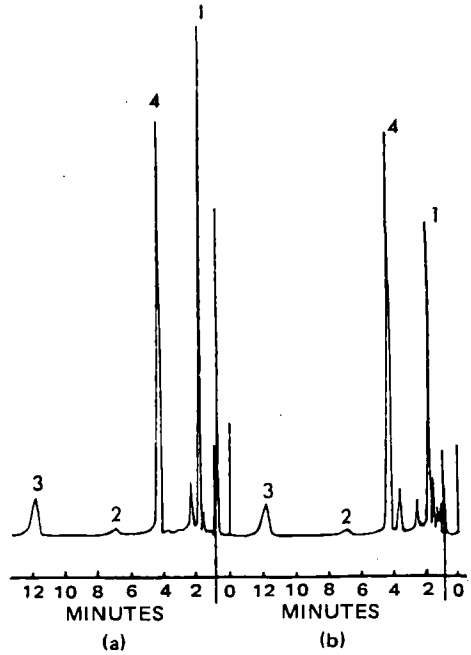

Figure 8—*Chromatograms of decomposed solutions of I in the presence (a) and absence (b) of EDTA. Key: (1) hydrocortisone; (2) I; (3) II (4) internal standard.*

Table X—Decomposition of Hydrocortisone Butyrate in the Presence and Absence of EDTA [a]

Starting Compound	Decomposition Rate Constant, $\times 10^3$ hr^{-1} With EDTA	Without EDTA	
Hydrocortisone	K_3 3.90	11.14	←
Hydrocortisone butyrate	K_1 274	292	
	K_2 14.4	16.1	
	K_3 5.2	15.3	←
	K_4 24.4	24.6	

[a] 0.05% w/v.

$$|B|_t = |A|_0 K_1 \left(\frac{1}{\gamma_2 - \gamma_1} e^{-\gamma_1 t} + \frac{1}{\gamma_1 - \gamma_2} e^{-\gamma_2 t}\right) \quad \text{(Eq. A6)}$$

$$|C|_t = |A|_0 K_1 K_2 \left[\frac{1}{(\gamma_2 - \gamma_1)(K_3 - \gamma_1)} e^{-\gamma_1 t} + \frac{1}{(\gamma_1 - \gamma_2)(K_3 - \gamma_2)} e^{-\gamma_2 t} + \frac{1}{(\gamma_1 - K_3)(\gamma_2 - K_3)} e^{-K_3 t}\right] \quad \text{(Eq. A7)}$$

where $\gamma_1 = \frac{1}{2}\{(K_1 + K_2 + K_4) - [(K_1 + K_2 + K_4)^2 - 4K_1K_2]^{1/2}\}$ (Eq. A8)

and

$$\gamma_2 = \frac{1}{2}\{(K_1 + K_2 + K_4) + [(K_1 + K_2 + K_4)^2 - 4K_1K_2]^{1/2}\} \quad \text{(Eq. A9)}$$

Integrated Rate Equations for Table VI—

$$|A|_t = |B|_0 K_4 \left(\frac{1}{\gamma_2 - \gamma_1} e^{-\gamma_1 t} + \frac{1}{\gamma_1 - \gamma_2} e^{-\gamma_2 t}\right) \quad \text{(Eq. A10)}$$

$$|B|_t = |B|_0 \left(\frac{K_1 - \gamma_1}{\gamma_2 - \gamma_1} e^{-\gamma_1 t} + \frac{K_1 - \gamma_2}{\gamma_1 - \gamma_2} e^{-\gamma_2 t}\right) \quad \text{(Eq. A11)}$$

$$|C|_t = |B|_0 K_2 \left[\frac{K_1 - \gamma_1}{(\gamma_2 - \gamma_1)(K_3 - \gamma_1)} e^{-\gamma_1 t} + \frac{K_1 - \gamma_2}{(\gamma_1 - \gamma_2)(K_3 - \gamma_2)} e^{-\gamma_2 t} + \frac{K_1 - K_3}{(\gamma_1 - K_3)(\gamma_2 - K_3)} e^{-K_3 t}\right] \quad \text{(Eq. A12)}$$

where γ_1 and γ_2 are as defined in Eqs. A8 and A9, respectively.

Integrated Rate Equations for Table VII—

$$|A|_t = |A|_0 \left(\frac{K_4 + K_2 - \gamma_1}{\gamma_2 - \gamma_1} e^{-\gamma_1 t} + \frac{K_4 + K_2 - \gamma_2}{\gamma_1 - \gamma_2} e^{-\gamma_2 t}\right) \quad \text{(Eq. A13)}$$

$$|B|_t = |A|_0 K_1 \left(\frac{1}{\gamma_2 - \gamma_1} e^{-\gamma_1 t} + \frac{1}{\gamma_1 - \gamma_2} e^{-\gamma_2 t}\right) \quad \text{(Eq. A14)}$$

$$|C|_t = |A|_0 \left[\frac{K_1K_2 + K_4K_5 + K_2K_5 - K_5\gamma_1}{(\gamma_2 - \gamma_1)(K_3 - \gamma_1)} e^{-\gamma_1 t} + \frac{K_1K_2 + K_4K_5 + K_2K_5 - K_5\gamma_2}{(\gamma_1 - \gamma_2)(K_3 - \gamma_2)} e^{-\gamma_2 t} + \frac{K_1K_2 + K_4K_5 + K_2K_5 - K_3K_5}{(\gamma_1 - K_3)(\gamma_2 - K_3)} e^{-K_3 t}\right] \quad \text{(Eq. A15)}$$

where

$$\gamma_1 = \frac{1}{2}\{(K_1 + K_2 + K_4 + K_5) - [(K_1 + K_2 + K_4 + K_5)^2 - 4(K_4K_5 + K_1K_2 + K_2K_5)]^{1/2}\} \quad \text{(Eq. A16)}$$

and

$$\gamma_2 = \frac{1}{2}\{(K_1 + K_2 + K_4 + K_5) + [(K_1 + K_2 + K_4 + K_5)^2 - 4(K_4K_5 + K_1K_5 + K_2K_5)]^{1/2}\} \quad \text{(Eq. A17)}$$

REFERENCES

(1) A. W. McKenzie and R. M. Atkinson, *Arch. Dermatol. Res.*, **89**, 741 (1964).

(2) W. P. Raab and B. M. Gmeiner, *Arch. Dermatol. Res.*, **253**, 113 (1975).

(3) R. C. O'Neill and J. E. Carless, *J. Pharm. Pharmacol.*, **32**, 10p (1980).

(4) R. Gardi, R. Vitali, and A. Ercoli, *Gazz. Chim. Ital.*, **93**, 431 (1963).

(5) Y. W. Yip and A. Li Wan Po, *J. Pharm. Pharmacol.*, **31**, 400 (1979).

(6) A. Li Wan Po, W. J. Irwin, and Y. W. Yip, *J. Chromatogr.*, **176**, 399 (1979).

(7) A. Li Wan Po, W. J. Irwin, and Y. W. Yip, *Proc. Anal. Div., Chem. Soc., London*, **16**, 333 (1979).

(8) P. J. Elving, J. M. Marketing, and Rosenthal, *J. Anal. Chem.*, **7**, 1179 (1956).

(9) K. J. Williams, A. Li Wan Po, and W. J. Irwin, *J. Chromatogr.*, **194**, 217 (1980).

(10) H. Bundgaard and J. Hansen, *Int. J. Pharm.*, **7**, 197 (1981).

(11) C. M. Metzler, G. L. Elfring, and A. J. McEwen "A User's Manual for Non-linear and Associated Programs," The Upjohn Co., Kalamazoo, Mich., 1974.

(12) J. Hansen and H. Bundgaard, *Arch. Pharm. Chem., Sci. Ed.*, **8**, 91 (1980).

(13) A. Li Wan Po and W. J. Irwin, *J. Pharm. Pharmacol.*, **27**, 512 (1979).

(14) A. Li Wan Po and W. J. Irwin, *J. Pharm. Pharmacol.*, **32**, 25 (1980).

(15) B. D. Anderson and V. Taphouse, *J. Pharm. Sci.*, **70**, 181 (1981).

(16) T. O. Oesterling and D. E. Guttman, *J. Pharm. Sci.*, **53**, 1189 (1964).

(17) H. Bundgaard, *Arch. Pharm. Chem., Sci. Ed*, **8**, 83 (1980).

Identification of *In Vitro* (Rat Liver Postmitochondrial S9 Fraction) Metabolites of the Antiprotozoal Agent 3a,4,5,6,7,7a-Hexahydro-3-(1-methyl-5-nitro-1*H*-imidazol-2-yl)-1,2-benzisoxazole

W. J. A. VANDENHEUVEL *[x], H. SKEGGS [‡], B. H. ARISON *, and P. G. WISLOCKI *

Received April 19, 1982 from *Merck Sharp & Dohme Research Laboratories, *Rahway, NJ 07065* and *‡West Point, PA 19486.* Accepted for publication June 29, 1982.

Abstract □ Twelve *in vitro* oxygenated metabolites of 3a,4,5,6,7,7a-hexahydro-3-(1-methyl-5-nitro-1*H*-imidazol-2-yl)-1,2-benzisoxazole (MK-0436) were produced by incubation of this antiprotozoal agent with the postmitochondriai supernatant (S9) fraction isolated from the livers of rats treated with phenobarbital. Metabolite structure elucidation was achieved using NMR and mass spectrometry. Seven monohydroxy and two dihydroxy metabolites were fully characterized; two other metabolites were partially characterized as dihydroxy derivatives of the drug. The major *in vitro* metabolite is the 5 axial hydroxy compound, and a minor metabolite is the corresponding ketone. In all cases metabolite formation involved biotransformation on the hexahydrobenzisoxazole ring.

Keyphrases □ 3a,4,5,6,7,7a - Hexahydro -3- (1-methyl-5-nitro-1*H*-imidazol-2-yl)-1,2-benzisoxazole—synthesis of *in vitro* oxygenated metabolites, characterization by NMR and mass spectrometry, biotransformations on the hexahydrobenzisoxazole ring □ Metabolites—of 3a,4,5,6,7,7a - hexahydro -3- (1-methyl-5-nitro-1*H*-imidazol -2- yl)-1,2-benzisoxazole, characterization by NMR and mass spectrometry □ Antiprotozoal agents—3a,4,5,6,7,7a-hexahydro-3-(1-methyl-5-nitro-1*H*-imidazol-2-yl)-1,2-benzisoxazole and its metabolites, characterization by NMR and mass spectrometry

Seven canine urinary metabolites of the antiprotozoal agent 3a,4,5,6,7,7a-hexahydro-3-(1-methyl-5-nitro-1*H*-imidazol-2-yl)-1,2-benzisoxazole (MK-0436, I) have been identified; all of the compounds (II–VIII) are formed by hydroxylation of the hexahydrobenzisoxazole ring (1, 2). Several dihydroxy analogues of I have been synthesized

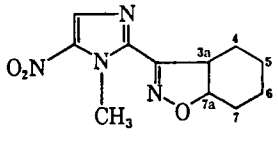

I

and at least one, the 6,7-*cis*-dihydroxy compound, exhibits higher antibacterial activity against *Salmonella schottmuelleri* in mice and greater trypanocidal activity *in vivo* against *Trypanosoma cruzi* (Brazil strain) than I (1). Incubation of I with the microsomal cytosol fraction (S9) from the livers of mice produced antibacterial activity not seen with the drug alone, suggesting the *in vitro* formation of antibacterial metabolites (1). The present study was undertaken to identify the metabolites of I generated *in vitro* by the rat liver postmitochondrial supernatant fraction (S9).

EXPERIMENTAL

***In Vitro* Incubations**—The postmitochondrial supernatant fraction was isolated from livers of rats that had been treated with phenobarbital. The 9–12-week-old rats were injected with phenobarbital for four consecutive days at a dose of 80 mg kg/day ip. Twenty-four hours after the last injection the rats were killed and the postmitochondrial S9 supernatant was isolated using the method of Ames (3).

The incubation mixture used was the same as that described by Ames for the S9 mixture (3) and used previously (1). It contained 0.1 *M* sodium phosphate (pH 7.4), 8 m*M* magnesium chloride, 33 m*M* potassium chloride, 5 m*M* glucose-6-phosphate, 4 m*M* nicotinamide adenine dinucleotide phosphate, homogenate equal to 0.78 g wet weight liver, and 4 mg of I (labeled with carbon-14 in the 3a and 7a positions) in 200 μl of dimethylsulfoxide with a total volume of 10.4 ml. The incubation was carried out in a 250-ml Erlenmeyer flask with shaking at room temperature. At the end of the 80-min incubation (determined to be optimum for metabolite production from preliminary experiments) an equal volume of cold methylene chloride was added.

Metabolite Isolation—The metabolites of I were isolated by dilution of the incubation mixture with 10 ml of water followed by three successive extractions with 20-ml portions of methylene chloride. This procedure resulted in the extraction of 80% of the radioactivity present in the incubation mixture. The organic phases were combined and the methylene chloride removed under a stream of nitrogen (water bath, 40°) to yield a tan residue. The latter was dissolved in methanol and subjected to TLC[1] (solvent system A; see below) to yield seven metabolite fractions. Further purification of these fractions, if necessary, was achieved by use of TLC with three other solvent systems (systems B–D; see below). Appropriate zones (visualized by radioscanning[2] or short-wavelength UV[3]) were scraped from the plate and the silica gel washed three times with ethyl acetate–methanol, 4:1. The eluates were combined and, following removal of solvent under a nitrogen stream at 40°, the residue was partitioned between ethyl acetate (2 ml) and water (0.1 ml) to minimize the amount of silica gel present in the isolated metabolite fraction.

TLC and Radioactivity Assay—Isolation of metabolite fractions *via* TLC involved the use of four solvent[4] systems: toluene–ethyl acetate, 3:1 (system A); methylene chloride (system B); methylene chloride–methanol, 9:1 (system C); and trimethylpentane–2-propanol, 4:1 (system D). Metabolite fractions were assayed for radioactivity by use of liquid scintillation counting[5] techniques.

Derivatization—Methoxime formation was carried out by dissolving an aliquot of the metabolite fraction in a pyridine solution of methoxyamine hydrochloride[6] (5 mg/ml) and allowing the reaction to proceed for 2 hr at room temperature. The trimethylsilyl derivative was prepared by dissolving an aliquot of the metabolite fraction in a 1:1 (v/v) mixture of *bis*(trimethylsilyl)trifluoroacetamide[7]–pyridine and allowing the reaction to proceed for 1 hr at room temperature.

NMR and Mass Spectrometry—NMR spectra[8] were obtained from metabolite fractions dissolved in deuterochloroform. Mass spectra[9] of metabolite fractions were obtained by use of the direct probe technique under the following operating conditions: 3.5 kV accelerating potential, 60 μA trap current, 70 eV ionizing energy, and 250° source temperature. Capillary column GLC–mass spectrometry[10] was carried out using a 15 m × 0.25-mm i.d. SE-30 column operated at 220° (helium carrier gas, 1

[1] Quanta/Gram QIF plates, Quantum Industries.
[2] BID System 100 Radioisotope Imaging System.
[3] Chromato-Vue.
[4] Burdick and Jackson, distilled in glass.
[5] Packard Tricarb Liquid Scintillation Spectrometer.
[6] Eastman.
[7] Supelco.
[8] Varian SC-300 MHz spectrometer equipped with a Fourier transform accessory.
[9] LKB 9000 instrument.
[10] Finnigan 3200 instrument.

0022-3549/83/0700-0782$01.00/0

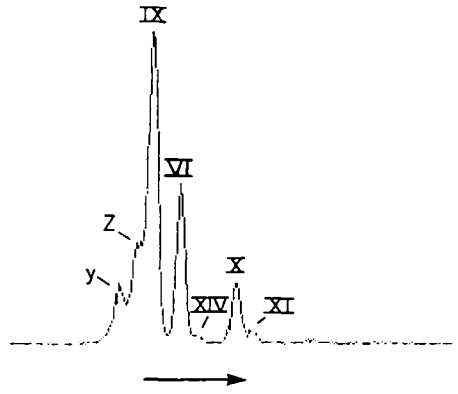

Figure 1—*Radioactivity profile*[11] *arising from TLC (silica gel; toluene–ethyl acetate, 3:1) of the methylene chloride extract from an* in vitro *reaction (rat liver S9 fraction) of [*^{14}*C]I.*

ml/min) interfaced with a spectrometer operated at 70 eV ionizing energy, 0.8 mA emission current, and 1800 V electron multiplier.

RESULTS AND DISCUSSION

The nitroimidazole I and its known hydroxyl group-containing metabolites exhibit strong short-wavelength UV absorption (254 nm) which facilitates their detection on a TLC plate. Further, as the drug used in these studies was ^{14}C-labeled, radioscanning of a developed TLC plate also allowed the detection of metabolites. The electron impact mass spectra of these compounds normally possess intense fragment ions at *m/z* 153 and 195 (1), and these, plus the presence of molecular ions at *m/z* 266 or 282 (16 and 32 AMU greater than the molecular ion of I, respectively), facilitate recognition of the unknown compounds as mono- or dihydroxylated analogues of I. When the metabolites are trimethylsilylated, their molecular ions increase by 72 AMU for each hydroxyl group present to yield signals at *m/z* 338 and 426 (molecular ions, low intensity) and *m/z* 323 and 411 (the corresponding M-15 ions).

Analytical TLC (solvent system A) with UV and/or radioscanning and capillary column GLC–mass spectrometry (as trimethylsilyl derivatives) of a methylene chloride extract of the incubation mixture (~80% of the radioactivity was extractable) demonstrated that it was multicomponent in nature, containing at least seven compounds related to I (Fig. 1, Table I). None of the parent drug was present. Preparative scale TLC (solvent system A) was employed to isolate the seven metabolite fractions in quantities suitable for structure elucidation. These were examined by mass and NMR spectrometry. In all cases the mass spectrometric data showed the metabolites to be mono- or dioxygenated derivatives of I, with the metabolic transformation occurring on the hexahydrobenzisoxazole ring (Table II).

One of the isolated metabolites was shown to be the 7-equatorial hydroxy compound, previously identified as a canine urinary metabolite of I (2) and is thus referred to as metabolite VI (the previous designation). This is the second most abundant of the *in vitro* metabolites.

The major *in vitro* metabolite, IX, is also a monohydroxy derivative of I (molecular ion, *m/z* 266). On the basis of NMR data [4.60 ddd, 7.5, 4.0, 4.0 (H_{7a}); 4.17 br s, $w_{1/2}$: 11 H_3 (H_{5eq}); 3.82 dt, 10.0, 7.5, 7.5 (H_{3a})] the hydroxyl group is assigned to the 5-position with an axial conformation.

Metabolite X is the third most abundant metabolite arising from the S9 incubation. It also possesses a molecular weight of 266, as determined by mass spectrometry. The location of the hydroxyl group was shown by NMR to be at C_{7a}, since the characteristic H_{7a} signal was absent. Other pertinent NMR data included the signal at 3.47 dd, 10.5, 7.5 (H_{3a}). This metabolite was found to dehydrate on prolonged exposure to silica gel to yield an olefin (molecular weight 248) identified as the $\Delta^{3a,7a}$ compound.

Metabolite XI, the fourth of the monohydroxy metabolites, was shown by NMR [key features include signals at 4.66 m (H_{7a}); 3.22 t, 8.3 (H_{3a}); and 3.59 ddd, 11.5, 8.0, 5.0 (H_{4ax})] to possess an equatorial hydroxyl group at C-4. Although hydroxylation at C-4 of I has been recognized previously for an *in vivo* metabolite [4,5-di-equatorial dihydroxy, II (2)], this is the first instance of monohydroxylation at this position.

The minor metabolite fractions Y and Z were found, on the basis of NMR (presence of several N—CH_3 signals) and mass spectrometry (interscan variation of relative ion intensities), to be multicomponent in nature. Preparative scale TLC (solvent system D; Table I) was employed to isolate two metabolites (one major, one minor) from Y and three metabolites (two major, one minor) from Z. The two major components of Z were shown to be the 5- and 6-equatorial monohydroxy metabolites, both previously found as canine urinary metabolites of I (2) and are thus designated (as before) metabolites IV and VII.

The minor components of Y and Z and the major component of Y all possess molecular ions of *m/z* 282 and are thus dihydroxy metabolites of I. As with all of the other known metabolites of this drug, their mass spectrometric behavior indicated that hydroxylation had occurred on the hexahydrobenzisoxazole ring. The exact positions and stereochemistry of the two hydroxyl groups of the major Y metabolite (VIII) were shown by NMR to be 5-axial and 7a. The NMR spectrum of VIII is characterized by the absence of an H_{7a} signal and the presence of a new *H*COH peak of 4.16δ. An equatorial configuration for the 4.16δ methine is inferred based on the broad singlet character and relatively narrow linewidth ($w_{1/2}$10 Hz). Since the coupling patterns of H_{3a} and H_{7a} axial exclude C-4 and C-6 as possible sites, VIII is assigned as the 5-axial,7a-dihydroxy analogue. The minor components of Y (XII) and Z (XIII) were not further characterized.

A very minor metabolite (XIV) was found by mass spectrometry to possess a molecular weight of 264 (*versus* 250 for I). This shift of 14 mass units suggested that the metabolic transformation involved formation of a ketone. Compound XIV was exposed to methoxime-forming conditions (4); mass spectrometry showed a shift in molecular weight from 264 to 293, demonstrating the ketonic nature of the metabolite. The exact site of the keto group on the hexahydrobenzisoxazole ring was shown by NMR [5.19 dt, 11.5, 3.5, 3.5 (H_{7a}); 4.38 ddd, 11.3, 7.3, 3.5 (H_{3a}); 2.96 dd 16.4, 3.5; 2.77 dd 16.4, 7.5 (4-CH_2); 2.44 m, 2.32 m (6,7-CH_2)] to be the 5-position. This metabolite presumably arises from IX *via* oxidation of the 5-axial hydroxyl group.

When the 6,7-epoxide of I is incubated under the conditions that yield the metabolites discussed above, the major metabolite is the 5-axial hydroxy derivative of the 6,7-epoxide. The mass spectrum of this metabolite contains a molecular ion at *m/z* 280 with *m/z* 195 as base peak, the same base peak as found in the mass spectrum of IX (which also possesses an axial hydroxyl group at C-5). The NMR of the hydroxylated epoxide showed peaks at 5.13 d, 11.0 (H_{7a}); 4.10 ddd, 11.0, 5.0, 3.0 (H_{3a}); 3.88 dd, 11.5, 5.0 (H_{5a}); 3.42 br s ($H_{6,7}$); 2.72 ddd, 14.0, 5.0, 4.0 (H_{4eq}); 1.95 ddd, 11.5, 11.5, 5.5 (H_{4ax}).

A preliminary incubation, in which only 10% of the radioactivity was extractable from the aqueous system by methylene chloride, gave six metabolites isolated by TLC (Table I)[12]. Again, no I was found in the extract (as measured by TLC). Four of these compounds were shown by TLC, mass spectrometry, and/or NMR to be metabolites IV, VI, VII, and IX. The two others are newly recognized *in vitro* metabolites of I. One is the 7-axial hydroxy analogue (metabolite V, previously found as a conjugate in dog urine); the second is the 4-equatorial,5-axial dihydroxy analogue (metabolite XV, not found in dog urine). The mass spectrum of this latter metabolite exhibits a molecular ion at *m/z* 282 and fragment

Table I—TLC R_f Values for *In Vitro* Metabolites of I

Compound	Substitution	Solvent System[a] A	B	C	D
I	—	0.72	—	—	—
IV	5-Eq-OH	0.09	—	—	0.28
V	7-Ax-OH	0.14	—	0.51	—
VI	7-Eq-OH	0.22	0.07	—	—
VII	6-Eq-OH	0.09	—	—	0.32
VIII	5-Ax,7a-$(OH)_2$	0.04	—	—	0.39
IX	5-Ax-OH	0.14	—	0.42	—
X	7a-OH	0.38	—	—	—
XI	4-Eq-OH	0.43	—	—	—
XII	$(OH)_2$	0.04	—	—	0.28
XIII	$(OH)_2$	0.09	—	—	0.39
XIV	5-Keto	0.27	—	—	—
XV	4-Eq,5-Ax-$(OH)_2$	0.22	0.11	—	—

[a] (A) Toluene–ethyl acetate, 3:1; (B) methylene chloride; (C) methylene chloride–methanol, 7:1; (D) trimethylpentane-2-propanol, 4:1.

[11] Bioscan BIII System 100/Hewlett-Packard 85.

[12] When incubation of ^{14}C-labeled I in the presence of S9 is carried out with a limited amount of air (without shaking) most of the radioactivity does not extract into methylene chloride following termination of the incubation but is associated with water-soluble species. (H. Skeggs and W. J. A. VandenHeuvel, unpublished data.)

Table II—Major Ions Found in the Mass Spectra of *In Vitro* Metabolites of I

Compound	Substitution	Ion and Relative Intensity											
		m/z 282	*m/z* 266	*m/z* 265	*m/z* 249	*m/z* 247	*m/z* 231	*m/z* 221	*m/z* 195	*m/z* 169	*m/z* 153	*m/z* 149	*m/z* 107
IV	5-Eq-OH	—	77	—	79	—	—	36	54	35	100	—	34
V	7-Ax-OH[a]	—	20	—	9	19	—	2	42	35	100	—	14
VI	7-Eq-OH[b]	—	41	—	54	90	20	16	60	10	100	—	32
VII	6-Eq-OH	—	95	—	80	12	—	—	96	35	100	—	43
VIII	5-Ax,7a-$(OH)_2$[c]	30	—	100	—	26	—	29	28	—	67	—	28
IX	5-Ax-OH[d]	—	29	—	28	22	5	—	100	10	48	—	10
X	7a-OH[e]	—	48	—	100	4	—	—	44	15	36	—	10
XI	4-Eq-OH	—	4	—	2	—	—	—	100	—	3	15	4
XII	$(OH)_2$	28	—	20	—	10	—	—	57	—	100	—	19
XIII	$(OH)_2$	3	—	2	—	—	—	—	6	—	100	—	19
XIV	5-Keto[f]	—	—	—	—	15	—	—	6	25	53	—	—
XV	4-Eq,5-Ax-$(OH)_2$	5	—	1	—	—	—	—	100	4	1	17	7

[a] *m/z* 210, 4%. [b] *m/z* 210, 2%. [c] *m/z* 237, 30%; *m/z* 223, 37%. [d] *m/z* 96, 30%. [e] *m/z* 210, 54%; *m/z* 207, 37%; *m/z* 204, 20%; *m/z* 193, 32%. [f] *m/z* 264, 100%.

ions characteristic of hydroxylation at C-4 and C-7 of the hexahydrobenzisoxazole ring. The NMR of this compound is characterized by signals at 4.68 m (H_{7a}); 3.54 dd, 8.0, 3.5 (H_{4ax}); 4.10 br s, $w_{1/2}$10 Hz (H_{5eq}); and 3.40 t, 8.0 (H_{3a}).

The outcome of this preliminary experiment (which yielded metabolites IV–VII, IX,and XV) might have resulted from a lack of sufficient air in the reaction flask during the incubation or possibly from secondary metabolism resulting from a high enzyme to substrate ratio and extended incubation. In any event, it is clear that routes and extent of *in vitro* metabolism of I are heavily dependent on the incubation conditions. Whether a radically different metabolism (*e.g.*, transformations of the nitro group or the heterocyclic rings) occurs or whether further oxidative metabolism of the hexahydrobenzisoxazole ring leads to highly polar, ring-opened derivatives is not known at present.

Earlier work demonstrated that at least four dihydroxy metabolites (two fully characterized) and at least five monohydroxy metabolites of I are found (free and/or conjugated) in dog urine (1, 2). The current study shows that monohydroxylation is by far the major *in vitro* pathway, but that dihydroxylation is not precluded. A total of 14 *in vivo* and *in vitro* metabolites of I resulting from introduction of one or two oxygen atoms into the hexahydrobenzisoxazole ring have now been recognized.

The extensive oxidative metabolism of I is another example of the ability of the hepatic microsomal mixed-function oxidases to metabolize a compound at several sites (5–7). It is of interest that the alicyclic carbons of the saturated benzisoxazole ring are the targets of metabolism, whereas the N—CH_3 group appears resistent to metabolic attack under the conditions used. Likewise, to date no metabolism has been found to occur at the 3a-position. So although extensive, the metabolism is quite selective. Other nitroimidazoles undergo metabolism on their hydrocarbon moieties. Metronidazole and ipronidazole are hydroxylated on the 2-CH_3 group (8) and the 2-isopropyl group (9), respectively, misonidazole undergoes *O*-demethylation (10), and 5-isopropyl-1-methyl-2-nitro-1*H*-imidazole undergoes extensive metabolism at the isopropyl group (11). Although reduction of the nitro group is considered the mechanism by which nitroimidazoles exert their therapeutic activity, modification of other parts of the molecules can enhance or diminish this therapeutic activity, as shown previously (1).

REFERENCES

(1) W. J. A. VandenHeuvel *et al.*, *J. Pharm. Sci.*, **68**, 1156 (1979).

(2) W. J. A. VandenHeuvel, D. Onofrey, J. S. Zweig, J. Pile, N. Kirkman-Bey, and B. H. Arison, *ibid.*, **69**, 1288 (1980).

(3) B. N. Ames, J. McCann, and E. Yamasaki, *Mutat. Res.*, **31**, 347 (1975).

(4) H. M. Fales and T. Luukkainen, *Anal. Chem.*, **37**, 955 (1965).

(5) G. Holder, H. Yagi, P. Dansette, D. M. Jerina, W. Levin, A. Y. H. Lu, and A. H. Conney, *Proc. Natl. Acad. Sci. USA*, **71**, 4356 (1974).

(6) S. K. Yang, J. K. Selkirk, E. V. Plotkin, and H. V. Gelboin, *Cancer Res.*, **35**, 3642 (1975).

(7) L. B. Pohl, S. D. Nelson, W. R. Porter, W. F. Trager, M. J. Fasco, F. D. Baker, and J. W. Fenton, II, *Biochem. Pharmacol.*, **25**, 2153 (1976).

(8) J. E. Stambaugh, L. G. Feo, and R. W. Manthei, *J. Pharmacol. Exp. Ther.*, **161**, 373 (1968).

(9) J. Fellig, A. MacDonald, E. Meseck, and H. Laurencot, *Poult. Sci.*, 48, 1806 (1969).

(10) I. R. Flockhart, P. Lange, D. Troup, S. L. Malcolm, and T. R. Martes, *Xenobiotica*, **8**, 97 (1978).

(11) A. Assandri, A. Perazzi, L. F. Zerilli, P. Ferrari, and E. Martinelli, *Drug Metab. Dispos.*, **6**, 109 (1978).

ACKNOWLEDGMENTS

We are grateful to Drs. B. M. Miller and F. J. Wolf for their interest in and support of this work, to G. J. Gatto for synthesizing the [^{14}C]-labeled I, and to C. E. Heiss for obtaining the radioactivity profile in Fig. 1.

Metabolism of Isosorbide Dinitrate in the Isolated Perfused Rabbit Lung

PHILIP R. MAYER*, WILLIAM C. LUBAWY, PATRICK J. MCNAMARA, and HARRY B. KOSTENBAUDER ˣ

Received February 1, 1982, from the *College of Pharmacy, University of Kentucky, Lexington, KY 40536.* Accepted for publication June 25, 1982. *Present address: School of Pharmacy and Pharmacal Sciences, Purdue University, West Lafayette, IN 47907.

Abstract □ The uptake and metabolism of isosorbide dinitrate was investigated in the recirculating isolated perfused rabbit lung and in lung homogenate 9000×*g* supernatant. Concentration *versus* time profiles from the isolated lung experiments indicate rapid metabolism of isosorbide dinitrate and corresponding increases in the metabolites 5-isosorbide mononitrate, 2-isosorbide mononitrate, and isosorbide. The data suggest that the mononitrates formed in the lung tissue were converted to isosorbide at an extraordinarily high rate. Surprisingly, the rate of appearance of completely denitrated isosorbide was greater when isosorbide dinitrate was administered to the lung than when the mononitrate metabolites of isosorbide dinitrate were administered. The results suggest rapid metabolism of a substantial portion of the mononitrates formed endogenously from isosorbide dinitrate before partitioning of mononitrates into the perfusion medium could occur. The metabolism of isosorbide dinitrate in lung homogenate 9000×*g* supernatant exhibited a metabolic scheme kinetically different from the intact lung studies, as isosorbide was formed slowly from a mononitrate intermediate and not by a near-simultaneous cleavage of both nitrate ester groups. Intravascular multiple-dose studies did not demonstrate any inhibition between isosorbide dinitrate and the mononitrates.

Keyphrases □ Isosorbide dinitrate—metabolism in isolated perfused rabbit lung, kinetic profiles □ Metabolism—of isosorbide dinitrate and metabolites in isolated perfused rabbit lung, kinetic profiles □ Metabolites—of isosorbide dinitrate, kinetic profiles in isolated perfused rabbit lung

The lung has been evaluated previously for many functions other than the physiological exchange of gases. The lung is now known to absorb many drugs, filter the air and blood, and serve in fibrinologic, endocrinologic, and metabolic capacities (1, 2). Uptake of a drug into the lung may be by passive diffusion (3) or carrier-mediated transport (4) and may have reversible, competitive, or saturable components (5). The lung can metabolize efficiently many biologically active substances once they are distributed in the lung (2, 3, 6).

Isosorbide dinitrate is a vasodilator used primarily in the treatment of angina pectoris and congestive heart failure (7, 8). Organic nitrates including isosorbide dinitrate are metabolized extensively by the enzyme glutathione organic nitrate reductase (9, 10), and their oral effectiveness has been questioned due to extensive first-pass liver metabolism (11, 12). The objective of this study was to investigate the uptake and metabolism of isosorbide dinitrate in the isolated perfused rabbit lung, and to evaluate in a preliminary manner this organ as a route of administration.

EXPERIMENTAL

Materials—Randomly labeled [^{14}C]isosorbide dinitrate (168 mCi/mmole)[1] was purified by the chromatographic procedure described in *Analytical Methods* and extracted from the silica gel with methanol. A working solution of >96% purity was obtained and checked at 6-month intervals. Radiolabeled metabolites were recovered in the same manner. Nonlabeled isosorbide dinitrate was obtained as a 25% lactose mixture[2], and the pure compound was recovered by extraction with ethyl acetate and evaporation of the solvent. Nonlabeled 5-isosorbide mononitrate[3], 2-isosorbide mononitrate[4], and isosorbide[5] were used without further purification. All other solvents and reagents were reagent grade.

Isolated Perfused Rabbit Lung Experiments—The isolated lung preparation has been modified slightly from procedures described previously (6, 13). The isolated lung was perfused at 225 ml/min by 100 ml of an artificial medium prepared the day of or day before an experiment. The perfusion medium was composed of Krebs–Henseleit bicarbonate buffer (500 ml) with 4.5% bovine serum albumin (22.5 g)[6] and 5 mmoles of glucose (90 mg)[7]. The pH, adjusted to 7.4, was maintained during the experiment by a constant 0.005-ml/min infusion of a 1.0 meq/ml sodium bicarbonate solution containing 10% glucose and by appropriate adjustments in an air–carbon dioxide ventilating mixture supplied to the lungs.

For intravascular bolus administration, the compounds were presented to the lung by addition to the upper reservoir. Generally ~8 μCi of the compound was added in each study, and supplementary unlabeled compounds were added to achieve the required dose. Doses ranged from 10^{-7} to 10^{-5} mole for isosorbide dinitrate and were 10^{-6} mole for the mononitrates. Each experiment was performed in duplicate. One-milliliter perfusion medium samples were withdrawn from the upper reservoir at appropriate intervals during the 1–2 hr experiment. In the multiple-dose studies, a second (10^{-7}-mole) dose of isosorbide dinitrate was given 60 min after the first (10^{-5}-mole) dose, with subsequent metabolism followed for an additional 60 min.

Lung 9000×*g* Homogenate Experiments—The lungs of New Zealand rabbits were separated from all extraneous tissue, weighed, and

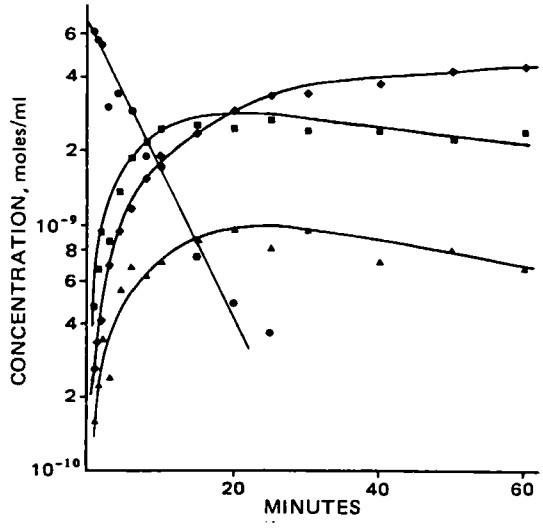

Figure 1—*Semilogarithmic perfusion medium concentration* versus *time profiles following a 10^{-6}-mole iv administration of isosorbide dinitrate. Key: (●) isosorbide dinitrate; (■) 5-isosorbide mononitrate; (▲) 2-isosorbide mononitrate; (◆) isosorbide. Lines are visual aids only.*

[1] New England Nuclear, Boston, Mass.

[2] Lot D-40-177, Wyeth Laboratories, Philadelphia, Pa.
[3] Lot 3369-17-2, Wyeth Laboratories, Philadelphia, Pa.
[4] Lot 82-1, Wyeth Laboratories, Philadelphia, Pa.
[5] Riches-Nelson, Greenwich, Conn.
[6] Rhesus Chemical Co., Phoenix, Ariz.
[7] Eastman Organic Chemicals, Rochester, N.Y.

0022-3549/83/0700-0785$01.00/0

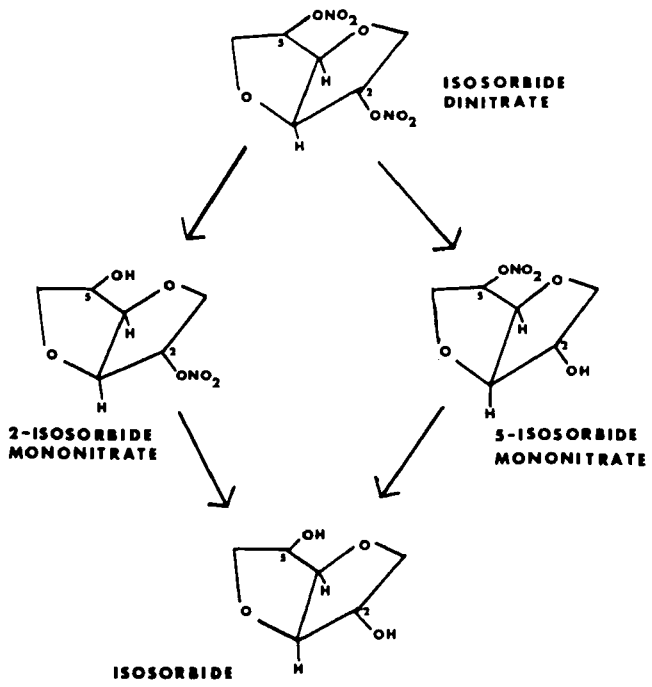

Scheme I—Pathways of isosorbide dinitrate metabolism.

added to a beaker containing two volumes of 0.04 *M* phosphate buffer, pH 7.4. The lungs were homogenized and centrifuged at 9000×*g* for 15 min in a centrifuge kept at 0°. For the incubations, 24 separate culture tubes were arranged containing 10^{-9} mole of isosorbide dinitrate, 5-isosorbide mononitrate, or 2-isosorbide mononitrate to allow a more precise quantitation of each metabolic step. Reduced glutathione[8] and sodium cyanide[9] were added in quantities of 2×10^{-9} moles each, according to the method of Needleman and Krantz (9). The experiment was initiated by the addition of 0.5 ml of the 9000×*g* supernatant. The culture tubes were placed in a shaker incubator kept at 37°, and one culture tube containing each compound was removed at every time interval for analysis. A control experiment was conducted to measure the hydrolysis of isosorbide dinitrate in the presence of glutathione, cyanide, and phosphate buffer. Each experiment was performed in duplicate.

Analytical Methods—The perfusion medium and homogenate samples were extracted with 10 ml of ether, and the organic phase was evaporated to dryness in a water bath not allowed to exceed 40°. Residues were reconstituted in 100 μl of methanol; half of this solution was streaked across 250-μm silica gel TLC plates[10]. Chromatograms were developed 15 cm with dichloromethane–ethyl acetate (4:1). A radiochromatogram scanner[11] was used to locate the radioactive zones on the TLC plates corresponding to isosorbide dinitrate, 5-isosorbide mononitrate, and 2-isosorbide mononitrate, which had R_f values of 0.63, 0.19, and 0.32, respectively. Appropriate bands were scraped into a scintillation vial[12] and dispersed with 15 ml of a scintillation gel prior to counting in a liquid scintillation counter[13]. The gel was composed of 112 g of naphthalene, 14 g of 2,5-diphenyloxazole (PPO), and 0.7 g of 1,4-bis[2-(4-methyl-5-phenyloxazolyl)-benzene] (dimethyl POPOP) dissolved in 1400 ml of a mixture of xylene (1 part), dioxane (3 parts), and ethylene glycol monoethyl ether (3 parts), followed by the addition of 84 g of a thixotropic gelling agent[14]. All samples were corrected for quenching by an external standardization method.

Isosorbide was measured by suspending 0.1 ml of the perfusion medium remaining after the ether extraction in a toluene–ethoxyoctylphenol[15] scintillation cocktail (6). To confirm that only isosorbide was measured, perfusion medium samples from a lung experiment were streaked on TLC plates and developed with a solvent system of 2-propanol–ammonium hydroxide (4:1) (14). The plates were scanned, scraped, and counted in 15 ml of the silicon dioxide cocktail. Unlabeled, authentic isosorbide was visualized by spraying the plates with a reagent composed of sodium metaperiodate, potassium permanganate, and sodium carbonate (15). Isosorbide concentrations found in the 2-propanol–ammonium hydroxide TLC system corresponded within 15% to those seen by direct measurement of the 0.1 ml postextraction perfusion-medium sample.

[8] Sigma Chemical Co., St. Louis, Mo.
[9] Fisher Scientific Co., Pittsburgh, Pa.
[10] Analtech Inc., Newark, Del.
[11] Model 7201, Packard Instrument Co., Downers Grove, Ill.
[12] Research Products International, Elk Grove Village, Ill.
[13] Model 2425, Packard Instrument Co., Downers Grove, Ill.
[14] Cabosil, Research Products International, Elk Grove Village, Ill.
[15] Triton X-100, Research Products International, Elk Grove Village, Ill.

Table I—Pharmacokinetic Parameters Obtained After Intravascular Administration of Isosorbide Dinitrate to Isolated Perfused Lung

Dose, moles	AUC, moles min/ml	*CL*, ml/min	$k_{\text{Isosorbide Dinitrate}}$, min^{-1}	Half-life, min
10^{-5}	1.1×10^{-6}	8.8	0.061	11.4
10^{-5}	1.2×10^{-6}	8.4	0.054	12.8
10^{-6}	5.2×10^{-8}	19.0	0.118	5.9
10^{-6}	6.0×10^{-8}	16.6	0.116	6.0
10^{-7}	5.0×10^{-9}	20.1	0.128	5.4
10^{-7}	3.6×10^{-9}	27.6	0.149	4.7

RESULTS AND DISCUSSION

The perfusion medium concentrations obtained after a 10^{-6}-mole iv dose of isosorbide dinitrate are shown in Fig. 1. The metabolites (5- and 2-isosorbide mononitrate) show increasing perfusion medium levels which peak after 40 min and have a slight decline when there is virtually no isosorbide dinitrate left to be converted. The 2-isosorbide mononitrate levels are only half those attained by the 5-isosorbide mononitrate, probably due to the stereoselective cleavage of the 2-nitrate group (Scheme I). The isosorbide concentration shows the same rapid increase, but no tendency to decline at the end of the experiment.

Similar concentration *versus* time profiles were obtained for the 10^{-5}- and 10^{-7}-mole doses of isosorbide dinitrate. Pharmacokinetic parameters for isosorbide dinitrate disposition obtained from these studies are given in Table I. Areas under the isosorbide dinitrate perfusion medium concentration *versus* time curve (AUC) were obtained by the trapezoidal rule. Clearances were calculated as the dose divided by the respective AUC. Rate constants and half-lives were obtained from the slope of a line determined from a least-squares analysis of the isosorbide dinitrate concentrations. Linear first-order kinetics appeared to be in effect at the

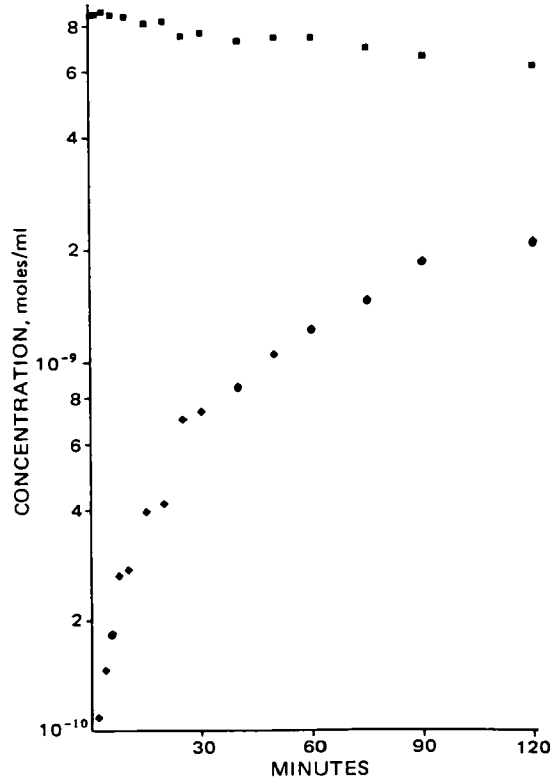

Figure 2—*Semilogarithmic perfusion medium concentration* versus *time profiles following a 10^{-6}-mole iv administration of 5-isosorbide mononitrate. Key: (■) 5-isosorbide mononitrate; (◆) isosorbide.*

Table II—Apparent First-Order Rate Constants for the Formation of 5-Isosorbide Mononitrate, 2-Isosorbide Mononitrate, and Isosorbide after Isosorbide Dinitrate Administration to Isolated Perfused Lung [a]

Dose, moles	$k_{5\text{-Isosorbide Mononitrate}}$ min^{-1}	$k_{2\text{-Isosorbide Mononitrate}}$ min^{-1}	$k_{\text{Isosorbide}}$ min^{-1}
10^{-5}	0.030	0.014	0.018
10^{-5}	0.028	0.015	0.021
10^{-6}	0.056	0.017	0.038
10^{-6}	0.055	0.027	0.041
10^{-7}	0.069	0.024	0.035
10^{-7}	0.084	0.032	0.039

[a] Based on initial rate data.

lower two doses, as demonstrated by the closeness in the clearance values. Lower clearances at high concentrations suggest some saturation of the organic nitrate reductase enzyme at the largest dose.

The role of the lung in the metabolism of isosorbide dinitrate in relationship to the overall disposition of the drug can be elucidated by comparison of the clearance and flow rate of the perfusion medium. The fraction of the dose which passes through the lung vasculature but is not eliminated would be calculated by:

$$F = 1 - \frac{CL}{Q_B}$$

where CL is the perfusion medium clearance (ml/min) and Q_B is the perfusion flow rate (ml/min) (16). For the case of isosorbide dinitrate, nearly 90% of the drug entering the lung would escape first-pass pulmonary metabolism. This relatively slight metabolism suggests that lung metabolism would not be a major factor in the overall elimination of this compound compared with the rapid hepatic denitration demonstrated by isolated, perfused rat liver experiments (17).

Initial rates of formation for the individual metabolites after administration of isosorbide dinitrate were determined from rectilinear plots using a tangent drawn to the respective data points collected in the first 2 min of the experiment. The corresponding apparent first-order rate constants were calculated by dividing these initial rates by the average isosorbide dinitrate concentration in the same time period. Rate constants for the formation of each of the individual metabolites are presented in Table II. In all cases, 5-isosorbide mononitrate was formed more rapidly than isosorbide, which in turn was formed more rapidly than 2-isosorbide mononitrate. The rapid monoexponential decline of the parent drug (Table I) corresponded to the rate of increase in metabolite levels as determined from the sum of the rate constants for the appearance of the three metabolites (Table II). The mean difference of these rate constants was 6.1% ($SD \pm 6.6\%$).

The profiles following administration of 10^{-6}-mole doses of 5- and 2-isosorbide mononitrate are shown in Figs. 2 and 3, respectively. The

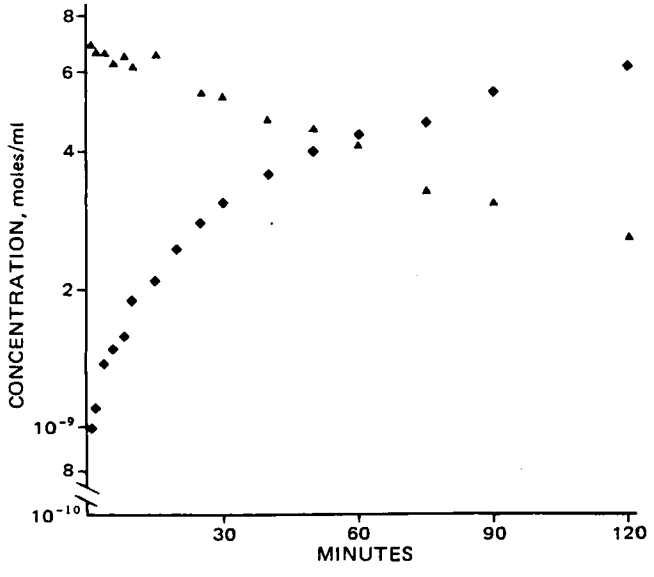

Figure 3—*Semilogarithmic perfusion medium concentration* versus *time profiles following a 10^{-6}-mole iv administration of 2-isosorbide mononitrate. Key: (▲) 2-isosorbide mononitrate; (◆) isosorbide.*

Table III—Apparent First-Order Rate Constants for the Formation of Isosorbide from Isosorbide Dinitrate, 5-Isosorbide Mononitrate, and 2-Isosorbide Mononitrate in Isolated Perfused Lung [a]

Compound	Rate Constant, min^{-1}
Isosorbide dinitrate	0.038 ± 0.003 [b]
5-Isosorbide mononitrate	0.0025 ± 0.0005 [c]
2-Isosorbide mononitrate	0.0073 ± 0.0011 [c]

[a] Mean ± *SD*. [b] $n = 4$. [c] $n = 2$.

2-isosorbide mononitrate shows a more rapid disposition (0.0073 min^{-1}) than the 5-isosorbide mononitrate (0.0025 min^{-1}), probably due to the exo positioning of the 2-nitrate group. In both cases, the rate constants were determined from semilogarithmic rate plots of the ascending isosorbide concentrations. The slight decrease in mononitrate levels appeared also to correlate well with the terminal slopes of the mononitrates in the isosorbide dinitrate experiments.

In Table III, rate constants for the formation of isosorbide from the two mononitrates (as determined from the terminal slopes of the semilogarithmic mononitrate plots) are compared with the apparent first-order rate constant calculated from initial rates of appearance of isosorbide after administration of 10^{-6}- and 10^{-7}-mole doses of isosorbide dinitrate to the lung. These results indicate that the isosorbide was formed much more rapidly when isosorbide dinitrate was given as the dose rather than 5- or 2-isosorbide mononitrate. The rate constants for formation of isosorbide when mononitrates were added to the lung account for <25% of that formed when isosorbide dinitrate was added. These data show that the large amount of isosorbide formed in the isosorbide dinitrate experiments could not have been formed by either mononitrate that had partitioned from the lung into the perfusion medium. The rapid formation of isosorbide from these experiments was not typical of a two-step metabolic process. There is no indication from the mononitrate concentration–time profiles in the perfusion medium that these compounds serve as intermediates to the completely denitrated molecule. Therefore, the rapid formation of isosorbide following isosorbide dinitrate administration appears to be the result of a high intrinsic clearance of the mononitrates formed in the metabolizing organ prior to their diffusion into the perfusion medium.

The differences in the rate of elimination of the mononitrates following

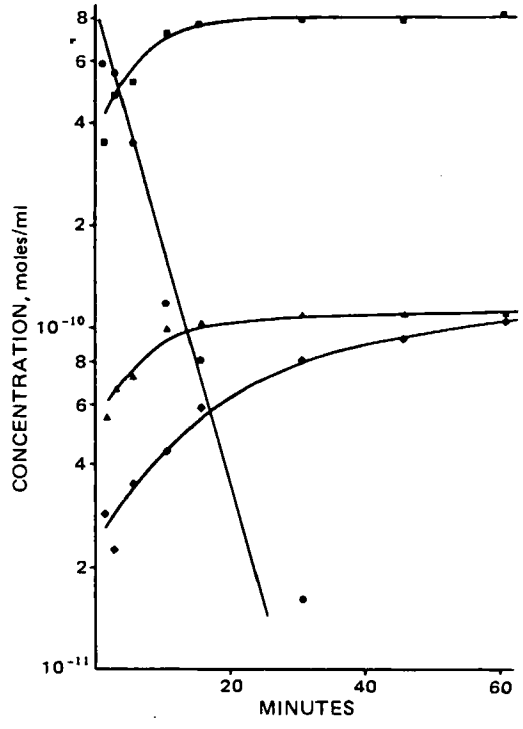

Figure 4—*Semilogarithmic concentration* versus *time profiles showing metabolism of 10^{-9} mole of isosorbide dinitrate in lung homogenate 9000×g supernatant. Key: (●) isosorbide dinitrate; (■) 5-isosorbide mononitrate; (▲) 2-isosorbide mononitrate; (◆) isosorbide. Lines are visual aids only.*

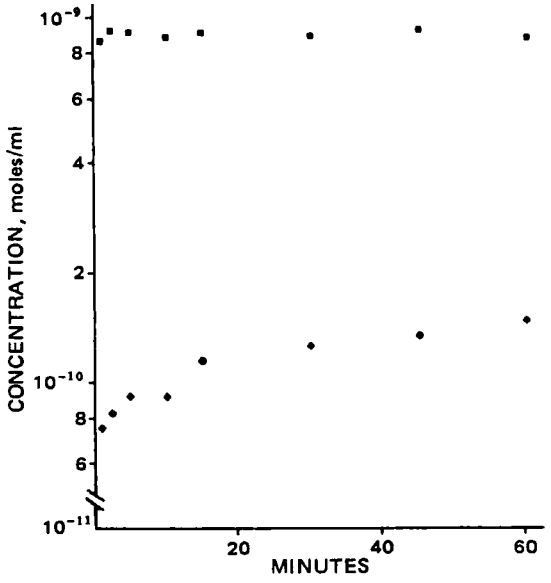

Figure 5—*Semilogarithmic concentration* versus *time profiles showing metabolism of 10^{-9} mole of 5-isosorbide mononitrate in lung homogenate 9000×g supernatant. Key: (■) 5-isosorbide mononitrate; (◆) isosorbide.*

administration of preformed mononitrates to the isolated perfused lung and the rate of production of isosorbide following administration of isosorbide dinitrate may be attributed to the different distribution characteristics of the mononitrates and the dinitrate. As a precursor, isosorbide dinitrate may deliver the 5- and 2-isosorbide mononitrates to sites in the proximity of the metabolizing tissue of the lung, to which the mononitrates themselves have relatively poor access. The second nitrate ester could be quickly denitrated at that point. The mononitrates formed in the lung may also diffuse into the perfusion medium, where their distribution characteristics lead to the slower metabolism seen after an intravascular dose of the mononitrates. Thus, the accessibility to the enzymatic site will directly affect the metabolism of the mononitrates to isosorbide.

There is other evidence that the rate at which a metabolite formed in a metabolizing organ achieves its fate cannot be assumed to be the same as a preformed metabolite presented to that organ. In the studies of Brazzell and Kostenbauder (18), greater metabolism of isoproterenol in the lung was observed when it was formed by the hydrolysis of two diester prodrugs than when it was delivered to the isolated perfused rabbit lung as isoproterenol. The extensive experiments of Pang and Gillette (19) demonstrated the sequential elimination of acetaminophen as it was

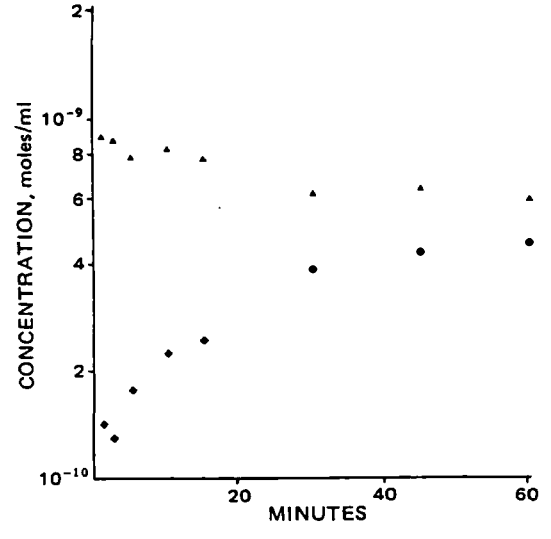

Figure 6—*Semilogarithmic concentration* versus *time profiles showing metabolism of 10^{-9} mole of 2-isosorbide mononitrate in lung homogenate 9000×g supernatant. Key: (▲) 2-isosorbide mononitrate; (◆) isosorbide.*

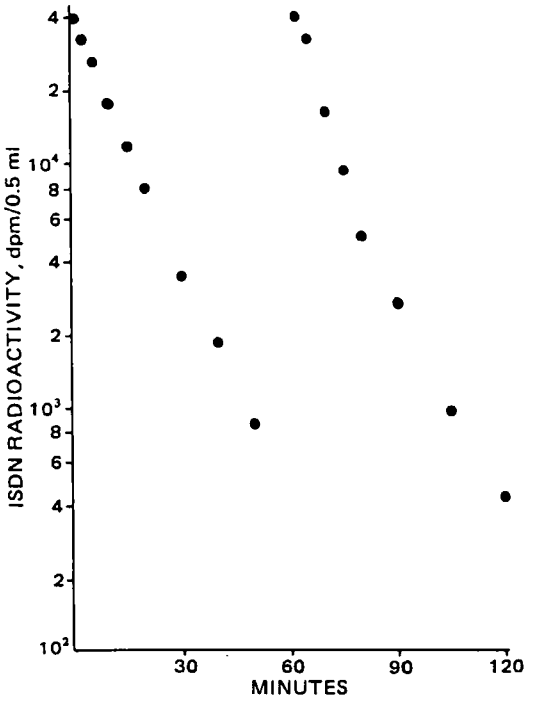

Figure 7—*Semilogarithmic radioactivity* versus *time profile of isosorbide dinitrate following successive doses of 10^{-5} and 10^{-7} mole.*

being formed from phenacetin in a single pass through the isolated perfused liver. Although diffusional barriers were not needed for an explanation of the differences in the metabolism of preformed acetaminophen and acetaminophen formed from phenacetin, these types of barriers to metabolism were hypothesized (20). Rate-limiting diffusional parameters have also been shown to affect metabolism and subsequent elimination in the isolated perfused rat kidney (21). Due to diffusion into renal tubular cells, salicylic acid was cleared more rapidly when it was formed in the kidney from salicyluric acid than when it was presented to the kidney as intact salicylic acid.

The 9000×*g* lung homogenate studies were designed to investigate the rates of metabolism of these organic nitrates independent of any cell wall barriers that might exist. In these experiments, isosorbide dinitrate was rapidly metabolized to the mononitrates in the lung supernatant (Fig. 4). The rate of appearance of isosorbide lagged behind that of both mononitrates and was consistent with sequential first-order dinitrate-to-mononitrate-to-isosorbide metabolism. This concentration *versus* time profile is markedly different from the virtually simultaneous appearance of mononitrate and isosorbide following administration of isosorbide dinitrate to the isolated perfused lung.

Figures 5 and 6 show examples of the slow metabolism of the 5- and 2-isosorbide mononitrates, respectively, in 9000×*g* supernatant. There is only a slight increase in isosorbide levels as these mononitrates are slowly denitrated. Further, the amount of isosorbide formed from the mononitrates in these lung homogenate experiments confirms that the isosorbide formed in the isosorbide dinitrate experiments is a direct product of the metabolism of the mononitrate intermediates alone. Therefore, in the homogenate studies, unlike the intact lung studies, isosorbide formation kinetics are not altered quantitatively by administering isosorbide dinitrate instead of a mononitrate. In a control experiment, isosorbide dinitrate was not hydrolyzed in the presence of reduced glutathione and sodium cyanide, so the metabolism was a direct result of the lung supernatant. The homogenate studies were interesting in the requirement of cyanide for the metabolism of isosorbide dinitrate. In the presence of lung 9000×*g* supernatant and reduced glutathione alone, the drug was not metabolized. The addition of sodium cyanide kept glutathione in its reduced form (9), and isosorbide dinitrate was metabolized quite rapidly.

The multiple-dose experiments were designed to investigate the possibility of product inhibition of the organic nitrate reductase enzyme. A constant infusion of the mononitrates, with coadministration of isosorbide dinitrate, would be inappropriate to demonstrate inhibition, since only small amounts of the mononitrates would reach the enzymatic site. By administering the parent compound, the mononitrates could reach that site by virtue of lung metabolism. Therefore, two separate intra-

vascular doses of isosorbide dinitrate, 10^{-5} and 10^{-7} moles, were given 60 min apart, and the rate of elimination was ascertained for each dose. Plots of isosorbide dinitrate radioactivity for the two doses of the drug in one experiment are shown in Fig. 7. Two parallel lines, representing a half-life of 8 min, indicated that there was no increase in the half-life exhibited with the second dose. There was thus no indication from these studies that the mononitrate metabolites could inhibit denitration of isosorbide dinitrate, whether the mononitrates were preformed or formed *in situ*.

In summary, this paper illustrates how access to selected organs or tissues may alter the expected metabolism of a drug. Release of a drug from a precursor in the proximity of metabolizing tissue may lead to more rapid metabolism than seems likely from studies involving presentation of the preformed drug to that organ or tissue.

REFERENCES

(1) A. P. Fishman and G. G. Pietra, *N. Engl. J. Med.*, **291**, 884 (1974).

(2) M. W. Anderson and T. E. Eling, *Environ. Health Perspect.*, **16**, 77 (1976).

(3) B. W. Blase and T. A. Loomis, *Toxicol. Appl. Pharmacol.*, **37**, 481 (1976).

(4) H. J. Hawkins, A. G. E. Wilson, M. W. Anderson, and T. E. Eling, *Prostaglandins*, **14**, 251 (1977).

(5) M. W. Anderson, T. C. Orton, R. D. Pickett, and T. E. Eling, *J. Pharmacol. Exp. Ther.*, **189**, 456 (1974).

(6) J. P. McGovren, W. C. Lubawy, and H. B. Kostenbauder, *ibid.*, **199**, 198 (1976).

(7) P. Needleman and E. Johnson, in "The Pharmacological Basis of Therapeutics," 6th ed., A. G. Gilman, L. S. Goodman, and A. Gilman, Eds., Macmillan, New York, N.Y., 1980, p. 819.

(8) J. A. Franciosa, L. A. Nordstrorm, and J. N. Cohn, *J. Am. Med. Assoc.*, **240**, 443 (1978).

(9) P. Needleman and J. C. Krantz, *Biochem. Pharmacol.*, **14**, 1225 (1965).

(10) P. Needleman and F. E. Hunter, *Mol. Pharmacol.*, **1**, 77 (1965).

(11) P. Needleman, S. Lang, and E. Johnson, *J. Pharmacol. Exp. Ther.*, **181**, 489 (1972).

(12) J. C. Krantz and C. D. Leake, *Am. J. Cardiol.*, **36**, 407 (1975).

(13) R. W. Neimeier and E. Bingham, *Life Sci.*, **11**, 807 (1972).

(14) S. F. Sisenwine and H. W. Ruelius, *J. Pharmacol. Exp. Ther.*, **176**, 296 (1971).

(15) F. J. DiCarlo, J. M. Hartigan, and G. E. Phillips, *Anal. Chem.*, **36**, 2301 (1964).

(16) M. Rowland, L. Z. Benet, and G. G. Graham, *J. Pharmacokinet. Biopharm.*, **1**, 123 (1973).

(17) E. M. Johnson, A. B. Harkey, D. J. Blehm, and P. Needleman, *J. Pharmacol. Exp. Ther.*, **182**, 56 (1972).

(18) R. K. Brazzell and H. B. Kostenbauder, *J. Pharm. Sci.*, **71**, 1274 (1982).

(19) K. S. Pang and J. R. Gillette, *J. Pharmacol. Exp. Ther.*, **207**, 178 (1978).

(20) K. S. Pang and J. R. Gillette, *J. Pharmacokinet. Biopharm.*, **7**, 275 (1979).

(21) I. Berkersky, L. Fishman, S. A. Kaplan, and W. A. Colburn, *J. Pharmacol. Exp. Ther.*, **212**, 309 (1980).

ACKNOWLEDGMENTS

This work was presented in part at APhA Academy of Pharmaceutical Sciences meeting (the Basic Pharmaceutics Section) in Washington, D.C., April 1980.

Abstracted from a dissertation submitted by P. R. Mayer to the University of Kentucky in partial fulfillment of the Doctor of Philosophy requirements.

Age-Related Pharmacokinetics of *N*-Acetylprocainamide in Rats

AVRAHAM YACOBI ‡×, BURDE L. KAMATH *, HERMAN F. STAMPFLI, ZEE M. LOOK, and CHII-MING LAI

Received April 19, 1982, from the *Department of Pharmaceutical Development, Research and Development Department, American Critical Care, McGaw Park, IL 60085.* Accepted for publication June 18, 1982.

Present Address: *Xavier University, College of Pharmacy, New Orleans, LA 70125. ‡Lederle Laboratories, Pharmacodynamics Dept., Pearl River, N.Y. 10965.

Abstract □ The pharmacokinetics of *N*-acetylprocainamide, administered orally or intravenously, were studied in 3-, 6-, and 12-month-old rats using a two-way crossover study design. At 3, 6, and 12 months of age, the half-life values of *N*-acetylprocainamide were 1.66, 1.82, and 2.29 hr, respectively; the apparent volumes of distribution were 4.75, 3.35, and 1.98 liter/kg, respectively. The elimination rate constant, clearance, and absolute bioavailability of the drug (determined by AUC measurements and the amounts excreted unchanged in the urine) decreased significantly with age. The rate of absorption remained unchanged. The amounts of *N*-acetylprocainamide in the liver and kidneys were significantly higher in the 12-month-old animals. These results clearly demonstrate a significant alteration with age in the bioavailability, distribution, and elimination of *N*-acetylprocainamide in rats. In long-term toxicity studies of this and other drugs that show age-dependent pharmacokinetics, an adjustment in the chronically administered dose is essential.

Keyphrases □ *N*-Acetylprocainamide—oral and intravenous pharmacokinetics in rats, bioavailability, age-related changes □ Pharmacokinetics—*N*-acetylprocainamide in rats after oral and intravenous administrations, age-related changes □ Bioavailability—*N*-acetylprocainamide in rats after oral and intravenous administrations, age-related changes

It has been established that many physiological changes are associated with aging. Lean body mass, plasma albumin, and total body water decrease with age. In humans, the cardiac output decreases 1%/year from ages 19 to 86, and the blood flow to the kidneys is also reduced with age (1). In rats, there are pronounced decreases (>30%) in the cardiac index and in hepatic, renal, and GI tract blood flow at 11–12 months of age (2). These changes can account for significant alterations in the pharmacokinetics and pharmacodynamics of drugs. In toxicity and oncogenicity studies in animals, which are conducted over a long period of time (1 year or more), aging may account for (3, 4): (*a*) diminished absorption of drugs through the GI tract; (*b*) diminished rate of metabolism and renal excretion of drugs; (*c*) accumulation of drugs in blood and receptor sites; (*d*) changes in affinity and sensitivity of the receptor sites to drug molecules; and (*e*) an increased rate of mortality. For these reasons, it was considered prudent to

0022-3549/83/0700-0789$01.00/0

vascular doses of isosorbide dinitrate, 10^{-5} and 10^{-7} moles, were given 60 min apart, and the rate of elimination was ascertained for each dose. Plots of isosorbide dinitrate radioactivity for the two doses of the drug in one experiment are shown in Fig. 7. Two parallel lines, representing a half-life of 8 min, indicated that there was no increase in the half-life exhibited with the second dose. There was thus no indication from these studies that the mononitrate metabolites could inhibit denitration of isosorbide dinitrate, whether the mononitrates were preformed or formed *in situ*.

In summary, this paper illustrates how access to selected organs or tissues may alter the expected metabolism of a drug. Release of a drug from a precursor in the proximity of metabolizing tissue may lead to more rapid metabolism than seems likely from studies involving presentation of the preformed drug to that organ or tissue.

REFERENCES

(1) A. P. Fishman and G. G. Pietra, *N. Engl. J. Med.*, **291**, 884 (1974).

(2) M. W. Anderson and T. E. Eling, *Environ. Health Perspect.*, **16**, 77 (1976).

(3) B. W. Blase and T. A. Loomis, *Toxicol. Appl. Pharmacol.*, **37**, 481 (1976).

(4) H. J. Hawkins, A. G. E. Wilson, M. W. Anderson, and T. E. Eling, *Prostaglandins*, **14**, 251 (1977).

(5) M. W. Anderson, T. C. Orton, R. D. Pickett, and T. E. Eling, *J. Pharmacol. Exp. Ther.*, **189**, 456 (1974).

(6) J. P. McGovren, W. C. Lubawy, and H. B. Kostenbauder, *ibid.*, **199**, 198 (1976).

(7) P. Needleman and E. Johnson, in "The Pharmacological Basis of Therapeutics," 6th ed., A. G. Gilman, L. S. Goodman, and A. Gilman, Eds., Macmillan, New York, N.Y., 1980, p. 819.

(8) J. A. Franciosa, L. A. Nordstrorm, and J. N. Cohn, *J. Am. Med. Assoc.*, **240**, 443 (1978).

(9) P. Needleman and J. C. Krantz, *Biochem. Pharmacol.*, **14**, 1225 (1965).

(10) P. Needleman and F. E. Hunter, *Mol. Pharmacol.*, **1**, 77 (1965).

(11) P. Needleman, S. Lang, and E. Johnson, *J. Pharmacol. Exp. Ther.*, **181**, 489 (1972).

(12) J. C. Krantz and C. D. Leake, *Am. J. Cardiol.*, **36**, 407 (1975).

(13) R. W. Neimeier and E. Bingham, *Life Sci.*, **11**, 807 (1972).

(14) S. F. Sisenwine and H. W. Ruelius, *J. Pharmacol. Exp. Ther.*, **176**, 296 (1971).

(15) F. J. DiCarlo, J. M. Hartigan, and G. E. Phillips, *Anal. Chem.*, **36**, 2301 (1964).

(16) M. Rowland, L. Z. Benet, and G. G. Graham, *J. Pharmacokinet. Biopharm.*, **1**, 123 (1973).

(17) E. M. Johnson, A. B. Harkey, D. J. Blehm, and P. Needleman, *J. Pharmacol. Exp. Ther.*, **182**, 56 (1972).

(18) R. K. Brazzell and H. B. Kostenbauder, *J. Pharm. Sci.*, **71**, 1274 (1982).

(19) K. S. Pang and J. R. Gillette, *J. Pharmacol. Exp. Ther.*, **207**, 178 (1978).

(20) K. S. Pang and J. R. Gillette, *J. Pharmacokinet. Biopharm.*, **7**, 275 (1979).

(21) I. Berkersky, L. Fishman, S. A. Kaplan, and W. A. Colburn, *J. Pharmacol. Exp. Ther.*, **212**, 309 (1980).

ACKNOWLEDGMENTS

This work was presented in part at APhA Academy of Pharmaceutical Sciences meeting (the Basic Pharmaceutics Section) in Washington, D.C., April 1980.

Abstracted from a dissertation submitted by P. R. Mayer to the University of Kentucky in partial fulfillment of the Doctor of Philosophy requirements.

Age-Related Pharmacokinetics of *N*-Acetylprocainamide in Rats

AVRAHAM YACOBI ‡×, BURDE L. KAMATH *, HERMAN F. STAMPFLI, ZEE M. LOOK, and CHII-MING LAI

Received April 19, 1982, from the *Department of Pharmaceutical Development, Research and Development Department, American Critical Care, McGaw Park, IL 60085.* Accepted for publication June 18, 1982.

Present Address: *Xavier University, College of Pharmacy, New Orleans, LA 70125. ‡Lederle Laboratories, Pharmacodynamics Dept., Pearl River, N.Y. 10965.

Abstract □ The pharmacokinetics of *N*-acetylprocainamide, administered orally or intravenously, were studied in 3-, 6-, and 12-month-old rats using a two-way crossover study design. At 3, 6, and 12 months of age, the half-life values of *N*-acetylprocainamide were 1.66, 1.82, and 2.29 hr, respectively; the apparent volumes of distribution were 4.75, 3.35, and 1.98 liter/kg, respectively. The elimination rate constant, clearance, and absolute bioavailability of the drug (determined by AUC measurements and the amounts excreted unchanged in the urine) decreased significantly with age. The rate of absorption remained unchanged. The amounts of *N*-acetylprocainamide in the liver and kidneys were significantly higher in the 12-month-old animals. These results clearly demonstrate a significant alteration with age in the bioavailability, distribution, and elimination of *N*-acetylprocainamide in rats. In long-term toxicity studies of this and other drugs that show age-dependent pharmacokinetics, an adjustment in the chronically administered dose is essential.

Keyphrases □ *N*-Acetylprocainamide—oral and intravenous pharmacokinetics in rats, bioavailability, age-related changes □ Pharmacokinetics—*N*-acetylprocainamide in rats after oral and intravenous administrations, age-related changes □ Bioavailability—*N*-acetylprocainamide in rats after oral and intravenous administrations, age-related changes

It has been established that many physiological changes are associated with aging. Lean body mass, plasma albumin, and total body water decrease with age. In humans, the cardiac output decreases 1%/year from ages 19 to 86, and the blood flow to the kidneys is also reduced with age (1). In rats, there are pronounced decreases (>30%) in the cardiac index and in hepatic, renal, and GI tract blood flow at 11–12 months of age (2). These changes can account for significant alterations in the pharmacokinetics and pharmacodynamics of drugs. In toxicity and oncogenicity studies in animals, which are conducted over a long period of time (1 year or more), aging may account for (3, 4): (*a*) diminished absorption of drugs through the GI tract; (*b*) diminished rate of metabolism and renal excretion of drugs; (*c*) accumulation of drugs in blood and receptor sites; (*d*) changes in affinity and sensitivity of the receptor sites to drug molecules; and (*e*) an increased rate of mortality. For these reasons, it was considered prudent to

0022-3549/83/0700-0789$01.00/0

Table I—Effect of Age on Pharmacokinetics after Intravenous Administration of *N*-Acetylprocainamide Hydrochloride in Rats [a]

Parameter [b]	Age [c] 3 Months Mean	3 Months CV, %	6 Months Mean	6 Months CV, %	12 Months Mean	12 Months CV, %
Plasma C_0 [d], μg/ml	19.0	12.1	27.7	21.6	46.9	21.8
AUC, μg·hr/ml	45.2	18.2	72.6	27.0	156	51.4
β, hr^{-1}	0.423	11.5	0.388	12.8	0.334	26.2
$t_{1/2}$, hr	1.66	12.1	1.82	14.2	2.29	42.3
V_d, ml/kg	4750	11.2	3350	22.0	1980	24.9
CL_{tot}, ml/min/kg	33.5	14.8	21.5	23.5	11.1	71.4

[a] The dose was 100 mg/kg. [b] Determined by model-independent equations. [c] The values for all parameters were significantly different ($p < 0.05$, Duncan's t test) at 6 months (*versus* 3 months) and 12 months (*versus* 3 and 6 months). The sample size was 7 at 3 and 12 months and 11 at 6 months. [d] Extrapolated time zero plasma concentration.

conduct age-dependent disposition studies in parallel with the long-term oncogenicity testing of *N*-acetylprocainamide in rats.

EXPERIMENTAL

Two-hundred Charles River CD rats[1] were randomly selected from large populations intended for long-term toxicity and oncogenicity testing. Each animal was housed in an individual stainless steel cage with free access to food[2] and water. The animals weighed 260–390 g (mean 320 g) at 3 months, 381–576 g (mean 481 g) at 6 months, and 512–735 g (mean 587 g) at 12 months. At each interval, a group of 12 rats was randomly selected from the population, and the pharmacokinetics of absorption, distribution, and elimination were studied.

A cannula was inserted surgically into a jugular vein of each rat under light ether anesthesia 1 day before drug administration. The preparation of the cannulas and the surgical procedures were described elsewhere (5). Food was withheld for 15 hr prior to drug administration and during the blood sampling period (10 hr). Water was freely accessible to the animals at all times.

The rats were divided into two groups, and the study was conducted according to a balanced two-way crossover design. One group received 100 mg/kg iv of *N*-acetylprocainamide hydrochloride[3] in distilled water through the jugular cannula; the other group received the same amount of drug by oral gavage. After 3 days, the crossover experiment was conducted. A solution containing 100 mg/ml of *N*-acetylprocainamide hydrochloride in distilled water was used for both administration routes. The volume of the administered solution ranged from 0.260 to 0.735 ml. Because of the difficulty in maintaining patent cannulas, the study was completed for 7, 11, and 7 rats at 3, 6, and 12 months, respectively.

Serial blood samples (0.4 ml each) were drawn at 0.5, 1, 1.5, 2, 4, 6, 8, and 10 hr postdose. After collection of each sample, 0.4–0.5 ml of normal saline containing 1% heparin sodium solution (5000 USP U/ml) was infused to flush the cannula and to replace the lost volume. Plasma was separated and frozen immediately. Urine and feces were collected quantitatively at 24 and 48 hr. At each urinary collection time, the animals were induced to empty their bladder by ether inhalation. Feces samples were homogenized[4] in distilled water. Aliquots of urine and feces homogenates were frozen immediately.

After completion of the crossover study, four animals received an additional 100 mg/kg iv of *N*-acetylprocainamide. One-half hour later, the animals were sacrificed by exsanguination *via* the portal vein under ether anesthesia. Plasma, liver, heart, and kidneys were harvested. Immediately after removal, the organs were sliced, blotted in tissue paper to remove excess blood, and weighed. A known volume of saline (3–5 times the weight of the organ) was added to the tissues. The mixture was homogenized[4] in an ice-water bath. An aliquot of each homogenate was frozen immediately.

Concentrations of *N*-acetylprocainamide in plasma, serum, and urine were determined in duplicate by a specific high-performance liquid chromatographic (HPLC) method (6). This procedure was modified for analysis of the drug in tissue homogenates (7) and in feces (8). The pharmacokinetic parameters describing the absorption, distribution, and elimination of *N*-acetylprocainamide were estimated as follows. Biological half-life was calculated from the terminal disposition rate constant (β) which was determined by regression analysis of the logarithm of the plasma concentration *versus* time curve at the postabsorption distribution phase. Area under the plasma concentration *versus* time curve (AUC) was determined by the trapezoidal method. Total clearance (CL_{tot}) was determined by dividing the administered intravenous dose (or amount absorbed) by the AUC. For oral administration, the ratio of AUC_{oral}/AUC_{iv} was used to account for the amount absorbed. The volume of distribution (V_d) was calculated by CL_{tot}/β.

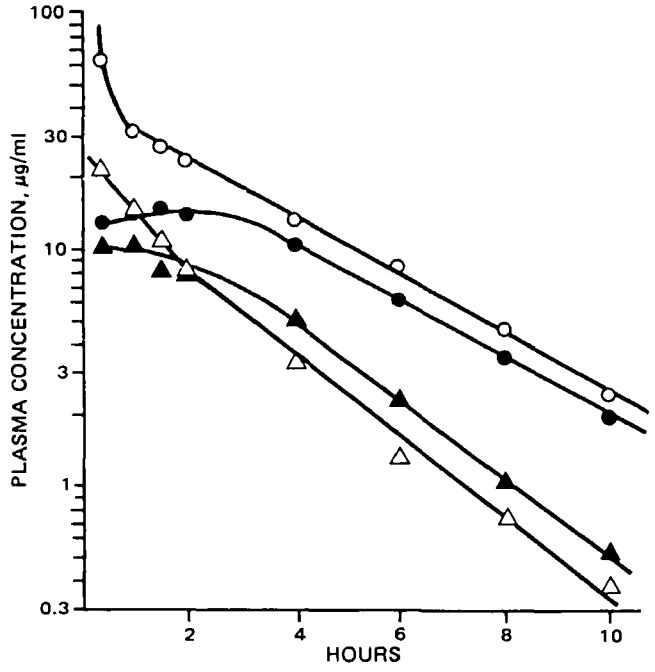

Figure 1—*Time course of* N-*acetylprocainamide in plasma after administration by intravenous injection and by oral gavage. Key: (△) 3-month-old rats, intravenous (n = 7); (▲) 3-month-old rats, oral (n = 7); (○) 12-month-old rats, intravenous (n = 6); (●) 12-month-old rats, oral (n = 6).*

RESULTS

Figure 1 depicts the time course of *N*-acetylprocainamide in plasma after administration by intravenous injection and by oral gavage in 3- and 12-month-old rats. These profiles show: (*a*) higher plasma concentrations of the drug in 12-month-old animals after administration by either route; (*b*) that the ratio of oral–intravenous plasma concentrations decreased with age, suggesting a decline in the bioavailability of *N*-acetylprocainamide; and (*c*) that the rate of decline of the postabsorption distribution plasma concentration was slower in older rats, indicating a longer elimination half-life following administration of the drug by either route.

Table I summarizes the pharmacokinetic parameters for distribution and elimination of *N*-acetylprocainamide in 3-, 6-, and 12-month-old rats following intravenous administration of the drug. The extrapolated time zero plasma concentrations and the AUC values increased significantly with age. Consistent with this, there was a significant decrease (58%) in the volume of distribution, from 4.75 liter/kg at 3 months to 1.98 liter/kg at 12 months of age. There was also a significant elongation of the biological half-life (38%) and a significant decrease in the total clearance (67%) in the 12-month-old animals as compared with the 3-month-old rats. In general, the coefficients of variation in all parameters increased with age: 11–18% in the 3-month-old rats to 22–71% in the 12-month-old animals.

Table II lists the parameters describing the absorption and excretion of unchanged *N*-acetylprocainamide in 3-, 6-, and 12-month-old rats. There was essentially no significant difference in the absorption half-life among the three age-groups. The elimination half-life became significantly longer with age after either intravenous or oral administration of the drug. Also, the ratio of the half-lives (oral–intravenous) increased from 1.05 after 3 months to 1.29 after 12 months, probably impacted by the changes in the absorption of the drug in the older rats. The AUC

[1] Charles River Breeding Laboratories, Inc., Portage, Mich.
[2] Purina Rodent Chow, Ralston Purina, St. Louis, Mo.
[3] American Critical Care Laboratories, McGaw Park, Ill.
[4] Polytron Homogenizer: Brinkmann Instruments, Inc., Westbury, N.Y.

Table II—Effect of Age on Pharmacokinetics Following Intravenous and Oral Administration of *N*-Acetylprocainamide Hydrochloride in Rats [a]

Parameter	Age [b] 3 Months Oral	3 Months iv	3 Months Ratio (Oral/iv)	6 Months Oral	6 Months iv	6 Months Ratio (Oral/iv)	12 Months Oral	12 Months iv	12 Months Ratio (Oral/iv)
Absorption $t_{1/2}$, hr	0.493	—	—	0.563	—	—	0.505	—	—
Elimination $t_{1/2}$, hr	1.74	1.66	1.05	1.92	1.82	1.08	2.66	2.29	1.29
AUC, μg·hr/ml	45.2	45.3	1.01	56.2	72.6	0.835	93.5	156	0.747
X_{tot}, % of Dose	85.1	76.6	1.29	89.2	97.0	0.930	69.0	87.1	0.815
X_u, % of Dose	77.1	76.4 [c]	1.04 [c]	83.6	92.2	0.918	64.3	77.9	0.812
X_f, % of Dose	7.99	10.1	0.674	5.65	4.75	1.29	6.83	6.81 [d]	1.19

[a] The dose was 100 mg/kg. [b] The sample size was 7 at 3 and 12 months and 11 at 6 months. [c] Without one unusually high value ($n = 6$). One urine sample after intravenous injection was very low, presumably due to incomplete collection. [d] $n = 6$.

Table III—Effect of Age on Tissue Distribution Following Intravenous Administration of *N*-Acetylprocainamide in Rats [a]

Tissue	Drug Concentration [b] 3 Months Mean	3 Months *SD*	6 Months Mean	6 Months *SD*	12 Months Mean	12 Months *SD*
Plasma	34.7	5.24	37.8	2.31	43.6	5.44
Liver	83.0	3.00	82.0	4.55	197	12.7
Heart	76.0	5.00	108	12.7	101	8.67
Kidney	294	90.0	299	47.9	528	256
Liver–Plasma Ratio	2.44	0.390	2.12	0.211	4.55	0.552
Heart–Plasma Ratio	2.24	0.370	2.80	0.208	2.33	0.0932
Kidney–Plasma Ratio	8.34	1.27	7.72	0.900	12.0	5.50

[a] The dose was 100 mg/kg. The animals were sacrificed 0.5 hr after receiving the drug. [b] The concentration is expressed as μg/g except for plasma, which is reported as μg/ml. The sample size is 4 at all time intervals.

values increased with age after intravenous and oral administrations. The ratio of the oral AUC to intravenous AUC decreased from 1.01 after 3 months to 0.747 after 12 months, showing a 25% decrease in bioavailability. Consistent with this finding, the oral–intravenous ratio of the percentage of unchanged *N*-acetylprocainamide excreted in the urine (X_u) also showed a decrease (from 1.04 to 0.812), a change of 22%. The oral–intravenous ratio of the amount eliminated in the feces (X_f), however, increased from 0.674 to 1.19 (a change of 77%), which might indicate poor GI absorption in the older rats.

Table III summarizes the effect of age on the distribution in heart, liver, and kidneys following intravenous administration of *N*-acetylprocainamide in rats. There was a significant increase in the tissue concentrations with increasing age, which is consistent with a decrease in the percentage of lean body mass in older rats. The tissue–plasma concentration ratios for liver and kidneys increased significantly ($p < 0.05$, Student's t test) after 12 months. The heart–plasma concentration ratios remained unchanged.

DISCUSSION

This study was conducted in conjunction with a long-term oncogenicity study of *N*-acetylprocainamide in rats. The goal was to determine the age-related changes in the pharmacokinetics of absorption, distribution, and elimination of the drug, which will allow a better understanding of the toxicological effects. For example, if there is a decrease in the GI absorption of the drug, the plasma concentration will decrease accordingly and, thus, a lesser exposure of tissues and organs to the drug will be expected. The opposite situation, however, may occur if the elimination is diminished. In this case, the plasma concentrations will be elevated, which may lead to augmentation of the pharmacological and toxicological response.

Consistent with previous findings in rats (7–9), *N*-acetylprocainamide was found to be: (*a*) primarily eliminated unchanged in the urine (Table II) by an active renal process in rats; (*b*) eliminated in the feces by biliary excretion to a small extent with the remainder eliminated in the urine, presumably after biotransformation to more polar compounds; (*c*) rapidly distributed in the body showing a higher affinity for heart, kidney, and liver tissues than plasma proteins; and (*d*) rapidly and completely absorbed from oral solution in young rats. These parameters were determined repeatedly in the same rats over a period of 12 months.

The data observed in this study show that the rate of absorption of *N*-acetylprocainamide from the GI tract is not age dependent. Similar results have been reported for intestinal absorption of sulfamethazole, paracetamol, amino acids, and glucose (10–14). The data from the present study, however, also indicate that the extent of absorption of *N*-acetylprocainamide (as reflected by the decrease in the oral–intravenous ratios of AUC values and the amounts of unchanged drug excreted in the urine) decreased significantly in the older rats. The fact that the GI blood flow diminished significantly would suggest that the rate of drug absorption should be affected proportionally. These conflicting results, however, may be due partially to the effect of changes in gastric pH, permeability of the GI wall, gastric emptying, and GI motility and, in part, to the simplified pharmacokinetic model used to analyze the data. In any case, the lower bioavailability did not result in a decrease in plasma concentrations of *N*-acetylprocainamide. The elimination rate and the clearance of the drug declined to a greater extent, and this presumably caused a pronounced accumulation of the drug in the body.

The age-related changes in the pharmacokinetic parameters obtained in this study are consistent with the age-related changes in other physiological parameters (2), *e.g.*, significant diminution in renal function in older rats (15, 16). Yates and Hiley (2) reported several hemodynamic parameters in young-adult (3–4 months) and middle-aged rats (11–12 months). Table IV summarizes some of these parameters as well as

Table IV—Effect of Age on Tissue Blood Flow and Related Pharmacokinetic Parameters of *N*-Acetylprocainamide

Parameters	Young Adult Rats 3–4 Months n	Young Adult Rats 3–4 Months Mean	Young Adult Rats 3–4 Months *SD*	Middle-Aged Rats 11–12 Months n	Middle-Aged Rats 11–12 Months Mean	Middle-Aged Rats 11–12 Months *SD*	Ratio of Means Middle-Aged/ Young Adult
Physiological [a]							
Cardiac index, ml/min/kg	10	210	63.2	10	123	34.8	0.586
Heart blood flow, ml/min	10	4.26	1.71	10	3.74	2.59	0.878
Liver blood flow [b], ml/min	10	0.13	0.063	10	0.09	0.032	0.692
Kidney blood flow, ml/min	10	5.70	1.26	10	3.00	1.26	0.562
Hepatosplanchnic [c], ml/min	10	1.10	0.32	10	0.44	0.095	0.400
Pharmacokinetics							
Volume of distribution, ml/kg	7	4750	530	7	1980	493	0.417
Total clearance, ml/min/kg	7	33.5	5.00	7	11.1	7.90	0.330
Renal clearance, ml/min/kg	7	22.2	7.87	6	7.13	1.55	0.322
Nonrenal clearance, ml/min/kg	7	11.3	9.42	6	5.02	2.88	0.444
AUC Ratio (Oral/iv)	7	1.01	—	7	0.747	—	0.740
X_u Ratio (Oral/iv)	6	1.04	—	6	0.841	—	0.809

[a] Physiological parameters taken from Ref. 2. [b] Hepatic artery. [c] Hepatic artery, spleen, pancreas, and GI tracts.

pharmacokinetic parameters, which might have been impacted directly by the physiological changes. There were significant decreases in the cardiac index (41%), hepatic blood flow (31%), renal blood flow (44%), and GI tract blood flow (60%) in older animals. These changes may account for the decreased renal clearance (68%), total clearance (67%), volume of distribution (57%), and bioavailability (25%). The renal clearance values were 3.9 and 2.4 times larger than the respective renal blood flow in young-adult and middle-aged rats indicating a significant active renal secretion of *N*-acetylprocainamide, consistent with previous findings (9). The nonrenal clearance values were 82 and 52 times larger than the respective hepatic blood flow in young-adult and middle-aged rats, indicating a combination of active biliary secretion and biotransformation of the drug in the liver. The decrease in the volume of distribution might have been due also to a change in body composition in the older animals. While the fatty tissue and skin account for a larger percentage of the body weight in older animals, the percentages of lean body mass and body water decrease.

The distribution of *N*-acetylprocainamide in the liver and kidneys was also affected by age. The liver–plasma and kidney–plasma concentration ratios increased with age (86 and 44%, respectively). This elevation of the drug level in the organs seems to be inversely proportional to the decrease in liver and kidney blood flow (31 and 44%, respectively) in the older rats. The drug accumulation in the organs of the older rats probably is caused by: (*a*) higher plasma levels of *N*-acetylprocainamide (initial concentrations of 19 and 46 μg/ml in 3- and 12-month-old animals, respectively); (*b*) the diminution in the blood flow to the organs (the redistribution of *N*-acetylprocainamide from the tissues was affected to a greater extent by this than by the actual distribution of the drug in the organs); and (*c*) changes in the composition of the liver and kidney tissues which favored a larger drug uptake. Interestingly, with the minor change in heart blood flow (12%), the heart–plasma concentration ratio did not change much with age.

In conclusion, the data show an age-dependent reduction in the bioavailability of orally administered *N*-acetylprocainamide solution in rats. The elimination of the drug, however, is impaired to a greater extent with age, which results in significant accumulations in the plasma and tissues after chronic administration. This finding indicates that in long-term toxicity testings of this and other drugs which show age-dependent pharmacokinetics, an adjustment in the chronically administered dose is essential.

REFERENCES

(1) A. D. Bender, *J. Am. Geriat. Soc.*, **13**, 192 (1965).

(2) M. S. Yates and C. R. Hiley, *Experientia*, **35**, 78 (1979).

(3) D. L. Schmucker, *Am. Pharmacol. Exp. Ther.*, **30**, 445 (1979).

(4) K. Wilson and J. Hanson, *Methods Find. Exp. Clin. Pharmacol.*, **2**, 303 (1980).

(5) P. G. Harms and S. R. Ojeda, *J. Appl. Physiol.*, **36**, 391 (1974).

(6) C.-M. Lai, B. L. Kamath. Z. M. Look, and A. Yacobi, *J. Pharm. Sci.*, **69**, 982 (1980).

(7) A. Yacobi, H. F. Stampfli, C.-M. Lai, and B. L. Kamath, *Drug. Metal. Dispos.*, **9**, 193 (1981).

(8) B. L. Kamath, A. Yacobi, S. D. Gupta, H. Stampfli, M. Durrani, and C.-M. Lai, *Res. Commun. Chem. Pathol. Pharmacol.*, **32**, 299 (1981).

(9) B. L. Kamath, C.-M. Lai, S. D. Gupta, M. J. Durrani, and A. Yacobi, *J. Pharm. Sci.*, **70**, 299 (1981).

(10) E. J. Triggs, R. L. Nation, A. Long, and J. J. Ashley, *Eur. J. Clin. Pharmacol.*, **8**, 55 (1975).

(11) L. Penzes, G. Simon, and M. Winter, *Exp. Gerontol.*, **3**, 607 (1968).

(12) L. Penzes and M. Boross, *Exp. Gerontol.*, **9**, 253 (1974).

(13) L. Penzes and M. Boross, *Exp. Gerontol.*, **9**, 259 (1974).

(14) J. Klimas, *J. Gerontol.*, **23**, 529 (1968).

(15) D. F. Davies and N. W. Shock, *J. Clin. Invest.*, **29**, 496 (1950).

(16) S. A. Friedman, A. E. Raizner, H. Rosen, N. A. Solomon, and W. Sy, *Ann. Intern. Med.*, **76**, 41 (1972).

Synthesis and Antiallergenic Properties of 3-*n*-Pentadecyl- and 3-*n*-Heptadecylcatechol Esters

MAHMOUD A. EISOHLY ˣ, DANIEL A. BENIGNI, LOLITA TORRES, and E. SUE WATSON

Received February 12, 1982, from the *Research Institute of Pharmaceutical Sciences, School of Pharmacy, University of Mississippi, University, MS 38677.* Accepted for publication June 11, 1982.

Abstract □ A synthetic procedure is described for the preparation of 3-*n*-pentadecyl- and 3-*n*-heptadecylcatechols and their acetate and alaninate esters. The Wittig reagent prepared from 2,3-dimethoxybenzyltriphenylphosphonium bromide (III) was coupled with 1-tetradecanal or 1-hexadecanal to give the olefins IV and V, respectively. Catalytic reduction of IV and V followed by demethylation with boron tribromide afforded VIII and IX. The acetates were prepared using acetic anhydride and pyridine, while the alaninates were prepared using *N*-(*tert*-butoxycarbonyl)-L-alanine and dicyclohexylcarbodiimide followed by removal of the *tert*-butoxycarbonyl group with hydrogen chloride gas. The esters were active in guinea pigs in the production of tolerance and desensitization or hyposensitization to poison ivy-type contact dermatitis.

Keyphrases □ Synthesis—3-*n*-pentadecyl- and 3-*n*-heptadecylcatechols, acetate and alaninate esters □ Urushiols—poison ivy and poison oak, synthesis of saturated congeners □ 3-*n*-Pentadecylcatechol—synthesis, acetate and alaninate esters □ 3-*n*-Heptadecylcatechol—synthesis, acetate and alaninate esters

Poison ivy (*Toxicodendron radicans*), poison oak (*T. diversilobum*), and poison sumac (*T. vernix*) are the primary cause of occupational dermatitis in the United States. Other genera of the plant family Anacardiaceae with dermatogenic constituents include *Anacardium* (cashew nuts), *Semicarpus* (india ink tree), *Metopium* (poison wood), and *Mangifera* (mango). The allergenic components in most of these plants are 3-*n*-alk-(en)-yl catechols with C-15 or C-17 side chains and different degrees of unsaturation (0–3 olefinic bonds) (1–5).

Extracts of poison ivy, poison oak, and poison sumac have been used for diagnosis and prophylactic treatment of poison ivy, oak, and sumac dermatitis (6–8). However, the efficacy of these extracts in producing desensitization is questionable (9). Kligman (10) found that, in humans, only hyposensitization was possible by oral or intramuscular injection of either poison ivy oleoresin or pentadecylcatechol. Oleoresin produced hyposensitization after intramuscular injection of 2–2.5 g or after oral administration of 3.5–4.0 g in multiple doses. The hyposensitization was temporary, and the individuals regained their original sensitivity within 6–10 months after cessation of the treatment.

A previous publication (11) reported a new method for

0022-3549/83/0700-0792$01.00/0

pharmacokinetic parameters, which might have been impacted directly by the physiological changes. There were significant decreases in the cardiac index (41%), hepatic blood flow (31%), renal blood flow (44%), and GI tract blood flow (60%) in older animals. These changes may account for the decreased renal clearance (68%), total clearance (67%), volume of distribution (57%), and bioavailability (25%). The renal clearance values were 3.9 and 2.4 times larger than the respective renal blood flow in young-adult and middle-aged rats indicating a significant active renal secretion of *N*-acetylprocainamide, consistent with previous findings (9). The nonrenal clearance values were 82 and 52 times larger than the respective hepatic blood flow in young-adult and middle-aged rats, indicating a combination of active biliary secretion and biotransformation of the drug in the liver. The decrease in the volume of distribution might have been due also to a change in body composition in the older animals. While the fatty tissue and skin account for a larger percentage of the body weight in older animals, the percentages of lean body mass and body water decrease.

The distribution of *N*-acetylprocainamide in the liver and kidneys was also affected by age. The liver–plasma and kidney–plasma concentration ratios increased with age (86 and 44%, respectively). This elevation of the drug level in the organs seems to be inversely proportional to the decrease in liver and kidney blood flow (31 and 44%, respectively) in the older rats. The drug accumulation in the organs of the older rats probably is caused by: (*a*) higher plasma levels of *N*-acetylprocainamide (initial concentrations of 19 and 46 μg/ml in 3- and 12-month-old animals, respectively); (*b*) the diminution in the blood flow to the organs (the redistribution of *N*-acetylprocainamide from the tissues was affected to a greater extent by this than by the actual distribution of the drug in the organs); and (*c*) changes in the composition of the liver and kidney tissues which favored a larger drug uptake. Interestingly, with the minor change in heart blood flow (12%), the heart–plasma concentration ratio did not change much with age.

In conclusion, the data show an age-dependent reduction in the bioavailability of orally administered *N*-acetylprocainamide solution in rats. The elimination of the drug, however, is impaired to a greater extent with age, which results in significant accumulations in the plasma and tissues after chronic administration. This finding indicates that in long-term toxicity testings of this and other drugs which show age-dependent pharmacokinetics, an adjustment in the chronically administered dose is essential.

REFERENCES

(1) A. D. Bender, *J. Am. Geriat. Soc.*, **13**, 192 (1965).

(2) M. S. Yates and C. R. Hiley, *Experientia*, **35**, 78 (1979).

(3) D. L. Schmucker, *Am. Pharmacol. Exp. Ther.*, **30**, 445 (1979).

(4) K. Wilson and J. Hanson, *Methods Find. Exp. Clin. Pharmacol.*, **2**, 303 (1980).

(5) P. G. Harms and S. R. Ojeda, *J. Appl. Physiol.*, **36**, 391 (1974).

(6) C.-M. Lai, B. L. Kamath. Z. M. Look, and A. Yacobi, *J. Pharm. Sci.*, **69**, 982 (1980).

(7) A. Yacobi, H. F. Stampfli, C.-M. Lai, and B. L. Kamath, *Drug. Metal. Dispos.*, **9**, 193 (1981).

(8) B. L. Kamath, A. Yacobi, S. D. Gupta, H. Stampfli, M. Durrani, and C.-M. Lai, *Res. Commun. Chem. Pathol. Pharmacol.*, **32**, 299 (1981).

(9) B. L. Kamath, C.-M. Lai, S. D. Gupta, M. J. Durrani, and A. Yacobi, *J. Pharm. Sci.*, **70**, 299 (1981).

(10) E. J. Triggs, R. L. Nation, A. Long, and J. J. Ashley, *Eur. J. Clin. Pharmacol.*, **8**, 55 (1975).

(11) L. Penzes, G. Simon, and M. Winter, *Exp. Gerontol.*, **3**, 607 (1968).

(12) L. Penzes and M. Boross, *Exp. Gerontol.*, **9**, 253 (1974).

(13) L. Penzes and M. Boross, *Exp. Gerontol.*, **9**, 259 (1974).

(14) J. Klimas, *J. Gerontol.*, **23**, 529 (1968).

(15) D. F. Davies and N. W. Shock, *J. Clin. Invest.*, **29**, 496 (1950).

(16) S. A. Friedman, A. E. Raizner, H. Rosen, N. A. Solomon, and W. Sy, *Ann. Intern. Med.*, **76**, 41 (1972).

Synthesis and Antiallergenic Properties of 3-*n*-Pentadecyl- and 3-*n*-Heptadecylcatechol Esters

MAHMOUD A. EISOHLY ˣ, DANIEL A. BENIGNI, LOLITA TORRES, and E. SUE WATSON

Received February 12, 1982, from the *Research Institute of Pharmaceutical Sciences, School of Pharmacy, University of Mississippi, University, MS 38677.* Accepted for publication June 11, 1982.

Abstract □ A synthetic procedure is described for the preparation of 3-*n*-pentadecyl- and 3-*n*-heptadecylcatechols and their acetate and alaninate esters. The Wittig reagent prepared from 2,3-dimethoxybenzyltriphenylphosphonium bromide (III) was coupled with 1-tetradecanal or 1-hexadecanal to give the olefins IV and V, respectively. Catalytic reduction of IV and V followed by demethylation with boron tribromide afforded VIII and IX. The acetates were prepared using acetic anhydride and pyridine, while the alaninates were prepared using *N*-(*tert*-butoxycarbonyl)-L-alanine and dicyclohexylcarbodiimide followed by removal of the *tert*-butoxycarbonyl group with hydrogen chloride gas. The esters were active in guinea pigs in the production of tolerance and desensitization or hyposensitization to poison ivy-type contact dermatitis.

Keyphrases □ Synthesis—3-*n*-pentadecyl- and 3-*n*-heptadecylcatechols, acetate and alaninate esters □ Urushiols—poison ivy and poison oak, synthesis of saturated congeners □ 3-*n*-Pentadecylcatechol—synthesis, acetate and alaninate esters □ 3-*n*-Heptadecylcatechol—synthesis, acetate and alaninate esters

Poison ivy (*Toxicodendron radicans*), poison oak (*T. diversilobum*), and poison sumac (*T. vernix*) are the primary cause of occupational dermatitis in the United States. Other genera of the plant family Anacardiaceae with dermatogenic constituents include *Anacardium* (cashew nuts), *Semicarpus* (india ink tree), *Metopium* (poison wood), and *Mangifera* (mango). The allergenic components in most of these plants are 3-*n*-alk-(en)-yl catechols with C-15 or C-17 side chains and different degrees of unsaturation (0–3 olefinic bonds) (1–5).

Extracts of poison ivy, poison oak, and poison sumac have been used for diagnosis and prophylactic treatment of poison ivy, oak, and sumac dermatitis (6–8). However, the efficacy of these extracts in producing desensitization is questionable (9). Kligman (10) found that, in humans, only hyposensitization was possible by oral or intramuscular injection of either poison ivy oleoresin or pentadecylcatechol. Oleoresin produced hyposensitization after intramuscular injection of 2–2.5 g or after oral administration of 3.5–4.0 g in multiple doses. The hyposensitization was temporary, and the individuals regained their original sensitivity within 6–10 months after cessation of the treatment.

A previous publication (11) reported a new method for

0022-3549/83/0700-0792$01.00/0

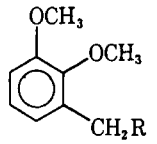

I: R = OH
II: R = Br
III: R = $\overset{+}{P}$—$(C_6H_5)_3\bar{B}r$

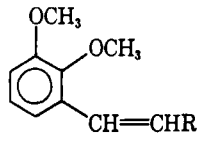

IV: R = $C_{13}H_{27}$
V: R = $C_{15}H_{31}$

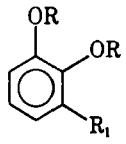

VI: R = CH_3, R_1 = $C_{15}H_{31}$
VII: R = CH_3, R_1 = $C_{17}H_{35}$
VIII: R = H, R_1 = $C_{15}H_{31}$
IX: R = H, R_1 = $C_{17}H_{35}$
X: R = $COCH_3$, R_1 = $C_{15}H_{31}$
XI: R = $COCH_3$, R_1 = $C_{17}H_{35}$
XII: R = $COCH(CH_3)NHCO_2C(CH_3)_3$, R_1 = $C_{17}H_{35}$
XIII: R = $COCH(CH_3)NH_2 \cdot HCl$, R_1 = $C_{17}H_{35}$
XIV: R = $COCH(CH_3)NHCO_2C(CH_3)_3$, R_1 = $C_{15}H_{31}$
XV: R = $COCH(CH_3)NH_2$ HCl, R_1 = $C_{15}H_{31}$

the induction of tolerance to poison ivy and oak urushiol in guinea pigs by intravenous injection of pentadecylcatechol-associated autologous red blood cells 2 weeks prior to attempted contact sensitization. It was also reported (12) that intravenous administration of the esterified urushiol (poison ivy or poison oak urushiol acetate) was effective in producing immune tolerance in naive guinea pigs and desensitization or hyposensitization in already sensitized animals. This paper reports the improved synthesis of the saturated congeners of poison ivy and poison oak urushiol acetates (diacetyl-3-*n*-pentadecylcatechol and diacetyl-3-*n*-heptadecylcatechol), and their efficacy in the production of tolerance and hyposensitization. In addition, the synthesis and activity of a water-soluble ester of heptadecylcatechol (heptadecylcatechol-dialaninate dihydrochloride) is described.

EXPERIMENTAL[1]

Synthesis—*2,3-Dimethoxybenzyl Bromide (II)*—A solution of 25 g (148.8 mmoles) of 2,3-dimethoxybenzyl alcohol (I) in 400 ml of dry ether was stirred at room temperature for 2.5 hr with 8 ml of phosphorus tribromide. The organic layer was washed with water, dried (anhydrous sodium sulfate), and the solvent removed at reduced pressure to give 33.7 g of II (98% yield); IR: ν_{max} (liquid film) 2940, 2830, 1585, and 1480 cm^{-1}; UV: λ_{max} (log ϵ) 219 (4.10) and 286 (3.24) nm; ^{1}H-NMR: δ 7.03–6.72 (3, m), 4.53 (2, s), 3.97 (3, s), and 3.80 (3, s) ppm; mass spectrum: *m/z* (%): 230 (35), 232 (M^+ +2, 34), 151 (88), and 136 (100).

2,3-Dimethoxybenzyltriphenylphosphonium Bromide (III)—A solution of 28 g of II (120 mmoles) in 500 ml of benzene containing 32 g (121 mmoles) of triphenylphosphine was allowed to reflux for 5 hr, whereupon a copious white precipitate formed. The precipitate was removed by filtration, washed with benzene, and dried to give 59 g (99% yield) of III; mp 233–234°; IR: ν_{max} (KBr) 2940, 2830, 2780, 1580, 1480, 1470, and 1430 cm^{-1}; UV: λ_{max} (log ϵ) 225 (4.46), 265 (sh, 3.61), 268 (3.67), 275 (3.66), and 282 (sh, 3.37) nm; ^{1}H-NMR: δ 8.00–7.50 (15, m), 7.00–6.60 (3, m), 5.13 (2, br, d, J = 14 Hz), 3.77 (3, s), and 3.50 (3, s).

2,3-Dimethoxy-$\Delta^{1'}$-pentadecenylbenzene (IV)—A dispersion of 5 g (10 mmoles) of the aforementioned phosphonium salt (III) in 100 ml of tetrahydrofuran (dried over sodium hydride) was stirred under nitrogen while 6 ml (10.2 mmoles) of a 1.7 *M* solution of *n*-butyllithium in hexane was added slowly. After 10 min the solution developed a deep-red color, at which time a solution of 2.65 g (10 mmoles) of 80% tetradecyl aldehyde[2] in 10 ml of tetrahydrofuran was added in a dropwise manner. The mixture slowly turned yellow and was stirred at room temperature for 2 hr. The mixture was refluxed for 16 hr and then cooled to room temperature. TLC (hexane–ethyl acetate, 95:5) on silica gel showed one spot (R_f 0.90) and no starting aldehyde (R_f 0.75). The solvent was removed under reduced pressure, and the residue was added to ethyl acetate (150 ml) and water (50 ml). The organic phase was washed with water (50 ml) and then dried over anhydrous sodium sulfate. The solvent was removed under reduced pressure to give 7.0 g of a pale amorphous solid which was filtered through 15 g of silica gel-60 (hexane–ethyl acetate, 97:3) to yield 3.3 g of a colorless solid. GC (2% OV-17) showed two peaks (*cis* and *trans* isomers of IV in a 2:3 ratio, respectively). GC/MS analysis showed the following ions: *cis m/z* 346 (M^+, 91%), 177 (100%), and 151 (83%); *trans m/z* 346 (M^+, 100%), 177 (90%), and 151 (70%).

2,3-Dimethoxy-pentadecylbenzene (VI)—The *cis* and *trans* isomeric mixture of IV (3.3 g) was dissolved in 40 ml of *tert*-butyl alcohol and 640 mg of 10% palladium-on-carbon was added. The mixture was hydrogenated on a Parr hydrogenator at 1.41 kg/cm^2 for 16 hr. Filtration of the product through diatomaceous earth[3] followed by evaporation of the solvent resulted in 3.3 g of VI as a white solid, mp 35–36°; IR: ν_{max} (liquid film) 2920, 2855, 1597, 1583, 1478, 1272, 1087, 1015, and 747 cm^{-1}; UV: λ_{max} (log ϵ) 207 (3.99), 213 (sh, 3.84), 270 (3.01), and 276 (3.00) nm; ^{1}H-NMR: δ 0.90 (3, t, J = 5 Hz), 1.28 (26, br, s), 2.62 (2, t, J = 6 Hz), 3.80 (6, s), and 6.82–6.46 (3, m) ppm; mass spectrum: *m/z* 348 (M^+, 40%), 151 (100%), and 136 (90%).

3-n-Pentadecylcatechol (VIII)—A solution of 2,3-dimethoxy-pentadecylbenzene (VI) (500 mg, 1.44 mmoles) in 30 ml of methylene chloride was cooled to 0° under nitrogen. A solution of boron tribromide in methylene chloride (1.1 ml of 12% v/v) was added and the mixture was allowed to slowly come to room temperature. After standing for 90 min, 3 ml of water was added followed by sodium bicarbonate (until no more gas evolution was noticeable). The organic layer was dried over anhydrous sodium sulfate, and the solvent was evaporated to yield a light brown residue (408 mg). Crystallization from hexane–isooctane yielded colorless needles of VIII, mp 55–56°; IR: ν_{max} 3400, 2910, 2840, 1615, 1590, 1475, 1285, 1055, 942, 827, and 725 cm^{-1}; UV: λ_{max} (log ϵ) 278 (3.23) and 230 (3.19) nm; ^{1}H-NMR (FT): δ 0.90 (3, t, J = 5 Hz), 1.26 (26, br, s), 2.55 (s, t, J = 6 Hz), 5.10 (2, br, s, exchangeable with D_2O), and 6.72 (3, br, s) ppm; mass spectrum: *m/z* 320 (M^+, 4%) and 123 (base peak).

Diacetyl-3-n-pentadecylcatechol (X)—Acetylation of VIII was carried out by stirring 400 mg with 1 ml each of acetic anhydride and pyridine at room temperature for 4 hr. The mixture was poured onto ice, and then extracted with chloroform (3 × 30 ml). The combined chloroform extract was washed successively with 20 ml of ice water, 20 ml of chilled 10% H_2SO_4, 20 ml of water, saturated sodium bicarbonate solution, and then 30 ml of water. The chloroform layer was dried over anhydrous sodium sulfate, and the solvent was evaporated to give a white solid (502 mg). Recrystallization from chloroform–ethanol afforded rosette crystals of X, mp 51–52°; IR: ν_{max} 2910, 2840, 1770, 1760, and 1470 cm^{-1}; UV: λ_{max} (log ϵ) 278 (sh, 1.65), 258 (2.45), and 210 (4.11) nm; ^{1}H-NMR: δ 7.30–7.00 (3, m), 2.50 (2, t, J = 6 Hz), 2.28 (3, s), 2.22 (3, s), 1.27 (26, br, s), and 0.88 (3, t, J = 6 Hz) ppm; mass spectrum: *m/z* 404 (M^+, 0.3%), 320 (48%), and 123 (100%).

2,3-Dimethoxy-$\Delta^{1'}$-heptadecenylbenzene (V)—Compound V was prepared from 5 g (10 mmoles) of the phosphonium salt (III) and 2.8 g (11.6 mmoles) of *n*-hexadecylaldehyde[4] following the same procedure used for the synthesis of IV. The reaction was filtered, the filtrate evaporated under reduced pressure, and the residue partitioned between chloroform (150 ml) and water (3 × 30 ml). The organic layer was dried over anhydrous sodium sulfate, and the solvent was removed under reduced pressure. The residue was dissolved in 15 ml of hexane, filtered, and the filtrate chromatographed on silica gel-60 (50 g, hexane–ethyl acetate, 95:5) to yield 3.6 g of a colorless solid. GC and GC/MS examination showed a mixture of *cis* and *trans* isomers (2:3, respectively); mass

[1] Melting points are uncorrected and were determined on a Thomas-Hoover Unimelt apparatus. The UV absorption spectra were obtained in methanol using a Beckman-Acta Model IV recording spectrophotometer. IR absorption spectra were recorded using a Perkin-Elmer 281B infrared spectrophotometer. ^{1}H-NMR spectra were recorded on a JEOL Model C-60 HL spectrometer. Fourier transform ^{1}H- and ^{13}C-NMR spectra were obtained on a JEOL NJM-FX60 spectrometer. Chemical shifts were reported in δ units with tetramethylsilane as the internal standard and deuterochloroform as the solvent. Mass spectral analyses were performed on a Finnigan 3200 GC/MS/DS. GC analyses were performed on a Beckman GC-65 using a 3% OV-17 or 5% OV-225 column and FID detector with 30 ml/min carrier gas (nitrogen).

[2] Aldrich Chemical Co., Milwaukee, Wis.

[3] Celite.

[4] Prepared from palmitic acid following the procedure described in Ref. 13.

Table I—^{13}C-NMR Chemical Shifts (ppm) for Compounds I–XI [a]

Carbon Number	Compound										
	I	II	III[b]	IV[c] *trans*	IV[c] *cis*	VI	VII	VIII	IX	X[d]	XI[e]
1	152.6	152.8	152.4	153.2	153.0	152.9	152.9	143.3	143.2	142.8	142.8
2	147.2	147.8	147.8	146.7	147.6	147.6	147.7	142.1	142.0	140.8	140.9
3	135.1	131.8	123.8	132.3	132.4	136.8	136.8	129.8	129.7	136.8	136.9
4	124.1	124.0	123.7	124.3	124.4	123.6	123.6	122.3	122.3	127.2	127.2
5	120.8	122.6	114.1	123.8	123.8	122.2	122.2	120.4	120.3	126.0	126.1
6	112.5	113.4	120.8	110.0	111.6	110.5	110.5	113.2	113.1	120.9	120.9
1-OCH_3	55.9	55.8	56.3	55.9	55.8	55.7	55.7				
2-OCH_3	60.6	60.6	60.3	60.6	60.3	60.4	60.7				
1′	60.6	28.1		132.5	133.6	30.9	30.9	29.8	29.8	29.7	30.2
2′				118.4	122.4	30.0	30.0	29.8	29.8	29.7	29.8
3′				33.5	33.5	29.8	29.8	29.8	29.8	29.7	29.8
4′-11′				29.8	29.8	29.8	29.8	29.8	29.8	29.7	29.8
12′				29.4	29.4	29.5	29.8	29.4	29.8	29.4	29.8
13′				32.0	32.0	32.0	29.8	32.0	29.8	32.0	29.8
14′				22.7	22.7	22.7	29.5	22.7	29.4	22.7	29.8
15′				14.1	14.1	14.0	32.0	14.1	32.0	14.0	32.0
16′							22.7		22.7		22.7
17′							14.0		14.0		14.1

[a] ^{13}C-NMR data on the alaninate derivatives are provided in *Experimental*. [b] In the proton-decoupled spectrum, the benzylic methylene carbon appeared at δ 25.7 ppm as a doublet (J = 48.8 Hz) as a result of coupling with phosphorus. The aromatic carbons of the triphenylphosphine residue of III also appeared as doublets at δ 135.1, 134.1, 130.2, and 118.1. We have also observed long-range coupling between phosphorus and carbons 1, 2, 3, 5, and 6. [c] The *trans* isomer of IV was separated by column chromatography; ^{13}C-NMR was recorded on the mixture and on the *trans* isomer. The data obtained on the *cis* isomer was by subtraction. No attempt was made to separate the *trans* isomer of V. [d] The carbonyl carbon atoms of the acetate groups were observed at δ 168.0 and 167.9 ppm while the methyl signals were observed at δ 20.5 and 20.1 ppm. [e] The carbonyl carbon atoms of the acetate groups were observed at δ 168.1 ppm (double intensity) and the methyl signals were observed at δ 20.6 and 20.2 ppm.

spectrum: *cis* m/z 374 (M^+, 56%), 177 (100%), and 151 (78%); *trans* m/z 374 (M^+, 61%), 177 (100%), and 151 (58%). The ^{1}H-NMR spectrum of the mixture showed peaks at δ 0.90 (3, t, J = 6 Hz), 1.30 (26, br, s), 2.48–2.10 (2, br, d), 3.88, 3.85 and 3.83 (6, 3s), and 5.48–7.15 (5, m).

2,3-Dimethoxy-heptadecylbenzene (*VII*)—Catalytic hydrogenation of V (3.6 g) was carried out as outlined for the preparation of VI to give a quantitative yield of VII as a colorless solid, mp 44–46°; IR: ν_{max} 1595, 1580, 1470, 1270, 1083, 1013, 737, and 717 cm^{-1}; UV: λ_{max} (log ε) 231 (3.16), 271 (3.03), and 276 (3.02) nm; ^{1}H-NMR: δ 0.90 (3, t, J = 5 Hz), 1.30 (30, br, s), 2.18 (2, t, J = 6 Hz), 3.85 (3, s), 3.83 (3, s), and 6.62–7.00 (3, m); mass spectrum: m/z 376 (M^+, 50%), 151 (97%), and 136 (100%).

3-n-Heptadecylcatechol (*IX*)—2,3-Dimethoxy-heptadecylbenzene (VII), 3.01 g, was demethylated with boron tribromide, following the procedure described for the preparation of VIII, to give 2.16 g (78% yield) of a colorless solid. Recrystallization from hexane–isooctane gave fine needles of IX, mp 63–64°; IR: ν_{max} 3380, 2920, 2847, 1617, 1592, 1475, 1468, 1282, 1190, and 720 cm^{-1}; UV: λ_{max} (log ε) 230 (3.19) and 275 (3.21) nm; ^{1}H-NMR: δ 0.89 (3, t, J = 6 Hz), 1.26 (30, br, s), 2.63 (2, t, J = 6 Hz), 4.99 (1, s, exchangeable with D_2O), 5.09 (1, s, exchangeable with D_2O), and 6.72 (3, s); mass spectrum: m/z 348 (M^+, 30%) and 123 (base peak).

Diacetyl-3-n-heptadecylcatechol (*XI*)—Compound XI was prepared by acetylation of IX following the same procedure as used for preparation of X. Crystallization from chloroform–ethanol afforded rosettes, mp 56–57°; IR: ν_{max} 2930, 2855, 1785, 1770, and 1480 cm^{-1}; UV: λ_{max} (log ε) 276 (sh, 1.64), 257 (2.47), and 210 (4.08) nm; ^{1}H-NMR: δ 7.30–7.00 (3, m), 2.50 (2, t, J = 6 Hz), 2.28 (3, s), 2.22 (3, s), 1.26 (30, br, s), and 0.88 (3, t, J = 5 Hz); mass spectrum: m/z 432 (M^+, 0.2%), 348 (15%), and 123 (100%).

3-n-Heptadecylcatechol-dialaninate Dihydrochloride (XIII)—A solution of dicyclohexylcarbodiimide (2.11 g, 10.2 mmoles) in 120 ml of acetonitrile was cooled in an ice bath for 10 min and then 1.94 g (10.3 mmoles) of *N*-(*tert*-butoxycarbonyl)-L-alanine was added. This solution was stirred in an ice bath for 30 min during which time a cloudy white precipitate appeared. Two portions of IX were then added (618 mg and 1.22 g) and the mixture was stirred at room temperature for 2 hr after each addition. TLC analysis of the reaction product using 2% methanol in chloroform showed some starting material (R_f 0.3, blue black with ferric chloride) an appreciable amount of the diester (XII) (R_f 0.75, yellow with chlorine tolidine reagent), and some monoester (R_f 0.70, yellow with chlorine tolidine reagent). Therefore, 1.03 g (5 mmoles) of dicyclohexylcarbodiimide in 30 ml of acetonitrile (cooled to 0°) and 950 mg (5 mmoles) of *N*-(*tert*-butoxycarbonyl)-L-alanine was stirred in an ice bath for 20 min and then was added to the above mixture. After stirring overnight, the reaction was filtered, and the solvent was removed by evaporation. The residue was chromatographed on 50 g of silica gel-60 (chloroform) to yield 3.25 g (4.7 mmoles) of XII as an oil (94% yield); $[\alpha]_D^{22°}$ − 19° (c 0.59, $CHCl_3$); UV: λ_{max} (log ε) 257 (2.40) and 220 (3.40) nm; IR: ν_{max} ($CHCl_3$); 3440, 3370, 2915, 2860, 1770, 1705, and 1500 cm^{-1}; ^{1}H-NMR: δ 1.30 (30, br, s), 1.50 (18, s), 2.70 (2, br, t, J = 6 Hz), 4.60–4.50 (2, br, s), 5.50 (1, br, s), 5.63 (1, br, s), and 7.10–7.00 (3, m); ^{13}C-NMR: δ 14.0 (q), 17.9 (q), 18.1 (q), 22.7 (t), 28.5 (q), 29.4 (t), 29.7 (t), 32.0 (t), 49.5 (d), 49.8 (d), 79.9 (s), 120.7 (d), 126.2 (d), 127.3 (d), 136.9 (s), 140.5 (s), 142.7 (s), 155.6 (s), 170.8 (s), and 171.0 (s) ppm.

Conversion of XII to XIII—A solution of XII (2.75 g) in ethyl acetate (50 ml) was chilled at 0° for 25 min, and then was saturated with hydrogen chloride for 3 min. The mixture was stirred for 20 min at 0° and then the solvent was evaporated to yield 1.81 g of XIII, mp 204–205° (dec); $[\alpha]_D^{25}$ + 107° (c 0.52, $CHCl_3$); UV: λ_{max} (log ε) 264 (2.54) and 210 (4.04) nm; IR: ν_{max} (KBr) 3420, 2920, 2840, 1790, and 1600 cm^{-1}; mass spectrum: m/z 419 (3%), 348 (23%), 136 (10%), and 123 (100%). Due to the insolubility of the material, the ^{1}H and ^{13}C-NMR spectra were not obtained.

3-n-Pentadecylcatechol-dialaninate Dihydrochloride (XV)—Reaction of VIII with *N*-(*tert*-butoxycarbonyl)-L-alanine in the manner previously described for the preparation of XIII afforded XIV; UV: λ_{max} (log ε) 280 nm (sh, 2.02), 258 (2.47), and 219 (3.40) nm; IR: ν_{max} ($CHCl_3$) 3440, 3370, 2930, 1770, 1700, and 1500 cm^{-1}; ^{1}H-NMR: δ 7.22–7.17 (3, m), 5.70 (1, br, s), 5.55 (1, br, s), 4.63 (2, br, q, J = 6 Hz), 2.60 (2, t, J = 6 Hz), 1.50 (18, s), 1.28 (26, br, s), and 0.92 (3, t, J = 6 Hz); ^{13}C-NMR: δ 171.1 (s), 170.8 (s), 155.5 (s), 142.6 (s), 140.5 (s), 136.9 (s), 127.3 (d), 126.3 (d), 120.7 (d), 80.0 (s), 49.8 (d), 49.4 (d), 32.0 (t), 30.1 (t), 30.0 (t), 29.7 (t), 29.5 (t), 29.4 (t), 28.5 (q), 22.7 (t), 18.1 (q), 17.9 (q), and 14.0 (q). The *tert*-butyloxycarbonyl protecting groups of XIV were removed with hydrogen chloride in ethyl acetate in the aforementioned manner to yield the dialaninate dihydrochloride XV.

Biological Studies—*Animals*—Female Hartley line-bred guinea pigs weighing 450–500 g were used; guinea pig food and water supplemented with vitamin C were offered *ad libitum*. Groups of 6–12 animals were used, and in all cases a sensitive control group was administered the vehicle only. Sensitization and skin testing were carried out using procedures previously described (11, 12).

Dosing—Doses of 1 or 10 mg of 3-*n*-pentadecylcatechol diacetate (X) per animal were administered intravenously. Emulsions containing the acetates were prepared using polyoxyethylene (20), sorbitan monostearate, and sorbitan monooleate[5] in saline as previously described (12). For tolerance studies, the drug was given to the animals 2 weeks prior to the attempted sensitization. Emulsions of either X or XI were given orally after sensitization of the guinea pigs for desensitization studies. The water-soluble ester (XIII) was given in aqueous solution. The animals were given a cumulative dose equivalent to 52.5 mg of the free catechols (VIII or IX) in the ester form over a period of 3 weeks as follows: (*a*) three doses of 2.5 mg each given on alternate days during the first week; (*b*) three doses of 5 mg each during the second week; and (*c*) three doses of 10 mg each during the third week. The animals were sensitized and skin

[5] Atlas Chemical Industries Inc., Wilmington, Del.

tested prior to dosing, and their sensitivity was measured again the week after the last dose.

RESULTS AND DISCUSSION

Poison ivy dermititis is a major problem among outdoor workers in the U.S. It is estimated that over 1.5 million cases of poison ivy dermatitis are encountered every year with a loss of over 152,000 work days in the United States[6].

In our search for ways to control contact dermatitis caused by the urushiols of poison ivy, oak, and sumac, two successful procedures were developed in this laboratory using guinea pigs as the animal model (11, 12). Of particular interest was the discovery that the esterified urushiol (urushiol acetate) had the ability to block the development of sensitivity in guinea pigs if administered prior to the attempted sensitization (tolerance induction), as well as the ability to desensitize or hyposensitize already sensitive animals (12). This study described the synthesis of the saturated congeners of poison ivy and poison oak urushiols and the ability of their esters to induce tolerance and desensitization or hyposensitization. The synthesis of VIII and IX (the saturated components of poison ivy and oak urushiols, respectively) have been previously described (14–17). These methods involved initially a Grignard reaction of the appropriate alkylmagnesium halide with either 2,3-dimethoxybenzaldehyde or 2,3-dimethoxybenzyl chloride. In addition, the reaction of the Grignard reagent with the phenolic aldehyde was investigated (18).

However, these procedures provided inconsistent results, and the final products were difficult to purify. Use of the Wittig reaction afforded high yields of products which were easy to purify. The Wittig reagent was prepared from 2,3-dimethoxybenzyl halide since the long-chain alkyl halide failed to form the phosphonium salt. The use of boron tribromide in methylene chloride for the demethylation was superior to previously used reagents such as hydrochloric acid, hydroiodic acid, or pyridinium chloride. Demethylation took place in two steps *via* the monomethyl ether, with demethylation of the more sterically hindered group occurring first.

In addition to the acetate esters, the water-soluble dialaninate ester dihydrochlorides (XIII and XV) were prepared. Spectral data are given in *Experimental*. Table I shows the ^{13}C-NMR data on compounds I–XI.

The synthetic compounds were tested for their ability to induce tolerance or desensitization to poison ivy and poison oak urushiols. Guinea pigs were used as the animal model, and immune tolerance was produced by a single- or 10-mg iv dose of X. Over 90% of the animals treated with X were completely tolerant (not reactive to ≤ 3.2-μg test doses of VIII for 6 weeks); none of the control animals were tolerant to VIII. The esters X, XI, and XIII were tested orally (gastric gavage) for their ability to desensitize or hyposensitize guinea pigs which were previously sensitized to poison ivy or oak urushiol. The dosage schedule consisted of consecutive escalating doses for 3 weeks: an amount of the ester equivalent to 2.5 mg of the parent catechol 3 times a week for the first week, doubling each week thereafter. The animals were tested with poison ivy or oak urushiol the week following the last dose and again 4 weeks later. Thity-eight percent of the guinea pigs receiving X were desensitized to 3-μg doses of poison ivy urushiol. There was also significant reduction of the sensitivity (hyposensitization) of the remaining animals as judged by the Driaze method (19) of evaluating skin erythema and edema. Compounds XI and XIII were also found to hyposensitize guinea pigs to poison oak urushiol.

A more detailed comparison of the toxicity and efficacy of free urushiols and their corresponding esters will be published[7].

[6] These figures were obtained from the Public Health Service for 1969, the last year for which there are figures available.

[7] E. S. Watson *et al.*, submitted for publication to *J. Invest. Dermatol.*

REFERENCES

(1) W. F. Symes and C. R. Dawson, *J. Am. Chem. Soc.*, **76**, 2959 (1954).

(2) S. V. Sunthankar and C. R. Dawson, *J. Am. Chem. Soc.*, **76**, 5070 (1954).

(3) K. H. Markiewitz and C. R. Dawson, *J. Org. Chem.*, **30**, 1610 (1965).

(4) M. D. Corbett and S. Billets, *J. Pharm. Sci.*, **64**, 1715 (1975).

(5) S. Billets, J. C. Craig, M. D. Corbett, and J. F. Vickery, *Phytochemistry*, **15**, 533 (1976).

(6) C. H. Ducan, *N.Y. Med. J.*, **104**, 901 (1916).

(7) G. A. Gellin, C. R. Wolf, and H. Milby, *Arch. Environ. Health*, **2**, 280 (1971).

(8) H. S. Mason and A. Lada, *J. Invest. Dermatol.*, **22**, 457 (1975).

(9) F. A. Stevens, *J. Am. Med. Assoc.*, **127**, 912 (1945).

(10) A. M. Kligman, *Arch. Dermatol.*, **78**, 47 (1958).

(11) E. S. Watson, J. C. Murphy, P. W. Wirth, M. A. ElSohly, and P. Skierkowski, *J. Pharm. Sci.*, **70**, 785 (1981).

(12) E. S. Watson, J. C. Murphy, C. W. Waller, and M. A. ElSohly, *J. Invest. Dermatol.*, **76**, 164 (1981).

(13) W. P. Campbell and D. Todd, *J. Am. Chem. Soc.*, **64**, 928 (1942).

(14) H. S. Mason, *J. Am. Chem. Soc.*, **67**, 1538 (1945).

(15) B. Loev and C. Dawson, *J. Am. Chem. Soc.*, **78**, 1180 (1956).

(16) A. P. Kurtz and C. Dawson, *J. Med. Chem.*, **14**, 729 (1971).

(17) J. S. Byck and C. R. Dawson, *J. Org. Chem.*, **33**, 2451 (1968).

(18) B. Loev and C. R. Dawson, *J. Am. Chem. Soc.*, **78**, 4083 (1956).

(19) J. H. Draize, G. Woodward, and H. O. Calvery, *J. Pharmacol. Exp. Ther.*, **82**, 377 (1944).

ACKNOWLEDGMENTS

This work was supported by the Research Institute of Pharmaceutical Sciences, School of Pharmacy, University of Mississippi.

The authors are grateful to Mr. Roger Seidel for providing the mass spectral analysis and Ms. Paula Smith for her technical assistance.

Acrylic Microspheres *In Vivo* VIII: Distribution and Elimination of Polyacryldextran Particles in Mice

PETER EDMAN and INGVAR SJÖHOLM ˣ

Received March 22, 1982, from the *National Board of Health and Welfare, Department of Drugs, Division of Pharmacy, S-751 25 Uppsala, Sweden.* Accepted for publication June 21, 1982.

Abstract □ The disposition of different ^{14}C-labeled, biodegradable polyacryldextran microparticles after intravenous injection has been studied in the mouse. The particles were rapidly cleared from the circulatory system by the reticuloendothelial system. They were predominantly (60–80%) found in the liver and spleen and to some extent in the bone marrow. Large particle aggregates were found in the lungs 6 hr postinjection. After redistribution, the particles were eliminated from the organs with an apparent $t_{1/2}$ of 12–30 weeks, depending on the composition of the particles. Highly cross-linked particles with 2% acrylic groups (DTC = 11-2-75) had a half-life similar to that of polyacrylamide particles (TC = 8-25). The metabolism rate was also correlated with the degradation *in vitro* with isolated rat lysosomes. After intravenous injection of small ^{14}C-labeled polyacrylamide particles (0.2–0.5 μm), significant amounts of radioactivity were detected in the bile and gallbladder.

Keyphrases □ Polyacryldextran—microparticles, *in vitro* degradation, *in vivo* metabolism and elimination in mice □ Microparticles—of polyacryldextran, *in vitro* degradation, *in vivo* metabolism and elimination in mice □ Metabolism—of polyacryldextran microparticles in mice following intravenous injection □ Elimination—of polyacryldextran microparticles in mice by the reticuloendothelial system following intravenous injection

Previous studies have revealed that proteins immobilized in microparticles of polyacrylamide can retain biological properties (1). The particles are small enough (0.2–1 μm in diameter) to be injected intravenously without respiratory problems (2). When such particles were injected parenterally, they were cleared rapidly from the circulatory system by cells of the reticuloendothelial system (RES), predominantly *via* the liver and spleen, where the particles were localized in the lysosomal vacuome (3). The spheres were eliminated from these organs with a half-life of ~20–25 weeks (2).

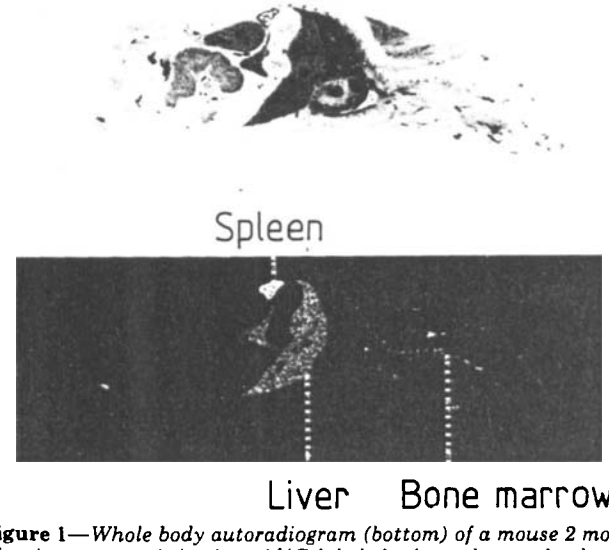

Figure 1—*Whole body autoradiogram (bottom) of a mouse 2 months after intravenous injection of ^{14}C-labeled microspheres of polyacryldextran, DTC = 11-1-75 (48,200 dpm in 2.6 mg). The top is the corresponding stained section, 20 μm.*

Derivatized natural polymers (*e.g.*, acryldextrans) recently have been introduced as a matrix for the preparation of microparticles, particularly for use *in vivo* (4), as substantially fewer synthetic polymer threads are then needed to form the microspheres. The total concentration of acrylic groups is only 0.5–2% in the water phase prior to the polymerization and formation of polyacryldextran. Moreover, the amount of protein immobilized in the microparticles is increased without any significant loss of the biological properties of the immobilized protein, with improved stability against heat denaturation (4). Such particles carrying immobilized dextranase have been used successfully to treat an artificially induced storage disease in mice (5). The present paper will describe quantitatively the distribution of polyacryldextran microparticles in mice and the influence of the polyacryl chains on the degradation of the microparticles *in vivo* and by dextranase *in vitro*.

EXPERIMENTAL

Materials—Acrylamide[1], *N,N'*-methylenebisacrylamide (BIS)[1], *N,N,N',N'*-tetramethylethylenediamine[2], dextran[3], 4-methylumbelliferyl-2-acetamido-2-deoxy-β-D-glucopyranoside[2], 4-methylumbelliferone[2], and other chemicals were of analytical grade. Acrylic acid-glycidyl[4], dextranase[2] (E.C. 3.2.1.11), and [^{14}C]paraformaldehyde[5] were used without further purification. ^{14}C-Labeled *N,N'*-methylenebisacrylamide was prepared as described by Sjöholm and Edman (2).

Synthesis of Acrylic Dextran—Acrylic dextran was prepared using a reported method (4). Dextran (T-40, mol. wt. 40,000) was dissolved in 250 ml of 0.01 *M* phosphate buffer, pH 9.0. Acrylic acid-glycidyl (25 ml) was added, and the emulsion was stirred with a magnetic stirrer for 9–10 days at room temperature. The dextran was precipitated and washed with ethanol. The precipitated dextran was dissolved in phosphate buffer, precipitated again, and washed with ethanol. This procedure was repeated at least five times. The content of acrylic groups in the dextran was determined by halogenation of the double bonds, as described previously (4).

Preparation of Microparticles—^{14}C-Labeled microparticles (DTC = 11-1-75, DTC = 11-2-75, and TC = 8-25)[6] were prepared by the methods of Ekman *et al.* (1) and Edman *et al.* (4). In a typical example, the monomers (acrylamide, ^{14}C-labeled *N,N'*-methylenebisacrylamide, and acryldextran) were dissolved in 5 ml of 0.1 *M* phosphate buffer, pH 7.4. Oxygen was removed from the solution using nitrogen gas. At the same time, 200 ml of a mixture of toluene and chloroform (4:1), containing a detergent[7] (0.5 g), was flushed with nitrogen. After addition of the catalyst, ammonium peroxodisulfate (100 μl of a 0.5-g/ml solution), the

[1] Eastman Kodak Co.
[2] Sigma Chemical Co.
[3] Dextrans (T40 and T500) were obtained from Pharmacia Fine Chemicals, Uppsala, Sweden.
[4] Fluka AG.
[5] Radiochemical Centre, Amersham, England.
[6] The particles prepared are characterized using the nomenclature suggested by Hjertén (6) and Edman *et al.* (4). The first numeral denotes the concentration of derivatized dextran (D) participating in the particle formation (g/100 ml of solvent). The second numeral denotes the total amount (T) of acrylic monomers (g/100 ml of solvent) and the third, the amount of cross-linking agent (C), *N,N'*-methylenebisacrylamide, expressed as the percentage (w/w) of the total amount of monomers.
[7] Pluronics F-68 (polyoxyethylene-derived polyoxypropylene) was obtained from Trebac AB, Stockholm, Sweden.

0022-3549/83/0700-0796$01.00/0

Table I—Distribution of ^{14}C-Labeled Polyacryldextran Particles after Intravenous Administration to Mice [a]

Organ	Time Postdose	Organ Weight, g	Dpm	Percentage of Injected Dose
		DTC = 11-1-75		
Liver	6 hr	1.10 ± 0.05	18,750 ± 650	38.88 ± 1.4
Spleen	6 hr	0.07 ± 0.01	2550 ± 350	5.3 ± 1.7
Lung	6 hr	0.16 ± 0.01	10,460 ± 1340	21.69 ± 2.78
Kidneys	6 hr	0.16 ± 0.01	490 ± 70	1.02 ± 0.15
Liver	1 week	1.45 ± 0.08	25,970 ± 1440	53.85 ± 2.99
Spleen	1 week	0.16 ± 0.01	5940 ± 380	12.32 ± 0.79
Lung	1 week	0.17 ± 0.01	890 ± 220	1.85 ± 0.46
Kidneys	1 week	0.18 ± 0.02	440 ± 30	0.91 ± 0.06
Liver	2 weeks	1.50 ± 0.07	27,340 ± 1110	56.69 ± 2.30
Spleen	2 weeks	0.16 ± 0.01	5500 ± 180	11.40 ± 0.37
Liver	4 weeks	1.27 ± 0.04	21,800 ± 950	45.20 ± 1.97
Spleen	4 weeks	0.12 ± 0.01	4500 ± 200	9.33 ± 0.41
Liver	8 weeks	1.31 ± 0.07	18,480 ± 510	38.32 ± 1.06
Spleen	8 weeks	0.13 ± 0.01	4160 ± 200	8.63 ± 0.42
Liver	12 weeks	1.36 ± 0.06	13,500 ± 300	27.99 ± 0.64
Spleen	12 weeks	0.12 ± 0.01	2200 ± 160	4.55 ± 0.33
Liver	20 weeks	1.47 ± 0.08	11,350 ± 720	23.55 ± 1.50
Spleen	20 weeks	0.13 ± 0.01	1990 ± 90	4.13 ± 0.19
		DTC = 11-2-75		
Liver	1 day	1.33 ± 0.07	39,640 ± 1310	70.04 ± 2.31
Spleen	1 day	0.08 ± 0.01	3880 ± 1000	6.86 ± 0.18
Lung	1 day	0.14 ± 0.01	2120 ± 100	3.75 ± 0.18
Kidneys	1 day	0.13 ± 0.01	210 ± 10	0.37 ± 0.02
Liver	1 week	1.51 ± 0.03	46,240 ± 1620	81.70 ± 2.86
Spleen	1 week	0.15 ± 0.01	4040 ± 300	7.14 ± 0.53
Lung	1 week	0.16 ± 0.01	500 ± 10	0.88 ± 0.02
Kidneys	1 week	0.15 ± 0.01	190 ± 10	0.34 ± 0.02
Liver	2 weeks	1.46 ± 0.05	41,050 ± 410	72.53 ± 0.72
Spleen	2 weeks	0.12 ± 0.01	4260 ± 300	7.53 ± 0.53
Liver	4 weeks	1.33 ± 0.04	41,860 ± 610	73.96 ± 1.08
Spleen	4 weeks	0.13 ± 0.01	4300 ± 190	7.60 ± 0.34
Liver	8 weeks	1.23 ± 0.02	32,320 ± 1130	57.10 ± 2.00
Spleen	8 weeks	0.13 ± 0.01	3050 ± 130	5.39 ± 0.23
Liver	13 weeks	1.35 ± 0.03	35,900 ± 1490	63.43 ± 2.63
Spleen	13 weeks	0.12 ± 0.01	3330 ± 250	5.88 ± 0.44
Liver	27 weeks	1.42 ± 0.03	27,380 ± 350	48.38 ± 0.62
Spleen	27 weeks	0.12 ± 0.01	2570 ± 270	4.54 ± 0.65

[a] Distribution of ^{14}C-labeled polyacryldextran particles in the liver, spleen, lung, and kidneys after injection of 2.6 mg iv of polyacryldextran particles with compositions of DTC = 11-1-75 and DTC = 11-2-75 containing 48,300 and 56,600 dpm, respectively. Each value is the mean obtained from 4–5 animals ± *SE*.

water phase was homogenized in toluene–chloroform to produce a water-in-oil emulsion. The polymerization was started by adding 1 ml of the accelerator, *N,N,N′,N′*-tetramethylethylenediamine, to the emulsion. The suspension was stirred for 20 min, and the phases were separated by centrifugation. The organic phase was removed, and the microparticles located at the bottom of the water phase were washed several times with buffer and physiological saline. Under the conditions used, the polyacrylamide particles (TC = 8-25) had a mean diameter of 0.2–0.5 μm; the polyacryldextran particles (DTC = 11-1-75 and DTC = 11-2-75) had a mean diameter of 0.5–1.5 μm.

Determination of Particle Size—The size of the particles was determined from photographs taken by scanning electron microscopy, using a previously described method (2). With this method, 85.0% of the polyacryldextran particles with DTC values of 11-2-75 used in this study had a diameter of 0.2–1.2 μm, 1.7% were <0.2 μm, and 4.0% were >2.4 μm. Among the particles having DTC = 11-1-75, 72.8% had a diameter of 0.2–1.2 μm, 8.9% were <0.2 μm, 12.5% had a diameter of 1.2–2.1 μm, and 5.8% were >2.1 μm. More than 300 particles were measured from the photographs in each case.

Distribution and Elimination of Polyacryldextran Particles After Intravenous Injection—Male mice[8], weighing 18–20 g at the beginning of the experiments, were used. The radiolabeled particles were dispersed in physiological saline (0.1–0.2 ml) and then injected intravenously. The doses corresponded to 2.6 mg of lyophilized microparticles DTC = 11-1-75 and DTC = 11-2-75, containing 48,200 and 56,600 dpm, respectively. At different time intervals (6 hr, 1, 2, 4, 8, 12, and 20 or 27 weeks) animals were killed by cervical dislocation, and the liver, spleen, lung, and kidneys were removed and prepared for radioactivity measurements. Tissues (the spleen, both lungs, one kidney, or 0.2–0.3 g of the liver) were dissolved in 2 ml of a tissue solubilizer[9]. After digestion at 37° for 12–14 hr (yielding a clear solution), 2-propanol and hydrogen peroxide were added to bleach the samples and minimize color quenching. A scintillation cocktail was added, and the radioactivity was measured after appropriate equilibration. The counting efficiency, generally ~75–80%, was calculated with an external standard.

Determination of Dextranase Activity—The activity of the dextranase was determined photometrically by the method of Janson and Porath (7). The enzyme in free form (0.1 ml) was added to dextran in 0.1 *M* potassium phosphate buffer (1.9 ml). After incubation for 30 min at 37°, 1 ml of the incubation solution was mixed with 1.0 ml of a color reagent (5 g of 3,5-dinitrosalicylic acid, 1 g of phenol, 0.25 g of sodium sulfite, and 100 g of potassium sodium tartrate in 500 ml of 2% NaOH) and heated in a boiling water bath for 15 min. After dilution with 10 ml of water, the absorbance was measured at 540 nm. A standard curve was prepared with maltose: one unit of activity caused the release of 1.0 μmole of maltose/min under the aforementioned conditions.

Autoradiography—Whole-body autoradiography was performed using the method of Ullberg (8). ^{14}C-Labeled particles were injected intravenously in mice. After 2 months, the animals were killed with ether and frozen in a mixture of solid carbon dioxide and hexane (−78°). The mice were embedded in an aqueous carboxymethylcellulose gel, freeze-dried (−15°), and cut into 20- or 60-μm sagittal sections with a microtome. Autoradiograms were made by apposition of the freeze-dried sections to X-ray films, the time of exposure was 6 months.

Isolation of Lysosomes from Rat Liver Homogenate—The livers from untreated male adult Sprague-Dawley rats were removed immediately after sacrifice and immersed in a beaker containing ice-cold 0.25 *M* sucrose, pH 5.5. After weighing, the tissue was cut into pieces and dispersed in 3 volumes of the medium with a homogenizer[10]. The resulting mixture was centrifuged at 750×*g* and 4° for 10 min. The sediment was rehomogenized three times and centrifuged. The resulting supernatants were pooled and centrifuged at 12,000×*g* for 10 min. The supernatant was discarded, and the pellet was dissolved in 0.25 *M* sucrose and centrifuged for 10 min at 6500×*g*. The sediment was redispersed in approximately the same quantity of medium and centrifuged at 6500×*g*

[8] NMRI-mice, Anticimex, Stockholm, Sweden.
[9] Soluene 350, Packard.
[10] Potter-Elvehjelm, Kebo Grave, Stockholm, Sweden.

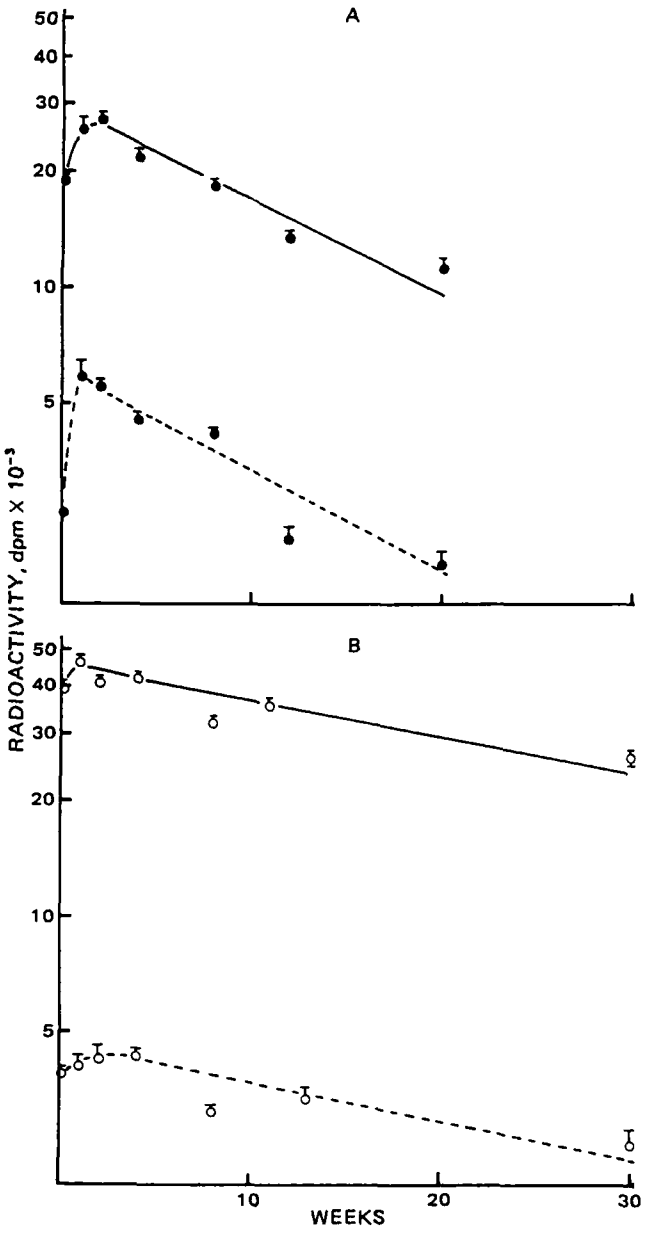

Figure 2—*Radioactivity content of the liver (—) and spleen (- - -) after a single 2.6-mg iv dose of ^{14}C-labeled polyacryldextran particles with composition of DTC = 11-1-75 (●) or DTC = 11-2-75 (○). Each point represents the mean ± SEM for 4–5 animals.*

for 10 min. This procedure was repeated three times. The supernatants from the washings were combined and centrifuged at 12,000×*g* for 15 min. The resulting pellet was redispersed in medium (pH 4.5) to a final volume equal to that of the original tissue. The isolated lysosomal fraction was usually preserved with benzylpenicillin and streptomycin. The described procedure follows that outlined by Beaufay *et al.* (9).

The concentration of lysosomes in the different supernatants and pellets during the preparation was determined by assay of a lysosomal enzyme, β-*N*-acetyl glucosaminidase (10). This enzyme was determined by using 1.5 m*M* 4-methylumbelliferyl-2-acetamido-2-deoxy-β-D-glucopyranoside as substrate in 1 ml of 0.15 *M* acetate–acetic acid buffer, pH 4.2. The sample (0.5 ml) was added, and the mixture was incubated at 37° for 15 min. The reaction was terminated by adding 3 ml of 0.5 *M* Na_2CO_3, pH 10.5, to each tube, and the free 4-methylumbelliferone was estimated by spectrophotometry at 360 nm. Standards containing 4-methylumbelliferone in buffer were included in every assay. The protein contents in the different fractions were estimated according to the method of Lowry *et al.* (11).

Preparation of Liver and Spleen Samples for Microscopic Studies—Tissue samples were cut from the organs immediately after sacrifice and immersed in chilled 5% formaldehyde in 0.15 *M* phosphate buffer, pH 7.2. The specimens were embedded in paraffin in a routine manner, cut at 2–3 μm, stained with hematoxylin and eosin, and examined under a light microscope.

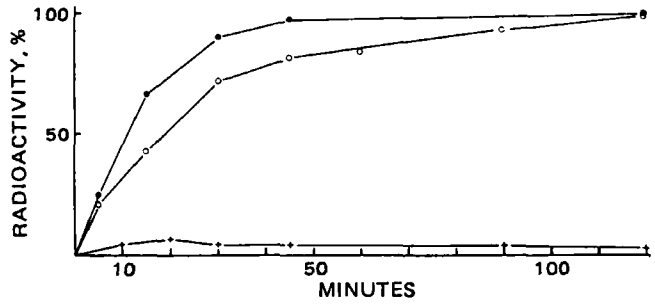

Figure 3—*Degradation of microparticles of polyacryldextran at 23° and pH 6.2 with 0.5 IU of dextranase/ml. Key: (●) DTC = 11-1-75; (○) DTC = 11-2-75; (+) TC = 8-25 (polyacrylamide).*

RESULTS

Distribution and Elimination of ^{14}C-Labeled Polyacryldextran Particles *In Vivo* After Intravenous Injection—On intravenous injection in mice, the microparticles were rapidly cleared from the circulatory system with a $t_{1/2}$ of ~60 min[11]. The distribution of the polyacryldextran particles (DTC = 11-1-75 and DTC = 11-2-75) was followed qualitatively and quantitatively in mice. The autoradiogram (Fig. 1) indicates, as expected, that the particles are phagocytosed by the macrophages belonging to the reticuloendothelial system (RES). The spheres were found in the liver, spleen, and bone marrow. Microparticles with 1% (DTC = 11-1-75) or 2% (DTC = 11-2-75) acrylic groups showed the same distribution pattern, which was also seen with particles containing no derivatized dextran (TC = 8-25) (2).

The quantitative distribution of the particles in the liver, spleen, kidneys, and lung was followed with time (Table I). Initially, some of the largest spheres and/or aggregates were entrapped in the lung capillaries, giving a higher radioactivity in the lungs than earlier noted with polyacrylamide particles (2). This phenomenon is due to the somewhat larger size of the polyacryldextran spheres. However, the aggregates were soon dissociated, and the radioactivity was <1% of the injected dose after 1–2 weeks. The values obtained from the lungs after 2 weeks, therefore, are not included in the table, nor are those from the kidneys which contained only very small amounts of radioactivity after 2 weeks.

The apparent half-life of the different microparticles in the liver and spleen was calculated from the curves in Fig. 2. As is evident, particles made of dextran containing a smaller number of acrylic groups (DTC = 11-1-75) were eliminated more rapidly than those containing more acrylic groups (DTC = 11-2-75). The terminal half-lives, as found by linear regression analysis, were 12.5 and 12 weeks and 33 and 29 weeks, respectively, in the liver and spleen. The figures also indicate that a redistribution took place after the first rapid elimination from the circulatory system, so that the maximal radioactivity was seen after 1–2 weeks in the liver and spleen, independent of the particle composition. About 70–80% of the total injected radioactivity was recovered in these tissues 2 weeks after injection. The uptake of the particles into the liver and spleen resulted in an enlargement of these organs. The weight increase compared with the control regressed after 4–8 weeks.

Ultrastructural Studies—Intravenous injection of a 2.6-mg dose of polyacryldextran particles (DTC = 11-1-75) produced pronounced changes in the liver and spleen. After 1–2 days, the sinusoids were dilated, and vacuolization of the liver parenchymal cells could be seen. The spleen showed an infiltration of inflammatory cells. Weight changes of the liver and spleen paralleled the ultrastructural changes seen microscopically. Formation of small abscesses and granulomas was observed after this period. After 4–8 weeks, the tissues appeared normal except for small granulomas. When a dose of <1 mg was given to the mice, only insignificant morphological changes could be detected in the liver and spleen.

Degradation of Polyacryldextran Particles *In Vitro* with Dextranase—To investigate the stability of the polymer polyacryldextran, ^{14}C-labeled particles of different polymer composition were incubated with dextranase (0.5 IU/ml of particle suspension) for up to 2 hr at 22° and pH 6.2. After centrifugation for 5 min at 4°, the supernatant was withdrawn and the dissolved radioactivity determined (Fig. 3). Micro-

[11] P. Artursson, T. Laakso, and P. Edman, unpublished observation, 1982.

particles of polyacrylamide (TC = 8-25) were not significantly affected. Polyacryldextran particles with composition DTC = 11-1-75 were rapidly hydrolyzed, and all the radioactivity was found in the supernatant after 45 min. Particles with a higher cross-linking degree, DTC = 11-2-75, were more stable, but were dissolved after digestion for 120 min.

Degradation of Different Polyacryldextran Particles *In Vitro* with Isolated Lysosomes from Rat Liver—^{14}C-Labeled particles (dry weight, 0.5 mg) of different gel-composition, (TC = 8-25, DTC = 11-1-75 and 11-2-75) were mixed with 1.0 ml of isolated lysosomes from rat liver homogenate in small plastic tubes. They were incubated at 37° for 1, 3, 6, 24, and 48 hr and then centrifuged for 10 min at 4°. The resulting supernatant was filtered through a filter[12] with 0.45-μm pore size. The radioactivity content in 300 μl of the filtrate was determined in the scintillation counter. Polyacrylamide particles (TC = 8-25) were not significantly affected during 48 hr: only background values were obtained. Polyacryldextran particles with DTC = 11-2-75 composition behaved in the same manner as the polyacrylamide particles. However, polyacryldextran particles with DTC = 11-1-75 were metabolized to some extent, and 0.56 ± 0.003% (mean ± *SD*, n = 4) of the radioactivity in the particles was recovered from the filtrate after incubation for 48 hr.

Excretion of Microparticles in Bile—The biliary excretion of microparticles was studied after a 4-mg iv injection of ^{14}C-labeled polyacrylamide microparticles (containing 400,000 dpm) in mice. The particles had a TC value of 8-25 and a diameter of 0.1–0.4 μm (92.6% of the particles had a diameter within this range, 2.2% were <0.1 μm, and 5.2% had a diameter of 0.4–0.5 μm). The particles were dispersed in physiological saline prior to injection to avoid aggregation. At different time intervals (3, 9, and 27 weeks), animals were killed, and the gallbladder with remaining bile was taken out and digested in 1 ml of 0.5 *M* quaternary ammonium hydroxide. Irrespective of the time elapsed after the injection of particles, the bile contained radioactivity (38, 91, and 34 dpm after 3, 9, and 27 weeks, respectively) after subtraction of background values obtained from untreated mice. The counting times used were long enough to minimize the statistical error to 2–3% for samples and blanks.

DISCUSSION

The most obvious conclusion which can be drawn from the results presented herein is the similarity of the disposition of polyacryldextran and polyacrylamide particles in mice. The half-life of the microparticles in the circulatory system and the general distribution of the microparticles in the mice are similar. They are predominantly taken up by the reticuloendothelial system (*i.e.*, liver, spleen, and bone marrow) as shown by autoradiography and quantitative meaurements in the tissues. Moreover, the morphological changes detected microscopically after intravenous administration of large doses (>50–100 mg dry weight/kg body weight) are similar (3) and parallel the weight changes observed. It is obvious that incorporation of cross-linked dextran in the microparticles does not change the distribution *in vivo*, and it is highly likely that the observations are representative for any uncharged particulates of the same size (*i.e.*, 0.2–1.0 μm in diameter) injected intravenously or intraperitoneally.

Similar effects—morphological changes in the liver—have also been detected with liposomes. A study with mice (12) on the effects of negatively charged liposomes given intravenously revealed that liposomes caused an enlargement of the Kupffer cells with vacuolization observed 7 hr postinjection.

The polyacryldextran particles exhibited a somewhat larger initial uptake in the lungs than seen with polyacrylamide particles. The uptake was reversible, and was detected only in the sample taken 6 hr after the injection. After a week, insignificant amounts of the radioactively labeled microparticles remained. This phenomenon may be due to the larger size of the polyacryldextran particles, with ~15% exceeding 1.2 μm in diameter; the polyacrylamide particles had diameters between 0.2 and 0.5 μm. The reason for the difference in size between the two different particle preparations is that the higher viscosity of the dextran aqueous solution makes it more difficult to prepare small polyacryldextran particles (<0.5 μm). It is important to stress that only small-sized particles should be used *in vivo* to avoid respiratory distress. This point was clearly illustrated in studies with dogs (13, 14), in which polystyrene particles (mean diameter 3 μm) injected intravenously resulted in death for three of four dogs, probably due to lung emboli.

The most significant advantages of the polyacryldextran particles over the polyacrylamide particles is the faster metabolism. Both the experiments *in vitro* with lysosomal enzymes or dextranase and those performed in the mice clearly showed that the degradation and elimination is related to the hydrocarbon content of the microparticles. The lysosomal preparations were able to release >0.5% of the radioactivity within the first 48 hr from particles containing 1% acryl groups. As expected, these particles were also degraded much faster with dextranase than those containing 2% acryl groups. The terminal half-lives *in vivo* in the liver and spleen were also significantly shorter for the polyacryldextran particles with 1% acryl groups (~12 weeks) than for the other particles. The results suggest that it is possible to control elimination by changing the composition of the microparticles, which is of great value when the particles are used as enzyme carriers. In such cases, the composition of the carrier should be chosen such that the degradation of the particles agrees with the denaturating rate of the enzyme. It is, however, also obvious that the size of the particles is a decisive factor for the rate of elimination, and it should be remembered that the polyacryldextran particles used in this study were larger than the polyacrylamide particles used previously (2).

An earlier report from this laboratory indicated that microparticles after intravenous injection were identified in two layers of the gut lumen, the microvilli region and the basal membrane, as judged by the whole-body autoradiograms (2). The reason for such a specific localization was unclear, but long-term studies have now shown that small but significant amounts of radioactivity—originating from the polyacrylamide particles—were found in the gallbladder. Thus the radioactivity in or at the microvilli may be radioactive metabolites excreted from the liver.

[12] Millipore Corp.

REFERENCES

(1) B. Ekman, C. Lofter, and I. Sjöholm, *Biochemistry*, **15**, 5115 (1975).

(2) I. Sjöholm and P. Edman, *J. Pharmacol. Exp. Ther.*, **211**, 656 (1979).

(3) P. Edman, I. Sjöholm, and U. Brunk, *J. Pharm. Sci.*, **72**, 658 (1983).

(4) P. Edman, B. Ekman, and I. Sjöholm, *ibid.*, **69**, 838 (1980).

(5) P. Edman and I. Sjöholm, *Life Sci.*, **30**, 327 (1982).

(6) S. Hjertén, *Arch. Biochem. Biophys., Suppl.*, **1**, 147 (1962).

(7) J.-C. Janson and J. Porath, *Methods Enzymol.*, **VIII**, 615 (1966).

(8) S. Ullberg, *Acta Radiol. (Suppl)*, **118**, 1 (1954).

(9) H. Beaufay, D. S. Bendall, P. Baudhuin, R. Wattiaux, and C. de Duve, *Biochem. J.*, **73**, 628 (1959).

(10) "Lysosomes: A Laboratory Handbook," 2nd ed., I. T. Dingle, Ed., Elsevier/North-Holland Biomedical Press, 1977, p. 118.

(11) O. Lowry, N. Rosebrough, L. Farr, and R. Randall, *J. Biol. Chem.*, **193**, 265 (1951).

(12) T. de Barsy, P. Devos, and F. Van Hoof, *Lab. Invest.*, **34**, 273 (1976).

(13) H. G. Schroeder, G. H. Simmons, and P. P. DeLuca, *J. Pharm. Sci.*, **67**, 504 (1978).

(14) H. G. Schroeder, B. A. Bivins, G. P. Sherman, and P. P. DeLuca, *J. Pharm. Sci.*, **67**, 508 (1978).

ACKNOWLEDGMENTS

Supported by the Swedish Board for Technical Development and the I.F. Foundation for Pharmaceutical Research.

The authors thank Miss Siv Larsson for technical assistance.

Transition-State Alkylation Geometries of 7,8-Dihydroxy-9,10-epoxy-7,8,9,10-tetrahydrobenzo[*a*]pyrene Enantiomeric Isomers with Nucleic Acid Dimers

O. KIKUCHI *§, R. PEARLSTEIN *, A. J. HOPFINGER *¶x, and D. R. BICKERS ‡

Received June 18, 1981, from the **Department of Macromolecular Science, Case Institute of Technology* and the ‡*Department of Dermatology, School of Medicine, Case Western Reserve University, Cleveland, OH 44106.* Accepted for publication June 25, 1982. §Permanent address: Department of Chemistry, The University of Tsukuba, Sakura-mura, Ibaraki, 305 Japan. ¶Alternate address: Department of Drug Design, G. D. Searle and Co., Chicago, IL 60080.

Abstract □ The steric contact spaces associated with the reaction of the enantiomeric isomers of 7,8-dihydroxy-9,10-epoxy-7,8,9,10-tetrahydrobenzo[*a*]pyrene (I) with the exocyclic amino group of guanine of dinucleoside dimer structures were examined for a fixed transition-state geometry. This reaction is sterically prohibited for the B form DNA conformation. If, however, the nucleic acid structure is deformed, such that the distance between two adjacent base pairs (one containing guanine and cytosine) is maximized, sterically allowed transition-state geometries can be identified. It was not possible to uniquely identify the preferred transition-state complex with respect to nucleic acid structure or isomer of I. However, two types of general transition-state geometries were observed. In one, I was located "outside" the nucleic acid structure; in the other geometry, I was intercalated between adjacent base pairs in the transition state. The intercalation process might serve as a physical catalyst for the alkylation of NH_2-guanine by I.

Keyphrases □ 7,8-Dihydroxy-9,10-epoxy-7,8,9,10-tetrahydrobenzene[*a*]pyrene—enantiomeric isomers, alkylation of dinucleoside dimers, transition-state geometry □ Dinucleoside dimers—alkylation by enantiomeric isomers of 7,8-dihydroxy-9,10-epoxy-7,8,9,10-tetrahydrobenzo[*a*]pyrene, transition-state geometry □ Transition-state geometry—of the alkylation of dinucleoside dimers by enantiomeric isomers of 7,8-dihydroxy-9,10-epoxy-7,8,9,10-tetrahydrobenzo[*a*]pyrene, intercalation

The chemical carcinogen benzo[*a*]pyrene (II) is metabolized to a diol-epoxide derivative (I) which is enzymatically formed in two stereoisomeric forms: 7β,8α-dihydroxy-9α,10α-epoxy-7,8,9,10-tetrahydrobenzo[*a*]-pyrene [III, designated *anti* or *trans*(eq,eq′)] and 7β,8α-dihydroxy-9β,10β-epoxy-7,8,9,10-tetrahydrobenzo[*a*]pyrene [IV, designated *syn* or *cis*(ax,ax′)] (1–6). Each has a complement, *trans*(ax,ax′) and *cis*(eq,eq′), respectively, and each of these four isomers can exist as a (+) or (−) enantiomer. The eight possible enantiomeric isomers are shown in Fig. 1, described in terms of our previous nomenclature (7).

Evidence to support the concept that activated metabolites of II are important for carcinogenesis has been presented (8–10). These studies have shown that NADPH-dependent mixed-function oxidases in liver microsomes produce reactive intermediates (epoxides) which can bind covalently to nucleic acids and proteins. Further studies have shown that epoxides are cleaved by a second microsomal enzyme, epoxide hydratase, to form dihydrodiols (11). The dihydrodiols are substrates for aryl hydrocarbon hydroxylase, which then generates diol-epoxides. It is the diol-epoxides of selected polycyclic aromatic hydrocarbon carcinogens that are thought to be the ultimate carcinogenic metabolites, binding to macromolecules to initiate tumor formation. Specific diol-epoxides of II such

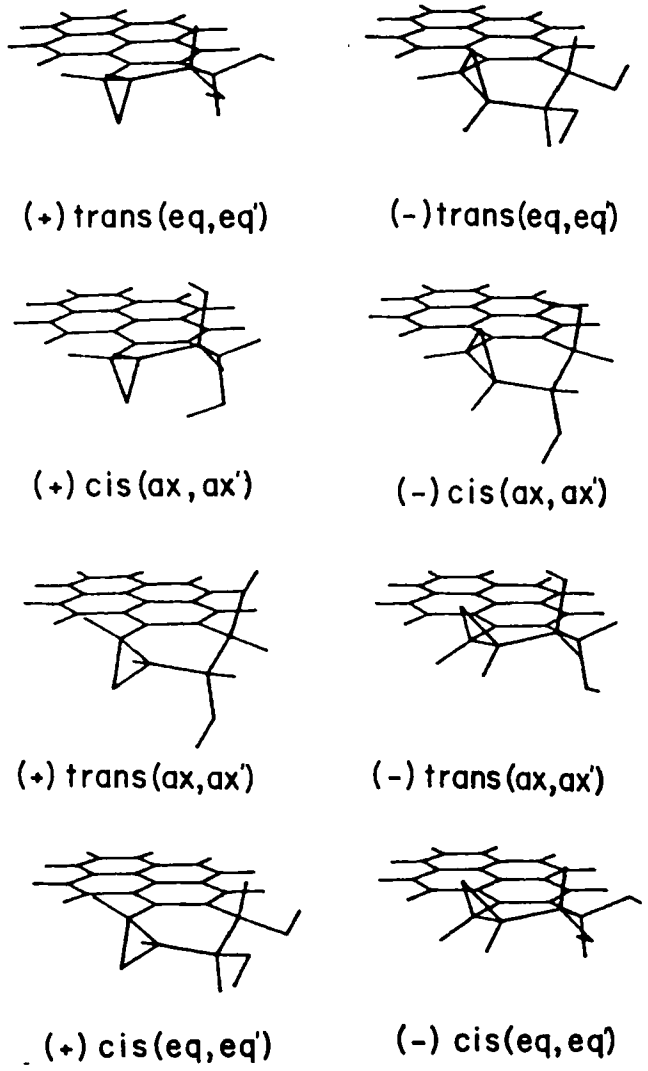

Figure 1—*Computer-drawn representations of the structure-optimized geometries of the eight enantiomeric isomers of I.*

as (+)-7β,8α-dihydroxy-9α,10α-epoxy-7,8,9,10-tetrahydrobenzo[*a*]pyrene have been shown to be potent inducers of neoplasia in mouse skin (12, 13). This pattern of metabolic reaction has been shown to occur in the skin and in cultured keratinocytes (14).

There is also considerable evidence that III residues bind covalently to both RNA (6) and DNA (15) predominantly at the 2-amino group of guanine. Cytosine and adenosine residues in nucleic acids are also alkylation targets to a

0022-3549/83/0700-0800$01.00/0

Table I—Optimized Molecular Parameters of the Four Isomers of I

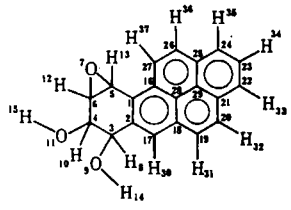

Bond	Isomer *cis* (ax,ax')	*trans* (eq,eq')	*trans* (ax,ax')	*cis* (eq,eq')
	Bond Distance, Å			
C(1)—C(2)	1.412	1.412	1.411	1.412
C(2)—C(3)	1.477	1.471	1.472	1.470
C(3)—C(4)	1.487	1.485	1.485	1.484
C(1)—C(5)	1.457	1.456	1.459	1.457
C(5)—C(6)	1.453	1.452	1.452	1.451
C(6)—O(7)	1.406	1.405	1.406	1.405
C(3)—O(9)	1.394	1.386	1.389	1.386
C(4)—O(11)	1.387	1.387	1.385	1.387
C(3)—H(8)	1.131	1.136	1.132	1.137
C(4)—H(10)	1.134	1.133	1.132	1.132
C(6)—H(12)	1.122	1.122	1.122	1.123
C(5)—H(13)	1.121	1.121	1.123	1.123
O(9)—H(14)	1.043	1.034	1.033	1.034
O(11)—H(15)	1.033	1.033	1.032	1.033
C(1)—C(16)				
	Bond Angle, °			
C(1)—C(2)—C(3)	120.2	120.3	120.7	120.6
C(2)—C(3)—C(4)	115.8	116.3	116.0	116.5
C(2)—C(1)—C(5)	118.1	119.1	118.4	118.8
C(1)—C(5)—C(6)	118.7	118.0	119.2	118.8
C(5)—C(6)—97	59.0	59.0	58.9	59.0
C(2)—C(3)—H(8)	111.3	105.3	110.4	104.5
C(2)—C(3)—O(9)	106.1	114.6	108.6	114.9
C(3)—C(4)—H(10)	108.5	108.6	108.9	109.1
C(3)—C(4)—O(11)	109.6	107.4	107.6	107.1
C(5)—C(6)—H(12)	119.0	118.9	119.2	119.1
C(6)—C(5)—H(13)	116.4	117.1	118.2	118.4
C(3)—O(9)—H(14)	102.8	107.9	107.2	108.0
C(4)—O(11)—H(15)	107.6	107.6	107.4	107.8
C(2)—C(1)—C(16)				
	Dihedral Angle, °			
C(1)—C(2)—C(3)—C(4)	−31.7	−29.0	28.7	28.2
C(2)—C(1)—C(5)—C(6)	18.0	17.5	−13.0	−13.7
C(1)—C(5)—C(6)—O(7)	−106.2	−108.1	−108.7	−109.7
C(1)—C(2)—C(3)—H(8)	−159.1	88.9	153.0	−89.6
C(1)—C(2)—C(3)—O(9)	86.0	−154.2	−90.5	153.7
C(2)—C(3)—C(4)—H(10)	163.1	−80.8	−162.6	80.8
C(2)—C(3)—C(4)—O(11)	−79.4	162.6	81.5	−163.2
O(7)—C(5)—C(6)—H(12)	−100.6	−100.0	−99.0	−98.5
O(7)—C(6)—C(5)—H(13)	99.1	99.3	99.4	99.0
C(4)—C(3)—O(9)—H(14)	57.5	179.4	180.1	180.4
C(3)—C(4)—O(11)—H(15)	180.3	179.4	180.7	181.0

smaller extent, both *in vitro* (15–17) and *in vivo* (15, 18). The three bases contain an exocyclic amino group which presumably is the common alkylation site. This is relatively unusual since alkylation usually occurs at the N(7) position of guanine (19).

It has been reported (20) that 60–80% of the total adduct formed by (±)III with DNA involves the (+) enantiomer with the 2-amino group of *d*-guanine residues. A minor adduct is formed from the reaction of the (−) enantiomer with DNA. This minor adduct is present in greater amounts in denatured DNA than in native DNA. Small amounts of III–*d*-adenosine and III–*d*-cytosine adducts are also detected for both single- and double-stranded DNA. No differences in the total extent of (±)III binding to double- and single-stranded calf thymus DNA have been detected. It is thus of interest to identify I–DNA

Table II—Relative Energy and Net-Charge Distribution of the Four Isomers of I [a]

Atom	Isomer *cis*(ax,ax')	*trans*(eq,eq')	*trans*(ax,ax')	*cis*(eq,eq')
	Relative Energy, kcal/mole			
	0.00	1.20	4.48	4.64
	Net-Charge, AMU			
C(1)	−0.011	−0.010	−0.007	−0.024
C(2)	0.006	0.001	0.004	0.003
C(3)	0.155	0.165	0.161	0.164
C(4)	0.143	0.155	0.153	0.149
C(5)	0.129	0.125	0.129	0.123
C(6)	0.104	0.098	0.095	−0.093
O(7)	−0.229	−0.221	−0.218	−0.219
H(8)	−0.023	−0.022	−0.038	−0.033
O(9)	−0.274	−0.253	−0.250	−0.250
H(10)	−0.031	−0.035	−0.033	−0.021
O(11)	−0.249	−0.239	−0.244	−0.242
H(12)	−0.015	−0.016	−0.017	−0.012
H(13)	−0.014	−0.015	−0.020	−0.019
H(14)	0.162	0.126	0.125	0.126
H(15)	0.124	0.122	0.131	0.124
C(16)	0.034	0.033	0.038	0.033
C(17)	−0.018	−0.021	−0.022	−0.020
C(18)	0.031	0.032	0.033	0.040
C(19)	−0.009	−0.010	−0.011	−0.011
C(20)	−0.008	−0.007	−0.006	−0.003
C(21)	0.033	0.032	0.032	0.031
C(22)	−0.011	−0.011	−0.011	−0.006
C(23)	0.005	0.005	0.004	0.005
C(24)	−0.011	−0.011	−0.011	−0.006
C(25)	0.032	0.032	0.032	0.031
C(26)	−0.006	−0.006	−0.006	0.002
C(27)	−0.013	−0.013	−0.011	−0.018
C(28)	0.011	0.009	0.011	0.003
C(29)	0.013	0.014	0.015	0.012
H(30)	−0.005	−0.009	−0.008	−0.009
H(31)	−0.007	−0.008	−0.008	−0.008
H(32)	−0.008	−0.007	−0.008	−0.007
H(33)	−0.007	−0.007	−0.007	−0.007
H(34)	−0.009	−0.008	−0.008	−0.009
H(35)	−0.008	−0.007	−0.007	−0.007
H(36)	−0.008	−0.007	−0.007	−0.007
H(37)	−0.008	−0.006	−0.004	−0.003

[a] Using the numbering scheme presented in Table I.

stereochemical reaction models that are consistent with these experimental observations. Such theoretical models are essential for working hypotheses to explain the chemical reactivity of these carcinogenic species and, perhaps, their relative tumor induction potencies.

EXPERIMENTAL

The electronic structure of four isomers of I have been investigated and previously reported (7). In this study several approximations were employed for the estimation of the molecular structures of isomers of I. The substructure of the epoxy group was assumed to be the same as that of ethylene oxide. The local conformation of the two hydroxyl groups was fixed at that of ethylene glycol. Moreover, the "L" version (21) of the

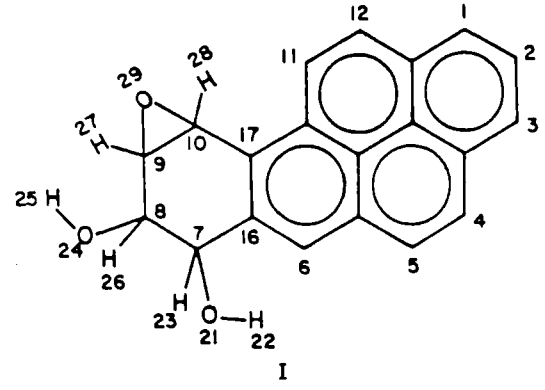

I

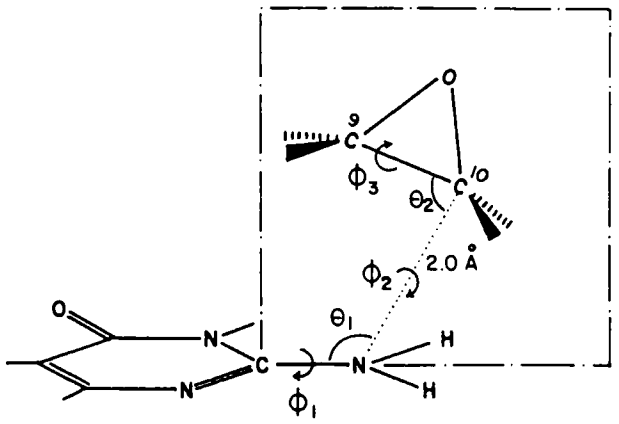

Figure 2—*Transition-state geometry used to perform the steric reaction calculations. In the specific I–NH_3 transition-state geometry (7) used as the starting point in these calculations, $\phi_1 = 100°$, $\theta_1 = 110°$, $\phi_2 = 90°$, $\theta_2 = 80°$, and $\phi_3 = 0$ or $180°$.*

semiempirical CNDO/2 method was employed in which only π-electrons were explicitly taken into account for the conjugated subsystem.

In the present study, the conjugated part of the molecule was fixed at the idealized structure (C—C = 1.40 Å, C—H = 1.10 Å, angles = 120°). All other structural parameters were optimized using the CNDO/2 method. The optimized molecular parameters for each isomer are reported in Table I. Computer-drawn representations of the structure-optimized geometries of the eight enantiomeric isomers are shown in Fig. 1. The charge distributions and total energies for the structure-optimized molecules are reported in Table II. As found in the previous study (7), the *trans*(eq,eq′) isomer (III) is more stable than the *trans*(ax,ax′) isomer, and the *cis*(ax,ax′) isomer (IV) is more stable than the *cis*(eq,eq′) isomer. The angle between the epoxy group and the conjugated hydrocarbon ring system is larger in the more stable *trans* and *cis* isomers than in the corresponding less stable isomers. The longer C(3)—O(9) and O(9)—H(14) bond lengths (Table I) for IV are due to hydrogen bonding between the hydroxyl group and the epoxy oxygen. These results are consistent with those obtained in our previous study (7), although small differences in valence geometry exist.

In the previous study (7), the reactivity of the four isomers of I with the simple nucleophile ammonia was modeled. Isomer IV was found to be the most reactive. These calculations allowed the identification of a unique transition-state geometry for alkylation. The transition state of I with ammonia corresponds to $\phi_1 = 100°$, $\theta_1 = 110°$, $\phi_2 = 90°$, $\theta_2 = 80°$, $\phi_3 = 0$ or $180°$, and $r = 2.0$ Å (Fig. 2).

Table III—Least Number of Bad-Contacts at Three Nucleophilic Sites in Four Base-Pair Sequences Using (+)III

Site	Base-Pair Sequence			
	C—G / G—C / C—G	G—C / G—C / G—C	T—A / G—C / T—A	A—T / G—C / A—T
N(7)	8	9	10	11
O(6)	9	10	8	14
2-NH_2	34	38	31	37

The calculations involving I and ammonia indicated that III and IV are both more stable, and also more reactive with the nucleophile, than the respective isomer complements, *trans*(ax,ax′) and *cis*(eq,eq′). This may explain why III is observed to be the major metabolic isomer relative to *trans*(ax,ax′). Unfortunately, corresponding experimental studies of isomers of I with ammonia are not reported in the literature. The current studies have focused on (±)III and (±)IV, since biochemical observations have clearly indicated their particular importance.

The large size of I would be expected to impose steric constraints regarding its capacity to alkylate DNA. These steric constraints may limit the ways in which a transition-state geometry may be realized between an enantiomeric isomer of I and the exocyclic amino group of guanine in DNA. Therefore, it is necessary to examine intermolecular reaction geometries for the I–DNA complex. To do this it was assumed that the transition-state geometry for I–NH_2-guanine is the same as that found for the complex of I and ammonia (7). The "bad-contacts" between pairs of atoms from I and DNA were sought for the transition-state geometry shown in Fig. 2.

A bad-contact is assigned to an atom pair if the distance is shorter than a critical distance. If a specific conformation has one or more bad-contacts, it is assumed to have a high energy and cannot be realized. The critical distance, r_c, was selected to be the van der Waals distance for all interactions involving atoms of the aromatic rings of I. Smaller values than the corresponding van der Waals distances were chosen for interactions involving epoxide, diol, and saturated ring atoms (including hy-

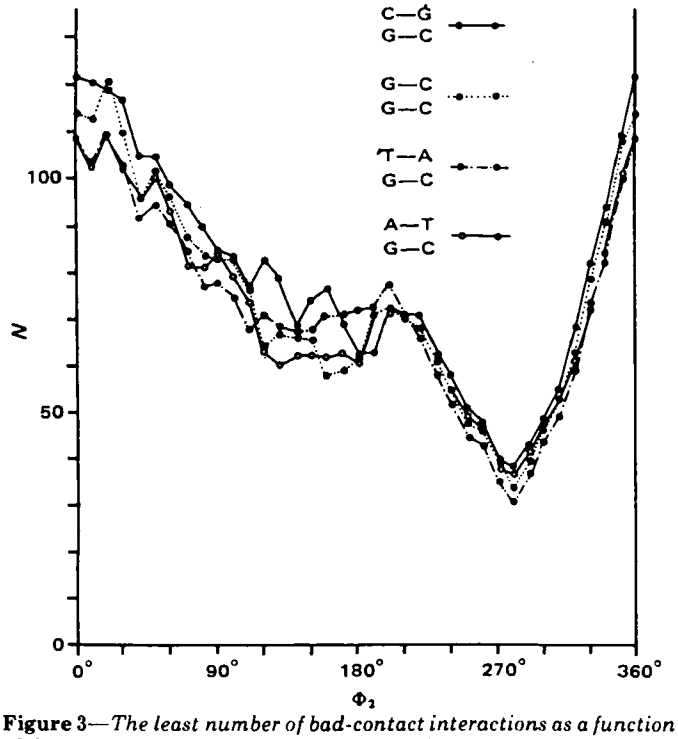

Figure 3—*The least number of bad-contact interactions as a function of the transition-state geometry variable ϕ_2 for (+)III interacting with four sequences of B form DNA.*

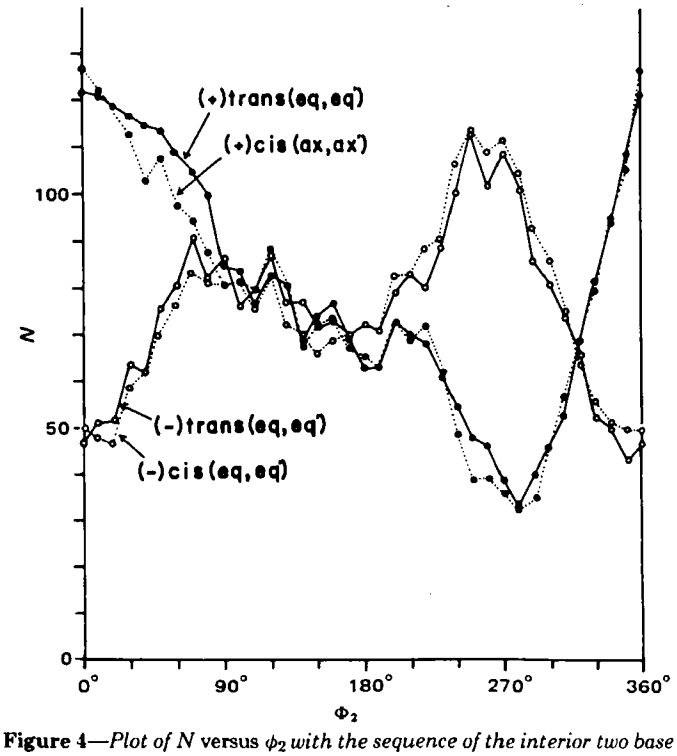

Figure 4—*Plot of N versus ϕ_2 with the sequence of the interior two base pairs of the B form structure fixed at* $\left|\begin{matrix}C-G\\G-C\end{matrix}\right|\uparrow$.

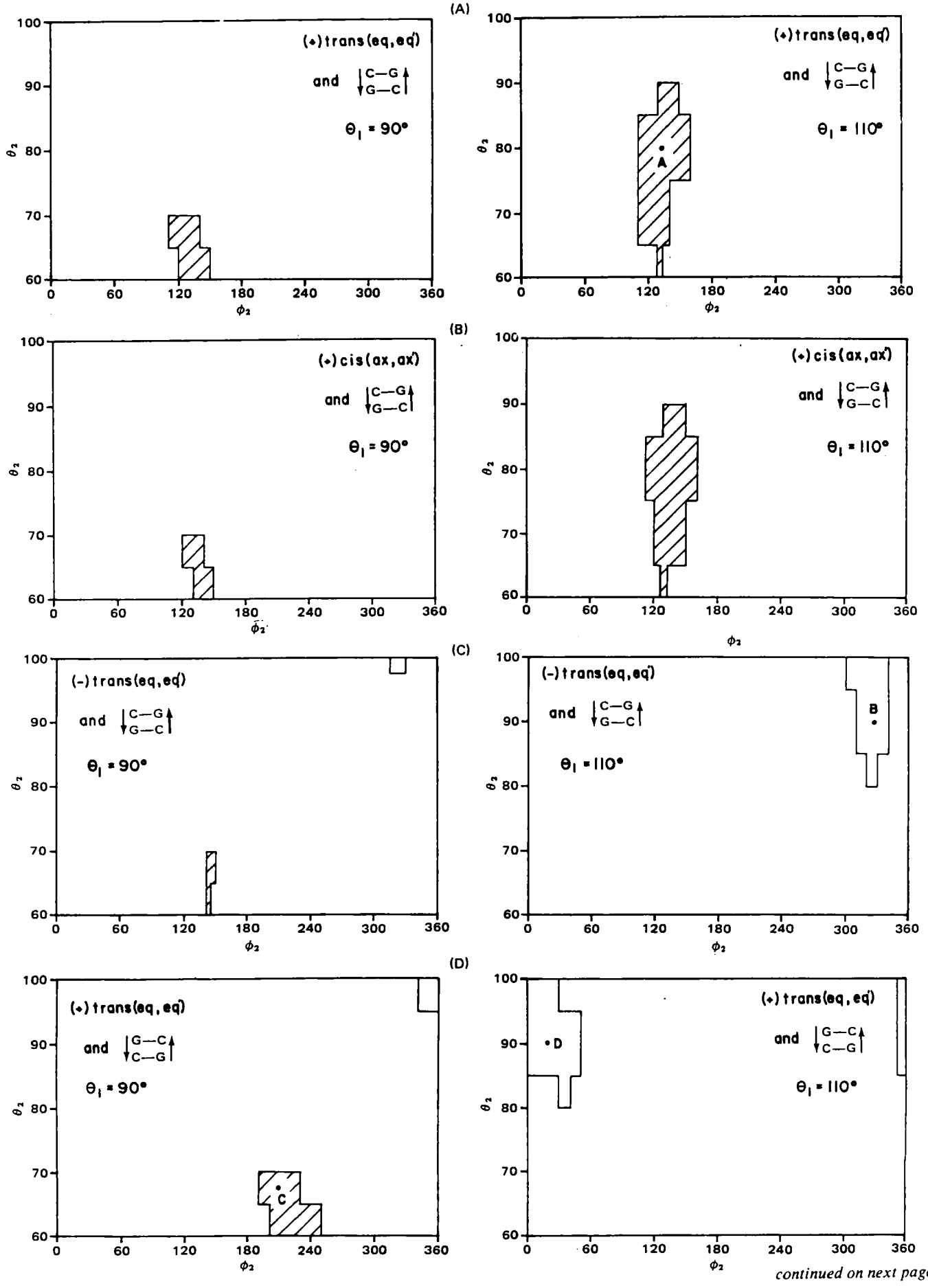

continued on next page

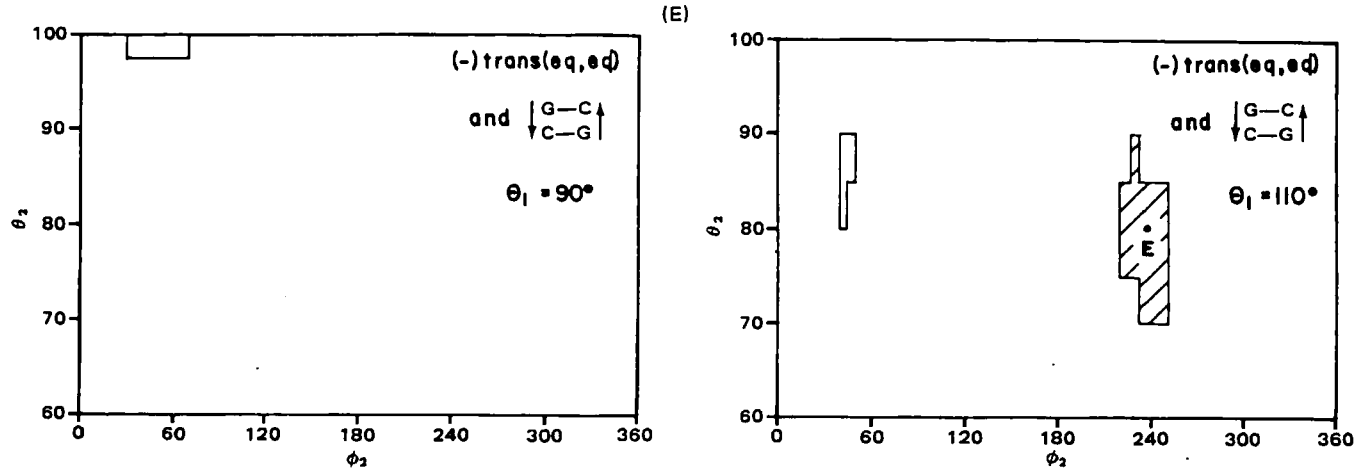

Figure 5—*Steric contact plots of θ_2 versus ϕ_2 for different sequences of unwound dinucleoside dimer, (±)III, (±)IV, and two different values of θ_1. The shaded regions correspond to allowed intercalation transition-state geometries. The open regions identify transition-state geometries in which I is outside the dinucleoside dimer. The letters A through E on the steric contact maps define the (ϕ_2,θ_2) values used to construct the stereo model figures in Fig. 7. The criteria for constructing the steric boundaries are given in* Experimental.

Table IV—Atomic Coordinates of the Deformed DNA Structure and Intercalated (+)III

DNA

C	1	3	-2.6680	8.7040	-3.3510	0.2400	2	3	4	25	0
H	2	1	-1.8640	9.4160	-3.5410	0.0520	1	0	0	0	0
H	3	1	-3.5880	9.2500	-3.5570	0.0520	1	0	0	0	0
C	4	3	-2.6420	7.4200	-4.1770	-0.0410	1	5	6	7	0
H	5	1	-2.2500	7.5600	-5.1830	0.0420	4	0	0	0	0
H	6	1	-3.6440	7.0040	-4.2870	0.0420	4	0	0	0	0
C	7	3	-1.6600	6.5480	-3.3770	0.1140	4	8	9	24	0
H	8	1	-0.6840	6.6760	-3.8010	0.0540	7	0	0	0	0
N	9	4	-2.0400	5.1020	-3.3770	-0.1030	7	10	22	0	0
C	10	2	-1.0453	4.1577	-3.3790	0.2210	11	20	9	0	0
N	11	4	0.2858	4.4269	-3.3790	-0.3730	12	10	0	0	0
C	12	2	1.0219	3.3203	-3.3790	0.4000	16	13	11	0	0
N	13	4	2.3602	3.3928	-3.3790	-0.2540	12	14	15	0	0
*H	14	1	2.8498	4.3550	-3.3790	0.1230	13	0	0	0	0
*H	15	1	2.9484	2.4882	-3.3790	0.1390	13	0	0	0	0
N	16	4	0.4840	2.0518	-3.3790	-0.2100	18	17	12	0	0
*H	17	1	1.1349	1.1911	-3.3790	0.1230	16	0	0	0	0
C	18	2	-0.8636	1.7512	-3.3790	0.3550	16	19	20	0	0
O	19	7	-1.2530	0.5766	-3.3790	-0.3790	18	0	0	0	0
C	20	2	-1.6724	2.9297	-3.3790	-0.0950	18	10	21	0	0
N	21	4	-3.0518	3.0870	-3.3790	-0.1720	20	22	0	0	0
C	22	2	-3.2188	4.3838	-3.3790	0.1190	21	23	9	0	0
H	23	1	-4.1651	4.9016	-3.3790	-0.0230	22	0	0	0	0
O	24	6	-1.6740	6.9380	-1.9130	-0.2710	7	25	0	0	0
C	25	3	-2.5420	6.1860	-1.9190	0.0940	1	24	26	27	0
H	26	1	-2.0420	8.9340	-1.3010	0.0510	25	0	0	0	0
C	27	3	-3.8400	7.7960	-1.2430	0.2090	25	28	29	30	0
H	28	1	-4.6720	8.2660	-1.7470	0.0530	27	0	0	0	0
H	29	1	-3.7720	8.2360	-0.2490	0.0530	27	0	0	0	0
O	30	6	-4.0580	6.3800	-1.3730	-0.3500	27	31	0	0	0
P	31	10	-5.1480	5.6720	-0.4410	0.1640	30	32	34	35	0
O	32	7	-6.2780	6.4620	-0.3630	-0.5220	31	33	0	0	0
ZH	33	20	-6.3360	7.4140	-0.8910	0.0000	32	0	0	0	0
O	34	7	-5.3520	4.3240	-0.8770	-0.5220	31	0	0	0	0
O	35	6	-4.4020	5.6720	0.9730	-0.3500	31	36	0	0	0
C	36	3	-4.0900	4.4300	1.5890	0.2400	35	37	38	59	0
H	37	1	-4.3440	3.6160	0.9130	0.0520	36	0	0	0	0
C	38	3	-2.6200	4.4280	2.0070	-0.0410	36	39	40	41	0
H	39	1	-2.1680	5.4160	2.0670	0.0420	38	0	0	0	0
H	40	1	-2.0360	3.8560	1.2870	0.0420	38	0	0	0	0
C	41	3	-2.6840	3.7700	3.3810	0.1140	38	42	58	43	0
H	42	1	-2.0680	4.3320	4.0810	0.0540	41	0	0	0	0
N	43	4	-2.2700	2.3380	3.3770	-0.1750	41	44	53	0	0
C	44	2	-0.9623	1.8769	3.3770	0.4220	43	45	46	0	0
O	45	7	-0.0403	2.7059	3.3770	-0.4190	44	0	0	0	0
N	46	4	-0.7378	0.5375	3.3770	-0.3440	44	47	0	0	0
C	47	2	-1.7635	-0.3234	3.3770	0.3240	46	48	51	0	0
N	48	4	-1.4960	-1.6148	3.3770	-0.2220	47	49	50	0	0
*H	49	1	-2.3038	-2.3320	3.3770	0.1170	48	0	0	0	0
*H	50	1	-0.4699	-1.9539	3.3770	0.1300	48	0	0	0	0

continued

Table IV—*continued*

DNA

C	51	2	-3.1186	0.1269	3.3770	-0.1630	47	52	53	0	0
CH	52	1	-3.9645	-0.5454	3.3770	0.0200	51	0	0	0	0
CCH	53	2	-3.3193	1.4717	3.3770	0.1900	51	54	43	0	0
CCH	54	1	-4.3310	1.8492	3.3770	-0.0030	53	55	56	57	0
CCC	55	20	1.5576	-1.6042	3.3770	0.0000	54	0	0	0	0
CCC	56	20	1.5576	-1.6042	3.3770	0.0000	54	0	0	0	0
CCC	57	20	1.5576	-1.6042	3.3770	0.0000	54	0	0	0	0
CCCH	58	6	-4.1140	3.6860	3.8230	-0.2710	41	59	0	0	0
CCCH	59	3	-4.7740	4.2800	2.9470	0.0940	58	36	60	61	0
CCHH	60	1	-4.8460	5.2560	3.4290	0.0510	59	0	0	0	0
CCHH	61	1	-5.7740	3.8680	2.8090	0.0510	59	62	0	0	0
CCCC	62	20	0.0000	0.0000	-3.3770	0.0000	61	63	0	0	0
CCCC	63	20	0.0000	0.0000	-3.3770	0.0000	62	64	0	0	0
CCCH	64	3	9.7260	-0.6300	3.3570	0.2400	63	65	66	67	88
CCHH	65	1	10.1880	0.3380	3.5470	0.0520	64	0	0	0	0
CCHH	66	1	10.5060	-1.3640	3.5630	0.0520	64	0	0	0	0
CCCH	67	3	8.4860	-0.9600	4.1830	-0.0410	64	68	69	70	0
CCHH	68	1	8.5180	-0.5420	5.1870	0.0420	67	0	0	0	0
CCHH	69	1	8.3660	-2.0380	4.2930	0.0420	67	0	0	0	0
CCCH	70	3	7.3800	-0.2780	3.3830	0.1140	67	71	87	72	0
CCCH	71	1	7.2240	0.7140	3.8070	0.0540	70	0	0	0	0
CCCN	72	4	6.0900	-1.0240	3.3830	-0.1030	70	73	85	0	0
CCCN	73	2	4.9562	-0.2523	3.3850	0.2210	74	83	72	0	0
CCCN	74	4	4.9369	1.1056	3.3850	-0.3730	75	73	0	0	0
CCCN	75	2	3.6993	1.5902	3.3850	0.4000	79	76	74	0	0
CCCN	76	4	3.4861	2.9134	3.3850	-0.2540	75	77	78	0	0
*CHH	77	1	4.3226	3.5960	3.3850	0.1230	76	0	0	0	0
*CHH	78	1	2.4774	3.2963	3.3850	0.1390	76	0	0	0	0
*CHN	79	4	2.5737	0.7954	3.3850	-0.2100	81	80	75	0	0
*CHC	80	1	1.5946	1.2489	3.3850	0.1230	79	0	0	0	0
CCCC	81	2	2.5702	-0.6049	3.3850	0.3550	79	82	83	0	0
CCCC	82	7	1.5007	-1.2151	3.3850	-0.3790	81	0	0	0	0
CCCN	83	2	3.8892	-1.1257	3.3850	-0.0950	81	73	84	0	0
CCCN	84	4	4.3356	-2.4403	3.3850	-0.1720	83	85	0	0	0
CCCH	85	2	5.6383	-2.3284	3.3850	0.1190	84	86	72	0	0
CCCH	86	1	6.3450	-3.1432	3.3850	-0.0230	85	0	0	0	0
CCCC	87	6	7.7560	-0.1600	1.9210	-0.2710	88	70	0	0	0
CCCH	88	3	9.1940	-0.6500	1.9270	0.0940	89	64	87	90	0
CCCH	89	1	9.7740	0.0360	1.3130	0.0510	88	0	0	0	0
CCCH	90	3	9.1600	-2.0060	1.2510	0.2090	88	91	92	93	0
CCCH	91	1	9.8800	-2.6700	1.7550	0.0530	90	0	0	0	0
CCCH	92	1	9.5960	-1.8200	0.2570	0.0530	90	0	0	0	0
CCCC	93	6	7.8800	-2.6080	1.3790	-0.3500	90	94	0	0	0
CCCC	94	10	7.5020	-3.8500	0.4470	0.1640	93	95	97	98	0
CCCC	95	7	8.5720	-4.7160	0.3690	-0.5520	94	96	0	0	0
ZHCCC	96	20	9.5020	-4.5060	0.8970	0.0000	95	0	0	0	0
CCCCC	97	7	6.2640	-4.4180	0.8830	-0.5520	94	0	0	0	0
CCCCC	98	6	7.2980	-3.1320	-0.9670	-0.3500	94	99	0	0	0
CCCCC	99	3	6.0200	-3.1780	-1.5830	0.2400	98	100	101	122	0
CCCCH	100	1	5.3060	-3.6460	-0.9070	0.0520	99	0	0	0	0
CCCCH	101	3	5.6120	-1.7680	-2.0030	-0.0410	99	102	103	104	0
CCCCH	102	1	6.4380	-1.0580	-2.0630	0.0420	101	0	0	0	0
CCCCH	103	1	4.9000	-1.3660	-1.2650	0.0420	101	0	0	0	0
CCCCH	104	3	5.0000	-2.0100	-3.3750	0.1140	105	106	101	121	0
CCCCN	105	1	5.3680	-1.2620	-4.0750	0.0540	104	0	0	0	0
CCCCN	106	4	3.5100	-2.0080	-3.3710	-0.1750	104	107	116	0	0
CCCCN	107	2	2.7385	-0.8558	-3.3710	0.4220	106	108	109	0	0
CCCCN	108	7	3.3126	0.2432	-3.3710	-0.4190	107	0	0	0	0
CCCCN	109	4	1.3654	-0.9710	-3.3710	-0.3440	107	110	0	0	0
CCCCN	110	2	0.8062	-2.1784	-3.3710	0.3240	109	111	114	0	0
CCCCN	111	4	-0.5111	-2.2401	-3.3710	-0.2220	110	112	113	0	0
*CHCC	112	1	-1.0053	-3.2007	-3.3710	0.1170	111	0	0	0	0
*CHCC	113	1	-1.0945	-1.3303	-3.3710	0.1300	111	0	0	0	0
CCHCC	114	2	1.5790	-3.3792	-3.3710	-0.1630	110	115	116	0	0
CCHCC	115	1	1.1378	-4.3655	-3.3710	0.0200	114	0	0	0	0
CCHCC	116	2	2.9315	-3.2396	-3.3710	0.1900	114	117	106	0	0
CCHZC	117	1	3.5484	-4.1258	-3.3710	-0.0030	116	118	119	120	0
CCZZC	118	20	-1.2594	0.7205	-3.3710	0.0000	117	0	0	0	0
CCZZC	119	20	-1.2594	0.7205	-3.3710	0.0000	117	0	0	0	0
CCZZC	120	20	-1.2594	0.7205	-3.3710	0.0000	117	0	0	0	0
CCCCC	121	6	5.3160	-3.4060	-3.8150	-0.2210	104	122	0	0	0
CCCCH	122	3	6.0640	-3.8760	-2.9390	0.0940	99	121	123	124	0
CCCCH	123	1	7.0200	-3.6740	-3.4210	0.0510	122	0	0	0	0
CCCHZ	124	1	5.9440	-4.9520	-2.8010	0.0510	122	0	0	0	0
	125	20	13.9341	14.3471	0.0000	0.0000	0	0	0	0	0

Intercalated (+)III

C	126	6	5.0571	3.8294	0.1434	-0.2280	127	128	0	0	0
CC	127	3	5.4544	3.2476	-1.0658	0.1120	126	128	129	137	0
CC	128	3	4.0629	3.4498	-0.7643	0.1270	126	127	130	131	0

continued on next page

Table IV—*continued*

Intercalated (+)III

H	129	1	6.0113	3.9185	-1.7631	-0.0160	127	0	0	0	0
H	130	1	3.4752	4.2843	-1.2126	-0.0110	128	0	0	0	0
C	131	2	3.2975	2.2902	-0.3413	-0.0160	128	132	152	0	0
C	132	2	3.9585	1.1315	0.0836	0.0080	131	133	141	0	0
C	133	3	5.4160	1.0886	0.1013	0.1550	132	134	136	137	0
O	134	6	5.8602	1.6040	1.3562	-0.2730	133	135	0	0	0
*H	135	1	5.5698	2.5245	1.4086	0.1620	134	0	0	0	0
H	136	1	5.7342	0.0197	0.0031	-0.0190	133	0	0	0	0
C	137	3	6.0105	1.8839	-0.9972	0.1340	127	133	138	140	0
O	138	6	5.6991	1.2723	-2.2497	-0.2630	137	139	0	0	0
*H	139	1	6.1002	1.6147	-2.9428	0.1360	138	0	0	0	0
H	140	1	7.1222	1.9261	-0.8684	-0.0280	137	0	0	0	0
C	141	2	3.2206	0.0143	0.4915	-0.0150	132	142	155	0	0
C	142	2	1.8208	0.0554	0.4745	0.0330	141	143	153	0	0
C	143	2	1.0828	-1.0618	0.8824	-0.0080	142	144	156	0	0
C	144	2	-0.3169	-1.0207	0.8654	-0.0090	143	145	157	0	0
C	145	2	-0.9779	0.1380	0.4405	0.0330	144	146	154	0	0
C	146	2	-2.3768	0.1795	0.4234	-0.0110	145	147	158	0	0
C	147	2	-3.0378	1.3382	-0.0016	0.0060	146	148	159	0	0
C	148	2	-2.2998	2.4553	-0.4094	-0.0120	147	149	160	0	0
C	149	2	-0.9001	2.4143	-0.3925	0.0320	148	150	154	0	0
C	150	2	-0.1621	3.5314	-0.8003	-0.0040	149	151	161	0	0
C	151	2	1.2377	3.4904	-0.7834	-0.0190	150	152	162	0	0
C	152	2	1.8986	2.3317	-0.3584	0.0210	131	151	153	0	0
C	153	2	1.1598	1.2141	0.0496	0.0080	142	152	154	0	0
C	154	2	-0.2391	1.2556	0.0325	0.0090	145	149	153	0	0
H	155	1	3.7304	-0.8795	0.8193	-0.0020	141	0	0	0	0
H	156	1	1.5927	-1.9556	1.2102	-0.0060	143	0	0	0	0
H	157	1	-0.8862	-1.8825	1.1801	-0.0060	144	0	0	0	0
H	158	1	-2.9461	-0.6823	0.7380	-0.0060	146	0	0	0	0
H	159	1	-4.1170	1.3702	-0.0148	-0.0080	147	0	0	0	0
H	160	1	-2.9097	3.3492	-0.7373	-0.0060	148	0	0	0	0
H	161	1	-0.6720	4.4253	-1.1282	-0.0060	150	0	0	0	0
H	162	1	1.8069	4.3522	-1.0980	-0.0040	151	0	0	0	0

drogens) to qualitatively account for the uncertainty in molecular geometry and flexibility at the transition state. A set of r_c values that give a 5 kcal/mole repulsive energy in the 6–12 potential (22) for each unique atom pair was chosen subjectively in this work.

Four base-pair sequences of trinucleoside dimers in the B conformation (23) were considered:

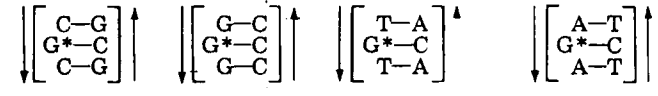

The reaction of the central guanine (G*) with (±)III and (±)IV was investigated. In each case the isomer was located "above" the central base pair, as shown in Fig. 2. In the first series of calculations, all conformational variables, except ϕ_2, were held fixed. ϕ_2 was allowed to fully rotate in each case. For completeness, transition-state conformational analyses were also performed for the N(7) and O(6) positions on guanine. Transition-state geometries found in earlier studies (24) for these two sites were used as constraints in the analyses.

The transition-state I-NH_2-guanine conformational analyses were next repeated for two deformed dinucleoside dimer sequences:

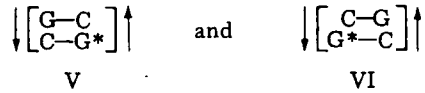

V VI

The particular deformed conformation selected is that with the largest possible base-pair separation distance, d = 6.76 Å; it has been used previously in nucleic acid–drug intercalation studies (25). The atomic coordinates of this structure (along with (+)III intercalated between base pairs) are in Table IV. The nitrogen atom of the 2-amino group in the lower guanine, G*, is attacked by the C(10) atom of I using the transition-state geometry shown in Fig. 2. Once again the conformational studies are characterized in terms of bad contacts. Since the N—C(10) distance is fixed at 2.0 Å and d = 6.76 Å, the upper base pair has minimal influence on specifying bad contacts. The conformational degrees of freedom, defined in Fig. 2, were varied over the same range of values as used in the calculations for B form DNA.

RESULTS

The least number of bad contacts (N) was determined for each of the N(7), O(6), and 2-amino reactions with (±)III and (±)IV. As an example, these least numbers are reported in Table III for (+)III [(+)*trans*(eq,eq') isomer]. Relative magnitudes in Table III may not be important. The essential observation is that in all cases bad contacts were found to exist. Figure 3 is a more detailed steric description of the 2-amino alkylation by (+)III. Nucleic acid sequence does not appear to alter the steric repulsions occurring in the transition state of the reaction. Figure 4 shows the dependence of N for 2-amino alkylation by (±)III and (±)IV as a function of transition-state conformation for d-(cytosine–guanine)$_2$. The steric effects in the 2-amino alkylation process by the (+) enantiomers are different from those of the (−) enantiomers. Nevertheless, alkylation by each form of I at the 2-amino position in guanine appears to be sterically unlikely from a study of Fig. 4. Alkylation at the N(7) or O(6) of guanine was also found to be sterically prohibited. It can be concluded from these conformational analyses that the B form of DNA cannot react with I because of steric hindrance for the selected transition-state geometries. Thus the experimental evidence (6, 8) which indicates 2-amino alkylation of guanine must be explained in terms of a deformation of the B form DNA structure. Of course, these results are dependent on the calculated transition-state geometry.

The two conformational degrees of freedom most critical to generating a stereochemically acceptable alkylation complex are θ_2 and ϕ_2. Steric maps that define complexing geometries that are possible for the transition state are shown in Fig. 5. The shaded areas correspond to intermolecular geometries in which I is intercalated between base pairs. The other areas correspond to structures in which the I isomer is located outside the dinucleoside dimer. Several typical complex structures are shown in stereo-stick model representation in Fig. 6.

Both (+)III and (+)IV can react with the 2-amino group of guanine for V. Reaction with VI is more restricted for both these isomers. There is little difference in the steric constraints for (+)III and (+)IV alkylation to V. The results suggest that (+)*trans*(eq,eq') and (+)*cis*(ax,ax') alkylation with V should occur subsequent to intercalation.

There is no difference between the electronic structures of (+)III and (−)IV. However, experiments indicate that the (+) enantiomer alkylates guanine more efficiently than (−)III (20). Thus the intercalation and chemical reaction may be controlled by the absolute configurations of these enantiomers. Figures 5A and 5C indicate a large difference in the steric effect due to the enantiomeric properties of III. The (−) enantiomer is not expected to react with the 2-amino group of guanine in the V dimer through intercalation. However, for VI, different possible reaction geometries are predicted for (+) and (−)III (Figs. 5D and 5E). The (+) enantiomer is expected to intercalate and react with the 2-amino group

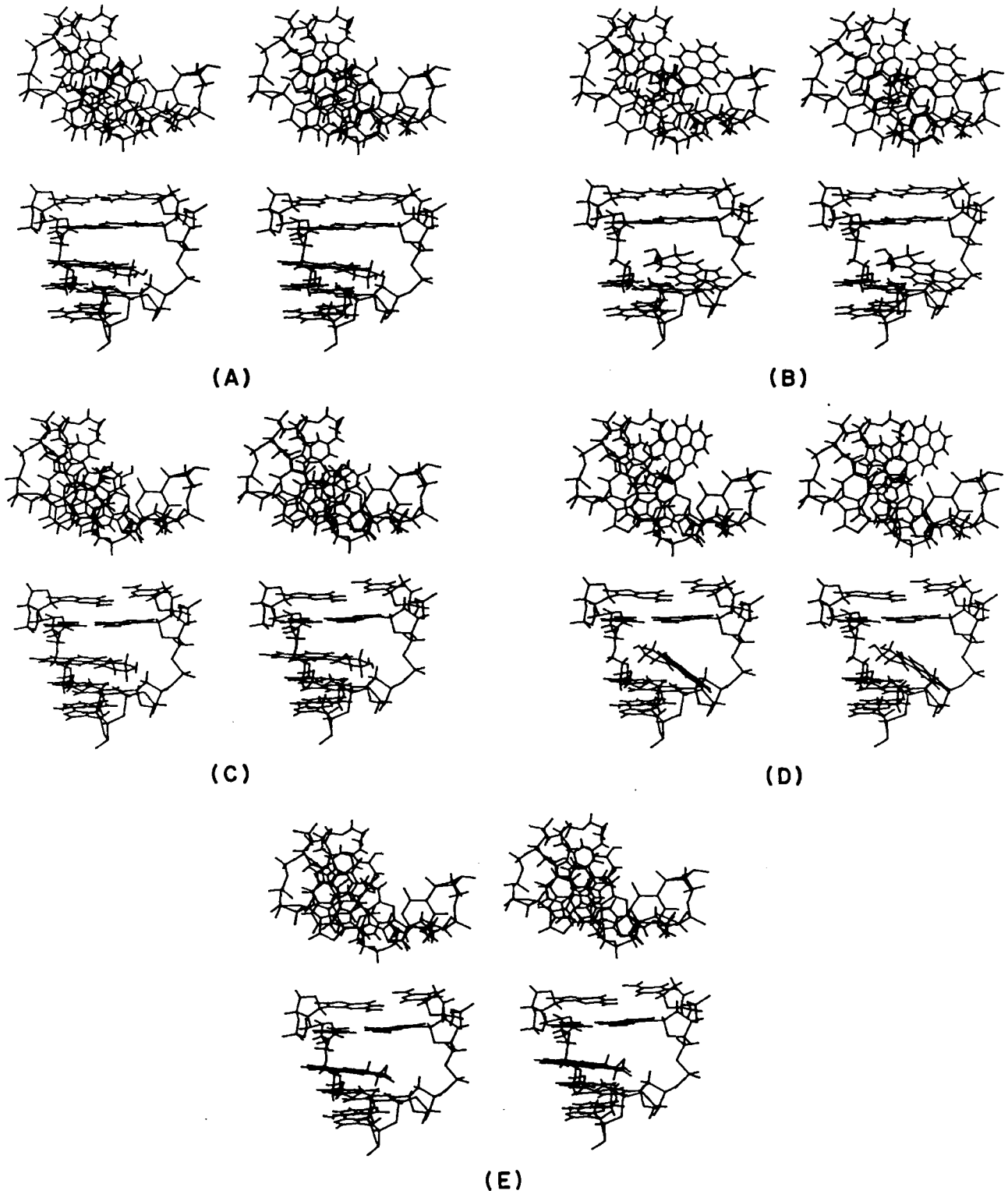

Figure 6—*Stereo-stick models of sterically allowed I–dinucleoside dimer transition-state geometries defined in Fig. 6 (A–E on the steric contact maps). The top views are looking down the helix axis of the nucleic acid structure; the bottom figures are side views.*

of guanine just above the nitrogen atom ($\theta_1 = 90°$, Fig. 5D). The intercalated (−) enantiomer can reach the reaction site from slightly outside the dimer ($\theta_1 = 110°$, Fig. 5C). Both the (+) and (−) enantiomers of III can react from outside the dimer helix. It is, however, not possible to deduce which reaction geometry is preferred since energetics are not included in the analysis.

The intercalation of isomers of I as a prerequisite for alkylation of the 2-amino of guanine is an interesting hypothesis. The intercalation process could be conceptualized as a physical catalyst which stabilizes the reaction geometry in a manner analogous to enzyme–substrate–inhibitor interactions. However, the intercalation model requires that the I component of the reaction product remains between the base pairs. Experimental studies indicate, however, that the adduct involving I is located outside the DNA structure (26). The conformational analysis of the I open-form model of DNA indicates that the part of the reaction product involving I cannot come outside of the base pairs by rotation about the adduct C(10)—N bond unless the hydrogen bond involving the exocyclic amino group of guanine and the cytosine oxygen is broken.

Thus the change in the hydrogen bonding energy for such a reaction process (Scheme I) was examined, and the relative energies of the three

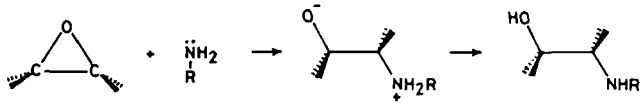

Scheme I

states of the G–C base pair (Fig. 7) were compared. The CNDO/2 method was used (27). The methyl group attached at the nitrogen atom was placed above the base-pair plane to fit the reaction product model with I held between base pairs. The results of these calculations suggest that if the hydrogen bond between the 2-amino group of guanine and the O of cytosine is broken during the alkylation process, allowing I to rotate out from between the base pairs, the resultant base-pairing structure could be of lower, or at least comparable, energy to that of the intercalation structure (Fig. 8).

DISCUSSION

Two major hypotheses were made in this study: (*a*) the transition-state geometries of isomers of I with the exocyclic amino group of guanine are identical to that calculated for isomers of I interacting with ammonia (7), and (*b*) the sterically allowed transition-state geometries of isomers of I with dinucleoside dimers can be identified using the aforementioned stereochemical model (*Experimental*).

The most clear-cut finding from the investigation is that neither (±)III or (±)IV can alkylate the 2-amino group of guanine for B form DNA. This reaction is stereochemically prohibited based on the postulated transition-state geometries. The deformation in the conformation of double-stranded DNA that is associated with this alkylation process has not been uniquely identified. However, if a dinucleoside dimer is unwound, so that the distance between base pairs is maximized (d = 6.76 Å), two possible geometric reaction models result. In one, alkylation occurs when I is located outside the nucleic acid structure; in the other, I is intercalated between base paris for the alkylation transition state. Intercalation of I could serve as a physical catalyst, or provide at least substrate stabilization, for NH_2-guanine alkylation. The alkalyation transition-state geometry is sensitive to nucleic acid sequence for both the isomeric and enantiomeric forms of I.

The choice of the deformed structure of the double-stranded DNA model is somewhat arbitrary. However, the structure selection should correspond to that in which one strand exerts the least steric influence on the interaction between I and the other strand. This is an important consideration since the total extent of (±) binding to I to single- and double-stranded DNA is the same (20). Conversely, this observation also requires that the stereochemical constraints for NH_2-guanine alkylation in double-stranded structures are no more severe than in the single-stranded DNA. This study has focused on double-stranded DNA because its local conformational properties are better understood, and because the double-stranded structure introduces more steric repulsive sites than a single strand.

The calculations reported here are based in part on "soft" steric contact distances (those atoms of the diols, epoxide, and saturated ring of I). As such, this model cannot be used to identify the preferred transition-state geometry. The following paper explores in detail the physical interaction of I with nucleic acid structures to better quantify allowed intermolecular geometries, with special emphasis on possible intercalation mechanisms.

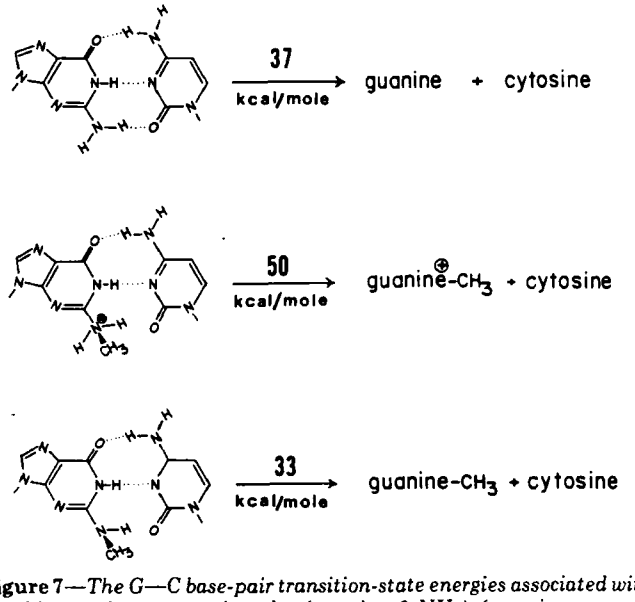

Figure 7—*The G—C base-pair transition-state energies associated with breaking and restructuring the (guanine 2-NH_2)-(cytosine oxygen) base-pair hydrogen bond.*

REFERENCES

(1) A. Borgen, H. Darvey, N. Castagnoli, T. T. Crocker, R. E. Rasmussen, and I. Y. Wang, *J. Med. Chem.*, **16**, 502 (1973).

(2) P. Sims, P. L. Grover, A. Swaisland, K. Pal, and A. Hewer, *Nature (London)*, **252**, 326 (1974).

(3) P. Daudel, M. Duquesne, P. Viqny, P. L. Grover, and P. Sims, *FEBS Lett.*, **57**, 250 (1975).

(4) H. W. S. King, S. R. Osborne, F. A. Beland, R. G. Harvey, and P. Brookes, *Proc. Natl. Acad. Sci. USA*, **73**, 2679 (1976).

(5) V. Ivanovic, N. E. Geacintov, and I. B. Weinstein, *Biochem. Biophys. Res. Commun.*, **70**, 1172 (1976).

(6) I. B. Weinstein, A. M. Jeffrey, K. W. Jennette, S. H. Blobstein, R. G. Harvey, C. Harris, H. Autrup, H. Kasai, and K. Nakanishi, *Science*, **193**, 592 (1976).

(7) O. Kikuchi, A. J. Hopfinger, and G. Klopman, *Cancer Biochem. Biophys.*, **4**, 1 (1979).

(8) J. A. Miller and E. C. Miller, in "Environmental Carcinogenesis," P. P. Kemmelot and E. Kriek, Eds., Elsevier, Amsterdam, 1979, p. 228.

(9) D. M. Jerina and J. W. Doly, *Science*, **185**, 573 (1974).

(10) P. L. Grover and P. Sims, *Biochem. J.*, **110**, 154 (1968).

(11) F. Olsch, *Ciba Found. Symp.*, **76**, 169 (1980).

(12) T. J. Slaga, W. M. Bracken, A. Biaje, W. Levin, H. Yagi, D. M. Jerina, and A. H. Conney, *Cancer Res.*, **39**, 67 (1979).

(13) M. Koreeda, P. D. Moore, P. G. Wislocki, W. Levin, A. H. Conney, H. Yagi, and D. M. Jerina, *Science*, **199**, 778 (1978).

(14) E. K. Parkinson and R. F. Newbold, *Int. J. Cancer*, **26**, 289, 1980.

(15) A. M. Jeffrey, K. W. Jennette, K. Gvzeskowiak, K. Nakanishi, R. G. Harvey, H. Autrup, and C. Harris, *Nature (London)*, **269**, 348 (1977).

(16) T. Meehan and K. Straub, *ibid.*, **277**, 410 (1979).

(17) A. M. Jeffrey, K. Gvzeskowiak, I. B. Weinstein, K. Nakanishi, P. Roller, and R. G. Harvey, *Science*, in press.

(18) V. Ivanovic, N. E. Geacintov, H. Yamasaki, and I. B. Weinstein, *Biochemistry*, **17**, 1597 (1978).

(19) P. D. Lawley, in "Chemical Carcinogens ACS Monograph 173," C. E. Searle, Ed., American Chemical Society, Washington, D.C., 1976, p. 83.

(20) P. Pulkrabek, S. Leffler, D. Grunberger, and I. B. Weinstein, *Biochemistry*, **18**, 5128 (1979).

(21) O. Kikuchi, A. J. Hopfinger, G. Klopman, *J. Theor. Biol.*, **77**, 129 (1979).

(22) A. J. Hopfinger, "Conformational Properties of Macromolecules," Academic, New York, N.Y., 1973.

(23) J. N. Davidson, "The Biochemistry of the Nucleic Acids," 8th ed., Academic, New York, N.Y., 1976, p. 94.

(24) O. Kikuchi, A. J. Hopfinger, and G. Klopman, *Biopolymers*, **19**, 325 (1980).

(25) Y. Nakata and A. J. Hopfinger, *Biochem. Biophys. Res. Commun.*, **95**, 583 (1980).

(26) N. E. Geacintov, A. Gagliano, V. Ivanovic, and I. B. Weinstein, *Biochemistry*, **17**, 5256 (1978).

(27) J. A. Pople and D. L. Beveridge, "Approximate Molecular Orbital Theory," McGraw-Hill, New York, N.Y., 1970.

ACKNOWLEDGMENTS

This work was supported by the National Cancer Institute (Contract N01-CP-65927), the National Institutes of Health (Grants ES-1900 and OH-1147), the Research Service of the Veterans Administration, and Adria Laboratories of Columbus, Ohio.

We appreciate the helpful discussions with D. Malhotra of our laboratory and Dr. S. Yang of the Uniformed Services University of the Health Sciences.

Intercalation of 7,8-Dihydroxy-9,10-epoxy-7,8,9,10-tetrahydrobenzo[a]pyrene Enantiomeric Isomers with Dinucleoside Dimers: A Basis for Alkylation of the 2-Amino Group in Guanine

Y. NAKATA *§, D. MALHOTRA *, A. J. HOPFINGER *¶x, and D. R. BICKERS ‡

Received June 18, 1981, from the *Department of Macromolecular Science, Case Institute of Technology and the ‡Department of Dermatology, School of Medicine, Case Western Reserve University, Cleveland, OH 44106. Accepted for publication June 25, 1982. §Permanent address: Department of Chemistry, Faculty of General Studies, Gunma University, Aramaki-cho, Maebashishi 371, Japan. ¶Alternate address: Department of Drug Design, G. D. Searle and Co., Chicago, IL 60080.

Abstract □ The minimum-energy intercalation-complex geometries of the (±)enantiomers of 7,8-dihydroxy-9,10-epoxy-7,8,9,10-tetrahydrobenzo[a]pyrene (I) with two dinucleoside dimers were determined. The purpose of these calculations was to see if I could intercalate into DNA in such a way that the observed alkylation of the 2-amino group of guanine could occur subsequent to intercalation. For both dinucleoside dimer sequences, it was found that the (+)-(9α,10α) isomer could form a stable intercalation complex in which the orientation and distance of the epoxide of I to the 2-amino group of guanine was close to the calculated critical transition-state geometry for the alkylation reaction. The (−)enantiomers can intercalate, but not in a manner close to the transition-state geometry necessary for the alkylation of the 2-amino group of guanine.

Keyphrases □ 7,8-Dihydroxy-9,10-epoxy-7,8,9,10-tetrahydrobenzo[a]pyrene—enantiomeric isomers, alkylation of dinucleoside dimers, intercalation-complex geometry and energetics □ Dinucleoside dimers—alkylation by enantiomeric isomers of 7,8-dihydroxy-9,10-epoxy-7,8,9,10-tetrahydrobenzo[a]pyrene, intercalation-complex geometry and energetics □ Intercalation—of 7,8-dihydroxy-9,10-epoxy-7,8,9,10-tetrahydrobenzo[a]pyrene into dinucleoside dimers, energetics, complex geometry

The previous paper (1) reported that a sterically acceptable transition-state geometry for the alkylation of the amino group of guanine by 7β,8α-dihydroxy-9α,10α-epoxy-7,8,9,10-tetrahydrobenzo[a]pyrene (II) and 7β,8α-dihydroxy-9β,10β-epoxy-7,8,9,10-tetrahydrobenzo[a]pyrene (III) could involve intercalation. Also, a noncovalent complex formation between benzo[a]pyrene and calf thymus DNA has been observed recently (2). This interaction is postulated to involve intercalation of the aromatic hydrocarbon between adjacent base pairs. An equivalent type of intermolecular geometry could also be expected for single-stranded DNA in which the isomeric forms of I are associated with a nucleic acid base or a pair of adjacent bases. This is an important consideration since the total extent of the alkylation of the 2-amino group of guanine by (±)II is observed to be the same for both single- and double-stranded DNA (3). In addition, (+)III forms the major adduct (60–80% of total adducts) with the amino group of guanine (3).

These findings have prompted the exploration of the possibility that the intercalation process might occur as a prior step to alkylation of the 2-amino group of guanine by I in double-stranded DNA. The energetics of the intercalation of (±)II and (±)III (Fig. 1) with dinucleoside dimer sequences was investigated using molecular mechanics energy calculations (4). The results of these calculations are reported herein.

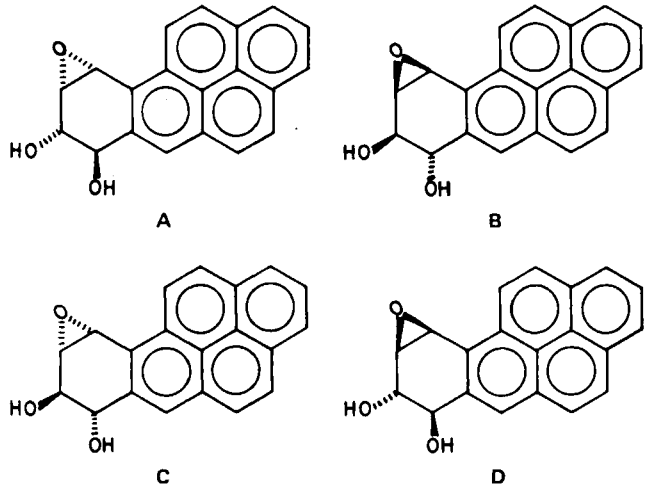

Figure 1—*The enantiomeric isomers of I. Key: (A) (+)II; (B) (−)II; (C) (+)III; (D) (−)III.*

EXPERIMENTAL

The overall procedure for these calculations is identical to that employed previously for the intercalation investigation of doxorubicin (5); a summary of the procedure follows. The DNA structure was represented by a dinucleoside dimer containing guanine. The same geometries used in the doxorubicin study were assigned to the dinucleoside dimers. There are seven unique ways of interacting I with guanine bases in dinucleoside dimers (Fig. 2). One sequence, has two possible 2-amino alkylation sites. Thus eight intermolecular complexes should be studied. However, if

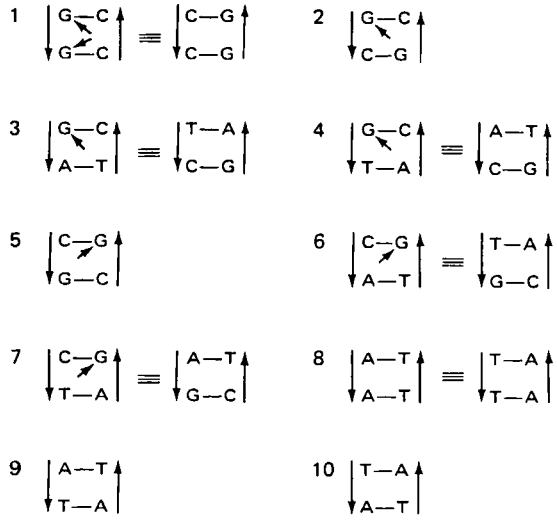

Figure 2—*The I-guanine interaction sites (indicated by the arrows) for dinucleoside dimer base sequences.*

0022-3549/83/0700-0809$01.00/0

Table I—Intercalation Properties of Isomers of I with Dinucleoside Dimers

Dinucleoside Dimer	Isomer	Intercalation Energy, kcal/moles/complex	Mode[b]	Position of I[a] r, Å	θ_1, °	θ_2, °	ϕ_1, °	ϕ_2, °	ϕ_3, °
↓(C—G)↑	(+)II	−88.27	d–e	3.7	126	118	97	161	160
		−84.00	a–b	7.6	52	112	140	13	−125
	(−)II	−89.02	e–f	4.2	97	82	80	−77	156
		−88.55	a	5.5	42	126	113	24	−162
	(+)III	−85.94	c	6.8	90	142	143	81	−178
		−85.07	d–e	3.1	123	110	90	168	−148
	(−)III	−88.65	e–f	4.2	100	81	79	−79	151
		−88.12	d	4.8	107	79	126	−179	125
↓(T—A)↑	(+)II	−89.70	d–e	3.7	104	115	−56	80	175
		−82.58	f	4.2	94	78	−123	−167	−154
	(−)II	−88.79	a	5.2	71	126	−138	−69	−168
		−83.54	d	4.0	63	86	−65	126	145
	(+)III	−86.90	d–e	3.1	111	105	−63	84	176
		−84.43	f	4.2	97	80	−118	−171	−159
	(−)III	−89.00	d	3.9	62	86	−65	126	146
		−80.87	a	5.6	55	139	−145	−48	−173

[a] The transition-state geometric variables. The geometry for I–NH_3 is r = 2.0 Å, θ_1 = 110°, θ_2 = 80°, ϕ_1 = 100°, ϕ_3 = 0 or 180°, with ϕ_2 variable. [b] As defined by the intercalation complex geometries in Fig. 5. The designation i–j indicates a reaction-state geometry between two of the designated complexes.

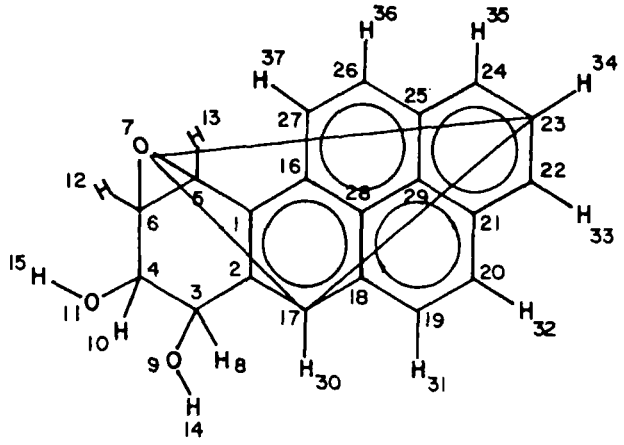

Figure 3—*Structure of I (indicating the internal atomic numbering used) with the descriptive intercalation triangle superimposed.*

detailed sequence specificity is set aside, there are only two cases to consider for the position of an isomer of I. One case involves an isomer of I interacting with guanine from the 3′-side of the base-pair plane, the other case an interaction from the 5′-side of the base-pair plane. Only these two possibilities were considered in this study. Two dinucleoside sequences were employed in the intercalation analyses:

↓(C—G)↑ (5′ side) IV ↓(T—A)↑ (3′ side) V

A specialized version of the MASS (Molecular Assembly Software System) option in the CHEMLAB software package (6, 7) was used to carry out the molecular mechanics calculations. The molecular and electronic structures of (±)II and (±)III used in the study are based on previous calculations (1, 8). The valence geometries of these molecules were held rigid in the intercalation calculations. The structure of I with a superimposition of the descriptive intercalation triangle, involving atoms O(7), C(17), and C(23) as vertices, is shown in Fig. 3. The descriptive intercalation triangle makes it possible to visualize easily the orientation of an isomer of I relative to a dinucleoside dimer. The atomic coordinates of II and V have been given previously (1).

The complexing energy was minimized as a function of the six intermolecular degrees of freedom defined in Fig. 4. Each enantiomer of II and III was placed such that the epoxide ring was above or below the guanine base. Six selected starting positions were chosen in each energy minimization (Fig. 5). It is seen from Fig. 5 that both major and minor groove intercalation were considered.

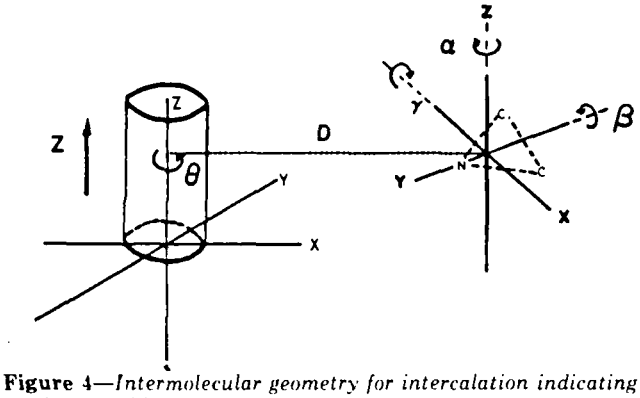

Figure 4—*Intermolecular geometry for intercalation indicating the six degrees of freedom (from Ref. 7).*

RESULTS

The minimum energy complexes for both dinucleoside dimer sequences are reported in Table I. The preferred intercalation structures are vir-

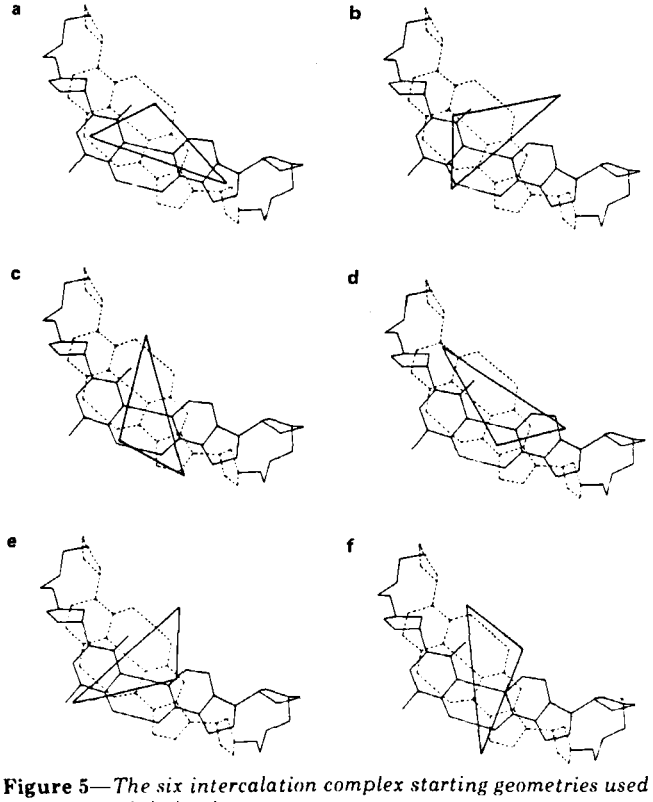

Figure 5—*The six intercalation complex starting geometries used in the energy minimizations.*

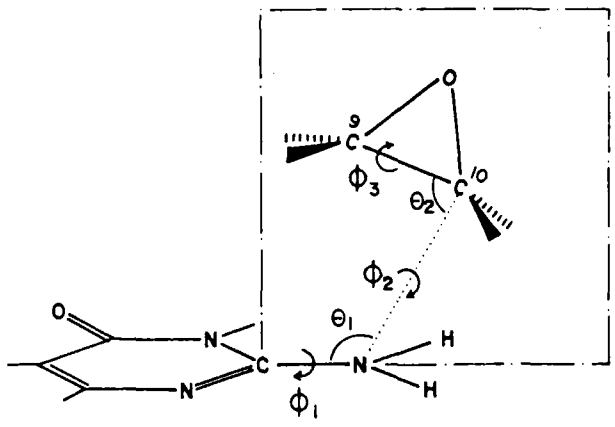

Figure 6—*The I-NH_2-guanine transition-state geometry (from Ref. 1).*

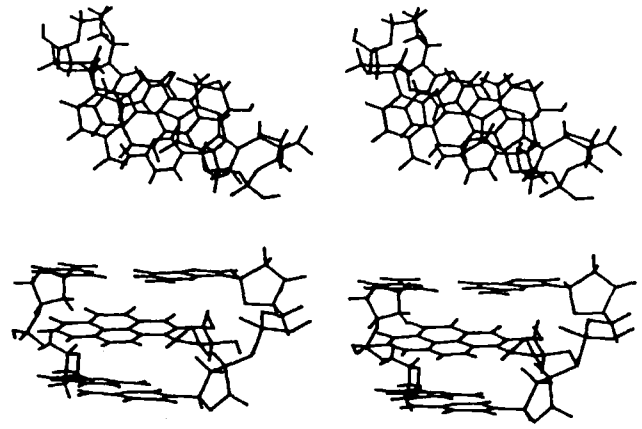

Figure 7—*Stereo-stick models of the (+)II–IV intercalation complex in which the epoxide group of II is close to the 2-amino group of guanine and in the transition-state orientation. The top figures are looking down at the base-pair planes; the bottom figures are looking into the dinucleoside dimer.*

tually independent of the approach of I from either the major or minor groove. The position of each enantiomeric isomer is reported in terms of the geometric variables of the transition state (1, 8). Many of the complex energies are close to one another (~1 kcal/mole). Consequently, it is not possible to identify the most stable intermolecular complex as a function of isomer and/or base sequence. The uncertainty in these computed energies is probably larger than several of the corresponding differences, thus negating such a structural assignment. However, the important observation is that intercalation geometries predisposed for NH_2-alkylation are among the most stable intermolecular structures.

The minimum-energy transition-state geometry has been computed for isomers of I with ammonia as $r = 2.0$ Å, $\theta_1 = 110°$, $\theta_2 = 80°$, $\phi_1 = 100°$, and $\phi_3 = 0$ or 180°, with ϕ_2 variable (8). This model system (Fig. 6) should be a reasonable approximation for I alkylating the 2-amino group of guanine and has been used to evaluate the reactive potential of the various intermolecular complexes.

The complexing energies show a moderate sensitivity to both choice of isomer and base-pair sequence. One consistent observation is that (+)III forms the least stable intercalation complex with the two dinucleoside dimers. The (+)III intercalation complex also possesses the minimum C(10)—NH_2 interaction distance of all complex structures. The second smallest interaction distance occurs in the (+)II–dinucleoside dimer complexes. However, (+)III undergoes a steric repulsion involving its 7-hydroxyl group with an upper base if it approaches closer than 3.1 Å to the amino group of guanine.

DISCUSSION

Intercalation complexes having isomers of I oriented toward the amino group of guanine close to the model transition-state geometry should be particularly reactive. From Table I it is seen that the (+) isomers of both II and III have their epoxide groups oriented toward the 2-amino group of guanine, similar to the model transition-state geometry for both dinucleoside dimers. Moreover, these two intercalated stereoisomers also have the minimum distances between the atoms involved in the alkylation process: C(10) of I (defined as atom number 5 in Fig. 3) and the nitrogen of the amino group of guanine. The distances are 3.7 and 3.1 Å for (+)II and (+)III, respectively. Thus, the (+) enantiomers should be more reactive toward DNA if intercalation is a prereactive step in the alkylation process. This conclusion is consistent with experimental observation (3).

The intercalation complex involving (+)II should be expected from these calculations to be the most reactive state if intercalation is part of the reaction process. Table II summarizes the relationship between the mode of intercalation and location of (+)II relative to the base alkylation sites for IV. Clearly, mode d–e is critical to the explanation of the experimental observations (3). It should be noted also that the second most stable intercalation complex corresponds to the epoxide of II being close to the amino group of cytosine. The exocyclic amino group of cytosine is postulated to be the alkylation site for the minor cytosine–II adducts that are observed (9–12). These intercalation calculations may provide both a geometric and energetic base for this assumed reaction site. Stereo-stick models of the (+)II–IV complex are shown in Fig. 7. The transition-state orientation of the epoxide group relative to the 2-amino group of guanine is easily seen.

Table II—Intercalation Modes of (+)II with IV

Mode[a]	Intercalation Energy, kcal/mole	Position of Epoxide to Base
a–b	−84.00	cytosine-NH_2
c	−82.96	cytosine ring
d–e	−88.27	guanine-NH_2
f	−81.33	guanine-N(3)

[a] As defined in Fig. 5. The designation *i–j* indicates a transition-state geometry between two of the designated complexes.

REFERENCES

(1) O. Kikuchi, R. Pearlstein, A. J. Hopfinger, and D. R. Bickers, *J. Pharm. Sci.*, **72**, 800 (1983).

(2) J. F. Becker, K. Straub, and T. Meehan, "Temperature-Jump Relaxation Rates of Intercalation Complexes Between Benzo(a)pyrene Derivatives and DNA," ASBC/BS Meeting (1980).

(3) P. Pulkrabek, S. Leffler, D. Grunberger, and I. B. Weinstein, *Biochemistry*, **18**, 5128 (1979).

(4) A. J. Hopfinger, "Conformational Properties of Macromolecules," Academic, New York, N.Y., 1973.

(5) Y. Nakata and A. J. Hopfinger, *Biochem. Biophys. Res. Commun.*, **95**, 583 (1980).

(6) R. P. Potenzone, Jr., E. Cavicchi, H. J. R. Weintraub, and A. J. Hopfinger, *Comput. Chem.*, **1**, 187 (1977).

(7) R. A. Pearlstein, S. K. Tripathy, R. Potenzone, Jr., D. Malhotra, A. J. Hopfinger, G. Klopman, and N. Max, *Biopolymers*, **19**, 311 (1980).

(8) O. Kikuchi, A. J. Hopfinger, and G. Klopman, *Cancer Biochem. Biophys.*, **4**, 1 (1979).

(9) A. M. Jeffrey, K. W. Jennette, K. Gvzeskowiak, K. Nakanishi, R. G. Harvey, H. Autrup, and C. Harris, *Nature (London)*, **269**, 348 (1977).

(10) T. Meehan and K. Straub, *Nature (London)*, **277**, 410 (1979).

(11) A. M. Jeffrey, K. Gvzeskowiak, I. B. Weinstein, K. Nakanishi, P. Roller, and R. G. Harvey, *Science*, in press.

(12) V. Ivanovic, N. E. Geacintov, H. Yamasaki, and I. B. Weinstein, *Biochemistry*, **17**, 1597 (1978).

ACKNOWLEDGMENTS

This work was supported by the National Cancer Institute (Contract N01-CP-65927), the National Institutes of Health (Grants ES-1900 and OH-1147), the Research Service of the Veterans Administration, and Adria Laboratories of Columbus, Ohio.

We appreciate the helpful discussions with R. Pearlstein of our laboratory and Dr. S. Yang of the Uniformed Services University of the Health Sciences.

Hypolipidemic Activity of Substituted 2-Pyrrolidinones in Rodents

GEORGE H. COCOLAS, JAMES M. CHAPMAN, Jr., P. JOSÉE VOORSTAD, and IRIS H. HALL[x]

Received March 11, 1982, from the *Division of Medicinal Chemistry, School of Pharmacy, The University of North Carolina at Chapel Hill, Chapel Hill, NC 27514.* Accepted for publication June 25, 1982.

Abstract □ A series of substituted 2-pyrrolidinones was evaluated for hypolipidemic activity at 20 and 30 mg/kg/day in CF_1 male mice. 4-Phenyl-5,5-dicarbethoxy-2-pyrrolidinone was the most potent compound at 30 mg/kg/day, reducing serum triglyceride levels 52% after 14 days of dosing and serum cholesterol levels 48% after 16 days of dosing. 4-Phenyl-5-carbethoxy-2-pyrrolidinone and 4-phenyl-3,5,5-tricarbethoxy-2-pyrrolidinone also demonstrated significant activity. Those compounds which contained a phenyl substituent were more potent than either the unsubstituted, the alkyl, or the dicarbethoxy 2-pyrrolidinone analogues.

Keyphrases □ 2-Pyrrolidinones—synthesis of substituted analogues, hypolipidemic activity in mice □ Antihyperlipidemic agents—substituted 2-pyrrolidinone analogues, synthesis, hypolipidemic activity in mice □ Succinimide—2-pyrrolidinone congeners, synthesis of substituted analogues, hypolipidemic activity in mice

Studies on the antihyperlipidemic activity of *N*-substituted phthalimides (1) and related imide analogues (2) revealed a wide variety of imides which caused a reduction in serum cholesterol and triglyceride levels in rodents. Succinimide was observed to be active at a dose of 20 mg/kg/day ip, affording a 27% reduction in serum cholesterol levels after 16 days and a 32% reduction of serum triglyceride levels after 14 days in mice (2). As an extension of these studies, the hypolipidemic activity of a series of 2-pyrrolidinone derivatives as congeners of succinimide was examined; those results are reported herein.

EXPERIMENTAL

Chemistry—Of the 18 compounds studied (Table I), 2-pyrrolidinone[1] (I) and L-pyroglutamic acid[2] (IV) were purchased commercially. 5-Carboxy-2-pyrrolidinone (III), 4-phenyl-5-carboxy-2-pyrrolidinone (used to prepare XIV), 5,5-dicarbethoxy-2-pyrrolidinone (V), and 5,5-dicarboxy-2-pyrrolidinone (VI) were prepared by the method of Cocolas and Hartung (3). 5-Carbethoxy-2-pyrrolidinone (II) was prepared by esterification of D,L-5-carboxy-2-pyrrolidinone (III) with ethanol–hydrochloric acid. The four alkyl-5,5-dicarbethoxy-2-pyrrolidinones (VII–XIII) were prepared by a Michael addition of an α,β-unsaturated ester to diethyl acetamidomalonate and subsequent cyclization as reported by Kim and Cocolas (4).

4-Phenyl-5,5-dicarbethoxy-2-pyrrolidinone (XIV)—The method of Kim and Cocolas (4) was used. To 400 mg (0.019 g-atom) of sodium dissolved in 200 ml of absolute ethanol of alcohol was added 21.7 g (0.1 mole) of diethyl acetamidomalonate and 22 g (0.125 mole) of ethyl cinnamate. The mixture was refluxed overnight (10–12 hr), cooled to room temperature, and then neutralized with glacial acetic acid. The solvent was removed under reduced pressure to give solid material which was recrystallized from toluene to give 16 g of product, mp[3] 96–97°.

Anal.—Calc.[3] for $C_{16}H_{12}NO_5$: C, 62.95; H, 6.23; N, 4.59. Found[3]: C, 62.82; H, 6.19; N, 4.74.

4-Phenyl-5-carbethoxy-2-pyrrolidinone (XV)—4-Phenyl-5,5-dicarbethoxy-2-pyrrolidinone (XIV), 26.9 g (0.088 mole), was dissolved in 125 ml of absolute ethanol, and 250 ml of 20% ethanolic potassium hydroxide solution was added slowly. The resulting solution was refluxed for 9 hr and allowed to cool, and the white solid precipitate was collected and dissolved in 150 ml of hot water. The solution was made strongly acidic with 6 *N* HCl and the resulting precipitate filtered to give 10.8 g of 4-phenyl-5,5-dicarboxy-2-pyrrolidinone. Decarboxylation at 160–165° under vacuum and recrystallization from ethanol gave 3.04 g of 4-phenyl-5-carboxy-2-pyrrolidinone, mp 180°. Esterification with ethanolic hydrochloric acid yielded 4-phenyl-5-carbethoxy-2-pyrrolidinone, mp 140–141°.

Anal.—Calc. for $C_{13}H_{15}NO_3$: C, 66.94; H, 6.48; N, 6.00. Found: C, 66.79; H, 6.67; N, 6.03.

4-Phenyl-3,5,5-tricarbethoxy-2-pyrrolidinone (XVI)—The method of Kim and Cocolas (4) was used. A solution containing 1.15 g (0.05 g-atom) of sodium metal, 10.85 g (0.05 mole) diethyl acetamidomalonate, and 12.5 g (0.05 mole) diethyl benzalmalonate in 100 ml absolute ethanol was maintained at room temperature for 3 days. The reaction mixture was then neutralized with glacial acetic acid and cooled to precipitate 20 g of XVI. The product was recrystallized from 95% ethanol, mp[3] 107–109°.

Anal.—Calc.[3] for $C_{19}H_{23}NO_7$: C, 60.47; H, 6.14; N, 3.71. Found[3]: C, 60.81; H, 6.22; N, 3.54.

4-Isopropyl-3,5-dicarbethoxy-2-pyrrolidinone (XVII)—Compound XVII was prepared according to the procedure of Kim and Cocolas (5).

3-Methyl-5,5-dicarbethoxy-2-pyrrolidinone (XVIII)—Compound XVIII was prepared according to the method of Cocolas *et al.* (6).

Biological Testing—Compounds were tested at 20 and 30 mg/kg/day ip in CF_1 male mice (~25 g). On days 9 and 16, blood was collected *via* a tail vein, and the serum was separated by centrifugation. Serum cholesterol was determined by a modification of the Leibermann–Burchard reaction (8). A separate group of mice were bled on day 14 and their serum triglyceride levels were determined using a commercial kit[4].

RESULTS AND DISCUSSION

The 2-pyrrolidinone derivatives were potent hypolipidemic agents in mice after dosing for 14–16 days at 20 and 30 mg/kg/day (Table II). The unsubstituted compounds demonstrated very poor activity. 4-Phenyl-5,5-dicarbethoxy-2-pyrrolidinone (XIV) gave the best anticholesteremic activity resulting in a 42% reduction of serum cholesterol levels at 20 mg/kg/day and a 48% reduction at 30 mg/kg/day. At the latter dose, serum triglycerides were reduced 52%. The other two derivatives containing a phenyl substituent, XV and XVI, also reduced cholesterol serum levels significantly but to a lesser degree. 4-Phenyl-5-carbethoxy-2-pyrrolidinone XV was more effective than 4-phenyl-3,5,5-tricarbethoxy-2-pyrrolidinone XVI, causing cholesterol reductions of 37 and 24%, respectively, at 20 mg/kg/day and 35 and 42%, respectively, at 30 mg/kg/day. Compound XV reduced serum triglyceride content 44%.

4-Alkyl substitution on the 5,5-dicarbethoxy-2-pyrrolidinone nucleus improved the reduction of serum triglycerides and cholesterol in mice.

[1] Aldrich Chemical Co.
[2] Mann Chemical Co.
[3] Determined at M-H-W Laboratories, Phoenix, Ariz.
[4] Fisher, Hycel Triglyceride Test (1975), Hycel, Inc.

0022-3549/83/0700-0812$01.00/0

Table I—Physical Characteristics of 2-Pyrrolidinone Analogues

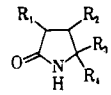

Compound	Name	R_1	R_2	R_3	R_4	Melting Point, Found	Melting Point, Lit. (ref.)
I	2-Pyrrolidinone	H	H	H	H	—	—
II	5-Carbethoxy-2-pyrrolidinone	H	H	$COOC_2H_5$	H	57–59°	61° (7)
III	D,L-5-Carboxy-2-pyrrolidinone	H	H	COOH	H	187–189°	183–185° (4)
IV	L-5-Carboxy-2-pyrrolidinone	H	H	COOH	H	158–159°	—
V	5,5-Dicarbethoxy-2-pyrrolidinone	H	H	$COOC_2H_5$	$COOC_2H_5$	82–83°	82–83° (3)
VI	5,5-Dicarboxy-2-pyrrolidinone	H	H	COOH	COOH	152–153°	152.5–153° (3)
VII	4-Methyl-5,5-dicarbethoxy-2-pyrrolidinone	H	CH_3	$COOC_2H_5$	$COOC_2H_5$	77–78°	77.5–78° (3)
VIII	4-Ethyl-5,5-dicarbethoxy-2-pyrrolidinone	H	C_2H_5	$COOC_2H_5$	$COOC_2H_5$	113–115°	113–115° (4)
IX	4-*n*-Propyl-5,5-dicarbethoxy-2-pyrrolidinone	H	*n*-C_3H_7	$COOC_2H_5$	$COOC_2H_5$	88–89°	88–89° (4)
X	4-Isopropyl-5,5-dicarbethoxy-2-pyrrolidinone	H	*i*-C_3H_7	$COOC_2H_5$	$COOC_2H_5$	98–99°	98–99° (4)
XI	4-*n*-Butyl-5,5-dicarbethoxy-2-pyrrolidinone	H	*n*-C_4H_9	$COOC_2H_5$	$COOC_2H_5$	104–105°	104–105° (4)
XII	4-Isobutyl-5,5-dicarbethoxy-2-pyrrolidinone	H	*i*-C_4H_9	$COOC_2H_5$	$COOC_2H_5$	108–109°	109° (4)
XIII	4-*n*-Pentyl-5,5-dicarbethoxy-2-pyrrolidinone	H	*n*-C_5H_9	$COOC_2H_5$	$COOC_2H_5$	104–105°	104–105° (4)
XIV	4-Phenyl-5,5-dicarbethoxy-2-pyrrolidinone	H	C_6H_5	$COOC_2H_5$	$COOC_2H_5$	96–97°	—
XV	4-Phenyl-5-carbethoxy-2-pyrrolidinone	H	C_6H_5	$COOC_2H_5$	H	140–141°	—
XVI	4-Phenyl-3,5,5-tricarbethoxy-2-pyrrolidinone	$COOC_2H_5$	C_6H_5	$COOC_2H_5$	$COOC_2H_5$	107–109°	—
XVII	4-Isopropyl-3,5-dicarbethoxy-2-pyrrolidinone	$COOC_2H_5$	*i*-C_3H_7	$COOC_2H_5$	H	107–109°	106–108° (5)
XVIII	3-Methyl-5,5-dicarbethoxy-2-pyrrolidinone	CH_3	H	$COOC_2H_5$	$COOC_2H_5$	113–115°	113–115° (6)

Table II—Effects of 2-Pyrrolidinone Analogues on Serum Cholesterol and Triglyceride Levels of CF_1 Male Mice [a]

Compound	Dose	Serum Triglyceride, % of Control, Day 14	Serum Cholesterol, % of Control, Day 9	Serum Cholesterol, % of Control, Day 16
Succinimide		68 ± 7[b]	78 ± 9[b]	73 ± 10[b]
I	20 mg/kg/day	80 ± 6[b]	86 ± 7[c]	83 ± 6[c]
II	20 mg/kg/day	62 ± 6	89 ± 6	72 ± 5
III	20 mg/kg/day	85 ± 7[c]	80 ± 6[b]	83 ± 7[c]
IV	20 mg/kg/day	88 ± 9	84 ± 7[c]	84 ± 6[c]
V	20 mg/kg/day	87 ± 10	94 ± 8	82 ± 5[b]
VI	20 mg/kg/day	82 ± 4[b]	92 ± 5	71 ± 3[b]
VII	20 mg/kg/day	76 ± 4[b]	84 ± 4[b]	79 ± 4[b]
VIII	20 mg/kg/day	75 ± 3[b]	81 ± 7[b]	73 ± 9[b]
	30 mg/kg/day	68 ± 6[b]	72 ± 6[b]	58 ± 5[b]
IX	20 mg/kg/day	63 ± 7[b]	77 ± 8[b]	73 ± 5[b]
X	20 mg/kg/day	70 ± 3[b]	78 ± 6[b]	75 ± 3[b]
	30 mg/kg/day	54 ± 4[b]	91 ± 8	55 ± 6[b]
XI	20 mg/kg/day	57 ± 7	80 ± 8	68 ± 3
XII	20 mg/kg/day	70 ± 7[b]	96 ± 7	62 ± 5[b]
	30 mg/kg/day	67 ± 6[b]	80 ± 7[b]	58 ± 6[b]
XIII	20 mg/kg/day	72 ± 3[b]	79 ± 7[b]	79 ± 7[b]
	30 mg/kg/day	61 ± 5[b]	86 ± 8[c]	68 ± 4[b]
XIV	20 mg/kg/day	83 ± 9	94 ± 4	58 ± 8[b]
	30 mg/kg/day	48 ± 5[b]	55 ± 6[b]	52 ± 5[b]
XV	20 mg/kg/day	82 ± 7[c]	91 ± 6	63 ± 9[b]
	30 mg/kg/day	56 ± 6[b]	97 ± 7	65 ± 6[b]
XVI	20 mg/kg/day	88 ± 4[c]	101 ± 5	76 ± 3[b]
	30 mg/kg/day	89 ± 6	89 ± 9	58 ± 5[b]
XVII	20 mg/kg/day	98 ± 9	85 ± 6[c]	68 ± 3[b]
	30 mg/kg/day	62 ± 7[b]	83 ± 8[c]	70 ± 7[b]
XVIII	20 mg/kg/day	84 ± 8[c]	94 ± 5	88 ± 10
1% Carboxymethyl cellulose		100 ± 6	100 ± 5	100 ± 6

[a] $n = 6$. [b] $p \leq 0.001$. [c] $p \leq 0.010$.

Reduction of serum cholesterol ranged from 21 to 38% at 20 mg/kg/day and 32 to 48% at 30 mg/kg/day compared with the control. 4-Isobutyl-5,5-dicarbethoxy-2-pyrrolidinone (XII) caused the greatest reduction of these 4-alkyl derivatives, 38% at 20 mg/kg/day and 42% at 30 mg/kg/day. The serum triglyceride levels were reduced 33% by XII at 30 mg/kg/day, 46% by X at 30 mg/kg/day, and 43% by XI at 20 mg/kg/day.

4-Isopropyl-3,5-dicarbethoxy-2-pyrrolidinone (XVII) reduced serum cholesterol levels by 32% on day 16 at 20 mg/kg/day, being slightly more active than the 4-isopropyl-5,5-dicarbethoxy analogue (X) which suppressed serum cholesterol levels by 25% at this dose level. However, X was more active than XVII at 30 mg/kg/day in lowering serum cholesterol.

3-Methyl-3,5-dicarbethoxy-2-pyrrolidinone (XVIII) was less effective in reducing both triglyceride and serum cholesterol levels than the 4-methyl analogue (VII).

The 4-*n*-propyl-5,5-dicarbethoxy-2-pyrrolidinone (IX) gave the best antitriglyceridemic activity of all the compounds when tested at 20 mg/kg/day, reducing serum levels by 37%. L-Pyroglutamic acid (IV) was one of the less effective compounds tested and had the same level of hypolipidemic activity as the racemic compound, III.

These studies demonstrate that the 2-pyrrolidinones possess antihyperlipidemic effects in mice. The compounds appear to be more potent than clofibrate which is inactive in the 20–30 mg/kg/day dose range. The hypolipidemic activity of these pyrrolidinones is, in general, equal to succinimide and similar imide-containing structures.

REFERENCES

(1) J. M. Chapman, G. H. Cocolas, and I. H. Hall, *J. Med. Chem.*, **22**, 1399 (1979).

(2) I. H. Hall, J. M. Chapman, and G. H. Cocolas, *J. Pharm. Sci.*, **70**, 326 (1981).

(3) G. H. Cocolas and W. H. Hartung, *J. Am. Chem. Soc.*, **79**, 5203 (1957).

(4) Y. C. Kim and G. H. Cocolas, *J. Med. Chem.*, **8**, 509 (1965).

(5) Y. C. Kim and G. H. Cocolas, *Can. J. Chem.*, **45**, 83 (1967).

(6) G. H. Cocolas, S. Avakian, and G. J. Martin, *J. Org. Chem.*, **26**, 1313 (1961).

(7) I. Heilbron and H. M. Bunbunty, "Dictionary of Organic Compounds," vol. 2, Oxford University Press, New York, N.Y., 1953, p. 607.

(8) A. T. Ness, J. V. Pastewka, and A. C. Peacock, *Clin. Chem. Acta*, **10**, 229 (1964).

ACKNOWLEDGMENTS

Supported by Grant HL25680 from the National Heart, Lung, and Blood Institute, National Institutes of Health.

The authors thank Melba Gibson, Jerry McKee, and Mary Dorsey for their technical assistance.

Potential Antitumor Agents IX: Synthesis and Antitumor Activity of Two Analogues of Ketocaine

ALDO ANDREANI *x, GIANCARLO SCAPINI *, IRAKLIS GALATULAS ‡, and ROSARIA BOSSA ‡

Received November 3, 1981, from the **Istituto di Chimica Farmaceutica e Tossicologica, University of Bologna* and the ‡*Istituto di Farmacologia, University of Milan, Italy.* Accepted for publication June 14, 1982.

Abstract □ The reaction between *o*-hydroxybutyrophenone and tris(2-chloroethyl)amine gave two analogues (II, V) of the well-known local anesthetic ketocaine (I). Compounds II and V showed interesting antitumor activity in mice implanted with Ehrlich ascites tumor cells (% T/C = 149 at 5 mg/kg and 171 at 50 mg/kg, respectively). Further studies on the pharmacological behavior of these new compounds are in progress.

Keyphrases □ Antitumor agents—synthesis and antitumor activity of two analogues of ketocaine, potential □ Ketocaine—potential antitumor agents, synthesis and antitumor activity of two analogues

The antimitotic properties associated with the bis(2-chloroethyl)amino group is well known, and a number of compounds bearing this group are of therapeutic interest. The choice of a suitable supporting moiety for this pharmacophoric group is very important (1). The local anesthetic ketocaine (I) (2) at high concentrations reduces the oxygen consumption by cerebral tissue, while at lower concentrations is able to stimulate intensely this consumption, not only by cerebral tissue, but also by tissues with prevailing anaerobic metabolism (HeLa cells, KB cells) (3–6). In particular, ketocaine inhibits the mitosis of lymphocytes in culture stimulated by phytohemoagglutinine, a process which has been correlated with the stimulating effect of this local anesthetic on oxygen consumption by tissues with prevailing anaerobic metabolism (7).

These observations prompted us to attach the bis(2-chloroethyl)amino group to the phenolic group in *o*-hydroxybutyrophenone, in order to potentiate and/or specialize the antimitotic action of the parent drug, ketocaine. Such a compound also is in agreement with the N—O—O triangulation hypothesis recently proposed for some antineoplastic agents (8).

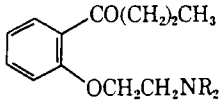

I R = —$CH(CH_3)_2$
II R = —CH_2CH_2Cl

RESULTS AND DISCUSSION

Replacement of the two isopropyl groups of ketocaine (I) with two 2-chloroethyl groups was effected by treating *o*-hydroxybutyrophenone(III) with one equivalent of tris(2-chloroethyl)amine (IV) in ethanolic sodium ethoxide. This not only furnished the expected *N*-[2-(2-butanoyl)phenoxyethyl]-*N*,*N*-di(2-chloroethyl)amine (II) but also *N*,*N*-di[2-(2-butanoyl)phenoxyethyl]-*N*-(2-chloroethyl)amine (V) (Scheme I). The IR and ^{1}H-NMR spectra of compounds II and V are in agreement with the assigned structures (see *Experimental*).

For antitumor testing, female Swiss mice (average weight 21 ±1 g) were implanted on day 0 with 10^6 Ehrlich ascites tumor cells from donor mice. After 24 hr the animals were treated with compound II dissolved in water (1, 5, or 20 mg/kg, i.p.) or compound V dissolved in dimethyl sulfoxide (10, 50, or 200 mg/kg, i.p.). The amount of dimethyl sulfoxide used was shown previously, in analogous experiments, not to affect tumor growth. Deaths were recorded for the 60-day period. The activities were measured as the ratio of the mean survival time of the test animals to that of the control animals expressed as a percentage (% T/C). Significant activity is achieved with an increased life span of 25% (T/C ≥ 125).

Both compounds prolonged the life span of mice bearing Ehrlich ascites carcinoma beyond that of untreated animals: increase for compound II was 48.7% at a 5 mg/kg, i.p. dose and for compound V was 71.2% at 50 mg/kg, 24 hr after tumor implantation (Table I).

The activity of compounds II and V is related to toxicity. While compound II may act as a cross-linking agent (similar to melphalan, chlorambucil, and cyclophosphamide), the antitumor activity of compound V may be due only to its alkylating properties; its lower toxicity is in agreement with the data reported for other monofunctional agents (1).

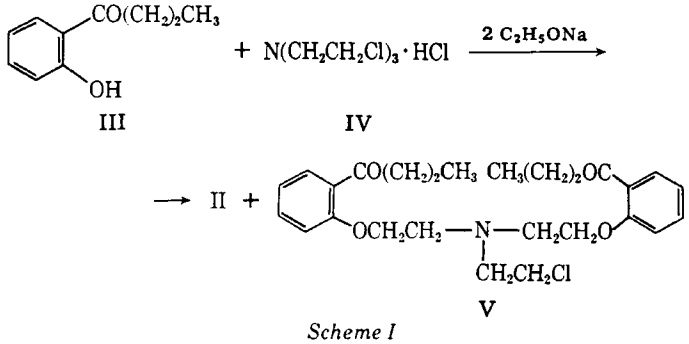

III IV

II + V

Scheme I

0022-3549/83/0700-0814$01.00/0

REFERENCES

(1) J. M. Chapman, G. H. Cocolas, and I. H. Hall, *J. Med. Chem.*, **22**, 1399 (1979).

(2) I. H. Hall, J. M. Chapman, and G. H. Cocolas, *J. Pharm. Sci.*, **70**, 326 (1981).

(3) G. H. Cocolas and W. H. Hartung, *J. Am. Chem. Soc.*, **79**, 5203 (1957).

(4) Y. C. Kim and G. H. Cocolas, *J. Med. Chem.*, **8**, 509 (1965).

(5) Y. C. Kim and G. H. Cocolas, *Can. J. Chem.*, **45**, 83 (1967).

(6) G. H. Cocolas, S. Avakian, and G. J. Martin, *J. Org. Chem.*, **26**, 1313 (1961).

(7) I. Heilbron and H. M. Bunbunty, "Dictionary of Organic Compounds," vol. 2, Oxford University Press, New York, N.Y., 1953, p. 607.

(8) A. T. Ness, J. V. Pastewka, and A. C. Peacock, *Clin. Chem. Acta*, **10**, 229 (1964).

ACKNOWLEDGMENTS

Supported by Grant HL25680 from the National Heart, Lung, and Blood Institute, National Institutes of Health.

The authors thank Melba Gibson, Jerry McKee, and Mary Dorsey for their technical assistance.

Potential Antitumor Agents IX: Synthesis and Antitumor Activity of Two Analogues of Ketocaine

ALDO ANDREANI *x, GIANCARLO SCAPINI *, IRAKLIS GALATULAS ‡, and ROSARIA BOSSA ‡

Received November 3, 1981, from the **Istituto di Chimica Farmaceutica e Tossicologica, University of Bologna* and the ‡*Istituto di Farmacologia, University of Milan, Italy.* Accepted for publication June 14, 1982.

Abstract □ The reaction between *o*-hydroxybutyrophenone and tris(2-chloroethyl)amine gave two analogues (II, V) of the well-known local anesthetic ketocaine (I). Compounds II and V showed interesting antitumor activity in mice implanted with Ehrlich ascites tumor cells (% T/C = 149 at 5 mg/kg and 171 at 50 mg/kg, respectively). Further studies on the pharmacological behavior of these new compounds are in progress.

Keyphrases □ Antitumor agents—synthesis and antitumor activity of two analogues of ketocaine, potential □ Ketocaine—potential antitumor agents, synthesis and antitumor activity of two analogues

The antimitotic properties associated with the bis(2-chloroethyl)amino group is well known, and a number of compounds bearing this group are of therapeutic interest. The choice of a suitable supporting moiety for this pharmacophoric group is very important (1). The local anesthetic ketocaine (I) (2) at high concentrations reduces the oxygen consumption by cerebral tissue, while at lower concentrations is able to stimulate intensely this consumption, not only by cerebral tissue, but also by tissues with prevailing anaerobic metabolism (HeLa cells, KB cells) (3–6). In particular, ketocaine inhibits the mitosis of lymphocytes in culture stimulated by phytohemoagglutinine, a process which has been correlated with the stimulating effect of this local anesthetic on oxygen consumption by tissues with prevailing anaerobic metabolism (7).

These observations prompted us to attach the bis(2-chloroethyl)amino group to the phenolic group in *o*-hydroxybutyrophenone, in order to potentiate and/or specialize the antimitotic action of the parent drug, ketocaine. Such a compound also is in agreement with the N—O—O triangulation hypothesis recently proposed for some antineoplastic agents (8).

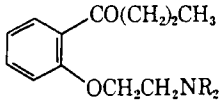

I R = —$CH(CH_3)_2$
II R = —CH_2CH_2Cl

RESULTS AND DISCUSSION

Replacement of the two isopropyl groups of ketocaine (I) with two 2-chloroethyl groups was effected by treating *o*-hydroxybutyrophenone(III) with one equivalent of tris(2-chloroethyl)amine (IV) in ethanolic sodium ethoxide. This not only furnished the expected *N*-[2-(2-butanoyl)phenoxyethyl]-*N*,*N*-di(2-chloroethyl)amine (II) but also *N*,*N*-di[2-(2-butanoyl)phenoxyethyl]-*N*-(2-chloroethyl)amine (V) (Scheme I). The IR and ^{1}H-NMR spectra of compounds II and V are in agreement with the assigned structures (see *Experimental*).

For antitumor testing, female Swiss mice (average weight 21 ±1 g) were implanted on day 0 with 10^6 Ehrlich ascites tumor cells from donor mice. After 24 hr the animals were treated with compound II dissolved in water (1, 5, or 20 mg/kg, i.p.) or compound V dissolved in dimethyl sulfoxide (10, 50, or 200 mg/kg, i.p.). The amount of dimethyl sulfoxide used was shown previously, in analogous experiments, not to affect tumor growth. Deaths were recorded for the 60-day period. The activities were measured as the ratio of the mean survival time of the test animals to that of the control animals expressed as a percentage (% T/C). Significant activity is achieved with an increased life span of 25% (T/C ≥ 125).

Both compounds prolonged the life span of mice bearing Ehrlich ascites carcinoma beyond that of untreated animals: increase for compound II was 48.7% at a 5 mg/kg, i.p. dose and for compound V was 71.2% at 50 mg/kg, 24 hr after tumor implantation (Table I).

The activity of compounds II and V is related to toxicity. While compound II may act as a cross-linking agent (similar to melphalan, chlorambucil, and cyclophosphamide), the antitumor activity of compound V may be due only to its alkylating properties; its lower toxicity is in agreement with the data reported for other monofunctional agents (1).

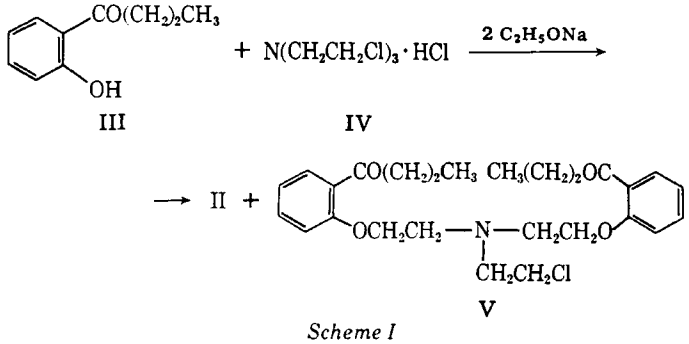

III IV

II + V

Scheme I

0022-3549/83/0700-0814$01.00/0

Table I—Antitumor Activity of Ketocaine Analogues Against Ehrlich Ascites Carcinoma in Mice

Compound	Dose, mg/kg i.p.	Number per Group	MST[a]	%,T/C[b]
Control[c]	—	10	16.0	—
II	1	5	15.0	93.7
	5	5	23.8	148.7
	20	5	—[d]	—
V	10	5	19.6	122
	50	5	27.4	171.2
	200	5	—[d]	—

[a] Mean Survival Time (days). [b] % T/C ≥ 125 denotes significant activity. [c] Saline. [d] Death due to drug-related toxicity.

EXPERIMENTAL[1]

Synthesis of Compounds II and V—*o*-Hydroxybutyrophenone (III: 16.4 g, 0.1 mole) and tris(2-chloroethyl)amine hydrochloride (IV: 24.1 g, 0.1 mole) were added to a solution of sodium ethoxide (0.2 mole) in absolute ethanol (150 ml). The mixture was refluxed for 3 hr, and the solvent was evaporated under reduced pressure. The residue was treated with water and a few drops of 34% ammonium hydroxide until alkaline, then extracted with chloroform, dried with anhydrous sodium sulfate, and evaporated under reduced pressure. Column chromatography of the residue gave 6 g of starting material (III), then 12 g of II, and finally 3 g of V. Compounds II and V, oily at room temperature, were then converted into the corresponding hydrochlorides: II HCl: mp 113–115° (absolute ethanol).

Anal.—Calc. for $C_{16}H_{23}Cl_2NO_2$·HCl: C, 52.11; H, 6.56; N, 3.80. Found: C, 52.19; H, 6.44; N, 3.72. IR (cm^{-1}): 2400–2300, 1690, 1600, 1580, 975, 760. ^{1}H-NMR (δ): 0.96 (t, 3, CH_3); 1.68 (m, 2, CH_2—CH_3); 2.84 (t, 2, $COCH_2$); 3.86 (m, 6, 3 $CH_2N^{(+)}\lesssim$), 4.10 (m, 4, 2 CH_2Cl); 4.61 (t, 2, O—CH_2); 6.9–7.7 (m, 4 aromatic).

V·HCl: mp 83–85° (toluene). *Anal.*—Calc. for $C_{26}H_{34}ClNO_4$·HCl: C, 62.90; H, 7.11; N, 2.82. Found: C, 63.18; H, 7.32; N, 2.81. IR (cm^{-1}): 2400–2300, 1670, 1600, 1580, 1125, 750. ^{1}H-NMR (δ): 0.95 (t, 6, 2 CH_3); 1.66 (m, 4, 2 CH_2—CH_3); 2.82 (t, 4, 2 $COCH_2$); 3.88 (m, 6, 3 $CH_2N^{(+)}\lesssim$); 4.12 (t, 2, CH_2Cl); 4.67 (t, 4, 2 O—CH_2); 6.9–7.7 (m, 8, aromatic).

[1] Melting points are uncorrected. Bakerflex plates (Silica-gel IB2-F) were used for TLC. For column chromatography, Kieselgel 60 (Merck) was used, activated at 120° for 2 hr: the eluent was a mixture of petroleum ether (bp 60–80°)–acetone 80:20. The IR spectra were recorded in Nujol with a Perkin-Elmer 298 spectrometer. ^{1}H-NMR spectra were recorded in $CDCl_3$ (10% w/v) with a 90-MHz spectrometer (Varian EM 390) using TMS as an internal standard.

REFERENCES

(1) W. B. Pratt and R. W. Ruddon, "The Anticancer Drugs," Oxford University Press, New York, N.Y., 1979, J. A. Stock, in "Drug Design Vol. II," E. J. Ariëns, Ed., Academic, New York, N.Y., 1971, p. 531.

(2) P. Da Re, L. Verlicchi, and I. Setnikar, *J. Med. Chem.*, **10**, 266 (1967).

(3) F. Ardizzone, M. Ariano, and I. Galatulas, *Boll. Soc. Ital. Biol. Sper.*, **44**, 60 (1967).

(4) I. Galatulas, F. Piccinini, and P. Pomarelli, *Atti Accad. Med. Lomb.*, **23**, 851 (1968).

(5) I. Galatulas, A. Nicolin, F. Piccinini, and P. Pomarelli, *Arch. Ital. Patol. Clin. Tumori*, **13**, 141 (1970).

(6) F. Ardizzone, I. Galatulas, A. Longhi, and P. Pomarelli, *Arzneim.-Forsch.*, **20**, 1794 (1970).

(7) R. Bossa, F. Dubini, I. Galatulas, and M. Taniguchi, *Arch. Ital. Patol. Clin. Tumori*, **13**, 135 (1970).

(8) C. C. Cheng and R. K. Y. Zee-Cheng, *Heterocycles*, **15**, 1275 (1981).

ACKNOWLEDGMENTS

Presented in part at the 21st Congress of the Italian Pharmacological Society in Naples, June 2–5, 1982.

Dedicated to Prof. M. Amorosa on the occasion of his 70th birthday.

Section VIII: A. Andreani, M. Rambaldi, D. Bonazzi, G. Fabbri, L. Greci, I. Galatulas, and R. Bossa, *Arch. Pharm.*, **316**, 141 (1983).

GLC Determination of (−)-1-Cyclopropylmethyl-4-(3-trifluoromethylthio-5*H*-dibenzo[*a*,*d*]cyclohepten-5-ylidene)piperidine in Human Plasma and Urine

H. B. HUCKER ˣ and J. E. HUTT

Received July 30, 1981, from the *Merck Institute for Therapeutic Research, West Point, PA 19486.* Accepted for publication June 18, 1982.

Abstract □ (−)-1-Cyclopropylmethyl-4-(3-trifluoromethylthio-5*H*-dibenzo[*a*,*d*]cyclohepten-5-ylidene)piperidine (MK-160) was extracted from human plasma and urine with petroleum ether and quantitated by GLC using a nitrogen-sensitive detector. A homologue of the drug served as the internal standard. The method is specific for the drug in the presence of potential metabolites and is capable of measuring concentrations in plasma as low as 6 ng/ml.

Keyphrases □ GLC determination—(−)-1-Cyclopropylmethyl-4-(3-trifluoromethylthio-5*H*-dibenzo[*a*,*d*]cyclohept-5-ylidene)piperidine (MK-160) in plasma and urine

(−)-1-Cyclopropylmethyl-4-(3-trifluoromethylthio-5*H*-dibenzo[*a*,*d*]cyclohepten-5-ylidene)piperidine (I)[1] shows stereospecific antipsychotic, antidopaminergic, and anticholinergic activities in the mouse, rat, and squirrel monkey (1, 2). Clinical trials in human subjects necessitated an analytical method capable of measuring low nanogram concentrations of I in plasma without interference from potential metabolites of the drug. This report describes a GLC method using a nitrogen–phosphorus detector which meets these requirements with acceptable precision and accuracy.

EXPERIMENTAL

Chemicals and Reagents—Heptane, petroleum ether (35–60°), and methanol were reagent grade; isoamyl alcohol was spectroscopic quality. Stock solutions of I HCl and II were prepared in methanol and serially diluted with methanol to the desired concentrations. All concentrations are expressed as the free base of I.

Apparatus—GLC analysis was performed with a gas chromatograph[2] equipped with a nitrogen–phosphorus detector and a 91-cm × 2-mm column packed with 3% OV-17 on Gas Chrom Q (80–100 mesh)[3]. The

[1] This compound is designated as MK-160 by Merck & Co., Inc.

[2] Hewlett-Packard Model 5840A.

[3] Supelco.

0022-3549/83/0700-0815$01.00/0

Table I—Antitumor Activity of Ketocaine Analogues Against Ehrlich Ascites Carcinoma in Mice

Compound	Dose, mg/kg i.p.	Number per Group	MST[a]	%,T/C[b]
Control[c]	—	10	16.0	—
II	1	5	15.0	93.7
	5	5	23.8	148.7
	20	5	—[d]	—
V	10	5	19.6	122
	50	5	27.4	171.2
	200	5	—[d]	—

[a] Mean Survival Time (days). [b] % T/C ≥ 125 denotes significant activity. [c] Saline. [d] Death due to drug-related toxicity.

EXPERIMENTAL[1]

Synthesis of Compounds II and V—*o*-Hydroxybutyrophenone (III: 16.4 g, 0.1 mole) and tris(2-chloroethyl)amine hydrochloride (IV: 24.1 g, 0.1 mole) were added to a solution of sodium ethoxide (0.2 mole) in absolute ethanol (150 ml). The mixture was refluxed for 3 hr, and the solvent was evaporated under reduced pressure. The residue was treated with water and a few drops of 34% ammonium hydroxide until alkaline, then extracted with chloroform, dried with anhydrous sodium sulfate, and evaporated under reduced pressure. Column chromatography of the residue gave 6 g of starting material (III), then 12 g of II, and finally 3 g of V. Compounds II and V, oily at room temperature, were then converted into the corresponding hydrochlorides: II HCl: mp 113–115° (absolute ethanol).

Anal.—Calc. for $C_{16}H_{23}Cl_2NO_2$·HCl: C, 52.11; H, 6.56; N, 3.80. Found: C, 52.19; H, 6.44; N, 3.72. IR (cm^{-1}): 2400–2300, 1690, 1600, 1580, 975, 760. ^{1}H-NMR (δ): 0.96 (t, 3, CH_3); 1.68 (m, 2, CH_2—CH_3); 2.84 (t, 2, $COCH_2$); 3.86 (m, 6, 3 $CH_2N^{(+)}\lesssim$), 4.10 (m, 4, 2 CH_2Cl); 4.61 (t, 2, O—CH_2); 6.9–7.7 (m, 4 aromatic).

V·HCl: mp 83–85° (toluene). *Anal.*—Calc. for $C_{26}H_{34}ClNO_4$·HCl: C, 62.90; H, 7.11; N, 2.82. Found: C, 63.18; H, 7.32; N, 2.81. IR (cm^{-1}): 2400–2300, 1670, 1600, 1580, 1125, 750. ^{1}H-NMR (δ): 0.95 (t, 6, 2 CH_3); 1.66 (m, 4, 2 CH_2—CH_3); 2.82 (t, 4, 2 $COCH_2$); 3.88 (m, 6, 3 $CH_2N^{(+)}\lesssim$); 4.12 (t, 2, CH_2Cl); 4.67 (t, 4, 2 O—CH_2); 6.9–7.7 (m, 8, aromatic).

[1] Melting points are uncorrected. Bakerflex plates (Silica-gel IB2-F) were used for TLC. For column chromatography, Kieselgel 60 (Merck) was used, activated at 120° for 2 hr: the eluent was a mixture of petroleum ether (bp 60–80°)–acetone 80:20. The IR spectra were recorded in Nujol with a Perkin-Elmer 298 spectrometer. ^{1}H-NMR spectra were recorded in $CDCl_3$ (10% w/v) with a 90-MHz spectrometer (Varian EM 390) using TMS as an internal standard.

REFERENCES

(1) W. B. Pratt and R. W. Ruddon, "The Anticancer Drugs," Oxford University Press, New York, N.Y., 1979, J. A. Stock, in "Drug Design Vol. II," E. J. Ariëns, Ed., Academic, New York, N.Y., 1971, p. 531.

(2) P. Da Re, L. Verlicchi, and I. Setnikar, *J. Med. Chem.*, **10**, 266 (1967).

(3) F. Ardizzone, M. Ariano, and I. Galatulas, *Boll. Soc. Ital. Biol. Sper.*, **44**, 60 (1967).

(4) I. Galatulas, F. Piccinini, and P. Pomarelli, *Atti Accad. Med. Lomb.*, **23**, 851 (1968).

(5) I. Galatulas, A. Nicolin, F. Piccinini, and P. Pomarelli, *Arch. Ital. Patol. Clin. Tumori*, **13**, 141 (1970).

(6) F. Ardizzone, I. Galatulas, A. Longhi, and P. Pomarelli, *Arzneim.-Forsch.*, **20**, 1794 (1970).

(7) R. Bossa, F. Dubini, I. Galatulas, and M. Taniguchi, *Arch. Ital. Patol. Clin. Tumori*, **13**, 135 (1970).

(8) C. C. Cheng and R. K. Y. Zee-Cheng, *Heterocycles*, **15**, 1275 (1981).

ACKNOWLEDGMENTS

Presented in part at the 21st Congress of the Italian Pharmacological Society in Naples, June 2–5, 1982.

Dedicated to Prof. M. Amorosa on the occasion of his 70th birthday.

Section VIII: A. Andreani, M. Rambaldi, D. Bonazzi, G. Fabbri, L. Greci, I. Galatulas, and R. Bossa, *Arch. Pharm.*, **316**, 141 (1983).

GLC Determination of (−)-1-Cyclopropylmethyl-4-(3-trifluoromethylthio-5*H*-dibenzo[*a*,*d*]cyclohepten-5-ylidene)piperidine in Human Plasma and Urine

H. B. HUCKER ˣ and J. E. HUTT

Received July 30, 1981, from the *Merck Institute for Therapeutic Research, West Point, PA 19486.* Accepted for publication June 18, 1982.

Abstract □ (−)-1-Cyclopropylmethyl-4-(3-trifluoromethylthio-5*H*-dibenzo[*a*,*d*]cyclohepten-5-ylidene)piperidine (MK-160) was extracted from human plasma and urine with petroleum ether and quantitated by GLC using a nitrogen-sensitive detector. A homologue of the drug served as the internal standard. The method is specific for the drug in the presence of potential metabolites and is capable of measuring concentrations in plasma as low as 6 ng/ml.

Keyphrases □ GLC determination—(−)-1-Cyclopropylmethyl-4-(3-trifluoromethylthio-5*H*-dibenzo[*a*,*d*]cyclohept-5-ylidene)piperidine (MK-160) in plasma and urine

(−)-1-Cyclopropylmethyl-4-(3-trifluoromethylthio-5*H*-dibenzo[*a*,*d*]cyclohepten-5-ylidene)piperidine (I)[1] shows stereospecific antipsychotic, antidopaminergic, and anticholinergic activities in the mouse, rat, and squirrel monkey (1, 2). Clinical trials in human subjects necessitated an analytical method capable of measuring low nanogram concentrations of I in plasma without interference from potential metabolites of the drug. This report describes a GLC method using a nitrogen–phosphorus detector which meets these requirements with acceptable precision and accuracy.

EXPERIMENTAL

Chemicals and Reagents—Heptane, petroleum ether (35–60°), and methanol were reagent grade; isoamyl alcohol was spectroscopic quality. Stock solutions of I HCl and II were prepared in methanol and serially diluted with methanol to the desired concentrations. All concentrations are expressed as the free base of I.

Apparatus—GLC analysis was performed with a gas chromatograph[2] equipped with a nitrogen–phosphorus detector and a 91-cm × 2-mm column packed with 3% OV-17 on Gas Chrom Q (80–100 mesh)[3]. The

[1] This compound is designated as MK-160 by Merck & Co., Inc.

[2] Hewlett-Packard Model 5840A.

[3] Supelco.

0022-3549/83/0700-0815$01.00/0

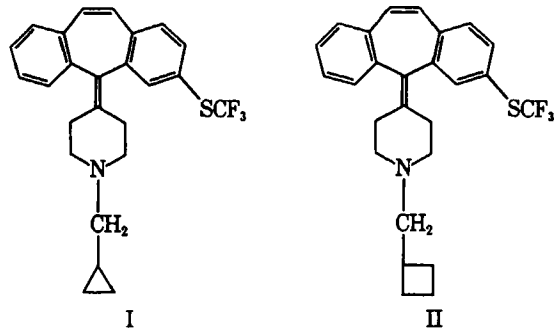

instrument was operated isothermally with column oven, detector, and injection port temperatures of 250, 275, and 300°, respectively. The carrier gas (helium), hydrogen, and air flow rates were 30, 3, and 50 ml/min, respectively. With daily use, the usable lifespan of the rubidium bead detector was ~2 months.

Procedure—To 1 ml of plasma or urine in a 13-ml glass-stoppered centrifuge tube were added 100 ng of II in 50 μl of methanol and, for plasma analysis only, 1 ml of 0.1 *N* HCl. Eight milliliters of petroleum ether–isoamyl alcohol (100:1) was added, and the tube was shaken for 10 min and centrifuged (600×*g*). Approximately 6.5 ml of the organic layer was transferred to a 13-ml centrifuge tube. The bulk of the solvent was evaporated in a stream of nitrogen in a water bath at 45°, leaving a small volume of isoamyl alcohol. The contents were dissolved in 50 μl of heptane, and 3 μl was injected into the GLC column. A standard curve was prepared by analysis of control human plasma or urine samples containing 6.25, 12.5, 25, 50, and 100 ng of I/ml and 100 ng of II/ml in a total volume of 50 μl of methanol. The ratios of the peak areas of I–II were plotted *versus* nanograms of I added.

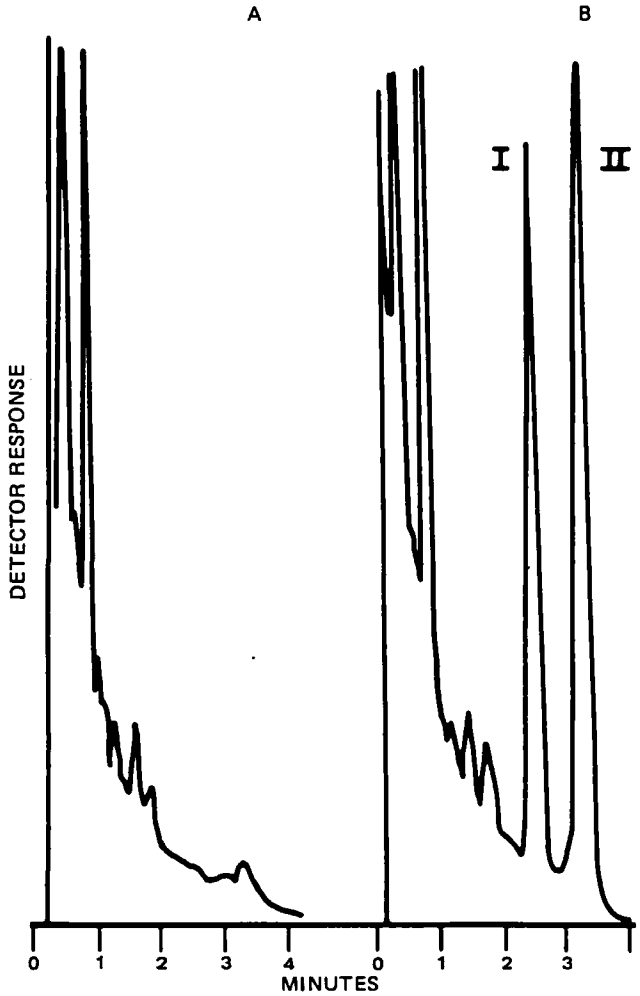

Figure 1—*Gas-liquid chromatograms (nitrogen detector) of human plasma extracts. Key: A, 0-hr human plasma; B, human plasma, containing 100 ng of I/ml to which was added 100 ng of II.*

Table I—Precision and Accuracy of the GLC Assay for I in Plasma

I Added, ng/ml	I Found[a], ng/ml	RSD, %	Relative Error, %
6.25	6.0 ± 1.1	18.3	−4.0
12.5	12.2 ± 1.7	13.9	−2.0
25	25.0 ± 2.4	9.6	0.0
50	50.3 ± 3.3	6.6	+0.6
100	99.1 ± 2.9	2.9	−0.9

[a] N = 40–48 for each concentration except at 100 ng/ml where N = 9.

Table II—Plasma Levels of I in a Human Subject after a Single Oral 120-mg Dose

Hours Postdose	Plasma I, ng/ml
1	8
2	100
4	61
6	31
8	29
24	8
32	4[a]

[a] Estimated value since 6.25 ng/ml was the lowest standard concentration analyzed.

RESULTS AND DISCUSSION

As shown in Fig. 1, I and II were adequately separated by the method, with retention times of 2.4 and 3.2 min, respectively. Control plasma or urine samples assayed concurrently gave no significant interfering peaks. Several potential metabolites of I (its sulfoxide, sulfone, and descyclopropylmethyl analogues) had retention times of 5.7, 4.9, and 1.3 min, respectively, and thus would not interfere in the determination of I.

The precision and accuracy of the method were demonstrated by analysis of replicate plasma samples containing known concentrations of I. The results are shown in Table I. The reproducibility of the method was indicated by the relative standard deviations of 18.3, 13.9, 9.6, 6.6, and 2.9%, respectively, for 6.25, 12.5, 25, 50, and 100 ng of I/ml. The accuracy of the procedure was demonstrated by the relative errors of −4, 2, 0, +0.6, and −0.9%, respectively, for 6.25, 12.5, 25, 50, and 100 ng of I/ml. The precision and accuracy of urine analyses were similar to that observed for plasma. The relative standard deviations were 15.9, 2, and 2.9%, respectively, for 6.25, 12.5, and 25 ng of I/ml of urine. The relative errors were +0.8, −4, and 3.2%, respectively, for the same concentrations. The overall recoveries for plasma and urine were ~92 and 78%, respectively.

Although I is a basic compound, its recovery from plasma was considerably higher at slightly acidic, rather than alkaline, pH values. A similar phenomenon has been reported for cinnarizine, a basic substituted piperazine with antihistaminic properties (3).

Plasma levels of I in a human subject are listed in Table II. Peak levels of drug were present at 2 hr postdose; only very low concentrations were observed after 24 or 32 hr. The urine contained no detectable amounts of I at any time after drug administration, nor was any detected in the urine of volunteers given multiple oral doses of I[4]. These results suggest that I is extensively metabolized in humans; studies with [^{3}H]I in animals indicated that I was well absorbed after oral administration. Approximately 10–30% of the dose was excreted in the urine but little or no unchanged I was present in the urine or feces[5].

This report describes a method which has adequate sensitivity to determine I in human plasma after therapeutic dosing. The use of a structurally similar internal standard obviated any need to correct the results for extraction volumes or for incomplete recovery of I from plasma or urine. Lack of interference in the assay by several potential metabolites of the drug was demonstrated.

REFERENCES

(1) D. C. Remy *et al.*, *J. Med. Chem.*, **20**, 1013 (1977).

[4] H. B. Hucker and J. E. Hutt, unpublished studies.
[5] H. B. Hucker and S. C. Stauffer, unpublished studies.

(2) B. V. Clineschmidt, M. A. McKendry, N. L. Papp, A. B. Pflueger, C. A. Stone, J. A. Totaro, and M. Williams, *J. Pharmacol. Exp. Ther.*, 208, 460 (1979).

(3) H. K. L. Hundt, L. W. Brown, and E. C. Clark, *J. Chromatogr.*, 183, 378 (1980).

ACKNOWLEDGMENTS

The authors thank Dr. D. C. Remy for a sample of the internal standard and Drs. J. D. Arnold and J. D. Irwin for supplying the human plasma samples.

Oral Bioavailability and Intravenous Pharmacokinetics of Amrinone in Humans

GEORGE B. PARK *, RONALD P. KERSHNER *, JON ANGELLOTTI *, ROGER L. WILLIAMS ‡, LESLIE Z. BENET ‡, and JEROME EDELSON *x

Received April 19, 1982, from the **Department of Drug Metabolism, Sterling-Winthrop Research Institute, Rensselaer, NY 12144* and the ‡*Drug Studies Unit, University of California, San Francisco, CA 94143.* Accepted for publication June 24, 1982.

Abstract □ Fourteen healthy males received two 75-mg doses of amrinone as a single capsule and as an intravenous solution in a single-dose crossover study. The mean (±*SD*) bioavailability, based on the area under the plasma concentration *versus* time curves, was 0.93 ± 0.12. The plasma data for these subjects during the intravenous phase was described by an open two-compartment body model with a mean (±*SD*) apparent first-order terminal elimination rate constant, β, of 0.19 ± 0.06 hr^{-1}, which corresponds to a half-life of 3.6 hr.

Keyphrases □ Amrinone—plasma levels in humans after oral and intravenous doses, pharmacokinetics, bioavailability □ Pharmacokinetics—amrinone after an intravenous dose, described by an open two-compartment body model □ Bioavailability—amrinone after oral and intravenous doses, plasma levels, pharmacokinetics

Amrinone[1], 5-amino[3,4′-bipyridin]-6(1*H*)-one, is a novel cardiotonic agent (1–4) which has demonstrated inotropic activity after both oral and parenteral administration to patients suffering from congestive heart failure (5–8). Previous investigations into the relationship between intravenous and peroral amrinone doses have suggested that it required twice as much amrinone by the oral route to achieve the same inotropic response as with an intravenous bolus (9). This report describes the results of our investigations into the bioavailability of amrinone, and includes a nonlinear least-squares estimate of the pharmacokinetic parameters of amrinone following intravenous administration.

EXPERIMENTAL

Study in Human Volunteers—In this single-dose crossover study, 14 healthy male volunteers each received two 75-mg doses of amrinone, as a single oral capsule and as an intravenous solution, with a 1-week washout interval between medications. The sequence of drug administration for each subject was determined by random assignment. Appropriate institutional review and approval were obtained. No subject had a history suggestive of renal, hepatic, or cardiac dysfunction. The mean (±*SEM*) age of these volunteers was 28.9 ± 1.2 years; the mean weight was 77.4 ± 3.4 kg and the mean height was 180 ± 1.7 cm. Blood samples were collected (potassium oxalate) before medication and at 0.17, 0.33, 0.50, 0.75, 1.0, 1.25, 1.5, 2.0, 3.0, 4.0, 5.0, 6.0, 8.0, 10.0, 12.0, 15.0, and 24.0 hr postdose. The blood was centrifuged; plasma was separated and frozen until it was assayed.

Assay Procedure—The analysis of plasma amrinone followed a published procedure (10) with the following minor changes: a 40° water bath was used to evaporate the residual ethyl acetate and ~2.3% (by volume) of tetrahydrofuran was added to the mobile phase. Plasma standards, which were prepared in normal human plasma, were extracted and analyzed with each set of plasma samples from the subjects in the study. The concentration of amrinone in plasma was determined by comparison with the regression line of the peak height ratios of the standards. The minimum quantifiable level of amrinone was estimated as the concentration whose lower 80% confidence limit just encompassed zero[2] and was ~0.02 μg/ml.

Five separate high-performance liquid chromatographic (HPLC)

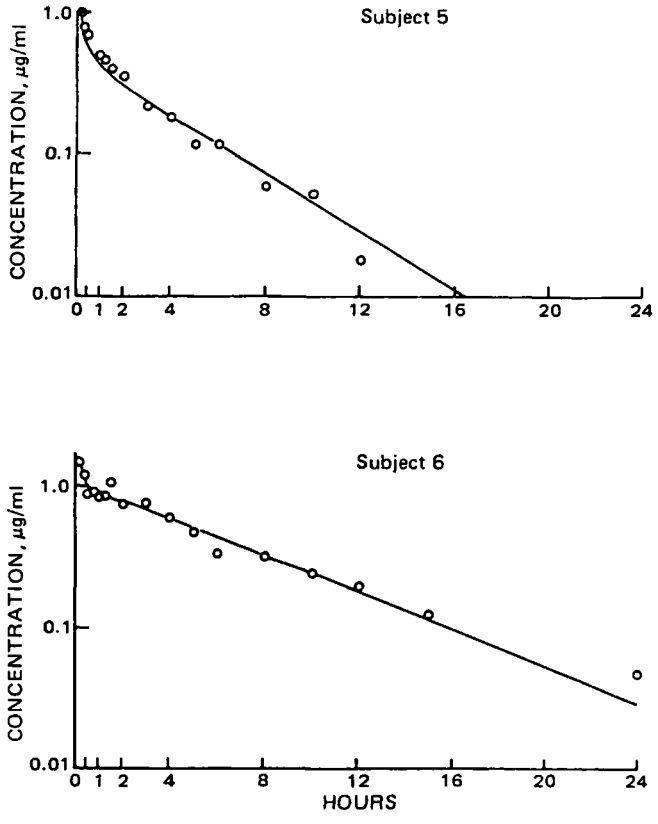

Figure 1—*Plasma concentration of amrinone in human volunteers after intravenous administration of a solution containing 75 mg of amrinone. Plasma concentrations observed (○) in two subjects with widely divergent clearance rates, and concentrations predicted by the open two-compartment body model (—).*

[1] Inocor; Sterling Drug, Inc., New York, N.Y.

[2] R. W. Ross and H. Stander, "Some Statistical Problems in Drug Metabolism," paper presented at the Princeton Conference on Applied Statistics, December 1975.

0022-3549/83/0700-0817$01.00/0

(2) B. V. Clineschmidt, M. A. McKendry, N. L. Papp, A. B. Pflueger, C. A. Stone, J. A. Totaro, and M. Williams, *J. Pharmacol. Exp. Ther.*, 208, 460 (1979).

(3) H. K. L. Hundt, L. W. Brown, and E. C. Clark, *J. Chromatogr.*, 183, 378 (1980).

ACKNOWLEDGMENTS

The authors thank Dr. D. C. Remy for a sample of the internal standard and Drs. J. D. Arnold and J. D. Irwin for supplying the human plasma samples.

Oral Bioavailability and Intravenous Pharmacokinetics of Amrinone in Humans

GEORGE B. PARK *, RONALD P. KERSHNER *, JON ANGELLOTTI *, ROGER L. WILLIAMS ‡, LESLIE Z. BENET ‡, and JEROME EDELSON *x

Received April 19, 1982, from the **Department of Drug Metabolism, Sterling-Winthrop Research Institute, Rensselaer, NY 12144* and the ‡*Drug Studies Unit, University of California, San Francisco, CA 94143.* Accepted for publication June 24, 1982.

Abstract □ Fourteen healthy males received two 75-mg doses of amrinone as a single capsule and as an intravenous solution in a single-dose crossover study. The mean (±*SD*) bioavailability, based on the area under the plasma concentration *versus* time curves, was 0.93 ± 0.12. The plasma data for these subjects during the intravenous phase was described by an open two-compartment body model with a mean (±*SD*) apparent first-order terminal elimination rate constant, β, of 0.19 ± 0.06 hr^{-1}, which corresponds to a half-life of 3.6 hr.

Keyphrases □ Amrinone—plasma levels in humans after oral and intravenous doses, pharmacokinetics, bioavailability □ Pharmacokinetics—amrinone after an intravenous dose, described by an open two-compartment body model □ Bioavailability—amrinone after oral and intravenous doses, plasma levels, pharmacokinetics

Amrinone[1], 5-amino[3,4′-bipyridin]-6(1*H*)-one, is a novel cardiotonic agent (1–4) which has demonstrated inotropic activity after both oral and parenteral administration to patients suffering from congestive heart failure (5–8). Previous investigations into the relationship between intravenous and peroral amrinone doses have suggested that it required twice as much amrinone by the oral route to achieve the same inotropic response as with an intravenous bolus (9). This report describes the results of our investigations into the bioavailability of amrinone, and includes a nonlinear least-squares estimate of the pharmacokinetic parameters of amrinone following intravenous administration.

EXPERIMENTAL

Study in Human Volunteers—In this single-dose crossover study, 14 healthy male volunteers each received two 75-mg doses of amrinone, as a single oral capsule and as an intravenous solution, with a 1-week washout interval between medications. The sequence of drug administration for each subject was determined by random assignment. Appropriate institutional review and approval were obtained. No subject had a history suggestive of renal, hepatic, or cardiac dysfunction. The mean (±*SEM*) age of these volunteers was 28.9 ± 1.2 years; the mean weight was 77.4 ± 3.4 kg and the mean height was 180 ± 1.7 cm. Blood samples were collected (potassium oxalate) before medication and at 0.17, 0.33, 0.50, 0.75, 1.0, 1.25, 1.5, 2.0, 3.0, 4.0, 5.0, 6.0, 8.0, 10.0, 12.0, 15.0, and 24.0 hr postdose. The blood was centrifuged; plasma was separated and frozen until it was assayed.

Assay Procedure—The analysis of plasma amrinone followed a published procedure (10) with the following minor changes: a 40° water bath was used to evaporate the residual ethyl acetate and ~2.3% (by volume) of tetrahydrofuran was added to the mobile phase. Plasma standards, which were prepared in normal human plasma, were extracted and analyzed with each set of plasma samples from the subjects in the study. The concentration of amrinone in plasma was determined by comparison with the regression line of the peak height ratios of the standards. The minimum quantifiable level of amrinone was estimated as the concentration whose lower 80% confidence limit just encompassed zero[2] and was ~0.02 μg/ml.

Five separate high-performance liquid chromatographic (HPLC)

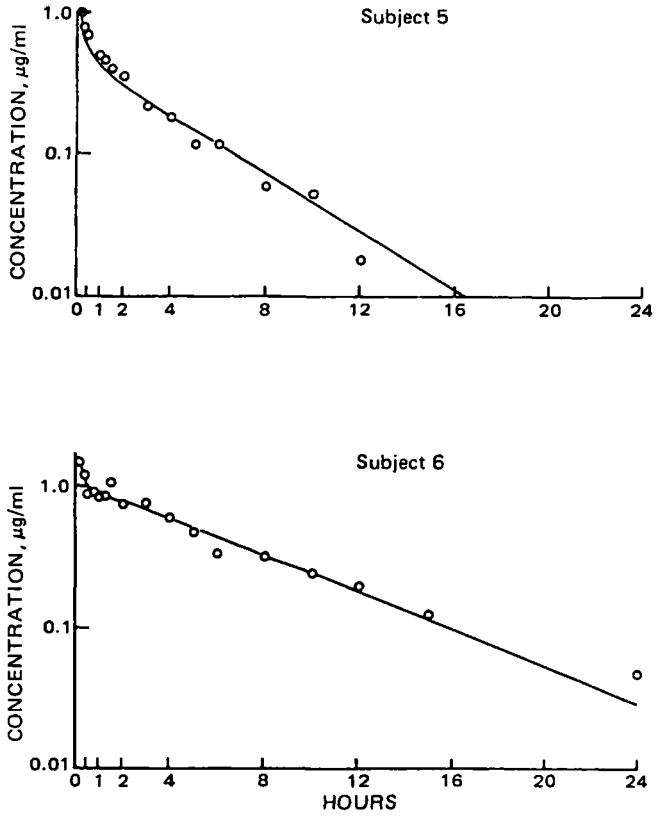

Figure 1—*Plasma concentration of amrinone in human volunteers after intravenous administration of a solution containing 75 mg of amrinone. Plasma concentrations observed (○) in two subjects with widely divergent clearance rates, and concentrations predicted by the open two-compartment body model (—).*

[1] Inocor; Sterling Drug, Inc., New York, N.Y.

[2] R. W. Ross and H. Stander, "Some Statistical Problems in Drug Metabolism," paper presented at the Princeton Conference on Applied Statistics, December 1975.

0022-3549/83/0700-0817$01.00/0

Table I—Pharmacokinetic Parameters in Humans Following a 75-mg iv Dose of Amrinone

Subject	Regression Dependent							Model Independent		
	α, hr^{-1}	β, hr^{-1}	A, $\mu g/ml$	B, $\mu g/ml$	CL, liter/hr	V_β, liter	Vd_{ss}, liter	CL, liter/hr	AUC_0^{24}, $\mu g\ hr/ml$	AUC_0^∞, $\mu g\ hr/ml$
1	9.08	0.14	0.93	0.65	16.1	113	110	16.1	4.78	5.13
2	4.13	0.23	1.30	0.50	30.1	132	116	30.2	2.59	2.59
3	8.06	0.20	2.59	0.64	21.2	106	96.9	20.8	3.86	3.96
4	3.26	0.13	1.32	0.55	16.2	125	114	16.2	4.36	4.36
5	4.29	0.24	1.22	0.50	31.3	132	117	31.4	2.23	2.23
6	7.58	0.15	1.09	1.06	10.1	69.7	68.2	10.1	7.34	7.69
7	4.00	0.17	1.20	0.62	19.4	112	104	19.4	4.28	4.45
8	18.4	0.25	46.4	0.51	16.6	65.4	29.6	16.6	1.89	1.89
9	51.4	0.14	2.20	0.73	14.0	102	101	14.0	5.48	5.85
10	0.33	0.08	0.57	0.35	12.5	151	120	12.4	5.44	6.06
11	4.87	0.29	2.54	0.59	29.1	102	82.4	29.1	2.49	2.49
12	2.04	0.14	0.78	0.73	13.0	96.2	90.3	13.0	5.68	5.98
13	3.19	0.24	0.75	0.74	22.6	94.8	88.7	22.6	3.53	3.62
14	4.45	0.29	1.91	0.74	25.1	86.9	75.2	25.1	2.88	2.88
Mean	8.94	0.19	4.62	0.64	19.8	106	93.9	19.8	4.06	4.23
$\pm SD$	13.0	0.06	12.0	0.17	6.9	23.9	24.6	7.0	1.58	1.74

Table II—Regression-Independent Parameters in Humans Following a Single Oral Capsule Containing 75 mg of Amrinone

Subject	t_{max}, min	C_{max}, g/ml	k_t, hr^{-1}	AUC_0^{24}, $\mu g\ hr/ml$	AUC_0^∞, $\mu g\ hr/ml$	Bioavailability Ratio[a], %
1	30	0.89	0.10	4.61	5.10	99
2	30	1.04	0.20	2.22	2.22	86
3	75	0.84	0.12	3.51	3.76	95
4	60	0.95	0.13	3.91	3.91	90
5	45	0.87	0.25	1.91	1.91	86
6	120	0.81	0.11	6.96	7.48	97
7	45	1.24	0.12	4.13	4.37	98
8	90	0.44	0.24	1.55	1.55	82
9	120	0.78	0.10	6.79	7.50	128
10	90	0.86	0.12	4.63	5.06	83
11	60	0.93	0.26	1.99	1.99	80
12	30	0.92	0.12	4.86	5.20	87
13	30	1.04	0.14	3.57	3.57	99
14	30	1.66	0.27	2.63	2.63	91
Mean	61	0.95	0.16	3.80	4.02	93
$\pm SD$	33	0.27	0.07	1.70	1.92	12

[a] Oral AUC_0^∞ divided by model-independent AUC_0^∞ during the intravenous phase, multiplied by 100.

systems were used. Each contained an automatic injector, a pump, a precolumn[3], a column[4], and an UV detector scanning the effluent from the column at 340 nm.

Pharmacokinetic Calculations—The data obtained from the analysis of the human plasma samples during the intravenous phase of the study was described by an open two-compartment body model by means of an unweighted nonlinear regression (NLIN) procedure (11). An attempt was made to describe the plasma concentration data obtained during the oral phase of the study by either an open one- or two-compartment body model with first-order absorption.

In addition to the regression-dependent parameters, the plasma concentration data also was analyzed with respect to the following model-independent parameters: the maximum observed plasma concentration (C_{max}), the time at which the maximum concentration was observed (t_{max}), and the area under the plasma concentration *versus* time curve (AUC_0^{24}). The latter was calculated by trapezoidal rule, including all of the data for the study period. For those subjects who had detectable concentrations of amrinone in the last sample examined, the AUC was extrapolated to infinite time.

RESULTS AND DISCUSSION

The concentrations of amrinone in the plasma samples from each of the volunteers were determined. After intravenous medication, the plasma concentrations declined biexponentially with time, suggesting that a two-compartment body model would be appropriate. Pharmacokinetic parameters for each subject were estimated after computer-fitting the plasma data by an iterative nonlinear least-squares regression technique (11); results are shown in Table I.

The mean apparent first-order terminal elimination half-life for amrinone was ~3.6 hr. The mean apparent volume of distribution at steady state was 94 liters or, dividing by the mean body weight, 1.2 liters/kg. This value suggests that amrinone may be bound to, or partition favorably into tissues. The mean value for α, 8.94 hr^{-1}, corresponds to a half-life of <5 min. The model-independent clearance (dose/AUC_0^∞) is in reasonable agreement with the clearance calculated from the open two-compartment body model (Table I). Although there is a threefold difference between the highest (subject 5) and lowest (subject 6) clearances, the observed concentration data during the intravenous phase was described adequately by the model for both of these subjects; a comparison of the observed and predicted concentrations is shown in Fig. 1. The agreement between the observed values and those predicted by the open two-compartment body model is apparent. The AUC during the intravenous phase of the study was estimated by the trapezoidal method (Table I). The mean ($\pm SD$) value was 4.23 ± 1.74 μg hr/ml.

The plasma concentration data obtained during the oral phase of the study was not described adequately by either the open one- or two-compartment body model with first-order absorption; several weighting schemes were tried. The AUC was determined by the trapezoidal method and, if necessary, extrapolated to infinite time by use of the plasma concentration in the last observed sample and the apparent first-order terminal elimination rate (Table II).

The mean ($\pm SD$) absolute bioavailability, or oral–parenteral ratio (defined as the ratio of the AUC_0^∞ for the capsule to the regression-independent AUC_0^∞ for the intravenous solution) is 0.93 ± 0.12. Analysis of variance shows that the AUC_0^∞ values for medication by either the intravenous or oral route are not significantly different ($p = 0.24$).

Although no rigorous pharmacokinetic analysis was performed, estimates of the terminal elimination half-life of amrinone from the bloodstream of healthy volunteers have been reported (12). The mean values were 2.6 hr after intravenous medication and 3.7 hr after oral treatment. These previously reported values are less than those obtained in the present study, probably due to the shorter time period during which

[3] Phenyl-Corasil; Waters Associates, Milford, Mass.
[4] μ-Bondapak phenyl; Waters Associates, Milford, Mass.

meaningful observations were made. Converting the mean terminal elimination rate constants generated in this study to half-lives results in values of 3.6 and 4.3 hr for the intravenous and oral treatments, respectively. In contrast, chronic congestive heart failure patients who received oral amrinone had a mean terminal elimination half-life of 8.3 hr (7). Since these patients all had symptoms that were sufficient to place them in class III or IV of the New York Heart Association classification, it is not surprising that their low cardiac output should result in a relatively long half-life for amrinone. Therefore, from the pharmacokinetic considerations discussed above, it would seem that an oral dosage regimen involving medication every 8 hr should be adequate for the treatment of patients with congestive heart failure.

REFERENCES

(1) A. A. Alousi, A. E. Farah, G. Y. Lesher, and C. J. Opalka, Jr., *Fed. Proc. Fed. Am. Soc. Exp. Biol*, **37**, 914 (1978).

(2) A. A. Alousi, A. E. Farah, G. Y. Lesher, and C. J. Opalka, Jr., *Circ. Res.*, **45**, 666 (1979).

(3) A. A. Alousi and J. Edelson, in "Pharmacological and Biochemical Properties of Drug Substances," vol. 3, M. E. Goldberg, Ed., American Pharmaceutical Association, Washington, D.C., 1981, p. 120.

(4) A. E. Farah and A. A. Alousi, *Life Sci.*, **22**, 1139 (1978).

(5) J. R. Benotti, W. Grossman, E. Braunwald, D. D. Davolos, and A. A. Alousi, *N. Engl. J. Med.*, **299**, 1373 (1978).

(6) J. R. Benotti, W. Grossman, E. Braunwald, and B. A. Carabello, *Circulation*, **62**, 28 (1980).

(7) J. Edelson, T. H. LeJemtel, A. A. Alousi, C. E. Biddlecome. C. S. Maskin, and E. H. Sonnenblick, *Clin. Pharmacol. Ther.*, **29**, 723 (1981).

(8) J. Wynne, R. F. Malacoff, J. R. Benotti, G. D. Curfman, W. Grossman, B. L. Holman, T. W. Smith, and E. Braunwald, *Am. J. Cardiol.*, **45**, 1245 (1980).

(9) T. H. LeJemtel, E. C. Keung, W. J. Schwartz, C. S. Maskin, M. A. Greenberg, R. S. Davis, R. Forman, H. S. Ribner, and E. H. Sonnenblick, *Trans. Assoc. Am. Physicians*, **92**, 325 (1979).

(10) M. P. Kullberg, B. Dorrbecker, J. Lennon, R. Rowe, and J. Edelson, *J. Chromatogr.*, **187**, 264 (1980).

(11) J. T. Helwig and K. A. Council, Eds., "SAS User's Guide," SAS Institute, Raleigh, N.C., 1979, p. 317.

(12) M. P. Kullberg, G. B. Freeman, C. Biddlecome, A. A. Alousi, and J. Edelson, *Clin. Pharmacol. Ther.*, **29**, 394 (1981).

Influence of Food on Aspirin Absorption from Tablets and Buffered Solutions

WILLIAM D. MASON[x] and NATHANIEL WINER

Received May 3, 1982, from the *Pharmacokinetics Laboratory, University of Missouri-Kansas City, Schools of Pharmacy and Medicine, Kansas City MO 64108.* Accepted for publication July 14, 1982.

Abstract □ After a standard meal, 12 normal volunteers received three aspirin dosage forms in a single-dose, complete crossover study. The three dosage forms were an unbuffered tablet, an effervescent solution with 16 meq of buffer, and an effervescent solution with 34 meq of buffer. Plasma and urine aspirin, salicylic acid, and salicyluric acid were measured for 10 hr. Significant differences in the absorption kinetics of aspirin were observed, with aspirin from the two solutions being absorbed faster than from the tablet. Urine pH and renal clearance for all three acid compounds were influenced by the buffer during the first 2 hr only. Area under the curve (AUC) and urine accumulation comparisons suggest that 15–20% more aspirin reaches the general circulation after the tablet, but that the total salicylate absorbed is not different. Comparison with an earlier study indicates the solution with 34 meq of buffer is virtually unaffected by the presence of the meal while the solution with 16 meq buffer and the tablet are more slowly absorbed in the nonfasted state.

Keyphrases □ Aspirin absorption—influence of food, comparison of tablets and buffered solutions □ Absorption—aspirin, influence of food

Aspirin is the drug of choice when a mild analgesic–antipyretic is required, and it is also a primary agent used in the chronic management of rheumatoid arthritis and osteoarthritis. After oral administration, rapid absorption is desirable to provide the rapid onset of effects and to reduce contact time with the gastric mucosa. The potential influence of food on the absorption kinetics of aspirin from two different buffered effervescent solutions and an unbuffered tablet dosage form is the subject of this report.

BACKGROUND

A recent report (1) from this laboratory describes the kinetics of aspirin absorption after oral administration of a tablet and two buffered solutions in fasting subjects. It was noted that while the solution with 16 meq of buffer was absorbed more rapidly than the one with 34 meq of buffer, both provided more rapid and less variable absorption than the tablet dosage form. Because the formulation with 34 meq of buffer is frequently used to treat the combined symptoms of headache and upset stomach associated with overindulgence in food and drink, the absorption kinetics of the same three formulations in nonfasted subjects were evaluated.

A recent review (2) describes the effects of food on drug bioavailability in general. Aspirin absorption from two conventional tablet dosage forms is clearly delayed and slowed when administered after a meal (3). Studies of salicylic acid kinetics suggest dispersed dosage forms such as granules (4) and effervescent solutions (5) are less subject to delayed absorption when food is present in the stomach.

Clearly the composition, quantity, and time of aspirin dosing relative to a meal can be significant factors (2, 3) in evaluating the effects of food on drug absorption kinetics. The meal chosen for the present study was previously evaluated (6) to characterize the associated physiological responses of the stomach including emptying rate, pH, and total acid production. Because the titratable acid reaches a maximal plateau between 1 and 2 hr after eating, a dose time 1 hr postcibus should provide a maximal test of the buffered solutions. The study described herein is identical to the one reported previously (1) in all aspects except the subjects in the present study ate a standard meal 1 hr prior to dosing. Two subjects were used in both studies.

EXPERIMENTAL

Dosage Forms—Three commercially available dosage forms were used to provide approximately equal doses of aspirin: two unbuffered tablets[1], each containing 325 mg of aspirin (T); one effervescent tablet[2] containing 640 mg of aspirin, 1.825 g of sodium bicarbonate, and 1.079 g of citric acid (16 meq of buffer) (S-16); and two effervescent tablets[3], each containing 324 mg of aspirin, 1.904 g of sodium bicarbonate, and 1.0 g of citric acid (34 meq of buffer) (S-34).

[1] Bayer Aspirin, Glenbrook Laboratories, Division of Sterling Drug Inc., New York, N.Y.

[2] Aspirvess, Miles Laboratory, Inc., Elkhart, Ind.

[3] Alka-Seltzer, Miles Laboratories, Inc., Elkhart, Ind.

0022-3549/83/0700-0819$01.00/0

meaningful observations were made. Converting the mean terminal elimination rate constants generated in this study to half-lives results in values of 3.6 and 4.3 hr for the intravenous and oral treatments, respectively. In contrast, chronic congestive heart failure patients who received oral amrinone had a mean terminal elimination half-life of 8.3 hr (7). Since these patients all had symptoms that were sufficient to place them in class III or IV of the New York Heart Association classification, it is not surprising that their low cardiac output should result in a relatively long half-life for amrinone. Therefore, from the pharmacokinetic considerations discussed above, it would seem that an oral dosage regimen involving medication every 8 hr should be adequate for the treatment of patients with congestive heart failure.

REFERENCES

(1) A. A. Alousi, A. E. Farah, G. Y. Lesher, and C. J. Opalka, Jr., *Fed. Proc. Fed. Am. Soc. Exp. Biol*, **37**, 914 (1978).

(2) A. A. Alousi, A. E. Farah, G. Y. Lesher, and C. J. Opalka, Jr., *Circ. Res.*, **45**, 666 (1979).

(3) A. A. Alousi and J. Edelson, in "Pharmacological and Biochemical Properties of Drug Substances," vol. 3, M. E. Goldberg, Ed., American Pharmaceutical Association, Washington, D.C., 1981, p. 120.

(4) A. E. Farah and A. A. Alousi, *Life Sci.*, **22**, 1139 (1978).

(5) J. R. Benotti, W. Grossman, E. Braunwald, D. D. Davolos, and A. A. Alousi, *N. Engl. J. Med.*, **299**, 1373 (1978).

(6) J. R. Benotti, W. Grossman, E. Braunwald, and B. A. Carabello, *Circulation*, **62**, 28 (1980).

(7) J. Edelson, T. H. LeJemtel, A. A. Alousi, C. E. Biddlecome. C. S. Maskin, and E. H. Sonnenblick, *Clin. Pharmacol. Ther.*, **29**, 723 (1981).

(8) J. Wynne, R. F. Malacoff, J. R. Benotti, G. D. Curfman, W. Grossman, B. L. Holman, T. W. Smith, and E. Braunwald, *Am. J. Cardiol.*, **45**, 1245 (1980).

(9) T. H. LeJemtel, E. C. Keung, W. J. Schwartz, C. S. Maskin, M. A. Greenberg, R. S. Davis, R. Forman, H. S. Ribner, and E. H. Sonnenblick, *Trans. Assoc. Am. Physicians*, **92**, 325 (1979).

(10) M. P. Kullberg, B. Dorrbecker, J. Lennon, R. Rowe, and J. Edelson, *J. Chromatogr.*, **187**, 264 (1980).

(11) J. T. Helwig and K. A. Council, Eds., "SAS User's Guide," SAS Institute, Raleigh, N.C., 1979, p. 317.

(12) M. P. Kullberg, G. B. Freeman, C. Biddlecome, A. A. Alousi, and J. Edelson, *Clin. Pharmacol. Ther.*, **29**, 394 (1981).

Influence of Food on Aspirin Absorption from Tablets and Buffered Solutions

WILLIAM D. MASON[x] and NATHANIEL WINER

Received May 3, 1982, from the *Pharmacokinetics Laboratory, University of Missouri-Kansas City, Schools of Pharmacy and Medicine, Kansas City MO 64108.* Accepted for publication July 14, 1982.

Abstract □ After a standard meal, 12 normal volunteers received three aspirin dosage forms in a single-dose, complete crossover study. The three dosage forms were an unbuffered tablet, an effervescent solution with 16 meq of buffer, and an effervescent solution with 34 meq of buffer. Plasma and urine aspirin, salicylic acid, and salicyluric acid were measured for 10 hr. Significant differences in the absorption kinetics of aspirin were observed, with aspirin from the two solutions being absorbed faster than from the tablet. Urine pH and renal clearance for all three acid compounds were influenced by the buffer during the first 2 hr only. Area under the curve (AUC) and urine accumulation comparisons suggest that 15–20% more aspirin reaches the general circulation after the tablet, but that the total salicylate absorbed is not different. Comparison with an earlier study indicates the solution with 34 meq of buffer is virtually unaffected by the presence of the meal while the solution with 16 meq buffer and the tablet are more slowly absorbed in the nonfasted state.

Keyphrases □ Aspirin absorption—influence of food, comparison of tablets and buffered solutions □ Absorption—aspirin, influence of food

Aspirin is the drug of choice when a mild analgesic–antipyretic is required, and it is also a primary agent used in the chronic management of rheumatoid arthritis and osteoarthritis. After oral administration, rapid absorption is desirable to provide the rapid onset of effects and to reduce contact time with the gastric mucosa. The potential influence of food on the absorption kinetics of aspirin from two different buffered effervescent solutions and an unbuffered tablet dosage form is the subject of this report.

BACKGROUND

A recent report (1) from this laboratory describes the kinetics of aspirin absorption after oral administration of a tablet and two buffered solutions in fasting subjects. It was noted that while the solution with 16 meq of buffer was absorbed more rapidly than the one with 34 meq of buffer, both provided more rapid and less variable absorption than the tablet dosage form. Because the formulation with 34 meq of buffer is frequently used to treat the combined symptoms of headache and upset stomach associated with overindulgence in food and drink, the absorption kinetics of the same three formulations in nonfasted subjects were evaluated.

A recent review (2) describes the effects of food on drug bioavailability in general. Aspirin absorption from two conventional tablet dosage forms is clearly delayed and slowed when administered after a meal (3). Studies of salicylic acid kinetics suggest dispersed dosage forms such as granules (4) and effervescent solutions (5) are less subject to delayed absorption when food is present in the stomach.

Clearly the composition, quantity, and time of aspirin dosing relative to a meal can be significant factors (2, 3) in evaluating the effects of food on drug absorption kinetics. The meal chosen for the present study was previously evaluated (6) to characterize the associated physiological responses of the stomach including emptying rate, pH, and total acid production. Because the titratable acid reaches a maximal plateau between 1 and 2 hr after eating, a dose time 1 hr postcibus should provide a maximal test of the buffered solutions. The study described herein is identical to the one reported previously (1) in all aspects except the subjects in the present study ate a standard meal 1 hr prior to dosing. Two subjects were used in both studies.

EXPERIMENTAL

Dosage Forms—Three commercially available dosage forms were used to provide approximately equal doses of aspirin: two unbuffered tablets[1], each containing 325 mg of aspirin (T); one effervescent tablet[2] containing 640 mg of aspirin, 1.825 g of sodium bicarbonate, and 1.079 g of citric acid (16 meq of buffer) (S-16); and two effervescent tablets[3], each containing 324 mg of aspirin, 1.904 g of sodium bicarbonate, and 1.0 g of citric acid (34 meq of buffer) (S-34).

[1] Bayer Aspirin, Glenbrook Laboratories, Division of Sterling Drug Inc., New York, N.Y.

[2] Aspirvess, Miles Laboratory, Inc., Elkhart, Ind.

[3] Alka-Seltzer, Miles Laboratories, Inc., Elkhart, Ind.

0022-3549/83/0700-0819$01.00/0

Table I—Mean Plasma/Urine Aspirin Data and Computed Parameters

Parameter	Mean ± SD, mg/liter[a] T	S-16	S-34
Time, min			
5	0.51 ± 0.57 b	3.32 ± 2.64 c	3.09 ± 1.79 c
10	1.24 ± 0.95 b	6.91 ± 2.14 c	6.17 ± 3.41 c
15	1.90 ± 1.31 b	9.12 ± 3.71 c	8.66 ± 3.14 c
20	2.77 ± 1.92 b	9.41 ± 2.03 c	9.70 ± 2.12 c
30	3.65 ± 3.27 b	7.07 ± 1.28 c	7.47 ± 2.17 c
45	4.42 ± 2.37 b	4.22 ± 1.09 b	4.82 ± 1.66 b
60	4.33 ± 1.52 b	2.95 ± 1.01 c	2.90 ± 1.05 c
90	3.24 ± 1.27 b	1.33 ± 0.52 c	1.25 ± 0.61 c
120	2.29 ± 0.86 b	0.54 ± 0.30 c	0.51 ± 0.29 c
AUC to 120 min, (mg min)/liter	380 ± 124 b	434 ± 60.0 bc	460 ± 70.8 c
Time of maximum concentration, min	60.6 ± 28.2 b	18.6 ± 6.0 c	22.8 ± 5.4 c
Maximum concentration, mg/liter	5.47 ± 2.60 b	10.36 ± 3.13 c	10.0 ± 2.18 c
AUC to infinity, (mg min)/liter	545 ± 101 b	462 ± 61.8 c	479 ± 78.0 c
MRT[b], min	85.2 ± 20.0 b	44.4 ± 10.0 c	41.3 ± 8.4 c
MAT[b], min	62.7 ± 20.0 b	21.9 ± 10.0 c	18.8 ± 8.4 c
VRT, hr	50.7 ± 26.8 b	16.6 ± 8.7 c	16.6 ± 8.7 c
Urine pH 0–2 hr	5.90 ± 0.54 b	6.14 ± 0.45 b	6.70 ± 0.57 c
Renal Clearance 0–2 hr, liter/hr	1.19 ± 0.45 b	1.67 ± 0.60 c	1.76 ± 0.43 c
Terminal log-linear half-life, min	39.0 ± 13.8 b	30.6 ± 14.4 c	23.4 ± 5.4 c

[a] A common letter following the standard deviation indicates no significant difference ($p < 0.05$) (*i.e.*, for AUC to 120 min T and S-16 do not differ and S-16 and S-34 do not differ; however, T and S-34 do differ). [b] MRT is the mean residence time and MAT is the mean absorption time per refs. 7 and 8. MAT computation assumes MRT_{IV} to be 15.6 min for all subjects.

Subjects—Twelve healthy male volunteers, 21–27 years old and weighing 56.9–88.6 kg, were evaluated by a comprehensive physical examination, blood chemistry profile (including blood count and differential), and complete urinalysis. None of the subjects had a history of GI disease or surgery. All were free of any active disease process and none had any medication for 14 days prior to the study.

Methods—A Latin-square design for three treatment in 12 subjects over three consecutive weekends was employed. A 10-hr fast (overnight) was followed by a standard meal (6) consisting of 90 g (uncooked weight) of tenderloin steak, 0.1 g of salt, 25 g of white bread, 8 g of butter, 60 g of vanilla ice cream, 35 g of chocolate syrup, and 240 ml of water. The total caloric value was 458 with approximately 40% fat, 40% carbohydrate, and 20% protein. If blended, the meal provided 540 mosmoles at pH 6.0.

One hour after completing the meal, which was eaten evenly over 30 min, predose blood and urine samples were collected and the aspirin doses administered. A total volume of 240 ml of water, as described previously (1), was given with each dose. After dosing, 100 ml of water was administered at 1, 2, and 3 hr, and each subject ate a uniform meal after the 4-hr blood sample. Subjects remained standing or sitting throughout the day, and exercise was limited to walking about the room. Blood and urine collection and the method of analysis were identical to those used in the preceding study (1).

RESULTS

The mean plasma concentrations and computed parameters for aspirin and salicylic acid are presented in Tables I and II, respectively. The rank order and profile projected in the tables was the same in all 12 subjects except the tablets frequently showed two or three maxima. Urine pH, flow rate, and drug recovery were almost identical to that reported without the meal (1) and, therefore, are not presented in detail herein. From the accumulation as aspirin, salicylic acid, and salicyluric acid in the urine over 10 hr the recovery (projected to infinity) ranged between 65 and 71% for the 36 doses, with no differences among the three dosage forms. Also, the renal clearance of aspirin, salicylic acid, and salicyluric acid agreed with the previously reported fasting study (1), with the salicylurate clearance between 33 and 38 liter/hr for all treatments.

Statistical moments as described by Yamaoka *et al.* (7) and Riegelman and Collier (8) were used and computed as in the previous report (1), with one change. Comparison of the terminal log linear half-lives for aspirin (*i.e.*, 39 ± 13.8, 30.6 ± 14.4, and 23.4 ± 5.4 min) in Table I are longer than previously reported: 14.9 min by Rowland and Riegelman (9) and 15.6 min by Mason and Winer (1), for the elimination half life of aspirin, thus indicating a flip-flop model. Therefore the terminal half-life cannot be used to estimate the elimination rate for aspirin or be used to compute the mean absorption time (MAT). The MAT values in Table I were computed by assuming that each subject has an aspirin elimination half-life of 15.6 min (*i.e.*, MRT_{IV} = 22.5 min), which was the mean estimate in the previous study (1). Computed in this manner the MAT values are estimates of the actual MAT values and represent the differences among the three dosage forms if the total aspirin clearance is constant over the 3 weeks.

DISCUSSION

Although the urine recovery shows the total salicylate absorbed to be about the same for all three dosage forms, there are significant differences in the rate and extent of bioavailability. After the meal, the plasma aspirin curves produced by the two effervescent solutions are almost identical, while the tablets produced later and lower maximum concentrations. The maximal aspirin concentrations for two effervescent solutions are nearly twice that for the tablet dosage form with higher aspirin concentrations by the 5-min sampling time. In addition, the maxima occurs in approximately one-third the time for the effervescent solutions compared with the tablets. These differences and the greater area under the curve (AUC) for the first 2 hr indicate the delaying effect of food on the rate of aspirin absorption from tablets but not on aspirin absorption from effervescent solutions. The areas under the aspirin and salicylic acid curves (when extrapolated to infinity) are ~15% greater for the tablets than for either of the solutions. Consistent with the earlier report (1), greater salicylic acid areas for the tablet dosage form can be attributed to the higher renal clearance with the buffered solutions. The larger aspirin area for the tablet suggests more drug has undergone gastric absorption, thus escaping intestinal metabolism. This hypothesis is supported by the fact that only a small proportion (1–2%) of aspirin clearance is renal, and thus even the observed twofold changes cannot significantly alter the plasma time curve.

Aspirin absorption kinetics can be complex with tablet dissolution, gastric absorption, and gastric emptying all being rate-determining processes. The statistical moment approach makes no assumption concerning the absorption kinetics and treats aspirin kinetics as a purely stochastic process. The MRT values for the tablet are almost twice those for the two solutions and reflect the longer residence time for aspirin in the body after the tablets. If the total aspirin clearance is constant for the three treatments then the greater MRT for the tablets is due to its remaining in the GI tract longer. The MAT values show that a longer time interval (about 40 min) is required for 63.2% of the aspirin to be absorbed after administration of the tablets than after administration of the solutions. These results primarily reflect the rate at which aspirin leaves the stomach and enters the intestine and/or the continued dissolution of the tablets. As noted above, the acid gastric contents and longer residence in the stomach result in some absorption occurring through the gastric mucosa and less intestinal metabolism.

In the fasting subjects S-16 was absorbed more rapidly than S-34 and

Table II—Mean Plasma/Urine Salicylic Acid Data and Computed Parameters

Parameter	Mean ± *SD*, mg/liter[a]		
	T	S-16	S-34
Time			
5 min	0.55 ± 0.45 b	4.09 ± 3.66 c	4.46 ± 1.69 c
10 min	1.29 ± 0.91 b	9.55 ± 4.83 c	10.21 ± 3.97 c
15 min	2.82 ± 1.91 b	17.42 ± 6.38 c	18.16 ± 5.66 c
20 min	4.36 ± 2.70 b	21.07 ± 5.78 c	24.61 ± 6.99 c
30 min	8.19 ± 5.97 b	27.02 ± 5.38 c	31.83 ± 5.58 d
45 min	13.91 ± 8.54 b	30.78 ± 4.12 c	35.64 ± 5.78 d
1 hr	19.11 ± 9.05 b	32.78 ± 3.41 c	37.14 ± 5.32 d
1.5 hr	26.81 ± 10.55 b	33.35 ± 3.94 c	37.36 ± 5.11 c
2 hr	31.57 ± 10.58 b	30.84 ± 4.09 b	35.01 ± 5.46 b
3 hr	33.26 ± 6.30 b	26.34 ± 3.40 c	29.71 ± 4.55 d
4 hr	32.01 ± 3.92 b	22.87 ± 3.60 c	25.52 ± 4.71 d
6 hr	21.97 ± 3.74 b	14.83 ± 2.75 c	16.94 ± 5.63 d
8 hr	15.39 ± 4.49 b	9.02 ± 2.49 c	9.92 ± 3.19 c
10 hr	10.38 ± 4.18 b	5.42 ± 1.95 c	6.11 ± 2.38 c
AUC to 2 hr, (mg hr)/liter	34.58 ± 14.00 b	56.82 ± 6.39 c	62.72 ± 8.22 c
Time of maximum concentration, hr	3.00 ± 0.74 b	1.25 ± 0.32 c	1.15 ± 0.34 c
Maximum concentration, mg/liter	36.79 ± 5.38 b	34.17 ± 3.72 c	38.35 ± 4.91 b
AUC to infinity, (mg hr)/liter	275.17 ± 61.46 b	218.52 ± 49.39 c	233.65 ± 45.76 c
Urine pH, 0–2 hr	5.90 ± 0.54 b	6.14 ± 0.45 b	6.70 ± 0.57 c
Renal Clearance[b] 0–2 hr, liter/hr	0.11 ± 0.14 b	0.19 ± 0.12 b	0.39 ± 0.25 c
Terminal log-linear half-life, hr.	3.55 ± 1.06 b	2.76 ± 0.63 c	2.76 ± 0.62 c

[a] A common letter following the standard deviation indicates no significant difference ($p < 0.05$) (*i.e.*, at the 4-hr salicylate concentration all three means are significantly different as none share a common letter). [b] Although the renal clearance for S-16 and T do not differ significantly at $p < 0.05$ one can reject the null hypothesis if the willingness to accept a Type I error is increased to about 10% (*i.e.*, $p < 0.1$).

had a greater AUC (1). The presence of a meal has eliminated these differences. The more highly buffered solution (S-34) has the same profile and almost identical estimated kinetic parameters (MAT_{meal} = 18.8 min; $MAT_{fasting}$ = 19.81 min) for absorption with and without a meal, while the S-16 solution is absorbed more slowly with a meal present (MAT_{meal} = 21.9 min, $MAT_{fasting}$ = 15 min).

The report by one group (3) that very little aspirin is bioavailable (*i.e.*, 5–8% nonfasting and 16–18% fasting) is not consistent with the 68% estimated by Rowland and Riegelman (9). The difference probably results from the application of a compartment model (3) to estimate elimination and absorption rate constants when delayed and/or continued absorption rendered such modeling inappropriate (flip-flop model). As discussed previously (1) the bioavailability of aspirin is influenced by the ratio of gastric emptying rate to gastric absorption rate, with the absolute bioavailability in the ~50–60% range.

In summary, the absorption of aspirin from tablets after a meal is significantly slower than from buffered effervescent solutions. Both 16 and 34 meq of soluble buffer produce relatively rapid absorption with similar peak aspirin plasma concentration. Comparisons with an earlier work show the 34 meq of buffer to provide plasma aspirin and salicylate profiles which are the same for fasted and nonfasted subjects. These data suggest that for occasional therapy intended to produce high plasma aspirin concentrations rapidly in both fasted and nonfasted individuals, buffered effervescent solutions are significantly better than nonbuffered aspirin tablets.

REFERENCES

(1) W. D. Mason and N. Winer, *J. Pharm. Sci.*, **70**, 262 (1981).

(2) R. Toothaker and P. Welling, *Annu. Rev. Pharmacol. Toxicol.*, **20**, 173 (1980).

(3) P. Koch, C. Schultz, J. Wills, S. Hallquist, and P. Welling, *J. Pharm. Sci.*, **67**, 1533 (1978).

(4) C. Bogentoft, I. Carlsson, G. Ekenved, and A. Magnusson, *Eur. J. Clin. Pharmacol.*, **14**, 351 (1978).

(5) G. Volans, *Br. J. Clin. Pharmacol.*, **1**, 137 (1974).

(6) J. Malagelada, G. Longstreth, W. Summerskill, and V. Go, *Gastroenterology*, **70**, 203 (1976).

(7) K. Yamaoka, T. Nakagawa, T. Uno, *J. Pharmacokinet. Biopharm.*, **6**, 547 (1978).

(8) S. Riegelman and P. Collier, *J. Pharmacokinet. Biopharm.*, **8**, 509 (1980).

(9) N. Rowland and S. Riegelman, *J. Pharm. Sci.*, **57**, 1313 (1968).

Rapid and Simplified Assay for Thyroid in Pharmaceutical Preparations by Potentiometric Titration

STEVEN L. RICHHEIMER ˣ **and MERL S. SCHACHET**

Received April 12, 1982, from the *Quality Control Division, Pharmaceutical Basics, Inc., Denver, CO 80223.* Accepted for publication July 1, 1982.

Abstract □ A procedure for the determination of thyroid (thyroid hormone) in pharmaceutical preparations by titration with 1 m*M* silver nitrate using an ion-selective electrode was developed and evaluated. Samples were combusted according to the USP procedure and analyzed with a minimum of work-up for iodine content. The results obtained by this method were compared with those obtained by the official methods. The recovery of iodide from spiked placebo samples was investigated. The method is applicable to content uniformity analyses as well as to bulk material and to the analysis of organically bound iodide in other pharmaceutical preparations such as sodium levothyroxine tablets. The method is fast, simple, accurate, applicable to automation, and is suitable for routine quality control use.

Keyphrases □ Thyroid—determination in pharmaceutical preparations, potentiometric titration of iodide □ Thyroid and sodium levothyroxine analyses—assay by potentiometric titration, content uniformity analyses

The USP XX method (1) for the assay of thyroid (thyroid hormone) in tablets and bulk material involves combustion of the samples at 675–700° with potassium carbonate followed by oxidation under acidic conditions to iodate by heating with excess bromine. The addition of potassium iodide converts the iodate to iodine, which is then titrated with sodium thiosulfate (2). The method for content uniformity analyses involves oxygen flask combustion followed by conversion of the iodine to triiodide ion and spectrophotometric determination. These methods are lengthy and filled with difficulties.

This report describes a simplified method for the assay of organically bound iodide, which uses an iodide-selective electrode (3–6). The method is applicable to the analysis of not only thyroid in tablets and bulk material but also to other pharmaceutical preparations in which organically bound iodine is determined.

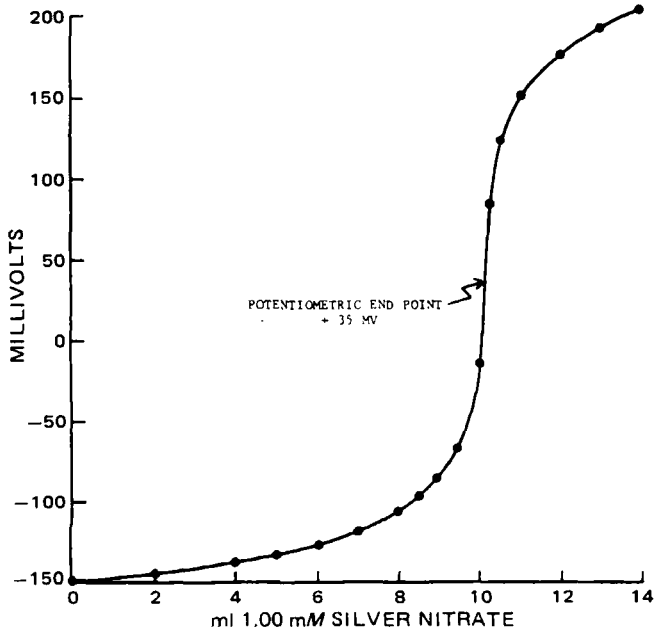

Figure 1—*Titration curve of a titrated thyroid sample containing ~0.01 meq of iodide with 1.00 m*M *silver nitrate using an iodide-sensing electrode, pH 2.5. Arrow indicates potentiometric end point + 35 mV.*

EXPERIMENTAL

Reagents and Materials—Sodium iodide reference standard (0.100 *M*)[1] was used as received or diluted as required with water; 1.00 m*M* silver nitrate solution was prepared by dilution of 0.100 *M* silver nitrate solution[2] and standardized by potentiometric titration against 1.00 m*M* iodide standard. This solution is quite stable if protected from light. Anhydrous potassium carbonate[3] was technical grade; dilute phosphoric acid was made by 1:1 dilution of reagent grade (85%) phosphoric acid[4]; deionized water[5] was used throughout; crucibles were porcelain[6] and all other tablet excipients were pharmaceutical grade and obtained commercially. The thyroid tablets were manufactured by Pharmaceutical Basics, Inc.

Apparatus and Equipment—A muffle furnace[7] was used for sample combustion. The specific ion electrodes used were an iodide-sensing electrode[8] and a silver-sulfide-sensing electrode[9]; the reference electrode was a double-junction type[10]. The potentiometric titrations were performed either automatically or manually to a predetermined millivolt end point using an end-point titrator fitted with a 20-ml dispensing buret unit and an antidiffusion buret tip[11].

Sample Preparation—*Uncoated Tablets and Bulk Material*—Twenty tablets were ground to a fine powder and a portion equivalent to ~635 mg of thyroid (proportionately less should be used if the iodine content is >0.2%) was weighed into a large crucible; this portion was mixed with ~8 g of anhydrous potassium carbonate, compressed, and then overlayed with 16 g of carbonate. The mixture was ignited at 675–700° in a preheated muffle furnace for 25 min. The cooled char was transferred to a 600-ml beaker, using water to facilitate the transfer, and then acidified to pH 2.5 ± 1 with dilute phosphoric acid while stirring vigorously with a magnetic stirrer. Water was added to bring the volume to 400 ml, and the mixture was titrated immediately with 1 m*M* silver nitrate to the potentiometric end point using an iodide-sensing electrode and a suitable reference electrode. (Each milliliter of 1 m*M* silver nitrate is equivalent to 0.1269 mg of iodine.)

Coated Tablets—The coated sample was prepared in the same way as the uncoated tablets except that the char was treated with hot water, filtered and then acifidied with dilute phosphoric acid, and the volume brought to 400 ml with water. (If calcium sulfate is used in the formulation, the acidified solution is boiled for at least 30 min.) The solution was cooled to room temperature and titrated with 1 m*M* silver nitrate to the potentiometric end point.

Content Uniformity Analyses—The procedure for uncoated or coated tablets was followed, except that 10 tablets were individually analyzed.

Sodium Levothyroxine Tablets—Twenty tablets were finely powered and an amount equivalent to 1–2 mg of sodium levothyroxine was weighed into a crucible. The procedure for uncoated tablets was followed

[1] Orion Research, Cambridge, Mass.
[2] Dilut-It, J. T. Baker Chemical Co., Phillipsburg, N.J.
[3] Diamond Shamrock Corp., Irving, Tex.
[4] J. T. Baker Chemical Co., Phillipsburg, N.J.
[5] Continental Water Conditioning Corp., Denver, Colo.
[6] Coors Porcelain, Golden, Colo.
[7] Thermolyne 2000, Sybron Corp., Dubuque, Iowa.
[8] Orion Research, Model 94-53.
[9] Orion Research Model 94-16.
[10] Orion Research Model 90-20.
[11] Metrohm/Brinkmann model E526 Titrator and model 655 Dosimat, Westbury, N.Y.

0022-3549/83/0700-0822$01.00/0

Table I—Percentage of Iodine in a 130-mg Thyroid Tablet by the USP XX Method and by the Proposed Method in the Presence and Absence of Charcoal

	USP XX Method	Proposed Method No Charcoal	Proposed Method With Charcoal
Iodine, %	0.190	0.190	0.190
Number of determinations	12	16	11
Range, %	0.175–0.199	0.180–0.202	0.180–0.201
RSD, %	4.6	3.6	3.4

except that each milliliter of 1 m*M* silver nitrate was equivalent to 0.1997 mg of sodium levothyroxine.

RESULTS AND DISCUSSION

Figure 1 shows the titration curve obtained with a typical thyroid sample containing ~0.01 meq of iodide is titrated with 1 m*M* silver nitrate using an iodide-sensing electrode and a suitable reference electrode. The end point occurs at about +35 milivolts mV in this sample but may vary according to the electrode pair used. A similar curve is obtained using a silver-sensing electrode. The iodide electrode can also be used to quantitatively measure inorganic iodide in thyroid preparations. Changing the pH of the solution from 1.5 to 3.5 has very little effect on the overall titration curve and the end point (± 5 mV). For content uniformity determinations of low-strength thyroid preparations (16–65 mg), the curve is shifted somewhat to a lower millivolt end point. Therefore, it is advisable to determine the end point of such samples in advance by titrating a representative sample and plotting the titration curve. Since the break in the curve near the end point is sharp, and since there is a change of almost 200 mV within ±0.5 ml of the end point, it is practical to titrate thyroid samples automatically using either an end-point titrator or recording titrator. It is also possible to perform the titrations manually using a pH–mV meter and buret to the predetermined end point.

Comparison of the USP XX Method—A 130-mg (2 gr) uncoated thyroid tablet was assayed by potentiometric titration and by the USP XX method. The results are shown in Table I and indicate that this method gives results equivalent to the USP method. Filtration of the charcoal produced in the combustion process is not necessary for ordinary compressed tablets if the sample is titrated immediately. However, stirring the sample in the presence of charcoal at pH 2.5 slowly oxidizes the iodide. In addition to this tablet, numerous lots of thyroid tablets (both coated and uncoated) and capsules and bulk material were assayed by both the USP and potentiometric titration methods. The two methods agreed closely, although the proposed method gave somewhat more consistent results, which were also closer to the theoretical input.

Recovery of Iodide from Spiked Placebos—Placebo mixtures containing excipients found in typical coated and uncoated thyroid tablets were prepared and spiked with iodide over the range of 0.0085–0.0115 meq (equivalent to 0.17–0.23% iodine). The recovery of iodide from the spiked samples was quantitative, and the relative standard deviations (*RSD*) of the recoveries varied from 0.58 to 1.24%. Linearity was excellent (r = 1.00), and placebo blanks showed that there was no interference from the tablet excipients (millivolt reading past the end point). The results are summarized in Table II.

Table II—Recovery of Iodide Added to Placebo Preparations

	Coated Tablet with Calcium Sulfate	Coated Tablet with Calcium Carbonate	Uncoated Tablet
Mean recovery, %	99.5	99.8	100.0
Number of determinations	10	13	16
Range, %	97.3–101.2	97.7–101.3	98.7–100.6
RSD, %	1.24	1.40	0.58

Table III—Recovery of Iodide Added to Content Uniformity Placebo Preparations

	16-mg Uncoated Tablet, 0.00025 meq Iodide Spike	65-mg Coated Tablet, 0.001 meq Iodide Spike	195-mg Uncoated Tablet, 0.003 meq Iodide Spike
Average recovery, %	98.9	100.9	100.7
Number of determinations	10	10	10
Range, %	96.0–104.0	98.8–103.7	98.4–101.9
RSD, %	3.33	1.60	1.60

Effect of Calcium Sulfate—When calcium sulfate is used in the formulation of coated tablets, sulfide is produced in the combustion process. Since sulfide interferes with both the iodide and silver-sensing electrodes, methods were investigated to remove this interfering ion. The addition of heavy metals, such as Ni(II), was not successful in removing the interference, while addition of hydrogen peroxide oxidized the sulfide but also slowly oxidized the iodide. Boiling of the filtered, acidified solution was found to be an acceptable method for removing the interfering sulfide. However, in samples with less sulfide, such as content uniformity samples, the boiling step can be eliminated by acidifying the char before filtration. Apparently the charcoal produced in the combustion process oxidizes the sulfide to a noninterfering form (possibly persulfide), since the addition of ascorbic acid again generates sulfide.

Content Uniformity Assays—The described method has been successfully applied to routine quality control work for content uniformity determinations of tablets ranging in potency from 16 to 324 mg of thyroid. For low-potency tablets the volume of titrant is small and the electrode response is slower; such samples may require manual titration. Table III summarizes the results obtained when placebo samples spiked with 0.00025, 0.001, and 0.003 meq of iodide (corresponding to 16-, 65-, and 195-mg tablets) are assayed by the present method. The results indicate that recovery of the added iodide is quantitative and that reproducibility is good.

Analysis of Sodium Levothyroxine Tablets—The above procedure provides a fast and accurate method for the analysis of sodium levothyroxine (I) in tablets. Sample preparation is the same as for uncoated thyroid tablets, except that an amount of powered tablets equivalent to 1–2 mg of I is used. Mean recoveries of I added to placebo mixtures were 99.8% (11 determinations; *RSD* 1.8%) for a 0.1-mg preparation and 99.2% (six determinations; *RSD* 0.7%) for a 0.3 mg tablet. Linearity of the method in both cases was excellent (r = 0.99).

REFERENCES

(1) "The United States Pharmacopeia," 20th rev., U.S. Pharmacopieal Convention, Rockville, Md., 1980, pp. 800–801.

(2) A. H. Beckett and J. B. Stenlake, "Practical Pharmaceutical Chemistry," Athlone, London, 1962, pp. 141–142.

(3) W. L. Hoover, J. R. Melton, and P. A. Howard, *J. Assoc. Off. Agric. Chem.*, **54**, 760 (1971).

(4) B. Paletta and K. Panzebeck, *Clin. Chim. Acta*, **26**, 11 (1969).

(5) B. Paletta, *Mikrochim. Acta*, **6**, 1210 (1969).

(6) U. Westerlune-Helmerson, *Anal. Chem.*, **43**, 1120 (1971).

Cobaltous Chloride-Induced Hypothermia in Mice III: Effect of Pretreatment with 5-Hydroxytryptaminergic Agents

DAVID H. BURKE ˣ, JACK C. BROOKS, and SUZANNE B. TREML

Received June 10, 1982, from the *Divisions of Pharmacology and Physiology, Marquette University School of Dentistry, Milwaukee, WI 53233.* Accepted for publication July 1, 1982.

Abstract □ The influence of various 5-hydroxytryptaminergic agonist and antagonist drugs on body-temperature response to cobaltous chloride in mice was noted. Pretreatment with *p*-chloroamphetamine, *p*-chlorophenylalanine, and *p*-iodoamphetamine antagonized the body-temperature response to cobalt. *p*-Chloroamphetamine and *p*-chlorophenylalanine reduced, while *p*-iodoamphetamine elevated, brain serotonin levels. The uptake inhibitor agents, fluoxetine and nisoxetine, failed to modify the ability of *p*-chloroamphetamine to antagonize cobalt hypothermia. Cyproheptadine, methergoline, and xylamidine pretreatment enhanced rather than antagonized body-temperature depression by cobalt. Tryptophan hydroxylase inhibitors antagonized cobalt hypothermia, but receptor-blocking agents were without influence, indicating that antagonism was mediated through mechanisms other than the depletion of serotonin. Elevation rather than depletion of brain serotonin by *p*-iodoamphetamine and failure of uptake inhibitors to modify *p*-chloroamphetamine antagonism of cobalt hypothermia lend further support for a nonserotonergic role of these amines in their ability to antagonize body-temperature depression by cobaltous chloride in mice.

Keyphrases □ Cobaltous chloride—induced hypothermia in mice, pretreatment with 5-hydroxytryptaminergic agents □ Hypothermia—induction in mice with cobaltous chloride, effects of pretreatment with 5-hydroxytryptamingeric agents

Cobaltous chloride has been reported to produce a dose-dependent depression of body temperature in several species, apparently through a centrally mediated decrease in heat production (1). Subsequent studies in this laboratory revealed that chlorpromazine was capable of antagonizing cobalt-induced hypothermia in mice, and it was concluded that central α-receptor blockade and/or peripheral antihistaminic activity, but not anticholinergic activity, may have contributed to this partial antagonism (2). Most recently, *p*-chloroamphetamine hydrochloride has been shown to attenuate markedly the body temperature response to cobalt in this same species (approximately 60% antagonism) (3). Although this compound has not been extensively studied in mice, it appeared possible that its well-known antiserotonin qualities may contribute to antagonism of the body temperature depression. The present report describes the influence of various 5-hydroxytryptaminergic agonists and antagonists on the body-temperature response to cobaltous chloride in mice.

EXPERIMENTAL

Male Swiss albino mice (20–30 g) were used in this investigation. The animals were housed in groups of 6–20 with *ab libitum* access to food[1] and water for at least 3 days prior to use. The mice were kept in a draft-free room under constant-temperature conditions (23 ± 1°) and maintained on a 12-hr light/dark cycle. All drugs were freshly prepared with distilled water in concentrations (calculated as the salt) such that a volume of 0.01 ml/g was delivered. Methergoline was solubilized with distilled water acidified to pH 3.8 with ascorbic acid. All injections were delivered by the intraperitoneal route.

A thermistor thermometer[2] was used for obtaining rectal temperature. Temperatures were recorded with a thermistor probe inserted 2.5 cm and held in position until constant readings were attained.

At the beginning of each experiment the mice were placed in individual circular wire-mesh cages, and weights were obtained with a triple-beam balance[3], after which initial temperatures were recorded and the treatment was administered. Temperatures were recorded again at various intervals. Control animals received distilled water (0.01 ml/g). To study the influence of various serotonergic agonist and antagonist agents on cobalt-induced hypothermia, pretreatment injections (water, *p*-chloroamphetamine HCl[4], *p*-iodoamphetamine HCl[5], *p*-chlorophenylalanine methyl ester HCl[4], fluoxetine HCl[5], nisoxetine HCl[5], cyproheptadine HCl[6], methergoline[7], and xylamidine tosylate[8]) were given at specified intervals prior to recording the initial temperatures.

Serotonin levels were recorded with a spectrophotofluorometer[9] according to the method of Curzon and Green (4), modified by Hyyppä *et al.* (5), with a standard curve relating relative fluorescence to serotonin concentration.

To compare mean temperature changes (*i.e.*, the difference between temperature immediately prior to and at the appropriate interval following treatment), statistical significance was determined by use of Student's *t* test. Temperature differences were considered significant at the probability level of 5% or less.

RESULTS

Cobaltous chloride (25 mg/kg ip) was administered at the appropriate interval following pretreatment with *p*-chloroamphetamine, *p*-iodoamphetamine, and *p*-chlorophenylalanine in groups of at least eight animals; body temperatures were monitored for a 4-hr period. The results of this experiment are shown in Fig. 1. Pretreatment with a single daily dose of 100 mg/kg of *p*-chlorophenylalanine for 3 consecutive days prior to the intraperatoneal administration of cobaltous chloride resulted in a reduction in the intensity and duration of the body temperature response. This antagonism was similar, but of less magnitude, to that seem in the case of *p*-chloroamphetamine (10 kg/kg ip 1 hr prior to cobalt). *p*-Iodoamphetamine pretreatment (10 mg/kg ip 1 hr before cobalt) also antagonized cobalt hypothermia and was less potent than *p*-chloroamphetamine.

Whole-brain serotonin levels were determined 2 hr following administration of *p*-chloroamphetamine and *p*-iodoamphetamine and 24 hr following the last of three single daily doses of 100 mg/kg of *p*-chlorophenylalanine in mice. *p*-Chloroamphetamine and *p*-chlorophenylalanine both significantly reduced whole-brain serotonin levels, while *p*-iodoamphetamine increased serotonin levels at the 2-hr interval (Table I).

The influence of fluoxetine and nisoxetine on the ability of *p*-chloroamphetamine to antagonize cobalt body temperature depression is presented in Table II. These uptake inhibitor agents both failed to modify the *p*-chloroamphetamine antagonism in doses known to reduce *p*-chloroamphetamine-induced serotonin depletion.

The body-temperature response to cobaltous chloride (25 mg/kg ip) was monitored at various intervals following the administration of 1 mg/kg each of cyproheptadine, methergoline, and xylamidine. In every

[1] Wayne Lab Blox.

[2] Model 46 Tele-thermometer, Yellow Springs Instrument Co., Yellow Springs, Ohio.
[3] Ohaus.
[4] Sigma Chemical Co.
[5] Eli Lilly and Co. Research Laboratories.
[6] Merck Sharp and Dohme Laboratories.
[7] Framitalia.
[8] Wellcome Research Laboratories.
[9] Aminco-Bowman.

0022-3549/83/0700-0824$01.00/0

Table I—Effect of Intraperitoneal *p*-Chloroamphetamine, *p*-Chlorophenylalanine, and *p*-Iodoamphetamine on Serotonin Concentration in Mice Brains

Drug	Serotonin, μg/g ± *SE*[a]		
	Controls	Treated[b]	Change, %
p-Chloroamphetamine	0.6585 ± 0.012	0.4413 ± 0.015	−32.98
p-Chlorophenylalanine	0.6612 ± 0.025	0.5904 ± 0.020	−10.71
p-Iodoamphetamine	0.6549 ± 0.022	0.7208 ± 0.021	+10.06

[a] Brains were removed from groups of at least eight mice 2 hr following the injection of 10 mg/kg of *p*-chloroamphetamine and *p*-iodoamphetamine and 24 hr following the third of three consecutive daily injections of 100 mg/kg of *p*-chlorophenylalanine. Control animals received 0.01 ml/g body weight of water instead of drug treatment. [b] Compared with appropriate water-treated control, $p < 0.05$.

case, 5-hydroxytryptaminergic receptor-blocking agent pretreatment enhanced rather than antagonized body temperature depression (Table III). The ascorbic acid vehicle for solubilizing methergoline did not alter body temperature, nor did it influence the body temperature response to cobaltous chloride.

DISCUSSION

The nature of body temperature response to cobaltous chloride in mice at present is poorly understood. However, the recent observation that cobalt hypothermia could be antagonized in part by pretreatment with *p*-chloroamphetamine suggests a possible serotonergic involvement (3). For example, cobalt may have acted indirectly in the CNS to release serotonin from neuronal storage sites into the vicinity of postsynaptic serotonergic receptors involved in the regulation of body temperature. One problem, however, with the use of *p*-chloroamphetamine as a pharmacological tool in the short term is its lack of specificity. For example, in addition to depletion of serotonin, this halogenated arylalkylamine has been shown to alter dopamine and norepinephrine synthesis in the rat (6). Thus, it is conceivable that other (nonserotonergic) mechanisms might also contribute to the development of hypothermia following the administration of cobaltous chloride.

The influence of *p*-chloroamphetamine on serotonergic nerve function has been extensively studied in the rat. Pletscher *et al.* (7) first reported that this compound causes a marked reduction in brain concentrations of 5-HT and 5-hydroxyindoleacetic acid in this species. Several mechanisms have been proposed to explain the action of this agent at the cellular level. Of these mechanisms, the inhibition of the rate-limiting enzyme tryptophan hydroxylase might possibly account for the rapid depletion of serotonin by *p*-chloroamphetamine in the short term. *p*-Iodoamphetamine also has been reported to decrease serotonin synthesis through the inhibition of tryptophan hydroxylase (8). One of the most commonly employed tryptophan hydroxylase inhibitors is *p*-chlorophenylalanine (9). The present investigation has shown that all three tryptophan hydroxylase inhibitors were capable of reducing the intensity and duration of cobalt hypothermia. These findings suggest that antagonism was accomplished through serotonin depletion, perhaps through inhibition of the rate-limiting enzyme in the synthesis of serotonin. However, similar antagonism of cobalt-induced hypothermia with central or peripheral serotonin receptor-blocking agents could not be demonstrated. The latter observations do not support the suggestion that *p*-chloroamphetamine antagonism of cobalt hypothermia was mediated through an antiserotonin influence.

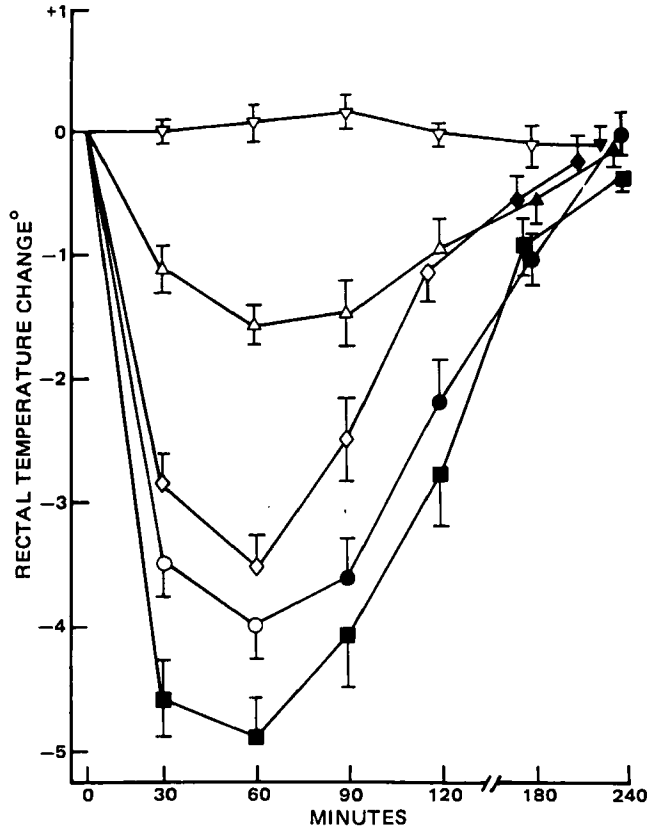

Figure 1—*Time course of the effect of 0.01 ml/g ip of distilled water (-▼-); 25 mg/kg ip of cobaltous chloride (-■-); 10 mg/kg ip of* p-*chloroamphetamine hydrochloride 1 hr prior to 25 mg/kg ip of cobaltous chloride (-▲-); three consecutive daily doses of 100 mg/kg ip of* p-*chlorophenylalanine methyl ester hydrochloride 24 hr prior to 25 mg/kg ip of cobaltous chloride (-●-); 10 mg/kg ip of* p-*iodoamphetamine 1 hr prior to 25 mg/kg ip of cobaltous chloride (-◆-) on the rectal temperature in mice. Water and cobaltous chloride were administered at time zero. Open symbols denote significant difference ($p < 0.05$) from cobalt treatment at the corresponding time interval. Each point represents the average of at least eight determinations. Vertical bars represent standard errors.*

Little information exists in the literature with respect to halogenated amphetamine effects on serotonergic neuronal function in mice, particularly in the case of *p*-iodoamphetamine. A previous study showed that *p*-chloroamphetamine causes depletion of serotonin from the brains of mice (3). In the present study we were unable to demonstrate a similar depletion with *p*-iodoamphetamine. In contrast, serotonin levels were significantly increased at the 2-hr interval following the intraperitoneal injection of *p*-iodoamphetamine. These observations suggest that mechanisms other than depletion of serotonin are involved in antagonism of cobalt-induced hypothermia by the halogenated arlalkylamines, *p*-

Table II—Interaction of Fluoxetine and Nisoxetine with *p*-Chloroamphetamine on the Body Temperature Response to Cobaltous Chloride in Mice

Pretreatment[a]	Treatment[b]			
	Water		Cobaltous Chloride	
	Initial Temperature °[c]	Temperature Change °[d] (Mean ± *SE*)	Initial Temperature °[c]	Temperature Change °[d] (Mean ± *SE*)
Water–Water	36.82	+0.10 ± 0.09	36.88	−4.38 ± 0.24[e]
Water–*p*-Chloroamphetamine	37.04	+0.04 ± 0.13	36.82	−1.13 ± 0.19[f]
Fluoxetine–Water	36.95	+0.29 ± 0.21	36.90	−4.79 ± 0.47
Fluoxetine –*p*-Chloroamphetamine	36.74	−0.07 ± 0.14	36.89	−1.29 ± 0.28[f]
Nisoxetine–Water	37.07	+0.03 ± 0.27	37.16	−4.62 ± 0.40
Nisoxetine–*p*-Chloroamphetamine	37.03	+0.01 ± 0.27	36.97	−0.73 ± 0.51[f]

[a] Fluoxetine hydrochloride (10 mg/kg ip), nisoxetine hydrochloride (10 mg/kg ip), or water (0.01 ml/g ip) were administered 2 hr prior to *p*-chloroamphetamine hydrochloride (10 mg/kg ip) or water (0.01 ml/g ip) to groups of 10 mice. [b] Intraperitoneal water (0.01 ml/g) and cobaltous chloride (25 mg/kg) treatments were given 1 hr following the final pretreatment injection. [c] Initial temperatures were recorded immediately prior to water or cobalt treatment. [d] Temperature changes represent the difference between body temperature recorded initially and that obtained 30 min after treatment. [e] Compared with water–water (pretreatment) water (treatment), $p < 0.05$. [f] Compared with water–water (pretreatment) cobalt (treatment), $p < 0.05$.

Table III—Effect of Pretreatment with 5-Hydroxytryptaminergic Receptor Blocking Agents on the Body Temperature Response to Cobaltous Chloride in Mice

Pretreatment[a]	Treatment[b]			
	Water		Cobaltous Chloride	
	Initial Temperature °[c]	Temperature Change °[d] (Mean ± SE)	Initial Temperature °[c]	Temperature Change °[d] (Mean ± SE)
Water	36.83	+0.13 ± 0.09	36.96	−4.73 ± 0.33[e]
Methergoline[f]	36.83	+0.25 ± 0.14	37.02	−6.12 ± 0.47[g]
Cyproheptadine	37.28	+0.03 ± 0.23	37.22	−5.97 ± 0.48[g]
Xylamadine	36.85	+0.22 ± 0.13	36.74	−5.56 ± 0.34[g]

[a] Water (0.01 ml/g), methergoline (1 mg/kg), cyproheptadine hydrochloride (1 mg/kg), and xylamidine tosylate (1 mg/kg) were administered intraperitoneally to groups of 10 animals. [b] Intraperitoneal water (0.01 ml/g) and cobaltous chloride (25 mg/kg) treatments were given 4 hr following pretreatment injection. [c] Initial temperatures were recorded immediately prior to water or cobalt treatment. [d] Temperature changes represent the difference between body temperature recorded initially and that obtained 30 min after treatment. [e] Compared with water–water (Pretreatment–Treatment), $p < 0.05$. [f] Methergoline was solubilized in distilled water acidified to pH 3.8 with ascorbic acid. [g] Compared with water–cobalt (Pretreatment–Treatment), $p < 0.05$.

chloroamphetamine and *p*-iodoamphetamine. In addition, the finding that uptake inhibitors (fluoxetine and nisoxetine) failed to modify halogenated amphetamine reversal of cobalt hypothermia further supports an extraserotonergic role of these amines in their ability to antagonize body temperature depression by cobaltous chloride.

The results presented in this report do not support the suggestion that cobaltous chloride hypothermia is mediated through the release of serotonin from intraneuronal storage sites. For example, the serotonin receptor-blocking agents, cyproheptadine, methergoline, and xylamidine, were incapable of attenuating the body temperature response. While it seems inviting to postulate an influence of cobalt on the neuronal storage of dopamine and/or norepinephrine, previous studies utilizing 6-hydroxydopamine failed to reveal catecholaminergic involvement (2). It is likely that cobalt produces hypothermia through a mechanism or mechanisms which are at present undefined.

REFERENCES

(1) D. H. Burke, *J. Pharm. Sci.*, 67, 799 (1978).

(2) D. H. Burke and J. C. Brooks, *J. Pharm. Sci.*, 68, 693 (1979).

(3) D. H. Burke, J. C. Brooks, and S. B. Treml, *Eur. J. Pharmacol.*, 60, 241 (1980).

(4) G. Curzon and A. R. Green, *Br. J. Pharmacol.*, 39, 653 (1970).

(5) M. T. Hyyppä, D. P. Cardinale, H. G. Baumgarten, and R. J. Wurtman, *J. Neural. Transm.*, 34, 111 (1973).

(6) L. Steranka and E. Sanders-Bush, *Eur. J. Pharmacol.*, 45, 83 (1977).

(7) A. Pletscher, G. Bartholini, H. Bruderer, W. P. Burkard, and K. F. Gey, *J. Pharmacol. Exp. Ther.*, 145, 344 (1964).

(8) R. W. Fuller, H. D. Snoddy, A. M. Snoddy, S. K. Hemrick, D. T. Wong, and B. B. Molloy, *J. Pharmacol. Exp. Ther.*, 212, 115 (1980).

(9) E. Sanders-Bush and V. J. Massari, *Fed. Proc. Fed. Am. Soc. Exp. Biol.*, 36, 2149 (1977).

ACKNOWLEDGMENTS

Presented at the Pharmacology and Toxicology Section, APhA Academy of Pharmaceutical Sciences Meeting, Orlando, Florida, November 1981.

Supported in part by National Institutes of Health Grant RR-09016.

The authors are indebted to Laura Huspen and Deborah Redford for assistance, and to Mary Jonas Owen for typing this manuscript. The authors thank Dr. R. W. Fuller of Eli Lilly and Company and Dr. P. J. McHale of the Wellcome Research Laboratories for their generosity in supplying *p*-iodoamphetamine and xylamidine.

Effect of Cimetidine on the Pharmacokinetics of Quinidine and Lidocaine in the Rat

RICHARD J. FRUNCILLO ˣ, G. JOHN DiGREGORIO, and ADAM SOLL

Received March 23, 1982, from the *Department of Pharmacology, Hahnemann Medical College and Hospital, Philadelphia, PA 19102.* Accepted for publication July 9, 1982.

Abstract □ Because of previously reported drug interactions involving cimetidine and liver-metabolized drugs, the intravenous pharmacokinetics of quinidine (25 mg/kg) and lidocaine (15 mg/kg) were investigated in anesthetized rats pretreated with a single intraperitoneal dose of cimetidine (60 mg/kg) and compared with saline pretreated controls. Significant reductions of 35 and 23% in the respective total clearances of quinidine and lidocaine were observed in the presence of cimetidine. The quinidine volume of distribution was significantly decreased in the cimetidine-treated rats, while the lidocaine volume of distribution was not altered significantly. There was no significant change in the elimination half-life for either drug in the presence of cimetidine. These results suggest cautious use of quinidine or lidocaine when cimetidine is prescribed concurrently.

Keyphrases □ Cimetidine—inhibition of lidocaine and quinidine clearances in the rat, kinetics □ Lidocaine—inhibition of clearance in the rat by cimetidine, kinetics □ Quinidine—inhibition of clearance in the rat by cimetidine, kinetics □ Kinetics—of the inhibition of lidocaine and quinidine clearances in the rat by cimetidine

Cimetidine, a histamine H_2-receptor antagonist, is prescribed widely for the therapy of peptic ulcers. Human pharmacokinetic studies have demonstrated that cimetidine in therapeutic doses impairs the elimination of drugs metabolized by cytochrome P-450-dependent pathways, such as antipyrine (1), theophylline (1), diazepam (2),

0022-3549/83/0700-0826$01.00/0

Table III—Effect of Pretreatment with 5-Hydroxytryptaminergic Receptor Blocking Agents on the Body Temperature Response to Cobaltous Chloride in Mice

Pretreatment[a]	Treatment[b]			
	Water		Cobaltous Chloride	
	Initial Temperature °[c]	Temperature Change °[d] (Mean ± SE)	Initial Temperature °[c]	Temperature Change °[d] (Mean ± SE)
Water	36.83	+0.13 ± 0.09	36.96	−4.73 ± 0.33[e]
Methergoline[f]	36.83	+0.25 ± 0.14	37.02	−6.12 ± 0.47[g]
Cyproheptadine	37.28	+0.03 ± 0.23	37.22	−5.97 ± 0.48[g]
Xylamadine	36.85	+0.22 ± 0.13	36.74	−5.56 ± 0.34[g]

[a] Water (0.01 ml/g), methergoline (1 mg/kg), cyproheptadine hydrochloride (1 mg/kg), and xylamidine tosylate (1 mg/kg) were administered intraperitoneally to groups of 10 animals. [b] Intraperitoneal water (0.01 ml/g) and cobaltous chloride (25 mg/kg) treatments were given 4 hr following pretreatment injection. [c] Initial temperatures were recorded immediately prior to water or cobalt treatment. [d] Temperature changes represent the difference between body temperature recorded initially and that obtained 30 min after treatment. [e] Compared with water–water (Pretreatment–Treatment), $p < 0.05$. [f] Methergoline was solubilized in distilled water acidified to pH 3.8 with ascorbic acid. [g] Compared with water–cobalt (Pretreatment–Treatment), $p < 0.05$.

chloroamphetamine and *p*-iodoamphetamine. In addition, the finding that uptake inhibitors (fluoxetine and nisoxetine) failed to modify halogenated amphetamine reversal of cobalt hypothermia further supports an extraserotonergic role of these amines in their ability to antagonize body temperature depression by cobaltous chloride.

The results presented in this report do not support the suggestion that cobaltous chloride hypothermia is mediated through the release of serotonin from intraneuronal storage sites. For example, the serotonin receptor-blocking agents, cyproheptadine, methergoline, and xylamidine, were incapable of attenuating the body temperature response. While it seems inviting to postulate an influence of cobalt on the neuronal storage of dopamine and/or norepinephrine, previous studies utilizing 6-hydroxydopamine failed to reveal catecholaminergic involvement (2). It is likely that cobalt produces hypothermia through a mechanism or mechanisms which are at present undefined.

REFERENCES

(1) D. H. Burke, *J. Pharm. Sci.*, 67, 799 (1978).

(2) D. H. Burke and J. C. Brooks, *J. Pharm. Sci.*, 68, 693 (1979).

(3) D. H. Burke, J. C. Brooks, and S. B. Treml, *Eur. J. Pharmacol.*, 60, 241 (1980).

(4) G. Curzon and A. R. Green, *Br. J. Pharmacol.*, 39, 653 (1970).

(5) M. T. Hyyppä, D. P. Cardinale, H. G. Baumgarten, and R. J. Wurtman, *J. Neural. Transm.*, 34, 111 (1973).

(6) L. Steranka and E. Sanders-Bush, *Eur. J. Pharmacol.*, 45, 83 (1977).

(7) A. Pletscher, G. Bartholini, H. Bruderer, W. P. Burkard, and K. F. Gey, *J. Pharmacol. Exp. Ther.*, 145, 344 (1964).

(8) R. W. Fuller, H. D. Snoddy, A. M. Snoddy, S. K. Hemrick, D. T. Wong, and B. B. Molloy, *J. Pharmacol. Exp. Ther.*, 212, 115 (1980).

(9) E. Sanders-Bush and V. J. Massari, *Fed. Proc. Fed. Am. Soc. Exp. Biol.*, 36, 2149 (1977).

ACKNOWLEDGMENTS

Presented at the Pharmacology and Toxicology Section, APhA Academy of Pharmaceutical Sciences Meeting, Orlando, Florida, November 1981.

Supported in part by National Institutes of Health Grant RR-09016.

The authors are indebted to Laura Huspen and Deborah Redford for assistance, and to Mary Jonas Owen for typing this manuscript. The authors thank Dr. R. W. Fuller of Eli Lilly and Company and Dr. P. J. McHale of the Wellcome Research Laboratories for their generosity in supplying *p*-iodoamphetamine and xylamidine.

Effect of Cimetidine on the Pharmacokinetics of Quinidine and Lidocaine in the Rat

RICHARD J. FRUNCILLO ˣ, G. JOHN DiGREGORIO, and ADAM SOLL

Received March 23, 1982, from the *Department of Pharmacology, Hahnemann Medical College and Hospital, Philadelphia, PA 19102.* Accepted for publication July 9, 1982.

Abstract □ Because of previously reported drug interactions involving cimetidine and liver-metabolized drugs, the intravenous pharmacokinetics of quinidine (25 mg/kg) and lidocaine (15 mg/kg) were investigated in anesthetized rats pretreated with a single intraperitoneal dose of cimetidine (60 mg/kg) and compared with saline pretreated controls. Significant reductions of 35 and 23% in the respective total clearances of quinidine and lidocaine were observed in the presence of cimetidine. The quinidine volume of distribution was significantly decreased in the cimetidine-treated rats, while the lidocaine volume of distribution was not altered significantly. There was no significant change in the elimination half-life for either drug in the presence of cimetidine. These results suggest cautious use of quinidine or lidocaine when cimetidine is prescribed concurrently.

Keyphrases □ Cimetidine—inhibition of lidocaine and quinidine clearances in the rat, kinetics □ Lidocaine—inhibition of clearance in the rat by cimetidine, kinetics □ Quinidine—inhibition of clearance in the rat by cimetidine, kinetics □ Kinetics—of the inhibition of lidocaine and quinidine clearances in the rat by cimetidine

Cimetidine, a histamine H_2-receptor antagonist, is prescribed widely for the therapy of peptic ulcers. Human pharmacokinetic studies have demonstrated that cimetidine in therapeutic doses impairs the elimination of drugs metabolized by cytochrome P-450-dependent pathways, such as antipyrine (1), theophylline (1), diazepam (2),

0022-3549/83/0700-0826$01.00/0

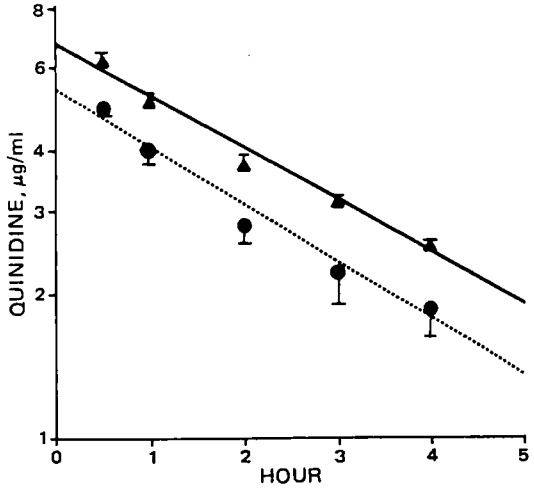

Figure 1—*Plasma disappearance curves of quinidine in rats pretreated with cimetidine (▲) or saline (●) intraperitoneally 30 min prior to the quinidine injection. Values are mean ± SE with n = 4–5 at each point.*

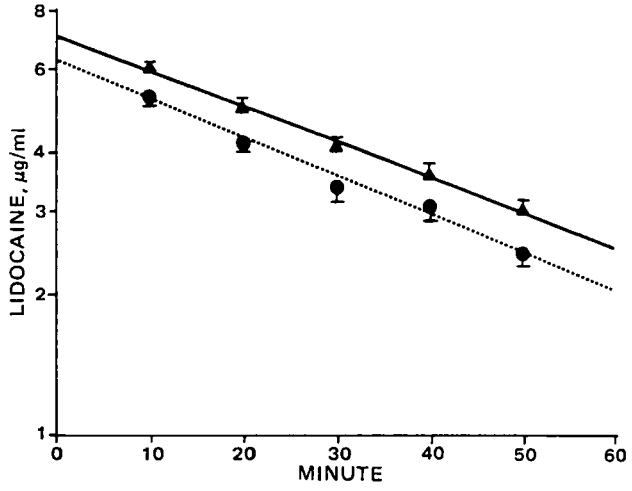

Figure 2—*Plasma disappearance curves of lidocaine in rats pretreated with cimetidine (▲) or saline (●) intraperitoneally 30 min prior to the lidocaine injection. Values are mean ± SE with n = 5–6 at each point.*

chlordiazepoxide (3), propranolol (4), warfarin (5), and phenytoin (6). The clearances of drugs such as lorazepam and oxazepam, which are eliminated by glucuronidation, are unaffected by cimetidine (7). Studies using *in vitro* rat liver homogenates have revealed that cimetidine inhibits aminopyrine *N*-demethylation and benzo[*a*]pyrene hydroxylation in a concentration-dependent manner (8). Similar results were found in homogenates obtained from human liver biopsies (9). Quinidine and lidocaine are two popular antiarrhythmic agents dependent on cytochrome P- 450 liver metabolism for inactivation (10). This present study investigates the effect of cimetidine on the pharmacokinetics of these drugs in the rat.

EXPERIMENTAL

Male Sprague–Dawley rats[1], weighing 220–250 g on the day of the study, were used. They were housed in groups of four in plastic cages over corn cob bedding in a well-ventilated room (24° ± 0.5°) with alternate 12-hr periods of light and dark. Food[2] and water were provided *ad libitum*.

After being acclimated to their cages for at least 5 days, the rats were anesthetized with 1.7 g/kg of urethane, an anesthetic that does not inhibit drug metabolism (11) and which has been reported to maintain hepatic blood flow at a level equal to that of an awake animal (12). The right and left jugular veins were surgically exposed by superficial skin incisions above both clavicles, and either 60 mg/kg of cimetidine or 1 ml/kg of saline was injected intraperitoneally. Thirty minutes after the injections, both groups of rats received either 15 mg/kg (free base) of lidocaine or 25 mg/kg (free base) of quinidine intravenously through the right jugular vein. Blood samples (0.4 ml) were taken at 10, 20, 30, 40, and 50 min postinjection (lidocaine) or at 0.5, 1, 2, 3, and 4 hr postinjection (quinidine). Samples were obtained by needle puncture of the left jugular vein using heparinized tuberculin syringes. Plasma lidocaine and quinidine concentrations were measured by commercially available enzyme immunoassay kits[3], as described previously (13).

The plasma disappearance of both drugs was treated as a one-compartment model and considered to follow the exponential function $C(t) = Ae^{-\lambda t}$ where $C(t)$ is the plasma concentration at time t, A is the time zero intercept, and λ is the elimination rate constant. The elimination half-life was calculated by $t_{1/2} = 0.693/\lambda$, the volume of distribution by V_D = dose/A, and the clearance by $CL = V_D\lambda$. The parameters were calculated for each animal by least-squares analysis of a semilogarithmic plot of drug concentrations *versus* time. Statistical calculations were performed using the two-tailed Student's t test.

[1] Charles River Breeding Laboratories, Wilmington, Mass.
[2] Rodent Chow, Ralston Purina Inc., St. Louis, Mo.
[3] EMIT System, Syva Co., Palo Alto, Calif.

RESULTS AND DISCUSSION

Figures 1 and 2 illustrate the respective average plasma disappearance curves for quinidine and lidocaine in cimetidine- and saline-pretreated rats; Table I shows the derived pharmacokinetic parameters. The administration of cimetidine caused a 35% reduction in quinidine clearance compared with saline-treated rats (significant at the $p < 0.05$ level). Likewise, cimetidine produced a significant (23%) reduction in lidocaine clearance ($p < 0.05$). There was a significant decrease in the quinidine volume of distribution in the cimetidine-treated rats ($p < 0.05$); however, the lidocaine volume of distribution was not significantly altered. There was no significant change in elimination half-life for either drug.

These results demonstrate that cimetidine, in a single dose, will prolong the clearance of either quinidine or lidocaine in the rat. They are similar to the findings of Desmond *et al.* (14), in which a single dose of cimetidine significantly prolonged the half-life of aminopyrine in the rat. All of the human pharmacokinetic studies reported to date were done after multiple doses of cimetidine; however, Patwardhan *et al.* (15) reported a decreased clearance of chlordiazepoxide as early as 24 hr after treatment with cimetidine, with recovery to baseline clearance 48 hr after discontinuing the cimetidine. Thus, it appears that a certain level of cimetidine is needed in the organism to manifest the inhibitory affect on drug metabolism. The exact mechanism by which cimetidine exerts its effect at the enzyme level is not entirely certain. Both competitive and noncompetitive inhibition of *in vitro* drug-metabolizing enzymes has been shown for various substrates (16).

There has been speculation that H_2-receptor blockade may play a role in the observed depression of drug clearances. However, a recent report demonstrated that the new H_2-receptor antagonist ranitidine did not inhibit drug metabolism (16). This fact supports the concept that the imidazole structure of cimetidine is responsible for its inhibitory effects, since similar structures are known to depress drug metabolism (17); ranitidine has a furan ring structure.

Table I—Effect of Cimetidine on the Pharmacokinetics of Quinidine and Lidocaine

Parameter	Quinidine[b] Treated: Saline Pretreatment (5)	Quinidine[b] Treated: Cimetidine Pretreatment (4)
$t_{1/2}$, hr	2.53 ± .25	3.09 ± .26
V_D, liter/kg	4.68 ± .21	3.82 ± .19[c]
CL liter/hr/kg	1.33 ± .13	0.86 ± .04[c]
	Lidocaine[b] Treated	
	Saline Pretreatment (5)	Cimetidine Pretreatment (6)
$t_{1/2}$, min	36.9 ± 1.2	42.4 ± 2.8
V_D liter/kg	2.45 ± .13	2.17 ± .07
CL ml/min/kg	46.5 ± 3.8	36.0 ± 2.1[c]

[a] Animals were pretreated with cimetidine 60 mg/kg ip or saline and received the test drug 30 min later. Results are means ± *SEM* with the number of animals in parentheses. [b] Dosage levels were 25 and 15 mg/kg iv, respectively, for quinidine and lidocaine. [c] $p < 0.05$ *versus* saline-treated animals, two-tailed Student's t test.

Quinidine and lidocaine are drugs that have intermediate-to-high hepatic extraction ratios and metabolites formed by the hepatic mixed-function oxidase system (10). Therefore, their clearances should be dependent both on liver blood flow and drug-metabolizing enzyme activity (18). The most likely explanation for the decreased clearances observed in this study is inhibited drug metabolism; however, decreased liver blood flow may play a role since a single dose of cimetidine has been shown to reduce hepatic blood flow 25% in humans (4). Since quinidine and lidocaine are drugs with narrow therapeutic ranges, decreases in their clearances could potentially lead to drug accumulation with resultant toxicity. Evaluated blood levels of quinidine have been associated with cinchonism, arrhythmias, and syncope, while increased lidocaine levels have been linked to confusion, seizures, and respiratory arrest (10). Therefore, frequent measurement of quinidine and lidocaine serum levels are recommended when cimetidine is prescribed concurrently, pending human pharmacokinetic studies on these interactions.

REFERENCES

(1) R. K. Roberts, J. Grice, L. Wood, V. Petroff, and C. McGuffie, *Gastroenterology*, **81**, 19 (1981).

(2) V. Klotz and I. Reimann, *N. Engl. J. Med.*, **302**, 1012 (1980).

(3) P. V. Desmond, R. V. Patwardhan, S. Schenker, and K. V. Speeg, *Ann. Intern. Med.*, **93**, 266 (1980).

(4) J. Feely, G. R. Wilkinson, and A. J. Wood, *N Engl. J. Med.*, **304**, 692 (1981).

(5) M. J. Serlin, R. G. Sibeon, S. Mossman, A. M. Breckenridge, J. B. Williams, J. L. Atwood, and J. T. Willoughby, *Lancet*, **ii**, 317 (1979).

(6) P. J. Neuvonen, R. A. Tokola, and M. Kaste, *Eur. J. Clin. Pharmacol.*, **21**, 215 (1981).

(7) R. V. Patwardhan, G. W. Yarborough, P. V. Desmond, R. F. Johnson, S. Schenker, and K. V. Speeg, *Gastroenterology*, **79**, 912 (1980).

(8) O. Pelkonen and J. Puurunen, *Biochem. Pharmacol.*, **29**, 3075 (1980).

(9) J. Puurunen, E. Sotaniemi, and O. Pelkonen, *Eur. J. Clin. Pharmacol.*, **18**, 185 (1980).

(10) J. T. Bigger and B. F. Hoffman, in "The Pharmacological Basis of Therapeutics," 6th ed., A. G. Goodman, L. S. Goodman, and A. Gilman, Eds. Macmillan, New York, N.Y., 1980, p. 761.

(11) T. Umeda and T. Inaba, *Can. J. Physiol. Pharmacol.*, **56**, 241 (1978).

(12) C. R. Hiley, M. S. Yates, and D. J. Black, *Experientia*, **34**, 1061 (1978).

(13) R. J. Bastiani, R. C. Phillips, R. S. Schneider, and E. F. Ullman, *Am. J. Med. Technol.*, **39**, 211 (1973).

(14) P. V. Desmond, R. Patwardhan, R. Parker, S. Schenker, and K. V. Speeg, *Life Sci.*, **26**, 1261 (1980).

(15) R. V. Patwardhan, R. F. Johnson, A. P. Sinclair, S. Schenker, and K. V. Speeg, *Gastroenterology*, **81**, 547 (1981).

(16) R. G. Knodell, J. L. Holtzman, D. L. Crankshaw, N. M. Steele, and L. N. Stanley, *Gastroenterology*, **82**, 84 (1982).

(17) C. F. Wilkinson, K. Hetnarski, and T. O. Yellin, *Biochem. Pharmacol.*, **21**, 3187 (1972).

(18) D. Shand and P. Turner, in "Recent Advances in Clinical Pharmacology," P. Turner and D. G. Shand, Eds., Churchill Livingstone, New York, N.Y., 1978, p. 1.

Acetaminophen–Aluminum Hydroxide Interaction in Rabbits

MING-MEEI CHEN *, CHARLES LEE ‡, YORISHIGE IMAMURA *, and JOHN H. PERRIN *x

Received March 25,1982, from the **Department of Pharmaceutics, College of Pharmacy, University of Florida, Gainesville, FL 32610*, and the ‡*Pharmaceutics Department, College of Pharmacy, University of Houston, Houston, TX 77030.* Accepted for publication July 8, 1982.

Abstract □ Acetaminophen–aluminum hydroxide interaction was investigated in a crossover study using six rabbits. Blood samples were collected at various time intervals for up to 6 hr following the oral administration of acetaminophen alone or in combination with aluminum hydroxide. Aluminum hydroxide at a 40-mg/kg dose did not appear to affect the rate and extent of acetaminophen absorption. The influence of aluminum hydroxide on gastric emptying could be compromised by gastric absorption of acetaminophen, resulting in a negligible effect on the overall bioavailability of acetaminophen.

Keyphrases □ Acetaminophen and aluminum hydroxide interaction—crossover study in rabbits, pharmacokinetics □ Aluminum hydroxide—effect on rate and extent of acetaminophen absorption in rabbits □ Pharmacokinetics—rate and extent of acetaminophen absorption in rabbits with and without aluminum hydroxide administration

Retarded drug absorption in the presence of aluminum hydroxide has been demonstrated in animals and humans (1). This pharmacokinetic interaction probably results from a slowed gastric emptying (1). *In vitro*, aluminum ion inhibits the contractile response of human and rat gastric strips to acetylcholine (2). This effect is possibly due to the antagonization by aluminum of calcium influx into smooth muscle cells during depolarization, leading to a delay in muscle contractions (3).

Acetaminophen (weak acid, pK_a 9.5) is a common, nonprescription, analgesic drug. It is not clear whether acetaminophen is completely free of damaging effects on the gastric mucosa, although minimal or no gastric structural damage has been found to be induced by acetaminophen in marked contrast to aspirin (4). Since acetaminophen is believed to cause less damaging effects, it has replaced aspirin as the analgesic of choice in many situations. However, acetaminophen is frequently used in combination with aspirin in nonprescription drugs (5), necessitating the use of antacids to avoid the gastric damage induced by aspirin, or perhaps acetaminophen.

Table I—Mean Plasma Acetaminophen Concentrations Following Oral Administrations of Acetaminophen Alone (100 mg/kg) and in Combination with Aluminum Hydroxide (40 mg/kg) to Rabbits

Time, hr	Acetaminophen		Acetaminophen Plus Aluminum Hydroxide	
	Mean[a]	*SEM*	Mean[a]	*SEM*
0.25	35.77	2.38	31.37	3.15
0.50	27.39	1.65	27.17	1.18
0.75	23.53	2.05	22.89	1.79
1.0	18.77	1.51	16.95	1.86
1.5	11.54	1.16	11.06	1.40
2.0	7.84	0.62	7.65	0.96
3.0	4.74	0.60	4.65	0.62
4.0	2.82	0.47	2.57	0.36
5.0	1.77	0.28	1.81	0.26
6.0	1.29	0.24	1.41	0.21

[a] Mean data of six rabbits.

0022-3549/83/0700-0828$01.00/0

Quinidine and lidocaine are drugs that have intermediate-to-high hepatic extraction ratios and metabolites formed by the hepatic mixed-function oxidase system (10). Therefore, their clearances should be dependent both on liver blood flow and drug-metabolizing enzyme activity (18). The most likely explanation for the decreased clearances observed in this study is inhibited drug metabolism; however, decreased liver blood flow may play a role since a single dose of cimetidine has been shown to reduce hepatic blood flow 25% in humans (4). Since quinidine and lidocaine are drugs with narrow therapeutic ranges, decreases in their clearances could potentially lead to drug accumulation with resultant toxicity. Evaluated blood levels of quinidine have been associated with cinchonism, arrhythmias, and syncope, while increased lidocaine levels have been linked to confusion, seizures, and respiratory arrest (10). Therefore, frequent measurement of quinidine and lidocaine serum levels are recommended when cimetidine is prescribed concurrently, pending human pharmacokinetic studies on these interactions.

REFERENCES

(1) R. K. Roberts, J. Grice, L. Wood, V. Petroff, and C. McGuffie, *Gastroenterology*, **81**, 19 (1981).

(2) V. Klotz and I. Reimann, *N. Engl. J. Med.*, **302**, 1012 (1980).

(3) P. V. Desmond, R. V. Patwardhan, S. Schenker, and K. V. Speeg, *Ann. Intern. Med.*, **93**, 266 (1980).

(4) J. Feely, G. R. Wilkinson, and A. J. Wood, *N Engl. J. Med.*, **304**, 692 (1981).

(5) M. J. Serlin, R. G. Sibeon, S. Mossman, A. M. Breckenridge, J. B. Williams, J. L. Atwood, and J. T. Willoughby, *Lancet*, **ii**, 317 (1979).

(6) P. J. Neuvonen, R. A. Tokola, and M. Kaste, *Eur. J. Clin. Pharmacol.*, **21**, 215 (1981).

(7) R. V. Patwardhan, G. W. Yarborough, P. V. Desmond, R. F. Johnson, S. Schenker, and K. V. Speeg, *Gastroenterology*, **79**, 912 (1980).

(8) O. Pelkonen and J. Puurunen, *Biochem. Pharmacol.*, **29**, 3075 (1980).

(9) J. Puurunen, E. Sotaniemi, and O. Pelkonen, *Eur. J. Clin. Pharmacol.*, **18**, 185 (1980).

(10) J. T. Bigger and B. F. Hoffman, in "The Pharmacological Basis of Therapeutics," 6th ed., A. G. Goodman, L. S. Goodman, and A. Gilman, Eds. Macmillan, New York, N.Y., 1980, p. 761.

(11) T. Umeda and T. Inaba, *Can. J. Physiol. Pharmacol.*, **56**, 241 (1978).

(12) C. R. Hiley, M. S. Yates, and D. J. Black, *Experientia*, **34**, 1061 (1978).

(13) R. J. Bastiani, R. C. Phillips, R. S. Schneider, and E. F. Ullman, *Am. J. Med. Technol.*, **39**, 211 (1973).

(14) P. V. Desmond, R. Patwardhan, R. Parker, S. Schenker, and K. V. Speeg, *Life Sci.*, **26**, 1261 (1980).

(15) R. V. Patwardhan, R. F. Johnson, A. P. Sinclair, S. Schenker, and K. V. Speeg, *Gastroenterology*, **81**, 547 (1981).

(16) R. G. Knodell, J. L. Holtzman, D. L. Crankshaw, N. M. Steele, and L. N. Stanley, *Gastroenterology*, **82**, 84 (1982).

(17) C. F. Wilkinson, K. Hetnarski, and T. O. Yellin, *Biochem. Pharmacol.*, **21**, 3187 (1972).

(18) D. Shand and P. Turner, in "Recent Advances in Clinical Pharmacology," P. Turner and D. G. Shand, Eds., Churchill Livingstone, New York, N.Y., 1978, p. 1.

Acetaminophen–Aluminum Hydroxide Interaction in Rabbits

MING-MEEI CHEN *, CHARLES LEE ‡, YORISHIGE IMAMURA *, and JOHN H. PERRIN *x

Received March 25,1982, from the **Department of Pharmaceutics, College of Pharmacy, University of Florida, Gainesville, FL 32610*, and the ‡*Pharmaceutics Department, College of Pharmacy, University of Houston, Houston, TX 77030.* Accepted for publication July 8, 1982.

Abstract □ Acetaminophen–aluminum hydroxide interaction was investigated in a crossover study using six rabbits. Blood samples were collected at various time intervals for up to 6 hr following the oral administration of acetaminophen alone or in combination with aluminum hydroxide. Aluminum hydroxide at a 40-mg/kg dose did not appear to affect the rate and extent of acetaminophen absorption. The influence of aluminum hydroxide on gastric emptying could be compromised by gastric absorption of acetaminophen, resulting in a negligible effect on the overall bioavailability of acetaminophen.

Keyphrases □ Acetaminophen and aluminum hydroxide interaction—crossover study in rabbits, pharmacokinetics □ Aluminum hydroxide—effect on rate and extent of acetaminophen absorption in rabbits □ Pharmacokinetics—rate and extent of acetaminophen absorption in rabbits with and without aluminum hydroxide administration

Retarded drug absorption in the presence of aluminum hydroxide has been demonstrated in animals and humans (1). This pharmacokinetic interaction probably results from a slowed gastric emptying (1). *In vitro*, aluminum ion inhibits the contractile response of human and rat gastric strips to acetylcholine (2). This effect is possibly due to the antagonization by aluminum of calcium influx into smooth muscle cells during depolarization, leading to a delay in muscle contractions (3).

Acetaminophen (weak acid, pK_a 9.5) is a common, nonprescription, analgesic drug. It is not clear whether acetaminophen is completely free of damaging effects on the gastric mucosa, although minimal or no gastric structural damage has been found to be induced by acetaminophen in marked contrast to aspirin (4). Since acetaminophen is believed to cause less damaging effects, it has replaced aspirin as the analgesic of choice in many situations. However, acetaminophen is frequently used in combination with aspirin in nonprescription drugs (5), necessitating the use of antacids to avoid the gastric damage induced by aspirin, or perhaps acetaminophen.

Table I—Mean Plasma Acetaminophen Concentrations Following Oral Administrations of Acetaminophen Alone (100 mg/kg) and in Combination with Aluminum Hydroxide (40 mg/kg) to Rabbits

Time, hr	Acetaminophen		Acetaminophen Plus Aluminum Hydroxide	
	Mean[a]	*SEM*	Mean[a]	*SEM*
0.25	35.77	2.38	31.37	3.15
0.50	27.39	1.65	27.17	1.18
0.75	23.53	2.05	22.89	1.79
1.0	18.77	1.51	16.95	1.86
1.5	11.54	1.16	11.06	1.40
2.0	7.84	0.62	7.65	0.96
3.0	4.74	0.60	4.65	0.62
4.0	2.82	0.47	2.57	0.36
5.0	1.77	0.28	1.81	0.26
6.0	1.29	0.24	1.41	0.21

[a] Mean data of six rabbits.

0022-3549/83/0700-0828$01.00/0

Table II—Distribution Parameter (α), Elimination Parameter (β), and AUC of Acetaminophen Following Treatments with Acetaminophen Alone and in Combination with Aluminum Hydroxide

Rabbit	Acetaminophen Alone			Acetaminophen Plus Aluminum Hydroxide		
	α, hr^{-1}	β, hr^{-1}	AUC, $\mu g \cdot hr/ml$	α, hr^{-1}	β, hr^{-1}	AUC, $\mu g \cdot hr/ml$
1	1.93	0.38	38.30	3.03	0.36	31.83
2	3.06	0.38	51.99	2.50	0.29	42.44
5	1.90	0.38	43.72	2.02	0.44	35.18
6	1.27	0.31	55.45	1.83	0.40	55.80
9	2.12	0.53	43.46	1.15	0.34	43.80
12	1.55	0.26	39.20	1.77	0.54	50.53
Mean[a]	1.97	0.37	45.39	2.05	0.40	43.26
SEM	0.25	0.04	2.83	0.27	0.04	3.68

[a] Mean data of six rabbits. Statistical difference of the mean was tested by Student's paired t test, $p > 0.8$ for α, $p > 0.75$ for β, and $p > 0.55$ for AUC.

The delayed absorption of salicylic acid from tablets buffered with aluminum hydroxide has been documented previously (6). A recent review of drug interactions with acetaminophen and aspirin was presented by Hayes (7). This study is undertaken to verify the drug interaction between acetaminophen and aluminum hydroxide using the rabbit model.

EXPERIMENTAL

Materials—Acetaminophen[1] and aluminum hydroxide[2] were reagent grade and were used without further purification. Appropriate strengths of acetaminophen alone or in combination with aluminum hydroxide were prepared in warm deionized water (37°) prior to oral administration to rabbits.

Animal Studies—The validity of the rabbit model for drug absorption has been discussed in a previous publication (8). Six male New Zealand rabbits weighing 2.8–4.6 kg were studied in a crossover design, with a 2-week washout period allowed between studies. Rabbits were fasted for 38–42 hr prior to the experiment, but water was allowed *ad libitum*. Food and water were withheld during the experiment. Acetaminophen (100 mg/kg) alone or in combination with aluminum hydroxide (40 mg/kg) was dissolved in 70 ml of warm deionized water and was administered orally to the rabbit by intubation. The intubation line was flushed with 30 ml of warm water to ensure complete delivery of the drugs to the stomach. Blood samples (0.5 ml each) were collected from the ear vein in heparinized tubes[3] at 0 (just before experiment), 0.25, 0.5, 0.75, 1.0, 1.5, 2, 3, 4, 5, and 6 hr. After centrifugation of the blood samples, plasma aliquots were obtained for analysis of acetaminophen content.

Drug Assay—Plasma acetaminophen was assayed by a high-performance liquid chromatographic method (9). Vanillin[4] was used as an internal standard. The assay method provided a minimum detectable concentration of 0.5 μg/ml in plasma. However, since 0.2-ml aliquots of plasma were the maximal volume available for analysis, the minimum detectable quantity was 0.1 μg.

RESULTS AND DISCUSSION

Acetaminophen, alone or in combination with aluminum hydroxide, was rapidly absorbed in rabbits, with the peak plasma concentration occurring within 15 min of drug administration. Mean plasma data obtained from the two crossover studies are presented in Table I. Following the administration of acetaminophen alone and in combination with aluminum hydroxide, similar plasma levels of acetaminophen were observed at corresponding time intervals for all the rabbits. Since plasma concentrations of acetaminophen appeared to decay biexponentially, data were fitted to a biexponential function using the NONLIN program (10). The distribution parameter (α) and the elimination parameter (β) thus obtained from the curve fitting are presented in Table II. The mean parameter values are not significantly different from each other ($p > 0.8$ for α; $p > 0.75$ for β). The lack of difference in mean values of α and β was expected, since aluminum hydroxide presumably affected drug absorption but not the distribution and/or elimination.

Values for area under the plasma concentration–time curve (AUC) were estimated according to the trapezoidal rule and the extrapolation method. Values for mean AUC were similar, 45.39 μg hr/ml for acetaminophen alone and 43.26 μg hr/ml for acetaminophen in combination, indicating no significant difference in the extent of acetaminophen absorption between the two treatments ($p > 0.55$). Since blood sampling was not carried out during the first 15 min after drug administration, it was not clear whether aluminum hydroxide affected the rate of acetaminophen absorption. However, a drug interaction of this magnitude would be of minimal clinical significance if it indeed occurred. By the same token, since areas covering 0–15 min constituted <10% of the total estimated areas, the effect of aluminum hydroxide, if indeed seen in the first 15 min, would not affect the overall bioavailability of acetaminophen. Therefore, it is to be concluded, based on these data, that aluminum hydroxide affected neither the rate nor the extent of acetaminophen absorption.

Aluminum salts have been known to delay the absorption of various drugs in animals and in humans. *In vitro* experiments have demonstrated that aluminum ion antagonizes the contractile response of human and rat gastric strips to acetylcholine. Although *in vitro* experiments demonstrating the antagonizing effect of aluminum ion have not been conducted in rabbits, a similar conclusion to that found for the human and rat would be drawn. At the 40-mg/kg dose used in this study, aluminum hydroxide did not appear to affect the rate and extent of acetaminophen absorption. This dose, on a weight basis, was approximately three times the therapeutic dose of the antacid used in humans. Acetaminophen is an acidic compound, a fact that favors its absorption from the stomach according to the pH partition theory. Although the gastric emptying might be delayed in the presence of aluminum hydroxide, the effect could be compromised by the gastric absorption of acetaminophen. The acetaminophen dose used in this study, 100 mg/kg, was approximately three times the recommended maximal daily dose for humans; whereas, the 40-mg/kg dose of aluminum hydroxide was similar to that used in a drug–antacid interaction study in humans (11).

Hurwitz (1) proposed that only drug products in which absorption is not rate limited by dissolution are subject to a significant gastric emptying effect. Acetaminophen is in this category. To eliminate the dissolution factor, a solution of acetaminophen instead of solid dosage forms was used in this study. Therefore, any interaction found in this study was the exclusive effect of gastric emptying and gastric absorption of the interactants. Since acetaminophen is available as solid dosage forms for human use, direct extrapolation of rabbit data to the human situation is not deemed appropriate. However, it is felt that any acetaminophen–aluminum hydroxide interaction, if indeed one occurs in humans, will be of minimal clinical significance based on results of this study in rabbits. The proof awaits further investigation in humans.

[1] Aldrich Chemical Co., Milwaukee, Wis.
[2] J. T. Baker Chemical Co., Hayward, Calif.
[3] Vacutainers.
[4] Matheson Coleman and Bell Manufacturing Chemists, Norwood, Ohio.

REFERENCES

(1) A. Hurwitz, "Drug Interactions," P. Morselli, J. Cohn, and E. Garattini, Eds. Raven, New York, N.Y., 1974, p. 21.

(2) M. Hava and A. Hurwitz, *Eur. J. Pharmacol.*, **22**, 156 (1973).

(3) M. Hava and A. Hurwitz, *Arch. Int. Pharmacodyn. Ther.*, **214**, 213 (1975).

(4) K. J. Ivey and P. Settree, *Gut*, **17**, 916 (1976).

(5) W. T. Beaver, *Arch. Int. Med.*, **141**, 293 (1981).

(6) M. Linnoila and J. Lehtola, *Int. J. Clin. Pharmacol. Biopharm.*, **15**, 61 (1972).

(7) A. H. Hayes, *Arch. Int. Med.*, **141**, 301 (1981).

(8) Y. Imamura, L. H. Wang, C. S. Lee, and J. H. Perrin, *Int. J. Pharmaceut.*, 5, 25 (1980).
(9) Y. Imamura, L. H. Wang, C. S. Lee, J. H. Perrin, K. Shiozu, and H. Ichibagase, *Int. J. Pharmaceut.*, 8, 277 (1981).
(10) C. M. Metzler, G. L. Elfring, and A. T. McGwen, *Biometrics*, 30, 562 (1974).
(11) M. J. Mattila, L. T. Seppala, and R. Koskinen, *Br. J. Clin. Pharmacol.*, 5, 161 (1978).

High-Yield Synthesis of Warfarin and Its Phenolic Metabolites: New Compounds

ERNIE BUSH and WILLIAM F. TRAGER ˣ

Received April 15, 1982, from the *Department of Medicinal Chemistry, University of Washington, Seattle, WA 98195.* Accepted for publication June 29, 1982.

Abstract □ A novel synthesis of warfarin and phenolic warfarin metabolites is presented which results in higher yields than previous methods.

Keyphrases □ Warfarin—phenolic metabolites, new high-yield synthetic method □ Synthesis—warfarin and its phenolic metabolites, new high-yield method

The oral anticoagulant warfarin [4-hydroxy-3-(1-phenyl-3-oxobutyl)-2*H*-1-benzopyran-2-one] (I) has found extensive clinical use in the treatment of such pathological conditions as thrombophlebitis, pulmonary emboli, and myocardial infarction (1). It is also used widely as a rodenticide to help control rat populations (2) and more recently has been used as a probe to investigate the multiplicity and catalytic activity of microsomal and purified cytochrome P-450 preparations (3–7). Because of its clinical and pharmacological importance, considerable effort has been expended to develop analytical methods to quantitate both warfarin and its metabolites from biological matrices (8–11). However, one of the impediments to progress in this area has been the lack of a high-yield synthetic procedure for these materials. Since mechanistic work in this laboratory on cytochrome P-450 required the synthesis and optical resolution of specifically deuterated warfarin analogues as substrates and multideuterated metabolites as GC–MS assay internal standards, the need for a reproducible, high-yield synthesis for these compounds was evident.

Although successful synthetic routes to these materials are documented in the literature, the reported yields are poor to moderate at best (12). Warfarin has been synthesized by the Michael addition of 4-hydroxycoumarin to benzalacetone under a number of acid- or base-catalyzed conditions (13). Traditionally, the reaction has most often been run in water containing a catalytic amount of triethylamine (~5 mole %). Hermodson *et al.* (12), using essentially the same conditions, extended this synthesis to the phenolic metabolites of warfarin by condensing benzalacetone with the appropriately substituted 4-hydroxycoumarin. Fasco *et al.* (14) followed a similar route, but to obtain a homogeneous system substituted dioxane as the solvent and piperidine as the catalyst. A further refinement was reported by Cook *et al.* (15) who, in their synthesis of 3′-bromowarfarin, heated a solution of *m*-bromobenzalacetone and 4-hydroxycoumarin in pyridine at reflux. However, rarely was the overall yield of warfarin or hydroxywarfarin >65%. In the case of 7-hydroxywarfarin, it was invariably much lower.

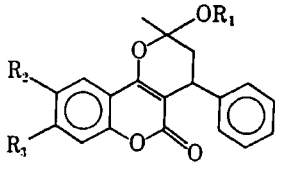

		R_1	R_2	R_3
I:	Warfarin	H	H	H
II:	Warfarin Ethyl Ether	C_2H_5	H	H
III:	Cyclocoumarol	CH_3	H	H
IV:	6-Hydroxywarfarin	H	OH	H
V:	7-Hydroxywarfarin	H	H	OH
VI:	6-Hydroxycyclocoumarol	CH_3	OH	H
VII:	7-Hydroxycyclocoumarol	CH_3	H	OH

RESULTS AND DISCUSSION

Numerous attempts in this laboratory to improve previous yields by alternate reaction pathways failed. A new approach was conceived when it was found that warfarin was quantitatively converted to its ethyl ether (II) by refluxing in absolute ethanol. This observation suggested that in absolute ethanol, the acidity of 4-hydroxycoumarin might be sufficient to catalyze its condensation with benzalacetone to generate warfarin. Once formed, the reaction would be driven to completion by the subsequent and essentially irreversible formation of the ethyl ether under these conditions. Initial experiments investigating this possibility proved successful. Complete removal of the ethanol, however, proved to be difficult; therefore, methanol was substituted as the solvent, with equal success. This extended the necessary reaction time, presumably because of the lower reaction temperature; however, the lower temperature also allowed the relatively unstable starting material (4,7-dihydroxycoumarin) to be converted to the warfarin methyl ether (VII) in high yield.

The reaction involved stirring an appropriate coumarin analogue with benzalacetone in refluxing methanol. After 4–24 hr, as determined by TLC, the corresponding methyl ether was obtained in high yield. The ether can be quantitatively converted back to the warfarin analogue by acid hydrolysis. Typically, overall yields are >70%, and often yields as high as 95% are obtained. This dramatic increase in reaction yields should significantly aid in the development of warfarin as a tool to probe metabolic pathways.

EXPERIMENTAL[1]

Warfarin [4-Hydroxy-3-(1-phenyl-3-oxobutyl)-2*H*-1-benzopyran-2-one] (I)—4-Hydroxycoumarin (1.0 g, 0.0069 mole) was stirred

[1] Melting points were determined on a Thomas-Hoover melting point apparatus and are uncorrected. NMR spectra were recorded on a Varian EM-360A spectrometer using tetramethylsilane as internal standard. 4-Hydroxycoumarin was purchased from the Aldrich Chemical Co., and benzalacetone was purchased from MCB Reagents. 4,6- and 4,7-Dihydroxycoumarin were gifts from Dr. Lawrence Low, University of Washington. TLC was performed on EM Reagents analytical silica gel chromatography plates with flourescent indicator (no. 5539). All other solvents and reagents were of reagent purity.

0022-3549/83/0700-0830$01.00/0

(8) Y. Imamura, L. H. Wang, C. S. Lee, and J. H. Perrin, *Int. J. Pharmaceut.*, 5, 25 (1980).
(9) Y. Imamura, L. H. Wang, C. S. Lee, J. H. Perrin, K. Shiozu, and H. Ichibagase, *Int. J. Pharmaceut.*, 8, 277 (1981).
(10) C. M. Metzler, G. L. Elfring, and A. T. McGwen, *Biometrics*, 30, 562 (1974).
(11) M. J. Mattila, L. T. Seppala, and R. Koskinen, *Br. J. Clin. Pharmacol.*, 5, 161 (1978).

High-Yield Synthesis of Warfarin and Its Phenolic Metabolites: New Compounds

ERNIE BUSH and WILLIAM F. TRAGER ˣ

Received April 15, 1982, from the *Department of Medicinal Chemistry, University of Washington, Seattle, WA 98195.* Accepted for publication June 29, 1982.

Abstract □ A novel synthesis of warfarin and phenolic warfarin metabolites is presented which results in higher yields than previous methods.

Keyphrases □ Warfarin—phenolic metabolites, new high-yield synthetic method □ Synthesis—warfarin and its phenolic metabolites, new high-yield method

The oral anticoagulant warfarin [4-hydroxy-3-(1-phenyl-3-oxobutyl)-2*H*-1-benzopyran-2-one] (I) has found extensive clinical use in the treatment of such pathological conditions as thrombophlebitis, pulmonary emboli, and myocardial infarction (1). It is also used widely as a rodenticide to help control rat populations (2) and more recently has been used as a probe to investigate the multiplicity and catalytic activity of microsomal and purified cytochrome P-450 preparations (3–7). Because of its clinical and pharmacological importance, considerable effort has been expended to develop analytical methods to quantitate both warfarin and its metabolites from biological matrices (8–11). However, one of the impediments to progress in this area has been the lack of a high-yield synthetic procedure for these materials. Since mechanistic work in this laboratory on cytochrome P-450 required the synthesis and optical resolution of specifically deuterated warfarin analogues as substrates and multideuterated metabolites as GC–MS assay internal standards, the need for a reproducible, high-yield synthesis for these compounds was evident.

Although successful synthetic routes to these materials are documented in the literature, the reported yields are poor to moderate at best (12). Warfarin has been synthesized by the Michael addition of 4-hydroxycoumarin to benzalacetone under a number of acid- or base-catalyzed conditions (13). Traditionally, the reaction has most often been run in water containing a catalytic amount of triethylamine (~5 mole %). Hermodson *et al.* (12), using essentially the same conditions, extended this synthesis to the phenolic metabolites of warfarin by condensing benzalacetone with the appropriately substituted 4-hydroxycoumarin. Fasco *et al.* (14) followed a similar route, but to obtain a homogeneous system substituted dioxane as the solvent and piperidine as the catalyst. A further refinement was reported by Cook *et al.* (15) who, in their synthesis of 3′-bromowarfarin, heated a solution of *m*-bromobenzalacetone and 4-hydroxycoumarin in pyridine at reflux. However, rarely was the overall yield of warfarin or hydroxywarfarin >65%. In the case of 7-hydroxywarfarin, it was invariably much lower.

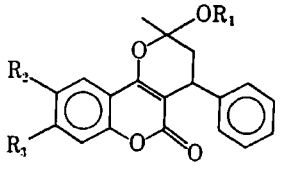

		R_1	R_2	R_3
I:	Warfarin	H	H	H
II:	Warfarin Ethyl Ether	C_2H_5	H	H
III:	Cyclocoumarol	CH_3	H	H
IV:	6-Hydroxywarfarin	H	OH	H
V:	7-Hydroxywarfarin	H	H	OH
VI:	6-Hydroxycyclocoumarol	CH_3	OH	H
VII:	7-Hydroxycyclocoumarol	CH_3	H	OH

RESULTS AND DISCUSSION

Numerous attempts in this laboratory to improve previous yields by alternate reaction pathways failed. A new approach was conceived when it was found that warfarin was quantitatively converted to its ethyl ether (II) by refluxing in absolute ethanol. This observation suggested that in absolute ethanol, the acidity of 4-hydroxycoumarin might be sufficient to catalyze its condensation with benzalacetone to generate warfarin. Once formed, the reaction would be driven to completion by the subsequent and essentially irreversible formation of the ethyl ether under these conditions. Initial experiments investigating this possibility proved successful. Complete removal of the ethanol, however, proved to be difficult; therefore, methanol was substituted as the solvent, with equal success. This extended the necessary reaction time, presumably because of the lower reaction temperature; however, the lower temperature also allowed the relatively unstable starting material (4,7-dihydroxycoumarin) to be converted to the warfarin methyl ether (VII) in high yield.

The reaction involved stirring an appropriate coumarin analogue with benzalacetone in refluxing methanol. After 4–24 hr, as determined by TLC, the corresponding methyl ether was obtained in high yield. The ether can be quantitatively converted back to the warfarin analogue by acid hydrolysis. Typically, overall yields are >70%, and often yields as high as 95% are obtained. This dramatic increase in reaction yields should significantly aid in the development of warfarin as a tool to probe metabolic pathways.

EXPERIMENTAL[1]

Warfarin [4-Hydroxy-3-(1-phenyl-3-oxobutyl)-2*H*-1-benzopyran-2-one] (I)—4-Hydroxycoumarin (1.0 g, 0.0069 mole) was stirred

[1] Melting points were determined on a Thomas-Hoover melting point apparatus and are uncorrected. NMR spectra were recorded on a Varian EM-360A spectrometer using tetramethylsilane as internal standard. 4-Hydroxycoumarin was purchased from the Aldrich Chemical Co., and benzalacetone was purchased from MCB Reagents. 4,6- and 4,7-Dihydroxycoumarin were gifts from Dr. Lawrence Low, University of Washington. TLC was performed on EM Reagents analytical silica gel chromatography plates with flourescent indicator (no. 5539). All other solvents and reagents were of reagent purity.

0022-3549/83/0700-0830$01.00/0

at reflux for 20 hr with benzalacetone (1.0 g, 0.0069 mole) in 50 ml of methanol. At this time, TLC (cyclohexane–ether, 1:1) indicated that all of the starting material had been converted to cyclocoumarol (III). The solvent was removed under reduced pressure and the residue was dissolved in 50 ml of acetone. An equal volume of 5 *N* HCl was added, and the solution was agitated in a 37° water bath for 4 hr or until TLC indicated complete hydrolysis to warfarin. Saturated aqueous NaCl (10 ml) was added and the mixture was extracted three times with 50 ml of ether. The combined ether extracts were back-extracted three times with 20 ml of 10% NaOH; the aqueous layer was filtered and reacidified to pH 2 with 5 *N* HCl. The resulting precipitate was collected by filtration, triturated with ether, and dried. Recrystallization from acetone–water (13) gave 1.98 g (93% yield) of I, mp 159–161° [lit. (12) 161°]. The NMR (dimethyl sulfoxide-d_6) was identical to that of authentic warfarin.

6-Hydroxywarfarin [4,6-Dihydroxy-3-(1-phenyl-3-oxobutyl)-2*H*-1-benzopyran-2-one] (VI)—6-Hydroxywarfarin was synthesized following the aforementioned procedure using 4,6-dihydroxycoumarin (0.5 g, 0.0028 mole) and benzalacetone (0.5 g, 0.0034 mole) in 30 ml of methanol. The product was recovered as described above and recrystallized from acetone–chloroform (12) to give 0.83 g (91% yield) of VI, mp 217–220° [lit. (12) 219–220°].

7-Hydroxywarfarin [4,7-Dihydroxy-3-(1-phenyl-3-oxobutyl)-2*H*-1-benzopyran-2-one] (VII)—7-Hydroxywarfarin was synthesized following the aforementioned procedure using 4,7-dihydroxycoumarin (0.2 g, 0.0011 mole) and benzalacetone (0.2 g, 0.0014 mole) in 20 ml of methanol. The product was recovered as described above and recrystallized from acetone–chloroform (12) to give 0.27 g (77% yield) of VII, mp 206–209° [lit. (12) 208–210°].

REFERENCES

(1) R. A. O'Reilly and P. M. Aggeler, *Pharmacol. Rev.*, **22**, 35 (1970).

(2) W. B. Jackson, P. J. Spear, and C. G. Wright, *Pest Control*, **39**, 13 (1971).

(3) W. R. Porter, C. Wheeler, and W. F. Trager, *Biochem. Pharmacol.*, **30**, 3099 (1981).

(4) M. J. Fasco, K. P. Vatsis, L. S. Kaminsky, and M. J. Coon, *J. Biol. Chem.*, **253**, 7813 (1978).

(5) L. S. Kaminsky, M. J. Fasco, and F. P. Guengerich, *J. Biol. Chem.*, **254**, 9657 (1979).

(6) M. J. Fasco, L. J. Piper, and L. S. Kaminsky, *Biochem. Pharmacol.*, **28**, 97 (1978).

(7) L. R. Pohl, S. D. Nelson, W. R. Porter, W. F. Trager, M. J. Fasco, F. D. Baker, and J. W. Fenton II, *Biochem. Pharmacol.*, **25**, 2153 (1976).

(8) W. N. Howald, E. D. Bush, W. F. Trager, R. A. O'Reilly, and C. H. Motley, *Biomed. Mass Spectrom.*, **7**, 35 (1980).

(9) M. J. Fasco, M. J. Cashin, and L. S. Kaminsky, *J. Liq. Chromatogr.*, **2**, 565 (1979).

(10) A. M. Duffield, P. H. Duffield, D. J. Birkett, M. Kennedy, and D. N. Wade, *Biomed Mass Spectrom.*, **6**, 209 (1979).

(11) C. E. Cook, N. H. Ballentine, T. B. Seltzman, and C. R. Tallent, *J. Pharmacol. Exp. Ther.*, **210**, 391 (1979).

(12) M. A. Hermodson, W. M. Barker, and L. P. Link, *J. Med. Chem.*, **14**, 167 (1971).

(13) C. Schroeder, Ph.D. Thesis, University of Wisconsin, Madison, Wis. (1955).

(14) M. J. Fasco, L. J. Piper, and L. S. Kaminsky, *J. Chromatogr.*, **131**, 365 (1977).

(15) C. E. Cook, R. Tallent, N. H. Ballentine, G. F. Taylor, and J. A. Kepler, *J. Label. Comp. Radiopharm.*, **16**, 623 (1979).

ACKNOWLEDGMENTS

This investigation was supported by the National Institutes of Health Grant IR01GM25136 (W.F.T.).

Synthesis of 4-Substituted *N*-[(Dimethylamino)methyl]benzamides: New Compounds

NILO ZANATTA and ROBERTO RITTNER *x

Received November 23, 1981 from the Instituto de Química, Universidade de São Paulo, C.P. 20.780, São Paulo, Brazil. Accepted for publication June 16, 1982. *Present address: Instituto de Química—UNICAMP, Caixa Postal 6154, 13.100—Campinas—São Paulo, Brazil.

Abstract □ Nine 4-substituted-*N*-[(dimethylamino)methyl]benzamides were obtained in high yield from the corresponding 4-substituted benzoic acids *via* the corresponding benzamides.

Keyphrases □ *N*-[(Dimethylamino)methyl]benzamides—4-substituted synthesis *via* Mannich–Einhorn reaction □ Amidomethylation reaction—synthesis of 4-substituted *N*-[(dimethylamino)methyl]benzamides

To investigate the possible relationship between electronic structure and local anesthetic properties, simple model compounds were required. The 4-substituted *N*-[(dimethylamino)methyl]benzamides[1] (I) were chosen as models since they are closely related to the procainamides, which are widely used as local anesthetics (1). These compounds have the advantage of being readily available from the 4-substituted benzamides (II) in a single step, using the Mannich–Einhorn reaction (2, 3). The 4-substituted benzamides (II) are either commercially available (4), or are readily prepared by conventional methods (5–9).

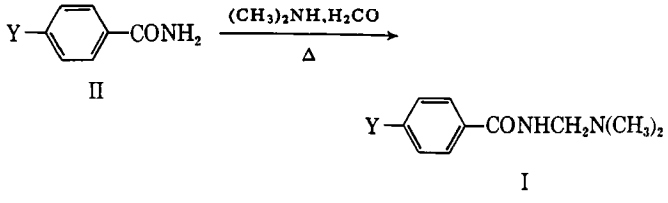

Y = H,F,Cl,Br,I,OCH$_3$,CH$_3$,N(CH$_3$)$_2$.

Scheme I

This study reports the application of the Mannich–Einhorn reaction (Scheme I) to the synthesis of I, and discusses the preparation of the starting materials (II), which were not commercially available.

EXPERIMENTAL[2]

4-Substituted *N*-[(dimethylamino)methyl]benzamide (I) was prepared by refluxing a mixture of a 4-substituted benzamide (II) (0.071 mole), 40% aqueous dimethylamine (17.4 ml; 0.142 mole), 35% aqueous formaldehyde (12.2 ml; 0.142 mole), and water (15 ml) with stirring for 4 hr.

[1] The key to the labeling of the 4-substituted amides (I) is in Table I.

[2] Melting points were determined in a Kofler apparatus and are uncorrected. IR spectra were determined in a Perkin-Elmer 457A spectrophotometer. NMR spectra were obtained with a Varian T-60 spectrometer using tetramethylsilane as the internal standard. Elemental analyses were performed at the Microanalysis Laboratories of the Instituto de Química—USP, São Paulo.

0022-3549/83/0700-0831$01.00/0

at reflux for 20 hr with benzalacetone (1.0 g, 0.0069 mole) in 50 ml of methanol. At this time, TLC (cyclohexane–ether, 1:1) indicated that all of the starting material had been converted to cyclocoumarol (III). The solvent was removed under reduced pressure and the residue was dissolved in 50 ml of acetone. An equal volume of 5 *N* HCl was added, and the solution was agitated in a 37° water bath for 4 hr or until TLC indicated complete hydrolysis to warfarin. Saturated aqueous NaCl (10 ml) was added and the mixture was extracted three times with 50 ml of ether. The combined ether extracts were back-extracted three times with 20 ml of 10% NaOH; the aqueous layer was filtered and reacidified to pH 2 with 5 *N* HCl. The resulting precipitate was collected by filtration, triturated with ether, and dried. Recrystallization from acetone–water (13) gave 1.98 g (93% yield) of I, mp 159–161° [lit. (12) 161°]. The NMR (dimethyl sulfoxide-d_6) was identical to that of authentic warfarin.

6-Hydroxywarfarin [4,6-Dihydroxy-3-(1-phenyl-3-oxobutyl)-2*H*-1-benzopyran-2-one] (VI)—6-Hydroxywarfarin was synthesized following the aforementioned procedure using 4,6-dihydroxycoumarin (0.5 g, 0.0028 mole) and benzalacetone (0.5 g, 0.0034 mole) in 30 ml of methanol. The product was recovered as described above and recrystallized from acetone–chloroform (12) to give 0.83 g (91% yield) of VI, mp 217–220° [lit. (12) 219–220°].

7-Hydroxywarfarin [4,7-Dihydroxy-3-(1-phenyl-3-oxobutyl)-2*H*-1-benzopyran-2-one] (VII)—7-Hydroxywarfarin was synthesized following the aforementioned procedure using 4,7-dihydroxycoumarin (0.2 g, 0.0011 mole) and benzalacetone (0.2 g, 0.0014 mole) in 20 ml of methanol. The product was recovered as described above and recrystallized from acetone–chloroform (12) to give 0.27 g (77% yield) of VII, mp 206–209° [lit. (12) 208–210°].

REFERENCES

(1) R. A. O'Reilly and P. M. Aggeler, *Pharmacol. Rev.*, **22**, 35 (1970).

(2) W. B. Jackson, P. J. Spear, and C. G. Wright, *Pest Control*, **39**, 13 (1971).

(3) W. R. Porter, C. Wheeler, and W. F. Trager, *Biochem. Pharmacol.*, **30**, 3099 (1981).

(4) M. J. Fasco, K. P. Vatsis, L. S. Kaminsky, and M. J. Coon, *J. Biol. Chem.*, **253**, 7813 (1978).

(5) L. S. Kaminsky, M. J. Fasco, and F. P. Guengerich, *J. Biol. Chem.*, **254**, 9657 (1979).

(6) M. J. Fasco, L. J. Piper, and L. S. Kaminsky, *Biochem. Pharmacol.*, **28**, 97 (1978).

(7) L. R. Pohl, S. D. Nelson, W. R. Porter, W. F. Trager, M. J. Fasco, F. D. Baker, and J. W. Fenton II, *Biochem. Pharmacol.*, **25**, 2153 (1976).

(8) W. N. Howald, E. D. Bush, W. F. Trager, R. A. O'Reilly, and C. H. Motley, *Biomed. Mass Spectrom.*, **7**, 35 (1980).

(9) M. J. Fasco, M. J. Cashin, and L. S. Kaminsky, *J. Liq. Chromatogr.*, **2**, 565 (1979).

(10) A. M. Duffield, P. H. Duffield, D. J. Birkett, M. Kennedy, and D. N. Wade, *Biomed Mass Spectrom.*, **6**, 209 (1979).

(11) C. E. Cook, N. H. Ballentine, T. B. Seltzman, and C. R. Tallent, *J. Pharmacol. Exp. Ther.*, **210**, 391 (1979).

(12) M. A. Hermodson, W. M. Barker, and L. P. Link, *J. Med. Chem.*, **14**, 167 (1971).

(13) C. Schroeder, Ph.D. Thesis, University of Wisconsin, Madison, Wis. (1955).

(14) M. J. Fasco, L. J. Piper, and L. S. Kaminsky, *J. Chromatogr.*, **131**, 365 (1977).

(15) C. E. Cook, R. Tallent, N. H. Ballentine, G. F. Taylor, and J. A. Kepler, *J. Label. Comp. Radiopharm.*, **16**, 623 (1979).

ACKNOWLEDGMENTS

This investigation was supported by the National Institutes of Health Grant IR01GM25136 (W.F.T.).

Synthesis of 4-Substituted *N*-[(Dimethylamino)methyl]benzamides: New Compounds

NILO ZANATTA and ROBERTO RITTNER *x

Received November 23, 1981 from the Instituto de Química, Universidade de São Paulo, C.P. 20.780, São Paulo, Brazil. Accepted for publication June 16, 1982. *Present address: Instituto de Química—UNICAMP, Caixa Postal 6154, 13.100—Campinas—São Paulo, Brazil.

Abstract □ Nine 4-substituted-*N*-[(dimethylamino)methyl]benzamides were obtained in high yield from the corresponding 4-substituted benzoic acids *via* the corresponding benzamides.

Keyphrases □ *N*-[(Dimethylamino)methyl]benzamides—4-substituted synthesis *via* Mannich–Einhorn reaction □ Amidomethylation reaction—synthesis of 4-substituted *N*-[(dimethylamino)methyl]benzamides

To investigate the possible relationship between electronic structure and local anesthetic properties, simple model compounds were required. The 4-substituted *N*-[(dimethylamino)methyl]benzamides[1] (I) were chosen as models since they are closely related to the procainamides, which are widely used as local anesthetics (1). These compounds have the advantage of being readily available from the 4-substituted benzamides (II) in a single step, using the Mannich–Einhorn reaction (2, 3). The 4-substituted benzamides (II) are either commercially available (4), or are readily prepared by conventional methods (5–9).

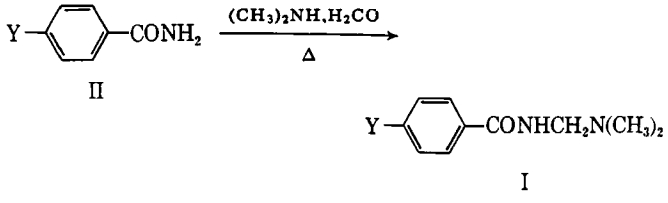

Y = H,F,Cl,Br,I,OCH$_3$,CH$_3$,N(CH$_3$)$_2$.

Scheme I

This study reports the application of the Mannich–Einhorn reaction (Scheme I) to the synthesis of I, and discusses the preparation of the starting materials (II), which were not commercially available.

EXPERIMENTAL[2]

4-Substituted *N*-[(dimethylamino)methyl]benzamide (I) was prepared by refluxing a mixture of a 4-substituted benzamide (II) (0.071 mole), 40% aqueous dimethylamine (17.4 ml; 0.142 mole), 35% aqueous formaldehyde (12.2 ml; 0.142 mole), and water (15 ml) with stirring for 4 hr.

[1] The key to the labeling of the 4-substituted amides (I) is in Table I.

[2] Melting points were determined in a Kofler apparatus and are uncorrected. IR spectra were determined in a Perkin-Elmer 457A spectrophotometer. NMR spectra were obtained with a Varian T-60 spectrometer using tetramethylsilane as the internal standard. Elemental analyses were performed at the Microanalysis Laboratories of the Instituto de Química—USP, São Paulo.

0022-3549/83/0700-0831$01.00/0

Table I—Physical Data of 4-Substituted *N*-[(Dimethylamino)methyl]benzamides

Compound	Y	Melting Point	Yield[a], %	Molecular Formula	Analysis, %	Calc.	Found
Ia	H	59–60°	48	$C_{10}H_{14}N_2O$	C	67.39	67.10
					H	7.92	8.06
					N	15.72	16.04
Ib	F[b]	—	86	$C_{10}H_{13}FN_2O$	C	61.21	55.22
					H	6.68	6.33
					N	14.28	12.27
Ic	Cl	82–83°	82	$C_{10}H_{13}ClN_2O$	C	56.47	56.16
					H	6.16	6.10
					N	13.17	13.51
Id	Br	107–108°	83	$C_{10}H_{13}BrN_2O$	C	46.71	47.37
					H	5.10	5.04
					N	10.89	11.19
Ie	I	123–125°	90	$C_{10}H_{13}IN_2O$	C	39.49	39.34
					H	4.31	5.15
					N	9.21	9.38
If	OCH_3	68–70°	82	$C_{11}H_{16}N_2O_2$	C	63.44	63.09
					H	7.74	7.93
					N	13.45	13.72
Ig	CH_3	56–58°	88	$C_{11}H_{16}N_2O$	C	68.72	68.43
					H	8.39	8.38
					N	14.57	14.51
Ih	$N(CH_3)_2$	95–97°	81	$C_{12}H_{19}N_3O$	C	65.13	64.83
					H	8.65	8.53
					N	18.99	19.01
Ii	NO_2	78–80°	41	$C_{10}H_{13}N_3O_3$	C	53.80	53.98
					H	5.87	5.89
					N	18.82	18.87

[a] Yields were based on the benzamides (II), recrystallized from benzene–*n*-hexane. [b] The oil did not crystallize. More accurate analytical data could not be obtained.

Table II—Spectral Data of 4-Substituted *N*-[(Dimethylamino)methyl]benzamides

Compound	Y	IR, (nujol), ν cm^{-1}	^{1}H-NMR ($CDCl_3$), δ H-2,6	H-3,5	N—H	CH_2	CH_3	Others
Ia	H	3340, 1640, 1600, 795, 685	7.84	7.46	6.88	4.26	2.40	
Ib	F	3300, 1650, 1605, 842	7.83	7.07	7.43	4.20	2.31	
Ic	Cl	3318, 1640, 1598, 840	7.75	7.35	7.05	4.18	2.31	
Id	Br	3310, 1640, 1590, 840	7.78	7.56	6.82	4.31	2.44	
Ie	I	3300, 1640, 1590, 827	7.90	7.58	6.86	4.32	2.46	
If	OCH_3	3372, 1635, 1605, 1250, 1020, 831	7.81	6.92	6.76	4.21	2.33	3.84
Ig	CH_3	3300, 1630, 830	7.73	7.23	6.76	4.21	2.33	2.38
Ih	$N(CH_3)_2$	3340, 1628, 1605, 817	7.79	6.73	6.73	4.25	2.35	3.05
Ii	NO_2	3145, 1670, 1600, 1512, 1343, 851	7.95	8.30	6.81	4.25	2.35	

The cooled solution was poured into a saturated aqueous sodium carbonate solution (50 ml), extracted with diethyl ether (3 × 30 ml), and dried over magnesium sulfate. The solvent was evaporated *in vacuo*, and the residue was recrystallized from benzene–petroleum ether to give a 40–90% yield of product.

DISCUSSION

The syntheses of the starting materials (II) for the Mannich–Einhorn reaction, were carried out as described previously (5–9). Oxidation of 4-anisaldehyde, 4-tolualdehyde, and 4-*N*-dimethylaminobenzaldehyde with an aqueous solution of silver nitrate–sodium hydroxide (10) gave the corresponding benzoic acids in yields of 40, 53, and 81%, respectively. The alternative procedure using silver oxide–ammonium hydroxide (5) failed and led to an explosive mixture. The 4-fluoro-, 4-bromo-, and 4-iodobenzoic acids were prepared as described previously (6–8) in yields of 86, 52, and 50%, respectively, following the diazotization of 4-aminobenzoic acid. Benzoic, 4-chlorobenzoic, and 4-nitrobenzoic acids were commercial products. All 4-substituted benzoic acids were converted to the corresponding benzoyl chlorides using thionyl chloride and catalytic amounts of dimethylformamide (11). The crude products were poured onto an excess of concentrated ammonium hydroxide (9) which led to the formation of the corresponding benzamides in yields of 70–80%. These 4-substituted benzamides, when treated with 35% aqueous formaldehyde and 40% aqueous dimethylamine gave the corresponding Mannich bases (I) (12), which were characterized by physical and spectral data (Tables I and II, respectively).

REFERENCES

(1) J. Büchi and X. Perlia, in "Drug Design," vol. 3, E. J. Ariëns, Ed., Academic, New York, N.Y., 1972, p. 243.

(2) H. Hellmann, *Angew. Chem.*, **69**, 463 (1957).

(3) M. Tramontini, *Synthesis*, **1973**, 703.

(4) "1981–1982 Aldrich Catalog Handbook of Fine Chemicals," Aldrich Chemical Co., Milwaukee, Wis., 1980.

(5) B. S. Furniss, A. J. Hannaford, V. Rogers, P. W. G. Smith, and A. R. Tatchell, "Vogel's Textbook of Practical Organic Chemistry," 4th ed., Longman, London, 1978, p. 1072.

(6) B. S. Furniss, A. J. Hannaford, V. Rogers, P. W. G. Smith, and A. R. Tatchell, *ibid.*, p. 705.

(7) B. S. Furniss, A. J. Hannaford, V. Rogers, P. W. G. Smith, and A. R. Tatchell, *ibid.*, p. 700.

(8) B. S. Furniss, A. J. Hannaford, V. Rogers, P. W. G. Smith, and A. R. Tatchell, *ibid.*, p. 695.

(9) B. S. Furniss, A. J. Hannaford, V. Rogers, P. W. G. Smith, and A. R. Tatchell, *ibid.*, p. 517.

(10) E. Campaigne and W. M. Le Suer, in "Organic Syntheses," vol. IV, N. Rabjohn, Ed., Wiley, New York, N.Y., 1963, p. 919.

(11) H. H. Bosshard, R. Mory, M. Schmid, and H. Zollinger, *Helv. Chim. Acta*, **42**, 1653 (1959).

(12) H. Hellmann and G. Haas, *Chem. Ber.*, **90**, 50 (1957).

ACKNOWLEDGMENTS

The authors thank the Conselho Nacional de Pesquisas for a grant to Roberto Rittner and a scholarship to Nilo Zanatta.

Estimating the Accumulation of Drugs

Keyphrases □ Drug accumulation—estimation during chronic dosing, theoretical *versus* empirical calculations □ Accumulation ratios—impact of lag time, effect of dosing

To the Editor:

Several methods are available to estimate the accumulation (R) of drugs during chronic dosing. The following equations are the ones most commonly used:

$$R_1 = \frac{AUC^1_{0-\infty}}{AUC^1_{0-\tau}} = \frac{AUC^{ss}_{0-\tau}}{AUC^1_{0-\tau}} \quad \text{(Eq. 1)}$$

$$R_2 = \frac{C_{min(ss)}}{C_{min(1)}} \quad \text{(Eq. 2)}$$

$$R_3 = 1/1 - e^{-\beta\tau} \quad \text{(Eq. 3)}$$

where $AUC^1_{0-\tau}$ and $AUC^1_{0-\infty}$ are the areas under the plasma concentration–time curves during a dosing interval and from time 0 to ∞ following a single dose, and $AUC^{ss}_{0-\tau}$ is the area under the plasma concentration–time curves during a dosing interval at steady state. $C_{min(1)}$ and $C_{min(ss)}$ are the plasma concentrations immediately prior to the administration of the second dose and any dose at steady state, respectively; and β and τ are the elimination rate constant and dosing interval, respectively.

Equations 1 and 2 can be determined empirically, whereas equation 3 is a theoretical calculation. If the pharmacological effect of the drug is a function of the plasma concentration, the R_1 values reflect the relevant accumulation, in that R_1 is a simple ratio of the observed concentrations during a dosing interval after a dose at steady state divided by the observed concentrations during the dosing interval after the first dose. R_2 values would be expected to closely approximate the relevant accumulation ratio (R_1) when k_a is larger compared with β but diverge as k_a approaches β, since the time of the maximum plasma concentration (C_{max}) moves closer to the time of drug administration during multiple dosing (1), and this will result in differences in C_{min} during multiple dosing. In general, the equation that uses β as the sole determinant of R (R_3) would be expected to deviate the most from R_1 and, in fact, only truly represents the accumulation during intravenous bolus administration.

Accumulation ratios (R) were estimated with a dosing interval equal to the half-life under known conditions using each of these equations with and without a lag time (t_{lag}) prior to the onset of absorption. The results of these calculations are presented in Table I. R_1 is always larger than R_2 and R_3. As the absorption half-life increases and k_a/β decreases these differences become more pronounced. In addition, when a lag time is incorporated the deviations among the three methods become more obvious. The reason for this deviation due to a lag time is displayed graphically in Fig. 1. Following the first dose, the lag time reduces the area during a dosing interval, whereas at steady state the lag time does not affect the area during a dosing interval.

Table I—Accumulation Ratios (R) Estimated by Various Commonly Used Methods with a Dosing Interval of 24 hr [a]

Parameter	k_a/β 24		12		4		2		1.1	
t_{lag}, hr	0	2	0	2	0	2	0	2	0	2
R_1	2.1	2.2	2.2	2.4	2.8	3.1	4.0	4.5	6.1	6.9
R_2	2.0	2.0	2.0	2.0	2.1	2.2	2.7	2.8	3.7	4.0
R_3	2.0	2.0	2.0	2.0	2.0	2.0	2.0	2.0	2.0	2.0

[a] $t_{1/2}\,k_a$ = 1, 2, 6, 12, and 21.8 hr; $t_{1/2}\,\beta$ = 24 hr; τ = 24 hr.

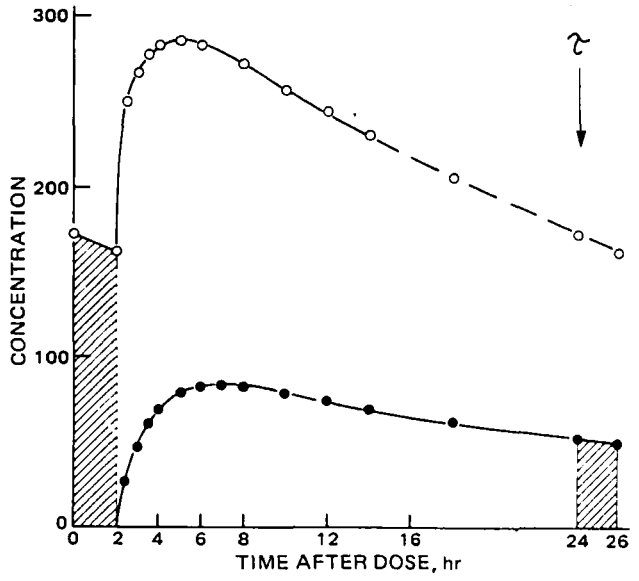

Figure 1—*Concentration–time profiles during a 24-hr dosing interval following first (—) and steady-state (- - -) doses when an absorption lag time occurs. The area that affects the prediction of accumulation is shaded. No area is lost at steady state, whereas the AUC from 24 to 26 hr is lost after a single dose.*

R values simulated when the same k_a/β ratios are employed but the dosing interval (τ) is altered are presented in Table II. It is apparent that the dosing interval significantly influences the deviations from R_1. Shorter dosing intervals cause greater deviations from the relevant accumulation ratio (R_1).

A composite view shows that several factors including lag time, dosing interval, and the ratio of k_a/β can influence the predictive capacity of Eqs. 2 and 3 compared with the true accumulation ratio estimated by Eq. 1. Although the need to use Eqs. 2 and 3 with caution and under specific conditions has been recognized (2), the impact of lag time and the actual deviations observed under appropriate use has been generally overlooked (3, 4). When one doses every

Table II—Accumulation Ratios (R) Estimated by Various Commonly Used Methods with a Dosing Interval of 12 or 48 hr [a]

Parameter	k_a/β 24		12		4		2		1.1	
τ, hr	12	48	12	48	12	48	12	48	12	48
R_1	3.8	1.4	4.3	1.4	7.1	1.5	11.6	1.8	19.8	2.4
R_2	3.4	1.3	3.5	1.3	4.6	1.3	6.8	1.4	10.8	1.7
R_3	3.4	1.3	3.4	1.3	3.4	1.3	3.4	1.3	3.4	1.3

[a] $t_{1/2}\,k_a$ = 1, 3, 6, 12, and 21.8 hr; $t_{1/2}\beta$ = 24 hr.

0022-3549/83/0700-0833$01.00/0

half-life, as is generally accepted as optimum therapy from a pharmacokinetic point of view, deviations occur even when k_a/β is large. When the dosing interval is decreased the deviations become greater. When k_a/β approached unity, as would be expected from certain controlled-release dosage forms, the deviations become enormous. In addition, it must be realized that although R_2 more closely reflects R_1 values than does R_3, it is not a predictive method, in that one must achieve steady state to determine $C_{min(ss)}$, whereas R_1 and R_3 can be used predictively following a single dose. These variables must be kept in mind when one is attempting to anticipate or predict drug accumulation and consequent pharmacological effects from single-dose data.

(1) J. H. Hull, *J. Clin. Pharmacol.*, **20**, 644 (1980).
(2) M. Gibaldi and D. Perrier, in "Pharmacokinetics," Dekker, New York, N.Y. 1975, p. 115.
(3) D. J. Greenblatt, M. Divoll, J. S. Harmatz, D. S. MacLaughlin, and R. I. Shader, *Clin. Pharmacol. Ther.*, **30**, 475 (1981).
(4) P. J. Perry, B. Alexander, F. J. Dunner, R. D. Schoenwald, B. Pfohl, and D. Miller, *J. Clin. Psychopharmacol.*, **2**, 114 (1982).

Wayne A. Colburn
Department of Pharmacokinetics and Biopharmaceutics
Hoffmann-La Roche Inc.
Nutley, NJ 07110

Received September 20, 1982.
Accepted for publication February 2, 1983.

Fraction Unbound in Interstitial Fluid

Keyphrases □ Pharmacokinetics—fraction unbound in interstitial fluid, relationship between binding in interstitial and vascular space

To the Editor:

The influence of protein binding of drugs on their pharmacological effect and pharmacokinetic disposition has been widely studied (1–3). However, most of the experimental observations have involved the interaction of drugs with plasma or serum proteins and not extravascular proteins. The lack of useful, experimental observations in this area is a result of the difficulty in obtaining representative tissue samples and the inadequate methods for performing tissue-binding studies (4). A mathematical approach has been derived (5) for estimating the fraction unbound in the "tissue" space utilizing a calculated volume of distribution term and anticipating physiological spaces. However, this approach is limited and only provides a complex average fraction unbound located outside the vascular space. Therefore, alternative theoretical approaches, as well as experimental methods need to be developed.

Nowhere is the role of plasma and tissue binding of greater interest than in the area of antibiotic therapy (6, 7). In general, β-lactam antibiotics are restricted in their distribution to the vascular space and the interstitial fluids; they do not penetrate intracellularly. Attempts to study the tissue (interstitial) binding of these antibiotics have centered on the collection of fluid from tissue cages (8), but the physiological character of the collected fluid has been questioned (9). The purpose of the present communication is to derive a theoretical relationship that relates the binding of a drug in the extravascular–extracellular or interstitial space to the binding in the vascular space. The original model on which this work is based was put forth by Øie *et al.* (10) and was recently used to describe the distribution of ceftriaxone (11). This theoretical relationship is used to explain the lack of distributional changes occurring with ceftriaxone despite the dramatic changes in the fraction unbound in the plasma (11).

The interaction of drugs with plasma proteins is usually described by the following Langmuir binding isotherm:

$$C_{BP} = \sum_{i=1}^{m} \frac{n_i P^* C_U}{Kd_i + C_U} \qquad \text{(Eq. 1)}$$

where C_{BP} is the plasma concentration of bound drug, m is the number of classes in binding sites, n_i is the number of binding sites for the ith class of binding sites, P is the concentration of the binding protein located in the vascular space, C_U is the concentration of unbound drug, and Kd_i is the equilibrium dissociation constant for the ith class of binding sites.

The presence of plasma proteins (*i.e.*, albumin) in the interstitial fluids has been well documented (12). If one assumes that the drug–protein interaction in the interstitial space is identical to the interaction in the vascular space (equivalent capacity and affinity constants), then a similar Langmuir relationship can be written for the interstitial binding:

$$C_{BE} = \sum_{i=1}^{m} \frac{n_i E^* C_U}{Kd_i + C_U} \qquad \text{(Eq. 2)}$$

where C_{BE} is the interstitial concentration of the bound drug and E is the concentration of binding protein in the interstitial space.

Equation 1 can be rewritten to factor out the protein and unbound concentration to yield:

$$C_{BP} = P^* C_U^* \sum_{i=1}^{m} \frac{n_i}{Kd_i + C_U} \qquad \text{(Eq. 3)}$$

For ease of manipulation, let a new parameter, S, replace the summation term:

$$C_{BP} = P^* C_U^* S \qquad \text{(Eq. 4)}$$

Given the assumptions concerning equivalent binding proteins in the vascular and interstitial spaces, and the additional assumptions of: (*a*) equal unbound drug concentration in both physiological spaces; (*b*) Kd_i does not change at lower protein concentrations; (*c*) other mechanisms of tissue distribution such as active transport, selective membrane permeability, and ion trapping are not present, then the S term for both C_{BP} and C_{BE} are equal, and a similar rearrangement and substitution can be written for C_{BE}:

$$C_{BE} = E^* C_U^* S \qquad \text{(Eq. 5)}$$

By definition, the fraction unbound in the plasma or vascular space (f_P) may be written as:

$$f_P = \frac{C_U}{C_U + C_{BP}} = \frac{1}{1 + P^* S} \qquad \text{(Eq. 6)}$$

A similar fraction unbound in the interstitial space (f_E) may be written as:

0022-3549/83/0700-0834$01.00/0

half-life, as is generally accepted as optimum therapy from a pharmacokinetic point of view, deviations occur even when k_a/β is large. When the dosing interval is decreased the deviations become greater. When k_a/β approached unity, as would be expected from certain controlled-release dosage forms, the deviations become enormous. In addition, it must be realized that although R_2 more closely reflects R_1 values than does R_3, it is not a predictive method, in that one must achieve steady state to determine $C_{min(ss)}$, whereas R_1 and R_3 can be used predictively following a single dose. These variables must be kept in mind when one is attempting to anticipate or predict drug accumulation and consequent pharmacological effects from single-dose data.

(1) J. H. Hull, *J. Clin. Pharmacol.*, **20**, 644 (1980).
(2) M. Gibaldi and D. Perrier, in "Pharmacokinetics," Dekker, New York, N.Y. 1975, p. 115.
(3) D. J. Greenblatt, M. Divoll, J. S. Harmatz, D. S. MacLaughlin, and R. I. Shader, *Clin. Pharmacol. Ther.*, **30**, 475 (1981).
(4) P. J. Perry, B. Alexander, F. J. Dunner, R. D. Schoenwald, B. Pfohl, and D. Miller, *J. Clin. Psychopharmacol.*, **2**, 114 (1982).

Wayne A. Colburn
Department of Pharmacokinetics and Biopharmaceutics
Hoffmann-La Roche Inc.
Nutley, NJ 07110

Received September 20, 1982.
Accepted for publication February 2, 1983.

Fraction Unbound in Interstitial Fluid

Keyphrases □ Pharmacokinetics—fraction unbound in interstitial fluid, relationship between binding in interstitial and vascular space

To the Editor:

The influence of protein binding of drugs on their pharmacological effect and pharmacokinetic disposition has been widely studied (1–3). However, most of the experimental observations have involved the interaction of drugs with plasma or serum proteins and not extravascular proteins. The lack of useful, experimental observations in this area is a result of the difficulty in obtaining representative tissue samples and the inadequate methods for performing tissue-binding studies (4). A mathematical approach has been derived (5) for estimating the fraction unbound in the "tissue" space utilizing a calculated volume of distribution term and anticipating physiological spaces. However, this approach is limited and only provides a complex average fraction unbound located outside the vascular space. Therefore, alternative theoretical approaches, as well as experimental methods need to be developed.

Nowhere is the role of plasma and tissue binding of greater interest than in the area of antibiotic therapy (6, 7). In general, β-lactam antibiotics are restricted in their distribution to the vascular space and the interstitial fluids; they do not penetrate intracellularly. Attempts to study the tissue (interstitial) binding of these antibiotics have centered on the collection of fluid from tissue cages (8), but the physiological character of the collected fluid has been questioned (9). The purpose of the present communication is to derive a theoretical relationship that relates the binding of a drug in the extravascular–extracellular or interstitial space to the binding in the vascular space. The original model on which this work is based was put forth by Øie *et al.* (10) and was recently used to describe the distribution of ceftriaxone (11). This theoretical relationship is used to explain the lack of distributional changes occurring with ceftriaxone despite the dramatic changes in the fraction unbound in the plasma (11).

The interaction of drugs with plasma proteins is usually described by the following Langmuir binding isotherm:

$$C_{BP} = \sum_{i=1}^{m} \frac{n_i P^* C_U}{Kd_i + C_U} \qquad \text{(Eq. 1)}$$

where C_{BP} is the plasma concentration of bound drug, m is the number of classes in binding sites, n_i is the number of binding sites for the ith class of binding sites, P is the concentration of the binding protein located in the vascular space, C_U is the concentration of unbound drug, and Kd_i is the equilibrium dissociation constant for the ith class of binding sites.

The presence of plasma proteins (*i.e.*, albumin) in the interstitial fluids has been well documented (12). If one assumes that the drug–protein interaction in the interstitial space is identical to the interaction in the vascular space (equivalent capacity and affinity constants), then a similar Langmuir relationship can be written for the interstitial binding:

$$C_{BE} = \sum_{i=1}^{m} \frac{n_i E^* C_U}{Kd_i + C_U} \qquad \text{(Eq. 2)}$$

where C_{BE} is the interstitial concentration of the bound drug and E is the concentration of binding protein in the interstitial space.

Equation 1 can be rewritten to factor out the protein and unbound concentration to yield:

$$C_{BP} = P^* C_U^* \sum_{i=1}^{m} \frac{n_i}{Kd_i + C_U} \qquad \text{(Eq. 3)}$$

For ease of manipulation, let a new parameter, S, replace the summation term:

$$C_{BP} = P^* C_U^* S \qquad \text{(Eq. 4)}$$

Given the assumptions concerning equivalent binding proteins in the vascular and interstitial spaces, and the additional assumptions of: (*a*) equal unbound drug concentration in both physiological spaces; (*b*) Kd_i does not change at lower protein concentrations; (*c*) other mechanisms of tissue distribution such as active transport, selective membrane permeability, and ion trapping are not present, then the S term for both C_{BP} and C_{BE} are equal, and a similar rearrangement and substitution can be written for C_{BE}:

$$C_{BE} = E^* C_U^* S \qquad \text{(Eq. 5)}$$

By definition, the fraction unbound in the plasma or vascular space (f_P) may be written as:

$$f_P = \frac{C_U}{C_U + C_{BP}} = \frac{1}{1 + P^* S} \qquad \text{(Eq. 6)}$$

A similar fraction unbound in the interstitial space (f_E) may be written as:

0022-3549/83/0700-0834$01.00/0

$$f_E = \frac{1}{1 + E^*S} \quad \text{(Eq. 7)}$$

One can rearrange Eq. 6 to obtain the S parameter in terms of f_P and P via:

$$S = \frac{1 - f_P}{P^* f_P} \quad \text{(Eq. 8)}$$

Substituting Eq. 8 into Eq. 7, one can now write an expression for f_E in terms of f_P, P, and E:

$$f_E = \frac{1}{1 + \frac{E}{P}\left(\frac{1 - f_P}{f_P}\right)} \quad \text{(Eq. 9)}$$

Figure 1 illustrates the theoretical relationship between f_P and f_E, when the ratio of protein concentration (E/P) is normal (0.32), less than normal (0.10), or greater than normal (0.64) (12). Two distinct trends are apparent from the data. As might be expected, decreasing or increasing the relative concentration of interstitial protein results in a larger or smaller fraction unbound in the interstitial space (f_E) relative to the vascular space (f_P). A second trend is the observation that as f_P values <0.1 the relationship between f_E and f_P becomes linear, irrespective of the value of E/P. This fixed ratio of f_E to f_P can be explained readily if one evaluates Eq. 9 as f_P approaches zero.

In this case:

$$f_E = \frac{P}{E} {}^* f_P \quad \text{(Eq. 10)}$$

Therefore, for drugs that are highly bound, the ratio of their fraction unbound in the interstitial and vascular spaces (f_E/f_P) is inversely related to the ratio of the concentration of binding protein located in those physiological spaces (E/P). Furthermore, any increases in f_P will result in proportional changes in f_E, such that the ratio of the two drugs (f_E/f_P) will remain relatively constant at f_P values <0.1.

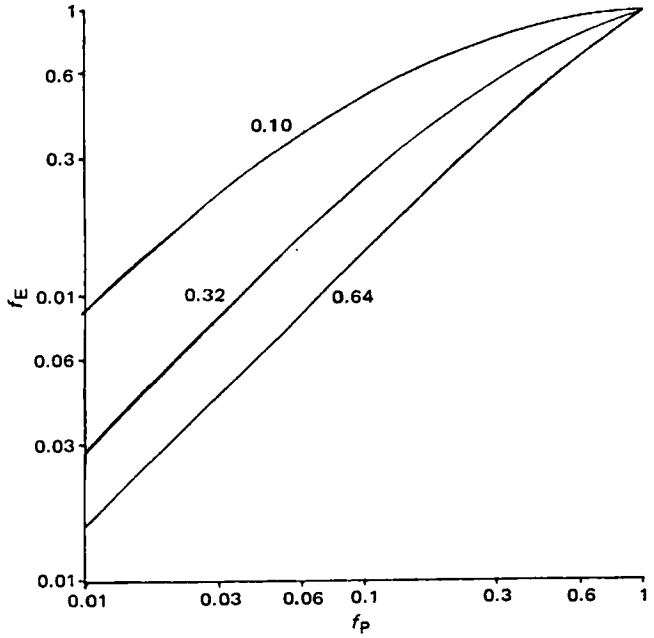

Figure 1—*Interrelationship of f_E and f_P as defined by Eq. 9; inset numbers refer to* E/P *values.*

One of the important implications for this theoretical observation lies in the distribution of drug mass. The pharmacokinetic parameter which best reflects shifts in drug distribution is the apparent volume of distribution at steady state calculated with reference to total drug levels (V_{ss}^T). As mentioned above, we have previously put forth a conceptual model or approach based on the work of Gillette (13) which relates V_{ss}^T to drug binding and physiological spaces (5). The following equation represents a modification of the original work:

$$V_{ss}^T = V_P + \frac{f_P}{f_E} V_E \quad \text{(Eq. 11)}$$

where V_P and V_E are the physiological volumes of the plasma and interstitial spaces, respectively.

Table I illustrates the influence of the ratio of the fractions unbound (f_E/f_P) on V_{ss}^T as f_P increases. In agreement with the observed ceftriaxone data (where f_P increased from 0.03 to 0.1), the change in V_{ss}^T is very small. Therefore, for this particular system under the stated conditions, one should expect no substantial shift in drug mass out of the vascular compartment as a result of an increase in f_P.

The stable nature of V_{ss}^T is contrasted by the large changes that occur in the parameter V_{ss}^U (Table I). The V_{ss}^U parameter can be derived experimentally from the analysis of the unbound concentration *versus* time profile (11) and has been theoretically described by the following equation:

$$V_{ss}^U = \frac{V_P}{f_P} + \frac{V_E}{f_E} \quad \text{(Eq. 12)}$$

As f_P and f_E increase, V_{ss}^U decreases strikingly. These dramatic changes in V_{ss}^U **do not** reflect any changes in the distributional space. They merely reflect the substantial shift in the ratio of unbound concentration in the plasma to the amount of drug in the body (*i.e.*, dose). The utility of V_{ss}^U is described elsewhere (11).

In conclusion, we have presented a conceptually useful equation which describes the fraction unbound in the interstitial space and provides a theoretical explanation for the observed behavior of the apparent volume of distribution for ceftriaxone. The equation was developed for

Table I—Influence of Increasing f_P Values and Various Ratios of E/P on V_{ss}^T and V_{ss}^U as Calculated by Eqs. 9, 11, and 12 [a]

		V_{ss}^T ml/kg		
f_P	E/P	0.10	0.32	0.64
0.001		59.2	96.5	147.
0.005		59.8	97.0	148.
0.01		60.5	97.6	148.
0.05		66.7	102.	151.
0.1		74.3	108.	154.
0.5		136.	154.	180.
1.0		212.	212.	212.
		V_{ss}^U liter/kg		
f_P	E/P	0.10	0.32	0.64
0.001		59.2	96.6	147.
0.005		12.0	19.4	30.2
0.01		6.05	9.76	15.1
0.05		1.33	2.04	3.08
0.1		0.75	1.08	1.57
0.5		0.27	0.31	0.36
1.0		0.21	0.21	0.21

[a] V_P = 42 ml/kg; V_E = 170 ml/kg.

antibiotics, but may have wider application. However, this application must be preceded by an appreciation (and if possible the testing) of the underlying assumptions of this relationship. The major assumption remains that the only binding that occurs outside the vascular space is to plasma proteins located there, and that the binding constants remain the same.

(1) G. R. Wilkinson and D. G. Shand, *Clin. Pharmacol. Ther.*, **18**, 377 (1975).
(2) A. Yacobi and G. Levy, *J. Pharm. Sci.*, **64**, 1660 (1975).
(3) G. H. Evans, A. S. Nies, and D. G. Shand, *J. Pharmacol. Exp. Ther.*, **180**, 114 (1973).
(4) W. J. Jusko and M. Gretch, *Drug Metab. Rev.*, **5**, 43 (1976).
(5) M. Gibaldi and P. J. McNamara, *J. Pharm. Sci.*, **66**, 1211 (1977).
(6) W. A. Craig and C. M. Kunin, *Annu. Rev. Med.*, **27**, 287 (1976).
(7) W. A. Craig and P. G. Welling, *Clin. Pharmacokinet.*, **2**, 252 (1977).
(8) G. D. Chisholm, *Scand. J. Infect. Dis. Suppl.*, **14**, 118 (1978).
(9) H.-U. Eickenberg, *Scand. J. Infect. Dis. Suppl.*, **14**, 166 (1978).
(10) S. Øie, T. W. Guentert, and T. N. Tozer, *J. Pharm. Pharmacol.*, **32**, 471 (1980).
(11) P. J. McNamara, M. Gibaldi, and K. Stoeckel, *Eur. J. Clin. Pharmacol.*, submitted.
(12) T. Kawai, in "Clinical Aspects of the Plasma Proteins," Lippincott, Philadelphia, Pa., 1973, pp. 114–130.
(13) J. R. Gillette, *Ann. N.Y. Acad. Sci.*, **179**, 43 (1971).

Patrick J. McNamara ˣ
College of Pharmacy
University of Kentucky
Lexington, KY 40536-0053
Milo Gibaldi
School of Pharmacy
University of Washington
Seattle, WA 98195
Klaus Stoeckel
Biological Pharmaceutical Research Department
F. Hoffmann-LaRoche & Co.
Basel, Switzerland

Received December 23, 1982.
Accepted for publication March 9, 1983.

Creatinine XII: Comparison of Assays of Low Serum Creatinine Levels Using High-Performance Liquid Chromatography and Two Picrate Methods

Keyphrases □ Creatinine—assay in serum using HPLC, automated picrate method, modified picrate method, comparison of methods □ High-performance liquid chromatography—creatinine assay in serum, comparison with two picrate methods

To the Editor:

Endogenous creatinine has been commonly employed to estimate the glomerular filtration rate for the study of renal function or for modifying dosages in patients with renal impairment (1–5). Clinically, the automated picrate method[1], based on a complex color reaction between creatinine and picrate in the alkaline medium, is probably most widely used to assay creatinine in plasma or serum (6–10). This method, however, is known to be nonspecific due to potential interferences by endogenous and/or exogenous substances, and often results in an overestimate of "true" creatinine levels (7–9). It appears that to date most of assay comparisons between this method and the more specific high-performance liquid chromatographic (HPLC) method were carried out in samples containing higher levels (such as >0.8 mg%) of creatinine (10, 11). Since lower levels are often found in patients, it would seem important to evaluate potential discrepancies using low-level samples. The modified picrate method of Yatzidis (12, 13) was also chosen for the present evaluation, since it has been reported to be highly specific.

A total of 30 random serum samples from patients determined by the automated picrate method in a clinical laboratory[2] and found to contain less than 0.8 mg% of creatinine, were employed in the study. The HLPC method (14) used in the present study is a slight modification of the method developed earlier in our laboratory (3). Briefly, the method involved the deproteinization of 0.1 ml of serum with 0.25 ml of acetonitrile. After vortexing and centrifugation, 50 μl of the supernatant was injected directly into the cation-exchange column[3]. The recovery in the above sample preparation is essentially 100% (3). The mobile phase with a flow rate of 3 ml/min contained 0.035 *M* monobasic ammonium phosphate adjusted to pH 4.8 with 0.01 *N* NaOH. The creatinine was monitored at 254 nm using a fixed wavelength detector[4] with a sensitivity setting of 0.005 AUFS. The retention time for creatinine was about 4.5 min. The present assay has a detection limit of 0.05 mg% (based on a signal/noise ratio of 3.0), and has a coefficient of variation for both interassay and intraassay between 1.2 and 3.0%. No interferences were found in the present and earlier (14) studies with samples obtained from patients or volunteers. It should be noted that the variable wavelength UV detector (without a noise damper) used in our earlier studies (3, 10) was much less sensitive; it had a larger base-line noise even at a previously used sensitivity setting of 0.05 AUFS. Duplicate analyses were performed using both the HPLC method and the Yatzidis method.

The results of the serum creatinine measured by the above three methods are summarized in Table I. The automated method overestimated serum creatinine by an average of 15.2% with a −16.7 to 66.7% range when compared with the HPLC method. Although the mean overestimation found in the present study is similar to the previous study (14.5%, $n = 30$) using samples with generally much higher serum levels (10), it is of interest to note (Table I) that for two samples the overestimations were >50%, and for eight samples the results were essentially identical. The above results suggest that the amount and nature of interfering substances may vary considerably with individuals.

The overestimations of serum creatinine by the modified picrate method were much higher with an average of 55.2% (ranging from −58.3 to 168%). In the previous report (10), a similar modified method (15) was found to overestimate

[1] Auto Analyzer SMA 6/60, Technicon Instruments, Tarrytown, N.Y.

[2] University of Illinois Hospital, Chicago, Ill.
[3] Partisil PXS 10/25 SCX, 30 cm, Whatman Inc., Clifton, N.J.
[4] Model 440, Waters Associates, Milford, Mass.

0022-3549/83/0700-0836$01.00/0

antibiotics, but may have wider application. However, this application must be preceded by an appreciation (and if possible the testing) of the underlying assumptions of this relationship. The major assumption remains that the only binding that occurs outside the vascular space is to plasma proteins located there, and that the binding constants remain the same.

(1) G. R. Wilkinson and D. G. Shand, *Clin. Pharmacol. Ther.*, **18**, 377 (1975).
(2) A. Yacobi and G. Levy, *J. Pharm. Sci.*, **64**, 1660 (1975).
(3) G. H. Evans, A. S. Nies, and D. G. Shand, *J. Pharmacol. Exp. Ther.*, **180**, 114 (1973).
(4) W. J. Jusko and M. Gretch, *Drug Metab. Rev.*, **5**, 43 (1976).
(5) M. Gibaldi and P. J. McNamara, *J. Pharm. Sci.*, **66**, 1211 (1977).
(6) W. A. Craig and C. M. Kunin, *Annu. Rev. Med.*, **27**, 287 (1976).
(7) W. A. Craig and P. G. Welling, *Clin. Pharmacokinet.*, **2**, 252 (1977).
(8) G. D. Chisholm, *Scand. J. Infect. Dis. Suppl.*, **14**, 118 (1978).
(9) H.-U. Eickenberg, *Scand. J. Infect. Dis. Suppl.*, **14**, 166 (1978).
(10) S. Øie, T. W. Guentert, and T. N. Tozer, *J. Pharm. Pharmacol.*, **32**, 471 (1980).
(11) P. J. McNamara, M. Gibaldi, and K. Stoeckel, *Eur. J. Clin. Pharmacol.*, submitted.
(12) T. Kawai, in "Clinical Aspects of the Plasma Proteins," Lippincott, Philadelphia, Pa., 1973, pp. 114–130.
(13) J. R. Gillette, *Ann. N.Y. Acad. Sci.*, **179**, 43 (1971).

Patrick J. McNamara ˣ
College of Pharmacy
University of Kentucky
Lexington, KY 40536-0053
Milo Gibaldi
School of Pharmacy
University of Washington
Seattle, WA 98195
Klaus Stoeckel
Biological Pharmaceutical Research Department
F. Hoffmann-LaRoche & Co.
Basel, Switzerland

Received December 23, 1982.
Accepted for publication March 9, 1983.

Creatinine XII: Comparison of Assays of Low Serum Creatinine Levels Using High-Performance Liquid Chromatography and Two Picrate Methods

Keyphrases □ Creatinine—assay in serum using HPLC, automated picrate method, modified picrate method, comparison of methods □ High-performance liquid chromatography—creatinine assay in serum, comparison with two picrate methods

To the Editor:

Endogenous creatinine has been commonly employed to estimate the glomerular filtration rate for the study of renal function or for modifying dosages in patients with renal impairment (1–5). Clinically, the automated picrate method[1], based on a complex color reaction between creatinine and picrate in the alkaline medium, is probably most widely used to assay creatinine in plasma or serum (6–10). This method, however, is known to be nonspecific due to potential interferences by endogenous and/or exogenous substances, and often results in an overestimate of "true" creatinine levels (7–9). It appears that to date most of assay comparisons between this method and the more specific high-performance liquid chromatographic (HPLC) method were carried out in samples containing higher levels (such as >0.8 mg%) of creatinine (10, 11). Since lower levels are often found in patients, it would seem important to evaluate potential discrepancies using low-level samples. The modified picrate method of Yatzidis (12, 13) was also chosen for the present evaluation, since it has been reported to be highly specific.

A total of 30 random serum samples from patients determined by the automated picrate method in a clinical laboratory[2] and found to contain less than 0.8 mg% of creatinine, were employed in the study. The HLPC method (14) used in the present study is a slight modification of the method developed earlier in our laboratory (3). Briefly, the method involved the deproteinization of 0.1 ml of serum with 0.25 ml of acetonitrile. After vortexing and centrifugation, 50 μl of the supernatant was injected directly into the cation-exchange column[3]. The recovery in the above sample preparation is essentially 100% (3). The mobile phase with a flow rate of 3 ml/min contained 0.035 *M* monobasic ammonium phosphate adjusted to pH 4.8 with 0.01 *N* NaOH. The creatinine was monitored at 254 nm using a fixed wavelength detector[4] with a sensitivity setting of 0.005 AUFS. The retention time for creatinine was about 4.5 min. The present assay has a detection limit of 0.05 mg% (based on a signal/noise ratio of 3.0), and has a coefficient of variation for both interassay and intraassay between 1.2 and 3.0%. No interferences were found in the present and earlier (14) studies with samples obtained from patients or volunteers. It should be noted that the variable wavelength UV detector (without a noise damper) used in our earlier studies (3, 10) was much less sensitive; it had a larger base-line noise even at a previously used sensitivity setting of 0.05 AUFS. Duplicate analyses were performed using both the HPLC method and the Yatzidis method.

The results of the serum creatinine measured by the above three methods are summarized in Table I. The automated method overestimated serum creatinine by an average of 15.2% with a −16.7 to 66.7% range when compared with the HPLC method. Although the mean overestimation found in the present study is similar to the previous study (14.5%, $n = 30$) using samples with generally much higher serum levels (10), it is of interest to note (Table I) that for two samples the overestimations were >50%, and for eight samples the results were essentially identical. The above results suggest that the amount and nature of interfering substances may vary considerably with individuals.

The overestimations of serum creatinine by the modified picrate method were much higher with an average of 55.2% (ranging from −58.3 to 168%). In the previous report (10), a similar modified method (15) was found to overestimate

[1] Auto Analyzer SMA 6/60, Technicon Instruments, Tarrytown, N.Y.

[2] University of Illinois Hospital, Chicago, Ill.
[3] Partisil PXS 10/25 SCX, 30 cm, Whatman Inc., Clifton, N.J.
[4] Model 440, Waters Associates, Milford, Mass.

0022-3549/83/0700-0836$01.00/0

Table I—Comparison of Serum Creatinine Levels Using Three Different Methods

HPLC, mg%	Automated Picrate Method[a], mg%	Deviation from HPLC, %	Modified Picrate Method, mg%	Deviation from HPLC, %
0.44	0.5	13.6	—	—
0.42	0.5	19.0	0.72	71.4
0.41	0.5	22.0	0.65	58.5
0.52	0.5	−3.8	0.75	44.2
0.59	0.5	−15.3	0.98	66.1
0.48	0.5	4.2	0.89	85.4
0.60	0.5	−16.7	0.88	46.7
0.47	0.5	6.4	0.80	70.2
0.57	0.6	5.3	0.91	59.6
0.47	0.6	27.7	0.95	102.1
0.48	0.6	25.0	0.83	72.9
0.48	0.6	25.0	0.20	−58.3
0.51	0.6	17.6	0.86	68.6
0.56	0.6	7.1	0.87	55.4
0.55	0.6	9.1	1.26	129.1
0.38	0.6	57.9	1.02	168.0
0.52	0.6	15.4	0.90	73.1
0.62	0.6	−3.2	0.54	−12.9
0.61	0.6	−1.6	0.84	37.7
0.49	0.6	22.4	0.86	75.5
0.64	0.7	9.4	0.92	43.8
0.62	0.7	12.9	1.11	79.0
0.51	0.7	37.3	1.10	115.7
0.61	0.7	14.8	0.88	44.3
0.61	0.7	14.8	0.46	−24.6
0.66	0.7	6.1	0.84	27.3
0.42	0.7	66.7	0.71	69.0
0.67	0.8	19.4	1.05	56.7
0.68	0.8	17.6	0.71	4.4
0.67	0.8	19.4	0.49	−26.9
Mean		15.2		55.2
±*SD*		±17.5		±47.2

[a] Only one significant figure was provided for concentrations <1.0 mg% by the printout of the instrument.

by an average of 32% in serum samples with a wider range of creatinine levels (0.62–18.5 mg% based on the HPLC method). However, for samples (n = 3) with serum levels in the range of 0.6–0.7 mg% (10) the mean overestimation was 88.2%. Thus, both of the modified picrate methods (12, 13, 15) resulted in consistently much higher creatinine values. The reason for the apparent discrepancy between their claimed specificity (12, 15) and the present as well as the previous (10, 16) findings remains to be investigated.

The results of the present study indicate that one should be cautious in using the automated and modified picrate methods for creatinine determinations. Since the HPLC method is generally considered to be more specific (3), its use should be preferred when accurate determinations are required.

It has been recently reported that creatinine might be extensively secreted and reabsorbed by renal tubules in both humans (17, 18) and animals (18, 19), and there might also be a significant nonrenal elimination in normal humans (19, 20) and normal rabbits (19). The full implications of these findings in the use of creatinine remain to be explored.

(1) W. L. Chiou and F. H. Hsu, *J. Clin. Pharmacol.*, **15**, 427 (1975).

(2) W. L. Chiou and F. H. Hsu, *Res. Commun. Chem. Pathol. Pharmacol.*, **10**, 315 (1975).

(3) W. L. Chiou, M. A. F. Gadalla, and G. W. Peng, *J. Pharm. Sci.*, **67**, 182 (1978).

(4) R. S. Lott and W. L. Hayton, *Drug Intel. Clin. Pharm.*, **12**, 140 (1978).

(5) T. D. Bjornsson, *Clin. Pharmacokinet.*, **4**, 200 (1979).

(6) A. L. Chasson, H. J. Grady, and M. A. Stanley, *Am. J. Clin. Pathol.*, **35**, 83 (1961).

(7) H. D. Lauson, *J. Appl. Physiol.*, **4**, 227 (1951).

(8) J. G. H. Cook, *Annu. Clin. Biochem.*, **12**, 219 (1975).

(9) S. Narayanan and H. D. Appleton, *Clin. Chem.*, **26**, 1119 (1980).

(10) W. L. Choiu, G. W. Peng, and M. A. F. Gadalla, *J. Pharm. Sci.*, **67**, 292 (1978).

(11) F. W. Spierto, L. MacNeil, P. Culbreth, I. Duncan, and C. A. Burtis, *Clin. Chem.*, **26**, 286 (1980).

(12) H. Yatzidis, *Clin. Chem.*, **20**, 1131 (1974).

(13) H. Yatzidis, *Clin. Chem.*, **21**, 157 (1975).

(14) W. L. Chiou and F. S. Pu, *Clin. Pharmacol. Ther.*, **25**, 777 (1979).

(15) H. Yatzidis, *Clin. Chem.*, **21**, 1848 (1975).

(16) W. L. Chiou, F. H. Hsu, and G. W. Peng, *Clin. Chem.*, **23**, 1374 (1977).

(17) W. L. Chiou, *Res. Commun. Chem. Pathol. Pharmacol.*, **36**, 349 (1982).

(18) W. L. Chiou, in "Pharmacokinetics: A Modern View," L. Z. Benet and G. Levy, Eds., Plenum, New York, N.Y., 1982.

(19) Y. C. Huang, "Pharmacokinetics of Creatinine," Ph.D. thesis, University of Illinois, 1981.

(20) Y. C. Huang, S. M. Huang, and W. L. Chiou, *Int. J. Clin. Pharmacol. Ther. Toxicol.*, **20**, 343 (1982).

*Yih-Chain Huang**
Win L. Chiou[x]

Departments of Pharmacodynamics and Pharmaceutics
College of Pharmacy
University of Illinois at Chicago
Chicago, IL 60612

Received June 15, 1981.
Accepted for publication March 13, 1983.

* Present address: College of Pharmacy, Rutgers–The State University, Piscataway, NJ 08854.

Crystalline Anhydrous–Hydrate Phase Changes of Caffeine and Theophylline in Solvent–Water Mixtures

Keyphrases □ Phase changes—in crystals, anhydrous to hydrate, caffeine, theophylline, solubility studies □ Caffeine—crystalline phase changes, anhydrous to hydrate, solubility studies □ Theophylline—crystalline phase changes, anhydrous to hydrates solubility studies

To the Editor:

The extended Hildebrand solubility approach (1–3) was recently developed and evaluated for calculation of solubilities in solvent–water systems that are not adequately described by the regular solution theory (4). The approach is based on regression analysis of solubility data to calculate solute–activity coefficients as a function of the solubility parameter of the solvent mixture.

A problem exists with several of the solutes used in the evaluation of the extended Hildebrand approach: crystalline anhydrous–hydrate phase transformation as the water content of the solvent mixture is changed. In the dry solvent it is clear that only a nonhydrated (anhydrous or solvated) form can be present at equilibrium (5); but in aqueous solvent mixtures the equilibrium form may be anhydrous solvated or hydrated crystals. This was recently demonstrated for cholesterol in water–glyceryl-1-monooctanoate solutions (6). The transition between anhydrous and monohydrate forms occurred at 5% water (37°) and was temperature dependent. In this system the max-

0022-3549/83/0700-0837$01.00/0

Table I—Comparison of Serum Creatinine Levels Using Three Different Methods

HPLC, mg%	Automated Picrate Method[a], mg%	Deviation from HPLC, %	Modified Picrate Method, mg%	Deviation from HPLC, %
0.44	0.5	13.6	—	—
0.42	0.5	19.0	0.72	71.4
0.41	0.5	22.0	0.65	58.5
0.52	0.5	−3.8	0.75	44.2
0.59	0.5	−15.3	0.98	66.1
0.48	0.5	4.2	0.89	85.4
0.60	0.5	−16.7	0.88	46.7
0.47	0.5	6.4	0.80	70.2
0.57	0.6	5.3	0.91	59.6
0.47	0.6	27.7	0.95	102.1
0.48	0.6	25.0	0.83	72.9
0.48	0.6	25.0	0.20	−58.3
0.51	0.6	17.6	0.86	68.6
0.56	0.6	7.1	0.87	55.4
0.55	0.6	9.1	1.26	129.1
0.38	0.6	57.9	1.02	168.0
0.52	0.6	15.4	0.90	73.1
0.62	0.6	−3.2	0.54	−12.9
0.61	0.6	−1.6	0.84	37.7
0.49	0.6	22.4	0.86	75.5
0.64	0.7	9.4	0.92	43.8
0.62	0.7	12.9	1.11	79.0
0.51	0.7	37.3	1.10	115.7
0.61	0.7	14.8	0.88	44.3
0.61	0.7	14.8	0.46	−24.6
0.66	0.7	6.1	0.84	27.3
0.42	0.7	66.7	0.71	69.0
0.67	0.8	19.4	1.05	56.7
0.68	0.8	17.6	0.71	4.4
0.67	0.8	19.4	0.49	−26.9
Mean		15.2		55.2
±*SD*		±17.5		±47.2

[a] Only one significant figure was provided for concentrations <1.0 mg% by the printout of the instrument.

by an average of 32% in serum samples with a wider range of creatinine levels (0.62–18.5 mg% based on the HPLC method). However, for samples (n = 3) with serum levels in the range of 0.6–0.7 mg% (10) the mean overestimation was 88.2%. Thus, both of the modified picrate methods (12, 13, 15) resulted in consistently much higher creatinine values. The reason for the apparent discrepancy between their claimed specificity (12, 15) and the present as well as the previous (10, 16) findings remains to be investigated.

The results of the present study indicate that one should be cautious in using the automated and modified picrate methods for creatinine determinations. Since the HPLC method is generally considered to be more specific (3), its use should be preferred when accurate determinations are required.

It has been recently reported that creatinine might be extensively secreted and reabsorbed by renal tubules in both humans (17, 18) and animals (18, 19), and there might also be a significant nonrenal elimination in normal humans (19, 20) and normal rabbits (19). The full implications of these findings in the use of creatinine remain to be explored.

(1) W. L. Chiou and F. H. Hsu, *J. Clin. Pharmacol.*, **15**, 427 (1975).

(2) W. L. Chiou and F. H. Hsu, *Res. Commun. Chem. Pathol. Pharmacol.*, **10**, 315 (1975).

(3) W. L. Chiou, M. A. F. Gadalla, and G. W. Peng, *J. Pharm. Sci.*, **67**, 182 (1978).

(4) R. S. Lott and W. L. Hayton, *Drug Intel. Clin. Pharm.*, **12**, 140 (1978).

(5) T. D. Bjornsson, *Clin. Pharmacokinet.*, **4**, 200 (1979).

(6) A. L. Chasson, H. J. Grady, and M. A. Stanley, *Am. J. Clin. Pathol.*, **35**, 83 (1961).

(7) H. D. Lauson, *J. Appl. Physiol.*, **4**, 227 (1951).

(8) J. G. H. Cook, *Annu. Clin. Biochem.*, **12**, 219 (1975).

(9) S. Narayanan and H. D. Appleton, *Clin. Chem.*, **26**, 1119 (1980).

(10) W. L. Choiu, G. W. Peng, and M. A. F. Gadalla, *J. Pharm. Sci.*, **67**, 292 (1978).

(11) F. W. Spierto, L. MacNeil, P. Culbreth, I. Duncan, and C. A. Burtis, *Clin. Chem.*, **26**, 286 (1980).

(12) H. Yatzidis, *Clin. Chem.*, **20**, 1131 (1974).

(13) H. Yatzidis, *Clin. Chem.*, **21**, 157 (1975).

(14) W. L. Chiou and F. S. Pu, *Clin. Pharmacol. Ther.*, **25**, 777 (1979).

(15) H. Yatzidis, *Clin. Chem.*, **21**, 1848 (1975).

(16) W. L. Chiou, F. H. Hsu, and G. W. Peng, *Clin. Chem.*, **23**, 1374 (1977).

(17) W. L. Chiou, *Res. Commun. Chem. Pathol. Pharmacol.*, **36**, 349 (1982).

(18) W. L. Chiou, in "Pharmacokinetics: A Modern View," L. Z. Benet and G. Levy, Eds., Plenum, New York, N.Y., 1982.

(19) Y. C. Huang, "Pharmacokinetics of Creatinine," Ph.D. thesis, University of Illinois, 1981.

(20) Y. C. Huang, S. M. Huang, and W. L. Chiou, *Int. J. Clin. Pharmacol. Ther. Toxicol.*, **20**, 343 (1982).

*Yih-Chain Huang**
Win L. Chiou[x]

Departments of Pharmacodynamics and Pharmaceutics
College of Pharmacy
University of Illinois at Chicago
Chicago, IL 60612

Received June 15, 1981.
Accepted for publication March 13, 1983.

* Present address: College of Pharmacy, Rutgers–The State University, Piscataway, NJ 08854.

Crystalline Anhydrous–Hydrate Phase Changes of Caffeine and Theophylline in Solvent–Water Mixtures

Keyphrases □ Phase changes—in crystals, anhydrous to hydrate, caffeine, theophylline, solubility studies □ Caffeine—crystalline phase changes, anhydrous to hydrate, solubility studies □ Theophylline—crystalline phase changes, anhydrous to hydrates solubility studies

To the Editor:

The extended Hildebrand solubility approach (1–3) was recently developed and evaluated for calculation of solubilities in solvent–water systems that are not adequately described by the regular solution theory (4). The approach is based on regression analysis of solubility data to calculate solute–activity coefficients as a function of the solubility parameter of the solvent mixture.

A problem exists with several of the solutes used in the evaluation of the extended Hildebrand approach: crystalline anhydrous–hydrate phase transformation as the water content of the solvent mixture is changed. In the dry solvent it is clear that only a nonhydrated (anhydrous or solvated) form can be present at equilibrium (5); but in aqueous solvent mixtures the equilibrium form may be anhydrous solvated or hydrated crystals. This was recently demonstrated for cholesterol in water–glyceryl-1-monooctanoate solutions (6). The transition between anhydrous and monohydrate forms occurred at 5% water (37°) and was temperature dependent. In this system the max-

0022-3549/83/0700-0837$01.00/0

imum cholesterol solubility coincided with the anhydrous–hydrate crystalline phase change.

The water content at which a given compound has the potential to convert to its hydrate is not predictable. A metastable form may remain supersaturated for long periods, particularly if the degree of supersaturation is not large. In addition, little is known about the effects of such crystal changes on solubility profiles in mixed solvents. Based on these and other considerations discussed below, compounds subject to such phase changes are not appropriate for modeling by the extended Hildebrand approach. Caffeine, theophylline, and theobromine all form hydrates, although they have been used as model compounds for evaluation of the extended Hildebrand approach (1–3). The purpose of this communication is to point out that knowledge of the crystal phase present at equilibrium is essential for the study of solubility. Furthermore it is especially important to identify the solid phase at equilibrium in mixed solvents.

To illustrate these points we examined the solid phases present when caffeine or theophylline were equilibrated at 25° in 0–50% water–dioxane solutions for 3–5 days[1]. These conditions were similar to those employed previously (1, 2). To avoid compositional bias, separate samples were equilibrated which contained either the anhydrous or monohydrate forms. At equilibrium the solid phases were filtered, dried under ambient conditions, and analyzed by differential scanning calorimetry (DSC)[2]. The hydrates were prepared by aqueous recrystallization and found to be monohydrates using Karl Fischer titrimetry[3]. At ambient conditions the hydrates were stable for at least 24 hr with respect to dehydration (7), and the anhydrous forms did not react with atmospheric moisture to form the hydrates. For some samples, solubilities were measured spectrophotometrically after 0.2-μm membrane filtration[4]. When heated in the DSC at 10°/min, the presence of water crystallization was verified by the broad dehydration endotherm centered at about 80° (caffeine) and 90° (theophylline). In these experiments the heat of dehydration was not measured and, thus, samples with the hydrate peak could also contain some anhydrous material. The solubilities were consistent with the previously reported data (1–3) except as described below.

For theophylline systems above ~5% water, the hydrate was always present at equilibrium. Below this concentration the anhydrous form was isolated. These findings were independent of the solid form initially added to the solvent, indicating that equilibrium was achieved with the more stable form. With a few exceptions, samples of caffeine equilibrated with 10–50% water, however, remained in the crystal form initially added. This apparent resistance to nucleation and crystallization of caffeine monohydrate led to significant differences in solubility. For example, at 50% water the solubilities were 71 mg/ml (hydrate) and 86 mg/ml (anhydrous). As the solvent water content decreased the solubilities became more similar [49 mg/ml (hydrate) *versus* 51 mg/ml (anhydrous)]. This behavior may explain the irregularity of the reported solubility profile in water–dioxane (3). With 0–5% water, samples initially prepared with hydrate were found to be anhydrous at equilibrium. There was no correlation between maximum solubility [at ~30–50% water (3)] and the crystal form change (at 5–10% water) in these systems. This is probably related to the extensive self-association of caffeine in water (8).

The regular solution theory (4) was developed to describe the solubility of molecular crystals, *i.e.*, single component substances. For solubility calculations the heat (or entropy) of fusion and the melting point of the solute are required. In the previous work these constants were obtained for the anhydrous forms by DSC (1–3). Since the equilibrium crystal form was most often the hydrate, these values should not have been used for calculation of solubility. The different calorimetric heats of solution (25°) in water for anhydrous caffeine (3.4 kcal/mole) and the hydrate (5.0 kcal/mole) show that the forms have quite different crystal energies (8). Further work will be required to develop the appropriate equations and physical constants for solubility modeling of hydrated (or solvated) crystalline compounds.

[1] Vibromixer E1, Chemapec Inc.
[2] DSC-1B, Perkin-Elmer.
[3] Auto-aquatrator, Precision Scientific Co.
[4] Alpha Metricel, Gelman.

(1) A. Martin, J. Newburger, and A. Adjei, *J. Pharm. Sci.*, **69**, 487 (1980).
(2) A. Adjei, J. Newburger, and A. Martin, *ibid.*, **69**, 659 (1980).
(3) A. Martin, A. N. Paruta and A. Adjei, *ibid.*, **70**, 1115 (1981).
(4) J. H. Hildebrand and R. L. Scott, "Regular Solutions," Prentice Hall, New York, N.Y., 1962.
(5) R. R. Pfeiffer, K. S. Yang, and M. A. Tucker, *J. Pharm. Sci.*, **59**, 1809 (1970).
(6) J. B. Bogardus, *J. Pharm. Sci.*, **71**, 370 (1982).
(7) E. Shefter and G. Kmack, *ibid.*, **56**, 1028 (1967).
(8) A. Cesaro, E. Russo, and V. Crescenzi, *J. Phys. Chem.*, **80**, 335 (1976).

Joseph B. Bogardus
College of Pharmacy
University of Kentucky
Lexington, KY 40506

Received January 10, 1983.
Accepted for publication February 18,1983.

Pharmacokinetic Absorption Plots from Oral Data Alone or Oral/Intravenous Data and An Exact Loo–Riegelman Equation

Keyphrases □ Deconvolution—amount absorbed as a function of time for all common disposition models; amount of drug in peripheral compartments of mammillary model from measurement in central compartment □ Wagner-Nelson equation—drug absorption □ Loo–Riegelman equation—drug absorption

To the Editor:

The purposes of this Communication are: (*a*) to give exact absorption equations when drug disposition is described by one, two, or three exponential terms; (*b*) when disposition is described by two exponential terms to show that one of the new absorption equations is an exact Loo–Riegelman equation and simpler and easier to use than the latter; and (*c*) to describe and illustrate use of the equations in a preliminary manner only.

The models to be considered are shown as models I, II, and III below.

0022-3549/83/0700-0838$01.00/0

imum cholesterol solubility coincided with the anhydrous–hydrate crystalline phase change.

The water content at which a given compound has the potential to convert to its hydrate is not predictable. A metastable form may remain supersaturated for long periods, particularly if the degree of supersaturation is not large. In addition, little is known about the effects of such crystal changes on solubility profiles in mixed solvents. Based on these and other considerations discussed below, compounds subject to such phase changes are not appropriate for modeling by the extended Hildebrand approach. Caffeine, theophylline, and theobromine all form hydrates, although they have been used as model compounds for evaluation of the extended Hildebrand approach (1–3). The purpose of this communication is to point out that knowledge of the crystal phase present at equilibrium is essential for the study of solubility. Furthermore it is especially important to identify the solid phase at equilibrium in mixed solvents.

To illustrate these points we examined the solid phases present when caffeine or theophylline were equilibrated at 25° in 0–50% water–dioxane solutions for 3–5 days[1]. These conditions were similar to those employed previously (1, 2). To avoid compositional bias, separate samples were equilibrated which contained either the anhydrous or monohydrate forms. At equilibrium the solid phases were filtered, dried under ambient conditions, and analyzed by differential scanning calorimetry (DSC)[2]. The hydrates were prepared by aqueous recrystallization and found to be monohydrates using Karl Fischer titrimetry[3]. At ambient conditions the hydrates were stable for at least 24 hr with respect to dehydration (7), and the anhydrous forms did not react with atmospheric moisture to form the hydrates. For some samples, solubilities were measured spectrophotometrically after 0.2-μm membrane filtration[4]. When heated in the DSC at 10°/min, the presence of water crystallization was verified by the broad dehydration endotherm centered at about 80° (caffeine) and 90° (theophylline). In these experiments the heat of dehydration was not measured and, thus, samples with the hydrate peak could also contain some anhydrous material. The solubilities were consistent with the previously reported data (1–3) except as described below.

For theophylline systems above ~5% water, the hydrate was always present at equilibrium. Below this concentration the anhydrous form was isolated. These findings were independent of the solid form initially added to the solvent, indicating that equilibrium was achieved with the more stable form. With a few exceptions, samples of caffeine equilibrated with 10–50% water, however, remained in the crystal form initially added. This apparent resistance to nucleation and crystallization of caffeine monohydrate led to significant differences in solubility. For example, at 50% water the solubilities were 71 mg/ml (hydrate) and 86 mg/ml (anhydrous). As the solvent water content decreased the solubilities became more similar [49 mg/ml (hydrate) *versus* 51 mg/ml (anhydrous)]. This behavior may explain the irregularity of the reported solubility profile in water–dioxane (3). With 0–5% water, samples initially prepared with hydrate were found to be anhydrous at equilibrium. There was no correlation between maximum solubility [at ~30–50% water (3)] and the crystal form change (at 5–10% water) in these systems. This is probably related to the extensive self-association of caffeine in water (8).

The regular solution theory (4) was developed to describe the solubility of molecular crystals, *i.e.*, single component substances. For solubility calculations the heat (or entropy) of fusion and the melting point of the solute are required. In the previous work these constants were obtained for the anhydrous forms by DSC (1–3). Since the equilibrium crystal form was most often the hydrate, these values should not have been used for calculation of solubility. The different calorimetric heats of solution (25°) in water for anhydrous caffeine (3.4 kcal/mole) and the hydrate (5.0 kcal/mole) show that the forms have quite different crystal energies (8). Further work will be required to develop the appropriate equations and physical constants for solubility modeling of hydrated (or solvated) crystalline compounds.

[1] Vibromixer E1, Chemapec Inc.
[2] DSC-1B, Perkin-Elmer.
[3] Auto-aquatrator, Precision Scientific Co.
[4] Alpha Metricel, Gelman.

(1) A. Martin, J. Newburger, and A. Adjei, *J. Pharm. Sci.*, **69**, 487 (1980).
(2) A. Adjei, J. Newburger, and A. Martin, *ibid.*, **69**, 659 (1980).
(3) A. Martin, A. N. Paruta and A. Adjei, *ibid.*, **70**, 1115 (1981).
(4) J. H. Hildebrand and R. L. Scott, "Regular Solutions," Prentice Hall, New York, N.Y., 1962.
(5) R. R. Pfeiffer, K. S. Yang, and M. A. Tucker, *J. Pharm. Sci.*, **59**, 1809 (1970).
(6) J. B. Bogardus, *J. Pharm. Sci.*, **71**, 370 (1982).
(7) E. Shefter and G. Kmack, *ibid.*, **56**, 1028 (1967).
(8) A. Cesaro, E. Russo, and V. Crescenzi, *J. Phys. Chem.*, **80**, 335 (1976).

Joseph B. Bogardus
College of Pharmacy
University of Kentucky
Lexington, KY 40506

Received January 10, 1983.
Accepted for publication February 18,1983.

Pharmacokinetic Absorption Plots from Oral Data Alone or Oral/Intravenous Data and An Exact Loo–Riegelman Equation

Keyphrases □ Deconvolution—amount absorbed as a function of time for all common disposition models; amount of drug in peripheral compartments of mammillary model from measurement in central compartment □ Wagner-Nelson equation—drug absorption □ Loo–Riegelman equation—drug absorption

To the Editor:

The purposes of this Communication are: (*a*) to give exact absorption equations when drug disposition is described by one, two, or three exponential terms; (*b*) when disposition is described by two exponential terms to show that one of the new absorption equations is an exact Loo–Riegelman equation and simpler and easier to use than the latter; and (*c*) to describe and illustrate use of the equations in a preliminary manner only.

The models to be considered are shown as models I, II, and III below.

0022-3549/83/0700-0838$01.00/0

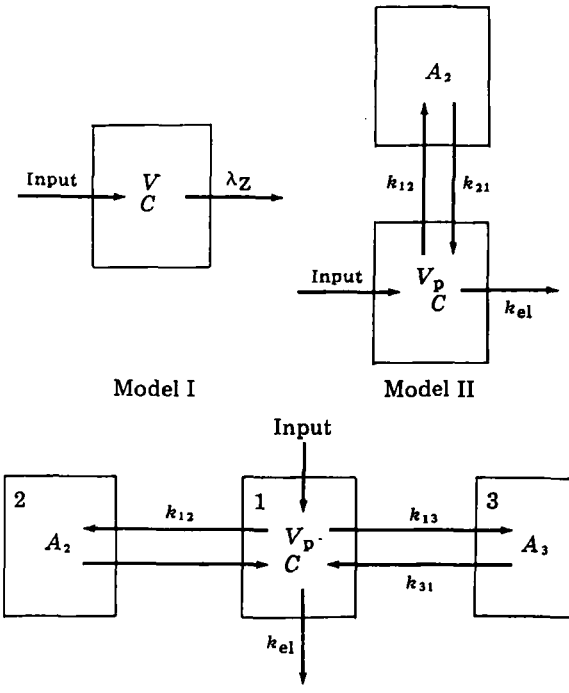

The bolus intravenous (disposition) equations corresponding to models I–III are given as Eqs. 1–3, respectively.

Model I: $$C = C_1 e^{-\lambda_z t} \quad \text{(Eq. 1)}$$

Model II: $$C = C_1 e^{-\lambda_1 t} + C_2 e^{-\lambda_2 t} \quad (\lambda_1 < \lambda_2) \quad \text{(Eq. 2)}$$

Model III: $$C = C_1 e^{-\lambda_1 t} + C_2 e^{-\lambda_2 t} + C_3 e^{-\lambda_3 t} \quad (\lambda_1 < \lambda_2 < \lambda_3) \quad \text{(Eq. 3)}$$

In Eqs. 1–3, C is the plasma (serum or whole blood) concentration of unchanged drug at time t, λ_z is the slope of the least-squares line when $y = \ln C$ and $x = t$, and C_i and λ_i are coefficients and exponents obtained by nonlinear least-squares fitting of C,t data. If the drug is administered by infusion and appropriate polyexponential functions fitted to the pre- and/or postinfusion C,t data, then the coefficients can be converted to those corresponding to a bolus intravenous injection as described by Wagner (1). There are 3 two-compartment disposition models (2) and model II is one of these. There are 21 three-compartment disposition models (3a, 4) and model III is one of these. The parameters k_{12}, k_{21}, and k_{el} of model I are estimated from the C_1, C_2, λ_1, and λ_2 of eq. 2 and the dose administered (3b). The parameters k_{12}, k_{21}, k_{13}, k_{31}, and k_{el} of model III are estimated from C_1, C_2, C_3, λ_1, λ_2, and λ_3 of Eq. 3 and the dose (5). In using the absorption equations given below it is extremely important to derive the microscopic rate constants for models I to III, which have central compartment input and elimination, and not for one of the other possible models whose disposition is also described by eqs. 2 and 3. Erroneous absorption data would be obtained if one used microscopic rate constants, derived for one of the other two- or three-compartment disposition models, with the absorption equations given below. However, Vaughan and Dennis (6) and Wagner (3c) have shown that the Loo–Riegelman equations (7) is model independent, and for similar reasons, the new absorption equations are also model independent, providing input is into the central compartment. (But elimination need not be from the central compartment.) It is also assumed that the central compartment is the one sampled. Thus, if oral data were generated from one of the two- or three-compartment disposition models other than model II or III, and one derived the parameters of model I or III and used these in the absorption equations below, one would obtain the correct input data as has been shown formerly by Wagner (3c) for the Loo–Riegelman equation.

The equations giving the amount absorbed per unit volume are:

Model I: $$\frac{A_T}{V} = C_T + \lambda_z \int_0^T C dt \quad \text{(Eq. 4)}$$

Model II: $$\frac{A_T}{V_p} = C_T + k_{el} \int_0^T C dt + k_{12} e^{-k_{21} T} \int_0^T C e^{k_{21} t} dt \quad \text{(Eq. 5)}$$

Model III: $$\frac{A_T}{V_p} = C_T + k_{el} \int_0^T C dt + k_{12} e^{-k_{21} T} \int_0^T C e^{+k_{21} t} dt + k_{13} e^{-k_{31} T} \int_0^T C e^{k_{31} t} dt \quad \text{(Eq. 6)}$$

In Eqs. 4–6, A_T is the amount of drug absorbed between time zero (time of administration) and the blood sampling time, T ($0 \le T \le t$), after a single dose of drug, t is clock time, V is the volume of the compartment of model I, V_p is the volume of the central compartment of models II and III, C_T (or C) is the plasma (serum or whole blood) concentrations of unchanged drug at time T, and the λ_Z and subscripted k parameters are first-order rate constants. Equation 4 is the Wagner–Nelson equation (8), and Eqs. 5 and 6 are new as written. Equation 5 is derived in the Appendix and Eq. 6 may be derived in a similar manner. The Loo–Riegelman equation provides approximate A_T/V_p data for model II, since it assumes a linear segment between any two C,t points where the differences are ΔC and Δt. Equations 7 and 8 are the long form of the Loo–Riegelman equation in the symbolism of this article.

$$\frac{A_T}{V_p} = C_T + k_{el} \int_0^T C dt + \left(\frac{A_2}{V_p}\right)_{T_n} \quad \text{(Eq. 7)}$$

$$\left(\frac{A_2}{V_p}\right)_{T_n} = \left(\frac{A_T}{V_p}\right)_{T_{n-1}} e^{-k_{21}\Delta t} + \frac{k_{12}}{k_{21}} C_{T_{n-1}} [1 - e^{-k_{21}\Delta t}] + \frac{k_{12}}{k_{21}} \Delta C - \frac{k_{12}}{k_{21}} \cdot \frac{\Delta C}{\Delta t} [1 - e^{-k_{21}\Delta t}] \quad \text{(Eq. 8)}$$

Equation 5 is an exact Loo–Riegelman equation. The third term on the right-hand side of Eq. 5 is an exact equation for $(A_2/V_p)_T$ and replaces the entire right-hand side of Eq. 8. In Eqs. 7 and 8 $(A_2)_{T_n}$ is the amount of drug in the peripheral compartment of model II at time T_n, and $(A_2)_{T_{n-1}}$ is the amount at the previous sampling time T_{n-1}. Similarly Eq. 6 is an exact equation for model III, and the last two terms of the right-hand side give the amounts of drug in the peripheral compartments 2 and 3 of model III divided by the volume V_p, *i.e.*, $(A_2/V_p)_T$ and $(A_3/V_p)_T$.

When estimating A_T/V or A_T/V_p with Eqs. 4 to 6, the areas (*i.e.*, integrals) may be determined by segmenting each area into trapezoids using the regular trapezoidal rule when concentrations are increasing or remaining constant and the logarithmic trapezoidal rule when the concentrations are decreasing (9).

The apparent fraction of drug absorbed to time T, F_a, is given as:

$$F_a = \frac{A_T/V_p}{A_\infty/V_p} = \frac{A_T}{A_\infty} \qquad \text{(Eq. 9)}$$

where A_∞/V_p is the asymptotic value of A_T/V_p and is given as:

$$\frac{A_\infty}{V_p} = k_{el}\int_0^\infty C dt \qquad \text{(Eq. 10)}$$

When using Eq. 4 it is usually preferable to obtain A_∞/V_p by averaging the values of the right side of Eq. 4 for those points used to estimate the apparent elimination rate constant, λ_z (3d). When using Eqs. 5, 6, 9, and 10 the subscripted k parameters would be obtained from intravenous data, and the remainder of the variables in the equations would be obtained from extravascular data.

The differential forms of Eqs. 4–6 are shown as:

Model I:
$$\left(\frac{dA}{dt}\right)_T = V\left(\frac{dC}{dt}\right)_T + V\lambda_z C_T \qquad \text{(Eq. 11)}$$

Model II:
$$\left(\frac{dA}{dt}\right)_T = (k_{12}+k_{el})V_p C_T + V_p\left(\frac{dC}{dt}\right)_T - k_{12}k_{21}e^{-k_{21}T}V_p\int_0^T Ce^{k_{21}t}dt \qquad \text{(Eq. 12)}$$

Model III:
$$\left(\frac{dA}{dt}\right)_T = (k_{12}+k_{13}+k_{el})V_p C_T + V_p\left(\frac{dC}{dt}\right)_T - k_{12}k_{21}e^{-k_{21}T}V_p\int_0^T Ce^{k_{21}t}dt - k_{13}k_{31}e^{+k_{el}T}\int_0^T Ce^{k_{31}t}dt \qquad \text{(Eq. 13)}$$

In Eqs. 11–13, $(dA/dt)_T$ is the rate of absorption at the specific time T, $(dC/dt)_T$ is the rate of change of drug concentration with respect to time at T, and other symbols have been defined formerly. Equation 11 has been derived formerly (8, 3e). Equations 12 and 13 in different form were derived by a deconvolution technique (10, 11) (see *Appendix*). Use of Eqs. 11–13 requires an estimate of the derivative $(dC/dt)_T$ at each sampling time T; such estimates may be obtained by fitting C,t data with a cubic spline function as described by Pedersen (10, 11) or a spline and Akima method as described by Wagner (3f). Equations 5–8, 12, and 13 require prior intravenous data for application. Equations 4 and 11 may be applied to extravascular data without intravenous data, and such application is appropriate when bolus intravenous data are fitted well to Eq. 1 as is sometimes the case (12–15). A special application of Eqs. 4 and 9 when input obeys zero-order kinetics will be the subject of a subsequent article.

Oral and intravenous data were simulated using Model II with first-order input and parameter values of $k_{12} = 1.5\ hr^{-1}$, $k_{21} = 0.5\ hr^{-1}$, $k_{el} = 0.5\ hr^{-1}$, $k_a = 4\ hr^{-1}$, $V_p = 10$ liters, $FD_{po} = 1000$ mg. These parameters with Model II gave $\lambda_1 = 0.15669\ hr^{-1}$ and $\lambda_2 = 2.3933\ hr^{-1}$. Equation 14 corresponds to Eq. 2 for this simulation. The simulated

$$C_{iv} = 17.2675e^{-0.10436t} + 82.7325e^{-2.3956t} \qquad \text{(Eq. 14)}$$

oral data were given by:

$$C_T = 17.7301e^{-0.10436T} + 206.2640e^{-2.3956T} - 223.9941e^{-4T} \qquad \text{(Eq. 15)}$$

For this example the actual F_a values, shown in the last column of Table I, are given as:

$$F_a = 1 - e^{-k_a T} = [1 - e^{-4T}] \qquad \text{(Eq. 16)}$$

Table I lists the sampling times, T, the C_T values obtained with Eq. 15, and the stepwise calculation of the component parts of Eq. 5 in columns 3–8. Note that a number in column 8 is the product of the numbers in the same row of columns 6 and 7 and that a number in column 9 is the sum of the numbers in the same row of columns 2, 4, and 8. Numbers in columns 3 and 6 were obtained by applying a combination of the regular and logarithmic trapezoidal rules (see text) to the numbers in columns 2 and 5, respectively, and the time values in column 1.

Table I—Simulation Example

		Components of Eq. 5							Calculated[b]	Actual
T, hr	C_T Eq. 15, μg/ml	$\int_0^T C dt$,[a] μg hr/ml	$k_{el}\int_0^T C dt$ μg/ml	$C_T e^{+k_{21}T}$, μg/ml	$\int_0^T C_T e^{+k_{21}T}dt$,[a] μg hr/ml	$k_{12}e^{-k_{21}T}$, hr^{-1}	$k_{12}e^{-k_{21}T}\int_0^T C_T e^{+k_{21}T}dt$, μg/ml	A_T/V_p, μg/ml	F_a (Eq. 5, 9)	F_a (Eq. 16)
0	0	0	0	0	0	0	0	0	0	0
0.05	17.23	0.43	0.22	17.67	0.44	1.46	0.64	18.09	0.181	0.181
0.1	29.72	1.60	0.80	31.24	1.66	1.39	2.31	32.83	0.328	0.330
0.2	44.46	5.31	2.66	49.14	5.68	1.36	7.72	54.84	0.547	0.551
0.3	50.25	10.05	5.03	58.38	11.06	1.29	14.27	69.55	0.694	0.699
0.4	50.90	15.11	7.56	62.17	17.09	1.23	21.02	79.48	0.793	0.798
0.5	47.78	20.09	10.05	62.63	23.33	1.17	27.30	86.13	0.860	0.865
0.6	45.33	24.79	12.40	61.19	29.52	1.11	32.77	90.50	0.903	0.909
0.75	39.45	31.14	15.57	57.40	38.41	1.03	39.56	94.58	0.944	0.950
1	30.67	39.86	19.93	50.57	51.89	0.910	47.22	97.82	0.976	0.982
1.5	20.28	52.42	26.21	42.93	75.21	0.758	57.01	103.50	1.03	0.9975
2	16.03	61.46	30.73	43.57	96.84	0.552	53.46	100.22	1.00	0.9997
3	13.12	75.98	37.99	58.80	148.02	0.335	49.59	100.70	1.00	1.00
4	11.69	88.37	44.19	86.38	220.61	0.203	44.78	100.66	1.00	1.00
6	9.48	109.47	54.74	190.41	497.40	0.0747	37.16	101.38	1.01	1.00
12	5.07	151.74	75.87	2045.38	7204.77	0.00372	26.80	107.74	1.08	1.00
18	2.71	174.35	87.18	21959.36	9774.89	0.000185	1.81	91.70	0.92	1.00

[a] A combination of the regular and logarithmic trapezoidal rules (see text) was used to estimate these integrals using data in the adjacent columns and the time values. [b] Estimation of AUC $0-\infty$ by the usual method (ref. 3g) directly from the T,C_T data gave AUC $0-\infty = 200.33$ μg hr/ml, hence $A_\infty/V_p = k_{el}(\text{AUC } 0-\infty) = (0.5)(200.33) = 100.2$ μg/ml, and this value was used to calculate the F_a values using Eq. 9.

Table II compares the F_a values estimated by the new Eq. 5 and Eq. 9 with those calculated by the long form of the Loo–Riegelman equation (Eqs. 7 and 8) and Eq. 9. For this example with error-free data the accuracy of the two methods are essentially identical as the percent errors in Table II indicate. In using Eqs. 5 and 6 one must be careful to carry enough decimal places since at the higher time values one is multiplying a very large number ($\int_0^T Ce^{k_{21}t}dt$) by a very small number ($k_{12}e^{-k_{21}T}$). Care must be taken also to estimate the asymptote A_∞/V_p correctly with Eq. 10 and not average terminal A_T/V_p values as done in application of the Wagner–Nelson method.

If absorption is first order then one can obtain an estimate of the absorption rate constant, k_a, by applying the method described by Wagner and Ayres (16). With reference to Table II one performs linear least-squares regression using the $x = \Delta F_a$ (second column of Table II) and $y = F_a$ (column 3); *i.e.*, the x,y pairs for this example are: 0.219, 0.328; 0.147, 0.547; 0.099, 0.694; 0.067, 0.793; and 0.043, 0.860. For this example the equally spaced $\Delta t = 0.1$ hr. The equation of such a line is:

$$(F_a)_i = (F_a)_\infty - \left[\frac{1}{1 - e^{-k_a \Delta t}}\right] \cdot \Delta F_a \qquad \text{(Eq. 17)}$$

ordinate: $(F_a)_i$; intercept: $(F_a)_\infty$; slope: $\left[\frac{1}{1 - e^{-k_a \Delta t}}\right]$; abscissa: ΔF_a

For the above data set the intercept was 0.994 (instead of the theoretical 1.00) and the slope was −3.0368.

$$k_a = \frac{-\ln\left[1 - \frac{1}{\text{slope}}\right]}{\Delta t} = \frac{-\ln\left[1 - \frac{1}{3.0368}\right]}{0.1} = 3.99 \text{ hr}^{-1} \qquad \text{(Eq. 18)}$$

where the known value was 4.0 hr^{-1}.

More extensive applications of the equations in this article will be published subsequently.

APPENDIX

Derivation of Eq. 5—Let D = the dose, and, at some time T let A_r = the amount of drug remaining at the absorption site, A_T = the amount absorbed, A_1 = amount in the central compartment of model II, A_2 = the amount in the peripheral compartment, and A_e = the amount of drug which has been eliminated by metabolism and excretion. Then mass balances give:

$$D = A_r + A_1 + A_2 + A_e \qquad \text{(Eq. 19)}$$

$$A_T = D - A_r \qquad \text{(Eq. 20)}$$

$$A_T = A_1 + A_2 + A_e \qquad \text{(Eq. 21)}$$

Now:

$$A_1 = V_p C_1 \qquad \text{(Eq. 22)}$$

The clearance equation for model II is:

$$\frac{dAe}{dt} = V_p k_{el} C_1 \qquad \text{(Eq. 23)}$$

which, upon integration between the limits $t = 0$ and $t = T$ yields:

Table II—Comparison of Results with Eqs. 5 and 9 *versus* Eqs. 7–9

Time, hr	ΔF_a	F_a Eqs. 5, 9	F_a Eqs. 7–9	% Error in F_a Eqs. 5, 9	% Error in F_a Eqs. 7–9
0.05		0.181	0.181	0	0
0.1		0.328	0.328	−0.61	−0.61
	0.219				
0.2		0.547	0.547	−0.54	−0.54
	0.147				
0.3		0.694	0.694	−0.72	−0.72
	0.099				
0.4		0.793	0.792	−0.63	−0.75
	0.067				
0.5		0.860	0.859	−0.58	−0.69
	0.043				
0.6		0.903	0.903	−0.66	−0.66
0.75		0.944	0.944	−0.63	−0.63
1		0.976	0.977	−0.61	−0.51
1.5		1.03	0.999	Mean −0.62	−0.64
2		1.00	1.00		
3		1.00	1.01		
4		1.00	1.00		
6		1.01	1.00		
12		1.08	1.00		
18		0.92	1.00		

$$A_e = V_p k_{el} \int_0^T C_1 dt \qquad \text{(Eq. 24)}$$

The differential equation for the peripheral compartment of model II is:

$$\frac{dA_2}{dt} = k_{12} V_p C_1 - k_{21} A_2 \qquad \text{(Eq. 25)}$$

Rearrangement of Eq. 25 and multiplication of both sides by $e^{k_{21}t}$ gives:

$$e^{k_{21}t}\left[\frac{dA_2}{dt} + k_{21}A_2\right] = k_{12}V_p C_1 e^{k_{21}t} \qquad \text{(Eq. 26)}$$

But Eq. 26 may be written as:

$$\frac{d(A_2 e^{k_{21}t})}{dt} = k_{12} V_p C_1 e^{k_{21}t} \qquad \text{(Eq. 27)}$$

Integrating Eq. 27 between the limits $t = 0$ and $t = T$ yields:

$$A_2 e^{k_{21}T} = k_{12} V_p \int_0^T C_1 e^{k_{21}t} dt \qquad \text{(Eq. 28)}$$

hence

$$A_2 = k_{12} e^{-k_{21}T} V_p \int_0^T C_1 e^{k_{21}t} dt \qquad \text{(Eq. 29)}$$

Substituting for A_1, A_2, and A_e from Eqs. 22, 29, and 24, respectively, into Eq. 21, followed by dividing by V_p gives:

$$\frac{A_T}{V_p} = C_1 + k_{el} \int_0^T C_1 dt + k_{12} e^{-k_{21}T} \int_0^T C_1 e^{k_{21}t} dt \qquad \text{(Eq. 30)}$$

Equation 30 is the same as Equation 5, since C_1 of Eq. 30 is equivalent to C_T or C of Eq. 5 and $e^{-k_{21}T}$ and $e^{k_{21}t}$ of Eq. 30 are equivalent to $e^{-k_{21}T}$ and $e^{k_{21}t}$, respectively, of Eq. 5.

Derivation of Eq. 12—To convert Eq. 67 of Veng-Pedersen (10) to Eq. 12, one must use the equalities shown below:

$$-\frac{a_1\lambda_1 + a_2\lambda_2}{(a_1 + a_2)^2} = \frac{V_p}{D_{iv}}(k_{12} + k_{el}) \qquad \text{(Eq. 31)}$$

$$\frac{a_1a_2(\lambda_1 - \lambda_2)^2}{(a_1 + a_2)^3} = \frac{V_p}{D_{iv}}(k_{12}k_{21}) \qquad \text{(Eq. 32)}$$

$$\frac{a_1\lambda_2 + a_2\lambda_1}{a_1 + a_2} = \frac{V_p}{D_{iv}}k_{21} \qquad \text{(Eq. 33)}$$

$$-\frac{\lambda_1\lambda_2}{a_1\lambda_2 + a_2\lambda_1} = \frac{V_p}{D_{iv}}k_{el} \qquad \text{(Eq. 34)}$$

Derivation of Eq. 13—Using similar equalities based on model III (5, 10) Veng-Pedersen's Eq. 74 may be converted to Eq. 13.

(1) J. G. Wagner, *J. Pharmacokinet. Biopharm.*, **4**, 443 (1976).
(2) J. G. Wagner, *J. Pharmacokinet. Biopharm.*, **3**, 457 (1975).
(3) J. G. Wagner, "Fundamentals of Clinical Pharmacokinetics," 2nd ed., Drug Intelligence Publications, Hamilton, Ill., 1979; (a) pp. 114, 116; (b) p. 88; (c) p. 196; (d) p. 175, Eq. 4–10; (e) p. 174; (f) p. 419; (g); p. 344.
(4) Von G. Heinzel, M. Wolf, R. Hammer, F.-W. Koss, and G. Bozler, *Arzneim.-Forsch.*, **27**, 912 (1977).
(5) M. Gibaldi and D. Perrier, "Pharmacokinetics," 2nd ed., Dekker, New York, N.Y., 1982, p. 92.
(6) D. P. Vaughan and M. Dennis, *J. Pharmacokinet. Biopharm.*, **8**, 83 (1980).
(7) J. C. K. Loo and S. Riegelman, *J. Pharm. Sci.*, **57**, 918 (1968).
(8) J. G. Wagner and E. Nelson, *ibid.*, **52**, 610 (1963).
(9) W. L. Chiou, *J. Pharmacokinet. Biopharm.*, **6**, 539 (1978).
(10) P. Veng-Pedersen, *J. Pharm. Sci.*, **69**, 298 (1980).
(11) P. Veng-Pedersen, *J. Pharm. Sci.*, **69**, 305 (1980).
(12) D. L. Smith, J. G. Wagner, and G. C. Geritsen, *J. Pharm. Sci.*, **56**, 1150 (1967).
(13) L. Endrenyi, T. Inabi, and W. Kalow, *Clin. Pharmacol. Ther.*, **20**, 701 (1976).
(14) J. J. MacKichan, M. S. Dubrinska, P. G. Welling, and J. G. Wagner, *ibid.*, **22**, 609 (1977).
(15) B. H. Dvorchik and E. S. Vesell, *ibid.*, **23**, 617 (1978).
(16) J. G. Wagner and J. W. Ayres, *J. Pharmacokinet. Biopharm.*, **5**, 533 (1977).

John G. Wagner
College of Pharmacy and Upjohn Center for Clinical Pharmacology
The University of Michigan
Ann Arbor, MI 48109

Received October 25, 1982.
Accepted for publication February 7, 1983.

BOOKS

REVIEWS

Good Manufacturing Practices for Pharmaceuticals—A Plan for Total Quality Control. 2nd Ed. By SIDNEY H. WILLIG, MURRAY M. TUCKERMAN, and WILLIAM S. HITCHINGS IV. Marcel Dekker, New York, NY 10016. 1982. 259 pp. 15 × 23 cm. Price $49.75 (20% higher outside the U.S. and Canada)

In the preface to the second edition of this book, the authors state the following:

> "This volume is a revised and expanded second edition. Substantial changes have been made in organization in order to have the text follow 21 CFR 210 and 211 (43 FR 54076, September 29, 1978). Many examples of violations which led to recall have been added to the text in order to illustrate problems encountered by the industry and to suggest ways in which they could have been avoided. In addition, several new chapters, which are not direct comments on the regulations but which are, nevertheless, pertinent to compliance, have been added. These chapters deal with repackaging and relabeling; FDA inspection; recalls; safeguarding controlled substances; and how the manufacturer is designated on the label, as well as an appendix giving the standards for potable water. These additions, made in response to users of the first edition, should make this second edition even more useful."

This statement fulfills the promises of this excellent book. The authors present each of the parts of the Current Good Manufacturing Practices (CGMP) with clear explanations and discussions. They present, in detail, not only their own interpretation of the regulations, but relevant interpretations by others. The authors also include both their own and FDA views of the underlying CGMP regulations, specifically and overall, in a philosophical vein, a most refreshing approach. In addition, practical examples and court cases are presented where relevant.

Particularly useful are the authors' clear discussion and clarification of the intent of the regulations. These discussions frequently include additional information which can be very useful for professionals in the pharmaceutical industry. Some examples should give an idea of the kinds of material included in this volume:

- Details of screening, hiring, and administrating quality control personnel.
- Details of building specifications and segregation of pharmaceutical manufacturing facilities.
- A comprehensive list of raw material specifications.
- Details of paperwork including records, procedures, flow of records, assignment of control numbers, and storage.
- Receipt of raw materials and certificates of analysis.
- Analytical production and quality control procedures and controls.
- Description of labels.
- In-process controls.
- Laboratory controls: containers (glass and otherwise) and stability (physical, chemical, and container).
- Requirements and recommendations for records and reports. Design of records and reports—what kinds and how long to keep them.
- Numbering system for quality control records and systems.
- Problems with returned or salvaged product.
- FDA inspections and legal aspects.
- Recalls.

The CGMP regulations often are broad in their definitions. This book clarifies the regulations with many practical examples. The authors expand on the regulations, demonstrating their relation and applicability to the function and implementation of the Quality Control department. The authors further expand the discussion by freely offering their own opinions. Although one may not agree with their views all of the time, they are always stimulating and provocative. For example, the philosophy behind the following statement (page 22) could be fuel for a very interesting discussion:

> "The quality control supervisor must have a questioning nature. Some say a supervisor must be naturally distrustful. This applies to all matters in his or her area, including calculations and conclusions reached by peers and superiors from an organization viewpoint. It certainly applies to findings submitted by vendors and vendees of the operation and by its subcontractors. If the supervisor is other than such, the reputation will be that of a buck passer."

This unique and information-packed book should be an indispensable part of the libraries of all industrial pharmaceutical quality control, manufacturing, pharmacy, and legal departments.

Reviewed by Sanford Bolton
College of Pharmacy
St. John's University
Jamaica, NY 11439

$$\frac{a_1a_2(\lambda_1 - \lambda_2)^2}{(a_1 + a_2)^3} = \frac{V_p}{D_{iv}}(k_{12}k_{21}) \qquad \text{(Eq. 32)}$$

$$\frac{a_1\lambda_2 + a_2\lambda_1}{a_1 + a_2} = \frac{V_p}{D_{iv}}k_{21} \qquad \text{(Eq. 33)}$$

$$-\frac{\lambda_1\lambda_2}{a_1\lambda_2 + a_2\lambda_1} = \frac{V_p}{D_{iv}}k_{el} \qquad \text{(Eq. 34)}$$

Derivation of Eq. 13—Using similar equalities based on model III (5, 10) Veng-Pedersen's Eq. 74 may be converted to Eq. 13.

(1) J. G. Wagner, *J. Pharmacokinet. Biopharm.*, **4**, 443 (1976).
(2) J. G. Wagner, *J. Pharmacokinet. Biopharm.*, **3**, 457 (1975).
(3) J. G. Wagner, "Fundamentals of Clinical Pharmacokinetics," 2nd ed., Drug Intelligence Publications, Hamilton, Ill., 1979; (a) pp. 114, 116; (b) p. 88; (c) p. 196; (d) p. 175, Eq. 4–10; (e) p. 174; (f) p. 419; (g); p. 344.
(4) Von G. Heinzel, M. Wolf, R. Hammer, F.-W. Koss, and G. Bozler, *Arzneim.-Forsch.*, **27**, 912 (1977).
(5) M. Gibaldi and D. Perrier, "Pharmacokinetics," 2nd ed., Dekker, New York, N.Y., 1982, p. 92.
(6) D. P. Vaughan and M. Dennis, *J. Pharmacokinet. Biopharm.*, **8**, 83 (1980).
(7) J. C. K. Loo and S. Riegelman, *J. Pharm. Sci.*, **57**, 918 (1968).
(8) J. G. Wagner and E. Nelson, *ibid.*, **52**, 610 (1963).
(9) W. L. Chiou, *J. Pharmacokinet. Biopharm.*, **6**, 539 (1978).
(10) P. Veng-Pedersen, *J. Pharm. Sci.*, **69**, 298 (1980).
(11) P. Veng-Pedersen, *J. Pharm. Sci.*, **69**, 305 (1980).
(12) D. L. Smith, J. G. Wagner, and G. C. Geritsen, *J. Pharm. Sci.*, **56**, 1150 (1967).
(13) L. Endrenyi, T. Inabi, and W. Kalow, *Clin. Pharmacol. Ther.*, **20**, 701 (1976).
(14) J. J. MacKichan, M. S. Dubrinska, P. G. Welling, and J. G. Wagner, *ibid.*, **22**, 609 (1977).
(15) B. H. Dvorchik and E. S. Vesell, *ibid.*, **23**, 617 (1978).
(16) J. G. Wagner and J. W. Ayres, *J. Pharmacokinet. Biopharm.*, **5**, 533 (1977).

John G. Wagner
College of Pharmacy and Upjohn Center for Clinical Pharmacology
The University of Michigan
Ann Arbor, MI 48109

Received October 25, 1982.
Accepted for publication February 7, 1983.

BOOKS

REVIEWS

Good Manufacturing Practices for Pharmaceuticals—A Plan for Total Quality Control. 2nd Ed. By SIDNEY H. WILLIG, MURRAY M. TUCKERMAN, and WILLIAM S. HITCHINGS IV. Marcel Dekker, New York, NY 10016. 1982. 259 pp. 15 × 23 cm. Price $49.75 (20% higher outside the U.S. and Canada)

In the preface to the second edition of this book, the authors state the following:

> "This volume is a revised and expanded second edition. Substantial changes have been made in organization in order to have the text follow 21 CFR 210 and 211 (43 FR 54076, September 29, 1978). Many examples of violations which led to recall have been added to the text in order to illustrate problems encountered by the industry and to suggest ways in which they could have been avoided. In addition, several new chapters, which are not direct comments on the regulations but which are, nevertheless, pertinent to compliance, have been added. These chapters deal with repackaging and relabeling; FDA inspection; recalls; safeguarding controlled substances; and how the manufacturer is designated on the label, as well as an appendix giving the standards for potable water. These additions, made in response to users of the first edition, should make this second edition even more useful."

This statement fulfills the promises of this excellent book. The authors present each of the parts of the Current Good Manufacturing Practices (CGMP) with clear explanations and discussions. They present, in detail, not only their own interpretation of the regulations, but relevant interpretations by others. The authors also include both their own and FDA views of the underlying CGMP regulations, specifically and overall, in a philosophical vein, a most refreshing approach. In addition, practical examples and court cases are presented where relevant.

Particularly useful are the authors' clear discussion and clarification of the intent of the regulations. These discussions frequently include additional information which can be very useful for professionals in the pharmaceutical industry. Some examples should give an idea of the kinds of material included in this volume:

- Details of screening, hiring, and administrating quality control personnel.
- Details of building specifications and segregation of pharmaceutical manufacturing facilities.
- A comprehensive list of raw material specifications.
- Details of paperwork including records, procedures, flow of records, assignment of control numbers, and storage.
- Receipt of raw materials and certificates of analysis.
- Analytical production and quality control procedures and controls.
- Description of labels.
- In-process controls.
- Laboratory controls: containers (glass and otherwise) and stability (physical, chemical, and container).
- Requirements and recommendations for records and reports. Design of records and reports—what kinds and how long to keep them.
- Numbering system for quality control records and systems.
- Problems with returned or salvaged product.
- FDA inspections and legal aspects.
- Recalls.

The CGMP regulations often are broad in their definitions. This book clarifies the regulations with many practical examples. The authors expand on the regulations, demonstrating their relation and applicability to the function and implementation of the Quality Control department. The authors further expand the discussion by freely offering their own opinions. Although one may not agree with their views all of the time, they are always stimulating and provocative. For example, the philosophy behind the following statement (page 22) could be fuel for a very interesting discussion:

> "The quality control supervisor must have a questioning nature. Some say a supervisor must be naturally distrustful. This applies to all matters in his or her area, including calculations and conclusions reached by peers and superiors from an organization viewpoint. It certainly applies to findings submitted by vendors and vendees of the operation and by its subcontractors. If the supervisor is other than such, the reputation will be that of a buck passer."

This unique and information-packed book should be an indispensable part of the libraries of all industrial pharmaceutical quality control, manufacturing, pharmacy, and legal departments.

Reviewed by Sanford Bolton
College of Pharmacy
St. John's University
Jamaica, NY 11439

JOURNAL OF PHARMACEUTICAL SCIENCES

August 1983
Volume 72 Number 8

A publication of the American Pharmaceutical Association

The *Journal of Pharmaceutical Sciences* (ISSN 0022-3549) is published monthly by the American Pharmaceutical Association (APhA) at 2215 Constitution Ave., N.W., Washington, DC 20037. Second-class postage paid at Washington, D.C. and at additional mailing office.

All expressions of opinion and statements of supposed fact appearing in articles or editorials carried in this journal are published on the authority of the writer over whose name they appear and are not to be regarded as necessarily expressing the policies or views of APhA.

Offices—Editorial, Advertising, and Subscription: 2215 Constitution Ave., N.W., Washington, DC 20037. All Journal staff may be contacted at this address. Printing: 20th & Northampton Streets, Easton, PA 18042.

Annual Subscriptions—United States and foreign, industrial and government institutions $75; educational institutions $75; individuals *for personal use only* $40; single copies $10. APhA and SAPhA members may subscribe to *J. Pharm. Sci.* for $20.00 per year. All foreign subscriptions add $10 for postage. Subscription rates are subject to change without notice.

Claims—Missing numbers will not be supplied if dues or subscriptions are in arrears for more than 60 days or if claims are received more than 60 days after the date of the issue, or if loss was due to failure to give notice of change of address. APhA cannot accept responsibility for foreign delivery when its records indicate shipment was made.

Change of Address—Members and subscribers should notify at once both the Post Office and APhA of any change of address.

Photocopying—The code at the foot of the first page of an article indicates that APhA has granted permission for copying of the article beyond the limits permitted by Sections 107 and 108 of the U.S. Copyright Law provided that the copier sends the per copy fee stated in the code to the Copyright Clearance Center, Inc., 21 Congress St., Salem, MA 01970. Copies may be made for personal or internal use only and not for general distribution.

Microfilm—Available from University Microfilms International, 300 N. Zeeb Road, Ann Arbor, MI 48106.

Science, Objectivity, and Judgment Uncompromised

From time to time, the public press and health care news publications have widely reported on investigations of alleged financial improprieties involving some prominent individual in either the public or the private sector.

Generally, the financially-related incidents involved were relatively insignificant or inconsequential in themselves. They might have involved gifts, honoraria, director's fees, or similar perquisites. However, it was because of the particular office of the person or his or her high position of public trust, or corporate responsibility, or overall general authority that made the matter a special concern. Even an appearance of secret favors or undisclosed benefits throws into question the objectivity and impartiality of a supposedly neutral individual in rendering decisions or taking actions.

This, then, brings us to our current concern: namely, the hidden biases or allegiances of scientists who volunteer or are called upon to participate in some proceeding as impartial, but knowledgeable, experts. The activity involved may cover the gamut from serving on a high-brow committee of some distinguished scientific society to testifying before some legislative or judicial body.

The July–August issues of *Science 83*, a publication of the American Association for the Advancement of Science carried in its "Advice and Dissent" section, a column entitled "When Scientists Testify for Hire." The article was written by Michael F. Jacobson, executive director of the Center for Science in the Public Interest—an organization that describes itself as a Washington-based consumer advocacy group.

"Of all the values that pervade science," writes Jacobson, *"one of the highest is objectivity, which I take to mean judgment uncompromised . . . . But scientific objectivity is sometimes invoked more for appearance than for substance. Whenever science moves into the commercial world, scientists come face-to-face with Mammon and manufacturers. When profits are threatened by legislation, lawsuits, or bad publicity, many companies like to have their positions bolstered by academic scientists. A professor's utterances are far more persuasive than those of the corporate chemist who developed the suspect 2,4,6-super-oxo-kleptane, or whatever."*

Jacobson then goes on to cite a number of examples in which individual companies or an industry trade organization will recruit academic scientists whose opinions they like or scientists who will willingly espouse opinions that are favorable to those companies or industry. These scientists may be "recruited" in any number of ways; for example, the industry "recruiters" might hire them as consultants, sponsor their research, offer employment to their graduate students, appoint them to their corporate boards, endow their teaching positions or professorships, or otherwise get them into a position of indebtedness.

Jacobsen brings out very nicely that it is not usually the positions *per se* that these scientists take that is wrong. What is objectionable is that they voice those positions while wearing a cloak of professed neutrality. And in this regard, Jacobson states that, *"The public is cheated by being given the appearance but not the substance of objective scientific analysis. Individuals and governments may make poor decisions based on one-sided information. The biggest loser in the long run, though, could be the scientific community itself, including the vast majority of scientists who do not testify for hire. The public supports research in the belief that scientists seek the truth, uncompromised by conflicts of interest."*

And then Jacobson concludes by expressing a view that we have stated previously in this column. It is a view that was not original with us, but which we repeated when the National Academy of Sciences did some gutsy housecleaning after it came to light that several members of one of its committees had strong, but concealed, ties to firms in an industry that was favored by the conclusions drawn by that same NAS committee.

If we are to utilize experts and their expertise, of necessity, we are going to draw upon people who have ties to groups, industries, or institutions with biased views or positions on the subject. What is important is: (*a*) to have a very clear and open record as to what are each individual's connections, obligations, and commitments, and (*b*) to balance, as carefully as possible, the make-up of each panel or committee by including a good cross-section of people with an appropriate range of views on the matter and with approximately equal distribution of advocates from the respective opposing sides.

When a scientist speaks out on a public issue, the populace expects that the scientist will feel obligated to explicitly disclose any links that he or she has to the affected company or industry.

Only in this manner will science and the scientific community continue to maintain integrity, and only through such integrity will science be able to continue to command the confidence and trust of the public at large. In its own way, that message is equally pertinent to each and every scientist.

—EDWARD G. FELDMANN
American Pharmaceutical Association
Washington, DC 20037

0022-3549/83/0800-0843$01.00/0

JOURNAL OF PHARMACEUTICAL SCIENCES

AUGUST 1983
VOLUME 72 NUMBER 8

RESEARCH ARTICLES

Antihyperlipidemic Activity of Phthalimide Analogues in Rodents

I. H. HALL ˣ, P. JOSÉE VOORSTAD, JAMES M. CHAPMAN, and G. H. COCOLAS

Received April 25, 1982, from the *Division of Medicinal Chemistry, School of Pharmacy, University of North Carolina, Chapel Hill, NC 27514.* Accepted for publication July 30, 1982.

Abstract □ Phthalimide analogues have been shown to effectively lower serum cholesterol and triglyceride levels in rats and mice. The mode of action of these agents was not to suppress the appetite of animals, but rather to reduce the activities of key enzymes in the early synthesis of liver cholesterol and fatty acids in the triglyceride pathway. Phthalimide analogues were effective in accelerating biliary excretion of cholesterol and blocking its absorption from the gut. After 16 days dosing, it was evident that higher levels of lipids were being excreted than in control mice. The major serum lipoprotein fractions were reduced in cholesterol, triglyceride, and neutral lipid content, but not phospholipid content in rats after 14 days of administration.

Keyphrases □ Phthalimide—analogues, antihyperlipidemic activity, cholesterol and triglyceride reduction □ Antihyperlipidemic agents—phthalimide analogues, cholesterol and triglyceride reduction □ Cholesterol—antihyperlipidemic effect of phthalimide analogues □ Triglyceride—antihyperlipidemic effect of phthalimide analogues

Continued investigation for new hypolipidemic agents has revealed that phthalimide analogues are potent in lowering serum lipids in rodents (1). In mice phthalimide lowers serum cholesterol 43% after 16 days of dosing at 20 mg/kg ip. Serum triglyceride levels were reduced 56% after 14 days of drug administration. Although phthalimide was the most active member of the series, other analogues demonstrate similar magnitudes of hypolipidemic activity (2). Preliminary *in vitro* studies indicate that phthalimide analogues suppressed the activity of liver enzymes involved in the early *de novo* synthesis of cholesterol and fatty acids. A more detailed study of the effects of these agents on lipid distribution and metabolism was undertaken.

EXPERIMENTAL

Source of Compounds—Phthalimide was purchased commercially[1]. The synthesis and chemical characterization of 1-*N*-phthalimidobutan-3-one and 3-*N*-phthalimidopropionic acid has been reported previously (1).

Antihyperlipidemic Screens in Normogenic Rodents—Compounds to be tested were suspended in 1% carboxymethylcellulose in water and administered to male CF_1 (~25 g) mice intraperitoneally or male Holtzman rats (~200 g) orally by an intubation needle for 16 days. On days 9 and 16 blood was obtained by tail vein bleeding, and the serum was separated by centrifugation for 3 min. The serum cholesterol levels were determined by a modification of the Liebermann–Burchard reaction (3). Serum was also collected on day 14, and the triglyceride content was determined using a commercial kit[2] (4). Animals were maintained on standard rodent food[3] throughout the experiment.

Hyperlipidemic-Induced Mice—Male CF_1 mice (~25 g) were placed on a commercial diet[4] which contained butter fat (400 g), cellulose[5] (60 g), cholesterol (53 g), choline dihydrogen citrate (4 g), salt mixture oil[6] (40 g), sodium cholate (40 g), sucrose (223 g), vitamin-free casein (200 g), and total vitamin supplement for a 2-week period. After the cholesterol and triglyceride levels were assayed and observed to be elevated, the mice were administered test drugs at 20 mg/kg/day ip for an additional 2-week period. Serum cholesterol and triglyceride levels were measured after 14 days of drug administration.

Animal Weights and Food Intake—Periodic animal weights were obtained during the experiments and expressed as a percentage of the animal's weight on day 0. After dosing for 16 days with test drugs, a number of organs were excised, trimmed of fat, and weighed. The organ weights were expressed as a percentage of the total body weight of the animal. The average food intake[3] in g/rat/day was determined over the 16-day period of dosing.

Toxicity Studies—The acute toxicity (LD_{50} value) (5) was determined in male CF_1 mice by administering test drugs intraperitoneally from 100 mg to 2 g/kg as a single dose. The number of deaths in the group was determined for each dosage.

Enzymatic Studies—*In vitro* enzymatic studies used 10% homogenates of male CF_1 mouse liver with 2.5 μmoles of the test drugs and male Holtzman rat liver with 0.100–10 m*M* concentration of the test drugs. *In vivo* enzymatic studies used 10% homogenates of livers from male CF_1 mice obtained after administering the agents intraperitoneally for 16 days at 10–60 mg/kg/day. The liver homogenates for both *in vitro* and *in vivo*

[1] Ruger Chemical Co., Inc.

[2] Fisher, Hycel Triglyceride Test Kit.
[3] Wayne Blox Rodent Chow.
[4] U.S. Biochemical Corporation Basal Atherogenic Test Diet.
[5] Celufil.
[6] Wesson Oil.

0022-3549/83/0800-0845$01.00/0

Table I—Effects of Phthalimide Analogues on Serum Cholesterol and Triglyceride Levels of Male Holtzman Rats and Male CF_1 Mice [a]

Compound	Rats: Dose, mg/kg/day	Rats: Serum Cholesterol Day 9	Rats: Serum Cholesterol Day 16	Rats: Triglyceride Day 14	Mice: Dose, mg/kg/day	Mice: Serum Cholesterol Day 9	Mice: Serum Cholesterol Day 14	Mice: Triglyceride Day 14
Control (1% carboxymethylcellulose)		100 ± 9[d]	100 ± 7[e]	100 ± 8[f]		100 ± 5[g]	100 ± 6[h]	100 ± 6[i]
Phthalimide	5	91 ± 8	79 ± 5[b]	66 ± 5[b]	10	67 ± 7[b]	43 ± 4[b]	46 ± 4[b]
	10	81 ± 9[c]	66 ± 7[b]	56 ± 5[b]	20	62 ± 5[b]	59 ± 5[b]	44 ± 3[b]
	20	72 ± 6[b]	57 ± 4[b]	58 ± 4[b]	40	49 ± 6[b]	45 ± 3[b]	52 ± 6[b]
	50	70 ± 4[b]	62 ± 5[b]	62 ± 6[b]	60	51 ± 4[b]	40 ± 5[b]	56 ± 7[b]
1-*N*-Phthalimidobutan-3-one	10	70 ± 8[b]	59 ± 8[b]	59 ± 13[b]	10	73 ± 9[b]	66 ± 5[b]	—
	20	67 ± 5[b]	51 ± 5[b]	68 ± 3[b]	20	67 ± 9[b]	63 ± 9[b]	58 ± 7[b]
	—	—	—	—	30	66 ± 7[b]	54 ± 6[b]	—
3-*N*-Phthalimidopropionic acid	—	—	—	—	10	84 ± 6[b]	80 ± 6[b]	52 ± 4[b]
	20	67 ± 5[b]	51 ± 5[b]	68 ± 3[b]	20	74 ± 8[b]	55 ± 4[b]	53 ± 5[b]
	—	—	—	—	40	84 ± 7[c]	74 ± 5[b]	58 ± 7[b]
	—	—	—	—	60	87 ± 6[b]	76 ± 6[b]	56 ± 6[b]

[a] Percent of control, expressed as mean ± *SD*; $n = 6$. [b] $p \leq 0.001$. [c] $p \leq 0.010$. [d] 73 mg %. [e] 78 mg %. [f] 110 mg %. [g] 118 mg %. [h] 122 mg %. [i] 137 mg %.

Table II—Effects of Phthalimide Analogues on Serum Cholesterol and Triglyceride Levels in Hyperlipidemic-Induced Mice [a]

Compound	Serum Cholesterol: 2-week Diet	Serum Cholesterol: 14 Days of Dosing	Serum Triglyceride: 2-week Diet	Serum Triglyceride: 14 Days of Dosing
Control (1% carboxymethylcellulose)	100 ± 6[c]	100 ± 7[d]	100 ± 5[e]	100 ± 4[f]
Control (hyperlipidemic diet)	289 ± 9[b]	290 ± 9[b]	131 ± 5[b]	131 ± 5[b]
Phthalimide	289 ± 8[b]	137 ± 7[b]	132 ± 6[b]	57 ± 5[b]
1-*N*-Phthalimidobutan-3-one	288 ± 9[b]	130 ± 6[b]	135 ± 6[b]	86 ± 5[b]
3-*N*-Phthalimidopropionic acid	288 ± 10[b]	126 ± 5[b]	130 ± 5[b]	75 ± 5[b]

[a] Percent of control, expressed as mean ± *SD*; $n = 6$. [b] $p \leq 0.001$. [c] 74 ± 4 mg %. [d] 76 ± 5 mg %. [e] 136 ± 7 mg %. [f] 139 ± 5 mg %.

studies were prepared in 0.25 *M* sucrose and 0.001 *M* EDTA [(ethylenedinitrilo)tetraacetic acid].

Acetyl coenzyme A synthetase (6) and adenosine triphosphate-dependent citrate lyase (7) activities were determined spectrophotometrically at 540 nm as the hydroxamate of acetyl coenzyme A formed after 30 min at 37°. Mitochondrial citrate exchange was determined by the procedure of Robinson *et al.* (8, 9) using sodium [^{14}C]bicarbonate (41 mCi/mmole) which was incorporated into mitochondrial [^{14}C]citrate after isolating rat mitochondria (9000×*g* for 10 min) from the homogenates. The exchange of the [^{14}C]citrate was determined after incubating the mitochondrial fraction, which was loaded with labeled citrate, with the test drugs for 10 min. Then the radioactivity was measured in the mitochondrial and supernatant fraction in scintillation fluid[7] and expressed as a percentage. Cholesterol side-chain oxidation was determined by the method of Kritchevsky *et al.* (10) using [26-^{14}C]cholesterol (50 mCi/mmole) and mitochondria isolated from rat liver homogenates. After an 18-hr incubation at 37° with the test drugs, the generated $^{14}CO_2$ was trapped in the center well in [2-[2-(*p*-1,1,3,3-tetramethylbutylcresoxy)-ethoxy]ethyl]dimethylbenzylammonium hydroxide[8] and counted. 3-Hydroxy-3-methylglutaryl coenzyme A reductase (HMG CoA reductase) was measured using [1-^{14}C]acetate (56 Ci/mmole) using a postmitochondrial supernatant (9000×*g* for 20 min) for 60 min at 37° (11). The digitonide derivative of cholesterol was isolated and counted (12). Acetyl coenzyme A carboxylase activity was measured by the method of Greenspan and Lowenstein (13). Initially, the enzyme had to be polymerized for 30 min at 37°, and then the assay mixture containing sodium [^{14}C]bicarbonate (41.0 mCi/mmole) was added and incubated for 30 min at 37° with the test drugs. Fatty acid synthetase activity was determined by the method of Brady *et al.* (14) using [2-^{14}C]malonyl-coenzyme A (37.5 mCi/mmole) incorporated into newly synthesized fatty acids, which were extracted with ether and counted. Acyl transferase activity was determined with L-[2-^{3}H]glycerol-3-phosphate (7.1 Ci/mmole) and the microsomal fraction of the liver homogenates (15). The reaction was terminated after 10 min, and the lipids were extracted with chloroform–methanol (1:2) containing 1% 1 *N* HCl and counted.

Phosphatidate phosphohydrolase activity was measured as the inorganic phosphate released after 30 min from phosphatidic acid by the method of Mavis *et al.* (16). The released inorganic phosphate after development with ascorbic acid and ammonium molybdate was determined at 820 nm.

The *in vitro* oxidative phosphorylation process in male CF_1 mouse liver was also examined with an oxygen electrode[9] connected to an oxygraph[10] at 37°. The reaction vessel contained 55 μmoles of sucrose, 22 μmoles of monobasic potassium phosphate, 22 μmoles of potassium chloride, 90 μmoles of succinate or 60 μmoles of α-ketoglutarate as substrate, 2 μmoles of adenosine triphosphate, and 2.5 μmoles of the test compounds in a total volume of 1.8 ml. After the basal metabolic (state 4) rate was obtained, 0.257 μmole of adenosine diphosphate was added to obtain the adenosine diphosphate stimulated respiration (state 3) rate (17). The rates were calculated as μl of oxygen consumed/mg of liver/hr.

Liver, Small Intestine, and Fecal Lipid Extraction—In male CF_1 mice that had been administered test drugs for 16 days, the liver, small intestine, and fecal materials (24-hr collection) were removed and a 10% homogenate in 0.25 *M* sucrose and 0.001 *M* EDTA was prepared. An aliquot (2 ml) of the homogenate was extracted by the Folch *et al.* (18) and Bligh and Dyer (19) methods and the number of milligrams of lipid weighed. The lipid was dissolved in methylene chloride, and the cholesterol level (3), triglyceride levels[11], neutral lipid content (20), and phospholipid content (21) were determined.

[^{14}C]Cholesterol Distribution in Mice and Rats—Male CF_1 mice (~25 g) were administered test agents intraperitoneally for 14 days and rats were administered test agents orally. On day 13, 10 μCi of [4-^{14}C]-cholesterol (52.5 mCi/mmole) was administered, and feces were collected for 0–6, 6–12, and 12–24 hr postadministration. Twenty-four hours after cholesterol administration, the major organs were excised and samples of blood, chyme, and urine were collected. Homogenates (10%) were prepared of the tissues which were combusted[12] and counted. Some tissue samples were plated on filter paper[13], dried, and digested for 24 hr in base[8] at 40° and counted. Results were expressed as dpm/mg of wet tissue and dpm/mg of total organ.

Cholesterol Absorption Study—Male Holtzman rats (~400 g) were administered test drugs intraperitoneally for 14 days at 20 mg/kg/day.

Table III—Effects of Phthalimide Analogues on Body Weight and Food Consumption of Rats after 14 Days of Dosing [a]

	Body Weight Increase Over 14 Days, %	Food Consumed Per Day, g
Control	138 ± 3	22.5
Phthalimide	142 ± 4	22.3
1-*N*-Phthalimidobutan-3-one	136 ± 3	21.5
3-*N*-Phthalimidopropionic acid	137 ± 3	20.0

[a] $n = 6$.

[7] Fisher, SOX-1 Scintiverse; Packard Scintillation Counter.
[8] Hyamine hydroxide; New England Nuclear.
[9] Clark electrode.
[10] Gilson Instruments.
[11] Bio-Dynamics/bmc Triglyceride Kit.
[12] Packard Tissue Oxidizer.
[13] Whatman No. 3.

Table IV—Effects of Phthalimide Analogues on Rat Organ Weights after 14 Days of Administration [a]

	Liver	Lung	Heart	Kidney	Spleen
Control	100 ± 5	100 ± 4	100 ± 3	100 ± 4	100 ± 6
Phthalimide	85 ± 6[c]	100 ± 5	93 ± 3[c]	89 ± 5[c]	73 ± 5[b]
3-*N*-Phthalimidopropionic acid	84 ± 7[c]	91 ± 4[c]	87 ± 2[b]	88 ± 5[c]	60 ± 5[b]
	Brain	Adrenals	Stomach	Small Intestine	Large Intestine
Control	100 ± 5	100 ± 8	100 ± 12	100 ± 10	100 ± 8
Phthalimide	100 ± 6	95 ± 7	98 ± 9	92 ± 11	108 ± 10
3-*N*-Phthalimidopropionic acid	110 ± 7	106 ± 8	97 ± 13	101 ± 9	109 ± 5

[a] Percent of control, expressed as mean ± *SD*; $n = 6$. [b] $p \leq 0.001$. [c] $p \leq 0.010$.

Table V—*In Vitro* Effects of Phthalimide Analogues (2.5 μmoles) on Mouse Liver Enzyme Activities after 16 Days of Dosing [a]

Compound	Mitochondrial Citrate Exchange	Acetyl Coenzyme A Synthetase	Citrate Lyase	HMG CoA Reductase	Cholesterol Side Chain
1% Carboxymethylcellulose	100 ± 10[d]	100 ± 11[e]	100 ± 9[f]	100 ± 7[g]	100 ± 8[h]
Phthalimide	19 ± 7[b]	70 ± 8[b]	42 ± 6[b]	85 ± 7	111 ± 9
1-*N*-Phthalimidobutan-3-one	10 ± 4[b]	53 ± 7[b]	34 ± 4[b]	72 ± 7[b]	90 ± 7
3-*N*-Phthalimidopropionic acid	6 ± 3[b]	57 ± 7[b]	87 ± 6[b]	86 ± 4[b]	75 ± 5[b]

Compound	Acetyl Coenzyme A Carboxylase	Fatty Acid Synthetase	Phosphatidate Phosphohydrolase	*sn*-Glycerol-3-*P*-acyl Transferase
1% Carboxymethylcellulose	100 ± 6[i]	100 ± 7[j]	100 ± 7[k]	100 ± 8[l]
Phthalimide	8 ± 4[b]	105 ± 8	55 ± 5[b]	28 ± 8[b]
1-*N*-Phthalimidobutan-3-one	17 ± 3[b]	109 ± 7	65 ± 3[b]	46 ± 5[b]
3-*N*-Phthalimidopropionic acid	18 ± 4[b]	107 ± 7	59 ± 4[b]	11 ± 5[b]

	Oxidative Phosphorylation			
	α Ketoglutarate		Succinate	
Compound	State 4	State 3	State 4	State 3
1% Carboxymethylcellulose	100 ± 6[m]	100 ± 7[n]	100 ± 5[o]	100 ± 6[p]
Phthalimide	64 ± 4[b]	65 ± 6[b]	64 ± 7[b]	65 ± 5[b]
1-*N*-Phthalimidobutan-3-one	79 ± 6[b]	76 ± 7[b]	83 ± 5[b]	58 ± 4[b]
3-*N*-Phthalimidopropionic acid	69 ± 5[b]	64 ± 5[b]	68 ± 6[b]	59 ± 3[b]

[a] Percent of control, expressed as mean ± *SD*; $n = 6$. [b] $p \leq 0.001$. [c] $p \leq 0.010$. [d] 30.8 ± 3.1 mg % exchange of mitochondrial citrate. [e] 28.5 ± 3.14 mg of acetyl coenzyme A formed/g wet tissue/30 min. [f] 30.5 ± 2.74 mg of citrate hydrolyzed/g wet tissue/30 min. [g] 384,900 ± 26,943 dpm of cholesterol formed/g wet tissue/60 min. [h] 6080 ± 5.58 dpm of CO_2 formed/g wet tissue/18 hr. [i] 32,010 ± 1921 dpm/g wet tissue/30 min. [j] 37,656 ± 2635 dpm/g wet tissue/30 min. [k] 16.70 ± 1.16 μg Pi/g wet tissue/15 min. [l] 537,800 ± 43,024 dpm of triglyceride formed/g wet tissue/10 min. [m] 3.51 ± 0.21 μl of oxygen consumed/hr/mg of tissue. [n] 5.21 ± 0.36 μl of oxygen consumed/hr/mg of tissue. [o] 5.92 ± 0.30 μl of oxygen consumed/hr/mg of tissue. [p] 11.31 ± 0.67 μl of oxygen consumed/hr/mg of tissue.

On day 13, 10 μCi of 1,2-[^{3}H]-cholesterol (40.7 Ci/mmole) was administered to the rat orally. Twenty-four hours later, the blood was collected, and the serum was separated by centrifugation (22). Both the serum and the precipitate were counted.

Bile Cannulation Study—Male Holtzman rats (~400 g) were treated with test drugs at 20 mg/kg/day orally for 14 days; the rats were anesthetized with chlorpromazine (25 mg/kg) followed after 30 min by pentobarbital (22 mg/kg ip). The duodenum section of the small intestine was isolated and ligatures were placed around the pyloric sphincter and at a site distally approximately one-third of the way down the duodenum. Sterile isotonic saline was injected into the sectioned off duodenum segment. The saline expanded the duodenum and the common bile duct. Once the bile duct was identified, a loose ligature was placed around the bile duct, and a nich was introduced into the duct immediately before it enters the duodenum. Plastic tubing[14] was introduced into the duct, passing the ligature, and tied in place. The ligatures around the duodenum were then removed. Once bile was freely moving down the cannulated tube, [1,2-^{3}H]cholesterol (40.7 Ci/mmole) was injected intravenously into the rats. The bile was collected over the next 6 hr and measured (in ml). Aliquots were counted as well as analyzed for cholesterol content (3).

Plasma Lipoprotein Fractions—Male Holtzman rats (~400 g) were administered test drugs at 20 mg/kg/day for 14 days. On day 14, blood was collected from the abdominal aorta. Serum was separated from whole blood by centrifugation at 3500 rpm. Aliquots (3 ml) were separated by density gradient ultracentrifugation according to the methods of Hatch and Lees (23) and Havel *et al.* (24) into the chylomicrons, very low-density lipoproteins, high-density lipoproteins, and low-density lipoproteins. Each of the fractions were analyzed for cholesterol (3), triglyceride[11], neutral lipids (20), phospholipids (21), and protein levels (25).

[14] PE-10 Intramedic Polyethylene tubing.

RESULTS

Clearly, phthalimide, 1-*N*-phthalimidobutan-3-one, and 3-*N*-phthalimidopropionic acid were effective in lowering serum cholesterol and triglycerides in rats and mice. The 20-mg/kg dose appeared to be the most effective dose in rodents (Table I). The phthalimide analogues were not only effective in normogenic mice, but also in hyperlipidemic-induced mice where serum cholesterol was reduced ~150% and triglyceride levels were reduced to below normal levels (Table II). The phthalimide analogues essentially had no effect on body weight increase in rats over the period of drug administration or the consumption of food compared with the control (Table III). Organ weights of the treated rats after 14 days of dosing were suppressed slightly in the case of the liver and moderately in the case of the spleen (Table IV). All other organs appeared to be within the normal range.

Examination of mouse liver enzymatic activities (Table V) showed that phthalimide analogues present at 2.5 μmoles suppressed mitochondrial exchange of citrate to the cytoplasm and cytoplasmic acetyl coenzyme

Table VI—*In Vitro* Inhibition of Rat Liver Lipid Enzymes

Enzyme	ID_{50} Values (10^{-3} *M*) Phthalimide	1-*N*-Phthalimidobutan-3-one	3-*N*-Phthalimidopropionic Acid
Acetyl Coenzyme A Synthetase	1.285	1.333	1.361
Acetyl Coenzyme A Carboxylase	1.221	2.100	2.227
Phosphatidate Phosphohydrolase	0.168	7.440	2.800
sn-Glycerol-3-*P*-acyl Transferase	5.174	7.616	7.168

Table VII—*In Vivo* Effects of Phthalimide Analogues on Male CF_1 Mouse Liver Enzymes [a]

Compound	Dose mg/kg/day	Acetyl Coenzyme A Synthetase	HMG CoA Reductase	Acetyl Coenzyme A Carboxylase	Phosphatidate Phosphohydrolase	Fatty Acid Synthetase	Liver Lipids	Small Intestine Lipids
Control (1% carboxymethylcellulose)	—	100 ± 7[d]	100 ± 6[e]	100 ± 5[f]	100 ± 8[g]	100 ± 6[h]	100 ± 9[i]	100 ± 7
Phthalimide	10	76 ± 5[b]	89 ± 9	60 ± 5[b]	91 ± 9	79 ± 8[b]	70 ± 8[b]	106 ± 8
	20	76 ± 6[b]	89 ± 10	62 ± 6[b]	67 ± 8[b]	78 ± 7[b]	70 ± 7[b]	58 ± 5
	40	75 ± 4[b]	88 ± 8	56 ± 5[b]	29 ± 5[b]	82 ± 4[b]	68 ± 8[b]	77 ± 6
	60	84 ± 5[b]	105 ± 10	57 ± 4[b]	3 ± 2[b]	76 ± 6[b]	64 ± 6[b]	88 ± 7
3-*N*-Phthalimidopropionic acid	10	76 ± 6[b]	68 ± 6[b]	79 ± 6[b]	69 ± 6[b]	91 ± 5	73 ± 5[b]	96 ± 7
	20	79 ± 7[b]	59 ± 5[b]	66 ± 5[b]	76 ± 7[b]	96 ± 6	67 ± 4[b]	76 ± 6
	40	82 ± 8[c]	79 ± 4[b]	58 ± 4[b]	88 ± 8	107 ± 7	66 ± 5[b]	77 ± 6
	60	82 ± 6[c]	84 ± 6[c]	47 ± 4[b]	83 ± 8[c]	109 ± 5	62 ± 6[b]	92 ± 8

[a] Percent of control, expressed as mean ± *SD*; $n = 6$. [b] $p \leq 0.001$. [c] $p \leq 0.010$. [d] 28.5 ± 3.14 mg of acetyl coenzyme A formed/g wet tissue/30 min. [e] 384,900 ± 26,943 dpm of cholesterol formed/g wet tissue/60 min. [f] 32,010 ± 1921 dpm/g wet tissue/30 min. [g] 37,656 ± 2635 dpm/g wet tissue/30 min. [h] 16.70 ± 1.16 μg Pi released/g wet tissue/15 min. [i] 79.5 ± 5.56 mg/g wet tissue.

A synthetase and adenosine triphosphate-dependent citrate lyase activities significantly. 3-Hydroxy-3-methylglutaryl coenzyme A reductase activity and side-chain oxidation of cholesterol were unaffected by the agents. Acetyl coenzyme A carboxylase, phosphatidate phosphohydrolase, and *sn*-glycerol-3-phosphate acyl transferase activities were suppressed by the phthalimide analogues, whereas fatty acid synthetase activity was unaffected. Both the basal and adenosine diphosphate-stimulated respiration states of oxidative phosphorylation of liver were reduced in the presence of the analogues. ID_{50} values obtained from rat liver assays are noted in Table VI for acetyl coenzyme A synthetase, acetyl coenzyme A carboxylase, phosphatidate phosphohydrase, and *sn*-glycerol-3-phosphate acyl transferase. ID_{50} values for 3-hydroxy-3-methylglutaryl coenzyme A reductase and fatty acid synthetase could not be obtained in the concentration range employed for these studies. When the same enzyme activities were tested *in vivo* in mice, it can readily be seen that the same enzyme activities were inhibited significantly (Table VII) after 16 days of dosing. In addition, suppression of 3-hydroxy-3-methyl glutaryl coenzyme A reductase activity was observed; in particular 3-*N*-phthalimidopropionic acid produced significant reduction of 3-hydroxy-3-methylglutaryl coenzyme A reductase activity. Dose-related suppression of acetyl coenzyme A carboxylase and phosphatidate phosphohydrolase activities and lipid content was observed for phthalimide, and acetyl coenzyme A carboxylase activity and lipid content suppression was observed for the 3-*N*-phthalimidopropionic acid.

Analysis of the lipid content (Table VIII) revealed that cholesterol, neutral lipids, and triglyceride content were reduced in liver homogenate with an elevation in phospholipid content. In the small intestine, cholesterol content was elevated and neutral lipid, triglyceride, and phospholipid content was reduced at the optimum dose, 20 mg/kg.

Table VIII—Effects of Phthalimide Analogues on Lipid Content of Mouse Liver and Small Intestine after 16 Days of Dosing [a]

Dosage	Liver: Phthalimide	Liver: 3-*N*-Phthalimidopropionic Acid	Small Intestine: Phthalimide	Small Intestine: 3-*N*-Phthalimidopropionic Acid
		Total Cholesterol		
Control	100 ± 7[d]	100 ± 7[d]	100 ± 7[h]	100 ± 7[h]
10 mg/kg	74 ± 6[b]	63 ± 6[b]	113 ± 6	108 ± 6
20 mg/kg	34 ± 4[b]	48 ± 5[b]	194 ± 8[b]	242 ± 8[b]
40 mg/kg	56 ± 5[b]	76 ± 7[b]	169 ± 9[b]	204 ± 7[b]
60 mg/kg	63 ± 5[b]	58 ± 6[b]	169 ± 8[b]	95 ± 6
		Neutral Lipids		
Control	100 ± 4[e]	100 ± 4[e]	100 ± 5[i]	100 ± 5[i]
10 mg/kg	51 ± 5[b]	25 ± 3[b]	113 ± 6[c]	78 ± 6[b]
20 mg/kg	36 ± 5[b]	22 ± 2[b]	45 ± 5[b]	48 ± 5[b]
40 mg/kg	18 ± 4[b]	22 ± 3[b]	45 ± 4[b]	55 ± 6[b]
60 mg/kg	15 ± 5[b]	32 ± 2[b]	105 ± 7	70 ± 5[b]
		Triglycerides		
Control	100 ± 5[f]	100 ± 5[f]	100 ± 6[j]	100 ± 6[j]
10 mg/kg	37 ± 7[b]	54 ± 4[b]	70 ± 5[b]	109 ± 6
20 mg/kg	31 ± 6[b]	39 ± 3[b]	47 ± 4[b]	62 ± 5[b]
40 mg/kg	38 ± 6[b]	40 ± 4[b]	48 ± 3[b]	70 ± 5[b]
60 mg/kg	30 ± 7[b]	44 ± 4[b]	70 ± 5[b]	93 ± 6
		Phospholipids		
Control	100 ± 8[g]	100 ± 8[g]	100 ± 8[k]	100 ± 8[k]
10 mg/kg	74 ± 7	128 ± 7[b]	88 ± 7	101 ± 7
20 mg/kg	144 ± 8	121 ± 4[b]	62 ± 6[b]	48 ± 5[b]
40 mg/kg	139 ± 8	128 ± 9[b]	84 ± 7[c]	44 ± 4[b]
60 mg/kg	137 ± 9	127 ± 7[b]	85 ± 8	74 ± 6[b]

[a] Percent of control, expressed as mean ± *SD*; $n = 6$. [b] $p \leq 0.001$. [c] $p \leq 0.010$. [d] 12.24 mg/g tissue. [e] 28.35 mg/g tissue. [f] 4.77 mg/g tissue. [g] 4.39 mg/g tissue. [h] 7.81 mg/g tissue. [i] 7.18 mg/g tissue. [j] 1.06 mg/g tissue. [k] 2.02 mg/g tissue.

Radiolabeled cholesterol studies (Tables IX and X) demonstrate that lipids removed from the blood compartment were not being deposited in major organs: *i.e.*, liver, heart, brain, kidney, and lung in rats (where the cholesterol was administered orally) and mice (where the cholesterol was administered intraperitoneally). The labeled cholesterol in the treated animals was found in higher concentrations in the intestine, chyme, and feces. Cholesterol absorption (Table XI) from the gut over a 24-hr period was reduced by phthalimide and the propionic analogue. In conjunction with this observation, it can also be seen that the agents accelerated bile flow and biliary secretion of cholesterol (Table XII). The increase in cholesterol secretion is also reflected in the lipid extractions from feces of mice after treatment with phthalimide (Table XIII). Elevations in neutral lipids and phospholipids were also noted in the fecal excretion at all doses employed. Significant reduction of the lipid and protein content of serum lipoprotein fractions (Table XIV) were observed in rats after treatment with all three agents. Cholesterol, neutral lipids, and triglycerides were reduced in the chylomicron, very low-, low- and high-density lipoproteins. Phospholipid content was elevated in the chylomicron, very low-, and high-density lipoprotein fractions. Protein content was reduced in the chylomicron and very low-density fraction for all three agents. However, only phthalimide treatment resulted in a reduction of the protein of the low- and high-density lipoprotein fractions.

Data are expressed in Tables I–VIII, XIII, and XIV as percent of control (mean ± the standard deviation). The probable significant level (p) between each test group and the control group was determined by the Student's t test.

DISCUSSION

A positive correlation between elevated serum cholesterol and triglycerides and the subsequent development of atherosclerosis has been made (26). Over the years, diet and chemotherapy have been the treatments of choice. However, the number of drugs distributed commercially for the treatment of hyperlipidemic states has been decreasing due to incurred hepatotoxicity, cardiovascular changes, and GI disturbances or due to the fact that the agents did not effectively reduce both serum cholesterol and triglycerides in humans.

The required doses to elicit hypolipidemic activity for phthalimide analogues are in a safe therapeutic range compared with the LD_{50} of >2 g/kg (2). The agents were more active than clofibrate in reducing both serum cholesterol and triglyceride levels in rodents (27). Clofibrate reduced total lipid and cholesterol by 15–20% of the control values at doses of 100–200 mg/kg daily by oral or subcutaneous routes of administration (27).

The suppression of cholesterol synthesis by the phthalimide analogues was not exclusively at the regulatory site of the cholesterol pathway, *e.g.*, clofibrate blocks 3-hydroxy-3-methylglutaryl coenzyme A reductase activity. Rather, earlier steps in the *de novo* synthesis of acetyl coenzyme A appeared to be blocked by phthalimide analogues. Reduction of available citrate from the mitochondria, where it is generated from glycolysis, may be a critical factor in the synthesis of cytoplasmic acetyl coenzyme A. Reduction of mitochondrial citrate exchange in the rat liver has been shown with other agents, *e.g.*, 1,2,3-benzenetricarboxylate and 2-*p*-iodobenzylmalonate (8). The inhibition of acetate incorporation into

Table IX—Effects of Phthalimide Analogues after 14 Days of Dosing on [^{3}H]Cholesterol Distribution 24 hr after Administration [a]

Organ	Control		Phthalimide		3-*N*-Phthalimidopropionic Acid	
	Total Organ dpm	Recovery, %	Total Organ dpm	Recovery, %	Total Organ dpm	Recovery, %
Brain	42,412	1.21	23,394	0.64	21,694	0.62
Heart	37,638	1.07	26,593	0.76	25,893	0.74
Lung	100,584	2.87	80,827	2.31	75,229	2.15
Liver	901,785	23.77	627,374	17.93	534,300	15.27
Spleen	67,760	1.93	56,684	1.62	41,638	1.19
Kidney	69,192	1.97	47,237	1.35	58,783	1.68
Stomach	127,446	3.64	80,477	2.30	52,835	1.51
Small Intestine	851,406	24.33	862,507	24.65	1,067,550	30.51
Large Intestine	246,924	7.05	500,709	14.31	244,581	6.99
Chyme	163,977	4.68	220,088	6.29	269,074	7.69
Feces	889,892	25.43	974,126	27.84	1,106,389	31.62

[a] $n = 6$.

fatty acids in neonatal chicks has also been shown for 1,2,3-benzenetricarboxylate. Reduction of cytoplasmic levels of acetyl coenzyme A would markedly affect both cholesterol and fatty acid synthesis. Hepatic triglyceride synthesis appeared to be blocked at the regulatory sites, *i.e.*, *sn*-glycerol-3-phosphate acyl transferase and phosphatidate phosphohydrase. The inhibition of phosphatidate phosphohydrolase activity by the phthalimide analogues may explain the elevation in levels of phospholipids observed in the liver and lipoprotein fractions. A number of agents have been identified that inhibit these two enzymes [*e.g.*, 1,3-bis(substituted phenoxy)-2-propanone, 1-methyl-4-piperidyl bis(*p*-chlorophenoxy)acetate, and clofibrate (28)] with a concomitant reduction of serum triglycerides (15). ID_{50} values obtained for inhibition of these enzyme activities in the rat liver seem to be realistic considering the *in vivo* dose required for potent hypolipidemic activity of the phthalimide analogues.

The phthalimide analogues did not uncouple liver oxidative phosphorylation processes, as has been observed for clofibrate (29) and which is probably due to the detergent action of clofibrate causing disruption of the mitochondrial membranes. The phthalimide did suppress both basal and adenosine diphosphate-stimulated respiration, which may reduce available energy for synthetic processes. The phthalimide analogues, like clofibrate (30), accelerated the excretion of cholesterol and probably cholesterol esters through the biliary route; these probably are not reabsorbed from the gut *via* the extrahepatic circulation process. Data from the biliary study suggest that this mode of action of the phthalimide analogues may be of sufficient importance to account for some of the observed reduction of serum lipids.

The lipids removed from the blood compartment are not being deposited in the major organs of the body, which should be an ideal characteristic of a hypolipidemic agent. Other studies have indicated that the reduction of serum cholesterol and triglycerides after 16 and 14 days of dosing, respectively, were returned to predrug administration levels (31), indicating that the pharmacological effects of the phthalimide analogues are freely reversible after 2 weeks. Low-density lipoprotein, derived from intravascular very low-density lipoprotein, is the major lipoprotein that

Table X—[^{3}H]Cholesterol Content 24 hr after Injection of 10 μCi in CF_1 Mice Administered Drug (20 mg/kg/day) for 14 Days [a]

Organ	Control		Phthalimide	
	Total dpm	Tritium Recovered, %	Total dpm	Tritium Recovered, %
Brain	8305	0.124	7042	0.105
Lung	33,949	0.506	20,589	0.307
Heart	23,774	0.354	7041	0.105
Liver	436,066	6.502	302,133	4.505
Spleen	54,303	0.810	55,329	0.825
Kidney	82,954	1.237	45,672	0.681
Stomach	266,464	3.973	146,941	2.191
Small Intestine	607,318	9.056	737,660	10.999
Large Intestine	791,297	11.799	542,437	8.0881
Subtotal		34.361		27.806
Feces				
0–6 hr	374,855	5.589	1,013,973	15.119
6–12 hr	2,126,220	31.703	2,333,767	34.798
12–24 hr	1,901,108	28.333	1,494,109	22.277
Total excreted in 24 hr		65.625		72.194
Plasma/ml	256,730		197,092	

[a] $n = 6$.

Table XI—Effects of Phthalimide Analogues on 24-hr [^{3}H]-Cholesterol Absorption in Rats After 14 Days of Dosing

Compound	Plasma[a]	Percent of Control
Control	14280	
Phthalimide	6283	44[b]
3-*N*-Phthalimidopropionic acid	5569	39[b]

[a] dpm assuming 17 ml total volume/rat; $n = 6$. [b] $p \leq 0.001$.

transports cholesterol (60–70%) to the peripheral tissue and in most species back to the liver (32, 33). Low-density lipoproteins are deposited in the atherosclerotic plaque shedding their cholesterol into the form cells (34–36). An increase in dietary cholesterol is reflected as an increase in cholesterol levels of low-density and, to a less extent, high-density and intermediate-density lipoproteins (37). High-density lipoproteins, which originate from the liver and intestine, play an important role in the interconversion of lipid components to various lipoprotein fractions and in the return of lipids from the peripheral tissue to the liver. Both the low- and high-density lipoproteins are actively taken up by the liver low-density lipoprotein receptors (33, 38). High-density lipoproteins may participate in the transport of cholesterol out of the atherosclerotic plaque or may slow down the atherogenic process (39). Studies have suggested that high-density lipoproteins are inversely related to the incidence of coronary heart disease (*e.g.*, Troms study) (40–43). However, other studies in humans dispute these findings (44–46). Other workers have proposed that the ratio of low-density to high-density lipoprotein is more important in predicting the incidence of atherosclerosis (46, 47). The cholesterol content of each fraction or the ratio of high-density lipoprotein cholesterol to total cholesterol has also been discussed as possible parameters for predicting coronary heart disease (46, 47).

Treatment with clofibrate does not significantly alter the high-density lipoprotein fraction in humans, but lowers the cholesterol of this fraction slightly; however, clofibrate does not protect against coronary heart disease (46). Treatment with probucol for short periods of time reduces the high-density lipoproteins as well as the ratio of cholesterol content of the high-density lipoproteins to total cholesterol content with no increase in the incidence of heart disease (44). A number of preliminary studies have alluded to the fact that high-density lipoproteins are taken up by the liver where the cholesterol is released from the apoprotein and acts as a precursor for bile acids and biliary cholesterol (33, 48, 49).

Treatment with phthalimide derivatives for a 2-week period lowers cholesterol and triglyceride levels of chylomicrons, very low-, low-, and high-density lipoprotein fractions of the rat. Although the lipid distribution among the lipoproteins fractions in the rat is different from the human, some analogies may be drawn. The reduction of cholesterol and

Table XII—Effects of Phthalimide Analogues on Bile Flow and Biliary [^{3}H]Cholesterol Excretion in Rats After 14 Days of Dosing [a]

	6-hr Bile Flow	Total cpm	Cholesterol, mg%
Control	3.36 ± 0.16	1016 ± 81	111 ± 8
Phthalimide	7.60 ± 0.40[b]	1686 ± 144[b]	201 ± 12[b]
3-*N*-Phthalimidopropionic acid	5.23 ± 0.57[b]	1554 ± 103[b]	171 ± 10[b]

[a] $n = 6$. [b] $p \leq 0.001$.

Table XIII—Effects of Phthalimide on Lipid Content of Fecal Material Collected after 16 Days of Dosing [a]

Dosage	Total Cholesterol	Neutral Lipids	Triglycerides	Phospholipids
		0–6-hr Fecal Collection		
Control	100 ± 7[d]	100 ± 8[e]	100 ± 6[f]	100 ± 5[g]
10 mg/kg	139 ± 8[b]	121 ± 8[c]	96 ± 5	166 ± 6[b]
20 mg/kg	134 ± 7[b]	151 ± 6[b]	90 ± 4	192 ± 8[b]
40 mg/kg	188 ± 9[b]	156 ± 7[b]	91 ± 6	177 ± 7[b]
60 mg/kg	115 ± 5[c]	128 ± 6	99 ± 8	116 ± 6[c]
		6–12-hr Fecal Collection		
Control	100 ± 7[h]	100 ± 8[i]	100 ± 6[j]	100 ± 6[k]
10 mg/kg	150 ± 7[b]	137 ± 7[b]	100 ± 6	112 ± 6
20 mg/kg	157 ± 8[b]	204 ± 8[b]	102 ± 5	145 ± 7[b]
40 mg/kg	140 ± 6[b]	162 ± 7[b]	106 ± 6	182 ± 7[b]
60 mg/kg	144 ± 6[b]	161 ± 8[b]	112 ± 7	125 ± 6[b]
		12–24-hr Fecal Collection		
Control	100 ± 8[l]	100 ± 6[m]	100 ± 7[n]	100 ± 6[o]
10 mg/kg	148 ± 6[b]	133 ± 5[b]	97 ± 6	148 ± 8[b]
20 mg/kg	146 ± 7[b]	230 ± 8[b]	98 ± 7	190 ± 7[b]
40 mg/kg	133 ± 6[b]	216 ± 7[b]	98 ± 7	150 ± 6[b]
60 mg/kg	99 ± 7	154 ± 6[b]	97 ± 7	129 ± 5[b]

[a] Percent of control, expressed as mean ± *SD*; $n = 6$. [b] $p \leq 0.001$. [c] $p \leq 0.010$. [d] 19.77 mg/g tissue. [e] 17.62 mg/g tissue. [f] 1.74 mg/g tissue. [g] 1.85 mg/g tissue. [h] 29.47 mg/g tissue. [i] 33.94 mg/g tissue. [j] 1.86 mg/g tissue. [k] 1.61 mg/g tissue. [l] 28.47 mg/g tissue. [m] 33.94 mg/g tissue. [n] 1.86 mg/g tissue. [o] 1.39 mg/g tissue.

Table XIV—Effects of Phthalimide Analogues on Holtzman Lipoprotein Fraction after 14 Days of Dosing [a]

Compound	Cholesterol	Neutral Lipids	Triglycerides	Phospholipids	Protein
			Chylomicrons		
1% Carboxymethylcellulose	100 ± 9[b]	100 ± 8[c]	100 ± 6[d]	100 ± 10[e]	100 ± 7[f]
Phthalimide	42 ± 4[v]	57 ± 6[v]	49 ± 4[v]	374 ± 13[v]	61 ± 5[v]
1-*N*-Phthalimidobutan-3-one	53 ± 4[v]	73 ± 6[v]	52 ± 5[v]	99 ± 11	61 ± 6[v]
3-*N*-Phthalimidopropionic acid	66 ± 5[v]	17 ± 3[v]	51 ± 6[v]	197 ± 15[v]	57 ± 6[v]
			Very Low-Density Lipoprotein		
1% Carboxymethylcellulose	100 ± 8[g]	100 ± 9[h]	100 ± 7[i]	100 ± 7[j]	100 ± 8[k]
Phthalimide	47 ± 5[v]	75 ± 7[v]	33 ± 4[v]	205 ± 10[v]	43 ± 3[v]
1-*N*-Phthalimidobutan-3-one	75 ± 6[v]	78 ± 6[w]	78 ± 7[v]	213 ± 9[v]	86 ± 7
3-*N*-Phthalimidopropionic acid	85 ± 8	85 ± 6	40 ± 4[v]	359 ± 5[v]	43 ± 5[v]
			Low-Density Lipoprotein		
1% Carboxymethylcellulose	100 ± 9[l]	100 ± 7[m]	100 ± 8[n]	100 ± 7[o]	100 ± 8[p]
Phthalimide	42 ± 3[v]	68 ± 6[v]	44 ± 4[v]	81 ± 6[v]	67 ± 7[v]
1-*N*-Phthalimidobutan-3-one	55 ± 5[v]	77 ± 5[v]	49 ± 4[v]	42 ± 4[v]	101 ± 9
3-*N*-Phthalimidopropionic acid	57 ± 7[v]	73 ± 5[v]	50 ± 4[v]	71 ± 6[v]	98 ± 8
			High-Density Lipoprotein		
1% Carboxymethylcellulose	100 ± 8[q]	100 ± 9[r]	100 ± 4[s]	100 ± 6[t]	100 ± 8[u]
Phthalimide	44 ± 5[v]	48 ± 4[v]	51 ± 3[v]	212 ± 7[v]	66 ± 6[v]
1-*N*-Phthalimidobutan-3-one	56 ± 5[v]	52 ± 3[v]	65 ± 5[v]	324 ± 12[v]	101 ± 7
3-*N*-Phthalimidopropionic acid	52 ± 8[v]	64 ± 5[v]	53 ± 4[v]	225 ± 8[v]	104 ± 8

[a] Percent of control, expressed as mean ± *SD*; $n = 6$. [b] 337 μg/ml. [c] 67 μg/ml. [d] 420 μg/ml. [e] 149 μg/ml. [f] 221 μg/ml. [g] 190 μg/ml. [h] 98 μg/ml. [i] 221 μg/ml. [j] 26 μg/ml. [k] 50 μg/ml. [l] 210 μg/ml. [m] 10 μg/ml. [n] 45 μg/ml. [o] 41 μg/ml. [p] 122 μg/ml. [q] 544 μg/ml. [r] 620 μg/ml. [s] 27 μg/ml. [t] 153 μg/ml. [u] 657 μg/ml. [v] $p \leq 0.001$. [w] $p \leq 0.010$.

triglyceride content of low- and high-density lipoproteins was approximately of the same magnitude after drug treatment which probably did not change the low-density to high-density lipoprotein ratio during drug treatment. The reduction of cholesterol in both lipoprotein fractions may reflect the increase in cholesterol excretion in the bile after phthalimide treatment. Supposedly, the cholesterol esters are exchanged between high- and low-density lipoproteins (50), so a reduction of one by drug therapy should reflect in the other fraction ultimately.

After phthalimide treatment it was noted that the phospholipid content of the very low-density and chylomicron fractions were elevated. Clofibrate is also known to increase the phospholipid content of liver and serum (51). The very low-density and chylomicron remnants have their phospholipid content enzymatically removed before they can be taken up by the liver. If the phospholipid, *e.g.*, phosphatidyl choline, remains on these remnants then the remnants are not taken up by the liver (52). The inability to take up these fractions may be critical to the regulation of liver cholesterol synthesis, since in hyperlipidemic patients and rats the cholesterol released from very low-density lipoproteins inhibit 3-hydroxy-3-methylglutaryl coenzyme A reductase activity (53). However, the cholesterol release from very low-density lipoproteins of normal rats did not inhibit the enzyme, suggesting that the actual content of cholesterol in the very low-density lipoprotein fraction may be the one decisive factor in the regulation of liver cholesterol synthesis (54).

Mixed results have been observed regarding the cholesterol content of high- and low-density lipoprotein fractions. In the fibroblast system, they inhibit the regulatory enzyme of cholesterol synthesis. However, in the hepatocyte tissue culture system, the high cholesterol content of high- and low-density lipoprotein did not inhibit 3-hydroxy-3-methylglutaryl coenzyme A reductase activity (54). Further studies are being conducted with the relationship of lipoprotein fractions of rats after phthalimide treatment.

REFERENCES

(1) J. M. Chapman, G. H. Cocolas, and I. H. Hall, *J. Med. Chem.*, **11**, 1399 (1979).

(2) I. H. Hall, J. M. Chapman, and G. H. Cocolas, *J. Pharm. Sci.*, **70**, 326 (1981).

(3) A. T. Ness, J. V. Pastewka, and A. C. Peacock, *Clin. Chem. Acta*, **10**, 229 (1964).

(4) M. Fletcher, *J. Clin. Chem. Acta*, **22**, 393 (1968).

(5) J. T. Litchfield and F. Wilcoxon, *J. Pharmacol. Exp. Ther.*, **96**, 99 (1949).

(6) A. G. Goodridge, *J. Biol. Chem.*, **248**, 4318 (1973).

(7) M. Hoffman, L. Weiss, and O. H. Weiland, *Anal. Biochim.*, **84**, 441 (1978).

(8) B. H. Robinson, G. R. Williams, M. L. Halperin, and C. C. Leznoff, *J. Biol. Chem.*, **246**, 5280 (1971).

(9) B. H. Robinson, G. R. Williams, M. L. Halperin, and C. C. Leznoff, *Eur. J. Biochem.*, **15**, 263 (1970).

(10) D. Kritchevsky, E. R. Kolman, M. W. Whitehouse, M. C. Cottrell, and E. Staple, *J. Lipid Res.*, **1**, 83 (1959).
(11) G. T. Haven, J. R. Krzemien, and T. T. Nguyen, *Res. Commun. Chem. Pathol. Pharmacol.*, **6**, 253 (1973).
(12) F. Wada, K. Kirata, and Y. Sakameto, *J. Biochem. (Tokyo)*, **65**, 171 (1969).
(13) M. D. Greenspan and J. M. Lowenstein, *J. Biol. Chem.*, **243**, 6273 (1968).
(14) R. O. Brady, R. M. Bradley, and E. G. Trams, *J. Biol. Chem.*, **235**, 3093 (1960).
(15) R. G. Lamb, S. D. Wyrick, and C. Piantadosi, *Atherosclerosis*, **27**, 147 (1977).
(16) R. D. Mavis, J. N. Finkelstein, and B. P. Hall, *J. Lipid Res.*, **19**, 467 (1978).
(17) I. H. Hall and G. L. Carlson, *J. Med. Chem.*, **19**, 1257 (1976).
(18) J. Folch, M. Lees, and G. H. S. Stanley, *J. Biol. Chem.*, **226**, 497 (1957).
(19) E. G. Bligh and W. J. Dyer, *Can. J. Biochem. Physiol.*, **37**, 911 (1959).
(20) J. H. Bragdon, *J. Biol. Chem.*, **190**, 513 (1951).
(21) C. P. Stewart and E. G. Hendry, *Biochem. J.*, **29**, 1683 (1935).
(22) A. Adam, J. van Cantfort, and J. Gielen, *Lipids*, **ii**, 610 (1976).
(23) F. T. Hatch and R. S. Lees, *Adv. Lipid Res.*, **6**, 1 (1968).
(24) R. J. Havel, H. A. Eder, and J. H. Bragdon, *J. Clin. Invest.*, **34**, 1345 (1955).
(25) O. H. Lowry, N. J. Rosebrough, A. L. Farr, and R. J. Randall, *J. Biol. Chem.*, **193**, 265 (1957).
(26) E. G. Smith, *J. Lipid Res.*, **12**, 1 (1974).
(27) J. M. Thorpe and W. S. Waring, *Nature (London)*, **194**, 948 (1962).
(28) R. G. Lamb and H. J. Fallon, *J. Biol. Chem.*, **247**, 1281 (1972).
(29) S. L. Katyal, J. Saha, and J. T. Kabara, *Biochem. Pharmacol.*, **21**, 747 (1972).
(30) G. Fredi, M. Cenet, P. Cucket, F. Rousselet, and C. Roze, *Digestion*, **19**, 228 (1979).
(31) J. M. Chapman, P. J. Voorstad, G. H. Cocolas, and I. H. Hall, *J. Med. Chem.* **28**, 237 (1983).
(32) G. S. Getz and R. V. Hay, in "The Biochemistry of Atherosclerosis," A. M. Scanu, R. W. Wissler, and G. S. Getz, Eds., Dekker New York, N.Y., 1979, p. 151.
(33) B. Lewis, *Annu. Rev. Clin. Biochem.*, **1**, 139 (1980).
(34) D. Kritchevsky and H. V. Kothari, *Adv. Lipid Res.*, **16**, 221 (1978).
(35) D. W. Crawford and D. H. Blankenhorn, *Annu. Rev. Med.*, **30**, 289 (1979).
(36) B. Eisele, S. R. Bates, and R. W. Wissler, *Atherosclerosis*, **36**, 9 (1980).
(37) P. Mistry, *Protides Biol. Fluids, Proc. Colloq.*, **25**, 349 (1978).
(38) J. F. Oram, J. J. Albers, M. C. Cheng, and E. L. Bierman, *J. Biol. Chem.*, **256**, 8348 (1981).
(39) T. E. Carew, T. Kochinsky, S. B. Hayes, and D. Steinberg, *Lancet*, **i**, 315 (1976).
(40) D. P. Barr, E. M. Russ, and H. A. Eder, *Am. J. Med.*, **11**, 480 (1951).
(41) E. A. Nikkila, *J. Clin. Lab. Invest. Suppl.*, **5**, 8 (1953).
(42) G. J. Miller and N. E. Miller, *Lancet*, **i**, 16 (1975).
(43) K. Berg, A. L. Borreson, and G. Dahlén, *Lancet*, **i**, 499 (1976).
(44) N. E. Miller, O. H. Forde, D. S. Thelle, and O. Mjos, *Lancet*, **i**, 965 (1977).
(45) T. A. Miettinen, J. K. Huttunen, T. Strandberg, V. Naukkarinen, S. Mattila, and T. Kumlin, *Lancet*, **ii**, 478 (1981).
(46) V. Manninen, M. Mälkönen, and S. Tuomilehto, *Am. Heart J.*, **97**, 674 (1979).
(47) G. J. Miller and N. E. Miller, in "High Density Lipoproteins and Atherosclerosis," A. M. Gotto, Jr., N. E. Miller, and M. F. Oliver, Eds., Elsevier-North Holland, Amsterdam, 1978, p. 85.
(48) C. A. Drevon, T. Berg, and K. R. Novum, *Biochim. Biophys. Acta*, **529**, 309 (1978).
(49) C. C. Schwartz, L. G. Halloran, Z. R. Vlahavic, D. H. Gregory, and L. Swell, *Science*, **200**, 62 (1978).
(50) J. J. Barter and M. E. Jones, *Atherosclerosis*, **34**, 67 (1979).
(51) D. Azurnoff, D. R. Tucker, and G. A. Barr, *Metabolism*, **14**, 959 (1965).
(52) P. S. Bachorik, P. O. Kwiterovich, and J. C. Cooke, *Biochemistry*, **17**, 5287 (1978).
(53) M. R. Lakshmanan, R. A. Muesings, and J. C. LaRosa, *J. Biol. Chem.*, **256**, 3037 (1981).
(54) J. L. Breslow, D. R. Spaulding, D. A. Lothrop, and A. W. Clowers, *Biochem. Biophys. Res. Commun.*, **67**, 119 (1975).

ACKNOWLEDGMENTS

This research was supported by NIH Grant HL 26580.
We thank Mellie Gibson, Jerry McKee, Mary Dorsey, and Kathy Wright for their technical assistance on this project.

Structure–Activity Studies on Sulfamate Sweetners III: Structure–Taste Relationships for Heterosulfamates

WILLIAM J. SPILLANE *x, **GRÁINNE McGLINCHEY** *, **IOGNAID Ó MUIRCHEARTAIGH** ‡, and **G. ANTHONY BENSON** §

Received May 22, 1981, from the *Department of Chemistry and the ‡Department of Statistics, University College, Galway, Ireland and the §Chemistry Department, Regional Technical College, Sligo, Ireland. Accepted for publication June 8, 1982.

Abstract □ Eleven heterosulfamates have been synthesized, characterized, and evaluated for sweetness. Measurements of the molecular dimensions (x, y, z, and V) of these sulfamates and 22 others that had been reported previously and evaluated for sweetness have been made using Corey–Pauling–Koltun space-filling models. The first-order molecular connectivities ($^1\chi^v$) of all the heterosulfamates have been calculated. The statistical technique of linear discriminant analysis was applied to the complete set of 33 compounds and to a reduced set of 27 compounds. The analysis was performed using the above five variables (x, y, z, V, and $^1\chi^v$) and various subsets thereof. For the complete set of compounds, seven variable subsets were identified which yielded correct classifications of 27 and 28 compounds. A similar analysis of the reduced set did not improve the misclassification rate.

Keyphrases □ Heterosulfamates—synthesis, classification by linear discriminant analysis, structure–taste relationship □ Sweetners, sulfamate—structure–taste relationship, classification by linear discriminant analysis □ Linear discriminant analysis—classification of heterosulfamates, molecular connectivity correlations

Previous studies (1–4) on heterosulfamates have shown that when one of the ring carbons of cyclohexylsulfamate is replaced by an oxygen or nitrogen atom, sweetness is lost, whereas replacement by a moiety containing a sulfur atom results in the retention of sweetness. Compounds X (1), XVIII (2), and XX (1) are nonsweet while IX (2), XI (3), and IV (4) are sweet.

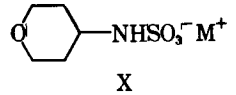

X

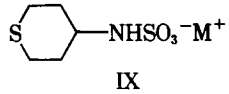

IX

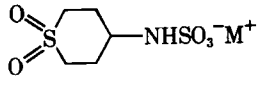

XI

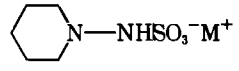

XVIII

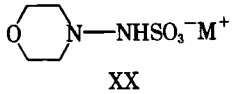

XX

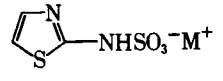

IV

Furthermore, one of the basic structure–taste rules found for carbosulfamates does not appear to apply to heterosulfamates, namely, that the presence of a free hydrogen on the nitrogen of the sulfamate function was essential for sweetness (5). This was shown by the taste evaluation of the series of cyclic sulfides (IX, XXIV, XXI, and XXV) and sulfones (XI, XXIII, and XXII) which are sweet (3).

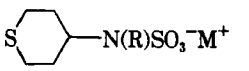

IX: R = H
XXIV: R = —CH_2CH_3
XXI: R = —$(CH_2)_3CH_3$
XXV: R = —CH_2CH_2OH

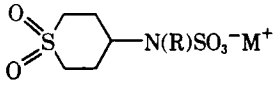

XI: R = H
XXIII: R = —CH_2CH_3
XXII: R = —$(CH_2)_3CH_3$

Since only a few other heterosulfamates have been reported, 11 new heterosulfamates (both cyclic and open-chain) were synthesized and several structure–taste relationships were established from measurements of the molecular dimensions and molecular connectivities of these and other heterosulfamates reported previously.

EXPERIMENTAL

Synthesis—All sulfamates except VII and XII were synthesized by previously described methods (5, 6).

5-Methylisoxazolo-3-sulfamate (VII)—A solution of 3-amino-5-methylisoxazole (5 g, 0.05 mole) in dry nitrobenzene (40 ml) was cooled to 0°. Chlorosulfonic acid (4.5 g, 0.05 mole) was added with stirring at a rate such that the temperature did not rise above 5°. The mixture was stirred at room temperature for 3 hr. Ether (20 ml) was added and the orange solid that precipitated from the solution was removed by filtration, dissolved in 0.05 *M* sodium hydroxide (20 ml), and the solution was extracted with ether (2 × 20 ml). On removal of the ether under reduced pressure, an oily residue remained. On chilling this gave rise to a white solid which was the amine salt of the required sulfamate. Attempts to prepare this compound by the method of Hurd and Kharasch (4) failed. By employing the dipolar aprotic solvent nitrobenzene, a small yield (2.4%) was obtained. Possibly in this solvent protonation of the ring nitrogen of the isoxazole and consequent reduced basicity of the amino group is inhibited. The basicity of the oxazole was such that the sulfamate formed was the oxazole salt rather than the sodium salt.

3-Thia-3,3-dioxocyclopentylsulfamate (XII)—A solution of 3-thia-3,3-dioxocyclopentylamine (5 g, 0.037 mole) in ethanol (40 ml) was cooled to ~0°. Chlorosulfonic acid (3.52 g, 0.03 mole) was added in a dropwise manner with stirring. The mixture was stirred at room temperature for 3 hr, and then ethanol was removed under reduced pressure. The resulting yellow solid was dissolved in 2 *M* sodium hydroxide, and the liberated amine was extracted with ether (3 × 25 ml). The aqueous layer was then concentrated to ~10 ml and the precipitated amine salt of the sulfamate was removed by filtration and then recrystallized from 95% ethanol. Again the amine was sufficiently basic to form this salt rather than the expected sodium salt. The yields of the sulfamates synthesized were 2–20%.

Analysis and Characterization—The sulfamates prepared gave satisfactory (within ±0.5%) C, H, and N analyses except for I, II, VII, XXVI, and XXVII. Analytical data (C, H, and N) for all new compounds are given in Table I. It should be noted that occluded solvent of recrystallization is a common problem with sulfamates (5, 7, 8). Despite repeated recrystallization, the elemental analysis for I could not be improved; however, this compound displayed the sulfamate properties described below.

IR spectra of all the sulfamates prepared were recorded[1]. The sulfamates gave the following characteristic bands (9): 3400–3190 (NH), 1240–1210 (asymSO_3), 1203–1170 (symSO_3), 1072–1040 (symSO_3), and 730–660 cm^{-1} (NS). All the prepared sulfamates gave a positive "sulfamate" test (2).

Taste Analysis—Analysis was carried out as previously described (10). Two of the sulfamates (VII and XII) were isolated and purified as their amine salts ($RHNSO_3^-NH_3^+R$) and were tasted as such, since it is known that the salt-forming group does not influence the taste of sulfamates (5, 11).

Measurements with Models and Molecular Connectivity Measurements—The measurements with the Corey–Pauling–Koltun models were carried out as previously described (10), and the parameters x, y,

[1] Perkin-Elmer 337 spectrophotometer using Nujol mulls.

0022-3549/83/0800-0852$01.00/0

Table I—Analytical Data for New Sulfamates

Compound	Found, % C	H	N	Formula	Required, % C	H	N
I	19.38	4.12	6.89	$C_5H_{10}NSO_4Na{\cdot}3H_2O$	23.42	6.22	5.44
II	29.22	3.02	7.11	$C_5H_6NSO_4Na$	30.15	3.02	7.03
III	28.21	11.13	5.14	$C_6H_{13}N_2SO_3Na{\cdot}2H_2O$	27.69	10.76	5.00
VII	35.32	5.97	19.8	$C_8H_{12}N_4SO_5$[a]	34.8	4.4	20.3
XII	27.38	5.44	7.82	$C_8H_{18}N_2S_3O_7$[a]	27.42	5.14	8.00
XIII	36.52	6.63	12.27	$C_7H_{15}N_2SO_3Na$	36.52	6.52	12.27
XIV	49.13	5.83	9.80	$C_{12}H_{17}N_2SO_3Na$	49.32	5.82	9.59
XV	34.38	6.23	11.51	$C_7H_{15}N_2SO_4Na$	34.14	6.23	11.38
XIX	30.66	6.47	12.03	$C_6H_{13}N_2SO_3Na{\cdot}1H_2O$	30.76	6.41	11.96
XXVI	28.22	5.49	5.75	$C_5H_{12}NSO_4Na{\cdot}\frac{1}{2}H_2O$	28.00	6.09	6.54
XXVII	24.98	5.44	11.75	$C_5H_{13}N_2SO_3Na{\cdot}2H_2O$	25.00	7.08	11.66

[a] Isolated as the amine salt of the sulfamate.

z, and V (*i.e.*, x-y-z) were determined as before (Table II). The values for the molecular connectivity (χ) for the different sulfamates were determined by considering the valence electrons, whether bonded or nonbonded. The δ values are considered to be the difference between the number of valence electrons z^v and the number of hydrogen atoms h_i:

$$\delta_i^v = z^v - h_i \qquad \text{(Eq. 1)}$$

Thus, applying this to oxygen in an alcohol $\delta^v = z^v - h_i = 6 - 1 = 5$. The δ^v values for heteroatoms are given in Table III (12). δ^v can be used to calculate a valence chi-term of the first order ($^1\chi^v$) by the expression:

$$^1\chi^v = \Sigma(\delta_i^v\delta_j^v)^{-1/2} \qquad \text{(Eq. 2)}$$

For example, the chi-term (of the first order) for the sulfamate anion XXVII was calculated as follows:

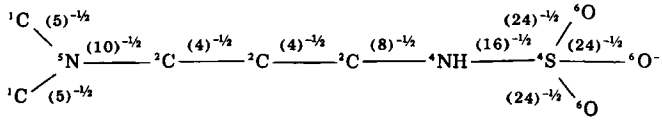

$$\begin{array}{r} 2 \times 0.447 \\ 0.316 \\ 2 \times 0.500 \\ 0.354 \\ 0.250 \\ 3 \times 0.204 \\ \hline {}^1\chi^v = 3.43 \end{array}$$

When cyclic compounds are considered, a ring correction factor must be used because of the presence of an additional edge (bond). This is accommodated for by the use of 0.5 as a modifying term to be subtracted from $^1\chi^v$. For example, the chi-term for the 4-oxacyclohexylsulfamate (χ) was calculated as follows:

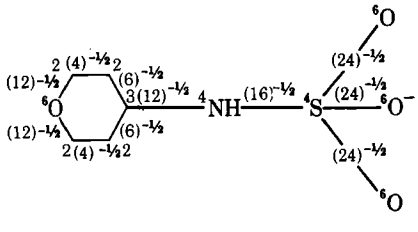

$$\begin{array}{r} 2 \times 0.289 \\ 2 \times 0.500 \\ 2 \times 0.408 \\ 0.289 \\ 0.250 \\ 3 \times 0.204 \\ \hline 3.545 \\ \text{Correction factor} - 0.5 \\ \hline {}^1\chi^v \quad 3.05 \end{array}$$

THEORETICAL

The technique used to facilitate determination of structure–taste relationships is that of linear discriminant analysis. This method is applied when M(≥1) measurements (variables) are available for each member of two clearly defined groups and yields a linear function of the variables which best separates the two groups.

The theory of the linear discriminant function is described in many statistical tests (17, 18). Conceptually the method is identical for all values of M (the number of variables observed for each member of each group), but the essential ideas are most easily expanded for the case M = 2. In this case, we have two measurements, say X and Y, for each member of each group. Each member can therefore be represented as a point in the X,Y plane. The linear discriminant function in this case is the line that, in a certain sense, best separates the two groups. If the equation of this line is:

$$aX + bY = k \qquad \text{(Eq. 3)}$$

then mathematically the problem is to use the given (X,Y) data to estimate constants a, b, and k such that the line given by (Eq. 3) separates the two groups in some optimal sense. The extension to the case of M > 2 variables is mathematically straightforward, but conceptually more difficult. We now seek a linear combination:

$$l(X_1,X_2,\ldots X_M) = a_1X_1 + a_2X_2 + \ldots + a_MX_M = a^1X \qquad \text{(Eq. 4)}$$

where $a^1 = (a_1, a_2, \ldots a_n)$ and $X^1 = (X_1, \ldots X_M)$ such that an equation of the form:

$$l(X) = k \qquad \text{(Eq. 5)}$$

optimally separates the two groups. In the case M = 3, this is equivalent to finding the plane that best separates the two groups in the three-dimensional space in which they can be represented. For M > 3, we obtain a hyper-plane separating the two groups. Although the geometrical representation breaks down for the case M > 3, the mathematical method is straightforward.

Most statistical packages used on computers will perform this analysis. The package BMDP (19) was used in this case, and it yields the constants $a_1, a_2, \ldots a_M$ of Eq. 4. The constant k is then chosen to optimize the discriminatory power of the discriminant function $l(X)$. The criterion of optimality usually used involves stochastic assumptions concerning the multivariate normal distribution of the underlying data. Given the nature of this particular data set, the more *ad hoc* criterion of minimizing the number of misclassifications using the discriminant function $l(X)$ has been adopted in this paper.

Suppose one has two groups of compounds and has recorded the values of each of M variables for n_1 members of group 1 and n_2 members of group 2.

Let $X_{ijk}\{i = 1,2; j = 1,2 \ldots n_i; k = 1,2 \ldots M\}$ be the value of the k^{th} variable for the j^{th} member of the i^{th} group. Let:

$$\overline{X}_{ik} = \sum_j X_{ijk}/n_i \qquad \begin{matrix} i = 1,2 \\ k = 1,2,\ldots M \end{matrix} \qquad \text{(Eq. 6)}$$

and define the mean vectors of the two groups to be, respectively:

$$\overline{X}_1^1 = (\overline{X}_{11}, \overline{X}_{12}, \ldots \overline{X}_{1M}) \qquad \text{(Eq. 7)}$$

$$\overline{X}_2^1 = (\overline{X}_{21}, \overline{X}_{22}, \ldots \overline{X}_{2M}) \qquad \text{(Eq. 8)}$$

Further let:

$$S_{kl} = \frac{\sum_i \sum_j (X_{ijk} - \overline{X}_{ik})(X_{ijl} - \overline{X}_{il})}{n_1 + n_2 - 2} \qquad \text{(Eq. 9)}$$

so that:

$$S = (S_{kl}) \qquad \text{(Eq. 10)}$$

is the M × M pooled estimate of the (assumed) common covariance matrix. Then the elements of the vector a of Eq. 4 are given by:

$$a = (\overline{X}_1 - \overline{X}_2)^1 \cdot S^{-1} \qquad \text{(Eq. 11)}$$

Table II—Spatial Parameters for R Groups, Chi-Values, and Taste of Heterosulfamates ($R—SO_3^-M^+$)

Compound	R[a]	Name of Sulfamate[b]	Taste[c]	x	y	z	V	$^1\chi^{vd}$	Reference
I	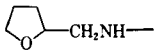	2-Tetrahydrofurfuryl-	N	7.40	4.99	5.92	219.0	3.06	—[e]
II	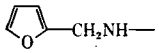	2-Furfuryl-	N	5.96	4.89	5.72	167.0	2.47	—
III	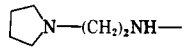	*N*-pyrrolidino-2-ethyl-	N	9.64	4.85	5.92	277.0	3.66	—
IV	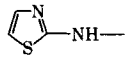	2-Thiazolyl-	S	7.08	3.66	5.84	151.0	1.97	4
V	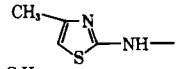	4-Methyl-2-thiazolyl-	S	7.08	3.80	6.96	187.0	2.39	4
VI	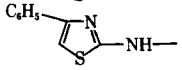	4-Phenyl-2-thiazolyl-	N	7.08	7.20	8.56	436.0	4.05	4
VII	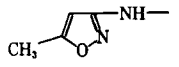	5-Methylisoxazolo-3-	N	7.80	3.88	5.44	165.0	2.30	—
VIII	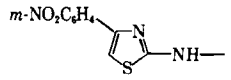	4-*m*-Nitrophenyl-2-thiazolyl-	N	7.08	8.48	9.24	555.0	4.50	4
IX	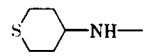	4-Thiacyclohexyl-	S	5.80	5.44	6.80	215.0	3.18	1
X	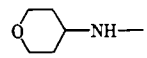	4-Oxacyclohexyl-	N	5.52	5.36	6.40	189.0	3.05	1
XI	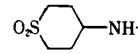	4-Thia-4,4-dioxocyclohexyl-	S	7.72	5.64	6.56	286.0	3.58	3
XII	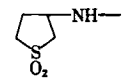	3-Thia-3,3-dioxocyclopentyl-	B	6.00	5.64	6.56	222.0	2.99	—
XIII	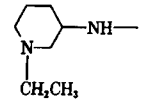	1-Ethylpiperidinyl-3-	N	6.08	5.68	8.24	285.0	4.12	—
XIV	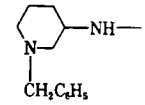	1-Benzylpiperidinyl-3-	N	11.50	6.80	6.32	494.0	5.68	—
XV	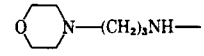	*N*-*n*-Propylmorpholino-	N	9.88	5.28	6.40	334.0	4.24	—
XVI	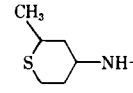	3-Methyl-4-thiacyclohexyl-	S	6.20	5.33	7.88	259.0	3.60	13
XVII	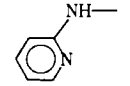	Pyridyl-2-	N	7.72	3.76	6.40	186.0	2.38	4
XVIII	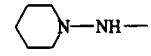	Piperidino-1-	N	7.00	5.30	6.50	241.0	3.22	2
XIX	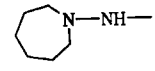	Azacycloheptyl-	N	7.16	5.04	7.20	260.0	3.72	—
XX	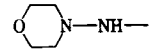	Morpholino-4-	N	5.68	5.36	6.24	190.0	2.80	2
XXI	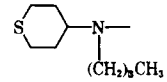	*N*-*n*-butyl-4-thiacyclohexyl-	S	12.72	5.20	6.60	437.0	5.14	3
XXII	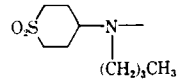	*N*-*n*-butyl-4-thia-4,4-dioxocyclohexyl-	S	13.56	6.24	6.52	552.0	5.55	3
XXIII	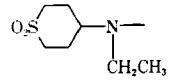	*N*-ethyl-4-thia-4,4-dioxocyclohexyl-	S	10.56	5.92	6.32	395.0	4.55	3
XXIV	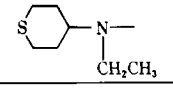	*N*-ethyl-4-thiacyclohexyl-	S	9.84	5.44	6.40	343.0	4.14	3

continued

Table II—*Continued*

Compound	R[a]	Name of Sulfamate[b]	Taste[c]	x	y	z	V	$^1\chi^{v d}$	Reference
XXV	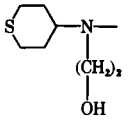	*N*-(2-hydroxyethyl)-4-thiacyclohexyl-	S	11.24	5.28	6.80	404.0	4.24	3
XXVI	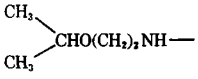	3-Isopropoxyethyl-	N	7.64	5.05	6.32	244.0	3.40	—
XXVII	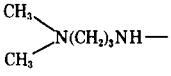	3-Dimethylamino-1-propyl-	B	8.52	4.80	6.12	250.0	3.43	—
XXVIII	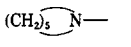	Piperidino-1-	N	5.38	5.30	6.40	182	3.49	14, 15
XXIX	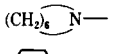	Azacycloheptyl-	N	6.44	5.04	7.20	234	3.47	16
XXX	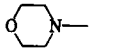	Morpholino-4-	N	4.48	4.48	6.32	127	2.59	15
XXXI	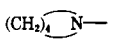	Pyrrolo-1-	N	4.88	4.32	6.00	126	2.47	14, 16
XXXII	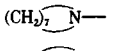	Azacyclooctyl-	N	6.48	5.12	7.76	257	3.97	16
XXXIII	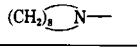	Azacyclononyl-	N	6.05	5.20	8.40	264	4.47	16

[a] Measurements were made on the structures indicated. [b] Compounds XXVIII–XXXIII are sulfonates, but may be regarded as secondary sulfamates and are thus included. [c] Key: (S) sweet; (N) nonsweet; (B) bitter. [d] Molecular connectivities were calculated for the total sulfamate anion, *i.e.*, the $-SO_3^-$ moiety was included in the calculations (see *Experimental*). [e] — Values obtained from this work.

and the classification rule is:

$$\text{classify as group 1 if } a^1X > k$$
$$\text{classify as group 2 if } a^1X \leq k$$

The choice of k is then made to minimize the number misclassified by this rule.

RESULTS AND DISCUSSION

In a previous paper, measurements using Corey–Pauling–Koltun (CPK) space-filling models were carried out on carbosulfamates and a semiquantitative structure–taste relationship was established (10). The approach was similar here and measurements of length (x), height (y), and width (z) of R—NH (or R—NR^1) in R—$NHSO_3^-$ (R—$NR^1SO_3^-$) were made using CPK models. V (in Å^3) may be thought of as a measure of the size or three-dimensional structure of R—NH(R—NR^1) and was calculated as previously described. In addition, a molecular connectivity term ($^1\chi^v$) has been calculated (see *Experimental*). The values of x, y, z, V, and $^1\chi^v$ as well as the test data are given for all the heterosulfamates in Table II.

The mathematical analysis has been performed twice: with the complete set of 33 compounds and with a reduced set of 27 compounds (omitting the last six compounds of Table II). Since six compounds of Table II are sulfonates that could be regarded as secondary sulfamates, the analysis has been tried with and without these compounds. As the analysis involving the reduced set did not improve the misclassification rate, it is not described further.

The linear discriminant analysis could be performed using any subset of the five variables. There are 31 such subsets and, to save computation time, a preliminary analysis using a statistically equivalent technique, stepwise logistic analysis (19), enabled identification of the 14 subsets most likely to provide effective discrimination. The discriminant analysis was then performed using these subsets. For the complete set (33 compounds), the most effective variable subset of each (2, 3, 4, 5), the discriminant function a^1X for each of those subsets, the corresponding constant k, and the number of compounds misclassified by the optimal classification rule so derived are given in Table IV.

A discussion of the discriminant analysis applied to the complete data set and using the variable subset (x,$^1\chi^v$) will be utilized to highlight the main points of this type of analysis. From Table IV it can be seen that the dividing line in this case is:

$$-0.63x + 0.58\,^1\chi^v = -3.95 \qquad \text{(Eq. 12)}$$

It can be seen from Table IV that, with the exception of IV, V, IX, XI, XVI, and XXIV, all the sweet compounds lie above and all the nonsweet compounds lie below this line. The mathematically equivalent results for this case are given in Table V, which presents the values of:

$$d = -0.63x + 0.58\,^1\chi^v \qquad \text{(Eq. 13)}$$

for each compound. It can be seen that for all the sweet compounds (with the aforementioned exceptions), $d < k\{-3.95\}$, whereas for all the nonsweet compounds $d > k$.

Detailed results are not presented for the discriminant analyses based on the other variable subsets given in Table IV. From Table IV it can be seen that, although the inclusion of additional variables does not dramatically affect the discriminatory performance, the number of misclassified compounds does decrease (to 5) when one uses the subset x,z,$^1\chi^v$. For this particular case, the discriminant function is:

$$d = -0.86x - 0.81z + 1.31\,^1\chi^v \qquad \text{(Eq. 14)}$$

and the corresponding classification rule is:

$$\text{classify as sweet if } d < -8.18$$
$$\text{classify as nonsweet if } d > -8.18$$

In fact three sweet compounds (IX, XI, and XVI) have values of $d > -8.18$, and two nonsweet compounds (III, XVII) have values of $d < -8.18$. The remaining subsets in Table IV misclassify six compounds in each case. Thus, an accuracy of 85% can be attained for the subset involving the variables x, z, and $^1\chi^v$ with 81% accuracy for all other subsets. For the carbosulfamates an accuracy of >90% could be achieved using the variables x and V only (10). Here the accuracy is not as good but, considering the wide diversity of heterocompounds in Table II, the present correlation can be regarded as reasonable.

A weakness of the x,$^1\chi^v$ subset correlation seems to be that all six misclassified compounds come from the group of 10 sweet compounds, while the 23 nonsweet compounds are classified correctly. One would prefer to see a more even spread of misclassified compounds from the sweet and nonsweet groups as in some of the four or five variable subsets in Table

Table III—Heteroatom Valence Delta-Values

Group	δ^v	Group	δ^v
		—OH	5
—NH	4	—O—	6
		=O	6
|		O (both nitro)	
—N—	5	O (both carboxylate)	6
=N—(pyridine)	5		
—N=(nitro)	6		
—S—	4		
=S=	4		

Table IV—Discriminant Analysis for Best Subsets

Subset	a^1X	k	Compounds Misclassified: Sweet	Compounds Misclassified: Nonsweet	Total Misclassified
$x,{}^1\chi^v$	$-0.63x + 0.58{}^1\chi^v$	−3.95	IV, V, IX, XI, XVI, XXIV		6
$y,V,{}^1\chi^v$	$1.62y - 0.02V + 0.65{}^1\chi^v$	+4.21	IX, XI, XVI, XXIII, XXIV	XVII	6
$x,z,{}^1\chi^v$	$-0.86x - 0.81z + 1.31{}^1\chi^v$	−8.18	IX, XI, XVI	III, XVII	5
$x,z,V,{}^1\chi^v$	$-1.01x - 1.08z + 0.01V + 1.06{}^1\chi^v$	−10.50	IX, XI, XVI	III, XV, XVII	6
$x,y,z,{}^1\chi^v$	$-0.81x + 0.34y - 0.88z + 1.01{}^1\chi^v$	−7.49	IX, XI, XVI	III, XV, XVII	6
x,y,z,V	$-0.37x + 1.05y - 0.41z - 0.01V$	−2.37	IV, IX, XI, XVI	XV, XVII	6
$x,y,z,V,{}^1\chi^v$	$-1.06x - 0.08y - 1.12z + 0.01V + 1.08{}^1\chi^v$	−11.17	IX, XI, XVI	III, XV, XVII	6

IV (*e.g.*, the $x,z,{}^1\chi^v$ subset which has three sweet and two nonsweet compounds misclassified).

If one uses the number misclassified and the spread of misclassified compounds between sweet and nonsweet groupings as criteria of significance, then one may concentrate on the last five subsets of Table IV. The importance of spatial or volume effects at the receptor site is clear when one observes that x and either z or y or both are involved in all these subsets. ${}^1\chi^v$ Encodes both volume and electronic effects of bonds (20), and it is noteworthy that this variable occurs in four of these five subsets. With the carbosulfamates, electronic influences were probably small and, hence, a correlation was possible using only spatial parameters. However, with the introduction of various heteroatoms into the sulfamates, electronic effects of bonds could be important, and a more complicated type of correlation would thus be expected.

Molecular connectivity terms have been used in recent years to correlate the sweetness of substituted nitroanilines (21) and the percent sweet/bitter taste of aldoximes, RCH=NOH (22). Thus, ${}^1\chi^v$ was introduced since a correlation with our spatial parameters only was not possible.

In the listing of misclassified compounds, the same compounds appeared: III, IX, XI, XV, XVI, and XVII. It is instructive to look at these more closely in the hope of finding a common factor that may cause their deviation. Compounds IX, XI, and XVI all have a sulfur atom in a six-membered ring in either the disulfide or sulfone form. Compounds IV–VI and VIII also have sulfur atoms in five-membered rings, but these atoms are involved in the aromaticity of the rings. Compound XII has sulfur in a five-membered saturated ring system, and one may regard compounds XXI–XXV as special cases since they all have disubstituted sulfamate nitrogens. It thus seems that the correlations established will consistently misclassify six-membered saturated sulfur ring systems. The reason(s) for the deviation of the three nonsweet compounds III, XV, and XVII are less clear.

Table V—Discriminant Function [a] Values for Subset ($x,{}^1\chi^v$)

Sweet Compounds: Compound	Sweet Compounds: d	Nonsweet Compounds: Compound	Nonsweet Compounds: d
IV	−3.31[b]	I	−2.88
V	−3.06[b]	II	−2.31
IX	−1.80[b]	III	−3.94
XI	−2.78[b]	VI	−2.10
XVI	−1.81[b]	VII	−3.57
XXI	−5.01	VIII	−1.84
XXII	−5.31	X	−1.70
XXIII	−4.00	XII	−2.04
XXIV	−3.78[b]	XIII	−1.43
XXXV	−4.61	XIV	−3.93
		XV	−3.75
		XVII	−3.47
		XVIII	−2.53
		XIX	−2.34
		XX	−1.95
		XVI	−2.83
		XVII	−3.37
		XVIII	−1.36
		XXIX	−2.03
		XXX	−1.31
		XXXI	−1.63
		XXXII	−1.77
		XXXIII	−1.21

[a] Discriminant function $d = -0.63x + 0.58\,{}^1\chi^v < -3.95$ sweet, > -3.95 nonsweet. [b] Misclassified.

REFERENCES

(1) R. Unterhalt and L. Boschemeyer, *Naturwissenschaften*, **271**, 59 (1972).

(2) G. A. Benson and W. J. Spillane, *J. Med. Chem.*, **19**, 869 (1976).

(3) G. R. Wendt and M. W. Winkley, U.S. Pat. 3,787,442 (1974).

(4) C. D. Hurd and N. Kharasch, *J. Am. Chem. Soc.*, **68**, 653 (1946).

(5) L. F. Audrieth and M. Sveda, *J. Org. Chem.*, **9**, 89 (1944).

(6) E. Boyland, D. Manson, and S. F. D. Orr, *Biochem. J.*, **65**, 417 (1957).

(7) C. Nofre and F. Pautet, *Bull. Soc. Chim. Fr.*, **1975**, 686.

(8) W. F. Beech, *J. Chem. Soc. (C)*, **1970**, 515.

(9) A. M. Vuagnat and E. C. Wagner, *J. Chem. Phys.*, **26**, 77 (1957).

(10) W. J. Spillane and G. McGlinchey, *J. Pharm. Sci.*, **70**, 933 (1981).

(11) K. M. Beck, U.S. Pat. 2,785,195 (1957).

(12) L. B. Kier and L. H. Hall, in "Medical Chemistry, Vol. 14: Molecular Connectivity in Chemistry and Drug Research," George de Stevens, Ed., Academic, New York, N.Y., 1976.

(13) B. Unterhalt and L. Boschemeyer, *Z. Lebensm. Unters.-Forsch.*, **161**, 275 (1976).

(14) W. W. Thompson, U.S. Pat. 2,805,124 (1957).

(15) H. Yamaguchi, Japanese Pat. 13,056 (1963).

(16) F. Blicke, H. E. Millson, Jr., and N. J. Doorenbos, *J. Am. Chem. Soc.*, **76**, 2489 (1954).

(17) D. F. Morrison, "Multivariate Statistical Methods," McGraw-Hill, Kogakusha, Japan, 1976, chap. 6.

(18) M. G. Kendall, "A Course in Multivariate Analysis," Griffin, 1961, chap. 9.

(19) W. J. Dixon and M. B. Brown, Eds., BMDP-79. Biomedical Computer Programs; P-Series, University of California Press, 1979.

(20) L. B. Kier and L. H. Hall, *J. Pharm. Sci.*, **70**, 583 (1981).

(21) L. H. Hall and L. B. Kier, *J. Pharm. Sci.*, **66**, 642 (1977).

(22) L. B. Kier, *J. Pharm. Sci.*, **69**, 416 (1980).

ACKNOWLEDGMENTS

The authors wish to thank the National Board for Science and Technology and the Department of Education for grants.

Percutaneous Absorption of Flufenamic Acid in Rabbits: Effect of Dimethyl Sulfoxide and Various Nonionic Surface-Active Agents

CHIAW-CHI HWANG and AUGUST G. DANTI ˣ

Received December 21, 1981, from the *School of Pharmacy, Northeast Louisiana University, Monroe, LA 71209.* Accepted for publication July 14, 1982.

Abstract □ Eight nonionic surface-active agents were each incorporated at a concentration of 10% into a white petrolatum ointment base containing 10% flufenamic acid with or without dimethyl sulfoxide. Percutaneous absorption was studied by determining the plasma concentration of flufenamic acid in New Zealand White rabbits at regular intervals for 8 hr following application of the ointment. The percutaneous absorption of flufenamic acid was significantly increased when sorbitan trioleate, polyoxyl 8 stearate, or polyoxyethylene 2 oleyl ether were added to the ointment containing flufenamic acid and white petrolatum. The percutaneous absorption of flufenamic acid was increased significantly when sorbitan monopalmitate, sorbitan trioleate, polyoxyl 8 stearate, polyoxyethylene 20 cetyl ether, or polyoxyethylene 2 oleyl ether were added to the ointment containing dimethyl sulfoxide, flufenamic acid, and white petrolatum.

Keyphrases □ Flufenamic acid—percutaneous absorption, effect of nonionic surfactants and/or dimethyl sulfoxide □ Dimethyl sulfoxide—effect on the percutaneous absorption of flufenamic acid, synergism with nonionic surfactants □ Surfactants, nonionic—effect on the percutaneous absorption of flufenamic acid, synergism with dimethyl sulfoxide □ Absorption, percutaneous—of flufenamic acid, effect of dimethyl sulfoxide and/or nonionic surfactants

The anti-inflammatory and analgesic actions of flufenamic acid, *N*-(α,α,α-trifluoro-*m*-tolyl)-anthranilic acid, have been reported previously (1–4). The side effects shown on oral administration of flufenamic acid are predominantly GI disorders such as diarrhea, nausea, and vomiting. Cutaneous application of flufenamic acid for rheumatic disorders could have numerous advantages. A highly potent preparation could be used without causing the aforementioned GI disturbances. The active ingredients diffuse directly through the skin at the application site, and the concentration of the active ingredients in the subcutis and the superficial musculature are considerably higher with a longer duration of action than after oral administration. Percutaneous absorption of flufenamic acid and the resulting anti-inflammatory activity has been shown using animal and human models (5–10).

The use of dimethyl sulfoxide as a penetrant carrier has been suggested (11). Stoughton *et al.* (12, 13) reported that dimethyl sulfoxide increased the rate of penetration of naphazoline hydrochloride, hexopyrronium bromide, and fluocinolone acetonide through the human skin. Dimethyl sulfoxide also has been found to accelerate the penetration of water (14), hydrocortisone, and testosterone (15) through the skin *in vivo*.

Surfactants are one of the most important groups of adjuvants in pharmaceutical preparations. For topically applied preparations, surfactant-induced dissolution or emulsification of active ingredients and changes in ointment viscosity may modify the absorption process. Higuchi (16) suggested that the surfactants generally possess a particular affinity for membranous structure. As a result of this affinity, a nonionic surfactant could possibly emulsify the sebum, enhance the thermodynamic activity of drugs, or change the diffusion constant and activity coefficient of drugs, all of which would permit easier penetration of the drug into the cells.

Shen *et al.* (17) studied the effects of 15 nonionic surfactants on the percutaneous absorption of salicylic acid in white petrolatum containing dimethyl sulfoxide. They found that the plasma salicylate levels in rabbits were increased significantly when sorbitan trioleate, sorbitan monopalmitate, poloxamer 231, poloxamer 182, polyoxyethylene 4 lauryl ether, polyoxyethylene 2 oleyl ether, or polyoxyl 8 stearate was added to the ointment. As a continuation of this work, the effect of selected nonionic surfactants on the percutaneous absorption of flufenamic acid in the presence of dimethyl sulfoxide was studied in rabbits.

EXPERIMENTAL

Materials—The following ointments were used: 10% flufenamic acid[1] in white petrolatum[2], 10% flufenamic acid plus 5% dimethyl sulfoxide[3] in white petrolatum, 10% flufenamic acid plus 10% surfactant in white petrolatum, and 10% flufenamic acid plus 10% surfactant plus 5% dimethyl sulfoxide in white petrolatum. The nonionic surfactants selected [with hydrophilic–lipophilic balance (HLB) values in brackets] were sorbitan monopalmitate[4] [6.7], sorbitan trioleate[5] [1.8], polyoxyl 8 stearate[6] [11.1], polyoxyl 40 stearate[7] [16.9], polyoxyethylene 20 cetyl ether[8] [15.7], polyoxyethylene 2 oleyl ether[9] [4.9], poloxamer 184[10] [15], and poloxamer 231[11] [2]. The absorption of topically applied flufenamic acid was compared for white petrolatum preparations containing the acid (with or without dimethyl sulfoxide) *versus* the acid (with or without dimethyl sulfoxide) plus a surfactant.

Ointment Preparation—Flufenamic acid, in a fine powder form, was dried at 50° in a heated vacuum desiccator for at least 48 hr before use. The prepared ointments contained 10% (w/w) flufenamic acid and 10% (w/w) surfactant with or without 5% dimethyl sulfoxide. Each ingredient was weighed on an analytical balance[12] and incorporated into the white petrolatum by the fusion method.

Test Animals—Each ointment was applied to the skin of a New Zealand white rabbit weighing 3.3–4.3 kg. Each rabbit was used four times and received the same group of surfactants in each test. Not more than three rabbits were utilized during any one experimental day, due to space and time limitations. The rabbits receiving ointments containing dimethyl sulfoxide for the first test run received the ointment without dimethyl sulfoxide for the second run and *vice versa*, with a 7-day rest period before reapplication. The animals were offered food[13] and water *ad libitum* and were housed individually in an animal room maintained

[1] Reagent grade, lot 0715KE; Aldrich Chemical Co.
[2] Reagent grade, lot 5M05; Matheson Coleman & Bell.
[3] Reagent grade, lot 755838; Fisher Scientific Co.
[4] Span 40; Atlas.
[5] Span 85; Atlas.
[6] Myrj 45; Atlas.
[7] Myrj 52; Atlas.
[8] Brij 58; Atlas.
[9] Brij 93; ICI.
[10] Pluronic L64; Wyandotte.
[11] Pluronic L81; Wyandotte.
[12] Model EA-1; Torsion Balance Co., Clifton, N.J.
[13] Purina rabbit chow; Ralston-Purina Co., St. Louis, Mo.

0022-3549/83/0800-0857$01.00/0

Table I—AUC_{0-8} for Plasma Concentration(s) of Flufenamic Acid *Versus* Time for Formulations With and Without Dimethyl Sulfoxide [a]

Surfactant	I [b]	II [c]
None	7.400 ± 1.332	21.784 ± 4.369
Sorbitan monopalmitate	5.421 ± 0.730	38.721 ± 1.016
Sorbitan trioleate	38.511 ± 12.976	123.194 ± 1.096
Polyoxyl 8 stearate	16.532 ± 4.131	64.462 ± 3.662
Polyoxyl 40 stearate	7.456 ± 0.373	11.751 ± 0.254
Polyoxyethylene 20 cetyl ether	1.789 ± 0.266	37.753 ± 5.044
Polyoxyethylene 2 oleyl ether	23.066 ± 8.460	109.314 ± 19.114
Poloxamer 184	2.610 ± 0.610	10.023 ± 0.608
Poloxamer 231	8.455 ± 2.749	26.384 ± 6.538

[a] Percutaneous absorption in rabbits; average of three determinations. [b] Flufenamic acid, surfactant, and white petrolatum. [c] Flufenamic acid, surfactant, dimethyl sulfoxide, and white petrolatum.

at a temperature of 25°. Fifteen to eighteen hours prior to the application of the ointment, the hair was removed from the back of the rabbit (8 × 12-cm^2 area) with an animal clipper[14] and depilatory cream[15]. The skin was examined under low-power magnification for damage resulting from the shaving procedure, and the animal was not used if the skin barrier was disrupted.

Application of Ointment—The rabbits were immobilized in a rack (stock) during treatment to prevent them from ingesting the ointment after application. The selected ointment was uniformly spread over the shaved back in a variety of doses (1 g ointment/kg). The ointment remained in contact with the skin for 8 hr, during which time the rabbit did not receive food or water.

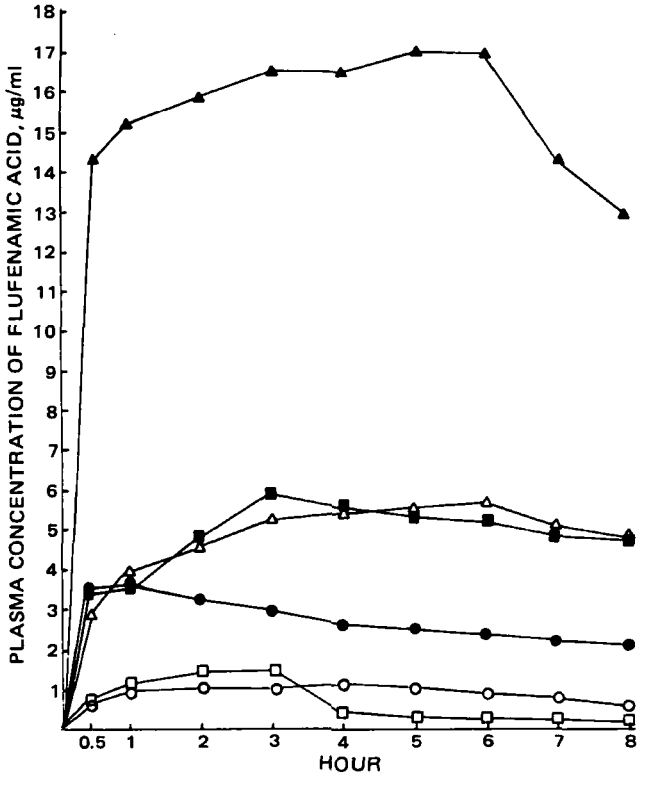

Figure 1—*Effect of sorbitan surfactants on the percutaneous absorption of flufenamic acid with or without dimethyl sulfoxide. Flufenamic acid in white petrolatum (○) with (□) sorbitan monopalmitate, (△) sorbitan trioleate, (●) dimethyl sulfoxide, (■) sorbitan monopalmitate plus dimethyl sulfoxide, and (▲) sorbitan trioleate plus dimethyl sulfoxide.*

[14] Oster Co.
[15] Neet; Whitehall Laboratory Inc., New York, N.Y.

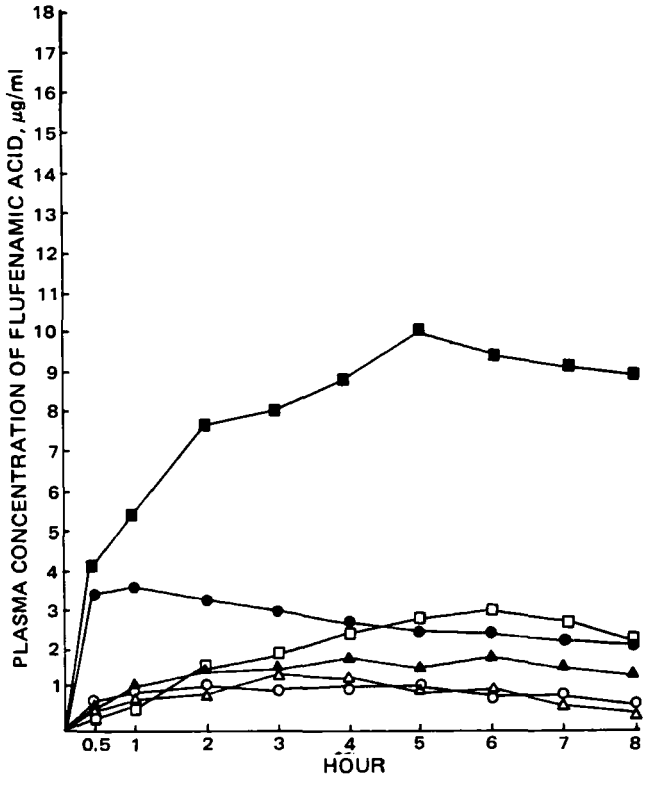

Figure 2—*Effect of polyoxyethylene ester surfactants on the percutaneous absorption of flufenamic acid with or without dimethyl sulfoxide. Flufenamic acid in white petrolatum (○) with (□) polyoxyl 8 stearate, (△) polyoxyl 40 stearate, (●) dimethyl sulfoxide, (■) polyoxyl 8 stearate plus dimethyl sulfoxide, and (▲) polyoxyl 40 stearate plus dimethyl sulfoxide.*

Procedure of Sample Collection—Blood samples were collected and analyzed for flufenamic acid. One-half milliliter of blood was withdrawn from the marginal ear vein of the rabbit prior to application of the ointment, at 0.5 hr after ointment application, and at hourly intervals for 8 hr after application. The blood was collected with a sterile 26-gauge, 0.9-cm needle[16] in a 1-ml disposable tuberculin syringe containing 0.05 ml of sodium heparin[17]. This blood–heparin mixture was placed in a 15-ml glass-stoppered centrifuge tube containing 0.5 ml of 0.2 *M* acetate buffer and 6 ml of ethyl acetate.

The concentration of flufenamic acid was analyzed using the spectrofluorometric[18] method described by Hattori *et al.* (18). Concentrations were determined using a standard curve obtained by analysis of heparinized (0.05 ml) blood samples with added known amounts of flufenamic acid. The plasma sample obtained from each rabbit prior to the drug application was used as a blank to determine the background fluorescence for that animal.

Statistical Analysis of Data—Three replications were made of each determination. A *t* test with four degrees of freedom at the 95% significance level was used to test the null hypothesis.

RESULTS AND DISCUSSION

The altered percutaneous absorption patterns of flufenamic acid obtained on the addition of surfactants to flufenamic acid, with or without dimethyl sulfoxide, in white petrolatum ointments are shown in Figs. 1–4. The areas under the curves (AUC) for the plasma concentration of flufenamic acid *versus* time of the different treatments were evaluated from 0 to 8 hr postdose (AUC_{0-8}) using the trapezoidal rule (Table I). The *t* test results for the comparison of the AUC_{0-8} between flufenamic acid (with or without dimethyl sulfoxide) plus a surfactant and flufenamic acid (with or without dimethyl sulfoxide) are shown in Table II.

Statistical analyses of the results of this study indicated that some of the surfactants functioned as penetrant carriers, enhancing the percu-

[16] Lot No. 327322, Sherwood Medical Industries Inc.
[17] 10,000 U/ml, lot No. 4CS09A; Eli Lilly & Co.
[18] Spectrophotofluorometer, Serial No. D223-62155; American Instrument Co., Silver Spring, Md.

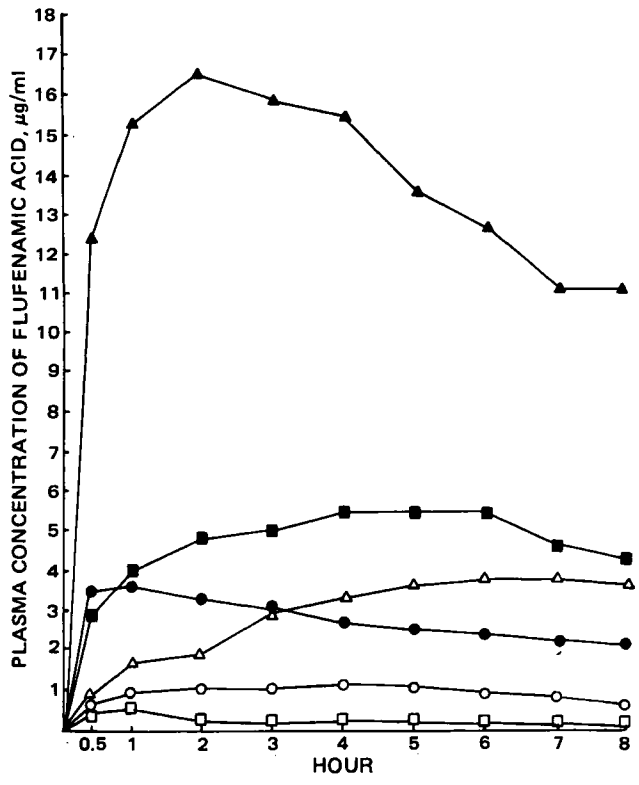

Figure 3—*Effect of polyoxyethylene surfactants on the percutaneous absorption of flufenamic acid with or without dimethyl sulfoxide. Flufenamic acid in white petrolatum (○) with (□) polyoxyethylene 20 cetyl ether, (△) polyoxyethylene 2 oleyl ether, (■) polyoxyethylene 20 cetyl ether plus dimethyl sulfoxide, (▲) polyoxyethylene 2 oleyl ether plus dimethyl sulfoxide, and (●) dimethyl sulfoxide.*

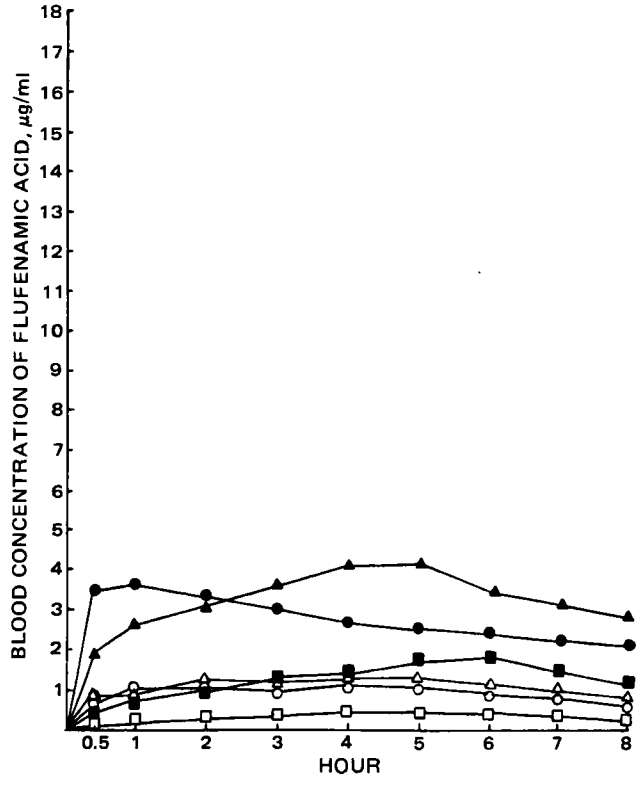

Figure 4—*Effect of poloxamer surfactants on the percutaneous absorption of flufenamic acid with or without dimethyl sulfoxide. Flufenamic acid in white petrolatum (○) with (□) poloxamer 184, (△) poloxamer 231, (●) dimethyl sulfoxide, (■) poloxamer 184 plus dimethyl sulfoxide, and (▲) poloxamer 231 plus dimethyl sulfoxide.*

taneous absorption of flufenamic acid. When these surfactants were added to an ointment containing flufenamic acid and dimethyl sulfoxide, percutaneous absorption of flufenamic acid was significantly increased throughout the 8-hr experimental period. The data suggest that this was a synergistic effect between the surfactant and dimethyl sulfoxide.

The percutaneous absorption of flufenamic acid was increased when dimethyl sulfoxide was added to the ointment. Since dimethyl sulfoxide (11) and flufenamic acid have been used alone in the treatment of musculoskeletal disorders, it was deemed worthwhile to conduct a further pharmacological study using concomitant cutaneous application of these two substances.

Dimethyl sulfoxide exhibited an unusual concentration dependence. Some investigators have pointed out that at least 60% dimethyl sulfoxide was required for a measurable permeability change in the skin (19). In this study, the percutaneous absorption of flufenamic acid was increased significantly by the addition of 5% dimethyl sulfoxide. The lower percutaneous absorption of flufenamic acid with certain surfactants may be due to the lowering of the thermodynamic activity of flufenamic acid by complexation or by other interactions with the skin (20) or by miceller trapping of the active ingredient (21).

Both the mechanism by which the percutaneous absorption of flufenamic acid is increased on addition of nonionic surfactants in the presence of dimethyl sulfoxide and the mechanism of action of dimethyl sulfoxide itself are unknown. However, it can be concluded that ultrastructural modifications of the stratum corneum caused by dimethyl sulfoxide and/or the surfactants, associated with altered skin permeability (22) do occur. Higuchi (16) suggested that the activity coefficient plays a major role in percutaneous absorption. Flufenamic acid may be held firmly by the white petrolatum, which exhibits a low activity coefficient. When dimethyl sulfoxide and the surfactants are added to the flufenamic acid in white petrolatum, the release rate of flufenamic acid could be increased by forming high activity coefficient complexes such as dimethyl sulfoxide–drug, surfactant–drug, or dimethyl sulfoxide–surfactant–drug.

Table II—*t* Test Comparisons of AUC_{0-8} for Plasma Concentrations of Flufenamic Acid for Formulations With *Versus* Without Surfactant [a]

Surfactant	I[b]	II[c]
Sorbitan monopalmitate	2.256[d]	6.543[e]
Sorbitan trioleate	4.131[e]	39.009[e]
Polyoxyl 8 stearate	3.644[e]	12.970[e]
Polyoxyl 40 stearate	0.070	3.972[d]
Polyoxyethylene 20 cetyl ether	7.155[d]	4.145[e]
Polyoxyethylene 2 oleyl ether	3.169[e]	7.732[e]
Poloxamer 184	5.663[d]	4.620[d]
Poloxamer 231	0.598	1.013

[a] $t = 5.457$ for the comparison of flufenamic acid in white petrolatum with *versus* without dimethyl sulfoxide. [b] Flufenamic acid in white petrolatum with *versus* without surfactant. [c] Flufenamic acid plus dimethyl sulfoxide in white petrolatum with *versus* without surfactant. [d] Statistically significantly less, $p < 0.05$. [e] Statistically significantly greater, $p < 0.05$.

REFERENCES

(1) E. L. Coodley, *West. J. Med.*, **4**, 228 (1963).

(2) P. Young, *Arthritis Rheum.*, **6**, 307 (1963).

(3) M. R. Simpson, N. R. W. Simpson, and H. C. Masheter, *Ann. Phys. Med.*, **8**, 208 (1966).

(4) C. A. Winter, *Int. Congr. Ser.—Excerpta Med.*, **82**, 190 (1966).

(5) P. Panse, P. Zeiller, and K. H. Sensch, *Arzneim.-Forsch.*, **21**, 1605 (1971).

(6) P. Panse, P. Zeiller, and K. H. Sensch, *Arzneim.-Forsch.*, **24**, 1298 (1974).

(7) E. St. von Batky, *Fortschr. Med.*, **90**, 1121 (1972).

(8) H. Feldmann, K. Kimiai, C. Fondermann, M. Haas, and R. Herwig, *Med. Monatsschr.*, **29**, 406 (1975).

(9) P. Fotiades and G. L. Bach, *Fortschr. Med.*, **94**, 1036 (1976).

(10) H. G. Jäckle, *Dtsch. Med. J.*, **23**, 245 (1972).

(11) S. W. Jacob, M. Bischel, and R. J. Herschler, *Curr. Ther. Res.*, **6**, 134 (1964).
(12) R. B. Stoughton and W. Fritsch, *Arch. Dermatol.*, **90**, 512 (1965).
(13) R. B. Stoughton, *Arch. Dermatol.*, **91**, 657 (1965).
(14) H. Baker, *J. Invest. Dermatol.*, **50**, 283 (1968).
(15) H. I. Maibach and R. J. Feldmann, *Ann. N.Y. Acad. Sci.*, **141**, 423 (1976).
(16) T. Higuchi, Presented to the Society of Cosmetic Chemists, Seminar, New York, N.Y., Sept. 23, 1959.
(17) W. Shen, A. G. Danti, and F. N. Bruscato, *J. Pharm. Sci.*, **65**, 1780 (1976).
(18) Y. Hattori, T. Arai, T. Mori, and E. Fujihira, *Chem. Pharm. Bull.*, **18**, 1063 (1970).
(19) T. M. Sweeney, A. M. Downes, and A. G. Matoltsy, *J. Invest. Dermatol.*, **46**, 300 (1966).
(20) Z. T. Chowhan and R. Pritchard, *J. Pharm. Sci.*, **67**, 1272 (1978).
(21) H. Shinkai and I. Tanaka, *J. Pharm. Soc. (Jpn)*, **89**, 1283 (1969).
(22) M. Mezei and A. K. Y. Lee, *J. Pharm. Sci.*, **59**, 858 (1970).

ACKNOWLEDGMENTS

Abstracted in part from a dissertation submitted by Chiaw-Chi (George) Hwang to the School of Pharmacy, Northeast Louisiana University, in partial fulfillment of the Master of Science degree requirements.

Steady-State Determination of the Contribution of Lung Metabolism to the Total Body Clearance of Drugs: Application to Carbamazepine

PETER J. WEDLUND, SHIH-LING CHANG, and RENÉ H. LEVY[x]

Received January 7, 1982, from the *Departments of Pharmaceutics and Neurological Surgery, Schools of Pharmacy and Medicine, University of Washington, Seattle, WA 98195.* Accepted for publication July 8, 1982.

Abstract □ A steady-state approach is proposed to examine the contribution that the lung makes to the total body elimination of medium- to high-clearance drugs. Carbamazepine, a potential candidate of pulmonary metabolism, was investigated by infusion into the femoral vein in seven unrestrained Sprague–Dawley rats (250–300 g). Blood samples (0.45 ml), taken simultaneously from the jugular vein and carotid artery in each rat during the infusion (2–5 days), were assayed in duplicate for carbamazepine by GLC/CI/MS. Venous blood concentrations were used to calculate the total body clearance of carbamazepine, 440 ± 38 ml/hr (mean ± *SEM*), and the difference between simultaneous venous and arterial blood concentrations were used to calculate the extraction ratio of carbamazepine by the lung. The mean extraction ratio of 0.0058 (n = 28) suggests that the lung only contributes ~5% to the total body clearance of carbamazepine. It is proposed that this technique could be useful in examining the importance of the lung in the total body clearance of other drugs, and that it has several advantages over some currently used techniques.

Keyphrases □ Carbamazepine—elimination *via* pulmonary metabolism in the rat, steady-state determination □ Metabolism, pulmonary—of carbamazepine in the rat, steady-state determination of drug elimination *via* the lungs □ Drug clearance—contribution to lung metabolism, steady-state determination using carbamazepine in the rat

Numerous articles and reviews have appeared over the last 10 years establishing the xenobiotic-metabolizing capability of *in vitro* lung preparations (1–5). However, the extrapolation of *in vitro* data on pulmonary metabolism to drug elimination by the lungs *in vivo* is fraught with difficulties and limitations (6–8). Several approaches are available for quantitation of lung metabolism *in vivo*, including isolated lung perfusion (6–9), ratios of area under the curve following venous and arterial bolus doses (10), and measurement of the extraction of drug across the lung at steady state (11). While each approach has advantages and disadvantages, measurement of drug extraction across the lung following achievement of steady-state drug levels constitutes a reliable and convenient method of delineating the contribution of the lung to the total body clearance of drugs. In the present study, the steady-state approach was used in rats to investigate the possible contribution of the lung to the total body clearance of the antiepileptic drug,

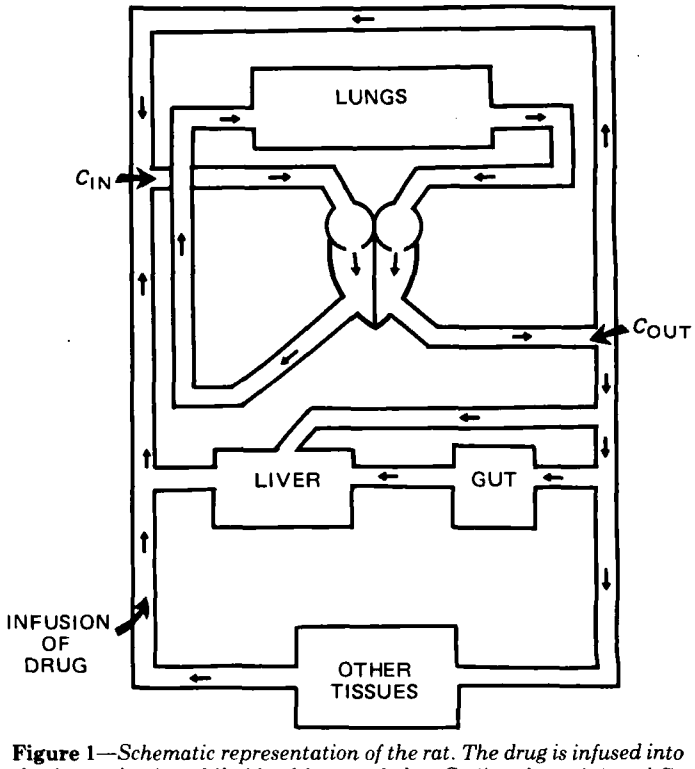

Figure 1—*Schematic representation of the rat. The drug is infused into the femoral vein, while blood is sampled at* C_i *(jugular vein) and* C_o *(carotid artery).* $CL_L = Q_B \times ER$ *[lung clearance = lung blood flow ×* $(C_i - C_o)/C_i$*].*

0022-3549/83/0800-0860$01.00/0

(11) S. W. Jacob, M. Bischel, and R. J. Herschler, *Curr. Ther. Res.*, **6**, 134 (1964).
(12) R. B. Stoughton and W. Fritsch, *Arch. Dermatol.*, **90**, 512 (1965).
(13) R. B. Stoughton, *Arch. Dermatol.*, **91**, 657 (1965).
(14) H. Baker, *J. Invest. Dermatol.*, **50**, 283 (1968).
(15) H. I. Maibach and R. J. Feldmann, *Ann. N.Y. Acad. Sci.*, **141**, 423 (1976).
(16) T. Higuchi, Presented to the Society of Cosmetic Chemists, Seminar, New York, N.Y., Sept. 23, 1959.
(17) W. Shen, A. G. Danti, and F. N. Bruscato, *J. Pharm. Sci.*, **65**, 1780 (1976).
(18) Y. Hattori, T. Arai, T. Mori, and E. Fujihira, *Chem. Pharm. Bull.*, **18**, 1063 (1970).
(19) T. M. Sweeney, A. M. Downes, and A. G. Matoltsy, *J. Invest. Dermatol.*, **46**, 300 (1966).
(20) Z. T. Chowhan and R. Pritchard, *J. Pharm. Sci.*, **67**, 1272 (1978).
(21) H. Shinkai and I. Tanaka, *J. Pharm. Soc. (Jpn)*, **89**, 1283 (1969).
(22) M. Mezei and A. K. Y. Lee, *J. Pharm. Sci.*, **59**, 858 (1970).

ACKNOWLEDGMENTS

Abstracted in part from a dissertation submitted by Chiaw-Chi (George) Hwang to the School of Pharmacy, Northeast Louisiana University, in partial fulfillment of the Master of Science degree requirements.

Steady-State Determination of the Contribution of Lung Metabolism to the Total Body Clearance of Drugs: Application to Carbamazepine

PETER J. WEDLUND, SHIH-LING CHANG, and RENÉ H. LEVY[x]

Received January 7, 1982, from the *Departments of Pharmaceutics and Neurological Surgery, Schools of Pharmacy and Medicine, University of Washington, Seattle, WA 98195.* Accepted for publication July 8, 1982.

Abstract □ A steady-state approach is proposed to examine the contribution that the lung makes to the total body elimination of medium- to high-clearance drugs. Carbamazepine, a potential candidate of pulmonary metabolism, was investigated by infusion into the femoral vein in seven unrestrained Sprague–Dawley rats (250–300 g). Blood samples (0.45 ml), taken simultaneously from the jugular vein and carotid artery in each rat during the infusion (2–5 days), were assayed in duplicate for carbamazepine by GLC/CI/MS. Venous blood concentrations were used to calculate the total body clearance of carbamazepine, 440 ± 38 ml/hr (mean ± *SEM*), and the difference between simultaneous venous and arterial blood concentrations were used to calculate the extraction ratio of carbamazepine by the lung. The mean extraction ratio of 0.0058 (n = 28) suggests that the lung only contributes ~5% to the total body clearance of carbamazepine. It is proposed that this technique could be useful in examining the importance of the lung in the total body clearance of other drugs, and that it has several advantages over some currently used techniques.

Keyphrases □ Carbamazepine—elimination *via* pulmonary metabolism in the rat, steady-state determination □ Metabolism, pulmonary—of carbamazepine in the rat, steady-state determination of drug elimination *via* the lungs □ Drug clearance—contribution to lung metabolism, steady-state determination using carbamazepine in the rat

Numerous articles and reviews have appeared over the last 10 years establishing the xenobiotic-metabolizing capability of *in vitro* lung preparations (1–5). However, the extrapolation of *in vitro* data on pulmonary metabolism to drug elimination by the lungs *in vivo* is fraught with difficulties and limitations (6–8). Several approaches are available for quantitation of lung metabolism *in vivo*, including isolated lung perfusion (6–9), ratios of area under the curve following venous and arterial bolus doses (10), and measurement of the extraction of drug across the lung at steady state (11). While each approach has advantages and disadvantages, measurement of drug extraction across the lung following achievement of steady-state drug levels constitutes a reliable and convenient method of delineating the contribution of the lung to the total body clearance of drugs. In the present study, the steady-state approach was used in rats to investigate the possible contribution of the lung to the total body clearance of the antiepileptic drug,

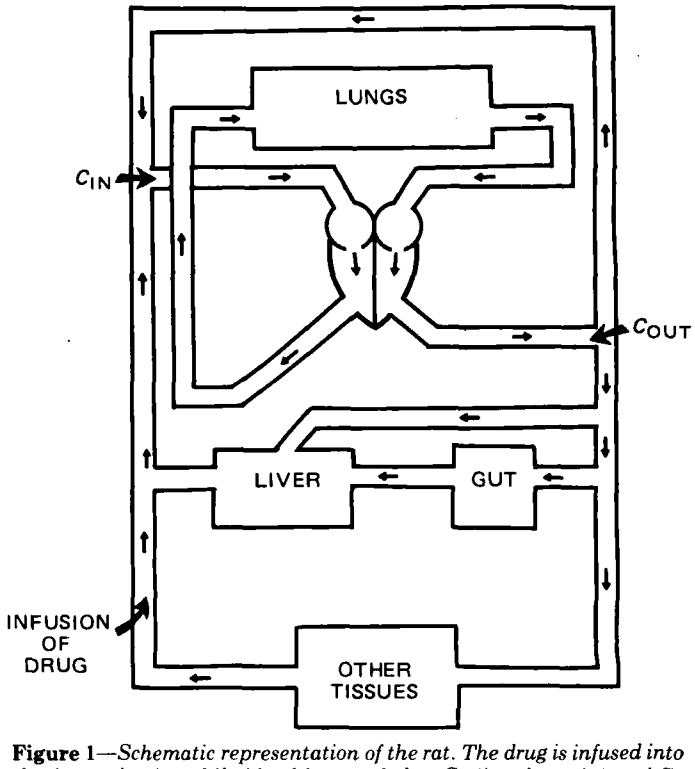

Figure 1—*Schematic representation of the rat. The drug is infused into the femoral vein, while blood is sampled at* C_i *(jugular vein) and* C_o *(carotid artery).* $CL_L = Q_B \times ER$ *[lung clearance = lung blood flow ×* $(C_i - C_o)/C_i$*].*

0022-3549/83/0800-0860$01.00/0

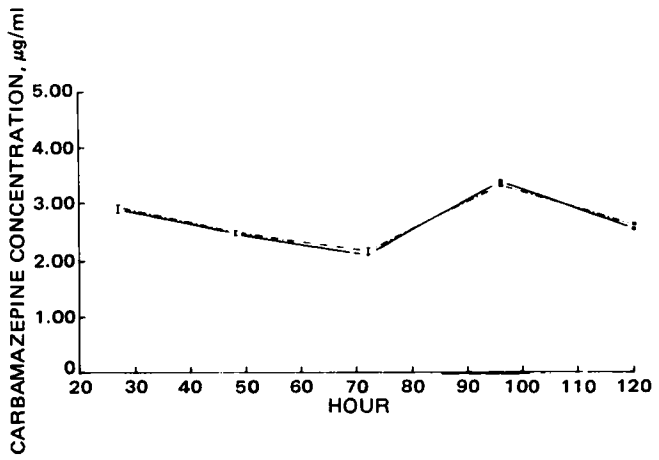

Figure 2—*Arterial (—) and venous (- - -) carbamazepine blood levels in rat 13 during a long-term carbamazepine infusion.*

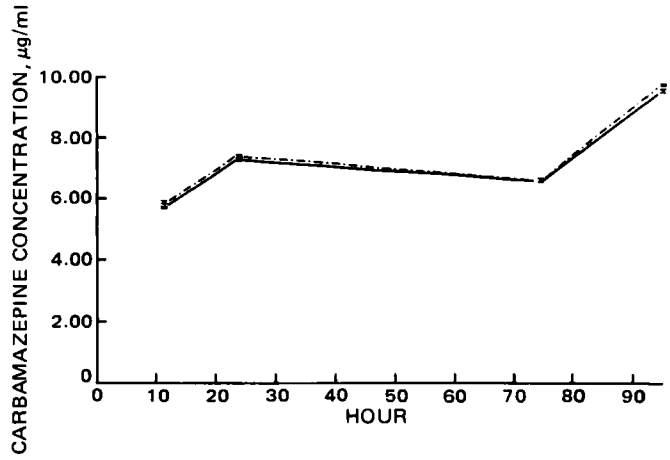

Figure 3—*Arterial (—) and venous (- - -) carbamazepine blood levels in rat 27 during a long-term carbamazepine infusion.*

carbamazepine. Carbamazepine has a large total body clearance in rats with a very small fraction (2%) eliminated unchanged in urine (12–14). Also, the reported clearance of carbamazepine in rat liver perfusions is too low to account for the large total body clearance observed (15, 16). Therefore, the potential contribution of the lungs to carbamazepine elimination was investigated.

THEORETICAL

Based on mass balance principles, the clearance of a drug by an organ can be defined by the relationship:

$$CL_o = Q_B \times ER = Q_B \times \frac{C_i - C_o}{C_i} \quad \text{(Eq. 1)}$$

where CL_o is the organ clearance, Q_B is the blood flow through the organ, and ER, estimated from the blood concentration before (C_i) and after (C_o) the organ circulation, represents the extraction ratio of the drug across the organ (17, 18). By placing cannulas in the jugular vein and carotid artery, one can measure the change in drug levels across the heart and lungs (Fig. 1). With the assumption that the heart does not metabolize the drug, one can calculate the pulmonary clearance of the drug at steady state using Eq. 1.

EXPERIMENTAL

Materials—Infusion solutions of carbamazepine (5 mg/ml) were made by dissolving the drug in 60% polyethylene glycol 400. The solutions were filtered and autoclaved before use. Harnesses and swivel joints for long-term infusions in unrestrained rats were purchased[1]. Constant-rate infusion pumps[2] were used for drug delivery. Cannulas were made of a short piece of silicone tubing[3] (for insertion into the veins and artery) connected to a longer section of polyethylene-50 tubing. Ether (USP grade) was used as the anesthetic.

Animals—Seven male Sprague–Dawley rats (250–300 g) were cannulated under ether anesthesia. Cannulations were performed on the right carotid artery and jugular vein for blood sampling and on the femoral vein for drug infusion. The polyethylene-50 section of the cannula was run subcutaneously beneath the skin and out through a small incision in the back of the neck. All operations were performed under aseptic conditions using sterilized instruments and cannulas. Rats were then attached for unrestrained long-term infusions using previously described methods (19–21).

Following the operation, animals were infused with sterile saline for 3 days. During this time, the carotid artery and jugular vein cannulas were flushed once a day with sterile saline solution (without heparin) to prevent blood clotting in the line.

[1] Instech Laboratories, Pittsburg, Pa.
[2] Sage pump models 352 and 355. Harvard pump model 2620.
[3] Silastic Medical-Grade tubing, i.d. 0.020 in., o.d. 0.037 in., Dow-Corning, Midland, Mich.

Drug Treatment and Blood Sampling—Three days after the cannula implantation, the rats were started on a carbamazepine infusion (0.25–0.30 ml/hr). Blood samples (0.45 ml) were drawn simultaneously from jugular vein and carotid artery once every 12–24 hr after the beginning of the infusion. The blood was frozen immediately and maintained at −20° until assayed.

Analytical Procedure—Whole blood (200 µl) was assayed for carbamazepine using a GLC/CI/MS assay developed in this laboratory (22). Each sample was assayed in duplicate, and the average values were used for all calculations.

RESULTS AND DISCUSSION

The concentration–time profiles of carbamazepine from jugular vein and carotid artery blood samples in rats 13 and 27 are shown in Figs. 2 and 3, respectively. Little, if any, difference in carbamazepine blood levels were found between these sampling sites.

A plot of the arterial *versus* venous carbamazepine blood levels for 28 simultaneous samples in all seven rats is given in Fig. 4. Theoretically, any slope from zero (reflecting complete extraction) to 1.0 (no pulmonary extraction) could result. The slope of 0.992 (not significantly different than 1.0) suggests very little or no carbamazepine elimination during passage through the pulmonary circulation.

The mean (± *SEM*) extraction ratio of carbamazepine by the lung was 0.0058 (±0.004) based on the 28 pairs of arterial–venous blood levels. Assuming a mean cardiac output of 62.5 ml/min in rats (23–25), the average lung clearance of carbamazepine would be approximately 22 ml/hr. The total body clearance of the drug (CL_T) was calculated using the infusion rate (Ko) and steady-state concentration (C_v) in the venous blood:

$$CL_T = \frac{Ko}{C_v} \quad \text{(Eq. 2)}$$

Based on a mean (± *SEM*) total body clearance of carbamazepine of 440 (± 38) ml/hr, the lung appears to contribute only ~5% to the total elimination of carbamazepine *in vivo*. The lack of significant lung metabolism of carbamazepine and the failure of liver perfusion experiments to account for its large total body clearance suggest either the presence of some other extrahepatic sites of drug metabolism or an error in the total liver clearance of carbamazepine determined by liver perfusion.

While the steady-state approach may be a useful technique to quantitate the role that lung metabolism plays in the total body clearance of drugs, several aspects of the present study design need further consideration before an appreciation can be gained for the limits of this approach. The blood flow through the pulmonary circulation is 3–4 times larger than the blood flow through other organs that are capable of drug elimination. Hence, even a small drug extraction ratio by the lungs can contribute significantly to the total elimination of a drug. To measure a potentially small pulmonary extraction ratio of a drug, a very sensitive and accurate assay is required in addition to a large number of samples. These problems were overcome in the present experiment by: (*a*) the use of a GLC/CI/MS assay for carbamazepine with a median percent difference between duplicate determinations of only 1.4% and (*b*) the inclusion of 28 pairs of observations from a group of seven rats.

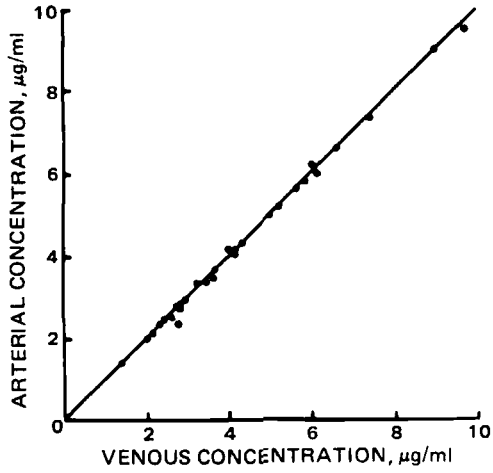

Figure 4—*Relationship between venous and arterial carbamazepine blood levels during long-term infusions in seven rats. The slope is 0.992 (not significantly different than 1.000);* $R^2 = 0.997$.

Despite the need for an accurate and reproducible assay, the steady-state approach has several advantages over other available techniques for quantitating the importance of lung metabolism. First, it does not require measuring the amounts of metabolites formed by the lung. This may be advantageous, from an analytical point of view, when there are a large number of potential metabolites which could be formed or novel metabolites specific to lung metabolism. Second, it allows a quantitation of the contribution of the lung to the total body clearance of drugs in the intact animal rather than under low pulmonary blood flow rates or other conditions optimal to *in vitro* systems. Third, it eliminates problems of intraanimal variability in drug metabolism (a potential problem with single bolus doses given by different routes) by using instantaneous differences in blood levels. Fourth, the contribution of lung metabolism to the total body clearance of drugs can be determined at drug concentrations of therapeutic importance.

The results of this study suggest that the steady-state approach can be a reliable and simple means of quantitating the contribution of lung metabolism to the total body clearance of drugs. This may be particularly important for drugs that are metabolized extensively, and where significant extrahepatic elimination is suspected. In addition, the steady-state approach can be a useful and direct means for examining the role of pulmonary metabolism for medium- to high-clearance drugs or model compounds which, based on other approaches, are postulated or appear to undergo significant lung metabolism.

Finally, it should be noted that although a number of substances are metabolized by isolated perfused lungs or lung homogenates (26, 27), little work has been directed toward quantitating the importance of lung metabolism to the total body clearance of these substances (11, 28). Despite the role played by lung metabolism in lung cancer and its induction by cigarette smoke (29–32), the importance of pulmonary metabolism in the overall elimination of drugs and its potential for producing toxic metabolites has only just begun to be appreciated (28, 33).

ADDENDUM

Following submission of this manuscript for publication, a theoretical treatment of the importance of lung metabolism to total body clearance by Collins and Dedrick was published (34).

REFERENCES

(1) W. W. Oppelt, M. Zange, W. E. Ross, and H. Remmer, *Res. Commun. Chem. Path. Pharmacol.*, **1**, 43 (1970).

(2) T. E. Gram, *Drug Metab. Rev.*, **2**, 1 (1973).

(3) E. A. B. Brown, *Drug Metab. Rev.*, **3**, 33 (1974).

(4) C. L. Litterst, E. G. Mimnaugh, R. L. Reagan, and T. E. Gram, *Drug. Metab. Dispos.*, **3**, 259 (1975).

(5) G. E. R. Hook and J. R. Bend, *Life Sci.*, **18**, 279 (1976).

(6) T. C. Orton, M. W. Anderson, R. D. Pickett, T. E. Eling, and J. R. Fouts, *J. Pharmacol. Exp. Ther.*, **188**, 482 (1973).

(7) F. C. P. Law, T. E. Eling, J. R. Bend, and J. R. Fouts, *Drug Metab. Dispos.*, **2**, 433 (1974).

(8) D. A. Wiersma and R. A. Roth, *J. Pharmacol. Exp. Ther.*, **212**, 97 (1980).

(9) B. Liseman, L. Bryant, and T. Waltuch, *J. Thorac. Cardiovas. Surg.*, **48**, 798 (1969).

(10) M. K. Cassidy and J. B. Houston, *J. Pharm. Pharmacol.*, **32**, 57 (1980).

(11) G. K. Gourlay, L. E. Mather, and K. S. Parkin, *Drug Metab. Dispos.*, **8**, 452 (1980).

(12) K. M. Baker, J. Csetenyi, A. Frigerio, and P. L. Morselli, *J. Med. Chem.*, **16**, 302 (1973).

(13) A. Frigerio and P. L. Morselli, *Adv. Neurol.*, **11**, 279 (1975).

(14) M. Theisohn, M. Sigmund, G. Heimann, and B. Roth, *Epilepsia*, **20**, 182 (1979).

(15) A. Rane, D. G. Shand, and G. R. Wilkinson, *Drug Metab. Dispos.*, **5**, 179 (1977).

(16) A. Rane, G. R. Wilkinson, and D. G. Shand, *J. Pharmacol. Exp. Ther.*, **200**, 420 (1977).

(17) M. Rowland, L. Z. Benet, and G. G. Graham, *J. Pharmacokinet. Biopharm.*, **1**, 123 (1973).

(18) G. R. Wilkinson and D. G. Shand, *Clin. Pharmacol. Ther.*, **18**, 377 (1975).

(19) A. N. Epstein and P. Teitelbaum, *J. Appl. Physiol.*, **17**, 171 (1962).

(20) D. W. Thomas and J. Mayer, *Physiol. Behav.*, **3**, 499 (1968).

(21) A. B. Steffens, *Physiol. Behav.*, **4**, 833 (1969).

(22) W. F. Trager, R. H. Levy, I. H. Patel, and J. M. Neal, *Anal. Lett.*, **B11**, 119 (1978).

(23) R. A. Roth and R. J. Rubin, *Drug Metab. Dispos.*, **4**, 460 (1976).

(24) A. S. Nies, G. R. Wilkinson, B. D. Rush, J. T. Strother, and D. G. McDevitt, *Biochem. Pharmacol.*, **25**, 1991 (1976).

(25) M. S. Yates, C. R. Hiley, P. J. Roberts, D. J. Back, and F. E. Crawford, *Biochem. Pharmacol.*, **27**, 2617 (1978).

(26) E. Whitnack, D. R. Knapp, J. C. Holmes, N. O. Fowler, and T. E. Gaffney, *J. Pharmacol. Exp. Ther.*, **181**, 288 (1972).

(27) D. M. Kornhauser, R. E. Vestal, and D. G. Shand, *Pharmacology*, **20**, 275 (1980).

(28) R. A. Roth and D. A. Wiersma, *Clin. Pharmacokinet.*, **4**, 355 (1979).

(29) P. L. Grover, A. Hewer, and P. Sims, *FEBS Lett.*, **34**, 63 (1973).

(30) H. Vadi, B. Jernström, and S. Orrenius, in "Carcinogenesis," R. I. Freudenthal and P. W. Jones, Eds., Raven, New York, N.Y. 1976, p. 45.

(31) K. Vahakangas, K. Nevasaari, O. Pelkonen, and N. T. Karki, *Acta Pharmacol. Toxicol.*, **41**, 129 (1977).

(32) R. E. Kouri, L. H. Billups, T. H. Rude, C. E. Whitmire, B. Sass, and C. J. Henry, *Cancer Lett.*, **9**, 277 (1980).

(33) G. O. Emerole and M. I. Thabrew, *Res. Commun. Chem. Pathol. Pharmacol.*, **31**, 567 (1981).

(34) J. M. Collins and R. L. Dedrick, *J. Pharm. Sci.*, **71**, 66 (1982).

Chemical Aspects of Propranolol Metabolism: 1,1-Diethoxy-3-(1-naphthoxy)-2-propanol and Related Ring-Closure Products *cis*- and *trans*-4-Ethoxy-3-hydroxy-3,4-dihydro-2*H*-naphtho[1,2-*b*]pyran

CHING-HSIU CHEN and WENDEL L. NELSON ˣ

Received March 22, 1982, from the *Department of Medicinal Chemistry, School of Pharmacy, University of Washington, Seattle, WA 98195.* Accepted for publication July 1, 1982.

Abstract □ 1,1-Diethoxy-3-(1-naphthoxy)-2-propanol (V), the diethyl acetal of an important aldehyde intermediate in the metabolic *N*-dealkylation of propranolol, was prepared from compound X, the product of the reaction of the lithium salt of methyl methylsulfinylmethyl sulfide with 2-(1-naphthoxy)-acetaldehyde. Compound X, as a mixture of three diastereomeric α-hydroxydithioacetal derivatives, when treated with ethyl orthoformate afforded the desired acetal V as well as two ring-closure products, the dihydronaphtho[1,2-*b*]pyrans VI and VII. Compounds VI and VII were characterized on the basis of mass spectral and ^{1}H- and ^{13}C-NMR data. The stereochemistry of these compounds was assigned on the basis of the 300-MHz ^{1}H-NMR spectra of their acetate esters (XI and XII).

Keyphrases □ Propranolol—metabolite synthesis, 1,1-diethoxy-3-(1-naphthoxy)-2-propanol □ Metabolism—of propranolol, synthesis of the diethyl acetal of an aldehyde intermediate, 1,1-diethoxy-3-(1-naphthoxy)-2-propanol □ 1,1-Diethoxy-3-(1-naphthoxy)-2-propanol—synthesis, diethyl acetal of an aldehyde intermediate in propranolol metabolism

Propranolol (I) is a β-adrenergic receptor antagonist used extensively in the treatment of various cardiovascular disorders, including hypertension and angina pectoris (1–3). In humans, a major metabolic process is oxidative *N*-dealkylation, which consists of at least two multistep pathways that result in the ultimate formation of both 3-(1-naphthoxy)-2-hydroxypropionic acid (II) and 3-(1-naphthoxy)propane-1,2-diol (III) (4–6). These metabolites are thought to arise from the oxidation and reduction of a common intermediate, 3-(1-naphthoxy)-2-hydroxypropionaldehyde (IV) (7). This aldehyde (IV) probably arises to a small extent directly from propranolol, but to a much greater extent by way of desisopropylpropranolol (7–10). Preparation of an easily characterized derivative of IV to be used in the further study of these *N*-dealkylation pathways was sought. In this paper, the synthesis of the diethyl acetal of IV (V) and the characterization of two dihydronaphtho[1,2-*b*]pyrans (VI and VII), ring-cyclized products formed during the synthesis of V, are reported.

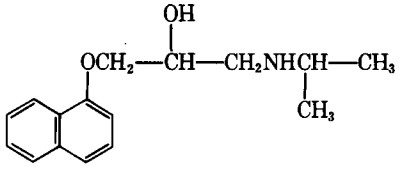

I

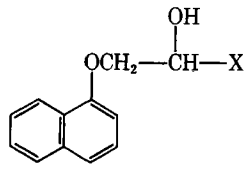

II: X = COOH
III: X = CH_2OH
IV: X = CHO
V: X = $CH(OEt)_2$

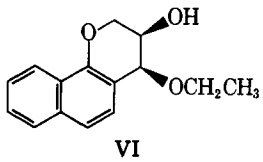

VI

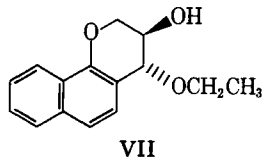

VII

RESULTS AND DISCUSSION

The initial attempt to prepare V was based on partial reduction of the cyanohydrin of 2-(1-naphthoxy)acetaldehyde (VIII), suitably protected as a dihydropyranyl ether. Sodium bis(2-methoxyethoxy)aluminum hydride has been reported to be successful in the partial reduction of some cyanohydrin acetals to form α-hydroxyaldehydes (11). However, over-reduction occurred and 1-naphthol, a product of ring cleavage, was formed, thus requiring an alternate approach.

The successful synthesis of the desired acetal V was accomplished by allowing VIII to react with an anionic formaldehyde equivalent, the lithium salt of methyl methylsulfinylmethyl sulfide (IX) (12). Three diastereomers of X were formed, which were separated. Each of these diastereomers (X*a*, X*b*, and X*c*), when treated with ethyl orthoformate, gave the desired acetal V, as well as cyclized products VI and VII. The most successful and direct method for preparation of V, however, was to subject the mixture of the diastereomers of X, without prior separation, to these conditions. Conversion of the mixture of diastereomers of X to the acetal V (ethyl orthformate and acid catalysis) was attempted to prevent possible isomerization of the α-hydroxyaldehyde, expected from direct hydrolysis of X, to an α-hydroxyketone, as reported in related systems by Ogura and Tsuchihashi (12).

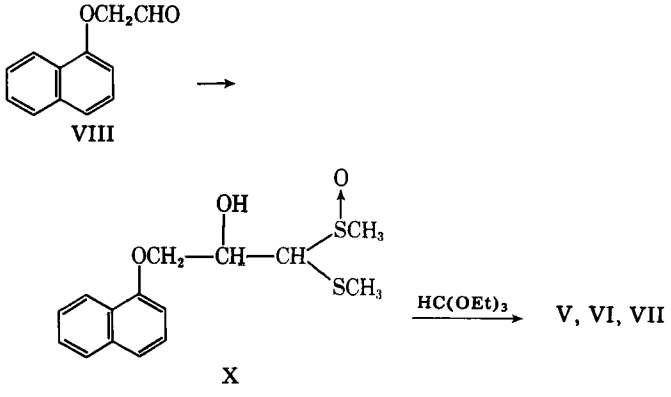

VIII

X

Crystallization and chromatographic separation of the products of the conversion of X to V afforded a 58% yield of the desired acetal V and two other components, which were characterized as VI and VII, obtained in 9 and 30% yields, respectively. Attempts to use milder conditions or shorter times for the conversion of X to V failed to reduce the relative amounts of VI and VII formed, suggesting that the activation energies for their formation are similar to that for formation of the desired acetal V.

The structures of compounds VI and VII were assigned on the basis of CI–MS data, ^{1}H- and ^{13}C-NMR data, and elemental analysis. Methane CI–MS of VI and VII each demonstrated the loss of the elements of ethanol. QM = *m/z* 245 rather than *m/z* 291; their 60-MHz ^{1}H-NMR spectra also showed the loss of one ethoxy substituent. In the aromatic region of the ^{1}H-NMR spectra, the signal of H_8 (the most downfield proton in V and other 1-alkoxynaphthalenes) was retained and the signal of H_2 (the most upfield aromatic proton in V and other 1-alkoxynaphthalenes) was lost, indicating cyclization at C_2 of the naphthalene ring. Comparison of the ^{13}C-NMR spectrum of VII with the spectrum of V

0022-3549/83/0800-0863$01.00/0

(Table I), confirmed the structural assignment. Assignment of the signals of all the carbons in the naphthalene ring was accomplished by comparison with published spectra of 1-methoxynaphthalene and 2-methylnaphthalene (13). The most distinguishing feature was the difference in the chemical shift of C_2 in the aromatic ring of V and the corresponding carbon atom C_{4a} of VII. This signal was shifted upfield in the dihydronaphtho[1,2-*b*]pyran VII. A similar upfield shift was noted for the signal of the acetal carbon $C_{1'}$ when it was converted to the benzylic carbon C_4 in VII.

The assignment of the relative stereochemistry of VI and VII was not apparent from their ^{1}H-NMR spectra because of similarities in the chemical shifts of the dihydropyran ring protons. The 300-MHz ^{1}H-NMR spectra of their acetate esters (XI and XII, respectively) provided sufficient signal separation to allow assignment of the stereochemistry of the esters and thus of VI and VII. The 300-MHz ^{1}H-NMR data of the dihydropyran ring protons of XI and XII are given in Table II. Comparison with ^{1}H-NMR data of the related structures *cis*- and *trans*-3,4-diacetoxy-3,4-dihydro-2*H*-pyran (15) and some related 3,4-substituted flavans (16–19) aided in assignment of the relative stereochemistry.

Several spectral similarities were noted when these data were compared with data from the model dihydropyrans. In the spectra of XI and XII, $J_{3,4}$ = 3.7 and 2.6 Hz, respectively, compared with $J_{3,4}$ = 4.12 and 2.87 Hz for *cis- and trans*-3,4-diacetoxy-dihydro-2*H*-pyran, respectively (15). In XI, assigned the *cis* stereochemistry, $J_{3,2}$ = 7.2 Hz. In both XI and XII, other $J_{2,3}$ and $J_{2',3}$ coupling constants are small (2.9 Hz in XI, 2.6 and 1.5 Hz *in XII*), *consistent* with data from the model dihydropyrans (15). Also, a larger long-range coupling ($J_{2,4}$ = 1.6 Hz) is observed in the spectrum of XII and in the reported data for the *trans* model dihydropyran, likely due to the contribution of a zigzag or W conformation (20).

Both XI and XII seem likely to exist in solution as a mixture of half-chair and/or twist boat conformations. In a series of structurally related conformationally flexible flavans with similar substituents in the 3- and 4-positions (16–19), the values of $J_{3,4}$ are of similar size. In these model flavans, $J_{3,4}$ of 3.2–4.5 Hz are observed in the spectra of *cis*-3,4-disubstituted compounds, and $J_{3,4}$ is ~2.3 Hz in the spectra of *trans*-3,4-disubstituted compounds. These comparisons, and those in the flexible dihydropyrans, strongly indicate the relative stereochemistry of the 3- and 4-substituents is *cis* in XI and *trans* in XII. Thus, VI and VII are assigned the *cis* and *trans* relative stereochemistry, respectively.

The synthesis and characterization of the acetal V and related naphtho[1,2-*b*]pyrans VI and VII will facilitate additional experiments on the metabolic *N*-dealkylation of propranolol. Compound V has been used successfully in experiments to trap intermediate aldehyde IV as an *O*-methyloxime (21).

EXPERIMENTAL[1]

2-(1-Naphthoxy)acetaldehyde (VIII)—This aldehyde was prepared from 1-naphthol and α-bromoacetaldehyde diethyl acetal as previously reported (22).

1-Methylthio-1-methylsulfinyl-3-(1-naphthoxy)-2-propanol (X)—To a solution of 1.24 g (1.1 ml, 10 mmoles) of methyl methylsulfinylmethyl sulfide (IX) in 20 ml of tetrahydrofuran at 0° was added slowly 6.6 ml (10.3 mmoles) of 1.55 *M* methyllithium solution, followed by 1.86 g (10 mmoles) of 2-(1-naphthoxy)acetaldehyde (VIII) in 5 ml of tetrahydrofuran. The mixture was stirred at 0° for 1 hr, water was added, and the mixture was extracted with ether. The ether extract was dried (magnesium sulfate) and evaporated to dryness. The residue, containing three diastereomers (X*a*, X*b*, and X*c*), was fractionally crystallized from a mixture of ethyl acetate–methanol (19:1) affording 200 mg (6.5%) of X*a* (R_f 0.30 ethyl acetate–methanol, 19:1) and 359 mg (11%) of X*c* (R_f 0.21). X*a*, mp 172–173.5°; ^{1}H-NMR (DMSO-d_6): δ 2.20 (s, 3, SCH_3), 2.80 (s, 3, $SOCH_3$), 3.35 (s, 1, OH), 3.97–4.16 (m, 1, C*H*OH), 4.16–4.50 (m, 2, OCH_2), 4.57–4.96 (m, 1, C*H*SCH_3), and 6.85–8.50 (m, 7, naphthalene protons); CI–MS: *m/z* 311 (QM), 293, 246, and 229. X*c*, mp 147–152°; ^{1}H-NMR (methanol-d_4): δ 2.25 (s, 3, SCH_3), 2.84 (s, 3, $SOCH_3$), 4.02–4.30 (m, 1, C*H*OH), 4.30–4.50 (m, 1, C*H*SCH_3), 4.60 (d, 2, OCH_2), and 6.90–8.65 (m, 7, naphthalene protons); CI–MS: *m/z* 311 (QM), 293, 246, and 229.

The combined mother liquors were evaporated and the residue purified by column chromatography on 100 g of silica gel eluting with 500 ml of ethyl acetate–methanol (19:1) to give 1.18 g (38%) of a mixture of X*a*, X*b*, and X*c* and 127 mg (4%) of X*b* as a liquid (R_f 0.25); ^{1}H-NMR (DMSO-d_6): δ 2.30 (s, 3, SCH_3), 2.68 (s, 3, $SOCH_3$), 3.38 (s, 1, OH), 4.17–4.57 (broad s, 4, $CH_2CHOHCHSCH_3$), and 6.67–8.54 (m, 7, naphthalene protons); CI–MS: *m/z* 311 (QM), 293, 246, and 229.

Anal.—Calc. for $C_{15}H_{18}O_3S_2$ (X*c*): C, 58.04; H, 5.85. Found: C, 58.35; H, 5.96.

1,1-Diethoxy-3-(1-naphthoxy)-2-propanol (V)—To a solution of the mixture of diastereomers of X (10.18 g, 32.8 mmoles) in 30 ml of ethanol was added 6.3 ml (38.1 mmoles) of ethyl orthoformate and 0.60 g of concentrated sulfuric acid. The mixture was heated at 60° for 24 hr. The reaction mixture was neutralized with 1.0 ml of concentrated aqueous ammonia and evaporated to dryness. The mixture was partitioned between water and ether, and the ether extract was evaporated to dryness. The residue was purified by column chromatography on 200 g of silica gel. Elution with 1 liter of chloroform–ethanol (99:1) gave 0.750 g (9.3%) of VI (R_f 0.39 in chloroform–ethanol, 99:1), 5.50 g (58%) of V (R_f 0.29), and 2.43 g (30%) of VII (R_f 0.18).

An analytical sample of the acetal V was obtained by rechromatographing crude V on 150 g of silica gel. Elution with 500 ml of benzene–ethyl acetate (4:1) afforded V as an oil; ^{1}H-NMR ($CDCl_3$): δ 0.85–1.40 [2t, 6, $CH(OCH_2CH_3)_2$], 2.80–3.18 (broad s, 1, OH), 3.28–3.90 [m, 4, $CH(OCH_2CH_3)_2$], 3.90–4.30 (m, 3, OCH_2CHOH), 4.74 [d, J = 5 Hz, 1, $CH(OCH_2CH_3)_2$], 6.75 (dd, J = 6 and 3 Hz, 1, naphthalene H_2), 7.15–7.55 (m, 4, naphthalene H_3, H_4, H_6, H_7), 7.70 (m, 1, naphthalene H_5), and 8.30 (distorted dd, J = 5 and 3 Hz, 1, naphthalene H_8); ^{13}C-NMR ($CDCl_3$): see Table I; CI–MS: *m/z* 291 (QM), 245, 227, and 199.

Anal.—Calc. for $C_{17}H_{18}O_4$: C, 70.32; H, 7.64. Found: C, 70.21; H, 7.67.

Compound V, in the presence of semicarbazide hydrochloride at pH 4–5 (ethanol, 60°, 2.5 hr), afforded the semicarbazone of IV as a white solid, mp 205–207°; CI–MS: *m/z* 274 (QM).

Anal.—Calc. for $C_{14}H_{15}N_3O_3$: C, 61.35; H, 5.33; N, 15.38. Found: C, 61.49; H, 5.72; N, 15.31.

***cis*-4-Ethoxy-3-hydroxy - 2*H*-3,4-dihydronaphtho[1,2-*b*]pyran (VI)**—Compound VI further purified twice by column chromatography on 15 g of silica gel eluting with 70 ml of chloroform–ethanol (199:1) was obtained as a colorless oil; ^{1}H-NMR ($CDCl_3$) δ 1.20 (t, J = 7 Hz, 3, OCH_2CH_3), 2.60–2.90 (broad d, J = 7 Hz, 1, OH), 3.68 (q, J = 7 Hz, 2, OCH_2CH_3), 4.10–4.30 (m, 3, OCH_2CHOH), 4.42 (m, 1, $CHOC_2H_5$), 7.06–7.92 (m, 5, naphthalene H_3, H_4, H_5, H_6, H_7), and 8.20 (distorted dd, J = 5.5 and 2.5 Hz, 1, naphthalene H_8); CI–MS: *m/z* 245 (QM).

Anal.—Calc. for $C_{15}H_{16}O_3$: C, 73.75; H, 6.60. Found: C, 73.50; H, 6.60.

Table I—^{13}C-NMR Data for 1,1-Diethoxy-3-(1-naphthoxy)-2-propanol (V) and *trans*-4-Hydroxy-3-ethoxy-3,4-dihydro-2*H*-naphtho[1,2-*b*]pyran (VII)

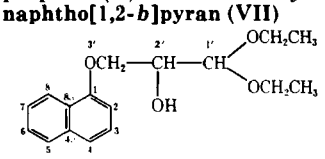

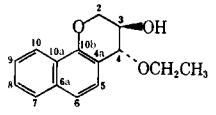

Compound V		Compound VII	
Carbon	Chemical shift, ppm	Carbon	Chemical shift, ppm
C_1	154.44	C_{10b}	149.46
C_2	105.03	C_{4a}	113.42
C_3	125.82	C_5	126.80
C_4	120.60	C_6	120.55
C_{4a}	134.51	C_{6a}	134.47
C_5	127.50	C_7	128.32
C_6	126.41	C_8	127.44
C_7	125.20	C_9	124.90
C_8	121.92	C_{10}	122.17
C_{8a}	125.68	C_{10a}	125.49
$C_{3'}$	71.14[a]	C_2	66.70, 65.63
$C_{2'}$	68.50[a]	C_3	
$C_{1'}$	102.53	C_4	74.66
OCH_2CH_3	64.16, 63.57	OCH_2CH_3	64.64
OCH_2CH_3	15.36, 15.20	OCH_2CH_3	15.62

[a] Tentative assignment consistent with the reported ^{13}C-NMR chemical shift assignments of carbons in the propanolamine side chain of propranolol (14).

[1] Melting points were determined on a Thomas-Hoover melting point apparatus and are uncorrected. IR spectra were recorded on a Perkin-Elmer 727B spectrophotometer. Routine ^{1}H-NMR spectra were recorded on a Varian EM-360A spectrometer, using TMS as internal standard. Notations used in the ^{1}H-NMR descriptions are as follows: (s) singlet; (d) doublet; (t) triplet; (q) quartet; (m) multiplet. High-field ^{1}H-NMR spectra were recorded on the Brucker 300-MHz spectrometer, using TMS as internal standard. ^{13}C-NMR spectra were recorded on the Varian CFT-20 spectrometer, using TMS as internal standard. Mass spectra were recorded on a Biospect mass spectrometer, operated in the CI mode with methane (0.5 torr) as the reagent gas. Microanalyses were performed by Galbraith Laboratories, Inc., Knoxville, Tenn.

Table II—300-MHz ^{1}H-NMR Data for the Dihydropyran Ring Protons of XI and XII

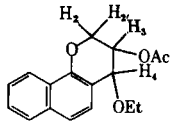

Proton	Chemical Shift (δ)	Apparent Coupling Constants
		Compound XI (*cis*)
H_4	4.74	$J_{3,4}$ = 3.7 Hz, line broadening[a]
H_3	5.47	$J_{3,2}$ = 7.4 Hz, $J_{3,4}$ = 3.7 Hz, $J_{3,2'}$ = 2.9 Hz
H_2	4.55	J_{gem} = 11.1 Hz, $J_{2,3}$ = 7.4 Hz
$H_{2'}$	4.36	J_{gem} = 11.1 Hz, $J_{2',3}$ = 2.9 Hz, $J_{2',4}$ = 1.0 Hz
		Compound XII (*trans*)
H_4	4.32	$J_{3,4}$ = 2.6 Hz, $J_{2,4}$ = 1.6 Hz
H_3	5.25	$J_{3,4}$ = 2.6 Hz, $J_{3,2}$ = 2.6 Hz, $J_{3,2'}$ = 1.5 Hz
H_2	4.56	J_{gem} = 12.1 Hz, $J_{2,3}$ = 2.6 Hz, $J_{2,4}$ = 1.6 Hz
$H_{2'}$	4.43	J_{gem} = 12.1 Hz, $J_{2',3}$ = 1.5 Hz

[a] Coupling constant $J_{2',4}$ was assigned on the basis of decoupling experiments and from the signal for $H_{2'}$.

***cis*-3-Acetoxy-4-ethoxy - 2*H*-3,4-dihydronaphtho[1,2-*b*]pyran (XI)**—To a solution of VI (120 mg, 0.49 mmole) in 5 ml of ether at room temperature was added triethylamine (717 mg, 7.1 mmoles), followed by the addition of acetyl chloride (569 mg, 7.1 mmoles). The reaction mixture was stirred for 2 hr, filtered, and evaporated to dryness. The residue was purified by column chromatography on 10 g of silica gel. Elution with 60 ml of chloroform gave 65 mg (46%) of XI as a colorless oil. An analytical sample was obtained by rechromatographing on 10 g of silica gel, eluting with 40 ml of chloroform; ^{1}H-NMR ($CDCl_3$): δ 1.27 (t, J = 7 Hz, 3, OCH_2CH_3), 2.10 (s, 3, $COCH_3$), 3.72 and 3.75 (overlapping q, J = 7 Hz, 2, OCH_2CH_3), 4.30–4.60 (m, 2, OCH_2), 4.70 (d, J = 3.5 Hz, 1, $CHOC_2H_5$), 5.25–5.65 (dt, J = 7, 3.5, and 3.5 Hz, 1, $CHOCOCH_3$), 7.00–7.97 (m, 5, naphthalene H_3, H_4, H_5, H_6, H_7), and 8.20 (dd, J = 6.5 and 3 Hz, 1, naphthalene H_8); partial 300-MHz ^{1}H-NMR spectrum: see Table II; CI-MS: m/z 287 (QM).

Anal.—Calc. for $C_{17}H_{18}O_4$: C, 71.31; H, 6.34. Found: C, 71.15; H, 6.57.

***trans*-4-Ethoxy-3-hydroxy - 2*H*-3,4-dihydronaphtho[1,2-*b*]pyran (VII)**—Compound VII further purified by column chromatography on 60 g of silica gel, eluting with 300 ml of benzene–ethyl acetate (4:1) was obtained as a colorless oil; ^{1}H-NMR ($CDCl_3$): δ 1.10 (t, J = 7 Hz, 3, OCH_2CH_3), 2.53–3.00 (broad d, 1, OH), 3.50 (q, J = 7 Hz, 2, OCH_2CH_3), 3.65–3.96 (m, 1, $CHOH$), 4.06 (d, J = 2 Hz, 1, $CHOC_2H_5$), 4.16 (d, J = 2 Hz, 2, OCH_2), 7.03–7.94 (m, 5, naphthalene H_3, H_4, H_5, H_6, H_7), and 8.17 (distorted dd, J = 5 and 2.5 Hz, 1, naphthalene H_8); ^{13}C-NMR ($CDCl_3$): see Table I; CI-MS: m/z 245 (QM).

Anal.—Calcd. for $C_{15}H_{16}O_3$: C, 73.75; H, 6.60. Found: C, 73.60; H, 6.89.

***trans*-3-Acetoxy-4-ethoxy - 2*H*-3,4-dihydronaphtho[1,2-*b*]pyran (XII)**—To a solution of VII (280 mg, 1.15 mmoles) in 10 ml of $CHCl_3$ at 0° was added triethylamine (1.74 g, 17.2 mmoles), followed by the addition of acetyl chloride (1.35 g, 17.2 mmoles). The reaction mixture was stirred at room temperature for 4 hr and quenched with ice. The chloroform layer was separated, dried (magnesium sulfate), and evaporated to dryness. The residue was purified by column chromatography on 15 g of silica gel. Elution with 80 ml of chloroform gave 70 mg (21%) of XII as a colorless oil. An analytical sample was obtained by rechromatographing on 10 g of silica gel eluting with 40 ml of chloroform; ^{1}H-NMR ($CDCl_3$): δ 1.25 (t, J = 7 Hz, 3, OCH_2CH_3), 1.95 (s, 3, $COCH_3$), 3.77 (q, J = 7 Hz, 2, OCH_2CH_3), 4.20–4.40 (m, 1, $CHOC_2H_5$), 4.40–4.55 (m, 2, OCH_2), 5.26 (q, J = 2 Hz, 1, $CHOCHOCH$), 6.95–8.05 (m, 5, naphthalene H_3, H_4, H_5, H_6, H_7), and 8.25 (dd, J = 6 and 2.5 Hz, 1, naphthalene H_8 proton); partial 300-MHz ^{1}H-NMR spectrum: see Table II; CI-MS: m/z 287 (QM).

Anal.—Calc. for $C_{17}H_{18}O_4$: C, 71.31; H, 6.34. Found: C, 71.40; H, 6.52.

REFERENCES

(1) T. F. Blaschke and K. L. Melmon in "The Pharmacological Basis of Therapeutics," 6th ed., A. G. Gilman, L. S. Goodman, and A. Gilman, Eds. MacMillan, New York, N.Y., 1980, p. 739–819.

(2) R. E. Buckingham and T. C. Hamilton, *Gen. Pharmacol.*, **10**, 1 (1979).

(3) F. O. Simpson, *Drugs*, **20**, 69 (1980).

(4) P. A. Bond, *Nature (London)*, **1967**, 721.

(5) J. W. Paterson, M. E. Connolly, C. T. Dollery, A. Hayes, and R. G. Cooper, *Pharmacol. Clin.*, **2**, 127 (1970).

(6) J. F. Pritchard, D. W. Schneck, and A. H. Hayes, Jr., *J. Chromatogr. Biomed. Appl.*, **162**, 47 (1979).

(7) W. L. Nelson and T. R. Burke, Jr., *Res. Commun. Chem. Pathol. Pharmacol.*, **21**, 77 (1978).

(8) T. Walle, T. Ishizaki, and T. E. Gaffney, *J. Pharmacol. Exp. Ther.*, **183**, 508 (1972).

(9) J. L. Tindell, T. Walle, and T. E. Gaffney, *Life Sci.*, Part II, **11**, 1029 (1972).

(10) O. M. Bakke, D. S. Davies, L. Davies, and C. T. Dollery, *Life Sci.*, **13**, 1665 (1973).

(11) M. Schlosses and A. Birch, *Helv. Chem. Acta*, **61**, 1903 (1978).

(12) K. Ogura and G. Tsuchihashi, *Tetrahedron Lett.*, **1972**, 2681.

(13) J. Secta, J. Sandstrom, and T. Drackenberg, *Org. Mag. Reson.*, **11**, 239 (1978).

(14) S. J. Pasaribu and G. C. Brophy, *Aust. J. Chem.*, **31**, 2629 (1978).

(15) J. Runsink, in "Handbook of NMR Spectral Parameters," W. Brügel, Ed., Heyden and Son, London, 1979, Table 68.1.4., p. 541.

(16) B. J. Bolger, A. Hirwe, K. G. Marathe, E. M. Philbin, M. A. Vickers, and C. P. Lillya, *Tetrahedron*, **22**, 621 (1966).

(17) J. W. Clark-Lewis, *Aust. J. Chem.*, **22**, 425 (1968).

(18) B. J. Bolger, K. G. Marathe, E. M. Philbin, T. S. Wheeler, and C. P. Lillya, *Tetrahedron*, **23**, 341 (1967).

(19) W. Brügel, "Handbook of NMR Spectral Parameters," Heyden and Son, London, 1979, Table 24.3.1(b–c), p. 168.

(20) L. M. Jackman and S. Sternhell, "Applications of Nuclear Magnetic Resonance Spectroscopy in Organic Chemistry," 2nd ed., Pergamon, Oxford, 1969, pp. 334–341.

(21) C.-H. Chen and W. L. Nelson, *Drug Metab. Disp.*, **10**, 277 (1982).

(22) W. L. Nelson and M. J. Bartels, *J. Org. Chem.*, **47**, 1574 (1982).

ACKNOWLEDGMENTS

This work was supported in part by U.S. Public Health Service Grant NIGMS 25373.

The authors thank Mr. James Christie for the ^{13}C-NMR spectra (University of Washington) and Dr. Duane Miller and Mr. John Fowble, (Ohio State University) for the 300-MHz ^{1}H-NMR spectra.

Solubility and Partitioning VI: Octanol Solubility and Octanol–Water Partition Coefficients

S. H. YALKOWSKY *x, S. C. VALVANI, and T. J. ROSEMAN

Received March 4, 1982, from the *Pharmacy Research Unit, The Upjohn Company, Kalamazoo, MI 49001.* Accepted for publication July 12, 1982. *Present address: College of Pharmacy, University of Arizona, Tucson, AZ 85721.

Abstract □ A simple equation for the estimation of the aqueous solubility of crystalline solutes was previously derived based on the assumption that the presence of water does not significantly alter the crystal properties of the solute. The data presented verify the solubility equation for a set of 36 nonelectrolytes and weak electrolytes. Using the same set of solutes, the two major assumptions used to derive the equation were also verified: that the octanol solubility of nonelectrolytes is exponentially proportional to the melting point of the solute and that the octanol–water solubility ratio is a good approximation of the octanol–water partition coefficient.

Keyphrases □ Solubility—of nonelectrolytes and weak electrolytes in octanol, determination using melting points and partition coefficients □ Partition coefficient—of nonelectrolytes and weak electrolytes in octanol–water, use with melting point to determine solubility □ Octanol—determination of the solubility of nonelectrolytes and weak electrolytes, partition coefficients with water

In previous publications (1–6) a simple equation for the estimation of the aqueous solubility of crystalline solutes was derived on the basis of the following rationale:

1. The solubility of nonpolar and semipolar solutes in octanol is approximately equal to the ideal solubility.
2. The ideal solubility can be estimated from the melting point and entropy of fusion of the solute.
3. The entropy of fusion of the solute is constant for rigid molecules.
4. The octanol–water solubility ratio of a solute is equivalent to the octanol–water partition coefficient.
5. The aqueous solubility is equal to the octanol solubility divided by the octanol–water partition coefficient.

The above strategy is based on the assumption that the presence of water does not significantly alter the crystal properties of the solute. This assumption is usually valid; however, its failure can occasionally be the source of an incorrect estimate of the aqueous solubility of a semipolar substance.

THEORETICAL

An equation enables the estimation of the aqueous solubility (S_w in moles/liter) of rigid organic compounds from melting point (mp) and octanol–water partition coefficient (PC) data. This equation has the simple form:

$$\log S_w(\text{calc}) = -0.01\ \text{mp} - \log \text{PC} + 1.05 \qquad \text{(Eq. 1)}$$

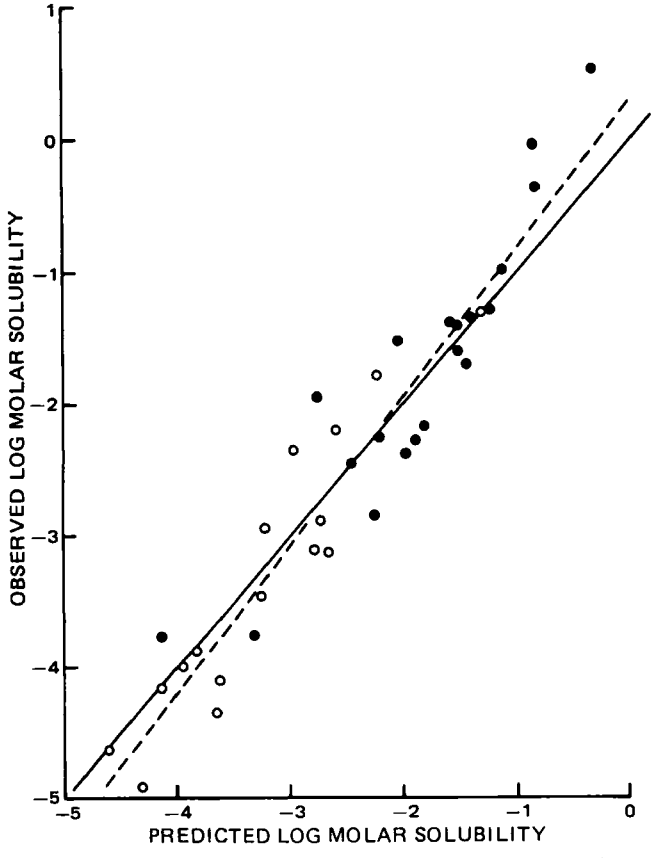

Figure 1—*Observed and predicted aqueous solubilities of nonelectrolytes (○) and weak electrolytes (●). Key: (—) theoretical line described by Eq. 1; (- - - -) regression line described by Eq. 6.*

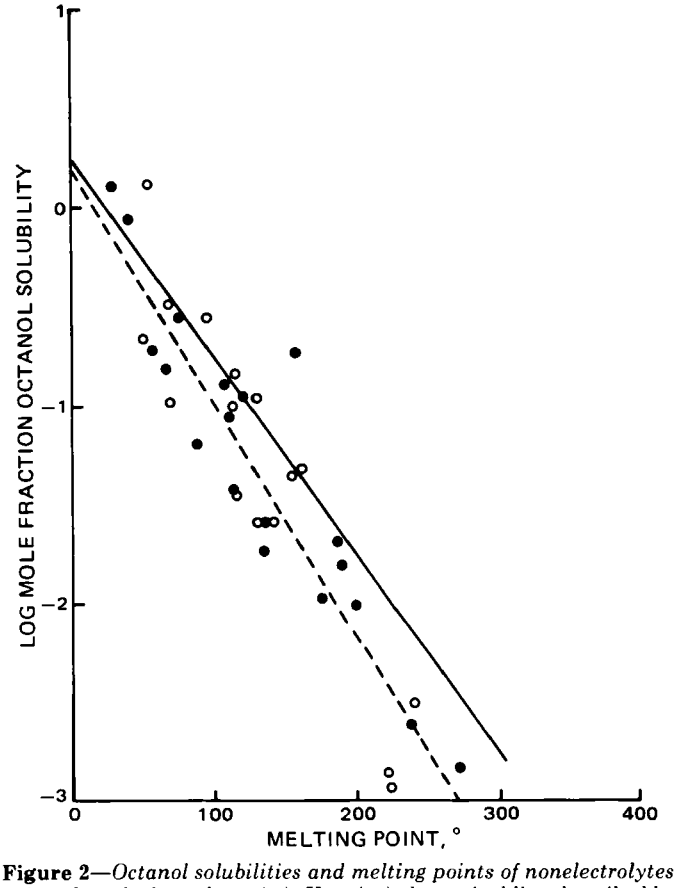

Figure 2—*Octanol solubilities and melting points of nonelectrolytes (○) and weak electrolytes (●). Key: (—) theoretical line described by Eq. 2; (- - - -) regression line described by Eq. 11.*

0022-3549/83/0800-0866$01.00/0

Table I—Estimation of Aqueous Solubility [a]

Solute	log PC (obs)	mp°, [b]	log S_w (obs)	log S_w (calc)	Difference
Acetylsalicylic acid	(1.21)	135	(−1.60)[c]	−1.51	0.094
p-Aminobenzoic acid	(0.58)	187	−1.35	−1.40	−0.048
Aminopyrine	(0.80)	108	(−0.36)[d]	−0.83	−0.470
Antipyrine	(0.26)	112	0.53	−0.33	−0.865
Barbital	(0.67)	190	(−1.41)[e]	−1.52	−0.106
Benzoic acid	(1.87)	122	−1.53	−2.04	−0.507
Butyl-*p*-aminobenzoate	2.72	58	−2.84	−2.25	0.593
Caffeine	−0.20	238	−0.98	−1.13	−0.154
Flurbiprofen	3.26	111	−3.74	−3.32	0.424
Ethyl-*p*-aminobenzoate	1.96	89	−2.17	−1.80	0.368
Fumaric acid	0.28	200	−1.29	−1.23	0.062
Ibuprofen	4.43	76	−3.76	−4.14	−0.382
Methyl-*p*-aminobenzoate	1.35	114	−1.70	−1.44	0.259
Phenobarbital	(1.48)	176	−2.26	−2.19	0.072
Phenacetin	(1.58)	135	−2.28	−1.88	0.399
Phenol	(1.48)	41	(−0.04)[f]	−0.84	−0.796
Prostaglandin E_2	2.82	67	−2.47	−2.44	0.017
Prostaglandin $F_{2\alpha}$	2.72	30	−2.38	−1.97	0.409
Salicylic acid	(2.23)	158	−1.95	−2.76	−0.813
Theophylline	−0.09	272	−1.38	−1.58	−0.200
Acetanilide	(1.21)	114	−1.31	−1.30	0.007
Biphenyl	(3.98)	70	−4.34	−3.63	0.710
Butyl-*p*-hydroxybenzoate	3.57	69	−2.93	−3.21	−0.283
Cortisone	1.47	222	−3.12	−2.64	0.479
Desoxycorticosterone	2.88	142	(−3.45)[g]	−3.25	0.201
Ethyl-*p*-hydroxybenzoate	2.47	116	−2.20	−2.58	−0.380
Fluorene	4.18	117	−4.91	−4.30	0.607
Methyl-*p*-hydroxybenzoate	1.96	131	−1.78	−2.22	−0.438
15-*s*-15-Methyl prostaglandin $F_{2\alpha}$ methyl ester	3.21	55	−2.88	−2.71	0.173
Methyltestosterone	3.36	163	−3.99	−3.94	0.046
Prednisolone	(1.42)	240	−3.10	−2.77	0.335
Propyl-*p*-hydroxybenzoate	(3.04)	96	−2.35	−2.95	−0.600
Progesterone	3.87	131	(−4.15)[h]	−4.13	0.023
Testosterone	3.32	155	(−3.87)[h]	−3.82	0.048
Triazolam	2.42	224	−4.09	−3.61	0.485

[a] *Values in parentheses were obtained from the literature.* [b] Melting point data taken from Ref. 8 or the manufacturers' specifications. [c] L. J. Edwards, *Trans. Faraday Soc.*, **57**, 1191 (1951). [d] R. Charonnat, *Compt. Rend.*, **185**, 284 (1927). [e] F. A. Long and W. F. McDevitt, *Chem. Rev.*, **51**, 119 (1952). [f] L. Erichsen and E. Dobbert, *Brennstoff Chem.*, **36**, 338 (1955). [g] H. Tomida, T. Yotsuyanagi, and K. Ikeda, *Chem. Pharm. Bull. Tokyo*, **26**, 2832 (1978). [h] K. Uekema, T. Fujinaga, F. Hirayama, M. Otagiri, and M. Tamasaki, *Int. J. Pharm.*, **10**, 1 (1982).

In the derivation of this equation, several important assumptions were made:

1. Octanol is a nearly ideal solvent for the solutes of interest, so that the octanol solubility (X_o in moles fraction) is given by:

$$\log X_o(\text{calc}) = -0.01\ \text{mp} + 0.25 \qquad \text{(Eq. 2)}$$

2. The octanol–water partition coefficient is equal to the octanol–water solubility ratio (SR), which is defined as the octanol solubility (S_o in moles/liter) divided by the aqueous solubility (S_w in moles/liter):

$$\text{PC} = \text{SR} = S_o/S_w \qquad \text{(Eq. 3)}$$

or

$$\log (S_w/S_o) = -\log \text{PC} = -\log \text{SR} \qquad \text{(Eq. 4)}$$

3. The melting point of the drug in equilibrium with octanol is the same as the melting point of the drug in equilibrium with water. The overall strategy of this approach can be expressed as:

$$S_w = S_o\,(S_w/S_o) \qquad \text{(Eq. 5)}$$

with S_o and the solubility ratio being determined by Eqs. 2 and 4, respectively.

In this report, an attempt was made to extend Eq. 1 to include some pharmaceutically important solutes and to verify the assumptions that were used in its derivation. A single set of solutes was chosen for these purposes, including both nonelectrolytes and weak electrolytes of widely varying chemical structure.

EXPERIMENTAL

Materials—The octanol was reagent grade[1]. All other compounds were of the purest grade available from commercial sources[2] and were used as received.

[1] Aldrich.
[2] Aldrich, Eastman, Fluka.

Solubilities—The aqueous solubilities of some of the solutes were taken from the literature or previous work in this laboratory[3]. Only values in the 20–30° range were used. Solubilities for those compounds for which literature data were not available were determined experimentally in the following manner. An excess amount of solute was allowed to equilibrate with water in a sealed vial for 24 hr at 30°. After equilibration the samples were filtered through either a 0.22-μm porous filter[4] or a 1.2-μm silver membrane filter[5] which was preequilibrated at 30°. Analysis of the filtrate was performed using UV spectrophotometry[6]. Octanol solubilities were determined in the same manner as the aqueous solubilities, except that dilutions were made with 2-propanol.

Partition Coefficients—For many of the solutes the partition coefficients were taken from the literature (7). For selected solutes, the partition coefficients were determined in the following manner. A known amount of solute was dissolved in water-saturated octanol or octanol-saturated water. The two phases were shaken for 3 hr and then allowed to equilibrate at 30° for 3–6 days. The phases were separated by centrifugation at 1500 rpm for 15 min, and the concentration in each phase was determined spectrophotometrically.

Solubility Ratio in Mutually Saturated Solvents—Water-saturated octanol and octanol-saturated water were prepared by shaking an excess of water or octanol with the pure solvent for 8 hr. After equilibration, the two layers in each of the solvent mixtures were separated to yield the mutually saturated octanol and water. These solvents were used to determine the aforementioned saturation solubilities for antipyrine, ethyl-*p*-aminobenzoate, caffeine, and theophylline. All determinations were run in duplicate.

RESULTS AND DISCUSSION

Water Solubility—The logarithms of the aqueous solubilities calculated by Eq. 1 for the solutes studied are listed in Table I, along with

[3] S. H. Yalkowsky and S. C. Valvani, unpublished compilation.
[4] Millipore.
[5] Selas.
[6] Zeiss DMR 21.

Table II—Estimation of Octanol Solubility

Solute	mp°, [a]	log X_o (obs)	log X_o (calc)	Difference
Acetylsalicylic acid	135	−1.58	−0.30	0.395
p-Aminobenzoic acid	187	−1.68	−0.82	−0.023
Aminopyrine	108	−0.89	−0.03	−0.029
Antipyrine	112	−1.06	−0.07	0.122
Barbital	190	−1.80	−0.85	0.071
Benzoic acid	122	−0.95	−0.17	−0.109
Butyl-*p*-aminobenzoate	58	−0.72	0.47	0.340
Caffeine	238	−2.61	−1.33	0.395
Flurbiprofen	111	−1.05	−0.06	0.140
Ethyl-*p*-aminobenzoate	89	−1.19	0.16	0.469
Fumaric acid	200	−2.00	−0.95	0.169
Ibuprofen	76	−0.55	0.29	0.017
Methyl-*p*-aminobenzoate	114	−1.42	−0.09	0.444
Phenobarbital	176	−1.97	−0.71	0.382
Phenacetin	135	−1.73	−0.30	0.543
Phenol	41	−0.06	0.64	−0.300
Prostaglandin E_2	67	−0.81	).38	0.406
Prostaglandin $F_{2\alpha}$	30	0.11	0.75	0.263
Salicylic acid	158	−0.73	−0.53	−0.679
Theophylline	272	−2.83	−1.67	0.276
Acetanilide	114	−1.00	−0.09	0.027
Biphentl	70	−0.98	0.35	0.448
Butyl-*p*-hydroxybenzoate	69	−0.48	0.36	0.021
Cortisone	222	−2.85	−1.17	0.797
Desoxycorticosterone	142	−1.58	−0.37	0.340
Diphenylethane	52	−0.66	0.53	0.337
Ethyl-*p*-hydroxybenzoate	116	−0.83	−0.11	−0.150
Fluorene	117	−1.45	−0.12	0.445
Methyl-*p*-hydroxybenzoate	131	−0.96	−0.26	−0.182
15-*s*-15-Methyl prostaglandin $F_{2\alpha}$, methyl ester	55	0.12	0.50	0.046
Methyltestosterone	163	−1.31	−0.58	−0.130
Prednisolone	240	−2.50	−1.35	0.270
Propyl-*p*-hydroxybenzoate	96	−0.55	0.09	−0.267
Progesterone	131	−1.58	−0.26	0.447
Testosterone	155	−1.35	−0.50	−0.013
Triazolam	224	−2.93	−1.19	0.856

[a] Melting point data taken from Ref. 8 or the manufacturers' specifications.

the experimentally determined values (log S_w and log PC) and the melting point data; the last column lists the difference between the observed and calculated solubilities. In no case is the error in the estimate greater than an order of magnitude, and in over three-quarters of the examples it is less than a factor of 3.

The relationship between the observed and predicted values is shown in Fig. 1. The regression line is described by:

$$\log S_w = 1.129 \log S_w(\text{calc}) + 0.32$$
$$r = 0.954 \quad s = 0.400 \quad n = 36 \qquad \text{(Eq. 6)}$$

It is clear that there is no systematic deviation from the regression line for the nonelectrolytes or the weak electrolytes. The regression lines for the weak electrolytes [log S_w = 1.124 log S_w(calc) + 0.308] and for the nonelectrolytes [log S_w = 1.143 log S_w(calc) + 0.371] are both in good agreement with the line described by Eq. 6.

The multiple-regression equation for the aqueous solubility in terms of the melting point and the octanol–water partition coefficient is:

$$\log S_w = -0.012\ \text{mp} - 1.13 \log \text{PC} + 1.62$$
$$r = 0.955 \quad s = 0.402 \quad n = 36 \qquad \text{(Eq. 7)}$$

This compares favorably with the theoretical line from Eq. 1. In spite of an added parameter, Eq. 7 is virtually equivalent to Eq. 6 in estimating the aqueous solubilities of the compounds studied.

Octanol Solubility—If octanol is an ideal solvent for a drug, then the mole fractional solubility of that drug in octanol (X_o) should be equal to the ideal mole fractional solubility (X_i) as given by the van't Hoff equation:

$$\log X_o = \log X_i = [\Delta S_f/(2.303\,RT)]\,(T_m - T) \qquad \text{(Eq. 8)}$$

where ΔS_f is the entropy of fusion of the solute, T_m is the solute melting point in °K, R is the gas constant, and T is the temperature of interest in °K. It has been shown that, for rigid molecules (molecules with little or no conformational flexibility), the entropy of fusion can be approximated by 13.5 eu (9). Thus, for rigid molecules at room temperature (298 °K), Eq. 8 becomes:

$$\log X_o = -0.01\,(T_m - 298) \qquad \text{(Eq. 9)}$$

If the melting point and temperature in Eq. 9 are converted to the centigrade scale (by subtracting 273 from T_m and from 298°), Eq 9 becomes identical to Eq. 2.

If the intercept is expressed in moles per liter rather than in mole fraction, then 0.80 (the logarithm of the molarity of pure octanol) must be added to the left hand side of Eq. 9, so that it becomes:

$$\log S_o = -0.01\,(T_m - 298) + 0.8 = -0.01\,(T_m - 378) \qquad \text{(Eq. 10)}$$

The use of 0.80 is only an approximation of log $\{[(1000\rho - M{\cdot}W)/130.22] + M\}$, where ρ is the density of solution, M is the molarity of the solute, W is the molecular weight of the solute, and 130.22 is the molecular weight of octanol. When the solute molarity (M) is low or when the molecular weight of the solute (W) is close to that of octanol, the exact expression reduces to 0.80. The mole fractional solubilities in octanol (X_o) can be estimated by assuming that the density of the solution (ρ) is equal to the density of octanol (ρ_o) by:

$$X_o = \frac{M}{\left(\frac{1000\,\rho_o - M{\cdot}W}{130.22}\right)+M}$$

Regression analysis of the octanol solubility data (Table II) against melting point for the 36 solutes gives:

$$\log X_o = -0.012\ \text{mp} + 0.26$$
$$r = 0.92 \quad s = 0.32 \quad n = 36 \qquad \text{(Eq. 11)}$$

which is in good agreement with Eq. 2. The relationship between the octanol solubilities and the predicted values is illustrated in Fig. 2. No adjustable parameters were used in the analyses. The data cover three orders of magnitude, and there is no systematic difference in the data for nonelectrolytes and weak electrolytes.

The regression equations for the 21 weak electrolytes (log X_o = −0.011 mp + 0.15) and for the 15 nonelectrolytes (log X_o = −0.013 mp + 0.44) are both consistent with Eq. 11. This confirms the applicability of the first assumption to the solutes selected for this study. The reason for the near ideal solubility of this wide range of solutes in octanol has been explained on the basis of regular solution theory and the fact that the sol-

Table III—Estimation of Partition Coefficient [a]

Solute	log S_o (obs)	log S_w (obs)	log PC (obs)	log SR (calc)	Difference
Acetylsalicylic acid	−0.69	(−1.60)[b]	1.21	0.91	0.301
p-Aminobenzoic acid	−0.80	−1.35	(0.58)	0.56	0.024
Aminopyrine	−0.00	(−0.36)[c]	(0.80)	0.36	0.441
Antipyrine	−0.19	0.53	(0.26)	−0.73	0.987
Barbital	−0.92	(−1.41)[d]	(0.67)	0.49	0.177
Benzoic acid	−0.06	−1.53	(1.87)	1.47	0.399
Butyl-*p*-aminobenzoate	0.13	−2.84	2.72	2.97	−0.253
Caffeine	−1.72	−0.98	−0.20	−0.75	0.548
Flurbiprofen	−0.20	−3.74	3.26	3.54	−0.284
Ethyl-*p*-aminobenzoate	−0.31	−2.17	1.96	1.86	0.101
Fumaric acid	−1.12	−1.29	0.28	0.17	0.107
Ibuprofen	0.27	−3.76	4.43	4.03	0.399
Methyl-*p*-aminobenzoate	−0.53	−1.70	1.35	1.17	0.185
Phenobarbital	−1.09	−2.26	(1.48)	1.17	0.310
Phenacetin	−0.84	−2.28	(1.58)	1.44	0.145
Phenol	0.94	(−0.04)[e]	(1.48)	0.98	0.496
Prostaglandin E_2	−0.03	−2.46	2.82	2.43	0.389
Prostaglandin $F_{2\alpha}$	0.49	−2.38	2.72	2.87	−0.146
Salicylic acid	0.15	−1.95	2.23	2.10	0.134
Theophylline	−1.95	−1.38	−0.09	−0.57	0.476
Acetanilide	−0.12	−1.31	(1.21)	1.19	0.021
Biphenyl	−0.10	−4.34	(3.98)	4.24	−0.262
Butyl-*p*-hydroxybenzoate	0.34	−2.93	3.57	3.27	0.304
Cortisone	−1.97	−3.12	1.47	1.15	0.318
Desoxycorticosterone	−0.71	(−3.45)[f]	2.88	2.74	0.139
Diphenylethane	0.19	−4.63	5.12	4.82	0.299
Ethyl-*p*-hydroxybenzoate	0.04	−2.20	2.47	2.24	0.229
Fluorene	−0.56	−4.91	4.18	4.34	−0.162
Methyl-*p*-hydroxybenzoate	−0.08	−1.78	1.96	1.70	0.256
15-*s*-15-Methyl prostaglandin $F_{2\alpha}$ methyl ester	0.45	−2.88	3.21	3.34	−0.127
Methyltestosterone	−0.45	−3.99	3.36	3.54	−0.176
Prednisolone	−1.62	−3.10	1.42	1.49	−0.065
Propyl-*p*-hydroxybenzoate	0.36	−2.35	(3.04)	2.71	0.333
Progesterone	−0.71	(−4.15)[g]	3.87	3.45	0.424
Testosterone	−0.49	(−3.87)[g]	3.32	3.38	−0.061
Triazolam	−2.05	−4.09	2.42	2.05	0.371

[a] Values in parentheses taken from the literature. [b] L. J. Edwards, *Trans. Faraday Soc.*, **57**, 1191 (1951). [c] R Charonnat, *Compt. Rend.*, **185**, 284 (1927). [d] F. A. Long and W. F. McDevitt, *Chem. Rev.*, **51**, 119 (1952). [e] L. Erichsen and E. Dobbert, *Brennstoff Chem.*, **36**, 338 (1955). [f] H. Tomida, T. Yotsuyanagi, and K. Ikeda, *Chem. Pharm. Bull., Tokyo*, **26**, 2832 (1978). [g] K. Uekema, T. Fujinaga, F. Hirayama, M. Otagiri, and M. Yamasaki, *Int. J. Pharm.*, **10**, 1 (1982).

ubility parameter of octanol (10.3) is within 3.3 units of the solubility parameter of each compound.

Solubility Ratio and Partition Coefficient—The second major assumption that is used to obtain Eq. 1 is that the octanol–water partition coefficient is equivalent to the octanol–water solubility ratio. Regression analysis clearly indicates a linear relationship between the logarithms of the two parameters:

$$\log PC = 0.900 \log SR + 0.390 \qquad \text{(Eq. 12)}$$
$$r = 0.985 \quad s = 0.233 \quad n = 36$$

For most of the compounds studied, the solubility ratio does not differ greatly from the partition coefficient (Table III). Antipyrine is a notable and inexplainable exception; this difference is concentration dependent.

Figure 3 shows the observed partition coefficients and solubility ratios for the solutes studied. If the regression line is forced through the origin, it becomes:

$$\log PC = 1.027 \log SR \qquad \text{(Eq. 13)}$$
$$r = 0.992 \quad s = 0.326 \quad n = 36$$

which is in agreement with the theoretical expectation. Again the weak electrolytes and the nonelectrolytes conform to regression equations similar to the equation for the entire data set. For weak electrolytes the equation is log PC = 0.868 log SR + 0.421; for nonelectrolytes it is log PC = 0.942 log SR + 0.281.

Experimentally the octanol–water partition coefficient is the ratio of the concentrations of the solute in each of the two phases determined in dilute solution, *i.e.*, PC = C_o/C_w. This differs from the solubility ratio in two respects. The solubility ratio (SR) is the ratio of the solubilities determined in pure octanol and pure water (or buffer), whereas the partition coefficient is based on the concentration ratio determined in water-saturated octanol and octanol-saturated water. The solute–solute interactions, which are concentration dependent, are more significant in the solute-saturated solutions used to determine the solubility ratio than in the dilute solutions used to determine the partition coefficient.

Fortunately these factors are not usually large, and for nonpolar and semipolar solutes (log PC > 0) they tend to negate each other. For polar solutes (log PC < 0), however, these effects amplify each other and increase the difference between the solubility ratio and the partition coefficient.

The effect of self-association of polar solutes at high concentration in octanol will generally increase the partition coefficient by increasing the ability of the octanol to accomodate the solute. This can be seen from a comparison of the partition coefficients determined in dilute solution and at saturation in Table IV. The effect of increasing the concentration of nonpolar solutes is to encourage their self-association in the aqueous phase. This, in turn, usually decreases the octanol–water partition coefficient by increasing the relative proportion of solute in the water. The effect of mutual saturation of the partitioning phases is to decrease the partition coefficient compared to the solubility ratio for nonpolar and semipolar solutes. Mutual saturation makes the octanol more water-like and the water more octanol-like. This tends to decrease the absolute value of log PC by bringing the partition coefficient closer to unity. For three of the four solutes in Table IV, the solubility ratio determined in mutually saturated solvents is closer to unity than the value determined in pure solvents. The mutual cancellation of the above effects can also be seen from the data in Table III, where the partition coefficients determined in dilute solution are quite close to the solubility ratio.

State of Undissolved Solute—The third assumption used for Eq. 1

Table IV—Effect of Mutual Saturation on Solubility Ratio

Solute	log (S_o/S_w) (pure phases)[a]	log (S_o/S_w) (mutually saturated)	log (C_o/C_w) (dilute)[b]
Antipyrine	−0.73	−0.50	0.26
Ethyl-*p*-aminobenzoate	1.86	2.21	1.96
Caffeine	−0.75	−0.42	−0.20
Theophylline	−0.57	−0.08	−0.09

[a] log SR. [b] log PC.

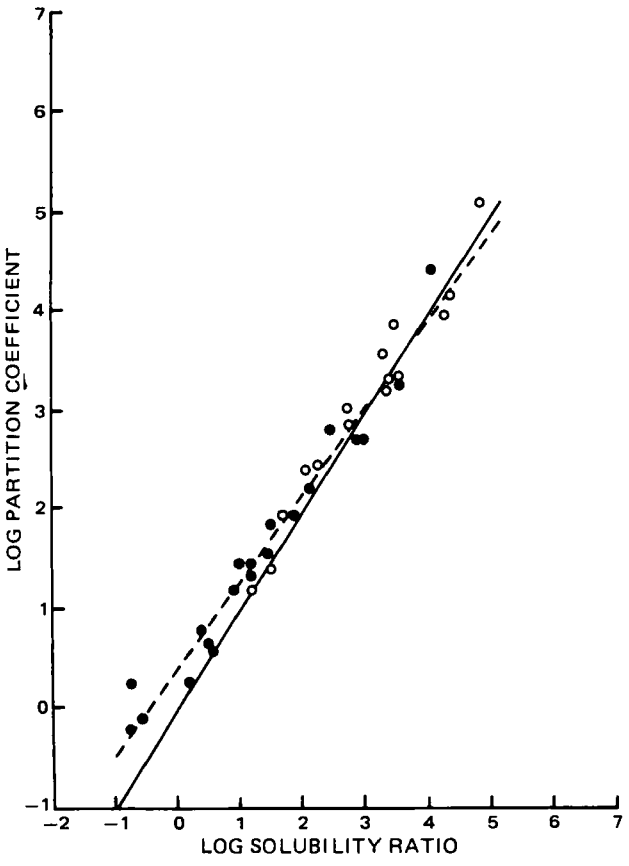

Figure 3—*Partition coefficients and solubility ratios of nonelectrolytes* (○) *and weak electrolytes* (●). *Key:* (—) *theoretical line described by Eq. 3;* (- - - -) *regression line described by Eq. 13.*

is that the melting point of the pure solute is the same as the melting point of the solute in equilibrium with its saturated solution in water. If this is not true, then the melting point used in Eq. 1 would be wrong. Fortunately, most organic compounds do not take up sufficient amounts of water to invalidate this assumption. Some compounds, however, can accomodate large enough amounts of water to significantly alter their physical properties. Phenol, for example, can take up enough water to cause liquification. The use of the normal melting point of phenol in Eq. 1 introduces a systematic error which results in an underestimation of the aqueous solubility of phenol. Still other organic compounds form crystalline hydrates which have melting points that are significantly different from the anhydrous parent compounds. If a substance is known to form a hydrate, the melting point of the hydrate should be used in Eq. 1. If a substance forms an undetected hydrate and if the melting point of this hydrate is different from the melting point of the unequilibrated material, then the use of the melting point of the latter would result in an erroneous estimation of the aqueous solubility.

It is not always feasible to isolate the exact species of a solute that is in equilibrium with its saturated solution. Recrystallization and drying can alter the water content and even the crystal form of the solute. Even the act of determining the melting point can alter the crystal in favor of a more anhydrous or a more stable form. For these reasons it appears likely that the use of an inappropriate melting point is the most likely source of error in the use of Eq. 1.

Fortunately, melting point alterations caused by water are rarely a problem with nonpolar solutes and are only infrequently significant for semipolar solutes. This is confirmed by the highly successful application of Eq. 1 to nonpolar solutes (1) and to a mixture of nonpolar and semipolar solutes (2), as well as to the compounds used herein.

REFERENCES

(1) S. H. Yalkowsky, S. C. Valvani, and D. Mackay, *Residue Rev.*, **85**, 43 (1983).

(2) S. H. Yalkowsky and S. C. Valvani, *J. Pharm. Sci.*, **69**, 912 (1980).

(3) S. C. Valvani and S. H. Yalkowsky, in "Physical Chemical Properties of Drugs," S. H. Yalkowsky, A. A. Sinkula, and S. C. Valvani, Eds., Dekker, New York, N.Y., 1980.

(4) S. H. Yalkowsky and S. C. Valvani, *J. Chem. Eng. Data*, **24**, 127 (1979).

(5) S. H. Yalkowsky, R. J. Orr, and S. C. Valvani, *I&EC Fundam.*, **18**, 351 (1979).

(6) S. Banerjee, S. H. Yalkowsky, and S. C. Valvani, *Environ. Sci. Technol.*, **14**, 1227 (1980).

(7) C. Hansch and A. Leo, "Substituent Constants for Correlation Analysis in Chemistry and Biology," Wiley-Interscience, New York, N.Y., 1979.

(8) M. Windholz, Ed., "The Merck Index," 9th ed., Merck & Co., Rahway, N.J., 1976.

(9) S. H. Yalkowsky, *I&EC Fundam.*, **18**, 108 (1979).

Effects of Organic Anions on the Uptake of 1-Anilino-8-naphthalenesulfonate by Isolated Liver Cells

YUICHI SUGIYAMA [x], SEIICHI KIMURA, JIUNN HUEI LIN [*], MAKOTO IZUKURA, SHOJI AWAZU [‡], and MANABU HANANO

Received January 5, 1982, from the *Faculty of Pharmaceutical Sciences, University of Tokyo, Hongo, Bunkyo-ku, Tokyo 113, Japan.* Accepted for publication July 15, 1982. *Present Address: Drug Metabolism Section, Merck Sharp & Dohme Research Laboratory, West Point, PA 19486. ‡Present Address: Department of Biopharmacy, Tokyo College of Pharmacy, Horinouchi, Hachioji, Tokyo 192-03, Japan.

Abstract □ Uptake of the fluorescent probe, 1-anilino-8-naphthalenesulfonate (I) into isolated rat liver cells was studied using both fluorescence and filtration methods. The time course of the fluorescence enhancement of I after addition to the isolated liver cells was analyzed in terms of rapid, medium, and slow phases. The slow phase (half-time ~7 min) was characteristic of viable cells. The fluorescence enhancement was proportional to the amount of I taken into the cells, as measured by the filtration method. The uptake of I followed Michaelis–Menten kinetics with an apparent K_m of 39 μM and V_{max} of 1.4 nmole/10^6 cells/min. The temperature coefficient (Q_{10}) of the uptake of I was found to be ~1.9. No pH optimum was observed, and various metabolic inhibitors did not affect the uptake of I. Among the amino acid reagents used, only 2,4-dinitrofluorobenzene decreased the uptake of I (by ~45%). The effects of various organic anions on the uptake of I were measured. The inhibition of the uptake of I by sulfobromophthalein could be analyzed in terms of competitive inhibition; the slight inhibition by sodium taurocholate could not. It is concluded that the uptake of I is a carrier-mediated facilitated process, and that the carrier is common to both I and sulfobromophthalein.

Keyphrases □ Fluorescence—measurement of 1-anilino-8-naphthalenesulfonate uptake into isolated rat liver cells, effect of organic anions, comparison with filtration method □ 1-Anilino-8-naphthalenesulfonate—determination of uptake into isolated rat liver cells using fluorescence enhancement, effect of organic anions, kinetics □ Kinetics—of 1-anilino-8-naphthalenesulfonate uptake into isolated rate liver cells, fluorescence enhancement, effect of organic anions

Sulfobromophthalein (II) and indocyanine green (III) are anionic drugs used to test liver function. The uptake mechanism responsible for the rapid and relatively selective hepatic clearance of these anions has been studied using whole animals (1–3), isolated perfused rat liver (3–5), liver slices (6), and isolated liver cells (7, 8). These studies suggested that the hepatic uptake of these anionic drugs is a carrier-mediated process.

Bile acids, endogenous compounds that are anionic at physiological pH, are also readily extracted from the plasma by the liver. Many investigators (9–11) have suggested that a carrier-mediated process might be responsible for the hepatic uptake of bile acids. If this is true, the question then arises as to whether the aforementioned anionic dyes and bile acids are transported by a common carrier. Studies on the inhibition of the uptake of one compound by another in isolated perfused rat liver (3, 5) and isolated rat liver cells (7) led to the suggestion that bile acids and other organic anions such as II and III are transported into the liver by two different systems.

The anionic fluorescent probe, 1-anilino-8-naphthalenesulfonate anion (I) has been used to study the membrane structure of several isolated membrane systems (12–14) since the large changes in its fluorescence parameters are observed in different environments (15, 16). Compound I also is an effective probe in the study of anion transport in erythrocytes (17) and Ehrlich ascites cells (18). Recently, Cheng and Levy (19) described the interaction of I with isolated rat liver cells, observing that the transport of I into liver cells was a carrier-mediated process. In the present study, we have attempted to clarify the mechanism of the uptake of I into isolated liver cells and to determine whether the transport system of I is shared by other organic anions, such as II, III, and the bile acid salts.

EXPERIMENTAL

Materials—The following analytical grade materials were used: sodium 1-anilino-8-naphthalenesulfonate[1], bromophenol[1], rose bengal[2], *p*-aminohippuric acid[2], sulfobromophthalein[3], indocyanine green[3], phenolsulfonphthalein[3], sodium taurocholate[4], sodium oleate[1], potassium cyanide[2], *n*-ethylmaleimide[2], 2,4-dinitrofluorobenzene[2], rotenone[4], carbonylcyanide *m*-chlorophenylhydrazone[4], *p*-hydroxymercuribenzoate[4], trypan blue[2], and collagenase (type I)[4].

Isolation of Liver Cells—Liver cells were isolated using a modification of the procedure of Baur *et al.* (20). Male Wistar rats (260–330 g), given free access to food and water, were used. During preparation, the liver was perfused with a calcium-free perfusion buffer at 37° *via* the vena portae (35 ml/min for 15 min). After preparation of the liver, perfusion was continued with a recirculating medium containing 4 m*M* calcium and 0.05% collagenase. After 15–20 min, the vena portae began to leak; the perfusion was continued *via* the vena cava for another 10–15 min. After perfusion for ~30 min, the liver disintegrated. Subsequently, the tissue was transferred to a round-bottomed flask and enzymatic treatment was continued for another 10 min with slow stirring. After washing, the cells were stored as a suspension (5×10^6 cells/ml) at 0° in a standard buffer saturated with 95% O_2 and 5% CO_2[5]. The composition of the perfusion buffer was: 121 m*M* NaCl, 6 m*M* KCl, 0.6 m*M* $MgSO_4$, 12 m*M* $NaHCO_3$, 0.74 m*M* KH_2PO_4, and 5 m*M* glucose (pH 7.2–7.1). The composition of the standard buffer was: 131 m*M* NaCl, 5.2 m*M* KCl, 0.9 m*M* $MgSO_4$, 0.12 m*M* $CaCl_2$, 3 m*M* Na_2HPO_4, and 10 m*M* Tris/HCl (pH 7.4).

Cell viability for each experiment was determined by the trypan blue exclusion test; the value obtained usually ranged from 93–98%. Damaged liver cells (<9% viability) were prepared by treatment in an automatic mixer for >5 min.

Uptake Studies—*Filtration Method*—Aliquots of the stock cell suspensions were diluted in 5 ml of the standard buffer to a final concentration of 5×10^5 cells/min. After preincubation for 3 min at 25°, small aliquots (3–35 μl) of a 5 m*M* solution of I were added, and the mixtures were incubated for various times. The uptake process was terminated by vacuum filtration of 1 ml of the suspension using a glass-fiber membrane[6]. After washing the cells on the filter three times with 3 ml of the ice-cold standard buffer, the content of I in the cells was analyzed spectrofluorometrically[7]. The cells were extracted with 4 ml of solvent (methanol–1 *N* NaOH, 8:1) for 1 hr. After centrifugation[8] at 3000 rpm for 15 min, the supernatant solution was analyzed spectrofluorometrically at 500 nm (excitation at 390 nm). The recovery of I from the liver cells was nearly 100%.

Fluorescence Method—The fluorescence measurements[7] were performed at room temperature (20–22°), unless otherwise stated, with 10-nm slit widths for both excitation and emission channels and a 430-nm

[1] Tokyo Chemical Industries, Co., Tokyo, Japan.
[2] Wako Pure Chemical Co., Tokyo, Japan.
[3] Daiichi Chemical Co., Tokyo, Japan.
[4] Sigma Chemical Co., St. Louis, Mo.
[5] Carbogen, Takachiho Shoji Co., Tokyo, Japan.
[6] GF/F membrane, Whatman.
[7] Hitachi MPF-4 fluorescence spectrometer.
[8] Kubota centrifuge.

0022-3549/83/0800-0871$01.00/0

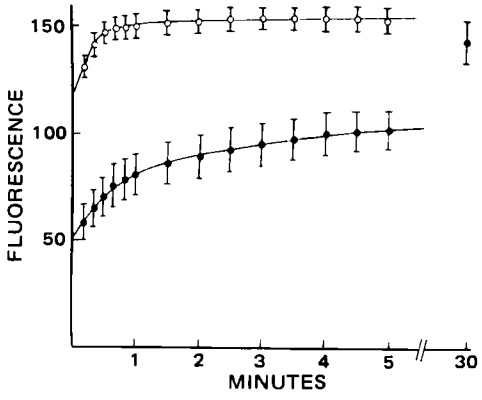

Figure 1—*Time course of the fluorescence enhancement of I (38 μM) added to isolated liver cells (5 × 10^5 cells/ml) in the standard buffer (pH 7.4) at room temperature. Excitation is at 400 nm; emission is at 480 nm; fluorescence is in arbitrary units. Each point is the mean of five experiments; bars represent the standard error. Key: (●) intact cells (93–98% cell viability); (○) damaged cells (3–9% cell viability).*

cutoff filter. The excitation and emission wavelengths for I were 400 and 480 nm, respectively. If necessary, fluorescence intensities were corrected for the inner filter effect according to the method of Chignell (21).

Small aliquots of a solution of I were added to the cell suspension (5 × 10^5 cells/ml) in the standard buffer. The solution was preincubated for 5 min and quickly mixed with a small stirring rod, and the fluorescence intensity was recorded at a chart speed of 12 cm/min. The mixing procedure could be performed in <4–6 sec. In some experiments, after the time course of uptake had been recorded for 30 sec after the addition of I, the zero point was lowered by adjusting the zero-suppression knob, and the sensitivity was increased so that the change of fluorescence could be monitored more closely.

In the experiments on inhibition by other organic anions, inhibitors were added 10 sec before the addition of I. In the experiments on inhibition by metabolic inhibitors and amino reagents, the reagents were added at the beginning of the 5-min preincubation.

Kinetic Analysis of the Data Obtained by the Fluorescence Method—For reasons discussed subsequently, the initial uptake rate of I was obtained from the initial slope of the slow component of fluorescence enhancement (40–100 sec). If the change of fluorescence (ΔF_{cell}) is assumed to be proportional to the change of I content within the cells (ΔA_{cell}), then:

$$\Delta F_{cell} = q_{cell} \cdot \Delta A_{cell} \qquad \text{(Eq. 1)}$$

where q_{cell} is the proportionality coefficient, which corresponds to the quantum yield of I bound to the intracellular components. [The validity of this assumption will be demonstrated later (*Results*).] The initial uptake rate in a carrier-mediated transport system can be expressed by the Michaelis–Menten-type equation:

$$\overline{\Delta A}_{cell} = \frac{V_{max} \cdot (A)}{K_m + (A)} \qquad \text{(Eq. 2)}$$

where $\overline{\Delta A}_{cell}$ is the initial uptake rate (40–100 sec), K_m is the apparent Michaelis constant, V_{max} is the maximum rate of uptake, and (A) is the concentration of I in the medium. Substituting Eq. 2 into Eq. 1 gives:

$$\overline{\Delta F}_{cell} = \frac{\overline{\Delta F}^{max}_{cell} \cdot (A)}{K_m + (A)} \qquad \text{(Eq. 3)}$$

where:

$$\overline{\Delta F}^{max}_{cell} = q_{cell} \cdot V_{max} \qquad \text{(Eq. 4)}$$

and $\overline{\Delta F}_{cell}$ is the initial rate of fluorescence enhancement (40–100 sec).

The binding of I to the plasma membrane of liver cells was determined by extrapolating the uptake curves to time zero, as described previously (7, 9, 11, 22). The kinetic analysis was carried out in a similar way, using:

$$F_{zero} = \frac{F^{max}_{zero} \cdot (A)}{K_{pm} + (A)} \qquad \text{(Eq. 5)}$$

and

$$F^{max}_{zero} = n \cdot q_{membrane}(P_{cell}) \qquad \text{(Eq. 6)}$$

Here, F_{zero} is the fluorescence intensity obtained by extrapolating the uptake curves to time zero, $q_{membrane}$ is the proportionality coefficient

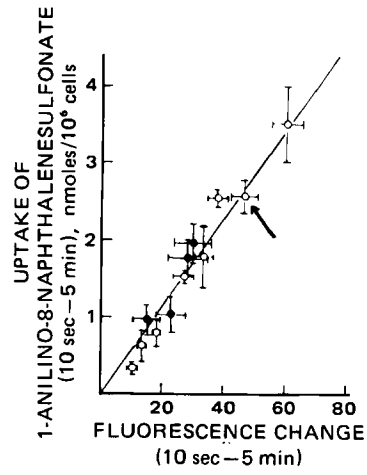

Figure 2—*Comparison of measurements of I uptake by the fluorescence and filtration methods using the same cell preparation. Small aliquots (3–35 μl) of I were added to the cell suspension (5 × 10^5 cells/ml), and the fluorescence change from 10 sec to 5 min was measured (abscissa), as described in Fig. 1. The amount of I taken into the cells during the same period was measured by the filtration method (ordinate). Each point is the mean of 4–5 experiments; bars represent the standard error. Key: (○) in the absence of II (concentration of I, 4.7–54 μM); (●) in the presence of II, added 10 sec before the addition of I (concentration of I, 38 μM; concentration of II, 20–60 μM). The arrow shows the result at a I concentration of 38 μM in the absence of II (control).*

(which corresponds to the quantum yield of I bound to the plasma membrane), K_{pm} is the dissociation constant, (P_{cell}) is the concentration of cells, (A) is the concentration of I in the medium, and n is the number of binding sites for I on a cell. Kinetic parameters were calculated with a program (23) for least-squares fitting, using a computer[9].

RESULTS

Time Course of I Uptake into Intact and Damaged Cells—When 38 μM I was added to hepatocytes (5 × 10^5 cells/ml), a marked enhancement of the fluorescence of I was observed. The fluorescence of I in buffer alone was negligible when compared with that obtained in the presence of hepatocytes. Figure 1 shows the time course of fluorescence enhancement of I both in intact and damaged cells. The time course in damaged cells (viability <9%) showed a rapid phase (half-time less than the mixing time) and a time-dependent (medium) phase which had almost reached a plateau within 40 sec. In the case of intact cells, a new time-dependent kinetic phase (slow phase) appeared, and the fluorescence intensity continued to increase up to 30 min. This slow phase, which is characteristic of intact cells, is thought to reflect the uptake of I and subsequent binding to intracellular components, while the rapid phase may correspond to the binding of I to plasma membrane. On this basis, the initial uptake rate was calculated from the initial slope of the slow phase of fluorescence enhancement (40–100 sec), as shown in Fig. 1.

Comparison of the Data Obtained by the Fluorescence and the Filtration Methods—To analyze the uptake of I by the fluorescence method, the validity of Eq. 1 must be demonstrated. Therefore, the changes of the fluorescence of I (10 sec–5 min) were compared with the amounts of I transported into cells during that period, as directly measured by the filtration method (Fig. 2). Figure 2 shows that the change of fluorescence (ΔF_{cell}) is proportional to that of I content within cells (ΔA_{cell}). The q_{cell} value in Eq. 1 was calculated to be 18.7/nmole of I from the data in Fig. 2.

The cell–medium ratio (C/M) of I after the establishment of equilibrium between the cells and the medium (~30 min after the addition of I) was calculated both from the data in Fig. 1 and from the q_{cell} value. In calculating the intracellular concentration of I, an intracellular volume of 4.2 μl/10^6 cells was used (24). C/M values of 45 ± 4 and 36 ± 2 were calculated for initial I concentrations of 4.7 μM and 39 μM, respectively.

Kinetic Analysis of the Initial Uptake Rate and Binding to Plasma Membrane at Various Concentrations of I—The initial rates (40–100 sec) of I uptake at concentrations ranging from 4.7 to 78.5 μM

[9] Hitachi 8700/8800 computer.

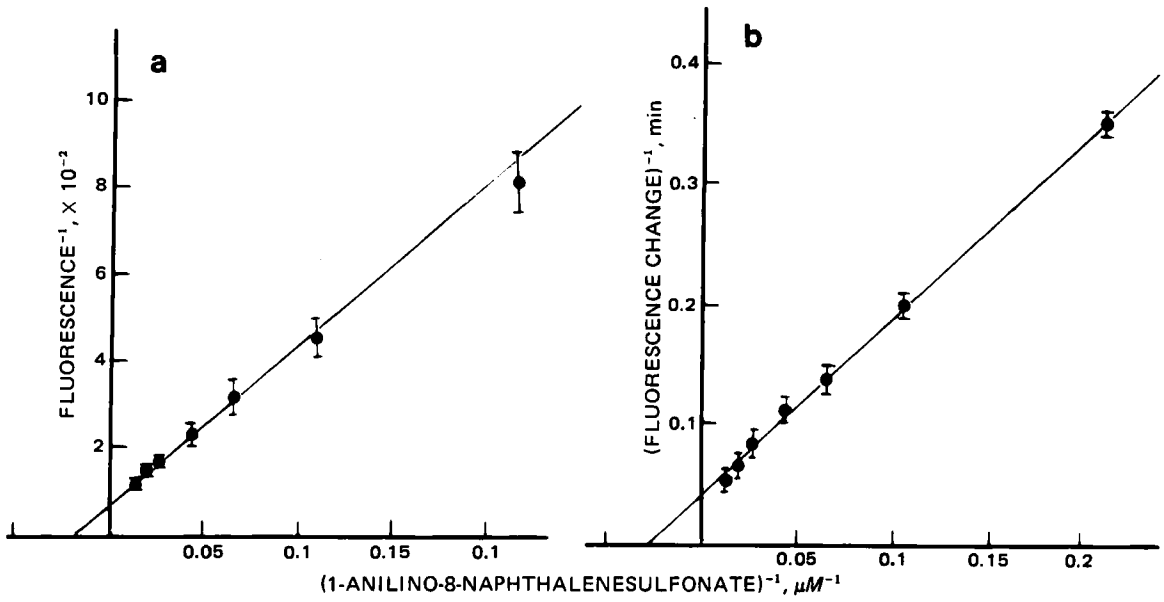

Figure 3—*(a) Double-reciprocal plot of I binding to the plasma membrane, determined by extrapolating the curve of fluorescence enhancement to time zero. The line represents the regression line calculated using Eq. 5. (b) Lineweaver–Burk plot of I uptake with the initial rate calculated from the initial slope (40–100 sec) of the slow phase (Fig. 1). The line represents the regression line calculated using Eq. 3. The fluorescence was measured at room temperature in the standard buffer with a cell concentration of 5 × 10^5 cells/ml. Each point is the mean of 5–9 experiments; bars represent the standard error.*

were measured by the fluorescence method. Figure 3b shows a Lineweaver–Burk plot of the uptake rates based on Eq. 3. An apparent K_m of 38.8 ± 5.2 μM and $\overline{\Delta F}^{max}_{cell}$ of 26 ± 2.8 min^{-1} were obtained. A V_{max} of 1.39 ± 0.15 nmole/10^6 cells/min was calculated from the $\overline{\Delta F}^{max}_{cell}$ and the q_{cell} values (18.7/nmole of I).

The binding of I to the plasma membrane of liver cells was determined by extrapolating the uptake curves to time zero. The data thus obtained were analyzed by means of a double-reciprocal plot based on Eq. 5, as shown in Fig. 3a. A dissociation constant (K_{pm}) of 56.7 ± 5.5 μM was obtained.

Effects of Metabolic Inhibitors and Amino Acid Reagents—To determine whether the uptake of I is dependent on metabolic energy, 19 μM I was added to cell suspensions preincubated for 5 min with one of four metabolic inhibitors, and the initial enhancement of fluorescence (40–100 sec) was measured. The inhibitors were potassium cyanide (1 mM), which blocks electron transport at the final step; rotenone (10 μM), which blocks electron transport near the initial step; ouabain[4] (1 mM), which inhibits Na^+-K^+ ATPase and the oxidative phosphorylation uncoupler carbonylcyanide *m*-chlorophenylhydrazone (10 μM). None of the inhibitors had a detectable effect on the initial uptake of I. Consequently, the concentrative uptake of I (C/M = 36–45) described previously is not due to the active transport of I, but to its binding to intracellular components.

The effects of amino acid reagents, which have been successfully used in membrane and cell research to inhibit carrier-mediated processes, were measured by the fluorescence method. *p*-Hydroxymercuribenzoate (100 μM) and *n*-ethylmaleimide (100 μM), which bind covalently to free sulfhydryl groups, did not significantly reduce the initial uptake of I (concentration of I, 19 μM); 2,4-dinitrofluorobenzene (100 μM), which binds covalently to free amino groups, decreased the initial uptake of I by 47 ± 7% (mean ± *SE* for three separate experiments). To confirm its effect, 2,4-dinitrofluorobenzene was also studied by the filtration method, which gave similar results, *i.e.*, a reduction ratio of 43% (n = 2).

Effect of Temperature and pH—In viable cells, the initial enhancement of fluorescence (40–100 sec) at 35° was higher than that at 25° (Fig. 4). The temperature coefficient ($\Delta F_{35°}/\Delta F_{25°}$) was 1.43 ± 0.12 ($n$ = 3). The dependence of the initial uptake of I on temperature was also measured by the filtration method, and a temperature coefficient (Q_{10}) of 1.9 ± 0.3 (n = 3) was obtained. The methods seem to give slightly different coefficients. The most likely explanation for this discrepancy is that the q_{cell} value in Eq. 1 changes with temperature. In damaged cells, the fluorescence intensity obtained after establishment of equilibrium at 25° was higher than that at 35° ($F_{35°}/F_{25°}$ = 0.83 ± 0.05). This result

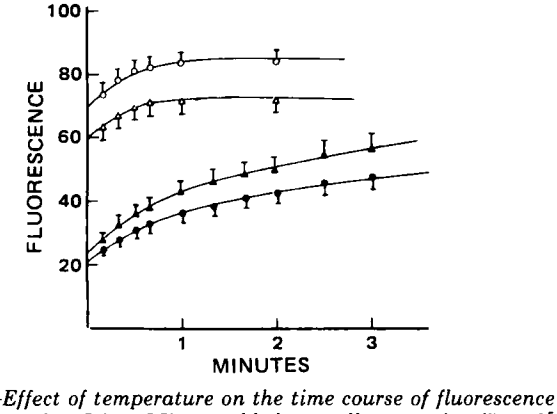

Figure 4—*Effect of temperature on the time course of fluorescence enhancement when I (19 μM) was added to a cell suspension (5 × 10^5 cells/ml) in the standard buffer. Each point is the mean of three experiments; bars represent the standard error. Key: (●) intact cells, 25°; (▲) intact cells, 35°; (○) damaged cells, 25°; (△) damaged cells, 35°.*

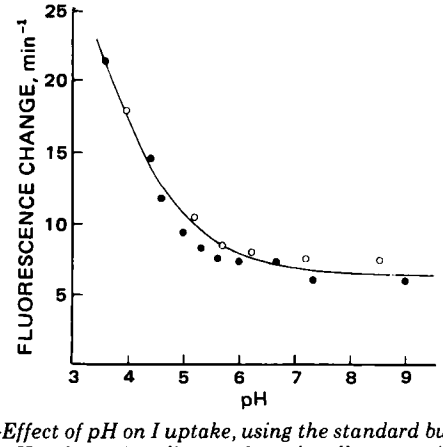

Figure 5—*Effect of pH on I uptake, using the standard buffer brought to various pH values. An aliquot of stock cell suspension (1 × 10^8 cells/ml) was diluted with the medium at each pH to yield a final concentration of 5 × 10^5 cells/ml prior to the addition of I (19 μM). The initial rates of uptake were measured by the fluorescence method as described in Fig. 3b. After the fluorescence measurement, the pH of each suspension was remeasured. Open and closed circles represent results using different cell preparations.*

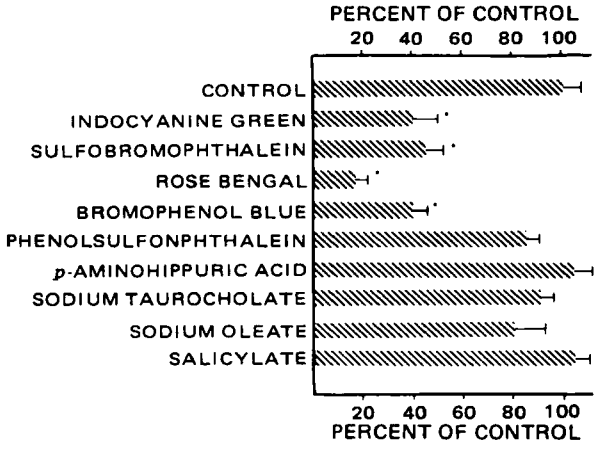

Figure 6—*Inhibitory effects of various organic anions at concentrations of 20 μM. Inhibitors were added to the cell suspension in the standard buffer (5 × 10^5 cells/ml) 10 sec before the addition of I (19 μM). Initial rates of uptake were measured by the fluorescence method as described in Fig. 3b. Fluorescence intensities were corrected as necessary for the inner filter effect. Each point is the mean for 3–4 experiments; bars represent the standard error; asterisks indicate statistical significance at the* $p < 0.05$ *level.*

in damaged cells might reflect a change of q_{cell} with temperature. On this basis, the Q_{10} obtained by the fluorescence method was recalculated as 1.75 (1.43/0.83), which is in good agreement with the value obtained by the filtration method.

Figure 5 shows the pH dependence of the initial uptake rate of I (concentration, 19 μM) measured by the fluorescence method. Between pH 6 and 9, the fluorescence was considerably increased.

Effects of Organic Anions—The initial uptake rate of 19 μM I was determined by the fluorescence method in the presence of various organic anions, each at 20 μM concentration (Fig. 6). Four organic anions (II, III, bromophenol blue, and rose bengal), which are thought to act as substrates for an organic anion transport system in the liver, inhibited the uptake of I by >50%; sodium taurocholate, which is thought to be transported into the liver by a different system (3, 5), did not show significant inhibition. *p*-Aminohippuric acid and phenolsulfonphthalein, which are known to act as substrates for an organic anion transport system in the kidney, did not have a significant effect.

Compound II and sodium taurocholate were selected as typical anions transported into the liver by different systems, and kinetic investigations of the inhibition of I uptake using these compounds were carried out. First, the effect of the addition of II on the q_{cell} value in Eq. 1 was examined (Fig. 2). Although both the fluorescence and filtration methods showed inhibition of I uptake by II, the q_{cell} value was not significantly altered by II. This finding indicates that it is possible to analyze the inhibition of I uptake kinetically by the fluorescence method.

In Fig. 7, the reciprocal of the initial rate of fluorescence enhancement

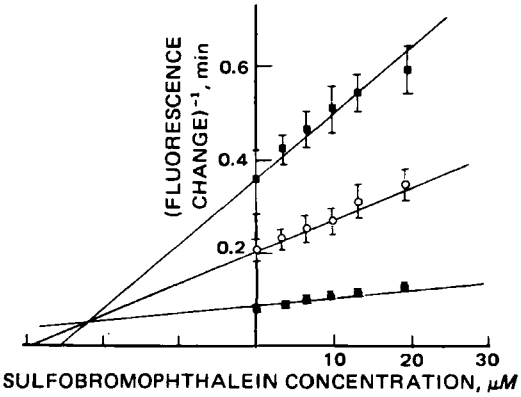

Figure 7—*Dixon plot of I uptake in the presence of II, measured by the fluorescence method, as described in Fig. 3b. Compound II was added 10 sec before the addition of I to the cell suspension (5 × 10^5 cells/ml). Each point is the mean of three experiments; bars represent the standard error. The lines represent the regression lines calculated using Eq. 7. Key: concentration of I (■) 4.7 μM; (○) 9.4 μM; (●) 38 μM.*

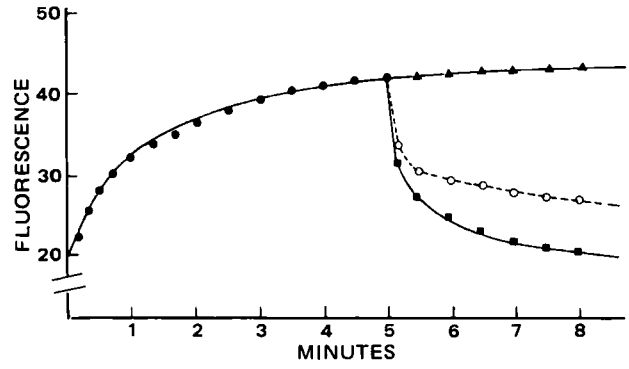

Figure 8—*Countertransport study using a small aliquot of buffer (▲), 20 μM II (○), or 20 μM III (■) added to the cell suspensions (5 × 10^5 cells/ml) after incubation with 19 μM I for 5 min. Each point is the mean of two experiments. The data points (●) before 5 min are means taken from the uptake experiments.*

of I (40–100 sec) is plotted *versus* the concentration of II. This Dixon plot shows that the uptake of I is inhibited competitively by II. The kinetic parameters $K_m = 32.7 \pm 6.5$ μM, $K_i = 22.2 \pm 2.7$ μM, and $\overline{\Delta F}^{max}_{cell} = 22.2 \pm 4.3$ min^{-1} were obtained by fitting the data to an equation that corresponds to competitive inhibition:

$$\overline{\Delta F}_{cell} = \frac{\overline{\Delta F}^{max}_{cell} \cdot (A)}{K_m(1 + i/K_i) + (A)} \qquad \text{(Eq. 7)}$$

where i is the concentration of inhibitor (II), K_i is the inhibition constant, and the other symbols are the same as those in Eqs. 3 and 4. The kinetic parameters thus obtained ($K_m = 32.7$ μM and $\overline{\Delta F}^{max}_{cell} = 22.2$ min^{-1}) are in good agreement with those ($K_m = 38.8$ μM and $\overline{\Delta F}^{max}_{cell} = 26.0$ min^{-1}) obtained from an independent uptake study of I (Fig. 3a).

On the other hand, inhibition by sodium taurocholate could not be detected in Fig. 5, so the inhibition of I uptake (19 μM) at a higher concentration of sodium taurocholate was measured. Even 170 μM sodium taurocholate inhibited the uptake of I by only 20% (mean of two separate experiments). If it is assumed that the uptake of I is competitively inhibited by sodium taurocholate and that the K_i value is 19 μM, 20 and 170 μM sodium taurocholate should inhibit the uptake of I by 41 and 86%, respectively[10]. A Michaelis constant of 19 μM was obtained by Schwarz *et al.* (9) in a study of taurocholate uptake into isolated liver cells. Marked discrepancies between the observed and calculated values suggest that the uptake system of sodium taurocholate is different from that of I.

Countertransport—Compound II was added to the cell suspension after addition of I (Fig. 8). The addition of II induced a rapid decrease of fluorescence which was complete within 10 sec, followed by a slower decrease. The rapid decrease suggests the inhibition of the plasma membrane binding of I by II. The slower decrease of fluorescence may represent the efflux of I previously taken into the cells, reflecting countertransport (1, 25, 26). A similar effect was also seen when III was added instead of II.

DISCUSSION

Many studies on the hepatic uptake of various compounds utilize isolated liver cells, and the advantage of their use has been discussed (7, 8, 27). In most of these studies, cells were separated from the incubation medium by centrifugation or filtration. The present study, using a fluorescence probe (I) as a substrate, has the advantage that the uptake of I can be determined simply by measuring the fluorescence change, without separation. This method has already been adopted in studies of anion transport in erythrocytes (17), Ehrlich ascites cells (18), and isolated liver cells (19).

The time course of fluorescence enhancement of I (Fig. 1) was analyzed by means of a semilogarithmic plot of log [fluorescence change (total

[10] Equation 7 yields the following equation:
Ratio of fluorescence change (R)

$$= \frac{\overline{\Delta F}_{cell} \text{ in the presence of sodium taurocholate}}{\overline{\Delta F}_{cell} \text{ in the absence of sodium taurocholate}}$$

$$= \frac{K_m + (A)}{K_m(1 + [\text{sodium taurocholate}]/K_i) + (A)}$$

where $K_m = 38.8$ μM, $(A) = 19$ μM, and $K_i = 19$ μM.

minus partial)] against time. This method is known to give good fits to kinetic data obtained in experiments with erythrocyte ghosts (28) or submitochondrial particles (29). The plot in the case of intact cells could be analyzed in terms of a three-exponential equation (not shown): *i.e.*, the fluorescence enhancement consisted of a rapid phase (half-time less than the mixing time), a medium phase (half-time of ~15 sec), and a slow phase (half-time of ~7 min). The rapid, medium, and slow phases comprised ~35, 20, and 45% of the overall fluorescence enhancement, respectively. Damaging the cells by vigorous shaking (viability <9%) hardly affected the half-time of the medium phase, but abolished the slow phase. A half-time (~15 sec) corresponding to the medium phase in the present study was also found in studies of the interaction of I with erythrocyte ghosts (28) and plasma membranes of hepatoma tissue culture cells (19), both of which lack intracellular components. Our findings and those of other workers suggest that the rapid phase corresponds to the binding to superficial sites of the plasma membrane, the medium phase to the binding to deep sites within the plasma membrane, and the slow phase to the uptake and subsequent binding to intracellular components. We assumed that the permeability barrier to I would be destroyed in damaged cells, and used the slow phase for measurement of the initial uptake of I. Cheng and Levy (19) used the period from 30 to 120 sec in uptake studies of I into isolated liver cells. However, in the present studies, we used 40–100 sec for measurement of the initial rate of uptake as the plot of fluorescence enhancement against time showed curvature after 100 sec (Fig. 1). Furthermore, we used 40 sec as the starting time of the slow phase to avoid the contribution of the medium phase.

Before the fluorescence method can be accepted for the measurement of I uptake, it must be demonstrated that the fluorescence change is proportional to the amount of I taken into the cells, *i.e.*, the q_{cell} value in Eq. 1 should be constant regardless of the I concentration within the cell. The results shown in Fig. 2, which demonstrate the validity of Eq. 2, confirm this method. The q_{cell} value (18.7/nmole of I) was obtained from the data between 10 sec and 5 min (Fig. 2); however, strictly speaking, the q_{cell} value should be obtained using only the slow phase, which is thought to reflect the true uptake phase. On the other hand, we also compared the changes of I fluorescence (0–10 sec) at several concentrations of I in a similar way. This period is thought to reflect the binding to the plasma membrane. A $q_{membrane}$ of 23/nmole of I was obtained in this experiment (unpublished data). This $q_{membrane}$ value, which corresponds to the quantum yield of I bound to the plasma membrane of liver cells, is not very different from the q_{cell} value (18.7/nmole of I). This result suggests that the quantum yields of I are essentially the same whether I is bound to the plasma membrane or to the intracellular components. Therefore, the q_{cell} value obtained from the data between 10 sec and 5 min may be considered to represent the true q_{cell} value. Moreover, the q_{cell} value was not altered by II (Fig. 2), and this result made it possible to investigate the inhibition of I uptake by II using the fluorescence method. To our knowledge, this is the first experiment demonstrating the validity of the fluorescence method.

Several specific criteria must be met to demonstrate the presence of carrier-mediated transport across biological membranes: the transport system must be saturable, structurally similar compounds should inhibit the transport process, and the system should show countertransport. These criteria are common to both active-transport and facilitated-diffusion processes. To differentiate between these two types of transport, other criteria are required.

By definition, active transport differs from facilitated diffusion in two ways: (*a*) transport of a substrate can occur against a chemical potential and (*b*) an expenditure of metabolic energy is required and the process generally is associated with a temperature coefficient (Q_{10}) of ≥3 (25). Each of these criteria was investigated in detail for the I uptake into isolated liver cells. The saturability (Fig. 3b) and the competitive inhibition by II (Fig. 7) suggest that a carrier-mediated transport system may be responsible for the uptake of I; saturability of I uptake was also suggested by Cheng and Levy (19). A countertransport study was undertaken to confirm the presence of carrier-mediated transport. The results obtained with II and III suggest countertransport (Fig. 8). However, these results should be interpreted with caution, since the phenomena shown in Fig. 8 might occur if II and III simply displace I from the binding sites of I on the intracellular components. This displacement would increase the unbound concentration of I within the cells and, thus, accelerate the efflux of I to the medium. Therefore, the fluorescence change caused by II and III shown in Fig. 8 is necessary but not sufficient to demonstrate true countertransport.

In addition to these findings, the inhibition of I uptake by 2,4-dinitrofluorobenzene, which combines with free amino groups on the carrier molecule, strongly suggests the countribution of a carrier-mediated process to uptake of I. It has been shown that sulfhydryl reagents can inhibit the uptake of cortisol (30) and procainamide ethobromide (31) into isolated liver cells. In the present study, *p*-hydroxymercuribenzoate and *n*-ethylmaleimide did not have a significant inhibitory effect. This may indicate the absence of a functional sulfhydryl group at the active site of the carrier protein for I. However, the uptake of I was unaffected by various metabolic inhibitors, suggesting that active transport is not involved. Independence of metabolic energy has also been demonstrated by Schwenk *et al.* (7) in the uptake of II into isolated liver cells. Furthermore, the relatively small dependence of I uptake on temperature (Q_{10} = 1.9) also suggests a facilitated-diffusion process. A similar temperature dependency (activation energy of 11 kcal/mole, Q_{10} of ~2) was reported in the uptake of II into isolated liver cells (7). Based on these findings, which suggest the facilitated diffusion of I, the accumulation of I in the cells (C/M of 36–45) found in the present study could be regarded as due to the binding of I to the intracellular components. In fact, I is bound to the cytoplasmic binding proteins (X, Y, and Z fraction) in the liver, especially to the Z-protein (32).

With regard to pH, the uptake of I (Fig. 5) is similar to that of II (7). Both have no pH optimum, though the uptake was considerably increased below pH 6. As described above, the uptake of I resembles that of II in many respects, namely the effect of metabolic inhibitors, the temperature dependence, and the pH profile. On the other hand, the uptake of sodium taurocholate was inhibited by metabolic inhibitors (carbonylcyanide *m*-chlorophenylhydrazone, ouabain, and antimycin A), the activation energy amounted to 29 kcal/mole which corresponds to a Q_{10} of ~5, and the uptake showed a pH optimum between pH 6.5 and pH 8.0 (9).

The similarity of the uptake of I to that of II raised the possibility that both compounds share a common carrier. To test this possibility, the effect of II on the uptake of I was studied kinetically (Fig. 7). A Dixon plot showed that uptake of I is inhibited competitively by II, indicating a common carrier for the uptake of both compounds. The K_i value (22 μM) of II obtained in the present study is comparable with the K_m value (7 μM) for II obtained by Schwenk *et al.* (7). On the other hand, the slight inhibition of I uptake by a high concentration of sodium taurocholate (170 μM) could not be explained by competitive inhibition. These findings indicate that I and II are transported by the same carrier, and that this carrier is different from that for sodium taurocholate. This result supports the hypothesis of Paumgartner and Reichen (3, 5) that there are at least two transport systems for organic anions: one for bile acids and the other for organic anions such as II and III.

Recently, a high-affinity binding protein for II (thought to be the carrier protein) has been isolated from the plasma membrane of the rat liver (33–35). During this isolation, the binding activity at each step was evaluated by gel-filtration using a small column (33) or equilibrium dialysis (34). The present result that I and II share a common carrier raised the possibility that fluorescence measurements of I could provide a simple and novel method for detecting binding protein for organic anions such as II and III during the isolation procedures.

REFERENCES

(1) B. F. Scharschmidt, J. G. Waggoner, and P. D. Berk, *J. Clin. Invest.*, **56**, 1280 (1975).

(2) C. A. Goresky, *Am. J. Physiol.*, **207**, 13 (1964).

(3) G. Paumgartner and J. Reichen, *Experientia (Basel)*, **31**, 306 (1975).

(4) J. Reichen and G. Paumgartner, *Am. J. Physiol.*, **231**, 734 (1976).

(5) G. Paumgartner and J. Reichen, *Clin. Sci. Mol. Med.*, **51**, 169 (1976).

(6) G. Barber-Riley, *S. Afr. J. Med. Sci.*, **26**, 91 (1961).

(7) M. Schwenk, R. Burr, L. Schwarz, and E. Pfaff, *Eur. J. Biochem.*, **64**, 189 (1976).

(8) R. J. Vonk, P. A. Jekel, D. K. F. Meijer, and M. J. Hardonk, *Biochem. Pharmacol.*, **27**, 397 (1978).

(9) L. R. Schwarz, R. Burr, M. Schwenk, E. Pfaff, and H. Greim, *Eur. J. Biochem.*, **55**, 617 (1975).

(10) J. C. Glasinovic, M. Dumont, M. Duval, and S. Erlinger, *Digestion*, **8**, 423 (1973).

(11) M. Anwer, R. Kroker, and D. Hegner, *Hoppe-Seyler's Z. Physiol. Chem.*, **357**, 1477 (1976).

(12) P. A. G. Fortes and J. F. Hoffman, *J. Membr. Biol.*, **5**, 154 (1971).

(13) D. H. Haynes and H. Staerk, *J. Membr. Biol.*, **17**, 313 (1974).

(14) B. Rabalcava, D. Martinez de Munoz, and C. Gitler, *Biochemistry*, **8**, 2742 (1969).

(15) L. Stryer, *Science*, **162**, 526 (1968).
(16) R. B. Freedman, D. J. Hancock, and G. K. Radda, in "Probes of Structure and Function of Macromolecules and Membranes," Vol. 1, B. Chance *et al.*, Eds., Academic, New York and London, 1969, p. 325.
(17) P. A. G. Fortes and J. F. Hoffman, *J. Membr. Biol.*, **16**, 79 (1974).
(18) C. Levinson and M. L. Villereal, *J. Cell. Physiol.*, **86**, 143 (1975).
(19) S. Cheng and D. Levy, *Biochim. Biophys. Acta*, **511**, 419 (1978).
(20) H. Baur, S. Kasperek, and E. Pfaff, *Hoppe-Seyler's Z. Physiol. Chem.*, **356**, 827 (1975).
(21) C. F. Chignell, in "Methods in Pharmacology," Vol. 2, C. F. Chignell, Ed., Appleton-Century-Crofts, New York, N.Y., 1972, p. 33.
(22) T. Iga, D. L. Eaton, and C. D. Klaassen, *Am. J. Physiol.*, **236**, C9 (1979).
(23) T. Nakagawa and Y. Koyanagi, in "SALS Riyo no Tebiki," Kisohen, SALS Kenkyukai Eds., Computer Center at Tokyo University, 1978.
(24) D. L. Eaton, Ph.D. thesis, University of Kansas, (1978).
(25) H. N. Christensen, in "Biological Transport," 2nd ed., N. A. Benjamin, Reeding, Mass., 1975.
(26) W. Wilbrandt and T.-Rosenberg, *Pharmacol. Rev.*, **13**, 109 (1961).
(27) D. L. Eaton and C. D. Klaassen, *J. Pharmacol. Exp. Ther.*, **205**, 480 (1978).
(28) G. K. Radda and D. S. Smith, *Biochim. Biophys. Acta*, **318**, 197 (1973).
(29) N. Grains and A. P. Dawson, *Biochem. J.*, **158**, 295 (1976).
(30) G. S. Rao, K. Schulze-Hagen, M. L. Rao, and H. Breuer, *J. Steroid Biochem.*, **7**, 1123 (1976).
(31) D. L. Eaton and C. D. Klaassen, *J. Pharmacol. Exp. Ther.*, **206**, 595 (1978).
(32) Y. Sugiyama, T. Iga, S. Awazu, and M. Hanano, *Chem. Pharm. Bull.*, **26**, 199 (1978).
(33) C. Tiribelli, G. Lunazzi, M. Luciani, E. Panfili, B. Gazzin, G. Liuz, G. Sandri, and G. Sottocasa, *Biochim. Biophys. Acta*, **532**, 105 (1978).
(34) G. Lunazzi, C. Tiribelli, B. Gazzin, and G. Sottocasa, *Biochim. Biophys. Acta*, **685**, 117 (1982).
(35) A. W. Wolkoff and C. T. Chung, *J. Clin. Invest.*, **65**, 1152 (1980).

ACKNOWLEDGMENTS

The authors are much indebted to Dr. Tatsuji Iga for his helpful suggestions and advice in the isolation of liver cells.

Thiazides VIII: Dissolution Survey of Marketed Hydrochlorothiazide Tablets

LARRY L. AUGSBURGER *x, RALPH F. SHANGRAW *, R. P. GIANNINI *§, VINOD P. SHAH ‡, VADLAMANI K. PRASAD ‡, and DANIEL BROWN ‡

Received April 12, 1982, from the **Department of Pharmaceutics, University of Maryland School of Pharmacy, Baltimore, MD 21201* and the ‡*Biopharmaceutics Laboratory Branch, Washington, D.C. 20204.* Accepted for publication, July 20, 1982. §Present address: Wyeth Laboratories, Philadelphia, PA 19101

Abstract □ The dissolution profiles of 50-mg hydrochlorothiazide tablets representing all approved manufacturers (at the time of the study) were determined in two vehicles [purified water and dilute (1:100) hydrochloric acid] by three methods (rotating basket at 150 rpm; spin filter at 300 rpm; paddle method at 50 rpm). The paddle method was preferred on the basis of overall ease of operation, reproducibility, and discrimination. The paddle data were validated in both vehicles on the same lots of tablets by a second laboratory. A standard of not <80% dissolution in 60 min by the paddle method in water is proposed for hydrochlorothiazide tablets.

Keyphrases □ Hydrochlorothiazide tablets—dissolution studies, paddle method, basket method, spin filter method □ Dissolution—paddle method, basket method, spin-filter method, hydrochlorothiazide tablets □ Paddle method—dissolution of hydrochlorothiazide tablets □ Basket method—dissolution studies of hydrochlorothiazide tablets □ Spin-filter method—dissolution studies of hydrochlorothiazide tablets

Hydrochlorothiazide is a member of the benzothiadiazine class of orally effective diuretics widely used in the treatment of hypertension, congestive heart failure, and other edematous conditions. As a class, these compounds generally are poorly wetted and have limited solubility. Thus, it is not surprising that they have been identified in the Federal Register (1) as a class of drugs with a potential for bioavailability/bioequivalency problems and for which dissolution standards should be developed. For such standards to be meaningful and reflect bioavailability performance, the dissolution system must be capable of generating data that consistently correlate with *in vivo* performance. However, the dissolution of a drug from its dosage form is dependent on many factors, which include not only the physicochemical properties of the drug, but also how the dosage form is formulated and processed. Thus, even in the absence of a correlation between *in vivo* and *in vitro* data, dissolution data provide a desirable aid in controlling formulation and manufacturing variables and should be a reliable indicator of uniformity of manufacture. The objectives of this study were to (*a*) survey the dissolution performance of marketed hydrochlorothiazide products by various methods, (*b*) select an appropriate dissolution method, and (*c*) develop acceptable dissolution standards based on the performance of the marketed products. The results of this study should form a basis for the consideration of other members of the benzothiadiazine class.

EXPERIMENTAL

Materials—Commercial 50-mg hydrochlorothiazide tablets[1] (representing all approved manufacturers at the time of the study) were used.

Reagents and Chemicals—Distilled water was used throughout, and all other chemicals or reagents were either official grade or reagent grade. Hydrochlorothiazide USP was the reference standard.

[1] Product 1, Abbott Laboratories Lot No. 55-116AF22; Product 2, Barr Lot No. 6C02013; Product 3, Ciba Lot No. 10721; Product 4, Danbury Lot No. 12357; Product 5, Heather Lot No. 61088; Product 6, Merck Sharp and Dohme Lot No. V2487; Product 7, Towne Paulsen Lot No. 037652; Product 8, Zenith Lot No. A208313.

0022-3549/83/0800-0876$01.00/0

(15) L. Stryer, *Science*, **162**, 526 (1968).
(16) R. B. Freedman, D. J. Hancock, and G. K. Radda, in "Probes of Structure and Function of Macromolecules and Membranes," Vol. 1, B. Chance *et al.*, Eds., Academic, New York and London, 1969, p. 325.
(17) P. A. G. Fortes and J. F. Hoffman, *J. Membr. Biol.*, **16**, 79 (1974).
(18) C. Levinson and M. L. Villereal, *J. Cell. Physiol.*, **86**, 143 (1975).
(19) S. Cheng and D. Levy, *Biochim. Biophys. Acta*, **511**, 419 (1978).
(20) H. Baur, S. Kasperek, and E. Pfaff, *Hoppe-Seyler's Z. Physiol. Chem.*, **356**, 827 (1975).
(21) C. F. Chignell, in "Methods in Pharmacology," Vol. 2, C. F. Chignell, Ed., Appleton-Century-Crofts, New York, N.Y., 1972, p. 33.
(22) T. Iga, D. L. Eaton, and C. D. Klaassen, *Am. J. Physiol.*, **236**, C9 (1979).
(23) T. Nakagawa and Y. Koyanagi, in "SALS Riyo no Tebiki," Kisohen, SALS Kenkyukai Eds., Computer Center at Tokyo University, 1978.
(24) D. L. Eaton, Ph.D. thesis, University of Kansas, (1978).
(25) H. N. Christensen, in "Biological Transport," 2nd ed., N. A. Benjamin, Reeding, Mass., 1975.
(26) W. Wilbrandt and T.-Rosenberg, *Pharmacol. Rev.*, **13**, 109 (1961).
(27) D. L. Eaton and C. D. Klaassen, *J. Pharmacol. Exp. Ther.*, **205**, 480 (1978).
(28) G. K. Radda and D. S. Smith, *Biochim. Biophys. Acta*, **318**, 197 (1973).
(29) N. Grains and A. P. Dawson, *Biochem. J.*, **158**, 295 (1976).
(30) G. S. Rao, K. Schulze-Hagen, M. L. Rao, and H. Breuer, *J. Steroid Biochem.*, **7**, 1123 (1976).
(31) D. L. Eaton and C. D. Klaassen, *J. Pharmacol. Exp. Ther.*, **206**, 595 (1978).
(32) Y. Sugiyama, T. Iga, S. Awazu, and M. Hanano, *Chem. Pharm. Bull.*, **26**, 199 (1978).
(33) C. Tiribelli, G. Lunazzi, M. Luciani, E. Panfili, B. Gazzin, G. Liuz, G. Sandri, and G. Sottocasa, *Biochim. Biophys. Acta*, **532**, 105 (1978).
(34) G. Lunazzi, C. Tiribelli, B. Gazzin, and G. Sottocasa, *Biochim. Biophys. Acta*, **685**, 117 (1982).
(35) A. W. Wolkoff and C. T. Chung, *J. Clin. Invest.*, **65**, 1152 (1980).

ACKNOWLEDGMENTS

The authors are much indebted to Dr. Tatsuji Iga for his helpful suggestions and advice in the isolation of liver cells.

Thiazides VIII: Dissolution Survey of Marketed Hydrochlorothiazide Tablets

LARRY L. AUGSBURGER *x, RALPH F. SHANGRAW *, R. P. GIANNINI *§, VINOD P. SHAH ‡, VADLAMANI K. PRASAD ‡, and DANIEL BROWN ‡

Received April 12, 1982, from the **Department of Pharmaceutics, University of Maryland School of Pharmacy, Baltimore, MD 21201* and the ‡*Biopharmaceutics Laboratory Branch, Washington, D.C. 20204.* Accepted for publication, July 20, 1982. §Present address: Wyeth Laboratories, Philadelphia, PA 19101

Abstract □ The dissolution profiles of 50-mg hydrochlorothiazide tablets representing all approved manufacturers (at the time of the study) were determined in two vehicles [purified water and dilute (1:100) hydrochloric acid] by three methods (rotating basket at 150 rpm; spin filter at 300 rpm; paddle method at 50 rpm). The paddle method was preferred on the basis of overall ease of operation, reproducibility, and discrimination. The paddle data were validated in both vehicles on the same lots of tablets by a second laboratory. A standard of not <80% dissolution in 60 min by the paddle method in water is proposed for hydrochlorothiazide tablets.

Keyphrases □ Hydrochlorothiazide tablets—dissolution studies, paddle method, basket method, spin filter method □ Dissolution—paddle method, basket method, spin-filter method, hydrochlorothiazide tablets □ Paddle method—dissolution of hydrochlorothiazide tablets □ Basket method—dissolution studies of hydrochlorothiazide tablets □ Spin-filter method—dissolution studies of hydrochlorothiazide tablets

Hydrochlorothiazide is a member of the benzothiadiazine class of orally effective diuretics widely used in the treatment of hypertension, congestive heart failure, and other edematous conditions. As a class, these compounds generally are poorly wetted and have limited solubility. Thus, it is not surprising that they have been identified in the Federal Register (1) as a class of drugs with a potential for bioavailability/bioequivalency problems and for which dissolution standards should be developed. For such standards to be meaningful and reflect bioavailability performance, the dissolution system must be capable of generating data that consistently correlate with *in vivo* performance. However, the dissolution of a drug from its dosage form is dependent on many factors, which include not only the physicochemical properties of the drug, but also how the dosage form is formulated and processed. Thus, even in the absence of a correlation between *in vivo* and *in vitro* data, dissolution data provide a desirable aid in controlling formulation and manufacturing variables and should be a reliable indicator of uniformity of manufacture. The objectives of this study were to (*a*) survey the dissolution performance of marketed hydrochlorothiazide products by various methods, (*b*) select an appropriate dissolution method, and (*c*) develop acceptable dissolution standards based on the performance of the marketed products. The results of this study should form a basis for the consideration of other members of the benzothiadiazine class.

EXPERIMENTAL

Materials—Commercial 50-mg hydrochlorothiazide tablets[1] (representing all approved manufacturers at the time of the study) were used.

Reagents and Chemicals—Distilled water was used throughout, and all other chemicals or reagents were either official grade or reagent grade. Hydrochlorothiazide USP was the reference standard.

[1] Product 1, Abbott Laboratories Lot No. 55-116AF22; Product 2, Barr Lot No. 6C02013; Product 3, Ciba Lot No. 10721; Product 4, Danbury Lot No. 12357; Product 5, Heather Lot No. 61088; Product 6, Merck Sharp and Dohme Lot No. V2487; Product 7, Towne Paulsen Lot No. 037652; Product 8, Zenith Lot No. A208313.

0022-3549/83/0800-0876$01.00/0

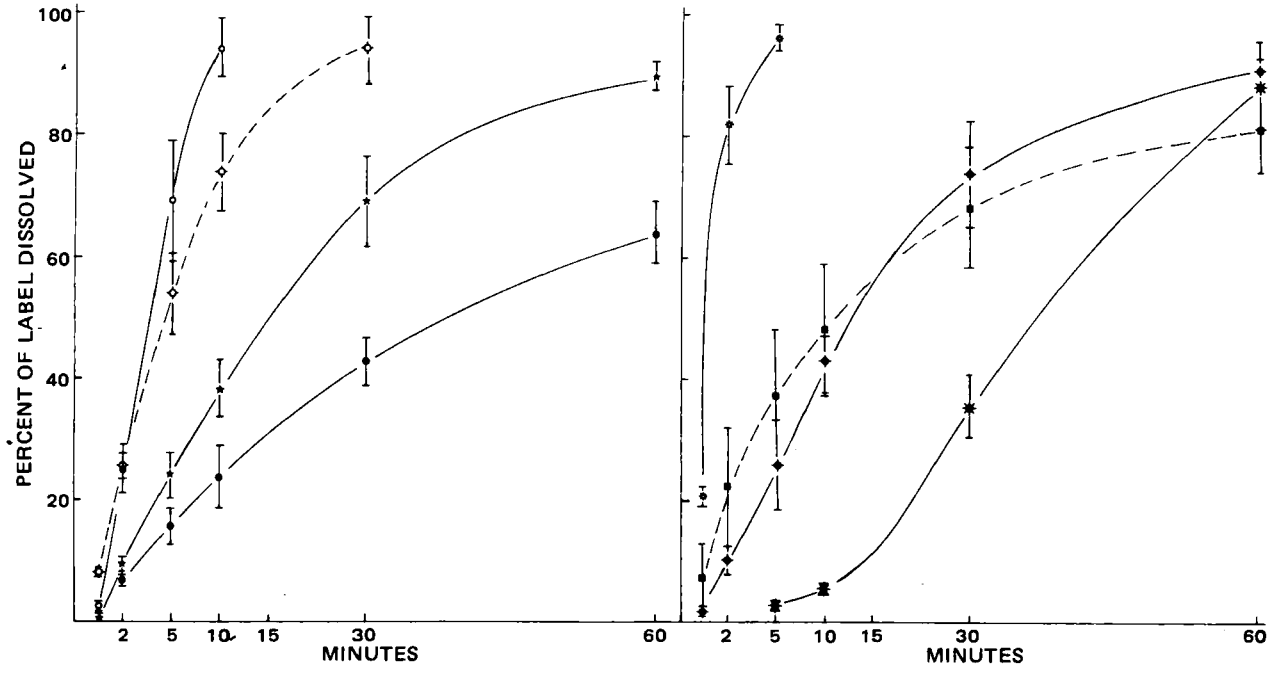

Figure 1—*Dissolution of hydrochlorothiazide tablets in purified water—paddle method (50 rpm). Key: product 1 (★); product 2 (☼); product 3 (○); product 4 (◇); product 5 (■); product 6 (●); product 7 (◆); product 8 (✹).*

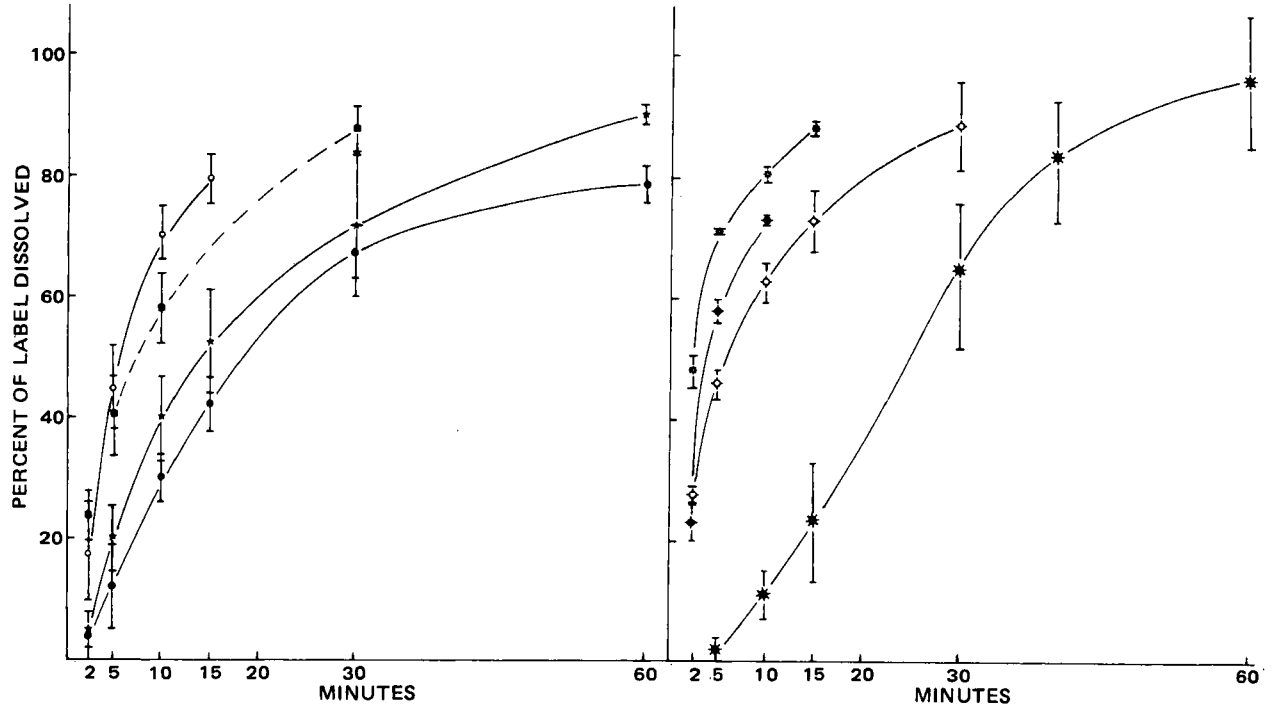

Figure 2—*Dissolution of hydrochlorothiazide tablets in purified water—rotating basket method (150 rpm). See Fig. 1 for key to graph.*

Dissolution Methods—The dissolution tests were carried out in two laboratories using UV spectrophotometry[2]. Dissolution was monitored by continuously circulating the filtered medium from each flask to and through a 0.1-cm path-length flow cell mounted in the spectrophotometer, and then back to the flask. The filter was mounted on the intake end of the hosing and consisted of a 13-mm fiberglass pad held in a plastic holder.

Dissolution was carried out in distilled water and in dilute (1:100) hydrochloric acid: 900 ml at 37°.

Rotating Basket (USP XIX, Method 1)—The basket assemblies were rotated in resin flasks by means of a multiple-spindle drive system[3]. Official specifications (2) were adhered to, including the 150-rpm stirring rate noted in the hydrochlorothiazide monograph.

Paddle Method (USP XX, Method 2)—The paddles were rotated in round-bottom flasks by suitable adaptation of the multiple-stirrer head. All official specifications (2) were followed. A paddle speed of 50 rpm was selected.

Spin-Filter Method—This method is essentially the stationary basket, spinning-filter method described by Shah *et al.* (3). The apparatus[4] was obtained commercially. The geometry relating the position of the basket to the filter is fixed by the apparatus design; however, the filter unit was always set 2 mm from the bottom of the flask, as recommended (3). Filter rotational speed was 300 rpm.

[2] Beckman 25/7 Spectrophotometer, Beckman Instruments, Fullterton, Calif.

[3] Easilift Dissolution Test Station Model 63-734-100, Hanson Research Corp., Northridge, Calif.

[4] Magne-Drive Dissolution Test Apparatus, Series 74, Coffman Industries, Inc., Kansas City, Kan.

Table I—Dissolution of 50-mg Hydrochlorothiazide Tablets by Paddle Method at 50 rpm in Water and Acid

Product	% Dissolved in Water				% Dissolved in Acid			
	30 min		60 min		30 min		60 min	
	Mean	*SD*	Mean	*SD*	Mean	*SD*	Mean	*SD*
1	68.9	7.4	89.4	2.5	86.7	2.3	95.3	1.4
2	95.8[a]	2.2	—	—	94.3[a]	5.9	—	—
3	93.7[a]	5.3	—	—	94.1[a]	4.6	—	—
4	93.7	4.9	—	—	91.5	5.3	—	—
5	68.4	10.3	81.1	6.7	86.3	9.6	—	—
6	42.5	3.9	63.8	4.9	66.0	11.0	78.0	6.9
7	73.5	8.6	90.5	2.3	97.8	2.2	—	—
8	35.5	5.3	88.0	7.3	80.0	4.5	95.5	3.2

[a] — 15-min value.

Except for the spin-filter runs, the media were not deaerated. Concentrations were determined at 272 nm. Laboratory I used all three methods; laboratory II validated laboratory I results using only the paddle method. Six or more tablets from each lot were evaluated by each laboratory.

Stability of Hydrochloride in the Dissolution Media—Stability studies were conducted in purified water and dilute hydrochloric acid (1:100) for 90 min at 37°. The samples were analyzed for diazotizable substances (hydrolyzed product) using both the Bratton–Marshall colorimetric technique (4) and a specific high-performance liquid chromatographic (HPLC) method. For the HPLC method, a C_{18} reverse-phase column, a 254-nm detector, and a methanol–water eluant (60:40) were used.

Table II—Dissolution of 50-mg Hydrochlorothiazide Tablets by Basket Method at 150 rpm in Water and Acid

Product	Water % Dissolved in 30 min		Acid % Dissolved in 30 min	
	Mean	*SD*	Mean	*SD*
1	71.8	12.4[a]	83.2	2.9[b]
2	88.3[c]	1.4	94.3[c]	4.3
3	79.2[c]	4.5	94.0[c]	5.7
4	88.7	7.2	81.0[c]	5.3
5	87.7	3.9	87.0[c]	5.6
6	67.5	4.6[d]	90.8	7.1
7	73.3[c]	0.5	78.8	4.0[e]
8	64.8	12.0[f]	93.2	1.9

[a] 90.5 ± 2.1 in 60 min. [b] 94.5 ± 2.3 in 60 min. [c] In 15 min. [d] 88.8 ± 3.5 in 60 min. [e] 88.3 ± 3.7 in 60 min. [f] 83.2 ± 10.3 in 60 min.

For the purposes of identity and determining the extent of hydrolysis under dissolution conditions, USP reference hydrolyzed products were used. Less than 5% hydrolysis was found in either medium after 90 min.

RESULTS AND DISCUSSION

One of the first requirements of a dissolution study is to determine the equilibrium solubility of the compound. The solubility test gives the maximum expected dissolution of less soluble compounds and provides information as to whether sink conditions are being approximated in the test or not. In earlier investigations, it was accepted that the maintenance of sink conditions (or the approximation) increases the chances for *in vitro–in vivo* correlation, although lack of sink conditions does not necessarily prohibit such a correlation. Equilibrium solubility studies carried out showed that hydrochlorothiazide is soluble to the extent of 1.05 mg/ml in water and 1.06 mg/ml in dilute hydrochloric acid, which approximates to only 5.3% saturation for a 50-mg tablet in 900 ml of the medium.

The dissolution of all marketed hydrochlorothiazide tablets was surveyed using both dilute (1:100) hydrochloric acid and water as the dissolution media: water is the simplest possible medium, and dilute acid has physiological significance owing to the pH of the gastric contents.

The USP rotating basket at 150 rpm was selected since it was the official method used for hydrochlorothiazide tablets in USP XIX. The paddle method has been gaining popularity in recent years and is currently recognized as Method 2 in the official compendia. The paddle speed of 50 rpm was selected on the basis of preliminary experiments and the experience of the Food and Drug Administration with this method. It was felt that this low degree of agitation would not only enhance the chances for *in vitro–in vivo* correlation, but also enhance discrimination between brands. The stationary basket-spinning filter method was se-

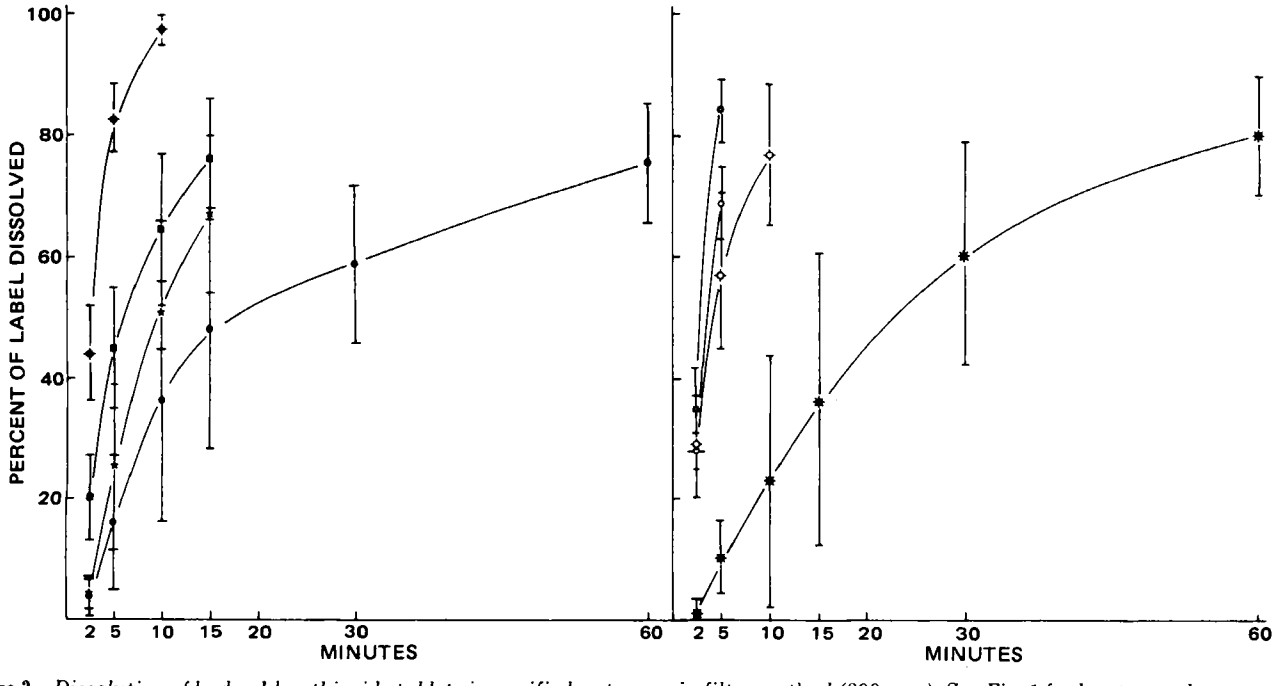

Figure 3—*Dissolution of hydrochlorothiazide tablets in purified water—spin filter method (300 rpm). See Fig. 1 for key to graph.*

Table III—Dissolution of 50-mg Hydrochlorothiazide Tablets by Spin-Filter Method at 300 rpm in Water and Acid

Product	Water % Dissolved			Acid % Dissolved		
	Minutes	Mean	*SD*	Minutes	Mean	*SD*
1	15	67.3	13.4	15	80.2	5.5
2	5	84.2	5.4	5	85.3	5.5
3	5	69.0	6.2	10	94.7	3.2
4	10	76.7	11.8	10	79.0	12.6
5	15	75.9	10.4	10	96.4	5.3
6	30	59.4	13.4[a]	15	83.6	3.4
7	5	82.7	5.8	10	80.0	4.9
8	30	58.4	18.1[b]	15	65.5	11.5

[a] 75.7 ± 10.0 in 60 min. [b] 78.0 ± 9.6 in 60 min.

lected largely on the basis of the encouraging results reported by Shah *et al.* (3).

The dissolution results by all three methods in both media are summarized in Tables I–III and Figs. 1–6. The final procedure for validation in laboratory II was selected based on the reproducibility of the method, its ability to discriminate brands, and ease of operation.

The data in Tables I–III show that the dissolution results in water and acid were similar, although some products (1, 5, 6, and 8) apparently contain acid-soluble excipients and, therefore, tend to show faster dissolution in this medium. For example, with the paddle method, the eight hydrochlorothiazide products dissolved in the range of 35–96% in 30 min in water, whereas in acid the same products dissolved in the range of 66–97% in 30 min (Table I). However, all products exhibited at least 60% dissolution in 60 min in both media. Dissolution by the basket method at 150 rpm was faster than the paddle method, but the spin-filter method showed the fastest dissolution. Most of the products showed 70–80% dissolution in 10 min by the spin-filter method.

The same lots were evaluated by each of the methods. The relative standard deviations were comparable for the paddle and basket methods; however, variability tended to be somewhat higher in the spin-filter apparatus. Furthermore, a comparison of the percent-dissolved figures reveals that both the paddle and basket methods tended to separate the tablet brands reasonably well. A somewhat more distinct separation was realized with the paddle method. In the case of the spin-filter apparatus, the dissolution rates of nearly all tablets were quite high, but the separation of brands was somewhat poorer. These distinctions can be visualized by comparing the dissolution profiles of the products in Figs. 1–6. The bar around each point represents the standard deviation. The results in Tables I–IV also show that regardless of the method, a somewhat clearer separation of the brands results when water is the dissolution medium.

In general, the paddle method was easier to set up and use. The disintegrated-tablet components tended to remain localized under the paddle in the concavity of the round-bottomed flask, where they presumably received a uniform degree of agitation during the course of the run. In addition, the paddle method was the easiest of the three methods to clean up.

In contrast, the basket method required insertion of the tablets into individual baskets prior to starting. As particles from the disintegrated tablet gradually pass through the basket screen during the test, it appeared that not all of the tablet material received uniform agitation.

The most difficult method to set up and use was the spin-filter apparatus. This method requires careful adjustment of the spinning filter to maintain a clearance of 2 mm from the bottom of the flask. Even after careful tightening of the lock nuts, the filter was found to drop at times to the bottom of the flask. This alters the rotational speed and contributes to variability. The most troublesome problem was the tendency of the

Table IV—Validation Studies on 50-mg Hydrochlorothiazide Tablets (Paddle Method, 50 rpm)

Product	% Dissolved in 60 min			
	Water		Acid	
	Mean	*SD*	Mean	*SD*
1	94	1.4	94	1.0
2	100	1.9	99	0.8
3	99	1.5	100	1.9
4	90	8.1	97	1.4
5	90	7.8	99	1.3
6	59	9.1	101	2.6
7	100	1.6	101	3.0
8	87	7.2	97	2.6

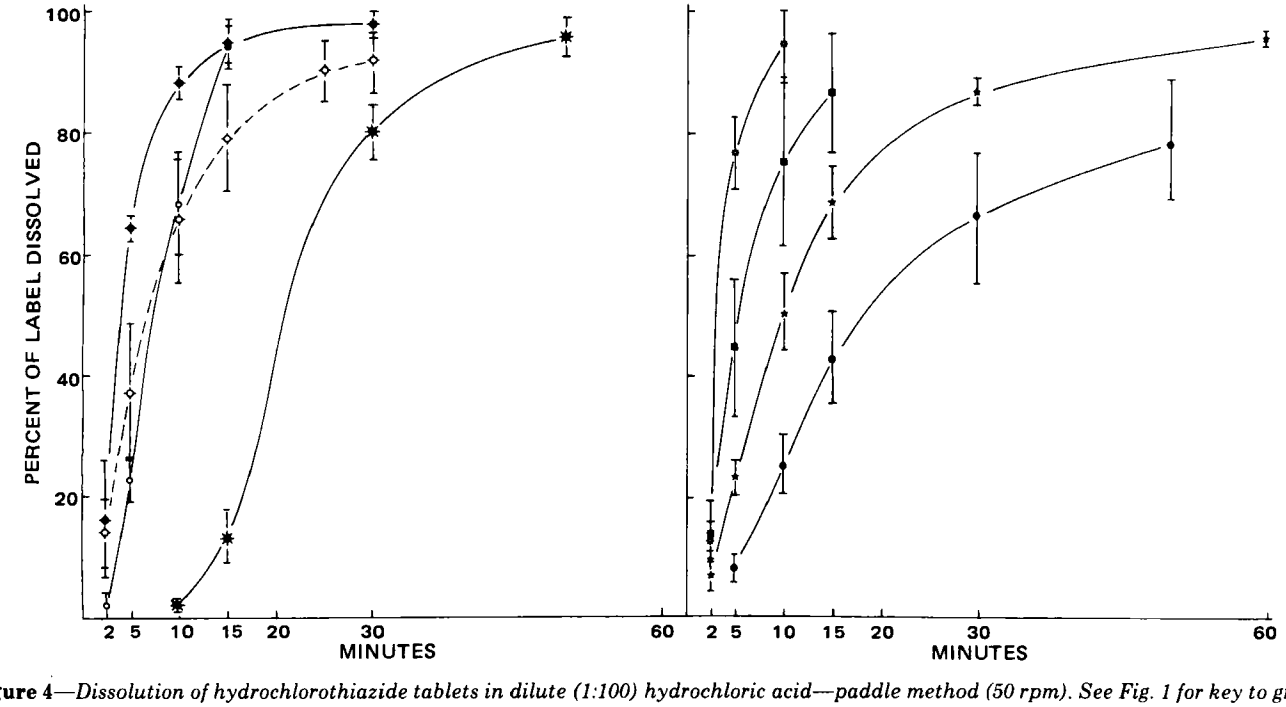

Figure 4—*Dissolution of hydrochlorothiazide tablets in dilute (1:100) hydrochloric acid—paddle method (50 rpm). See Fig. 1 for key to graph.*

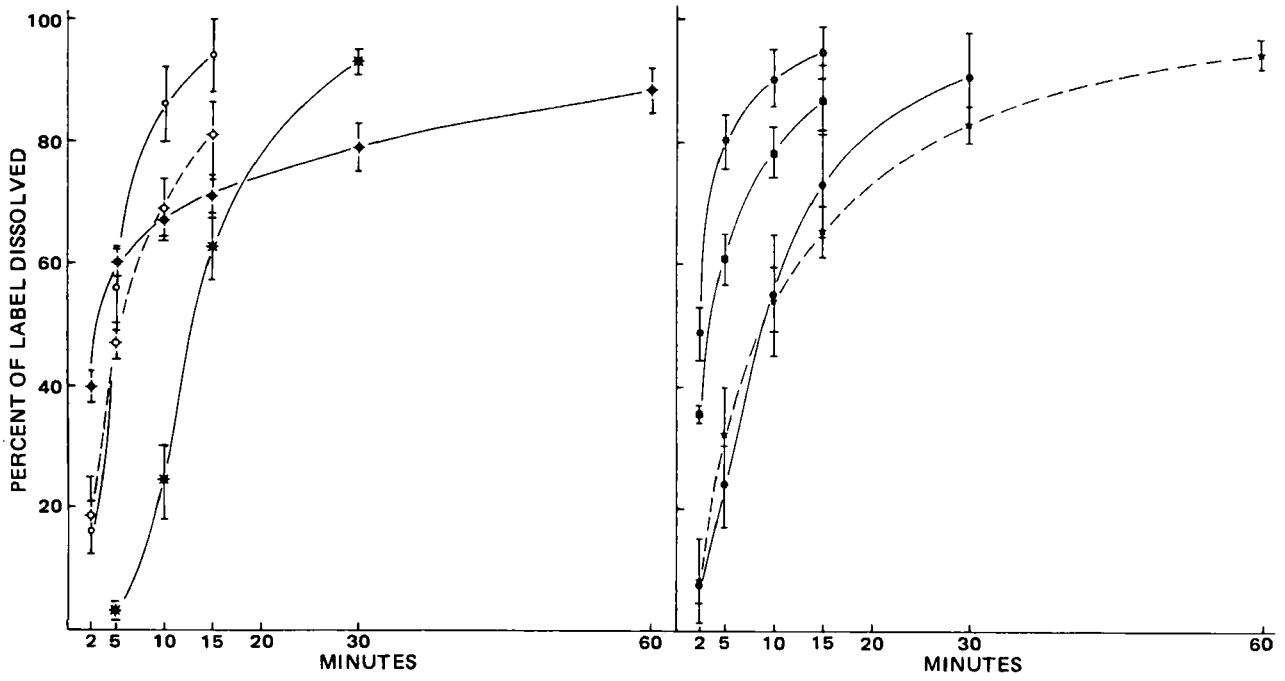

Figure 5—*Dissolution of hydrochlorothiazide tablets in dilute (1:100) hydrochloric acid—rotating basket method (150 rpm). See Fig. 1 for key to graph.*

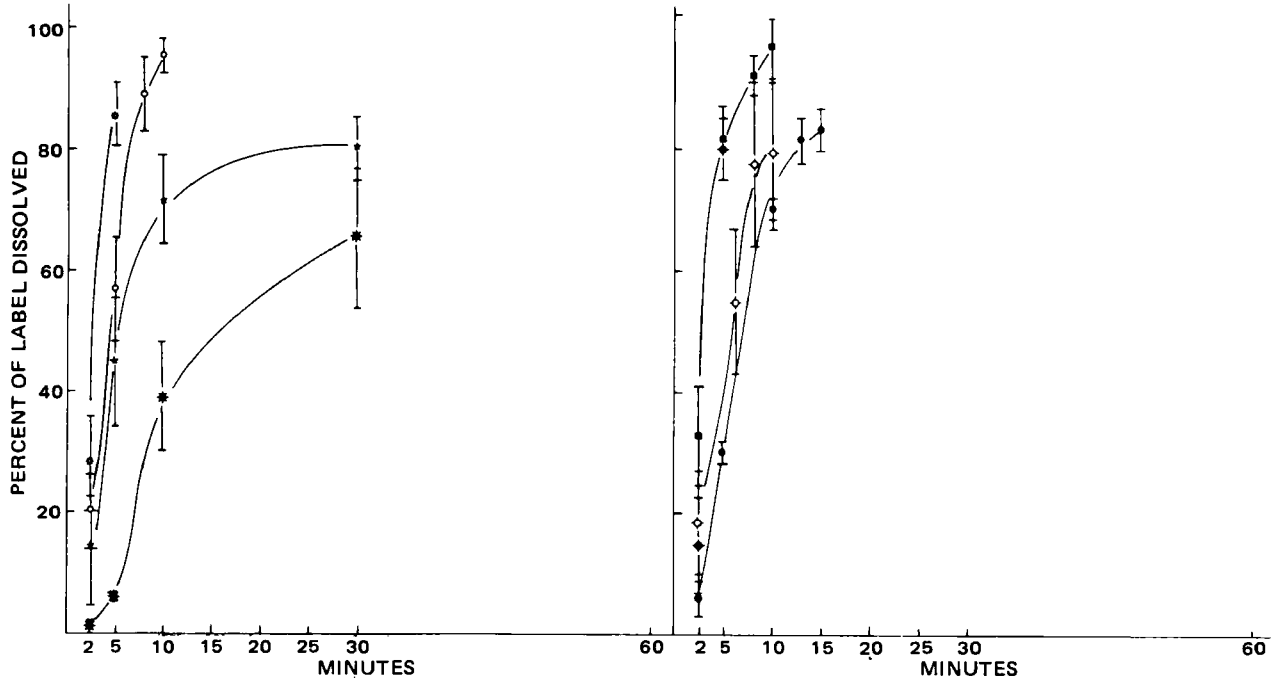

Figure 6—*Dissolution of hydrochlorothiazide tablets in dilute (1:100) hydrochloric acid—spin filter method (300 rpm). See Fig. 1 for key to graph.*

spinning filter to create air bubbles in the flow lines which interfered with spectrophotometric readings. Careful cleaning of the filters in an ultrasonic bath and thorough deaeration of the medium reduced the air bubble problem to manageable levels; however, they could not be eliminated entirely.

In conclusion, on the basis of data reproducibility (lower standard deviation) and ease of operation, as well as enhanced separation of the dissolution results for all products tested, the paddle method at 50 rpm was selected (preferred) over the basket method at 150 rpm and the spin-filter method at 300 rpm.

The same lots of hydrochlorothiazide tablets were validated by another laboratory using the paddle method with water and dilute hydrochloric acid as the dissolution media. The results from these studies (Table IV) show good agreement between data from the two laboratories. All eight products studied show a good dissolution profile. Additional batches of products 6 and 8 were also studied, and they showed faster dissolution.

At present, there is no documented evidence of any bioavailability problem from the marketed products studied. The dissolution survey described herein indicated that it is possible to manufacture products that dissolve not <80% in 60 min by the paddle method at 50 rpm in water. The dissolution methodology presented herein is simple. In addition, it is evident that the limit specified is achievable. These two facts show that the method could be useful in a quality assurance program.

REFERENCES

(1) *Fed. Regis.*, Jan. 7, 1977.

(2) "United States Pharmacopeia XX," United States Pharmacopeial

Convention, Inc., Rockville, Md., 1980.
(3) A. C. Shah, C. B. Peot, and J. F. Ochs, *J. Pharm. Sci.*, **62**, 671 (1973).
(4) "National Formulary XIV," U.S. Pharmacopeial Convention, Rockville, Md., 1975.

ACKNOWLEDGMENT

The research work was supported by FDA Contract 223-76-3009. The very capable technical assistance of Mr. Melford Henderson is gratefully acknowledged.

Synthesis and Structural Study of *N*-Substituted Nortropane Spirohydantoins

E. GALVEZ *, M. MARTINEZ *, J. GONZALEZ *, G. G. TRIGO *x, P. SMITH-VERDIER ‡, F. FLORENCIO ‡, and S. GARCIA-BLANCO ‡

Received February 22, 1982, from the **Department of Organic and Pharmaceutical Chemistry, School of Pharmacy, Universidad Compultense, Madrid-3, Spain* and the ‡*Department of X-Ray, Rocasolano Institute of Physical Chemistry, C.S.I.C., Serrano 119, Madrid-6, Spain.* Accepted for publication June 29, 1982.

Abstract □ A series of N^8-alkyloxycarbonylalkyl-nortropane-3-spiro-5′-hydantoins has been synthesized and studied by spectral and crystallographic methods. The crystal and molecular structure of one [8(γ-ethoxycarbonylpropyl)nortropane-3-spiro-5′-hydantoin, VI] was determined by X-ray diffraction. The preferred conformations of these compounds and subsequent changes on protonation were determined from ^{1}H-NMR and ^{13}C-NMR data.

Keyphrases □ *N*-Substituted nortropane spirohydantoins—synthesis, structural studies using IR, NMR, and X-ray crystallography □ NMR spectroscopy—analysis of *N*-substituted nortropane spirohydantoins □ IR spectroscopy—analysis of *N*-substituted nortropane spirohydantoins □ X-Ray crystallography—analysis of *N*-substituted nortropane spirohydantoins

In a previous paper (1), ^{1}H- and ^{13}C-NMR studies of a pharmacologically interesting series of tropane- and *N*-substituted nortropane-3-spiro-5′-hydantoins were reported. The structure of tropane-3-spiro-5′-hydantoin (determined by X-ray methods) also has been described (2). In this study the synthesis and structural determination of a series of N^8-ethoxycarbonylalkyl-nortropane-3-spiro-5′-hydantoins and their corresponding hydrochlorides is reported (Scheme I). Treatment of the appropriate N^8-substituted nortropinone[1] with potassium cyanide and ammonium carbonate in aqueous ethanol gave the desired hydantoins.

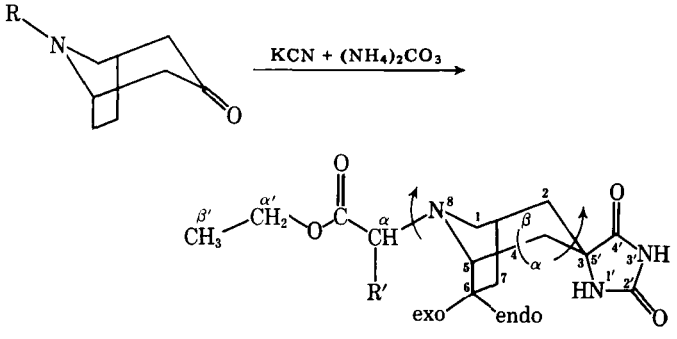

I: R′ = H
II: R′ = $-CH_3$
III: R′ = $-CH_bH_cC_6H_5$
IV: R′ = $-CH_2CH_2CO_2CH_2CH_3$
V: R′ = $-CH(CH_3)_2$
VI: $>N^8-CH_2CH_2CH_2CO_2CH_2CH_3$
VII: $>N^8-C_6H_4$-*p*-$CO_2CH_2CH_3$

Scheme I

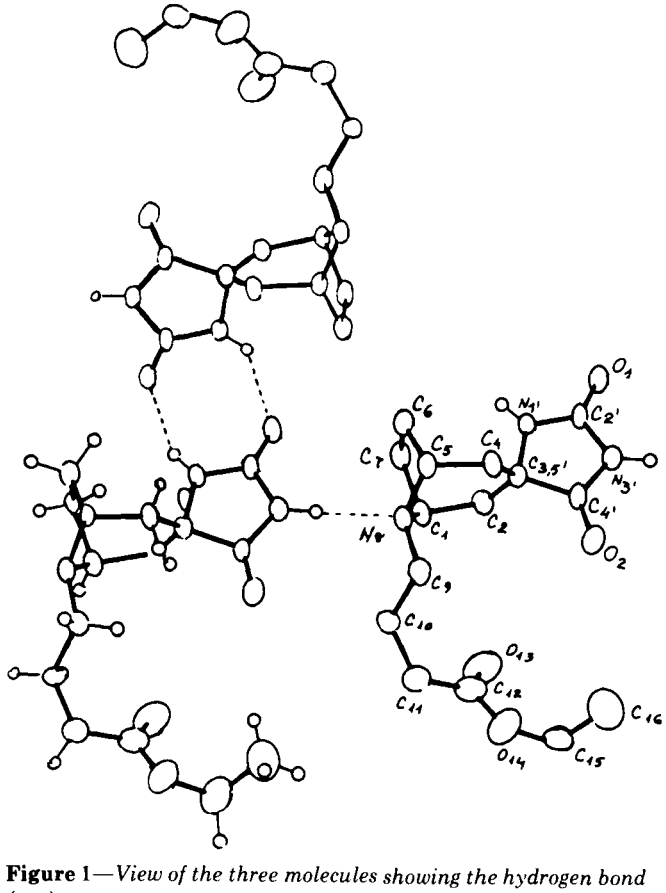

Figure 1—*View of the three molecules showing the hydrogen bond (---).*

[1] G. G. Trigo, M. Martinez and E. Galvez, unpublished results.

0022-3549/83/0800-0881$01.00/0

Convention, Inc., Rockville, Md., 1980.
(3) A. C. Shah, C. B. Peot, and J. F. Ochs, *J. Pharm. Sci.*, **62**, 671 (1973).
(4) "National Formulary XIV," U.S. Pharmacopeial Convention, Rockville, Md., 1975.

ACKNOWLEDGMENT

The research work was supported by FDA Contract 223-76-3009. The very capable technical assistance of Mr. Melford Henderson is gratefully acknowledged.

Synthesis and Structural Study of *N*-Substituted Nortropane Spirohydantoins

E. GALVEZ *, M. MARTINEZ *, J. GONZALEZ *, G. G. TRIGO *x, P. SMITH-VERDIER ‡, F. FLORENCIO ‡, and S. GARCIA-BLANCO ‡

Received February 22, 1982, from the **Department of Organic and Pharmaceutical Chemistry, School of Pharmacy, Universidad Compultense, Madrid-3, Spain* and the ‡*Department of X-Ray, Rocasolano Institute of Physical Chemistry, C.S.I.C., Serrano 119, Madrid-6, Spain.* Accepted for publication June 29, 1982.

Abstract □ A series of N^8-alkyloxycarbonylalkyl-nortropane-3-spiro-5′-hydantoins has been synthesized and studied by spectral and crystallographic methods. The crystal and molecular structure of one [8(γ-ethoxycarbonylpropyl)nortropane-3-spiro-5′-hydantoin, VI] was determined by X-ray diffraction. The preferred conformations of these compounds and subsequent changes on protonation were determined from ^{1}H-NMR and ^{13}C-NMR data.

Keyphrases □ *N*-Substituted nortropane spirohydantoins—synthesis, structural studies using IR, NMR, and X-ray crystallography □ NMR spectroscopy—analysis of *N*-substituted nortropane spirohydantoins □ IR spectroscopy—analysis of *N*-substituted nortropane spirohydantoins □ X-Ray crystallography—analysis of *N*-substituted nortropane spirohydantoins

In a previous paper (1), ^{1}H- and ^{13}C-NMR studies of a pharmacologically interesting series of tropane- and *N*-substituted nortropane-3-spiro-5′-hydantoins were reported. The structure of tropane-3-spiro-5′-hydantoin (determined by X-ray methods) also has been described (2). In this study the synthesis and structural determination of a series of N^8-ethoxycarbonylalkyl-nortropane-3-spiro-5′-hydantoins and their corresponding hydrochlorides is reported (Scheme I). Treatment of the appropriate N^8-substituted nortropinone[1] with potassium cyanide and ammonium carbonate in aqueous ethanol gave the desired hydantoins.

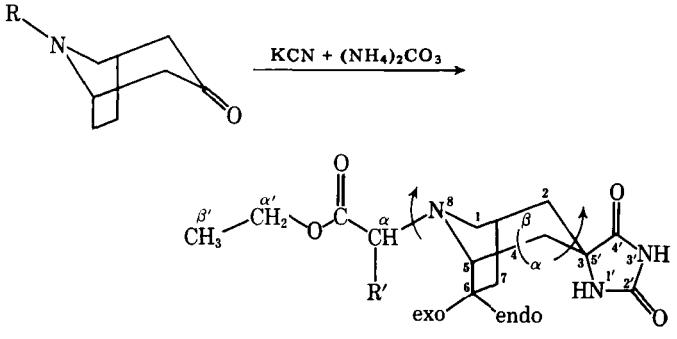

I: R′ = H
II: R′ = $-CH_3$
III: R′ = $-CH_bH_cC_6H_5$
IV: R′ = $-CH_2CH_2CO_2CH_2CH_3$
V: R′ = $-CH(CH_3)_2$
VI: $>N^8-CH_2CH_2CH_2CO_2CH_2CH_3$
VII: $>N^8-C_6H_4$-*p*-$CO_2CH_2CH_3$

Scheme I

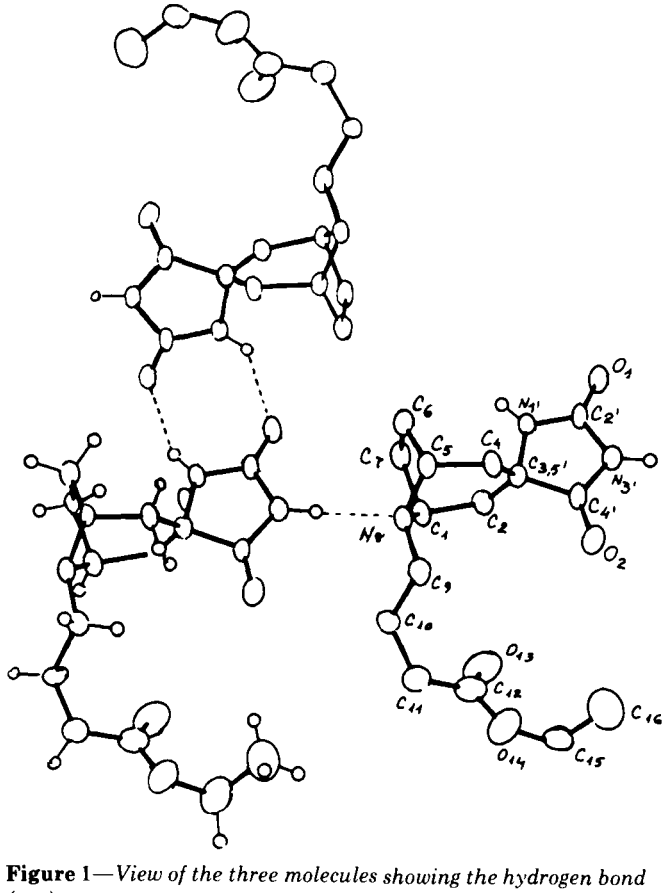

Figure 1—*View of the three molecules showing the hydrogen bond (---).*

[1] G. G. Trigo, M. Martinez and E. Galvez, unpublished results.

0022-3549/83/0800-0881$01.00/0

Table I—Bond Distances and Angles of VI

Bond	Distance, Å	Bond	Angle, °
C(1—C(2)	1.533(3)	C(2)—C(1)—N(8)	112.3(3)
C(1)—C(7)	1.541(4)	C(2)—C(1)—C(7)	112.4(3)
C(1)—N(8)	1.487(4)	C(7)—C(1)—N(8)	100.8(2)
C(2)—C(3,5′)	1.545(4)	C(1)—C(8)—C(5)	101.1(2)
C(3,5′)—C(4)	1.544(4)	C(2)—C(3,5′)—C(4)	111.6(2)
C(4)—C(5)	1.529(4)	C(2)—C(3,5′)—N(1′)	112.6(2)
C(5)—C(6)	1.537(4)	C(2)—C(3,5′)—C(4′)	109.0(2)
C(5)—N(8)	1.487(4)	C(4)—C(3,5′)—N(1′)	112.7(2)
N(8)—C(9)	1.467(3)	C(4)—C(3,5′)—C(4′)	109.9(2)
C(9)—C(10)	1.528(5)	N(1′)—C(3,5′)—C(4′)	100.4(2)
C(11)—C(12)	1.504(6)	C(3,5′)—C(4)—C(5)	112.6(3)
C(12)—O(13)	1.198(5)	C(4)—C(5)—N(8)	112.7(2)
C(12)—O(14)	1.333(4)	C(4)—C(5)—C(6)	113.4(3)
O(14)—C(15)	1.457(6)	C(6)—C(5)—N(8)	100.4(2)
C(15)—C(16)	1.488(8)	C(5)—C(6)—C(7)	104.7(3)
C(3,5′)—N(1′)	1.468(3)	C(1)—C(7)—C(6)	104.0(3)
N(1′)—C(2′)	1.340(3)	C(1)—N(8)—C(5)	101.1(2)
C(2′)—N(3′)	1.400(3)	C(1)—N(8)—C(9)	114.4(3)
C(2′)—O(1)	1.223(3)	C(5)—N(8)—C(9)	116.8(3)
N(3′)—C(4′)	1.370(4)	N(8)—C(9)—C(10)	111.8(3)
C(4′)—O(2)	1.198(3)	C(9)—C(10)—C(11)	110.8(3)
C(4′)—C(3,5′)	1.536(3)	C(10)—C(11)—C(12)	112.1(4)
		C(11)—C(12)—O(13)	124.7(4)
		C(11)—C(12)—O(14)	111.2(4)
		O(13)—C(12)—O(14)	124.1(4)
		C(12)—O(14)—C(15)	116.5(4)
		C(14)—C(15)—C(16)	110.3(5)

EXPERIMENTAL

IR spectra were recorded on a double-beam spectrophotometer[2] using indene and polystyrene for calibration. The ^{1}H-NMR spectra were recorded at 60 MHz[3], 90 MHz[4], and 250 MHz[5]. The ^{13}C-NMR spectra were determined at 20 MHz[6] in the Fourier transform mode at room temperature. Both broad-band decoupled and single-frequency off-resonance decoupled spectra were determined. Mass spectral determinations were made[7]. Elemental analyses were determined[8].

N^8-Substituted Nortropane Spirohydantoins (I–VII)—A solution of potassium cyanide (0.15 mole) and ammonium carbonate (0.3 mole) in water (115 ml) was added to a solution of the corresponding racemic *N*-substituted nortropinone[1] (0.1 mole) in ethanol (35 ml). The mixture was heated at 60° in a sealed flask for 24 hr. After cooling, the precipitated solid was removed by filtration. The mother liquors were concentrated (~50%) under reduced pressure and cooled, and the resulting solid was removed by filtration and added to the first material obtained.

Hydrochlorides of I–VI—Solutions of I–VI (0.01 mole) in ethanol (10 ml) were added to hydrogen chloride dissolved in ethanol (2 ml, 5 *N*). The resulting mixtures were heated at reflux for 10 min and then allowed to cool. The solvent was removed under reduced pressure, and each residue was recrystallized from ethanol.

RESULTS AND DISCUSSION

Structure Determination and Refinement of VI—The cell parameters a = 8.191 (1), b = 9.380 (2), and c = 10.752 Å (2) and α = 105.45 (2), β = 98.68 (1), and γ = 97.00° (1) were obtained from a least-squares calculation of the setting angles of 30 reflections measured on an automatic four-circle diffractometer[9]. The calculated density was 1.325 g/cm^3 with Z = 2. The intensities were collected from a crystal of 0.30 × 0.40 × 0.25 mm in the range $2 \leq 2\theta \leq 60°$ in the $\theta/2\theta$ scan mode with MoK$_\alpha$ radiation monochromatized by a graphite crystal; 4478 independent reflections were measured of which 2598 had $I \geq 2\sigma$ (I), σ being calculated from counting statistics. No systematic absences were observed; therefore, the possible space groups were P1 and P$\bar{1}$.

A centrosymmetric structure was suggested by normalized structure factor statistics. The structure was solved by direct methods [MULTAN 77 (3)]. The best E map revealed all the nonhydrogen atoms. Anisotropic full-matrix least-squares refinement with unit weights led to R = 0.10.

[2] Perkin-Elmer 577.
[3] Hitachi/Perkin-Elmer R-24 B spectrometer.
[4] Varian EM 390 spectrometer.
[5] Bruker WM 250 SY spectrometer.
[6] Bruker WM 80 SY spectrometer.
[7] Hitachi/Perkin Elmer RMU-6M spectrometer.
[8] Carlo Erba Elemental Analyzer model 1104.
[9] Philips PW 1100.

Table II—Atomic Parameters of VI

	x/a	y/b	z/c	Ueq
		Nonhydrogen Atoms[a]		
C(1)	0.1901(3)	0.8132(3)	0.2776(3)	318(9)
C(2)	0.3822(3)	0.8438(3)	0.3078(3)	294(8)
C(3,5′)	0.4600(3)	0.7014(3)	0.3056(2)	279(8)
C(4)	0.3581(3)	0.5954(3)	0.3648(3)	316(9)
C(5)	0.1691(3)	0.5894(3)	0.3279(3)	312(8)
C(6)	0.1035(3)	0.5451(3)	0.1787(3)	405(10)
C(7)	0.1184(3)	0.6941(4)	0.1446(3)	383(10)
N(8)	0.1190(3)	0.7395(3)	0.3688(2)	298(7)
C(9)	0.1711(3)	0.8245(3)	0.5083(3)	350(9)
C(10	0.0785(4)	0.7524(4)	0.5953(3)	488(12)
C(11)	0.1623(4)	0.8191(5)	0.7397(3)	553(14)
C(12)	0.3229(5)	0.7624(4)	0.7714(3)	474(12)
O(13)	0.3574(4)	0.6479(4)	0.7086(3)	724(13)
O(14)	0.4215(4)	0.8548(3)	0.8803(3)	623(11)
C(15)	0.5737(6)	0.8048(5)	0.9287(4)	644(16)
C(16)	0.7171(7)	0.8660(7)	0.8774(6)	850(24)
O(1)	0.7119(2)	0.5600(3)	0.0785(2)	459(8)
O(2)	0.6823(2)	0.8149(3)	0.4978(2)	441(8)
N(1′)	0.4891(2)	0.6248(3)	0.1749(2)	313(7)
C(2′)	0.6514(3)	0.6202(3)	0.1722(3)	321(9)
N(3′)	0.7441(2)	0.7006(3)	0.2971(2)	342(8)
C(4′)	0.6410(3)	0.7480(3)	0.3832(3)	306(8)
		Hydrogen Atoms		
H(11)	0.162(7)	0.915(6)	0.291(5)	
H(21)	0.414(6)	0.911(5)	0.396(5)	
H(22)	0.424(6)	0.893(6)	0.247(5)	
H(41)	0.394(6)	0.634(6)	0.464(5)	
H(42)	0.390(6)	0.502(6)	0.335(5)	
H(51)	0.118(6)	0.522(6)	0.369(5)	
H(61)	0.020(7)	0.494(6)	0.153(5)	
H(62)	0.162(7)	0.474(6)	0.134(5)	
H(71)	0.191(7)	0.700(6)	0.078(5)	
H(72)	0.005(7)	0.712(6)	0.110(5)	
H(91)	0.149(7)	0.932(6)	0.516(5)	
H(92)	0.290(7)	0.838(6)	0.539(5)	
H(101)	0.084(8)	0.638(7)	0.568(6)	
H(102)	0.033(8)	0.768(7)	0.585(6)	
H(111)	0.094(9)	0.791(8)	0.799(7)	
H(112)	0.188(9)	0.927(8)	0.773(7)	
H(151)	0.578(10)	0.680(9)	0.888(8)	
H(152)	0.612(10)	0.863(9)	1.022(7)	
H(1′,1)	0.426(6)	0.580(5)	0.109(5)	
H(3′,1)	0.853(7)	0.713(6)	0.319(5)	
H(161)	0.737(12)	0.984(11)	0.916(9)	
H(162)	0.688(12)	0.827(11)	0.779(9)	
H(163)	0.811(12)	0.833(11)	0.926(9)	

[a] Coordinates and thermal parameters as Ueq = $(1/3)\cdot\Sigma[U_{ij} = a_i^* a_j^* a_i a_j \cos(a_i,a_j)]$ pm^2.

Table III—Torsion Angles of VI

Bonds	Angle, °
C(3,5′)—C(2)—C(1)—N(8)	56.4(3)
C(2)—C(1)—N(8)—C(5)	−68.5(3)
C(1)—N(8)—C(5)—C(4)	69.5(3)
N(8)—C(5)—C(4)—C(3,5′)	−57.5(3)
C(5)—C(4)—C(3,5′)—C(2)	38.3(3)
C(4)—C(3,5′)—C(2)—C(1)	−38.1(3)
C(1)—N(8)—C(5)—C(6)	−51.5(3)
N(8)—C(5)—C(6)—C(7)	31.3(3)
C(5)—C(6)—C(7)—C(1)	−0.5(3)
C(6)—C(7)—C(1)—N(8)	−30.4(3)
C(7)—C(1)—N(8)—C(5)	51.3(3)
N(1′)—C(2′)—N(3′)—C(4′)	4.4(3)
C(2′)—N(3′)—C(4′)—C(3,5′)	−3.3(3)
N(3′)—C(4′)—C(3,5′)—N(1′)	1.1(3)
C(4′)—C(3,5′)—N(1′)—C(2′)	1.7(3)
C(3,5′)—N(1′)—C(2′)—N(3′)	−3.7(3)

A difference synthesis showed all hydrogen atoms. Final refinement, with the isotropic temperature factor for hydrogen, gave R = 0.070 and $R_w = (\Sigma w \Delta^2/\Sigma w |F_0|^2)^{1/2}$ = 0.079. A final difference synthesis showed no significant electron density[10].

Description of the Structure—The molecular conformation of the

[10] The structure factor lists are deposited in the Division of Drug Chemistry, Food and Drug Administration, Washington, DC 20204; copies are available on request to the authors.

Table IV—Physical Data and Spectral Properties of I–VII and the Corresponding Hydrochlorides

Compound	R^1 [a]	Yield, %	Melting Point[b], °	IR[c] (KBr), cm^{-1}	MS, *m/z*	Formula	Analysis, % Calc.	Found
I	—H	47	225–226	3358 (m), 2720 (vw), 1765 (s), 1745 (s), 1710 (vs) 1760 (w), 1730 (s)[d]	281 (M^+), 208, 181, 96, 80, 55, 44	$C_{13}H_{19}N_3O_4$	C 55.50 H 6.80 N 14.93	55.60 6.68 14.57
I · HCl		95	185	1720, 1745, 1760		$C_{13}H_{20}ClN_3O_4$	C 49.13 H 6.34 N 13.22	48.95 6.26 13.20
II	$-CH_3$	58	239–240	3250 (m), 2720 (m), 1770 (s), 1740 (vs), 1720 (vs) 1760 (w), 1720 (s)[d]	295 (M^+), 222, 168, 136, 70, 68, 56, 55, 44	$C_{14}H_{21}N_3O_4$	C 56.94 H 7.17 N 14.23	56.60 7.10 14.16
II · HCl		83	199	1730, 1768		$C_{14}H_{22}ClN_3O_4$	C 50.68 H 6.68 N 12.66	50.43 6.93 12.58
III	$-CH_bH_cC_6H_5$	39	228–229	3240 (m), 2720 (w), 1765 (s), 1735 (sh), 1720 (vs) 1760 (w), 1720 (s)[d]	342 ($M^+ - 29$), 299, 280, 159, 130, 103, 91, 89, 67, 55, 54, 44	$C_{20}H_{25}N_3O_4$	C 64.67 H 6.78 N 11.31	64.30 6.93 11.70
III · HCl		72	248	1735, 1768		$C_{20}H_{26}ClN_3O_4$	C 58.89 H 6.42 N 10.30	58.80 6.29 10.12
IV	$-CH_2CH_2CO_2-CH_2CH_3$	72	135–136	3300 (w), 2712 (w), 1762 (m), 1750 (s), 1720 (vs) 1760 (w), 1730 (s)[d]	281 (M^+), 336, 234, 151, 134, 63, 55, 54	$C_{18}H_{27}N_3O_6 \cdot H_2O$	C 54.12 H 7.31 N 10.51	54.37 7.45 10.82
IV · HCl		96	198–199	1736, 1770		$C_{18}H_{28}ClN_3O_6$	C 51.73 H 6.75 N 10.05	51.79 7.06 9.79
V	$-CH(CH_3)_2$	57	206	3365 (m), 3190 (m), 1775 (s), 1728 (vs), 1710 (vs) 1760 (w), 1725 (s)[d]	280 ($M^+ - 43$), 250, 138, 96, 83, 55, 54, 44	$C_{16}H_{25}N_3O_4$	C 59.61 H 7.50 N 13.03	60.00 7.85 12.75
V · HCl		87	235–236	1730, 1767		$C_{16}H_{26}ClN_3O_4$	C 53.40 H 7.28 N 11.67	53.32 7.26 11.77
VI	$>NCH_2CH_2CH_2-CO_2CH_2CH_3$	37	180	3270 (m), 2710 (m), 1765 (m), 1730 (vs), 1715 (vs) 1765 (w) 1725 (s)[d]	309 (M^+), 264, 208, 182, 124, 82, 64, 55, 54, 44	$C_{15}H_{23}N_3O_4$	C 58.23 H 7.49 N 13.58	58.26 7.80 14.00
VI · HCl		82	250–252	1732, 1770		$C_{15}H_{24}ClN_3O_4$	C 52.09 H 6.99 N 12.15	51.78 6.89 12.09
VII	$>N-C_6H_4$-*p*-$CO_2-CH_2CH_3$	24	320–321	3400 (m), 3195 (m), 1770 (s), 1730 (vs), 1700 (vs) 1770 (w), 1732 (s)[d]		$C_{18}H_{21}N_3O_4$	C 62.96 H 6.16 N 12.23	62.65 6.10 12.57

[a] R^1 is the same in each compound for the free base and corresponding hydrochloride salt. [b] All compounds were recrystallized from ethanol except for III, which was recrystallized from methanol. [c] The N—H and C=O stretching frequencies are listed for the free bases. The C=O stretching frequencies are listed for the hydrochloride salts. Key: (s) strong; (w) weak; (sh) shoulder; (vs) very strong; (vw) very weak. [d] Spectra were run in dimethyl sulfoxide (DMSO) solution.

Table V—Chemical Shifts of I–VII in Dimethyl Sulfoxide [a]

Group	I	II	III[b]	IV	V	VI	VII
$H_{2,4\alpha}$	1.50(a)	1.40(a)	1.43(a)	1.40(a)	1.40(a)	1.40(a)	1.53(a)
$H_{2,4\beta}$	2.20(a)	2.30(a) 2.20(a)	2.27(a) 2.21(a)	~2.1(b)[c]	2.18(a) 2.10(a)	2.16(a)	2.20(a)
$H_{1,5}$	3.31(c)	3.40(c)	3.35(c)	3.26(c)	3.15(c)	3.20(c)	4.4(c)
$H_{6,7}$	1.90(c)	1.90(c)	1.90(c)	1.84(c)	1.80(c)	1.86(c)	2.10(c)
$N^{1'}$—H	8.25(d)	8.30(d)	8.22(d)	8.0(d)	8.0(d)	8.14(d)	8.36(d)
$N^{3'}$—H	10.80(c)	10.40(c)	10.72(c)	10.70(c)	10.50(c)	10.45(c)	10.50(c)
CH_α	3.30(d)	3.40(e)	3.52(a)	~3.3(b)[c]	3.05(f)	2.36(g)	
CH_β		1.18(f)	2.73(a) 3.08(a)	~2.2(b)[c]	~1.8(b)[c]	1.70(h)	
CH_γ				~2.4(b)[c]	0.88(f) 0.83(f)	2.33(g)	
$CH_{\alpha'}$	4.15(e)	4.15(e)	3.88(e)	4.06(e)	4.0(e)	4.10(e)	4.20(e)
$CH_{\beta'}$	1.20(g)	1.20(g)	0.92(g)	1.12(g)	1.14(g)	1.16(g)	1.30(g)
$CH_{\alpha''}$				4.04(e)			
$CH_{\beta''}$				1.12(g)			
Aromatic $H_{2'(6')}$			7.1–7.3(b)				6.83(f)
Aromatic $H_{3'(5')}$							7.76(f)

[a] Spectra recorded at 90 MHz unless otherwise indicated; tetramethylsilane was used as the internal standard. Key: (a) doublet of doublets; (b) multiplet; (c) wide singlet; (d) singlet; (e) quartet; (f) doublet; (g) triplet; (h) quintuplet. [b] Spectra recorded at 250 MHz. [c] Not resolved.

Table VI—Coupling Constants of I–VII in Dimethyl Sulfoxide [a]

Identification	I	II	III	IV	V	VI	VII[b]
$JH_{2,4\alpha}$—$H_{2,4\beta}$	14	15	14	14	14	14	14
$JH_{2,4\beta}$—$H_{1,5}$	3	3	3		3	3	3
$JH_{2,4\alpha}$—$H_{1,5}$	<1	1	<1	~1	<1	<1	<1
$JH_{1,5}(W_{1/2})$	8	9	10	10		9	9
JH_{α}—H_{β}		7	[c]		6	6	
JH_{β}—H_{γ}					6	6	
$JH_{\alpha'}$—$H_{\beta'}$	7	7	7	7	7	7	7
$JH_{\alpha''}$—$H_{\beta''}$				7			

[a] Hertz values; tetramethylsilane was used as the internal reference. [b] Aromatic $^3J = 7$. [c] In the molecular fragment >N—CH_a—C(—H_b)(—H_c)—ϕ; JH_a—H_b = 10, JH_a—H_c = 4, and JH_b—H_c = 12.

compound reported here provides a comparison with some of the derivatives already studied (2, 4, 5). Figure 1 shows the structural formula. Table I lists the bond lengths and angles; Table II shows the final parameters for the atoms; Table III lists the torsion angles.

The molecule consists of a piperidine ring and a five-membered ring joined by a common C—N—C bridge, with an ethoxycarbonylpropyl group attached to the N-8 atom and a hydantoin ring substituted at the C-3,5′ atom. The piperidine ring adopts a distorted chair conformation. The asymmetry parameters (6) are $\Delta C_s^{(3,5')} = 0.9$, $\Delta C_2^{(2\text{-}3,5')} = 15.0$, and $\Delta C_2^{(1\text{-}2)} = 30.8$, showing that mirror symmetry is dominant with an approximate C_s-plane passing through C-3,5′ and N-8. The displacements of C-3,5′ and N-8 from the plane through the remaining atoms of the piperidine ring are 0.496 and −0.818 Å, respectively: larger than the corresponding deviations of the C-3,5′ and N-6 in N^3-ethyl-3-azabicyclo(3.2.1)octane-8-spiro-5′-hydantoin (4), −0.897 and 0.575 Å, respectively. The nonbonded distances C-7 · · · C-3,5′ and N-8 · · · C-3,5′ are 3.04 and 3.01 Å, respectively, similar to the corresponding distances found in N^8-methyl-nortropane-3-spiro-5′-hydantoin (2).

The five-membered ring adopts a puckering N^8-envelope conformation. This conformation has been studied in terms of the torsion angles (7). The pseudo-rotation parameters Δ and ϕ are −35.0 and 53.7°, respectively, and the deviation of N-8 atom from the plane through C-1, C- 5, C-6, and C-7 is −0.750 Å, similar to the value found previously (4) for the C-3,5′ atom.

The configuration of N-8 is pyramidal, as in other mentioned cases (2, 4), and the ethoxycarbonylpropyl radical is attached to the N-8 in an axial position as previously described (2). Two hydrogen bonds of the types N—H · · ·O and N—H · · ·N link the molecules together (Fig. 1). The geometry of these hydrogen bonds are N(1′) · · ·O(1)(−x + 1, −y + 1, −z) = 2.932 Å, N(3′) · · ·N(8)(x + 1, y,z) = 3.005 Å, N—H · · ·O = 163.0°, and N—H · · ·N = 178.3°.

IR Spectra—The IR data of I–VII (Table IV) were compared with analogous azabicyclospirohydantoins studied previously (8, 9). The IR spectrum of VI in the solid state shows a medium band at 3270 cm^{-1} and a broad band at 2710 cm^{-1}. The band at 3270 cm^{-1} is due to the stretching of the $N^{1'}$—H bond belonging to the intermolecular bonding system, $N^{1'}$—H · · ·O=$C^{2'}$ formed between pairs of molecules related by a center of symmetry. The band at 2710 cm^{-1} is explained by the existence of a strong intermolecular hydrogen bond formed between the weak acid $N^{3'}$—H group and the basic piperidine nitrogen atom. Both structural facts are in good agreement with the results obtained by X-ray diffraction. The spectrum of VI in solid state shows a medium band at 1765 cm^{-1} and two strong bands at 1730 and 1715 cm^{-1} in the carbonyl region. The bands at 1765 and 1715 cm^{-1} are attributed to the symmetrical and asymmetrical modes of the pseudo-ring system formed between molecules shown in Fig. 1. The band corresponding to the $C^{4'}$=O stretching vibration did not appear in the IR spectrum. As in related systems, this fact is explained by overlapping of the band corresponding to the $C^{2'}$=O asymmetric stretching mode of the dimer. The band at 1730 cm^{-1} is attributed to the stretching of the ester carbonyl group. The spectra of II and III in solid state also showed bands similar to those found in VI.

The spectra of V and VII in solid state are different from those of II, III, and VI (in which the intermolecular hydrogen bonds deduced from IR data were confirmed by the X-ray study of VI). Therefore the intermolecular hydrogen bonds in V and VII are different; there is no $N^{3'}$—H · · ·N bond which can be attributed to the great size of the N-substituent in the case of V and to the low basicity of the piperidine nitrogen atom in the case of VII.

The carbonyl region shows the same pattern as those found in II, III, and VI. The spectra of I–VII showed the same absorption pattern in the carbonyl region in solid state as in solution in dimethyl sulfoxide; consequently, the N^1—· · ·O=$C^{2'}$ bonds remain in solution.

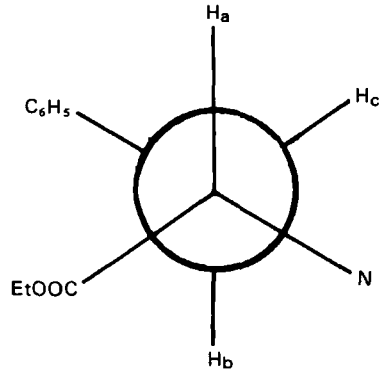

Figure 2—*Newman projection showing the conformation about C_α—C_β bond in III.*

NMR Spectra—The ^{1}H- and ^{13}C-NMR data of I–VII[11] are summarized in Tables V–XI. In all cases, broad-band decoupled and single-frequency off-resonance decoupling spectra were obtained. Assignments of the carbon resonances were made by the multiplicity of signals in the single-frequency off-resonance decoupled spectra, the peak intensity of the broad-band decoupled spectra, and the literature data (1, 10–18).

From the ^{1}H- and ^{13}C-NMR data of I–VII and the crystal structure of VI, the following general features were deduced: (*a*) the pyrrolidine and piperidine rings in these compounds all have a flattened N^8-envelope and distorted chair conformation puckered at N-8 and flattened at C-3,5′ similar to that observed in the crystal structure of VI; (*b*) the $C^{4'}$=O group is attached to the piperidine ring in an equatorial position (Scheme I), in good agreement with the X-ray results for VI; and (*c*) the radical attached to the piperidine nitrogen adopts an equatorial position; however, in the solid state (according to X-ray and IR data for II, III, and VI), the corresponding radical is attached in an axial position.

These conclusions are supported by the following. In the ^{1}H-NMR spectra, the $W_{1/2}$ value (1) for the C-1 and C-5 hydrogen signals of ~10 Hz corresponds to a tropane system with the piperidine ring in a flattened chair conformation (1, 19). The J $H_{2,4}$—$H_{1,5}$ values (Table VI) correspond to dihedral angles of ~60°. In all cases J $H_{2,4\beta}$—$H_{1,5}$ is greater than J $H_{2,4\alpha}$—$H_{1,5}$; consequently, the dihedral angle $H_{2,4\alpha}$—C—C—$H_{1,5}$ is greater than $H_{2,4\beta}$—C—C—$H_{1,5}$. The C-6 and C-7 hydrogen signal appears in all cases as a wide singlet; in an ideal chair, the C-6 and C-7 endo hydrogen atoms would be deshielded by the anisotropic effect due to the hydantoin ring. The C-2β and C-4β hydrogen signals are shifted to lower field, with respect to the C-2α and C-4α hydrogen signals, because of the anisotropic deshielding effect due to the equatorial $C^{4'}$=O group (1).

In the ^{13}C-NMR spectra, the chair conformation adopted by the piperidine ring is confirmed by the C-2 and C-4δ values (Table IX). For a boat conformation, these carbon signals would be shifted to higher field because of the steric compressing effect due to the eclipsing between the C-2(4)β and C-1(5) hydrogen atoms (16). The different radicals are attached to the piperidine nitrogen atom in an equatorial position. For an axial position of the radical, the γ-effect exerted on H-2α and H-4α would shift to higher field to the C-2 and C-4 carbon signals (16). The puckering of the piperidine ring at N-8 is deduced from the γ-shielding effect exerted by the equatorial N-group on H-6 exo and H-7 exo. This γ-effect is ~3 ppm[12], smaller than that expected for an ideal envelope conformation of the pyrrolidine ring.

The hydrochlorides of I–IV, which are the usual species in pharmacological studies, have also been studied. The main features found in the protonated forms are: (*a*) the puckering at N-8 is decreased, and (*b*) the proton attached to the N-piperidine atoms is in the axial position.

These results are supported by the following. In the ^{13}C-NMR, the carbon signals corresponding to the C-2 and C-4 in the hydrochlorides of I–IV are shifted to higher fields with respect to the same carbon signals of the corresponding bases. This fact is due to the *syn*-diaxial effect of the N^+—H proton. The mentioned decreasing of the puckering is sup-

[11] Copies of the ^{13}C-NMR spectra of II, II·HCl, III, III·HCl, V, and VI and the ^{1}H-NMR spectrum of III are deposited in the Division of Drug Chemistry, Food and Drug Administration, Washington, DC 20204 and are available on request to the authors.

[12] This value is the difference between the C-6 and C-7δ values of compounds I–VII and the C-6 and C-7δ value of nortropane (10).

Table VII—Chemical Shifts of the Hydrochlorides of I–VI [a]

Group	I[b,d]	I[c,e]	II[b,e]	II[c,e]	III[c,e]	IV[b,d]	IV[c,e]	V[b,d]	VI[c,e]
$H_{2,4\alpha}$	2.02(a)	2.08(a)	1.93(a)	2.26(a)	2.20(a)	2.05(a)	2.20(a)	1.95(a)	1.8–2.1(b)[f]
$H_{2,4\beta}$	2.60(a)	2.60(a)	2.5–2.8(b)[f]	2.69(a)	2.70(a)	~2.7(b)[f]	~2.7(b)[f]	2.5–2.7(b)[f]	2.55(a)
$H_{1,5}$	4.15(c)	4.05(c)	4.26(c)	4.30(c)	4.40(c)	4.1(c)	4.0(c)	4.0(c)	4.1(c)
$H_{6,7}$	2.25(c)	2.27(c)	2.26(c)	2.35(c)	2.35(c)	2.30(c)	2.34(c)	2.30(c)	2.20(c)
$N_{1'}$—H	8.58(c)		8.63(c)			8.60(c)		8.50(c)	
CH_α	4.15(d)	3.9(d)	~4.2(b)[f]	4.28(c)	4.23(a)	~4.2(b)[f]	~4.0(b)[f]	4.30(f)	3.0(g)
CH_β			1.60(f)	1.67(f)	3.17(a)	2–2.7(b)[f]	2.60(c)	~2.0(b)[f]	2.0(h)
CH_γ						2–2.7(b)[f]	2.60(c)	1.05(f) 1.06(f)	2.4(g)
$CH_{\alpha'}$	4.30(e)	4.27(e)	4.26(e)	4.35(e)	4.10(e)	4.33(e)	4.36(e)	4.30(e)	4.05(e)
$CH_{\beta'}$	1.28(g)	1.27(g)	1.36(g)	1.33(g)	1.06(g)	1.23(g)	1.32(g)	1.20(g)	1.16(g)
$CH_{\alpha''}$						4.02(e)	4.20(e)		
$CH_{\beta''}$						1.12(g)	1.31(e)		
Aromatic					7.2–7.4(b)				

[a] Key: (a) doublet of doublets; (b) multiplet; (c) wide singlet; (d) singlet; (e) quartet; (f) doublet; (g) triplet; (h) quintuplet. [b] In dimethyl sulfoxide. [c] In deuterium oxide. [d] Spectra recorded at 60 MHz. [e] Spectra recorded at 90 MHz. [f] Not resolved.

Table VIII—Coupling Constants of the Hydrochlorides of I–VI [a]

Identification	I[b]	I[c]	II[b]	II[c]	III[c]	IV[b]	IV[c]	V[b]	VI[c]
$JH_{2,4\alpha}$—$H_{2,4\beta}$	16	16	15	16	15	14	16	14	14
$JH_{2,4\beta}$—$H_{1,5}$	~3	3		3	3		~3		~3
$JH_{2,4\alpha}$—$H_{1,5}$	<1	<1	<1	<1	<1	~1	~1	<1	
$JH_{1,5}(W_{1/2})$	~10	~10	~12		~12			~12	
JH_α—H_β				7	[d]			6	8
JH_β—H_γ								6	7
$JH_{\alpha'}$—$H_{\beta'}$	7	7	7	7	7	7	7	7	7
$JH_{\alpha''}$—$H_{\beta''}$						7	7		

[a] Hertz values; tetramethylsilane was used as the internal reference. [b] In dimethyl sulfoxide. [c] In deuterium oxide. [d] In the molecular fragment 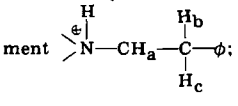 ; JH_a—H_b = 10, JH_a—H_c = 5, and JH_b—H_c = 15.

ported by the increased γ-effect exerted by the *N*-group on the C-6 and C-7 exo hydrogen atoms, so that the C-6 and C-7 carbon signals are shifted to higher fields.

To give a detailed account of the former results, several pairs of base–hydrochloride compounds were studied. For solubility reasons, it was not possible to run the spectra of the bases and the hydrochlorides in the same solvent; however, medium-induced shifts are often negligibly small in ^{13}C-NMR because the nuclei studied are buried in the molecular framework.

Compound I—In this case, the decreasing of the puckering on protonation is noticeable $\Delta\delta$(C-6, C-7) = −4.5 ppm.

Compound II—In this case, the decreasing of the *N*-puckering is less than that observed in I, $\Delta\delta$(C-6, C-7) ≃ −2.5 ppm. The proton-coupled spectral data of II hydrochloride are in Table XI; from the J C$^{4'}$—$H_{2,4\beta}$ value of 3 Hz, a value near 0° can be deduced for the dihedral angle C$^{4'}$—C^3—C^2—$H_{2,4\beta}$ in good agreement with values found in the literature (20, 21).

Compounds III and IV—For these compounds, the decreasing of N-8 puckering on protonation is remarkable, $\Delta\delta$(C-6,7) ≃ −5 ppm. From the ^1H—NMR spectra of III resolved at 250 MHz, it can be deduced that the *N*-piperidine group adopts the preferred conformation represented in Fig. 2. This fact can be explained as:

1. The vicinal coupling constants (Table VI) of the ϕ—CH_2—CH—N< fragment.
2. Hc resonates at a lower field with respect to Hb; this is due to the anisotropic effect exerted by the phenyl group.
3. The aromatic proton resonance is a complex multiplet, showing a distinct conformational preference about the aryl-Cβ bond.
4. In the proposed conformation, the ethyl ester protons resonate at a higher field position than those of related compounds (Table V) since they are shielded by the π-electron cloud of the phenyl group.

The deshielding of the C-1 and C-5 carbon signals on protonation (≈5 ppm, Tables IX and X) remains unexplained. It could be explained by the enhancement of the N-σ-effect on protonation, but it had been shown (22) that, in *N*-methyl piperidine, the *N*-protonation effect on the α-carbon is quite irregular (−1.7–26.1 ppm).

Table IX—^{13}C-Chemical Shifts for I–VII in Dimethyl Sulfoxide

Carbon Position	Multiplicity[a]	I	II	III[b]	IV[b]	V	VI[b]	VII[b]
1,5	d	57.09(d)	55.70	54.43 54.82	54.34 54.70	53.87 55.70	56.70	51.90
2,4	t	38.58	37.41	37.50	38.01	38.47	38.92	35.41
3	s	59.28	59.24	59.55	59.01	59.75	59.70	60.15
6,7	t	24.97	25.48 25.01	25.87	25.60	25.88 26.03	25.14	26.43
C—α		52.70(t)	54.39(d)	63.58(d)	59.82(d)	66.78(d)	49.79(t)	
C—β			16.28(q)	37.50(t)	25.60(t)	28.14(d)	23.65(t)	
C—γ					29.14(t)	16.79(q) 19.53(q)	31.62(t)	
C—*C*=O	s	170.73	172.63	171.83	172.13	171.72	172.80	165.55
C—*C*=O	s				172.73			
C—α′	t	59.68	60.41	59.76	60.13	59.53	59.52	59.49
C—β′	q	13.91	13.98	13.75	13.87	13.98	14.02	14.17
C—α″	t				60.13			
C—β″	q				13.87			
C—2′	s	156.68	156.79	156.84	156.84	156.72	156.81	156.81
C—4′	s	178.84	178.70	178.92	178.77	178.80	178.95	177.82
Aromatic								
C—1	s			137.30				149.02
C—2,6	d			126.70				130.92
C—3,5	d			128.03				117.01
C—4	d			126.25				113.36

[a] Signal multiplicity obtained from single-frequency off-resonance decoupling spectra. Key: (s) singlet; (d) doublet; (t) triplet; (q) quartet. [b] In 10% deuterated chloroform.

Table X—^{13}C-Chemical Shifts for the Hydrochlorides of I–IV in Deuterium Oxide

Position	Carbon Multiplicity[a]	I	II	III[b]	IV
1.5	d	59.09	57.60 61.20	58.10 60.16	57.70 58.16
2.4	t	35.41 36.25	37.50 37.71	34.32	34.28
3	s	55.85	58.46	55.43	55.61
6.7	t	20.44	22.96 23.55	20.50 20.80	20.39 20.93
C—α		51.17(t)	58.46(d)	56.58(d)	56.31(d)
C—β			13.92(q)	31.68(t)	20.93(t)
C—γ	t				26.78
C_α—C=O	s	167.34	169.45	165.41	165.50
C_γ—C=O	s				171.13
C—α'	t	61.25	64.04	61.37	61.70
C—β'	q	10.77	13.44	10.39	10.85
C—α''	t				59.61
C—β''	q				10.69
C—2′	s	155.80	158.30	155.66	155.63
C—4′	s	176.06	178.44	176.01	175.90

[a] Signal multiplicity obtained from single-frequency off-resonance decoupling spectra. Key: (s) singlet; (d) doublet; (t) triplet; (q) quartet. [b] Aromatic: C-1, 130.70; C-2 and C-6[c], 126.70; C-3 and C-5[c], 126.58; C-4, 125.52. [c] Values may be interchanged.

Table XI—^{13}C—H Coupling Constants of the Hydrochloride of II in Deuterium Oxide [a]

JC_1—H_1: 154; JC_5—H_5: 150; JC_2—H_2 and JC_4—H_4: 130; JC_6—H_6 and JC_7—H_7: 138; JC_α—H_α: 150; JC_β—H_β: 126; JC_β—H_α: 5; $JC_{\alpha'}$—$H_{\alpha'}$: 150; $JC_{\alpha'}$—$H_{\beta'}$: 4.5; $JC_{\beta'}$—$H_{\beta'}$: 126; $JC_{\beta'}$—$H_{\alpha'}$: 2.8; $JC_{4'}$—$H_{2,4_{ax}}$: 3

[a] Hertz values.

Compounds V and VI—The ^{1}H- and ^{13}C-NMR data for these compounds are analogous to those of I–IV.

Compound VII—Because of the π-releasing conjugative effect of the *N*-piperidine atom, the phenyl group is essentially located on a plane approximately parallel to the C^1—C^2—C^4—C^5 plane; consequently, a β-compressing effect on H-6 exo and H-7 exo is exerted, and the ^{13}C-NMR signal of C-1 and C-5 carbon atoms are shifted to higher field ($\Delta \simeq -4$ ppm) with respect to the same C-signal of the parent compounds.

CONCLUSIONS

In the crystalline state, the cyclohexane ring of VI adopts a deformed chair conformation with a flattening at C-3,5′. This deformation is probably due to the steric interaction between the ethylene bridge and the hydantoin group. The opposite puckering at N-8 and the axial position of the *N*-substituent make the formation of the intramolecular $N^{3'}$—H···N^8 bond easy. Compounds I–VII in dimethyl sulfoxide solution show the same deformation in the cyclohexane rings, but the N—H···N bond disappears, and the *N*-radical adopts the equatorial position to avoid the *syn*-diaxial effect on the C-2 and C-4 axial hydrogen atoms. In III and VII the N^8-group shows a distinct conformational preference. The N^8-puckering of I–VII in dimethylsulfoxide solution is governed by the steric effect of the N^8-group on the C-6 and C-7 exo hydrogen atoms. In deuterium oxide solution, the N^8-protonation of I–IV takes place in an axial position. An equatorial protonation would produce the aforementioned syn-diaxial effect. The decreasing of *N*-puckering on protonation would decrease the N^+—H *syn*-diaxial effect on the C-2 and C-4 axial hydrogen atoms and facilitate the N^+—H solvation.

REFERENCES

(1) G. G. Trigo, M. Martínez, and E. Galvez, *J. Pharm. Sci.*, **70,** 87 (1981).

(2) P. Smith-Verdier, F. Florencio, and S. Garcia-Blanco, *Acta Crystallogr. Sect. B*, **33,** 3381 (1977).

(3) P. Main, M. M. Woolfson, L. Lessinger, G. Germain, and J. P. Declercq, MULTAN 77, (1977) (A system of computer programs for the automatic solution of crystal structures from X-ray diffraction data). University of York, England, and University of Louvain, Belgium.

(4) P. Smith-Verdier, F. Florencio, and S. García-Blanco, *Acta Crystallogr. Sect. B* **35,** 1911 (1979).

(5) J. Vilches, F. Florencio, and S. García-Blanco, *Acta Crystallogr. Sect. B* **37,** 361 (1981).

(6) W. L. Duax and D. A. Norton, "Atlas of Steroid Structure," Plenum, New York, N.Y., 1975, pp. 13, 25.

(7) C. Altona, H. J. Geise, and C. Romers, *Tetrahedron*, **24,** 13 (1968).

(8) J. Bellanato, C. Avendaño, P. Ballesteros, and M. Martínez, *Spectrochim. Acta*, **35A,** 807 (1979).

(9) J. Bellanato, E. Galvez, M. Espada, and G. G. Trigo, *J. Mol. Struct.*, **67,** 1417 (1980).

(10) E. Wenkert, J. S. Bindra, C. J. Chang, D. W. Cochran, and F. M. Schell, *Acc. Chem. Res.*, **7,** 46 (1974).

(11) L. Simeral and G. E. Maciel, *Org. Magn. Reson.*, **6,** 226 (1974).

(12) S. J. Daum, C. M. Martini, R. K. Kullnig, and R. L. Clark, *J. Med. Chem.*, **18,** 496 (1975).

(13) K. Pook, W. Schulz, and R. Banholzer, *Ann. Chem.*, **1975,** 1499.

(14) P. M. Workulich and E. Wenkert, *J. Org. Chem.*, **40,** 3694 (1975).

(15) H. Scheider and L. Sturn, *Angew. Chem. Int. Ed.*, **15,** 545 (1976).

(16) P. Hanisch, A. J. Jones, A. F. Casy, and J. E. Coates, *J. Chem. Soc., Perkin II.*, **1977,** 1202.

(17) J. Feeney, R. Foster, and E. A. Piper, *J. Chem. Soc. Perkin II.*, **1977,** 2016.

(18) A. M. Taha and G. Rucker, *J. Pharm. Sci.*, **67,** 775 (1978).

(19) A. F. Casy and J. E. Coates, *Org. Magn. Reson.*, **6,** 441 (1974).

(20) J. A. Scharcz and A. S. Perlin, *Can. J. Chem.*, **50,** 3667 (1972).

(21) P. E. Hansen, J. Feeney, and G. C. K. Roberts, *J. Magn. Reson.*, **17,** 249 (1975).

(22) J. B. Lambert, D. A. Netzel, H. N. Sun, and K. K. Lilianstrom, *J. Am. Chem. Soc.*, **98,** 3778 (1976).

Evaluation of Some Mannich Bases Derived from Substituted Acetophenones Against P-388 Lymphocytic Leukemia and on Respiration in Isolated Rat Liver Mitochondria

J. R. DIMMOCK *x, K. SHYAM *, N. W. HAMON *, B. M. LOGAN *, S. K. RAGHAVAN *, D. J. HARWOOD *, and P. J. SMITH ‡

Received March 1, 1982, from the **College of Pharmacy* and ‡*Department of Chemistry and Chemical Engineering, College of Arts and Science, University of Saskatchewan, Saskatoon, Saskatchewan, S7N 0W0, Canada.* Accepted for publication July 7, 1982.

Abstract □ Series of 3-dimethylamino-1-aryl-1-propanone hydrobromides (IV) and 3-dimethylamino-2-dimethylaminomethyl-1-aryl-1-propanone dihydrobromides (V) were synthesized. Evaluation of these derivatives against P-388 lymphocytic leukemia growth revealed that two compounds show promise as antineoplastic agents. Compounds of the V series were unstable in phosphate buffer (in contrast to series IV), and when the same nuclear substituent was present in both series of compounds, V was ~100 times more active than IV in both the stimulation and inhibition of respiration of mitochondria isolated from rat liver cells. Representatives from both series showed that respiration in mitochondria was affected by changing the pH of the aqueous buffer from 7.4 to 6.9 or 6.4 and by reducing the temperature from 37° to 20°. The compounds showed reactivity toward a biomimetic thiol.

Keyphrases □ 3-Dimethylamino-1-aryl-1-propanone hydrobromides—synthesis, activity against P-388 lymphocytic leukemia growth, effect on mitochondrial respiration □ 3-Dimethylamino-2-dimethylaminomethyl-1-aryl-1-propanone dihydrobromides—synthesis, activity against P-388 lymphocytic leukemia growth, effect on mitochondrial respiration □ Antineoplastic agents—potential, 3-dimethylamino-1-aryl-1-propanone hydrobromides, 3-dimethylamino-2-dimethylaminomethyl-1-aryl-1-propanone dihydrobromides, activity against P-388 lymphocytic leukemia growth

When arylalkyl ketones such as propiophenone (I) are attacked by nucleophiles such as thiols, thiohemiketals are formed (1). While the rate of nucleophilic attack may be increased by electron-withdrawing substituents on the aromatic ring, other molecular modifications of these compounds, such as the formation of the corresponding Mannich bases (*e.g.*, II), allow the possibility of increased nucleophilic attack at the carbonyl carbon atom. First, the proton attached to the quadrivalent nitrogen in II is acidic and therefore intramolecular proton transfer to the carbonyl oxygen may occur, expediting nucleophilic attack at the carbonyl carbon atom. Second, such additions as in III, exemplified by the attack of a thiol, lead to a reaction intermediate where there is relief from dipole repulsion between the carbonyl and onium groups.

There are, however, two other ways the Mannich bases could interact with cellular nucleophiles, *per se* or after undergoing molecular modification to give reactive derivatives. First, the strong positive inductive effect of the ammonium group [Taft σ^* value for $(H_3C)_3\overset{+}{N}$ is 1.90 (2)] renders the carbon atom of the adjacent methylene group susceptible to nucleophilic attack. Instances may be cited where thiol displacements have occurred (3) although, on occasion, vigorous conditions have been required (4). In the second case, instances have been described whereby Mannich bases have undergone elimination to give the corresponding enones (5, 6); such compounds readily undergo nucleophilic attack (7). Treatment of a variety of 3-dialkylaminopropiophenones with thiophenols gave the corresponding sulfides, possibly formed by an elimination–addition mechanism (8). For these reasons the synthesis of the series of IV compounds for antineoplastic evaluation was contemplated.

When a second dimethylaminomethyl group is introduced into the molecule, as in V, the proton of the methine group adjacent to the carbonyl group is more acidic than the methylene protons adjacent to the carbonyl group in IV. Hence, compounds of the V series have a greater tendency to undergo elimination than IV compounds. Furthermore, after the loss of one onium group in V, the olefin formed may react in a facile manner with nucleophiles, and expedition of the loss of the remaining quaternary ammonium group could occur generating a further center for nucleophilic attack.

Some of a series of Mannich bases (VI) have activity in the P-388 screen. These compounds, which resemble IV, except that an olefinic linkage separates the aromatic ring from the keto function, affected basal respiration in mitochondria isolated from liver cells of male Wistar rats at concentrations as low as 1–5 μmoles (9, 10). One of these compounds [VI, R^1 = 3-OH; R^2 = H; R^3 = $(CH_2)_4CH_3$] elicited a biphasic response: at low dose levels (*e.g.*, 1.25 μmoles), stimulation of respiration occurred, while at higher doses (5 μmoles), inhibition of respiration was noted (11). The stimulation of respiration was shown to be due to the uncoupling of oxidative phosphorylation, while the inhibition was due to the blocking of the electron transport chain between cytochromes b and c_1 (11). Thus, it was considered of interest to evaluate the antineoplastic activity and the effect on mitochondrial respiration of series IV and V compounds and to determine whether a corre-

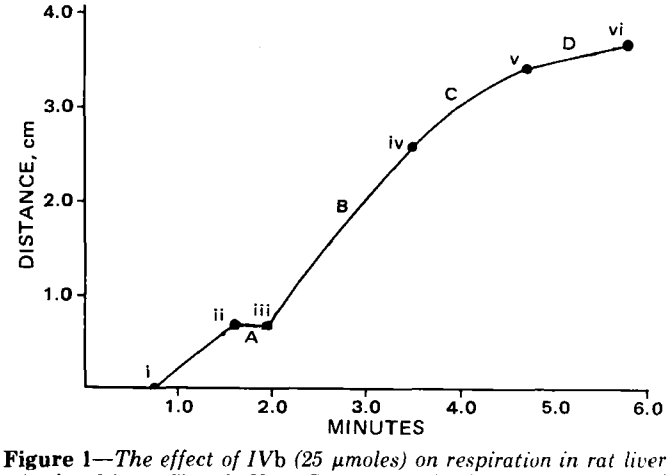

Figure 1—*The effect of IVb (25 μmoles) on respiration in rat liver mitochondria at 37° and pH 7.4. Succinate and IVb were added at* i *and* ii, *respectively. The periods A (between* ii *and* iii) *and C (between* iv *and* v) *represent lag periods prior to the constant maximal stimulation (phase B) and constant maximal inhibition (phase D) of respiration.*

0022-3549/83/0800-0887$01.00/0

Table I—Physical Data, Activity Against P-388 Lymphocytic Leukemia in Mice, and Murine Toxicity of the Amine and Diamine Hydrobromides IV and V

Compound	Yield, %	Melting Point, °	Formula	Analysis, % Calc. C	Calc. H	Calc. N	Found C	Found H	Found N	T/C%[a] (dose in mg/kg)	Murine Toxicity[b] (dose in mg/kg)
IV*a*	60	180–181	$C_{11}H_{16}BrNO$	51.17	6.24	5.43	50.76	6.17	5.41	110(100)	0(200), 6(100)
IV*b*	63	183–184	$C_{11}H_{15}BrClNO$	45.14	5.17	4.79	45.11	5.26	4.79	106(50)	1(200), 5(100), 6(50)
IV*c*	54	199–200	$C_{11}H_{14}BrCl_2NO$	40.39	4.31	4.28	40.43	4.48	4.17	107(50)	1(200), 5(100), 6(50)
IV*d*	41	164–166	$C_{12}H_{18}BrNO$	52.94	6.67	5.15	52.63	6.68	5.12	107(100)	0(200), 6(100)
IV*e*	51	178–179	$C_{12}H_{18}BrNO_2$	50.01	6.29	4.86	50.08	6.39	4.73	104(50)	5(200, 100), 6(50)
V*a*	23	187–188	$C_{14}H_{24}Br_2N_2O$	42.44	6.11	7.07	42.32	6.29	7.03	117(25)	2(50), 6(25)
V*b*	15	180–181	$C_{14}H_{23}Br_2ClN_2O$	39.04	5.38	6.51	38.91	5.57	6.48	116(25)	3(50), 6(25)
V*c*	11	188–189	$C_{14}H_{22}Br_2Cl_2N_2O$	36.15	4.77	6.02	36.09	4.81	5.96	108(12.5)	3(100), 6(50)
V*d*	12	184–185	$C_{15}H_{26}Br_2N_2O$	43.92	6.39	6.83	43.68	6.64	6.82	138(25)	0(50), 6(25)
V*e*	24	204–206	$C_{15}H_{26}Br_2N_2O_2$	42.27	6.15	6.57	41.82	6.08	6.57	136(25)	4(50), 6(25)

[a] Anticancer activity is expressed as the ratios of the survival time of the treated animals to control animals expressed as a percentage. All of the compounds were initially screened at 200, 100, and 50 mg/kg; if mortalities occurred at these doses, they were reduced to nonlethal levels. A compound should increase the median survival time by ≥20% to be considered active. [b] These figures are survivors out of six mice on the fifth day after commencement of the dosage schedule (nine daily doses given intraperitoneally) except V*b* and *c* in which cases the compounds were administered for five consecutive days only.

lation between these two biological parameters exists. In addition, a comparison of the general bioactivity of IV and V could reveal molecular features associated with efficacy against the growth of P-388 lymphocytic leukemia and effect on mitochondrial function.

The effect of temperature on the pattern of respiration was considered of interest since recent reports indicate alterations in mitochondrial function with changes in temperature (12, 13). The compounds could serve as biochemical tools. For example, if both stimulation and inhibition of mitochondrial respiration occurs at 37° and only inhibition occurs when the temperature is lowered to 20°, the effects of concentration can be determined for inhibition of respiration alone.

A number of investigators have shown that the pH of certain tumors is ~7.0 (14, 15), and in addition, the administration of glucose to tumor-bearing animals has lowered the pH of the neoplasm to 6.4 while the pH of normal tissue was unaffected (14, 15). Earlier work was shown that certain compounds in series VI had increased respiratory-inhibiting properties in mitochondria obtained from both rat liver cells and from the Morris 5123 TCH tumor (16) as the pH was lowered from 7.4 to 6.9 and then from 6.9 to 6.4. The question was posed as to whether a similar variation in effect in mitochondria would occur with series IV and V compounds.

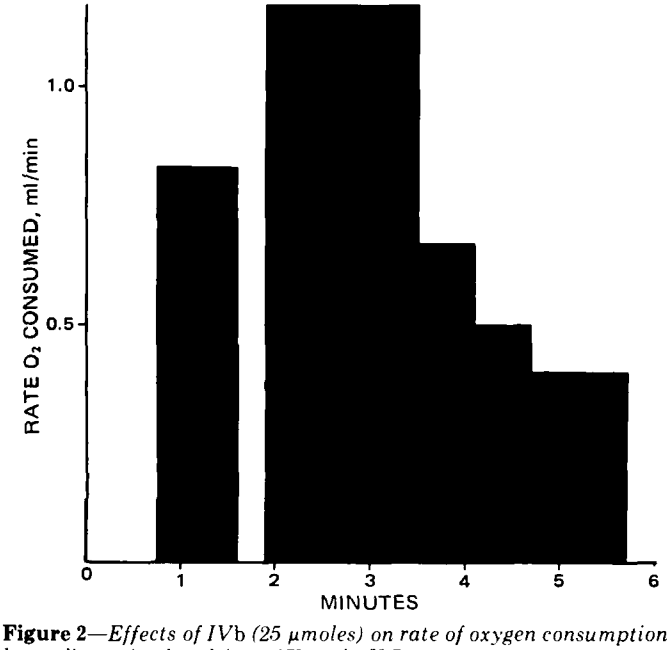

Figure 2—*Effects of IV*b *(25 μmoles) on rate of oxygen consumption by rat liver mitochondria at 37° and pH 7.4.*

RESULTS AND DISCUSSION

The two series of compounds (IV and V) were prepared and assessed for activity against P-388 lymphocytic leukemia growth (Table I). The dose schedule was constant for compounds of both series except fewer doses of V*b* and *c* were administered. From the data available, it may be seen that, while the monobasic compounds of series IV were uniformly inactive against murine P-388 lymphocytic leukemia growth, variation in antineoplastic activity in series V compounds was found. Compounds V*d* and *e* showed significant activity in this screen, V*a* and *b* displayed marginal potencies, and V*c* was inactive. The compounds were less active than 5-fluorouracil, which has a T/C% of 182 at 25 mg/kg (20 daily doses) in the P-388 murine screen (17). All of the compounds in Table I showed toxicity; but, whereas no mortalities were found at 50 mg/kg in series IV, only the inactive diamine of the V series (V*c*) did not cause deaths at this dose level. No animals died when V*a–e* were administered at a dose of 25 mg/kg. Thus, with the exception of V*c*, greater antineoplastic activity accompanied by greater murine toxicity was found with series V than with series IV.

The reasons for the differences in bioactivities between series IV and V were then considered. Lability of a number of Mannich bases to produce the corresponding α,β-unsaturated ketones is well documented (6, 18) and, on occasions, this property has been invoked to explain the bioactivities of a number of Mannich bases (19, 20). Such deamination processes are possible in both IV and V, leading to the formation of substituted acrylophenones which could undergo attack with cellular nucleophiles such as thiols of proteins. Since the rate of deamination is dependent on the nature of the Hammett σ value in the aromatic ring, the stabilities of the compounds with the most divergent σ values namely IV*c* and V*c* ($\sigma = +0.60$) and IV*e* and V*e* ($\sigma = -0.27$) were examined under simulated physiological conditions (buffer of pH 7.4 and 37°). Both IV*c* and *e* were stable for at least 1.5 hr; after 5 min, degradation of V*c* and *e* to VII*a* and *b* occurred as evidenced by extraction of the reaction medium and analysis by NMR. When the temperature was reduced to 5°, V*c* gave rise to a mixture of VII*a* and V*c* as the free base in a ratio of 10:1 after 5 min, while V*e* gave rise to the free base and no olefin. After 1 hr at 5°, V*e* gave a mixture of VII*b* and the free base of V*e* in a ratio of 7:4. Hence, the comparative rates of deamination of V*c* and *e* follow that predicted by a consideration of the electronic effects of the nuclear substituents. The difference between IV and V in ability to undergo elimination, producing the corresponding α,β-unsaturated ketones, is probably due to variation in the acidity of the protons in the β-position to the dimethylamino group, since the rate-determining step in such elimination reactions is the attack of the hydroxyl anion at the methylene carbon atom adjacent to the keto function. This facile elimination could permit reaction with cellular nucleophiles, and reaction of V*c* with a biomimetic thiol (2-mercaptoethanol) was undertaken. Preliminary experiments involving incubation of V*c* and 2-mercaptoethanol in buffer at 37° followed by extraction with chloroform gave a mixture of compounds, as revealed by TLC. However, when V*c* and the thiol were incubated for a short period of time in a mixture of buffer and chloroform, the product

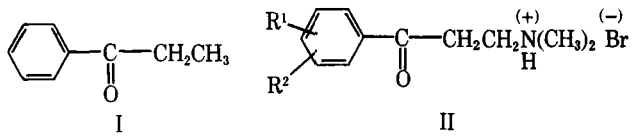

I II

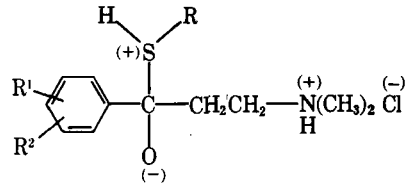

III

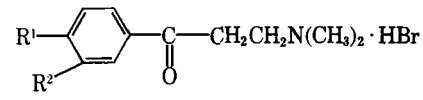

IV

a: $R^1 = R^2 = H$ *d*: $R^1 = CH_3$; $R^2 = H$
b: $R^1 = Cl$; $R^2 = H$ *e*: $R^1 = OCH_3$; $R^2 = H$
c: $R^1 = R^2 = Cl$

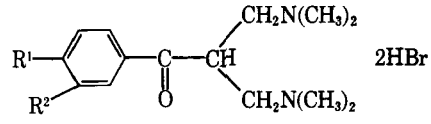

V

a: $R^1 = R^2 = H$ *d*: $R^1 = CH_3$; $R^2 = H$
b: $R^1 = Cl$; $R^2 = H$ *e*: $R^1 = OCH_3$; $R^2 = H$
c: $R^1 = R^2 = Cl$

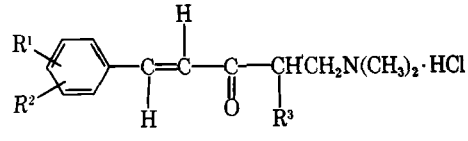

VI

$R^1 = R^2 = H$, Cl, OH
$R^3 = H$, $(CH_2)_4CH_3$

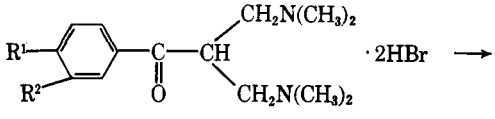

Vc,e

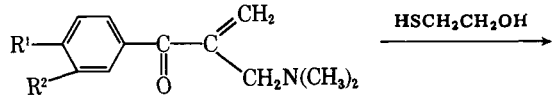

VII

a: $R^1 = R^2 = Cl$
b: $R^1 = OCH_3$; $R^2 = H$

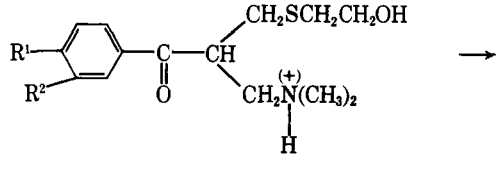

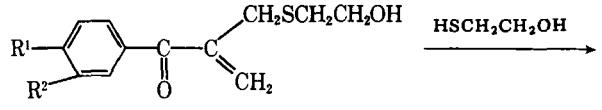

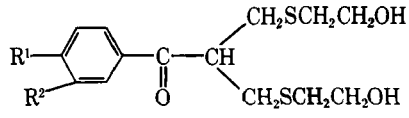

VIII

a: $R^1 = R^2 = Cl$

Scheme I

isolated was shown by NMR to be VIII*a*, which could arise as shown in Scheme I. The mass spectral (MS) fragmentation pattern was consistent with the structure of VIII*a*; in particular, a molecular ion corresponding to the dithioether was observed and the absence of a prominent peak at *m/z* 58, which is often the base peak in Mannich bases due to the dimethylmethyleneimmonium ion, was noted. It was considered that the stability of IV compounds in buffer, and hence lack of formation of the corresponding olefins, may have led to inactivity of these compounds towards thiols. The least reactive member of the series, IV*e*, was incubated with 2-mercaptoethanol in the presence of chloroform and buffer, and the mixture was shown by NMR and MS to be principally 3-(2-hydroxyethylthio)-1-(*p*-methoxyphenyl)-1-propanone, *i.e.*, the dimethylamino group had been replaced by a 2-hydroxyethylthio function. Control experiments showed that the reaction between IV*e* and 2-mercaptoethanol occurred in the buffer and not in the organic solvent. Hence, elimination in series IV may occur in the presence of stronger nucleophiles than the hydroxide anion found in the aqueous buffer. It is conceivable, however, that the Mannich bases of IV and V could interact with thiols by a substitution reaction on the carbon atom adjacent to the dimethylamino group, but the synthesis of such derivatives is often accomplished in the presence of virtually nonpolar solvents and elevated temperatures (4). Hence, the elimination–addition mechanism seems more feasible.

The effect of IV and V compounds on respiration in rat liver mitochondria is given in Table II. At low concentrations in both series of compounds, stimulation of respiration occurs. In general, as the concentration is increased, stimulation of respiration increases and then diminishes while inhibition of respiration increases. In addition, the elevation of concentration shortens the time period prior to inhibition by IV and V compounds. A typical result is illustrated in Figs. 1 and 2. While from a qualitative viewpoint, both series of compounds exert similar effects, a quantitative evaluation of IV*a–e* with the compounds bearing a similar nuclear substituent in series V, indicates that IV requires ~100 times the concentration to elicit the same increases in both stimulation and inhibition of respiration as V. For example, doses of 25 μmoles of IV*a–e* cause similar percentage inhibitions of respiration in mitochondria as 0.25-μmole concentrations of V*a–e*. At comparable concentration levels, the olefins VII*a* and *b* have similar respiration-inhibiting properties as their progenitors V*c* and *e*, although the effect on stimulation of respiration appears somewhat different. Two representative compounds in series IV and V were examined for their effect on mitochondria at 20° and, in general, stimulation of respiration was increased and inhibition of respiration diminished at this temperature compared with 37° (Table III). The respiration-inhibitory data generated for V*a* and *c* are comparable to the olefinic analogues VI ($R^1 = R^2 = H$) and VI (R^1 = 3-CL; R^2 = 4-CL), respectively (9).

A comparison of the effect on respiration in mitochondria between a compound displaying significant activity against P-388 lymphocytic leukemia (V*e*) and an inactive analogue (V*c*) at pH values of 6.9 and 6.4 is summarized in Table IV. With the exception of the 1.0-μmole dose for V*c*, the largest increase in stimulation of respiration is at the pH of normal cells (7.4) in the case of V*c*, while the maximal increase in stimulation for the active compound V*e* is at pH 6.4. If antineoplastic activity is influenced by the effect on stimulation of respiration (*e.g.*, by the uncoupling of oxidative phosphorylation impairing the synthesis of adenosine triphosphate), selective toxicity under the acidic conditions of the tumorous cells is conceivable. When inhibition of respiration was examined, an alternate situation was found; *i.e.*, minimal percentage inhibition of respiration occurs with both V*c* and *e* at pH 6.4. Hence, the bioactivity of V*e* in contrast to V*c* is explicable only in terms of the effect on stimulation and not inhibition of respiration if the effect on mitochondrial function is associated with anticancer properties and the pH of malignant cells is much lower than that of the corresponding normal cells.

In conclusion, the following generalizations regarding chemical structure and bioactivity may be made. First, series V was found to be more active against P-388 lymphocytic leukemia growth and to display greater murine toxicity than series IV, possibly due to the greater fragility

Table II—Effect on Respiration in Rat Liver Mitochondria Using Succinate as the Substrate at pH 7.4 and 37°

Compound	Concentration, μmoles	Stimulation, %	*SE*	Time Prior to Constant Inhibition of Respiration, min	*SE*	Inhibition, %	*SE*
IV*a*	10	37.32	13.22	—	—	0	—
	25	35.57	6.09	6.72	0.90	54.18	12.21
	50	28.22	5.10	7.76	0.86	57.44	4.87
	100	28.62	2.86	4.43	0.35	72.38	2.19
IV*b*	5	35.26	7.67	3.68	0.18	48.75	8.92
	10	45.03	12.18	3.36	0.16	50.36	11.79
	25	57.24	4.69	3.08	0.16	63.96	1.88
	35	27.79	5.79	3.38	0.20	86.09	2.11
IV*c*	5	68.48	15.13	3.89	0.36	84.86	2.73
	10	63.27	6.26	2.22	0.19	63.38	4.73
	25	0	—	1.00	0.09	87.76	3.91
IV*d*	10	39.93	7.96	1.50	0.92	4.31	3.28
	25	92.89	6.54	5.60	0.27	62.27	3.95
	50	34.23	8.47	3.58	0.29	46.83	9.68
	100	0	—	2.95	0.34	78.93	3.67
IV*e*	10	35.46	1.08	—	—	0	—
	25	52.18	7.82	—	—	0	—
	50	64.69	8.45	6.02	0.17	29.75	15.11
	100	49.11	5.61	5.22	0.21	56.58	2.26
V*a*	0.01	64.72	7.43	—	—	0	—
	0.1	38.65	5.29	2.81	1.05	9.81	4.21
	0.25	33.68	4.25	3.64	0.64	53.94	5.22
	1.0	20.02	1.97	5.14	1.10	70.60	4.37
	5.0	34.60	4.29	1.90	0.11	85.27	1.37
	10.0	12.22	3.23	1.28	0.12	87.58	2.79
	25.0	0	—	1.25	0.06	96.62	1.02
V*b*	0.01	32.14	9.19	—	—	0	—
	0.1	27.41	2.28	4.84	0.23	34.90	4.65
	0.25	37.56	5.44	3.64	0.27	70.97	5.78
	1.0	24.19	3.47	2.32	0.10	83.30	1.97
	10	16.48	1.54	0.84	0.02	89.33	2.46
	25	0	—	0	—	94.47	2.31
V*c*	0.01	38.58	8.65	—	—	0	—
	0.1	63.90	8.60	4.76	0.21	79.78	1.24
	0.25	79.86	9.44	1.66	0.79	79.08	4.61
	1.0	0	—	1.17	0.03	89.98	1.09
	10	0	—	0.20	0.03	97.35	1.16
V*d*	0.01	63.32	1.03	—	—	0	—
	0.1	28.87	6.94	3.32	0.68	23.65	5.67
	0.25	57.85	5.01	6.40	0.38	51.14	1.68
	1.0	56.67	4.47	2.82	0.10	64.88	4.33
	10	0	—	1.22	0.07	82.82	1.37
	25	0	—	0.87	0.07	97.36	0.57
V*e*	0.01	54.77	14.25	—	—	0	—
	0.1	18.41	1.99	—	—	0	—
	0.25	27.75	5.37	4.29	0.37	21.58	4.27
	1.0	34.00	5.99	3.88	0.21	55.60	1.63
	10	33.17	3.32	2.20	0.19	75.62	4.24
	12.5	60.08	7.05	1.88	0.12	78.97	6.61
	15	36.92	3.44	2.32	0.30	80.52	3.12
	25	17.25	7.77	1.64	0.10	90.54	0.99
	50	0	—	1.57	0.30	97.78	0.78
VII*a*	1.0	68.71	7.14	2.18	0.14	84.70	2.50
	10	0	—	0.65	0.04	90.25	1.76
VII*b*	1.0	37.00	8.37	6.94	0.30	36.25	7.10
	10	69.46	4.07	2.52	0.18	74.70	2.89
	25	49.34	4.84	1.42	0.02	81.85	3.06

of V in aqueous media in which decomposition to the corresponding enones occurred. The only exception was V*c*, which was inactive against the particular tumor under consideration and appeared to be less toxic than V*a*, *b*, *d*, and *e*. Retrospectively, the five substitution patterns in the aromatic ring in V were the ones recommended for a Topliss analysis (21), and the order of activity found in this series of compounds is claimed by such an approach to indicate the greater importance of the Hammett σ value over the Hansch π parameter. Second, murine toxicity in both IV and V compounds may be associated, at least partially, with interaction with cellular nucleophiles. Third, both series of compounds affected respiration in mitochondria isolated from rat liver cells, but compounds bearing the same nuclear substituents differed ~100-fold in the doses required to elicit similar effects. A direct correlation between antineoplastic activity and the effect on respiration in mitochondria was absent. Fourth, maximum antineoplastic activity is found with V*d* and *e*, although these do not represent the extremes in regard to either rate of decomposition or effect on respiration in mitochondria. Thus, if decomposition is proportional to the Hammett σ value, V*a–c* liberate the corresponding acrylophenones faster than V*d* and *e* while the IV compounds appeared to be stable in aqueous media. In isolated mitochondria, a similar generalization appears valid, *i.e.*, V*a–c* are more active and IV is less active than V*d* and *e*. It is conceivable, therefore, that an optimal rate of breakdown is required for good activity against P-388 lymphocytic leukemia; *e.g.*, although V*c* is rapidly converted to VII*a*, which can affect mitochondria at very low dose levels, it may be inactivated prior to reaching a site of action. On the other hand, the absence of formation of

the acrylophenone or formation at a very slow rate could lead to insufficient compound for anticancer efficacy, which may involve the mitochondria as one of the targets. Relationships between the optimal chemical reactivity required for anticancer activity have been described previously (22), and the evolution of V*d* and *e* from this study permits these compounds to serve as lead compounds (23) in the design of further anticancer molecules.

EXPERIMENTAL

Melting points are uncorrected. Elemental analyses were undertaken locally[1] and when necessary both solvents and organic extracts were dried with anhydrous magnesium sulfate. No attempt was made to optimize the percentage yields of compounds unless otherwise stated. TLC was carried out using sheets of silica gel with fluorescent indicator[2] and a solvent mixture of chloroform–methanol (10:1). Mass spectra[3] were run at 70 eV and the 60-MHz NMR spectra[4] were determined using tetramethylsilane as the internal standard. High-performance liquid chromatography (HPLC)[5] was undertaken using a column[6] eluted with acetate buffer (0.04 *M*) in acetonitrile.

Synthesis—*3-Dimethylamino-1-aryl-1-propanone Hydrobromides* (*IV*a, d, *and* e)—The crude hydrochloride salts of the Mannich bases derived from acetophenone, *p*-methylacetophenone, and *p*-methoxyacetophenone were prepared as previously described (24). The yields obtained for the hydrochloride salts corresponding to IV*b* and *c* were 42 and 16%, respectively. The crude hydrochloride salts of IV*a*, *d*, and *e* were converted to the hydrobromide salts by the procedure described below to give IV*a*, *d*, and *e* as colorless crystals from acetone–methanol. In an attempt to improve the yield of 1-(3,4-dichlorophenyl)-3-dimethylamino-1-propanone hydrochloride, a mixture of 3,4-dichloroacetophenone (9.45 g, 0.05 mole), paraformaldehyde (1.80 g, 0.06 mole) dimethylamine hydrochloride (5.30 g, 0.065 mole), hydrochloric acid (0.1 ml), and 1,2-dimethoxyethane (35 ml) was heated under reflux for 24 hr. The solid that separated on cooling was removed by filtration, dried, and recrystallized from ether–ethanol to give 1-(3,4-dichlorophenyl)-3-dimethylamino-1-propanone hydrochloride (4.2 g, 30%) as colorless crystals; mp 193–195° [lit. (25) mp 193–195°].

1-(p-Chlorophenyl)-3-dimethylamino-1-propanone Hydrobromide (*IV*b)—An excess of acetyl chloride was added to *N,N,N′,N′*-tetramethyldiaminomethane[7] (10.2 g, 0.1 mole) in dry methylene chloride (100 ml) at 0° with vigorous stirring. The precipitated Mannich reagent was removed by filtration, washed with methylene chloride, and dried *in vacuo* to give *N,N*-dimethyl(methylene)ammonium chloride (8.5 g). This compound was used without purification.

A solution of *p*-chloroacetophenone (15.50 g, 0.1 mole) in dry acetonitrile (40 ml) was added to the *N,N*-dimethyl(methylene)ammonium chloride (9.35 g, 0.1 mole), and the mixture was stirred at room temperature for 2 hr. The precipitate was removed by filtration, dried, and recrystallized from ether–methanol to give 1-(*p*-chlorophenyl)-3-dimethylamino-1-propanone hydrochloride (21.5 g, 84%) as colorless crystals, mp 173–175° (26).

An aqueous solution of 1-(*p*-chlorophenyl)-3-dimethylamino-1-propanone hydrochloride (6.20 g, 0.025 mole) was basified with aqueous sodium carbonate solution (10% w/v) and extracted with chloroform (3 × 15 ml). The chloroform extracts were combined, washed with water (2 × 5 ml), and dried with anhydrous magnesium sulfate; removal of the chloroform gave a viscous oil which was dissolved in acetone–ether (1:1) and treated with dry hydrogen bromide gas. The crude hydrobromide (5.0 g) which precipitated was removed, and recrystallization from ether–methanol gave 1-(*p*-chlorophenyl)-3-dimethylamino-1-propanone hydrobromide, IV*b* (5.5 g), as colorless crystals. The yield of IV*b* was 63% based on the quantity of *p*-chloroacetophenone utilized.

1-(3,4-Dichlorophenyl)-3-dimethylamino-1-propanone Hydrobromide (*IV*c)—This compound was prepared in the same manner as IV*b*. The yield for the formation of 1-(3,4-dichlorophenyl)-3-dimethylamino-1-propanone hydrochloride, mp 193–194° [lit. (25) mp 193–195°] was 72%, and the overall yield for the formation of IV*c* from 3,4-dichloroacetophenone was 54%.

3-Dimethylamino- 2 -dimethylaminomethyl -1-aryl-1-propanone Dihydrobromides (*V*)—The general procedure for preparing V is illustrated by the synthesis of V*a*. A mixture of acetophenone (6.0 g, 0.05 mole), an aqueous solution of formaldehyde (37% w/v, 12 ml, 0.15 mole), dimethylamine (25% w/v, 27 ml, 0.15 mole), and ethanol (25 ml) was heated under reflux for 3 hr. After removal of the ethanol *in vacuo*, the mixture was cooled and extracted with ether (3 × 20 ml). The combined ether extracts were washed with water and dried with anhydrous magnesium sulfate; evaporation of the ether gave the crude ketone as a viscous oil. A solution of this oil in dry acetone was treated with hydrogen bromide gas to give a colorless solid which was removed by filtration, washed with acetone, dried, and recrystallized from methanol to give 3-dimethylamino-2-dimethylaminomethyl-1-phenyl-1-propanone hydrobromide, V*a* (4.5 g), as colorless crystals. Compound V*d* was prepared in an identical manner as V*a*, while the times of heating under reflux for V*b*, *c*, and *e* were 16, 30, and 6 hr, respectively. The structures of V*a–e* were confirmed by NMR, and the data generated for a representative compound, V*e*, are as follows: δ 8.1 (d, 2, aromatic protons at C_2 and C_6), 7.15 (d, 2, aromatic protons at C_3 and C_5), 3.95 (s, 3, OCH_3), 3.2–3.9 [m, 5, $C^2H(CH_2)_2$] and 2.95 [s, 12, $2N(CH_3)_2$]. The base peak in the MS was at 58 AMU.

2-Dimethylaminomethyl-1-aryl-2-propen-1-ones (*VII*a *and* b)—Chloroform (20 ml) was added to a solution of V*c* (0.500 g) in 40 ml of Sørensen's phosphate buffer, pH 7.4, (27) and the mixture was incubated at 37° with vigorous shaking. After 1 hr, the chloroform layer was removed and dried with anhydrous magnesium sulfate; evaporation of the organic solvent gave 2-dimethylaminomethyl-1-(3,4-dichlorophenyl)-2-propen-1-one, VII*a* (0.155 g, 56%) as a light yellow semisolid. HPLC showed one major peak (95.3%) plus two minor peaks. NMR: δ 7.85 (s, 1, aromatic proton at C_5), 7.7 (s, 2, aromatic protons at C_2 and C_6), 6.05 (s, 1, $=C^3H_2$), 5.7 (s, 1, $=C^3H_2$), 3.4 (s, 2, $-CH_2N$), and 2.4 [s, 6, $N(CH_3)_2$]; MS: *m/z* 257 (M^+, 5%), 173 (9%), and 58 (100%).

Anal.—Calc. for $C_{12}H_{13}Cl_2NO$: N, 5.43. Found: N, 5.37.

2-Dimethylaminomethyl-1-(*p*-methoxyphenyl)-2-propen-1-one, VII*b*, was prepared in the same way as a light yellow semisolid in 63% yield. HPLC showed one major peak (94.7%). NMR: δ 7.85 (d, 2, aromatic protons at C_2 and C_6), 6.9 (d, 2, aromatic protons at C_3 and C_5), 6.05 (s, 1, $=C^3H_2$), 5.7 (s, 1, $=C^3H_2$), 3.9 (s, 3, OCH_3), 3.4 (s, 2, CH_2N), and 2.4 [s, 6, $N(CH_3)_2$]; MS: *m/z* 219 (M^+, 19%).

Anal.—Calc. for $C_{13}H_{17}NO_2$: N, 6.38. Found: N, 5.94.

Stabilities in Phosphate Buffer—*Compounds IV*c *and* e—Chloroform (5 ml) was added to a solution of IV*c* (100 mg, 0.306 mmole) in phosphate buffer (pH 7.4, 2 ml), and the mixture was incubated at 37° on a shaking constant-temperature bath[8]. After 1.5 hr, the chloroform layer was separated and dried; removal of the solvent afforded a colorless solid (0.081 g, 95%) identified as the free base of IV*c*. NMR: δ 8.2–7.5 (m, 3, aromatic), 3.3–2.6 (m, 4, C^2H_2 and C^3H_2), and 2.3 [s, 6, $N(CH_3)_2$].

Similarly IV*e* gave the free base corresponding to IV*e* in 90% yield. NMR: δ 7.9 (d, 2, aromatic protons at C_2 and C_6), 6.9 (d, 2, aromatic protons at C_3 and C_5), 3.8 (s, 3, OCH_3), 3.4–2.6 (m, 4, C^2H_2 and C^3H_2), and 2.4 [s, 6, $N(CH_3)_2$].

Compounds Vc and e—Compound V*c* (100 mg, 0.215 mmole) was dissolved in a mixture of phosphate buffer (pH 7.4, 2 ml) and chloroform (5 ml) at 37° using a constant-temperature bath[8]. After 5 min, the chloroform layer was separated and dried; removal of the solvent afforded a semisolid which was identified by NMR as predominantly (>95%) VII*a*. Similarly V*e* gave rise to VII*b*.

The experiment was repeated except that V*c* was added to a mixture of buffer and chloroform in an ice bath (5°) and the resultant mixture shaken manually for 5 min. The chloroform layer was separated and dried; removal of the solvent gave a semisolid which was shown from the NMR spectra to be a mixture of VII*a* and V*c* as the free base in a ratio of 10:1. The ratio of these two compounds was determined from the NMR spectra using the following simultaneous equations: $AX_0 + BX_b = Y$ and $CX_0 + DX_b = Z$ where *A* and *B* are the number of aromatic protons in VII*a* and V*c*, respectively, as the free bases; X_0 and X_b are the mole fractions of VII*a* and V*c*, respectively, as the free bases; *C* and *D* are the number of protons in the dimethylamino group of VII*a* and V*c*, respectively, as the free bases; and *Y* and *Z* are the respective integrals. When the experiment was repeated with V*e* (100 mg, 0.2346 mmole) at 5° and for 5 min, only the free base of V*e* was obtained. However if the length of time was increased to 1 hr, a mixture of VII*b* and V*e* as the free bases was obtained which was shown by the NMR spectra and the use of the aforementioned simultaneous equations to be in a ratio of 7:4.

[1] Mr. R. E. Teed, Department of Chemistry and Chemical Engineering, University of Saskatchewan.

[2] Eastman-Kodak Co.

[3] AEI MS-12 mass spectrometer, Picker X-Ray Engineering Ltd.; VG Micromass MM16F mass spectrometer with 2025 data system.

[4] Varian T-60 spectrometer, Varian Associates of Canada Ltd.

[5] Waters Associates Model 440 fitted with a UV absorbance detector (254 nm) and a Beckman 110A pump.

[6] Ultrasphere cyanocolumn.

[7] Aldrich Chemical Co.

[8] Dubnoff Metabolic Shaking Incubator.

Table III—Effect of IV*c, e* and V*c, e* on Respiration in Rat Liver Mitochondria Using Succinate as the Substrate at pH 7.4 and 20°

Compound	Concentration, μmoles	Stimulation, %	*SE*	Time prior to Constant Inhibition of Respiration, min	*SE*	Inhibition, %	*SE*
IV*c*	5	27.03	11.26	—	—	—	—
	10	70.00	18.45	—	—	—	—
	25	68.56	9.50	10.76	1.09	39.70	6.73
IV*e*	25	42.35	3.89	—	—	—	—
	50	60.80	6.18	—	—	—	—
	100	66.45	4.58	—	—	—	—
V*c*	0.1	25.70	4.62	7.62	0.17	43.98	2.98
	0.25	46.54	10.50	3.46	0.16	50.62	11.57
	1.0	29.64	1.92	2.04	0.10	69.16	2.50
	10	—	—	0.62	0.13	82.75	2.46
V*e*	0.1	5.19	1.80	—	—	—	—
	0.25	21.17	3.54	—	—	—	—
	10	49.86	5.87	5.78	0.45	48.30	6.69
	15	51.36	7.28	3.62	0.27	61.25	4.76
	25	49.96	8.73	2.98	0.41	68.37	4.45
	50	—	—	1.34	0.40	84.37	3.17

Reaction of IV*e* with 2-Mercaptoethanol—Chloroform (10 ml) was added to a solution of IV*e* (200 mg, 0.694 mmole) and 2-mercaptoethanol (167 mg, 2.1 mmoles) in phosphate buffer (pH 7.4, 4 ml), and the mixture was incubated at 37° on a shaking constant-temperature bath[8]. After 1 hr, the chloroform layer was separated and dried; removal of the organic solvent and excess of 2-mercaptoethanol under reduced pressure gave a bright-yellow viscous oil, the NMR spectrum of which showed the retention of the aromatic and methoxy protons but the absence of the dimethylamino protons. Other unidentified peaks were present and the oil appeared to be a mixture of compounds, although predominantly 3-(2-hydroxyethylthio)-1-(*p*-methoxyphenyl)-1-propanone. MS gave a parent peak corresponding to this ketone (*m/z* 240, 0.4%) with major ions at *m/z* 222:

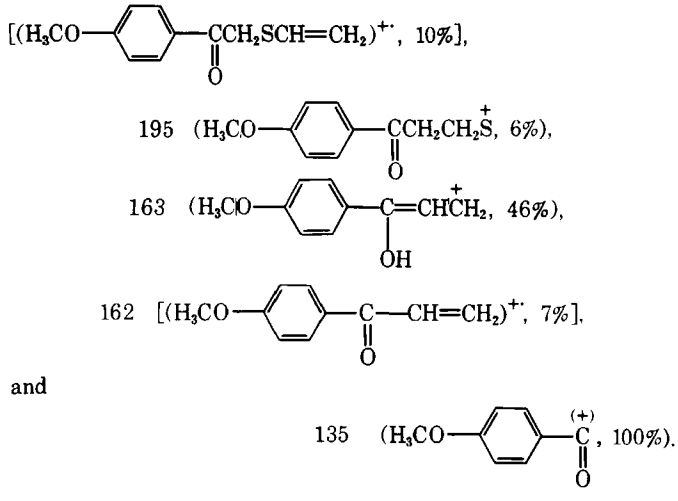

The intensity of the peak at *m/z* 58 was 1%.

The experiment was repeated twice: in the absence of phosphate buffer and when chloroform was omitted. In the absence of buffer, a 98% recovery of IV*e*, identified by NMR and melting point, was found. In the absence of chloroform, IV*e* and 2-mercaptoethanol were incubated at 37° in buffer (5 ml) for 1 hr, and the mixture was extracted with chloroform (3 × 10 ml). The organic extract was saturated with dry hydrogen chloride gas and dried. Removal of the chloroform gave a residue which, when triturated with dry ether, gave IV*e* as the hydrochloride salt (0.042 g), identified by NMR. Evaporation of the ether gave a residue which was shown by NMR to contain 3-(2-hydroxyethylmercapto)-1-(*p*-methoxyphenyl)-1-propanone along with minor amounts of contaminants.

Preparation of 3-(2-Hydroxyethyl)mercapto-2-[(2-hydroxyethyl)mercapto]methyl-1-(3,4-dichlorophenyl) - 1 - propanone (VIII*a*)—A solution of 2-mercaptoethanol (125 mg, 1.6 mmoles) in phosphate buffer, pH 7.4 (13 ml), was added to a solution of V*c* (250 mg, 0.538 mmole) in phosphate buffer, pH 7.4 (10 ml). After the addition of chloroform (50 ml), the mixture was incubated for 15 min at 37° with vigorous stirring. The chloroform layer was removed, washed with water, and dried with anhydrous magnesium sulfate, and both chloroform and excess 2-mercaptoethanol were removed *in vacuo* to give a yellow viscous oil (0.120 g) which was predominantly 3-(2-hydroxyethyl)mercapto-2-[(2-hydroxyethyl)mercapto]methyl-1-(3,4-dichlorophenyl)-1-propanone. MS: *m/z* 368:

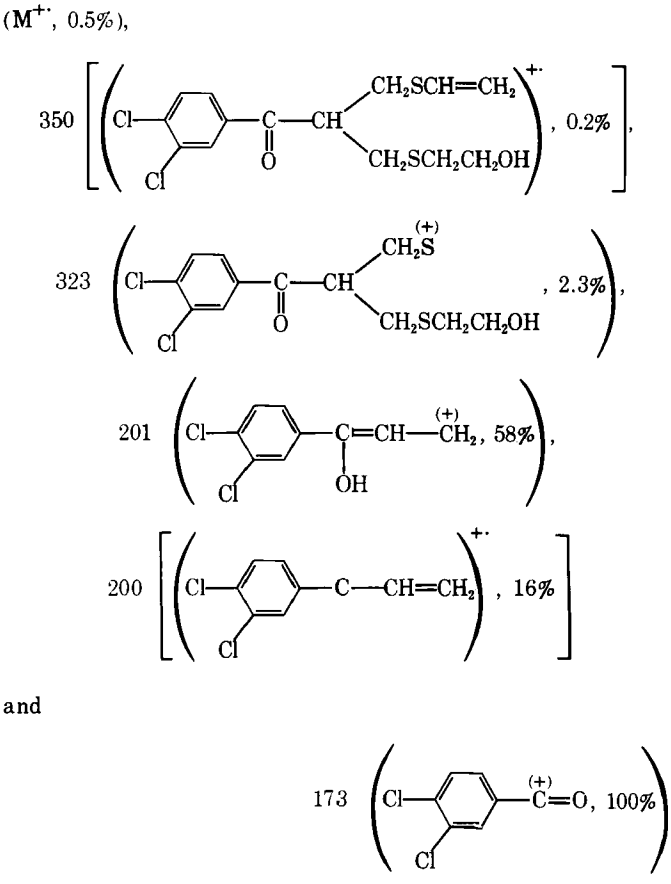

58 AMU (4%) was noted.

Anal.—Calc. for $C_{14}H_{18}Cl_2O_3S_2$: C, 45.53; H, 4.91; N, 0.00. Found: C, 44.43; H, 5.18; N, 0.27.

Effect of IV and V on Respiration in Rat Liver Mitochondria—Compounds IV and V were dissolved in Sørensen's buffer and kept ice-cold prior to the addition to the previously prepared mitochondrial suspension. The mitochondria were obtained from male Wistar rats (200–250 g) and the effect of IV and V on respiration was measured using a previous procedure (9). The buffer used in isolating the mitochondria and the

Table IV—Effect of Vc and e on Respiration in Rat Liver Mitochondria Using Succinate as the Substrate at pH 6.9 and 6.4 and 37°

Compound	Concentration, μmoles	Stimulation: pH 6.9 %	pH 6.9 SE	pH 6.4 %	pH 6.4 SE	Levels of Significance (p) Between pH Values of: 7.4 & 6.9	6.9 & 6.4	7.4 & 6.4
Vc	0.01	12.23	2.71	30.41	7.15	0.05	0.10	0.50
	0.1	0	—	34.47	7.06	<0.001	0.005	0.01
	0.25	0	—	40.76	6.73	<0.001	<0.001	<0.001
	1.0	0	—	49.53	7.96	>0.50	<0.001	<0.001
Ve	0.25	19.57	4.11	54.22	1.85	0.20	<0.001	0.005
	1.0	17.48	2.98	58.65	6.86	0.10	<0.001	0.01
	10	9.27	4.97	43.33	6.89	0.25	0.005	0.50

Compound	Concentration, μmoles	Time Prior to Constant Inhibition of Respiration: pH 6.9 min	pH 6.9 SE	pH 6.4 min	pH 6.4 SE	Levels of Significance (p) Between pH Values of: 7.4 & 6.9	6.9 & 6.4	7.4 & 6.4
Vc	0.01	4.74	0.26	0	0	<0.001	<0.001	>0.50
	0.1	3.42	0.11	10.22	0.41	0.005	<0.001	<0.001
	0.25	3.50	0.21	6.20	0.25	<0.001	<0.001	<0.001
	1.0	1.90	0.09	3.65	0.13	<0.001	<0.001	<0.001
Ve	0.25	1.78	1.11	0	0	0.10	0.10	0.01
	1.0	3.26	0.97	0	0	0.50	0.005	<0.001
	10	3.93	0.31	7.97	0.19	<0.001	<0.001	<0.001

Compound	Concentration, μmoles	Inhibition: pH 6.9 %	pH 6.9 SE	pH 6.4 %	pH 6.4 SE	Levels of Significance (p) Between pH Values of: 7.4 & 6.9	6.9 & 6.4	7.4 & 6.4
Vc	0.01	11.35	2.49	0	—	<0.001	<0.001	>0.50
	0.1	67.43	3.79	24.13	9.30	0.20	<0.001	<0.001
	0.25	87.56	2.00	46.09	5.36	0.20	<0.001	<0.001
	1.0	94.45	1.45	82.29	3.04	0.20	0.005	0.025
Ve	0.25	7.33	4.51	0	—	0.05	0.50	0.025
	1.0	12.14	4.57	0	—	<0.001	0.005	<0.001
	10	73.01	1.87	49.30	6.72	<0.50	0.005	0.005

respiration media employed were those described previously (9), except that Sørensen's buffer and not tromethamine hydrochloride was used. The data generated at 37° (Table II) and the percentage stimulation and inhibition of respiration are both in relation to the original respiration rate. A minimum of five determinations were made at each concentration; in the case of IVc (5.0 μmoles), Va (0.1 μmole), Vd (0.1 μmole) and Ve (0.25 and 25 μmoles) a total of 12 determinations were performed.

In both Figs. 1 and 2, the data shown indicate differences in oxygen uptake compared with control mitochondria (no succinate or compound added). The lag period (A) was also found with IVa (10 μmoles), IVd (10 μmoles), IVe (10, 25, and 50 μmoles), Va (0.01, 0.1, and 0.25 μmole), Vb (0.01 μmole), Vc (0.001, 0.01, 0.1, and 0.25 μmole), Vd (0.01, 0.1, 0.25, and 1.0 μmole), Ve (0.01, 0.1, 0.25, 1.0, and 10 μmoles), and VIIb (1.0 μmole). In some cases, during interval A the slope of the line was identical to that after the addition of succinate; *i.e.*, no difference in oxygen utilization was noted after addition of the compound. This phenomenon occurred with IVb (5 and 10 μmoles), Va (1.0 μmole), Ve (12.5 and 15 μmoles), and VIIa (1.0 μmole). Inhibition of respiration occurred prior to stimulation of respiration during interval A in the case of IVa (25 μmoles), IVb (25 μmoles), IVc (5 and 10 μmoles), IVd (25 and 50 μmoles), IVe (100 μmoles), Va (10 μmoles), Vb (0.01 and 0.1 μmole), and VIIb (10 and 25 μmoles). In the remaining cases, the lag period (A) was absent and addition of the compound led to effects noted in one or more of the time periods B, C, and D.

The effect on respiration at pH values of 6.9 and 6.4 is given in Table III. At pH 6.9, respiration continued at the same rate as after addition of succinate during interval A in the case of Vc (0.01 μmole) and Ve (0.25 and 1.0 μmoles). Inhibition of respiration during interval A occurred with Ve (10 μmoles). The lag period was absent at concentrations of 0.1, 0.25, and 1.0 μmole of Vc. At pH 6.4, submaximal stimulation of respiration was noted with Vc (0.01 and 0.1 μmole) and Ve (0.25 and 1.0 μmole). Inhibition of respiration during interval A was found with Vc (0.25 and 1.0 μmole) and Ve (10 μmoles).

Table IV indicates the effect of various concentrations of IVc and e, Vc and e on respiration in rat liver mitochondria at 20°. The same procedure (9) was employed, using a constant-temperature bath[9]. Submaximal stimulation occurred during the lag period for IVc (5 μmoles) and Vc (0.1, 0.25, 10, 15, and 25 μmoles). Respiration was identical to that after the addition of succinate for IVe (25 μmoles) and Vc (0.25 μmoles). Inhibition of respiration during interval A was noted for IVc (10 and 25 μmoles), IVe (50 and 100 μmoles), and Vc (1.0 μmole). The lag period was absent in the cases of Vc (10 μmoles) and Ve (50 μmoles).

Screening of Compounds—The anticancer screening was carried out by the Drug Research and Development Division of the National Cancer Institute, Bethesda, Md., using their protocols (28). Male or female CD_2F_1 mice were used. The compounds were administered by the intraperitoneal route in saline except for IVc, for which hydroxypropylcellulose was employed.

REFERENCES

(1) D. S. Kemp and F. Vellaccio, "Organic Chemistry," Worth, New York, N.Y., 1980, p. 295.

(2) K. B. Wiberg, "Physical-Organic Chemistry," Wiley, New York, N.Y., 1964, p. 410.

(3) M. Tramontini, *Synthesis*, **1973**, 703 and references cited therein.

(4) J. R. Dimmock, L. M. Smith, and P. J. Smith, *Can. J. Chem.*, **58**, 984 (1980).

(5) J. R. Dimmock and M. L. C. Wong, *Can. J. Pharm. Sci.*, **11**, 35 (1976).

(6) J. A. Mollica, J. B. Smith, I. M. Nunes, and H. K. Govan, *J. Pharm. Sci.*, **59**, 1770 (1970) and references cited therein.

(7) R. C. Fahey, P. A. Myers, and D. L. Distefano, *Bioorg. Chem.*, **9**, 293 (1980).

(8) R. Andrisano, A. S. Angeloni, P. De Maria, and M. Tramontini, *J. Chem. Soc. (C)*, **1967**, 2307.

[9] Lauda K2R instrument, Messgeräte-Werk Lauda, West Germany.

(9) N. W. Hamon, D. L. Bassendowski, D. E. Wright, J. R. Dimmock, and L. M. Noble, *J. Pharm. Sci.*, **67**, 1539 (1978).
(10) J. R. Dimmock, N. W. Hamon, L. M. Noble, and D. E. Wright, *J. Pharm. Sci.*, **68**, 1033 (1979).
(11) N. W. Hamon, D. L. Kirkpatrick, E. W. K. Chow, and J. R. Dimmock, *J. Pharm. Sci.*, **71**, 25 (1982).
(12) T. Psenakova and J. Kolek, *Biologia*, **36**, 1109 (1981).
(13) I. A. Goroshinskay, A. A. Krichevskaya, and Z. G. Bronovitskaya, *Bull. Exp. Biol. Med.*, **91**, 464 (1981).
(14) M. Eden, B. Haines, and H. Kahler, *J. Natl. Cancer Inst.*, **16**, 541 (1956).
(15) H. Kahler and W. B. Robertson, *J. Natl. Cancer Inst.*, **3**, 495 (1943).
(16) J. R. Dimmock, N. W. Hamon, E. W. K. Chow, D. L. Kirkpatrick, L. M. Smith, and M. G. Prior, *Can. J. Pharm. Sci.*, **15**, 84 (1980).
(17) J. H. Burchenal, E. A. D. Holmberg, J. J. Fox, S. C. Hemphill, and J. A. Reppert, *Cancer Res.*, **19**, 494 (1959).
(18) J. R. Dimmock and W. G. Taylor, *J. Pharm. Sci.*, **63**, 69 (1974).
(19) P. N. Gordon, J. D. Johnston, and A. R. English, in "Antimicrobial Agents and Chemotherapy," G. L. Hobby, Ed., American Society for Microbiology, Ann Arbor, Mich., 1965, p. 165.
(20) H. Schönenberger, T. Bastug, L. Bindl, A. Adam, D. Adam, A. Petter, and W. Zwez, *Pharm. Acta Helv.*, **44**, 691 (1969).
(21) J. G. Topliss, *J. Med. Chem.*, **20**, 463 (1977).
(22) W. C. J. Ross, "Biological Alkylating Agents," Butterworths and Co. Ltd., London, 1962, p. 107.
(23) E. J. Ariens in "Drug Design," Vol. 1, E. J. Ariens, Ed., Academic, New York, N.Y., 1971, p. 42 seq.
(24) C. E. Maxwell, *Org. Syn.*, **23**, 30 (1943).
(25) Italian pat. 637,371, (March 29, 1962); through *Chem. Abstr.*, **60**, 479e (1964).
(26) D. W. Adamson and J. W. Billinghurst, *J. Chem. Soc.*, **1950**, 1039.
(27) D. L. Deardoff in "Remington's Pharmaceutical Sciences," 14th ed., Mack Publishing Company, Easton, Pa. 1970, p. 1554.
(28) R. I. Geran, N. H. Greenberg, M. M. MacDonald, A. M. Schumacher, and B. J. Abbott, *Cancer Chemother. Rep.* (Part 3), **3**, (Sept., 1972).

ACKNOWLEDGMENTS

The authors thank the Medical Research Council of Canada for the award of an operating grant (MA-5538) to J. R. Dimmock and for providing a Summer Undergraduate Research Scholarship to D. J. Harwood. The receipt of Graduate Scholarships from the University of Saskatchewan to K. Shyam and S. K. Raghavan is acknowledged gratefully.

Appreciation is accorded to Dr. S. M. Wallace of the College of Pharmacy, University of Saskatchewan, for assistance in the statistical evaluation of some of the results obtained from experimentation with mitochondria and also to the National Cancer Institute, Bethesda, Md., which undertook the antineoplastic evaluation of some of the compounds reported in this investigation.

Pharmacokinetics of Piperacillin and Gentamicin Following Intravenous Administration to Dogs

VIJAY K. BATRA ˣ, JOHN A. MORRISON, and THOMAS R. HOFFMAN

Received February 5, 1982, from the *Pharmacodynamics Department and Statistical Design and Analysis Department, Medical Research Division, American Cyanamid Co., Pearl River, NY 10965.* Accepted for publication July 30, 1982.

Abstract □ Piperacillin sodium was administered intravenously to dogs, alone or in combination with gentamicin, twice a day (~5 hr apart) for 36–37 days. The pharmacokinetics of neither drug changed in the presence of the other; however, the percentage of the gentamicin dose recovered in the urine decreased significantly when coadministered with piperacillin. The data demonstrate that interaction between the two drugs in urine is feasible.

Keyphrases □ Piperacillin—pharmacokinetics in the dog, effect of concomitant administration of gentamicin □ Gentamicin—pharmacokinetics in the dog, effect of concomitant administration of piperacillin □ Pharmacokinetics—of piperacillin and gentamicin in the dog, effect of concomitant administration

Piperacillin[1], sodium (2*S*, 5*R*, 6*R*)-6-[(*R*)-2-(4-ethyl-2,3-dioxo-1-piperazinecarboxamido)-2-phenylacetamido]-3,3-dimethyl-7-oxo-4-thia-1-azabicyclo[3.2.0]heptane-2-carboxylate, is a novel semisynthetic penicillin that possesses broad spectrum antibacterial activity against Gram-negative and Gram-positive pathogenic bacteria, including anaerobes. Results of *in vitro* studies (1) have shown piperacillin to be superior to ampicillin, carbenicillin, and cephalosporins against Gram-negative bacteria, particularly *Klebsiella*, *Proteus*, and *Serratia* species and *Pseudomonas aeruginosa*. In certain cases, a piperacillin and gentamicin combination would be preferred to obtain a synergistic effect. To evaluate the toxicity of these two drugs when administered alone or in combination, a 1-month study was undertaken in dogs. Since aminoglycosides can interact with β-lactam antibiotics (2–4), the study was designed to allow the serum concentrations to be analyzed pharmacokinetically. This paper describes the pharmacokinetics of piperacillin and gentamicin when given alone or in combination.

EXPERIMENTAL

Animal Studies—Six groups of 18–20-month-old beagle dogs[2] (two males and two females in each group) were utilized for the study. The weight range was 9.4–12.3 kg for the males and 7.9–9.6 kg for the females. The dogs were assigned to groups using a table of random numbers. They were housed individually in a room maintained at 21–24°, with a 12-hr on/off light cycle. Food[3] (250–300 g) was offered to each dog daily, ~30 min after the last dose; water was available *ad libitum*.

Drug solutions, made prior to each dose, were administered twice daily (~5 hr apart) over a 5-min period with an infusion pump[4] calibrated using the specific syringes, solutions, and tubing employed. Doses, adjusted to the body weight twice a week, were administered according to the schedule shown in Table I. The concentration of the piperacillin solution in sterile water for injection, expressed as free acid, was 250 mg/ml. The gentamicin solution was made in concentrations of 1 and 2 mg/ml (expressed as base equivalent activity) using sterile isotonic saline. For dogs

[1] Pipracil; American Cyanamid Co.

[2] Marshall Research Animals, North Rose, N.Y.
[3] Respond 2000, Country Foods Div., Agway, Hauppauge, N.Y.
[4] Model 355, Sage Instrument, Cambridge, Mass.

0022-3549/83/0800-0894$01.00/0

(9) N. W. Hamon, D. L. Bassendowski, D. E. Wright, J. R. Dimmock, and L. M. Noble, *J. Pharm. Sci.*, **67**, 1539 (1978).
(10) J. R. Dimmock, N. W. Hamon, L. M. Noble, and D. E. Wright, *J. Pharm. Sci.*, **68**, 1033 (1979).
(11) N. W. Hamon, D. L. Kirkpatrick, E. W. K. Chow, and J. R. Dimmock, *J. Pharm. Sci.*, **71**, 25 (1982).
(12) T. Psenakova and J. Kolek, *Biologia*, **36**, 1109 (1981).
(13) I. A. Goroshinskay, A. A. Krichevskaya, and Z. G. Bronovitskaya, *Bull. Exp. Biol. Med.*, **91**, 464 (1981).
(14) M. Eden, B. Haines, and H. Kahler, *J. Natl. Cancer Inst.*, **16**, 541 (1956).
(15) H. Kahler and W. B. Robertson, *J. Natl. Cancer Inst.*, **3**, 495 (1943).
(16) J. R. Dimmock, N. W. Hamon, E. W. K. Chow, D. L. Kirkpatrick, L. M. Smith, and M. G. Prior, *Can. J. Pharm. Sci.*, **15**, 84 (1980).
(17) J. H. Burchenal, E. A. D. Holmberg, J. J. Fox, S. C. Hemphill, and J. A. Reppert, *Cancer Res.*, **19**, 494 (1959).
(18) J. R. Dimmock and W. G. Taylor, *J. Pharm. Sci.*, **63**, 69 (1974).
(19) P. N. Gordon, J. D. Johnston, and A. R. English, in "Antimicrobial Agents and Chemotherapy," G. L. Hobby, Ed., American Society for Microbiology, Ann Arbor, Mich., 1965, p. 165.
(20) H. Schönenberger, T. Bastug, L. Bindl, A. Adam, D. Adam, A. Petter, and W. Zwez, *Pharm. Acta Helv.*, **44**, 691 (1969).
(21) J. G. Topliss, *J. Med. Chem.*, **20**, 463 (1977).
(22) W. C. J. Ross, "Biological Alkylating Agents," Butterworths and Co. Ltd., London, 1962, p. 107.
(23) E. J. Ariens in "Drug Design," Vol. 1, E. J. Ariens, Ed., Academic, New York, N.Y., 1971, p. 42 seq.
(24) C. E. Maxwell, *Org. Syn.*, **23**, 30 (1943).
(25) Italian pat. 637,371, (March 29, 1962); through *Chem. Abstr.*, **60**, 479e (1964).
(26) D. W. Adamson and J. W. Billinghurst, *J. Chem. Soc.*, **1950**, 1039.
(27) D. L. Deardoff in "Remington's Pharmaceutical Sciences," 14th ed., Mack Publishing Company, Easton, Pa. 1970, p. 1554.
(28) R. I. Geran, N. H. Greenberg, M. M. MacDonald, A. M. Schumacher, and B. J. Abbott, *Cancer Chemother. Rep.* (Part 3), **3**, (Sept., 1972).

ACKNOWLEDGMENTS

The authors thank the Medical Research Council of Canada for the award of an operating grant (MA-5538) to J. R. Dimmock and for providing a Summer Undergraduate Research Scholarship to D. J. Harwood. The receipt of Graduate Scholarships from the University of Saskatchewan to K. Shyam and S. K. Raghavan is acknowledged gratefully.

Appreciation is accorded to Dr. S. M. Wallace of the College of Pharmacy, University of Saskatchewan, for assistance in the statistical evaluation of some of the results obtained from experimentation with mitochondria and also to the National Cancer Institute, Bethesda, Md., which undertook the antineoplastic evaluation of some of the compounds reported in this investigation.

Pharmacokinetics of Piperacillin and Gentamicin Following Intravenous Administration to Dogs

VIJAY K. BATRA ˣ, JOHN A. MORRISON, and THOMAS R. HOFFMAN

Received February 5, 1982, from the *Pharmacodynamics Department and Statistical Design and Analysis Department, Medical Research Division, American Cyanamid Co., Pearl River, NY 10965.* Accepted for publication July 30, 1982.

Abstract □ Piperacillin sodium was administered intravenously to dogs, alone or in combination with gentamicin, twice a day (~5 hr apart) for 36–37 days. The pharmacokinetics of neither drug changed in the presence of the other; however, the percentage of the gentamicin dose recovered in the urine decreased significantly when coadministered with piperacillin. The data demonstrate that interaction between the two drugs in urine is feasible.

Keyphrases □ Piperacillin—pharmacokinetics in the dog, effect of concomitant administration of gentamicin □ Gentamicin—pharmacokinetics in the dog, effect of concomitant administration of piperacillin □ Pharmacokinetics—of piperacillin and gentamicin in the dog, effect of concomitant administration

Piperacillin[1], sodium (2*S*, 5*R*, 6*R*)-6-[(*R*)-2-(4-ethyl-2,3-dioxo-1-piperazinecarboxamido)-2-phenylacetamido]-3,3-dimethyl-7-oxo-4-thia-1-azabicyclo[3.2.0]heptane-2-carboxylate, is a novel semisynthetic penicillin that possesses broad spectrum antibacterial activity against Gram-negative and Gram-positive pathogenic bacteria, including anaerobes. Results of *in vitro* studies (1) have shown piperacillin to be superior to ampicillin, carbenicillin, and cephalosporins against Gram-negative bacteria, particularly *Klebsiella*, *Proteus*, and *Serratia* species and *Pseudomonas aeruginosa*. In certain cases, a piperacillin and gentamicin combination would be preferred to obtain a synergistic effect. To evaluate the toxicity of these two drugs when administered alone or in combination, a 1-month study was undertaken in dogs. Since aminoglycosides can interact with β-lactam antibiotics (2–4), the study was designed to allow the serum concentrations to be analyzed pharmacokinetically. This paper describes the pharmacokinetics of piperacillin and gentamicin when given alone or in combination.

EXPERIMENTAL

Animal Studies—Six groups of 18–20-month-old beagle dogs[2] (two males and two females in each group) were utilized for the study. The weight range was 9.4–12.3 kg for the males and 7.9–9.6 kg for the females. The dogs were assigned to groups using a table of random numbers. They were housed individually in a room maintained at 21–24°, with a 12-hr on/off light cycle. Food[3] (250–300 g) was offered to each dog daily, ~30 min after the last dose; water was available *ad libitum*.

Drug solutions, made prior to each dose, were administered twice daily (~5 hr apart) over a 5-min period with an infusion pump[4] calibrated using the specific syringes, solutions, and tubing employed. Doses, adjusted to the body weight twice a week, were administered according to the schedule shown in Table I. The concentration of the piperacillin solution in sterile water for injection, expressed as free acid, was 250 mg/ml. The gentamicin solution was made in concentrations of 1 and 2 mg/ml (expressed as base equivalent activity) using sterile isotonic saline. For dogs

[1] Pipracil; American Cyanamid Co.

[2] Marshall Research Animals, North Rose, N.Y.
[3] Respond 2000, Country Foods Div., Agway, Hauppauge, N.Y.
[4] Model 355, Sage Instrument, Cambridge, Mass.

0022-3549/83/0800-0894$01.00/0

Table I—Dosing Schedule of Animals Administered Intravenous Piperacillin and Gentamicin Alone or in Combination

Group[a]	Dose, mg/kg BID		Animal	Sex	Samples Collected		Day of Collection		Number of Doses Administered[b]
	Piperacillin	Gentamicin			Serum	Urine	Serum	Urine	
2	500	0	015945	M	X	X	2, 37	5, 6, 34, 35	73
			015966	M	—	X	—	5, 6, 34, 35	71
			015998	F	X	X	2, 37	5, 6, 34, 35	73
			016024	F	—	X	—	5, 6, 34, 35	71
3	0	2	015943	M	X	X	3, 37	5, 6, 34, 35	73
			015956	M	—	X	—	5, 6, 34, 35	71
			015994	F	X	X	3, 37	5, 6, 34, 35	73
			016022	F	—	X	—	5, 6, 34, 35	71
4	0	4	015937	M	X	X	1, 36	5, 6, 34, 35	73
			015952	M	—	X	—	5, 6, 34, 35	71
			016006	F	X	X	1, 36	5, 6, 34, 35	73
			016021	F	—	X	—	5, 6, 34, 35	71
5	500	2	015963	M	X	X	2, 37	5, 6, 34, 35	73
			015965	M	—	X	—	5, 6, 34, 35	71
			016007	F	X	X	2, 37	5, 6, 34, 35	73
			016014	F	—	X	—	5, 6, 34, 35	71
6	500	4	015917	M	X	X	1, 36	5, 6, 34, 35	73
			015953	M	—	X	—	5, 6, 34, 35	71
			016005	F	X	X	1, 36	5, 6, 34, 35	73
			016015	F	—	X	—	5, 6, 34, 35	71

[a] Group 1 is not included as the dogs received no drug and served only as control for the toxicological evaluation. [b] No dose was administered on day 13 and in the evening of day 14 for reasons which were not drug related.

Table II—Mean Serum Concentrations of Piperacillin Following Intravenous Administration Alone or in Combination with Gentamicin [a]

Dose of Piperacillin, mg/kg BID	Dose of Gentamicin, mg/kg BID	Phase	Mean Serum Concentration, μg/ml						
			5 min	10 min	20 min	40 min	60 min	120 min	240 min
500	0	1	2475	1825	1305	715	530	167	13
		2	4200	2188	1380	775	615	154	17
500	2	1	2475	1514	1145	855	510	165	15
		2	2650	1625	1005	780	533	137	18
500	4	1	2700	1763	1325	870	613	179	17
		2	3000	1870	1410	965	825	232	26

[a] $n = 2$ for each group.

that received both drugs, the solutions of piperacillin and gentamicin were prepared independently and mixed in the infusion flow during administration, as illustrated in Fig. 1.

Serum samples were obtained from one dog per sex-group prior to the infusion and at 5 (end of the infusion), 10, 20, 40, 60, 120, and 240 min following the commencement of the infusion during the first (phase I) and last (phase 2) week of dosing. Urine samples (0–24 hr) were collected for 2 consecutive days from all dogs during the first and last weeks of the study.

Antibiotic Assay—Antibiotic concentrations were determined by the disk diffusion method. The assays for piperacillin were performed with *Sarcina lutea* ATCC 9341 (indicator organism) grown on antibiotic medium No. 1[5] to which 0.6% sodium polyanetholesulfonate was added to inhibit gentamicin activity (5). This concentration of sodium polyanetholesulfonate was sufficient to inactivate 50 μg/ml of gentamicin in the solutions containing 2.5–0.16 μg/ml of piperacillin used for the standard curve. The recovery from samples of known piperacillin concentration, alone or combined with gentamicin, was 95–108%; the limit of detection was 0.16 μg/ml.

The assays for gentamicin were performed with *Bacillus subtilis* ATCC 6633 grown on mycin agar[5] to which 1000 kinetic units of pencillinase[6] were added per milliliter of medium to inactivate the piperacillin. This concentration of the enzyme was sufficient to inactivate >440 μg/ml of piperacillin in the solutions containing 2.5–0.16 μg/ml of gentamicin used for the standard curve. Samples were diluted to the range of concentrations in the standard curve. The recovery from samples of known gentamicin concentration, alone or combined with piperacillin, was 96–107%; the limit of detection was 0.16 μg/ml. All samples were assayed twice, and the precision of the assays was ±15%.

Pharmacokinetic Analysis—Pharmacokinetic analysis of the data was performed using the digital computer program AUTOAN (6) in conjunction with the nonlinear regression analysis program NONLIN (7). The serum concentrations were weighted according to the square of their reciprocals. The excretion rate constant (k_u) was computed using:

$$\frac{X_u^\infty}{\text{Dose}} = \frac{k_u}{K_{el}}$$

where X_u^∞ is the amount of unchanged drug excreted in the urine and K_{el} is the overall elimination rate constant of the drug. Renal clearance was estimated by multiplying k_u by the volume of distribution of the central compartment. The other pharmacokinetic parameters were obtained by previously published pharmacokinetic equations (8).

Statistical Methods—The pharmacokinetic model parameters were

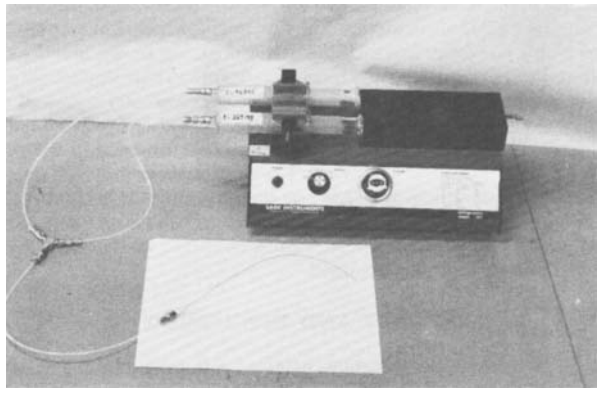

Figure 1—*Apparatus used to combine the piperacillin and gentamicin doses during infusion.*

[5] Difco Laboratories, Detroit, MI 48201.
[6] Baltimore Biological Laboratory, Cockeysville, MD 21050

Table III—Mean Serum Concentration of Gentamicin Following Intravenous Administration Alone or in Combination with Piperacillin [a]

Dose of Piperacillin, mg/kg BID	Dose of Gentamicin, mg/kg BID	Phase	Mean Serum Concentration, μg/ml						
			5 min	10 min	20 min	40 min	60 min	120 min	240 min
0	2	1	9.6	6.0	4.4	2.8	2.2	1.1	0.5
		2	12.4	7.7	6.2	5.1	3.4	1.9	0.8
0	4	1	25.5	18.4	12.9	9.7	7.3	3.5	1.0
		2	29.0	19.6	12.9	8.6	6.8	3.4	1.0
500[b]	2	1	8.1	6.7	5.0	3.5	2.5	1.2	0.4
		2	7.7	6.2	4.6	3.9	3.0	1.6	0.5
500	4	1	17.9	15.3	12.1	8.9	6.9	3.6	1.3
		2	15.4	10.9	8.6	7.5	5.9	3.8	1.3

[a] $n = 2$ unless otherwise noted. [b] $n = 1$; data from dog 016007 (female) was rejected as an outlier.

Table IV—Mean Pharmacokinetic Parameters of Piperacillin and Gentamicin

Drug	Dose, mg/kg BID	Phase	Half-life, min		V_c, ml/kg	Vd, ml/kg	Vd_{ss}, ml/kg	Clearance, ml/min		k_u, min^{-1}
			α	β				Body	Renal	
Piperacillin[a]	500	1	3.9	32.8	154	256	236	50	22	0.016
		2	3.2	35.6	87	263	219	47	21	0.026
Gentamicin[b]	2 or 4	1	5.4	70.1	163	391	347	36	18	0.011
		2	4.1	70.7	123	307	280	30	19	0.015

[a] $n = 2$. [b] $n = 4$.

Table V—Effect of the Piperacillin–Gentamicin Combination on the Pharmacokinetics of Piperacillin [a]

Dose, mg/kg BID		Phase	Half-life, min		V_c, ml/kg	Vd, ml/kg	Vd_{ss}, ml/kg	Clearance, ml/min		k_u, min^{-1}	AUC, μg·min/ml
Piperacillin	Gentamicin		α	β				Body	Renal		
500	0	1	3.9	32.8	154	256	236	50	22	0.016	96,918
	2		1.2	34.8	121	320	302	57	31	0.029	94,134
	4		1.5	34.9	128	314	295	58	32	0.027	105,624
500	0	2	3.2	35.6	87	263	219	47	21	0.026	113,086
	2		2.8	37.1	138	351	312	59	13	0.011	90,823
	4		4.8	37.8	145	254	234	43	13	0.013	124,870

[a] $n = 2$.

Table VI—Effect of the Piperacillin–Gentamicin Combination on the Pharmacokinetics of Gentamicin [a]

Dose, mg/kg BID		Phase	Half-life, min		V_c, ml/kg	Vd, ml/kg	Vd_{ss}, ml/kg	Clearance, ml/min		k_u, min^{-1}	AUC, μg·min/ml
Gentamicin	Piperacillin		α	β				Body	Renal		
2	0	1	5.6	76.5	187	504	440	43	20.9	0.012	425
	500[b]		14.2	76.8	258	486	407	41	1.5	0.0006	468
4	0		5.1	63.7	139	278	255	30	14.3	0.010	1318
	500		10.9	79.9	266	419	378	34	1.5	0.0008	1242
2	0	2	3.1	74.7	126	303	285	27	16.2	0.015	660
	500		4.2	71.4	245	402	387	35	2.3	0.001	523
4	0		5.1	66.7	121	311	274	33	22.1	0.014	1293
	500		2.9	81.4	209	430	413	34	7.4	0.004	1090

[a] $n = 2$ unless otherwise noted. [b] $n = 1$; data from dog 016007 (female) was rejected as an outlier.

subjected to three separate ANOVA to compare the pharmacokinetics of piperacillin with gentamicin, determine the effects of gentamicin on piperacillin pharmacokinetics, and determine the effects of piperacillin on gentamicin pharmacokinetics. The first analysis included animals that received only one drug. The effects tested were drug, phase, and the drug by phase interaction; the dose level of gentamicin was not considered. The second analysis included animals that received 500 mg/kg of piperacillin, alone or in combination with gentamicin at either 2 or 4 mg/kg. The effects tested were dose level of gentamicin, phase, and the interaction between dose level and phase. The final analysis included animals that received gentamicin at either 2 or 4 mg/kg, alone or in combination with 500 mg/kg of piperacillin. The effects tested were dose levels of both drugs, phase, and all interactions. Homogeneity of variance within the male and female dogs was assumed.

RESULTS AND DISCUSSION

The mean serum concentrations attained following administration of 500 mg/kg of piperacillin and 2 or 4 mg/kg of gentamicin (alone or in combination) during phase 1 (day 1, 2, or 3) and phase 2 (day 36 or 37) are shown in Tables II and III. Following administration of 500 mg/kg of piperacillin alone, the mean serum concentration at the end of the infusion in phase 1 was 2475 μg/ml; after 5 min, it declined rapidly and biexponentially. The mean serum concentrations at 10, 20, 40, 60, 120, and 240 min after administration were 1825, 1305, 715, 530, 167, and 12.5 μg/ml, respectively. In phase 2, no detectable levels of piperacillin were present before the start of the infusion. At the end of the infusion, the serum concentration was 4200 μg/ml, a level higher than seen in phase 1. After 5 min, serum concentrations were about the same magnitude as observed in phase 1. Simultaneous administration of gentamicin did not change the serum piperacillin levels to any significant extent.

Following 2 mg/kg of gentamicin alone, the serum concentration at the end of the infusion in phase 1 was 9.6 μg/ml; after 5 min, it declined in a biexponential manner. The respective serum levels at 10, 20, 40, 60, 120, and 240 min were 6.0, 4.4, 2.8, 2.2, 1.1, and 0.5 μg/ml. In phase 2, no detectable levels of gentamicin were present before the start of the infusion. At the end of the infusion, the serum level was 12.4 μg/ml and was higher than that in phase 1. Following the 4-mg/kg dosage regimen, the serum levels in both phases 1 and 2 were about two- to threefold the corresponding serum levels observed following the 2-mg/kg dosage regimen.

The time course of both piperacillin and gentamicin in the dog serum

Table VII—Percentage of Dose Excreted in the Urine Following Intravenous Administration of Piperacillin Alone or in Combination with Gentamicin

Dose, mg/kg BID			Mean[a] Percent of Dose Excreted	
Piperacillin	Gentamicin	Animal	Phase 1	Phase 2
500	0	015945	45.20	39.73
		015998	42.44	49.70
		015966	16.52[b]	1.56[b]
		016024	50.53	30.10
		Mean	46.06	39.84
500	2	015963	57.74	18.61
		016007	51.09	24.45
		015965	60.51	26.55
		016014	55.39	37.13
500	4	015917	51.57	10.21
		016005	59.08	49.88
		015953	49.47	39.03
		016015	58.92	24.54
		Mean[c]	55.47	28.81

[a] Mean of two 0–24-hr collections from 2 consecutive days. [b] Values of 16.52 and 1.56 are considered outliers and were not used in calculating the mean. [c] Mean of 2- and 4-mg/kg dose levels together.

Table VIII—Percentage of Dose Excreted in the Urine Following Intravenous Administration of Gentamicin Alone or in Combination with Piperacillin

Dose, mg/kg BID			Mean[a] Percent of Dose Excreted	
Piperacillin	Gentamicin	Animal	Phase 1	Phase 2
0	2	015943	63.88	60.40
		015994	32.66	59.05
		015956	52.24	68.52
		016022	61.80	43.37
	4	015937	51.01	49.00
		016006	43.83	57.34
		015952	56.89	84.62
		016021	67.83	54.41
		Mean[b]	53.77	59.59
500	2	015963	3.71	5.17
		016007	5.15	8.13
		015965	0.83	17.72
		016014	2.58	12.55
	4	015917	1.11	20.06
		016005	9.25	23.33
		015953	4.88	6.25
		016015	6.67	14.02
		Mean[b]	4.28	13.41

[a] Mean of two 0–24-hr collections from 2 consecutive days. [b] Mean of 2- and 4-mg/kg dose levels together.

could be described by a two-compartment open model. The relevant mean pharmacokinetic parameters estimated based on this model are given in Table IV. Table V shows the effect of gentamicin administration on the pharmacokinetics of piperacillin; Table VI shows the effect of piperacillin administration on the pharmacokinetics of gentamicin.

The pharmacokinetic parameters, except the volume of distribution of the central compartment (V_c), of both of the drugs in phase 2 were not different from those in phase 1. Even though V_c dropped significantly in phase 2, no statistically significant change was observed either in the volume of distribution at steady state (Vd_{ss}) or the overall volume of distribution, Vd. The reason for the lower V_c in the second phase is not known.

Since the two drugs were given in combination, it was considered of interest to compare the pharmacokinetics of piperacillin with that of gentamicin. Based on data from both phases, the half-life of piperacillin was 34 min, the body and renal clearances were 49 and 22 ml/min, respectively, and the volume of distribution at steady state was 228 ml/kg. The corresponding values for gentamicin were 70 min, 33 and 19 ml/min, and 314 ml/kg, respectively. Compared with gentamicin, piperacillin had a shorter half-life and a larger body clearance. There were no statistically significant differences in the volume of distribution nor in the renal clearance of the two drugs.

The percentages of the piperacillin and gentamicin doses excreted in the urine are given in Tables VII and VIII, respectively. The excretion data of dog 015966 were not used in averaging because of the exceptionally low values obtained: these values are considered to be outliers[7]. When piperacillin was administered alone, ~46% of the dose was recovered in 0–24 hr during phase 1 and ~40% in phase 2. The two urinary recoveries were not statistically different ($p > 0.05$). These recoveries remained unaffected when gentamicin was administered concurrently ($p > 0.05$). Following administration of gentamicin alone, ~54% of the dose was excreted in the urine in 0–24 hr in phase 1 and ~60% in phase 2; again, no statistical differences were observed between the two recoveries ($p > 0.05$). Simultaneous administration of piperacillin reduced ($p < 0.05$) the phase recovery by 92% (from 53.8 to 4.3) and the phase 2 recovery by 78% (from 59.6 to 13.4).

Gentamicin did not affect the pharmacokinetics of piperacillin to any large extent, nor were the pharmacokinetics of gentamicin changed significantly when piperacillin was administered simultaneously. The serum levels, area under serum concentration–time curve (AUC), body clearance, and half-life of gentamicin were not affected by the combination. However, the urinary recovery of gentamicin decreased significantly when it was coadministered with piperacillin.

The similarity of the pharmacokinetic parameters of gentamicin administered alone or in combination with piperacillin clearly indicate that the interaction between piperacillin and gentamicin occurred after excretion, *i.e.*, either in the urinary bladder or the collection container. The *in vitro* inactivation of aminoglycoside antibiotics by β-lactam antibiotics has been documented (2–4, 9, 10). It has been proposed (3, 9) that the two interact to form a biologically inactive conjugate linked between the amino group of the aminoglycoside and the β-lactam ring of the penicillin. Piperacillin in high concentrations has been shown to inactivate gentamicin in serum *in vitro*, but less rapidly than carbenicillin (11). It has also been shown that the inactivation of gentamicin proceeds at a much faster rate in saline or distilled water than in serum (9). Since both piperacillin and gentamicin are excreted in the urine rapidly and in high concentrations, the interaction could take place in the urinary system, especially if voiding does not occur for a long time. Inactivation of gentamicin by piperacillin either during infusion or *in vivo* would have resulted in an area under the gentamicin serum concentration–time curve lower than that in dogs given gentamicin alone. Statistically, there was no difference between the AUC values. Thus, the drop seen in the excretion rate constant and the renal clearance is probably an artifact of the computation process since the equation to calculate these parameters utilizes the amount of unchanged drug excreted in the urine. Results very similar to ours were observed by Waitz and coworkers (3) with carbenicillin. They showed that an intravenous administration of carbenicillin had no effect on gentamicin serum levels in dogs, but did result in reduced urinary excretion of gentamicin. Young *et al.* (4) have also investigated the inactivation of gentamicin by carbenicillin. In dogs whose urine flow was obstructed surgically, they were able to demonstrate that an interaction between carbenicillin and gentamicin could take place in the urinary bladder.

An *in vitro* study was conducted to confirm the interaction of the two drugs in urine. Piperacillin and gentamicin, alone and in combination, were incubated in dog urine at 37° at approximately the same concentration levels as were encountered in the urine of dogs receiving piperacillin or gentamicin alone. Aliquots of urine were removed at predetermined intervals and assayed for piperacillin and gentamicin activity

Table IX—Concentrations of Piperacillin and Gentamicin in Dog Urine as a Function of Time Following Incubation at 37° Either Alone or in Combination

Time, hr	Concentration in Urine, μg/ml			
	Piperacillin		Gentamicin	
	Alone	In Combination	Alone	In Combination
0	4270	5120	69.9	60.4
0.5	4350	4790	67.8	47.0
1	4070	4820	65.4	48.8
2	4120	4730	64.9	48.4
4	4110	4670	34.7[a]	40.7
6	4050	4920	64.0	35.2
8	4020	4630	64.2	32.1

[a] An apparent outlier.

[7] Inclusion of data of this animal in the analysis did not affect the results or conclusions.

(Table IX). There was no loss in piperacillin activity whether incubated alone or with gentamicin; however, a 47% loss of the initial activity of gentamicin was noted when it was incubated with piperacillin. The data clearly demonstrate that interaction between the two drugs in urine is feasible.

REFERENCES

(1) N. A. Kuck and G. S. Redin, *J. Antibiot.*, **31**, 1175 (1978).

(2) J. E. McLaughlin and D. S. Reeves, *Lancet*, **i**, 261 (1971).

(3) J. A. Waitz, C. G. Drube, L. M. Eugene, Jr., E. M. Oden, J. V. Bailey, G. H. Wagmen, and M. J. Weinstein, *J. Antibiot.*, **25**, 219 (1972).

(4) L. S. Young, G. Decker, and W. L. Hewitt, *Chemotherapy*, **20**, 212 (1974).

(5) S. C. Edberg, C. J. Bohenbley, and K. Gam, *Antimicrob. Agents Chemother.*, **9**, 414 (1976).

(6) A. Sedman and J. G. Wagner, "A Decision Making Pharmacokinetic Computer Program," University of Michigan Press, Ann Arbor, Mich., 1974.

(7) C. M. Metzler, G. L. Elfring, and A. J. McEwen, "A User's Manual for NONLIN and Associated Programs," The Upjohn Co., Kalamazoo, Mich., 1974.

(8) M. Gibaldi and D. Perrier, "Pharmacokinetics," Dekker, New York, N.Y., 1975.

(9) L. J. Riff and G. G. Jackson, *Arch. Intern. Med.*, **130**, 887 (1972).

(10) B. Lynn, *Eur. J. Cancer*, **9**, 425 (1973).

(11) D. C. Hale, R. Jenkins, and J. M. Matsen, *Am. J. Clin. Pathol.*, **74**, 316 (1980).

ACKNOWLEDGMENTS

The authors gratefully acknowledge the assistance of Mr. E. Pelcak of the Department of Microbiology Research, Lederle Laboratories for performing the microbiological assays.

Potential Tumor- or Organ-imaging Agents XXIV: Chylomicron Remnants as Carriers for Hepatographic Agents

N. S. DAMLE, R. H. SEEVERS, S. W. SCHWENDNER, and R. E. COUNSELL ˣ

Received April 15, 1982, from the *Departments of Pharmacology and Medicinal Chemistry, The University of Michigan, Ann Arbor, MI 48109.* Accepted for publication September 7, 1982.

Abstract □ This paper describes the possible utility of plasma lipoproteins for the site-specific delivery of diagnostic agents. The class of lipoproteins known as chylomicrons was selected for this preliminary study, since they are known to be rapidly metabolized and taken up by the liver. Cholesteryl iopanoate (II), an iodinated analogue of a normal constituent of the hydrophobic core of chylomicrons, was synthesized from cholesterol and iopanoic acid (I) and subsequently radiolabeled with ioidine-125. Whereas intravenous administration of II in physiological saline resulted in the appearance of ~31% of the dose in the liver at 0.5 hr, prior incorporation of II into chylomicrons resulted in an almost threefold (87%) increase in the liver accumulation of II in the same time period. A more gradual appearance of II in steroid-secreting tissues was consistent with the association of II with high-density lipoproteins following administration.

Keyphrases □ Chylomicron—remnants as carriers for hepatographic agents, potential tumor- or organ-imaging agents □ Tumor-imaging agents—potential, chylomicron remnants as carriers for hepatographic agents □ Organ-imaging agents—potential, chylomicron remnants as carriers for hepatographic agents

The early detection of small metastatic lesions in the liver has been a long-term goal of radiology and nuclear medicine. Among the noninvasive diagnostic approaches, radionuclide scintiscanning, ultrasonography, and computed tomography (CT) have all enjoyed variable success (1). Over the past several years, one of the goals of this laboratory has been to devise approaches for the selective delivery of radiopharmaceuticals or radiopaque agents to the liver on the premise that specific uptake of these agents in either normal or abnormal tissue will significantly improve image resolution of small lesions. While others have employed liposomes as delivery vehicles for radiopharmaceuticals (2) and radiopaque contrast agents (3), the focus of this study is on those naturally occurring macromolecules responsible for the transport of lipophilic substances in the plasma—the lipoproteins.

It has been known for many years that the liver plays a major role in lipoprotein catabolism. This is especially true for the class of lipoproteins known as chylomicrons (4, 5). The chylomicrons are synthesized in the intestinal mucosa during fat absorption and are responsible for the transport of dietary fats to sites of utilization and storage. Structurally they are the largest (800–5000 Å) and the lightest (<0.95 g/ml) of the lipoproteins, and consist of an apolar core of lipid surrounded by a phospholipid monolayer (Fig. 1). The lipophilic core is composed of triglycerides and cholesteryl esters. Free cholesterol and apoproteins are associated with the outer phospholipid membrane.

Once in the circulation, these native chylomicrons are acted on by tissue lipoprotein lipase, the enzyme responsible for hydrolyzing triglycerides and providing free fatty acids for cellular metabolism. The resulting triglyceride-depleted, cholesteryl ester-enriched chylomicrons are referred to as chylomicron remnants. In humans, these smaller remnants (300–800 Å) are rapidly taken up by the liver, and their plasma half-life is in the range of 4–5 min (6).

The uptake of chylomicron remnants by liver cells has been shown to occur by a saturable high-affinity process, suggesting the existence of receptors on the surface of liver cells capable of specificially binding these particles (7, 8). Moreover, the presence of apoprotein E on the surface of the remnants has been shown to be important for the recognition and uptake of these particles (9, 10).

0022-3549/83/0800-0898$01.00/0

(Table IX). There was no loss in piperacillin activity whether incubated alone or with gentamicin; however, a 47% loss of the initial activity of gentamicin was noted when it was incubated with piperacillin. The data clearly demonstrate that interaction between the two drugs in urine is feasible.

REFERENCES

(1) N. A. Kuck and G. S. Redin, *J. Antibiot.*, **31**, 1175 (1978).

(2) J. E. McLaughlin and D. S. Reeves, *Lancet*, **i**, 261 (1971).

(3) J. A. Waitz, C. G. Drube, L. M. Eugene, Jr., E. M. Oden, J. V. Bailey, G. H. Wagmen, and M. J. Weinstein, *J. Antibiot.*, **25**, 219 (1972).

(4) L. S. Young, G. Decker, and W. L. Hewitt, *Chemotherapy*, **20**, 212 (1974).

(5) S. C. Edberg, C. J. Bohenbley, and K. Gam, *Antimicrob. Agents Chemother.*, **9**, 414 (1976).

(6) A. Sedman and J. G. Wagner, "A Decision Making Pharmacokinetic Computer Program," University of Michigan Press, Ann Arbor, Mich., 1974.

(7) C. M. Metzler, G. L. Elfring, and A. J. McEwen, "A User's Manual for NONLIN and Associated Programs," The Upjohn Co., Kalamazoo, Mich., 1974.

(8) M. Gibaldi and D. Perrier, "Pharmacokinetics," Dekker, New York, N.Y., 1975.

(9) L. J. Riff and G. G. Jackson, *Arch. Intern. Med.*, **130**, 887 (1972).

(10) B. Lynn, *Eur. J. Cancer*, **9**, 425 (1973).

(11) D. C. Hale, R. Jenkins, and J. M. Matsen, *Am. J. Clin. Pathol.*, **74**, 316 (1980).

ACKNOWLEDGMENTS

The authors gratefully acknowledge the assistance of Mr. E. Pelcak of the Department of Microbiology Research, Lederle Laboratories for performing the microbiological assays.

Potential Tumor- or Organ-imaging Agents XXIV: Chylomicron Remnants as Carriers for Hepatographic Agents

N. S. DAMLE, R. H. SEEVERS, S. W. SCHWENDNER, and R. E. COUNSELL ˣ

Received April 15, 1982, from the *Departments of Pharmacology and Medicinal Chemistry, The University of Michigan, Ann Arbor, MI 48109.* Accepted for publication September 7, 1982.

Abstract □ This paper describes the possible utility of plasma lipoproteins for the site-specific delivery of diagnostic agents. The class of lipoproteins known as chylomicrons was selected for this preliminary study, since they are known to be rapidly metabolized and taken up by the liver. Cholesteryl iopanoate (II), an iodinated analogue of a normal constituent of the hydrophobic core of chylomicrons, was synthesized from cholesterol and iopanoic acid (I) and subsequently radiolabeled with ioidine-125. Whereas intravenous administration of II in physiological saline resulted in the appearance of ~31% of the dose in the liver at 0.5 hr, prior incorporation of II into chylomicrons resulted in an almost threefold (87%) increase in the liver accumulation of II in the same time period. A more gradual appearance of II in steroid-secreting tissues was consistent with the association of II with high-density lipoproteins following administration.

Keyphrases □ Chylomicron—remnants as carriers for hepatographic agents, potential tumor- or organ-imaging agents □ Tumor-imaging agents—potential, chylomicron remnants as carriers for hepatographic agents □ Organ-imaging agents—potential, chylomicron remnants as carriers for hepatographic agents

The early detection of small metastatic lesions in the liver has been a long-term goal of radiology and nuclear medicine. Among the noninvasive diagnostic approaches, radionuclide scintiscanning, ultrasonography, and computed tomography (CT) have all enjoyed variable success (1). Over the past several years, one of the goals of this laboratory has been to devise approaches for the selective delivery of radiopharmaceuticals or radiopaque agents to the liver on the premise that specific uptake of these agents in either normal or abnormal tissue will significantly improve image resolution of small lesions. While others have employed liposomes as delivery vehicles for radiopharmaceuticals (2) and radiopaque contrast agents (3), the focus of this study is on those naturally occurring macromolecules responsible for the transport of lipophilic substances in the plasma—the lipoproteins.

It has been known for many years that the liver plays a major role in lipoprotein catabolism. This is especially true for the class of lipoproteins known as chylomicrons (4, 5). The chylomicrons are synthesized in the intestinal mucosa during fat absorption and are responsible for the transport of dietary fats to sites of utilization and storage. Structurally they are the largest (800–5000 Å) and the lightest (<0.95 g/ml) of the lipoproteins, and consist of an apolar core of lipid surrounded by a phospholipid monolayer (Fig. 1). The lipophilic core is composed of triglycerides and cholesteryl esters. Free cholesterol and apoproteins are associated with the outer phospholipid membrane.

Once in the circulation, these native chylomicrons are acted on by tissue lipoprotein lipase, the enzyme responsible for hydrolyzing triglycerides and providing free fatty acids for cellular metabolism. The resulting triglyceride-depleted, cholesteryl ester-enriched chylomicrons are referred to as chylomicron remnants. In humans, these smaller remnants (300–800 Å) are rapidly taken up by the liver, and their plasma half-life is in the range of 4–5 min (6).

The uptake of chylomicron remnants by liver cells has been shown to occur by a saturable high-affinity process, suggesting the existence of receptors on the surface of liver cells capable of specificially binding these particles (7, 8). Moreover, the presence of apoprotein E on the surface of the remnants has been shown to be important for the recognition and uptake of these particles (9, 10).

0022-3549/83/0800-0898$01.00/0

The parenchymal cells, which comprise the majority of cells in the liver, have been shown to be the most intimately involved in the clearance of chylomicron remnants from the circulation (11, 12). Of particular interest was the finding that remnant-incorporated cholesteryl esters are not taken up to any significant extent by nonparenchymal cells (Kupffer and endothelial) of the rat liver (13). Since radioactive colloids currently used for imaging of liver function are phagocytized by Kupffer cells, chylomicron remnants offer an alternate mechanism for the localization of imaging agents in the liver.

Since cholesteryl esters are a major constituent of chylomicron remnants, it seemed reasonable that incorporation of polyiodinated esters of cholesterol into remnant vesicles could give rise to a new class of hepatographic agents. The iodine of these polyiodinated esters would confer sufficient electron density to serve as radiopaques, or the iodine could be substituted with any one of its various radioisotopic forms (*e.g.*, iodine-123) for radionuclide imaging. To test this hypothesis, iopanic acid (I), an established cholecystographic agent was esterified with cholesterol to afford the highly lipophilic cholesteryl iopanoate (II). This new ester was then labeled with iodine-125 to assist in the measurement of chylomicron incorporation and subsequent tissue distribution analysis.

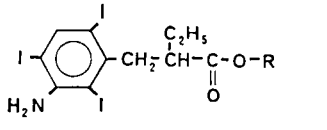

I. R = H = IOPANOIC ACID

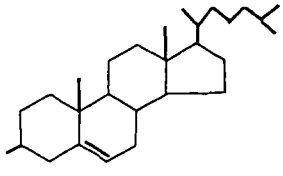

II. R =

EXPERIMENTAL[1]

Cholesteryl Iopanoate (II)—A solution of iopanoic acid (I, 571 mg, 1 mmole) and 1,1′-carbonyldiimidazole (170 mg, 1.05 mmoles) in dry tetrahydrofuran (5 ml) was heated at reflux for 10 min. Cholesterol (425 mg, 1.1 mmoles) was added along with a catalytic amount of sodium hydride. The mixture was stirred at room temperature for 1 hr, whereupon the solvent was removed using a rotatory evaporator. Water (10 ml) was carefully added to the residue and the mixture was extracted with benzene. The benzene extracts were combined, the solvent was removed under reduced pressure, and the residue was chromatographed on silica gel (benzene). The fractions containing the ester were combined, the solvent was removed under reduced pressure, and the residue was crystallized from ethanol–water to give II, mp 128–130° (dec) in 58.5% yield. IR(KBr): 3465, 3370, and 1738 cm^{-1}; ^1H-NMR: 4.8 (m, 3 H), 4.85 (s, NH_2), 5.45 (m, 6 vinyl H), and 8.15 ppm (s, Ar 1 H).

Anal.—Calc. for $C_{38}H_{56}I_3NO_2$: C, 48.58; H, 6.01; I, 40.52. Found: C, 48.71; H, 5.97; I, 40.23.

Isotope Exchange of II—The ester (5 mg) and acetamide (100 mg) were placed in a flask containing 10^{-9} *M* NH_4Cl (1.0 eq based on the amount of pH 9 $Na^{125}I$ solution to be added) and 10^{-7} *M* $Na_2S_2O_7$ (1.3–1.5 eq based on $^{125}I^-$ with a specific activity of 2.5×10^9 mCi/mole). $Na^{125}I$ (15 mCi) was added and rinsed in with acetone (0.15 ml). The flask was heated at 170° under a slight positive nitrogen pressure for 1 hr to evaporate the acetone and water present. Heating at 170° was continued for an additional 12 hr, and the flask was allowed to cool. The solid residue was dissolved in benzene, washed with water, and chromatographed on silica gel with benzene to afford [^{125}I]II (3 mg; 2.4 mCi). Radiochemical purity was established by TLC with unlabeled ester as the standard: R_f 0.50 (C_6H_6); R_f 0.08 (CCl_4).

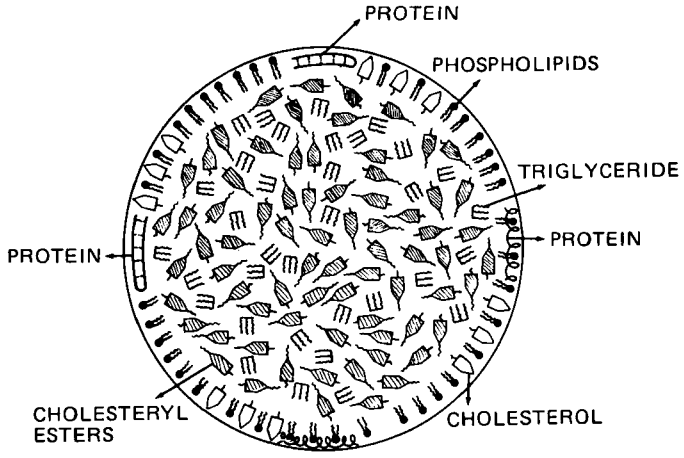

Figure 1—*General structure of a plasma lipoprotein.*

Animals—Sprague–Dawley rats (200–250 g), maintained on a standard rat food, were used for all studies. They were housed in temperature- and light-controlled quarters and had free access to food and water.

Isolation of Chylomicrons—To maximize the yield of chylomicrons from blood samples, the animals were given corn oil intragastrically (2 ml) three times at 3-hr intervals with a fourth dose (3 ml) administered 20 min prior to exsanguination. Blood was drawn by cardiac puncture in heparinized evacuated tubes[2] while the rats were under ether anesthesia (each rat gave approximately 6 ml of blood). The blood was immediately centrifuged at 3000 rpm for 10 min at 4° to separate plasma from packed cells. The plasma was divided into 6.25-ml fractions and layered beneath an equal volume of 0.15 *M* NaCl solution containing 0.002 *M* EDTA [(ethylene dinitrilo)tetraacetic acid] in cellulose nitrate tubes. These tubes were placed in an ultracentrifuge[3] with a Type 40 rotor and spun at 37,000 rpm (114,000×*g*) at 12° for 20 hr. The top, milky white, flocculant layer containing the chylomicrons was carefully separated from the remaining solution and stored at 4°. Lipid analysis of this fraction showed it to contain 281 meq/liter of triglycerides and 15.5 meq/liter of cholesterol[4].

Chylomicron Incorporation—Radioiodinated II (2.0 mg, 420 μCi) was dissolved in benzene (1 ml) to which was added polysorbate 20 (0.2

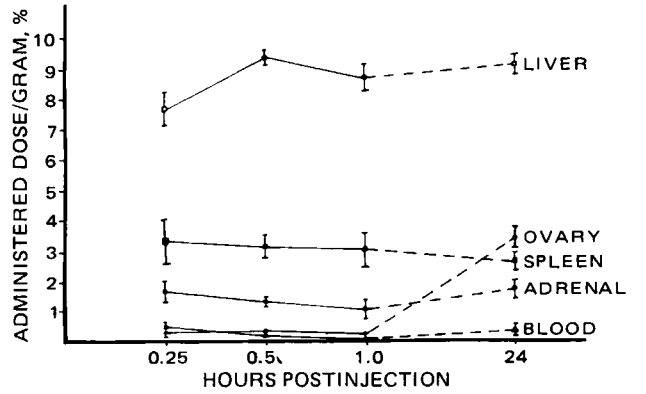

Figure 2—*Tissue distribution of radioactivity following administration of chylomicrons labeled with [^{125}I]cholesteryl iopanoate as a function of time.*

[1] NMR spectra were obtained on a Varian EM360A spectrometer in $CDCl_3$ containing tetramethylsilane as an internal reference. IR spectra were taken in KBr pellets on a Perkin-Elmer 281 spectrophotometer. Elemental analyses were performed by Midwest Microlab, Ltd., Indianapolis, Ind. TLC was performed on Eastman polyethylene-backed silica gel plates with a fluorescent indicator. Cholesterol and 1,1′-carbonyldiimidazolde were obtained from the Aldrich Chemical Co., Milwaukee, Wis. Iopanoic acid was a gift from the Sterling-Winthrop Research Institute, Rensselaer, N.Y. Sodium iodide-125 was purchased from Union Carbide, Tuxedo, N.Y. Polysorbate 20 (Tween 20) was obtained from Sigma Chemical Co., St. Louis, Mo. Rats were obtained from Spartan Research Animals, Inc., Haslett, Mich. Rat food was purchased from Ralston Purina Co., St. Louis, Mo. Agarose gel (Biogel A-50M) was obtained from Bio-Rad Laboratories, Richmond, Calif.

[2] Vacutainer; Bectin, Dickinson and Co.

[3] Beckman LS200.

[4] Analysis provided by Dr. Walter Block of the University of Michigan School of Public Health.

Table I—Distribution of Radioactivity 0.5 and 24 hr after Intravenous Administration of Cholesteryl [^{125}I]Iopanoate in Polysorbate 20–Saline Vehicle or Chylomicrons

Tissue	% Administered Dose/g of Tissue ± *SEM*			
	Polysorbate 20–Saline		Chylomicrons	
	0.5 hr[a]	24 hr[a]	0.5 hr[b]	24 hr[b]
Adrenal cortex	4.903 ± 0.718	11.029 ± 2.172	1.293 ± 0.126	1.921 ± 0.207
Blood	5.191 ± 0.441	0.696 ± 0.048	0.062 ± 0.008	0.231 ± 0.047
Liver	4.035 ● 0.543	6.587 ± 0.316	9.220 ± 0.251	9.151 ± 0.315
Lung	1.340 ± 0.126	0.599 ± 0.078	0.286 ± 0.062	0.252 ± 0.050
Ovary	5.161 ± 0.716	24.542 ± 2.964	0.118 ± 0.019	3.464 ± 0.773
Plasma	10.369 ± 0.862	1.345 ± 0.082	0.133 ± 0.027	0.388 ± 0.104
Spleen	0.777 ± 0.073	2.001 ± 0.134	3.136 ± 0.447	2.735 ± 0.344
Thyroid	0.868 ± 0.098	3.571 ± 0.218	0.075 ± 0.014	1.319 ± 0.317

[a] $N = 5$. [b] $N = 4$.

ml). This mixture was vortexed and the benzene evaporated. Physiological saline (1.0 ml) was added, and the solution was vortexed for 5 min. This solution was added to the chylomicron suspension (2.5 ml) in an Erlenmeyer flask, and the mixture was incubated in a water bath at 37° with shaking for 24 hr. At the end of the incubation period, an aliquot was taken for radioactivity determination and the remainder was placed on an agarose-gel (1.5 × 90 cm) column. The column was eluted with 0.20 *M* NaCl solution containing 0.002 *M* EDTA and 0.02% sodium azide. The column was run at a flow rate of 2.5 ml/min, the fractions were collected in a fraction collector[5] (150 drops/tube). The fractions were assayed for optical density (280 nm) and radioactivity[6] (50-μl aliquots) (Fig. 3). The fractions in the void volume were pooled, concentrated to a final volume of 13 ml in an ultrafiltration unit[7], and analyzed for total radioactivity.

Tissue Distribution—Rats were injected with radiolabeled chylomicrons (0.6 ml, 2.5 μCi per animal) intravenously through the tail vein. Groups of four animals were sacrificed by cardiac puncture under ether anesthesia at 0.25, 0.5, 1.0, and 24 hr. The tissues were excised, placed in preweighed cellulose acetate capsules, weighed, and assayed for radioactivity as previously described (14). The tissue concentrations at 0.5 and 24 hr are tabulated in Table I; the results for five key tissues are graphed in Fig. 2.

Tissue Extraction—Adrenal, liver, and plasma were extracted according to the method of Folch *et al.* (15). The percentage of radioactivity in the aqueous and organic phases was measured. The organic phase was streaked on a TLC plate and chromatographed using a petroleum ether–diethyl ether (7:2) system. The TLC plates were sliced and counted in a γ-counter to determine the amount of original ester remaining in the tissues.

Polyacrylamide Gel Electrophoresis (PAGE)—PAGE analysis of plasma samples was performed according to the method of Narayan *et al.* (16), as previously described (17). The amount of radioactivity associated with each lipoprotein class was determined by sectioning the gels and counting each section in a γ-counter. The radioactivity associated with each lipoprotein class was expressed as a percentage of the total radioactivity applied to the gel (Table II).

RESULTS AND DISCUSSION

As has been shown in previous papers in this series (18, 19), cholesterol is efficiently esterified by acid imidazolides. Using this mild procedure, cholesteryl iopanoate (II) was obtained in 58.5% yield from cholesterol and iopanoic acid. This product was readily radioiodinated with iodine-125 by using the isotope exchange method in acetamide (19).

Incorporation of II into chylomicron remnants also proved successful. Similar to previous studies (20) with radiolabeled cholesteryl oleate, II was found to diffuse from the saline solution into the lipophilic core of the chylomicrons during incubation. Incorporated ester was readily separated from unincorporated ester by gel filtration. The elution profile exhibited two peaks when assayed for radioactivity and absorbance at 280 nm (Fig. 3). Since the molecular mass exclusion limit of the gel was 50×10^6 daltons and the approximate molecular mass of chylomicrons is $\sim 200 \times 10^6$ daltons, the radioactivity appearing in the void volume represented II associated with chylomicrons and the radioactivity in the later fractions represented unincorporated ester. Extraction of the labeled chylomicrons and TLC analysis of the extract demonstrated that all of the radioactivity was still associated with II. Moreover, PAGE analysis was consistent with incorporation of II into chylomicrons. The overall process is outlined in Fig. 4. Following this procedure, ~40% of II was incorporated into chylomicron remnants.

Table II—PAGE[a] Analysis of Rat Plasma at Various Times Postinjection of Cholesteryl [^{125}I]Iopanoate in Polysorbate 20–Saline or Incorporated into Chylomicron Remnants[b]

Preparation	Region[c]	Total Radioactivity in Gel, %				
		0 hr[d]	0.25 hr	0.50 hr	1.00 hr	24 hr
Polysorbate 20–Saline	Stacking gel	80.0	—	1.1	—	5.1
	VLDL/LDL	16.8	—	23.5	—	27.2
	HDL/albumin	2.2	—	75.2	—	66.7
	Below albumin	1.0	—	0.2	—	0.9
Chylomicron remnants	Stacking gel	97.0	90.6	38.2	40.6	32.4
	VLDL/LDL	0.8	5.7	21.2	18.4	15.3
	HDL/albumin	1.1	2.4	21.2	22.3	35.2
	Below albumin	1.1	1.3	19.4	18.7	17.1

[a] PAGE is polyacrylamide gel electrophoresis. [b] $n = 3$–5. [c] LDL = low-density lipid; HDL = high-density lipid. [d] Analysis of dose prior to administration.

The disposition of II administered in saline was compared with II administered in chylomicron remnants. The tissue distribution of radioactivity at 0.5 and 24 hr after intravenous administration of these two preparations is summarized in Table I. When the ester was given in saline, high levels of radioactivity remained in the plasma at 0.5 hr. Plasma levels declined with time and at 24 hr, the adrenal and ovaries were the tissues containing the highest concentration of radioactivity. Lipid extraction and TLC analysis of these tissues demonstrated that the radioactivity was still associated with cholesteryl iopanoate.

Administration of II incorporated into chylomicron remnants, on the other hand, led to a marked increase in the amount of ester reaching the liver within 0.5 hr. Based on organ weights, ~87% of II was present in the liver following administration in chylomicrons as opposed to ~31% when given in saline. This result agrees very closely with that obtained earlier (20) using chylomicron remnants labeled with cholesteryl oleate. A major difference from cholesteryl oleate, however, was that the concentration of II in the liver remained essentially unchanged over the 24-hr period (Fig. 2). TLC analysis of the lipid extracted from the liver revealed that the radioactivity was still in the form of cholesteryl iopanoate (II). Unlike the naturally occurring esters of cholesterol, II is apparently a poor substrate for cholesteryl ester hydrolase (EC 3.1.1.13) present in the liver. In all likelihood, this *in vivo* stability accounts for its ability to persist in the liver.

The increased radioactivity in the steroid-secreting tissues (adrenals and ovaries) with time (Fig. 2) suggests redistribution of II from chylomicron remnants to other lipoproteins. In the rat, the major cholesterol carrier is high-density lipoproteins (HDL), and steroid-secreting tissues have been shown to acquire their cholesterol by an HDL receptor-mediated process (21). Thus, the high levels in the ovary and adrenal may result from the transfer of II from chylomicron remnants to HDL. Support for such a sequence comes from the PAGE analysis of the plasma (Table II). At 0 hr, 97% of II is in the chylomicron band (stacking gel), but by 0.5 hr, 21.2% is found to be associated with HDL. At 24 hr, the amount of II associated with HDL is 35.2%. By contrast, when II is administered in normal saline, it rapidly becomes associated with HDL such

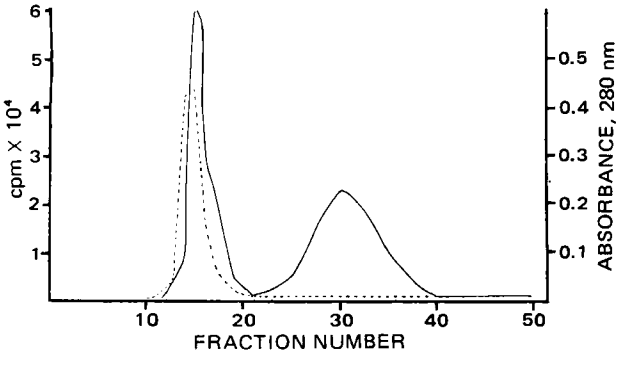

Figure 3—*Gel filtration profile of incubation medium containing rat chylomicrons and [^{125}I]cholesteryl iopanoate. The solid line represents radioactivity in cpm and the dotted line represents absorbance at 280 nm.*

[5] LKB 2070 Ultra Rac II.
[6] Searle 1185 γ-Counter (84.5% efficiency).
[7] Diaflo YM-30; Amicon Corporation, Lexington, Mass.

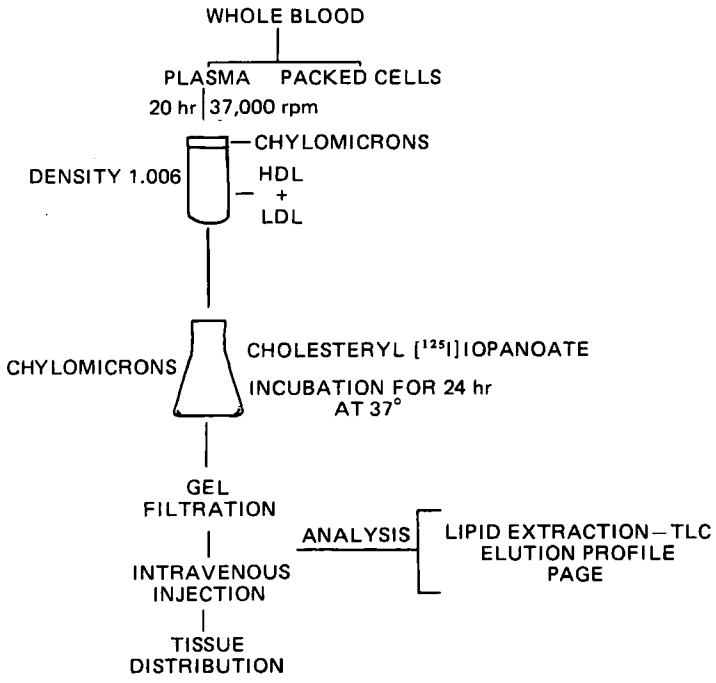

Figure 4—*Outline of procedures employed for the isolation of rat plasma chylomicrons, the incorporation of radioiodinated cholesteryl iopanoate, and the subsequent purification and analysis of the radioiodinated chylomicron preparation.*

that >75% is associated with this lipoprotein fraction at 0.5 hr. This could account for the higher concentration of ester appearing in the adrenals and ovaries following administration of II in saline.

The purpose of this preliminary study was to determine whether foreign lipid molecules could be introduced into chylomicron remnants and delivered selectively to the liver. This study has demonstrated that, at least in radiotracer amounts, cholesteryl iopanoate (II) can be incorporated into chylomicron remnants in a manner similar to that shown previously for cholesteryl oleate. Moreover, it has been shown that such remnant incorporation of II markedly increased its ability to selectively accumulate in the liver. These results suggest a potential use of lipoproteins as carriers of radiopharmaceuticals for liver imaging. Even in this instance, however, the procedures described in this paper would have to be modified in order to use radionuclides such as iodine-123, which has a half-life of 13 hr. Moreover, to be useful as vehicles for the delivery of radiopaques to the liver, it would be necessary to develop methods capable of incorporating radiologic concentrations of radiopaques into chylomicrons. Studies aimed at answering these and related questions are now in progress.

REFERENCES

(1) R. Williams and W. M. Melia, *Clin. Radiol.*, **31**, 1 (1980).

(2) V. J. Caride, W. Taylor, J. A. Cramer, and A. Gottschalk, *J. Nucl. Med.*, **17**, 1067 (1976).

(3) A. Havron, S. E. Seltzer, M. A. Davis, and P. Shulkin, *Radiology*, **140**, 507 (1981).

(4) T. G. Redgrave, *J. Clin. Invest.*, **49**, 465 (1970).

(5) A. D. Cooper, S. K. Erickson, R. Nutik, and M. A. Shrewsbury, *J. Lipid Res.*, **23**, 42 (1982).

(6) M. S. Brown, P. T. Kovanen, and J. L. Goldstein, *Science*, **212**, 628 (1981).

(7) B. C. Sherrill and J. M. Dietschy, *J. Biol. Chem.*, **253**, 1859 (1978).

(8) A. D. Cooper and P. Y. S. Yu, *J. Lipid Res.*, **19**, 635 (1978).

(9) B. C. Sherrill, T. L. Innerarity, and R. M. Mahley, *J. Biol. Chem.*, **255**, 1804 (1980).

(10) E. Windler, Y. Chao, and R. J. Havel, *J. Biol. Chem.*, **255**, 8303 (1980).

(11) C. H. Florén and A. Nilsson, *J. Biochem.*, **168**, 483 (1977).

(12) M. R. El-Maghrabi, M. Waite, L. L. Rudel, and V. L. King, *Biochim. Biophys. Acta*, **572**, 52 (1979).

(13) P. M. Lippiello, J. Dijkstra, M. van Galen, G. Scherphof, and B. M. Waite, *J. Biol. Chem.*, **256**, 7454 (1981).

(14) N. Korn, G. Nordblom, E. Floyd, and R. E. Counsell, *J. Pharm. Sci.*, **69**, 1014 (1980).

(15) J. Folch, M. Lees, and G. H. Sloane-Stanley, *J. Biol. Chem.*, **226**, 497 (1957).

(16) K. A. Narayan, H. L. Creinin, and F. A. Kummerow, *J. Lipid Res.*, **7**, 150 (1966).

(17) R. E. Counsell, L. W. Schappa, N. Korn, and R. J. Huler, *J. Nucl. Med.*, **21**, 852 (1980).

(18) R. E. Counsell, R. H. Seevers, N. Korn, and S. W. Schwendner, *J. Med. Chem.*, **24**, 5 (1981).

(19) R. H. Seevers, S. W. Schwendner, S. L. Swayze, and R. E. Counsell, *J. Med. Chem.*, **25**, 618 (1982).

(20) S. H. Quarfordt and D. S. Goodman, *J. Lipid Res.*, **8**, 264 (1967).

(21) J. T. Gwynne, D. Mahaffee, H. B. Brewer, Jr., and R. L. Ney, *Proc. Natl. Acad. Sci. USA*, **73**, 4329 (1976).

ACKNOWLEDGMENTS

This research was supported in part by the Michigan Heart Association and U.S. Public Health Service Grant CA-08349. R. H. Seevers was the recipient of an NIH traineeship under Grant T32-GM-07767.

The authors thank Sterling-Winthrop Laboratories for providing the iopanoic acid used in these studies and Dr. Walter Block of the University of Michigan for the lipid analyses. The authors acknowledge the technical assistance of Miss Sandra Swayze and Miss Kim Bergner.

Enhancement of the Antitumor Activity of N^6-(Δ^2-Isopentenyl)adenosine Against Cultured L-1210 Leukemia Cells by Pentostatin Using a Polymeric Delivery System

BRUCE HACKER and YUNIK CHANG*x

Received April 20, 1982, from the *Departments of Pharmacology-Toxicology and Pharmaceutics, Northeast Louisiana University, Monroe, LA 71209.* Accepted for publication July 14, 1982. *Present address: The College of Pharmacy, University of Oklahoma, Oklahoma City, OK 73190.

Abstract □ The adenosine deaminase inhibitor pentostatin (I), recently shown to be effective in the treatment of several types of acute and chronic human leukemias, was impregnated in a silicone polymer monolithic disk device for release *in vitro* in the presence of the antitumor nucleoside N^6-(Δ^2-isopentenyl)adenosine (II) against mouse L-1210 lymphocytic leukemia cells. Although I is ineffective alone against L-1210 cells, controlled release from the polymeric delivery matrix potentiates the antiproliferative effects of II during the midlog phase of growth (48 hr). Cytotoxicity is prolonged, leading to total cell death during the stationary phase of growth (96 hr). The present study suggests that polymeric delivery systems be used for controlled release of oncologic agents, alone or in combination with inhibitors, especially where lability is a concern.

Keyphrases □ Pentostatin—use to potentiate antineoplastic activity of N^6-(Δ^2-isopentenyl)adenosine against L-1210 leukemia cells, polymeric delivery system □ N^6-(Δ^2-Isopentenyl)adenosine—antineoplastic agent, potentiation by pentostatin against L-1210 leukemia cells □ Delivery systems—impregnated silicone polymer, pentostatin

The clinical use of several adenosine analogues for the treatment of various types of cancer as well as some immunodeficiency diseases has been hindered by inactivation of the oncologic agent. Elevated adenosine deaminase (adenosine aminohydrolase, E.C. 3.5.4.4), responsible for enzymatically deaminating adenosine nucleosides, has been reported in patients with acute or chronic (T-cell) lymphocytic leukemia (1–3). Certain of these patients have also been unresponsive to other conventional courses of chemotherapy (3). Treatment with pentostatin (I) (4), a tight-binding inhibitor of adenosine deaminase, has been shown to result in a successful level of clinical remission when used in single-agent therapy (1, 3, 5). It has been suggested that the antineoplastic activity of I alone when used in Phase I clinical trials is the result of accumulation of deoxyadenosine-5′-triphosphate (2, 6). The latter then interferes with DNA synthesis and/or the accumulation of 2′-deoxyadenosine which, in turn, is capable of blocking critical methylation reactions (6). Whatever the exact biochemical locus, it is clear that I potentiates certain adenosine analogues such as the antiviral agent vidarabine (9-β-D-arabinofuranosyladenine) (3, 7) and the antitumor nucleoside N^6-(Δ^2-isopentenyl)adenosine (II) (8–10) used in the present investigation. Nucleoside II has been shown to be immunosuppressive (11) as well as capable of interfering with the transmembrane translocation of unmodified nucleosides in several mammalian systems (12).

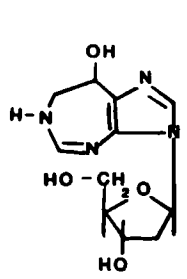

I

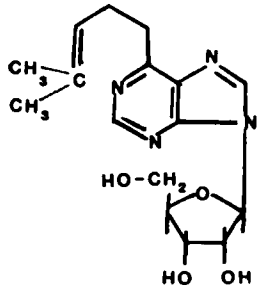

II

Recently, this laboratory demonstrated that controlled release of II from a monolithic silicone polymeric delivery system results in more effective cytotoxic action against cultured L-1210 leukemia cells (8, 9). Current studies have revealed that the adenosine deaminase inhibitor pentostatin (I), itself marginally active against L-1210 leukemia, is capable of potentiating and prolonging the cytotoxic activity of II. The present investigation has sought to take advantage of both the ability of I to act as an inhibitor of adenosine deaminase and the properties of the silicone monolithic polymeric delivery system for the controllable release of I to provide maximal potentiation and regulation of the cytotoxic effects of II against cultured L-1210 leukemia cells.

EXPERIMENTAL

Drug Agents—Pentostatin (I), (*R*)-3-(2-deoxy-β-D-*erythro*-pentofuranosyl)-3,6,7,8-tetrahydroimidazo[4,5-*d*][1,3]diazepin-8-ol, (2′-deoxycoformycin; NSC-218321) was supplied[1]. The preparation of N^6-(Δ^2-isopentenyl)adenosine (II) was as previously described (6, 9, 12). Both agents are routinely stored at −20° over silica gel.

Culturing of L-1210 Cells and Determination of the Antileukemic Activity of I and II—Mouse lymphocytic L-1210 leukemia cells were routinely cultured in RPMI-1640 medium with L-glutamine plus 10% fetal bovine serum[2] in tissue culture flasks[3] at 37° under controlled conditions using a digital incubator[4] containing a 5% carbon dioxide–air atmosphere, and grown to various densities as previously described (8, 9). Total cell number and cell viability values were determined using Turk's solution and trypan blue exclusion, respectively (8, 9). After the addition of I, I–silicone polymer, or II (singly or in combination), aliquots of each type of cell suspension were aseptically removed at various intervals for the determination of cell number. In addition, a portion of each cell suspension was centrifuge-filtered[5] to produce cell-free filtrates for high-performance liquid chromatographic (HPLC) analyses as previously described (8, 9), with certain modifications.

HPLC Analyses for I and II in L-1210 Cell Culture Medium—HPLC using a reverse-phase column[6] eluted at designated flow rates with various concentrations of aqueous or phosphate-buffer methanolic solutions was used to quantitatively analyze I and II in each cell-free culture

[1] Natural Products Branch, Division of Cancer Treatment, National Cancer Institute, Bethesda, Md.
[2] Grand Island Biological Co., Grand Island, N.Y.
[3] Corning No. 25100; 25 ml.
[4] Forma Scientific, Marietta, Ohio (Model 3029).
[5] Bioanalytical System, Inc., West Lafayette, Ind.
[6] Micropak MCH-10 (300 mm × 0.4 mm i.d.), Varian Instrument Co., Palo Alto, Calif.

0022-3549/83/0800-0902$01.00/0

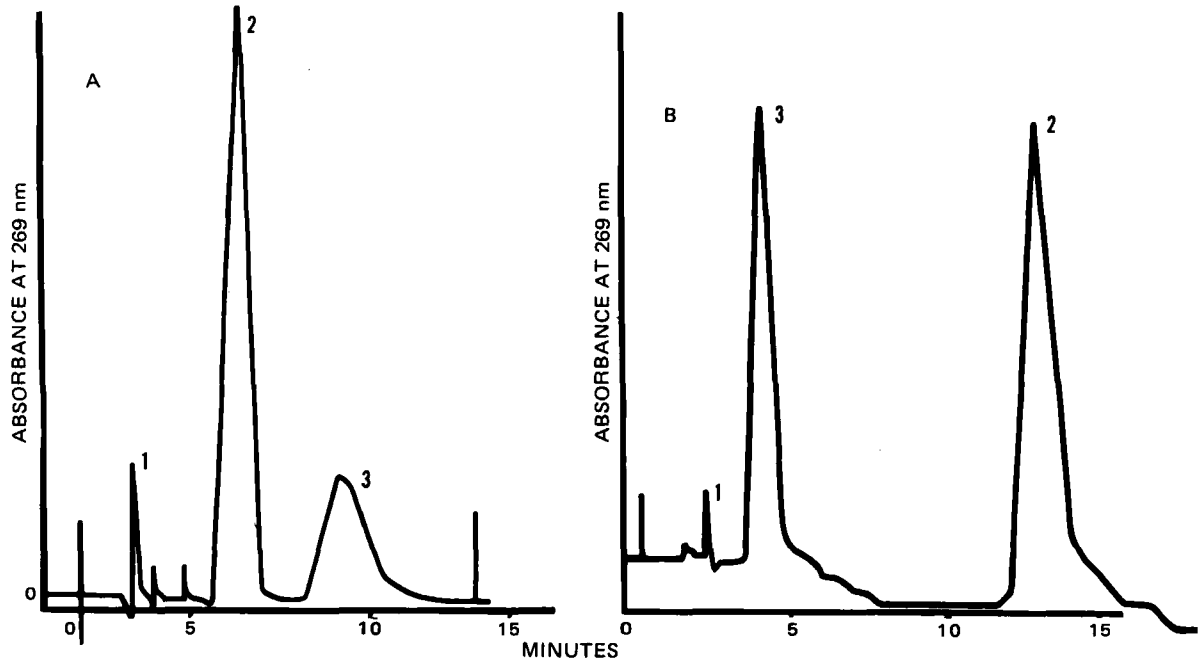

Figure 1—*Representative reverse-phase chromatograms of cell-free growth medium fractions from cultured L-1210 leukemia cells: (A) mobile phase, 60% methanol–water; column temperature, 25°; injection volume, 30 μl; (B) programmed mobile phase, 25% methanol–3 mM phosphate buffer, pH 7.0, increased to 70% methanol–3 mM phosphate buffer, pH 7.0, at a rate of 4.5%/min. Key: (1) inosine or adenosine; (2) II; (3) I.*

extract. Representative chromatograms are given in Fig. 1A and B. Three different calibration curves (stored in computer memory) were established to quantitate the results using a spectrophotometric–computer interface system[7] as previously described (8, 9). Standard curves for both I and II constructed using a detector sensitivity of 0.05–0.5 AUFS were found to be linear over the concentration ranges detected in the samples. Correlation coefficients for the standard curves were usually 0.99 (n = 7). The preparation of samples for HPLC employed cellulose prefilters, as detailed previously (9).

RESULTS AND DISCUSSION

The nucleoside N^6-(Δ^2-isopentenyl)adenosine has been shown to interfere with the transport of unmodified nucleosides in several types of mammalian cells at the level of transmembrane translocation (11). Following its metabolism in mouse spleen lymphocytes, II, or its phosphorylated form, interferes with the transport of unmodified nucleosides thereby resulting in inhibition of cellular RNA and DNA synthesis (12). It has been possible to prepare a serologically specific antibody to II (13) as well as to demonstrate an immunosuppressive response to the parent nucleoside (12). Although at first II appeared to be potentially useful for treating leukemia in humans (10), its antitumor activity was found subsequently to be limited by its low solubility and short half-life (14) due to rapid deamination to inosine by adenosine deaminase (15, 16).

This laboratory recently demonstrated (8, 9) that it is possible to use a silicone polymeric delivery system to control the release rate of II against cultured L-1210 leukemia cells, avoiding the usual peak and trough concentrations encountered with direct single additions of antitumor agents. Moreover, information was acquired in that study concerning the interaction of II and silicone polymers. In other recent studies using pentostatin, information has been acquired showing that I potentiates the antileukemic effects of II when added in combination directly to L-1210 cells grown in culture[8]. The enhanced cytotoxicity of this synergistic combination has not only been demonstrated in these studies *in vitro*, but has also been shown to substantially increase the mean survival time (MST) using tumorgenicity assays in CD2F1 mice *in vivo*[9].

In the present investigation, analyses for I and II in cell-free extracts from serum-containing growth medium have been accomplished using two separate reverse-phase HPLC systems (Fig. 1). When 60% aqueous methanol was used as described previously (8, 9), it was possible to resolve I and II with a retention time difference of ~3 min (Fig. 1A). On occasion, the peak for II had a tendency to broaden in that system, thereby reducing the sensitivity for detecting I and obtaining less than satisfactory results. Use of a computer-programmed gradient, initially at a concentration of 25% methanol in 3 m*M* phosphate buffer, pH 7.0, and increased to 70% methanol at a methanol rate change of 4.5%/min, gave much greater sensitivity for detecting I (Fig. 1B). In addition to increasing the retention time difference to 13 min, II became more lipophilic, thereby reversing the elution order for I and II when using the programmed gradient system. Use of the programmed mobile phase system, however, gave some tailing of the peak of II. In practice both systems were used throughout this investigation for routinely separating I and II to confirm and generate the data given in Table I and elsewhere.

Experiments conducted to assess the antileukemic effects of I alone and in combination with II revealed some profound information. Al-

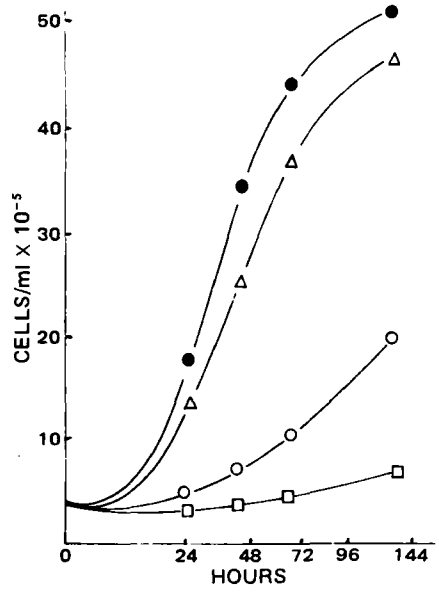

Figure 2—*Effects of I and II on the proliferation of L-1210 mouse leukemia cells. Aliquots of each cell suspension were removed at designated intervals for HPLC and determination of cell number. Key: (●) no additions; (○) plus 25 μg/ml of II; (△) plus 2 μg/ml of I; (□) plus 2 μg/ml of I and 25 μg/ml of II.*

[7] UV-50, Varian Instrument Co., Palo Alto, Calif.

[8] B. Hacker and Y. Chang (presented at the 73rd American Association of Cancer Research, St. Louis, Mo., April 1982); *Cancer Treat. Reports* (submitted for publication).

[9] B. Hacker and Y. Chang, unpublished results.

Table I—HPLC Determination of N^6-(Δ^2-Isopentenyl)adenosine and Pentostatin in Medium from Cultured L-1210 Leukemia Cells

Addition at Time Zero[a]	Sample Time, hr: 0		72		96		144	
	Concentration in Growth Medium[b], μg/ml: I	II	I	II	I	II	I	II
None	0	0	0	0	0	0	0	0
I (10 μg/ml)	8.6	0	5.1	0	3.5	0	2.8	0
I (3 μg/ml) plus II (25 μg/ml)	2.3	25.3	3.0	24.2	1.3	19.2	0.9	17.1
I (10 μg/ml) plus II (25 μg/ml)	9.4	20.6	5.4	21.9	4.3	14.0	3.0	13.3
II (25 μg/ml)	0	21.2	0	25.3	0	25.1	0	19.3
Silicone–I (1.96 mg of I per 88.8 mg silicone device; 1 × 7 cm)	11.7	0	90.3	0	80.6	0	76.8	0
Silicone–I (2.18 mg of I per 98.6 mg silicone device; 1 × 7 cm) plus II (25 μg/ml)	23.0	27.2	98.7	20.0	79.2	21.8	75.4	16.0

[a] Each T-flask contained 5 ml of growth medium (RPMI-1640 plus 10% fetal bovine serum) plus 1 × 10^5 L-1210 leukemia cells. The experiments were initiated (time zero) by the addition of each agent in RPMI-1640 without serum in a volume of 0.05–0.10 ml with prior sterile-filtration before their introduction into the cell cultures. [b] Aliquots (0.20 ml) of each cell suspension were removed at each designated sample time for the determination of cell number, viability, and HPLC analyses. Values reflect the results of duplicate determinations.

though I is a tight-binding inhibitor of adenosine deaminase and has demonstrated antitumor effects against certain human lymphocytic leukemias (3, 6), it is by itself marginally inhibitory (≤4%) toward cultured L-1210 cells (Figs. 2 and 3). On the other hand, when I (2 μg/ml) is added directly to cultured L-1210 lymphocytic leukemia cells, it dramatically potentiates the effects of II (25 μg/ml) within 24 hr. At 144 hr after each addition of I and II in combination, 85% inhibition is achieved. This represents an additional 30% compared with II used alone (Fig. 2). The most dramatic result here is that without concurrent use of I and II, the ability of II to be cytostatic gradually declines from a 73% value at 24 hr to 56% at 144 hr. The combined use of I and II not only potentiates the latter, but also prolongs its cytostatic effects against L-1210 cells in culture. Recently, Cass *et al.* (17) have shown that several sugar-substituted homologues of tubercidin and adenosine, which are deaminase-sensitive, were also active in combination with I.

In subsequent experiments, when the concentration of I was increased to 5 μg/ml and given in combination with II, it was found to further potentiate the latter to an ~96% level within 144 hr (Fig. 3). The few cells which remained had viability values <50%. Use of higher concentrations of I did not result in significantly greater cytotoxicity[10]. If the addition of II (25 μg/ml) is delayed for 24 hr after the introduction of I into the cultured L-1210 cell suspension, inhibition is reduced by about one-fourth compared with the inhibition when both agents are added simultaneously (Fig. 3). This suggests the importance of administering I at the onset to maximize its inhibition of adenosine deaminase, thereby reducing the overall deamination of II. When this occurs the antileukemic effects of II are potentiated and prolonged. Under these conditions it may be possible to reduce the concentration or dose of II required for maximally effective cytotoxicity as an antitumor agent.

With these initial observations, experiments were designed to establish the feasibility of preparing a silicone polymeric delivery form for I that was perhaps similar to the system used previously for II (8, 9). The underlying rationale was that the controlled release (if possible) of I from such a device might serve to block the deamination of II, thereby making

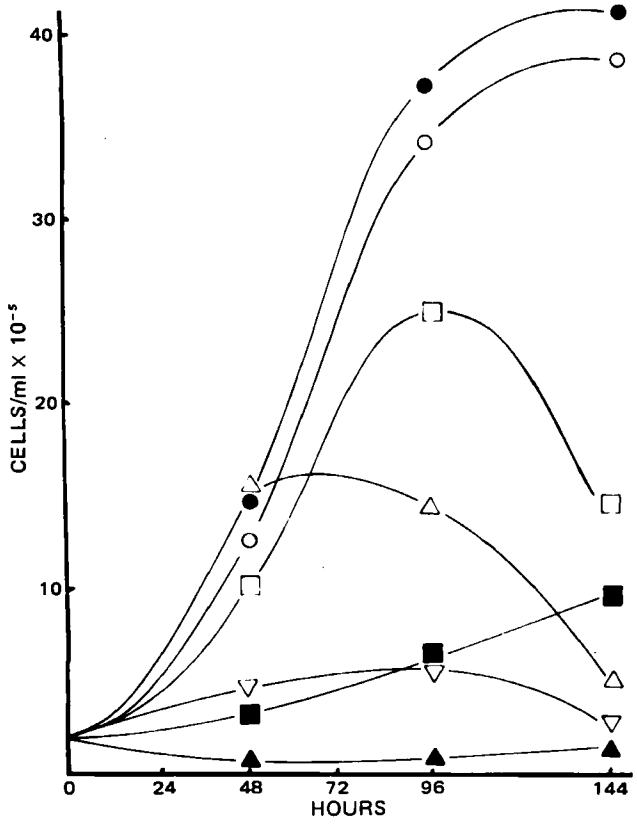

Figure 3—*Effects of pretreatment of cultured L-1210 cells. Additions of I (5 μg/ml) and II (25 μg/ml) to cultures of L-1210 cells were made at time zero and 48 hr. Aliquots of each cell suspension were removed at designated intervals for HPLC and determination of cell number. Key: (●) no additions; (○) plus I at time zero; (□) plus I at time zero and II at 48 hr; (■) plus II at time zero; (▲) plus I and II at time zero; (▽) plus II at time zero and I at 48 hr; (△) plus I and II at 48 hr.*

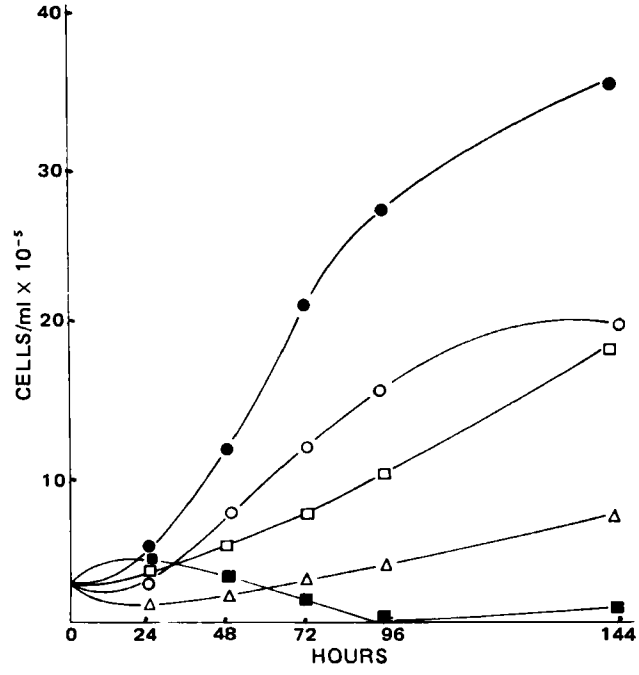

Figure 4—*Enhancement of antiproliferative activity of II against cultured L-1210 leukemia cells by I and I–silicone polymeric monolithic membrane (SPMM) in the presence of II. Aliquots of each cell suspension were removed at designated intervals for HPLC and determination of cell number. Key: (●) no additions; (○) plus 25 μg/ml of II; (□) plus 25 μg/ml of II and 2 μg/ml of I; (△) plus 25μg/ml of II and 5 μg/ml of I; (■) plus 25 μg/ml of II and I–SPMM (2.18 mg of I/98.6 mg of SPMM, 1 × 7 cm).*

[10] B. Hacker, unpublished results.

II a more potent cytotoxic agent. As the release of I begins to occur (Fig. 4 and Table I), its protective effect *via* binding and inhibition of adenosine deaminase is initiated. This occurs within 48 hr with the concurrent potentiation of the cytotoxic property of II. At 72 hr, inhibition by II is almost complete with remaining cells at 30% viability. At 96 hr, when the silicone polymer–I is present initially, inhibition by II is total. Although it was not possible to achieve total cell death when I was added directly (at concentrations as high as 100 μg/ml) with II (Figs. 2 and 3), that end was reached when lower concentrations of I were released into the growth medium from the silicone polymeric delivery device in the presence of II. The few remaining cells at 144 hr were found to be nonviable (Fig. 4) when the combination of the I–silicone polymer plus II was used.

Although both I and II are separately stable when incubated in cell-free medium, analyses of the data using HPLC (Table I) suggest that L-1210 cells have the capacity to metabolize I and/or II. Concentrations of I and II gradually decrease at longer sample times. Previously it was demonstrated that cell-free enzyme extracts of L-1210 cells converted II to its nucleoside monophosphate (18). Similarly, recent studies by Venner and Glazer (19) have shown that L-1210 cells convert I to its mononucleotide to the extent of ≤16%, while most of the parent drug is excreted unchanged in the urine of tumor-bearing mice. Studies by two groups have sought to develop models and data for I alone to describe the pharmacokinetics in normal and leukemic (L-1210) mice (20, 21).

The present study has demonstrated that the adenosine deaminase inhibitor I is capable of greatly potentiating the antileukemic effects of II, particularly when the former is released at a controllable rate from a silicone monolithic polymeric matrix. The clinical application of protection labile oncologic agents in this manner will be explored in the near future.

REFERENCES

(1) A. Yu, B. Bakay, S. Matsumoto, W. Nyhan, M. Green, and I. Rayston, *Proc. Am. Assoc. Cancer Res.*, **22**, 226 (1981).

(2) D. G. Poplack, S. E. Sallan, G. Rivera, *Cancer Res.*, **41**, 3343 (1981).

(3) D. P. Gray, M. R. Grever, M. F. E. Slaw, M. S. Coleman, and S. P. Balcerzak, *Cancer Treat. Rep.*, **66**, 253 (1982).

(4) P. W. K. Woo, H. W. Dion, S. M. Lange, and D. F. Dahl, *J. Heterocycl. Chem.*, **11**, 641 (1974).

(5) D. D. Von Hoff, J. Kuhn, and G. J. Harris, "New Anticancer Drugs in Cancer Chemotheropy Annual 2," H. M. Pinedo, Ed., Elsevier, New York, N.Y. 1981, pp. 122, 130.

(6) R. L. Wortmann, J. Holcenberg, and D. G. Poplack, *Cancer Treat. Rep.*, **66**, 387 (1982).

(7) C. E. Cass and T. H. Au-Yeung, *Cancer Res.*, **36**, 1486 (1976).

(8) B. Hacker and Y. Chang, *Proc. J. Pharm. Sci.*, **11**, 136 (1981).

(9) Y. Chang and B. Hacker, *J. Pharm. Sci.*, **71**, 328 (1982).

(10) J. T. Grace, M. T. Hakala, R. H. Hall, and J. Blakeslee, *Proc. Am. Assoc. Cancer Res.*, **8**, 23 (1967).

(11) D. Hare and B. Hacker, *Phys. Chem. Phys.*, **4**, 275 (1972).

(12) B. Hacker and T. L. Feldbush, *Cancer*, **27**, 1384 (1971).

(13) B. Hacker, H. Vunakis and L. Levine, *J. Immunol.*, **108**, 1726 (1972).

(14) G. B. Chheda and A. Mittelman, *Biochem. Pharmacol.*, **21**, 27 (1972).

(15) B. M. Chassy and R. J. Suhadolnik, *J. Biol. Chem.*, **242**, 3655 (1967).

(16) R. H. Hall and G. Mintsioulis, *J. Biochem.*, **73**, 739 (1973).

(17) C. E. Cass, M. Seiner, T. H. Tan, W. H. Muhs, and M. J. Robins, *Cancer Treat. Rep.*, **66**, 317 (1982).

(18) B. Hacker, *Biochim. Biophys. Acta*, **224**, 635 (1970).

(19) P. M. Venner and R. I. Glazer, *Biochem. Pharmacol.*, **28**, 3239 (1979).

(20) W. R. McConnell, R. L. Furner, and D. L. Hill, *Drug Metab. Dispos.*, **7**, 11 (1979).

(21) F. G. King and R. L. Dedrick, *J. Pharmacokinet. Biopharm.*, **9**, 519 (1981).

ACKNOWLEDGMENTS

Supported in part by Faculty Research Grants from the State of Louisiana to B. Hacker and Y. Chang.

The authors wish to acknowledge the Lord Jesus Christ who inspired and directed this investigation (Proverbs 3:6). We thank Mrs. Beverly Coody for typing the manuscript.

Time-Dependent Kinetics VII: Effect of Diurnal Oscillations on the Time Course of Carbamazepine Autoinduction in the Rhesus Monkey

PETER J. WEDLUND and RENÉ H. LEVY ×

Received January 7, 1982, from the *Departments of Pharmaceutics and Neurological Surgery, Schools of Pharmacy and Medicine, University of Washington, Seattle, WA 98195.* Accepted for publication July 8, 1982.

Abstract □ Extensive blood sampling and repeated long-term carbamazepine infusions were carried out in four rhesus monkeys to examine the time course of carbamazepine autoinduction in detail and assess the intraanimal variability in the rate constant of induction. Diurnal oscillations in carbamazepine blood levels were observed during all infusions and these prevented a good data fit for the biochemical model previously proposed for describing the decline in drug blood levels during induction by carbamazepine. An attempt at fitting only selected blood samples to the model resulted in variable (and perhaps questionable) induction rate constants, even in the same animal. Previous variability in calculated induction rate constants may be due to the presence of diurnal oscillations superimposed on the autoinduction phenomenon. It is proposed that the simultaneous expression of diurnal oscillations and autoinduction are the result of effects on drug metabolism at two independent levels.

Keyphrases □ Carbamazepine—autoinduction in the rhesus monkey, rate constant determination, effect of diurnal oscillations on drug metabolism □ Metabolism—of carbamazepine in the rhesus monkey, autoinduction rate constants, effect of diurnal oscillations □ Diurnal Oscillation—effect on metabolism of carbamazepine in the rhesus monkey

The ability of carbamazepine to induce self-elimination during chronic administration in the rat, dog, monkey, and human is well established (1–10). This increased elimination is reflected in a decline in carbamazepine steady-state blood levels. To describe this time-dependent decline, equations have been proposed based on a biochemical model of exponentially increasing levels of drug-metabolizing enzymes in the liver (11–14). These equations have

0022-3549/83/0800-0905$01.00/0

II a more potent cytotoxic agent. As the release of I begins to occur (Fig. 4 and Table I), its protective effect *via* binding and inhibition of adenosine deaminase is initiated. This occurs within 48 hr with the concurrent potentiation of the cytotoxic property of II. At 72 hr, inhibition by II is almost complete with remaining cells at 30% viability. At 96 hr, when the silicone polymer–I is present initially, inhibition by II is total. Although it was not possible to achieve total cell death when I was added directly (at concentrations as high as 100 μg/ml) with II (Figs. 2 and 3), that end was reached when lower concentrations of I were released into the growth medium from the silicone polymeric delivery device in the presence of II. The few remaining cells at 144 hr were found to be nonviable (Fig. 4) when the combination of the I–silicone polymer plus II was used.

Although both I and II are separately stable when incubated in cell-free medium, analyses of the data using HPLC (Table I) suggest that L-1210 cells have the capacity to metabolize I and/or II. Concentrations of I and II gradually decrease at longer sample times. Previously it was demonstrated that cell-free enzyme extracts of L-1210 cells converted II to its nucleoside monophosphate (18). Similarly, recent studies by Venner and Glazer (19) have shown that L-1210 cells convert I to its mononucleotide to the extent of ≤16%, while most of the parent drug is excreted unchanged in the urine of tumor-bearing mice. Studies by two groups have sought to develop models and data for I alone to describe the pharmacokinetics in normal and leukemic (L-1210) mice (20, 21).

The present study has demonstrated that the adenosine deaminase inhibitor I is capable of greatly potentiating the antileukemic effects of II, particularly when the former is released at a controllable rate from a silicone monolithic polymeric matrix. The clinical application of protection labile oncologic agents in this manner will be explored in the near future.

REFERENCES

(1) A. Yu, B. Bakay, S. Matsumoto, W. Nyhan, M. Green, and I. Rayston, *Proc. Am. Assoc. Cancer Res.*, **22**, 226 (1981).

(2) D. G. Poplack, S. E. Sallan, G. Rivera, *Cancer Res.*, **41**, 3343 (1981).

(3) D. P. Gray, M. R. Grever, M. F. E. Slaw, M. S. Coleman, and S. P. Balcerzak, *Cancer Treat. Rep.*, **66**, 253 (1982).

(4) P. W. K. Woo, H. W. Dion, S. M. Lange, and D. F. Dahl, *J. Heterocycl. Chem.*, **11**, 641 (1974).

(5) D. D. Von Hoff, J. Kuhn, and G. J. Harris, "New Anticancer Drugs in Cancer Chemotheropy Annual 2," H. M. Pinedo, Ed., Elsevier, New York, N.Y. 1981, pp. 122, 130.

(6) R. L. Wortmann, J. Holcenberg, and D. G. Poplack, *Cancer Treat. Rep.*, **66**, 387 (1982).

(7) C. E. Cass and T. H. Au-Yeung, *Cancer Res.*, **36**, 1486 (1976).

(8) B. Hacker and Y. Chang, *Proc. J. Pharm. Sci.*, **11**, 136 (1981).

(9) Y. Chang and B. Hacker, *J. Pharm. Sci.*, **71**, 328 (1982).

(10) J. T. Grace, M. T. Hakala, R. H. Hall, and J. Blakeslee, *Proc. Am. Assoc. Cancer Res.*, **8**, 23 (1967).

(11) D. Hare and B. Hacker, *Phys. Chem. Phys.*, **4**, 275 (1972).

(12) B. Hacker and T. L. Feldbush, *Cancer*, **27**, 1384 (1971).

(13) B. Hacker, H. Vunakis and L. Levine, *J. Immunol.*, **108**, 1726 (1972).

(14) G. B. Chheda and A. Mittelman, *Biochem. Pharmacol.*, **21**, 27 (1972).

(15) B. M. Chassy and R. J. Suhadolnik, *J. Biol. Chem.*, **242**, 3655 (1967).

(16) R. H. Hall and G. Mintsioulis, *J. Biochem.*, **73**, 739 (1973).

(17) C. E. Cass, M. Seiner, T. H. Tan, W. H. Muhs, and M. J. Robins, *Cancer Treat. Rep.*, **66**, 317 (1982).

(18) B. Hacker, *Biochim. Biophys. Acta*, **224**, 635 (1970).

(19) P. M. Venner and R. I. Glazer, *Biochem. Pharmacol.*, **28**, 3239 (1979).

(20) W. R. McConnell, R. L. Furner, and D. L. Hill, *Drug Metab. Dispos.*, **7**, 11 (1979).

(21) F. G. King and R. L. Dedrick, *J. Pharmacokinet. Biopharm.*, **9**, 519 (1981).

ACKNOWLEDGMENTS

Supported in part by Faculty Research Grants from the State of Louisiana to B. Hacker and Y. Chang.

The authors wish to acknowledge the Lord Jesus Christ who inspired and directed this investigation (Proverbs 3:6). We thank Mrs. Beverly Coody for typing the manuscript.

Time-Dependent Kinetics VII: Effect of Diurnal Oscillations on the Time Course of Carbamazepine Autoinduction in the Rhesus Monkey

PETER J. WEDLUND and RENÉ H. LEVY ×

Received January 7, 1982, from the *Departments of Pharmaceutics and Neurological Surgery, Schools of Pharmacy and Medicine, University of Washington, Seattle, WA 98195.* Accepted for publication July 8, 1982.

Abstract □ Extensive blood sampling and repeated long-term carbamazepine infusions were carried out in four rhesus monkeys to examine the time course of carbamazepine autoinduction in detail and assess the intraanimal variability in the rate constant of induction. Diurnal oscillations in carbamazepine blood levels were observed during all infusions and these prevented a good data fit for the biochemical model previously proposed for describing the decline in drug blood levels during induction by carbamazepine. An attempt at fitting only selected blood samples to the model resulted in variable (and perhaps questionable) induction rate constants, even in the same animal. Previous variability in calculated induction rate constants may be due to the presence of diurnal oscillations superimposed on the autoinduction phenomenon. It is proposed that the simultaneous expression of diurnal oscillations and autoinduction are the result of effects on drug metabolism at two independent levels.

Keyphrases □ Carbamazepine—autoinduction in the rhesus monkey, rate constant determination, effect of diurnal oscillations on drug metabolism □ Metabolism—of carbamazepine in the rhesus monkey, autoinduction rate constants, effect of diurnal oscillations □ Diurnal Oscillation—effect on metabolism of carbamazepine in the rhesus monkey

The ability of carbamazepine to induce self-elimination during chronic administration in the rat, dog, monkey, and human is well established (1–10). This increased elimination is reflected in a decline in carbamazepine steady-state blood levels. To describe this time-dependent decline, equations have been proposed based on a biochemical model of exponentially increasing levels of drug-metabolizing enzymes in the liver (11–14). These equations have

0022-3549/83/0800-0905$01.00/0

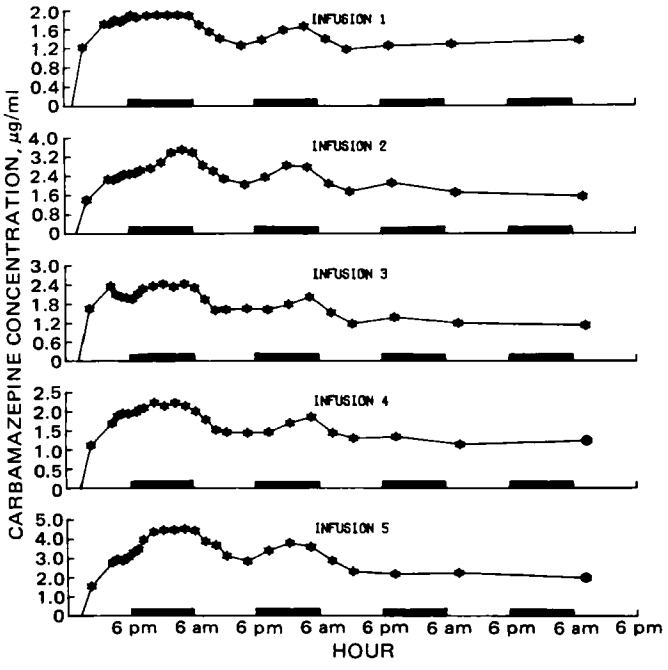

Figure 1—*Carbamazepine concentration* versus *time for five infusions in monkey 202.*

been used to fit the plasma concentration–time data during auto- and heteroinduction by carbamazepine and to calculate a first-order rate constant (induction rate constant) which characterizes the time course of the decline in plasma drug levels (15–18). Recently, further support for this model was provided by the finding of a close correlation between the change in liver enzymes responsible for drug metabolism (cytochrome P-450) and the change in metabolic clearance of carbamazepine in monkeys during long-term infusions (19).

An interesting result of the application of this model has been the remarkable interanimal variability in the induction rate constant (twofold or more) (15–18). Although

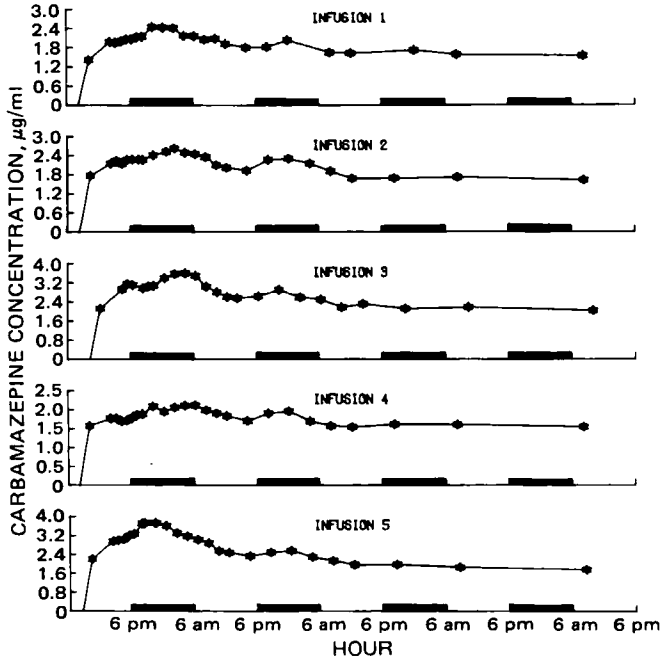

Figure 2—*Carbamazepine concentration* versus *time for five infusions in monkey 204.*

Table I—Calculated Induction Half-Life [a] During Carbamazepine Long-Term Infusions

Monkey	Infusion	Infusion Rate, ml/hr	r^b	Calculated Induction Half-Life, hr
202	1	1.00	0.866	4.0
202	2	1.41	1.000	10.4
202	3	1.19	0.965	13.8
202	4	1.07	0.941	6.9
202	5	1.69	0.988	16.5
203	1	1.45	0.946	13.4
203	2	1.54	0.994	13.9
203	3	1.76	0.964	9.3
203	4	1.54	0.957	7.8
203	5	1.58	0.995	20.1
204	1	1.40	0.892	6.6
204	2	1.39	0.926	7.2
204	3	1.23	0.995	10.5
204	4	1.41	0.962	11.4
204	5	1.54	0.944	11.0
60409	1	1.63	0.868	7.2
60409	2	1.56	0.947	10.1
60409	3	1.47	—[c]	—
60409	4	1.60	0.979	32.9
60409	5	1.49	0.931	302.0

[a] Calculated using only the blood samples collected at 18, 20, 22, 24, 26, 28, 32, 52, 72, and 96 hr, fitting the calculated intrinsic clearance at these times to a model that predicts a monoexponential increase in intrinsic clearance (12, 13). [b] Correlation coefficient from fitting intrinsic clearances to a monoexponential equation. [c] — Lost due to technical difficulties.

it is tempting to speculate about the meaning of this observation, such speculation should be limited until the reproducibility of the rate constant in a given animal can be determined. Following an assessment of intraanimal variability in this parameter, the interanimal variability in the induction rate constant and the possible contribution of genetic factors could be evaluated. The present study was undertaken: (*a*) to characterize in greater detail the time course of carbamazepine autoinduction in the rhesus monkey, (*b*) to quantitate the intraanimal variability in the rate constant of autoinduction, and (*c*) to examine factors that may affect the rate constant determination.

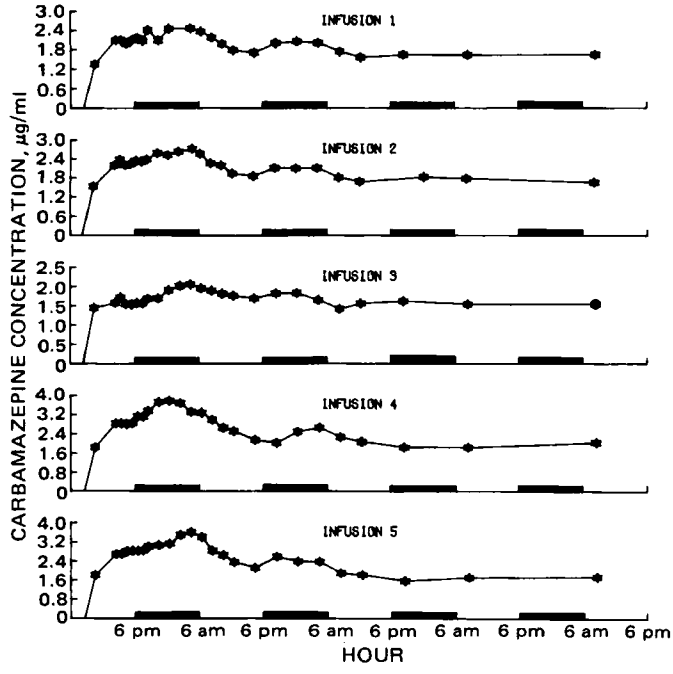

Figure 3—*Carbamazepine concentration* versus *time for five infusions in monkey 203.*

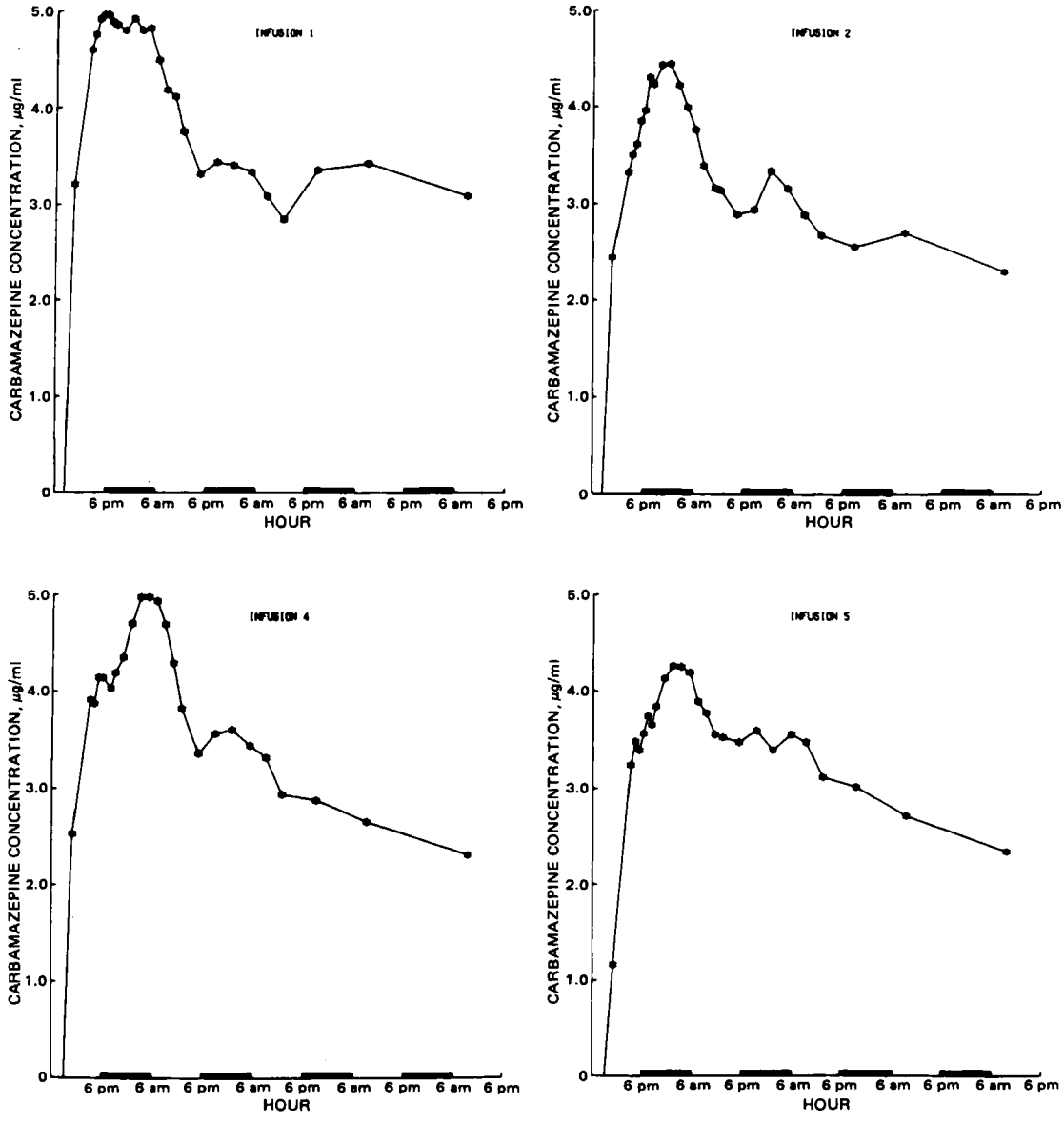

Figure 4—*Carbamazepine concentration* versus *time for four infusions in monkey 60409. (The third infusion was lost due to technical difficulties.)*

EXPERIMENTAL

Animals—This study was conducted in five restraint chair-adapted normal rhesus monkeys (*Macaca mulatta*). Each animal was equipped with two chronic indwelling catheters (femoral for drug infusions and jugular for blood sampling).

Dosing—Four animals received five 96-hr carbamazepine infusions, a fifth animal received a single 96-hr carbamazepine infusion. Infusions were separated by at least a 3-week period, during which time no drugs were administered. Sterile carbamazepine solutions (10 mg/ml) in 60% polyethylene glycol 400 were used for drug administration. Carbamazepine was infused at rates of 1.0–1.8 ml/hr with an infusion pump[1].

Blood Sampling—Blood samples (1.4 ml) were obtained at 2, 6, 7, 8, 9, 10, 11, 12, 14, 16, 18, 20, 22, 24, 26, 28, 32, 36, 40, 44, 48, 52, 60, 72, and 96 hr during the carbamazepine infusion. Each sample was divided and stored at −20° until assayed.

Liver Biopsies—To investigate the relationship between the cytochrome P_{450} level and the diurnal changes in carbamazepine clearance observed in this study, an additional but limited investigation of diurnal change in the cytochrome P_{450} level was undertaken. Liver biopsies were obtained in three of the five monkeys at 1:00 a.m. and 1:00 p.m. Monkeys received only saline (no carbamazepine) during this phase of the study, with a 3-week rest period between biopsy samples. The liver tissue was immediately placed on ice, blood clots were eased away from the tissue, and the biopsy was blotted dry and weighed. The liver tissue was homogenized in 20% glycerol phosphate buffer to give 10 mg of liver tissue/ml of buffer. The homogenate was centrifuged at 200×*g*, and the supernatant was removed and assayed for cytochrome P_{450} and protein.

Analytical Procedures—Whole blood samples were assayed in duplicate for carbamazepine by GC interfaced with a mass spectrometer in chemical ionization mode (20). Cytochrome P_{450} measurements were performed with a scanning spectrophotometer[2] by using the sodium dithionite difference technique reported by Estabrook *et al.* (21) and Joly *et al.* (22). Protein was determined with the sodium anazolene[3] assay reported by Spector (23).

RESULTS AND DISCUSSION

Plots of the time course of carbamazepine blood levels from replicate infusions in four monkeys are given in Figs. 1–4. These curves appear to show two types of phenomena: (*a*) an overall decrease in steady-state carbamazepine blood levels between the first and the fourth day and (*b*)

[1] Holter model 905; Extracorporeal Medical Specialties, Inc., King of Prussia, PA 19406.

[2] Aminco DW-2 UV-VIS spectrophotometer; American Instruments Co., Silver Spring, MD 20910.

[3] Comassie Blue; Pierce, Rockford, IL 61125.

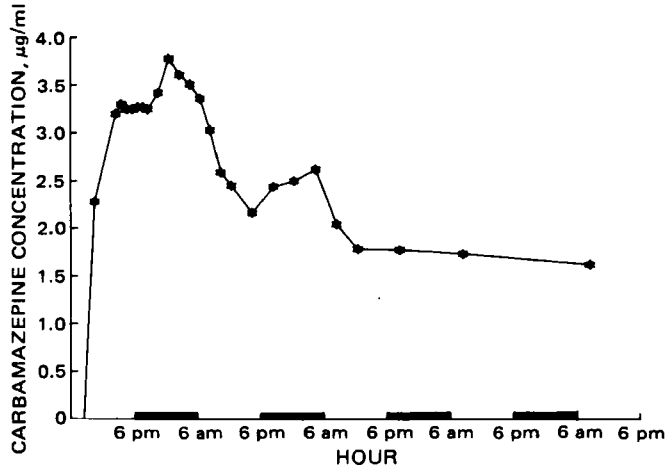

Figure 5—*Carbamazepine concentration* versus *time for a single infusion in monkey N436.*

oscillations in blood levels (increase followed by decrease) during the first two dark periods. This pattern in carbamazepine blood levels was reproducible in replicate studies in four monkeys and was also found in the single infusion of monkey N436 (Fig. 5).

The decrease in carbamazepine blood levels during the 4-day infusions involves a chemically induced, time-dependent increase in clearance (24) (autoinduction) which has been observed consistently during long-term infusions of carbamazepine in the rhesus monkey (16, 25). The oscillations in carbamazepine levels during the dark periods are probably the expression of a diurnal phenomenon. Diurnal oscillations in steady-state levels of several drugs (valproic acid, ethosuximide, and carbamazepine) have been observed in the rhesus monkey (26–28) and are most likely the result of an endogenous physiological process (24). This study shows that these two different types of time-dependent phenomena can occur simultaneously. As a result, the blood level data could not be fitted to previous equations describing the time course of induction (12, 13).

In an effort to separate the diurnal oscillations from the autoinduction phenomenon, carbamazepine blood samples taken at 18, 20, 22, 24, 26, 28, 32, 52, 72, and 96 hr were used to describe the time course of induction. The systemic clearance of carbamazepine at each of these times was computed by dividing the rate of infusion by the respective blood concentration. Each systemic clearance was then used in conjunction with an estimated liver blood flow rate [2.735 liters/hr/kg (29, 30)] to calculate the intrinsic clearance at these respective times. Both the intrinsic and systemic clearance values were fitted with the BMDX85 computer program to the equation (13, 14):

$$CL_t = CL_0 + P(1)\{1 - e^{-[P(2)(t-\theta)]}\} \quad \text{(Eq. 1)}$$

where CL_t represents the clearance at any time t, CL_0 represents the initial clearance calculated from the steady-state blood levels, P(1) represents the change between the initial and final clearance values, P(2) represents the rate constant of induction, and θ is the time lag before the start of the induction process. The induction half-lives obtained by dividing ln 2 by the rate constant of induction exhibited large variability (intra- and interanimal) whether intrinsic (Table I) or systemic clearance values were used. The poor reproducibility in induction half-lives probably reflects the inability to accurately separate the diurnal oscillations from the autoinduction process. The variability observed in the past may also be a reflection of this problem (15–18, 31). However, other biochemical factors which may also vary and influence the time course of induction cannot be ruled out.

The diurnal phenomenon observed in this study is consistent with what has been reported for other drugs in the rat and human (32–40). Factors that could contribute to this phenomenon include a decrease in liver blood flow, enterohepatic recycling, and/or a decrease in the carbamazepine free fraction during the night. However, there are a number of reasons to suspect that the oscillations are more likely due to changes in intrinsic drug clearance by the liver. First, carbamazepine is extensively metabolized and only a small amount is eliminated unchanged in the monkey (41). Second, the liver appears to be the predominant eliminating organ based on intravenous and portal vein catheter experiments in this laboratory[4]. Third, liver blood flow would have to decrease an average of 40% each night to explain the observed decrease in drug clearance and elevation of carbamazepine levels. Fourth, ethosuximide and valproic acid, which are extensively metabolized in the monkey and have clearances insensitive to changes in liver blood flow, also exhibit pronounced diurnal oscillations (26, 27). Fifth, the time course of change in carbamazepine blood levels overnight is too slow to be compatible with an enterohepatic recycling process. The absence of elevated carbamazepine levels following meals during the day also suggests that the oscillations are probably not due to an enterohepatic recycling process. Sixth, in view of the linear binding (free fraction 0.35 ± 0.02) of carbamazepine in monkey plasma between 1 and 10 μg/ml, a large decrease in this parameter during the night seems unlikely.

[4] Unpublished data.

Table II—Cytochrome P_{450} Determination in Liver Homogenates [a]

Monkey	Cytochrome P_{450} Levels, nmoles/g liver 1:00 a.m.	1:00 p.m.
204	32	36
N436	32	28
203	—[b]	33
Mean ± *SD*	32 ± 0	32 ± 4

[a] Monkeys 202 and 60409 were not available for P_{450} determinations. [b] — P_{450} could not be determined due to the small amount of liver tissue available.

If the diurnal oscillations observed in the present study are due to changes in hepatic metabolic activity, the lack of any apparent change in cytochrome P_{450} (Table II) suggests that the diurnal variations are not due to changes in this enzyme. This is consistent with other observations in rats, which also exhibit pronounced diurnal oscillations in drug metabolism but little diurnal change in cytochrome P_{450} levels (42, 43). This hypothesis is further supported by the consistent observation in this study that diurnal oscillations are unaffected by the process of induction which is known to involve an increase in liver cytochrome P_{450} enzymes.

An alternative mechanism for the diurnal oscillations in this study may be concurrent oscillations in cytochrome P_{450} reductase activity. The levels of the reductase are one-tenth to one-twentieth those of cytochrome P_{450} levels (44, 45), and reductase levels have been found to be a rate-limiting component in microsomal monoxygenase systems (44, 46). Furthermore, several studies in rats have shown diurnal oscillations in cytochrome P_{450} reductase activity (42, 43, 47). In addition, the formation of at least one major metabolite of carbamazepine (carbamazepine-10,11-epoxide) in the human has been shown to be dependent on the activity of this enzyme (48). If the reductase activity undergoes diurnal oscillations in the monkey and is also a rate-limiting component in some of the pathways of carbamazepine elimination, the two time-dependent phenomena observed in this study could be the result of effects on separate components of the drug metabolizing system (diurnal oscillations related to oscillations in cytochrome P_{450} reductase activity and autoinduction related to increase in cytochrome P_{450} enzymes).

It should be noted that endogenous steroids are also known to exhibit diurnal variations in both the rat and human. Whether these steroids are responsible for changes in drug metabolism or just spuriously related is unknown. Whatever the relationship between endogenous steroids and the diurnal phenomena noted for drug metabolism, it is probable that a key to the mechanism lies in understanding the factors responsible for changes in drug metabolism at the cellular level.

This study provides the first evidence that two types of time-dependent phenomena, diurnal oscillations and autoinduction, can occur simultaneously. As a result, blood level data cannot be fitted to previous equations for describing the time course of induction. Use of selected blood samples resulted in variable induction rate constants, even in the same animal. In view of the observed intraanimal variability, the first-order rate constants of induction computed in the past should be interpreted with some caution. We propose that the autoinduction and diurnal phenomena seen in this study may be the result of effects on drug metabolism at two independent levels.

REFERENCES

(1) P. L. Morselli and A. Frigerio, *Drug Metab. Rev.*, **4**, 97 (1975).

(2) M. Eichelbaum, K. Ekbom, L. Bertilsson, V. A. Ringberger, and A. Rane, *Eur. J. Clin. Pharmacol.*, **8**, 337 (1975).

(3) R. H. Levy, W. H. Pitlick, A. S. Troupin, and J. R. Green, in "The Effect of Disease States on Drug Pharmacokinetics," L. Benet, Ed., American Pharmaceutical Assoc. Academy of Pharmaceutical Sciences, Washington, D.C., 1976, p. 87.

(4) F. Hasson, B. M. Assael, L. Bossi, S. Garattini, M. Gerna, R. Gomeni, and P. L. Morselli, *Arch. Int. Pharmacodyn. Ther.*, **220,** 125 (1976).

(5) A. P. Gerardin, F. V. Abadie, J. A. Campestrini, and W. Theobald, *J. Pharmacokinet. Biopharm.*, **4,** 521 (1976).

(6) L. Bertilsson, *Clin. Pharmacokinet.*, **3,** 128 (1978).

(7) M. Theisohn, M. Sigmund, G. Heimann, and B. Roth, *Epilepsia*, **20,** 182 (1979).

(8) L. Bertilsson, B. Höjer, G. Tybring, J. Osterloh, and A. Rane, *Clin. Pharmacol. Ther.*, **27,** 83 (1980).

(9) H. H. Frey and W. Loscher, *Arch. Int. Pharmacodyn. Ther.*, **243,** 180 (1980).

(10) S. Pynnonen, H. Frey, and M. Sillanpaa, *Int. J. Clin. Pharmacol. Ther. Toxicol.*, **18,** 247 (1980).

(11) W. H. Pitlick, R. H. Levy, A. S. Troupin, and J. R. Green, *J. Pharm. Sci.*, **65,** 462 (1976).

(12) R. H. Levy, A. A. Lai, and M. S. Dumain, *J. Pharm. Sci.*, **68,** 398 (1979).

(13) R. H. Levy, M. S. Dumain, and J. L. Cook, *J. Pharmacokinet. Biopharm.*, **1,** 557 (1979).

(14) R. H. Levy and A. A. Lai, in "Antiepileptic Therapy: Advances in Drug Monitoring," S. I. Johannessen *et al.*, Eds., Raven, New York, N.Y., 1980, p. 315.

(15) P. H. Corbisier and R. H. Levy, APhA/Academy of Pharmaceutical Sciences Abstracts, **1,** 134 (1977).

(16) W. H. Pitlick and R. H. Levy, *J. Pharm. Sci.*, **66,** 647 (1977).

(17) A. A. Lai and R. H. Levy, *J. Pharm. Sci.*, **68,** 416 (1979).

(18) J. W. Warren, J. B. Benmaman, B. B. Wannamaker, and R. H. Levy, *Clin. Pharmacol. Ther.*, **28,** 646 (1980).

(19) P. J. Wedland, S. D. Nelson, S. Nickelson, and R. H. Levy, *Drug Metab. Dispos.*, **10,** 480 (1982).

(20) W. F. Trager, R. H. Levy, I. H. Patel, and J. M. Neal, *Anal. Lett.*, **B11,** 119 (1978).

(21) R. W. Estabrook, J. Peterson, J. Baron, and A. Hildebrant, *Methods Pharmacol.*, **2,** 303 (1972).

(22) J. G. Joly, C. Doyon, and Y. Pesant, *Drug Metab. Dispos.*, **3,** 577 (1975).

(23) T. Spector, *Anal. Biochem.*, **86,** 142 (1978).

(24) R. H. Levy, in "International Encyclopedia of Pharmacology and Therapeutics: Pharmacokinetics—Theory and Methodology," Pergamon, Oxford, 1982, pp. 383–397.

(25) I. H. Patel, R. H. Levy, and W. F. Trager, *J. Pharmacol. Exp. Ther.*, **206,** 607 (1978).

(26) J. S. Lockard, R. H. Levy, L. L. DuCharme, W. C. Congdon, and I. H. Patel, *Epilepsia*, **20,** 169 (1979).

(27) I. H. Patel, R. H. Levy, and J. S. Lockard, *J. Pharm. Sci.*, **66,** 650 (1977).

(28) J. S. Lockard, R. H. Levy, L. L. DuCharme, W. C. Congdon, and I. H. Patel, *Epilepsia*, **18,** 183 (1977).

(29) R. P. Forsyth, A. S. Nies, F. Wyler, J. Neutze, and K. L. Melmon, *J. Appl. Physiol.*, **25,** 736 (1969).

(30) R. A. Branch, D. G. Shand, G. R. Wilkinson, and A. S. Nies, *J. Clin. Invest.*, **53,** 1101 (1974).

(31) P. J. McNamara, W. A. Colburn, and M. Gibaldi, *J. Pharmacokinet. Biopharm.*, **7,** 63 (1979).

(32) F. M. Radzialowski and W. F. Bousquet, *J. Pharmacol. Exp. Ther.*, **163,** 229 (1968).

(33) A. Jori, E. DiSalle, and V. Santini, *Biochem. Pharmacol.*, **20,** 2965 (1971).

(34) J. Swoyer, D. J. LaKatua, E. Haus, T. Warner, and L. Sackett, *Chronobiologia Suppl.*, **1,** 71 (1975).

(35) C. A. Shively and E. S. Vesell, *Clin. Pharmacol. Ther.*, **18,** 413 (1976).

(36) J. Clench, A. Reinberg, J. Dziewanoska, J. Ghata, and J. Dupont, *Chronobiologia*, **4,** 1 (1977).

(37) E. S. Vesell, C. A. Shively, and G. T. Passananti, *Clin. Pharmacol. Ther.*, **22,** 843 (1977).

(38) L. Carosella, P. DiNardo, R. Bernabei, A. Cocchi, and P. Carbonin, in "Advances in the Biosciences, 7th Intl. Congr. Pharmacol., Symposium on Chronopharmacology," A. Reinberg and F. Halberg, Eds., Pergamon, Oxford 1978, p. 125.

(39) G. M. Kyle, M. H. Smolensky, and J. P. McGovern, in "Advances in the Biosciences, 7th Intl. Congr. Pharmacol., Symposium Chronopharmacology," A. Reinberg and F. Halberg, Eds., Pergamon, Oxford 1978, p. 219.

(40) J. N. Pinkston, K. F. A. Soliman, and C. A. Walker, in "Advances in the Biosciences, 7th Intl. Congr. Pharmacol., Symposium on Chronopharmacology," A. Reinberg and F. Halberg, Eds., Pergamon, Oxford 1978, p. 337.

(41) R. H. Levy, J. S. Lockard, J. R. Green, P. Friel, and L. Martis, *J. Pharm. Sci.*, **64,** 302 (1975).

(42) J. A. Castro, F. E. Greene, P. Gigon, H. Sasame, and J. R. Gillette, *Biochem. Pharmacol.*, **19,** 2461 (1970).

(43) J. M. Tredger and R. S. Chhabra, *Xenobiotica*, **1,** 481 (1977).

(44) M. Kitada, H. Kitagawa, and T. Kamataki, *Biochem. Pharmacol.*, **28,** 2670 (1979).

(45) J. E. Gander and G. J. Mannering, *Pharmacol. Ther.*, **10,** 191 (1980).

(46) G. T. Miwa, S. B. West, and A. Y. H. Lu, *J. Biol. Chem.*, **253,** 1921 (1978).

(47) M. A. Miller, J. M. Parker, and A. E. Colas, *Life Sci.*, **23,** 217 (1978).

(48) C. VonBahr, C. G. Groth, H. Jansson, G. Lundgren, M. Lind, and H. Glaumann, *Clin. Pharmacol. Ther.*, **27,** 711 (1980).

Systematic Error Associated with Apparatus 2 of the USP Dissolution Test III: Limitations of Calibrators and the USP Suitability Test

DON C. COX ˣ, WILLIAM B. FURMAN, LARRY K. THORNTON, TERRY W. MOORE, and EVERETT H. JEFFERSON

Received April 19, 1982, from the *National Center for Drug Analysis, Food and Drug Administration, St. Louis, MO 63101.* Accepted for publication July 22, 1982.

Abstract □ The calibrator tablets now used in the USP suitability test do not reveal common sources of systematic error associated with Apparatus 2. When the apparatus was operated under conditions near or beyond USP tolerances, changes in the results of the USP calibrators were slight, whereas those of several samples of commercial prednisone tablets were significant. Thus, the USP calibrators and requirements do not guarantee suitability of the equipment for general dissolution testing of drug products.

Keyphrases □ Dissolution—systematic error associated with Apparatus 2 of the USP dissolution test using calibrator tablets □ Calibrator tablets, USP—systematic error associated with Apparatus 2 of the dissolution test □ Apparatus 2—of the USP dissolution test, systematic error using calibrator tablets

The USP provides an Apparatus Suitability Test (1) to ensure that a dissolution apparatus operates satisfactorily and is free from significant extraneous vibration (2). Two official calibrators, both compressed tablets, are available[1] for use in the test. The nondisintegrating calibrator is labeled to contain 300 mg of salicylic acid; the disintegrating calibrator is labeled to contain 50 mg of prednisone. The test conditions for use of the tablets and the ranges within which the results must fall appear in information sheets provided with the calibrators.

Before a given piece of equipment is considered suitable for use as Apparatus 2, it must pass a four-point test. Dissolution results from both calibrators must fall within the established ranges at 50 and 100 rpm. If the equipment fails the test, alignment, speed, vibration, *etc.* should be checked and corrected. If the requirements cannot be met, the equipment is judged unsuitable for use as Apparatus 2 (3). Thus, equipment suitability is determined by the response of the calibrator tablets to variations in the USP test conditions.

Some of the test conditions are defined in terms of numerical tolerances, *e.g.*, the shaft rotation speed is to be maintained within ±4% of a specified value, and the shaft axis is to be positioned not more than 2 mm from the vertical axis of the vessel. Others are defined in absolute terms, *e.g.*, the vessel is cylindrical with a spherical bottom, and the paddle blade forms a section of a circle of specified diameter subtended by parallel chords of specified length. Certain other test conditions are not clearly defined, but rather are to be controlled so that they do not significantly influence the results, *e.g.*, no part of the assembly (vessel, paddle, and variable-speed drive) or the surrounding environment should contribute significant motion, agitation, or vibration beyond that which is due to the smoothly rotating paddle, and dissolved gases are to be removed from the dissolution medium if they change the dissolution results.

Results from commercial prednisone tablets can be influenced by minor variations in equipment alignment (4) and small differences in vessel curvature (5). Both of these conditions may cause systematic error among laboratories. Another possible source of error, recognized in the USP, is the effect of excess gas in the medium.

Two studies (6, 7) indicate that the USP calibrator tablets do not respond to certain variations in test conditions associated with Apparatus 2. Such lack of response normally would lead to the conclusions that the test is rugged, and that similar results for these tablets could be obtained among laboratories. However, the collaborative study results used to derive the acceptance ranges (3) show that similar results were not obtained among the laboratories.

Because the calibrator tablets respond only slightly to variations in test conditions, the purpose of the suitability test is not achieved. Comparisons of the responses of the USP calibrators and certain commercial prednisone tablets to variations in selected test conditions are presented in this paper.

EXPERIMENTAL

Apparatus and Samples—Two analysts, each using a separate commercial apparatus[2], performed the USP suitability test with 50-mg prednisone tablets[1] and 300-mg salicylic acid tablets[1]. A commercial 10-mg prednisone tablet, previously identified as Tablet 2 (5), was studied in a similar manner using the appropriate USP methodology (8).

Each analyst, working independently, adjusted the apparatus to conform to the USP test conditions as closely as practical. One analyst worked with an apparatus that possessed parallel shafts; the other worked with an apparatus known to have two shafts that were not parallel to the other four (4, 5). Although the shaft alignment in the vessels in these two positions differed from the shaft alignment in the vessels in the other four positions, the apparatus could be adjusted to pass the USP requirements.

Six tablets from each of the three samples were tested. A third analyst measured the absorbances of the filtered aliquots, thus minimizing systematic error in this step of the test. These results became a benchmark to which other results were compared; benchmark results were obtained before and after test conditions were varied.

Variations in Test Conditions—Selected test conditions were changed from the USP requirements, one at a time. Six additional tablets from each sample were tested after each change.

Paddle Rotation—The motor drive was operated at least 15 min to allow it to stabilize. The drive was then adjusted to give the desired number of revolutions in 60 (+1, −0) sec by manual count and use of a stopwatch. The rotational speed was again measured after the aliquots were obtained and filtered. In this way the benchmark results were obtained at 50 (± 0.8) and 100 (± 1.6) rpm. For comparison, data were also obtained at 54 (± 0.9) and 108 (+ 3.3, − 1.8) rpm.

[1] USP–NF reference standards (prednisone, Lot F; salicylic acid, Lot G), U.S. Pharmacopeial Convention, Inc., Rockville, MD 20852.

[2] Model 72RL, Hanson Research Corp., Northridge, CA 91324.

0022-3549/83/0800-0910$01.00/0

Table I—Response of USP Nondisintegrating Calibrator Tablets [a] to Changes in Test Conditions [b]

Test Condition [c]	50 rpm [d]				100 rpm [d]			
	Analyst 1		Analyst 2		Analyst 1		Analyst 2	
	Mean	*SD*	Mean	*SD*	Mean	*SD*	Mean	*SD*
Benchmark [e]	15.9	2.3	15.2	2.0	21.0	1.2	21.2	1.1
A	16.6	1.4	16.1	1.7	20.6	0.8	21.0	1.2
B	16.5	1.8	15.6	0.8	19.9	0.6	21.0	0.8
C	19.2	2.1	16.9	2.7	20.0	0.8	20.1	1.0
D	17.2	2.1	17.2	1.2	20.2	0.8	21.2	0.9
E	18.5	3.2	19.3	2.4	21.5	1.2	22.2	0.3
F	18.3	2.7	16.0	1.7	20.2	0.7	20.3	1.8
G	16.1	1.6	14.9	0.7	19.5	1.4	20.6	1.7
H	16.9	1.5	16.6	0.8	23.4	1.8	23.1	1.3
I	15.7	1.6	18.8	3.0	20.4	0.6	20.6	1.4
J	—	—	18.7	1.4	—	—	20.7	1.3
Benchmark [f]	17.0	3.4	16.9	3.1	20.1	1.1	21.5	1.3

[a] Salicylic acid, 300 mg, Lot G. [b] Expressed in percent of label claim; $n = 6$. [c] (A) 54 or 108 rpm; (B) irregular glass vessels; (C) paddle rotating before tablet dropped; (D) vessel axis displaced 2 mm from paddle axis; (E) vessel axis displaced 4 mm from paddle axis; (F) nonvertical shafts (test 1); (G) nonvertical shafts (test 2); (H) medium not deaerated; (I) paddle depth 2.0 cm; (J) probe present throughout test. [d] Except results obtained under test condition A. [e] Obtained before any variation in test conditions. [f] Obtained after variations in test procedures were completed.

Table II—Response of USP Disintegrating Calibrator Tablets [a] to Changes in Test Conditions [b]

Test Condition [c]	50 rpm [d]				100 rpm [d]			
	Analyst 1		Analyst 2		Analyst 1		Analyst 2	
	Mean	*SD*	Mean	*SD*	Mean	*SD*	Mean	*SD*
Benchmark [e]	68.8	1.5	67.2	3.1	76.7	1.2	74.6	1.1
A	71.9	0.7	68.5	1.4	77.0	1.2	76.0	0.8
B	69.1	1.0	64.3	2.9	75.7	2.0	75.4	1.2
C	68.6	3.1	67.4	2.3	77.6	0.8	74.4	1.2
D	67.7	1.9	65.8	1.1	77.6	0.9	74.6	1.1
E	70.4	0.9	68.8	1.2	78.7	1.1	75.9	0.8
F	69.6	1.3	69.2	1.3	77.9	1.5	75.0	1.7
G	69.3	0.7	68.0	1.2	79.6	0.8	75.5	0.9
H	67.3	1.5	64.6	3.3	74.8	1.5	73.4	0.6
I	70.2	1.2	66.6	1.0	76.8	1.3	75.1	0.7
J	—	—	67.5	2.8	—	—	77.1	1.1
Benchmark [f]	69.3	1.4	67.3	1.2	77.6	1.0	75.9	1.2

[a] Prednisone, 50 mg, Lot F. [b] Expressed in percent of label claim; $n = 6$. [c] As in Table I. [d] Except results obtained under test condition A. [e] Obtained before any variation in test conditions. [f] Obtained after variations in test procedures were completed.

Vessels—Six plastic vessels[3] were used by each analyst to obtain the benchmark results. For comparison, one set of irregular glass vessels[4] was used by both analysts. The inside bottom curvatures of these glass vessels did not conform to USP specifications (5).

Tablet Immersion—For benchmark results, each tablet was allowed to sink to the bottom of the vessel before the clutch controlling the paddle rotation was engaged. Results for comparison were obtained with the tablet dropped into the vessel while the paddle was rotating.

Centering of Vessels—The tops of the plastic vessels were centered precisely around the paddle shafts when the benchmark results were obtained, using a specially designed centering tool (9). For comparison, results were obtained with each paddle shaft set either 2 or 4 mm from the center of the top of its vessel. To measure these offsets, an overlay of concentric circles 9.5, 13.5, 17.5, and 21.5 mm in diameter was placed over the centering tool with the innermost circle coinciding with the top of the hole in the centering tool. The tool was placed in the top of one of the centered, rigidly held vessels. The paddle shafts were inverted in the chucks of the dissolution apparatus drive head, and the drive head was repositioned until the paddle shafts were either 2 or 4 mm off-center with respect to the tops of the vessels.

Shaft Verticality—For benchmark conditions, the collars on the stand of the dissolution apparatus were adjusted to 136 mm between the bottom of the drive head and the top of the leveled base of the stand. This distance was chosen because it equals the distance from the top of the stand base to the bottom of the paddles when the paddles are set 2.5 cm above the bottom of the plastic vessels. To facilitate measurements, the paddles were inserted in their inverted (paddle at the top) positions. The drive head was adjusted until a torpedo level (bubble indicators at right angles) placed on the paddle shafts showed that they were vertical. The shafts were then inserted in their normal (paddle down) positions, and the benchmark results were obtained.

Two tests were performed with nonvertical shafts. In the first (test 1), the equipment was misaligned so that each paddle shaft intersected the vertical axis of its vessel at the top of the vessel and was displaced 2 mm from the vertical axis 2.5 cm from the bottom of the vessel. For the second (test 2), the equipment was misaligned so that the paddle shaft axis was displaced 2 mm to the front of the vertical axis of the vessel at the top of the vessel and 2 mm to the rear of the vertical axis 2.5 cm above the bottom of the vessel. Results of both misalignments were compared to the benchmark results.

Deaeration of Media—Water from a commercial deionizer system was mist-sprayed[5] into a 19-liter (5-gallon) glass carboy under vacuum to obtain benchmark results for the prednisone calibrators. For the salicylic acid tablets, the prepared buffer was drawn by vacuum through a 30-mm coarse-porosity glass frit into a 19-liter glass carboy. For comparison, water taken directly from the deionizer system was used for the prednisone samples, and buffer, originally prepared in deionized water and then allowed to equilibrate with the atmosphere at room temperature, was used for the salicylic acid tablets. Both of the latter media released excess gas as bubbles at 37°.

Paddle Depth—The lower edge of the paddle was placed 2.5 cm above the bottom of the vessel as the benchmark and 2.0 cm above the bottom of the vessel for comparison.

Effect of Probes—All aliquots were taken manually with 50-ml syringes fitted with 4-mm o.d. glass tubes cut to lengths that allowed the aliquots to be taken from a standardized position (midway between the top of the medium and the top of the paddle blade and midway between the shaft and the wall of the vessel). For the benchmark condition, the tubes were inserted in the medium only as aliquots were obtained.

To assess the effect of probes, such as those often used with automatic analyzers, a 4-mm o.d. glass tube fitted with a filter tip[6] was placed in the vessel so that the filter was at the standardized position throughout the test. Otherwise, the aliquots were taken as described for the benchmark condition. Only one analyst collected data on the effect of probes in the medium because more thorough studies (10, 11) have been reported on commercial tablets.

Analysis of Commercial Tablets—The two analysts each tested five samples of 5-mg prednisone tablets from four manufacturers. Benchmark results were obtained as described above. Analyst 1 also obtained comparative results with the paddle shafts 2 mm off-center, while analyst 2 obtained comparative results by (*a*) substituting the set of irregular glass vessels for the plastic vessels and (*b*) using the dissolution medium containing excess gas instead of the deaerated dissolution medium.

RESULTS AND DISCUSSION

When possible, test conditions were varied in such a way to theoretically give a higher result: the rotational rate of the paddle was increased, not decreased, and the location of the paddle in the vessel was lower, not higher. The bottom curvature of the irregular glass vessels was flatter than that of a sphere. Any misalignment of the vertical axis of the paddle with that of the vessel tends to raise the results. Because it takes a finite time for motion from the paddle to produce motion in the liquid, dropping the tablet into the vessel with the paddle rotating tends to raise the results.

Whether air dissolved in the dissolution medium will influence test results is difficult to predict. Often, little or no effect is seen; but at times, the effect is dramatic. If the dissolution medium is not deaerated properly, small air bubbles are released from the medium during the test. These bubbles collect on all solid surfaces in contact with the medium, including the tablet or disintegrated tablet particles. Air bubbles adhering to the surface of tablet particles may act as a barrier between the solid drug and the medium. This tends to lower the dissolution results because the drug must contact the medium to dissolve.

Certain tablet products give disintegrated particles with a density such that the particles are lifted from the vessel bottom and circulated by the swirling medium in the absence of air bubbles. With such products the presence of air bubbles tends to lower the dissolution results due to the barrier effect. Furthermore, air bubbles attached to particles may synchronize the particle's motion with that of the medium; in this case, the

[3] Eli Lilly and Co., Indianapolis, IN 46206.
[4] Kimble Div., Owens-Illinois, Inc., Vineland, NJ 08360.
[5] Taken from a three-spray nozzle, available from Fogg-It Nozzle Co., San Francisco, CA 94116.
[6] Centaur Chemical Co., Stamford, CT 06902.

Table III—Response of Tablet 2 [a] to Changes in Test Conditions [b]

Test Condition [c]	50 rpm [d]				100 rpm [d]			
	Analyst 1		Analyst 2		Analyst 1		Analyst 2	
	Mean	*SD*	Mean	*SD*	Mean	*SD*	Mean	*SD*
Benchmark [e]	37.9	3.0	36.2	5.0	79.8	3.1	80.9	6.2
A	41.9	3.0	39.7	5.4	83.6	1.6	82.8	8.3
B	34.8	1.8	35.4	2.1	86.5	5.2	90.6	4.0
C	39.3	1.9	38.8	3.0	78.2	3.7	78.5	6.1
D	40.2	4.0	41.6	4.8	86.8	4.1	88.5	1.7
E	45.7	3.1	45.7	3.3	92.8	1.7	90.3	2.1
F	37.3	4.5	34.9	3.2	78.8	8.2	76.6	7.6
G	37.6	4.6	39.5	5.7	81.6	8.2	80.2	6.3
H	83.0	4.2	83.2	3.9	96.0	1.7	96.4	0.8
I	37.2	2.0	34.6	4.0	80.9	3.9	80.8	5.8
J	—	—	41.2	4.2	—	—	90.9	2.8
Benchmark [f]	34.9	2.5	34.3	5.1	78.2	2.3	75.4	8.0

[a] Prednisone, 10 mg. [b] Expressed as percent of label claim; $n = 6$. [c] As in Table I. [d] Except results obtained under test condition A. [e] Obtained before any variation in test conditions. [f] Obtained after variations in test procedures were completed.

concentration gradients near the particles could increase, also lowering the dissolution results.

Other tablet products disintegrate into particles of sufficient density to collect in a compact, cone-shaped mass on the bottom of the vessel in a region of relatively low liquid agitation. If the density of the tablet particles is changed sufficiently by the presence of air bubbles, the aggregate of particles on the vessel bottom is disrupted and more particles are lifted into regions of higher liquid agitation. Considered alone, this effect raises the dissolution results because more particles are brought into contact with more liquid in a given time. In practice, however, the net result of this effect plus the barrier effect is observed for such products.

The mean results of the USP calibrator tablets change only slightly with variations in individual test conditions (Tables I and II). If a variation in test conditions truly affects the dissolution behavior of these tablets, a bias will be present in the results at both 50 and 100 rpm. Statistical techniques suggested by Steiner (12) were used to analyze the mean results.

The means obtained by each analyst at each rotational rate were ranked from low to high, without the results obtained when probes were present in the dissolution medium. The ranks of all mean results obtained under the particular test conditions (specified in Tables I and II) were summed. The rank sums were then compared with values representing upper and lower limits that would not be exceeded by chance at the 95% confidence level.

When the means obtained from the salicylic acid tablets (Table I) were analyzed by this technique, it was found that a small upward bias may have existed in the results when the USP tolerance for centering was doubled (test variation E). The statistical test gave a borderline result at the 95% confidence level. The means obtained by test variation E were removed, and the means remaining in the table were ranked a second time. The remaining test variations did not give a consistent bias to the results. Individual means were then tested for bias. The means obtained by test variation H at 100 rpm were found to be significantly high at the 95% confidence level. Thus, air bubbles accumulating on the tablets produced a small bias in the results at 100 rpm, but not at 50 rpm.

When the means obtained from the USP disintegrating calibrator tablets (Table II) were ranked and the ranks were summed across the table, test variation H was found to produce a downward bias. Thus, air bubbles accumulating on these tablets lower the dissolution results. After the means from test variation H were removed, no consistent bias was found for the other test variations. No individual means were found to contain a bias significant at the 95% confidence level.

The means obtained from Tablet 2 (Table III) were analyzed in a similar manner. The means obtained under the last benchmark conditions were found to have a downward bias, and test variation H was found to produce an upward bias. After these means were removed, test variation E was found to produce an upward bias, test variation D produced a high bias with borderline significance at the 95% confidence level, and test variation A produced a high bias. No consistent bias was found for the remaining means obtained under the first benchmark conditions and test variations B, C, F, G, and I. When these means were analyzed individually, the two means obtained from test condition B at 100 rpm were found to be significantly high at the 95% confidence level. Thus, a bias is produced in the results from Tablet 2 by not deaerating the medium, by not centering the paddles in the vessels, by doubling the USP tolerance for rotational rate of the paddle, and, at 100 rpm, by using glass vessels with flattened bottom curvatures. The magnitude of the bias is large when there is excess gas present in the medium. The magnitude of the bias is noticeable when the USP tolerance for centering is doubled and, at 100 rpm, when the paddles are shifted 2 mm from the vessel centers. The bias from the glass vessels is noticeable at 100 rpm.

Probes, used in many laboratories to take aliquots automatically, can influence the dissolution results of tablets (10, 11). The USP calibrator tablets do not respond noticeably to changes in the hydrodynamics of the test generated by the probes (Tables I and II).

Five samples of 5-mg prednisone tablets from four manufacturers were subjected to selected changes in test conditions (Table IV). Analyst 1 used an apparatus previously described (4) and discussed (5). Because the paddle shafts in positions 4 and 6 were not parallel to the other four shafts, tablets from each of the samples gave higher results in these two positions. All shafts in the apparatus used by analyst 2 were parallel. This difference in equipment is the major cause of the differences between the benchmark results collected by the two analysts. The response to changes in test conditions is considerably greater for the commercial tablets than for the calibrator tablets. These commercial tablets fail the USP dissolution test when the test is performed under benchmark conditions, but may easily pass the test when the conditions are only slightly altered.

The official acceptance ranges for the USP calibrator tablets are based on results of collaborative studies (Table V) that involved 20 laboratories (3). Two independent studies of the 50-mg prednisone tablets at 50 rpm have also been reported—one by 5 (6) and the other by 11 FDA laboratories (13).

The official ranges show considerable overlap: the equipment could give identical results at 50 and 100 rpm and yet pass the requirements. This paradox arises from the large systematic errors of unknown origin among the 20 collaborating laboratories. However, only a small part of the wide spread in collaborative results can be ascribed to malfunctioning equipment (Tables I and II).

The official ranges are much too wide. According to the USP calibrators and ranges, the equipment used to collect the data in Tables I–IV is suitable for use, even when the measurable official tolerances (rotation and geometry) are exceeded. Narrowing the official calibrator ranges will not help, however, because the USP calibrators do not respond to the variables of interest (Tables I and II).

Tablet 2 has been used in several FDA laboratories as a performance standard for Apparatus 2, complementing, but not replacing, the USP calibrators. The acceptance ranges for Tablet 2 (Table V) were derived from a collaborative study by 11 FDA laboratories (13). Although Tablet 2 shows excellent sensitivity to excess gas in the dissolution medium, it does not respond adequately to irregularities in vessel curvature or to equipment misalignment. Nevertheless, Tablet 2 often has revealed subtle differences among sets of dissolution equipment that appeared equivalent when tested with the USP calibrators.

Roles of Disintegration and Density—Tablets that do not disintegrate during the test usually show little response to malfunctioning equipment or excess gas in the medium. Tablets that disintegrate within 2–3 min and give disintegrated particles that are lifted and circulated throughout the medium are usually immune to minor variations in equipment alignment and vessel curvature. Tablets that disintegrate within 2–3 min into granules that remain on the vessel bottom are likely to respond to such minor variations and, thus, are candidates as calibrators for the test.

Tablet Position Effect—The behavior of a tablet that disintegrates after 5–7 min is influenced by its position in the vessel[7]. If such a tablet settles at the center of the vessel, it will take longer to disintegrate and will exhibit a slower dissolution rate than a similar tablet that settles some distance away from the center. The latter tablet will disintegrate faster, and the disintegrated tablet material will be pulled toward the center by the circular liquid flow generated by the rotating paddle. For prednisone tablets of this nature, differences of 10–20% of label claim are commonly seen among the dissolution results of individual tablets. If the tablets settle at widely different locations in the dissolution vessels, the mean result will be higher than it should be and the standard deviation will be large. The wide range of results usually is blamed on the "inherent standard deviation" of the tablets when, in fact, it is due to the scattered positions of the tablets at the start of the test. The two samples of tablets from manufacturer B (Table IV) take from 10–15 min to disintegrate and exhibit this position effect. Ideally such tablets should be positioned at

[7] This effect has also been observed in Food and Drug Administration laboratories in Chicago, Ill., and Winchester, Mass.

Table IV—Response of Commercial 5-mg Prednisone Tablets to Changes in Test Conditions [a]

Condition [c]	Manufacturer A Mean	A SD	B_1 [b] Mean	B_1 SD	B_2 Mean	B_2 SD	C Mean	C SD	D Mean	D SD
Benchmark [d]	68.4	12.2	69.2	16.3	77.2	14.7	75.3	7.5	79.7	5.4
Benchmark [e]	70.8	5.3	64.6	9.0	71.0	7.2	74.0	4.2	76.4	4.3
B [e]	76.3	8.0	77.6	13.3	80.3	11.9	82.5	10.7	82.5	6.3
D [d]	88.0	3.5	94.2	2.3	95.8	2.9	90.4	3.0	87.0	3.2
H [e]	98.9	1.4	97.2	1.7	95.7	2.1	97.3	1.6	95.5	2.7

[a] Expressed in percent of label claim; $n = 6$. [b] Two different lots from manufacturer B were used. [c] As in Table I. [d] Performed by Analyst 1. [e] Performed by Analyst 2.

the bottom of the vessel at the start of each test. Tablets whose results depend on their initial position in the vessel should not be considered as potential calibrators.

Role of Calibrators—The ideal calibrator is easily defined, but has yet to be found. It should warn of incorrect shaft-rotation speed, equipment misalignment, irregularities in vessel curvature, *etc.* The calibrator results must leave no doubt about equipment suitability. A reproducible way to manufacture the calibrator must exist so that it may be distributed widely. These requirements will not soon be met. A simple suitability test for correct equipment setup is highly desirable, but its benefits may be outweighed by the expense of developing and manufacturing the required calibrator.

Meanwhile, most of the requirements for suitability of equipment can be met without using calibrator tablets. Alignment of equipment can be ensured by careful measurement with centering tools, calipers, and bubble levels. Uniform vessels are available. Control of shaft-rotation speed and temperature is trivial. Drug manufacturers can easily test whether deaerating the media influences the results for their products.

CONCLUSIONS

Large systematic errors existed among the laboratories that contributed the data from which the USP acceptance ranges for the official calibrators were derived. The sources of these errors are unknown; however, the USP calibrators do not warn of common equipment malfunctions. Thus, the USP suitability test cannot ensure correct equipment operation.

The general chapter on dissolution testing in the USP recognizes many of the test conditions that require control and gives an idealized concept of how the test is to be conducted. Unfortunately, control of equipment tolerances is not well defined in some cases and not fully adequate in others. The effect of changes in some of these equipment conditions on the dissolution results obtained from certain commercial tablets has been demonstrated.

Although equipment alignment and shaft-rotation speed may be controlled with simple measurements, a calibrator tablet is very useful when checking for test conditions that are difficult to measure (*e.g.*, excess gas) or that require sophisticated equipment (*e.g.*, vibration). One cannot rely totally on calibrator tablets to establish that the dissolution test conditions remain unchanged from day to day unless these requirements are met: (*a*) the tablets must respond to changes in critical test conditions, (*b*) the tablet response must be measured under rigidly controlled and well-defined test conditions, and (*c*) an acceptance range must be established within which variations in results due to minor fluctuations in test conditions can safely be ignored.

Table V—Acceptance Ranges for Tablets Used in the Apparatus 2 Suitability Test

Tablet	rpm	Acceptable Range of Means [a]	Maximum Acceptable *SD* [a]
Salicylic acid	50	14.1–22.5	3.7
Lot G [b]	100	17.6–30.0	3.7
Prednisone, 50 mg	50	56.6–77.0	4.5
Lot F [b]	100	67.9–84.3	3.2
Lot F [c]	50	63.1–73.2	3.3
Lot F [d]	50	62.4–69.8	4.1
Tablet 2 [d]	50	32.5–45.3	5.9

[a] Expressed in percent of label claim; $n = 6$. [b] Basis for official USP values, derived from results collected by 20 Pharmaceutical Manufacturers Association laboratories (3). [c] Derived from results collected by 5 FDA laboratories (6). [d] Derived from results collected by 11 FDA laboratories (13).

REFERENCES

(1) "The United States Pharmacopeia," 20th rev., United States Pharmacopeial Convention, Rockville, Md., 1980, p. 959.

(2) *Pharmacopeial Forum*, **4**, 120 (1978).

(3) A. C. Sarapu, A. R. Lewis, and M. F. Grostic, *Pharmacopeial Forum*, **6**, 172 (1980).

(4) D. C. Cox and W. B. Furman, *J. Pharm. Sci.*, **71**, 451 (1982).

(5) D. C. Cox, C. E. Wells, W. B. Furman, T. S. Savage, and A. C. King, *J. Pharm. Sci.*, **71**, 395 (1982).

(6) D. J. Schuirmann, *Pharmacopeial Forum*, **6**, 75 (1980).

(7) K. D. Thakker, N. C. Naik, V. A. Gray, and S. Sun, *Pharmacopeial Forum*, **6**, 177 (1980).

(8) "The United States Pharmacopeia," 20th rev., United States Pharmacopeial Convention, Rockville, Md., 1980, p. 655.

(9) A. A. Serino, *J. Pharm. Sci.*, **71**, 725 (1982).

(10) C. E. Wells, *J. Pharm. Sci.*, **70**, 232 (1981).

(11) T. S. Savage and C. E. Wells, *J. Pharm. Sci.*, **71**, 670 (1982).

(12) W. J. Youden and E. H. Steiner, "Statistical Manual of the Association of Official Analytical Chemists," Association of Official Analytical Chemists, Washington, D.C., 1975, pp. 74–76.

(13) D. C. Cox and W. B. Furman, *J. Pharm. Sci.*, in press.

ACKNOWLEDGMENTS

The authors thank John C. Black for constructing the overlay of concentric circles.

Radioimmunoassay of the Immunomodulator *erythro*-9-(2-Hydroxy-3-nonyl)-hypoxanthine in Human Serum and Urine

E. H. PFADENHAUER ˣ, C. E. JONES, and K. W. MAXWELL

Received April 5, 1982, from *Newport Pharmaceuticals International, Inc., Newport Beach, CA 92660.* Accepted for publication July 30, 1982.

Abstract □ A radioimmunoassay was developed for the measurement in human serum and urine of *erythro*-9-(2-hydroxy-3-nonyl)-hypoxanthine. Antisera were produced in rabbits by immunization with an *erythro*-9-(2-hydroxy-3-nonyl)-hypoxanthine hemisuccinate–bovine serum albumin conjugate. The competitive antigen was *erythro*-9-(2-hydroxy-3-nonyl)-hypoxanthine labeled with carbon-14 on the purine ring. Cross-reactivities were measured against three metabolites and the naturally occurring purine bases inosine and hypoxanthine. Sensitivity of the method was 1 ng/ml in serum and 10 ng/ml in urine. Precision at clinical levels was ±15% in serum at 2 ng/ml and ±3% in urine at 200 ng/ml.

Keyphrases □ *erythro*-9-(2-Hydroxy-3-nonyl)-hypoxanthine—immunomodulator, quantitation in human serum and urine by radioimmunoassay □ Radioimmunoassay—of *erythro*-9-(2-hydroxy-3-nonyl)-hypoxanthine, quantitation in human serum and urine □ Immunomodulators—*erythro*-9-(2-hydroxy-3-nonyl)-hypoxanthine, quantitation by radioimmunoassay, human serum and urine

A considerable amount of interest in the academic and industrial community is currently being directed at the emerging discipline of immunopharmacology. The cellular immunological component of this pharmacological category includes both natural and synthetically derived substances with biological activity. Paramount among the former category are the thymic hormones (1), bacterial agents [BCG (2), *Corynebacterium parvum* (3)], transfer factor (4), and interferon (5). Levamisole (6), inosiplex (7), krestin (8), and interferon inducers (5) are examples of synthetic entities that possess a number of interesting immunomodulatory properties that have been defined in both *in vitro* and *in vivo* systems.

erythro-9-(2-Hydroxy-3-nonyl)-hypoxanthine[1] (I) is an immunopharmacologically active substance (9, 10) which is intended for use in the treatment of acquired or genetically determined deficiencies in cell-mediated immune function. Since the minimum effective dose of this compound was relatively small (0.01 mg/kg), serum and urine levels were expected to be correspondingly low. Initial analytical development, utilizing high-performance liquid chromatographic (HPLC) reverse-phase techniques and UV detection, indicated a lower limit of detectability on the order of 0.5 μg/ml in plasma. The detectability in urine, however, was even less sensitive due to interferences from normal urine constituents. Extractive procedures using various organic phases were of limited utility in improving the levels of detectability.

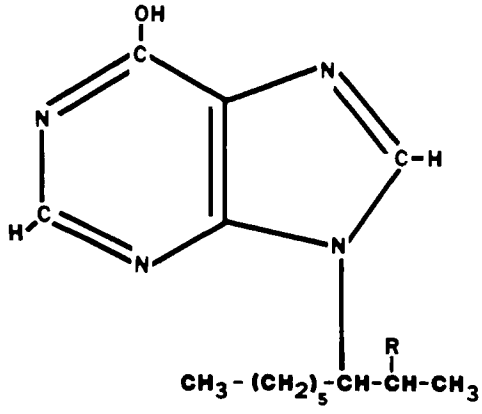

I: R = OH
II: R = $CO_2(CH_2)_2COOH$
III: R = $CO_2(CH_2)_2CONH$-Albumin

This paper describes a radioimmunoassay (RIA) for I. The assay is of sufficient specificity and sensitivity to determine relevant pharmacological parameters (*e.g.*, bioavailability, elimination, and absorption) at the expected therapeutic doses which would be used in clinical investigations.

EXPERIMENTAL

Chemicals and Materials—Reagent-grade solvents and chemicals were used except for the HPLC solvents, which were HPLC grade. Freund's adjuvant[2] (complete and incomplete) was purchased in sealed glass ampules. Bovine serum albumin[3] was RIA grade. Sodium [^{14}C]-formate[4] (99+% radiopure, specific activity 51 mCi/mm) was packaged in a glass ampule in 70% ethanol under a nitrogen atmosphere. *erythro*-5-Amino-4-chloro-6-(2-hydroxy-3-nonyl)-pyrimidine[5] contained 1.5% of the *threo* isomer. The *erythro*-9-(2-hydroxy-3-nonyl)-hypoxanthine used in these assays was reference standard grade, containing 0.2% of the *threo* isomer.

Chromatographic Systems—Preparative TLC was performed on 2-mm silica plates[6] using *n*-butyl alcohol–2 *N* ammonia (5:1) as a solvent (system A). TLC systems were silica[7] with *n*-butyl alcohol–acetic acid–water (4:1:2) (system B) and cellulose F-254 with isopropyl alcohol–water (4:1) (system C).

HPLC separations were carried out using a gradient liquid chromatograph[8], a 5-μm reverse-phase 250 × 4.6-mm column[9], and a detector[10] operating at 254 nm. The eluant used was typically 0.05 *M* H_3PO_4 in water–methanol (60:40) (system D).

Scintillation Counting—Radioactivity measurements were performed on a liquid scintillation counter[11]. An open channel was used for the carbon-14 counts. Scintillation fluid[12] (2.5 ml) was added to 15 × 45-mm glass vials containing the [^{14}C]protein precipitate from the urine assay. For the serum assay precipitate, 10 ml of cocktail was added to 21 × 68-mm glass vials.

Preparation of the Immunogen—*Synthesis of Erythro-9-(2-hydroxy-3-nonyl)-hypoxanthine Hemisuccinate (II)*—Compound I (300

[1] NPT 15392.

[2] Grand Island Biological Co., Grand Island, N.Y.
[3] Sigma Chemical Co., St. Louis, Mo.
[4] Rosechem Products, Los Angeles, Calif.
[5] Dr. A. Giner-Sorolla, Sloan-Kettering Institute for Cancer Research, Rye, N.Y.
[6] Silica 60 F-254, E. Merck, Darmstadt, West Germany.
[7] Silica IB-F, J. T. Baker, Phillipsburg, N.J.
[8] Altex Model 332, Beckman Instruments, Irvine, Calif.
[9] Ultrasphere, Beckman Instruments, Irvine, Calif.
[10] Model LS-8000, Beckman Instruments, Irvine, Calif.
[11] Waters Associates, Milford, Mass.
[12] Aquasol, New England Nuclear, Boston, Mass.

0022-3549/83/0800-0914$01.00/0

Table I—Recoveries of I from Human Serum

Amount of I Added, ng/ml	Estimated I Recovered, ng/ml						Mean	CV^b, %
	A[a]	B	C	D	E	F		
1	1.0	0.8	0.5	1.1	1.1	1.2	0.95	27.2
2	2.3	2.2	1.8	1.9	1.5	1.9	1.93	14.9
5	4.2	4.5	3.4	4.8	4.2	5.0	4.35	13.0

[a] Individuals providing serum samples. [b] Coefficient of variation for six individual observations.

mg) and succinic anhydride (2 g) were dissolved in 4 ml of pyridine. The mixture was stirred overnight at 40°. The pyridine was removed under reduced pressure, and the residue was dissolved in a minimum amount of ethanol. Concentrated ammonium hydroxide was added until precipitation ceased. The supernatant was removed, and the precipitate was washed three times with small volumes of ethanol. The supernatant and ethanol washes were pooled and applied to chromatographic system A. After a 15-hr development, the major UV-absorbing band at R_f 0.34 was isolated and eluted with 15 ml of ethanol. This elution was repeated three times. The ethanol was removed under reduced pressure, and the residue was dissolved in 50% ethanol–water prior to ultrafiltration[13]. The solvent was again removed under reduced pressure to give 124 mg (30% yield) of the hemisuccinate II. The identity of II was confirmed by base hydrolysis (1 *N* NaOH, 70° for 1 hr), which gave total conversion to the parent compound, I.

Preparation of the Bovine Serum Albumin Conjugate (III)—A solution of bovine serum albumin (23 mg) in 1.5 ml of water was stirred and room temperature and the pH was adjusted to 5.5 with a dilute sodium hydroxide solution. The hemisuccinate II was added (11 mg in 0.5 ml of water) and the pH was readjusted to 5.5. 1-Cyclohexyl-3-(2-morpholinoethyl)-carbodiimide metho-*p*-toluenesulfonate (21 mg) was added to the aforementioned solution and the resulting turbid mixture was stirred overnight at room temperature. The suspension was removed and dialyzed against phosphate-buffered saline at 4°. The dialysate was changed frequently.

The product was characterized in the following manner:

1. An aliquot of the product was ultrafiltered, and the ultrafiltrate was analyzed by system D for I. Only a trace amount was found.
2. The ultrafiltrate was hydrolyzed with base and then analyzed for I. Again, only a trace amount of the drug was found.

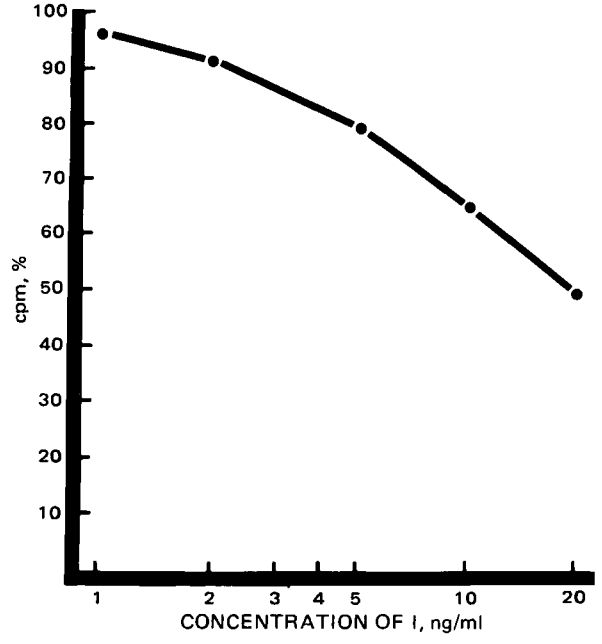

Figure 1—*Serum RIA standard curve. Known amounts of I were added to control serum at 0, 1, 2, 5, 10, and 20 ng/ml, the RIA was carried out, and the percent cpm was calculated. Percent cpm was defined as cpm sample ÷ cpm control (×100).*

[13] CF-50 Membrane Cone, Amicon Corp., Lexington, Mass.

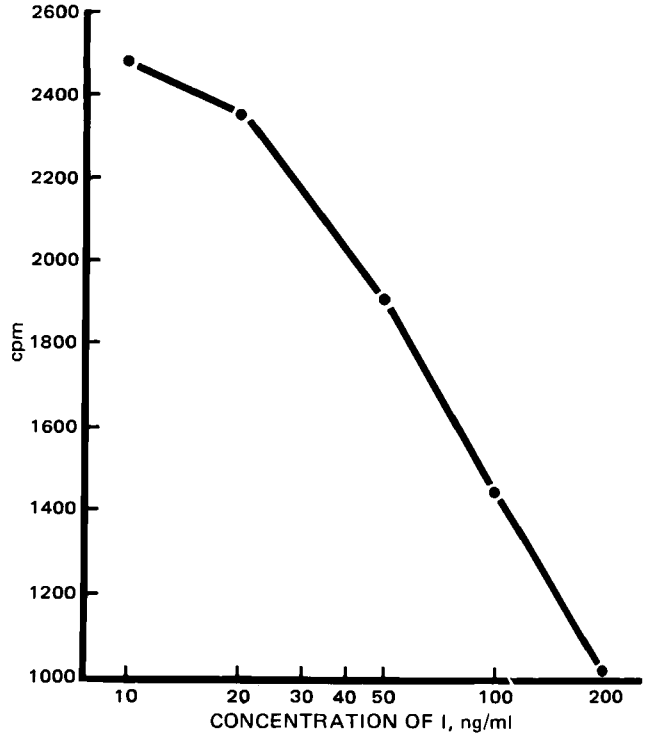

Figure 2—*Urine RIA standard curve. Known amounts of I were added to water at 10, 20, 50, 100, and 200 ng/ml, and the RIA was carried out as described in the text.*

3. An aliquot of the product was hydrolyzed with base and ultrafiltered. A large amount of I was found in the ultrafiltrate, corresponding to 4.21 μmoles or ~13 molecules bound to a molecule of bovine serum albumin in the product.
4. Base hydrolysis of bovine serum albumin alone did not interfere with the HPLC assay. The results of the first two experiments indicated only small amounts (<1 μg) of I and II were present in the product. Two other coupling agents used under various conditions did not yield a conjugate. Agents found not to be effective were 1-ethyl-3-(3-dimethylaminopropyl)-carbodiimide and *N*-ethyl-5-phenylisoxazolium-3′-sulfonate.

The conjugate (III) was diluted with sterile phosphate-buffered saline to a final concentration of 1 mg/ml and frozen in aliquots. It was determined by the aforementioned HPLC procedure that a freeze–thaw cycle did not alter the integrity of the conjugate.

Immunization—The solution of III was thawed and emulsified thoroughly with an equal volume of Freund's complete adjuvant. Subcutaneous injections of the emulsion (1.6 ml) were made to the back area of each of four New Zealand White rabbits. After 3 weeks, a second injection was administered with incomplete Freund's adjuvant. Four weeks after the second injection, all rabbits showed a workable titer of antibodies to I. Blood was removed from the ear vein, allowed to clot at room temperature for 1 hr, and stored overnight at 4°. The serum was removed and used in the RIA. Periodic booster shots of the original preparation of III were administered to the rabbits for over 1 year, and each time the antiserum titer showed a anamnestic (2-week) rise to original levels.

Preparation of [8-^{14}C]*erythro*-9-(2-Hydroxy-3-nonyl)-hypoxanthine (IV)—The 70% ethanol solvent was removed under reduced pressure from sodium [^{14}C]formate (5 mCi, 51 mCi/mm). The sodium [^{14}C]formate was then dissolved in 100 μl of phosphoric acid, and an excess of *erythro*-5-amino-4-chloro-6-(2-hydroxy-3-nonylamino)-pyrimidine (55 mg) was added with vortexing. The reaction was heated at 95–100° in an oil bath for 4 hr, and then cooled. Methanol (300 μl) and then concentrated ammonium hydroxide (180 μl) were added with vortexing. This solution was applied to system A and developed overnight. The UV-absorbing band corresponding to I (R_f 0.51) was isolated and eluted into 175 ml of methanol. Analysis by HPLC (system D) determined a chemical purity of 97.9% IV, which contained 1.4% of the *threo* isomer; yield was 13.7 mg of IV (50%). Radiochemical purity analyses using the same system showed 96.5% of IV and 1.6% of the *threo* isomer. Analyses in systems B and C revealed 99.6 and 98.6% overall radiopurity, respectively. The TLC systems were unable to resolve the *threo* isomer.

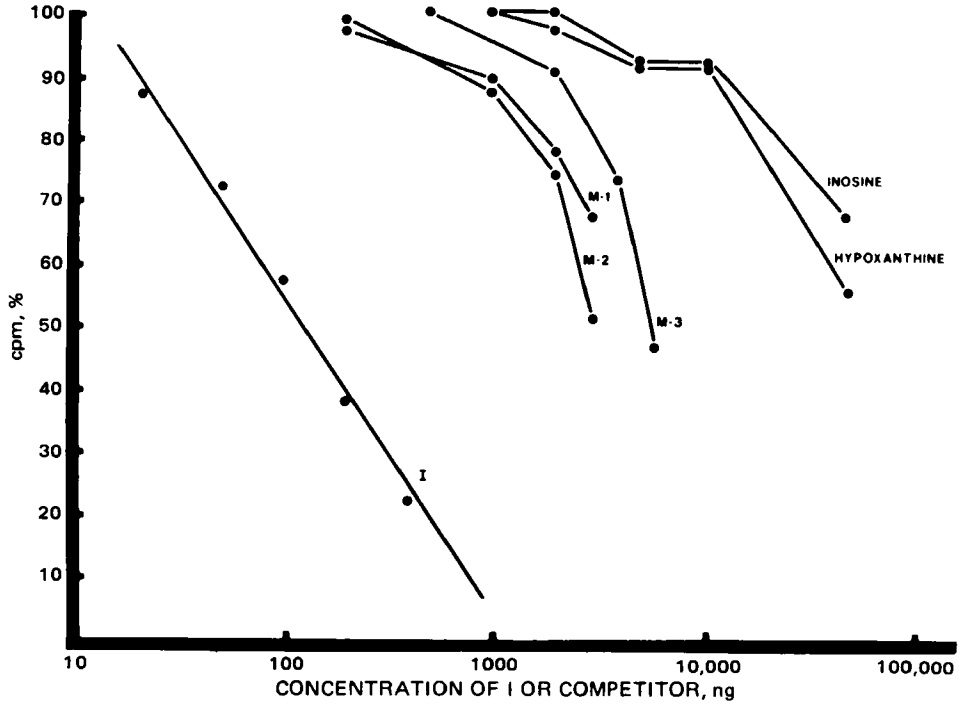

Figure 3—*RIA competition curves for the drug (I), three of its metabolites (M-1, M-2, M-3), inosine, and hypoxanthine. The serum RIA was carried out as described, and either I, a metabolite, inosine, or hypoxanthine was added as a competitor.*

RIA from Human Serum—A stock solution of IV was prepared in water at an activity of ~2×10^7 dpm/ml. A stock solution of 0.5 *M* sodium phosphate buffer, pH 7.5, was also made.The assay mixture was prepared by mixing 1.6 μl of stock solution IV, 2 ml of buffer, 50 μl of antiserum, and diluting to a final 10 ml volume. This mixture was freshly prepared and used immediately. In practice, the antiserum was diluted to give a total binding of IV in the presence of control serum of 70%.

The assay mixture (1 ml) was added to 2 ml of serum, and each sample was run in duplicate. Standards of I were prepared in serum at 0, 1, 2, 5, 10, and 20 ng/ml (also in duplicate) and analyzed concurrently. The solutions were thoroughly mixed and allowed to incubate overnight at 4°. After warming to room temperature, saturated ammonium sulfate was added slowly with vortexing to a final dilution of 40% saturation. The precipitate was allowed to stand 5 min, then centrifuged. The supernatant was aspirated, and the precipiate was washed with 1 ml of 50% saturated ammonium sulfate. Water (0.5 ml) was used to dissolve the precipitate, and the radioactivity (in cpm) was measured.

Quantitation of the amount of drug present in serum was determined from a standard curve of percent cpm *versus* ng/ml of I added. Percent cpm for a given sample was calculated by dividing the sample cpm by the control cpm and multiplying by 100. A typical standard curve is illustrated in Fig. 1.

RIA from Human Urine—The assay mixture was identical to that for the serum RIA except human control serum was also added (ml serum per 10 ml assay mixture) to ensure adequate levels of precipitable protein. To duplicate 1-ml urine samples, 2 ml of ethyl acetate was added; this was vortexed over a 5-min period. Duplicate standards of 0, 10, 20, 50, 100, and 200 ng/ml of I in water were prepared, extracted, and run concurrently. One milliliter of the top layer was removed, and the solvent was evaporated under a stream of nitrogen. The assay mixture (1.5 ml) was added and incubated at 4° overnight. After warming to room temperature, 1 ml of saturated ammonium sulfate was added slowly while vortexing. The precipitate was allowed to stand for 5 min, then centrifuged to a pellet. The supernatant was aspirated and discarded. Water (0.2 ml) was used to dissolve the precipitate, and the radioactivity (in cpm) present in the pellet was measured. Quantitation of the amount of drug present in the urine was derived from a graph of the standard curve of cpm *versus* ng/ml of I added. A typical standard curve is illustrated in Fig. 2.

Table II—Recoveries of I from Human Urine

Amount of I added, ng/ml	Estimated I Recovered, ng/ml					Mean	CV^b, %
	A[a]	B	C	D	E		
0	<10	<10	<10	<10	13		
10	10.5	23	12.5	8	24	15.6	47.4
20	14	32	21.5	11	39	23.5	50.5
50	41	63	51	56	66	55.4	18.0
100	112	112	108	103	120	111	5.6
200	205	210	202	215	220	210	3.5

[a] Individuals providing urine samples. [b] Coefficient of variation for five individual observations.

RESULTS AND DISCUSSION

The accuracy and precision of the immunoassays were evaluated and the results are given in Tables I and II. For the serum RIA, samples were collected from six untreated individuals, and I was added at levels of 1, 2, and 5 ng/ml. Control serum was also run for each individual. Percent cpm (cpm sample/cpm control × 100) was calculated, and the concentration of drug present (in ng/ml) was read from a graph of a standard curve. The standard curve was generated from similarly treated pooled human sera. Average recoveries in serum at levels of 1, 2, and 5 ng/ml were 95, 97, and 87%, respectively. Precision was directly related to the concentration. The coefficient of variation (*CV*) decreased from 27% at 1 ng/ml (the sensitivity of the assay) to 15% at 2 ng/ml and 13% at 5 ng/ml. The method clearly discriminates between control (blank) serum and drug-treated serum at low levels (1 ng/ml) and yields quantitatively acceptable results at higher levels.

Various statistical methods were attempted to improve the accuracy of quantitation in serum. These methods include linear regression of log ng/ml *versus* percent cpm and polynomial least-squares fit to ng/ml *versus* percent cpm. Simple graphical interpolation gave results comparable to the computer-generated data.

The serum RIA requires a control sample from each individual for the calculation of percent cpm. However, it was possible to obtain quantitative results without the control sample by a plot of cpm *versus* ng/ml of the standard and deriving the concentration from the uncorrected cpm of the sample. These results were considerably less accurate than those obtained from the percent cpm method, probably due to variable amounts of competing materials in the individual sera. The interference was not removed by solvent extraction or chemical or membrane deproteinization. Since control sera are generally available from pharmacological studies, their requirement is not a great limitation. A calculation of percent cpm was not necessary for the standard curve of the urine RIA. Acceptable results were obtained from a plot of uncorrected cpm *versus* ng/ml of I in water for the urine quantitation.

The urine RIA recovery data are given in Table II. For this study, urine from five individuals was sampled, and I was added at levels of 10, 20, 50, 100, and 200 ng/ml. Control urine was also analyzed for each individual. The assays were carried out over a period of several weeks, with each

individual being analyzed on a separate day using a concurrent standard curve. The urine assay standards of I were made in water, extracted, and treated identically to the urine samples.

Average recoveries of drug in urine at levels of 10, 20, 50, 100, and 200 ng/ml were 156, 118, 111, 111, and 105%, respectively. The high recovery values were due to small constant amounts of background in the normal urine (5–10 ng/ml) and were mostly due to two individuals (B and E). The interference, of course, becomes less important at higher drug levels (100–200 ng/ml). The precision also improves considerably at higher levels, ranging from a *CV* of 50% at 10–20 ng/ml to 3% at 200 ng/ml.

For the urine RIA, an extraction was necessary to increase the sensitivity level. Without an ethyl acetate extraction, a background of 50–100 ng/ml was present in control urine. The cause of this interference has not been determined. The highest background level noted in this study was in subject E at 13 ng/ml, which has subsequently been found to be the highest level observed in any normal urine examined. In every other normal urine assayed, the amount of interference was well below the lowest concentration on the standard curve (usually 10 ng/ml).

The specificity of the RIA was also investigated. Three metabolites of I, designated as M-1, M-2, and M-3, were isolated from rabbits. UV spectra of the metabolites indicated the purine base was unchanged, so the amount of metabolites could be estimated using the molar absorptivity of the parent compound. These metabolites and other possible competitors containing a similar purine ring (hypoxathine and inosine) were added to an assay in varying amounts and compared with the competitive effects of I (Fig. 3). Metabolite M-2 was the most effective competitor in the assay, having a cross-reactivity of 2–4%. Metabolite M-1 had a cross-reactivity of 1.5–2%, and M-3 was the least effective competitive metabolite at 0.8–2%. Hypoxanthine and inosine were cross-reactive at ~0.1%. Percent cross-reactivity was defined as the ng of I ÷ ng of competitor (×100) when each was at a level producing the same reduction in percent cpm.

The various rabbit antisera were screened for usability. Of the four immunized rabbits, the serum from one particular animal was extremely sensitive to changes in I. When used in the serum RIA, this rabbit's antiserum gave the curve illustrated in Fig. 1, whereas the other rabbits' antiserum produced no measurable reduction in percent cpm up to a drug concentration of 10 ng/ml. At some concentrations (2–10 ng/ml), the percent cpm actually significantly increased compared with the control. This effect has been noted in other systems and has been ascribed to increasing amounts of hapten producing a conformational change in the antibody, thus increasing its binding affinity (11).

Various approaches to assay optimization were used. Incubation times from 2 to 24 hr were explored. The shorter times were usable, but the 24-hr incubation time yielded the maximum slope (sensitivity) at lower concentrations. Reversing the order of the addition of IV and sample to the antiserum had no effect. The pH of the assay buffer was incrementally varied from 5 to 7.5, but binding remained constant throughout this range. Since hypoxanthine and inosine were slightly competitive in the assay and are present in normal plasma at a level of ~600 ng/ml (12) and ~200 ng/ml (13), respectively, the effect of their enzymatic removal from the serum was studied. Purine nucleoside phosphorylase, xanthine oxidase, and uricase were added to normal serum and compared by an RIA standard curve to the same untreated serum. There were no apparent differences between the standard curves generated.

Attempts to synthesize an ^{125}I-labeled derivative of I yielded apparently unstable products. Attachment of tyrosine or tyrosine methyl ester to II gave multiple UV-absorbing products by TLC analysis. Attachment of iodine-125 to tyrosine methyl ester, then conjugating the labeled ester to II also yielded multiple-labeled products. These products were isolated and tested in the RIA, but would not bind to the antiserum. Since the ^{14}C-labeled drug gave acceptable sensitivity and excellent chemical and radiochemical stability, neither iodine-125 or tritium labeling efforts were pursued.

The RIA described in this article has been used to assess serum and urine drug levels in human volunteers participating in a tolerance trial. Patients were administered a single oral dose of either 0.7, 3.0, or 9.0 mg of I. Assays were performed on 24-hr pooled urine collections and on serum at 2 hr postdose.

Urinary levels obtained after administration of 0.7 mg of I ranged from 64 to 290 ng/ml (n = 5); after 3.0 mg the range was 190 to 640 ng/ml (n = 7); and after 9.0 mg the range was 437 to 1425 ng/ml (n = 6). Urine samples were diluted with water when necessary to bring the drug concentration into the standard curve range. Corrections were made for urine volume, and the amount and percent of dose excreted were calculated (± standard deviation). From the 0.7-, 3.0-, and 9.0-mg dose groups, 196 ± 62 μg (28.0% of dose), 355 ± 102 μg (9.6% of dose), and 850 ± 241 μg (9.4% of dose) were excreted, respectively. The percentage of dose excreted unchanged from the 0.7-mg group is significantly higher than the other two groups (ANOVA, $p < 0.001$).

The 2-hr postdose serum levels were also analyzed from the three dosage groups. The 0.7-mg group attained a mean serum level of 1.24 ng/ml (n = 4), the 3.0-mg group a level of 5.43 ng/ml (n = 6), and the 9.0-mg group had an average level of 10.7 ng/ml (n = 4). The RIA techniques, therefore, appear to possess adequate sensitivity for their intended purpose.

REFERENCES

(1) R. H. Levy, N. Trainin, and L. W. Law, *J. Natl. Cancer Inst.*, **31**, 199 (1963).

(2) B. N. Halpern, G. Biozzi, G. Stiffel, and D. Mouton, *C. R. Seances Soc. Biol. Ses Fil.*, **153**, 919 (1959).

(3) A.-R. Prevot, J. Levaditti, O. Nazimov, and H. Thouvenot, *Ann. Inst. Pasteur*, **94**, 405 (1958).

(4) H. S. Lawrence, *J. Clin. Invest.*, **34**, 219 (1955).

(5) M. Ho and J. A. Armstrong, *Annu. Rev. Microbiol.*, **29**, 131 (1975).

(6) G. Renoux and M. Renoux, *C. R. Hebd. Seances Acad. Sci.*, **272**, 349 (1971).

(7) J. W. Hadden, E. M. Hadden, and R. G. Coffey, *Infect. Immun.*, **13**, 382 (1976).

(8) K. Nomoto, C. Yoshikumi, K. Matsunaga, T. Fujii, and K. Takeya, *Gann*, **66**, 365 (1975).

(9) J. W. Hadden, and J. Wybran, in "Advances in Immunopharmacology," J. W. Hadden, L. Chedid, P. Mullen, and F. Spreafico, Eds., Pergamon, New York, N.Y., 1981.

(10) S. Ikehara, J. W. Hadden, R. A. Good, D. G. Lunzer, and R. N. Pahwa, *Thymus*, **3**, 87 (1981).

(11) C. W. Parker, "Radioimmunoassay of Biologically Active Compounds," Prentice-Hall, Englewood Cliffs, N.J., 1976.

(12) E. H. Pfadenhauer, *J. Chromatogr.*, **81**, 85 (1973).

(13) E. H. Pfadenhauer and S. Tong, *J. Chromatogr.*, **162**, 585 (1979).

Improved Procedure for the Determination of Protein Binding by Conventional Equilibrium Dialysis

COLIN J. BRIGGS ˣ, JOHN W. HUBBARD, CATHERINE SAVAGE, and DIANE SMITH

Received October 7, 1981, from the *Faculty of Pharmacy, University of Manitoba, Winnipeg, Manitoba, Canada, R3T 2N2.* Accepted for publication July 30, 1982.

Abstract □ The binding of drugs to plasma proteins has been studied extensively using a variety of methods, including equilibrium dialysis. Published information on controls used in these studies is frequently inadequate; in other cases, there are deficiencies in the experimental design for the controls. A method is described that eliminates many of the problems associated with artifactual errors in dialysis studies. Multiple replicated controls are performed at the same time as the test, under identical conditions. The controls are used to correct for concentration-dependent binding of drug to the membrane or other equipment. The method was used to determine the binding of sulfadimethoxine to CF-IV-1 α-globulin at therapeutic concentrations. The level of binding was low (9–13%), but the stringent control technique permitted statistical analysis which showed each mean test value to be significantly different from its corresponding control. Furthermore, there was a linear relationship between the control-corrected percentage binding values and total drug concentration, whereas there was no correlation between total drug concentration and the uncorrected percentage binding values.

Keyphrases □ Equilibrium dialysis—measurement of low-level protein binding, elimination of artifactual error, multiple replicated controls □ Protein binding—low levels measured by equilibrium dialysis, use of multiple replicated controls to eliminate artifactual error, correction for concentration-dependent binding □ Sulfadimethoxine—binding to CF-IV-1 α-globulin at therapeutic doses, equilibrium dialysis with multiple replicated controls

The binding of drugs and xenobiotic agents to blood proteins is an important parameter in pharmacokinetic studies, since the extent and affinity of this binding influences distribution of the compound in the body (1, 2). The concentration of unbound drug in the plasma can affect rates of metabolism and elimination (3). Numerous qualitative and quantitative techniques have been used to study the interaction between drugs and macromolecules. Equilibrium dialysis is the classical procedure and remains the most popular method (4). In the conventional method, the drug–protein mixture is contained within a sealed tube of semipermeable membrane, with protein-free buffer solution outside the membrane. At equilibrium the concentration of drug in the dialysate equals that of the unbound drug inside the dialysis tube. If a suitable range of drug concentrations is used, it is also possible to determine the extent of binding, the binding constants, and the number of binding sites on an isolated pure protein (5). A comprehensive study also should include an appropriate range of protein concentrations to detect any differences in binding due to changes in protein concentration.

Good controls are essential in any dialysis study since many drugs bind to the semipermeable membranes and apparatus (6), reducing the apparent concentration of free drug. Other factors influencing the extent of binding measured include temperature (7, 8), pH (9), and variation in the physicochemical properties of the protein (10). Additional influences are those parameters inherent in the design of the experiment, such as the nature and concentration of proteins present (11) and the drug used. Artifactual errors in the determination of protein binding can be minimized through adequate controls and consideration of experimental design. Literature reports of equilibrium dialysis studies for the determination of free drug concentrations are frequently deficient in details concerning the controls used.

All methods for determination of free drug concentrations in plasma, serum, or solutions of macromolecules at normal biological concentrations have some inherent problems that may influence the results (4). The most commonly used techniques involve separation of a fraction of the unbound drug from the bound component. One of the advantages of dialysis is that the free component retains access to the bound component when equilibrium is reached. Concentrations of free and bound drug are not affected to the same extent as in ultrafiltration, where a portion of the free drug is removed from the system. Ultrafiltration also results in some concentration of the protein solution, which may influence the binding (12).

Inadequacy of controls is a major contributor to the variations found in binding studies reported in the literature. Nonspecific adsorption to the semipermeable membrane is a problem in the dialysis of many compounds (13). The extent of adsorption to membranes is frequently <10% of the total drug present, but may exceed 50% (6) and vary according to the method of preparation and storage of the membrane (14). It can occur with all types of membrane and is a source of potential error in free drug determination. Nevertheless, a commonly used technique is to run limited preliminary controls which are used to generate a correction factor to be applied to all subsequent results obtained with solutions containing protein (15). In many cases, the binding to apparatus and membranes is considered negligible. But variations in these losses may become highly significant when working at low concentrations such as those encountered with many drugs at therapeutic doses. Furthermore, the variability in results obtained with conventional dialysis procedures often

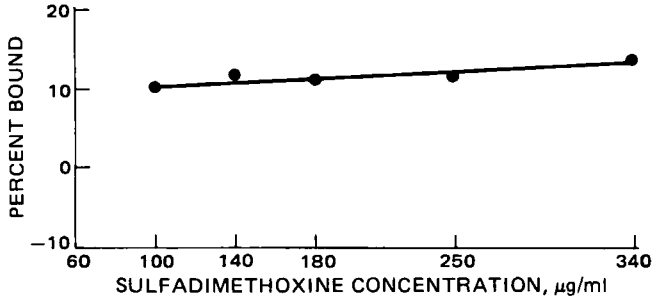

Figure 1—*Plot of percentage binding* versus *concentration of sulfadimethoxine. Percentage binding values are calculated directly from the optical density mean values shown in Table I.*

0022-3549/83/0800-0918$01.00/0

Table I—Percentage Protein Binding of Sulfadimethoxine Calculated Directly from the Mean Optical Density Values (First Method) [a]

Initial Concentration, μg/ml	Mean Optical Density		Protein Binding, [b] %
	Control (Y_c)	Test (Y_t)	
100	0.3783 ± 0.0025	0.3394 ± 0.0041	10.28 ± 1.09
140	0.5338 ± 0.0066	0.4710 ± 0.0082	11.76 ± 1.54
180	0.7170 ± 0.0129	0.6378 ± 0.0096	11.05 ± 1.33
250	1.049 ± 0.0051	0.9276 ± 0.0084	11.57 ± 0.80
340	1.452 ± 0.0080	1.253 ± 0.0094	13.71 ± 0.65
	r = 0.9997	r = 0.9994	r = 0.8811

[a] Expressed as mean ± SE; n = 5. [b] $[(Y_c - Y_t)/Y_c] \times 100$.

precludes accurate determination of binding for drugs that show a low percentage bound.

In the present study, an equilibrium dialysis method is described which employs calibration and control procedures that minimize artifactual errors and permit statistical evaluation of control, as well as test data. The method permits compensation to be made for concentration-dependent binding to apparatus and membranes and allows for variations in conditions in individual experiments. Sulfadimethoxine and Cohn fraction (CF) IV-1 α-globulin were selected as a model drug–protein system that gives a low percentage binding. The concentration of the protein was constant at the normal blood level of 0.81% w/v, with the drug present in amounts equivalent to those found in therapeutic application.

EXPERIMENTAL

Equilibrium dialysis was performed using 20-cm strips of dialysis tubing[1] (1-cm diameter, 4.8-nm pore diameter) with a molecular weight cut-off not greater than 12,000. These membranes were immersed in boiling water and stirred for 2 hr as the water cooled. The tubing was then stirred with 70% methanol for 30 min, stored in 50% methanol overnight, rinsed with distilled water, and soaked in phosphate buffer (pH 7.4) for 2–3 hr prior to use. The membranes were used immediately after preparation. The tubing was tied with a double knot at one end and filled with 2 ml of protein solution (CF-IV-1 α-globulin[2] in phosphate buffer, 0.81% w/v; pH 7.4) containing sulfadimethoxine. The drug concentration range was 100–340 μg/ml. The tubing was sealed and placed in a glass culture tube (16 × 125 mm) with a polytetrafluoroethylene cap. Four milliliters of phosphate buffer (pH 7.4) was placed in each culture tube, and the solutions were dialyzed for 24 hr at 37°[3]. The tubes were rotated 12 times per minute using a rotary mixer[4]. The protein solution and dialysate were assayed for sulfadimethoxine using the Bratton–Marshall method (16). Absorbance was measured at 420 nm; five replicates of each test concentration were dialyzed. A set of five controls was prepared for each concentration studied and placed in the rotary mixer with the test samples. Controls were identical to the test samples, except the solution inside the dialysis membrane contained no protein. Glassware and buffer were sterilized by autoclave[5] prior to use. Preparation and transfer of solutions were carried out under aseptic conditions in a laminar-airflow hood[6]. The dialysate was tested for the absence of protein both visually (absence of frothing) and by means of a semiquantitative colorimetric indicator[7].

RESULTS AND DISCUSSION

The mean optical density values (n = 5) for control and test solutions are shown in Table I. Each set of controls is an exact replicate of the corresponding set of test solutions, except that the dialysis bags in the control tubes contained no protein. The controls therefore take into account any spurious loss of drug due to adsorption to the tubes, cap liners, membrane, transfer pipets, or any other equipment. Furthermore, the controls obviate any day-to-day variation in the assay procedure or experimental conditions because they are run in parallel with the tests, and they may be subjected to the same statistical analyses as the tests.

Table II—Percentage Protein Binding of Sulfadimethoxine Calculated by a Regression Equation (Second Method) [a]

Initial Concentration, μg/ml	Protein Binding, %		Corrected Protein Binding, % [d]
	Test [b]	Control [c]	
100	5.53 ± 0.81	−3.06 ± 0.47	8.59 ± 0.91
140	11.75 ± 1.16	1.84 ± 0.94	9.91 ± 1.30
180	10.87 ± 1.05	1.16 ± 1.42	9.71 ± 1.18
250	10.22 ± 0.66	−0.51 ± 0.40	10.73 ± 0.74
340	12.84 ± 0.54	−0.097 ± 0.46	12.93 ± 0.61
	r = 0.6842	r = 0.2243	r = 0.9670

[a] Expressed as mean ± SE; n = 5. [b] $[(X_0 - \hat{X}_t)/X_0] \times 100$. [c] $[(X_0 - \hat{X}_c)/X_0] \times 100$. [d] $[(\hat{X}_c - \hat{X}_t)/X_0] \times 100$.

Calculation of Protein Binding—*First Method*—The difference in mean optical density values between the test and its corresponding control ($Y_c - Y_t$) is attributable to binding of the drug to protein since artifactual discrepancies are represented in the control value. The control value is the optical density reading that would be obtained in the corresponding test if there were no binding of drug to the protein. Thus, the value obtained by subtracting the test optical density from that of the control, expressed as a percentage of the control $[100\ (Y_c - Y_t)/Y_c]$, corresponds to the percentage binding of the drug to protein (Table I). The percentage binding in the present experiment was ~10% throughout the concentration range studied (Fig. 1). Nevertheless, the stringent control technique permits statistical analysis, which showed each test optical density mean to be significantly different from its corresponding control (Student's two-tailed t test; $p < 0.001$ except for the 180-μg/ml concentration where the limit was $p < 0.01$). It is interesting to note that there is a linear relationship between the percentage drug bound and concentration ($y = 0.01183x + 9.279$; $r = 0.8811$, $p' = 0.05$). We would point out however that the y-intercept value of 9.279% is meaningless because we have no data for concentrations <100 μg/ml, and there is no reason to presume that linearity in the relationship would continue to hold at very low drug concentrations.

Second Method—As an alternate approach to the calculation, the controls (Table I) may be used to generate a calibration curve ($y = 0.004525x - 0.08808$; $r = 0.9970$) from which the test optical density values (Y_t) may be converted to percentage binding values. In this procedure, the experimental test optical density mean value (Y_t) is inserted in the regression equation to calculate a value ($\hat{X}_t$) for the concentration of free drug in the test solution at equilibrium. The percentage drug bound to the protein is then calculated by the expression $100\ (X_0 - \hat{X}_t)/X_0$, where X_0 is the initial concentration of the drug (Table II). There is no correlation (Fig. 2) between these uncorrected percentage binding values and initial drug concentration (r = 0.6842, not significant).

However, the present experimental design also permits the control optical density mean value (Y_c) to be converted similarly to a value ($\hat{X}_c$) for the concentration of free drug in the control solution at equilibrium. The percentage "spurious" binding in the control is then given by the expression $100\ (X_0 - \hat{X}_c)/X_0$. The "spurious" binding values calculated by this method are shown in Table II. Theoretically, the controls should show no binding because they contain no protein. In practice, positive

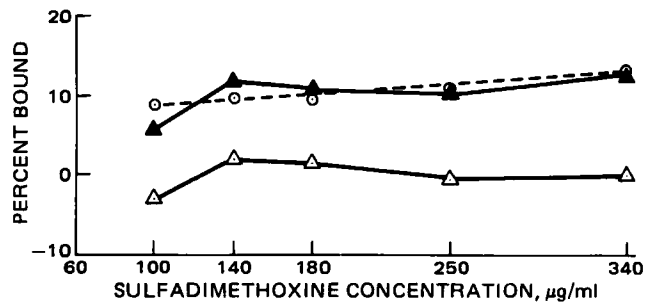

Figure 2—*Plots of percentage binding* versus *concentration of sulfadimethoxine. Key: (▲) mean test values; (△) mean control values; (⊙) adjusted test values (test less control).*

[1] Fisher Scientific Co., Toronto, Ontario, Canada.
[2] United States Biochemical Corp., Cleveland, Ohio.
[3] Thelco Model 4 Incubator, Fisher Scientific Co., Toronto, Ontario, Canada.
[4] Hematology/Chemistry Mixer Model 346, Fisher Scientific Co., Toronto, Ontario, Canada.
[5] Castle Autoclave, Fisher Scientific Co., Toronto, Ontario, Canada.
[6] Enviralab Sterility Module, Bio-Dynamics, Burlington, Ontario, Canada.
[7] Albustix, Ames Co. Division, Miles Laboratories, Rexdale, Ontario, Canada.

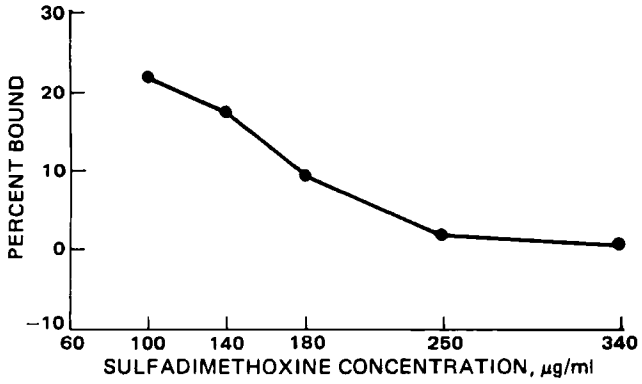

Figure 3—*Erroneous percentage binding values calculated from the regression equation of an unpaired calibration curve.*

or negative deviations from 0% binding reflect nonideal behavior in the system, brought about by the binding of drug to the equipment or other experimental error. Thus, the control ("spurious") binding values were subtracted from the corresponding test (uncorrected) binding values to give the percent binding. The simplified expression for the calculation of percent binding values by this method is 100 $(\hat{X}_c - \hat{X}_t)/X_0$. There is a good correlation between the corrected percentage binding and initial concentration of drug ($y = 0.01650x + 7.042$; $r = 0.9670$, $p' = 0.01$).

Comparison of data in Tables I and II reveals that the percentage binding values calculated by the two methods are similar, but not identical. The disparity arises because of the different types of arithmetic manipulation of data employed. In the first method (Table I), the experimental optical density mean values of the test and control are used directly to calculate percentage binding values. By contrast, the second method (Table II) depends on the ability of the regression equation to predict the drug concentration ($\hat{X}$) which corresponds to an experimentally determined optical density value (Y). Thus the numerical difference between the percentage binding values generated by the two methods may be predicted by the expression 100 $(1/Y_c - 1/mX_0)(Y_c - Y_t)$, where m is the slope of the regression equation. Full details of the derivation of this expression will be published elsewhere.

The percentage binding values calculated by the second method are consistently smaller than those calculated by the first method. This results in high t values (>7.0 with 4 degrees of freedom) when individual results contributing to a pair of mean values are compared, term by term, in a paired t test. However, the scatter of results about each mean is sufficiently wide to produce low t values (<1.0 with 8 degrees of freedom) in an unpaired t test. This means that, for practical purposes, there is no significant difference between mean percentage binding calculated by the two methods. We therefore prefer the first method because it is simple and direct.

Variability in the System—To assess day-to-day variability in the system, control-calibration experiments were run on nine different occasions by the same technician. Slope values generated from this data varied considerably (mean, 0.003970; *SD*, 0.0004974; coefficient of variation, 12.53%). This reflects not only variation in the analytical method, but also any day-to-day differences in the adsorption of drug to the membrane. The latter is suspect because the membranes have to be prepared for each run (see *Experimental*) and it is possible that there is interbatch variation in the extent of drug adsorption.

To illustrate the distortion that may be brought about by the use of an unpaired calibration curve, the test optical density mean values in Table I were converted to percent protein binding values by means of a calibration curve ($y = 0.003522x + 0.06394$; $r = 0.9981$) selected at random from the nine calibration-control experiments described above. The resulting percentage binding–drug concentration plot (Fig. 3) has a negative slope ($y = -0.09193x + 28.81$; $r = -0.9406$) and bears little resemblance to the authentic uncorrected plot (Fig. 2).

In the execution of the experiments, care was taken to standardize the manipulative procedures to minimize experimental error. The use of tubes with polytetrafluoroethylene-lined caps avoided the problem of leaching from rubber- or polyvinylchloride-lined caps, which can cause displacement of drugs from protein binding sites (17). All solutions and glassware were sterilized before use, and solution transfers were made under aseptic conditions in a laminar-airflow hood. This eliminates the possibility of microbial growth during dialysis and permits the experiments to be conducted for 24 hr without the use of preservatives that could influence binding characteristics. All dialysates were checked for

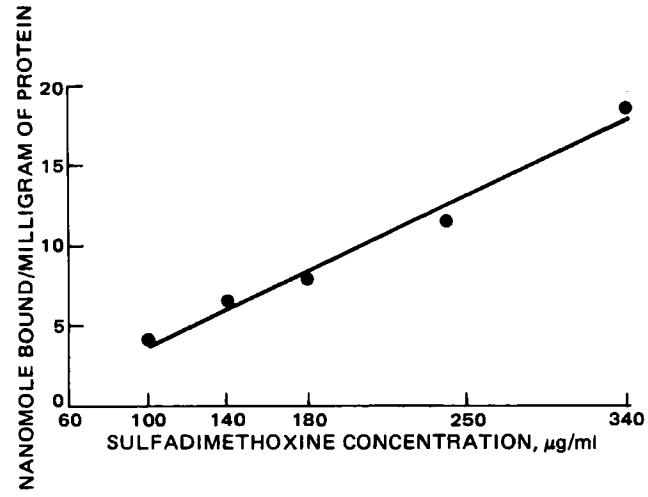

Figure 4—*Relationship between nanomoles of sulfadimethoxine bound per milligram of protein and total drug concentration.*

the absence of protein, both visually (absence of frothing) and by the use of a semiquantitative colorimetric indicator.

The majority of protein-binding experiments described in the literature are concerned with drugs which have a high percentage binding to plasma proteins and with protein fractions that transport a major fraction of a drug in the blood. The significance of minor proteins may increase in disease or other conditions, and it can be important to know their contribution to the overall binding of drugs in the blood.

The variability in results obtained with conventional dialysis procedures often precludes accurate determination of the binding of drugs which show a low percentage bound or a low affinity for proteins. The results (Fig. 1) obtained by the present method however, reveal a low, but statistically significant percentage binding throughout the drug concentration range studied. Conventional percentage binding–drug concentration plots can be difficult to interpret when the slope is shallow as in Fig. 1 ($y = 0.01183x + 9.297$). However, if the percentage binding is expressed in terms of nanomoles of drug bound per milligram of protein, it is clear that the amount of drug bound increases with total drug concentration in a linear manner ($y = 0.05866x - 2.116$, $r = 0.9913$; Fig. 4).

CONCLUSION

The method developed in this study provides an accurate technique for the minimization of errors that arise in equilibrium dialysis and is particularly suitable for use when the percentage binding is low. The stringent control technique permits correction to be made for concentration-dependent binding of drug to the membrane or other equipment. Most significant in the present study is the linear relationship between total drug concentration and control-corrected percentage binding, whereas there was no correlation between total drug concentration and conventional (uncorrected) percentage binding. The method may be adapted to other experimental designs (*e.g.*, fixed concentration of drug *versus* varied concentration of protein) and can be employed with any suitable method of drug analysis.

REFERENCES

(1) J. J. Vallner, *J. Pharm. Sci.*, **66**, 447 (1977).

(2) T. F. Blaschke, *Clin. Pharmacokinet.*, **2**, 32 (1977).

(3) A. Yacobi and G. Levy, *J. Pharm. Sci.*, **68**, 742 (1979).

(4) M. Rowland, *Ther. Drug Monit.*, **2**, 29 (1980).

(5) J. E. Fletcher and A. A. Spector, *Mol. Pharmacol.*, **13**, 387 (1977).

(6) H. Kurz, H. Trunk, and B. Weitz, *Arzneim.-Forsch.*, **27**, 1373 (1977).

(7) W. D. Hooper, D. K. Dubetz, F. Bochner, L. M. Colter, G. A. Smith, M. J. Eadie, and T. H. Tyrer, *Clin. Pharmacol. Ther.*, **17**, 433 (1975).

(8) J. F. Zaroslinski, S. Keresztes-Nagy, R. F. Mais, and Y. T. Oester, *Biochem. Pharmacol.*, **23**, 1767 (1974).

(9) J. J. Vallner, W. A. Speir, R. C. Kolbeck, G. N. Morrison, and E. D. Bransome, *Am. Rev. Resp. Dis.*, **120**, 83 (1979).

(10) J. Koch-Weser and E. M. Sellers, *N. Engl. J. Med.*, **294**, 311 (1976).
(11) K. M. Piafsky and O. Borga, *Clin. Pharmacol. Ther.*, **22**, 545 (1977).
(12) R. Geddes and P. M. White, *Biochem. Pharmacol.*, **28**, 2285 (1979).
(13) C. F. Chignell, *CRC Crit. Rev. Toxicol.*, **1**, 413 (1972).
(14) E. Woo and D. J. Greenblatt, *J. Pharm. Sci.*, **68**, 466 (1979).
(15) E. M. Sellers and J. Koch-Weser, *Biochem. Pharmacol.*, **23**, 553, (1974).
(16) A. C. Bratton and E. K. Marshall, *J. Biol. Chem.*, **128**, 537 (1939).
(17) K. K. Midha, J. K. Cooper, Y. D. Lapierre, and J. W. Hubbard, *Can. Med. J.*, **124**, 264 (1980).

ACKNOWLEDGMENTS

The authors acknowledge the financial support from the University of Manitoba Research Board and the Medical Research Council of Canada for the award of a summer studentship to Catherine Savage.

We also thank Dr. B. Johnston of the Department of Statistics, University of Manitoba, for helpful discussions and suggestions.

Stereospecific High-Performance Liquid Chromatographic Analysis of Warfarin in Plasma

CHRISTOPHER BANFIELD and MALCOLM ROWLAND ˣ

Received March 9, 1982, from the *Department of Pharmacy, University of Manchester, Manchester M13 9PL, England.* Accepted for publication August 5, 1982.

Abstract □ A stereospecific high-performance liquid chromatographic assay has been developed to determine *R*(+)- and *S*(−)-warfarin simultaneously in plasma. The method involved the formation of diastereoisomeric esters, using carbobenzyloxy-L-proline, with subsequent separation using silica as the stationary phase. The method permits characterization of the pharmacokinetics of warfarin enantiomers following administration of racemic drug.

Keyphrases □ Warfarin—stereospecific quantitation in plasma, high-performance liquid chromatography □ Stereoisomers—of warfarin, quantitation in plasma using the racemate, high-performance liquid chromatography □ High-performance liquid chromatography—of warfarin in plasma, quantitation of the stereoisomers using the racemate

Warfarin (I) is administered clinically as a racemic mixture. In humans, *S*(−)-warfarin is five times more potent and is more rapidly eliminated than the *R*-isomer (1, 2). Consequently, the concentration of each isomer in plasma varies with time within an individual and also between individuals following a dose of racemic warfarin. The response to warfarin is also variable (3). Drugs interact with the isomers differently (4–6). Thus, a more complete understanding of the sources of variability in response to warfarin, and the nature of interactions of drugs with warfarin, requires either giving each isomer separately (a rare clinical procedure) or determining the concentration of each isomer in plasma following administration of the prescribed racemic drug.

Stereospecific analysis of a mixture of enantiomers is difficult. Several specialized analytical techniques, including the synthesis of stable isotopes (pseudo-racemates) coupled with mass spectrometry (7, 8) and a stereospecific radioimmunoassay (9) have been developed to overcome this difficulty.

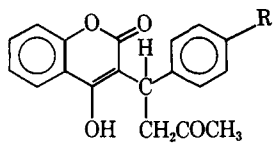

I R = H
II R = F

Chromatographic separation of enantiomers is possible if a diastereoisomeric relationship is established between them either through the use of chiral solvents (10–12) or derivatization with a suitable chiral reagent (13–15). This paper describes a simple method for the quantitative estimation of the isomers of warfarin in plasma using carbobenzyloxy-L-proline to form diastereoisomeric esters, which can be separated by high-performance liquid chromatography (HPLC) using silica as the stationary phase.

EXPERIMENTAL

Reagents and Materials—Racemic warfarin was obtained from its sodium salt[1] by precipitation with 0.1 *M* HCl. The dried material was recrystallized from absolute ethanol. *R*(+)- and *S*(−)-warfarin[2], the internal standard[3] (3-[α-(4′-fluorophenyl-)-β-acetylethyl]-4-hydroxycoumarin; 4′-fluorowarfarin) (II), imidazole[4], dicyclohexylcarbodiimide[5], carbobenzyloxy-L-proline[5], hexane (HPLC grade)[6], methanol[7], and ethyl acetate (HPLC grade)[6] were used as supplied. Peroxide-free ether[8] was prepared by passage through a column of activated alumina[9] (45 g, Brockman type 1 alkaline).

Extraction of *RS*-Warfarin—Plasma (0.2 ml) and internal standard (0.1 ml; 0.846 μg/0.1 ml of water) were added to a clean culture tube[10] (16 × 125 mm). The solution was made alkaline with 0.1 *M* K_2CO_3 (1 ml), shaken manually for 3 min with ether (4 ml), and separated by centrifugation[11] at 3000 rpm for 5 min. After aspiration of the organic layer, the aqueous layer was acidified with 1 *M* HCl (1.5 ml) and shaken manually for 3 min with ether (6 ml), followed by centrifugation at 3000 rpm for 3 min. The aqueous layer was quickly frozen by immersion in liquid nitrogen (40–60 sec) to allow the organic layer to be decanted into a culture tube whose tip was drawn out to a capacity of 0.2 ml. An antibumping

[1] Sorex, U.K.
[2] Gifts from Endo Laboratories, Inc., U.S.A.
[3] Gifts from Ciba Geigy Ltd., Switzerland.
[4] Sigma Chemical Co., U.S.A.
[5] Aldrich Chemical Co., U.S.A.
[6] Rathburn, Scotland.
[7] Analar; Fisons, U.K.
[8] May and Baker, Dagenham, U.K.
[9] B.D.H., U.K.
[10] Corning, U.S.A.
[11] MSE, Super Minor Centrifuge, No. 533A: MSE, U.K.

0022-3549/83/0800-0921$01.00/0

(10) J. Koch-Weser and E. M. Sellers, *N. Engl. J. Med.*, **294**, 311 (1976).
(11) K. M. Piafsky and O. Borga, *Clin. Pharmacol. Ther.*, **22**, 545 (1977).
(12) R. Geddes and P. M. White, *Biochem. Pharmacol.*, **28**, 2285 (1979).
(13) C. F. Chignell, *CRC Crit. Rev. Toxicol.*, **1**, 413 (1972).
(14) E. Woo and D. J. Greenblatt, *J. Pharm. Sci.*, **68**, 466 (1979).
(15) E. M. Sellers and J. Koch-Weser, *Biochem. Pharmacol.*, **23**, 553, (1974).
(16) A. C. Bratton and E. K. Marshall, *J. Biol. Chem.*, **128**, 537 (1939).
(17) K. K. Midha, J. K. Cooper, Y. D. Lapierre, and J. W. Hubbard, *Can. Med. J.*, **124**, 264 (1980).

ACKNOWLEDGMENTS

The authors acknowledge the financial support from the University of Manitoba Research Board and the Medical Research Council of Canada for the award of a summer studentship to Catherine Savage.

We also thank Dr. B. Johnston of the Department of Statistics, University of Manitoba, for helpful discussions and suggestions.

Stereospecific High-Performance Liquid Chromatographic Analysis of Warfarin in Plasma

CHRISTOPHER BANFIELD and MALCOLM ROWLAND ˣ

Received March 9, 1982, from the *Department of Pharmacy, University of Manchester, Manchester M13 9PL, England.* Accepted for publication August 5, 1982.

Abstract □ A stereospecific high-performance liquid chromatographic assay has been developed to determine *R*(+)- and *S*(−)-warfarin simultaneously in plasma. The method involved the formation of diastereoisomeric esters, using carbobenzyloxy-L-proline, with subsequent separation using silica as the stationary phase. The method permits characterization of the pharmacokinetics of warfarin enantiomers following administration of racemic drug.

Keyphrases □ Warfarin—stereospecific quantitation in plasma, high-performance liquid chromatography □ Stereoisomers—of warfarin, quantitation in plasma using the racemate, high-performance liquid chromatography □ High-performance liquid chromatography—of warfarin in plasma, quantitation of the stereoisomers using the racemate

Warfarin (I) is administered clinically as a racemic mixture. In humans, *S*(−)-warfarin is five times more potent and is more rapidly eliminated than the *R*-isomer (1, 2). Consequently, the concentration of each isomer in plasma varies with time within an individual and also between individuals following a dose of racemic warfarin. The response to warfarin is also variable (3). Drugs interact with the isomers differently (4–6). Thus, a more complete understanding of the sources of variability in response to warfarin, and the nature of interactions of drugs with warfarin, requires either giving each isomer separately (a rare clinical procedure) or determining the concentration of each isomer in plasma following administration of the prescribed racemic drug.

Stereospecific analysis of a mixture of enantiomers is difficult. Several specialized analytical techniques, including the synthesis of stable isotopes (pseudo-racemates) coupled with mass spectrometry (7, 8) and a stereospecific radioimmunoassay (9) have been developed to overcome this difficulty.

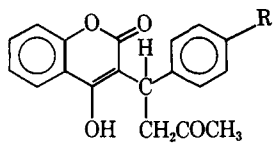

I R = H
II R = F

Chromatographic separation of enantiomers is possible if a diastereoisomeric relationship is established between them either through the use of chiral solvents (10–12) or derivatization with a suitable chiral reagent (13–15). This paper describes a simple method for the quantitative estimation of the isomers of warfarin in plasma using carbobenzyloxy-L-proline to form diastereoisomeric esters, which can be separated by high-performance liquid chromatography (HPLC) using silica as the stationary phase.

EXPERIMENTAL

Reagents and Materials—Racemic warfarin was obtained from its sodium salt[1] by precipitation with 0.1 *M* HCl. The dried material was recrystallized from absolute ethanol. *R*(+)- and *S*(−)-warfarin[2], the internal standard[3] (3-[α-(4′-fluorophenyl-)-β-acetylethyl]-4-hydroxycoumarin; 4′-fluorowarfarin) (II), imidazole[4], dicyclohexylcarbodiimide[5], carbobenzyloxy-L-proline[5], hexane (HPLC grade)[6], methanol[7], and ethyl acetate (HPLC grade)[6] were used as supplied. Peroxide-free ether[8] was prepared by passage through a column of activated alumina[9] (45 g, Brockman type 1 alkaline).

Extraction of *RS*-Warfarin—Plasma (0.2 ml) and internal standard (0.1 ml; 0.846 μg/0.1 ml of water) were added to a clean culture tube[10] (16 × 125 mm). The solution was made alkaline with 0.1 *M* K_2CO_3 (1 ml), shaken manually for 3 min with ether (4 ml), and separated by centrifugation[11] at 3000 rpm for 5 min. After aspiration of the organic layer, the aqueous layer was acidified with 1 *M* HCl (1.5 ml) and shaken manually for 3 min with ether (6 ml), followed by centrifugation at 3000 rpm for 3 min. The aqueous layer was quickly frozen by immersion in liquid nitrogen (40–60 sec) to allow the organic layer to be decanted into a culture tube whose tip was drawn out to a capacity of 0.2 ml. An antibumping

[1] Sorex, U.K.
[2] Gifts from Endo Laboratories, Inc., U.S.A.
[3] Gifts from Ciba Geigy Ltd., Switzerland.
[4] Sigma Chemical Co., U.S.A.
[5] Aldrich Chemical Co., U.S.A.
[6] Rathburn, Scotland.
[7] Analar; Fisons, U.K.
[8] May and Baker, Dagenham, U.K.
[9] B.D.H., U.K.
[10] Corning, U.S.A.
[11] MSE, Super Minor Centrifuge, No. 533A: MSE, U.K.

0022-3549/83/0800-0921$01.00/0

Table I—Chromatographic Parameters for the Carbobenzyloxy-L-prolyl Esters of Warfarin on Various Stationary Phases

Solvent Composition	Stationary[a] Phase	k_S[b]	k_R[c]	R[d]	α[e]
Acetonitrile–water–acetic acid (43:66:1)	Spherisorb 5 ODS	26.2	23.3	1.13	1.12
Ethyl acetate–hexane (15:85)	Spherisorb 5 CN	8.3	10.5	1.44	1.26
Ethyl acetate–hexane (25:75)	Spherisorb 5 Si	5.0	7.0	2.74	1.40

[a] Column size was 4.6-mm i.d. × 10 cm. [b] Capacity factor for the carbobenzyloxy-L-prolyl ester of *S*-warfarin. [c] Capacity factor for the carbobenzyloxy-L-prolyl ester of *R*-warfarin. [d] Resolution factor. [e] Selectivity.

granule was added to the organic layer, which was evaporated to dryness on a heating block at 45° under a stream of nitrogen. The inside of the tube was washed several times with small (100–200 μl) volumes of ether, with vortexing and evaporating to dryness between additions.

For each day of analysis a calibration curve was prepared using the above extraction procedure on blank plasma (0.2 ml) spiked with an aqueous solution (0.1 ml) containing 0.2–2.0 μg of *RS*-warfarin and internal standard (0.8 μg, 0.1 ml).

Derivatization—The derivatization procedure involves esterification with carbobenzyloxy-L-proline using imidazole as catalyst and dicyclohexylcarbodiimide as the condensing agent. To the plasma extract in the modified culture tubes was added carbobenzyloxy-L-proline (10 μl; 100 mg/ml of acetonitrile), imidazole (10 μl; 1 mg/ml of acetonitrile), and dicyclohexylcarbodiimide (10 μl; 100 mg/ml of acetonitrile). The mixture was vortexed for ~10 sec, during which time a precipitate formed. The reaction was allowed to proceed for 2 hr. The tubes were centrifuged at 3000 rpm for 5 min, and aliquots (3–10 μl) of the supernatant were analyzed by HPLC.

High-Performance Liquid Chromatography—For HPLC discrimination of the diastereoisomers, a pump[12], fitted to a stainless steel column (250 mm × 5 mm-i.d.) packed with silica[13] was used with ethyl acetate–hexane–methanol–acetic acid (25:74.75:0.25:0.4) as mobile phase, at a flow rate of 1 ml/min (~600 psi). Test samples were applied by means of an on-column injector, and the effluent was monitored at 313 nm (0.005 AUFS) using a UV detector[14]. All analyses were performed at ambient temperature. Chromatographic tracings were obtained on a strip chart recorder[15] at a chart speed of 1 cm/2 min. The concentrations of the isomers in the unknown samples were calculated by reference to the appropriate calibration curves, constructed by plotting the peak height ratios obtained (using either ester of the internal standard) *versus* the known amounts of isomer per sample of plasma.

Synthesis of the Diastereoisomeric Esters—To *RS*-warfarin (100 mg) in a conical flask (10 ml) was added dichloromethane[8] (3.0 ml) and carbobenzyloxy-L-proline (300 mg). This was sonicated to effect solution, and dicyclohexylcarbodiimide (300 mg in 1 ml of dichloromethane) was added. A precipitate formed immediately, but the reaction was allowed to proceed for ~14 hr at room temperature. The mixture was then filtered, and the filtrate was stored in the dark until TLC separation was performed.

Isolation of Diastereoisomers—Prior to sample application, the TLC plates (silica gel GF 254/G60) were chromatographed in methanol, dried, and rerun in the solvent system, ethyl acetate–hexane–acetic acid (30:70:0.2), used for the separation of the diastereoisomers. The filtered solution containing the diastereoisomers was applied as a narrow band ~2 cm from the bottom edge of the plate. The bands were detected using short-wavelength (254-nm) UV light. Identification of the spots was made by chromatographing each ester formed by independently reacting *R*(+)-warfarin and *S*(−)-warfarin with carbobenzyloxy-L-proline. The average time to complete an analysis (15 cm) was 1.5 hr in a nonequilibrated tank. Care was taken not to overload the plate, since this led to band broadening. In the advent of overlap, lines were drawn across the plate a few millimeters above and below where the overlap had occurred. The material contained within this area was used as racemic diastereoisomeric ester. The regions above and below these lines were scraped into tubes labeled *SS* ester and *RS* ester, respectively, and eluted by manually shaking for 2 min with ethyl acetate or dichloromethane (2 ml). The materials were transferred to microcentrifuge tubes (1.5 ml), centrifuged at 12,000×*g* for 1 min, and the supernatant was transferred to a clean vial. An aliquot of each supernatant was chromatographed using the same solvent system used to separate the diastereoisomeric esters. Those fractions chromatographing as either *SS* ester, *RS* ester, or racemic ester were pooled in appropriately labeled vials. The entire process was then repeated using several plates.

A sample of silica gel was taken from an area free from UV-absorbing material and processed as for the diastereoisomers. Mass spectral[16] and IR[17] (solution) analyses were performed on both the silica gel blank and the diastereoisomers.

Table II—Within-Assay Variability of Peak Height Ratios at Various Amounts of *RS*-Warfarin

Amount of Isomer, μg	Relative Standard Deviation, %			
	SS[1 a]	*RS*[1 a]	*SS*[2 b]	*RS*[2 b]
1.0[c]	3.2	3.5	3.25	3.7
0.4[c]	6.3	6.7	5.1	6.6
0.1[d]	9.8	8.4	11.9	11.8

[a] Peak height ratios determined relative to the first eluting ester of the internal standard. [b] Peak height ratios determined relative to the second eluting ester of the internal standard. [c] $n = 6$. [d] $n = 4$.

RESULTS AND DISCUSSIONS

The proposed structures of the carbobenzyloxy-L-prolyl diastereoisomeric esters of warfarin (III) were established (after separation of the diastereoisomers by semipreparative TLC) by low-resolution electron impact (EI) and chemical ionization (CIMS, ammonia as carrier) mass spectrometry (MS) and IR analysis. The chemical ionization MS data, in conjunction with EI studies, verified the predicted molecular weight (CIMS: *m/z* 557, $[M + NH_4]^+$; EI: *m/z* 539, $[M^+]$). These molecular ions were not present in the background sample of silica gel. As expected the MS of the *R*(+)- and *S*(−)-warfarin esters were similar. The IR spectra (chloroform) of the diastereoisomeric esters showed an absorption at 1780 cm^{-1} consistent with vinylic esters (1800–1770 cm^{-1}).

Not all apparently good candidates for the formation of diastereoisomers with *RS*-warfarin gave favorable results. Thus, *N*-acetyl-L-alanine[5] and *N*-acetyl-L-phenylalanine[5] did not form derivatives with *RS*-warfarin using dicyclohexylcarbodiimide as the activating agent. Also, although both *R*(−)-2-methoxy-2-phenylacetic acid[18] and L-menthoxyacetic acid[5] formed derivatives, chromatographic conditions could not be found to achieve resolution of the resultant diastereoisomeric esters on either silica[13] or Spherisorb 5 ODS[13] stationary phases. In contrast, successful derivatization and resolution of *RS*-warfarin was achieved using *N*-acetyl-L-proline (16) and carbobenzyloxy-L-proline (*Z*-L-proline). The latter was eventually chosen because of its higher (>99%) optical purity.

The effectiveness of the derivative for resolution is subject to several criteria: conformational rigidity of groups attached to the asymmetric center [a center as part of a ring system can improve resolution (17)], *e.g.*, *N*-acetyl-L-proline and carbobenzyloxy-L-proline; a minimum distance of 3–4 atoms between the chiral centers of the reagent and solute (18–20); and polar or polarizable groups in close proximity to the asymmetric centers (21). In *R*(−)-2-methoxy-2-phenylacetic acid the asymmetric center is not part of a ring system. Although the asymmetric center of L-menthoxyacetic acid is in a ring sytem, the asymmetric centers of the proposed derivative are six atoms apart. These results suggest that all of the above criteria must be met if adequate resolution is to be effected. The lack of reactivity of the *N*-acyl derivatives of L-alanine and L-phenylalanine may be due to formation of oxazolones (22, 23) when dicyclohexylcarbodiimide is used as the activating agent.

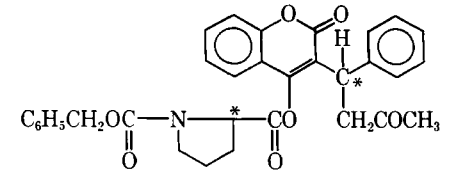

III

[12] Altex Model 100A, Anachem Ltd., U.K.
[13] Spherisorb Si 5 μm, Phase Sep., U.K.
[14] Waters Model 440, Waters Associates, U.S.A.
[15] Servoscribe 210, Smiths Instruments, U.K.
[16] Kratos, MS25.
[17] Perkin-Elmer 237 Infra-red Spectrophotometer, Perkin-Elmer, U.S.A.
[18] Fluka, A.G., Switzerland.

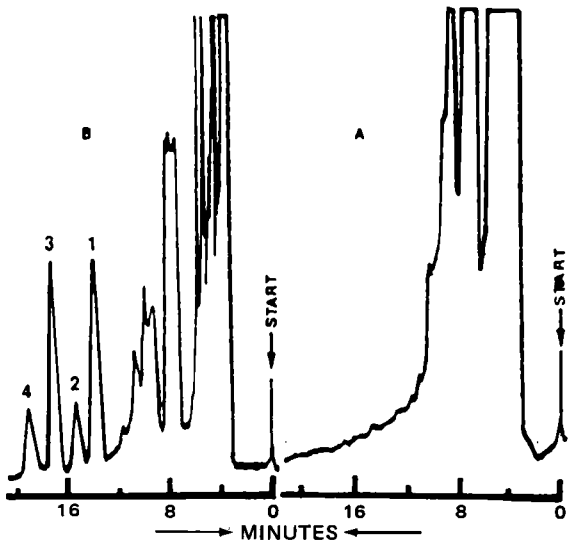

Figure 1—*Chromatograms obtained after derivatization with carbobenzyloxy-L-proline of (A) control human plasma and (B) human plasma spiked with* RS-*warfarin (2 μg). Key: (1)* SS-*warfarin ester; (2) first eluting ester of the internal standard; (3)* RS-*warfarin ester; (4) second eluting ester of the internal standard.*

N,N'-Dicyclohexylurea, a byproduct in the activation of carboxyl functions by dicyclohexylcarbodiimide (24) is soluble only to a certain extent in most organic solvents. To overcome the purification problem caused by the formation of *N,N'*-dicyclohexylurea and *N*-acyl ureas, water-soluble carbodiimides are often used (25). However ester formation with carbobenzyloxy-L-proline in the presence of such water-soluble carbodiimides as 1-cyclohexyl-3-(2-morpholinoethyl)-carbodiimide methoxy-*p*-toluenesulfonate[5] or 1-(3-dimethyl-aminopropyl)-3-ethyl carbodiimide[5] was inferior to that in the presence of dicyclohexylcarbodiimide. With the first, derivative formation did not occur; with the second, derivatization was incomplete. Even so, as the technique is being developed specifically for analytical purposes, the lack of the option for removal of the urea-type impurities is not a serious disadvantage, because the impurities lack good chromophores at the wavelength (313 nm) used in the analysis of warfarin, so that minimal interference is observed.

Reverse-phase HPLC is popular partly because of the wide variety of stationary phases available and partly because the ability to inject aqueous samples reduces the number of prechromatographic steps required. From preliminary investigations with the stationary phases Hypersil-5 ODS[19], Spherisorb 5 ODS[13], Spherisorb 5 phenyl[13], and Spherisorb 5 CN[13] in the reverse-phase mode only Spherisorb 5 ODS and Spherisorb 5 CN gave sufficient promise to warrant further study. Improved performance was seen, however, when Spherisorb 5 CN was used in the normal-phase mode. Under optimal conditions, using the solvent combinations shown in Table I, Spherisorb 5 ODS showed both low selectivity and resolution. In general, normal-phase chromatography on silica gave the highest selectivity and resolution. Although the maximum difference in selectivity between Spherisorb 5 CN and Spherisorb 5 Si was ~11%, this resulted in a 90% increase in resolution for the diastereoisomeric esters. Addition of acetic acid to the mobile phase when Spherisorb 5 Si is used as stationary phase decreases retention time without adversely affecting resolution or selectivity for the diastereoisomeric carbobenzyloxy-L-prolyl esters (Table I).

The rate of derivatization of *RS*-warfarin (2 mg/ml of ethyl acetate, 10 μl) by carbobenzyloxy-L-proline (100 mg/ml of ethyl acetate, 10 μl) in the presence of dicyclohexylcarbodiimide (100 mg/ml of ethyl acetate, 15 μl), measured by the disappearance of *RS*-warfarin, was followed for 12 hr. The rate is first order with a half-life of disappearance of 3.5 hr. With completion (99%) of the reaction not anticipated before 24 hr, this reaction time was considered too long. In the presence of pyridine (24.5 μl in ethyl acetate) as catalyst, the reaction was complete within 1 hr, and the resultant diastereoisomers remained stable for at least 9 hr. However, the detection of a large peak attributed to pyridine, eluting after the diastereoisomers, limited its use as catalyst because the number of HPLC analyses would be restricted to only two samples per hour. Pyridine absorbs strongly in the 305–315-nm region, which coincides with the wavelength (313 nm) used for detection of the diastereoisomeric esters. Imidazole, which has a lower maximum wavelength of absorption (207 nm), proved to be just as good a catalyst as pyridine; the mechanism of catalysis of esterification is similar (26). Apparently, the presence of a basic nitrogen alone is not sufficient, since triethylamine failed to catalyze the reaction.

[19] Shandon, Southern Products Ltd., U.K.

Table III—Between-Assay Variability of Peak Height Ratios at Various Concentrations of *RS*-Warfarin over a 6-Week Period

Amount of Isomer, μg	Relative Standard Deviation, %			
	$SS^{1\,a}$	$RS^{1\,a}$	$SS^{2\,b}$	$RS^{2\,b}$
1.0[c]	3.8	3.6	6.0	5.1
0.8[d]	3.1	2.9	5.9	4.2
0.6[d]	6.05	7.8	4.7	6.8
0.4[e]	7.7	7.4	7.5	7.9
0.2[d]	9.0	8.3	9.4	9.9
0.1[f]	13.7	17.1	14.4	13.7

[a] Peak height ratios determined relative to the first eluting ester of the internal standard. [b] Peak height ratios determined relative to the second eluting ester of the internal standard. [c] $n = 26$. [d] $n = 10$. [e] $n = 23$. [f] $n = 16$.

Initially, 4-hydroxycoumarin was chosen as the internal standard; it produced a single ester with carbobenzyloxy-L-proline, eluting just after the *RS*-warfarin ester. However, there was a high degree of variability in the subsequent assay procedure which was identified with an instability of the carbobenzyloxypropyl ester of 4-hydroxycoumarin, probably due to imadazole-catalyzed hydrolysis. The absence of a 3-substituent in 4-hydroxycoumarin (*cf.* warfarin) would make attack of the ester carbonyl more facile, due to lack of steric hindrance, for this ester than for the warfarin ester. Of the many others examined, 4'-fluorowarfarin proved the most suitable with respect to retention time and stability, although being a racemate, diastereoisomeric esters are formed.

A typical chromatogram obtained after derivatization of an ethereal extract from human plasma spiked with *RS*-warfarin and internal standard (4'-fluorowarfarin) is shown in Fig. 1. Identification of the retention times of *RS*- and *SS*-warfarin esters was made by chromatographing each of the esters formed by independently reacting *R*(+)-

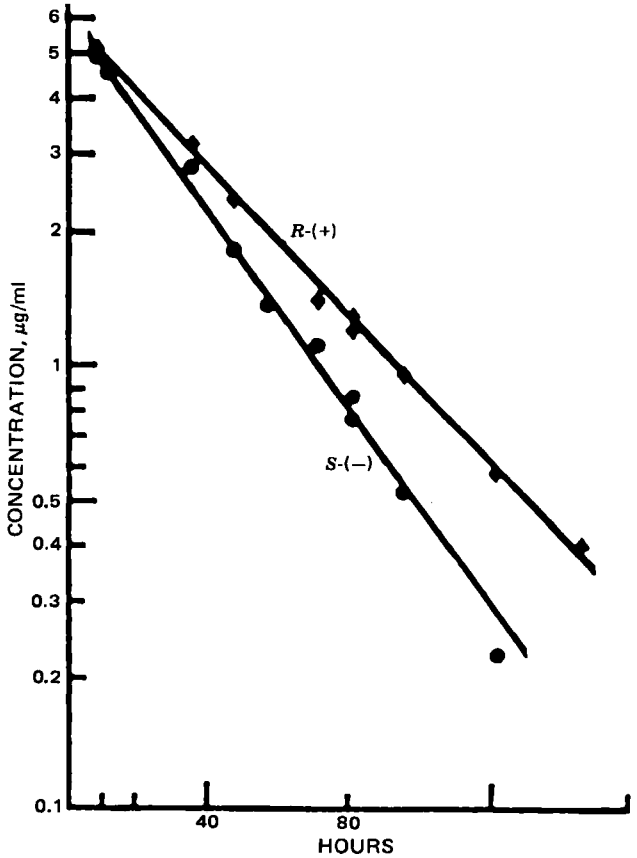

Figure 2—*Plasma concentration–time profile of* R(+)-*warfarin (◆) and* S(−)-*warfarin (●) following oral administration of* RS-*warfarin (1.56 mg/kg) to a human subject.*

warfarin and S(−)-warfarin with carbobenzyloxy-L-proline. The S(−)-warfarin carbobenzyloxy-L-prolyl ester elutes before the ester of R(+)-warfarin, with a separation factor of 3.0. A similar elution order is assumed for the internal standard, but could not be verified because this compound has never been resolved. Repeated analyses with time indicated that the derivatives were stable for at least 48 hr in the final reaction mixture.

The recovery of *RS*-warfarin investigated by taking *RS*-warfarin (0.8 μg) spiked with [^{14}C]*RS*-warfarin through the extraction, derivatization, and HPLC analysis was 70% (n = 3). The major losses occurred during evaporation of the sample, therefore the inside of the tube must be washed to concentrate the extracted material in the tip of the tube.

Linear calibration plots for either isomer ($r^2 > 0.99$) were obtained over the range 0.1–1.0 μg/isomer. As shown in Table II, based on either of the internal standard esters (*RS* or *SS*), the relative standard deviations of the peak height ratios were between 11.9 and 3.2% for 0.1 and 1.0 μg warfarin isomer, respectively. Table III summarizes the results of a similar assessment of between-assay variability for studies performed over a 6-week period using 0.1–1.0 μg of warfarin isomer. Satisfactory precision (<10%) is observed over a fivefold concentration range of warfarin isomers. The results indicate that the assay is accurate and reproducible.

The determination limit of the assay with a 10% coefficient of variation was computed from the expression (27):

$$X_0 = 10\sqrt{V(X_0)}$$

where X_0 is the determination limit at the preselected coefficient of variation, and $V(X_0)$ is the variance associated with X_0. Using the above procedure, the determination limits (10% *CV*) of the UV assay for *S*- and *R*-warfarin are 0.16 and 0.096 μg, respectively, using the first eluting standard. Similar values were obtained when using the second eluting standard. The difference in determination limits of the esters of warfarin may be ascribed to the greater potential for interference between the *SS*-ester of warfarin and the first internal standard, due to changes in retention as a result of column deterioration, or day-to-day variability in eluant composition.

Figure 2 shows the plasma concentration–time profiles for the *R*- and *S*-isomers (using 200-μl plasma samples) following administration of *RS*-warfarin (1.5 mg/kg po) to a normal volunteer. At this dose level the plasma concentration can be monitored for at least 5 days for the *S*-isomer or 6 days for the *R*-isomer. The more rapid elimination of the *S*-isomer confirms the findings using the stereospecific MS methods (7, 8) or following the administration of the separate enantiomers (2).

REFERENCES

(1) A. Breckenridge, M. Orme, H. Wesseling, R. J. Lewis, and R. Gibbons, *Clin. Pharmacol. Ther.*, **15**, 424 (1974).

(2) R. A. O'Reilly, *Clin. Pharmacol. Ther.*, **16**, 384 (1974).

(3) J. Koch-Weser, *Eur. J. Clin. Pharmacol.*, **9**, 1 (1975).

(4) R. J. Lewis, W. F. Trager, K. K. Chan, A. Breckenridge, M. Orme, M. Rowland, and W. Schary, *J. Clin. Invest.*, **53**, 1607 (1974).

(5) R. A. O'Reilly, *N. Engl. J. Med.*, **295**, 354 (1976).

(6) R. A. O'Reilly, *N. Engl. J. Med.*, **302**, 33 (1980).

(7) W. N. Howald, E. D. Busch, W. F. Trager, R. A. O'Reilly, and C. H. Motely. *Biomed. Mass Spectrom.*, **7**, 35 (1980).

(8) C. Hignite, J. Vetrecht, C. Tschanz, and D. Arzanoff, *Clin. Pharmacol. Ther.*, **28**, 99 (1980).

(9) C. E. Cooke, N. A. Ballentine, T. B. Seltzman, and C. R. Tallent, *J. Pharmacol. Exp. Ther.*, **210**, 391 (1979).

(10) P. E. Hare and E. Gil-av, *Science*, **204**, 1226 (1979).

(11) C. Gilon, R. Leshman, and E. Goushka, *Anal. Chem.*, **52**, 1206 (1980).

(12) Y. Ta'uhi, N. Miller, and B. L. Karger, *J. Chromatogr.*, **205**, 325 (1981).

(13) B. Silben and S. Riegelman, *J. Pharmacol. Exp. Ther.*, **215**, 643 (1980).

(14) R. W. Souter, *J. Chromatogr.*, **221**, 109 (1980).

(15) K. Imai, S. Mammo, and T. Ohtaki, *Tetrahedron Lett.* **15**, 1211 (1976).

(16) V. du Vigneaud and C. Meyer, *J. Biol. Chem.* **98**, 295 (1932).

(17) B. L. Karger, R. L. Stern, E. Keane, B. Halpern, and J. W. Westley, *Anal. Chem.*, **39**, 228 (1967).

(18) G. Helmchen and G. Nill, *Angew. Chem. Int. Ed. Engl.*, **18**, 65 (1979).

(19) C. G. Scott, M. J. Petrin, and R. McCorkle, *J. Chromatogr.*, **125**, 157 (1976).

(20) H. C. Rose, R. L. Stern, and B. L. Karger, *Anal. Chem.*, **38**, 469 (1966).

(21) G. Halmchen, G. Nill, D. Flockenzi, W. Schükle, and M. S. K. Youssef, *Angew. Chem. Int. Ed. Engl.*, **18**, 62, (1979).

(22) M. Goodman and L. Levine, *J. Am. Chem. Soc.*, **86**, 2918 (1964).

(23) M. Goodman and W. J. McGahren, *Tetrahedron*, **23**, 2031 (1967).

(24) F. Kurzer and K. Douraghi-Zadeh, *Chem. Rev.*, **67**, 107 (1967).

(25) Y. S. Klansner and M. Bodansky, *Synthesis*, **453** (1972).

(26) W. P. Jencks and J. Canivola, *J. Biol. Chem.*, **234**, 1272 (1959).

(27) L. Aarons, *Analyst*, **106**, 1249 (1981).

ACKNOWLEDGMENTS

Supported by Grant G977/249 from the British Medical Research Council.

Stability-Indicating Assay for Chlorthalidone Formulation: Evaluation of the USP Analysis and a High-Performance Liquid Chromatographic Analysis

JOHN BAUER ˣ, JOHN QUICK, SUZANNE KROGH, and DOUGLAS SHADA

Received March 22, 1982, from *Abbott Laboratories, North Chicago, IL 60064.* Accepted for publication July 30, 1982.

Abstract □ An investigation of the USP assay of chlorthalidone tablets showed that variable degradation of chlorthalidone occurred during assay preparation. The degradation products were isolated and identified. A stability-indicating high-performance liquid chromatographic (HPLC) assay which separates the degradation products from chlorthalidone was developed and used to examine the present USP preparation. The HPLC assay is suggested as an alternate.

Keyphrases □ Chlorthalidone—high-performance liquid chromatography, stability-indicating assay, comparison with the USP analysis □ Degradation products—of chlorthalidone, high-performance liquid chromatographic determination, comparison with the USP analysis □ USP analysis—for chlorthalidone and degradation products, comparison to a high-performance liquid chromatographic assay

Chlorthalidone (I) is a monosulfamyl diuretic used in the treatment of hypertension. The official analysis of chlorthalidone tablets, as prescribed in the United States Pharmacopeia, is a spectrophotometric assay (1). Chlorthalidone has been quantitated in various media using a variety of methodologies (2–8). The major techniques in

0022-3549/83/0800-0924$01.00/0

warfarin and S(−)-warfarin with carbobenzyloxy-L-proline. The S(−)-warfarin carbobenzyloxy-L-prolyl ester elutes before the ester of R(+)-warfarin, with a separation factor of 3.0. A similar elution order is assumed for the internal standard, but could not be verified because this compound has never been resolved. Repeated analyses with time indicated that the derivatives were stable for at least 48 hr in the final reaction mixture.

The recovery of *RS*-warfarin investigated by taking *RS*-warfarin (0.8 μg) spiked with [^{14}C]*RS*-warfarin through the extraction, derivatization, and HPLC analysis was 70% (n = 3). The major losses occurred during evaporation of the sample, therefore the inside of the tube must be washed to concentrate the extracted material in the tip of the tube.

Linear calibration plots for either isomer ($r^2 > 0.99$) were obtained over the range 0.1–1.0 μg/isomer. As shown in Table II, based on either of the internal standard esters (*RS* or *SS*), the relative standard deviations of the peak height ratios were between 11.9 and 3.2% for 0.1 and 1.0 μg warfarin isomer, respectively. Table III summarizes the results of a similar assessment of between-assay variability for studies performed over a 6-week period using 0.1–1.0 μg of warfarin isomer. Satisfactory precision (<10%) is observed over a fivefold concentration range of warfarin isomers. The results indicate that the assay is accurate and reproducible.

The determination limit of the assay with a 10% coefficient of variation was computed from the expression (27):

$$X_0 = 10\sqrt{V(X_0)}$$

where X_0 is the determination limit at the preselected coefficient of variation, and $V(X_0)$ is the variance associated with X_0. Using the above procedure, the determination limits (10% *CV*) of the UV assay for *S*- and *R*-warfarin are 0.16 and 0.096 μg, respectively, using the first eluting standard. Similar values were obtained when using the second eluting standard. The difference in determination limits of the esters of warfarin may be ascribed to the greater potential for interference between the *SS*-ester of warfarin and the first internal standard, due to changes in retention as a result of column deterioration, or day-to-day variability in eluant composition.

Figure 2 shows the plasma concentration–time profiles for the *R*- and *S*-isomers (using 200-μl plasma samples) following administration of *RS*-warfarin (1.5 mg/kg po) to a normal volunteer. At this dose level the plasma concentration can be monitored for at least 5 days for the *S*-isomer or 6 days for the *R*-isomer. The more rapid elimination of the *S*-isomer confirms the findings using the stereospecific MS methods (7, 8) or following the administration of the separate enantiomers (2).

REFERENCES

(1) A. Breckenridge, M. Orme, H. Wesseling, R. J. Lewis, and R. Gibbons, *Clin. Pharmacol. Ther.*, **15**, 424 (1974).

(2) R. A. O'Reilly, *Clin. Pharmacol. Ther.*, **16**, 384 (1974).

(3) J. Koch-Weser, *Eur. J. Clin. Pharmacol.*, **9**, 1 (1975).

(4) R. J. Lewis, W. F. Trager, K. K. Chan, A. Breckenridge, M. Orme, M. Rowland, and W. Schary, *J. Clin. Invest.*, **53**, 1607 (1974).

(5) R. A. O'Reilly, *N. Engl. J. Med.*, **295**, 354 (1976).

(6) R. A. O'Reilly, *N. Engl. J. Med.*, **302**, 33 (1980).

(7) W. N. Howald, E. D. Busch, W. F. Trager, R. A. O'Reilly, and C. H. Motely. *Biomed. Mass Spectrom.*, **7**, 35 (1980).

(8) C. Hignite, J. Vetrecht, C. Tschanz, and D. Arzanoff, *Clin. Pharmacol. Ther.*, **28**, 99 (1980).

(9) C. E. Cooke, N. A. Ballentine, T. B. Seltzman, and C. R. Tallent, *J. Pharmacol. Exp. Ther.*, **210**, 391 (1979).

(10) P. E. Hare and E. Gil-av, *Science*, **204**, 1226 (1979).

(11) C. Gilon, R. Leshman, and E. Goushka, *Anal. Chem.*, **52**, 1206 (1980).

(12) Y. Ta'uhi, N. Miller, and B. L. Karger, *J. Chromatogr.*, **205**, 325 (1981).

(13) B. Silben and S. Riegelman, *J. Pharmacol. Exp. Ther.*, **215**, 643 (1980).

(14) R. W. Souter, *J. Chromatogr.*, **221**, 109 (1980).

(15) K. Imai, S. Mammo, and T. Ohtaki, *Tetrahedron Lett.* **15**, 1211 (1976).

(16) V. du Vigneaud and C. Meyer, *J. Biol. Chem.* **98**, 295 (1932).

(17) B. L. Karger, R. L. Stern, E. Keane, B. Halpern, and J. W. Westley, *Anal. Chem.*, **39**, 228 (1967).

(18) G. Helmchen and G. Nill, *Angew. Chem. Int. Ed. Engl.*, **18**, 65 (1979).

(19) C. G. Scott, M. J. Petrin, and R. McCorkle, *J. Chromatogr.*, **125**, 157 (1976).

(20) H. C. Rose, R. L. Stern, and B. L. Karger, *Anal. Chem.*, **38**, 469 (1966).

(21) G. Halmchen, G. Nill, D. Flockenzi, W. Schükle, and M. S. K. Youssef, *Angew. Chem. Int. Ed. Engl.*, **18**, 62, (1979).

(22) M. Goodman and L. Levine, *J. Am. Chem. Soc.*, **86**, 2918 (1964).

(23) M. Goodman and W. J. McGahren, *Tetrahedron*, **23**, 2031 (1967).

(24) F. Kurzer and K. Douraghi-Zadeh, *Chem. Rev.*, **67**, 107 (1967).

(25) Y. S. Klansner and M. Bodansky, *Synthesis*, **453** (1972).

(26) W. P. Jencks and J. Canivola, *J. Biol. Chem.*, **234**, 1272 (1959).

(27) L. Aarons, *Analyst*, **106**, 1249 (1981).

ACKNOWLEDGMENTS

Supported by Grant G977/249 from the British Medical Research Council.

Stability-Indicating Assay for Chlorthalidone Formulation: Evaluation of the USP Analysis and a High-Performance Liquid Chromatographic Analysis

JOHN BAUER ˣ, JOHN QUICK, SUZANNE KROGH, and DOUGLAS SHADA

Received March 22, 1982, from *Abbott Laboratories, North Chicago, IL 60064.* Accepted for publication July 30, 1982.

Abstract □ An investigation of the USP assay of chlorthalidone tablets showed that variable degradation of chlorthalidone occurred during assay preparation. The degradation products were isolated and identified. A stability-indicating high-performance liquid chromatographic (HPLC) assay which separates the degradation products from chlorthalidone was developed and used to examine the present USP preparation. The HPLC assay is suggested as an alternate.

Keyphrases □ Chlorthalidone—high-performance liquid chromatography, stability-indicating assay, comparison with the USP analysis □ Degradation products—of chlorthalidone, high-performance liquid chromatographic determination, comparison with the USP analysis □ USP analysis—for chlorthalidone and degradation products, comparison to a high-performance liquid chromatographic assay

Chlorthalidone (I) is a monosulfamyl diuretic used in the treatment of hypertension. The official analysis of chlorthalidone tablets, as prescribed in the United States Pharmacopeia, is a spectrophotometric assay (1). Chlorthalidone has been quantitated in various media using a variety of methodologies (2–8). The major techniques in

0022-3549/83/0800-0924$01.00/0

Table I—Precision Study of USP Chlorthalidone Assay

Lot No.	Concentration	HPLC Assay, %	USP Assay, % Lab 1	Lab 2	Lab 3	Lab 4
16-910-AR	25 mg/tab	101.8	94.8	100.4	96.7	104.0
			95.2		95.6	102.3
Mean			98.43			
SD			±3.75			
RSD			±3.81%			
16-911-AR	50 mg/tab	100.5	96.4	101.4	104.8	106.8
			94.5		106.1	106.5
Mean			102.36			
SD			±2.65			
RSD			±2.58%			

Table II—Standard Addition and Recovery of Chlorthalidone 25-mg and 50-mg Tablets

Chlorthalidone Added, mg	Placebo for 25-mg Tablets mg Found	Recovery,%	Placebo for 50-mg Tablets mg Found	Recovery,%
12.54	12.38	98.7	12.44	99.2
25.08	24.74	98.6	24.87	99.2
37.62	37.12	98.7	37.20	98.9
50.16	49.45	98.6	49.64	99.0
62.70	61.68	98.4	62.10	99.0

biological materials involve extractive alkylation and GLC (6–8) or deamination followed by UV spectrophotometric quantitation (2, 3, 5). Although a high-performance liquid chromatographic (HPLC) method using a polyamide column (9) has been published for chlorthalidone formulations, the USP still officially requires a UV spectrophotometric assay. An investigation of the precision of this analysis indicated erratic results (Table I). Two lots of chlorthalidone tablets were analyzed by the USP method in four separate testing laboratories with varying results.

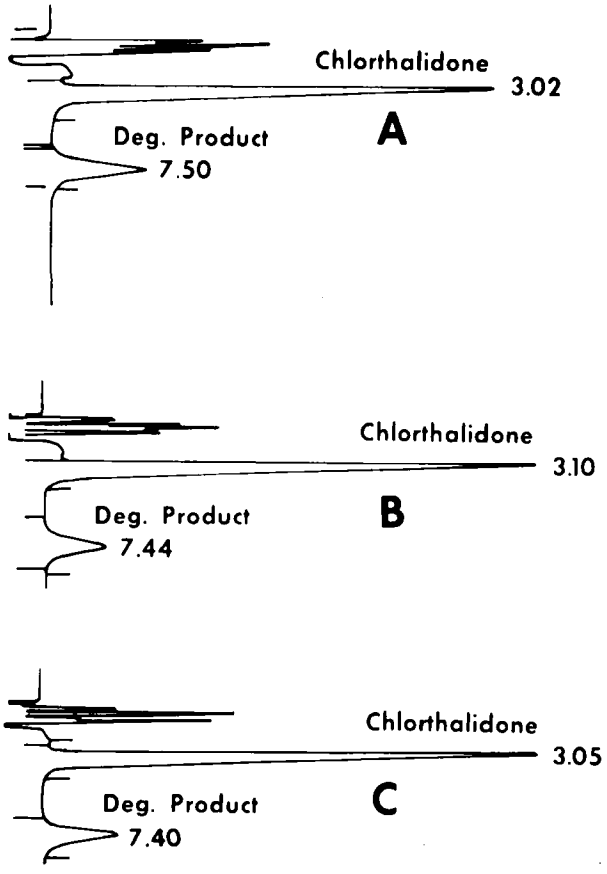

Figure 1—*Chromatograms of USP assay preparations. Key: (A) USP standard lot G immediately after acidification; (B) current marketed product immediately after acidification; (C) chlorthalidone (generic 25 mg) immediately after acidification.*

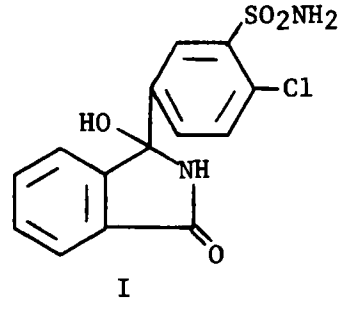

I

2-Chloro-5-(2,3-dihydro-1-hydroxy-3-oxo-1*H*-isoindol-1-yl)benzenesulfonamide

Since the UV absorbance of chlorthalidone is known to conform to Beer's law in the concentration region used for the assay, the possibility that chlorthalidone is unstable in the acidic assay preparation was investigated. The USP analysis is not stability indicating; therefore, development

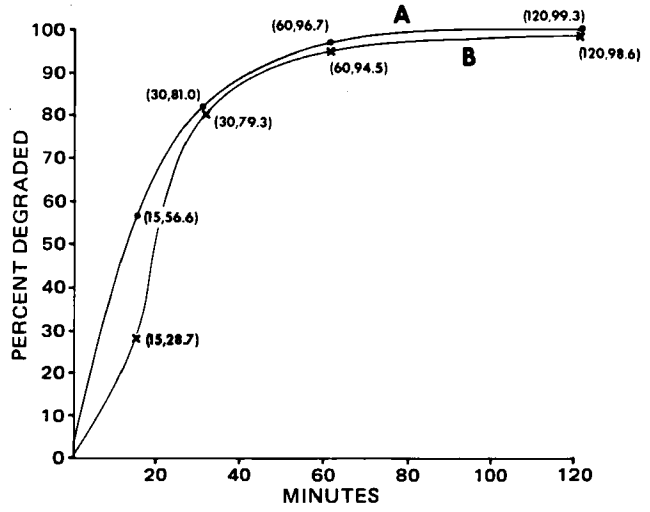

Figure 2—*Rate of degradation of chlorthalidone in USP assay medium. Key: (A) standard preparation; (B) sample preparation.*

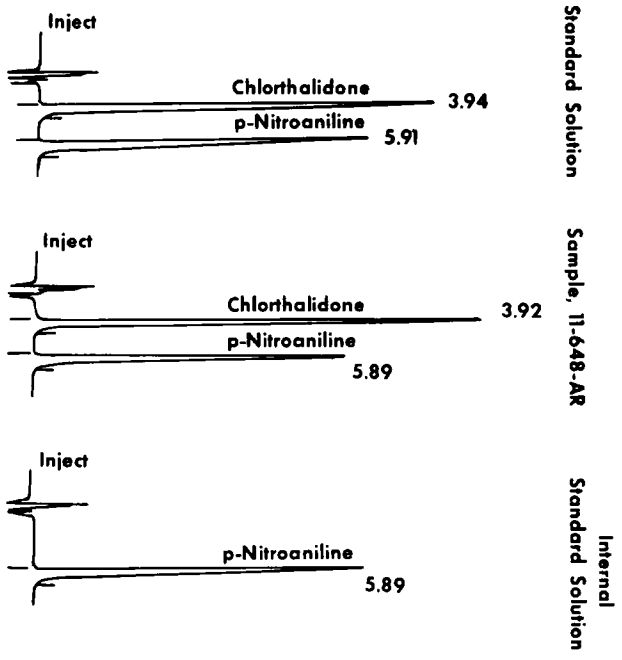

Figure 3—*Typical chlorthalidone chromatograms.*

of an HPLC assay using a less specialized and sensitive column than previously reported (9) was undertaken. The HPLC system was used to evaluate the current USP methodology and is suggested as an alternate assay.

BACKGROUND

The USP assay for chlorthalidone consists of an acetone extraction followed by filtration and evaporation of the extract. The residue is then dissolved in acidic methanol and quantitated by UV spectrophotometry. The analytical wavelength is 275 nm.

When the final acidic methanol solutions from the USP assay were examined by HPLC (Fig. 1) they were found to contain mixtures of chlorthalidone and one or both of the degradation products (II and III), which coelute, shown below:

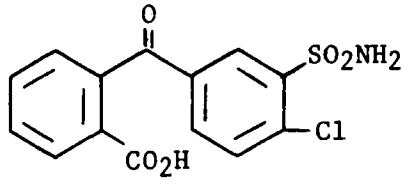

II

2-(3-aminosulfonyl-4-chlorobenzoyl)benzoic acid

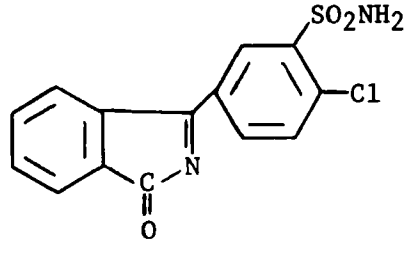

III

3-[(4-chloro-3-aminosulfonyl)phenyl]-1*H*-isoindol-1-one

Both compounds II and III have larger extinction coefficients at the analytical wavelength than does chlorthalidone. This study reports the occurrence of a noncontrolled degradation of chlorthalidone in the USP

Table III—Precision Study for the Chlorthalidone HPLC Assay

~25 mg/tablet		~50 mg/tablet	
mg Found	mg Found	mg Found	mg Found
23.77	23.97	47.91	47.26
23.92	23.74	48.04	47.04
23.88	23.49	47.92	47.04
23.87	23.98	47.54	47.39
23.80	23.58	47.81	47.03
Mean	23.80 mg/tablet		47.50 mg/tablet
SD	±0.16 mg/tablet		±0.40 mg/tablet
RSD	±0.68%		±0.84%

sample and standard preparations and details an HPLC analysis for chlorthalidone, which is stability indicating in so far as the degradation products are separated from the parent drug. These products can be quantitated independently if desired. Kinetic studies of the standard preparation and the tablet preparation during the USP assay show that, although similar, the rates of degradation of the sample and standard are different (Fig. 2). Since the degradation is not quantitative, the samples assayed are heterogeneous mixtures and errors result in both directions.

The use of a mineral acid in the USP assay causes chlorthalidone to degrade. The HPLC analysis presented here does not use strong acid during sample preparation.

EXPERIMENTAL

Materials—Acetonitrile[1], acetic acid[1], methanol[2], and *p*-nitroaniline[3] were used as received. The chlorthalidone used was USP reference standard lot G.

A high-performance liquid chromatograph[4], a scanning spectrophotometer[5], a UV-visible spectrophotometer[6], and a mechanical shaker[7] were used. A microparticulate octadecylsilane column[8] was used. The

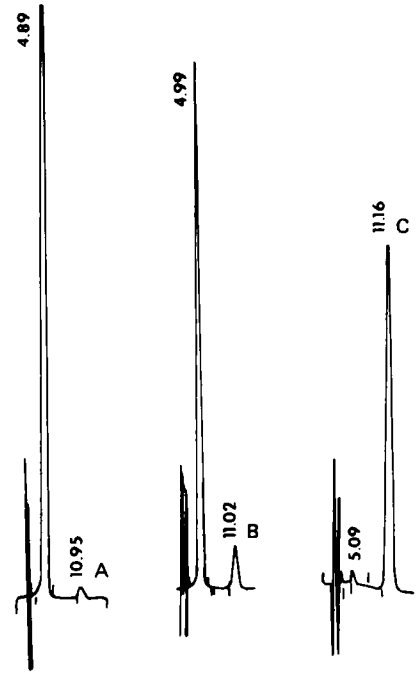

Figure 4—*Time study of USP assay using HPLC. Key: (A) immediately after preparation; (B) 10 min after; (C) 30 min after.*

[1] Glass Distilled, Burdick and Jackson.
[2] Mallinckrodt.
[3] Aldrich Chemical Co.
[4] Waters Model 6000A liquid chromatographic pump; Spectra-Physics Model 4100 computing integrator; DuPont variable-wavelength UV detector; Rheodyne Model 7120 injector with a 20 μl loop.
[5] Cary/Varian 219 recording spectrophotometer.
[6] Beckman DU spectrophotometer with Gilford Model 222 photometer update attachment.
[7] Shaker in the round Model S-500, Kraft Apparatus Inc.
[8] Waters Associates C_{18} μ-Bondapak.

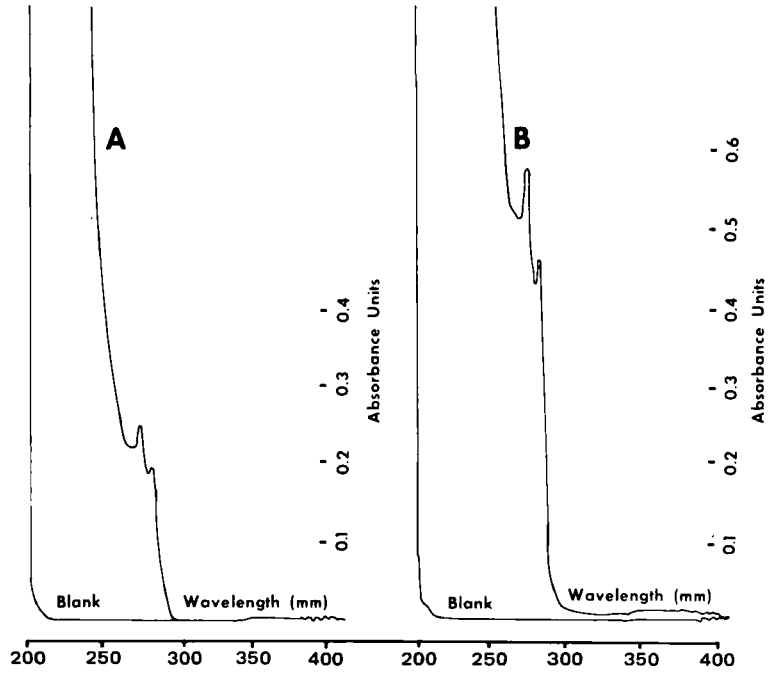

Figure 5—*UV scans of acidified* versus *neutral solution. Key: (A) chlorthalidone in methanol; (B) USP assay preparation.*

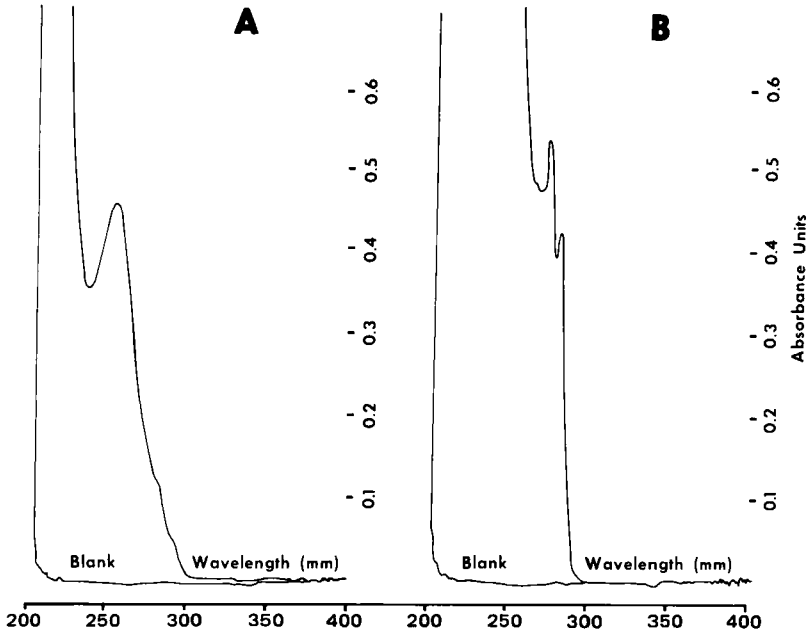

Figure 6—*UV scans of chlorthalidone degradation products. Key: (A) 2-(3-aminosulfonyl-2-chlorobenzoyl)benzoic acid 9.9 μg/ml in acidified MeOH; (B) 3-[(4-chloro-3-aminosulfonyl)-phenyl]-1H-isoindol-1-one 10 μg/ml in acidified MeOH.*

mobile phase was acetonitrile–2% acetic acid (30:70) at a flow rate of 1.5 ml/min. The analytical wavelength was 280 nm.

Reagent Preparation—The internal standard solution was 5 mg/ml of *p*-nitroaniline in methanol.

Approximately 40 mg of chlorthalidone USP standard was accurately weighed and dissolved in 100.0 ml of methanol containing 5.0 ml of the internal standard solution. The solution was diluted 1:1 with water before injection into the liquid chromatograph.

Sample Preparation—Twenty intact tablets were weighed to determine an average tablet weight, finely ground, and a quantity equivalent of 40 mg of chlorthalidone was weighed into a 100-ml volumetric flask. Approximately 50 ml of methanol was added, and the mixture was shaken mechanically for 1 hr. After shaking, 5.0 ml of the internal standard solution was added; the solution was diluted to volume with methanol. A portion of this solution was filtered and diluted 1:1 with water before injection into the liquid chromatograph.

Calculations—The percent of label claim was calculated on the basis of peak height ratios as follows.

$$\frac{(\text{peak height chlorthalidone})_{spl}}{(\text{peak height internal standard})_{spl}} \times \frac{(\text{peak height internal standard})_{std}}{(\text{peak height chlorthalidone})_{std}} \times \frac{\text{Conc. of std.}}{(\text{mg/ml})} \times \frac{100}{\text{Sample Wt}} \times 2 \times \frac{\text{av. tablet wt.}}{(\text{mg/tablet})_{theory}} = \% \text{ Label Claim}$$

RESULTS AND DISCUSSION

The precision data for the HPLC analysis and the precision study conducted on the USP assay (Tables I and III) demonstrate that the HPLC analysis is significantly better than the current compendial method.

When spiked samples were analyzed, recoveries ranged from 98.4 to

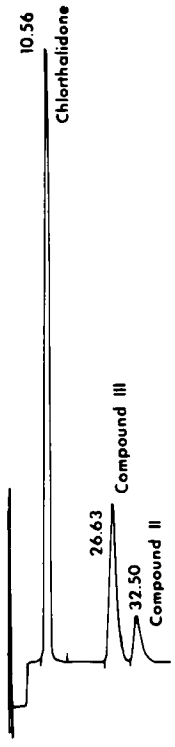

Figure 7—*HPLC system for both degradation products.*

99.2% (Table II). The HPLC method had a relative standard deviation of 0.68% for the analysis of 25 mg of chlorthalidone and 0.84% for 50-mg tablets (Table III). These data were obtained by separate analysts in three laboratories. *p*-Nitroaniline was used as the internal standard. Typical chromatograms for the analysis are shown in Fig. 3.

HPLC analysis of the USP preparation indicated that the solutions being analyzed were mixtures of compounds I, II, and III. The degradation products were isolated from the USP preparation using HPLC. Compound II was identified by comparison with an authentic sample[9] and compound III was identified by spectroscopic techniques[10].

The extent to which chlorthalidone degrades in the acidic methanol appears to depend on pH, water content, and time, although these factors were not all studied in depth. Both of the degradation compounds (II and III) have larger extinction coefficients at the wavelength used for the USP assay than does chlorthalidone. Consequently, the extent of degradation has a marked effect on the assay results and can cause errors in either direction. Figure 4 shows the decrease in chlorthalidone and increase in III with time. Since the degradation is not quantitative and no restraints are prescribed in the USP for pH or time, the absorbance recorded cannot be attributable to any single component.

Comparison of the UV curve for the USP assay preparation with that of chlorthalidone (Figs. 5 and 6) shows substantially the same maxima and minima with slightly greater absorbances. The UV spectrum of compound III is strikingly similar to that of chlorthalidone except for the increased absorptivity for compound III (Fig. 6). The large absorption of chlorthalidone below 260 nm could easily mask the maxima of compound II. This juxtaposition explains how the degradation of chlorthalidone under the USP assay conditions could have been misinterpreted simply as an increase in absorbance due to pH.

The HPLC method described here was designed to quantitate chlorthalidone only. It is stability indicating in so far as chlorthalidone is separated from its degradation products. If a quantitation of the degradation products is desired, a modification of the mobile phase to 85% of 2% acetic acid and 15% acetonitrile flowing at 2 ml/min will allow analysis of I, II, and III concomitantly (Fig. 7).

Close examination of the current compendial assay for chlorthalidone tablets reveals that the drug degrades during analysis. The extent of the degradation is neither quantitative nor reproducible, making the USP assay unreliable. The HPLC method developed in our laboratory is stability indicating and provides a rapid, reliable assay of chlorthalidone. Slight changes in the mobile phase also allow quantitation of the individual degradation products.

[9] Two authentic samples were used: one prepared by Abbott Laboratories, characterized by MS, NMR, IR, CHN; a second obtained as a USP standard. Comparison was done by HPLC and MS to the impurities found in the USP assay preparation.

[10] Compound III was identified by high-resolution mass spectroscopy.

REFERENCES

(1) "The United States Pharmacopeia," 19th rev., U.S. Pharmacopeial Convention, Rockville, Md., 1975, p. 91.

(2) R. Pulver, H. Wirtz, and E. G. Stenger, *Schweiz. Med. Wochenschr.*, **89**, 1130 (1959).

(3) G. Beisenherz, F. W. Koss, L. Klatt, and B. Binder, *Arch. Intern. Pharmacodyn.*, **161**, 76 (1966).

(4) R. Maes, M. Gijbels, and L. Laruelle, *J. Chromatogr.*, **53**, 408 (1970).

(5) M. G. Tweeddale and R. I. Ogilvie, *J. Pharm. Sci.*, **63**, 1065 (1974).

(6) A. Brandstrom and K. Gustavii, *Acta Chem. Scand.*, **23**, 1215 (1969).

(7) M. Ervik and K. Gustavii, *Anal. Chem.*, **46**, 39 (1974).

(8) P. H. Degen and A. Schweizer, *J. Chromatogr.*, **142**, 549 (1977).

(9) M. O'Hare and E. Tan, *J. Pharm. Sci.*, **68**, 106 (1979).

ACKNOWLEDGMENTS

The authors thank Mr. Joseph Martin and Ms. Diane Horgen for assistance in the preparation of this paper.

Thermochemical Investigations of Associated Solutions: Calculation of Solute–Solvent Equilibrium Constants from Solubility Measurements

WILLIAM E. ACREE, Jr., DANNY R. McHAN, and J. HOWARD RYTTING ˣ

Received May 13, 1982, from the *Pharmaceutical Chemistry Department, University of Kansas, Lawrence, KS 66045.* Accepted for publication July 29, 1982.

Abstract □ A simple solution model that has lead to successful predictive equations for the partial molar excess properties of a solute in simple binary solvent mixtures containing only nonspecific interactions is extended to include association between the solute and one of the solvent components. An expression is derived and tested for its ability to describe anthracene solubilities in binary solvent mixtures containing benzene. The best description of the experimental solubilities requires the formation of a 1:1 anthracene–benzene complex, with a molarity-based equilibrium constant of $K^c_{AC} \approx 0.107\ M^{-1}$. In comparison, a stoichiometric complexation model which attributes all solubility enhancement to the formation of anthracene–benzene complexes requires a somewhat larger equilibrium constant ($K^c_{AC} \approx 0.228\ M^{-1}$) to describe the solubility behavior of anthracene in the benzene–*n*-heptane system. The results of these calculations illustrate that the determination of solute–solvent equilibrium constants from solubility data depends on the theoretical model used and the manner in which nonspecific interactions are incorporated into the model.

Keyphrases □ Solute–solvent interactions—determination of equilibrium constants from solubility measurements, comparison of the stoichiometric and nearly ideal binary solvent models □ Solvent systems—binary, anthracene solubility determinations in benzene mixtures using the nearly ideal binary solvent model □ Solubility—binary solvent systems, extension of the nearly ideal binary solvent model to include solute–solvent complexation

Current approaches for predicting solubility often overlook the role of specific interactions in determining the solubilities of organic solids in organic solvents. As part of a continuing study on the thermochemical properties of a solute at high dilution in binary solvent mixtures (1–8), this paper considers the calculation of solute–solvent equilibrium constants from solubility measurements.

Historically, the interpretation of solution nonideality has followed two dissimilar lines of reasoning: the physical approach originated by van Laar (9) and the chemical approach proposed by Dolezalek (10). The physical approach may be described by a random distribution of molecules throughout the entire solution, while the chemical approach may be characterized by a specific geometric orientation of one molecule with respect to an adjacent molecule. Even in systems known to contain specific interactions, the need to properly account for nonspecific interactions is recognized.

Arnett *et al.* (11, 12) attempted a classical separation of specific and nonspecific interactions with their "pure" base calorimetric method for determining enthalpies of hydrogen bond formation. The sensitivity of the numerical results to the selection of the model compound and inert solvent (13) points out the difficulty in separating the physical and chemical contributions of solution nonideality. Christian *et al.* (14, 15) proposed a model for relating the thermodynamic properties of polar solutes involved in complex equilibria to those of analogous nonpolar solutes in the same solvent media. In the nonpolar analogue method, the polar solute is replaced by a hypothetical nonpolar molecule which has the same molecular volume and the same total energy of interaction with a nonpolar solvent as does the polar solute. Saluja *et al.* (16) used a somewhat similar rationale in their comparison of enthalpies of transfer of alkenes and the corresponding alkanes from the vapor state to methanol, dimethylformamide, benzene, and cyclohexane, with the more exothermic values for the alkenes in methanol and dimethylformamide attributed to dipole-induced dipole interactions between the solvent and the polarizable π-bond.

Many of the remaining methods for studying association phenomena can be classified as solubility methods. That is, the increase in solubility of a solute at constant fugacity in a complexing-inert solvent mixture, relative to the solubility in pure inert solvent, is generally attributed to the formation of molecular complexes. This primary assumption is common to several thermodynamic methods, such as the partition of solutes between two immiscible liquid phases, the measurement of infinite dilution GC partition coefficients, and the increased solubility of solids. The techniques for calculating formation constants are essentially identical for all solubility methods, as are the difficulties in properly assessing what portion of the observed solubility enhancement is due to nonspecific interactions.

In earlier papers, the experimental solubilities for benzil (5) and *p*-benzoquinone (6) in binary solvent mixtures containing carbon tetrachloride were reported, in which the mole fraction solubility of benzil and *p*-benzoquinone cover a 14- and 6-fold range, respectively. The experimental data were interpreted with solution models developed previously for solubility in systems containing specific solute–solvent interactions and with models of purely nonspecific interactions. A stoichiometric complexation model based entirely on specific interactions (nonspecific interactions ignored) required several equilibrium constants to mathematically describe the experimental results, while the simple nearly ideal binary solvent (NIBS) model based on nonspecific interactions adequately described the observed solubilities without introducing a single equilibrium constant.

The success of the NIBS approach in predicting the binary solvent effect on benzil and *p*-benzoquinone solubilities suggests the possibility that this model may provide a foundation for approximations of the physical interactions even in a system containing chemical interactions such as association between the solute and a complexing solvent. To pursue this idea further, the basic NIBS model

0022-3549/83/0800-0929$01.00/0

is extended to complexing systems and an expression is derived for the calculation of solute–solvent equilibrium constants from solubility measurements. Equilibrium constants for presumed benzene–anthracene complexes are calculated from the newly derived expression and are compared with values calculated from a stoichiometric complexation model based entirely on specific interactions. Although the magnitude of the calculated equilibrium constants are relatively small, and perhaps meaningless, the calculations do illustrate the importance of including nonspecific interactions, particularly in the case of weak association complexes.

THEORETICAL

Stoichiometric Complexation Model—Stoichiometric complexation models have been used frequently to quantitatively explain enhanced solubilities of a polar organic solute in binary mixtures containing an inert hydrocarbon and a polar cosolvent. The basic model assumes complexation between the solute, A, and an interacting cosolvent, C (17–21):

$$A_1 + C_1 \rightleftharpoons AC \overset{+C_1}{\rightleftharpoons} AC_2 \overset{+C_1}{\rightleftharpoons} AC_3 \ldots AC_n$$

Each reaction is described by an appropriate equilibrium constant with concentrations expressed in molarities:

$$K^c_{AC} = \frac{C_{AC}}{C^{sat}_{A_1} C_{C_1}} \qquad \text{(Eq. 1)}$$

$$K^c_{AC_n} = \frac{C_{AC_n}}{C_{AC_{n-1}} C_{C_1}} \qquad \text{(Eq. 2)}$$

where $C^{sat}_{A_1}$ is the saturation solubility of solute in pure inert hydrocarbon (assumed to represent the free solute concentration in binary mixtures as well) and C_{C_1} is the free (uncomplexed) ligand concentration. This particular model assumes only a single solute molecule is present in each complex, but the mathematical form of the resulting equations is not significantly altered by additional solute molecules per complex.

The total solubility of solute in any system, C^{sat}_A, can be expressed as:

$$C^{sat}_A = C^{sat}_{A_1} + K^c_{AC} C^{sat}_{A_1} C_{C_1} + K^c_{AC} K^c_{AC_2} C^{sat}_{A_1} C^2_{C_1} + \ldots \qquad \text{(Eq. 3)}$$

and the total concentration of complexing agent, C_C, as:

$$C_C = C_{C_1} + K^c_{AC} C^{sat}_{A_1} C_{C_1} + 2K^c_{AC} K^c_{AC_2} C^{sat}_{A_1} C_{C_1} + \ldots \qquad \text{(Eq. 4)}$$

If only 1:1 solute–solvent complexes are present, Eqs. 3 and 4 can be combined to give:

$$\text{Fractional change in solubility} = \frac{C^{sat}_A - C^{sat}_{A_1}}{C^{sat}_{A_1}} = \frac{K^c_{AC} C_C}{1 + K^c_{AC} C^{sat}_{A_1}} \qquad \text{(Eq. 5)}$$

and a plot of the fractional change in solubility *versus* added ligand gives a straight line, with the equilibrium constant calculated from the slope.

Direct graphical evaluation of equilibrium constants is also possible for systems having both 1:1 and 1:2 solute–solvent complexes. Suitable mathematical manipulations of Eqs. 3 and 4 result in:

$$\frac{C^{sat}_A - C^{sat}_{A_1}}{C_C - 2(C^{sat}_A - C^{sat}_{A_1})} = \alpha + \beta[C_C - 2(C^{sat}_A - C^{sat}_{A_1})] \qquad \text{(Eq. 6)}$$

where $\alpha = K^c_{AC} C^{sat}_{A_1}/(1 - K^c_{AC} C^{sat}_{A_1})$ and $\beta = K^c_{AC_2} C^{sat}_{A_1}/(1 - K^c_{AC} C^{sat}_{A_1})^2$. Plots of the left-hand side of Eq. 6 *versus* $C_C - 2(C^{sat}_A - C^{sat}_{A_1})$ gives a straight line. The two equilibrium constants, K^c_{AC} and $K^c_{AC_2}$, are easily calculated from the slope and intercept.

Graphical determination of the association constants is depicted in Figs. 1 and 2 for anthracene solubilities in binary solvent mixtures containing benzene, as reported previously (8). Inspection of the two figures reveal that the solubility data can be described adequately throughout most of the concentration region. The model, however, does not describe the solubility in pure benzene. Equilibrium constants calculated from the various slopes and intercepts are small in magnitude, *e.g.*, linear least-squares analysis of the anthracene solubilities in benzene–*n*-heptane mixtures *via* Eq. 6 gives $K^c_{AC} = 0.228\ M^{-1}$ and $K^c_{AC_2} = 0.034\ M^{-1}$. By reporting these numerical values, we do not intend to imply that anthracene–benzene complexes actually exist in solution. Rather, the experimental solubilities are being used to illustrate the calculation of solute–solvent equilibrium constants from solubility data and to show that the numerical values of these constants depend on how nonspecific interactions are incorporated into the theoretical model. This is particularly true for weak association complexes.

Although the stoichiometric complexation model mathematically describes the experimental solubilities, one is naturally suspicious of whether the calculated values of $K^c_{AC_n}$ truly represent specific solute–solvent interactions or the failure of the model to properly describe nonspecific interactions. As demonstrated in an earlier paper (5), experimental solubilities of benzil in simple hydrocarbon mixtures do vary with solvent composition, and there is no reason to expect the free solute concentration to be independent of solvent composition in more complex systems. The failure of Eqs. 5 and 6 to allow for variation in free solute concentration has been one of the main criticisms of this model.

A second limitation of this particular complexation model becomes apparent on writing the solubility expressions in terms of the solubility in the two pure solvents: $(C^{sat}_A)B$ and $(C^{sat}_A)C$[1]. The complete description of experimental solubility in the pure complexing solvent through Eq. 5 requires:

$$\frac{(C^{sat}_A)_C - (C^{sat}_A)_B}{(C^{sat}_A)_B} = \frac{K^c_{AC} C^*_C}{1 + K^c_{AC}(C^{sat}_A)_B} \qquad \text{(Eq. 7)}$$

where C^*_C refers to the concentration of pure complexing solvent in the saturated solution. Within limitations of the approximate relationships:

$$C_i = 10^3\, X^0_i/(X^0_B \overline{V}_B + X^0_C \overline{V}_C) \qquad \text{(Eq. 8)}$$

and

$$(C^{sat}_A)_i = 10^3\, (X^{sat}_A)_i/\overline{V}_i \qquad \text{(Eq. 9)}$$

combination of Eq. 5 and 7–9 enables the solubility in binary solvent mixtures to be expressed as a mole fraction average of the values in the two pure solvents:

$$X^{sat}_A = X^0_B (X^{sat}_A)_B + X^0_C (X^{sat}_A)_C \qquad \text{(Eq. 10)}$$

$$X^0_B = 1 - X^0_C = X_B/(X_B + X_C)$$

Predictions using Eq. 10 are off by as much as 50% for *p*-benzoquinone in *n*-heptane–carbon tetrachloride mixtures (6) and are off by a factor of two for benzil in the isooctane–carbon tetrachloride system (5). It is difficult to attribute the failure of Eq. 10 to specific solute–solvent interactions between the solutes and carbon tetrachloride or to the departure from infinite dilution, as the nearly ideal binary solvent approach describes these experimental solubilities to within a maximum deviation of 6% without introducing a single equilibrium constant.

Equation 10 was derived specifically for binary solvent systems containing both a complexing and inert solvent, but comparable equations have been derived from quite dissimilar models. Sytilin (22) described solubility in mixed solvents as:

$$C^{sat}_A = K_B C_B + K_C C_C \qquad \text{(Eq. 11)}$$

$$K_i = (C^{sat}_A)/C^*_i \qquad i = B, C$$

Equation 11 becomes identical to Eq. 10 when the saturation solubility is sufficiently small. Sytilin's expression is based on the assumption of solvational complexes between the solute and solvent and has been applied to systems in which true association is generally not considered to exist (*i.e.*, iodine–*n*-alkane mixtures). While Eq. 10 does provide reasonable predictions for a rather large number of systems, the expression is obviously incapable of describing systems containing either a maximum or minimum mole fraction solubility. Classic examples are found in studies of phenanthrene (23) and 2-nitro-5-methylphenol (24) in cyclohexane–methylene iodide mixtures where the observed solubilities show maximum values that are almost twice that predicted by Eq. 10. Extension of Eq. 11 to include mixed solvates has been proposed by Sytilin (25) as a means of explaining maximum solubilities, but even this explanation seems unsatisfactory since the existence of maximum solubility in these two systems is predicted by solubility parameter theory.

In a series of papers devoted to infinite dilution solubility of volatile third components in binary mixtures of relatively nonvolatile liquids, Purnell and coworkers (26, 27) have shown that a majority of published

[1] The solubility of the solute in the inert solvent $(C^{sat}_A)_B$ equals the solubility of the uncomplexed solute in the inert solvent $(C^{sat}_{A_1})_B$.

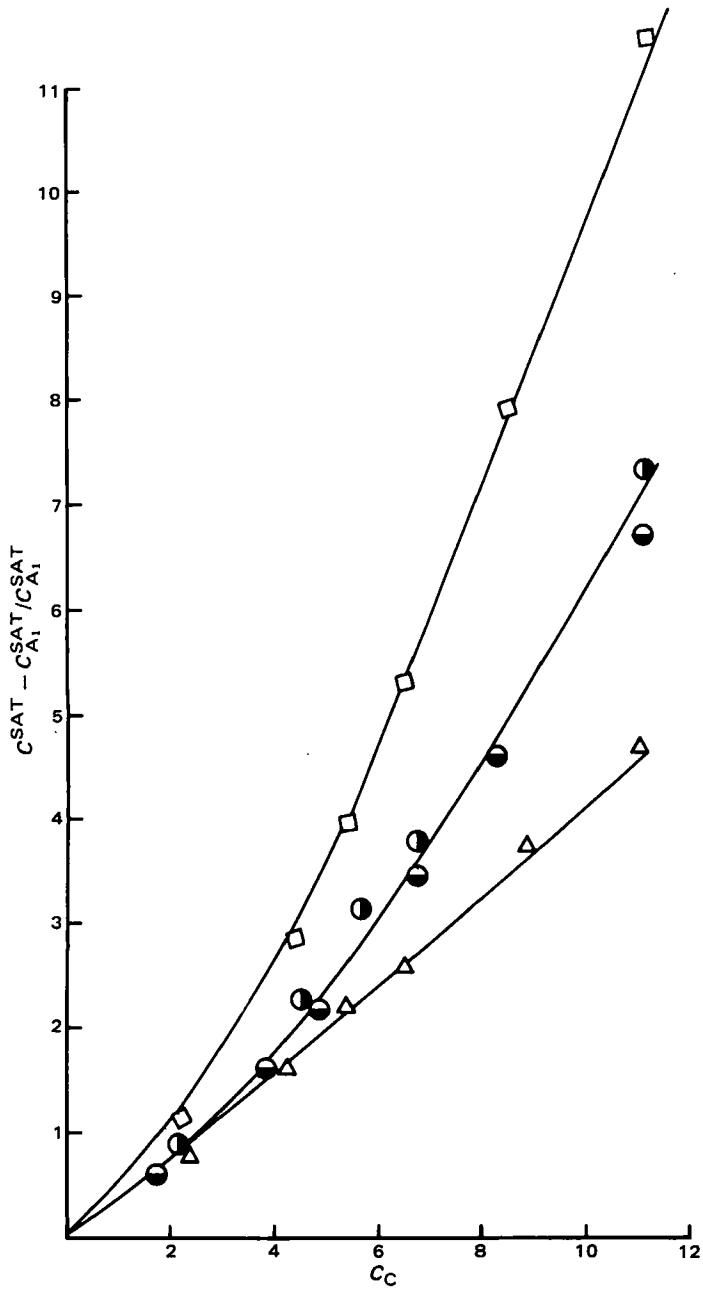

Figure 1—*Graphical determination of* K^c_{AC} *from plots of the fraction change in solubility* versus *benzene molarity in several binary solvents consisting of benzene and* n-*hexane* (◑), n-*heptane* (◒), *cyclohexane* (△), *or isooctane* (□). *The basic model requires additional solute–solvent complexes to explain the nonlinear behavior (see Eqs. 3 and 4).*

data can be described by a simple linear relationship between the volume fraction and partition coefficient:

$$K^0_R = \phi_B(K^0_R)_B + \phi_C(K^0_R)_C \qquad \text{(Eq. 12)}$$

irrespective of the complexing nature of the solvents. ϕ_B and ϕ_C are volume fractions of solvents B and C, respectively, K^0_R is the infinite dilution gas–liquid partition coefficient in the mixted solvent, and $(K^0_R)_B$ and $(K^0_R)_C$ refer to the corresponding values of K^0_R in the pure liquids. Using standard definitions relating partition and activity coefficients, Purnell and Vargas de Andrade (26) have shown that Eq. 12 is equivalent to:

$$\frac{1}{\gamma^\infty_A} = \frac{X^0_B}{(\gamma^\infty_A)_B} + \frac{X^0_C}{(\gamma^\infty_A)_C} \qquad \text{(Eq. 13)}$$

where γ^∞_A is the infinite dilution activity coefficient of the solute (relative to Raoult's law), with only the ideal molar volume approximation.

The activity coefficient of the solute can be related to the solubility of a solid through the thermodynamic relationship:

$$a^{solid}_A = X^{sat}_A \gamma^{sat}_A \qquad \text{(Eq. 14)}$$

in which the activity of the solid depends on temperature only and is determined relative to the pure supercooled liquid. If the solubility is sufficiently small, the activity coefficient of the solute at infinite dilution may be approximated directly as the activity coefficient at saturation:

$$\gamma^{sat}_A = \gamma^\infty_A \qquad \text{(Eq. 15)}$$

Combination of Eqs. 13–15 yields an expression which is identical to Eq. 10.

The fact that several dissimilar solution models reduce to a common mathematical expression in the limits of low solute solubility suggests that there is often more than one interpretation of solution nonideality that will describe the observed solubility data. Each solution model, therefore, must be judged not only on its ability to describe a particular set of experimental data, but also on the validity and limitations of its underlying assumptions and simplifying approximations.

Extension of the NIBS Approach to Solubility in Complexing Systems—The NIBS treatment has been shown to be quite dependable for estimating heats of solution (28, 29), gas–liquid partition coefficients (1–3), and solubilities (4–8) in binary solvent systems that are free of

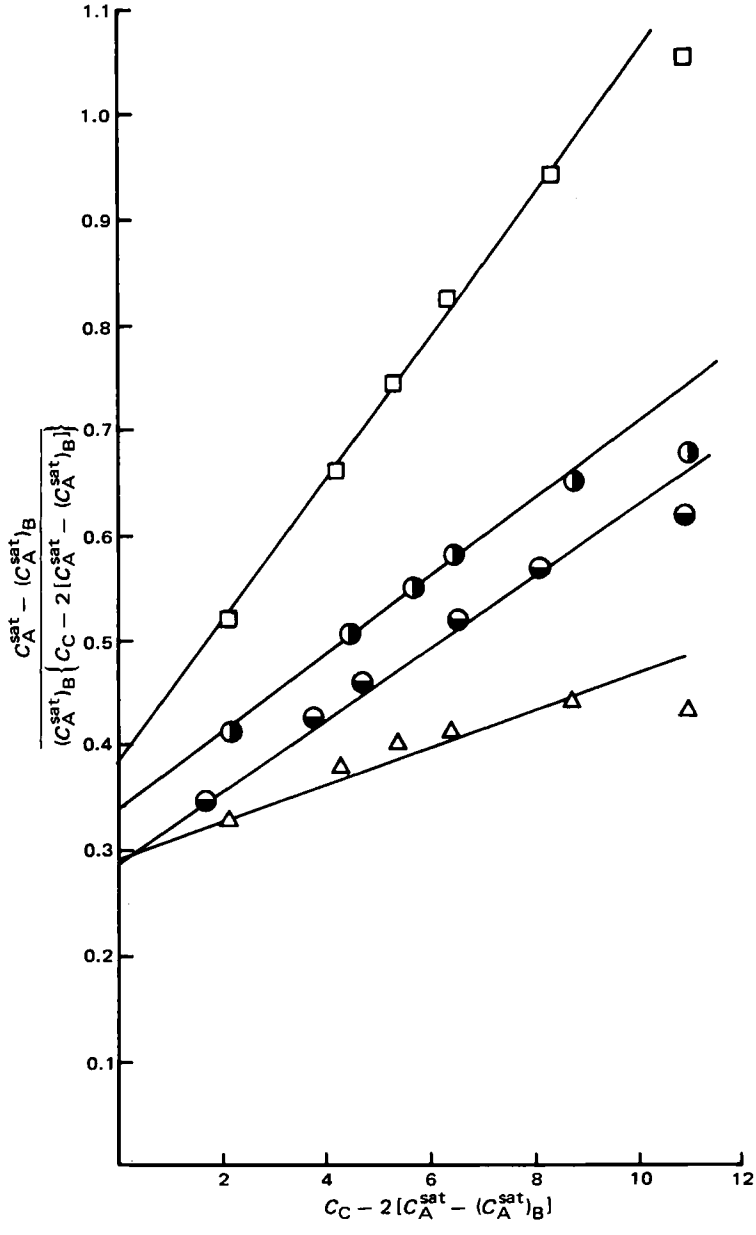

Figure 2—*Graphical determination of* K^c_{AC} *and* $K^c_{AC_2}$ *for anthracene in several binary solvents at 25°. The binary mixtures contained benzene and* n-*hexane* (◑), n-*heptane* (◒), *cyclohexane* (△), *or isooctane* (□).

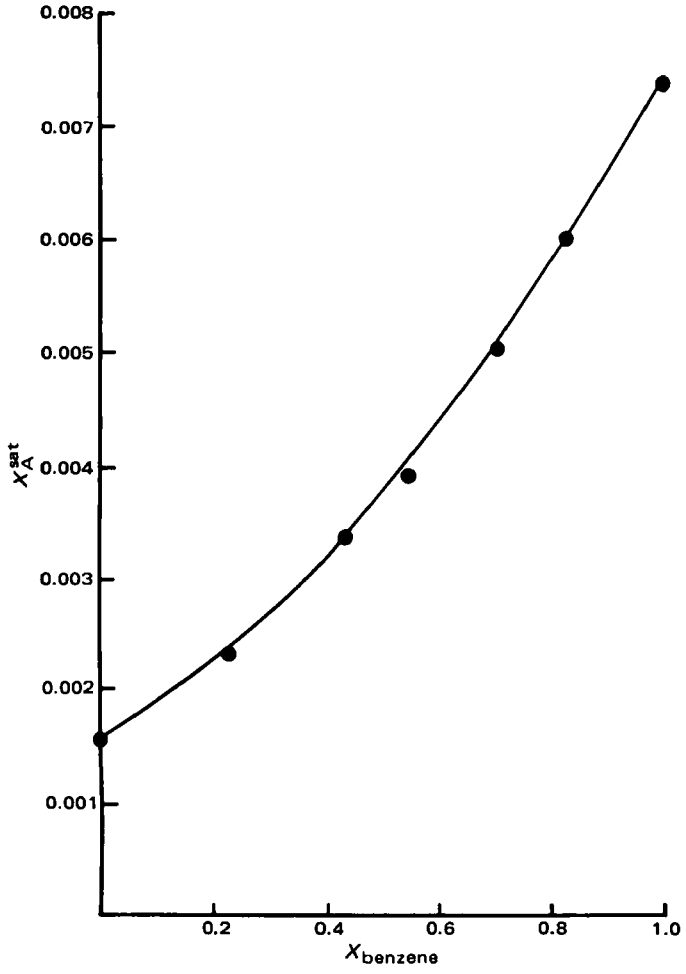

Figure 3—*Comparison between experimental solubilities (●) and the predictions of Eq. 30 (——) for anthracene in binary mixtures of benzene–n-heptane. The free energy of mixing data for the binary solvent ($\Delta\overline{G}^{ex}_{BC}$) is taken from measurements by Harris and Dunlop (32).*

association. The form of the NIBS equation which has been most successful for describing the excess chemical potential of solutes is based on a simple mixing model of a multicomponent system:

$$\Delta G^{mix}_{1,2,\ldots N} = RT \sum_{i=1}^{N} n_i \ln \phi_i + \left(\sum_{i=1}^{N} n_i \overline{V}_i\right)\left(\sum_{i=1}\sum_{j>i} \phi_i \phi_j A_{ij}\right) \quad \text{(Eq. 16)}$$

in which n_i is the number of moles of component i, $\overline{V}_i$ is the molar volume of a pure liquid, ϕ_i is the volume fraction, and A_{ij} is a binary interaction parameter that is independent of solvent composition. The application of Eq. 16 to the quaternary system (A_1, B, C_1, and AC) takes the form of:

$$\Delta G^{mix} = RT(n_{A_1}\ln \phi_{A_1} + n_B \ln \phi_B + n_{C_1}\ln \phi_{C_1} + n_{AC}\ln \phi_{AC}) + (n_{A_1}\overline{V}_A + n_B\overline{V}_B + n_{C_1}\overline{V}_{C_1} + N_{AC}\overline{V}_{AC})(\phi_{A_1}\phi_B A_{A_1B} + \phi_{A_1}\phi_{C_1}A_{A_1C_1} + \phi_{A_1}\phi_{AC}A_{A_1AC} + \phi_B\phi_{C_1}A_{BC_1} + \phi_B\phi_{AC}A_{BAC} + \phi_{C_1}\phi_{AC}A_{C_1AC}) \quad \text{(Eq. 17)}$$

The only assumption is that the molar volume of the AC complex equals the sum of the molar volumes of components A and C, *i.e.*, $\overline{V}_{AC} = \overline{V}_A + \overline{V}_C$. The chemical potentials of the individual components relative to the pure liquids (μ_i^*) are obtained through the appropriate differentiation:

$$\mu_{A_1} - \mu_A^* = RT\left(\ln \phi_{A_1} + 1 - \frac{\overline{V}_A}{\hat{V}_{solution}}\right) + \overline{V}_A[\phi_B(1-\phi_{A_1})A_{A_1B} + \phi_{C_1}(1-\phi_{A_1})A_{A_1C_1} + \phi_{AC}(1-\phi_{A_1})A_{A_1AC} - \phi_B\phi_{C_1}A_{BC_1} - \phi_B\phi_{AC}A_{BAC} - \phi_{C_1}\phi_{AC}A_{C_1AC}] \quad \text{(Eq. 18)}$$

$$\mu_B - \mu_B^* = RT\left(\ln \phi_B + 1 - \frac{\overline{V}_B}{\hat{V}_{solution}}\right) + \overline{V}_B[\phi_{A_1}(1-\phi_B)A_{A_1B} + \phi_{C_1}(1-\phi_B)A_{BC_1} + \phi_{AC}(1-\phi_B)A_{BAC} - \phi_{A_1}\phi_{C_1}A_{A_1C_1} - \phi_{A_1}\phi_{AC}A_{A_1AC} - \phi_{C_1}\phi_{AC}A_{C_1AC}] \quad \text{(Eq. 19)}$$

and

$$\mu_{C_1} - \mu_C^* = RT\left(\ln \phi_{C_1} + 1 - \frac{\overline{V}_C}{\hat{V}_{solution}}\right) + \overline{V}_C[\phi_{A_1}(1-\phi_{C_1})A_{A_1C_1} + \phi_B(1-\phi_{C_1})A_{BC_1} + \phi_{AC}(1-\phi_{C_1})A_{C_1AC} - \phi_{A_1}\phi_B A_{A_1B} - \phi_{A_1}\phi_{AC}A_{A_1AC} - \phi_{B_1}\phi_{AC}A_{B_1AC}] \quad \text{(Eq. 20)}$$

where $\hat{V}_{solution}$ is the molar volume of the true solution and:

$$\frac{1}{\hat{V}_{solution}} = \frac{\phi_{A_1}}{\overline{V}_A} + \frac{\phi_B}{\overline{V}_B} + \frac{\phi_{C_1}}{\overline{V}_C} + \frac{\phi_{AC}}{\overline{V}_A + \overline{V}_C} \quad \text{(Eq. 21)}$$

As shown in many thermodynamic textbooks [*e.g.*, Prigogine and Defay (30)], the chemical potential of stoichiometric component C (and also A) is equal to the chemical potential of the monomeric (uncomplexed) species in the solution:

$$\mu_C = \mu_{C_1} \quad \text{(Eq. 22)}$$

Combining Eqs. 18–22, the Gibbs free energy of mixing can be written as:

$$\Delta G^{mix} = RT\left[n_A\ln \phi_{A_1} + n_B\ln \phi_B + n_C\ln \phi_{C_1} + n_A + n_B + n_C - \frac{(n_A\overline{V}_A + n_B\overline{V}_B + n_C\overline{V}_C)}{\hat{V}_{solution}}\right] + (n_A\overline{V}_A + n_B\overline{V}_B + n_C\overline{V}_C)(\phi_A\phi_B A_{A_1B} + \phi_A\phi_{C_1}A_{A_1C_1} + \phi_A\phi_{AC}A_{A_1AC} + \phi_C\phi_{A_1}A_{A_1C_1} + \phi_C\phi_B A_{BC_1} + \phi_C\phi_{AC}A_{C_1AC} - \phi_{A_1}\phi_{C_1}A_{A_1C_1} - \phi_{A_1}\phi_{AC}A_{A_1AC} - \phi_{C_1}\phi_{AC}A_{C_1AC}) \quad \text{(Eq. 23)}$$

where $n_A = n_{A_1} + n_{AC}$ and $n_C = n_{C_1} + n_{AC}$. Equation 23 obviously contains far too many parameters for useful applications, but reasonable assumptions enable the number of parameters to be greatly reduced. Treatment of all interaction parameters involving the AC complex in a manner similar to that employed by Bertrand (31) for the chloroform–triethylamine complex leads to:

$$A_{A_1AC} = \overline{V}_C^2(\overline{V}_A + \overline{V}_C)^{-2}A_{A_1C_1} \quad \text{(Eq. 24)}$$

and

$$A_{C_1AC} = \overline{V}_A^2(\overline{V}_A + \overline{V}_C)^{-2}A_{A_1C_1} \quad \text{(Eq. 25)}$$

Substitution of these approximations into Eq. 23, after suitable mathematical manipulations, yields the following expression for the Gibbs free energy:

$$\Delta G^{mix} = RT\left[n_A \ln \phi_{A_1} + n_B \ln \phi_B + n_C \ln \phi_{C_1} + n_A + n_B + n_C - \frac{(n_A\overline{V}_A + n_B\overline{V}_B + n_C\overline{V}_C)}{\hat{V}_{solution}}\right] + (n_A\overline{V}_A + n_B\overline{V}_B + n_C\overline{V}_C)(\phi_A\phi_B A_{A_1B} + \phi_B\phi_C A_{BC_1} + \phi_A\phi_C A_{A_1C_1}) \quad \text{(Eq. 26)}$$

Using the equilibrium condition defined by:

$$A_1 + C_1 \rightleftharpoons AC$$

$$K^{\phi}_{AC} = \frac{\phi_{AC}}{\phi_{A_1}\phi_{C_1}} \quad \text{(Eq. 27)}$$

it can be easily shown that the chemical potential of the solid solute (at saturation) is:

$$\mu_A - \mu_A^* = RT\ln a_A^{solid} = RT\left(\ln \phi_{A_1}^{sat} + 1 - \frac{\overline{V}_A}{\hat{V}_{solution}}\right) + \overline{V}_A(1-\phi_A^{sat})^2(\phi_B^0 A_{A_1B} + \phi_C^0 A_{A_1C_1} - \phi_B^0\phi_C^0 A_{BC_1}) \quad \text{(Eq. 28)}$$

where $\phi_B^0 = 1 - \phi_C^0 = \phi_B/(\phi_B + \phi_C)$ and a_A^{solid} is the activity of the solid solute. This activity is defined as the ratio of the fugacity of the solid to the fugacity of the pure supercooled liquid and is calculated from:

$$\ln a_A^{solid} = \int_{T_m}^{T} (\Delta H_A^{fus}/RT^2)dT \quad \text{(Eq. 29)}$$

with the molar enthalpy of fusion (ΔH_A^{fus}) at the normal melting point (T_m).

Inspection of Eq. 28 reveals that, for model systems obeying this expression, the A_1B and $A_{A_1C_1}$ interaction parameters can be eliminated from the basic model *via* the saturation solubilities in the pure solvents, and the A_{BC_1} parameter can be eliminated *via* the excess Gibbs free en-

ergy of the binary solvent mixture calculated according to Eq. 16. Performing these substitutions:

$$RT\left[\ln (a_A^{solid}/\phi_{A1}^{sat}) - 1 + \frac{\overline{V}_A}{\overline{V}_{solution}}\right] = (1 - \phi_A^{sat})^2[\phi_B^0(\Delta\overline{G}_A^{fh})_B^\infty + \phi_C^0(\Delta\overline{G}_A^{fh})_C^\infty - \overline{V}_A(X_B\overline{V}_B + X_C\overline{V}_C)^{-1}\Delta\overline{G}_{BC}^{fh}] \quad \text{(Eq. 30)}$$

where:

$$(\Delta\overline{G}_A^{fh})_B^\infty = (1 - \phi_A^{sat})^{-2} RT\left[\ln (a_A^{solid}/\phi_A^{sat}) - (1 - \phi_A^{sat})\left(1 - \frac{\overline{V}_A}{\overline{V}_B}\right)\right] \quad \text{(Eq. 31)}$$

and

$$(\Delta\overline{G}_A^{fh})_C^\infty = (1 - \phi_A^{sat})^{-2} RT\left[\ln (a_A^{solid}/\phi_{A1}^{sat}) - 1 + \overline{V}_A\left(\frac{\phi_{A1}^{sat}}{\overline{V}_A} + \frac{\phi_C}{\overline{V}_C}\right)\right] \quad \text{(Eq. 32)}$$

The liquid-phase compositions for Eqs. 31 and 32 refer to the saturated pure solvents. In the absence of solute–solvent complexation ($K_{AC}^{\phi} = 0$), the above expression reduces to an equation derived earlier (Eq. VV of Ref. 4) for systems containing only nonspecific interactions.

Despite the complex appearance of Eq. 30, its predictive application to solubilities in mixed solvents is relatively straightforward and is similar in concept to the numerical example presented in an earlier paper (8) for systems containing only nonspecific interactions. The quantities $(\Delta\overline{G}_A^{fh})_B^\infty$ and $(\Delta\overline{G}_A^{fh})_C^\infty$ are calculated from the volume fraction solubility of the solid in the pure solvents using an assumed value for the equilibrium constant. These quantities, with the excess Gibbs free energy of the binary solvent mixture (usually obtained from the literature), are then used in Eq. 30 to calculate ϕ_{A1}^{sat} using a reiterative approach. The overall volume fraction solubility, ϕ_A^{sat}, can be calculated from the solubility of the uncomplexed solute and the equilibrium constant:

$$\phi_A^{sat} = \phi_{A1}^{sat}[1 + \overline{V}_A K_{AC}^{\phi}\phi_{C_1}/(\overline{V}_A + \overline{V}_C)] \quad \text{(Eq. 33)}$$

The entire procedure can be repeated until the numerical value of K_{AC}^{ϕ} that best describes the experimental solubility in a particular binary solvent system is obtained.

Graphical comparison between the experimental solubilities and predictions of Eq. 30 (with $K_{AC}^{\phi} = 1.91$) are shown in Figs. 3 and 4 for anthracene in *n*-heptane–benzene and isooctane–benzene mixtures. Properties of the pure components were taken from a previous tabulation (8). Examination of these two figures indicates Eq. 30 can describe adequately the experimental data using a single equilibrium constant[2]. Readers are reminded that the calculation of association constants for a presumed anthracene–benzene complex does not imply the authors believe such a complex actually exists in solution. As in all cases, the presence of molecular complexes should be supported by independent measurements involving spectroscopy, calorimetry, *etc.*

Although the numerical value of $K_{AC}^{\phi} = 1.91$ is much larger than the equilibrium constant used in Eq. 6, direct comparison requires both constants to be based on an identical concentration scale. Doing this conversion:

$$K_{AC}^{c} = K_{AC}^{\phi}\frac{\overline{V}_A\overline{V}_C}{(\overline{V}_A + V_C)} \quad \text{(Eq. 34)}$$

one finds that the molarity-based equilibrium constant of Eq. 6 ($K_{AC}^{c} = 0.228\ M^{-1}$) is actually two times greater than the molarity-based equilibrium constant of Eq. 30 ($K_{AC}^{c} = 0.107\ M^{-1}$). These calculations further support our earlier observation (5) that equilibrium constants determined from solution models based entirely on specific interactions may not truly represent specific solute–solvent interactions, but rather, in some cases, the failure of the particular solution model to properly describe nonspecific interactions.

RESULTS AND DISCUSSION

A simple solution model that has led to successful predictive equations for the thermochemical properties of a solute in simple binary solvent systems containing only nonspecific interactions has been extended to include association between the solute and one of the solvent components. An expression has been derived and tested for its ability to describe anthracene in binary solvent mixtures containing benzene. The best description of the experimental solubilities required the postulation of a 1:1 anthracene–benzene complex, with a molarity-based equilibrium constant of $K_{AC}^{c} = 0.107\ M^{-1}$. In comparison, a stoichiometric complexation model that attributes all solubility enhancement to the formation of anthracene–benzene complexes required a larger equilibrium constant ($K_{AC}^{c} = 0.228\ M^{-1}$) to describe the six-fold mole fraction range of anthracene solubilities in the benzene–*n*-heptane system. That the two equilibrium constants differ by a factor of two demonstrates the importance of including nonspecific interactions in equilibrium constant calculations, particularly in the case of weak association complexes.

Furthermore, it has been shown that several dissimilar solution models, developed previously for predicting solubility in binary solvent mixtures, reduce to a common mathematical expression in the limits of low solute solubility. Based on this observation, we conclude that there may be more than one interpretation of solution nonideality that will describe the observed solubility data. As criteria for selecting the best description of solution nonideality, we suggest that each solution model should be judged on its ability to describe the thermochemical properties of the solute (in this case, solubility) and on the validity of the model's underlying assumptions and simplifying approximations.

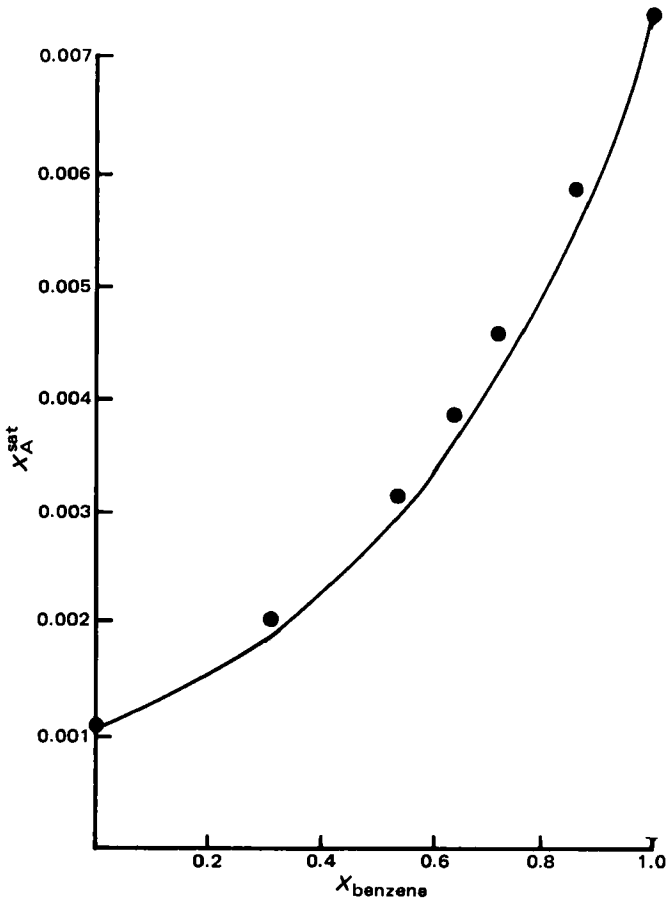

Figure 4—*Comparison between experimental solubilities (●) and the predictions of Eq. 30 (—) for anthracene in binary mixtures of benzene–isooctane. The free energy of mixing data for the binary solvent is taken from an article by Weissman and Wood (33).*

REFERENCES

(1) W. E. Acree, Jr. and G. L. Bertrand, *J. Phys. Chem.*, **83**, 2355 (1979).

(2) W. E. Acree, Jr. and J. H. Rytting, *Anal. Chem.*, **52**, 1764 (1980).

(3) W. E. Acree, Jr., *J. Phys. Chem.*, in press.

(4) W. E. Acree, Jr. and G. L. Bertrand, *J. Phys. Chem.*, **81**, 1170 (1977).

[2] Improvements in the descriptive ability of Eq. 30 could be obtained by permitting the equilibrium constant to vary from one solvent system to another. For example, the best description of the benzene–isooctane system required a slightly larger value for K_{AC}^{ϕ}. This fact is not too disturbing as many of the prevailing solution theories predict that complex formation constants will not be constant in different solvents, even if a maximum-randomness criterion is met by all the species involved in the formation reaction in each of the solvents (34, 35). The numerical value quoted in the text is for the benzene–*n*-heptane system.

(5) W. E. Acree, Jr. and J. H. Rytting, *J. Pharm. Sci.*, **71**, 201 (1982).
(6) W. E. Acree, Jr. and J. H. Rytting, *Int. J. Pharm.*, **10**, 231 (1982).
(7) W. E. Acree, Jr. and G. L. Bertrand, *J. Pharm. Sci.*, **70**, 1033 (1981).
(8) W. E. Acree, Jr. and J. H. Rytting, *J. Pharm. Sci.*, **72**, 292 (1983).
(9) J. J. van Laar, *Z. Phys. Chem.*, **72**, 723 (1910).
(10) F. Dolezalek, *Z. Phys. Chem.*, **64**, 727 (1908).
(11) E. M. Arnett, T. S. S. R. Murty, P. v. R. Schleyer, and L. Joris, *J. Am. Chem. Soc.*, **89**, 5955 (1967).
(12) E. M. Arnett, L. Joris, E. Mitchell, T. S. S. R. Murty, T. M. Gorrie, and P. v. R. Schleyer, *J. Am. Chem. Soc.*, **92**, 2365 (1970).
(13) W. C. Duer and G. L. Bertrand, *J. Am. Chem. Soc.*, **92**, 2587 (1970).
(14) S. D. Christian, R. Frech, and K. O. Yeo, *J. Phys. Chem.*, **77**, 813 (1973).
(15) S. D. Christian, K. O. Yeo, and E. E. Tucker, *J. Phys. Chem.*, **75**, 2413 (1971).
(16) P. P. S. Saluja, T. M. Young, R. F. Rodewald, F. H. Fuchs, D. Kohli, and R. Fuchs, *J. Am. Chem. Soc.*, **99**, 2949 (1977).
(17) B. D. Anderson, J. H. Rytting, and T. Higuchi, *J. Pharm. Sci.*, **69**, 676 (1980).
(18) H. L. Fung and T. Higuchi, *J. Pharm. Sci.*, **60**, 1782 (1971).
(19) B. D. Anderson, Ph.D. Dissertation, University of Kansas, Lawrence, Kans. 1977.
(20) H. L. Fung, Ph.D. Dissertation, University of Kansas, Lawrence, Kans. 1970.
(21) K. Iga, A. Hussain, and T. Kashihara, *J. Pharm. Sci.*, **70**, 108 (1981).
(22) M. S. Sytilin, *Russ. J. Phys. Chem.*, **48**, 1091, 1353, 1500 (1974).
(23) L. J. Gordon and R. L. Scott, *J. Am. Chem. Soc.*, **74**, 4138 (1952).
(24) H. Buchowski, U. Domanska, and A. Ksiazczak, *Polish J. Chem.*, **53**, 1127 (1979).
(25) M. S. Sytilin, *Russ. J. Phys. Chem.*, **52**, 1671 (1978).
(26) J. H. Purnell and J. M. Vargas de Andrade, *J. Am. Chem. Soc.*, **97**, 3585, 3590 (1975).
(27) R. J. Laub and J. H. Purnell, *J. Am. Chem. Soc.*, **98**, 30, 35 (1976).
(28) T. E. Burchfield and G. L. Bertrand, *J. Solut. Chem.*, **4**, 205 (1975).
(29) T. E. Burchfield, Ph.D. Dissertation, University of Missouri-Rolla, Rolla, Mo. 1977.
(30) I. Prigogine and R. Defay, "Chemical Thermodynamics," Wiley, New York, N.Y. 1954.
(31) G. L. Bertrand, *J. Phys. Chem.*, **79**, 48 (1975).
(32) K. R. Harris and P. J. Dunlop, *J. Chem. Thermodyn.*, **2**, 805 (1970).
(33) S. Weissman and S. E. Wood, *J. Chem. Phys.*, **32**, 1153 (1960).
(34) H. Buchowski, J. Devaure, P. V. Huong, and J. Lascombe, *Bull. Soc. Chim. Fri.*, **1966**, 2532.
(35) P. V. Huong, N. Platzer, and M. L. Josien, *J. Am. Chem. Soc.*, **91**, 3669 (1969).

ACKNOWLEDGMENTS

This work was supported in part by Grant GM22357 and Biomedical Research Support Grant RR 5606 from the National Institutes of Health.

Physicochemical and Topological Correlates of the Enzymatic Acetyltransfer Reaction

S. C. BASAK, D. P. GIESCHEN, D. K. HARRISS, and V. R. MAGNUSON ˣ

Received April 26, 1982, from the *Department of Chemistry, University of Minnesota–Duluth, Duluth, MN 55812.* Accepted for publication August 4, 1982.

Abstract □ The relative potencies of a series of substituted anilines as acetyl acceptors in the enzymatic *N*-acetylation reaction have been correlated using physicochemical substituent constants (π, σ^-), molecular connectivity indices ($^1\chi$, $^1\chi^v$), and newly formulated information–theoretic topological indices (IC, SIC). Results indicate a predominant role of the topological steric parameters in determining the rates of the *N*-acetyltransferase reaction.

Keyphrases □ *p*-Nitroaniline—determination of the *N*-acetylation reaction, topological indices □ Topological indices—information–theoretic, rate determination of the *N*-acetylation reaction, comparison with physicochemical constants and molecular connectivity indices, substituted anilines □ *N*-Acetylation reaction—of substituted anilines, enzymatic acetyltransferase, rate determination using information–theoretic topological indices

The biochemical acetyl transfer reaction is important not only for normal physiological processes, but also in the extramicrosomal metabolism of therapeutically active compounds like isoniazid (1, 2), *p*-aminosalicylic acid (3), sulfonamides (4, 5), and anticancer drugs–*viz.*, 6-aminonicotinamide (4). Acetyltransferase is capable of catalyzing the transfer of the acetyl moiety from acetyl CoA (CoASAc) to aliphatic and aromatic amines as well as the reversible transfer of an acetyl group between different aromatic amines (6, 7). Therefore, one of the probable ways of elucidating the molecular basis of this reaction might arise from the study of acetyl group transfer rates from a particular acetylated amine (donor) to other variously substituted amines (acceptor) that vary in their physicochemical and geometrical characteristics in a well-defined manner.

Jacobson (6) studied the rates of acetyl transfer from *p*-(*p*-acetylaminophenylazo)benzenesulfonate to a series of substituted anilines in the presence of purified pigeon liver acetyltransferase. The electronegativity of the substituent(s) was conjectured to have an overwhelming role on the rates of the reaction. This notion gained support from the quantum chemical studies of Perault and Pullman (8) where the electronic charge on the amine nitrogen (ϵ) of the acceptor was shown to parallel the acetylation rate. Further studies by Hansch *et al.* (9) using substituent constants derived from physical organic model systems showed that a biparametric relationship using hydrophobic (π) and electronic (σ^- or ϵ) parameters could adequately correlate the biological data.

0022-3549/83/0800-0934$01.00/0

(5) W. E. Acree, Jr. and J. H. Rytting, *J. Pharm. Sci.*, **71**, 201 (1982).
(6) W. E. Acree, Jr. and J. H. Rytting, *Int. J. Pharm.*, **10**, 231 (1982).
(7) W. E. Acree, Jr. and G. L. Bertrand, *J. Pharm. Sci.*, **70**, 1033 (1981).
(8) W. E. Acree, Jr. and J. H. Rytting, *J. Pharm. Sci.*, **72**, 292 (1983).
(9) J. J. van Laar, *Z. Phys. Chem.*, **72**, 723 (1910).
(10) F. Dolezalek, *Z. Phys. Chem.*, **64**, 727 (1908).
(11) E. M. Arnett, T. S. S. R. Murty, P. v. R. Schleyer, and L. Joris, *J. Am. Chem. Soc.*, **89**, 5955 (1967).
(12) E. M. Arnett, L. Joris, E. Mitchell, T. S. S. R. Murty, T. M. Gorrie, and P. v. R. Schleyer, *J. Am. Chem. Soc.*, **92**, 2365 (1970).
(13) W. C. Duer and G. L. Bertrand, *J. Am. Chem. Soc.*, **92**, 2587 (1970).
(14) S. D. Christian, R. Frech, and K. O. Yeo, *J. Phys. Chem.*, **77**, 813 (1973).
(15) S. D. Christian, K. O. Yeo, and E. E. Tucker, *J. Phys. Chem.*, **75**, 2413 (1971).
(16) P. P. S. Saluja, T. M. Young, R. F. Rodewald, F. H. Fuchs, D. Kohli, and R. Fuchs, *J. Am. Chem. Soc.*, **99**, 2949 (1977).
(17) B. D. Anderson, J. H. Rytting, and T. Higuchi, *J. Pharm. Sci.*, **69**, 676 (1980).
(18) H. L. Fung and T. Higuchi, *J. Pharm. Sci.*, **60**, 1782 (1971).
(19) B. D. Anderson, Ph.D. Dissertation, University of Kansas, Lawrence, Kans. 1977.
(20) H. L. Fung, Ph.D. Dissertation, University of Kansas, Lawrence, Kans. 1970.
(21) K. Iga, A. Hussain, and T. Kashihara, *J. Pharm. Sci.*, **70**, 108 (1981).
(22) M. S. Sytilin, *Russ. J. Phys. Chem.*, **48**, 1091, 1353, 1500 (1974).
(23) L. J. Gordon and R. L. Scott, *J. Am. Chem. Soc.*, **74**, 4138 (1952).
(24) H. Buchowski, U. Domanska, and A. Ksiazczak, *Polish J. Chem.*, **53**, 1127 (1979).
(25) M. S. Sytilin, *Russ. J. Phys. Chem.*, **52**, 1671 (1978).
(26) J. H. Purnell and J. M. Vargas de Andrade, *J. Am. Chem. Soc.*, **97**, 3585, 3590 (1975).
(27) R. J. Laub and J. H. Purnell, *J. Am. Chem. Soc.*, **98**, 30, 35 (1976).
(28) T. E. Burchfield and G. L. Bertrand, *J. Solut. Chem.*, **4**, 205 (1975).
(29) T. E. Burchfield, Ph.D. Dissertation, University of Missouri-Rolla, Rolla, Mo. 1977.
(30) I. Prigogine and R. Defay, "Chemical Thermodynamics," Wiley, New York, N.Y. 1954.
(31) G. L. Bertrand, *J. Phys. Chem.*, **79**, 48 (1975).
(32) K. R. Harris and P. J. Dunlop, *J. Chem. Thermodyn.*, **2**, 805 (1970).
(33) S. Weissman and S. E. Wood, *J. Chem. Phys.*, **32**, 1153 (1960).
(34) H. Buchowski, J. Devaure, P. V. Huong, and J. Lascombe, *Bull. Soc. Chim. Fri.*, **1966**, 2532.
(35) P. V. Huong, N. Platzer, and M. L. Josien, *J. Am. Chem. Soc.*, **91**, 3669 (1969).

ACKNOWLEDGMENTS

This work was supported in part by Grant GM22357 and Biomedical Research Support Grant RR 5606 from the National Institutes of Health.

Physicochemical and Topological Correlates of the Enzymatic Acetyltransfer Reaction

S. C. BASAK, D. P. GIESCHEN, D. K. HARRISS, and V. R. MAGNUSON ˣ

Received April 26, 1982, from the *Department of Chemistry, University of Minnesota–Duluth, Duluth, MN 55812.* Accepted for publication August 4, 1982.

Abstract □ The relative potencies of a series of substituted anilines as acetyl acceptors in the enzymatic *N*-acetylation reaction have been correlated using physicochemical substituent constants (π, σ^-), molecular connectivity indices ($^1\chi$, $^1\chi^v$), and newly formulated information–theoretic topological indices (IC, SIC). Results indicate a predominant role of the topological steric parameters in determining the rates of the *N*-acetyltransferase reaction.

Keyphrases □ *p*-Nitroaniline—determination of the *N*-acetylation reaction, topological indices □ Topological indices—information–theoretic, rate determination of the *N*-acetylation reaction, comparison with physicochemical constants and molecular connectivity indices, substituted anilines □ *N*-Acetylation reaction—of substituted anilines, enzymatic acetyltransferase, rate determination using information–theoretic topological indices

The biochemical acetyl transfer reaction is important not only for normal physiological processes, but also in the extramicrosomal metabolism of therapeutically active compounds like isoniazid (1, 2), *p*-aminosalicylic acid (3), sulfonamides (4, 5), and anticancer drugs–*viz.*, 6-aminonicotinamide (4). Acetyltransferase is capable of catalyzing the transfer of the acetyl moiety from acetyl CoA (CoASAc) to aliphatic and aromatic amines as well as the reversible transfer of an acetyl group between different aromatic amines (6, 7). Therefore, one of the probable ways of elucidating the molecular basis of this reaction might arise from the study of acetyl group transfer rates from a particular acetylated amine (donor) to other variously substituted amines (acceptor) that vary in their physicochemical and geometrical characteristics in a well-defined manner.

Jacobson (6) studied the rates of acetyl transfer from *p*-(*p*-acetylaminophenylazo)benzenesulfonate to a series of substituted anilines in the presence of purified pigeon liver acetyltransferase. The electronegativity of the substituent(s) was conjectured to have an overwhelming role on the rates of the reaction. This notion gained support from the quantum chemical studies of Perault and Pullman (8) where the electronic charge on the amine nitrogen (ϵ) of the acceptor was shown to parallel the acetylation rate. Further studies by Hansch *et al.* (9) using substituent constants derived from physical organic model systems showed that a biparametric relationship using hydrophobic (π) and electronic (σ^- or ϵ) parameters could adequately correlate the biological data.

0022-3549/83/0800-0934$01.00/0

Table I—Partitioning of *p*-Nitroaniline

Partition Class	Coordinate	Number of Atoms in the Partitioned Class[a]	Probability ($p_i = n_i/n$)
I	1^4	4	4/16
II	1^3	2	2/16
III	2^5	2	2/16
IV	$1^4 2^2 2^2$	1	1/16
V	$1^1 1^1 1^4$	1	1/16
VI	$1^1 1^4 2^4$	4	4/16
VII	$1^4 1^5 2^4$	1	1/16
VIII	$1^3 1^4 2^4$	1	1/16

[a] Total number of atoms in the molecule = 16.

One of the important outcomes of the Hansch analysis in this area was that the steric factor is insignificant in enzymatic acetyl transfer process, a conclusion drawn from a study of six compounds. Jacobson (6) studied the *N*-acetylation of 10 substituted anilines. Although the physicochemical substituent constants for the remaining four compounds were not available then (9), some of them can be derived today. Moreover, in recent years, a number of information–theoretic (10–14) and molecular connectivity-type (15–20) topological indices have been derived and found to be of use in biological correlations. While valence molecular connectivity ($^m\chi^v$) indices are excellent electronic parameters (21), simple connectivity indices ($^m\chi$) and information–theoretic indices derived from the topological neighborhood of vortices (atoms) in the molecular graph (structure) are steric parameters that encode information regarding the topological shape of the molecule (11–15, 22). Although the action of nonspecific bioactive molecules is mainly guided by their hydrophobicity, the *in vivo* and *in vitro* activity of specific biologically active agents, *i.e.*, molecules which act by virtue of being recognized by an enzyme or a physiological receptor, is highly dependent on stereoelectronic makeup associated with the molecular architecture (23, 24).

Hence it was of interest to examine whether steric parameters have any role in the mechanism of action of *N*-acetyltransferase. To this end, correlations of the rates of enzymatic acetylation of amines with the physicochemical substituent constants (π, σ^-), molecular connectivity indices ($^1\chi$, $^1\chi^v$), as well as information–theoretic topological indices (11), *i.e.*, information content (IC) and structural information content (SIC), have been attempted. Also, a comparative study of the role of physicochemical *versus* theoretical parameters in the correlation of biological data has been undertaken using multiparametric regression equations.

EXPERIMENTAL

Calculation of the Hydrophobic Constant (π)—The hydrophobic parameter for the various substituents in the aniline derivatives are taken from Hansch and Leo (25). In cases where more than one substituent is present, the combined lipophilic effect is calculated by the addition of the individual contributions of the groups with respect to lipophilicity.

Calculation of the Electronic Parameter (σ^-)—The σ^- values for the various groups in the aniline system are taken from Hansch *et al.* (9, 25), Hoefnagel *et al.* (26), and Zeng (27). Since the simple additivity rule is obeyed with respect to electronic parameters of the Hammett type from a single system (28), the electronic effects (σ^-) of more than one substituent in the ring is taken to be the sum of their individual contributions in the aniline system.

Calculation of Molecular Connectivity ($^1\chi$)—To each atom of the hydrogen-suppressed graph a δ value is assigned corresponding to the number of nonhydrogen atoms bonded to it. No consideration is made to the class of atom or type of bond. A connectivity value for a bond C_k (connecting atoms i and j) is computed as follows (15):

$$C_k = (\delta_i \delta_j)^{-1/2} \qquad \text{(Eq. 1)}$$

And $^1\chi$ is calculated as the sum of all connectivity terms:

$$^1\chi = \sum_k C_k \qquad \text{(Eq. 2)}$$

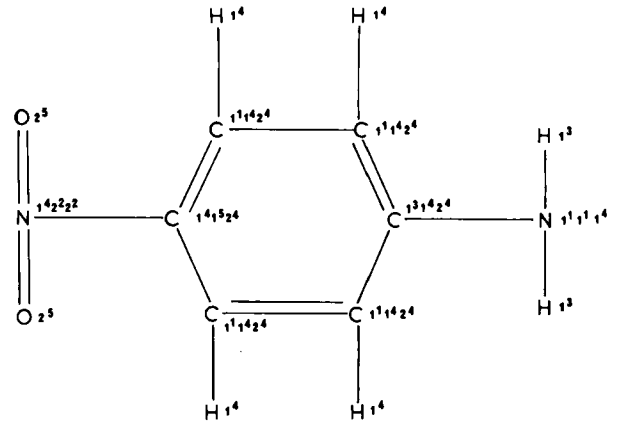

Figure 1—*Coordinate-attached structure of* p-*nitroaniline.*

Calculation of Valence Molecular Connectivity ($^1\chi^v$)—To each atom of the hydrogen-depleted skeleton a δ^v value is assigned as follows (15, 21):

$$\delta^v = Z_i^v - h_i \qquad \text{(Eq. 3)}$$

where Z_i^v is the number of valence electrons and h_i is the number of hydrogen atoms attached to the particular atom. Thereafter, $^1\chi^v$ is calculated in a similar manner as $^1\chi$ by substituting δ^v for δ in Eq. 1.

Calculation of Information Content (IC) and Structural Information Content (SIC) from the Molecular Graph—In this graph–theoretic formalism, the total (nonhydrogen-suppressed) molecular graph is considered to define the various topological indices. The method is sufficiently general to include the linear graphs as well as multigraphs. If G is a molecular graph with vertex set $X(G)$ and $A_i (i = 1, 2, \ldots, k)$ is a partition of $X(G)$, then a probability scheme is given by:

$$\begin{pmatrix} A_1, A_2, \ldots, A_k \\ p_1, p_2, \ldots, p_k \end{pmatrix}$$

where $p_i = n_i/n$, and n_i and n are the cardinalities of A_i and $X(G)$, respectively. Then, the information content (IC) of the graph G with respect to this mode of partition of $X(G)$ is given by Shannon's formula (29):

$$IC(X(G)) = -\sum_k p_i \log_2 p_i \text{ bits} \qquad \text{(Eq. 4)}$$

The logarithm is taken at a basis 2 to measure the information in bits. By defining a first-order topological neighborhood and an equivalence relation on the vertex set $X(G)$ of a molecular graph, Sarkar *et al.* (10) computed the first-order topological information content of various molecular graphs. Subsequently Basak *et al.* (30) defined another information–theoretic topological index, structural information content (SIC):

$$SIC = IC/\log_2 n \qquad \text{(Eq. 5)}$$

Let us take a member of the series of anilines, *p*-nitroaniline (Fig. 1), to exemplify the partitioning of atoms into disjoint classes (Table I) and also the calculation of IC and SIC. In this graph–theoretic treatment, which is patterned after the work of Sarkar *et al.* (10), all four hydrogen atoms attached to the aromatic ring lie in the same disjoint subset. This partitioing scheme differs from that proposed by Kier (14) where chemical intuition is also used in the decomposition of the vertex set of the molecular graph into disjoint subsets.

RESULTS AND DISCUSSION

Table II shows the π and σ^- values of the substituents, $^1\chi$ and $^1\chi^v$ indices from the hydrogen-suppressed molecular graphs, IC and SIC indices

Table II—Biological Properties and Molecular Descriptors for Aniline Derivatives

Compound	Relative Rate (A_x)	σ^-	π	$^1\chi$	$^1\chi^v$	IC (bits)	SIC
Aniline	0.70	0.00	0.00	3.3938	2.1994	2.0060	0.5269
p-Me-Aniline	1.00	−0.17	0.48	3.7877	2.6100	2.3432	0.5733
p-Cl-Aniline	1.09	0.23	0.93	3.7877	2.7120	2.0138	0.5289
p-Br-Aniline	1.12	0.23	1.13	3.7877	3.1021	2.0185	0.5301
p-NO_2-Aniline	0.34	1.27	0.50	4.6984	2.6988	2.7500[a]	0.6875[b]
Sulfanilamide	0.18	0.91	−1.16	4.9900	3.1110	2.8795	0.6778
p-NH_2-Salicylic acid	0.15	0.38	−0.99	5.1091	2.9280	3.3083	0.7934
p-NH_2-Benzoic acid	0.03	0.77	−0.32	4.6984	2.7878	3.0286	0.7409
Sulfanilic acid	0.01	0.48	−4.76	4.9980	3.0422	3.0588	0.7335

[a] $IC = 2 \times 4/16 \log_2(16/4) + 2 \times 2/16 \log_2(16/2) + 4 \times 1/16 \log_2(16/1) = 2.7500$ bits. [b] $SIC = IC/\log_2(16) = 0.6875$.

from the total chemical graphs, and the relative rates of enzymatic acetylation (A_x) for a series of substituted anilines; the experimental data was taken from the work of Jacobson (6). Since our approach was to have a comparative study between the physicochemical and theoretical descriptors in the correlation of acetylation rates, *p*-aminohippuric acid was not considered for correlation because the σ^- value for the *para* substituent was not available.

Table III shows the correlation matrix (31) for A_x and the six molecular descriptors under study. High correlations are observed between the variables A_x, IC, SIC,and $^1\chi$. The parameters $^1\chi^v$, π, and σ^- are poorly correlated with A_x and the other three descriptors. Linear correlation results of each of the six descriptors with A_x are:

$$A_x = -0.616\,(^1\chi) + 3.20 \qquad \text{(Eq. 6)}$$
$$n = 9 \quad r = 0.88 \quad s = 0.24 \quad F_{1,7} = 23\ (p < 0.002)$$

$$A_x = -0.473\,(^1\chi^v) + 1.84 \qquad \text{(Eq. 7)}$$
$$n = 9 \quad r = 0.30 \quad s = 0.48 \quad F_{1,7} = 0.68\ (p < 0.439)$$

$$A_x = -0.830\,(\text{IC}) + 2.67 \qquad \text{(Eq. 8)}$$
$$n = 9 \quad r = 0.91 \quad s = 0.20 \quad F_{1,7} = 35\ (p < 0.001)$$

$$A_x = -4.07\,(\text{SIC}) + 3.13 \qquad \text{(Eq. 9)}$$
$$n = 9 \quad r = 0.92 \quad s = 0.20 \quad F_{1,7} = 36\ (p < 0.001)$$

$$A_x = 0.181\,(\pi) + 0.598 \qquad \text{(Eq. 10)}$$
$$n = 9 \quad r = 0.70 \quad s = 0.36 \quad F_{1,7} = 6.7\ (p < 0.036)$$

$$A_x = -0.648\,(\sigma^-) + 0.807 \qquad \text{(Eq. 11)}$$
$$n = 9 \quad r = 0.64 \quad s = 0.38 \quad F_{1,7} = 4.8\ (p < 0.065)$$

Here n is the number of data points, r the correlation coefficient, s the standard deviation, and F is the F-ratio between the variances of the observed and calculated values.

Equations 6–11 account for 76.8, 8.7, 83.4, 83.7, 48.7, and 40.6% of the variance (r^2) in A_x, respectively. It is clear from these results that steric (topological) parameters like $^1\chi$, IC, and SIC have a very important role in determining the rates of enzymatic acetylation as compared with the hydrophobic (π) or electronic (σ^- or $^1\chi^v$) parameters. The same trend is obtained with the parabolic correlations of A_x with $^1\chi$, $^1\chi^v$, IC, SIC, and π:

$$A_x = 0.462\,(\pi) + 0.0761\,(\pi)^2 + 0.494 \qquad \text{(Eq. 12)}$$
$$n = 9 \quad r = 0.87 \quad s = 0.26 \quad F_{2,6} = 9.8\ (p < 0.013)$$

$$A_x = 2.97\,(^1\chi) - 0.418\,(^1\chi)^2 - 4.34 \qquad \text{(Eq. 13)}$$
$$n = 9 \quad r = 0.90 \quad s = 0.23 \quad F_{2,6} = 12\ (p < 0.007)$$

$$A_x = -0.782\,(^1\chi^v) + 0.0574\,(^1\chi^v)^2 + 2.25 \qquad \text{(Eq. 14)}$$
$$n = 9 \quad r = 0.30 \quad s = 0.51 \quad F_{2,6} = 0.29\ (p < 0.759)$$

Table III—Correlation Matrix

	A_x	π	$^1\chi$	$^1\chi^v$	IC	SIC	σ^-
A_x	1.00						
π	0.70	1.00					
$^1\chi$	−0.88	−0.62	1.00				
$^1\chi^v$	−0.30	−0.36	0.63	1.00			
IC	−0.91	−0.63	0.95	0.46	1.00		
SIC	−0.92	−0.60	0.94	0.43	0.99	1.00	
σ^-	−0.64	−0.16	0.69	−0.37	0.55	0.53	1.00

$$A_x = -1.73\,(\text{IC}) + 0.174\,(\text{IC})^2 + 3.79 \qquad \text{(Eq. 15)}$$
$$n = 9 \quad r = 0.92 \quad s = 0.224 \quad F_{2,6} = 16\ (p < 0.004)$$

$$A_x = -17.60\,(\text{SIC}) + 10.5\,(\text{SIC})^2 + 7.39 \qquad \text{(Eq. 16)}$$
$$n = 9 \quad r = 0.93 \quad s = 0.20 \quad F_{2,6} = 18\ (p < 0.003)$$

Of the nine compounds in Table II, the last seven are homogeneous in the sense that each of them has an electron-withdrawing substituent in the position *para* to the amino group. Therefore, it is expected that steric fit may better correlate the biological data for such a homogeneous group of compounds. Regression equations (Eqs. 17–20) show this to be the case:

$$A_x = -6.67\,(^1\chi) + 0.666\,(^1\chi)^2 + 16.8 \qquad \text{(Eq. 17)}$$
$$n = 7 \quad r = 0.98 \quad s = 0.13 \quad F_{2,4} = 41\ (p < 0.002)$$

$$A_x = -4.49\,(\text{IC}) + 0.695\,(\text{IC})^2 + 7.35 \qquad \text{(Eq. 18)}$$
$$n = 7 \quad r = 0.99 \quad s = 0.09 \quad F_{2,4} = 93\ (p < 0.001)$$

$$A_x = -28.5\,(\text{SIC}) + 18.6\,(\text{SIC})^2 + 11.0 \qquad \text{(Eq. 19)}$$
$$n = 7 \quad r = 0.99 \quad s = 0.10 \quad F_{2,4} = 69\ (p < 0.001)$$

$$A_x = 0.451\,(\pi) + 0.0781\,(\pi)^2 + 0.411 \qquad \text{(Eq. 20)}$$
$$n = 7 \quad r = 0.90 \quad s = 0.25 \quad F_{2,4} = 9.0\ (p < 0.033)$$

The addition of the hydrophobic parameter, π, to Eqs. 17 and 18 made only marginal improvement in the correlation coefficient.

It is evident from the above that topological indices reveal a predominant role of steric factor in determining the rate of the enzymatic *N*-acetyltransferase reaction, although Hansch *et al.* (9) could assign no role of the steric descriptor with a smaller subset of these compounds. With nine compounds a topological parameter such as $^1\chi$, IC, or SIC emerged to be the single variable best suited for correlation of this type of bioactive agent. The significant relationships developed above may be utilized in the rational design of substrates for *N*-acetyltransferase.

REFERENCES

(1) W. Johnson, *Nature (London)*, **174**, 744 (1954).

(2) H. B. Hughes, *J. Pharmacol. Exp. Ther.*, **109**, 444 (1953).

(3) W. Johnson and G. Corte, *Proc. Soc. Exp. Biol. Med.*, **92**, 446 (1956).

(4) W. Johnson, *Can. J. Biochem. Physiol.*, **33**, 107 (1955).

(5) L. S. Goodman and A. Gilman, "The Pharmacological Basis of Therapeutics," Macmillan, New York and London, 1975.

(6) K. B. Jacobson, *J. Biol. Chem.*, **236**, 343 (1961).

(7) S. P. Bessman and F. Lipmann, *Arch. Biochem. Biophys.*, **46**, 252 (1953).

(8) A. M. Perault and B. Pullman, *Biochim. Biophys. Acta*, **66**, 86 (1963).

(9) C. Hansch, E. W. Deutsch, and R. N. Smith, *J. Am. Chem. Soc.*, **87**, 2738 (1965).

(10) R. Sarkar, A. B. Roy, and P. K. Sarkar, *Math. Biosci.*, **39**, 299 (1978).

(11) S. K. Ray, S. C. Basak, C. Raychaudhury, A. B. Roy, and J. J. Ghosh, *Ind. J. Chem.*, **20B**, 894 (1981).

(12) S. C. Basak, S. K. Ray, C. Raychaudhury, A. B. Roy, and J. J. Ghosh, *IRCS Med. Sci.-Biochem.*, **10**, 145 (1982).

(13) S. K. Ray, S. C. Basak, C. Raychaudhury, A. B. Roy, and J. J. Ghosh, *Arzneim.-Forsch.*, **32**, 322 (1982).

(14) L. B. Kier, *J. Pharm. Sci.*, **69**, 807 (1980).

(15) L. B. Kier and L. H. Hall, "Molecular Connectivity in Chemistry

and Drug Research," Academic, New York and London, 1976.
(16) L. B. Kier and L. H. Hall, *J. Med. Chem.*, **20**, 1631 (1977).
(17) J. S. Millership and A. D. Woolfson, *J. Pharm. Pharmacol*, **30**, 483, (1978).
(18) L. B. Kier, R. J. Simons, and L. H. Hall, *J. Pharm. Sci.*, **67**, 725 (1978).
(19) B. K. Evans, K. C. James, and D. K. Luscombe, *J. Pharm. Sci.*, **68**, 370 (1979).
(20) B. van't Riet, L. B. Kier, and H. L. Elford, *J. Pharm. Sci.*, **69**, 856 (1980).
(21) L. B. Kier and L. H. Hall, *J. Pharm. Sci.*, **70**, 583 (1981).
(22) A. T. Balaban, A. Chiriac, I. Motoc, and Z. Simon, "Steric Fit in Quantitative Structure–Activity Relations, Lecture Notes in Chemistry," vol. 15, Springer–Verlag, Berlin–Heidelberg–New York, 1980.
(23) E. J. Ariens, "Drug Design," vol. 1, Academic, New York and London, 1971.
(24) C. Hansch, *Drug Metab. Rev.*, **1**, 1 (1972).
(25) C. Hansch and A. J. Leo, "Substituent Constants for Correlation Analysis in Chemistry and Biology," Wiley, New York–Brisbane–Toronto, 1979.
(26) A. J. Hoefnagel, M. A. Hoefnagel, and G. M. Wepster, *J. Org. Chem.*, **43**, 4720 (1978).
(27) G. Z. Zeng, *Acta Chim. Sinica*, **32**, 107 (1966).
(28) K. Kalfus, J. Kroupa, M. Vecera, and O. Exner, *Collect. Czech. Chem. Commun.*, **40**, 3009 (1975).
(29) C. E. Shannon and W. Weaver, "The Mathematical Theory of Communication," University of Illinois Press, Urbana, Ill., 1949.
(30) S. C. Basak, A. B. Roy, and J. J. Ghosh, "Proceedings of the II International Conference on Mathematical Modelling," vol. 2, University of Missouri, Rolla, Mo., 1979, p. 851.
(31) N. H. Nie, C. H. Hull, J. G. Jenkins, K. Steinbrenner, and D. H. Benf, "Statistical Package for Social Sciences," McGraw-Hill, New York, N.Y., 1975.

ACKNOWLEDGMENTS

The authors wish to express their appreciation to the U.S. Environmental Protection Agency (Contract CR 807566) for support of this work and to the University of Minnesota, Duluth Computer Center for partial financial assistance.

Pharmacokinetics and Anesthetic Potency of a Thiopental Isomer

DONALD R. STANSKI[x], PATRICK G. BURCH, SANDRA HARAPAT, and RICHARD K. RICHARDS[†]

Received March 9, 1982, from the *Departments of Anesthesia and Medicine (Clinical Pharmacology), Stanford University School of Medicine, Stanford, CA 94305* and the *Palo Alto Veterans Administration Hospital, Palo Alto, CA 94304.* Accepted for publication July 29, 1982. [†] Deceased

Abstract □ In developing a high-performance liquid chromatographic assay for thiopental [5-ethyl-5-(1-methylbutyl)-2-thiobarbituric acid], a thiopental isomer [5-ethyl-5-(1-ethylpropyl)-2-thiobarbituric acid] was found. This isomer occurs (6–7%) in supposedly pure thiopental and in the commercially available thiopental sodium administered to patients for induction of anesthesia. A similar type of isomer also occurs in pentobarbital, the oxybarbiturate analogue of thiopental. Because the disposition and anesthetic potency of the isomer is unknown, its pharmacokinetic properties were determined in humans and its anesthetic potency in mice. In five surgical patients, the terminal elimination half-life, clearance, and volume of distribution at steady state of the isomer were not statistically different from those of thiopental. In mice, the isomer proved to be as effective as thiopental for induction of anesthesia. The LD_{50} and sleep time at one-half the LD_{50} did not statistically differ between the two compounds in mice. The close structural similarity of thiopental and the isomer results in similar pharmacokinetic and anesthetic properties. It does not appear critical that the isomer be separated from thiopental in subsequent pharmacological research.

Keyphrases □ Thiopental—isomer determination in serum by high-performance liquid chromatography, pharmacokinetics in humans, anesthetic potency in mice □ Pharmacokinetics—of a thiopental isomer in humans, comparison with thiopental □ Anesthetic agents—potency of a thiopental isomer in mice, comparison with thiopental

Previous high-performance liquid chromatographic (HPLC) assays for thiopental apparently lacked the chromatographic resolution to separate thiopental from any side-chain isomer (1–4). This paper describes an HPLC assay that separates thiopental, 5-ethyl-5-(1-methylbutyl)-2-thiobarbituric acid, from this isomeric material, 5-ethyl-5-(1-ethylpropyl)-2-thiobarbituric acid (see Fig. 1). The isomer was found both in standard thiopental obtained from the manufacturer and the commercially available thiopental sodium used for the induction of anesthesia in patients. It apparently is formed during the manufacture of thiopental[1]. The presence of a similar isomer has been described for pentobarbital [5-ethyl-5-(1-methylbutyl) barbituric acid], the oxybarbiturate analogue of thiopental (5).

EXPERIMENTAL

Apparatus and Reagents—A liquid chromatograph[2] was equipped with a variable-wavelength detector[3] and column heater. The phosphoric acid, monobasic potassium phosphate, sodium hydroxide, and sodium carbonate were certified ACS grade[4]; anhydrous ethyl ether was reagent grade[5]; acetonitrile was HPLC grade[6]. The sodium salt of thiopental[7] and the thiopental isomer[8] were used for preparation of the standard curves. The thiopental contained 9.0% of the isomer, based on peak heights from a sample separated on the HPLC assay. The isomer did not contain thiopental; only a single peak was seen when the isomer was chromatographed on the HPLC assay. Thiamylal acid[9] was used as an internal standard for measurement of thiopental and the isomer.

Thiopental Protein Precipitation and Chromatography—The HPLC assay described by Kabra *et al.* (6) was modified. For thiopental concentrations >200 ng/ml, an equal volume of acetonitrile containing the internal standard (2.5 or 25 μg/ml) was added to human serum (200 μl) and mixed on a vortex mixer. Following two sequential centrifugations, the acetonitrile supernatant was injected into the chromatograph.

[1] Personal communication, Abbott Laboratories, North Chicago, Ill.
[2] Model 5020, Varian, Palo Alto, Calif.
[3] Model UV-50, Varian, Palo Alto, Calif.
[4] Fisher Scientific Co., Fair Lawn, N.J.
[5] J. T. Baker Chemical Co., Phillipsburg, N.J.
[6] Distilled in glass; Burdick & Jackson Laboratories, Muskegon, Mich.
[7] Lot 845-7283, Abbott Laboratories, North Chicago, Ill.
[8] Abbott 13750, Lot No. 16-859-AX, Abbott Laboratories, North Chicago, Ill.
[9] Lot 7274 x 24-6, Parke-Davis & Co., Detroit, Mich.

0022-3549/83/0800-0937$01.00/0

and Drug Research," Academic, New York and London, 1976.
(16) L. B. Kier and L. H. Hall, *J. Med. Chem.*, **20**, 1631 (1977).
(17) J. S. Millership and A. D. Woolfson, *J. Pharm. Pharmacol*, **30**, 483, (1978).
(18) L. B. Kier, R. J. Simons, and L. H. Hall, *J. Pharm. Sci.*, **67**, 725 (1978).
(19) B. K. Evans, K. C. James, and D. K. Luscombe, *J. Pharm. Sci.*, **68**, 370 (1979).
(20) B. van't Riet, L. B. Kier, and H. L. Elford, *J. Pharm. Sci.*, **69**, 856 (1980).
(21) L. B. Kier and L. H. Hall, *J. Pharm. Sci.*, **70**, 583 (1981).
(22) A. T. Balaban, A. Chiriac, I. Motoc, and Z. Simon, "Steric Fit in Quantitative Structure–Activity Relations, Lecture Notes in Chemistry," vol. 15, Springer–Verlag, Berlin–Heidelberg–New York, 1980.
(23) E. J. Ariens, "Drug Design," vol. 1, Academic, New York and London, 1971.
(24) C. Hansch, *Drug Metab. Rev.*, **1**, 1 (1972).
(25) C. Hansch and A. J. Leo, "Substituent Constants for Correlation Analysis in Chemistry and Biology," Wiley, New York–Brisbane–Toronto, 1979.
(26) A. J. Hoefnagel, M. A. Hoefnagel, and G. M. Wepster, *J. Org. Chem.*, **43**, 4720 (1978).
(27) G. Z. Zeng, *Acta Chim. Sinica*, **32**, 107 (1966).
(28) K. Kalfus, J. Kroupa, M. Vecera, and O. Exner, *Collect. Czech. Chem. Commun.*, **40**, 3009 (1975).
(29) C. E. Shannon and W. Weaver, "The Mathematical Theory of Communication," University of Illinois Press, Urbana, Ill., 1949.
(30) S. C. Basak, A. B. Roy, and J. J. Ghosh, "Proceedings of the II International Conference on Mathematical Modelling," vol. 2, University of Missouri, Rolla, Mo., 1979, p. 851.
(31) N. H. Nie, C. H. Hull, J. G. Jenkins, K. Steinbrenner, and D. H. Benf, "Statistical Package for Social Sciences," McGraw-Hill, New York, N.Y., 1975.

ACKNOWLEDGMENTS

The authors wish to express their appreciation to the U.S. Environmental Protection Agency (Contract CR 807566) for support of this work and to the University of Minnesota, Duluth Computer Center for partial financial assistance.

Pharmacokinetics and Anesthetic Potency of a Thiopental Isomer

DONALD R. STANSKI[x], PATRICK G. BURCH, SANDRA HARAPAT, and RICHARD K. RICHARDS[†]

Received March 9, 1982, from the *Departments of Anesthesia and Medicine (Clinical Pharmacology), Stanford University School of Medicine, Stanford, CA 94305* and the *Palo Alto Veterans Administration Hospital, Palo Alto, CA 94304.* Accepted for publication July 29, 1982. [†] Deceased

Abstract □ In developing a high-performance liquid chromatographic assay for thiopental [5-ethyl-5-(1-methylbutyl)-2-thiobarbituric acid], a thiopental isomer [5-ethyl-5-(1-ethylpropyl)-2-thiobarbituric acid] was found. This isomer occurs (6–7%) in supposedly pure thiopental and in the commercially available thiopental sodium administered to patients for induction of anesthesia. A similar type of isomer also occurs in pentobarbital, the oxybarbiturate analogue of thiopental. Because the disposition and anesthetic potency of the isomer is unknown, its pharmacokinetic properties were determined in humans and its anesthetic potency in mice. In five surgical patients, the terminal elimination half-life, clearance, and volume of distribution at steady state of the isomer were not statistically different from those of thiopental. In mice, the isomer proved to be as effective as thiopental for induction of anesthesia. The LD_{50} and sleep time at one-half the LD_{50} did not statistically differ between the two compounds in mice. The close structural similarity of thiopental and the isomer results in similar pharmacokinetic and anesthetic properties. It does not appear critical that the isomer be separated from thiopental in subsequent pharmacological research.

Keyphrases □ Thiopental—isomer determination in serum by high-performance liquid chromatography, pharmacokinetics in humans, anesthetic potency in mice □ Pharmacokinetics—of a thiopental isomer in humans, comparison with thiopental □ Anesthetic agents—potency of a thiopental isomer in mice, comparison with thiopental

Previous high-performance liquid chromatographic (HPLC) assays for thiopental apparently lacked the chromatographic resolution to separate thiopental from any side-chain isomer (1–4). This paper describes an HPLC assay that separates thiopental, 5-ethyl-5-(1-methylbutyl)-2-thiobarbituric acid, from this isomeric material, 5-ethyl-5-(1-ethylpropyl)-2-thiobarbituric acid (see Fig. 1). The isomer was found both in standard thiopental obtained from the manufacturer and the commercially available thiopental sodium used for the induction of anesthesia in patients. It apparently is formed during the manufacture of thiopental[1]. The presence of a similar isomer has been described for pentobarbital [5-ethyl-5-(1-methylbutyl) barbituric acid], the oxybarbiturate analogue of thiopental (5).

EXPERIMENTAL

Apparatus and Reagents—A liquid chromatograph[2] was equipped with a variable-wavelength detector[3] and column heater. The phosphoric acid, monobasic potassium phosphate, sodium hydroxide, and sodium carbonate were certified ACS grade[4]; anhydrous ethyl ether was reagent grade[5]; acetonitrile was HPLC grade[6]. The sodium salt of thiopental[7] and the thiopental isomer[8] were used for preparation of the standard curves. The thiopental contained 9.0% of the isomer, based on peak heights from a sample separated on the HPLC assay. The isomer did not contain thiopental; only a single peak was seen when the isomer was chromatographed on the HPLC assay. Thiamylal acid[9] was used as an internal standard for measurement of thiopental and the isomer.

Thiopental Protein Precipitation and Chromatography—The HPLC assay described by Kabra *et al.* (6) was modified. For thiopental concentrations >200 ng/ml, an equal volume of acetonitrile containing the internal standard (2.5 or 25 μg/ml) was added to human serum (200 μl) and mixed on a vortex mixer. Following two sequential centrifugations, the acetonitrile supernatant was injected into the chromatograph.

[1] Personal communication, Abbott Laboratories, North Chicago, Ill.
[2] Model 5020, Varian, Palo Alto, Calif.
[3] Model UV-50, Varian, Palo Alto, Calif.
[4] Fisher Scientific Co., Fair Lawn, N.J.
[5] J. T. Baker Chemical Co., Phillipsburg, N.J.
[6] Distilled in glass; Burdick & Jackson Laboratories, Muskegon, Mich.
[7] Lot 845-7283, Abbott Laboratories, North Chicago, Ill.
[8] Abbott 13750, Lot No. 16-859-AX, Abbott Laboratories, North Chicago, Ill.
[9] Lot 7274 x 24-6, Parke-Davis & Co., Detroit, Mich.

0022-3549/83/0800-0937$01.00/0

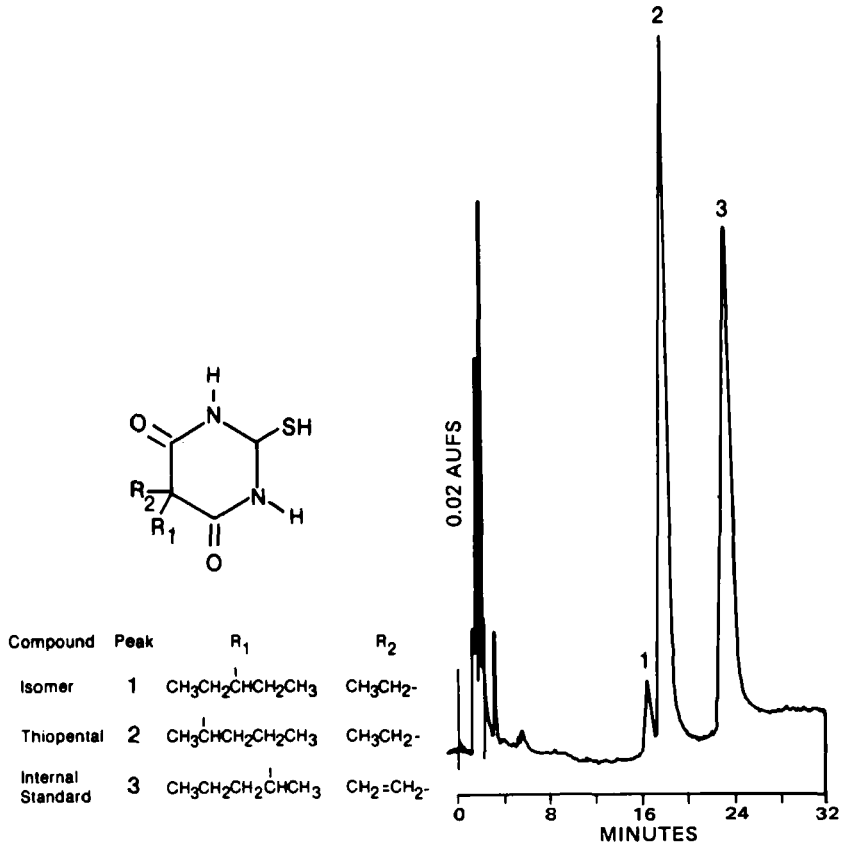

Figure 1—*A chromatogram demonstrating the presence of the isomer in a sample of supposedly pure thiopental. The structures of thiopental, the isomer, and the internal standard (thiamylal) are as indicated.*

Appropriate concentrations of the internal standard were added before the protein precipitation. To increase the sensitivity of the assay to 25 ng/ml, the ether extraction procedure described for the thiopental isomer can be used. Because the thiopental concentrations were >200 ng/ml for the duration of the study, it was not necessary to use the extraction.

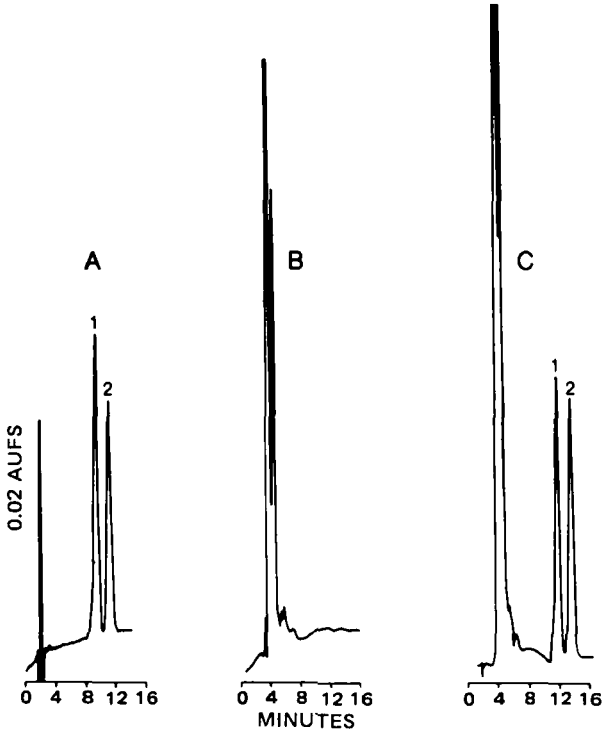

Figure 2—*Typical chromatograms obtained using the assay described for measurement of thiopental. Key: (A) separation of thiopental (peak 1) and the internal standard (peak 2) when both are injected directly onto the chromatograph; (B) a human serum blank; (C) separation of 1.25 μg of thiopental and 2.5 μg of the internal standard from 1.0 ml of human serum.*

The HPLC mobile phase was acetonitrile–phosphate buffer (38:62). The buffer was prepared by adding 175 μl of 1 *M* KH_2PO_4 and 50 μl of 1 *M* H_3PO_4 to 1 liter of glass-distilled and filtered water. The pH of the phosphate buffer was 4.5, and the molarity was 4.5×10^{-4} *M* acid and 1.75×10^{-4} *M* salt. The flow rate was 1.2 ml/min with a C_{18} reverse-phase column[10] (4-mm i.d. × 30 cm) at 50°. The detector wavelength was 290 nm and ranged from 0.01 to 0.05 AUFS.

To prepare standard curves, aliquots of thiopental in methanol were evaporated to dryness and diluted to volume with serum. The standard was then handled as described above. Standard curves were linear at all concentrations from 200 ng/ml to 50 μg/ml. The retention times of thiopental and the internal standard were 9.2 and 11.2 min, respectively (Fig. 2). The assay does not separate the isomer from thiopental and therefore measures both compounds.

Isomer Extraction and Chromatography—For analysis of isomer concentrations between 25 and 500 ng/ml, variable volumes of serum (0.1–1.0 ml) were extracted with 200 ng of thiamylal as the internal standard. Following acidification with 1 *M* phosphoric acid two-thirds saturated with potassium phosphate, an extraction with ether (3 ml) was performed. The ether phase was removed and evaporated to dryness. The residue was reconstituted in 100 μl of the HPLC assay eluant and injected into the chromatograph. The HPLC mobile phase was acetonitrile–dilute phosphate buffer (33:67). The flow rate was 1.2 ml/min on a C_{18} reverse-phase column[11] (4-mm i.d. × 30 cm) at 50°. The detector wavelength was 290 nm and 0.01 or 0.02 AUFS.

Standard curves for the isomer assay were prepared by evaporating to dryness aliquots of the pure isomer in methanol and diluting to volume with serum. The standard was then prepared using the aforementioned acidification and ether extraction. Standard curves were linear from 25 to 500 ng/ml of the pure isomer. Retention times were: isomer, 16.7 min; thiopental, 18.1 min; and the internal standard, 23.6 min (Fig. 3).

Isomer Identification—The isomer was identified by addition of pure 5-ethyl-5-(1-ethylpropyl)-2-thiobarbituric acid to a sample of thiopental. When chromatographed using the aforementioned assay that separated the two compounds, addition of the isomer resulted in an increase of the isomer peak height in the thiopental sample, with an identical retention time. The UV spectra of thiopental and the isomer were identical, showing a maximum absorption at 290 nm. The structure of the isomer

[10] Varian MCH-10, Varian, Palo Alto, Calif.
[11] μ-Bondpack C_{18}, Waters Associates Inc., Milford, Mass.

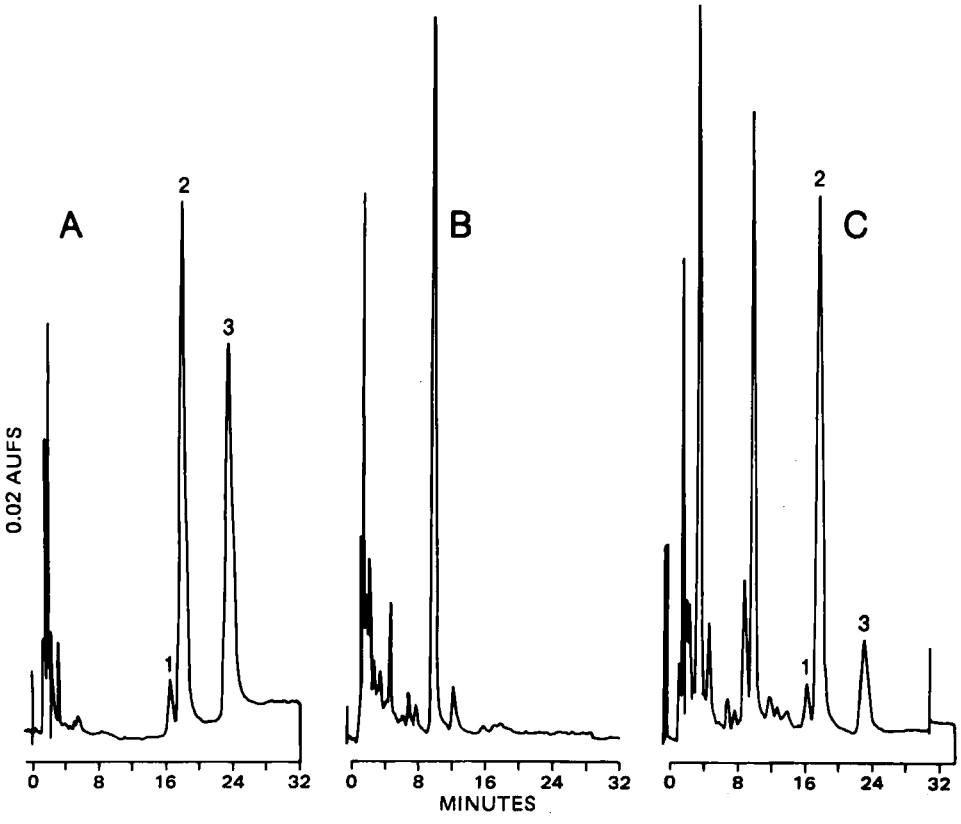

Figure 3—*Typical chromatograms obtained using the assay for measurement of the isomer. Key: (A) separation of the isomer (peak 1) from thiopental (peak 2) and the internal standard (peak 3) when thiopental and internal standard are injected directly onto the chromatograph; (B) a human serum blank; (C) separation of the compounds from human serum. Peak 1 in chromatogram C represents 56 ng of the isomer, peak 2 is 781 ng of thiopental, and peak 3 is 200 ng of internal standard extracted from 0.5 ml of serum.*

also was characterized using ^{13}C- and ^{1}H-NMR[12]. No evidence of interconversion of the two compounds was found during the extraction and HPLC chromatography.

Pharmacokinetics in the Human—One female and four male patients undergoing elective surgical procedures were studied. An institution review board approval was obtained along with consent from each patient. Subject age, weight, and thiopental dose are indicated in Table I. Commercially available thiopental sodium was used to induce anesthesia; therefore, both thiopental and the isomer were administered to the patients. A sample of the thiopental sodium administered was analyzed for the amount of isomer present (Table I).

Following rapid intravenous injection of the thiopental sodium for induction of anesthesia, blood samples were obtained from a catheter inserted into a radial artery or an antecubital vein. Arterial blood samples were obtained at 1, 2, 3, 5, 10, 15, 30, 45, 60, 90, and 120 min; venous blood samples were obtained at 3, 4, 6, 8, 10, 12, 14, 16, 18, 20, 22, and 24 hr. This protocol allows accurate characterization of the distribution and elimination phases of thiopental and the isomer. Serum samples were frozen and subsequently analyzed using two assays: one that collectively measured the thiopental and isomer, and one that measured only the isomer. Following the administration of thiopental sodium, anesthesia was maintained with nitrous oxide–oxygen (60:40) and enflurane (1–2%) for 1–3 hr.

The pharmacokinetic data analysis used only the serum concentration *versus* time data. Linear regression of the postdistribution log serum concentration *versus* time data was used to determine the terminal elimination half-life. The dose divided by the area under the curve (linear trapezoid rule) was used to determine total body clearance. The area under the first-moment curve, as described by Benet and Galleazzi (7), was used to determine the volume of distribution at steady state. A two-tailed paired t test at a significance level of $p < 0.05$ was used to statistically compare the pharmacokinetic parameters for thiopental and the isomer.

Anesthetic Potency in Mice—Thiopental and the isomer were compared for anesthetic potency in male white Swiss mice[13] weighing 18–24 g. Thiopental was used as the commercially available sodium salt containing 8.3% sodium carbonate. The free acid isomer was converted to the sodium salt by adding 1 meq of NaOH and 8.3% Na_2CO_3 to 1 meq of the free acid. Both compounds were used as a 0.4% solution.

Because the anesthetic effect of these compounds is influenced by the peak blood level achieved, the speed of intravenous injection into the tail vein was rigidly controlled at 0.01 ml/5 sec. Sleep occurred immediately, during, or at the end of the injection. The anesthetized animals were placed on their backs and left undisturbed until they righted themselves.

In the fatal-dose range, death was due to respiratory arrest a few minutes after the drug injection. After the initial dose-ranging studies,

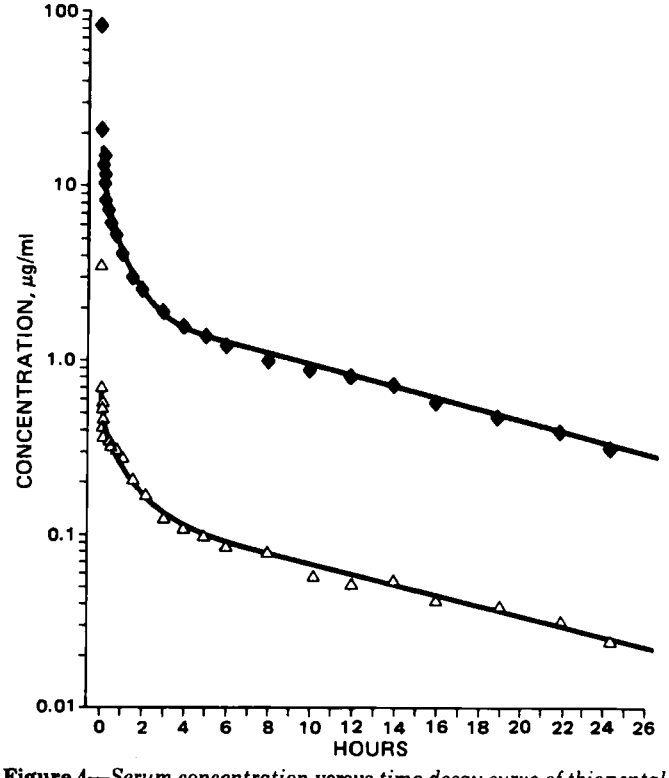

Figure 4—*Serum concentration* versus *time decay curve of thiopental (◆) and the isomer (△) for subject 5 in Table I.*

[12] Varian XL100, Varian, Palo Alto, Calif.

[13] Simson, Gilroy, Calif.

Table I—Demographic and Pharmacokinetic Data

Patient	Age, year	Weight, kg	Isomer, %	Dose, mg/kg	Elimination Half-Life, min		Clearance, ml/kg/min		Volume of Distribution at Steady State, liter/kg	
					Thiopental	Isomer	Thiopental	Isomer	Thiopental	Isomer
1	30	55	6.1	8.2	409	291	3.3	3.4	1.52	1.30
2	23	79	6.1	5.9	932	835	3.1	4.9	2.82	4.32
3	30	81	6.2	5.4	566	636	2.6	2.4	1.66	1.85
4	28	67	6.1	6.6	378	752	4.4	3.9	2.01	2.6
5	35	82	6.0	5.6	465	396	3.1	2.7	1.4	1.4
Mean	29.2	72.8	6.10	6.3	550	582	3.3	3.8	1.88	2.29
±*SD*	4.3	11.6	0.07	1.1	225	231	0.6	1.0	0.57	1.24

the LD_{50} was determined for both drugs using groups of eight mice at three dosage levels for each drug. The LD_{50} and 95% confidence limits were determined using the method of Litchfield and Wilcoxon (8). In addition to the LD_{50}, the sleep time at one-half the LD_{50} was also determined using eight mice per drug. A third study was performed with an additional eight mice per drug to determine if cumulative properties of these two barbiturates were the same. One-half of the LD_{50} dose was given to a mouse and a second injection $\frac{1}{8}$ of the LD_{50} dose was given when the animal righted itself. The sleep times from the first and second doses were compared using a two-tailed unpaired t test at a significance level of $p < 0.05$.

RESULTS AND DISCUSSION

Assay Sensitivity, Reproducibility, and Chromatography—With the acetonitrile protein precipitation, the assay sensitivity for thiopental was 200 ng/ml. Analysis of the same serum sample 6–8 times on the same day gave the following coefficients of variation: 300 ng/ml, 4.2%; 1.1 μg/ml, 3.7%; and 15.4 μg/ml, 1.8%. The between-day coefficient of variation at a thiopental concentration of 2.5 μg/ml was 5.0%. The isomer assay was sensitive to 25 ng/ml. Analysis of the same serum sample for the isomer 6–8 times on the same day gave the following coefficients of variation: 25 ng/ml, 7.9%; 125 ng/ml, 7.8%, and 500 ng/ml, 5.4%. The between-day coefficient of variation at an isomer concentration of 125 ng/ml was 5.1%. Figure 1 indicates the chemical structures of thiopental and the isomer, along with a chromatogram showing the presence of the isomer peak in a sample of thiopental obtained from the manufacturer[7]. Analysis of 10 different lots of commercially available thiopental sodium showed that the isomer comprised 6–7% of the total drug content. Figure 2 is a representative chromatogram obtained with the thiopental assay where thiopental and the isomer are not separated. Figure 3 demonstrates a representative chromatogram of the isomer assay where thiopental and the isomer are effectively separated.

Pharmacokinetics in the Human—Table I summarizes the derived pharmacokinetic parameters for thiopental and the isomer in each patient. Figure 4 displays the serum concentration *versus* time data for patient 5. Simultaneous arterial and venous samples in three patients demonstrated minimal thiopental concentration differences due to sample site, which had no effect on the derived pharmacokinetic variables. There was no statistical difference between the terminal elimination half-life, clearance, or volume of distribution at steady state when thiopental was compared with the isomer. The variability occurs because the isomer serum concentrations are 10–15 times lower than the thiopental concentrations and measurement varies more at the low isomer concentrations. While not formally characterized in this analysis, there was no visible difference in the initial distribution phases of thiopental relative to the isomer. Thus, in humans, the distribution and elimination of thiopental and the isomer are similar. This would be expected given the close structural similarity and (presumably) physicochemical properties of thiopental and the isomer.

Table II—LD_{50} and Anesthetic Potency in Mice

Drug	LD_{50}, mg/kg	Sleep Time[a] min	Cumulative Sleep Times, min	
			1st Dose[a]	2nd Dose[b]
Thiopental	90 (84.9–95.4)[c]	25.4 ± 17.3	25.3 ± 15.5	32.3 ± 20.9
Isomer	90 (84.9–85.4)	38.0 ± 18.3	31.3 ± 33.0	52.7 ± 22.1

[a] Dosed at 45 mg/kg; mean ± *SD*. [b] Dosed at 11.5 mg/kg; mean ± *SD*. [c] Range in parentheses.

Anesthetic Potency in Mice—Thiopental and the isomer had an identical fatal dose as judged by the LD_{50} studies (Table II). With one-half of the LD_{50}, the duration of sleep (as judged by return of the righting reflex) was not statistically different. Additionally, there was no evidence of a statistical difference in the cumulative duration of sleep when the anesthetic was administered a second time. Thus, it appears that the thiopental isomer is an anesthetic of potency comparable with that of thiopental in mice.

In summary, there is a 6–7% level of an isomer form present in thiopental. In the human, this isomer has distribution and elimination characteristics similar to thiopental. It also has, in mice, a degree of anesthetic potency similar to that of thiopental. It is therefore not critical that subsequent analytical technology used for thiopental pharmacokinetic or pharmacodynamic research quantitate or separate this isomer from thiopental.

REFERENCES

(1) J. H. Christensen and F. Andreasen, *Acta Pharmacol. Toxicol.*, **44**, 260 (1979).

(2) A. N. Masoud, G. A. Scratchley, S. H. Stahs, and D. W. Wingard, *J. Liq. Chromatogr.*, **1**, 607 (1978).

(3) W. Toner, P. J. Howard, J. W. Dundee, and P. D. A. McIlroy, *Anesthesia*, **34**, 657 (1979).

(4) G. L. Blackman and G. J. Jordan, *J. Chromatogr.*, **145**, 492 (1978).

(5) J. Hoogmartens, E. Rolts, and H. Vanderhaeghe, *J. Chromatogr.*, **219**, 431 (1981).

(6) P. M. Kabra, H. Y. Koo, and L. J. Marton, *Clin. Chem.*, **24**, 657 (1978).

(7) L. Z. Benet and R. L. Galeazzi, *J. Pharm. Sci.*, **68**, 1071 (1979).

(8) J. T. Litchfield and W. F. Wilcoxon, *J. Pharmacol. Exp. Ther.*, **96**, 99 (1948).

ACKNOWLEDGMENTS

Supported in part by National Institutes of Health Grant 1R23-GM28032, the Parker B. Francis Foundation, and the Veterans Administration Research Fund.

The authors are obliged to Mr. D. E. Williamson and Dr. O. Geisler of Abbott Laboratories, North Chicago, Ill. for the supply of the thiopental isomer and to Ms M. Schuler, Institute of Pharmacology, Syntex Research, Palo Alto, Calif. for assistance in the animal experiments.

Diphenhydramine Determination in Human Plasma by Gas–Liquid Chromatography using Nitrogen–Phosphorus Detection: Application to Single Low-Dose Pharmacokinetic Studies

DARRELL R. ABERNETHY ˣ **and DAVID J. GREENBLATT**

Received April 5, 1982, from the *Division of Clinical Pharmacology, Departments of Psychiatry and Medicine, Tufts University School of Medicine and New England Medical Center Hospital, Boston, MA 02111.* Accepted for publication July 23, 1982.

Abstract □ A highly sensitive method (≤1 ng/ml) for single-dose pharmacokinetic studies of diphenhydramine which utilizes GLC with nitrogen–phosphorus detection is described. Standard curves, using orphenadrine as the internal standard, were linear for diphenhydramine concentrations from 1.0 to 300 ng/ml. Applicability of the method was demonstrated by a pharmacokinetic study in a normal volunteer who received 25 mg iv of diphenhydramine.

Keyphrases □ Diphenhydramine—determination in human plasma using GLC with nitrogen–phosphorus detection, application to single low-dose pharmacokinetic studies □ GLC—with nitrogen–phosphorus detection, determination of diphenhydramine in human plasma, single-dose pharmacokinetic study □ Pharmacokinetics—of diphenhydramine in the human, detection after a single dose using GLC with nitrogen–phosphorus detection

Diphenhydramine, widely used in the treatment of allergic conditions (1) and as a sedative–hypnotic in the elderly (2), has been measured by GLC using flame-ionization detection (3), GLC–MS (4), UV spectrophotometry (5), and by a fluorescent dye procedure (6). With the exception of GLC–MS, these methods lack adequate specificity and sensitivity. A method using GLC with nitrogen–phosphorus detection that is rapid, specific, and sensitive to 1 ng/ml is described. Following a straightforward plasma extraction requiring 3–4 hr, up to 150 samples per 24 hr can be analyzed if an automated injection system is used. This method is valuable since, in some subject populations (particularly the elderly), a diphenhydramine dose small enough to cause little sedative or anticholinergic effect but large enough to permit a blood level determination for the time needed to complete a single-dose pharmacokinetic study is necessary.

EXPERIMENTAL

Apparatus and Chromatographic Conditions—A gas chromatograph[1] equipped with a nitrogen–phosphorus detector and an electronic integrator was used. The column was coiled glass (1.83 m × 2-mm i.d.) packed with 3% SP-2250 on 80/100 mesh Supelcoport[2]. The carrier gas was ultra-high purity helium[3] at a flow rate of 30 ml/min. The detector purge was ultra-high purity hydrogen[3] at 3 ml/min mixed with dry air[3] at 50 ml/min. Operating temperatures were: injection port, 310°; column, 205°; and detector, 275°. Before being connected to the detector, new columns were conditioned at 270° for 48 hr with a carrier flow of 30 ml/min. At the beginning of each work day, the column was primed with 2 μg of phospholipid (asolectin) in benzene.

Reagents—Certified *n*-hexane[4] (99% pure) and isoamyl alcohol[4] were used. The toluene[5], methanol[4], concentrated hydrochloric acid[5], sodium hydroxide[5], sodium carbonate[5], and sodium bicarbonate[5] were analytical reagent grade. The isoamyl alcohol was glass-distilled prior to use; other organic solvents were used without further distillation. All aqueous solvents (0.25 *M* NaOH, 0.1 *M* HCl, and 1 *M* carbonate–bicarbonate buffer) were washed five times with hexane–isoamyl alcohol (98:2) prior to use.

Reference Standards—Pure standards of diphenhydramine hydrochloride[6] and orphenadrine citrate[7] were provided by the manufacturers. Standard solutions of each were prepared by dissolving the appropriate quantity of the salt to yield 100 mg of base in 100 ml of methanol. Sequential dilutions to 1 μg/ml were made. The solutions were stored in the dark in glass-stoppered bottles at 4° and were stable for at least 4 months.

Preparation of Samples—Orphenadrine was used as the internal standard for all analyses. A 100-μl volume of stock solution (1 μg/ml), containing 100 ng of orphenadrine, was added to 15-ml tubes, with poly-

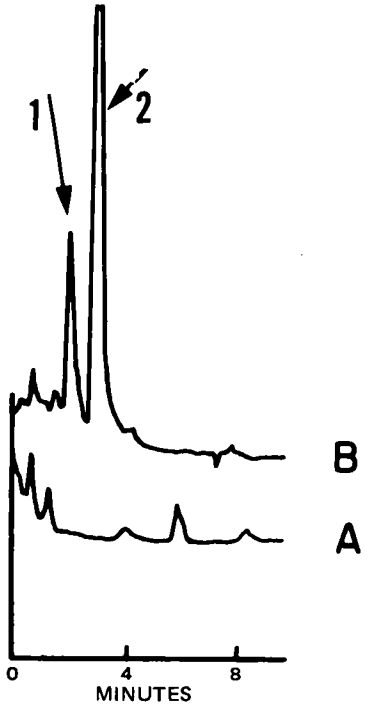

Figure 1—*Chromatogram of the extract of a 1-ml plasma blank (A) and plasma with 25 ng/ml of diphenhydramine and 100 ng of orphenadrine added (B). Key: (1) diphenhydramine; (2) orphenadrine.*

[1] Hewlett-Packard Model 5840A.
[2] Packing 1-1767, Supelco, Bellefonte, Pa.
[3] Matheson Gas Products, Gloucester, Mass.
[4] Fisher Scientific, Fair Lawn, N.J.
[5] Mallinckrodt, St. Louis, Mo.
[6] Benadryl; Parke-Davis Div., Warner-Lambert Co., Ann Arbor, Mich.
[7] Riker Laboratories, Inc., Northridge, Calif.

0022-3549/83/0800-0941$01.00/0

Table I—Representative Calibration Data

Diphenhydramine Concentration, ng/ml	Peak Height Ratio[a]
1.0	0.00615 ± 0.00025
5.0	0.03831 ± 0.00354
10.0	0.07177 ± 0.00372
25.0	0.30977 ± 0.01362
50.0	0.64632 ± 0.01118
200.0	2.5786 ± 0.0341
Correlation coefficient	0.9998
Slope	0.01303
Intercept	−0.02341
Slope corrected through origin	0.01287

[a] Mean ± *SD*; $n = 5$.

tef-faced, rubber-lined, screw-top caps. A 0.25–2.0 ml test sample of plasma was added to each tube. Calibration standards for diphenhydramine were prepared by adding 1, 2.5, 5, 10, 25, 50, 100, 200, and 300 ng of drug to consecutive tubes. Drug-free control plasma was added to each of the calibration tubes. One plasma sample, taken from the subject prior to drug administration, was analyzed with the calibration standards and each set of unknown samples as a blank.

Extraction Procedure—One milliliter of 0.25 *M* NaOH solution was added to each tube. To this was added 5 ml of hexane–isoamyl alcohol (98:2), and the tubes were agitated gently in the upright position on a vortex mixer for 15 min. The samples were centrifuged at room temperature for 5 min at 400×*g*[8]. The organic layer was transferred to another 15-ml tube that contained 1.2 ml of 0.1 *M* HCl. This mixture was agitated gently in the upright position on a vortex mixer for 10 min. The samples were centrifuged again at room temperature for 5 min at 400×*g*, and the upper, organic layer was discarded. The aqueous layer was carefully transferred to another tube, and to this was added 0.5 ml of 1 *M* carbonate–bicarbonate buffer (pH 11.5). To the mixture was added 200 μl of toluene–isoamyl alcohol (85:15). This mixture was agitated gently in the upright position on a vortex mixer for 15 min, and the samples were centrifuged again at room temperature for 5 min at 400×*g*. Using a 23-cm disposable pipet passed through the organic layer, the entire aqueous layer was removed leaving the organic phase (150 μl) containing diphenhydramine and the internal standard. This was transferred to a 2-ml automatic sampling vial.[9] Six microliters was injected into the gas chromatograph using the automatic-injection sampling system.

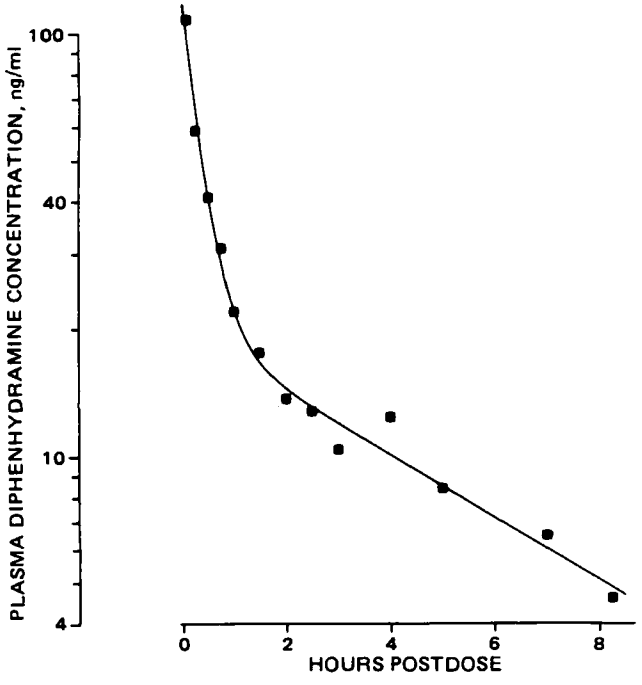

Figure 2—*Plasma diphenhydramine concentrations and the derived pharmacokinetic function following intravenous diphenhydramine administration to a healthy 32-year-old male subject. The elimination half-life is 4.1 hr (see Table I).*

Table II—Derived Diphenhydramine Pharmacokinetic Parameters in a Healthy Male Subject[a]

Subject Characteristics	
Age/Sex	32/male
Weight, kg	70.5
Diphenhydramine Kinetic Variables	
Distribution half-life, min	14.3
Elimination half-life, hr	4.06
Central compartment volume, liters/kg	2.66
Total volume of distribution, liters/kg	12.17
Total metabolic clearance, ml/min/kg	34.7

[a] Diphenhydramine dose of 25 mg iv.

Single-Dose Pharmacokinetic Study—A healthy 32-year-old male volunteer participated after giving written informed consent. Diphenhydramine hydrochloride (25 mg) was administered by intravenous bolus injection. The drug solution (50 mg/ml) was administered through a glass syringe. Multiple venous blood samples were drawn into heparin-containing tubes[10] over 8 hr postdose. Concentrations of diphenhydramine were determined by the aforementioned method.

Plasma diphenhydramine concentrations were analyzed by iterative, weighted, nonlinear, least-squares regression analysis (7, 8). After correction of the dose to diphenhydramine base, the following pharmacokinetic variables were determined: distribution half-life, elimination half-life, total volume of distribution, and total clearance.

RESULTS

Under the described conditions, retention times for diphenhydramine and orphenadrine were 3.41 and 4.32 min, respectively. A chromatogram of a typical blank plasma sample compared with a sample containing diphenhydramine and orphenadrine (internal standard) is shown in Fig. 1.

The relationship between diphenhydramine concentration and the area ratio (*versus* internal standard) is linear to at least 300 ng/ml. Analysis of more than 20 standard curves over a month always afforded a correlation coefficient ≥0.99. The day-to-day coefficient of variation in the slopes of the calibration curves was 5.9% (Table I).

The sensitivity limit of the method is 1 ng/ml using a 2-ml extracted plasma sample. The within-day coefficient of variation for identical samples ($n = 5$) were: 1 ng/ml, 4%; 5 ng/ml, 9.2%; 10 ng/ml, 5.2%; 25 ng/ml, 4.4%; 50 ng/ml, 1.7%; 100 ng/ml, 1.7%; 200 ng/ml, 1.3%; and 300 ng/ml, 2.8%. Residue analysis indicated the extraction of diphenhydramine is 97.3% at a plasma concentration of 25 ng/ml.

Figure 2 shows the plasma diphenhydramine concentration and pharmacokinetic function for the test subject. The derived pharmacokinetic parameters are listed in Table II.

DISCUSSION

This report describes a reliable, sensitive, and specific method for the quantitation of diphenhydramine in plasma using GLC with nitrogen–phosphorus detection. This method is an advance over previously reported methods in that the sensitivity is adequate for single-dose pharmacokinetic studies with very low doses, permitting safe study in widely varying subject populations. Addition of a dilute sodium hydroxide–hexane–isoamyl alcohol mixture to the plasma samples followed by an acid extraction of the organic phase, readjustment of the aqueous phase to pH 11.5, and reextraction with toluene–isoamyl alcohol afforded blank samples suitable for direct injection into the GC that were consistently free of contaminants in the area corresponding to the retention time for diphenhydramine. Known basic metabolites will not elute from the GLC column without derivatization, and acidic metabolites are not coextracted by the procedure used (9). The value of this GLC with nitrogen–phosphorus detection method includes the reasonable time required for sample preparation, as well as a sensitivity that is adequate for single low-dose pharmacokinetic studies.

[8] Portable refrigerated centrifuge Model PR-2, Head No. 269; International Equipment, Boston, Mass.

[9] Wheaton Scientific, Millville, N.J.

[10] Venoject.

REFERENCES

(1) V. J. Cirillo and K. F. Tempero, *Drug Ther. Rev.*, **2**, 24 (1979).

(2) G. Teutsch, D. L. Mahler, C. R. Brown, W. H. Forrest, K. E. James, and B. W. Brown, *Clin. Pharmacol. Ther.*, **17**, 195 (1975).

(3) W. Bilzer and V. Gundert-Remy, *Eur. J. Clin. Pharmacol.*, **6**, 268 (1973).

(4) S. G. Carruthers, D. W. Shoeman, C. E. Hignite, and D. L. Azarnoff, *Clin. Pharmacol. Ther.*, **23**, 375 (1968).

(5) J. E. Wallace, J. D. Biggs, and E. V. Dahl, *Anal. Chem.*, **38**, 831 (1966).

(6) A. J. Glazko, W. A. Dill, R. M. Young, T. C. Smith, and R. I. Ogilvie, *Clin. Pharmacol. Ther.*, **16**, 1066 (1974).

(7) D. W. Marquardt, *J. Soc. Ind. Appl. Math.*, **11**, 431 (1963).

(8) R. A. Usanis, Library Services Series Document No. LSR-089-1, Triangle Universities Computation Center, Research Triangle Park, N.C. (1972).

(9) T. Chang, R. A. Okerholm, and A. J. Glazko, *Res. Commun. Chem. Pathol. Pharmacol.*, **9**, 391 (1974).

ACKNOWLEDGMENTS

Supported in part by Grant MH-34223 from the U.S. Public Health Service.

The authors are grateful for the assistance of Ann Locniskar, Christopher Willis, Jerold S. Harmatz, Dr. Richard I. Shader, and the Staff of the Clinical Study Unit, New England Medical Center Hospital (which is supported by U.S. Public Health Service Grant RR-24040).

Intestinal Absorption of Amino Acid Derivatives: Structural Requirements for Membrane Hydrolysis

G. L. AMIDON*x, M. LEE, and H. LEE

Received April 14, 1982, from the *University of Wisconsin, School of Pharmacy, Madison, WI 53706.* Accepted for publication August 5, 1982.

* Present address: College of Pharmacy, The University of Michigan, Ann Arbor, MI 48109.

Abstract □ The intestinal absorption of L-lysine-*p*-nitroanilide, L-alanine-*p*-nitroanilide, and glycine-*p*-nitroanilide was studied in perfused rat intestine in the presence of a variety of potential competitive inhibitors. The results indicate that the hydrolysis site(s) show side-chain specificity, and that inhibitors require a free amino group in the α-position and must be in the L-configuration to be effective. Glycyl-L-proline, a peptide transport inhibitor, had no effect on the absorption rate.

Keyphrases □ Absorption, intestinal—amino acid derivatives, structural requirements for membrane hydrolysis, rats □ Hydrolysis, membrane—structural requirements, intestinal absorption of amino acid derivatives, rats □ Amino acid derivatives—intestinal absorption, structural requirements for membrane hydrolysis, rats

Previous reports (1, 2) have demonstrated that intestinal membrane (or brush-border) enzymes may serve as useful prodrug reconversion sites. For example, compounds that are insoluble, unstable, or have other undesirable pharmaceutical properties may be derivatized so as to improve these properties with the regeneration of the active drug occurring just prior to entry into the systemic circulation. Clearly the specificity of the enzymes in the brush-border region sets a boundary for this strategy. In this report the intestinal absorption of L-lysine-, L-alanine-, and glycine-*p*-nitroanilides is studied in the presence of a variety of potential competitive inhibitors to more clearly define the specificities of the surface peptidases.

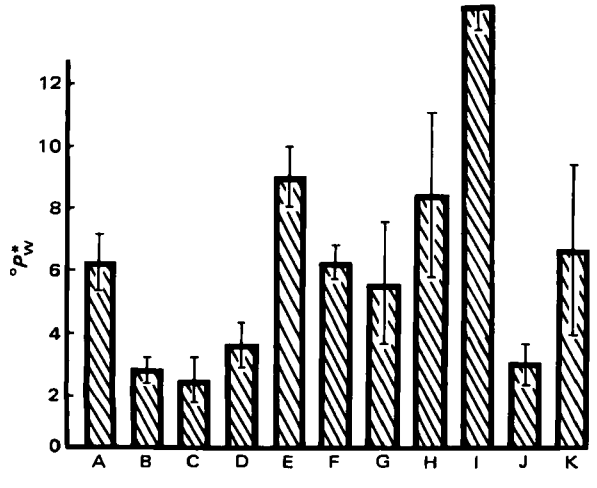

Figure 1—*Intestinal wall permeability (°P^*_w) of L-lysine-p-nitroanilide alone (A) and with L-lysine methyl ester (B), L-arginine-β-naphthylamide (C), L-arginine methyl ester (D), α-N-acetyl-L-lysine methyl ester (E), L-lysine (F), L-phenylalanine methyl ester (G), L-alanine methyl ester (H), glycine methyl ester (I), L-prolylglycine (J), or glycyl-L-proline (K).*

EXPERIMENTAL

Materials—L-lysine-*p*-nitroanilide[1], L-alanine-*p*-nitroanilide[2], and glycine-*p*-nitroanilide[1] were used as received. The inhibitors L-lysine[3], L-lysine methyl ester[2], α-*N*-acetyl-L-lysine methyl ester[3], L-alanine methyl ester[2], L-alanine amide[1], β-alanine methyl ester[1], D-alanine methyl ester[1], L-phenylalanine methyl ester[3], L-phenylalanine amide[1], glycine methyl ester[2], L-arginine methyl ester[1], L-arginine-β-naphthylamide[1], L-prolylglycine[1], and glycyl-L-proline[1] were used as received.

Perfusion Experiments—Rat intestinal perfusion experiments were carried out as previously described (1, 2). Inlet (*Co*) and exit (*Cm*,) concentrations of the perfused segment were measured by determining the *p*-nitroaniline concentration after a 12-hr hydrolysis. The *Cm/Co* ratio was determined using a three-point spectral analysis to account for any background absorbance due to protein in the perfusate. Experiments were carried out with the substrate concentration at 4×10^{-5} *M* and the inhibitor concentration at 4×10^{-3} *M*. Each permeability is the average result from 6–10 rats.

RESULTS AND DISCUSSION

The dimensionless intestinal wall permeability, °P^*_w, was calculated as previously described (3). Tests for significance were done using the two-sample *t* test for samples with unequal variance[4] (95% confidence level). The results are shown in Table I and Figs. 1–3.

L-Lysine methyl ester, L-arginine-β-naphthylamide, and L-arginine

[1] U.S. Biochemical Corp., Cleveland, Ohio
[2] Sigma Chemical Co., St. Louis, Mo.
[3] Aldrich Chemical Co., Milwaukee, Wis.
[4] MINITAB, University of Pennsylvania, Philadelphia, Pa.

0022-3549/83/0800-0943$01.00/0

REFERENCES

(1) V. J. Cirillo and K. F. Tempero, *Drug Ther. Rev.*, **2**, 24 (1979).

(2) G. Teutsch, D. L. Mahler, C. R. Brown, W. H. Forrest, K. E. James, and B. W. Brown, *Clin. Pharmacol. Ther.*, **17**, 195 (1975).

(3) W. Bilzer and V. Gundert-Remy, *Eur. J. Clin. Pharmacol.*, **6**, 268 (1973).

(4) S. G. Carruthers, D. W. Shoeman, C. E. Hignite, and D. L. Azarnoff, *Clin. Pharmacol. Ther.*, **23**, 375 (1968).

(5) J. E. Wallace, J. D. Biggs, and E. V. Dahl, *Anal. Chem.*, **38**, 831 (1966).

(6) A. J. Glazko, W. A. Dill, R. M. Young, T. C. Smith, and R. I. Ogilvie, *Clin. Pharmacol. Ther.*, **16**, 1066 (1974).

(7) D. W. Marquardt, *J. Soc. Ind. Appl. Math.*, **11**, 431 (1963).

(8) R. A. Usanis, Library Services Series Document No. LSR-089-1, Triangle Universities Computation Center, Research Triangle Park, N.C. (1972).

(9) T. Chang, R. A. Okerholm, and A. J. Glazko, *Res. Commun. Chem. Pathol. Pharmacol.*, **9**, 391 (1974).

ACKNOWLEDGMENTS

Supported in part by Grant MH-34223 from the U.S. Public Health Service.

The authors are grateful for the assistance of Ann Locniskar, Christopher Willis, Jerold S. Harmatz, Dr. Richard I. Shader, and the Staff of the Clinical Study Unit, New England Medical Center Hospital (which is supported by U.S. Public Health Service Grant RR-24040).

Intestinal Absorption of Amino Acid Derivatives: Structural Requirements for Membrane Hydrolysis

G. L. AMIDON*x, M. LEE, and H. LEE

Received April 14, 1982, from the *University of Wisconsin, School of Pharmacy, Madison, WI 53706.* Accepted for publication August 5, 1982.

* Present address: College of Pharmacy, The University of Michigan, Ann Arbor, MI 48109.

Abstract □ The intestinal absorption of L-lysine-*p*-nitroanilide, L-alanine-*p*-nitroanilide, and glycine-*p*-nitroanilide was studied in perfused rat intestine in the presence of a variety of potential competitive inhibitors. The results indicate that the hydrolysis site(s) show side-chain specificity, and that inhibitors require a free amino group in the α-position and must be in the L-configuration to be effective. Glycyl-L-proline, a peptide transport inhibitor, had no effect on the absorption rate.

Keyphrases □ Absorption, intestinal—amino acid derivatives, structural requirements for membrane hydrolysis, rats □ Hydrolysis, membrane—structural requirements, intestinal absorption of amino acid derivatives, rats □ Amino acid derivatives—intestinal absorption, structural requirements for membrane hydrolysis, rats

Previous reports (1, 2) have demonstrated that intestinal membrane (or brush-border) enzymes may serve as useful prodrug reconversion sites. For example, compounds that are insoluble, unstable, or have other undesirable pharmaceutical properties may be derivatized so as to improve these properties with the regeneration of the active drug occurring just prior to entry into the systemic circulation. Clearly the specificity of the enzymes in the brush-border region sets a boundary for this strategy. In this report the intestinal absorption of L-lysine-, L-alanine-, and glycine-*p*-nitroanilides is studied in the presence of a variety of potential competitive inhibitors to more clearly define the specificities of the surface peptidases.

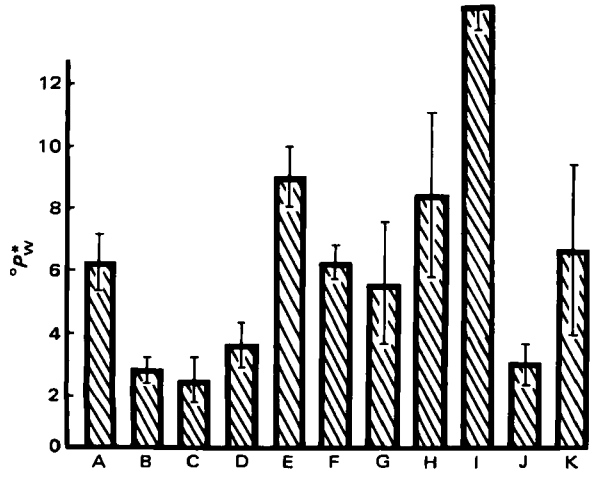

Figure 1—*Intestinal wall permeability (°P^*_w) of L-lysine-p-nitroanilide alone (A) and with L-lysine methyl ester (B), L-arginine-β-naphthylamide (C), L-arginine methyl ester (D), α-N-acetyl-L-lysine methyl ester (E), L-lysine (F), L-phenylalanine methyl ester (G), L-alanine methyl ester (H), glycine methyl ester (I), L-prolylglycine (J), or glycyl-L-proline (K).*

EXPERIMENTAL

Materials—L-lysine-*p*-nitroanilide[1], L-alanine-*p*-nitroanilide[2], and glycine-*p*-nitroanilide[1] were used as received. The inhibitors L-lysine[3], L-lysine methyl ester[2], α-*N*-acetyl-L-lysine methyl ester[3], L-alanine methyl ester[2], L-alanine amide[1], β-alanine methyl ester[1], D-alanine methyl ester[1], L-phenylalanine methyl ester[3], L-phenylalanine amide[1], glycine methyl ester[2], L-arginine methyl ester[1], L-arginine-β-naphthylamide[1], L-prolylglycine[1], and glycyl-L-proline[1] were used as received.

Perfusion Experiments—Rat intestinal perfusion experiments were carried out as previously described (1, 2). Inlet (*Co*) and exit (*Cm*,) concentrations of the perfused segment were measured by determining the *p*-nitroaniline concentration after a 12-hr hydrolysis. The *Cm/Co* ratio was determined using a three-point spectral analysis to account for any background absorbance due to protein in the perfusate. Experiments were carried out with the substrate concentration at 4×10^{-5} *M* and the inhibitor concentration at 4×10^{-3} *M*. Each permeability is the average result from 6–10 rats.

RESULTS AND DISCUSSION

The dimensionless intestinal wall permeability, °P^*_w, was calculated as previously described (3). Tests for significance were done using the two-sample *t* test for samples with unequal variance[4] (95% confidence level). The results are shown in Table I and Figs. 1–3.

L-Lysine methyl ester, L-arginine-β-naphthylamide, and L-arginine

[1] U.S. Biochemical Corp., Cleveland, Ohio
[2] Sigma Chemical Co., St. Louis, Mo.
[3] Aldrich Chemical Co., Milwaukee, Wis.
[4] MINITAB, University of Pennsylvania, Philadelphia, Pa.

0022-3549/83/0800-0943$01.00/0

Table I—Inhibition Results for the Various Substrates [a]

Inhibitor	Substrate		
	L-Lysine-*p*-nitroanilide	L-Alanine-*p*-nitroanilide	Glycine-*p*-nitroanilide
L-Lysine methyl ester	Yes	No	No
L-Arginine-β-naphthylamide	Yes	—	—
L-Arginine methyl ester	Yes	No	—
L-Phenylalanine methyl ester	No	No	—
Glycine methyl ester	No	No	No
L-Lysine	No	—	—
α-*N*-Acetyl-L-lysine methyl ester	No	—	—
L-Alanine methyl ester	No	Yes	—
β-Alanine methyl ester	—	No	—
D-Alanine methyl ester	—	No	—
L-Alanine amide	—	No	—
L-Phenylalanine amide	—	No	—
L-Prolylglycine	Yes	Yes	Yes
Glycyl-L-proline	No	No	No

[a] Using a *t* test at the 95% confidence level.

methyl ester reduced the permeability of L-lysine-*p*-nitroanilide, while L-phenylalanine methyl ester, glycine methyl ester, *N*-acetyl-L-lysine methyl ester, and L-alanine methyl ester did not. This suggests that the hydrolysis site for lysine-*p*-nitroanilide shows a preference for positively charged side chains (lysine, arginine) and a lower affinity for the nonpolar side chains (alanine, glycine). The fact that *N*-acetyl-L-lysine methyl ester is not an inhibitor while L-lysine methyl ester is a good inhibitor demonstrates the requirement for a free L-amino group.

The results for L-alanine-*p*-nitroanilide indicate that, of the compounds studied, only L-alanine methyl ester is a good competitive inhibitor. Since the methyl esters of lysine, arginine, phenylalanine, and glycine did not show significant inhibition, the site of L-alanine-*p*-nitroanilide hydrolysis must be relatively specific for small nonpolar amino acid side chains. The fact that β-alanine methyl ester and D-alanine methyl ester were not inhibitors suggests that the free amino group must be in the α-position and that the stereochemistry is important. This is

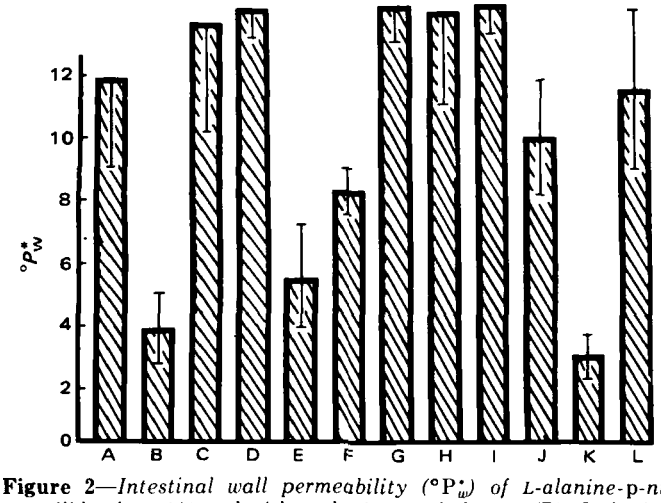

Figure 2—*Intestinal wall permeability ($^{\circ}P_w^*$) of L-alanine-p-nitroanilide alone (A) and with L-alanine methyl ester (B), β-alanine methyl ester (C), D-alanine methyl ester (D), L-lysine methyl ester (E), L-phenylalanine methyl ester (F), L-arginine methyl ester (G), glycine methyl ester (H), L-alanine amide (I), L-phenylalanine amide (J), L-prolylglycine (K), or glycyl-L-proline (L).*

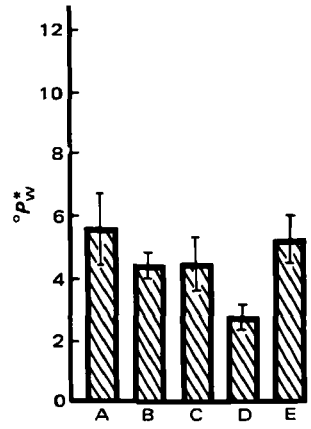

Figure 3—*Intestinal wall permeability ($^{\circ}P_w^*$) of glycine-p-nitroanilide alone (A) and with glycine methyl ester (B), L-lysine methyl ester (C), L-prolylglycine (D), or glycyl-L-proline (E).*

what one would expect for an enzymatic reaction, where the free α-amino group was located in the primary binding site. If the free amino group is located in any other position, the carbonyl carbon that is the subject of attack during hydrolysis would be improperly located with respect to the catalytic groups on the enzyme. The fact that L-alanine amide is not a good competitive inhibitor is somewhat surprising. However, as is the case with α-chymotrypsin substrates (4), it would appear that the amide of alanine has a higher K_m (weaker binding) than the corresponding ester.

The results for glycine-*p*-nitroanilide suggest that the affinity of glycine for the hydrolysis site is weak since glycine methyl ester was not an inhibitor of glycine-*p*-nitroanilide uptake.

The results using the dipeptides glycyl-L-proline and L-prolylglycine show that L-prolylglycine inhibited the absorption of all three amino acid anilides studied. It has been shown that glycyl-L-proline has a high affinity for the intestinal peptide transport process and is not a substrate nor inhibitor of brush-border amino peptidase (5, 6). Since this compound did not inhibit absorption of any of the substrates studied, the result suggests that direct uptake by the peptide transport process does not occur for these compounds. On the other hand, L-prolylglycine appears to be a general amino peptidase inhibitor.

Further studies on the specificity of the intestinal brush-border peptidases in an intestinal perfusion system show that, in addition to the required presence of an α-amino group, the enzymes show specificity for the amino acid side chains as well. The results clearly demonstrate that the absorption mechanism for these compounds is not simple passive diffusion and that the hydrolysis site is probably of the amino peptidase type.

REFERENCES

(1) G. L. Amidon, M. Chang, D. Fleisher, and R. Allen, *J. Pharm. Sci.*, **71**, 1138 (1982).

(2) G. L. Amidon, G. D. Leesman, and R. L. Elliott, *J. Pharm. Sci.*, **69**, 1363 (1980).

(3) R. L. Elliott, G. L. Amidon, and E. N. Lightfoot, *J. Theor. Biol.*, **87**, 757 (1980).

(4) P. K. Banerjee and G. L. Amidon, *J. Pharm. Sci.*, **70**, 1304 (1981).

(5) F. Wojnarowska and G. M. Gray, *Biochim. Biophys. Acta*, **403**, 147 (1975).

(6) E. M. Rosen-Leoin, K. W. Smithson, and G. M. Gray, *Biochim. Biophys. Acta*, **629**, 126 (1980).

ACKNOWLEDGMENTS

This work was supported by Grant GM 27680 from the National Institutes of Health.

Cardiac Inhibitory Action of Constituents of the Marine Green Alga *Ulva pertusa*

K. YAMADA *x, Y. SHIZURI *, Y. ISHIDA ‡, and S. SHIBATA ¶

Received March 9, 1982, from the **Department of Chemistry, Faculty of Science, Nagoya University, Chikusa, Nagoya, Japan*, and the ‡*Mitsubishi-Kasei Institute of Life Science and Department of Pharmacology*, ¶*School of Medicine, University of Hawaii, Honolulu, HI 96822.* Accepted for publication July 9, 1982.

Abstract □ As part of a search for substances from marine organisms, which exhibit inotropic effects, the chemical constituents of the marine green alga, *Ulva pertusa* were investigated. The fractionated extract was tested for inotropic effects on the isolated guinea pig atria. The aqueous layer obtained from the acetone extract of fresh algae was concentrated, and the residue was extracted with methanol. The methanolic extract was fractionated by chromatography using mixtures of aqueous methanol. Elution with 50% aqueous methanol afforded material that had a significant negative inotropic effect. Further purification of this material by high-performance liquid chromatography (HPLC) using methanol–water (2:5) afforded crystalline adenosine, which was shown to be the active substance of *U. pertusa*, causing a negative inotropic action.

Keyphrases □ Cardioinhibitory effects—of extracts of the marine green alga (*Ulva pertusa*), adenosine □ *Ulva pertusa*—inotropic effects of extract fractions (adenosine), cardioinhibitory effects □ Adenosine—extracted from the marine green alga (*Ulva pertusa*), cardioinhibitory effects

The marine green alga, *Ulva pertusa*, is cultivated around the seashore in all parts of Japan, especially in the intertidal zone. This alga is also cultured *in vitro* (1). The green alga possesses only type I aldolase, which is also present in the animals and higher terrestrial plants, but not in bacteria which have the type II aldolase (2). It has been reported that a water-soluble fraction from the green alga had antimicrobial activity (3).

A screening program was designed to assess the biological activity of various marine organisms. In such screening tests, extracts of the marine green alga have produced cardioinhibitory action on the isolated guinea pig atria. A cardiotonic fraction (4) was extracted from a sea weed, *Undaria pinnatifida*, but the chemical nature of the active substance was not reported. Therefore, the purpose of this work was to investigate the chemical constituents and pharmacological properties of the active substance (causing the negative inotropic effect) of the green alga.

EXPERIMENTAL

Isolation—An acetone extract of *U. pertusa*[1] (5.6 kg) was concentrated under reduced pressure, washed successively with hexane (2 × 1.5 liters) and ethyl acetate (1.8 liters), and then concentrated *in vacuo* to dryness. The resulting brown powder was extracted with methanol to remove inorganic salts. After filtration the yellow methanolic solution was concentrated to give a light-brown oil (45 g), which showed a negative inotropic effect on the isolated guinea pig atria at concentrations $>10^{-4}$ g/ml. The crude oil was subjected to column chromatography on TSK-Gel G-3000 S[2] (220 ml). The column was developed successively with water (600 ml, fractions 1–6), aqueous methanol (80:20 200 ml, fractions 7 and 8), aqueous methanol (50:50, 200 ml, fractions 9 and 10), and methanol (400 ml, fraction 11). Fraction 9 (365 mg) was found to have inotropic activity; this fraction was purified by high-performance liquid chromatography (HPLC)[3] using a Megapack SIL C_8 column, a mobile phase of methanol–water (v/v 2:5), and a UV detector at 210 nm. The fraction corresponding to the major peak gave pale yellow crystals (46.3 mg, 8.3 × 10^{-4}% yield), which showed a negative inotropic effect at concentrations $>10^{-5}$ g/ml. Recrystallization from water gave colorless needles (32 mg): $C_{10}H_{13}N_5O_4$, mp 233–235°; UV[4] (methanol): 260 nm (ϵ 14,800); IR[5] (KBr): 1665, 1610, and 1580 cm^{-1}; ^{1}H-NMR[6] (deuterium oxide): δ 3.92 (3, m), 4.30–4.50 (2, m), 6.06 (1, d, J = 6 Hz), 8.16 (1, s), and 8.31 (1, s). The above data, as well as the chromatographic properties (TLC, HPLC) of the crystals, were in agreement with those of authentic adenosine[7].

Bioassay—The bioassay of fractions was performed on isolated guinea pig heart. The left atrium was separated from the rest of the heart and suspended in a 50-ml tissue bath containing physiological salt solution of the following composition (mM): NaCl, 120.3; KCl, 48; $CaCl_2$, 1.2; $MgSO_4$, 1.3; KH_2PO_4, 1.2; $NaHCO_3$, 25.2; and glucose, 5.5. The solution was bubbled continuously with a gas mixture of oxygen–carbon dioxide (19:1) and maintained at 30°, pH 7.4. Contractile response was recorded isometrically through a force-displacement transducer[8] and displayed on a polygraph[9]. The atrium was driven by an electrical stimulator[10] at a frequency of 2 Hz with square-wave pulses of 5 msec duration at 100% above threshold voltage. The atrium was allowed to equilibrate under 0.5-g tension for 60 min prior to beginning each measurement.

RESULTS AND DISCUSSION

Table I shows the negative inotropic effect of fractions extracted from the green alga *U. pertusa* on the guinea pig left atria driven electrically. The crude oil caused a negative inotropic effect at a concentration of 4 × 10^{-4} g/ml while fraction 9 (TSK-Gel filtration) showed an effect at 4 × 10^{-5} g/ml and the purified crystalline material at 10^{-5} g/ml. The potency of the purified crystalline material was essentially equivalent to

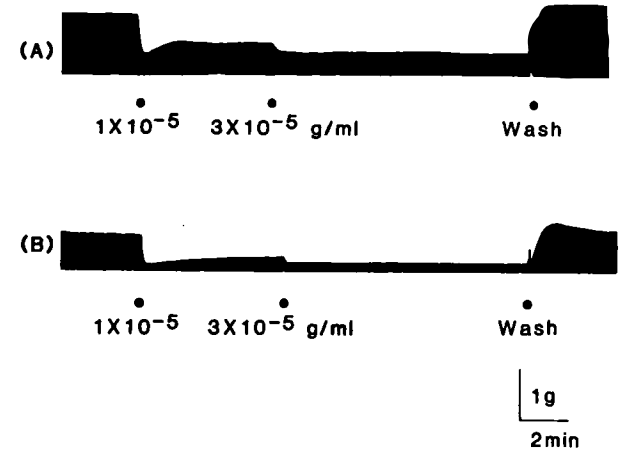

Figure 1—*Inhibitory effects of the final crystals (A) from* U. pertusa *and authentic adenosine (B) on the guinea pig atria driven electrically (2 Hz, 5 V, and 5 msec duration). The final crystals and adenosine at concentrations of 1 × 10^{-5} and 3 × 10^{-5} g/ml were applied to the muscle and then washed out of the solution.*

[1] Collected at Himaka-Jima, Aichi, Japan in August 1981. The alga was identified as *Ulva pertusa* (Chlorophyceae) by Professor W. Kida, Mie University, Japan. A voucher specimen (No. KY-15) representing material collected for this investigation is available for inspection at the Herbarium of Laboratory of Organic Chemistry, Department of Chemistry, Nagoya University, Nagoya, Japan.

[2] Toyo Soda Manufacturing Co., Ltd.

[3] JASCO TRI ROTAR-II liquid chromatograph.

[4] JASCO UVIDEC 510 spectrophotometer.

[5] JASCO Model IRS instrument.

[6] Varian HA-100D spectrometer.

[7] Kohjin Co., Ltd.

[8] Toyo Baldwin model T-7-30, Tokyo.

[9] Nihon Kohden model RM6000, Tokyo.

[10] Nihon Kohden model SEN7103, Tokyo.

0022-3549/83/0800-0945$01.00/0

Table I—Inhibitory Effect of Adenosine and Fractions Extracted from *U. pertusa* on the Contractility of Isolated Guinea Pig Atria [a]

Substance	Concentration, g/ml	Inhibition, [b] %
Crude oil	4×10^{-4}	6.9
Fraction 9[c]	4×10^{-5}	40.4
Final crystals	1×10^{-5}	63.6
Adenosine	1×10^{-5}	69.0

[a] The guinea pig left atria was electrically driven with square pulses (2 Hz, 5 msec duration, and 5 V). [b] Inhibition was expressed by percent decrease in the systolic tension development of the atria. [c] Purified using column chromatography (TSK-Gel).

that of authentic adenosine, 1×10^{-5} g/ml. Figure 1 is representative of the negative inotropic effect of the purified crystalline material (1×10^{-5} and 3×10^{-5} g/ml) on the atria.

When the crystalline material was washed out of the tissue bath, the negative inotropic action of the agent disappeared. The contractility was restored to the control level within 1 min after washout, similar to the effect of the removal of adenosine reported by Baumann *et al.* (5). Furthermore, negative inotropic effects of the purified crystalline material and adenosine were not affected by the β-blocker propranolol (1×10^{-6} *M*) or the α-blocker phentolamine (1×10^{-6} *M*). Thus, the inhibitory action of the purified crystalline material is not mediated through the activation of adrenoceptors. In conclusion, the chemical and pharmacolgical results indicate that the cardioinhibitory substance isolated from the green alga *U. pertusa* is adenosine, which had not been found previously in marine organism.

REFERENCES

(1) M. Ohno and S. Arasaki, *Rec. Oceanogr. Work*, **9**, 130 (1967).

(2) W. J. Rutter, *Fed. Proc. Fed. Am. Soc. Exp. Biol.*, **23**, 1248 (1964).

(3) K. Saito and M. Samejima, *No Ka*, **29**, 427 (1955).

(4) P. B. Searl, T. R. Norton, and B. K. B. Lum, *Proc. West. Pharmacol. Soc.*, **24**, 63 (1981).

(5) G. Baumann, J. Schrader, and E. Gerlach, *Circ. Res.*, **48**, 259 (1981).

ACKNOWLEDGMENTS

Supported in part by the Hawaii Heart Association.

Degradation of Fenprostalene in Aqueous Solution

DAVID M. JOHNSON ˣ, WILLIAM F. TAYLOR, GEOFFREY F. THOMPSON, and RAYMOND A. PRITCHARD

Received May 17, 1982, from the *Institute of Pharmaceutical Sciences, Syntex Research, Palo Alto, CA 94304.* Accepted for publication August 24, 1982

Abstract □ The degradation of the prostaglandin fenprostalene (III) was studied in aqueous solution. The reaction was both specific acid and base catalyzed. The only reaction found to occur was hydrolysis of the methyl ester at C-1. Activation energies for the acid- and base-catalyzed reactions were determined and are nearly identical to that for the hydrolysis of ethyl acetate, a model ester. A competing acid-catalyzed reaction of the C-1 free acid of III was found to be ~ 10 times slower than the hydrolysis of III.

Keyphrases □ Degradation—fenprostalene, prostaglandins, high-performance liquid chromatography, kinetics, ester hydrolysis □ Fenprostalene—degradation, prostaglandins, high-performance liquid chromatography, kinetics, ester hydrolysis □ High-performance liquid chromatography—degradation of fenprostalene, kinetics, ester hydrolysis □ Ester hydrolysis—fenprostalene degradation, high-performance liquid chromatography, kinetics

The degradation of prostaglandin $F_{2\alpha}$ in aqueous solution is known to be acid catalyzed (1, 2). No evidence of degradation under alkaline conditions has been reported. Recently, the degradation of two $F_{2\alpha}$-type aryloxy prostaglandins (I and II) was reported by Jones *et al.* (3). The authors found that the degradation of these luteolytic agents in aqueous solution was acid catalyzed, and the rate of degradation as well as the type of products formed were dependent on the presence of oxygen in the solution. No degradation of these compounds was observed at pH values >5.

Fenprostalene (III)[1] is a new prostaglandin developed for use as an abortifacient and for estrus synchronization in cattle (4, 5). The likely degradation route of this F-type prostaglandin at high pH is hydrolysis of the C-1 methyl ester group. However, we were interested to see whether acid-catalyzed decomposition reactions analogous to those found for I and II (3) or $PGF_{2\alpha}$ itself (1, 2) might compete with acid-catalyzed hydrolysis of the ester moiety in III at low pH. Accordingly, we have studied the degradation of fenprostalene (III) and its C-1 free acid (IV) in aqueous solution as a function of pH.

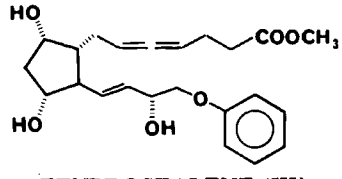

FENPROSTALENE (III)

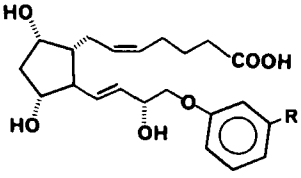

I: R = CF_3
II: R = Cl

EXPERIMENTAL

Materials—The fenprostalene (6) used was 99% pure by high-performance liquid chromatographic (HPLC) area normalization. The methanol was glass-distilled HPLC grade, and the water was purified through a filtration and ion exchange system[2]. All other chemicals were reagent grade quality.

Kinetics Methods—Buffer solutions contained 0.025 *M* total buffer,

[1] Fenprostalene is the generic name for methyl 7-[3,5-dihydroxy-2-(3-hydroxy-4-phenoxy-1-butenyl)cyclopentyl]-4,5-heptadienoate.

[2] Barnstead Nanopure System.

0022-3549/83/0800-0946$01.00/0

Table I—Inhibitory Effect of Adenosine and Fractions Extracted from *U. pertusa* on the Contractility of Isolated Guinea Pig Atria [a]

Substance	Concentration, g/ml	Inhibition, [b] %
Crude oil	4×10^{-4}	6.9
Fraction 9[c]	4×10^{-5}	40.4
Final crystals	1×10^{-5}	63.6
Adenosine	1×10^{-5}	69.0

[a] The guinea pig left atria was electrically driven with square pulses (2 Hz, 5 msec duration, and 5 V). [b] Inhibition was expressed by percent decrease in the systolic tension development of the atria. [c] Purified using column chromatography (TSK-Gel).

that of authentic adenosine, 1×10^{-5} g/ml. Figure 1 is representative of the negative inotropic effect of the purified crystalline material (1×10^{-5} and 3×10^{-5} g/ml) on the atria.

When the crystalline material was washed out of the tissue bath, the negative inotropic action of the agent disappeared. The contractility was restored to the control level within 1 min after washout, similar to the effect of the removal of adenosine reported by Baumann *et al.* (5). Furthermore, negative inotropic effects of the purified crystalline material and adenosine were not affected by the β-blocker propranolol (1×10^{-6} *M*) or the α-blocker phentolamine (1×10^{-6} *M*). Thus, the inhibitory action of the purified crystalline material is not mediated through the activation of adrenoceptors. In conclusion, the chemical and pharmacolgical results indicate that the cardioinhibitory substance isolated from the green alga *U. pertusa* is adenosine, which had not been found previously in marine organism.

REFERENCES

(1) M. Ohno and S. Arasaki, *Rec. Oceanogr. Work*, **9**, 130 (1967).

(2) W. J. Rutter, *Fed. Proc. Fed. Am. Soc. Exp. Biol.*, **23**, 1248 (1964).

(3) K. Saito and M. Samejima, *No Ka*, **29**, 427 (1955).

(4) P. B. Searl, T. R. Norton, and B. K. B. Lum, *Proc. West. Pharmacol. Soc.*, **24**, 63 (1981).

(5) G. Baumann, J. Schrader, and E. Gerlach, *Circ. Res.*, **48**, 259 (1981).

ACKNOWLEDGMENTS

Supported in part by the Hawaii Heart Association.

Degradation of Fenprostalene in Aqueous Solution

DAVID M. JOHNSON ˣ, WILLIAM F. TAYLOR, GEOFFREY F. THOMPSON, and RAYMOND A. PRITCHARD

Received May 17, 1982, from the *Institute of Pharmaceutical Sciences, Syntex Research, Palo Alto, CA 94304.* Accepted for publication August 24, 1982

Abstract □ The degradation of the prostaglandin fenprostalene (III) was studied in aqueous solution. The reaction was both specific acid and base catalyzed. The only reaction found to occur was hydrolysis of the methyl ester at C-1. Activation energies for the acid- and base-catalyzed reactions were determined and are nearly identical to that for the hydrolysis of ethyl acetate, a model ester. A competing acid-catalyzed reaction of the C-1 free acid of III was found to be ~ 10 times slower than the hydrolysis of III.

Keyphrases □ Degradation—fenprostalene, prostaglandins, high-performance liquid chromatography, kinetics, ester hydrolysis □ Fenprostalene—degradation, prostaglandins, high-performance liquid chromatography, kinetics, ester hydrolysis □ High-performance liquid chromatography—degradation of fenprostalene, kinetics, ester hydrolysis □ Ester hydrolysis—fenprostalene degradation, high-performance liquid chromatography, kinetics

The degradation of prostaglandin $F_{2\alpha}$ in aqueous solution is known to be acid catalyzed (1, 2). No evidence of degradation under alkaline conditions has been reported. Recently, the degradation of two $F_{2\alpha}$-type aryloxy prostaglandins (I and II) was reported by Jones *et al.* (3). The authors found that the degradation of these luteolytic agents in aqueous solution was acid catalyzed, and the rate of degradation as well as the type of products formed were dependent on the presence of oxygen in the solution. No degradation of these compounds was observed at pH values >5.

Fenprostalene (III)[1] is a new prostaglandin developed for use as an abortifacient and for estrus synchronization in cattle (4, 5). The likely degradation route of this F-type prostaglandin at high pH is hydrolysis of the C-1 methyl ester group. However, we were interested to see whether acid-catalyzed decomposition reactions analogous to those found for I and II (3) or $PGF_{2\alpha}$ itself (1, 2) might compete with acid-catalyzed hydrolysis of the ester moiety in III at low pH. Accordingly, we have studied the degradation of fenprostalene (III) and its C-1 free acid (IV) in aqueous solution as a function of pH.

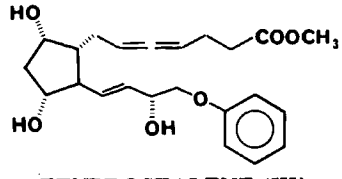

FENPROSTALENE (III)

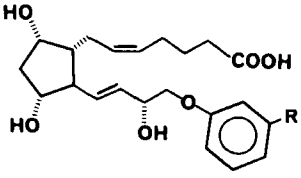

I: R = CF_3
II: R = Cl

EXPERIMENTAL

Materials—The fenprostalene (6) used was 99% pure by high-performance liquid chromatographic (HPLC) area normalization. The methanol was glass-distilled HPLC grade, and the water was purified through a filtration and ion exchange system[2]. All other chemicals were reagent grade quality.

Kinetics Methods—Buffer solutions contained 0.025 *M* total buffer,

[1] Fenprostalene is the generic name for methyl 7-[3,5-dihydroxy-2-(3-hydroxy-4-phenoxy-1-butenyl)cyclopentyl]-4,5-heptadienoate.

[2] Barnstead Nanopure System.

0022-3549/83/0800-0946$01.00/0

Table I—Observed Rate Constants for the Decomposition of III and IV in Aqueous Solution

Compound	pH	Buffer[a]	Temperature	$k_{obs} \times 10^7$ (sec^{-1})
III	1.15	HCl	80°	3360
	2.99[b]	Formate	80°	35.0
	3.21	Formate	80°	22.1
	3.22[c]	Formate	80°	21.6
	5.13	Acetate	80°	1.43
	6.51[d]	Phosphate	80°	18.6
	6.57[e]	Phosphate	80°	21.4
	7.21	Phosphate	80°	84.5
	9.22	Carbonate	80°	8350
	1.03	HCl	60°	855
	9.26	Carbonate	60°	1331
	1.20	HCl	30°	42.7
	9.31	Carbonate	30°	35.3
IV	1.1	HCl	80°	302
	3.10	Formate	80°	2.0
	4.98	Acetate	80°	0.11
	7.05	THAM	80°	<0.05[f]

[a] Buffer concentration 0.025 *M* except for HCl (0.1 *M*). [b] Contains 10^{-3} *M* Fe^{3+}. [c] Contains 10^{-3} *M* Cu^{2+}. [d] Contains Fe^{3+}. [e] Contains Cu^{2+}. [f] No degradation was observed after 104 days at 80°.

and potassium chloride was added to make the ionic strength 0.10 (0.20 for solutions of IV). Metal ions (10^{-3} *M*) were added to some buffer solutions; however, precipitation occurred with both iron and copper at pH 6.5. These solutions were filtered at room temperature, and the rate constants were thus measured in solutions saturated with these metals.

The pH of all solutions was measured at the reaction temperature (30, 60, or 80°)[3]. Reaction solutions were typically prepared by adding 4 ml of a 2.5-mg/ml methanol solution of III to 96 ml of buffer to give a final solution containing 100 μg/ml of III and ~4% methanol. The solutions

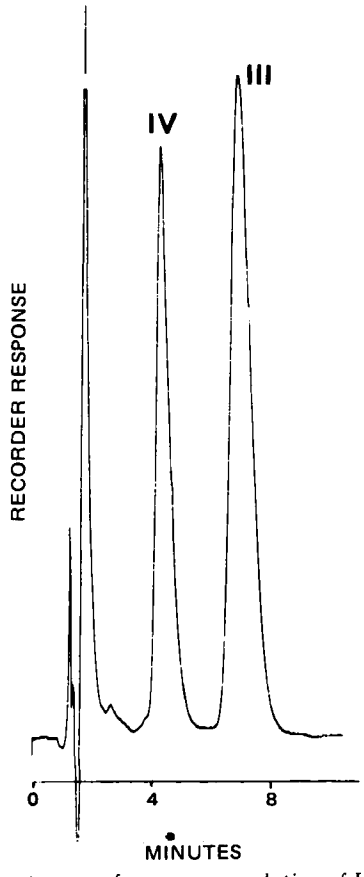

Figure 1—*Chromatogram of an aqueous solution of III after partial hydrolysis to IV at pH 1.03, 60°.*

[3] Radiometer model PHM 64 pH meter equipped with a Radiometer model GK2401C electrode.

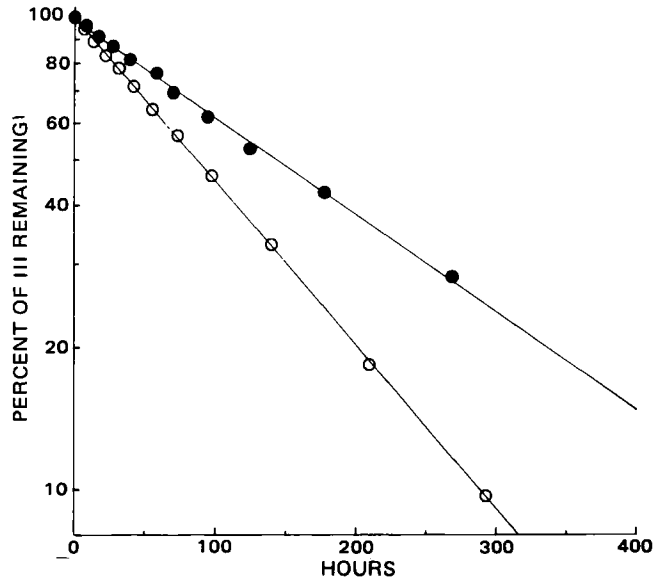

Figure 2—*First-order plot for the degradation of III at 60° in a pH 9.26 buffer solution (○) and a pH 1.03 buffer solution (●).*

were stored in sealed amber glass ampules and placed in a constant-temperature water bath at 80, 60, or 30° for the appropriate period of time. They were then removed, and in the case of the 30° samples the ampules were frozen until they were assayed. The 80 and 60° samples were refrigerated (4°) until assayed. The solutions were then diluted 2:5 with mobile phase and analyzed by HPLC for the amount of III (or IV) remaining compared with an initial sample kept at 4°.

HPLC Method—An HPLC system consisting of a pump[4], a variable-wavelength detector[5] and a 100-μl fixed-loop injector[6] was used. A 10-μm ODS column[7] was used with a mobile phase of methanol–0.02 *M* acetic acid (55:45) and detection wavelength of either 270 or 219 nm to achieve baseline separation of compounds III and IV (Fig. 1). Quantitation by peak area integration[8] gave excellent linearity for III over the range of concentrations investigated in the kinetics. The mobile phase in the above method was modified slightly (45:55 ratio of methanol to 0.02 *M* acetic acid) to follow the degradation of IV.

RESULTS AND DISCUSSION

The rate of disappearance of fenprostalene (III) in aqueous solution was followed using HPLC. At 80° the reaction was studied over the pH range 1.1–9.2, while at 30 and 60° the reaction was studied only at the extremes of this pH range. The degradation reaction obeyed pseudo-first-order kinetics as evidenced by the linear log percent remaining *versus* time plot shown in Fig. 2 for pH 9.26 and 1.03 at 60°. The observed pseudo-first-order rate constants (k_{obs}) are listed in Table I.

Degradation of III throughout the entire pH region was found to give the corresponding acid (IV) of fenprostalene as the only observable product by HPLC (Fig. 1). Mass balance was determined by comparing the combined area of the peaks representing III and IV throughout the time course of the reaction with the initial area of III. Greater than 94% mass balance was found for both acid- and base-catalyzed decomposition of III by this method. These results are consistent with hydrolysis of the ester group at C-1 as the exclusive reaction occurring in aqueous solution.

The log k_{obs} *versus* pH profile for the hydrolysis of III in aqueous solution at 80° is shown in Fig. 3. The line drawn through the experimental points represents the rate law described in Eq. 1 where $k_{H^+} = 3.94 \times 10^{-3}$ M^{-1} sec^{-1} and $k_{HO^-} = 2.16$ M^{-1} sec^{-1}:

$$k_{obs} = k_{H^+}[H^+] + k_{HO^-}[HO^-] \qquad \text{(Eq. 1)}$$

This simple rate law contains only two terms: a specific acid term and a specific base term. The excellent fit of the theoretical line to the data

[4] Altex model 110 A.
[5] Cecil model CE 212.
[6] Rheodyne model 70-10.
[7] Spherisorb ODS particles (10 μm) were packed under high pressure in a 250 mm × 3.2-mm i.d. column.
[8] Spectra-Physics model SP-4000.

Table II—Second-Order Rate Constants for the Acid- and Base-Catalyzed Decomposition of III [a]

Temperature	$k_{H^+} \times 10^5$, M^{-1} sec^{-1}	k_{HO^-}, M^{-1} sec^{-1}
80°	394	2.16
60°	81.0	0.761
30°	6.72	0.118

[a] Calculated from the data in Table I.

indicates no other catalytic terms are necessary to explain the observed data. This also implies that it is likely that no significant buffer catalysis occurred in these solutions. It is also apparent from Fig. 3 that the presence of Cu^{2+} and Fe^{3+} had no effect on the rate of degradation of III.

The rate equation describing the pH dependence for the degradation of III (Eq. 1) is likely to hold at low temperatures as well as at 80°. The second-order rate constants k_{HO^-} and k_{H^+} at 60 and 30° were thus obtained by determining k_{obs} at high pH (9.3) and low pH (1.1) and calculating k_{HO^-} and k_{H^+} from Eqs. 2 and 3, respectively:

$$k_{HO^-} = \frac{k_{obs}[H^+]}{K_w} \quad \text{(Eq. 2)}$$

$$k_{H^+} = \frac{k_{obs}}{[H^+]} \quad \text{(Eq. 3)}$$

The second-order rate constants at 80, 60, and 30° are shown in Table II and were used to calculate the activation energies for the specific acid- (17 kcal/mole) and base-catalyzed (12 kcal/mole) hydrolysis of III[9].

The degradation kinetics of IV were also investigated at 80° from pH 1 to 7. The degradation reaction followed pseudo-first-order kinetics, and the observed rate constants obtained are shown in Table I. From the plot in Fig. 3 one can see that the degradation rate of IV is acid catalyzed and is significantly slower than that of its methyl ester (III) in the acidic pH region. The degradation rate for IV at pH 7.0 was too slow to measure. If the assumption is made that the degradation reaction of IV does not involve the C-1 carboxyl group[10], then this acid-catalyzed pathway is probably available to fenprostalene (III) itself. Hydrolysis of the C-1 methyl ester, however, is preferred by ~10-fold over this alternate degradation pathway for III at 80° in the acidic pH region.

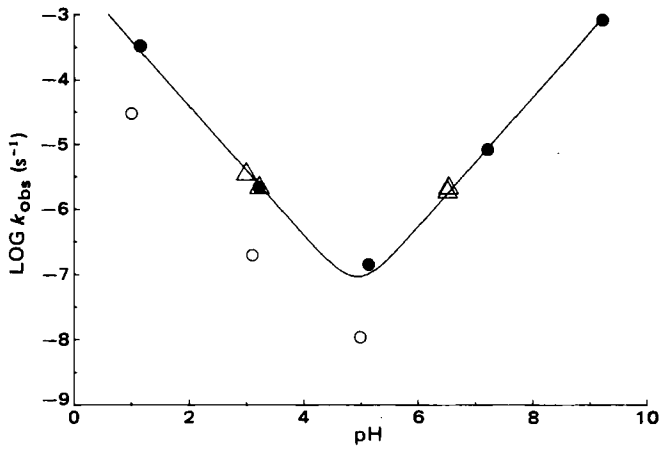

Figure 3—*Log* k_{obs} *versus pH profile for the hydrolysis of III at 80°. Key: solid circles represent simple buffer solutions, open triangles represent buffer solutions containing* Cu^{2+} *and* Fe^{3+} *ions, and the reaction of IV in aqueous solution at 80° is shown by the open circles.*

[9] These results are nearly identical to those reported for the hydrolysis of ethyl acetate (7).

[10] Jones *et al.* (3) studied the degradation of II in acidic solution under aerobic conditions. The products were a complex mixture of compounds, and no major products were identified. We have not identified the degradation products of IV in acidic media but have observed on HPLC that several products are formed.

REFERENCES

(1) S. M. M. Karim, J. Devlin, and K. Hillier, *Eur. J. Pharmacol.*, **4**, 416 (1968).

(2) T. J. Roseman, B. Sims, and R. G. Stehle, *Am. J. Hosp. Pharm.*, **30**, 236 (1973).

(3) M. F. Jones, E. Crundwell, and P. J. Taylor, *Int. J. Pharm.*, **4**, 1 (1979).

(4) B. H. Vickery, G. I. McRae, J. S. Kent, and R. V. Tomlinson, *Prostaglandins Med.*, **5**, 93 (1980).

(5) R. C. Herschler, *Agri. Pract.*, **4**, 28 (1983).

(6) J. M. Muchowski and J. H. Fried, U.S. pat. 3,985,791 (1976).

(7) T. C. Bruice and S. J. Benkovic, "Bio-organic Mechanisms," Vol. I, W. A. Benjamin, New York, N.Y., 1966, p. 272.

Determination of Hydrazine in Pharmaceuticals III: Hydralazine and Isoniazid Using GLC

F. MATSUI ˣ, D. L. ROBERTSON, and E. G. LOVERING

Received February 26, 1982, from the *Bureau of Drug Research, Health Protection Branch, Ottawa, Ontario K1A OL2.* Accepted for publication July 30, 1982.

Abstract □ A GLC procedure has been developed for the determination of hydrazine in hydralazine and isoniazid drug raw materials, single and multicomponent tablets, injectables, and syrups. The method is based on the derivatization of hydrazine with benzaldehyde to form benzalazine. The minimum detectable amount of hydrazine in hydralazine and isoniazid raw materials and formulations is ~0.0003%. No hydrazine was found in the hydralazine raw material specimens examined. Traces of hydrazine (~0.0003%) were found in some tablet lots and ~0.02% was found in an injectable product. A trace of hydrazine was found in one lot of isoniazid raw material and low levels (0.0012 and 0.0029%) were found in isoniazid tablet products. An isoniazid syrup contained ~0.2% hydrazine.

Keyphrases □ Hydrazine—determination in hydralazine and isoniazid by GLC □ Hydralazine—GLC, determination of hydrazine □ Isoniazid—GLC, determination of hydrazine □ GLC—determination of hydrazine in pharmaceutics, hydralazine, isoniazid

Previous papers in this series described high-performance liquid chromatographic (HPLC) methods for the determination of hydrazine in isoniazid and phenelzine products and reported typical amounts found in commercial formulations (1, 2). Since hydrazine is a mutagen (3) and a carcinogen in laboratory animals (4), concern over its presence in drug products resulted in proposed regulatory action in the United States (5) and to the recall of

0022-3549/83/0800-0948$01.00/0

Table II—Second-Order Rate Constants for the Acid- and Base-Catalyzed Decomposition of III [a]

Temperature	$k_{H^+} \times 10^5$, M^{-1} sec^{-1}	k_{HO^-}, M^{-1} sec^{-1}
80°	394	2.16
60°	81.0	0.761
30°	6.72	0.118

[a] Calculated from the data in Table I.

indicates no other catalytic terms are necessary to explain the observed data. This also implies that it is likely that no significant buffer catalysis occurred in these solutions. It is also apparent from Fig. 3 that the presence of Cu^{2+} and Fe^{3+} had no effect on the rate of degradation of III.

The rate equation describing the pH dependence for the degradation of III (Eq. 1) is likely to hold at low temperatures as well as at 80°. The second-order rate constants k_{HO^-} and k_{H^+} at 60 and 30° were thus obtained by determining k_{obs} at high pH (9.3) and low pH (1.1) and calculating k_{HO^-} and k_{H^+} from Eqs. 2 and 3, respectively:

$$k_{HO^-} = \frac{k_{obs}[H^+]}{K_w} \quad \text{(Eq. 2)}$$

$$k_{H^+} = \frac{k_{obs}}{[H^+]} \quad \text{(Eq. 3)}$$

The second-order rate constants at 80, 60, and 30° are shown in Table II and were used to calculate the activation energies for the specific acid- (17 kcal/mole) and base-catalyzed (12 kcal/mole) hydrolysis of III[9].

The degradation kinetics of IV were also investigated at 80° from pH 1 to 7. The degradation reaction followed pseudo-first-order kinetics, and the observed rate constants obtained are shown in Table I. From the plot in Fig. 3 one can see that the degradation rate of IV is acid catalyzed and is significantly slower than that of its methyl ester (III) in the acidic pH region. The degradation rate for IV at pH 7.0 was too slow to measure. If the assumption is made that the degradation reaction of IV does not involve the C-1 carboxyl group[10], then this acid-catalyzed pathway is probably available to fenprostalene (III) itself. Hydrolysis of the C-1 methyl ester, however, is preferred by ~10-fold over this alternate degradation pathway for III at 80° in the acidic pH region.

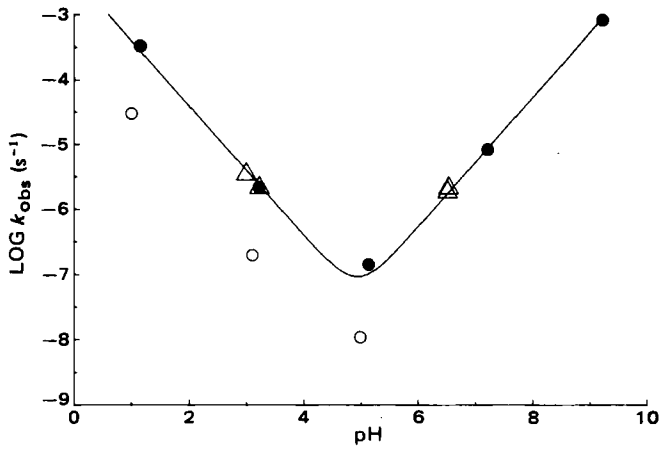

Figure 3—*Log* k_{obs} *versus pH profile for the hydrolysis of III at 80°. Key: solid circles represent simple buffer solutions, open triangles represent buffer solutions containing* Cu^{2+} *and* Fe^{3+} *ions, and the reaction of IV in aqueous solution at 80° is shown by the open circles.*

[9] These results are nearly identical to those reported for the hydrolysis of ethyl acetate (7).

[10] Jones *et al.* (3) studied the degradation of II in acidic solution under aerobic conditions. The products were a complex mixture of compounds, and no major products were identified. We have not identified the degradation products of IV in acidic media but have observed on HPLC that several products are formed.

REFERENCES

(1) S. M. M. Karim, J. Devlin, and K. Hillier, *Eur. J. Pharmacol.*, **4**, 416 (1968).

(2) T. J. Roseman, B. Sims, and R. G. Stehle, *Am. J. Hosp. Pharm.*, **30**, 236 (1973).

(3) M. F. Jones, E. Crundwell, and P. J. Taylor, *Int. J. Pharm.*, **4**, 1 (1979).

(4) B. H. Vickery, G. I. McRae, J. S. Kent, and R. V. Tomlinson, *Prostaglandins Med.*, **5**, 93 (1980).

(5) R. C. Herschler, *Agri. Pract.*, **4**, 28 (1983).

(6) J. M. Muchowski and J. H. Fried, U.S. pat. 3,985,791 (1976).

(7) T. C. Bruice and S. J. Benkovic, "Bio-organic Mechanisms," Vol. I, W. A. Benjamin, New York, N.Y., 1966, p. 272.

Determination of Hydrazine in Pharmaceuticals III: Hydralazine and Isoniazid Using GLC

F. MATSUI ˣ, D. L. ROBERTSON, and E. G. LOVERING

Received February 26, 1982, from the *Bureau of Drug Research, Health Protection Branch, Ottawa, Ontario K1A OL2.* Accepted for publication July 30, 1982.

Abstract □ A GLC procedure has been developed for the determination of hydrazine in hydralazine and isoniazid drug raw materials, single and multicomponent tablets, injectables, and syrups. The method is based on the derivatization of hydrazine with benzaldehyde to form benzalazine. The minimum detectable amount of hydrazine in hydralazine and isoniazid raw materials and formulations is ~0.0003%. No hydrazine was found in the hydralazine raw material specimens examined. Traces of hydrazine (~0.0003%) were found in some tablet lots and ~0.02% was found in an injectable product. A trace of hydrazine was found in one lot of isoniazid raw material and low levels (0.0012 and 0.0029%) were found in isoniazid tablet products. An isoniazid syrup contained ~0.2% hydrazine.

Keyphrases □ Hydrazine—determination in hydralazine and isoniazid by GLC □ Hydralazine—GLC, determination of hydrazine □ Isoniazid—GLC, determination of hydrazine □ GLC—determination of hydrazine in pharmaceutics, hydralazine, isoniazid

Previous papers in this series described high-performance liquid chromatographic (HPLC) methods for the determination of hydrazine in isoniazid and phenelzine products and reported typical amounts found in commercial formulations (1, 2). Since hydrazine is a mutagen (3) and a carcinogen in laboratory animals (4), concern over its presence in drug products resulted in proposed regulatory action in the United States (5) and to the recall of

0022-3549/83/0800-0948$01.00/0

an isoniazid product in Canada (6). Determination of hydrazine has now been extended to hydralazine, an antihypertensive drug.

Hydrazine contamination of hydralazine may occur during synthesis (7) or by degradation of the drug. Hydrazine is a metabolite of hydralazine in humans, and a GLC method for its identification and quantitation in urine has been described (8). Methods for the determination of hydrazine as a metabolite of isoniazid have also been reported (9, 10). Since attempts to determine hydrazine in hydralazine by the HPLC methods developed for isoniazid and phenelzine (1, 2) led to irreproducible results, a GLC method was developed. The sensitivity and stability of this method prompted its extension to isoniazid products as an alternative to the HPLC procedure (1).

EXPERIMENTAL

Materials—Hydrazine dihydrochloride[1], hydralazine hydrochloride[1], benzalazine[2], 5-chloro-2-methylaminobenzophenone[2], and benzaldehyde[3] were used as received. Solvents and reagents were commercial analytical reagent grade, except for *n*-heptane[4] which was HPLC grade.

Apparatus—The gas chromatograph[5] was equipped with a nitrogen–phosphorus alkali thermionic detector and a coiled-glass column (0.91-m × 4-mm i.d.) packed with 2% OV-101[6] on Chromosorb G-HP[7] (80/100 mesh). Instrument temperatures were: injector port, 275°; column, 250°; and detector, 300°. Gas flows were: nitrogen, 40 ml/min; air, 60 ml/min; and hydrogen, 1.75 ml/min.

Standard Solutions and Reagents—A stock solution of 5-chloro-2-methylaminobenzophenone in *n*-heptane (12 μg/ml) was diluted daily with *n*-heptane to obtain the working internal standard solution (1.2 μg/ml). The benzaldehyde reagent was prepared by dissolving benzaldehyde in a solution of equal parts (by volume) of methanol and water to yield a final concentration of 35 mg/ml.

Preparation of the Calibration Curve—An 80-μg/ml aqueous solution of hydrazine dihydrochloride (equivalent to 24.4 μg/ml of hydrazine) was diluted with distilled water to obtain five standard solutions ranging from 0.080 to 2 μg/ml of hydrazine dihydrochloride (representing 0.005–0.122 ng of hydrazine on-column). To a 2.0-ml aliquot of each solution, pipetted into separate 150 × 20-mm culture tubes fitted with polytef-lined screw caps, was added 1.0 ml of benzaldehyde reagent solution. The tubes were rotated for 10 min at 30 rpm, 10.0 ml of the working internal standard solution was added to each tube, and the tubes were rotated again for 30 min at 30 rpm. Duplicate 1-μl aliquots of the upper phase were chromatographed, and the slope was calculated from the ratio of the area counts of the benzalazine peaks to the area counts of the internal standard peaks *versus* the corresponding weight ratio.

Day-to-Day Calibration—Two hydrazine dihydrochloride standards, usually ~0.40 and 1.20 μg/ml, were prepared daily. Two-milliliter aliquots of these standards were derivatized as described above, and 1-μl aliquots were injected onto the chromatograph at regular intervals.

Analysis of Drug Raw Materials and Tablet Formulations—An accurately weighed amount of hydralazine hydrochloride, isoniazid drug raw material, or a powdered tablet composite equivalent to 50 mg of drug substance was tumbled for 30 min in a screw-capped culture tube with 5.0 ml of distilled water. After centrifugation, a 2.0-ml aliquot of the aqueous extract was derivatized as described above, and 1-μl aliquots were injected onto the chromatograph.

Analysis of Liquid Formulations—An aliquot of hydralazine hydrochloride injectable or isoniazid syrup equivalent to 20 mg of drug was pipetted into a 150 × 20-mm culture tube with 1.0 ml of distilled water, if necessary, to bring the total volume to 2.0 ml. The solution was derivatized and chromatographed as described above.

Quantitation—Hydrazine was estimated by comparison of the benzalazine to internal standard peak area ratio of the sample to the corresponding ratio of the standard. When the area ratio of the sample was less than that of the daily calibration standard, a new standard was prepared to approximate the concentration of the sample in question. When the area ratio exceeded that of the daily calibration standard, the sample was diluted with the working internal standard solution to approximate the concentration of the standard.

[1] Sigma Chemical Co., St. Louis, Mo.
[2] K&K—ICN Pharmaceutical, Plainview, N.Y.
[3] Aldrich Chemical Co., Milwaukee, Wis.
[4] Burdick and Jackson Laboratories, Muskegon, Mich.
[5] Hewlett-Packard Model 5880A.
[6] Pierce Chemical Co., Rockford, Ill.
[7] Johns-Manville, Celite Division, Denver, Colo.

Table I—Hydrazine Levels in Hydralazine Hydrochloride Products

Products	Lot No.	Hydralazine Strength	Hydrazine, %[a]
Drug raw material	(4 lots)	—	ND
Tablet	A	10 mg/tab	Trace
Tablet	B	25 mg/tab	ND
Tablet	C	50 mg/tab	Trace
Injectable	D	20 mg/ml	0.0327; 0.0326
Tablet	E	50 mg/tab	Trace
Tablet (lot E, stressed[b])			0.0017; 0.0018; 0.0013
Tablet (with 0.2 mg of reserpine)	F	50 mg/tab	ND
Tablet (lot F, stressed[b])			0.0045[f]
Tablets (with 0.1 mg of reserpine and 25 mg of hydrochlorothiazide)	G	25 mg/tab	ND
Tablet (lot G, stressed[c])			ND
Injectable	H	20 mg/ml	0.0217; 0.0215; 0.0240
Injectable (lot H, stored[d])			0.0422; 0.0409; 0.0394; 0.0387
Injectable (lot H, stressed[e])			0.1083[g]

[a] Expressed as weight percent of the labeled amount of hydralazine hydrochloride. Key: (ND) none detected; (Trace) minimum amount detectable (~0.0003%). [b] Stressed at 37° and 75% relative humidity for 221 days. [c] Stressed at 22° (room temperature) and 75% relative humidity for 221 days. [d] Stored at room temperature for 221 days. [e] Stressed at 37° for 221 days. [f] Mean of five determinations; relative *SD* 7.0%. [g] Mean of four determinations; relative *SD* 0.83%.

RESULTS AND DISCUSSION

Hydrazine in hydralazine and isoniazid raw materials and formulations was determined as the benzaldehyde derivative by GC. Hydrazine dihydrochloride was chosen as the calibration standard because it is more stable in aqueous solution (50 days) than the sulfate (7 days) or the hydrate (1 day).

Concomitant with the formation of benzalazine in the derivatization step is the formation of a hydrazone from the condensation of hydralazine with benzaldehyde. This compound is not separated from benzalazine by extraction and appears at ~4.3 and 8.1 min, well after the appearance of benzalazine and the internal standard at 1.2 and 1.6 min, respectively. It is the presence of this compound which leads to the requirement for a GLC method: the compound accumulated on the HPLC column, only to elute after a time with a resultant baseline shift and other undesirable chromatographic features. Similar compounds form from phenelzine and isoniazid. In the former case the compound elutes from the HPLC column, while in the latter it does not enter the partitioning solvent.

Derivatization Reaction—*Hydralazine*—Water was used as the medium for dissolution of the hydralazine and the derivatization reaction. The final pH values associated with dissolution of the drug were similar for all raw materials and formulated products (pH 2.9–3.2) and had no apparent effect on the derivatization reaction. The sodium acetate buffer (pH 6) used for sampling in the method for hydrazine in phenelzine (2) could not be used for hydralazine because it gave rise to an unidentified peak on the chromatogram that interfered with the internal standard peak. The time required for complete derivatization and the stability of the benzalazine formed were determined by measuring the GLC response due to benzalazine as a function of the time during which the derivatization was allowed to proceed. The derivatization of the hydrazine dihydrochloride standard was complete within 3–5 min, and the benzalazine formed was stable for at least 35 min. Hydralazine hydrochloride was stable under the derivatization conditions for 30 min after which time a peak due to a trace (0.0003%) of benzalazine appeared in the chromatogram. Neither hydralazine nor reserpine and/or hydrochlorothiazide (sometimes formulated with hydralazine) interfered with the derivatization reaction.

In contrast to the behavior of hydrazine dihydrochloride, the benza-

Table II—Hydrazine Levels in Isoniazid Products

Product	Lot No.	Isoniazid Strength	Hydrazine, %[a] Mean	Hydrazine, %[a] Range[b]
Drug raw material	(1 lot)	—	Trace	—
Tablet (stressed[c])	I	100 mg/tab	0.0012	0.0012–0.0013(2)
Tablet (with 50 mg pyridoxine hydrochloride[d])	J	300 mg/tab	0.0582	0.0571–0.0595(4)
Tablet (with 50 mg pyridoxine hydrochloride)	K	300 mg/tab	0.0029	0.0026–0.0034(5)
Tablet (lot K, stressed[e])			0.0199	0.0192–0.0210(4)
Tablet (lot K, stressed[f])			0.0052	0.0050–0.0055(3)
Tablet (lot K, stressed[g])			0.0671	0.0619–0.0757(3)
Syrup	L	10 mg/ml	0.235	0.234–0.236 (2)
Syrup	M	10 mg/ml	0.200	0.188–0.210 (3)
Syrup (lot M, stored[h])			0.349	0.326–0.378 (3)

[a] Expressed as weight percent of the labeled amount of isoniazid. Trace means the minimum detectable amount (~0.0003%). [b] Number of determinations is in parentheses. [c] Stressed at 45° and ambient humidity for 3 years. [d] Expired product. [e] Stressed at 22° (room temperature) and 75% relative humidity for 228 days. [f] Stressed at 37° and ambient humidity for 228 days. [g] Stressed at 37° and 75% relative humidity for 228 days. [h] Stored at room temperature for 228 days.

lazine derivative formed from hydrazine sulfate in water or acetate buffer was stable for only 10 or 20 min, respectively (2). There was no difference in the time required for the derivatization to go to completion.

Isoniazid—Either water or acetate buffer can be used for the sampling and derivatization of hydrazine from isoniazid products: the rate of derivatization of hydrazine dihydrochloride was the same in both solvents. Neither isoniazid nor pyridoxine interfered with the derivatization reaction. The mole ratio of benzaldehyde to hydralazine required to achieve quantitative derivatization of hydrazine in the presence of hydralazine, determined as previously described (1, 2), was 2.5:1. The method provides for a mole ratio of 3.0:1.

Neither hydralazine nor isoniazid decomposed to hydrazine during extraction and derivatization. This is demonstrated by the nondetectable and trace levels found in some drug raw materials and formulations (Tables I and II) and by the complete recovery of hydrazine from spiked samples (Table III).

Extraction and Partition—The extraction was done with *n*-heptane because it was free of interfering impurities and was a good solvent for the internal standard. To show that benzalazine was completely extracted from the derivatization medium, the latter was shaken with *n*-heptane in ratios of 1:20; 1:10; 2:10, and 3:10. The peak area ratios of derivative to internal standard divided by the corresponding weight ratios were 11.064, 11.028, 11.112, and 11.052, respectively, showing that partition was virtually complete. In addition, there was no significant change in the chromatographic response of internal standard solutions containing benzalazine after they had been extracted with the aqueous derivatization medium. The ratios of aqueous to the organic phase examined were 1:5, 2:5, and 4:5.

Tablet extraction conditions were verified by shaking portions of an isoniazid–pyridoxine tablet composite equivalent to 50 mg with 3.0, 5.0, 10.0, and 20.0 ml of water. After derivatization and extraction, hydrazine levels were found to be 0.0640, 0.0662, 0.0654, and 0.0602%, respectively. To check the time required for extraction, an isoniazid–pyridoxine tablet product was shaken with 5 ml of water for 10 and 30 min. Hydrazine levels, after derivatization and extraction, were 0.0060 and 0.0065%, respectively, identical within the experimental error.

The amount of *n*-heptane required to extract the hydrazine derivative from the aqueous phase was established by experiments with a hydralazine injectable and an isoniazid elixir. For the injectable, aqueous to organic phase ratios of 2:5, 2:10, 2:15, and 2:20 gave apparent hydrazine levels of 0.0257, 0.0240, 0.0256, and 0.0260%, respectively. For the isoniazid syrup formulation, the hydrazine levels were 0.374, 0.370, 0.363, and 0.389%, respectively, for the same solvent ratios. The method calls for a ratio of 2:10.

Linearity, Reproducibility, and Accuracy—A standard curve was prepared by derivatizing, extracting, and chromatographing known amounts of hydrazine dihydrochloride. Over the range from 0.005 to 0.122 ng of hydrazine injected (as benzalazine), the slope of the area count ratio of benzalazine to internal standard *versus* the corresponding weight ratio was 11.7121 and the intercept did not differ significantly from zero (7.2×10^{-3}). The standard deviation of the slope was 0.2131, and the correlation coefficient was 0.9987. This range represents hydrazine levels from 0.0003 to 0.0061% for 2000 ng of drug injected.

The chromatographic reproducibility was established by injecting seven aliquots of each of three solutions of derivatized and extracted hydrazine dihydrochloride. The amounts of hydrazine injected (as benzalazine) were 0.0264, 0.0486, and 0.0972 ng, and the relative standard deviations of the count/weight ratios were 1.60, 0.63, and 0.89%, respectively. The reproducibility of the procedure as applied to formulated drug products can be gauged from the data in Tables I and II. Relative standard deviations ranged from 4.0% for a hydralazine injectable (4 replicates, 0.0403% hydrazine) to 10.3% for isoniazid tablets (5 replicates, 0.0029% hydrazine).

The recovery of hydrazine in the presence of formulation matrices was determined by adding known amounts of hydrazine dihydrochloride at the extraction step and carrying the assay through to completion. Recoveries ranged between 93.4 and 103.2% (Table III).

The minimum detectable amount of hydrazine, as benzalazine on-column, is ~0.005 ng, with the minimum quantifiable level about three times this amount. This permits detection of hydrazine at the level of ~0.0003% in drugs. This method is 20 times as sensitive as the previously described HPLC methods (1, 2).

Hydrazine in Drug Raw Materials and Formulations—No hydrazine was found in raw material lots of hydralazine. Traces of hydrazine were found in some tablet lots and these amounts increased in tablets subjected to stress (Table I). Hydrazine levels in injectable hydralazine products were higher than in tablets and increased with time and temperature stress (Table I). It would appear that hydrazine is a degradation product of hydralazine.

Only a trace of hydrazine was found in the isoniazid raw material lot examined, but the formulated products examined contained hydrazine. The levels increased in products subjected to temperature and humidity stress (Table II). Again, it appears that hydrazine is a degradation product of the drug.

Table III—Hydrazine Recoveries

Product	Hydrazine, ng/injection Original	Added	Found	Recovery, %
Hydralazine hydrochloride drug raw material	0	1.305	1.285	98.5
	0	2.18	2.19	101.0
	0	3.44	3.45	100.1
	0	5.74	5.68	98.9
Hydralazine hydrochloride and reserpine tablet (lot F)	0	0.350	0.327	93.4
	0	0.606	0.606	100.3
Hydralazine hydrochloride, reserpine, an hydrochlorothiazide tablet (lot G)	0	0.0263	0.0263	100.0
	0	0.584	0.556	95.2
Isoniazid syrup	2.289	0.315	2.61	100.2
	2.289	0.315	2.65	102.0
Isoniazid and pyridoxine hydrochloride tablet (lot K)	0.253	0.715	0.949	98.0
	0.261	1.072	1.265	94.9
Isoniazid and pyridoxine hydrochloride tablet (lot J)	0.0243	0.0210	0.0443	97.8
	0.0493	0.0552	0.1078	103.2
	0.582	0.1071	0.696	101.0

REFERENCES

(1) A. G. Butterfield, N. M. Curran, E. G. Lovering, F. Matsui, D. L. Robertson, and R. W. Sears, *Can. J. Pharm. Sci.*, **16**, 15 (1981).

(2) F. Matsui, A. G. Butterfield, N. M. Curran, E. G. Lovering, R. W. Sears, and D. L. Robertson, *Can. J. Pharm. Sci.*, **16**, 20 (1981).

(3) B. Ames, "Chemical Mutagens. Principles and Methods for Their Detection," Vol. 1, Plenum, New York, N.Y. 1976, pp. 267–282.

(4) IARC Monographs, "Evaluation of Carcinogenic Risk of Chemicals to Man." Vol. 4. International Agency for Research on Cancer, Lyon, 1974, p. 127.

(5) "Protection," Health Protection Branch, Ottawa *1*, 4 (1977).

(6) Fed. Regist. 44(114), 33694 (1979).

(7) J. Druey and B. H. Ringier, *Helv. Chim. Acta*, **34**, 195 (1951).

(8) J. A. Timbrell and S. J. Harland, *Clin. Pharmacol. Ther.*, **26**, 81 (1979).

(9) S. Iguchi, T. Goromaru, A. Noda, K. Matsuyama, and K. Sogabe, *Pharm. Bull.*, **25**, 2796 (1977).

(10) J. A. Timbrell, J. M. Wright, and C. M. Smith, *J. Chromatogr.*, **138**, 165 (1977).

Theophylline Blood–Brain Barrier Transfer Kinetics in Dogs

P. VENG-PEDERSEN *[x], R. E. BRASHEAR [‡], and M. D. KAROL *

Received April 28, 1982, from the **Division of Pharmacokinetics, School of Pharmacy and Pharmacal Sciences, Purdue University, West Lafayette, IN 47907* and the [‡]*Department of Medicine, Indiana University, Indianapolis, IN 46223.* Accepted for publication August 6, 1982.

Abstract □ A simple diffusion-based pharmacokinetic model is proposed relating blood–brain barrier transfer kinetics of theophylline to the difference in the free concentrations of the drug in serum and cerebrospinal fluid (CSF). The model predicts that the CSF drug level is proportional to the serum drug level convoluted by $\exp(-kt)$, where k is the blood–brain barrier diffusion rate constant. An excellent agreement was found by nonlinear regression analysis between serum and CSF theophylline data in eight dogs and the proposed model for the blood–brain barrier transfer kinetics of theophylline. The ratio of the free fractions of theophylline in serum and CSF predicted from the model also agrees with the value determined experimentally.

Keyphrases □ Theophylline—blood–brain barrier transfer in dogs, kinetics □ Kinetics—of theophylline, blood–brain barrier transfer in dogs □ Blood–brain barrier—theophylline transfer in dogs, kinetics

The narrow therapeutic range of theophylline and the substantial intersubject variability in its disposition have resulted in extensive studies of the pharmacokinetics and clinical dosage management of the drug (1–8). Several investigations have related the bronchodilator effect of theophylline to its serum concentration level (5, 6, 9–13). However, it is the adverse effects rather than the therapeutic effect that dictates the dose administered and limits the therapeutic efficacy. The main adverse effects appear to be of CNS origin. It may be misleading, therefore, to use serum levels as a guide for the clinical management of the drug without any *a priori* knowledge of the kinetics of the blood–brain barrier transfer of theophylline. The theophylline concentration in the cerebrospinal fluid (CSF), should provide a better correlation to the CNS effects. The object of this study is to investigate the serum–CSF disposition of theophylline and the blood–brain barrier transfer kinetics. By establishing the kinetic relationship between the serum and CSF drug levels, a more rational approach to the usage of serum theophylline determinations can be established.

Although it was recognized early that theophylline enters the cerebrospinal fluid, neither the rate of equilibration with serum nor the serum–CSF concentration ratio have been defined adequately. In fact, little is known about the kinetics of transfer of drugs across the blood–brain barrier. The few CSF samples that have been correlated with serum samples in humans provide only a very limited insight into the kinetics (14–17). The use of dogs in the present study allowed comprehensive CSF sampling enabling a proper pharmacokinetic analysis of the serum–CSF theophylline disposition. Animals are often a poor predictor of human pharmacokinetics mainly due to substantial differences in the elimination processes. However, the present manner of analysis of the serum–CSF transfer kinetics is not influenced by absorption or elimination or other disposition processes. Furthermore, the tissues that constitute the blood–brain barrier apparently do not differ significantly between dogs and humans (18). The results from this study should therefore be of clinical interest.

EXPERIMENTAL

Study Design—After an 18-hr fast, eight dogs were anesthetized with 30 mg/kg iv of sodium pentobarbital; supplemental doses were given as needed during the remainder of the experiment. A polyethylene catheter in the left lateral saphenous vein was used for the infusion of aminophylline. Aminophylline[1] for intravenous use was utilized containing 25 mg of aminophylline (20.63 mg of anhydrous theophylline)/ml of solution. Aminophylline, 9 mg/kg (7.43 mg/kg theophylline) was diluted with saline to 19.4 ml and infused with a constant-infusion pump over a total of 20 min.

Blood samples for theophylline level determination were taken from a catheter in the left external jugular vein. An 18-gauge needle was percutaneously placed in the cisterna magna for obtaining the CSF samples. Cerebrospinal fluid and blood for theophylline levels were obtained at time zero (start of the infusion) and 20 (end of infusion), 50, 80, 140, 200, 260, 320, 350, and 380 min. The dogs were ventilated through a cuffed endotracheal tube using a constant-volume ventilator[2] with periodic hyperinflation to prevent atelectasis.

Theophylline Assay—The serum from 2–3 ml of blood and 0.5 ml of CSF were frozen and later assayed for theophylline, usually within 1–3 days. Theophylline concentrations were determined by the GC method of Least and coworkers (19) using 100-μl samples and substituting iodobutane for iodopentane in the derivation procedure. Theophylline concentrations were calculated using peak height ratios of theophylline to internal standards.

Protein Binding—The protein binding of theophylline was deter-

[1] Searle Laboratories.
[2] Harvard model 607.

0022-3549/83/0800-0951$01.00/0

REFERENCES

(1) A. G. Butterfield, N. M. Curran, E. G. Lovering, F. Matsui, D. L. Robertson, and R. W. Sears, *Can. J. Pharm. Sci.*, **16**, 15 (1981).

(2) F. Matsui, A. G. Butterfield, N. M. Curran, E. G. Lovering, R. W. Sears, and D. L. Robertson, *Can. J. Pharm. Sci.*, **16**, 20 (1981).

(3) B. Ames, "Chemical Mutagens. Principles and Methods for Their Detection," Vol. 1, Plenum, New York, N.Y. 1976, pp. 267–282.

(4) IARC Monographs, "Evaluation of Carcinogenic Risk of Chemicals to Man." Vol. 4. International Agency for Research on Cancer, Lyon, 1974, p. 127.

(5) "Protection," Health Protection Branch, Ottawa *1*, 4 (1977).

(6) Fed. Regist. 44(114), 33694 (1979).

(7) J. Druey and B. H. Ringier, *Helv. Chim. Acta*, **34**, 195 (1951).

(8) J. A. Timbrell and S. J. Harland, *Clin. Pharmacol. Ther.*, **26**, 81 (1979).

(9) S. Iguchi, T. Goromaru, A. Noda, K. Matsuyama, and K. Sogabe, *Pharm. Bull.*, **25**, 2796 (1977).

(10) J. A. Timbrell, J. M. Wright, and C. M. Smith, *J. Chromatogr.*, **138**, 165 (1977).

Theophylline Blood–Brain Barrier Transfer Kinetics in Dogs

P. VENG-PEDERSEN *[x], R. E. BRASHEAR [‡], and M. D. KAROL *

Received April 28, 1982, from the **Division of Pharmacokinetics, School of Pharmacy and Pharmacal Sciences, Purdue University, West Lafayette, IN 47907* and the [‡]*Department of Medicine, Indiana University, Indianapolis, IN 46223.* Accepted for publication August 6, 1982.

Abstract □ A simple diffusion-based pharmacokinetic model is proposed relating blood–brain barrier transfer kinetics of theophylline to the difference in the free concentrations of the drug in serum and cerebrospinal fluid (CSF). The model predicts that the CSF drug level is proportional to the serum drug level convoluted by $\exp(-kt)$, where k is the blood–brain barrier diffusion rate constant. An excellent agreement was found by nonlinear regression analysis between serum and CSF theophylline data in eight dogs and the proposed model for the blood–brain barrier transfer kinetics of theophylline. The ratio of the free fractions of theophylline in serum and CSF predicted from the model also agrees with the value determined experimentally.

Keyphrases □ Theophylline—blood–brain barrier transfer in dogs, kinetics □ Kinetics—of theophylline, blood–brain barrier transfer in dogs □ Blood–brain barrier—theophylline transfer in dogs, kinetics

The narrow therapeutic range of theophylline and the substantial intersubject variability in its disposition have resulted in extensive studies of the pharmacokinetics and clinical dosage management of the drug (1–8). Several investigations have related the bronchodilator effect of theophylline to its serum concentration level (5, 6, 9–13). However, it is the adverse effects rather than the therapeutic effect that dictates the dose administered and limits the therapeutic efficacy. The main adverse effects appear to be of CNS origin. It may be misleading, therefore, to use serum levels as a guide for the clinical management of the drug without any *a priori* knowledge of the kinetics of the blood–brain barrier transfer of theophylline. The theophylline concentration in the cerebrospinal fluid (CSF), should provide a better correlation to the CNS effects. The object of this study is to investigate the serum–CSF disposition of theophylline and the blood–brain barrier transfer kinetics. By establishing the kinetic relationship between the serum and CSF drug levels, a more rational approach to the usage of serum theophylline determinations can be established.

Although it was recognized early that theophylline enters the cerebrospinal fluid, neither the rate of equilibration with serum nor the serum–CSF concentration ratio have been defined adequately. In fact, little is known about the kinetics of transfer of drugs across the blood–brain barrier. The few CSF samples that have been correlated with serum samples in humans provide only a very limited insight into the kinetics (14–17). The use of dogs in the present study allowed comprehensive CSF sampling enabling a proper pharmacokinetic analysis of the serum–CSF theophylline disposition. Animals are often a poor predictor of human pharmacokinetics mainly due to substantial differences in the elimination processes. However, the present manner of analysis of the serum–CSF transfer kinetics is not influenced by absorption or elimination or other disposition processes. Furthermore, the tissues that constitute the blood–brain barrier apparently do not differ significantly between dogs and humans (18). The results from this study should therefore be of clinical interest.

EXPERIMENTAL

Study Design—After an 18-hr fast, eight dogs were anesthetized with 30 mg/kg iv of sodium pentobarbital; supplemental doses were given as needed during the remainder of the experiment. A polyethylene catheter in the left lateral saphenous vein was used for the infusion of aminophylline. Aminophylline[1] for intravenous use was utilized containing 25 mg of aminophylline (20.63 mg of anhydrous theophylline)/ml of solution. Aminophylline, 9 mg/kg (7.43 mg/kg theophylline) was diluted with saline to 19.4 ml and infused with a constant-infusion pump over a total of 20 min.

Blood samples for theophylline level determination were taken from a catheter in the left external jugular vein. An 18-gauge needle was percutaneously placed in the cisterna magna for obtaining the CSF samples. Cerebrospinal fluid and blood for theophylline levels were obtained at time zero (start of the infusion) and 20 (end of infusion), 50, 80, 140, 200, 260, 320, 350, and 380 min. The dogs were ventilated through a cuffed endotracheal tube using a constant-volume ventilator[2] with periodic hyperinflation to prevent atelectasis.

Theophylline Assay—The serum from 2–3 ml of blood and 0.5 ml of CSF were frozen and later assayed for theophylline, usually within 1–3 days. Theophylline concentrations were determined by the GC method of Least and coworkers (19) using 100-μl samples and substituting iodobutane for iodopentane in the derivation procedure. Theophylline concentrations were calculated using peak height ratios of theophylline to internal standards.

Protein Binding—The protein binding of theophylline was deter-

[1] Searle Laboratories.
[2] Harvard model 607.

0022-3549/83/0800-0951$01.00/0

Table I—Pharmacokinetic Parameters Obtained by Fitting Eqs. 5 and 8 Simultaneously to Theophylline Serum and Cerebrospinal Fluid Concentration Data

Dog	k, min^{-1}	R	$t_{1/2}(\alpha)$, min	$t_{1/2}(\beta)$, min	r_T[a]	r_s[a]	r_c[a]
1	0.0135	0.690	0.00865	419	0.9906	0.9913	0.9716
2	0.0151	0.664	0.0489	634	0.9902	0.9943	0.9505
3	0.0668	0.674	0.0135	416	0.9963	0.9965	0.9771
4	0.0194	0.614	0.0144	617	0.9939	0.9963	0.9489
5	0.0323	0.670	0.0327	450	0.9918	0.9980	0.9391
6	0.0340	0.610	0.0172	587	0.9945	0.9923	0.9458
7	0.0158	0.642	0.00671	326	0.9971	0.9975	0.9777
8	0.0143	0.632	0.0249	560	0.9928	0.9980	0.9164
Mean	0.0264	0.600	0.0208	501	0.9934	0.9955	0.9533
SD	0.0182	0.029	0.0141	113	0.0025	0.0026	0.0212

[a] Correlation coefficients between observed and calculated theophylline levels: (r_T) total (serum and CSF), (r_s) serum, and (r_c) CSF.

mined by filtering serum and CSF samples through filter membrane cones[3] to yield an ultrafiltrate free of molecules with molecular weights >50,000. A 2-ml aliquot was centrifuged at 2000 rpm (not exceeding 1000×g) for 30 min yielding ~1 ml of filtrate. Both the filtrate and original sample were assayed for theophylline. The amount of theophylline bound to protein was determined by subtracting the amount of theophylline in the protein-free ultrafiltrate sample from the amount of theophylline in the original sample. The percent of protein-bound theophylline was calculated by dividing the amount of protein-bound theophylline by the amount of theophylline in the original sample. The free fractions of theophylline in serum were 0.86, 0.85, 0.89, 0.86, 0.91, 0.79, 0.80, and 0.83 and the cerebrospinal fluid 1.00, 1.00, 0.92, 1.00, 0.99, 1.00, 1.00, and 0.95 for dogs 1–8, respectively.

PHARMACOKINETIC ANALYSIS

The object of the pharmacokinetic analysis is to elucidate the blood–brain barrier transfer kinetics of theophylline on the basis of serum and CSF concentration data. Compounds may pass the blood–brain barrier by different mechanisms such as simple diffusion, facilitated passive diffusion with carrier substances, and active transport (20). The latter two are saturable processes. However, due to the narrow therapeutic range of theophylline, it may not be possible to establish kinetically if the drug crosses the blood–brain barrier by simple diffusion or by a saturable facilitated transport. For a diffusional process the rate of transfer of drug across the blood–brain barrier would be proportional to the difference between the free drug concentrations on the two sides of the barrier, *i.e.*:

$$\frac{d}{dt}\{V_cC_c(t)\} = k_1[F_sC_s(t) - F_cC_c(t)] \qquad \text{(Eq. 1)}$$

where subscripts c and s denote cerebrospinal fluid and serum, respectively; V, C, and F stand for volume, total drug concentration, and free (unbound) fraction, respectively; and k_1 is a positive diffusion constant. Equation 1 assumes that the drug is not metabolized in the CSF, which is consistent with our current knowledge about the metabolic systems present on the CNS side of the blood–brain barrier (20).

Equation 1 can be written simply as:

$$\frac{dC_c(t)}{dt} = k[RC_s(t) - C_c(t)] \qquad \text{(Eq. 2)}$$

where $k = F_ck_1/V_c$ is a diffusion rate constant with dimension time^{-1} and $R = F_s/F_c$ is the free fraction ratio. Laplace transformation of Eq. 2 yields, after rearrangement (bars denote transformed functions):

$$\bar{C}_c(s) = kR\bar{C}_s(s)\frac{1}{s+k} \qquad \text{(Eq. 3)}$$

which back-transformed gives:

$$C_c(t) = kRC_s(t) * e^{-kt} \qquad \text{(Eq. 4)}$$

where * denotes convolution. Equation 4 expresses how the concentration of theophylline in the CSF relates to the concentration of the drug in serum if the transfer of the drug across the blood–brain barrier is by simple diffusion. The diffusional transport hypothesis is tested kinetically in the following manner according to Eq. 4:

A suitable arbitrary function is chosen to approximate the $C_s(t)$ response by nonlinear least-squares curve fitting. The fitting of the arbitrary function to the serum data is done simultaneously with a fitting to the CSF data of a second function resulting from convoluting the first function with e^{-kt} and multiplying by a constant (kR) according to Eq. 4. The two constants k and R are treated as unknown parameters and determined in the simultaneous curve fitting.

The following empirical function was used to approximate the serum data resulting from a short ($t = 0$ to $t = T$) constant rate infusion:

$$C_s(t) = A\,[e^{-\alpha(t-T)_+} - e^{-\alpha t}] + B[e^{-\beta(t-T)_+} - e^{-\beta t}] \qquad \text{(Eq. 5)}$$

$$A, \alpha, B, \beta > 0$$

where:

$$(t-T)_+ = t - T \text{ for } t > T \qquad \text{(Eq. 6)}$$

$$(t-T)_+ = 0 \text{ for } t \le T \qquad \text{(Eq. 7)}$$

and A, α, B, β are positive constants that are adjusted in the curve fitting to provide a least-squares approximation of the serum level data by the $C_s(t)$ function.

Convoluting Eq. 5 according to Eq. 4 yields:

$$C_c(t) = kR\left\{\left[\frac{A\alpha}{k(\alpha-k)} + \frac{B\beta}{k(\beta-k)}\right][e^{-k(t-T)_+} - e^{-kt}] + \frac{A}{k-\alpha}[e^{-\alpha(t-T)_+} - e^{-\alpha t}] + \frac{B}{k-\beta}[e^{-\beta(t-T)_+} - e^{\beta t}]\right\} \qquad \text{(Eq. 8)}$$

Equations 5 and 8 were fitted simultaneously to serum and CSF theophylline data for each dog using the interactive nonlinear regression program FUNFIT (21).

RESULTS AND DISCUSSION

The present method of pharmacokinetic analysis differs in several aspects from classical pharmacokinetic approaches:

1. The study focuses on a single disposition process (the blood–brain barrier transfer kinetics) which is analyzed without interference from other pharmacokinetic processes.
2. The kinetic model for the process is physiologically meaningful.
3. The analysis does not rely on the many often unrealistic assumptions and concepts of classical pharmacokinetic approaches such as linear disposition, abstract multicompartmental drug transfer, rate processes that are proportional to the amount rather than the concentration of the drug, *etc.*
4. With the exception of the specific process under investigation, the method is completely model independent. No attempts are made to derive kinetic models to account for the drug's disposition and elimination kinetics.

The approach may perhaps best be characterized as a "response approximation approach" where the concentration response is estimated by fitting a suitable arbitrary function (Eq. 5) to the data. It is not necessary to attach any kinetic significance to the approximating function and its parameters. Its purpose is not to model the pharmacokinetics but to estimate (approximate) the concentration profile so it can be used to investigate changes in the theophylline concentrations in the serum and CSF in a way that is consistent with the proposed kinetic model for transfer of the drug across the blood–brain barrier (Eqs. 1 and 4).

The serum and cerebrospinal fluid data for each of the eight dogs showed excellent agreement with the proposed diffusion model for the transfer of theophylline across the blood–brain barrier (Fig. 1, Table I).

[3] Type CF50A Centriflo, Americon Corp.

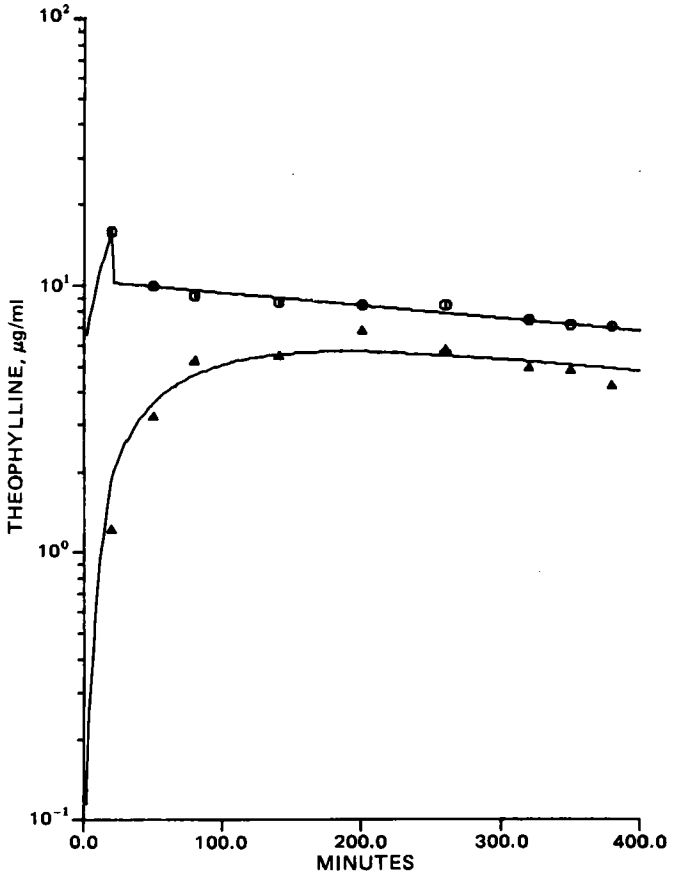

Figure 1—*Simultaneous least-squares fit of Eqs. 5 and 8 to serum (⊙) and CSF (▲) theophylline data resulting from a 20-min constant-rate intravenous infusion for dog 2. This fit has the smallest total correlation coefficient of the eight dogs studied (Table I).*

The k values are all of the same order of magnitude. Since $k = F_c k_1/V_c$ depends on both V_c, the volume of the CSF and F_c, the free fraction of theophylline in the CSF, this parameter is naturally expected to show greater intersubject variability than the more intrinsic diffusion parameter, k_1 (defined in Eq. 1). The determination of k_1 would have required V_c to be experimentally determined which was not done in the present study. The free fraction ratio $R = F_s/F_c$ differs remarkably little from subject to subject. The mean value of 0.60 ±0.03 (*SD*) for R comes fairly close to the ratio of 0.86 ± 0.06 (*SD*) calculated from experimentally determined values. The difference may well be due to the inherent inaccuracy of binding determination by ultrafiltration and to the fact that the free fraction is dependent on the total drug concentration. The microenvironment where the diffusion takes place may also have a different protein composition than that found in serum and CSF.

The binding of theophylline in serum is not likely to be affected by the presence of pentobarbital, because a significant change in the free fraction of a drug by competitive binding is usually only seen for drugs that are highly bound (>95%).

Theophylline serum data are used in clinical monitoring for dosage adjustments and in the management of overdose cases. However, since the side effects are of a CNS origin, the CSF drug level should provide a better basis for monitoring. In the postdistribution phase of a drug input where the ratio between the theophylline serum and CSF levels remains fairly constant (Fig. 1), the serum level should be a good indicator of the CNS level of the drug. However, in the distribution phase (lasting 1–1.5 hr after a rapid drug input), there appears to be a significant divergence in the serum and CSF drug levels[4]. In fact, during this phase the serum level may drop while the CSF level increases (Fig. 1). Evidently it is of great clinical significance to understand this kinetic phenomenon. During the distribution phase of a case of theophylline overdosing, it would be inappropriate to rely on serum levels for safety predictions. A decline in the serum level may not guarantee improvement; it would be wise to be prepared for delayed severe toxic effects. In a study of overdose cases resulting in seizure, it was reported that the most noteworthy phenomenon was the apparent absence of adverse effects in seven of the eight patients prior to the seizure (13). That study is consistent with what could be predicted from our pharmacokinetic investigation when the toxic effects are related to the CSF drug level rather than the serum level. Undoubtedly there is a need to further study the serum–CSF disposition of theophylline so a proper pharmacodynamic basis can be established for the rational clinical use of theophylline serum data.

REFERENCES

(1) J. W. Jenne, M. S. Wyze, F. S. Rood, and F. M. McDonald, *Clin. Pharmacol. Ther.*, **13**, 349 (1972).

(2) J. W. Jenne, H. T. Nagasawa, and R. D. Thomson, *Clin. Pharmacol. Ther.*, **19**, 375 (1976).

(3) P. A. Miteuko and R. I. Ogilvie, *Clin. Pharmacol. Ther.*, **14**, 509 (1973).

(4) L. Lendeles, M. Weinberger, and L. Bidhley, *Am. Rev. Resp. Dis.*, **118**, 97 (1978).

(5) M. M. Weinberger, R. A. Matthay, E. J. Ginchansky, C. A. Chidsey, and T. L. Petty, *J. Am. Med. Assoc. A*, **235**, 2110 (1976).

(6) P. A. Mitenko and R. I. Ogilvie, *N. Engl. J. Med*, **289**, 600 (1973).

(7) P. A. Mitenko and R. I. Ogilvie, *Clin. Pharmacol. Ther.*, **13**, 329 (1978).

(8) L. Hendeles, M. Weinberger, and R. Wyatt, *Am. J. Dis. Child*, **132**, 876 (1978).

(9) L. Hendeles, L. Bighley, R. H. Richardson, C. D. Hepler, and J. Carmichael, *Drug Intell. Clin. Pharm.*, **11**, 12 (1977).

(10) G. Levy and R. Koysooko, *J. Pediatr.*, **86**, 789 (1975).

(11) J. Pollock, F. Kiechel, D. Cooper, and M. Weinberger, *Pediatrics*, **60**, 840 (1977).

(12) C. W. Bierman, G. G. Shapiro, and W. E. Pierson, *Pediatrics*, **60**, 848 (1977).

(13) C. W. Zwillich, F. D. Sutton, T. A. Neff, W. M. Cohn, R. A. Matthay, and M. M. Weinberger, *Am. Intern. Med.*, **82**, 748 (1975).

(14) S. M. Somani, N. N. Khanna, and H. S. Bada, *J. Pediatr.*, **96**, 1091 (1980).

(15) H. J. Teschemacher, A. Hertz, A. Hess, and G. Novozek, *Experienta*, **24**, 54 (1968).

(16) T. Turneu, T. A. Lourides, and J. V. Aranda, *J. Pediatr.*, **95**, 644 (1979).

(17) A. A. Tiu, S. M. Somani, H. S. Bada, and N. N. Khanna, *J. Anal. Toxicol.*, **3**, 26 (1979).

(18) W. H. Oldendorf, *Annu. Rev. Pharmacol. Toxicol.*, **14**, 239 (1974).

(19) C. J. Least, G. F. Johnson, and H. M. Soloman, *Clin. Chem.*, **22**, 765 (1976).

(20) W. H. Oldendorf, *Exp. Eye Res. Suppl.*, **25**, 177 (1977).

(21) P. Veng-Pedersen, *J. Pharmacokinet. Biopharm.*, **5**, 513 (1977).

[4] The distribution phase in the present context is defined in reference to the CSF. Thus, although the distribution of theophylline to compartments other than the cerebrospinal fluid appears very rapid judged from the short α-phase in the serum, this is not the case for the CSF (Fig. 1).

Allergenic Properties of Naturally Occurring Cannabinoids

EDNA S. WATSON ˣ, JAMES C. MURPHY, and CARLTON E. TURNER

Received June 14, 1982, from the *Research Institute of Pharmaceutical Sciences, School of Pharmacy, University of Mississippi, University, MS 38677.* Accepted for publication August 4, 1982.

Abstract □ The guinea pig maximization test was used to determine the potential of seven cannabinoids to produce allergic contact dermatitis. Δ^9-Tetrahydrocannabinol and cannabinol were found to be extreme (Grade V) sensitizers. Cannabidiol, Δ^8-tetrahydrocannabinol, and cannabichromene were moderate (Grade III) sensitizers. Cannabigerol and cannabinol methyl ether were not sensitizers. Most of the cannabinoids were found to be allergenically cross-reactive. Additionally, it was shown that the presence of a free 1′-hydroxyl group was required for sensitization, but not to elicit a response in sensitive animals.

Keyphrases □ Cannabinoids—naturally occurring, allergenic properties, determined by the guinea pig maximization test for skin sensitivity □ Allergenicity—of naturally occurring cannabinoids, guinea pig maximization test for skin sensitivity □ Sensitizers, skin—allergenic properties of naturally occurring cannabinoids, guinea pig maximization test

Δ^9-Tetrahydrocannabinol (I) was shown to be a potent skin sensitizer in the guinea pig, and serum from sensitive animals sensitized guinea pig mast cells for degranulation (1). Tetrahydrocannabivarol, a Δ^9-tetrahydrocannabinol homologue, was also found to be a potent skin sensitizer (2). In view of these findings, a systematic study comparing the sensitizing potential of I to six other cannabinoids was conducted utilizing the guinea pig maximization test. The cross-allergenicity of these cannabinoids was also studied.

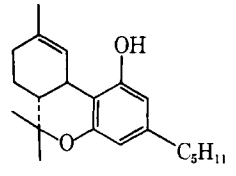

Δ^9-Tetrahydrocannabinol
I

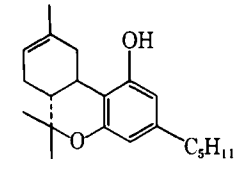

Δ^8-Tetrahydrocannabinol
II

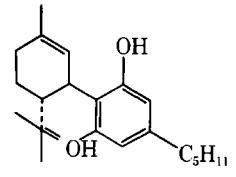

Cannabidiol
III

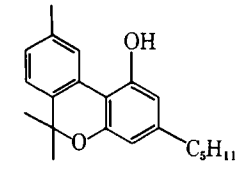

Cannabinol
IV

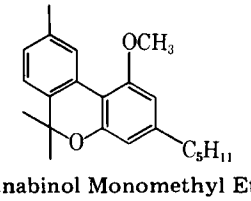

Cannabinol Monomethyl Ether
V

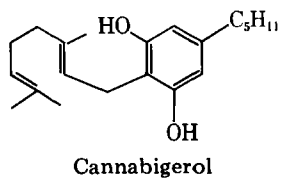

Cannabigerol
VI

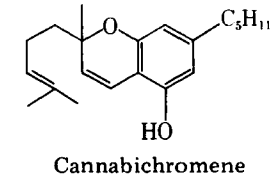

Cannabichromene
VII

EXPERIMENTAL

Female Hartley guinea pigs, weighing 350–400 g, were used[1]. Food[2] and water supplemented with vitamin C were available *ad libitum*. Δ^9-Tetrahydrocannabinol (I), Δ^8-tetrahydrocannabinol (II), cannabidiol (III), and cannabinol (IV) were obtained from the National Institute on Drug Abuse, Rockville, Md. Cannabigerol (VI) was synthesized according to the literature procedure (3); cannabinol monomethyl ether (V) was synthesized from cannabinol as previously reported (4); cannabichromene (VII) was synthesized by the literature procedure (5). The purity of each cannabinoid was shown to be >95% by GC analysis.

Ten guinea pigs were used for maximization testing of cannabigerol and cannabinol methyl ether. Twenty guinea pigs were used for maximization testing of the remaining cannabinoids. The maximization method of Magnusson and Kligman (6) was used to determine the sensitizing capacity of each cannabinoid. A 5% water-in-oil emulsion of each cannabinoid (50 mg/ml of emulsion) was prepared by dissolving the cannabinoid in complete Freund's Adjuvant[3] and emulsifying using adjuvant–sterile water (1:1, v/v). A 5% solution of each cannabinoid was dissolved in sterile paraffin oil. Guinea pigs were sensitized by duplicate 0.1-ml intradermal (id) injections of cannabinoid emulsion, cannabinoid in paraffin oil, and adjuvent alone.

Topical induction sites were prepared by application of 10% sodium lauryl sulfate in petrolatum over the intradermal induction sites, 6 days after intradermal induction. Forty-eight-hour occlusive patches of the cannabinoid in petrolatum (0.03% w/w) were applied directly over the intradermal induction sites on day 7, after removal of the sodium lauryl sulfate. On day 23 the animals and nonsensitive control animals were given topical open epicutaneous skin tests with 100 and 50 μg of each cannabinoid in 10 μl of alcohol. The sites were observed 24, 48, and 72 hr later for erythema and edema. The Draize scoring system (7) was used to rank the intensity of erythema and edema based on a 0 to +4 rating scale. The mean erythema and edema scores from the three test readings were summed to provide an intensity score for each animal. The intensity scores of the 20 animals in each group were averaged to provide an average score. Animals demonstrating sensitivity to homologous sensitizing cannabinoids were skin tested with the other cannabinoids to determine if cross-allergenicity occurred.

RESULTS AND DISCUSSION

All of the cannabinoids subjected to maximization testing were sensitizers except cannabinol methyl ether and cannabigerol. Δ^9-Tetrahydrocannabinol and cannabinol were rated as extreme sensitizers (Table I), while cannabidiol, Δ^8-tetrahydrocannabinol, and cannabichromene were found to be moderate sensitizers. The allergenic potency of the cannabinoids (in descending order) was I = IV > III > VII > II > VI = V.

The cross-allergenicity of some cannabinoids and eugenol are shown in Table II. The extreme sensitizers, I and IV, provided the greater number of cross-reactions to the other cannabinoids. All cannabinoids tested were cross-reactive with other cannabinoids. However, the moderate sensitizers produced fewer cross-reactions than did the extreme

[1] Kentucky Cavies, Fern Creek, Ky.
[2] Purina guinea pig chow, Ralston-Purina, St. Louis, Mo.
[3] Complete Freund's Adjuvant, Difco Laboratories, Detroit, Mich.

0022-3549/83/0800-0954$01.00/0

Table I—Maximization Grading of Cannabinoids

Cannabinoid	Sensitization Rate	Grade	Average Draize Score
I	100	V, Extreme	3.75
IV	100	V, Extreme	3.29
III	60	III, Moderate	1.69
VII	40	III, Moderate	0.38
II	30	III, Moderate	0.70
VI	0	Inactive	0
V	0	Inactive	0

sensitizers. Eugenol did not elicit cross-reactions in any animals. Since cannabinol methyl ether failed to sensitize, but did produce reactions in animals sensitized with cannabinol and cannabidiol, it appeared that a free hydroxyl group in position one was required for sensitization, but not to elicit a reaction in animals already sensitized. The failure of cannabinol methyl ether to elicit reactions in Δ^9-tetrahydrocannabinol-sensitized animals is not understood.

Although many of the biological effects of Δ^9-tetrahydrocannabinol are shared by all naturally occurring cannabinoids, the psychoactive effects are not. Desoize *et al.* (8) found that six natural cannabinoids (I, II, III, IV, VII, and cannabicyclol) suppressed phytohemagglutinin-induced DNA synthesis in normal human peripheral-blood lymphocytes, an *in vitro* model for cell-mediated immune function. In addition, the inhibitory effects of five of these six natural cannabinoids on the passive cutaneous anaphylaxis reaction in rats has been reported (9). Compound I, however, was a more potent inhibitor of passive cutaneous anaphylaxis than the other cannabinoids, and III was least active. Zimmerman *et al.* (10) reported that cannabidiol and cannabinol did not reduce hemagglutination titers to sheep red blood cells in mice at doses of 25 mg/kg, while Δ^9-tetrahydrocannabinol did.

The olivetol moiety of the molecule appeared, in the above studies, to be the portion of the molecule required for the shared activities. Olivetol was found by Desoize *et al.* (8) to inhibit phytohemagglutinin-induced lymphocyte transformation.

In this study, most cannabinoids containing the olivetol moiety were found to be skin sensitizers. Cannabinol methyl ether, which has its hydroxyl function blocked with a methyl ether, was not a sensitizer. The cross-allergenicity of these compounds is likely to be directly related to the presence of the olivetol component.

Table II—Immunological Cross-Reactivity of Cannabinoids

Sensitizing Substance	Skin Test Substance[a] I	IV	III	II	VII	VI	V	Eugenol
I	9/9	4/9	1/9	3/9	3/9	0/7	0/7	0/9
IV	2/9	9/9	0/9	3/9	1/9	4/9	4/9	0/10
III	0/6	0/6	6/10	0/6	0/10	2/6	2/6	0/6
II	0/3	0/3	0/3	3/10	0/3	NT	NT	NT

[a] Expressed as the number of animals with positive reactions to the skin test substance over the number tested.

REFERENCES

(1) H. de Lecorsier, N. Hoellinger, and E. Fournier, *C. R. Acad. Sci. Ser. D*, **285**, 1351 (1977).

(2) F. Braut-Boucher, M. Paris, H. Hoellinger, Nguyen-Hoang-Nan, and E. Fournier, *Toxicol. Eur. Res.* **2**, 175 (1979).

(3) R. Mechoulam and B. Yagen, *Tetrahedron Lett.*, **1969**, 5349.

(4) F. S. El-Feraly, M. A. ElSohly, and C. E. Turner, *Acta. Pharm. Jugoslav.*, **27**, 43, 1977.

(5) M. A. ElSohly, E. G. Boeren, and C. E. Turner, *J. Heterocycl. Chem.*, **15**, 699, 1978.

(6) B. Magnusson and A. M. Kligman, *J. Invest. Dermatol.*, **52**, 268 (1969).

(7) H. H. Draize, G. Woodward, and H. O. Calvery, *J. Pharmacol. Exp. Ther.*, **82**, 377 (1944).

(8) B. Desoize, G. G. Nahas, C. Leger, and J. Banchereau, *Dermatol. Considerations Toxicol.*, **2**, 61 (1981).

(9) E. S. Watson, M. A. ElSohly, C. E. Turner, and J. R. Koutny, "Abstracts," Southeastern Pharmacology Society 1st Annual Meeting, Medical College of Georgia, Augusta, Georgia, 1980, p. 49.

(10) S. Zimmerman, A. M. Zimmerman, E. L. Cameron, and H. L. Laurence, *Pharmacology*, **15**, 10 (1977).

ACKNOWLEDGMENTS

The authors wish to thank Ms. Paula Whatley for technical assistance with the manuscript. Appreciation is extended to Drs. Hala and Mahmoud ElSohly for synthesis of some of the cannabinoids used in this study.

Absolute and Relative Bioavailability of Oral Acetaminophen Preparations

BARBARA AMEER *x, MARCIA DIVOLL ‡, DARRELL R. ABERNETHY ‡, DAVID J. GREENBLATT ‡, and LEON SHARGEL *

Received February 5, 1982, from the **College of Pharmacy and Allied Health Professions, Northeastern University, Boston, MA 02115* and the ‡*Division of Clinical Pharmacology, Tufts-New England Medical Center, Boston, MA 02111.* Accepted for publication August 11, 1982.

Abstract □ Eighteen healthy volunteers received single 650-mg doses of acetaminophen by 5-min intravenous infusion, in tablet form by mouth in the fasting state, and in elixir form orally in the fasting state in a three-way crossover study. An additional eight subjects received two 325-mg tablets from two commercial vendors in a randomized crossover fashion. Concentrations of acetaminophen in multiple plasma samples collected during the 12-hr period after each dose were determined by high-performance liquid chromatography. Following a lag time averaging 3–4 min, absorption of oral acetaminophen was first order, with apparent absorption half-life values averaging 8.4 (elixir) and 11.4 (tablet) min. The mean time-to-peak concentration was significantly longer after tablet (0.75 hr) than after elixir (0.48 hr) administration. Peak plasma concentrations and elimination half-lives were similar following both preparations. Absolute systemic availability of the elixir (87%) was significantly greater than for the tablets (79%). Two commercially available tablet formulations did not differ significantly in peak plasma concentrations, time-to-peak, or total area under the plasma concentration curve and therefore were judged to be bioequivalent.

Keyphrases □ Bioavailability—absolute and relative, oral acetaminophen preparations, determined by high-performance liquid chromatography □ Acetaminophen—absolute and relative bioavailability of oral preparations, determination by high-performance liquid chromatography □ High-performance liquid chromatography—oral acetaminophen preparations, determination of absolute and relative bioavailability

Acetaminophen (paracetamol) is used extensively as a nonprescription analgesic and antipyretic agent (1). Over 40 oral acetaminophen preparations are available commercially (2). The present study evaluated the absolute bioavailability of orally administered acetaminophen in elixir and tablet forms. Also assessed was the relative

0022-3549/83/0800-0955$01.00/0

Table I—Maximization Grading of Cannabinoids

Cannabinoid	Sensitization Rate	Grade	Average Draize Score
I	100	V, Extreme	3.75
IV	100	V, Extreme	3.29
III	60	III, Moderate	1.69
VII	40	III, Moderate	0.38
II	30	III, Moderate	0.70
VI	0	Inactive	0
V	0	Inactive	0

sensitizers. Eugenol did not elicit cross-reactions in any animals. Since cannabinol methyl ether failed to sensitize, but did produce reactions in animals sensitized with cannabinol and cannabidiol, it appeared that a free hydroxyl group in position one was required for sensitization, but not to elicit a reaction in animals already sensitized. The failure of cannabinol methyl ether to elicit reactions in Δ^9-tetrahydrocannabinol-sensitized animals is not understood.

Although many of the biological effects of Δ^9-tetrahydrocannabinol are shared by all naturally occurring cannabinoids, the psychoactive effects are not. Desoize *et al.* (8) found that six natural cannabinoids (I, II, III, IV, VII, and cannabicyclol) suppressed phytohemagglutinin-induced DNA synthesis in normal human peripheral-blood lymphocytes, an *in vitro* model for cell-mediated immune function. In addition, the inhibitory effects of five of these six natural cannabinoids on the passive cutaneous anaphylaxis reaction in rats has been reported (9). Compound I, however, was a more potent inhibitor of passive cutaneous anaphylaxis than the other cannabinoids, and III was least active. Zimmerman *et al.* (10) reported that cannabidiol and cannabinol did not reduce hemagglutination titers to sheep red blood cells in mice at doses of 25 mg/kg, while Δ^9-tetrahydrocannabinol did.

The olivetol moiety of the molecule appeared, in the above studies, to be the portion of the molecule required for the shared activities. Olivetol was found by Desoize *et al.* (8) to inhibit phytohemagglutinin-induced lymphocyte transformation.

In this study, most cannabinoids containing the olivetol moiety were found to be skin sensitizers. Cannabinol methyl ether, which has its hydroxyl function blocked with a methyl ether, was not a sensitizer. The cross-allergenicity of these compounds is likely to be directly related to the presence of the olivetol component.

Table II—Immunological Cross-Reactivity of Cannabinoids

Sensitizing Substance	Skin Test Substance[a] I	IV	III	II	VII	VI	V	Eugenol
I	9/9	4/9	1/9	3/9	3/9	0/7	0/7	0/9
IV	2/9	9/9	0/9	3/9	1/9	4/9	4/9	0/10
III	0/6	0/6	6/10	0/6	0/10	2/6	2/6	0/6
II	0/3	0/3	0/3	3/10	0/3	NT	NT	NT

[a] Expressed as the number of animals with positive reactions to the skin test substance over the number tested.

REFERENCES

(1) H. de Lecorsier, N. Hoellinger, and E. Fournier, *C. R. Acad. Sci. Ser. D*, **285**, 1351 (1977).

(2) F. Braut-Boucher, M. Paris, H. Hoellinger, Nguyen-Hoang-Nan, and E. Fournier, *Toxicol. Eur. Res.* **2**, 175 (1979).

(3) R. Mechoulam and B. Yagen, *Tetrahedron Lett.*, **1969**, 5349.

(4) F. S. El-Feraly, M. A. ElSohly, and C. E. Turner, *Acta. Pharm. Jugoslav.*, **27**, 43, 1977.

(5) M. A. ElSohly, E. G. Boeren, and C. E. Turner, *J. Heterocycl. Chem.*, **15**, 699, 1978.

(6) B. Magnusson and A. M. Kligman, *J. Invest. Dermatol.*, **52**, 268 (1969).

(7) H. H. Draize, G. Woodward, and H. O. Calvery, *J. Pharmacol. Exp. Ther.*, **82**, 377 (1944).

(8) B. Desoize, G. G. Nahas, C. Leger, and J. Banchereau, *Dermatol. Considerations Toxicol.*, **2**, 61 (1981).

(9) E. S. Watson, M. A. ElSohly, C. E. Turner, and J. R. Koutny, "Abstracts," Southeastern Pharmacology Society 1st Annual Meeting, Medical College of Georgia, Augusta, Georgia, 1980, p. 49.

(10) S. Zimmerman, A. M. Zimmerman, E. L. Cameron, and H. L. Laurence, *Pharmacology*, **15**, 10 (1977).

ACKNOWLEDGMENTS

The authors wish to thank Ms. Paula Whatley for technical assistance with the manuscript. Appreciation is extended to Drs. Hala and Mahmoud ElSohly for synthesis of some of the cannabinoids used in this study.

Absolute and Relative Bioavailability of Oral Acetaminophen Preparations

BARBARA AMEER *x, MARCIA DIVOLL ‡, DARRELL R. ABERNETHY ‡, DAVID J. GREENBLATT ‡, and LEON SHARGEL *

Received February 5, 1982, from the **College of Pharmacy and Allied Health Professions, Northeastern University, Boston, MA 02115* and the ‡*Division of Clinical Pharmacology, Tufts-New England Medical Center, Boston, MA 02111.* Accepted for publication August 11, 1982.

Abstract □ Eighteen healthy volunteers received single 650-mg doses of acetaminophen by 5-min intravenous infusion, in tablet form by mouth in the fasting state, and in elixir form orally in the fasting state in a three-way crossover study. An additional eight subjects received two 325-mg tablets from two commercial vendors in a randomized crossover fashion. Concentrations of acetaminophen in multiple plasma samples collected during the 12-hr period after each dose were determined by high-performance liquid chromatography. Following a lag time averaging 3–4 min, absorption of oral acetaminophen was first order, with apparent absorption half-life values averaging 8.4 (elixir) and 11.4 (tablet) min. The mean time-to-peak concentration was significantly longer after tablet (0.75 hr) than after elixir (0.48 hr) administration. Peak plasma concentrations and elimination half-lives were similar following both preparations. Absolute systemic availability of the elixir (87%) was significantly greater than for the tablets (79%). Two commercially available tablet formulations did not differ significantly in peak plasma concentrations, time-to-peak, or total area under the plasma concentration curve and therefore were judged to be bioequivalent.

Keyphrases □ Bioavailability—absolute and relative, oral acetaminophen preparations, determined by high-performance liquid chromatography □ Acetaminophen—absolute and relative bioavailability of oral preparations, determination by high-performance liquid chromatography □ High-performance liquid chromatography—oral acetaminophen preparations, determination of absolute and relative bioavailability

Acetaminophen (paracetamol) is used extensively as a nonprescription analgesic and antipyretic agent (1). Over 40 oral acetaminophen preparations are available commercially (2). The present study evaluated the absolute bioavailability of orally administered acetaminophen in elixir and tablet forms. Also assessed was the relative

0022-3549/83/0800-0955$01.00/0

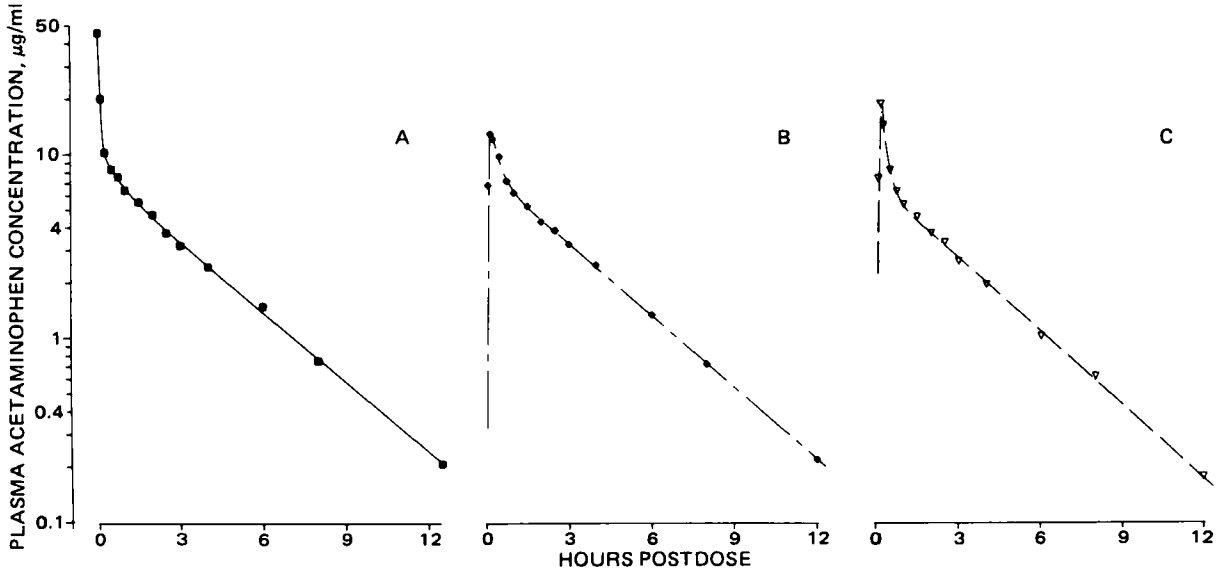

Figure 1—*Plasma acetaminophen concentrations and pharmacokinetic functions in a representative subject following 650-mg doses by three modes of administration. Key: (A) intravenous; (B) elixir; (c) tablet.*

bioavailability of two brands of oral acetaminophen tablets.

EXPERIMENTAL

Three-way Crossover Study of Acetaminophen Dosage Forms—Eighteen healthy male and female volunteers, aged 22–36 years, participated after giving informed written consent. All participants were ambulatory, were taking no other medications, and had no history of chronic disease. All subjects received a single 650-mg dose of acetaminophen on three occasions separated by at least 1 week. The sequence of the three trials was randomized. The modes of administration were:

1. Intravenous acetaminophen, administered as a sterile solution[1] infused into an antecubital vein over a period of 5 min;
2. Acetaminophen elixir[2] administered as 19.5 ml of a 33.3-mg/ml solution and followed by 20 ml of water;
3. Two 325-mg oral tablets[3] administered with 100–200 ml of water.

For the two oral dosage trials, subjects were fasted overnight prior to and for 3 hr following drug administration.

Venous blood samples were drawn from an indwelling butterfly catheter, or by separate venipuncture, and placed in heparinized tubes. Samples were collected prior to intravenous acetaminophen infusion, immediately at the end of the infusion, and at 5, 15, 30, and 45 min, 1, 1.5, 2, 2.5, 3, 4, 6, 8, and 12 hr postinfusion. In the oral acetaminophen trials, a sample was drawn prior to dosage, at 5, 10, 15, 30, and 45 min, and thereafter as described for intravenous acetaminophen. Whole-blood samples were centrifuged, and the plasma was separated and stored until the time of assay.

Concentrations of acetaminophen in all plasma samples were determined by high-performance liquid chromatography (HPLC) (3). The sensitivity of this method was 0.1–0.2 μg of acetaminophen/ml of plasma. For six identical samples at concentration points ranging from 0.25–15 μg/ml, the coefficient of variation was <5%. The mean deviation between pairs of duplicate samples (n = 45) analyzed during pharmacokinetic studies was 2.4%.

Plasma acetaminophen concentrations after intravenous dosage were analyzed by iterative nonlinear least-squares techniques as described in detail previously (4, 5). Plasma levels were fitted to a linear sum of 2 or 3 exponential terms. Coefficients, corrected for the infusion period (6), and exponents from the fitted function were used to determine the total area under the plasma concentration curve from time zero to infinity ($AUC_{0\text{-}\infty}$). After oral dosage, plasma concentrations likewise were fitted to a linear sum of 2 or 3 exponential terms. Coefficients and exponents from the fitted function were used to determine the apparent lag time prior to the start of absorption, the first-order absorption half-life, and the elimination half-life (7). The plasma concentration AUC from time zero until the final detectible acetaminophen concentration was determined by the trapezoidal method. To this value was added the residual area extrapolated to infinity, calculated as the final plasma concentration divided by the terminal exponent. The sum of these two areas represent the total AUC (7, 8).

Absolute bioavailability of both oral acetaminophen preparations for each subject was determined as the AUC following oral administration divided by the AUC following intravenous dosage to the same subject. Statistical methods included Student's t test and ANOVA.

Two-way Crossover Study of Two Acetaminophen Tablets—The

Table I—Pharmacokinetics of Intravenous Acetaminophen

Subject	Age	Sex	Volume of Distribution, liters/kg	β Half-life, hr	Clearance, mg/min/kg	$AUC_{0\text{-}\infty}$, μg/ml · hr
1	25	F	1.27	2.65	5.55	41.0
2	25	F	0.76	2.70	3.27	50.3
3	33	F	0.90	2.15	4.85	44.7
4	25	F	0.66	2.78	2.73	72.8
5	23	F	1.07	2.94	4.20	47.3
6	32	F	0.88	2.32	4.37	48.8
7	29	F	0.95	3.06	3.59	53.2
8	26	F	0.99	2.83	4.06	49.8
9	22	M	0.97	2.64	4.24	31.2
10	33	M	1.02	3.02	3.92	42.0
11	24	M	1.36	2.21	7.11	21.6
12	24	M	1.13	1.88	6.94	22.2
13	39	M	0.99	2.55	4.48	28.0
14	39	M	1.34	2.90	5.53	22.6
15	30	M	1.09	2.54	4.93	32.2
16	26	M	1.00	2.61	4.45	35.7
17	22	M	0.91	2.39	4.36	34.2
18	25	M	1.52	3.19	5.50	31.0
Mean	27.9		1.05	2.63	4.67	39.37
± SE	1.3		0.05	0.08	0.27	3.12

Table II—Pharmacokinetic Parameters for Two Oral Preparations of Acetaminophen [a]

Parameter	Mean ± SE Values		Student's t test
	Elixir	Tablet	
Peak plasma concentration, μg/ml	12.41 ± 1.22	11.99 ± 1.02	0.34
Time-to-peak concentration, hr	0.48 ± 0.06	0.76 ± 0.12	2.54[b]
Lag time, hr	0.06 ± 0.01	0.07 ± 0.01	0.58
Absorption half-life, hr	0.14 ± 0.02	0.19 ± 0.04	1.03
Elimination half-life, hr	2.74 ± 0.13	2.55 ± 0.14	1.78
Systemic availability[c]	0.87 ± 0.02	0.79 ± 0.02	4.47[d]

[a] In the three-way crossover study. [b] Significance level = $p < 0.025$. [c] Fraction of intravenous. [d] Significance level = $p < 0.001$.

[1] Thirteen milliliters of a 50-mg/ml solution [propylene glycol–ethyl alcohol–5% dextrose (40:10:50, v/v)] diluted to 50 ml with 5% dextrose.
[2] McNeil, Fort Washington, Pa.
[3] Parke-Davis, Ann Arbor, Mich.

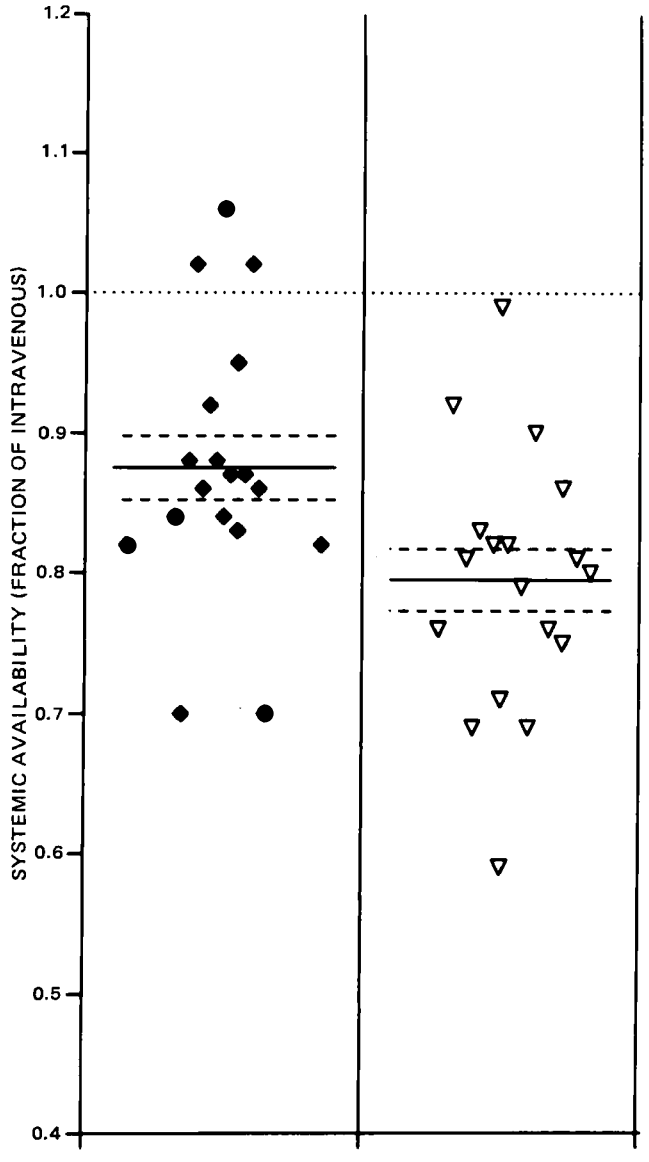

Figure 2—*Absolute bioavailability of oral acetaminophen in the elixir (◆) and tablet (▽) preparations. Horizontal lines represent means (—), standard errors (- - -), and 100% of the intravenous bioavailability (·····).*

relative bioavailability of two oral acetaminophen tablet preparations was evaluated in a two-way randomized crossover study involving seven male and one female volunteer. All subjects received a single 650-mg dose (two 325-mg tablets) of oral acetaminophen on two occasions separated by at least one week, using two commercially available[4] products (A and B).

Plasma samples were obtained as described above following both oral acetaminophen trials. Acetaminophen concentrations in all samples were determined by HPLC (3). Pharmacokinetic and statistical analyses were as described above. Differences between the two oral preparations were evaluated by Students's t test.

RESULTS

Comparison of Intravenous, Elixir, and Tablet Dosage Forms—Following intravenous acetaminophen administration, disappearance of drug from plasma was described by a linear sum of exponential terms (Fig. 1 and Table I). Iterative solutions were possible for 15 subjects following acetaminophen elixir administration and for 11 subjects following acetaminophen dosing by tablet (Fig. 1).

[4] Brand A was Tylenol tablets, lot HP2588, McNeil Consumer Products Co., Fort Washington, Pa.; Brand B was Tapar tablets, lot 2C246, Parke-Davis, Ann Arbor, Mich.

Table III—Pharmacokinetic Parameters for Two Tablet Formulations of Acetaminophen

Parameter	Mean ± *SE* Values Brand A	Brand B	Student's Paired t
Peak plasma concentration, μg/ml	8.56 ± 1.22	8.89 ± 0.78	0.221
Time-to-peak concentration, hr	1.06 ± 0.27	0.78 ± 0.10	0.986
Elimination half-life, hr	2.62 ± 0.10	2.43 ± 0.11	2.30[a]
Total $AUC_{0\to\infty}$, μg/ml × hr	26.82 ± 1.44	27.37 ± 0.94	0.468

[a] Significance level $0.05 < p < 0.10$.

Peak plasma concentrations following the elixir preparation administration were slightly higher than that for tablets, but the difference was not significant (Table II). The time-to-peak concentration averaged 0.48 hr after dosage with elixir *versus* 0.75 hr with the tablet ($p < 0.025$). The two preparations did not differ significantly in apparent half-life of absorption or in lag time prior to the start of absorption.

Absolute systemic availability of both oral preparations was significantly less than 100% complete (Table II, Fig. 2). Absolute availability of the elixir (87%) was significantly greater than that for tablets (79%). The elimination half-lives were similar following both preparations (Table II).

Comparison of Two Acetaminophen Tablet Formulations—The kinetics of acetaminophen absorption following dosing with brand B were very close to that reported in the three-way crossover study. Peak plasma concentration averaged 8.9 μg/ml and was reached an average of 0.78 hr after dosing. These values were similar to those observed for brand A (8.6 μg/ml and 1.1 hr after dosing, respectively), and the differences did not approach significance. The total AUC was nearly identical for both preparations (Fig. 3, Table III). The elimination half-life following brand B administration (2.43 hr) was shorter than with brand A (2.62 hr) although the magnitude of the mean difference was only 8%.

DISCUSSION

The results of the three-way crossover study concur with reports of other investigators (9) and indicate that absorption of acetaminophen from both tablet and elixir preparations is relatively rapid, with peak plasma concentrations generally attained within 1 hr postdose. The time-to-peak concentration was significantly shorter with the elixir than with the tablet, but differences in other absorption kinetic parameters did not reach statistical significance. Generally, drug absorption from an elixir preparation will be somewhat more rapid than from the same dose administered as a tablet. Absorption of acetaminophen from oral tablet preparations can be dissolution rate limited (10), probably explaining why the time-to-peak concentration was earlier following the elixir than with the tablet.

Neither preparation showed complete (100%) systemic availability;

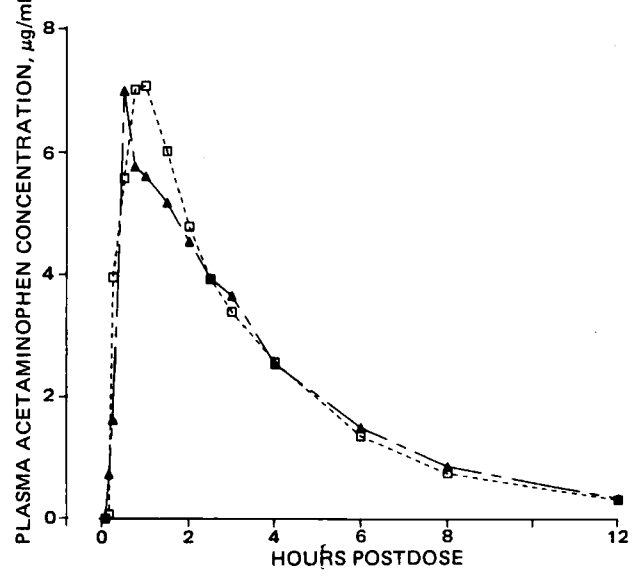

Figure 3—*Plasma concentrations following 650-mg doses of two brands of acetaminophen. Each point is the mean for all subjects at that time point. Key: (▲) Brand A; (□) Brand B.*

the elixir had significantly greater bioavailability than did the tablet. The incomplete systemic availability of oral acetaminophen could be explained either by incomplete absorption or presystemic biotransformation, (*e.g.*, first-pass hepatic extraction or metabolism in the epithelium and/or lumen of the GI tract), or by a combination of these two factors (11). Differentiation between these two possible mechanisms could be achieved through an examination of route-dependent differences in the pattern of drug metabolism, as described by Harris and Riegelman (12). In a previous study of systemic availability (13), Rawlins *et al.* reported the bioavailability of acetaminophen tablets in a 500-mg dose to be only 63% compared with 79% in our study of a 650-mg dose. Bioavailability increased to 89 and 87% following 1,000- and 2,000-mg doses, respectively (13). The discrepancy in results of the two studies may be due to saturation of presystemic biotransformation at doses >500 mg.

The comparative bioavailability studies of two widely used acetaminophen tablets suggest that they have essentially similar systemic availability and therefore should be therapeutically equivalent.

REFERENCES

(1) B. Ameer and D. J. Greenblatt, *Ann. Intern. Med.*, **87**, 202 (1977).

(2) N. F. Billups and S. M. Billups, "American Drug Index 1981," J. B. Lipincott, Philadelphia, Pa., 1981.

(3) B. Ameer, D. J. Greenblatt, M. Divoll, D. R. Abernethy, and L. Shargel, *J. Chromatogr.*, **226**, 224 (1981).

(4) D. W. Marquardt, *J. Soc. Ind. Appl. Math.*, **11**, 431 (1963).

(5) R. A. Usanis, "NLIN—Nonlinear Least Squares Estimation of Parameters (Library Services Series Document No. LSR-089-1)," Triangle Universities Computation Center, Research Triangle Park, N.C., 1972.

(6) J. C. K. Loo and S. Riegelman, *J. Pharm. Sci.*, **59**, 53 (1970).

(7) M. Gibaldi, and D. Perrier, "Pharmacokinetics," Dekker, New York, N.Y., 1975.

(8) D. J. Greenblatt and J. Koch-Weser, *N. Engl. J. Med.*, **293**, 702, 964 (1975).

(9) G. Levy, *Arch. Intern. Med.*, **141**, 279 (1981).

(10) J. B. Sotiropoulus, T. Deutsch, and F. M. Plakogiannis, *J. Pharm. Sci.*, **70**, 422 (1981).

(11) C. F. George, *Clin. Pharmacokinet.*, **6**, 259 (1981).

(12) L. Harris and S. Riegelman, *J. Pharm. Sci.*, **58**, 71 (1969).

(13) M. D. Rawlins, D. B. Henderson, and A. R. Hijab, *Eur. J. Clin. Pharmacol.*, **11**, 283 (1977).

ACKNOWLEDGMENTS

Presented in part at the APhA Academy of Pharmaceutical Sciences meeting in Las Vegas, April 1982.

The authors are grateful for the assistance of Lawrence J. Moschitto, Jerold S. Harmatz, Dr. Dean S. MacLaughlin, and the staff of the Clinical Study Unit, New England Medical Center Hospital. Supported by Grants RR-24040, RR-05830-1, and MH-34223 from the United States Public Health Service.

Simultaneous Determinations of Cefsulodin and Cefotiam in Serum and Bone Marrow Blood by High-Performance Liquid Chromatography

KEIKO YAMAMURA *x, MAKOTO NAKAO *, JUN-ICHIRO YAMADA *, and TOSHIHISA YOTSUYANAGI ‡

Received March 17, 1982, from the **Pharmacy Department, Nagoya University Branch Hospital, Higashi-ku, Nagoya 461* and the ‡*Faculty of Pharmaceutical Sciences, Nagoya City University, Mizuho-ku, Nagoya 467 Japan.* Accepted for publication August 9, 1982.

Abstract □ A high-performance liquid chromatographic method is described for the simultaneous determinations of cefsulodin and cefotiam in serum and bone marrow blood samples. After extraction with acetonitrile, the cephalosporins were applied to a reverse-phase column with an internal standard, cefazolin; the mobile phase was a mixture of 0.005 *M* tetrabutylammonium phosphate and methanol (35:65, v/v). The method yielded satisfactory resolutions for these agents, and the results were compared with those obtained using the microbiological method. The statistical analysis of the relationship between the methods gave a good correlation for all of these agents and samples. The concentrations of cefsulodin and cefotiam, concurrently administered by the intravenous route to patients subjected to artificial total joint prosthesis, in serum and bone marrow blood collected at 0.5 and 1 hr postinjection were almost equivalent.

Keyphrases □ Cefsulodin—simultaneous determination with cefotiam in serum and bone marrow blood, high-performance liquid chromatography □ Cefotiam—simultaneous determination with cefsulodin in serum and bone marrow blood, high-performance liquid chromatography □ High-performance liquid chromatography—simultaneous determination of cefsulodin and cefotiam in serum and bone marrow blood

Cefsulodin, sodium 4-carbamoyl-1-[(6*R*,7*R*)-2-carboxy-8-oxo-7- [(2*R*) -2-phenyl-2-sulfoacetamido] -5-thia-1-azabicyclo[4.2.0]oct-2-en-3-yl]methylpyridium hydroxide, a potent cephalosporin derivative, is superior to sulbenicillin and carbenicillin and comparable to gentamicin in activity against *Pseudomonas aeruginosa*. The drug is stable to *P. aeruginosa*-specific cephalosporinase (1–3). Cefotiam, (6*R*,7*R*)-7-[2-(2-amino-4-thiazolyl)-acetamido]-3-[[[1-[2-(dimethylamino)ethyl]-1*H*-tetrazol-5-yl]thio]methyl]-8-oxo-5-thia-1-azabicyclo[4.2.0]-oct-2-ene-2-carboxylic acid dihydrochloride, also shows broad-spectrum antibacterial activity against both Gram-positive and Gram-negative bacteria (4). Combined administration of these agents is frequently used to treat systemic infections in which a broader anti-infective spectrum is needed. A simple, specific high-performance liquid chromatographic (HPLC) method was developed which determines both cefsulodin and cefotiam in biological fluids. A comparison is made with the previously used microbiological method.

EXPERIMENTAL

Materials—Cefsulodin[1] and cefotiam[2] were used as received. Cefazolin[3], employed as an internal standard, was used as received. HPLC-quality methanol[4] and acetonitrile[5] were used. Tetrabutylammonium

[1] Tilmapor, Ciba-Geigy, Basle, Switzerland.
[2] Halospor, Ciba-Geigy, Basle, Switzerland.
[3] Cefamezin, Fujisawa Pharmaceutical Co., Osaka, Japan.
[4] Wako Chemical Co., Osaka, Japan.
[5] Tokyo Kasei Chemical Co., Tokyo, Japan.

0022-3549/83/0800-0958$01.00/0

the elixir had significantly greater bioavailability than did the tablet. The incomplete systemic availability of oral acetaminophen could be explained either by incomplete absorption or presystemic biotransformation, (*e.g.*, first-pass hepatic extraction or metabolism in the epithelium and/or lumen of the GI tract), or by a combination of these two factors (11). Differentiation between these two possible mechanisms could be achieved through an examination of route-dependent differences in the pattern of drug metabolism, as described by Harris and Riegelman (12). In a previous study of systemic availability (13), Rawlins *et al.* reported the bioavailability of acetaminophen tablets in a 500-mg dose to be only 63% compared with 79% in our study of a 650-mg dose. Bioavailability increased to 89 and 87% following 1,000- and 2,000-mg doses, respectively (13). The discrepancy in results of the two studies may be due to saturation of presystemic biotransformation at doses >500 mg.

The comparative bioavailability studies of two widely used acetaminophen tablets suggest that they have essentially similar systemic availability and therefore should be therapeutically equivalent.

REFERENCES

(1) B. Ameer and D. J. Greenblatt, *Ann. Intern. Med.*, **87**, 202 (1977).

(2) N. F. Billups and S. M. Billups, "American Drug Index 1981," J. B. Lipincott, Philadelphia, Pa., 1981.

(3) B. Ameer, D. J. Greenblatt, M. Divoll, D. R. Abernethy, and L. Shargel, *J. Chromatogr.*, **226**, 224 (1981).

(4) D. W. Marquardt, *J. Soc. Ind. Appl. Math.*, **11**, 431 (1963).

(5) R. A. Usanis, "NLIN—Nonlinear Least Squares Estimation of Parameters (Library Services Series Document No. LSR-089-1)," Triangle Universities Computation Center, Research Triangle Park, N.C., 1972.

(6) J. C. K. Loo and S. Riegelman, *J. Pharm. Sci.*, **59**, 53 (1970).

(7) M. Gibaldi, and D. Perrier, "Pharmacokinetics," Dekker, New York, N.Y., 1975.

(8) D. J. Greenblatt and J. Koch-Weser, *N. Engl. J. Med.*, **293**, 702, 964 (1975).

(9) G. Levy, *Arch. Intern. Med.*, **141**, 279 (1981).

(10) J. B. Sotiropoulus, T. Deutsch, and F. M. Plakogiannis, *J. Pharm. Sci.*, **70**, 422 (1981).

(11) C. F. George, *Clin. Pharmacokinet.*, **6**, 259 (1981).

(12) L. Harris and S. Riegelman, *J. Pharm. Sci.*, **58**, 71 (1969).

(13) M. D. Rawlins, D. B. Henderson, and A. R. Hijab, *Eur. J. Clin. Pharmacol.*, **11**, 283 (1977).

ACKNOWLEDGMENTS

Presented in part at the APhA Academy of Pharmaceutical Sciences meeting in Las Vegas, April 1982.

The authors are grateful for the assistance of Lawrence J. Moschitto, Jerold S. Harmatz, Dr. Dean S. MacLaughlin, and the staff of the Clinical Study Unit, New England Medical Center Hospital. Supported by Grants RR-24040, RR-05830-1, and MH-34223 from the United States Public Health Service.

Simultaneous Determinations of Cefsulodin and Cefotiam in Serum and Bone Marrow Blood by High-Performance Liquid Chromatography

KEIKO YAMAMURA *x, MAKOTO NAKAO *, JUN-ICHIRO YAMADA *, and TOSHIHISA YOTSUYANAGI ‡

Received March 17, 1982, from the **Pharmacy Department, Nagoya University Branch Hospital, Higashi-ku, Nagoya 461* and the ‡*Faculty of Pharmaceutical Sciences, Nagoya City University, Mizuho-ku, Nagoya 467 Japan.* Accepted for publication August 9, 1982.

Abstract □ A high-performance liquid chromatographic method is described for the simultaneous determinations of cefsulodin and cefotiam in serum and bone marrow blood samples. After extraction with acetonitrile, the cephalosporins were applied to a reverse-phase column with an internal standard, cefazolin; the mobile phase was a mixture of 0.005 *M* tetrabutylammonium phosphate and methanol (35:65, v/v). The method yielded satisfactory resolutions for these agents, and the results were compared with those obtained using the microbiological method. The statistical analysis of the relationship between the methods gave a good correlation for all of these agents and samples. The concentrations of cefsulodin and cefotiam, concurrently administered by the intravenous route to patients subjected to artificial total joint prosthesis, in serum and bone marrow blood collected at 0.5 and 1 hr postinjection were almost equivalent.

Keyphrases □ Cefsulodin—simultaneous determination with cefotiam in serum and bone marrow blood, high-performance liquid chromatography □ Cefotiam—simultaneous determination with cefsulodin in serum and bone marrow blood, high-performance liquid chromatography □ High-performance liquid chromatography—simultaneous determination of cefsulodin and cefotiam in serum and bone marrow blood

Cefsulodin, sodium 4-carbamoyl-1-[(6*R*,7*R*)-2-carboxy-8-oxo-7- [(2*R*) -2-phenyl-2-sulfoacetamido] -5-thia-1-azabicyclo[4.2.0]oct-2-en-3-yl]methylpyridium hydroxide, a potent cephalosporin derivative, is superior to sulbenicillin and carbenicillin and comparable to gentamicin in activity against *Pseudomonas aeruginosa*. The drug is stable to *P. aeruginosa*-specific cephalosporinase (1–3). Cefotiam, (6*R*,7*R*)-7-[2-(2-amino-4-thiazolyl)-acetamido]-3-[[[1-[2-(dimethylamino)ethyl]-1*H*-tetrazol-5-yl]thio]methyl]-8-oxo-5-thia-1-azabicyclo[4.2.0]-oct-2-ene-2-carboxylic acid dihydrochloride, also shows broad-spectrum antibacterial activity against both Gram-positive and Gram-negative bacteria (4). Combined administration of these agents is frequently used to treat systemic infections in which a broader anti-infective spectrum is needed. A simple, specific high-performance liquid chromatographic (HPLC) method was developed which determines both cefsulodin and cefotiam in biological fluids. A comparison is made with the previously used microbiological method.

EXPERIMENTAL

Materials—Cefsulodin[1] and cefotiam[2] were used as received. Cefazolin[3], employed as an internal standard, was used as received. HPLC-quality methanol[4] and acetonitrile[5] were used. Tetrabutylammonium

[1] Tilmapor, Ciba-Geigy, Basle, Switzerland.
[2] Halospor, Ciba-Geigy, Basle, Switzerland.
[3] Cefamezin, Fujisawa Pharmaceutical Co., Osaka, Japan.
[4] Wako Chemical Co., Osaka, Japan.
[5] Tokyo Kasei Chemical Co., Tokyo, Japan.

0022-3549/83/0800-0958$01.00/0

Table I—Recoveries of Cefsulodin, Cefotiam, and Cefazolin from Serum

Drug	Concentration, μg/ml	Recovery[a], %
Cefsulodin	100	103.0 ± 2.7
	50	98.0 ± 1.2
	10	98.5 ± 3.2
	5	98.1 ± 2.0
Cefotiam	100	99.6 ± 2.1
	50	102.1 ± 4.1
	10	99.9 ± 1.3
	5	98.5 ± 1.8
Cefazolin	100	101.8 ± 2.3
	50	103.2 ± 1.1
	10	99.4 ± 3.2
	5	98.8 ± 3.3

[a] Recovery calculated as (serum value/water control value) × 100. Each value is the mean ± *SD* of six determinations.

phosphate[6] was used as a constituent of the mobile phase. All other reagents were of analytical grade.

Serum and Bone Marrow Blood Samples—Cefsulodin (1 g) and cefotiam (2 g) were administered concurrently by intravenous injection to 16 patients immediately before beginning surgery. Serum and bone marrow blood samples were collected from each subject at 0.5 and 1 hr after injection (a total of 64 samples). Samples were centrifuged immediately at 3000 rpm for 15 min. The serum fractions were separated and stored frozen at −60° until assayed.

Chromatographic Conditions—An HPLC apparatus[7] equipped with a UV-absorbance detector[8] and a reverse-phase column[9] (10 μm, 30 cm × 3.9-mm i.d.) were used. Peak areas were obtained by a data analyzer[10]. The mobile phase was a mixture of methanol–water (35:65, v/v) and 0.005 *M* tetrabutylammonium phosphate. The flow-rate was 1.5 ml/min with an operating pressure of 220 kg/cm². The column eluate was continuously monitored at 280 nm, with a sensitivity of 0.08 AUFS and a chart speed of 5 mm/min.

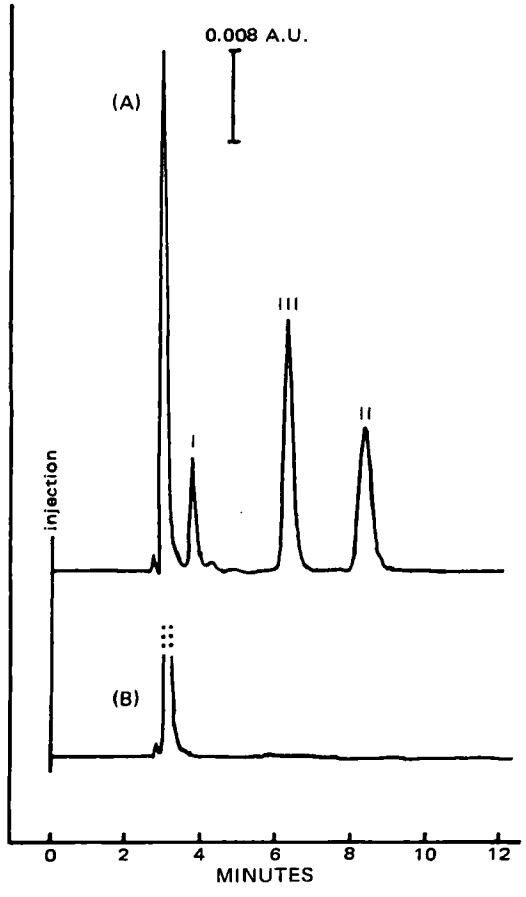

Figure 1—*Chromatograms of cefsulodin (I), cefotiam (II), and cefazolin (internal standard, III) in human serum, at concentrations of 25 μg/ml for I, 40 μg/ml for II, and 50 μg/ml for III. Key: (A) spiked serum sample; (B) serum blank. Chromatograph was run at 0.08 AUFS with a chart speed of 5 mm/min.*

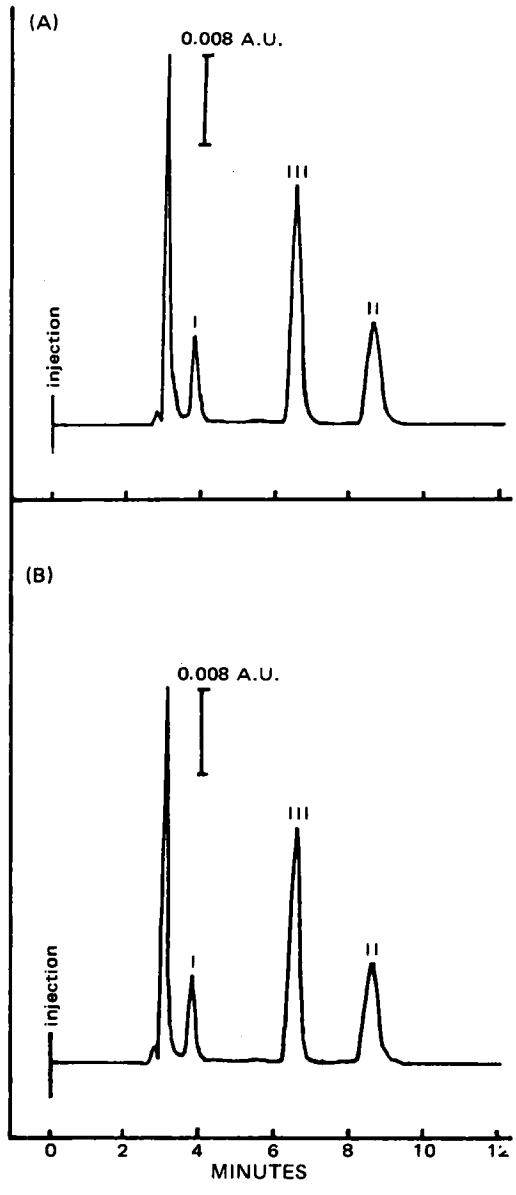

Figure 2—*Typical chromatograms of human serum (A) and bone marrow blood (B) samples collected from a patient 0.5 hr after intravenous injection of both drugs. Key: (I) cefsulodin; (II) cefotiam; (III) cefazolin.*

Assay Procedures—A 0.2-ml serum sample was mixed with acetonitrile (0.2 ml) containing a known amount of the internal standard on a vortex mixer for 10 sec and then contrifuged at 12,000 rpm for 5 min. The supernatant was passed through a membrane filter (0.45 μm)[11] and a 10-μl aliquot was injected into a port of the HPLC column.

Calibration Curves of Cefsulodin, Cefotiam, and Cefazolin—Calibration curves were constructed using a known concentration of the drugs (10–100 μg/ml) dissolved in human serum. The relationship between the concentration (ordinate) and the peak area (abscissa) showed good linearity for each: respective intercepts, slopes, and correlation coefficients, 0.558, 0.0106, and 0.998 for cefsulodin; 0.030, 0.0088, and 0.999 for cefotiam; and 0.558, 0.0059, and 0.998 for cefazolin (internal standard). The ratios (R) of the slopes of cefsulodin and cefotiam to that

[6] Waters Associates, Milford, Mass.
[7] Model 520, GASUKURO KOGYO, Tokyo, Japan.
[8] UVIDEC 100-II, JASCO, Tokyo, Japan.
[9] μBondapak C_{18}, Waters Associates, Milford, Mass.
[10] C-R1A CHROMATOPAC, Shimadzu, Kyoto, Japan.
[11] TM-2P, Toyo Scientific Inc., Tokyo, Japan.

Table II—Concentrations of Cefsulodin and Cefotiam in Serum and Bone Marrow Blood Determined by the HPLC Method

Sample	Time[b], hr	Concentration[a], μg/ml	
		Cefsulodin	Cefotiam
Serum	0.5	44.2 ± 20.8	79.8 ± 33.1
	1	34.1 ± 16.8	46.4 ± 14.5
Marrow	0.5	39.6 ± 16.8	76.1 ± 34.7
	1	30.1 ± 13.4	44.4 ± 22.1

[a] Mean ± *SD* of 16 subjects. [b] Blood samples were collected with 0–10-min variance.

of the internal standard were 1.80 and 1.49, respectively, from which the sample concentration (C_a) was calculated as: C_a = (peak area ratio between sample and internal standard) × (concentration of internal standard)/R.

Microbiological Assay—The microbiological assay was performed according to a modified method of Fugono *et al.* (5). The concentrations of cefsulodin and cefotiam were determined by the cup plate method (6), using *P. aeruginosa*[12] and *Proteus mirabilis*[13] as test organisms. The minimum inhibitory concentrations of these agents are: 1.56 and >100 μg/ml against *P. aeruginosa* for cefsulodin and cefotiam, respectively,and >100 and 0.01 μg/ml against *P. mirabilis* for cefsulodin and cefotiam, respectively, with an inoculation of 10^6 cells/ml (7, 8). The culture medium was prepared from an agar base[14] containing 0.1% sodium acetate (w/v). A series of dilutions for the calibration curve were made with normal human serum.

RESULTS AND DISCUSSION

Recovery and Separation of Cephalosporins—Recovery of cefsulodin, cefotiam, and cefazolin from injected solutions in serum was established by comparing the peak areas for samples with those from water solutions in the range of 5–100 μg/ml. As shown in Table I, the recoveries were regarded as 100% for these cephalosporins.

The liquid chromatograms of cefsulodin, cefotiam, and the internal standard in serum are shown in Fig. 1. The retention times were found to be 3.8, 6.3, and 8.3 min, respectively. The peaks of the control serum had low retention times and were completely separated from those of the antibacterial agents. Also, the separation of peaks among cefsulodin, cefotiam, and the internal standard was established with satisfactory resolutions for simultaneous determination.

Determinations of Cephalosporins in Serum and Bone Marrow Blood—The HPLC method was applied for the simultaneous determinations of cefsulodin and cefotiam in serum and bone marrow blood samples. Figure 2 shows typical chromatograms of serum and bone marrow blood samples collected from a patient 0.5 hr after intravenous injection. There was little difference in the retention time between serum and bone marrow blood samples that originated from different sources of body fluids.

Table II indicates the average concentrations and standard deviations of cefsulodin and cefotiam in serum and bone marrow blood samples that were collected from 16 subjects. There were no significant differences in the concentrations between the different samples for each agent, although there was a tendency for the average concentration in serum to be slightly higher than that in bone marrow blood. The results indicate that very fast movement of these agents from the peripheral to the bone marrow blood was always established.

Correlation of the HPLC and Microbiological Methods—To examine the reliability of the HPLC method, the same biological samples containing cefsulodin and cefotiam were also assayed by the microbiological method in general use, and the correlation between both the methods was studied. The great difference in the minimum inhibitory concentration enabled these agents to be determined individually even when concurrently administered, even though cefsulodin and cefotiam are categorized in the same family of cephalosporins.

The calculation of the correlation coefficient and regression analysis were conducted for both serum and bone marrow blood samples irrespective of the sampling time. The statistical values were: in cefsulodin, y(HPLC) = 0.91x(microbiological) + 1.71, r = 0.974 (n = 32) in serum and y = 0.91x − 1.52, r = 0.961 (n = 32) in bone marrow blood; in cefotiam, y = 1.07x −8.99, r = 0.971 (n = 32) in serum and y = 1.01x − 4.05, r = 0.978 (n = 32) in bone marrow blood.

The intercepts of the regression lines of cefsulodin gave values closer to the origin than those of cefotiam, while the regression coefficients were very close to unity for each agent, indicating that the sensitivity of the HPLC procedure described here was almost equivalent to the microbiological method. Therefore, the HPLC method is accurate enough to use within the putative range of effective concentrations in biological fluids as well as enabling the simultaneous determination of these cephalosporins. The HPLC method, furthermore, was more rapid and easier to perform than the microbiological method.

[12] IFO 12582, Institute of Fermentation of Osaka, Osaka, Japan.
[13] IFO 3849, Institute of Fermentation of Osaka, Osaka, Japan.
[14] Diagnostic Sensitivity Test, Code CM 261, Oxoid Ltd., England.

REFERENCES

(1) K. Tsuchiya, M. Kondoh, and H. Nagatomo, *Antimicrob. Agents Chemother.*, **13**, 137 (1978).

(2) K. Tsuchiya and M. Kondo, *Antimicrob. Agents Chemother.*, **13**, 536 (1978).

(3) M. Kondo and K. Tsuchiya, *Antimicrob. Agents Chemother.*, **14**, 151 (1978).

(4) K. Tsuchiya, M. Kida, M. Kondo, H. Ono, M. Takeuchi, and T. Nishi, *Antimicrob. Agents Chemother.*, **14**, 557 (1978).

(5) T. Fugono and K. Maeda, *Chemotherapy (Tokyo)*, **27**(s-2), 120 (1979).

(6) "Commentary of Antibiotics Standard of Japan (KIJUN KAISETSU)," Ministry of Public Health and Welfare of Japan, YAKUGYO JIHO, Tokyo, 1978, p. 593.

(7) S. Goto, M. Ogawa, A. Tsuji, Y. Kaneko, and S. Kuwahara, *Chemotherapy (Tokyo)*, **27**(s-2), 1 (1979).

(8) T. Nishino and T. Iwahi, *Chemotherapy (Tokyo)*, **27**(s-3), 45 (1979).

Analysis of Doxylamine in Plasma by High-Performance Liquid Chromatography

KENNETH J. KOHLHOF ˣ, DECHERD STUMP, and JOSEPH A. ZIZZAMIA

Received March 9, 1981, from *Clinical Research Associates, New York, NY 10010.* Accepted for publication July 28, 1982.

Abstract □ A rapid and sensitive high-performance liquid chromatographic (HPLC) assay for the quantitative determination of doxylamine in plasma is described. The drug levels of doxylamine in plasma were monitored after the oral administration of a single 25-mg tablet of doxylamine succinate to each of 20 male volunteers. The compound was extracted from the plasma samples, concentrated under a nitrogen stream, and analyzed by HPLC using normal-phase chromatography with detection at 254 nm. The detection limit is ~5 ng/ml.

Keyphrases □ Doxylamine—in human plasma, determination by high-performance liquid chromatography □ High-performance liquid chromatography—quantitation of doxylamine in human plasma □ Antihistamines—doxylamine succinate, determination of doxylamine in human plasma by high-performance liquid chromatography

Doxylamine, one of the oldest drugs exhibiting antihistaminic properties, also possesses impressive hypnotic properties. Although the characteristic activity of the antihistamines is their ability to antagonize the effects of histamine on various peripheral structures (1), these compounds are known to have a wide spectrum of pharmacological and therapeutic effects. Since many of these drugs cause sedation, they are frequently used as hypnotic agents or sedatives, in spite of their mixed excitatory and depressant actions within the CNS (2). According to Sjöqvist and Lasagna, 25–50 mg of doxylamine is more effective as a sedative than 100 mg of secobarbital (3), and it is often used as a hypnotic antihistamine at bedtime (4).

A previous method, tested by the Food and Drug Administration in 1972, describes a doxylamine assay in urine using GC (5). This paper describes a simple, sensitive, high-performance liquid chromatographic (HPLC) method for the measurement of doxylamine in plasma using normal-phase chromatography.

EXPERIMENTAL

Materials—Reagent grade sodium hydroxide, ammonium hydroxide, and ammonium chloride; HPLC grade acetonitrile, chloroform, methanol, and dichloromethane; and USP reference standard dextroamphetamine sulfate and doxylamine succinate were used.

Standard Preparation—A set of standard samples was prepared by adding 80, 50, 30, 20, and 10 μl of a 10-ng/μl solution of doxylamine succinate in water to 3.0-ml plasma blanks with a microliter syringe. The

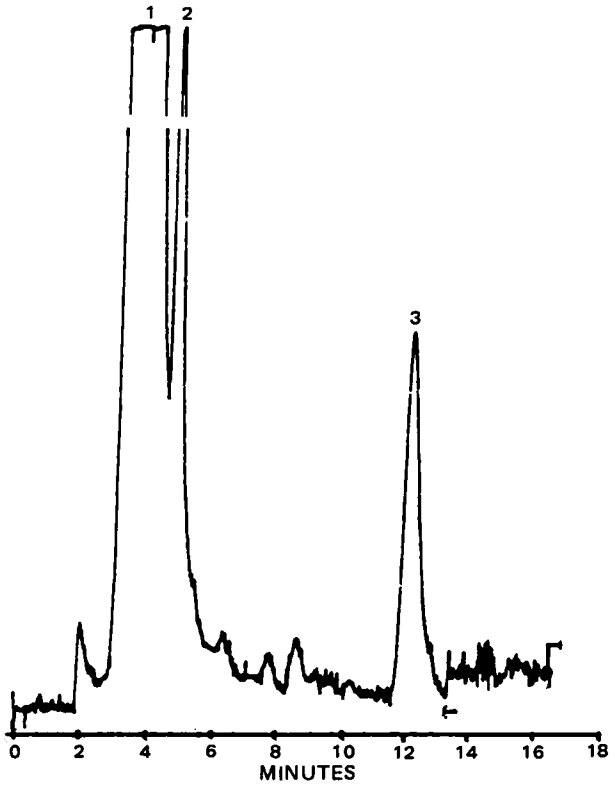

Figure 1—*Chromatogram of a plasma blank. Key: (1) and (2) unidentified components of plasma; (3) amphetamine peak.*

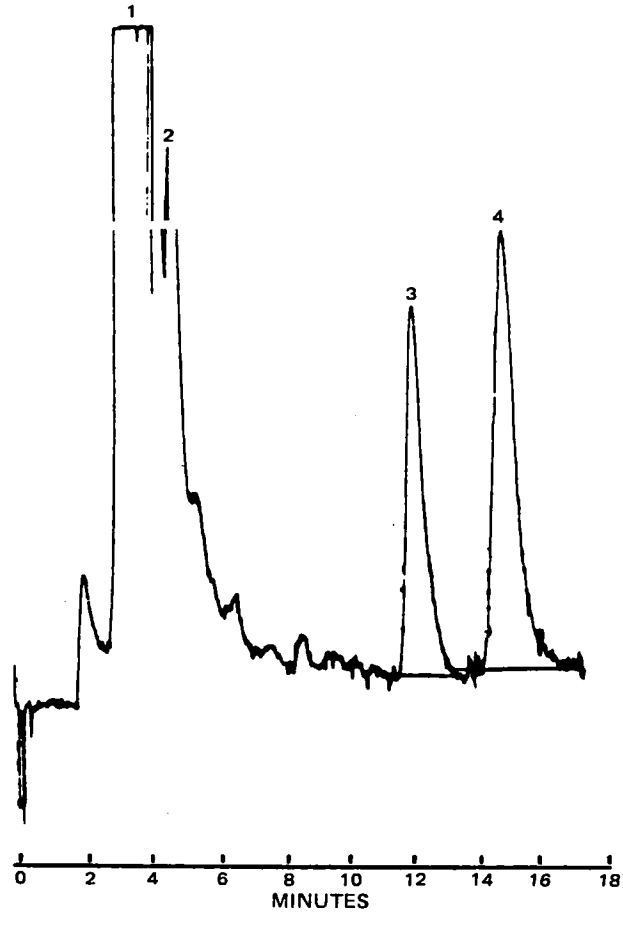

Figure 2—*Chromatogram of a plasma sample taken from a human volunteer 2 hr after oral administration of 25 mg of doxylamine succinate in tablet form. Key: (1) and (2) unidentified components of plasma; (3) amphetamine; (4) doxylamine.*

0022-3549/83/0800-0961$01.00/0

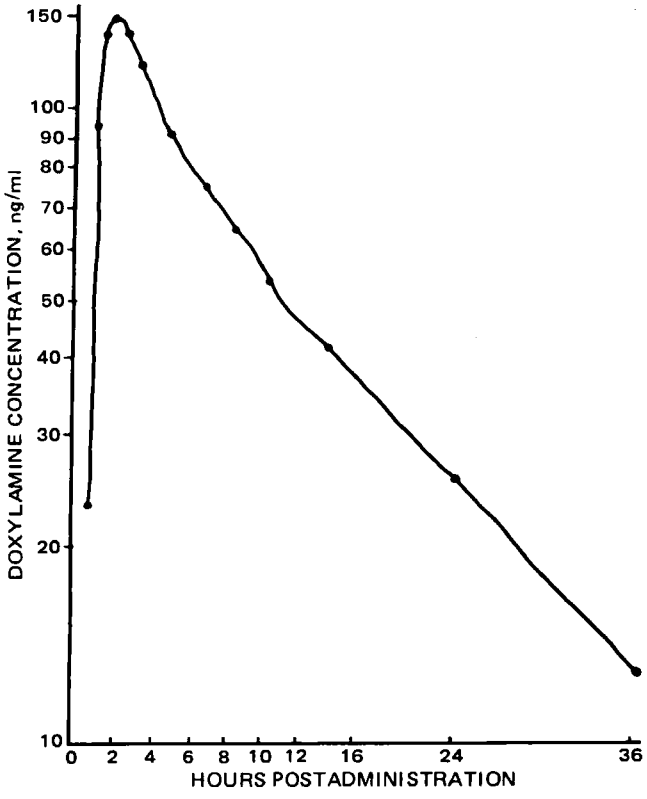

Figure 3—*Plasma levels of doxylamine in a human volunteer following the oral administration of 25 mg of doxylamine succinate in tablet form.*

internal standard was prepared by adding 10 ml of 0.3 *N* NaOH and 20 ml of dichloromethane to 20 mg of dextroamphetamine sulfate in a 125-ml separatory funnel and shaking manually for 5 min. After the layers separated, the organic layer was collected in a 50-ml volumetric flask. The extraction was repeated with 20 ml of dichloromethane, and the organic phase was combined with the first extract. This was diluted to volume with dichloromethane to obtain a 300-μg/ml concentrated solution of dextroamphetamine in dichloromethane. A 5-ml aliquot of this solution was transferred to a 50-ml volumetric flask and diluted to volume with the eluting solvent. The concentration of the resulting solution was 30 μg/ml.

Subjects—After an overnight fast, 20 healthy male volunteers (20–50 years old, 59–68 kg) were administered a single 25-mg dose of doxylamine succinate in tablet form. Blood samples of sufficient volume to obtain 10 ml of plasma were drawn prior to administration and at regular intervals postadministration. All samples were collected in heparinized evacuated containers[1] and centrifuged at 2500 rpm. The separated plasma was stored at −20° until analysis.

Plasma Extraction—Plasma (3.0 ml) was pipetted into a 20-ml screw-cap[2] test tube, and 10 ml of 0.3 *N* NaOH and 5 ml of dichloromethane were added. The tubes were placed on a rocking shaker[3] at a slow speed for 15 min and then centrifuged. Any emulsion formed was broken up by lightly tapping the tubes and the samples were centrifuged again. The organic layer was transferred to a 12-ml glass-stoppered conical-tip tube using a Pasteur pipet. The extraction of the aqueous layer was repeated with an additional 5 ml of dichloromethane. This was centrifuged, the organic layer was combined with the first extract in the conical-tip tube, and the tubes were placed in a water bath with the temperature maintained at 40°. The combined extracts were evaporated under a nitrogen stream, and 200 μl of the dilute dextroamphetamine solution was added with a 100-μl syringe. The tube was capped with the glass stopper, vortexed[4], and centrifuged.

Chromatographic Analysis—The HPLC system[5] consisted of a solvent delivery pump, a fixed-wavelength UV detector at 254 nm, and a μPorasil column (10 μm, 3.9 mm × 30 cm). The eluting solvent was 8 parts chloroform, 1 part acetonitrile, and 1 part of a mixture of methanol–ammonium hydroxide–ammonium chloride (57:2:1); the flow rate was 1.5 ml/min. The UV absorption was monitored using an electronic integrator[6] with an attenuation of 2^4–2^5, as necessary.

Eighty microliters of the plasma extract was introduced into the column using an automatic injector[7]. Retention times for doxylamine and amphetamine were 14.6 and 12.1 min, respectively. The peak height ratio of doxylamine to the internal standard in the sample plasma was measured and compared with the peak height ratio in the standards to achieve quantitation.

Calibration Curve—The linearity of the calibration curve was determined by adding 100–800 ng of doxylamine succinate[8] to 3-ml plasma blanks. The coefficients of variation were determined using replicate plasma standards spiked with doxylamine succinate.

Table I—Reproducibility of Doxylamine Determination in Human Plasma [a]

Doxylamine Succinate Concentration, ng/ml	Doxylamine–Amphetamine Peak Height Ratio, ng/ml	*CV*, %
268	1.600	2.5
167	0.982	3.8
100	0.598	2.5
67	0.406	3.2
34	0.203	6.2

[a] n = 20 for all concentrations.

RESULTS AND DISCUSSION

The method was evaluated in terms of extraction efficiency, interference, linearity, and precision. Preliminary experiments demonstrated the need for adding amphetamine at the end of the extraction steps. When known amounts of amphetamine were added to the dichloromethane solution in the beginning of the extraction procedure, its recovery was negligible. To ensure the availability of a fixed amount of amphetamine in the sample solution, 200 μl of amphetamine was added to each tube after the dichloromethane was evaporated.

The peaks observed for doxylamine and amphetamine were well separated from any naturally occurring plasma constituents or any metabolites of the drug. With the blank plasma, when the standard doxylamine was eliminated from the assay, no peaks absorbing at 254 nm that had the same retention time as doxylamine were observed (Fig. 1). Figure 2 shows plasma extracted from a typical subject 2 hr after the administration of 25 mg of doxylamine succinate. From 0.5–36 hr postadministration, the concentration of doxylamine in plasma was generally in the range of 10 to 150 ng/ml (Fig. 3). The peaks encountered for doxylamine and the internal standard were symmetrical and well defined.

The mean values of the peak height ratio of doxylamine to amphetamine obtained from 20 calibration curves are given in Table I. The method exhibits excellent linearity: the correlation coefficient of the doxylamine to amphetamine peak height ratio *versus* doxylamine succinate added to plasma was 0.99 over the range of values obtained (Table I). The absolute recovery when 570 ng of doxylamine succinate was added to 3 ml of plasma was 84.8% (based on three determinations). The assay is suitable for the study of doxylamine succinate pharmacokinetics, representing a reproducible and accurate method for the detection of doxylamine in plasma to 5 ng/ml.

REFERENCES

(1) "United States Dispensatory & Physicians's Pharmacology," 26th ed., Lippincott, Philadelphia, Pa., 1967, p. 155.

(2) L. S. Goodman and A. Gilman, "The Pharmacological Basis of Therapeutics," 4th ed., Macmillan, New York, N.Y., 1970, p. 132.

(3) F. Sjöqvist and L. Lasagna, *Clin. Pharmacol. Ther.*, 8, 48 (1967).

(4) L. S. Goodman and A. Gilman, "The Pharmacological Basis of Therapeutics," 4th ed., Macmillan, New York, N.Y., 1970, pp. 640, 642.

(5) "Dextromethorphan, *O*-Desmethyldextromethorphan, Doxylamine Assay in Urine," Food and Drug Administration, Washington, D.C., November 16, 1972. (Analytical Method No. 1652E.)

[1] Vacutainer; Becton, Dickinson & Co., Oxnard, Calif.
[2] Teflon-lined screw cap, No. 9826; Pyrex.
[3] Buchler Instruments, Fort Lee, N.J.
[4] Vortex-Genie, Model K-550-G, Scientific Industries, Bohemia, N.Y.
[5] Solvent delivery pump Model M6000, UV detector Model 440, Waters Associates, Milford Mass.
[6] Automation System No. 3385A, Hewlett-Packard, Palo Alto, Calif.
[7] WISP Model 710B, Waters Associates, Milford, Mass.
[8] The plasma levels of doxylamine were calculated as doxylamine succinate.

High-Performance Liquid Chromatographic Determination of Nitroglycerin in Sublingual, Sustained-Release, and Ointment Dosage Forms

CAROLYN S. OLSEN ˣ **and HENRY S. SCROGGINS**

Received March 5, 1982, from the *Food and Drug Administration, New Orleans, LA 70122.* Accepted for publication August 12, 1982. Address correspondence to: Miss Helen L. Reynolds, Technical Editor, Food and Drug Administration, Bureau of Foods, Washington, DC 20204.

Abstract □ A rapid, precise, sensitive, and specific assay for nitroglycerin in sublingual, sustained-release, and ointment dosage forms using high-performance liquid chromatography is described. The nitroglycerin dosage forms were dissolved in methanol, filtered, and injected directly into the liquid chromatograph. A variable-wavelength UV detector operated at 220 nm and a C_{18} microporous silica column were employed. The mobile phase was methanol–water (40:60).

Keyphrases □ Nitroglycerin—high-performance liquid chromatographic determination in sublingual, sustained-release, and ointment dosage forms □ Dosage forms—ointment, sublingual, sustained-release, high-performance liquid chromatographic determination of nitroglycerin □ High-performance liquid chromatography—determination of nitroglycerin in sublingual, sustained-release, and ointment dosage forms

Several techniques for the determination of nitroglycerin in commercial dosage forms have been reported (1–5). Some limitations of these methods include: the time-consuming and nonspecific determination of the compendial assay (1), the poor sensitivity and lack of precision of the IR method (2, 3), possible decomposition in the GC method (4), and the inability to distinguish among the decomposition products using the polarographic method (5).

High-performance liquid chromatography (HPLC) as a determinative technique appears to offer the best approach (6, 7). As reported here, it is both rapid and stability indicating. A single procedure is applicable to more than one dosage form, and individual tablets can be analyzed at low dosage levels. The latter is necessary when analyzing nitroglycerin products because nitroglycerin migrates from tablet to tablet on exposure to air (8, 9). The use of HPLC eliminates interferences from other organic or inorganic nitrates and allows nitroglycerin to be distinguished from its mono- and dinitrate degradation products.

EXPERIMENTAL

Reagents—HPLC-grade methanol[1] and water[1] were used. All other chemicals and solvents were reagent grade and were used without further purification. A 10% nitroglycerin in lactose triturate[2] was used as a reference standard and was assayed by the USP phenoldisulfonic acid method (1). Authentic 1,2- and 1,3-dinitroglycerin and 1- and 2-mononitroglycerin[3] were used to determine the presence of any degradation products; pentaerythritol tetranitrate[4] and isosorbide dinitrate[5] were used as internal standards.

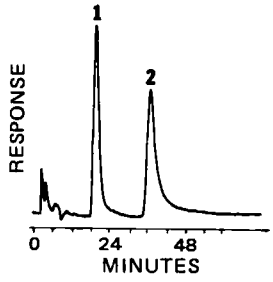

Figure 1—*Chromatogram of sublingual tablet sample. Key: (1) nitroglycerin; (2) pentaerythritol tetranitrate.*

Apparatus—The liquid chromatographic system consisted of a dual-head reciprocating piston positive-displacement pump[6], a septumless syringe-loaded loop injector with a 20-μl loop[7], a variable-wavelength UV detector[8] operated at 220 nm, a 10-mV recorder[9], and a 3.9 mm × 30-cm C_{18} microparticulate column[10] with a 4 cm × 4.6-mm guard column packed with pellicular octadecyl reverse-phase material[11]. The solvent system was methanol–water (40:60). The flow rate was 1 ml/min with a pressure of ~1600 psi.

Nitroglycerin Standard Solution—An accurately weighed quantity of nitroglycerin reference standard was dissolved in the internal standard solution (0.1 mg of pentaerythritol tetranitrate/ml of methanol) to obtain a concentration of ~0.075 mg/ml.

Extraction—*Sublingual Tablets*—Sufficient powdered tablet composite or individual powdered tablets (if individual tablet assays were required) were transferred to a 25-ml glass-stoppered Erlenmeyer flask and diluted with internal standard solution to give a nitroglycerin concentration of 0.075 mg/ml. The mixture was sonicated for 2 min then mechanically shaken for 30 min. The resulting solution was filtered through 0.7-μm filter paper[12] and injected into the chromatograph.

Ointment—Sufficient ointment was transferred to a 25-ml glass-stoppered Erlenmeyer flask and diluted with internal standard solution to give a nitroglycerin concentration of 0.075 mg/ml. The mixture was warmed in a 50° water bath and shaken intermittently until the ointment dispersed. The ointment solidified after being removed from the bath and shaken vigorously. The heating and shaking operation was then repeated. The solution was filtered through a 0.7-μm filter paper[12] and injected into the chromatograph.

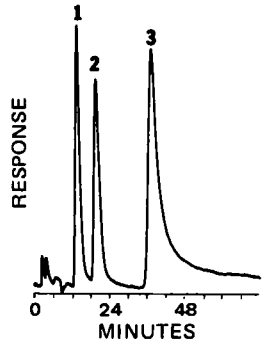

Figure 2—*Chromatogram of sustained-release tablet sample that contains phthalates. Key: (1) isosorbide dinitrate; (2) nitroglycerin; (3) phthalate excipient.*

[1] J. T. Baker Chemical Co., Phillipsburg, N.J.

[2] ICI Americas, Wilmington, Del.
[3] Arnar-Stone Labs, McGaw Park, Ill.
[4] Atlas Chemical Industries, Wilmington, Del.
[5] USP Reference Standard, United States Pharmacopeial Convention, Rockville, Md.
[6] Model 100A, Altex Scientific, Berkeley, Calif.
[7] Model 210 injector with 210-06 loop, Altex Scientific, Berkeley, Calif.
[8] Model 155-40, Altex Scientific, Berkeley, Calif.
[9] B-D-41, Kipp & Zonen, Delft, The Netherlands.
[10] μBondapak C_{18}, Waters Associates, Milford, Mass.
[11] μBondapak C_{18}/Corasil, Waters Associates, Milford, Mass.
[12] Gilman Instrument Co., Ann Arbor, Mich.

0022-3549/83/0800-0963$01.00/0

Table I—Nitroglycerin Found in Sublingual, Sustained-Release, and Ointment Dosage Forms and in Synthetic Mixtures

Manufacturer	Tablet Concentration, mg	Found, %	Spike Added, mg	Spike Recovery, %	Synthetic Mixture Added, mg	Synthetic Mixture Recovery, %
			Sublingual Tablets[a]			
1	0.15	104.4	0.079	99.3	0.147	100.0
	0.30	108.7	0.193	100.7	0.302	100.3
	0.40	103.3	0.204	100.9	0.423	100.9
	0.60	108.7	0.335	99.7	0.615	100.9
2	0.15	98.0	0.081	99.3	0.146	99.3
	0.30	106.7	0.169	99.7	0.298	100.9
	0.40	102.3	0.192	101.0	0.421	100.9
	0.60	105.0	0.337	100.9	0.614	99.7
			Sustained-Release Tablets and Capsules[b]			
1	6.5	93.2	4.29	101.8	0.602	100.9
2	2.5	90.1	1.15	100.9	0.248	99.8
	6.5	94.8	3.10	101.8	0.500	100.5
	9.0	92.5	3.65	99.8	0.896	99.7
3	2.5	114.0	0.251	98.3	—[c]	—[c]
	6.5	106.5	0.643	99.4	—[c]	—[c]
4	2.6	91.0	0.243	97.2	—[c]	—[c]
	6.5	93.1	0.635	98.1	—[c]	—[c]
			2% Ointments[d]			
1		101.0	1.01	99.7	1.745	99.5
2		113.3	0.925	99.2	2.037	99.7
3		110.0	1.127	99.4	1.975	99.3

[a] Average recovery for all manufacturers, 100.2%; coefficient of variation, 0.753%; correlation coefficient, 0.9998. [b] Average recovery for all manufacturers, 99.4%; coefficient of variation, 1.83%; correlation coefficient, 0.9999. [c] Formulations not available for preparation of synthetic mixtures. [d] Average recovery for all manufacturers, 99.4%; coefficient of variation, 0.253%; correlation coefficient, 0.9997.

Sustained-Release Tablets or Capsules—This procedure required an alternate internal standard (isosorbide dinitrate) be used if phthalates were present as an excipient since phthalates have approximately the same retention time (R_t) as pentaerythritol tetranitrate under the conditions described. The presence of phthalates was detected by injecting a portion of sample dissolved in methanol into the chromatograph (a peak with the same R_t as that of pentaerythritol tetranitrate indicated the presence of phthalates). In such cases, isosorbide dinitrate (0.1 mg/ml of methanol) was used as the internal standard solution. Sufficient powdered sustained-release composite was transferred to a 25-ml glass-stoppered Erlenmeyer flask and diluted with the appropriate internal standard solution, giving a nitroglycerin concentration of 0.075 mg/ml. The mixture was sonicated for 2 min, then mechanically shaken for 30 min. The solution was filtered through 0.7-μm filter paper[12] and injected into the chromatograph.

Quantitation—The drug was quantitated by using the internal standard method, which compares peak height ratios. The internal standard for the sublingual tablets, ointments, and sustained-release dosage forms that did not contain phthalates was pentaerythritol tetranitrate; isosorbide dinitrate was used for the sustained-release dosage forms that contained phthalates.

RESULTS AND DISCUSSION

Figure 1 shows a typical chromatogram of 1.5 μg of nitroglycerin from a composite of sublingual tablets. Figure 2 shows a chromatogram of 1.5 μg of nitroglycerin from a composite of sustained-release tablets employing isosorbide dinitrate as the internal standard. Ointment and sustained-release capsules not containing phthalates gave chromatograms similar to those of the sublingual tablets because they contain no excipient interferences in the area of either nitroglycerin or pentaerythritol tetranitrate. The R_t with 40% methanol in water was ~12 min for isosorbide dinitrate, 18 min for nitroglycerin, and 32 min for pentaerythritol tetranitrate.

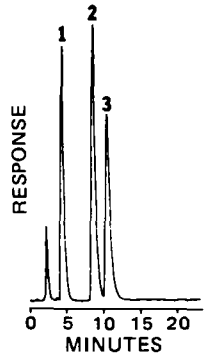

Figure 3—*Chromatogram of degradation products of nitroglycerin. Key: (1) 1- and 2-mononitroglycerin; (2) 1,3-dinitroglycerin; (3) 1,2-dinitroglycerin.*

During the development of this assay, a number of variations were tried. Methanol was chosen as the extracting solvent because of its ability to separate nitroglycerin and its mono- and dinitroglyceryl degradation products from the excipients in the various dosage forms. Methanol gave a cleaner solution than dimethyl sulfoxide; the latter dissolved the active ingredient as well as the excipients. Methanol and acetonitrile performed equally well as the mobile phase; methanol was chosen because it is less costly. Pentaerythritol tetranitrate was chosen as the internal standard because a number of samples contained excipients whose R_t value was the same or slightly different from that of isosorbide dinitrate, thereby causing peak distortion. One manufacturer's sustained-release tablets contained a phthalate with the same R_t as pentaerythritol tetranitrate, necessitating the use of isosorbide dinitrate as the internal standard.

The HPLC method described is capable of separating nitroglycerin from its mono- and dinitroglyceryl degradation products. Since these degradation products are more polar than nitroglycerin, they travel through the reverse-phase column faster and are eluted soon after the solvent front. To determine the degradation products, the methanol concentration of the mobile phase must be decreased, thereby increasing the R_t value of the other nitrate esters.

While detection at 254 nm may be possible when assaying nitroglycerin in a composite sample, it is not suitable for determining individual sublingual tablet uniformity because of the small quantity of active ingredient present in a single tablet. Detection at 220 nm gives a 60-fold enhancement in sensitivity with quantitative results comparable to those obtained at 254 nm, thus making individual tablet analysis possible.

The internal standard method of calculation was applied to the quantitative determination of nitroglycerin in the various dosage forms. The relative percentage of nitroglycerin found in the various dosage forms as well as the recovery data appear in Table I.

Synthetic mixtures (analogous to commercial formulations) were prepared by adding known amounts of the nitroglycerin triturate to the excipients according to the manufacturer's specifications. With these synthetic mixtures, the method demonstrated linearity from 0.05 to 1.5 mg/ml of original sample solution with a correlation coefficient >0.999 (10). Spiked samples of each dosage form were prepared using standard addition procedures. Weighed amounts of the triturate were added to previously assayed dosages containing the active ingredient. These preparations were then analyzed as described above (Table I).

This assay provides a rapid, sensitive, and specific method for the

determination of nitroglycerin in various dosage forms. The degradation products of nitroglycerin can be determined by a simple change of the mobile solvent system (methanol–water, 20:80) (Fig. 3). The assay is faster, more specific, and provides more stability-indicating information than the USP method.

REFERENCES

(1) "The United States Pharmacopeia," 20th rev., U.S. Pharmacopeial Convention, Rockville, Md., 1980, p. 552.

(2) F. Pristera, M. Halik, M. Castelli, and W. Fredericks, *Anal. Chem.*, **32**, 495 (1960).

(3) J. Carol, *J. Assoc. Off. Agric. Chem.*, **43**, 259 (1960).

(4) B. J. Alley and H. W. Dykes, *J. Chromatogr.*, **71**, 23 (1972).

(5) B. Flann, *J. Pharm. Sci.*, **58**, 122 (1969).

(6) W. G. Crouthamel and B. J. Dorsch, *J. Pharm. Sci.*, **68**, 237 (1979).

(7) D. M. Baske, J. E. Carter, and A. H. Amann, *J. Pharm. Sci.*, **68**, 481 (1979).

(8) C. D. Chandler, G. R. Gibson, and W. T. Bolleter, *J. Chromatogr.*, **100**, 185 (1974).

(9) R. Dalton, C. D. Chandler, and W. T. Bolleter, *J. Chromatogr. Sci.*, **13**, 40 (1973).

(10) R. G. D. Steel and J. H. Torrie, "Principles and Procedures of Statistics," McGraw-Hill, New York, N.Y., 1960, p. 188.

ACKNOWLEDGMENTS

The authors gratefully acknowledge the technical and editorial assistance of Dr. Jack Stocker, Science Advisor, New Orleans District.

Hydrazine Levels in Formulations of Hydralazine, Isoniazid, and Phenelzine Over a 2-Year Period

E. G. LOVERING, F. MATSUI ˣ, N. M. CURRAN, D. L. ROBERTSON, and R. W. SEARS

Received March 29, 1982, from the *Bureau of Drug Research, Health Protection Branch, Health and Welfare Canada, Tunney's Pasture, Ottawa, Ontario K1A 0L2.* Accepted for publication August 10, 1982.

Abstract □ Hydrazine levels in formulations of hydralazine, isoniazid, and phenelzine have been measured over a 2-year period under ambient conditions and under temperature and humidity stress. Hydralazine tablets are stable under ambient conditions, but the hydrazine level in an injectable formulation increased from 4.5 to 10 μg/ml over a 23-month period. Isoniazid tablets are also stable, but hydrazine levels in an elixir and a pyridoxine combination product doubled to 44 μg/ml and 19 μg/tablet, respectively. Levels in phenelzine tablets appeared to remain constant at ~60 μg/tablet, with considerable tablet-to-tablet variation.

Keyphrases □ Hydrazine—levels in formulations of hydralazine, isoniazid, and phenelzine over a 2-year period □ Hydralazine—hydrazine levels in formulations over a 2-year period □ Isoniazid—hydrazine levels in formulations over a 2-year period □ Phenelzine—hydrazine levels in formulations over a 2-year period

Previous work demonstrated the presence of hydrazine in an isoniazid injectable product (1) and showed that isoniazid may hydrolyze to hydrazine (2, 3). Because hydrazine poses a risk of cancer in humans (4, 5), these observations prompted an assessment of other drugs derived from hydrazine that are available in Canada. These include carbidopa, hydralazine, isocarboxazid, and phenelzine, in addition to isoniazid. Hydrazine levels in isoniazid single-component tablet formulations were determined by TLC (2) and high-performance liquid chromatography (HPLC) (6) and by modifying a GLC procedure originally developed for the determination of phenelzine in urine (7). Methods for the determination of hydrazine in formulations of hydralazine (8), isoniazid elixir, isoniazid–pyridoxine combination tablets (8), and phenelzine (9) have also been developed. A 2-year normal and accelerated aging study of hydrazine formation in formulated products of hydralazine, isoniazid, and phenelzine has been completed and the results are reported in this paper.

Hydrazine is used in some syntheses of hydralazine (10), isoniazid (11), and phenelzine (12), and its presence in a formulated drug product may result from improper purification of the drug. All three drugs are known to degrade to hydrazine in solution (6, 9, 11), but there does not appear to be any published information on the formation of hydrazine in formulations of these drugs.

EXPERIMENTAL

Sample Preparation—Drug formulations were obtained directly from the manufacturer. All tablet samples were transferred to amber bottles for storage with at least five tablets in each bottle, and 1.0-ml aliquots of the elixir were transferred to culture tubes and securely capped. Phenelzine tablets from lot D were sealed in glass tubes (22 × 220 mm) by drawing out the top of the tube in a flame. The 100% relative humidity condition was achieved by sealing a 12-ml centrifuge tube containing 4 ml of water in with the tablets; tablets were not in direct contact with the water.

Storage Conditions—All formulations were aged under the temperature and humidity conditions given in Tables I, II, and III. Except as noted above, the humidity was controlled by placing silica gel (0% relative humidity) or an aqueous solution of sodium chloride (75 and 80% relative humidity) (13) in desiccators along with the product to be aged. The desiccators were placed in ovens[1] at the appropriate temperatures. Temperature variations were within 1.0° over the time of the experiments.

Procedure—All products were analyzed for hydrazine at the start of each study and at appropriate times thereafter. Assays were done in duplicate, usually on composites of five tablets, or composites of three ampules of an injectable or elixir or, for phenelzine, on single tablets. Hydrazine content (as the benzaldehyde derivative) in hydralazine (8), isoniazid–pyridoxine tablets, and isoniazid elixir (8) was determined by GLC using a 2% OV-101 column and a nitrogen–phosphorus detector. In phenelzine products and for some isoniazid analyses, hydrazine content (as the benzaldehyde derivative) was determined by HPLC (9) on a 5-μm silica gel column with a mobile phase of 6% chloroform in *n*-hexane and detection at 313 mm. In isoniazid single-component tablets after 2.5 and 6.8 months, hydrazine, as the acetone derivative, was determined by GLC on a 3% OV-225 column with a flame-ionization detector (7). The initial assessment of hydrazine in isoniazid tablets was made by TLC with

[1] Thelco Model 6 M and Freas Model 815, Precision Scientific.

0022-3549/83/0800-0965$01.00/0

determination of nitroglycerin in various dosage forms. The degradation products of nitroglycerin can be determined by a simple change of the mobile solvent system (methanol–water, 20:80) (Fig. 3). The assay is faster, more specific, and provides more stability-indicating information than the USP method.

REFERENCES

(1) "The United States Pharmacopeia," 20th rev., U.S. Pharmacopeial Convention, Rockville, Md., 1980, p. 552.

(2) F. Pristera, M. Halik, M. Castelli, and W. Fredericks, *Anal. Chem.*, **32**, 495 (1960).

(3) J. Carol, *J. Assoc. Off. Agric. Chem.*, **43**, 259 (1960).

(4) B. J. Alley and H. W. Dykes, *J. Chromatogr.*, **71**, 23 (1972).

(5) B. Flann, *J. Pharm. Sci.*, **58**, 122 (1969).

(6) W. G. Crouthamel and B. J. Dorsch, *J. Pharm. Sci.*, **68**, 237 (1979).

(7) D. M. Baske, J. E. Carter, and A. H. Amann, *J. Pharm. Sci.*, **68**, 481 (1979).

(8) C. D. Chandler, G. R. Gibson, and W. T. Bolleter, *J. Chromatogr.*, **100**, 185 (1974).

(9) R. Dalton, C. D. Chandler, and W. T. Bolleter, *J. Chromatogr. Sci.*, **13**, 40 (1973).

(10) R. G. D. Steel and J. H. Torrie, "Principles and Procedures of Statistics," McGraw-Hill, New York, N.Y., 1960, p. 188.

ACKNOWLEDGMENTS

The authors gratefully acknowledge the technical and editorial assistance of Dr. Jack Stocker, Science Advisor, New Orleans District.

Hydrazine Levels in Formulations of Hydralazine, Isoniazid, and Phenelzine Over a 2-Year Period

E. G. LOVERING, F. MATSUI ˣ, N. M. CURRAN, D. L. ROBERTSON, and R. W. SEARS

Received March 29, 1982, from the *Bureau of Drug Research, Health Protection Branch, Health and Welfare Canada, Tunney's Pasture, Ottawa, Ontario K1A 0L2.* Accepted for publication August 10, 1982.

Abstract □ Hydrazine levels in formulations of hydralazine, isoniazid, and phenelzine have been measured over a 2-year period under ambient conditions and under temperature and humidity stress. Hydralazine tablets are stable under ambient conditions, but the hydrazine level in an injectable formulation increased from 4.5 to 10 μg/ml over a 23-month period. Isoniazid tablets are also stable, but hydrazine levels in an elixir and a pyridoxine combination product doubled to 44 μg/ml and 19 μg/tablet, respectively. Levels in phenelzine tablets appeared to remain constant at ~60 μg/tablet, with considerable tablet-to-tablet variation.

Keyphrases □ Hydrazine—levels in formulations of hydralazine, isoniazid, and phenelzine over a 2-year period □ Hydralazine—hydrazine levels in formulations over a 2-year period □ Isoniazid—hydrazine levels in formulations over a 2-year period □ Phenelzine—hydrazine levels in formulations over a 2-year period

Previous work demonstrated the presence of hydrazine in an isoniazid injectable product (1) and showed that isoniazid may hydrolyze to hydrazine (2, 3). Because hydrazine poses a risk of cancer in humans (4, 5), these observations prompted an assessment of other drugs derived from hydrazine that are available in Canada. These include carbidopa, hydralazine, isocarboxazid, and phenelzine, in addition to isoniazid. Hydrazine levels in isoniazid single-component tablet formulations were determined by TLC (2) and high-performance liquid chromatography (HPLC) (6) and by modifying a GLC procedure originally developed for the determination of phenelzine in urine (7). Methods for the determination of hydrazine in formulations of hydralazine (8), isoniazid elixir, isoniazid–pyridoxine combination tablets (8), and phenelzine (9) have also been developed. A 2-year normal and accelerated aging study of hydrazine formation in formulated products of hydralazine, isoniazid, and phenelzine has been completed and the results are reported in this paper.

Hydrazine is used in some syntheses of hydralazine (10), isoniazid (11), and phenelzine (12), and its presence in a formulated drug product may result from improper purification of the drug. All three drugs are known to degrade to hydrazine in solution (6, 9, 11), but there does not appear to be any published information on the formation of hydrazine in formulations of these drugs.

EXPERIMENTAL

Sample Preparation—Drug formulations were obtained directly from the manufacturer. All tablet samples were transferred to amber bottles for storage with at least five tablets in each bottle, and 1.0-ml aliquots of the elixir were transferred to culture tubes and securely capped. Phenelzine tablets from lot D were sealed in glass tubes (22 × 220 mm) by drawing out the top of the tube in a flame. The 100% relative humidity condition was achieved by sealing a 12-ml centrifuge tube containing 4 ml of water in with the tablets; tablets were not in direct contact with the water.

Storage Conditions—All formulations were aged under the temperature and humidity conditions given in Tables I, II, and III. Except as noted above, the humidity was controlled by placing silica gel (0% relative humidity) or an aqueous solution of sodium chloride (75 and 80% relative humidity) (13) in desiccators along with the product to be aged. The desiccators were placed in ovens[1] at the appropriate temperatures. Temperature variations were within 1.0° over the time of the experiments.

Procedure—All products were analyzed for hydrazine at the start of each study and at appropriate times thereafter. Assays were done in duplicate, usually on composites of five tablets, or composites of three ampules of an injectable or elixir or, for phenelzine, on single tablets. Hydrazine content (as the benzaldehyde derivative) in hydralazine (8), isoniazid–pyridoxine tablets, and isoniazid elixir (8) was determined by GLC using a 2% OV-101 column and a nitrogen–phosphorus detector. In phenelzine products and for some isoniazid analyses, hydrazine content (as the benzaldehyde derivative) was determined by HPLC (9) on a 5-μm silica gel column with a mobile phase of 6% chloroform in *n*-hexane and detection at 313 mm. In isoniazid single-component tablets after 2.5 and 6.8 months, hydrazine, as the acetone derivative, was determined by GLC on a 3% OV-225 column with a flame-ionization detector (7). The initial assessment of hydrazine in isoniazid tablets was made by TLC with

[1] Thelco Model 6 M and Freas Model 815, Precision Scientific.

0022-3549/83/0800-0965$01.00/0

Table I—Hydrazine Levels in Hydralazine Products

Product	Time, months	Hydrazine Level, μg/tablet[a] RT, AH[b]	RT, 80%	37°, AH	37°, 80%
Tablets (10 mg)	0	Tr.[c]	Tr.	Tr.	Tr.
	7.5	0.03	0.22	0.03	0.06
	16	0.05	0.12	0.05	n.d.
	23	0.06	0.05	0.24	n.d.
Tablets (50 mg)	0	Tr.	Tr.	Tr.	Tr.
	7.5	n.d.	0.15	n.d.	0.8
	16	n.d.	n.d.	n.d.	1.3
	23	0.1	0.17	0.1	3.8
Injection (20 mg/ml;	0	4.5 μg/ml[d]	—	4.5 μg/ml[d]	—
hydrazine levels in	7.5	8	—	22	—
μg/ml)	16	12	—	76	—
	23	10	—	42[e]	—
Tablets (50 mg with	0	Tr.	Tr.	Tr.	Tr.
0.2-mg reserpine)	7.5	0.2	n.d.	n.d.	2.2
	16	n.d.	0.8	n.d.	3.2
	23	0.1	0.6	0.1	0.2
Tablets (25 mg with	0	Tr.	Tr.	Tr.	Tr.
0.1-mg reserpine and	7.5	n.d.	n.d.	n.d.	0.35
15-mg hydrochloro-	16	n.d.	n.d.	n.d.	0.35
thiazide)	23	0.05	0.05	0.07	0.15

[a] Minimum quantifiable amounts at 0, 7.5, 16, and 23 months were 0.001, 0.0005, 0.00025, and 0.000125%, respectively. Measurements were made with a Perkin-Elmer Model 3920 and Hewlett-Packard Models 5880 and 5840 gas chromatographs at 0, 7.5 and 16, and 23 months respectively. The amounts of drug injected on column were 10.0, 1.0, 2.0, and 4.0 μg, respectively. [b] RT = room temperature; AH = ambient humidity. [c] Tr. = trace, borders on the minimum detectable level (7×10^{-5} %). [d] This product is an aqueous solution. [e] Mean hydrazine level in five vials was 42 μg/ml, *RSD* 7.3%, range 42–57 μg/ml.

silica gel plates, run first in a solvent of methanol–chloroform (1:1) and then in acetone–methanol–glacial acetic acid (50:50:10) (2).

RESULTS AND DISCUSSION

Hydralazine—A preliminary examination of hydralazine products revealed traces of hydrazine in some tablet products and ~5 μg/ml in an injectable formulation. These results prompted a stability assessment of this drug. The products assessed, the test conditions, and the hydrazine levels at intervals over a 23-month period are presented in Table I. Over this period the sensitivity of the test method increased due to changes in the equipment available for the work and slight modifications made in the sampling procedure. Minimum quantifiable amounts are also given in Table I. Many of the results are close to the minimum quantifiable level of the method. This, coupled with the instability of hydrazine, probably accounts for the lack of a clear trend in hydrazine levels with time in some products.

The results show that there is no significant change in the hydrazine level in tablets stored under normal room conditions or at 37° and ambient humidity. At 80% relative humidity hydrazine levels increased in some products, more noticeably at 37°; but even at 37° not all tablet products were affected. At 37° and 80% relative humidity, the maximum level observed was ~3.8 μg in a 50-mg tablet after ~2 years. In the injectable product at room temperature and 37°, the hydrazine level increased from 4.5 to 12 and 76 μg/ml, respectively, in 16 months and then decreased, possibly due to decomposition of hydrazine rather than vial-to-vial variation in the hydrazine content. More rapid degradation to hydrazine in a liquid product would be expected. There is no indication that the presence of reserpine and/or hydrochlorothiazide had any effect on the formation of hydrazine from hydralazine.

Isoniazid—The isoniazid stability study was done in two parts. In the first, samples from two lots of tablets were stressed for 8 months under the conditions given in Table II. This work was undertaken before the analytical methodology was firmly established. The hydrazine assays were by TLC (initial), GLC (2.5 and 6.8 months), and HPLC (8.2 months). The GLC procedure (7) was modified to provide for the reaction of hydrazine with acetone to form an acetonide which was partitioned between water and ether and chromatographed at 45° on 3% OV-225 on Chromosorb WHP (100/120 mesh). The results (Table II) indicate only low levels of hydrazine contamination in products kept at room temperature and 0% relative humidity. Hydrazine formation is promoted at higher humidity, as would be anticipated, but the effect is not pronounced except in one product at 60° and 75% relative humidity.

In the second part of the work, an isoniazid–pyridoxine combination product and an isoniazid elixir were evaluated (Table II). The hydrazine level in tablets at ambient humidity (room temperature and 37°) rose to a constant value of ~20 μg/tablet. At 80% relative humidity, hydrazine levels were much higher, but again there was some indication of the attainment of a steady-state hydrazine level. In the elixir at room temperature, the hydrazine level increased to a steady level of ~40 μg/ml, but at 37° it declined to a steady level of 2–4 μg/ml. A temperature-dependent steady-state level of hydrazine would result when the rate of formation of hydrazine and its rate of decomposition are in balance.

Phenelzine—The stability study of phenelzine tablets began when samples from lot C were tested under the temperature and humidity conditions given in Table III. After 4 months it was observed that the cores of individual tablets varied in color from white to beige. Single tablets were analyzed for hydrazine, and it was found that hydrazine levels increased roughly with the color of the tablet, with a range of 34–82 μg/tablet. The data obtained from the sample stored at 37° and 80% relative humidity indicated a loss of hydrazine due to volatilization and/or chemical breakdown. In view of these uncertainties, a second lot (D) of tablets were obtained, repackaged in sealed containers, and tested to find out what became of the hydrazine (Table III).

The first observation that can be made from the data is that hydrazine levels decreased during storage at 80 and 100% relative humidity. The levels decreased sharply at 100% relative humidity and the tablets showed extensive deterioration. Hydrazine levels also decreased at 80% relative humidity and 37°. The data obtained from the samples stored in sealed containers show that these decreases can be attributed to chemical degradation rather than evaporation of the hydrazine. At ambient humidity, both at room temperature and 37°, there may have been some increase in the hydrazine content to a steady level, but once this state was reached (after a few months) there did not appear to be any further increase.

Table II—Hydrazine Levels in Isoniazid Products

Product	Time, months	Hydrazine Level, μg/tablet RT, 0%	RT, 75%	45°, 0%	45°, 75%	60°, 0%	60°, 75%
Tablets (100 mg)	0[a]	Tr.	Tr.	Tr.	Tr.	Tr.	Tr.
(Lot A)	2.5	<2	2	—[c]	5	1	—
	6.8	2	3	1	6	2	47
	8.2	1[b]	3.6[b]	1.5[b]	7[b]	3[b]	70[b]
Tablets (100 mg)	0[a]	n.d.[d]	n.d.	n.d.	n.d.	n.d.	n.d.
(Lot B)	2.5	—	—	—	—	—	—
	8.2	2.4[b]	2.5[b]	3.4[b]	6[b]	4.4[b]	6[b]
		RT, AH	RT, 80%	37°, AH	37°, 80%		
Tablets (300 mg	0	8	8	8	8		
with 15 mg	7.5	12	58	15	201		
pyridoxine HCl)	16	n.d.	96	21	257		
	23	19	112	22	189		
Elixir (10 mg/ml)	0	19.5 μg/ml	—	19.5 μg/ml	—		
	7.5	36	—	4	—		
	16	43	—	5	—		
	23	44	—	2	—		

[a] *Determinations at time zero were by* TLC. The minimum quantifiable level was 0.006%. Trace is ~0.003%. [b] Determination by HPLC. The minimum quantifiable amount was 0.0002%. [c] Not determined. [d] None detected.

Table III—Hydrazine Levels in Phenelzine Products

Product	Time, months	Hydrazine Level, μg/tablet[a] RT, AH Mean (CV)[a]	RT, AH Range (n)[b]	RT, 80% Mean (CV)	RT, 80% Range (n)	37°, AH Mean (CV)	37°, AH Range (n)	37°, 80% Mean (CV)	37°, 80% Range (n)
Tablets (15 mg) (Lot C)	0	47[c]	—[d]	47[c]	—	47[c]	—	47[c]	—
	4	51(44)	34–82 (4)	37[c]	—	—	—	23[c]	—
	13	79(36)	43–110(5)	40(37)	27–59(5)	—	—	5.5(40)	1.8–9.1(12)
	19	72(57)	43–135(5)	—	—	—	—	—	—
	24	63(49)	23–128(20	—	—	—	—	—	—
Tablets (15 mg) (Lot D)	0	40(28)	28–64 (30)	40(28)	28–64(30)	40(28)	28–64 (30)	40(28)	28–64(30)
	4	63(46)	34–115(14)	2.7(45)[e]	1.5–4.8(5)[e]	58(35)	38–82 (5)	n.d.[e,f]	n.d.[e,f]
	11	47(29)	33–68 (10)	1.3[e,g]	—	61(40)	35–101(10)	—	—
	16	56(37)	30–86 (20)	—	—	68(45)	38–122(10)	—	—

[a] Coefficient of variation. [b] Number of tablets assayed. [c] Composite of 10 tablets. [d] — Not determined. [e] 100% relative humidity. [f] n.d. = none detected. [g] Composite of 15 tablets.

Table IV—Distribution of Hydrazine[a] in Phenelzine Tablets

Time of Assay, Months[b]	Number of Tablets Assayed	Percentage of Tablets in each Range of Hydrazine Level <30 μg	30–45 μg	45–60 μg	60–75 μg	75–90 μg	90–105 μg	>105 μg
	Lot C							
5	4	—	50	25	—	25	—	—
13	5	—	20	—	40	—	20	20
19	5	—	60	—	—	—	20	20
24	20	5	40	20	5	5	10	15
	Lot D							
0	30	3	74	10	13	—	—	—
4	14	—	43	14	7	7	22	7
11	10	—	50	30	20	—	—	—
16	20	—	45	10	15	30	—	—

[a] Tablets stored at ambient temperature and humidity. [b] Time elapsed since tablets were assayed at the start of the study.

The intertablet variation in hydrazine level is presented in Table IV. The variation appeared to be present in the tablets as they were obtained from the manufacturer, and the data do not support the view that there were significant changes in hydrazine levels as the study progressed. The tablet-to-tablet variation suggests that hydrazine is formed during manufacture under local reaction conditions, but specific conditions are unknown.

The work described herein was done to identify major stability problems with respect to increases in the hydrazine levels with time in the drugs examined. Other facets of the stability of these products, such as degradation of the drug itself, were not included in this work. Except for samples stored at ambient temperature and humidity, samples were repacked so that they would be fully exposed to the conditions of the experiment. This was done because the objective of the work was to examine the behavior of the formulated products, not the ability of the packaging to protect the product from the environment.

The results show that hydrazine itself decomposes in some formulations, *e.g.*, the isoniazid elixir at 37° (Table II) and phenelzine tablets at 37° and 80% relative humidity (Table III). Some data, like that for isoniazid–pyridoxine tablets indicate the hydrazine concentration increases to a fixed level and remains constant. This and the results at two temperatures for the isoniazid elixir suggest that hydrazine levels in some products are steady-state levels. The actual value of the steady-state level would depend on the nature of the formulation excipients, the rates of hydrazine formation and decomposition, and the relative effect of temperature on these rates.

Hydrazine is a metabolite of isoniazid (14–16) and hydralazine (17) in humans. It may also be a metabolite of phenelzine[2]. Any assessment of hydrazine contamination in formulated products should include an evaluation of the metabolic data.

[2] Personal communication, S. Sved and I. J. McGilveray.

REFERENCES

(1) "Protection," Health and Welfare Canada, Ottawa, **1**, 4 (1977).

(2) F. Matsui, K. M. McErlane, E. G. Lovering, and D. L. Robertson, *Can. J. Pharm. Sci.*, **13**, 71 (1978).

(3) E. Pawelczyk, T. Hermann, and R. Sukowski, *Diss. Pharm. Pharmacol.*, **21**, 481 (1969).

(4) Fed. Regist., **44**, 33694, June 12, 1979.

(5) *IARC Monographs* (Lyons, France), **4**, 127 (1974).

(6) A. G. Butterfield, N. M. Curran, E. G. Lovering, F. Matsui, D. L. Robertson, and R. W. Sears, *Can. J. Pharm. Sci.*, **16**, 15 (1981).

(7) B. Caddy, W. J. Tilstone, and E. C. Johnstone, *Br. J. Clin. Pharmacol.*, **3**, 633 (1976).

(8) F. Matsui, D. L. Robertson and E. G. Lovering, *J. Pharm. Sci.*, **72**, 948 (1983).

(9) F. Matsui, A. G. Butterfield, N. M. Curran, E. G. Lovering, R. W. Sears, and D. L. Robertson, *Can. J. Pharm. Sci.*, **16**, 20 (1981).

(10) J. Druey and B. H. Ringier, *Helv. Chem. Acta*, **34**, 195 (1951); Chem. Abs., **45**, 10248c.

(11) G. A. Brewer, in "Analytical Profiles of Drug Substances," Vol. 6, K. Florey, Ed., Academic, New York, N.Y. 1977.

(12) R. E. Daly, in "Analytical Profiles of Drug Substances," Vol. 2, K. Florey, Ed., Academic, New York, N.Y. 1973.

(13) "Annual Book of ASTM Standards," Part 35, American Society for Testing and Materials, Philadelphia, Pa. (1975).

(14) S. Iguchi, T. Goromaru, A. Noda, K. Matsuyama, and K. Sogabe, *Chem. Pharm. Bull.*, **25**, 2796 (1977).

(15) A. Noda, T. Goromaru, K. Matsuyama, K. Sogabe, K. Y. Hsu, and S. Iguchi, *J. Pharm. Dyn.*, **1**, 132 (1978).

(16) J. A. Timbrell, J. M. Wright, and C. M. Smith, *J. Chromatogr.*, **138**, 165 (1977).

(17) J. A. Timbrell and S. J. Harland, *Clin. Pharmacol. Ther.*, **26**, 81 (1979).

Comparative Controlled Skin Permeation of Nitroglycerin from Marketed Transdermal Delivery Systems

Keyphrases □ Transdermal delivery—nitroglycerin, hairless mouse skin, comparison of three marketed systems □ Nitroglycerin—permeation of, comparison of marketed transdermal delivery systems □ Skin, hairless mouse—permeation of nitroglycerin, transdermal delivery systems

To the Editor:

The antianginal activity of nitroglycerin was discovered over 100 years ago by Murrel (1). Since then, nitroglycerin use has increased and it is now widely prescribed for the prevention and treatment of angina pectoris. Several types of pharmaceutical dosage forms, mainly the oral sustained-release capsules and tablets, sublingual tablets, topical ointments, and intravenous fluids, are available commercially. Unfortunately, oral administration of nitroglycerin leads to extensive hepatic first-pass metabolism to give several inactive metabolites (2). When administered sublingually, first-pass metabolism is eliminated, however the antianginal activity is of such short duration (10–30 min.), due to the inherently rapid elimination (half-life = 1.9–4.4 min.) of nitroglycerin (3), that repeated dosing every 5 min is recommended until the symptoms are relieved. On the other hand, the duration of antianginal activity of nitroglycerin can be substantially prolonged to 3–4 hr by topical administration of ointment formulations; however, the area covered and thickness of the ointment is variable and it is messy and inconvenient.

Recently, three one-a-day-type transdermal nitroglycerin delivery systems[1] (Products A, B, and C) were developed for transdermal-controlled administration of nitroglycerin over a 24-hr period. They were recently approved for marketing by the U.S. Food and Drug Administration for treatment of angina pectoris (4). Several articles have been published to compare these new delivery systems with the sublingual tablets and/or the topical ointment formulations (3, 5–7). However, the only data available to date are the results of studies conducted independently and under different conditions and protocols by the manufacturers, and controversy has surfaced concerning the interchangeability of these three nitroglycerin-releasing transdermal delivery systems (8, 9).

Since no results are available from studies that are designed to evaluate the performance of these transdermal delivery systems under identical conditions, the purpose of this investigation was to establish an *in vitro* skin permeation system to study and compare the controlled skin-permeation kinetics of nitroglycerin delivered by these controlled-release transdermal delivery systems. In our studies, pieces (3.5 × 3.5 cm each) of full-thickness abdominal skin were freshly excised from 5–7-week-old hairless mice[2] (10) and mounted individually on the 8-cell Franz diffusion assembly[3] (Fig. 1). After soaking the dermal side of the skin in the elution solution overnight (as the time-zero sample), the transdermal delivery system was applied to the stratum corneum side of the skin, and the skin permeation profile of nitroglycerin was followed by sampling and assaying the nitroglycerin concentration in the elution solution. A sensitive reverse-phase high-performance liquid chromatographic (HPLC) method was used with samples taken at 1, 2, 4, 8, 12, 16, 20, 24, and 30 hr postapplication. The elution solution was prepared from normal saline solution containing 20% polyethylene glycol 400 to enhance aqueous solubility of nitroglycerin for simulating the biological sink (11, 12). At least four experiments on each type of transdermal delivery system were performed in each run of the drug release and skin permeation studies.

The results of the skin permeation studies indicated that nitroglycerin penetrates through the abdominal skin of the hairless mouse at a rate profile which can be described fairly well by zero-order kinetics (Fig. 2). It appears that the rate of skin permeation for nitroglycerin delivered by system A (18.15 $\mu g/cm^2/hr$) is significantly greater than system C (14.55 $\mu g/cm^2/hr$). Interestingly, the rate of skin permeation of nitroglycerin from system B is between systems A and C rates, but it shows a shift at 12 hr from 16.67 $\mu g/cm^2/hr$ to 10.56 $\mu g/cm^2/hr$. However, a constant skin permeation is maintained in both phases. The rates determined in this investigation are quite in agreement with the data (10–25 $\mu g/cm^2/hr$) generated from human cadaver skins (13).

The release kinetics of nitroglycerin from the transdermal delivery systems were also evaluated under the same conditions without the hairless mouse skin. Results indicated that nitroglycerin is released at a constant rate profile from system C but not from systems A nor B (Fig. 3). System C is a membrane permeation-controlled drug delivery system in which a rate-determining microporous

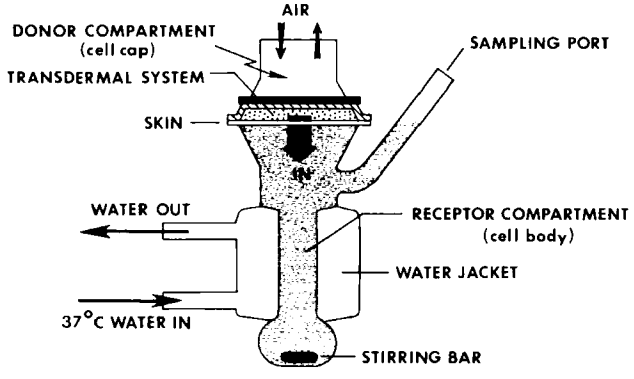

Figure 1—*Schematic illustration of the* in vitro *skin permeation system with skin sample and transdermal system sandwiched in between the donor and receptor compartments of the Franz diffusion cell assembly. The stratum corneum of the skin sample faces the donor compartment and is in close contact with the transdermal system. The dermal tissue faces the receptor compartment and is soaked in an elution solution at 37°.*

[1] System A, Nitrodisc, G. D. Searle & Co.; System B, Nitro Dur, Key Pharmaceuticals; System C, Transderm-Nitro, Ciba Pharmaceuticals.

[2] Male, HRS/J strain, Jackson Laboratories, Bar Harbor, Maine.

[3] Crown Glass Co., Somerville, N.J.

0022-3549/83/0800-0968$01.00/0

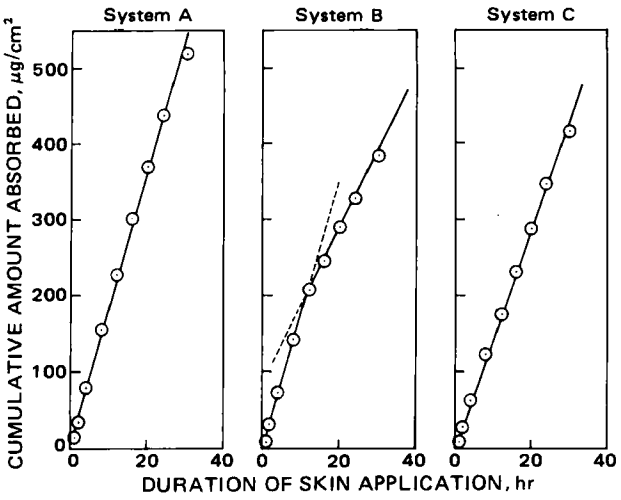

Figure 2—*Permeation profiles of nitroglycerin through the abdominal skin of the hairless mouse, following its controlled release from each of the three commercial transdermal delivery systems (each data point is the mean of at least eight determinations). The rate of skin permeation for nitroglycerin is calculated to be 18.15 μg/cm²/hr (system A), 16.67 (<12 hr) and 10.56 (>12 hr) μg/cm²/hr (system B), and 14.55 μg/cm²/hr (system C).*

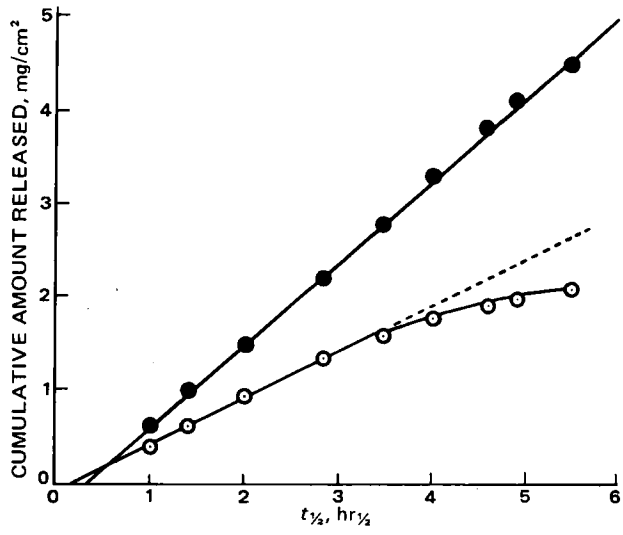

Figure 4—*Linear* Q versus $t^{1/2}$ *relationship for the controlled release of nitroglycerin from system B (●) and system A (○). (The* $Q \sim t^{1/2}$ *linearity is followed in system A for up to 12 hr in which 78% of the loading nitroglycerin dose is released, as compared with 30 hr duration and 89% release in system B). Each data point is the mean value of four determinations.*

ethylene–vinyl acetate membrane controls the release of nitroglycerin from a suspension-type drug reservoir (5, 6), and, as expected (11), a constant drug-release profile results. It is interesting to note that nitroglycerin is released from system C at a rate (35.8 μg/cm²/hr) which is more than two times greater than the rate of skin permeation (14.55 μg/cm²/hr). These results suggest that the skin tissues provide an additional diffusional barrier for the permeation of nitroglycerin.

On the other hand, the release profiles of nitroglycerin from systems A and B can be better defined by a *Q versus* $t^{1/2}$ relationship (Fig. 4), indicating that nitroglycerin is released under a matrix diffusion-controlled process from both systems A and B (11, 12, 14–16). System A is, in its original development (17–19), a partition-controlled drug delivery system with the drug reservoir microsealed as microscopic liquid compartments homogeneously dispersed in a cross-linked polymer matrix, and a constant drug release profile is expected (20). The incorporation of a hydrophobic solvent, like isopropyl palmitate (21), which is a good solvent for nitroglycerin, into the polymer matrix during fabrication, could affect the interfacial partitioning kinetics of nitroglycerin from the microscopic *liquid* compartment, leading to the shift in drug-release kinetics from the partition-controlled process to the matrix-controlled process (11, 22).

Similarly, system B is a matrix diffusion-controlled drug delivery system in which nitroglycerin–lactose triturate is homogeneously dispersed in a hydrophilic gel matrix (23); and, as expected (11), the release profile of nitroglycerin from system B follows the *Q versus* $t^{1/2}$ linearity. Again, the drug release fluxes from both systems A and B are maintained at magnitudes that are much greater than

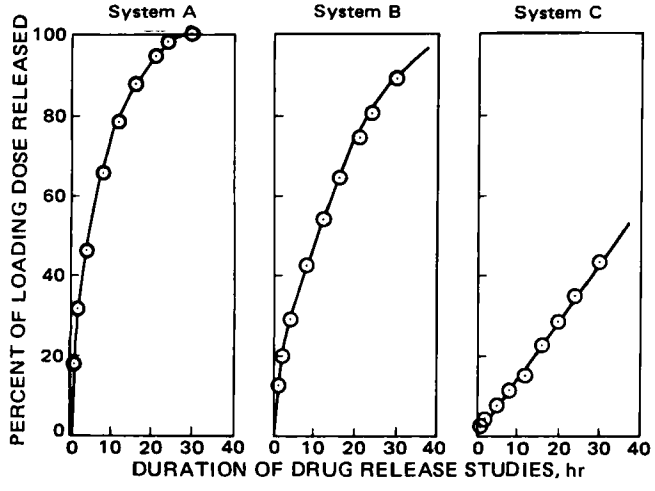

Figure 3—*Release profiles of nitroglycerin from the transdermal delivery systems into normal saline solution at 37° as drug elution solution (containing 20% polyethylene glycol 400 w/w to maintain a sink condition). Each data point is a mean value of four determinations.*

Table I—Comparison in Drug Release Kinetics and Skin Permeation Profiles of Nitroglycerin from Commercial Transdermal Delivery Systems

	System A	System B	System C
System Characteristics			
Surface area, cm²	8	10	10
Loading dose, mg	16	51	25
Release Kinetics			
Flux or rate of release	500 μg/cm²/hr 1/2	875 μg/cm²/hr 1/2	35.8 μg/cm²/hr
Dose released (24 hr)[a]			
Percent	98.1 (±0.1)	80.3 (±0.2)	34.4 (±1.4)
Milligrams	15.7 (±0.02)	40.9 (±0.1)	8.6 (±0.35)
Skin Permeation Profiles			
Rate of permeation, μg/cm²/hr	18.15	16.67 (<12 hr) 10.56 (>12 hr)	14.55
Dose absorbed (24 hr)			
Percent	21.93 (±3.86)[b]	6.41 (±1.19)[b]	13.88 (±2.65)[c]
Milligrams	3.51 (±0.62)[b]	3.27 (±0.60)[b]	3.47 (±0.66)[c]

[a] Mean (± standard deviation) of four determinations. [b] Mean (± standard deviation) of eight determinations. [c] Mean (± standard deviation) of 12 determinations.

the rate of skin permeation (Table I), so a constant skin-permeation profile can be achieved. By calculation, systems A and B release nitroglycerin at a flux ($Q/t^{1/2}$) of 500 and 875 $\mu g/cm^2/hr^{1/2}$, respectively (Fig. 4). The difference in release fluxes between these two systems is expected from the difference in drug-loading doses in the devices (11).

In summary, the results generated from the present investigation suggest that even though nitroglycerin is released at different rate profiles from these three transdermal delivery systems (Figs. 3 and 4), it penetrates through the hairless mouse skin under, basically, the same rate process (Fig. 2). Additionally, the total nitroglycerin dose delivered through the abdominal skin at 24 hr by each of these transdermal delivery systems is fairly close in magnitude and the difference is statistically insignificant [$F = 0.33$, $F_{0.95}(2,25) = 3.39$] (Table I), although the loading dose varies greatly from one system to another, and the percentage of the loading doses released during a 24-hr elution study is substantially different.

Additional studies are currently underway to generate evidence on the feasibility of using hairless mouse skin as the viable substitute for human skin in studying the transdermal controlled administration of systemically active drugs from novel drug delivery systems. A more detailed report will be written when more data become available.

(1) M. M. Tjoeng, *Pharmacy International*, **2**, 88 (1981).

(2) J. R. Boyd, "Drug: Facts and Comparisons," 1982 ed., Lippincott, St. Louis, Mo., 1982, p. 419.

(3) J. F. Dasta and D. R. Geraets, *Am. Pharmacy*, **NS22**(2), 28 (1982).

(4) *Med. Lett.*, **24**, 35 (1982).

(5) Y. W. Chien, "Logics of Transdermal Controlled Drug Administration, 1982 Industrial Pharmaceutical Research and Development Symposium, Rutgers University, College of Pharmacy, Piscataway, N.J., January 1982.

(6) W. R. Good, "Transderm-Nitro: Controlled Delivery of Nitroglycerin *via* The Transdermal Route," 1982 Industrial Pharmaceutical Research and Development Symposium, Rutgers University, College of Pharmacy, Piscataway, N.J., January 1982.

(7) A. Karim, "Transdermal Absorption: A Unique Opportunity for Constant Delivery of Nitroglycerin," 1982 Industrial Pharmaceutical Research and Development Symposium, Rutgers University, College of Pharmacy, Piscataway, N.J., January 1982.

(8) J. E. Shaw and H. Benson, *Am. Pharmacy*, **NS22**(5), 2 (1982).

(9) A. Karim, *Am. Pharmacy*, **NS22**(8), 4 (1982).

(10) H. Durrheim, G. L. Flynn, W. I. Higuchi, and C. R. Behl, *J. Pharm. Sci.*, **69**, 781 (1980).

(11) Y. W. Chien, "Novel Drug Delivery Systems: Fundamentals, Developmental Concepts, Biomedical Assessments," Dekker, New York, N.Y. 1982, Chap. 9.

(12) Y. W. Chien, H. J. Lambert, and D. E. Grant, *J. Pharm. Sci.*, **63**, 365 (1974).

(13) A. S. Michaels, S. K. Chandrasekaran, and J. E. Shaw, *AIChE J.*, **21**, 985 (1975).

(14) Y. W. Chien, S. E. Mares, J. Berg, S. Huber, H. J. Lambert, and K. F. King, *J. Pharm. Sci.*, **64**, 1776 (1975).

(15) Y. W. Chien and E. P. K. Lau, *J. Pharm. Sci.*, **65**, 488 (1976).

(16) Y. W. Chien, H. J. Lambert, and L. F. Rozek, *ACS Symp. Ser.*, **33**, 72 (1976).

(17) Y. W. Chien and H. J. Lambert, U.S. pat. no. 3,946,106 (March 23, 1976).

(18) Y. W. Chien and H. J. Lambert, U.S. pat. no. 3,992,518 (November 16, 1976).

(19) Y. W. Chien and H. J. Lambert, U.S. pat. no. 4,053,580 (October 11, 1977).

(20) Y. W. Chien, L. F. Rozek, and H. J. Lambert, *J. Pharm. Sci.*, **67**, 214 (1978).

(21) D. R. Sanvordeker, J. G. Cooney, and R. C. Wester, U.S. pat. no. 4,336,243 (June 22, 1982).

(22) Y. W. Chien, H. J. Lambert, and T. K. Lin, *J. Pharm. Sci.*, **64**, 1643 (1975).

(23) A. D. Keith and W. Snipes, Eur. pat. no. 0,013,606 (July 23, 1980).

Yie W. Chien[x]
Prakash R. Keshary
Yih C. Huang
Pramod P. Sarpotdar
College of Pharmacy
Rutgers University
Piscataway, NJ 08854

Received October 4, 1982.
Accepted for publication January 13, 1983.

The authors extend their appreciation to Dr. F. W. Goodhart and Ms. S. Belsale for securing the nitroglycerin materials for this investigation, and to Ms. M. Kiger for manuscript preparation.

Organ Perfusion Studies

Keyphrases □ Organ perfusion—pharmacokinetics, importance of volume replenishment □ Pharmacokinetics—organ perfusion studies, importance of volume replenishment

To the Editor:

Single-pass and recirculating perfused organ systems have been used to study how specific organs of the body handle drugs. The single-pass system has been used extensively to study the influx and efflux of drugs by various organs, whereas recirculating systems have been used more commonly to study metabolism and/or excretion of drugs by these organs. Although both systems are useful, the conservation of drug and perfusion media associated with the recirculating system makes it more economical and allows for longer perfusion experiments even with limited volumes of perfusion medium. However, in recirculating perfusion systems, there are problems associated with volume depletion due to excretion in open systems (*i.e.*, liver and kidney) and sample withdrawal in both closed (*i.e.*, heart, muscle, and lung) and open systems, which must be considered when performing pharmacokinetic analyses of the data derived from these experiments. The following discussion will address these problems.

It has been shown that the rate of elimination of a drug from an isolated organ perfusion system is a function of the perfusate volume (1) according to the following equation:

$$\frac{dC_i}{dt} = \frac{Q}{V_R}(C_i - C_o) \qquad \text{(Eq. 1)}$$

where C_i and C_o are the inflow and outflow concentrations, Q is the perfusate flow, and V_R is the reservoir volume. The elimination rate constant (K) varies inversely with perfusate volume changes since $K = Q/V_R$. Several authors have published on this observation (1–5), and some have attempted to correct the elimination rate for perfusate volume changes (2–5). Other authors have discussed perfusate volume and nutrient replenishment as a means of maintaining the viability of open perfused organ systems, such as the kidney or liver, where there is loss of water and energy sources due to urine and bile excretion (6–8). Two

0022-3549/83/0800-0970$01.00/0

the rate of skin permeation (Table I), so a constant skin-permeation profile can be achieved. By calculation, systems A and B release nitroglycerin at a flux ($Q/t^{1/2}$) of 500 and 875 $\mu g/cm^2/hr^{1/2}$, respectively (Fig. 4). The difference in release fluxes between these two systems is expected from the difference in drug-loading doses in the devices (11).

In summary, the results generated from the present investigation suggest that even though nitroglycerin is released at different rate profiles from these three transdermal delivery systems (Figs. 3 and 4), it penetrates through the hairless mouse skin under, basically, the same rate process (Fig. 2). Additionally, the total nitroglycerin dose delivered through the abdominal skin at 24 hr by each of these transdermal delivery systems is fairly close in magnitude and the difference is statistically insignificant [$F = 0.33$, $F_{0.95}(2,25) = 3.39$] (Table I), although the loading dose varies greatly from one system to another, and the percentage of the loading doses released during a 24-hr elution study is substantially different.

Additional studies are currently underway to generate evidence on the feasibility of using hairless mouse skin as the viable substitute for human skin in studying the transdermal controlled administration of systemically active drugs from novel drug delivery systems. A more detailed report will be written when more data become available.

(1) M. M. Tjoeng, *Pharmacy International*, **2**, 88 (1981).

(2) J. R. Boyd, "Drug: Facts and Comparisons," 1982 ed., Lippincott, St. Louis, Mo., 1982, p. 419.

(3) J. F. Dasta and D. R. Geraets, *Am. Pharmacy*, **NS22**(2), 28 (1982).

(4) *Med. Lett.*, **24**, 35 (1982).

(5) Y. W. Chien, "Logics of Transdermal Controlled Drug Administration, 1982 Industrial Pharmaceutical Research and Development Symposium, Rutgers University, College of Pharmacy, Piscataway, N.J., January 1982.

(6) W. R. Good, "Transderm-Nitro: Controlled Delivery of Nitroglycerin *via* The Transdermal Route," 1982 Industrial Pharmaceutical Research and Development Symposium, Rutgers University, College of Pharmacy, Piscataway, N.J., January 1982.

(7) A. Karim, "Transdermal Absorption: A Unique Opportunity for Constant Delivery of Nitroglycerin," 1982 Industrial Pharmaceutical Research and Development Symposium, Rutgers University, College of Pharmacy, Piscataway, N.J., January 1982.

(8) J. E. Shaw and H. Benson, *Am. Pharmacy*, **NS22**(5), 2 (1982).

(9) A. Karim, *Am. Pharmacy*, **NS22**(8), 4 (1982).

(10) H. Durrheim, G. L. Flynn, W. I. Higuchi, and C. R. Behl, *J. Pharm. Sci.*, **69**, 781 (1980).

(11) Y. W. Chien, "Novel Drug Delivery Systems: Fundamentals, Developmental Concepts, Biomedical Assessments," Dekker, New York, N.Y. 1982, Chap. 9.

(12) Y. W. Chien, H. J. Lambert, and D. E. Grant, *J. Pharm. Sci.*, **63**, 365 (1974).

(13) A. S. Michaels, S. K. Chandrasekaran, and J. E. Shaw, *AIChE J.*, **21**, 985 (1975).

(14) Y. W. Chien, S. E. Mares, J. Berg, S. Huber, H. J. Lambert, and K. F. King, *J. Pharm. Sci.*, **64**, 1776 (1975).

(15) Y. W. Chien and E. P. K. Lau, *J. Pharm. Sci.*, **65**, 488 (1976).

(16) Y. W. Chien, H. J. Lambert, and L. F. Rozek, *ACS Symp. Ser.*, **33**, 72 (1976).

(17) Y. W. Chien and H. J. Lambert, U.S. pat. no. 3,946,106 (March 23, 1976).

(18) Y. W. Chien and H. J. Lambert, U.S. pat. no. 3,992,518 (November 16, 1976).

(19) Y. W. Chien and H. J. Lambert, U.S. pat. no. 4,053,580 (October 11, 1977).

(20) Y. W. Chien, L. F. Rozek, and H. J. Lambert, *J. Pharm. Sci.*, **67**, 214 (1978).

(21) D. R. Sanvordeker, J. G. Cooney, and R. C. Wester, U.S. pat. no. 4,336,243 (June 22, 1982).

(22) Y. W. Chien, H. J. Lambert, and T. K. Lin, *J. Pharm. Sci.*, **64**, 1643 (1975).

(23) A. D. Keith and W. Snipes, Eur. pat. no. 0,013,606 (July 23, 1980).

Yie W. Chien[x]
Prakash R. Keshary
Yih C. Huang
Pramod P. Sarpotdar
College of Pharmacy
Rutgers University
Piscataway, NJ 08854

Received October 4, 1982.
Accepted for publication January 13, 1983.

The authors extend their appreciation to Dr. F. W. Goodhart and Ms. S. Belsale for securing the nitroglycerin materials for this investigation, and to Ms. M. Kiger for manuscript preparation.

Organ Perfusion Studies

Keyphrases □ Organ perfusion—pharmacokinetics, importance of volume replenishment □ Pharmacokinetics—organ perfusion studies, importance of volume replenishment

To the Editor:

Single-pass and recirculating perfused organ systems have been used to study how specific organs of the body handle drugs. The single-pass system has been used extensively to study the influx and efflux of drugs by various organs, whereas recirculating systems have been used more commonly to study metabolism and/or excretion of drugs by these organs. Although both systems are useful, the conservation of drug and perfusion media associated with the recirculating system makes it more economical and allows for longer perfusion experiments even with limited volumes of perfusion medium. However, in recirculating perfusion systems, there are problems associated with volume depletion due to excretion in open systems (*i.e.*, liver and kidney) and sample withdrawal in both closed (*i.e.*, heart, muscle, and lung) and open systems, which must be considered when performing pharmacokinetic analyses of the data derived from these experiments. The following discussion will address these problems.

It has been shown that the rate of elimination of a drug from an isolated organ perfusion system is a function of the perfusate volume (1) according to the following equation:

$$\frac{dC_i}{dt} = \frac{Q}{V_R}(C_i - C_o) \qquad \text{(Eq. 1)}$$

where C_i and C_o are the inflow and outflow concentrations, Q is the perfusate flow, and V_R is the reservoir volume. The elimination rate constant (K) varies inversely with perfusate volume changes since $K = Q/V_R$. Several authors have published on this observation (1–5), and some have attempted to correct the elimination rate for perfusate volume changes (2–5). Other authors have discussed perfusate volume and nutrient replenishment as a means of maintaining the viability of open perfused organ systems, such as the kidney or liver, where there is loss of water and energy sources due to urine and bile excretion (6–8). Two

0022-3549/83/0800-0970$01.00/0

situations can arise during sampling and/or replenishment in organ perfusion studies:

1. The elimination rate constant (K) increases when the perfusate volume is depleted by samples being taken and not replenished or by excretion of urine/bile in an open system, since $K = Q/V_R$.
2. The concentration of drug in the perfusate decreases by dilution as lost volume is replenished. As the concentration in the perfusate is diluted, the concentration in the organ decreases to reestablish an equilibrium.

Volume replenishment for the purpose of maintaining the viability of the organ is essential, whereas volume correction either by replenishment or mathematical manipulation is not necessary for pharmacokinetic purposes. This reflects the fact that the elimination rate of a drug in a perfused organ has little meaning unless the volumes and flow rates used mimic those observed *in vivo*. Even if these requirements are met, elimination rate is a function of reservoir volume and will thus change with changes in volume.

The pharmacokinetic parameter that should be determined in organ perfusion studies is clearance, since this parameter describes the intrinsic ability of the isolated organ to eliminate or metabolize the drug independent of extraneous variables such as binding to other tissues or clearance by other organs. Organ clearance, however, is independent of reservoir volume, as shown:

$$CL_o = Q\left(\frac{C_{in} - C_o}{C_{in}}\right) \qquad \text{(Eq. 2)}$$

Similarly in the case of the liver and kidney, the biliary and renal clearance of intact drug (CL_{id}) is also independent of perfusate volume:

$$CL_{id} = \frac{\Delta X}{C_{mid}} \qquad \text{(Eq. 3)}$$

where ΔX is the amount of intact drug excreted and C_{mid} is the perfusate concentration at the midpoint of the excretion interval. Both equations are clearly independent of perfusate volume changes.

Therefore, if the primary pharmacokinetic objective of an organ perfusion study is to determine the organ clearance, it becomes apparent that volume correction for the purpose of pharmacokinetic calculations is not warranted. On the other hand, volume replenishment for the purpose of maintaining hydration, nutrient supply, energy sources, and, therefore, organ viability is important and must be considered during the design of organ perfusion studies. In addition, it must be realized that replenishment may be more critical for open systems such as the kidney and liver (where losses occur not only during sample withdrawal but in the urine and bile) than for closed systems such as the heart, lung, muscle, *etc.*

(1) M. Rowland, L. Z. Benet, and G. G. Graham, *J. Pharmacokinet. Biopharm.*, **1**, 123 (1973).
(2) R. Nagashima, G. Levy, and E. J. Sarcione, *J. Pharm. Sci.*, **57**, 1881 (1968).
(3) R. Nagashima and G. Levy, *ibid.*, **57**, 1991 (1968).
(4) C. J. Timmer and H. P. Wijnand, *J. Pharmacokinet. Biopharm.*, **5**, 335 (1977).
(5) W. L. Hayton and T. Chen, *J. Pharm. Sci.*, **71**, 820 (1982).
(6) G. Reach, H. Nakane, Y. Nakane, C. Auzan, and P. Corvol, *Steroids*, **30**, 621 (1977).
(7) H. Nakane, Y. Nakane, G. Reach, P. Corvol, and J. Menard, *Am. J. Physiol.*, **234**, E472 (1978).
(8) I. Bekersky, A. C. Popick, and W. A. Colburn, *Drug Metab. Disp.* (Submitted).

Wayne A. Colburn[x]
Romulus K. Brazzell
Ihor Bekersky
Department of Pharmacokinetics and Biopharmaceutics
Hoffmann-La Roche Inc.
Nutley, NJ 07110

Received September 20, 1982.
Accepted for publication February 18, 1983.

Rebound Phenomenon Observed During the Compaction of Samples in the Fisher Subsieve Sizer for Measuring Specific Surface Area of Griseofulvin

Keyphrases □ Specific surface area—Fisher subsieve sizer, rebound phenomenon observed during compaction, griseofulvin □ Compaction, tablet—rebound phenomenon, Fisher subsieve sizer, specific surface area of griseofulvin

To the Editor:

The air-permeability technique for measuring the specific surface area of powders is a well-recognized technique. It has been used for more than 30 years by the cement industry. The American Society of Testing Materials (1) as well as various European societies have adopted it as a standard method for measuring the fineness of cement by means of the Blaine apparatus, using the measurement of the resistance offered to the air flow by a packed bed of powder at a defined porosity level.

Recently the air-permeability method has also been included in the USP XX for measuring the fineness of griseofulvin in terms of its specific surface area (SSA). The USP monograph on griseofulvin specifies SSA limits between 1.30–1.70 m^2/g. For making the measurements, however, a procedure based on measuring at a range of porosities and using a Fisher subsieve sizer (FSS) apparatus is described. In the normal use of FSS-apparatus, it is common to take a sample weight equal to the density value of the sample material. The USP XX, however, suggests the use of 1.25 times the weight of material density as sample weight. This recommendation is based on an assumption that the SSA-value should be determined at very low porosities (down to 0.25 range), which cannot be reached easily when using the FSS-chart scale and sample weight equal to the density of a material. The basis of this recommendation is an earlier study by Edmundson and Tootil (2) who advanced an hypothesis that very low porosities are desirable for achieving a uniform packing of the powder bed and for getting a maximum SSA value which may be considered a unique value for a given powder sample.

A series of SSA measurements were made on a number of griseofulvin samples using the FSS apparatus and taking

0022-3549/83/0800-0971$01.00/0

situations can arise during sampling and/or replenishment in organ perfusion studies:

1. The elimination rate constant (K) increases when the perfusate volume is depleted by samples being taken and not replenished or by excretion of urine/bile in an open system, since $K = Q/V_R$.
2. The concentration of drug in the perfusate decreases by dilution as lost volume is replenished. As the concentration in the perfusate is diluted, the concentration in the organ decreases to reestablish an equilibrium.

Volume replenishment for the purpose of maintaining the viability of the organ is essential, whereas volume correction either by replenishment or mathematical manipulation is not necessary for pharmacokinetic purposes. This reflects the fact that the elimination rate of a drug in a perfused organ has little meaning unless the volumes and flow rates used mimic those observed *in vivo*. Even if these requirements are met, elimination rate is a function of reservoir volume and will thus change with changes in volume.

The pharmacokinetic parameter that should be determined in organ perfusion studies is clearance, since this parameter describes the intrinsic ability of the isolated organ to eliminate or metabolize the drug independent of extraneous variables such as binding to other tissues or clearance by other organs. Organ clearance, however, is independent of reservoir volume, as shown:

$$CL_o = Q\left(\frac{C_{in} - C_o}{C_{in}}\right) \qquad \text{(Eq. 2)}$$

Similarly in the case of the liver and kidney, the biliary and renal clearance of intact drug (CL_{id}) is also independent of perfusate volume:

$$CL_{id} = \frac{\Delta X}{C_{mid}} \qquad \text{(Eq. 3)}$$

where ΔX is the amount of intact drug excreted and C_{mid} is the perfusate concentration at the midpoint of the excretion interval. Both equations are clearly independent of perfusate volume changes.

Therefore, if the primary pharmacokinetic objective of an organ perfusion study is to determine the organ clearance, it becomes apparent that volume correction for the purpose of pharmacokinetic calculations is not warranted. On the other hand, volume replenishment for the purpose of maintaining hydration, nutrient supply, energy sources, and, therefore, organ viability is important and must be considered during the design of organ perfusion studies. In addition, it must be realized that replenishment may be more critical for open systems such as the kidney and liver (where losses occur not only during sample withdrawal but in the urine and bile) than for closed systems such as the heart, lung, muscle, *etc.*

(1) M. Rowland, L. Z. Benet, and G. G. Graham, *J. Pharmacokinet. Biopharm.*, **1**, 123 (1973).
(2) R. Nagashima, G. Levy, and E. J. Sarcione, *J. Pharm. Sci.*, **57**, 1881 (1968).
(3) R. Nagashima and G. Levy, *ibid.*, **57**, 1991 (1968).
(4) C. J. Timmer and H. P. Wijnand, *J. Pharmacokinet. Biopharm.*, **5**, 335 (1977).
(5) W. L. Hayton and T. Chen, *J. Pharm. Sci.*, **71**, 820 (1982).
(6) G. Reach, H. Nakane, Y. Nakane, C. Auzan, and P. Corvol, *Steroids*, **30**, 621 (1977).
(7) H. Nakane, Y. Nakane, G. Reach, P. Corvol, and J. Menard, *Am. J. Physiol.*, **234**, E472 (1978).
(8) I. Bekersky, A. C. Popick, and W. A. Colburn, *Drug Metab. Disp.* (Submitted).

Wayne A. Colburn[x]
Romulus K. Brazzell
Ihor Bekersky
Department of Pharmacokinetics and Biopharmaceutics
Hoffmann-La Roche Inc.
Nutley, NJ 07110

Received September 20, 1982.
Accepted for publication February 18, 1983.

Rebound Phenomenon Observed During the Compaction of Samples in the Fisher Subsieve Sizer for Measuring Specific Surface Area of Griseofulvin

Keyphrases □ Specific surface area—Fisher subsieve sizer, rebound phenomenon observed during compaction, griseofulvin □ Compaction, tablet—rebound phenomenon, Fisher subsieve sizer, specific surface area of griseofulvin

To the Editor:

The air-permeability technique for measuring the specific surface area of powders is a well-recognized technique. It has been used for more than 30 years by the cement industry. The American Society of Testing Materials (1) as well as various European societies have adopted it as a standard method for measuring the fineness of cement by means of the Blaine apparatus, using the measurement of the resistance offered to the air flow by a packed bed of powder at a defined porosity level.

Recently the air-permeability method has also been included in the USP XX for measuring the fineness of griseofulvin in terms of its specific surface area (SSA). The USP monograph on griseofulvin specifies SSA limits between 1.30–1.70 m^2/g. For making the measurements, however, a procedure based on measuring at a range of porosities and using a Fisher subsieve sizer (FSS) apparatus is described. In the normal use of FSS-apparatus, it is common to take a sample weight equal to the density value of the sample material. The USP XX, however, suggests the use of 1.25 times the weight of material density as sample weight. This recommendation is based on an assumption that the SSA-value should be determined at very low porosities (down to 0.25 range), which cannot be reached easily when using the FSS-chart scale and sample weight equal to the density of a material. The basis of this recommendation is an earlier study by Edmundson and Tootil (2) who advanced an hypothesis that very low porosities are desirable for achieving a uniform packing of the powder bed and for getting a maximum SSA value which may be considered a unique value for a given powder sample.

A series of SSA measurements were made on a number of griseofulvin samples using the FSS apparatus and taking

0022-3549/83/0800-0971$01.00/0

the sample weight suggested in the USP XX. Difficulty was experienced in compressing certain samples to powder bed porosities below the 0.50 range. Not only was an unusually high amount of force required, but it was almost impossible to compress some of the samples below 0.45 porosity by manual force.

The ASTM-Standard C 204-79 (1) (under its Note [7]) contains instructions for selecting the "Size of Test Sample" to be used with the Blaine permeameter:

> "The weight of sample shall be adjusted so that a firm, hard bed is produced by the compacting process. In no case, however should more than thumb pressure be used to secure the proper bed, nor should such thumb pressure be used that the plunger "rebounds" from the cell top when the plunger is removed."

To examine the influence of high force required to achieve sample-bed porosities of the lower range (<0.50) and any associated "rebound" phenomena, we compressed the griseofulvin samples to different porosity levels, as indicated on the FSS-chart line. After withdrawal of the FSS compressing plunger, the sample height in the FSS cell was measured by using a slide-gauge. The mean particle diameter and the corresponding SSA were then obtained from the FSS chart. Before compressing the bed to the next porosity level, the FSS cell was attached to a modified Blaine permeameter, the time of flow of air measured, and the corresponding SSA calculated according to the basic Kozeny-Carman equation (3), using the calculated porosity from the powder bed dimensions.

The results summarized in Table I show that the use of a higher sample weight of griseofulvin, as suggested in the USP XX, and its compression to bed porosities <0.50 level can lead to a rebound and expansion of the powder bed. This is seen in columns 2 and 3 of Table I where there is shown an appreciable difference between the corrected porosity and the calculated porosity (ϵ_3) obtained from the powder height measurements. These data imply that due to this rebound effect at the porosity range of 0.45 the SSA values read from the FSS chart will also be in error. This is also reflected in a greater deviation between the SSA values obtained with the FSS and Blaine apparatuses.

Table I [a]—SSA-Values of Griseofulvin Sample Measured at Different Porosities using FSS and Blaine Permeameter [a]

ϵ_1 [b] Indicated Porosity	ϵ_2 [c] Corrected Porosity	ϵ_3 [d] Calculated Porosity	L, cm [e] Sample Height Measured	S_{w1} [f] (m^2/g) from FSS	S_{w2} [g] (m^2/g) Blaine permeameter	S_{w2} [h]/S_{w1}
		0.6422	2.78	0.884	0.885	1.00
0.72	0.65	0.6447	2.80	0.844	0.907	0.07
		0.6460	2.81	0.844	0.898	1.06
		0.5940	2.45	1.116	1.161	1.04
0.68	0.60	0.5948	2.45	1.093	1.163	1.06
		0.5965	2.46	1.093	1.164	1.06
		0.5405	2.16	1.420	1.447	1.02
0.64	0.55	0.5458	2.19	1.314	1.410	1.07
		0.5468	2.19	1.383	1.421	1.03
		0.5001	1.99	1.619	1.680	1.04
0.60	0.50	0.5001	1.99	1.568	1.690	1.08
		0.5136	2.04	1.520	1.595	1.05
		0.4594	1.84	1.584	1.758	1.11
0.56	0.45	0.4737	1.89	1.584	1.715	1.08
		0.4859	1.93	1.397	1.685	1.21

[a] Griseofulvin, ρ = 1.455 g/cm³ FSS-sample cell; sample weight used (1.455 × 1.25) = 1.819 g; supplied by Leo Pharmaceutical Products, Copenhagen, Denmark. [b] ϵ_1, indicated porosity on the FSS chart. [c] ϵ_2, corrected porosity due to higher sample weight (= $\rho \times 1.25$). [d] ϵ_3, calculated porosity from the measured sample height. [e] L, measured sample height. [f] S_{w1}, specific surface area obtained from particle diameter read at the FSS chart. [g] S_{w2}, specific surface area calculated from the ϵ_3-porosity value and measurement with Blaine-permeameter. [h] S_{w2}/S_{w1}, ratio of the SSA values from Blaine permeameter and Fisher subsieve sizer.

It is therefore proposed that the USP should adopt the procedure of measuring the SSA values at one defined porosity level, such as $\epsilon \sim 0.50$ used in the ASTM Standard. Another proposal is to leave the choice of permeameter open, provided a suitable calibration of the apparatus has been undertaken, more particularly of the sample cells.

In the calculation of SSA from air-permeability data, use is made of the Kozeny-Carman equation. In using this equation, it is important to know the accurate and precise values of the bed porosity as well as the length, diameter, and the volume of the compacted powder bed. For some permeability cells, such as that for the Blaine permeameter, a so-called mercury displacement method of calibration is frequently employed, and its details are also specified in the ASTM-Standard (1). The Fisher subsieve sizer, however, does not use any particular technique to calibrate its cell dimensions or the porosity setting. Edmundson (3) used a traveling microscope for this purpose, but it cannot be suggested for routine purposes.

We used a simple method to calibrate the permeability cells. The powder samples were compressed in the permeability cells and then ejected out carefully, by means of a suitable rod. The plug dimensions such as height and diameter were measured by means of a precision micrometer and the bulk volume was then calculated from these dimensions. Table II summarizes comparative values of such dimensions for some Blaine permeability cells, using the direct dimensions measurement and the mercury displacement methods.

A separate measurement of the metal components of the cells by means of a gauge confirm the directly measured dimensions of the powder plug. The direct measurement method is of more relevance to the actual state of the compressed powder plug used during the permeability measurements and it is easier to use. This method can be employed with different types of cells, including the Fisher subsieve sizer cell or the small bore tubes (~0.6 cm diameter) where the mercury-displacement method is not only tedious but impractical. Therefore, the direct measurement method is preferred for calibration.

For routine calibration purposes, it is advisable to use malleable materials for preparing the compressed powder plugs. The plugs should be compressed to porosities that are low enough to give firm plugs which can withstand handling, but not so low that expansion of the powder bed occurs because of "relaxation" after ejection from the cell.

Table II—Dimensions of Blaine Permeameter Cells Determined by Two Calibration Methods

Blaine cells	Mercury Displacement Method [a] Length, cm	Diameter, cm	Volume, cm^3	Direct Measurement of Dimensions [b] Length, cm	Diameter, cm	Volume, cm^3
A	(1.419) [c]	(1.270)	1.798	1.478	1.272	(1.878)
B	(1.450)	(1.270)	1.838	1.500	1.268	(1.895)

[a] Means of two measurements as stated in ASTM C-204-79. [b] Means of 10 measurements using separate compactions for each determination (*RSD* <0.4%). [c] Parentheses indicate values not experimentally determined.

Using very fine particle size materials, self-supporting plugs can be formed without the use of any additional binders. We found the addition of a mixture of micronized lactose and 5% magnesium stearate is suitable to improve flow properties.

(1) ASTM-Standard C-204-79 "Standard Test Method for Fineness of Portland Cement by Air-Permeability Apparatus," American Society for Testing Materials, Philadelphia, Pa. 1979.

(2) I. C. Edmundson and J. P. R. Tootil, *Analyst*, **88**, 805 (1963).

(3) I. C. Edmundson, *Analyst*, **91**, 306 (1966).

P. Seth[x]
Mepha Ltd.
CH-4143 Dornach, Switzerland

N. Møller
Royal Danish School of Pharmacy
Department of Pharmaceutics
DK-2100 Copenhagen, Denmark

J. C. Tritsch
A. Stamm
Faculty of Pharmacy
Louis Pasteur University
F-67048 Strasbourg, France

Received September 3, 1982.
Accepted for publication March 29, 1983.

Physicochemical Interpretation of pH-Stat Titration of Amorphous Aluminum Hydroxycarbonate

Keyphrases □ Amorphous aluminum hydroxycarbonate—pH-stat titration, physicochemical interpretation, fiber optic Doppler anemometer analysis, dissolution data □ pH-stat titration—correlation between the *in vitro* test and *in vivo* acid neutralization, amorphous aluminum hydroxycarbonate, fiber optic Doppler anemometer analysis, dissolution data

To the Editor:

The pH-stat titration of antacids (1) is a valuable *in vitro* test because it has been correlated with *in vivo* acid neutralization (2). In contrast to the acid-neutralizing capacity test and the acid-consuming capacity test, which are essentially indirect assays, the pH-stat titration measures the rate of acid neutralization (3). The pH-stat titration has provided insights into (*a*) the structure of aluminum hydroxycarbonate (4, 5); (*b*) the adsorption of polybasic acids (6), polyols (7), polymers (8), and surface-active agents (8) by aluminum hydroxycarbonate; and (*c*) the interaction of aluminum hydroxycarbonate and magnesium hydroxide (9, 10).

The pH-stat titrigram of aluminum hydroxycarbonate contains three phases rather than the linear rate of acid neutralization expected for an acid–base titration (1). As seen in Fig. 1, the reaction is characterized by an initial rapid reaction (phase I) which abruptly converts into a slow zero-order reaction (phase II) which gradually transforms into a more rapid zero-order reaction (phase III). In contrast, antacids such as sodium bicarbonate, calcium carbonate, magnesium hydroxide, and hydrotalcite exhibit the expected linear pH-stat titrigram (9, 10). The purpose of this communication is to describe the

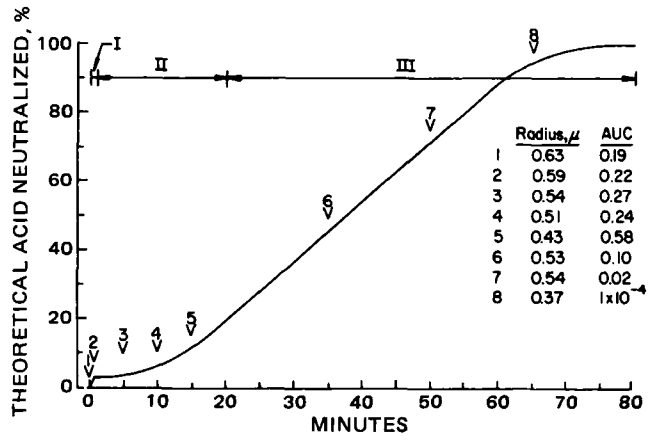

Figure 1—*pH-Stat titration at pH 3, 25° of aluminum hydroxycarbonate gel, which was examined at the indicated points by FODA.*

physicochemical reactions that are responsible for the three phases of the pH-stat titration of aluminum hydroxycarbonate.

The pH-stat titration at pH 3, 25° was interrupted periodically, as indicated in Fig. 1, and the apparent particle size was determined by fiber optic Doppler anemometry (FODA)[1] (11). The apparent mean hydrodynamic radius decreased from an initial value of 0.63 μm to 0.59 μm during phase I. A further decline to 0.43 μm was observed during the second phase. The apparent particle size initially increased during the third phase but decreased at the end of phase III.

The fiber optic Doppler anemometer determines particle size based on the measurement of the Brownian motion of colloidal particles. Thus, particle interactions that reduce the Brownian motion of particles will cause the apparent hydrodynamic radius, as measured by the fiber optic Doppler anemometer, to increase. In fact, if particle interactions cause Brownian motion to cease, the particle(s) will not be detected by FODA. Therefore, the apparent mean hydrodynamic radius data should be interpreted in conjunction with measurements of the total signal intensity. This is readily accomplished by integration of the power spectrum [area under the voltage squared *versus* frequency curve (AUC)] (12, 13). Thus, the AUC will be related to the total number of freely diffusing particles. The AUC increased from 0.19 to 0.22 during phase I and further increased to 0.58 during the slow, second phase. The AUC went to zero during phase III. The AUC data suggest that the number of particles exhibiting Brownian motion increased during phases I and II and decreased sharply during phase III.

It was hypothesized recently that aluminum hydroxide and aluminum hydroxycarbonate are composed of three types of particles: primary particles, secondary particles, and aggregates (14, 15). The primary particle is the basic unit: platy crystallites composed of fused six-membered rings of aluminum joined by double hydroxide bridges. The secondary particles are formed from primary particles arranged in a turbostratic type of arrangement due to the cohesive strength of van der Waals forces. Aggregates are composed of secondary particles formed in response to the balance of attractive and repulsive forces described by

[1] SIRA Institute Ltd., Kent, England.

0022-3549/83/0800-0973$01.00/0

Using very fine particle size materials, self-supporting plugs can be formed without the use of any additional binders. We found the addition of a mixture of micronized lactose and 5% magnesium stearate is suitable to improve flow properties.

(1) ASTM-Standard C-204-79 "Standard Test Method for Fineness of Portland Cement by Air-Permeability Apparatus," American Society for Testing Materials, Philadelphia, Pa. 1979.

(2) I. C. Edmundson and J. P. R. Tootil, *Analyst*, **88**, 805 (1963).

(3) I. C. Edmundson, *Analyst*, **91**, 306 (1966).

P. Seth[x]
Mepha Ltd.
CH-4143 Dornach, Switzerland

N. Møller
Royal Danish School of Pharmacy
Department of Pharmaceutics
DK-2100 Copenhagen, Denmark

J. C. Tritsch
A. Stamm
Faculty of Pharmacy
Louis Pasteur University
F-67048 Strasbourg, France

Received September 3, 1982.
Accepted for publication March 29, 1983.

Physicochemical Interpretation of pH-Stat Titration of Amorphous Aluminum Hydroxycarbonate

Keyphrases □ Amorphous aluminum hydroxycarbonate—pH-stat titration, physicochemical interpretation, fiber optic Doppler anemometer analysis, dissolution data □ pH-stat titration—correlation between the *in vitro* test and *in vivo* acid neutralization, amorphous aluminum hydroxycarbonate, fiber optic Doppler anemometer analysis, dissolution data

To the Editor:

The pH-stat titration of antacids (1) is a valuable *in vitro* test because it has been correlated with *in vivo* acid neutralization (2). In contrast to the acid-neutralizing capacity test and the acid-consuming capacity test, which are essentially indirect assays, the pH-stat titration measures the rate of acid neutralization (3). The pH-stat titration has provided insights into (*a*) the structure of aluminum hydroxycarbonate (4, 5); (*b*) the adsorption of polybasic acids (6), polyols (7), polymers (8), and surface-active agents (8) by aluminum hydroxycarbonate; and (*c*) the interaction of aluminum hydroxycarbonate and magnesium hydroxide (9, 10).

The pH-stat titrigram of aluminum hydroxycarbonate contains three phases rather than the linear rate of acid neutralization expected for an acid–base titration (1). As seen in Fig. 1, the reaction is characterized by an initial rapid reaction (phase I) which abruptly converts into a slow zero-order reaction (phase II) which gradually transforms into a more rapid zero-order reaction (phase III). In contrast, antacids such as sodium bicarbonate, calcium carbonate, magnesium hydroxide, and hydrotalcite exhibit the expected linear pH-stat titrigram (9, 10). The purpose of this communication is to describe the

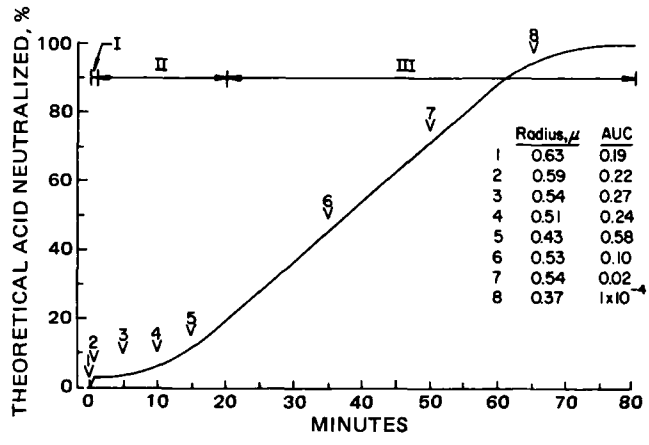

Figure 1—*pH-Stat titration at pH 3, 25° of aluminum hydroxycarbonate gel, which was examined at the indicated points by FODA.*

physicochemical reactions that are responsible for the three phases of the pH-stat titration of aluminum hydroxycarbonate.

The pH-stat titration at pH 3, 25° was interrupted periodically, as indicated in Fig. 1, and the apparent particle size was determined by fiber optic Doppler anemometry (FODA)[1] (11). The apparent mean hydrodynamic radius decreased from an initial value of 0.63 μm to 0.59 μm during phase I. A further decline to 0.43 μm was observed during the second phase. The apparent particle size initially increased during the third phase but decreased at the end of phase III.

The fiber optic Doppler anemometer determines particle size based on the measurement of the Brownian motion of colloidal particles. Thus, particle interactions that reduce the Brownian motion of particles will cause the apparent hydrodynamic radius, as measured by the fiber optic Doppler anemometer, to increase. In fact, if particle interactions cause Brownian motion to cease, the particle(s) will not be detected by FODA. Therefore, the apparent mean hydrodynamic radius data should be interpreted in conjunction with measurements of the total signal intensity. This is readily accomplished by integration of the power spectrum [area under the voltage squared *versus* frequency curve (AUC)] (12, 13). Thus, the AUC will be related to the total number of freely diffusing particles. The AUC increased from 0.19 to 0.22 during phase I and further increased to 0.58 during the slow, second phase. The AUC went to zero during phase III. The AUC data suggest that the number of particles exhibiting Brownian motion increased during phases I and II and decreased sharply during phase III.

It was hypothesized recently that aluminum hydroxide and aluminum hydroxycarbonate are composed of three types of particles: primary particles, secondary particles, and aggregates (14, 15). The primary particle is the basic unit: platy crystallites composed of fused six-membered rings of aluminum joined by double hydroxide bridges. The secondary particles are formed from primary particles arranged in a turbostratic type of arrangement due to the cohesive strength of van der Waals forces. Aggregates are composed of secondary particles formed in response to the balance of attractive and repulsive forces described by

[1] SIRA Institute Ltd., Kent, England.

0022-3549/83/0800-0973$01.00/0

DLVO theory. This type of particle structure has also been proposed for carbon black (16).

It is proposed that the pH-stat titrigram can be interpreted in light of the recently proposed particle structure of aluminum hydroxycarbonate (14, 15). The point of zero charge of aluminum hydroxide is 9.6 and ranges from 6 to 9 for aluminum hydroxycarbonate (17). The aluminum hydroxycarbonate gel shown in Fig. 1 had a point of zero charge of 6.5. Acid was consumed very rapidly during the initial phase. Kerkhof *et al.* (1) observed that the rate of acid neutralization during the first phase exceeds the capability of the autoburet to add compensating acid. This rapid proton consumption is primarily due to protonation of the hydroxyl groups and carbonate surface sites as the pH of the system is instantaneously adjusted to 3, well below the point of zero charge. During this phase Al—OH—Al and Al—OCO_2 bonds are not believed to react. Rather, rapid charging due to proton adsorption leads to a positive surface charge. The first phase is very brief, which is expected for a protonation reaction.

The initial phase, which will be referred to as the proton loading phase, quickly shifts into a second phase in which the rate of proton consumption is much slower. The rate of acid neutralization increases gradually during phase II. It is hypothesized that the gradual increase in the rate of acid neutralization is due to an increase in surface area. The increase in surface area is compatible with the hypothesis that aluminum hydroxycarbonate is composed of primary particles, secondary particles, and aggregates. Protonation during phase I caused the development of a strong, positive surface potential. Therefore, large coulombic repulsive forces develop, which are believed to cause the aggregates to disperse into secondary particles and the secondary particles to disperse into primary particles. As peptization proceeds, the exposed surface area will increase, and in turn, the rate of acid neutralization will increase. Therefore, phase II will be termed the peptization phase.

The FODA analysis (Fig. 1) during the first two phases supports the hypothesis that proton loading and peptization occur during phases I and II, respectively. The mean hydrodynamic radius decreased to 0.43 μm by the end of phase II (point 5 in Fig. 1) with the consumption of only 11% of the acid necessary to neutralize the sample. The volume of a 0.43-μm sphere is only 31% of the volume of a 0.63-μm sphere. Therefore, if the decrease in mean hydrodynamic radius had occurred solely by acid dissolution, approximately 70% of the theoretical acid would have been required. Thus, a dispersion effect has taken place.

The decrease in mean hydrodynamic radius during phase I and phase II must be considered in light of the concurrent changes in the AUC: the number of particles exhibiting Brownian movement. The AUC increased by a factor of 3 during phases I and II. Thus, a decrease in mean hydrodynamic radius and an increase in the number of particles exhibiting Brownian motion is occurring simultaneously. In view of the fact that only a small fraction of the acid necessary to dissolve the particles has been added, the observed trends in particle size and AUC are consistent with a proton loading and peptization process.

The rapid rate of acid neutralization which is characteristic of the third phase of the pH-stat titration of aluminum hydroxycarbonate is believed to be due to the high surface area produced by the peptization of the aggregates and secondary particles. Evidence of dissolution is seen in the FODA analysis by the decrease in the AUC during the third phase. The increase in the mean hydrodynamic radius during the early part of phase III (points 6 and 7 in Fig. 1) is believed to arise because of the greater dissolution rate of smaller particles, which causes the mean particle size of the remaining particles to increase. Since the acid dissolution reaction predominates during phase III, it will be referred to as the dissolution phase.

In most aluminum hydroxycarbonate gels, the third phase of the pH-stat titration terminates with the neutralization of the theoretical amount of acid based on the stoichiometric reaction of three protons per aluminum. However, some aluminum hydroxycarbonate gels do not complete the theoretical reaction during phase III, and a very slow rate of acid neutralization proceeds until the reaction is complete. The slow-reacting material is believed to have a very large primary particle size, approaching, in some cases, the crystalline state. On the other hand, an occasional aluminum hydroxycarbonate gel neutralizes more than three protons per aluminum. Gels of this type usually contain a high level of sodium and the superpotency is due to contamination with dawsonite [crystalline sodium aluminum hydroxycarbonate, $NaAl(OH)_2CO_3$] which neutralizes four protons per aluminum (18).

Antacid materials such as sodium bicarbonate, calcium carbonate, magnesium hydroxide, and hydrotalcite which exhibit a linear pH-stat titration are all crystalline materials with a particle size usually in excess of the colloidal range. Therefore, they probably do not exist as primary particles, secondary particles, or aggregates.

An examination of the changes in the pH-stat titrigram during the aging of amorphous aluminum hydroxycarbonate gel further supports the proposed interpretation. IR and X-ray studies indicate that the primary particle size increases during aging (19–21). In some cases the degree of aggregation will also increase during aging due to the consolidating effects of gravitational settling. As seen in Fig. 2, the pH-stat titrigram of a freshly precipitated aluminum hydroxycarbonate gel is dominated by phase I (proton loading) and phase III (dissolution of peptized particles). Most of the aggregates and secondary particles in the freshly precipitated sample are readily dispersed

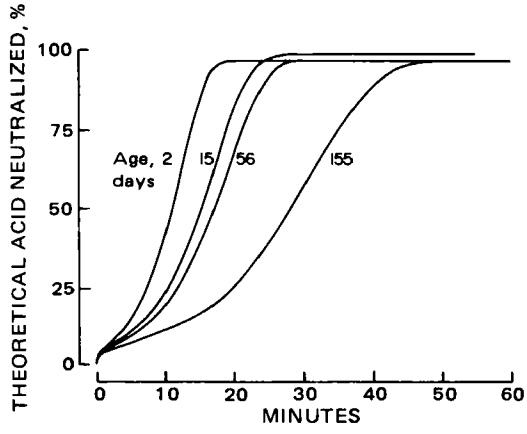

Figure 2—*Effect of aging of aluminum hydroxycarbonate gel at 25° on the pH-stat titration at pH 3, 25°.*

when the pH is lowered to 3. Since no significant particle growth has occurred, the relatively small primary particle size of the fresh gel gives a rapid rate of acid neutralization.

Phase II becomes more evident as the aluminum hydroxycarbonate gel ages. Both the primary particle size and the degree of aggregation increases during aging. Therefore, peptization becomes more important and the slow, second phase becomes more prominent. The rate of acid neutralization during phase III decreases during aging (day 2 *versus* day 155 in Fig. 2), which reflects the increase in primary particle size.

An understanding of the physicochemical processes required for the *in vitro* acid neutralization of aluminum hydroxycarbonate gel is necessary, because similar reactions occur in the GI tract when aluminum hydroxycarbonate gel is used as an antacid.

(1) N. J. Kerkhof, R. K. Vanderlaan, J. L. White, and S. L. Hem, *J. Pharm. Sci.*, **66**, 1528 (1977).

(2) J. S. Fordtran, S. G. Morawski, and C. T. Richardson, *N. Engl. J. Med.*, **288**, 923 (1973).

(3) S. L. Hem, J. L. White, J. D. Buehler, J. R. Luber, W. M. Grim, and E. A. Lipka, *Am. J. Hosp. Pharm.*, **39**, 1925 (1982).

(4) N. J. Kerkhof, J. L. White, and S. L. Hem, *J. Pharm. Sci.*, **66**, 1533 (1977).

(5) C. J. Serna, J. L. White, and S. L. Hem, *J. Pharm. Sci.*, **67**, 1144 (1978).

(6) M. K. Wang, J. L. White, and S. L. Hem, *J. Pharm. Sci.*, **69**, 668 (1980).

(7) D. N. Shah, J. L. White, and S. L. Hem, *J. Pharm. Sci.*, **70**, 1101 (1981).

(8) M. I. Zapata, J. R. Feldkamp, G. E. Peck, J. L. White, and S. L. Hem, *J. Pharm. Sci.*, in press.

(9) R. K. Vanderlaan, J. L. White, and S. L. Hem, *J. Pharm. Sci.*, **68**, 1498 (1979).

(10) R. K. Vanderlaan, J. L. White, and S. L. Hem, *J. Pharm. Sci.*, **71**, 780 (1982).

(11) D. A. Ross, H. S. Dhadwal, and R. B. Dyott, *J. Colloid Interface Sci.*, **64**, 533 (1978).

(12) B. J. Berne and R. Pecora, "Dynamic Light Scattering," Wiley, New York, N.Y., 1976, pp. 28, 60.

(13) A. M. Jamieson and M. E. McDonnell, *Adv. Chem. Ser.*, **174**, 163 (1979).

(14) E. C. Scholtz, Ph.D. Thesis, Purdue University, 1981.

(15) J. C. Liu, Ph.D. Thesis, Purdue University, 1982.

(16) F. A. Heckman, *Rubber Chem. Technol.*, **37**, 1245 (1964).

(17) J. R. Feldkamp, D. N. Shah, S. L. Meyer, J. L. White, and S. L. Hem, *J. Pharm. Sci.*, **70**, 638 (1981).

(18) C. J. Serna, J. L. White, and S. L. Hem, *J. Pharm. Sci.*, **67**, 324 (1978).

(19) S. L. Nail, J. L. White, and S. L. Hem, *J. Pharm. Sci.*, **64**, 1166 (1975).

(20) S. L. Nail, J. L. White, and S. L. Hem, *J. Pharm. Sci.*, **65**, 231 (1976).

(21) S. L. Nail, J. L. White, and S. L. Hem, *J. Pharm. Sci.*, **65**, 1192 (1976).

Edward C. Scholtz
Mary I. Zapata
Stanley L. Hem[x]
Department of Industrial and Physical Pharmacy
Joseph R. Feldkamp
Joe L. White
Department of Agronomy
Purdue University
West Lafayette, IN 47907

Received August 23, 1982.
Accepted for publication March 16, 1983.
Supported in part by William H. Rorer, Inc.
This report is Journal Paper 9165, Purdue University Agricultural Experiment Station, West Lafayette, IN 47907.

Simplified Method for Intravenous Dosing and Serial Blood Sampling of Unanesthetized Guinea Pigs

Keyphrases □ Blood sampling—serial collection from unanesthetized guinea pigs □ Guinea pigs—dosing and serial blood sampling without anesthesia □ Vacuum bleeding apparatus—serial blood collection from unanesthetized guinea pigs

To the Editor:

Ascorbic acid (vitamin C) levels can influence oxidative demethylation processes in the guinea pig (1), the only common laboratory animal unable to synthesize ascorbic acid endogenously (2). Thus, the guinea pig is an especially popular model for studying the effects of ascorbic acid on drug metabolism. Because of this, it is important to define methods for drug administration and repetitive blood sampling when using this species for pharmacokinetic studies. The following procedures were developed during a recent investigation of the effect of ascorbic acid on caffeine pharmacokinetics in young and aged guinea pigs.

A large towel was effective in quieting and immobilizing the animals during both drug dosing and blood sampling. The animals were prepared for dosing, by removing the hair over the injection site with an electric clipper. The prominent superficial vein on the medial side of the thigh (the medial saphenous vein) was used for all drug injections. The injection site was dabbed with ethanol and then the vein was enlarged using a finger to block venous return, and a small (21 gauge) needle was inserted in the direction of blood flow. A small quantity of blood was drawn *into the* 1-ml syringe to ensure correct insertion of the needle in the vein. Following a bolus injection of the drug solution, the needle was withdrawn quickly and pressure placed on the puncture with a finger to prevent venous backflow and avoid loss of some of the injected dose.

The method used here for repeated blood sampling was modified from that of Dolence and Jones (3) and found to be highly effective, producing a minimum of stress or pain in the guinea pigs. Similar to the procedure for caffeine dosing, the guinea pigs were wrapped in a towel exposing only the hind legs, which kept them comfortable yet immobilized. The leg not used for drug injection was extended and the hair removed using an electric clipper. A thin layer of silicone grease[1] was applied to the leg to form a tight seal with the vacuum bleeding apparatus and to prevent loose hair from contaminating the blood sample. One of the toenails was clipped, cutting into the vein and producing a flow of blood. Using this method alone only a small quantity of blood could be collected before coagulation stopped the flow. To circumvent this problem the prepared leg was positioned in the bleeding apparatus, as shown in Fig. 1, and the vacuum adjusted to produce a steady blood flow. The blood was collected in a 3-ml heparinized tube attached to the bottom of the vacuum-bleeding apparatus with a plastic[2] collar. The vacuum was adjusted to either increase or decrease the blood flow.

[1] Dow Corning, Midland, MI 48640.
[2] Tygon (R3603) tubing, Cole-Parmer, Chicago, IL 60648.

0022-3549/83/0800-0975$01.00/0

when the pH is lowered to 3. Since no significant particle growth has occurred, the relatively small primary particle size of the fresh gel gives a rapid rate of acid neutralization.

Phase II becomes more evident as the aluminum hydroxycarbonate gel ages. Both the primary particle size and the degree of aggregation increases during aging. Therefore, peptization becomes more important and the slow, second phase becomes more prominent. The rate of acid neutralization during phase III decreases during aging (day 2 *versus* day 155 in Fig. 2), which reflects the increase in primary particle size.

An understanding of the physicochemical processes required for the *in vitro* acid neutralization of aluminum hydroxycarbonate gel is necessary, because similar reactions occur in the GI tract when aluminum hydroxycarbonate gel is used as an antacid.

(1) N. J. Kerkhof, R. K. Vanderlaan, J. L. White, and S. L. Hem, *J. Pharm. Sci.*, **66**, 1528 (1977).

(2) J. S. Fordtran, S. G. Morawski, and C. T. Richardson, *N. Engl. J. Med.*, **288**, 923 (1973).

(3) S. L. Hem, J. L. White, J. D. Buehler, J. R. Luber, W. M. Grim, and E. A. Lipka, *Am. J. Hosp. Pharm.*, **39**, 1925 (1982).

(4) N. J. Kerkhof, J. L. White, and S. L. Hem, *J. Pharm. Sci.*, **66**, 1533 (1977).

(5) C. J. Serna, J. L. White, and S. L. Hem, *J. Pharm. Sci.*, **67**, 1144 (1978).

(6) M. K. Wang, J. L. White, and S. L. Hem, *J. Pharm. Sci.*, **69**, 668 (1980).

(7) D. N. Shah, J. L. White, and S. L. Hem, *J. Pharm. Sci.*, **70**, 1101 (1981).

(8) M. I. Zapata, J. R. Feldkamp, G. E. Peck, J. L. White, and S. L. Hem, *J. Pharm. Sci.*, in press.

(9) R. K. Vanderlaan, J. L. White, and S. L. Hem, *J. Pharm. Sci.*, **68**, 1498 (1979).

(10) R. K. Vanderlaan, J. L. White, and S. L. Hem, *J. Pharm. Sci.*, **71**, 780 (1982).

(11) D. A. Ross, H. S. Dhadwal, and R. B. Dyott, *J. Colloid Interface Sci.*, **64**, 533 (1978).

(12) B. J. Berne and R. Pecora, "Dynamic Light Scattering," Wiley, New York, N.Y., 1976, pp. 28, 60.

(13) A. M. Jamieson and M. E. McDonnell, *Adv. Chem. Ser.*, **174**, 163 (1979).

(14) E. C. Scholtz, Ph.D. Thesis, Purdue University, 1981.

(15) J. C. Liu, Ph.D. Thesis, Purdue University, 1982.

(16) F. A. Heckman, *Rubber Chem. Technol.*, **37**, 1245 (1964).

(17) J. R. Feldkamp, D. N. Shah, S. L. Meyer, J. L. White, and S. L. Hem, *J. Pharm. Sci.*, **70**, 638 (1981).

(18) C. J. Serna, J. L. White, and S. L. Hem, *J. Pharm. Sci.*, **67**, 324 (1978).

(19) S. L. Nail, J. L. White, and S. L. Hem, *J. Pharm. Sci.*, **64**, 1166 (1975).

(20) S. L. Nail, J. L. White, and S. L. Hem, *J. Pharm. Sci.*, **65**, 231 (1976).

(21) S. L. Nail, J. L. White, and S. L. Hem, *J. Pharm. Sci.*, **65**, 1192 (1976).

Edward C. Scholtz
Mary I. Zapata
Stanley L. Hem[x]
Department of Industrial and Physical Pharmacy
Joseph R. Feldkamp
Joe L. White
Department of Agronomy
Purdue University
West Lafayette, IN 47907

Received August 23, 1982.
Accepted for publication March 16, 1983.
Supported in part by William H. Rorer, Inc.
This report is Journal Paper 9165, Purdue University Agricultural Experiment Station, West Lafayette, IN 47907.

Simplified Method for Intravenous Dosing and Serial Blood Sampling of Unanesthetized Guinea Pigs

Keyphrases □ Blood sampling—serial collection from unanesthetized guinea pigs □ Guinea pigs—dosing and serial blood sampling without anesthesia □ Vacuum bleeding apparatus—serial blood collection from unanesthetized guinea pigs

To the Editor:

Ascorbic acid (vitamin C) levels can influence oxidative demethylation processes in the guinea pig (1), the only common laboratory animal unable to synthesize ascorbic acid endogenously (2). Thus, the guinea pig is an especially popular model for studying the effects of ascorbic acid on drug metabolism. Because of this, it is important to define methods for drug administration and repetitive blood sampling when using this species for pharmacokinetic studies. The following procedures were developed during a recent investigation of the effect of ascorbic acid on caffeine pharmacokinetics in young and aged guinea pigs.

A large towel was effective in quieting and immobilizing the animals during both drug dosing and blood sampling. The animals were prepared for dosing, by removing the hair over the injection site with an electric clipper. The prominent superficial vein on the medial side of the thigh (the medial saphenous vein) was used for all drug injections. The injection site was dabbed with ethanol and then the vein was enlarged using a finger to block venous return, and a small (21 gauge) needle was inserted in the direction of blood flow. A small quantity of blood was drawn *into the* 1-ml syringe to ensure correct insertion of the needle in the vein. Following a bolus injection of the drug solution, the needle was withdrawn quickly and pressure placed on the puncture with a finger to prevent venous backflow and avoid loss of some of the injected dose.

The method used here for repeated blood sampling was modified from that of Dolence and Jones (3) and found to be highly effective, producing a minimum of stress or pain in the guinea pigs. Similar to the procedure for caffeine dosing, the guinea pigs were wrapped in a towel exposing only the hind legs, which kept them comfortable yet immobilized. The leg not used for drug injection was extended and the hair removed using an electric clipper. A thin layer of silicone grease[1] was applied to the leg to form a tight seal with the vacuum bleeding apparatus and to prevent loose hair from contaminating the blood sample. One of the toenails was clipped, cutting into the vein and producing a flow of blood. Using this method alone only a small quantity of blood could be collected before coagulation stopped the flow. To circumvent this problem the prepared leg was positioned in the bleeding apparatus, as shown in Fig. 1, and the vacuum adjusted to produce a steady blood flow. The blood was collected in a 3-ml heparinized tube attached to the bottom of the vacuum-bleeding apparatus with a plastic[2] collar. The vacuum was adjusted to either increase or decrease the blood flow.

[1] Dow Corning, Midland, MI 48640.
[2] Tygon (R3603) tubing, Cole-Parmer, Chicago, IL 60648.

0022-3549/83/0800-0975$01.00/0

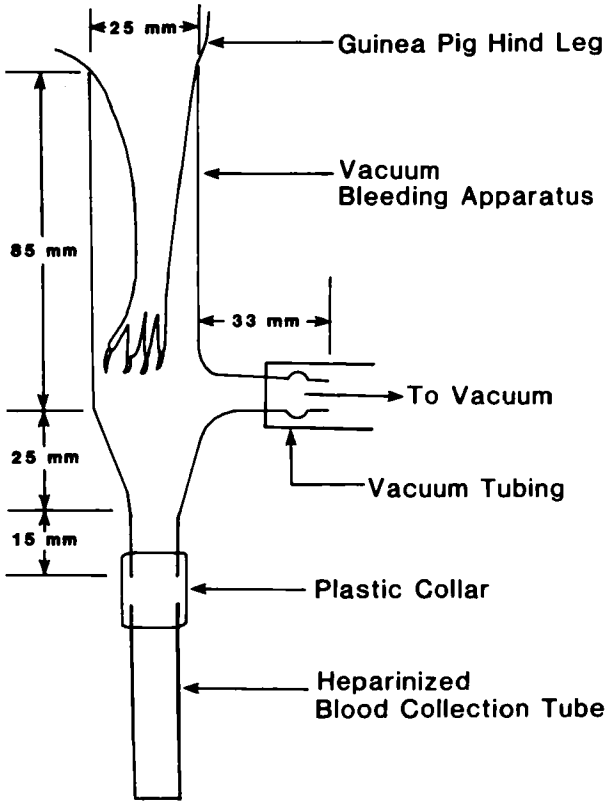

Figure 1—*Schematic diagram of the vacuum bleeding apparatus.*

When a 1- to 2-ml volume of whole blood was collected for each timed sample, the vacuum was turned off and the leg carefully removed from the apparatus. Bleeding usually ceased promptly, but it was sometimes necessary to place a gauze bandage over the toenail until all bleeding had stopped, usually within 1 min. For repeated blood collection from the same animal the nail was cut progressively more proximally at each sampling; the nails on both legs were used. The guinea pigs were not distressed by a sampling of up to 3 ml, and since no anesthetic was used, the animals had normal mobility when returned to their cages. The problem of blood clotting in the collection apparatus was minimized by using silicone grease on the inside glass surfaces.

Previous researchers have sampled guinea pig blood from the ear veins, penis vein, superficial thigh vein, jugular vein, orbital venous plexus and by the methods of heart puncture, indwelling vascular cannulation, cutting the toenail bed, and cutting the lateral saphenous vein or lateral metatarsal vein (4, 5). None of these methods proved completely satisfactory for the purposes of this study, since in most cases, an anesthetic was needed which could confound the observed results by affecting caffeine metabolism and/or plasma ascorbic acid levels (6, 7) if the study involved ascorbic acid supplementation, depletion, *etc.* We believe that the simplified procedure described here can be applied with similar success to studies involving other rodent species, in which anesthesia may be undesirable.

(1) V. G. Zannoni and M. M. Lynch, *Drug Metab. Rev.*, **2**, 57 (1973).
(2) L. E. Anthony, C. G. Kurahara, and K. B. Taylor, *Am. J. Clin. Nutr.*, **32**, 1691 (1979).
(3) D. Dolence and H. E. Jones, *Lab. Anim. Sci.*, **25**, 106 (1975).
(4) S. Schermer, "The Blood Morphology of Laboratory Animals," P. A. Davis, Philadelphia, Pa., 1967, p. 25.
(5) H. Lopez and J. M. Navia, *Lab. Anim. Sci.*, **27**, 522 (1977).
(6) B. I. Sikic, E. G. Mimnaugh, and T. E. Gram, *Biochem. Pharmacol.*, **26**, 2037 (1977).
(7) W. A. Behrens and R. Madere, *Nutr. Reports Inter.*, **19**, 419 (1979).

David Hochman
James Blanchard[x]
Department of Pharmaceutical Sciences
College of Pharmacy
University of Arizona
Tucson, AZ 85721

Received December 27, 1982.
Accepted for publication March 21, 1983.
Supported by Biomedical Research Support Grant No. 829750 from the University of Arizona.

An Automated Sampling Device for Dissolution Testing

Keyphrases □ Dissolution testing—automated sampling device

To the Editor:

Many automated sampling devices have been designed for commercially available dissolution units[1]. The major criticism of some of these units is that the sampling probes remain in the dissolution medium during the duration of the test, thereby disturbing the hydrodynamics of the solution (1). This can cause dissolution results other than those intrinsic to the dosage form. We have designed a simple sampling device which eliminates this problem while still allowing the convenience of automation. The device is made from a commercially available air-actuated, solenoid-controlled valve[2] and brackets that can be easily made in-house. The design and orientation of the brackets are shown in Figs. 1 and 2. Dimensional and installational information is presented in Fig. 3. Air is supplied to the device at 20 psi. Either house air or an air pump can be used. The unit is connected to a computer-controlled pump-fraction collecter[2] which provides contact closure to the solenoid through its internal-timing sequences which also control the pump-fraction collector's prime, sample, and purge cycles. However, this unit need only be connected to a 110 V contact closure and external air supply to actuate the valve. Once actuated, any suitable multiple-channel pump and collector can provide samples.

As previously indicated, we have chosen a combination pump-fraction collector with computerized timing sequences. A program is entered using a hand-held pad, and at program-designated intervals contact closure is made, the device is actuated, and samples are collected during a three-part 60-sec sequence: for 20 sec the lines are washed with sample to waste; the sample tray is then advanced and the next 20-sec sample is collected; and for 20 sec the pumps reverse to purge the lines. The sample tray then

[1] Hanson Research Corp., Northridge, CA 91324; Applied Analytical Industries, Wilmington, NC 28403; Technicon Industrial Systems, Tarrytown, NY 10591.
[2] Bimba Manufacturing Co., Monee, IL 60449.

0022-3549/83/0800-0976$01.00/0

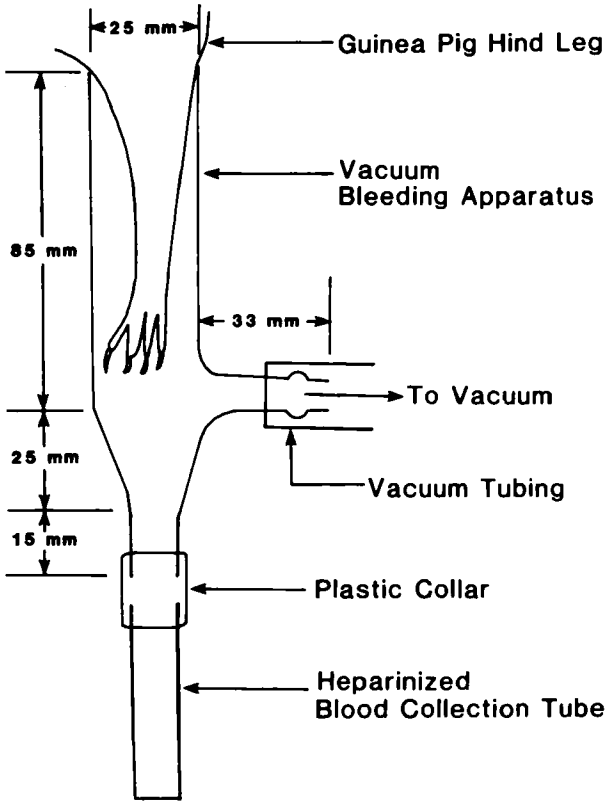

Figure 1—*Schematic diagram of the vacuum bleeding apparatus.*

When a 1- to 2-ml volume of whole blood was collected for each timed sample, the vacuum was turned off and the leg carefully removed from the apparatus. Bleeding usually ceased promptly, but it was sometimes necessary to place a gauze bandage over the toenail until all bleeding had stopped, usually within 1 min. For repeated blood collection from the same animal the nail was cut progressively more proximally at each sampling; the nails on both legs were used. The guinea pigs were not distressed by a sampling of up to 3 ml, and since no anesthetic was used, the animals had normal mobility when returned to their cages. The problem of blood clotting in the collection apparatus was minimized by using silicone grease on the inside glass surfaces.

Previous researchers have sampled guinea pig blood from the ear veins, penis vein, superficial thigh vein, jugular vein, orbital venous plexus and by the methods of heart puncture, indwelling vascular cannulation, cutting the toenail bed, and cutting the lateral saphenous vein or lateral metatarsal vein (4, 5). None of these methods proved completely satisfactory for the purposes of this study, since in most cases, an anesthetic was needed which could confound the observed results by affecting caffeine metabolism and/or plasma ascorbic acid levels (6, 7) if the study involved ascorbic acid supplementation, depletion, *etc.* We believe that the simplified procedure described here can be applied with similar success to studies involving other rodent species, in which anesthesia may be undesirable.

(1) V. G. Zannoni and M. M. Lynch, *Drug Metab. Rev.*, **2**, 57 (1973).
(2) L. E. Anthony, C. G. Kurahara, and K. B. Taylor, *Am. J. Clin. Nutr.*, **32**, 1691 (1979).
(3) D. Dolence and H. E. Jones, *Lab. Anim. Sci.*, **25**, 106 (1975).
(4) S. Schermer, "The Blood Morphology of Laboratory Animals," P. A. Davis, Philadelphia, Pa., 1967, p. 25.
(5) H. Lopez and J. M. Navia, *Lab. Anim. Sci.*, **27**, 522 (1977).
(6) B. I. Sikic, E. G. Mimnaugh, and T. E. Gram, *Biochem. Pharmacol.*, **26**, 2037 (1977).
(7) W. A. Behrens and R. Madere, *Nutr. Reports Inter.*, **19**, 419 (1979).

David Hochman
James Blanchard[x]
Department of Pharmaceutical Sciences
College of Pharmacy
University of Arizona
Tucson, AZ 85721

Received December 27, 1982.
Accepted for publication March 21, 1983.
Supported by Biomedical Research Support Grant No. 829750 from the University of Arizona.

An Automated Sampling Device for Dissolution Testing

Keyphrases □ Dissolution testing—automated sampling device

To the Editor:

Many automated sampling devices have been designed for commercially available dissolution units[1]. The major criticism of some of these units is that the sampling probes remain in the dissolution medium during the duration of the test, thereby disturbing the hydrodynamics of the solution (1). This can cause dissolution results other than those intrinsic to the dosage form. We have designed a simple sampling device which eliminates this problem while still allowing the convenience of automation. The device is made from a commercially available air-actuated, solenoid-controlled valve[2] and brackets that can be easily made in-house. The design and orientation of the brackets are shown in Figs. 1 and 2. Dimensional and installational information is presented in Fig. 3. Air is supplied to the device at 20 psi. Either house air or an air pump can be used. The unit is connected to a computer-controlled pump-fraction collecter[2] which provides contact closure to the solenoid through its internal-timing sequences which also control the pump-fraction collector's prime, sample, and purge cycles. However, this unit need only be connected to a 110 V contact closure and external air supply to actuate the valve. Once actuated, any suitable multiple-channel pump and collector can provide samples.

As previously indicated, we have chosen a combination pump-fraction collector with computerized timing sequences. A program is entered using a hand-held pad, and at program-designated intervals contact closure is made, the device is actuated, and samples are collected during a three-part 60-sec sequence: for 20 sec the lines are washed with sample to waste; the sample tray is then advanced and the next 20-sec sample is collected; and for 20 sec the pumps reverse to purge the lines. The sample tray then

[1] Hanson Research Corp., Northridge, CA 91324; Applied Analytical Industries, Wilmington, NC 28403; Technicon Industrial Systems, Tarrytown, NY 10591.
[2] Bimba Manufacturing Co., Monee, IL 60449.

0022-3549/83/0800-0976$01.00/0

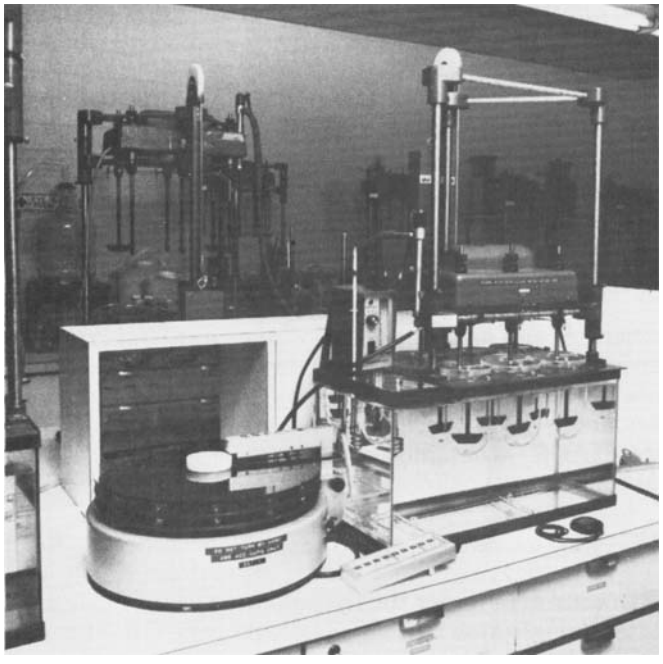

Figure 1—*Automated sampling device, fraction collector and dissolution unit.*

advances in preparation for the next sampling time. During the final 20 sec the probes are not in solution. Sample size can be adjusted by varying pump piston displacement.

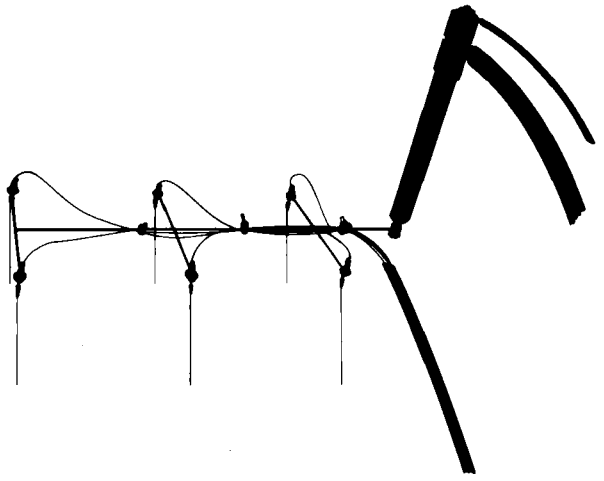

Figure 2—*Automated sampling device.*

During sampling, 50 μl-capillary tube probes are inserted into the medium for only 40 sec. The sampling location of the probes is as recommended in USP XX, and they retract above the surface of the medium after the 40-sec interval.

It has been shown by Savage and Wells that is is advantageous to minimize sample-probe size to reduce the influence on hydrodynamics (1). This design not only uses minimal probe size, but has the additional advantage of limiting the time the sample probes are inserted into the

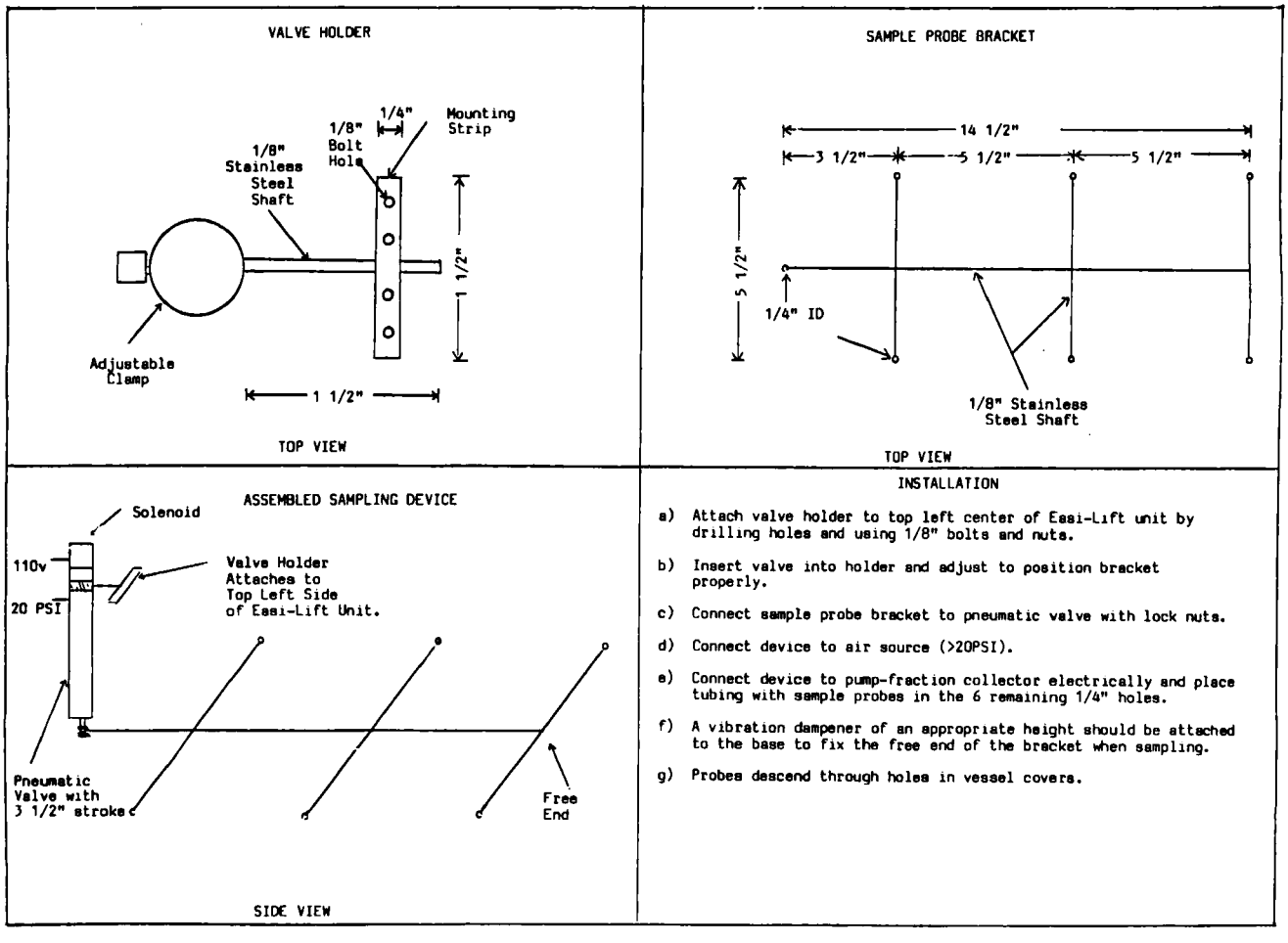

Figure 3—*Dimensional and installational information.*

dissolution medium to 40 sec/sampling time. This combination of reduced probe size and minimal contact with the dissolution medium results in minimal disturbance of the hydrodynamics of the medium.

In summary, this design offers these advantages for adaptation to Hanson Easi-Lift dissolution units:

1. The device does not disturb the hydrodynamics of the dissolution test, and the sampling probes are inserted in the solution only while sampling.
2. There is easy access to the dissolution unit because probes and brackets retract.
3. The sampling device is inexpensive to make and could be linked to a variety of dissolution pump-sample collection devices.

This device has proven to be reliable and essentially carryover-free in our laboratory and is in routine use.

(1) T. S. Savage and C. E. Wells, *J. Pharm. Sci.*, **71**, 670, (1982).
(2) "U.S. Pharmacopeia," 20th rev., U.S. Pharmacopeial Convention, Rockville, Md., p. 959, 1980.

T. R. Carrie[x]
G. A. Sanders
Mead Johnson & Co.
Evansville, IN 47721

Received November 15, 1982.
Accepted for publication April 18, 1983.

Computation of Model-Independent Pharmacokinetic Parameters During Multiple Dosing

Keyphrases □ Pharmacokinetics—computation of model-independent parameters, multiple dosing

To the Editor:

Pharmacokinetic analysis by means of traditional compartmental methods is slowly giving way to model-independent or noncompartmental approaches. Computational simplicity and, in some cases, more useful information are among the reasons for this trend. Methods that use the area under the drug concentration *versus* time curve (AUC) and the area under the first moment of drug concentration *versus* time curve (AUMC) are available to determine clearance (CL), mean residence time ($\bar{t}$), and apparent volume of distribution at steady state (V_{ss}) from data obtained after a single dose of drug (1, 2).

Often, the need arises to calculate pharmacokinetic parameters after several doses or at steady state; this is particularly true when patients are being treated with the study drug, and doses may not be manipulated for the purposes of the investigation. With the limited exception of the determination of clearance at steady state, noncompartmental methods have not been considered for this purpose.

Following repeated administration of a fixed dose of a drug at fixed intervals, the AUC during a dosing interval at steady state is equal to the total AUC after the first dose (3). Therefore, drug clearance can be calculated at steady state. On the other hand, AUMC during a dosing interval at steady state ($AUMC_{ss}$) is less than the total AUMC after a single dose. Therefore, $\bar{t}$ and V_{ss} cannot be calculated directly from steady-state data.

The inequivalence of $AUMC_{ss}$ and AUMC (single dose) can be demonstrated by considering multiple intravenous bolus doses of a drug with linear multicompartmental characteristics. Drug concentration (C) after a single dose is given by:

$$C = \sum_{i=1}^{n} A_i \exp(-k_i t) \qquad \text{(Eq. 1)}$$

where A_i and k_i are drug specific constants with units of concentration and reciprocal time, respectively; k_i values are independent of dose; $k_1 > k_2 \ldots > k_n$. The total area under the drug concentration–time curve after a single dose (AUC) is obtained by integrating Eq. 1 with respect to time:

$$\text{AUC} = \int_0^\infty C\,dt = \sum_{i=1}^{n} A_i/k_i \qquad \text{(Eq. 2)}$$

The total area under the first moment *versus* time curve after a single dose (AUMC) is given by the following integral:

$$\text{AUMC} = \int_0^\infty Ct\,dt = \sum_{i=1}^{n} A_i/(k_i)^2 \qquad \text{(Eq. 3)}$$

The analogous equations that apply to a dosing interval at steady state are as follows:

$$C_{ss} = \sum_{i=1}^{n} A_i \exp(-k_i t)/[1 - \exp(-k_i \tau)] \qquad \text{(Eq. 4)}$$

$$\text{AUC}_{ss} = \int_0^\tau C_{ss}dt = \sum_{i=1}^{n} A_i/k_i \qquad \text{(Eq. 5)}$$

$$\text{AUMC}_{ss} = \int_0^\tau C_{ss}t\,dt = \sum_{i=1}^{n} \frac{A_i}{(k_i)^2} \times \frac{[1 - \exp(-k_i\tau)] - k_i\,\tau \exp(-k_i\tau)}{1 - \exp(-k_i\tau)} \qquad \text{(Eq. 6)}$$

where τ is the fixed dosing interval. Note that Eqs. 2 and 5 are equivalent.

However, the relationship between $AUMC_{ss}$ and AUMC is given by the following ratio:

$$\frac{\text{AUMC}_{ss}}{\text{AUMC}} = \sum_{i=1}^{n} \frac{A_i}{(k_i)^2} \times \left[1 - \frac{k_i\,\tau \exp(-k_i\,\tau)}{[1 - \exp(-k_i\,\tau)]}\right] \Big/ \sum_{i=1}^{n} A_i/(k_i)^2 \qquad \text{(Eq. 7)}$$

Clearly, attempting to calculate t or V_{ss} by replacing AUMC with $AUMC_{ss}$ would provide incorrect answers, because $AUMC_{ss} < AUMC$.

We wish to propose an alternate, noncompartmental method to calculate pharmacokinetic parameters during repetitive dosing. This method may be called reverse superposition because a single dose curve is derived from data obtained during the second, third, or nth dosing interval. It is not limited to steady state but does require that subsequent doses be given during the postabsorptive, postdistributive phase of the previous dose. Each data point on the single-dose curve is calculated by means of the following equation:

$$C(t) = C_i(t) - C_i(0) \exp(-k_n t) \qquad \text{(Eq. 8)}$$

0022-3549/83/0800-0978$01.00/0

dissolution medium to 40 sec/sampling time. This combination of reduced probe size and minimal contact with the dissolution medium results in minimal disturbance of the hydrodynamics of the medium.

In summary, this design offers these advantages for adaptation to Hanson Easi-Lift dissolution units:

1. The device does not disturb the hydrodynamics of the dissolution test, and the sampling probes are inserted in the solution only while sampling.
2. There is easy access to the dissolution unit because probes and brackets retract.
3. The sampling device is inexpensive to make and could be linked to a variety of dissolution pump-sample collection devices.

This device has proven to be reliable and essentially carryover-free in our laboratory and is in routine use.

(1) T. S. Savage and C. E. Wells, *J. Pharm. Sci.*, **71**, 670, (1982).
(2) "U.S. Pharmacopeia," 20th rev., U.S. Pharmacopeial Convention, Rockville, Md., p. 959, 1980.

T. R. Carrie[x]
G. A. Sanders
Mead Johnson & Co.
Evansville, IN 47721

Received November 15, 1982.
Accepted for publication April 18, 1983.

Computation of Model-Independent Pharmacokinetic Parameters During Multiple Dosing

Keyphrases □ Pharmacokinetics—computation of model-independent parameters, multiple dosing

To the Editor:

Pharmacokinetic analysis by means of traditional compartmental methods is slowly giving way to model-independent or noncompartmental approaches. Computational simplicity and, in some cases, more useful information are among the reasons for this trend. Methods that use the area under the drug concentration *versus* time curve (AUC) and the area under the first moment of drug concentration *versus* time curve (AUMC) are available to determine clearance (CL), mean residence time ($\bar{t}$), and apparent volume of distribution at steady state (V_{ss}) from data obtained after a single dose of drug (1, 2).

Often, the need arises to calculate pharmacokinetic parameters after several doses or at steady state; this is particularly true when patients are being treated with the study drug, and doses may not be manipulated for the purposes of the investigation. With the limited exception of the determination of clearance at steady state, noncompartmental methods have not been considered for this purpose.

Following repeated administration of a fixed dose of a drug at fixed intervals, the AUC during a dosing interval at steady state is equal to the total AUC after the first dose (3). Therefore, drug clearance can be calculated at steady state. On the other hand, AUMC during a dosing interval at steady state ($AUMC_{ss}$) is less than the total AUMC after a single dose. Therefore, $\bar{t}$ and V_{ss} cannot be calculated directly from steady-state data.

The inequivalence of $AUMC_{ss}$ and AUMC (single dose) can be demonstrated by considering multiple intravenous bolus doses of a drug with linear multicompartmental characteristics. Drug concentration (C) after a single dose is given by:

$$C = \sum_{i=1}^{n} A_i \exp(-k_i t) \qquad \text{(Eq. 1)}$$

where A_i and k_i are drug specific constants with units of concentration and reciprocal time, respectively; k_i values are independent of dose; $k_1 > k_2 \ldots > k_n$. The total area under the drug concentration–time curve after a single dose (AUC) is obtained by integrating Eq. 1 with respect to time:

$$\text{AUC} = \int_0^\infty C\,dt = \sum_{i=1}^{n} A_i/k_i \qquad \text{(Eq. 2)}$$

The total area under the first moment *versus* time curve after a single dose (AUMC) is given by the following integral:

$$\text{AUMC} = \int_0^\infty Ct\,dt = \sum_{i=1}^{n} A_i/(k_i)^2 \qquad \text{(Eq. 3)}$$

The analogous equations that apply to a dosing interval at steady state are as follows:

$$C_{ss} = \sum_{i=1}^{n} A_i \exp(-k_i t)/[1 - \exp(-k_i \tau)] \qquad \text{(Eq. 4)}$$

$$\text{AUC}_{ss} = \int_0^\tau C_{ss}dt = \sum_{i=1}^{n} A_i/k_i \qquad \text{(Eq. 5)}$$

$$\text{AUMC}_{ss} = \int_0^\tau C_{ss}t\,dt = \sum_{i=1}^{n} \frac{A_i}{(k_i)^2} \times \frac{[1 - \exp(-k_i\tau)] - k_i\,\tau \exp(-k_i\tau)}{1 - \exp(-k_i\tau)} \qquad \text{(Eq. 6)}$$

where τ is the fixed dosing interval. Note that Eqs. 2 and 5 are equivalent.

However, the relationship between $AUMC_{ss}$ and AUMC is given by the following ratio:

$$\frac{\text{AUMC}_{ss}}{\text{AUMC}} = \sum_{i=1}^{n} \frac{A_i}{(k_i)^2} \times \left[1 - \frac{k_i\,\tau \exp(-k_i\,\tau)}{[1 - \exp(-k_i\,\tau)]}\right] \Big/ \sum_{i=1}^{n} A_i/(k_i)^2 \qquad \text{(Eq. 7)}$$

Clearly, attempting to calculate t or V_{ss} by replacing AUMC with $AUMC_{ss}$ would provide incorrect answers, because $AUMC_{ss} < AUMC$.

We wish to propose an alternate, noncompartmental method to calculate pharmacokinetic parameters during repetitive dosing. This method may be called reverse superposition because a single dose curve is derived from data obtained during the second, third, or nth dosing interval. It is not limited to steady state but does require that subsequent doses be given during the postabsorptive, postdistributive phase of the previous dose. Each data point on the single-dose curve is calculated by means of the following equation:

$$C(t) = C_i(t) - C_i(0) \exp(-k_n t) \qquad \text{(Eq. 8)}$$

0022-3549/83/0800-0978$01.00/0

Table I—Simulated Data for a 500-mg Dose every 2 hr [a]

Time, hr	Single Dose Concentration, μg/ml	Steady-State Concentration, μg/ml	Concentration Converted to Single Dose, μg/ml[b]
0	—	11.6	—
0.083	85.2	96.4	85.3
0.167	61.8	72.5	61.8
0.25	46.3	56.6	46.4
0.5	23.8	32.8	23.8
0.75	16.1	24.1	16.1
1.0	12.8	19.9	12.9
1.5	9.5	15.0	9.5
2	7.4	11.6	7.3
AUC[c]	56.159	—	55.996
AUMC[c]	84.198	—	83.391
V_{ss}[d]	13.3 liter	—	13.3 liter
CL[d]	8.9 liter/hr	—	8.9 liter/hr
$\bar{t}$[d]	1.5 hr	—	1.5 hr

[a] Single dose described by $C = 100e^{-5t} + 20e^{-0.5t}$. [b] Computed as $C = C_{sst} - 11.6e^{-0.5t}$. [c] Computed using trapezoidal rule. [d] V_{ss} = [Dose(AUMC)]/AUC^2, CL = Dose/AUC, $\bar{t}$ = AUMC/AUC.

where $C(t)$ is the calculated concentration after a single dose at time t, $C_i(t)$ is the observed concentration during the ith dosing interval at time t, $C_i(0)$ is the postabsorptive, postdistributive drug concentration at the start of the ith dosing interval, and k_n is the terminal rate constant.

To illustrate this method, data were simulated (4) for two different sets of conditions. The first data set represented concentration–time values after an intravenous bolus dose (Table I). The second set of data are values representative of extravascular administration (Table II). The last data set consists of concentration–time values for intermittant intravenous infusion (Table III). In all cases, a single-dose curve was constructed by means of Eq. 8 from the steady-state values. The AUC and AUMC values between the single dose situation and the curve derived using reverse superposition varied slightly because of rounding-off errors, but no appreciable differences were apparent between respective pharmacokinetic parameters.

Since reverse superposition applies also during multiple dosing before steady state occurs, this method could be applied at any time during therapy. This approach could be useful when patients receiving the study drug are investigated, since it is often difficult to ensure steady-state conditions (*i.e.*, compliance, errors in administration time, *etc.*) Caution must be used when the dosing interval is short relative to the terminal half-life of the drug. Under these conditions half-life may be difficult to calculate, and errors may occur in the estimation of $C(t)$ as well as in the estimation of AUC and AUMC from the derived single dose curve.

Table II—Simulated Data for a 500-mg Dose every 6 hr [a]

Time, hr	Single Dose Concentration, μg/ml	Steady-State Concentration, μg/ml	Concentration Converted to Single Dose, μg/ml[b]
0	0	15.4	0
0.25	4.4	19.4	4.4
0.5	7.3	21.8	7.3
1.0	10.3	24.1	10.1
2.0	11.5	23.7	11.5
3.0	10.8	21.7	10.8
4.0	9.7	19.4	9.7
5.0	8.7	17.3	8.7
6.0	7.7	15.4	7.7
AUC[c]	122.49	—	122.57
AUMC[c]	1140.68	—	1140.76
$\bar{t}$[d]	8.6 hr	—	8.6 hr

[a] Single dose described by $C = 15.5e^{-0.116t} - 15.5e^{-1.5t}$ assuming complete bioavailability. [b] Computed as $C = C_{sst} - 15.4e^{-0.116t}$. [c] Computed using trapezoidal rule. [d] $\bar{t}$ = AUMC/AUC, the mean residence time after oral administration.

Table III—Simulated Data for a 500-mg Dose Infused Over 0.5 hr Administered every 2 hr [a]

Time, hr	Single Dose Concentration, μg/ml	Steady-State Concentration, μg/ml	Concentration Converted to Single Dose, μg/ml[b]
0	0	12.5	—
0.25	41.9	52.7	41.7
0.5	58.3	68.0	58.2
0.583	42.4	51.9	42.6
0.667	32.5	41.5	32.5
0.75	26.1	34.8	26.2
1.0	17.1	24.6	17.0
1.25	13.5	20.2	13.5
1.5	11.4	17.3	11.4
2.0	8.8	13.4	8.8
AUC[c]	62.49	—	62.45
AUMC[c]	104.30	—	104.30
V_{ss}[d]	11.4 liter	—	11.4 liter
CL[d]	8.0 liter/hr	—	8.0 liter/hr
$\bar{t}$[d]	1.7 hr	—	1.7 hr

[a] Single intraveneous bolus dose described by $C = 100e^{-5t} + 20e^{-0.5t}$. [b] Computed as $C = C_{sst} - 12.5e^{-0.5t}$. [c] Computed using trapezoidal rule. [d] V_{ss} = [Dose(AUMC)/(AUC)^2] − [T(Dose)]/2AUC, where T = Infusion duration. See Table I for other equations.

(1) L. Z. Benet and R. L. Galeazzi, *J. Pharm. Sci.*, **68**, 1071 (1979).

(2) D. Perrier and M. Mayersohn, *J. Pharm. Sci.*, **71**, 372 (1982).

(3) J. G. Wagner, J. I. Northam, C. D. Alway, and O. S. Carpenter, *Nature (London)*, **1965**, 207.

(4) J. R. Koup and D. R. Benjamin, *Ther. Drug Monitor.*, **1980**, 243.

Larry A. Bauer [x]
Milo Gibaldi
School of Pharmacy
University of Washington
Seattle, WA 98195

Received January 24, 1983.
Accepted for publication April 20, 1983.

Test for Selection of Erythromycin Stearate Bulk Drug for Tablet Preparation

Keyphrases □ Bioavailability—erythromycin stearate tablet formulation, dissolution rate, high-performance liquid chromatography □ Erythromycin stearate—bioavailability, tablet formulations, dissolution rate, high-performance liquid chromatography □ High-performance liquid chromatography—erythromycin stearate tablet formulation, bioavailability

To the Editor:

Bioavailability testing of experimental erythromycin stearate tablet formulations showed significant differences between tablets declaring 250 and 500 mg, where the concentrations of antibiotic and excipients were identical and the tablets differed only in fill weight and geometry. Different lots of erythromycin stearate were used in these formulations. It was learned, subsequently, that the dissolution rate (and presumably bioavailability) of erythromycin from the tablets could be correlated with the intrinsic dissolution rate of the batch of erythromycin stea-

0022-3549/83/0800-0979$01.00/0

Table I—Simulated Data for a 500-mg Dose every 2 hr [a]

Time, hr	Single Dose Concentration, μg/ml	Steady-State Concentration, μg/ml	Concentration Converted to Single Dose, μg/ml[b]
0	—	11.6	—
0.083	85.2	96.4	85.3
0.167	61.8	72.5	61.8
0.25	46.3	56.6	46.4
0.5	23.8	32.8	23.8
0.75	16.1	24.1	16.1
1.0	12.8	19.9	12.9
1.5	9.5	15.0	9.5
2	7.4	11.6	7.3
AUC[c]	56.159	—	55.996
AUMC[c]	84.198	—	83.391
V_{ss}[d]	13.3 liter	—	13.3 liter
CL[d]	8.9 liter/hr	—	8.9 liter/hr
$\bar{t}$[d]	1.5 hr	—	1.5 hr

[a] Single dose described by $C = 100e^{-5t} + 20e^{-0.5t}$. [b] Computed as $C = C_{sst} - 11.6e^{-0.5t}$. [c] Computed using trapezoidal rule. [d] V_{ss} = [Dose(AUMC)]/AUC^2, CL = Dose/AUC, $\bar{t}$ = AUMC/AUC.

where $C(t)$ is the calculated concentration after a single dose at time t, $C_i(t)$ is the observed concentration during the ith dosing interval at time t, $C_i(0)$ is the postabsorptive, postdistributive drug concentration at the start of the ith dosing interval, and k_n is the terminal rate constant.

To illustrate this method, data were simulated (4) for two different sets of conditions. The first data set represented concentration–time values after an intravenous bolus dose (Table I). The second set of data are values representative of extravascular administration (Table II). The last data set consists of concentration–time values for intermittant intravenous infusion (Table III). In all cases, a single-dose curve was constructed by means of Eq. 8 from the steady-state values. The AUC and AUMC values between the single dose situation and the curve derived using reverse superposition varied slightly because of rounding-off errors, but no appreciable differences were apparent between respective pharmacokinetic parameters.

Since reverse superposition applies also during multiple dosing before steady state occurs, this method could be applied at any time during therapy. This approach could be useful when patients receiving the study drug are investigated, since it is often difficult to ensure steady-state conditions (*i.e.*, compliance, errors in administration time, *etc.*) Caution must be used when the dosing interval is short relative to the terminal half-life of the drug. Under these conditions half-life may be difficult to calculate, and errors may occur in the estimation of $C(t)$ as well as in the estimation of AUC and AUMC from the derived single dose curve.

Table II—Simulated Data for a 500-mg Dose every 6 hr [a]

Time, hr	Single Dose Concentration, μg/ml	Steady-State Concentration, μg/ml	Concentration Converted to Single Dose, μg/ml[b]
0	0	15.4	0
0.25	4.4	19.4	4.4
0.5	7.3	21.8	7.3
1.0	10.3	24.1	10.1
2.0	11.5	23.7	11.5
3.0	10.8	21.7	10.8
4.0	9.7	19.4	9.7
5.0	8.7	17.3	8.7
6.0	7.7	15.4	7.7
AUC[c]	122.49	—	122.57
AUMC[c]	1140.68	—	1140.76
$\bar{t}$[d]	8.6 hr	—	8.6 hr

[a] Single dose described by $C = 15.5e^{-0.116t} - 15.5e^{-1.5t}$ assuming complete bioavailability. [b] Computed as $C = C_{sst} - 15.4e^{-0.116t}$. [c] Computed using trapezoidal rule. [d] $\bar{t}$ = AUMC/AUC, the mean residence time after oral administration.

Table III—Simulated Data for a 500-mg Dose Infused Over 0.5 hr Administered every 2 hr [a]

Time, hr	Single Dose Concentration, μg/ml	Steady-State Concentration, μg/ml	Concentration Converted to Single Dose, μg/ml[b]
0	0	12.5	—
0.25	41.9	52.7	41.7
0.5	58.3	68.0	58.2
0.583	42.4	51.9	42.6
0.667	32.5	41.5	32.5
0.75	26.1	34.8	26.2
1.0	17.1	24.6	17.0
1.25	13.5	20.2	13.5
1.5	11.4	17.3	11.4
2.0	8.8	13.4	8.8
AUC[c]	62.49	—	62.45
AUMC[c]	104.30	—	104.30
V_{ss}[d]	11.4 liter	—	11.4 liter
CL[d]	8.0 liter/hr	—	8.0 liter/hr
$\bar{t}$[d]	1.7 hr	—	1.7 hr

[a] Single intraveneous bolus dose described by $C = 100e^{-5t} + 20e^{-0.5t}$. [b] Computed as $C = C_{sst} - 12.5e^{-0.5t}$. [c] Computed using trapezoidal rule. [d] V_{ss} = [Dose(AUMC)/(AUC)^2] − [T(Dose)]/2AUC, where T = Infusion duration. See Table I for other equations.

(1) L. Z. Benet and R. L. Galeazzi, *J. Pharm. Sci.*, **68**, 1071 (1979).

(2) D. Perrier and M. Mayersohn, *J. Pharm. Sci.*, **71**, 372 (1982).

(3) J. G. Wagner, J. I. Northam, C. D. Alway, and O. S. Carpenter, *Nature (London)*, **1965**, 207.

(4) J. R. Koup and D. R. Benjamin, *Ther. Drug Monitor.*, **1980**, 243.

Larry A. Bauer [x]
Milo Gibaldi
School of Pharmacy
University of Washington
Seattle, WA 98195

Received January 24, 1983.
Accepted for publication April 20, 1983.

Test for Selection of Erythromycin Stearate Bulk Drug for Tablet Preparation

Keyphrases □ Bioavailability—erythromycin stearate tablet formulation, dissolution rate, high-performance liquid chromatography □ Erythromycin stearate—bioavailability, tablet formulations, dissolution rate, high-performance liquid chromatography □ High-performance liquid chromatography—erythromycin stearate tablet formulation, bioavailability

To the Editor:

Bioavailability testing of experimental erythromycin stearate tablet formulations showed significant differences between tablets declaring 250 and 500 mg, where the concentrations of antibiotic and excipients were identical and the tablets differed only in fill weight and geometry. Different lots of erythromycin stearate were used in these formulations. It was learned, subsequently, that the dissolution rate (and presumably bioavailability) of erythromycin from the tablets could be correlated with the intrinsic dissolution rate of the batch of erythromycin stea-

0022-3549/83/0800-0979$01.00/0

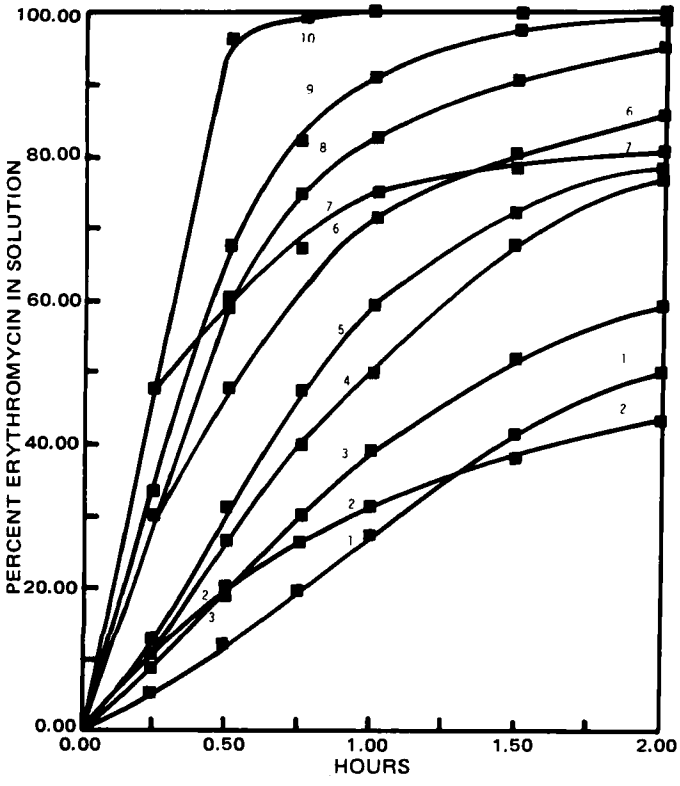

Figure 1—*Dissolution profile of various lots of erythromycin stearate as a function of time (0.05 M pH 6.6 phosphate buffer).*

rate used. A dissolution test method was developed for erythromycin stearate bulk drug and tablets using conditions under which decomposition of the antibiotic does not occur.

Erythromycin, its esters, salts, and their preparations have been reported to show significant differences in bioavailability (1). Stavchansky *et al.* (2) described attempts to correlate the known bioavailability of erythromycin stearate tablets from various sources with different *in vitro* test methods, including disintegration, dissolution, and dissolution–dialysis. Their findings were inconclusive, perhaps because their dissolution experiments were confounded by the decomposition of the antibiotic under the conditions used: their test method did not discriminate between intact and decomposed erythromycin.

Tsuji and Goetz (3) described a high-performance liquid chromatographic (HPLC) method for erythromycin which is selective for the intact drug and correlates with microbiological potency assay. In this laboratory, the method afforded a single peak for erythromycin at about 7.9 min. At 37°, the conventional temperature used in dissolution testing, erythromycin decomposition was rapid as evidenced by the decrease of its peak height and appearance of a new peak at about 12.5 min. Dissolution of the drug increases with increased acidity. However, acidity and temperature promote decomposition of erythromycin. On the basis of these considerations, the dissolution test method developed used pH 6.6 phosphate buffer at room temperature for the dissolution medium.

The dissolution studies were performed in a USP Apparatus 2 (4), equilibrating 500 ml of 0.05 *M* pH 6.6 phosphate buffer at 22°. The paddle was rotated at 50 rpm and 500 mg of erythromycin stearate (dispersing it with a micro spatula to ensure that it is wetted) or an erythromycin stearate tablet was added to the medium. A 5.0-ml aliquot was withdrawn after 60 min. The test sample was filtered through a membrane filter[1] and assayed immediately for erythromycin by the HPLC method (3). Under these test conditions, no decomposition of erythromycin was detected on the chromatograms. (The HPLC assay was used to obtain the data reported below; however, any convenient method could be employed after establishment of the validity of the test conditions.) Decomposition of erythromycin becomes evident after prolonged residence (several hours) in the dissolution medium; hence the injunction to assay the test sample immediately after completion of the test.

Table I—Dissolution of Erythromycin Stearate Bulk Drug and Corresponding Tablets

Curve No.[a]	Percent Dissolution After 1.0 Hr		
	Bulk Drug	500-mg Tablet	250-mg Tablet
4	49	44	
6	72	70	
7	75	70	
—	78	—	80
8	82	78	
9	92	88	

[a] Dissolution curves from Fig. 1.

Ten lots of erythromycin stearate from two domestic and six foreign sources were found to vary from 27 to 100% dissolution in 1 hr. A plot of the dissolution rate as a function of time is shown for these lots in Fig. 1. In general, dissolution of the bulk drug was similar to that of the tablets made from it. The dissolution rates of bulk drug and corresponding tablets are shown in Table I.

Bioavailability studies showed that the tablets made from bulk drugs of 72 and 78% dissolution were acceptable, while those made from bulk drug of 49% dissolution were unacceptable. For this reason, 70% dissolution for the bulk drug has been arbitrarily set as acceptable.

Erythromycin stearate is a mixture of the stearate salt of erythromycin with varying amounts of free stearic acid, medium stearate, and water. The chemical and physical properties that affect its dissolution have not been elucidated; attempts to correlate dissolution with particle size, shape, and crystal forms of the drug have failed. However, the test method proposed affords a facile empirical means for selecting suppliers.

(1) C. H. Nightingale, L. W. Dittert, and T. N. Tozer, *J. Am. Pharm. Assoc. NS*, **16**, 203 (1976).

(2) S. Stavchansky, J. T. Doluisio, A. Martin, C. Martin, B. Cabana, S. Dighe, and A. Loper, *J. Pharm. Sci.*, **69**, 1307 (1980).

(3) K. Tsuji and J. F. Goetz, *J. Chromatogr.*, **147**, 359 (1978).

(4) "The United States Pharmacopeia," 20th rev., U.S. Pharmacopeial Convention, Rockville, Md., 1980, p. 959.

Jose Philip [x]
Robert E. Daly
Product Development Laboratories
Warner Lambert Pharmaceutical Research
Warner Lambert Company
Morris Plains, NJ 07950

Received July 26, 1982.
Accepted for publication April 22, 1983.

[1] Metricel Membrane filter, 0.45 μm; Gelman Instrument Co., Ann Arbor, MI 48106.

JOURNAL OF PHARMACEUTICAL SCIENCES

September 1983
Volume 72 Number 9

A publication of the American Pharmaceutical Association

The *Journal of Pharmaceutical Sciences* (ISSN 0022-3549) is published monthly by the American Pharmaceutical Association (APhA) at 2215 Constitution Ave., N.W., Washington, DC 20037. Second-class postage paid at Washington, D.C. and at additional mailing office.

All expressions of opinion and statements of supposed fact appearing in articles or editorials carried in this journal are published on the authority of the writer over whose name they appear and are not to be regarded as necessarily expressing the policies or views of APhA.

Offices—Editorial, Advertising, and Subscription: 2215 Constitution Ave., N.W., Washington, DC 20037. All Journal staff may be contacted at this address. Printing: 20th & Northampton Streets, Easton, PA 18042.

Annual Subscriptions—United States and foreign, industrial and government institutions $75; educational institutions $75; individuals *for personal use only* $40; single copies $10. APhA and SAPhA members may subscribe to *J. Pharm. Sci.* for $20.00 per year. All foreign subscriptions add $10 for postage. Subscription rates are subject to change without notice.

Claims—Missing numbers will not be supplied if dues or subscriptions are in arrears for more than 60 days or if claims are received more than 60 days after the date of the issue, or if loss was due to failure to give notice of change of address. APhA cannot accept responsibility for foreign delivery when its records indicate shipment was made.

Change of Address—Members and subscribers should notify at once both the Post Office and APhA of any change of address.

Scientific Manpower—Supply *versus* Demand

A very popular and apparently successful business magazine is entitled "*Changing Times.*" Today that title, more than ever before, seems to reflect what is happening all around us.

During the past several decades, government and its handmaiden, government regulation—particularly at the federal level—have expanded tremendously. Much of this expansion can be attributed to the desire of citizens and legislators to minimize sudden and upsetting shifts in the economic, trade, business, and employment arenas by establishing controls over the forces believed to be responsible for such shifts.

However, the record of performance and experience is anything but convincing or even satisfactory.

For example, just a year ago, the country struggled through a period of one of the highest inflation rates and interest rates in its entire history; and this happened despite more prevailing fiscal, monetary, and banking regulatory authority than ever before. As another example, within a matter of less than three years, we went from mass warnings of an oil and energy "crunch" to a situation now described as a "glut."

So the times do change; and they change rapidly; and they change in spite of considerable efforts to plan, control, and channel the directions of the forces that are behind those changes.

It should not be too surprising, therefore, that changes of a comparably upsetting magnitude are now taking place in the field of health care delivery.

Just a few short years ago, the popular and almost universally repeated theme was the impending shortage of all constituent elements of health care: hospitals, physicians, and all other health care practitioners. Every suggestion of expanding public benefits *via* legislation was couched in fears of overburdening the capacity of the already overstrained health care system by trying to accommodate anticipated additional demands placed upon it.

Now that, too, has all changed.

In virtually each issue of every medical, dental, pharmacy, and other health care related news publication, there is at least some reference to the existing or impending *oversupply* of physicians, dentists, pharmacists, nurses, or other practitioners. And the latest predictions are that hospitals are going to be next on "the hit list." In fact, a nationally known hospital consulting firm has just predicted that "1,000 of the existing 6,000 hospitals in the country will close by 1985, due to cutbacks in government funding and patients' inability to pay their bills." Furthermore, "the remaining 5,000 hospitals will be controlled by 400 ownerships," suggesting that a lot of constriction and belt-tightening will take place in order to maintain the economic viability of the surviving hospitals.

In the professional practice arena, this has begun to trigger a good deal of preliminary "jockeying" on the part of each group to stake out new roles or expanded areas of practice involvement. All of this is in an effort to maintain as large as possible a share of the health care dollar *via* future demand for their professional services. But, conversely, to other groups, this often is perceived as "trespassing" on their territory. Hence, the so-called "turf battles" are just now beginning to shape up, and undoubtedly they will become more severe as the situation itself grows more difficult.

Our pharmaceutical scientist readers may find all this only incidentally interesting, and wonder how—if at all—it affects them.

But affect them, it most likely will; and that warning is the underlying message of this editorial.

Approximately 10 years ago, employers such as drug companies, government laboratories, health sciences schools, and so on, found it very difficult to lure graduating pharmacists and physicians into their employment. The financial rewards as practitioners were better and more immediate. Hence, at that time, there was relatively less competition for the industry, government, and academic jobs than there is now; and today there is much less competition than will probably be the case in the near future.

Such a threat of intense job competition might appear farfetched to many pharmaceutical scientists, but when considered against the backdrop of current physician fears of inroads being made by nurse-practitioners, of pharmacist concerns of physicians turning to drug product dispensing, and dentist efforts to curb expansion by dental hygienists, the potential threat becomes far more believable. Physicians who are unable to establish a viable practice may be even receptive to taking jobs as laboratory scientists. And, in doing so, they will displace a corresponding number of technical people.

And lest the Ph.D.-level, senior scientists assume that they will be immune, one only has to think back to about the early 1970s when there was a reverse type of situation.

At that time, the physician shortage and the lure of bigger financial rewards—coupled with a downturn in the demand for scientific and technical personnel—prompted so much interest among Ph.D. people, that a number of medical schools established a specially tailored curriculum for such people who wanted to obtain an M.D. degree. Is it not just as reasonable to project that sizable numbers of today's and tomorrow's graduates from medical schools, as well as pharmacy schools—when faced with poor employment prospects—will opt for Ph.D. degrees as their admission ticket into pharmaceutical research?

Consequently, the alternately rising and ebbing tide of health care manpower does, indeed, impact upon everyone in the field: on some more than others, on some more directly than others.

"Preparation" is the byword of success in any endeavor. Hence, it would be well for pharmaceutical scientists to prepare themselves for this situation; moreover, the signs clearly indicate that it is not too early now to begin such planning and preparations.

—EDWARD G. FELDMANN
American Pharmaceutical Association
Washington, DC 20037

0022-3549/83/0900-0981$01.00/0

JOURNAL OF PHARMACEUTICAL SCIENCES

SEPTEMBER 1983
VOLUME 72 NUMBER 9

RESEARCH ARTICLES

Effect of Intergranular *versus* Intragranular Cornstarch on Tablet Friability and *In Vitro* Dissolution

Z. T. CHOWHAN [x] **and I.-C. YANG**

Received March 22, 1982, from the *Institute of Pharmaceutical Sciences, Syntex Research, Palo Alto, CA 94304.* Accepted for publication August 18, 1982.

Abstract □ The effect of blending dry cornstarch *versus* wet granulation with the drug and other excipients on friability and *in vitro* dissolution of a ticlopidine hydrochloride tablet formulation was studied. The friability of the tablets was reduced by wet granulating cornstarch with the drug and other excipients compared with the dry blending. The dissolution rate and the tablet-to-tablet variability was improved by incorporating cornstarch in the wet-granulation stage. The lactose placebo tablets, which were wet granulated with either a binder solution or without a binder, also showed reduced tablet friability due to the incorporation of cornstarch in the wet-granulation step. Examination of the tablet cross sections under the scanning electron microscope indicated clumping of starch grains when starch was blended in the dry form. Starch grains were well embedded in the other materials of the tablet and not readily visible when starch was wet granulated with the other excipients. This results in better bonding, fewer weak points, and better homogeneity of the starch disintegrator within the tablet, which accounts for better friability and improved dissolution.

Keyphrases □ Ticlopidine hydrochloride—tablet friability, *in vitro* dissolution, effect of inter- *versus* intragranular cornstarch □ Cornstarch—inter- *versus* intragranular, effect on tablet friability and *in vitro* dissolution, ticlopidine hydrochloride □ Dissolution—*in vitro*, ticlopidine hydrochloride, effect of inter- *versus* intragranular corn starch, friability

Starch USP is a common excipient in compressed tablets, both as a disintegrator and as a binder. Cornstarch is one of the most common disintegrating agents used in tablet formulations today. When added in the dry state to the dry granulation, it acts as a disintegrator. In the paste or dry form, when added before wet granulation, its function is that of a disintegrator and binder.

The mechanism of action of starches is not well understood. In aspirin tablets (1) where contact of starch grains was continuous in the interparticle spaces, disintegration was rapid and effective even when void spaces were eliminated. Where contact was not continuous, disintegration was slower, and appeared to depend on the degree of contact between starch grains and aspirin particles and on the size of interparticle spaces. The primary mechanism appeared to be a swelling action. Capillarity *per se* did not appear to have a disintegrating effect. Ingram and Lowenthal (2) could not find any measurable correlations between starch grain damage and disintegration time or between starch swelling and compressional force. Outside of compressional force, the inherent effect of the tablet ingredients was the only factor that appeared to affect disintegration. In a later study, Lowenthal and Burruss (3) discounted pore diameter and porosity of the tablet as a mechanism of action of starch as a disintegrator. A significant swelling of the starch grains was not observed (4) when pressure-deformed grains were moistened with water. Thus, the regaining of the shape of starch grains was apparently not the mechanism of action as a tablet disintegrator. Observations by scanning electron microscope (5) indicated that rupture of the tablet surface occurred where starch agglomerates were found. It was postulated that water hydrates the hydroxyl groups of the starch molecules, causing them to move apart. The slight swelling that occurs is due to a rapid hydration step and a slower sorption step after the addition of water. Channels or pores lined with starch were not evident. The conditions for rapid tablet disintegration were sufficient agglomerates, low pressure, and presence of water.

In wet-granulated tablet formulations, starch is usually added in the dry form prior to compression. This general practice is based perhaps on the swelling theory of the mechanism of action of starch as a disintegrator which is generally discounted. The data in the literature strongly suggest that disintegration is influenced by a wide variety

0022-3549/83/0900-0983$01.00/0

Table I—Formulations Used in This Study [a]

Ingredients	Formulation A	Formulation B	Formulation C
Ticlopidine hydrochloride	250.00	—	—
Microcrystalline cellulose	87.35	—	87.35
Lactose	—	337.35	255.85
Citric acid	3.90	3.90	3.90
Starch	39.00	39.00	39.00
Povidone	7.80	7.80	—
Stearic acid	—	—	3.90
Magnesium stearate	1.95	1.95	—

[a] Milligrams of ingredient per tablet.

of factors that are specific only for a given tablet formulation; it is difficult to determine the mechanism of action of starch as a tablet disintegrator.

Recent studies from these laboratories (6) suggested that the friability of compressed tablets was reduced by incorporating 80% cornstarch in the wet-granulation step compared with the dry blending. This paper examines the effects of intragranular *versus* intergranular cornstarch on tablet friability and *in vitro* dissolution.

EXPERIMENTAL

Materials—The drug, ticlopidine hydrochloride[1], was ≥99.0% pure. The excipients used were microcrystalline cellulose[2] NF, povidone[3] USP, citric acid[4] USP, stearic acid[5] powder NF, cornstarch[6] NF, lactose[7] USP, and magnesium stearate[4] NF.

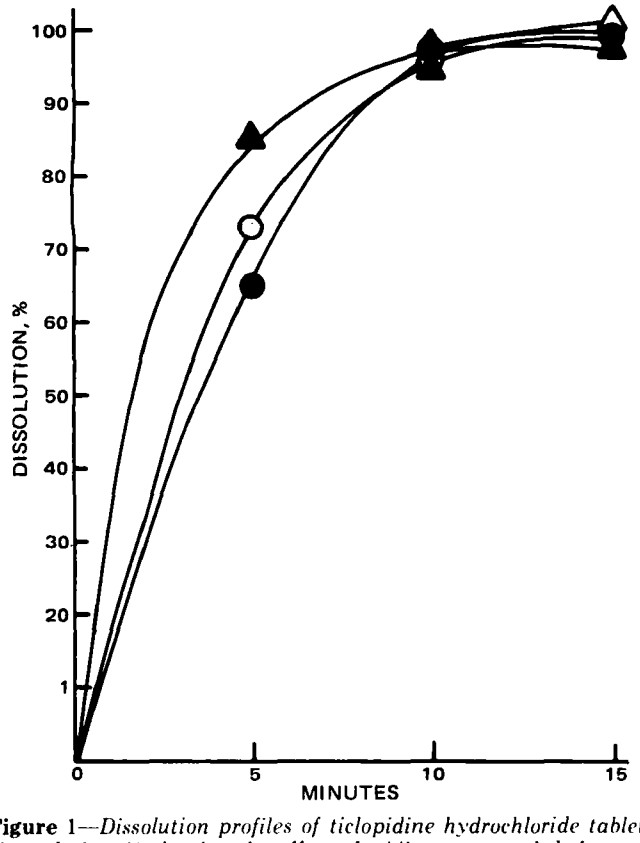

Figure 1—*Dissolution profiles of ticlopidine hydrochloride tablets (formulation A) showing the effect of adding cornstarch before wet granulation* versus *blending it with the dry granulation. The granulation moisture content was 2.1%, and tablet crushing strength was 15 Strong Cobb units. Key: (○) starch dry blended, with extra-deep concave punches; (●) starch dry blended, with standard concave punches; (△) starch wet granulated, with extra-deep concave punches; (▲) starch wet granulated, with standard concave punches.*

[1] 5-(o-Chlorobenzyl)-4,5,6,7-tetrahydrothieno-[3,2-c]pyridine hydrochloride; Sanofi Research Co., New York, NY 10019.
[2] Avicel pH 101; FMC Corp.
[3] GAF Corp., New York, NY 10020.

Table II—Effect of the Addition of Starch During Wet Granulation or Blending with the Dry Granulation on Friability of Tablets Compressed with Standard Concave Punches [a]

Punch	Tablet Friability, % Starch Blended with Dry Granulation	Tablet Friability, % Starch Wet Granulated with Other Materials
Standard concave	0.27	0.0925
Extra-deep concave	0.135	0.0165

[a] Using formulation A with a granulation moisture of 2.1% and tablet crushing strength of 15 Strong Cobb units.

Granulation—The formulations used in this study are given in Table I. The drug and the appropriate excipients were mixed together in a small, planetary mixer for 10 min. Citric acid and povidone in formulations A and B and citric acid alone in formulation C were dissolved in water. These solutions were used to granulate the powder mixture. After 10 min of mixing, the granulation was passed through a 1.4-mm aperture and dried in a forced-air oven at 50° until the desired moisture levels were obtained. The dried granulation was forced through a 1.2-mm aperture screen. The lubricant and the disintegrator were blended with the granulation for 5 min. The granulations were stored in tightly closed, glass bottles. The moisture content of the final granulation was determined prior to compression.

Compression—The compression was carried out by means of a single-punch tablet machine[8]. The punches and die were 10.32 mm in diameter. Standard concave and extra-deep concave punches were used for compression. The target compression weight was 390 mg/tablet. The tablet crushing strength was determined[9] immediately after compression. For each determination, 10 tablets were tested and the mean was calculated.

Granulation Moisture—The granulation was exposed to a 125-W

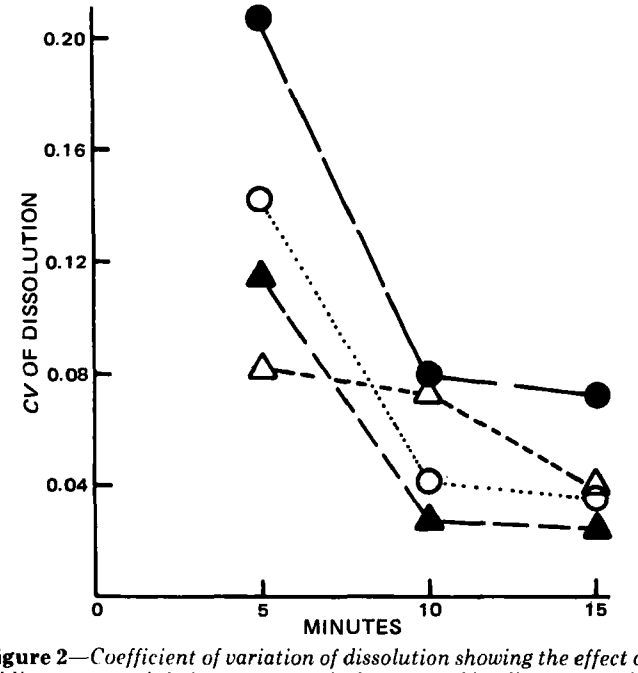

Figure 2—*Coefficient of variation of dissolution showing the effect of adding cornstarch before wet granulation* versus *blending it with the dry granulation (formulation A). The granulation moisture content was 2.1%, and the tablet crushing strength was 15 Strong Cobb units. Key: (○) starch dry blended, with extra-deep concave punches; (●) starch dry blended, with standard concave punches; (△) starch wet granulated, with extra-deep concave punches; (▲) starch wet granulated, with standard concave punches.*

[4] Mallinckrodt, Inc., St. Louis, MO 63147.
[5] Emery Industries, Inc., Cincinnati, OH 45232.
[6] Staley Manufacturing Co., Decatur, Ill.
[7] Regular Grade; Foremost Co., San Francisco, CA 94104.
[8] Stokes Model F4.
[9] Schleuniger-2E Hardness Tester; Vector Corp., Marion, IA 52303.

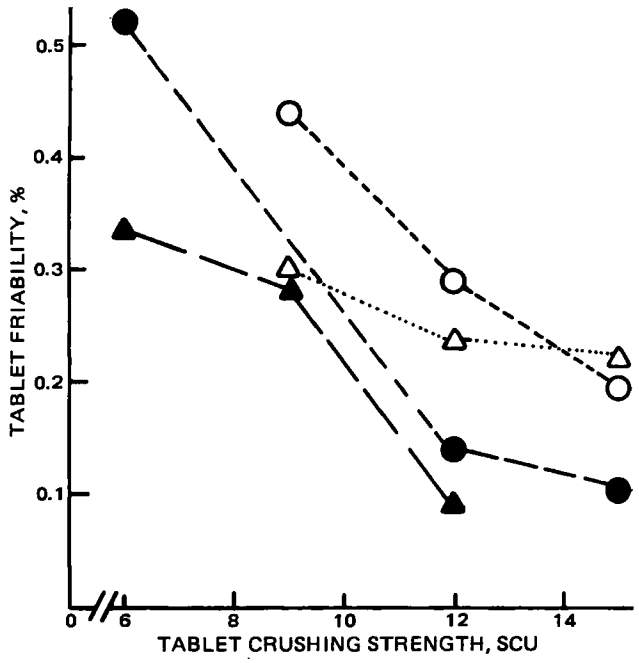

Figure 3—*Effect of adding cornstarch during wet granulation* versus *blending with the dry granulation on friability of placebo tablets (formulation B). The granulation moisture content was 2.0%. Key: (○) starch dry blended, with standard concave punches; (●) starch dry blended with extra-deep concave punches; (△) starch wet granulated, with standard concave punches; (▲) starch wet granulated, with extra-deep concave punches.*

IR lamp for 15 min at a 90-V setting in a moisture balance[10]. The percent weight loss on drying was read directly from the instrument.

Tablet Friability—A Roche-type friabilator was used. Twenty tablets were brushed with a soft, camel's hair brush to remove all adhering particles. After accurate weighing, the tablets were placed in the drum. The drum was rotated for 4 min (100 revolutions), the tablets were removed, brushed to remove adhering particles, and accurately weighed. The test was carried out in duplicate, and the mean percent friability was calculated.

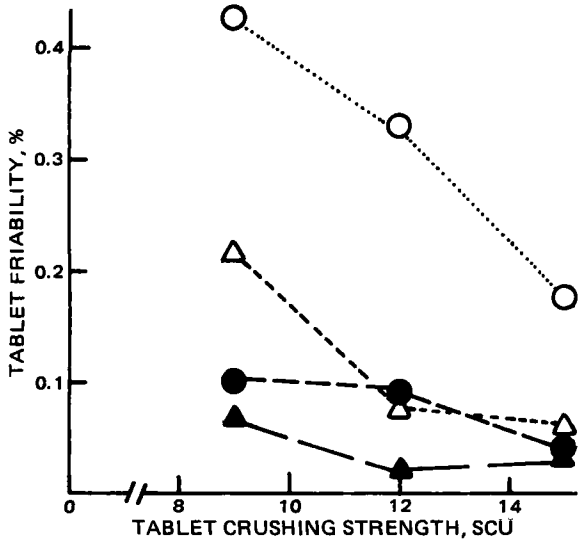

Figure 4—*Effect of adding cornstarch during wet granulation* versus *blending with the dry granulation on friability of placebo tablets (formulation C). The granulation moisture content was 2.0%. Key: (○) starch dry blended, with standard concave punches; (●) starch dry blended, extra-deep concave punches; (△) starch wet granulated, with standard concave punches; (▲) starch wet granulated, with extra-deep concave punches.*

[10] Cenco Central Scientific Co., Chicago, IL 60623.

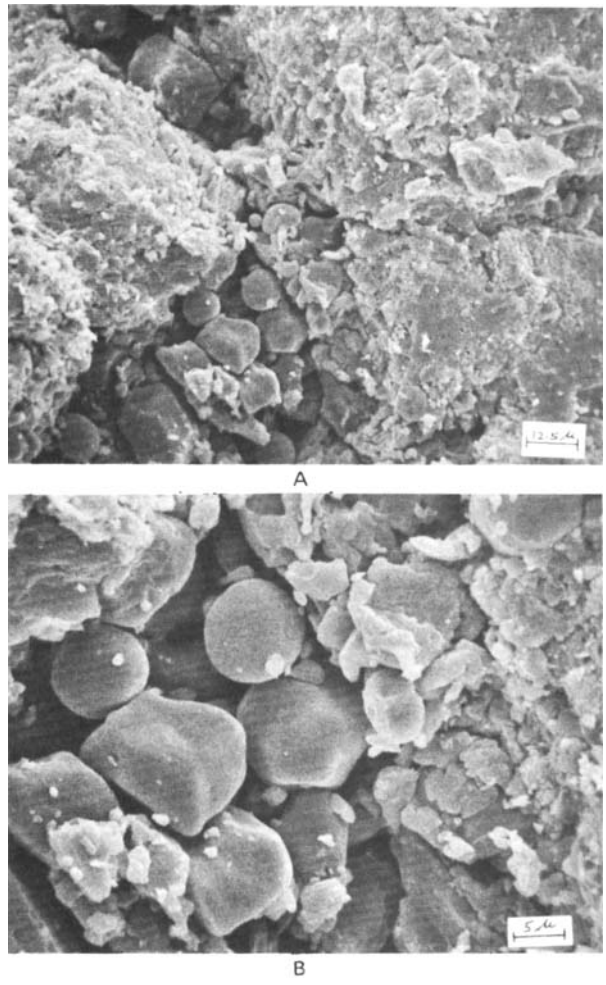

Figure 5—*Cross-sectional view of ticlopidine hydrochloride tablets compressed with the standard concave punches using formulation A. Starch was dry blended. Key: (A) ~800× (original magnification); (B) ~2000× (original magnification).*

***In Vitro* Dissolution**—The *in vitro* dissolution was determined by the USP Method II as reported earlier (6). For each determination, six tablets were tested. This apparatus consisted of USP paddles driven by a multiple-spindle drive with a variable-speed control[11]; round-bottom, plastic resin kettles[12] measuring 1 liter; and a water bath. The dissolution

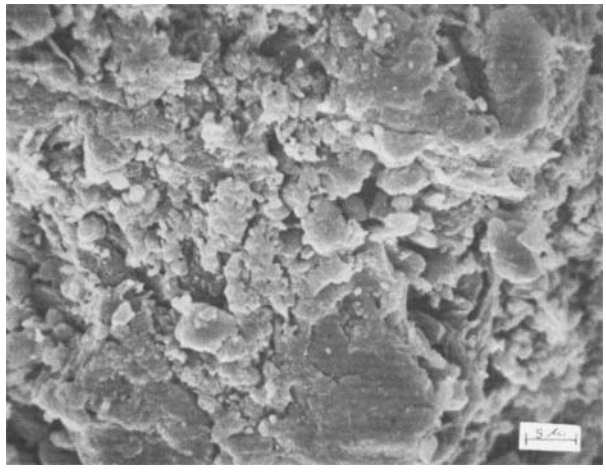

Figure 6—*Cross-sectional view of ticlopidine hydrochloride tablets compressed with the standard concave punches using formulation A. Starch was wet granulated [~2000× (original magnification)].*

[11] Model 72R; Hanson Research Corp., Northridge, Calif.
[12] Elanco, Indianapolis, Ind.

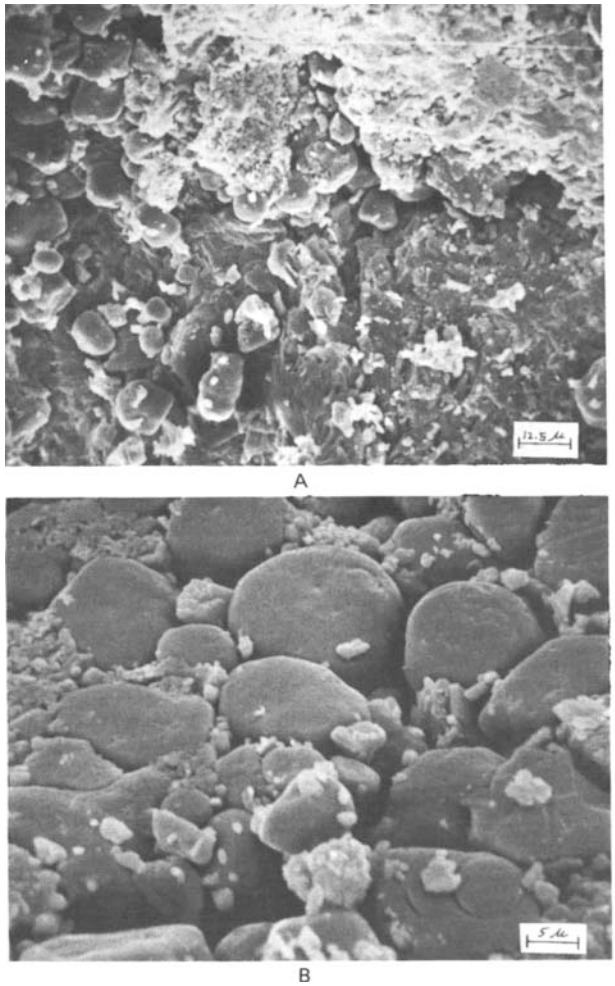

Figure 7—*Cross-sectional view of ticlopidine hydrochloride tablets compressed with the extra-deep concave punches using formulation A. Starch was dry blended. Key: (A) ~800× (original magnification); (B) ~2000× (original magnification).*

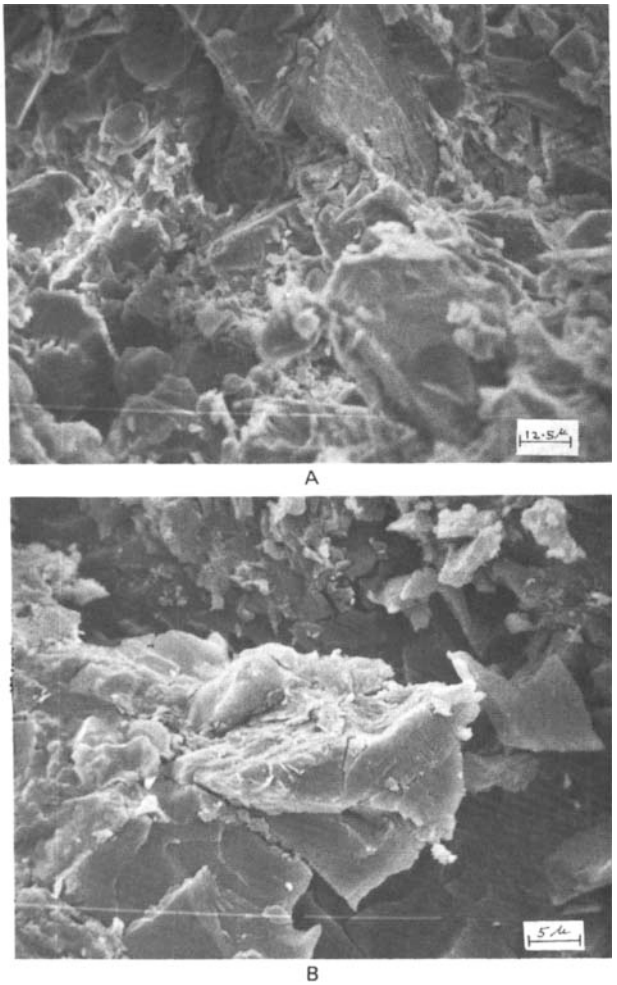

Figure 9—*Cross-sectional view of the placebo tablets compressed with extra-deep concave punches using formulation B. Starch was (A) dry blended or (B) wet granulated [~2000× (original magnification)].*

medium was 700 ml of deaerated water equilibrated at 37° and stirred at 50 rpm. The dissolved drug was analyzed by recording the absorbance at 236 nm, using an automated monitoring system consisting of a peristaltic pump[13], 1-mm spectrophotometer flow cells, and automatic sample changer/spectrophotometer[14]. The absorbances were plotted on a recorder every minute until complete dissolution was achieved. The dissolution apparatus was calibrated using USP dissolution calibrator tablets (prednisone, 50 mg). The mean dissolution and the standard deviations were within the required range.

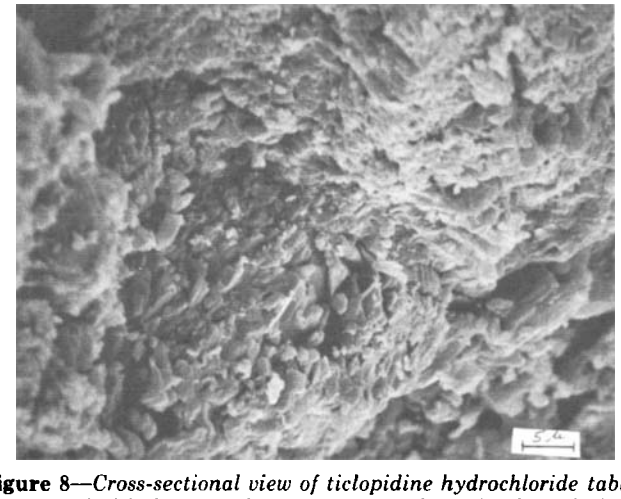

Figure 8—*Cross-sectional view of ticlopidine hydrochloride tablets compressed with the extra-deep concave punches using formulation A. Starch was wet granulated [~2000× (original magnification)].*

Scanning Electron Micrographs—Cross sections of the tablets were obtained by cutting tablets axially with a sharp razor blade. The tablet cross sections were mounted on cylindrical specimen stubs with double-stick tape[15] with the inner side surface up. Surface conductivity on the tablet sample was obtained with a silver paste in a vacuum evaporator. The samples were viewed at an oblique angle of 30° in a scanning electron microscope[16]. The photographs were taken using self-developing film[17].

RESULTS AND DISCUSSION

The results of the friability of ticlopidine hydrochloride tablets (formulation A) are given in Table II. The starch was either added during the wet-granulation process or blended in the dry form with the dry granules. The tablet crushing strength and the granulation moisture were both controlled in these studies[18]. The compression was carried out with standard concave and extra-deep concave punches. The results indicate that the friability of the tablets compressed from granulations in which starch was incorporated in the wet-granulation process was lower compared with the friability of the tablets containing starch in the dry-blended form. Extra-deep concave punches showed a much larger effect

[13] Model 1210; Haryard Apparatus, Millis, Mass.
[14] Model 25; Beckman Instruments, Fullerton, Calif.
[15] Scotch Tape; Minnesota Mining and Manufacturing Co., St. Paul, MN 55101.
[16] SEM Model Alpha-9; International Scientific Instruments, Inc., Santa Clara, CA 95050.
[17] Type 52 Polapan; Polaroid Corp.
[18] Data to be published.

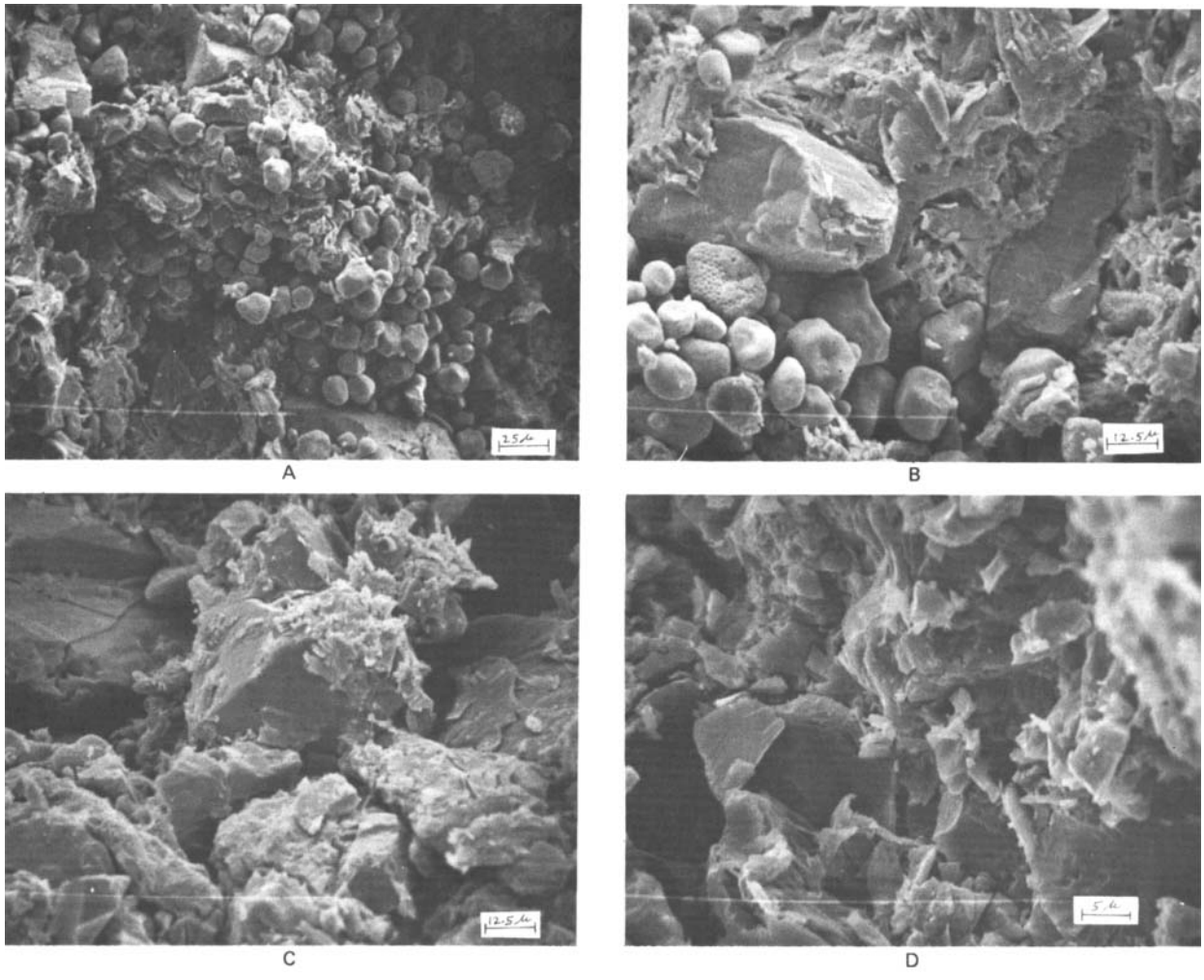

Figure 10—*Cross-sectional view of the placebo tablets compressed with the standard concave punches using formulation C. Key: (A) Starch was dry blended [~400× (original magnification)]; (B) starch was dry blended [~800× (original magnification)]; (c) starch was wet granulated [~800× (original magnification)]; (D) starch was wet granulated [~2000× (original magnification)].*

in reducing tablet friability compared with the standard concave punches as a result of the differences in processing starch.

Figure 1 gives the dissolution profiles of ticlopidine hydrochloride tablets (formulation A) resulting from granulations in which starch was either blended in the dry form or wet granulated with the drug and other excipients. For both punch tip geometries, the initial dissolution rate of the tablets compressed from granulations containing starch in the wet-granulation stage was higher compared with the tablets that were compressed from granulations containing starch in the dry form.

The coefficients of variation (CV) of these tablets as a function of the dissolution time are given in Fig. 2. At all time points studied, the dissolution coefficient of variation of standard convex tablets was smaller for tablets containing starch in the wet-granulated form compared with the tablets containing starch in the dry-blended form. The dissolution coefficient of variation of extra-deep convex tablets compressed from granules containing wet-granulated starch was smaller only at the 5-min time point. At later time points, the punch tip geometry effects discussed earlier (6) override, at least in part, the starch-processing effects.

Placebo tablets (formulations B and C) were compressed with both punch tip geometries to confirm the nonspecificity of the effect on tablet friability caused by the mode of the addition of starch. The results of the friability of formulation B placebo tablets at various crushing strengths under controlled granulation moisture are given in Fig. 3. The tablets compressed with the granulation containing wet-granulated starch were less friable compared with the tablets compressed from granulations containing starch in the dry-blended form. At higher crushing strengths, these differences were small. This was true with both punch tip geometries. In agreement with an earlier report (6), the friability of extra-deep convex tablets was smaller than the friability of standard convex tablets.

Granulations were made without a wet binder (formulation C) to study the influence of the mode of the starch addition on tablet friability. Figure 4 gives the results of the tablet friability at various crushing strengths at a controlled moisture content. For both punch tip geometries, the friability of the tablets compressed from granulations containing wet-granulated starch was smaller than the tablets compressed from granulations containing starch in the dry-blended form. The friability of the extra-deep convex tablets was much smaller than the friability of the standard convex tablets.

These results suggest definite advantages of incorporating starch as a disintegrator in the wet-granulated part of the formulation of tablets containing soluble drugs and/or soluble major excipients for improving tablet friability and *in vitro* dissolution. It is also important to point out that the wet granulations containing starch must be dried below 60° to prevent gelatinization of the starch.

To investigate the mechanism by which the incorporation of starch in the wet granulation improved tablet friability and *in vitro* dissolution, a scanning electron microscope was used to examine the cross sections of the tablets. Figure 5 is a cross-sectional view of ticlopidine hydrochloride tablets (formulation A) containing starch in the dry-blended form compressed with the standard concave punches. Starch grains, mostly deformed, appeared in clumps with some loose, fine granules. The clumping of the starch grains was not observed when cross sections of the tablet containing starch as a part of the wet granulation were examined (Fig. 6). The starch grains were well distributed in the drug–excipient granules showing good contact with the powders.

Because of the dependence of the axial and radial movement of the powders on punch tip geometry, cross sections of the extra-deep convex tablets were examined to study its effect on the distribution of starch granules within the tablet. Clumps of starch grains with some loose, fine granules were observed (Fig. 7) when starch was dry blended with the dry granules. Starch did not appear to adhere to itself or to the other materials

in the tablet. This results in weaker points within the tablets and fine cracks around the agglomerates. Higher tablet friability and higher tablet-to-tablet variability in dissolution could be explained as resulting from clumping of starch grains and weaker points around these agglomerates. The cross-sectional view of the tablet compressed from granules containing starch in the wet-granulation stage is shown in Fig. 8. No clumping of the starch grains was seen. The materials were well distributed in the tablet matrix. Comparisons of the two punch tip geometries revealed no major differences in the distribution of starch resulting from the differential particle movement during compression (compare Figs. 5 and 6 with Figs. 7 and 8).

Figure 9 gives cross-sectional views of the placebo tablet compressed with the standard concave punches (formulation B). Tablets containing dry-blended starch showed only a few starch grains (Fig. 9A) compared with the largely fused lactose (Fig. 9B) for tablets compressed from wet-granulated starch.

The cross-sectional views of the tablets compressed from formulation C without a wet binder are shown in Fig. 10. Similar to ticlopidine hydrochloride tablets, clumping of starch grains was observed when starch was dry blended (Fig. 10A and B). Starch grains do not adhere to themselves or to the other materials in the tablet. This is in contrast to the case when starch was wet granulated with other excipients using water (Fig. 10C and D). Agglomerates or even isolated starch grains were not observed. The starch was well embedded in the soluble excipient, lactose, which on drying crystallized out.

In conclusion, this study suggests that the tablet friability and *in vitro* dissolution improved by incorporating starch in the wet-granulation stage of formulations containing a soluble drug and/or a soluble major excipient. This improvement in tablet friability and *in vitro* dissolution is due to a better bonding, fewer weak points, and better homogeneity of the disintegrator, starch, within the tablet.

REFERENCES

(1) N. R. Patel and R. Hopponen, *J. Pharm. Sci.*, **55**, 1065 (1966).

(2) J. T. Ingram and W. Lowenthal, *J. Pharm. Sci.*, **57**, 393 (1968).

(3) W. Lowenthal and R. A. Burruss, *J. Pharm. Sci.*, **60**, 1325 (1971).

(4) W. Lowenthal, *J. Pharm. Sci.*, **61**, 455 (1972).

(5) W. Lowenthal and J. H. Wood, *J. Pharm. Sci.*, **62**, 287 (1973).

(6) Z. T. Chowhan, I.-C Yang, A. A. Amaro, L.-H. Chi, and Y. P. Chow, *J. Pharm. Sci.*, **71**, 1371 (1982).

Application of the Ammonia Gas-Sensing Electrode: Determination of Drugs Having a Carbothionamido Group by Decomposition with Acid

SHOICHIRO TAGAMI ˣ **and HIROMI MAEDA**

Received April 19, 1982, from the *Toyama Medical and Pharmaceutical University, Sugitani, Toyama, Japan.* Accepted for publication August 4, 1982.

Abstract □ A method to determine drugs having a carbothionamido group using an ammonia gas-sensing electrode is described. To obtain analytical accuracy, the effect of factors that influence the potential is also discussed. Ethionamide or prothionamide was refluxed with 20% HCl to give ammonium chloride, hydrogen sulfide, and a carboxylic acid. The ammonia, which evolved at pH > 11, was determined. A linear calibration plot was obtained within the drug concentration range of 2×10^{-5}–1×10^{-2} *M*.

Keyphrases □ Ammonia gas-sensing electrode—determination of carbothionamido groups, acid decomposition of ethionamide and prothionamide □ Ethionamide—carbothionamido group, determination using ammonia gas-sensing electrode, acid decomposition □ Prothionamide—carbothionamido group, determination using ammonia gas-sensing electrode, acid decomposition

In recent years, the development of gas-permeable membrane electrodes has led to their widespread use in the analytical field (1). Although electrodes that use immobilized enzymes on the membrane are employed for the determination of organic and biological compounds, few applications to drug analysis have been reported in the literature, and no pharmacopeia has yet introduced their use for assays. Therefore, a previous paper (2) described procedures for the determination of drugs having a carboxyamido group (ethenzamide, niacinamide, pyrazinamide, and salicylamide).

The present paper describes the determination of drugs having a carbothionamido group in an analogous way and describes in detail the operations and handling of the ammonia gas-sensing electrode. The carbothionamido group decomposes into ammonium chloride, hydrogen sulfide, and a carboxylic acid on heating with hydrochloric acid (Scheme I). It may thus be possible to utilize the ammonia gas-sensing electrode to determine the ammonia derived from the ammonium chloride during the decomposition.

EXPERIMENTAL

Apparatus and Reagents—Direct potentiometric measurements were made at 20° in an 80-ml cell equipped with a magnetic stirrer, using a pH/mV meter[1] with a recorder[2] and ammonia gas-sensing electrodes A[3] and B[4]. Ethionamide[5], prothionamide[6], and ammonium chloride[7] were analytical grade or certified quality and were dried *in vacuo* at room temperature for 5 hr. Other chemicals used were reagent grade. Ammonium chloride solutions of 0.001–1 *M* and ammonium chloride solutions of 0.01–0.1 *M* saturated with ammonium picrate were used as internal filling solutions.

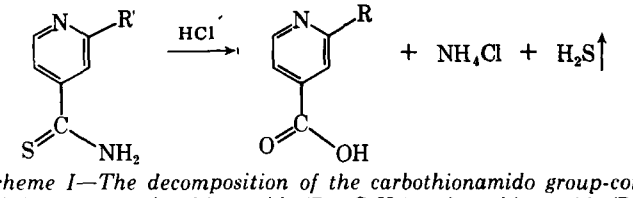

Scheme I—The decomposition of the carbothionamido group-containing compounds ethionamide ($R = C_2H_5$) and prothionamide ($R = C_3H_7$).

[1] Model F-7ss, Hitachi-Horiba Instruments, Horiba Co., Kyoto.
[2] Model EPR-22A, Toa-Denpa Co., Tokyo.
[3] Model 5002-05T, Horiba Co., Kyoto.
[4] Model 95-10, Orion Research Inc., Cambridge.
[5] Daiichi Seiyaku Co., Tokyo (lot CA 7921806).
[6] Lederle Japan Ltd., Tokyo (lot CA 7917603; assay, 100.2%).
[7] E. Merck, Darmstadt (lot 0074534; assay, 99.8%).

0022-3549/83/0900-0988$01.00/0

in the tablet. This results in weaker points within the tablets and fine cracks around the agglomerates. Higher tablet friability and higher tablet-to-tablet variability in dissolution could be explained as resulting from clumping of starch grains and weaker points around these agglomerates. The cross-sectional view of the tablet compressed from granules containing starch in the wet-granulation stage is shown in Fig. 8. No clumping of the starch grains was seen. The materials were well distributed in the tablet matrix. Comparisons of the two punch tip geometries revealed no major differences in the distribution of starch resulting from the differential particle movement during compression (compare Figs. 5 and 6 with Figs. 7 and 8).

Figure 9 gives cross-sectional views of the placebo tablet compressed with the standard concave punches (formulation B). Tablets containing dry-blended starch showed only a few starch grains (Fig. 9A) compared with the largely fused lactose (Fig. 9B) for tablets compressed from wet-granulated starch.

The cross-sectional views of the tablets compressed from formulation C without a wet binder are shown in Fig. 10. Similar to ticlopidine hydrochloride tablets, clumping of starch grains was observed when starch was dry blended (Fig. 10A and B). Starch grains do not adhere to themselves or to the other materials in the tablet. This is in contrast to the case when starch was wet granulated with other excipients using water (Fig. 10C and D). Agglomerates or even isolated starch grains were not observed. The starch was well embedded in the soluble excipient, lactose, which on drying crystallized out.

In conclusion, this study suggests that the tablet friability and *in vitro* dissolution improved by incorporating starch in the wet-granulation stage of formulations containing a soluble drug and/or a soluble major excipient. This improvement in tablet friability and *in vitro* dissolution is due to a better bonding, fewer weak points, and better homogeneity of the disintegrator, starch, within the tablet.

REFERENCES

(1) N. R. Patel and R. Hopponen, *J. Pharm. Sci.*, **55**, 1065 (1966).

(2) J. T. Ingram and W. Lowenthal, *J. Pharm. Sci.*, **57**, 393 (1968).

(3) W. Lowenthal and R. A. Burruss, *J. Pharm. Sci.*, **60**, 1325 (1971).

(4) W. Lowenthal, *J. Pharm. Sci.*, **61**, 455 (1972).

(5) W. Lowenthal and J. H. Wood, *J. Pharm. Sci.*, **62**, 287 (1973).

(6) Z. T. Chowhan, I.-C Yang, A. A. Amaro, L.-H. Chi, and Y. P. Chow, *J. Pharm. Sci.*, **71**, 1371 (1982).

Application of the Ammonia Gas-Sensing Electrode: Determination of Drugs Having a Carbothionamido Group by Decomposition with Acid

SHOICHIRO TAGAMI ˣ **and HIROMI MAEDA**

Received April 19, 1982, from the *Toyama Medical and Pharmaceutical University, Sugitani, Toyama, Japan.* Accepted for publication August 4, 1982.

Abstract □ A method to determine drugs having a carbothionamido group using an ammonia gas-sensing electrode is described. To obtain analytical accuracy, the effect of factors that influence the potential is also discussed. Ethionamide or prothionamide was refluxed with 20% HCl to give ammonium chloride, hydrogen sulfide, and a carboxylic acid. The ammonia, which evolved at pH > 11, was determined. A linear calibration plot was obtained within the drug concentration range of 2×10^{-5}–1×10^{-2} *M*.

Keyphrases □ Ammonia gas-sensing electrode—determination of carbothionamido groups, acid decomposition of ethionamide and prothionamide □ Ethionamide—carbothionamido group, determination using ammonia gas-sensing electrode, acid decomposition □ Prothionamide—carbothionamido group, determination using ammonia gas-sensing electrode, acid decomposition

In recent years, the development of gas-permeable membrane electrodes has led to their widespread use in the analytical field (1). Although electrodes that use immobilized enzymes on the membrane are employed for the determination of organic and biological compounds, few applications to drug analysis have been reported in the literature, and no pharmacopeia has yet introduced their use for assays. Therefore, a previous paper (2) described procedures for the determination of drugs having a carboxyamido group (ethenzamide, niacinamide, pyrazinamide, and salicylamide).

The present paper describes the determination of drugs having a carbothionamido group in an analogous way and describes in detail the operations and handling of the ammonia gas-sensing electrode. The carbothionamido group decomposes into ammonium chloride, hydrogen sulfide, and a carboxylic acid on heating with hydrochloric acid (Scheme I). It may thus be possible to utilize the ammonia gas-sensing electrode to determine the ammonia derived from the ammonium chloride during the decomposition.

EXPERIMENTAL

Apparatus and Reagents—Direct potentiometric measurements were made at 20° in an 80-ml cell equipped with a magnetic stirrer, using a pH/mV meter[1] with a recorder[2] and ammonia gas-sensing electrodes A[3] and B[4]. Ethionamide[5], prothionamide[6], and ammonium chloride[7] were analytical grade or certified quality and were dried *in vacuo* at room temperature for 5 hr. Other chemicals used were reagent grade. Ammonium chloride solutions of 0.001–1 *M* and ammonium chloride solutions of 0.01–0.1 *M* saturated with ammonium picrate were used as internal filling solutions.

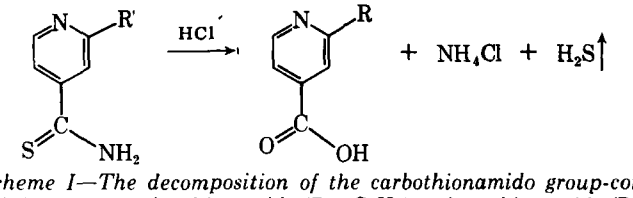

Scheme I—The decomposition of the carbothionamido group-containing compounds ethionamide ($R = C_2H_5$) and prothionamide ($R = C_3H_7$).

[1] Model F-7ss, Hitachi-Horiba Instruments, Horiba Co., Kyoto.
[2] Model EPR-22A, Toa-Denpa Co., Tokyo.
[3] Model 5002-05T, Horiba Co., Kyoto.
[4] Model 95-10, Orion Research Inc., Cambridge.
[5] Daiichi Seiyaku Co., Tokyo (lot CA 7921806).
[6] Lederle Japan Ltd., Tokyo (lot CA 7917603; assay, 100.2%).
[7] E. Merck, Darmstadt (lot 0074534; assay, 99.8%).

0022-3549/83/0900-0988$01.00/0

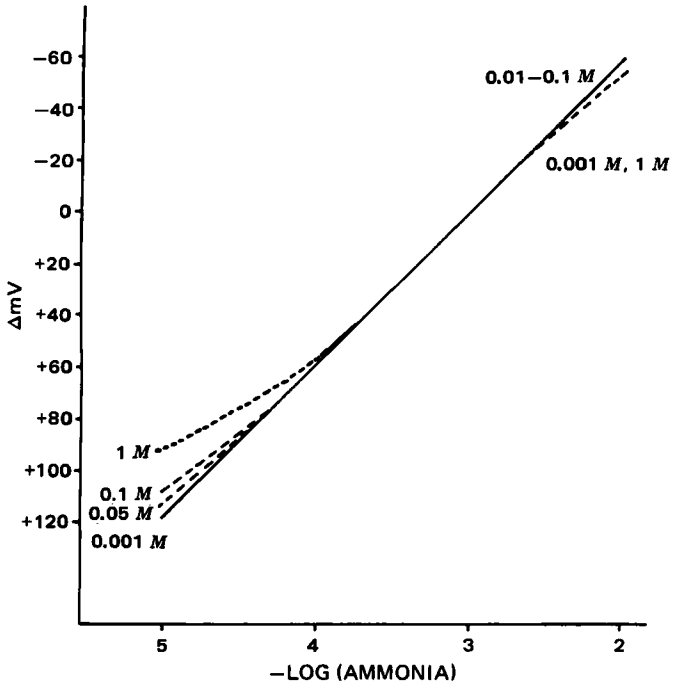

Figure 1—*Effect of internal filling solutions on the calibration plot.*

Standard Solution—To 25 ml of 0.1 *M* ammonium chloride solution in a 250-ml volumetric flask was added 50 ml of a 20% HCl solution which had been neutralized to pH 6.5 with sodium hydroxide, and the resulting solution was diluted to volume with distilled water. A working solution was prepared by diluting this stock solution to 1×10^{-2} *M* ammonium chloride.

Decomposition of Drugs—A mixture of 166.24 mg (1×10^{-3} mole) of ethionamide or 180.27 mg (1×10^{-3} mole) of prothionamide and 20 ml of 20% HCl was heated at reflux in an oil bath for 1 hr. The solution was cooled, poured into a 100-ml beaker, and diluted with ~50 ml of water. A drop of methyl orange was added while cooling the beaker continuously, and the acid was cautiously neutralized with 10 *N* NaOH solution until the indicator began to change color. The solution was then adjusted to pH 6.5 with dilute sodium hydroxide solution using a pH meter. The solution was poured into a 100-ml volumetric flask and diluted to volume with water. The concentrations of the final drug solutions were 1×10^{-2} *M*, corresponding to 1×10^{-2} *M* ammonia. Sample solutions for measurements were obtained by dilution of these solutions with water.

Assay Procedure—A 50-ml portion of the sample and standard solutions used was incubated for 30 min at 20°, and 1 ml of 5 *N* NaOH was added before the electrode was immersed in the solutions. (After alkalinization, the solutions are stable for several hours in the cell with a rubber stopper.) The standard procedure was as follows: The electrode with 0.05 *M* ammonium chloride internal filling solution was washed with water and immersed for ~5 min in fresh 0.05 *M* NaCl solution acidified with dilute hydrochloric acid at pH 4, and then the old internal filling solution was replaced with fresh 0.05 *M* ammonium chloride solution. The electrode was placed in the first standard, and the potential was measured. After washing the electrode as described above, the electrode was placed in the sample solution, and the potential was measured. After another washing, the electrode was placed in the second standard, and the potential was measured. The sample concentration was determined from the calibration curve.

Assay of Tablets—Twenty tablets were weighed and finely powdered. A portion of the powder (equivalent to ~166.24 mg of ethionamide or 180.27 mg of prothionamide) was accurately weighed, and 20 ml of acetone was added. The solution was stirred and then centrifuged. The supernatant acetone solution was removed, and 20 ml of acetone was added to the residue. The extraction procedure was repeated until the supernatant acetone solution was colorless. The acetone fractions were evaporated to dryness, and the resulting residue was refluxed for 1 hr with 20 ml of 20% HCl. As described above, the acidic solution was adjusted to pH 6.5 and diluted to 250 ml in a volumetric flask. The ammonia concentration in a 50-ml portion of the sample was determined from the calibration curve.

Table I—Effect of Dissolved Salts on the Electrode Potential

Salt	Salt Concentration,[a] *M*	Potential Shift, mV
Sodium chloride	1×10^{-4}	0
	1×10^{-3}	0
	1×10^{-2}	+0.1
	1×10^{-1}	−0.1
	5×10^{-1}	−0.1
	1	−0.6
Potassium chloride	1×10^{-4}	+0.2
	1×10^{-3}	−0.1
	1×10^{-2}	−0.1
	1×10^{-1}	−0.2
	5×10^{-1}	−0.6
	1	−2.2
Sodium sulfate	1×10^{-4}	0
	1×10^{-3}	+0.1
	1×10^{-2}	−0.1
	1×10^{-1}	−1.0
	5×10^{-1}	−4.0
	1	−8.4
Potassium sulfate	1×10^{-4}	+0.2
	1×10^{-3}	+0.1
	1×10^{-2}	0
	5×10^{-2}	−0.4
	1×10^{-1}	−0.8
	3×10^{-1}	−2.7
	5×10^{-1}	−4.7

[a] The given salt concentrations are the concentrations in 1×10^{-3} *M* ammonium chloride.

RESULTS AND DISCUSSION

Internal Filling Solution—The electrolyte solution in the reference electrode and the internal filling solution contained known amounts of ammonium chloride. Commercially available ammonia gas-sensing electrodes differ slightly from one another in the concentration of the internal filling solution and in their inner structure. The electrolyte solution in reference electrode A can be replaced by fresh electrolyte solution, but not in electrode B. By using both electrodes, the effect of internal filling solutions on the calibration plot was investigated. First, electrode A, in which the internal filling solution and the electrolyte solution are the same, was examined by employing filling solutions with 0.001–1 *M* ammonium chloride. The results are shown in Fig. 1, where the potential difference (ΔmV) from 1×10^{-3} *M* ammonia to each concentration of ammonia is plotted as the ordinate and the ammonia concentration is plotted as the abscissa. Using 0.1, 0.05, and 0.01 *M* filling solutions, a linear calibration plot was obtained for the concentration range of 1×10^{-4}–1×10^{-2} *M* ammonia. Using 0.001 *M* filling solution, a linear calibration plot was obtained at 1×10^{-5}–1×10^{-3} *M* ammonia.

Table II—Determination of Drugs Having a Carbothionamido Group

Drug	Determination	Label Claim, mg	Found, mg	Recovery, %
Ethionamide	1	0.831	0.829	99.8
	2	0.831	0.832	100.1
	3	0.831	0.832	100.1
	4	8.312	8.337	100.3
	5	8.312	8.320	100.1
	6	8.312	8.312	100.0
	7	8.312	8.304	99.9
	8	8.312	8.304	99.9
Mean ± *SD*				100.03 ± 0.15
Prothionamide	1	0.901	0.900	99.9
	2	0.901	0.901	100.0
	3	0.901	0.898	99.7
	4	0.901	0.902	100.1
	5	9.014	9.014	100.0
	6	9.014	9.005	99.9
	7	9.014	9.050	100.4
	8	9.014	9.032	100.2
Mean ± *SD*				100.03 ± 0.20

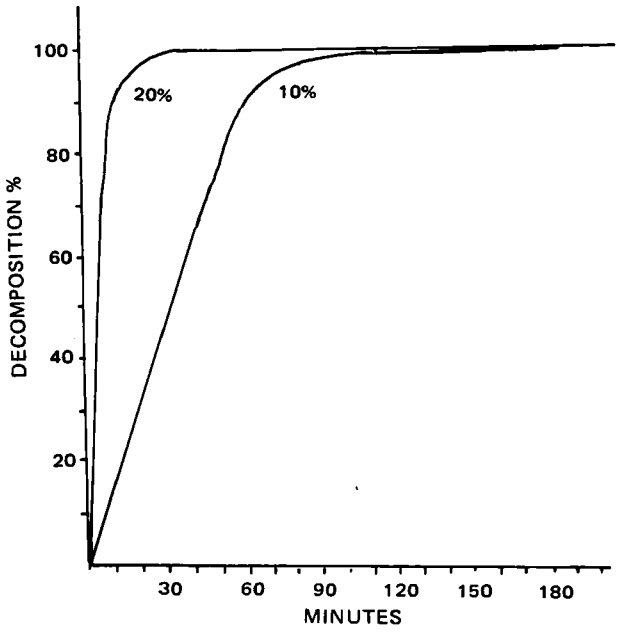

Figure 2—*Effect of hydrochloric acid concentrations on drug decomposition.*

The slope of the lines was 58 mV per decade increase in ammonia concentration. At a low concentration range of ammonia (from 1×10^{-5} to 1×10^{-4} *M*), the higher the concentration of the filling solution, the smaller ΔmV. At a high concentration range of ammonia (from 1×10^{-3} to 1×10^{-2} *M*), ΔmV became <58 mV when 0.001 *M* filling solution was used. With 1 *M* filling solution, the electrode potentials were unstable; the calibration plot was not linear, resulting in an S-curve. Based on the above data, 0.001 *M* filling solution is considered suitable for potential measurements of a low level of ammonia (1×10^{-5}–1×10^{-3} *M*). In the concentration range of 1×10^{-4}–1×10^{-2} *M* ammonia, 0.01–0.1 *M* filling solutions are suitable for the potential measurements. However, with a high level of ammonia (1×10^{-3}–1×10^{-2} *M*), the use of 0.1 *M* filling solution is preferred.

The electrolyte solution in electrode B consists of a saturated solution of ammonium picrate or ammonium purpurate. To provide a chloride concentration for the reference Ag–AgCl electrode, the electrolyte also contains a known amount of ammonium chloride (3). However, the concentration of ammonium chloride in this electrode is not obvious. Using an internal filling solution containing 0.05 *M* ammonium chloride saturated with ammonium picrate, a linear calibration plot was obtained in the concentration range of 1×10^{-4}–1×10^{-2} *M* ammonia, and the potential difference (ΔmV) was 58 mV per decade increase in ammonia concentration. However, using 0.01 or 0.1 *M* ammonium chloride saturated with ammonium picrate, the calibration plot was not linear.

On using the Instrumental Laboratory filling solution, a linear calibration plot was obtain in the ammonia concentration range of 1×10^{-4}–1×10^{-2} *M*. This indicates that the Instrumental Laboratory solution and the 0.05 *M* ammonium chloride solution saturated with ammonium picrate are the same.

Standard Solution—Water vapor resulting from the difference in concentrations of ions between the decomposition and internal filling solutions (osmotic strength) leads to error, and the partial pressure of the dissolved gas is also a function of the sample temperature and the level of dissolved species (4). In the present study, therefore, the effect of dissolved salts on the potential was examined more closely. The results are shown in Table I. In a given 1×10^{-3} *M* ammonium chloride solution, 1×10^{-1} *M* potassium or sodium sulfate caused an ~1-mV electrode shift. However, in sodium chloride, the amount of salt is negligibly small in a concentration <1 *M*. The experimental data indicated that the calibration plot of ammonium chloride standard solution coincided with that of the decomposition solution in the concentration range of 1×10^{-4}–1×10^{-2} *M*. Thus, the standard solution should use ammonium chloride standard instead of the drug standard.

To obtain analytical accuracy, a calibration curve should be prepared for every set of determinations. Since the potential of the glass electrode is stable for ~12 hr, but changes with after that time, the slope of the linear calibration plot is not constant.

Electrode Response—The response of the electrode is a function of the ammonia concentration, with a faster response at higher ammonia levels. In a given ammonia concentration it is also a function of the salt concentration, with a faster response at higher dissolved salt levels. On repeated use, the equilibrium time may become longer because of deterioration of the glass electrode. To activate the electrode, the electrode tip should be immersed in 2% ammonium fluoride for 3 min, then in 5 *N* HCl for several minutes, followed by exhaustive washing with water.

Another important factor that influences the electrode response is the working area of the gas-permeable membrane. Employing membranes with diameters of 4 mm^3 and 9 mm^4, the response times of the electrode were found to be 20–30 min and 1–3 min in 1×10^{-3} *M* ammonia, respectively.

When the electrode is immersed in water for storage overnight, the response time may become longer, as water vapor may condense in the hole in the gas-permeable membrane, hindering the passage of ammonia gas. For storage overnight or over the weekend, the electrode tip should be immersed in ammonium chloride solution, with the same level of ammonium chloride as in the internal filling solution to avoid wetting and change of internal filling solution concentration.

Contamination—The electrode is always contaminated by the ammonia adsorbed on the gas-permeable membrane and by the ammonia in the small gap between the bottom cap of the electrode and the gas-permeable membrane. Since the contaminating substance cannot be removed by washing with water, the electrode tip must be washed by immersion in freshly prepared sodium chloride solution (pH 4) of a similar concentration to the ammonium chloride in the internal filling solution. At a concentration $<10^{-4}$ *M* ammonia, the potential change resulting from contamination is much larger than in the concentration range of 10^{-3}–10^{-2} *M*. The electrode tip must be washed thoroughly. During washing of the electrode, the concentration of the internal filling solution is slightly changed. Thus, the internal filling solution should be replaced with fresh solution before making potential measurements.

Reproducibility—In a sample solution with a high level of dissolved salt, reproducibility is influenced by the mode of operation of the potential measurement. In the first procedure, after alkalinization of the sample solution with sodium hydroxide, the electrode is immersed in the sample solution and the potential measurements are determined. In the second procedure, following immersion of the electrode in the sample solution, the solution is alkalinized with sodium hydroxide after a few minutes, and then potential measurements determined. The potential values obtained by these different modes of operation are not equal. Results show that in the second procedure, the concentration of the internal filling solution changes with lapse of time due to water vapor caused by osmotic pressure. Small changes in the concentration of the filling solution influence the potential value. The potentiometric measurements should be determined using the first procedure.

Electrode B has a fast response time, but the large area of the gas-permeable membrane subjects it to influence from osmotic pressure. Therefore, electrode A was used.

Decomposition of Drugs—A mixture of ethionamide and 20% HCl was refluxed until complete decoloration had taken place. Hydrogen sulfide was evolved during the course of the reaction, and the yellow solution became colorless after 30 min. The resulting ammonia formed in the decomposition was determined at various times (Fig. 2). The electrode potential reached a maximum at a heating time of 30 min. In the case of decomposition with 10% HCl, the electrode potential reached a maximum at a heating time of 3 hr. After 1 and 2 hr, the recoveries were 87 and 99%, respectively. The decomposition time of prothionamide was the same

Table III—Determination of Tablets

Drug	Determination	Label Claim, mg	Found, mg	Recovery, %
Ethionamide	1	155.96	157.36	100.9
	2	166.24	167.07	100.5
	3	166.24	166.02	99.9
	4	164.34	165.29	100.6
	5	173.46	174.22	100.4
Mean ± *SD*				100.46 ± 0.36
Prothionamide	1	187.00	187.94	100.5
	2	180.12	181.15	100.6
	3	205.54	206.07	100.3
	4	195.41	195.49	100.0
	5	182.35	183.63	100.7
Mean ± *SD*				100.42 ± 0.28

as that of ethionamide. When the potential was plotted against the logarithm of the drug concentration, a linear calibration plot was obtained in the drug concentration range of 2×10^{-5}–1×10^{-2} M.

The amount of drug was first determined with the pure drug powder. According to USP XX (5), ethionamide contains ≥98.0% and ≤102.0% of $C_8H_{10}N_2S$, calculated on an anhydrous basis. Prothionamide is described only in the JP X (6), and not in the USP or British Pharmacopeia (7). According to the Japanese Pharmacopeia, prothionamide determined on a dry weight basis should be >98.0% pure.

The recovery of the drugs is shown in Table II. Determinations were performed on eight samples of both drugs. The amounts of ethionamide and prothionamide were estimated with the same average errors of 0.03%, and the standard deviations were 0.15 and 0.20, respectively. The recoveries were good and reproducible.

Determinations on both tablets were carried out. A suitable extraction solution was sought. Both drugs are very soluble in methanol and glacial acetic acid and are also soluble in ethanol and acetone; however, in the extraction it is necessary to avoid interference from extraneous compounds. Methanol is used in the USP procedure. The tablets were therefore extracted with methanol and after evaporation of the methanol, the residue was heated at reflux with 20% HCl. After heating for 3 hr, the solution became brown, and a brown precipitate separated out. Evidently the precipitate resulted from impurities dissolved in the methanol.

The tablets were then extracted with acetone. After dissolution in acetone, the solution was centrifuged. This was found to be the best method because filtration of the acetone solution proved to be difficult. The extraction was carried out four or five times until the extract was colorless. The solvent was evaporated, and the residue was heated at reflux for 1 hr with 20% HCl to give a light-brown precipitate and a pale-brown solution. The acidic solution was then neutralized with sodium hydroxide at pH 6.5, and the resulting mixture was subjected to potentiometric measurements. Determinations were performed on five samples of 20 tablets. According to the USP XX, ethionamide tablets contain ≥95.0% and ≤110% of the labeled amount of drug. The results obtained are shown in Table III. The mean recoveries for ethionamide and prothionamide tablets were 100.46 and 100.42%, respectively, and the respective standard deviations were 0.36 and 0.28. The labeled amount of drugs was 100 mg/tablet. The recoveries are given compared with the theoretical amount of ammonia in the drug tablets, and it is believed that one tablet indeed contains 100 mg.

CONCLUSION

The assay method for the drugs in JP X is based on the nonaqueous titration method using perchloric acid; however, the color change is not sharp. In the BP, the end-point is determined potentiometrically, which alleviates this problem. In USP XX, a colorimetric method is used for the determination of the pure powder and tablets. The procedure is accurate, but nonspecific.

The proposed method for the assay of drugs having a carbothionamido group is simple and specific. The recovery is satisfactory and lies within acceptable limits. In view of this, use of the ammonia gas-sensing electrode is recommended as a possible pharmacopeial method.

REFERENCES

(1) G. E. Baiulescu and V. V. Cosofret, "Applications of Ion-Selective Membrane Electrodes in Organic Analysis," Halsted Press (div. John Wiley & Sons), New York, N.Y., 1977.

(2) S. Tagami and M. Fujita, *J. Pharm. Sci.*, **71**, 523 (1982).

(3) J. H. Riseman and J. Krueger, U.S. Pat., 3,830,718 (1974).

(4) "Instruction Manual," Orion Research Inc., 1978, pp. 23 and 27.

(5) "The United States Pharmacopeia," 20th rev., U.S. Pharmacopeial Convention, Rockville, Md. 1980, p. 308.

(6) "The Japanese Pharmacopeia," 10th rev., Hirokawa Publishing Co., Tokyo, 1981, p. 1352.

(7) "The British Pharmacopeia," The University Printing House, Cambridge, England, 1973, p. 194.

ACKNOWLEDGMENTS

The authors are grateful to Professor Takenori Tanimura for his unfailing guidance throughout the course of this work.

Pharmacokinetics of Chlorzoxazone in Humans

RAVI K. DESIRAJU ˣ, NED L. RENZI, Jr., RAMCHANDRA K. NAYAK, and KUNG-TAT NG

Received March 5, 1982, from the *Department of Drug Metabolism, McNeil Pharmaceutical, Spring House, PA 19477.* Accepted for publication August 6, 1982.

Abstract □ Twenty-three normal male subjects received 900 mg of acetaminophen and 750 mg of chlorzoxazone as an oral suspension. Analysis of plasma samples indicated a rapid absorption and rapid elimination of chlorzoxazone. Average values of the elimination half-life and plasma clearance were 1.12 ± 0.48 hr and 148.0 ± 39.9 ml/min, respectively. Analysis of urine samples showed that chlorzoxazone was eliminated from the body as the glucuronide conjugate of the intermediate metabolite 6-hydroxychlorzoxazone, to the extent of 74% of the dose. The plasma and the urinary excretion data were fitted to theoretical equations, and excellent fits were obtained using a five-parameter pharmacokinetic model.

Keyphrases □ Chlorzoxazone—analysis in human plasma and urine, administration with acetaminophen; pharmacokinetics □ Pharmacokinetics—chlorzoxazone, analysis in human plasma and urine, concomitant administration with acetaminophen □ Acetaminophen—concomitant administration with chlorzoxazone, analysis in human plasma and urine, effect on pharmacokinetics

Chlorzoxazone (5-chloro-2(3*H*)-benzoxazolone) (I) is a potent skeletal muscle relaxant that is effective in the treatment of skeletal muscle spasms. Onset of therapeutic activity is observed within 1 hr, with a duration usually up to 6 hr (1). Chlorzoxazone exhibits minimal adverse effects and almost no GI irritation.

The data and results presented in this report are part of a study that was performed with 23 normal male subjects to determine the bioavailability of acetaminophen and chlorzoxazone from a commercial combination tablet formulation and an oral suspension. While there exists sufficient information in the literature regarding acetaminophen elimination kinetics (2–6), little has been reported on the disposition characteristics of chlorzoxazone in humans. This report deals primarily with the plasma levels and urinary excretion of chlorzoxazone following administration of a suspension of chlorzoxazone and acetaminophen.

In studies dealing with the metabolic fate of chlorzoxazone in humans, Conney and Burns (7) reported that <1% of the drug was excreted unchanged in urine. Chlorzoxazone was rapidly metabolized in humans to 6-hydroxy-

0022-3549/83/0900-0991$01.00/0

as that of ethionamide. When the potential was plotted against the logarithm of the drug concentration, a linear calibration plot was obtained in the drug concentration range of 2×10^{-5}–1×10^{-2} M.

The amount of drug was first determined with the pure drug powder. According to USP XX (5), ethionamide contains ≥98.0% and ≤102.0% of $C_8H_{10}N_2S$, calculated on an anhydrous basis. Prothionamide is described only in the JP X (6), and not in the USP or British Pharmacopeia (7). According to the Japanese Pharmacopeia, prothionamide determined on a dry weight basis should be >98.0% pure.

The recovery of the drugs is shown in Table II. Determinations were performed on eight samples of both drugs. The amounts of ethionamide and prothionamide were estimated with the same average errors of 0.03%, and the standard deviations were 0.15 and 0.20, respectively. The recoveries were good and reproducible.

Determinations on both tablets were carried out. A suitable extraction solution was sought. Both drugs are very soluble in methanol and glacial acetic acid and are also soluble in ethanol and acetone; however, in the extraction it is necessary to avoid interference from extraneous compounds. Methanol is used in the USP procedure. The tablets were therefore extracted with methanol and after evaporation of the methanol, the residue was heated at reflux with 20% HCl. After heating for 3 hr, the solution became brown, and a brown precipitate separated out. Evidently the precipitate resulted from impurities dissolved in the methanol.

The tablets were then extracted with acetone. After dissolution in acetone, the solution was centrifuged. This was found to be the best method because filtration of the acetone solution proved to be difficult. The extraction was carried out four or five times until the extract was colorless. The solvent was evaporated, and the residue was heated at reflux for 1 hr with 20% HCl to give a light-brown precipitate and a pale-brown solution. The acidic solution was then neutralized with sodium hydroxide at pH 6.5, and the resulting mixture was subjected to potentiometric measurements. Determinations were performed on five samples of 20 tablets. According to the USP XX, ethionamide tablets contain ≥95.0% and ≤110% of the labeled amount of drug. The results obtained are shown in Table III. The mean recoveries for ethionamide and prothionamide tablets were 100.46 and 100.42%, respectively, and the respective standard deviations were 0.36 and 0.28. The labeled amount of drugs was 100 mg/tablet. The recoveries are given compared with the theoretical amount of ammonia in the drug tablets, and it is believed that one tablet indeed contains 100 mg.

CONCLUSION

The assay method for the drugs in JP X is based on the nonaqueous titration method using perchloric acid; however, the color change is not sharp. In the BP, the end-point is determined potentiometrically, which alleviates this problem. In USP XX, a colorimetric method is used for the determination of the pure powder and tablets. The procedure is accurate, but nonspecific.

The proposed method for the assay of drugs having a carbothionamido group is simple and specific. The recovery is satisfactory and lies within acceptable limits. In view of this, use of the ammonia gas-sensing electrode is recommended as a possible pharmacopeial method.

REFERENCES

(1) G. E. Baiulescu and V. V. Cosofret, "Applications of Ion-Selective Membrane Electrodes in Organic Analysis," Halsted Press (div. John Wiley & Sons), New York, N.Y., 1977.

(2) S. Tagami and M. Fujita, *J. Pharm. Sci.*, **71**, 523 (1982).

(3) J. H. Riseman and J. Krueger, U.S. Pat., 3,830,718 (1974).

(4) "Instruction Manual," Orion Research Inc., 1978, pp. 23 and 27.

(5) "The United States Pharmacopeia," 20th rev., U.S. Pharmacopeial Convention, Rockville, Md. 1980, p. 308.

(6) "The Japanese Pharmacopeia," 10th rev., Hirokawa Publishing Co., Tokyo, 1981, p. 1352.

(7) "The British Pharmacopeia," The University Printing House, Cambridge, England, 1973, p. 194.

ACKNOWLEDGMENTS

The authors are grateful to Professor Takenori Tanimura for his unfailing guidance throughout the course of this work.

Pharmacokinetics of Chlorzoxazone in Humans

RAVI K. DESIRAJU ˣ, NED L. RENZI, Jr., RAMCHANDRA K. NAYAK, and KUNG-TAT NG

Received March 5, 1982, from the *Department of Drug Metabolism, McNeil Pharmaceutical, Spring House, PA 19477.* Accepted for publication August 6, 1982.

Abstract □ Twenty-three normal male subjects received 900 mg of acetaminophen and 750 mg of chlorzoxazone as an oral suspension. Analysis of plasma samples indicated a rapid absorption and rapid elimination of chlorzoxazone. Average values of the elimination half-life and plasma clearance were 1.12 ± 0.48 hr and 148.0 ± 39.9 ml/min, respectively. Analysis of urine samples showed that chlorzoxazone was eliminated from the body as the glucuronide conjugate of the intermediate metabolite 6-hydroxychlorzoxazone, to the extent of 74% of the dose. The plasma and the urinary excretion data were fitted to theoretical equations, and excellent fits were obtained using a five-parameter pharmacokinetic model.

Keyphrases □ Chlorzoxazone—analysis in human plasma and urine, administration with acetaminophen; pharmacokinetics □ Pharmacokinetics—chlorzoxazone, analysis in human plasma and urine, concomitant administration with acetaminophen □ Acetaminophen—concomitant administration with chlorzoxazone, analysis in human plasma and urine, effect on pharmacokinetics

Chlorzoxazone (5-chloro-2(3*H*)-benzoxazolone) (I) is a potent skeletal muscle relaxant that is effective in the treatment of skeletal muscle spasms. Onset of therapeutic activity is observed within 1 hr, with a duration usually up to 6 hr (1). Chlorzoxazone exhibits minimal adverse effects and almost no GI irritation.

The data and results presented in this report are part of a study that was performed with 23 normal male subjects to determine the bioavailability of acetaminophen and chlorzoxazone from a commercial combination tablet formulation and an oral suspension. While there exists sufficient information in the literature regarding acetaminophen elimination kinetics (2–6), little has been reported on the disposition characteristics of chlorzoxazone in humans. This report deals primarily with the plasma levels and urinary excretion of chlorzoxazone following administration of a suspension of chlorzoxazone and acetaminophen.

In studies dealing with the metabolic fate of chlorzoxazone in humans, Conney and Burns (7) reported that <1% of the drug was excreted unchanged in urine. Chlorzoxazone was rapidly metabolized in humans to 6-hydroxy-

0022-3549/83/0900-0991$01.00/0

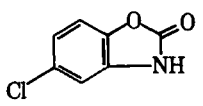

I

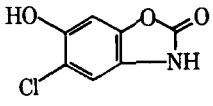

II

chlorzoxazone (5-chloro-6-hydroxy-2(3*H*)-benzoxazolone) (II) which was excreted in urine primarily as the glucuronide conjugate. They could not detect any 6-hydroxychlorzoxazone in the urine in the free form. Their *in vitro* experiments utilizing liver homogenates of rat, rabbit, mouse, and guinea pig established the liver as the principal site of metabolism and 6-hydroxychlorzoxazone as the major metabolite of the *in vitro* metabolism of chlorzoxazone. In this investigation, we have attempted to obtain the pharmacokinetic parameters of chlorzoxazone in humans when administered concomitantly with acetaminophen.

EXPERIMENTAL

Subject Selection—Twenty-three normal, healthy, adult male subjects (20–39 years of age) participated in this study. They were found to be in good health as determined by a screening procedure consisting of a physical examination, evaluation of clinical laboratory values (hematology, blood chemistry, and urinalysis), and determination of vital signs. None of the subjects had any serious diseases, and they refrained from taking drugs for a period of 2 weeks prior to this study.

Dose Administration—The subjects, after fasting for a minimum period of 12 hr, received 900 mg of acetaminophen and 750 mg of chlorzoxazone as an oral suspension. Each milliliter of the aqueous suspension contained 15 mg of chlorzoxazone, 18 mg of acetaminophen, and 5 mg of tragacanth (as a 0.5% solution).

Blood samples (10 ml) were drawn from the subjects at 0 (predose), 0.25, 0.5, 0.75, 1, 1.5, 2, 3, 4, 5, 6, 8, and 10 hr after dosing. The samples were collected in heparinized tubes[1], stored in ice, and centrifuged as soon as possible to obtain plasma.

Urine samples were obtained from pooled samples collected for the following time periods: 0 (predose), 0–2, 2–4, 4–6, 6–8, and 8–10 hr after dosing. The pH and total volume of the pooled sample for each time period were recorded. A 50-ml aliquot of each pooled sample was transferred to a container and frozen.

Analytical Procedures—*Analysis of Plasma Samples for Acetaminophen*—To a 2-ml plasma sample in a 35-ml screw-cap centrifuge tube were added 1 ml of phosphate buffer (pH 7.4), 1.0 ml of ethyl acetate solution containing 20 μg/ml of *N*-butyl-*p*-aminophenol (internal standard), 1.0 g of solid sodium chloride, and 9.0 ml of ethyl acetate. The tube was shaken for 10 min and centrifuged at 2000 rpm for 10 min. Nine milliliters of ethyl acetate was transferred to another 35-ml centrifuge tube containing 2.0 ml of 5% sodium phosphate (pH 11.9). After centrifugation, the ethyl acetate was aspirated off. To the aqueous layer, 1.0 ml of sodium phosphate monobasic buffer (pH 4.5) and 11.0 ml of ethyl acetate were added. The tube was shaken for 10 min and centrifuged for 10 min. Ten milliliters of the ethyl acetate (upper) layer was transferred to a 15-ml conical screw-cap centrifuge tube and evaporated to dryness under a nitrogen stream. The residue was dissolved in 5 μl of pyridine and 15 μl of acetic anhydride, and the tube was placed in a thermostated water bath at 42° for 20 min.

Two microliters of the resulting acetylated reaction mixture was injected into a gas chromatograph[2] using the following conditions: the glass column (91.5 cm × 2-mm i.d.) was packed with 3% OV-17 on 80/100 mesh Chromosorb G-HP. The injection port, column, and detector (FID) temperatures were 220°, 165°, and 220°, respectively. The carrier gas (nitrogen) flow rate was 25 ml/min; hydrogen and air flow rates were 25 and 300 ml/min, respectively. The retention times of acetaminophen and the internal standard were 8.5 and 15.0 min, respectively. The calibration curve was linear from 0.5 to 20.0 μg/ml.

Analysis of Plasma Samples for Chlorzoxazone—Sample preparation involved a single-step extraction and derivatization. One milliliter of plasma was pipetted into a 15-ml disposable bottle containing 1 ml of 0.5 *N* HCl. To this was added 10 ml of ethyl acetate containing 20 μg of the internal standard (*n*-hexadecane). The mixture was shaken for 10 min and centrifuged at 2000 rpm for 5 min. A 9-ml aliquot of the ethyl acetate layer was transferred to a 15-ml screw-cap centrifuge tube and evaporated to ~0.5 ml under a nitrogen stream. The sides of the tubes were rinsed with an additional 0.5 ml of ethyl acetate. The combined ethyl acetate solution was evaporated to dryness. To the residue were added 5 μl of pyridine and 15 μl of acetic anhydride. The tube was capped and placed in a water bath at 42° for 20 min.

A 2-μl aliquot of the resulting reaction mixture was injected into a gas chromatograph equipped with a dual flame-ionization detector. The columns were 1.83 m × 4-mm i.d. glass tubes packed with 3% OV-1 on 60/80 mesh Gas Chrom Q. Column temperature was maintained at 130°. The carrier gas (nitrogen) was held at a flow rate of 30 ml/min; the hydrogen and air flow rates were 30 and 300 ml/min, respectively. The retention times of chlorzoxazone and the internal standard were 3.25 and 4.5 min, respectively. The lower limit of quantitation was 0.5 μg/ml using 1 ml of plasma. The calibration curve was found to be linear between 0.5 and 25 μg/ml. Extraction efficiency for chlorzoxazone under the above conditions was 88 ± 8% (six determinations).

Table I—Mean Peak Plasma Concentrations, Peak Times, and AUC (0–10 hr) of Acetaminophen and Chlorzoxazone in 23 Normal Subjects Following Oral Administration of Acetaminophen and Chlorzoxazone [a]

Drug	Parameter, mean ± *SEM*		
	Peak Plasma Concentration, μg/ml	Peak Time, min	AUC (0–10 hr) μg·min/ml
Acetaminophen	16.7 ± 1.3	40 ± 9.4	2816 ± 170
Chlorzoxazone	36.3 ± 2.3	38 ± 3.3	4084 ± 284

[a] Administered as a suspension containing 900 mg of acetaminophen and 750 mg of chlorzoxazone.

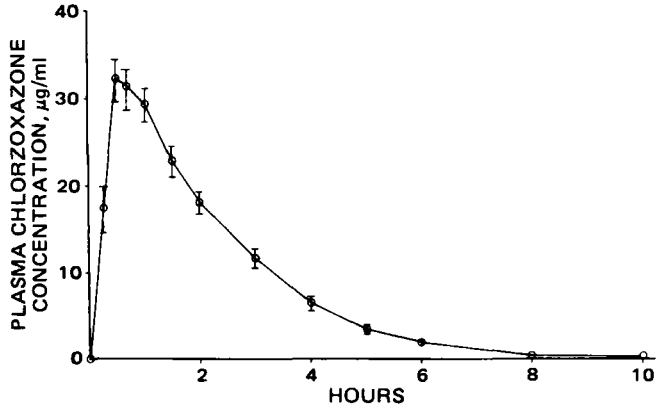

Figure 1—*Mean (±SEM) plasma concentrations of chlorzoxazone (μg/ml) in 23 human subjects following the oral administration of 900 mg of acetaminophen and 750 mg of chlorzoxazone.*

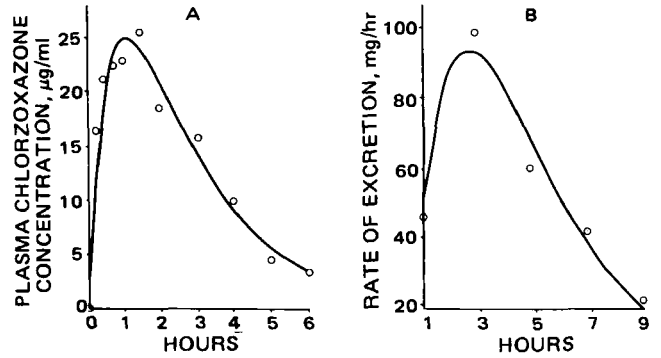

Figure 2—*Computer-fitted profiles (—) of plasma chlorzoxazone data (A) and urinary excretion data (B) of 6-hydroxychlorzoxazone glucuronide as chlorzoxazone equivalents obtained for a subject. Circles represent observed data.*

[1] Vacutainer, Becton, Dickinson and Co.

[2] Varian Aerograph (Model 2400).

Table II—Pharmacokinetic Parameters of Chlorzoxazone in Humans [a]

	V/f, liters	K, hr^{-1}	k_a, hr^{-1}	k_{m1}, hr^{-1}	k_{u2} hr^{-1}	$t_{1/2}$, hr	KV/f, ml/min [b]
Average of individual values [c]	13.70 ± 5.07	0.73 ± 0.29	2.28 ± 2.08	0.63 ± 0.31	0.60 ± 0.31	1.12 ± 0.48	148.0 ± 39.9
Evaluation of mean data [d]	13.89 ± 1.85	0.69 ± 0.13	1.96 ± 0.35	0.53 ± 0.10	0.42 ± 0.04	1.00	159.7

[a] Expressed as mean ± *SD*. [b] Clearance/*f*. [c] $n = 22$; one subject was excluded due to nonconvergence of k_a. [d] $n = 23$.

Analysis of Urine Samples for 6-Hydroxychlorzoxazone and Acetaminophen—The assay was designed to quantitate simultaneously total acetaminophen (intact plus glucuronide and sulfate conjugates) and total 6-hydroxychlorzoxazone (intact and glucuronide conjugate) in urine. Intact chlorzoxazone has been reported to be present in urine at ≤1% of the dose (7).

Aliquots (0.5 ml) of urine samples containing acetaminophen, 6-hydroxychlorzoxazone, their conjugates, and the added internal standard (*N*-butyl-*p*-aminophenol, 200 μg) were incubated overnight with β-glucuronidase[3] in an acetate buffer (pH 4.6) at 37°. The enzymatically hydrolyzed products were then extracted by adjusting the urine sample pH to 7.4 with 1 ml of phosphate buffer (pH 11.9) and extracting with 5 ml of ethyl acetate. A 4-ml aliquot of the ethyl acetate was then extracted with 3 ml of phosphate buffer (pH 11.9). The ethyl acetate was aspirated off and 1 ml of phosphate buffer (pH 4.5) was added to neutralize the solution. The neutralized solution was again extracted with 5 ml of ethyl acetate. Four milliliters of the ethyl acetate layer was evaporated to dryness under a nitrogen stream, and the residue was reconstituted with 50 μl of methanol.

Ten microliters of the methanolic solution was injected into a liquid chromatograph[4] equipped with a UV detector[5] at a wavelength of 280 nm. The reverse-phase analytical column[6] was 25 cm in length and 4.6-mm i.d. The mobile phase was water–methanol–pH 4.6 acetate buffer (3:1:1, v/v/v). The flow rate was held at 2 ml/min. The retention times for acetaminophen, 6-hydroxychlorzoxazone, and the internal standard were 3, 9, and 11 min, respectively. The calibration curve was linear from 20 to 1000 μg/ml for both acetaminophen and 6-hydroxychlorzoxazone. The extraction efficiencies for 6-hydroxychlorzoxazone and acetaminophen under the above conditions were 86 ± 6.5 and 95 ± 10.7%, respectively (six determinations).

RESULTS AND DISCUSSION

Table I lists a summary of acetaminophen peak plasma concentrations, peak times, and the area under the plasma concentration–time curve (AUC 0–10 hr) as calculated by the trapezoidal rule, observed in 23 normal subjects following the oral administration of 900 mg of acetaminophen and 750 mg of chlorzoxazone. Acetaminophen was rapidly absorbed with a mean peak plasma concentration of 16.7 μg/ml at a mean peak time of 40 min. These values are in the range of values obtained by other investigators (5), thus showing that the disposition kinetics of acetaminophen were not altered by the concurrent administration of chlorzoxazone.

Table I also lists the pharmacokinetic parameter values for chlorzoxazone. The mean (± *SEM*) plasma chlorzoxazone concentration–time profile is shown in Fig. 1. Chlorzoxazone was rapidly absorbed, attaining a mean (±*SEM*) peak level of 36.3 ± 2.3 μg/ml at a mean peak time of 38 ± 3.3 min after dosing. After reaching a peak, the plasma concentrations declined rapidly in a monoexponential manner, suggesting a rapid distribution. Plasma concentrations at the 8- and 10-hr time points for most subjects were either zero or were below the assay quantitation limit of 0.5 μg/ml, indicating that chlorzoxazone was rapidly eliminated from the body. The individual and mean plasma chlorzoxazone concentration–time profiles following the oral administration of chlorzoxazone were found to be characteristic of a one-compartment oral absorption model conforming to:

$$C_t = \frac{k_a f X_0}{V(k_a - K)}\left[e^{-Kt} - e^{-k_a t}\right] \qquad \text{(Eq. 1)}$$

where C_t is the concentration of chlorzoxazone in plasma at time t, k_a is the apparent first-order absorption rate constant, X_0 is the dose of chlorzoxazone (750 mg), f is the fraction of the administered dose reaching systemic circulation as unchanged chlorzoxazone, K is the apparent first-order elimination rate constant of the drug, and V is the apparent volume of distribution.

The urinary excretion data revealed that at the end of 10 hr, 74 ± 3.4% (mean ± *SEM*) of the dose was excreted as 6-hydroxychlorzoxazone glucuronide. Based on the information available in the literature (7), the biotransformation profile of chlorzoxazone could be explained by:

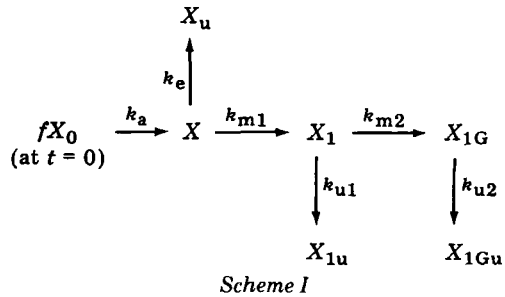

Scheme I

where X and X_u are the amounts of chlorzoxazone in the body and urine, respectively; X_1 and X_{1u} are the amounts of 6-hydroxychlorzoxazone in the body and urine, respectively; X_{1G} and X_{1Gu} are the amounts of 6-hydroxychlorzoxazone glucuronide in the body and urine, respectively; k_e, k_{u1}, and k_{u2} are the renal excretion rate constants for chlorzoxazone, 6-hydroxychlorzoxazone, and 6-hydroxychlorzoxazone glucuronide, respectively; and k_{m1} and k_{m2} are the respective metabolic rate constants for the formation in the body of 6-hydroxychlorzoxazone from chlorzoxazone and 6-hydroxychlorzoxazone glucuronide from 6-hydroxychlorzoxazone.

Under the conditions of the analytical procedure employed in this study, neither unchanged chlorzoxazone nor 6-hydroxychlorzoxazone could be detected in the urine samples. Although the lower limit of quantitation was established at 20 μg/ml, the assay was capable of detecting 5 μg/ml of 6-hydroxychlorzoxazone in urine. When the urine samples were hydrolyzed by β-glucuronidase and then assayed, 6-hydroxychlorzoxazone was detected indicating the presence of 6-hydroxychlorzoxazone glucuronide in the urine samples prior to hydrolysis.

Since 6-hydroxychlorzoxazone was not detected in the urine samples (or was present in negligible amounts), the biotransformation pathway in Scheme I was simplified to give:

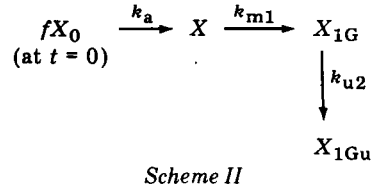

Scheme II

In proposing this simplified model, the following assumptions were made:

1. The absence of 6-hydroxychlorzoxazone in the urine samples is due to its rapid conversion in the body to the glucuronide conjugate, *i.e.*, $k_{m1} <<< k_{m2}$ or k_{m1} is the limiting rate constant.
2. The absence of 6-hydroxychlorzoxazone in urine is not due to its reabsorption from the kidney since 6-hydroxychlorzoxazone is sufficiently polar in nature to be excreted by the kidney, *i.e.*, $k_{u1} \simeq 0 <<< k_{m2}$. For this model, the amount of 6-hydroxychlorzoxazone glucuronide excreted in urine as a function of time is given as (8):

$$\frac{d(X_{1Gu})}{dt} = k_{u2}k_{m1}k_a f X_0 \left[\frac{e^{-k_a t}}{(K - k_a)(k_{u2} - k_a)} + \frac{e^{-Kt}}{(k_a - K)(k_{u2} - K)} + \frac{e^{-k_{u2}t}}{(k_a - k_{u2})(K - k_{u2})}\right] \qquad \text{(Eq. 2)}$$

[3] Glusulase, Endo Laboratories, Garden City, N.J.
[4] Waters Associates, Milford, Mass.
[5] Model 440.
[6] Hibar-II, LiChrosorb, RP-18; E. Merck.

Table III—F Test to Determine the Number of Parameters Needed to Describe Chlorzoxazone Data Obtained for a Subject

	Number of Parameters in Model	Remaining Degrees of Freedom	Total Sum of Weighted Squared Deviations
	4	16 − 4 = 12	1409.7
	5	16 − 5 = 11	135.9
Difference	1	1	1273.8

$$F = \frac{1273.8}{135.9} \times \frac{11}{1} = 103.10^{a}$$

$$0.05\,F^{1}_{11} = 4.84$$

[a] Observed F exceeds critical F at 0.05 level of significance; therefore, the number of parameters should be increased from 4 to 5.

The plasma chlorzoxazone concentration and urinary excretion rate data of 6-hydroxychlorzoxazone glucuronide (as chlorzoxazone equivalents) for each individual subject were then simultaneously fitted by the least-squares method to Eqs. 1 and 2 using NONLIN (9) and a digital computer[7] to obtain estimates for the parameters V/f, K, k_a, k_{m2}, and k_{u2}. The mean plasma and urine data were also similarly fitted to Eqs. 1 and 2.

The least-squares estimates for one subject resulted in poor correlation owing to nonconvergence of the parameter k_a; hence, this subject was not included in the calculation of the average values. The average values for 22 subjects along with the parameter values obtained by simultaneous fitting of the mean plasma concentration–time data and the mean urinary excretion data are listed in Table II with the elimination half-life and plasma clearance values. There was good agreement between the average values for 22 subjects and the values obtained using the mean plasma concentration–time data. Average elimination half-life was 1.12 ± 0.48 hr and the average plasma clearance was 148.0 ± 39.9 ml/min. These values agree very well with the elimination half-life of 1 hr and the plasma clearance of 159.7 ml/min derived from the mean data. Figure 2 shows the model-predicted plasma concentration–time curve and the rate of excretion *versus* time at the midpoint of the urine collection period (t-MID) plot for one subject. Figure 3 shows the predicted curves for the mean plasma concentration–time data and the mean rate of excretion *versus* time (t-MID) plot. From these curves, it can be seen that excellent fits were obtained for the observed data when fitted to Eqs. 1 and 2 and that the scatter of the observed data about the theoretical curves was randomly distributed.

Equation 2 describes the rate of excretion of 6-hydroxychlorzoxazone glucuronide and is composed of the exponentials of three parameters: (*a*) the absorption rate constant of chlorzoxazone, (*b*) the elimination rate constant of chlorzoxazone, and (*c*) the excretion rate constant of the glucuronide. To test whether a three-exponential equation was needed, the data were fitted to a model consisting of the exponentials of only two parameters:

$$\underset{(\text{at } t = 0)}{fX_0} \xrightarrow{k_a} X \xrightarrow{k_{m1}} X_{1Gu}$$

Scheme III

which uses:

$$\frac{dX_{1Gu}}{dt} = k_{m1}X = \frac{k_{m1}k_a f X_0}{(k_a - K)}\left[e^{-Kt} - e^{-k_a t}\right] \qquad \text{(Eq. 3)}$$

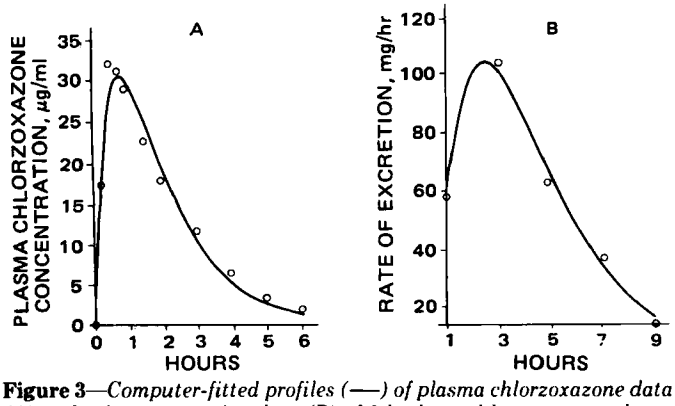

Figure 3—*Computer-fitted profiles (—) of plasma chlorzoxazone data (A) and urinary excretion data (B) of 6-hydroxychlorzoxazone glucuronide as chlorzoxazone equivalents obtained from the mean data. Circles represent observed means.*

[7] DEC 1099; Digital Equipment Corp.

Equation 3 resembles Eq. 1, *i.e.*, the rate of excretion of the glucuronide can also be described by only two exponentials, that describing absorption and that describing the overall elimination of the unchanged drug. The combined plasma and urine data were then fitted to Eqs. 1 and 3, and the parameters V/f, K, k_a, and k_{m1} were obtained.

As suggested by Boxenbaum *et al.* (10), an F ratio test was utilized to determine if it was justified to use four parameters instead of the original five to describe the data. Table III lists the number of parameters, the degrees of freedom, and the total sum of weighted, squared deviations obtained by fitting the combined plasma and urine data of one representative subject using four and five parameters. The results of the F test are also included and show that the observed F of 103.1 exceeds the critical F of 4.84, thereby suggesting that a minimum of five parameters are needed to define the data. Use of four parameters generally resulted in a relatively poor fit of the data and in higher values of total sum of weighted, squared deviations for all subjects and for the mean data. Application of Akaike's information criterion (11) confirmed the results of the F test, thus providing a strong justification for the use of five parameters instead of four.

A comparison of the least-squares estimates of the parameters V/f, K, k_a, k_{m1}, and k_{u2} (Table II) obtained by averaging the values for individual subjects and those obtained from the evaluation of the mean data showed a better correlation among the plasma parameters (V/f, K, and k_a) than among the urinary excretion rate parameters (k_{m1} and k_{u2}). This is probably because the urinary excretion data were described by only five samples, each obtained at intervals of 2 hr while plasma data were described by a minimum of 11 data points for each subject. This may have contributed to the variability observed in the urinary excretion parameters.

An apparent volume of distribution of ~ 14 liters (assuming complete systemic availability, $f = 1$) suggests that the drug is not widely distributed and that it would be confined to the circulatory system and possibly the extracellular fluid. Previous experiments (7) with dogs showed that the concentration of chlorzoxazone in the liver, muscle, brain, and kidney was approximately one-half or less that found in plasma. Chlorzoxazone concentration in fat was, however, twice that in plasma.

REFERENCES

(1) E. Settel, *Clin. Med.*, **6**, 1373 (1959).

(2) E. Nelson and T. Morioka, *J. Pharm. Sci.*, **52**, 864 (1963).

(3) A. J. Cummings, M. L. King, and B. K. Martin, *Br. J. Pharmacol. Chemother.*, **29**, 150 (1967).

(4) K. S. Albert, A. J. Sedman, and J. G. Wagner, *J. Pharmacokinet. Biopharm.*, **2**, 381 (1974).

(5) M. D. Rawlins, D. B. Henderson, and A. R. Hijab, *Eur. J. Clin. Pharmacol.*, **11**, 283 (1977).

(6) J. A. Clements, R. C. Heading, W. S. Nimmo, and L. F. Prescott, *Clin. Pharmacol. Ther.*, **24**, 420 (1978).

(7) A. H. Conney and J. J. Burns, *J. Pharmacol. Exp. Ther.*, **128**, 340 (1960).

(8) J. G. Wagner, "Biopharmaceutics and Relevant Pharmacokinetics," Drug Intelligence Publications, Hamilton, Ill., 1971, p. 293.

(9) C. M. Metzler, G. L. Elfring, and A. J. McEwen, "A User's Manual for NONLIN and Associated Programs," The Upjohn Co., Kalamazoo, Mich., 1974.

(10) H. G. Boxenbaum, S. Riegelman, and R. M. Elashoff, *J. Pharmacokinet. Biopharm.*, **2**, 123 (1974).

(11) K. Yamaoka, T. Nakagawa, and T. Uno, *J. Pharmacokinet. Biopharm.*, **6**, 165 (1978).

ACKNOWLEDGMENTS

The authors thank Ms. Susan Stellar for providing technical assistance.

Model-Independent Procedure for Area Estimation and Intergroup Comparisons

THOMAS CAPIZZI ˣ, HINA MEHTA, and LEONARD OPPENHEIMER

Received December 24, 1981, from *Biometrics Research, Merck Sharp & Dohme Research Laboratories, Rahway, NJ 07065.* Accepted for publication August 9, 1982.

Abstract □ A method is provided for estimating the area under a response–time curve for an experimental situation where independent observations are made at each time point. The procedure utilizes least-squares spline functions and the jackknife technique to provide area estimates, standard errors, and a statistical test for intergroup comparisons. The method is based on an empirical model and provides a means of analysis when no prior model can be specified or if the incorrect specification of a model will produce invalid results. The method is illustrated using data from a study comparing the pharmacokinetic behavior of a fasciolicide in rats having either a young or old parasitic infestation. The results obtained are comparable with those generated by a model-dependent approach.

Keyphrases □ Pharmacokinetics—area under response–time curve, model-independent estimation, intergroup comparisons □ Spline functions—use with jackknife technique to provide area under response–time curve estimations, model independent

In pharmacokinetics it is often necessary to calculate the area under the response–time curve (AUC) for a subject and then compare the AUC among subjects allocated to several experimental groups. For one type of experimental design, a drug is given to several groups of subjects and a response variable for each subject is then observed at fixed time points (Scheme I, type B). Each subject has its own response–time curve, and an estimate of a subject's AUC could be obtained by (*a*) fitting and then numerically integrating a pharmacokinetic model (1), or (*b*) utilizing a model-independent interpolation procedure such as the trapezoidal rule (2). However, in some situations a time–response curve is not available for each subject; instead independent observations are made at each time point (Scheme I, type A). For example, a drug may be given to several groups of animals with different experimental conditions, and the drug concentration in an organ of the animal is required at several points in time. Since the animals must be serially sacrificed to obtain this information, the measurements are made using different animals at each time point. A model-independent procedure for this experimental design (Scheme I, type A) is introduced which will provide area estimates, standard errors, and a statistical test for intergroup comparisons.

TYPE A STUDIES	TYPE B STUDIES
P experimental groups or treatments	P experimental groups or treatments
↓	↓
N_i subjects in each group	N_i subjects in each group
↓	↓
Drug is given to all the subjects at time t_0	Drug is given to all the subjects at time t_0
↓	↓
A random sample of subjects is selected from each group and the response variable is measured at time t_i, $i = 1, 2, \ldots, k$. Once selected, the subject is removed from the study	Response variable is measured for each subject at all subsequent times $t_1, t_2, \ldots, t_k$
↓	↓
Response–time curve for each group (not individual)	Each subject has a response–time curve
↓	↓
Area calculated for each group's response–time curve	Area calculated for each subject's response–time curve

Scheme I—Two Types of Experimental Designs

In these situations (Scheme I, type A) a model-dependent AUC estimate can be obtained by specifying a pharmacokinetic model. However, this model dependent approach could result in biased and unreliable area estimates in situations where the specific model used is not the correct functional form. In general, it is difficult to discriminate among competing models on the basis of prior biological information and/or statistical goodness-of-fit tests, and this is especially so with the addition of between-subject variability at each time point. Another alternative would be to apply an interpolation procedure to each group's mean response–time curve. However, no estimate of precision would be available and thus, no intergroup comparisons could be made.

This paper presents a model-independent method for estimation of an experimental group's AUC in type A studies, which also allows for intergroup hypothesis testing. The method utilizes least-squares spline functions (3) and the jackknife technique (4), and would appear to be the procedure of choice in obtaining AUC estimates for type A studies unless there is strong evidence for a specific pharmacokinetic model. The method is illustrated on data from a study (5) comparing the pharmacokinetic behavior of a fasciolicide in rats having either young or old parasitic infestations.

THEORETICAL

Estimation and Intergroup Comparison Procedure—The method presented in this paper can be outlined in three steps:

1. Fit an empirical function (spline, Eq. 2) using ordinary least squares to the group response–time curve.
2. Obtain an estimate of the AUC (the integral of the fitted function over time, Eq. 4) and its standard error by least squares or the jackknife procedure (4).
3. Use of the pseudovalues (Eq. 6) generated by the jackknife procedure to evaluate group differences *via* a t test or an ANOVA.

Fitting an Empirical Function (Spline) Using Ordinary Least Squares—In this method it is assumed that for each group and response variable there is a continuous (smooth) function, $g(t)$, which represents the average response *versus* time relationship, *i.e.*:

$$Y_{ism} = g(t_{is}) + e_{ism} \quad m = 1, 2, \ldots M_{is}, \quad s = 0, \ldots S_i, \quad i = 1, 2, \ldots P, \quad \sum_s M_{is} = N_i \qquad \text{(Eq. 1)}$$

where Y_{ism} is the response of the mth subject at the sth time of the ith group; $g(t)$ is a continuous function whose exact form is not known; e_{ism} are independent identically distributed random errors with mean 0 and variance σ^2; and N_i is the number of subjects in the ith group.

To obtain model-independent AUC estimates for each group, an em-

0022-3549/83/0900-0995$01.00/0

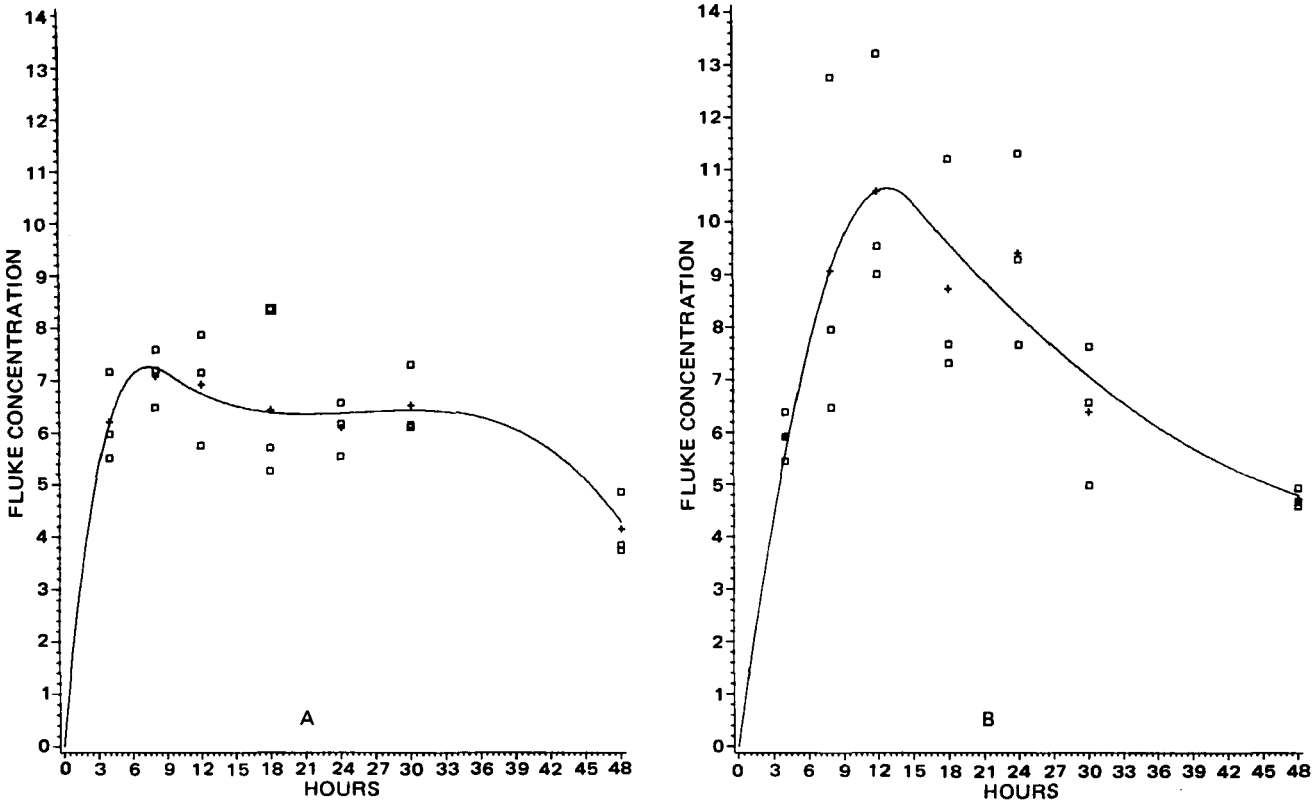

Figure 1—*Plot of observed individual drug concentration in the liver fluke of rats (□) and mean drug concentration (+)* versus *time (hr) for young (A) and old (B) infestation groups. Curves represent least-squares spline fit to the individual drug concentration* versus *time data (Table I).*

pirical function must be chosen that adequately describes the variation of response over time and gives a close approximation to $g(t)$. Spline functions, which are defined as piecewise continuous polynomials of degree n, are considered to be excellent empirical functions (3, 6, 7) for this purpose. The pieces of the spline are joined together at points called knots (abscissa values) in such a fashion that the function and the first $n-1$ derivatives agree at the join points. The degree of the polynomial pieces and the number and position of the knots may be varied in different situations to provide a good fit to the data. Quadratic and cubic splines (polynomial pieces of degree at most 2 or 3) are the most popular among practitioners because of their computational simplicity, smoothness, and flexibility, and have been used in a variety of biological and chemical applications (3, 7, 8–12).

There are several numerical methods for fitting splines to data (3). The method employed here is that of ordinary least squares (OLS). This method requires that the number of knots, as well as their location, be specified. The fitting of the spline to data is then accomplished by multiple linear regression techniques. The choice of the number and position of the knots is an important and difficult problem that has to be addressed. Knots should be chosen so as to correspond to the overall behavior of the data (number of time points, position of maxima and minima, *etc.*). Some rules of thumb for knot positioning have been presented by Wold (3). However, in most applications judgment and experience together with simulation results seem to be the only criteria for making these decisions.

Spline functions can be considered as a multiple linear regression model by employing the "+" function representation of a spline (7). For example, a cubic spline is given as follows: Let $S(t)$ for $t_0 \le t \le t_L$ be a cubic spline with knots at $k_2, \ldots k_{r-1}$. Then:

$$S(t) = b_0 + b_1 t + b_2 t^2 + b_3 t^3 + \sum_{j=2}^{r-1} b_{j+2}\,(t-k_j)_+^3 \qquad \text{(Eq. 2)}$$

where:

$$(t-k_j)_+ = \begin{cases} t-k_j, \text{ if } t > k_j \\ 0, \text{ otherwise} \end{cases} \qquad \text{(Eq. 3)}$$

and b_j are the parameters to be estimated. Notice that the parameters b_j appear linearly in Eq. 1 and thus can be estimated by OLS. A quadratic spline can be defined in an analogous manner (7).

Area Estimation Using Least-Squares Theory—Once the appropriate spline has been fitted to the time–response data for each experimental group, an estimate of the AUC can be obtained. Let the fitted spline function for a group be denoted by $S_i(\hat{t})$. An estimate of the area under the fitted function ($\hat{\text{AUC}}_i$) is given by the integral of $S_i(\hat{t})$ evaluated from t_0 to t_L, *i.e.*:

$$\hat{\text{AUC}}_i = \int_{t_0}^{t_L} S_i(\hat{t})\,dt \qquad \text{(Eq. 4)}$$

If $S_i(\hat{t})$ is a cubic spline, then:

$$\hat{\text{AUC}}_i = \hat{b}_{0i}t + \frac{\hat{b}_{1i}t^2}{2} + \frac{\hat{b}_{2i}t^3}{3} + \frac{\hat{b}_{3i}t^4}{4} + \sum_{j=2}^{r-1} \frac{\hat{b}_{ji+2}}{4}(t-k_j)_+^4 \Bigg|_{t_0}^{t_L} \qquad \text{(Eq. 5)}$$

Estimates of the AUC are linear combinations of the spline parameter estimates, $\hat{b}_{ji}$, so that an estimate of their standard error can be obtained using linear regression methods (13). Note that different spline functions ($\hat{b}_{ji}$) and area estimates ($\hat{\text{AUC}}_i$) are obtained for the different experimental groups.

Area Estimation and Measurements of Precision Using the Jackknife Procedure—If the residuals (observed values minus fitted values) obtained from the spline regression were normally distributed, then the estimated standard errors for AUC estimates computed by least squares could be used to calculate confidence intervals and test for group differences. However, in addition to the random variation, the residuals contain a degree of unknown bias. The bias occurs from fitting an empirical model [$S(t)$] and not the true functional form of the underlying model [$g(t)$]. Also, the random component of the residuals may not be normally distributed. Thus, the standard least-squares method when

Table I—Least-Squares Parameter Estimates for Spline Functions Fitted to Drug Uptake Data in the Liver Fluke in Rats

Parameter	Infestation Group	
	Young	Old
t	2.4767	1.6480
t^2	−0.2714	−0.06386
t^3	0.0093730	—
$(t-10)_+^3$	−0.0095835	—
$(t-15)_+^2$	—	0.06676
S^a	0.8624	1.8322

[a] Denotes root mean square error.

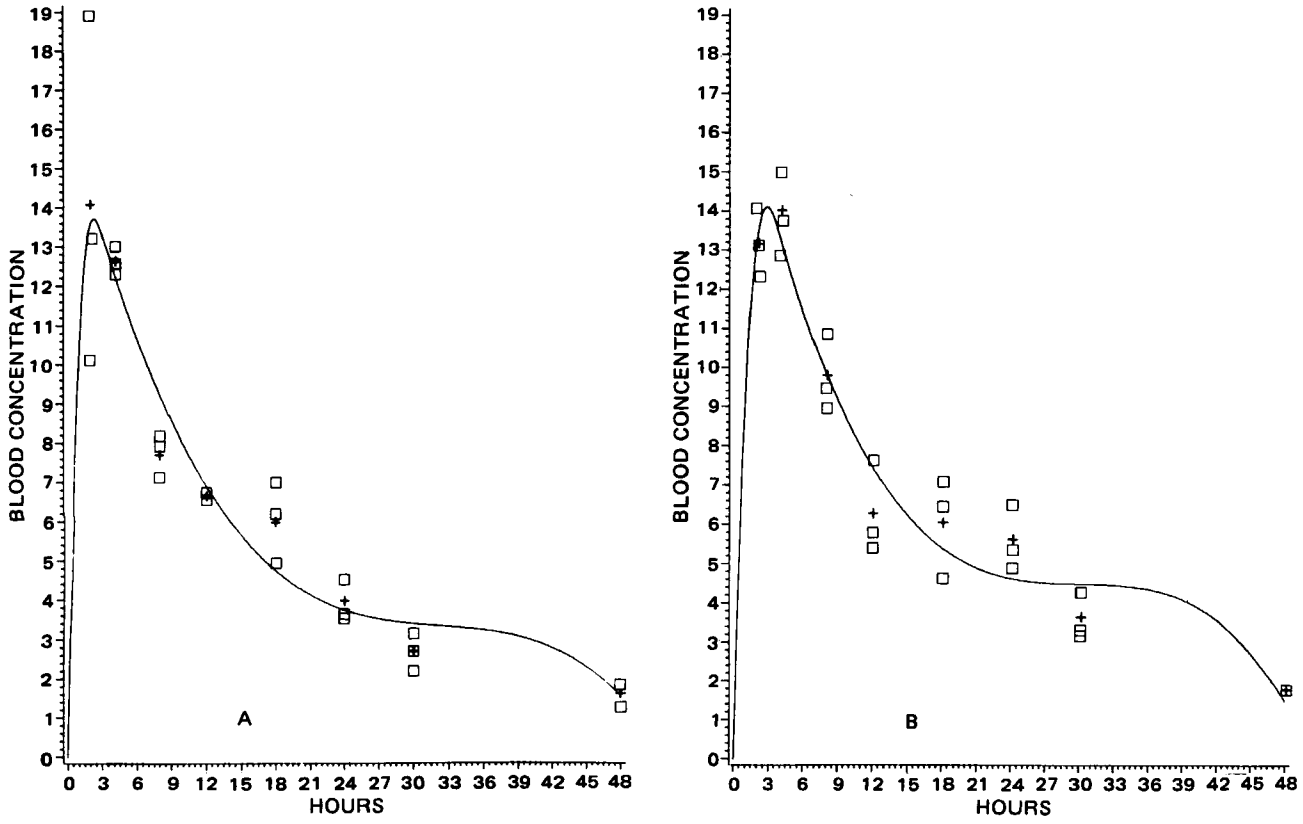

Figure 2—*Plot of observed individual drug concentration in blood of rats (□) and mean drug concentration (+) versus time (hr) for the young (A) and old (B) infestation groups. Curves represent least-squares spline fit to the individual drug concentration versus time data (Table III).*

used to test group differences could yield misleading results. In complex situations where standard methods might not be applicable, a useful statistical technique has been the jackknife procedure (4). The jackknife procedure was introduced by Quenouille (14) as a method for eliminating bias due to finite sample sizes in estimating parameters. Tukey (15) proposed that the jackknife be used for robust interval estimation. A clear nonmathematical exposition of the jackknife with examples is provided by Mosteller and Tukey (4), while an excellent review of the statistical literature dealing with the jackknife is presented by Miller (16).

In situations where linear least-squares methods are employed, there are two methods of jackknifing: the regular jackknife and the weighted jackknife (17). The weighted version provides improved bias reduction and variance estimation for nonlinear functions of linear regression parameters. However, in contrast to the regular jackknife, the weighted jackknife does not address the issue of bias for linear functions of the regression parameters. Since the AUC estimate for each group is a linear function of the fitted spline parameters, the regular jackknife is the procedure of choice for this situation.

To obtain the regular jackknife estimate of the AUC for each group, the function given by Eq. 4 is first calculated with all of the group's observations included. Let $A_{\text{all},i}$, $i = 1, 2, \ldots P$ denote this estimate of area. Next, let A_{ism} denote the estimate of area with the mth subject at the sth time deleted (*i.e.*, the $_{ism}$th subject is deleted, the spline function for the ith group is fitted, and the AUC is computed). Then, pseudovalues are defined as:

$$P_{ism} = N_i A_{\text{all},i} - (N_i - 1) A_{ism}, \quad \begin{matrix} i = 1, 2, \ldots, p \\ s = 1, 2, \ldots, S_i \\ m = 1, 2, \ldots, M_{is} \end{matrix} \qquad \text{(Eq. 6)}$$

The jackknife estimate of AUC for the ith group is then the mean of the pseudovalues:

$$J_i(\hat{\text{AUC}}) = \frac{1}{N_i} \sum_{sm} P_{ism} \qquad \text{(Eq. 7)}$$

with estimated variance:

$$s^2(\hat{J}_i) = \frac{1}{N_i(N_i - 1)} \sum_{sm} [P_{ism} - J_i(\hat{\text{AUC}})]^2 \qquad \text{(Eq. 8)}$$

For each group the pseudovalues can be treated as if they follow a Student's t distribution, and a $(1 - \alpha)$% confidence interval is given by:

$$J_i(\hat{\text{AUC}}) \pm t_{(1-\alpha/2),Ni-1} s(\hat{J}_i) \qquad \text{(Eq. 9)}$$

where $t_{(1-\alpha/2)}, N_i - 1$ is the $(1 - \alpha/2)$ percentage point of the Student's t distribution with $N_i - 1$ degrees of freedom.

Intergroup Comparisons—The pseudovalues for each group can be used as if they were identically distributed estimates of the AUC, and hence, standard statistical procedures can be applied to make intergroup comparisons (18). Various statistical analyses can be used depending on the experimental design, *e.g.*, a one-way or factorial ANOVA procedure. In addition, trend tests for factors with quantitative levels or comparisons of various linear functions of treatment groups using multiple-comparison procedures can be obtained easily.

EXPERIMENTAL

Data Description—A study (5) investigating the pharmacokinetic basis for increased efficacy of a fasciolicide against older liver flukes (*Fasciola hepatica*), *i.e.*, 39–44 weeks old, in rats led to the development of the model-independent estimation and hypothesis-testing procedure described above. The fasciolicide was administered as a single oral dose when the fluke infestation in the rats were either young (9–16 weeks) or

Table II—Area Under the Drug Uptake in Liver Fluke of Rats–Time Curve

		Model Independent[a]		Model Dependent	
Group	N^b	Least Squares[c]	Jackknife[c]	Least Squares[d]	Jackknife[c]
Young	21	289.31 (11.35)	289.83 (9.66)	278.89	277.66 (10.02)
Old	21	344.16 (19.96)	344.23 (18.94)	347.80	348.67 (17.32)
t statistic		—	-2.56^f (30)[e]	—	-3.55^g (32)[e]

[a] Results taken from Ref. 21. [b] Number of observations. [c] Number in parentheses are standard errors. [d] Standard errors were not computed. [e] Since the within-group variances were statistically significantly different ($p < 0.05$), a t test for unequal variances was applied to the pseudovalues and adjusted degrees of freedom are reported (in parentheses). [f] Statistically significant difference, $p < 0.05$ between young and old groups. [g] Statistically significant difference ($p < 0.001$) between young and old groups.

Table III—Least-Squares Parameter Estimates for Spline Functions Fitted to Blood Level Data of Drug in Rats

Parameter	Infestation Group	
	Young	Old
t	15.2758	12.1734
t^2	−5.4484	−3.3347
t^3	0.6090	0.2811
$(t-3)_+^3$	−0.6094	—
$(t-4)_+^3$	—	−0.2816
S^a	1.6970	1.1907

[a] Denotes root mean square error.

old (39–44 weeks). Twenty-one rats were started in each group, with three rats being sacrificed at each time point. The drug uptake in the liver fluke was one of the variables measured (Fig. 1). Blood levels of the rats were also taken at these time points (Fig. 2). It was hypothesized that the drug uptake in the liver fluke was greater in rats having the older infestation, while the drug concentrations in the blood profile were similar for both groups. The areas under the respective time–response curves were considered to be one of the parameters of interest.

Data Treatment—To apply the estimation procedure to these data, the degree of the spline and the number and position of the knots had to be determined. Based on the work of Wold (3) and previous studies[1], it was thought that a spline with a single knot situated near the peak of the response–time curve would provide an adequate fit in this kind of situation (where the response variable rises to a peak and slowly decreases toward zero). Thus, for each group and response variable, either a quadratic or cubic spline with one knot and no intercept term was fitted by OLS. The specific form of the spline was determined by varying the location of the knot and degree of the spline and choosing the result that gave the smallest sum of squared errors. The OLS AUC estimates were obtained by computing the definite integral of the fitted spline from 0 to 48 hr. The jackknife was applied to the AUC estimates. The old *versus* young infestation group comparison was accomplished by performing a two-sample Student's t test on the pseudovalues obtained with the jackknife.

For purposes of comparison, a model-dependent approach was also utilized. An open one-compartment model that is often used for these kind of data (19) was fitted using nonlinear regression. The least-squares and jackknifed AUC estimates were obtained in an analogous manner as described in the model-independent approach.

Computation—All necessary computations were made by utilizing the Statistical Analysis System (SAS) computer package (20). The spline functions were fitted with the SYSREG procedure and the no-intercept option. A SAS PROC MATRIX macro (21) was used to obtain the area estimates and to apply the jackknife procedure. The between-infestation group comparison was made with the TTEST procedure. The results for the model-dependent case were obtained by using the SAS NLIN (nonlinear least-squares) procedure. The plots (Figs. 1 and 2) were computer-generated using a ZETA 1536 plotter which was driven by the SAS/GRAPH package.

RESULTS

Liver Fluke Uptake—The spline function used for area estimation for the young infestation group was a cubic spline with a knot at 10 hr; the spline function for the old infestation group was a quadratic spline with a knot at 15 hr. The spline parameter estimates are given in Table I.

The OLS and jackknife estimates of the AUC are contained in Table II. The AUC estimates and standard errors are similar for the least-squares and jackknife procedures. The two-sample t test for unequal variances performed on the AUC pseudovalues showed that old infestation groups had a statistically significantly greater AUC ($p < 0.05$) after 48 hr than the young group. The AUC estimates obtained with the model-dependent approach gave results that were comparable to the model-independent approach.

Blood Level of Drug—The following splines were fitted: (*a*) for the young infestation group, a cubic spline with a knot at 3 hr and (*b*) for the old infestation group, a cubic spline with a knot at 4 hr. The spline estimates are given in Table III. Results of the AUC estimation procedure are presented in Table IV.

The least-squares and jackknife AUC estimates yield similar estimates and standard errors. Although the jackknife AUC estimates for the old infestation group of rats were higher than those for the young group, the two-sample t test using the pooled within-group variance showed that this result was not statistically significant ($p > 0.05$). The AUC estimates for the model-dependent approach are comparable (although smaller) to corresponding estimates obtained with the model-independent procedures.

[1] Unpublished data, Merck Sharp & Dohme.

Table IV—Area Under the Blood Level of Drug in Rats–Time Curves

Group	N^b	Model Independent[a]		Model Dependent	
		Least Squares[c]	Jackknife[c]	Least Squares[d]	Jackknife[c]
Young	24	251.20 (20.53)	250.01 (17.25)	239.94	242.68 (13.67)
Old	22	285.79 (15.18)	281.67 (15.41)	262.12	260.83 (15.61)
t statistic		—	−1.35[e]	—	−0.88[e]

[a] Results taken from Ref. 21. [b] Number of observations. [c] Number in parentheses are standard errors. [d] Standard errors were not computed. [e] No statistically significant difference, $p > 0.05$, between young and old groups based on a two-sample t test.

DISCUSSION

AUC estimation for type A studies is different from what is usually encountered, in that independent observations are made on different subjects at each point in time rather than each subject having its own time–response curve (type B studies). The model-independent approach developed for this situation can be considered as a viable option when there is no strong evidence for choosing a particular model. The flexibility in fitting least-squares spline functions could provide protection against the possibility of systematic bias resulting from the choice of an improper functional form. Simulation results (22) have shown that splines are competitive in situations where they are compared with the correct functional form and yield much better results when compared with an incorrect model specification. This flexibility of spline functions was also evident in the analysis of the illustrative data. For the liver fluke uptake data, the spline approach gave similar results to the more classical one-compartment open model. However, for the blood level of drug data, the paucity of data in the absorption phase of response–time curve would seem to make the spline approach more applicable than that of the one-compartment open model. This property of least-squares splines could prove extremely useful in situations where very complicated nonlinear models seem warranted, but are difficult to fit using the usual nonlinear regression techniques.

Fitting the spline function is somewhat subjective in that the number and position of the knots must be specified. However, this subjective process is also encountered in some pharmacokinetic situations where the number of terms of a multiexponential model must be chosen. With some experience, one should be able to select knots so that the resulting spline will give a good fit to the data. Also, it should be noted that because of the excellent local properties of spline functions, the effects of incorrect knot positioning should not cause difficulties.

Although the AUC estimates and standard errors are similar for the least-squares and jackknife procedures, the jackknife also gives protection against potentially unsatisfied assumptions. The advertised advantages of the jackknife in situations such as this are (*a*) bias reduction, (*b*) validity robustness, and (*c*) robustness against violation in homogeneity of variance. The jackknife is quite versatile and flexible and has been applied to problems in several biological settings, *e.g.*, toxicology (23) and enzyme kinetics (18). For this problem, standard errors, which were not readily obtainable for the model-dependent approach using least-squares theory, were relatively easy to compute using the jackknife.

In this situation, the usual least-squares techniques may be sensitive to the violation of the assumptions of normality and homogeneity of variance required in Eq. 1. The jackknife is an excellent tool for constructing nonparametric confidence intervals, since it is relatively insensitive to the manner in which the random errors are distributed. An added advantage of the jackknife is that one can use the pseudovalues to evaluate group differences, especially in situations involving more complicated experimental designs (18). Additional protection against violations of assumptions can be obtained by employing a transformation in conjunction with the jackknife (4, 16, 18). Since the distribution of the AUC estimates might be adversely affected by asymmetrical residuals (*e.g.*, log normal distribution) resulting from the spline regression, a logarithmic transformation might be required in conjunction with the jackknife. This can be accomplished by using log ($A_{\text{all},i}$) and log (A_{ism}) in Eq. 6 to compute pseudovalues. Such a transformation may also provide protection against variance heterogeneity, although the jackknife is considered robust against such a violation in assumptions (17).

For the above transformation, the spline function would still be fit to the untransformed response data. An alternative that might be necessary if the final concentrations are close to zero is to fit the spline function to a transformed response variable (3). However, the situation is more complicated[2] since the AUC becomes a nonlinear function of the spline parameters. In this case, the weighted jackknife (17) should be employed. Also note that this discussion relates to the within-experimental group analysis. The necessity for transformation for purposes of comparisons between experimental groups is a separate consideration. For instance, in the analysis of the study data, a log transformation was employed in the hope of achieving homogeneity of the within-infestation group variance for the liver fluke data. However, the results were similar to the untransformed case and, thus, were not reported.

The jackknife estimate of variance is known to be slightly inflated in theory (24)[1]. However, this is a minor defect since the standard error estimates from nonlinear regression procedures are often optimistically low (25)[1], and the jackknife precision estimates are closer to reality because they are data based. The results of a study which examined the jackknife estimation of rate constants for multiexponential functions fitted to biochemical data seemed to corroborate this claim (26).

The chief drawback to the widespread use of the jackknife has been concern about computational issues. However, with growing sophistication of computers, software packages, and more efficient jackknife procedures (18, 27), this may no longer be an issue. As noted above, the entire model estimation procedure developed in this paper can be automatically perfomed with a SAS macro (21).

In summary, the model-independent approach gave reasonable AUC estimates and allowed for intergroup comparisons in this study (type A design, two groups studied). Careful application of this procedure should prove to be a valuable technique for type A studies. This method should also be investigated for other parameters that can be computed by model-independent methods.

REFERENCES

(1) E. L. Frome and G. J. Yakatan, *Commun. Stat. Simula. Comput.*, **B9**, 201 (1980).

(2) K. C. Yeh and K. C. Kwan, *J. Pharmacokinet. Biopharm.*, **6**, 79 (1978).

(3) S. Wold, *Technometrics*, **16**, 1 (1974).

(4) F. Mosteller and J. W. Tukey, "Data Analysis and Regression," Addison-Wesley, Reading, Mass., 1977, pp. 133–162.

(5) M. Schulman, D. Valentino, S. Cifelli, and D. Ostlind, *J. Parasitol.*, **68**, 603 (1982).

(6) J. Ahlberg, F. N. Nilson, and J. L. Walsh, "The Theory of Splines and Other Applications," Academic, New York, N.Y., 1967, pp. 9–108.

(7) P. L. Smith, *Am. Statist.*, **33**, 57 (1979).

(8) T. P. Capizzi and R. D. Small, "1978 Proceedings of Stat. Comput. Sec.," American Statistical Association, Washington, D.C., 1978, pp. 218–222.

(9) L. G. Dunfield and J. F. Read, *J. Chem. Phys.*, **57**, 2178 (1971).

(10) K. C. Yeh and K. C. Kwan, *J. Pharm. Sci.*, **68**, 1120 (1979).

(11) S. Wold, *J. Phys. Chem.*, **76**, 369 (1972).

(12) P. Veng-Pedersen, *J. Pharm. Sci.*, **69**, 305 (1980).

(13) N. Draper and H. Smith, "Applied Regression Analysis," Wiley, New York, N.Y., 1981, pp. 70–124.

(14) M. J. Quenouille, *Biometrika*, **43**, 353 (1956).

(15) J. W. Tukey, *Ann. Math. Stat.*, **29**, 614 (1958).

(16) R. G. Miller, *Biometrika*, **61**, 1 (1974).

(17) D. V. Hinkley, *Technometrics*, **19**, 285 (1977).

(18) L. Oppenheimer, T. Capizzi, and G. Miwa, *Biochem. J.*, **197**, 721 (1981).

(19) B. E. Rodda, C. B. Sampson, and D. W. Smith, *J. R. Stat. Soc., C*, **24**, 309 (1975).

(20) SAS Users Guide, SAS Institute, Raleigh, N.C., 1979.

(21) H. Mehta, T. Capizzi, and L. Oppenheimer, "Proceedings of the Sixth Annual SAS Users Group International Conference," SAS Institute, Raleigh, N.C., 1981, pp. 211–216.

(22) T. P. Capizzi and R. D. Small, *Biometrics*, **35**, 855 (1979).

(23) B. Gladen, *J. Am. Stat. Assoc.*, **74**, 278 (1979).

(24) B. Efron and C. Stein, *Ann Stat.*, **9**, 586 (1981).

(25) H. Boxenbaum, S. Riegelman, and R. M. Elashoff, *J. Pharmacokinet., Biopharm.*, **2**, 123 (1974).

(26) I. A. Nimmo, A. Bauermeister, and J. E. Dale, *Anal. Biochem.*, **110**, 407 (1981).

(27) T. Fox, D. Hinkley, and K. Larntz, *Technometrics*, **22**, 29 (1980).

ACKNOWLEDGMENTS

Parts of this paper were presented at the Sixth Annual SAS Users Group International Conference, February 1980 and were included in the Conference Proceedings.

The authors thank an anonymous referee for an insightful review and for several suggestions which have been incorporated in this paper. The authors also thank B. Rodda, M. Tsianco, and K. C. Yeh for their thoughtful and helpful comments on previous drafts of the manuscript.

[2] As noted by a referee.

Synthesis and Antidiabetic Activity of Some Sulfonylurea Derivatives of 3,5-Disubstituted Pyrazoles

RAAFAT SOLIMAN *x, HASSAN MOKHTAR ‡, and HOSNY F. MOHAMED §

Received August 26, 1981, from the **Department of Pharmaceutical Chemistry*, the ‡*Department of Pharmacology, Faculty of Pharmacy*, and the §*Department of Chemistry Faculty of Science; University of Alexandria, Alexandria, Egypt.* Accepted for publication May 21, 1982.

Abstract □ Two series of 3,5-disubstituted pyrazolesulfonylurea derivatives were prepared and evaluated as hypoglycemic agents. Preliminary biological testing revealed that the new compounds possess potent hypoglycemic activity.

Keyphrases □ 3,5-Disubstituted pyrazolesulfonylurea derivatives—synthesis, potential hypoglycemic agents □ Potential hypoglycemic agents—preparation, antidiabetic activity of 3,5-disubstituted pyrazolesulfonylurea derivatives

Previous work showed that 3,5-dimethylpyrazole and its active metabolite, 5-methylpyrazole-3-carboxylic acid, had potent hypoglycemic activity (1–5). The present study, which is a continuation of previous work (6–11), describes the preparation of derivatives of 3,5-disubstituted pyrazolesulfonylureas and their evaluation as potential hypoglycemic agents.

Derivatives of *p*-[3-ethoxycarbonyl-5-α-phenyl-*p*-chlorostyryl)-1-pyrazolyl]benzenesulfonylurea and *p*-[3 - ethoxycarbonyl-5-(α-phenyl-*p*-methoxystyryl)-1-

0022-3549/83/0900-0999$01.00/0

For the above transformation, the spline function would still be fit to the untransformed response data. An alternative that might be necessary if the final concentrations are close to zero is to fit the spline function to a transformed response variable (3). However, the situation is more complicated[2] since the AUC becomes a nonlinear function of the spline parameters. In this case, the weighted jackknife (17) should be employed. Also note that this discussion relates to the within-experimental group analysis. The necessity for transformation for purposes of comparisons between experimental groups is a separate consideration. For instance, in the analysis of the study data, a log transformation was employed in the hope of achieving homogeneity of the within-infestation group variance for the liver fluke data. However, the results were similar to the untransformed case and, thus, were not reported.

The jackknife estimate of variance is known to be slightly inflated in theory (24)[1]. However, this is a minor defect since the standard error estimates from nonlinear regression procedures are often optimistically low (25)[1], and the jackknife precision estimates are closer to reality because they are data based. The results of a study which examined the jackknife estimation of rate constants for multiexponential functions fitted to biochemical data seemed to corroborate this claim (26).

The chief drawback to the widespread use of the jackknife has been concern about computational issues. However, with growing sophistication of computers, software packages, and more efficient jackknife procedures (18, 27), this may no longer be an issue. As noted above, the entire model estimation procedure developed in this paper can be automatically perfomed with a SAS macro (21).

In summary, the model-independent approach gave reasonable AUC estimates and allowed for intergroup comparisons in this study (type A design, two groups studied). Careful application of this procedure should prove to be a valuable technique for type A studies. This method should also be investigated for other parameters that can be computed by model-independent methods.

REFERENCES

(1) E. L. Frome and G. J. Yakatan, *Commun. Stat. Simula. Comput.*, **B9**, 201 (1980).

(2) K. C. Yeh and K. C. Kwan, *J. Pharmacokinet. Biopharm.*, **6**, 79 (1978).

(3) S. Wold, *Technometrics*, **16**, 1 (1974).

(4) F. Mosteller and J. W. Tukey, "Data Analysis and Regression," Addison-Wesley, Reading, Mass., 1977, pp. 133–162.

(5) M. Schulman, D. Valentino, S. Cifelli, and D. Ostlind, *J. Parasitol.*, **68**, 603 (1982).

(6) J. Ahlberg, F. N. Nilson, and J. L. Walsh, "The Theory of Splines and Other Applications," Academic, New York, N.Y., 1967, pp. 9–108.

(7) P. L. Smith, *Am. Statist.*, **33**, 57 (1979).

(8) T. P. Capizzi and R. D. Small, "1978 Proceedings of Stat. Comput. Sec.," American Statistical Association, Washington, D.C., 1978, pp. 218–222.

(9) L. G. Dunfield and J. F. Read, *J. Chem. Phys.*, **57**, 2178 (1971).

(10) K. C. Yeh and K. C. Kwan, *J. Pharm. Sci.*, **68**, 1120 (1979).

(11) S. Wold, *J. Phys. Chem.*, **76**, 369 (1972).

(12) P. Veng-Pedersen, *J. Pharm. Sci.*, **69**, 305 (1980).

(13) N. Draper and H. Smith, "Applied Regression Analysis," Wiley, New York, N.Y., 1981, pp. 70–124.

(14) M. J. Quenouille, *Biometrika*, **43**, 353 (1956).

(15) J. W. Tukey, *Ann. Math. Stat.*, **29**, 614 (1958).

(16) R. G. Miller, *Biometrika*, **61**, 1 (1974).

(17) D. V. Hinkley, *Technometrics*, **19**, 285 (1977).

(18) L. Oppenheimer, T. Capizzi, and G. Miwa, *Biochem. J.*, **197**, 721 (1981).

(19) B. E. Rodda, C. B. Sampson, and D. W. Smith, *J. R. Stat. Soc., C*, **24**, 309 (1975).

(20) SAS Users Guide, SAS Institute, Raleigh, N.C., 1979.

(21) H. Mehta, T. Capizzi, and L. Oppenheimer, "Proceedings of the Sixth Annual SAS Users Group International Conference," SAS Institute, Raleigh, N.C., 1981, pp. 211–216.

(22) T. P. Capizzi and R. D. Small, *Biometrics*, **35**, 855 (1979).

(23) B. Gladen, *J. Am. Stat. Assoc.*, **74**, 278 (1979).

(24) B. Efron and C. Stein, *Ann Stat.*, **9**, 586 (1981).

(25) H. Boxenbaum, S. Riegelman, and R. M. Elashoff, *J. Pharmacokinet., Biopharm.*, **2**, 123 (1974).

(26) I. A. Nimmo, A. Bauermeister, and J. E. Dale, *Anal. Biochem.*, **110**, 407 (1981).

(27) T. Fox, D. Hinkley, and K. Larntz, *Technometrics*, **22**, 29 (1980).

ACKNOWLEDGMENTS

Parts of this paper were presented at the Sixth Annual SAS Users Group International Conference, February 1980 and were included in the Conference Proceedings.

The authors thank an anonymous referee for an insightful review and for several suggestions which have been incorporated in this paper. The authors also thank B. Rodda, M. Tsianco, and K. C. Yeh for their thoughtful and helpful comments on previous drafts of the manuscript.

[2] As noted by a referee.

Synthesis and Antidiabetic Activity of Some Sulfonylurea Derivatives of 3,5-Disubstituted Pyrazoles

RAAFAT SOLIMAN *x, HASSAN MOKHTAR ‡, and HOSNY F. MOHAMED §

Received August 26, 1981, from the **Department of Pharmaceutical Chemistry*, the ‡*Department of Pharmacology, Faculty of Pharmacy*, and the §*Department of Chemistry Faculty of Science; University of Alexandria, Alexandria, Egypt.* Accepted for publication May 21, 1982.

Abstract □ Two series of 3,5-disubstituted pyrazolesulfonylurea derivatives were prepared and evaluated as hypoglycemic agents. Preliminary biological testing revealed that the new compounds possess potent hypoglycemic activity.

Keyphrases □ 3,5-Disubstituted pyrazolesulfonylurea derivatives—synthesis, potential hypoglycemic agents □ Potential hypoglycemic agents—preparation, antidiabetic activity of 3,5-disubstituted pyrazolesulfonylurea derivatives

Previous work showed that 3,5-dimethylpyrazole and its active metabolite, 5-methylpyrazole-3-carboxylic acid, had potent hypoglycemic activity (1–5). The present study, which is a continuation of previous work (6–11), describes the preparation of derivatives of 3,5-disubstituted pyrazolesulfonylureas and their evaluation as potential hypoglycemic agents.

Derivatives of *p*-[3-ethoxycarbonyl-5-α-phenyl-*p*-chlorostyryl)-1-pyrazolyl]benzenesulfonylurea and *p*-[3 - ethoxycarbonyl-5-(α-phenyl-*p*-methoxystyryl)-1-

0022-3549/83/0900-0999$01.00/0

Table I—Physical and Analytical Data for the 3-Carboxy-5-substituted Styrylpyrazolylsulfonylurea Derivatives

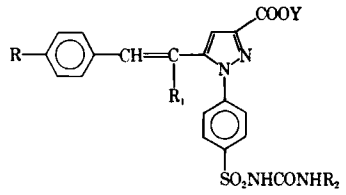

Compound	R	R_1	Y	R_2	Yield, %	Melting Point, °	Formula	Analysis, %	Calc.	Found
V*a*	H	H	C_2H_5	$(CH_2)_3CH_3$	80	205[a]	—		—	
V*b*	H	CH_3	C_2H_5	C_6H_{11}	80	225[a]	—		—	
V*c*	H	C_6H_5	C_2H_5	$(CH_2)_3CH_3$	75	128[a]	—		—	
V*d*	Cl	C_6H_5	C_2H_5	C_2H_5	70	199[b]	$C_{29}H_{27}ClN_4O_5S$	C	60.2	60.3
								H	4.7	5.0
								Cl	6.1	6.2
								N	9.7	9.7
V*e*	Cl	C_6H_5	C_2H_5	$(CH_2)_2CH_3$	75	102[c]	$C_{30}H_{29}ClN_4O_5S$	C	60.8	61.0
								H	4.9	5.0
								Cl	6.0	6.2
								N	9.5	9.5
V*f*	Cl	C_6H_5	C_2H_5	$(CH_2)_3CH_3$	70	209[d]	$C_{31}H_{31}ClN_4O_5S$	C	61.3	61.5
								H	5.1	5.1
								Cl	5.9	6.0
								N	9.2	9.2
V*g*	Cl	C_6H_5	C_2H_5	C_6H_{11}	80	229[e]	$C_{33}H_{33}ClN_4O_5S$	C	62.6	62.5
								H	5.2	5.5
								Cl	5.6	5.8
								N	8.9	9.0
V*h*	Cl	C_6H_5	C_2H_5	C_6H_5	78	238[e]	$C_{33}H_{27}ClN_4O_5S$	C	63.2	63.3
								H	4.3	4.5
								Cl	5.7	5.8
								N	8.9	9.0
VII*a*	Cl	C_6H_5	H	C_2H_5	75	200	$C_{27}H_{23}ClN_4O_5S$	C	58.9	59.1
								H	4.2	4.2
								Cl	6.4	6.3
								N	10.2	10.1
VII*b*	Cl	C_6H_5	H	$(CH_2)_2CH_3$	70	160	$C_{28}H_{23}ClN_4O_5S$	C	59.5	59.5
								H	4.4	4.5
								Cl	6.3	6.4
								N	9.9	10.0
VII*c*	Cl	C_6H_5	H	$(CH_2)_3CH_3$	68	218	$C_{29}H_{27}ClN_4O_5S$	C	60.2	60.1
								H	4.7	4.6
								Cl	6.1	6.0
								N	9.7	9.7
VII*d*	Cl	C_6H_5	H	C_6H_{11}	72	228	$C_{31}H_{29}ClN_4O_5S$	C	61.5	61.5
								H	4.8	5.0
								Cl	5.9	6.0
								N	9.3	9.5
VII*e*	Cl	C_6H_5	H	C_6H_5	78	230	$C_{31}H_{23}ClN_4O_5S$	C	62.2	62.4
								H	3.8	4.0
								Cl	5.9	6.0
								N	9.4	9.5
V*i*	OCH_3	C_6H_5	C_2H_5	C_2H_5	70	215[d]	$C_{30}H_{30}N_4O_6S$	C	62.7	63.0
								H	5.2	5.3
								N	9.8	10.0
								S	5.6	5.6
V*j*	OCH_3	C_6H_5	C_2H_5	$(CH_2)_2CH_3$	75	181[b]	$C_{31}H_{32}N_4O_6S$	C	63.3	63.5
								H	5.4	5.5
								N	9.5	9.5
								S	5.4	5.5
V*k*	OCH_3	C_6H_5	C_2H_5	$(CH_2)_3CH_3$	70	175[b]	$C_{32}H_{34}N_4O_6S$	C	63.8	63.6
								H	5.3	5.4
								N	9.3	9.5
								S	5.3	5.2
V*l*	OCH_3	C_6H_5	C_2H_5	C_6H_{11}	75	228[e]	$C_{34}H_{36}N_4O_6S$	C	65.0	65.0
								H	5.7	5.7
								N	8.9	9.0
								S	5.1	5.0
V*m*	OCH_3	C_6H_5	C_2H_5	C_6H_5	80	240[e]	$C_{34}H_{30}N_4O_6S$	C	65.6	65.7
								H	4.8	4.7
								N	9.0	9.1
								S	5.1	5.0
VII*f*	OCH_3	C_6H_5	H	C_2H_5	68	184	$C_{28}H_{26}N_4O_6S$	C	61.5	61.5
								H	4.8	5.0
								N	10.3	10.2
								S	5.9	6.0

continued

Table I—*continued*

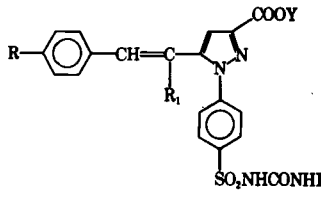

Compound	R	R_1	Y	R_2	Yield, %	Melting Point, °	Formula	Analysis, %	Calc.	Found
VII*g*	OCH_3	C_6H_5	H	$(CH_2)_2CH_3$	72	158	$C_{29}H_{28}N_4O_6S$	C	62.1	62.2
								H	5.0	5.0
								N	10.0	10.1
								S	5.7	5.9
VII*h*	OCH_3	C_6H_5	H	$(CH_2)_3CH_3$	75	190	$C_{30}H_{30}N_4O_6S$	C	62.7	63.0
								H	5.2	5.1
								N	9.8	10.0
								S	5.6	5.5
VII*i*	OCH_3	C_6H_5	H	C_6H_{11}	73	224	$C_{32}H_{32}N_4O_6S$	C	64.0	64.2
								H	5.3	5.1
								N	9.3	9.5
								S	5.3	5.4
VII*j*	OCH_3	C_6H_5	H	C_6H_5	78	236	$C_{32}H_{26}N_4O_6S$	C	64.6	64.7
								H	4.4	4.5
								N	9.4	9.3
								S	5.4	5.5

[a] Taken from Ref. 11. [b] Crystallized in ethanol–water. [c] Crystallized in benzene–petroleum ether. [d] Crystallized in chloroform–methanol. [e] Crystallized in methanol–benzene.

pyrazolyl]benzenesulfonylurea were prepared, and some were evaluated for hypoglycemic activity. Preliminary biological testing revealed that the new compounds possess potent hypoglycemic activity.

BACKGROUND

The pyrazole esters (III) were prepared by condensation of the appropriate ethyl 2,4-dioxo-6-(*p*-substituted phenyl)-5-phenyl-hex-5-enoate (I) with *p*-sulfamylphenylhydrazine (II). The resulting benzenesulfonamides (II), on treatment with the appropriate isocyanate or isothiocyanate in dry acetone, afforded the corresponding pyrazolesulfonylurea or thiourea derivatives (V and VI). Alkaline hydrolysis of the pyrazole esters III, V, or VI with ethanolic 2 *N* potassium hydroxide solution, afforded the corresponding pyrazole-3-carboxylic acids.

The physical and analytical data of these new pyrazoles are listed in Tables I and II. The antidiabetic activity of some of these compounds are given in Table III.

EXPERIMENTAL[1]

1 - (*p*-Sulfamylphenyl) -3- ethoxycarbonyl-5-(α-phenyl-*p*-chlorostyryl)pyrazole (III*a*)—A mixture of *p*-sulfamylphenylhydrazine (II) (0.1 mole) and ethyl 2,4-dioxo-6-(*p*-chlorophenyl)-5-phenyl-hex-5-enoate (I) (0.1 mole) in ethanol (150 ml) was refluxed for 6 hr on a steam bath, concentrated, and allowed to cool. The crude product was separated and recrystallized (65% yield) from ethanol, mp 196°.

The ^{1}H-NMR spectrum of III*a* showed absorption at 7.0–7.8 (m, aromatic H), 6.8 (s, 1, pyrazole H), 6.3 (s, 1, styryl H), 5.3 (s, 2, SO_2NH_2), 4.3 (q, J = 7.0 Hz, 2, $CO_2CH_2CH_3$), and 1.2 ppm (t, J = 7.0 Hz, 3 $CO_2CH_2CH_3$).

Anal.—Calc. for $C_{26}H_{22}ClN_3O_4S$: C, 61.5; H, 4.3; Cl, 7.0; N, 8.3. Found: C, 61.6; H, 4.5; Cl, 7.3; N, 8.0.

1-(*p*-Sulfamylphenyl)-3-carboxy-5-(α-phenyl-*p*-chlorostyryl)-pyrazole—A mixture of III*a* (1 g) in an ethanolic solution 2 *N* potassium hydroxide (25 ml) was refluxed for 1 hr. After concentration, cooling, and acidification with dilute hydrochloric acid, the crude pyrazole carboxylic acid crystallized. Recrystallization from ethanol gave the carboxylic acid (80% yield), mp 210°. IR showed bands at 1700–1725 (C=O), 1330–1350, and 1170–1190 cm^{-1} (SO_2N).

Anal.—Calc. for $C_{24}H_{18}ClN_3O_4S$: C, 60.1; H, 3.3; Cl, 7.4; N, 8.8. Found: C, 60.0; H, 3.5; Cl, 7.6; N, 9.1.

1 - (*p*-Sulfamylphenyl) -3- ethoxycarbonyl-5-(α-phenyl-*p*-methoxystyryl)pyrazole (III*b*)—A mixture of II (0.1 mole) and ethyl 2,4-dioxo-6-(*p*-methoxyphenyl)-5-phenyl-hex-5-enoate (0.1 mole) in ethanol (150 ml) was refluxed for 6 hr on a steam bath, concentrated, and allowed to cool. The crude product was separated and recrystallized (70% yield) from ethanol, mp 185°.

The ^{1}H-NMR spectrum of III*b* showed absorption at 6.8–7.7 (m, aromatic H), 6.7 (s, 1, pyrazole H), 6.4 (s, 1, styryl H), 5.0 (s, 2, SO_2NH_2), 4.3 (q, 2, $CO_2CH_2CH_3$), and 3.6 ppm (s, 3, OCH_3).

Anal.—Calc. for $C_{27}H_{25}N_3O_5S$: C, 64.4; H, 5.0; N, 8.3; S, 6.4. Found: C, 64.5; H, 5.0; N, 8.5; S, 6.5.

1 - (*p*-Sulfamylphenyl)-3-carboxy -5- (α-phenyl-*p*-methoxystyryl)pyrazole—A mixture of III*b* (1 g) in an ethanolic solution of potassium hydroxide (25 ml) was refluxed for 1 hr. After concentration, cooling, and acidification with dilute hydrochloric acid, the crude pyrazole carboxylic crystallized. Recrystallization from ethanol gave the carboxylic acid (78% yield), mp 108°. IR showed bands at 1700–1730 (C=O), 1330–1350, and 1170–1190 cm^{-1} (SO_2N).

Anal.—Calc. for $C_{25}H_{21}N_3O_5S$: C, 63.2; H, 4.4; N, 8.8; S, 6.7. Found: C, 63.4; H, 4.5; N, 9.0; S, 6.6.

***p*-[3-Ethoxycarbonyl -5- (α-phenyl-*p*-chlorostyryl) -1- pyrazolyl]benzenesulfonylurea Derivatives (V*d–h*)**—A mixture of III*a* (0.005 mole) and anhydrous potassium carbonate (0.01 mole) in dry acetone (50 ml) was stirred at reflux for 1.5 hr. At this temperature, a solution of the appropriate isocyanate (0.01 mole) in dry acetone (10 ml) was added in a dropwise manner. The mixture was stirred at reflux overnight and then the acetone was removed under reduced pressure. The resulting solid material was dissolved in water, and the solution was acidified with 2 *N* hydrochloric acid. Recrystallization of the resulting solid from the appropriate solvent (12) gave V*d–h*.

***p* - [3-Ethoxycarbonyl -5- (α-phenyl -*p*- methoxystyryl)-1-pyrazolyl]benzenesulfonylurea Derivatives (V*i–m*)**—A mixture of III*b* (0.005 mole) and anhydrous potassium carbonate (0.01 mole) in dry acetone (50 ml) was treated with the appropriate isocyanate (0.01 mole) in dry acetone (10 ml) and completed as mentioned above.

***p*-[3-Ethoxycarbonyl -5- (α-phenyl -*p*- chlorostyryl)-1-pyrazolyl]benzenesulfonylthiourea Derivatives (VI*a–e*)**—A mixture of III*a* (0.005 mole) and anhydrous potassium carbonate (0.01 mole) in dry acetone (50 ml) was stirred and treated with the appropriate isothiocyanate (0.006 mole). The mixture was stirred at reflux for 10 hr, and the acetone was removed under reduced pressure. The resulting solid was dissolved in water, and the mixture was acidified with 2 *N* hydrochloric acid. The

[1] Melting points were determined in open glass capillaries and are uncorrected. UV spectra were measured with a Perkin-Elmer 550 S spectrophotometer. IR spectra were determined as Nujol mulls with a Beckman IR-4210 spectrophotometer. ^{1}H-NMR spectra were recorded on a Varian EM-360 60-Hz NMR spectrophotometer. Microanalyses were performed by the Microanalytical Unit, Faculty of Science, University of Cairo, Cairo, Egypt.

Table II—Physical and Analytical Data for the 3-Carboxy-5-substituted Styrylpyrazolylsulfonylthiourea Derivatives

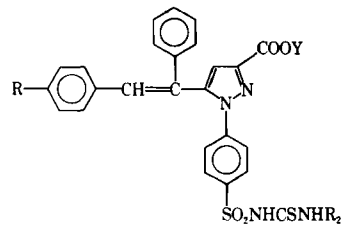

Compound[a]	R	Y	R_2	Yield, %	Melting Point, °	Formula	Analysis, %	Calc.	Found
VI*a*	Cl	C_2H_5	$(CH_2)_3CH_3$	80	220	$C_{31}H_{31}ClN_4O_4S_2$	C	59.8	60.0
							H	5.0	5.1
							Cl	5.7	5.6
							N	9.0	8.9
VI*b*	Cl	C_2H_5	C_6H_{11}	82	224	$C_{33}H_{33}ClN_4O_4S_2$	C	61.1	61.0
							H	5.1	5.1
							Cl	5.5	5.4
							N	8.6	8.8
VI*c*	Cl	C_2H_5	C_6H_5	78	162	$C_{33}H_{27}ClN_4O_4S_2$	C	61.6	61.8
							H	4.2	4.5
							Cl	5.5	5.5
							N	8.7	8.5
VI*d*	Cl	C_2H_5	$C_6H_5CH_2$	80	217	$C_{34}H_{29}ClN_4O_4S_2$	C	62.1	62.3
							H	4.4	4.5
							Cl	5.4	5.3
							N	8.5	8.7
VI*e*	Cl	C_2H_5	*p*-$CH_3C_6H_4$	75	185	$C_{34}H_{29}ClN_4O_4S_2$	C	62.1	62.0
							H	4.4	4.3
							Cl	5.4	5.5
							N	8.5	8.5
VIII*a*	Cl	H	$(CH_2)_3CH_3$	70	185	$C_{29}H_{27}ClN_4O_4S_2$	C	58.5	58.7
							H	4.5	4.6
							Cl	6.0	6.1
							N	9.4	9.2
VIII*b*	Cl	H	C_6H_{11}	75	230	$C_{31}H_{29}ClN_4O_4S_2$	C	60.0	60.0
							H	4.7	4.5
							Cl	5.7	5.9
							N	9.0	8.9
VIII*c*	Cl	H	C_6H_5	73	135	$C_{31}H_{23}ClN_4O_4S_2$	C	60.5	60.3
							H	3.7	3.8
							Cl	5.8	6.0
							N	9.1	9.0
VIII*d*	Cl	H	$C_6H_5CH_2$	78	>300	$C_{32}H_{25}ClN_4O_4S_2$	C	61.1	61.0
							H	4.0	4.0
							Cl	5.6	5.7
							N	8.9	9.0
VIII*e*	Cl	H	*p*-$CH_3C_6H_4$	80	>300	$C_{32}H_{25}ClN_4O_4S_2$	C	61.1	61.3
							H	4.0	3.9
							Cl	5.6	5.5
							N	8.9	9.0
VI*f*	OCH_3	C_2H_5	$(CH_2)_3CH_3$	70	228	$C_{32}H_{34}N_4O_5S_2$	C	62.1	62.0
							H	5.5	5.4
							N	9.1	9.3
							S	10.4	10.2
VI*g*	OCH_3	C_2H_5	C_6H_{11}	76	120	$C_{34}H_{36}N_4O_5S_2$	C	63.4	63.7
							H	5.6	5.8
							N	8.7	8.6
							S	9.9	10.0
VI*h*	OCH_3	C_2H_5	C_6H_5	73	176	$C_{34}H_{30}N_4O_5S_2$	C	63.9	64.0
							H	4.7	4.5
							N	8.8	8.9
							S	10.0	9.8
VI*i*	OCH_3	C_2H_5	$C_6H_5CH_2$	78	233	$C_{35}H_{32}N_4O_5S_2$	C	64.4	64.5
							H	4.9	5.0
							N	8.6	8.7
							S	9.8	9.6
VI*j*	OCH_3	C_2H_5	*p*-$CH_3C_6H_4$	80	170	$C_{35}H_{32}N_4O_5S_2$	C	64.4	64.7
							H	4.9	4.8
							N	8.6	8.5
							S	9.8	10.0
VIII*f*	OCH_3	H	$(CH_2)_3CH_3$	77	190	$C_{30}H_{30}N_4O_5S_2$	C	61.0	60.8
							H	5.1	5.1
							N	9.5	9.3
							S	10.8	10.6
VIII*g*	OCH_3	H	C_6H_{11}	80	165	$C_{32}H_{32}N_4O_5S_2$	C	62.3	62.1
							H	5.2	5.3
							N	9.1	9.0
							S	10.4	10.5

continued

Table II—*continued*

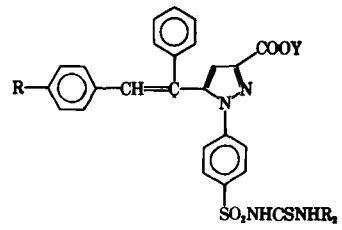

Compound[a]	R	Y	R_2	Yield, %	Melting Point, °	Formula	Analysis, %	Calc.	Found
VIII*h*	OCH_3	H	C_6H_5	75	160	$C_{32}H_{26}N_4O_5S_2$	C	63.0	62.7
							H	4.3	4.4
							N	9.2	9.1
							S	10.5	10.5
VIII*i*	OCH_3	H	$C_6H_5CH_2$	72	195	$C_{33}H_{28}N_4O_5S_2$	C	63.5	63.2
							H	4.5	4.5
							N	9.0	8.8
							S	10.3	10.5
VIII*j*	OCH_3	H	p-$CH_3C_6H_4$	78	>300	$C_{33}H_{28}N_4O_5S_2$	C	63.5	63.4
							H	4.5	4.6
							N	9.0	9.2
							S	10.3	10.1

[a] Application for a patent was made for the compounds described in this report.

crude product was purified by recrystallization from the appropriate solvent.

***p*-[3-Ethoxycarbonyl-5-(α-phenyl-*p*-methoxystyryl)-1-pyrazolyl]benzenesulfonylthiourea Derivatives (VI*f–j*)**—A mixture of III*b* (0.005 mole) and anhydrous potassium carbonate (0.01 mole) in dry acetone (50 ml) was stirred and treated with the appropriate isothiocyanate (0.006 mole) and completed as mentioned above.

***p*-[3-Carboxy-5-(α-phenyl-*p*-substituted styryl)-1-pyrazolyl]-benzenesulfonylurea (VII) or -thiourea (VIII) Derivatives**—A mixture of V or VI (1 g) in an ethanolic solution of 2 *N* potassium hydroxide (20 ml) was refluxed for 1 hr. The mixture was concentrated, cooled, and then acidified with dilute hydrochloric acid to give a crystalline material. Recrystallization from dilute ethanol gave either VII or VIII.

Spectra of V–VIII—The UV spectra of V–VIII showed absorption at 228–235 and 268–277 nm. The IR spectra of V–VIII showed absorption at 1700–1725 (C=O) and 1330–1360 cm^{-1} (2 bands) (SO_2N); compounds V and VII showed additional carbonyl absorption at 1650–1660 cm^{-1}, whereas compounds VI and VIII showed absorption at 1050–1200 cm^{-1}, indicative of the C=S group.

The ^1H-NMR spectrum of V*g* showed absorption at 7.8–8.2 (aromatic H), 6.8 (pyrazole H), 6.2 (s, styryl H), 4.2 (q, CH_2 of the ester), 1.5 (m, methylene H), and 1.0 ppm (t, CH_3 of the ester).

Biological Testing Method—Compounds IV, V*a–g,k,l*, VI*b,h*, VII*d,e,h* and VIII*a,g* were tested for hypoglycemic activity using alloxan-treated female albino mice with an average weight of 20 g. Alloxan (100 mg/kg) in a 10 mg/ml saline solution was injected into the tail vein. Three days later the mice were given the test compounds orally in suspension

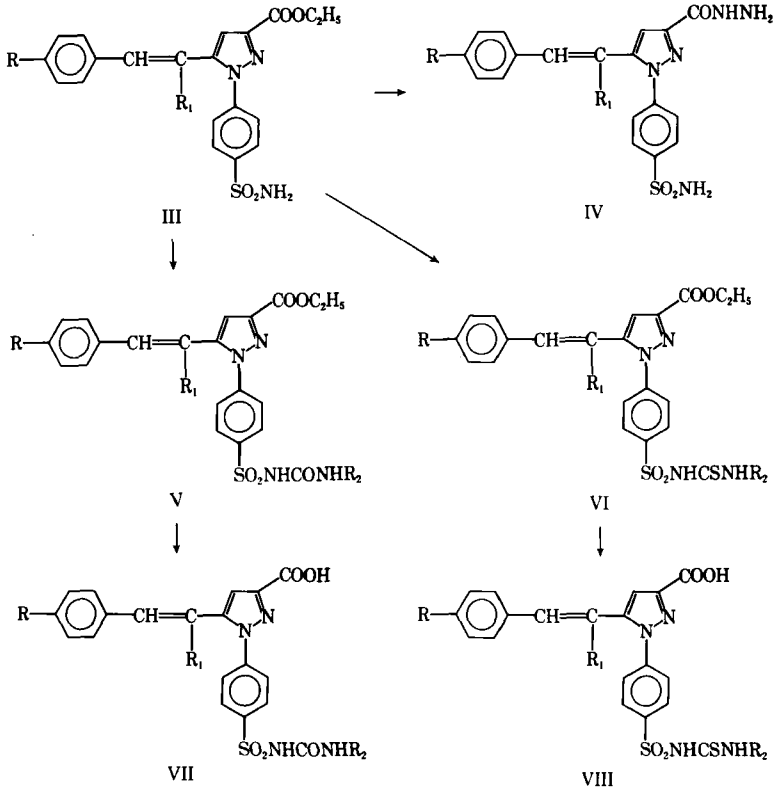

Scheme I

Table III—Antidiabetic Activity of 3-Carboxy-5-substituted Styrylpyrazolylsulfonylurea Derivatives

Compound	Reduction in Plasma Glucose Level[a], %
IV	12[b]
Va	18[b]
Vb	9[b]
Vc	8[b]
Vd	6.5[c]
Ve	3
Vf	4
Vg	3.5
Vk	2.5
Vl	6.5[c]
VIb	3.5
VIh	4
VIId	5[c]
VIIe	4.5
VIIh	4
VIIIa	2
VIIIg	1

[a] Tested using alloxan-treated mice (100 mg/kg). Phenformin (0.4 mmole/kg) was used as the positive control; the hypoglycemic activity of phenformin was 10% reduction (statistically significant when compared with the untreated controls, $p < 0.01$). [b] Statistically significantly different when compared with the untreated controls at $p < 0.01$. [c] Statistically significantly different when compared with the untreated controls at $p < 0.05$.

in 1% carboxymethylcellulose at the rate of 0.4 mmole/kg. On each day of the experiment, a group of four mice was used as the control; one group of four mice was given the standard 100 mg (0.4 mmole) of phenformin/kg. Up to five groups of four mice each received the test compounds. Blood samples were collected into 0.04% NaF solution at 0, 1, and 3 hr.

Glucose was determined by a microcolorimetric copper reduction technique used previously (13). Results are expressed as a percentage reduction of plasma glucose levels compared with the control value. Statistical significance was assessed by Student's t test, where the calculated t value exceeded the tabulated t value at the $p = 0.05$ level.

Compounds IV, Va,b,c,l, and VIIe possess marked hypoglycemic activity. The most active members are the α-unsubstituted styrylpyrazolesulfonylurea derivatives. The activity decreases from the α-methylstyryl to α-phenylstyryl analogues. Surprisingly, α-unsubstituted styrylpyrazolylsulfonamide-3-carbohydrazide showed marked hypoglycemic activity.

REFERENCES

(1) J. B. Wright, W. E. Dulin, and J. H. Markillie, *J. Med. Chem.*, **7**, 102 (1964).

(2) G. C. Gerritsen and W. E. Dulin, *Diabetes*, **14**, 507 (1965).

(3) D. L. Smith, A. A. Forist, and W. E. Dulin, *J. Med. Chem.*, **8**, 350 (1965).

(4) G. C. Gerritsen and W. E. Dulin, *J. Pharmacol. Exp. Ther.*, **150**, 491 (1965).

(5) D. L. Smith, A. A. Forist, and G. C. Gerritsen, *J. Pharmacol. Exp. Ther.*, **150**, 316 (1965).

(6) R. Soliman, H. Mokhtar, and E. S. El Ashry, *Pharmazie*, **33**, 184 (1978).

(7) H. Mokhtar and R. Soliman, *Pharmazie*, **33**, 649 (1978).

(8) R. Soliman, *J. Med. Chem.*, **22**, 321 (1979).

(9) R. Soliman and H. M. Feid-Allah, *J. Pharm. Sci.*, **70**, 602 (1981).

(10) R. Soliman, H. M. Feid-Allah, S. K. El Sadany, and H. F. Mohamed, *J. Pharm. Sci.*, **70**, 606 (1981).

(11) H. M. Feid-Allah, H. Mokhtar, and R. Soliman, *J. Heterocycl. Chem.*, **18**, 1561 (1981).

(12) F. J. Marshall, M. V. Sigal, and M. A. Root, *J. Med. Chem.*, **6**, 60 (1963).

(13) G. A. D. Haslewood and T. A. Strookman, *Biochem. J.*, **33**, 920 (1939).

Synthesis and Antidiabetic Activity of Some Sulfonylurea Derivatives of 3,4,5-Trisubstituted Pyrazoles

RAAFAT SOLIMAN *x, HASSAN MOKHTAR ‡, and HOSNY F. MOHAMED §

Received August 26, 1981, from the **Department of Pharmaceutical Chemistry*, the ‡*Department of Pharmacology, Faculty of Pharmacy*, and the §*Department of Chemistry Faculty of Science, University of Alexandria, Alexandria, Egypt.* Accepted for publication May 21, 1982.

Abstract □ Three series of 3,4,5-trisubstituted pyrazolesulfonylurea derivatives were prepared and evaluated as hypoglycemic agents. Preliminary biological testing revealed that the new compounds possess moderate hypoglycemic activity.

Keyphrases □ Pyrazolesulfonylurea derivatives—preparation, potential hypoglycemic agents □ Potential hypoglycemic agents—preparation of new trisubstituted pyrazolesulfonylurea derivatives

Since previous studies indicated that several substituted 3,5-dimethylpyrazoles possessed potent hypoglycemic activity (1–5), additional compounds were synthesized (6–10). The present study, which is a continuation of previous work (8–10), describes the preparation of derivatives of 3,4,5-trisubstituted pyrazolesulfonylureas and their evaluation as potential hypoglycemic agents.

Derivatives of *p*-(3,5-dimethyl-4-ethoxycarbonyl-1-pyrazolyl)-benzenesulfonylurea, *p*-(3-methyl-5-phenyl-4-carboxy-1-pyrazolyl)-benzenesulfonylurea, and *p*-(3-methyl - 5 - phenyl - 1 - pyrazolylcarbamoylbenzenesulfonylurea (in addition to the corresponding 4-bromo derivative) were prepared and some were evaluated for hypoglycemic activity. Preliminary biological testing revealed that the new compounds possess moderate hypoglycemic activity.

BACKGROUND

1-(*p*-Sulfamylphenyl)-3,5-dimethyl-4-ethoxycarbonylpyrazole (III) was prepared by treating *p*-sulfamylphenylhydrazine (II) with an equivalent amount of 3-ethoxycarbonyl-2,4-pentanedione (I). Similarly, 1 - (*p* - sulfamylphenyl) - 3 - methyl - 5 - phenyl - 4 - ethoxycarbonylpyrazole (VII) was prepared by treating *p*-sulfamylphenylhydrazine (II), with 1-phenyl-2-ethoxycarbonylbutane-1,3-dione (VI).

The IR absorption spectra of these trisubstituted pyrazoles (III and VII) showed an absorption band at 1700–1725 cm^{-1} due to the carbonyl of the ester group and two bands at 1330–1350 cm^{-1} and 1170–1190 cm^{-1} due to the $—SO_2N$ group.

Alkaline hydrolysis of the pyrazole esters (IV and VII) with ethanolic 2 *N* potassium hydroxide solution afforded the corresponding pyrazole-3-carboxylic acids (V and VIII). The IR spectra of the pyrazolylcarboxylic acid (VIII) showed an absorption band at 1675 cm^{-1} for the —COOH group.

p - (3,5 - Dimethyl - 4 - ethoxycarbonyl - 1 - pyrazolyl)benzenesulfonylurea (IV) and *p*-(4-carboxy-3-methyl-5-phenyl-1-pyrazolyl)benzenesulfonylurea (IX) derivatives were prepared by the reaction between III or VIII with the appropriate isocyanate in dry acetone (11). The

0022-3549/83/0900-1004$01.00/0

Table III—Antidiabetic Activity of 3-Carboxy-5-substituted Styrylpyrazolylsulfonylurea Derivatives

Compound	Reduction in Plasma Glucose Level[a], %
IV	12[b]
Va	18[b]
Vb	9[b]
Vc	8[b]
Vd	6.5[c]
Ve	3
Vf	4
Vg	3.5
Vk	2.5
Vl	6.5[c]
VIb	3.5
VIh	4
VIId	5[c]
VIIe	4.5
VIIh	4
VIIIa	2
VIIIg	1

[a] Tested using alloxan-treated mice (100 mg/kg). Phenformin (0.4 mmole/kg) was used as the positive control; the hypoglycemic activity of phenformin was 10% reduction (statistically significant when compared with the untreated controls, $p < 0.01$). [b] Statistically significantly different when compared with the untreated controls at $p < 0.01$. [c] Statistically significantly different when compared with the untreated controls at $p < 0.05$.

in 1% carboxymethylcellulose at the rate of 0.4 mmole/kg. On each day of the experiment, a group of four mice was used as the control; one group of four mice was given the standard 100 mg (0.4 mmole) of phenformin/kg. Up to five groups of four mice each received the test compounds. Blood samples were collected into 0.04% NaF solution at 0, 1, and 3 hr.

Glucose was determined by a microcolorimetric copper reduction technique used previously (13). Results are expressed as a percentage reduction of plasma glucose levels compared with the control value. Statistical significance was assessed by Student's t test, where the calculated t value exceeded the tabulated t value at the $p = 0.05$ level.

Compounds IV, Va,b,c,l, and VIIe possess marked hypoglycemic activity. The most active members are the α-unsubstituted styrylpyrazolesulfonylurea derivatives. The activity decreases from the α-methylstyryl to α-phenylstyryl analogues. Surprisingly, α-unsubstituted styrylpyrazolylsulfonamide-3-carbohydrazide showed marked hypoglycemic activity.

REFERENCES

(1) J. B. Wright, W. E. Dulin, and J. H. Markillie, *J. Med. Chem.*, **7**, 102 (1964).

(2) G. C. Gerritsen and W. E. Dulin, *Diabetes*, **14**, 507 (1965).

(3) D. L. Smith, A. A. Forist, and W. E. Dulin, *J. Med. Chem.*, **8**, 350 (1965).

(4) G. C. Gerritsen and W. E. Dulin, *J. Pharmacol. Exp. Ther.*, **150**, 491 (1965).

(5) D. L. Smith, A. A. Forist, and G. C. Gerritsen, *J. Pharmacol. Exp. Ther.*, **150**, 316 (1965).

(6) R. Soliman, H. Mokhtar, and E. S. El Ashry, *Pharmazie*, **33**, 184 (1978).

(7) H. Mokhtar and R. Soliman, *Pharmazie*, **33**, 649 (1978).

(8) R. Soliman, *J. Med. Chem.*, **22**, 321 (1979).

(9) R. Soliman and H. M. Feid-Allah, *J. Pharm. Sci.*, **70**, 602 (1981).

(10) R. Soliman, H. M. Feid-Allah, S. K. El Sadany, and H. F. Mohamed, *J. Pharm. Sci.*, **70**, 606 (1981).

(11) H. M. Feid-Allah, H. Mokhtar, and R. Soliman, *J. Heterocycl. Chem.*, **18**, 1561 (1981).

(12) F. J. Marshall, M. V. Sigal, and M. A. Root, *J. Med. Chem.*, **6**, 60 (1963).

(13) G. A. D. Haslewood and T. A. Strookman, *Biochem. J.*, **33**, 920 (1939).

Synthesis and Antidiabetic Activity of Some Sulfonylurea Derivatives of 3,4,5-Trisubstituted Pyrazoles

RAAFAT SOLIMAN *x, HASSAN MOKHTAR ‡, and HOSNY F. MOHAMED §

Received August 26, 1981, from the **Department of Pharmaceutical Chemistry*, the ‡*Department of Pharmacology, Faculty of Pharmacy*, and the §*Department of Chemistry Faculty of Science, University of Alexandria, Alexandria, Egypt.* Accepted for publication May 21, 1982.

Abstract □ Three series of 3,4,5-trisubstituted pyrazolesulfonylurea derivatives were prepared and evaluated as hypoglycemic agents. Preliminary biological testing revealed that the new compounds possess moderate hypoglycemic activity.

Keyphrases □ Pyrazolesulfonylurea derivatives—preparation, potential hypoglycemic agents □ Potential hypoglycemic agents—preparation of new trisubstituted pyrazolesulfonylurea derivatives

Since previous studies indicated that several substituted 3,5-dimethylpyrazoles possessed potent hypoglycemic activity (1–5), additional compounds were synthesized (6–10). The present study, which is a continuation of previous work (8–10), describes the preparation of derivatives of 3,4,5-trisubstituted pyrazolesulfonylureas and their evaluation as potential hypoglycemic agents.

Derivatives of *p*-(3,5-dimethyl-4-ethoxycarbonyl-1-pyrazolyl)-benzenesulfonylurea, *p*-(3-methyl-5-phenyl-4-carboxy-1-pyrazolyl)-benzenesulfonylurea, and *p*-(3-methyl - 5 - phenyl - 1 - pyrazolylcarbamoylbenzenesulfonylurea (in addition to the corresponding 4-bromo derivative) were prepared and some were evaluated for hypoglycemic activity. Preliminary biological testing revealed that the new compounds possess moderate hypoglycemic activity.

BACKGROUND

1-(*p*-Sulfamylphenyl)-3,5-dimethyl-4-ethoxycarbonylpyrazole (III) was prepared by treating *p*-sulfamylphenylhydrazine (II) with an equivalent amount of 3-ethoxycarbonyl-2,4-pentanedione (I). Similarly, 1 - (*p* - sulfamylphenyl) - 3 - methyl - 5 - phenyl - 4 - ethoxycarbonylpyrazole (VII) was prepared by treating *p*-sulfamylphenylhydrazine (II), with 1-phenyl-2-ethoxycarbonylbutane-1,3-dione (VI).

The IR absorption spectra of these trisubstituted pyrazoles (III and VII) showed an absorption band at 1700–1725 cm^{-1} due to the carbonyl of the ester group and two bands at 1330–1350 cm^{-1} and 1170–1190 cm^{-1} due to the $—SO_2N$ group.

Alkaline hydrolysis of the pyrazole esters (IV and VII) with ethanolic 2 *N* potassium hydroxide solution afforded the corresponding pyrazole-3-carboxylic acids (V and VIII). The IR spectra of the pyrazolylcarboxylic acid (VIII) showed an absorption band at 1675 cm^{-1} for the —COOH group.

p - (3,5 - Dimethyl - 4 - ethoxycarbonyl - 1 - pyrazolyl)benzenesulfonylurea (IV) and *p*-(4-carboxy-3-methyl-5-phenyl-1-pyrazolyl)benzenesulfonylurea (IX) derivatives were prepared by the reaction between III or VIII with the appropriate isocyanate in dry acetone (11). The

0022-3549/83/0900-1004$01.00/0

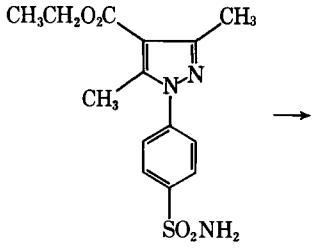

III

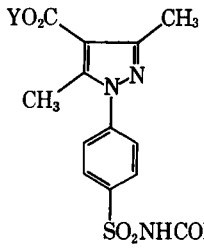

IVa: Y = CH_2CH_3, R = CH_2CH_3 Va: Y = H, R = CH_2CH_3
b: Y = CH_2CH_3, R = $(CH_2)_2CH_3$ b: Y = H, R = $(CH_2)_2CH_3$
c: Y = CH_2CH_3, R = $(CH_2)_3CH_3$ c: Y = H, R = $(CH_2)_3CH_3$
d: Y = CH_2CH_3, R = C_6H_{11} d: Y = H, R = C_6H_{11}
e: Y = CH_2CH_3, R = C_6H_5 e: Y = H, R = C_6H_5

Scheme I

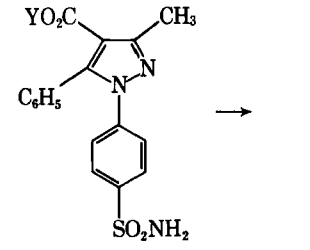

VII: Y = CH_2CH_3
VIII: Y = H

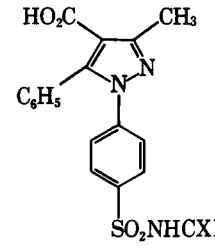

IXa: X = O, R = $(CH_2)_2CH_3$ Xa: X = S, R = $CH_2CH{=}CH_2$
b: X = O, R = $(CH_2)_3CH_3$ b: X = S, R = $(CH_2)_3CH_3$
c: X = O, C_6H_{11} c: X = S, R = C_6H_{11}
d: X = S, R = C_6H_5
e: X = S, R = $CH_2C_6H_5$

Scheme II

thiourea derivatives (X) were prepared in a similar manner treating VIII with the appropriate isothiocyanate in dry acetone.

p-(3-Methyl-5-phenylpyrazol-1-yl-carbamoyl)benzenesulfonamide (XIII) was prepared by fusing *p*-sulfamylphenylsemicarbazide (XII) with 1-phenylbutane-1,3-dione (XI) at 110°. Treatment of XIII with the appropriate isocyanate afforded *p*-(3-methyl-5-phenyl-1-pyrazolyl)carbamoylbenzenesulfonylurea (XIV), which on bromination with bromine in chloroform gave the corresponding 4-bromo derivatives. The IR spectra of these compounds revealed two absorption bands at 1350–1330 cm^{-1} and 1190–1170 cm^{-1} indicative of the $-SO_2N$ group as well as a urea carbonyl band at 1660 cm^{-1}.

The physical and analytical data of these new pyrazoles, as well as the antidiabetic activity of some of the compounds are listed in Table I.

EXPERIMENTAL[1]

1 - (*p* - Sulfamylphenyl) - 3,5 - dimethyl - 4 - ethoxycarbonylpyrazole (III)—A mixture of *p*-sulfamylphenylhydrazine (18.7 g, 0.1 mole) and 3-ethoxycarbonyl-2,4-pentanedione (17 g, 0.1 mole) in ethanol (150 ml) was refluxed for 4 hr on a steam bath, concentrated, and allowed to cool. The crude product was separated and recrystallized (65% yield) from ethanol, mp 232°.

Anal.—Calc. for $C_{12}H_{17}N_3O_4S$: C, 48.2; H, 5.7; N, 14.0; S, 10.7. Found: C, 48.4; H, 5.6; N, 14.1; S, 11.0.

Substituted *p*-(3,5-Dimethyl-4-ethoxycarbonyl-1-pyrazolyl)-benzenesulfonylurea Derivatives (IV)—A mixture of III (0.025 mole) and anhydrous potassium carbonate (0.05 mole) in dry acetone (50 ml) was stirred at reflux for 1.5 hr. At this temperature, a solution of the appropriate isocyanate (0.04 mole) in dry acetone (10 ml) was added, in a dropwise manner, the mixture was stirred at reflux overnight, the acetone was removed under reduced pressure, and the resulting solid residue was dissolved in water. The crude product was isolated by acidification with 2 *N* hydrochloric acid and purified by recrystallization from ethanol.

Substituted *p*-(4-Carboxy-3,5-dimethyl-1-pyrazolyl)benzenesulfonylurea Derivatives (V)—A mixture of IV (1 g) in an alcoholic solution of 2 *N* potassium hydroxide (25 ml) was refluxed for 1 hr. The mixture was concentrated, cooled, and acidified with dilute hydrochloric acid to give crystalline material.

1-(*p*-Sulfamylphenyl)-3-methyl-5-phenyl-4-ethoxycarbonylpyrazole (VII)—A mixture of *p*-sulfamylphenylhydrazine (18.7 g, 0.1 mole) and 1-phenyl-2-ethoxycarbonylbutane-1,3-dione (23.6 g, 0.1 mole) in ethanol (150 ml) was refluxed for 4–6 hr on a steam bath, concentrated, and allowed to cool. The crude product was separated and recrystallized (70% yield) from ethanol, mp 232°.

Anal.—Calc. for $C_{17}H_{19}N_3O_4S$: C, 56.5; H, 5.3; N, 11.6; S, 8.9. Found: C, 56.5; H, 5.5; N, 11.8; S, 9.1.

1 - (*p* - Sulfamylphenyl) - 3 - methyl - 5 - phenyl - 4 - carboxypyrazole (VIII)—A mixture of VII (5 g) in alcoholic solution of 2 *N* potassium hydroxide (100 ml) was refluxed for 1 hr. The mixture was concentrated, cooled, and then acidified with dilute hydrochloric acid to give a crystalline material. Recrystallization from ethanol, gave VIII (80% yield) mp 250°.

Anal.—Calc. for $C_{15}H_{15}N_3O_4S$: C, 54.1; H, 4.5; N, 12.6; S, 9.6. Found: C, 54.4; H, 4.4; N, 12.5; S, 9.8.

Substituted *p*-(4-Carboxy-3-methyl-5-phenyl-1-pyrazolyl)-benzenesulfonylurea Derivatives (IX)—A mixture of VIII (0.025 mole) and anhydrous potassium carbonate (0.05 mole) in dry acetone (50 ml) was refluxed for 1.5 hr. At this temperature, a solution of the appropriate isocyanate (0.04 mole) in dry acetone (10 ml) was added in a dropwise manner. After the mixture was stirred and refluxed overnight, the acetone was removed under reduced pressure, and the solid residue was dissolved in water. The crude product precipitated when the mixture was acidified with 2 *N* hydrochloric acid. Recrystallization from ethanol afforded the purified material.

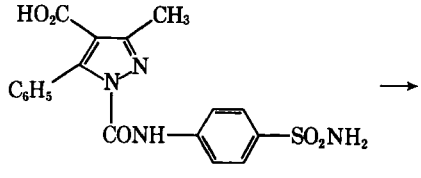

XIII

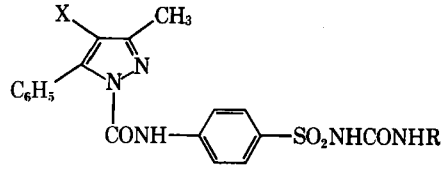

XIVa: X = H, R = CH_2CH_3 XVa: X = Br, R = $(CH_2)_2CH_3$
XIVb: X = H, R = $(CH_2)_2CH_3$ XVb: X = Br, R = $(CH_2)_3CH_3$
XIVc: X = H, R = $(CH_2)_3CH_3$ XVc: X = Br, R = C_6H_5
XIVd: X = H, R = C_6H_5

Scheme III

[1] Melting points were determined in open glass capillaries and are uncorrected. UV spectra were measured with a Perkin-Elmer 550 S spectrophotometer. The IR spectra were determined as Nujol mulls with a Beckman IR-4210 spectrophotometer. ^{1}H-NMR spectra were recorded on a Varian EM-360 60-Hz, NMR spectrophotometer. Microanalyses were performed by the Microanalytical Unit, Faculty of Science, University of Cairo, Cairo, Egypt.

Table I—Physical and Analytical Data and Hypoglycemic Activity of the Substituted Pyrazolesulfonylureas

Compound	Yield, %	Melting Point,°	Formula		Analysis, % Calc.	Found	Reduction in Plasma Glucose Level %,[a]
IV*a*	65	195	$C_{17}H_{22}N_4O_5S$	C	51.8	52.0	
				H	5.6	5.7	
				N	14.2	14.0	
				S	8.1	8.3	
IV*b*	60	145	$C_{18}N_{24}N_4O_5S$	C	52.9	53.1	
				H	5.9	6.2	
				N	13.7	13.5	
				S	7.8	8.0	
IV*c*	70	77	$C_{19}H_{26}N_4O_5S$	C	54.0	53.9	5[b]
				H	6.2	6.4	
				N	13.3	13.1	
				S	7.6	7.8	
IV*d*	73	204	$C_{21}H_{28}N_4O_5S$	C	56.3	56.1	
				H	6.3	6.4	
				N	12.5	12.5	
				S	7.1	7.0	
IV*e*	70	226	$C_{21}H_{22}N_4O_5S$	C	57.0	56.9	4[b]
				H	5.0	5.1	
				N	12.7	12.5	
				S	7.2	7.4	
V*a*	70	178	$C_{15}H_{18}N_4O_5S$	C	49.2	49.0	
				H	4.9	5.0	
				N	15.3	15.4	
				S	8.7	9.0	
V*b*	68	134	$C_{16}H_{20}N_4O_5S$	C	50.5	50.6	
				H	5.3	5.1	
				N	14.7	14.8	
				S	8.4	8.4	
V*c*	65	89	$C_{17}H_{22}N_4O_5S$	C	51.8	51.7	5
				H	5.6	5.8	
				N	14.2	14.0	
				S	8.1	8.3	
V*d*	72	218	$C_{19}H_{24}N_4O_5S$	C	54.3	54.1	3
				H	5.7	5.8	
				N	13.3	13.3	
				S	7.6	7.4	
V*e*	75	235	$C_{19}H_{18}N_4O_5S$	C	55.1	55.0	
				H	4.3	4.5	
				N	13.5	13.4	
				S	7.7	7.7	
IX*a*	65	170	$C_{21}H_{22}N_4O_5S$	C	57.0	57.1	2
				H	5.0	4.9	
				N	12.7	13.0	
				S	7.2	7.3	
IX*b*	70	72	$C_{22}H_{24}N_4O_5S$	C	57.8	58.0	
				H	5.3	5.4	
				N	12.3	12.5	
				S	7.0	7.1	
IX*c*	75	195	$C_{24}H_{26}N_4O_5S$	C	59.8	60.0	2
				H	5.4	5.5	
				N	11.6	11.8	
				S	6.6	6.5	
X*a*	65	140	$C_{21}H_{20}N_4O_4S_2$	C	55.3	55.5	
				H	4.4	4.5	
				N	12.3	12.4	
				S	14.0	13.8	
X*b*	68	239	$C_{22}H_{24}N_4O_4S_2$	C	55.9	56.1	
				H	5.1	5.0	
				N	11.9	12.1	
				S	13.6	13.3	
X*c*	66	255	$C_{24}H_{26}N_4O_4S_2$	C	57.8	58.1	3
				H	5.2	5.1	
				N	11.2	11.5	
				S	12.9	13.0	
X*d*	70	152	$C_{24}H_{20}N_4O_4S_2$	C	58.5	58.4	1
				H	4.1	4.1	
				N	11.4	11.6	
				S	13.0	12.9	
X*e*	65	252	$C_{25}H_{22}N_4O_4S_2$	C	59.3	59.5	
				H	4.3	4.4	
				N	11.1	11.2	
				S	12.6	12.5	
XIV*a*	70	128	$C_{20}H_{21}N_5O_4S$	C	56.2	56.0	
				H	4.9	5.0	
				N	16.4	16.5	
				S	7.5	7.4	
XIV*b*	65	108	$C_{21}H_{23}N_5O_4S$	C	57.1	57.0	
				H	5.2	5.1	
				N	15.9	16.1	
				S	7.3	7.3	

continued

Table I—*continued*

Compound	Yield, %	Melting Point,°	Formula		Analysis, % Calc.	Found	Reduction in Plasma Glucose Level %,[a]
XIV*c*	73	70	$C_{22}H_{25}N_5O_4S$	C	58.0	57.9	
				H	5.5	5.6	
				N	15.4	15.2	
				S	7.0	7.1	
XIV*d*	65	230	$C_{24}H_{21}N_5O_4S$	C	60.6	60.9	10[c]
				H	4.4	4.6	
				N	14.7	14.4	
				S	6.7	6.8	
XV*a*	80	100	$C_{21}H_{22}BrN_5O_4S$	C	48.5	48.4	
				H	4.2	4.1	
				Br	15.4	15.6	
				N	13.5	13.3	
XV*b*	88	74	$C_{22}H_{24}BrN_5O_4S$	C	49.4	49.1	8[c]
				H	4.5	4.5	
				Br	15.0	14.8	
				N	13.1	13.0	
XV*c*	84	220	$C_{24}H_{20}BrN_5O_4S$	C	52.0	52.1	
				H	3.6	3.8	
				Br	14.4	14.3	
				N	12.6	12.6	

[a] Tested using alloxan-treated mice (100 mg/kg). Phenformin (0.4 mmole/kg) was used as the positive control; the hypoglycemic activity of phenformin was 10% reduction (statistically significant when compared with the untreated controls at $p < 0.01$). [b] Statistically significantly different from the untreated controls at $p < 0.05$. [c] Statistically significantly different from the untreated controls at $p < 0.01$.

Substituted *p*-(4-Carboxy-3-methyl-5-phenyl-1-pyrazolyl)-benzenesulfonylthiourea Derivatives (X)—A mixture of VIII (0.025 mole) and anhydrous potassium carbonate (0.05 mole) in dry acetone (100 ml) was stirred and treated with the appropriate isothiocyanate (0.03 mole). The mixture was stirred at reflux for 10 hr, and then the acetone was removed under reduced pressure; the resulting solid residue was dissolved in water. Acidification with 2 *N* hydrochloric acid, followed by recrystallization of the resulting solid from dilute ethanol gave X.

***p*-(3-Methyl-5-phenyl-1-pyrazolyl)carbamoylbenzenesulfonamide (XIII)**—A mixture of XII (22.9 g, 0.1 mole) and 1-phenylbutane-1,3-dione (16.6 g, 0.1 mole) was stirred and fused at 110° for 1 hr, cooled, and crystallized from ethanol to give colorless crystals, mp 190°.

Anal.—Calc. for $C_{17}H_{16}N_4O_3S$: C, 57.3; H, 4.5; N, 15.7; S, 9.0. Found: C, 57.5; H, 4.5; N, 16.0; S, 8.8.

***p*-(3-Methyl-5-phenyl-1-pyrazolyl)carbamoylbenzenesulfonylurea (XIV)**—A mixture of XIII (0.025 mole) and anhydrous potassium carbonate (0.05 mole) in dry acetone (50 ml) was stirred at reflux for 1.5 hr. At this temperature, a solution of the appropriate isocyanate (0.04 mole) in dry acetone (10 ml) was added in a dropwise manner. The mixture was stirred at reflux overnight, and then the acetone was removed under reduced pressure to give a solid material. This material was dissolved in water, and the solution was acidified with 2 *N* hydrochloric acid. Recrystallization from methanol–benzene gave XIV.

***p*-(4-Bromo-3-methyl-5-phenyl-1-pyrazolyl)carbamoylbenzenesulfonylurea Derivatives (XV)**—A mixture of XIV (0.01 mole) in chloroform (10 ml) was stirred at room temperature and a solution of bromine was added with chloroform (0.011 mole) for a 1-hr period. The mixture was allowed to stand at room temperature overnight and the resulting solid was removed by filtration. Recrystallization from dilute ethanol gave colorless crystals of XV.

Spectra—The UV spectrum of IV showed two peaks at λ_{max} 230–237 and 272–277 nm. Compound IX showed two peaks at λ_{max} 210–214 and 260–268 nm. The IR spectra revealed bands at 1700–1730 (C=O), 1330–1350, and 1170–1190 cm^{-1} (SO_2N), whereas XIV and XV showed bands at 1650–1660 (amide), 1330–1350, and 1170–1190 cm^{-1} (SO_2N).

The ^{1}H-NMR spectrum of III showed absorption at 7.1–7.7 (m, aromatic H), 5.6 (s, 2, SO_2NH_2), 4.2 (q, J = 7.0 Hz, $CO_2CH_2CH_3$), 1.8 (s, CH_3), and 1.2 ppm (t, J = 7.0 Hz, $CO_2CH_2CH_3$). The ^{1}H-NMR spectrum of XIV*d* showed absorption at 7.6–8.2 (m aromatic H), 6.6 (s, 1, pyrazole H), and 1.6 ppm (s, CH_3).

Biological Testing Method—Compounds IV*c*,*e*, V*c*,*d*, IX*a*,*c*, X*c*,*d*, XIV*d*, and XV*b* were tested for hypoglycemic activity using alloxan-treated female albino mice with an average weight of 20 g. Alloxan (100 mg/kg) in a 10-mg/ml saline solution was injected into the tail vein. Three days later, the mice were given the test compounds orally in suspension in 1% carboxymethylcellulose at the rate of 0.4 mmole/kg. Each day of the experiment, a group of four mice was used as the control; one group of four mice was given the standard, 100 mg (0.4 mmole) of phenformin/kg. Up to five groups of four mice each received the test compounds. Blood samples were collected into 0.04% NaF solution at 0, 1, and 3 hr.

Glucose was determined by a previously used microcolorimetric copper reduction technique (12). Results are expressed as a percentage reduction of plasma glucose levels compared with the control value. Statistical significance was assessed by Student's t test, where the calculated t value exceeded the tabulated t value at the p = 0.05 level.

Compound XIV*d* possesses marked hypoglycemic activity (Table I); its potency is comparable with phenformin. The other compounds showed moderate hypoglycemic activity.

From the data presented previously (8–10) and in this report, it is obvious that pyrazole-3-carboxylic acids are much more potent hypoglycemics than the corresponding 4-carboxylic acid derivatives. 3,5-Disubstituted pyrazolebenzenesulfonylurea derivatives are much more active than the corresponding trisubstituted pyrazoles. The presence of a 4-ethoxycarbonyl or carboxy group in the pyrazole ring reduces the hypoglycemic activity. Generally, pyrazolesulfonylurea derivatives are much more active than the corresponding thiourea analogues.

REFERENCES

(1) J. B. Wright, W. E. Dulin, and J. H. Markillie, *J. Med. Chem.*, **7**, 102 (1964).

(2) G. C. Gerritsen and W. E. Dulin, *Diabetes*, **14**, 507 (1965).

(3) D. L. Smith, A. A. Forist, and W. E. Dulin, *J. Med. Chem.*, **8**, 350 (1965).

(4) G. C. Gerritsen and W. E. Dulin, *J. Pharmacol. Exp. Ther.*, **150**, 491 (1965).

(5) D. L. Smith, A. A. Forist, and G. C. Gerritsen, *J. Pharmacol. Exp. Ther.*, **150**, 316 (1965).

(6) R. Soliman, H. Mokhtar, and E. S. El Ashry, *Pharmazie*, **33**, 184 (1978).

(7) H. Mokhtar and R. Soliman, *Pharmazie*, **33**, 649 (1978).

(8) R. Soliman, *J. Med. Chem.*, **22**, 321 (1979).

(9) R. Soliman and H. M. Feid-Allah, *J. Pharm. Sci.*, **70**, 602 (1981).

(10) R. Soliman, H. M. Feid-Allah, S. K. El Sadany, and H. F. Mohamed, *J. Pharm. Sci.*, **70**, 606 (1981).

(11) F. J. Marshall, M. V. Sigal, and M. A. Root, *J. Med. Chem.*, **6**, 60 (1963).

(12) G. A. D. Haslewood and T. A. Strookman *Biochem. J.*, **33**, 920 (1939).

Antitumor Agents LXIII: The Effects of Microlenin on Nucleic Acid and Protein Syntheses of Ehrlich Ascites Cells

I. H. HALL ˣ, K. H. LEE, Y. IMAKURA, and D. SIMS

Received July 8, 1982, from the *Division of Medicinal Chemistry, School of Pharmacy, University of North Carolina at Chapel Hill, Chapel Hill, NC 27514.* Accepted for publication August 13, 1982

Abstract □ Microlenin, a novel dimeric sesquiterpene lactone isolated from Texas *Helenium microcephalum*, was shown to inhibit Ehrlich ascites carcinoma growth. Metabolic studies demonstrated that DNA synthesis and protein synthesis were significantly inhibited by two doses of microlenin at 5 mg/kg/day. DNA synthesis appeared to be blocked at several sites including DNA polymerase, purine synthesis, and dihydrofolate reductase. Thymidine nucleotide pools were significantly reduced by microlenin. Protein synthesis inhibition by microlenin appeared to occur during the initiation step of polypeptide synthesis. The metabolic effects of microlenin were similar to other sesquiterpene lactones in the Ehrlich ascites carcinoma cells. However, a lower dose of microlenin was required to bring about these metabolic effects when compared with other sesquiterpene lactones. Thus, microlenin may be a more likely therapeutic agent than helenalin which has demonstrated cellular toxicity.

Keyphrases □ Microlenin—sesquiterpene lactone, inhibition of DNA and protein syntheses, inhibition of Ehrlich ascites carcinoma growth □ Protein synthesis—effects of microlenin, Ehrlich ascites carcinoma growth

Microlenin was originally isolated from Texas *Helenium microcephalum* (1–3). The molecule appears to arise from a Diels-Alder type condensation involving the 11,13-double bond of helenalin and the enol form of the cyclopentenone ring of a norpseudoguaianolide. Preliminary antineoplastic screening demonstrated that microlenin was active against rat Walker 256 carcinosarcoma growth at 2.5 mg/kg/day affording a T/C% value equal to 172%. Further testing against the mouse P-388 lymphocytic leukemia growth demonstrated that at 12.5 mg/kg/day, a T/C% = 167 was obtained. Sesquiterpene lactones of varying structures have been shown to be potent inhibitors of nucleic acid and protein synthesis of tumor cells. Reported at this time are the effects of microlenin on the cellular metabolism of Ehrlich ascites cell carcinoma.

EXPERIMENTAL

Ehrlich Ascites Screen—Male CF_1 mice (30 g) were implanted with 2×10^6 Ehrlich ascites cells intraperitoneally on day 0. Microlenin was suspended by homogenization in 0.05% polysorbate 80–water and administered intraperitoneally at 5 and 10 mg/kg/day. The mice were sacrificed on day 10, and the ascites fluid was collected from the peritoneal cavity. The volume and ascrit (packed cell volume) were determined for each animal, and the percent inhibition of tumor growth was calculated (4).

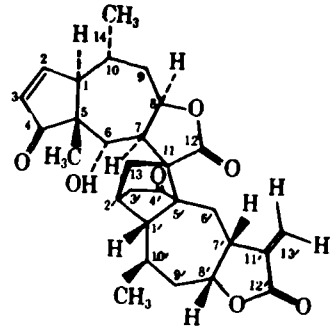

Structure of Microlenin

In vitro incorporation of [^{3}H]thymidine, [^{3}H]uridine, or [^{3}H]leucine was determined using 10^6 Ehrlich ascites cells, 1-μCi labeled precursor, minimum essential medium, and varying final concentrations of drug from 0.125 to 2.0 m*M* (5). The tubes were incubated at 37° for 60 min and inactivated by trichloroacetic acid. The acid-insoluble, labeled DNA, was collected on GF/F glass filter disks[1], and RNA and protein were precipitated on nitrocellulose filters[2] by vacuum suction. Results are expressed as dpm of incorporated precursor/hr/10^6 cells. For *in vitro* studies, cells were collected on day 10, and the microlenin was incubated at 0.25–1.0 m*M* concentration.

Ehrlich ascites cells (10^6) were injected intraperitoneally into CF_1 male mice (~22 g) on day 0. On days 8 and 9, microlenin (5 mg/kg/day in 0.05% polysorbate 80–water) was injected intraperitoneally. Incorporation of thymidine into DNA was determined by the method of Chae *et al.* (6). One hour prior to sacrifice on day 10, 10 μCi of [6-^{3}H]thymidine (21.5 Ci/mmole) was injected intraperitoneally. The DNA was isolated and the tritium content was determined in a toluene-based scintillation fluid[3]. The DNA concentration was determined by the diphenylamine reaction using calf thymus DNA as a standard. Uridine incorporation into RNA was determined using 10 μCi of [5,6-^{3}H]uridine (22.4 Ci/mmole). RNA was extracted by the method of Wilson *et al.* (7). Using yeast RNA as a standard, the RNA content was assayed by the orcinol reaction. Leucine incorporation into protein was determined by the method of Sartorelli (8) using 10 μCi of [4,5-^{3}H]leucine (52.2 Ci/mmole). Extracted protein was determined by the Lowry procedure using bovine albumin as a standard. *In vitro* and *in vivo* nuclear DNA polymerase activity was determined on isolated Ehrlich ascites cell nuclei (9). The incubation method was that described by Sawada *et al.* (10) except that [methyl-^{3}H]deoxythymidine triphosphate (82.4 Ci/mmole) was used. The acid-insoluble nucleic acid was collected on GF/F filters and counted.

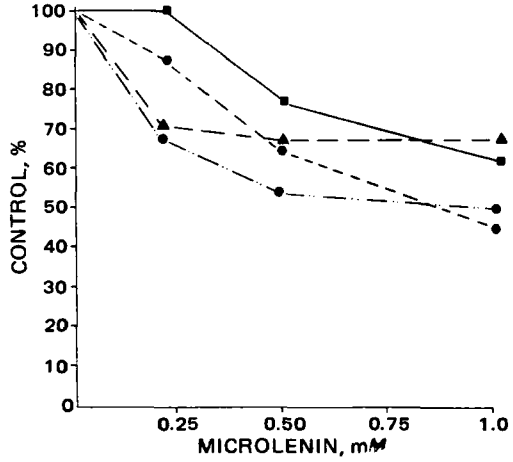

Figure 1—*The* in vitro *effects of microlenin on the incorporation of radiolabeled precursors into DNA, RNA, protein and purine of Ehrlich ascites cells. Key: (■) [^{3}H]leucine incorporation into protein; (▲) [^{3}H]uridine incorporation into RNA; (●) [^{3}H]thymidine incorporation into DNA; and (◆) [^{14}C]formate incorporation into purine.*

[1] Whatman GF/F.
[2] Millipore.
[3] Fisher ScintiVerse.

0022-3549/83/0900-1008$01.00/0

Table I—Antineoplastic Activity of Microlenin Against the Growth of Ehrlich Ascites Carcinoma Cells [a]

Compound	Survival at Day 10	Volume of Ascites	Ascrit Packed Cells Volume	Inhibition, %
Control (0.05% polysorbate 80)	6/6	6.68	43.1	—
Microlenin (5 mg/kg/day)	6/6	0.02	5.1	99.9
Microlenin (10 mg/kg/day)	6/6	0.75	36.8	90.4
Mercaptopurine	6/6	0.10	2.5	99.9

[a] Number of mice = 6.

Nuclear RNA polymerase activities were determined on enzymes isolated from nuclei (9). Messenger, ribosomal, and transfer RNA polymerases were isolated using 0.3 *M*, 0.04 *M*, and 0.0 *M* concentrations of ammonium sulfate in magnesium chloride, respectively. The incubation medium was that of Anderson *et al.* (11) using [^{3}H]uridine triphosphate (23.2 Ci/mmole). The acid-insoluble RNA was collected on nitrocellulose filters and counted.

Deoxythymidine as well as deoxythymidylate monophosphate and diphosphate kinase activities were measured spectrophotometrically at 340 nm for 20 min using reduced nicotinamide adenine dinucleotide (0.1 μmole) (12). [6-^{3}H]Thymidine (21.5 Ci/mmole) incorporation into the nucleotides was also measured using the reaction medium of Maley and Ochoa (12) and then plating the ether extract of the reaction medium on PEI cellulose F plates. The plates were eluted with 0.5 *N* formic acid–0.6 *N* LiCl (1:1). After identifying R_f values consistent with the standards, thymidine, thymidylate monophosphate, and thymidylate diphosphate, the areas on the plates were scraped and counted. Carbamyl phosphate synthetase activity was determined using the reaction medium of Kalman *et al.* (13) in the presence of ornithine and the enzyme ornithine transcarbamylase. Citrulline formed from ornithine was measured at 490 nm by the method of Archibald (14). Aspartate transcarbamylase activity was assayed using the incubation medium of Kalman *et al.* (13). The colorimetric determination of carbamyl aspartate was conducted by the procedure of Koritz and Cohen (15). Orotidine monophosphate decarboxylase activity was assayed by the method of Appel (16) using 0.1 μCi of [^{14}C]orotidine monophosphate (34.9 mCi/mmole). The $^{14}CO_2$ generated in 15 min was trapped in 1 *M* methanolic base[4] and counted. Thymidylate synthetase activity was determined using a postmitochondrial supernatant (9000×*g* for 10 min) and 5 μCi of [5-^{3}H]deoxyuridine monophosphate (14 Ci/mmole) according to the method of Kampf *et al.* (17). [^{14}C]Formate incorporation into purines was determined by the method of Spassova *et al.* (18), using 0.5 μCi of [^{14}C]formic acid (52.0 mCi/mmole). Purines were separated on silica gel TLC plates eluted with 1-butanol–acetic acid–water (4:1:5). After identifying R_f values consistent with the standards, adenine and guanine, the plates were scraped and the radioactive content determined. Phosphoribosyl-1-pyrophosphate amidotransferase activity was determined on a supernatant fraction (600×*g*, for 10 min) measuring the reduction of 0.6 μmole of nicotinamide adenine dinucleotide at 340 nm for 30 min (19). Inosinic acid dehydrogenase activity was determined by the method of Becker and Löhr (20) using a supernatant 7000×*g*, for 10 min and [8-^{14}C]inosine-5′ monophosphate (61 mCi/mmole). After plating on PEI cellulose F plastic precoated plates and eluting with 0.5 *M* $(NH_4)_2SO_4$, the spot corresponding to xanthine monophosphate was scraped and counted. Dihydrofolate reductase activity was determined at 340 nm for 30 min as the oxidation of reduced nicotinamide adenine dinucleotide phosphate (21). Ribonucleotide reductase activity was determined by the method of Moore and Hurlbert (22) using [5-^{3}H]cytidine-5-diphosphate (25 Ci/mmole). Ribose and deoxyribose nucleotide were separated on PEI cellulose F plastic precoated plates eluted with 4% boric acid–4 *M* LiCl (4:3) and scraped at the R_f values consistent with the standard deoxycytidine diphosphate. An *in vitro* method[5] using a lysate of Ehrlich ascites cells was used to determine if microlenin was an initiation or elongation inhibitor of protein synthesis by using the standards pyrocatechol violet (an initiation inhibitor) and emetine (an elongation inhibitor) using 1 μCi [^{3}H]leucine (24.7 Ci/mmole). Aliquots of the reaction medium were removed every 2 min, spotted on dried filter paper[5], treated for 10 min in boiling 5% trichloroacetic acid, and washed with cold 5% trichloroacetic acid, ether–ethanol (4:1), and ether. The disks were dried and counted[3].

[4] Hyamine Hydroxide, New England Nuclear.

[5] Whatman #3.

Table II—*In Vivo* Effects of Microlenin at 5 mg/kg/day ip on Ehrlich Ascites Carcinoma of CF_1 Male Mice

Biochemical Parameter or Enzyme (n = 6)	Control) (0,05%) Polysorbate 80 $\bar{X} \pm SD$	Microlenin (5 mg/kg/day) on Days 8 & 9 $\bar{X} \pm SD$
[^{3}H]Thymidine incorporation into DNA	100 ± 8	48 ± 5[a]
[^{3}H]Uridine incorporation into RNA	100 ± 9	98 ± 8
[^{3}H]Leucine incorporation into protein	100 ± 8	59 ± 7[a]
[^{14}C]Formate incorporation into purines	100 ± 12	58 ± 8[a]
DNA polymerase activity	100 ± 6	38 ± 3[a]
Messenger RNA polymerase activity	100 ± 8	104 ± 9
Ribosomal RNA polymerase activity	100 ± 9	82 ± 9[b]
Transfer RNA polymerase activity	100 ± 10	72 ± 9[a]
Ribonucleotide reductase activity	100 ± 6	102 ± 8
Thymidylate monophosphate levels	100 ± 10	47 ± 5[a]
Thymidylate diphosphate levels	100 ± 12	45 ± 6[a]
Thymidylate triphosphate levels	100 ± 9	52 ± 7[a]
Phosphoribosyl pyrophosphate amidotransferase activity	100 ± 9	37 ± 5[a]
Inosinic acid dehydrogenase activity	100 ± 10	86 ± 8
Dihydrofolate reductase activity	100 ± 8	62 ± 7[a]
Carbamyl phosphate synthetase activity	100 ± 10	104 ± 11
Aspartate transcarbamylase activity	100 ± 9	108 ± 10
Orotidine monophosphate decarboxylase activity	100 ± 10	82 ± 9
Thymidylate synthetase activity	100 ± 9	107 ± 10
Number of cells × 10^6/ml ascites fluid	100 ± 9	41 ± 4[a]

[a] $p \leq 0.001$. [b] $p \leq 0.010$.

Protein for enzymatic assay was determined by the Lowry *et al.* technique (23).

Probable (p) significant differences were determined by the Student's t test. Data are expressed in Tables I–II as percent of control with standard deviations.

RESULTS

Microlenin has potent activity against Ehrlich ascites carcinoma growth at 5 and 10 mg/kg/day with 99.9 and 90.4% inhibition, respectively (Table I). Preliminary *in vitro* studies demonstrated that DNA, RNA, and protein syntheses are effectively reduced by microlenin. An ID_{50} value of 1.0 μ*M* was obtained for DNA synthesis and protein synthesis at 1.42 m*M*. Formate incorporation into purine was significantly suppressed by microlenin with an ID_{50} value of 783 μ*M*. Phosphoribosyl pyrophosphate amido transferase activity was markedly reduced in the presence of microlenin, affording an ID_{50} value of 611 μ*M* concentration and for dihydrofolate reductase activity an ID_{50} value of 520 μ*M* was obtained. Marginal inhibition (28%) was observed by 100 μ*M* of microlenin on orotidine monophosphate decarboxylase activity. The thymidine nucleotide pools were reduced during *in vitro* incubation with microlenin. Thymidine monophosphate pools were reduced 45% at 25 μ*M*. DNA polymerase activity was suppressed with microlenin resulting in an ID_{50} value of 498 μ*M*. Deoxyribonuclease activity *in vitro* was inhibited 48% at 100 μ*M* of microlenin. A number of enzyme activities were not affected by microlenin. Those include messenger, ribosomal, and transfer RNA polymerases, ribonucleotide reductase, carbamyl phosphate synthetase, aspartate carbamyl transferase, thymidylate synthetase, and RNA synthesis. *In vivo* studies after 2 days dosing with microlenin at 5 mg/kg/day showed that DNA synthesis was markedly reduced. The control DNA synthesis rate is 107,533 dpm/hr/mg of isolated DNA, which was inhibited 52% by microlenin. Uridine incorporation into RNA for the 10-day control was 51,193 dpm/hr/mg of isolated RNA which was unaffected by drug treatment. Leucine incorporation for the control was 19,181 dpm/hr/mg of isolated protein, which was suppressed 41% by drug therapy. Formate incorporation into purines was 28,786 dpm/mg of protein, which was inhibited 42% by microlenin. Nuclear DNA polymerase activity for the control was 76,528 dpm/hr/mg of nucleoprotein, which was inhibited 62% by drug therapy. Messenger RNA polymerase activity for 10-day cells was 4867 dpm/hr/mg of nucleoprotein, ribosomal RNA polymerase activity was 8751 dpm/hr/mg of nucleoprotein, and transfer RNA polymerase activity was 10,792 dpm/hr/mg of nucleoprotein, which were inhibited 0, 28, and 18%, respectively, by administration of microlenin. Ribonucleotide reductase activity for the control was 153,791 dpm/mg of protein, which was not affected by drug treatment. Thymidine nu-

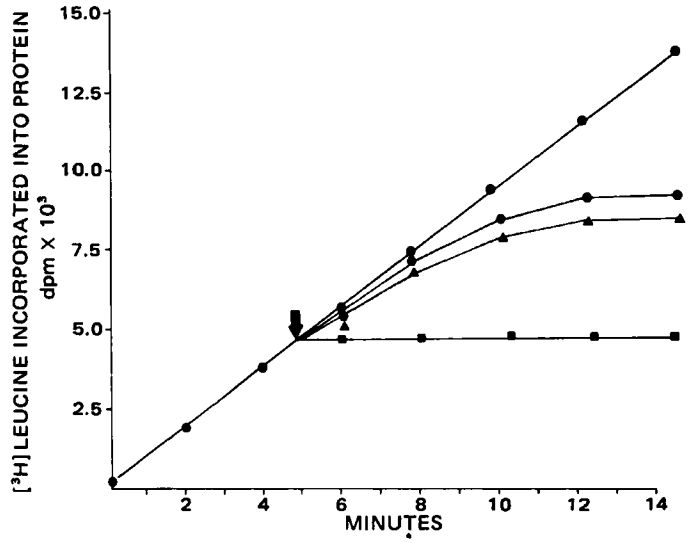

Figure 2—*Effects of microlenin on the initiation and elongation of protein synthesis of Ehrlich ascites carcinoma cells. Key: (●) control, (●) pyrocatechol violet, (■) emetine, and (▲) microlenin, (↓) addition of drug at 100 μM concentration.*

cleotide pools were altered by microlenin treatment. Thymidylate monophosphate pools were reduced 53%, thymidylate diphosphate pools 55%, and thymidylate triphosphate pools 48%.

Examination of the regulatory enzymes of *de novo* purine synthesis phosphoribosyl amido transferase activity for the control was 0.544 optical density units change/hr/mg of protein, which was reduced 63% by two doses of microlenin. Inosinic acid dehydrogenase activity for the 10-day control was 36,530 dpm/mg of protein, which was reduced 14% by microlenin administration. Dihydrofolate reductase activity for the untreated cells afforded a change of 0.514 optical units/hr/mg of protein which was suppressed 38% by drug administration. Examination of pyrimidine synthesis, the regulatory enzyme carbamyl phosphate synthetase activity for the control was 0.128 mg of carbamyl phosphate formed/hr/mg of protein and aspartate carbamyl transferase activity for the control was 7.526 mg of carbamyl aspartate formed/hr/mg of protein, which were not affected by drug treatment. Orotidine monophosphate decarboxylase activity for the control was 10,775 dpm of CO_2 generated for 15 min/mg of protein. Drug treatment reduced the activity 18%. Thymidylate synthetase activity for the control was 103,328 dpm/mg of protein, which was unaffected by drug therapy. Two days of treatment with microlenin at 5 mg/kg/day reduced the number of ascites cells/ml from 226×10^6 to 93×10^6.

DISCUSSION

Microlenin effectively suppressed Ehrlich ascites carcinoma growth as well as DNA synthesis and protein synthesis. Similar findings have also been observed for other sesquiterpene lactones. For example, helenalin at 33.3 mg/kg totally inhibited Ehrlich ascites growth (24) and at 12.5 mg/kg/day for 3 days significantly reduced DNA synthesis 88% (24–26). Tenulin produced a 97.3% reduction of Ehrlich ascites growth and a 91% inhibition of DNA synthesis at the same dose (24–26). Germacranolides [*i.e.*, eupahyssopin (27), eupaformosanin (28), and molephantinin (29)] produced similar effects in the Ehrlich tumor growth. However, the dose microlenin required to bring about the same degree of suppression of tumor growth was much lower: 6 mg/kg/day, compared with the higher doses of drugs, *i.e.*, 33.3 and 12.5 mg/kg/day, for the other derivatives. DNA polymerase activity was significantly reduced by microlenin. A number of pseudoguaianolides and germacranolides have been shown to inhibit both *in vivo* and *in vitro* DNA polymerase activity (24–29), basically at a higher dose than required by microlenin. Thymidylate synthetase activity was also suppressed by the pseudoguaianolides and germacranolides (24–26), but it should be noted that microlenin did not have any effect on thymidylate synthetase activity. These latter two enzymes contain sulfhydryl groups, which are supposedly alkylated by the α,β-unsaturated carbonyl moiety through a rapid Michael-type addition (25). The α,β-unsaturated carbonyl system in a ketone unit exists as the β-unsubstituted cyclopentenone moiety and as the α-methylene-γ-lactone in the structure of microlenin.

Formate incorporation into purines was significantly suppressed by microlenin. The activity of the regulatory enzyme of purine synthesis, phosphoribosyl pyrophosphate amido transferase, was also significantly reduced by microlenin. The magnitude of inhibition of the regulatory enzyme by the drug would account for the degree of reduction of purine synthesis. Nevertheless, microlenin marginally suppressed inosinic acid dehydrogenase activity, another regulatory enzyme of the purine pathway, and dihydrofolate reductase activity was moderately inhibited by microlenin. The latter enzyme plays a major role in the transfer of one carbon unit for purine and pyrimidine synthesis. The earlier regulatory enzymes of pyrimidine synthesis were not affected by drug treatment; however, a later regulatory enzyme, orotidine monophosphate decarboxylase, was marginally inhibited by *in vivo* administration. The nucleotide pools were reduced by microlenin with ~50% reduction. The reductions of monophosphate, diphosphate, and triphosphate pools will severely limit DNA synthesis of cells. Inhibition of formate incorporation, regulatory enzyme activities of the purine pathway, and nucleotide pools has been demonstrated previously with molephantinin in Ehrlich ascites cells.

Analysis of the protein data suggests that microlenin is an initiation inhibitor of protein synthesis of Ehrlich ascites carcinoma cells. Protein synthesis inhibition has been shown for helenalin, eupahyssopin, molephantinin. Recent studies in P-388 lymphocytic leukemia cells and rabbit reticulocyte cells demonstrated that helenalin and bis(henalinyl)malonate inhibit the formation of a 48S ribosomal complex during the initiation step of protein synthesis.

REFERENCES

(1) K. H. Lee, Y. Imakura, D. Sims, A. T. McPhail, and K. D. Onan, *J. Chem. Soc. Chem. Commun.*, **1976**, 341.

(2) Y. Imakura, K. H. Lee, D. Sims, and I. H. Hall, *J. Pharm. Sci.*, **67**, 1228 (1978).

(3) Y. Imakura, K. H. Lee, D. Sims, R. Y. Wu, I. H. Hall, H. Furukawa, M. Itoiguawa, and K. Yonaha, *J. Pharm. Sci.*, **69**, 1044 (1980).

(4) C. Piantadosi, C. S. Kim, and J. L. Irvin, *J. Pharm. Sci.*, **58**, 821 (1969).

(5) L. L. Liao, S. M. Kupchan, and S. B. Horwitz, *Mol. Pharmacol.*, **12**, 167 (1976).

(6) C. B. Chae, J. L. Irvin, and C. Piantadosi, *Proc. Am. Assoc. Cancer Res.*, **9**, 44 (1968).

(7) R. G. Wilson, R. H. Bodner, and G. E. MacHorter, *Biochim. Biophys. Acta*, **378**, 260 (1975).

(8) A. C. Sartorelli, *Biochim. Biophys. Res. Commun.*, **27**, 26 (1976).

(9) W. C. Hymer and E. L. Kuff, *J. Histochem. Cytochem.*, **12**, 359 (1964).

(10) H. Sawada, K. Tatsumi, M. Sasada, S. Shirakawa, T. Nakamura, and G. Wakisaka, *Cancer Res.*, **34**, 3341 (1974).

(11) K. M. Anderson, I. S. Mendelson, and G. Guzik, *Biochim. Biophys. Acta*, **383**, 56 (1975).

(12) F. Maley and S. Ochoa, *J. Biol. Chem.*, **233**, 1538 (1958).

(13) S. M. Kalman, P. H. Duffield, and T. Brzozowski, *J. Biol. Chem.*, **240**, 1871 (1966).

(14) R. M. Archibald, *J. Biol. Chem.*, **156**, 121 (1944).

(15) S. B. Koritz and P. P. Cohen, *J. Biol. Chem.*, **209**, 145 (1954).

(16) S. H. Appel, *J. Biol. Chem.*, **243**, 3929 (1968).

(17) A. Kampf, R. L. Barfknecht, P. J. Schaffer, S. Osaki, and M. P. Mertes, *J. Med. Chem.*, **19**, 903 (1976).

(18) M. K. Spassova, G. C. Russev, and E. V. Golovinsky, *Biochem. Pharmacol.*, **25**, 923 (1976).

(19) J. B. Wyngaarden and D. M. Ashton, *J. Biol. Chem.*, **234**, 1492 (1959).

(20) H. J. Becker and G. W. Löhr, *Klin. Wochenschr.*, **57**, 1109 (1979).

(21) Y. K. Ho, T. Kakala, and S. F. Zahrzewski, *Cancer Res.*, **32**, 1023 (1972).

(22) E. G. Moore and R. B. Hurlbert, *J. Biol. Chem.*, **241**, 4802 (1966).

(23) O. H. Lowry, N. J. Rosebrough, A. L. Farr, and R. J. Randall, *J. Biol. Chem.*, **193**, 265 (1951).

(24) I. H. Hall, K. H. Lee, E. C. Mar, C. O. Starnes, and T. G. Waddell, *J. Med. Chem.*, **20**, 33 (1977).

(25) K. H. Lee, I. H. Hall, E. C. Mar, C. O. Starnes, S. A. ElGebaly, T.

G. Waddell, R. I. Hadgraft, C. G. Ruffner, and I. Weidner, *Science*, **196**, 533 (1977).

(26) I. H. Hall, K. H. Lee, C. O. Starnes, S. A. ElGebaly, T. Ibuka, Y. S. Wu, T. Kimura, and M. Haruna, *J. Pharm. Sci.*, **67**, 1235 (1978).

(27) I. H. Hall, K. H. Lee, and S. A. ElGebaly, *J. Pharm. Sci.*, **67**, 1232 (1978).

(28) I. H. Hall, K. H. Lee, W. L. Williams, Jr., T. Kimura, and T. Hirayama, *J. Pharm. Sci.*, **69**, 294 (1980).

(29) I. H. Hall, Y. F. Liou and K. H. Lee, *J. Pharm. Sci.*, **71**, 687 (1982).

ACKNOWLEDGMENTS

Supported in part by National Cancer Institute Grant CA-17625. The authors thank Melba Gibson, Jerry McKee, and Colleen Gilbert for their technical assistance.

Quantum Mechanical Calculations Useful For Determining the Mechanism of Action of Fosfomycin

YVES G. SMEYERS *x, A. HERNANDEZ-LAGUNA *, and C. VON CARSTENN-LICHTERFELDE ‡

Received May 12, 1982, from the **Quantum Chemistry Laboratory, Instituto de Estructura de la Materia, C.S.I.C., c/Serrano, 119, Madrid-6, Spain* and the ‡*Instituto de Farmacologia Española, CEPA, c/Menendez-Alvaro, 57, Madrid-7, Spain.* Accepted for publication August 12, 1982.

Abstract □ CNDO/2 calculations were performed to determine at the molecular level the mechanism of action of the antibiotic fosfomycin, (−)-(1*R*,2*S*)-(1,2-epoxypropyl)phosphonic acid. Fosfomycin, a bacterial cell wall inhibitor, is known to act as a competitive inhibitor of *N*-acetylglucosamine-3-*O*-enolpyruvyl transferase, the normal substrate of which is phosphoenolpyruvate. Both compounds were studied, and the theoretical calculations revealed that the preferred conformations of phosphoenolpyruvate and fosfomycin presented the same spatial charge distributions on the active sites, the values of which are in complete agreement with the experimental observations. These results permit the projection of some details of the receptor, with implications for the modification of fosfomycin to increase its antibiotic activity.

Keyphrases □ Fosfomycin—preferred molecular conformation for biological activity, quantum mechanical calculations □ Phosphoenolpyruvate—preferred molecular conformation for biological activity, quantum mechanical calculations □ Structure–activity relationship—fosfomycin and phosphoenolpyruvate, molecular level mechanism of action, preferred conformation

Fosfomycin, (−)-(1*R*,2*S*)-(1,2-epoxypropyl)phosphonic acid, a relatively new low molecular weight antibiotic, contains both an epoxide ring and a carbon–phosphorus bond (Fig. 1) [found for the first time among natural products (1)]. Despite the presence of the epoxide ring, fosfomycin is quite stable, and its activity seems to be limited to the inhibition of *N*-acetylglucosamine-3-*O*-enolpyruvyl transferase, resulting in the formation of an irreversible adduct with the enzyme. The reaction seems to be stereospecific; (+)-(1*R*,2*S*)-, (−)-(2*R*,1*S*)-, and (+)-(2*R*,1*S*)-(1,2-epoxypropyl)phosphonic acids do not form stable adducts, as shown by their lack of biological activity. The absolute configuration of fosfomycin has been found to be (−)-(1*R*,2*S*) (2).

Fosfomycin is structurally similar to phosphoenolpyruvate (Fig. 2), an important substance for both bacterial and animal cells (3). Kahan *et al.* (4) have studied the mechanism of action of fosfomycin, which appears to be a competitive inhibitor of phosphoenolpyruvate in the cell wall biosynthesis of bacteria. The reactive sites on the enolpyruvyl transferase are a nucleophilic sulfur of a cysteine residue and a proton donor. The reaction is interpreted by the authors as a sulfhydryl addition across the C(2)—O(1) bond, analogous with the assumed sulfhydryl addition across the C(2)=C(3) double bond of phosphoenolpyruvate in the bacterial cell wall. In the present work, quantum mechanical conformational and charge distribution calculations for fosfomycin and phosphoenolpyruvate were performed to determine the mimetic action of fosfomycin at the molecular level.

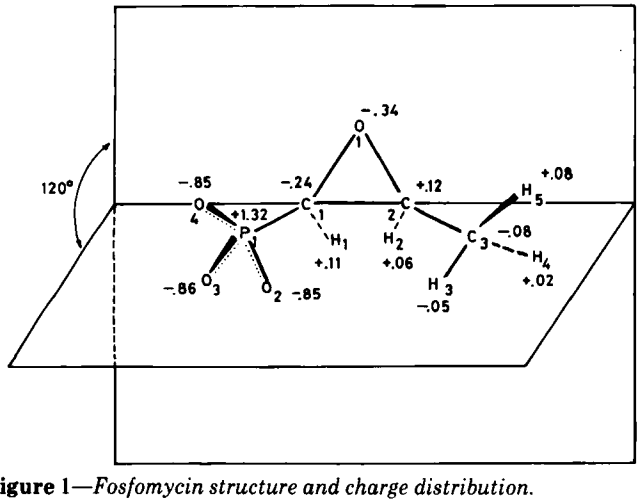

Figure 1—*Fosfomycin structure and charge distribution.*

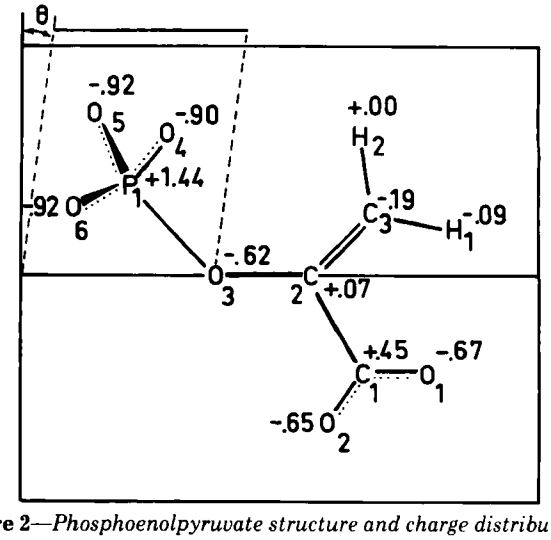

Figure 2—*Phosphoenolpyruvate structure and charge distribution.*

0022-3549/83/0900-1011$01.00/0

G. Waddell, R. I. Hadgraft, C. G. Ruffner, and I. Weidner, *Science*, **196**, 533 (1977).

(26) I. H. Hall, K. H. Lee, C. O. Starnes, S. A. ElGebaly, T. Ibuka, Y. S. Wu, T. Kimura, and M. Haruna, *J. Pharm. Sci.*, **67**, 1235 (1978).

(27) I. H. Hall, K. H. Lee, and S. A. ElGebaly, *J. Pharm. Sci.*, **67**, 1232 (1978).

(28) I. H. Hall, K. H. Lee, W. L. Williams, Jr., T. Kimura, and T. Hirayama, *J. Pharm. Sci.*, **69**, 294 (1980).

(29) I. H. Hall, Y. F. Liou and K. H. Lee, *J. Pharm. Sci.*, **71**, 687 (1982).

ACKNOWLEDGMENTS

Supported in part by National Cancer Institute Grant CA-17625. The authors thank Melba Gibson, Jerry McKee, and Colleen Gilbert for their technical assistance.

Quantum Mechanical Calculations Useful For Determining the Mechanism of Action of Fosfomycin

YVES G. SMEYERS *x, A. HERNANDEZ-LAGUNA *, and C. VON CARSTENN-LICHTERFELDE ‡

Received May 12, 1982, from the **Quantum Chemistry Laboratory, Instituto de Estructura de la Materia, C.S.I.C., c/Serrano, 119, Madrid-6, Spain* and the ‡*Instituto de Farmacologia Española, CEPA, c/Menendez-Alvaro, 57, Madrid-7, Spain.* Accepted for publication August 12, 1982.

Abstract □ CNDO/2 calculations were performed to determine at the molecular level the mechanism of action of the antibiotic fosfomycin, (−)-(1*R*,2*S*)-(1,2-epoxypropyl)phosphonic acid. Fosfomycin, a bacterial cell wall inhibitor, is known to act as a competitive inhibitor of *N*-acetylglucosamine-3-*O*-enolpyruvyl transferase, the normal substrate of which is phosphoenolpyruvate. Both compounds were studied, and the theoretical calculations revealed that the preferred conformations of phosphoenolpyruvate and fosfomycin presented the same spatial charge distributions on the active sites, the values of which are in complete agreement with the experimental observations. These results permit the projection of some details of the receptor, with implications for the modification of fosfomycin to increase its antibiotic activity.

Keyphrases □ Fosfomycin—preferred molecular conformation for biological activity, quantum mechanical calculations □ Phosphoenolpyruvate—preferred molecular conformation for biological activity, quantum mechanical calculations □ Structure–activity relationship—fosfomycin and phosphoenolpyruvate, molecular level mechanism of action, preferred conformation

Fosfomycin, (−)-(1*R*,2*S*)-(1,2-epoxypropyl)phosphonic acid, a relatively new low molecular weight antibiotic, contains both an epoxide ring and a carbon–phosphorus bond (Fig. 1) [found for the first time among natural products (1)]. Despite the presence of the epoxide ring, fosfomycin is quite stable, and its activity seems to be limited to the inhibition of *N*-acetylglucosamine-3-*O*-enolpyruvyl transferase, resulting in the formation of an irreversible adduct with the enzyme. The reaction seems to be stereospecific; (+)-(1*R*,2*S*)-, (−)-(2*R*,1*S*)-, and (+)-(2*R*,1*S*)-(1,2-epoxypropyl)phosphonic acids do not form stable adducts, as shown by their lack of biological activity. The absolute configuration of fosfomycin has been found to be (−)-(1*R*,2*S*) (2).

Fosfomycin is structurally similar to phosphoenolpyruvate (Fig. 2), an important substance for both bacterial and animal cells (3). Kahan *et al.* (4) have studied the mechanism of action of fosfomycin, which appears to be a competitive inhibitor of phosphoenolpyruvate in the cell wall biosynthesis of bacteria. The reactive sites on the enolpyruvyl transferase are a nucleophilic sulfur of a cysteine residue and a proton donor. The reaction is interpreted by the authors as a sulfhydryl addition across the C(2)—O(1) bond, analogous with the assumed sulfhydryl addition across the C(2)=C(3) double bond of phosphoenolpyruvate in the bacterial cell wall. In the present work, quantum mechanical conformational and charge distribution calculations for fosfomycin and phosphoenolpyruvate were performed to determine the mimetic action of fosfomycin at the molecular level.

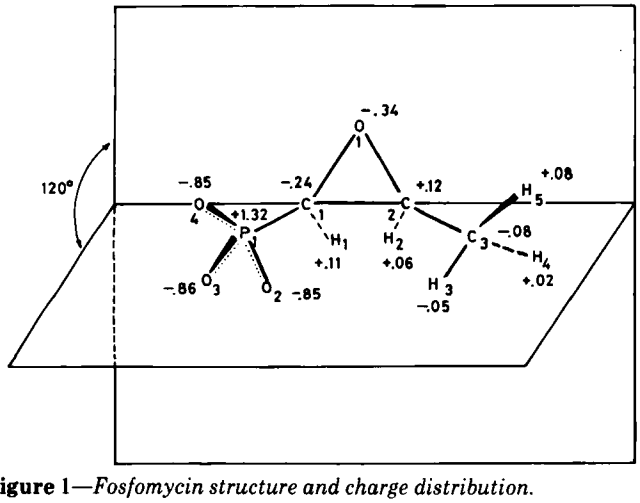

Figure 1—*Fosfomycin structure and charge distribution.*

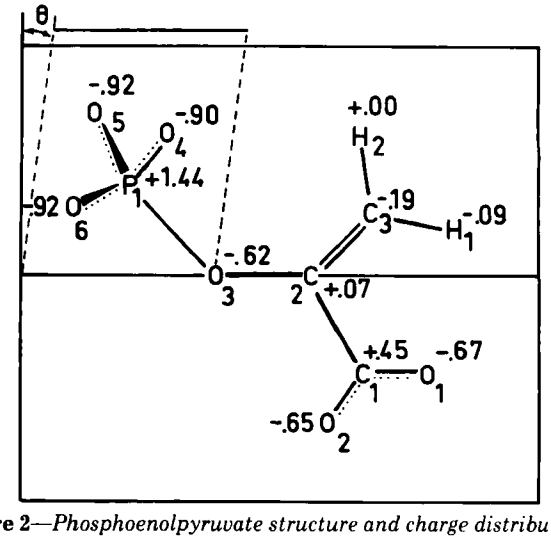

Figure 2—*Phosphoenolpyruvate structure and charge distribution.*

0022-3549/83/0900-1011$01.00/0

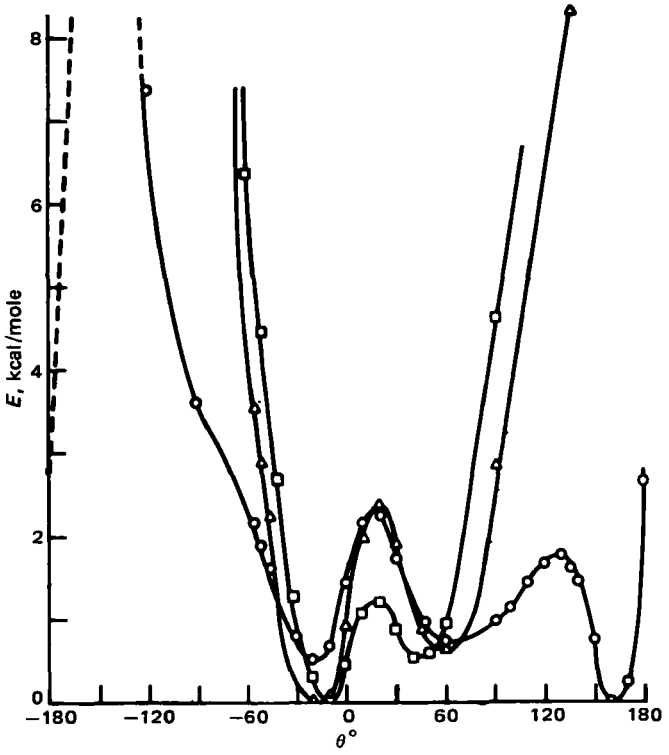

Figure 3—*Calculated relative potential energy curves for the one-* (○), *two-* (△), *and threefold* (□) *ionized species of phosphoenolpyruvate as a function of the rotation angle around the C—O bond of the ester bridge.*

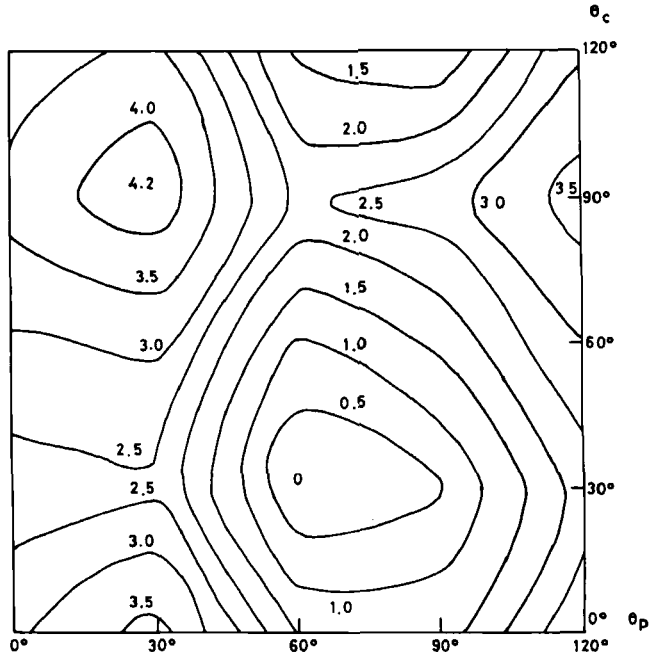

Figure 4—*Calculated potential energy (kcal/mole) map for the internal rotation in fosfomycin.* θ_p *and* θ_c *are the rotation angles of the phosphonium and carboxylic groups, respectively.*

THEORETICAL

Since fosfomycin and phosphoenolpyruvate are relatively large molecules to be approached by an *ab initio* method, the charge distribution calculations and conformational analysis were performed using the standard semiempirical CNDO/2 procedure (5). This method considers the system under study in the gas phase and needs only knowledge of the atomic number and the position coordinates of the atoms. Solvent effects can be introduced (6). These effects usually appear as a small increase in the charges, which will not modify the overall conclusions of this work. Therefore, solvent effects will not be considered explicitly.

Although the CNDO/2 method must be used with some caution in the conformational calculations (7), this procedure usually yields reasonable charge distributions. However, since it resorts to the zero differential overlap approximation (ZDO), the electronic charge distributions must be recalculated conveniently to obtain more reliable values (8).

In the ZDO approach, the electric charge of a given atom, A, with core charge Z_A, is expressed as:

$$Q_A = Z_A - 2\sum_{a}^{N}\sum_{i}^{n} C_{ia}^2 \qquad \text{(Eq. 1)}$$

where C_{ia} are the coefficients of the ath basis function in the ith molecular orbital, N is the number of basis functions centered on atom A, and n the number of occupied molecular orbitals. In this approximation, the basis functions may be regarded as atomic Slater orbitals orthogonalized by the Löwdin procedure. This orthogonalization involves a delocalization of the basis functions. To undo this transformation seems to be necessary in order to obtain localized charges on the atoms. So, according to the Löwdin transformation, the new coefficients are written as:

$$C' = CS^{-1/2}$$

where S is the overlap matrix between the Slater orbitals, and C and C' are the coefficient matrices before and after deorthogonalization, respectively. After this operation, the electric charges are given by the Mulliken population analysis formula:

$$Q_A = Z_A - 2\sum_{a}^{N}\sum_{b}^{M}\sum_{i}^{n} C'_{ia}C'_{ib}S_{ab} \qquad \text{(Eq. 2)}$$

where the summation on the index b must be extended to all the nonorthogonal basis orbitals.

EXPERIMENTAL

Phosphoenolpyruvic acid and fosfomycin should be ionized in a physiological medium. Essentially complete ionization of both compounds at pH ~7.4 is shown by the pK_a values of the carboxyl group (3.5) and the phosphoric acid groups (<2 and 6.4) of phosphoenolpyruvate acid and the phosphonic moiety (1.85 and 6.40) of fosfomycin (9). One-, two-, and threefold ionized species for fosfomycin were considered in the calculations.

To determine the coordinates of the ionized species, the bond lengths and bond angles were taken from the available crystallographic data, *i.e.*, X-ray measurements in solid phase on the monocyclohexylammonium salt of phosphoenolpyruvate (10) and monophenethylammonium salt of fosfomycin (11). Because the ions may show some conformational modifications in liquid phase, various possible conformations were taken into account.

Phosphoenolpyruvate Calculations—It appears that phosphoenolpyruvate has not been studied from a quantum point of view, except for two previous works on bond energy wealth (12, 13). X-ray measurements (10) show a roughly planar structure except for the phosphate group, which extends out from the plane of the enolpyruvate moiety. The P(1)—O(3) bond forms a tetrahedral angle (~109°) with the C(2)—O(3) bond of the ester bridge, and the P(1)—O(3)—C(2) plane forms a dihedral angle of 90° with the molecular planar frame. Because of the tetrahedral character of the P(1)—O(3) bond, the lack of steric effect, and its high symmetry, the phosphate group is expected to be able to rotate in the free molecule. Among the small irregularities of the planar frame, the carboxylic group appears somewhat twisted, and the oxygen atom (O-3), lies somewhat under the enolpyruvate plane. From a quantum point of view, it may be expected that the more ionized the molecule, the more planar it is because of a clear increasing of the conjugation of the π-electron system. This feature is especially true for the carboxylic group, which may be considered as rigorously coplanar in its ionized form.

Concerning the phosphoric rest, the question is whether the P(1)—O(3)—C(2) plane remains vertical up the enolpyruvic plane. Therefore, conformational calculations were performed around the O(3)—C(2) bond, taking as origin of rotations the conformation in which the phosphorus atom lies in the pyruvic plane side of the methylenic group. In these calculations, however, the O-3 atom is assumed to remain in its original location, slightly under the molecular plane.

The conformational dependencies of the three ionized species of phosphoenolpyruvic acid are reported in Fig. 3; they show a potential asymmetric double-well behavior, due to the out-of-plane O-3 atom. Minima are found at 60° and −20°, 60° and −20°, and 45° and −10° in the one-, two-, and threefold ionized species, respectively. The one-ionized

species has an extra minimum at 160°. As expected, at least to some extent, the more ionized the compound the more planar the ion. In the liquid phase, however, it may be expected that the solvent effect will damp this trend, because of its dielectric nature (6).

The preferred conformations appear also at lower angles. However, since the energy differences between the two branches of double wells are not too large (0.27, 0.66, and 0.54 kcal/mole), it may be expected that the ionized species will exist in both conformations at the physiological temperature. Furthermore, the barrier heights between the two branches are relatively low (1.8, 2.4, and 1.3 kcal/mole) so that the interconversion should be relatively easy through a switching of the O-3 atom.

The localized charge distributions were determined using Eq. 2 as a function of the torsion angle for the three ionized species. The distributions look qualitatively similar in the three species, although the more ionized the phosphoenolpyruvate species, the sharper the charge distribution, probably because of the increasing conjugation of the π-system. Their conformational dependencies, however, are not too large in the region of the minima. In Fig. 3, the charge distribution of the preferred conformation of the threefold ionized species in which the P(1)—O(3)—C(2) plane lies at −10° from the molecular plane is given.

Fosfomycin Calculations—Compared with phosphoenolpyruvate, fosfomycin presents a relatively rigid structure. In the X-ray measurements (11), fosfomycin may be regarded as a planar epoxide bearing a phosphonate and methyl groups in *cis* positions. Taking as rotation axis the C(1)—C(2) ring side and as origin of rotation the conformation in which the P atom lies in the epoxide half-plane, the phosphonate and methyl groups point rigidly out ~120° from the molecular plane. Only hindered internal rotations of the phosphonate and methyl radicals are possible. Therefore, the conformational calculations on the one- and twofold ionized species of fosfomycin were restricted to these two possibilities.

The conformational map for the twofold ionized species is given in Fig. 4, in which the threefold symmetry of the rotors is taken into account. In Fig. 4, the preferred conformation has the methyl and phosphonate groups rotated at 30° and 60°, respectively, taking as origin of rotation the conformation in which one atom of the rotating group lies in the plane formed by the rotation axis and the ring side. The conformational map, however, shows a valley corresponding to the single rotation of the methyl group, with a relatively low saddle point at 2 kcal/mole. This result reveals that the methyl group is able to rotate, though with some hindrance, regardless of the position of the phosphonate group.

The localized charge distributions of the two ionized species were calculated as a function of the two internal rotation angles. These distributions look very similar in the two species, and their conformational dependencies appear to be very small. In Fig. 1, the charge distribution of the twofold ionized species for the preferred conformation is also given.

RESULTS AND DISCUSSIONS

The results below are discussed assuming a neutral pH in the bacterial cell. These results also are valid, however, at lower pH values where local variations could occur in the reactive medium.

As has been seen, phosphoenolpyruvate and fosfomycin possess a central frame to which the PO_3^{2-} moiety is attached. Fosfomycin has a rigid structure; in contrast, phosphoenolpyruvate is a more flexible molecule which can adopt different conformations. The question arises whether fosfomycin may be considered as a rigid analogue of the natural compound.

As it is seen in Fig. 3, phosphoenolpyruvate has essentially two preferred conformations. To adopt the structure of fosfomycin ($\theta \sim 120°$) the fully ionized species needs more than 20 kcal/mole, which is a large energy requirement. On the other hand, in this conformation some distances between active sites such as P-1 and C-3 appear to be too large when compared with the corresponding distance between P-1 and O-1 in fosfomycin. In the more stable conformation of phosphoenolpyruvate (which appears for lower angles), all the distances between the active sites coincide approximately with those of fosfomycin (Fig. 5).

When considering the charges of the active sites, *i.e.*, the proton acceptor centers (the C-3 atom in phosphoenolpyruvate and the O-1 atom in fosfomycin) and the sulfhydryl acceptor centers (the C-2 atoms in both molecules), it is seen that the proton acceptor sites have a negative charge in both molecules. The sulfhydryl acceptor centers, C-2, have a positive charge in both molecules. Furthermore, the second carbon atom of the epoxide ring of fosfomycin (C-1), which could be a competitive acceptor center for the sulfhydryl residue, appears to be negatively charged, analogous with the oxygen atom (O-3) of the ester bridge in phosphoenolpyruvate. The charge distributions are similar in the PO_3^{2-} groups of both molecular systems.

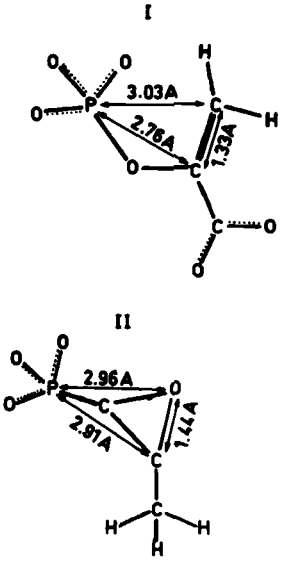

Figure 5—*Spatial distributions of the active sites (proposed receptor pattern) in the preferred conformation of the phosphoenolpyruvate (I) and fosfomycin (II).*

Therefore, fosfomycin should not be considered a rigid analogue of phosphoenolpyruvate. Nevertheless, this compound and fosfomycin appear to possess some local isosterism with a similar electric charge distribution at the active sites. This isosterism does not extend to the carboxylic group of phosphoenolpyruvate or methyl group of fosfomycin, which probably do not enter directly into the addition reaction. Fosfomycin, however, shows a high stereospecificity regarding the methyl group. This feature may be attributed to some steric hindrance, assuming that the reaction takes place in two steps: (*a*) fosfomycin is first adsorbed sideways by the PO_3^{2-} on the receptor and (*b*) the sulfhydryl addition reaction takes place on the opposite free face of the epoxide ring. Finally, it may be underlined that the knowledge of the charge distribution in fosfomycin suggests the possibility of selecting some structural modifications to increase the antibiotic activity of fosfomycin.

The present theoretical calculations confirm the assumed mechanism of action for the sulfhydryl and proton additions in fosfomycin as well as in phosphoenolpyruvate (4). The conformational analysis and electric charge distribution calculations indicate the same spatial charge distribution on the active sites in both molecular systems, the values of which are in accordance with the experimental data. Furthermore, taking into account the rigidity of fosfomycin and the stereospecificity involved, it may be stated that the active centers are probably located in a very small area on the receptor, limited approximately by the positions of three adjacent active centers, PO_3^{2-}, O-1, and C-2 (Fig. 5).

REFERENCES

(1) D. Hendlin *et al.*, *Science*, **166**, 122 (1969).

(2) B. G. Christensen, W. J. Leanza, T. R. Beattle, A. A. Patchett, B. H. Arison, R. E. Ormond, F. A. Kuehl, Jr., G. Albers-Schonberg, and O. Jardetzky, *Science*, **166**, 123 (1969).

(3) H. B. Woodruff, J. M. Mata, S. Hernández, S. Mochales, A. Rodriguez, E. O. Stapley, H. Wallick, A. K. Miller, and D. Hendlin, *Chemotherapy*, **23 S1**, 1 (1977).

(4) F. M. Kahan, J. S. Kahan, P. J. Cassidy, and H. Kropp, *Ann. N.Y. Acad. Sci.*, **235**, 364 (1974).

(5) J. A. Pople and D. L. Beveridge, "Approximate Molecular Orbital Theory," McGraw-Hill, New York, N.Y., 1970.

(6) O. Tapia, in "Molecular Interaction," vol. III, H. Ratajczak and W. J. Orville-Tomas, Eds., Wiley, New York, N.Y., 1982, p. 47.

(7) C. Sieiro, P. Gonzalez-Diaz, and Y. G. Smeyers, *J. Mol. Struct.*, **24**, 345 (1975).

(8) Y. G. Smeyers, A. De Bueren, and A. Hernández-Laguna, *Ann. Quim.*, **75**, 102 (1979).

(9) F. Wold and C. E. Ballou, *J. Biol. Chem.*, **227**, 301 (1957).

(10) D. G. Watson and O. Kennard, *Acta Crystallogr., Sect. 23*, **29**, 2358 (1973).
(11) A. Perales and S. Garcia Blanco, *Acta Crystallogr., Sect. B*, **34**, 238 (1978).
(12) B. Pullman and A. Pullman, "Quantum Biochemistry," Wiley Interscience, New York, N.Y., 1963, p. 335.
(13) D. M. Hayes, G. L. Kenyon, and P. A. Kollman, *J. Am. Chem. Soc.*, **100**, 4331 (1978).

ACKNOWLEDGMENTS

Y. G. Smeyers is indebted to Dr. A. Perales for valuable discussions and Prof. E. Galvez for reading the manuscript.

In Vitro Method for Detecting Precipitation of Parenteral Formulations After Injection

SAMUEL H. YALKOWSKY *x, SHRI C. VALVANI, and BENJAMIN W. JOHNSON

Received January 21, 1982, from *Pharmacy Research, The Upjohn Company, Kalamazoo, MI 49001.* Accepted for publication July 14, 1982. *Present address: College of Pharmacy, The University of Arizona, Tucson, AZ 85721.

Abstract □ Many injectable formulations currently on the market, including diazepam and alprazolam, utilize one or more cosolvents to solubilize the active constituents. On injection into an aqueous medium, some of these components tend to precipitate. A simple procedure is described for measuring the degree of precipitation that occurs when a solubilized drug is injected. This *in vitro* technique was used to show that alprazolam injection shows less precipitation than diazepam injection under all tested conditions, and that the precipitation observed with diazepam can be controlled by ensuring that the formulation is injected very slowly. This simple technique also can be used during preformulation development to evaluate the relative potential for precipitation of various formulations.

Keyphrases □ Diazepam—*in vitro* detection of precipitation for injectable formulations □ Alprazolam—*in vitro* detection of precipitation for injectable formulations □ Formulations, injectable—potential precipitation in aqueous media, *in vitro* detection using diazepam and alprazolam

It is often necessary to administer a drug parenterally at a concentration which exceeds its aqueous solubility. The use of water-miscible cosolvents is by far the most versatile means of increasing the solubility of drugs. Cosolvents in concentrations up to 50% v/v can produce solubility increases of several orders of magnitude for very insoluble drugs (1, 2).

In some cases, the injection of a formulation (in which the drug is solubilized by a cosolvent) into blood or some other aqueous fluid can result in precipitation of the drug (2–7). This precipitation, in turn, can result in erratic or reduced drug bioavailability, pain on injection, and/or thrombophlebitis (3–7). The amount of precipitation, and thus the severity of the above problems, often is related to the rate at which the drug is injected (3–7).

The elimination of precipitation on dilution not only can lead to a safer and more effective formulation, it can also

Table I—Some Parenteral Products Formulated with Cosolvents

Generic Name	Cosolvent Composition
Hydralazine HCl[a]	10% propylene glycol
Lorazepam[b]	80% propylene glycol 20% polyethylene glycol
Deslanoside[c]	9.8% ethanol 15% glycerin
Phenytoin sodium[d]	40% propylene glycol 10% ethanol
Dihydroergotamine mesylate[e]	6.1% ethanol 15% glycerin
Dimenhydrinate[f]	50% propylene glycol
Digoxin[g]	40% propylene glycol 10% ethanol
Chlordiazepoxide HCl[h]	20% propylene glycol
Phenobarbital sodium[i]	67.8% propylene glycol
Multiple vitamin infusion[j]	30% propylene glycol
Pentobarbital sodium[k]	40% propylene glycol 10% ethanol
Methocarbamol[l]	50% polyethylene glycol
Reserpine[m]	10% dimethylacetamide 5% polyethylene glycol
Diazepam[n]	40% propylene glycol 10% ethanol

[a] Apresoline (Ciba). [b] Ativan (Wyeth). [c] Cedilanid (Sandoz). [d] Dilantin (Parke-Davis). [e] DHE 45 (Sandoz). [f] Dramamine (Searle). [g] Lanoxin (Burroughs Wellcome). [h] Librium (Roche). [i] Luminal (Winthrop). [j] MVI (USV). [k] Nembutal (Abbott). [l] Robaxin (Robins). [m] Serpacil (Ciba). [n] Valium (Roche).

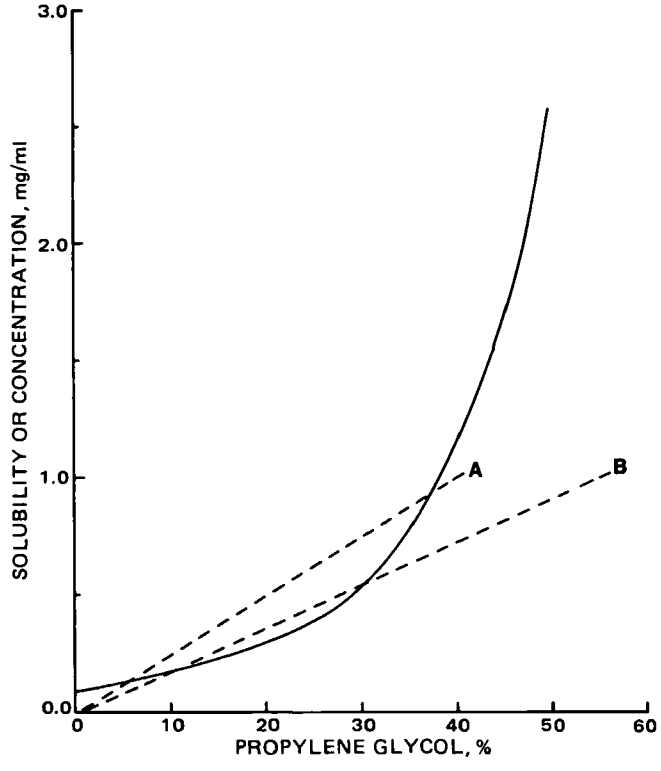

Figure 1—*Solubility (——) of alprazolam in propylene glycol–water mixtures containing 40% (A) and 55% (B) propylene glycol. The dilution lines (- - -) above the solubility curve represent conditions under which precipitation can occur.*

0022-3549/83/0900-1014$01.00/0

(10) D. G. Watson and O. Kennard, *Acta Crystallogr., Sect. 23*, **29**, 2358 (1973).
(11) A. Perales and S. Garcia Blanco, *Acta Crystallogr., Sect. B*, **34**, 238 (1978).
(12) B. Pullman and A. Pullman, "Quantum Biochemistry," Wiley Interscience, New York, N.Y., 1963, p. 335.
(13) D. M. Hayes, G. L. Kenyon, and P. A. Kollman, *J. Am. Chem. Soc.*, **100**, 4331 (1978).

ACKNOWLEDGMENTS

Y. G. Smeyers is indebted to Dr. A. Perales for valuable discussions and Prof. E. Galvez for reading the manuscript.

In Vitro Method for Detecting Precipitation of Parenteral Formulations After Injection

SAMUEL H. YALKOWSKY *x, SHRI C. VALVANI, and BENJAMIN W. JOHNSON

Received January 21, 1982, from *Pharmacy Research, The Upjohn Company, Kalamazoo, MI 49001.* Accepted for publication July 14, 1982. *Present address: College of Pharmacy, The University of Arizona, Tucson, AZ 85721.

Abstract □ Many injectable formulations currently on the market, including diazepam and alprazolam, utilize one or more cosolvents to solubilize the active constituents. On injection into an aqueous medium, some of these components tend to precipitate. A simple procedure is described for measuring the degree of precipitation that occurs when a solubilized drug is injected. This *in vitro* technique was used to show that alprazolam injection shows less precipitation than diazepam injection under all tested conditions, and that the precipitation observed with diazepam can be controlled by ensuring that the formulation is injected very slowly. This simple technique also can be used during preformulation development to evaluate the relative potential for precipitation of various formulations.

Keyphrases □ Diazepam—*in vitro* detection of precipitation for injectable formulations □ Alprazolam—*in vitro* detection of precipitation for injectable formulations □ Formulations, injectable—potential precipitation in aqueous media, *in vitro* detection using diazepam and alprazolam

It is often necessary to administer a drug parenterally at a concentration which exceeds its aqueous solubility. The use of water-miscible cosolvents is by far the most versatile means of increasing the solubility of drugs. Cosolvents in concentrations up to 50% v/v can produce solubility increases of several orders of magnitude for very insoluble drugs (1, 2).

In some cases, the injection of a formulation (in which the drug is solubilized by a cosolvent) into blood or some other aqueous fluid can result in precipitation of the drug (2–7). This precipitation, in turn, can result in erratic or reduced drug bioavailability, pain on injection, and/or thrombophlebitis (3–7). The amount of precipitation, and thus the severity of the above problems, often is related to the rate at which the drug is injected (3–7).

The elimination of precipitation on dilution not only can lead to a safer and more effective formulation, it can also

Table I—Some Parenteral Products Formulated with Cosolvents

Generic Name	Cosolvent Composition
Hydralazine HCl[a]	10% propylene glycol
Lorazepam[b]	80% propylene glycol 20% polyethylene glycol
Deslanoside[c]	9.8% ethanol 15% glycerin
Phenytoin sodium[d]	40% propylene glycol 10% ethanol
Dihydroergotamine mesylate[e]	6.1% ethanol 15% glycerin
Dimenhydrinate[f]	50% propylene glycol
Digoxin[g]	40% propylene glycol 10% ethanol
Chlordiazepoxide HCl[h]	20% propylene glycol
Phenobarbital sodium[i]	67.8% propylene glycol
Multiple vitamin infusion[j]	30% propylene glycol
Pentobarbital sodium[k]	40% propylene glycol 10% ethanol
Methocarbamol[l]	50% polyethylene glycol
Reserpine[m]	10% dimethylacetamide 5% polyethylene glycol
Diazepam[n]	40% propylene glycol 10% ethanol

[a] Apresoline (Ciba). [b] Ativan (Wyeth). [c] Cedilanid (Sandoz). [d] Dilantin (Parke-Davis). [e] DHE 45 (Sandoz). [f] Dramamine (Searle). [g] Lanoxin (Burroughs Wellcome). [h] Librium (Roche). [i] Luminal (Winthrop). [j] MVI (USV). [k] Nembutal (Abbott). [l] Robaxin (Robins). [m] Serpacil (Ciba). [n] Valium (Roche).

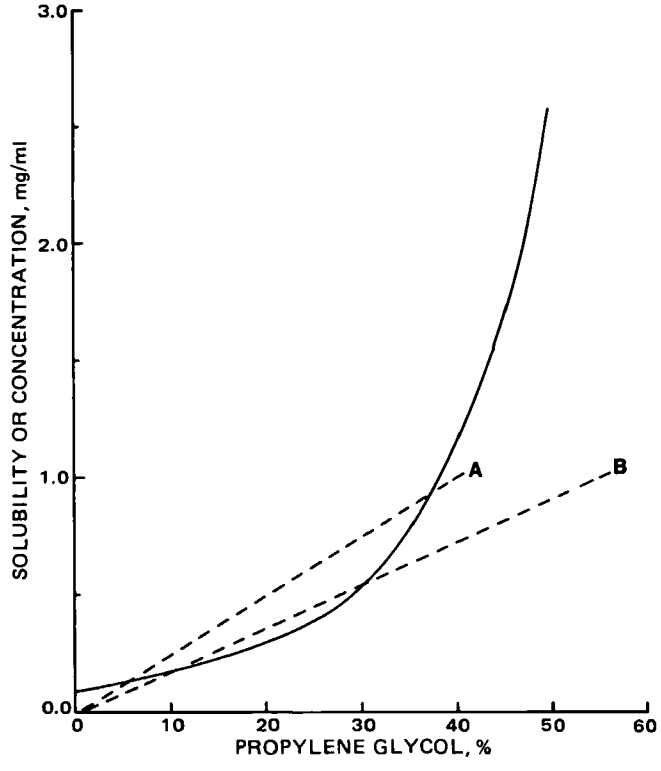

Figure 1—*Solubility (——) of alprazolam in propylene glycol–water mixtures containing 40% (A) and 55% (B) propylene glycol. The dilution lines (- - -) above the solubility curve represent conditions under which precipitation can occur.*

0022-3549/83/0900-1014$01.00/0

Table II—Some Properties of Diazepam and Alprazolam

	Diazepam	Alprazolam
Chemical name	7-Chloro-1,3-dihydro-1-methyl-5-phenyl-2*H*-1,4-benzodiazepin-2-one	8-Chloro-1-methyl-6-phenyl-4*H*-*s*-triazolo-[4,3-*a*][1,4]benzodiazepine
Formula	$C_{16}H_{13}ClN_2O$	$C_7H_{13}ClN_4$
Melting point	125–126°	226–234°
pK_a	3.50[b]	2.4 @ 25°
Solubility[a]	0.0414 (20°)[c]	0.114 (25°)
Water	0.048 (25°)[b]	
Propylene glycol	15.2 (10°)[c]	42 (25°)

[a] In g/liter. [b] From N. A. Mason, S. Cline, M. L. Hyneck, R. R. Bernardi, N. F. H. Ho, and G. L. Flynn, *Am. J. Hosp. Pharm.*, **38**, 1449 (1981). [c] From M. C. Neira, F. Jiminez, and L. F. Ponce de Leon, *Rev. Colmb. Cienc. Quim.-Farm.*, **3**, 37 (1980).

ensure more meaningful evaluations of new drugs. A simple *in vitro* dynamic system for evaluating the degree of precipitation on injection of a solubilized drug is presented. The technique also can be used during preformulation development to evaluate the relative potential for precipitation of various formulations.

BACKGROUND

Many parenteral products currently on the market utilize one or more water-miscible cosolvents (Table I). The tendency for this type of formulation to precipitate when injected or diluted with an aqueous medium has been explained (2) on the basis of the following:

1. When a formulation is diluted by blood or by an intravenous drip solution, the concentrations of drug and cosolvent(s) decrease proportionally to one another.
2. The solubility of the drug in the mixed solvent decreases exponentially as the concentration of cosolvent is decreased linearly.

This frequently results in a situation in which the drug concentration exceeds the solubility, as shown in Fig. 1. The curve in Fig. 1 represents the solubilization of alprazolam in the propylene glycol–water system. The shape of this curve indicates an exponential increase in solubility with increasing cosolvent composition. This commonly encountered dependency of solubility on cosolvent composition has been explained previously (8, 9). The dashed lines show dilution curves for two 1.0-mg/ml alprazolam formulations: the upper line represents a formulation containing 40% propylene glycol (minimum needed to solubilize the drug) and the lower line represents the alprazolam formulation used in this study (55% propylene glycol). When the concentration line is above the solubility curve, the solution is supersaturated. If the formulation is diluted further, the dilution line again crosses the solubility curve, and the solution becomes unsaturated as it approaches infinite dilution. The distance between the concentration line and the solubility curve is equal to the amount of supersaturation. The length of the dilution line between the crossover points is a measure of the time that the drug will be supersaturated when it is being diluted.

It is clear from the figure that the dilution line for the formulation containing 55% propylene glycol is much closer to the solubility curve than the line for the 40% propylene glycol formulation. Consequently, there is a much lower probability of drug precipitation in the former formulation on dilution. The excess cosolvent present also helps to prevent precipitation when the formulation is cooled (as can happen during shipping in the winter season).

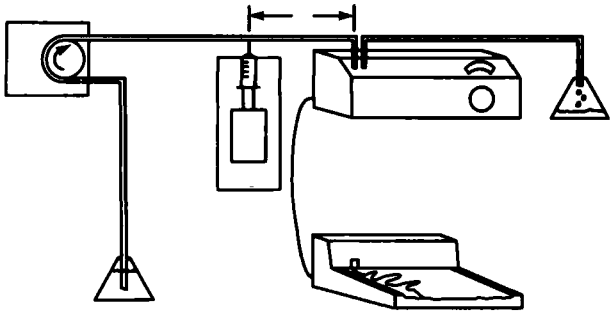

Figure 2—*Schematic of the apparatus used to detect precipitation.*

Table III—Composition of Diazepam and Alprazolam Injectable Formulations

Component	Diazepam	Alprazolam
Active ingredient	5.0 mg/ml	1.0 mg/ml
Benzyl alcohol	1.5%	—
Sodium benzoate–benzoic acid	5.0%	—
Ethanol	10%	—
Propylene glycol	40%	55%

As stated, both concentration lines fall below the solubility curve at high dilution. This indicates that any formed precipitate would redissolve on further dilution. It does not, however, give any indication as to the rapidity of the redissolution. In fact, this step is usually very slow. Therefore, it is not advisable to rely on redissolution as a means of avoiding precipitation.

Using the aforementioned technique, it is possible to estimate the precipitation potential of a drug on the basis of its solubility in water and in the cosolvents used. However, these estimates are based on equilibrium data and do not account for kinetic factors, such as crystal growth rate, fluid (or blood) flow rate, and injection rate. (The last two parameters determine the formulation dilution rate.) A more meaningful assessment of precipitation potential requires a dynamic system in which the above factors are controlled to the greatest extent possible.

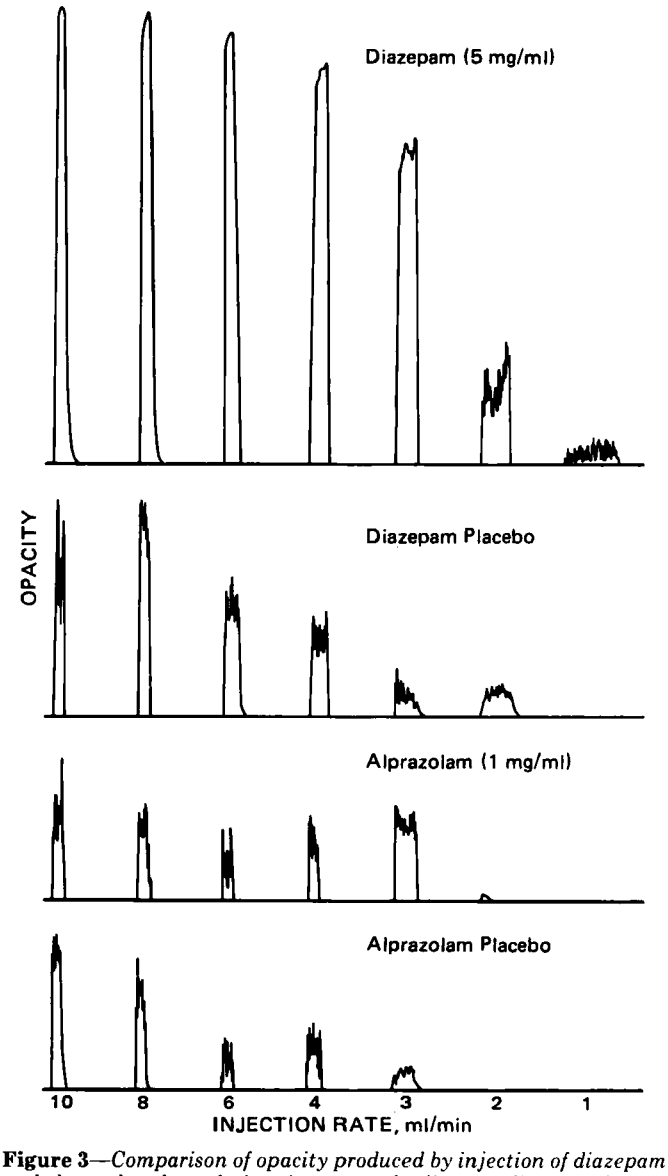

Figure 3—*Comparison of opacity produced by injection of diazepam and alprazolam formulations into normal saline at a distance of 15 cm from the flow cell.*

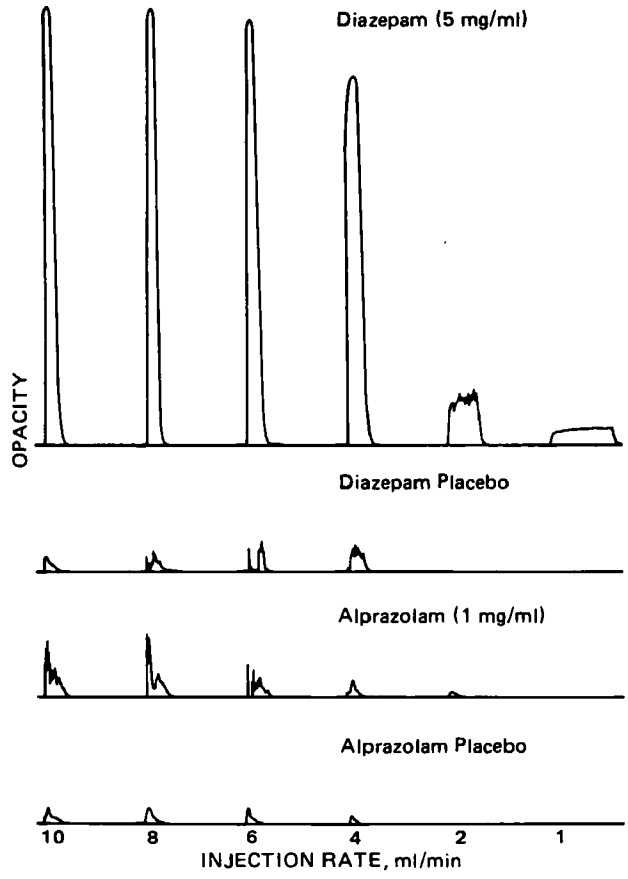

Figure 4—*Comparison of opacity produced by injection of diazepam and alprazolam formulations into normal saline at a distance of 30 cm from the flow cell.*

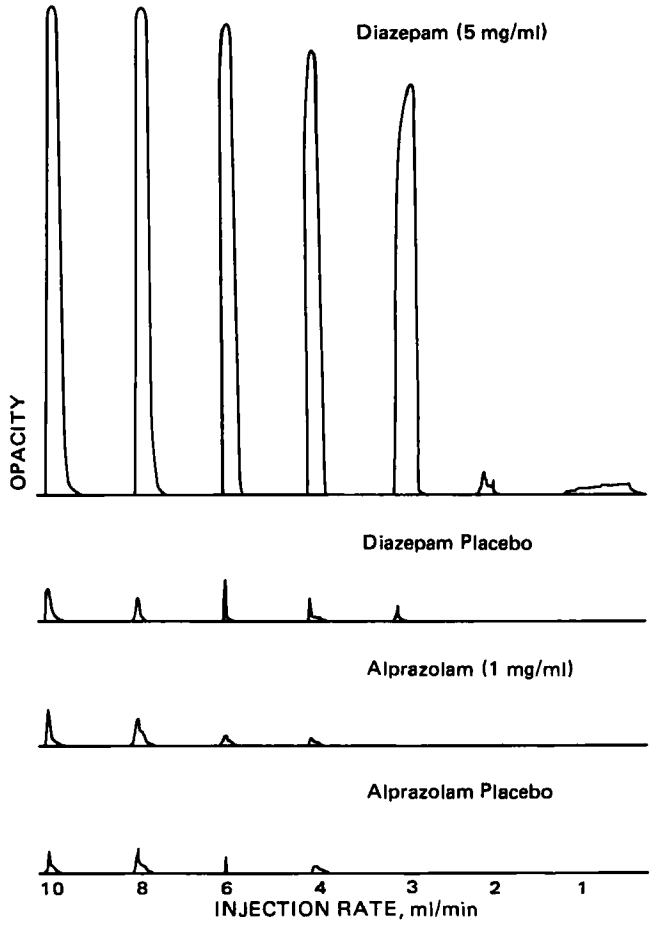

Figure 5—*Comparison of opacity produced by injection of diazepam and alprazolam formulations into normal saline at a distance of 45 cm from the flow cell.*

In this report a simple laboratory experiment is described that provides a semiquantitative evaluation of precipitation formation in a dynamic system. This is used to determine the effect of injection rate on precipitation and to compare parenteral formulations of the antianxiety drugs diazepam[1] and alprazolam[2]. Some of the important physicochemical properties of both drugs are presented in Table II.

This type of experiment is not intended to replace *in vivo* testing. It can, however, provide an early warning as to whether a precipitation problem should be anticipated.

EXPERIMENTAL

Methods—The apparatus used in this study is shown schematically in Fig. 2. It was developed to provide a reasonable simulation of the events that occur when a drug formulation solubilized with a cosolvent is injected into the venous system or into an intravenous drip tube.

A peristaltic pump provided flow of an aqueous phase at a rate of 30 ml/min through a 2.50-mm tube and a 2.0-mm quartz flow cell. The aqueous phases used were 0.9% sodium chloride (normal saline) in distilled water and 5.0% dextrose in deionized water (D5W). Drug formulation or placebo solution was injected into the tubing through a 20-gauge needle inserted 15, 30, or 45 cm upstream of the flow cell. A syringe pump[3] was used to control the rate of drug injection. The injection rate varied from 1.0 to 10 ml/min, but the total volume injected was kept constant at 1.0 ml. Injection rates of 10, 8, 6, 4, 3, 2, and 1 ml/min were attained by injecting 1 ml of solution in 6.0, 7.5, 10, 15, 20, 30, and 60 sec, respectively. The appearance of drug precipitate was detected by measuring the optical transmittance through the flow cell in a spectrophotometer. For both diazepam and alprazolam formulations, any absorption at 400 nm was attributed to the opacity caused by the passage of precipitate through the flow cell. Changes in absorbance were monitored on a strip-chart recorder (see *Results*). This study was conducted at room temperature (20–23°).

Materials—The sodium chloride, dextrose, propylene glycol, ethanol, sodium benzoate, benzoic acid, benzyl alcohol, and distilled water were USP quality and were obtained from commercial sources. Alprazolam injectable was prepared by dissolving the drug in propylene glycol and then adding the required quantity of water. Diazepam injectable[4] was purchased. The composition of the diazepam and alprazolam injectable formulations are given in Table III.

RESULTS

The recorder tracings generated by injecting diazepam and alprazolam formulations and their respective placebos into normal saline at distances of 15, 30, and 45 cm from the flow cell are shown in Figs. 3, 4, and 5, respectively. Those obtained by injecting the same formulations into D5W at a distance of 30 cm from the flow cell are shown in Fig. 6.

Replacing the following aqueous fluid with diazepam vehicle and injecting diazepam formulation produced no opacity under any of the above conditions. Likewise, injecting alprazolam into its own vehicle under the above conditions produced no opacity.

It is clear from Figs. 4 and 6 that there is no significant difference between the results obtained in normal saline at 30 cm and the results obtained in D5W at the same distance. Changing the tubing diameter had no significant effect on the opacity observed. Changing the rate of flow of the fluid into which the formulations were injected produced an effect similar to changing the distance from the injection site to the flow cell. The following trends are apparent in each of Figs. 3–6:

1. Short distances between the injection site and the flow cell tend to produce higher opacity readings.
2. The faster the injection rate, the greater the opacity.
3. The diazepam formulations show the greatest degree of opacity under all tested conditions.

[1] Valium; Roche, P.R.
[2] Xanax; The Upjohn Co., Kalamazoo, Mich.
[3] Sage.
[4] Valium Injectable; Roche, P.R.

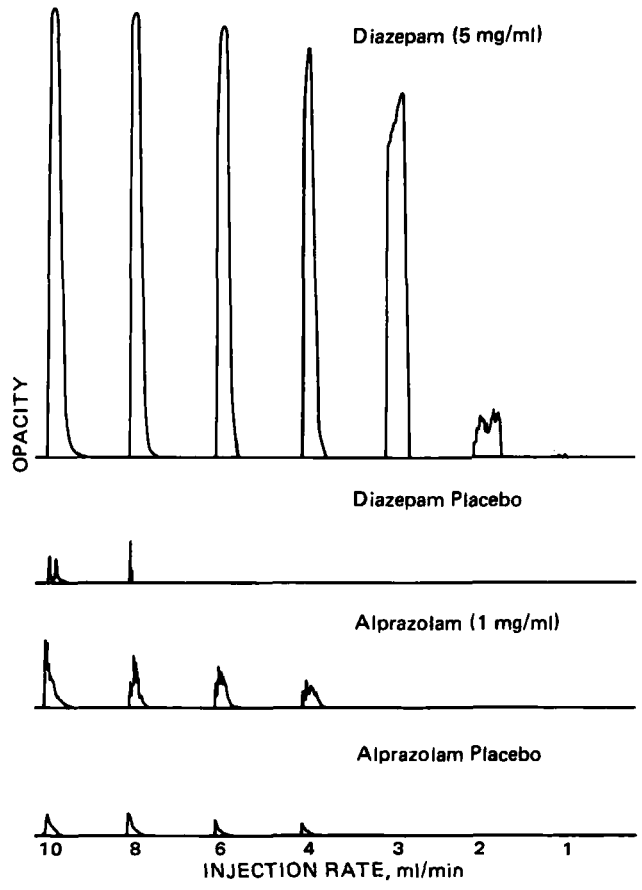

Figure 6—*Comparison of opacity produced by injection of diazepam and alprazolam formulations into 5% dextrose at a distance of 30 cm from the flow cell.*

DISCUSSION

Distance from Injection Site—In all cases, the placebo formulations produced little or no opacity when injected at distances of 30 and 45 cm from the flow cell. At 15 cm, however, the more rapid injection rates produced measurable changes in the transmission of light through the cell. Since the placebo formulations contained no material that is insoluble in the flowing aqueous fluid, the apparent opacity cannot be due to precipitation. The decrease in light transmission through the flow cell after rapid injection of placebo formulations at short distances is due to Schlieren patterns. These wavy patterns form when two liquids of different refractive indices are partially mixed; scattering light and, thus, reducing transmission. They are less prevalent at longer distances, which provide more time for the liquids to mix completely before passing through the flow cell. (This effect can be easily demonstrated by adding glycerin or propylene glycol to water. At first there are striations of Schlieren patterns in the mixture. As mixing progresses, these patterns disappear and the solution becomes clear.)

Injection Rate—Under all of the conditions considered, no opacity was produced when the formulations were injected at a rate <1.0 ml/min. At this slow rate of addition, the formulation is diluted very rapidly by the flowing aqueous phase. At more rapid injection rates, the formulation is diluted more slowly. The dilution ratio is equal to the rate of injection divided by the rate of flow of the aqueous fluid. If the formulation is injected at a rate of 1.0 ml/min and the fluid flowrate is 30 ml/min, the dilution ratio is equal to 30; if the injection rate is increased 10-fold, the dilution ratio is reduced 10-fold (to 3.0). When the dilution ratio is large and the dilution is rapid, there is little time for nucleation and crystal growth and, thus, less likelihood of precipitation. Rapid injection and the accompanying slow dilution provide more time for the formation and growth of crystal nuclei.

An additional explanation for the effect of injection rate on the amount of precipitate formation is as follows. The segment or plug of fluid containing the injected formulation tends to remain more or less intact as it flows through the tube to the flow cell: there is only poor lateral mixing in the narrow tube. The magnitude of precipitation in the plug of diluted formulation will depend on the degree of supersaturation in the plug. If the plug is highly supersaturated, the potential for precipitation is greater than if the drug concentration is only slightly above its solubility. Of course, if the concentration of drug in the plug is below the solubility limit, there is no potential for precipitation. This ideal situation is achieved when the drug is injected very slowly and the dilution ratio is very large. These results clearly show the advantage of slow intravenous administration of solubilized drugs.

Comparison of Diazepam and Alprazolam—It is obvious from Figs. 3–6 that diazepam has a high tendency to precipitate when injected, and that alprazolam shows little or no tendency to precipitate. This is not due to differences in pK_a (Table II) since both drugs are essentially completely un-ionized at physiological pH. The difference results from a combination of several factors: (*a*) the concentration of diazepam is much higher than that of alprazolam in the injection formulations, (*b*) diazepam is less soluble in water than alprazolam, and (*c*) the formulation of diazepam studied does not have excess cosolvent (as does the alprazolam formulation). This *in vitro* study indicates that formulation of a solubilized drug should be designed so that the solubility of the drug is not exceeded as it comes into contact with an aqueous environment. Based on the results of this study, excess cosolvent should be added to protect the drug against the solubility-reducing effect of the aqueous medium into which it is injected.

REFERENCES

(1) S. H. Yalkowsky in "Techniques of Solubilization of Drugs," S. H. Yalkowsky, Ed., Dekker, New York, N.Y., 1981, Chap. 1.

(2) S. H. Yalkowsky and S. C. Valvani, *Drug Intell. Clin. Pharm.*, **11**, 417 (1977).

(3) M. E. Morris, *Am. J. Hosp. Pharm.*, **35**, 669 (1978).

(4) K. Korttila, A. Sothman, and P. Anderson, *Acta. Pharm. Toxicol.*, **39**, 104 (1976).

(5) D. E. Langdon, J. R. Harlem, and R. L. Bailey, *J. Am. Med. Assoc.*, **223**, 184 (1973).

(6) C. W. Graham, R. P. Pagano, and R. L. Katz, *Curr. Res. Anesth. Analg.*, **56**, 409 (1977).

(7) H. G. Schroeder and P. P. DeLuca, *Bull. Parenter. Drug Assoc.*, **28**, 1 (1974).

(8) S. H. Yalkowsky, S. C. Valvani, and G. L. Amidon, *J. Pharm. Sci.*, **65**, 1488 (1976).

(9) S. H. Yalkowsky and T. J. Roseman, in "Techniques of Solubilization of Drugs," S. H. Yalkowsky, Ed., Dekker, New York, N.Y., 1981, Chap. 3.

Determination of Phenylpropanolamine in Serum and Urine by High-Performance Liquid Chromatography

R. DOWSE, J. M. HAIGH, and I. KANFER ˣ

Received June 18, 1982, from the *School of Pharmaceutical Sciences, Rhodes University, Grahamstown 6140, South Africa.* Accepted for publication August 13, 1982.

Abstract □ A high-performance liquid chromatographic analysis of phenylpropanolamine in human serum and urine without prior derivatization is presented. Using direct UV detection the method is sufficiently sensitive to detect 25 ng of drug/ml of serum or urine; the coefficients of variation at 25 ng/ml and 500 ng/ml were 5.16 and 2.12, respectively, in serum. The method involves serum and urine extraction at a basic pH with chloroform, a single back-extraction, and chromatography on a reverse-phase column. Serum and urine data following administration of a single 150-mg sustained-release tablet of phenylpropanolamine hydrochloride in six healthy volunteers demonstrates the suitability of the analytical method.

Keyphrases □ Phenylpropanolamine—determination by high-performance liquid chromatography without prior derivatization, human serum and urine □ High-performance liquid chromatography—phenylpropanolamine, determination in human serum and urine without prior derivatization

Phenylpropanolamine, a sympathomimetic amine, used to relieve congestion of the nasal mucosa and sinuses in the treatment of colds, sinusitus, rhinitis, and hay fever is also used as an appetite suppressant (1). Phenylpropanolamine has been determined in plasma by GLC following derivatization with pentafluorobenzaldehyde (2) and also as the heptafluorobutyryl derivative (3). Urine phenylpropanolamine levels have been analyzed by nitrogen-selective GLC (4, 5). High-performance liquid chromatography (HPLC) has been used for the determination of phenylpropanolamine alone and in pharmaceutical formulations (6–11), but little information has appeared on the HPLC analysis of phenylpropanolamine in biological fluids (12, 13).

Endo *et al.* (12) used a color reaction with sodium β-naphthoquinone-4-sulfonate after extraction from alkaline urine to determine phenylpropanolamine by HPLC, but this method is time consuming and no indication is given as to the levels of phenylpropanolamine determined. The HPLC method described by Mason and Amick (13) involved extraction from plasma, back-extraction, and *o*-phthalicdicarboxaldehyde derivatization after which fluorescence detection was used to determine concentrations of phenylpropanolamine as low as 5 ng/ml.

The purpose of this study was to develop a sensitive, reproducible, and rapid method to determine phenylpropanolamine in serum and urine without prior derivatization.

EXPERIMENTAL

Apparatus—The modular high-performance liquid chromatograph consisted of a constant-flow pump[1], an automated sample injector[2], a variable-wavelength UV detector[3], and a data module[4]. The separation was performed on a 30-cm × 4-mm i.d. column containing microparticulate-bonded (10-μm) octadecylsilane material[5]. The temperature of the column was maintained at 20° [6].

Reagents and Materials—Reagents were of at least analytical reagent grade quality and the acetonitrile[7] was distilled in glass. Phenylpropanolamine hydrochloride[8], ephedrine hydrochloride[9], chloroform[10], and sodium 1-heptanesulfonate[11] were obtained commercially. Water was deionized and then double-distilled in glass.

Chromatographic Conditions—The mobile phase was prepared by mixing acetonitrile (250 ml) with a 0.005 *M* solution of sodium 1-heptanesulfonate in water (750 ml) and adding 1 *M* HCl (2 ml). The solvent mixture (pH 2.5) was deaerated and filtered through a 0.6-μm filter[12]. This mobile phase was used at a flow rate of 1.3 ml/min for the analysis of both serum and urine samples, with a resulting pressure of 230 bar. The wavelength of detection was 220 nm.

Extraction—*Serum*—One milliliter of serum, 1 ml ephedrine hydrochloride solution (0.24 μg/ml), and 50 μl of a saturated solution of sodium carbonate, which adjusted the pH of the mixture to 10, were vortexed for 15 sec in a test tube[13] (16 × 100 mm). Five milliliters of chloroform were added and the tube was stoppered, vortexed for 1 min, and centrifuged at 2000×*g* for 5 min. A plug formed between the aqueous and organic phases, and the aqueous layer above this plug was removed by aspiration and discarded. A pasteur pipet was used to transfer the chloroform extract to a tapered centrifuge tube containing 100 μl of 5% (v/v) acetic acid. The pipet was rinsed with 2 ml of chloroform, which was then added to the original test tube, vortexed for 30 sec, and centrifuged at 2000×*g* for 5 min. The chloroform washings were added to the tapered centrifuge tube, vortexed for 1 min, and centrifuged at 600×*g* for an additional minute. The chloroform layer was reduced by aspiration to ~200 μl and discarded, and the tube was again centrifuged at 2000×*g* for 5 min.

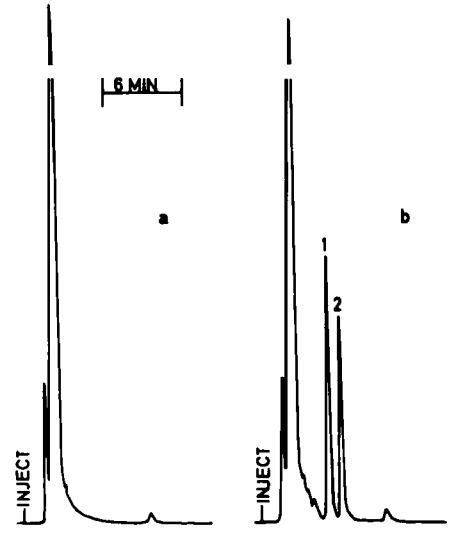

Figure 1—*HPLC chromatograms of (a) blank serum extract and (b) an extract of serum containing phenylpropanolamine (1) and ephedrine (2).*

[1] Model M6000A, Waters Associates, Milford, Mass.
[2] WISP model 710B, Waters Associates, Milford, Mass.
[3] Model LC3, Pye Unicam, Cambridge, England.
[4] Model 730, Waters Associates, Milford, Mass.
[5] μ-Bondapak C_{18}, Waters Associates, Milford, Mass.
[6] Model LC-22 Temperature Controller, Bioanalytical Systems Inc., West Lafayette, Ind.
[7] UV grade, Waters Associates, Milford, Mass.
[8] Chamberlains (Pty) Ltd., Cape Town, South Africa.
[9] E. Merck, Darmstadt, West Germany.
[10] B. D. H. Chemicals, Poole, England.
[11] Aldrich Chemical Co., Milwaukee, Wis.
[12] Type BD, Millipore Corp., Bedford, Mass.
[13] Vacutainer, Becton, Dickinson and Co., Rutherford, N.J.

0022-3549/83/0900-1018$01.00/0

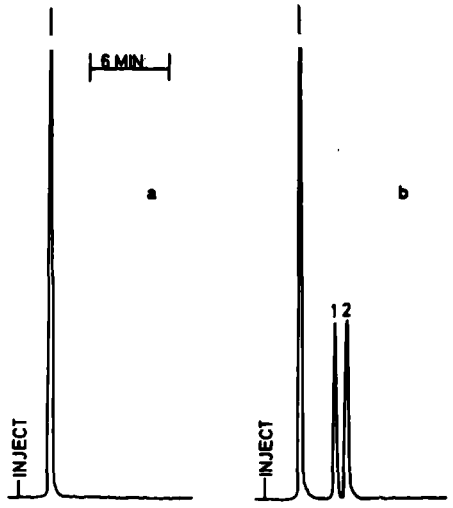

Figure 2—*HPLC chromatograms of (a) blank urine extract and (b) an extract of urine containing phenylpropanolamine (1) and ephedrine (2).*

Aliquots of 15–30 μl of the acetic acid extract were injected directly onto the column. Typical chromatograms are depicted in Fig. 1.

Urine—To 1 ml of urine in a test tube were added an aqueous solution of 1 ml of ephedrine hydrochloride (40 μg/ml) and 50 μl of a saturated solution of sodium carbonate (to adjust the pH to 10). The tube was vortexed for 15 sec, 5 ml of chloroform was added, and the tube was stoppered and vortexed again for 1 min. After centrifugation at 2000×*g* for 5 min, the chloroform extract was transferred with a pasteur pipet to a tapered centrifuge tube containing 1 ml of 5% (v/v) acetic acid. The pipet was rinsed with 2 ml of chloroform, which was then added to the original tube, vortexed for 30 sec, and centrifuged at 2000×*g* for 5 min. The chloroform washings were added to the centrifuge tube, vortexed for 1 minute and centrifuged at 2000×*g* for 5 min. Aliquots of 1–8 μl of the upper acetic acid extract were injected onto the column. Typical chromatograms are depicted in Fig. 2.

Clinical Study—As part of a bioavailability study, six normal healthy volunteers each received one sustained-release tablet containing 150 mg of phenylpropanolamine hydrochloride following an overnight fast. Blood samples were drawn at 0, 0.5, 1, 1.5, 2, 3, 4, 5, 6, 8, 9, 10, 12, and 24 hr after ingestion of the medication; the serum was separated by centrifugation and frozen until assayed. Urine samples were collected at 0, 2, 4, 6, 8, 12, and 24 hr, and representative samples were frozen until analysis. Urine voided at times other than those specified above was collected and treated in the same manner.

RESULTS

Linearity—Calibration curves using five different concentrations of phenylpropanolamine in serum and urine, obtained by plotting the ratio of the peak height of phenylpropanolamine to that of the internal standard (ephedrine) *versus* their respective concentrations, were linear over the concentration ranges studied. The calibration curve in serum (25–500 ng/ml) had a slope of 0.0039 and a *y*-intercept of 0.0509 with a correlation coefficient of 0.9997, while the curve in urine (10–200 μg/ml) had a slope of 0.0265 and a *y*-intercept of 0.0386 with a correlation coefficient of 0.9999.

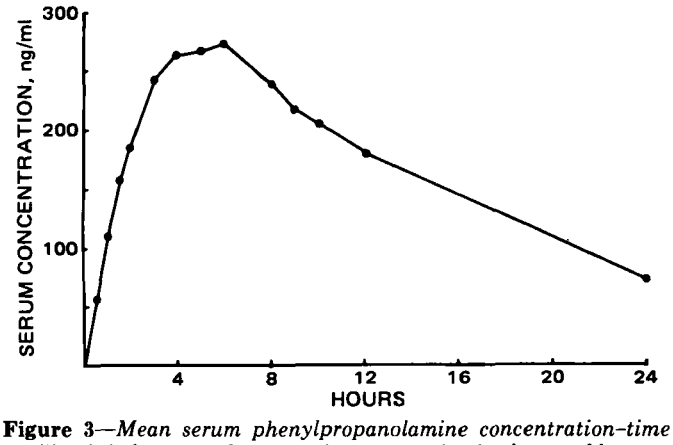

Figure 3—*Mean serum phenylpropanolamine concentration–time profile of six human volunteers given a sustained-release tablet containing 150 mg of drug.*

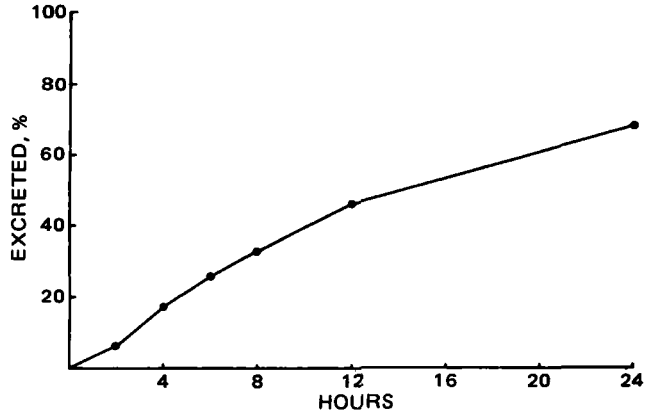

Figure 4—*Mean cumulative urinary phenylpropanolamine concentration–time profile of six human volunteers given a sustained-release tablet containing 150 mg of drug.*

Precision and Accuracy—Within-run precision was assessed by extracting five spiked serum and urine samples each at the upper and lower limits of the concentration ranges studied. The coefficients of variation were found to be 5.16% at 25 ng/ml and 2.12% at 500 ng/ml for serum and 1.66% at 10 μg/ml and 0.33% at 100 μg/ml for urine. Corresponding standard deviations for these samples were 1.26 ng/ml, 10.75 ng/ml, 0.155 μg/ml, and 0.324 μg/ml, respectively. Replicate assays in serum and urine samples determined over a period of 3 months (stored at −10°) revealed no significant differences in phenylpropanolamine concentrations.

Extraction Efficiency—Spiked serum and urine samples were assayed in triplicate at four different concentrations. All samples were extracted as described previously except that the internal standard was added as a final step to each extract. The results were compared with those obtained from the injection of equivalent concentrations of phenylpropanolamine in the internal standard solution. Mean values of 80.39 and 80.20% recovery were obtained for phenylpropanolamine from serum and urine, respectively.

Sensitivity and Detection Limit—Under the conditions of this assay, the detection limit for phenylpropanolamine was 25 ng/ml in serum and 10 μg/ml in urine. These lower limits can be extended, particularly in the case of urine, if smaller volumes of 5% (v/v) acetic acid are used in the back-extraction step.

Serum and Urine Profiles—The mean serum concentration–time profile is presented in Fig. 3. Figure 4 represents the cumulative urinary excretion profile for the six subjects who received one sustained-release tablet containing phenylpropanolamine hydrochloride (150 mg).

DISCUSSION

The method described involved a rapid, relatively simple extraction of phenylpropanolamine from urine and serum. Previous HPLC methods used to determine this drug in biological fluids have involved either derivatization with *o*-phthalicdicarboxaldehyde followed by fluorescence detection (13) or the use of a normal-phase column followed by reaction with sodium β-naphthoquinone-4-sulfonate and subsequent colorimetric determination (12). The latter method was applied to urinalysis only, and concentrations relating specifically to phenylpropanolamine were not reported. Both these methods are relatively time consuming and involve postcolumn manipulations.

Our method eliminates the derivatization step, thus allowing direct determination using a variable-wavelength UV detector. The method is sufficiently sensitive, accurate, and precise for the monitoring of phenylpropanolamine concentrations in small volumes of both serum and urine following oral doses of the drug. In addition, the resulting chromatograms are clean with no interfering peaks due to endogenous constituents. Metabolite interference did not present a problem since no significant metabolism of phenylpropanolamine occurs (14). Retention times of phenylpropanolamine and ephedrine were 4.8 min and 5.7 min,

respectively. In summary, the HPLC method presented here is rapid, precise, and extremely suitable for the determination of phenylpropanolamine in serum and urine.

REFERENCES

(1) "Remington's Pharmaceutical Sciences," 15th ed., Mack Publishing Co., Easton, Pa., 1975, p. 820.

(2) L. Neelakantan and H. B. Kostenbauder, *J. Pharm. Sci.*, **65**, 740 (1976).

(3) L. M. Cummins and M. J. Fourier, *Anal. Lett.*, **2**, 403 (1969).

(4) H. Kinsun, M. A. Moulin, and E. C. Savini, *J. Pharm. Sci.*, **67**, 118 (1978).

(5) E. Appel, *Eur. J. Clin. Pharmacol.*, **8**, 161 (1975).

(6) T. L. Sprieck, *J. Pharm. Sci.*, **63**, 591 (1974).

(7) V. Das Gupta and A. G. Ghanekar, *J. Pharm. Sci.*, **66**, 895 (1977).

(8) T. R. Koziol, J. T. Jacob, and R. G. Achari, *J. Pharm. Sci.*, **68**, 1135 (1979).

(9) A. G. Ghanekar and V. Das Gupta, *J. Pharm. Sci.*, **67**, 873 (1978).

(10) "Over the Counter Cough/Cold Remedies," L. C. du Pont, Technical Report, E 32022.

(11) "Analysis of Pharmaceutical Products," Waters Associates, Publication N68, 1976, p. 11.

(12) M. Endo, H. Imamichi, M. Moriyasu, and Y. Hashimoto, *J. Chromatogr.*, **196**, 334 (1980).

(13) W. D. Mason and E. N. Amick, *J. Pharm. Sci.*, **70**, 707 (1981).

(14) J. E. Sinsheimer, I. G. During, and R. T. Williams, *Biochem. J.*, **136**, 763 (1973).

ACKNOWLEDGMENTS

The authors gratefully acknowledge financial support from the South African Council for Scientific and Industrial Research.

High-Performance Liquid Chromatographic Determination of Aspirin and Its Metabolites in Plasma and Urine

SHAMSUL K. BAKAR and SARFARAZ NIAZI ˣ

Received December 3, 1981, from the *Department of Pharmacodynamics, College of Pharmacy, University of Illinois Health Sciences Center, Chicago, IL 60612.* Accepted for publication February 25, 1982.

Abstract □ A simple quantitative method for the rapid determination of aspirin and its metabolites, salicylic acid, salicyluric acid, and gentisic acid, in plasma and urine using *o*-toluic and *o*-anisic acids, respectively, as internal standards was developed. Plasma proteins were precipitated by the addition of acetonitrile and, after centrifugation, the supernatant fluid was injected directly onto a reverse-phase column. The mobile phase consisted of an isocratic mixture of water, methanol, and glacial acetic acid (64:35:1, v/v/v) and the separated components were detected at 238 nm using a UV detector. Concentrations ≥0.5 μg/ml could be quantitated for aspirin or its metabolites in plasma. The peak heights and peak height ratios to the internal standard, *o*-toluic acid, were linear for the concentration range of 0.5–200 μg/ml. The aspirin metabolites in urine were isolated by extracting the acidified urine with ether and then reextracting the material into an aqueous buffer solution at pH 7.0. Twenty microliters of the buffer extract was directly injected onto the column. The separated components were detected and quantitated at 305 nm. Concentrations ≥5 μg/ml of salicyluric acid, salicylic acid, and gentisic acid could be determined accurately. The peak heights and peak height ratios to the internal standard, *o*-anisic acid, were found to be linear for the concentration range of 5–200 μg/ml in urine.

Keyphrases □ Salicylates—aspirin and metabolites, quantitation in urine and plasma, high-performance liquid chromatography □ Metabolites—of aspirin, quantitation in urine and plasma, high-performance liquid chromatography □ High-performance liquid chromatography—quantitation of aspirin and metabolites, urine and plasma

Aspirin is one of the most extensively used drugs. Recently, the importance of monitoring plasma levels of salicylates has been reviewed (1). A number of high-performance liquid chromatographic (HPLC) methods for the analysis of aspirin and its metabolites in plasma and urine have been reported (2–7). Few of the reported methods (3, 6) can determine aspirin in plasma, and they employ time-consuming extraction procedures. Since aspirin is rapidly hydrolyzed in blood and plasma (8), extraction procedures which delay the analysis of the sample will yield inaccurate results, underestimating the quantity of aspirin. Therefore, this work was initiated to develop a method for the rapid analysis of plasma samples for aspirin, salicylic acid, salicyluric acid, and gentisic acid, which does not require an extraction step.

The analysis of urine for the metabolites of aspirin using a simple extraction procedure is also desirable since urine usually contains a large number of acidic components (9, 10). Better results are obtained by eliminating as many undesirable components from the sample as possible before analysis. Injecting the urine onto a column without extraction (7, 11) shortens the useful life of the chromatography column.

EXPERIMENTAL

Materials—Aspirin USP[1], salicylic acid[1], salicyluric acid[1], gentisic acid[1], *o*-toluic acid[1], *o*-anisic acid[1], glacial acetic acid[2], anhydrous ether[3], acetonitrile[4], and methanol[4] were obtained commercially. The mobile phase consisted of water–methanol–glacial acetic acid (64:35:1, v/v/v), filtered and deaerated under reduced pressure.

Instrumentation—A dual-pump high-performance liquid chromatograph[5] equipped with a variable-wavelength UV detector[6], a 20-μl loop injector[7], and a reverse-phase microparticulate column[8] was used. The UV detector was connected to a linear recorder[9].

Stock Solutions—For the standard curves in plasma, aspirin, salicylic acid, salicyluric acid, and gentisic acid were singly dissolved in water–

[1] Aldrich Chemical Co., Milwaukee, Wis.
[2] J. T. Baker Chemical Co., Phillipsburg, N.J.
[3] Mallinckrodt, St. Louis, Mo.
[4] Burdick and Jackson Laboratories, Muskegon, Mich.
[5] Perkin-Elmer Series 2 High-Pressure Liquid Chromatograph, Perkin-Elmer, Norwalk, Conn.
[6] Model LC-55 Variable Wavelength Detector, Perkin-Elmer, Norwalk, Conn.
[7] Model 7125 Rheodyne, Berkeley, Calif.
[8] μBondapak C_{18} column, Waters Associates, Milford, Mass.
[9] Linear Instruments, Model 261/MM, Irvine, Calif.

0022-3549/83/0900-1020$01.00/0

respectively. In summary, the HPLC method presented here is rapid, precise, and extremely suitable for the determination of phenylpropanolamine in serum and urine.

REFERENCES

(1) "Remington's Pharmaceutical Sciences," 15th ed., Mack Publishing Co., Easton, Pa., 1975, p. 820.

(2) L. Neelakantan and H. B. Kostenbauder, *J. Pharm. Sci.*, **65**, 740 (1976).

(3) L. M. Cummins and M. J. Fourier, *Anal. Lett.*, **2**, 403 (1969).

(4) H. Kinsun, M. A. Moulin, and E. C. Savini, *J. Pharm. Sci.*, **67**, 118 (1978).

(5) E. Appel, *Eur. J. Clin. Pharmacol.*, **8**, 161 (1975).

(6) T. L. Sprieck, *J. Pharm. Sci.*, **63**, 591 (1974).

(7) V. Das Gupta and A. G. Ghanekar, *J. Pharm. Sci.*, **66**, 895 (1977).

(8) T. R. Koziol, J. T. Jacob, and R. G. Achari, *J. Pharm. Sci.*, **68**, 1135 (1979).

(9) A. G. Ghanekar and V. Das Gupta, *J. Pharm. Sci.*, **67**, 873 (1978).

(10) "Over the Counter Cough/Cold Remedies," L. C. du Pont, Technical Report, E 32022.

(11) "Analysis of Pharmaceutical Products," Waters Associates, Publication N68, 1976, p. 11.

(12) M. Endo, H. Imamichi, M. Moriyasu, and Y. Hashimoto, *J. Chromatogr.*, **196**, 334 (1980).

(13) W. D. Mason and E. N. Amick, *J. Pharm. Sci.*, **70**, 707 (1981).

(14) J. E. Sinsheimer, I. G. During, and R. T. Williams, *Biochem. J.*, **136**, 763 (1973).

ACKNOWLEDGMENTS

The authors gratefully acknowledge financial support from the South African Council for Scientific and Industrial Research.

High-Performance Liquid Chromatographic Determination of Aspirin and Its Metabolites in Plasma and Urine

SHAMSUL K. BAKAR and SARFARAZ NIAZI ˣ

Received December 3, 1981, from the *Department of Pharmacodynamics, College of Pharmacy, University of Illinois Health Sciences Center, Chicago, IL 60612.* Accepted for publication February 25, 1982.

Abstract □ A simple quantitative method for the rapid determination of aspirin and its metabolites, salicylic acid, salicyluric acid, and gentisic acid, in plasma and urine using *o*-toluic and *o*-anisic acids, respectively, as internal standards was developed. Plasma proteins were precipitated by the addition of acetonitrile and, after centrifugation, the supernatant fluid was injected directly onto a reverse-phase column. The mobile phase consisted of an isocratic mixture of water, methanol, and glacial acetic acid (64:35:1, v/v/v) and the separated components were detected at 238 nm using a UV detector. Concentrations ≥0.5 μg/ml could be quantitated for aspirin or its metabolites in plasma. The peak heights and peak height ratios to the internal standard, *o*-toluic acid, were linear for the concentration range of 0.5–200 μg/ml. The aspirin metabolites in urine were isolated by extracting the acidified urine with ether and then reextracting the material into an aqueous buffer solution at pH 7.0. Twenty microliters of the buffer extract was directly injected onto the column. The separated components were detected and quantitated at 305 nm. Concentrations ≥5 μg/ml of salicyluric acid, salicylic acid, and gentisic acid could be determined accurately. The peak heights and peak height ratios to the internal standard, *o*-anisic acid, were found to be linear for the concentration range of 5–200 μg/ml in urine.

Keyphrases □ Salicylates—aspirin and metabolites, quantitation in urine and plasma, high-performance liquid chromatography □ Metabolites—of aspirin, quantitation in urine and plasma, high-performance liquid chromatography □ High-performance liquid chromatography—quantitation of aspirin and metabolites, urine and plasma

Aspirin is one of the most extensively used drugs. Recently, the importance of monitoring plasma levels of salicylates has been reviewed (1). A number of high-performance liquid chromatographic (HPLC) methods for the analysis of aspirin and its metabolites in plasma and urine have been reported (2–7). Few of the reported methods (3, 6) can determine aspirin in plasma, and they employ time-consuming extraction procedures. Since aspirin is rapidly hydrolyzed in blood and plasma (8), extraction procedures which delay the analysis of the sample will yield inaccurate results, underestimating the quantity of aspirin. Therefore, this work was initiated to develop a method for the rapid analysis of plasma samples for aspirin, salicylic acid, salicyluric acid, and gentisic acid, which does not require an extraction step.

The analysis of urine for the metabolites of aspirin using a simple extraction procedure is also desirable since urine usually contains a large number of acidic components (9, 10). Better results are obtained by eliminating as many undesirable components from the sample as possible before analysis. Injecting the urine onto a column without extraction (7, 11) shortens the useful life of the chromatography column.

EXPERIMENTAL

Materials—Aspirin USP[1], salicylic acid[1], salicyluric acid[1], gentisic acid[1], *o*-toluic acid[1], *o*-anisic acid[1], glacial acetic acid[2], anhydrous ether[3], acetonitrile[4], and methanol[4] were obtained commercially. The mobile phase consisted of water–methanol–glacial acetic acid (64:35:1, v/v/v), filtered and deaerated under reduced pressure.

Instrumentation—A dual-pump high-performance liquid chromatograph[5] equipped with a variable-wavelength UV detector[6], a 20-μl loop injector[7], and a reverse-phase microparticulate column[8] was used. The UV detector was connected to a linear recorder[9].

Stock Solutions—For the standard curves in plasma, aspirin, salicylic acid, salicyluric acid, and gentisic acid were singly dissolved in water–

[1] Aldrich Chemical Co., Milwaukee, Wis.
[2] J. T. Baker Chemical Co., Phillipsburg, N.J.
[3] Mallinckrodt, St. Louis, Mo.
[4] Burdick and Jackson Laboratories, Muskegon, Mich.
[5] Perkin-Elmer Series 2 High-Pressure Liquid Chromatograph, Perkin-Elmer, Norwalk, Conn.
[6] Model LC-55 Variable Wavelength Detector, Perkin-Elmer, Norwalk, Conn.
[7] Model 7125 Rheodyne, Berkeley, Calif.
[8] μBondapak C_{18} column, Waters Associates, Milford, Mass.
[9] Linear Instruments, Model 261/MM, Irvine, Calif.

0022-3549/83/0900-1020$01.00/0

Table I—Peak Heights and Peak Height Ratios of Aspirin (III) and Its Metabolites Gentisic Acid (I), Salicyluric Acid (II), Salicylic Acid (IV), and the Internal Standard *o*-Toluic Acid (V) in Plasma

Concentration Added, μg/ml					Peak Height					Peak Height Ratio[a]			
I	II	III	IV	V	I	II	III	IV	V	I	II	III	IV
0.5	0.5	0.5	0.5	10.0	3	5	3	3	41	0.07	0.12	0.12	0.07
1.25	1.25	1.25	1.25	10.0	7	12	4	6	42	0.17	0.29	0.10	0.14
2.5	2.5	2.5	2.5	10.0	12	20	7	10	46	0.26	0.43	0.15	0.22
5.0	5.0	5.0	5.0	10.0	24	37	15	25	43	0.56	0.86	0.35	0.58
12.5	12.5	12.5	12.5	10.0	60	89	42	59	44	1.40	2.02	0.95	1.34
25.0	25.0	25.0	25.0	100.0	123	171	87	120	450	2.72	3.80	1.93	2.67
50.0	50.0	50.0	50.0	100.0	246	353	184	255	441	5.58	8.00	4.17	5.78
100.0	100.0	100.0	100.0	100.0	480	670	360	460	436	11.01	15.37	8.26	10.55
200.0	200.0	200.0	200.0	100.0	970	1373	728	983	455	21.32	30.18	16.00	21.60

[a] Peak height of the drug/peak height of the internal standard.

Table II—Peak Heights and Peak Height Ratios of Gentisic Acid (I), Salicyluric Acid (II), Salicylic Acid (IV), and the Internal Standard *o*-Anisic Acid (VI) in Urine

Concentration Added, μg/ml				Peak Height				Peak Height Ratio[a]		
I	II	IV	VI	I	II	IV	VI	I	II	IV
6.0	6.0	6.0	10.0	10	16	9	23	0.43	0.70	0.39
10.0	10.0	10.0	10.0	19	21	14	21	0.90	1.00	0.67
20.0	20.0	20.0	10.0	39	45	33	21	1.86	2.14	1.57
40.0	40.0	40.0	100.0	91	100	79	225	3.57	3.92	3.10
80.0	80.0	80.0	100.0	174	185	150	242	7.19	7.64	6.20
120.0	120.0	120.0	100.0	276	272	219	237	11.65	11.48	9.24
160.0	160.0	160.0	100.0	362	363	301	228	15.88	15.92	13.20
200.0	200.0	200.0	100.0	455	451	372	235	19.36	19.19	15.83

[a] Peak height of the drug/peak height of the internal standard.

Table III—Regression Equations for Aspirin (III) and Its Metabolites Gentisic Acid (I), Salicyluric Acid (II), and Salicylic Acid (IV) in Plasma and Urine

Drug	Peak Height (y) *versus* Concentration (x)[a]	r^b	Peak Height Ratio (y) *versus* Concentration (x)[a]	r^b
		In plasma		
I	$y = 4.8410x + 0.4819$	0.9999	$y = 0.1070x + 0.0703$	0.9999
II	$y = 6.8261x + 2.4129$	0.9999	$y = 0.1509x + 0.1321$	0.9999
III	$y = 3.6457x - 1.9355$	0.9998	$y = 0.0806x - 0.0027$	0.9998
IV	$y = 4.8727x - 1.3624$	0.9995	$y = 0.1077x + 0.0251$	0.9997
		In urine		
I	$y = 2.2980x - 4.4384$	0.9998	$y = 0.0985x - 0.2269$	0.9994
II	$y = 2.2492x + 2.8104$	0.9996	$y = 0.0964x + 0.0873$	0.9996
IV	$y = 1.8771x - 2.1076$	0.9997	$y = 0.0805x - 0.1236$	0.9993

[a] Concentration in μg/ml. [b] Correlation coefficient.

acetonitrile (2:1) to produce solutions with final concentrations of 600 μg/ml. Due to the instability of aspirin in the solution, new solutions were prepared before each analysis. For the standard curves in urine, salicylic acid, salicyluric acid, and gentisic acid were dissolved together in water–acetonitrile (2:1) using a shaker[10] to yield a solution with a final concentration of 500 μg/ml for each of the components. The solution was kept refrigerated to avoid microbial degradation of the salicyluric and salicylic acids.

Internal Standards—The internal standard in plasma, *o*-toluic acid, was dissolved in water–acetonitrile (2:1) to yield solutions with concentrations of 50 and 500 μg/ml. For plasma samples containing 20–200 μg/ml of aspirin, salicylic, salicyluric, and gentisic acids, the concentration of the internal standard was 100 μg/ml; for plasma samples containing <20 μg/ml of the components, the internal standard concentration was 10 μg/ml.

The internal standard for urine, *o*-anisic acid, was dissolved in water to produce a solution with a concentration of 500 μg/ml. When the concentration of salicylic acid and its metabolites in urine was ≥40 μg/ml, the concentration of internal standard used was 100 μg/ml; when the salicylate concentration was <40 μg/ml in urine, the internal standard concentration was 20 μg/ml.

Standard Curves—*Plasma*—To 100 μl of rat plasma in a 500-μl polypropylene microcentrifuge tube[11], stock solution, the internal standard, water, and acetonitrile were added in such proportions that the final volume in each tube was 450 μl (300 μl of acetonitrile and 150 μl of a water–plasma mixture). The concentration of aspirin, salicylic acid, salicyluric acid, and gentisic acid ranged from 0.5 to 200 μg/ml in the water–plasma mixture. The internal standard concentration was 100 μg/ml in the mixture if the aspirin concentration was >20 μg/ml and 10 μg/ml if the aspirin concentration was ≤20 μg/ml.

The contents of the tube were vortexed[12] for 1 min and then centrifuged[13] for 5 min at 15,000 rpm. Twenty microliters of the supernatant was introduced directly onto the column at ambient temperature. The flow rate for the mobile phase was set at 2 ml/min (at 2800 psi), and the chart speed was 1 cm/min. The separated components were monitored at 238 nm, and the responses were recorded at 10 mV with proper attenuation of the recorder. The peak height and peak height ratio for each of the components in plasma were calculated.

For unknown samples, 50 μl of the plasma was precipitated with 100 μl of acetonitrile containing the internal standard in a 500-μl polypropylene microcentrifuge tube. This mixture was vortexed and centrifuged as described above for the standard curve. Twenty microliters was injected onto the column through the loop injector, and the peak height and peak height ratio of the separated components were calculated.

Urine—To 1 ml of urine contained in a 13-mm × 100-mm borosilicate glass culture tube with a polytef-lined screw cap, was added the salicylate

[10] Wrist Action Shaker, Burrell Corp., Pittsburgh, Pa.
[11] Eppendorf Micro Test Tube, Brinkmann Instruments Inc., Westbury, N.Y.
[12] Vortex Genie Mixer, Scientific Products, Evanston, Ill.
[13] Eppendorf Microcentrifuge, Model 5412, Brinkmann Instruments Inc., Westbury, N.Y.

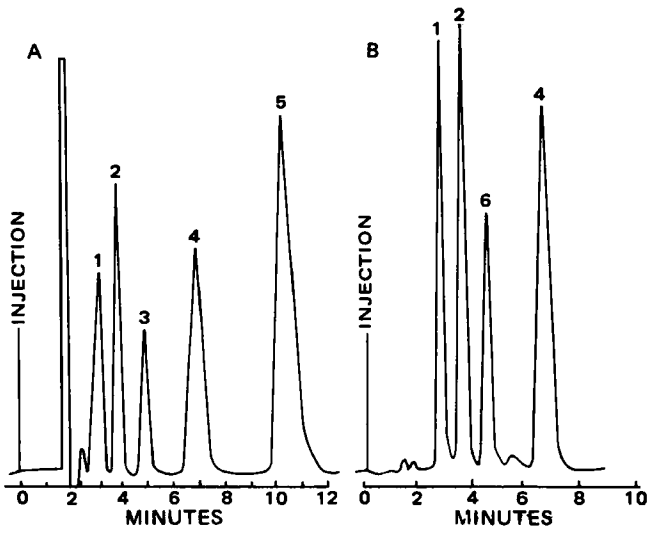

Figure 1—*Chromatograms of salicylic acid in blood (A) and urine (B). Key: (1) gentisic acid; (2) salicyluric acid; (3) aspirin; (4) salicylic acid; (5) o-toluic acid; (6) o-anisic acid. The concentrations for all components are 5 μg/ml in blood and 10 μg/ml in urine.*

mixture in aqueous solution to give concentrations ranging from 5 to 500 μg/ml. The concentration of *o*-anisic acid, the internal standard, was 100 μg/ml of urine when the salicylate concentration was ≥40 μg/ml and 10 μg/ml of urine if the salicylate concentration was <40 μg/ml in urine. One-half milliliter of 6 *N* HCl and 6 ml of anhydrous ether were also added, and the mixture was shaken for 15 min in a shaker and centrifuged for 10 min at 2000 rpm to separate the ether layer from the aqueous layer.

Five milliliters of the ether extract was transferred to another tube, and 1 ml of phosphate buffer (0.1 *M*, pH 7.0; prepared by dissolving 13.61 g of potassium dihydrogen phosphate and 2.38 g of NaOH pellets in water to make 1 liter) was added. The system was shaken for 15 min and then centrifuged at 2000 rpm for 10 min. The ether layer was aspirated, and 20 μl of the aqueous buffer solution was directly injected onto the column under conditions identical to those described earlier for plasma, except that the eluate was monitored at 305 nm.

For the unknown urine samples, 1 ml of urine was acidified with 0.5 ml of 6 *N* HCl. The rest of the procedure was the same as that described above.

Accuracy and Precision Studies—Both the plasma and urine were spiked with aspirin and its metabolites (salicylic acid, salicyluric acid, and gentisic acid) to yield mixtures with concentrations ranging from 25 to 200 μg/ml. Five samples from each of these concentrations were processed appropriately and analyzed as described earlier for the preparation of the standard curves in plasma and urine.

RESULTS AND DISCUSSION

Standard Curves in Plasma and Urine—Figure 1 shows a typical chromatogram of aspirin and its metabolites in spiked plasma and urine. The components were well separated both in plasma and urine. The peaks were identified by their retention times, determined for each component by injecting the compounds individually. Additional identifications were made by injecting different concentrations of the same compound and observing the proportional changes in the peak height and peak height ratio. The retention time for each component was found to be constant at all concentrations, and the values for gentisic acid, salicyluric acid, aspirin, *o*-anisic acid, salicylic acid, and *o*-toluic acid were 3.0, 3.7, 4.8, 5.0, 7.1, and 10.2 min, respectively.

Tables I and II list the peak heights and peak height ratios from the analysis of aspirin and its metabolites in plasma and urine, respectively. Both peak heights and peak height ratios were linear for the concentration range studied in plasma (0.5–200 μg/ml) and in urine (6–200 μg/ml). This was evident from the correlation coefficients (*r*) obtained for the regression line (Table III). The high values of *r* confirmed that there was an excellent linearity between the salicylate concentration and the peak height and peak height ratio, both in plasma and urine.

Recovery Studies in Plasma and Urine—Table IV shows the percent recovery of aspirin and its metabolites in plasma. The percent recoveries are similar at different concentrations. The greatest recovery was of aspirin (99%), followed by salicyluric acid (94%), salicylic acid (91%), and gentisic acid (62%).

It has been reported that salicylic acid and its metabolites, salicyluric acid and gentisic acid, are completely recovered in the aqueous acetonitrile phase following precipitation of plasma with an equal volume of acetonitrile (5). It has also been observed that one volume of acetonitrile is not sufficient to completely precipitate the protein in plasma (12). Preliminary experiments showed that two volumes of acetonitrile, rather than three, were sufficient to precipitate the proteins in plasma. This reduced the dilution of the components in plasma, thus increasing the sensitivity of the analytical method.

Ideally, the entire amount of the salicylates should be present in the plasma–acetonitrile supernatant. But the fact that not all the components were recovered completely from the plasma suggests that there was some kind of binding of the salicylates, especially gentisic acid (~38%), with the precipitated proteins.

The recovery studies with urine samples at different concentrations showed that all the components were equally extracted both from urine and water. When chloroform was used instead of ether, aspirin and salicylic acid were extracted almost completely, but the extraction of gentisic acid and salicyluric acid was poor (<50%). The overall recoveries from the urine using the proposed procedure were calculated to be 97, 95, 92, and 91% for gentisic, salicyluric, *o*-anisic, and salicylic acids, respectively.

Accuracy and Precision Studies in Plasma and Urine—The method proposed here eliminates the necessity of evaporating the organic phase, which is time consuming and involves a number of steps which may result in large variations in the analytical data (3, 6). Since the method described does not involve extraction steps, the variation in the data is considerably decreased; this is reflected by the data in Tables V and VI for plasma and urine, respectively. The low coefficients of variation (*CV*) and the narrow range in each of the concentrations studied suggest that the analytical method is precise and accurate.

This method has little dilution effect since 1 ml of the urine was finally extracted into 1 ml of buffer. In this respect, the method for urine analysis was more sensitive than that for plasma, since the plasma was diluted twice with acetonitrile.

Using this method, some sensitivity is lost because of the selection of 305 nm as the detection wavelength. At this wavelength, the absorptivity of different salicylate metabolites has been found to be less than at 238 nm. However, the latter wavelength cannot be used for urine samples because of numerous endogenous acidic components present in the urine (9, 10) that interfere with the analysis of the salicylate metabolites. At 305 nm the peaks are well separated and the metabolites are detected with sufficient sensitivity.

The proposed method could also be adapted for smaller urine samples (≤100 μl) or urine samples containing submicrogram quantities of aspirin metabolites simply by evaporating the 5 ml of ether extract and dissolving the residue in ~50 μl of the mobile phase.

Selection of Internal Standards—*o*-Anisic acid was used as the in-

Table IV—Recovery Study of Aspirin (III) and Its Metabolites Gentisic Acid (I), Salicyluric Acid (II), and Salicylic Acid (IV) in Plasma and Water

Concentration, μg/ml		Peak Height I	II	III	IV
48.78	Plasma	480	690	360	460
	Water	791	743	365	505
	Recovery, %	60.7	92.9	98.6	91.1
24.39	Plasma	246	353	184	237
	Water	395	376	185	258
	Recovery, %	62.3	93.9	99.5	91.9
12.195	Plasma	123	171	89	120
	Water	197	186	92	136
	Recovery, %	62.5	91.9	96.7	88.2
6.098	Plasma	60	89	42	59
	Water	98	93	41	65
	Recovery, %	61.2	95.7	102.4	90.8
2.439	Plasma	25	37	15	25
	Water	41	39	15	28
	Recovery, %	61.0	94.9	100.0	89.3
1.22	Plasma	13	20	8	13
	Water	21	21	8	14
	Recovery, %	61.9	95.2	100.0	92.9
	Average recovery, %	61.6	94.1	99.5	90.7
	SD	0.7	1.5	1.9	1.7
	CV	1.1	1.6	1.9	1.9

Table V—Accuracy and Precision Studies of the Analysis of Aspirin and Its Metabolites in Plasma

Compound	Concentration Added, μg/ml	Concentration Found[a], μg/ml		
		Mean + *SD*	Range	*CV*, %
Aspirin	25.0	25.02 + 1.04	23.91–26.26	4.2
	50.0	49.98 + 2.25	47.72–53.31	4.5
	100.0	101.47 + 2.53	98.95–104.16	2.5
Salicylic acid	25.0	24.66 + 0.80	24.50–26.70	3.1
	50.0	49.69 + 1.68	49.21–51.33	3.3
	100.0	100.12 + 2.19	97.32–102.68	2.2
Salicyluric acid	25.0	24.66 + 0.80	24.50–26.70	3.1
	50.0	49.69 + 1.68	49.21–51.33	3.3
	100.0	100.12 + 2.19	97.32–102.68	2.2
Gentisic acid	25.0	25.15 + 0.57	24.48–25.79	2.2
	50.0	49.63 + 2.20	46.16–51.58	4.4
	100.0	101.27 + 2.40	98.49–102.88	2.4

[a] $n = 5$.

Table VI—Accuracy and Precision Studies of the Analysis of Aspirin Metabolites in Urine

Compound	Concentration Added, μg/ml	Concentration Found[a], μg/ml		
		Mean + *SD*	Range	*CV*, %
Salicylic acid	40.0	41.37 + 1.14	39.80–42.66	2.9
	120.0	119.55 + 4.05	115.97–125.29	3.4
	200.00	200.23 + 3.49	196.48–204.80	1.8
Salicyluric acid	40.0	39.19 + 0.41	37.20–40.73	3.3
	120.0	120.23 + 1.51	117.49–123.30	2.0
	200.0	200.40 + 4.31	193.14–207.25	2.6
Gentisic acid	40.0	40.6 + 1.27	38.74–41.79	3.4
	120.0	119.54 + 2.30	116.70–122.80	2.0
	200.0	201.04 + 4.54	196.36–205.43	2.3

[a] $n = 5$.

ternal standard in urine. This compound has been used previously as an internal standard in plasma samples (5), but not in urine samples which had been processed by an extraction procedure. However, *o*-anisic acid could not be used for the analysis of aspirin because of the close proximity of their retention times (4.8 and 5.0 min for aspirin and *o*-anisic acid, respectively). This problem was solved by selecting *o*-toluic acid, which has a retention time of 10.2 min, well beyond the peak of salicylic acid. Its absorptivity at 237 nm is comparable with salicylic acid. However, in urine, *o*-anisic acid was used as an internal standard instead of *o*-toluic acid because of the long retention time of the latter.

In HPLC analyses of aspirin metabolites, the peaks for gentisic acid and salicyluric acid frequently overlap (7). In the present study, the mobile phase developed for the analysis was very efficient in separating the peaks for gentisic and salicyluric acids and in preventing the tailing of the salicylic acid peak.

REFERENCES

(1) M. Mandelli and G. Tognani, *Clin. Pharmacokinet.*, **5**, 424 (1980).

(2) C. P. Terweij-Groen, T. Vahlkamp, and J. C. Kraak, *J. Chromatogr.*, **145**, 115 (1978).

(3) G. W. Peng, M. A. F. Gadalla, V. Smith, A. Peng, and W. Chiou, *J. Pharm. Sci.*, **67**, 710 (1978).

(4) I. Bekersky, H. G. Boxenbaum, M. H. Whitson, C. V. Puglisi, R. Pocilinko, and S. A. Kaplan, *Anal. Lett.*, **10**, 539 (1977).

(5) B. E. Cham, D. Johns, F. Bochner, D. M. Imhoff, and M. Rowland, *Clin. Chem.*, **25**, 1420 (1979).

(6) L. I. Harrison, M. L. Funk, and R. E. Ober, *J. Pharm. Sci.*, **69**, 1268 (1980).

(7) D. L. Maulding and J. F. Young, *J. Pharm. Sci.*, **69**, 1224 (1980).

(8) A. M. Morgan and A. B. Truitt, Jr., *J. Pharm. Sci.*, **54**, 1640 (1965).

(9) M. Molnar and C. Horvath, *J. Chromatogr.*, **143**, 391 (1977).

(10) L. D. Mell, Jr., in "Biological/Medical Applications of Liquid Chromatography," vol. 10, G. H. Hawk, Ed., Dekker, New York, N.Y., 1977, pp. 619–636.

(11) B. E. Cham, F. Bochner, D. M. Imhoff, D. Johns, and M. Rowland, *Clin. Chem.*, **26**, 111 (1980).

(12) M. Bernardo, *Clin. Chem.*, **25**, 1861 (1979).

Stability of Aspirin in Different Media

SHAMSUL K. BAKAR and SARFARAZ NIAZI ˣ

Received December 3, 1981, from the *Department of Pharmacodynamics, College of Pharmacy, University of Illinois Health Sciences Center, Chicago, Ill 60612.* Accepted for publication May 12, 1982.

Abstract □ Aspirin rapidly hydrolyzes in various aqueous, organic, and biological media. The purpose of this investigation was to study the decomposition of aspirin in the media that comes in contact with it during analysis in biological fluids for pharmacokinetic studies. These media included water, water–polyethylene glycol 400, water–methanol–acetic acid, phosphate buffer, freshly drawn blood and plasma from control rats and rats deprived of water for 36 hr, and blood precipitated with acetonitrile. Studies were also conducted to determine the decomposition as a function of temperature and pH. Of the various solvent systems studied, aspirin was found most stable in water–polyethylene glycol (4:1, v/v), which provides an excellent medium for preparation of intravenous dosage forms. Phosphate buffer showed significant catalysis of aspirin hydrolysis. A more than fivefold increase in the hydrolysis of aspirin was noted when the temperature was raised to 37° from 22.5°. The hydrolysis of aspirin in rat blood was 13 times faster than that in plasma, with an average half-life in blood of ~13 min. This creates significant problems in aspirin disposition kinetic studies. Mixing the blood sample immediately after collection with twice the volume of acetonitrile and then centrifuging gives a plasma–acetonitrile mixture in which no lysis of blood cells is observed.

Keyphrases □ Aspirin—stability in media, human blood and plasma, hydrolysis kinetics □ Kinetics—aspirin hydrolysis in media, human blood and plasma, stability □ Stability—of aspirin in media, human blood and plasma, hydrolysis kinetics

The spontaneous hydrolysis of aspirin in suspensions can be stabilized by the addition of polyethylene glycol 6000, povidone, or sorbitol (1). The former two additives form viscous insoluble masses; sorbitol is therefore the only potential stabilizer of aspirin in suspensions. The hydrolysis rate constant of aspirin decreases in the presence of surfactants due to the migration of aspirin molecules into the micelles where they are unavailable for hydrolysis (2, 3), but the undissociated molecules of aspirin are often less stable in the micellar phase than in the aqueous bulk phase (4). The stability of aspirin in polyethylene glycols, both substituted and unsubstituted, has been studied in great detail (5–8). Aspirin is more stable in unsubstituted polyethylene glycols, where the hydrolysis occurs through transesterification which is retarded when the substituted polyethylene glycols are used.

Aspirin is also rapidly hydrolyzed by a group of enzymes broadly termed as aryl esterases. These enzymes are widely distributed in blood, plasma, liver, kidney, and GI tissues (9) and are present in lesser amounts in the other tissues (10). All organs of the human fetus exhibit aspirin-hydrolyzing esterase activity, with the activity increasing during intrauterine development (11).

Sex differences have been observed in the aspirin esterase activity in human serum: activity is more prolonged in males than in females (9,12). However, a sex difference has not been observed in the esterase activity of serum albumin (12). The aryl esterase activity is significantly reduced in chronic hepatitis, liver cirrhosis, and nephrosis (12). The differences between choline, pseudocholine, and the so-called aspirin esterases in serum have been reviewed by Morgan and Truitt (10). A recent finding shows that pseudocholine esterases also participate in the hydrolysis of aspirin in serum (12).

The *in vitro* hydrolysis of aspirin in dilute blood and serum shows significant inter- and intraspecies variability, probably due to differences in the aryl esterase activity (10). At 25° the half-life of aspirin in serum diluted 30 times is 8.1, 12.6, 13.1, 14.7, and 23.3 hr in the rat, rabbit, cat, human, and dog, respectively. Thus, the hydrolysis rate of aspirin in human serum is comparable with that in the rabbit and the cat, while rats and dogs are at the extreme ends of the range. In human blood diluted 30 times, the half-life is calculated to be ~10 hr at 25°.

Significant variations have been observed in the hydrolysis rate of aspirin in serum of different human individuals (10). In human blood or plasma, diluted by 10% with aspirin in isotonic saline, the hydrolysis of aspirin follows apparent first-order kinetics at body temperature with half-lives of 32 and 66 min in blood and plasma, respectively (13).

Compared with aspirin, the enzymatic hydrolysis of salsalate, a dimer of salicylic acid, is much slower in both plasma and blood (14). For example, the half-life of aspirin in 95% whole blood (95 ml of blood plus 5 ml of ethanol containing 10 mg of aspirin) is 50 min, which compares well with the previously reported value (13). But the half-life of salsalate hydrolysis under similar conditions is 854 min, 17 times longer than the half-life of aspirin.

The routine analysis of aspirin in biological fluids involves contact with blood, acetonitrile-precipitated blood, plasma, and other solvent systems such as water–methanol–glacial acetic acid mixtures for high-performance liquid chromatographic (HPLC) analysis, water–polyethylene glycol 400 mixtures, phosphate buffer, *etc.* Because of the instability of aspirin in solution, both biological or nonbiological, it was decided to investigate the rate of hydrolysis of aspirin in these media to estimate the loss of aspirin due to the time lag between blood sampling and analysis. This information would help devise proper storage conditions for blood and plasma samples, minimizing the loss of aspirin during sample preparation. The determination of the rate constants for the hydrolysis of aspirin in blood (both *in vivo* and *in vitro*), plasma, and precipitated plasma would also permit the estimation of the relative contribution of the liver (and other aspirin-hydrolyzing tissues), blood cells, and plasma to the overall disposition of aspirin in the body.

EXPERIMENTAL

Analytical Method—One-hundred microliters of the reaction mixture was diluted with 200 μl of acetonitrile[1], mixed thoroughly and centrifuged[2] for 5 min at 15,000 rpm. Twenty microliters of the supernatant

[1] Burdick and Jackson Laboratories, Muskegon, Mich.
[2] Eppendorf Microcentrifuge Model 5412, Brinkmann Instruments, Westbury, N.Y.

0022-3549/83/0900-1024$01.00/0

Table I—Half-Lives for the Hydrolysis of Aspirin in Different Solvent Systems

Solvent System	Temperature	N^a	Half-life ± SEM^b, hr	k_{obs} ± SEM^b, hr^{-1}
Distilled water, unbuffered	22.5°	4	153.30 ± 3.70	$4.53 \times 10^{-3} \pm 1.12 \times 10^{-4}$
Water–propylene glycol 400 (4:1), unbuffered	22.5°	4	359.80 ± 7.80	$1.92 \times 10^{-3} \pm 4.15 \times 10^{-5}$
Mobile phase (water–methanol–acetic acid; 64:35:1, v/v/v)	22.5°	4	178.50 ± 4.70	$3.89 \times 10^{-3} \pm 9.98 \times 10^{-5}$
Phosphate buffer, 0.1 *M*, pH 7.0	22.5°	4	75.30 ± 3.00	$9.25 \times 10^{-3} \pm 7.29 \times 10^{-4}$
Phosphate buffer, 0.1 *M*, pH 7.4	22.5°	4	82.40 ± 1.70	$8.43 \times 10^{-3} \pm 3.49 \times 10^{-4}$
Phosphate buffer, 0.1 *M*, pH 7.4	37.0°	4	15.40 ± 0.40	$4.50 \times 10^{-2} \pm 2.36 \times 10^{-3}$
Acetonitrile-precipitated blood	22.5°	6	105.70 ± 2.70	$6.58 \times 10^{-3} \pm 1.69 \times 10^{-4}$
Plasma from control rats[c]	22.5°	6	7.60 ± 0.50	$9.39 \times 10^{-2} \pm 7.01 \times 10^{-3}$
Plasma from control rats[c]	37.0°	6	2.80 ± 0.20	$2.55 \times 10^{-1} \pm 1.94 \times 10^{-2}$
Plasma from water-deprived rats[d]	37.0°	6	2.50 ± 0.10	$2.83 \times 10^{-1} \pm 1.08 \times 10^{-2}$
Blood from control rats[c]	22.5°	6	0.46 ± 0.04	$2.57 \times 10^{-2} \pm 1.91 \times 10^{-3}$
Blood from control rats[c]	37.0°	6	0.21 ± 0.01	$6.59 \times 10^{-2} \pm 5.94 \times 10^{-3}$
Blood from water-deprived rats[d]	37.0°	6	0.18 ± 0.02	$5.59 \times 10^{-2} \pm 3.52 \times 10^{-3}$

[a] Number of experiments. [b] Standard error of the mean. [c] Food and water *ad libitum*. [d] Deprived of water for 36 hr; food available *ad libitum*.

was analyzed by HPLC as described in the previous paper (15). The mobile phase was an isocratic mixture of water–methanol[1]–glacial acetic acid[3] (64:35:1, v/v/v), and the flow rate was 2 ml/min on a reverse-phase column[4]. The separated components were detected at 238 nm. The concentrations of aspirin and salicylic acid were calculated from the peak heights using appropriate standard curves.

Hydrolysis of Aspirin in Different Solvents—The solvent systems used to study the rate of hydrolysis of aspirin were: (*a*) water at 22.5°, (*b*) water–polyethylene glycol 400[5] (4:1, v/v) at 22.5°, (*c*) water–methanol–glacial acetic acid (64:35:1, v/v/v) at 22.5°, (*d*) phosphate buffer (0.1 *M*, pH 7.0) at 22.5°, and (*e*) phosphate buffer (0.1 *M*, pH 7.4) at 22.5 and 37°. The aspirin stock solution was prepared by dissolving 1 g of aspirin in 25 ml of polyethylene glycol 400, then diluting with sterile normal saline to 100 ml. Forty microliters of the aspirin stock solution was diluted with 1960 μl of the solvent system to make the final reaction mixture of volume 2 ml. Therefore, the concentration of aspirin was 10 mg/ml in the stock solution and 200 μg/ml in the reaction mixture. Samples were collected at appropriate intervals for up to 100 hr and analyzed by HPLC.

Hydrolysis of Aspirin in Plasma, Blood, and Precipitated Blood—Approximately 6 ml of blood was collected from each rat. Two milliliters of this sample was used for the study of aspirin hydrolysis in blood; from the remainder, ~2 ml of plasma was obtained to study the hydrolysis of aspirin in plasma. The following experimental media were used to study aspirin hydrolysis:

1. Fresh plasma from control rats (food and water *ad libitum*) at 22.5°.
2. Fresh plasma from control rats (food and water *ad libitum*) at 37°.
3. Fresh plasma from rats deprived of water for 36 hr (food *ad libitum*) at 37°.
4. Blood precipitated with acetonitrile at 22.5°. Whole blood was precipitated with two volumes of acetonitrile, mixed gently, centrifuged (5 min at 15,000×*g*), and the supernatant was used to prepare the reaction mixture.
5. Blood from control rats (food and water *ad libitum*) at 22.5 and 37°.
6. Blood from rats deprived of water for 36 hr (food *ad libitum*) at 37°.

The reaction mixture for all of the above kinetic determinations was 5 μl of heparin (10,000 U/ml), 40 μl of aspirin stock solution (10 mg/ml), and 1955 μl of plasma (or blood). Therefore, the final concentrations of heparin and aspirin in the reaction mixture was 25 U/ml and 200 μg/ml, respectively. The samples were collected at appropriate intervals, precipitated with two volumes of acetonitrile, and the supernatant was analyzed by HPLC (15).

[3] BASF, Wyandotte, Mich.
[4] J. T. Baker Chemical Co., Phillipsburg, N.J.
[5] C_{18} μBondapak Column, 30 cm long, 10 μm silica, Waters Associates, Milford, Mass.

RESULTS AND DISCUSSION

Hydrolysis of Aspirin in Different Solvent Systems—The rate of hydrolysis of aspirin was followed by direct measurement of the amount of intact aspirin remaining as a function of time. The hydrolysis of aspirin was found to follow apparent first-order kinetics in all solvent systems studied. A minimum of four and maximum of six replicate kinetic runs were conducted for each of the solvent systems used. The concentration–time data were fitted to the linear regression equation for pseudo-first-order kinetics.

Table I lists the observed rate constant (k_{obs}) and the half-lives of aspirin in different solvent systems at the specified temperature. Aspirin was found to be most stable in a water–polyethylene glycol 400 (4:1, v/v) mixture ($t_{1/2}$ = 360 ± 8 hr), followed by the mobile phase ($t_{1/2}$ = 179 ± 5 hr), distilled water ($t_{1/2}$ = 153 ± 4 hr), phosphate buffer at pH 7.4 ($t_{1/2}$ = 82 ± 2 hr), and phosphate buffer at pH 7.0 ($t_{1/2}$ = 75 ± 3 hr) at 22.5°. At 37.0°, the rate constant of aspirin hydrolysis in 0.1 *M* phosphate buffer (pH 7.4) was found to be more than five times the rate constant for the same buffer at 22.5°.

Although aspirin has been reported to be more stable in moisture-free polyethylene glycol (5), its stability data in a water–polyethylene glycol combination are not available in literature. In polyethylene glycol, aspirin is hydrolyzed by a process of transesterification with an activation energy of 20.1 Kcal/mole (5), resulting in much higher stability compared with water alone. Therefore, the water–polyethylene glycol 400 (4:1, v/v) solvent system is superior to water as a vehicle for aspirin in terms of both solubility and stability.

Since aspirin is highly unstable in phosphate buffer, any sample containing aspirin which is extracted with phosphate buffer should be analyzed as quickly as possible. The relatively higher stability of aspirin ($t_{1/2}$ = 179 ± 5 hr) in the mobile phase [an isocratic mixture of water, methanol, and glacial acetic acid (64:35:1, v/v/v)] compared with its stability in water ($t_{1/2}$ = 153 ± 4 hr) at room temperature ensures that there will be no significant on-the-column hydrolysis of aspirin during its analysis by the described HPLC method (15).

Hydrolysis of Aspirin in Plasma and Blood—The hydrolysis of aspirin in plasma and blood is mostly an enzymatic process caused by aryl esterases in plasma and blood cells. Although the enzymes retain their activity for at least 1 week when stored at 5° (15), only freshly drawn blood and plasma were used to conduct the hydrolysis studies of aspirin. The hydrolysis was also performed at two different temperatures, 22.5° and 37.0°, using plasma and blood from water-deprived rats (deprived

of water for 36 hr, but having access to food *ad libitum*). Since sex differences in the rate of hydrolysis of aspirin in blood have been reported (9, 12), only male rats weighing between 300 and 450 g were used in this study.

The hydrolysis of aspirin in blood and plasma follows apparent first-order kinetics. The rate constants (k_{obs}) and the half-lives are listed in Table I. The hydrolysis of aspirin in blood from control rats is more than 13 times faster than in plasma, both at 22.5° and 37.0°. For example, at 37.0°, the half-life of aspirin in blood is 0.21 hr (13 min) compared with 2.8 hr (168 min) in plasma. The corresponding values at 22.5° for blood and plasma are 28 and 456 min, respectively.

The activity of various enzymes such as acid phosphatase, β-glucosidase, β-glucuronidase, β-galactosidase, and *N*-arylamidase has been reported to increase in water-deprived rats (16). The hydrolysis rates of aspirin in both blood and plasma of water-deprived rats, however, were found to be about equal to that in the blood and plasma from control rats.

As expected, temperature had considerable effect on the rate of enzymatic hydrolysis of aspirin in blood and plasma. The half-lives at 22.5° in the blood and plasma of control rats were 0.46 and 7.6 hr, respectively, compared with 0.21 and 2.8 hr at 37.0°.

The rapid hydrolysis of aspirin in blood and plasma might create considerable problems in the handling and storage of samples for analysis. When the blood sample containing aspirin is drawn from the rat, it has a temperature of ~37°. At that temperature, the half-life of aspirin in blood is only 13 min (Table I). Unless frozen immediately, the aspirin in the sample will hydrolyze rapidly as the sample gradually cools to room temperature (~22.5°), where the half-life of aspirin is still merely 28 min. If blood at room temperature is centrifuged and the plasma separated, the half-life of aspirin in plasma at room temperature is 7.6 hr. Therefore, to avoid significant hydrolysis of aspirin in plasma samples, the enzymatic process should be stopped at the moment the blood is collected in the syringe. If the blood is collected in a syringe and transferred to a centrifuge tube to obtain plasma, considerable loss of aspirin is inevitable due to the time lag between blood collection and the end of centrifugation. This difficulty can be overcome by collecting the blood samples in a syringe containing twice the volume of acetonitrile. Acetonitrile instantly deactivates the aspirin-hydrolyzing enzymes, coagulates the blood, and precipitates the serum proteins, but does not cause hemolysis of red blood cells so that a colorless, clear solution is obtained from blood on centrifugation. Stability studies have shown that aspirin hydrolysis in blood–acetonitrile (1:2, v/v) supernatant follows pseudo-first-order kinetics with a half-life of 106 hr at room temperature (Table I), as compared with a half-life of 75 hr for aspirin in phosphate buffer, pH 7.0.

Pharmacokinetic studies of aspirin in blood or plasma have long had problems due to (*a*) rapid loss of aspirin in blood and plasma, (*b*) lack of an analytical procedure which directly measures the aspirin in blood or plasma samples, and (*c*) fast disposition of aspirin in the body. These problems have been obviated by instantly deactivating the aspirin-hydrolyzing enzymes by adding acetonitrile, developing a rapid and sensitive HPLC method for direct quantitation of aspirin in blood and plasma, and cannulating the rat permanently so that blood samples can be collected as frequently as ≤1 min.

The *in vitro* hydrolysis rate of aspirin in whole blood or serum of rats has been reported previously by Morgan and Truitt (10) using 30-fold dilute rat serum. The initial concentration of aspirin used in their study was 433 μg/ml, a toxic level. The hydrolysis rate was followed by measuring salicylic acid (not aspirin) spectrophotometrically at 300 nm. The half-life of aspirin was found to be 8.12 hr in 30-fold dilute rat serum at 25°. This value is much higher than the half-life of 168 min found in the present study in plasma, showing that the rate constant for the enzymatic hydrolysis of aspirin cannot be extrapolated to whole blood serum, or plasma from dilute-sample studies. Morgan and Truitt (10) failed to recognize that at high serum dilution and higher aspirin concentrations, the hydrolysis may follow a different order of reaction.

Harris and Riegelman (13) have reported half-lives of aspirin in human plasma and blood to be 32 and 66 min, respectively, corresponding to 13 and 168 min in rats in our study. The concentration of aspirin was ~20 times smaller than our study, and therefore no direct comparisons can be made. But if the dilution effect is extrapolated, it is observed that aspirin is hydrolyzed by rat blood faster than human blood, whereas the opposite finding is made when plasma is used. Thus, rat blood is not a good substitute for human blood in hydrolysis studies.

REFERENCES

(1) S. M. Blaug and J. W. Wesolowski, *J. Am. Pharm. Assoc., Sci. Ed.*, **48,** 691 (1959).

(2) H. Nogami, S. Awazu, and N. Nakajima, *Chem. Pharm. Bull.*, **10,** 503 (1962).

(3) A. G. Mitchell and J. F. Broadhead, *J. Pharm. Sci.*, **56,** 1261 (1967).

(4) K. S. Murthy and E. G. Rippie, *J. Pharm. Sci.*, **56,** 1026 (1967).

(5) H. W. Jun, C. W. Whiteworth, and L. A. Luzzi, *J. Pharm. Sci.*, **63,** 133 (1974).

(6) C. W. Whiteworth, H. W. Jun, and L. A. Luzzi, *J. Pharm. Sci.*, **62,** 1184 (1973).

(7) C. W. Whiteworth and A. F. Asker, *J. Pharm. Sci.*, **63,** 1790 (1974).

(8) C. W. Whiteworth and A. F. Asker, *J. Pharm. Sci.*, **64,** 2018 (1975).

(9) R. Mengay, L. Desbaillets, Y. F. Masters, and S. Okabe, *Nature (London)*, **239,** 102 (1972).

(10) A. M. Morgan and E. B. Truitt, Jr., *J. Pharm. Sci.*, **54,** 1640 (1965).

(11) A. Schroeder and I. Amon, *J. Biol. Res. Pregnancy*, **1,** 31 (1980).

(12) M. Morikawa, M. Inoue, M. Tsuboi, and M. Mamoru, *Jpn. J. Pharmacol.*, **29,** 581 (1979).

(13) P. A. Harris and S. Riegelman, *J. Pharm. Sci.*, **56,** 713 (1967).

(14) L. Harthon and M. Hedstrom, *Acta Pharmacol. Toxicol.*, **29,** 155 (1971).

(15) S. K. Bakar and S. Niazi, *J. Pharm. Sci.*, **72,** 1020 (1983).

(16) G. J. Boer and J. F. Jonkind, *J. Neurochem.*, **22,** 965 (1974).

Simple Reliable Method for Chronic Cannulation of the Jugular Vein for Pharmacokinetic Studies in Rats

SHAMSUL K. BAKAR and SARFARAZ NIAZI ˣ

Received December 3, 1981, from the *Department of Pharmacodynamics, College of Pharmacy, University of Illinois Health Sciences Center, Chicago, IL 60612.* Accepted for publication March 5, 1982.

Abstract □ A simple method for the preparation and implantation of silicone cannulas into the rat jugular vein is described. The implanted cannula can be used to administer drugs and collect blood samples at intervals of ≤1 min without causing stress to the animal. If necessary, the animals can be exanguinated within a few minutes using this cannula. With proper maintenance, the cannula is patent for weeks and could be used for repeated and crossover studies.

Keyphrases □ Sampling, blood—serial, chronic cannulation procedure, rat jugular vein, pharmacokinetic studies □ Cannulation—chronic, rat jugular vein, serial blood samples for pharmacokinetic studies □ Pharmacokinetics—serial blood sampling by chronic cannulation, rat jugular vein

Pharmacokinetic studies of drugs require sequential blood sampling. It is preferable that the blood samples are drawn from the animals with minimum trauma and stress to avoid any changes in the body physiology, which might alter the disposition characteristics of the drug (1–4). A number of methods are available for serial blood sampling (5, 6); these can be broadly classified into surgical and nonsurgical methods. The nonsurgical methods include cardiac puncture (5, 7), bleeding of the orbital plexus (8–10), and bleeding of the tail (5, 11). These methods are traumatic and may require anesthetizing the animals; the cardiac puncture method is not suitable for sequential blood sampling. Some methods do not involve surgery and are available for continuous intravenous drug infusion (12–14), but these methods cannot be used for serial blood sampling because the vein often collapses after a certain period of time.

The surgical approaches for obtaining serial blood samples mainly include cannulation of the jugular vein (15–19) or cardiac ventricle (20, 21). Other methods of cannulation in the rat for the study of first-pass effect have been reviewed elsewhere (6).

The cannulation of the external jugular vein is one of the most reliable methods for intravenous administration of drugs and rapid sequential blood sampling for prolonged periods of time. However, the complexity involved in the cannulation and maintenance of cannula patency for a sufficient length of time has limited the use of this technique in pharmacokinetic studies. The purpose of this study is to devise a simple method for the preparation of the cannula, for the introduction of the cannula into the vein, and for the maintenance of cannula patency for long-term use.

EXPERIMENTAL

Preparation of Cannula—Approximately 12 cm of medical-grade silicone rubber tubing (0.051-cm i.d. × 0.094-cm o.d.)[1] was gently wrapped around twice with silk thread[2] ~20 cm in length. A firm knot was tied in the thread, taking precaution that the lumen of the silicone tube was not occluded. The knot was made ~3 cm from one end of the silicone tubing, so that the other end was ~9 cm long (Fig. 1a).

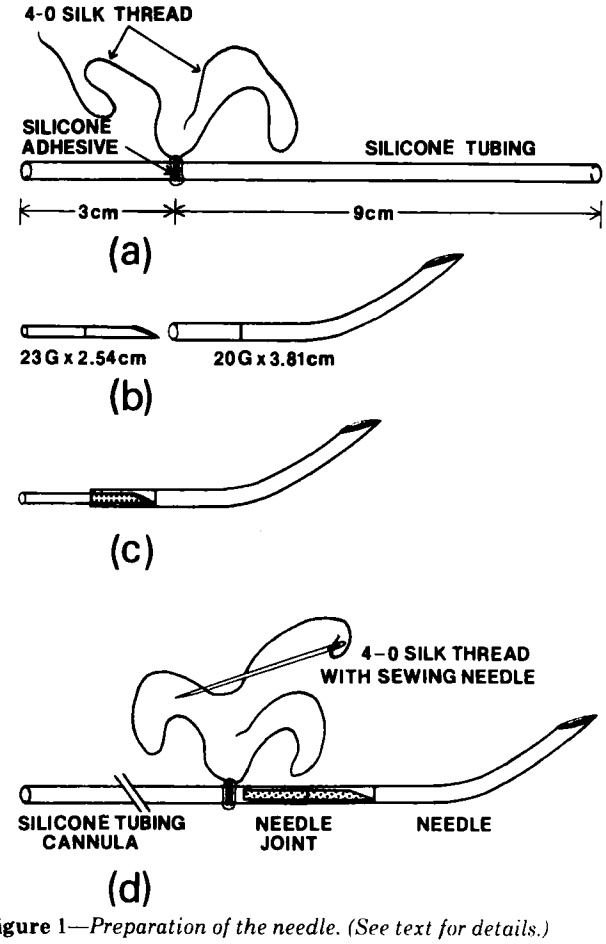

Figure 1—*Preparation of the needle. (See text for details.)*

A coat of silicone adhesive[3] was applied to the thread around the tubing and cured for at least 24 hr. The coating was not >1 mm thick so as to keep the thread firmly held on the silicone tubing without making the joint too bulky. After curing, the silicone cannula was checked for occlusion by flushing with sterile normal saline. The cannulas were cleaned and disinfected by soaking them in benzalkonium chloride antirust solution for at least 30 min before use. The lumen of the cannula was cleaned by flushing with 2 ml of sterile normal saline.

The short end of the cannula is inserted into the superior vena cava through the right external jugular vein, and the longer portion is passed subcutaneously to the back of the neck. The length of the short end can vary depending on the size of the rat: a 3-cm length is suitable for rats weighing between 300 and 450 g.

Preparation of the Implantation Needle—The needle used for the introduction of the cannula into the jugular vein was prepared using the method of Harms and Ojeda (17). The plastic hubs were removed from two thin-walled beveled hypodermic needles[4] (23-gauge × 2.54 cm and 20-gauge × 3.81 cm). Approximately 1.2 cm of the beveled end of the

[1] Silastic Medical-Grade Tubing, Dow Corning Corp., Medical Products, Midland, Mich.
[2] 4-0 Silk, Black Braided, Code A-53, Ethicon, Inc., Somerville, N.J.
[3] Silastic Medical Adhesive, Silicone Type A, Dow Corning Corp., Medical Products, Midland, Mich.
[4] Yale Sterile Disposable Needles, Becton, Dickinson and Co., Rutherford, N.J.

0022-3549/83/0900-1027$01.00/0

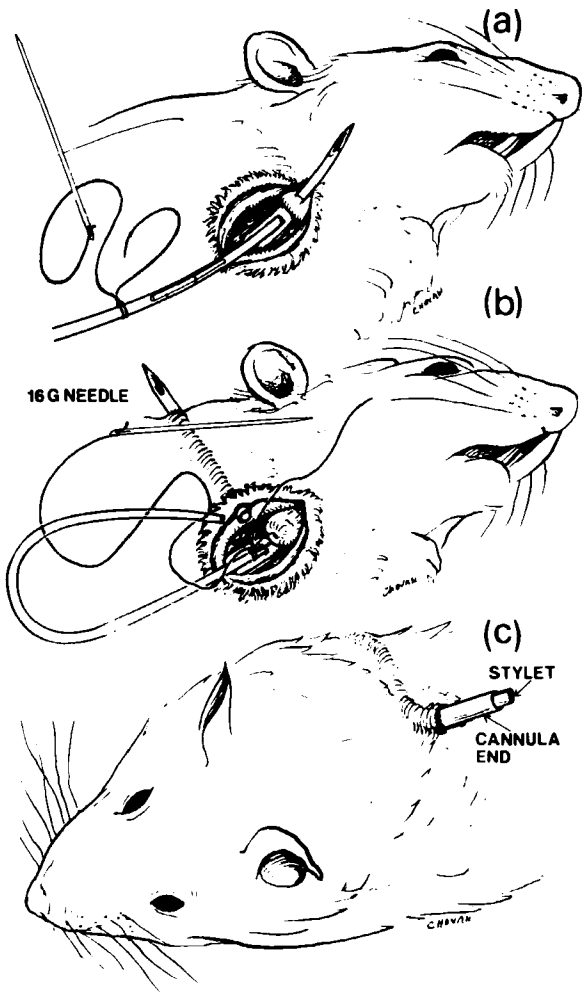

Figure 2—*Cannulation of the rat. Key: (a) insertion of the needle, (b) securing of the cannula, and (c) externalization of the cannula.*

23-gauge needle was forced into the opposite (nonbeveled) end of the 20-gauge needle, which had been bent (Fig. 1b). If the 23-gauge needle was too thick to be fitted snugly into the bore of the 20-gauge needle, the outer surface of the 23-gauge needle was rubbed on a rough surface (such as a sharpening stone) to make the outer diameter small enough to fit tightly into the lumen of the 20-gauge needle. The short end of the silicone cannula fit snugly over the protruding portion of the 23-gauge needle (Fig. 1c).

Surgical Implantation of the Cannula—All the instruments used for the animal surgery were cleaned and disinfected by immersing them into a benzalkonium chloride antirust solution for ~1 hr. Strict asepsis was not necessary, but a clean environment and neat handling of the animal were important.

The rat was anesthetized with ether in a desiccator. After removing the rat from the desiccator, the anesthesia was maintained throughout the implantation procedure by placing ether-impregnated cotton close to the nose of the rat. The hair on the back of the animal was clipped, and a point was marked at the center of the back of the neck to indicate the exteriorization point for the longer portion of the cannula. The rat was then placed on its back, and the hair on the area over the right external jugular vein was clipped. This area is recognized by observing the rapid pulsation of the jugular vein. The shaved area was cleaned by repeated wipings with sterile gauze saturated with 70% isopropyl alcohol.

A longitudinal incision, ~2 cm long, was made on the skin over the jugular vein, and the vein was exposed by clearing the surrounding tissues. To avoid unnecessary blood loss, care was taken not to damage any surrounding veins. The short end of the cannula was passed into and out of the jugular vein using the implantation needle–cannula assembly (Fig. 2a). This was done without loss of blood from the vein.

At this point, while the shorter end of the cannula was out of the jugular vein, a sterile disposable syringe (3- to 10-ml capacity) containing heparinized (20 U/ml) normal saline for injuection, was connected to the longer end of the silicone cannula by a blunt-ended 23-gauge sterile needle. This needle was prepared by clipping the beveled portion of a 23-gauge × 2.54-cm needle, smoothing out both the inside and outside of this cut-end needle, cleaning and sterilizing with benzalkonium chloride antirust solution, and rinsing several times with heparinized normal saline for injection. The flushing can be done with or without the implantation needle at the end of the cannula. However, it is a good practice to flush the initial portion of the normal saline with the implantation needle on, so that the needle is cleared of any blood that may have entered it during its short passage through the jugular vein. If the implantation needle is not flushed immediately, blood clots may form in the lumen of the needle; these clots often are difficult to remove.

The implantation needle was disconnected and the cannula was flushed again with ~0.5 ml of normal saline. Then the cannula was pushed slowly toward the heart until the junction of the silk thread was reached. The cannula was then fixed in place by suturing the silk thread to the muscle through which the implantation needle exited (Fig. 2b). The suturing was done using an ordinary sewing needle which had been sterilized.

Approximately 0.2 ml of heparinized normal saline was injected slowly from the syringe through the cannula into the vena cava. The plunger of the syringe was then pulled back slowly to observe the appearance of blood in the cannula. When blood was observed, another 0.2 ml of heparinized sterile normal saline was injected into the cannula. The longer end of the cannula was disconnected from the syringe and threaded with the aid of a 16-gauge needle (Fig. 2b), which was passed subcutaneously from the point marked at the back of the rat's neck to the point of incision. Blood loss through the cannula was minimized during this step either by putting a small clip close to the junction of the silk thread or by keeping the cannula pressed at that point with two fingers. After passing through the skin, the cannula was again filled with heparinized normal saline and closed with a 1-cm portion of nylon monofilament, the inner end of which had been tapered and smoothed.

The muscles at the incision were closed by a single suture, and the open skin was closed by 3 to 4 stitches using absorbable, surgical suture with a needle[5] and hemostat. The administration of ether to the rat was then discontinued, any blood around the skin incision was cleared with cotton gauze, and the rat was placed in a supine position in its cage. Within a few minutes, the rat turned over and started walking somewhat shakily. After 1 hr, the movements of the rat became normal, indicating that the rat had recovered from the anesthesia.

Serial Blood Collection—To avoid contamination of blood from one sample to the next, a 1- or 3-ml disposable plastic syringe was fitted with a 23-gauge × 2.54-cm needle (Fig. 3). The beveled portion of the needle had been cut off and smoothed, as mentioned earlier, to avoid damaging the cannula. The needle was fitted with two segments (A and B) of silicone rubber tubing, both ends of which had been smoothed (Fig. 3). At the end of the second tubing (B), another 23-gauge connector was fixed with half of its length protruding.

When blood was collected, the nylon stylet was removed from the implanted cannula, and the cannula was connected to the free end of the 23-gauge needle. When the plunger of the syringe was pulled back, first heparinized normal saline and then blood started entering the tubing and the syringe. As soon as the dead volume of normal saline and/or blood had crossed the joint of the two tubings, the first tubing (A) was disconnected along with its needle joint. Another syringe, fitted with a 23-gauge blunt-ended needle, was attached to the open end of the second tubing (B). Blood was drawn into the second tubing by pulling the plunger back slowly.

During the connecting and disconnecting processes, the open end of the cannula was firmly pressed between two fingers so that the blood remained immobile within the cannula. After drawing the required volume of blood, the syringe and its needle were removed, and the cannula was filled with heparinized normal saline and closed with the nylon stylet. If blood samples are withdrawn in quick succession, for example every minute, flushing the cannula each time with saline solution is unneces-

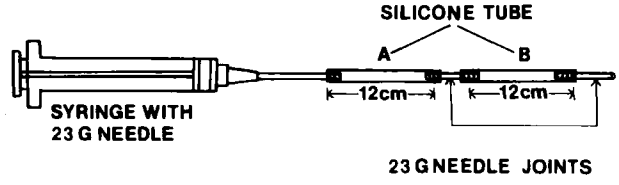

Figure 3—*Syringe and tubing assembly for the collection of uncontaminated serial blood samples from cannulated rats.*

[5] 4-0 Dexon, American Cyanamid Co., Pearl River, N.Y.

sary. The mixing of blood between samples can be avoided by adopting the above procedure.

Maintenance of the Cannula—Using the syringe and tubing arrangement, as described earlier for the collection of serial blood samples, the blood was first drawn into the tubing under negative pressure. If any clot had formed, it was removed from the cannula and not pushed into the systemic circulation. The cannula was then filled completely with heparinized (20 U/ml) normal saline for injection. Flushing of the cannula was done at least once, but preferably twice, a day.

DISCUSSION

The method described here for the chronic cannulation of the rat jugular vein is simple and reliable. More than 100 rats have been cannulated in our laboratory for pharmacokinetic studies of drugs whose half-lives ranged from a few minutes to several hours or days. With proper maintenance, the cannula remains patent for months. This method for the preparation of the cannula is simpler than the one described previously (17). The cannula preparation eliminates the use of silicone sheeting which is difficult to fabricate, causes discomfort to the rats, has a bulky appearance after the skin incision is closed and healed, and prolongs the healing time. Other methods of cannula preparation (16, 18) are even more complicated, needing many accessories and expertise to make and implant them.

Upton (19) described a cannulation method where the "tubing is secured by tying firmly around the vein," which blocks blood circulation through the jugular vein. The cannula can become blocked if tied too firmly, or dislodged from the vein if the knot is not firm enough. Insertion of the cannula through the jugular vein into the vena cava involves manipulation of the vein which can cause it to collapse, thus complicating further the insertion procedure. Unless the tube is inserted promptly on incision in the jugular vein (19), significant loss of venous blood may occur. However, the method described here involves minimal manipulation of the vein with little loss of blood.

The passage of the cannula into and out of the jugular vein should be accomplished in the first attempt. If the first attempt fails, the vein may collapse, making it somewhat difficult (but not impossible) to insert the implantation needle into the vein. It is recommended that while learning this cannulation technique, one should anesthetize the first few rats with pentobarbital, since ether anesthesia requires attention to maintain the optimum anesthesia of the rat, which may hamper the surgical procedure.

Monofilament nylon cord is used as a stylet to close the open end of the cannula because it is nonreactive with normal saline and the silicone tubing and is lighter than stainless steel. Although the medical-grade silicone tubing used is nonreactive with body tissue (22), it neither resists blood clotting nor is impervious to moisture. Thus, loss of water from the saline-filled cannula allows the blood to enter the cannula and form a clot. Initially, this clot is soft and could be aspirated easily. But if the clot remains for a longer period (>24 hr), it becomes hardened and strongly affixed to the inside wall of the cannula. In these cases, heparinized normal saline should be forced in to clear the cannula. The presence of these clots in the vena cava often damages this blood vessel, rendering the cannula inoperative. It is preferable that the clots be removed by aspiration before flushing the cannula rather than be forced into the general circulation. To reduce the microbial contamination during the flushing of the cannula, the exposed end of the cannula, the stylet, the needle of the syringe, and the finger tips which come in contact with the cannula should be thoroughly wiped with sterile gauze saturated with 70% isopropyl alcohol.

For the first few days, some rats may show some restlessness making it difficult to connect or disconnect the syringe with cannula for drawing the blood. In these situations, some confinement such as that described by Davis and Coleman (23) or any simpler version, should be used to limit the movements of the animal. After time the animal becomes used to this manipulation and offers no problems.

Unless the pharmacokinetic studies are complicated by the use of heparin (24), it is recommended that blood sample volumes should be replaced by heparinized (20–50 U/ml) normal saline. Also ~0.2 ml of heparinized (20–50 U/ml) normal saline should be injected a few minutes before the withdrawal of blood. If heparin poses problems, another anticoagulant may be used.

REFERENCES

(1) H. Chung and D. R. Brown, *Toxicol, Appl. Pharmacol.*, **37**, 313 (1976).

(2) P. Soubrie, M. H. Thiebot, A. Jobert, J. L. Montastruc, F. Hery, and M. Hamon, *Brain Res.*, **189**, 505 (1980).

(3) J. Culman, R. Kvetnansky, T. Torda, and K. Murgas, *Neuroscience*, **5**, 1503 (1980).

(4) G. Cassesn, M. Roffman, A. Kuruc, P. J. Orsulak, and J. J. Schldkraut, *Science*, **209** (4461), 1138 (1980).

(5) H. C. Grice, *Lab. Anim. Care*, **14**, 483 (1964).

(6) B. H. Migdalof, *Drug Metab. Rev.*, **5**, 295 (1976).

(7) S. O. Burhoe, *J. Hered.*, **31**, 445 (1940).

(8) S. H. Stone, *Science*, **119**, 100 (1954).

(9) V. Riley, *Proc. Soc. Exp. Biol. Med.*, **104**, 751 (1960).

(10) B. J. Sanders, *Am. J. Clin. Pathol.*, **40**, 46 (1963).

(11) S. T. Nerenberg and P. Zedler, *J. Lab. Clin. Med.*, **85**, 523 (1975).

(12) A. L. Kennan, *J. Appl. Physiol.*, **19**, 157 (1964).

(13) M. L. Rhodes and C. E. Patterson, *Lab. Anim. Sci.*, **29**, 82 (1979).

(14) P. A. Jones and J. W. Hynd, *Lab. Anim.*, **15**, 82 (1981).

(15) V. Popovic and P. Popovic, *J. Appl. Physiol.*, **15**, 727 (1960).

(16) J. R. Weeks and J. D. Davis, *J. Appl. Physiol.*, **19**, 540 (1964).

(17) P. G. Harms and S. R. Ojeda, *J. Appl. Physiol.*, **36**, 391 (1974).

(18) S. G. Smith and W. M. Davis, in "Methods in Narcotics Research," S. Ehrenpreis and A. Neidle, Eds., Dekker, New York, N.Y., 1975, pp. 3–15.

(19) R. A. Upton, *J. Pharm. Sci.*, **64**, 112 (1975).

(20) V. Popovic and P. Popovic, *Proc. Soc. Exp. Biol. Med.*, **113**, 599 (1963).

(21) S. M. Smith, J. H. Mayers, and H. M. Kaplan, *Lab. Anim.*, **13**, 15 (1979).

(22) A. C. Speirs and R. Blocksma, *Plast. Reconstr. Surg.*, **31**, 166 (1963).

(23) M. H. Davis, Jr. and T. J. Coleman, *Lab. Anim. Sci.*, **29**, 499 (1979).

(24) M. Wood, D. G. Shand, and A. J. J. Wood, *Clin. Pharmacol. Ther.*, **25**, 103 (1979).

Effect of Water Deprivation on Aspirin Disposition Kinetics

SHAMSUL K. BAKAR and SARFARAZ NIAZI[x]

Received December 3, 1981, from the *Department of Pharmacodynamics, College of Pharmacy, University of Illinois Health Sciences Center, Chicago, IL 60612.* Accepted for publication May 11, 1982.

Abstract □ Temporary water deprivation results in serious stress causing significant physiological, hormonal, and enzymatic changes in the body which can affect the disposition kinetics, toxicity, and activity of drugs. This study attempts to recognize the effect of water deprivation on drug disposition kinetics using aspirin. No significant effects were noted following 36-hr water deprivation in rats on the metabolism of aspirin; there was also no effect of heparinization on aspirin disposition kinetics. The disposition of salicylic acid, however, was altered significantly, with the half-life increased by ~72% concomitant with decreased total body clearance. The effect of two dose levels, 5 and 10 mg/kg, was also studied to elucidate nonlinearity in the disposition kinetic model. Almost complete urinary recovery of aspirin was obtained in the intact form or as metabolites. At the 10-mg/kg dose, the fraction of salicyluric acid excreted decreased significantly compared with the 5-mg/kg dose. However, the effect of water deprivation was uniform at the two dose levels without any effect on the excretion of salicyluric acid. It is suggested that, in view of the significant changes in the disposition characteristics of salicylates with water deprivation, due care must be exercised in adjusting doses giving proper consideration to body hydration levels.

Keyphrases □ Aspirin—disposition kinetics in rats, effect of water deprivation on metabolism □ Kinetics—aspirin metabolism, rats, effect of water deprivation □ Metabolism—of aspirin, effect of water deprivation in rats, kinetics

Dehydration in the body occurs due to circumstantial water deprivation, excessive sweating, and various disease states such as polyuria and diarrhea. A number of physiological and biochemical changes have been attributed to the short-term stress of water deprivation; these can significantly modify the disposition of drugs in the body.

The most prominent manifestations of water deprivation are loss of body weight and decrease of both blood and plasma volumes (1–6). This results in increased plasma osmotic pressure, plasma protein concentration, and hematocrit, while the pH and the acid–base status of blood remain essentially constant (1–10). The volume of the urine and the amount of electrolytes excreted in the urine also decrease significantly in water-deprived rats (5), with corresponding morphological and histochemical changes in the renal medulla (11).

The effects of starvation and nutrition on the drug-metabolizing enzymes of liver microsomes have been extensively investigated (12–22), but kinetic studies of drug disposition with short- and long-term water deprivation in humans or animals are almost nonexistent. Some empirical data exist indicating that water deprivation may influence the pharmacological effect of some drugs (23–27).

The fate and pharmacokinetics of aspirin (acetylsalicylic acid) and salicylic acid in human and animals have been extensively investigated (28–34). However, specific *in vivo* data on aspirin metabolism by rats and other common laboratory animals are lacking. The desert rodents, hopping mice (*Notomys alexis*, Family: Muridae), conserve body water with extreme economy and show high papillary-to-cortex ratios of salicylates along with longer biological half-lives of salicylates (100–120 min) when compared with nondesert mice (55 min). Also, only 9% of the salicylate in desert mice is metabolized to salicyluric acid, compared with 80% in humans and 50% in rats (35, 36). Thus water economy and species differences determine the biological half-life of circulatory salicylate and the nature and extent of its metabolites.

The primary purpose of this study was to investigate the effect of a 36-hr water deprivation on the disposition kinetics of aspirin. Aspirin was selected as a model drug because of its extensive protein binding, several pathways for metabolism and excretion, variable dose-dependent disposition, and clinical importance. Since *in vivo* heparinization of the circulatory system was done to facilitate the withdrawing and handling of blood samples from the rats, the effect of heparin on the pharmacokinetics of aspirin was also investigated.

EXPERIMENTAL

Animal Preparation—Male rats[1] weighing between 300 and 450 g were used. The rats were housed in individual cages[2] and allowed to become accustomed to the laboratory conditions for at least 7 days. The rats were cannulated in the right jugular vein as described in the previous paper (37) at least 3 days before the pharmacokinetic study began, thus allowing sufficient time for recovery from the surgery. The cannula was kept patent by flushing with heparinized (20 U/ml) sterile normal saline for injection[3] twice a day. Each study group was comprised of six rats, selected randomly.

For the treatment group of rats, water deprivation started at 7:00 pm, and the drug was given 36 hr later. During this 36-hr water deprivation, the rats had access to food all the time. The rats were weighed prior to the administration of aspirin to calculate the proper dose; they were also weighed before and after water deprivation to calculate the percent weight loss.

Preparation and Administration of the Aspirin Dose—One gram of aspirin was dissolved in 20 ml of polyethylene glycol 400[4] with constant shaking and diluted with sterile normal saline for injection to 100 ml, so that the final concentration of aspirin in the solution was 10 mg/ml. The resultant solution was passed through a sterile 0.22-μm filter for the removal of any particles or microorganisms. Each solution was freshly prepared due to the instability of aspirin in solution (38).

The sterilized, particle-free solution was aspirated into a 1-ml disposable hypodermic syringe[5], and the dose was administered intravenously through the jugular vein cannula. The dead volume in the cannula was flushed immediately with ~0.2 ml of heparinized (50 U/ml) sterile normal saline. When the effect of heparin on the pharmacokinetics of aspirin was studied, the cannulas of the control (nonheparinized) rats were flushed with sterile normal saline instead of heparinized normal saline.

Collection of Blood and Plasma Samples—For the pharmacokinetic study of intact aspirin, 200 μl of blood was collected in a 1-ml syringe containing 400 μl of acetonitrile[6] prior to the administration of the dose. The contents of the syringe were mixed gently, and this mixture served

[1] Sprague–Dawley strain, King Animals, Madison, Wis.
[2] Nalgene Metabolic Cage, Nage Co., Rochester, N.Y.
[3] Abbott Laboratories, North Chicago, Ill.
[4] BASF, Wyandotte, Mich.
[5] Becton, Dickinson and Co., Rutherford, N.J.
[6] Burdick and Jackson Laboratories, Muskegon, Mich.

0022-3549/83/0900-1030$01.00/0

Table I—Effects of Heparin on the Disposition Kinetics (Single Compartment) of Salicylic Acid in Rats [a]

Parameter	Control Rats[b] Mean ± *SEM*	Control Rats[b] Range	Heparinized Rats[b] Mean ± *SEM*	Heparinized Rats[b] Range
Body weight, g	363.0 ± 9.0	327.0–434.0	359.0 ± 10.0	332.0–426.0
Half-life, hr	2.38 ± 0.11	1.62–2.82	2.36 ± 0.15	1.63–3.05
Volume of distribution (V_d), ml/kg	146.8 ± 5.6	124.0–189.0	138.0 ± 6.0	106.0–176.0
Total body clearance, ml/kg·hr	45.4 ± 2.4	33.9–61.1	41.0 ± 2.4	26.6–52.1
AUC, μg·hr/ml	227.3 ± 11.1	162.8–290.3	244.3 ± 15.9	187.7–337.8

[a] Salicylic acid dose = 10 mg/kg; $n = 6$. [b] Rats received 0.3 ml of physiological normal saline (control) or physiological normal saline containing 6 U of heparin (treatment) as a replacement for each 0.3-ml blood sample drawn.

Table II—Effects of Water Deprivation on the Disposition Kinetics (*In Vivo* Hydrolysis) of Aspirin in Rats [a]

Parameter	Control Rats[b] Mean ± *SEM*	Control Rats[b] Range	Water-Deprived Rats[c] Mean ± *SEM*	Water-Deprived Rats[c] Range
Body weight, g	325.0 ± 20.0	285.0–420.0	350.0 ± 6.0	328.0–361.0
Half-life, min	1.8 ± 0.4	0.8–3.2	2.0 ± 0.4	1.6–3.9
Volume of distribution (V_d), ml/kg	994.0 ± 95.0	714.0–1285.0	794.0 ± 43.0	644.0–939.0
Total body clearance, ml/kg·min	465.0 ± 96.0	166.0–736.0	299.0 ± 29.0	166.0–364.0
AUC, μg·min/ml	31.0 ± 8.6	13.9–68.8	37.6 ± 5.5	27.3–64.4

[a] Aspirin dose = 10 mg/kg; $n = 6$. [b] Rats received food and water *ad libitum*. [c] Rats were deprived of water for 36 hr, but received food *ad libitum*.

as the blank. After administering aspirin intravenously through the jugular vein cannula, blood samples were collected every 1 min for 5 min and then every 2 min for another 6–10 min.

For the pharmacokinetic study of salicylic acid in the rats, ~200- to 300-μl blood samples were collected every 15 min for the first hour after the administration of the intravenous dose, every 30 min for the next 2 hr, and then every hour for the next 4 hr. Thereafter, blood samples were collected every 2 hr for another 4–6 hr. The volume of each blood sample collected from the rat was replaced with an equal volume of heparinized (50 U/ml) sterile normal saline.

When the effect of heparin itself on the pharmacokinetics of salicylic acid was investigated, the blood samples for the control (nonheparinized) group of rats were replaced with sterile normal saline rather than heparinized normal saline. Blood samples were collected from each rat for each pharmacokinetic study before administering the aspirin dose and were used as blanks.

Collection of Urine Samples—Rats were placed in metabolism cages, which allowed the collection of urine and feces in separated receptacles that could be removed without disturbing the animal. The urine deposited in the receptacle was collected every 12 hr, pooled, and stored in the refrigerator. The pooled urine was analyzed within 24 hr after the end of the collection. Urine samples from control rats (receiving food and water *ad libitum*) were collected for a total of 48 hr; samples for water-deprived rats were collected for 60 hr. The volume of the pooled urine and its pH were measured at the end of collection. Urine samples were also collected from each rat prior to the administration of aspirin; these samples served as blanks.

Analytical Procedure—*Blood*—The blood–acetonitrile (1:2) mixture was transferred to a 500-μl polypropylene microcentrifuge tube and centrifuged[7] for 5 min at 15,000 rpm. Twenty microliters of the supernatant was analyzed by the high-performance liquid chromatographic (HPLC) method described previously (39).

Plasma—Blood samples collected in the syringe were transferred to 250-μl polyethylene microcentrifuge tubes and centrifuged for 2 min at 15,000 rpm to separate the plasma from the cellular fraction. Aliquots of the separated plasma layer (100 μl) were transferred to a 500-μl polypropylene microcentrifuge tube and precipitated with 200 μl of acetonitrile. The mixture was vortexed for 30 sec, then centrifuged for 8 min (15,000 rpm). Twenty microliters of the supernatant was analyzed using the HPLC method described previously (39).

Urine—The refrigerated pooled urine was warmed to room temperature and mixed by shaking. A portion of the mixture was clarified by centrifugation for 10 min at 2500 rpm. One milliliter of the clarified urine was acidified with 0.5 ml of 6 *N* HCl[8] and extracted with 6 ml of ether[9]. Five milliliters of the ether extract were re-extracted with 1 ml of phosphate buffer (0.1 *M*, pH 7.0), and 20 μl of the buffer extract was analyzed by HPLC (39). The urine samples were prepared in duplicate, and each sample was chromatographed twice so that each analytical value reported was an average of four determinations.

[7] Eppendorf Microcentrifuge Model 5412, Brinkmann Instruments, Westbury, N.Y.
[8] J. T. Baker Chemicals Co., Phillipsburg, N.J.
[9] Mallinckrodt, St. Louis, Mo.

RESULTS AND DISCUSSION

Effect of Heparin on the Pharmacokinetics of Salicylic Acid—Table I lists the pharmacokinetic data for the 22 rats (11 rats in each group) used to study the effect of heparin on the disposition of salicylic acid administered intravenously as a solution of sodium salicylate. The elimination of salicylate by the body was described by first-order kinetics, as is evident from the excellent linear correlation coefficients obtained for each of the pharmacokinetic studies. Figure 1 shows the disposition kinetics of salicylic acid in two representative rats, one from the heparinized and the other from the nonheparinized groups of rats. No statistical significance was observed in the disposition kinetic data between the two study groups.

Similar findings were made at much higher doses of heparin (500–1000 U/kg). This finding is important since heparin decreases plasma protein binding of neutral and basic drugs and increases the binding of acidic drugs (40), except for salicylates where a decreased binding is noted at a 500-U/kg dose (41). The present finding suggests that the decrease in plasma protein binding of salicylate, as observed by Weigand and Levy (41), will not affect the disposition characteristics of salicylic acid.

Disposition of Aspirin in Control and Water-Deprived Rats—Table II lists the disposition kinetic parameters for aspirin after an in-

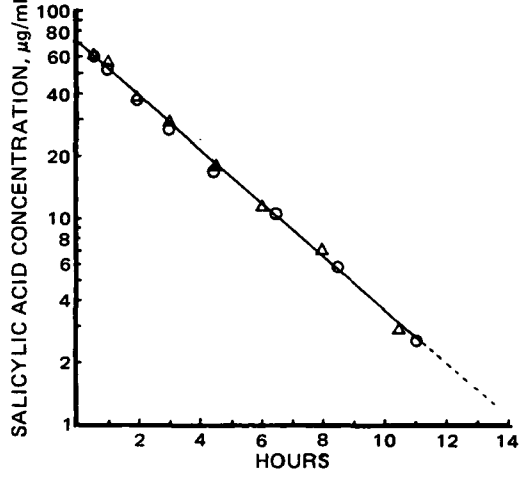

Figure 1—*Typical first-order plots for salicylic acid concentration in plasma* versus *time, after an intravenous dose of 10 mg of aspirin/kg of body weight in rats. Key: (○) control rats, 0.3 ml blood samples were replaced by 0.3 ml sterile normal saline; (△) heparinized rats, 0.3 ml blood samples were replaced by 0.3 ml sterile normal saline containing ~ 6 U of heparin.*

Table III—Effects of Water Deprivation on the Disposition Kinetics of Intravenously Administered Aspirin in Rats [a]

Parameter	Control Rats[b]		Water-Deprived Rats[c]	
	Mean ± *SEM*	Range	Mean ± *SEM*	Range
Body weight, g	393.0 ± 9.0	353.0–422.0	337.0 ± 13.0	270.0–381.0
Half-life, hr	2.1 ± 0.09	1.71–2.44	3.62 ± 0.41	2.39–5.81
Volume of distribution (V_d), ml/kg	176.3 ± 21.9	135.2–326.4	179.4 ± 5.6	160.4–205.5
Total body clearance, ml/kg·hr	50.7 ± 3.3	41.2–70.3	37.0 ± 3.6	24.5–50.9
AUC, μg·hr/ml	101.9 ± 6.2	66.5–121.7	166.4 ± 21.5	93.1–257.6

[a] Aspirin dose = 5 mg/kg; n = 6. [b] Rats received food and water *ad libitum*. [c] Rats were deprived of water for 36 hr, but received food *ad libitum*.

Table IV—Effects of Water Deprivation on the Disposition Kinetics of Salicylate in Rats [a]

Parameter	Control Rats[b]		Water-Deprived Rats[c]	
	Mean ± *SEM*	Range	Mean ± *SEM*	Range
Body weight, g	373.0 ± 6.0	341.0–405.0	374.0 ± 8.0	342.0–410.0
Half-life, hr	2.59 ± 0.15	1.86–3.22	4.37 ± 0.46	2.98–7.07
Volume of distribution (V_d), ml/kg	175.7 ± 7.0	141.0–196.1	178.2 ± 9.1	137.1–232.9
Total body clearance, ml/kg·hr	47.5 ± 1.5	40.8–52.7	30.1 ± 2.7	20.7–44.7
AUC, μg·hr/ml	207.4 ± 13.9	143.3–243.6	369.1 ± 38.9	235.3–555.8

[a] Salicylate dose = 10 mg/kg; n = 6. [b] Rats received food and water *ad libitum*. [c] Rats were deprived of water for 36 hr, but received food *ad libitum*.

travenous dose of 10 mg/kg of body weight in two groups of rats: a control group which had free access to food and water and a 36-hr water-deprived (treatment) group which had free access to food only. Figure 2 shows the first-order disposition kinetics of of aspirin in two rats which represent the control and treatment groups. The disposition constants for aspirin in the control group of rats were not statistically significant ($p < 0.05$) compared with the treatment group.

Therefore, in short-term water deprivation, the activity of the aryl esterases in blood and other organs, such as liver and kidneys, is not significantly altered. Based on the volume of distribution, the contribution of blood to the clearance of aspirin in rats is insignificant (<1%) compared with humans (~20%), despite the fact that the hydrolysis of aspirin in rat blood is faster than in human blood ($t_{1/2}$ = 30 and 12 min, respectively).

Disposition of Salicylic Acid in Control and Water-Deprived Rats—Since no detectable level of aspirin in the blood is found after 10 min following intravenous administration of aspirin, the blood samples collected 15 min after the administration of the intravenous dose and all subsequent sampling times represent the disposition kinetic study of salicylic acid. The two dose levels of aspirin (5 and 10 mg/kg) were selected to study the linearity of kinetics and the effect of dose on the disposition of salicylic acid both in the control and treatment groups.

Figure 3 shows the disposition of salicylic acid after an intravenous 5-mg/kg dose of aspirin in typical control and treatment rats. The disposition kinetics follow a first-order process (Table III). The time zero concentrations of salicylic acid in plasma were similar in both control and treatment rats (30.2 and 31.6 μg/ml, respectively). This implies that short-term water deprivation has little effect on the volume of distribution of salicylic acid.

Although the volume of distribution in both groups of rats was essentially the same (176 and 179 ml/kg), the biological half-life of salicylic acid in the treatment group of rats was 72% higher than the half-life in the control group. This increase in biological half-life is also reflected in the higher value of area under the curve (AUC) (166 *versus* 102 μg·hr/ml) and lower total body clearance (37 *versus* 51 ml/kg/hr).

The results obtained after the administration of a 10-mg/kg aspirin dose in control and treatment rats are listed in Table IV. The typical first-order plots for the disposition of salicylic acid are shown in Fig. 4. The disposition of salicylic acid at this dose level also follows apparent first-order kinetics in rats.

The biological half-life of salicylic acid in 36-hr water-deprived rats was ~70% higher (4.37 *versus* 2.59 hr) than in control rats, although the volume of distribution in both groups was essentially the same (176 and 178 ml/kg). The higher biological half-life of salicylic acid in treatment rats is consistent with the observed lower value (37%) of total body clearance (30.1 *versus* 47.5 ml/kg/hr) and higher value (78%) of the AUC (369.1 *versus* 207.4 μg·hr/ml).

The overall results for the two dose levels suggest that the biological half-life of salicylic acid in both groups of rats increases significantly (p

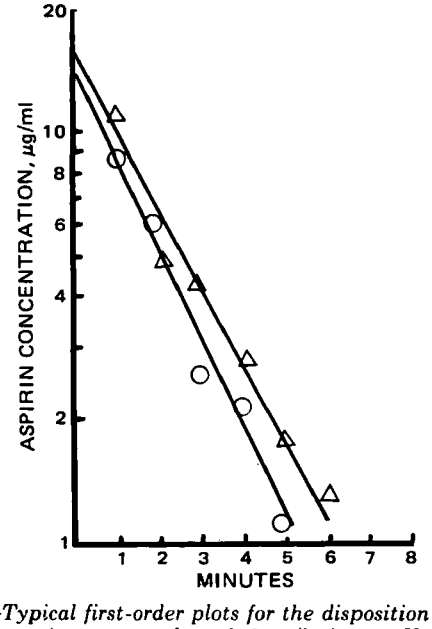

Figure 2—*Typical first-order plots for the disposition of aspirin in plasma after an intravenous dose of 10 mg/kg in rats. Key: (○) control rats (received food and water* ad libitum*); (△) treatment rats (deprived of water for 36 hr, but received food* ad libitum*).*

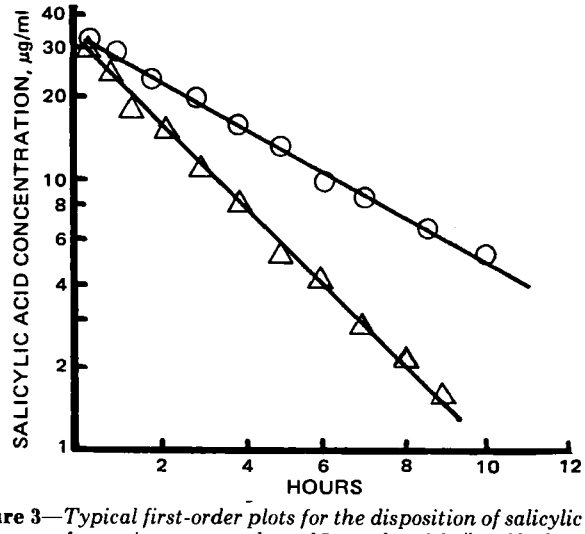

Figure 3—*Typical first-order plots for the disposition of salicylic acid in plasma after an intravenous dose of 5 mg of aspirin/kg of body weight in rats. Key: (△) control rats (received food and water* ad libitum*); (○) treatment rats (deprived of water for 36 hr, but received food* ad libitum*).*

Table V—Recovery of Aspirin Metabolites Salicylic Acid, Salicyluric Acid, and Gentisic Acid in Urine After Intravenous Administration of Aspirin in Two Doses to Control and Water-Deprived Rats

Aspirin Dose, mg/kg	Group	Recovery in Urine, % of Aspirin Dose						
		Salicylic Acid		Salicyluric Acid		Gentisic Acid		
		Mean ± *SEM*	Range	Mean ± *SEM*	Range	Mean ± *SEM*	Range	Total
5	Control[a]	48.6 ± 3.7	40.0–63.1	46.0 ± 3.0	34.9–55.2	—	—	94.6 ± 4.2
5	Water Deprived[b]	44.2 ± 5.7	24.5–65.0	53.6 ± 7.1	30.4–81.9	—	—	97.8 ± 1.8
10	Control	58.3 ± 5.0	31.2–81.3	38.0 ± 4.9	25.7–72.4	—	—	96.3 ± 4.0
10	Water Deprived	50.3 ± 1.7	40.6–55.6	36.9 ± 2.3	29.8–48.2	6.5 ± 0.9	3.6–10.8	93.6 ± 2.1

[a] The control group of rats (n = 6) received food and water *ad libitum*. [b] The rats (n = 9) were deprived of water for 36 hr, but received food *ad libitum*.

< 0.05) when the dose is doubled. This confirms the earlier finding in humans (28), that the disposition of salicylic acid is dose dependent. When the dose was doubled in the control rats, the half-life increased from 2.1 to 3.6 hr, an increase of ~72%. In water-deprived rats, the corresponding increase was 69% (2.59 to 4.37 hr).

The significant increase in the biological half-life of salicylic acid with water deprivation has important implications in the salicylate therapy of rheumatoid arthritis and inflammatory diseases, where aspirin is administered chronically at high dosages and where effective therapeutic levels of salicylate in these conditions approach toxic levels. Accumulation of salicylate due to increased biological half-life, as a result of short-term water deprivation, may produce toxic, possibly fatal effects.

Metabolites of Aspirin in Control and Water-Deprived Rats—Urine samples were analyzed for the major aspirin metabolites, salicylic and salicyluric acids, which account for >90% of the administered dose, and also for the minor metabolite, gentisic acid. The results are shown in Table V for a 5-mg/kg dose of aspirin in control and water-deprived (treatment) rats. The total recovery of aspirin in control rats is ~95% as compared with 97% for the treatment group. There was no significant difference in recovery of aspirin metabolites in these two groups of rats, and there also was no detectable gentisic acid in any of the urine samples. In both groups, approximately half of the aspirin was excreted as salicyluric acid. The fraction of aspirin excreted in the urine as salicyluric acid decreased significantly ($p < 0.05$) as the dose was increased from 5 to 10 mg/kg in both groups of rats. However, no effect of water deprivation was observed on the total percentage of aspirin metabolized to salicyluric acid. This finding is very interesting, since it would be expected that the percentage of salicyluric acid formed would increase in water-deprived rats because the long half-life of salicylic acid gives the liver more time to form salicyluric acid under conditions of metabolic saturation.

Since water deprivation produces no significant change in the excretion of salicyluric acid, the situation may be explained by one or both of two phenomena:

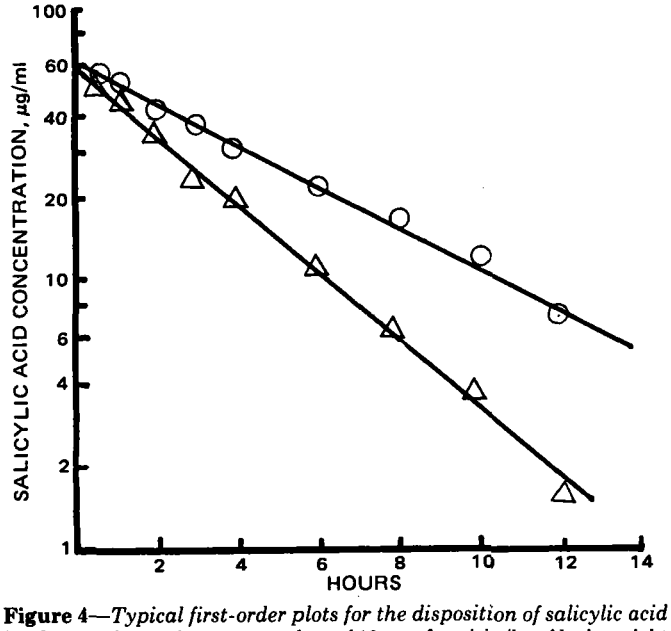

Figure 4—*Typical first-order plots for the disposition of salicylic acid in plasma after an intravenous dose of 10 mg of aspirin/kg of body weight in rats. Key: (△) control rats (received food and water* ad libitum*); (○) treatment rats (deprived of water for 36 hr, but received food* ad libitum*).*

1. If it is assumed that the drug-metabolizing enzymes are inhibited to some extent by water deprivation, the longer circulating half-life of salicylic acid could be balanced by the slower rate of formation of salicyluric acid. In the first step, the carboxylic group of salicylic acid binds with CoA to form the activated complex. In the second step, glycine conjugates with the reactive complex with the help of glycine-*N*-acylase. It is not presently known if one or both of these enzymes is inhibited by water deprivation.

2. The renal tubular conversion of salicyluric acid to salicylic acid (42) is a significant factor. The salicyluric acid formed in the liver from salicylic acid is transferred to the tubule cells of the kidneys, where it is metabolized back to salicylic acid and reabsorbed, thus prolonging the biological half-life of salicylic acid without increasing the proportion of salicyluric acid in the urine. Since with water deprivation, rats are more likely to conserve body water by reducing the formation of urine, the conversion of salicyluric acid to salicylic acid is more likely to occur.

Another interesting finding from the urinary studies is that at higher aspirin doses (10 mg/kg), ~6.5% of aspirin was metabolized to gentisic acid in water-deprived rats, suggesting that the enzyme system responsible for the hydroxylation of the aromatic ring (microsomal mixed-function oxidase) is somewhat stimulated by short-term water deprivation. No gentisic acid was found in the urine of control rats.

In conclusion, it might be stated that although there is no dramatic change in the excretion pattern of different metabolites of aspirin in the urine, the half-life of salicylic acid is significantly increased with water deprivation at both dose levels studied. This increased biological half-life of salicylic acid may have significant clinical impact in the treatment of rheumatoid arthritis and other diseases where the differences between the effective and toxic blood levels of salicylate are extremely narrow.

REFERENCES

(1) G. I. Hatton, *Physiol. Behav.*, **7**, 35 (1970).

(2) J. O. Barker and E. F. Adolph, *Am. J. Physiol.*, **173**, 495 (1953).

(3) C. L. Kutscher, *Comp. Biochem. Physiol.*, **25**, 929 (1968).

(4) P. Aarseth and D. King, *Acta Physiol. Scand.*, **85**, 277 (1972).

(5) C. Lucke, H. Erbler, T. Hating, and K. D. Dohler, *Contr. Nephrol.*, **19**, 63 (1980).

(6) S. A. Osman, J. D. Smith, L. E. Hanson, and R. J. Meade, *J. Nutr.*, **90**, 268 (1966).

(7) C. L. Kutscher, *Physiol. Behav.*, **7**, 283 (1971).

(8) J. J. Legros and J. J. Dreifuss, *Experimentia*, **31**, 603 (1975).

(9) H. G. Brazzuna and H. Pierce, *Acta Physiol. Lat. Am.*, **25**, 83 (1975).

(10) I. M. Libermann, H. Brazzuna, J. Rodriguez, A. Capano, and J. Neumark, *Pfluegers Arch.*, **365**, 191 (1976).

(11) L. N. Ivanoa, T. E. Goryunova, and V. P. Limova, *Dokl. Akad. Nauk SSR.*, **224**, 1209 (1975); through *Chem. Abstr.*, **84**, 26322r (1976).

(12) B. Ballantyne, *Cytobiosis*, **6**, 217 (1972).

(13) C. W. Jones and B. T. Pickering, *J. Physiol. (London)*, **203**, 449 (1969).

(14) G. J. Boer and J. F. Jonking, *J. Neurochem.*, **22**, 965 (1974).

(15) C. Popov, *Dokl. Bolg. Akad. Nauk.*, **29**, 715 (1976); through *Chem. Abstr.*, **85**, 120790j (1976).

(16) I. A. Alimova, Z. A. Ishkakov, and K. Raknimov, *Uzb. Biol. Zh.*, **17**, 32 (1973); through *Chem. Abstr.*, **80**, 118808z (1974).

(17) R. L. Dixon, R. W. Sultice, and J. R. Fouts, *Proc. Soc. Exp. Biol. Med.*, **103**, 333 (1960).

(18) R. Kato and J. R. Gillette, *J. Pharmacol. Exp. Ther.*, **150**, 279 (1965).

(19) R. Kato and J. R. Gillette, *J. Pharmacol. Exp. Ther.*, **150**, 285 (1965).

(20) T. W. Gram, A. M. Guarino, D. H. Schroeder, D. C. Davis, R. L. Reagan, and J. R. Gillette, *J. Pharmacol. Exp. Ther.*, **175**, 121 (1970).
(21) J. R. Gillette, *Ann. N.Y. Acad. Sci.*, **179**, 43 (1971).
(22) T. C. Campbell and J. R. Hays, *Pharmacol. Rev.*, **26**, 171 (1974).
(23) A. M. Baetjer, S. N. D. Joarder, and W. A. McQuary, *Arch. Environ. Health*, **1**, 463 (1960).
(24) A. M. Baetjer, *Arch. Environ. Health*, **19**, 784 (1969).
(25) A. M. Baetjer and R. J. Rubin, *J. Toxicol. Environ. Health*, **2**, 131 (1976).
(26) M. D. Maines and B. A. Westfall, *Comp. Gen. Pharmacol.*, **2**, 311 (1971).
(27) K. Thomsen and O. V. Olsen, *J. Pharmacol. Exp. Ther.*, **209**, 327 (1979).
(28) G. Levy, *J. Pharm. Sci.*, **54**, 959 (1965).
(29) M. Rowland and S. Riegelman, *J. Pharm. Sci.*, **57**, 1313 (1968).
(30) G. Levy, *Pediatrics*, **62**, 867 (1978).
(31) G. Levy, *Drug Metab. Rev.*, **9**, 3 (1979).
(32) W. D. Mason and N. Winer, *J. Pharm. Sci.*, **70**, 262 (1981).
(33) D. E. Furst, N. Gupta, and H. E. Paulas, *J. Clin. Invest.*, **60**, 32 (1977).
(34) T. Tsuchya and G. Levy, *J. Pharm. Sci.*, **61**, 800 (1972).
(35) R. E. MacMillen and A. K. Lee, *Science*, **158**, 383 (1967).
(36) A. L. Tonkin, J. F. Wheldrake, and R. V. Baudinette, *Comp. Biochem. Physiol.*, **1977**, 585.
(37) S. K. Bakar and S. Niazi, *J. Pharm. Sci.*, **72**, 1027 (1983).
(38) S. K. Bakar and S. Niazi, *J. Pharm. Sci.*, **72**, 1024 (1983).
(39) S. K. Bakar and S. Niazi, *J. Pharm. Sci.*, **72**, 1020 (1983).
(40) M. Wood, D. G. Shand, and A. J. J. Wood, *Clin. Pharmacol. Ther.*, **25**, 103 (1979).
(41) V. Weigand and G. Levy, *J. Pharm. Sci.*, **68**, 1483 (1979).
(42) I. Bekersky, L. Fishman, S. A. Kaplan, and W. A. Colburn, *J. Pharmacol. Exp. Ther.*, **212**, 309 (1980).

Effect of Dosage Form and Formulation Factors on the Adherence of Drugs to the Esophagus

MARTTI MARVOLA [‡x], **MARKKU RAJANIEMI, ESKO MARTTILA, KARI VAHERVUO, and ASLAK SOTHMANN**

Received June 15, 1982, from the [*]*Pharmaceutical Research Laboratories, Orion Pharmaceutical Co., SF-02101 Espoo, Finland*, and [‡]*School of Pharmacy, University of Helsinki, Helsinki, Finland.* Accepted for publication August 20, 1982.

Abstract □ In recent years, many case reports concerning esophageal injuries caused by drugs have been published. The primary cause has apparently been the adherence of the drug product to the esophagus. In the present study, the adherent tendency of a number of types of tablets and capsules were tested *in vitro* using a recently developed isolated porcine esophagus preparation. The results showed that the tendency of products to adhere to the esophageal mucosa can be modified to a great extent by shape and formulation. Products with low adherence can be obtained by film coating with aqueous dispersions or by sugarcoating. In contrast, gelatin capsules and some cellulose films appear to have a high tendency to adhere to the esophagus.

Keyphrases □ Tablet coatings—effect on adherence, isolated porcine esophagus, potassium chloride □ Potassium chloride—adherence to isolated porcine esophagus, effect of tablet shape, formulation, and coatings □ Drug formulations—effect of additives and coatings on adherence, isolated porcine esophagus

In recent years, many reports concerning esophageal injuries caused by drugs (*e.g.*, doxycycline, emepronium bromide, and potassium chloride) have been published (1–9). The primary cause has apparently been adherence of the drug product to the esophageal mucosa. The tendency to adhere has obviously been greatest for hard gelatin capsules, but differences between various tablet formulations have also been evident. In a previous paper, a study of the tendency of drug products to adhere to the esophageal wall, using the isolated porcine esophagus, was published (10). In the present investigation the effect of the pharmaceutical characteristics of dosage forms on the adherence was studied.

EXPERIMENTAL

Isolated Esophagus Preparation—The isolated porcine esophagus preparation and its usefulness has been described previously (10). Pigs of both sexes were of the Landrace or Yorkshire breeds, weighing 90–100 kg. Immediately after slaughter, the esophagi were removed and transported to the laboratory in Tyrode's solution. Segments (6–7 cm long) were cut from the esophagus and mounted in a classic organ bath for isolated preparations.

Recording of Adherence—A hole was drilled in the products to be tested. The product was attached to a copper wire and placed in the esophageal preparation for 2.0 min (gelatin capsules, 1.0 min). The force needed to detach the product was then measured using a modified prescription balance (10); the force used was taken as a measure of adherence.

Drug Products—Hard gelatin capsules[1] sizes 1, 2, 3, 4, and 5 were filled with lactose. Oval soft gelatin capsules[2] (length 12 or 15 mm) were left empty. The round soft gelatin capsule formulation studied was a commercially available product[3] (diameter 7 mm). The uncoated placebo tablets were compressed from a mixture of basic granules (96%), talc (3%), and magnesium stearate (1%). The basic granules contained 78% lactose, 19% cornstarch, and 3% gelatin. Potassium chloride tablets were compressed from pure potassium chloride. To obtain products with low adherent properties metal tablets were compressed from an alloy of bismuth, lead, tin, and cadmium (5:3:1:1). The shapes, diameters, and areas of all formulations are given in Tables I–III.

The sugar-coated tablets were all commercially available products[3]. The coating suspension used contained 47 g of sucrose, 4 g of polyethylene glycol 6000, 8 g of calcium sulfate, 2 g of titanium dioxide, 30 g of purified water, and 3 g of other ingredients. The dusting powder contained calcium sulfate and talc (1:1). The coating suspension and powder were used in an approximate ratio of 9:5.

To investigate the effect of film coatings on the adherence of drugs to the esophagus, biconvex tablets were coated with different film coatings. The compositions of the hydroxypropyl methyl cellulose-containing solutions (I–V) are given in Table I. The other coating solutions were as follows: VI, 10.0 g of cellulose acetate phthalate, 0.5 g of castor oil, and 89.5 g of acetone; VII, 14.0 g of polyethylene glycol 6000, 6.0 g of cellulose acetate phthalate, 1.0 g of stearic acid, 0.3 g of castor oil, 0.3 g of sorbitan

[1] Capsugel AG, Switzerland and Eli Lilly and Co.
[2] R. P. Scherer Ltd, England.
[3] Orion Pharmaceutical Co, Finland.

0022-3549/83/0900-1034$01.00/0

(20) T. W. Gram, A. M. Guarino, D. H. Schroeder, D. C. Davis, R. L. Reagan, and J. R. Gillette, *J. Pharmacol. Exp. Ther.*, **175**, 121 (1970).
(21) J. R. Gillette, *Ann. N.Y. Acad. Sci.*, **179**, 43 (1971).
(22) T. C. Campbell and J. R. Hays, *Pharmacol. Rev.*, **26**, 171 (1974).
(23) A. M. Baetjer, S. N. D. Joarder, and W. A. McQuary, *Arch. Environ. Health*, **1**, 463 (1960).
(24) A. M. Baetjer, *Arch. Environ. Health*, **19**, 784 (1969).
(25) A. M. Baetjer and R. J. Rubin, *J. Toxicol. Environ. Health*, **2**, 131 (1976).
(26) M. D. Maines and B. A. Westfall, *Comp. Gen. Pharmacol.*, **2**, 311 (1971).
(27) K. Thomsen and O. V. Olsen, *J. Pharmacol. Exp. Ther.*, **209**, 327 (1979).
(28) G. Levy, *J. Pharm. Sci.*, **54**, 959 (1965).
(29) M. Rowland and S. Riegelman, *J. Pharm. Sci.*, **57**, 1313 (1968).
(30) G. Levy, *Pediatrics*, **62**, 867 (1978).
(31) G. Levy, *Drug Metab. Rev.*, **9**, 3 (1979).
(32) W. D. Mason and N. Winer, *J. Pharm. Sci.*, **70**, 262 (1981).
(33) D. E. Furst, N. Gupta, and H. E. Paulas, *J. Clin. Invest.*, **60**, 32 (1977).
(34) T. Tsuchya and G. Levy, *J. Pharm. Sci.*, **61**, 800 (1972).
(35) R. E. MacMillen and A. K. Lee, *Science*, **158**, 383 (1967).
(36) A. L. Tonkin, J. F. Wheldrake, and R. V. Baudinette, *Comp. Biochem. Physiol.*, **1977**, 585.
(37) S. K. Bakar and S. Niazi, *J. Pharm. Sci.*, **72**, 1027 (1983).
(38) S. K. Bakar and S. Niazi, *J. Pharm. Sci.*, **72**, 1024 (1983).
(39) S. K. Bakar and S. Niazi, *J. Pharm. Sci.*, **72**, 1020 (1983).
(40) M. Wood, D. G. Shand, and A. J. J. Wood, *Clin. Pharmacol. Ther.*, **25**, 103 (1979).
(41) V. Weigand and G. Levy, *J. Pharm. Sci.*, **68**, 1483 (1979).
(42) I. Bekersky, L. Fishman, S. A. Kaplan, and W. A. Colburn, *J. Pharmacol. Exp. Ther.*, **212**, 309 (1980).

Effect of Dosage Form and Formulation Factors on the Adherence of Drugs to the Esophagus

MARTTI MARVOLA [‡x], **MARKKU RAJANIEMI, ESKO MARTTILA, KARI VAHERVUO, and ASLAK SOTHMANN**

Received June 15, 1982, from the [*]*Pharmaceutical Research Laboratories, Orion Pharmaceutical Co., SF-02101 Espoo, Finland*, and [‡]*School of Pharmacy, University of Helsinki, Helsinki, Finland.* Accepted for publication August 20, 1982.

Abstract □ In recent years, many case reports concerning esophageal injuries caused by drugs have been published. The primary cause has apparently been the adherence of the drug product to the esophagus. In the present study, the adherent tendency of a number of types of tablets and capsules were tested *in vitro* using a recently developed isolated porcine esophagus preparation. The results showed that the tendency of products to adhere to the esophageal mucosa can be modified to a great extent by shape and formulation. Products with low adherence can be obtained by film coating with aqueous dispersions or by sugarcoating. In contrast, gelatin capsules and some cellulose films appear to have a high tendency to adhere to the esophagus.

Keyphrases □ Tablet coatings—effect on adherence, isolated porcine esophagus, potassium chloride □ Potassium chloride—adherence to isolated porcine esophagus, effect of tablet shape, formulation, and coatings □ Drug formulations—effect of additives and coatings on adherence, isolated porcine esophagus

In recent years, many reports concerning esophageal injuries caused by drugs (*e.g.*, doxycycline, emepronium bromide, and potassium chloride) have been published (1–9). The primary cause has apparently been adherence of the drug product to the esophageal mucosa. The tendency to adhere has obviously been greatest for hard gelatin capsules, but differences between various tablet formulations have also been evident. In a previous paper, a study of the tendency of drug products to adhere to the esophageal wall, using the isolated porcine esophagus, was published (10). In the present investigation the effect of the pharmaceutical characteristics of dosage forms on the adherence was studied.

EXPERIMENTAL

Isolated Esophagus Preparation—The isolated porcine esophagus preparation and its usefulness has been described previously (10). Pigs of both sexes were of the Landrace or Yorkshire breeds, weighing 90–100 kg. Immediately after slaughter, the esophagi were removed and transported to the laboratory in Tyrode's solution. Segments (6–7 cm long) were cut from the esophagus and mounted in a classic organ bath for isolated preparations.

Recording of Adherence—A hole was drilled in the products to be tested. The product was attached to a copper wire and placed in the esophageal preparation for 2.0 min (gelatin capsules, 1.0 min). The force needed to detach the product was then measured using a modified prescription balance (10); the force used was taken as a measure of adherence.

Drug Products—Hard gelatin capsules[1] sizes 1, 2, 3, 4, and 5 were filled with lactose. Oval soft gelatin capsules[2] (length 12 or 15 mm) were left empty. The round soft gelatin capsule formulation studied was a commercially available product[3] (diameter 7 mm). The uncoated placebo tablets were compressed from a mixture of basic granules (96%), talc (3%), and magnesium stearate (1%). The basic granules contained 78% lactose, 19% cornstarch, and 3% gelatin. Potassium chloride tablets were compressed from pure potassium chloride. To obtain products with low adherent properties metal tablets were compressed from an alloy of bismuth, lead, tin, and cadmium (5:3:1:1). The shapes, diameters, and areas of all formulations are given in Tables I–III.

The sugar-coated tablets were all commercially available products[3]. The coating suspension used contained 47 g of sucrose, 4 g of polyethylene glycol 6000, 8 g of calcium sulfate, 2 g of titanium dioxide, 30 g of purified water, and 3 g of other ingredients. The dusting powder contained calcium sulfate and talc (1:1). The coating suspension and powder were used in an approximate ratio of 9:5.

To investigate the effect of film coatings on the adherence of drugs to the esophagus, biconvex tablets were coated with different film coatings. The compositions of the hydroxypropyl methyl cellulose-containing solutions (I–V) are given in Table I. The other coating solutions were as follows: VI, 10.0 g of cellulose acetate phthalate, 0.5 g of castor oil, and 89.5 g of acetone; VII, 14.0 g of polyethylene glycol 6000, 6.0 g of cellulose acetate phthalate, 1.0 g of stearic acid, 0.3 g of castor oil, 0.3 g of sorbitan

[1] Capsugel AG, Switzerland and Eli Lilly and Co.
[2] R. P. Scherer Ltd, England.
[3] Orion Pharmaceutical Co, Finland.

0022-3549/83/0900-1034$01.00/0

Table I—Compositions of Coating Solutions I–V

Ingredient	Amount in the Coating Solution, g I	II	III	IV	V
Hydroxypropyl methyl cellulose	7	5	6	6	7
Titanium dioxide	—	3	—	—	7
Talc	—	1	—	—	—
Sucrose	—	—	8	—	—
Lactose	—	—	—	8	—
Ethyl cellulose pseudolatex[a]	—	—	—	—	22
Triacetin	—	—	—	—	1
Purified water	—	—	66	66	63
Ethyl alcohol	68	71	20	20	—
Methylene chloride	25	20	—	—	—

[a] Aquacoat ECD-30; FMC Corp.

Table II—Effect of Tablet Shape on the Force Needed to Detach the Product from the Isolated Esophagus

Formulation	Force per Unit Area[a], $mN \cdot mm^{-2}$ Biconvex Tablets	Flat Tablets[b]	Capsule-Shaped Tablets[b]
Uncoated placebo	2.40 ± 0.72	2.92 ± 0.88*	1.77 ± 0.53**
Potassium chloride	0.56 ± 0.11	0.64 ± 0.13*	0.41 ± 0.09***
Metal	0.56 ± 0.08	0.66 ± 0.10***	0.44 ± 0.09***

[a] Means ± *SD*; $n = 20$. [b] Student's t test, compared with the corresponding value of the biconvex tablets: (*) $p < 0.05$, (**) $p < 0.01$, (***) $p < 0.001$.

Table III—Effect of Tablet Coatings on the Force Needed to Detach the Tablets from the Isolated Esophagus

Tablet Coating	Diameter, mm	Area, mm^2	Detaching Force[a], N	Force per Unit Area, $mN \cdot mm^{-2}$
Uncoated	7	160	0.41 ± 0.08	2.56
	9	223	0.53 ± 0.08	2.38
	10	259	0.65 ± 0.22	2.51
	11	299	0.71 ± 0.21	2.37
	12	358	0.86 ± 0.26	2.40
Sugarcoated	6	101	0.08 ± 0.02	0.65
	8	190	0.13 ± 0.03	0.68
	10	277	0.16 ± 0.02	0.58
Film coating I	9	226	0.55 ± 0.18	2.43
	11	350	0.64 ± 0.27	1.83
Film coating II	9	316	0.79 ± 0.20	2.50
	11	350	0.93 ± 0.20	2.66
Film coating III	7	127	0.20 ± 0.04	1.57
	9	240	0.33 ± 0.10	1.38
	11	336	0.47 ± 0.13	1.40
Film coating IV	7	127	0.38 ± 0.14	2.99
	9	209	0.55 ± 0.20	2.63
	11	316	0.78 ± 0.32	2.47
Film coating V	11	298	0.31 ± 0.08	1.04
Film coating VI	11	329	0.39 ± 0.15	1.19
Film coating VII	11	299	0.91 ± 0.24	3.04
Film coating VIII	12	379	0.31 ± 0.08	0.82
Film coating IX	10	259	0.18 ± 0.09	0.69
Film coating X	9	214	0.24 ± 0.05	1.12

[a] Mean ± *SD*; $n = 20$.

monooleate, 12.0 g of ethyl alcohol, and 64.0 g of acetone; VIII, 4.2 g of shellac, 1.4 g of polyethylene glycol 6000, 12.6 g of titanium dioxide, 4.2 g of talc, 1.4 g of povidone, 1.4 g of sorbitan monooleate, 4.2 g of iron oxide, and 40.6 g of isopropyl alcohol; and IX, 16.7 g of methacrylate copolymer[4], 8.0 g of talc, 3.5 g of titanium dioxide, 1.5 g of iron oxide, 0.5 g of hydroxypropyl methyl cellulose, and 68.3 g of purified water. In addition, a placebo product coated with a copolymer of vinyl acetate and crotonic acid[5] (X) was investigated. The product was supplied by the manufacturer.

In the final part of the present study, 10 commercially available potassium chloride products were studied. The coatings of these products are described on the basis of information given by the manufacturers or their Finnish agents.

[4] Eudragit E 30 D; Röhm Pharma, West Germany.
[5] BASF CE 5142; BASF, West Germany.

Table IV—Effect of Material, Size, and Shape of Gelatin Capsules on the Force Needed to Detach the Products from the Isolated Esophagus

Formulation	Area, mm^2	Detaching Force[a], N	Force per Unit Area, $mN \cdot mm^{-2}$
Hard gelatin capsule			
No. 2	330	1.30 ± 0.31	3.94
No. 3	283	1.10 ± 0.28	3.89
No. 4	220	0.85 ± 0.18	3.86
No. 5	160	0.64 ± 0.20	3.88
Oval soft gelatin capsule			
Length 15 mm	350	0.88 ± 0.27	2.51
Length 12 mm	268	0.80 ± 0.25	2.99
Round soft gelatin capsule (7 mm)	154	0.39 ± 0.14	2.53

[a] Mean ± *SD*; $n = 15$.

RESULTS AND DISCUSSION

The effect of shape on the force needed to detach the products from the isolated porcine esophagus is shown in Table II. Detachment force was greatest for flat tablets and lowest for capsule-shaped tablets. Capsule-shaped tablets may therefore be preferable for drugs known to cause esophageal ulceration.

The adherence of biconvex tablets of different surface areas and coatings is shown in Table III; the same data for various gelatin capsules are shown in Table IV. There were no significant differences in adherence to the esophagus between the hard gelatin capsules made by the two different manufacturers.

As the results show, the tendency to adhere was greatest for hard gelatin capsules. Calculated per unit area, it was six times as high as that for sugarcoated tablets, which had the lowest tendency to adhere. The force needed to detach the soft gelatin capsules was significantly lower than that for the hard gelatin capsules. However, soft gelatin capsules seemed to stick to the esophagus to the same degree as the most adherent tablet formulations in this study.

If the specific adherence of the film coatings is examined, it can be seen that the very common coating material hydroxypropyl methyl cellulose (I) belongs to the middle group of all formulations studied. The tendency of the hydroxypropyl methyl cellulose film to adhere could be adjusted by the use of additives. If sucrose (III) was added, the adherent tendency decreased significantly. The mixture of hydroxypropyl methyl cellulose and ethyl cellulose pseudolatex (V) led to a still lower adherence. In contrast, the addition of lactose (IV) or titanium dioxide and talc (II) increased the tendency to stick.

The common enteric coating cellulose acetate phthalate film (VI) had a fairly low adherent tendency, as did the coatings of shellac (VIII), methacrylate copolymer (IX), and the copolymer of vinyl acetate and crotonic acid (X). When polyethylene glycol 6000 (VII) was used as the main film-forming material, the adherence was, in contrast, considerable.

The results relating to the uncoated placebo tablets should not be interpreted as indicating that the adherent tendency of uncoated tablets is always high. The conclusion relates to the present situation in which tablets were compressed from granules containing lactose and cornstarch. Previous results have shown, however, that uncoated tablets containing other ingredients can have a very low tendency to adhere to the isolated esophagus (10).

The forces needed to detach the commercially available potassium chloride products from the esophagus are shown in Table V. Adherence of the worst formulation was ~3.2 times as great as that of the best formulation. The forces per unit area in Table V are in good agreement with the results in Table III. Sugarcoated tablets had a low adherent tendency, and the specific adherence of the hydroxypropyl methyl cellulose films were 2.1–2.4 $mN \cdot mm^{-2}$ as compared with 1.8–2.4 $mN \cdot mm^{-2}$ in Table III. It is noteworthy that the adherence of hydroxypropyl methyl cellulose decreased as a consequence of adding silicic acid. Ethyl cellulose seemed to have fairly substantial adherent properties.

Although gelatin capsules appeared to have the greatest tendency to adhere to the isolated porcine esophagus, the present results show that many tablet formulations could have a similar tendency to adhere. However, by selecting a proper coating material this tendency can be diminished. The classic sugarcoating seems to be a good choice in this respect. The addition of sucrose to film coatings also reduces adherence. Film coating with aqueous dispersions (IX and V) also results in products

Table V—Force Needed to Detach the Commercially Available Potassium Chloride Formulations from the Isolated Porcine Esophagus

Drug Product	Amount of Potassium Chloride, g	Coating Material	Detaching Force[a], N	Mean Force per Unit Area, $mN \cdot mm^{-2}$
A	1.0	Polyvinyl chloride; sucrose crystals	0.38 ± 0.03	0.9
B	0.6	Sugarcoating	0.39 ± 0.01	0.9
C	1.0	Hydroxypropyl methyl cellulose; silicic acid	0.54 ± 0.04	1.1
D	0.5	Hydroxypropyl methyl cellulose	0.78 ± 0.06	2.4
E	0.75	Hydroxypropyl cellulose	0.93 ± 0.09	2.6
F	0.75	Hydroxypropyl methyl cellulose	0.94 ± 0.12	2.2
G	1.0	Hydroxypropyl methyl cellulose	0.98 ± 0.13	2.1
H	0.75	Special wax; talc	1.00 ± 0.11	2.8
I	1.0	Special wax; talc	1.10 ± 0.13	2.4
J	0.75	Ethyl cellulose	1.20 ± 0.10	2.2

[a] Mean ± *SD*; $n = 18$.

with low adherence. In contrast, sparingly water-soluble ingredients (talc, titanium dioxide, and ethyl cellulose) and, in addition, lactose, mostly increase adherence.

On the basis of this research it seems possible to develop pharmaceutical products having a very low tendency to adhere to the esophageal mucosa. It seems desirable to develop such products in the case of drugs known to cause esophageal strictures or ulcerations, in particular.

REFERENCES

(1) L. Bokey and T. B. Hugh, *Med. J. Austr.*, **1**, 236 (1975).

(2) T. D. Crowson, L. H. Head, and W. A. Ferrante, *J. Am. Med. Assoc.*, **235**, 2747 (1976).

(3) B. Carlborg, A. Kumlien, and H. Olsson, *Läkartidningen*, **75**, 4609 (1978).

(4) H. Kavin, *Lancet*, **i**, 424 (1977).

(5) H. J. Puhakka, *J. Laryngol. Otol.*, **92**, 927 (1978).

(6) R. Hughes, *Br. Med. J.*, **2**, 132 (1979).

(7) J. Pemberton, *Br. Heart J.*, **32**, 267 (1970).

(8) T. Rosenthal, R. Adar, J. Militianu, and V. Deutsch, *Chest*, **65**, 463 (1974).

(9) J. R. Lambert and A. Newman, *Am. J. Gastroenterol.*, **73**, 508 (1980).

(10) M. Marvola, K. Vahervuo, A. Sothmann, E. Marttila, and M. Rajaniemi, *J. Pharm. Sci.*, **71**, 975 (1982).

High-Performance Liquid Chromatographic Analysis of Iodochlorohydroxyquin and Hydrocortisone in Ointments and Creams

F. W. EZZEDEEN *, S. J. STOHS *x, and A. N. MASOUD ‡

Received April 5, 1982, from the *Departments of *Biomedicinal Chemistry and ‡Anesthesiology, University of Nebraska Medical Center, Omaha, NE 68105.* Accepted for publication August 13, 1982.

Abstract □ A simple isocratic, high-performance liquid chromatographic (HPLC) assay procedure was developed for the simultaneous determination of iodochlorhydroxyquin and hydrocortisone in ointments and creams using phenyl salicylate as an internal standard. Ointment samples were extracted by direct dissolution in ether. Homogeneous suspensions of the creams were prepared in the mobile phase. The samples were spiked by the addition of standard iodochlorhydroxyquin, standard hydrocortisone, and the internal standard and subsequently extracted with the mobile phase. HPLC was performed using a reverse-phase microparticulate C-18 column, a precolumn, and a UV detector set at 256 nm. A mobile phase containing methanol and 0.05 *M* phosphoric acid (70:30) was employed at a flow rate of 1 ml/min. The percent iodochlorhydroxyquin and hydrocortisone found to be present in eight commercial products is reported.

Keyphrases □ Iodochlorhydroxyquin—simultaneous determination with hydrocortisone, ointment and cream, high-performance liquid chromatography □ Hydrocortisone—simultaneous determination with iodochlorhydroxyquin, ointment and cream, high-performance liquid chromatography □ High-performance liquid chromatography—simultaneous determination of iodochlorhydroxyquin and hydrocortisone, ointment and cream

Iodochlorhydroxyquin (I) is used alone or in combination with hydrocortisone (II) as an antimycotic, antibacterial, and anti-inflammatory agent in topical preparations. Because of its toxicity, several analytical procedures have been developed for the determination of I in biological fluids (1–7). The present pharmacopeial assay method for I in creams or ointments (8, 9) is time consuming, requires heating during the extraction procedures (which can lead to decomposition of I), and involves the use of an IR spectrophotometric assay procedure. Other IR spectrophotometeric procedures specific for I in pharmaceutical products have also been described (10, 11). However, these methods are cumbersome, require a large sample, and involve the use of carbon disulfide in the assay procedure. The pharmacopeial methods for assaying II in creams and ointments (12) depend on the oxidation of the α-ketol side chain by either triphenyltetrazolin chloride or blue tetrazolin. Base concentration, water, air, solvent, and light are known to interfere with color formation in the tetrazolin reaction (13). Excipients that interfere with color formation include sorbitan monooleate, lanolin, and stearic acid (14).

This work describes a high-performance liquid chro-

0022-3549/83/0900-1036$01.00/0

Table V—Force Needed to Detach the Commercially Available Potassium Chloride Formulations from the Isolated Porcine Esophagus

Drug Product	Amount of Potassium Chloride, g	Coating Material	Detaching Force[a], N	Mean Force per Unit Area, $mN \cdot mm^{-2}$
A	1.0	Polyvinyl chloride; sucrose crystals	0.38 ± 0.03	0.9
B	0.6	Sugarcoating	0.39 ± 0.01	0.9
C	1.0	Hydroxypropyl methyl cellulose; silicic acid	0.54 ± 0.04	1.1
D	0.5	Hydroxypropyl methyl cellulose	0.78 ± 0.06	2.4
E	0.75	Hydroxypropyl cellulose	0.93 ± 0.09	2.6
F	0.75	Hydroxypropyl methyl cellulose	0.94 ± 0.12	2.2
G	1.0	Hydroxypropyl methyl cellulose	0.98 ± 0.13	2.1
H	0.75	Special wax; talc	1.00 ± 0.11	2.8
I	1.0	Special wax; talc	1.10 ± 0.13	2.4
J	0.75	Ethyl cellulose	1.20 ± 0.10	2.2

[a] Mean ± *SD*; $n = 18$.

with low adherence. In contrast, sparingly water-soluble ingredients (talc, titanium dioxide, and ethyl cellulose) and, in addition, lactose, mostly increase adherence.

On the basis of this research it seems possible to develop pharmaceutical products having a very low tendency to adhere to the esophageal mucosa. It seems desirable to develop such products in the case of drugs known to cause esophageal strictures or ulcerations, in particular.

REFERENCES

(1) L. Bokey and T. B. Hugh, *Med. J. Austr.*, **1**, 236 (1975).

(2) T. D. Crowson, L. H. Head, and W. A. Ferrante, *J. Am. Med. Assoc.*, **235**, 2747 (1976).

(3) B. Carlborg, A. Kumlien, and H. Olsson, *Läkartidningen*, **75**, 4609 (1978).

(4) H. Kavin, *Lancet*, **i**, 424 (1977).

(5) H. J. Puhakka, *J. Laryngol. Otol.*, **92**, 927 (1978).

(6) R. Hughes, *Br. Med. J.*, **2**, 132 (1979).

(7) J. Pemberton, *Br. Heart J.*, **32**, 267 (1970).

(8) T. Rosenthal, R. Adar, J. Militianu, and V. Deutsch, *Chest*, **65**, 463 (1974).

(9) J. R. Lambert and A. Newman, *Am. J. Gastroenterol.*, **73**, 508 (1980).

(10) M. Marvola, K. Vahervuo, A. Sothmann, E. Marttila, and M. Rajaniemi, *J. Pharm. Sci.*, **71**, 975 (1982).

High-Performance Liquid Chromatographic Analysis of Iodochlorohydroxyquin and Hydrocortisone in Ointments and Creams

F. W. EZZEDEEN *, S. J. STOHS *x, and A. N. MASOUD ‡

Received April 5, 1982, from the *Departments of *Biomedicinal Chemistry and ‡Anesthesiology, University of Nebraska Medical Center, Omaha, NE 68105.* Accepted for publication August 13, 1982.

Abstract □ A simple isocratic, high-performance liquid chromatographic (HPLC) assay procedure was developed for the simultaneous determination of iodochlorhydroxyquin and hydrocortisone in ointments and creams using phenyl salicylate as an internal standard. Ointment samples were extracted by direct dissolution in ether. Homogeneous suspensions of the creams were prepared in the mobile phase. The samples were spiked by the addition of standard iodochlorhydroxyquin, standard hydrocortisone, and the internal standard and subsequently extracted with the mobile phase. HPLC was performed using a reverse-phase microparticulate C-18 column, a precolumn, and a UV detector set at 256 nm. A mobile phase containing methanol and 0.05 *M* phosphoric acid (70:30) was employed at a flow rate of 1 ml/min. The percent iodochlorhydroxyquin and hydrocortisone found to be present in eight commercial products is reported.

Keyphrases □ Iodochlorhydroxyquin—simultaneous determination with hydrocortisone, ointment and cream, high-performance liquid chromatography □ Hydrocortisone—simultaneous determination with iodochlorhydroxyquin, ointment and cream, high-performance liquid chromatography □ High-performance liquid chromatography—simultaneous determination of iodochlorhydroxyquin and hydrocortisone, ointment and cream

Iodochlorhydroxyquin (I) is used alone or in combination with hydrocortisone (II) as an antimycotic, antibacterial, and anti-inflammatory agent in topical preparations. Because of its toxicity, several analytical procedures have been developed for the determination of I in biological fluids (1–7). The present pharmacopeial assay method for I in creams or ointments (8, 9) is time consuming, requires heating during the extraction procedures (which can lead to decomposition of I), and involves the use of an IR spectrophotometric assay procedure. Other IR spectrophotometeric procedures specific for I in pharmaceutical products have also been described (10, 11). However, these methods are cumbersome, require a large sample, and involve the use of carbon disulfide in the assay procedure. The pharmacopeial methods for assaying II in creams and ointments (12) depend on the oxidation of the α-ketol side chain by either triphenyltetrazolin chloride or blue tetrazolin. Base concentration, water, air, solvent, and light are known to interfere with color formation in the tetrazolin reaction (13). Excipients that interfere with color formation include sorbitan monooleate, lanolin, and stearic acid (14).

This work describes a high-performance liquid chro-

0022-3549/83/0900-1036$01.00/0

matographic (HPLC) method that can be used routinely to assay I and II in ointments and creams. The method is simple and combines specificity and sensitivity not attainable by previously described methods.

EXPERIMENTAL

Apparatus—The HPLC system consisted of a reciprocating minipump[1]; a stainless steel tube, 6.35-mm o.d. and 4.76-mm i.d. × 1 m as a pulsation damper; a 34.5-MPa (5000 psi) pressure gauge[2]; a fixed-volume sample injector[3] with a 20-μl loop; and a variable-wavelength UV detector[4]. A multivoltage 25.4-cm strip chart recorder[5] was connected to the UV detector. A microparticulate reverse-phase chromatographic column (250 × 2.6 mm, packed with ODS-HC-SIL-X-1[6]) and a 5 × 40-mm guard column (RP-18-MPLC[7]) were connected to the HPLC system. The following chemicals were used: iodochlorhydroxyquin[8]; anhydrous ether (analytical reagent grade)[9]; methanol distilled in glass, residue free[10]; phenyl salicylate[11]; hydrocortisone[12]; and water, which was deionized, demineralized, and glass-distilled in our laboratory. No impurities were detected by HPLC in the iodochlorhydroxyquin (I) or hydrocortisone (II) reference standards or in the phenyl salicylate internal standard.

Ointments and Creams—The following products used were reported by the manufacturers to contain the indicated percentages of each drug: product A[13], 3% I; product B[14], 3% I; product C[15], 3% I and 1% II; product D[16], 3% I and 1% II; product E[17], 3% I, 1% II, and 0.5% pramoxine hydrochloride; product F[18], 3% I and 0.5% II; product G[19], 3% I and 0.5% II; and product H[20], 3% I and 1% II.

Standards—Stock solutions of I were prepared in methanol at 1.0 mg/ml. Solutions of II and phenyl salicylate were each prepared in the mobile phase (methanol–0.05 *M* phosphoric acid, 70:30) and contained 1.0 mg/ml. These solutions could be stored in the refrigerator for at least 2 weeks without deterioration. Working standards were prepared daily, using methanol–0.05 *M* phosphoric acid (70:30) to make the desired dilutions.

Chromatographic Conditions—The parameters used for this investigation included a reverse-phase column and precolumn, as previously described, and a 20-μl injector loop, with the recorder chart speed set at 0.254 mm/min. A mobile phase containing methanol–0.05 *M* phosphoric acid (70:30) was used at a flow rate of 1 ml/min. The mobile phase was filtered using a 0.20-μm filter[21], deaerated under vacuum, and maintained at 40° during chromatography. The UV detector was set at 256 nm. The column was flushed at the end of each day with methanol. Not more than 30 min was required for column equilibration prior to use each day.

Extraction Procedures—*Ointments*—Fifty milligrams of each ointment was dissolved in 10 ml of ether by vortexing. Aliquots (200 μl) were transferred to 20-ml screw-cap vials and spiked with varying amounts of I working standard. A fixed amount of the internal standard (phenyl salicylate) was added to each vial. In cases where the ointments contained II, the ointment solutions were spiked with standard II solution in addition to I and the internal standard. These solutions were evaporated to dryness at 40° under a stream of nitrogen. The contents of each vial were dissolved in 10.0 ml of mobile phase by warming for 1 min on a steam bath followed by vortexing for 1 min. After cooling to room temperature, aliquots of each solution were removed, diluted with mobile phase, and injected onto the column.

Creams—Fifty milligrams of each cream was uniformly suspended in 10 ml of mobile phase by vortexing. Aliquots were removed, spiked with the standard solutions and internal standard, and evaporated to dryness as described above for ointments. The contents of each vial were warmed, suspended in 10.0 ml of the mobile phase by warming on a steam bath followed by vortexing. Aliquots were subsequently diluted with mobile phase and assayed by HPLC.

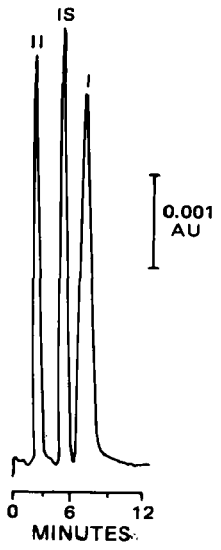

Figure 1—*Chromatogram of extracted product C to which the internal standard (IS), phenyl salicylate (4 μg/ml), had been added. The amounts of iodochlorhydroxyquin (I) and hydrocortisone (II) that were present in the product were 2.8 and 0.93%, respectively. The detector was set at 256 nm and 0.02 AUFS.*

RESULTS AND DISCUSSION

Iodochlorhydroxyquin (I) standard was scanned in methanol–0.05 *M* phosphoric acid (70:30) and exhibited maxima at 256 (α = 0.15) and 204 (α = 0.11) nm. For optimum sensitivity the detector was set at 256 nm.

The use of 4,7-dichloroquinoline[22], 10-chloro-9-anthracenemethanol[22], 2,4-quinolinediol[22], 3-quinolinecarbonitrile[22], 5,7-diiodo-8-hydroxyquinoline[23], and 5,7-dichloro-8-hydroxyquinoline[22] as internal standard was attempted without satisfactory results. 4,7-Dichloroquinoline, 5,7-diiodo-8-hydroxyquinoline, 10-chloro-9-anthracenemethanol, and 5,7-dichloro-8-hydroxyquinoline had retention times that overlapped with I, while 2,4-quinolinediol and 3-quinolinecarbonitrile had retention times that interfered with II. Phenyl salicylate was found to be suitable as an internal standard. It was easily separated from I, absorbed adequately at 256 nm, and produced consistent peak heights when extracted in conjunction with ointments or creams. Suitable retentions for I, II, and phenyl salicylate were obtained when a mobile phase containing methanol–0.05 *M* phosphoric acid (70:30) was used.

To determine whether the ointment and cream bases interfered with the HPLC of I, II, or the internal standard, the peak height ratios of the absorbances at two different wavelengths (256 and 246 nm) were determined on extracts from each product. These results were compared with the same ratios for the standard I, II, and internal standard. No differences were found when comparing the respective ratios, indicating that constituents in the bases that may have been extracted did not interfere with the analyses of the desired compounds.

Figure 1 is a chromatogram of an extracted ointment (product C) which contained I and II and was spiked with the internal standard. The capacity factor (k') for I was 2.94 and for the internal standard was 1.76,

[1] Milton Roy Model 326.
[2] Laboratory Data Control, Riviera Beach, FL 33404.
[3] Rheodyne Inc., Berkeley, CA 94710.
[4] Model Spectro-Monitor III; Laboratory Data Control, Riviera Beach, FL 33404.
[5] Beckman Instruments, Palo Alto, CA 94304.
[6] Serial No. 1303; Perkin-Elmer, Norwalk, CT 06858.
[7] Manufactured by Brownlee Lab and obtained from Rheodyne Inc., Berkeley, CA 94710.
[8] 5-Chloro-7-iodo-8-hydroxyquinoline, Vioform; Ciba Pharmaceutical, Summit, NJ 07901.
[9] Mallinckrodt Inc., St. Louis, MO 63147.
[10] Burdick and Jackson Labs Inc., Muskegan, MI 49442.
[11] Merck and Co., Rahway, NJ 07065.
[12] Sigma Chemical Co., St. Louis, MO 63178.
[13] Vioform Cream, Exp. date Aug. 82, Batch No. 13312; Ciba Pharmaceutical, Summit, NJ 07901.
[14] Vioform Ointment, Exp. date July 84, Batch No. 13642; Ciba Pharmaceutical, Summit, NJ, 07901.
[15] Vioform with Hydrocortisone Ointment, Exp. date July 83, Batch No. 16171; Ciba Pharmaceutical, Summit, NJ 07901.
[16] Vioform with Hydrocortisone Cream, Exp. date Sept 83, Batch No. 15503; Ciba Pharmaceutical, Summit NJ 07901.
[17] F-E-P Cream, Exp. date May 83, Batch No. 3967; Boots Pharmaceuticals, Inc., Shreveport, LA 71106.
[18] Racet LCD Cream, Exp. date May 83, Batch No. 6080; Lemmon Co., Sellersville, PA 18690.
[19] Racet Cream, Exp. date Jan 85, Batch No. 6626; Lemmon Co., Sellersville, PA 18690.
[20] Racet 1% Cream, Exp. date July 81, Batch No. 6084; Lemmon Co., Sellersville, PA 18690.
[21] Catalogue No. EGWP-04700; Millipore Corp., Bedford, MA 07130.
[22] Aldrich Chemical Co., Inc., Milwaukee, WI 53233.
[23] K and K Laboratories, Plainview, NY 11803.

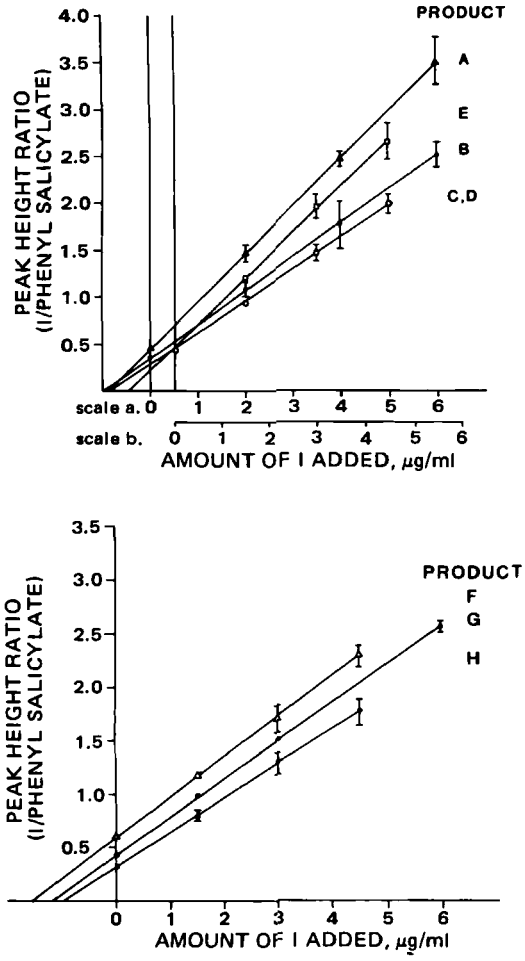

Figure 2—*Plots of I/phenyl salicylate peak height ratio* versus *amount of I added to products A–H. Extrapolation of the regression lines to the x-axis and multiplication by the appropriate dilution factor permits determination of I in each ointment or cream. The concentration of phenyl salicylate added to extracts from the products was 4.0 μg/ml. Each assay was performed in triplicate; standard deviations are shown only when >0.10.*

where the retention times for I (Rt_I) and phenyl salicylate were 7.50 and 5.25 min, respectively. The elution time of the solvent front (Rt_0) was 1.90 min and was determined by injecting methanol onto the column. In cases of ointments or creams which contained II, it was necessary to use the mobile phase in the extraction procedure and preparation of the standards to elminate the solvent front which interfered with the chromatographic peak of II (Rt_{II}, 2.50 min). As can be seen in Fig. 1, the peaks for I, II, and internal standard are well separated. Optimum extraction of I was obtained with the mobile phase (pH 2.8). Extraction of I from ointments and creams at other pH values was less efficient.

Figure 2 shows the regression lines of peak height ratio of iodochlorhydroxyquin (I)/phenyl salicylate *versus* concentration of I for the eight different products examined. Each product was spiked with varying concentrations of I, and the determinations were performed in triplicate. The mean values are presented with the standard deviations. Correlation coefficients for each of the lines for the eight products were >0.96. The regression lines for I in products C and D are identical and are presented as a single line in Fig. 2; only the largest standard deviations are given.

In Fig. 3 is plotted the peak height ratios of hydrocortisone (II)/phenyl salicylate against II concentration for five products that contained II. Determinations were performed in triplicate, and each value represents the mean with the standard deviation. The correlation coefficients for each of the plots are again >0.96. The regression lines for II in products F, G, and H are identical and are presented as a single line in the figure.

The concentrations of I and II found in the eight products, as determined by HPLC, are presented in Table I and were derived by using the regression lines presented in Figs. 2 and 3. These results are compared with the percentages of I and II claimed to be present in the products by

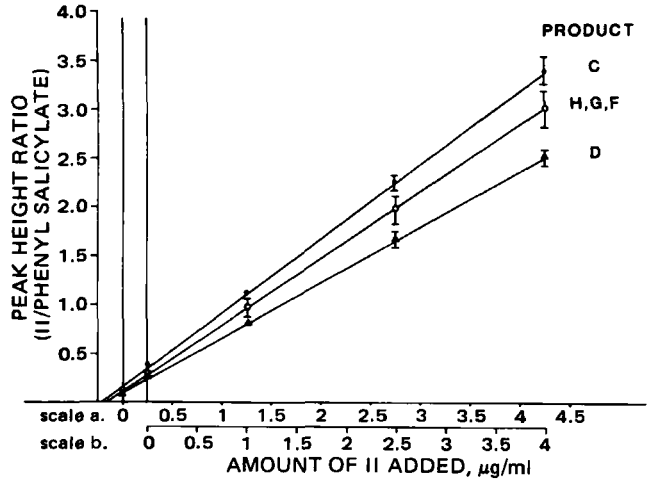

Figure 3—*Regression lines of II/phenylsalicylate peak height ratio* versus *amount of II added to products C, D, F, G, and H. The x-intercept of each regression line when multiplied by the appropriate dilution factor yields the concentration of II in the ointment or cream. The concentration of phenyl salicylate added to each product extract was 4.0 μg/ml. Each assay was performed in triplicate; standard deviations are shown only when >0.10.*

the manufacturers. As can be seen, the concentrations of I and II do not agree with the manufacturers' claims in all cases.

Products E and H were reported to contain 3% I, but were experimentally determined to contain only 2.0%; product G was purported to contain 3% I, but was experimentally found by HPLC to contain only 2.4%. These discrepancies may in part be due to the decomposition of I to products which were not extracted by the methods employed. No unidentified components were detected by HPLC (Fig. 1). The formation of unextracted complexes between I and constituents in the ointment bases is not likely based on the recovery data presented in Table II. The results obtained for products E, G, and H were reproducible on repeated analysis. As previously stated, for all other products containing I good agreement between the concentrations of I claimed by the manufacturers and the amounts determined by HPLC was obtained.

Compound II was present in six products; the concentration of II could be determined in five of the products. The concentrations of II determined experimentally by HPLC for two of the products contained 20% less than that claimed by the manufacturer. Better agreement was ob-

Table I—Results of HPLC Assay of Iodochlorhydroxyquin and Hydrocortisone in Ointments and Creams

Product	Claimed by Manufacturer, %		Determined by HPLC, %	
	Iodochlor-hydroxyquin	Hydro-cortisone	Iodochlor-hydroxyqin	Hydro-cortisone
A	3	—	2.8	—
B	3	—	3.0	—
C	3	1	2.8	0.93
D	3	1	2.8	0.88
E	3	1	2.0	ND[a]
F	3	0.5	3.1	0.40
G	3	0.5	2.4	0.40
H	3	1	2.0	0.88

[a] Not determined

Table II—Percent Recovery of Iodochlorhydroxyquin and Hydrocortisone from Extracted Ointments and Creams [a]

Product	Iodochlorhydroxyquin	Hydrocortisone
A	87.1 ± 4.6	—
B	95.3 ± 1.5	—
C	97.9 ± 0.9	91.2 ± 1.9
D	92.3 ± 0.0	63.4 ± 3.9
E	57.9 ● 3.4	ND[b]
F	94.0 ± 3.9	77.3 ± 5.7
G	90.0 ± 0.0	83.2 ± 5.5
H	79.9 ± 1.4	71.4 ± 0.0

[a] Each value is the mean with the standard deviation for three determinations. [b] Not determined.

tained for the other three products between our results and the purported concentrations of II. Product D contains pramoxine hydrochloride, which had a retention time on HPLC that overlapped with II, precluding the determination of II in this product.

Table II presents the percent recovery of I and II from each of the products as determined without the addition of the internal standard, phenyl salicylate. Approximately 58–98% of I was recovered, while 63–91% of II was recovered.

In summary a simple, precise, and accurate HPLC method has been developed that can be used for routine analysis and quality control for iodochlorhydroxyquin and hydrocortisone in creams and ointments.

REFERENCES

(1) Z. Tamura, M. Yoshioka, T. Imarari, J. Fukaya, J. Kusaka, and K. Samejima, *Clin. Chim. Acta.*, **47**, 13 (1973).

(2) C. T. Chen, K. Samejima, and Z. Tamura, *Chem. Pharm. Bull.*, **24**, 97 (1976).

(3) F. W. Ezzedeen, A. N. Masoud, S. J. Stohs, and S. J. Lerman, *J. Pharm. Sci.*, **70** 889 (1981).

(4) Y. Toyokura and T. Takasu, *Jpn. J. Med. Sci. Biol.*, **28**, 87 (1975).

(5) P. H. Degen, W. Schneider, I. P. Vuillard, U. P. Geiger, and W. Riess. *J. Chromatogr.*, **117**, 407 (1976).

(6) P. D. Saldato, *J. Pharm. Sci.*, **66**, 334 (1977).

(7) L. Bergren and O. Hansson, *Clin. Pharmacol. Ther.*, **9**, 67 (1968).

(8) "U.S. Pharmacopeia XX" and "National Formulary XV," U.S. Pharmacopeial Convention, Rockville, Md., 1980, p. 155.

(9) "U.S. Pharmacopeia XX" and "National Formulary XV," U.S. Pharmacopeial Convention, Rockville, Md., 1980, p. 156.

(10) T. Urbanyi, D. Sloniewsky, and F. Tishler, *J. Pharm. Sci.*, **55**, 570 (1966).

(11) T. Urbanyi and W. H. Stober, *J. Pharm. Sci.*, **58**, 232 (1969).

(12) "U.S. Pharmacopeia XX" and "National Formulary XV", U.S. Pharmacopeial Convention, Rockville, Md., 1980, p. 172.

(13) A. R. Lea, J. M. Kennedy, and G. K. C. Low, *J. Chromatogr.*, **198**, 41 (1980).

(14) R. E. Graham, P. A. Williams, and C. T. Kenner, *J. Pharm. Sci.*, **59**, 152, (1970).

Urinary Excretion of Methylparaben and Its Metabolites in Preterm Infants

K. W. HINDMARSH *§x, E. JOHN ‡, L. A. ASALI *, J. N. FRENCH *, G. L. WILLIAMS ‡, and W. G. McBRIDE *

Received June 15, 1982, from **Foundation 41, Foetal Pharmacology Laboratory*, and the ‡*Neonatal Unit, The Womens Hospital, Sydney, N.S.W. Australia 2010.* Accepted for publication August 6, 1982.

§Present address: College of Pharmacy, University of Saskatchewan Saskatoon, Saskatchewan, Canada S7N OWO.

Abstract □ A high-performance liquid chromatographic (HPLC) assay to quantitate methylparaben in urine was developed. Standard curves were linear and recovery of the paraben from urine averaged 82.6%. The urinary excretion of methylparaben in six preterm infants (≤31 weeks gestational age), who were receiving intramuscular injections of a paraben-containing gentamicin formulation, ranged from 13.2 to 88.1%. Small quantities of the metabolite, *p*-hydroxybenzoic acid, were detected by GC–MS.

Keyphrases □ Methylparaben—determination in human urine, preterm infants, high-performance liquid chromatography □ High-performance liquid chromatography—methylparaben in human urine, preterm infants, gentamicin formulations □ Preservatives—methylparaben, determination in human urine, preterm infants, high-performance liquid chromatography

Methylparaben (methyl *p*-hydroxybenzoate) and propylparaben (propyl *p*-hydroxybenzoate) are used in combination (in some medications) as preservatives. Reports that methylparaben can displace bilirubin from its binding sites on albumin *in vitro* has produced some concern regarding its use in medicinal formulations administered to the newborn and, in particular, the preterm infant (1–3). Displacement of bilirubin from its binding sites in infants with neonatal jaundice could lead to brain damage (kernicterus).

Gentamicin, an effective antibiotic for treatment of a neonatal Gram-negative sepsis, was also suspected of being a bilirubin displacer (4). Subsequent experiments have proven that gentamicin does not displace bilirubin (2, 5). However, some gentamicin formulations do contain methylparaben as a preservative. In an *in vivo* study a group of infants received a single intramuscular injection of a paraben-containing gentamicin formulation. No reduction in the albumin binding capacity for bilirubin was detected (3). The differences seen between this *in vivo* study and the *in vitro* studies may have been due to *in vivo* preservative catabolism or low paraben serum levels achieved after intramuscular injection. The concentrations of methylparaben used *in vitro* were relatively high, *e.g.*, 167 μg/ml of serum (2).

In this study, the excretion and metabolism of methylparaben was monitored in preterm infants after they had received multiple doses of a gentamicin formulation containing paraben preservatives.

EXPERIMENTAL

Materials—Methyl-, propyl-, and *n*-butylparabens[1], phosphoric acid[2], glacial acetic acid[3], and sodium hydroxide[4] were obtained commercially, and appropriate aqueous or methanolic solutions were prepared as required. Urine samples were extracted with freshly glass-distilled ether[5]. An acetate buffer (100 ml, pH 5.0) was prepared by mixing 0.2 *M* acetic acid (14.8 ml), 0.2 *M* sodium acetate[2] (35.2 ml), and water. A 1 *M* carbonate buffer (pH 9.5) was prepared by adding sodium carbonate[2] (5.3 g) and sodium bicarbonate[2] (4.2 g) to water (100 ml). Gentamicin[6] was obtained commercially; each vial (2 ml) contained gentamicin (80 mg), methylparaben (3.6 mg), and propylparaben (0.4 mg).

Patients—Six preterm babies (4 males, 2 females), with estimated gestatinal ages of 26–31 weeks and birth weights of 0.69–1.50 kg, were studied. Each infant was admitted to the neonatal intensive care unit and

[1] Sigma Chemical Co., St. Louis, Mo.
[2] Ajax Chemicals Ltd., Sydney, Australia.
[3] B.D.H. Chemicals (Aust) Pty. Ltd., Fairy, Vic., Australia.
[4] E. Merck, Darmstadt, West Germany.
[5] Anesthetic ether B.P.; Hoechst Australia Ltd., Melbourne, Vic., Australia.
[6] Gentamicin Injection, B.P.; David Bull Lab. Pty. Ltd., Mulgrave, Vic., Australia.

0022-3549/83/0900-1039$01.00/0

tained for the other three products between our results and the purported concentrations of II. Product D contains pramoxine hydrochloride, which had a retention time on HPLC that overlapped with II, precluding the determination of II in this product.

Table II presents the percent recovery of I and II from each of the products as determined without the addition of the internal standard, phenyl salicylate. Approximately 58–98% of I was recovered, while 63–91% of II was recovered.

In summary a simple, precise, and accurate HPLC method has been developed that can be used for routine analysis and quality control for iodochlorhydroxyquin and hydrocortisone in creams and ointments.

REFERENCES

(1) Z. Tamura, M. Yoshioka, T. Imarari, J. Fukaya, J. Kusaka, and K. Samejima, *Clin. Chim. Acta.*, **47**, 13 (1973).

(2) C. T. Chen, K. Samejima, and Z. Tamura, *Chem. Pharm. Bull.*, **24**, 97 (1976).

(3) F. W. Ezzedeen, A. N. Masoud, S. J. Stohs, and S. J. Lerman, *J. Pharm. Sci.*, **70** 889 (1981).

(4) Y. Toyokura and T. Takasu, *Jpn. J. Med. Sci. Biol.*, **28**, 87 (1975).

(5) P. H. Degen, W. Schneider, I. P. Vuillard, U. P. Geiger, and W. Riess. *J. Chromatogr.*, **117**, 407 (1976).

(6) P. D. Saldato, *J. Pharm. Sci.*, **66**, 334 (1977).

(7) L. Bergren and O. Hansson, *Clin. Pharmacol. Ther.*, **9**, 67 (1968).

(8) "U.S. Pharmacopeia XX" and "National Formulary XV," U.S. Pharmacopeial Convention, Rockville, Md., 1980, p. 155.

(9) "U.S. Pharmacopeia XX" and "National Formulary XV," U.S. Pharmacopeial Convention, Rockville, Md., 1980, p. 156.

(10) T. Urbanyi, D. Sloniewsky, and F. Tishler, *J. Pharm. Sci.*, **55**, 570 (1966).

(11) T. Urbanyi and W. H. Stober, *J. Pharm. Sci.*, **58**, 232 (1969).

(12) "U.S. Pharmacopeia XX" and "National Formulary XV", U.S. Pharmacopeial Convention, Rockville, Md., 1980, p. 172.

(13) A. R. Lea, J. M. Kennedy, and G. K. C. Low, *J. Chromatogr.*, **198**, 41 (1980).

(14) R. E. Graham, P. A. Williams, and C. T. Kenner, *J. Pharm. Sci.*, **59**, 152, (1970).

Urinary Excretion of Methylparaben and Its Metabolites in Preterm Infants

K. W. HINDMARSH *§x, E. JOHN ‡, L. A. ASALI *, J. N. FRENCH *, G. L. WILLIAMS ‡, and W. G. McBRIDE *

Received June 15, 1982, from **Foundation 41, Foetal Pharmacology Laboratory*, and the ‡*Neonatal Unit, The Womens Hospital, Sydney, N.S.W. Australia 2010.* Accepted for publication August 6, 1982.

§Present address: College of Pharmacy, University of Saskatchewan Saskatoon, Saskatchewan, Canada S7N OWO.

Abstract □ A high-performance liquid chromatographic (HPLC) assay to quantitate methylparaben in urine was developed. Standard curves were linear and recovery of the paraben from urine averaged 82.6%. The urinary excretion of methylparaben in six preterm infants (≤31 weeks gestational age), who were receiving intramuscular injections of a paraben-containing gentamicin formulation, ranged from 13.2 to 88.1%. Small quantities of the metabolite, *p*-hydroxybenzoic acid, were detected by GC–MS.

Keyphrases □ Methylparaben—determination in human urine, preterm infants, high-performance liquid chromatography □ High-performance liquid chromatography—methylparaben in human urine, preterm infants, gentamicin formulations □ Preservatives—methylparaben, determination in human urine, preterm infants, high-performance liquid chromatography

Methylparaben (methyl *p*-hydroxybenzoate) and propylparaben (propyl *p*-hydroxybenzoate) are used in combination (in some medications) as preservatives. Reports that methylparaben can displace bilirubin from its binding sites on albumin *in vitro* has produced some concern regarding its use in medicinal formulations administered to the newborn and, in particular, the preterm infant (1–3). Displacement of bilirubin from its binding sites in infants with neonatal jaundice could lead to brain damage (kernicterus).

Gentamicin, an effective antibiotic for treatment of a neonatal Gram-negative sepsis, was also suspected of being a bilirubin displacer (4). Subsequent experiments have proven that gentamicin does not displace bilirubin (2, 5). However, some gentamicin formulations do contain methylparaben as a preservative. In an *in vivo* study a group of infants received a single intramuscular injection of a paraben-containing gentamicin formulation. No reduction in the albumin binding capacity for bilirubin was detected (3). The differences seen between this *in vivo* study and the *in vitro* studies may have been due to *in vivo* preservative catabolism or low paraben serum levels achieved after intramuscular injection. The concentrations of methylparaben used *in vitro* were relatively high, *e.g.*, 167 μg/ml of serum (2).

In this study, the excretion and metabolism of methylparaben was monitored in preterm infants after they had received multiple doses of a gentamicin formulation containing paraben preservatives.

EXPERIMENTAL

Materials—Methyl-, propyl-, and *n*-butylparabens[1], phosphoric acid[2], glacial acetic acid[3], and sodium hydroxide[4] were obtained commercially, and appropriate aqueous or methanolic solutions were prepared as required. Urine samples were extracted with freshly glass-distilled ether[5]. An acetate buffer (100 ml, pH 5.0) was prepared by mixing 0.2 *M* acetic acid (14.8 ml), 0.2 *M* sodium acetate[2] (35.2 ml), and water. A 1 *M* carbonate buffer (pH 9.5) was prepared by adding sodium carbonate[2] (5.3 g) and sodium bicarbonate[2] (4.2 g) to water (100 ml). Gentamicin[6] was obtained commercially; each vial (2 ml) contained gentamicin (80 mg), methylparaben (3.6 mg), and propylparaben (0.4 mg).

Patients—Six preterm babies (4 males, 2 females), with estimated gestatinal ages of 26–31 weeks and birth weights of 0.69–1.50 kg, were studied. Each infant was admitted to the neonatal intensive care unit and

[1] Sigma Chemical Co., St. Louis, Mo.
[2] Ajax Chemicals Ltd., Sydney, Australia.
[3] B.D.H. Chemicals (Aust) Pty. Ltd., Fairy, Vic., Australia.
[4] E. Merck, Darmstadt, West Germany.
[5] Anesthetic ether B.P.; Hoechst Australia Ltd., Melbourne, Vic., Australia.
[6] Gentamicin Injection, B.P.; David Bull Lab. Pty. Ltd., Mulgrave, Vic., Australia.

0022-3549/83/0900-1039$01.00/0

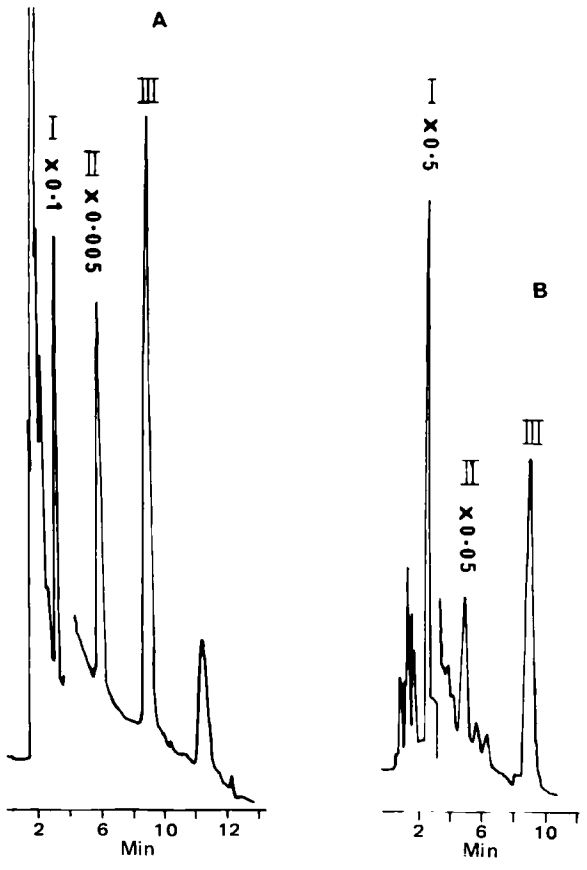

Figure 1—*Chromatograms (HPLC) of urine extracts. Key: (A) urine sample spiked with methylparaben (I), propylparaben (II), and butylparaben (III); (B) urine from a subject receiving a paraben-containing gentamicin formulation. Key: (I) methylparaben, (II) an endogenous substance, (III) butylparaben.*

was being treated for suspected sepsis with intramuscular gentamicin, 2.5 mg/kg every 18 hr or 3.0 mg/kg every 24 hr. Each infant was given gentamicin from the first day of extrauterine life. For infants on the 2.5-mg/kg dosage regimen, urine collection was 18 hr in duration and thus spanned the dosage interval. When the infant voided, time and volume were recorded and the collecting device[7] was replaced. With the two infants on the 3.0-mg/kg dosage regimen, urine was collected only when the collecting device was filled, and the total 24-hr urine was pooled prior to analysis. None of the infants were on any other drugs containing methylparaben as a preservative. Four of the infants were receiving electrolytes, vitamins, and amino acid nutrition (hyperalimentation, no paraben preservatives). The other two infants were on their first day of pooled breast milk.

Extraction of Urine Samples—Aliquots (1–2 ml) of urine from each collection period were diluted with an equal volume of acetate buffer and incubated in a water bath[8] at 37° for 18 hr with β-glucuronidase[9] (5 mg) and sulfatase[10] (5 mg). *n*-Butylparaben (800 mg) was added as the internal standard, and the hydrolyzed urine was adjusted first to pH 9 for extraction of methylparaben using carbonate buffer (400–600 μl) and then to pH 2 for extraction of metabolites with phosphoric acid. The urine samples (pH 9) were extracted[11] twice with ether (5 ml) for 1 min, and then centrifuged[12] at 1000×*g* for 5 min. The organic layers were back-extracted into a 0.1 *M* NaOH solution (300 μl) and the ethereal layer was discarded. The basic solution was acidified (pH 2) with phosphoric acid (1 drop) and subsequently extracted with ether (5 ml). After centrifugation (1000×*g*) the ether was transferred to a glass evaporation tube. A tapered pipet[13] with a sealed end was inserted and the tube placed in a 40° water bath[14]. Immediately after evaporation the tubes were stoppered and placed in an ice bath to allow the ether to condense and wash down the inner walls of the evaporation tube. The condensed ether was evaporated under a nitrogen stream. Before injection into the liquid chromatograph, the residue was reconstituted in 200 μl of mobile phase by mixing[11] (30 sec).

After extracting at pH 9, urine samples were adjusted to pH 2 and extracted twice with ether (5 ml) in a similar fashion to that described above. The ether was evaporated and the residues derivatized utilizing *N,N*-dimethylformamide di-*n*-butyl acetal[15] (20 μl) and acetonitrile[1] (10 μl; silylation grade). The stoppered tubes were heated (water bath, 48°) for 15 min before injection into the gas chromatograph–mass spectrometer.

High-Performance Liquid Chromatography (HPLC)—Methylparaben concentrations were determined utilizing a liquid chromatograph[16] equipped with a loop injection system[17] and a 30 cm × 3.9-mm (i.d.) octadecylsilane column[18]. A UV detector[19] equipped with a 254-nm filter and a dual-pen recorder[20] (with inputs set at 10 mV and chart speed of 20 cm/hr) was used. The mobile phase, HPLC-grade acetonitrile[21] and 0.05% phosphoric acid (40:60) was pumped through the column at 90 ml/hr, resulting in an inlet pressure of 900 psig.

Gas Chromatography–Mass Spectrometry (GC–MS)—GC–MS was performed on a GC–mass spectrometer equipped with a data system[22]. The chromatographic column was a 0.9 m × 2-mm (i.d.) coiled, glass column packed with 3% OV-17 on 100–120 mesh Gas Chromosorb Q[23]. The injection port temperature was 240°, and the helium flow rate 30 ml/min. The column was heated at 160° (1 min) and then increased to 220° (2 min) at a rate of 10°/min. A solvent wait period of 0.5 min was employed.

Methylparaben concentrations were calculated from standard curves made after extracting known quantities of methylparaben which had been added to urine. A standard curve was plotted as the peak height ratio of methylparaben to internal standard (butylparaben) against known methylparaben concentrations. Creatinine levels were determined using the Jaffe kinetic reaction[24].

Table I—Urinary Excretion of Methylparaben

Patient	Amount Administered, μg	Total Amount Detected, μg	Percent of Dose Excreted
A	70.0	9.24	13.2
B[a]	170.0	27.7	16.3
C	85.0	74.9	88.1
D	135.0	21.7	16.1
E[a]	190.0	67.9	35.7
F	160.0	54.6	34.1

[a] Urine collected over 24 hr.

RESULTS AND DISCUSSION

The gentamicin administered intramuscularly to the infants in this study contained both methyl- and propylparaben. HPLC analysis of spiked urine extracts gave two well-defined peaks adequately separated from the internal standard, butylparaben (peak III, Fig. 1A). Peaks I and II (Fig. 1A) are methyl- and propylparaben, respectively. The urine extracts from the infants in this study showed, on analysis, one major peak (peak I, Fig. 1B) other than the internal standard (peak III) which was not present on analysis of a control urine extract. The solvent eluant corresponding to the retention time of peak I (Fig. 1B) was collected, extracted, and identified by GC–MS as methylparaben (molecular ion, *m/z* 152). Peak II (Fig. 1B) was due to an endogenous substance. Although it was not the intention of this study to measure propylparaben levels,

[7] U-Bag, newborn size; Hollister Inc., Chicago, Ill.
[8] Gared Thermoline Pty. Ltd., Smithfield, N.S.W. Australia.
[9] No. G-0251, Type B-1; Sigma Chemical Co., St. Louis, Mo.
[10] No. S-8504, from limpets *Patella vulgata*, Type IV; Sigma Chemical Co., St. Louis, Mo.
[11] Vortex-Genie; Scientific Industries Inc., Springfield, Mass.
[12] *GS-200 centrifuge*; H. J. Clements Pty. Ltd., Sydney, Australia.
[13] Disposable Pasteur pipets (9″); Lab. Supply Pty. Ltd., Sydney, Australia.
[14] Ken Lab WBC_6; Townson & Mercer Distributors Pty. Ltd., Sydney, Australia.
[15] *n*-Butyl 8; Pierce Chemical Co., Rockford, Ill.
[16] Varian Aerograph 8500 Liquid Chromatograph; Varian Instruments, Palo Alto, Calif.
[17] Valco, Houston, Tex.
[18] C_{18} μ-Bondapak column; Waters Associates Inc., Milford, Mass.
[19] Model 440 ultraviolet detector; Waters Associates Inc., Milford, Mass.
[20] Model 585; Cole Parmer, Chicago, Ill.
[21] Waters Associates Inc., Milford, Mass.
[22] Model 5992 GC/MS system controlled by a Flexible Disc Software using the HP Model 9825 Desk Computer and HP 9885 Flexible Disc Drives; Hewlett-Packard, Avondale, Pa.
[23] Applied Science, Milton Roy Co., State College, Pa.
[24] Smith Kline Co., Sydney, Australia.

this paraben was detectable, and verified by GC–MS (molecular ion, m/z 166) in the pooled 24-hr urine extracts. The samples obtained at the time of urine void during the 18-hr collection period were not of sufficient volume for propylparaben analysis. The standard curve for the HPLC analysis of methylparaben was linear (r^2, coefficient of determination, 0.996) over a concentration range of 100–2000 ng/ml. The mean recovery of methylparaben from urine was 82.6 ± 4.9% (SD).

The percentage of the methylparaben dose accounted for in hydrolyzed urine samples (collected over 18 or 24 hr) after gentamicin administration varied from 13.2 to 88.1% (Table I). Of the methylparaben excreted in the urine the majority was in conjugated form. Extraction of nonhydrolyzed urine samples yielded <1% methylparaben. Analysis of a single urine sample divided into three aliquots and hydrolyzed with sulfatase, β-glucuronidase, or β-glucuronidase in combination with sulfatase indicated sulfate conjugates were more abundant (19% greater) than glucuronides. Levy *et al.* (6) noted the decreased phenolic glucuronidation of acetaminophen was partially compensated, in the full-term neonate, by a well-developed capacity for sulfate conjugation.

A number of factors may be responsible for the poor recovery of methylparaben in most of these infants. The patients may not have achieved a steady state with respect to parabens. However, each infant had been receiving gentamicin from the first day postpartum. The volume of distribution is increased due to a greater total water content in the newborn and a higher ratio of extracellular to intracellular water (7). Extracellular fluid in the newborn may be as high as 45% (8). The maximum urinary excretion rate of methylparaben in the infants varied, ranging from 1.5 to 17 hr (A, 4.5 hr; C, 6.25 hr; D, 1.5 hr; F, 17 hr). This variability may, in part, be due to differences in intramuscular absorption. Peripheral vasomotor instability, changes in relative blood flow of muscles (due to maturational adaptation), and relative insufficiency of muscular contractions account for variation in intramuscular absorption in the newborn (7).

One patient (C) who was 11 days of age excreted 88.1% of the administered methylparaben (Table I). Serum creatinine determinations (Table II) indicated renal function was adequate. Only two infants had creatinine levels within the normal range (<0.10 mmoles/liter). An improvement in glomerular filtration is usually seen within the first few days of the preterm infants' extrauterine life (7).

Methylparaben may be eliminated by routes other than renal excretion and/or metabolized by means other than conjugation. The only metabolite detected was p-hydroxybenzoic acid. GC–MS analysis of a pH 2, butylated, hydrolyzed urine extract revealed a small peak (R_T, 3.1 min) which gave prominent ions at m/z 194, 138, and 121. These latter ions were due to the loss of a C_4H_8 molecule and a C_4H_9O radical, respectively, from the molecular ion of n-butylparaben, m/z 194. The retention time and mass spectral data were identical to those obtained on GC–MS analysis of an authentic sample of p-hydroxybenzoic acid which had been treated with N,N-dimethylformamide di-n-butyl acetal. The recovery of this metabolite was not attempted because the peak was small and in some cases appeared only as a shoulder on an endogenous urine peak. Perhaps the small recovery of this metabolite is not surprising since esterase activity in preterm infants is low (8).

Glycine conjugation is evident in hepatic, renal, and intestinal tissue at relatively early stages of gestation (9). The glycine conjugate of p-hydroxybenzoic acid was not detected, but hippuric acid (glycine conjugate of benzoic acid) was seen in the butylated pH 2 urine extracts. GC–MS analysis of these extracts revealed a peak (R_T, 4.1 min) with a molecular ion at m/z 235 and prominent ions at m/z 134 and 105 due to the loss of $C_5H_9O_2$ and $C_6H_{12}NO_2$ fragments, respectively, from the molecular ion. p-Hydroxyhippuric acid, the glucuronide of p-hydroxybenzoic acid, and the ether sulfate of p-hydroxybenzoic acid were the main metabolites detected in the urine and bile of the rat after the administration of ethylparaben (10).

Table II—Patient Data

Patient	Birth Wt., kg	Gestational Age, weeks	Postpartum Age, days	Serum Creatinine, mmoles/liter
A	0.69	26	3	0.16
B	1.20	27	3	0.05
C	0.83	27	11	0.03
D	1.19	30	3	0.13
E	1.45	30	7	0.13
F	1.50	31	3	0.13

Although the number of infants studied is small, recovery of methylparaben appears to improve as gestational and postpartum age increase. Excluding patient C (discussed earlier), the recoveries were greatest in patients E and F (Table I). Both of these infants were 31 weeks conceptional (gestational plus postnatal) age.

In conclusion, the excretion of methylparaben by the urinary route, in preterm infants is variable during the first few days of extrauterine life. These infants are often on medications, such as gentamicin, that contain paraben preservatives for extended periods of time. Whether there is an accumulation of the preservatives in the body and whether after repeated injections the albumin binding capacity for bilirubin is affected remains to be determined. It is not uncommon for preterm infants to have neonatal jaundice. In fact, except for patient F the preterm infants in this study had jaundice which was treated with phototherapy. The differences seen between the *in vitro* and *in vivo* studies (1–3) cannot be explained by preservative metabolism or urinary excretion in the preterm infant as postulated by Woods *et al.* (3).

REFERENCES

(1) L. F. Rasmussen, C. E. Ahlfors, and R. P. Wennberg, *J. Pediatr.*, **89,** 475 (1976).

(2) C. J. Loria, P. Echeverria, and A. L. Smith, *J. Pediatr.*, **89,** 479 (1976).

(3) J. T. Woods, L. E. Bryan, G. Chan, and D. Schiff, *J. Pediatr.*, **89,** 483 (1976).

(4) G. B. Odell, *Ann. N.Y. Acad. Sci.*, **226,** 225 (1973).

(5) G. B. Odell, J. O. Cukier, and A. C. Moglalang, *J. Pediatr.*, **86,** 614 (1975).

(6) G. Levy, N. N. Khanna, D. M. Soda, O. Tsuzuki, and L. Stern, *Pediatrics*, **55,** 818 (1975).

(7) P. L. Morselli, R. Franco-Morselli, and L. Bossi, *Clin. Pharmacokinet.*, **5,** 485 (1980).

(8) D. R. Cook, L. B. Wingard, and F. L. Taylor, *Clin. Pharmacol. Ther.*, **20,** 493 (1976).

(9) M. R. Juchau, S. T. Chao, and C. J. Omiecinski, *Clin. Pharmacokinet.*, **5,** 320 (1980).

(10) H. Kiwada, S. Awazu, and M. Hanano, *J. Pharm. Dyn.*, **2,** 356 (1979).

ACKNOWLEDGMENTS

The assistance of the Medical Research Council in the form of travel assistance (for K.W.H.) is appreciated.

Dr. Roger Nation is gratefully acknowledged for helpful discussions.

Interaction of Povidone with Aromatic Compounds IV: Effects of Macromolecule Molecular Weight, Solvent Dielectric Constant, and Ligand Solubility on Complex Formation

J. A. PLAIZIER-VERCAMMEN

Received January 11, 1982, from the *Vrije Universiteit van Brussel, Farmaceutisch Instituut, B-1090 Brussels, Belgium.* Accepted for publication August 10, 1982.

Abstract □ Complex formation of ligand molecules with povidone was investigated to elucidate the effect of the molecular weight of the macromolecule and the influence of the solvent dielectric constant on the complexing tendency. The higher molecular weight polymers were more effective complexing agents than those with lower degrees of polymerization. When studying complex formation as a function of the dielectric constant (D), a linear relationship was noted between D and log B/F (B/F representing the ratio of bound to free ligand); the use of solvent mixtures to achieve a range of solvent dielectric constants enabled changes of the pH of the solvent, ligand dissociation, and solubility of the ligand and macromolecule. Of the variables under investigation, only the change in ligand solubility seemed to play an important role: a linear relationship was noted between the complexing tendency (log B/F) and the logarithm of the inverse of the ligand molecule solubility in the solvent mixtures (log $1/S$). It was concluded that the change in solubility of the ligand was the predominant factor in the decrease of the complexing tendency with decreasing dielectric constant.

Keyphrases □ Povidone—complex formation with salicylic acid, influence of molecular weight, solvent dielectric constant, and ligand solubility □ Salicylic acid—complex formation with povidone, influence of polymer molecular weight, solvent dielectric constant, and solubility □ Complex formation—salicylic acid and povidone, influence of polymer molecular weight, solvent dielectric constant, and ligand solubility

The effect of the molecular weight of povidone on the complexing tendency of ligand molecules has been studied (1–4). Either a positive effect (1, 2) or no effect at all was noted (3, 4). However, no interpretative statements were given. It was also observed (5) that the complexing tendency of ligand molecules with povidone decreases with a decrease of the dielectric constant. Such dependence as a function of dielectric constant is generally attributed to hydrophobic bondings (6–8). However, varying the dielectric constant also has an effect on the solubility of the ligand molecule. It was the purpose of this report to study the influence of the molecular weight of povidone on the complexing tendency of the ligand molecule and to investigate the possible relationships between the dielectric constant of the solvent, solubility of the ligand, and complex formation with povidone.

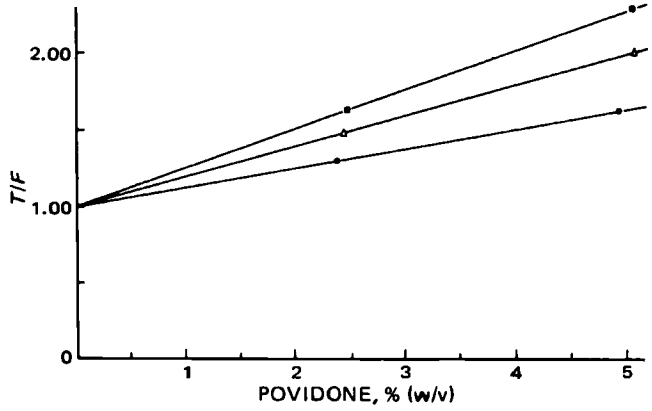

Figure 1—*Ratio of the total to free concentration of salicylic acid as a function of the concentration of povidone with molecular weights of 11,500 (●), 25,000 (△), and 700,000 (■). Initial salicylic acid concentration: 1.00 × 10⁻² M; pH 7.00; 25.0°.*

EXPERIMENTAL

Reagents—Povidone with molecular weights (weight average values) of 11,500[1] (batch I), 25,000[2] (batch II), and 700,000[3] (batch III) was used. It was oven-dried at 50° until constant weight was achieved. As ligand molecules, the following compounds were employed: salicylic acid[4], 4-hydroxysalicylic acid[5], and 5-hydroxysalicylic acid[4]. A phosphate buffer of pH 7.00 with a 0.25 ionic strength was used. The pH of the buffer was controlled with a potentiometric pH measurement[6] and adjusted as necessary. Different ethanol–water (from 0.0 to 20.0% v/v ethanol) and propylene glycol–water (from 0.0 to 50.0% v/v propylene glycol) mixtures were prepared, providing solvents with a wide range of dielectric constants.

Ultrafiltration—Ultrafiltration was used to investigate the ligand–macromolecule interactions. The equipment used was described previously (9).

Spectrophotometric Analysis—The concentration of unbound ligand was determined spectrophotometrically in the ultrafiltrate. Corrections for membrane adsorption effects were made, and the concentration of bound ligand was calculated from the difference between the concentration of total and unbound cosolute. The spectrophotometric measurements were performed with a double-beam spectrophotometer[7] at the respective λ_{max} of the ligand molecules, after appropriate dilution.

Effect of Molecular Weight of Povidone on Complex Formation—Two concentrations of the three batches of povidone were dissolved in a phosphate buffer (pH 7.00) containing 1.00×10^{-2} M salicylic acid. Ultrafiltration was carried out at 25.0°.

Effect of Dielectric Constants on Complex Formation—Salicylic acid, 4-hydroxysalicylic acid, and 5-hydroxysalicylic acid were dissolved in a range of ethanol–water mixtures (0.0 to 20.0% v/v ethanol), containing the macromolecule povidone (batch III). For 5-hydroxysalicylic acid, batch I povidone was also used. The latter ligand molecule was also dissolved in propylene glycol–water mixtures (0.0 to 50.0% v/v propylene glycol). The dielectric constants of the solvent mixtures were measured at 25.0° and 35.0°[8].

Solubility Measurements—The solubility data for salicylic acid and 4-hydroxysalicylic acid were obtained by placing amounts of the two compounds, in excess of their solubility, in 25 ml of the ethanol–water mixtures (0.0 to 20.0% v/v ethanol) in stoppered flasks. The suspensions were agitated at 25.0° and 35.0°, respectively, in a water bath. After equilibrium, the flasks were removed from the water bath, and the contents were quickly filtered through filter paper[9]. Suitable aliquots of the clear filtrate were pipetted, appropriately diluted with the respective solvent mixtures, and the absorbance of the samples was determined.

[1] Polyvinylpyrrolidone, Kollidon K_{17}, batch I, BASF, Brussels, Belgium.
[2] Polyvinylpyrrolidone, Kollidon K_{25}, batch II, BASF, Brussels, Belgium.
[3] Polyvinylpyrrolidone, Kollidon K_{90}, batch III, BASF, Brussels, Belgium.
[4] Merck, Darmstadt, West Germany.
[5] Merck-Suchardt.
[6] Radiometer Copenhagen, Denmark.
[7] Perkin-Elmer Model 124.
[8] Dekameter DK WTW Weilheim, West Germany.
[9] No. 2 Whatman.

0022-3549/83/0900-1042$01.00/0

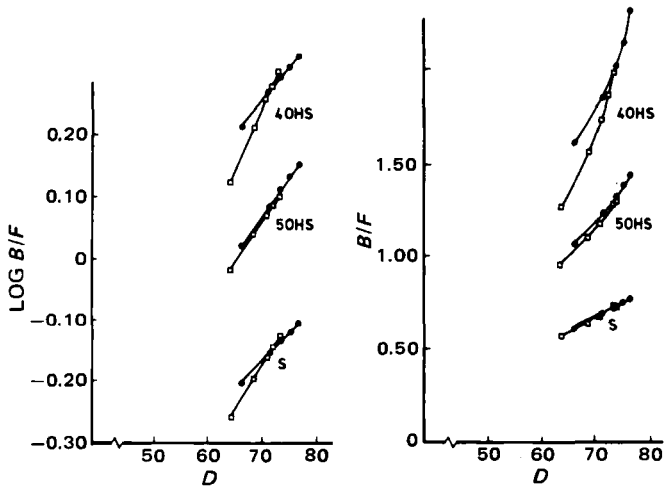

Figure 2—*Variation in the complexing tendency of ligand molecules with the dielectric constant of the solution (solvent: ethanol–water). Key: (●) 25.0°; (□) 35.0°; (4OHS) 4-hydroxysalicylic acid (5.00 × 10^{-3} M) plus 4.00% povidone, batch III; (5OHS) 5-hydroxysalicylic acid (5.00 × 10^{-3} M) plus 5.00% povidone, batch III; (S) salicylic acid (5.00 × 10^{-3} M) plus 4.00% povidone, batch III.*

Viscometric Analysis—Using capillary viscometers, the intrinsic viscosities of povidone dissolved in water, 20% (v/v) ethanol, and 50% (v/v) propylene glycol were determined at 25°. Temperature was controlled to ±0.05°. Povidone concentrations ranged from 0.2 to 1.0%.

RESULTS AND DISCUSSIONS

Theory of Multiple Equilibria—The principles and concepts fundamental to an understanding of macromolecular binding can be found elsewhere (10–16). In this report, the relative tendencies of several ligand molecules to form complexes are expressed as the ratio of the total ligand concentration (T) to the concentration of the free form (F) as a function of the percentage of povidone (17–19). This may be written as:

$$q = \frac{\text{concentration of total ligand}}{\text{concentration of free ligand}} = \frac{T}{F} = \frac{r}{F}[\text{PVP}] + 1 \quad \text{(Eq. 1)}$$

where r is moles of bound ligand/moles of macromolecule and [PVP] is the concentration of povidone in the solution. If r/F was constant, *i.e.*, if the same type of binding was taking place with increasing povidone concentration, T/F *versus* [PVP] plots resulted in straight lines (20).

Effect of Molecular Weight of Povidone on Complex Formation—The results expressed as T/F were plotted against the polymer concentration in Fig. 1. The higher molecular weight polymers are more efficient complexing agents than those with lower degrees of polymerization.

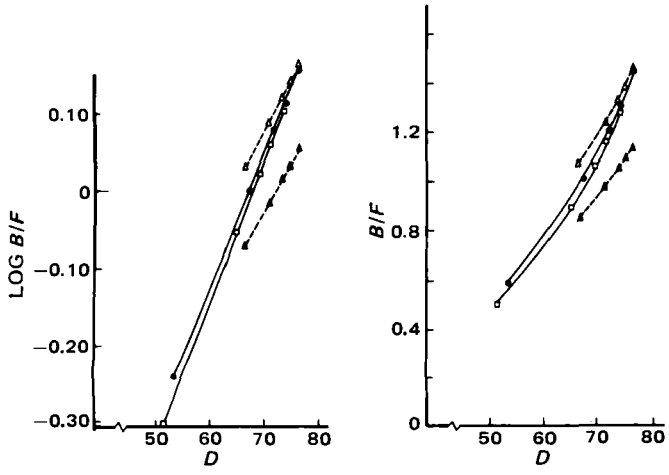

Figure 3—*Variation in the complexing tendency of 5-hydroxysalicylic acid with the dielectric constant of the solution [5-hydroxysalicylic acid (5.000 × 10^{-3} M) plus 5.00% povidone]. Key: (●) solvent propylene glycol–water, 25.0°, batch III; (□) solvent propylene glycol–water, 35.0°, batch III; (△) solvent ethanol–water, 25.0°, batch III; (▲) solvent ethanol–water, 25.0°, batch I.*

Table I—Intrinsic Viscosity of Povidone (Batch III) in Solvent Mixtures

Solvent	Intrinsic Viscosity, g/ml
Water	140
20% (v/v) Ethanol	150
50% (v/v) Propylene glycol	152

The two variables that can influence complex formation (*i.e.*, true solvation and the number of sites) are, however, independent of molecular weight for the same concentration of polymer (expressed in weight percent). On one hand, it is shown that for the same polymer, true solvation is independent of molecular weight if the active sites for solvent are equally accessible (12). On the other hand, if specific sites exist, according to the complexing theory they also will be independent of molecular weight for the same polymer percentage.

The difference in complexing tendency is in accordance with the existence of carboxylic end groups on the polymer (2, 21), as shown by IR spectroscopy. The end groups per unity weight polymer will be largest for the lower molecular weight, accompanied by an increase of solvation; this will result in a lower complexing tendency, as dehydration has a positive effect on the binding of ligand molecules onto povidone (22).

Effect of Dielectric Constant on Complex Formation—The results expressed as log B/F and B/F (the ratio of bound to free ligand concentration) were plotted in Figs. 2 and 3 as a function of the dielectric constant of the solvent, measured at the same temperatures as the ultrafiltration experiments. For all the derivatives, complex formation was diminished with decreasing dielectric constant (or increasing ethanol or propylene glycol concentration). Furthermore, the complexing tendency was diminished at higher temperatures. Comparing complex formation of 5-hydroxysalicylic acid onto povidone batch III and batch I (Fig. 3), the higher molecular weight macromolecule was the most effective complexing agent.

Figures 2 and 3 corresponded to the following equations:

$$\log \frac{B}{F} = b_1 + a_1 \cdot D \quad \text{(Eq. 2)}$$

where D is the dielectric constant and b_1 and a_1 are two constants, or:

$$\frac{B}{F} = 10^{b_1 + a_1 \cdot D} \quad \text{(Eq. 3)}$$

Using Eq. 2, it was noted that log B/F increased linearly with the dielectric constant of the solvent or diminished linearly with the percentage ethanol or propylene glycol.

In addition to the dielectric constant, temperature also played a role: for salicylic acid and 4-hydroxysalicylic acid (Fig. 2), the lines at 25.0° crossed those at 35.0°; for 5-hydroxysalicylic acid, the two lines are nearly parallel. That complex formation is not only dependent on dielectric constants could be observed from the results obtained with 5-hydroxysalicylic acid in ethanol–water and propylene glycol–water (Figs. 2 and 3, respectively). For the same dielectric constant, complex formation was

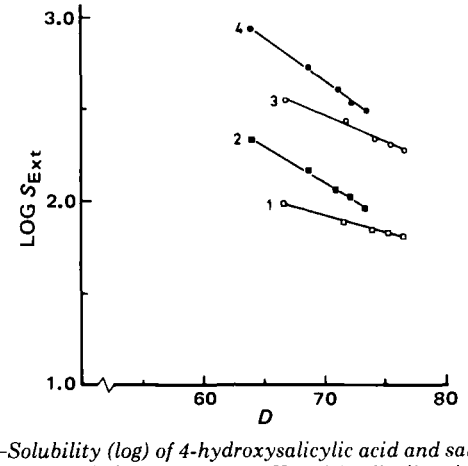

Figure 4—*Solubility (log) of 4-hydroxysalicylic acid and salicylic acid as a function of the dielectric constant. Key: (1) salicylic acid, 25.0°; (2) salicylic acid, 35.0°; (3) 4-hydroxysalicylic acid, 25.0°; (4) 4-hydroxysalicylic acid, 35.0°.*

lowest in the propylene glycol–water mixture. Thus, the nature of the solvent must also play a role.

A diminishing complexing tendency with lower dielectric constants is generally attributed to hydrophobic bonds (6–8). However, the use of ethanol–water mixtures in differing proportions to achieve a range of solvent dielectric constants changed the ionization of the ligand (23), the pH of the solution, and the solubility (hydration) (24) of the macro- and ligand molecules (23–25). These factors, which also could influence complex formation, were investigated.

Ionization and dissociation of ligand molecules are depressed under conditions of low dielectric constant of the medium (23). This factor cannot be very important, in view of experimental observations (22) where a decrease in the dissociation of ligand molecules enhanced complex formation; this is not observed for the ligand molecules under investigation.

The difference in hydration of povidone in water, ethanol, and propylene glycol solutions was investigated with viscometric measurements. The intrinsic viscosities are given in Table I. No attempts were made to interpret changes in the Huggins constant (26), since no good interpretation in small deviations of these constants exists (27, 28).

From Table I, it was observed that the parameters are not significantly affected by change in solvent composition; this may possibly indicate that the total solvation of povidone was not affected much by changes in solvent composition. After all, povidone is not only soluble in water, but also in alcohol and even in chloroform, and hence, presumably in propylene glycol as well. Therefore, alcohol and propylene glycol will also be bound to povidone, in addition to water.

From pH measurements, it is noted that the pH of the solutions is almost unaffected by changing the solvent composition from zero to 20.0% (v/v) ethanol. At constant pH, ethanol enhances the solubility of weak electrolytes, by lowering the polarity of the solvent (23). For povidone batches I and III, the solubility of the ligand molecule is not changed in the same solvent composition; therefore, the difference in complex formation must be due to the macromolecule. The difference in complex formation of 5-hydroxysalicylic acid onto the two povidone batches also is attributed to the lower hydration of povidone batch III, enhancing the complexing tendency.

The solubility of two ligand molecules, *i.e.*, salicylic acid and 4-hydroxysalicylic acid, as a function of solvent composition and dielectric constant was investigated. The results obtained at 25.0° and 35.0° are represented in Fig. 4. The values of the ordinate are extinction values.

The solubility (log) of the two ligand molecules is linearly decreasing with increasing dielectric constant of the solvent medium; the decrease is faster at 35.0° than at 25.0°. This can be written as:

$$\log S = b_2 - a_2 \cdot D \qquad \text{(Eq. 4)}$$

where S is the solubility of the compounds and b_2 and a_2 are two constants or:

$$\log \frac{1}{S} + b_2 = a_2 \cdot D \qquad \text{(Eq. 5)}$$

The relationship between the solubility of the ligand and the complexing tendency onto povidone can be obtained from Eqs. 2 and 5. Dividing the two equations results in:

$$\log \frac{B}{F} = \frac{a_1}{a_2} \log \frac{1}{S} + b_2 \frac{a_1}{a_2} + b_1 \qquad \text{(Eq. 6)}$$

or:

$$\log \frac{B}{F} = a_3 \log \frac{1}{S} + b_3 \qquad \text{(Eq. 7)}$$

with $a_1/a_2 = a_3$ and $b_3 = (b_2 \cdot a_1/a_2) + b_1$.

The correctness of Eq. 7 was checked with the experimental results: the data obtained for 4-hydroxysalicylic acid and salicylic acid (Fig. 2) expressed as log B/F were plotted as a function of log $1/S$. The deduced linear relationship between log B/F and log $1/S$ in Eq. 7 was confirmed experimentally. The corresponding values of a_3 and b_3 for salicylic acid are 0.492 and 0.823 at 25.0° and 0.534 and 0.612 at 35.0°; for 4-hydroxysalicylic acid these values are 0.435 and 1.35 at 25.0° and 0.365 and 1.23 at 35.0°. A similar relationship was obtained for the interaction of anilines to nylon (29).

Log $1/S$ is a partitioning term, as it is an equilibrium constant between drug (pure) $\rightleftarrows$ drug (H_2O) (30) and is correlated with another partitioning function. Indeed, B/F may also be considered a partitioning term expressing the partition of ligand between the macromolecule and the solvent; it is directly analogous to an organic solvent–water partition coefficient.

From our experiments, it can be concluded that the predominant effect of the decrease in complex formation in the solvent mixtures was caused by the increasing solubility of the ligand molecules. Correlation between complex formation to povidone and solubilities for the two derivatives provide additional support for the occurrence of complex formation by hydrophobic interactions.

REFERENCES

(1) E. Ullman, K. Thoma, and P. Mohrschulz, *Arch. Pharm.*, **302,** 756 (1969).

(2) W. Scholtan, *Makromol. Chem.*, **11,** 131 (1953).

(3) J. Ruedy and W. Chernecki, *Can. J. Physiol. Pharmacol.*, **46,** 829 (1968).

(4) R. Voigt, H. H. Schultze, and S. Keipert, *Pharmazie*, **3,** 863 (1976).

(5) J. A. Plaizier-Vercammen and R. De Nève, *J. Pharm. Sci.*, **71,** 552 (1982).

(6) W. Kauzmann, *Adv. Protein Chem.*, **14, 1** (1959).

(7) K. Nishida and W. Watanabe, *Kolloid Z.-Z. Polym.*, **244,** 346 (1971).

(8) S. Keipert, J. Becker, and R. Voigt, *Pharmazie*, **32,** 280 (1977).

(9) J. A. Plaizier-Vercammen and R. E. De Nève, *J. Pharm. Sci.*, **69,** 1403 (1980).

(10) C. Tanford, "Physical Chemistry of Macromolecules," Wiley, New York, N.Y., 1966.

(11) R. M. Rosenberg and I. M. Klotz in "A Laboratory Manual of Analytical Methods of Protein Chemistry," vol. 2, P. Alexander and R. J. Block, Eds., Pergamon, New York, N.Y., 1960.

(12) I. M. Klotz in "The Proteins," vol. 1, part B, H. Neurath and K. Bailey, Eds., Academic, New York, N.Y., 1953.

(13) J. T. Edsall and J. Wyman, "Biophysical Chemistry," vol. 1, Academic, New York, N.Y., 1958.

(14) J. Steinhardt and J. A. Reynolds, "Multiple Equilibria in Proteins," Academic, New York, N.Y., 1969.

(15) I. M. Klotz, *Arch. Biochem.*, **9,** 109 (1946).

(16) I. M. Klotz and D. L. Hunston, *J. Biol. Chem.*, **250,** 3001 (1975).

(17) C. K. Bahal and H. B. Kostenbauder, *J. Pharm. Sci.*, **53,** 1027 (1964).

(18) S. J. Blaug and P. S. Ebersman, *J. Pharm. Sci.*, **53,** 35 (1964).

(19) N. K. Patel and N. E. Foss, *J. Pharm. Sci.*, **53,** 94 (1964).

(20) G. Jürgensen Eide and P. Speiser, *Acta Pharm. Suec.*, **4,** 185 (1967).

(21) L. May, PH. Hines, L. Weintraub, M. Scudder, and S. Graff, *Surgery*, **35,** 191 (1954).

(22) J. A. Plaizier-Vercammen and R. E. De Nève, *J. Pharm. Sci.*, **70,** 1252 (1981).

(23) A. N. Martin, J. Swarbrick, and A. Cammarata, "Physical Pharmacy," 2nd ed., Lea and Febiger, Philadelphia, Pa., 1973.

(24) S. Glasstone, "Textbook of Physical Chemistry," 2nd ed., McMillan, Woodbridge, Ill., 1972.

(25) W. G. Gorman and G. D. Hall, *J. Pharm. Sci.*, **53,** 1017 (1964).

(26) M. L. Huggins, *J. Am. Chem. Soc.*, **64,** 2716 (1942).

(27) P. Molyneux and H. P. Frank, *J. Am. Chem. Soc.*, **83,** 3175 (1961).

(28) R. L. Darskus, D. O. Jordan, T. Kurucsev, and M. L. Martin, *J. Polym. Sci.*, **A3** (1941)

(29) T. M. Ward and R. P. Upchurch, *J. Agra. Food Chem.*, **13,** 334 (1965).

(30) C. Hansch and F. Helmer, *J. Polym. Sci.*, **6,** 3295 (1968).

ACKNOWLEDGMENTS

Abstracted from a thesis submitted by J. A. Plaizier-Vercammen to the Vrije Universiteit van Brussel, in partial fulfillment of the Doctor in Philosophy degree requirements.

The author thanks Mr. G. Hoogewijs for helpful discussion, Mr. G. Bultinck and M. Piret for technical assistance, and BASF Brussels for the batches of povidone.

Pharmacokinetics of Intravenous and Oral 1,2-*O*-Isopropylidene-3-*O*-3′-(*N*′,*N*′-dimethylamino-*n*-propyl)-D-glucofuranose Hydrochloride in the Dog as a Function of Dose and Characterization of Metabolites

EDWARD R. GARRETT ˣ **and ACHIEL VAN PEER**

Received April 16, 1982, from *The Beehive, College of Pharmacy, J. Hillis Miller Health Center, University of Florida, Gainesville, FL 32610.* Accepted for publication August 6, 1982.

Abstract □ The pharmacokinetics of 1,2-*O*-isopropylidene-3-*O*-3′-(*N*′,*N*′-dimethylamino-*n*-propyl)-D-glucofuranose hydrochloride (I) was studied in dogs at intravenous and oral doses of 1–50 mg/kg. There was no significant difference between the electron-capture GLC of the heptafluorobutyric derivative of I and the radiochemical assay of chloroform extracts of plasma and urine for 1- to 20-mg/kg doses. Urinary amounts of I measured by GLC were 20% lower than radioassays of chloroform extracts at the 50-mg/kg dose. The pharmacokinetics of intravenous I was described by a two-compartment body model with sequential plasma half-lives of 7.5 ± 0.7 and 136 ± 6 min. No apparent dose-dependent pharmacokinetics for I was observed on intravenous or oral administration. The apparent volume of distribution of the central compartment, 13.1 ± 0.7 liters, is approximately the volume of the total body water in a 20-kg dog. The apparent overall volume of distribution of 40.0 ± 1.5 liters exceeds the total body water, indicative of sequestration of I in tissues. Total and renal clearances were 205 ± 5 and 155 ± 5 ml/min, respectively. The high renal clearance of I indicated an excess of tubular secretion. Renal clearance of I was not dependent on urine flow nor urine pH. Recovery of radioactivity in the feces after I was intravenously administered was <1%. Plasma protein binding of I was <5%, and the erythrocyte–plasma water partition coefficient was approximately unity. Compounds excreted in urine were separated into chloroform-extractable (pH 12), ethyl acetate-extractable (pH 2), and unextractable fractions which were further characterized by TLC. A multiple-extraction system was developed to estimate relative amounts and intrinsic partition coefficients of these extractable compounds from radioactivity counts of scraped plates and was applied to the assay of these compounds in the urine after intravenous administration of I. There was a readily chloroform-extractable metabolite with an apparent partition coefficient of 3.3 and R_f 0.43 on TLC in the systems used. This apparent major metabolite could account for 8% of the administered radioactivity. Minor chloroform-extractable metabolites (0.8–3.3%) had lower apparent partition coefficients (0.26) but R_f values of 0.28 and 0.44. Ethyl acetate-extractable compounds (1.3–2.7%) had an apparent partition coefficient of 0.81 with R_f values of 0.52 and 0.68. Three unextractable compounds had R_f values of 0.20, 0.50, and 0.62 and accounted for 0.16, 2.8, and 0.9% of the administered radioactivity.

Keyphrases □ 1,2-*O*- Isopropylidene-3- *O*-3′- (*N*′,*N*′-dimethylamino-*n*-propyl)-D-glucofuranose—pharmacokinetics, intravenous and oral doses, dogs □ Metabolites—1,2-*O*-isopropylidene-3-*O*-3′-(*N*′,*N*′-dimethylamino-*n*-propyl)-D-glucofuranose, multiple extraction, radiochemical analysis in urine, dogs □ Pharmacokinetics—1,2-*O*-isopropylidene-3-*O*-3′-(*N*′,*N*′-dimethylamino-*n*-propyl)-D-glucofuranose and metabolites, dogs, intravenous and oral doses

The properties, stability, assay, and preliminary pharmacokinetics in a dog of the immunomodulatory 1,2-*O*-isopropylidene-3-*O*-3′ - (*N*′,*N*′-dimethylamino-*n*-propyl)-D-glucofuranose hydrochloride (I) were described previously (1). This initial pharmacokinetic study in a dog showed that 60–80% of I was renally excreted unchanged and 20–40% as unidentified metabolites at doses of 2 and 10 mg/kg iv. This contrasted with the urinary recovery of the GLC-assayed I in humans of 93 ± 2% in preliminary pharmacokinetic studies, indicative that only a small fraction was probably metabolized (2). Assays of chloroform-extracted radioactivity at pH 11 from plasma and urine appeared to be synonomous to electron-capture GLC assays of the heptafluorobutyric derivative of I, indicating the greater polarity of the unextracted metabolites.

This paper presents detailed studies on the pharmacokinetics of I in dogs after intravenous and oral administration as a function of dose (1–50 mg/kg). A fractionation and multiple-extraction system is presented that permits the quantitative assays of unidentified metabolites and the estimations of the partition coefficients of extractable metabolites from radioassays of sequential organic extracts.

EXPERIMENTAL

Materials—The following analytical grade materials were used: ammonium hydroxide[1], volumetric concentrations of sodium hydroxide[2] and hydrochloric acid[2], chloroform suitable for GC[3], ethyl acetate[3], isopropyl alcohol[3], methanol[3], *n*-propyl alcohol[4], 30% hydrogen peroxide[4], and a toluene-based scintillation cocktail[4]. 1,2-*O*-Isopropylidene-3-*O*-3′-(*N*′,*N*′-dimethylamino-*n*-propyl)-D-glucofuranose hydrochloride[5] (I) and radiolabeled I (randomly ^{14}C-labeled in the glucose component[6], 324.0 mCi/mmole) were used to prepare doses for the pharmacokinetic studies. The TLC plates used were silica gel G-coated glass plates[7].

Purity of ^{14}C-Labeled I—Radiolabeled [^{14}C]I applied on TLC and developed with *n*-propyl alcohol–ethyl acetate–water–ammonium hydroxide (6:1:4:1) had a 98% recovery of the administered radioactivity at the R_f (0.67) of I. No significant radioactivity over background was observed for its hydrolysis product, 3-*O*-3′-(*N*′,*N*′-dimethylamino-*n*-propyl)-D-glucofuranose hydrochloride, at R_f 0.30. In addition no significant radioactivity was observed over background at any other R_f value.

Plasma Protein Binding of I by Ultrafiltration—Fresh dog plasma was spiked with 0.1–100 μg/ml ^{14}C-labeled I (47,000 dpm). An aliquot (0.1 ml) was taken prior to filtration to determine total radioactivity. Spiked plasma (2.00 ml) was centrifuged through ultrafiltration cones[8] at 3000 rpm for 10 min for no more than 30% (usually 10%) filtration of the plasma. Aliquots (0.1 ml) of the ultrafiltrates were assayed by liquid scintillation counting (2). Membrane binding (3–29%) of ^{14}C-labeled I was found by ultrafiltration of spiked plasma water samples and subtracted from the studies of spiked plasma.

Red Blood Cell–Plasma Water Partitioning of I—Red blood cells obtained from centrifugation of fresh, heparinized dog blood were washed five times with isotonic saline[9], recentrifuged, and resuspended in plasma water obtained by ultrafiltration to give a hematocrit of 46. Aliquots (2.00 ml) of the suspensions were spiked with 0.01–100 μg/ml of ^{14}C-labeled I (47,000 dpm), incubated at 25° for 30 min, and centrifuged at 3000 rpm for 10 min. Aliquots (0.1 ml) of the original suspension and the separated

[1] Mallinckrodt, Saint Louis, MO 63147.
[2] Ricca Chemical Co., Arlington, TX 76012.
[3] Burdick and Jackson Laboratories, Muskegon, MI 49442.
[4] Scinti-Verse, Fisher Scientific Co., Fair Lawn, NJ 07410.
[5] Lots 3646 and 13553; Greenwich Pharmaceuticals, Greenwich, CT 06830.
[6] Lot 1141-220; New England Nuclear, Boston, MA 02118.
[7] Analtech, Newark, DE 19711.
[8] Centriflo ultrafiltration membrane cones, CF50; Amicon Corp., Lexington, MA 02173.
[9] Sodium Chloride Injection USP; McGaw Laboratories, Irvine, CA 92714.

0022-3549/83/0900-1045$01.00/0

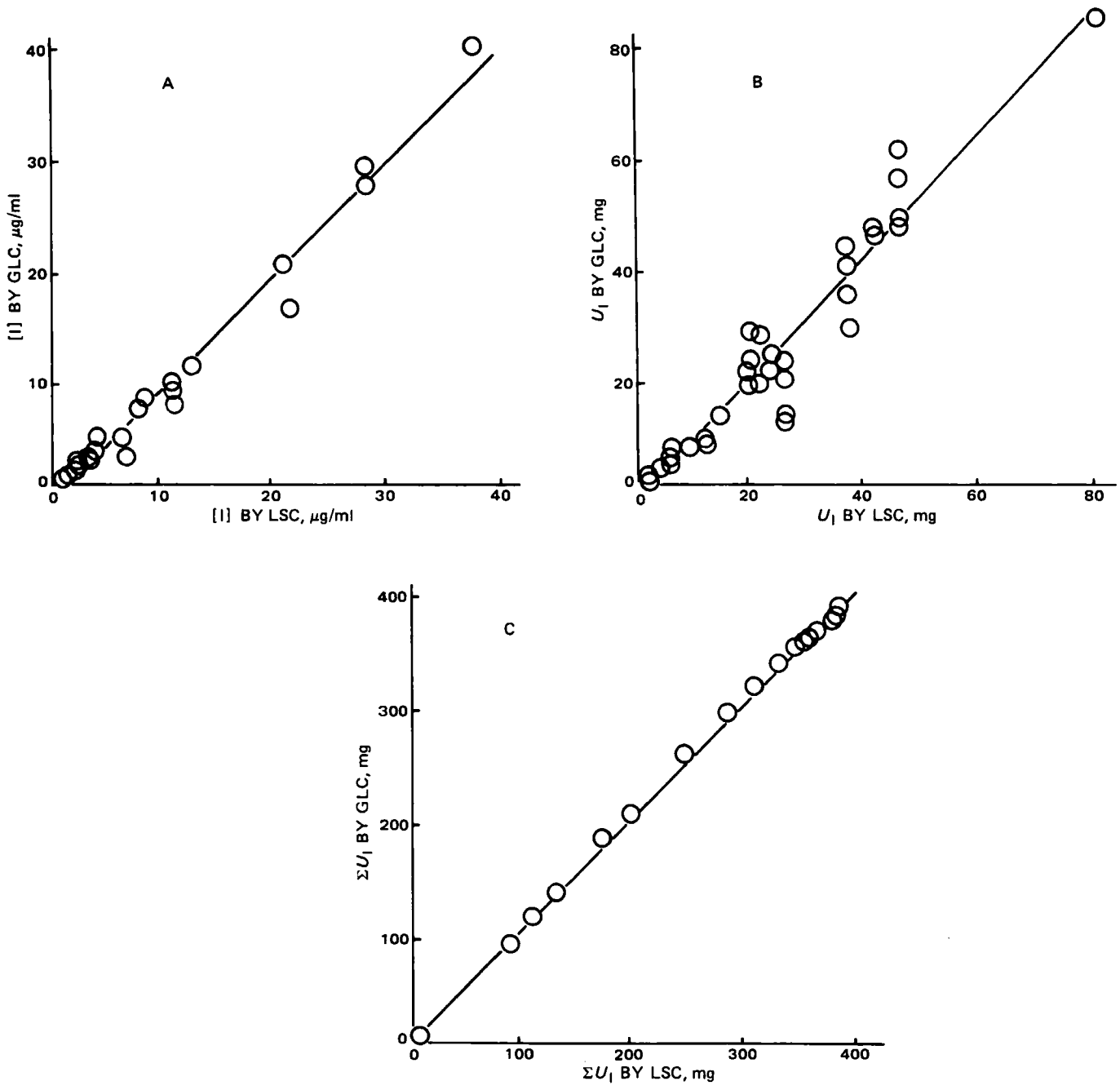

Figure 1—*Linear regressions of (A) concentrations of I ([I]) in plasma, (B) amounts of I (U_I) excreted in the urine in a given time interval, and (C) cumulative amounts of I (ΣU_I) excreted in the urine at a given time assayed by electron-capture GLC on the radioassay (LSC) of chloroform extracts. Dog A was administered 24.0 mg/kg iv of I.*

plasma water were assayed for radioactivity after digestion with 1.00 ml of a mixture of solubilizer[10]–isopropyl alcohol (1:1 v/v) and 0.5 ml of 30% hydrogen peroxide.

The partition coefficient, D, was calculated from the equation cited in the literature (3) where the fraction of bound I was taken as zero. Partition coefficients between red blood cells and plasma water were also determined as a function of time for a 1-μg/ml spiked red blood cell suspension.

Analysis of ^{14}C-Labeled I in Plasma and Urine—The electron-capture GLC assay of the heptafluorobutyric derivative of I and the radioassays after chloroform extraction of plasma and urine were described previously (1).

Pharmacokinetic Studies of I in Dogs—One male dog (A) received intravenous doses of 1.9, 2.0, 10.0, 24.0, and 48.4 mg/kg and oral doses of 5.1 and 20.0 mg/kg of ^{14}C-labeled I. Except for the 2.0 and 10.0 mg/kg iv studies, effected respectively 1 year and 6 months before the others (1), the studies had intervals of 3 weeks. Four other male dogs (B, C, D, and E) were intravenously injected with ~1, 5, and 10 mg/kg at ~3-week intervals. Intravenous doses of known specific activity were injected into the jugular catheter[11] by a three-way stopcock[12] over 10 sec. The dosing stopcock and catheter were flushed with 10.0 ml of isotonic saline. In the oral studies, a tube was placed into the stomach of dog A to administer 10.0 ml of the solution of ^{14}C-labeled I. The stomach tube was flushed twice with 50.0 ml of water before it was removed.

Blood samples after oral administration were withdrawn at 2 and 5 min, every 5 min up to 60 min, every 10 min up to 90 min, and then at the same times as previously reported for the intravenous studies (1). Urine samples in oral studies were collected at the same times as for intravenous studies (1). Further details of the treatment of the dogs, before and on the days of the experiments, the collection times of plasma and urine for

[10] Bio-Solv solubilizer; Beckman Instruments, Fullerton, CA 92634.

[11] Intracath, intravenous placement unit, catheter size 16 gauge, catheter length 12 inch, needle size 14 gauge; Deseret Pharmaceutical Co., Sandy, UT 84070.

[12] Pharmaseal Inc., Toa Alta, PR 00758.

Table I—Comparison of GLC (y) and LSC (x) Assays of Chloroform Extracts of Plasma and Urine With Time by Regression Analysis[a] of the Plasma Concentration of I after Intravenous and Oral Doses to Dog A

Assay	Dose, mg/kg	n	Range	$m \pm s_m$	$b \pm s_b$	$s_{y \cdot x}$	r
[I], μg/ml	24 iv	26	1–40	1.006 ± 0.032	−1.11 ± 0.43	1.52	0.988
	48.4 iv	39	0.5–120	0.724 ± 0.033	0.91 ± 1.29	6.13	0.963
		38[b]	0.5–85	0.941 ± 0.029	−2.36 ± 0.77	3.26	0.984
	20.0 po	30	0.3–15	1.161 ± 0.070	0.03 ± 0.46	1.40	0.952
U_I, mg	24 iv	51	0.4–85	1.074 ± 0.040	−1.89 ± 1.09	4.69	0.968
	48.4 iv	25	0.1–130	0.820 ± 0.013	−1.19 ± 0.72	2.62	0.997
	20.0 po	35	2–55	0.927 ± 0.094	1.23 ± 2.10	6.23	0.863
ΣU_I, mg	24 iv	18	5–380	0.992 ± 0.009	6.27 ± 2.61	4.46	0.999
	48.4 iv	25	81–920	0.795 ± 0.007	−4.11 ± 5.38	9.20	0.999
	20 iv	19	5–365	1.019 ± 0.008	−3.11 ± 1.91	4.06	0.999

[a] $y \pm s_{y \cdot x} = m (\pm s_m)_x + b (\pm s_b)$, where the constants m and b are the slope and intercept, respectively, of the regression of GLC assays of I (y) on LSC (x) assays of chloroform extracts of plasma and urine, and $s_{y \cdot x}$, s_m, and s_b are the respective standard errors of estimate; r is the correlation coefficient (4). [b] The 1-min plasma sample was excluded from the regression analysis.

the intravenous studies, and the handling of the samples were given previously (1).

Treatment of Feces—Feces were collected at 24-hr intervals and homogenized with a 10-fold volume of distilled water. An aliquot (0.2 ml) was transferred to a scintillation vial[13]; 0.5 ml of solubilizer[10] was added and the mixture was digested at 50° for 1 hr in a water bath. After cooling, 1 ml of 30% H_2O_2 was added dropwise, and the mixture was gently swirled for 30 min. After air bubbles were eliminated, 15 ml of liquid scintillation fluid was added. Samples were dark-adapted overnight before counting.

Extraction of Urine with Various Organic Solvents and at Different pH Values—The strategy of extractions is given in Scheme I. Aliquots of urine (0.5 ml), before and at various times after intravenous administration of 1017 and 43.1 mg of [^{14}C]I (48.4 and 1.9 mg/kg), from dog A were alkalinized to pH 12 with 0.1 ml of 1 N NaOH. Radioactivity before extraction was counted after addition of 10 ml of liquid scintillation fluid to 0.02 ml of the alkalinized urine. Alkalinized samples were then extracted sequentially 15 times with 5.0 ml of water-saturated chloroform. Each chloroform extract was transferred to a scintillation vial and evaporated under a nitrogen stream. The dried residues were each reconstituted in 10 ml of liquid scintillation fluid, and the radioactivity was counted.

The aqueous phase, previously extracted 15 times with chloroform, was acidified with 2 N HCl to pH 2, and then extracted seven times sequentially with 5.0 ml of water-saturated ethyl acetate. Each ethyl acetate extract was transferred to a scintillation vial and evaporated under a nitrogen stream. The dried residues were each reconstituted in 10 ml of liquid scintillation fluid to count radioactivity.

After all chloroform and ethyl acetate extractions, 10.0 ml of liquid scintillation fluid was added to 0.05 ml of the aqueous phase to count unextractable radioactivity. The remaining aqueous phase was neutralized with 2 N NaOH to pH ~7, and an aliquot (0.05 ml) was applied on a silica gel-coated TLC plate. Aliquots of solutions of the administered radiolabeled drug, 585 and 1056 ng in 0.6 ml of blank urine and distilled water, respectively, were treated similarly (Scheme I).

TLC Separation of Chloroform- and Ethyl Acetate-Extractable and Unextractable Radioactivity—An aliquot (0.05 ml) of the final aqueous phase, previously multiple extracted by chloroform and ethyl acetate, was neutralized, spotted on a silica gel G-coated glass plate, and developed with n-propyl alcohol–ethyl acetate–water–ammonium hydroxide (6:1:4:1). The TLC plate was scraped in 0.5-cm sections after development to 15 cm and being dried in air. The scrapings were transferred to scintillation vials and dissolved in 3.0 ml of water. Liquid scintillation fluid (10.0 ml) was added, and the vials were counted for radioactivity after overnight dark adapting.

Samples of repetitive chloroform and ethyl acetate extracts of a 20.0-ml combined sample of 120-, 180-, and 240-min urine and of 20.0 ml of 665-min urine were evaporated, reconstituted in 50–100 μl of solvent, spotted on TLC, and developed similarly. Similar studies were effected for the spiked blank urine solutions of radiolabeled I.

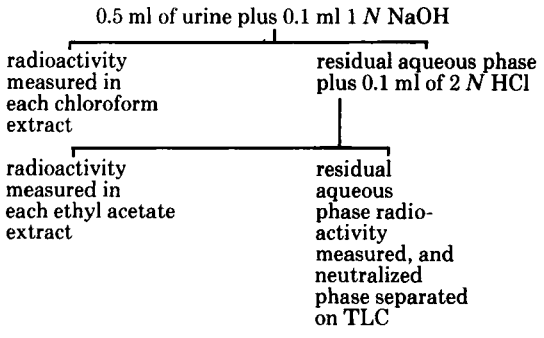

Scheme I—Multiple extractions of urine taken at various times after intravenous administration of 48.4 mg/kg of ^{14}C-labeled I to dog A.

[13] Kimble, Division of Owens-Illinois, Toledo, OH 43668.

RESULTS AND DISCUSSION

Plasma Protein Binding and Red Blood Cell–Plasma Water Partitioning of I—Plasma protein binding of I by ultrafiltration was 3.4 ± 2 (*SEM*)%, n = 4, when corrected for membrane binding and was independent of the spike concentration (0.1–100 μg/ml). This was similar to the plasma protein binding, 1.5 ± 1.9%, in humans (2). The red blood cell–plasma water partition coefficient, D, was not concentration dependent (0.01–100 μg/ml of red blood cell suspension), and was approximately unity [0.99 ± 0.08 (*SEM*), n = 5], close to the 0.95 ± 0.04 of human erythrocytes (2). There was also no time-dependent distribution of I in the erythrocytes, measured between 5 and 60 min at 1 μg/ml.

Recovery of Radioactivity in Feces—Negligible amounts (0.3 and 0.1%) of the administered radioactivity were found in the feces of dog A after intravenous administrations of 40 (0.3%) and 200 mg (0.1%) of radiolabeled I.

Comparison of Radiolabeled and GLC Assays of I—Plasma sampled from dog A as a function of time (1–600 min) after intravenous administration of 24.0 and 48.4 mg/kg and after oral administration of 20.0 mg/kg of ^{14}C-labeled I were analyzed for I by electron-capture GLC and by the radioassay of the single 5-ml chloroform extracts of 500 μl of solution containing 0.5–500 μl of plasma. The assays were linearly related (Fig. 1A). The regression coefficients, m, were not significantly different than unity, nor were the intercepts, b, different than zero (Table I) for the 24- (iv) and 20- (po) mg/kg doses. There is a possibly greater assay value by radioassay than GLC at the 48.4-mg/kg dose, indicating a small amount of chloroform-extractable metabolite, although elimination of the 1-min plasma sample increased the regression coefficient to 0.94 ± 0.03.

Similarly, the amount of I excreted in the urine, U_I and the amounts cumulatively excreted in the urine, ΣU_I, with time (15–900 min) were the same by the GLC assay and the radioactivity counting of the single 5-ml chloroform extracts of 500 μl of a solution containing 0.02–500 μl of urine (Fig. 1B and C) at 24.0-mg/kg iv and 20.0-mg/kg po doses. However, GLC assays of urinary I at the 48.4-mg/kg iv dose were 20% lower than radioassays of the chloroform extracts, as ascertained by regression analysis (Table I), indicating the presence of significant amounts of chloroform-extractable metabolites at this dose.

The good correlation between the GLC assays of I and the radioassays of chloroform extracts of plasma and urine at the 2- and 10-mg/kg iv doses in dog A had been reported previously (1). It can be concluded that any radiolabeled metabolite extracted in a single chloroform extraction of

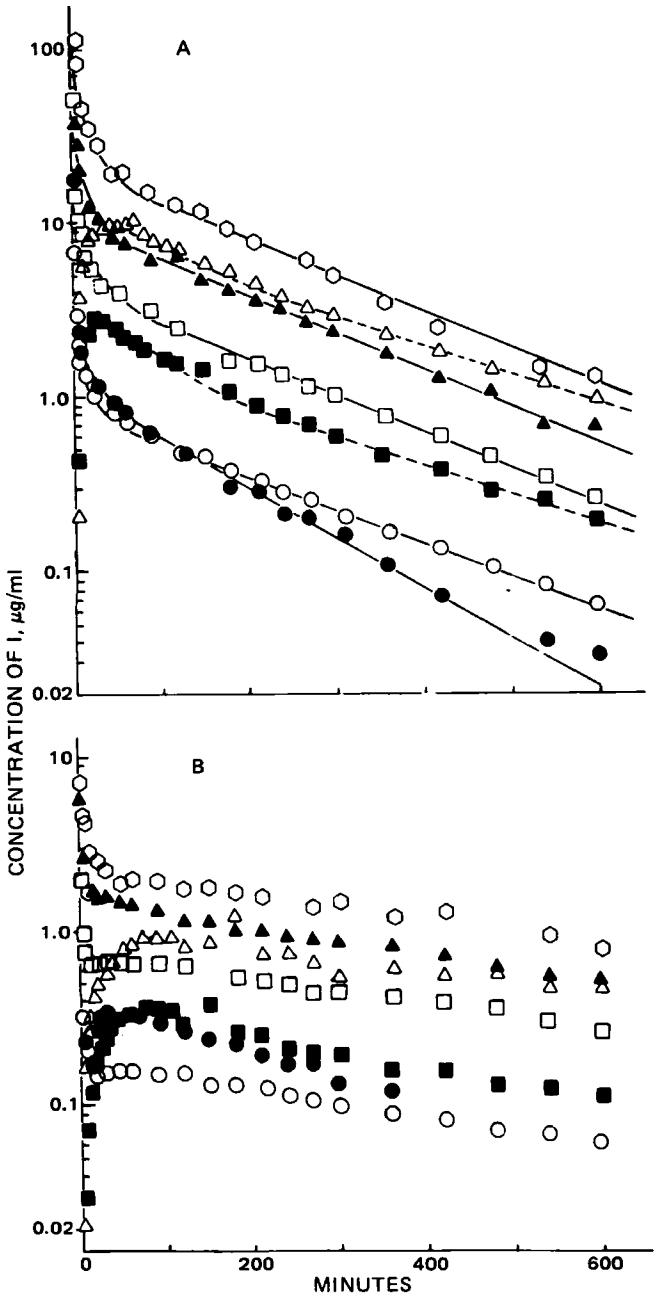

Figure 2—*Semilogarithmic plasma concentration* versus *time plots of (A) I determined by radioassay (LSC) of chloroform extracts and (B) total metabolites determined by direct radioassay of chloroform-extracted aqueous phases after administration of ^{14}C-labeled I to dog A at mg/kg doses of (○) 1.9 iv, (●) 2.0 iv, (□) 10.0 iv, (▲) 24.0 iv, (○) 48.4 iv, (■) 5.1 po, and (△) 20.0 po. Solid lines were drawn in accordance with [I] = $Ae^{-\alpha t} + Be^{-\beta t}$ where parameters are given in Table II.*

plasma or urine at pH 12 for low doses of I (2 to 24 mg/kg) did not disturb assays of I by LSC, although some radiolabeled metabolite(s) were extracted with chloroform at the high dose of 48 mg/kg iv.

Pharmacokinetics of Intravenously Administered I—The semilogarithmic plots of the plasma levels of I with time at doses of 1.9, 24.0, and 48.4 mg/kg iv and at the previously reported 2.0 and 10.0 mg/kg iv doses in dog A (Fig. 2A) and at doses of 1, 5, and 10 mg/kg iv in dogs B, C, D, and E showed primarily biphasic curves, indicative of a two-compartment body model for I. The lines drawn through the experimental points were calculated from the general equation $[I] = Ae^{-\alpha t} + Be^{-\beta t}$ in μg/ml of plasma where the parameters A, B, α, and β are listed in Tables II and III for the intravenous data. Similar curves were obtained for the studies in the other dogs.

In all intravenous studies the first 1-min data point after administration was omitted to fit the experimental plasma values to a sum of two

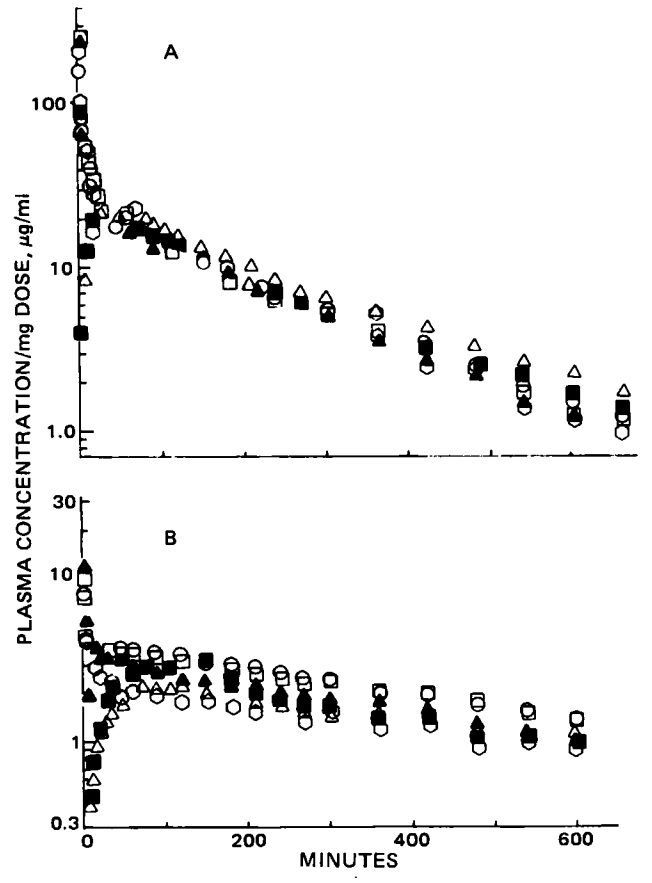

Figure 3—*Semilogarithmic plots of plasma concentrations with time of (A) I per milligram administered dose determined by radioassay (LSC) of chloroform extracts and (B) total metabolites, in equivalents of I per milligram administered dose, determined by direct radioassay of chloroform-extracted aqueous phases after administration to dog A of ^{14}C-labeled I in mg/kg doses of (○) 1.9 iv, (□) 10.0 iv, (▲) 24.0 iv, (○) 48.4 iv, (■) 5.1 po, and (△) 20.0 po. Drawn curves through iv data were in accordance with $[I]/D_0 = (A/D_0)e^{-\alpha t} + (B/D_0)e^{-\beta t}$.*

exponentials. This 1-min plasma concentration was significantly higher than the concentration calculated from this sum in all studies and indicated a possibly faster initial distribution phase with an apparent half-life of 0.5–1.0 min. It could not be explained by the first samples being contaminated with residual ^{14}C-labeled I, which was administered into the jugular catheter, since plasma levels of I obtained simultaneously from the jugular catheter and a leg vein catheter were identical in both the intravenous 48.4-mg/kg and 1.0-mg/kg doses of I administered to dogs A and C, respectively. Subsequent samples up to 1 hr from both sites also showed coincident plasma levels.

The average plasma half-lives of the distribution and elimination phases for all intravenous studies in dogs A, B, C, D, and E were, respectively, 7.5 ± 0.7 (*SEM*) and 136 ± 6 (*SEM*) min and were independent of dose in the range of 1–50 mg/kg (Tables II and III). The plasma levels calculated per milligram unit dose, $[I]/D_0$ with time were reasonably superimposable for all intravenous doses in dog A (Fig. 3A). This was also true for the different dose studies in the other dogs. These facts indicated dose-independent pharmacokinetics of I on intravenous administration.

The plasma levels of total metabolites as equivalents of I were estimated from the radioactivity in the aqueous phase after chloroform extraction of the plasma. The radioactivity was corrected for unextracted I (1), and the resultant curves of apparent total metabolite concentrations in plasma are given directly in Fig. 2B and per milligram of administered dose of I in Fig. 3B. The apparent metabolite plasma levels per milligram of dose (Fig. 3B) decreased slightly, but systematically, with increasing intravenous doses, indicating a possible dose dependence in metabolite formation in contrast to the plasma levels of I. This was also observed for other dog studies at different doses. Since metabolic clearance is only 13% of the total clearance, this apparently minor dose-dependent metabolism would not be expected to significantly affect the observed dose-independent overall pharmacokinetics of I.

Table II—Pharmacokinetic Parameters of I Administered Intravenously to Dog A

Parameter						Mean ± *SD*(*SEM*)
Dose (D_0), mg	40[a]	43.1	200[a]	480	1017	
Dose, mg/kg	2.0	1.9	10.0	24.0	48.4	
Specific activity, dpm/μg	50304	40898	9995	21707	7180	
A^b, μg/ml	3.4	2.6	11.5	28.9	87.4	
B^b	1.19	0.86	5.30	10.73	21.9	
α^b, min^{-1} ($t_{1/2}$, min)	0.195(3.6)	0.119(5.8)	0.160(4.3)	0.101(6.9)	0.082(8.4)	0.131 ± 0.046(0.020) [5.8 ± 1.9(0.9)]
$10^3\ \beta^b$, ($t_{1/2}$, min)	6.68(104)	4.44(156)	5.44(127)	4.98(139)	4.74(146)	5.26 ± 0.88(0.44) [134 ± 20(9)]
Clearances, ml/min						
CL^I_{tot}[c]	204	200	191	197	179	194 ± 10(4)
CL^I_{ren}[d]	135	152[o]	163[o]	162[o]	177[o], 141[n]	158 ± 16(7)[o]
Apparent volumes of distribution, liters						
V_c[e]	8.7	12.4	11.9	12.1	9.3	10.9 ± 1.7(0.8)
V^I_d[f]	30.6	45.0	35.1	39.5	37.8	37.6 ± 5.3(2.4)
$V^I_{dextrap}$[g]	33.6	50.1	37.7	44.7	46.5	42.5 ± 6.7(3.0)
Disposition, fraction of dose[h]						
ΣU^I_∞/Dose	0.60[n], 0.64[o]	0.796[o]	0.82[n], 0.85[o]	0.82[n], 0.82[o]	0.71[n], 0.90[o]	0.80 ± 0.10(0.04)[o]
ΣU^M_∞/Dose[i]	0.18	0.13	0.15	0.09	0.07	0.12 ± 0.04(0.02)
ΣU^{tot}_∞/Dose[j]	0.980	1.00	1.02	0.98	0.97	0.99 ± 0.02(0.01)
k^k_{TB}, min^{-1}	0.0555	0.0329	0.0542	0.0310	0.0202	0.0388 ± 0.0155(0.0069)
k^l_{BE}	0.0235	0.0161	0.0161	0.0162	0.0192	0.0182 ± 0.0032(0.0014)
k^m_{BT}	0.1227	0.0744	0.0951	0.0588	0.0473	0.0797 ± 0.0300(0.0134)

[a] Pharmacokinetic parameters of 2.0- and 10.0-mg/kg studies were reported previously (1). [b] Parameters estimated from best fit of LSC assay of I in plasma against time (Fig. 2) in accordance with $[I] = Ae^{-\alpha t} + Be^{-\beta t}$; LSC and GLC assays were coincident. The 1-min plasma level datum was omitted from consideration. [c] Total clearance of I, D_0/AUC_∞, where AUC_∞ is the total area under the I plasma level-time plot. [d] Renal clearance of I consistent with the $\Sigma U = CL_{ren}AUC_t$ (Figs. 4 and 6), where AUC_t is the area under the plasma level of I-time plot for the time when the cumulative amount of I in the urine, ΣU, was measured. At the highest dose of 48.4 mg/kg iv, GLC and LSC of extracts were not coincident. [e] Apparent volume of central compartment for I, $Dose/(A + B)$. [f] Apparent overall volume of distribution for I, CL^I_{tot}/β. [g] Apparent extrapolated volume of distribution for I on presumption of one-compartment body model, $Dose/B$. [h] Estimated from asymptotes of ΣU *versus* time plots of Fig. 6. [i] Based on LSC assay of radioactivity in aqueous phase after chloroform extraction of urine. [j] Based on LSC assay of total radioactivity in urine (1). [k] Transfer rate constant from the tissue compartment to the central compartment, $k_{TB} = (A\beta + B\alpha)/(A + B)$ (7). [l] Elimination rate constant from the central compartment, $k_{BE} = \alpha\beta/k_{TB}$ (7). [m] Transfer rate constant from the central compartment to the tissue compartment $k_{BT} = \alpha + \beta - k_{TB} - k_{BE}$ (7). [n] Based on GLC assay of urine. [o] Based on LSC assay of chloroform extract of urine.

Apparent Volumes of Distribution of I—The apparent volumes of distribution (Tables II and III) were referenced to the plasma concentration of I. The average apparent volume of distribution of the central compartment was 13.1 ± 0.7 (*SEM*) liters, $V_c = D_0/(A + B)$, which is equivalent to the total body water in a 20-kg dog (12–14 liters) (5). The average apparent overall volume of distribution, $V_d = CL_{tot}/\beta$, was 40.0 ± 1.5 (*SEM*) liters, which exceeded total body water and indicated tissue sequestration.

Clearances of I—The renal clearances (Tables II and III) were estimated from plots of the urinary excretion rates of I against the plasma concentrations at the midpoint time of each urine collection interval and from plots of the amounts of I cumulatively excreted in the urine at time t (ΣU_t) against the area under the plasma level–time curve at time t (AUC_t), according to the equation $\Sigma U_t = CL_{ren}AUC_t$ (Fig. 4). The presence of a possible initial distribution phase of 0.5–1-min half-life was supported by the fact that the positive intercepts frequently observed for renal clearance plots of ΣU_t against AUC_t when the initial 1-min datum was ignored did not exist when the additional area given by its inclusion was considered. Then the intercept was not significantly different from zero.

The renal clearances [155 ± 5 (*SEM*) ml/min] were independent of dose, urine flow, and urinary pH and indicated an excess of tubular secretion of the negligibly plasma protein-bound I in addition to glomerular filtration, which is in the range of the inulin clearance (85 ± 35 ml/min) in a 20-kg dog (6). Thus, at doses <24 mg/kg, dose-dependent renal clearances cannot be concluded. However, the possibility of lowered renal clearance at higher doses is still open, as the one study at 48.4 mg/kg did not show coincident LSC and GLC assays of extracts of urine, and the renal clearances from the latter assay appeared to be significantly lower (Table II).

Bioavailability on Oral Administration—The fact that no dose dependency was observed on intravenous administration of 1–48.4 mg/kg (Fig. 3A, Tables II and III) demonstrated that that systemic distribution and disposition of I followed first-order linear pharmacokinetics and permits us to estimate the absolute bioavailability of oral solutions of I with respect to intravenous administration by the ratio of areas under the plasma level–time curves. The areas under the plasma level–time curves (Table IV) were calculated by integration to time infinity according to $AUC_\infty = A/\alpha + B/\beta$ for the intravenous doses. They were calculated for the oral doses by the trapezoidal rule to time 900 min and by adding the terminal area estimated by dividing the plasma level at 900 min by the disposition rate constant. The area per milligram oral dose of 5.1 μg·min/ml at the 5.1-mg/kg dose was virtually identical to the averaged area of 5.2 μg·min/ml for the intravenous doses of 1.9–48.4 mg/kg. However, the area per milligram dose of 6.1 μg·min/ml at the 20.0-mg/kg oral dose was 10% higher than the highest area of 5.58 μg·min/ml found for the 48.4-mg/kg intravenous dose. This finding could indicate a possible saturable first-pass metabolism of I at high oral doses. This was also indicated by the fact that the plasma concentrations per unit dose were slightly higher for the higher oral dose (Fig. 3A).

Absorption Rates of Orally Administered I—The rates of absorption of I were determined by the Loo–Riegelman deconvolution method (7). The values of the apparent volume of distribution of the central compartment (V_c) and the parameters α, β, and A and B per milligram intravenous dose necessary for estimates of the microscopic rate constants between the central and tissue compartments, k_{BT} and k_{TB}, and the

Table III—Pharmacokinetic Parameters[a] of I Administered Intravenously to Dogs B, C, D, and E

Parameters	B			C			D		E		Mean ± *SD*(*SEM*)	Overall Mean ± *SD*(*SEM*) for Dogs A–E
Dose (D_0), mg	19.9	116.1	231.2	22.2	84.6	203.3	24.8	130.6	113.1	220.3	—	—
Dose, mg/kg	0.97	5.05	10.05	1.00	4.15	10.30	1.00	5.10	4.98	9.40	—	—
Specific activity dpm/μg	95691	14381	7531	78618	21797	7779	78746	12617	15229	7206	—	—
A^b, μg/ml	0.734	5.25	11.35	0.857	5.16	11.99	1.10	5.27	11.43	10.86	—	—
B^b	0.423	2.66	5.27	0.515	1.96	5.09	0.412	2.51	2.35	4.49	—	—
α^b, min^{-1} ($t_{1/2}$, min)	0.046(15)	0.087(8.0)	0.092(7.5)	0.074(9.4)	0.086(8.1)	0.094(7.3)	0.100(6.9)	0.094(7.4)	0.112(6.2)	0.084(8.3)	0.087 ± 0.013(0.005) [8.4 ± 2.5(0.8)]	0.102 ± 0.036(0.009) [7.54 ± 2.57(0.66)]
$10^3\ \beta^b$, ($t_{1/2}$, min)	5.24(132)	4.84(143)	5.24(132)	6.47(107)	5.96(116)	5.69(122)	3.83(181)	5.40(128)	5.05(137)	4.08(170)	5.18 ± 0.80(0.25) [137 ± 23(7)]	5.20 ± 0.79(0.20) [136 ± 21(6)]
Clearances, ml/min												
CL^{I}_{tot}[c]	205	190	205	243	218	203	209	251	200	179	210 ± 22(7)	205 ± 20(5)
CL^{I}_{ren}[d]	124	128	161	168	149	184	145	196	154	154	154 ± 20(6)	155 ± 19(5)
Apparent volumes of distribution, liters												
V^{I}_{c}[e]	17.2	14.7	13.9	16.1	11.9	12.1	16.3	16.8	8.2	14.4	14.2 ± 2.8(0.9)	13.1 ± 2.9(0.7)
V^{I}_{d}[f]	39.1	39.3	39.0	37.5	36.6	35.7	54.5	46.5	39.5	43.9	41.2 ± 5.7(1.8)	40.0 ± 5.7(1.5)
$V^{I}_{dextrap}$[g]	47.0	43.6	43.8	42.9	43.2	40.7	60.1	52.0	48.2	49.0	47.0 ± 5.7(1.8)	45.5 ± 6.2(1.6)
Disposition, fraction of dose[h]												
ΣU^{I}_{∞}/ Dose	0.660	0.795	0.831	0.751	0.741	0.810	0.789	0.799	0.839	0.888	0.79 ± 0.06(0.02)	0.79 ± 0.07(0.02)
ΣU^{M}_{∞}/ Dose[i]	0.233	0.161	0.115	0.193	0.181	0.154	0.160	0.117	0.169	0.103	0.16 ± 0.04(0.01)	0.15 ± 0.04(0.01)
ΣU^{tot}_{∞}/ Dose[i]	0.994	0.995	1.00	1.04	0.979	1.00	0.920	0.971	1.00	1.01	0.99 ± 0.03(0.01)	0.99 ± 0.03(0.01)

[a] Pharmacokinetic parameters were based on LSC. Refer to Table II for footnotes *b*–*j*.

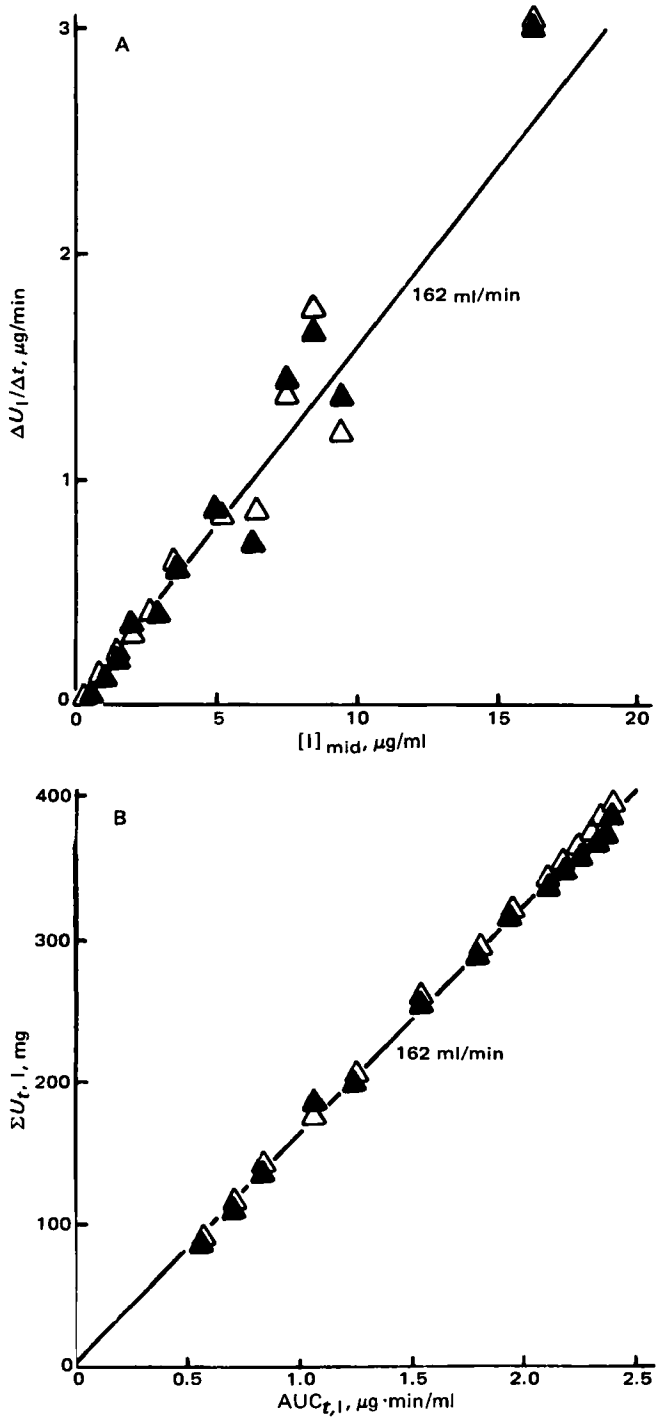

Figure 4—*Typical renal clearance plots for I assayed by GLC (▲) and LSC (△) of extracts, (A) plotting the urinary excretion rates* ($\Delta U/\Delta t$) versus *the plasma levels of I at the midpoint of the urine collection,* ($[I]_{mid}$) *and (B) the cumulative amounts of I excreted in the urine at time* t (ΣU_t) versus *the area under the plasma level–time curve to time* t (AUC_t) *after intravenous administration of 24.0 mg/kg of I to dog A.*

elimination rate constant from the central compartment, k_{BE}, were obtained from the average values of those parameters in the intravenous studies in dog A. The semilogarithmic plots of the percent unabsorbed I with time for the oral doses administered to dog A are given in Fig. 5 and were linear, indicating first-order absorption. First-order rate constants of absorption were 0.017 min^{-1} (absorption $t_{1/2}$ of 41 min) for the 5.1-mg/kg dose and 0.042 min^{-1} (absorption $t_{1/2}$ of 16 min) for the 20.0-mg/kg dose after negligible lag times of 5 and 2 min, respectively. The ratio of the first-order absorption rate constants to the dose was reasonably constant and indicates a possible dose dependence.

Table IV—Areas Under the Plasma Concentration–Time Curves (AUC_∞) of I for Various Intravenous and Oral Doses in Dog A

Dose, mg	AUC_∞, μg·min/ml	AUC_∞/Dose, μg·min/ml·mg
	Intravenous Studies	
40	196	4.90
43.1	215	5.00
200	1047	5.24
480	2442	5.09
1017	5677	5.58
		5.16 ± 0.26(0.12)[a]
	Oral Studies	
112.5	578	5.14
444	2708	6.10
		5.62 ± 0.68(0.48)[a]
		($p < 0.01$)[b]

[a] Mean ± *SD*(*SEM*) are given. [b] *t* Test for two means.

Urinary Recoveries of Intravenously and Orally Administered I—Unchanged I was recovered in the urine for 79 ± 2 (*SEM*)% of the intravenous doses (1–50 mg/kg). Chloroform-unextracted metabolites accounted for 15 ± 1% (Tables II and III, Fig. 6). There were no significant differences between renally excreted total radioactivity and the sum of the cumulative amounts of extracted and unextracted radioactivities (Tables II and III).

The total recovery of radioactivity from the cumulative total urine was 106 and 103% of the administered radiolabeled I for the 5.1- and 20.0-mg/kg oral doses, respectively, in dog A, implying complete absorption. The plots of the cumulative amounts of extracted and unextracted activities, expressed as the percentage of the orally administered 5.1- and 20.0-mg/kg doses in dog A, with time are also given in Fig. 6. The cumulative plots of I were fitted for constant renal clearances of 158 and 141 ml/min for the respective 5.1- and 20.0-mg/kg oral doses; these renal clearances were consistent with the renal clearances for the intravenous doses (2–48.4 mg/kg) in dog A (Table II). The urinary recoveries after 5.1- and 20.0-mg/kg oral doses in dog A were 84.5 and 87.2%, respectively, of the dose for extracted radioactivity and 11.5 and 8.1% for the unextracted radioactivity. The slightly lower yield of urinary metabolites (8.1%) at the 20.0-mg/kg oral dose than at the 5.1-mg/kg oral dose (11.5%) and a slightly higher area under the plasma level–time curve of unchanged I at the 20.0-mg/kg oral dose (6.10 μg·min/ml) than the area for the highest intravenous dose of 48.4 mg/kg (5.58 μg·min/ml) could indicate the possibility of saturable first-pass metabolism of I. However, these differences in metabolite recoveries in the urine and in area under the plasma level–time curves of I were small.

Theoretical Basis for Estimation of Number of Metabolites and Their Partition Coefficients from Multiple Extractions of Urine—The apparent partition coefficient (k) of any single radiolabeled compound can be defined as the ratio of the radioactivity (disintegrations per minute, dpm) in the organic phase (dpm_{org}) over the radioactivity in the aqueous phase (dpm_{aq}):

$$k = \frac{dpm_{org}}{dpm_{aq}} = \frac{dpm_{tot} - dpm_{aq}}{dpm_{aq}} \quad \text{(Eq. 1)}$$

where dpm_{tot} is the total radioactivity in the system and equal to the sum of the radioactivity in the aqueous and organic phases. On rearrangement of Eq. 1, the fraction of unextracted radioactivity after a single extraction can be expressed as:

$$\frac{dpm_{aq}}{dpm_{tot}} = \frac{1}{1+k} \quad \text{(Eq. 2)}$$

Thus, the radioactivity remaining in the aqueous phase after the first extraction ($dpm_{aq,1}$) is:

$$dpm_{aq,1} = \frac{dpm_{tot}}{1+k} \quad \text{(Eq. 3)}$$

and the solution can be extracted with organic solvent for a second time to give:

$$dpm_{aq,2} = \frac{dpm_{aq,1}}{1+k} \quad \text{(Eq. 4)}$$

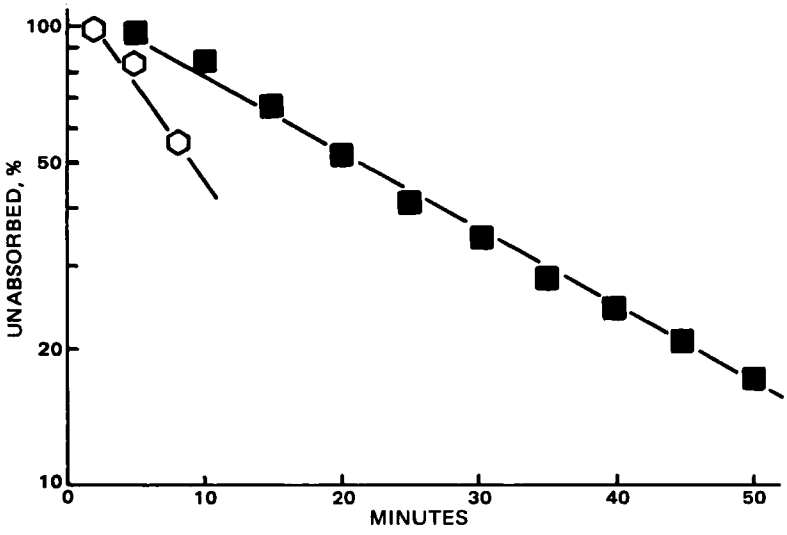

Figure 5—*Semilogarithmic plot of the percent unabsorbed I with time for oral doses of 5.1 (■) and 20.0 (○) mg/kg administered to dog A. Percent unabsorbed I was calculated by the Loo-Riegelman deconvolution method (7).*

Substitution of Eq. 3 into Eq. 4 gives:

$$\mathrm{dpm}_{aq,2} = \frac{\mathrm{dpm}_{tot}}{(1+k)^2} \qquad \text{(Eq. 5)}$$

Thus, the radioactivity left in the aqueous phase after n repetitive extractions is:

$$\mathrm{dpm}_{aq,n} = \frac{\mathrm{dpm}_{tot}}{(1+k)^n} \qquad \text{(Eq. 6)}$$

and

$$\log \mathrm{dpm}_{aq,n} = \log \mathrm{dpm}_{tot} - n\log(1+k) \qquad \text{(Eq. 7)}$$

and a plot of the logarithm of the radioactivity left in the aqueous phase and unextracted ($\mathrm{dpm}_{aq,n}$) *versus* the number of sequential extractions, n, will be linear. The intercept would be the logarithm of the total radioactivity (dpm_{tot}) of the compound before any extraction.

The linearity of the semilogarithmic plot of $\mathrm{dpm}_{aq,n}$ against n (Fig. 7, curves A and A′) implies the possibility of one extractable compound (or several with the same partition coefficient) on ethyl acetate extraction of the acidified chloroform pre-extracted urine samples obtained after intravenous administration of I (curve A) or on spiking blank urine with [^{14}C]I (Curve A′). The total radioactivity (dpm_{tot}) before any ethyl acetate extraction can be estimated from the intercept. This was 1.9% of the total radioactivity in the original urine collection of Fig. 7a, and corresponded to 1.04 mg of the total amount of material as I equivalents in this 370-min urine sample. The apparent partition coefficient of the compound, k, determined from the slope of the line, $\log(1+k)$, in Eq. 7 was 0.815.

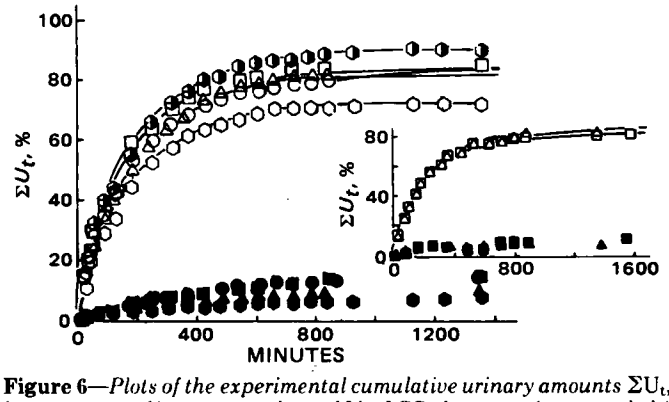

Figure 6—*Plots of the experimental cumulative urinary amounts ΣU_t, in percentage of intravenous dose, of I by LSC of extracts (open symbols) and of total metabolites by LSC of chloroform-extracted aqueous phase (solid symbols), for the 1.9- (○), 10.0- (□), and 24-mg/kg (△) doses of I administered to dog A, against time, where the GLC and LSC assays of urine extracts were coincident (Table I). The different values of the cumulative urinary amounts of I, by GLC (○) and LSC (◑) assays of chloroform extracts of urine after a 24.0-mg/kg dose to dog A, against time are both presented (Table I). Similar plots of the experimental cumulative urinary amounts of I, by LSC assay of extracts, which were coincident with the GLC assays (Table I) for the orally administered doses of 5.1 (□) and 20.0 (△) mg/kg to dog A, against time are given in the insert. Curves through the experimental points of I were fitted according to $\Sigma U = CL_{ren}AUC$ for the constant renal clearances summarized in Tables II and III.*

If there were two extractable compounds with significantly different partition coefficients, the radioactivity remaining in the aqueous phase after n extractions, $(\mathrm{dpm}_{aq,n})_{sum}$, would be the sum of the two radioactivities from each of compounds 1 and 2, $(\mathrm{dpm}_{aq,n})_1$ and $(\mathrm{dpm}_{aq,n})_2$, where each remaining activity could be defined by an equation of the form of Eq. 6, where $(\mathrm{dpm}_{tot})_1$, $(\mathrm{dpm}_{tot})_2$, and dpm_{tot} are the total radioactivities of compound 1, compound 2, and their sum, respectively, in the aqueous system before any extractions were made. Thus:

$$(\mathrm{dpm}_{aq,n})_{sum} = (\mathrm{dpm}_{aq,n})_1 + (\mathrm{dpm}_{aq,n})_2 = \frac{(\mathrm{dpm}_{tot})_1}{(1+k_1)^n} + \frac{(\mathrm{dpm}_{tot})_2}{(1+k_2)^n} \qquad \text{(Eq. 8)}$$

If compound 1 were more readily extracted than compound 2 as n increases to large numbers, there would be eventually no more of the former to be extracted and $(\mathrm{dpm}_{aq,n})_1$ would be equal to zero so that:

$$\lim_{n \to \infty} (\mathrm{dpm}_{aq,n})_{sum} = (\mathrm{dpm}_{aq,n})_2 = \frac{(\mathrm{dpm}_{tot})_2}{(1+k_2)^n} \qquad \text{(Eq. 9)}$$

and the logarithm of both sides would give an equation similar to Eq. 7. This can be seen in the examples of curves B and B′ in Fig. 7 for 15 sequential chloroform extractions at pH 12 of urine sampled 370 min after intravenous administration of ^{14}C-labeled I to dog A and for the [^{14}C]I spiked urine, respectively, where possibly two chloroform-extractable compounds may exist in the urine. The apparent partition coefficients (k_2) of this least readily extracted compound, calculated from the slopes of the terminal data, were 0.29 (curve B) and 0.24 (curve B′). The intercept of these extrapolated linear terminal data permitted the calculation of the radioactivity, $(\mathrm{dpm}_{tot})_2$ due to this compound that contributed to the total radioactivity in the original urine sample:

$$\lim_{n \to \infty} \log(\mathrm{dpm}_{aq,n})_{sum} = \log(\mathrm{dpm}_{aq,n})_2 = \log(\mathrm{dpm}_{tot})_2 - n\log(1+k_2) \qquad \text{(Eq. 10)}$$

Thus, the apparent metabolite 2 accounted for 2.24 mg (as I equivalents) or 4.1% of the total radioactivity in the urine collection of the example of curve B and 0.59% in the example of curve B′.

Since $(\mathrm{dpm}_{aq,n})_2$ can be calculated for any n by Eq. 9 from the estimated k_2 and $(\mathrm{dpm}_{tot})_2$, the logarithm of the difference between this value and the experimentally determined $(\mathrm{dpm}_{aq,n})_{sum}$ can be plotted against n (curve C in Fig. 7) to estimate k_1 and $(\mathrm{dpm}_{tot})_1$ (Eq. 8) from the straight line obtained in accordance with:

$$\log[(\mathrm{dpm}_{aq,n})_{sum} - (\mathrm{dpm}_{aq,n})_2] = \log(\mathrm{dpm}_{aq,n})_1 = \log(\mathrm{dpm}_{tot})_1 - n\log(1+k_1) \qquad \text{(Eq. 11)}$$

In the given example (Fig. 7a, curve C), the readily extractable compound, on the assumption that there was only one, had an apparent partition coefficient of 12.8 and accounted for 47.7 mg (as I equivalents) or 87.3% of the original radioactivity in the 370-min urine collection. For Fig. 7b, curve C′, the readily extractable compound had an apparent partition coefficient of 17.4 and accounted for 97.5% of the total radioactivity of

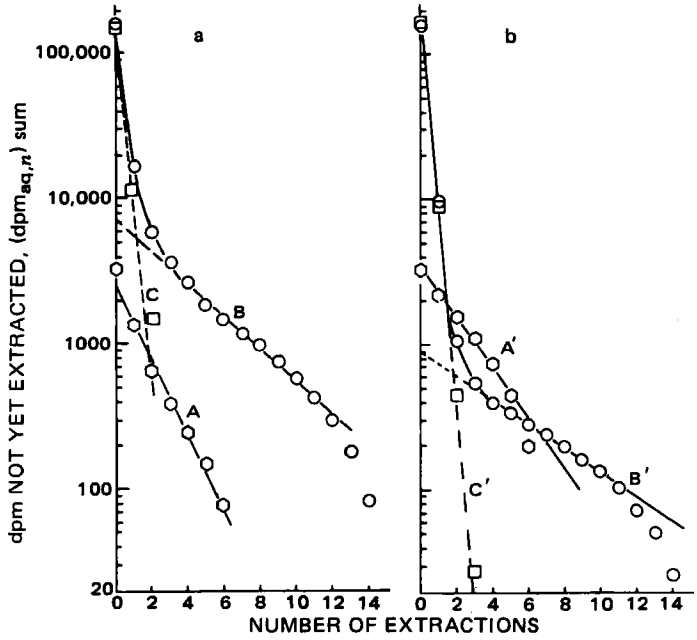

Figure 7—*Typical examples of semilogarithmic plots of not-yet-extracted urine radioactivity against the number of extractions for (a) the 310–370-min urine collection containing a total of 0.177 × 10⁶ dpm after administration of 1017 mg iv of [¹⁴C]I to dog A and for (b) the spiked blank urine containing 1.22 × 10⁶ dpm of standard [¹⁴C]I (585 ng). The ordinate values in (b) are scaled to 0.177/1.22 of their measured values for better comparison with (a). Curves A and A′ are for the 5-ml repetitive ethyl acetate extraction of the 0.6-ml acidified and previously exhaustively chloroform-extracted urines. Curves B and B′ are for the 5-ml repetitive chloroform extractions of the 0.6 ml of urine adjusted to pH 12. Curves C and C′ are the feathered lines obtained from the apparently biphasic curves B and B′.*

the standard [¹⁴C]I. It is evident that the $(dpm_{tot})_i$ and k_i values for each of a mixture of i different compounds of significantly different partition coefficients can be estimated by a series of such deconvolutions using this method, which is similar to the method of residuals used to estimate the parameters of a sum of exponentials.

Application and Limitations of the Method of Multiple Extractions of Urine on Dosing of Radiolabeled I—The semilogarithmic plots of $(dpm_{aq,n})_{sum}$ against the number (n) of sequential chloroform extractions appeared to be reasonably biphasic for the urine samples taken between 15 and 784 min after intravenous administrations of 1017-mg (Fig. 7, curves B and C) and 43-mg ¹⁴C-labeled I. Feathering of the semilogarithmic plots showed at least two radiolabeled chloroform-extractable compounds.

Possible Least Chloroform-Extractable Compound (II) as Metabolite—The least extractable compound (II), resolved from the terminal data, had an average apparent partition coefficient, k_{II}, of 0.264 ± 0.016 (0.004), n = 17, for the 1017-mg dose (Table V) and 0.268 ± 0.038 (0.009), n = 19, for the 43-mg dose (Table VI). It comprised increasing percentages of the urinary radioactivity with time, from 0.4% in the urine collected between 0 and 15 min to 6.4% in the urine collected between 665 and 725 min for the 1017-mg dose and from 0.9% in the urine collected between 0 and 15 min to 16.8% in the urine collected between 790 and 850 min for the 43-mg dose. This implies that II, relative to I, is formed later in the body and/or is eliminated more slowly.

When 0.6 ml of blank urine adjusted to pH 12 containing 1.22 × 10⁶ dpm of [¹⁴C]I[6] (585 ng of specific activity 324 mCi/mmole) was sequentially extracted 15 times, each time with 5 ml of fresh water-saturated chloroform, a semilogarithmic plot of amount radioactivity remaining in the aqueous phase against the number of extractions (n) was remarkably similar in its biphasic form (Fig. 7, curve B′) to that from the urines (Fig. 7, curve B). The slope of the terminal points paralleled that of the terminal points in the urine studies (Fig. 7, curve B) and gave a similar calculated apparent partition coefficient of 0.24 (Eq. 10) as compared with the average of 0.26 ± 0.02 (0.004) and 0.27 ± 0.04 (0.01) for the urine samples listed in Tables V and VI, respectively. A similar study for 950,000 dpm of [¹⁴C]I (0.56 ng of specific activity 137 mCi/mmole) in 0.6 ml of distilled water adjusted to pH 12 gave an apparent partition coefficient of 0.303.

Since the apparent partition coefficients for II in urine and in administered drug were similar, this could imply that this least chloroform-extractable compound II in the urine was a radiolabeled impurity in the original dose of intravenously administered I. The extrapolated intercept of this terminal phase (Fig. 7, curve B′) which permitted the estimation of the original amount of radioactivity of compound II that might contaminate the administered radiolabeled I, gave a value that could be interpreted as accounting for 0.59% of the total radioactivity of I for a radiolabeled purity of the administered I of 99.4%. In the similar aqueous study it accounted for 2.4% for a radiolabeled purity of the administered I of 97.6%, in agreement with the estimated chromatographic purity of I determined before the pharmacokinetic studies. The 2.4% was similar to an estimated 2.7% of II cumulatively excreted at infinite time (2.4% at 784 min) in the urine for the dog administered 1017 mg (Table V), but significantly less than a similar estimate of 8.0% of II for the administered 43-mg dose, (Table VI, 7.4% at 1378 min). This latter fact implies that a significantly greater amount of material of similar properties as the impurity II might result as a renally excreted biotransformation product in the dog.

TLC were made of the repetitive chloroform extracts of the mixed urine samples collected between 120 and 240 min and the urine collected at 605–665 min when the 1017-mg dose was administered intravenously. Definitive radioactivity was observed at R_f values of 0.29, 0.44, and 0.63 in all of the sequential extracts. However, sequential chloroform extracts of the spiked blank urine containing a solution of the administered dose showed radioactivity only at R_f 0.63, coincident with the R_f value of I but not necessarily I. This implied that compounds with R_f 0.33 and 0.47 can result from metabolic processes when the [¹⁴C]I is administered.

The fraction of radioactivity, F, extracted in each of n repetitive extractions of a single compound can be expressed as:

$$F = \frac{\text{dpm in } CHCl_3}{\text{Initial dpm in aqueous phase}} = \frac{k}{(1+k)^n} \qquad \text{(Eq. 12)}$$

Thus:

$$\log(\text{dpm extracted in } CHCl_3) = \log k(\text{initial dpm in aqueous phase}) - n\log(1+k) \qquad \text{(Eq. 13)}$$

The amount extracted into chloroform that appears at a given R_f value can be calculated from the product of the fraction of the total radioactivity applied on the TLC ($dpm_{R_f}/dpm_{applied}$) and the total dpm_{CHCl_3} in a given chloroform extract. This should be linear when plotted semilogarithmically against the number of extractions (n). When such plots were made for amounts at the several observed R_f values (Fig. 8) obtained from the 605–665-min urine sample from dog A after intravenous administration of 1017 mg of [¹⁴C]I, the materials at the three TLC spots all had terminal phases which indicated compounds with approximately equivalent partition values R_f, k: 0.29, 0.204; 0.44, 0.38; 0.63, 0.183. The percentage of these least extractable compounds in that particular urine sample can be estimated from the intercepts of the linearly extrapolated terminal data (Fig. 8, Eq. 13) and were R_f, percent of chloroform-extractable radioactivity, percent of radioactivity in total urine: 0.29, 0.96, 0.83; 0.44, 1.17, 1.02; 0.63, 3.33, 2.89. The 0.83 and 1.02% of total estimates of radioactivity in total urine at the given urine collection (R_f 0.29 and 0.44, respectively) do indicate small amounts of chloroform-extractable compounds produced by metabolism that cannot be assigned to the apparent radiolabeled impurity, II, in the administered radiolabeled dose of I. It is, of course, possible that the compounds at these R_f values are not metabolites of I, but of the apparent radiolabeled impurity, II, in the radiolabeled dose of I.

Possible Readily Chloroform-Extractable Compounds as Metabolites—The apparent partition coefficient of the more readily extractable chloroform compounds, k_{res}, systematically decreased from 19.8 in the 0–15-min urine to 10.9 in the 728–784-min urine for the 1017-mg study (Table V) and from 19.85 in the 15–30-min urine to 6.7 in the 850–1738-min urine for the 43.1-mg study (Table VI). These apparent k_{res} partition coefficients were estimated from the slopes based on first and second repetitive partitions of material from 0.6 ml of urine into 5 ml of $CHCl_3$ (Fig. 7, curve C). The apparent k_{res} partition coefficients for the radiolabeled dose added to urine (curve C′) and water, respectively, were 18.0 and 20.0. Inspection of curve C′ (Fig. 7b) shows no indication of changing partition coefficients for this residual line with increasing n. This strongly implies that not only I is readily chloroform extractable from the urine of dogs administered I, but also a compound, I′, with a slightly lower partition coefficient, and that I′, relative to I, is formed later in the body and/or is eliminated more slowly.

The TLC distribution of sequential chloroform extracts of the 605–

Table V—Data and Constants Estimated from Multiple Extractions of Collected Urines after Intravenous Administration of 1017 mg of I to Dog A[a]

Min[b]	U_{tot}, mg[c]	$U^{tot}_{CHCl_3}$, mg[d]	k_{II}[e]	U^{tot}_{II}, mg[f]	k_{res}[g]	U^{tot}_{res}, mg[h]	k_{ETAC}[i]	U^{tot}_{ETAC}, mg[j]	U^{tot}_{unext}, mg[k]	$U^{R_f\,0.20}_{unext}$, mg[l]	$U^{R_f\,0.50}_{unext}$, mg[l]	$U^{R_f\,0.62}_{unext}$, mg[l]
15	102.5	100.4	0.26	0.41	19.8	100.0	0.81	0.51	1.53	0.308	0.84	0.41
33	117.9	115.1	0.23	1.30	18.3	113.8	0.90	0.71	2.12	0.354	1.30	0.47
47	57.8	56.2	0.25	0.75	18.7	55.4	0.99	0.46	1.16	0.139	0.75	0.23
62	59.2	57.4	0.28	1.07	16.2	56.3	0.69	0.53	1.30	0.000	0.89	0.41
91	78.4	75.5	0.28	1.65	20.1	73.8	0.73	0.94	1.96	0.063	1.25	0.63
122	46.6	44.7	0.28	1.35	12.9	43.3	0.76	0.61	1.40	0.047	0.91	0.47
180	138.5	122.1	0.28	3.74	17.4	128.4	0.80	1.94	4.43	0.125	3.05	1.25
255	116.8	110.2	0.25	2.92	16.2	107.3	0.73	1.64	4.91	0.222	3.39	1.28
310	60.8	56.5	0.25	1.82	15.6	54.7	0.72	0.97	3.34	0.103	2.43	0.79
370	54.7	49.9	0.29	2.24	12.8	47.7	0.82	1.04	3.72	0.087	2.90	0.77
423	38.2	34.3	0.28	1.53	12.8	32.8	0.84	0.73	3.13	0.000	2.66	0.50
484	34.1	30.0	0.25	1.40	10.3	28.6	1.15	0.82	3.34	0.051	2.73	0.58
546	18.9	16.4	0.28	0.96	12.1	15.4	0.81	0.51	2.00	0.053	1.64	0.30
605	26.2	22.7	0.27	1.21	9.8	21.5	1.21	0.66	2.83	0.065	2.25	0.52
665	15.6	13.6	0.25	0.76	13.0	12.8	0.62	0.52	1.54	0.017	1.25	0.28
728	10.7	9.2	0.26	0.69	12.9	8.5	0.74	0.33	1.17	—[m]	—	—
784	5.9	5.0	0.26	0.36	10.9	4.6	0.70	0.21	0.71	—	—	—
Total, mg	982.8	929.2		24.15		904.9		13.12	40.59	1.67	28.24	8.89
Percent of ΣU_{tot}	100	94.5		2.46		92.1		1.33	4.13	0.17	2.87	0.90
Percent of Dose	96.6	91.4		2.37		89.0		1.29	3.99	0.16	2.78	0.87
Mean ± *SD* (*SEM*)			0.26 ± 0.016 (0.004)				0.82 ± 0.16 (0.04)					

[a] Dose of 7.30×10^9 dpm. $\Sigma U_{tot} = \Sigma U^{tot}_{CHCl_3}\ \Sigma U^{tot}_{ETAG} + \Sigma U^{tot}_{unext}$; $\Sigma U^{tot}_{CHCl_3} = \Sigma U^{tot}_{res} + \Sigma^{tot}_{II}$; $\Sigma U^{tot}_{unext} = \Sigma U^{R_f\,0.20}_{unext} + \Sigma U^{R_f\,0.50}_{unext} + \Sigma U^{R_f\,0.62}_{unext}$. [b] Final time of urine collection started at the time listed. [c] Total amount of excreted compound in urine collection, U_{tot}, in I equivalents as determined from total radioactivity in collection, $10^{-3}\,(V/v) \times \text{dpm}_{tot} \div$ specific activity of [^{14}C]I, where V is volume of urine collected, v is volume counted by LSC to obtain the dpm_{tot} values. The specific activity was 7180 dpm/μg. [d] Amount in each urine collection, $U^{tot}_{CHCl_3}$, that can be ultimately extracted into chloroform $10^{-3}\,(V/v) \times \text{dpm}_{CHCl_3} \div$ specific activity. dpm_{CHCl_3} is the total cumulative radioactivity extracted into all of the repetitive chloroform extracts. [e] Estimated from terminal slope, S, of log $(\text{dpm}_{aq,n})_{sum}$ *versus* n where $(\text{dpm}_{aq,n})_{sum}$ is the radioactivity not yet extracted into chloroform or log $(U^{tot}_{CHCl_3} - U^{n}_{CHCl_3})$ and where $U^{n}_{CHCl_3}$ is the cumulative amount extracted into chloroform from a given urine collection up to the nth extraction and k_{II} = antilog $(|S| - 1)$, in accordance with Eq. 10. [f] Estimated cumulative amounts of II that are chloroform extractable from a given urine collection and obtained from the intercept, dpm_{Int}, of the linear extrapolation of the plot of the terminal data as in footnote *e*; $U^{tot}_{II} = 10^{-3}\,(V/v) \times \text{dpm}_{Int} \div$ specific activity. [g] Obtained from slopes (S) of plots of log $[(\text{dpm}_{aq,n})_{sum} - (\text{dpm}_{aq,n})_{II}] = \log (\text{dpm}_{tot})_{res} - n\log (1 + k_{res})$, in accordance with Eq. 11 and calculated for the line through 0 and 1 values of n, where k_{res} = antilog $(|S| - 1)$. The $(\text{dpm}_{aq,n})_{II} = \text{dpm}_{Int}/(1 + k_{II})^n$ where dpm_{Int} is the total cumulative amount of II that is chloroform extractable from the given urine collection and was defined in footnote *f*. [h] Estimated amount of residual material that is not II and is more readily chloroform extractable obtained from the intercept $(\text{dpm}_{tot})_{res}$ of the plot described in footnote *g*, *i.e.*, $10^{-3}\,(V/v) \times (\text{dpm}_{tot})_{res} \div$ specific activity. [i] Estimated from slope, S, of log $(\text{dpm}_{aq,n})$ *versus* n where $(\text{dpm}_{aq,n})$ *versus* n where $(\text{dpm}_{aq,n})$ is the radioactivity not yet extracted into ethyl acetate or log $(U^{tot}_{ETAC} - U^{n}_{ETAC})$. U^{n}_{ETAC} is the cumulative amount extracted into ethyl acetate from a given chloroform pre-extracted urine collection up to the nth extraction and k_{ETAC} = antilog $(|S| - 1)$, in accordance with Eq. 7. [j] Estimated total ethyl acetate-extractable amounts, U^{tot}_{ETAC}, from a urine collection; obtained from the intercept, dpm_{Int}, of the linear plot of log U^{n}_{ETAC} *versus* n, as in footnote *i*. [k] Estimated amounts of unextractable compounds obtained from total radioactivity measurement (dpm_{unext}), in 50 μl of the aqueous phase previously sequentially chloroform and ethyl acetate extracted; $10^{-3}\,(V/v) \times \text{dpm}_{unext} \div$ specific activity. [l] Amounts that remained in urine collection after repetitive chloroform and ethyl acetate extractions and appearing at specified R_f values on TLC plates as determined by plate scraping and LSC counting where $U^{R_f}_{unext} = (\text{dpm}_{R_f}/\text{dpm}_{applied}) \times U^{tot}_{unext}$, where dpm_{R_f} and $\text{dpm}_{applied}$ are the counts measured at the R_f spot and the total counts applied on the plate respectively. [m] Not measured.

Table VI—Data and Constants Estimated from Multiple Extractions of Collected Urine after Intravenous Administration of 43.1 mg of I to Dog A[a]

Min[b]	U_{tot}, mg[c]	$U^{tot}_{CHCl_3}$, mg[d]	k_{II}[e]	U^{tot}_{II}, μg[f]	k_{res}[g]	U^{tot}_{res} mg[h]	k_{ETAC}[i]	U^{tot}_{ETAC}, μg[j]	U^{tot}_{unext}, μg[k]	$U^{R_f\,0.20}_{unext}$ μg[l]	$U^{R_f\,0.35}_{unext}$ μg[l,n]	$U^{R_f\,0.50}_{unext}$ μg[l,n]	$U^{R_f\,0.62}_{unext}$ μg[l]
15	6.30	6.17	0.34	0.57	25.30	6.11	0.52	31.5	101	0	0	101	0
30	3.69	3.56	0.35	137	19.85	3.42	0.65	33.2	100	0	0	38	63
45	2.32	2.23	0.33	125	17.02	2.10	0.73	32.5	67	0	0	38	30
60	2.14	2.03	0.29	124	14.91	1.91	0.81	34.2	73	0	14.1	30	28
90	3.56	3.35	0.27	224	13.92	3.13	0.86	71.2	139	0	21.0	72	46
120	2.85	2.50	0.27	217	15.04	2.28	0.83	57.0	291	3.7	0	157	100
180	5.02	4.64	0.25	377	14.50	4.26	0.84	130.5	251	0	47.7	121	105
250	3.97	3.64	0.24	361	14.59	3.28	0.87	119.1	202	0	47.6	127	64
310	2.74	2.47	0.26	296	15.10	2.17	0.78	95.9	184	0	43.8	104	36
370	1.98	1.77	0.25	218	16.70	1.55	0.83	69.3	139	0	27.7	87	24
430	1.56	1.37	0.23	156	15.37	1.21	0.83	60.8	134	0	23.4	83	28
490	1.52	1.30	0.31	170	13.91	1.13	0.83	65.4	150	0	31.1	102	17
550	1.04	0.877	0.24	121	13.00	0.756	0.84	47.8	115	3.4	0	92	21
610	0.77	0.611	0.24	96	12.26	0.515	0.83	40.8	118	4.5	0	91	22
670	0.59	0.443	0.24	89	9.75	0.354	0.81	36.0	111	6.9	0	84	20
725	0.57	0.415	0.25	76	11.08	0.339	0.82	37.6	118	6.3	0	89	23
790	0.40	0.285	0.24	53	7.47	0.232	0.80	27.2	84	5.0	0	64	16
850	0.37	0.264	0.27	62	8.81	0.202	0.82	26.6	80	4.1	0	61	14
1378	1.58	1.05	0.25	242	6.73	0.807	0.74	133.0	400	—[m]	—	—	—
Total, mg	42.97	38.98		3.20		35.8		1.15	2.86	0.034	0.26	1.54	0.66
Percent of ΣU_{tot}	100	90.7		7.45		83.2		2.68	6.66	0.08	0.61	3.59	1.54
Percent of Dose	99.7	90.4		7.42		82.9		2.67	6.64	0.08	0.60	3.57	1.53
Mean ± *SD* (*SEM*)			0.27 ± 0.04 (0.009)				0.79 ± 0.08 (0.02)						

[a] Dose of 1.76×10^9 dpm. $\Sigma U_{tot} = \Sigma U^{tot}_{CHCl_3} + \Sigma U^{tot}_{ETAC} + \Sigma U^{tot}_{unext}$; $\Sigma U^{tot}_{CHCl_3} = \Sigma U^{tot}_{res} + \Sigma U^{tot}_{II}$; $\Sigma U^{tot}_{unext} = \Sigma U^{R_f\,0.20}_{unext} + \Sigma U^{R_f\,0.35}_{unext} + \Sigma U^{R_f\,0.50}_{unext} + \Sigma U^{R_f\,0.62}_{unext}$. Refer to Table V for footnotes *b*–*m*. [n] These minor amounts of metabolites were found at different R_f values for different urine samples for unexplainable reasons.

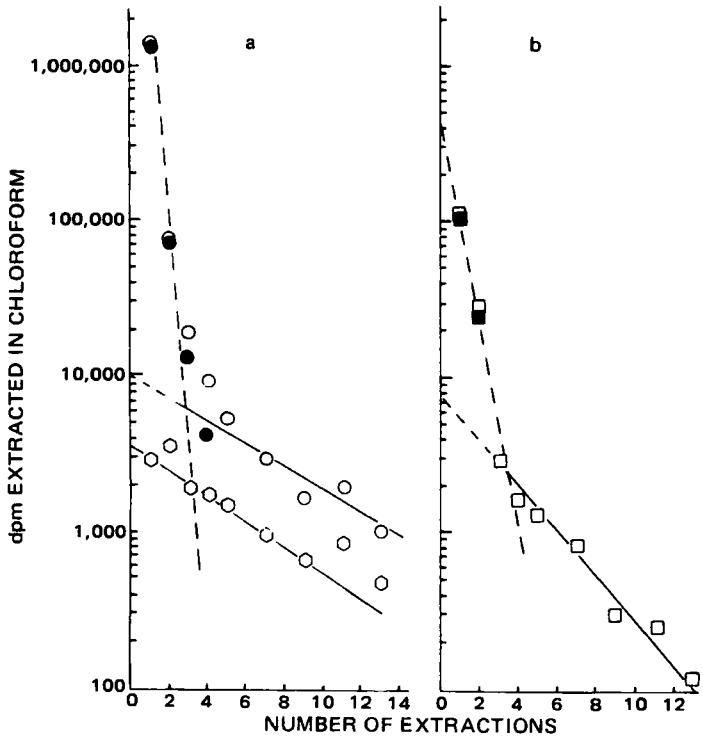

Figure 8—*Semilogarithmic plots against number of extractions (n) of radioactivities (dpm) of different TLC spots at* R_f (○) *0.60–0.69, (□) 0.40–0.47, and (○) 0.27–0.30 from 5.0-ml chloroform extracts of 0.6 ml of pH 12 urine. The urine was collected between 605 and 665 min when 1017 mg of [¹⁴C]I was intravenously administered to dog A. The amounts at each* R_f *value were calculated from* $dpm_{R_f}/dpm_{applied} \times dpm_{CHCl_3}$ *where* dpm_{R_f}, $dpm_{applied}$, *and* dpm_{CHCl_3} *are the radioactivities at the specified* R_f *values, total applied to the TLC plate, and the radioactivity extracted at the* n^{th} *chloroform extraction. The solid symbols are the feathered data.*

665-min urine collection from dog A after administration of 1017 mg of [¹⁴C]I gave the data for Fig. 8 with biphasic semilogarithmic plots. The data from the spot at R_f 0.63, when feathered, permitted the estimation of a partition coefficient of 18.0, consistent with I (Fig. 7, curve C'). The intercept of the feathered line permitted an estimation of 86.4% in the total urine collection that is chloroform extractable (75% of total radioactivity in urine samples) and can be assigned to I. The data from the spot at R_f 0.43, when feathered (Fig. 8) permitted the estimation of a partition coefficient of 3.3. The intercept of the feathered line permitted an estimation of 8.1% of this readily chloroform-extractable R_f 0.43 material of $k = 3.3$ in the total urine collection that is chloroform extractable (7.0% of total radioactivity in urine sample). This would be the possible metabolite I', that accounts for the greatest portion of the discrepancy between GLC and total radioactivity assays of I in urine at the 48.4-mg/kg iv dose (Table I).

When material found at R_f 0.43 was eluted, incubated at pH 12 or 7 for 2 hr at 50°, and rechromatographed on TLC, the radioactivity appeared at the same R_f value. When this material was incubated similarly at pH 2, the rechromatographed material appeared at R_f 0.10–0.23. This shift to much lower R_f values with acid hydrolysis is indicative of the loss of an isopropylidene group (1). This fact plus its ready alkaline chloroform extractability indicate that a possible structure assignment to I' is that it is a monodealkylated product of I.

Possible Ethyl Acetate-Extractable Compounds of Acidified Urines as Metabolites—The semilogarithmic plots of $(dpm_{aq,n})_{sum}$ against the number of sequential ethyl acetate extractions (n) of acidified chloroform-extracted urine indicated one radiolabeled extractable compound (Fig. 7, curve A) with an average apparent partition coefficient of 0.82 ± 0.16 (0.04), $n = 17$, for the 1017-mg dose (Table V) and 0.80 ± 0.08 (0.02), $n = 19$, for the 43-mg dose (Table VI). The cumulative amounts of such ethyl acetate-extractable material excreted in the total urine accounted for 1.29 and 2.67% of the administered doses, respectively. A similar analysis of ethyl acetate-extractable material for the [¹⁴C]I spiked into urine (Fig. 7, curve A') and water accounted for 0.6 and 0.7% of the administered compound, respectively, with respective apparent partition coefficients of 0.46 and 0.57 and a sole TLC spot at R_f 0.67. These facts imply that small, but additional, amounts of ethyl acetate-extractable material are formed in the animal. The ethyl acetate extracts of the 120–240-min urine from the 1017-mg dosed animal showed R_f values of 0.52 and 0.68, but only an R_f value of 0.68 in the 605–665-min urine indicates that the ethyl acetate-extractable material has the same R_f as I.

Possible Unextractable Materials as Metabolites—After the multiple extraction of urine with chloroform and ethyl acetate, 4.0% of the administered radioactivity from the 1017-mg dose of [¹⁴C]I was found in the accumulated urine (Table V), whereas 6.6% was found for the 43.1-mg study (Table VI). Only 1.4 and 1.2% of unextractable radioactivity was found in the [¹⁴C]I spiked urine and distilled water, respectively, implying that additional amounts of unextractable material were formed in the animal. The percentage of total unextractable radioactivity in the urine collections increased from 1.5% at 15 min to 12.1% at 784 min (Table V). The residual urine after multiple extractions with chloroform and ethyl acetate was applied to TLC plates, and sections were scraped for LSC counting. A major portion of the applied radioactivity (60–80%) appeared at R_f 0.47–0.53 with 15–30% at R_f 0.60–0.63 and a small amount (0.05%) at R_f 0.17–0.23. These comprised 2.8% (R_f 0.50), 0.87% (R_f 0.62), and 0.16% (R_f 0.20) of the total administered 1017-mg dose (Table V), and 3.6% (R_f 0.50), 1.5% (R_f 0.62), and 0.70% (R_f 0.20 and R_f 0.35) of the total administered 43.1-mg dose.

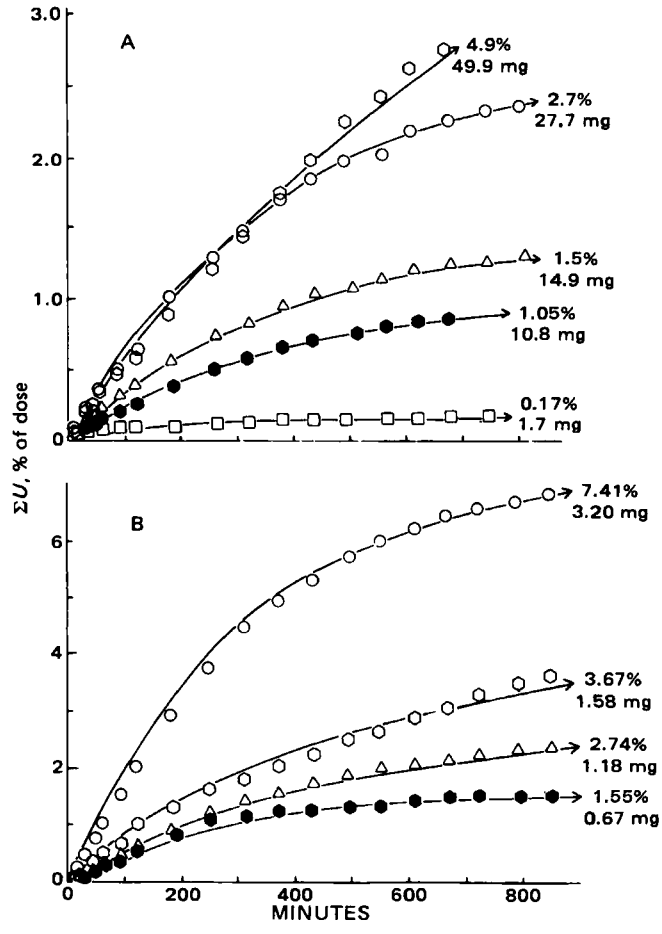

Figure 9—*Cumulative amounts (as percent of administered [¹⁴C]I dose) of variously characterized possible metabolites and/or impurities found in the urine of dog A intravenously administered (A) 1017 mg and (B) 43.1 mg of I. Key: (○) total amounts of II with a partition coefficient of ~0.24 transferred from pH 12 urine (0.6 ml) into repetitive 5-ml chloroform extractions; (△) total amounts of compound transferred from acidified and chloroform pre-extracted urine into repetitive 5-ml ethyl acetate extractions; and cumulative amounts of compounds at* R_f *0.50 (○),* R_f *0.62 (●), and* R_f *0.20 (□) that were unextracted by repetitive chloroform and ethyl acetate extractions. Each curve shows the total amounts of materials and percentage of administered dose estimated from their respective asymptotes. The lines drawn through the values for each curve were calculated from* $\Sigma U = \Sigma U_\infty (1 - e^{-\lambda t})$.

The cumulative amounts of non-I compounds (as percentage of administered radioactivity in the [^{14}C]I dose) are plotted against time in Fig. 9 for the 1017-mg (A) and 43.1-mg (B) doses. The lines drawn through the values were calculated from:

$$\Sigma U = \Sigma U_\infty (1 - e^{-\lambda t}) \qquad \text{(Eq. 13)}$$

The respective half-life values (0.693/λ) in min were: (A) ΣU_{II}, 266; ΣU_{ETAC}, 266; $\Sigma U_{Rf}^{0.2}$, 152; $\Sigma U_{Rf}^{0.5}$, 578; $\Sigma U_{Rf}^{0.62}$, 277; and (B) ΣU_{II}, 231; ΣU_{ETAC}, 300; $\Sigma U_{Rf}^{0.5}$, 278; and $\Sigma U_{Rf}^{0.62}$, 193. Most of these half-lives were approximately the same as I and may indicate the facile renal elimination of these compounds.

REFERENCES

(1) E. R. Garrett, A. Van Peer, H. Mahrous, and W. Schuermann, *J. Pharm. Sci.*, **71**, 387 (1982).

(2) E. R. Garrett, A. Van Peer, P. Altmayer, W. Schuermann, and P. Lücker, *J. Pharmacokinet. Biopharm*, **10**, 247 (1982).

(3) E. R. Garrett and H. J. Lambert, *J. Pharm. Sci.*, **62**, 550 (1973).

(4) Stat-1-22A "Linear Regression" HP-65 Stat Pac I, Hewlett-Packard, Cupertine, Calif., pp. 49–51.

(5) P. L. Altman and D. S. Dittmer, "Blood and Other Body Fluids," Biological Handbooks, Federation of American Societies for Experimental Biology, Washington, D.C., 1961, p. 352.

(6) H. M. Smith, "Principles of Renal Physiology," Oxford University Press, New York, N.Y., 1956, p. 32.

(7) M. Gibaldi and D. Perrier, "Pharmacokinetics," Dekker, New York, N.Y., 1975, pp. 55, 136–140.

ACKNOWLEDGMENTS

Supported in part by unrestricted grants from Greenwich Pharmaceuticals Inc., Greenwich, CT 06830 and Kali-Pharma Inc., Elizabeth, NJ 07207. A. Van Peer is grateful to the Belgian Foundation for Medicinal Scientific Research for their support.

The technical assistance of Kathy Eberst and Marjorie Rigby is gratefully acknowledged.

In Vitro Drug Release from Egg Albumin Microcapsules

TAKAFUMI ISHIZAKA ˣ and MASUMI KOISHI

Received February 12, 1982, from the *Faculty of Pharmaceutical Sciences and the Institute of Colloid and Interface Science, Science University of Tokyo, Shinjuku-ku, Tokyo, Japan.* Accepted for publication August 9, 1982.

Abstract □ The *in vitro* release of phenacetin from microcapsules prepared using egg albumin as the membrane material was investigated. It was shown by scanning electron microscopy that the albumin microcapsules have nonsmooth surfaces. The amount of phenacetin released is proportional to the square root of time up to 50–70% drug release. Increases in the albumin concentration and 1-vinyl-2-pyrrolidinone polymer content in the aqueous phases used in the microcapsule preparation have an effect on matrix porosity and channel tortuosity in the matrix of albumin microcapsules. The *in vitro* release rate was found to decrease with increasing albumin concentration and 1-vinyl-2-pyrrolidinone polymer content in the aqueous phases. The *in vitro* release rate per unit area also decreased with decreasing capsule size.

Keyphrases □ Phenacetin—albumin microcapsules, release rate, controlling factors □ Microcapsules, albumin—release rate of phenacetin, effects of albumin concentration, 1-vinyl-2-pyrrolidinone polymer content, capsule size □ Delivery systems—albumin microcapsules, release rate of phenacetin, effect of albumin concentration, 1-vinyl-2-pyrrolidinone polymer content, capsule size

Delivery of a chemotherapeutic agent to desired target sites with drug carriers could achieve effective local drug concentration and minimize systemic side effects by reducing the therapeutic dose of the chemotherapeutic agent. When a drug carrier, such as liposomes, microcapsules, and microspheres, is injected into the circulatory system, its distribution in the body is an important factor in drug delivery. The tissue distribution of albumin microspheres has been studied in detail (1–3). In addition, alteration in the tissue distribution of albumin microspheres was examined using magnetic guidance (4, 5). Albumin microspheres prepared using a water–oil emulsion have a hydrophilic matrix structure, consisting of albumin molecules, that is similar to that in albumin microcapsules (6).

However, despite many reports on the tissue distribution of albumin microspheres, the mechanism of drug release from minute drug carriers that have a hydrophilic matrix structure is not well known because there are few reports on drug release (7, 8). This paper describes *in vitro* drug release from albumin microcapsules having a hydrophilic matrix structure and some controlling factors.

EXPERIMENTAL

Materials—Isooctane, dibasic potassium phosphate, monobasic sodium phosphate, acetic acid, hydrochloric acid, and sodium acetate were reagent grade. Phenacetin powder (250–300 mesh) was used for microencapsulation as the core drug.

Egg albumin[1] solution was prepared as follows: Albumin was dissolved in buffer solution [0.033 *N* KH_2PO_4–0.033 *N* Na_2HPO_4, 1:16 (v/v); pH 8.0], and the solution was filtered after centrifugation at 16,000 × *g* for 30 min to remove the undissolved materials. The albumin concentration was either 10 or 20% (w/w). 1-Vinyl-2-pyrrolidinone polymer[2] was dissolved in the same buffer solution at 70°. The solution thus obtained (50% w/w) was stored in a refrigerator overnight and used for the preparation of aqueous albumin solutions containing the polymer.

Measurement of Viscosity—Viscosities of both the albumin and mixed polymer solutions [prepared from 20% (w/w) albumin solution and 50% (w/w) 1-vinyl-2-pyrrolidinone polymer solution] were measured at 25° with a cone-plate type viscometer[3] in a shear rate range of 50–3950 sec^{-1}. Viscosity values were calculated from the straight lines in rheograms.

Preparation of Microcapsules—Albumin microcapsules were prepared by a method similar to that described in a previous paper (6). Phenacetin powder (10% v/v) was previously dispersed in albumin solutions with and without the polymer. To 100 ml of isooctane containing 5.0% (v/v) sorbitan trioleate[4] as an emulsifier, in a three-necked flask, was added 15 ml of each of the aqueous dispersions, with stirring. After further stirring for 10 min, the flask was immersed in a water bath maintained at 85° for a given period to denature the egg albumin. The resultant dispersion was cooled to room temperature.

[1] Tokyo Kasei Kogyo Co., Tokyo, Japan.
[2] K-30; Tokyo Kasei Kogyo Co., Tokyo, Japan.
[3] Rheomat 30; Contraves AG, Zurich, Switzerland.
[4] Span 85; Nikko Chemicals Inc., Tokyo, Japan.

0022-3549/83/0900-1057$01.00/0

The cumulative amounts of non-I compounds (as percentage of administered radioactivity in the [^{14}C]I dose) are plotted against time in Fig. 9 for the 1017-mg (A) and 43.1-mg (B) doses. The lines drawn through the values were calculated from:

$$\Sigma U = \Sigma U_\infty (1 - e^{-\lambda t}) \qquad \text{(Eq. 13)}$$

The respective half-life values (0.693/λ) in min were: (A) ΣU_{II}, 266; ΣU_{ETAC}, 266; $\Sigma U_{Rf}^{0.2}$, 152; $\Sigma U_{Rf}^{0.5}$, 578; $\Sigma U_{Rf}^{0.62}$, 277; and (B) ΣU_{II}, 231; ΣU_{ETAC}, 300; $\Sigma U_{Rf}^{0.5}$, 278; and $\Sigma U_{Rf}^{0.62}$, 193. Most of these half-lives were approximately the same as I and may indicate the facile renal elimination of these compounds.

REFERENCES

(1) E. R. Garrett, A. Van Peer, H. Mahrous, and W. Schuermann, *J. Pharm. Sci.*, **71**, 387 (1982).

(2) E. R. Garrett, A. Van Peer, P. Altmayer, W. Schuermann, and P. Lücker, *J. Pharmacokinet. Biopharm*, **10**, 247 (1982).

(3) E. R. Garrett and H. J. Lambert, *J. Pharm. Sci.*, **62**, 550 (1973).

(4) Stat-1-22A "Linear Regression" HP-65 Stat Pac I, Hewlett-Packard, Cupertine, Calif., pp. 49–51.

(5) P. L. Altman and D. S. Dittmer, "Blood and Other Body Fluids," Biological Handbooks, Federation of American Societies for Experimental Biology, Washington, D.C., 1961, p. 352.

(6) H. M. Smith, "Principles of Renal Physiology," Oxford University Press, New York, N.Y., 1956, p. 32.

(7) M. Gibaldi and D. Perrier, "Pharmacokinetics," Dekker, New York, N.Y., 1975, pp. 55, 136–140.

ACKNOWLEDGMENTS

Supported in part by unrestricted grants from Greenwich Pharmaceuticals Inc., Greenwich, CT 06830 and Kali-Pharma Inc., Elizabeth, NJ 07207. A. Van Peer is grateful to the Belgian Foundation for Medicinal Scientific Research for their support.

The technical assistance of Kathy Eberst and Marjorie Rigby is gratefully acknowledged.

In Vitro Drug Release from Egg Albumin Microcapsules

TAKAFUMI ISHIZAKA ˣ and MASUMI KOISHI

Received February 12, 1982, from the *Faculty of Pharmaceutical Sciences and the Institute of Colloid and Interface Science, Science University of Tokyo, Shinjuku-ku, Tokyo, Japan.* Accepted for publication August 9, 1982.

Abstract □ The *in vitro* release of phenacetin from microcapsules prepared using egg albumin as the membrane material was investigated. It was shown by scanning electron microscopy that the albumin microcapsules have nonsmooth surfaces. The amount of phenacetin released is proportional to the square root of time up to 50–70% drug release. Increases in the albumin concentration and 1-vinyl-2-pyrrolidinone polymer content in the aqueous phases used in the microcapsule preparation have an effect on matrix porosity and channel tortuosity in the matrix of albumin microcapsules. The *in vitro* release rate was found to decrease with increasing albumin concentration and 1-vinyl-2-pyrrolidinone polymer content in the aqueous phases. The *in vitro* release rate per unit area also decreased with decreasing capsule size.

Keyphrases □ Phenacetin—albumin microcapsules, release rate, controlling factors □ Microcapsules, albumin—release rate of phenacetin, effects of albumin concentration, 1-vinyl-2-pyrrolidinone polymer content, capsule size □ Delivery systems—albumin microcapsules, release rate of phenacetin, effect of albumin concentration, 1-vinyl-2-pyrrolidinone polymer content, capsule size

Delivery of a chemotherapeutic agent to desired target sites with drug carriers could achieve effective local drug concentration and minimize systemic side effects by reducing the therapeutic dose of the chemotherapeutic agent. When a drug carrier, such as liposomes, microcapsules, and microspheres, is injected into the circulatory system, its distribution in the body is an important factor in drug delivery. The tissue distribution of albumin microspheres has been studied in detail (1–3). In addition, alteration in the tissue distribution of albumin microspheres was examined using magnetic guidance (4, 5). Albumin microspheres prepared using a water–oil emulsion have a hydrophilic matrix structure, consisting of albumin molecules, that is similar to that in albumin microcapsules (6).

However, despite many reports on the tissue distribution of albumin microspheres, the mechanism of drug release from minute drug carriers that have a hydrophilic matrix structure is not well known because there are few reports on drug release (7, 8). This paper describes *in vitro* drug release from albumin microcapsules having a hydrophilic matrix structure and some controlling factors.

EXPERIMENTAL

Materials—Isooctane, dibasic potassium phosphate, monobasic sodium phosphate, acetic acid, hydrochloric acid, and sodium acetate were reagent grade. Phenacetin powder (250–300 mesh) was used for microencapsulation as the core drug.

Egg albumin[1] solution was prepared as follows: Albumin was dissolved in buffer solution [0.033 *N* KH_2PO_4–0.033 *N* Na_2HPO_4, 1:16 (v/v); pH 8.0], and the solution was filtered after centrifugation at 16,000 × *g* for 30 min to remove the undissolved materials. The albumin concentration was either 10 or 20% (w/w). 1-Vinyl-2-pyrrolidinone polymer[2] was dissolved in the same buffer solution at 70°. The solution thus obtained (50% w/w) was stored in a refrigerator overnight and used for the preparation of aqueous albumin solutions containing the polymer.

Measurement of Viscosity—Viscosities of both the albumin and mixed polymer solutions [prepared from 20% (w/w) albumin solution and 50% (w/w) 1-vinyl-2-pyrrolidinone polymer solution] were measured at 25° with a cone-plate type viscometer[3] in a shear rate range of 50–3950 sec^{-1}. Viscosity values were calculated from the straight lines in rheograms.

Preparation of Microcapsules—Albumin microcapsules were prepared by a method similar to that described in a previous paper (6). Phenacetin powder (10% v/v) was previously dispersed in albumin solutions with and without the polymer. To 100 ml of isooctane containing 5.0% (v/v) sorbitan trioleate[4] as an emulsifier, in a three-necked flask, was added 15 ml of each of the aqueous dispersions, with stirring. After further stirring for 10 min, the flask was immersed in a water bath maintained at 85° for a given period to denature the egg albumin. The resultant dispersion was cooled to room temperature.

[1] Tokyo Kasei Kogyo Co., Tokyo, Japan.
[2] K-30; Tokyo Kasei Kogyo Co., Tokyo, Japan.
[3] Rheomat 30; Contraves AG, Zurich, Switzerland.
[4] Span 85; Nikko Chemicals Inc., Tokyo, Japan.

0022-3549/83/0900-1057$01.00/0

Table I—Effects of Albumin Concentration and Release Medium on Drug Release [a] from Albumin Microcapsules [b]

Release Medium	Cs^c, g/liter	Sample	Albumin, % (w/w)	Diameter, μm	Phenacetin Content, % (w/w)	$10^4 v_i$, g/sec	t_h, min	K, %/sec$^{1/2}$
Simulated gastric fluid	1.26	A-1	10	76.1 ± 25.9	56.4	3.75	1.1	7.69
		A-2	10	70.1 ± 22.3	55.8	3.64	0.9	8.09
		B-1	20	74.7 ± 25.3	43.5	2.80	1.8	6.60
		B-2	20	83.9 ± 31.5	44.1	3.16	1.6	6.74
Water	1.30	B-2	20	83.9 ± 31.5	44.1	2.53	2.4	5.22
Simulated intestinal fluid	1.10	B-2	20	83.9 ± 31.5	44.1	2.58	2.0	6.04

[a] Microcapsules containing 40 mg of phenacetin were dispersed in 200 ml of a test medium to obtain v_i, t_h, and K. [b] Each group of microcapsules was prepared on the same day. Speed setting and heating time in microencapsulation were 512 rpm and 10 min, respectively. [c] Solubility of phenacetin.

Table II—Size Effect on Drug Release [a] from Albumin Microcapsules [b]

Sample	Speed Setting, rpm	Diameter, μm	Phenacetin Content, % (w/w)	$10^4 v_i$, g/sec	t_h, min	K, %/sec$^{1/2}$	$10^7 V_i$[c], g·cm/sec	$10^3 K'$[d], %·cm/sec$^{1/2}$
D-1	313	239.9 ± 100.0	45.7	1.34	5.0	3.45	7.13	18.30
D-2	512	95.2 ± 28.0	46.9	2.60	2.1	5.10	4.87	9.55
D-3	848	55.6 ± 15.9	49.4	3.33	1.5	6.93	3.70	7.70

[a] Microcapsules containing 40 mg of phenacetin were dispersed in 200 ml of the simulated gastric fluid to obtain v_i, t_h, and K. [b] Microcapsules were prepared on the same day. Albumin concentration and heating time in microencapsulation were 20% (w/w) and 10 min, respectively. [c] $V_i = v_i/S_v$, where S_v is the specific surface area of the microcapsules. [d] $K' = K/S_v$.

The microcapsules separated by filtration were dispersed in 10 ml of buffer solution [0.1 *N* CH_3COOH–0.1 *N* CH_3COONa, 1:1 (v/v); pH 4.7], which was saturated with phenacetin and contained 10% (v/v) polyoxyethylene sorbitan monolaurate[5], with gentle agitation. The microcapsules were washed once with the pH 4.7 buffer solution and several times with water saturated with phenacetin. The microcapsules collected by decantation were freeze-dried.

Size measurement of the microcapsules was performed in the saturated phenacetin solution before freeze-drying. One thousand microcapsules were photographed under an optical microscope. Each of the developed film strips was projected onto a large-section paper by a slide projector. Enlarged images of the microcapsules were measured to the nearest 1.0 μm. The scale in the micrometer was used for calibration. To eliminate fluctuation in the denaturating procedures of egg albumin, the microcapsules in all experimental series (A–E) were prepared on the same day.

A scanning electron microscope[6] was used to observe the surface appearance of the albumin microcapsules. The original microcapsules and those sampled from a release test medium were dried at 50°. The dried microcapsules were vacuum-coated with gold in an ion coater[7].

Determination of Solubility of Phenacetin—Finely ground phenacetin powder was dispersed in three release test media in Erlenmeyer flasks. The dispersion in the stoppered flask, which was immersed in a water bath thermostated at 37 ± 0.1°, was vigorously agitated with a magnetic stirrer overnight to attain equilibrium. Membrane filters[8], holders, and syringes (maintained previously at 37 ± 0.1°) were used for the separation procedure of undissolved phenacetin particles. The phenacetin concentration in the filtrate was determined spectrophotometrically at 245 nm.

***In Vitro* Release of Microencapsulated Phenacetin**—The cylindrical glass cell used for the release test, 62 mm in diameter and 88 mm in depth, was equipped with a plastic cover to minimize the influence of vaporization. In the cell, 200 ml of a test medium was maintained at 37 ± 0.1°. At time zero, a given weight of albumin microcapsules containing 40 mg of phenacetin was added with stirring to this thermostated medium. Stirring was carried out with a six-blade impeller (50 mm in diameter) at a fixed rotation speed. The amount of phenacetin (40 mg) encapsulated was previously calculated to maintain the same sink condition for each *in vitro* release experiment during the test period. The dispersion was sampled at scheduled intervals and immediately filtered to remove the microcapsules. The drug concentration in the filtrate was determined by the same spectroscopic method described for the phenacetin analysis.

In release experiments, test media similar to those described in JP IX were employed. Simulated gastric fluid (pH 1.2) was a hydrochloric acid solution containing 0.1% (v/v) polyoxyethylene sorbitan monolaurate and 2 g/liter of sodium chloride; simulated intestinal fluid (pH 7.5) contained hydrochloric acid and 35.8 g/liter of monobasic sodium phosphate. Water obtained from a water purification apparatus[9] was also used as a test medium.

To attain reproducibility of the release experiments, a stirring rate of 313 rpm was employed. At stirring rates <200 rpm, no dispersion of microcapsules was observed, and the measured values were scattered widely. At rotating speeds >200 rpm, the release rates were reproducible.

RESULTS AND DISCUSSION

Properties of Microcapsules—As reported previously (6), the viscosity of the aqueous phase in the preparation of egg albumin microcapsules and microspheres markedly affects their size. Stirring speed in this experiment was determined for each preparation to obtain microcapsules within a given size range (70–110 μm) except for the microcapsule samples for the study of size effect on phenacetin release. Tables I–III show the preparation conditions of microcapsules, microcapsule size, and phenacetin content. Both the microcapsule size and phenacetin content were approximately constant in each series.

Surface Appearance of Microcapsules—Scanning electron micrographs of albumin microcapsules before and after the release experiments are shown in Fig. 1. Figure 1a–d shows that the increase of albumin concentration and the addition of 1-vinyl-2-pyrrolidinone polymer change the membrane appearance as compared with the original microcapsules (Fig. 1a). All albumin microcapsules had nonsmooth surfaces. Scanning electron micrographs (10,000×, unpublished) from a portion of the surfaces of four samples (Fig. 1a–d) showed no evidence of appearance changes due to the increase in albumin concentration and the addition of 1-vinyl-2-pyrrolidinone polymer in the preparation. Pores similar to those seen in polystyrene microcapsules prepared by an interfacial polymer deposition technique (9) could not be found in the albumin microcapsules. But a few microcapsules having some small cracks on their surfaces, which may be caused by shrinking in the freeze-drying process, existed in samples A-1 and A-2 (Table I). The undesirable surface cracks were not found in microcapsules prepared using 20% (w/w) albumin solution (B, C, and D series) or mixed polymer solutions (E series). Accordingly, increase of the albumin concentration and use of 1-vinyl-2-pyrrolidinone polymer should strengthen the microcapsule membrane.

The surface appearances of the microcapsules collected after *in vitro* release experiments were not different from those of the original capsules (Fig. 1e–h). As observation under a light microscope showed, the mixed polymer solution [10% (w/w) albumin, 20% (w/w) 1-vinyl-2-pyrrolidinone polymer], in contrast to the other solutions, gives a homogeneous

[5] Tween 20; Nikko Chemicals Inc., Tokyo, Japan.
[6] JSM-T20; JEOL, Tokyo, Japan.
[7] JFC-1100; JEOL, Tokyo, Japan
[8] Millipore filter BDWP02500; Millipore Co., Bedford, Mass.
[9] Milli-Q2; Millipore Co., Bedford, Mass.

Table III—Effect of 1-Vinyl-2-pyrrolidinone Polymer Concentration on Drug Release [a] from Albumin Microcapsules [b]

Sample	Polymer Concentration, % (w/w)	Viscosity of Aqueous Phase, cp	Speed Setting, rpm	Diameter, μm	Phenacetin Content, % (w/w)	$10^4 v_i$, g/sec	t_h, min	K, %/sec$^{1/2}$	$10^7 V_i$[c], g·cm/sec	$10^2 K'$[d], %·cm/sec$^{1/2}$
E-1	0	1.90	512	81.5 ± 27.5	62.9	3.27	1.6	6.30	5.48	1.06
E-2	5	5.22	512	94.3 ± 33.6	61.8	2.87	1.8	5.94	5.55	1.15
E-3	10	14.7	848	107.5 ± 35.0	59.4	2.40	2.4	4.88	5.21	1.06
E-4	20	68.5	1360	114.5 ± 40.7	62.7	2.02	3.0	4.34	4.72	1.01

[a] Microcapsules containing 40 mg of phenacetin were dispersed in 200 ml of the simulated gastric fluid to obtain v_i, t_h, and K. [b] Microcapsules were prepared on the same day. Albumin concentration and heating time were 10% (w/w) and 10 min, respectively. [c] $V_i = v_i/S_v$, where S_v is the specific surface area of microcapsules. [d] $K' = K/S_v$.

stripe-pattern. Many pores would be expected to be produced by the swelling and subsequent release of 1-vinyl-2-pyrrolidinone polymer dispersed in the membrane matrix during the *in vitro* release experiments; but, no pore was found in the membrane (Fig. 1g and h). On the other hand, fine white crystalline particles adhered to the outer surfaces of the microcapsules, as observed in Fig. 1e–h, which when collected from the release test medium were confirmed to be phenacetin particles.

Each of the albumin microcapsules shown in Fig. 1a, c, e, and g possessed a folded and invaginated surface. A similar surface structure has been reported by Matthews and Nixon with gelatin microcapsules prepared by a simple alcohol coacervation (10). Contrary to the findings with gelatin microcapsules, it was confirmed by light microscopy that the albumin microcapsules dispersed in the release test media appear almost spherical, suggesting hydration of the membrane materials; *i.e.*, folding and invaginating of the surfaces were caused by shrinking in the drying process. Therefore, as the membrane of the microcapsules was fully hydrated in the release test media and remained intact after release experiments, it was concluded that the drug molecules are released through channels in the fully hydrated albumin matrix.

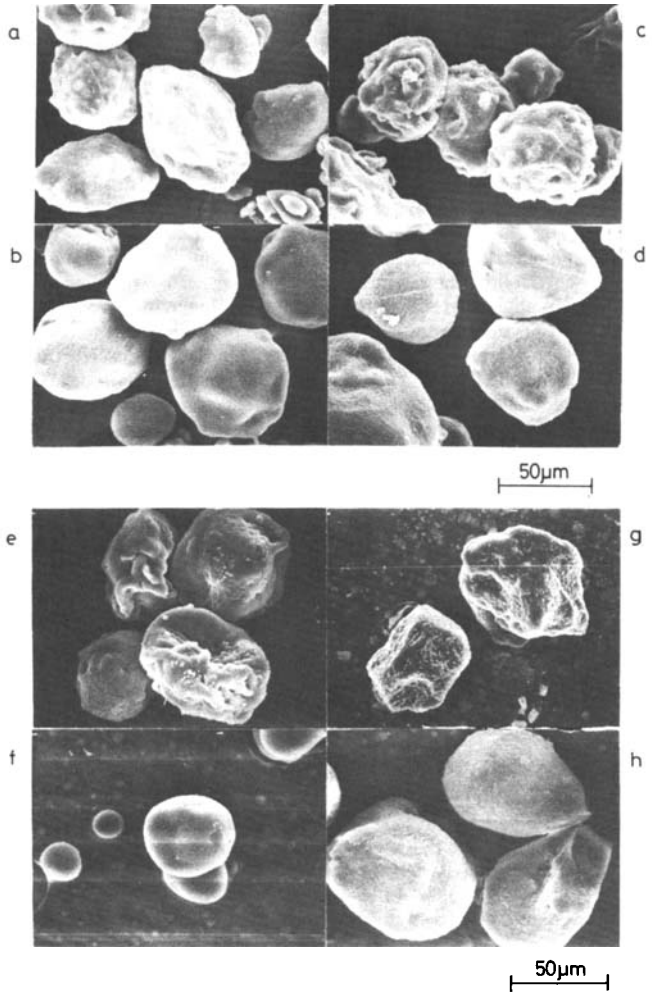

Figure 1—*Scanning electron micrographs of microcapsules prepared using (a,e) 10% (w/w) albumin solution (A-1); (b,f) 20% (w/w) albumin solution (B-1); (c,g) 10% (w/w) albumin solution containing 5% (w/w) 1-vinyl-2-pyrrolidinone polymer (E-2); and (d,h) 10% (w/w) albumin solution containing 20% (w/w) 1-vinyl-2-pyrrolidinone polymer (E-4) before and after the release tests.*

Effects of Albumin Concentration and Release Test Medium—The results of *in vitro* dissolutions of phenacetin powder and microencapsulated phenacetin prepared using a high albumin concentration [20% (w/w)] are shown in Fig. 2. In the simulated gastric fluid, a slower dissolution of phenacetin from the microcapsules in the initial stage was found, as expected. This observation suggests that the drug would be released effectively in drug diffusion. The Higuchi equation may be applied to the *in vitro* release of drugs from microcapsules if diffusion through their membranes is the rate-limiting step (11). Of the four samples of albumin microcapsules used in this study, series A and B gave a linear relationship in the initial stage of phenacetin release in the simulated gastric fluid when the percentage of drug released was plotted against the square root of time, sec$^{1/2}$ (Fig. 3). However, once 50–70% of phenacetin was released, the plots deviated negatively from linearity. This result was unexpected because, with the method of manufacture employed, these microcapsules have a suitable protective wall. But, after the initial stage of release, the core drug content appeared to have little effect on the total percentage of drug released. Accordingly, it is considered that this deviation in Fig. 3 could be attributed to exhaustion of the drug suspension phase, as described by Borodkin and Tucker (12), that is, the number of vacant microcapsules may increase in the latter stage of release.

As analysis over the whole release is difficult in this study, the initial release rate (v_i, g/sec) and the 50% release time (t_h, min), which are obtained by plotting the amount of drug released *versus* time (in min), and the slope (K) of the straight line obtained by plotting the percentage of drug released against the square root of time, sec$^{1/2}$, are used for evaluation of the *in vitro* drug release from albumin microcapsules. Table I shows v_i, t_h, and K obtained from the release profiles of the drug in the three test media. Although the difference was slight, the drug is released in the simulated gastric fluid faster from series A than from series B. As described above, the drug molecules appear to be released through the hydrated and intact membranes. Therefore, this result would be caused by decreased porosity in the membrane matrix and increased tortuosity of channels in which drug molecules diffuse.

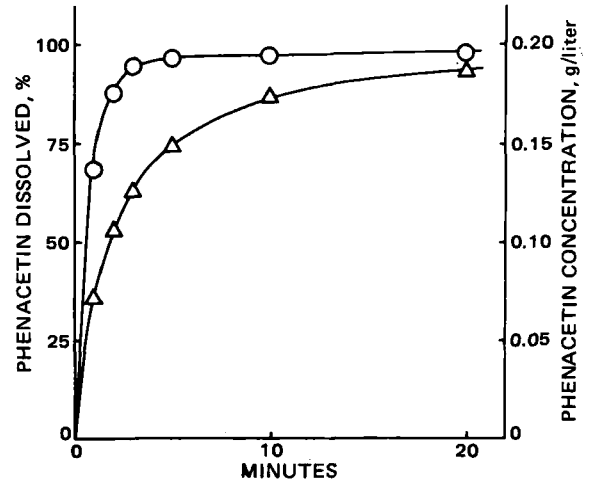

Figure 2—*Dissolution of phenacetin in the simulated gastric fluid. Key: (○) phenacetin; (△) phenacetin microencapsulated using 20% (w/w) albumin solution (B-2).*

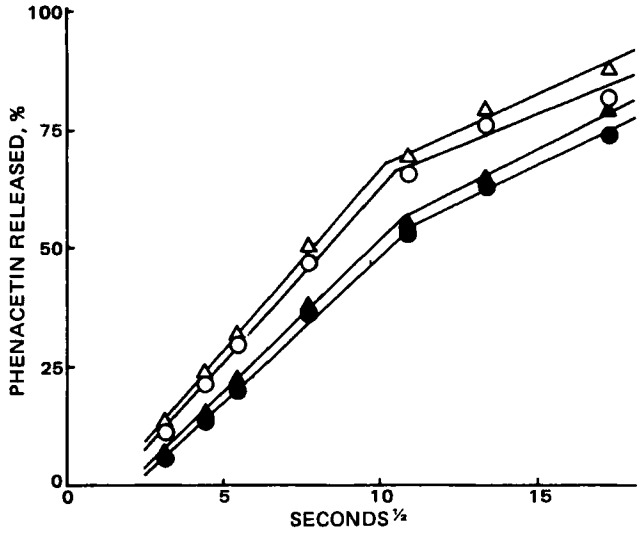

Figure 3—*Relationship between the percentage of drug release in the simulated gastric fluid and the square root of time. Microcapsules were prepared using 10% (w/w) albumin solution (○) A-1; (△) A-2 and 20% (w/w) albumin solution (●) B-1; (▲) B-2.*

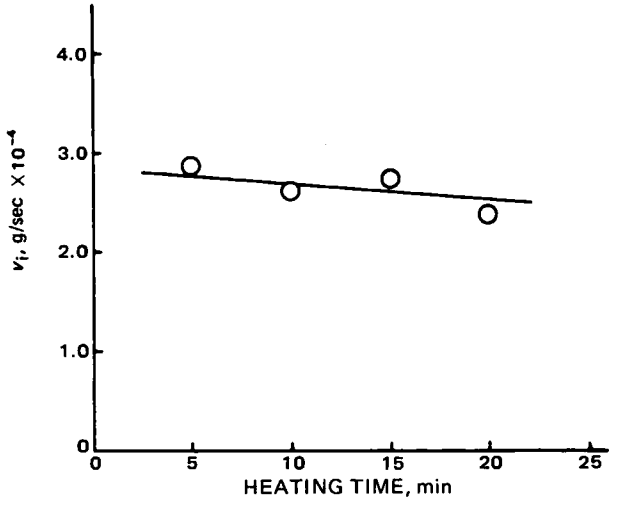

Figure 4—*Effect of heating time in the microencapsulation process on the drug release from albumin microcapsules prepared using 20% (w/w) albumin solution. As samples in the heating process at 85° were separated at scheduled intervals from the same batch (C series), capsule size was not measured. The phenacetin contents were 54.9% (w/w) at 5 min, 46.3% at 10 min, 42.9% at 15 min, and 42.7% at 20 min.*

The albumin microcapsules in sample B-2 released the drug faster in the simulated gastric fluid, though the release rates in both the simulated intestinal fluid and water were similar. Since the solubilities of phenacetin in the three test media were nearly equal, the sink condition was held constant in all *in vitro* release tests. Therefore, the condition for the albumin matrix in which drug molecules diffuse in the simulated gastric fluid seems to be different from those in the simulated intestinal fluid and in water. Furthermore, it is well known that the isoelectric point (pI) of egg albumin is 4.7. When the pH differs greatly from the pI, electrostatic repulsion of the ionized groups change the porosity and tortuosity of channels in the albumin matrix.

Effect of Heating Time in Microencapsulation—Albumin microcapsules were prepared using 20% (w/w) albumin solution. In a microcapsule dispersion sampled 2 min after the flask was immersed in a water bath maintained at 85°, albumin was still insufficiently denaturated in isooctane, and the particles collected by filtration resembled soft-boiled egg membranes. Albumin microcapsules having rigid membranes were obtained if heated >4 min. The microcapsules sampled at 5 min were white in isooctane; those obtained at 10, 15, and 20 min were light yellow.

Figure 4 shows the relationship between the initial release rate v_i and heating time in the microencapsulation. Prolonged heating time produced no appreciable difference in the release rate. Sugibayashi *et al.* have reported that an increase in the denaturing temperature of the microsphere preparation decreases matrix porosity and increases channel tortuosity in the matrix, leading to decreased drug release (8). However, the denaturing temperature of 85° in the microencapsulation used in this study is low when compared with those employed in their work (100–180°), and prolonged heating time may not affect the matrix porosity and channel tortuosity, as previously mentioned.

Effect of Capsule Size—Jalšenjak and Kondo found that the permeability of gelatin–acacia microcapsules toward sodium chloride decreased with increasing capsule size (13). The same trend was observed with the albumin microcapsules.

The effects of capsule size on drug release are given in Table II. The values of v_i and K decreased with increasing capsule size. These results are expected because (*a*) the total volume of the microcapsules containing 40 mg of phenacetin is almost constant and (*b*) the total surface area of the microcapsules increases with decreasing capsule size. But, V_i and K', which are obtained by dividing v_i and K by the specific surface area of the albumin microcapsules, increase with increasing capsule size. Contrary to the gelatin–acacia microcapsules, the albumin microcapsules are multinuclear and their membrane thickness cannot be determined theoretically. And if phenacetin particles are dispersed uniformly in the albumin matrix, it cannot be assumed that the distance along which solute molecules diffuse is shortened as the capsule size increases.

The explanation for V_i increasing with increasing capsule size is as follows: Water structure plays an important role in drug release from microcapsules, as reported previously (14). The structured water in and around the membrane affects the transport of solute molecules, and the amount of structured water is greater in a dispersion containing a large number of microcapsules than in that containing a small number of microcapsules. Another reason would be differences in the denatured state of albumin, due to increased capsule size. It can be assumed that the denaturation affects matrix porosity and channel tortuosity in the matrix.

Effect of Added 1-Vinyl-2-pyrrolidinone Polymer—The effects of the concentration of 1-vinyl-2-pyrrolidinone polymer added to the aqueous albumin solution in the microencapsulation process are shown in Table III. The values of v_i and K decrease, while t_h increases with increasing amounts of 1-vinyl-2-pyrrolidinone polymer. V_i decreases at high 1-vinyl-2-pyrrolidinone polymer concentrations, (10–20%, w/w; samples E-3, E-4). A slight increase in the capsule size due to increased viscosity of the aqueous polymer phase is also shown in Table III. However, even if V_i and K' decrease with increasing capsule size, as described in the previous section, it would be concluded that the increase in the 1-vinyl-2-pyrrolidinone polymer concentration decreases the *in vitro* release rate. Addition of the polymer to the aqueous albumin solution makes the matrix dense (Fig. 1c, d, g, and h), leading to a decreased matrix porosity and increased channel tortuosity in the matrix. Also, hydration of 1-vinyl-2-pyrrolidinone polymer may play an important role in controlling the diffusion of drug molecules. Nakagaki and Shimabayashi reported that the hydration number (water/base, mole) of 1-vinyl-2-pyrrolidinone polymer was calculated to be 2–5 by conductometry (15). Therefore, it is possible that the increase of polymer content decreases the amount of free water in unit volume of the matrix, making channels narrow and channel tortuosity higher.

CONCLUSIONS

Higuchi's equation could be applied to the phenacetin release from albumin microcapsules that have a hydrophilic matrix structure in their membranes, except in the later stages of drug release. The *in vitro* release rate was affected by capsule size, egg albumin concentration, and 1-vinyl-2-pyrrolidinone polymer content used in the microencapsulation process. It decreased with increasing capsule size and albumin and polymer concentrations. Matrix porosity and channel tortuosity in the albumin matrix played an important role in the phenacetin release.

REFERENCES

(1) K. Sugibayashi, Y. Morimoto, T. Nadai, and Y. Kato, *Chem. Pharm. Bull.*, **25**, 3433 (1977).

(2) P. L. Hagen, G. E. Krejcarek, A. Taylor, and N. Alazraki, *J. Nucl. Med.*, **19**, 1055 (1978).

(3) B. Ng, S. M. Shaw, W. V. Kessler, R. R. Landolt, G. E. Peck, and G. H. Dockerty, *Can. J. Pharm. Sci.*, **15**, 30 (1980).

(4) K. J. Widder, A. E. Senyei, and D. G. Scarpelli, *Proc. Soc. Exp. Biol. Med.*, **58**, 141 (1978).
(5) Y. Morimoto, K. Sugibayashi, M. Okamura, and Y. Kato, *J. Pharm. Dyn.*, **3**, 264 (1980).
(6) T. Ishizaka, K. Endo, and M. Koishi, *J. Pharm. Sci.*, **70**, 358 (1981).
(7) P. A. Kramer, *J. Pharm. Sci.*, **63**, 1646 (1974).
(8) K. Sugibayashi, M. Akimoto, Y. Morimoto, T. Nadai, and Y. Kato, *J. Pharm. Dyn.*, **2**, 350 (1979).
(9) A. Miyagishima, T. Fujimura, and F. Higashide, *Yakuzaigaku*, **38**, 53 (1978).
(10 B. R. Matthews and J. R. Nixon, *J. Pharm. Pharmacol.*, **26**, 383 (1974).
(11) H. Takenaka, Y. Kawashima, and S. Y. Lin, *Chem. Pharm. Bull.*, **27**, 3054 (1979).
(12) S. Borodkin and F. E. Tucker, *J. Pharm. Sci.*, **63**, 1359 (1974).
(13) I. Jalšenjak and T. Kondo, *J. Pharm. Sci.*, **70**, 456 (1981).
(14) T. Ishizaka, M. Koishi, and T. Kondo, *J. Membrane Sci.*, **5**, 283 (1979).
(15) M. Nakagaki and S. Shimabayashi, *Nipponkagakukaishi*, **1973**, 207.

ACKNOWLEDGMENTS

Supported in part by Grant 55-2016 from Science University of Tokyo.

Systematic Error Associated with Apparatus 2 of the USP Dissolution Test IV: Effect of Air Dissolved in the Dissolution Medium

DON C. COX ˣ, WILLIAM B. FURMAN, and DONALD P. PAGE

Received July 23, 1982, from the *National Center for Drug Analysis, Food and Drug Administration, St. Louis, MO 63101.* Accepted for publication August 20, 1982.

Abstract □ Acceptable concentrations of gases in a medium are not well defined in USP dissolution tests. A sample of 10-mg prednisone tablets, known to be sensitive to dissolved gases, was tested with batches of purified water that contained different concentrations of air. The data suggest that results from Apparatus 2 can be influenced by the concentration of air in the dissolution medium unless the medium remains unsaturated with air for the duration of the test. The repeatability of means of six results was markedly improved when the air concentration in the medium was accurately controlled at the beginning of the test.

Keyphrases □ USP dissolution test—correlation of air concentration in medium to dissolution results, Apparatus 2 □ USP Apparatus 2—repeatability of dissolution results, prednisone tablets, effect of dissolved air in medium □ Prednisone—dissolution, USP Apparatus 2, effect of dissolved air in medium

The USP (1) recognizes that gases dissolved in the dissolution medium may influence dissolution test results. In such cases the analyst is directed to remove the dissolved gases before conducting the test; however, no guidance concerning acceptable gas concentrations is given. Since purified water is used to prepare dissolution media, the dissolved gases are those found in air. Complete removal of air from water is not easy; even if "air-free" water were available, air would begin to redissolve as soon as the water again contacted the atmosphere. Thus, one must assume that the air in the dissolution medium is to be reduced to a concentration that no longer influences the dissolution results—a concentration which can be determined only by experiment.

In addition to the USP calibrator tablets, this laboratory has used a sample of commercial 10-mg prednisone tablets, identified as Tablet 2 in previous papers of this series (2, 3), as a "performance standard" for Apparatus 2. Tablet 2, which was also used as a practice sample in a recent collaborative study (4), is very sensitive to excess air in the dissolution medium. A dissolution medium whose air concentration does not influence dissolution results was desired. Various methods for controlling the concentration of dissolved air were studied, and the data are presented in this paper.

BACKGROUND

The first USP dissolution test for prednisone tablets (5) specified the use of deaerated water. Deaerated water (6) is purified water that has been treated to reduce the content of dissolved air by suitable means, such as by boiling it vigorously for 5 min and cooling or by applying ultrasonic vibration. This laboratory interpreted (7) the specification to mean that the water could not be supersaturated with air at 37°, the temperature at which the dissolution test is conducted, because this condition might result in the gradual formation of bubbles on all immersed solid objects, including the product being tested. For several years, dissolution media were prepared from purified water which was boiled, cooled to room temperature, and used within a 24-hr period. A vacuum technique (3) was then developed and used. The two treatments appeared to give equivalent results; however, boiling was less convenient and was gradually replaced by the vacuum treatment.

When the dissolution test for prednisone tablets was revised (8), the specification for the medium was changed from deaerated water to purified water. The USP monograph on purified water does not specify the quantity of dissolved air allowed. Freshly prepared purified water obtained by distillation contains only a fraction of the air contained in freshly prepared purified water obtained by ion-exchange or by reverse osmosis. Dissolution results for certain products are substantially changed when purified water obtained by ion-exchange treatment is substituted for deaerated water (9). The USP later inserted the current specification for dissolved gases in the dissolution medium in the general chapter on dissolution.

EXPERIMENTAL

The test conditions were those used in a recent collaborative study (4) with these exceptions. The six-spindle dissolution drive[1] was not commercially available. The volumes of dissolution medium were measured in volumetric flasks[2]. The dissolution test system was allowed to equilibrate for only 1–2 min before the test was started. Purified water was

[1] Built by the Winchester Engineering and Analytical Center, Food and Drug Administration, Winchester, MA 01890.
[2] 500-ml flasks marked T.D./T.C.; Kimble Products, Vineland, NJ 08360.

0022-3549/83/0900-1061$01.00/0

(4) K. J. Widder, A. E. Senyei, and D. G. Scarpelli, *Proc. Soc. Exp. Biol. Med.*, **58**, 141 (1978).
(5) Y. Morimoto, K. Sugibayashi, M. Okamura, and Y. Kato, *J. Pharm. Dyn.*, **3**, 264 (1980).
(6) T. Ishizaka, K. Endo, and M. Koishi, *J. Pharm. Sci.*, **70**, 358 (1981).
(7) P. A. Kramer, *J. Pharm. Sci.*, **63**, 1646 (1974).
(8) K. Sugibayashi, M. Akimoto, Y. Morimoto, T. Nadai, and Y. Kato, *J. Pharm. Dyn.*, **2**, 350 (1979).
(9) A. Miyagishima, T. Fujimura, and F. Higashide, *Yakuzaigaku*, **38**, 53 (1978).
(10 B. R. Matthews and J. R. Nixon, *J. Pharm. Pharmacol.*, **26**, 383 (1974).
(11) H. Takenaka, Y. Kawashima, and S. Y. Lin, *Chem. Pharm. Bull.*, **27**, 3054 (1979).
(12) S. Borodkin and F. E. Tucker, *J. Pharm. Sci.*, **63**, 1359 (1974).
(13) I. Jalšenjak and T. Kondo, *J. Pharm. Sci.*, **70**, 456 (1981).
(14) T. Ishizaka, M. Koishi, and T. Kondo, *J. Membrane Sci.*, **5**, 283 (1979).
(15) M. Nakagaki and S. Shimabayashi, *Nipponkagakukaishi*, **1973**, 207.

ACKNOWLEDGMENTS

Supported in part by Grant 55-2016 from Science University of Tokyo.

Systematic Error Associated with Apparatus 2 of the USP Dissolution Test IV: Effect of Air Dissolved in the Dissolution Medium

DON C. COX ˣ, WILLIAM B. FURMAN, and DONALD P. PAGE

Received July 23, 1982, from the *National Center for Drug Analysis, Food and Drug Administration, St. Louis, MO 63101.* Accepted for publication August 20, 1982.

Abstract □ Acceptable concentrations of gases in a medium are not well defined in USP dissolution tests. A sample of 10-mg prednisone tablets, known to be sensitive to dissolved gases, was tested with batches of purified water that contained different concentrations of air. The data suggest that results from Apparatus 2 can be influenced by the concentration of air in the dissolution medium unless the medium remains unsaturated with air for the duration of the test. The repeatability of means of six results was markedly improved when the air concentration in the medium was accurately controlled at the beginning of the test.

Keyphrases □ USP dissolution test—correlation of air concentration in medium to dissolution results, Apparatus 2 □ USP Apparatus 2—repeatability of dissolution results, prednisone tablets, effect of dissolved air in medium □ Prednisone—dissolution, USP Apparatus 2, effect of dissolved air in medium

The USP (1) recognizes that gases dissolved in the dissolution medium may influence dissolution test results. In such cases the analyst is directed to remove the dissolved gases before conducting the test; however, no guidance concerning acceptable gas concentrations is given. Since purified water is used to prepare dissolution media, the dissolved gases are those found in air. Complete removal of air from water is not easy; even if "air-free" water were available, air would begin to redissolve as soon as the water again contacted the atmosphere. Thus, one must assume that the air in the dissolution medium is to be reduced to a concentration that no longer influences the dissolution results—a concentration which can be determined only by experiment.

In addition to the USP calibrator tablets, this laboratory has used a sample of commercial 10-mg prednisone tablets, identified as Tablet 2 in previous papers of this series (2, 3), as a "performance standard" for Apparatus 2. Tablet 2, which was also used as a practice sample in a recent collaborative study (4), is very sensitive to excess air in the dissolution medium. A dissolution medium whose air concentration does not influence dissolution results was desired. Various methods for controlling the concentration of dissolved air were studied, and the data are presented in this paper.

BACKGROUND

The first USP dissolution test for prednisone tablets (5) specified the use of deaerated water. Deaerated water (6) is purified water that has been treated to reduce the content of dissolved air by suitable means, such as by boiling it vigorously for 5 min and cooling or by applying ultrasonic vibration. This laboratory interpreted (7) the specification to mean that the water could not be supersaturated with air at 37°, the temperature at which the dissolution test is conducted, because this condition might result in the gradual formation of bubbles on all immersed solid objects, including the product being tested. For several years, dissolution media were prepared from purified water which was boiled, cooled to room temperature, and used within a 24-hr period. A vacuum technique (3) was then developed and used. The two treatments appeared to give equivalent results; however, boiling was less convenient and was gradually replaced by the vacuum treatment.

When the dissolution test for prednisone tablets was revised (8), the specification for the medium was changed from deaerated water to purified water. The USP monograph on purified water does not specify the quantity of dissolved air allowed. Freshly prepared purified water obtained by distillation contains only a fraction of the air contained in freshly prepared purified water obtained by ion-exchange or by reverse osmosis. Dissolution results for certain products are substantially changed when purified water obtained by ion-exchange treatment is substituted for deaerated water (9). The USP later inserted the current specification for dissolved gases in the dissolution medium in the general chapter on dissolution.

EXPERIMENTAL

The test conditions were those used in a recent collaborative study (4) with these exceptions. The six-spindle dissolution drive[1] was not commercially available. The volumes of dissolution medium were measured in volumetric flasks[2]. The dissolution test system was allowed to equilibrate for only 1–2 min before the test was started. Purified water was

[1] Built by the Winchester Engineering and Analytical Center, Food and Drug Administration, Winchester, MA 01890.
[2] 500-ml flasks marked T.D./T.C.; Kimble Products, Vineland, NJ 08360.

0022-3549/83/0900-1061$01.00/0

Table I—Dissolution Results (Percent of Label Claim) for Tablet 2 from Water Equilibrated [a] with Air at Various Temperatures and then Brought to 37°

Equilibration Temperature, °	Uncorrected Barometric Pressure, mm Hg	Mean[b]	SD[b]
	754	78.8[c]	3.5
23	754	71.4[d]	4.2
23	754	70.9[e]	5.6
25	754	61.4	3.5
27	754	57.6	3.8
29	754	50.3	3.3
31	744	46.3	1.4
33	745	41.8	2.7
35	745	40.4	2.7
37	748	39.0	1.6
39	748	38.5	2.8
41	748	37.5	1.3
43	746	38.2	1.9
45	741	37.2	2.2
47	740	39.8	2.3
47	—[f]	36.8	2.5
49	742	35.2	1.6
49	—	36.3	3.1

[a] For 45 min unless otherwise indicated. [b] $n = 6$. [c] Result obtained from deionized water at 23° that had not been equilibrated with air. [d] Result obtained from deionized water that had been equilibrated with air for 90 min. [e] Result obtained from deionized water that had been equilibrated with air for 30 min. [f] — Not recorded.

obtained by reverse osmosis. A 19-liter carboy was filled daily and served as a reservoir. Before the water was subjected to the treatments described below, portions were siphoned into 500-ml volumetric flasks. The contents of the flasks were heated to 38° and transferred to the dissolution vessels. Six dissolution results were obtained with this water.

Control of Air Concentration by Temperature—Approximately 800 ml of water was added to each of six 900-ml volumetric flasks which were then placed in a water bath at room temperature. A 4-mm o.d. glass tube was inserted to the bottom of each flask and connected through a manifold to an air pump that delivered air at a rate of 4 liters/min. Air was bubbled through the water for 90 min. The temperature of the water and the barometric pressure were recorded. Six 500-ml volumetric flasks were filled to volume with the treated water from the 900-ml flasks and placed in a holding bath at 38°. After 30 min the contents of the 500-ml flasks were transferred to the dissolution vessels. In this way the temperature of the treated water was kept between 36.5° and 37° at the beginning of the dissolution test. Six dissolution results were obtained for Tablet 2.

This procedure was repeated under the same experimental conditions except that air was bubbled through the water for 30 min. The results from six tablets agreed closely with those obtained when the water was equilibrated with air for 90 min. Thereafter, air was bubbled through the water for a minimum of 45 min.

The temperature of the water bath holding the 900-ml flasks was increased from 23° to 49° in increments of 2° for each test of six tablets. Additional data were collected by equilibrating the water with air in the same manner over a narrow range of temperatures from 37.4° to 38.4°.

Ten units of Tablet 2 were dissolved in 17 liters of water. The tablet excipients were allowed to settle, and the clear solution was siphoned into a container. Portions of this solution were equilibrated with air at 37.1° and transferred to the dissolution vessels for testing of Tablet 2. Additional portions were used in the determinative step as solvent for the standard solution and as reference for the spectrophotometer. The experiment was then repeated with a solution prepared by dissolving 20 units of Tablet 2 in 20 liters of water.

The air pump was then replaced with a cylinder of compressed nitrogen with minimum purity of 99.7%. The nitrogen was bubbled for 1 hr through 3500 ml of water heated to 37.0°. Portions of the water were siphoned into six 500-ml flasks that had been flushed with nitrogen. The flasks were placed in a water bath at 38° for 30 min, and the contents of the flasks were then transferred to dissolution vessels that also had been flushed with nitrogen. During dissolution, a nitrogen atmosphere was maintained over the water in the vessels.

Control of the Air Concentration by Pressure—Approximately 3500 ml of water was added to a 4-liter reagent bottle equipped with a two-hole rubber stopper. A long tube (6-mm i.d.) was inserted through one hole of the stopper so that its end was close to the bottom of the bottle. A short tube was inserted through the other hole so that the end of the tube was flush with the lower side of the stopper. The air pump was connected to the long tube with the stopper in place in the bottle, and air was bubbled up through the water. A piece of rubber tubing connected to the short tube in the stopper was partially closed, and a positive pressure was developed over the water in the bottle while the water was agitated by the air bubbles. The bottle was placed in a water bath at 37.6° for 1 hr, and a positive pressure of 50 mm Hg above that of the prevailing atmosphere was maintained over the water. The water was then siphoned into 500-ml flasks, and the flasks were returned to the water bath for 10 min before being emptied into the dissolution vessels. Six units of Tablet 2 were tested. The experiment was then repeated with water prepared by maintaining a positive pressure of 10 mm Hg over the water instead of 50 mm Hg.

To obtain pressures below ambient, the short tube in the stopper was connected to a vacuum, and air was drawn down through the long tube (now open to the atmosphere) and up through 3500 ml of water. The vacuum over the water was adjusted by partial closure of a piece of rubber tubing connected to the long tube. The water in the bottle was heated to 37.5° for 1 hr under a pressure ~30 mm Hg below that of the prevailing atmosphere. The water in the bottle was then siphoned into the 500-ml flasks, the flasks were reheated, and the contents of the flasks were then transferred to the dissolution vessels. Six dissolution results were obtained. The experiment was conducted again at the same pressure and then repeated with the pressure adjusted to 57 mm Hg below ambient. The experiment was then conducted at pressures of 145, 80, 70, and 50 mm Hg. Dissolution results obtained in this manner were compared with dissolution results obtained with the use of water as it was routinely prepared in this laboratory, *i.e.*, the water was sprayed into a 19-liter carboy at room temperature under a pressure of ~145 mm Hg.

RESULTS AND DISCUSSION

The saturated concentration of air in water in a container open to the atmosphere depends on the temperature of the water and the pressure of the air above the water. Ideally, the equilibrium concentration of a gas in a liquid is proportional to the pressure of the gas over the liquid at a constant temperature (Henry's Law). Thus, the concentration of air in

Table II—Dissolution Results (Percent of Label Claim) for Tablet 2 from Water Equilibrated with Gas [a] under Various Conditions

Equilibration Temperature, °	Uncorrected Barometric Pressure, mm Hg	Mean[b]	SD[b]	Equilibration Temperature, °	Pressure, mm Hg[c]	Mean[b]	SD[b]
37.5	750	39.3	2.7	37.6	AP +50	56.3	4.3
37.5	750	41.2	2.5	37.6	AP +10	39.9	1.8
38.4	—[d]	39.1	2.0	37.6	AP −30	38.8	2.7
37.6	747	38.8	2.6	37.5	AP −30	37.3	2.4
				38.0	AP −57	37.8	1.8
37.4	—	39.7	4.0	36.8	145	35.6	1.8
				36.4	80	35.0	3.6
37.1	749	37.1[e]	3.0	39.0	70	35.2	2.2
37.1	751	38.3[f]	3.0	37.6	50	35.1	2.5
				RT[g]	~145	35.2	2.1
37.0	749	38.7[h]	3.0	RT	~145	35.6	2.7
				RT	~145	35.3	1.5

[a] Air in all instances except where otherwise indicated. [b] $n = 6$. [c] AP = atmospheric pressure. [d] — Not recorded. [e] Medium contained 10 tablets dissolved in 17 liters. [f] Medium contained 20 tablets dissolved in 20 liters. [g] RT = medium was sprayed into a carboy under reduced pressure at room temperature. [h] Medium was treated with nitrogen at atmospheric pressure instead of air.

water can be controlled over a very wide range by changing the air pressure over the water. Although there is no general relationship between temperature and the concentration of a gas in a liquid, the equilibrium concentrations in water of the four major components of air decrease as the temperature of the water increases (10). These four components are nitrogen, oxygen, argon, and carbon dioxide (78.08, 20.95, 0.93, and 0.03% by volume, respectively). Combined, they make up 99.99% of the gases found in air (11). Because the solubility (v/v) of air in water under 1 atm at 100° is ~65% of the solubility of air at 25° (10), the concentration of air in water can be controlled only over a narrow range by changing the temperature of the water.

The dissolution results obtained for Tablet 2 when the air concentration in the water was controlled by temperature at prevailing atmospheric pressures are given in Table I and Fig. 1. The means of six results agreed closely when batches of water equilibrated with air for 30 and 90 min at room temperature were used; this agreement indicated that the water was being equilibrated in a repeatable manner. These means were significantly lower ($p < 0.025$) than the mean of six results obtained when freshly drawn deionized water that had not been equilibrated with air at room temperature was used. Thus, the equilibration treatment had a definite effect on the air concentration in the water.

Since the dissolution test was carried out at 37° in all cases, the dissolution media equilibrated at <37° became supersaturated with air when heated to 37° and those equilibrated at >37° became unsaturated with air when cooled to 37°. Because of the manipulation of the medium after the original equilibration, the degree of saturation at the beginning of the dissolution test was related to, but probably not equal to, the difference in the equilibrium concentration of air at the equilibration temperature and at 37°.

The relationship (Fig. 1) between the amount of prednisone dissolved from Tablet 2 and the air concentration in the medium may be explained in terms of sorption of air by the tableted formulation after tablet disintegration takes place. Normally, the tablet particles stay on the bottom of the dissolution vessel and collect into a cone of material during the dissolution test. Sorption of air decreases the density of the particles so that they may be agitated to a greater extent by the dissolution medium. The cone is disrupted by this agitation, and shielding of the inner particles is lessened. The sorption of air can also partially block the medium from contact with the particles. In this case the dissolution results decrease as the quantity of excess air increases. This effect has been observed with another tableted formulation (3) whose disintegrated particles are normally lifted and circulated by the dissolution medium. The decrease in dissolution results was small when air prevented contact of the medium with the particles. However, the increase in dissolution results was large when air bubbles increased the agitation of the particles.

The curve in Fig. 1 appears to approach a lower limit of 35% of label claim. This lower limit does not coincide with the equilibrium concentration of air in water at 37°, but is obtained from water that has a lower concentration of air. Additional tests of Tablet 2 with water equilibrated with air at temperatures near 37° confirmed that mean dissolution results between 39 and 41% of label claim were obtained (Table II). One explanation is that the equilibrium concentration of air in the water is shifted downward when the tablet is introduced to the medium. Thus, excess air from the medium would be available for sorption. This explanation is not well supported by the slightly lower results obtained when the tablets were introduced to equilibrated solutions that already contained some dissolved tablet material (Table II). The decrease in results is not large enough to account for the total difference. Another explanation is that the tablet particles are in "competition" with the water for the dissolved air. In this case the sorption process could be described as a true equilibrium of air between the water and the tablet particles.

To see if one or more of the minor components of air could be preferentially sorbed by Tablet 2, the test was conducted under a nitrogen atmosphere. The dissolution results obtained by this procedure compare closely with those obtained by equilibrating water with air (Table II). Preferential sorption was not indicated.

The dissolution results obtained when the equilibrium air concentration was controlled by pressure (Table II) follow a predictable pattern. Dissolution medium equilibrated at 37° with air at a positive pressure of 50 mm Hg above atmospheric pressure gave results that indicated that the medium was supersaturated with air. Dissolution medium equilibrated with air at a positive pressure of 10 mm Hg gave results that were equivalent to those obtained from dissolution medium equilibrated at atmospheric pressure. Media equilibrated at pressures of 30–57 mm Hg below atmospheric pressure gave results that were equivalent to or slightly below those obtained at atmospheric pressure. When the pressure over the water was reduced to ≤145 mm Hg, sufficient air was removed to cause the dissolution results (means of six) to level off between 35 and 36% of label claim. This is the lower limit that the curve in Fig. 1 appears to approach. Results between 35 and 36% of label claim were also obtained when the test was conducted with water that had been sprayed into a carboy under a pressure of 145 mm Hg at room temperature.

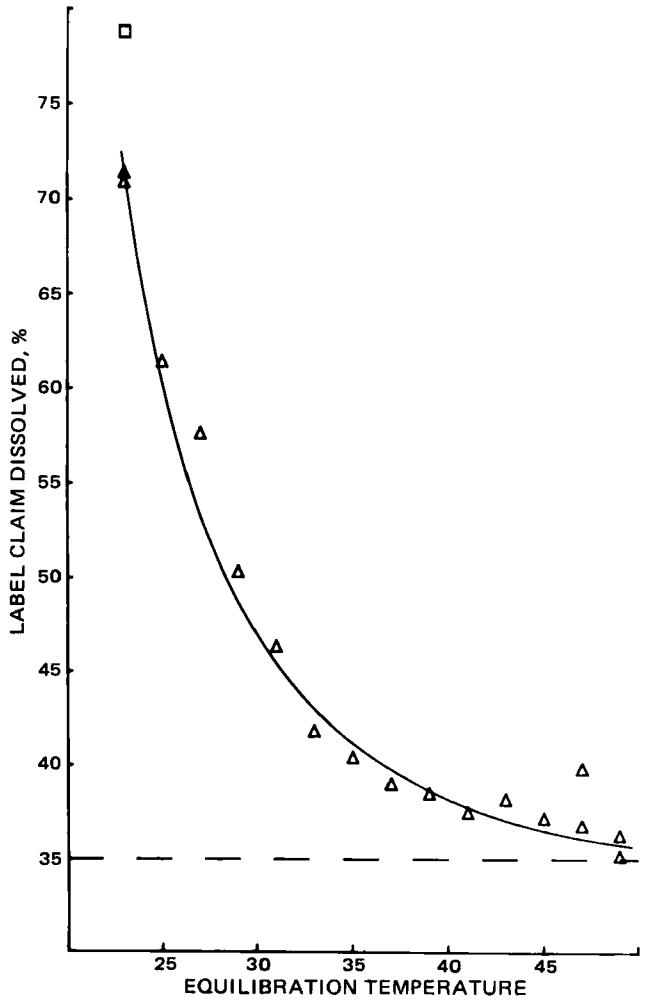

Figure 1—*Dissolution results for Tablet 2* versus *the temperature at which the dissolution medium was equilibrated with air; all results were obtained at 37°; (□) deionized water at room temperature.*

CONCLUSIONS

It is known that excess air from the dissolution medium can change the dissolution results obtained for certain tablets. The data presented in this paper show that results can be changed not only by air concentrations that exceed the saturation point in the dissolution medium but also by concentrations of air at the saturation point and below. To ensure that dissolved air does not influence dissolution results, the USP dissolution test should be conducted with dissolution media that contain different concentrations of air until a range of concentrations has been established that will not change the results. Although the concentration of air can be reduced to a low value at the beginning of a test, it is difficult to specify an air concentration below which no dissolution result could possibly be changed because of the variety of products subjected to the test, the conditions under which the test is made, and the differences in time requirements for the test. Nevertheless, repeatable dissolution results can be obtained by control of the air concentration. Thus, if the air concentration in the dissolution medium is repeatably controlled at the beginning of the test, the effect of the air on the solid dosage form should be reasonably constant from one laboratory to the next.

This laboratory has routinely reduced the air concentrations in the dissolution medium to low, but unknown, values by use of vacuum at room temperature. The medium thus treated has been considered adequate for dissolution tests within 8 hr of its preparation. When water prepared in this manner was used to test Tablet 2, an intralaboratory acceptance range of 35–43% of label claim was established for means of

six results[3]. From the data presented in this paper, a range of 35–41% of label claim is obtained from the use of water that contains air concentrations that do not exceed the saturation point of air in water at 37°. Thus, it should be possible to narrow the present acceptance range for these tablets, or at least to make the range more meaningful, if the air concentration in the water is controlled at the beginning of the test.

REFERENCES

(1) "The United States Pharmacopeia," 20th rev., U.S. Pharmacopeial Convention, Rockville, Md., 1980, p. 959.

(2) D. C. Cox, C. E. Wells, W. B. Furman, T. S. Savage, and A. C. King, *J. Pharm. Sci.*, **71**, 395 (1982).

(3) D. C. Cox, W. B. Furman, L. K. Thornton, T. W. Moore, and E. H. Jefferson, *J. Pharm. Sci.*, **72**, 910 (1983).

(4) D. C. Cox and W. B. Furman, *J. Pharm. Sci.*, in press.

(5) "The United States Pharmacopeia," 18th rev., U.S. Pharmacopeial Convention, Rockville, Md., 1970, p. 536.

(6) "The United States Pharmacopeia," 18th rev., U.S. Pharmacopeial Convention, Rockville, Md., 1970, p. 952.

(7) D. C. Cox, C. C. Douglas, W. B. Furman, R. D. Kirchhoefer, J. W. Myrick, and C. E. Wells, *Pharm. Technol.*, **2**(4), 41 (1978).

(8) "Fourth Interim Revision Announcement Pertaining to USP XIX and NF XIV," The United States Pharmacopeial Convention, Inc., Rockville, Md., 1977, p. 1.

(9) D. P. Page, D. C. Cox, M. L. Dow, M. A. Kreienbaum, P. A. McCullen, T. W. Moore, and L. K. Thornton, *FDA By-Lines*, **10**, 57 (1980).

(10) "Lange's Handbook of Chemistry," 12th ed., J. A. Dean, Ed., McGraw-Hill, New York, N.Y., 1979, pp. 10-3 to 10-6.

(11) "Handbook of Chemistry and Physics," 45th ed., R. C. Weast, Ed., The Chemical Rubber Co., Cleveland, Ohio, 1964, p. F-88.

[3] This acceptance range was calculated from data obtained by this laboratory.

Drug Interactions I: Detection of Inorganic Nitrite in Organic Nitrate Esters Under Acidic Conditions Simulating the Human Stomach

SUZANNE BORING, FRANCIS JOHNSON, JACK CHEN, ROBERT KLETT, and ILENE H. RAISFELD-DANSE *x

Received April 22, 1982, from the *Division of Clinical Pharmacology and Toxicology, Department of Pharmacological Sciences, Health Sciences Center, State University of New York at Stony Brook, Stony Brook, NY 11794.* Accepted for publication October 20, 1982. *Present address: Chevron Environmental Health Center, Inc., P.O. Box 4054, Richmond, CA 94804.

Abstract □ Both unformulated (bulk) and formulated (drugs) organic nitrate esters (isosorbide dinitrate, nitroglycerin, and pentaerythritol tetranitrate) were studied in the presence and absence of hydrochloric acid to determine if they could be sources of nitrite (and therefore lead to nitrosamine formation) under acidic conditions similar to those found in the stomach. The presence and generation of nitrite ion was detected by a modification of the Griess reaction. Bulk isosorbide dinitrate and nitroglycerin were found to be contaminated with 13.8–121.4 μmoles of inorganic nitrite per mole of nitrate ester. In addition, in the presence of hydrochloric acid, these preparations generated 0.52–1.18 μmoles of inorganic nitrite/mole of nitrate ester/min. Unformulated nitroglycerin generated nitrite at a rate roughly twice that of isosorbide dinitrate. In contrast, no evidence for nitrite contamination or generation by pentaerythritol tetranitrate was found. Tablets and capsules of isosorbide dinitrate contained ~27–216 μmoles of nitrite/mole of nitrate ester and, in the presence of hydrochloric acid, generated an average of 0.55 μmole nitrite/min. For isosorbide dinitrate, this rate was similar for bulk and formulated drug. In comparison to isosorbide dinitrate, the amount of nitrite initially present in tablets and capsules of nitroglycerin varied more widely (~25–2290 μmoles nitrite/mole of nitrate ester), and in this case nitrite was generated at higher rates than unformulated drug averaging ~4.7 μmoles nitrite/mole of nitrate ester/min. Contrary to a literature report, we found that nitrate ion is not reduced to nitrite by hydrochloric acid (pH 1–3). These data suggest that the continuous production of nitrite ion from isosorbide dinitrate and nitroglycerin is due to the hydrolysis of nitrite ester impurities, a reaction known to be strongly catalyzed by the chloride ion. Although the generation of inorganic nitrite from organic nitrate esters is of interest, the low levels of nitrite produced are unlikely to lead to intragastric nitrosamine formation.

Keyphrases □ Isosorbide dinitrate—presence and generation of inorganic nitrite, simulated gastric conditions, Griess reaction □ Nitroglycerin—presence and generation of inorganic nitrite, simulated gastric conditions, Griess reaction □ Pentaerythritol tetranitrate—presence and generation of inorganic nitrite, simulated gastric conditions, Griess reaction □ Inorganic nitrite—presence in and generation from the nitrate esters isosorbide dinitrate, nitroglycerin, and pentaerythritol tetranitrate, simulated gastric conditions, Griess reaction

Organic nitrate esters such as nitroglycerin have been used for many years on an intermittent basis to relieve the symptoms of angina pectoris. Recently, organic nitrates have been used on a continuing basis to prevent anginal attacks; they are often ingested with other medications such as tranquilizers or are prescribed concomitantly with β-adrenergic blocking drugs such as propranolol hydrochloride for an additive pharmacological effect (1). Since these medications are taken for many years, often for the lifetime of the patient, it is important to evaluate the safety of simultaneous ingestion of such drugs (2).

There has been much discussion regarding the potential hazards of nitrosamines formed from therapeutic drugs during their passage through the GI tract (3, 4). In fact, in studies where animals are fed inorganic nitrite along with various drugs such as chlordiazepoxide, the formation of carcinogenic nitrosamines has been demonstrated (5). To form nitrosamines, an acidic milieu, the presence of amines, and a source of nitrite are required. The human stomach provides such an appropriate acidic environment (6), and most antihypertensive, β-adrenergic blocking, and tranquilizing drugs are secondary or tertiary amines. Nitrosamine formation can occur from a tertiary amine, but an oxidative cleavage to a secondary amine is required first (7). Nitrosation of secondary amines is a well-established reaction (7).

0022-3549/83/0900-1064$01.00/0

six results[3]. From the data presented in this paper, a range of 35–41% of label claim is obtained from the use of water that contains air concentrations that do not exceed the saturation point of air in water at 37°. Thus, it should be possible to narrow the present acceptance range for these tablets, or at least to make the range more meaningful, if the air concentration in the water is controlled at the beginning of the test.

REFERENCES

(1) "The United States Pharmacopeia," 20th rev., U.S. Pharmacopeial Convention, Rockville, Md., 1980, p. 959.

(2) D. C. Cox, C. E. Wells, W. B. Furman, T. S. Savage, and A. C. King, *J. Pharm. Sci.*, **71**, 395 (1982).

(3) D. C. Cox, W. B. Furman, L. K. Thornton, T. W. Moore, and E. H. Jefferson, *J. Pharm. Sci.*, **72**, 910 (1983).

(4) D. C. Cox and W. B. Furman, *J. Pharm. Sci.*, in press.

(5) "The United States Pharmacopeia," 18th rev., U.S. Pharmacopeial Convention, Rockville, Md., 1970, p. 536.

(6) "The United States Pharmacopeia," 18th rev., U.S. Pharmacopeial Convention, Rockville, Md., 1970, p. 952.

(7) D. C. Cox, C. C. Douglas, W. B. Furman, R. D. Kirchhoefer, J. W. Myrick, and C. E. Wells, *Pharm. Technol.*, **2**(4), 41 (1978).

(8) "Fourth Interim Revision Announcement Pertaining to USP XIX and NF XIV," The United States Pharmacopeial Convention, Inc., Rockville, Md., 1977, p. 1.

(9) D. P. Page, D. C. Cox, M. L. Dow, M. A. Kreienbaum, P. A. McCullen, T. W. Moore, and L. K. Thornton, *FDA By-Lines*, **10**, 57 (1980).

(10) "Lange's Handbook of Chemistry," 12th ed., J. A. Dean, Ed., McGraw-Hill, New York, N.Y., 1979, pp. 10-3 to 10-6.

(11) "Handbook of Chemistry and Physics," 45th ed., R. C. Weast, Ed., The Chemical Rubber Co., Cleveland, Ohio, 1964, p. F-88.

[3] This acceptance range was calculated from data obtained by this laboratory.

Drug Interactions I: Detection of Inorganic Nitrite in Organic Nitrate Esters Under Acidic Conditions Simulating the Human Stomach

SUZANNE BORING, FRANCIS JOHNSON, JACK CHEN, ROBERT KLETT, and ILENE H. RAISFELD-DANSE *x

Received April 22, 1982, from the *Division of Clinical Pharmacology and Toxicology, Department of Pharmacological Sciences, Health Sciences Center, State University of New York at Stony Brook, Stony Brook, NY 11794.* Accepted for publication October 20, 1982. *Present address: Chevron Environmental Health Center, Inc., P.O. Box 4054, Richmond, CA 94804.

Abstract □ Both unformulated (bulk) and formulated (drugs) organic nitrate esters (isosorbide dinitrate, nitroglycerin, and pentaerythritol tetranitrate) were studied in the presence and absence of hydrochloric acid to determine if they could be sources of nitrite (and therefore lead to nitrosamine formation) under acidic conditions similar to those found in the stomach. The presence and generation of nitrite ion was detected by a modification of the Griess reaction. Bulk isosorbide dinitrate and nitroglycerin were found to be contaminated with 13.8–121.4 μmoles of inorganic nitrite per mole of nitrate ester. In addition, in the presence of hydrochloric acid, these preparations generated 0.52–1.18 μmoles of inorganic nitrite/mole of nitrate ester/min. Unformulated nitroglycerin generated nitrite at a rate roughly twice that of isosorbide dinitrate. In contrast, no evidence for nitrite contamination or generation by pentaerythritol tetranitrate was found. Tablets and capsules of isosorbide dinitrate contained ~27–216 μmoles of nitrite/mole of nitrate ester and, in the presence of hydrochloric acid, generated an average of 0.55 μmole nitrite/min. For isosorbide dinitrate, this rate was similar for bulk and formulated drug. In comparison to isosorbide dinitrate, the amount of nitrite initially present in tablets and capsules of nitroglycerin varied more widely (~25–2290 μmoles nitrite/mole of nitrate ester), and in this case nitrite was generated at higher rates than unformulated drug averaging ~4.7 μmoles nitrite/mole of nitrate ester/min. Contrary to a literature report, we found that nitrate ion is not reduced to nitrite by hydrochloric acid (pH 1–3). These data suggest that the continuous production of nitrite ion from isosorbide dinitrate and nitroglycerin is due to the hydrolysis of nitrite ester impurities, a reaction known to be strongly catalyzed by the chloride ion. Although the generation of inorganic nitrite from organic nitrate esters is of interest, the low levels of nitrite produced are unlikely to lead to intragastric nitrosamine formation.

Keyphrases □ Isosorbide dinitrate—presence and generation of inorganic nitrite, simulated gastric conditions, Griess reaction □ Nitroglycerin—presence and generation of inorganic nitrite, simulated gastric conditions, Griess reaction □ Pentaerythritol tetranitrate—presence and generation of inorganic nitrite, simulated gastric conditions, Griess reaction □ Inorganic nitrite—presence in and generation from the nitrate esters isosorbide dinitrate, nitroglycerin, and pentaerythritol tetranitrate, simulated gastric conditions, Griess reaction

Organic nitrate esters such as nitroglycerin have been used for many years on an intermittent basis to relieve the symptoms of angina pectoris. Recently, organic nitrates have been used on a continuing basis to prevent anginal attacks; they are often ingested with other medications such as tranquilizers or are prescribed concomitantly with β-adrenergic blocking drugs such as propranolol hydrochloride for an additive pharmacological effect (1). Since these medications are taken for many years, often for the lifetime of the patient, it is important to evaluate the safety of simultaneous ingestion of such drugs (2).

There has been much discussion regarding the potential hazards of nitrosamines formed from therapeutic drugs during their passage through the GI tract (3, 4). In fact, in studies where animals are fed inorganic nitrite along with various drugs such as chlordiazepoxide, the formation of carcinogenic nitrosamines has been demonstrated (5). To form nitrosamines, an acidic milieu, the presence of amines, and a source of nitrite are required. The human stomach provides such an appropriate acidic environment (6), and most antihypertensive, β-adrenergic blocking, and tranquilizing drugs are secondary or tertiary amines. Nitrosamine formation can occur from a tertiary amine, but an oxidative cleavage to a secondary amine is required first (7). Nitrosation of secondary amines is a well-established reaction (7).

0022-3549/83/0900-1064$01.00/0

We have been concerned as to whether or not organic nitrate drugs could be a source of nitrite ion and therefore give rise to nitroso compounds during dissolution in the stomach. Although organic nitrate esters are known to be converted to nitrite by hepatic enzymes (8), the conversion of organic nitrate esters to inorganic nitrite in actual or simulated gastric contents has not been described. Nevertheless, Oishis (9) has reported, on the basis of polarographic studies, a mechanism by which nitrite could arise from nitrate in the presence of hydrochloric acid. He found that even in dilute solution, the interaction of nitric acid and hydrochloric acid (aqua regia reaction: $HCl + HNO_3 \rightarrow HNO_2 + HOCl$) gave rise to an equilibrium that favored the products over starting compounds in the ratio 99:1.

Earlier studies in our laboratory showed that nitrosamines could be recovered from incubations of isosorbide dinitrate with hydroxyzine hydrochloride, a tertiary amine (2), or propranolol hydrochloride, a secondary amine (10). In this report, we examined whether or not organic nitrate esters are a source of inorganic nitrite, and if not, other possible origins of inorganic nitrite. Various preparations of isosorbide dinitrate, nitroglycerin, and pentaerythritol tetranitrate were examined for the presence of nitrite under acidic conditions simulating those found in the human stomach.

EXPERIMENTAL

Materials—Unformulated samples, tablets, and capsules of isosorbide dinitrate, nitroglycerin, and pentaerythritol tetranitrate were gifts from various manufacturers. Because of their explosive properties, organic nitrates are routinely stored and handled as either lactose or mannitol mixtures. When formulated as drugs, the active ingredients are combined with inert materials and lubricants. In the studies described here, samples of the bulk (unformulated) materials were used as received, and in addition, a bulk sample of isosorbide dinitrate (25% in mannitol) was purified by sublimation and also by recrystallization from absolute ethanol.

Sulfanilic acid[1] and 1-aminonaphthalene[1] were analytical reagent grade. All reagents, water, and glassware used in these studies were free of contaminating nitrite and periodically checked using the Griess test (11).

Bulk Organic Nitrates—Samples were incubated in hydrochloric acid, pH 1.0, at 37° accompanied by gentle shaking to simulate conditions of acidity, temperature, and pH found in the human stomach. Incubations were conducted for 60–90 min to determine the time course of inorganic nitrite production during the period that a drug is likely to remain in the stomach. Under these conditions, the free nitrite ion (nitrous acid) was found to be unstable. Therefore, the Griess test (11, 12) was modified in that sulfanilic acid was added at the outset to trap nitrite released from the nitrate esters as the diazo derivative. Under these conditions, diazotization is complete in <1 min.

The assay procedure was as follows: Sulfanilic acid (12.9 m*M*) in 0.12 *M* HCl was added to an aqueous solution of organic nitrate ester in a final concentration of 10% dimethylformamide in water. Aliquots (1.5 ml) of this incubation mixture were removed at specific times and allowed to react with 1-aminonaphthalene (15.7 m*M*), forming a red dye which gave maximal absorbance at 520 nm within 2 min. Nitrite concentrations were calculated as a function of the absorption of the dyestuff using a molar extinction coefficient of 33,000 liter/mole-cm at 520 nm. The minimum detectable amount of nitrite in the assay, based on an absorbance reading of 0.010 is ~0.5 nmole of nitrite. It should be noted that the Griess test is specific for the nitrite ion, and its sensitivity for nitrite detection is considerably better than other published methods (12) including chemiluminescence (13) and a recently reported high-performance liquid chromatographic (HPLC) technique (14).

Because the pH of human stomach contents varies, nitrite levels were measured at several hydrogen ion concentrations. The pH of the solution

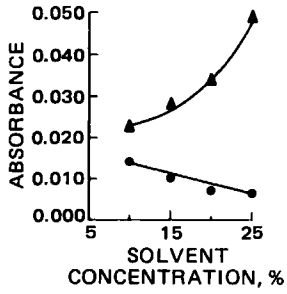

Figure 1—*Effect of organic solvents on absorbance. The Griess reaction was performed at pH 1.0 in solutions containing 8.47 mmoles/liter of isosorbide dinitrate; absorbance was measured after 90 min of incubation. Key: (▲) dimethylacetamide; (●) dimethylformamide. Points are mean values obtained from at least two experiments.*

was raised by adding sodium hydroxide to the sulfanilic acid reagent mixture such that the desired pH of 2.0 or 3.0 was achieved in the final incubation mixture. At pH 2.0 or 3.0 at 37°, diazotization and coupling times varied from 5 to 30 min. No studies were performed at pH >3.0 due to the insolubility of the components of the Griess reagents.

Organic nitrate esters were found to be only partially soluble in aqueous solutions as well as in the Griess reagent mixture. It was therefore necessary to use dimethylformamide as a cosolvent to ensure complete solubility and thus accurate measurement of nitrite under the experimental conditions described above. HPLC analysis was used to compare the quantity of organic nitrate ester added to the Griess reaction mixture and the amount of organic nitrate recovered from the incubation mixture. This was done by weighing organic nitrate esters mixed with sugars, extraction into 100% dimethylformamide, and injection onto a μ-Bondapak C-18 column. These samples were compared with companion samples that were added to the Griess reaction mixture and also with samples that were back-extracted from the Griess reaction incubation mixture into methylene chloride. Samples were separated by HPLC and detected by a UV detector at 254 and 280 nm. The retention time for isosorbide dinitrate separated by methanol–water (55:45), isocratic, flow rate 2 ml/min, was 3.3 min; for nitroglycerin in a 50–100% acetonitrile linear gradient, flow rate 1.5 ml/min, the retention time was 6 min. HPLC analysis of organic nitrate esters under the conditions described confirmed their complete solubility in the Griess reaction mixture at a final dimethylformamide concentration of 10%.

Formulated Organic Nitrates (Drugs)—Formulated tablets and the contents of capsules of isosorbide dinitrate, nitroglycerin, and pentaerythritol tetranitrate were ground using a mortar and pestle prior to testing. The resulting powder was dissolved in dimethylformamide and centrifuged at 2000×*g* for 10 min at 4° to separate the nitrate ester from insoluble components of the formulated preparations. Samples were diluted with water to contain 1.0, 1.5, and 2.0 mg of nitrate ester/ml in the final 10% dimethylformamide mixture. The concentration of organic nitrate ester actually present in the drug extract was confirmed by the aforementioned HPLC method. At time zero, sulfanilic acid and 1-aminonaphthalene in hydrochloric acid, pH 1.0, were simultaneously added to the drug extract and incubated at 37° with shaking. Aliquots were removed at various intervals up to 90 min, passed through a filter[2] to remove particles, and the absorbance was read at 520 nm. This procedure differs from that described above in that sulfanilic acid and 1-aminonaphthalene were added together instead of sequentially.

The effect of the sequence of addition of sulfanilic acid and 1-aminonaphthalene on detection of nitrite was evaluated as follows: In one case, sulfanilic acid was incubated with the reaction mixture and 1-aminonaphthalene was added at the end of the incubation period. In the second case, the sulfanilic acid and 1-aminonaphthalene were added together at the initiation of the incubation period. When scanned by spectrophotometry, absorption maxima (520 nm) were superimposable for sodium nitrite standards, sodium nitrite mixed with unformulated isosorbide dinitrate and nitroglycerin, and sodium nitrite mixed with isosorbide dinitrate and nitroglycerin extracted from tablets and capsules.

RESULTS

Effect of Organic Solvents—Bulk organic nitrate esters were found to be only partially soluble in aqueous solutions as well as in the Griess

[1] J. T. Baker Chemical Co., Phillipsburg, N.J.

[2] Millipore Corp.

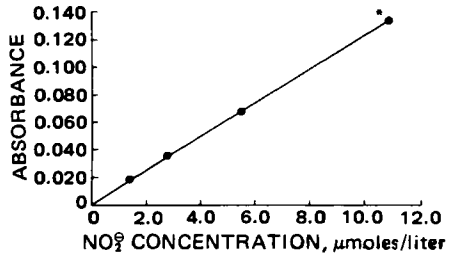

Figure 2—*Effect of 10% dimethylformamide on the measurement of inorganic nitrite by the Griess reaction. All points obtained for sodium nitrite in hydrochloric acid, pH 1.0, with and without 10% dimethylformamide, are completely superimposable. Points are mean values obtained from at least two experiments.*

reagent mixture. It was therefore necessary to use organic solvents to ensure complete solubility and thus accurate measurement of nitrite. Various cosolvents were tested and, surprisingly, were found to interfere with accurate measurement of the nitrite. For example, the addition of ethanol or acetone to a known quantity of inorganic nitrite lowered the apparent nitrite concentration as measured by the Griess test. Ethanol appeared to destroy nitrite itself while acetone appeared to destroy the diazonium ion intermediate. The aprotic solvents dimethylacetamide, dioxane, and dimethylformamide did not affect solutions of inorganic nitrite. However, when increasing concentrations of dimethylacetamide were added to solutions of isosorbide dinitrate of identical composition, the apparent nitrite concentration was increased. In contrast, increasing amounts of dimethylformamide slightly decreased absorbance readings (Fig. 1). Because of its negligible interaction with nitrites, nitrates, and the Griess reaction, dimethylformamide was used as the solvent in subsequent experiments (Fig. 2).

Presence of Nitrite in Bulk Organic Nitrate Esters—Two samples of isosorbide dinitrate were analyzed by the Griess reaction as previously described. Both preparations contained an initial level of nitrite that varied 10-fold between the two samples (Fig. 3A and B). In addition, in the presence of hydrochloric acid these preparations generated nitrite. Both the initial levels of nitrite as well as that generated in hydrochloric acid increased linearly with increasing concentrations of isosorbide dinitrate. The increase in the production of nitrite in the presence of hydrochloric acid was apparent for 6 hr. After this period, there was no further generation of nitrite. In contrast with the generation of nitrite in hydrochloric acid, initial levels of nitrite in phosphoric acid remained constant over time (Fig. 4).

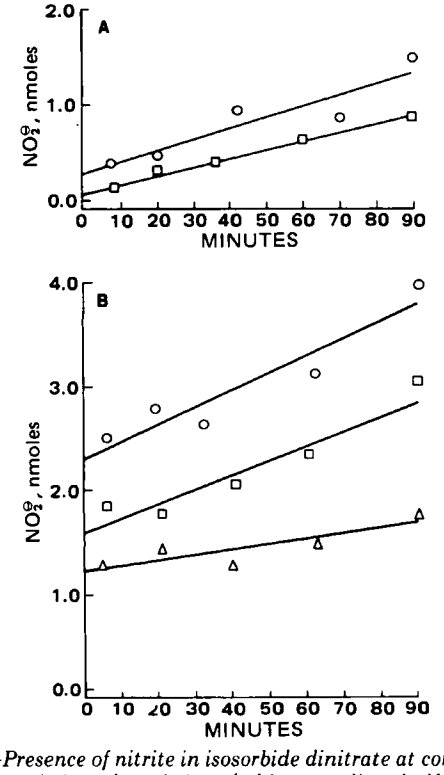

Figure 3—*Presence of nitrite in isosorbide dinitrate at concentrations of 2.0 (○), 1.5 (□), and 1.0 (△) mg/ml in 10% dimethylformamide in hydrochloric acid, pH 1.0, using formulations of 25% isosorbide dinitrate in lactose (A) or mannitol (B). Points are mean values obtained from at least two experiments.*

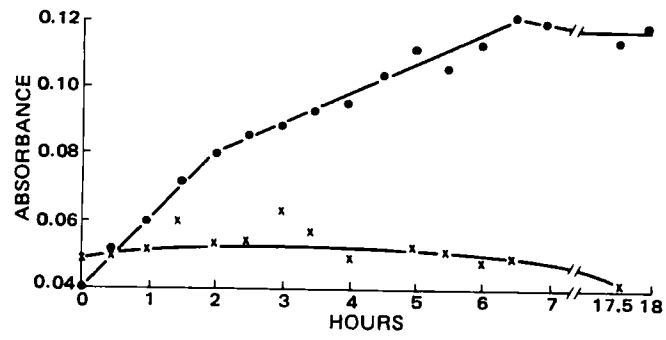

Figure 4—*Time course for generation of nitrite from isosorbide dinitrate, 25% in lactose. Points represent nitrite generated from isosorbide dinitrate (2.0 mg) in 10% dimethylformamide, pH 1.0, in hydrochloric acid (●) and phosphoric acid (×).*

Examination of samples of isosorbide dinitrate (25% in mannitol) purified by sublimation and by recrystallization, indicated the presence and generation of nitrite in amounts similar to the previously examined parent sample, except that initial levels of nitrite were lower (Table I). Thus, in hydrochloric acid, all preparations of isosorbide dinitrate generated nitrite at similar rates.

Samples of isosorbide dinitrate in lactose and mannitol were examined by the Griess reaction at pH 1, 2, and 3 under diazotization and coupling times ranging from 5 to 30 min. The amount of nitrite detected initially or generated within this range of pH was the same as that for isosorbide dinitrate samples described above (data not shown).

In comparison with isosorbide dinitrate, on a molar basis, nitroglycerin contained higher initial levels of nitrite, and nitrite was generated in hydrochloric acid at rates roughly twice that observed with isosorbide dinitrate (Table I, Fig. 5). Like isosorbide dinitrate, the production of nitrite is linear with time and the rates are essentially parallel for different concentrations of nitroglycerin. In hydrochloric acid, but not in phosphoric acid, nitrite was generated for 4 hr (Fig. 6). Because of its volatile and explosive properties, nitroglycerin was not purified further. Significantly, corresponding experiments performed on pentaerythritol tetranitrate failed to give absorbance readings above background levels; no evidence for the presence or generation of nitrite was obtained.

Finally, to eliminate the possibility that the nitrite ion could arise by reduction of the nitrate ion, we examined the action of hydrochloric acid (pH 1.0–3.0) on dilute solutions of sodium nitrate (40 m*M*) and nitric acid (40 m*M*) over 24 hr. Within the detection limits of the Griess test, no evidence of nitrite formation was obtained.

Presence of Nitrites in Formulated Organic Nitrate Vasodilators—The first studies on drugs containing isosorbide dinitrate and nitroglycerin using the sequential addition of Griess reagents (sulfanilic acid present during the incubation, followed by the addition of 1-aminonaphthalene) showed an initial level of nitrite present that appeared to decrease with time. This phenomenon may reflect destruction of the intermediate diazonium ion by an unidentified constituent(s) present in the formulated drugs. Therefore, the Griess reagents were added simultaneously so that immediately after its formation, the diazonium

Table I—Nitrite Detected in Bulk Organic Nitrate Ester Preparations

Compound	μmole of nitrite/mole of nitrate ester		
	After 2 min[a]	After 60 min[b]	Total[c]
Isosorbide dinitrate, sublimed	23.6	32.9	56.5
recrystallized	13.2	43.3	56.5
25% in lactose	13.8	30.9	44.7
25% in mannitol	114.6	44.9	159.5
Nitroglycerin, 10% in lactose	121.4	70.7	192.1
Pentaerythritol tetranitrate, 20% in lactose	—[d]	—	—

[a] The concentrations of nitrite initially detectable after 2 min in hydrochloric acid, pH 1.0. [b] The amount of nitrite generated in 60 min. [c] The sum of nitrite initially present plus nitrite generated over 60 min. [d] Not detected.

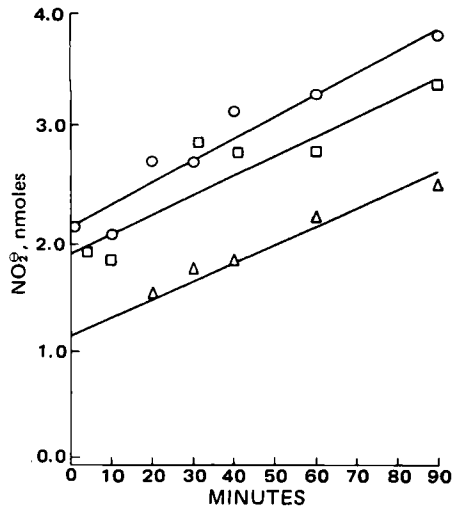

Figure 5—*Presence of nitrite in nitroglycerin, 10% in lactose, at concentrations of 2.0 (○), 1.5 (□), and 1.0 (△) mg/ml in hydrochloric acid, pH 1.0, in 10% dimethylformamide. Points are mean values obtained from at least two experiments.*

reagent could react with the coupling reagent, 1-aminonaphthalene. By this procedure, the production of inorganic nitrite was followed for 90 min, the longest time that a drug is likely to remain in the stomach. In contrast to isosorbide dinitrate and nitroglycerin, the green color of commercially formulated drugs that contained pentaerythritol tetranitrate obscured the absorbance of the dyestuff at 520 nm. Thus pentaerythritol tetranitrate-containing drugs were not analyzed for nitrite content.

At concentrations of nitrite <1 μmole/liter, the sequential and simultaneous addition of Griess reagents gave similar absorbance values. At higher concentrations of nitrite, in comparison with the sequential addition of reagents, the simultaneous addition of Griess reagents gave a decrease of 15–20% in absorbance readings for identical nitrite concentrations (Fig. 7).

Tablets and capsules of isosorbide dinitrate were found to contain varying amounts of nitrite initially (~27–216 μmoles of nitrite/mole of nitrate ester) and to generate an average of 0.55 μmole of nitrite/mole of nitrate ester/min (Fig. 8, Table II).

Tablets and capsules of nitroglycerin also varied widely in their nitrite content. Nitrite was present in initial concentrations of ~25–2290 μmoles of nitrite/mole of nitrate ester and was generated at an average rate of ~4.7 μmoles of nitrite/mole of nitrate ester/min (Fig. 8, Table II).

DISCUSSION

It is evident that most of the preparations that were examined contained small quantities of inorganic nitrite. In addition, it also appears that apart from pentaerythritol tetranitrate, these preparations probably

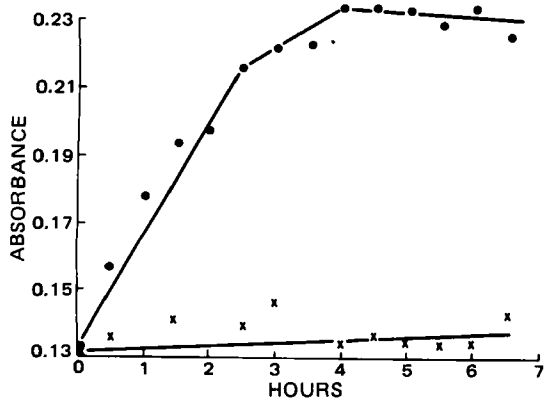

Figure 6—*Time course of generation of nitrite from nitroglycerin, 10% in lactose. Points represent nitrite generated from nitroglycerin (2.0 mg) in 10% dimethylformamide, pH 1.0, in hydrochloric acid (●) and phosphoric acid (×).*

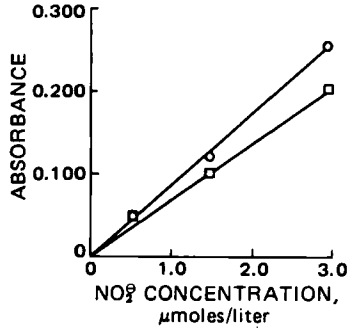

Figure 7—*Comparison of dye absorbance with sequential and simultaneous addition of Griess reagents using solutions with identical concentrations of nitrite in hydrochloric acid, pH 1.0, in 10% dimethylformamide. Key: (○) values obtained when only sulfanilic acid is present at time zero; (□) values obtained when sulfanilic acid and 1-aminonaphthalene are added together at time zero. Absorbance readings were taken 60 min later; points represent mean values from at least three experiments.*

contain small quantities of nitrite esters as impurities. These serve as the source of the continuous production of nitrite ion when the mixture is incubated with hydrochloric acid. Evidently a slow HCl-catalyzed hydrolysis is occurring; the sensitivity of nitrite esters to acidic hydrolysis is well documented (15).

In addition, acidic hydrolysis of nitrite esters is catalyzed by the presence of halide ions. Companion experiments were performed on all nitrate esters using phosphoric acid instead of hydrochloric acid to provide an acidic medium of identical pH. In all samples of isosorbide dinitrate and nitroglycerin, but not pentaerythritol tetranitrate, an initial level of nitrite was detected which corresponded to that seen in hydrochloric acid, but no further generation of nitrite was observed. These results are consistent with the findings of Allen, who showed that the rates of acid hydrolysis of propyl nitrite were increased by at least two orders of magnitude when equivalent concentrations of chloride ion were present (16).

The possibility exists, however, that the nitrite that is continually produced could come from the reduction of nitrate ion or nitrate ester by hydrochloric acid. If the claim by Oishis (9) that nitric acid is reduced to nitrous acid in dilute solution by hydrochloric acid is correct (the aqua regia mechanism), then it is difficult to explain the failure of pentaerythritol tetranitrate to yield nitrite. We have now examined dilute mixtures of both $NaNO_3$–HCl (1:4) and HNO_3–HCl (1:4) in water, over a time course of 24 hr and at pH values of 1 and 3. No evidence of nitrite (or nitrous acid) formation could be detected within the sensitivity range of the Griess reagent. These results are consistent with literature reports of hydrolysis of nitrate esters. Boschan (15) states that hydrolysis of nitrate esters predominantly yields nitrate ion, and that no subsequent reduction to nitrite occurs. However, nitrite esters containing an α-hydrogen can undergo elimination to directly form nitrite. Of course, nitric

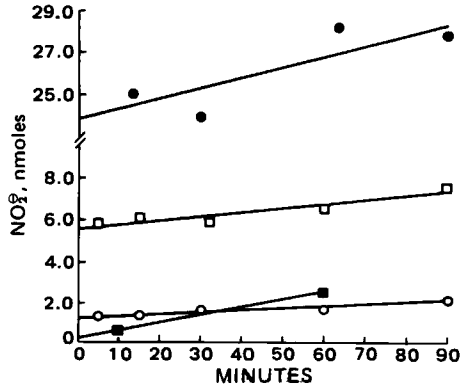

Figure 8—*Time course of nitrite production by some organic nitrate ester drug dosage forms. Drugs were incubated in hydrochloric acid, pH 1.0; points represent the mean values obtained from at least three experiments. Key: (●) 0.6-mg nitroglycerin tablet; (■) 6.5-mg sustained-action nitroglycerin capsule; (○) 40-mg sustained-action isosorbide dinitrate tablet; (□) 40-mg sustained-action isosorbide dinitrate capsule.*

Table II—Nitrite Detected in Organic Nitrate Ester Drug Formulations

Drug	μmole of nitrite/mole of nitrate ester		
	After 2 min[a]	After 60 min	Total[b]
Isosorbide dinitrate 40-mg tablet, SA[c]	63.6	28.0	91.6
40-mg capsule, SA	26.5	26.9	53.4
40-mg capsule, SA	216.0	44.0	260.0
Nitroglycerin, 6.5-mg capsule, SA	2290.0	299.0	2589.0
2.5-mg capsule, SA	1014.0	328.0	686.0
0.6-mg tablet	24.7	222.0	247.0

[a] Drugs were analyzed as described in *Experimental*. The 2-min time reflects absorbance values (520 nm) obtained 2 min after the simultaneous addition of Griess reagents and is assumed to reflect nitrite initially present. [b] Total of the nitrite initially present and the nitrite generated over 60 min. [c] SA = sustained-action or time-released preparation.

Table III—Calculated Maximal Nitrite Concentrations in Gastric Juice Arising from Dissolved Organic Nitrate Ester Drugs

Drug	μmole of nitrite/liter of gastric juice[a]	
	After 2 min	Total, After 60 min
Isosorbide dinitrate, 40-mg tablet, SA[b]	1.08	1.55
40-mg capsule, SA	0.45	0.91
40-mg capsule, SA	3.66	4.40
Nitroglycerin, 6.5-mg capsule, SA	13.10	14.80
2.5-mg capsule, SA	5.80	3.90
0.6-mg tablet	0.14	1.41

[a] Nitrite concentrations are calculated on the basis of actual levels of nitrite found (Table II). Calculations are based on the ingestion of 60 mg of isosorbide dinitrate or 19.5 mg of nitroglycerin dissolved in a 15-ml volume of gastric juice. [b] SA = sustained-action or time-released preparation.

acid and sodium nitrate could not form nitrites according to this scheme.

In comparison with unformulated isosorbide dinitrate and nitroglycerin, tablets and capsules of these drugs generally contained higher levels of nitrite initially. For isosorbide dinitrate, levels were twofold higher while two of three nitroglycerin drugs tested contained ten to twenty times more nitrite than comparable amounts of unformulated nitroglycerin. In addition, as discussed above, the values obtained for nitrite probably reflect a 15–20% underestimation of the nitrite actually present.

For isosorbide dinitrate, the amount of nitrite generated with time, 0.55 μmole of nitrite/mole of nitrate ester/min was comparable for both unformulated and formulated drug. In contrast, drugs containing nitroglycerin generated nitrite at faster rates than unformulated drug, averaging 4.7 μmoles of nitrite/mole of nitrate ester/min for formulated drug, a figure somewhat higher than that of 1.2 μmoles of nitrite/mole of nitrate ester/min given for nitroglycerin formulated with lactose alone. Again, as is discussed above, the nitrite initially present is assumed to be there as inorganic nitrite contamination, whereas nitrite which is generated with time in hydrochloric acid is believed to be due to the acid- and chloride-catalyzed hydrolysis of nitrite esters (15, 16), which are believed to be present as impurities in these drugs.

Because many nitrosamines pose a carcinogenic risk one might reasonably ask if the levels of nitrite in these drugs are sufficient to pose a risk of nitrosamine formation from other amine drugs while dissolution in the stomach is taking place. In Table III, nitrite levels actually detected in six different organic nitrate ester drug formulations (Table II) were used to calculate the nitrite concentration that would be present in gastric juice if all of the drug were completely soluble in 15.0 ml of gastric juice. It should be noted however, that these compounds are known to have limited solubility in aqueous solutions. The dosage used for these calculations are the upper limit of currently recommended single therapeutic doses of these compounds—60 mg of isosorbide dinitrate and 19.5 mg of nitroglycerin (17).

On the basis of these data, only the 6.5-mg sustained-action capsules of nitroglycerin provided more than the 10 μmoles of nitrite necessary, on a theoretical basis, to nitrosate 80 mg of propranolol hydrochloride, a secondary amine (18), or 100 mg of hydroxyzine hydrochloride, a tertiary amine[3]. Despite this, when these nitroglycerin capsules were actually incubated with propranolol hydrochloride, a nitrosamine product could not be recovered (19).

In conclusion, the organic nitrate ester vasodilator drugs, isosorbide dinitrate and nitroglycerin, contain varying amounts of inorganic nitrite and nitrite esters present as impurities. Although these nitrate esters may contain adventitious nitrite or nitrite ester, no hazard appears to be posed by the possibility that they themselves can give rise to nitrites *via* reduction with hydrochloric acid. These impurities may arise during the manufacture of the raw material, formulation into therapeutic dosage forms, and/or from decomposition during storage. In terms of the amount of nitrite provided daily by the average American diet (13 mg, 2.3 mmoles), the amount of nitrite provided by these drugs in absolute terms is quite small (20). Moreover, the risk of nitrosating secondary or tertiary amine drugs simultaneously ingested with organic nitrate esters appears to be negligible.

[3] Klett and I. Raisfeld-Danse, manuscript in preparation.

REFERENCES

(1) T. D. Giles, *Ration. Drug Ther.*, **15**, 1 (1981).

(2) I. H. Raisfeld and C. Lin, *Biochem. Pharmacol.*, **28**, 3451 (1979).

(3) S. S. Mirvish, *J. Natl. Cancer Inst.*, **44**, 633 (1970).

(4) T. J. Muscroft, D. J. Youngs, D. W. Burdon, and M. R. B. Keighley, *Lancet*, **i**, 408 (1981).

(5) W. Lijinsky, "The Potential Carcinogenicity of Nitrosatable Drugs," Ablex Publishing, Norwood, N.J., 1980, pp. 101–106.

(6) N. P. Sen, D. C. Smith, and L. Schwinghamer, *Food Cosmet. Toxicol.*, **1**, 301 (1969).

(7) S. S. Mirvish, *Toxicol. Appl. Pharmacol.*, **31**, 325 (1975).

(8) P. Needleman, S. Lang, and E. M. Johnson, Jr., *J. Pharmacol. Exp. Ther.*, **181**, 489 (1972).

(9) Y. Oishis, *J. Chem. Soc. Jpn.*, **53**, 417 (1950).

(10) I. H. Raisfeld, C. Lin, J. Cheng, and J. Brandys, *Fed. Proc. Fed. Am. Soc. Exp. Biol.* **38**, 680 (1979).

(11) B. F. Rider and M. G. Mellon, *Ind. Eng. Chem.*, **18**, 96 (1946).

(12) E. Sawicki, T. W. Stanley, J. Pfaff, and A. D'Amico, *Talanta*, **10**, 641 (1963).

(13) D. W. Joseph and C. W. Spicer, *Anal. Chem.*, **50**, 1400 (1978).

(14) D. J. Pietrzyk and Z. Iskandarani, *Am. Chem. Soc. Abstracts*, March 1982.

(15) R. Boschan, R. T. Merrow, and R. W. Van Dolah, *Chem. Rev.*, **55**, 485 (1955).

(16) A. D. Allen, *J. Chem. Soc.*, **76**, 198, (1954).

(17) J. Abrams, *N. Engl. J. Med.*, **302**, 1234 (1980).

(18) J. Chen and I. Raisfeld-Danse, *J. Pharmacol. Exp. Ther.*, in press.

(19) I. Raisfeld-Danse and J. Chen, *J. Pharmacol. Exp. Ther.*, in press.

(20) J. W. White, *J. Agric. Food Chem.*, **23**, 886 (1975).

ACKNOWLEDGMENTS

This work was supported by Research Grant NIA, R01 AG02033 from the National Institutes of Health.

Determination of Cyproheptadine in Plasma and Urine by GLC with a Nitrogen-Sensitive Detector

H. B. HUCKER[x] and J. E. HUTT

Received June 14, 1982, from the *Merck Institute for Therapeutic Research, West Point, PA 19486.* Accepted for publication August 24, 1982.

Abstract □ A method for the determination of cyproheptadine in plasma and urine was developed using the *N*-ethyl homologue as an internal standard. After extraction of the drug from an alkalinized sample into petroleum ether–isoamyl alcohol, back-extraction into 0.1 *N* HCl, washing the aqueous phase with fresh solvent, re-extraction into petroleum ether after alkalinization, the solvent was evaporated. The reconstituted residue was analyzed by GLC using a SP-2250 column and nitrogen-sensitive detector. Concentrations as low as 3 ng/ml could be determined. Plots of peak area of cyproheptadine–peak area of internal standard *versus* cyproheptadine concentration were linear over the range studied with correlation coefficients of 0.9945 and 0.9924 for plasma and urine, respectively. The method was used to determine the peak time (0.5 hr), peak concentration (33 ng/ml average), and apparent half-life (3 hr) in two dogs after oral administration of 1 mg of cyproheptadine/kg.

Keyphrases □ Cyproheptadine—GC determination in plasma and urine □ GC—cyproheptadine, determination in plasma and urine

Cyproheptadine[1], 4-(5*H*-dibenzo[*a*,*d*]cyclohepten-5-ylidene)-1-methylpiperidine (I, R = CH_3), is a potent antihistaminic and antiserotonergic agent (1) and inhibitor of platelet aggregation (2). Its disposition and metabolism in humans and animals have been described (3–9). Cyproheptadine has been quantitated in rat tissues by GC with a reported sensitivity of ~1 μg/g (3). The present report describes an analytical method suitable for the determination of cyproheptadine in low nanogram concentrations in plasma and urine.

EXPERIMENTAL

Reagents—Petroleum ether (35–60°) and all other chemicals were of analytical reagent grade and were used without further purification. Analytically pure cyproheptadine·HCl and the maleate salt of its *N*-ethyl analogue were synthesized in these laboratories. Stock solutions of the drug and the *N*-ethyl analogue used as an internal standard (II, R = C_2H_5) were prepared in methanol (1 mg/ml, as the free bases). The solution of cyproheptadine was diluted with methanol to give solutions containing 1, 0.5, 0.25, and 0.125 ng of drug/μl. The internal standard solution was diluted with methanol to give a solution containing 2 ng of the compound/μl.

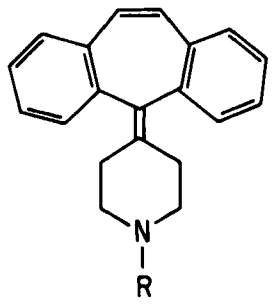

I: R = CH_3
II: R = C_2H_5

A solution of isoamyl alcohol in petroleum ether (99:1, v/v) was prepared.

Instrument—Analyses were performed on a GC[2] equipped with a nitrogen-sensitive detector. The column, 0.91 m × 2 mm (i.d.) was packed with 3% SP-2250 on Supelcoport (80–100 mesh)[3]. The column was conditioned by heating overnight at 260° under helium flow (30 ml/min). Chromatographic conditions were as follows: column oven, detector, and injection port temperatures of 230, 300, and 275°, respectively; helium, hydrogen, and air flows of 30, 3.6, and 50 ml/min, respectively.

Procedure for Plasma—To 1 ml of plasma in a 13-ml glass-stoppered centrifuge tube were added 3.12, 6.25, 12.5, 25, or 50 ng of cyproheptadine and 50 ng of internal standard in a total volume of 50 μl of methanol. After addition of 1 ml of 0.1 *N* NaOH and 8 ml of petroleum ether–isoamyl alcohol (99:1), the tube was shaken for 10 min and centrifuged. Most of the organic phase was transferred to a second tube containing 1 ml of 0.1 *N* HCl. The tube was shaken for 5 min and centrifuged. The organic phase was discarded and 8 ml of petroleum ether–isoamyl alcohol added. After shaking again for 5 min and centrifuging, the organic phase was aspirated. After addition of 0.2 ml of 1 *N* NaOH and 8 ml of petroleum ether–isoamyl alcohol, the tube was shaken for 10 min and centrifuged. The solvent was transferred to a 13-ml centrifuge tube and evaporated in a stream of nitrogen at 40°. The small volume of residual isoamyl alcohol was diluted with 50 μl of heptane and 3 μl was injected into the column. The peak areas of cyproheptadine and the internal standard were measured by the chromatograph terminal and the ratio of the areas plotted *versus* the concentration of cyproheptadine present. Cyproheptadine concentrations in the unknowns were obtained by reference to this standard curve.

Procedures for Urine—The procedure was the same as for plasma except that the standard samples contained 12.5, 25, 50, and 100 ng of cyproheptadine.

RESULTS AND DISCUSSION

As shown in Fig. 1, cyproheptadine and its ethyl homologue used as an internal standard were well separated under the conditions used, having retention times of 4.2 and 5.3 min, respectively. Blank plasma samples assayed by the same procedure showed no significant interfering peaks.

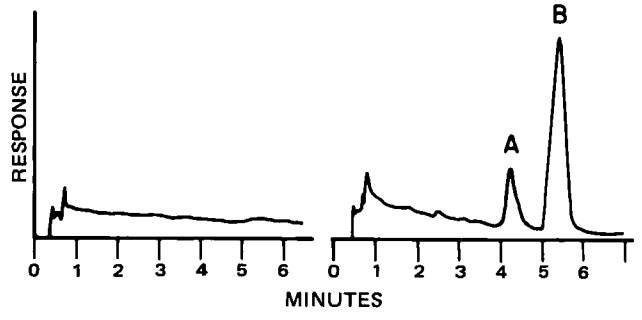

Figure 1—*Gas chromatograms of control dog plasma (left panel) and of plasma containing 12.5 ng of cyproheptadine (A) and 50 ng of internal standard (B) per milliliter (right panel).*

[1] Periactin is the registered trademark of Merck & Co., Inc. for its brand of cyproheptadine.

[2] Hewlett-Packard, Model 5840A.

[3] Supelco, Inc., Bellefonte, Pa.

0022-3549/83/0900-1069$01.00/0

Table I—Precision and Accuracy of the GLC Assay for Cyproheptadine in Plasma and Urine

Cyproheptadine Added, ng/ml	Cyproheptadine Found: Plasma N	Plasma Mean + SD, ng/ml	Plasma RSD, %	Plasma RE[a], %	Urine N	Urine Mean + SD, ng/ml	Urine RSD, %	Urine RE[a], %
3.12	12	3.8 ± 0.5	13.1	+21.8				
6.25	12	6.6 ± 0.7	10.6	+5.6				
12.5	12	13.2 ± 1.1	8.3	+5.6	8	11.2 ± 0.7	6.2	−10.4
25	18	24.0 ± 3.2	13.3	−4.0	8	25.4 ± 4.2	16.5	+ 1.6
50	6	48.8 ± 5.5	11.3	−2.4	8	46.9 ± 1.7	3.6	− 9.4
100					6	103.0 ± 7.3	7.1	+ 3.0

[a] Relative error.

Table II—Plasma Concentrations of Cyproheptadine in Dogs after Administration of a Single Oral Dose (1 mg/kg)

Time, hr	Plasma Concentration: Dog 1, ng/ml	Dog 2, ng/ml
0.5	32	34
1	22	32
2	20	24
4	14	14
6	8	8
12	2	3

Most of the known metabolites of cyproheptadine (*i.e.*, the 10-hydroxy, 10,11-epoxy, 10-ketodesmethyl-, and 10,11-dihydroxy analogues) did not interfere since their retention times were all longer than that of cyproheptadine (7.2, 7.5, 9.3, and 10.8 min, respectively). The *N*-oxide gave a peak at the same retention time as cyproheptadine, presumably from thermal loss of oxygen during GLC. However, it was found that the *N*-oxide was not extracted from plasma or urine under these conditions and, thus, would not interfere in the analysis. Similarly, *N*-desmethylcyproheptadine had the same retention time as the internal standard, but was very poorly extracted (<10% recovery) from plasma under the conditions used. In addition, plasma and urine from dogs dosed with cyproheptadine (see below) were analyzed without addition of the internal standard. No peak was seen at the retention time of desmethylcyproheptadine, indicating that this metabolite would not interfere in the determination of cyproheptadine. However, it would be advisable before using the method in multiple-dose studies to determine if the desmethyl metabolite is present in concentrations sufficient to cause interference. If this is indicated, use of another internal standard would be required.

The precision and accuracy of the method were demonstrated by replicate analyses of plasma and urine samples containing known concentrations of cyproheptadine (Table I). The overall relative standard deviations for plasma ranged from 8.3 to 13.3% and the relative error range was −4.0–21.8%. For urine, the overall relative standard deviation range was 3.6–16.5% and the relative error −10.4–3.0%. The within-day correlation coefficient for the plasma standard curve was 0.9945 and the between-day value was 0.9825. The correlation coefficient for urine was 0.9924.

Plasma levels and urinary excretion of cyproheptadine were measured in two dogs at various times after administration of a single oral dose of the drug (1 mg/kg). The results are shown in Table II. Maximal concentrations were present at the earliest time sampled (0.5 hr). The apparent plasma half-life was ~ 3 hr. Urine (0–24 hr) contained 0.4–0.5% of the dose as unchanged cyproheptadine.

In summary, the present method was shown to be sufficiently sensitive, specific, and reliable for pharmacokinetic studies in the dog and possibly other species as well. Use of an internal standard of similar structure served to minimize errors in quantitation resulting from sample manipulation.

REFERENCES

(1) C. A. Stone, H. C. Wenger, C. T. Ludden, J. M. Stavorski, and C. A. Ross, *J. Pharmacol. Exp. Ther.*, **131**, 73 (1961).

(2) B. Goldman, L. M. Aledort, E. Puszkin, and L. Burrows, *Circulation*, **44**, II–68 (1971).

(3) J. S. Wold and L. J. Fischer, *J. Pharmacol. Exp. Ther.*, **183**, 188 (1972).

(4) H. B. Hucker, A. J. Balletto, S. C. Stauffer, A. G. Zacchei, and B. H. Arison, *Drug Metab. Dispos.*, **2**, 406 (1974).

(5) A. Frigerio, N. Sossi, G. Belvedere, C. Pantarotto, and S. Garattini, *J. Pharm. Sci.*, **63**, 1536 (1974).

(6) K. L. Hintze, J. S. Wold, and L. J. Fischer, *Drug Metab. Dispos.*, **3**, 1 (1975).

(7) C. C. Porter, B. H. Arison, V. F. Gruber, D. C. Titus, and W. J. A. Vandenheuvel, *Drug Metab. Dispos.*, **3**, 189 (1975).

(8) K. A. Kennedy, K. A. Halmi, and L. J. Fischer, *Life Sci.*, **21**, 1813 (1977).

(9) L. J. Fischer, R. L. Thies, D. Charkowski, and K. J. Donham, *Drug Metab. Dispos.*, **8**, 422 (1980).

In Vivo–In Vitro Correlations for Trisulfapyrimidine Suspensions

LEO K. MATHUR *x, JOHN L. COLAIZZI ‡, JAMES M. JAFFE §, ROLLAND I. POUST ¶, and VINOD P. SHAH ‖

Received April 5, 1982, from **G. D. Searle & Co., Chicago, IL 60680;* ‡*College of Pharmacy, Rutgers–The State University, Piscataway, NJ 08854;* §*Sandoz Pharmaceuticals, East Hanover, NJ 07936;* ¶*Burroughs Wellcome Co., Greenville, NC 27834;* and the ‖*Division of Biopharmaceutics, Food and Drug Administration, Rockville, MD 20857.* Accepted for publication August 17, 1982.

Abstract □ A UV method is described for measuring total sulfa drug concentration in dissolution samples. This *in vitro* measurement was found to correlate well with several *in vivo* parameters obtained after administration of commercial trisulfapyrimidine suspensions to humans. The UV method, which is rapid, simple, inexpensive and easily automated, is recommended for studying the dissolution of trisulfapyrimidine suspensions.

Keyphrases □ Trisulfapyrimidine—*in vivo–in vitro* correlations, UV method for the measurement of the dissolution of trisulfapyrimidine suspensions

Several reports (1–8) have appeared in the literature dealing with the bioavailability and dissolution of sulfa drugs. We have observed (9) significant bioavailability differences among seven commercial trisulfapyrimidine suspensions and have reported a dissolution method that provided good *in vivo–in vitro* correlation. This method was subsequently recommended for *in vitro* screening of trisulfapyrimidine suspensions. However, the dissolution samples were analyzed by a specific high-performance liquid chromatographic (HPLC) method which measured the concentrations of each component [sulfadiazine (I), sulfamerazine (II), and sulfamethazine (III)] of trisulfapyrimidine suspensions. The present study was undertaken to determine the suitability of a more rapid and readily available UV spectrophotometric procedure for measuring dissolution samples of trisulfapyrimidine suspensions, and to determine whether dissolution data collected in terms of total sulfa drug could be correlated with the *in vivo* parameters reported previously.

EXPERIMENTAL

***In Vivo* Study**—Details of the *in vivo* study are given elsewhere (9). Briefly, seven commercially available trisulfapyrimidine suspensions (A–G)[1] were each administered to 14 healthy male volunteers in a complete cross-over study design. Fourteen blood samples were then collected over a 48-hr period, and serum was analyzed for I, II, and III by a specific HPLC procedure (10).

Dissolution Methodology—Details of the dissolution method employed have been reported previously (9). Studies were done using the rotating paddle method (11) at 25 rpm in 900 ml of 2.2×10^{-4} *M* HCl, pH 3.4 at 37°. Samples were analyzed spectrophotometrically as described below.

Analytical—For the *in vivo* study, all serum samples were analyzed for sulfadiazine, sulfamerazine, and sulfamethazine by an HPLC method described previously (9, 10). For the *in vitro* study, all dissolution samples were analyzed for total sulfa drug content by a UV spectrophotometric procedure. A solution of trisulfapyrimidines was prepared by dissolving 100 mg each of I[2], II[3], and III[4] in the dissolution medium and adjusting the volume to 100 ml in a volumetric flask. This solution was quantitatively diluted with dissolution medium to obtain a stock solution containing 30 μg of total sulfa drug per milliliter. Standards (1.5, 3.0, 4.5, 6.0, 7.5, and 9.0 μg/ml total sulfa drug) were prepared by further diluting the stock solution with the dissolution medium. The absorbance of each standard solution was measured[5] at 254 nm and a calibration plot constructed. Unknown dissolution samples were measured in similar fashion, dilutions being performed with the dissolution medium where necessary. Prior to use, the spectra of each commercial suspension were examined in the dissolution medium for possible interference by excipients. All preparations gave similar spectra, and no interfering peaks were observed.

Table I—Mean [a] (± SD) Percent of Total Sulfa Drug Dissolved in 15 and 30 Min as Measured by the UV Assay for Seven Commercial Trisulfapyrimidine Suspensions

Product	15 min	30 min
A	68.3 ± 1.1	88.4 ± 0.9
B	86.8 ± 1.3	95.9 ± 1.0
C	47.9 ± 3.2	69.2 ± 4.8
D	88.0 ± 1.4	97.8 ± 1.9
E	30.7 ± 0.9	35.8 ± 1.9
F	22.1 ± 2.5	42.1 ± 4.1
G	9.9 ± 1.2	28.3 ± 1.6

[a] Mean of three determinations.

RESULTS

***In Vivo* Study**—Detailed results of the observed maximum serum concentration (C_{max}), the time for maximum serum concentration (t_{max}), and normalized areas under the curve ($AUC_0^\infty \times K_e$), have been presented previously (9) for I, II, and III.

***In Vitro* Study**—The mean percentages of total sulfa drug (IV) dissolved in 15 and 30 min for the seven trisulfapyrimidine suspensions are shown in Table I. It is observed that there were large differences in the dissolution rate among the seven suspensions. Product G showed the slowest rate of dissolution, while products A, B, and D showed the most rapid dissolution.

***In Vivo–In Vitro* Correlations**—For the three drugs (I, II, and III), each *in vivo* parameter was correlated with the percent of total sulfa drug (IV) dissolved in 15 and 30 min. Significant values of the linear correlation coefficient were observed between: (*a*) percent of IV dissolved in 30 min and C_{max} for I ($r = 0.83$, $p < 0.05$); (*b*) percent of IV dissolved in 15 min and C_{max} for I ($r = 0.80$, $p < 0.05$); (*c*) percent of IV dissolved in 30 min and t_{max} for I ($r = -0.80$, $p < 0.05$); (*d*) percent of IV dissolved in 15 min and t_{max} for I ($r = -0.79$, $p < 0.05$); (*e*) percent of IV dissolved in 30 min and C_{max} for II ($r = 0.77$, $p < 0.05$); (*f*) percent of IV dissolved in 30 min and t_{max} for II ($r = -0.85$, $p < 0.02$); (*g*) percent of IV dissolved in 15 min and t_{max} for II ($r = -0.81$, $p < 0.05$). Other combinations of *in vivo* and *in vitro* parameters did not give significant correlations.

DISCUSSION

Significant bioavailability differences among the commercial trisulfapyrimidine suspensions have been reported (9). These differences were

[1] A, Trisem, lot C53747, Beecham-Massengill Pharmaceuticals, Bristol, Tenn.; B, Terfonyl, lot 60080, E. R. Squibb and Sons, Princeton, N.J.; C, Sulfaloid, lot 17612, Westerfield Laboratories, Cincinnati, Ohio; D. Trisureid, lot 5M249, Reid-Provident Laboratories, Atlanta, Ga.; E, Quad-Ramoid, lot 28431, Paul B. Elder Co., Bryan, Ohio; F, Sulfose, lot 1951619, Wyeth Laboratories, Philadelphia, Pa.; and G, Neotriazine, lot 9ND79A, Eli Lilly and Co., Indianapolis, Ind.

[2] Lot R02114, Eli Lilly and Co., Indianapolis, Ind.

[3] Lot M07059, Eli Lilly and Co., Indianapolis, Ind.

[4] Lot R02011, Eli Lilly and Co., Indianapolis, Ind.

[5] DB-G grating spectrophotometer, Beckman Instruments Inc., Irvine, Calif.

0022-3549/83/0900-1071$01.00/0

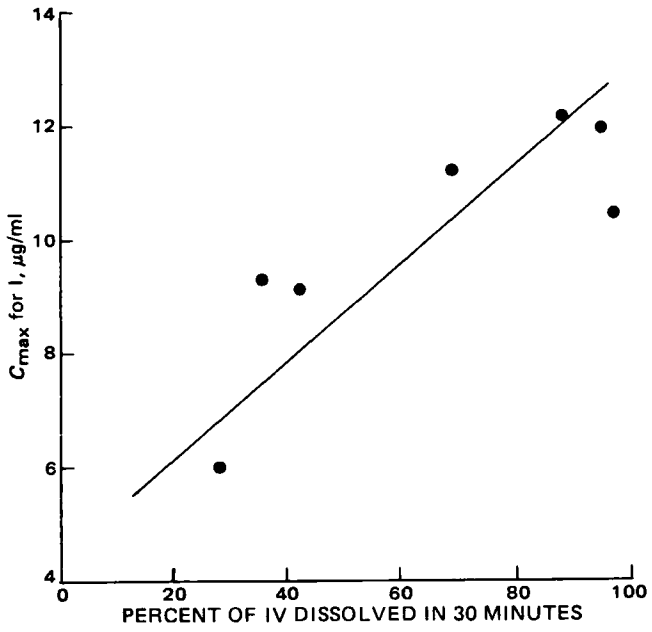

Figure 1—*Relationship between the* in vivo *measure of* C_{max} *for I and the* in vitro *measure of percent IV dissolved in 30 min for the seven trisulfapyrimidine suspensions, showing the regression line for the correlation coefficient of +0.83 (*$p < 0.05$*).*

observed in the rate and extent of absorption of individual suspension components. An *in vitro* dissolution test procedure was developed and dissolution samples analyzed by HPLC. Several significant correlations were reported between *in vivo* and *in vitro* parameters for individual sulfa components. Results of the present investigation show that when using the same dissolution procedure but a different method of detection (UV spectrophotometric) statistically significant correlations could be achieved between the *in vitro* values of percent of total sulfa drug dissolved (in 15 and 30 min) and the *in vivo* parameters reported previously for I and II.

As reported previously, the greatest bioavailability difference among the seven products was observed for the C_{max} parameter for I, for which good correlation was shown with the percent of I dissolved in 30 min (as measured by HPLC). The results of this study also show good correlation ($r = 0.83$, $p < 0.05$) between C_{max} for I and percent of IV dissolved in 30 min, as shown in Fig. 1. Thus, the UV method can be employed for studying the dissolution of trisulfapyrimidine suspensions. The method offers certain advantages over the HPLC procedure in that it is more rapid, less expensive, readily available in most laboratories, and more easily applicable to automation technology. Except for the fact that it could not detect differences in the individual sulfa components of trisulfapyrimidines, the UV method was found to be suitable for the determination of dissolution properties of commercial products.

ACKNOWLEDGMENTS

This work was supported by Food and Drug Administration contract 223-76-3010.

REFERENCES

(1) Y. Langlois, M. A. Gagnon, and L. Tetreault, *J. Clin. Pharmacol.*, **12**, 196 (1972).

(2) V. Bernareggi, G. Bugada, A. Cassola, G. Levi, and F. Moncalvo, *Boll. Chim. Farm.*, **112**, 177 (1973).

(3) S. A. Khalil, M. A. Moustafa, A. R. Ebian, and M. M. Motawi, *J. Pharm. Sci.*, **61**, 1615 (1972).

(4) M. J. Taraszka and R. A. Delor, *J. Pharm. Sci.*, **58**, 207 (1969).

(5) G. R. VanPetten, G. C. Becking, R. J. Withey, and H. F. Lettau, *J. Clin. Pharmacol.*, **11**, 27 (1971).

(6) G. R. VanPetten, G. C. Becking, R. J. Withey, and H. F. Lettau, *J. Clin. Pharmacol.*, **11**, 35 (1971).

(7) R. J. Withey, G. R. VanPetten, and H. F. Lettau, *J. Clin. Pharmacol.*, **12**, 190 (1972).

(8) G. L. Mattok and I. J. McGilveray, *J. Pharm. Sci.*, **61**, 746 (1972).

(9) L. Mathur, J. M. Jaffe, R. I. Poust, H. Barry, III, T. J. Goehl, V. P. Shah, and J. L. Colaizzi, *J. Pharm. Sci.*, **68**, 699 (1979).

(10) T. J. Goehl, L. Mathur, J. D. Strum, J. M. Jaffe, W. H. Pitlick, V. P. Shah, R. I. Poust, and J. L. Colaizzi, *J. Pharm. Sci.*, **67**, 404 (1978).

(11) "The United States Pharmacopeia," 20th rev., U.S. Pharmacopeial Convention, Rockville, Md., 1980, p. 959.

Quantitative Assessment of the Effect of Some Excipients on Nitrazepam Stability in Binary Powder Mixtures

P. R. PERRIER and U. W. KESSELRING ˣ

Received January 25, 1982, from the *Laboratoire d'Analyse Pharmaceutique, Ecole de Pharmacie, CH-1005 Lausanne, Switzerland.* Accepted for publication August 24, 1982.

Abstract □ The decomposition rate constants, normalized for dilution and relative specific surface effects, of nitrazepam in simple binary powder mixtures with talcum, lactose·H_2O, microcrystalline cellulose, corn starch, mannitol, and saccharose are shown to be linearly related to the nitrogen adsorption energy of the excipients.

Keyphrases □ Nitrazepam—effect of excipients on stability in binary powder mixtures □ Excipients—effect on nitrazepam stability in binary powder mixtures

Recently, considerable effort has been made to precisely describe the chemical properties of excipients and how these excipients influence the technical and biopharmaceutical characteristics of the dosage forms. Excellent reviews list the "inert compounds" of pharmaceutical preparations (1), describe the difficulties concerning the "choice of excipients for international use" (2), "the influence of excipients on the design and manufacture of tablets and capsules" (3), and the "problems of drug interactions with excipients" (4). Many studies describe the influence of excipients, *e.g.* the acid-catalyzed decomposition of digoxin by montmorillonite (5), the effect of water adsorption properties of silica gel on the stability and the biological availability of ascorbic acid (6), and the influence of the solubility of some excipients on *in vitro* and *in vivo* properties of bendroflumethiazide tablets (7). Additional references were cited by Carstensen (8, 9).

0022-3549/83/0900-1072$01.00/0

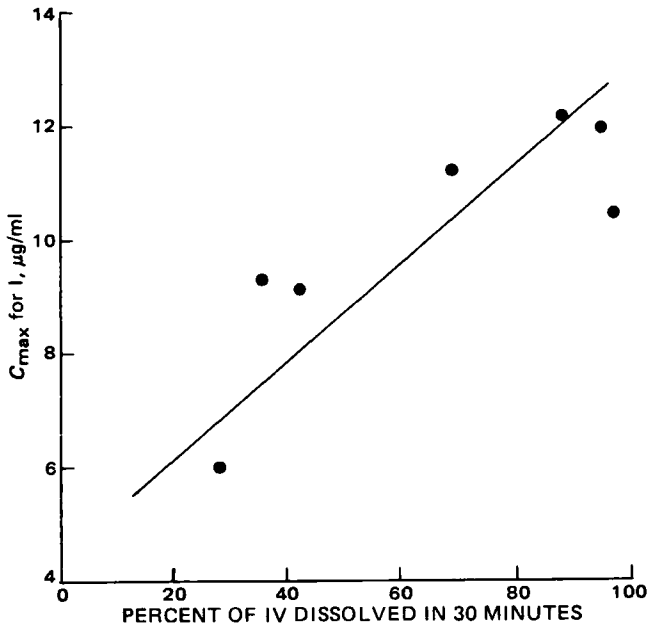

Figure 1—*Relationship between the* in vivo *measure of* C_{max} *for I and the* in vitro *measure of percent IV dissolved in 30 min for the seven trisulfapyrimidine suspensions, showing the regression line for the correlation coefficient of +0.83 (*$p < 0.05$*).*

observed in the rate and extent of absorption of individual suspension components. An *in vitro* dissolution test procedure was developed and dissolution samples analyzed by HPLC. Several significant correlations were reported between *in vivo* and *in vitro* parameters for individual sulfa components. Results of the present investigation show that when using the same dissolution procedure but a different method of detection (UV spectrophotometric) statistically significant correlations could be achieved between the *in vitro* values of percent of total sulfa drug dissolved (in 15 and 30 min) and the *in vivo* parameters reported previously for I and II.

As reported previously, the greatest bioavailability difference among the seven products was observed for the C_{max} parameter for I, for which good correlation was shown with the percent of I dissolved in 30 min (as measured by HPLC). The results of this study also show good correlation ($r = 0.83$, $p < 0.05$) between C_{max} for I and percent of IV dissolved in 30 min, as shown in Fig. 1. Thus, the UV method can be employed for studying the dissolution of trisulfapyrimidine suspensions. The method offers certain advantages over the HPLC procedure in that it is more rapid, less expensive, readily available in most laboratories, and more easily applicable to automation technology. Except for the fact that it could not detect differences in the individual sulfa components of trisulfapyrimidines, the UV method was found to be suitable for the determination of dissolution properties of commercial products.

ACKNOWLEDGMENTS

This work was supported by Food and Drug Administration contract 223-76-3010.

REFERENCES

(1) Y. Langlois, M. A. Gagnon, and L. Tetreault, *J. Clin. Pharmacol.*, **12**, 196 (1972).

(2) V. Bernareggi, G. Bugada, A. Cassola, G. Levi, and F. Moncalvo, *Boll. Chim. Farm.*, **112**, 177 (1973).

(3) S. A. Khalil, M. A. Moustafa, A. R. Ebian, and M. M. Motawi, *J. Pharm. Sci.*, **61**, 1615 (1972).

(4) M. J. Taraszka and R. A. Delor, *J. Pharm. Sci.*, **58**, 207 (1969).

(5) G. R. VanPetten, G. C. Becking, R. J. Withey, and H. F. Lettau, *J. Clin. Pharmacol.*, **11**, 27 (1971).

(6) G. R. VanPetten, G. C. Becking, R. J. Withey, and H. F. Lettau, *J. Clin. Pharmacol.*, **11**, 35 (1971).

(7) R. J. Withey, G. R. VanPetten, and H. F. Lettau, *J. Clin. Pharmacol.*, **12**, 190 (1972).

(8) G. L. Mattok and I. J. McGilveray, *J. Pharm. Sci.*, **61**, 746 (1972).

(9) L. Mathur, J. M. Jaffe, R. I. Poust, H. Barry, III, T. J. Goehl, V. P. Shah, and J. L. Colaizzi, *J. Pharm. Sci.*, **68**, 699 (1979).

(10) T. J. Goehl, L. Mathur, J. D. Strum, J. M. Jaffe, W. H. Pitlick, V. P. Shah, R. I. Poust, and J. L. Colaizzi, *J. Pharm. Sci.*, **67**, 404 (1978).

(11) "The United States Pharmacopeia," 20th rev., U.S. Pharmacopeial Convention, Rockville, Md., 1980, p. 959.

Quantitative Assessment of the Effect of Some Excipients on Nitrazepam Stability in Binary Powder Mixtures

P. R. PERRIER and U. W. KESSELRING ˣ

Received January 25, 1982, from the *Laboratoire d'Analyse Pharmaceutique, Ecole de Pharmacie, CH-1005 Lausanne, Switzerland.* Accepted for publication August 24, 1982.

Abstract □ The decomposition rate constants, normalized for dilution and relative specific surface effects, of nitrazepam in simple binary powder mixtures with talcum, lactose·H_2O, microcrystalline cellulose, corn starch, mannitol, and saccharose are shown to be linearly related to the nitrogen adsorption energy of the excipients.

Keyphrases □ Nitrazepam—effect of excipients on stability in binary powder mixtures □ Excipients—effect on nitrazepam stability in binary powder mixtures

Recently, considerable effort has been made to precisely describe the chemical properties of excipients and how these excipients influence the technical and biopharmaceutical characteristics of the dosage forms. Excellent reviews list the "inert compounds" of pharmaceutical preparations (1), describe the difficulties concerning the "choice of excipients for international use" (2), "the influence of excipients on the design and manufacture of tablets and capsules" (3), and the "problems of drug interactions with excipients" (4). Many studies describe the influence of excipients, *e.g.* the acid-catalyzed decomposition of digoxin by montmorillonite (5), the effect of water adsorption properties of silica gel on the stability and the biological availability of ascorbic acid (6), and the influence of the solubility of some excipients on *in vitro* and *in vivo* properties of bendroflumethiazide tablets (7). Additional references were cited by Carstensen (8, 9).

0022-3549/83/0900-1072$01.00/0

Table I—Sample Description, Nitrogen Adsorption Energies and Decomposition Rate Constants [a]

Excipient	Density, g/cm³	Specific Surface (Σ), m²/g	$\frac{\Sigma_I}{\Sigma_e}$	Dilution Factor[b], $\frac{C_e}{C_I} = \frac{100 - C_I}{C_I}$	10^3k, day⁻¹	$10^3k_{0.5}\frac{\Sigma_I}{\Sigma_e}$, day⁻¹	E_{ads} (N_2), kcal/g
Talcum	2.841	2.53	0.451	199.3	6.11	2.77	2.04
Lactose·H_2O	1.545	2.15	0.530	204.5	8.86	4.59	2.00
Microcrystalline cellulose	1.530	1.39	0.820	105.8	5.04	7.81	1.90
Corn starch	1.504	0.55	2.073	199.2	5.31	11.1	1.87
Mannitol	1.486	0.45	2.533	200.8	5.67	14.3	1.78
Saccharose	1.587	0.28	4.071	199.4	4.44	18.1	1.74
Nitrazepam	1.398	1.14					

[a] These data were normalized to 0.5% dilution, and corrected for surface effect, (Σ_I/Σ_e), of nitrazepam, I, mixed with various excipients, e, stored at 70° and 60% relative humidity. [b] Expressed in terms of C_I, mg of nitrazepam, and C_e, mg of excipient per 100 mg of sample.

BACKGROUND

No systematic approach has been made to quantitatively study the so-called "inertness" of excipients. The work reported here is a first attempt to assess quantitatively (under well-defined conditions) the influence of some commonly used excipients on nitrazepam stability to find some parameter(s) which permit an objective comparison of the inertness of excipients.

Assuming a pseudo-first-order degradation, it has been shown that the logarithm of the nitrazepam decomposition rate constant is proportionally related to the inverse of absolute temperature and to the relative humidity of the environment (10). Other parameters to be considered are the dilution of the active ingredients and the relative specific surface area of the components of the system.

It is assumed that the slight concentration differences in the individual samples used in this study (<5%, except for the cellulose system, where the nitrazepam concentration was 1%, as compared with 0.5% in the other samples) may be linearly normalized[1].

These parameters must all be known and taken into account for further discussion and eventual elucidation of their influence on reaction mechanism. Because direct chemical reaction with the so-called "inert" excipients can be excluded in most cases, the hypothesis is formulated that the solid-state nitrazepam decomposition might be treated in analogy to heterogeneous catalysis reactions (11) whose basic steps are:

1. diffusion of the reactant toward the catalyst;
2. adsorption of the reactant onto the catalyst;
3. reaction of the adsorption complex to yield the product;
4. desorption of the product from the catalyst;
5. diffusion of the product away from the catalyst.

Anyone of these steps can be rate controlling for a given process, but not all the steps are necessarily involved in all decomposition reactions encountered in solid-state pharmaceutical dosage forms.

Before elucidating reaction mechanisms it would seem reasonable to study the role of water and to find out whether the reacting water molecules are in the gaseous, liquid, or some intermediate state, and whether it is possible to define a quantity of "water available for reaction" according to the following equation:

$$A_{sol} + (H_2O)_n \cdot B \rightarrow C_{sol} + D_{sol} + B \cdot (H_2O)_{n-1}$$

The difficulty of evaluating hygroscopicity for pharmaceutical solids has recently been described by van Campen *et al.* (12).

Also, the adsorption properties of the aerosol play an important role in nitrazepam stability (13).

EXPERIMENTAL

Materials—Nitrazepam (1,3-dihydro-7-nitro-phenyl-2*H*-1,4-benzodiazepin-2-one)[2], microcrystalline cellulose[3], talcum[4], mannitol[4], lactose·H_2O[4], cornstarch[4], and saccharose[4] were supplied commercially. Microcrystalline cellulose was used as received, all other excipients were of Pharmacopoea Helvetica VI quality. Adsorption isotherms and specific surfaces were determined with nitrogen (purity: 99.998%)[5].

Sample Preparation and Storage Conditions—Individual 800-mg samples containing 4 mg (0.5%) of nitrazepam were prepared by carefully mixing the constituents and avoiding any alteration of the granulometric characteristics. The samples were stored in climatic chambers[6] at constant relative humidity (60 ± 2%) and temperature (70 ± 0.5°).

Density and Specific Surface Area Determinations—True density values were obtained by means of a commercial pycnometer[7] measuring the helium gas or air volume displacement by the dried sample with a precision of 0.02 ml for a total volume of 15 ml. The specific surface area and the nitrogen energy of adsorption on the excipients were obtained by means of a homemade manifold, calculated according to the BET theory (14). The precision of the surface values obtained by nitrogen adsorption at 77°K is 1% for surfaces smaller than 1 m^2g^{-1} and better than 1% for surfaces larger than 1 m^2g^{-1}.

Assay—The decomposition of nitrazepam has been followed by HPLC using a liquid chromatograph[8] with a dualwave UV detector linked to an electronic integrating recorder[9] and fitted with a silica-filled column

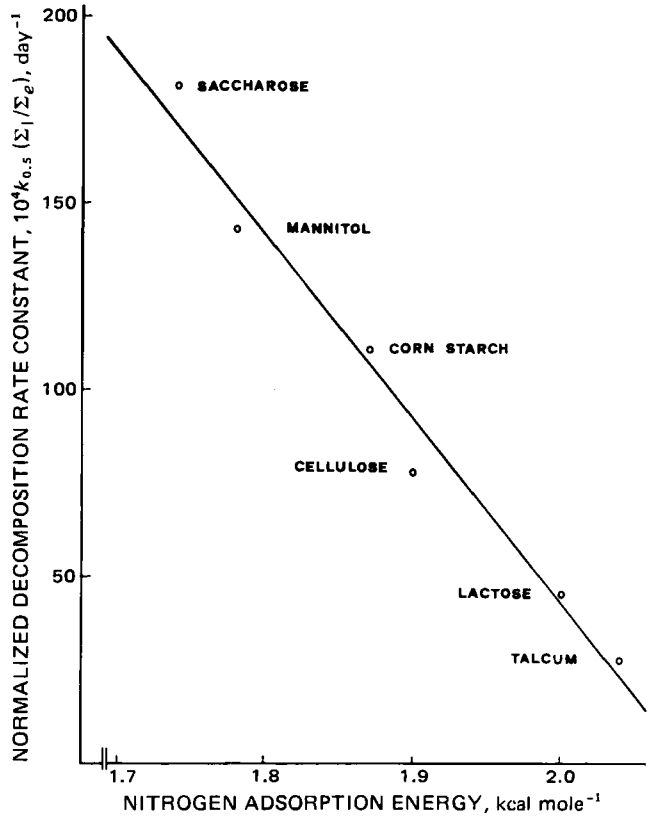

Figure 1—*Normalized decomposition rate constants of nitrazepam in relation to the nitrogen adsorption energy of various excipients.*

[1] Unpublished results from this laboratory; manuscript in preparation.
[2] F. Hoffmann-La Roche and Co. S.A., CH-4000 Basel, Switzerland.
[3] Avicel PH 101, Interchemie A.G., CH-8001 Zürich, Switzerland.
[4] Siegfried A.G., CH-4800 Zofingen, Switzerland.
[5] $N_2$48, Air Liquide Co., CH-1211 Genève, Switzerland.
[6] Voetsch VTKTR and VTKTR 125S, Heraeus-Laborgeräte S.A., CH-1227 Carouge-Genève, Switzerland.
[7] Air Comparison Pycnometer model 930, Instrumenten Gesellschaft A.G., CH-1227 Carouge-Genève, Switzerland.
[8] Liquid Chromatograph Spectra-Physics model 3500, Spectra-Physics A.G., CH-4054 Basel, Switzerland.
[9] Minigrator, Spectra-Physics A.G., CH-4054 Basel, Switzerland.

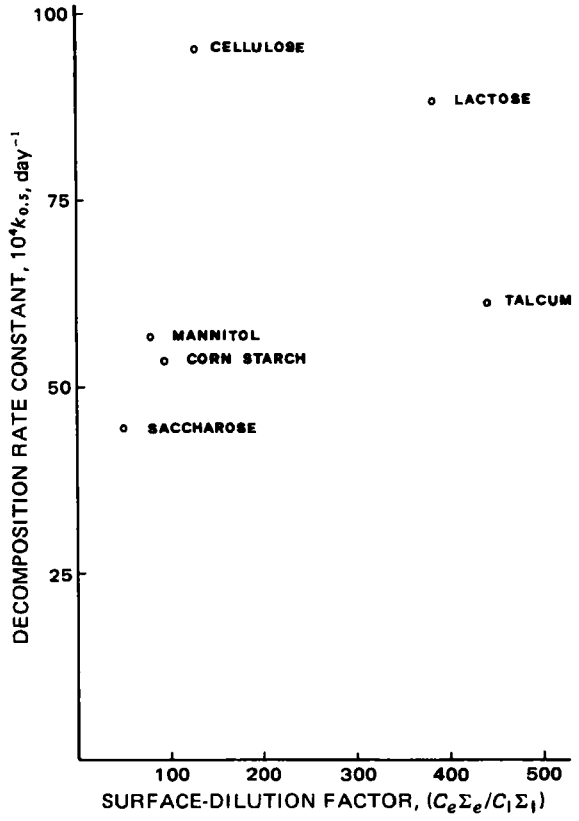

Figure 2—*Decomposition rate constants of nitrazepam as a function of the surface-dilution factor.*

(0.3 × 25 cm)[10]. To maintain column efficiency a precolumn of 0.3 × 5 cm, with identical filling, served as the filter. Operating conditions were as follows: mobile phase composition was *n*-hexane–chloroform–methanol (83.25:12.5:2.25), flow rate was 1.8 ml/min at a pressure of ~79 atm.

Antipyrine (2,3-dimethyl-1-phenyl-3-pyrazolin-5-one) at a concentration of 1.063×10^{-3} moles/liter served as the internal standard. The linearity range of nitrazepam was from 0.04 to 4 μg. Recovery of nitrazepam at 0.5% in microcrystalline cellulose was >98%, and the precision obtained was better than 1% for assays of amounts of I >0.04 μg and better than 2% for quantities <0.04 μg.

RESULTS AND DISCUSSION

Based on the experimental results obtained (Table I) the following linear relationship was established:

$$10^3 k_{0.5} \frac{\sum_I}{\sum_e} = 102 - 49.0\, E_{ads}(N_2) (r^2 = 0.976 \text{ for } n = 6)$$

where $k_{0.5}$ is the decomposition rate constant for a sample containing exactly 0.500% nitrazepam, Σ is the specific surface (m^2g^{-1}), (I is nitrazepam and *e* is the excipient), and $E_{ads}(N_2)$ is the nitrogen adsorption energies in which the nitrazepam decomposition constant decreases proportionally to the increase of nitrogen adsorption energy on the six excipients (Fig. 1).

If the contact surface were the only influence an excipient had, and assuming similar excipient surface coverage by the drug, then all decomposition rate constants of nitrazepam, once corrected for dilution and relative specific surface areas of the sample components, should be identical, whatever excipients are used. As can be seen in Fig. 2, this is not the case; each excipient has its own specific and/or nonspecific influence on the observed rate. In the case of hydrolytic decomposition and according to the law of mass action, the amount of water present as a reagent (as long as not in excess) has a direct influence on the reaction rate. At present there is no possibility of determining quantitatively and directly the amount of water available and usable for reaction in a solid-state sample and the exact physical state of the reacting water. There is, however, no doubt that both the physical and the structural states of the water are strongly influenced by adsorption properties of the excipients. In the case of nitrazepam decomposition, the reaction rate diminishes with increasing nitrogen adsorption energy of the excipients.

From structural considerations, there is no reason to expect that the nitrazepam adsorption energy would be affected by the various excipients used. Since the only other reactant is water, a hypothetical conclusion can be drawn that the availability, *i.e.* reactivity, of water is the important parameter in the experimental system considered and that the water-binding energy to the excipients is the important factor to look at. Since only adsorbed water molecules may react, and their reactivity is inversely related to their adsorption energy, it is necessary either to establish the relationship between E_{ads} (N_2) and E_{ads} (H_2O), the adsorption energy of (for the reaction available) water, and/or to determine the relative water binding forces to the excipient.

[10] Spherisorb Silica 5 μm, SS-3-250-S5W, Spectra-Physics A.G., CH-4054 Basel, Switzerland.

REFERENCES

(1) J. Cooper, *Drug Dev. Ind. Pharm.*, **5**, 293 (1979).

(2) H. Hess, *Drug Dev. Ind. Pharm.*, **3**, 491 (1977).

(3) T. M. Jones, *Drug Cosmet. Ind.*, **(1979)** 40.

(4) P. H. Stahl, "Proceedings of the 39th International Congress of Pharmaceutical Science," (FIP, Brighton, Sept. 3–7, 1979), Elsevier, North-Holland Biomedical Press, 1980, pp. 265–280.

(5) L. S. Porubcan, S. Born, J. L. White, and S. L. Hem, *J. Pharm. Sci.*, **68**, 358 (1979).

(6) E. de Ritter, L. Magid, M. Osadca, and S. Rubin, *J. Pharm. Sci.*, **59**, 229 (1970).

(7) M. H. Rubinstein and M. Birch, *Drug Dev. Ind. Pharm.*, **3**, 439 (1977).

(8) J. T. Carstensen, "Pharmaceutics of Solids and Solid Dosage Forms," Wiley, New York, N.Y., 1977, pp. 182–206.

(9) J. T. Carstensen, "Solid Pharmaceutics: Mechanical Properties and Rate Phenomena," Academic, New York, N.Y., 1980, pp. 237–245.

(10) D. Genton and U. W. Kesselring, *J. Pharm. Sci.*, **66**, 676 (1977).

(11) J. Fripiat, J. Chaussidon, and A. Jelli, "Chimie Physique des Phénomènes de Surface," Masson, Paris, 1971, pp. 201–227.

(12) L. van Campen, G. Zografi, and J. T. Carstensen, *Int. J. Pharm.*, **5**, 1 (1980).

(13) J. Czaja and J. B. Mielck, *Pharm. Acta Helv.*, **57**, 144 (1982).

(14) S. Brunauer, P. H. Emmet, and E. Teller, *J. Am. Chem. Soc.*, **60**, 309 (1938).

ACKNOWLEDGMENTS

The authors are indebted to F. Hoffmann-La Roche & Co. S.A., Basel, Switzerland, and to the Swiss National Foundation for Scientific Research (Grant 3.730.72) who in part supported this work.

Kinetics and Mechanism of the Basic Hydrolysis of Indomethacin and Related Compounds: A Reevaluation

ANTONIO CIPICIANI *, CYNTHIA EBERT ‡, PAOLO LINDA §x, FULVIO RUBESSA ‡, and GIANFRANCO SAVELLI *

Received June 18, 1982, from the *Dipartimento di Chimica, Università di Perugia, Italy, the ‡Istituto di Chimica Farmaceutica, and the §Istituto di Chimica, Università di Trieste, Italy. Accepted for publication August 25, 1982.

Abstract □ The kinetics of the hydrolysis of indomethacin and related compounds were studied in an alkaline medium at 25°. The pseudo-first-order rate constants were evaluated from log absorbance *versus* time plots in the ultraviolet. These compounds showed a second-order rate constant at low concentrations of hydroxide ion and a first-order rate constant at higher concentrations of hydroxide ion.

Keyphrases □ Indomethacin—kinetics of the hydrolysis in alkaline medium □ Kinetics—hydrolysis of indomethacin

The kinetics of the alkaline hydrolysis of indomethacin [1-(4-chlorobenzoyl)-5-methoxy-2-methyl-indole-3-acetic acid (I)] have been investigated in several studies.

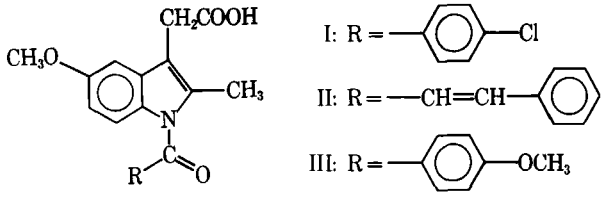

Hajratwala and Dawson (1) measured the apparent first-order rate constants in the pH 11–12 range at different temperatures, and suggested that the experimental data were in agreement with a mechanism involving the reaction of the monodissociated species of indomethacin with the hydroxide ion and postulated a rate law of the type: $k_{obs} = k_1[OH^-]$. Krasowska (2) described a linear relationship between log k_{obs} *versus* pH in the range of pH 7–10 at 50, 60, and 70°, but no conclusions were drawn on the mechanism of the hydrolysis of I.

The aim of this study was to reinvestigate the mechanism of the basic hydrolysis of I and to compare its behavior with that of simpler models in view of our previous results on related compounds (3–5).

A variety of amides undergo basic hydrolysis, as is shown in Scheme I.

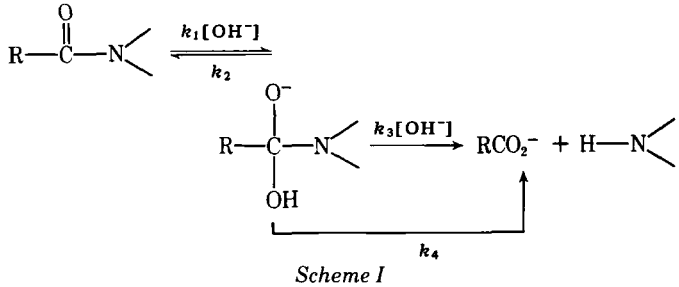

Scheme I

According to the structure of the amide and the pH of the medium, the rate-determining step of the reaction is (*a*) the attack of hydroxide ion on the amide (k_1) and (*b*) the decomposition of the tetrahedral intermediate to products either uncatalyzed (k_4) or catalyzed by hydroxide ion (k_3). Equation 1 represents the rate law for the mechanistic Scheme I.

$$k_{obs} = \frac{k_1k_4[OH^-] + k_1k_3[OH^-]^2}{k_2 + k_4 + k_3[OH^-]} \qquad \text{(Eq. 1)}$$

Many *N*-acyl derivatives of pyrroles, indoles, and carbazoles show a second-order rate constant at low concentrations of hydroxide ion, and a first-order rate constant at higher concentrations of base (3–5). Only the hydrolysis of *N*-(4-nitrobenzoyl)pyrrole was found to be first-order in hydroxide ion at all base concentrations (6). This behavior was ascribed to the electronic polarization by the nitro group destabilizing the carbonyl of the substrate, reducing k_2 and increasing k_1. These electronic effects enlarge the ratio k_3/k_2 and the formation of the tetrahedral intermediate becomes the rate-determining step.

EXPERIMENTAL

Materials—All materials were analytical grade; water double-distilled in glass was used throughout. Indomethacin[1], cinmetacin[2] (II), and 1-(4-methoxybenzoyl)-5-methoxy-2-methyl-indole-3-acetic acid (III)[3] were used without further purification.

1-(4-Chlorobenzoyl)indole (IV)—A solution of 1.2 g (10 mmoles) of indole and 34 mg (0.1 mmole) of tetrabutylammonium hydrogen sulfate in 30 ml of dichloromethane was stirred at room temperature while 1 g of finely powdered sodium hydroxide was added, followed by a solution of 2.6 g (15 mmoles) of 4-chlorobenzoyl chloride in 10 ml of dichloromethane over a 15-min period. The mixture was cooled in a water bath, stirred for 20 min, and the product was removed by filtration. This material was recrystallized from *n*-hexane to give IV as white crystals, mp 114–115° [lit. 114.5–115.5° (7, 8)] IR (mineral oil): 1680 cm^{-1} (C=O); NMR (deuterochloroform): 6.6 (d, J = 4 Hz, 1, indole-3 proton), 7.2–7.9 (m, 8, aromatic protons), 8.3–8.5 ppm (m, 1, indole-7 proton)[4].

Kinetic Studies—A stoppered quartz cell containing an aqueous sodium hydroxide solution (3 ml) was thermostated at 25 ± 0.1° for 20 min within the cell compartment. The reaction was initiated by adding 10–20 μl of the substance dissolved in acetonitrile. The initial concentration of the substrates in the reaction cell was in the order of 10^{-4}–10^{-5} *M*. An ionic strength of 0.2 was maintained constant by adding sodium chloride.

Absorbance (against an appropriate blank) was recorded as a function of time at 325 nm for I, 320 nm for II, 315 nm for III, and 305 nm for IV[5]. Pseudo-first-order rate constants (k_{obs}) were calculated using regression analysis. The correlation coefficients were between 0.993–0.999.

The products of hydrolysis were examined by comparing the final spectra with those obtained from a solution of indoles and appropriate carboxylic acid under conditions identical to those of the kinetic experiments.

Data Treatment—The rate constants for individual steps in the hydrolysis reaction were evaluated according to the method of Kershner and Schowen (9)[6].

RESULTS AND DISCUSSION

The effects of hydroxide ion concentration on the apparent first-order rate constant, k_{obs}, for the indole derivatives are shown in Table I.

[1] Merck Sharp & Dohme, Rahway, N.J.
[2] Chiesi Farmaceutici, Parma, Italy.
[3] Compagnia di Ricerca Chimica, San Giovanni al Natisone, Italy.
[4] IR spectra were recorded on a Perkin-Elmer model 399 spectrophotometer; NMR spectra were registered on a JEOL 60 MHz spectrometer.
[5] Perkin-Elmer model 552 spectrophotometer.
[6] Hewlett-Packard model 9825A Computer.

0022-3549/83/0900-1075$01.00/0

Table I—Effect of the Hydroxide Ion Concentration on the Pseudo-First-Order Rate Constant at 25.0 ± 0.1°

$[OH^-]$ 10^3 M	k_{obs} 10^4, sec^{-1} [a]			
	I	II	III	IV
1.0	2.21	0.471	0.269	15.1
1.5		0.906		
2.0	4.05	1.23	0.633	
2.5		1.63		40.9
3.0	6.49		0.978	
4.0	8.75	2.69	1.42	
5.0	13.2		1.81	96.3
6.0		4.31		
7.0	17.5			
7.5		5.51	2.74	151
10.0	27.4	7.58	3.98	209
12.4		10.0		
15.0	42.6		3.85	322
17.3		14.4		
20.0	60.3		8.51	427
21.8		18.2		
25.0	77.1	21.4	10.7	
30.0	89.6		12.8	633
31.7		27.8		
34.6			15.6	
40.0	128	35.6	17.5	
44.5		39.8	20.3	
50.0	162	45.1	22.9	1057

[a] Average of two or three runs.

Plots of rate constant–hydroxide ion concentration *versus* hydroxide ion concentration are shown in Fig. 1. The mechanism of hydrolysis shown in Scheme I is the most probable. Equation 1 represents the rate law for this mechanism. The rate constants for the single steps are reported in Table II together with relevant data presented in our previous papers [*i.e.*, 1-(4-chlorobenzoyl)pyrrole (V) and 1-(4-methoxybenzoyl)pyrrole (VI)] (3). The statistical treatment showed that k_4 (the rate constant for the water-catalyzed decomposition of the tetrahedral intermediate) is negligible.

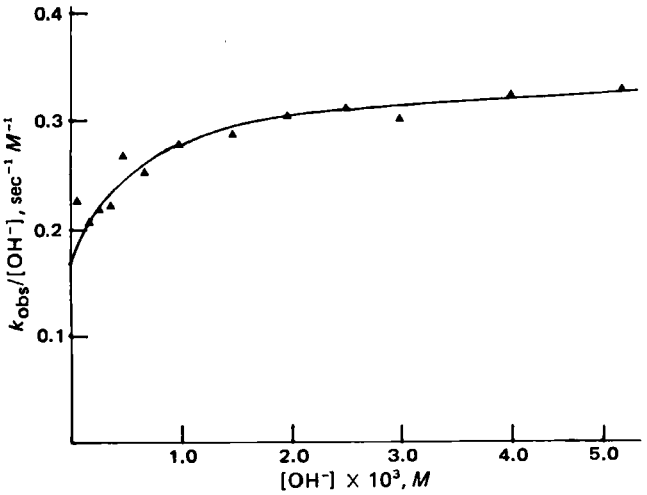

Figure 1—*Effect of concentration of hydroxide ion on the hydrolysis of indomethacin at 25.0 ± 0.1° and ionic strength 0.2.*

Table II—Rate Constants for the Hydroxide Ion-Catalyzed Hydrolysis in Water at 25.0 ± 0.1°

	k_1, M^{-1} sec^{-1}	$k_1k_3k_2$, M^{-2} sec^{-1}	k_3k_2, M^{-1}
I	0.34	120	350
II	0.09	54	600
III	0.05	35	700
IV	2.20	2200	1000
V[a]	5.50	4900	900
VI[a]	1.10	800	700

[a] Data from Ref. (3).

From the data one can observe that 1-(4-chlorobenzoyl)indole (IV) shows a value of k_1 (the rate constant of formation of the tetrahedral intermediate) about 7 times higher than I, and this can be ascribed to steric inhibition by the methyl group in the 2-position of I to the attack of the hydroxide ion, since this reaction appears to be more sensitive to steric effects than to electronic effects (3–5). Similarly steric effects affect the k_3/k_2 ratio favoring the decomposition of the intermediate rather than the return to the reactants. Furthermore, electronic effects resulting from substitution in the benzoyl ring of the indomethacin series closely parallel those in the pyrrole series, as shown by the fact that the k_1 relative ratio of I–III is ~7 and is quite similar to that of V–VI (~5). Finally, the fact that the k_3/k_2 values are of the same order of magnitude shows that partitioning of the tetrahedral intermediate to products is the result of a subtle balance among steric, electronic, and leaving-group effects.

In conclusion, the kinetics of hydrolysis of indomethacin and cinmetacin, are similar to that of analogous models used in this study. A knowledge of the mechanism of hydrolysis of simple molecules is important to rationalize the behavior of more complex compounds.

REFERENCES

(1) B. R. Hajratwala and J. E. Dawson, *J. Pharm. Sci.*, **66,** 27 (1977).

(2) H. Krasowska, *Acta Pharm. Jugoslav.*, **24,** 193 (1974).

(3) A. Cipiciani, P. Linda, and G. Savelli, *J. Heterocycl. Chem.*, **16,** 673 (1979).

(4) A. Cipiciani, P. Linda, and G. Savelli, *J. Heterocycl. Chem.*, **16,** 677 (1979).

(5) A. Cipiciani, P. Linda, and G. Savelli, *J. Heterocycl. Chem.*, **20,** 247 (1983).

(6) F. M. Menger and J. A. Donohue, *J. Am. Chem. Soc.*, **95,** 432 (1973).

(7) T. Itahara, *Synthesis*, **1979,** 151.

(8) D. R. Julian and G. D. Tringham, *J. Chem. Soc. Chem. Commun.*, **1973,** 13.

(9) L. D. Kershner and R. L. Schowen, *J. Am. Chem. Soc.*, **93,** 2014 (1971).

ACKNOWLEDGMENTS

The authors thank the various companies for the gift of the drug samples and the Consiglio Nazionale delle Ricerche (Roma) for financial support.

Noninvasive Assessments of the Percutaneous Absorption of Methyl Nicotinate in Humans

RICHARD H. GUY *x, RONALD C. WESTER ‡, ETHEL TUR ‡, and HOWARD I. MAIBACH ‡

Received June 11, 1982, from the **School of Pharmacy* and ‡*Department of Dermatology, School of Medicine, University of California–San Francisco, San Francisco, CA 94143.* Accepted for publication August 16, 1982.

Abstract □ Percutaneous penetration of the vasodilator methyl nicotinate (methyl 3-pyridinecarboxylate) has been monitored *in vivo* in humans with the noninvasive techniques of laser Doppler velocimetry and photopulse plethysmography. These optical methods use different technologies to generate a voltage output which is related to perfusion of the cutaneous microcirculation. The procedures are therefore sensitive to the pharmacologic stimulus and duration of local vasodilation. Following topical application of methyl nicotinate, excellent correlation was found between the response of both methods and the visual observation of erythema. Lower drug concentrations delayed the onset and magnitude of the response and shortened the time period for which elevated microperfusion was observed. These techniques appear to provide a useful noninvasive assessment of the time course of drug behavior in the region of skin to which topical application is made.

Keyphrases □ Methyl nicotinate—noninvasive assessments of percutaneous absorption, laser Doppler velocimetry, photopulse plethysmography, pharmacokinetics □ Absorption, percutaneous—of methyl nicotinate, noninvasive assessments by laser Doppler velocimetry and photopulse plethysmography, pharmacokinetics □ Pharmacokinetics—of percutaneous absorption of methyl nicotinate in humans, noninvasive assessments by laser Doppler velocimetry and photopulse plethysmography

Presently, there exists limited understanding of the kinetics associated with drug absorption into the skin, retention or metabolism of compounds within the tissue, and subsequent elimination into the systemic circulation. Such knowledge, however, is valuable both for devising rational dermatological chemotherapy and for topical dosage form design and optimization. In this paper two noninvasive procedures for monitoring blood perfusion through the cutaneous microcirculation are discussed, and methodology is suggested that may improve pharmacokinetic and pharmacologic measurement of percutaneous absorption.

The techniques employed are laser Doppler velocimetry (LDV) and photopulse plethysmography (PPG). The methodologies employ different optical principles to generate an output related to either velocity (LDV) or amount (PPG) of cutaneous blood vessel perfusion. In 1975, it was shown that LDV could indicate changes in microvascular perfusion (1). Validation and development of the method for clinical evaluation of local blood flow in the skin surface (2–4) was followed by its application to assess perfusion changes in response to injection trauma (5) and its employment as an indicator of skin blood flow (as compared with heater power) during transcutaneous oxygen monitoring (6). A recent review (7) has summarized the current technological and theoretical status of the procedure and has discussed possible clinical applications.

The PPG technique has been used for many years to assess skin blood flow (8), alone and in conjunction with other procedures, to assess various physiological functions. Although there are examples in the literature which have indicated the ability of PPG to demonstrate drug-induced changes in skin blood flow (9–12), there has been no attempt to apply the method specifically to follow the passage of drug into the body following topical administration.

To characterize and test the two techniques, the percutaneous absorption of methyl nicotinate in humans has been considered. This nicotinic acid ester crosses the skin rapidly and elicits a distinctive erythema (13), the time of onset of which is reportedly a function of drug concentration (14). After its appearance, erythema intensity first increases to a maximum, and the area of redness expands, before gradually fading away and becoming no longer visually detectable (15, 16).

EXPERIMENTAL

LDV experiments were performed with a recently developed capillary perfusion monitor[1]. The method uses the Doppler principle. Light at 632.8 nm from a 5-mW helium–neon laser is transmitted to the skin through a quartz optical fiber. The light is backscattered from stationary skin components and by erythrocytes moving in the dermal capillaries[2], which are encountered as the radiation penetrates to a depth of 1–1.5 mm. A second optical fiber collects the reflected light and the electronic configuration of the instrument then separates out the frequency-shifted (*i.e.*, Doppler) component and converts it to a single flow parameter, which is registered as a voltage output. That this quantity is related to peripheral cutaneous perfusion, as measured by other means, has been shown (4). The optical fibers supplying and detecting the radiation are supported in a small, essentially cylindrical probe (1.9-cm diameter, 0.5-cm height) which is held securely to the skin surface by double-sided adhesive tape.

Experiments with PPG utilized a photoplethysmograph[3] in conjunction with two photopulse probes[4] and a dual-channel recorder[5]. As with LDV, information is collected by a small (2 × 1 × 0.7-cm) probe attached with tape to the skin surface. In this case, however, the optical source is a diode (LED) emitting IR radiation at 800–940 nm. A phototransistor positioned in the probe beside the LED detects the reflected part of the incident source, and the photoplethysmograph then converts this information for display as a fluctuating voltage on the chart recorder. The frequency of the input radiation covers wavelengths strongly absorbed by hemoglobin. It follows that changes in blood volume in the region of skin under the probe cause the PPG output to change because the percentage of incident radiation absorbed is altered. The penetration depth of the light from the PPG probe is stated to be similar to that of the LDV apparatus, 1–2 mm. Whereas the recording displayed by the LDV unit can be damped so that output oscillations due to the heartbeat can be eliminated, this is not the case with the PPG instrument. The results from the latter appear as a series of pulses on which, at high sensitivities, the dicrotic notch may be observed (Fig. 1).

Percutaneous penetration experiments were carried out on two healthy male volunteers. Methyl nicotinate[6] (I) solutions of 150, 15, and 1.5 m*M* were prepared in distilled water and used directly. The application procedure was as follows: A 1-cm diameter standard test patch[7] was saturated

[1] Medpacific LD5000, Medpacific Corp., Seattle, Wash.
[2] Medpacific, technical information.
[3] Medasonics PPG-13, Medasonics, Mountain View, Calif.
[4] Medasonics PH77, Medasonics, Mountain View, Calif.
[5] Medasonics R12A, Medasonics, Mountain View, Calif.
[6] Sigma Chemical Co., St. Louis, Mo.
[7] Al-test, Imeco-ab, Södertälje, Sweden.

0022-3549/83/0900-1077$01.00/0

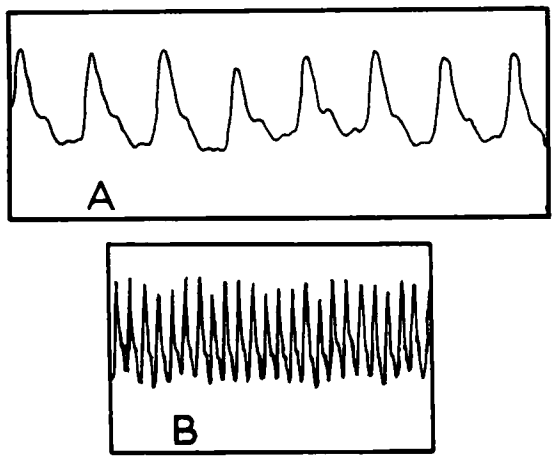

Figure 1—*Typical pulsatile output from the PPG apparatus (probe attached to the forefinger). The dicrotic notch is visible at both (A) fast (25 mm/sec) and (B) slow (5 mm/sec) chart recorder speeds.*

with the appropriate solution of I and applied with tweezers to the midpoint of the flexor aspect of the subject's forearm. The patch was in contact with the skin for 15 sec before being removed; any excess solution left on the skin was wiped away with a tissue.

The LDV or PPG probe was then placed directly over the drug application site (the center of the probe being coincident with the position occupied by the center of the patch) and recordings were made from this point. For LDV measurements, continuous readings were taken throughout the duration of an experiment (~1 hr). For PPG, data collection was continual for the first 10–15 min and thereafter, 30-sec recordings were made every 3–5 min for the remainder of the run. The PPG procedure is much more sensitive to subject movement than LDV and it was found that periodic measurement as described provided both volunteer comfort and measurement clarity.

With the PPG technique, for which there were two probes available, the second probe was positioned on the identical site on the other arm to which no drug was applied. This probe acted as a control to indicate whether any changes in the monitored outputs were induced by the apparatus alone in contact with the skin. On no occasion was there any change in output from the control site during the course of a normal experiment (of ~1-hr duration). Finally, in a separate set of experiments, the same drug application procedure was followed and the onset of erythema determined visually with no probe on the skin. Erythema onset was defined as the appearance of redness at the skin position to which the patch had been applied (14).

RESULTS AND DISCUSSION

The results are presented in Table I. Figure 2 shows a typical initial response to the drug observed with LDV, and in Fig. 3 the pattern of microperfusion changes detected by PPG during an experiment is summarized. Good correlation between erythema onset and instrument response was found for both techniques, and the expected concentration dependence of drug effect (*i.e.*, increased concentration, faster onset, and longer duration) was confirmed. Furthermore, there is potential to begin to quantify in an objective fashion both the initial response following

Table I—Summary of LDV and PPG Experimental Results [a]

Methyl Nicotinate Concentration, m*M*	Onset of LDV Response, sec	Onset of PPG Response, sec	Observed Onset of Erythema, sec	Decay Time of Response[b], min
Subject 1				
150	120	125	125	40–60
15	160	180	165	20–35
1.5	250	270	260	15–25
Subject 2				
150	135	150	180	40–60
15	300	325	370	30–50
1.5	615	635	645	20–35

[a] All data represent the average of duplicate or triplicate experiments (±10%). [b] Approximate time ranges covering the postapplication period between the start of the response decay and the return to baseline LDV or PPG output.

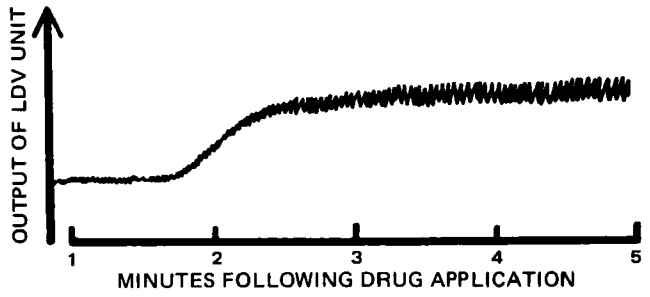

Figure 2—*Early time portion of a characteristic LDV response curve (Subject 1; applied concentration of methyl nicotinate = 150 m*M*).*

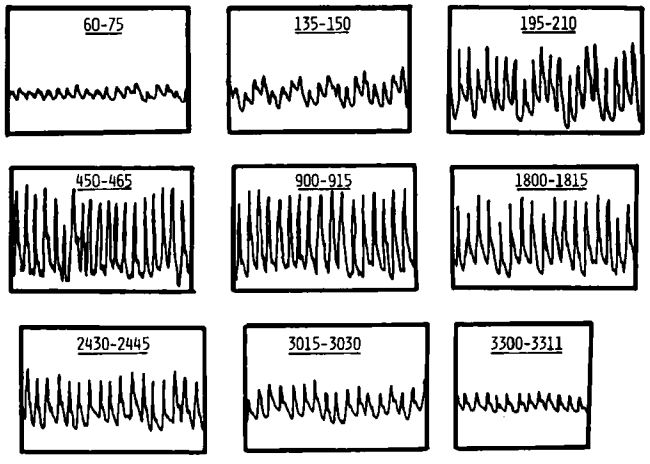

Figure 3—*PPG recording at various times (in seconds) after a 15-sec application of 150 m*M *methyl nicotinate to Subject 1.*

absorption (*e.g.*, Fig. 2) and the subsequent increase and eventual decay (Fig. 3) of the microcirculation stimulus. Certainly for the nicotinic acid esters, it is now possible to follow the latter part of the local time course of the drug.

An additional feature of the data is the demonstration that, within minutes, sufficient drug is able to penetrate and produce the threshold concentration necessary to elicit an observable pharmacological effect. Because of the design of these experiments, steady-state transport across the stratum corneum cannot be established, and conventional *in vivo–in vitro* penetration assessment parameters (*e.g.*, steady-state permeability coefficient and lag time) are not appropriate for describing the data. It is interesting, however, to note that classically measured lag times are often on the order of hours and always in significant excess of 2–10 min. It seems clear that the lag period between application and physiological response for methyl nicotinate must be quite different from the lag time necessary to establish a quasi-steady-state concentration profile across the barrier.

At present, it appears reasonable to suggest that the data reported here strongly hint that local cutaneous pharmacokinetics may prove accessible to study *in vivo* and that the noninvasive procedures described warrant further attention.

REFERENCES

(1) M. D. Stern, *Nature (London)*, **254**, 56 (1975).

(2) G. A. Holloway, Jr. and D. W. Watkins, *J. Invest. Dermatol.*, **69**, 306 (1977).

(3) D. W. Watkins and G. A. Holloway, Jr., *IEEE Trans. Biomed. Eng.*, **BME-25**, 28 (1978).

(4) M. D. Stern, D. L. Lappe, P. D. Bowen, J. E. Chimoskey, G. A. Holloway, Jr., H. R. Keiser, and R. L. Bowman, *Am. J. Physiol.*, **232**, H441 (1977).

(5) G. A. Holloway, Jr., *J. Invest. Dermatol.*, **74**, 1 (1980).

(6) L. Enkema, G. A. Holloway, Jr., D. W. Paraino, D. Harry, G. L. Zick, and M. A. Kenny, *Clin. Chem.*, **27**, 391 (1981).

(7) R. F. Bonner, T. R. Chen, P. D. Bowen, and R. L. Bowman, in "Scattering Techniques Applied to Supramolecular and Non-Equilibrium Systems," (NATO ASI Series B, Vol. 73), S. H. Chen, B. Chu, and R. Nossal, Eds., Plenum, New York, N.Y., 1981, pp. 685–702.

(8) A. V. J. Challoner, in "Non-Invasive Physiological Measurements, Vol. I," P. Rolfe, Ed., Academic, New York, N.Y., 1979, pp. 125–151.
(9) A. B. Hertzmann and W. C. Randall, *J. Appl. Physiol.*, **1**, 234 (1948).
(10) E. G. Cummings, *J. Invest. Dermatol.*, **53**, 64 (1969).
(11) P. Thune, *Acta Derm. Venerol.*, **51**, 261 (1971).
(12) C. Ramsay, *Br. J. Dermatol.*, **81**, 37 (1969).
(13) R. B. Stoughton, W. E. Clendenning, and D. Kruse, *J. Invest. Dermatol.*, **35**, 337 (1960).
(14) W. J. Albery and J. Hadgraft, *J. Pharm. Pharmacol.*, **31**, 140 (1979).
(15) R. B. Fountain, B. S. Baker, J. W. Hadgraft, and I. Sarkany, *Br. J. Dermatol.*, **81**, 202 (1969).
(16) R. H. Guy and H. I. Maibach, *Arch. Dermatol. Res.*, **273**, 91 (1982).

ACKNOWLEDGMENTS

Partial presentation of the work reported here was made at the 31st National Meeting of the APhA Academy of Pharmaceutical Sciences in Orlando, Florida, November 1981 and at the 43rd Annual Meeting of the Society for Investigative Dermatology in Washington, DC, May 1982.

The authors thank Medpacific, Inc. for the loan of the LDV apparatus and representatives of both Medpacific and Medasonics for their assistance and comments.

Stabilizing Effect of Fructose on Aqueous Solutions of Hydrocortisone

N. P. BANSAL, E. M. HOLLERAN, and C. I. JAROWSKI ˣ

Received July 1, 1982 from the *Department of Allied Health and Industrial Sciences, College of Pharmacy and Allied Health Professions and the School of Chemistry, St. John's University, Jamaica, NY 11439.* Accepted for publication August 26, 1982.

Abstract □ Accelerated stability studies (37°, 47°, and 57°) were conducted on buffered aqueous solutions (pH 7.4, 8.4, and 9.4) of hydrocortisone in the presence of various molar ratios of D-fructose. First-order degradation was observed. Significant improvement in hydrocortisone stability was seen in those solutions containing a 25 *M* excess of D-fructose. Hydrocortisone solutions containing dextrose, lactose, sucrose, sorbitol, propylene glycol, or glycerin in the same molar ratio were not stabilized.

Keyphrases □ Hydrocortisone—stability in aqueous buffers, stabilization by D-fructose □ Stability studies—hydrocortisone, stability in aqueous buffers, stabilization by D-fructose

A ketol side chain is present at the 17-position in the following therapeutically important glucocorticoids: cortisone, hydrocortisone, dexamethasone, prednisone, prednisolone, and 6-α-methylprednisolone. Removal of the ketol side chain results in a significant loss of therapeutic activity.

The reactivity of the ketol side chain of the adrenocorticosteroids is well documented. Base-catalyzed rearrangements and eliminations have been shown to occur under both aerobic and anaerobic conditions (1–5). Guttman and Meister (6) showed that at least three parallel first-order reactions were involved in the base-catalyzed degradation of prednisolone. Neutral and acidic degradation products were obtained. Caspi *et al.* (7) studied oxidative cleavage of the ketol side chain of cortisone with lead tetraacetate. Lewbart and Mattox (8) reported that trace amounts of copper in actinic glassware caused destruction of cortisone and related steroids.

Mauger *et al.* (9) followed the degradation of 21-hydrocortisone hemisuccinate at 70° in aqueous solutions buffered at pH 6.9, 7.2, and 7.6. The data obtained indicated that the overall kinetic pathway at each pH value could be interpreted as consecutive first-order reactions. The blue tetrazolium assay confirmed that the production of a species devoid of the ketol side chain at the 17-position occurred after the steroid alcohol was formed. The ketol group imparts reducing properties to the glucocorticoid molecules similar to those of fructose (Scheme I), which contains a similar ketol group. It was speculated that the presence of excess fructose in aqueous solutions of hydrocortisone (II) might retard the base-catalyzed degradation of the latter. The significance of the ketol group would be checked by using other polyols lacking this group.

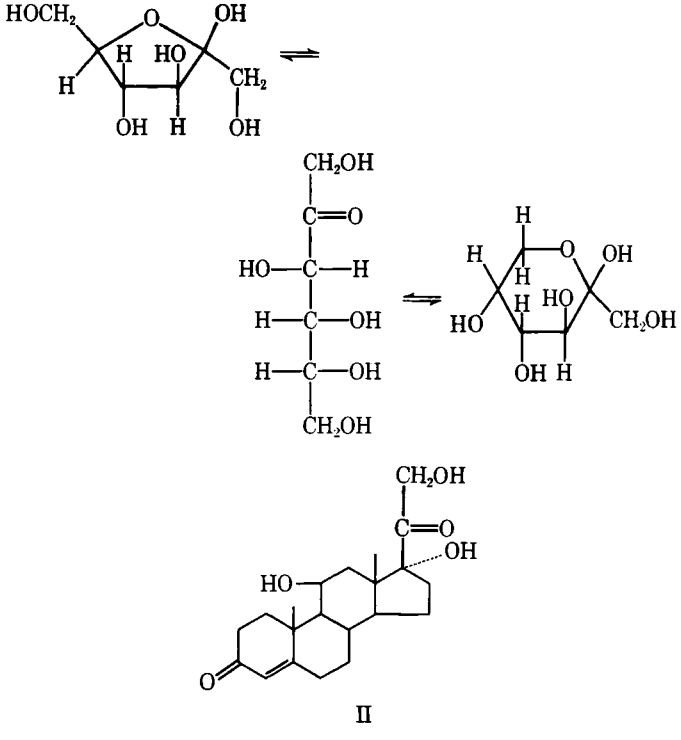

II

EXPERIMENTAL

Materials—The following were obtained from commercial sources: hydrocortisone, USP (lot 15C-6126)[1], blue tetrazolium[1], tetramethylammonium hydroxide[1], D-fructose[2], dextrose USP[3], glacial acetic acid

[1] Sigma Chemical Co., St. Louis, Mo.
[2] Pfaltz and Bauer, Inc., Flushing, N.Y.
[3] Mallinckrodt Chemical Works, St. Louis, Mo.

0022-3549/83/0900-1079$01.00/0

(8) A. V. J. Challoner, in "Non-Invasive Physiological Measurements, Vol. I," P. Rolfe, Ed., Academic, New York, N.Y., 1979, pp. 125–151.
(9) A. B. Hertzmann and W. C. Randall, *J. Appl. Physiol.*, **1**, 234 (1948).
(10) E. G. Cummings, *J. Invest. Dermatol.*, **53**, 64 (1969).
(11) P. Thune, *Acta Derm. Venerol.*, **51**, 261 (1971).
(12) C. Ramsay, *Br. J. Dermatol.*, **81**, 37 (1969).
(13) R. B. Stoughton, W. E. Clendenning, and D. Kruse, *J. Invest. Dermatol.*, **35**, 337 (1960).
(14) W. J. Albery and J. Hadgraft, *J. Pharm. Pharmacol.*, **31**, 140 (1979).
(15) R. B. Fountain, B. S. Baker, J. W. Hadgraft, and I. Sarkany, *Br. J. Dermatol.*, **81**, 202 (1969).
(16) R. H. Guy and H. I. Maibach, *Arch. Dermatol. Res.*, **273**, 91 (1982).

ACKNOWLEDGMENTS

Partial presentation of the work reported here was made at the 31st National Meeting of the APhA Academy of Pharmaceutical Sciences in Orlando, Florida, November 1981 and at the 43rd Annual Meeting of the Society for Investigative Dermatology in Washington, DC, May 1982.

The authors thank Medpacific, Inc. for the loan of the LDV apparatus and representatives of both Medpacific and Medasonics for their assistance and comments.

Stabilizing Effect of Fructose on Aqueous Solutions of Hydrocortisone

N. P. BANSAL, E. M. HOLLERAN, and C. I. JAROWSKI ˣ

Received July 1, 1982 from the *Department of Allied Health and Industrial Sciences, College of Pharmacy and Allied Health Professions and the School of Chemistry, St. John's University, Jamaica, NY 11439.* Accepted for publication August 26, 1982.

Abstract □ Accelerated stability studies (37°, 47°, and 57°) were conducted on buffered aqueous solutions (pH 7.4, 8.4, and 9.4) of hydrocortisone in the presence of various molar ratios of D-fructose. First-order degradation was observed. Significant improvement in hydrocortisone stability was seen in those solutions containing a 25 *M* excess of D-fructose. Hydrocortisone solutions containing dextrose, lactose, sucrose, sorbitol, propylene glycol, or glycerin in the same molar ratio were not stabilized.

Keyphrases □ Hydrocortisone—stability in aqueous buffers, stabilization by D-fructose □ Stability studies—hydrocortisone, stability in aqueous buffers, stabilization by D-fructose

A ketol side chain is present at the 17-position in the following therapeutically important glucocorticoids: cortisone, hydrocortisone, dexamethasone, prednisone, prednisolone, and 6-α-methylprednisolone. Removal of the ketol side chain results in a significant loss of therapeutic activity.

The reactivity of the ketol side chain of the adrenocorticosteroids is well documented. Base-catalyzed rearrangements and eliminations have been shown to occur under both aerobic and anaerobic conditions (1–5). Guttman and Meister (6) showed that at least three parallel first-order reactions were involved in the base-catalyzed degradation of prednisolone. Neutral and acidic degradation products were obtained. Caspi *et al.* (7) studied oxidative cleavage of the ketol side chain of cortisone with lead tetraacetate. Lewbart and Mattox (8) reported that trace amounts of copper in actinic glassware caused destruction of cortisone and related steroids.

Mauger *et al.* (9) followed the degradation of 21-hydrocortisone hemisuccinate at 70° in aqueous solutions buffered at pH 6.9, 7.2, and 7.6. The data obtained indicated that the overall kinetic pathway at each pH value could be interpreted as consecutive first-order reactions. The blue tetrazolium assay confirmed that the production of a species devoid of the ketol side chain at the 17-position occurred after the steroid alcohol was formed. The ketol group imparts reducing properties to the glucocorticoid molecules similar to those of fructose (Scheme I), which contains a similar ketol group. It was speculated that the presence of excess fructose in aqueous solutions of hydrocortisone (II) might retard the base-catalyzed degradation of the latter. The significance of the ketol group would be checked by using other polyols lacking this group.

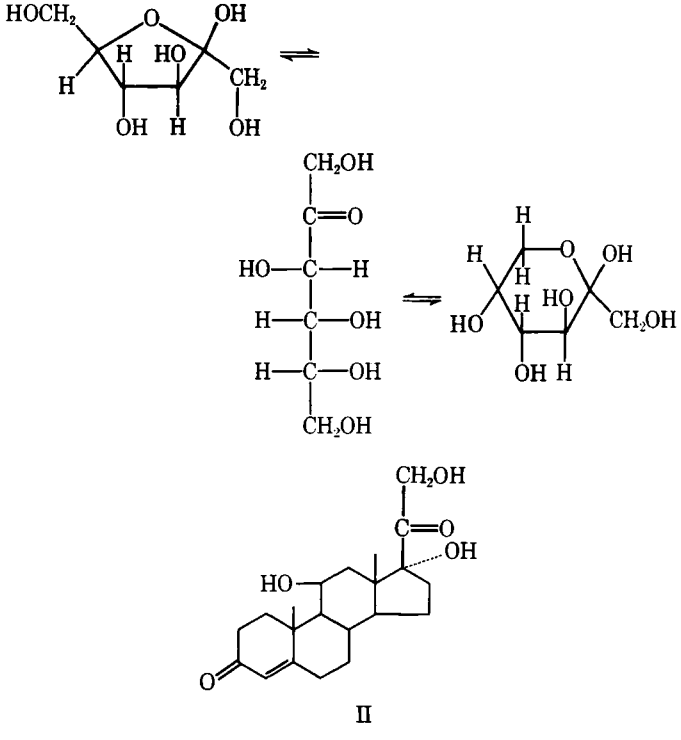

II

EXPERIMENTAL

Materials—The following were obtained from commercial sources: hydrocortisone, USP (lot 15C-6126)[1], blue tetrazolium[1], tetramethylammonium hydroxide[1], D-fructose[2], dextrose USP[3], glacial acetic acid

[1] Sigma Chemical Co., St. Louis, Mo.
[2] Pfaltz and Bauer, Inc., Flushing, N.Y.
[3] Mallinckrodt Chemical Works, St. Louis, Mo.

0022-3549/83/0900-1079$01.00/0

Table I—Rate of Degradation of Hydrocortisone at pH 7.4 in the Presence of D-Fructose at 37, 47, and 57°

Time, hr	Percent Remaining, Molar Ratio of Hydrocortisone–Fructose 1:0	1:1	1:5	1:10	1:25
		37°			
0	100	100	100	100	100
4	98.9	98.8	99.3	99.7	100
24	95.1	95.2	95.7	95.9	99.1
72	91.3	91.9	92.0	93.5	96.6
144	82.3	82.9	84.2	87.7	90.1
264	69.2	71.0	73.5	77.1	95.8
408	57.9	59.9	63.5	68.6	79.4
528	47.5	49.5	52.3	61.3	72.0
648	42.2	44.6	47.4	55.3	66.8
		47°			
0	100	100	100	100	100
14	97.2	96.8	97.1	98.6	98.2
50	81.1	79.8	87.0	89.8	94.6
72	74.9	73.8	81.7	84.5	90.1
120	62.9	62.0	71.9	77.3	84.9
168	48.6	51.1	63.3	69.2	79.0
216	38.2	39.7	54.6	59.5	75.0
264	30.5	33.8	48.1	54.3	68.1
336	21.7	22.6	36.1	49.0	63.0
384	19.0	20.0	34.4	44.5	61.5
		57°			
0	100	100	100	100	100
1	97.3	97.3	98.6	99.2	99.8
4	92.3	92.0	91.3	96.2	95.6
9	87.1	88.6	89.1	94.0	95.1
24	75.9	79.0	84.1	90.6	94.0
48	58.2	63.5	74.2	80.7	87.0
72	45.8	49.8	63.9	75.4	81.8
120	28.4	32.9	48.0	62.1	72.5
150	20.2	23.4	38.1	54.5	67.6
180	10.8	14.6	33.0	46.6	63.3

Table II—Rate of Degradation of Hydrocortisone at pH 8.4 in the Presence of D-Fructose at 37, 47, and 57°

Time, hr	Percent Remaining, Molar Ratio of Hydrocortisone–Fructose 1:0	1:1	1:5	1:10	1:25
		37°			
0	100	100	100	100	100
4	89.0	89.0	95.4	95.4	98.6
24	77.1	82.7	89.7	93.2	91.5
72	61.6	62.5	67.0	74.9	78.4
144	42.1	41.4	44.5	60.9	65.2
264	19.9	20.2	22.6	34.2	40.3
408	7.7	7.6	9.7	16.3	23.5
528	3.9	3.8	5.3	11.3	17.3
		47°			
0	100	100	100	100	100
2	95.3	95.6	95.9	95.6	98.4
14	82.0	83.0	88.0	90.0	94.8
50	63.8	63.9	66.0	73.2	82.8
72	51.3	53.2	56.1	63.5	74.5
120	35.3	35.2	42.9	51.3	64.6
168	23.9	24.2	29.8	38.3	51.6
216	15.9	16.2	21.7	28.8	43.0
264	10.6	11.3	15.7	22.4	36.2
336	5.8	6.5	9.2	14.7	25.6
384	3.6	4.1	6.6	11.8	23.1
		57°			
0	100	100	100	100	100
1	98.8	98.7	98.8	99.6	99.7
4	91.1	91.1	98.1	96.5	98.1
9	81.8	85.0	95.8	94.5	96.6
24	51.8	60.0	80.8	92.3	95.0
48	24.5	37.1	65.7	84.2	91.2
72	16.9	30.4	52.8	77.5	90.1
120	14.9	21.3	34.4	62.4	84.2
150	14.5	17.9	27.0	56.3	82.2
180	13.8	14.3	19.4	54.3	81.8

(reagent grade)[4], phosphoric acid (reagent grade)[4], hydrochloric acid (reagent grade)[4], monobasic potassium phosphate (reagent grade)[5], boric acid USP[5], potassium chloride (reagent grade)[6], sodium hydroxide (reagent grade)[6], citric acid USP[7], sorbitol USP[7], lactose USP[3], sucrose (reagent grade)[8], chloroform NF[9], absolute ethanol, (reagent grade)[9], glycerol (reagent grade)[10], propylene glycol (reagent grade)[10], and nitrogen, extra dry[10].

Equipment—The following pieces of equipment were used: a double beam spectrophotometer[11], a precision temperature-controlled oven[12], and a pH meter[13].

Preparation of the Buffer Solutions—The pH 7.4 buffer was prepared by dissolving monobasic potassium phosphate, (6.8045 g), and sodium hydroxide (1.564 g) in sufficient distilled water to make 1 liter. The buffer solution at pH 8.4 was prepared by dissolving boric acid (3.0915 g), potassium chloride (3.7277 g), and sodium hydroxide (0.344 g) in sufficient distilled water to make 1 liter. The pH 9.4 buffer solution contained similar quantities of boric acid and potassium chloride plus 1.284 g of sodium hydroxide.

Preparation of Hydrocortisone Solutions with and without D-Fructose—Stock solutions of hydrocortisone in absolute ethanol (5 mg/ml) and D-fructose in each of the buffer solutions (24.85 mg/ml, 0.14 *M*) were prepared. Control solutions were prepared by diluting 10 ml of the glucocorticoid stock solution (50 mg, 0.14 mmole) with the appropriate buffer solution to 100 ml. Blank solutions were also prepared by diluting the stock solutions of D-fructose (1, 5, 10, or 25 ml) to 100 ml with the appropriate buffer solution. Hydrocortisone–D-fructose solutions (molar ratios: 1:1, 1:5, 1:10, and 1:25) were prepared by adding various volumes of the D-fructose stock solutions to 10 ml of the hydrocortisone stock solution and diluting to 100 ml with the appropriate buffer. The solutions were analyzed in duplicate and placed in ovens set at 37, 47, and 57 ± 1°.

Preparation of Hydrocortisone Solutions with Various Polyols—The following polyols were added to hydrocortisone solutions

Table III—Rate of Degradation of Hydrocortisone at pH 9.4 in the Presence of D-Fructose at 37, 47, and 57°

Time hr	Percent Remaining, Molar Ratio of Hydrocortisone–Fructose 1:0	1:1	1:5	1:10	1:25
		37°			
0	100	100	100	100	100
4	96.6	97.3	98.5	98.7	99.6
24	87.0	89.7	94.4	96.7	96.2
72	71.6	73.8	80.9	87.4	93.0
144	52.3	54.1	68.4	75.3	86.2
264	28.8	31.7	47.3	58.8	77.4
408	15.0	17.1	32.4	43.9	67.9
528	8.5	9.1	22.3	33.8	62.9
648	4.1	4.5	16.7	26.9	51.7
		47°			
0	100	100	100	100	100
2	94.7	94.9	96.6	98.2	98.9
14	83.6	84.7	91.2	95.8	96.1
50	50.1	51.7	65.3	78.0	90.3
72	35.1	36.7	55.1	66.4	87.0
120	21.7	23.1	37.4	53.9	79.6
168	10.9	11.9	25.4	39.8	68.6
216	6.3	6.6	18.2	31.2	64.5
264	0	0	12.1	24.1	61.5
		57°			
0	100	100	100	100	100
1	97.6	97.3	98.2	99.1	99.4
4	86.9	88.7	87.1	93.4	94.3
10	63.0	64.9	75.8	78.7	89.0
24	40.7	40.8	47.9	51.3	64.5
48	19.7	19.7	25.1	26.1	28.9
72	18.1	18.7	19.5	23.7	28.9
120	15.7	15.7	19.5	22.5	27.5

[4] J. T. Baker Chemical Co., Phillipsburg, N.J.
[5] Merck & Co., Inc., Rahway, N.J.
[6] Fisher Scientific Co., Fair Lawn, N.J.
[7] Pfizer, Inc., New York, N.Y.
[8] Mann Research Labs., New York, N.Y.
[9] New York Laboratory Supply Co., New York, N.Y.
[10] Union Carbide Inc., New York, N.Y.
[11] Coleman-Hitachi, model No. 124, Coleman Instruments Division, Maywood, N.J.
[12] Precision Temperature Controlled Oven, model No. 18, New York Laboratory Supply Co., New York, N.Y.
[13] Will Scientific Co., Inc., New York, N.Y.

Table IV—Rate of Degradation of Hydrocortisone at pH 7.4 in the Presence of Various Polyols at 37° [a]

Time, hr	Percent Remaining						
	Control	Dextrose	Lactose	Sucrose	Sorbitol	Propylene Glycol	Glycerin
				1:10			
0	100	100	100	100	100	100	100
4	98.5	99.5	98.9	99.5	98.6	98.7	99.4
24	93.7	95.4	95.1	94.4	93.2	93.9	95.0
72	89.2	89.6	88.9	90.7	88.7	89.3	90.5
144	81.0	82.8	81.6	82.7	82.1	82.5	82.6
264	70.0	72.0	70.9	71.1	71.2	70.8	70.6
408	58.2	58.9	58.8	60.2	58.5	58.2	59.5
552	45.7	47.8	45.7	45.7	45.9	47.8	47.6
696	33.5	35.9	36.1	35.4	33.9	36.4	37.3
864	21.3	22.9	22.7	21.8	22.4	23.8	23.7
				1:25			
0	100	100	100	100	100	100	100
4	98.5	99.6	99.0	99.2	98.9	98.3	99.4
24	93.7	94.6	95.0	93.5	93.0	93.6	94.8
72	89.2	89.7	89.3	88.3	88.4	88.8	89.0
144	81.0	82.9	81.9	82.8	81.5	82.3	82.4
264	70.0	73.2	71.1	72.2	72.8	71.6	72.0
408	58.2	60.5	59.4	58.2	59.8	58.9	59.5
552	45.7	48.5	47.9	48.7	48.6	49.2	48.7
696	33.5	36.1	35.5	35.7	34.8	35.0	35.5
864	21.3	23.7	24.8	23.6	25.6	24.0	25.3

[a] Molecular ratios of hydrocortisone–polyol are 1:10 and 1:25.

buffered at pH 7.4 (molar ratios of hydrocortisone–polyol, 1:10 and 1:25): dextrose, sucrose, lactose, sorbitol, glycerin, and propylene glycol. The stability of these solutions was only studied at 37 ± 1°.

Assay Procedure for Hydrocortisone—At various time intervals, 10 ml of the sample was extracted with three 20-ml portions of chloroform. The chloroform extracts were passed through a glass wool pledget previously rinse with chloroform. The combined extracts were diluted to 100 ml and then evaporated to dryness in a stream of nitrogen at room temperature. The residue was dissolved in 20 ml of absolute ethanol and treated with 1 ml of blue tetrazolium solution (1% in absolute ethanol) plus 1 ml of tetramethylammonium hydroxide (1 ml of a 10% aqueous solution diluted to 10 ml with absolute ethanol). The color was allowed to develop in the dark for exactly 45 min. Color development was then quenched by the addition of 1 ml of glacial acetic acid. The absorbance was determined at 525 nm. A standard solution of hydrocortisone in absolute ethanol was carried through the identical procedure and was used as a color reference in calculating the concentration of steroid in the sample. Blank solutions were also subjected to the same procedure. The results are summarized in Tables I–IV.

RESULTS AND DISCUSSION

The stability data for the solutions of II plus I are summarized in Tables I–III. It is evident that an increase in the concentration of I results in an improvement in the stability of II. This relationship holds for the three pH values and three temperatures studied. The importance of the ketol group in I is also evident after inspection of the data in Table IV. None of the polyols at ratios of 1:10 or 1:25 showed any stabilization of II as compared with the control.

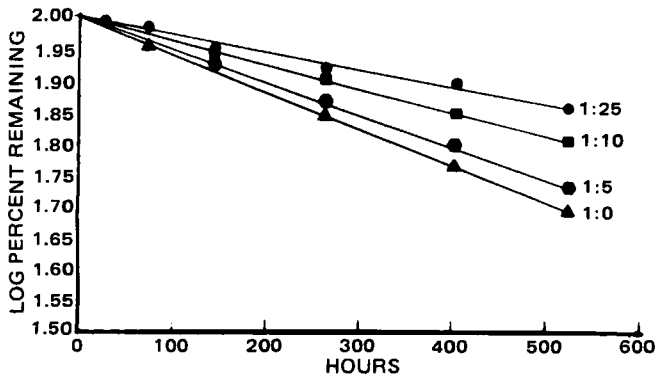

Figure 1—*Influence of molar concentrations of D-fructose on the stability of aqueous solutions of hydrocortisone (50 mg%) buffered at pH 7.4 and stored at 37° plotted in first-order fashion.*

The rate constants, *y*-intercepts, and correlation coefficients summarized in Table V were derived from first-order plots of the data shown in Tables I–III. Selected solutions buffered at pH 7.4 were plotted in first-order fashion (Fig. 1) to illustrate the linearity of the data.

A possible explanation for the stabilization observed is the complex formation between II and I. Such complexes could resist oxidative destruction more effectively than solutions of II alone. An alternative mechanism is that fructose competes with II for the oxygen present in the system and thus acts as an antioxidant. Failure of the other polyols to exert a protective effect could be attributed to the greater reaction speed of I as compared with the polyols studied. Thus, Singh *et al.* (10) reported that the order of the oxidative reaction speed catalyzed by bi-

Table V—Rate Constant (*k*), *y*-Intercept, and Correlation Coefficient (*r*) Values Derived from First-Order Plots of the Data in Tables I–III [a]

First-order Parameters	Molar Ratio of Hydrocortisone–Fructose				
	1:0	1:1	1:5	1:10	1:25
		pH 7.4			
k_{37}	1.35[a]	1.26	1.16	0.91	0.62
y-intercept	1.998	1.998	1.998	1.997	2.001
r	0.998	0.998	0.998	0.999	0.995
k_{47}	4.51	4.28	2.88	2.17	1.34
y-intercept	2.011	2.006	2.004	2.000	2.000
r	0.998	0.997	0.996	0.993	0.992
k_{57}	11.4	10.0	6.03	4.05	2.50
y-intercept	2.000	2.000	1.988	1.996	1.994
r	0.989	0.993	0.996	0.997	0.995
		pH 8.4			
k_{37}	6.06	6.13	5.62	4.40	3.41
y-intercept	1.978	1.987	2.000	2.014	2.002
r	0.999	0.999	0.999	0.996	0.997
k_{47}	8.45	8.15	6.98	5.57	3.89
y-intercept	1.987	1.982	1.986	1.988	2.000
r	0.999	0.999	0.999	0.999	0.998
k_{57}	11.9	10.9	9.03	3.57	1.15
y-intercept	1.882	1.934	2.005	1.996	1.992
r	0.827	0.946	0.999	0.991	0.965
		pH 9.4			
k_{37}	4.70	4.58	2.79	2.04	0.96
y-intercept	2.002	2.011	2.000	2.002	2.000
r	0.995	0.996	0.999	0.999	0.992
k_{47}	15.4	15.3	7.97	5.39	1.93
y-intercept	2.040	2.050	1.990	2.000	2.000
r	0.958	0.952	0.999	0.999	0.987
k_{57}	18.0	16.8	15.3	14.2	12.7
y-intercept	1.890	1.890	1.910	1.930	1.950
r	0.867	0.827	0.812	0.821	0.808

[a] All values for *k* must be multiplied by 10^{-3}. Units: hr^{-1}.

valent copper is fructose > glucose > galactose. Joslyn and Miller (11) reported that I was more effective than sucrose and dextrose in stabilizing ascorbic acid solutions against oxidative degradation. These authors concluded that no simple rate law governed the oxidation of ascorbic acid in the presence of sugars. They also observed that the temperature coefficients of the oxidation in the presence or absence of the sugars were similar. This observation would seem to indicate that complex formation was not occurring since the temperature coefficients would be expected to differ. Ashida (12) also reported that methylene blue was more easily reduced by a ketose such as fructose than by an aldose such as glucose.

The data and speculations serve as a stimulus for additional research to establish a mechanism for the stabilization observed. It will be of interest to learn if the redox potential of I is similar to that for II. Such similarity is anticipated because of the structural relationship between the portions of the two molecules where oxidation reactions have been shown to occur. The redox potentials of the other polyols are anticipated to differ significantly.

REFERENCES

(1) L. Velluz, A. Petit, M. Pesez, and R. Berret, *Bull Soc. Chim. France*, **1947**, 123.

(2) P. T. Herzig and M. Ehrenstein, *J. Org. Chem.*, **16**, 1050 (1951).

(3) H. L. Mason, C. S. Myers, and E. C. Kendall, *J. Biol. Chem.*, **116**, 267 (1936).

(4) H. L. Mason, *Proc. Staff Meetings Mayo Clinic*, **13**, 235 (1938).

(5) N. L. Wendler and R. P. Graber, *Chem. Ind. (London)*, **1956**, 549.

(6) D. E. Guttman and P. D. Meister, *J. Am. Pharm. Assoc., Sci. Ed.*, **47**, 773 (1958).

(7) E. Caspi, W. Schmid, and T. A. Wittstruck, *Tetrahedron*, **16**, 271 (1961).

(8) M. L. Lewbart and V. R. Mattox, *J. Org. Chem.*, **21**, 2001 (1963).

(9) J. W. Mauger, A. N. Paruta, and R. J. Gerraughty, *J. Pharm. Sci.*, **58**, 574 (1969).

(10) M.Pd. Singh, B. Krishna, and S. Ghosh, *Z. Phyzik. Chem. (Leipzig)*, **205**, 285 (1956).

(11) M. A. Joslyn and J. Miller, *Food Res.*, **14**, 340 (1949).

(12) K. Ashida, *Mem. Inst. Sci. Ind. Res., Osaka Univ.*, **10**, 205 (1953).

Cinchophen Analogues as Potential CNS Agents

A. KAR

Received October 20, 1981, from the *Department of Pharmaceutical Chemistry, University of Nigeria, Nsukka, Nigeria.* Accepted for publication June 1, 1982.

Abstract □ Several amides of cinchophen were prepared and evaluated as CNS agents. Compounds III, VII, XII, XIII, and XIV exhibited analgesic activity while I, III, and XIV acted as CNS depressants.

Keyphrases □ Cinchophen—amide analogue synthesis, evaluation of CNS activity in mice □ Analgesics—potential, amide analogues of cinchophen, evaluation of CNS activity in mice □ Central nervous system agents—amide analogues of cinchophen, evaluation of CNS activity in mice

Cinchophen (I) was formerly used for the treatment of gout (1, 2); however, it was withdrawn from the market because of its toxic effects (3–5). It was concluded that the quinoline ring, a carboxylic acid group in the C-3 or C-4 position, and an aryl residue at C-2 were essential for the physiological action of cinchophen (6). Many structural modifications of cinchophen have been reported [*i.e.*, neocinchophen, 2-phenyl-3-hydroxycinchonic acid, hexophan, and 2-phenyl-4-hydroxyacetyl-6-methoxyquinoline (1)]. Reversal of the phenyl and carboxyl groups afforded an inactive compound (I).

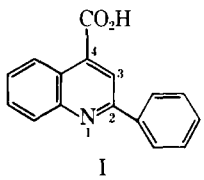

I

In this study 16 amides of I were synthesized and evaluated as CNS agents. Cinchophen has been synthesized either by the condensation of acetophenone with isatic acid in alcoholic potassium hydroxide solution (7) or by heating pyruvic acid with either aniline and benzaldehyde or with benzylidene aniline in absolute ethanol (8). In the present study, I was prepared by the condensation of pyruvic acid with aniline and benzaldehyde (9, 10). The desired amides were subsequently synthesized by treating the corresponding acid chloride with the appropriate amine.

EXPERIMENTAL

Synthesis—The amides II–XVII were prepared (11) by vigorously shaking for 30 min at room temperature a mixture of the appropriate amine (0.002 mole), a 10–15% molar excess of the acid chloride of cinchophen, and 10 ml of 10% aqueous sodium hydroxide solution. The resulting solid material was removed by filtration and purified, as indicated in Table I.

Analysis and Spectral Data—Melting points were determined in open capillary tubes in an electrothermal apparatus and are uncorrected. NMR[1] spectra were obtained in deuterated acetone using tetramethylsilane as the internal standard. The mass spectra[2] of the various compounds were determined. Microanalyses were within ±0.3% of the theoretical values (Table I).

Pharmacological Evaluation—The hot plate method was employed to evaluate the analgesic activity of the amides in mice. The CNS-depressant activity was studied *in vivo* by noting the effect of the amides on spontaneous motor activity, ptosis, and pentobarbital-induced hypnosis. Swiss albino mice of both sexes, weighing 20–30 g, were used; solutions of normal saline or 3% (w/v) aqueous polysorbate 80 were given to the untreated and vehicle controls, respectively. Cinchophen (50 or 100 mg/kg), pentobarbital sodium (40 mg/kg), and morphine hydrochloride (4 mg/kg) were used as reference drugs to evaluate the activity of the amides.

Analgesic Activity—Analgesic activity was measured by the hot plate method at 53 ± 2°. The normal reaction time (pain threshold) for each mouse was determined by placing the mouse on the hot plate and noting the amount of time (≤5 sec) required for the mouse to leave the hot plate platform. The pain threshold was measured 30 min postinjection and at hourly intervals for 4 hr.

[1] Perkin-Elmer R-32 spectrometer.
[2] VG-Micromass 16F (with a VG system 2000 computer).

0022-3549/83/0900-1082$01.00/0

valent copper is fructose > glucose > galactose. Joslyn and Miller (11) reported that I was more effective than sucrose and dextrose in stabilizing ascorbic acid solutions against oxidative degradation. These authors concluded that no simple rate law governed the oxidation of ascorbic acid in the presence of sugars. They also observed that the temperature coefficients of the oxidation in the presence or absence of the sugars were similar. This observation would seem to indicate that complex formation was not occurring since the temperature coefficients would be expected to differ. Ashida (12) also reported that methylene blue was more easily reduced by a ketose such as fructose than by an aldose such as glucose.

The data and speculations serve as a stimulus for additional research to establish a mechanism for the stabilization observed. It will be of interest to learn if the redox potential of I is similar to that for II. Such similarity is anticipated because of the structural relationship between the portions of the two molecules where oxidation reactions have been shown to occur. The redox potentials of the other polyols are anticipated to differ significantly.

REFERENCES

(1) L. Velluz, A. Petit, M. Pesez, and R. Berret, *Bull Soc. Chim. France*, **1947**, 123.

(2) P. T. Herzig and M. Ehrenstein, *J. Org. Chem.*, **16**, 1050 (1951).

(3) H. L. Mason, C. S. Myers, and E. C. Kendall, *J. Biol. Chem.*, **116**, 267 (1936).

(4) H. L. Mason, *Proc. Staff Meetings Mayo Clinic*, **13**, 235 (1938).

(5) N. L. Wendler and R. P. Graber, *Chem. Ind. (London)*, **1956**, 549.

(6) D. E. Guttman and P. D. Meister, *J. Am. Pharm. Assoc., Sci. Ed.*, **47**, 773 (1958).

(7) E. Caspi, W. Schmid, and T. A. Wittstruck, *Tetrahedron*, **16**, 271 (1961).

(8) M. L. Lewbart and V. R. Mattox, *J. Org. Chem.*, **21**, 2001 (1963).

(9) J. W. Mauger, A. N. Paruta, and R. J. Gerraughty, *J. Pharm. Sci.*, **58**, 574 (1969).

(10) M.Pd. Singh, B. Krishna, and S. Ghosh, *Z. Phyzik. Chem. (Leipzig)*, **205**, 285 (1956).

(11) M. A. Joslyn and J. Miller, *Food Res.*, **14**, 340 (1949).

(12) K. Ashida, *Mem. Inst. Sci. Ind. Res., Osaka Univ.*, **10**, 205 (1953).

Cinchophen Analogues as Potential CNS Agents

A. KAR

Received October 20, 1981, from the *Department of Pharmaceutical Chemistry, University of Nigeria, Nsukka, Nigeria.* Accepted for publication June 1, 1982.

Abstract □ Several amides of cinchophen were prepared and evaluated as CNS agents. Compounds III, VII, XII, XIII, and XIV exhibited analgesic activity while I, III, and XIV acted as CNS depressants.

Keyphrases □ Cinchophen—amide analogue synthesis, evaluation of CNS activity in mice □ Analgesics—potential, amide analogues of cinchophen, evaluation of CNS activity in mice □ Central nervous system agents—amide analogues of cinchophen, evaluation of CNS activity in mice

Cinchophen (I) was formerly used for the treatment of gout (1, 2); however, it was withdrawn from the market because of its toxic effects (3–5). It was concluded that the quinoline ring, a carboxylic acid group in the C-3 or C-4 position, and an aryl residue at C-2 were essential for the physiological action of cinchophen (6). Many structural modifications of cinchophen have been reported [*i.e.*, neocinchophen, 2-phenyl-3-hydroxycinchonic acid, hexophan, and 2-phenyl-4-hydroxyacetyl-6-methoxyquinoline (1)]. Reversal of the phenyl and carboxyl groups afforded an inactive compound (I).

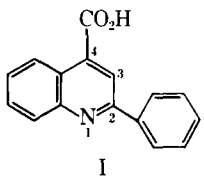

I

In this study 16 amides of I were synthesized and evaluated as CNS agents. Cinchophen has been synthesized either by the condensation of acetophenone with isatic acid in alcoholic potassium hydroxide solution (7) or by heating pyruvic acid with either aniline and benzaldehyde or with benzylidene aniline in absolute ethanol (8). In the present study, I was prepared by the condensation of pyruvic acid with aniline and benzaldehyde (9, 10). The desired amides were subsequently synthesized by treating the corresponding acid chloride with the appropriate amine.

EXPERIMENTAL

Synthesis—The amides II–XVII were prepared (11) by vigorously shaking for 30 min at room temperature a mixture of the appropriate amine (0.002 mole), a 10–15% molar excess of the acid chloride of cinchophen, and 10 ml of 10% aqueous sodium hydroxide solution. The resulting solid material was removed by filtration and purified, as indicated in Table I.

Analysis and Spectral Data—Melting points were determined in open capillary tubes in an electrothermal apparatus and are uncorrected. NMR[1] spectra were obtained in deuterated acetone using tetramethylsilane as the internal standard. The mass spectra[2] of the various compounds were determined. Microanalyses were within ±0.3% of the theoretical values (Table I).

Pharmacological Evaluation—The hot plate method was employed to evaluate the analgesic activity of the amides in mice. The CNS-depressant activity was studied *in vivo* by noting the effect of the amides on spontaneous motor activity, ptosis, and pentobarbital-induced hypnosis. Swiss albino mice of both sexes, weighing 20–30 g, were used; solutions of normal saline or 3% (w/v) aqueous polysorbate 80 were given to the untreated and vehicle controls, respectively. Cinchophen (50 or 100 mg/kg), pentobarbital sodium (40 mg/kg), and morphine hydrochloride (4 mg/kg) were used as reference drugs to evaluate the activity of the amides.

Analgesic Activity—Analgesic activity was measured by the hot plate method at 53 ± 2°. The normal reaction time (pain threshold) for each mouse was determined by placing the mouse on the hot plate and noting the amount of time (≤5 sec) required for the mouse to leave the hot plate platform. The pain threshold was measured 30 min postinjection and at hourly intervals for 4 hr.

[1] Perkin-Elmer R-32 spectrometer.
[2] VG-Micromass 16F (with a VG system 2000 computer).

0022-3549/83/0900-1082$01.00/0

Table I—Physical Properties of Cinchophen Amides

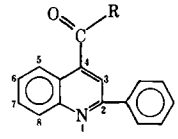

Compound	R	Yield,[a] %	mp, °	Formula	Analysis, % Calc.	Found	IR Spectra (KBr), cm^{-1}	^1H-NMR Spectra (acetone d_6), δ
II	2-Aminopyridino	85	119–121	$C_{21}H_{15}N_3O$	C 77.5 H 4.61 N 12.92	77.72 4.60 12.89	3300–3400 (m,—NH), 1660 (w,C=O), 1500 (aromatic), 1340 (s,aryl NH_2), 770 (s, pyridine, 2-mono-subst.)	8.7 (s,1,C—3); 8.3 (d, 4, C_5—C_8); 8.1 (s,1,—NH, C—9); 7.4 (d,5, C—2 phenyl)
III	2-Aminopyrimidino	21	183	$C_{20}H_{14}N_4O$	C 73.61 H 4.29 N 17.17	73.57 4.30 17.21	3400 (m,—NH), 1620 (m, C=O), 1320 (w, aryl-NH_2)	8.8 (s,1,C—3); 8.3 (d,4,C_5—C_8); 8.15 (s,1,—NH, C—9); 7.4 (d,5, C—2 phenyl)
IV	2-Nitroanilino	90	195–197	$C_{22}H_{15}N_3O_3$	C 71.54 H 4.06 N 11.38	71.22 4.03 11.35	3300–3400 (m,—NH), 1660 (w, C=O), 1600 (w, phenyl), 1320 (m, nitro), 700 (monosubst. aryl CH)	8.75 (s,1,C—3); 8.45 (d,4,C_5—C_8); 8.1 (s,1,—NH, C—9); 7.7 (d,4, C—3′ to C—6′); 7.4 (d,5, C—2 phenyl)
V	3-Nitroanilino	62	121–123	$C_{22}H_{15}N_3O_3$	C 71.54 H 4.06 N 11.38	71.64 4.08 11.40	3400 (m,—NH), 1660 (w, C=O), 1600 (w, phenyl), 1330 (m, NO_2), 720 (monosubst. aryl CH)	8.80 (s,1,C—3); 8.45 (d,4,C_5—C_8); 8.15 (s,1,—NH, C—9); 7.65 (d,4, C—3′ to C—6′); 7.4 (d,5,C—2 phenyl)
VI	2-Methyl-6-*tert*-butylanilino	85	214–216	$C_{27}H_{26}N_2O$	C 82.23 H 6.59 N 7.10	82.02 6.61 7.12	3400 (w,—NH), 1670 (m,C=O), 1600 (m,phenyl), 1340 (s, aryl —NH_2)	8.75 (s,1,C—3); 8.45 (d,4,C_5—C_8); 7.3 (d,5, C—2 phenyl), 2.1 (d,3, C—9,2—CH_3): 1.4 (t,9, C—9, 6 *tert*-butyl)
VII	2-Ethyl-6-*sec*-butylanilino	82	113	$C_{28}H_{28}N_2O$	C 82.35 H 6.86 N 6.86	82.17 6.88 6.84	3400 (m,—NH), 1670 (m,C=O), 1340 (s, aryl *sec* amino group), 700 (s, mono-subst. aryl CH)	8.7 (s,1,C—3); 8.1 (s,1,—NH); 7.7 (d,3,C—9, C—3′ to C—5′); 7.3 (d,5, C—2 phenyl); 2.8–2.4 (d, 5, C—9, —C_2H_5); 2.0 (t,9, C—9, 6 *sec*-butyl)
VIII	2-Ethyl-6-isopropylanilino	75	171–173	$C_{27}H_{26}N_2O$	C 82.23 H 6.59 N 7.10	82.31 6.57 7.09	3400 (m,—NH), 1670 (m,C=O), 1340 (s, aryl *sec* amino group)	8.7 (s,1,C—3); 8.4 (d,4, C—5 to C—8); 7.7 (d,3, C—9, C—3′ to C—5′); 7.45 (d,5, C—2 phenyl); 3.0 (s,1,C—6); 1.4–1.0 (d,6, C—9 isopropyl)
IX	2-Methyl-6-isopropylanilino	92	315–317	$C_{26}H_{24}N_2O$	C 82.10 H 6.31 N 7.37	81.89 6.29 7.34	3400 (m,—NH), 1500 (s, aromatic), 1380 (s, isopropyl)	8.7 (s,1,C—3); 8.2 (d,4,C_5—C_8); 7.8 (d, 3,C—3′ to C—5′); 7.4 (d, 5, C—2 phenyl)
X	Morpholino	42	199–201	$C_{20}H_{18}N_2O$	C 79.47 H 5.96 N 9.27	79.29 5.98 9.29	3420 (m,—NH), 1660 (m,C=O), 1510 (m, aromatic)	8.7 (s,1,C—3); 8.1 (d,4,C—5 to C—8); 7.6 (d,3,C—3′ to C—5′); 7.2 (d,5,C—2 phenyl)
XI	Pyrrolidino	25	195	$C_{20}H_{18}N_2O$	C 79.47 H 5.96 N 9.27	79.55 5.94 9.26	1670 (m,C=O), 1500 (m, aromatic), 720 (mono-subst. aryl CH)	8.75 (s,1,C—3); 8.1 (d,4,C_5—C_8); 7.9 (d,8,C—2′ to C—5′); 7.1 (d, 5,C—2 phenyl)
XII	Piperidino	38	189	$C_{21}H_{20}N_2O$	C 79.74 H 6.32 N 8.86	79.68 6.34 8.88	1640 (m,C=O), 1500 (m, aromatic), 730 (monosubst. aryl CH)	8.7 (s,1,C—3); 8.2 (d,4,C_5—C_8); 7.85 (d,10,C—2′ to C—6′); 7.1 (d,5,C—2 phenyl)
XIII	*p*-Toluidino	92	90–91	$C_{22}H_{18}N_2O$	C 80.98 H 5.52 N 8.58	81.10 5.53 8.57	3400(m,—NH), 1670 (w,C=O), 1620 (m, amide), 1600 (m, phenyl), 1500 (m, aromatic)	8.7 (s,1,C—3); 8.5 (d,4,C_5—C_8) 7.7 (d,4,C—2′,3′,5′ & 6′); 7.4 (d,5, C—2 phenyl); 2.1 (d,3, C—4′ methyl)
XIV	*p*-Anisidino	85	299–301	$C_{22}H_{18}N_2O_2$	C 77.19 H 5.26 N 8.18	77.27 5.25 8.20	3400 (m,—NH), 1670 (w,C=O) 1620 (m, amide), 1172 (m,—OCH_3), 700 (s, monosubst. aryl CH)	8.75 (s,1,C—3); 8.5 (d,4,C_5—C_8); 7.7 (d,4,C—2′,C—3′,C—5′ & C—6′); 6.65 (d,3, C—4′—OCH_3);
XV	2-Aminobenzo thiazolyl	88	110	$C_{23}H_{15}N_3OS$	C 72.44 H 3.93 N 11.02 S 8.39	72.14 3.92 10.99 8.41	3400 (m,—NH), 1650 (m,C=O), 1110 (m, aryl), 700 (s, monosubst. aryl CH)	8.70 (s,1,C—3); 8.5 (d,4,C—5 to C—8); 8.0 (s,1,—NH at C—9); 7.4 (d,5, C—2 phenyl); 7.1 (d,4 C—3′ to C—6′)
XVI	Diphenylamino	91	56–58	$C_{28}H_{20}N_2O$	C 84.00 H 5.00 N 7.00	83.88 5.02 7.02	1680–1630 (s, *tert* amide), 1660 (m,C=O), 1600 (w, phenyl), 1500 (s, aromatic)	8.3 (d,4,C_5—C_8); 7.4 (d,5 C—2 phenyl); 4.2 (d,10,C—9)
XVII	5-Nitroisatoic anhydride	85	248–250	$C_{24}H_{13}N_3O_6$	C 65.60 H 2.96 N 9.56	65.52 2.96 9.54	3400–3300 (m,—NH), 1650 (w,C=O), 1600 (w, phenyl), 1320 (m, nitro), 700 (monosubst. aryl CH)	8.25 (d,4,C_5—C_8); 7.4 (d,5,C—2 phenyl); 3.7 (d,3,C—9 aryl);

[a] All compounds were recrystallized from 95% ethanol except for XVII which was recrystallized from water.

Spontaneous Motor Activity—The increase in SMA was measured using an activity cage[3] 30 min postinjection and at hourly intervals for 4 hr. Any change in the activity levels was noted.

Pentobarbital-Induced Hypnosis—Fifteen minutes postinjection, all animals were treated with 40 mg/kg of pentobarbital sodium. The time to the loss of the righting reflex was noted for each mouse; the mice were then placed on their backs. When the animals regained their righting reflex (*i.e.*, starting moving around the cage) the time was again noted, and the duration of the pentobarbital-induced hypnosis was calculated.

[3] Activity Cage 7401, Ugo Basile, Biological Research Apparatus, Comerio-(va)-Italy.

RESULTS AND DISCUSSION

Of the 16 compounds synthesized, 12 were evaluated as CNS agents. The significant analgesic activity of the 2-nitroanilino analogue (IV)

Table II—Pharmacological Activity of Cinchophen Amides in Mice[a]

Compound	ED_{50} for Analgesic Activity, mg/kg ip	ED_{50} for Pentobarbital Induced Hypnosis, mg/kg ip	LD_{50}[b], mg/kg ip
II	>150	>50[c]	>600
IV	>50	>50	>600
V	>150	>100	>500
VII	>150	>100	>600
VIII	>50	>100	>500
IX	>150	>150	>600
XIII	>100	>100	>600
XIV	>100	>150	>600
XV	>50	>50[c]	>500
XVI	>100	>50	>500
XVII	>150	>100	>600

[a] Each value is the average of four replicate experiments. [b] Taken from the work of Miller and Tainter (12) for comparison. [c] Maximum effect observed.

compared with the inactive 3-nitroaniline isomer (V) suggested that the close proximity of the nitro group to the amino moiety in the phenyl ring is essential for analgesic activity and also that possible electronic interactions exist between them. Of the four closely related analogues (VI–IX), only VIII retained the significant analgesic activity of the parent molecule, while the others showed an opposite effect. This is possibly due to the presence of either a 2-methyl side chain (VI and IX) that undergoes rapid metabolism or to steric hinderance caused by the bulky *tert*-butylamino side chain (VI and VII). The 2-ethyl substituent in VIII could possibly resist metabolic oxidation thereby allowing VIII to reach the blood levels necessary to exhibit a pharmacological effect. Both the *p*-toluidino and *p*-anisidino analogues (XIII and XIV, respectively) showed greater analgesic activity than the parent molecule (I). It is interesting to note that the 2-aminobenzothiazolo analogue (XV) exhibitd a maximum analgesic effect at a dose of 50 mg/kg.

Considerable CNS-depressant activity, as observed by marked reduction in the spontaneous motor activity (SMA) and ptosis, was exhibited with IV but was absent with V, suggesting that the 2-nitroanilino analogue was pharmacologically active while the 3-nitroanilino analogue had no pharmacological effect. The *p*-toluidino analogue (XIII) exhibited CNS-depressant activity while the corresponding *p*-anisidino derivative (XIV) had no effect on the nervous system.

The significant potentiation of pentobarbital-induced hypnosis observed with XV suggests a possible correlation between analgesic activity and the CNS-depressant effect of the 2-aminobenzothiazolo analogue. The 2-aminopyridino analogue (II) also exhibited a maximum effect on the pentobarbital-induced sleeping time in mice (Table II). The presence of the pyridine moiety may be regarded as an essential component for the strong CNS effect of this compound.

REFERENCES

(1) A. Burger, "Medicinal Chemistry," 2nd ed., Interscience New York, N.Y., 1960, p. 349.

(2) J. C. Krantz and C. J. Carr, "The Pharmacological Principle of Medical Practice," 6th ed., Williams and Wilkins, Baltimore, Md., London, 1965, p. 826.

(3) W. D. M. Paton and J. Payne, "Pharmacologic Principles and Practice," Churchill A. Ltd., London, 1969, p. 107.

(4) P. J. Hanzlik, "Action and Uses of the Salicylates and Cinchophen in Medicine," William and Wilkins, Baltimore, Md., London, 1927, p. 3194.

(5) M. T. Bogert and E. M. Ambrahamson, *J. Am. Chem. Soc.*, **4**, 44,826 (1922).

(6) R. Meduedecky, J. Durinda, P. Zakova, and L. Kopacova, *J. Cask. Farm.*, **15**, 291 (1966).

(7) H. Pfitzinger, *J. Prakt., Chem.*, **38**, 582 (1882).

(8) G. Doebner, *Justus Liebigs Ann. Chem.*, **242**, 290 (1887).

(9) A. I. Vogel, "Practical Organic Chemistry," 3rd ed., English Library Book Society, London, 1946, p. 791.

(10) D. Lednicer and L. A. Mitscher, "The Organic Chemistry of Drug Synthesis," Interscience, London, 1977, p. 344.

(11) G. F. Mann and B. C. Saunders, "Practical Organic Chemistry," 5th ed., Longman Green, London, 1957, p. 242.

(12) L. C. Miller and M. L. Tainter, *Proc. Soc. Exp. Biol. Med.*, **57**, 261 (1944).

ACKNOWLEDGMENTS

The author is deeply indebted to E. C. Onyeji and C. N. Obijiofor for their valuable assistance in the pharmacological screening. In addition, the author thanks George McDonnough and Alan Passmoor of Chelsea College, University of London, for the spectral data.

Structure of the Isonicotinyl Hydrazone of Norethindrone

KEITH BAILEY ˣ, ALLAN MENZIES, and HISAKO WATANABE

Received January 6, 1982, from the *Bureau of Drug Research, Health Protection Branch, Tunney's Pasture, Ottawa, Canada, K1A 0L2.* Accepted for publication August 10, 1982.

Abstract □ The contraceptive steroid norethindrone reacts with isoniazid both *in vivo* and *in vitro* to give the corresponding hydrazone, which exists as *syn* and *anti* (with respect to C-4) isomers. These isomers rapidly interconvert, with the *anti* form predominating in solution. The identification of the isomers was based on an interpretation of ^{1}H- and ^{13}C-NMR spectroscopic data and corroborated by high-performance liquid chromatographic and UV spectrophotometric evidence. ^{1}H- and ^{13}C-NMR spectroscopic data for other derivatives of norethindrone hydrazone are presented and interpreted.

Keyphrases □ Norethindrone—isonicotinyl hydrazone, synthesis, characterization by NMR □ NMR—isonicotinyl hydrazone of norethindrone, characterization, synthesis □ Synthesis—isonicotinyl hydrazone of norethindrone, characterization by NMR

Isoniazid (isonicotinylhydrazine) (I) reacts with ketones and aldehydes under acidic conditions. The usual products are hydrazones, but the reaction with reducing sugars gives 1-glycosyl-2-isonicotinylhydrazines (1). Reactions of this type can take place *in vivo* (2), the pharmacological and toxicological consequences of which are largely unknown. We recently showed that isoniazid reacts with norethindrone (17-hydroxy-19-nor-17α-pregn-4-en-20-yn-3-one) (II) to give the hydrazone (III) when they are coadministered orally to the rat (3) and minipig[1]. The product is readily absorbed from the GI tract (4). The analytical procedures involved conversion of norethindrone hydrazone (IV), a metabolite of III (3), to the *p*-methoxybenzaldehyde derivative (V). Some properties of V were described (3). Spectroscopic evidence for the structures of

[1] Unpublished data.

0022-3549/83/0900-1084$01.00/0

Table II—Pharmacological Activity of Cinchophen Amides in Mice[a]

Compound	ED_{50} for Analgesic Activity, mg/kg ip	ED_{50} for Pentobarbital Induced Hypnosis, mg/kg ip	LD_{50}[b], mg/kg ip
II	>150	>50[c]	>600
IV	>50	>50	>600
V	>150	>100	>500
VII	>150	>100	>600
VIII	>50	>100	>500
IX	>150	>150	>600
XIII	>100	>100	>600
XIV	>100	>150	>600
XV	>50	>50[c]	>500
XVI	>100	>50	>500
XVII	>150	>100	>600

[a] Each value is the average of four replicate experiments. [b] Taken from the work of Miller and Tainter (12) for comparison. [c] Maximum effect observed.

compared with the inactive 3-nitroaniline isomer (V) suggested that the close proximity of the nitro group to the amino moiety in the phenyl ring is essential for analgesic activity and also that possible electronic interactions exist between them. Of the four closely related analogues (VI–IX), only VIII retained the significant analgesic activity of the parent molecule, while the others showed an opposite effect. This is possibly due to the presence of either a 2-methyl side chain (VI and IX) that undergoes rapid metabolism or to steric hinderance caused by the bulky *tert*-butylamino side chain (VI and VII). The 2-ethyl substituent in VIII could possibly resist metabolic oxidation thereby allowing VIII to reach the blood levels necessary to exhibit a pharmacological effect. Both the *p*-toluidino and *p*-anisidino analogues (XIII and XIV, respectively) showed greater analgesic activity than the parent molecule (I). It is interesting to note that the 2-aminobenzothiazolo analogue (XV) exhibitd a maximum analgesic effect at a dose of 50 mg/kg.

Considerable CNS-depressant activity, as observed by marked reduction in the spontaneous motor activity (SMA) and ptosis, was exhibited with IV but was absent with V, suggesting that the 2-nitroanilino analogue was pharmacologically active while the 3-nitroanilino analogue had no pharmacological effect. The *p*-toluidino analogue (XIII) exhibited CNS-depressant activity while the corresponding *p*-anisidino derivative (XIV) had no effect on the nervous system.

The significant potentiation of pentobarbital-induced hypnosis observed with XV suggests a possible correlation between analgesic activity and the CNS-depressant effect of the 2-aminobenzothiazolo analogue. The 2-aminopyridino analogue (II) also exhibited a maximum effect on the pentobarbital-induced sleeping time in mice (Table II). The presence of the pyridine moiety may be regarded as an essential component for the strong CNS effect of this compound.

REFERENCES

(1) A. Burger, "Medicinal Chemistry," 2nd ed., Interscience New York, N.Y., 1960, p. 349.

(2) J. C. Krantz and C. J. Carr, "The Pharmacological Principle of Medical Practice," 6th ed., Williams and Wilkins, Baltimore, Md., London, 1965, p. 826.

(3) W. D. M. Paton and J. Payne, "Pharmacologic Principles and Practice," Churchill A. Ltd., London, 1969, p. 107.

(4) P. J. Hanzlik, "Action and Uses of the Salicylates and Cinchophen in Medicine," William and Wilkins, Baltimore, Md., London, 1927, p. 3194.

(5) M. T. Bogert and E. M. Ambrahamson, *J. Am. Chem. Soc.*, **4**, 44,826 (1922).

(6) R. Meduedecky, J. Durinda, P. Zakova, and L. Kopacova, *J. Cask. Farm.*, **15**, 291 (1966).

(7) H. Pfitzinger, *J. Prakt., Chem.*, **38**, 582 (1882).

(8) G. Doebner, *Justus Liebigs Ann. Chem.*, **242**, 290 (1887).

(9) A. I. Vogel, "Practical Organic Chemistry," 3rd ed., English Library Book Society, London, 1946, p. 791.

(10) D. Lednicer and L. A. Mitscher, "The Organic Chemistry of Drug Synthesis," Interscience, London, 1977, p. 344.

(11) G. F. Mann and B. C. Saunders, "Practical Organic Chemistry," 5th ed., Longman Green, London, 1957, p. 242.

(12) L. C. Miller and M. L. Tainter, *Proc. Soc. Exp. Biol. Med.*, **57**, 261 (1944).

ACKNOWLEDGMENTS

The author is deeply indebted to E. C. Onyeji and C. N. Obijiofor for their valuable assistance in the pharmacological screening. In addition, the author thanks George McDonnough and Alan Passmoor of Chelsea College, University of London, for the spectral data.

Structure of the Isonicotinyl Hydrazone of Norethindrone

KEITH BAILEY ˣ, ALLAN MENZIES, and HISAKO WATANABE

Received January 6, 1982, from the *Bureau of Drug Research, Health Protection Branch, Tunney's Pasture, Ottawa, Canada, K1A 0L2.* Accepted for publication August 10, 1982.

Abstract □ The contraceptive steroid norethindrone reacts with isoniazid both *in vivo* and *in vitro* to give the corresponding hydrazone, which exists as *syn* and *anti* (with respect to C-4) isomers. These isomers rapidly interconvert, with the *anti* form predominating in solution. The identification of the isomers was based on an interpretation of ^{1}H- and ^{13}C-NMR spectroscopic data and corroborated by high-performance liquid chromatographic and UV spectrophotometric evidence. ^{1}H- and ^{13}C-NMR spectroscopic data for other derivatives of norethindrone hydrazone are presented and interpreted.

Keyphrases □ Norethindrone—isonicotinyl hydrazone, synthesis, characterization by NMR □ NMR—isonicotinyl hydrazone of norethindrone, characterization, synthesis □ Synthesis—isonicotinyl hydrazone of norethindrone, characterization by NMR

Isoniazid (isonicotinylhydrazine) (I) reacts with ketones and aldehydes under acidic conditions. The usual products are hydrazones, but the reaction with reducing sugars gives 1-glycosyl-2-isonicotinylhydrazines (1). Reactions of this type can take place *in vivo* (2), the pharmacological and toxicological consequences of which are largely unknown. We recently showed that isoniazid reacts with norethindrone (17-hydroxy-19-nor-17α-pregn-4-en-20-yn-3-one) (II) to give the hydrazone (III) when they are coadministered orally to the rat (3) and minipig[1]. The product is readily absorbed from the GI tract (4). The analytical procedures involved conversion of norethindrone hydrazone (IV), a metabolite of III (3), to the *p*-methoxybenzaldehyde derivative (V). Some properties of V were described (3). Spectroscopic evidence for the structures of

[1] Unpublished data.

0022-3549/83/0900-1084$01.00/0

Table I—Data from ^{1}H-NMR Spectra of II, III, V, and VI [a]

	Solvent	II	IIIa	IIIb	Va	Vb	VIa	VIb
HC=N	VII				8.34	8.34		
	VIII				8.33	8.30		
H-2′,6′	VII		8.75		7.74	7.80		
	VIII		8.72		7.76	7.74		
H-3′,5′	VII		7.74		6.93	7.00		
	VIII		7.76		7.01	7.03		
H-4	VII	5.84	6.31		6.11	6.95	6.11	6.25
	VIII	5.72	6.00	6.51	6.02	6.78	6.02	6.28
OCH_3	VII				3.85	3.85		
	VIII				3.81	3.81		
C≡CH	VII	2.57	2.57		2.56	2.60	2.57	
	VIII	3.29	3.28		3.27	3.29	3.28[b]	3.30[b]
18-CH_3	VII	0.91	0.91		0.91	0.94	0.92	
	VIII	0.79	0.79		0.79	0.79	0.79	
NH	VII						11.24[b]	11.35[b]
	VIII						11.01[b]	11.11[b]

[a] Chemical shifts in ppm downfield from tetramethylsilane. The isomers of V, but not of III or VI, were determined separately. [b] These assignments may be reversed between *a* and *b*.

Table II—Data from ^{13}C-NMR Spectra of II, III, V, and VI [a]

	Solvent	II	IIIa[b]	IIIb[b]	Va[c]	Vb[c]	VIa[d]	VIb[d]
C-3	VII	200.11	—[e]		167.50	164.95	161.09	
	VIII	198.53	—		165.83	163.19	160.82	
C-5	VII	166.71	—		155.90	156.81	154.74	155.59
	VIII	166.77	—		155.47	156.26	154.87	156.26
C-4	VII	124.86	122.50	112.25[f]	122.92	115.57	121.58	111.05
	VIII	123.83	121.43	113.39[f]	122.19	114.78	120.98	110.83
—C≡	VII	87.58	88.08		87.64	87.70	87.64	
	VIII	88.91	88.94		88.97	88.97	88.97	
C-17	VII	79.86	79.86		80.04	79.98	79.89	
	VIII	78.10	78.13		78.16	78.16	78.19	
≡CH	VII	74.28	74.21		74.21	74.21	74.24	
	VIII	74.94	74.88		74.97	74.94	74.94	
C-18	VII	12.75	12.75		12.75	12.75	12.72	
	VIII	12.57	12.57		12.60	12.63	12.63	

[a] Chemical shifts in ppm downfield from tetramethylsilane. The isomers of V, but not of III or VI, were determined separately. [b] The isonicotinic acid hydrazide moiety of III gave signals from C-2′,6′ and C-3′,5′ at 150.31 (150.04) and 122.50 (121.86) ppm, respectively, in VII(VIII); others were not detected. [c] The aryl moiety of Va and Vb gave signals from C-4′, C-2′,6′, C-1′, C-3′,5′, OCH_3, and HC=N at 161.97 (161.52), 130.09 (129.78), 128.20 (127.51), 114.42 (114.42), 55.51 (55.36), and 157.72 (156.84) and at 162.03 (161.49), 130.15 (129.75), 128.08 (127.45), 114.42 (114.39), 55.51 (55.36), and 157.72 (156.69) ppm, respectively, in VII(VIII). [d] The aryl moiety of VI gave double signals from C-1′, C-4′, C-5′, C-2′, C-3′, and C-6′ centered at 145.13 (144.45), 137.81 (136.83), 130.12 (130.17), 129.27 (129.16), 123.83 (123.13), and 116.55 (116.06) ppm, respectively, in VII(VIII). [e] Signals were broad and weak or not detected. [f] Weak signal.

III, V, and the 2,4-dinitrophenylhydrazone of II (VI, prepared as a model compound) is presented here.

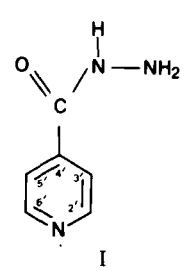

I

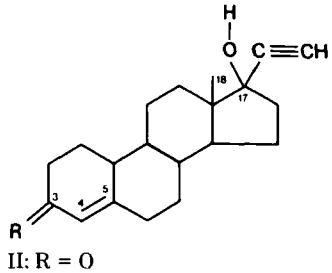

II: R = O
III: R = $C_5H_4NCONHN$
IV: R = H_2NN
V: R = $C_6H_4(OCH_3)CH{=}N{-}N$
VI: R = $C_6H_3(NO_2)_2NHN$

EXPERIMENTAL

Isoniazid[2], *p*-methoxybenzaldehyde[3], hydrazine[4], 2,4-dinitrophenylhydrazine[3], and norethindrone[5] were used to prepare III, V, and VI by general or previously described methods (3). ^{1}H-NMR and broad-band decoupled ^{13}C-NMR spectra were recorded at 80 and 20.1 MHz, respectively, on a Fourier-transform spectrometer[6] at ambient temperature. The deuterium resonance of the solvent, $CDCl_3$[7] (VII) or DMSO-d_6[7] (VIII), provided an internal lock and TMS[8] was the internal reference from which downfield chemical shifts (δ) are expressed in ppm. Interferograms of 4K Fourier-transformed output data points (latterly 8K) and sweepwidths of 1000 and 5000 Hz gave separations in memory addresses of 0.004 and 0.06 (latterly 0.03) ppm for ^{1}H- and ^{13}C-NMR spectra, respectively.

RESULTS AND DISCUSSION

As described previously, hydrazone V is easily separated into isomers Va and Vb, respectively (3). IR spectra of these (KBr pellet) show minor differences in the fingerprint region, but none are helpful in making structural assignments. Their mass spectra are essentially identical, while the UV absorption maximum of Va is at 323 nm and Vb is at 315 nm (3).

^{1}H-NMR spectroscopic data for II, III, Va, Vb, and VI are presented in Table I. Two isomers (~1:1, VIa–VIb) could be detected in the spectra of VI and in the spectrum of III determined in DMSO-d_6 (~2:1, IIIa–IIIb). Signals of isomers have closely similar chemical shifts except for the signal assigned to H-4, which has a width at half-height ($w_{1/2}$) of ~5 Hz in each case. The chemical shifts and widths of these signals are appropriate for Δ^4 rather than Δ^5 structures (5). ^{1}H-NMR data for *syn* and *anti* (with respect to C-4) oximes of some 3 keto-Δ^4 steroids show that H-4 appears at ~6.5 and 5.9 ppm, respectively (6), suggesting that the *a* forms are the *anti* isomers.

Data from the ^{13}C-NMR spectra are presented in Table II. It is beyond our present scope to assign all of the signals, especially the 14 signal (steroidal) appearing between ~20 and 50 ppm, but assignments of the remainder have been made by comparison with compiled data (7). Limited quantities of III, the presence of both isomers in DMSO-d_6, and

[2] Sigma Chemical Co., St. Louis, Mo.
[3] BDH Chemicals Ltd., Poole, England.
[4] Fisher Scientific Co., Fair Lawn, N.J.
[5] Supplied by G. D. Searle, Chicago, Ill.
[6] Bruker WP80; Bruker Spectrospin (Canada) Ltd., Mississauga, Ont.
[7] Merck Sharpe & Dohme (Canada) Ltd., Montréal, Québec.
[8] Stohler Isotope Chemicals, Montréal, Québec.

its low solubility in $CDCl_3$ prevented us from detecting all of the signals. It is also possible that the rates of interconversion of the two forms are such that while the proton chemical shifts are time-averaged in $CDCl_3$, although distinct in DMSO-d_6, certain of the ^{13}C-NMR signals are broadened by these processes and hence obscured (8). Variable temperature studies that might answer these questions are beyond our present capabilities. The ^{13}C-NMR spectra showed differences at C-3, C-4, and C-5 of ~2.5 and 7 ppm downfield and 1 ppm upfield, respectively, for V*a* in comparison with V*b*. Comparable differences were also found between the unseparated forms of III and VI and so have been assigned to *a* and *b* isomers in Tables I and II by comparison with V*a* and V*b* data. The resonances of carbons *anti* to hydrazones and oximes appear 6–12 ppm downfield from the positions of the corresponding *syn* carbons (9), again in agreement with assignment of the *anti* configuration to the *a* forms.

In further support, the order of elution (V*a* followed by V*b*) on high-performance liquid chromatography (HPLC) (3) is compatible with this assignment (6), and the UV data also suggest that the conjugated double bonds are more extended in V*a* than in V*b* (10, 11). Thus, the structures depicted are initially proposed for this series of compounds (the most stable rotational conformation about the N—N bond is shown).

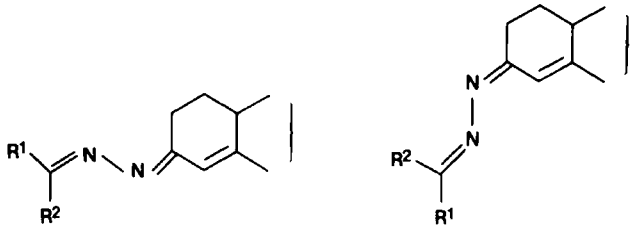

V*a*,V*a*′ V*b*,V*b*′

V*a*,V*b*: R^1 = *p*-$(OCH_3)C_6H_4$, R^2 = H
V*a*′,V*b*′: R^1 = H, R^2 = *p*-$(OCH_3)C_6H_4$

A particularly interesting feature of the spectra of VI was that the aromatic carbon-13 signals were all doubled (except for C-3′ and C-5′ in $CDCl_3$). The signals, separated by 0.1–0.2 ppm, presumably arise from the *syn* and *anti* isomers, and were assigned (Table II) by comparison with the spectrum of the 2,4-dinitrophenylhydrazone of cyclohexanone in which they are not, of course, doubled. The additional possibility in azine V of *anti*/*syn* isomerism about the aldimino double bond (HC=N) leads to alternative structures V*a*′ and V*b*′, which are expected to have very similar NMR and UV absorption properties to those of V*a* and V*b*, respectively. It does not seem that mixtures are present, and it is very unlikely that the two forms of V are V*a* with V*b*′ or V*a*′ with V*b*, as neither the ^1H-NMR nor the ^{13}C-NMR shifts of the HC=N function differ between isomers (Tables I and II). The stable *anti* aldimino configuration (V*a* and V*b*) is favored.

It is evident that hydrazine-based derivatives of norethindrone can be produced *in vivo* by interaction with isoniazid. We have found that the metabolic disposition of the steroid is thereby altered[1]. Other pharmacologically important steroids and possibly other hydrazine-derived drugs may undergo similar interactions. *Syn* and *anti* isomers of norethindrone hydrazones arise and can be identified. They undergo rapid interconversion in some cases, but may be separated in others. Whether tissue enzymes, which further metabolize the hydrazones (3), are selective for *syn*/*anti* isomers remains to be determined. If such selectivity were to occur, one might expect that the rate of metabolism of various hydrazones would be dependent, *inter alia*, on the relative degree of interconvertibility of the isomers.

REFERENCES

(1) K. Bailey and A. G. Butterfield, *Can. J. Chem.*, **59**, 641 (1981).

(2) J. P. O'Donnell, W. J. Proveaux, and J. K. H. Ma, *J. Pharm. Sci.*, **68**, 1524 (1979).

(3) H. Watanabe, J. A. Menzies, N. Jordan, and J. C. K. Loo, *Res. Commun. Chem. Path. Pharmacol.*, **31**, 435 (1981).

(4) H. Watanabe, J. A. Menzies, and J. C. K. Loo, *Experientia*, **37**, 883 (1981).

(5) N. S. Bhacca and D. H. Williams, "Applications of NMR Spectroscopy in Organic Chemistry," Holden-Day, San Francisco, Calif., 1964, pp. 87–90.

(6) M. Patthy and E. Tomori, *J. Chromatogr.*, **191**, 145 (1980).

(7) E. Breitmaier, G. Haas, and W. Voelter, "Atlas of Carbon-13 NMR Data," Vol. 2, Heyden, Philadelphia, Pa., 1979, entries 2673–84.

(8) F. W. Wehrli and T. Wirthlin, "Interpretation of Carbon-13 NMR Spectra," Heyden, New York, N.Y., 1976, pp. 197–215.

(9) C. A. Bunnell and P. L. Fuchs, *J. Org. Chem.*, **42**, 2614 (1977).

(10) J. R. Dyer, "Applications of Absorption Spectroscopy of Organic Compounds," Prentice-Hall, Englewood Cliffs, N.J., 1965, pp. 19, 20.

(11) D. J. Cram and G. S. Hammond, "Organic Chemistry," McGraw-Hill, New York, N.Y., 1959, p. 618.

ACKNOWLEDGMENTS

The authors thank Mr. H. W. Avdovich for determining NMR spectra.

Effect of the Nonionic Surfactant Poloxamer 338 on the Fate and Deposition of Polystyrene Microspheres Following Intravenous Administration

LISBETH ILLUM * **and STANLEY S. DAVIS** ‡

Received December 11, 1981, from the **Department of Pharmaceutics, The Royal Danish School of Pharmacy, DK-2100 Copenhagen, Denmark*, and the ‡*Department of Pharmacy, University of Nottingham, University Park, Nottingham, NG7 2RD, U.K.* Accepted for publication August 25, 1982.

Abstract □ The blood clearance and organ deposition of polystyrene microspheres in the rabbit following intravenous injection has been investigated using the technique of gamma scintigraphy, blood and organ level measurements, and histology. Uncoated microspheres of 1.27-μm diameter were cleared rapidly from the blood and were taken up primarily by the reticuloendothelial system in the liver. Coating of the microspheres with the nonionic surface-active agent poloxamer 338 reduced the uptake in the liver and gave a corresponding increase in the lungs.

Keyphrases □ Microspheres, polystyrene—effect of nonionic surfactants on blood clearance and deposition, intravenous administration □ Nonionic surfactants—effect on blood clearance and deposition of polystyrene microspheres, intravenous administration □ Deposition, tissue—polystyrene microspheres following intravenous administration, effect of nonionic surfactants □ Blood clearance—polystyrene microspheres following intravenous administration, effect of nonionic surfactants

Colloidal systems such as liposomes, microspheres, nanospheres, and emulsions have been investigated as potential drug-targeting devices (1–4). The fate of such particles in the body following administration is deter-

0022-3549/83/0900-1086$01.00/0

its low solubility in $CDCl_3$ prevented us from detecting all of the signals. It is also possible that the rates of interconversion of the two forms are such that while the proton chemical shifts are time-averaged in $CDCl_3$, although distinct in DMSO-d_6, certain of the ^{13}C-NMR signals are broadened by these processes and hence obscured (8). Variable temperature studies that might answer these questions are beyond our present capabilities. The ^{13}C-NMR spectra showed differences at C-3, C-4, and C-5 of ~2.5 and 7 ppm downfield and 1 ppm upfield, respectively, for V*a* in comparison with V*b*. Comparable differences were also found between the unseparated forms of III and VI and so have been assigned to *a* and *b* isomers in Tables I and II by comparison with V*a* and V*b* data. The resonances of carbons *anti* to hydrazones and oximes appear 6–12 ppm downfield from the positions of the corresponding *syn* carbons (9), again in agreement with assignment of the *anti* configuration to the *a* forms.

In further support, the order of elution (V*a* followed by V*b*) on high-performance liquid chromatography (HPLC) (3) is compatible with this assignment (6), and the UV data also suggest that the conjugated double bonds are more extended in V*a* than in V*b* (10, 11). Thus, the structures depicted are initially proposed for this series of compounds (the most stable rotational conformation about the N—N bond is shown).

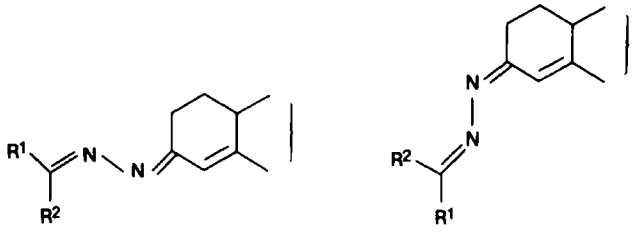

V*a*,V*a*′ V*b*,V*b*′

V*a*,V*b*: R^1 = *p*-$(OCH_3)C_6H_4$, R^2 = H
V*a*′,V*b*′: R^1 = H, R^2 = *p*-$(OCH_3)C_6H_4$

A particularly interesting feature of the spectra of VI was that the aromatic carbon-13 signals were all doubled (except for C-3′ and C-5′ in $CDCl_3$). The signals, separated by 0.1–0.2 ppm, presumably arise from the *syn* and *anti* isomers, and were assigned (Table II) by comparison with the spectrum of the 2,4-dinitrophenylhydrazone of cyclohexanone in which they are not, of course, doubled. The additional possibility in azine V of *anti*/*syn* isomerism about the aldimino double bond (HC=N) leads to alternative structures V*a*′ and V*b*′, which are expected to have very similar NMR and UV absorption properties to those of V*a* and V*b*, respectively. It does not seem that mixtures are present, and it is very unlikely that the two forms of V are V*a* with V*b*′ or V*a*′ with V*b*, as neither the ^1H-NMR nor the ^{13}C-NMR shifts of the HC=N function differ between isomers (Tables I and II). The stable *anti* aldimino configuration (V*a* and V*b*) is favored.

It is evident that hydrazine-based derivatives of norethindrone can be produced *in vivo* by interaction with isoniazid. We have found that the metabolic disposition of the steroid is thereby altered[1]. Other pharmacologically important steroids and possibly other hydrazine-derived drugs may undergo similar interactions. *Syn* and *anti* isomers of norethindrone hydrazones arise and can be identified. They undergo rapid interconversion in some cases, but may be separated in others. Whether tissue enzymes, which further metabolize the hydrazones (3), are selective for *syn*/*anti* isomers remains to be determined. If such selectivity were to occur, one might expect that the rate of metabolism of various hydrazones would be dependent, *inter alia*, on the relative degree of interconvertibility of the isomers.

REFERENCES

(1) K. Bailey and A. G. Butterfield, *Can. J. Chem.*, **59**, 641 (1981).

(2) J. P. O'Donnell, W. J. Proveaux, and J. K. H. Ma, *J. Pharm. Sci.*, **68**, 1524 (1979).

(3) H. Watanabe, J. A. Menzies, N. Jordan, and J. C. K. Loo, *Res. Commun. Chem. Path. Pharmacol.*, **31**, 435 (1981).

(4) H. Watanabe, J. A. Menzies, and J. C. K. Loo, *Experientia*, **37**, 883 (1981).

(5) N. S. Bhacca and D. H. Williams, "Applications of NMR Spectroscopy in Organic Chemistry," Holden-Day, San Francisco, Calif., 1964, pp. 87–90.

(6) M. Patthy and E. Tomori, *J. Chromatogr.*, **191**, 145 (1980).

(7) E. Breitmaier, G. Haas, and W. Voelter, "Atlas of Carbon-13 NMR Data," Vol. 2, Heyden, Philadelphia, Pa., 1979, entries 2673–84.

(8) F. W. Wehrli and T. Wirthlin, "Interpretation of Carbon-13 NMR Spectra," Heyden, New York, N.Y., 1976, pp. 197–215.

(9) C. A. Bunnell and P. L. Fuchs, *J. Org. Chem.*, **42**, 2614 (1977).

(10) J. R. Dyer, "Applications of Absorption Spectroscopy of Organic Compounds," Prentice-Hall, Englewood Cliffs, N.J., 1965, pp. 19, 20.

(11) D. J. Cram and G. S. Hammond, "Organic Chemistry," McGraw-Hill, New York, N.Y., 1959, p. 618.

ACKNOWLEDGMENTS

The authors thank Mr. H. W. Avdovich for determining NMR spectra.

Effect of the Nonionic Surfactant Poloxamer 338 on the Fate and Deposition of Polystyrene Microspheres Following Intravenous Administration

LISBETH ILLUM * **and STANLEY S. DAVIS** ‡

Received December 11, 1981, from the **Department of Pharmaceutics, The Royal Danish School of Pharmacy, DK-2100 Copenhagen, Denmark*, and the ‡*Department of Pharmacy, University of Nottingham, University Park, Nottingham, NG7 2RD, U.K.* Accepted for publication August 25, 1982.

Abstract □ The blood clearance and organ deposition of polystyrene microspheres in the rabbit following intravenous injection has been investigated using the technique of gamma scintigraphy, blood and organ level measurements, and histology. Uncoated microspheres of 1.27-μm diameter were cleared rapidly from the blood and were taken up primarily by the reticuloendothelial system in the liver. Coating of the microspheres with the nonionic surface-active agent poloxamer 338 reduced the uptake in the liver and gave a corresponding increase in the lungs.

Keyphrases □ Microspheres, polystyrene—effect of nonionic surfactants on blood clearance and deposition, intravenous administration □ Nonionic surfactants—effect on blood clearance and deposition of polystyrene microspheres, intravenous administration □ Deposition, tissue—polystyrene microspheres following intravenous administration, effect of nonionic surfactants □ Blood clearance—polystyrene microspheres following intravenous administration, effect of nonionic surfactants

Colloidal systems such as liposomes, microspheres, nanospheres, and emulsions have been investigated as potential drug-targeting devices (1–4). The fate of such particles in the body following administration is deter-

0022-3549/83/0900-1086$01.00/0

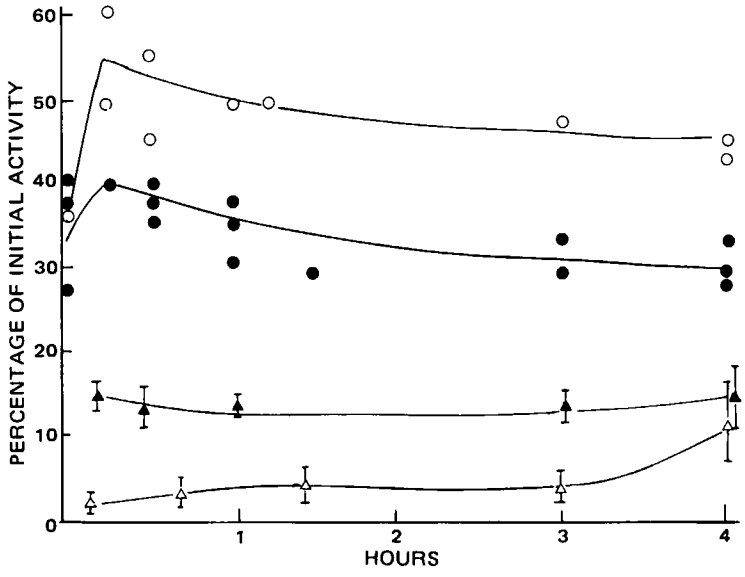

Figure 1—*Activity-time profiles for blood and liver following intravenous administration of ^{131}I-labeled polystyrene microspheres. Key: uncoated, (○) liver, (△) blood; coated with poloxamer 338, (●) liver, (▲) blood.*

mined by the chemical nature of the colloid and its physical characteristics such as particle size and surface charge (5). The reticuloendothelial system plays a major role in clearing small particles from the circulation following intravenous administration, while larger particles are trapped in the capillary beds of the lungs. Studies on emulsion systems have indicated the important role of the surface layer of the emulsifier. The use of nonionic emulsifiers (*e.g.*, poloxamer) leads to slow clearance from the bloodstream and an altered distribution pattern to organ sites (6).

In this work such effects have been investigated further in rabbits using a model colloidal system, polystyrene microspheres. This material has been well characterized physically, including studies involving the adsorption of nonionic surfactants (7, 8). In addition, polystyrene microspheres labeled with a gamma ray-emitting radionuclide have been used to study the distribution, fate, and acute and semichronic effects of microspheres in animal models (9–11).

EXPERIMENTAL

Administration of Microspheres—Polystyrene microspheres (1.27 μm) were obtained from a commercial supplier[1]. The particle size was verified using an electronic particle counter[2] with a 30-μm orifice tube. The particles were surface-labeled with iodine-131 by a process of irradiation using a cobalt-60 source with the microspheres suspended in a solution of 2-mCi $Na^{131}I$; the total irradiation dose was 5 Mrad. The particles were dialyzed free from $Na^{131}I$. Preliminary experiments *in vitro* and *in vivo* indicated that the integrity of the label was satisfactory, although some free iodide was detectable after dialysis for 120-hr against rabbit plasma.

In each experiment, 50–75 μCi of labeled material was administered. The particles ($\sim 2 \times 10^8$) were suspended in saline and rapidly injected. One group received microspheres that had been equilibrated for 24-hr in a saline solution containing 1% w/v poloxamer 338[3], molecular weight of poloxypropylene moiety 3250, polyoxyethylene content 80–90% (8).

The surface charge on the microspheres over the pH range 2–10 was determined using cell-microelectrophoresis[4] (12). The microspheres were also equilibrated at 25° at pH 7.4 with a 1% poloxamer 338 solution for 24 hr in the presence or absence of rabbit plasma (1:1 mixture with the microsphere suspension). All samples were diluted with 1.54×10^{-4} *M* NaCl solution before measurement of the surface charge at pH 7.4. Any adjustment in pH was carried out using hydrochloric acid or sodium hydroxide. The state of aggregation of the microspheres was examined using the light microscope. The adsorption of poloxamer 338 on the surface of polystyrene microspheres of the same approximate size and the same surface characteristics has been investigated in detail by Kayes and Rawlins (5). Equilibration was reached in 24 hr. The isotherms were Langmuirian, and the thickness of the adsorbed layer was 26 nm.

Animal Experiments—New Zealand White rabbits 2–4 kg in weight were randomly divided into two groups of three. The microspheres were injected into the marginal ear vein. The distribution of the microspheres in various body organs was followed using external scintigraphic imaging[5]. Dynamic and static views were recorded at suitable times during a 10-day period and processed by computer[6]. Blood samples were removed at suitable intervals and were analyzed for radioactivity using a gamma counter[7]. At the end of 11 days the animals were sacrificed and the organs removed. Small samples were taken for histological investigation, and the total organ activity in the remainder was determined using a well-type gamma counter[8]. The histological samples were fixed, dehydrated, and mounted in wax. Microtome sections were stained using hematoxylin–eosin.

RESULTS

Properties of the Microspheres—The electrophoretic mobility–pH relationship for the polystyrene microspheres showed that at a physiological pH value (7.4) in 1.54×10^{-4} *M* NaCl, the particles carried a net negative charge (zeta potential) of −35 mV. In the presence of 1% poloxamer 338, the surface charge was reduced to −8 mV. This is due to the presence of an adsorbed layer of polymer on the surface of the particles (8). Incubation of polystyrene microspheres with rabbit plasma caused a reduction of surface charge to −15 mV. The presence of poloxamer on the surface of the particle prior to incubation with plasma caused the surface charge to be reduced to almost zero. The reduction in charge brought about by added plasma is thought to be due to the adsorption of plasma proteins (*e.g.*, albumin or globulin) or more specific substances such as fibronectin (13–15). Microscopic examination showed that added plasma caused aggregation of the microspheres, but this was prevented by the presence of poloxamer 338.

Gamma Scintigraphy—The processed computer images showed that the small microspheres were rapidly taken up by the liver of the rabbit (Fig. 1). No other body organs were visualized on the scintiscans except small quantities of activity that were observed in the thyroid and/or bladder, which can be attributed to the presence of small quantities of free iodide. There was no evidence of large numbers of particles being taken up by the lungs. The presence of an adsorbed layer of poloxamer 338 on the microspheres reduced the uptake in the liver. This difference,

[1] Dow Diagnostics, Dow Co., Indianapolis, Ind.
[2] Coulter Counter TAII, Coulter Electronics, Harpended, U.K.
[3] Pluronic F108 (poloxyethylene–polyoxypropylene copolymer), Ugine Kuhlmann Ltd., Bolton, U.K.
[4] Rank Mk. II Microelectrophoresis apparatus, Rank Bros., Cambridge, U.K.
[5] Maxi Camera II—gamma camera—General Electric, Milwaukee, Wis.
[6] Gammascope, Link Systems Ltd., High Wycombe, U.K.
[7] Intertechnique CG4000 gamma counter, Intertechnique, Uxbridge, U.K.
[8] Bucket Counter, Ortec, Bracknell, U.K.

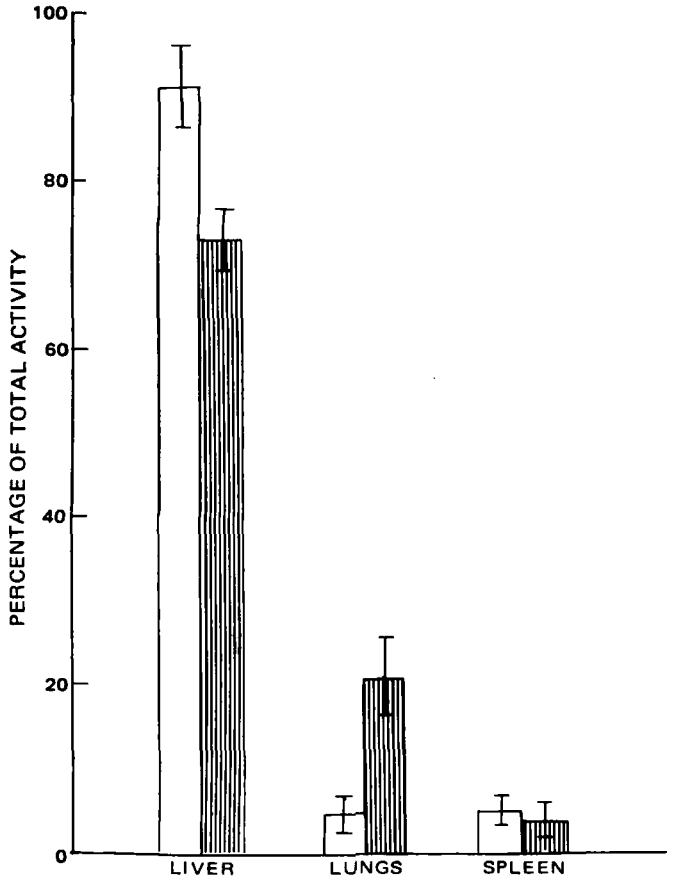

Figure 2—*Tissue distribution of iodine-131 11 days after administration of ^{131}I-labeled polystyrene microspheres. Key: (□) uncoated; (■) coated with poloxamer 338.*

caused by the presence of the nonionic surfactant, was still evident after 11 days of imaging.

Blood Levels—The blood level–time profiles (Fig. 1) show that clearance of the microspheres from the blood is affected by the presence of poloxamer 338. In the absence of the surfactant, the particles are cleared rapidly and the blood levels are low. In contrast, in the presence of poloxamer 338 significant sustained levels of activity were observed over a period of many hours.

Organ Levels—The distribution of activity after 11 days postadministration is shown in Fig. 2 for the three major sites of uptake. The majority of the activity was in the liver, with much smaller quantities in the lung and spleen. The group that received microspheres coated with poloxamer had less activity in the liver and more activity in the lungs compared with the control group which received microspheres alone.

Histology—Conventional histological techniques would not be expected to show small individual microspheres of 1.27 μm in body tissues. Histological examinations were undertaken, therefore, to reveal aggregated particles. None were observed.

DISCUSSION

Effect of Poloxamer on the Deposition of Microspheres—The results from scintigraphic imaging, blood level determinations, and organ uptake studies all show clearly that the adsorption of a layer of poloxamer 338 onto the surface of polystyrene microspheres affects their deposition in the rabbit following intravenous administration. Differential leaching of the radiolabel from the particles prior and subsequent to administration would be expected to alter the absolute values for deposition, but not their relative magnitudes. The uncoated particles were deposited mainly in the liver; it is well known that small colloidal particles will be cleared rapidly from the bloodstream by the reticuloendothelial system of this organ, *i.e.*, the Kupffer cells (16). Larger particles (normally those >7 μm) will be cleared by the lungs by a process of filtering or mechanical obstruction (10).

The coating of colloidal particles with polymers and macromolecules can alter organ uptake considerably. Wilkins and coworkers (17, 18) have demonstrated the importance of surface modification as well as surface charge. Negatively charged particles are removed from the circulatory system quite rapidly, whereas positive and neutral particles have different clearance patterns. Certain positively charged particles can be taken up by the lungs and then rapidly redistributed to the spleen rather than the liver (17). The important process controlling the fate and deposition of colloidal particles would seem to be one of the interaction of a foreign surface with the blood and the coating of that surface with various components such as albumin, globulin, *etc;* the exact coating material being determined by the nature of the particle itself. The coating then influences the interaction of the particle with cells of the reticuloendothelial system (5). Certain blood components (termed opsonins) can enhance phagocytic uptake (16). Van Oss *et al.* (19) have discussed the role of surface hydrophobicity in phagocytic engulfment and cell adhesiveness. Particles with low contact angles are taken up much less rapidly by phagocytes than particles with high contact angles. Poloxamer 338 causes a very significant reduction in the contact angle of the hydrophobic polystyrene particles.

Studies that have dealt specifically with nonionic surface-active agents have employed both polystyrene microspheres and emulsion systems. For example, Singer *et al.* (5) found that microspheres coated with polysorbate 80 showed the slowest decline in blood concentration. Similarly, Jeppsson and Rossner (20) using fat emulsions demonstrated the importance of the molecular weight of the adsorbed surfactant, poloxamer 338 (mol wt 3250) being much more effective at reducing the clearance rate of droplets than poloxamer 188 (mol wt 1750). Such differences could be due to the different thicknesses of the adsorbed layers (26 and 14 nm, respectively, for 338 and 188) and/or to differences in surface charge (8).

The increased uptake of the coated microspheres in the lungs (after 11 days) is more difficult to explain. One obvious reason would be aggregation, and the entrapment of the larger entities so created, in the lungs. Kanke *et al.* (10) have reported "clusters" of microspheres in histological preparations. However, no aggregates of a size that would be trapped in lung capillaries were seen in the histological specimens, and the *in vitro* studies showed that the nonionic surfactant brought about deaggregation even though the microsphere system with adsorbed poloxamer and plasma components had the lowest surface charge. It is recognized that a different type of aggregation–deaggregation process could occur *in vivo*, since the microspheres are exposed to different environments and the poloxamer could be modified by metabolic changes.

The critical minimum particle size for deposition in the lungs is usually regarded as being ~7–10 μm, depending on the nature of the particle and its shape (21). However, a recent report by Findler *et al.* (22) has shown that efficient localization of liposomes in the capillary bed of the lungs could be achieved using negatively charged multilamellar liposomes 1–2 μm in diameter. This size range covers the microspheres used in the present work. Furthermore, uptake of technetium-99m–sulfur colloid (particle size 400–600 nm) in the lungs has been reported in clinical diagnostic studies (23).

The pathophysiology of such increased uptake of colloid in the lung is poorly understood, but evidence from human and animal studies does not support the hypothesis that *in vivo* microaggregation results in the formation of microemboli that are trapped in the lung. The evidence does support the possibilities of increased phagocytic activity in the pulmonary capillary bed or adherence of colloid to altered endothelium in the pulmonary capillaries (23, 24). Thus, the modified surface properties of the microspheres coated by poloxamer could potentiate their uptake in the lungs.

REFERENCES

(1) D. Papahadjopoulos, *Ann. N.Y. Acad. Sci.*, **308**, 1 (1978).

(2) H. Teder, K. F. Aronsen, K. F. Lindell, and U. Rothman, *Acta Chir. Scand.*, **144** Suppl. 487, 71 (1978).

(3) P. Speiser, in "Optimisation of Drug Delivery," H. Bundgaard, A. Bagger-Hansen, and H. Kofod, Eds., Munksgaard, Copenhagen, 1982, p. 305.

(4) S. S. Davis, in "Optimisation of Drug Delivery," H. Bundgaard, A. Bagger-Hansen, and H. Kofod, Eds., Munksgaard, Copenhagen, 1982, p. 198.

(5) J. M. Singer, S. Lavie, L. Adlersberg, E. Ende, E. M. Hoenig, and Y. Tchorsh, in "The Reticuloendothelial System and Atherosclerosis," N. R. DiLuzio and R. Paoletti, Eds., Plenum, New York, N.Y., 1967, p. 18.

(6) S. S. Davis and P. K. Hansrani, in "Radionuclide Imaging in Drug

Research," C. G. Wilson, J. G. Hardy, M. Frier, and S. S. Davis, Eds., Croom Helm, London, 1981.
(7) R. H. Ottewill and J. N. Shaw, *Electroanal. Chem.*, **37**, 133 (1972).
(8) J. B. Kayes and D. A. Rawlins, *Colloid Polym. Sci.*, **257**, 622 (1979).
(9) H. G. Schroeder, G. H. Simmons, G. P. Sherman, and P. P. DeLuca, *J. Pharm. Sci.*, **67**, 508 (1978).
(10) M. Kanke, G. H. Simmons, D. L. Weiss, B. A. Bivins, and P. P. DeLuca, *J. Pharm. Sci.*, **69**, 755 (1980).
(11) J. D. Slack, M. Kanke, G. H. Simmons, and P. P. DeLuca, *J. Pharm. Sci.*, **70**, 660 (1981).
(12) A. D. Bangham, D. H. Heard, R. Flemans, and G. V. F. Seaman, *Nature (London)*, **182**, 642 (1958).
(13) J. Zborowski, F. Roerdink, and G. Scherphof, *Biochim. Biophys. Acta*, **497**, 183 (1977).
(14) J. Molnar, S. McLain, C. Allen, H. Laga, A. Gara, and F. Gelder, *Biochim. Biophys. Acta*, **493**, 37 (1977).
(15) A. Vaheri and D. F. Mosher, *Biochim. Biophys. Acta*, **516**, 1 (1978).
(16) A. E. Stuart, "The Reticuloendothelial System," Livingstone, Edinburgh, 1970.
(17) D. J. Wilkins, in "The Reticuloendothelial System," N. R. DiLuzio and R. Paoletti, Eds., Plenum, New York, N.Y., 1967, p. 25.
(18) D. J. Wilkins and P. A. Myers, *Br. J. Expl. Pathol.*, **47**, 568 (1966).
(19) C. J. Van Oss, C. F. Gillman, and A. W. Neumann, "Phagocytic Engulfment and Cell Adhesiveness as Surface Phenomena," Dekker, New York, N.Y., 1975.
(20) R. Jeppsson and S. Rossner, *Acta Pharm. Toxicol.*, **37**, 134 (1975).
(21) L. Illum, S. S. Davis, C. G. Wilson, N. W. Thomas, M. Frier, and J. G. Hardy, *Intern. J. Pharmaceut.*, **12**, 135 (1982).
(22) I. J. Findler, A. Raz, W. E. Fogler, R. Kirsh, P. Bugelski, and G. Poste, *Cancer Res.*, **40**, 4460 (1980).
(23) W. C. Klingensmith, S. L. Yang, and H. N. Wagner, *J. Nucl. Med.*, **19**, 31 (1978).
(24) W. C. Klingensmith and T. W. Ryerson, *J. Nucl. Med.*, **14**, 201 (1973).

ACKNOWLEDGMENTS

The authors thank the NATO Science Fellowships Programme for financial assistance. The advice and expertise of Drs. M. Frier, J. G. Hardy, C. G. Wilson, and N. Thomas of the Medical School, University of Nottingham, are gratefully acknowledged. Helpful assistance in experimental work was obtained from S. N. Mills, A. Robinson, S. K. Wong, and J. Ratcliffe.

Application of Postcolumn Ionization in the High-Performance Liquid Chromatographic Analysis of Butabarbital Sodium Elixir

EDITH P. SCOTT

Received February 16, 1982, from the *Food and Drug Administration, Atlanta, GA 30309.* Accepted for publication August 16, 1982.

Abstract □ A sensitive postcolumn ionization high-performance liquid chromatographic (HPLC) method for the quantitative determination of butabarbital sodium in butabarbital sodium elixir is described. The procedure employs a octadecylsilane column chemically bonded to porous silica microparticles. The mobile phase is a mixture of methanol and water (typically 35:65), adjusted to provide separation of butabarbital from two degradation compounds and other formulation ingredients. A buffer (pH 10) added between the column and detector provides for the primary ionization of the barbiturate necessary for optimum UV-detector sensitivity at ~240 nm. Determinations are made using the sodium salt; thus the need for extraction of the free base is eliminated. The procedure is linear over the 0.3–0.9-mg/ml concentration range of butabarbital sodium. Reproducibility values for 10 injections of a single reference standard range from 100.2 to 100.8% of theoretical with a mean of 100.5% and a coefficient of variation of 0.23%. An interlaboratory precision study for blind duplicates of one simulated product formulation and two commercial elixers produced coefficients of variation of 1.4, 1.3, and 1.1%, respectively. Recovery determinations for the drug in simulated product formulations ranged from 98.4 to 99.0%, intralaboratory, and 97.7 to 102.2%, interlaboratory. The HPLC procedure is stability indicating with respect to two decomposition products.

Keyphrases □ Butabarbital sodium—application of postcolumn ionization in higher-performance liquid chromatographic analysis, elixir □ Ionization—postcolumn, application in high-performance liquid chromatographic analysis of butabarbital sodium elixir □ High-performance liquid chromatography—application of postcolumn ionization, analysis of butabarbital sodium elixir

The chromaphoric characteristics of barbiturates establish them as prime compounds for high-performance liquid chromatographic (HPLC) analysis using a combination of reverse-phase chromatography and postcolumn ionization with a pH 10 buffer. Clark and Chan (1) have reported the advantages of combining conventional reverse-phase chromatography and postcolumn ionization into a single system. In this study, their analytical approach has been successfully employed in the assay of butabarbital sodium elixir. The procedure eliminates the need for extraction of butabarbital free acid. No sample cleanup was required because a suitable chromatographic system was found that would resolve the phenobarbital internal standard, butabarbital, placebo ingredients, and one decomposition product, capuride.

Table I—Typical HPLC Standard Curve Data [a] for Butabarbital Sodium

Butabarbital Sodium Added, mg/50 ml	Butabarbital Sodium, Found, mg/50 ml	Percent of Theoretical
16.73	16.54	98.9
23.24	23.19	99.8
30.36	30.27	99.7
38.00	38.00	100.0
46.00	45.82	99.6

[a] Correlation coefficient = 0.9999.

EXPERIMENTAL

Apparatus—The liquid chromatograph[1] consisted of a solvent pump with flow controller; an injector with flowing-stream, valve-controlled

[1] Waters Liquid Chromatograph; Model 6000-A Solvent Delivery System, Model 720 System Controller, Model U6K Injector, Model 440 Absorbance Detector with 254 nm filter, Model 730 Data Module; Waters Associates, Milford, Mass.

0022-3549/83/0900-1089$01.00/0

Research," C. G. Wilson, J. G. Hardy, M. Frier, and S. S. Davis, Eds., Croom Helm, London, 1981.
(7) R. H. Ottewill and J. N. Shaw, *Electroanal. Chem.*, **37**, 133 (1972).
(8) J. B. Kayes and D. A. Rawlins, *Colloid Polym. Sci.*, **257**, 622 (1979).
(9) H. G. Schroeder, G. H. Simmons, G. P. Sherman, and P. P. DeLuca, *J. Pharm. Sci.*, **67**, 508 (1978).
(10) M. Kanke, G. H. Simmons, D. L. Weiss, B. A. Bivins, and P. P. DeLuca, *J. Pharm. Sci.*, **69**, 755 (1980).
(11) J. D. Slack, M. Kanke, G. H. Simmons, and P. P. DeLuca, *J. Pharm. Sci.*, **70**, 660 (1981).
(12) A. D. Bangham, D. H. Heard, R. Flemans, and G. V. F. Seaman, *Nature (London)*, **182**, 642 (1958).
(13) J. Zborowski, F. Roerdink, and G. Scherphof, *Biochim. Biophys. Acta*, **497**, 183 (1977).
(14) J. Molnar, S. McLain, C. Allen, H. Laga, A. Gara, and F. Gelder, *Biochim. Biophys. Acta*, **493**, 37 (1977).
(15) A. Vaheri and D. F. Mosher, *Biochim. Biophys. Acta*, **516**, 1 (1978).
(16) A. E. Stuart, "The Reticuloendothelial System," Livingstone, Edinburgh, 1970.
(17) D. J. Wilkins, in "The Reticuloendothelial System," N. R. DiLuzio and R. Paoletti, Eds., Plenum, New York, N.Y., 1967, p. 25.
(18) D. J. Wilkins and P. A. Myers, *Br. J. Expl. Pathol.*, **47**, 568 (1966).
(19) C. J. Van Oss, C. F. Gillman, and A. W. Neumann, "Phagocytic Engulfment and Cell Adhesiveness as Surface Phenomena," Dekker, New York, N.Y., 1975.
(20) R. Jeppsson and S. Rossner, *Acta Pharm. Toxicol.*, **37**, 134 (1975).
(21) L. Illum, S. S. Davis, C. G. Wilson, N. W. Thomas, M. Frier, and J. G. Hardy, *Intern. J. Pharmaceut.*, **12**, 135 (1982).
(22) I. J. Findler, A. Raz, W. E. Fogler, R. Kirsh, P. Bugelski, and G. Poste, *Cancer Res.*, **40**, 4460 (1980).
(23) W. C. Klingensmith, S. L. Yang, and H. N. Wagner, *J. Nucl. Med.*, **19**, 31 (1978).
(24) W. C. Klingensmith and T. W. Ryerson, *J. Nucl. Med.*, **14**, 201 (1973).

ACKNOWLEDGMENTS

The authors thank the NATO Science Fellowships Programme for financial assistance. The advice and expertise of Drs. M. Frier, J. G. Hardy, C. G. Wilson, and N. Thomas of the Medical School, University of Nottingham, are gratefully acknowledged. Helpful assistance in experimental work was obtained from S. N. Mills, A. Robinson, S. K. Wong, and J. Ratcliffe.

Application of Postcolumn Ionization in the High-Performance Liquid Chromatographic Analysis of Butabarbital Sodium Elixir

EDITH P. SCOTT

Received February 16, 1982, from the *Food and Drug Administration, Atlanta, GA 30309.* Accepted for publication August 16, 1982.

Abstract □ A sensitive postcolumn ionization high-performance liquid chromatographic (HPLC) method for the quantitative determination of butabarbital sodium in butabarbital sodium elixir is described. The procedure employs a octadecylsilane column chemically bonded to porous silica microparticles. The mobile phase is a mixture of methanol and water (typically 35:65), adjusted to provide separation of butabarbital from two degradation compounds and other formulation ingredients. A buffer (pH 10) added between the column and detector provides for the primary ionization of the barbiturate necessary for optimum UV-detector sensitivity at ~240 nm. Determinations are made using the sodium salt; thus the need for extraction of the free base is eliminated. The procedure is linear over the 0.3–0.9-mg/ml concentration range of butabarbital sodium. Reproducibility values for 10 injections of a single reference standard range from 100.2 to 100.8% of theoretical with a mean of 100.5% and a coefficient of variation of 0.23%. An interlaboratory precision study for blind duplicates of one simulated product formulation and two commercial elixers produced coefficients of variation of 1.4, 1.3, and 1.1%, respectively. Recovery determinations for the drug in simulated product formulations ranged from 98.4 to 99.0%, intralaboratory, and 97.7 to 102.2%, interlaboratory. The HPLC procedure is stability indicating with respect to two decomposition products.

Keyphrases □ Butabarbital sodium—application of postcolumn ionization in higher-performance liquid chromatographic analysis, elixir □ Ionization—postcolumn, application in high-performance liquid chromatographic analysis of butabarbital sodium elixir □ High-performance liquid chromatography—application of postcolumn ionization, analysis of butabarbital sodium elixir

The chromaphoric characteristics of barbiturates establish them as prime compounds for high-performance liquid chromatographic (HPLC) analysis using a combination of reverse-phase chromatography and postcolumn ionization with a pH 10 buffer. Clark and Chan (1) have reported the advantages of combining conventional reverse-phase chromatography and postcolumn ionization into a single system. In this study, their analytical approach has been successfully employed in the assay of butabarbital sodium elixir. The procedure eliminates the need for extraction of butabarbital free acid. No sample cleanup was required because a suitable chromatographic system was found that would resolve the phenobarbital internal standard, butabarbital, placebo ingredients, and one decomposition product, capuride.

Table I—Typical HPLC Standard Curve Data [a] for Butabarbital Sodium

Butabarbital Sodium Added, mg/50 ml	Butabarbital Sodium, Found, mg/50 ml	Percent of Theoretical
16.73	16.54	98.9
23.24	23.19	99.8
30.36	30.27	99.7
38.00	38.00	100.0
46.00	45.82	99.6

[a] Correlation coefficient = 0.9999.

EXPERIMENTAL

Apparatus—The liquid chromatograph[1] consisted of a solvent pump with flow controller; an injector with flowing-stream, valve-controlled

[1] Waters Liquid Chromatograph; Model 6000-A Solvent Delivery System, Model 720 System Controller, Model U6K Injector, Model 440 Absorbance Detector with 254 nm filter, Model 730 Data Module; Waters Associates, Milford, Mass.

0022-3549/83/0900-1089$01.00/0

Table II—HPLC Assay Results for Commercial Butabarbital Sodium Elixir and Recovery Data for Corresponding Product Control [a]

	Manufacturer			
	A	B	C	D
Assay of drug in commercial products				
Butabarbital sodium found (mg/5 ml)	29.2	32.9	29.0	31.7
Butabarbital sodium declared (mg/5 ml)	30.0	33.3	30.0	33.0
Percent of declared	97.3	98.8	96.7	96.1
Recovery for drug in authentic formulations				
Butabarbital sodium found (mg/5 ml)	30.48	31.26	30.09	30.87
Butabarbital sodium added (mg/5 ml)	30.92	31.59	30.47	31.36
Recovery, %	98.6	99.0	98.8	98.4

[a] Small batch of commercial product, accurately prepared in the laboratory according to the manufacturer's master formulation.

specimen loop; a UV-detector capable of monitoring absorbance at ~240 nm; a digital integrator–recorder; and a 10-μm micropellicular octadecylsilane column[2]. To achieve postcolumn ionization, a second solvent pump[3] was connected to the HPLC apparatus by means of a 1.58 mm union tee[4] installed in the line between the column and the detector.

Reagents—The methanol[5] was distilled in glass. The boric acid[6], potassium chloride[7], and sodium hydroxide[5] were ACS grade. Phenobarbital[8] was USP grade; the butabarbital[9] was USP reference standard[9].

HPLC Operating Conditions—The mobile phase consisted of methanol–distilled water (35:65), and the flow rate was 1.5 ml/min. The ionization solvent was a borate buffer (pH 10.0 ± 0.05) prepared by mixing 250 ml of 0.2 *M* boric acid, 250 ml of 0.2 *M* potassium chloride, and 220 ml of 0.2 *M* sodium hydroxide and diluting to 1 liter with distilled water. The buffer was pumped into the mobile phase at a flow rate of 0.1 ml/min. The UV detector was operated with a 254-nm filter and a sensitivity setting of 0.1 AUFS. Injection volume for sample and standard solutions was ~7.5 μl; injections were made in triplicate. A resolution value, R[10], of ≮1.5 was established to evaluate system suitability.

Preparation of Solutions—A solution of phenobarbital in methanol was prepared at a concentration of ~3 mg/ml for the internal standard. Aliquots of the internal standard solution and butabarbital sodium elixir were combined to produce a mixed solution containing ~0.3 mg/ml of phenobarbital and 0.7 mg/ml of butabarbital sodium in methanol. Butabarbital and an aliquot of the internal standard solution were combined to produce a mixed solution (standard) containing ~0.3 mg/ml of phenobarbital and 0.6 mg/ml of butabarbital in methanol.

Chromatographic Separation and Analysis—A printer–plotter–integrator[11] which automatically integrates chromatographic peaks and calculates results was employed in the liquid chromatograph apparatus. The data processor calculated peak areas and response factors resulting from injection of a standard solution and stored the data in a calibration table. Similarly, the data processor calculated areas and response factors for injections of sample solutions and compared sample data with standard data in the calibration table for calculation of sample amounts. Phenobarbital elution time was ~9 min, and butabarbital elution was ~13 min (Fig. 1).

RESULTS AND DISCUSSION

The HPLC procedure described herein was subjected to validation studies for linearity, precision, and accuracy. Linearity was determined at five concentrations which would be equivalent to butabarbital sodium elixir products with assay values ranging from 50 to 150% of declared butabarbital sodium. Assay results ranged from 98.9 to 100.0% of theoretical, with a correlation coefficient of 0.9999 (Table I). Reproducibility for 10 injections of a butabarbital sodium standard solution ranged from 100.2 to 100.8% of theoretical, with a mean of 100.5% and a coefficient of variation of 0.23% (Table III).

Four brands of butabarbital sodium elixir were assayed by the HPLC procedure. Recoveries were determined using product controls prepared for these four brands of elixir. A product control is defined here as a small batch of commercial product accurately prepared in the laboratory according to the manufacturer's master formulation. Assay results and recoveries for the corresponding product controls are shown in Table II.

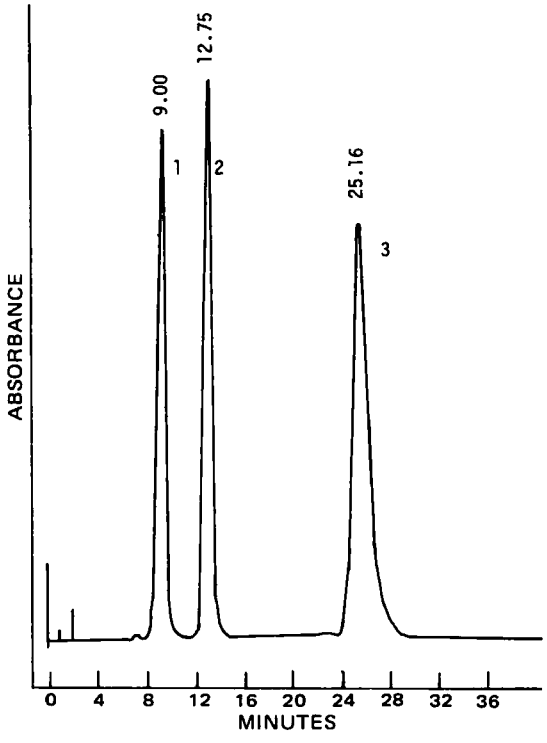

Figure 1—*HPLC response for (1) phenobarbital, (2) butabarbital, and (3) capuride. The column was μBondapak C_{18}; the mobile phase was methanol–distilled water (35:65); ionization solvent was borate buffer (pH 10).*

An interlaboratory collaborative study of the procedure was conducted using blind duplicate samples of one simulated product formulation and

Table III—Precision Data for Multiple HPLC Injections of Butabarbital Sodium [a]

Butabarbital Sodium Found by HPLC, mg/50 ml	Percent of Theoretical
34.85	100.2
35.03	100.7
35.00	100.7
35.04	100.8
34.92	100.4
34.95	100.5
34.86	100.2
34.89	100.3
34.98	100.6
34.93	100.5
Mean	100.5
SD	0.23
CV	0.23

[a] Butabarbital sodium added: 34.77 mg/50 ml.

[2] μBondapak C_{18}, 3.9 mm × 30 cm, Waters Associates, Milford, Mass.
[3] Model 6000-A Solvent Delivery System; Waters Associates, Milford, Mass.
[4] Swagelok Union Tee, SS-100-3, Crawford Fitting Co., Solon, Ohio.
[5] ACS grade, Burdick and Jackson Laboratories, Inc., Muskegon, Mich.
[6] J. T. Baker Chemical Co., Phillipsburg, N.J.
[7] Fisher Scientific Co., Fair Lawn, N.J.
[8] ACS grade; City Chemical Corp., New York, N.Y.
[9] USP grade; U.S. Pharmacopeial Convention, Inc., Rockville, Md.
[10] USP Reference standard; U.S. Pharmacopeia XX, (621) Chromatography, Glossary of Symbols, p. 946.
[11] Waters Model 730 Data Module.

Table IV—Interlaboratory Analysis of Blind Duplicate Samples of Butabarbital Sodium Elixir

Laboratory	Sample A[a] Recovered, %		Sample B[b] Percent of Declared		Sample C[c] Percent of Declared	
1	101.2	100.1	98.7	98.0	97.0	96.7
2	99.1	98.0	95.3	95.7	95.2	95.8
3	100.8	100.5	97.7	97.7	94.9	95.2
4	100.8	102.2	97.0	97.0	97.3	97.9
5	99.1	97.7	94.7	95.7	94.9	96.4
6	101.2	100.5	98.3	97.3	96.1	97.3
Mean	100.1%		96.9		96.2%	
SD	±1.36		±1.28		±1.03	
CV	1.4%		1.3%		1.1%	

[a] Simulated product formulation with 28.36 mg/5 ml of butabarbital sodium added. [b] Commercial product with 30 mg of butabarbital sodium per 5 ml declared. [c] Commercial product with 33.3 mg of butabarbital sodium per 5 ml declared.

two commercial elixirs. Coefficients of variation were 1.4, 1.3, and 1.1%, respectively, for the three samples. Recovery values for the authentic sample ranged from 97.7 to 102.2%. Results of interlaboratory testing are presented in Table IV.

A placebo was prepared for each of the four butabarbital sodium elixir products analyzed. None of the placebos interfered with the assay (Fig. 2). Solutions of butabarbital sodium and butabarbital in methanol were found to be stable over a prolonged period in laboratory fluorescent light and laboratory temperature (generally 20–25°). Stability determinations were made after 11 and 56 days of exposure time.

Limited data on HPLC response for decomposition products was obtained. No commercial source for butabarbital decomposition compounds was available; thus, an attempt was made to prepare the compounds through thermal degradation of butabarbital sodium in this laboratory. Breakdown products due to hydrolysis of barbiturates (Scheme I) have been established (2–5).

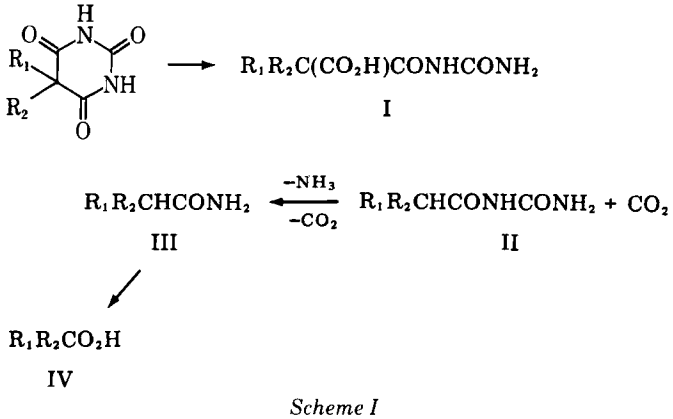

Scheme I

Two approaches to thermal decomposition were employed. With the Watson and Pernarowski procedure (5) only one compound, capuride (II), was obtained in sufficient quantity for analytical testing. Thermal decomposition using a pressure bottle (6) was also attempted to isolate additional decomposition products. This procedure also produced capuride and, additionally, a compound which was identified as valnoctamide (III). Both the capuride and valnoctamide which were produced were identified by means of melting point, IR spectrophotometry, and mass spectroscopy.

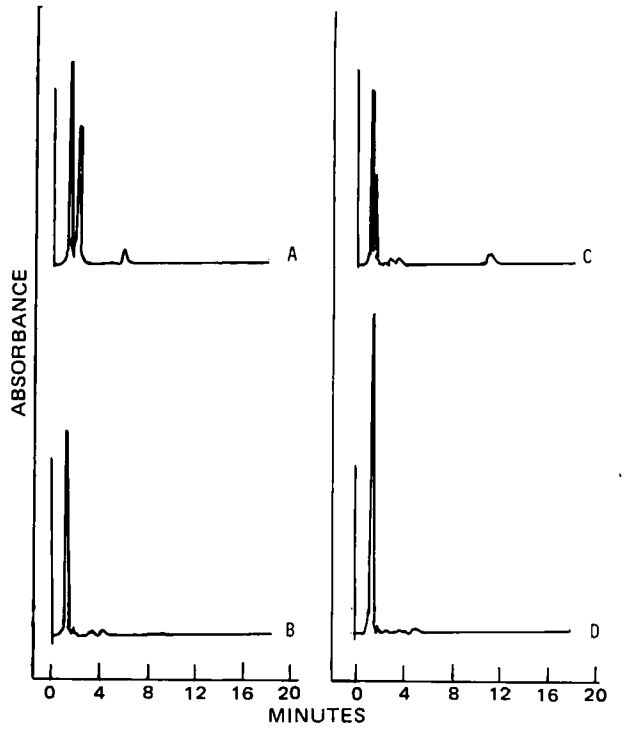

Figure 2—*HPLC responses for placebo ingredients from manufacturers A–D (see Table II).*

Capuride eluted from the HPLC column at 25.16 min. (Fig. 1). An injection of ~10 μg produced a pen deflection of ~1.5 cm at 0.02 AUFS. No HPLC response was produced for a 35-μg injection of valnoctamide at 0.02 AUFS.

Chromatograms of phenobarbital, butabarbital, and product placebos from injections made on six octadecylsilane columns representing five commercial sources and one in-laboratory preparation were evaluated. Columns that met the system suitability criterion gave satisfactory resolution of phenobarbital, butabarbital, and placebo ingredients.

REFERENCES

(1) C. R. Clark and J. Chan, *Anal. Chem.*, **50**, 635 (1978).

(2) F. A. Rotondaro, *J. Assoc. Off. Anal. Chem.*, **23**, 777 (1940).

(3) F. A. Rotondaro, *J. Assoc. Off. Anal. Chem.*, **38**, 809 (1955).

(4) A. H. Bailey, *Pharm. J.*, **136**, 620 (1936).

(5) J. R. Watson and M. Pernarowski, *J. Assoc. Off. Anal. Chem.*, **45**, 609 (1962).

(6) M. Freifelder, A. O. Geiszler, and G. R. Stone, *J. Org. Chem.*, **26**, 203 (1961).

Rapid Gas Chromatographic Determination of Serum Salicylates After Silylation

Keyphrases □ GLC analysis—Simultaneous determination of acetylsalicylic acid and salicylic acid in plasma, serum and whole blood, formation of trimethylsilyl derivatives

To the Editor:

Both acetylsalicylic acid and salicylic acid are pharmacologically active, but there are qualitative and quantitative differences in the analgesic and antiplatelet effects and in their inhibition of prostaglandin synthetase (1, 2). Gas–liquid chromatographic (GLC) methods for quantifying acetylsalicylic acid and salicylic acid simultaneously are time consuming, requiring extraction prior to the formation of the corresponding trimethylsilyl derivatives (3–5). Furthermore, the analyses are complicated by some hydrolysis of acetylsalicylic acid to salicylic acid during derivatization (6).

The GLC methods available for the quantitation of acetylsalicylic acid and salicylic acid require prior silylation at 50° for 60 min (3–5). Silylation of salicylic acid with hexamethyldisilazane in acetone gave two peaks with retention times of 1.5 and 2.2 min when chromatographed at 135° under our conditions. These peaks were considered to be the mono- and bis-trimethylsilyl derivatives of salicylic acid, respectively, since the intensity of the 1.5-min peak decreased with time with concomitant increase in the height of the 2.2-min peak (4). Therefore, a more appropriate system of derivatization was sought. Table I gives the effect of time on the silylation of acetylsalicylic acid, salicylic acid, and *p*-hydroxybenzoic acid at 23° and 60° with *N,O*-bis(trimethylsilyl)trifluoroacetamide in acetonitrile. *p*-Hydroxybenzoic acid was chosen as the internal standard since it readily forms a bis-trimethylsilyl derivative (7). Acetonitrile was chosen as the solvent, since it has been reported to be suitable for the silylation of catecholamines and related compounds (8). The results show that under these conditions of silylation[1] the maximum peak area ratio was obtained almost immediately at both temperatures and that the ratio was stable for at least 60 min, even at 60°. The mean peak area ratio obtained for salicylic acid at the various times after the addition of *N,O*-bis(trimethylsilyl)trifluoroacetamide was 0.96 ± 0.10 (*SD*) at 23° and 1.02 ± 0.05 (*SD*) at 60°, representing coefficients of variation of 10.4 and 5.0%, respectively. Similarly, the mean values of the peak area ratio for acetylsalicylic acid were 0.56 ± 0.01 (*SD*) at 23° and 0.55 ± 0.03 (*SD*) at 60°, giving coefficients of variation of 2.6 and 6.1%, respectively. The peak with a retention time of 1.5 min, considered to be the monosilylation product of salicylic acid, was not observed under these conditions. For rapid silylation of acetylsalicylic acid and salicylic acid, dry acetone can be substituted for acetonitrile. Also, the rate of silylation was faster when *N,O*-bis(trimethylsilyl)trifluoroacetamide was used instead of hexamethyldisilazane.

Table I—Effects of Time and Temperature on the Silylation of Acetylsalicylic Acid, Salicylic Acid, and *p*-Hydroxybenzoic Acid in Acetonitrile Using *N,O*-bis(trimethylsilyl)trifluoroacetamide as the Silylating Reagent [a]

	Peak Area Ratio of Disilylated Salicylic Acid or Monosilylated Acetylsalicylic Acid/Disilylated *p*-Hydroxybenzoic Acid			
	Acetylsalicylic Acid		Salicylic Acid	
Minutes [b]	23°	60°	23°	60°
0.2–1	0.57	—	1.08	—
10	0.56	0.60	1.04	1.07
20	0.56	0.56	0.90	1.02
30	0.56	0.56	0.87	1.06
40	0.54	0.57	0.83	0.94
50	0.59	0.49	1.03	0.98
60	0.56	0.54	1.00	1.03

[a] One ml of an ethereal solution containing 10 μg of each compound was evaporated to dryness; the residue was dissolved in 10 μl of acetonitrile and reacted with 5 μl of *N,O*-bis(trimethylsilyl)trifluoroacetamide. A 2–3-μl aliquot was injected into the gas chromatograph. [b] After addition of silylating reagent.

Figure 1 shows typical chromatograms of ethereal extracts of drug-free serum carried through the analytical procedure (A); of drug-free serum to which 15 μg of acetylsalicylic acid, salicylic acid, and the internal standard *p*-hydroxybenzoic acid were added (B); and of a mixture of acetanilide, methyl salicylate, salicylic acid, *p*-hydroxy-

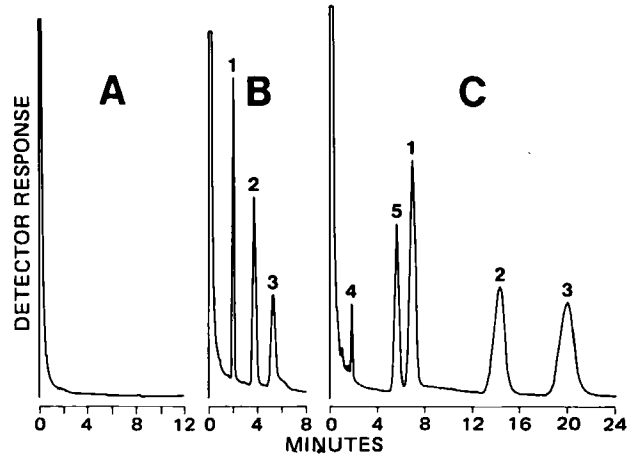

Figure 1—*Chromatograms of drug-free serum carried through the procedure (A), drug-free serum to which 15 μg of acetylsalicylic acid, salicylic acid, and p-hydroxybenzoic acid were added and analyzed, as described in the procedure (B), and of a mixture of acetanilide, methyl salicylate, salicylic acid, p-hydroxybenzoic acid, and acetylsalicylic acid analyzed at 110° (C). The derivatization was carried out in acetonitrile using* N,O-*bis(trimethylsilyl)trifluoroacetamide as silylating reagent. Key: (1) salicylic acid; (2)* p-*hydroxybenzoic acid; (3) acetylsalicylic acid; (4) acetanilide; (5) methyl salicylate.*

[1] Sample formulation: To each 0.10-ml aliquot of serum, plasma, or whole blood, 2 ml of 1 *N* HCl was added; *p*-hydroxybenzoic acid (15 μg in 1 ml of water) was added as the internal standard; and the mixture was extracted twice with 5 ml of freshly distilled ether. The organic phase was transferred to another tube and evaporated to dryness under a stream of nitrogen in a water bath at 42–44°. The residue was dissolved in 10 μl of acetonitrile and derivatized with 5 μl of *N,O*-bis(trimethylsilyl)trifluoroacetamide (Pierce Chemical Co.). A 2–3-μl sample was injected into a gas chromatograph (Hewlett-Packard model 5710A) equipped with a flame-ionization detector and a chart recorder-integrator (Hewlett-Packard model 3380s). The column was 1.2 m long ×4-mm i.d. glass tubing packed with 2% OV-225 on 80–100 mesh Gas Chrom W (Chromatographic Specialities, Ltd.) It was conditioned overnight at 225° and treated with hexamethyldisilazane before use. The operating conditions were: injection port temperature, 250°; oven temperature (isothermal), 135 or 110°; detector temperature, 300°. The nitrogen (carrier gas), air, and hydrogen flow rates were 60, 100, and 30 ml/min, respectively.

0022-3549/83/0900-1092$01.00/0

benzoic acid, and acetylsalicylic acid (C). Parts A and B were determined at 135° with part C determined at 110° in order to have base line resolution of all the peaks. The ethereal extract of control serum sample (A) did not give any peak that interfered with the GLC analysis of acetylsalicylic acid, salicylic acid, and *p*-hydroxybenzoic acid. Similar results were obtained using samples of either rat or human plasma. The retention times of the trimethylsilyl derivatives of salicylic acid, *p*-hydroxybenzoic acid, and acetylsalicylic acid were 2.2, 4.4, and 5.4, respectively at 135°. Under these conditions, the retention times of the trimethylsilyl derivatives of methyl salicylate, ibuprofen, salicylamide, and acetaminophen were 1.9, 3.7, 10.8, and >30 min, respectively. Acetanilide and phenacetin did not form a trimethylsilyl derivative, but each compound produced a single peak with retention time values of 0.9 and 4.7 min, respectively, when chromatographed at 135°. Other nonsteroid anti-inflammatory drugs such as ketoprofen, indomethacin, and naproxen did not produce a peak when silylated under identical conditions. Complete separation between the peak of the trimethylsilyl derivatives of methylsalicylic acid and salicylic acid was obtained at 110° (Fig. 1C). Under these conditions, the retention time values of underivatized acetanilide and of the trimethylsilyl derivatives of methylsalicylic acid, salicylic acid, *p*-hydroxybenzoic acid, and acetylsalicylic acid were 2.0, 5.1, 7.1, 14.35, and 20.05 min, respectively. Salicyluric acid (2-hydroxyhippuric acid), the major metabolite of salicylic acid, did not give a peak under the analytical conditions used. The chromatographic conditions determined at 135° were suitable for the simultaneous analysis of acetylsalicylic acid and salicylic acid in serum samples. There was no interference from the commonly used analgesics often prescribed in combination with acetylsalicylic acid, except for phenacetin, which gave a peak of similar retention time value close to that of the trimethylsilyl derivative of *p*-hydroxybenzoic acid. In cases where phenacetin is also being administered, 4-chlorophenylacetic acid can be used as a reference standard since its trimethylsilyl derivative has a retention time value of 2.9 min.

Table II gives the coefficient of variation and the recovery of different concentrations of acetylsalicylic acid and salicylic acid added to the control serum. The coefficients of variation of triplicate analysis varied from 0.0 to 6.9% for acetylsalicylic acid and from 1.1 to 6.4% for salicylic acid. The mean values for the coefficient of variation of the eight concentrations of acetylsalicylic acid and salicylic acid used were 2.6 ± 2.6 and 3.7 ± 1.8 (*SD*%) respectively. The recovery of these two compounds was essentially quantitative. The overall recovery for acetylsalicylic acid was 104.0 ± 8.4 (*SD*)%, while that of salicylic acid was 98.2 ± 5.3 (*SD*)%. Calibration curves were obtained for acetylsalicylic acid ($y = 0.03 + 0.0474x$ and $r = 0.996$) and for salicylic acid ($y = 0.20 + 0.064x$ and $r = 0.997$) in the range of concentrations of 2.5–25 μg/0.1 ml of serum, *i.e.*, within the concentrations determined in pharmacokinetic studies. It should be pointed out that the hydrolysis of acetylsalicylic acid to salicylic in blood samples at 37° is rapid (9–11) and, therefore, it is necessary to extract the acetylsalicylic acid as soon as possible to avoid its breakdown in storage. There was no breakdown of acetylsalicylic acid to salicylic acid during the extraction, evaporation, and derivatization processes described herein.

Table II—Recovery of Different Amounts of Acetylsalicylic Acid and Salicylic Acid Added to Control Serum

Amount Added, μg/0.1 ml	Acetylsalicylic Acid: Amount Recovered[a], μg/0.1 ml ± *SD*	*CV*, %[b]	Recovery, %	Salicylic Acid: Amount Recovered[a], μg/0.1 ml ± SD	CV, %[b]	Recovery, %
2.5	2.25 ± 0.13	5.8	90.0	2.7 ± 0.1	3.3	108.0
7.5	9.1 ± 0.6	6.9	121.0	7.4 ± 0.3	5.3	98.7
10.0	10.5 ± 0.0	0.0	105.0	9.7 ± 0.3	3.2	97.0
12.5	12.9 ± 0.2	1.6	103.2	11.7 ± 0.55	4.7	93.6
15.0	15.6 ± 0.2	1.3	104.0	13.8 ± 0.6	4.5	92.0
17.5	17.9 ± 0.7	4.1	102.3	16.6 ± 0.2	1.4	94.8
20.0	21.1 ± 0.0	0.0	105.5	19.7 ± 0.2	1.1	98.5
25.0	25.3 ± 0.2	0.8	101.2	25.8 ± 1.6	6.4	103.2

[a] Mean value ± *SD* of triplicate analyses. [b] Coefficient of variation = *SD*/mean × 100.

The proposed GLC assay of acetylsalicylic acid and salicylic acid in serum is simpler and faster than other methods that have been published for the same purpose.

(1) C. Patrono, G. Ciabattoni, F. Pugliese, E. Pinca, G. Castrucci, A. De Salvo, M. A. Satla, and M. Parachini, *Agents Actions*, **4** (Suppl.), 138 (1979).

(2) D. C. Atkinson and H. O. J. Collier, *Adv. Pharmacol. Chemother.*, **17**, 233 (1981).

(3) B. H. Thomas, G. Solomonraj, and B. B. Caldwell, *J. Pharm. Pharmacol.*, **25**, 201 (1973).

(4) L. J. Walter, D. F. Biggs, and R. T. Coutts, *J. Pharm. Sci.*, **63**, 1754 (1974).

(5) M. J. Rance, B. J. Jordan, and J. D. Nichols, *J. Pharm. Pharmacol.*, **27**, 425 (1975).

(6) S. L. Ali, *Chromatographia*, **8**, 33 (1975).

(7) C. E. Dalgliesh, E. C. Horning, M. G. Horning, K. L. Knox, and K. Yarger, *Biochem. J.*, **101**, 792 (1966).

(8) M. G. Horning, A. M. Moss, and E. C. Horning, *Biochim. Biophys. Acta*, **148**, 597 (1967).

(9) E. B. Truitt, Jr. and A. M. Morgan, *Arch. Int. Pharmacodyn. Ther.*, **135**, 105 (1962).

(10) P. A. Harris and S. Riegelman, *J. Pharm. Sci.*, **56**, 713 (1967).

(11) M. Rowland and S. Riegelman, *J. Pharm. Sci.*, **56**, 717 (1967).

Pierre M. Bélanger *x
Marcel Lalande *
François Doré ‡
Gaston Labrecque ‡

*Ecole de Pharmacie and
‡ Département de Pharmacologie
Université Laval
Ste-Foy, Québec, Canada G1K 7P4

Received May 11, 1982.

Accepted for publication March 16, 1983.

Supported in part by grants from the Medical Research Council (MA-6469) and the Arthritis Society of Canada and by a F.C.A.C. studentship to M. Lalande.

Is Aspirin Phenylalanine Ethyl Ester a Prodrug for Aspirin?

Keyphrases □ Aspirin—high-performance liquid chromatography, phenylalanine ethyl ester as prodrug

To the Editor:

It is known that oral administration of aspirin induces gastric irritation and bleeding because of local irritation

benzoic acid, and acetylsalicylic acid (C). Parts A and B were determined at 135° with part C determined at 110° in order to have base line resolution of all the peaks. The ethereal extract of control serum sample (A) did not give any peak that interfered with the GLC analysis of acetylsalicylic acid, salicylic acid, and *p*-hydroxybenzoic acid. Similar results were obtained using samples of either rat or human plasma. The retention times of the trimethylsilyl derivatives of salicylic acid, *p*-hydroxybenzoic acid, and acetylsalicylic acid were 2.2, 4.4, and 5.4, respectively at 135°. Under these conditions, the retention times of the trimethylsilyl derivatives of methyl salicylate, ibuprofen, salicylamide, and acetaminophen were 1.9, 3.7, 10.8, and >30 min, respectively. Acetanilide and phenacetin did not form a trimethylsilyl derivative, but each compound produced a single peak with retention time values of 0.9 and 4.7 min, respectively, when chromatographed at 135°. Other nonsteroid anti-inflammatory drugs such as ketoprofen, indomethacin, and naproxen did not produce a peak when silylated under identical conditions. Complete separation between the peak of the trimethylsilyl derivatives of methylsalicylic acid and salicylic acid was obtained at 110° (Fig. 1C). Under these conditions, the retention time values of underivatized acetanilide and of the trimethylsilyl derivatives of methylsalicylic acid, salicylic acid, *p*-hydroxybenzoic acid, and acetylsalicylic acid were 2.0, 5.1, 7.1, 14.35, and 20.05 min, respectively. Salicyluric acid (2-hydroxyhippuric acid), the major metabolite of salicylic acid, did not give a peak under the analytical conditions used. The chromatographic conditions determined at 135° were suitable for the simultaneous analysis of acetylsalicylic acid and salicylic acid in serum samples. There was no interference from the commonly used analgesics often prescribed in combination with acetylsalicylic acid, except for phenacetin, which gave a peak of similar retention time value close to that of the trimethylsilyl derivative of *p*-hydroxybenzoic acid. In cases where phenacetin is also being administered, 4-chlorophenylacetic acid can be used as a reference standard since its trimethylsilyl derivative has a retention time value of 2.9 min.

Table II gives the coefficient of variation and the recovery of different concentrations of acetylsalicylic acid and salicylic acid added to the control serum. The coefficients of variation of triplicate analysis varied from 0.0 to 6.9% for acetylsalicylic acid and from 1.1 to 6.4% for salicylic acid. The mean values for the coefficient of variation of the eight concentrations of acetylsalicylic acid and salicylic acid used were 2.6 ± 2.6 and 3.7 ± 1.8 (*SD*%) respectively. The recovery of these two compounds was essentially quantitative. The overall recovery for acetylsalicylic acid was 104.0 ± 8.4 (*SD*)%, while that of salicylic acid was 98.2 ± 5.3 (*SD*)%. Calibration curves were obtained for acetylsalicylic acid ($y = 0.03 + 0.0474x$ and $r = 0.996$) and for salicylic acid ($y = 0.20 + 0.064x$ and $r = 0.997$) in the range of concentrations of 2.5–25 μg/0.1 ml of serum, *i.e.*, within the concentrations determined in pharmacokinetic studies. It should be pointed out that the hydrolysis of acetylsalicylic acid to salicylic in blood samples at 37° is rapid (9–11) and, therefore, it is necessary to extract the acetylsalicylic acid as soon as possible to avoid its breakdown in storage. There was no breakdown of acetylsalicylic acid to salicylic acid during the extraction, evaporation, and derivatization processes described herein.

Table II—Recovery of Different Amounts of Acetylsalicylic Acid and Salicylic Acid Added to Control Serum

Amount Added, μg/0.1 ml	Acetylsalicylic Acid: Amount Recovered[a], μg/0.1 ml ± *SD*	*CV*, %[b]	Recovery, %	Salicylic Acid: Amount Recovered[a], μg/0.1 ml ± SD	CV, %[b]	Recovery, %
2.5	2.25 ± 0.13	5.8	90.0	2.7 ± 0.1	3.3	108.0
7.5	9.1 ± 0.6	6.9	121.0	7.4 ± 0.3	5.3	98.7
10.0	10.5 ± 0.0	0.0	105.0	9.7 ± 0.3	3.2	97.0
12.5	12.9 ± 0.2	1.6	103.2	11.7 ± 0.55	4.7	93.6
15.0	15.6 ± 0.2	1.3	104.0	13.8 ± 0.6	4.5	92.0
17.5	17.9 ± 0.7	4.1	102.3	16.6 ± 0.2	1.4	94.8
20.0	21.1 ± 0.0	0.0	105.5	19.7 ± 0.2	1.1	98.5
25.0	25.3 ± 0.2	0.8	101.2	25.8 ± 1.6	6.4	103.2

[a] Mean value ± *SD* of triplicate analyses. [b] Coefficient of variation = *SD*/mean × 100.

The proposed GLC assay of acetylsalicylic acid and salicylic acid in serum is simpler and faster than other methods that have been published for the same purpose.

(1) C. Patrono, G. Ciabattoni, F. Pugliese, E. Pinca, G. Castrucci, A. De Salvo, M. A. Satla, and M. Parachini, *Agents Actions*, **4** (Suppl.), 138 (1979).

(2) D. C. Atkinson and H. O. J. Collier, *Adv. Pharmacol. Chemother.*, **17**, 233 (1981).

(3) B. H. Thomas, G. Solomonraj, and B. B. Caldwell, *J. Pharm. Pharmacol.*, **25**, 201 (1973).

(4) L. J. Walter, D. F. Biggs, and R. T. Coutts, *J. Pharm. Sci.*, **63**, 1754 (1974).

(5) M. J. Rance, B. J. Jordan, and J. D. Nichols, *J. Pharm. Pharmacol.*, **27**, 425 (1975).

(6) S. L. Ali, *Chromatographia*, **8**, 33 (1975).

(7) C. E. Dalgliesh, E. C. Horning, M. G. Horning, K. L. Knox, and K. Yarger, *Biochem. J.*, **101**, 792 (1966).

(8) M. G. Horning, A. M. Moss, and E. C. Horning, *Biochim. Biophys. Acta*, **148**, 597 (1967).

(9) E. B. Truitt, Jr. and A. M. Morgan, *Arch. Int. Pharmacodyn. Ther.*, **135**, 105 (1962).

(10) P. A. Harris and S. Riegelman, *J. Pharm. Sci.*, **56**, 713 (1967).

(11) M. Rowland and S. Riegelman, *J. Pharm. Sci.*, **56**, 717 (1967).

Pierre M. Bélanger *x
Marcel Lalande *
François Doré ‡
Gaston Labrecque ‡

*Ecole de Pharmacie and
‡ Département de Pharmacologie
Université Laval
Ste-Foy, Québec, Canada G1K 7P4

Received May 11, 1982.

Accepted for publication March 16, 1983.

Supported in part by grants from the Medical Research Council (MA-6469) and the Arthritis Society of Canada and by a F.C.A.C. studentship to M. Lalande.

Is Aspirin Phenylalanine Ethyl Ester a Prodrug for Aspirin?

Keyphrases □ Aspirin—high-performance liquid chromatography, phenylalanine ethyl ester as prodrug

To the Editor:

It is known that oral administration of aspirin induces gastric irritation and bleeding because of local irritation

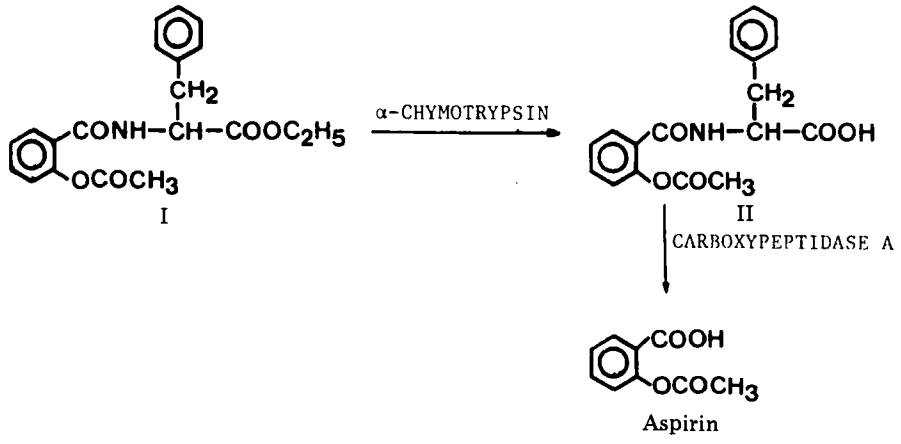

Scheme I

of the gastric mucosal membrane by the very acidic aspirin particles (1–3). One approach to minimizing this side effect is to mask the acidic carboxyl group of aspirin reversibly *via* a prodrug. Upon administration, the neutral derivative dissolves first, then hydrolyzes either in the GI tract or in the plasma, generating aspirin. It has been shown that classical esterification of the carboxyl group results in nonirritating but insoluble species which do not revert to aspirin but rather to the corresponding salicylate derivative (4). Thus, a prerequisite for any aspirin prodrug is that the masking group cleave much faster than the acetyl group. Prodrugs that cleave to aspirin have been reported (5–7). The compounds were aspirin derivatives in which the carboxyl group was masked *via* an acylal linkage.

Banerjee and Amidon (8–10) have recently proposed aspirin phenylalanine ethyl ester (I) as a possible prodrug for aspirin. It was rationalized that, because of the specificity of certain enzymes such as α-chymotrypsin and carboxypeptidase A, I would first be cleaved by α-chymotrypsin to aspirin phenylalanine (II) and subsequently to aspirin by carboxypeptidase A. To support their hypothesis, the authors studied the rate of hydrolysis of I at pH values of 7.5 and 8 in the presence of α-chymotrypsin and separately determined the rate of hydrolysis of II at pH 8.5 in the presence of carboxypeptidase A. In their kinetic studies, the reactions were followed by measuring the consumption of sodium hydroxide using a pH-stat titration. Aspirin was detected using TLC from a reaction mixture containing I and the two enzymes at pH 7.5. Based on this information, the authors proposed Scheme I for the stepwise enzymatic hydrolysis of I.

In this communication we report recent studies conducted using a specific high-performance liquid chromatographic (HPLC) assay and TLC assay which indicate that the work reported by these authors is in error. In disagreement with their conclusions, the new data indicate that (*a*) compound I does not generate aspirin in the presence of the two enzymes, (*b*) the hydrolysis of II is not catalyzed by carboxypeptidase A, and (*c*) compound I *does* hydrolyze to II in the presence of carboxypeptidase A.

Compound I was prepared according to the procedure of Banerjee and Amidon (8). Compound II was prepared from I using the reported procedure, but with slight modification; namely, treating I with α-chymotrypsin for longer than the reported 2 min to ensure complete conversion to II. The compounds were characterized by their melting points, NMR spectroscopy, and elemental analysis.

The activity of carboxypeptidase A[1] was redetermined in our laboratories and found to be 39.4 U/mg of protein, in close agreement with the labeled value of 41 U/mg of protein. The buffers used in our studies were 0.1 *M* phosphate adjusted to the desired pH values. The pH values of all the solutions were redetermined at the end of the experiments and found to be unchanged. An HPLC was equipped with a UV detector[2] set at 254 nm and 0.02–0.1 AUFS. Samples were analyzed on a 3.9-mm × 30-cm reverse-phase[3] column. The mobile phase was acetic acid–methanol–water (2:40:58), and the flow rate[4] was 2 ml/min. The injection volume[5] was 20 μl.

Figure 1 is a chromatogram of a mixture of equimolar concentrations (1.57×10^{-4} *M*) of I, II, aspirin, salicylic acid, salicyl phenylalanine, and salicyl phenylalanine ethyl ester. With this technique, the hydrolysis of I, even to the extent of 20%, would result in aspirin levels that are easily detectable. The enzymatic hydrolysis rates of I and II were examined using this HPLC method.

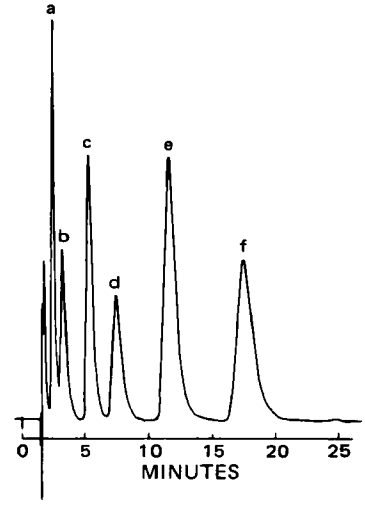

Figure 1—*HPLC chromatograms for (a) aspirin, (b) salicylic acid, (c) aspirin phenylalanine, (d) salicyl phenylalanine, (e) aspirin phenylalanine ethyl ester, and (f) salicyl phenylalanine ethyl ester.*

[1] Lot 12F-8185, Sigma Chemical Co., St. Louis, Mo.
[2] LDC III, Milton Roy Corp., Riviera Beach, Fla.
[3] μBondapak C_{18}, Waters Associates, Milford, Mass.
[4] Delivered by a Model 110A pump, Beckman Instruments, Inc., Irvine, Calif.
[5] Model 7125, Rheodyne Inc., Berkeley, Calif.

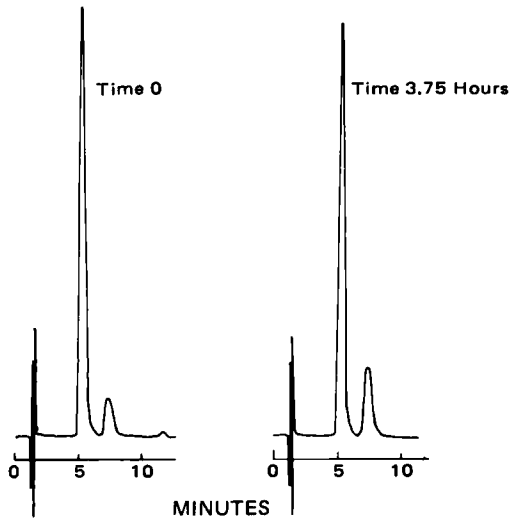

Figure 2—*HPLC chromatograms of aspirin phenylalanine (8.5×10^{-4} M) in the presence of carboxypeptidase A (1.0×10^{-5} M) at pH 8.5. Key: Aspirin phenylalanine, 5.0 min; Salicyl phenylalanine, 7.0 min.*

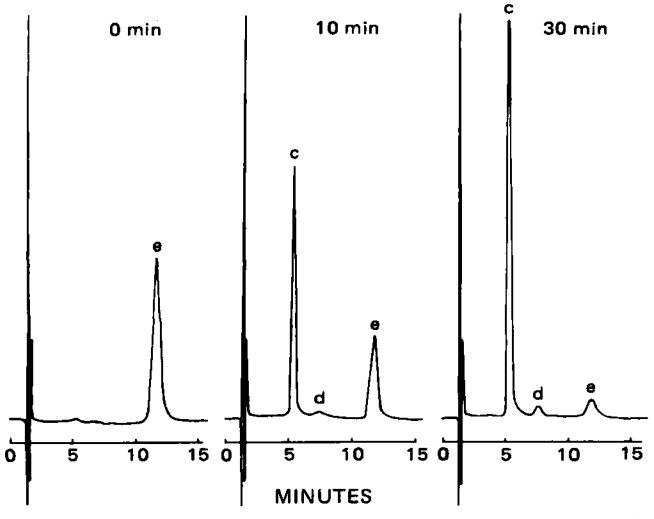

Figure 3—*HPLC chromatograms showing the disappearance of the prodrug and the appearance of aspirin phenylalanine as a function of time in the presence of 1×10^{-5} M carboxypeptidase A at pH 8.5. Key: (c) aspirin phenylalanine, (d) salicyl phenylalanine, and (e) prodrug.*

minor peak corresponding to salicyl phenylalanine. This experiment confirms that I does indeed cleave to II in the presence of α-chymotrypsin (8). However, when a mixture of α-chymotrypsin (3.9×10^{-6} *M*) and carboxypeptidase A (1×10^{-5} *M*) was added to I (8×10^{-4} *M*) at pH values of 7.4 and 8.5 and the solution immediately analyzed by HPLC, the same two peaks were observed and no peak corresponding to aspirin was detected even after 30 min. Therefore, aspirin is not liberated from II in the presence of carboxypeptidase A. To support this conclusion, the hydrolysis of II itself (8.5×10^{-4} *M*) in the presence of carboxypeptidase A (1×10^{-5} *M*) at pH 8.5 (the pH used by the previous authors to study this reaction) was determined by HPLC. When the mixture was immediately injected into the HPLC, two peaks, corresponding to II and salicyl phenylalanine were observed. As shown in Fig. 2, no additional peaks were observed, even after 3.75 hr. The same result was observed when the carboxypeptidase A concentration was increased 20-fold.

On the other hand, and contrary to the hypothesis of the authors, I was found to cleave to II in the presence of carboxypeptidase A. Figure 3 shows the time course for the appearance of II in a solution containing I (8×10^{-4} *M*) and carboxypeptidase A at pH 8.5.

To confirm the HPLC results, the same TLC system reported previously (8) was used to examine the mixture containing I and the two enzymes. Again, no aspirin spot was observed.

The results obtained by the authors which led to their conclusions appear to be in error for two reasons:

1. The aspirin spot appearing on the TLC plates (8) may have been the result of the hydrolysis of aspirin anhydride contaminating their prodrug. This is quite possible, since preparation of the prodrug involves the intermediate formation of aspirin anhydride, as shown in Scheme II. The half-life of the conversion of aspirin anhydride to aspirin is known to be ~8 min at pH 7.4 and 25°[7].

2. The consumption of sodium hydroxide observed previously when carboxypeptidase A was added to II may have been due to the hydrolysis of I, a very likely contaminant of the preparation. This is quite possible, since II was obtained by treating I with α-chymotrypsin for only 2 min and the purity of II was determined only by NMR (8). If this were the case, then I itself would, as shown

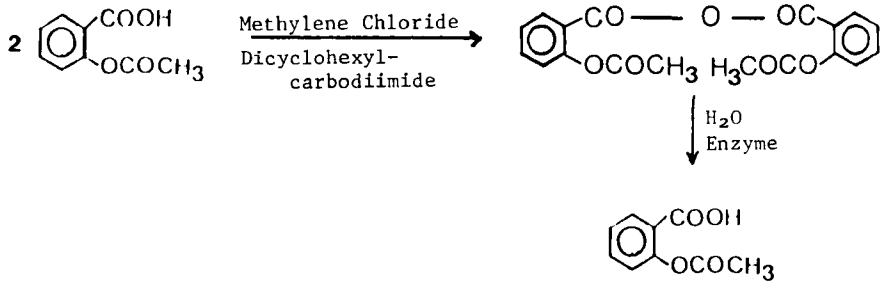

Scheme II

above, hydrolyze in the carboxypeptidase A preparation. The hydrolysis of I by carboxypeptidase A follows Michaelis–Menten kinetics. Linear Lineweaver–Burk plots

When a solution at pH 8 containing I (8×10^{-4} *M*) and α-chymotrypsin[6] was analyzed by HPLC, only two peaks were observed: a major peak corresponding to II and a

[6] Lot 70F-8000, Sigma Chemical Co., St. Louis, Mo.

[7] M. N. Khawam, J. B. Bogardus, and A. A. Hussain, unpublished results.

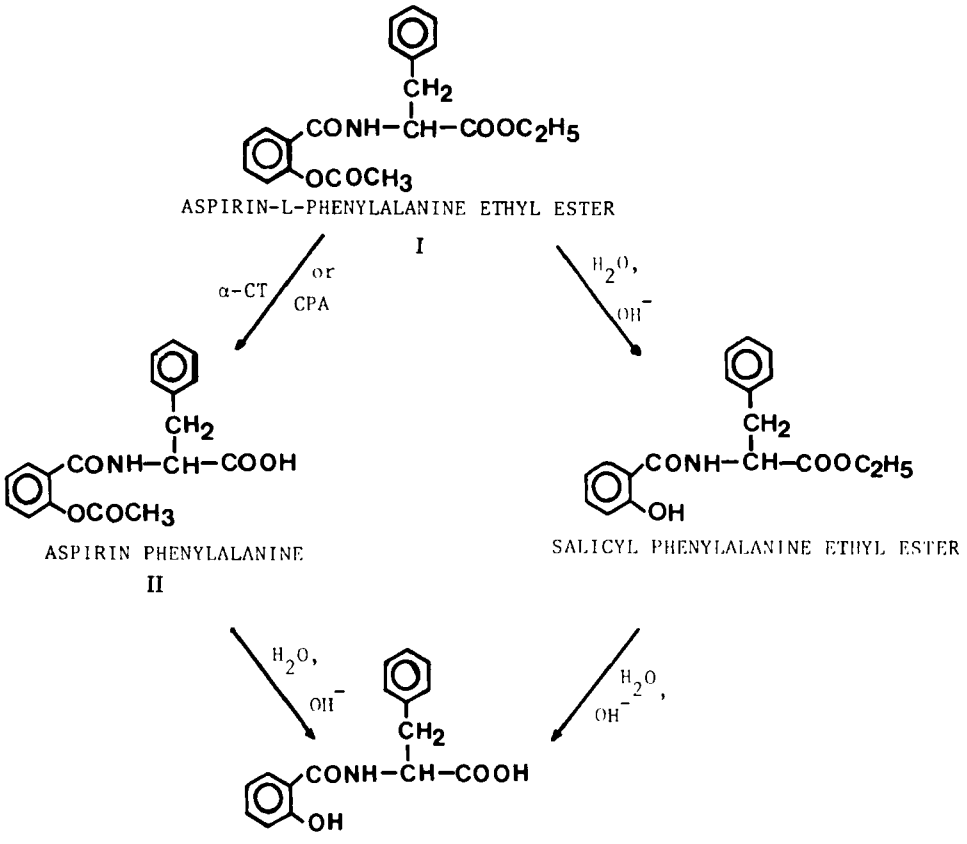

Scheme III

at concentrations ranging from 4.4×10^{-4} to 1.2×10^{-3} *M* were obtained in the presence of 1×10^{-5} *M* enzyme. The details of these experiments will be published in a later paper.

Since I is hydrolyzed to II by α-chymotrypsin and II does not cleave to aspirin in the presence of carboxypeptidase A, I is not a prodrug for aspirin.

Based on the previous work (8–10) and the additional data obtained in this laboratory, Scheme III is proposed for the hydrolysis of aspirin phenylalanine ethyl ester.

(1) J. P. Leonards and G. Levy, *J. Pharm. Sci.*, **59**, 1151 (1970).
(2) K. W. Anderson, *Arch. Int. Pharmacodyn. Ther.*, **152**, 379 (1964).
(3) C. Davison, D. H. Hertig, and R. DeVine, *Clin. Pharmacol. Ther.*, **7**, 329 (1966).
(4) T. St. Pierre and W. P. Jencks, *J. Am. Chem. Soc.*, **90**, 3817 (1968).
(5) A. A. Hussain, M. Yamasaki, and J. E. Truelove, *J. Pharm. Sci.*, **63**, 627 (1974).
(6) A. A. Hussain, J. E. Truelove, and H. Kostenbauder, *J. Pharm. Sci.*, **68**, 299 (1979).
(7) J. E. Truelove, A. A. Hussain, and H. B. Kostenbauder, *J. Pharm. Sci.*, **69**, 231 (1980).
(8) P. K. Banerjee and G. L. Amidon, *J. Pharm. Sci.*, **70**, 1299 (1981).
(9) P. K. Banerjee and G. L. Amidon, *J. Pharm. Sci.*, **70**, 1304 (1981).
(10) P. K. Banerjee and G. L. Amidon, *J. Pharm. Sci.*, **70**, 1307 (1981).

M. Kawahara

Z. Muhi-Eldeen
A. Hussain ˣ
College of Pharmacy
University of Kentucky
Lexington, KY 40536-0053

Received June 24, 1982.
Accepted for publication March 4, 1983.

Comment on a Second-Degree Polynomial Mathematical Model for Tablet Friability and *In Vitro* Dissolution

Keyphrases □ Dissolution—*in vitro*, polynomial mathematical model, effect of moisture and crushing strength □ Friability—effect of moisture and crushing strength, mathematical model

To the Editor:

In a recent report, Chowhan *et al.* (1) have used a function of a two-variable model to describe the effect of moisture and crushing strength on tablet friability and *in vitro* dissolution. Elliptical shape and ridge contour curves were unfortunately not reproduced on a computer[1] using all published data. Further examination of the mathematical equation (Eq. 1) using SAS contour plot procedure[2] on the same computer showed indeed that Figs. 5 and 6 contour plots in the article did not agree with the analytical expression.

[1] IBM 3033.
[2] SAS Institute Inc., Cary, NC 27511.

0022-3549/83/0900-1096$01.00/0

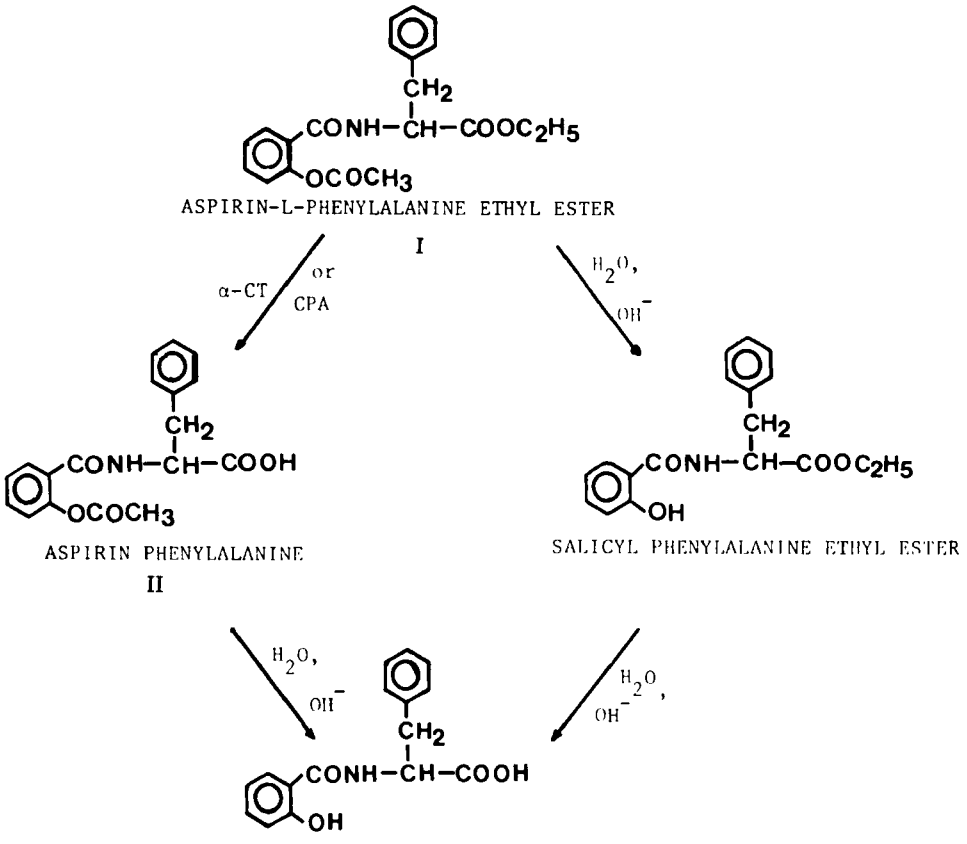

Scheme III

at concentrations ranging from 4.4×10^{-4} to 1.2×10^{-3} *M* were obtained in the presence of 1×10^{-5} *M* enzyme. The details of these experiments will be published in a later paper.

Since I is hydrolyzed to II by α-chymotrypsin and II does not cleave to aspirin in the presence of carboxypeptidase A, I is not a prodrug for aspirin.

Based on the previous work (8–10) and the additional data obtained in this laboratory, Scheme III is proposed for the hydrolysis of aspirin phenylalanine ethyl ester.

(1) J. P. Leonards and G. Levy, *J. Pharm. Sci.*, **59**, 1151 (1970).
(2) K. W. Anderson, *Arch. Int. Pharmacodyn. Ther.*, **152**, 379 (1964).
(3) C. Davison, D. H. Hertig, and R. DeVine, *Clin. Pharmacol. Ther.*, **7**, 329 (1966).
(4) T. St. Pierre and W. P. Jencks, *J. Am. Chem. Soc.*, **90**, 3817 (1968).
(5) A. A. Hussain, M. Yamasaki, and J. E. Truelove, *J. Pharm. Sci.*, **63**, 627 (1974).
(6) A. A. Hussain, J. E. Truelove, and H. Kostenbauder, *J. Pharm. Sci.*, **68**, 299 (1979).
(7) J. E. Truelove, A. A. Hussain, and H. B. Kostenbauder, *J. Pharm. Sci.*, **69**, 231 (1980).
(8) P. K. Banerjee and G. L. Amidon, *J. Pharm. Sci.*, **70**, 1299 (1981).
(9) P. K. Banerjee and G. L. Amidon, *J. Pharm. Sci.*, **70**, 1304 (1981).
(10) P. K. Banerjee and G. L. Amidon, *J. Pharm. Sci.*, **70**, 1307 (1981).

M. Kawahara

Z. Muhi-Eldeen
A. Hussain ˣ
College of Pharmacy
University of Kentucky
Lexington, KY 40536-0053

Received June 24, 1982.
Accepted for publication March 4, 1983.

Comment on a Second-Degree Polynomial Mathematical Model for Tablet Friability and *In Vitro* Dissolution

Keyphrases □ Dissolution—*in vitro*, polynomial mathematical model, effect of moisture and crushing strength □ Friability—effect of moisture and crushing strength, mathematical model

To the Editor:

In a recent report, Chowhan *et al.* (1) have used a function of a two-variable model to describe the effect of moisture and crushing strength on tablet friability and *in vitro* dissolution. Elliptical shape and ridge contour curves were unfortunately not reproduced on a computer[1] using all published data. Further examination of the mathematical equation (Eq. 1) using SAS contour plot procedure[2] on the same computer showed indeed that Figs. 5 and 6 contour plots in the article did not agree with the analytical expression.

[1] IBM 3033.
[2] SAS Institute Inc., Cary, NC 27511.

0022-3549/83/0900-1096$01.00/0

The mathematical model (2):

$$Y = b_0 + b_1X_1 + b_2X_2 + b_3X_1^2 + b_1X_1X_2 + b_5X_2^2 + \text{Error} \quad \text{(Eq. 1)}$$

can be rearranged and rewritten as shown below:

$$Y = b_3X_1^2 + b_4X_1X_2 + b_5X_2^2 + b_1X_1 + b_2X_2 + b_0 + \text{Error} \quad \text{(Eq. 1)}$$

$$Z = AX^2 + BXY + CY^2 + DX + EY + F \quad \text{(Eq. 2)}$$

According to a well-known theorem (3), the surface (Eq. 2) is an elliptic parabaloid which has ellipses for horizontal cross sections if $B^2 - 4AC$ is negative, a hyperbolic parabaloid if $B^2 - 4AC$ is positive, and a parabolic cylinder if $B^2 - 4AC$ is zero. The type of a parabaloid can, therefore, be obtained by computing the discriminant $B^2 - 4AC$ in the equation. Using those suggested coefficients b_0, b_1, b_2 . . . b_5 to substitute for Eq. 1 for the case of tablet friability response, the discriminant $B^2 - 4AC$ is positive, the level curves (contour curves) are hyperbolas, and the surface is a hyperbolic parabaloid; for the dissolution response, the discriminant $B^2 - 4AC$ is negative and A and C are negative, the level curves are ellipses, and the surface is an elliptic parabaloid that opens downward. No evidence was given showing that the mathematical model had been tested. No explanation or reference was provided to show how the contour curves were derived and drawn. No examination was given to discuss whether the part of error in the equation (Eq. 1) was due to lack-of-fit.

By definition (3), a level curve (or contour curve) of a function $f(x,y)$ is the curve $f(x,y) = C$ in the XY-plane. It consists of the points (x,y) where the function has the value C. In a real situation, it appears to be difficult for tablet friability and dissolution response to satisfy the necessary conditions for the curve $f(x,y) = C$, respectively. In other words, no tablets can be obtained with zero crushing strength; however, if $x = 0, y = 0$, the tablet friability response curve should remain $f(x,y) = C$. As a consequence, the quadratic response model does not adequately represent the true response surface.

In addition, the authors stated that "The friability contour plot consists of a series of ellipsoidal curves" (p. 1375) in the *Results* and *Discussions* section. There was no proof or test for ellipsoids, $Z^2 = AX^2 + BY^2 + C$. An ellipsoid is defined (4) as a surface, all plane sections of which are ellipses or circles. Mathematically speaking, $Z^2 = AX^2 + BY^2 + C$, if A and B are negative, the cross sections are all ellipses, and the surface is an ellipsoid. The Eq. 1 mathematical form does not automatically equate with the equation $Z^2 = AX^2 + BY^2 + C$.

It is a suitable approach to sketch a graph geometrically for the range of tablet specifications to obtain a desired quality product. A particularly chosen mathematical model should be carefully examined and thoroughly tested to determine the suitability and validity of the model for explaining scientific observations.

(1) Z. T. Chowhan, I. C. Yang, A. A. Amaro, and Li-Hua Chi, *J. Pharm. Sci.*, **71**, 1371 (1982).

(2) The RSREG Procedure, SAS Technical Report P115 (1982), SAS Institute, Inc., Cary, NC 27511.

(3) A. Shenk, "Calculus and Analytical Geometry," 2nd ed., 1979.

(4) "Webster's New Collegiate Dictionary," Merriam, Springfield, Mass.

Liang-Lii Huang
Wm. H. Rorer, Inc.
Fort Washington, PA 19034

Received March 7, 1983.
Accepted for publication May 3, 1983.

A Rebuttal on a Second-Degree Polynomial Mathematical Model Used to Evaluate the Effect of Moisture and Crushing Strength on Tablet Friability and *In Vitro* Dissolution

Keyphrases □ Dissolution—*in vitro*, effect of moisture and crushing strength, friability □ Crushing strength—effect on tablet friability and *in vitro* dissolution □ Friability—effect of moisture and crushing strength

To the Editor:

Huang's communication (1) refers critically to the report of Chowhan *et al.* (2); the basis of his criticism stems from his attempt to reproduce the response surface contour plots in Figs. 5 and 6 using the regression coefficients given in Table I (1) by means of a program package[1], RSREG, on a computer[2]. To confirm our results, the experimental data were evaluated by the same program package[1] and computer[2] and a completely separate data analysis package, RSM[3]. The results from both analyses were consistent with the results reported earlier (2) in Figs. 5 and 6. Closer scrutiny of the published regression coefficients in Table I (2) revealed a printing error; coefficient b_3 for tablet friability should read (positive) +0.06228 rather than (negative) −0.06228. This makes the discriminant $B^2 - 4AC$ negative, which corresponds to an elliptical level curve with an elliptical parabaloid surface that opens upwards. These results are completely consistent with the model chosen over the ranges evaluated. The tablet crushing strength and the granulation moisture were evaluated only within the practical limitations of tableting. It was stated clearly that within the practical ranges of tablet crushing strength and granulation moisture content, the data could be analyzed using a general quadratic response surface model. Within the practical limitations of tableting, the usefulness of this method in establishing *rational* specifications for the in-process variables, such as granulation moisture (x) and initial tablet crushing strength (y), to ensure proper control of the tablet friability and *in vitro* dissolution was also discussed. Since the experimental data were evaluated within the practical limitations of tableting, and this point was emphasized in the discussion, there is no justification for Huang to be critical of conditions such as $f(x,y) = C$ with $x = 0, y = 0$, which are unrealistic and of no consequence for optimizing *in vitro* dissolution and tablet friability.

Table I (2) gives the values of multiple correlation coefficients. The model was tested using lack-of-fit, F ratio, and t test. It was stated in the report that contour curves

[1] SAS Institute, Inc. Cary, NC 27511.
[2] IBM 3033.
[3] Compuserve, Santa Clara, CA 95054.

0022-3549/83/0900-1097$01.00/0

The mathematical model (2):

$$Y = b_0 + b_1X_1 + b_2X_2 + b_3X_1^2 + b_1X_1X_2 + b_5X_2^2 + \text{Error} \quad \text{(Eq. 1)}$$

can be rearranged and rewritten as shown below:

$$Y = b_3X_1^2 + b_4X_1X_2 + b_5X_2^2 + b_1X_1 + b_2X_2 + b_0 + \text{Error} \quad \text{(Eq. 1)}$$

$$Z = AX^2 + BXY + CY^2 + DX + EY + F \quad \text{(Eq. 2)}$$

According to a well-known theorem (3), the surface (Eq. 2) is an elliptic parabaloid which has ellipses for horizontal cross sections if $B^2 - 4AC$ is negative, a hyperbolic parabaloid if $B^2 - 4AC$ is positive, and a parabolic cylinder if $B^2 - 4AC$ is zero. The type of a parabaloid can, therefore, be obtained by computing the discriminant $B^2 - 4AC$ in the equation. Using those suggested coefficients b_0, b_1, b_2 . . . b_5 to substitute for Eq. 1 for the case of tablet friability response, the discriminant $B^2 - 4AC$ is positive, the level curves (contour curves) are hyperbolas, and the surface is a hyperbolic parabaloid; for the dissolution response, the discriminant $B^2 - 4AC$ is negative and A and C are negative, the level curves are ellipses, and the surface is an elliptic parabaloid that opens downward. No evidence was given showing that the mathematical model had been tested. No explanation or reference was provided to show how the contour curves were derived and drawn. No examination was given to discuss whether the part of error in the equation (Eq. 1) was due to lack-of-fit.

By definition (3), a level curve (or contour curve) of a function $f(x,y)$ is the curve $f(x,y) = C$ in the XY-plane. It consists of the points (x,y) where the function has the value C. In a real situation, it appears to be difficult for tablet friability and dissolution response to satisfy the necessary conditions for the curve $f(x,y) = C$, respectively. In other words, no tablets can be obtained with zero crushing strength; however, if $x = 0, y = 0$, the tablet friability response curve should remain $f(x,y) = C$. As a consequence, the quadratic response model does not adequately represent the true response surface.

In addition, the authors stated that "The friability contour plot consists of a series of ellipsoidal curves" (p. 1375) in the *Results* and *Discussions* section. There was no proof or test for ellipsoids, $Z^2 = AX^2 + BY^2 + C$. An ellipsoid is defined (4) as a surface, all plane sections of which are ellipses or circles. Mathematically speaking, $Z^2 = AX^2 + BY^2 + C$, if A and B are negative, the cross sections are all ellipses, and the surface is an ellipsoid. The Eq. 1 mathematical form does not automatically equate with the equation $Z^2 = AX^2 + BY^2 + C$.

It is a suitable approach to sketch a graph geometrically for the range of tablet specifications to obtain a desired quality product. A particularly chosen mathematical model should be carefully examined and thoroughly tested to determine the suitability and validity of the model for explaining scientific observations.

(1) Z. T. Chowhan, I. C. Yang, A. A. Amaro, and Li-Hua Chi, *J. Pharm. Sci.*, **71**, 1371 (1982).

(2) The RSREG Procedure, SAS Technical Report P115 (1982), SAS Institute, Inc., Cary, NC 27511.

(3) A. Shenk, "Calculus and Analytical Geometry," 2nd ed., 1979.

(4) "Webster's New Collegiate Dictionary," Merriam, Springfield, Mass.

Liang-Lii Huang
Wm. H. Rorer, Inc.
Fort Washington, PA 19034

Received March 7, 1983.
Accepted for publication May 3, 1983.

A Rebuttal on a Second-Degree Polynomial Mathematical Model Used to Evaluate the Effect of Moisture and Crushing Strength on Tablet Friability and *In Vitro* Dissolution

Keyphrases □ Dissolution—*in vitro*, effect of moisture and crushing strength, friability □ Crushing strength—effect on tablet friability and *in vitro* dissolution □ Friability—effect of moisture and crushing strength

To the Editor:

Huang's communication (1) refers critically to the report of Chowhan *et al.* (2); the basis of his criticism stems from his attempt to reproduce the response surface contour plots in Figs. 5 and 6 using the regression coefficients given in Table I (1) by means of a program package[1], RSREG, on a computer[2]. To confirm our results, the experimental data were evaluated by the same program package[1] and computer[2] and a completely separate data analysis package, RSM[3]. The results from both analyses were consistent with the results reported earlier (2) in Figs. 5 and 6. Closer scrutiny of the published regression coefficients in Table I (2) revealed a printing error; coefficient b_3 for tablet friability should read (positive) +0.06228 rather than (negative) −0.06228. This makes the discriminant $B^2 - 4AC$ negative, which corresponds to an elliptical level curve with an elliptical parabaloid surface that opens upwards. These results are completely consistent with the model chosen over the ranges evaluated. The tablet crushing strength and the granulation moisture were evaluated only within the practical limitations of tableting. It was stated clearly that within the practical ranges of tablet crushing strength and granulation moisture content, the data could be analyzed using a general quadratic response surface model. Within the practical limitations of tableting, the usefulness of this method in establishing *rational* specifications for the in-process variables, such as granulation moisture (x) and initial tablet crushing strength (y), to ensure proper control of the tablet friability and *in vitro* dissolution was also discussed. Since the experimental data were evaluated within the practical limitations of tableting, and this point was emphasized in the discussion, there is no justification for Huang to be critical of conditions such as $f(x,y) = C$ with $x = 0, y = 0$, which are unrealistic and of no consequence for optimizing *in vitro* dissolution and tablet friability.

Table I (2) gives the values of multiple correlation coefficients. The model was tested using lack-of-fit, F ratio, and t test. It was stated in the report that contour curves

[1] SAS Institute, Inc. Cary, NC 27511.
[2] IBM 3033.
[3] Compuserve, Santa Clara, CA 95054.

0022-3549/83/0900-1097$01.00/0

were derived and drawn using the SAS contour plot procedure, RSREG. No further clarification was deemed necessary.

Since the model tested in the paper is $Z = AX^2 + BXY + CY^2 + DX + EY + F$, the possible contour surfaces are hyperbolic paraboloid, elliptic paraboloid, and an elliptic cylinder, depending on the sign of the coefficients of the equation. The dictionary definition (3) of the suffix "-oid" is, "having the form or appearance of." In the two-dimensional representation of the contour surface, the dictionary definition is implicit and the term ellipsoidal translates into elliptical as it is stated in the article. It does not imply that the resulting contour level curves for tablet friability are ellipsoidal in the mathematical sense, but rather is the elliptical projection onto a plane of the response surface at a fixed value of Z.

In conclusion, we iterate that a general multiple linear regression analysis, if used within the practical limitations of tableting, is helpful in understanding the role of the granulation moisture and tablet crushing strength on tablet friability and *in vitro* dissolution. Rational in-process specifications for the granulation moisture content and tablet crushing strength may be established by superimposing the contour plots of tablet friability and drug dissolution.

(1) L. Huang, *J. Pharm. Sci.*, **72**, 1096 (1983).

(2) Z. T. Chowhan, I. C. Yang, A. A. Amaro, and L.-H. Chi, *J. Pharm. Sci.* **71**, 1371 (1982).

(3) "Webster's New Collegiate Dictionary," Merriam, Springfield, Mass.

Z. T. Chowhan ˣ
I.-C. Yang
A. A. Amaro
Li-hua Chi
Institute of Pharmaceutical Sciences
Syntex Research
Palo Alto, CA 94304

Received April 8, 1983
Accepted for publication May 3, 1983

Model-Independent Method of Predicting Peak, Trough, and Mean Steady-State Levels in Multiple Intravenous Bolus Dosing in Nonlinear Pharmacokinetics

Keyphrases □ Pharmacokinetics—nonlinear, model-independent method, use of simulated data

To the Editor:

Nonempirical methods for dosage predictions and adjustments of drugs showing nonlinear pharmacokinetics are apparently all based on nonlinear pharmacokinetic models. However, the disproportional behavior of such drugs necessitates particularly reliable calculations, which are generally not provided by structured pharmacokinetic models, due to their inherent nonuniqueness and often unrealistic kinetic assumptions. The model-independent method proposed here should overcome some of the disadvantages of such methods.

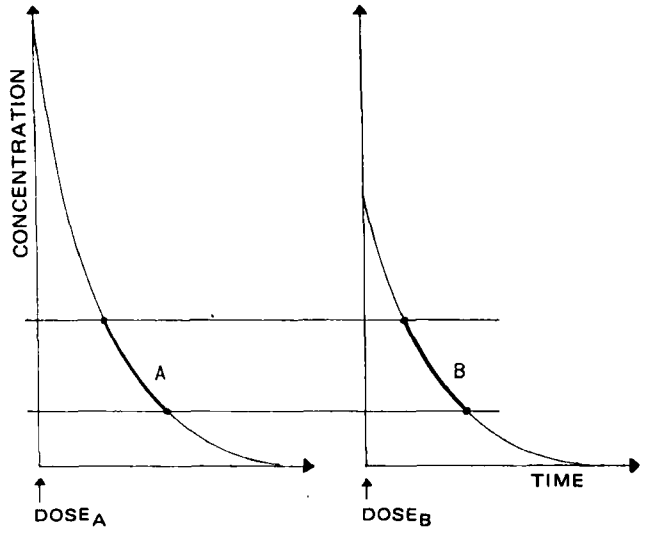

Figure 1—*Illustration of the congruence property of a pharmacokinetic system satisfying the differential equation, Eq. 1: Curve segment A = curve segment B.*

In nonlinear pharmacokinetics it is often observed that the slopes of the drug concentration *versus* time profiles at arbitrary drug levels are independent of the intravenous bolus dose given, which results in the congruence property illustrated in Fig. 1. Such kinetic behavior will be found for any nonlinear (or linear) pharmacokinetic system when the rate of change of the drug level depends only on the drug level, *i.e.*:

$$\frac{dC}{dt} = f(C) \qquad \text{(Eq. 1)}$$

where $f(\ )$ can be any function only dependent on the concentration C. For example, a parallel first-order and Michaelis–Menten elimination:

$$\frac{dC}{dt} = -kC - \frac{V_m C}{K_m + C} \qquad \text{(Eq. 2)}$$

will result in this behavior; so will any other system incorporating nonlinear binding, excretion, metabolism, *etc.*, as long as the kinetics can be described in the general form of Eq. 1. Due to the model-independent nature of the method proposed, there is of course no need to postulate a specific kinetic relationship. The congruence property (Fig. 1) makes drug level predictions particularly simple: Once drug level data from an intravenous bolus injection have been well approximated by an arbitrary function then this function can serve as a base function for drug level predictions. For example, to predict the drug level profile at steady state starting at point P (Fig. 2), the corresponding point P′ on the base curve is found. The base curve segment starting at P′ and stretching over a time interval of length T (where T is the dosing period) then defines the steady-state profile (Fig. 2).

The peak and trough levels at steady state can be derived from the base function as follows: The difference between the peak and trough levels at steady state is equal to the concentration increment, ΔC_D, resulting from the dose injected at the completion of the dosing period:

$$C_{ss}^{max} - C_{ss}^{min} = \Delta C_D \qquad \text{(Eq. 3)}$$

Equation 3 can be transformed into the equivalent base

0022-3549/83/0900-1098$01.00/0

were derived and drawn using the SAS contour plot procedure, RSREG. No further clarification was deemed necessary.

Since the model tested in the paper is $Z = AX^2 + BXY + CY^2 + DX + EY + F$, the possible contour surfaces are hyperbolic paraboloid, elliptic paraboloid, and an elliptic cylinder, depending on the sign of the coefficients of the equation. The dictionary definition (3) of the suffix "-oid" is, "having the form or appearance of." In the two-dimensional representation of the contour surface, the dictionary definition is implicit and the term ellipsoidal translates into elliptical as it is stated in the article. It does not imply that the resulting contour level curves for tablet friability are ellipsoidal in the mathematical sense, but rather is the elliptical projection onto a plane of the response surface at a fixed value of Z.

In conclusion, we iterate that a general multiple linear regression analysis, if used within the practical limitations of tableting, is helpful in understanding the role of the granulation moisture and tablet crushing strength on tablet friability and *in vitro* dissolution. Rational in-process specifications for the granulation moisture content and tablet crushing strength may be established by superimposing the contour plots of tablet friability and drug dissolution.

(1) L. Huang, *J. Pharm. Sci.*, **72**, 1096 (1983).

(2) Z. T. Chowhan, I. C. Yang, A. A. Amaro, and L.-H. Chi, *J. Pharm. Sci.* **71**, 1371 (1982).

(3) "Webster's New Collegiate Dictionary," Merriam, Springfield, Mass.

Z. T. Chowhan ˣ
I.-C. Yang
A. A. Amaro
Li-hua Chi
Institute of Pharmaceutical Sciences
Syntex Research
Palo Alto, CA 94304

Received April 8, 1983
Accepted for publication May 3, 1983

Model-Independent Method of Predicting Peak, Trough, and Mean Steady-State Levels in Multiple Intravenous Bolus Dosing in Nonlinear Pharmacokinetics

Keyphrases □ Pharmacokinetics—nonlinear, model-independent method, use of simulated data

To the Editor:

Nonempirical methods for dosage predictions and adjustments of drugs showing nonlinear pharmacokinetics are apparently all based on nonlinear pharmacokinetic models. However, the disproportional behavior of such drugs necessitates particularly reliable calculations, which are generally not provided by structured pharmacokinetic models, due to their inherent nonuniqueness and often unrealistic kinetic assumptions. The model-independent method proposed here should overcome some of the disadvantages of such methods.

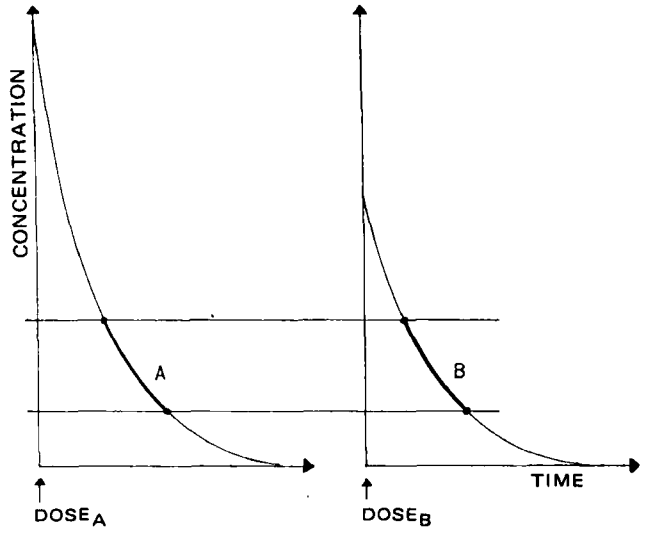

Figure 1—*Illustration of the congruence property of a pharmacokinetic system satisfying the differential equation, Eq. 1: Curve segment A = curve segment B.*

In nonlinear pharmacokinetics it is often observed that the slopes of the drug concentration *versus* time profiles at arbitrary drug levels are independent of the intravenous bolus dose given, which results in the congruence property illustrated in Fig. 1. Such kinetic behavior will be found for any nonlinear (or linear) pharmacokinetic system when the rate of change of the drug level depends only on the drug level, *i.e.*:

$$\frac{dC}{dt} = f(C) \qquad \text{(Eq. 1)}$$

where $f(\ )$ can be any function only dependent on the concentration C. For example, a parallel first-order and Michaelis–Menten elimination:

$$\frac{dC}{dt} = -kC - \frac{V_m C}{K_m + C} \qquad \text{(Eq. 2)}$$

will result in this behavior; so will any other system incorporating nonlinear binding, excretion, metabolism, *etc.*, as long as the kinetics can be described in the general form of Eq. 1. Due to the model-independent nature of the method proposed, there is of course no need to postulate a specific kinetic relationship. The congruence property (Fig. 1) makes drug level predictions particularly simple: Once drug level data from an intravenous bolus injection have been well approximated by an arbitrary function then this function can serve as a base function for drug level predictions. For example, to predict the drug level profile at steady state starting at point P (Fig. 2), the corresponding point P′ on the base curve is found. The base curve segment starting at P′ and stretching over a time interval of length T (where T is the dosing period) then defines the steady-state profile (Fig. 2).

The peak and trough levels at steady state can be derived from the base function as follows: The difference between the peak and trough levels at steady state is equal to the concentration increment, ΔC_D, resulting from the dose injected at the completion of the dosing period:

$$C_{ss}^{max} - C_{ss}^{min} = \Delta C_D \qquad \text{(Eq. 3)}$$

Equation 3 can be transformed into the equivalent base

0022-3549/83/0900-1098$01.00/0

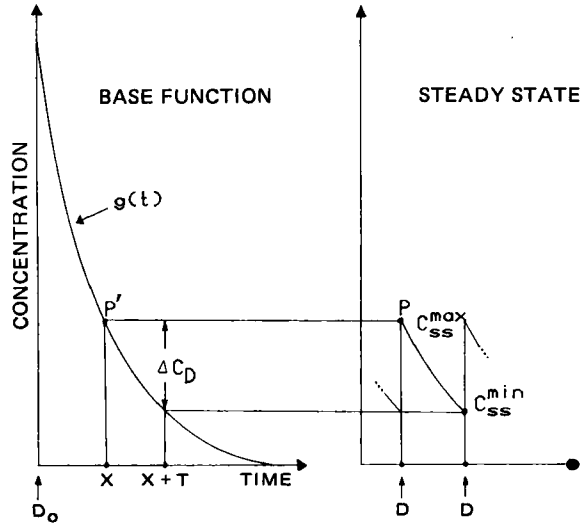

Figure 2—*Base function approach to obtain peak, trough, and mean steady-state levels in multiple intravenous bolus dosing in nonlinear pharmacokinetics.*

function relationship (Fig. 2):

$$g(x) - g(x + T) = \Delta C_D \qquad \text{(Eq. 4)}$$

The basic principle behind the methodology expressed by Eq. 4 is simply to find a certain level $g(x)$ (point P′, Fig. 2) on the base function, which over a period (x to $x + T$) equal to the dosing period T results in a reduction $g(x) - g(x + T)$, which is equal to the concentration increment Δc_D resulting from the maintenance dose. The particular curve segment on the base curve with the property expressed by Eq. 4 is determined numerically by finding the particular value of the unknown quantity x which satisfies Eq. 4. The method assumes that the pharmacokinetics show a dose linear boundary condition, so that c_D is proportional to the dose:

$$\Delta C_D = D/V \qquad \text{(Eq. 5)}$$

This appears to be a reasonable assumption, since the nonlinearity of the drug is more likely due to secretion and metabolic processes than to its initial distribution. The proportionality term, V, in Eq. 4 can be estimated from the base function and its intravenous bolus dose D_0:

$$V = D_0/g(0) \qquad \text{(Eq. 6)}$$

Substituting Eqs. 5 and 6 into Eq. 4 yields the following final expression:

$$g(x + T) + \frac{D}{D_0} g(0) - g(x) = 0 \qquad \text{(Eq. 7)}$$

If the function g fitted to the single-dose data is monotonically decreasing and D_0 has been chosen slightly larger than a normal loading dose so that $g(0) > C_{ss}^{max}$, then Eq. 7 can be solved for x to subsequently give the steady-state peak and trough levels (Fig. 2):

$$C_{ss}^{max} = g(x) \qquad \text{(Eq. 8)}$$

$$C_{ss}^{min} = g(x + T) \qquad \text{(Eq. 9)}$$

Thus, the procedure to determine the steady-state peak and trough levels resulting from intravenous bolus doses D, injected at regular dosing intervals T, can be summarized as follows: Plasma level data from an intravenous bolus dose $D_0 (D_0 > D$, *e.g.*, a loading dose) is obtained and an arbitrary, monotonically decreasing function is fitted to the data to give the base function g. The dose D_0 should be chosen sufficiently large to ensure that the initial base function value $g(0)$ is larger than the expected steady-state peak level. Equation 7 is then solved numerically for x. Most computer program libraries for scientific computations will have programs suitable for this task (1, 2). The peak and trough levels are subsequently calculated from the base function according to Eqs. 8 and 9.

The mean steady-state level, $\bar{C}_{ss}$, can also be calculated from the base function once x has been found:

$$\bar{C}_{ss} = \int_x^{x+T} g(t)dt/T \qquad \text{(Eq. 10)}$$

The sum of exponential functions which are fitted so successfully to intravenous bolus data in linear pharmacokinetics apparently do not fit nonlinear pharmacokinetic data properly. Preliminary investigations were, therefore, carried out to identify a suitable type of function that could be used. It was found that the following empirical function:

$$g(t) = \frac{p_1 e^{-p_2 t}}{1 + e^{p_3 - p_4 t}} \qquad p_i > 0 \qquad \text{(Eq. 11)}$$

produced excellent fit to all typical Michaelis–Menten type data investigated. Extension of the numerator and denominator (Eq. 11) to include more exponential terms may perhaps be fairly universally applicable to most nonlinear pharmacokinetic data.

The following example using simulated data illustrates the methodology. Fifteen concentration–time data with 10% normally distributed errors added were generated from the arbitrarily chosen nonlinear model, Eq. 2. The kinetic parameters $V_m = 12$, $K_m = 27$, $k = 0.08$, $C(0) = D/V = 70$, $t = 0.2,, 0.4, 0.6, 0.8, 1.0, 1.2, 1.4, 1.6, 1.8, 2.0, 2.5, 3.0, 3.5, 4$, and 8 were chosen to produce a pronounced nonlinearity indicated by a typical Michaelis–Menten type semilogarithmic concavity. Using the nonlinear regression program FUNFIT (3), the empirical equation Eq. 11 produced an excellent least-squares fit to the simulated data with $p_1 = 494$, $p_2 = 0.532$, $p_3 = 1.88$, and $p_4 = 0.414$.

Equation 7 was subsequently used to make steady-state predictions for a maintenance dose half the size of the above loading dose when given every 4 hours. This was done by inserting Eq. 11 into Eq. 7 with $D/D_0 = 0.5$ and $T = 4$ to give:

$$\frac{p_1 e^{-p_2(x+4)}}{1 + e^{p_3 - p_4(x+4)}} + 0.5 \frac{p_1}{1 + e^{p_3}} - \frac{p_1 e^{-p_2 x}}{1 + e^{p_3 - p_4 x}} = 0 \qquad \text{(Eq. 12)}$$

This equation was solved numerically for x with the above least-squares p-values using a fairly standard, commonly used root-finding algorithm (1). The peak, trough, and mean steady-state levels $C_{ss}^{max} = 47.7$, $C_{ss}^{min} = 15.0$, and $\bar{C}_{ss} = 29.8$ were calculated from the obtained x value ($x = 1.64$) according to:

$$C_{ss}^{max} = \frac{p_1 e^{-p_2 x}}{1 + e^{p_3 - p_4 x}} \qquad \text{(Eq. 13)}$$

$$C_{ss}^{min} = \frac{p_1 e^{-p_2(x+4)}}{1 + e^{p_3 - p_4(x+4)}} \qquad \text{(Eq. 14)}$$

$$\bar{C}_{ss} = \frac{1}{4}\int_x^{x+4} \frac{p_1 e^{-p_2 t}}{1 + e^{p_3 - p_4 t}}\, dt \qquad \text{(Eq. 15)}$$

The integral in Eq. 15 was evaluated numerically by a commonly used integration algorithm (4).

Special caution must be taken in applying a loading dose of a nonlinear drug. It may not be desirable to use a loading dose for a drug showing a narrow therapeutic index. However, in certain clinical situations it may be necessary to quickly establish high therapeutic levels by a loading dose. For example, the treatment of an epileptic emergency may call for an intravenous loading dose of phenytoin (5). The loading dose required for the method only needs to be slightly larger than a normal loading dose.[1] It should, therefore, not add much additional risk to the administration of such a loading dose. The method may also be used in dosing adjustments requiring lower steady-state drug levels, in which case the drug level data needed to make the predictions may be obtained from the later part of the dosing period.

[1] However, if the function $g(\ )$ is well chosen, it can be used to extrapolate to required levels and a loading dose may not be required.

(1) ZBRENT, IMSL, Houston, Texas.

(2) G. Dahlquist and A. Björk, "Numerical Methods," Prentice-Hall, Inglewood Cliffs, N.J., 1974, Chap. 6.

(3) P. Veng-Pedersen, *J. Pharmacokinet. Biopharm.*, **5**, 513 (1977).

(4) C. deBoor, in "Mathematical Software," J. Rice, Ed., Academic, New York, N.Y., 1971, Chap. 7.

(5) M. E. Winter, "Basic Clinical Pharmacokinetics," Applied Therapeutics Inc., San Francisco, Calif., 1980, p. 183.

Peter Veng-Pedersen[x]
Luis Suarez
Division of Pharmacokinetics
School of Pharmacy and Pharmacal Sciences
Purdue University
West Lafayette, IN 47907

Received December 30, 1982.
Accepted for publication June 6, 1983.

BOOKS

Progress in Medicinal Chemistry, Vol. 19. Edited by G. P. ELLIS and G. B. WEST. Elsevier Biomedical Press BV, Amsterdam, The Netherlands. 1982. 345 pp. 14 × 21 cm. Price $93.50 (Dfl. 220).

Contained in this volume are six reviews of independent topics covering a variety of subjects. Chapter I, "Immunopharmacology of Gold," by A. J. Lewis and D. T. Walz denotes the pathology of rheumatoid arthritis, the historical use of gold for therapeutic purposes, pharmacokinetics of gold compounds, and gold–protein interaction with tissue sulfhydryl groups, hydrolytic enzyme, prostaglandin synthetase complement, and collagen. The response systems as well as their current clinical uses in rheumatoid arthritis, pemphigus, asthma, and cancer are described.

Chapter II, "Calcium and Histamine Secretion from Mast Cells," by F. L. Pearce deals with the role of calcium in histamine release, membrane ionophones, phospholipid vesicles and permeability, and calcium pools inside and outside the cell. The activation of vasoamine release by the mast cell *via* the translocation of calcium was related to membrane phosphatidylinositol metabolism, phospholipid methylation, and cAMP levels. Known inhibitors of these processes were evaluated.

Chapter III, "Biological and Pharmacological Properties of Phospholipids," by A. Bruni and P. Palatini is a discussion of the phospholipid bilayer model including flexibility, stability, asymmetry, head groups, and fusion of the components. Phospholipid–protein interrelations, including lipid-binding proteins, mode of association, specificity of the interreaction, mutual influence of components in the membrane, and structural models are presented. The pharmacological aspects of liposomes or bilayer envelopes including pharmacokinetics; interaction with cells; delivery of drugs, genetic material, or immune components; and lipid chemical mediators were presented by the authors.

Chapter IV, "Cyclophosphamide Analogues," by G. Zon includes a cursory historical review of cyclophosphamide as an antineoplastic agent including novel chemical substitutions, related conformational effects, prodrug models, structure–activity relationships of active metabolites, and miscellaneous analogues.

Chapter V, "Chartruesin, a Glycosidic Antitumor Antibiotic from *Streptomyces*," by J. A. Beisler covers the natural, microbial, and biochemical sources and structure determination of chartruesin. Partial and total synthetic routes of aglycones are reviewed. The antitumor activity, mode of action, and toxicity of chartruesin are briefly eluded to in the discussion.

Chapter VI, "Recent Progress in the Medicinal Chemistry of 2,4-Diaminopyrimidines," by B. Roth and C. C. Cheng covers the classical aspects of antimetabolites of folic acid and descriptions of dihydrofolate reductase enzymes from bacteria and vertebrate sources. Pharmacological action was discussed in three areas: (*a*) antibacterial action of diaminopyrimidines of the 2,4-diamino-5-(substituted benzyl) pyrimidines, 6-substituted 2,4-diamino-5-benzyl pyrimidines, isosteres of the benzylpyrimidines, dihydro-*sym*-triazines, and bicyclic analogues of diamino-pyrimidines; (*b*) antimalarial dihydrofolate reductase inhibitors—pyrimethamine and cycloguanil, monocyclic 2,4-diamino-pyrimidines and isosteres, dihydro-*sym*-triazines, and quinazolines; (*c*) anticancer—dihydrofolate reductase inhibitions by methotrexate, modifications of the glutamic acid, benzene ring, bridge atoms between the rings, and pteridine portions. Miscellaneous and nonclassical dihydrofolate reductase inhibitors are included in the chapter.

Whereas all six of these topics are relevant to medicinal chemistry, this reviewer found the text somewhat disappointing from two aspects: (*a*) much of the material was redundant with basic conceptual ideas presented on numerous occasions in the literature; (*b*) the topics selected were not those that would be at the forefront of current research today. However, the chapters are well referenced with a number of figures, tables, and diagrams, and the text is organized and clearly written for understanding by the reader. The major use of the text as a reference book would be for graduate students and individuals not versed in these areas of research. The current status of each of the six topics is accurately assessed by the authors, and the text is an excellent overview of both chemical and biological ideas regarding the topics, which is important in medicinal chemistry because of the diversity of the field.

Reviewed by Iris H. Hall
Division of Medicinal Chemistry and Natural Products
The University of North Carolina at Chapel Hill
Chapel Hill, NC 27514

$$C_{ss}^{min} = \frac{p_1 e^{-p_2(x+4)}}{1 + e^{p_3 - p_4(x+4)}} \qquad \text{(Eq. 14)}$$

$$\bar{C}_{ss} = \frac{1}{4}\int_x^{x+4} \frac{p_1 e^{-p_2 t}}{1 + e^{p_3 - p_4 t}}\, dt \qquad \text{(Eq. 15)}$$

The integral in Eq. 15 was evaluated numerically by a commonly used integration algorithm (4).

Special caution must be taken in applying a loading dose of a nonlinear drug. It may not be desirable to use a loading dose for a drug showing a narrow therapeutic index. However, in certain clinical situations it may be necessary to quickly establish high therapeutic levels by a loading dose. For example, the treatment of an epileptic emergency may call for an intravenous loading dose of phenytoin (5). The loading dose required for the method only needs to be slightly larger than a normal loading dose.[1] It should, therefore, not add much additional risk to the administration of such a loading dose. The method may also be used in dosing adjustments requiring lower steady-state drug levels, in which case the drug level data needed to make the predictions may be obtained from the later part of the dosing period.

[1] However, if the function $g(\ )$ is well chosen, it can be used to extrapolate to required levels and a loading dose may not be required.

(1) ZBRENT, IMSL, Houston, Texas.

(2) G. Dahlquist and A. Björk, "Numerical Methods," Prentice-Hall, Inglewood Cliffs, N.J., 1974, Chap. 6.

(3) P. Veng-Pedersen, *J. Pharmacokinet. Biopharm.*, **5**, 513 (1977).

(4) C. deBoor, in "Mathematical Software," J. Rice, Ed., Academic, New York, N.Y., 1971, Chap. 7.

(5) M. E. Winter, "Basic Clinical Pharmacokinetics," Applied Therapeutics Inc., San Francisco, Calif., 1980, p. 183.

Peter Veng-Pedersen[x]
Luis Suarez
Division of Pharmacokinetics
School of Pharmacy and Pharmacal Sciences
Purdue University
West Lafayette, IN 47907

Received December 30, 1982.
Accepted for publication June 6, 1983.

BOOKS

Progress in Medicinal Chemistry, Vol. 19. Edited by G. P. ELLIS and G. B. WEST. Elsevier Biomedical Press BV, Amsterdam, The Netherlands. 1982. 345 pp. 14 × 21 cm. Price $93.50 (Dfl. 220).

Contained in this volume are six reviews of independent topics covering a variety of subjects. Chapter I, "Immunopharmacology of Gold," by A. J. Lewis and D. T. Walz denotes the pathology of rheumatoid arthritis, the historical use of gold for therapeutic purposes, pharmacokinetics of gold compounds, and gold–protein interaction with tissue sulfhydryl groups, hydrolytic enzyme, prostaglandin synthetase complement, and collagen. The response systems as well as their current clinical uses in rheumatoid arthritis, pemphigus, asthma, and cancer are described.

Chapter II, "Calcium and Histamine Secretion from Mast Cells," by F. L. Pearce deals with the role of calcium in histamine release, membrane ionophones, phospholipid vesicles and permeability, and calcium pools inside and outside the cell. The activation of vasoamine release by the mast cell *via* the translocation of calcium was related to membrane phosphatidylinositol metabolism, phospholipid methylation, and cAMP levels. Known inhibitors of these processes were evaluated.

Chapter III, "Biological and Pharmacological Properties of Phospholipids," by A. Bruni and P. Palatini is a discussion of the phospholipid bilayer model including flexibility, stability, asymmetry, head groups, and fusion of the components. Phospholipid–protein interrelations, including lipid-binding proteins, mode of association, specificity of the interreaction, mutual influence of components in the membrane, and structural models are presented. The pharmacological aspects of liposomes or bilayer envelopes including pharmacokinetics; interaction with cells; delivery of drugs, genetic material, or immune components; and lipid chemical mediators were presented by the authors.

Chapter IV, "Cyclophosphamide Analogues," by G. Zon includes a cursory historical review of cyclophosphamide as an antineoplastic agent including novel chemical substitutions, related conformational effects, prodrug models, structure–activity relationships of active metabolites, and miscellaneous analogues.

Chapter V, "Chartruesin, a Glycosidic Antitumor Antibiotic from *Streptomyces*," by J. A. Beisler covers the natural, microbial, and biochemical sources and structure determination of chartruesin. Partial and total synthetic routes of aglycones are reviewed. The antitumor activity, mode of action, and toxicity of chartruesin are briefly eluded to in the discussion.

Chapter VI, "Recent Progress in the Medicinal Chemistry of 2,4-Diaminopyrimidines," by B. Roth and C. C. Cheng covers the classical aspects of antimetabolites of folic acid and descriptions of dihydrofolate reductase enzymes from bacteria and vertebrate sources. Pharmacological action was discussed in three areas: (*a*) antibacterial action of diaminopyrimidines of the 2,4-diamino-5-(substituted benzyl) pyrimidines, 6-substituted 2,4-diamino-5-benzyl pyrimidines, isosteres of the benzylpyrimidines, dihydro-*sym*-triazines, and bicyclic analogues of diamino-pyrimidines; (*b*) antimalarial dihydrofolate reductase inhibitors—pyrimethamine and cycloguanil, monocyclic 2,4-diamino-pyrimidines and isosteres, dihydro-*sym*-triazines, and quinazolines; (*c*) anticancer—dihydrofolate reductase inhibitions by methotrexate, modifications of the glutamic acid, benzene ring, bridge atoms between the rings, and pteridine portions. Miscellaneous and nonclassical dihydrofolate reductase inhibitors are included in the chapter.

Whereas all six of these topics are relevant to medicinal chemistry, this reviewer found the text somewhat disappointing from two aspects: (*a*) much of the material was redundant with basic conceptual ideas presented on numerous occasions in the literature; (*b*) the topics selected were not those that would be at the forefront of current research today. However, the chapters are well referenced with a number of figures, tables, and diagrams, and the text is organized and clearly written for understanding by the reader. The major use of the text as a reference book would be for graduate students and individuals not versed in these areas of research. The current status of each of the six topics is accurately assessed by the authors, and the text is an excellent overview of both chemical and biological ideas regarding the topics, which is important in medicinal chemistry because of the diversity of the field.

Reviewed by Iris H. Hall
Division of Medicinal Chemistry and Natural Products
The University of North Carolina at Chapel Hill
Chapel Hill, NC 27514

JOURNAL OF PHARMACEUTICAL SCIENCES

October 1983
Volume 72 Number 10

A publication of the American Pharmaceutical Association

The *Journal of Pharmaceutical Sciences* (ISSN 0022-3549) is published monthly by the American Pharmaceutical Association (APhA) at 2215 Constitution Ave., N.W., Washington, DC 20037. Second-class postage paid at Washington, D.C. and at additional mailing office.

All expressions of opinion and statements of supposed fact appearing in articles or editorials carried in this journal are published on the authority of the writer over whose name they appear and are not to be regarded as necessarily expressing the policies or views of APhA.

Offices—Editorial, Advertising, and Subscription: 2215 Constitution Ave., N.W., Washington, DC 20037. All Journal staff may be contacted at this address. Printing: 20th & Northampton Streets, Easton, PA 18042.

Annual Subscriptions—United States and foreign, industrial and government institutions $75; educational institutions $75; individuals *for personal use only* $40; single copies $10. APhA and SAPhA members may subscribe to *J. Pharm. Sci.* for $20.00 per year. All foreign subscriptions add $10 for postage. Subscription rates are subject to change without notice.

Claims—Missing numbers will not be supplied if dues or subscriptions are in arrears for more than 60 days or if claims are received more than 60 days after the date of the issue, or if loss was due to failure to give notice of change of address. APhA cannot accept responsibility for foreign delivery when its records indicate shipment was made.

Change of Address—Members and subscribers should notify at once both the Post Office and APhA of any change of address.

Photocopying—The code at the foot of the first page of an article indicates that APhA has granted permission for copying of the article beyond the limits permitted by Sections 107 and 108 of the U.S. Copyright Law provided that the copier sends the per copy fee stated in the code to the Copyright Clearance Center, Inc., 21 Congress St., Salem, MA 01970. Copies may be made for personal or internal use only and not for general distribution.

Microfilm—Available from University Microfilms International, 300 N. Zeeb Road, Ann Arbor, MI 48106.

Neither Black Nor White, But Very Gray

Undoubtedly, every reader of this *Journal* has heard the observation stated that "no drug is completely safe." Indeed, most of our readers have probably articulated this point themselves on one or more occasion.

Generally, the need to bring out this fact comes up in discussions with the general public. The average lay person does not have the training, background, or sophistication to understand or grasp the concept that there are no real absolutes in the case of either safety or toxicity.

Although we might cringe a bit at the simplification involved, this writer once heard a pharmacologist try to explain this point to a lay audience; he stated that "chemotherapeutic agents are virtually nothing more than selective poisons that are administered to humans in carefully controlled quantities."

In this, the pharmacologist was simply paraphrasing Paracelsus (1493–1541) who is quoted as having written: "All substances are poisons; there is none which is not a poison. The right dose differentiates a poison and a remedy."

Virtually every substance known has some element of hazard associated with it, depending upon the form of exposure, duration of exposure, concentration of the substance, total intake involved, and similar considerations. And the more active or effective the substance is for some desired purpose, usually the more that its untoward effects or negative properties increase as well.

All of this gives rise to risk–benefit analysis or evaluations. Scientists and health care practitioners deal with these concepts countless times each day, and the concepts therefore should be almost second nature to them.

But on rare occasions, not only individual scientists but even relatively large groups of scientifically or medically trained people will react or overreact with apparently the same lack of understanding and judgment that we associate with the lay public.

About twenty years ago, Rachel Carson published her classic work titled "Silent Spring." This book had as its central theme a thesis that our indiscriminate use of pesticides was having a totally disastrous side effect on all animal life and particularly on the bird population.

Granted, she was guilty of some over-exaggeration, and she wrote with the high intensity of a typical crusader. But there also was a very significant element of truth in her position—truth that was later brought out by the DDT problems of the 1960's and infamous Kepone revelations of the mid-1970's.

Unfortunately, however, the scientific community as a whole did not assess her contentions in a calm, cool, and deliberate manner. Instead, scientists—and, in particular, chemists active in the American Chemical Society—scoffed at Carson's contentions and subjected her personally to the severest degree of ridicule. It wasn't until years later that the error of these unfortunate actions, which were prompted out of a misguided or excessive sense of loyalty to the chemical industry, was generally acknowledged.

Over the years, there have been other regrettable instances of knee-jerk reactions by scientists and scientifically trained people: groups that should really know better than to allow themselves to act either precipitiously or without appropriate balance.

One of the most recent of such incidents occurred this past June when the House of Delegates of the American Medical Association, by voice vote, approved the adoption of "an active public information campaign to prevent irrational reaction and unjustified public fright and to prevent the dissemination of possibly erroneous information" about the health hazards of dioxin. The language included with the resolution also spoke of "hysterical malreporting" and "a witch hunt" of dioxin.

Certainly, the facts presently known about the toxicity and hazards of dioxin do not justify the sensationalist press treatment and some of the extreme actions being recommended or taken with respect to controlling potential exposure to the agent. But, on the other hand, sufficient information is known to justify significant caution in dealing with it.

The regrettable aspect of the AMA policy action was to deal with the exaggerations by overreacting in the opposite direction. And the eager press and broadcast media were quick to publicize the action with stories carrying titles such as "AMA Votes to Fight Dioxin 'Witch Hunt.' "

Fortunately, cooler heads quickly prevailed at the AMA, and efforts were promptly taken to put their position in better public perspective—but, sadly, AMA credibility had already been damaged by the initial press reports.

Without citing additional examples, let it suffice to say that other areas of science, including the pharmaceutical sciences, have also had their share of such moments of embarrassment.

Hopefully, we will all learn from these experiences that while others may adopt positions that we see as extremist, scientists must avoid the temptation to take opposite positions that are equally extreme. Rather, the correct position—which is rarely, if ever, either black or white—must be sought and identified.

As one wag put it to us recently, "Scientists must keep their heads while all about them are losing theirs!"

—EDWARD G. FELDMANN
American Pharmaceutical Association
Washington, DC 20037

0022-3549/83/1000-1101$01.00/0

JOURNAL OF PHARMACEUTICAL SCIENCES

OCTOBER 1983
VOLUME 72 NUMBER 10

LITERATURE SURVEY

Physiologically Based Pharmacokinetic Modeling: Principles and Applications

LEONARD E. GERLOWSKI and RAKESH K. JAIN ˣ

Received March 25, 1982, from the *Department of Chemical Engineering, Carnegie-Mellon University, Pittsburgh, PA 15213.*

Pharmacokinetic models are used to describe the time-dependent distribution and disposition of a substance in a living system and, as such, have numerous uses in clinical applications and drug design. For medicinal purposes, pharmacokinetics can be used to estimate optimal drug scheduling and dosage regimens. For industrial toxins, pharmacokinetics can be used to aid in determining safe working environments. The modeling procedure is useful in animal and clinical applications, and for obtaining fundamental knowledge of the transport and metabolism of a substance *in vivo*. In this paper we present a review of physiologically based pharmacokinetics in the hope of understanding and increasing the use of this modeling technique. Recent review articles on the subject have primarily focused on the use of physiologically based pharmacokinetics in cancer treatment. The most comprehensive of these articles discusses proper formulation of a model and development of the equations in detail (1). Other reviews on the subject discuss the application of this modeling technique to certain chemotherapeutic agents (2, 3). We present a rather extensive compilation of the literature on all substances modeled to date with this technique and discuss formulation of the equations, limitations of the modeling process, and areas of future applications to provide a unified framework for the understanding of physiologically based pharmacokinetics.

BACKGROUND

The term pharmacokinetics refers to prediction of the time-dependent concentrations of a substance in a living system. Two approaches currently in use are based on classical and physiological models. The classical approach utilizes a lumped-compartmental system and fits exponential functions to time-dependent plasma concentration data. The physiologically based approach separates the body into a number of anatomical compartments, each compartment interconnected through the body fluid systems. The physiologically based approach also has the advantages of interspecies scalability, specific organ metabolism, specific organ transport, and specific organ binding properties.

Classical pharmacokinetic techniques are used to describe drug uptake with one- or multiple-compartmental systems. The solutions of differential equations that describe the time-dependent concentration behavior of the system consist of a series of decaying exponentials. The coefficients of the exponentials are fit to plasma, urinary, or some other obtainable tissue concentration data (4). Although these models are useful in many clinical situations (5), this modeling procedure does not describe a physiological system with large tissue-to-tissue concentration differences. In instances where the drug concentration is of the same order of magnitude over a large number of body organs, or certain other constraints are satisfied, a multiple-organ body system may indeed be simplified to a two-compartment model (6). For example, this intercompartmental variation is tolerable for drugs with a low therapeutic index; but substances that show high affinities for certain organs, are toxic to certain tissues, or have a specific target organ are not well described by the classical pharmacokinetic modeling technique (7).

The uptake of a drug is known to be dependent on organ perfusion rate, tissue volume, and many other biochemical and physiological parameters. The physiological parameters such as tissue volume, *etc.*, are scalable from species to species by a proportionality constant times body weight to some power (8, 9). If the uptake mechanisms are similar in small and large species, the biochemical and physiochemical parameters should be scalable through the species. However, the parameters obtained from classical

0022-3549/83/1000-1103$01.00/0

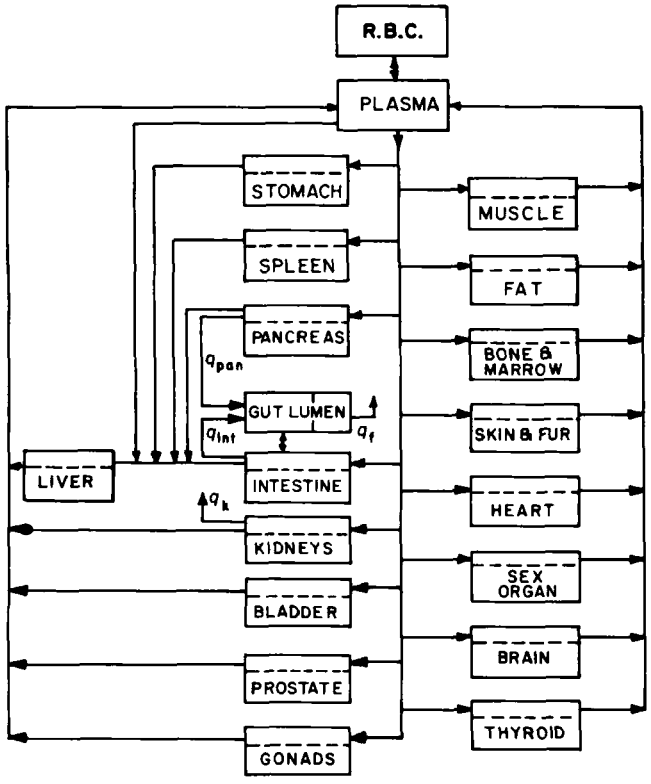

Figure 1—*Example of a comprehensive physiologically based pharmacokinetic model flow scheme (15). Reprinted from the* Annals of Biomedical Engineering *with permission; copyright 1982, Pergamon Press, Ltd.*

pharmacokinetics contain little physiological basis and, hence, show no scalability from species to species. Therefore, to describe a highly toxic substance with classical pharmacokinetics, all experimentation must be performed on a particular species (*e.g.*, humans). The ability to scale-up a model to humans based on experiments with smaller species (mice, rats, dogs, *etc.*), could lead to the safer use of drugs.

The limitations of the classical approach have led to the need for a physiologically based approach. The first use of physiological parameters in modeling appeared in the 1930's when Teorell (10) included mass balances on specific tissues, with specific tissue volume and specific organ perfusion rates. In 1960, Bellman *et al.* (11) included capillary, interstitial, and cellular subcompartments in the modeling of drug distribution in organs. In this work, a perfused compartment with vascular, interstitial, and cellular spaces was solved analytically and applied to chemotherapy (11). In the late 1960's, Bischoff and Brown proposed a model which adapted and extended these ideas to predict drug distribution in mammals (12). This approach was later improved to describe time-dependent concentration profiles in various organs and interspecies scale-up. This physiologically based modeling technique has since been applied to numerous substances with much success.

DEVELOPMENT OF A MODEL

Compartmental analysis of a system requires a rational basis for selection of the size and number of compartments. In the classical pharmacokinetic approach, certain tissues of the body are lumped together to form one large compartment (such as a rapidly equilibrated compartment). The physical existence of such compartments does not realistically occur and is not easily visualized (13). In physiologically based pharmacokinetics, each compartment represents a particular organ or tissue and has anatomical significance. One approach in physiologically based pharmacokinetic modeling would be to model a whole body by performing mass balances on each organ and tissue. However, besides the cost of developing such an extensive model, such detailed distribution information is not required for most substances. For example, certain substances are known to accumulate primarily in a few organs [*e.g.*, cadmium accumulates primarily in the liver and kidneys (14)]. Other substances are specifically toxic to certain organs (*e.g.*, doxorubicin is a known cardiotoxin). Still other agents are desired to be toxic to a specific tissue (*e.g.*, anticancer agents to tumors) or are desired to accumulate in a target organ (*e.g.*, general anesthetics in the nervous system). This information is applied with physiological (tissue volumes and blood flow rates), physicochemical (binding, lipid solubility, ionization, *etc.*), and pharmacological (mechanism of transport, sites of action, *etc.*) knowledge of the substance in the body to simplify the model.

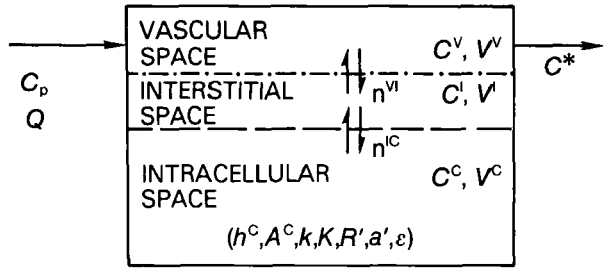

Figure 2—*Schematic representation of the vascular, interstitial, and intracellular spaces of an organ. The flux of the substance occurs across the dashed lines; the arrows represent the direction of blood flow.*

In the development of a physiological model, a flow scheme is assumed with the desired organs describing the species anatomically. Figure 1 is an interpretation of the circulatory flow scheme of a rat used to describe zinc uptake (15). Each organ is represented by a compartment, and all compartments are interconnected through the circulatory system as in the body. The physiological basis is maintained in the enterohepatic system with the liver, gut, spleen, and pancreas interconnected anatomically. Also, the substance is tranferred from the liver to the gut lumen by the biliary system. The large number of organs incorporated in this flow scheme represents an attempt to develop a comprehensive model.

Each compartment is considered to consist of three well-mixed phases (referred to as subcompartments): (*a*) a vascular section through which the compartment (organ) is perfused with blood; (*b*) an interstitial space in the tissue which forms a matrix for the tissue cells; and (*c*) a cellular space consisting of the tissue cells that comprise the compartment (organ). This type of compartment is shown schematically in Fig. 2. Following injection, *via* any route of administration, the uptake of the substance in the compartment occurs through influx with the afferent blood in the vascular subcompartment. Each subcompartment is considered to be a well-mixed phase; therefore, the efferent blood has the same concentration as the vascular

subcompartment. The substance crosses the capillary wall and diffuses into the interstitial subcompartment. Then, the substance moves across the cellular membrane from the interstitial fluid into the cells. In each of the subcompartments, the agent may degrade by metabolic action or bind to an endogenous substance. Specific binding to a particular enzyme or cellular component may occur to allow for the therapeutic or toxic action of the agent. To form the model, mass balance equations on the substance in vascular, interstitial, and cellular subcompartments of organ i, respectively, are written as:

$$V_i^{\mathrm{V}} \frac{dC_i^{\mathrm{V}}}{dt} = Q_i C_{\mathrm{p}} - Q_i C_i^{\mathrm{V}} - n_i^{\mathrm{V-I}} \qquad \text{(Eq. 1)}$$

$$V_i^{\mathrm{I}} \frac{dC_i^{\mathrm{I}}}{dt} = n_i^{\mathrm{V-I}} - n_i^{\mathrm{I-C}} \qquad \text{(Eq. 2)}$$

$$V_i^{\mathrm{C}} \frac{dC_i^{\mathrm{C}}}{dt} = n_i^{\mathrm{I-C}} \qquad \text{(Eq. 3)}$$

The flux (n_i) in the above equations is used to describe either passive or carrier-mediated transport across the capillary wall ($n_i^{\mathrm{V-I}}$) or cellular membrane ($n_i^{\mathrm{I-C}}$). These mass balance equations are written for each organ. A mass balance on the substance is made on the plasma compartment to close the balance on the system:

$$V_{\mathrm{p}} \frac{dC_{\mathrm{p}}}{dt} = \sum_i Q_i C_i^{\mathrm{V}} - Q_{\mathrm{p}} C_{\mathrm{p}} + g(t) \qquad \text{(Eq. 4)}$$

where $g(t)$ is the intravenous injection function. The mathematical form of $g(t)$ will depend on the form of injection, *e.g.*, pulse, step input (16, 17). Injection into some other area of the body can easily be incorporated in such a model. These equations (Eqs. 1–4) are simplified in that metabolism, transport, binding, and excretion terms are not included. These processes are described in detail later in this article.

The uptake of a substance in a system thus can be described by a set of equations modeling the drug uptake in each subcompartment as a function of time. Although these subcompartments have a physiological basis, it is possible to measure reliably only total tissue concentration. [Jain *et al.* measured the concentration of methotrexate in the tumor interstitial fluid (18).] The total compartment (organ) concentration, C_i, thus is described by volume averaging the subcompartment concentrations:

$$C_i = \frac{C_i^{\mathrm{V}} V_i^{\mathrm{V}} + C_i^{\mathrm{I}} V_i^{\mathrm{I}} + C_i^{\mathrm{C}} V_i^{\mathrm{C}}}{V_i} \qquad \text{(Eq. 5)}$$

Flow Limitation (One Compartment)—When one of the steps in mass transfer is rate limiting, a compartment may be simplified from the three-subcompartment model to a model with one or two subcompartments. The flow-limited assumption to mass transfer is made for organs not well perfused by the circulatory system. This assumption implies that the transfer across the capillary wall and across the cellular membrane is very rapid when compared with the perfusion rate of the tissue. In essence, the vascular, interstitial, and cellular subcompartments are in equilibrium, and the mass balance on the compartment is written as:

$$V_i \frac{dC_i}{dt} = Q_i \left(C_{\mathrm{p}} - \frac{C_i}{R_i} \right) \qquad \text{(Eq. 6)}$$

The term R_i in Eq. 6 is the partition coefficient and is the ratio of the drug concentration in the tissue to the drug concentration in the plasma at equilibrium.

Membrane Limitation (Two Subcompartments)—Another simplification occurs when the transfer across the cell membrane is the rate-limiting step; a two-subcompartmental model is assumed for the tissue. The two subcompartments are the cellular space, which consists of the tissue cells, and the extracellular space, which consists of the vascular and interstitial subcompartments in equilibrium, separated by a cellular membrane across which transport occurs. A mass balance on the extracellular space is:

$$V_i^{\mathrm{E}} \frac{dC_i^{\mathrm{E}}}{dt} = Q_i (C_{\mathrm{p}} - C_i^{\mathrm{E}}) - n_i^{\mathrm{E-C}} \qquad \text{(Eq. 7)}$$

The flux across the cell membrane ($n_i^{\mathrm{E-C}}$) accounts for net transfer to the cellular space; therefore, the accumulation in the cellular space can be described as:

$$V_i^{\mathrm{C}} \frac{dC_i^{\mathrm{C}}}{dt} = n_i^{\mathrm{E-C}} \qquad \text{(Eq. 8)}$$

Again, the concentration of the whole organ (tissue) is volume averaged as:

$$C_i = \frac{V_i^{\mathrm{E}} C_i^{\mathrm{E}} + V_i^{\mathrm{C}} C_i^{\mathrm{C}}}{V_i} \qquad \text{(Eq. 9)}$$

Thus, Eqs. 7–9 and Eq. 4 are written over the system of organs to describe a complete mass balance of the agent being studied.

If the limitation to transfer of the agent is across the capillary wall, then the transfer is assumed to be capillary membrane limited. In this instance, the interstitial and cellular spaces are assumed in equilibrium, and a two-subcompartmental model is obtained similar to the cell membrane limitation. Equations similar to Eqs. 7–9 are written for the vascular and extravascular spaces to describe such organs.

Transport Mechanism—The transport of a substance across a biological membrane is complex and may occur by passive diffusion, carrier-mediated transport, or both (19). Here, we discuss the mathematical formulation of two simple cases. For the case of passive diffusion the flux across the cell membrane is described by a mass transfer coefficient (h_i) times a concentration driving force:

$$n_i^{\mathrm{E-C}} = h_i \left(C_i^{\mathrm{E}} - \frac{C_i^{\mathrm{C}}}{R_i} \right) \qquad \text{(Eq. 10)}$$

However, in many biological systems the transport across a cell membrane is facilitated by carrier molecules. When this is the case, the flux is described by a saturable form:

$$n_i^{\mathrm{E-C}} = \frac{a_i C_i^{\mathrm{E}}}{b_i + C_i^{\mathrm{E}}} - \frac{\dfrac{a_i C_i^{\mathrm{C}}}{R_i}}{b_i + \dfrac{C_i^{\mathrm{C}}}{R_i}} \qquad \text{(Eq. 11)}$$

When both transport mechanisms exist, the flux term is a linear combination of Eqs. 10 and 11.

For more in-depth studies on transport mechanisms, the reader is referred to treatises on the subject (20, 21).

Binding—Substances are known to bind to plasma,

interstitial, or subcellular proteins, and red blood cells and many other biological components. Details of binding can be found elsewhere (22, 23), but one simple case will be discussed. Binding of most substances follows a Langmuir-type isotherm, and the total amount of drug in a compartment can be expressed as the sum of the free and bound drug:

$$C_i = C_i^* + \frac{a_i' C_i^*}{\epsilon_i + C_i^*} \qquad \text{(Eq. 12)}$$

which can be solved for the free drug concentration (C_i^*). When binding occurs in a subcompartment, only the free agent is available for mass transfer.

Excretion—The excretion of the agent must be taken into account to maintain a complete mass balance of the agent. For compartments such as the liver and kidneys, biliary and urinary excretion must be included, respectively. For example, Eq. 6 for a flow-limited compartment is modified to include an excretion rate term q_i (amount of drug excreted per unit time):

$$V_i \frac{dC_i}{dt} = Q_i \left(C_p - \frac{C_i}{R_i} \right) - q_i \qquad \text{(Eq. 13)}$$

In many cases, the excretion process can be described by a first-order approximation:

$$q_i = k_i C_i \qquad \text{(Eq. 14)}$$

In some cases, the plasma concentration is used instead of the tissue concentration. The linearity constant can be estimated from experimental data; the fraction of the initial dose excreted over a given amount of time (t_O) must satisfy the following equation:

$$\text{(fraction excreted)} \times \text{(initial dose)} = \int_0^{t_O} k_i C_i \, dt \qquad \text{(Eq. 15)}$$

If the excretion kinetics are assumed to be saturable, then:

$$q_i = \frac{v_{max} C_i}{K_e + C_i} \qquad \text{(Eq. 16)}$$

The Michaelis–Menten constant must be determined by fitting the model to the excretion data.

Metabolism—In many biological environments, an agent is unstable and may be altered by chemical reaction. This degradation or change of the agent, referred to as metabolism, must be taken into account to completely describe the distribution and disposition of an agent. In specific instances, the metabolite may be the actual agent of interest (24). The metabolism of an agent in the model is described by a reaction rate $[r_i(t)]$. In most cases of interest, the metabolism reactions are assumed to follow either first-order or Michaelis–Menten saturable kinetics. For first-order kinetics in a flow-limited compartment i, Eq. 6 would become:

$$V_i \frac{dC_i}{dt} = Q_i \left(C_p - \frac{C_i}{R_i} \right) - k_i C_i \qquad \text{(Eq. 17)}$$

For Michaelis–Menten kinetics, Eq. 6 would be:

$$V_i \frac{dC_i}{dt} = Q_i \left(C_p - \frac{C_i}{R_i} \right) - \frac{C_i v_{max}}{K_m + C_i} \qquad \text{(Eq. 18)}$$

The order, rate, and rate constants for metabolism are normally determined from *in vitro* studies. Whenever possible, these *in vitro* rate constants are used to describe metabolism *in vivo*. On many occasions the metabolism of a drug occurs primarily in a particular organ for which the kinetic data may not be readily available. In these instances the constants are obtained as best-fit parameters to pharmacokinetic data. Based on the flow-, capillary-, or membrane-limitation assumptions, equations similar to those of the parent compound are written to describe the pharmacokinetics of the metabolites.

Parameter Estimation—Time-dependent concentration data are obtained from laboratory animals sacrificed at predetermined intervals following an injection. To describe these data, the model parameters must be specified or estimated. The physiological parameters such as blood flow rate (Q_i) and tissue volume (V_i) can be determined from various experimental methods. For most species these values can be readily found in the literature. Kinetic parameters may be determined from separate experiments *in vivo* or *in vitro*. In some cases, the tissue-to-plasma binding constants are measured experimentally following long-term constant infusion. In other cases, the binding constants (R_i) and the passive diffusion coefficients (h_i) are estimated from the long- and short-term data, respectively (25), following a pulse injection. If *in vivo–in vitro* correlations are not available or appropriate, these parameters are determined from best fits of the concentration profile simulations to tissue concentration data. Once all parameter values are specified, the coupled, ordinary, and sometimes nonlinear first-order differential equations which describe the mass balance on the system need to be solved numerically to simulate the data (28).

For details of parameter estimation the reader is referred elsewhere (26, 27).

MODELS FOR SPECIFIC AGENTS

The pharmacokinetics of many substances have been described by this modeling technique. We have divided these models into six categories: (*a*) anticancer agents, (*b*) antibiotics, (*c*) anesthetics, (*d*) single elements (trace metals and ions), (*e*) environmental hazards and toxic substances, and (*f*) others. We realize that in this classification system, some anticancer agents are also antibiotics. Table I is an outline of 37 substances indicating the molecular structure, biological action, several treatment usages (for anticancer agents), the species modeled, and comments about the assumptions and limitations of the particular model. These models are described in more detail in the following section. The physiological parameters for each species are listed in Table II; the physicochemical and biological parameters for each model are tabulated throughout the text.

Anticancer Agents—Most drugs used to treat cancer are toxic to both normal and neoplastic tissues. These drugs are used for therapy in various dosages and schedules, usually given in combination with other antineoplastic agents to obtain optimal therapeutic effects in cancer patients. The high toxicity of these drugs makes it desirable to quantify their intake, distribution, metabolism, and excretion in various tissues of the body. To this extent, physiologically based pharmacokinetics has been

applied to study these processes. These models may be useful in estimating dosages and schedules which ensure that tissue concentrations remain below the toxic level for normal tissue and above the toxic level for neoplastic tissue. Initially, these models are developed for small animals and then scaled-up to humans in hopes of being able to prescribe dosage levels and administration schedules that ensure patient safety and optimal drug usage.

Dactinomycin—Actinomycin is a naturally occurring crystalline antibiotic of which all forms have been synthesized. Dactinomycin (actinomycin D) has been used to treat various neoplasms, including gestational carcinoma, testicular neoplasm, and Wilms tumor. The mechanism of action of dactinomycin includes binding to DNA, thus preventing progression of RNA polymerase along the DNA template. Lethal damage from dactinomycin occurs along the intestinal mucosa. A flow-limited physiologically based pharmacokinetic model was developed by Lutz *et al.* to describe the distribution of dactinomycin in the beagle dog (29) at doses of 0.03 and 0.135 mg/kg iv. The 13-compart-

Table I—Agents Modeled by Physiologically Based Pharmacokinetics

Agent	Chemical Structure	Biological Effect[a]	Model: Reference	Model: Species	Model: Comments
		Chemotherapeutic Agents			
Dactinomycin	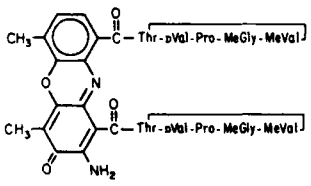	-blocks RNA synthesis by binding to DNA -gestational carcinoma, testicular neoplasm, Wilms tumor	(29)	dog	Flow and diffusion limitation
Doxorubicin	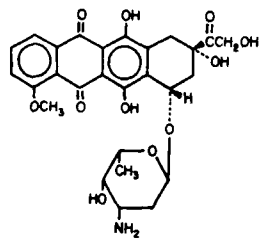	-binds to DNA, interferes with DNA function and RNA synthesis	(31)	rabbit, human	Flow limited
		-acute lymphoblastic and acute myeloblastic leukemias, Wilms tumor, neuroblastoma, breast and ovarian carcinomas	(32)	human	Applied previous model (31) to human
			(34)	hamster	Membrane limited
			(33)	mouse	Membrane limited with flow-limited tumor
Ancitabine	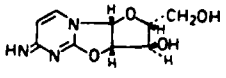	-leukemia	(24)	human	Flow limited, Michaelis–Menten kinetics
Cytarabine	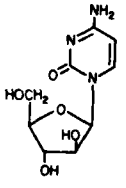	-blocks DNA synthesis and introduces moieties into the DNA coding sequence -ovarian cancer	(35)	human	Flow limited, nonlinear metabolism
			(36)	mouse, dog, monkey	Flow limited, nonlinear metabolism
			(38)	mouse	Extends Dedrick model (37) to include intracellular metabolism
			(37)	human	Flow limited, nonlinear metabolism
Pentostatin	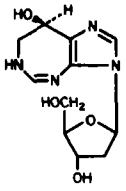	-binding inhibitor of adenosine deaminase -leukemia	(39)	mouse	Flow limited
5-Fluorouracil	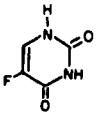	-anabolic: blocks the methylation reaction of deoxyuridylic acid to thymidic acid, interferes with DNA synthesis; catabolic: degeneration to CO_2 and urea -carcinomas of the colon, rectum, breast, stomach, and pancreas	(40)	rat	Flow limited, saturable excretion, hybrid model
Mercaptopurine	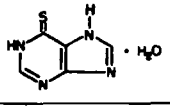	-acute lymphocytic leukemia	(42)	rat	Flow limited

Continued on next page

Table I–*Continued*

Agent	Chemical Structure	Biological Effect[a]	Model: Reference	Model: Species	Model: Comments
Methotrexate	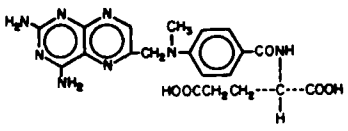	-strongly binds to intracellular dihydrofolate and inhibits conversion to tetrahydrofolate (an inhibitor in DNA synthesis) -leukemia, lung tumor, choriocarcinoma, Burkett's lymphoma	(44)	mouse	Flow limited, nonlinear
			(43)	mouse, rat, dogs, monkey, human	Flow limited, nonlinear excretion
			(45)	sting ray	Flow limited
			(25)	rat	Membrane limited, nonlinear transport
			(46)	mouse	Flow limited, hybrid model
			(47)	dog	Hybrid model, nonlinear transport
			(48)	mouse	Hybrid model, membrane limited
			(37)	human	Membrane limited, nonlinear transport
			(18)	rat	Flow limited, nonlinear transport, solid tumor
Cisplatin	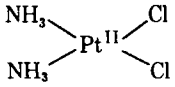 I	-produces intra- and interstrand crosslinks in DNA -metastatic testicular and ovarian tumors	(50)	dog	Flow limited, linear binding, first-order metabolism
Streptozocin	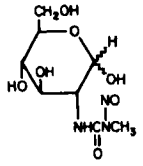	-inhibits DNA synthesis by alkylation of cell components -pancreatic tumor	(51)	mouse	Membrane limited
2-Amino-1,3,4-thiadiazole	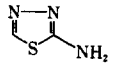	-inhibits the action of inosine-5-phosphate dehydrogenase in leukemia cells -melanoma, glioblastoma, lymphosarcoma, leukemia	(52)	mouse, dog, monkey	Flow limited, linear and saturable metabolism
		Antibiotics			
Cephalosporins	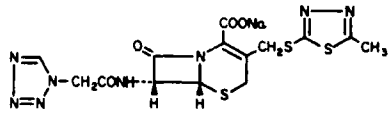 (cefazolin)	-antibiotic	(53)	human	Flow limited
	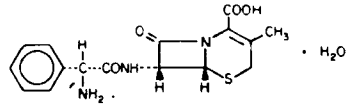 (cephalexin)				
	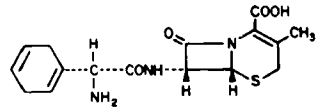 (cephradine)				
Tetracycline	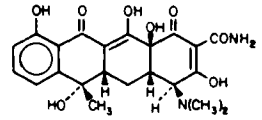	-antibiotic; exhibits maternal and fetal toxic effects	(16)	rat	Flow limited with placenta compartment
β-Lactam antibiotics	(various)	-antibiotic	(54)	rat	Flow and membrane limited, linear and nonlinear binding (depending on drug)

continued

Table I–*Continued*

Agent	Chemical Structure	Biological Effect[a]	Model: Reference	Model: Species	Model: Comments
		Anesthetics			
Halothane		-general anesthetic	(57) (17) (58) (59)	human human human human	Nonlinear Flow limited Flow limited Nonlinear, flow limited
Lidocaine	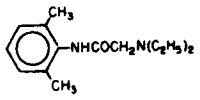	-local anesthetic	(65)	monkey, human	Flow limited
Methohexital	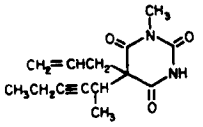	-short-acting, local anesthetic	(63)	human	Nonlinear
Pentobarbital	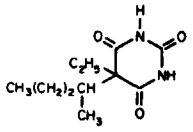	-sedative, anticonvulsant	(61)	human	Application of the thiopental model to humans
Phenobarbital	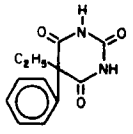	-anticonvulsant, hypnotic, sedative	(64)	rat	Flow limited
Hexobarbital	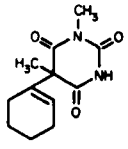	-hypnotic, sedative	(64)	rat	Flow limited
Procaine	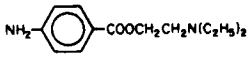	-local anesthetic	(67)	human	Nonlinear binding and metabolism, flow limited
Thiopental sodium	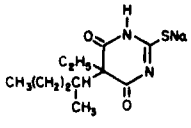	-local anesthetic	(60) (61) (62) (63) (64)	dog, human dog, human dog human human	Flow limited, nonlinear Flow limited Flow limited, nonlinear metabolism and binding Nonlinear Flow limited
		Trace Metals and Other Ions			
Bromide	Br^-	-toxic at high doses leading to mental and neurological disorders -used to measure extracellular space	(69)	rat	Flow and membrane limited
Cadmium	Cd	-toxic at high doses leading to hypertension and necrosis of testicles	(73)	mouse	Flow and membrane limited
Chloride	Cl^-	-essential electrolyte, osmotic balance gastric hydrochloride	(74)	cat	Flow limited
Lithium	Li^+	-potentially toxic at high doses -preferred drug for treating manic-depressive illness	(75)	human	Nonlinear uptake
Zinc	Zn	-essential trace element for DNA and protein synthesis -effects carbohydrate metabolism, lipid peroxidation, bone formation	(15)	rat	Membrane limited

continued on next page

Table I–*Continued*

Agent	Chemical Structure	Biological Effect[a]	Model: Reference	Model: Species	Comments
		Environmental Hazards and Toxic Substances			
Acetonylacetone	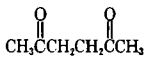	-neurotoxic	(76)	mouse	Flow limited
Chlordecone	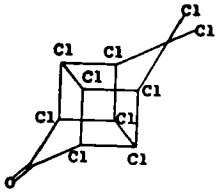	-toxic	(78)	rat	Membrane limited
Nitrite	$(CH_3)_2NNO$ (*n*-nitrosodimethylamine)	-carcinogenic	(79)	human	Accounts for nitrite formed endogenously to the carcinogen nitrosamine
Polychlorinated biphenyls	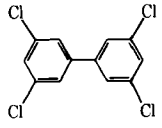	-environmental contaminants, possible toxicants	(80)	rat	Flow limited
		-accumulation in adipose tissue	(81)	rat	Flow limited, includes
	(3,3′,5,5′-tetrachlorobiphenyl)		(82)	rat	Flow limited
		Others			
2-Butanol	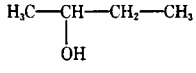	-pretreatment can potentiate the toxicity of carbon tetrachloride	(83)	rat	Flow limited, metabolites, nonlinear metabolism, oral administration
Digoxin	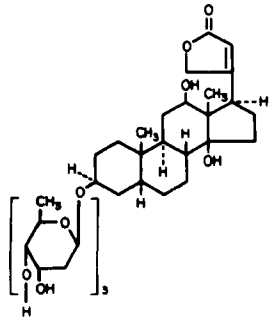	-cardiotonic: increases myocardial contraction force; depressant: decreases cardiac rate	(84)	rat	Flow limited
			(85)	dog, human	Flow limited
Ethanol	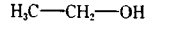	-depressant	(86)	rat	Hybrid, flow limited
			(87)	dog	Hybrid, flow limited
Phenolsulfonphthalein	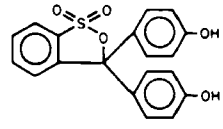	-renal function test	(88)	shark	Flow limited
Salicylates	 (salicylic acid)	-antipyretic and analgesic	(89)	dog	Flow limited, Michaelis–Menten metabolism
Sulfobromophthalein	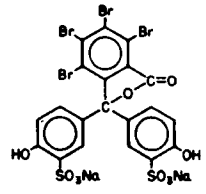	-liver function test	(90)	rat, human	Flow limited
			(91)	rat	Flow limited
Tetraethylammonium ion	$(C_2H_5)_4N^{\oplus}$	-ganglion blocking agent, antihypertensive, peripheral vasodilator	(92)	rat	Membrane limited, nonlinear

[a] Biologic mechanism and several uses (treatments).

Table II—Physiological Parameters

Parameter	Mouse[a]	Hamster[b]	Rat[c]	Rabbit[d]	Monkey[a]	Dog[e]	Human[f]
Body weight, g	22	150	500	2330	5000	12,000	70,000
Volume, ml							
Plasma	1.0	6.48	19.6	70	220	500	3000
Muscle	10.0	—	245	1350	2500	5530	35,000
Kidney	0.34	1.36	3.65	15	30	60	280
Liver	1.3	6.89	19.55	100	135	480	1350
Gut	1.5	12.23	11.25	120	230	480	2100
Gut Lumen	1.5	—	8.8	—	230	—	2100
Heart	0.095	0.63	1.15	6	17	120	300
Lungs	0.12	0.74	2.1	17	—	120	—
Spleen	0.1	0.54	1.3	1	—	36	160
Fat	—	—	34.9	—	—	—	10,000
Marrow	0.6	—	—	47	135	120	1400
Bladder	—	—	1.05	—	—	—	—
Brain	—	—	—	—	—	—	1500
Pancreas	—	—	2.15	—	—	24	—
Prostate	—	—	6.4	—	—	—	—
Thyroid	—	—	0.85	—	—	—	20
Plasma Flow Rate, ml/min							
Plasma	4.38	40.34	84.6	520	379	512	3670
Muscle	0.5	—	22.4	155	50	138	420
Kidney	0.8	5.27	12.8	80	74	90	700
Liver	1.1	6.5	4.7	177	92	60	800
Gut	0.9	5.3	14.6	111	75	81.5	700
Heart	0.28	0.14	1.6	16	65	60	150
Lungs	4.38	28.4	2.25	520	—	512	—
Spleen	0.05	0.25	0.95	9	—	13.5	240
Fat	—	—	3.6	—	—	—	200
Marrow	0.17	—	—	11	23	20	120
Bladder	—	—	1.0	—	—	—	—
Brain	—	—	0.95	—	—	—	380
Pancreas	—	—	1.1	—	—	21.3	—
Prostate	—	—	0.5	—	—	—	—
Thyroid	—	—	0.8	—	—	—	20

[a] Data (43) reprinted from the *Journal of Pharmaceutical Sciences* with permission; © 1971, American Pharmaceutical Association. [b] Data taken from Ref. 34. [c] Data (15) reprinted from the *Annals of Biomedical Engineering* with permission; © 1982, Pergamon Press, Inc. [d] Data taken from Ref. 31. [e] Data (29) reprinted from the *Journal of Pharmacology and Experimental Therapeutics* with permission; © 1977, American Society for Pharmacology and Experimental Therapeutics. [f] Data taken from Ref. 1.

mental model with linear binding in the tissue used the transport and binding parameters listed in Table III. The authors have compared the cell mass transfer coefficient with blood flow rate per unit volume of normal tissues and have found that both are of the same order of magnitude, thus indicating the appropriateness of the flow-limited assumptions. An exception to the flow-limited assumption was the testis compartment where the perfusion rate was much larger than the mass transfer coefficient, suggesting that the testes, analogous to the brain, have a low permeability membrane barrier. This result has important implications in the treatment of testicular neoplasms.

Doxorubicin—The anthracycline antibiotic doxorubicin hydrochloride[1] has been used in chemotherapeutic treatment of various solid tumors, lymphomas, and sarcomas (*e.g.*, acute lymphoblastic and myeloblastic leukemia, Wilms tumor, neuroblastoma, breast carcinoma, ovarian carcinoma). Doxorubicin exhibits neoplastic effects through interference with DNA functions and RNA synthesis. However, recent studies indicate that binding of the drug to cell membranes may be the lethal step (30). Toxic effects include depression of cell production in bone marrow and dose-dependent cardiomyopathy, thereby limiting dosages to low levels. To this end, Harris and Gross have modeled doxorubicin pharmacokinetics in the rabbit (31), Chan *et al.* in humans (32), Townsend in the hamster (33), and Gerlowski in the mouse (34) (Table IV). The rabbit model of Harris and Gross contains 10 flow-limited compartments. Their model overestimates concentration data at times <5 hr, indicating that a diffusion limitation may exist. These authors have also compared the model simulations with human plasma data and found underprediction at early intervals and overprediction at 24–48 hr. Chan *et al.* adapted the Harris and Gross model to simulate human plasma data. The authors were able to show consistent agreement with normal patients and, in some cases, in patients with significant hepatic dysfunction who show prolonged doxorubicin levels. The human plasma data also exhibited a short-term (2–4 hr) behavior not predicted by a flow-limited model, suggesting the need

Table III—Model Parameters for Dactinomycin in the Dog [a]

Compartment	Flow-Limited Binding Constant (R)	Membrane Limited: Mass Transfer Coefficient (h), hr^{-1}	Membrane Limited: Drug–DNA Dissociation Constant (D), μg/ml
Lung	53	7.7	0.5
Heart	11	7.7	0.5
Spleen	55	7.7	0.5
Stomach	25	7.7	0.5
GI tract	42	7.7	0.5
Liver	30	7.7	0.5
Kidney	45	7.7	0.5
Testes	18	0.2	0.5
Salivary gland	44	7.7	0.5
Thymus	47	7.7	0.5
Bone marrow	20	7.7	0.5
Pancreas	45	7.7	0.5
Muscle	8	7.7	0.5

[a] Data (29) reprinted from the *Journal of Pharmacology and Experimental Therapeutics* with permission; © 1977, American Society for Pharmacology and Experimental Therapeutics.

[1] Adriamycin; Adria Laboratories, Columbus, Ohio.

Table IV—Model Parameters for Doxorubicin in the Human, Rabbit, Hamster, and Mouse

Tissue	Human[a] and Rabbit[b] Linear Binding Constant (R)[e]	Hamster[c] Mass Transfer Coefficient (h)[f], min^{-1}	Hamster[c] Linear Binding Constant (R')[f]	Mouse[d] Mass Transfer Coefficient (h)[f], min^{-1}	Mouse[d] Linear Binding Constant (R')[f]
Plasma	0.5	—	—	—	—
Adipose tissue	19	—	—	—	—
Lean tissue	29	—	—	—	—
Liver	45	0.26	300	0.023	400
Gut	51	0.082	35	0.082	35
Heart	57	0.027	12	0.004	0.5
Bone marrow	91	—	—	—	—
Lungs	155	0.041	27	0.0009	7
Kidney	512	0.13	90	0.0044	1000
Spleen	556	0.046	40	0.046	40
Tumor	—	0.0075	15	—	0.5[e]
Other values, ml/min					
k_{el}	70	—		—	
Liver clearance (k_l)	—	0.011		0.0085	
Kidney clearance (k_k)	—	0.0074		0.0004	

[a] Data taken from Ref. 32. [b] Data taken from Ref. 31. [c] Data taken from Ref. 33. [d] Data taken from Ref. 34. [e] Flow limited. [f] Membrane limited.

to incorporate metabolism and membrane-limited assumptions into such a model.

The mouse and hamster models contain seven organs, all membrane limited, except the tumor compartment in the mouse, which was assumed to be flow limited (33, 35). It is known that doxorubicin metabolizes primarily in the intracellular space. Since the metabolite has similar antineoplastic effects, it was lumped with the drug as doxorubicin equivalents in these models. Good agreement was obtained with both early- and late-interval data, supporting the existence of a membrane limitation. In addition to the lumped doxorubicin analysis, Townsend (33) tried to model the metabolism as saturable intracellular reactions in the liver and kidney using parameters determined *in vitro*. Although no comparison with data for the metabolite was shown, simulations indicate that the metabolite concentrations in the hamster are at least one order of magnitude below the parent drug concentration levels, in contrast to the human data.

Cytarabine—Cytarabine (ara-C) is a neoplastic agent which provides an excellent example of the usefulness of *in vitro* enzyme kinetics in physiologically based pharmacokinetic modeling. Cytarabine is known to metabolize in the liver *via* pyrimidine nucleotide deaminase to 1-β-D-furanosyluracil. For antineoplastic action, cytarabine must be phosphorylated to the nucleotide. It is the nucleotide that is considered to act as an inhibitor of DNA polymerase by incorporation into the DNA template. Cytarabine and its metabolites were modeled in the mouse, dog, monkey, and human by Dedrick *et al.* (35–37) and in the mouse by Morrison *et al.* (38). A six-compartment flow-limited model was developed by Dedrick *et al.* to describe cytarabine distribution and its metabolism to 1-β-D-furanosyluracil by saturable kinetics. This study was one of the first models in the literature to apply *in vitro* saturable kinetic parameters to describe *in vivo* human data (35). In physiologically based pharmacokinetics, models are usually developed for small animals and then scaled-up to humans. In this case, the human model was developed first and then extended to mice, monkeys, and dogs (36) to study interspecies differences in pharmacokinetic modeling. The kidney clearance constant was found to exhibit essentially the same variation with body weight as seen for inulin. This model was later extended by Dedrick *et al.* (37) to include a peritoneal cavity compartment and was used successfully to develop rational protocols to treat patients with ovarian cancer.

The model of cytarabine in the mouse by Morrison *et al.* (38) extends the Dedrick model to include intracellular metabolism of the drug to the active metabolite, arabinoside cytosine triphosphate. The authors applied *in vitro* reaction constants for saturable kinetics to determine cytarabine and triphosphate cytarabine concentration profiles in various tissues. The kinetics of this reaction are strain dependent (as shown in the mouse), perhaps due to different levels of liver deaminase among strains. When scaling-up to humans, these effects must be incorporated with the higher pyrimidine activity in human marrow (relative to other tissue sites) than in murine systems. Also, the Michaelis constant of human pyrimidine deaminase is much lower than that found in mice, thus increasing the importance of deoxycytine and cytidine as inhibitors. The results indicate quite different concentration profiles of these substances, suggesting that the kinetics of reaction must be determined for the prediction of DNA inhibition by these substances.

Ancitabine—Ancitabine (cyclocytidine) is known to hydrolyze *in vivo* to the effective anticancer agent cytarabine. This drug is known to have a slower urinary clearance than cytarabine, by metabolism and kidney clearance, leading to an enhanced cytotoxic effect in tumor-bearing animals. Following the models of Dedrick *et al.* for cytarabine (35, 36), Himmelstein and Gross have developed a six-compartment model to predict this effect in humans (24). All compartments were assumed to be flow limited, and the hydrolysis reaction was considered to occur by saturable kinetics in all compartments. *In vitro*-determined values were used for hydrolysis rate constants, and clearance values were calculated from cumulative urinary data assuming linear excretion for both ancitabine and cytarabine (Table V). Based on good agreement with the plasma data in humans, the authors conclude that ancitabine can act as an *in vivo* reservoir for cytarabine, and therefore, its pharmacokinetics should be considered in developing treatment schedules.

Pentostatin—Pentostatin (2′-deoxycoformycin) is a bacterial fermentation product which is used primarily in combination chemotherapy with other antineoplastic

Table V—Model Parameters for Cytarabine in the Mouse, Monkey, Dog, and Human and Ancitabine in the Human

Parameter	Cytarabine[a]				Ancitabine[b]
	Mouse	Monkey	Dog	Human	Human
Michaelis constant (K_m), μg/ml H_2O	283	39	115	39	—
Heart	—	—	—	—	31
Liver	—	—	—	—	27
Kidney	—	—	—	—	32
Deaminase activity (v_{max}), μg/g·min					
Blood	—	1.6	—	—	—
Liver	4.6	80.2	7	119	119
Gut	8.3	—	—	—	—
Heart	—	57	—	6	6
Kidney	91.5	71.8	—	20	20
Lean tissue	—	34.3	—	—	—
Kidney clearance (k_k), ml/min	0.18	14	32	90	90

[a] Data (36) reprinted from *Biochemical Pharmacology* with permission; © 1973, Pergamon Press, Ltd. [b] Data (24) reprinted from the *Journal of Pharmaceutical Sciences* with permission © 1977, American Pharmaceutical Association.

agents. When applied with vidarabine (ara-A), increased antitumor activity is found in laboratory animals. Pentostatin is a tight-binding inhibitor of intracellular adenosine deaminase in the liver, kidney, and L-1210 tumor cells. King and Dedrick developed a five-compartment model to describe pentostatin pharmacokinetics in normal and leukemic mice (Table VI) (39). The authors used both linear and nonlinear binding in a flow-limited model to account for tissue distribution at high pentostatin concentrations and for the tight binding to adenosine deaminase, respectively. Since blood flow rate to L-1210 tumors is not known, these authors have estimated the blood flow rate to be 0.22 min^{-1} by fitting their model to the tumor data. Pharmacokinetic parameters for normal tissues were determined by decomposing the model into a series of hybrid models which could be solved individually. The model indicated that the primary means of drug elimination was through the urinary tract, although the model was not able to predict this data well at high dosages. These authors suggest that a more comprehensive model should include the detailed kinetics of the inhibition of adenosine deaminase by pentostatin and the dissociation rate of the pentostatin–adenosine deaminase complex based on experimental data.

5-Fluorouracil—The pharmacokinetics of 5-fluorouracil are of interest since the drug is known to be metabolized by two pathways in the body. The anticancer effect of 5-fluorouracil results from an anabolic pathway where the drug incorporates into nucleosides and nucleotides. A

Table VI—Model Parameters for Pentostatin in the Mouse[a]

Tissue	Linear Binding Constant (R)	Dissociation Constant μg/ml	Specific Binding Parameter, μg/ml	
			Normal Mice	Leukemic Mice
Gut	1.0	0.7	82	101
Liver	1.24	0.7	18	61
Kidney	2.8	0.7	16	32
Tumor	0.72	0.7	—	92
Carcass	0.56	0.7	45	45
Other values, ml/min				
Glomerular filtration rate			0.30	0.26
Secretion clearance			0.35	0.30

[a] Data (39) reprinted from the *Journal of Pharmacokinetics and Biopharmaceutics* with permission; © 1981, Plenum Publishing Corp.

Table VII—Model Parameters for Mercaptopurine in the Rat and Human[a]

Tissue	Rat		Human	
	Linear Binding Constant (R)	Strong Binding Constant (a) μg/ml	Linear Binding Constant (R)	Strong Binding Constant (a), μg/ml
Muscle	1.4	0.0	1.4	0.0
Kidney	2.4	0.35	2.4	0.35
Liver	4.0	0.6	4.0	0.6
Gut	3.0	0.1	3.0	0.1
Spleen	1.7	0.2	1.7	0.2
Bone marrow	0.35	0.2	0.35	0.2
Other values				
Kidney clearance (k_k) ml/min	1.2		315	
Biliary clearance (k_l) ml/min	1.2		500	
Time constants				
bile duct (τ_B)	1.0		10	
GI tract (τ_{GI})	100		1000	

[a] Data (42) reprinted from the *Journal of Pharmaceutical Sciences* with permission; © 1977, American Pharmaceutical Association.

catabolic pathway for metabolism also exists, where the drug undergoes degradation ultimately to carbon dioxide and urea. A two-compartmental flow-limited hybrid model around the pulmonary system was developed by Collins *et al.* (40) for humans. The authors did not differentiate between the two metabolic pathways in the model, but presented a framework on which to build. The novel aspect of this work results from the route- and schedule-dependent drug clearance. The model included saturable clearances and was used for the intravenous bolus, intravenous infusion, and intraperitoneal injection routes. Because of the good fit to data for the different modes of administration, the authors concluded that the simple physiologically based pharmacokinetic model with nonlinear terms is sufficient for use in clinical situations.

Mercaptopurine—The primary use of mercaptopurine is in combination therapy for treatment of leukemia and certain sarcomas (41). Mercaptopurine is most toxic to rapidly multiplying cells; therefore, the intestine, bone marrow, and spleen are more susceptible to mercaptopurine and are of primary interest in the modeling of this drug. Tterlikkis *et al.* (42) have developed a six-compartment flow-limited model with a complete hepatic system to describe the pharmacokinetics of mercaptopurine in the rat (Table VII). The model, similar to one developed by Bischoff *et al.* (43), includes linear binding and excretion, a three-compartment biliary tract, and a four-compartment gut lumen. The rat concentration data were simulated well by the model. The authors also scaled-up their model to humans and have obtained general agreement with the data despite large patient-to-patient differences. A more comprehensive model of mercaptopurine should include detailed kinetics of metabolism analogous to the models for cytarabine, cisplatin, *etc.* When this kinetic framework is determined, a clinically applicable model can be made available based on the structure presented in this work.

Methotrexate—Methotrexate has been the most studied drug in the area of physiologically based pharmacokinetics. The antineoplastic mechanism of methotrexate results from its binding to the enzyme dihydrofo-

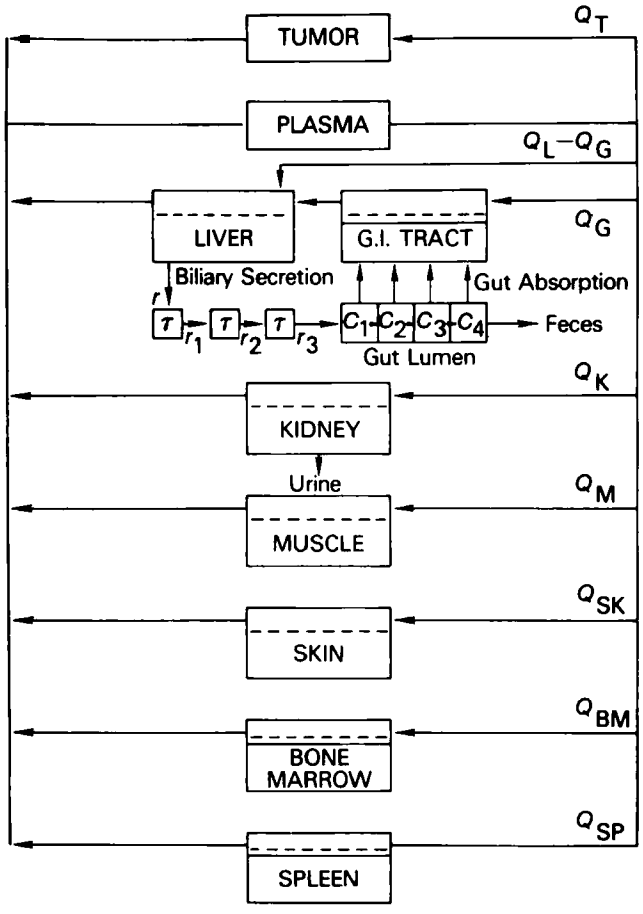

Figure 3—*Location of the biliary and gut lumen compartments represented by well-mixed subcompartments connected in series.*

late reductase which inhibits conversion of dihydrofolate to tetrahydrofolate. Tetrahydrofolate is used to produce a coenzyme required for thymidylate formation, which in turn, is required for DNA synthesis. Preliminary pharmacokinetic work on methotrexate began with a six-compartment model that was simplified to a two-compartment model by Bischoff *et al.* (43). The analytical solutions of this simple model were used to obtain initial estimates of mass transfer coefficients and clearance constants. The equations for the six-compartment flow-limited model were solved with a numerical technique, and good agreement with data for the six tissues was found.

Bischoff *et al.* then extended their model by incorporating saturable binding and excretion, multicompartmental representation of biliary excretion, and movement of drug through the GI tract with partial reabsorption (Fig. 3) (44). The model was able to predict successfully detailed distribution and excretion of methotrexate in the mouse, rat, monkey, dog, and human over a wide range of doses.

Dedrick *et al.* (25) determined membrane resistance to transport in bone marrow, the spleen, and the small intestine of rats by plotting the drug concentrations in various tissues as functions of the plasma concentration. The transport parameters estimated from the membrane-limited model were found to be in general agreement with *in vitro* results obtained in many mammalian cells. The mathematical treatment presented in this paper was general and has been adapted by many investigators of physiologically based pharmacokinetics.

Zaharko *et al.* (45) used the flow-limited model to predict the distribution of methotrexate in the sting ray and found the blood circulation velocity to be approximately one-sixteenth of that in the mouse. Dedrick *et al.* (37) used the membrane-limited model to simulate plasma and peritoneal fluid concentrations following single and repeated intraperitoneal injections of methotrexate in humans. This work led to the conclusion that a significantly greater concentration of methotrexate in the peritoneal cavity than in the plasma following intraperitoneal injection could be exploited in the treatment of patients with microscopic residual cancer confined to the peritoneal cavity.

Table VIII—Model Parameters for Methotrexate in the Mouse, Rat, Dog, Monkey, and Human [a]

Tissue	Linear Binding Constant (R)				
	Mouse	Rat	Dog (5 kg), Monkey	Dog (17 kg)	Human
Muscle	0.15	0.15	0.15	0.15	0.15
Kidney	3.0	3.0	14	14	3.0
Liver	10	3.0	2.0	2.0	3.0
Gut	1.0	1.0	1.0	1.0	1.0
Clearance rate, ml/min					
kidney (k_k)	0.2	1.1	20	56	190
bile (k_b)	0.4	3.0	2.0	8	200

[a] Data (43) reprinted from the *Journal of Pharmaceutical Sciences* with permission; © 1971, American Pharmaceutical Association.

Zaharko *et al.* (46) and Lutz *et al.* (47) (Table VIII) developed hybrid models to simulate concentrations of methotrexate in Lewis lung carcinoma in mice and spontaneous lymphosarcoma in dogs, respectively. These investigators found the transport in tumors to be best modeled by the membrane-limited assumption. Similarly, Weissbrod *et al.* (48) used a hybrid model to calculate the membrane permeability of L-1210 leukemia cells in mice and found these values comparable to *in vitro* values. In contrast, Jain *et al.* (18) used the whole-body model and found the transport of methotrexate in hepatoma 5123 and Walker 256 carcinoma in rats to be flow limited. Jain also estimated the extent of drug metabolism during constant infusion and found the fraction of drug metabolized to be ~20% at the end of a 3-day infusion (49). Further extensions of these models should incorporate synthesis of dihydrofolate reductase in the presence of drug and details of the drug metabolism.

Cisplatin—The antineoplastic activity of cisplatin occurs from its ability to produce intrastrand and interstrand crosslinks in DNA molecules. Cisplatin is known to metabolize by a complex scheme of reactions. The metabolites of the parent compound are considered also to have antineoplastic effects. To this end, parent drug and metabolites represented by one species were modeled with a

Table IX—Model Parameters for Cisplatin in a 10-kg Dog [a]

Tissue	Linear Binding Constant (R)	Other Values	Cisplatin	Metabolite
Muscle	0.7	Kidney clearance (k_k), ml/min	0.5	0.6
Skin	3.5			
Ovaries	1	Bile clearance (k_b), ml/min	0	0.035
Liver	6			
Kidney	8	Metabolism constant, min^{-1}	0.00416	
GI tract	1			

[a] Data taken from Ref. 50.

Table X—Model Parameters for Streptozocin in the Mouse [a]

Tissue	Linear Binding Constant (R')		Mass Transfer Coefficient (h), min^{-1}		Metabolism Constant (k), min^{-1}	
	Bioassay	Chemoassay	Bioassay	Chemoassay	Bioassay	Chemoassay
Liver	23.6	19.7	0.0164	0.1392	0.0086	0.0041
Kidney	5.6	7.7	0.0305	0.1625	0.0096	0.0041
Pancreas	—	15.8	—	0.0063	—	0.0041

[a] Data (51) reprinted from the *Journal of Pharmaceutical Sciences* with permission; © 1980, American Pharmaceutical Association.

flow-limited scheme containing six compartments in the beagle dog by LeRoy *et al.* (Table IX) (50). Linear binding and first-order metabolism were incorporated using *in vitro* reaction rate constants. The flow-limited model was able to provide an adequate simulation of most of the tissue data. However, disagreement with muscle data, especially at early intervals, might be due to a diffusion limitation.

Streptozocin—Streptozocin is known to inhibit primary DNA synthesis by alkylation of cell components. The drug has a selective toxicity for pancreatic β-cells and is therefore useful in treating pancreatic tumors (*e.g.*, metastatic insulinoma). Weissbrod and Jain have applied a physiogically based hybrid model to describe streptozocin distribution in mice (Table X) (51). This model incorporates three membrane-limited compartments with linear binding and first-order intracellular metabolism. Tissue data obtained by bioassay to determine parent streptozocin and by chemoassay to determine parent streptozocin and its metabolites were compared with simulations. The fit to the parent compound and metabolites was adequate in this work, although the authors suggested that more data were required to describe the transport and metabolism in greater detail.

2-Amino-1,3,4-Thiadiazole—The antineoplastic action of 2-amino-1,3,4-thiadiazole includes inhibition of inosine-5-phosphate dehydrogenase in cells. For this reason, 2-amino-1,3,4-thiadiazole retards the growth of melanomas, lymphosarcomas, and leukemias. A physiologically based pharmacokinetic model was developed by King and Dedrick (Table XI) (52) to describe 2-amino-1,3,4-thiadiazole in the mouse, dog, and monkey. The authors used a flow-limited system with four compartments and represented all metabolites as one species. The rate of metabolism was described as a first-order linear process in mice and as a saturable process in dogs and monkeys. Binding and kidney clearance were considered linear. The authors obtained partition coefficients based on long-term experimental values of serum and tissue concentations. The metabolic parameters were obtained by best fit of the model to tissue concentration data. The major excretory pathways were found to be kidney clearance in the mouse and saturable metabolism in the dog and monkey. It seems that because of these interspecies differences, scale-up to humans would be difficult for this substance.

Antibiotics—Antibiotics are prescribed to treat infection. The wide applicability of antibiotics raises questions as to the disposition of these substances in the body. Physiologically based pharmacokinetics provide a tool that can aid in answering these questions.

Cephalosporin Antibiotics—Three cephalosporin antibiotics (cefazolin, cephalexin, and cephradine) were studied by Greene *et al.* (53) These antibiotics show *in vitro* activity against penicillin-resistant staphylococci and are considered to bind to plasma proteins. The authors compared the simulations using a six-compartmental perfusion model with a classical two-compartmental model, with and without protein binding. Plasma binding, described by the Scatchard equation, was used to fit the models to human plasma data for each cephalosporin administered. The authors obtained good simulations of the plasma data for cefazolin at a 1-g iv dose and for cephalexin at a 0.5-g iv dose, but underpredicted the plasma concentration at times >1.5 hr for cephradine at a 2-g iv dose. The authors attributed this disagreement to a possible overestimate of the cephradine clearance value.

β-Lactam Antibiotics—β-Lactam antibiotics include ampicillin, cefazolin, dicloxacillin, methicillin, penicillin G, penicillin V, and others. The uptake, distribution, and elimination of various antibiotics and the model test substance inulin were studied in a 12-compartment model in rats (54). The lung, heart, muscle, skin, gut, and carcass were modeled as cell membrane limited, the liver and kidney as flow limited, and the bone compartment was broken down into bone marrow (flow-limited) and bone cortex (membrane-limited) compartments. Tissue-to-plasma partition coefficients of penicillin V, dicloxacillin, cefazolin, and inulin were determined by *in vivo* experi-

Table XI—Model Parameters for 2-Amino-1,3,4-thiadiazole in the Dog and Monkey [a]

Tissue	Linear Binding Constant (R)					
	Mouse		Dog		Monkey	
	Drug	Metabolites	Drug	Metabolites	Drug	Metabolites
Liver	0.9	1.3	0.9	2.8	0.6	1.8
Gut	1.0	1.1	1.0	0.4	0.4	1.3
Kidney	0.9	2.0	1.6	2.0	0.6	3.6
Lean tissue	0.9	0.5	1.0	0.2	0.9	0.3
Kidney clearance (k_k), ml/min						
Drug		0.066		8.8		1.5
Metabolites		0.215		18.3		4.6
Metabolism						
v_{max}, μg/min		—		19.2		6.3
K_m, μg/ml		—		0.2		0.5
k, ml/min		0.017		95.0		12.5

[a] Data taken from Ref. 52.

Table XII—Model Parameters for Several β-Lactam Antibiotics in the Rat [a]

Tissue	Linear Binding Constant (R)		
	Penicillin V	Dicloxacillin	Cefazolin
Lung	0.157	0.123	0.154
Heart	0.095	0.074	0.101
Muscle	0.062	0.051	0.077
Bone	—	—	0.111
Skin	—	—	0.303
Spleen	0.096	0.088	—
Gut	0.966	1.357	0.114
Liver	0.250	0.430	0.788
Kidney	3.70	1.27	2.79

[a] Data taken from Ref. 54.

ments after constant infusion of these substances. Renal and hepatic clearance constants were also determined from independent experiments. Binding to serum proteins (albumin) was considered to be nonlinear for cefazolin and penicillin V, whereas linear binding was used for penicillin G, methicillin, dicloxacillin, and ampicillin (Table XII). Although partition coefficients, binding constants, and elimination parameters were measured for several antibiotics, these authors compared their model to tissue distribution data for cefazolin and inulin only and found good agreement.

Tetracycline—The antibiotic tetracycline is highly active against Gram-positive and Gram-negative organisms. This drug is recommended for treatment of pneumonia, actinomycosis, brucellosis, urinary infections, Rocky Mountain spotted fever, and typhus fever (41). When tetracycline is given to rats during pregnancy, it is known to lead to acute fatty liver syndrome in the mother and teratogenic effects in the fetus. To this end, Olanoff *et al.* developed a physiologically based pharmacokinetic model of tetracycline in nonpregnant (55) and pregnant rats (16) (Table XIII). This model included seven flow-limited compartments in both the maternal section and the fetal section, including a placenta compartment for maternal-to-fetal transfer of the drug. The authors applied linear binding in all compartments and allowed for fetal growth over 21 days. The model was used to determine the controlled release of tetracycline using a trilaminate drug delivery device. The model described the data well and was able to predict the constant tissue concentrations desired of a controlled-release device. The authors had to use uniformly lower values of the partition coefficients in the pregnant rats when compared with the nonpregnant rats. The inclusion of a fetus in such a model represents a significant advance in physiologically based pharmacokinetics.

Table XIII—Model Parameters for Tetracycline in the Pregnant Rat [a]

Tissue	Flow-Limited Linear Binding Constant (R)	
	Maternal	Fetal [b]
Liver	0.97	1.0
Kidney	0.97	1.4
Bone	1.68	4.55
Muscle	1.03	—
GI tract	1.06	1.32
Placenta	—	1.23
Amniotic fluid	—	0.46
Fat	0.7	—

[a] Data (16) reprinted from the *Journal of Pharmacokinetics and Biopharmaceutics*; © 1980, Plenum Publishing Corp. [b] Ratio of fetal tissue concentration to maternal plasma concentration at equilibrium.

Anesthetics—Anesthetics are used for temporary suppression of pain, normally during surgery. Based on the knowledge of the uptake, distribution, metabolism, *etc.*, of these substances in the body, physiologically based pharmacokinetics provide an excellent technique to determine dosage regimens to ensure that proper amounts are delivered to the desired region of the body. Biomedical equipment that is used in the delivery of anesthetics can be designed based on pharmacokinetic simulations, thus limiting the danger of experimentation with new equipment.

Halothane—Halothane is a widely used, potent, noninflammable, and nonexplosive inhalation anesthetic with rapid onset and rapid reversal. Since the pioneering work of Mapleson (56), several flow-limited hybrid models have appeared in the literature to describe the uptake and distribution of halothane in humans (17, 57–59). Since changes in halothane concentration influence cardiac output and distribution, and *vice versa*, many investigations have tried to incorporate this interrelationship in their models. Ashman *et al.* (57) assumed that a uniformly distributed reduction in cardiac output occurred as anesthetic concentration in the viscera increased. After comparing the results of constant and variable cardiac output models, the authors concluded that the differences in these two models were insignificant for the first few minutes, but progressively increased during the first hour to 6%. Zwart *et al.* (17) and Smith *et al.* (58) improved this model by making changes in the cardiac output and its distribution a function of halothane concentration in one or two of the three most important compartments, *i.e.*, brain, myocardium, and arterial blood (Table XIV). The results of this model differed significantly from those models with constant cardiac output and gave new insight into halothane-induced changes in the circulation. Munson *et al.* (59) divided the body into five flow-limited compartments and modeled the effects of reduced ventilation rate and cardiac output on halothane pharmacokinetics. Using this model, these authors were able to predict limits to which

Table XIV—Model Parameters for Halothane in the Human and Lidocaine in the Monkey and Human

Tissue	Flow-Limited Linear Binding Constant (R)	
	Halothane (Human) [a]	Lidocaine (Monkey and Human) [b]
Arterial	2.3	—
Brain		
Grey matter	5.4	1.21
White matter	8.3	
Heart	8.1	—
Well-perfused organs	3.7	—
Poorly perfused organs	5.3	—
Fat (and fatty marrow)	138	2.0
Splanchnic	6.0	—
Muscle	8.1	0.65
Lung	5.3	3.08
Liver	—	0.61
Rapidly equilibrating tissue	—	2.02
Slowly equilibrating tissue	—	0.60
Portal	—	1.53

[a] Data (58) reprinted from *Anesthesiology* with permission; © 1972, Lippincott/Harper and Row. [b] Data (65) reprinted from *Clinical Pharmacology and Therapeutics* with permission; © 1974, American Society for Pharmacology and Experimental Therapeutics.

Table XV—Model Parameters for Methohexital, Pentobarbital, and Thiopental in the Human

Parameter	Methohexital[a]	Pentobarbital[b]	Thiopental[b]
Effective fraction			
f_B	ramp functions 0–1.0	0.985	0.985
f_V		0.963	0.963
f_L		0.980	0.980
f_V		0.200	0.200
Binding sites, μmole/liter			
B_1	52 (mg/liter)	5,900	18,400
B_2	870 (mg/liter)	317,000	305,400
Binding equilibrium constant (liter/μmole)			
k_1	3.3×10^{-2} (liter/mg)	0.2117	0.06
k_2	1.2×10^{-3} (liter/mg)	0.00016	0.000625
Lipid solubility (BA)	65	9.0	100
Michaelis–Menten constants			
K_m, μmole/liter	—	4.0	4.0
v_{max} μmole/min	—	2.63	26.3

[a] Data (63) reprinted from the *Journal of Pharmaceutical Sciences* with permission; © 1976, American Pharmaceutical Association. [b] Data (60) reprinted from "Pharmakinetics in Applications of the Artificial Kidney" with permission; © 1968, Chemical Engineering Progress Symposium Series.

anesthetic drugs and techniques could be used safely.

Hexobarbital, Pentobarbital, Phenobarbital, and Thiopental—These four drugs are the most common barbiturates used in medicine. Thiopental, a local anesthetic used in dental patients, has biological effects similar to methohexital. Hexobarbital and thiopental are short- and ultrashort-acting anesthetics, respectively. This rapidity results from metabolic degradation and physical redistribution. Phenobarbital has a slower rate of action on the brain compared with hexobarbital and thiopental. Pentobarbital is a fast-acting sedative useful in the treatment of insomnia, nausea, *etc.* The drug is also useful in controlling convulsions such as those which occur in eclampsia, epilepsy, tetany, and strychnine poisoning. Overdoses of barbiturates can lead to death by respiratory failure (41).

To this end, Bischoff and Dedrick (60, 61) developed a four-compartment model (blood, viscera, lean tissue, and adipose tissue) to describe the pharmacokinetics of barbiturates in dogs and humans. By incorporating parameters characterizing lipid solubility, protein binding, and metabolism of thiopental, these authors were able to simulate the tissue data in dogs and plasma data in humans. These authors later applied the thiopental model to pentobarbital which has a lower lipid solubility, less protein binding, and is metabolized at about one-tenth the rate of thiopental (60). By including these changes, a suicidal dose in the human (43 mg/kg) was simulated (Table XV). These authors also simulated the effect of treatment with an artificial kidney, and using this model, were able to predict the well-known rebound effect in blood, lean tissue, and viscera.

Since Bischoff and Dedrick combined brain, heart, kidneys, liver, *etc.* as a viscera component, their model can not predict thiopental concentrations in the brain, which is valuable information for optimal therapy. To this end, Chen and Andrade (62) developed a seven-compartment model to predict thiopental kinetics in the brain, plasma, liver, GI tract, lean tissue, adipose tissue, and viscera and obtained good agreement with the data obtained in dogs. A detailed sensitivity analysis indicated the values for fractions of bound drug in various tissues were more sensitive parameters than the others in the model and, therefore, must be determined precisely. Similar to methohexital, the four-compartment model of Bischoff and Dedrick was also extended by Gillis *et al.* (63) to account for the slow approach to equilibrium in human tissues.

The most comprehensive model of barbiturates (hexobarbital, phenobarbital, and thiopental) has been developed recently by Igari *et al.* (Table XVI) (64a). These authors have developed an 11-compartment model which includes lung, venous and arterial plasma, liver, brain, heart, GI tract, kidney, muscle, skin, and adipose tissue. Except for the brain, all tissues were assumed to be flow limited. Partition coefficients, Michaelis–Menten constants for drug metabolism, and binding constants were determined *in vitro* and compared with *in vivo* data. The *in vitro* partition coefficients did not lead to good agreement with the plasma and brain data. When partition coefficients obtained from *in vivo* experiments were used instead, the authors were able to describe the data well. [In a later publication, these authors use a similar model to predict ethenzamide (ethoxybenzamide) concentrations in nine compartments in rats, scaled-up to rabbits (64b), from K_p (partition coefficient) values obtained *via* intravenous bolus injection, constant-rate infusion, and *in vitro* determinations (64c).]

Lidocaine—Lidocaine is a potent anesthetic agent used for infiltration and block anesthesia. It is also used topically for anesthesia of accessible mucous membranes. The action of lidocaine on nerves is considered similar to that of procaine (41). Congestive heart failure patients, when given standard intravenous doses of lidocaine, show ele-

Table XVI—*In Vitro* and *In Vivo* Model Parameters for Hexobarbital, Phenobarbital, and Thiopental[a]

Tissue	Thiopental		Hexobarbital		Phenobarbital	
	In Vitro	*In Vivo*	*In Vitro*	*In Vivo*	*In Vitro*	*In Vivo*
Lung	2.71	1.16	1.49	3.26	1.14	0.816
Heart	1.91	1.07	1.86	1.12	1.93	0.97
Liver	2.10	5.28	1.45	5.96	1.87	1.92
GI tract	2.02	1.18	1.91	1.26	1.75	1.66
Kidney	2.50	1.18	2.31	1.51	2.03	0.78
Muscle	2.32	0.664	1.34	0.625	1.60	1.05
Skin	3.42	1.94	0.984	0.909	1.88	1.28
Adipose tissue	11.3	2.86	4.13	1.64	0.926	0.318
Liver kinetics						
$K_m, M \times 10^{-3}$	0.103		1.32		—	
v_{max}, μmole/min/0.25 kg	0.099		8.48		—	

[a] Data (64a) reprinted from the *Journal of Pharmacokinetics and Biopharmaceutics* with permission; © 1982, Plenum Publishing Corp.

vated blood levels presumably due to decreased circulation and clearance. A physiologically based pharmacokinetic model can be useful in predicting the lidocaine levels of patients suffering from cardiovascular diseases. An eight-compartment flow-limited model to describe the pharmacokinetics of lidocaine in humans and monkeys was developed by Benowitz *et al.* (Table XIV) (65). The authors assumed equilibrium was obtained after 24 hr to obtain experimental tissue-to-plasma partition coefficients in rhesus monkeys. The model was then scaled-up to humans with the same binding parameters as found in the rhesus monkey. Good agreement was found between human plasma data and model predictions. In a later study by Benowitz *et al.* (66), the effects of hemorrhagic shock and sympathomimetic drugs (isoproterenol and norepinephrine) on lidocaine kinetics and regional blood flow in the rhesus monkey were examined. The results obtained have many interesting clinical implications.

Methohexital—Methohexital is a local anesthetic used primarily in dental surgery. Dosage requirements can change from alterations in body distribution processes. Alterations can result from dehydration, uremia, peripheral circulatory failure, increased cardiac output, electrolyte disturbances, hepatic failure, and chronic renal failure.

Using the approach developed by Bischoff and Dedrick for thiopental pharmacokinetics, Gillis *et al.* (63) developed a flow-limited model to describe the distribution of methohexitol in the human. Similar to the model of Bischoff and Dedrick, it included details of protein binding and liver metabolism (Table XV). Unlike that of Bischoff and Dedrick, this model used a ramp function to describe the approach to equilibrium in tissue, with characteristic times determined by the perfusion rates. The model described the available data adequately and was used to predict the influence of body alterations (*e.g.*, obesity) on drug distribution.

Procaine—Procaine[2] is a local anesthetic used primarily in dental surgery. The drug blocks the function of the nerves near an injection site by attaching to and preventing sodium transfer across the nerve cell membrane, thus hindering the formation and propagation of the action potential on the membrane. The process is reversible, so the effects on the cell are only temporary (19). A nine-compartment flow-limited model was developed by Smith *et al.* (67) to describe procaine pharmacokinetics in humans. Independently determined nonlinear binding and nonlinear metabolism terms were incorporated into the model. Model simulations showed good agreement with human data in the arterial plasma, brain, muscle, adipose tissue, and viscera regions. The model was also applied to lidocaine in humans and compared well with the human plasma data.

Trace Metals and Other Ions—Trace metals and other ions are studied for various reasons. Certain endogenous metals and ions are essential for body growth, development, and many daily functions. Several exogenous metals and ions are also required nutritionally by the body (*e.g.*, iodine, chromium) and must be taken in the diet. Other exogenous substances can be lethal at high doses (*e.g.*, cadmium, lithium). To this end, physiologically based pharmacokinetic models can be used to determine proper dietary intake, to predict maximum dosages to ensure against toxicity in high-accumulation or target organs, and also to develop detoxification strategies.

[2] Novocain; Breon Laboratories, Inc., New York, N.Y.

Table XVII—Model Parameters for Bromide in the Rat and Human [a]

Tissue	Flow-Limited Linear Binding Constant (R)	Membrane-Limited Linear Binding Constant (R')	Mass Transfer Coefficient (h), ml/min
Skin	—	0.35	0.015
Kidney	—	0.21	0.0004
Liver	—	0.085	0.0009
Muscle	0.150	—	—
Spleen	0.240	—	—
GI tract	—	0.37	0.0058
Brain	—	0.14	0.00073
Lung	0.376	—	—
Thyroid	0.480	—	—
Heart	0.150	—	—
Adipose tissue	—	0.22	0.0002
Red blood cell compartments			
1	0.30	—	5.0
2	2.79	—	0.019
Residual carcass	0.08	—	—

[a] Data (69) reprinted from the *American Journal of Physiology* with permission; © 1978, The American Physiology Society.

Bromide—Bromide is an essential element for the body. Small amounts are found in table salt and several vegetables. Natural intake of bromide occurs primarily by GI absorption from these sources. Bromide passes through the various body fluids, penetrates red blood cell membranes, and is eliminated *via* the kidneys. Bromide also displaces chloride in extracellular fluid, which may lead to a sedative effect on nerve tissue (68). In this manner, bromide can be used as a tracer to measure the volume of extracellular water (69). The model by Pierson *et al.* (69) applied physiologically based pharmacokinetics to predict the distribution of bromide in rats and then scaled-up to humans (Table XVII). Twelve compartments were included in this model; the muscle, lung, heart, spleen, thyroid, and body compartments were assumed to be flow limited and the skin, adipose tissue, kidney, brain, liver, GI tract, and red blood cell compartments were assumed to be membrane limited. The authors computed the linear binding parameters from steady-state bromide distribution data. The rat model predictions of extracellular volume were compared with known values along with the concentration data. The authors found adequate agreement within the inherent statistical limitations of the data. Identical thermodynamic and transport parameters were used in the scaled-up model and led to good agreement with plasma, skin, muscle, and adipose tissue data in humans. This model and these experiments indicated that bromide was an imperfect tracer for extracellular water because of consistent overprediction of the extravascular water volume.

Cadmium—Cadmium, an exogenous substance, is toxic when present at high levels. Because of this toxicity, cadmium is of primary concern to the metals industry for environmental reasons. Low cadmium doses are found to result in hypertension (70). Accumulation of cadmium in

Table XVIII—Model Parameters for Cadmium in the Mouse [a]

Tissue	Flow-Limited Linear Binding Constant (R)	Membrane-Limited Linear Binding Constant (R')	Mass Transfer Coefficient (h), min^{-1}
Spleen	0.55	—	—
GI tract	0.53	—	—
Liver	—	19.0	0.16
Kidney	—	7.0	0.03
Red blood cell	—	0.5	0.002
Carcass	0.34	—	—

[a] Data taken from Ref. 73.

the testicles of laboratory animals leads to necrosis of this tissue (71). The similarities and dependence in transport and uptake of cadmium to zinc has led to many comparative studies of these two elements (72). Following intake, cadmium is found to clear rapidly from the plasma, bind to subcellular proteins, and accumulate readily in the liver and kidneys (14). The Gerlowski and Jain model (73) combines both membrane-limited and flow-limited compartments to study cadmium uptake in mice (Table XVIII). Membrane-limited liver and kidney compartment simulations show good agreement with the data, which account for 60% of the initial dose. The fit was not as good in the other compartments, especially in the residual carcass compartment where many organs were lumped into one flow-limited compartment. Further improvements can be made in this model when short-term data become available for various organs.

Chloride—Chloride, an endogenous trace element, is essential for electrolytic, osmotic, and acid balances and other bodily functions. Dietary chloride is obtained in animal foods, absorbed through the GI tract, and excreted primarily through the urinary tract (68). Chloride depletion may be a useful treatment for brain edema (74). Gabelnick *et al.* (74) have developed a three-compartment hybrid model (Fig. 4) representing brain, well-perfused, and poorly perfused compartments to study mass transfer of chloride in cats undergoing hemodialysis. Transfer to the brain was considered to occur by diffusion from the well-perfused compartment, by convection from cerebrospinal fluid (CSF), and by mediated transport from the well-perfused compartment. Brain tissue was assumed to be in equilibrium with the CSF. The mass transfer coefficient from the well-perfused compartment to the brain was estimated to be 0.037 ml/min. The transport rate of chloride into the CSF was found to be a constant (0.55 μeq/ml · min) for 60–120-meq/liter plasma chloride concentrations. This behavior indicated the existence of a "saturated pump" and was modeled as a constant infusion term (2.8 μeq/min). The authors noted agreement with the data, except for the brain compartment, which experimentally indicates a steady-state equilibrium concentration, unlike the model predictions. This disagreement may have resulted from a possible change in flow rate of the CSF or mediated transport into the brain during hemodialysis.

Lithium—Lithium, an exogenous substance, is used in the treatment of manic-depressive illness. Problems that arise from dosage levels and schedules of lithium have led to the use of pharmacokinetics in determining proper regimens. A model presented by Ehrlich (75) applies a three-compartment scheme representing plasma and extracellular fluid, red blood cells, and muscle-like cells to

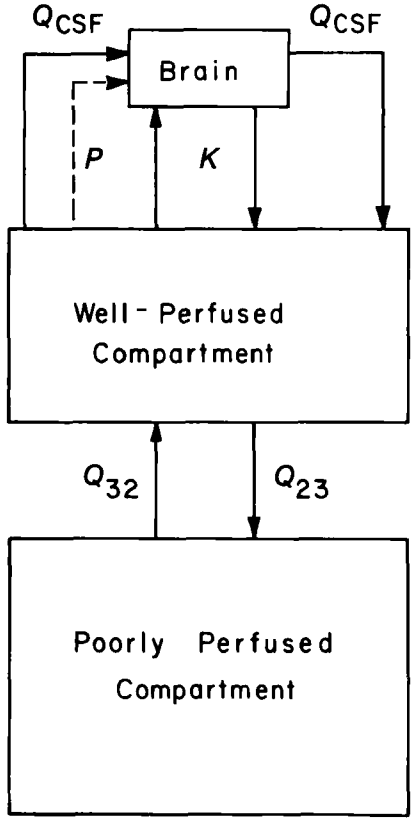

Figure 4—*Location of the brain compartment (74). Reprinted from the* Journal of Applied Physiology *with permission; copyright 1980, American Physiological Society.*

describe lithium distribution in four human subjects (Table XIX). Linear transport and Michaelis–Menten excretion parameters were incorporated in the hybrid model. The model simulated the data well and suggests that the Li^+ countertransport efflux mechanism of the red blood cell may be shared with the muscle. However, variations in the intercompartment concentrations, because of high concentrations in the liver and kidneys, suggest the need of a larger model consisting of several more compartments when the data become available.

Zinc—Zinc, an endogenous substance, is essential in that DNA and protein syntheses are zinc dependent; also, carbohydrate metabolism, lipid peroxidation, and bone formation require zinc. Deficiencies in zinc may lead to growth retardation and failure of sexual maturation. A comprehensive model (17 tissues, plasma, and red blood cells) was developed to describe zinc distribution in rats (15). In this model, membrane-limited compartments were incorporated with linear binding, transport, and excretion.

Table XIX—Model Parameters for Lithium in the Human [a]

Tissue	Absorption Rate, hr^{-1}
GI tract	
Absorption rate	0.36–1.88
Renal excretion rate	0.09–0.18
Muscle	
Influx	0.26–0.38
Efflux	0.19–0.36
Red blood cells	
Influx	0.12–0.29
Efflux	0.35–0.80

[a] Data (75) reprinted from the *Journal of Pharmacokinetics and Biopharmaceutics* with permission; © 1980, Plenum Publishing Corp.

Table XX—Model Parameters for Zinc in the Rat [a]

Tissue	Membrane-Limited Linear Binding Constant (R')	Mass Transfer Coefficient (h), hr^{-1}
Skin and fur	6.5	0.0339
Muscle	11.0	0.0171
Liver	28.0	0.4076
Intestine	14.8	0.3132
Stomach	18.0	0.1181
Fat	0.7	0.0037
Thyroid	11.3	0.1815
Bone and bone marrow	25.0	0.0799
Heart	13.0	0.1216
Bladder	17.0	0.0739
Prostate	6.0	0.0633
Spleen	15.0	0.2083
Pancreas	20.0	0.1884
Kidney	20.0	0.3278
Brain	11.4	0.0191
Gonads	15.0	0.05
Sex organ	8.0	0.04
Gut lumen	16.0	0.1274
Red blood cell	5.5	0.0376 (ml/hr)
Clearance rate, ml/hr		
Fecal (k_f)	0.14	
Urinary (k_k)	0.15	
Intestinal (k_i)	7.21	
Pancreatic (k_{pan})	2.41	

[a] Data (15) reprinted from the *Annals of Biomedical Engineering* with permission; © 1982, Pergamon Press Inc.

Table XXI—Model Parameters for Acetonylacetone in the Rat [a]

Tissue	Linear Binding Constant (R)		Tissue–Plasma Turnover Ratio
	Parent Drug	Metabolite	
Liver	1.7	3.4	0.7
Kidney	0.6	3.1	0.75
Lung	0.6	2.5	0.55
Lean tissue	0.4	0.8	1.0
Brain	0.4	0.5	1.4
Sciatic nerve	0.4	0.4	3.0
Spinal cord	0.4	0.5	5.0 (k_{sc} 11.5)
Other values			
Peritoneal permeability, ml/hr		12.0	
Linear kidney clearance, ml/hr			
Parent drug		10.0	
Metabolite		30.0	
First-order metabolism constant, ml/hr		150.0	
Carbon-14 incorporation rate constant (plasma), hr^{-1}		0.03	

[a] Data (76) reprinted with permission of the author.

The physicochemical parameters were estimated by decomposing this model into hybrid models and minimizing the error between data and model for each issue (Table XX) (15). Excellent agreement with data was found (average error <10%); however, only a limited number of data were used in estimating the model parameters. A more complete model should incorporate zinc speciation, nonlinear transport and binding, and intercompartmental diffusion.

Environmental Hazards and Toxic Substances—The uptake of many chemicals by the body can lead to harmful effects. Various regulatory agencies impose tolerance levels for hazardous chemicals to ensure safe working conditions. These levels are usually obtained from experiments over short periods of time and formulate an opinion on only one tissue concentration value (*e.g.*, plasma concentration). But, tissue concentrations are known to vary over a wide range throughout the body. Therefore, to ensure that all tissues remain below toxic levels at all times, physiologically based pharmacokinetics may be incorporated into such decision-making processes to set more precise levels.

Acetonylacetone—Acetonylacetone (2,5-hexanedione) is a neurotoxic metabolite of the industrial solvents *n*-hexane and methyl *n*-butyl ketone. Action of acetonylacetone on the sciatic nerves causes axonal damage which characterizes central–peripheral distal axonopathy. Recently, a nine-compartment flow-limited physiologically based pharmacokinetic model was constructed by Angelo and Bischoff (76) to simulate the detailed pharmacokinetics and metabolism in rats (Table XXI). These authors determined equilibrium tissue–plasma distribution ratios based on *in vivo* data determined by constant intravenous infusion of acetonylacetone using a surgically implanted infusion pump. Metabolism of acetonylacetone was simplified to a three-step series reaction scheme, and the rate constant for the second reaction was considered to be organ specific. Very good agreement with data was found for single-dose exposures of 0.8 and 8.0 mg/kg ip for the plasma, sciatic nerve, liver, kidney, lung, and lean compartments in the elimination phase; however, the absorption phase was somewhat underpredicted in each case up to 1 hr. Additionally, the spinal cord compartment exhibited a dose-dependent partition coefficient. The model also described the concentrations of metabolites in the plasma, liver, and urine adequately. In multiple dosing (8.0 mg/kg/day ip), simulations reproduced the tissue data well except for plasma data. These data were overpredicted, perhaps due to kinetics of the radioisotope uptake and release by plasma constituents. The early interval behavior suggested the need for a diffusion-limited model with precise blood kinetics.

Chlordecone—Chlordecone[3] is a chlorinated organic insecticide which is toxic to most life forms. In industrial sites, workers in contact with chlordecone are found to contract severe cases of tremors. From tests performed on laboratory mice, chlordecone has been found to be a carcinogen. Boylan *et al.* (77) and Bungay *et al.* (78) have shown evidence for bidirectional transport of chlordecone between blood and gut contents in mice. Bungay *et al.* (78) have developed a physiologically based pharmacokinetic model with a detailed enteric transport model to describe the distribution and excretion of a nonadsorbable tracer and parent chlordecone in rats (Table XXII). The GI tract was modeled to include stomach, small intestine, cecum, and large intestine; each organ was represented by a series of well-mixed subcompartments. This model was able to predict the short-term transport kinetics of parent chlordecone as well as substances that are unabsorbed or passively transported across the gut wall. The scaled-up model also provided a rational basis for cholestyramine therapy for victims of chlordecone poisoning.

Nitrate and Nitrite—Nitrosamines, which are known to be potent carcinogens, can be formed endogenously from dietary nitrate. Nitrate enters the body in the diet and also is formed from reduced nitrogen compounds. In addition,

[3] Kepone.

Table XXII—Model Parameters for Chlordecone in the Rat[a]

Tissue	Membrane-Limited Linear Binding Constant (R)			Mass Transfer Coefficient (h), ml/min		
	Capillary	Mucosa	Lumen	Capillary	Mucosa	Lumen
Stomach	7	1	0.031	0.2	0.002	0.002
Small intestine						
I	8	0.5	0.030	0.3	0.05	0.1
II	7	0.4	0.078	0.26	0.04	0.1
III	6	0.3	0.013	0.25	0.02	0.07
Cecum	5	0.2	0.006	0.09	0.006	0.03
Large intestine	4	0.2	0.005	0.10	0.004	0.02
Fat	15	—	—	—	—	—
Liver	55	—	—	11	—	—
Muscle	5	—	—	—	—	—
Skin	6	—	—	0.54	—	—

[a] Data (78) reprinted from the *Journal of Pharmacokinetics and Biopharmaceutics* with permission; © 1981, Plenum Publishing Corp.

the salivary glands transport nitrate from the blood to saliva. By bacterial reaction, nitrate is converted in the oral cavity to nitrite, which is then available to form nitrosamines in the stomach. Therefore, to determine the safe amount of dietary nitrate intake, an understanding of the distribution and metabolic fate of nitrate and nitrite would be useful. To this end, Deen *et al.* (79) developed a physiologically based pharmacokinetic model to simulate nitrate and nitrite concentrations in humans following an oral dose of nitrate (Table XXIII). The model consisted of an oral cavity, stomach, small and large intestines, blood and well-perfused tissues, and lean tissues. Transport between the digestive system, blood pool, and well-perfused tissues was modeled to occur by diffusive and convective means *via* bile, saliva, and gastric and pancreatic juices. The authors were able to simulate data adequately for plasma and salivary nitrate and salivary nitrite. The authors found individual variations in values of the renal clearance constant among groups of subjects. The model was not able to predict in detail the fate of reduced nitrogen, *e.g.*, reabsorption from the GI tract, exhalation of gaseous products, *etc.* Denitrification in the oral cavity is also known to occur, but was not incorporated in this model and needs to be further investigated along with the fate of the nitrite presented to the stomach.

Polychlorinated Biphenyls—Polychlorinated biphenyls (PCB's) are widely recognized as a highly toxic environmental hazard. These substances appear throughout the food chains of all animals. Highly chlorinated biphenyl molecules are known to persist in the body for long periods of time (10–15 years) and are potent inducers of microsomal enzyme activity. Metabolism of polychlorinated biphenyls occurs primarily in the liver, and the metabolites are known to have carcinogenic effects. Polychlorinated biphenyls are known to accumulate primarily in the adipose tissue. Anderson *et al.* (80) and Lutz *et al.* (81) each applied a six-compartment flow-limited model to describe the disposition and metabolism of polychlorinated biphenyls (1-, 2-, 5-, and 6-chlorinated biphenyls) in rats. These authors concluded that a membrane-limited model may be more appropriate for pharmacokinetics of polychlorinated biphenyls in the skin compartment. The alternative would have been to divide the skin into a number of compartments to model the heterogeneous perfusion rate in the skin. The pharmacokinetics of 3,3′,5,5′-tetrachlorobiphenyl (4-chlorinated biphenyl) and its metabolites were also studied in rats by Tuey and Mathews (Table XXIV) (82) using the framework developed by Lutz *et al.* Except for 4-chlorinated biphenyl, the rate of metabolism of four polychlorinated biphenyls (1-, 2-, 5-, and 6-chlorinated biphenyls) decreased as the degree of chlorination increased. The rate of metabolism of 4-chlorinated biphenyl was found to be less than that of 5-chlorinated biphenyl and greater than that of 6-chlorinated biphenyl. However, the relative rates of various polychlorinated biphenyls could be ordered according to the number of adjacent unsubstituted carbon atom pairs they contained. These authors, therefore, suggested that the chlorine po-

Table XXIII—Model Parameters for Nitrite in the Human[a]

Tissue	First-Order Rate Constant, hr^{-1}	Reaction Rate Constant for Nitrate, hr^{-1}	P/V, hr^{-1}
Intestinal segment			
1	0.21	0.84	5.1
2	0.21	0.84	5.1
3	0.21	0.84	2.0
4	2.1	8.4	1.1
5	2.1	8.4	1.1
6	2.1	8.4	1.1
Gastric emptying	2.0–9.0	—	—
Liver	0–0.038	—	—
Oral cavity	4.8	0–50	—
G1	0.8		
G2	0		
Other values			
Renal clearance liter/hr	1.6–2.5		
K_m, mM	1.5		
V_{max}/K_m, hr^{-1}	38		
Fraction of nitrite lost in stomach by reaction	0.4		
R (gastric juice to plasma)	18–28		
R (saliva to plasma)	20		

[a] Data (79) reprinted with permission of the authors.

Table XXIV—Model Parameters for 3,3′,5,5′-Tetrachlorobiphenyl in the Rat[a]

Tissue	Flow-Limited Linear Binding Constant (R)	
	Parent Drug	Metabolite
Liver	6	2
Muscle	1	0.1
Skin	7	0.3
Adipose tissue	220	0.5
Gut lumen	—	1
Others, ml/hr		
Liver metabolism constant (k)	14.7	
Kidney clearance (k_k)	0.7	
Biliary clearance (k_b)	12.1	
Fecal transport	0.05	
Gut reabsorption	0.01	

[a] Data (82) reprinted from *Drug Metabolism and Disposition* with permission; © 1977, American Society for Pharmacology and Experimental Therapeutics.

Table XXV—Model Parameters for Digoxin in the Rat, Dog, and Human

Tissue	Flow-Limited Linear Binding Constant (R)		
	Rat[a]	Dog[b]	Human[b]
Heart	1.6	40	40
Skeletal muscle	1.4	9	9
Skin, fat, *etc.*	1.0	9	9
Kidney	1.9	200	200
Liver	7.9	15	15
GI tract			
Tissues	30.0	30	30
Contents	—	—	—

[a] Data (84) reprinted from the *Journal of Pharmaceutical Sciences* with permission; © 1977, American Pharmaceutical Association. [b] Data (85) reprinted from the *Journal of Pharmaceutical Sciences* with permission; © 1977, American Pharmaceutical Association.

sition is more important than the degree of chlorination.

Other Substances—*2-Butanol*—Pretreatment with 2-butanol and its metabolites is known to potentiate the hepatotoxicity of carbon tetrachloride. Assuming that the only important site of 2-butanol metabolism is in the liver, a two-compartment model consisting of a volume of distribution compartment and a flow-limited liver compartment was developed for 2-butanol and its metabolites butanone, 3-hydroxy-2-butanone, and 2,3-butanediol by Dietz *et al.* (83) The model included transport to the site of metabolism, inhibition of the transformation of butanone to 3-hydroxy-2-butanone, reabsorption of the latter in the liver, and elimination of all four compounds from the animal. The model adequately described the blood data for each of these species after intravenous injections of 3-hydroxy-2-butanone and 2,3-butanediol and following oral administration of 2,3-butanediol and 2-butanol. These simulations also suggested that a 28–30% molar dose of 2,3-butanediol relative to 2-butanol and butanone gave comparable 2,3-butanediol blood kinetics. These authors suggested that there is need for incorporating saturable transport, both linear and saturable binding, and the interactions of 2-butanol and its metabolites with enzymes and other cellular components when appropriate data become available.

Digoxin—Digoxin is one of the cardiac glycosides used in the treatment of heart diseases. As a cardiotonic, digoxin increases myocardial contraction force, and as a depressant, digoxin decreases cardiac rate. A physiologically based pharmacokinetic study was performed on digoxin and its metabolite by Harrison and Gilbaldi (Table XXV) (84). Eight flow-limited compartments were considered with metabolism in the liver, linear tissue binding, and linear excretion in rats. Good agreement was found with plasma, heart, muscle, and liver tissue data and urinary excretion data following an intravenous dose. The model was then altered to include cholestasis and renal failure by setting biliary secretion and renal clearance rates equal to zero, respectively. Plasma and urinary excretion data from rats with ligated bile ducts or ligated ureters were found to be in good agreement with model simulations. The same model was then modified for dogs and scaled-up to humans (85). The simulations agreed well with urinary excretion data and kidney, heart, liver, and muscle tissue data in the dog. When scaled-up to humans the model underpredicted early interval plasma data, but adequately described the urinary excretion data following a single intravenous dose. This discrepancy in plasma data may be due to differences in binding parameters between dogs and humans, or a diffusion limitation may exist in this system. Steady-state concentration levels predicted were in the same range as those found postmortem in human plasma, heart, and skeletal muscle; however, liver and kidney concentrations were predicted to be 1.5–2 times and 2–3 times the patient data, respectively. While the model described the plasma data in patients with moderate renal impairment, the model underpredicted the plasma data in anuric patients. This discrepancy may have resulted from an effect on the transport and binding parameters by uremia.

Table XXVI—Model Parameters for Ethanol in the Dog and Rat

Parameter	Dog[a]	Rat[b]
v_{max}, mg/ml·hr	0.1992	11.64
Michaelis constant (K_m), mg/ml	0.0095	0.000041
Distribution rate		
k_{13}	0.0005	—
k_{31}	0.1782	—

[a] Data (87) reprinted from the *Journal of Pharmacokinetics and Biopharmaceutics* with permission; © 1981, Plenum Publishing Corp. [b] Data (86) reprinted from *Biochemical Pharmacology* with permission; © 1973, Pergamon Press Inc.

Ethanol—Ethyl alcohol is known to act on the central nervous system causing excitation followed by a depressed state. On ingestion, ethanol is rapidly absorbed from the small intestine and is rapidly metabolized to acetic acid by active acetyl oxidative enzymes in the liver (41). Thus, the primary concern for ethanol in the body from a modeling point of view is in the hepatic system. A two-compartment hybrid model consisting of the liver and the remainder of the body, which were interconnected by the hepatic artery and vein, was developed by Dedrick and Forrester for rats (Table XXVI) (86). The authors concluded that *in vitro* Michaelis–Menten kinetic parameters for the liver alcohol dehydrogenase agreed well with the model parameters; however, a significant artifact may be introduced if the body is considered to be a single compartment. A three-compartment hybrid model was recently developed by Rheingold *et al.* (87) to account for the observed vascular concentration gradients, blood flow limitations, and liver metabolism. These compartments included: the liver; the peripheral circulation represented by the femoral artery, peripheral capillaries, and femoral vein in series; and a deep compartment. The model was fitted to femoral artery and vein data following a 10-min constant infusion of ethanol *via* the cephalic vein at doses of 0.13 and 0.26 g/kg. The values of the metabolism parameters did not agree with those of Dedrick and Forrester.

Phenolsulfonphthalein — Phenolsulfonphthalein (phenol red) is useful as a diagnostic agent to determine the functional activity of the kidney; *i.e.*, intravenous injection of phenolsulfonphthalein has a longer residence time in impaired kidneys (41). A physiologically based pharmacokinetic model was developed in the dogfish shark (*Squalus acanthias*) by Bungay *et al.* (Table XXVII) (88). The dogfish shark was chosen to study physiologically based pharmacokinetics in aquatic animals because of the large amounts of pollutants in the ocean, the scalability of pharmacokinetics to lower species, and the abundance of experimental methodology available in fish. This model consisted of three flow-limited compartments representing the kidney, liver, and muscle, a two-subcompartment bile duct, and a plasma compartment. The linear binding constants for the liver and muscle were obtained from the

Table XXVII—Model Parameters for Phenolsulfonphthalein in the Dogfish Shark [a]

Tissue	Flow-Limited Linear Binding Constant (R)	Clearance Constant (k), ml/min·kg
Kidney	8	0.36
Liver	4	0.62
Muscle	0.1	—
Other		
Bile duct subcompartments	retention time (τ), 120 min (n = 2)	

[a] Data (88) reprinted from the *Journal of Pharmacokinetics and Biopharmaceutics* with permission; © 1976, Plenum Publishing Corp.

equilibrium data; the kidney constants were determined by trial and error. Clearance constants were determined from experimental data. Although agreement between the model and data was good, the concentrations predicted in the liver and kidneys were lower than the measured values during the distribution phase, while plasma predictions were higher than data at early intervals. This discrepancy indicates the possibility of higher plasma flow rates than reported in the literature. The agreement between predictions and urine data was good over the entire 48 hr following injection; however, the bile data were lower than the predicted values at 24 and 48 hr. Incorporation of enterohepatic circulation might reduce this discrepancy, as suggested by these authors.

Salicylates—Salicylates have been found to produce marked antipyretic and analgesic effects, and are used to treat rheumatic fever and rheumatic tonsilitis. These substances are easily absorbed from the upper GI tract and spread readily through the tissues. Seventy to eighty percent is usually excreted through the kidneys as free acid (41). A seven-compartment flow-limited model was applied to study the pharmacokinetics of salicylates in the plasma, brain, liver, GI tract, muscle, visceral region, and adipose tissue of dogs by Chen *et al.* (Table XXVIII) (89). The CSF concentration of salicylates was determined by mass balance around the brain, CSF, and blood. Three markedly different dosages, from therapeutic to severely intoxicating levels, were given to determine the appropriateness of dosage regimens. The model was able to predict the data extremely well over all dosages. In addition, comparison of the model with dogs treated with hemoperfusion to remove salicylates was presented. In all cases the predicted concentrations agreed well with the data.

Sulfobromophthalein and Warfarin—Sulfobromophthalein dramatically decreases the elimination of warfarin, an anticoagulant, in the bile. The kinetics of this effect are well known and concentration of both drugs can

Table XXVIII—Model Parameters for Salicylates in the Dog [a]

Tissue	Ratio of Blood Volume in Organ Capillaries to Total Blood Volume (R)
Blood pool	0.46
Brain	0.007
Liver	0.087
Viscera	0.091
GI tract	0.163
Muscle	0.164
Adipose tissue	0.028

[a] Data (89) reprinted from the *Journal of Pharmaceutical Sciences* with permission; © 1978, American Pharmaceutical Association.

Table XXIX—Model Parameters for Sulfobromophthalein and Warfarin in the Rat [a]

Tissue	Flow-Limited Linear Binding Constant (R)	
	Sulfobromophthalein	Warfarin
Muscle	0.10	0.060
Kidney	1.20	0.48
Liver	2456	1.08
Elimination constants		
Primary		
v_{max}, 10^{-9} mole/min·ml (liver)	23.6	0.051
K_m, 10^{-9} mole/ml	174.0	65.0
Secondary		
v_{max}	15.0	—
K_m	64.1	—

[a] Data (91) reprinted from the *Journal of Pharmacokinetics and Biopharmaceutics* with permission; © 1979, Plenum Publishing Corp.

be easily measured (41). These properties make sulfobromophthalein a useful agent for a physiologically based pharmacokinetic study. Montandon *et al.* (90) have developed a model to describe total sulfobromophthalein (unchanged plus conjugated) in the hepatic system of rats and have scaled it to humans (Table XXIX). Two flow-limited compartments for liver and extrahepatic tissue with linear binding, a three-subcompartment bile duct, and a plasma compartment were incorporated. The model simulations compared well with data from the bile, liver, and plasma following a 200-nmoles/min/kg iv infusion in rats. The scaled-up model also agreed with human plasma data following a constant intravenous infusion with or without a rapid intravenous priming dose. The relative inaccuracy between the model and data for the first 10 min following rapid intravenous injection may be corrected by including different kinetics of conjugated and unconjugated sulfobromophthalein in the model. A recent rat model by Luecke and Wosilait (91) improved the aforementioned model by replacing the extrahepatic compartment with the kidney compartment and using the Michaelis–Menten equations for enzymatic processes involved in the drug elimination *via* two pathways (Table XXIX). The model described the plasma and bile data of warfarin and sulfobromophthalein following a 1-mg/kg iv dose of warfarin at time zero and a 50-mg/kg dose of sulfobromophthalein at 60 min. This model provides a framework to study drug interaction using single-drug models.

Tetraethylammonium chloride—The tetraethylammonium cation is effective in blocking vasomotor impulses to blood vessels, thus producing reduction of gastric acidity, GI motility, and partial or complete block of impulses to structures innervated by the autonomic nervous system such as the eye, sweat gland, and bladder (41). An eight-compartment model was developed to describe transport of the tetraethylammonium ion in the rat by Mintun *et al.* (Table XXX) (92). In the development of the model the authors first assumed a flow limitation. However, the data showed no steady-state concentration of tetraethylammonium ion, which the model predicted should occur after a few hours. The authors then incorporated a passive-diffusion membrane limitation. This type of model was not able to predict either the early interval peak or the late interval high concentration associated with the data. On the other hand, the authors were able to predict the data well by incorporating both passive

Table XXX—Model Parameters for Tetraethylammonium Chloride in the Rat [a]

Tissue	Half Saturation Concentration for Transport (K_m), μg/ml	Maximum Transport Velocity (v_{max}), μg/min	Permeability (k_i), ml/min
Liver	3.0	75.0	2.0
Kidney	1.0	60.0	0.8
Gut	2.0	9.0	0.3
Lung	0.3	0.5	0.05
Heart	0.065	0.32	0.03
Carcass			
rapid	—	—	400
slow	—	—	0.5

[a] Data (92) reprinted from the *Journal of Pharmacokinetics and Biopharmaceutics* with permission; © 1980, Plenum Publishing Corp.

and saturable transport across the capillary membrane. Since *in vitro* estimates of drug transport and permeability parameters led to poor agreement with the *in vivo* data, these parameters were fitted with a semiempirical curve-fitting technique. Although the model led to an adequate representation of the intravenous data, these authors questioned the assumption of unidirectional active transport in their model. The incorporation of bidirectional transport and the division of the carcass compartment into subcompartments representing various tissues were improvements suggested by these authors.

CONCLUSIONS

The objective of this review article was to present a unified theoretical framework for physiologically based pharmacokinetics. To this end, historical and technical developments in this area of research were discussed briefly. The comparison between experimental and theoretical results on the distribution of over 37 agents in various mammals were summarized according to their applications. Several important and poorly understood problems were pointed out at various places in the text in the hope of stimulating interest in the investigations involved in this area of research.

Some important problems that deserve further attention are:

1. While simplified models of various organs (*e.g.*, lungs, heart, brain, enterohepatic system, kidneys) appear to give adequate results in several applications, a more complete anatomical description is needed. In reality, lungs receive the cardiac output *via* the pulmonary circulation for oxygenation and a small amount *via* the bronchial circulation for the lung tissue. In most analyses, however, the lung component is placed in series with a single plasma compartment (Fig. 5A) (29, 31). In a limited number of analyses the plasma compartment is divided into the arterial and veinous pools with the lung placed between them, consistent with the anatomy (54, 64). A more complete model would include the bronchial circulation as well (Fig. 5B). Similarly, a complete model of the heart would include both the coronary and cardiac flows. Detailed models of the kidneys (93), brain, eyes (94–96), and enterohepatic system (43, 78), which have been discussed elsewhere, should be of help in developing more comprehensive physiologically based pharmacokinetic models (Figs. 1 and 3).

2. The modeling of the uptake of a substance that binds to the red blood cells presents anatomical queries,

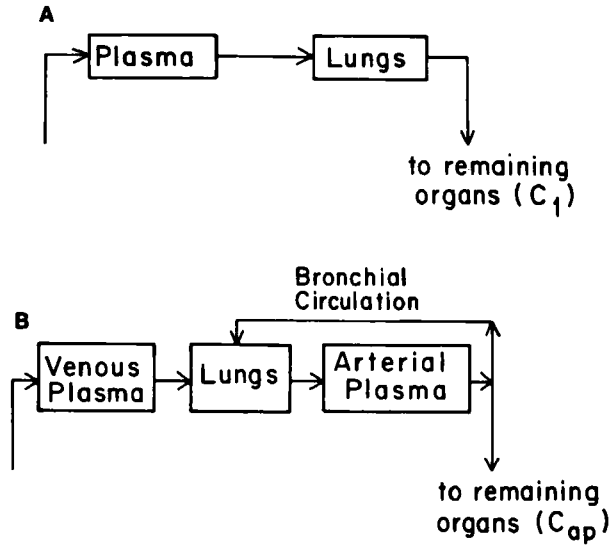

Figure 5—*Physiological location of the lung compartment with (A) only one plasma compartment and no bronchial circulation and (B) two plasma compartments with bronchial circulation.*

since red blood cells are present in every tissue throughout the body. As shown in Fig. 1, the red blood cells are lumped into one compartment and connected to the plasma compartment where transport is considered to occur, normally by diffusion. A first-order approximation is made by assuming that the transfer of the substance occurs only from the plasma compartment and that the red blood cells occupy dead space for transfer. This method is able to describe the data well, but a detailed model should account for the presence of erythrocytes in each tissue.

3. Although the assumption of no intercompartmental transfer by diffusion is valid for major organs such as the liver, kidneys, heart, *etc.*, the assumption does not realistically apply to poorly perfused organs and tissues. The bone, muscle, and fat organs are usually considered to be separate components with no diffusional transfer; however, this may not be the case for some agents. A first-order approximation to alleviate this limitation would be to assume diffusional mass transfer across these compartments. To date no physiologically based model has used or required this approach to describe data.

4. For many tissues, *e.g.*, solid tumors, the intratissue concentration gradients can be large and each compartment or subcompartment may not behave as a well-mixed phase (97). When this is the case, the lumped-compartment approach applied to date in physiologically based pharmacokinetic modeling may not be applicable, and a distributed parameter approach may be preferred to describe spatial concentration profiles in various tissues (97–101). However, detailed descriptions of convective and diffusive mass transfer in tissues are mathematically intractible. The boundary conditions, due to the complex geometries of the tissue, may also be difficult. Finally, the solution of the partial differential equations may require an enormous amount of computer time. To achieve this end, finite difference or finite element numerical techniques could alleviate some of these problems.

5. Effect of the disease state can significantly alter the pharmacokinetics of an agent by changing its transport, excretion, or metabolism. As discussed in this review article, some models have been able to simulate the effects

of renal and/or hepatic impairment and hemodialysis in uremic patients.

6. Use of multiple drugs is common for the treatment of various diseases, *e.g.*, combination chemotherapy for cancer. Interaction of various drugs can lead to significant alterations in the excretion kinetics if they share the same biochemical mechanism (91). Models for drug interaction need to be developed on the basis of single-drug models.

7. A novel application for physiologically based pharmacokinetics would be in cancer treatment when chemotherapy is used in conjunction with other methods of cancer therapy, *e.g.*, radiation, hyperthermia, immunotherapy, and surgery. In multimodal therapy, both the physicochemical (*e.g.*, mass transfer coefficient and binding constants) and the physiological parameters (*e.g.*, tissue volume and perfusion rates) may change. The effects of temperature on the physiological properties have been studied, but such information has not been incorporated in physiologically based pharmacokinetic models to date (101, 102).

8. Use of certain agents may lead to changes in the cell-cycle parameters involved with enzyme synthesis, drug resistance, or cell death (103). Incorporation of cytokinetics and detailed biochemical processes in physiologically based models remains a challenging problem with useful applications.

9. Although sophisticated numerical techniques are available for parameter estimation, most investigators have estimated the physicochemical parameters not measured independently by "eye-balling." One reason for this procedure is, perhaps, that the estimation of a large number of parameters is expensive. The problem can, however, be alleviated by dividing the whole body into a number of hybrid models, and estimating parameters for each tissue by using plasma as the forcing function. Such a sequential optimization approach has been successfully applied for zinc and pentostatin pharmacokinetics (15, 39).

10. While the ultimate goal of physiologically based pharmacokinetics is to scale-up small animal data to humans and to develop rational clinical protocols, such applications have been limited (37). Perhaps the paucity of human data and the large amount of information needed to develop these models prohibit their use in the clinical situation. Utilization of hybrid models, however, offers an attractive alternative to both classical and physiological approaches (40). Unless this approach is widely applied in clinical situations, its full potential will not be realized.

APPENDIX: GLOSSARY

a = maximum facilitated transport rate (mole/min)
a' = strong-binding constant (mole/ml)
b = Michaelis constant for saturable transport (mole/min)
C = tissue concentration (mole/ml)
ϵ = dissociation constant (mole/ml)
$g(t)$ = injection function (mole/min)
h = mass transfer coefficient (ml/min)
k = first-order kinetic rate constant (ml/min)
K_c = elimination saturation concentration (mole/ml)
K_m = Michaelis metabolism saturation constant (mole/ml)
n = flux across capillary or cell membrane (mole/min)
R = flow-limited linear binding constant (dimensionless)
$r_i(t)$ = rate of drug disappearance by metabolism in compartment i (mole/min)
R' = membrane-limited linear binding constant (dimensionless)
Q = tissue plasma flow rate (ml/min)
q = excretion rate (mole/min)
t = time (min)
V = tissue volume (ml)
v_{max} = maximum reaction velocity (mole/min)

subscripts
i = ith organ (compartment)
p = plasma compartment

superscripts
C = cellular compartment
E = extracellular compartment
I = interstitial compartment
V = vascular compartment
$*$ = free drug

REFERENCES

(1) K. B. Bischoff, *Cancer Chemother. Rep.*, **59**, 777 (1975).

(2) K. J. Himmelstein and R. J. Lutz, *J. Phamacokinet. Biopharm.*, **7**, 127 (1979).

(3) H.-S. G. Chen and J.F. Gross, *Cancer Chemother. Pharmocol.*, **2**, 85 (1979).

(4) J. G. Wagner, "Biopharmaceutics and Relevant Pharmacokinetics," Drug Intelligence Publications, Hamilton, Ill. 1971.

(5) J. G. Wagner, "Fundamentals of Clinical Pharmacokinetics," Drug Intelligence Publications, Hamilton, Ill. 1975.

(6) L. Sharney, L. R. Wasserman, and N. R. Geritz, *Am. J. Med. Electron.*, **3**, 249 (1964).

(7) S. Riegelman, J. Loo, and M. Rowland, *J. Pharm. Sci.*, **57**, 117 (1968).

(8) K. Schmidt-Nielson, *Fed. Proc. Fed. Am. Soc. Exp. Biol.*, **29**, 1524 (1970).

(9) R. L. Dedrick, *J. Pharmacokinet. Biopharm.*, **1**, 435 (1973).

(10) T. Teorell, *Arch. Intern. Pharmacodyn.*, **57**, 205 (1937).

(11) R. Bellman, J. A. Jaquez, and R. Kabala, *Bull. Math. Biophys.*, **22**, 181 (1960).

(12) K. B. Bischoff and R. G. Brown, *Chem. Eng. Prog. Symp. Ser.*, **62**, 33 (1966).

(13) D. J. Cutler, *J. Theor. Biol.*, **73**, 329 (1978).

(14) L. Friberg, M. Piscator, G. F. Nordberg, and T. Kjellstrom, "Cadmium in the Environment," Cleveland Rubber Co., Cleveland, Ohio, 1974.

(15) R. K. Jain, L. E. Gerlowski, J. M. Weissbrod, J. Wang, and R. N. Pierson Jr.. *Ann. Biomed. Eng.*, **9**, 347 (1982).

(16) L. S. Olanoff and J. M. Anderson, *J. Pharmacokinet. Biopharm.*, **8**, 599 (1980).

(17) A. Zwart, N. T. Smith, and J. E. W. Beneken, *Comput. Biomed. Res.*, **5**, 228 (1972).

(18) R. K. Jain, J. Wei, and P. M. Gullino, *J. Pharmacokinet. Biopharm.*, **7**, 181 (1979).

(19) E. E. Selkurt, "Basic Physiology for the Health Sciences," Little, Brown and Co., Boston, Mass. 1975.

(20) W. D. Stein, "The Movement of Molecules Across Cell Membranes", Academic, New York, N.Y., 1967.

(21) E. N. Lightfoot, "Transport Phenomena and Living Systems—Biomedical Aspects of Momentum and Mass Transport," Wiley, New York, N.Y., 1974.

(22) A. Goldstein, L. Aronow, and S. M. Kalman, "Principles of Drug Action," Harper and Row, New York, N.Y., 1969.

(23) E. M. Ariens (Ed.), in "Molecular Pharmacology," Academic, New York, N.Y., 1964.

(24) K. J. Himmelstein and J. F. Gross, *J. Pharm. Sci.*, **66,** 1441 (1977).
(25) R. L. Dedrick, D. S. Zaharko, and R. J. Lutz, *J. Pharm. Sci.*, **62,** 882 (1973).
(26) R. F. Brown, *Trans. Biomed. Eng.*, **27,** 1 (1980).
(27) Y. Bard, "Nonlinear Parameter Estimation," Academic, New York, N.Y., 1974.
(28) B. Carnahan, H. A. Luther, and J. O. Wilkes, "Applied Numerical Methods," Wiley, New York, N.Y., 1969.
(29) R. J. Lutz, W. M. Galbraith, R. L. Dedrick, R. Shrager, and L. B. Mellett, *J. Pharmacol. Exp. Ther.*, **200,** 469 (1977).
(30) T. R. Tritton and G. Yee, *Science*, **217** (July), 248 (1982).
(31) P. A. Harris and J. F. Gross, *Cancer Chemother., Rep.*, **59,** 819 (1975).
(32) K. K. Chan, J. L. Cohen, J. F. Gross, K. J. Himmelstein, J. R. Bateman, Y. Tsu-Lee, and A. S. Marlis, *Cancer Treatment Rep.*, **62,** 1161 (1978).
(33) J. G. Townsend, "Physiologically Based Pharmacokinetics of Anti-Cancer Drugs and Toxic Substances—Applications to Adriamycin and Ethylene Glycol," Master's Thesis, Carnegie-Mellon University, April 1980.
(34) L. E. Gerlowski, "Physiologically Based Pharmacokinetics of Anti-Cancer Agents and Trace Metals—Adriamycin, Zinc, and Cadmium," Master's Thesis, Carnegie-Mellon University, May 1982.
(35) R. L. Dedrick, D. D. Forrester, and D. H. W. Ho, *Biochem. Pharmacol.*, **21,** 1 (1972).
(36) R. L. Dedrick, D. D. Forrester, J. N. Cannon, S. M. El Dareer, and L. B. Mellett, *Biochem. Pharmacol.*, **22,** 2405 (1973).
(37) R. L. Dedrick, C. E. Meyers, P. M. Bungay, and V. T. DeVita, Jr., *Cancer Treatment Rep.*, **62,** 1 (1978).
(38) P. F. Morrison, T. L. Lincoln, and J. Aroesty, *Cancer Chemother. Rep.* **59,** 861 (1975).
(39) F. G. King and R. L. Dedrick, *J. Pharmacokinet. Biopharm.*, **9,** 519 (1981).
(40) J. M. Collins, R. L. Dedrick, F. G. King, J. L. Speyer, and C. E. Meyers, *Clin. Pharmacol. Ther.*, **28,** 235 (1980).
(41) G. L. Jenkins, W. H. Hartung, K. E. Hamlin, and J. B. Data, "The Chemistry of Organic Medicinal Products," Wiley, New York, N.Y., 1975.
(42) L. Tterlikkis, E. Ortega, R. Solomon, and J. L. Day, *J. Pharm. Sci.*, **66,** 1454 (1977).
(43) K. B. Bischoff, R. L. Dedrick, and D. S. Zaharko, *J. Pharm. Sci.*, **59,** 149 (1970).
(44) K. B. Bischoff, R. L. Dedrick, D. S. Zaharko, and J. A. Longstreth, *J. Pharm. Sci.*, **60,** 1128 (1971).
(45) D. S. Zaharko, R. L. Dedrick, and V. T. Oliverio, *Comp. Biochem. Physiol.*, **42A,** 183 (1972).
(46) D. S. Zaharko, R. L. Dedrick, A. L. Peal, J. C. Drake, and R. J. Lutz, *J. Pharmacol. Exp. Ther.*, **189,** 585 (1974).
(47) R. J. Lutz, R. L. Dedrick, J. A. Straw, M. M. Hart, P. Klubes, and D. S. Zaharko, *J. Pharmacokinet. Biopharm.*, **3,** 77 (1975).
(48) J. M. Weissbrod, R. K. Jain, and F. M. Sirotnak, *J. Pharmacokinet. Biopharm.*, **6,** 487 (1978).
(49) R. K. Jain, "Dynamics of Drug Distribution in Solid Tumors," PhD Dissertation, University of Delaware, 1976.
(50) A. F. LeRoy, R. J. Lutz, R. L. Dedrick, C. L. Litterst, and A. M. Guarino, *Cancer Treatment Rep.*, **63,** 59 (1979).
(51) J. M. Weissbrod, and R. K. Jain, *J. Pharm. Sci.*, **69,** 691 (1980).
(52) F. G. King, R. L. Dedrick, *Cancer Treatment Rep.*, **63,** 1939 (1979).
(53) D. S. Greene, R. Quintiliani, and C. H. Nightingale, *J. Pharm. Sci.*, **67,** 191 (1978).
(54) A. Tsuji, T. Yoshikawa, K. Nishide, H. Minami, M. Kimura, E. Nakashima, T. Terasaki, E. Miuamoto, C. H. Nightingale, and T. Yamana, *J. Pharm. Sci.* (In Press).
(55) L. Olanoff, T. Koinis, and J. M. Anderson, *J. Pharm. Sci.*, **68,** 1151 (1979).
(56) W. W. Mapleson, *J. Appl. Physiol.*, **18,** 197 (1963).
(57) M. N. Ashman, W. B. Blesser, and R. M. Epstein, *Anesthesiology*, **33,** 419 (1970).
(58) N. T. Smith, A. Zwart, and J. E. W. Beneken, *Anesthesiology*, **37,** 47 (1972).
(59) E. S. Munson, E. I. Eger, and D. L. Bowers, *Anesthesiology*, **38,** 251 (1973).
(60) R. L. Dedrick, and K. B. Bischoff, *Chem. Eng. Prog. Sym. Ser.*, **64,** 32 (1968).
(61) K. B. Bischoff and R. L. Dedrick, *J. Pharm. Sci.*, **57,** 1346 (1968).
(62) C. N. Chen, and J. D. Andrade, *J. Pharm. Sci.*, **65,** 717 (1976).
(63) P. P. Gillis, R. J. DeAngelis, and R. L. Wynn, *J. Pharm. Sci.*, **65,** 1001 (1976).
(64) (a) Y. Igari, Y. Sugiyama, S. Awazu, and M. Hanaro, *J. Pharmacokinet. Biopharm.*, **10,** 53 (1982). (b) J. H. Lin, Y. Sugiyama, S. Awazu, and M. Hanaro, *J. Pharmacokinet. Biopharm.*, **10,** 649 (1982). (c) J. H. Lin, S. Awazu, and M. Hanaro, *J. Pharmacokinet. Biopharm.*, **10,** 637 (1982).
(65) N. Benowitz, R. P. Forsyth, K. L. Melmon, and M. Rowland, *Clin. Pharmacol. Ther.*, **16,** 87 (1974).
(66) N. Benowitz, R. P. Forsyth, K. L. Melmon, and M. Rowland, *Clin. Pharmacol. Ther.*, **16,** 99 (1974).
(67) R. H. Smith, D. H. Hunt, A. B. Seifen, A. Ferrari, and D. S. Thompson, *J. Pharm. Sci.*, **68,** 1016 (1979).
(68) J. M. Orten and O. W. Neuhaus, "Biochemistry," C. V. Mosby, St. Louis, Mo., 1970.
(69) R. N. Pierson, Jr., D. C. Price, J. Wang, and R. K. Jain, *Am. J. Physiol.*, **235,** F254 (1978).
(70) G. F. Nordberg, *Environ. Physiol. Biochem.*, **1,** 171 (1971).
(71) H. A. Schroeder and W. H. Vinton, Jr., *Am. J. Physiol.*, **202,** 315 (1962).
(72) B. S. Kingsley and J. M. Frazier, *Am. J. Physiol.*, **236,** C139 (1979).
(73) L. E. Gerlowski and R. K. Jain, "Pharmacokinetics of Trace Metals: Zinc and Cadmium," presented at AIChE conference, New Orleans, La., 1981.
(74) H. L. Gabelnick, R. L. Dedrick, and R. S. Bourke, *J. Appl. Physiol.*, **28,** 636 (1970).
(75) B. E. Ehrlich, C. Clausen, and J. M. Diamond, *J. Pharmacokinet. Biopharm.*, **8,** 497 (1980).
(76) M. J. Angelo and K. B. Bischoff, "Pharmacokinetics of the Neurotoxin 2,5-Hexanedione: Distribution, Elimination and Model Prediction," presented at AIChE conference, New Orleans, La., 1981.
(77) J. J. Boylan, J. L. Egle, and P. S. Guzelian, *Science*, **199,** 893 (1978).
(78) P. M. Bungay, R. L. Dedrick and H. B. Mathews, *J. Pharmacokinet. Biopharm.*, **9,** 309 (1981).
(79) D. S. Schultz and W. M. Deen, personal communication.
(80) M. W. Anderson, T. E. Eling, R. J. Lutz, R. L. Dedrick, and H. B. Mathews, *Clin. Pharmacol. Ther.*, **22,** 765 (1977).
(81) R. J. Lutz, R. L. Dedrick, H. B. Mathews, T. E. Eling, and M. W. Anderson, *Drug Metab. Dispos.*, **5,** 386 (1977).
(82) D. B. Tuey and H. B. Mathews, *Drug Metab. Dispos.*, **5,** 444 (1977).
(83) F. K. Dietz, M. Rodriguez-Giaxola, G. J. Traiger, V. J. Stella, and K. J. Himmelstein, *J. Pharmacokinet. Biopharm.*, **9,** 553 (1981).
(84) L. I. Harrison and M. Gibaldi, *J. Pharm. Sci.*, **66,** 1138 (1977).
(85) L. I. Harrison and M. Gibaldi, *J. Pharm. Sci.*, **66,** 1679 (1977).
(86) R. L. Dedrick and D. D. Forrester, *Biochem. Pharmacol.*, **22,** 1133 (1973).
(87) J. L. Rheingold, R. E. Lindstrom, and P. K. Wilkinson, *J. Pharmacokinet. Biopharm.*, **9,** 261 (1981).
(88) P. M. Bungay, R. L. Dedrick, A. M. Guarino, *J. Pharmacokinet. Biopharm.*, **4,** 377 (1976).
(89) C. N. Chen, D. L. Coleman, J. D. Andrade, and A. R. Temple, *J. Pharm. Sci.*, **67,** 38 (1978).
(90) B. Montandon, R. J. Roberts, and L. J. Fischer, *J. Pharmacokinet. Biopharm.*, **3,** 277 (1975).
(91) R. H. Luecke and W. D. Wosilait, *J. Pharmacokinet. Biopharm.*, **7,** 629 (1979).
(92) M. Mintun, K. J. Himmelstein, R. L. Schroder, M. Gibaldi, and D. D. Shen, *J. Pharmacokinet. Biopharm.*, **8,** 373 (1980).
(93) P. Hekman and C. A. M. van Ginneken, *J. Pharmacokinet. Biopharm.*, **10,** 77 (1982).
(94) K. J. Himmelstein, I. Guvenir, and T. F. Patton, *J. Pharm. Sci.*, **68,** 435 (1979).
(95) V. H. L. Lee and J. R. Robinson, *J. Pharm. Sci.*, **68,** 673 (1979).
(96) S. C. Miller, K. J. Himmelstein, and T. F. Patton, *J. Pharmacokinet. Biopharm.*, **9,** 653 (1981).
(97) R. K. Jain and J. Wei, *J. Bioeng.*, **1,** 313 (1977).
(98) R. B. Bird, W. E. Stewart, and E. N. Lightfoot, "Transport Phenomena," Wiley, New York, N.Y., 1960.

(99) E. F. Leonard and S. B. Jorgensen, *Annu. Rev. Biophys. Bioeng.*, **3**, 293 (1974).
(100) R. K. Jain, J. M. Weissbrod, and J. Wei, *Adv. Cancer Res.*, **33**, 251 (1980).
(101) R. K. Jain, in "Advances in Transport Processes," vol. 3 Wiley, New Delhi, 1983, pp. 205–339.
(102) R. K. Jain, in "Hyperthermia in Cancer Treatment," F. K. Storm, Ed., G. K. Hall, Boston, Mass., 1983, Chap. 2, pp. 9–46.
(103) R. A. Bender and R. L. Dedrick, *Cancer Chemother. Rep.*, **59**, 805 (1975).

ACKNOWLEDGMENTS

This work was supported by grants from the National Science Foundation and the American Cancer Society, an NIH predoctoral traineeship (LEG), and an NIH Research Career Development Award (RKJ).

The authors wish to thank Dr. Robert Dedrick for his helpful comments.

RESEARCH ARTICLES

Dose-Dependent Pharmacokinetics and Biliary Excretion of Bromophenol Blue in the Rat

ROBERT J. WILLS *, RANDALL B. SMITH ‡, and GERALD J. YAKATAN x§

Received December 31, 1981, from the *Drug Dynamics Institute, College of Pharmacy, University of Texas at Austin, Austin, TX 78712.* Accepted for publication August 26, 1982. Present addresses: *Department of Pharmacokinetics and Biopharmaceutics, Hoffmann-La Roche, Nutley, NJ 07110; ‡Clinical Bioavailability Unit, The Upjohn Company, Kalamazoo, MI 49001; §Warner-Lambert/Parke-Davis, Pharmaceutical Research Division, Morris Plains, NJ 07950.

Abstract □ Concentrations of bromophenol blue (I) in plasma, urine, and bile were determined spectrophotometrically after intravenous bolus injections and infusions in rats. The plasma concentrations were found to decrease monoexponentially after all doses except the highest, where the decrease was biexponential. Although the disposition kinetics of I were apparently first-order at all doses, the half-life increased with increasing dose. The area under the plasma concentration–time curve ($AUC_{0-\infty}$) increased disproportionately with increasing dose. The binding of I to rat plasma proteins, as determined by equilibrium dialysis, showed that the fraction bound (96%) remained constant in the concentration range of 10–300 μg/ml. Plasma concentrations were determined at time zero after intravenous administration and after a second dose administered 20 min later when plasma concentrations from the first dose were minimal. The apparent first-order elimination rate constant for the plasma concentration decline following the second dose was significantly less than after the first dose, indicating that the residual dye in the liver altered the elimination of I after the second dose. The fraction of the dose in the liver decreased with increasing dose, indicating a saturable uptake process. The biliary excretion profile reflected the uptake saturation that occurred in the liver and demonstrated that the biliary excretion of I depended on the amount present in the liver. When liver damage was induced by exposure to carbon tetrachloride, dye concentrations in the plasma, liver, and kidney increased markedly.

Keyphrases □ Bromophenol blue—in rat urine, plasma, and bile, dose-dependent pharmacokinetics, biliary excretion □ Pharmacokinetics—bromophenol blue, rat plasma, urine, and bile, biliary excretion □ Biliary excretion—bromophenol blue, rat urine, plasma, and bile, dose-dependent pharmacokinetics

Bromophenol blue (I) is a high molecular weight anionic sulfonephthalein dye (670 g/mole, pK_a 4.0). Several reports (1–3) have shown that I is extensively excreted in the bile and is not metabolized in a variety of species including the rat.

Takada *et al.* (4, 5) conducted studies aimed at characterizing the role of the intracellular protein fractions Y and Z in the uptake and transport of I in rat hepatocytes, and also developed a linear pharmacokinetic model for the biliary excretion of I after intravenous administration in rats (6). The model adequately described a single low-dose plasma and bile profile, but could not describe the observed nonlinearity at higher doses. The overall aim of these authors was to evaluate I as a model organic anionic compound by characterizing the pharmacokinetics at three different doses. Their report did not fully characterize the pharmacokinetics at any dose. Liver concentrations and plasma protein binding were not measured, and the observed nonlinearity was not addressed.

Studies on the pharmacokinetics of drugs excreted in the bile have increased in recent years as investigators have become more interested in the effects of liver disease on drug clearance, the effects of first-pass liver clearance on drug bioavailability, the effects of enterohepatic recirculation on drug disposition, and the nonlinear excretion of drugs (7–11). Usually these studies have not considered the extent of protein binding, liver-to-plasma and bile-to-liver drug concentration ratios, hepatic blood flow, and bile flow. These factors contribute to the interpretation of hepatobiliary elimination. In addition, the interpretation has been complicated by the use of compounds such as sulfobromophthalein that undergo metabolism. Ideally, a model compound used in studying hepatobiliary elimination would not undergo metabolism, nor enterohepatic recirculation, and would not be pharmacologically active.

The organic anion, bromophenol blue (I), possesses these qualities (2, 4). Therefore, the present investigation was undertaken to: (*a*) determine the pharmacokinetic profile

0022-3549/83/1000-1127$01.00/0

(99) E. F. Leonard and S. B. Jorgensen, *Annu. Rev. Biophys. Bioeng.*, **3**, 293 (1974).
(100) R. K. Jain, J. M. Weissbrod, and J. Wei, *Adv. Cancer Res.*, **33**, 251 (1980).
(101) R. K. Jain, in "Advances in Transport Processes," vol. 3 Wiley, New Delhi, 1983, pp. 205–339.
(102) R. K. Jain, in "Hyperthermia in Cancer Treatment," F. K. Storm, Ed., G. K. Hall, Boston, Mass., 1983, Chap. 2, pp. 9–46.
(103) R. A. Bender and R. L. Dedrick, *Cancer Chemother. Rep.*, **59**, 805 (1975).

ACKNOWLEDGMENTS

This work was supported by grants from the National Science Foundation and the American Cancer Society, an NIH predoctoral traineeship (LEG), and an NIH Research Career Development Award (RKJ).

The authors wish to thank Dr. Robert Dedrick for his helpful comments.

RESEARCH ARTICLES

Dose-Dependent Pharmacokinetics and Biliary Excretion of Bromophenol Blue in the Rat

ROBERT J. WILLS *, RANDALL B. SMITH ‡, and GERALD J. YAKATAN x§

Received December 31, 1981, from the *Drug Dynamics Institute, College of Pharmacy, University of Texas at Austin, Austin, TX 78712.* Accepted for publication August 26, 1982. Present addresses: *Department of Pharmacokinetics and Biopharmaceutics, Hoffmann-La Roche, Nutley, NJ 07110; ‡Clinical Bioavailability Unit, The Upjohn Company, Kalamazoo, MI 49001; §Warner-Lambert/Parke-Davis, Pharmaceutical Research Division, Morris Plains, NJ 07950.

Abstract □ Concentrations of bromophenol blue (I) in plasma, urine, and bile were determined spectrophotometrically after intravenous bolus injections and infusions in rats. The plasma concentrations were found to decrease monoexponentially after all doses except the highest, where the decrease was biexponential. Although the disposition kinetics of I were apparently first-order at all doses, the half-life increased with increasing dose. The area under the plasma concentration–time curve ($AUC_{0-\infty}$) increased disproportionately with increasing dose. The binding of I to rat plasma proteins, as determined by equilibrium dialysis, showed that the fraction bound (96%) remained constant in the concentration range of 10–300 μg/ml. Plasma concentrations were determined at time zero after intravenous administration and after a second dose administered 20 min later when plasma concentrations from the first dose were minimal. The apparent first-order elimination rate constant for the plasma concentration decline following the second dose was significantly less than after the first dose, indicating that the residual dye in the liver altered the elimination of I after the second dose. The fraction of the dose in the liver decreased with increasing dose, indicating a saturable uptake process. The biliary excretion profile reflected the uptake saturation that occurred in the liver and demonstrated that the biliary excretion of I depended on the amount present in the liver. When liver damage was induced by exposure to carbon tetrachloride, dye concentrations in the plasma, liver, and kidney increased markedly.

Keyphrases □ Bromophenol blue—in rat urine, plasma, and bile, dose-dependent pharmacokinetics, biliary excretion □ Pharmacokinetics—bromophenol blue, rat plasma, urine, and bile, biliary excretion □ Biliary excretion—bromophenol blue, rat urine, plasma, and bile, dose-dependent pharmacokinetics

Bromophenol blue (I) is a high molecular weight anionic sulfonephthalein dye (670 g/mole, pK_a 4.0). Several reports (1–3) have shown that I is extensively excreted in the bile and is not metabolized in a variety of species including the rat.

Takada *et al.* (4, 5) conducted studies aimed at characterizing the role of the intracellular protein fractions Y and Z in the uptake and transport of I in rat hepatocytes, and also developed a linear pharmacokinetic model for the biliary excretion of I after intravenous administration in rats (6). The model adequately described a single low-dose plasma and bile profile, but could not describe the observed nonlinearity at higher doses. The overall aim of these authors was to evaluate I as a model organic anionic compound by characterizing the pharmacokinetics at three different doses. Their report did not fully characterize the pharmacokinetics at any dose. Liver concentrations and plasma protein binding were not measured, and the observed nonlinearity was not addressed.

Studies on the pharmacokinetics of drugs excreted in the bile have increased in recent years as investigators have become more interested in the effects of liver disease on drug clearance, the effects of first-pass liver clearance on drug bioavailability, the effects of enterohepatic recirculation on drug disposition, and the nonlinear excretion of drugs (7–11). Usually these studies have not considered the extent of protein binding, liver-to-plasma and bile-to-liver drug concentration ratios, hepatic blood flow, and bile flow. These factors contribute to the interpretation of hepatobiliary elimination. In addition, the interpretation has been complicated by the use of compounds such as sulfobromophthalein that undergo metabolism. Ideally, a model compound used in studying hepatobiliary elimination would not undergo metabolism, nor enterohepatic recirculation, and would not be pharmacologically active.

The organic anion, bromophenol blue (I), possesses these qualities (2, 4). Therefore, the present investigation was undertaken to: (*a*) determine the pharmacokinetic profile

0022-3549/83/1000-1127$01.00/0

of I elimination from plasma after intravenous administration of different doses; (*b*) evaluate the effect of prior administration of I on the plasma decline of a subsequent intravenous administration; (*c*) determine the liver concentration of I after intravenous administration; (*d*) assess the plasma protein binding of I; (*e*) analyze the biliary excretion profile of I after intravenous bolus and infusion administrations; and (*f*) evaluate the utility of I pharmacokinetics in assessing liver damage.

EXPERIMENTAL

Animal Preparation—Fasted male Sprague–Dawley rats (260–470 g) were anesthetized with 50 mg/kg ip of sodium secobarbital followed by cannulation of the left jugular vein and the right carotid artery with polyethylene tubing[1]. Doses of I[2] were administered as a bolus or infusion through the jugular vein catheter. Blood samples were withdrawn from the carotid artery cannula at selected times after administration, collected in heparinized tubes[3], and centrifuged; the plasma was removed and stored frozen at −20° until assayed. The blood collected did not exceed 10% of the total blood volume. Urine was collected as produced and then frozen. All bile was collected in preweighed, screw-cap vials[4] and frozen *until* assayed. Bile collection was at 5-min intervals for 2 hr and then at 15-min intervals for the duration of the experiment. The body temperatures of the rats were maintained at 37 ± 0.5° with a heat lamp and monitored by a rectal thermistor probe[5].

Intravenous Studies—Doses of 5.6, 11.2, 22.4, and 33.6 mg/kg of I dissolved in 0.5 ml of isotonic phosphate buffer (pH 7.4) were administered to four rats per dose as an intravenous bolus through the jugular vein catheter followed by a 0.3-ml saline wash. Blood samples, 0.2–0.4 ml, were withdrawn from the carotid artery cannula at various times after dosing, collected in heparinized tubes, centrifuged, and the plasma removed for assay.

In six other rats, additional surgery exposed the common bile duct through a small midline abdominal incision (2–3 cm) followed by the insertion of a polyethylene[6] cannula for bile collection. Two doses of I, 5.6 and 11.2 mg/kg, were administered to three rats each as an intravenous bolus. Blood, urine, and bile were collected after administration.

In another experiment, three rats were administered an 11.2-mg/kg dose of I as an intravenous bolus through the jugular cannula followed by the administration of a second 11.2-mg/kg dose 20 min later. Blood samples, 0.2 ml, were withdrawn from the carotid artery at selected intervals after each administration of I.

Infusion Studies—Twenty-four rats were prepared for drug administration and blood withdrawal as described above. Twelve rats received an 11.2-mg/kg dose of I and twelve rats received a 22.4-mg/kg dose of I. At selected times after the dye administration, 4.0–6.0 ml of blood was drawn from the inferior vena cava followed by excision of the liver. The liver was rinsed in normal saline, dried, weighed, and stored frozen at −20° until assayed. A 2-ml plasma sample was subjected to equilibrium dialysis as described below, and the remainder of the sample was frozen until assayed.

Four additional rats were prepared for blood, urine, and bile collection as outlined. Bromophenol blue was infused through a jugular cannula with an infusion pump at rates of 3.0, 6.0, 10.0, and 24.0 mg/hr for 2 hr. The time to reach steady state was approximated at 1–1.5 hr using data from the intravenous studies. The approximation was based on linear pharmacokinetics, so an additional 0.5 hr of infusion time was allotted as an adjustment for the observed nonlinearity bringing the total time of infusion to 2 hr. Blood, urine, and bile were collected during and after the infusion of I.

Liver Dysfunction Studies—Undiluted carbon tetrachloride was given by intubation at a dose of 2.5 ml/kg, followed by the immediate infusion of I, to three rats which had been fasted for 24 hr. Three additional rats were used as a control. The rats were then allowed food and water *ad libitum* for the next 24 hr. At this time the rats were anesthetized with ether and blood (4–6 ml) was drawn from the inferior vena cava; both the liver and kidneys were quickly excised, rinsed in normal saline, blotted dry, and weighed. The rate of bile production was used as an index of liver dysfunction.

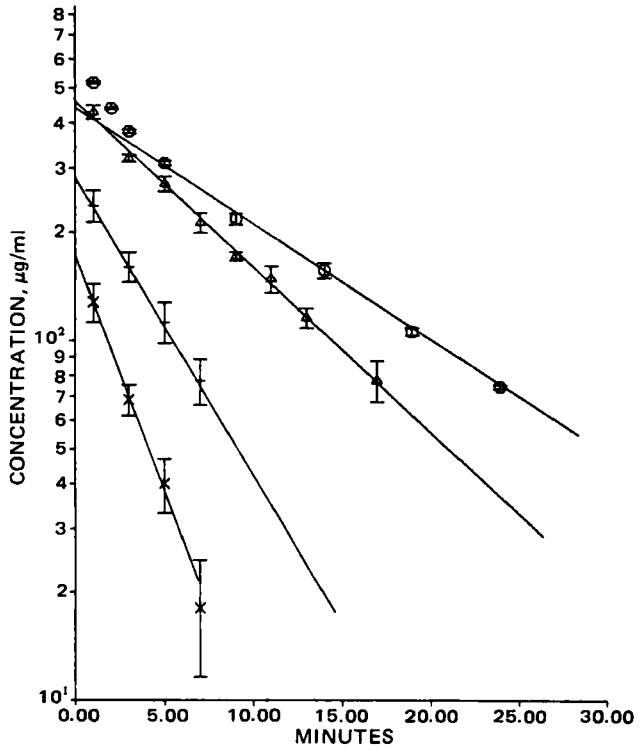

Figure 1—*Semilogarithmic plot of mean ± SD (bars) plasma levels of I as a function of time after intravenous bolus administration of 5.6 mg/kg (×); 11.2 mg/kg (+); 22.4 mg/kg (△); and 33.6 mg/kg (○).*

Protein Binding—The binding of I to plasma proteins was determined by equilibrium dialysis. Dialysis tubing, average pore diameter 24 Å, was prepared by boiling twice for 20 min in distilled water. Fresh rat plasma, 2 ml, was placed in the dialysis bag and allowed to equilibrate with I in isotonic phosphate buffer (pH 7.4) for 24 hr at 37°.

Assays—Plasma or urine (25–200 μl) was diluted with 1–2 ml of phosphate buffer (pH 8), and the absorbance was measured at 595 nm with a microsample spectrophotometer[7]. Bile was diluted with 2–10 ml of phosphate buffer (pH 8.0) and measured with a double-beam spectrophotometer[8]. The specific gravity of bile was determined by weighing known volumes of bile. Standard curves were prepared daily from rat plasma, urine, or bile spiked with appropriate concentrations of I. The amount of I in the liver and kidneys was measured after each organ was homogenized with twice its weight of isotonic phosphate buffer (pH 7.4) in an homogenizer[9]. Six milliliters of acetone was added to 5 ml of homogenate, mixed, and shaken for 15 min in a mechanical shaker[10]. The final mixture was centrifuged for 20 min at 2500 rpm. The supernatant was collected, centrifuged again, diluted with phosphate buffer (pH 8), and then measured at 595 nm with a spectrophotometer[7].

Standard curves were prepared on each day of analysis by adding known amounts of I to rat liver or kidney cytoplasm diluted in phosphate buffer (pH 8.0). The standard curves were linear ($r = 0.9998$) from 1 to 12 μg/ml with assay sensitivity limits in plasma, urine, bile, and tissue of 0.6, 0.6, 0.8, and 0.6 μg/ml, respectively.

RESULTS

Intravenous Studies—A semilogarithmic plot of the mean plasma concentration–time curves after intravenous bolus injections of 5.6, 11.2, 22.4, and 33.6 mg/kg of I is shown in Fig. 1. The elimination of I from plasma appeared to be monoexponential in the dose range of 5.6–22.4 mg/kg. The data for these doses were fit by NONLIN (12) to the equation:

$$C_p = \frac{D}{V}\exp(-\beta t) \qquad \text{(Eq. 1)}$$

[1] PE-50; Clay-Adams, Parsippany, N.J.
[2] Allied Chemical Co., New York, N.Y.
[3] Vacutainer; Becton, Dickinson & Co., Rutherford, N.J.
[4] Kimble, Toledo, Ohio.
[5] Yellow Springs Instruments, Yellow Springs, Ohio.
[6] PE-10; Clay-Adams, Parsippany, N.J.
[7] Gilford Instruments Laboratories Inc., Oberlin, Ohio.
[8] Coleman Model 124, Perkin-Elmer Corp., Marywood, Il.
[9] Polytron; Brinkmann Instruments, Westbury, N.Y.
[10] Precision Instruments, Chicago, Ill.

Table I—Mean (±*SD*) Pharmacokinetic Parameters After Intravenous Bolus Administration of I in Rats

Dose, mg/kg	$t_{1/2}$[a], min	V[b], ml/kg	$AUC_{0-\infty}$[c], μg min/ml	CL_p[d], ml/min	β[e], min^{-1}
5.6[f]	2.28	32.7 ± 2.5	574 ± 107	3.68 ± 0.88	0.304 ± 0.030
11.2[g]	3.66	40.1 ± 4.8	1489 ± 191	2.77 ± 0.35	0.190 ± 0.008
22.4[f]	6.54	49.0 ± 3.5	4349 ± 231	2.21 ± 0.45	0.106 ± 0.013
33.6[f]	9.43	78.2 ± 6.1	6275 ± 43	1.43 ± 0.01	0.073 ± 0.004

[a] Harmonic mean. [b] Volume of distribution per kg of body weight. [c] Area under the plasma concentration–time curve (time zero to infinity). [d] CL_p = dose/$AUC_{0-\infty}$. [e] Apparent elimination rate constant. [f] n = 3. [g] n = 4.

where C_p is the plasma concentration at time t, D is the dose, V is the apparent volume of distribution, and β is the apparent first-order disposition rate constant. The plasma concentration–time curve for the 33.6-mg/kg dose of I appeared to be biexponential and β was determined from the terminal log-linear segment.

The plasma clearance of I was calculated for each dose by:

$$CL_p = D/AUC_{0-\infty} \quad \text{(Eq. 2)}$$

Where CL_p is the plasma clearance and $AUC_{0-\infty}$ is the area under the plasma concentration–time curve from zero to infinity. The trapezoidal rule was used to calculate the AUC from time zero to the time of the last measurable concentration–time point and a β correction was then added to the trapezoidal AUC to approximate the $AUC_{0-\infty}$. The volume of distribution per kilogram of body weight was determined from:

$$V = CL_p/\beta \cdot W \quad \text{(Eq. 3)}$$

where CL_p and β are as defined previously and W is the weight of the rat in kilograms. The results of these calculations are shown in Table I. The elimination rate constant (β), the plasma clearance (CL_p), and the volume of distribution (V) were not constant over the range of doses administered. The $AUC_{0-\infty}$ deviated positively from a linear relationship (Fig. 2) when plotted against the dose.

Plasma concentrations of I were determined following two intravenous injections of 11.2 mg/kg separated by 20 min. At 20 min after the first dose, most of the dye was eliminated from the plasma (Fig. 3). The apparent elimination rate constant following the first dose was 0.176 ± 0.011 min^{-1} (n = 3). The plasma concentrations of I following the second dose deviated from the predicted values and declined monoexponentially. The apparent elimination rate constant following the second dose was 0.134 ± 0.018 min^{-1}, which was significantly different from the first dose using the paired-value t test ($p < 0.01$). The line in Fig. 3 is the theoretical line based on linear kinetics using the parameters derived from the first dose.

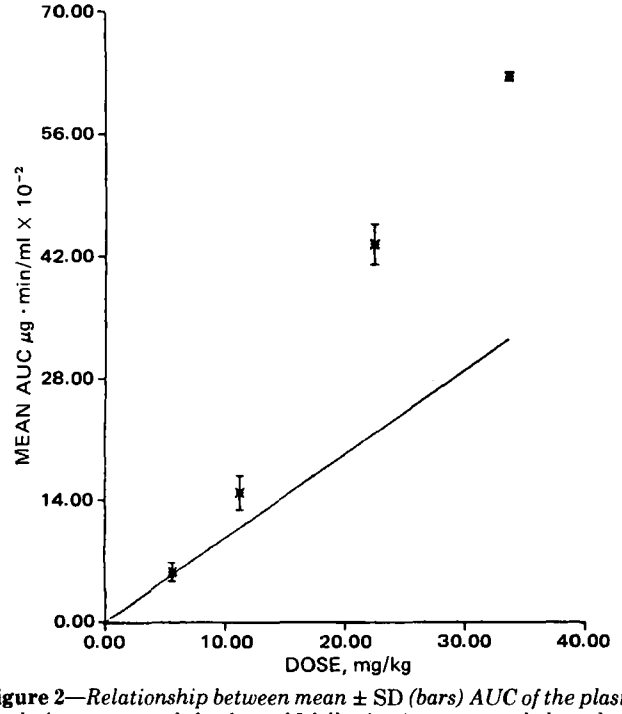

Figure 2—*Relationship between mean ± SD (bars) AUC of the plasma level–time curve and the dose of I following intravenous bolus administration in rats with cannulated bile ducts. The solid line represents the relationship that would be expected if linear kinetics were operable.*

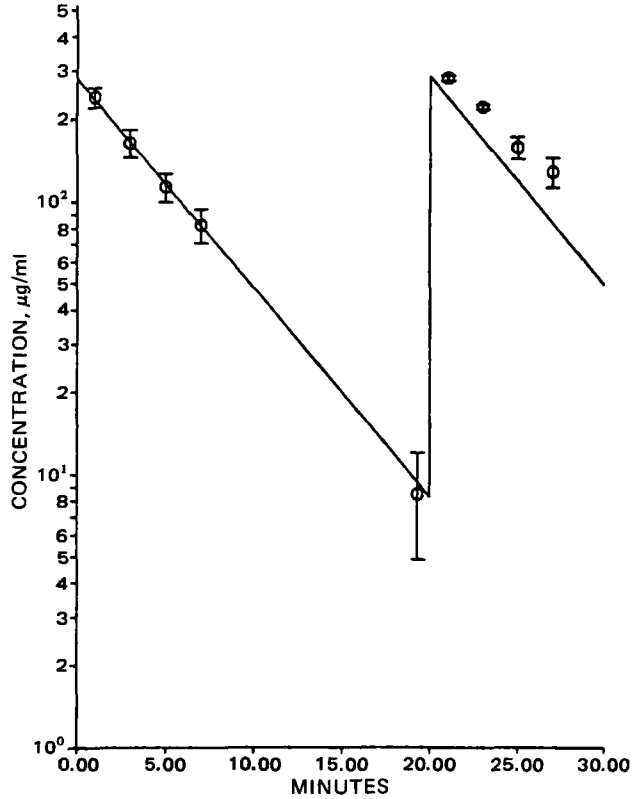

Figure 3—*Semilogarithmic plot of mean ± SD (bars) plasma levels (n = 3) of I after intravenous bolus administration of 11.2 mg/kg at t = 0 and a second dose at t = 20 min. The line is the theoretical line based on the elimination rate constant for the first dose and assuming linear kinetics.*

The fraction of the dose in the plasma and liver at selected times after the administration of 5.6- and 11.2-mg/kg doses of I are shown in Fig. 4. The fraction of the dose in the liver was lower after the 22.4-mg/kg dose than after the 11.2-mg/kg dose for times >3 min. The concentration of I in the liver did not reach equilibrium with the concentration in the plasma until 30 min after drug administration (Fig. 4).

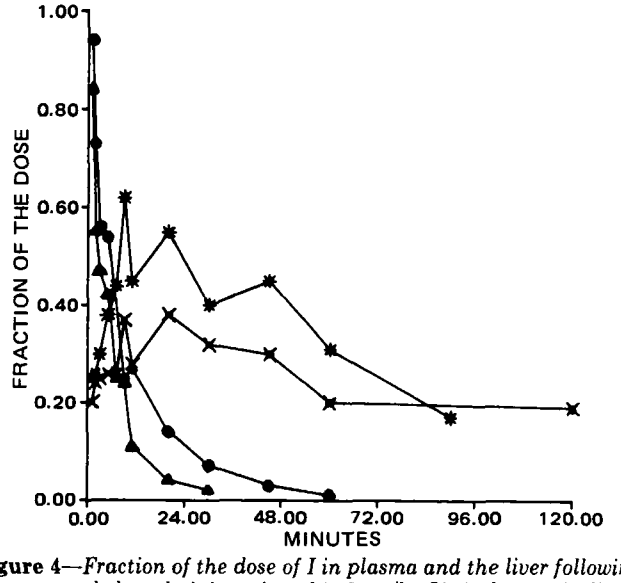

Figure 4—*Fraction of the dose of I in plasma and the liver following intravenous bolus administration of 11.2 mg/kg [(▲) plasma, (*) liver] and 22.4 mg/kg [(●) plasma, (■) liver]. Each set of plasma and liver points that correspond in time are from one rat.*

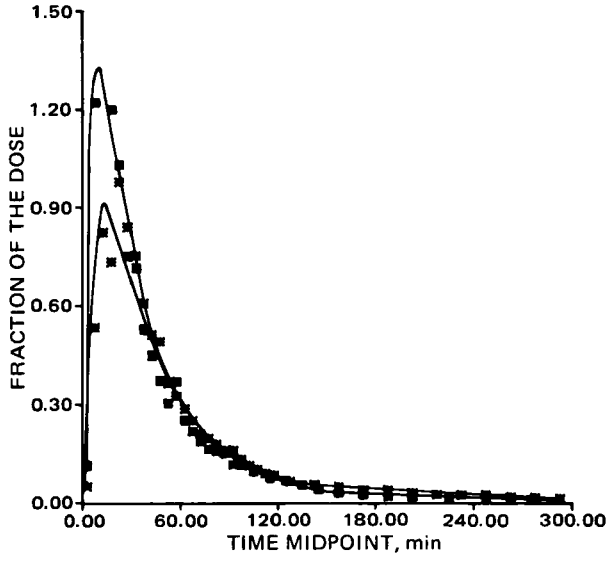

Figure 5—*Mean fraction (n = 3) of 5.6-mg/kg (■) and 11.2-mg/kg (*) doses expressed as the percent of the dose of I excreted per hour in bile after intravenous bolus administration. The solid lines were simulated and serve as definition of the data points.*

The total mean fraction of the dose excreted following a 5.6-mg/kg dose (0.93) was greater than the total mean fraction of the dose excreted following an 11.2-mg/kg dose (0.86). The mean rate of excretion (mean fraction per hour) of I in the bile following 5.6- and 11.2-mg/kg doses are shown in Fig. 5. The mean fractional rate of excretion of I in the bile was greater after the 5.6-mg/kg dose than after the 11.2-mg/kg dose at ≤25 min. When body temperature was not controlled, a reduction in the cumulative fraction of the dose excreted in the bile (0.76) following an 11.2-mg/kg dose was observed. The cumulative amount of I collected in the urine accounted for 2.5% of the dose, and the amount excreted was not dose related.

Infusion Studies—The amounts of I excreted per hour in bile during intravenous infusion at rates of 3.0, 6.0, 10.0, and 24.0 mg/hr are shown in Fig. 6. Saturation of the excretion of I in bile occurred with the 10.0- and 24.0-mg/hr rates. The maximum excretion rate was 8.5 mg/hr. Again, the amount of I excreted in the urine was small in proportion to the dose administered and was not dose related.

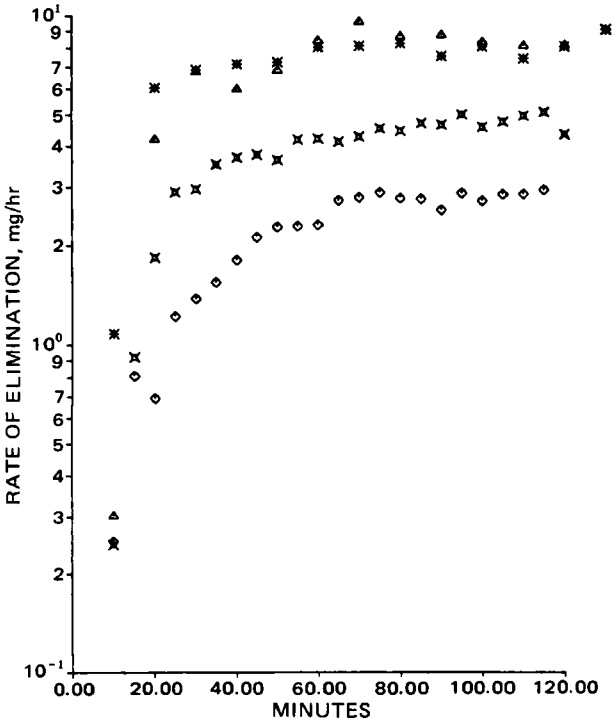

Figure 6—*Amount of I excreted per hour in bile during constant intravenous infusion at the rates of 3.0 mg/hr (◇), 6.0 mg/hr (✕), 10.0 mg/hr (△), and 24.0 mg/hr (*). The concentration of I in the infusion solution was adjusted so that the volume infused was the same for all infusion rates.*

Table II—Tissue Concentration, Concentration Ratios, and Bile Production of I During Constant Intravenous Infusion in Control and Carbon Tetrachloride-Treated Rats [a]

Tissue	Drug Concentration[b] Control	Drug Concentration[b] Treated[c]	*t* Test
Plasma (μg/ml)	62 ± 15	240 ± 9	$p < 0.05$
Liver (μg/g)	89 ± 38	119 ± 25	$p < 0.05$
Bile (μg/ml)	2567 ± 402	1652 ± 613	$p < 0.05$
Kidney (μg/g)	58 ● 8	203 ± 12	$p < 0.05$
Concentration Ratios			
Liver/Plasma	1.3 ± 0.1	0.5 ± 0.1	$p < 0.05$
Bile/Liver	33 ± 10	14 ± 2.2	$p < 0.05$
Kidney/Plasma	1.3 ± 0.8	0.8 ± 0.1	n.s.
Mean bile production rate[d], μl/min·kg	78 ± 1	22 ± 1	$p < 0.05$

[a] Mean ± *SD*; $n = 3$. [b] At 3 hr during a 5.7-mg/hr infusion; normalized to a 300-g rat. [c] Carbon tetrachloride dose of 2.5 ml/kg po. [d] During a 16-mg/hr·kg infusion.

Liver Dysfunction Studies—The results of the carbon tetrachloride treatment are presented in Table II. The carbon tetrachloride treatment reduced the rate of bile production to one-third that of the control group. Liver-to-plasma and bile-to-liver ratios of I decreased by 60% in the treated rats. It is interesting to note the kidney concentrations increased by 200% in the treated rats.

Protein Binding—The plasma protein binding of I was determined by equilibrium dialysis of pooled rat plasma against I in isotonic phosphate buffer. The percentage of I bound to plasma proteins was 96.0 ± 0.5% at 37° and was constant over the range of 10–300 μg/ml.

DISCUSSION

The clearance of I from plasma is not a linear process in the dose range investigated. Changes in the binding of I to plasma proteins did not explain these observations since the binding was constant. Referring to Fig. 1, the plasma profiles appear to be first order. Perrier *et al.* (13) presented theoretical curves which are very similar in nature to the curves in Fig. 1. However, the theoretical curves are the result of either Michaelis–Menten kinetics, substrate inhibition, or product inhibition. Any suggestions regarding applicability of I disposition to biotransformation kinetics are inappropriate since I is not metabolized, but adaptation to a Michaelis–Menten type saturable binding equation may be appropriate for successful modeling.

Recently, Stoeckel *et al.* (11) developed a compartmental model to describe the plasma profile of indocyanine green in rabbits. The model incorporated Michaelis–Menten transfer from the central compartment to the peripheral compartment. However, these authors failed to fit indocyanine green data from rats and cited experimental difficulties as an explanation. It is likely that the indocyanine green data from the rat do not conform to Michaelis–Menten kinetics. In fact, the actual plasma profile of indocyanine green in rats (Fig. 6 in Ref. 11) appears to be biexponential and first order. It is conceivable that a combination of fast distribution and dose-dependent saturation described herein may result in the nonlinear and apparent first-order profiles observed by Stoeckel *et al.* (11), since indocyanine green is in the same chemical class as I and it is not metabolized nor enterohepatically recycled (14).

The consecutive dose administration study showed that the plasma profile after the second injection differed significantly from the plasma profile after the first injection, even though the plasma concentrations after the first injection were approaching zero prior to the second injection (Fig. 3). The difference in the plasma profiles following repeated intravenous injections of I indicated that the nonlinearity depends not only on the dose of I but also on the residual amount of I in the liver and a rapid distribution from plasma. Smith *et al.* (3) reported a dye concentration in the liver of rats 20 times the plasma concentration at 5 min after dosing, confirming a rapid distribution from plasma. Thus, the nonlinear plasma elimination of I is related to either differences in liver uptake with increasing dose or differences in biliary secretion with increasing dose.

Takada *et al.* (4) had previously shown that the liver-to-plasma concentration ratio of I decreased as the dose was increased from 11.2 to 66.7

mg/kg in rats, indicating that saturation occurred and caused a decrease in the distribution from plasma. There was no change in the bile-to-liver concentration ratio over the same dose range, suggesting that nonlinear plasma elimination was due to saturable liver uptake only.

The data from the liver studies support the data of Takada (4) because a partial saturation of the transfer process (uptake) from the plasma to the liver occurred at the higher dose (Fig. 4). It has been previously hypothesized that the saturability of the uptake process is due to the limited binding capacity on the hepatic intracellular macromolecules (Y and Z), which have been shown to be instrumental in the hepatobiliary transport of I (4, 5). Nagashima *et al.* (15) suggested that saturable tissue binding can be responsible for the type of nonlinearity observed with this data. If the macromolecular binding sites for I become saturated at higher doses, the fraction of free drug in the liver should increase. Classically, only free drug can transfer across membranes. Therefore, I could then transfer back into plasma resulting in an increase in the apparent elimination (β-phase) half-life. The same result would occur if a very tight binding site for I was saturated and more dye was bound to a protein for which it normally has less affinity. The data from this study and from previous studies (3–6) support the hypothesis that the plasma nonlinearity is due to the saturation of the hepatic protein binding sites for I.

The saturation of the liver at higher doses of I was reflected in the bile as well (Fig. 5). Takada *et al.* (4) reported that the excretion of I in bile was not saturable over the dose range of 11.2–66.7 mg/kg because the bile-to-liver concentration ratio remained unchanged. Therefore, the observed differences in the cumulative amount excreted and in the excretion rate of I in the bile after 5.6- and 11.2-mg/kg doses must be a direct result of the saturation of the uptake process in the liver (Fig. 5). The same result occurred with the infusion data; *i.e.*, the amount of I excreted per hour in the bile plateaued at 8.5 mg/hr at the two highest infusion rates, indicating a dependence on the amount of I present in the liver (Fig. 6). Overall, the excretion of I in bile was linear.

When liver injury was induced by carbon tetrachloride administration, a significant reduction in the rate of excretion of I in bile occurred (Table II). The excretion of I in bile in carbon tetrachloride-treated rats decreased to the extent that it is doubtful that a linear model would apply. The extent of parameter changes that would be calculated from the data may be a reflection of both the liver damage produced by the carbon tetrachloride treatment and the nonlinear behavior of I.

In summary, the disposition of I in the rat was characterized. The apparent first-order elimination kinetics of I in plasma were nonlinear because the liver uptake process was saturable. This was evident from the increase in elimination half-life and disproportionate increase in area under the plasma concentration–time curve with increase in dose. The nature of the saturation was not determined in this study, but it does appear that it is not a Michaelis–Menten effect because I is neither metabolized (2) nor does it demonstrate the appropriate plasma concentration–time profiles with ascending doses (*i.e.*, parallel slopes at concentrations below K_m). It is also not a facilitated transport effect because metabolic inhibitors do not influence the uptake of I by liver cells (4). The amount of I excreted in bile was dependent on the amount present in the liver reflecting the uptake saturability.

These findings could be applied to other nonmetabolizing organic anions and, with adaptations, to compounds that are metabolized. Further work regarding the nature of the saturation and regarding the disposition in higher animals is suggested in order to completely evaluate the use of I as a general index for hepatobiliary function.

REFERENCES

(1) P. C. Hirom, P. Millburn, R. L. Smith, and R. T. Williams, *Biochem. J.*, **129**, 1071 (1972).

(2) T. H. Kim and S. K. Hong, *Am. J. Physiol.*, **202**, 174 (1962).

(3) R. B. Smith, L. McWhorter, and J. W. Triplett, *Int. J. Nucl. Med. Biol.*, **7**, 37 (1980).

(4) K. Takada, Y. Mizobuchi, and S. Muranishi, *Chem. Pharm. Bull.*, **22**, 922 (1974).

(5) K. Takada, M. Ueda, M. Ohno, and S. Muranishi, *Chem. Pharm. Bull.*, **22**, 1477 (1974).

(6) K. Takada, S. Muranishi, and H. Sezaki, *J. Pharmacokinet. Biopharm.*, **2**, 495 (1974).

(7) S. K. Lin, A. A. Moss, R. Motson, and S. Riegelman, *J. Pharm. Sci.*, **67**, 930 (1978).

(8) P. Chelvan, J. M. T. Hamilton-Miller, and J. N. Brumfit, *Br. J. Clin. Pharmacol.*, **8**, 233 (1979).

(9) W. A. Colburn, P. C. Hirom, R. J. Parker, and P. Millburn, *Drug Metab. Dispos.*, **1**, 100 (1979).

(10) R. A. Zito and P. R. Reid, *J. Clin. Pharmacol.*, **21**, 100 (1981).

(11) K. Stoeckel, P. J. McNamara, A. J. McLean, P. duSouich, D. Lalka, and M. Gibaldi, *J. Pharmacokinet. Biopharm.*, **8**, 483 (1980).

(12) C. M. Metzler, G. L. Elfring, and A. J. McEwen, "A Users Manual for NONLIN and Associated Programs," The Upjohn Co., Kalamazoo, Mich., 1974.

(13) D. Perrier, J. I. Ashley, and G. Levy, *J. Pharmacokinet. Biopharm.*, **1**, 231 (1973).

(14) F. Barbier and G. A. DeWeerdt, *Clin Chim. Acta*, **10**, 549 (1964).

(15) R. Nagashima, G. Levy, and E. J. Sarcione, *J. Pharm. Sci.*, **57**, 1881 (1968).

ACKNOWLEDGMENTS

The authors thank Mrs. Judy Webster for typing this manuscript.

Picrotoxin-Like Lactones

JAMES D. McCHESNEY *x and ALAN F. WYCPALEK

Received April 26, 1982, from the *Department of Medicinal Chemistry, School of Pharmacy, The University of Kansas, Lawrence, KS 66045.* Accepted for publication July 23, 1982.

*Present address: Department of Pharmacognosy, School of Pharmacy, University of Mississippi, University, MS 38677.

Abstract □ Preparation of some simple lactone analogues of picrotoxin and their biological evaluation is reported. Certain analogues possessed activity, but at potencies insufficient to warrant further work.

Keyphrases □ Picrotoxin—lactone analogue synthesis, CNS activity □ Analogues—of picrotoxin, synthesis, CNS activity □ CNS activity—of picrotoxin lactone analogues, synthesis

Although picrotoxin [an equimolar mixture of picrotin (I) and picrotoxinin (II)] was used as early as the 18th century as a fish toxin and clinically in humans during the 1930s and 1940s, only in the last decade has an understanding of its mode of action as a CNS stimulant begun to emerge. It was first recognized as a γ-aminobutyric acid antagonist (1), but more recently its mechanism of antagonism has been shown to be inhibition of chloride ion permeability in neuronal preparations (2). Jarboe and coworkers (3) have examined aspects of the structure–activity relationship (SAR) of these materials and concluded that in order to possess activity, certain features were required: (*a*) a free bridgehead hydroxyl group, (*b*) a lactone ring connecting carbons 3 and 5, and (*c*) an isopropenyl group (which appears to govern potency).

0022-3549/83/1000-1131$01.00/0

mg/kg in rats, indicating that saturation occurred and caused a decrease in the distribution from plasma. There was no change in the bile-to-liver concentration ratio over the same dose range, suggesting that nonlinear plasma elimination was due to saturable liver uptake only.

The data from the liver studies support the data of Takada (4) because a partial saturation of the transfer process (uptake) from the plasma to the liver occurred at the higher dose (Fig. 4). It has been previously hypothesized that the saturability of the uptake process is due to the limited binding capacity on the hepatic intracellular macromolecules (Y and Z), which have been shown to be instrumental in the hepatobiliary transport of I (4, 5). Nagashima *et al.* (15) suggested that saturable tissue binding can be responsible for the type of nonlinearity observed with this data. If the macromolecular binding sites for I become saturated at higher doses, the fraction of free drug in the liver should increase. Classically, only free drug can transfer across membranes. Therefore, I could then transfer back into plasma resulting in an increase in the apparent elimination (β-phase) half-life. The same result would occur if a very tight binding site for I was saturated and more dye was bound to a protein for which it normally has less affinity. The data from this study and from previous studies (3–6) support the hypothesis that the plasma nonlinearity is due to the saturation of the hepatic protein binding sites for I.

The saturation of the liver at higher doses of I was reflected in the bile as well (Fig. 5). Takada *et al.* (4) reported that the excretion of I in bile was not saturable over the dose range of 11.2–66.7 mg/kg because the bile-to-liver concentration ratio remained unchanged. Therefore, the observed differences in the cumulative amount excreted and in the excretion rate of I in the bile after 5.6- and 11.2-mg/kg doses must be a direct result of the saturation of the uptake process in the liver (Fig. 5). The same result occurred with the infusion data; *i.e.*, the amount of I excreted per hour in the bile plateaued at 8.5 mg/hr at the two highest infusion rates, indicating a dependence on the amount of I present in the liver (Fig. 6). Overall, the excretion of I in bile was linear.

When liver injury was induced by carbon tetrachloride administration, a significant reduction in the rate of excretion of I in bile occurred (Table II). The excretion of I in bile in carbon tetrachloride-treated rats decreased to the extent that it is doubtful that a linear model would apply. The extent of parameter changes that would be calculated from the data may be a reflection of both the liver damage produced by the carbon tetrachloride treatment and the nonlinear behavior of I.

In summary, the disposition of I in the rat was characterized. The apparent first-order elimination kinetics of I in plasma were nonlinear because the liver uptake process was saturable. This was evident from the increase in elimination half-life and disproportionate increase in area under the plasma concentration–time curve with increase in dose. The nature of the saturation was not determined in this study, but it does appear that it is not a Michaelis–Menten effect because I is neither metabolized (2) nor does it demonstrate the appropriate plasma concentration–time profiles with ascending doses (*i.e.*, parallel slopes at concentrations below K_m). It is also not a facilitated transport effect because metabolic inhibitors do not influence the uptake of I by liver cells (4). The amount of I excreted in bile was dependent on the amount present in the liver reflecting the uptake saturability.

These findings could be applied to other nonmetabolizing organic anions and, with adaptations, to compounds that are metabolized. Further work regarding the nature of the saturation and regarding the disposition in higher animals is suggested in order to completely evaluate the use of I as a general index for hepatobiliary function.

REFERENCES

(1) P. C. Hirom, P. Millburn, R. L. Smith, and R. T. Williams, *Biochem. J.*, **129**, 1071 (1972).

(2) T. H. Kim and S. K. Hong, *Am. J. Physiol.*, **202**, 174 (1962).

(3) R. B. Smith, L. McWhorter, and J. W. Triplett, *Int. J. Nucl. Med. Biol.*, **7**, 37 (1980).

(4) K. Takada, Y. Mizobuchi, and S. Muranishi, *Chem. Pharm. Bull.*, **22**, 922 (1974).

(5) K. Takada, M. Ueda, M. Ohno, and S. Muranishi, *Chem. Pharm. Bull.*, **22**, 1477 (1974).

(6) K. Takada, S. Muranishi, and H. Sezaki, *J. Pharmacokinet. Biopharm.*, **2**, 495 (1974).

(7) S. K. Lin, A. A. Moss, R. Motson, and S. Riegelman, *J. Pharm. Sci.*, **67**, 930 (1978).

(8) P. Chelvan, J. M. T. Hamilton-Miller, and J. N. Brumfit, *Br. J. Clin. Pharmacol.*, **8**, 233 (1979).

(9) W. A. Colburn, P. C. Hirom, R. J. Parker, and P. Millburn, *Drug Metab. Dispos.*, **1**, 100 (1979).

(10) R. A. Zito and P. R. Reid, *J. Clin. Pharmacol.*, **21**, 100 (1981).

(11) K. Stoeckel, P. J. McNamara, A. J. McLean, P. duSouich, D. Lalka, and M. Gibaldi, *J. Pharmacokinet. Biopharm.*, **8**, 483 (1980).

(12) C. M. Metzler, G. L. Elfring, and A. J. McEwen, "A Users Manual for NONLIN and Associated Programs," The Upjohn Co., Kalamazoo, Mich., 1974.

(13) D. Perrier, J. I. Ashley, and G. Levy, *J. Pharmacokinet. Biopharm.*, **1**, 231 (1973).

(14) F. Barbier and G. A. DeWeerdt, *Clin Chim. Acta*, **10**, 549 (1964).

(15) R. Nagashima, G. Levy, and E. J. Sarcione, *J. Pharm. Sci.*, **57**, 1881 (1968).

ACKNOWLEDGMENTS

The authors thank Mrs. Judy Webster for typing this manuscript.

Picrotoxin-Like Lactones

JAMES D. McCHESNEY *x and ALAN F. WYCPALEK

Received April 26, 1982, from the *Department of Medicinal Chemistry, School of Pharmacy, The University of Kansas, Lawrence, KS 66045.* Accepted for publication July 23, 1982.

*Present address: Department of Pharmacognosy, School of Pharmacy, University of Mississippi, University, MS 38677.

Abstract □ Preparation of some simple lactone analogues of picrotoxin and their biological evaluation is reported. Certain analogues possessed activity, but at potencies insufficient to warrant further work.

Keyphrases □ Picrotoxin—lactone analogue synthesis, CNS activity □ Analogues—of picrotoxin, synthesis, CNS activity □ CNS activity—of picrotoxin lactone analogues, synthesis

Although picrotoxin [an equimolar mixture of picrotin (I) and picrotoxinin (II)] was used as early as the 18th century as a fish toxin and clinically in humans during the 1930s and 1940s, only in the last decade has an understanding of its mode of action as a CNS stimulant begun to emerge. It was first recognized as a γ-aminobutyric acid antagonist (1), but more recently its mechanism of antagonism has been shown to be inhibition of chloride ion permeability in neuronal preparations (2). Jarboe and coworkers (3) have examined aspects of the structure–activity relationship (SAR) of these materials and concluded that in order to possess activity, certain features were required: (*a*) a free bridgehead hydroxyl group, (*b*) a lactone ring connecting carbons 3 and 5, and (*c*) an isopropenyl group (which appears to govern potency).

0022-3549/83/1000-1131$01.00/0

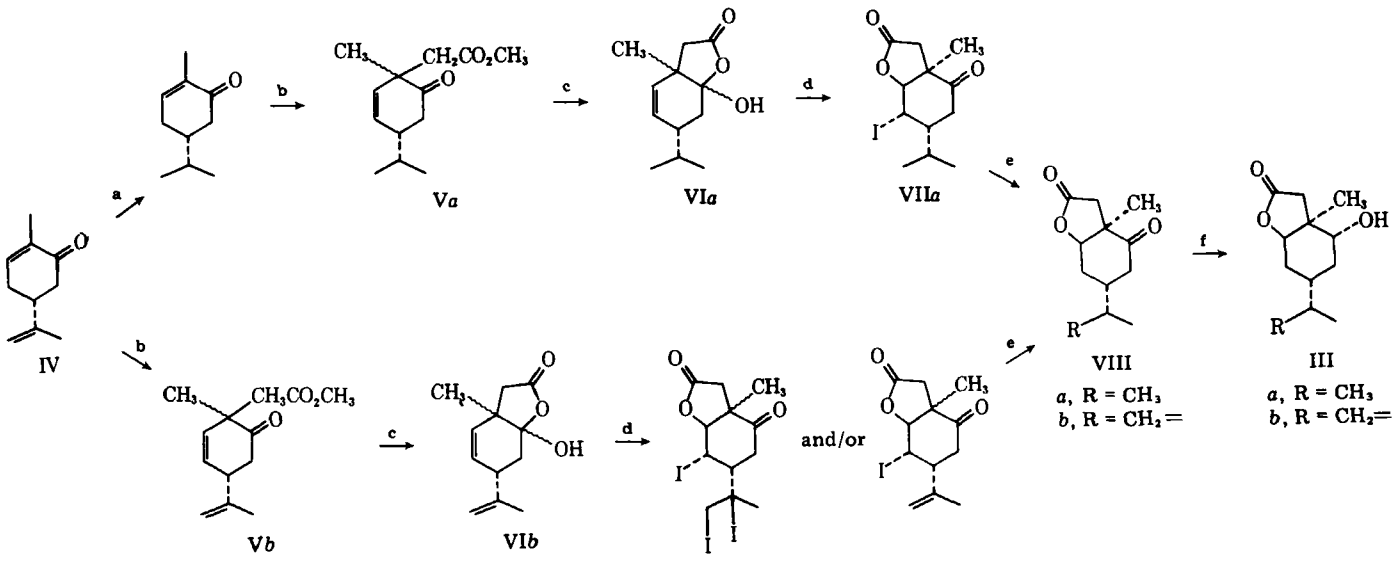

Scheme I—Synthesis of lactones III. Key: (a) *tris*-triphenylphosphine rhodium chloride–hydrogen; (b) potassium-*tert*-amylate–methyl bromoacetate; (c) potassium hydroxide; (d) iodine–potassium iodide, sodium bicarbonate; (e) triphenyltin hydride; (f) sodium borohydride.

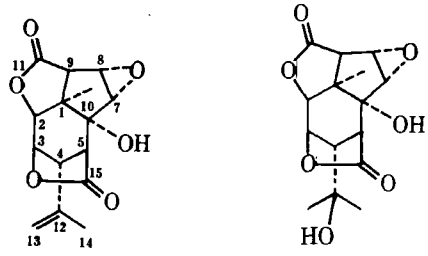

I II

To ascertain if a simpler agent might possess picrotoxin-like activity, *i.e.*, if the lactone ring connecting carbons 3 and 5 is essential while the lactone connecting carbons 2 and 11 plays no role (as previously suggested), we set about to prepare analogous lactones (III) and determine if they showed CNS stimulatory activity similar to picrotoxin in rodents.

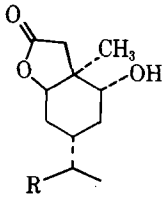

III

a R = CH_3
b R = CH_2=

RESULTS AND DISCUSSION

The most convenient preparation of the target compounds with asymmetric centers of the same configuration as picrotoxin seemed to reside in choosing a starting material with at least some of these centers already established. Then one may rely on the particular features of the molecule, such as steric factors and conformation, to control the course of reactions which would be, thereby, regio- and stereoselective. With these factors in mind, it can be seen that the most suitable starting material is the known natural product (−)-carvone (IV).

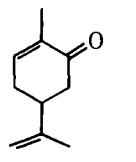

IV

The desired lactones (III) should be available from carvone *via* introduction of a suitable two-carbon side chain α to the ketone, lactonization, and subsequent reduction of the ketone function. A convenient approach for the introduction of the two-carbon side chain was expected to be the alkylation of the enolate generated by base abstraction of a γ proton of an α,β-unsaturated ketone. There is ample precedent for this expected alkylation in polycyclic systems (4). However, Theobald (5) reported dimerization of carvone under the projected reaction conditions. Initial attempts in our laboratory at direct base-catalyzed alkylation of carvone afforded only over-alkylated products. Finally, careful investigation of the effects of the nature of the alkoxide anion, metal cation, solvent, and temperature conditions[1] of the base-catalyzed alkylation afforded a convenient direct procedure. It was found that alkylation of carvone with potassium *tert*-amylate–methyl bromoacetate in a mixture of dimethoxyethane and dimethylformamide afforded acceptable yields of the desired product, methyl-2-[1(*R*,*S*)-methyl-2-oxo-4(*S*)-isopropenyl-5-cyclohexenyl]acetate (V*b*). Alternatively, prior reduction of the isopropenyl group of carvone followed by alkylation under the same conditions afforded V*a*. The keto esters were then hydrolyzed in base producing lactols VI, which were lactonized under iodolactonization conditions to a mixture of iodo lactones VII. Iodo lactone VII*b* was not characterized fully because it darkened rapidly on isolation, apparently due to the presence of triiodo lactone formed by iodination of the isopropenyl group during the lactonization sequence. The iodo lactones were deiodinated by reduction with triphenyltin hydride and the resultant keto lactones VIII were reduced to the hydroxy lactones III with sodium borohydride (Scheme I).

The structural assignments were based on the following:

1. The sequence was initiated with a starting material of known absolute configuration. Selective reduction of the isopropenyl group should not modify any centers of stereochemistry.
2. The base-catalyzed alkylation would be expected to produce a mixture with β-alkylation (*trans* to the isopropyl and isopropenyl group) predominating (6).
3. Hydrolysis of the acetate ester mixture and iodolactonization produced a mixture (3:1 ratio) of γ-lactones, showing carbonyl absorption at 1780 cm^{-1} in the IR spectrum.
4. The major iodo lactone isomer was assigned structure VII based on its carbonyl absorption and by an examination of the coupling pattern of the methine hydrogen α to the lactone ether linkage, showing one proton doublet, δ 5.1 ppm (J = 4 Hz). This proton is clearly diequatorially coupled to the adjacent methine α to the iodine function. This is consistent with the usual transdiaxial iodolactonization mechanism.

[1] H. N. Edwards; unpublished work.

5. Deiodination does not alter stereochemistry at any centers, so structure VIII represents the keto lactones.

6. Sodium borohydride reductions of cyclohexanones proceed with introduction of hydrogen from the less hindered face, in this case from the β face, to produce hydroxy lactones III.

Biological evaluation was made with a screening procedure which attempts to selectively utilize available techniques to identify major types of central nervous system (CNS) activity. It is not definitive, but rather a qualitative evaluation. Generally, it is a comparison of activity between an unknown and a control vehicle. The detection screen employs direct visual observation of behavior plus measures of simple reflex activities. In this particular case attention was given to muscle tonus. The animals were placed in an observation arena, which is a large metal tray lined with bedding[2]. The animals were provoked to walk and were gently handled to judge body tonus. Compounds III*a*, III*b*, VIII*a*, and VIII*b* were evaluated at doses of 1, 10, 100 (and higher, if quantities permitted) mg/kg in female Wistar rats. Compound III*a* produced no effect at doses of ≤200 mg/kg (the highest dose tested). Compound III*b* produced no effect at doses of ≤100 mg/kg, but caused death within 24 hr at 150 mg/kg, the highest dose evaluated. It is unknown if picrotoxin-like convulsions were produced. At doses of <100 mg/kg, ketolactone VIII*a* caused no observable effect, but caused the animal to die within 4 days after a 100-mg/kg dose. At a dose of 200 mg/kg this ketolactone produced onset of tonic convulsions within 3 min followed by clonic convulsions by 10 min, with pilorection and salivation. The animals died within a 20-min period. Keto lactone VIII*b* produced no effects at doses <100 mg/kg, but at a dose of 125 mg/kg (the highest dose tested) the animals died within 12–15 hr. It is unknown if convulsions were produced. Because doses >100 mg/kg were required to produce biological effects, the potency of this series was not sufficient to develop further.

EXPERIMENTAL[3]

Preparation of Potassium-*tert*-amyloxide—To 60 ml of *tert*-amyl alcohol (44.5 g, 0.55 mole) contained in 500 ml of dimethoxyethane under argon was added potassium (23.45 g, 0.6 g-atom), and the mixture was heated to reflux for 2 days. The contents were allowed to cool to room temperature, and the reflux condenser was replaced with a rubber septum. The resulting stock solution was standardized by titration with 2.42 × 10^{-2} *N* potassium acid phthalate solution (phenophthalein as indicator) before each base reaction was carried out.

Alkylation Reactions Using Potassium-*tert*-amyloxide—To 0.1 mole of enone in 250 ml of dimethylformamide stirring in an ice bath under argon was added 0.086–0.14 mole of freshly prepared base solution over a period of 10 min. To the resultant mixture was added 0.2 mole of alkylating agent, and the contents were allowed to stir an additional 45 min at room temperature. The reaction was quenched with ice water and extracted with ether. The ether layer was washed 5 times with equal volumes of water and dried over sodium sulfate. The ether was removed, and the resulting oil was chromatographed or distilled.

Methyl 2-[1(*R,S*)-Methyl-2-oxo-4(*S*)-isopropenyl-5-cyclohexenyl]acetate, (V*b*)—*l*-Carvone (30.04 g, 0.20 mole) in 500 ml of dimethylformamide was alkylated with 62 ml of potassium-*tert*-amylate base solution (0.20 eq) and methyl bromoacetate (61.2 g, 0.40 mole). The resulting oil was distilled to give (V*b*) (8.6 g, 20%): bp 86–88° (0.05 mm); IR (neat) 1745, 1720, and 890; NMR ($CDCl_3$) 1.22 (3, s, CH_3), 1.78 (3, s, vinyl CH_3), 3.62 (3, s, OCH_3), 4.81 (2, m, $=CH_2$), and 5.73 ppm (2, m, H—C=C—H); $M^{\oplus}$ *m/z* 222; n_D^{22} 1.4955.

***l*-Carvotanacetone, 5(*R*)-Isopropyl-2-methyl-2-cyclohexanone**—The procedure used was that of Birch and Walker (7). Modifications were made in the percent of catalyst and the hydrogenation apparatus used. To *l*-carvone (80 g, 0.53 mole) in 150 ml of absolute ethanol contained in a Parr bottle was added *tris*-triphenylphosphine rhodium chloride. The hydrogenation was carried out at room temperature and 30 psi over a period of 6 hr. The bottle was refilled with hydrogen twice during this period. The ethanol was removed, and the crude oil was distilled to produce *l*-carvotanacetone (77.4 g, 95%): bp 54–60° (0.4–0.6 mm); IR (neat) 1680, 1380, and 1365; NMR (CCl_4) 0.72 (6, d, *J* = 6 Hz, 2 CH_3), 1.72 (3, s, CH_3), and 6.6 ppm (1, br s, =CH); n_D^{28} 1.4760 [lit (8) bp 227–228°; n_D^{19} 1.4822].

Methyl 2-[1(*R,S*)-Methyl-2-oxo-4(*R*)-isopropyl-5-cyclohexenyl]acetate, (V*a*)—*l*-Carvotanacetone (15.2 g, 0.10 mole) in 250 ml of dimethylformamide was alkylated with 100 ml of potassium-*tert*-amylate solution (0.11 eq) and methyl bromoacetate (30.6 g, 0.20 mole). Chromatography (alumina; 10% ethyl acetate in cyclohexane) produced V*a* (6.75 g, 35%): bp 86–88° (0.075 mm); IR (neat) 1745, 1720, 1387, 1368, and 735; NMR ($CDCl_3$) 0.99 (6, d, *J* = 6 Hz, 2 CH_3), 1.2 (3, s, CH_3), 3.68 (3, s, OCH_3), and 5.84 ppm (2, m, HC=CH); $M^{\oplus}$, *m/z* 224; n_D^{24} 1.4744.

Ester Hydrolyses—The procedure used was that of Allen and Kalm (9) modified by shortening the reaction time to 2 hr. To 1 mmole of the keto ester in 2 ml of 95% ethanol was added 1.5 mmoles solid 85% KOH, and the mixture was heated to reflux for 2 hr. The ethanol was removed by evaporation, and the resulting oil was diluted with 5 volumes of ice water and acidified (pH 1) with 5 *N* sulfuric acid. The organic portion was extracted with ether, and the ether extract was dried over sodium sulfate.

2-[1(*R,S*)-Methyl-2-oxo-4(*S*)-isopropenyl-5-cyclohexenyl]-acetic acid-γ-lactol, (VI*b*)—The keto ester (V*b*) (6.3 g, 28 mmoles) in 55 ml of 95% ethanol was hydrolyzed with 85% KOH (3.0 g, 45 mmoles). The ether was removed to give 5.8 g of (VI*b*): IR (neat) 3400, 1780–1720 (br), 1650, and 890; NMR (CCl_4) 1.21 (3, s, CH_3), 2.75 (3, s, CH_3), 4.79 (2, m, $=CH_2$), and 6.6 ppm (2, m, HC=CH); $M^{\oplus}$, *m/z* 208; n_D^{26} 1.5088.

2-[1(*R,S*)-Methyl-2-oxo-4(*R*)-isopropyl-5-cyclohexenyl]-acetic acid-γ-lactol, (VI*a*)—The keto ester V*a* (4.92 g, 22 mmoles) in 40 ml of 95% ethanol was hydrolyzed with 85% KOH (2.2 g, 33 mmoles). The ether was removed affording 4.2 g of (VI*a*): IR (neat) 3440, 1775, and 1720; NMR (CCl_4) 0.95 (6, d, *J* = 6 Hz, 2 CH_3, 1.23 (3, s, CH_3), 5.6 (2, m, HC=CH), and 6.9 ppm (1, s, lactol H); $M^{\oplus}$, *m/z* 210; n_D^{24} 1.4990.

Procedure for Iodolactonization—The procedure used was that of Van Tamelen and Shamma (10). The only modification made was a one-fold increase of iodine and potassium iodide in the doubly unsaturated lactol. To a solution of 5 mmoles of the lactol in 30 ml of 0.5 *N* $NaHCO_3$ was added 30 mmoles of potassium iodide in 15 ml of water and 10 mmoles of iodine. The mixture was allowed to stand in the dark for 24 hr. The contents of the reaction was transferred to a separatory funnel and diluted with ether. The mixture was shaken with a saturated solution of sodium thiosulfate until two almost colorless phases were obtained. The ether layer was concentrated and the iodo lactones were allowed to crystallize.

2-[1 (*R*)-Methyl-2-oxo-4 (*S*)-(1′,2′-diiodo)-isopropyl-5 (*S*)-iodo-6(*S*)-hydroxycyclohexyl-acetic acid-γ-lactone or 2-[1 (*R*)-Methyl-2-oxo-4 (*R*)-isopropenyl-5 (*S*)-iodo-6 (*S*)-hydroxycyclohexyl]-acetic acid-γ-lactone (VII*b*)—The lactol (VI*b*) (4.25 g, 20 mmoles) in 60 ml of 0.5 *N* $NaHCO_3$ was lactonized with iodine (20.0 g, 79 mmoles) and potassium iodide (2.0 g, 12 mmoles). The ether extract was concentrated, and the mixture was treated with triphenyltin hydride without purification.

2-[1 (*R*)-Methyl-2-oxo-4 (*R*)-isopropyl-5 (*S*)-iodo-6 (*S*)-hydroxycyclohexyl]-acetic acid-γ-lactone, (VII*a*)—The lactol VI*a* (4.8 g, 23 mmoles) in 130 ml of 0.5 *N* $NaHCO_3$ was lactonized with iodine (10.44 g, 41 mmoles) and potassium iodide (2.16 g, 13 mmoles). Fractional crystallization afforded the major isomer, VII*a* (2.16 g, 36.5%): mp 113–114°; IR ($CHCl_3$) 1780 and 1712; NMR ($CDCl_3$) 0.98 (3, d, *J* = 6 Hz, CH_3), 1.05 (3, d *J* = 6 Hz, CH_3), 1.55 (3, s CH_3), 4.79 (1, m, I—C—H), and 5.15 ppm (1, d *J* = 2 Hz, O—C—H); $M^{\oplus}$, *m/z* 336; $[\alpha]_D^{25}$($CHCl_3$) −13.5°.

Anal.—Calc. for $C_{12}H_{17}IO_3$: C, 42.86; H, 5.06. Found: C, 43.04; H, 5.21.

Preparation of Triphenyltin Hydride—The preparation used was that of Kuivila (11) without modification. To 150 ml of dry ether containing lithium aluminum hydride (1.56 g, 41 mmoles) was added slowly triphenyltin chloride (32.5 g, 100 mmoles). The mixture was stirred at room temperature under argon for 3 hr and then hydrolyzed with 100 ml of ice water while cooling in an ice bath. The ether layer was washed twice with ice water then dried over magnesium sulfate. The ether was removed, and the hydride was distilled rapidly with a bath preheated to 200°; yield 19.5 g (69%); bp 144–152° (0.2–0.3 mm) [lit. (11) 162–168° (0.5 mm)].

Triphenyltin Hydride Reduction of Iodolactones—The procedure used was that of Kuivila (11). The only modification which was made was a onefold increase of the hydride in the iodo lactones of the doubly unsaturated γ-lactol. To 1 mmole of the iodo lactone contained in 10 ml of dry benzene stirring under argon was added 1 mmole of triphenyltin hydride. The mixture was stirred at room temperature overnight, and then the benzene was removed. The resulting product was either fractionally sublimed or fractionally distilled.

[2] Sanicel.

[3] All melting points were taken on a Thomas-Hoover Unimelt and are corrected. Analyses were performed by either Midwest Microlab, Inc., Indianapolis, Ind., or on an F and M Model 185, C, H, N, Analyzer, University of Kansas. IR data were recorded on Beckman IR-8, IR-10, and IR-33 spectrophotometers and are reported in cm^{-1}. ^1H-NMR data were recorded on Varian A-60, A-60A, and T-60 analytical spectrometers with tetramethylsilane as the internal standard. ^1H-NMR data are reported as δ-values (ppm). Mass spectra were recorded on a Varian-Atlas CH-5 at 70 eV at a resolution of ~4000.

2-[1(*R*)-Methyl-2-oxo-4(*R*)-isopropenyl-6(*R*)-hydroxycyclohexyl]-acetic acid-γ-lactone, (VIII*b*)—The iodo lactone(s) VII*b* (3.8 g) in 100 ml of dry benzene was reduced with triphenyltin hydride (6.72 g, 0.02 mole). Distillation (150–154° and 0.1 mm) provided VIII*b* (975 mg, 72% based on monoiodo starting material, 91% based on triiodo starting material): IR ($CHCl_3$) 1795 and 1720; NMR ($CDCl_3$) 1.35 (3, s, CH_3), 1.75 (3, s, CH_3), 4.68 (1, t, J = 2 Hz, O—C—H), and 4.82 ppm (2, m, $=CH_2$); $M^{\oplus}$, m/z 208; $[\alpha]_D^{26}$ ($CHCl_3$) +114.2°.

Anal.—Calc. for $C_{12}H_{16}O_3$: C, 69.20; H, 7.68. Found: C, 68.95; H, 7.79.

2-[1(*R*)-Methyl -2- oxo-4(*R*)-isopropyl-6(*R*)-hydroxycyclohexyl]-acetic acid-γ-lactone, (VIII*a*)—The iodo lactone VII*a* (1.0 g, 3 mmoles) in 30 ml of dry benzene was reduced with triphenyltin hydride (0.98 g, 2.8 mmoles). The benzene was removed, and the resulting gum was fractionally sublimed [67° (0.05 mm)] to yield VIII*a* (200 mg, 32%): IR ($CHCl_3$) 1785 and 1715; NMR ($CDCl_3$) 0.95 (6, d, J = 6 Hz, 2 CH_3), 1.35 (3, s, CH_3), and 4.67 ppm (1, t, J = 2 Hz, O—C—H); $M^{\oplus}$, m/z 210; $[\alpha]_D^{26}$ ($CHCl_3$) +127°; mp 84–85°.

Anal.—Calc. for $C_{12}H_{18}O_3$: C, 68.55; H, 8.57. Found: C, 68.33; H, 8.52.

Sodium Borohydride Reductions—The procedure used was that of Elisberg *et al.* (12) modified by length of reaction time and solvent. To 0.5 mmole of the keto lactone in 30 ml of 95% ethanol stirring in an ice bath was added 1 mmole of sodium borohydride. Ice water was added to the mixture, the solution was extracted with ether three times, and the organic layer was dried over sodium sulfate.

2-[1(*S*)-Methyl-2(*R*)-hydroxy -4(*S*)- isopropenyl-6(*R*)-hydroxycyclohexyl]-acetic acid-γ-lactone, (III*b*)—The keto lactone (VIII*b*) (560 mg, 2.69 mmoles) in 40 ml of 95% ethanol was reduced with sodium borohydride (200 mg, 5.38 mmoles). Workup after a 6-hr reaction time and distillation produced III*b* (270 mg, 48%): IR (neat) 3500 and 1770; NMR ($CDCl_3$) 1.1 (3, s, CH_3), 1.74 (3, s, CH_3), 4.35 (1, t, J = 3 Hz, O—C—H), and 4.73 ppm (2, s, $=CH_2$); $M^{\oplus}$, m/z 210.

Anal.—Calc. for $C_{12}H_{18}O_3$: C, 68.59; H, 8.57. Found: C, 68.34; H, 8.63.

2-[1(*S*)-Methyl-2(*R*)-hydroxy-4(*S*)-isopropyl-6(*R*)-hydroxycyclohexyl]-acetic acid-γ-lactone, (III*a*)—The keto lactone, VIII*a* (315 mg, 1.5 mmoles) in 30 ml of 95% ethanol was reduced with sodium borohydride (113 mg, 3.0 mmoles). Workup after a period of 7 hr and distillation gave III*a* (130 mg, 41%): IR (neat) 3500 and 1775; NMR ($CDCl_3$) 0.85 (3, d, J = 5 Hz, CH_3), 1.1 (3, d, J = 4 Hz, CH_3), 1.22 (3, s, CH_3), and 4.3 ppm (1, s, O—C—H); $M^{\oplus}$, m/z 212.

Anal.—Calc. for $C_{12}H_{20}O_3$: C, 67.94; H, 9.43. Found: C, 67.85; H, 9.49.

REFERENCES

(1) G. A. R. Johnston, *Annu. Rev. Pharmacol. Toxicol.*, **18**, 269 (1978).

(2) M. K. Ticker and R. W. Olsen, *Biochim. Biophys. Acta*, **464**, 519 (1977).

(3) C. H. Jarboe, L. A. Porter, and R. T. Buckler, *J. Med. Chem.*, **11**, 729, (1968).

(4) H. D. House, "Modern Synthetic Reactions," 2nd ed., W. A. Benjamin, Menlo Park, Calif., 1972, chap. 9.

(5) D. W. Theobald, *Tetrahedron*, **23**, 2767 (1967).

(6) R. S. Matthews, S. J. Girgenti, and E. A. Folkers, *J. Chem. Soc., Chem. Comm.*, **1970**, 738.

(7) A. J. Birch and K. Walker, *J. Chem. Soc., C*, **1964**, 1894.

(8) O. Wallach., *Ann. Chem.*, **336**, **1901**, 1.

(9) C. F. Allen and M. J. Kalm, *Org. Syn. Coll.*, **4**, 608 (1963).

(10) E. E. Van Tamelen and M. Shamma, *J. Am. Chem. Soc.*, **76**, 2315 (1954).

(11) H. G. Kuivila, *Synthesis*, **1970**, 499.

(12) E. Elisberg, H. Vanderhaege, and T. F. Gallager, *J. Am. Chem. Soc.*, **74**, 2814 (1952).

ACKNOWLEDGMENTS

Taken in part from the dissertation presented by A. F. Wycpalek to the Graduate School of the University of Kansas in partial fulfillment of the requirements for the Doctor of Philosophy degree in 1972.

The authors gratefully acknowledge the financial support of the National Institutes of Health. We wish to thank the Department of Pharmacology and Toxicology, University of Kansas Medical Center, Kansas City, Kansas through whose cooperation the biological evaluations were made.

Influence of Ionic Strength on Rectal Absorption of Gentamicin Sulfate in the Presence and Absence of Sodium Salicylate

JOSEPH A. FIX ˣ, PAULA S. LEPPERT, PATRICIA A. PORTER, and LARRY J. CALDWELL

Received November 20, 1981, from *INTERx Research Corporation*, a subsidiary of *Merck Sharp & Dohme Research Laboratories, Lawrence, KS 66044.* Accepted for publication August 16, 1982.

Abstract □ The rectal absorption of gentamicin sulfate in rats, both in the presence and absence of sodium salicylate, was facilitated by the use of high ionic strength aqueous formulations. The relative order of effectiveness in promoting gentamicin absorption was sodium dihydrogen phosphate ≃ sodium chloride ≫ potassium chloride, indicating a preferential effect of sodium ions. The increased gentamicin bioavailability in response to sodium salicylate adjuvant activity appeared to be independent of and additive to the increased gentamicin absorption due to high ionic strength conditions. The inability of sorbitol to increase gentamicin bioavailability above control levels indicated that elevated osmotic pressure was not a major determinant of rectal gentamicin absorption.

Keyphrases □ Gentamicin—rectal absorption, effect of ionic strength and specificity, sodium salicylate adjuvant □ Sodium salicylate—as adjuvant, rectal absorption of gentamicin, effect of ionic strength and specificity □ Absorption, rectal—gentamicin, sodium salicylate adjuvant, effect of ionic strength and specificity

Sodium salicylate has been reported to enhance the rectal absorption of water-soluble compounds (1, 2). Two types of formulations were used in the salicylate studies, an aqueous microenema and a fatty-base suppository. The influence of variations in ionic strength and ionic specificity on salicylate-enhanced rectal absorption has not been thoroughly examined in either formulation.

The effect of sodium concentration on absorption of fluid, as classically illustrated by the active transport of sodium from the large intestine and the concomitant water

0022-3549/83/1000-1134$01.00/0

2-[1(*R*)-Methyl-2-oxo-4(*R*)-isopropenyl-6(*R*)-hydroxycyclohexyl]-acetic acid-γ-lactone, (VIII*b*)—The iodo lactone(s) VII*b* (3.8 g) in 100 ml of dry benzene was reduced with triphenyltin hydride (6.72 g, 0.02 mole). Distillation (150–154° and 0.1 mm) provided VIII*b* (975 mg, 72% based on monoiodo starting material, 91% based on triiodo starting material): IR ($CHCl_3$) 1795 and 1720; NMR ($CDCl_3$) 1.35 (3, s, CH_3), 1.75 (3, s, CH_3), 4.68 (1, t, J = 2 Hz, O—C—H), and 4.82 ppm (2, m, $=CH_2$); $M^{\oplus}$, m/z 208; $[\alpha]_D^{26}$ ($CHCl_3$) +114.2°.

Anal.—Calc. for $C_{12}H_{16}O_3$: C, 69.20; H, 7.68. Found: C, 68.95; H, 7.79.

2-[1(*R*)-Methyl -2- oxo-4(*R*)-isopropyl-6(*R*)-hydroxycyclohexyl]-acetic acid-γ-lactone, (VIII*a*)—The iodo lactone VII*a* (1.0 g, 3 mmoles) in 30 ml of dry benzene was reduced with triphenyltin hydride (0.98 g, 2.8 mmoles). The benzene was removed, and the resulting gum was fractionally sublimed [67° (0.05 mm)] to yield VIII*a* (200 mg, 32%): IR ($CHCl_3$) 1785 and 1715; NMR ($CDCl_3$) 0.95 (6, d, J = 6 Hz, 2 CH_3), 1.35 (3, s, CH_3), and 4.67 ppm (1, t, J = 2 Hz, O—C—H); $M^{\oplus}$, m/z 210; $[\alpha]_D^{26}$ ($CHCl_3$) +127°; mp 84–85°.

Anal.—Calc. for $C_{12}H_{18}O_3$: C, 68.55; H, 8.57. Found: C, 68.33; H, 8.52.

Sodium Borohydride Reductions—The procedure used was that of Elisberg *et al.* (12) modified by length of reaction time and solvent. To 0.5 mmole of the keto lactone in 30 ml of 95% ethanol stirring in an ice bath was added 1 mmole of sodium borohydride. Ice water was added to the mixture, the solution was extracted with ether three times, and the organic layer was dried over sodium sulfate.

2-[1(*S*)-Methyl-2(*R*)-hydroxy -4(*S*)- isopropenyl-6(*R*)-hydroxycyclohexyl]-acetic acid-γ-lactone, (III*b*)—The keto lactone (VIII*b*) (560 mg, 2.69 mmoles) in 40 ml of 95% ethanol was reduced with sodium borohydride (200 mg, 5.38 mmoles). Workup after a 6-hr reaction time and distillation produced III*b* (270 mg, 48%): IR (neat) 3500 and 1770; NMR ($CDCl_3$) 1.1 (3, s, CH_3), 1.74 (3, s, CH_3), 4.35 (1, t, J = 3 Hz, O—C—H), and 4.73 ppm (2, s, $=CH_2$); $M^{\oplus}$, m/z 210.

Anal.—Calc. for $C_{12}H_{18}O_3$: C, 68.59; H, 8.57. Found: C, 68.34; H, 8.63.

2-[1(*S*)-Methyl-2(*R*)-hydroxy-4(*S*)-isopropyl-6(*R*)-hydroxycyclohexyl]-acetic acid-γ-lactone, (III*a*)—The keto lactone, VIII*a* (315 mg, 1.5 mmoles) in 30 ml of 95% ethanol was reduced with sodium borohydride (113 mg, 3.0 mmoles). Workup after a period of 7 hr and distillation gave III*a* (130 mg, 41%): IR (neat) 3500 and 1775; NMR ($CDCl_3$) 0.85 (3, d, J = 5 Hz, CH_3), 1.1 (3, d, J = 4 Hz, CH_3), 1.22 (3, s, CH_3), and 4.3 ppm (1, s, O—C—H); $M^{\oplus}$, m/z 212.

Anal.—Calc. for $C_{12}H_{20}O_3$: C, 67.94; H, 9.43. Found: C, 67.85; H, 9.49.

REFERENCES

(1) G. A. R. Johnston, *Annu. Rev. Pharmacol. Toxicol.*, **18**, 269 (1978).

(2) M. K. Ticker and R. W. Olsen, *Biochim. Biophys. Acta*, **464**, 519 (1977).

(3) C. H. Jarboe, L. A. Porter, and R. T. Buckler, *J. Med. Chem.*, **11**, 729, (1968).

(4) H. D. House, "Modern Synthetic Reactions," 2nd ed., W. A. Benjamin, Menlo Park, Calif., 1972, chap. 9.

(5) D. W. Theobald, *Tetrahedron*, **23**, 2767 (1967).

(6) R. S. Matthews, S. J. Girgenti, and E. A. Folkers, *J. Chem. Soc., Chem. Comm.*, **1970**, 738.

(7) A. J. Birch and K. Walker, *J. Chem. Soc., C*, **1964**, 1894.

(8) O. Wallach., *Ann. Chem.*, **336**, **1901**, 1.

(9) C. F. Allen and M. J. Kalm, *Org. Syn. Coll.*, **4**, 608 (1963).

(10) E. E. Van Tamelen and M. Shamma, *J. Am. Chem. Soc.*, **76**, 2315 (1954).

(11) H. G. Kuivila, *Synthesis*, **1970**, 499.

(12) E. Elisberg, H. Vanderhaege, and T. F. Gallager, *J. Am. Chem. Soc.*, **74**, 2814 (1952).

ACKNOWLEDGMENTS

Taken in part from the dissertation presented by A. F. Wycpalek to the Graduate School of the University of Kansas in partial fulfillment of the requirements for the Doctor of Philosophy degree in 1972.

The authors gratefully acknowledge the financial support of the National Institutes of Health. We wish to thank the Department of Pharmacology and Toxicology, University of Kansas Medical Center, Kansas City, Kansas through whose cooperation the biological evaluations were made.

Influence of Ionic Strength on Rectal Absorption of Gentamicin Sulfate in the Presence and Absence of Sodium Salicylate

JOSEPH A. FIX ˣ, PAULA S. LEPPERT, PATRICIA A. PORTER, and LARRY J. CALDWELL

Received November 20, 1981, from *INTERx Research Corporation*, a subsidiary of *Merck Sharp & Dohme Research Laboratories, Lawrence, KS 66044.* Accepted for publication August 16, 1982.

Abstract □ The rectal absorption of gentamicin sulfate in rats, both in the presence and absence of sodium salicylate, was facilitated by the use of high ionic strength aqueous formulations. The relative order of effectiveness in promoting gentamicin absorption was sodium dihydrogen phosphate ≃ sodium chloride ≫ potassium chloride, indicating a preferential effect of sodium ions. The increased gentamicin bioavailability in response to sodium salicylate adjuvant activity appeared to be independent of and additive to the increased gentamicin absorption due to high ionic strength conditions. The inability of sorbitol to increase gentamicin bioavailability above control levels indicated that elevated osmotic pressure was not a major determinant of rectal gentamicin absorption.

Keyphrases □ Gentamicin—rectal absorption, effect of ionic strength and specificity, sodium salicylate adjuvant □ Sodium salicylate—as adjuvant, rectal absorption of gentamicin, effect of ionic strength and specificity □ Absorption, rectal—gentamicin, sodium salicylate adjuvant, effect of ionic strength and specificity

Sodium salicylate has been reported to enhance the rectal absorption of water-soluble compounds (1, 2). Two types of formulations were used in the salicylate studies, an aqueous microenema and a fatty-base suppository. The influence of variations in ionic strength and ionic specificity on salicylate-enhanced rectal absorption has not been thoroughly examined in either formulation.

The effect of sodium concentration on absorption of fluid, as classically illustrated by the active transport of sodium from the large intestine and the concomitant water

0022-3549/83/1000-1134$01.00/0

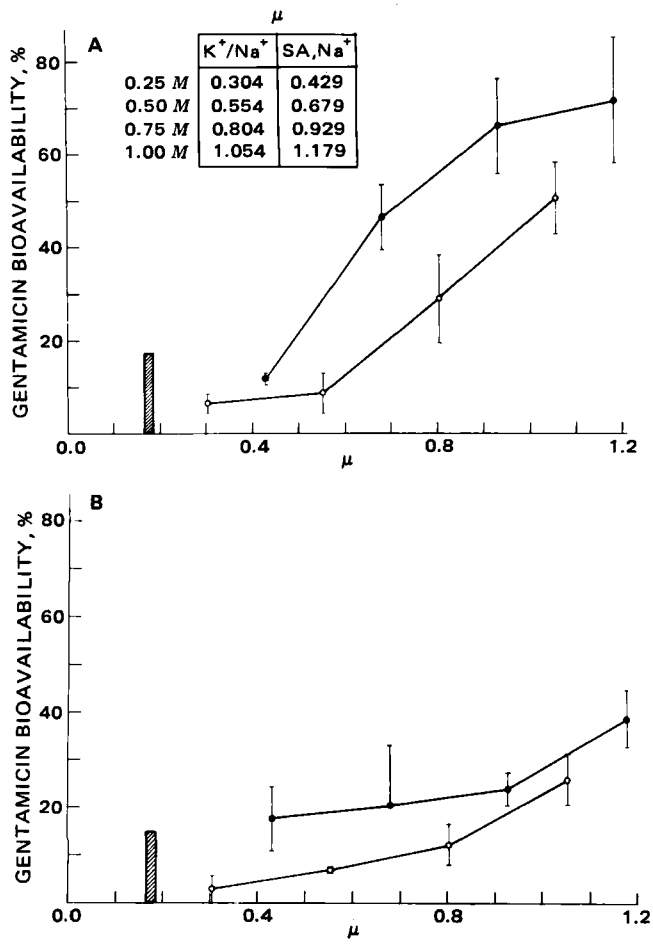

Figure 1—*Gentamicin bioavailability in the presence (●) or absence (○) of sodium salicylate following administration of aqueous microenemas of varying ionic strength (μ) to the unligated rectal compartment. Sodium chloride (A) or potassium chloride (B) at 0.25, 0.50, 0.75, and 1.00* M *was the major determinant of ionic strength, with minor contributions from sodium salicylate (SA) and gentamicin sulfate. Bars (▨) represent ionic strength of standard physiological solutions. Error bars represent standard deviations for* n = 3–6.

absorption, is well documented (3, 4). Recent studies have demonstrated a direct link between the transport of sodium ions and macromolecules in the rat small intestine (5, 6). Sodium ions have also been shown to influence calcium transport in the small intestine (7). However, the influence of ionic strength on adjuvant-assisted rectal absorption of water-soluble compounds has not been reported.

In the present study, the effect of various ionic species on the rectal absorption of gentamicin, a model water-soluble compound, in the presence and absence of sodium salicylate are examined. The purpose of the study is threefold: (*a*) to determine the effect, if any, of ionic strength on rectal absorption of a water-soluble compound; (*b*) to examine possible ionic specificity with regard to promoting rectal absorption; and (*c*) to determine if the absorption-promoting activity of sodium salicylate is influenced by alterations in ionic species or total ionic strength.

EXPERIMENTAL

Adult male Sprague-Dawley rats (200–250 g) were fasted, with free access to water, for 18–24 hr prior to the experiments. Animals were anesthetized by intramuscular injections of urethane (0.1 ml of 43% ethylcarbamate[1] in distilled water/100 g of body weight).

Experimental formulations were administered as aqueous microenemas, given with a 1-ml syringe at an intrarectal depth of 2.5 cm. Each animal received a 250-μl microenema, pH 5.0, containing 2.5 mg of gentamicin sulfate[1] with or without 5 mg of sodium salicylate. Ionic strength was controlled by the addition of various salts, as indicated in each individual set of experiments. Total ionic strength included contributions from the drug and adjuvant, as well as from the added salts, and was determined by the following formula:

$$I = \tfrac{1}{2}\sum m_i z_i^2 \qquad \text{(Eq. 1)}$$

where I is the ionic strength, m_i is the molality of i, and z_i is the charge of i.

In some experiments, designed to minimize effects due to possible movement of the microenema solution away from the site of administration, the rectum was ligated 4 cm from the anal opening. With care taken not to restrict the vasculature, this procedure ensured retention of the microenema in the distal 4 cm of the rectal compartment.

Blood samples (0.5 ml) were taken from the external jugular vein at 15, 30, 60, and 90 min following rectal administration of the microenema. Serum was isolated and frozen until assayed within 1–2 weeks. For determination of intravenous serum profiles, each animal received 2.5 mg of gentamicin sulfate in 250 μl of 0.1 *M* Tris-HCl buffer, pH 7.5. Blood samples (0.5 ml) were collected at 5, 10, 20, 30, 60, and 90 min and processed as described for rectal administration. Serum gentamicin was determined by microbiological assay using *Bacillus subtilis* (ATCC #6633) as the target organism (8). Results are expressed as percent bioavailability, calculated as:

$$\%\ \text{Bioavailability} = \frac{(\text{AUC})_{\text{rectal}}(\text{Dose})_{\text{iv}}}{(\text{Dose})_{\text{rectal}}(\text{AUC})_{\text{iv}}} \times 100 \qquad \text{(Eq. 2)}$$

The area under the serum concentration–time curve from 0 to 90 min, AUC_0^{90}, was calculated by a summation of trapezoidal areas. For the calculation of the intravenous AUC_0^{90}, the linear portion of the log serum concentration *versus* time profile was extrapolated to $t = 0$ min to correct for the drug distribution phase. Three to six animals were used for determining mean AUC_0^{90} values for both rectal and intravenous serum profiles. Following rectal administration, the absorption of gentamicin sulfate was virtually complete by 30–60 min, and the serum $t_{1/2}$ value (220–240 min) was the same as that observed after intravenous administration.

RESULTS

The effect of sodium chloride on unligated rectal delivery of gentamicin, with and without sodium salicylate as the adjuvant, is shown in Fig. 1A. Without adjuvant, no apparent sodium chloride effect is observed until the ionic strength (μ) in the microenema exceeds 0.55. A linear increase in percent bioavailability occurred from $\mu = 0.544$ to $\mu = 1.054$ ($r = 0.9998$ by regression analysis). At 1.0 *M* NaCl ($\mu = 1.054$), gentamicin bioavailability was 51 ± 7.9%. Solutions of greater sodium chloride ionic strength were not examined, so it is not known whether the sodium chloride effect on bioavailability would plateau prior to reaching 100% gentamicin delivery. At all ionic strengths examined, gentamicin bioavailability was greater in the presence of sodium salicylate. At higher ionic strengths with sodium salicylate, the effect of sodium chloride was no longer linear and appeared to plateau around 70–80% bioavailability.

Figure 1B shows the results of a similar set of experiments using unligated rectum in which potassium chloride was substituted for sodium chloride as the major contributor to total ionic strength. The effect of potassium chloride alone (26 ± 5.6% at $\mu = 1.054$) on gentamicin delivery was significantly less than the corresponding response observed with sodium chloride (51 ± 7.9% at $\mu = 1.054$). In the presence of sodium salicylate, the gentamicin bioavailability using potassium chloride was 39 ± 5.9% at $\mu = 1.179$, whereas with sodium chloride the bioavailability was 72 ± 13.4%.

In the absence of adjuvant and added salts, gentamicin sulfate bioavailability was 12 ± 4.5%. The inclusion of 2–10% sorbitol in the formulation caused a slight decrease in gentamicin sulfate absorption (Table I). Including 30% sorbitol in microenemas containing gentamicin sulfate and adjuvant did not significantly increase bioavailability (36 ± 14.8%) above that seen with sorbitol-free microenemas containing adjuvant and drug along (29 ± 7.4%).

[1] Sigma Chemical Co., St. Louis, Mo.

Table I—Effect of Sorbitol on Rectal Gentamicin Sulfate Absorption from Aqueous Formulations

Formulation[a]		Gentamicin Sulfate
Adjuvant, %	Sorbitol, %	Bioavailability, %[b]
0	0	12 ± 4.5
0	2	5 ± 3.4
0	5	3 ± 0.3
0	10	4 ± 2.3
2	0	29 ± 7.4
2	30	36 ± 14.8

[a] All formulations contained 1% gentamicin sulfate. [b]Based on $n = 3$ animals.

The use of potassium chloride or potassium dihydrogen phosphate with ligated tissue produced somewhat equivocal results (Fig. 2A). There was no apparent difference between the gentamicin bioavailability after the administration of potassium chloride alone compared with that of potassium chloride administered with sodium salicylate, except at very high ionic strengths ($\mu > 1.0$). Potassium dihydrogen phosphate, in conjunction with sodium salicylate, yielded the highest gentamicin bioavailability in the potassium series (63 ± 9.4% at $\mu = 1.179$), although this value was significantly less than the bioavailability observed with sodium dihydrogen phosphate and sodium salicylate (88 ± 13.2% at $\mu = 0.929$) (Fig. 2B). As seen in the experiments with unligated rectal tissue, bioavailabilities attained with sodium chloride and sodium salicylate were greater than those observed with sodium chloride alone.

DISCUSSION

The ability of salicylate-type adjuvants to enhance the GI absorption of water-soluble compounds has been previously established (1, 2). In this study, the ionic contributions of sodium and potassium salts to rectal absorption of a model water-soluble compound, gentamicin, were examined. Ionic strength and specificity were found to significantly affect the rectal absorption of gentamicin.

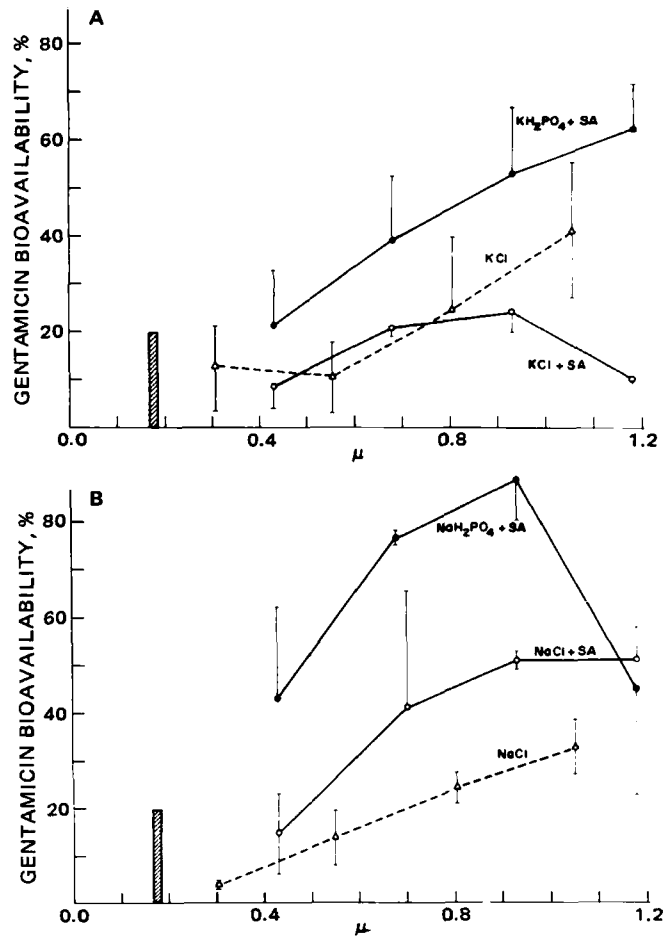

Figure 2—*Gentamicin bioavailability in the presence (—) or absence (- - -) of sodium salicylate (SA) following administration of aqueous microenemas of varying ionic strength (μ) to the ligated rectal compartment. The potassium (A) or sodium (B) salts were the major determinants of ionic strength, with minor contributions from sodium salicylate and gentamicin sulfate. Bars (▨) represent ionic strength of standard physiological solutions. Error bars represent standard deviations for* n = *3–6.*

Sodium chloride significantly increased gentamicin absorption, even in the absence of sodium salicylate. It is not possible to determine, from the present data, the precise mechanism involved in the sodium chloride enhancement of drug permeability across the rectal mucosa. However, several possibilities exist: (*a*) high sodium or chloride concentrations may activate some undefined transport mechanism for gentamicin; (*b*) active transport of sodium out of the rectal lumen, with concomitant water movement, may establish mass transfer conditions favoring absorption of gentamicin; or (*c*) high ionic strength solutions may damage or disrupt the normal epithelial barrier and allow concentration-dependent movement of gentamicin through the disrupted barrier.

The mucosal layer in the rectum and lower portion of the large intestine is not classically viewed as an absorptive area except for the absorption of water and small ions (*e.g.*, sodium). This does not preclude the possible existence of specific transport mechanisms for water-soluble compounds (*e.g.*, gentamicin), although it is unlikely that such a system exists. The apparent inability of the rectal tissue to absorb gentamicin in the absence of the salicylate adjuvant further refutes the existence of a specific transport system which could be affected by the sodium or chloride ion.

Possible tissue damage at very high concentrations of sodium chloride may account for part of the observed increase in gentamicin absorption, although comparable gentamicin serum levels were not observed at higher concentrations of potassium chloride or sorbitol. The inability of sorbitol to increase gentamicin bioavailability indicates that the osmotic pressures generated by high sodium chloride or potassium chloride solutions are unlikely causes of the increased delivery. The fact that sodium chloride was twice as effective as potassium chloride in both the presence and absence of sodium salicylate (at comparable ionic strengths) suggests certain ionic specificities, possibly implicating the involvement of the membrane sodium–potassium pump.

Sodium dihydrogen phosphate and potassium dihydrogen phosphate were tested in the ligated rectum to determine if the absorption promoting potential of the salts was influenced by the anionic species. Maximal effects in the ligated rectum were observed at lower ionic strengths than in the unligated rectum. This is probably due to the increased effective concentration of drug and salt in the limited exposed surface area of the ligated rectum. With both sodium and potassium, the dihydrogen phosphate salts appeared to be more effective than the chloride salts in promoting gentamicin delivery. While this increased absorption using dihydrogen phosphate salts may be a real effect, it is also possible that alterations in rectal pH may have caused ionic strengh changes that were responsible for promoting absorption. All microenemas were administered as buffered solutions (pH 5) with sodium dihydrogen phosphate predominately existing in solution as sodium and dihydrogen phosphate. The rectal compartment in the rat is capable of some buffering activity and tends to adjust the pH of aqueous solutions to a range of pH 7–8 (unpublished observations). If the pH of the microenema is buffered *in vivo* to the pH 7–8 range, a significant portion of the dihydrogen phosphate may be ionized to monohydrogen phosphate. Since the ionic strength is a function of charge squared, this would significantly increase the total ionic strength of the solution and could account for the greater effect of sodium dihydrogen phosphate as compared with sodium chloride. Sodium chloride ionic strength is unaffected by pH. Since the buffering effect of the rectal compartment is not instantaneous, the relative concentrations of the two ionized species of the phosphate salts will be continually changing. To determine if the buffering capacity of the rectum changes the ionic strength of the formulation, and therefore the absorption of gentamicin sulfate, controlled pH perfusion studies will be required. At this point, the possibility that phosphate has a greater effect on gentamicin sulfate absorption than chloride cannot be precluded.

An important deduction that can be made from this study is that the absorption-promoting activity of sodium salicylate is not solely attributed to ionic strength. In the data presented in the figures, ionic contributions from sodium salicylate were included in the calculations of total ionic strength in the microenemas. The increase in gentamicin bioavailability due to the adjuvant activity of sodium salicylate is significantly greater than the bioavailability achieved with adjuvant-free microenemas at the same total ionic strength (adjusted by sodium chloride). Sodium salicylate, therefore, possesses an absorption-enhancing potential above that which can be attributed to sodium ionic strength alone.

Ionic strength and ionic specificity were found to have a significant influence on the rectal absorption of gentamicin. Sodium was more effective than potassium in promoting rectal absorption, but the enhancing effect of sodium salicylate could not be totally explained on the basis of ionic strength. These data, while helping to elucidate some parameters that affect rectal drug absorption, may offer potential insights into new formulation designs for systemic delivery of water-soluble drugs from the rectal compartment.

REFERENCES

(1) T. Nishihata, J. H. Rytting, and T. Higuchi, *J. Pharm. Sci.*, **69**, 744 (1980).

(2) T. Nishihata, J. H. Rytting, and T. Higuchi, *J. Pharm. Sci.*, **70**, 71 (1981).

(3) C. O. Billich and R. Levitan, *J. Clin. Invest.*, **48**, 1336 (1969).

(4) C. J. Edmonds, *Gut*, **12**, 356 (1971).

(5) F. Alvarado, *Biochim. Biophys. Acta*, **109**, 478 (1965).

(6) G. A. Kimmich, *Biochim. Biophys. Acta*, **300**, 31 (1973).

(7) D. L. Martin and H. F. DeLuca, *Am. J. Physiol.*, **216**, 1351 (1969).

(8) L. D. Sabath, J. I. Casey, P. A. Ruch, L. L. Stumpf, and M. Finland, *J. Lab. Clin. Med.*, **78**, 457 (1971).

Effect of Quinidine on Digoxin Distribution and Elimination in Guinea Pigs

JUN SATO, YASUFUMI SAWADA, TATSUJI IGA ˣ, and MANABU HANANO

Received June 4, 1982, from the *Faculty of Pharmaceutical Sciences, Department of Pharmaceutics, University of Tokyo, Hongo, Bunkyo-ku, Tokyo 113, Japan.* Accepted for publication August 20, 1982.

Abstract □ The effect of quinidine on the distribution and elimination of digoxin was examined by comparing the change in the steady-state volume of distribution (Vd_{ss}), determined both from *in vivo* plasma elimination and tissue distribution and *in vitro* serum binding studies, with that in the total body clearance (CL_{tot}) determined from biliary, renal, and metabolic clearances in guinea pigs. The plasma disappearance of digoxin after a 250-μg/kg iv dose followed a triexponential decline in both the control and quinidine-treated guinea pigs. In the quinidine-treated guinea pigs, the pharmacokinetic parameters Vd_{ss} and CL_{tot} significantly decreased to approximately half of that for the control guinea pigs. The tissue-to-plasma partition coefficients (K_p) of all tissues studied, *i.e.* liver, heart, muscle, and brain, at 6 hr after bolus injection of digoxin decreased in the presence of quinidine. The serum free fraction and the plasma-to-blood concentration ratio of digoxin in the therapeutic range did not show a significant alteration in the presence of quinidine. This suggested that the decrease of K_p is due mainly to the inhibition of tissue distribution of digoxin by quinidine. The biliary clearance (CL_B) and renal clearance (CL_R) also significantly decreased in the presence of quinidine. It was concluded that quinidine caused a inhibition of digoxin in the tissue binding or uptake, which significantly decreased the K_p values of digoxin; this result may explain the significant decrease of Vd_{ss}. Moreover quinidine may be the cause of a reduction of biliary, renal, and metabolic clearances, which significantly decrease the CL_{tot} of digoxin.

Keyphrases □ Quinidine—effect on the distribution and elimination of digoxin, guinea pigs □ Digoxin—pharmacokinetics, effect of quinidine coadministration, guinea pigs □ Pharmacokinetics—digoxin in the guinea pig, effect of quinidine coadministration

When quinidine is given to patients (1–5), dogs (6), or guinea pigs (7) receiving digoxin, the serum digoxin concentration increases. Reduction in the total body clearance (CL_{tot}) (5, 6) and the volume of distribution (Vd) (5, 6, 8) of digoxin has been observed and accounts for the elevated digoxin concentration. Quinidine has been reported to diminish the renal clearance (CL_R) of digoxin in humans (2, 4, 5, 8, 9) and dogs (10, 11) without significantly altering the glomerular filtration rate as measured by the creatinine clearance. Doherty *et al.* (12) reported that quinidine reduced the canine skeletal and heart muscle concentrations of digoxin, while increasing concentrations in the plasma and brain. Straub *et al.* (13) showed that quinidine reduced the number of digitalis-binding sites, as determined by *in vitro* binding studies with Na^+,K^+-ATPase from bovine heart membrane. Evidence has been reported that quinidine was capable of decreasing the affinity for digoxin of cardiac glycoside receptor sites on purified Na^+,K^+-ATPase in guinea pigs and on intact human erythrocyte membranes (14).

The present study examined the effect of quinidine on the distribution and elimination of digoxin by comparing the changes in Vd and CL_{tot} *in vivo*, which were determined from the tissue distribution, metabolism, excretion, serum protein binding, and plasma-to-blood distribution ratio. As a model animal for digoxin–quinidine interaction in the human, the guinea pig, a species in which digoxin distribution appears similar to that observed in the human, was selected.

EXPERIMENTAL

Digoxin[1] and quinidine sulfate[2] were used. Tritiated digoxin, labeled at the 12α-position (14.0 Ci/mmole)[3], which was found to be at least 99% pure by TLC, was used as the radioactive compound. All other reagents were commercially available and analytical grade.

Animal Experiments—Adult male Hartley guinea pigs[4], weighing 280–300 g, were used. Under light ether anesthesia, the jugular vein and carotid artery were cannulated with polyethylene tubing[5]. For the biliary and urinary excretion studies, bile fistula and urinary bladder cannulation were used to collect samples of bile and urine, respectively. Cannulated animals were kept in restraining cages with access to water under normal housing conditions prior to the experiments.

The guinea pigs were simultaneously given 250 μg/kg of digoxin (containing 100 μCi/kg of 12α-[^{3}H]digoxin) in 40% ethanol solution and 25 mg/kg of quinidine sulfate in physiological saline through the jugular vein cannula. The digoxin solution containing 40% ethanol was administered alone to the control guinea pigs. Blood samples (0.25 ml) were obtained for the determination of digoxin at 1, 5, 30, 60, 120, 180, 240, 300, and 360 min, and for the determination of quinidine (in different animals) at 5, 10, 15, 20, 30, 45, 60, 90, 120, 180, and 240 min in heparinized poly-

[1] Sigma Chemical Co., St. Louis, Mo.
[2] Tokyo Kasei Co., Tokyo, Japan.
[3] New England Nuclear Co., Boston, Mass.
[4] Nihon Seibutsu Zairyo, Tokyo, Japan.
[5] PE-10 for jugular vein and PE-50 for carotid artery: Clay Adams, Becton, Dickinson & Co., Parsippany, N.J.

0022-3549/83/1000-1137$01.00/0

Ionic strength and ionic specificity were found to have a significant influence on the rectal absorption of gentamicin. Sodium was more effective than potassium in promoting rectal absorption, but the enhancing effect of sodium salicylate could not be totally explained on the basis of ionic strength. These data, while helping to elucidate some parameters that affect rectal drug absorption, may offer potential insights into new formulation designs for systemic delivery of water-soluble drugs from the rectal compartment.

REFERENCES

(1) T. Nishihata, J. H. Rytting, and T. Higuchi, *J. Pharm. Sci.*, **69**, 744 (1980).

(2) T. Nishihata, J. H. Rytting, and T. Higuchi, *J. Pharm. Sci.*, **70**, 71 (1981).

(3) C. O. Billich and R. Levitan, *J. Clin. Invest.*, **48**, 1336 (1969).

(4) C. J. Edmonds, *Gut*, **12**, 356 (1971).

(5) F. Alvarado, *Biochim. Biophys. Acta*, **109**, 478 (1965).

(6) G. A. Kimmich, *Biochim. Biophys. Acta*, **300**, 31 (1973).

(7) D. L. Martin and H. F. DeLuca, *Am. J. Physiol.*, **216**, 1351 (1969).

(8) L. D. Sabath, J. I. Casey, P. A. Ruch, L. L. Stumpf, and M. Finland, *J. Lab. Clin. Med.*, **78**, 457 (1971).

Effect of Quinidine on Digoxin Distribution and Elimination in Guinea Pigs

JUN SATO, YASUFUMI SAWADA, TATSUJI IGA ˣ, and MANABU HANANO

Received June 4, 1982, from the *Faculty of Pharmaceutical Sciences, Department of Pharmaceutics, University of Tokyo, Hongo, Bunkyo-ku, Tokyo 113, Japan.* Accepted for publication August 20, 1982.

Abstract □ The effect of quinidine on the distribution and elimination of digoxin was examined by comparing the change in the steady-state volume of distribution (Vd_{ss}), determined both from *in vivo* plasma elimination and tissue distribution and *in vitro* serum binding studies, with that in the total body clearance (CL_{tot}) determined from biliary, renal, and metabolic clearances in guinea pigs. The plasma disappearance of digoxin after a 250-μg/kg iv dose followed a triexponential decline in both the control and quinidine-treated guinea pigs. In the quinidine-treated guinea pigs, the pharmacokinetic parameters Vd_{ss} and CL_{tot} significantly decreased to approximately half of that for the control guinea pigs. The tissue-to-plasma partition coefficients (K_p) of all tissues studied, *i.e.* liver, heart, muscle, and brain, at 6 hr after bolus injection of digoxin decreased in the presence of quinidine. The serum free fraction and the plasma-to-blood concentration ratio of digoxin in the therapeutic range did not show a significant alteration in the presence of quinidine. This suggested that the decrease of K_p is due mainly to the inhibition of tissue distribution of digoxin by quinidine. The biliary clearance (CL_B) and renal clearance (CL_R) also significantly decreased in the presence of quinidine. It was concluded that quinidine caused a inhibition of digoxin in the tissue binding or uptake, which significantly decreased the K_p values of digoxin; this result may explain the significant decrease of Vd_{ss}. Moreover quinidine may be the cause of a reduction of biliary, renal, and metabolic clearances, which significantly decrease the CL_{tot} of digoxin.

Keyphrases □ Quinidine—effect on the distribution and elimination of digoxin, guinea pigs □ Digoxin—pharmacokinetics, effect of quinidine coadministration, guinea pigs □ Pharmacokinetics—digoxin in the guinea pig, effect of quinidine coadministration

When quinidine is given to patients (1–5), dogs (6), or guinea pigs (7) receiving digoxin, the serum digoxin concentration increases. Reduction in the total body clearance (CL_{tot}) (5, 6) and the volume of distribution (Vd) (5, 6, 8) of digoxin has been observed and accounts for the elevated digoxin concentration. Quinidine has been reported to diminish the renal clearance (CL_R) of digoxin in humans (2, 4, 5, 8, 9) and dogs (10, 11) without significantly altering the glomerular filtration rate as measured by the creatinine clearance. Doherty *et al.* (12) reported that quinidine reduced the canine skeletal and heart muscle concentrations of digoxin, while increasing concentrations in the plasma and brain. Straub *et al.* (13) showed that quinidine reduced the number of digitalis-binding sites, as determined by *in vitro* binding studies with Na^+,K^+-ATPase from bovine heart membrane. Evidence has been reported that quinidine was capable of decreasing the affinity for digoxin of cardiac glycoside receptor sites on purified Na^+,K^+-ATPase in guinea pigs and on intact human erythrocyte membranes (14).

The present study examined the effect of quinidine on the distribution and elimination of digoxin by comparing the changes in Vd and CL_{tot} *in vivo*, which were determined from the tissue distribution, metabolism, excretion, serum protein binding, and plasma-to-blood distribution ratio. As a model animal for digoxin–quinidine interaction in the human, the guinea pig, a species in which digoxin distribution appears similar to that observed in the human, was selected.

EXPERIMENTAL

Digoxin[1] and quinidine sulfate[2] were used. Tritiated digoxin, labeled at the 12α-position (14.0 Ci/mmole)[3], which was found to be at least 99% pure by TLC, was used as the radioactive compound. All other reagents were commercially available and analytical grade.

Animal Experiments—Adult male Hartley guinea pigs[4], weighing 280–300 g, were used. Under light ether anesthesia, the jugular vein and carotid artery were cannulated with polyethylene tubing[5]. For the biliary and urinary excretion studies, bile fistula and urinary bladder cannulation were used to collect samples of bile and urine, respectively. Cannulated animals were kept in restraining cages with access to water under normal housing conditions prior to the experiments.

The guinea pigs were simultaneously given 250 μg/kg of digoxin (containing 100 μCi/kg of 12α-[^{3}H]digoxin) in 40% ethanol solution and 25 mg/kg of quinidine sulfate in physiological saline through the jugular vein cannula. The digoxin solution containing 40% ethanol was administered alone to the control guinea pigs. Blood samples (0.25 ml) were obtained for the determination of digoxin at 1, 5, 30, 60, 120, 180, 240, 300, and 360 min, and for the determination of quinidine (in different animals) at 5, 10, 15, 20, 30, 45, 60, 90, 120, 180, and 240 min in heparinized poly-

[1] Sigma Chemical Co., St. Louis, Mo.
[2] Tokyo Kasei Co., Tokyo, Japan.
[3] New England Nuclear Co., Boston, Mass.
[4] Nihon Seibutsu Zairyo, Tokyo, Japan.
[5] PE-10 for jugular vein and PE-50 for carotid artery: Clay Adams, Becton, Dickinson & Co., Parsippany, N.J.

0022-3549/83/1000-1137$01.00/0

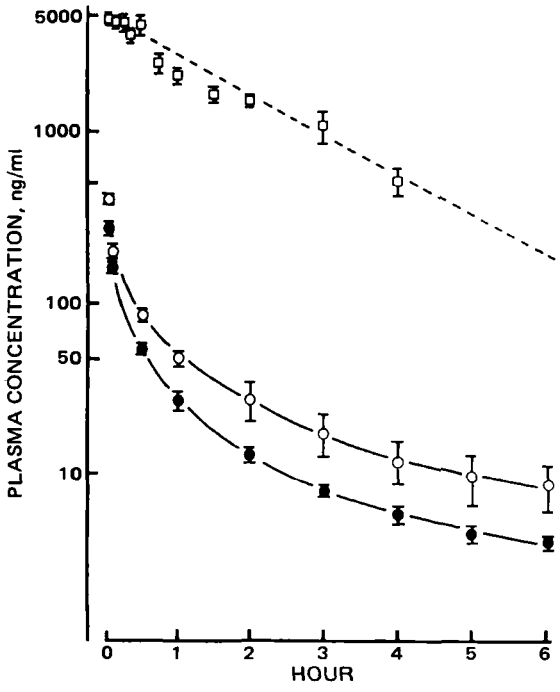

Figure 1—*Plasma disappearance curves of digoxin after a 250-μg/kg iv dose. Each point and vertical bar represent the mean and standard error of four (control) or three (quinidine-treated) guinea pigs. Curves were calculated by the least-squares method (17) using a digital computer. Key: (●) plasma digoxin concentration of control guinea pigs; (○) plasma digoxin concentration of quinidine-treated guinea pigs (digoxin simultaneously administered with 25 mg/kg of quinidine); (□) plasma concentration of quinidine.*

ethylene centrifuge tubes[6]. Bile samples were obtained at 15, 30, or 60 min, while the urine sample was collected for 360 min. The body temperature was kept at 37° using a heat lamp. Plasma was separated by centrifugation for 20 sec[7].

For the tissue distribution study the animals were sacrificed at 1 and 6 hr after digoxin administration by an injection of air into the carotid artery. After removal of blood samples, the brain, heart, liver, and muscle were quickly excised, rinsed with cold saline, blotted, and weighed. All tissues and plasma were stored at −40° until assayed. Tissue samples were homogenized with a three-fold excess of physiological saline[8]. The separation of the metabolites from digoxin was carried out using the method of Harrison and Gibaldi (15). A 100-μl quantity of the plasma sample and 1 ml of the tissue homogenate were shaken for 10 min and then extracted twice with 2 ml of chloroform–methanol (1:1, v/v). The pooled extracts were then streaked on silica gel plates and chromatographed. Glass sheets precoated with silica gel 60[9] of 0.25 mm thickness were developed twice in ethyl acetate–chloroform–acetic acid (90:5:5, v/v/v). Digoxin was visualized by spraying the plate with 3,5-dinitrobenzoic acid and 2 *N* KOH in methanol to develop a violet color. The spots attributable to digoxin from chromatograms of biological samples were scraped into scintillation vials containing 10 ml of scintillation fluid[10]. The extraction coefficients of digoxin from plasma, brain, heart, liver, and muscle were 0.85, 0.45, 0.68, 0.55, and 0.86, respectively. The concentration of ^{3}H-labeled digoxin was determined[11]. Quinidine concentration was determined by the double-extraction method according to Crámer and Isaksson (16).

Serum Protein Binding—Serum was separated from the blood, obtained through the carotid artery, by centrifugation for 10 min at 3000 rpm after standing for 60 min at room temperature. The serum free fraction of digoxin was determined by equilibrium dialysis at 37° for 16 hr using *semimicrocells*[12] and a semipermeable membrane[13] against

[6] Beckman Instruments, Fullerton, Calif.
[7] Table-top microfuge; Beckman Instruments, Fullerton, Calif.
[8] Teflon glass homogenizer.
[9] Without F; E. Merck, Darmstadt, West Germany.
[10] 0.1 g of 1,4-bis(4-methyl-5-phenyloxazol-2-yl)benzene, 4.0 g of 2,5-diphenyloxazole, and 500 ml of Triton X-100/liter of toluene.
[11] Aloka Tri-Carb counter; Aloka Instruments Co., Tokyo.
[12] *Kokugo-Gomu* Co., Tokyo, Japan.
[13] Type 36/32; Visking Co., Chicago, Ill.

Table I—Digoxin Pharmacokinetics in Guinea Pigs [a]

Parameter	Control (Digoxin)	Digoxin plus Quinidine
P, μg/ml	158.6 ± 13.3	575.3 ± 204.2
π, min^{-1}	0.126 ± 0.042	0.764 ± 0.442
A, μg/ml	68.6 ± 23.6	134.9 ± 5.9
α, min^{-1}	0.022 ± 0.005	0.0308 ± 0.0041
B, μg/ml	11.5 ± 2.5	33.2 ± 11.8
β, min^{-1}	0.00313 ± 0.00067	0.00388 ± 0.00035
Vd_{ss}, liter/kg[b]	5.25 ± 0.78	2.76 ± 0.31[f]
CL^p_{tot}, ml/(min kg)[c]	31.5 ± 2.6	17.3 ± 3.6[f]
CL_R, ml/(min kg)[d]	3.4 ± 0.8	0.9 ± 0.5[f]
CL_B, ml/(min kg)[d]	4.9 ± 0.5	0.9 ± 0.1[f]
CL_M, ml/(min kg)[e]	23.2	15.5

[a] Results are given as the mean ± *SE* of three or four animals. [b] The volume of distribution at steady state (Vd_{ss}) was calculated by a conventional equation (18) using triexponential equation constants from plasma disappearance curves. [c] The total plasma clearance (CL^p_{tot}) was calculated using CL^p_{tot} = dose/AUC. [d] The biliary clearance (CL_B) and the renal clearance (CL_R) were calculated using the equation in the text. [e] The mean metabolic clearance (CL_M) was calculated by $CL_M = CL_{tot} - CL_B - CL_R$ (see text). [f] Significantly different ($p < 0.05$) from the control guinea pigs.

Krebs–Ringers buffer (pH 7.4), containing 0.6–46.8 ng/ml of [^{3}H]digoxin and 1 and 10 μg/ml of quinidine. The protein binding of digoxin to serum was unchanged between 16 and 20 hr of dialysis at 37°. The quinidine concentration in the protein chamber after dialysis was in the same range as that of the *in vivo* concentration of quinidine (0.5–5 μg/ml) in plasma.

Plasma-to-Blood Concentration Ratio of Digoxin—All procedures were carried out immediately after the blood collection. The blood was incubated with 1 μCi/ml of [^{3}H]digoxin and various amounts of nonlabeled digoxin (1–300 ng/ml as blood concentration) at 37° for 20 min in the presence of quinidine (1 and 10 μg/ml). Preliminary experiments indicated that equilibration was attained within 30 sec between plasma and red blood cells (unpublished data). After centrifugation, an aliquot of the plasma was removed and the concentration of [^{3}H]digoxin was determined as described above. An analytical blank without substrate was determined in the same manner. The hemolysis during the incubation was negligible.

Data Analysis—The digoxin concentration data for individual animals were fitted to the equation $C_t = Pe^{-\pi t} + Ae^{-\alpha t} + Be^{-\beta t}$ for the plasma concentration C_t at time t by nonlinear least-squares regression (17). Pharmacokinetic constants (Table I) were determined from the three-exponential equation constants, *i.e.*, P, π, A, α, B, and β, using conventional equations (18). All means are presented with their standard error (the mean ± *SE*). The Student's t test was utilized to determine significant differences between the control and the quinidine-treated groups.

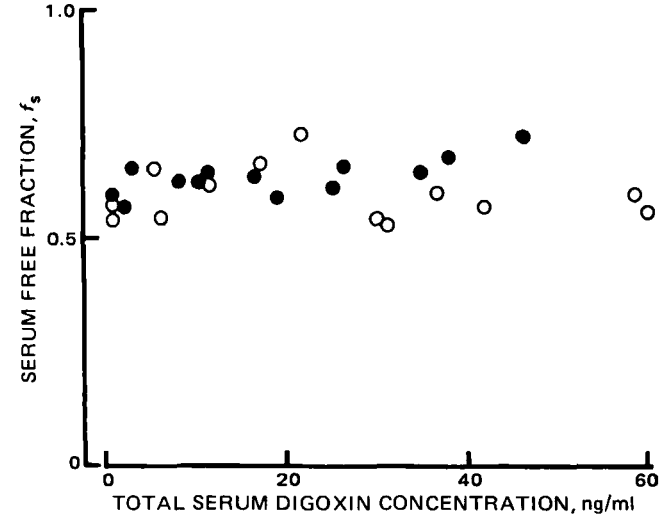

Figure 2—*Serum free fraction as a function of total blood concentration of digoxin with (○) and without (●) quinidine. Equilibrium dialysis was performed at 37° for 16 hr against Krebs–Ringer buffer (pH 7.4) containing 0.61–46.8 ng/ml of [^{3}H]digoxin. The concentration of quinidine was 1 and 10 μg/ml.*

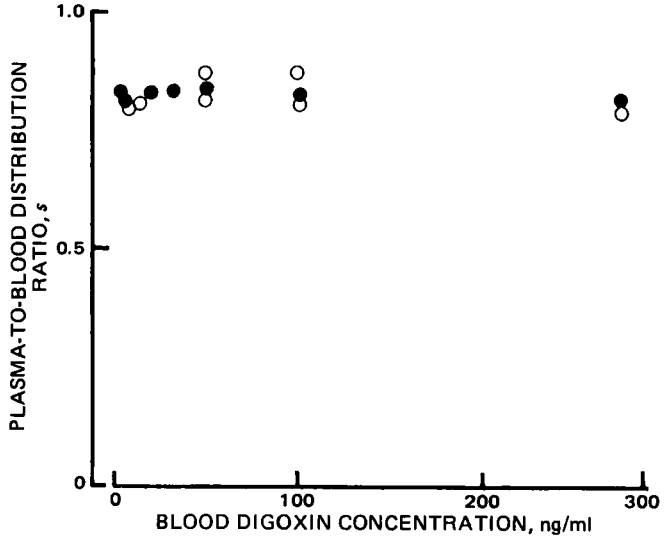

Figure 3—*Plasma-to-blood concentration ratio of digoxin as a function of total plasma concentration with (○) and without (●) quinidine. The blood was incubated with 1–300 ng/ml of [^{3}H]digoxin (as the blood concentration) at 37° for 20 min. The concentration of quinidine was 1 and 10 μg/ml.*

RESULTS

Effect of Quinidine on Digoxin Elimination from Plasma—The plasma disappearance of digoxin after intravenous administration of 250 μg/kg in the presence and absence of quinidine is shown in Fig. 1. The disappearance of digoxin followed three-exponential curves in both the control and quinidine-treated guinea pigs. The range of the plasma quinidine concentration was 0.5–5 μg/ml during the sampling period of 4 hr. The pharmacokinetic constants were computed by a nonlinear iterative least-squares method (17) and are listed in Table I. In the quinidine-treated guinea pigs, a significant decrease was observed in the total body plasma clearance (CL^p_{tot}). The Vd_{ss} was decreased significantly by quinidine.

Effect of Quinidine on Serum Protein Binding of Digoxin—The results from serum protein binding experiments are shown in Fig. 2. In both the experiments, *i.e.*, with and without quinidine, the serum binding of digoxin exhibited apparent linear relationships. The serum free fraction (f_s) did not show a significant alteration in the presence of quinidine.

Plasma-to-Blood Concentration Ratio of Digoxin—The plasma-to-blood concentration ratio of digoxin in the dose range from 1 to 300 ng/ml were determined in the presence and absence of quinidine (Fig. 3). The ratio seems to be constant over the dose range studied and did not show a significant alteration in the presence of quinidine.

Effect of Quinidine on Tissue Distribution of Digoxin—Table II demonstrates the changes in the tissue concentrations of digoxin at 1 and 6 hr after intravenous bolus administration of 250 μg/kg. It is apparent that the tissue concentration of digoxin did not show a significant alteration in the quinidine-treated guinea pigs. There are two exceptions: the liver, with a 50% decrease (significantly different from the control group, $p < 0.05$) in the quinidine-treated group and the brain, where a 370% increase (significantly different from the control, $p < 0.05$) occurred in the same group at 1 hr after intravenous bolus administration of digoxin. The apparent tissue-to-plasma partition coefficients (K_p) at 1 and 6 hr after intravenous bolus administration of digoxin in the presence and absence of quinidine are shown in Table II. The K_p values of most tissues studied significantly decreased in the quinidine-treated group, while the apparent brain-to-plasma concentration ratio at 1 hr significantly ($p < 0.05$) increased in the same group.

Effect of Quinidine on Biliary and Renal Excretion of Digoxin—In the quinidine-treated guinea pigs, no significant difference was observed in the mean bile flow rate for 6 hr when compared with that in the control animals (138.3 ± 16.1 μl/min/kg for the quinidine-treated group, $n = 3$, and 133.8 ± 17.4 for the control, $n = 3$). The biliary excretion rates of digoxin are shown in Fig. 4A; significant decreases ($p < 0.05$) were observed, except at 3 and 4 hr. Cumulative biliary excretion curves of digoxin are shown in Fig. 4B. The amount of digoxin excreted during 6 hr in the control guinea pigs was 13.8 ± 1.1% of the dose ($n = 3$), while that of the quinidine-treated group was 5.6 ± 1.1% ($n = 3$). The cumulative amount of digoxin excreted in urine during 6 hr after intravenous bolus administration in the control guinea pigs was 9.9 ± 2.3% of the dose ($n = 3$), while that of the quinidine-treated group was 5.2 ± 2.9% ($n = 3$). The mean biliary (CL_B) and renal clearances (CL_R) were calculated by:

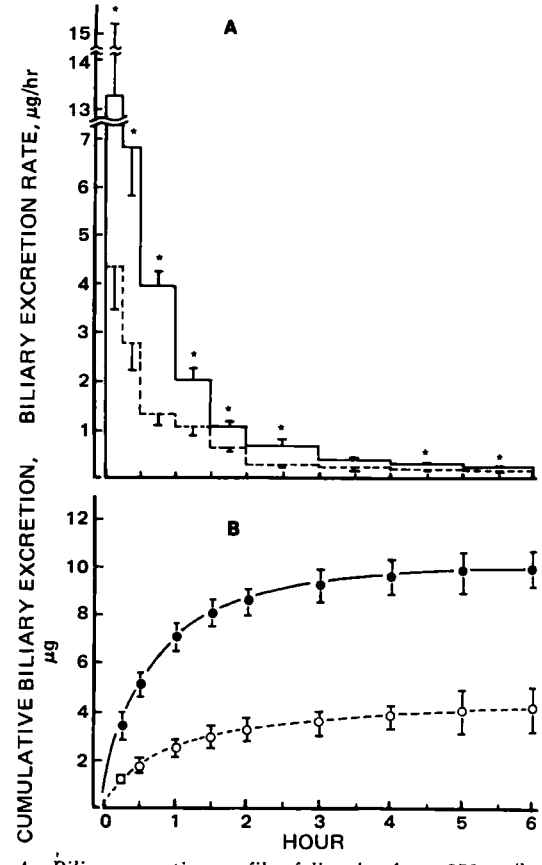

Figure 4—*Biliary excretion profile of digoxin after a 250-μg/kg iv dose. (A) Biliary excretion rate. Each datum and bar represents the mean and standard error of three control (—) quinidine-treated (---) guinea pigs; (*) statistically significant at p = 0.05 when compared with the biliary excretion rate of the control guinea pigs. (B) Cumulative biliary excretion curves. Each point and bar represents the mean and standard error of three control (●) or quinidine-treated (○) guinea pigs.*

$$CL_B \text{ or } CL_R = \frac{\text{Cumulative amount of digoxin excreted for 360 min}}{AUC_{0\text{–}360\ min}}$$

where AUC is the area under the plasma concentration *versus* time curve calculated from pharmacokinetic parameters listed in Table I. The CL_B and CL_R calculated by this equation in the presence and absence of quinidine are also listed in Table I. Both clearances significantly decreased in the presence of quinidine.

From the digoxin content in plasma, liver, and bile, the liver-to-plasma and the bile-to-liver concentration ratios were calculated (Table III). These ratios indicated that the transport of digoxin from plasma to liver and from liver to bile were against a large concentration gradient in the control guinea pigs. But after quinidine treatment, the liver-to-plasma concentration ratio significantly decreased, while the bile-to-liver concentration ratio did not show a significant alteration.

DISCUSSION

The results of this study in guinea pigs are in agreement with previous studies, in which the increases in the serum (plasma) concentrations of digoxin were observed in the presence of quinidine in humans (1–5), dogs (6), and guinea pigs (7). Many investigators have reported that quinidine decreased Vd and CL_{tot} of digoxin in humans (5) and dogs (6). In this study the decreases of both parameters were also observed in guinea pigs (Table I). The lack of a substantial change in the elimination half-life ($t_{1/2}$) of digoxin suggested that the parallel changes in Vd and CL_{tot} tend to counterbalance each other. In plasma protein binding, no significant difference was observed in the serum free fraction of digoxin with or without quinidine (Fig. 2). This finding suggests that quinidine does not

Table II—Tissue Distribution of Digoxin in Guinea Pigs [a]

		1 hr[b]		6 hr[b]	
		Concentration, ng/g	K_p[c]	Concentration, ng/g	K_p[c]
Control (Digoxin)	Brain	2.3 ± 1.2	0.09 ± 0.05	12.5 ± 1.1	3.42 ± 0.31
	Muscle	168.3 ± 4.1	6.63 ± 0.16	108.7 ± 6.0	29.81 ± 1.65
	Heart	170.0 ± 6.6	6.69 ± 0.26	34.1 ± 5.3	9.36 ± 1.47
	Liver	94.9 ± 12.8	3.74 ± 0.50	36.0 ± 1.5	9.88 ± 0.40
Digoxin + Quinidine	Brain	8.5 ± 1.0[d]	0.17 ± 0.02[d]	15.0 ± 0.6	1.76 ± 0.20[d]
	Muscle	208.7 ± 31.2	4.14 ± 0.62[d]	157.0 ± 25.5	18.38 ± 2.98[d]
	Heart	212.0 ± 15.3	4.21 ± 0.30[d]	42.5 ± 7.5	4.98 ± 0.87[d]
	Liver	—[e]	—[e]	16.6 ± 5.2[d]	1.95 ± 0.61[d]

[a] Results are given as the mean ± *SE* of three guinea pigs. [b] At 1 and 6 hr after bolus intravenous administration of 250 μg/kg of digoxin. [c] The apparent tissue-to-plasma partition coefficient. [d] Significantly different ($p < 0.05$) from the control guinea pigs. [e] — Not determined.

alter the binding of digoxin to serum (plasma) proteins. A possible reason for this effect might be that digoxin binds mainly to albumin in serum (plasma), but the basic drug quinidine binds not only to albumin but also to lipoprotein or α_1-acid glycoprotein (19).

The plasma-to-blood concentration ratio (s) of digoxin did not show a significant change when coadministered with quinidine in guinea pigs (Fig. 3). Using ^{86}Rb-labeled human erythrocytes, Doering *et al.* (20) recently showed that quinidine did not interfere with the glycoside receptor. Thus, changes in s in the presence of quinidine cannot be explained by this mechanism. The decrease in Vd at steady state may be compatible with the hypothesis that quinidine displaces digoxin from the tissue binding sites (14). As shown in Table II, digoxin extensively binds to tissues such as skeletal muscle, liver, and heart, and the K_p values significantly decreased in the presence of quinidine. Straub *et al.* (13) recently reported that high concentrations of quinidine displace digoxin from bovine heart ATPase preparations. However, similar studies by Doering (2) failed to demonstrate the displacement of ouabain by quinidine from the sarcolemma fraction of lamb ventricular myocardium. Recent *in vitro* studies by Ball *et al.* (14) showed that quinidine competes for the binding site on Na^+,K^+-ATPase with digoxin. The effect of quinidine on Na^+,K^+-ATPase, however, occurred at considerably higher concentrations of quinidine than those in the therapeutic range found in humans. Thus, it is uncertain whether quinidine displaces digoxin from Na^+,K^+-ATPase in therapeutic serum concentrations. It has also been reported that another cinchona alkaloid, quinine, decreases the initial uptake rate of ouabain, a cardiac glycoside, by isolated rat hepatocytes (21). In a similar way, digoxin uptake may be inhibited by quinidine.

The renal clearance (CL_R) significantly decreased in the presence of quinidine (Table I). This suggested that quinidine may reduce digoxin secretion or increase digoxin reabsorption as shown in dogs (11), but it is difficult to determine which is the predominant factor from the restricted findings to date.

Koup *et al.* (22) reported the mean value of CL_{tot} for digoxin, which was significantly higher than that of the CL_R of digoxin in the human, and Fenster *et al.* (23) also reported a similar result. Furthermore, considerable biliary excretion of digoxin was evident in guinea pigs (24) and rats (25). It has been suggested that the CL_{tot} of digoxin in rats essentially reflected the sum of CL_R and the hepatic clearance (CL_H) which involves the biliary and metabolic clearance (25). Therefore, the mean metabolic clearance (CL_M) was estimated by the difference calculated by $CL_M = CL_{tot} - CL_B - CL_R$ (Table I). The decrease of CL_M in the quinidine-treated guinea pigs was not so remarkable when compared with the decreases in CL_B or CL_R.

The hepatic transport of digoxin may occur in at least two discernible steps: the uptake from plasma into liver and the transport from liver into bile. As shown in Table III, quinidine may suppress the carrier-mediated transport of digoxin from plasma to liver or the tissue binding, but the transport from liver to bile may not be affected by quinidine.

Table III—Liver-to-Plasma and Bile-to-Liver Concentration Ratios for Digoxin in Control and Quinidine-Treated Guinea Pigs [a]

	Control (Digoxin)	Digoxin plus Quinidine
Liver-to-Plasma	9.88 ± 0.40	1.95 ± 0.61[b]
Bile-to-Liver	4.25 ± 0.53	5.49 ± 3.10

[a] Results are given as the mean ± *SE* of three guinea pigs. The mean digoxin concentrations in the liver and plasma at 6 hr, and in the bile from 5 to 6 hr after bolus intravenous administration of 250 μg/kg of digoxin were used for the calculation of the ratios. [b] Significantly different ($p < 0.05$) from the control guinea pigs.

The distribution of digoxin to the CNS is of interest in view of the suggestion that some of the effects of cardiac glycosides may occur as a result of the effect on the CNS (26). As shown in Table II, the concentration of digoxin measured in the brain was low in guinea pigs (this study), and in humans (27) digoxin seems to gradually enter the spinal fluid. But the concentration of digoxin in the choroid plexus of the human has been found to be at least as high as that in the ventricular myocardium (27). The slow entry of digoxin into the brain may be due to an efflux mechanism through the choroid plexus. Thus, the increase of digoxin distribution to the brain at 1 hr after bolus intravenous administration in the presence of quinidine might be due to the inhibition of the transport system from the cerebrospinal fluid to blood through the choroid plexus for digoxin. On the contrary, the decrease of the apparent brain-to-plasma concentration ratio (K_p) at 6 hr after bolus intravenous administration of digoxin might be due mainly to the displacement of the glycosides from the binding sites (Na^+,K^+-ATPase) in the brain cells.

In conclusion, the quinidine–digoxin interaction was demonstrated in guinea pigs. Quinidine caused an inhibition in the tissue distribution of digoxin, which was shown in the significant decrease of the K_p values of digoxin, and this result may explain the significant decrease of Vd_{ss}. Furthermore, quinidine may cause a reduction of biliary, renal, and metabolic clearances, which significantly decrease the CL_{tot} of digoxin.

REFERENCES

(1) G. Ejvinsson, *Br. Med. J.*, **1**, 279 (1978).

(2) W. Doering, *N. Engl. J. Med.*, **301**, 400 (1979).

(3) E. B. Leahey, Jr., J. A. Reiffel, R. E. Drusin, R. H. Heissenbuttel, W. P. Lovejoy, and J. T. Bigger, Jr., *J. Am. Med. Assoc.*, **240**, 533 (1978).

(4) E. B. Leahey, Jr., J. T. Bigger, Jr., V. P. Butler, Jr., J. A. Reiffel, G. C. O'Connel, L. E. Scaffidi, and J. N. Rottman, *Am. J. Cardiol.*, **48**, 1141 (1981).

(5) K. Shenk-Gustafsson and R. Dahlqvist, *Br. J. Clin. Pharmacol.*, **11**, 181 (1981).

(6) T. P. Gibson and H. A. Nelson, *J. Lab. Clin. Med.*, **95**, 417 (1980).

(7) D. H. Kim, T. Akera, and T. M. Brody, *J. Pharmacol. Exp. Ther.*, **217**, 559 (1981).

(8) W. D. Hager, P. Fenster, M. Mayerson, D. Perrier, P. Graves, F. I. Marcus, and S. Goldman, *N. Engl. J. Med.*, **300**, 1238 (1979).

(9) P. M. Hooymans and F. W. H. M. Merkus, *Br. Med. J.*, **2**, 1022 (1978).

(10) E. B. Leahey, Jr., J. A. Carson, J. T. Bigger, Jr., and V. P. Butler, Jr., *Circulation* (Suppl. 2), **59–60**, 16 (1979).

(11) T. P. Gibson and A. Quintanilla, *J. Lab Clin. Med.*, **96**, 1062 (1980).

(12) J. E. Doherty, K. D. Straub, M. L. Murrhy, N. de Soyza, J. K. Bissett, and J. J. Kane, *Am. J. Cardiol.*, **45**, 1196 (1980).

(13) K. D. Straub, J. J. Kane, J. K. Bissett, and J. E. Doherty, *Circulation* (Suppl. 2), **58**, II-58 (1978).

(14) W. J. Ball, Jr., D. Tse-Eng, E. T. Wallick, J. P. Bilezikian, A. Schwartz, and V. P. Butler, Jr., *J. Clin. Invest.*, **68**, 1065 (1981).

(15) L. I. Harrison, and M. Gibaldi, *Drug. Metab. Dispos.*, **4**, 88 (1976).

(16) G. Cramér and B. Isaksson, *Scand. J. Clin. Lab. Invest.*, **15**, 553 (1963).

(17) T. Nakagawa, Y. Koyanagi, and H. Togawa, "SALS, a Computer Program for Statistical Analysis with Least Squares Fitting," Library Program of the University of Tokyo Computer Center, Tokyo, Japan,

1978.
(18) M. Gibaldi and D. Perrier, "Pharmacokinetics," Dekker, New York, N.Y., 1975.
(19) H. R. Ochs, D. J. Greenblatt, and E. Woo, *Clin. Pharmacokinet.*, **5**, 150 (1980).
(20) W. Doering and G. G. Belz, *Klin. Wochenschr.*, **59**, 95 (1981).
(21) D. L. Eaton and C. D. Klaassen, *J. Pharmacol. Exp. Ther.*, **205**, 480 (1978).
(22) J. R. Koup, D. J. Greenblatt, W. J. Jusko, T. W. Smith, and J. Koch-Weser, *J. Pharmacokinet. Biopharm.*, **3**, 181 (1975).
(23) P. E. Fenster, J. R. Powell, P. E. Graves, K. A. Conrad, W. D. Hager, S. Goldman, and F. I. Marcus, *Ann. Intern. Med.*, **93**, 698 (1980).
(24) A. Marzo and P. Ghirardi, *Naunyn-Schmiedeberg's Arch. Pharmacol.*, **298**, 51 (1977).
(25) L. I. Harrison and M. Gibaldi, *J. Pharm. Sci.*, **66**, 1138 (1977).
(26) B. Levitt, N. Cagin, J. Kleid, J. Somberg, and R. Gillis, *Am. J. Cardiol.*, **37**, 1111 (1976).
(27) R. Krakauer and E. Steiness, *Clin. Pharmacol. Ther.*, **24**, 454 (1978).

Pharmacokinetics of Heparin V: *In Vivo* and *In Vitro* Factors Affecting the Relationship Between Concentration and Anticoagulant Effect of Heparin in Rat Plasma

LLOYD R. WHITFIELD and GERHARD LEVY ˣ

Received June 21, 1982, from the *Department of Pharmaceutics, School of Pharmacy, State University of New York at Buffalo, Amherst, NY 14260.* Accepted for publication August 25, 1982.

Abstract □ There are appreciable interindividual variations in rats of baseline activated partial thromboplastin time (APTT) and of the anticoagulant effect of heparin added to plasma (as reflected by the slope of the regression line describing the essentially linear relationship between ln APTT and heparin concentration). Determination of baseline APTT and slope value on two occasions, 7 days apart, in the same rats revealed that (unlike in humans) these characteristics were subject also to considerable intraindividual variation. To explore the possible reasons for the observed variability, the effect of citrate concentration (acid citrate solution is used as a blood anticoagulant in the collection of plasma), calcium concentration (in the recalcifying solution used to initiate coagulation), and plasma incubation time (for activating the coagulation system) was determined. All three variables had pronounced effects on the anticoagulant response to heparin. Since rat erythrocytes are almost totally impermeable to citrate, hematocrit is a determinant of plasma citrate concentration when acid citrate solution is added in constant proportion to rat blood. Accordingly, inter- and intraindividual differences in baseline APTT and slope values were measured in another experiment in which the citrate solution to plasma (rather than blood) volume ratio was held constant and blood samples were obtained 30 days apart to permit the return of hematocrit values to normal. Intraindividual variation of the coagulation characteristics was appreciably decreased under these conditions. There are important differences between rats and humans with respect to the effect of citrate concentration and plasma incubation time on baseline APTT and on the anticoagulant action of heparin, as well as with respect to the relationship between these two characteristics.

Keyphrases □ Heparin—pharmacokinetics, concentration and anticoagulant effect, *in vivo* and *in vitro* factors □ Pharmacokinetics—heparin, concentration and anticoagulant effect, *in vivo* and *in vitro* factors □ Anticoagulants—heparin, effect of concentration, *in vivo* and *in vitro* factors, pharmacokinetics

Safe and effective anticoagulant therapy with heparin is complicated by the chemical and pharmacological heterogeneity of this natural product (1–3), by inter- and intraindividual differences in anticoagulant response (4–8) that necessitate individualization and frequent changes of the dosing rate of this drug, and by questions concerning the suitability of the various *in vitro* clotting tests used as intermediate therapeutic end points to serve as indices of therapeutic efficacy (prevention of thrombosis) and safety (absence of hemorrhagic episodes due to excessive anticoagulation) (9, 10). An individual's anticoagulant response to a given dose or dosing rate of heparin is subject to two sources of considerable variation, one pharmacokinetic and the other pharmacodynamic: the disposition (systemic clearance and biological half-life) of the drug and the relationship between heparin concentration in plasma (the site of anticoagulant action) and the magnitude of anticoagulant effect (6). Practical and ethical considerations impose limitations on exploration of these problems in humans and make it desirable to use animal models for certain pharmacokinetic and pharmacodynamic studies of heparin. The rat appears to be promising for this purpose. Like humans, rats exhibit dose-dependent elimination kinetics of heparin (11). The anticoagulant response to this drug as reflected by the activated partial thromboplastin time (APTT) is log-linearly related to the concentration of added heparin in plasma over a wide concentration range in both humans and rats (4, 11).

Studies in normal human adults (4) have shown a significant correlation between hematocrit and an index of the anticoagulant response of plasma to added heparin (the slope of the essentially linear relationship between ln APTT and the concentration of heparin added to plasma, to be referred to in this article as the slope or slope value). It has also been observed that there are pronounced interindividual differences in both baseline APTT (*i.e.*, APTT of plasma without added heparin) and slope value, but that intraindividual differences are relatively small in humans (4).

Contrary to these findings, it was found in the initial phase of the present study that baseline APTT and slope values in individual rats, while exhibiting similar interindividual differences as in humans, were poorly reproducible when measured again 7 days later. To explore the reasons for these intraindividual differences in rats, the relationship of hematocrit, citrate concentration (acid citrate solution is added to blood to prevent coagulation),

0022-3549/83/1000-1141$01.00/0

1978.
(18) M. Gibaldi and D. Perrier, "Pharmacokinetics," Dekker, New York, N.Y., 1975.
(19) H. R. Ochs, D. J. Greenblatt, and E. Woo, *Clin. Pharmacokinet.*, **5**, 150 (1980).
(20) W. Doering and G. G. Belz, *Klin. Wochenschr.*, **59**, 95 (1981).
(21) D. L. Eaton and C. D. Klaassen, *J. Pharmacol. Exp. Ther.*, **205**, 480 (1978).
(22) J. R. Koup, D. J. Greenblatt, W. J. Jusko, T. W. Smith, and J. Koch-Weser, *J. Pharmacokinet. Biopharm.*, **3**, 181 (1975).
(23) P. E. Fenster, J. R. Powell, P. E. Graves, K. A. Conrad, W. D. Hager, S. Goldman, and F. I. Marcus, *Ann. Intern. Med.*, **93**, 698 (1980).
(24) A. Marzo and P. Ghirardi, *Naunyn-Schmiedeberg's Arch. Pharmacol.*, **298**, 51 (1977).
(25) L. I. Harrison and M. Gibaldi, *J. Pharm. Sci.*, **66**, 1138 (1977).
(26) B. Levitt, N. Cagin, J. Kleid, J. Somberg, and R. Gillis, *Am. J. Cardiol.*, **37**, 1111 (1976).
(27) R. Krakauer and E. Steiness, *Clin. Pharmacol. Ther.*, **24**, 454 (1978).

Pharmacokinetics of Heparin V: *In Vivo* and *In Vitro* Factors Affecting the Relationship Between Concentration and Anticoagulant Effect of Heparin in Rat Plasma

LLOYD R. WHITFIELD and GERHARD LEVY ˣ

Received June 21, 1982, from the *Department of Pharmaceutics, School of Pharmacy, State University of New York at Buffalo, Amherst, NY 14260.* Accepted for publication August 25, 1982.

Abstract □ There are appreciable interindividual variations in rats of baseline activated partial thromboplastin time (APTT) and of the anticoagulant effect of heparin added to plasma (as reflected by the slope of the regression line describing the essentially linear relationship between ln APTT and heparin concentration). Determination of baseline APTT and slope value on two occasions, 7 days apart, in the same rats revealed that (unlike in humans) these characteristics were subject also to considerable intraindividual variation. To explore the possible reasons for the observed variability, the effect of citrate concentration (acid citrate solution is used as a blood anticoagulant in the collection of plasma), calcium concentration (in the recalcifying solution used to initiate coagulation), and plasma incubation time (for activating the coagulation system) was determined. All three variables had pronounced effects on the anticoagulant response to heparin. Since rat erythrocytes are almost totally impermeable to citrate, hematocrit is a determinant of plasma citrate concentration when acid citrate solution is added in constant proportion to rat blood. Accordingly, inter- and intraindividual differences in baseline APTT and slope values were measured in another experiment in which the citrate solution to plasma (rather than blood) volume ratio was held constant and blood samples were obtained 30 days apart to permit the return of hematocrit values to normal. Intraindividual variation of the coagulation characteristics was appreciably decreased under these conditions. There are important differences between rats and humans with respect to the effect of citrate concentration and plasma incubation time on baseline APTT and on the anticoagulant action of heparin, as well as with respect to the relationship between these two characteristics.

Keyphrases □ Heparin—pharmacokinetics, concentration and anticoagulant effect, *in vivo* and *in vitro* factors □ Pharmacokinetics—heparin, concentration and anticoagulant effect, *in vivo* and *in vitro* factors □ Anticoagulants—heparin, effect of concentration, *in vivo* and *in vitro* factors, pharmacokinetics

Safe and effective anticoagulant therapy with heparin is complicated by the chemical and pharmacological heterogeneity of this natural product (1–3), by inter- and intraindividual differences in anticoagulant response (4–8) that necessitate individualization and frequent changes of the dosing rate of this drug, and by questions concerning the suitability of the various *in vitro* clotting tests used as intermediate therapeutic end points to serve as indices of therapeutic efficacy (prevention of thrombosis) and safety (absence of hemorrhagic episodes due to excessive anticoagulation) (9, 10). An individual's anticoagulant response to a given dose or dosing rate of heparin is subject to two sources of considerable variation, one pharmacokinetic and the other pharmacodynamic: the disposition (systemic clearance and biological half-life) of the drug and the relationship between heparin concentration in plasma (the site of anticoagulant action) and the magnitude of anticoagulant effect (6). Practical and ethical considerations impose limitations on exploration of these problems in humans and make it desirable to use animal models for certain pharmacokinetic and pharmacodynamic studies of heparin. The rat appears to be promising for this purpose. Like humans, rats exhibit dose-dependent elimination kinetics of heparin (11). The anticoagulant response to this drug as reflected by the activated partial thromboplastin time (APTT) is log-linearly related to the concentration of added heparin in plasma over a wide concentration range in both humans and rats (4, 11).

Studies in normal human adults (4) have shown a significant correlation between hematocrit and an index of the anticoagulant response of plasma to added heparin (the slope of the essentially linear relationship between ln APTT and the concentration of heparin added to plasma, to be referred to in this article as the slope or slope value). It has also been observed that there are pronounced interindividual differences in both baseline APTT (*i.e.*, APTT of plasma without added heparin) and slope value, but that intraindividual differences are relatively small in humans (4).

Contrary to these findings, it was found in the initial phase of the present study that baseline APTT and slope values in individual rats, while exhibiting similar interindividual differences as in humans, were poorly reproducible when measured again 7 days later. To explore the reasons for these intraindividual differences in rats, the relationship of hematocrit, citrate concentration (acid citrate solution is added to blood to prevent coagulation),

0022-3549/83/1000-1141$01.00/0

and calcium concentration (calcium chloride is added to the citrated plasma to initiate the clotting process) to baseline APTT and slope value were determined. Based on the results of these experiments, the assessment of inter- and intraindividual differences in baseline APTT and slope value was repeated under conditions in which the volume ratio of citrate solution to *plasma* (rather than blood, as is the usual practice) was kept constant. Since citrate is almost totally excluded from erythrocytes (12), this prevents any variation of plasma citrate concentration due to differences in hematocrit. Another variable studied in this investigation was the effect of the incubation time of citrated plasma with APTT reagent (before recalcification) on baseline APTT and on slope. The results of these studies (*a*) serve to identify those variables which have to be carefully controlled in pharmacodynamic and pharmacokinetic (based on bioassay) experiments on rats, (*b*) provide an indication of the magnitude of inter- and intraindividual differences of baseline APTT and anticoagulant effect of heparin in rats, and (*c*) permit a comparison of differences between humans and rats with respect to inter- and intraindividual variations of baseline APTT and slope, and the relationship of these two indices to one another and to certain other physiological and methodological variables.

EXPERIMENTAL

Adult, male Sprague–Dawley rats[1] were used in this investigation. They had free access to food[2] and water at all times. The APTT was determined as described previously (11): Samples of frozen citrated plasma were thawed at 37° and the tubes were then transferred to an ice-water bath. Within 1 hr, 0.25 ml of the plasma was transferred to a 0.75-ml polypropylene tube containing 10 μl of normal saline solution. One-tenth milliliter of this plasma was mixed with 0.1 ml of APTT reagent[3], and this mixture was incubated at 37° for exactly 15 min (except when incubation time was studied as a variable). One-tenth milliliter of calcium chloride solution (0.025 *M* except when calcium concentration was studied as a variable) was then added to initiate clotting. The incubation and subsequent determination of APTT were done with a coagulation timer[4]. All samples were prepared and APTT was measured in duplicate. The duplicate values, which usually varied by <4%, were averaged.

To determine the effect of added heparin on APTT, the 10 μl of normal saline solution added to a plasma sample for determination of baseline APTT was replaced by 10 μl of sodium heparin (bovine lung origin)[5] in normal saline solution. The heparin concentration in this solution was varied such as to yield plasma heparin concentrations of 0.05–1.0 U/ml, usually in nine increments. The slope of the relationship between ln APTT and heparin concentration was determined by least-squares linear regression analysis of APTT values obtained from plasma samples in the 0.1 to 1.0-U/ml heparin concentration range. The statistical significance of differences between slope values of plasma obtained on different days from the same animal was determined by analysis of covariance (13).

To determine the effect of plasma citrate concentration on baseline APTT and on the anticoagulant activity of heparin, 10-ml blood samples were collected from each of seven rats, weighing 470–567 g. The blood was drawn from the abdominal aorta, during ether anesthesia, into a plastic syringe containing 0.6 ml of 0.1 *M* acid citrate solution (14). The blood samples were pooled in a plastic beaker immersed in an ice-water bath and kept well mixed by magnetic stirring. Aliquots (9.6 ml) of the pooled, citrated blood were transferred by polypropylene pipet to screw-capped polycarbonate centrifuge tubes containing 0.45 ml of either isotonic saline solution or acid citrate solution of six different (66–330 m*M*) concentrations. Since citrate is almost totally excluded from rat erythrocytes (12), the plasma citrate concentration was calculated from the known whole blood citrate concentration and the hematocrit. Plasma was obtained by centrifuging the blood samples at 14,000×*g* for 5 min in a temperature-controlled centrifuge at 15°, and baseline APTT and slope value were determined as described in the preceding paragraphs.

The effect of calcium chloride concentration in the recalcifying solution used to initiate plasma clotting was determined at a constant citrate concentration (*i.e.*, changing calcium–citrate concentration ratio) and at a constant calcium–citrate concentration ratio[6]. Pooled citrated plasma was obtained from eight rats, weighing 442–530 g, using the aforementioned procedure except that the final citrate concentration in half of the plasma samples was kept constant. The calcium chloride concentration in the recalcifying solution ranged from 12.5 to 46.6 m*M*, in six increments. Baseline APTT and slope values were determined.

To determine the effect of incubation time on baseline APTT and slope, 10-ml blood samples were obtained from each of 15 rats weighing 344–382 g. A 30-μl sample of blood was first drawn from the tail artery into a heparinized microhematocrit tube; the tube was centrifuged (4) and the hematocrit determined. A sufficient volume of acid citrate solution was then drawn into a plastic syringe such that on collection of 10 ml of blood from an animal, the volume ratio of citrate solution to plasma was 1:6. Individual plasma samples from five of the rats were divided into three equal volumes, and plasma samples from the other 10 rats were divided into two equal volumes. One of the plasma aliquots from each of the initial five rats was used to determine the time required for maximum activation of the intrinsic coagulation pathway. This was done by incubating the citrated plasma–APTT reagent mixture at 37° in covered tubes for 1–20 min before recalcification. Except for the variation of incubation time, the APTT measurements were performed by the standard procedure. Based on the results of the five-animal study, baseline APTT and slope value determinations on plasma from the other 10 rats were made after 3 and 15 min of incubation. (It should be noted that these experiments were not done with pooled plasma, but with individual plasma samples from a total of 15 animals.)

Inter- and intraindividual differences of baseline APTT and slope values were determined in two experiments. All rats had a silicone rubber cannula implanted in the right jugular vein under ether anesthesia 3 days before the start of the experiment (15). Their body weight and hematocrit were determined on each study day. Thirteen animals were used in the first experiment. On day 1, 4 ml of blood was collected through the cannula in a plastic syringe containing 0.44 ml of 0.1 *M* acid citrate solution using the technique previously described (11). On day 7, 9 ml of blood was obtained from the abdominal aorta, under ether anesthesia, in a plastic syringe containing 1 ml of the acid citrate solution. The second experiment, with 12 rats, consisted of blood withdrawals on days 1 and 30. In this experiment, hematocrit was determined first from a microsample of blood taken from the tail artery, and the volume of acid citrate solution was individualized to yield a constant acid citrate solution–plasma volume ratio of 1:6. In all cases, the blood and citrate anticoagulant solution were mixed gently and platelet-poor plasma was separated by centrifugation at 14,000×*g* for 5 min at 15° in polycarbonate tubes. These plasma samples were transferred to stoppered polypropylene tubes, frozen in a dry ice–methanol bath, and stored at −80° until assayed.

RESULTS

The baseline APTT in a group of 13 rats ranged from 11.1 to 27.1 sec, averaging 19.5 sec. Identical average APTT and a similar range of individual values were found in the same animals 7 days later, but there was no significant correlation between the day 1 and day 7 baseline APTT values in individual rats (Table I). An essentially linear correlation between ln APTT and the concentration of heparin added to plasma was consistently found over a heparin concentration range from 0.1 to 1.0 U/ml. However, the APTT at a heparin concentration <0.1 U/ml and the baseline APTT were usually above the linear regression line (Fig. 1). Slope values ranged from 1.14 to 2.31 ml/U on day 1 and from 1.36 to 2.49 ml/U on day 7; 7 of the 13 animals had significantly different slope values on these 2 days and there was no apparent correlation between day 1 and day 7 slope values for individual rats (Table I). On day 1, baseline APTT showed a positive correlation with hematocrit; on days 1 and 7, the slope correlated negatively with hematocrit (Table II).

[1] Blue Spruce Farms, Altamont, N.Y.
[2] Formula R-1000; Charles River, Syracuse, N.Y.
[3] Automated APTT; General Diagnostics, Morris Plains, N.J.
[4] Fibrometer; Baltimore Biological Laboratories, Cockeysville, Md.
[5] Lot No. 955FW; The Upjohn Co., Kalamazoo, Mich.

[6] The constant calcium–citrate concentration ratio was chosen to be similar to the ratio obtained when 1 part of 0.1 *M* acid citrate solution is used to anticoagulate 6 parts of plasma and 0.025 *M* calcium chloride solution is used to recalcify the plasma.

Table I—Baseline APTT, Slope, Hematocrit, and Body Weight of Rats Determined Twice, 7 Days Apart When the Citrate Solution–Blood Volume Ratio was Constant

Rat	Baseline APTT, sec		Slope, ml/U		Hematocrit, %		Body Weight, g	
	Day 1	Day 7	Day 1	Day 7	Day 1	Day 7	Day 1	Day 7
1	26.8	17.7	1.14	1.80[a]	49	—[b]	464	—[b]
2	15.8	25.3	1.51	1.95[a]	47	—[b]	324	—[b]
3	18.3	19.0	1.67	1.86[a]	46	41	424	395
4	11.1	17.8	1.95	1.85	41	40	547	539
5	13.6	15.3	1.86	1.82	40	41	350	361
6	27.1	16.3	1.64	2.48[a]	50	36	312	381
7	20.0	22.5	1.61	1.68	51	44	548	552
8	16.5	18.3	2.26	2.49[a]	40	37	423	467
9	23.8	23.8	1.59	1.36	50	40	444	456
10	20.8	23.8	1.81	1.67	47	41	410	422
11	22.3	19.3	1.44	1.55	49	43	392	414
12	20.6	18.1	2.31	2.02[a]	44	40	388	402
13	16.2	16.8	1.97	2.32[a]	43	40	408	432
Mean	19.5	19.5	1.75	1.91	46	40	418	438
SD	4.8	3.2	0.32	0.34	4	2	72	61
Significance of difference between means	N.S.[c]		N.S.		$p < 0.01$		N.S.	
Correlation coefficient	0.04		0.44		0.29		0.94	
Significance	N.S.		N.S.		N.S.		$p < 0.001$	

[a] Significantly different ($p < 0.05$) from slope value on day 1. [b] Missing data. [c] N.S. = not significant.

Table II—Correlations of Data in Table I

Data Pair	Correlation Coefficient	Significance, p
Baseline APTT *versus* slope, day 1	−0.50	N.S.[a]
Baseline APTT *versus* slope, day 7	−0.66	<0.05
Baseline APTT *versus* hematocrit, day 1	0.79	<0.01
Baseline APTT *versus* hematocrit, day 7	0.42	N.S.
Slope *versus* hematocrit, day 1	−0.73	<0.01
Slope *versus* hematocrit, day 7	−0.75	<0.01

[a] N.S. = not significant.

The baseline APTT and slope values were found to be extensively affected by the concentration of citrate added as an anticoagulant to the blood to permit separation of plasma. The baseline APTT increased with increasing citrate concentration while the slope decreased (Table III). The opposite relationships were observed with respect to the concentration of calcium used to initiate the clotting process: baseline APTT decreased and slope increased with increasing calcium concentration (Table IV). When citrate and calcium concentrations were increased simultaneously, at a constant ratio, the citrate effect predominated with respect to the baseline APTT (which increased with increasing concentration), while the calcium effect predominated with respect to slope (which also increased with increasing concentration) (Table V).

Incubation time of citrated plasma with APTT reagent (before addition of calcium to initiate clotting), intended to activate the intrinsic coagulation pathway, had a pronounced effect on APTT. As reflected by the decreasing APTT, the activation process predominated during the first 3 min (Fig. 2). At longer incubation times, APTT gradually increased, suggesting degradation of one or more components of the coagulation system. Comparing the results obtained after 3 and 15 min of incubation, the change in slope values was relatively more pronounced than the change in baseline APTT (Table VI). However, the 3- and 15-min values for the same animals correlated strongly, and the ratio of the 15- to 3-min values varied little between animals (Table VI). The intercept of the ln APTT *versus* heparin concentration regression lines at zero heparin concentration determined in this experiment is lower, on the average, than baseline APTT (Fig. 1).

Based on the preceding results, the reproducibility of individual baseline APTT and slope values was reexamined in another experiment (Table VII). Compared with the first experiment (Table I), the citrate solution–plasma volume ratio rather than the citrate solution–blood volume ratio was held constant, and the time interval between repeated measurements was lengthened from 7 to 30 days. The mean baseline APTT values and standard deviations obtained in the two studies are similar. The slope values in the second experiment are slightly higher than those in the first experiment, but the coefficients of variation are similar.

Table III—Effect of Added Citrate on the Baseline APTT of Pooled Rat Plasma and on the Anticoagulant Response to Added Heparin[a]

Citrate Concentration in Plasma, m*M*	Baseline APTT[b], sec	Slope[c], ml/U
8.75	11.6	2.31
13.5	17.8	2.42
17.5	24.6	1.87
20.9	27.1	1.59
24.3	31.4	1.55
32.7	38.6	1.33

[a] Calcium concentration in recalcifying solution was constant at 25 m*M*. [b] Significantly correlated with citrate concentration ($r = 0.991$, $p < 0.001$). [c] Significantly correlated with citrate concentration ($r = -0.923$, $p < 0.01$).

Table IV—Effect of Added Calcium Concentration on the Baseline APTT of Pooled Rat Plasma and on the Anticoagulant Response to Added Heparin[a]

Calcium Chloride Concentration[b], m*M*	Baseline APTT[c], sec	Slope[d], ml/U
12.5	37.6	0.85
19.0	24.8	1.09
25.0	28.6	1.38
29.8	22.6	2.57
34.6	21.8	2.14
46.6	21.8	2.46

[a] Citrate concentration in plasma was constant at 18.75 m*M*. [b] Refers to concentration in the recalcifying solution added to plasma. [c] Not significantly correlated with calcium concentration ($r = -0.78$). [d] Significantly correlated with calcium concentration ($r = 0.864$, $p < 0.05$).

Based on the preceding results, the reproducibility of individual baseline APTT and slope values was reexamined in another experiment (Table VII). Compared with the first experiment (Table I), the citrate solution–plasma volume ratio rather than the citrate solution–blood volume ratio was held constant, and the time interval between repeated measurements was lengthened from 7 to 30 days. The mean baseline APTT values and standard deviations obtained in the two studies are similar. The slope values in the second experiment are slightly higher than those in the first experiment, but the coefficients of variation are similar.

Table V—Effect of Added Citrate and Calcium Concentrations[a] on the Baseline APTT of Pooled Rat Plasma and on the Anticoagulant Response to Added Heparin

Concentration, m*M*		Baseline APTT[b], sec	Slope[c], ml/U
Citrate in Plasma	Calcium Chloride in Recalcifying Solution		
8.74	12.5	9.7	1.47
13.5	19.0	15.8	1.83
17.5	25.0	19.0	1.92
20.9	29.8	25.6	1.92
24.3	34.6	27.0	2.59
32.7	46.6	39.0	2.75

[a] At a constant concentration ratio. [b] Significantly correlated with citrate and calcium concentrations ($r = 0.994$, $p < 0.001$). [c] Significantly correlated with citrate and calcium concentrations ($r = 0.943$, $p < 0.01$).

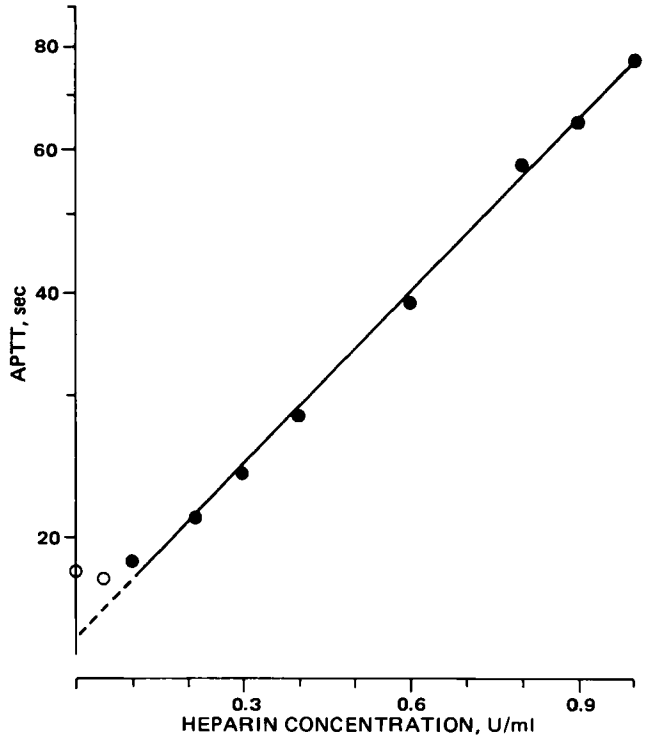

Figure 1—*Relationship between APTT and concentration of added heparin in plasma of a rat. The ordinate scale is logarithmic. The open circles at zero and very low heparin concentrations are usually above the regression line, which was calculated without these two data points. The incubation time was 15 min.*

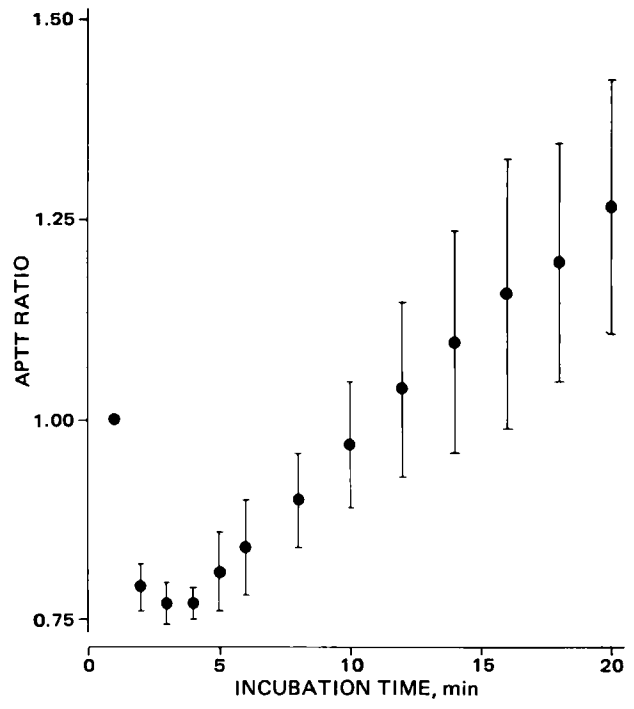

Figure 2—*Effect of incubation time on the baseline APTT of plasma from five rats. Plotted are the APTT ratios (APTT at a given time/APTT at 1 min), as mean ±SD, against incubation time. The APTT at 1 min ranged from 15.4 to 23.9 sec.*

The correlation coefficients for the baseline APTT and slope values, respectively, of the first and last day of each study were higher in the second study. Only the second study showed a statistically significant correlation between slope values obtained on different days from the same animals. During the 30-day interval of the second study, hematocrit values returned to normal, and body weight of the animals increased significantly (Table VII).

DISCUSSION

The magnitude of interindividual variation of baseline APTT and slope values observed in this investigation is similar to that found previously in another investigation on rats (11)[7] and is similar also to the magnitude of interindividual variation of these characteristics in humans (4, 5). All of the cited studies were carried out, at various times, in this laboratory with reagents from the same sources and with the same coagulation timer and are therefore readily comparable. However, unlike the situation in humans (4), the reproducibility of baseline APTT and slope values determined twice, on different days, in the rats was poor (Table I). An examination of the results of the first crossover experiment in rats (Tables I and II) suggested that one reason for the relatively poor reproducibility of individual results may be related to the inter- and intraindividual variation of hematocrit values.

Baseline APTT and slope values were significantly correlated with hematocrit (Table II). Since the permeability of rat erythrocytes to citrate is almost negligible (13) and the standard method of blood collection for plasma APTT determinations involves the addition of acid citrate anticoagulant solution to *blood* in a constant volume ratio, increasing hematocrit values are associated with increasing citrate concentration in *plasma*. As citrate concentrations are increased (all else being constant by use of pooled blood), baseline APTT increases and slope values decrease (Table III). The positive correlation between hematocrit and baseline APTT and the negative correlation between slope and hematocrit, obtained by statistical analysis of individual results from 13 rats (Table II), are consistent with these observations. Thus, a modification of the experimental methodology whereby the citrate solution–blood volume ratio is individualized on the basis of the animal's hematocrit such as to assure a constant citrate solution–plasma volume ratio was indicated. Moreover, a 7-day interval between blood withdrawals was apparently not sufficient for the animals to regenerate the considerable volume of blood that was taken on the first day of the experiment, as reflected by the significantly lower hematocrit values on the seventh day (Table I). It is possible also that the levels of certain clotting factors, which are likely to have been lowered by the first blood withdrawal, may not have returned to normal within 7 days. It was therefore deemed advisable to increase the time interval between blood withdrawals considerably.

In the second experiment to determine inter- and intraindividual differences in baseline APTT and slope value, the citrate solution–plasma volume ratio was held constant, and the interval between the two blood withdrawals was 30 days. The results of this experiment (Table VII) yielded higher correlation coefficients for the individual pairs of baseline APTT and slope values, respectively, than in the first experiment. The hematocrit values had returned to normal within the 30-day period. However, while intraindividual variation was decreased relative to the first experiment, interindividual variation was not appreciably different. The correlation between slope values and hematocrit was no longer statistically significant (Table VIII). On the other hand, there remains a significant correlation between hematocrit and baseline APTT, but this correlation is now negative rather than positive. The reason for this is

Table VI—Effect of Incubation Time on the Baseline APTT of Plasma from Rats and on the Anticoagulant Response to Added Heparin [a]

	Incubation Time, min		Ratio	Correlation Coefficient	
	3	15	15:3 min		
Baseline APTT, sec	18.6 ± 2.8	24.5 ± 3.0	1.32 ± 0.08	0.933	$p < 0.001$
Ordinate Intercept, sec	17.3 ± 2.4	20.5 ± 2.5[b]	1.19 ± 0.09	0.855	$p < 0.001$
Slope, ml/U	0.98 ± 0.13	1.74 ± 0.26	1.78 ± 0.13	0.872	$p < 0.001$

[a] Data and ratio values are expressed as mean ± *SD*, $n = 15$. [b] Significantly different from baseline APTT, $p < 0.001$.

[7] The slope values reported by Bjornsson and Levy (11) are based on heparin concentrations in plasma before it was diluted 10-fold for APTT determination. The slope values in the present study are based on heparin concentration in plasma that was used undiluted for APTT determination. For comparison with the results of this investigation, the slope values reported by Bjornsson and Levy (11) must be multiplied by 10.

Table VII—Baseline APTT, Slope, Hematocrit, and Body Weight of Rats Determined Twice, 30 Days Apart When the Citrate Solution–Plasma Volume Ratio was Constant at 1:6

Rat	Baseline APTT, sec		Slope, ml/U		Hematocrit, %		Body Weight, g	
	Day 1	Day 30	Day 1	Day 30	Day 1	Day 30	Day 1	Day 30
14	10.6	12.9	3.12	3.12	46	47	394	477
15	24.3	20.8	1.83	2.32[a]	46	47	412	485
16	17.1	19.6	2.48	2.78	45	47	422	492
17	16.6	16.6	1.94	2.56[a]	49	50	397	458
18	22.3	15.6	2.49	2.87[a]	47	51	456	508
19	14.0	20.3	3.23	2.73	45	41	478	538
20	16.6	19.2	2.30	2.34	44	45	397	455
21	20.7	18.2	2.13	2.45	45	47	417	468
22	16.1	15.3	2.21	2.24	48	47	421	462
23	20.0	22.8	1.94	1.66	42	42	485	524
24	17.3	17.0	2.61	2.54	48	49	356	422
25	22.3	20.3	2.21	1.90	46	44	342	422
Mean	18.2	18.2	2.37	2.46	46	46	415	476
SD	3.9	2.8	0.44	0.41	2	3	43	36
Significance of difference between means	N.S.[b]		N.S.		N.S.		$p < 0.001$	
Correlation coefficient	0.50		0.68		0.73		0.95	
Significance	N.S.		$p < 0.05$		$p < 0.01$		$p < 0.001$	

[a] Significantly different ($p < 0.05$) from slope value on day 1. [b] N.S. = not significant.

unknown; it could reflect differences in dilution (by the addition of acid citrate solution to blood in variable proportions) of one or more endogenous substances that distribute readily between plasma and erythrocytes and whose concentration is relevant to the clotting of plasma.

One potential alternative to individualization of the citrate solution–blood volume ratio (to achieve a constant citrate solution–plasma volume ratio) is to adjust the concentration of calcium chloride in the recalcifying solution such as to achieve a constant molar ratio of citrate to calcium. Increasing the concentration of calcium while citrate concentration was held constant did in fact cause an increase in slope and may also have decreased baseline APTT, although the latter effect was not statistically significant (Table IV). However, maintaining a constant molar ratio of citrate to calcium did not abolish the citrate concentration dependency of baseline APTT and indicated a predominance of the calcium effect over the citrate effect on the slope (Table V).

It has been the practice in this laboratory to incubate the plasma–APTT reagent mixture 15 min, rather than the customary 3 or 5 min, for activation of the intrinsic coagulation pathway. This change was made to increase the sensitivity of the APTT to changes of heparin concentration. A detailed study of the relationship between APTT and incubation time revealed considerable complexity (Fig. 2), with the activation process predominating initially and degradation of component(s) of the clotting process predominating at later times (after ~3 min). Increased incubation time had a more pronounced effect on slope than on baseline APTT (Table VI) and contributed to a more pronounced difference between the actual and apparent baseline APTT, determined by back-extrapolation of the ln APTT–heparin concentration regression line to a heparin concentration of zero (Fig. 1, Table VI). Since there is a relatively constant relationship between baseline APTT and slope values, respectively, obtained after 3 and 15 min of incubation, the time variable should have little or no effect on the analysis and interpretation of the results of heparin studies such as the one described here. The 15-min procedure is more sensitive to heparin concentration (due to the increased slope value) and is more convenient.

The results of this investigation, assessed in conjunction with the results of corresponding clinical studies also performed in this laboratory (4, 5) provide interesting information concerning species differences between rats and humans (Table IX). These differences should be appreciated in the context of the two major similarities between these species: the pharmacokinetics of heparin are dose dependent and there is an essentially linear relationship between ln APTT and heparin concentration in both humans and rats (11). On the other hand, citrate concentration in plasma has a pronounced effect on baseline APTT and slope in rats, but not in humans. Both human and rat erythrocytes are essentially impermeable to citrate (12). In view of the pronounced citrate concentration effect in rats, the human experiments were repeated recently and the previously observed lack of a citrate concentration effect was reconfirmed (unpublished data).

Another striking difference between rats and humans is the effect of plasma incubation time on APTT. The APTT of human plasma decreased and eventually reached a constant value during incubation for up to 21 min (5), indicative of activation of the clotting system without noticeable degradation of clotting factors. On the other hand, the APTT of rat plasma first decreases (indicative of activation) and then increases,

Table VIII—Correlations of Data in Table VII

Data Pair	Correlation Coefficient	Significance, p
Baseline APTT *versus* slope, day 1	−0.70	<0.05
Baseline APTT *versus* slope, day 30	−0.67	<0.05
Baseline APTT *versus* hematocrit, day 1	−0.10	N.S.[a]
Baseline APTT *versus* hematocrit, day 30	−0.66	<0.05
Slope *versus* hematocrit, day 1	0.01	N.S.
Slope *versus* hematocrit, day 30	0.48	N.S.

[a] N.S. = not significant.

Table IX—Comparison of Healthy Humans and Rats with Respect to the Coagulation of Plasma and the Anticoagulant Effect of Heparin [a]

Characteristics	Humans	Rats[b]
Relationship between ln APTT and added heparin concentration	Linear	Linear
Effect of incubation time on APTT	Decreases asymptotically	First decreases, then increases
Effect of citrate concentration	No effect on baseline APTT or slope	Significant positive correlation with baseline APTT and significant negative correlation with slope
Slope–hematocrit correlation	Significant, negative	(*a*) Often significant, negative (*b*) no correlation
Slope–baseline APTT correlation	Significant, positive	(*b*) Significant, negative
Baseline APTT–hematocrit correlation	Not significant[c]	Variable
Citrate uptake by erythrocytes	Negligible	Negligible
Reproducibility of baseline APTT values on repeated testing at different times	Excellent	Very poor
Reproducibility of slope values on repeated testing at different times	Excellent	Poor

[a] Based on our previous studies (4, 5, 13) and on the results of the present study. [b] Different results were observed in some cases depending on whether plasma was obtained from animals with (*a*) citrate solution–blood volume ratio held constant or (*b*) citrate solution–plasma volume ratio held constant. [c] Significant negative correlation in patients (5, 7).

apparently due to the opposing effects of activation and subsequent degradation of coagulation factors. In a search for factors that may be useful for predicting an individual patient's response to heparin, baseline APTT has emerged as the variable which consistently correlates positively with slope value (4, 5, 8). Unlike humans, rats exhibit a negative correlation between baseline APTT and slope value. The reason for this species difference is not known.

In summary, coagulation studies in rats require considerably more attention to the control of the variables examined in this investigation than do similar studies in humans. The volume of blood required to determine baseline APTT and slope represents a significant fraction of a rat's total blood volume, but is negligible compared with the human blood volume. This is an additional complicating factor in studies on rats. The observed species variation may, however, be useful for exploring various aspects of the blood coagulation process. Parallel and coordinated studies on humans and rats, and perhaps also on other species, may facilitate the elucidation of important pharmacokinetic and pharmacodynamic aspects of the anticoagulant action of heparin.

REFERENCES

(1) L. B. Jaques and L. W. Kavanagh, *Thromb. Diath. Haemorrh. (Stuttg.), Suppl.*, **56**, 171 (1973).

(2) L. B. Jaques, L. W. Kavanagh, and S. H. Kuo, *Thromb. Res.*, **3**, 295 (1973).

(3) H. B. Nader, H. K. Takahashi, and J. A. Guimarães, *Int. J. Biol. Macromolec.*, **3**, 356 (1981).

(4) L. R. Whitfield and G. Levy, *Clin. Pharmacol. Ther.*, **28**, 509 (1980).

(5) L. R. Whitfield, J. J. Schentag, and G. Levy, *Clin. Pharmacol. Ther.*, **32**, 503 (1982).

(6) J. Hirsh, W. G. van Aken, A. S. Gallus, C. T. Dollery, J. F. Cade, and W. L. Yung, *Circulation* **53**, 691 (1973).

(7) R. J. Cipolle, R. D. Seifert, B. A. Neilan, D. E. Zaske, and E. Haus, *Clin. Pharmacol. Ther.*, **29**, 387 (1981).

(8) T. D. Bjornsson and K. M. Wolfram, *Ann. N.Y. Acad. Sci.*, **370**, 656 (1980).

(9) H. N. Teien and U. Abildgaard, *Thromb. Haemostas. (Stuttg.)*, **35**, 592 (1976).

(10) W. B. Forman and G. Bayer, *Am. J. Hematol.*, **11**, 277 (1981).

(11) T. D. Bjornsson and G. Levy, *J. Pharmacol. Exp. Ther.*, **210**, 237 (1979).

(12) L. R. Whitfield and G. Levy, *Thromb. Res.*, **21**, 681 (1981).

(13) R. R. Sokal and F. J. Rohlf, "Biometry," W. H. Freeman, San Francisco, Calif., 1969, p. 450

(14) R. R. Proctor and S. I. Rapaport, *Am. J. Clin. Path.*, **36**, 212 (1961).

(15) J. R. Weeks and J. D. Davis, *J. Appl. Physiol.*, **19**, 540 (1964).

ACKNOWLEDGMENTS

Supported in part by Grant GM 20852 from the National Institute of General Medical Sciences, National Institutes of Health, by Biomedical Research Support Grant 2S07RR05454-19, and by a Graduate Fellowship from the State University of New York for L.R.W.

The previous (fourth) part of this series was L. R. Whitfield, J. J. Schentag, and G. Levy, *Clin. Pharmacol. Ther.*, **32**(5), 503 (1982).

Distribution and Elimination of Poly(methyl methacrylate) Nanoparticles After Subcutaneous Administration to Rats

JÖRG KREUTER *x, **M. NEFZGER** ‡, **E. LIEHL** ‡, **R. CZOK** ‡, and **R. VOGES** §

Received June 14, 1982, from the *School of Pharmacy, Federal Institute of Technology, CH 8092 Zurich, Switzerland, ‡SANDOZ Forschungsinstitut, A 1235 Vienna, Austria, and §SANDOZ LTD., CH 4002 Basle, Switzerland. Accepted for publication August 25, 1982.

Abstract □ Poly(methyl [1-^{14}C]methacrylate) nanoparticles were injected subcutaneously into rats. Almost all of the radioactivity stayed at the injection site. After an initial urinary and fecal excretion of ~1% of the administered dose per day, the rate of elimination dropped to a low level (~0.005%/day *via* the feces and ~0.0005%/day *via* the urine) within 70 days. After 200 days, the fecal elimination increased exponentially until a >100-fold increase was observed after 287 days in one rat. After this time, a tendency for an increase in fecal elimination was also observed in the other animals, and the radioactivity in all organs and tissue increased by ~100 times in all animals in comparison with the organ radioactivity determinations at earlier times.

Keyphrases □ Poly(methyl methacrylate)—^{14}C-labeled nanoparticles, distribution and elimination in rats, subcutaneous administration □ Distribution—^{14}C-labeled poly(methyl methacrylate) nanoparticles, subcutaneous administration in rats □ Elimination—^{14}C-labeled poly(methyl methacrylate) nanoparticles, subcutaneous administration in rats

Poly(methyl [1-^{14}C]methacrylate) nanoparticles were shown to be promising adjuvants for vaccines (1–4). In contrast to the rapidly biodegradable cyanoacrylates, they achieve a good adjuvant effect. The reproducibility of the adjuvant effect was much better than that of the presently widely used aluminum hydroxide (5). Moreover, in preliminary experiments (2), poly(methyl [1-^{14}C]methacrylate) nanoparticles seem to cause much milder tissue reactions than aluminum hydroxide.

However, the distribution and elimination of these nanoparticles after subcutaneous administration so far has not been studied. In a previous study (6) concerning the fate of poly(methyl [1-^{14}C]methacrylate) nanoparticles after intravenous administration, a strong affinity of the nanoparticles to the reticuloendothelial system, especially to the liver, was observed.

The elimination of radioactivity after implantation of poly(methyl [1-^{14}C]methacrylate) films was investigated in two studies (7, 8). In one study (7), an elevated elimination rate of radioactivity was observed in the urine between 2 and 8 weeks, decreasing to minimal values after this time. This elimination was probably caused by residual monomers or low-molecular weight components present in the polymer films. After 54 weeks, however, considerable radioactivity suddenly started to be eliminated (8), indicating a degradation of the polymer. This study investigates the elimination pattern and distribution

[1] Unpublished observation.

0022-3549/83/1000-1146$01.00/0

apparently due to the opposing effects of activation and subsequent degradation of coagulation factors. In a search for factors that may be useful for predicting an individual patient's response to heparin, baseline APTT has emerged as the variable which consistently correlates positively with slope value (4, 5, 8). Unlike humans, rats exhibit a negative correlation between baseline APTT and slope value. The reason for this species difference is not known.

In summary, coagulation studies in rats require considerably more attention to the control of the variables examined in this investigation than do similar studies in humans. The volume of blood required to determine baseline APTT and slope represents a significant fraction of a rat's total blood volume, but is negligible compared with the human blood volume. This is an additional complicating factor in studies on rats. The observed species variation may, however, be useful for exploring various aspects of the blood coagulation process. Parallel and coordinated studies on humans and rats, and perhaps also on other species, may facilitate the elucidation of important pharmacokinetic and pharmacodynamic aspects of the anticoagulant action of heparin.

REFERENCES

(1) L. B. Jaques and L. W. Kavanagh, *Thromb. Diath. Haemorrh. (Stuttg.), Suppl.*, **56**, 171 (1973).

(2) L. B. Jaques, L. W. Kavanagh, and S. H. Kuo, *Thromb. Res.*, **3**, 295 (1973).

(3) H. B. Nader, H. K. Takahashi, and J. A. Guimarães, *Int. J. Biol. Macromolec.*, **3**, 356 (1981).

(4) L. R. Whitfield and G. Levy, *Clin. Pharmacol. Ther.*, **28**, 509 (1980).

(5) L. R. Whitfield, J. J. Schentag, and G. Levy, *Clin. Pharmacol. Ther.*, **32**, 503 (1982).

(6) J. Hirsh, W. G. van Aken, A. S. Gallus, C. T. Dollery, J. F. Cade, and W. L. Yung, *Circulation* **53**, 691 (1973).

(7) R. J. Cipolle, R. D. Seifert, B. A. Neilan, D. E. Zaske, and E. Haus, *Clin. Pharmacol. Ther.*, **29**, 387 (1981).

(8) T. D. Bjornsson and K. M. Wolfram, *Ann. N.Y. Acad. Sci.*, **370**, 656 (1980).

(9) H. N. Teien and U. Abildgaard, *Thromb. Haemostas. (Stuttg.)*, **35**, 592 (1976).

(10) W. B. Forman and G. Bayer, *Am. J. Hematol.*, **11**, 277 (1981).

(11) T. D. Bjornsson and G. Levy, *J. Pharmacol. Exp. Ther.*, **210**, 237 (1979).

(12) L. R. Whitfield and G. Levy, *Thromb. Res.*, **21**, 681 (1981).

(13) R. R. Sokal and F. J. Rohlf, "Biometry," W. H. Freeman, San Francisco, Calif., 1969, p. 450

(14) R. R. Proctor and S. I. Rapaport, *Am. J. Clin. Path.*, **36**, 212 (1961).

(15) J. R. Weeks and J. D. Davis, *J. Appl. Physiol.*, **19**, 540 (1964).

ACKNOWLEDGMENTS

Supported in part by Grant GM 20852 from the National Institute of General Medical Sciences, National Institutes of Health, by Biomedical Research Support Grant 2S07RR05454-19, and by a Graduate Fellowship from the State University of New York for L.R.W.

The previous (fourth) part of this series was L. R. Whitfield, J. J. Schentag, and G. Levy, *Clin. Pharmacol. Ther.*, **32**(5), 503 (1982).

Distribution and Elimination of Poly(methyl methacrylate) Nanoparticles After Subcutaneous Administration to Rats

JÖRG KREUTER *x, **M. NEFZGER** ‡, **E. LIEHL** ‡, **R. CZOK** ‡, and **R. VOGES** §

Received June 14, 1982, from the *School of Pharmacy, Federal Institute of Technology, CH 8092 Zurich, Switzerland, ‡SANDOZ Forschungsinstitut, A 1235 Vienna, Austria, and §SANDOZ LTD., CH 4002 Basle, Switzerland. Accepted for publication August 25, 1982.

Abstract □ Poly(methyl [1-^{14}C]methacrylate) nanoparticles were injected subcutaneously into rats. Almost all of the radioactivity stayed at the injection site. After an initial urinary and fecal excretion of ~1% of the administered dose per day, the rate of elimination dropped to a low level (~0.005%/day *via* the feces and ~0.0005%/day *via* the urine) within 70 days. After 200 days, the fecal elimination increased exponentially until a >100-fold increase was observed after 287 days in one rat. After this time, a tendency for an increase in fecal elimination was also observed in the other animals, and the radioactivity in all organs and tissue increased by ~100 times in all animals in comparison with the organ radioactivity determinations at earlier times.

Keyphrases □ Poly(methyl methacrylate)—^{14}C-labeled nanoparticles, distribution and elimination in rats, subcutaneous administration □ Distribution—^{14}C-labeled poly(methyl methacrylate) nanoparticles, subcutaneous administration in rats □ Elimination—^{14}C-labeled poly(methyl methacrylate) nanoparticles, subcutaneous administration in rats

Poly(methyl [1-^{14}C]methacrylate) nanoparticles were shown to be promising adjuvants for vaccines (1–4). In contrast to the rapidly biodegradable cyanoacrylates, they achieve a good adjuvant effect. The reproducibility of the adjuvant effect was much better than that of the presently widely used aluminum hydroxide (5). Moreover, in preliminary experiments (2), poly(methyl [1-^{14}C]methacrylate) nanoparticles seem to cause much milder tissue reactions than aluminum hydroxide.

However, the distribution and elimination of these nanoparticles after subcutaneous administration so far has not been studied. In a previous study (6) concerning the fate of poly(methyl [1-^{14}C]methacrylate) nanoparticles after intravenous administration, a strong affinity of the nanoparticles to the reticuloendothelial system, especially to the liver, was observed.

The elimination of radioactivity after implantation of poly(methyl [1-^{14}C]methacrylate) films was investigated in two studies (7, 8). In one study (7), an elevated elimination rate of radioactivity was observed in the urine between 2 and 8 weeks, decreasing to minimal values after this time. This elimination was probably caused by residual monomers or low-molecular weight components present in the polymer films. After 54 weeks, however, considerable radioactivity suddenly started to be eliminated (8), indicating a degradation of the polymer. This study investigates the elimination pattern and distribution

[1] Unpublished observation.

0022-3549/83/1000-1146$01.00/0

Table I—Total Radioactivity Found after 287 Days in Percent of the Administered Dose

Animal No.	903	906	910	912
Sex	M	M	M	F
Weight at start of study, g	197	207	173	206
Weight at end of study, g	574	490	458	262
Virus	−[a]	−[a]	+[b]	+[b]
Injection site	69.4	71.1	61.9	55.4
Excreted *via* urine	6.4	6.2	6.5	6.8
(within 7 days)	(5.7)	(5.8)	(6.1)	(6.5)
Excreted *via* feces	7.1	6.9	24.9	6.9
(within 7 days)	(4.9)	(4.8)	(4.5)	(4.5)
Residual body (estimated)	3–11	5–11	4–14	3–9
Total	86–94	89–95	97–107	72–78

[a] No virus present in the injected sample. [b] Inactivated influenza virions present in the injected sample.

of radioactivity in the body after subcutaneous administration of poly(methyl methacrylate) nanoparticles.

EXPERIMENTAL

Preparation of Poly(methyl [1-^{14}C]methacrylate) Nanoparticles—Methyl [1-^{14}C]methacrylate was prepared in a three-step reaction sequence starting from barium [^{14}C]carbonate. Carboxylation of isopropylmagnesium iodide, bromination of the resulting [1-^{14}C]isobutyric acid, and subsequent methanolysis gave methyl 2-bromo[1-^{14}C]isobutyrate (9). Hydrogen bromide elimination in 1,5-diazabicyclo[5.4.0]-undec-5-ene at 110° led to methyl [1-^{14}C]methacrylate, which was continuously removed from the reaction mixture by a slow stream of helium, and collected at −196°. The ester was vacuum-transferred into phosphate-buffered saline to give a 0.5% solution. The chemical identity and chemical and radiochemical purity (>95%) were confirmed by GC after ether extraction.

The monomeric methyl [1-^{14}C]methacrylate saline solution was used for the preparation of two nanoparticle suspensions, with and without influenza virions, for subcutaneous administration. The nanoparticles were produced by γ-irradiation-initiated polymerization with 500 krad (2.2 krad/min) in a ^{60}Co-source. Thus, the following suspensions were obtained:

1. Polymerization in the presence of influenza virions afforded a 0.35% suspension at a specific activity of (5.30 ± 0.82) × 10^8 dpm/ml in which all virions were incorporated into the nanoparticles.

2. Polymerization in the absence of influenza virions afforded a 0.35% suspension of virus-free nanoparticles at a specific activity of (5.22 ± 0.46) × 10^8 dpm/ml.

That the nanoparticles tended to flocculate led to difficulties in the reproducibility of the radioactivity measurements and the determination of the exact amount of the administered nanoparticles. Although the suspensions were permanently stirred during sampling of the aliquots for calibration or administration, the relative standard deviations were 14% for 0.1-ml samples of the virus-free nanoparticle suspension (26 determinations) and 9% for 0.1-ml samples containing the virion-incorporated nanoparticles (14 determinations). The addition of substituted methyl cellulose[2] as a stabilizer did not reduce the variation. The previously used technique of freeze-drying the suspensions (6) to obtain a homogeneous distribution of radioactivity within the resulting nanoparticle powder was not applicable because the virions would have been destroyed by this technique.

Although the animals obtained a fivefold higher volume than that used for calibration, similar variations in the dose actually administered have to be taken into consideration. Nevertheless, the material balance (the mean from the calibration experiments) is satisfactory (Table I). Since no apparent differences in the distribution and elimination of the nanoparticle preparations could be observed, both preparations were treated together as one set of data.

Excretion and Tissue Distribution after Subcutaneous Administration—A 0.5-ml aliquot of the thoroughly stirred suspension was subcutaneously injected into the neck of Sprague–Dawley rats, weighing 170–207 g, at the beginning of the study. One group of five male and five female rats received the virus-containing preparation and a second group of the same composition received the preparation with virus-free nanoparticles. The animals were kept in metabolism cages and had free access to water and food.

The elimination of radioactivity of two animals per group was measured in urine and feces up to 287 days after administration. For the determination of radioactivity in the organs, two animals per group were sacrificed at 15, 45, 66, 157, and 287 days after dosing.

Urine was collected separately from feces and stored at ~ −60°. The storage container contained 100 μl of diethylamine to maintain the urine at a pH ≥ 9, thus ensuring the binding of the radioactivity excreted as carbonate. After each collection period, the cage was rinsed with water (30–40 ml) to wash out dried urine residues. The collected feces were homogenized with approximately the same weight of water. Three samples (200–400 mg) of each homogenate were analyzed.

The radioactivity in the organs was measured after sacrificing the animals by an ~0.5 ml ip injection of euthanasia solution[3]. From the adrenal glands, epididymis, ovary, thyroid gland, lymph nodes, and bone marrow one sample of 7–130 mg was taken; from the other organs two samples of 50–400 mg each were taken. At the application site, remaining depots were dissected and combusted[4]. The resulting carbon dioxide was absorbed in a mixture of absorber solution and scintillation cocktail[5] and diluted up to 100 times before counting with the same mixture.

The radioactivity of the excreta, blood, plasma, and organs was determined after predrying and combustion in oxygen using a sample oxidizer (recovery of radioactivity 92–100%). The resulting [^{14}C]carbon dioxide was absorbed in the aforementioned scintillation cocktail. The samples were then counted in a liquid scintillation counter for 20 min. The counting efficiency was determined by the external standard method; the detection limit was 4 ng/g for the bone marrow, lymph nodes, and thyroid gland and 2 ng/g for all other organs and tissue.

RESULTS AND DISCUSSION

The organ and tissue distribution after subcutaneous administration of the poly(methyl [1-^{14}C]methacrylate) nanoparticles is shown in Table II. With the exception of the injection site, <0.1% of the administered dose could be found in the rest of the body within 15 and 157 days. The major amount of the radioactive material remained at the injection site (Tables I and III), where a hard yellow disk, ~5 mm, was found. The formation of this disk is probably caused by encapsulation with collagenous tissue, which represents the normal reaction of the body (10–12). Even after 287 days, 55–71% of the administered dose remained at the site of injection. This finding confirms previous macroautoradiographic studies in mice, in which radioactivity was detectable only at the injection site for 70 days.

In the rest of the body, the highest amounts of radioactivity were observed in the liver, spleen, lymph nodes, bone marrow, renal fatty tissue, skin, and pancreas. The comparatively high radioactivity levels in the liver, spleen, and bone marrow were not unexpected, since this was also

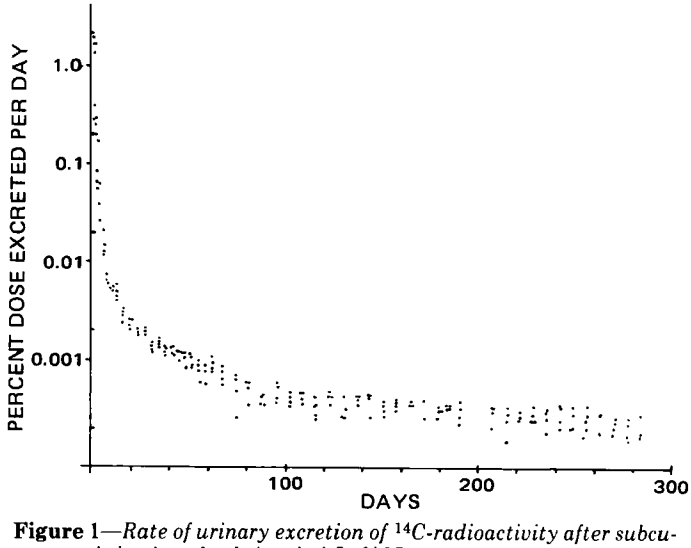

Figure 1—*Rate of urinary excretion of ^{14}C-radioactivity after subcutaneous injection of poly(methyl [1-^{14}C]methacrylate) nanoparticles into rats (n = 4).*

[2] Tylose MH 1000; Kalle & Co., Wiesbaden-Biebrich, West Germany.

[3] T61; Farbwerke Hoechst, Frankfurt/Main, West Germany.
[4] Sample Oxydizer; Packard Instrument, Downers Grove, Ill.
[5] Carbosorb and Permafluor; Packard Instrument, Downers Grove, Ill.

Table II—Distribution of ^{14}C-Radioactivity in Organs after Subcutaneous Administration of ^{14}C-Labeled Poly(methyl methacrylate) Nanoparticles to Rats [a]

Organ or Tissue	Days 15	45	66	157	287
Blood	4.5 ± 1.5	1.6 ± 0.6	0.2 ± 0.4	0.4 ± 0.5	107.4 ± 108.5
Plasma	—[b]	—	—	—	114.4 ± 167.0
Liver	8.2 ± 6.2	1.9 ± 0.4	3.1 ± 3.7	1.2 ± 0.8	255.3 ± 220.7
Spleen	3.7 ± 2.7	2.7 ± 1.3	10.9 ± 13.4	2.9 ± 3.3	122.6 ± 106.8
Pancreas	2.9 ± 1.0	2.0 ± 0.9	1.5 ± 0.6	—	605.5 ± 418.1
Kidneys	4.1 ± 0.7	1.4 ± 0.4	0.7 ± 0.3	—	104.0 ± 72.3
Adrenals	—	—	—	—	244.9 ± 215.0
Fatty renal tissue	4.3 ± 1.6	2.8 ± 1.0	1.8 ± 0.9	—	461.6 ± 102.6
Testes	1.6	—	—	—	40.0 ± 21.4
Uterus	—	—	—	—	56.4
Epididymis	1.6	—	—	—	109.0 ± 73.2
Ovary	1.6	—	—	—	115.7
Colon	1.8 ± 1.0	1.7 ± 0.6	0.8 ± 1.0	—	79.3 ± 18.4
Stomach	1.1 ± 0.5	—	—	—	51.5 ± 25.2
Small intestine	2.6 ± 0.4	1.1 ± 0.5	0.6 ± 0.1	0.4 ± 0.3	84.4 ± 42.8
Salivary glands	—	—	—	—	119.2 ± 76.0
Lymph nodes	6.8 ± 10.0	6.6 ± 7.3	543 ± 812	—	277.0 ± 55.2
Thyroid glands	—	—	—	—	153.2 ± 59.8
Lungs	3.2 ± 1.0	1.4 ± 0.6	0.7 ± 0.3	—	28.1 ± 19.8
Heart	1.8 ± 1.0	0.7 ± 0.2	0.4 ± 0.3	—	96.5 ± 44.8
Muscles	1.7 ± 0.3	1.2 ± 0.3	0.6 ± 0.1	—	105.5 ± 6.1
Bone marrow	—	—	—	—	847.4 ± 197.9
Skin	4.7 ± 2.1	3.1 ± 0.5	2.2 ± 0.7	—	205.4 ± 48.3
Brain	0.9 ± 0.4	—	—	—	90.0 ± 28.6

[a] Mean (ng/g) ± *SD*; $n = 4$. Administered dose = ~8 mg/kg. [b] — Less than the detection limit (<4 ng/g for bone marrow, lymph nodes, and thyroid; <2 ng/g for all other organs and tissues).

Table III—Residual Radioactivity at the Injection Site in Percent of the Injected Dose

Days	Samples without Virus		Samples with Virus	
15	41.5	41.7	56.2	70.0
45	79.1	74.0	49.5	55.2
66	59.0	91.8	65.3	55.2
157	88.3	76.1	68.6	68.6
287	69.4	71.1	61.9	55.4

seen after intravenous administration. In contrast to the intravenous study, the radioactivity in the lymph nodes was high in some cases.

The radioactivity in the organs decreased from day 15 until day 157. Between day 157 and day 287, a sudden ~100-fold increase in radioactivity occurred in all organs of all animals. The ratio of blood radioactivity to organ radioactivity, however, remained largely unaltered (Table IV). This indicates that nanoparticles or their degradation products were transported *via* the blood.

The excretion of the radioactivity in the urine of four rats is shown in Fig. 1; the excretion in the feces is shown in Fig. 2. Initially, the excretion of radioactivity was rapid: approximately 1% of the administered dose was excreted per day in the urine, with approximately the same amount excreted in the feces. Consequently, ~6% of the dose was eliminated *via* the urine and 5% *via* the feces within 7 days. However, the excretion rate dropped very rapidly until a very slow constant logarithmic decline of the excretion rate was reached after ~70 days. At this stage, only ~0.005% of the administered dose was eliminated per day, mainly *via* the feces ($t_{1/2}$ ~ 140 days) where the level of excretion was ~10 times higher than in the urine ($t_{1/2}$ ~ 170 days). After ~200 days, however, the rate of excretion started to increase continuously in one rat until a >100-fold increase was reached after 287 days. At this stage, the elimination rate amounted to 1% of the administered dose per day. A tendency for an increase in the excretion rate also could be observed in the three other animals at the end of the observation period.

The observed increases in the excretion rate do not seem to be coincidental, since they were accompanied by the aforementioned 100-fold increase in the radioactivity level of all organs in all four rats. The ob-

Table IV—Ratio of Organ Radioactivity to Blood Radioactivity

Organ or Tissue	Days 15	45	66	157	187
Plasma	0.15	—[a]	—	—	0.79
Liver	—	1.36	16.08	3.48	3.58
Spleen	1.13	1.85	60.93	6.35	1.78
Pancreas	0.70	1.26	5.91	—	8.47
Kidneys	0.97	0.92	2.51	—	1.39
Adrenals	—	—	—	—	2.91
Fatty renal tissue	1.08	1.82	6.66	—	7.92
Testes	0.37	—	1.44	—	0.56
Uterus	—	—	—	—	0.89
Epididymis	0.41	—	2.50	—	1.41
Ovary	0.29	—	—	—	1.83
Colon	0.43	1.01	2.83	—	1.42
Stomach	0.27	—	1.64	—	0.77
Small intestine	0.65	0.68	1.98	2.36	1.25
Salivary glands	—	—	1.54	—	1.60
Lymph nodes	1.47	4.09	3174.50	—	5.90
Thyroid glands	—	—	2.63	—	2.32
Lungs	0.89	0.82	2.57	—	0.72
Heart	0.45	0.34	1.13	—	1.56
Muscles	0.43	0.71	2.32	—	2.06
Bone marrow	—	—	13.48	—	16.22
Skin	1.36	2.03	8.97	—	3.38
Brain	0.25	—	1.40	—	1.66

[a] — Radioactivity in the tissue below the detection limit.

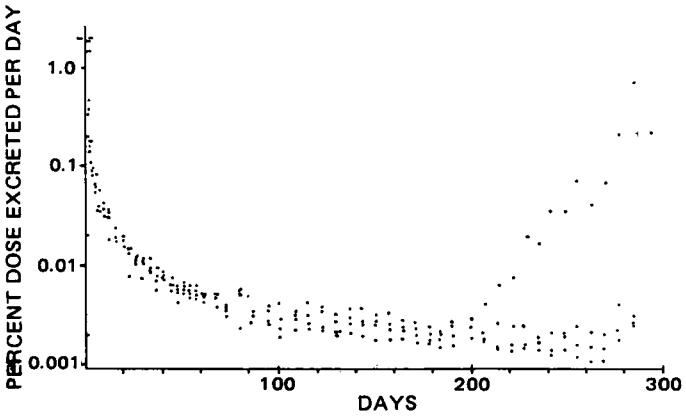

Figure 2—*Rate of fecal excretion of ^{14}C-radioactivity after subcutaneous injection of poly(methyl [1-^{14}C]methacrylate) nanoparticles into rats (n = 4).*

servation of a lag phase for the elimination of implanted material is not new. In 1955, Oppenheimer *et al.* (8) observed a lag period of 54 weeks after implantation of poly(methyl [1-^{14}C]methacrylate) films into rats, until suddenly the excretion of radioactivity started and continued for 40 weeks. When the films were removed, the excretion of radioactivity disappeared. Schindler *et al.* (13) observed with polylactide implants that degradation of the polymer, measured by the decrease in the molecular weight *via* the viscosity of the implant, started soon after administration. The removal of material from the administration site, however, occurred only after a certain molecular weight was reached. After implantation of poly(ε-caprolactone-co-DL-lactic acid) capsules for instance, the viscosity decreased by 75%, while only 1% of the injected capsule material was removed from the injection site. Since the viscosity is directly related to the molecular weight, a comparable reduction of ~75% in the molecular weight has to be assumed. Over the following 8 weeks, the residual polymer disappeared totally from the site of administration, while the viscosity decreased only slowly.

A similar process possibly occurred after subcutaneous administration of poly(methyl [1-^{14}C]methacrylate) nanoparticles and films. The degradation might have started rather early after injection or implantation, but the removal from the site of administration and the excretion began only when a certain molecular weight of the degradation products was reached. The faster excretion rate during the first couple of days can also be explained by the limitation of the transportation and excretion process by the molecular weight. The initially excreted total amount of ~13% far exceeds the possible amount of residual monomers. As mentioned previously, ≤1% residual monomers are contained in the polymer. However, as shown by gel permeation chromatography (14), the molecular weight distribution of the poly(methyl [1-^{14}C]methacrylate) nanoparticles prepared by γ-irradiation is rather wide, allowing for a considerable amount of low-molecular weight polymer, some of which could be readily excreted.

REFERENCES

(1) J. Kreuter and P. P. Speiser, *Infect. Immun.*, **13**, 204 (1976).

(2) J. Kreuter, R. Mauler, H. Gruschkau, and P. P. Speiser, *Exp. Cell Biol.*, **44**, 12 (1976).

(3) J. Kreuter and E. Liehl, *Med. Microbiol. Immunol.*, **165**, 111 (1978).

(4) J. Kreuter and E. Liehl, *J. Pharm. Sci.*, **70**, 367 (1981).

(5) J. Kreuter and I. Haenzel, *Infect. Immun.*, **19**, 667 (1978).

(6) J. Kreuter, U. Täuber, and V. Illi, *J. Pharm. Sci.*, **68**, 1443 (1979).

(7) L. Tomatis, *Tumori*, **52**, 165 (1966).

(8) B. S. Oppenheimer, E. T. Oppenheimer, I. Danishefsky, A. P. Stout, and F. R. Eirich, *Cancer Res.*, **15**, 333 (1955).

(9) A. Murray and D. L. Williams, "Organic Synthesis with Isotopes, Part I," Interscience, New York, N.Y., 1958.

(10) P. Edman and I. Sjöholm, *J. Pharm. Sci.*, **70**, 684 (1981).

(11) M. Barvic, K. Kliment, and M. Zaradil, *J. Biomed. Mater. Res.*, **1**, 313 (1967).

(12) L. Sprincl, J. Kopecek, and D. Lim, *J. Biomed. Mater. Res.*, **4**, 447 (1971).

(13) A. Schindler, R. Jeffcoat, G. L. Kimmel, C. G. Pitt, M. E. Wall, and R. Zweidinger, in "Contemporary Topics in Polymer Science," Vol. 2, E. M. Pearce and J. F. Schaefgen, Eds., Plenum, New York, N.Y., 1977, pp. 251–289.

(14) V. Bentele, U. E. Berg, and J. Kreuter, *Int. J. Pharm.* **13**, 109 (1983).

Solid-State Decomposition of Alkoxyfuroic Acids in the Presence of Microcrystalline Cellulose

J. T. CARSTENSEN ˣ and ROHIT C. KOTHARI *

Received April 9, 1982, from the *School of Pharmacy, University of Wisconsin, Madison, WI 53706.* Accepted for publication August 24, 1982. * Present address: Riker Laboratories, St. Paul, MN 55119.

Abstract □ A solid–solid interaction between alkoxyfuroic acids and microcrystalline cellulose has been studied. The decomposition of the mixture differs from that of the drug(s) alone, in that carbon monoxide (not carbon dioxide) is the high-temperature decomposition product. A model is proposed in which interaction occurs at contact points. A liquid decomposition product, dissolving part of the alkoxyfuroic acid (to the extent of its solubility) serves as a carrier, so that the number of contact points increases, thus accelerating the reaction. Both the main and ancillary parameters have calculated values that are consistent with the model.

Keyphrases □ Alkoxyfuroic acid—solid-state interactions with microcrystalline cellulose, decomposition model □ Microcrystalline cellulose—solid-state interactions with alkoxyfuroic acids, decomposition model □ Decomposition—alkoxyfuroic acids with microcrystalline cellulose, model, solid-state interactions

The interaction between solid drugs and solid excipients is of great theoretical and practical interest. Most studies deal with multicomponent systems, but even when only two solid components are present, the presence of air complicates the interpretation of data. Nevertheless, good direct conclusions have frequently been derived (1, 2).

This study describes the interaction between a drug (5-alkyloxy-2-furoic acid)[1] and a common pharmaceutical excipient (microcrystalline cellulose). Interactions between drugs and this excipient have been reported in the past (3) and present a challenging field of investigation.

EXPERIMENTAL

The 5-alkoxy-2-furoic acids were synthesized and purified as described by Carstensen and Kothari (4). The microcrystalline cellulose used[2] was

[1] A few studies were carried out with the C_8 derivative as well.

[2] Avicel; FMC Corp., West Point, Pa.

0022-3549/83/1000-1149$01.00/0

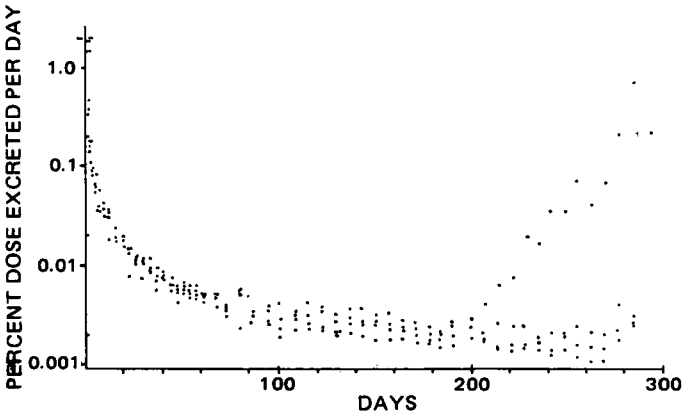

Figure 2—*Rate of fecal excretion of ^{14}C-radioactivity after subcutaneous injection of poly(methyl [1-^{14}C]methacrylate) nanoparticles into rats (n = 4).*

servation of a lag phase for the elimination of implanted material is not new. In 1955, Oppenheimer *et al.* (8) observed a lag period of 54 weeks after implantation of poly(methyl [1-^{14}C]methacrylate) films into rats, until suddenly the excretion of radioactivity started and continued for 40 weeks. When the films were removed, the excretion of radioactivity disappeared. Schindler *et al.* (13) observed with polylactide implants that degradation of the polymer, measured by the decrease in the molecular weight *via* the viscosity of the implant, started soon after administration. The removal of material from the administration site, however, occurred only after a certain molecular weight was reached. After implantation of poly(ε-caprolactone-co-DL-lactic acid) capsules for instance, the viscosity decreased by 75%, while only 1% of the injected capsule material was removed from the injection site. Since the viscosity is directly related to the molecular weight, a comparable reduction of ~75% in the molecular weight has to be assumed. Over the following 8 weeks, the residual polymer disappeared totally from the site of administration, while the viscosity decreased only slowly.

A similar process possibly occurred after subcutaneous administration of poly(methyl [1-^{14}C]methacrylate) nanoparticles and films. The degradation might have started rather early after injection or implantation, but the removal from the site of administration and the excretion began only when a certain molecular weight of the degradation products was reached. The faster excretion rate during the first couple of days can also be explained by the limitation of the transportation and excretion process by the molecular weight. The initially excreted total amount of ~13% far exceeds the possible amount of residual monomers. As mentioned previously, ≤1% residual monomers are contained in the polymer. However, as shown by gel permeation chromatography (14), the molecular weight distribution of the poly(methyl [1-^{14}C]methacrylate) nanoparticles prepared by γ-irradiation is rather wide, allowing for a considerable amount of low-molecular weight polymer, some of which could be readily excreted.

REFERENCES

(1) J. Kreuter and P. P. Speiser, *Infect. Immun.*, **13**, 204 (1976).

(2) J. Kreuter, R. Mauler, H. Gruschkau, and P. P. Speiser, *Exp. Cell Biol.*, **44**, 12 (1976).

(3) J. Kreuter and E. Liehl, *Med. Microbiol. Immunol.*, **165**, 111 (1978).

(4) J. Kreuter and E. Liehl, *J. Pharm. Sci.*, **70**, 367 (1981).

(5) J. Kreuter and I. Haenzel, *Infect. Immun.*, **19**, 667 (1978).

(6) J. Kreuter, U. Täuber, and V. Illi, *J. Pharm. Sci.*, **68**, 1443 (1979).

(7) L. Tomatis, *Tumori*, **52**, 165 (1966).

(8) B. S. Oppenheimer, E. T. Oppenheimer, I. Danishefsky, A. P. Stout, and F. R. Eirich, *Cancer Res.*, **15**, 333 (1955).

(9) A. Murray and D. L. Williams, "Organic Synthesis with Isotopes, Part I," Interscience, New York, N.Y., 1958.

(10) P. Edman and I. Sjöholm, *J. Pharm. Sci.*, **70**, 684 (1981).

(11) M. Barvic, K. Kliment, and M. Zaradil, *J. Biomed. Mater. Res.*, **1**, 313 (1967).

(12) L. Sprincl, J. Kopecek, and D. Lim, *J. Biomed. Mater. Res.*, **4**, 447 (1971).

(13) A. Schindler, R. Jeffcoat, G. L. Kimmel, C. G. Pitt, M. E. Wall, and R. Zweidinger, in "Contemporary Topics in Polymer Science," Vol. 2, E. M. Pearce and J. F. Schaefgen, Eds., Plenum, New York, N.Y., 1977, pp. 251–289.

(14) V. Bentele, U. E. Berg, and J. Kreuter, *Int. J. Pharm.* **13**, 109 (1983).

Solid-State Decomposition of Alkoxyfuroic Acids in the Presence of Microcrystalline Cellulose

J. T. CARSTENSEN ˣ and ROHIT C. KOTHARI *

Received April 9, 1982, from the *School of Pharmacy, University of Wisconsin, Madison, WI 53706.* Accepted for publication August 24, 1982. * Present address: Riker Laboratories, St. Paul, MN 55119.

Abstract □ A solid–solid interaction between alkoxyfuroic acids and microcrystalline cellulose has been studied. The decomposition of the mixture differs from that of the drug(s) alone, in that carbon monoxide (not carbon dioxide) is the high-temperature decomposition product. A model is proposed in which interaction occurs at contact points. A liquid decomposition product, dissolving part of the alkoxyfuroic acid (to the extent of its solubility) serves as a carrier, so that the number of contact points increases, thus accelerating the reaction. Both the main and ancillary parameters have calculated values that are consistent with the model.

Keyphrases □ Alkoxyfuroic acid—solid-state interactions with microcrystalline cellulose, decomposition model □ Microcrystalline cellulose—solid-state interactions with alkoxyfuroic acids, decomposition model □ Decomposition—alkoxyfuroic acids with microcrystalline cellulose, model, solid-state interactions

The interaction between solid drugs and solid excipients is of great theoretical and practical interest. Most studies deal with multicomponent systems, but even when only two solid components are present, the presence of air complicates the interpretation of data. Nevertheless, good direct conclusions have frequently been derived (1, 2).

This study describes the interaction between a drug (5-alkyloxy-2-furoic acid)[1] and a common pharmaceutical excipient (microcrystalline cellulose). Interactions between drugs and this excipient have been reported in the past (3) and present a challenging field of investigation.

EXPERIMENTAL

The 5-alkoxy-2-furoic acids were synthesized and purified as described by Carstensen and Kothari (4). The microcrystalline cellulose used[2] was

[1] A few studies were carried out with the C_8 derivative as well.

[2] Avicel; FMC Corp., West Point, Pa.

0022-3549/83/1000-1149$01.00/0

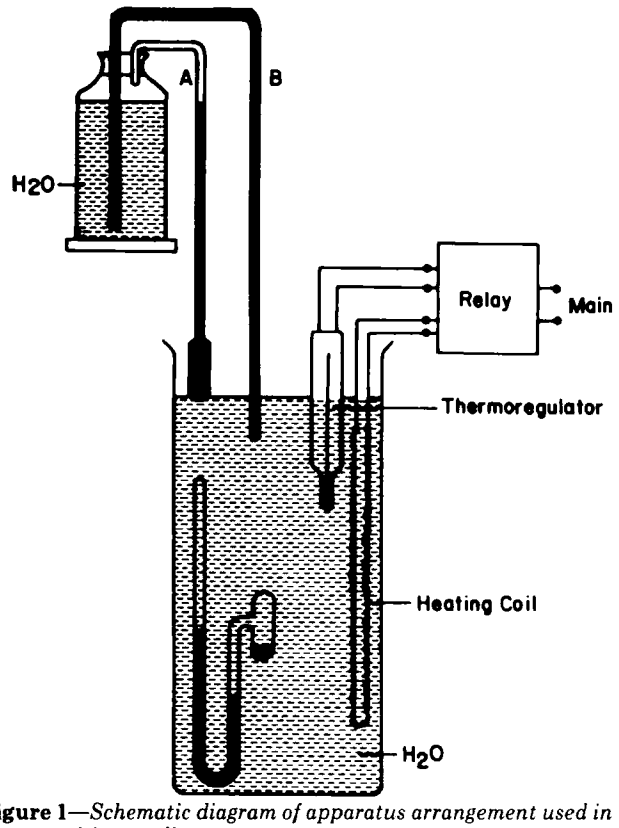

Figure 1—*Schematic diagram of apparatus arrangement used in the decomposition studies.*

found to contain 3% water as determined by (*a*) use of a vacuum electrobalance and (*b*) Karl Fischer titration. To eliminate the effect of water, the microcrystalline cellulose was dried *in vacuo* on a high-vacuum rack for 10 hr just prior to the preparation of the sample for kinetic studies.

The kinetic studies were carried out by mixing furoic acid with microcrystalline cellulose (see below) and placing the powder mixture in the sidearm of a fused manometer as described by Carstensen and Kothari (5). This was then placed in a constant-temperature bath as shown in Fig. 1, and the level of the mercury was determined as a function of time. The volumes of sample bulb and of the high-pressure side of the manometer (as a function of level) were determined as described by Carstensen and Musa (6). Knowledge of the density of mercury at the temperature in question allows conversion of mercury level to pressure, and hence the number of moles of gas produced can be calculated by means of the ideal gas law.

Although the decomposition of the two solids takes place in the absence of air, there is mercury vapor in the atmosphere above the solids which has been shown to effect some systems (7). The decomposition was, therefore, carried out in breakseal tubes (7) for certain samples. In a breakseal tube sample there is no mercury vapor in the head space. No significant difference was observed in decomposition rates, so that, unless otherwise noted, the studies were done in the fused manometer as shown in Fig. 1.

Since intimacy of mixing is important, a variety of mixing methods were tested:

1. Physical mixtures of the two compounds were made in various proportions and were mixed using a quartering technique. Some samples were ground in a ball mill. The ratios used are shown in Table I.

2. The alkoxyfuroic acid was weighed and dissolved in a solvent (methanol or acetone). Weighed amounts of microcrystalline cellulose were then added, and the suspension was stored in a closed container for 12 hr. The solvent was evaporated and then the samples were tested by the fused manometer and breakseal techniques. The surface area of the samples was tested by krypton adsorption[3]. The Brunauer–Emmett–Teller equation (8) was used for calculation of the surface from the adsorption data.

The gas evolved was carbon monoxide (not carbon dioxide) at elevated temperatures[4]. This identification was carried out in two ways. At the end of the kinetic study the sample bulb was immersed in a toluene slush (9) in a Dewar flask. The toluene slush (a mixture of ~80% solid toluene and 20% liquid toluene at the melting point of toluene, 178°K) was prepared by adding liquid nitrogen to toluene in a Dewar flask while stirring the liquid. The toluene eventually started freezing, and addition of liquid nitrogen was stopped when a "slush" was obtained giving a constant temperature reservoir as long as solid toluene was present. If the evolved gas is condensable at 178°K (*e.g.*, carbon dioxide), then the gas in the head space should condense and the pressure in the manometer equilibrate to zero. The gas, however, was not condensable at 178°K. Samples of the head space gas were analyzed by MS and identified as carbon monoxide.

[3] Quantasorb; Quantachrome Corp. Syosset, NY 11791.

[4] The conclusions refer to the temperatures used here only. It is doubtful that measurable amounts of carbon monoxide would be formed at room temperature.

Table I—Statistical Comparison of the Models According to Eqs. 1A, 2, and 3A

Derivative[a]	Furoic Acid, %	Temperature	s^2_{yx} for Model		
			Eq. 2	Eq. 3A	Eq. 1A
C_{14}	60	90°	0.00234	0.00380	0.00106
C_{14}	40[b]	90°	0.00159	0.00956	0.00006
C_{14}	80	90°	0.00143	0.00457	0.00004
C_{14}	40	90°	0.00027	0.00025	0.00008
C_{14}	20[b]	90°	0.00093	0.01230	0.00014
C_{14}	20	90°	0.00018	0.00333	0.00125
C_{14}	10	90°	0.00000	0.00192	0.00001
C_{14}	30[c]	90°	0.00197	0.00321	0.00000
C_{14}	47[c]	90°	0.01132	0.02179	0.00189
C_{14}	18[c]	90°	0.00016	0.00238	0.00051
C_{14}	40[d]	90°	0.00140	0.00639	0.00004
C_{14}	20[d]	90°	0.00002	0.00232	0.00000
C_8	20	90°	0.00000	0.00145	0.00000
C_8	40	90°	0.00016	0.00033	0.00003

[a] Number of side-chain carbons. [b] Ground in ball mill. [c] Applied as a methanolic solution. [d] Applied as a solution in acetone.

RESULTS AND DISCUSSION

A typical pattern of decomposition of alkoxyfuroic acid in the presence of microcrystalline cellulose is shown in Fig. 2. The fraction decomposed (x) as a function of time (t) is a sigmoid curve, as in the case of the pure furoic acids themselves (4). A few obvious possibilities for this are delineated below. As for the case of the pure furoic acids, the decomposition could be directed by Bawn kinetics (10) in which case:

$$\ln(1 + Ax) = Kt + c'' \qquad \text{(Eq. 1)}$$

where A, K, and c'' are constants. This model relies on decomposition

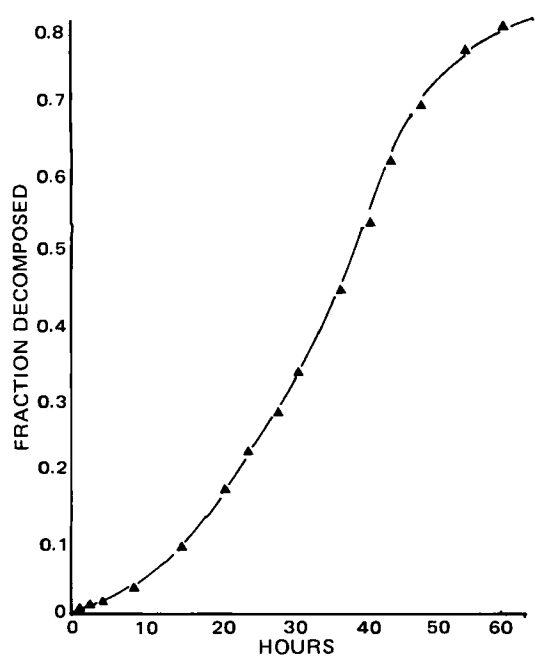

Figure 2—*Typical decomposition profile of an alkoxyfuroic acid–microcrystalline cellulose mixture, with 40% alkoxyfuroic acid (C_{18}) at 90°.*

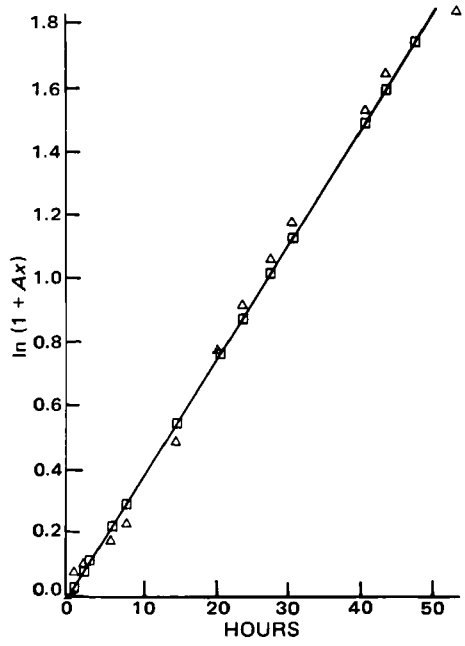

Figure 3—*Data in Fig. 2 plotted according to Eq. 1. In the ordinate,* x *is fraction decomposed and* A *(Eq. 1 and Table IV) is a floating parameter. Key: (△) = actual values; (□) = values according to least-squares fit.*

of the furoic acid in the solid state as well as in solution of the furoic acid in its (liquid) decomposition product. There is also the possibility that the decomposition occurs *via* the vapor phase, which results in zero-order kinetics (11), *i.e.*:

$$x = kt + c \qquad \text{(Eq. 2)}$$

where k and c are constants. That this is not the case is graphically obvious (Fig. 2), but it has been included as a possibility in the statistical evaluation in Table I. Finally, there is the possibility of Prout–Tompkins-type kinetics (12) where:

$$\ln|x/(1-x)| = -k't + c' \qquad \text{(Eq. 3)}$$

Unlike the decomposition of the pure furoic acids, the presence of a liquid phase was not visually obvious. This, however, could be due to adsorptive and absorptive properties of the microcrystalline cellulose. For decompositions where a solid decomposes to a solid plus a gas, Eq. 3 could be expected to hold.

For the sake of comparison, least-squares fits were performed of all data according to the three equations, and the residual sum of squares (s_{yx}^2) calculated for fits *via* Eq. 2 and from Eqs. 1 and 3 in the forms:

$$x = \exp(Kt + c'') - 1 \qquad \text{(Eq. 1A)}$$

$$x = \exp(-k't + c')/\{1 + \exp(-k't + c')\} \qquad \text{(Eq. 3A)}$$

In this manner the values of s_{yx}^2 are comparable (being in the same dimensionless unit). It is obvious from Table I (Fig. 3) that Eq. 1 (Eq. 1A) fits the data better than the two other equations. Values of K and c from the various mixtures of furoic acid and microcrystalline cellulose studied are shown in Table II. For reasons that will be dealt with later, these evaluations were carried out only through 80% of the decomposition. Beyond this point there was distinct deviation from all three models.

Solid-state interactions have been covered in the past in descriptive and qualitative fashions (13–15), but in a quantitative sense physical models of interactions between two solids have only occurred infrequently in the literature (16, 17). In the following an explanation for the kinetic scheme is sought using models. The first point to notice is that the decomposition of the furoic acids (RCOOH) differs when microcrystalline cellulose (R'CHOHR") is present. Furoic acids alone decompose in the following manner:

$$\text{RCOOH} \rightarrow \text{RH(liquid)} + \text{CO}_2\text{(gas)} \qquad \text{(Eq. 4)}$$

i.e., carbon dioxide is formed. Part of the decomposition occurs in the solid RCOOH and part in a saturated solution of RCOOH in RH. In the presence of microcrystalline cellulose, however, carbon monoxide is

Table II—Parameter Values for Decomposition of Furoic Acids in Contact With Microcrystalline Cellulose [a]

Derivative	Furoic Acid, %	Temperature	$\ln(1+Ax) = Kt + c''$ Slope (K or q)	Intercept (c'')	R^2 [b]
C_{14}	60	90°	0.066	−0.0008	0.98
C_{14}	40[c]	90°	0.057	0.00009	0.97
C_{14}	80	90°	0.035	0.00002	0.98
C_{14}	40	90°	0.036	0.00008	0.99
C_{14}	20[d]	90°	0.107	0.00010	0.99
C_{14}	20	90°	0.049	−0.00005	0.97
C_{14}	30[e]	90°	0.043	−0.00001	0.98
C_{14}	10	90°	0.016	0.00005	0.99
C_{14}	47[e]	90°	0.042	0.00004	0.93
C_{14}	18[e]	90°	0.008	0.00000	0.97
C_{14}	40[f]	90°	0.017	−0.00004	0.99
C_{14}	20[f]	90°	0.013	0.00007	0.99
C_8	20	90°	0.004	−0.00001	0.99
C_8	40	90°	0.016	−0.00002	0.99
C_{14}	40	85°	0.0039	−0.06168	0.98
C_{14}	40	95°	0.0688	−0.01793	0.99
C_{14}	40	100°	0.5836	0.02268	0.99

[a] Data treated according to Eq. 1. [b] Correlation coefficient squared. [c] Ground in ball mill. [d] Hand ground with a mortar and pestle. [e] Applied as a methanolic solution. [f] Applied as a solution in acetone.

formed. Without any kind of speculation as to the actual interaction between the two solids, it may be stated generally that:

$$\text{RCOOH} + \text{R'CHOHR''} \rightarrow \text{Q}_1 + \text{Q}_2 + \text{CO} \qquad \text{(Eq. 5)}$$

where Q_1 and Q_2 are decomposition products. One of these (or both of them) could be liquid.

Cellulose, of course, decomposes at elevated temperatures, but usually not until >140° (18) within the time periods used in this study. The usual decomposition path is one of loss of water, leading to the formation of dehydrocellulose.

It is possible to visualize reaction schemes including microcrystalline cellulose, such as:

$$\text{RCOOH} + \text{R'CHOHR''} \rightarrow \text{RH} + \text{CO} + \text{H}_2\text{O} + \text{R'(C:O)R''} \qquad \text{(Eq. 6)}$$

where RH is liquid. It is also possible to visualize schemes where the microcrystalline cellulose does not take part in the overall reaction, *i.e.*, where it serves as a catalyst:

$$\text{RCOOH(+ R'CHOHR'')} \rightarrow \text{ROH} + \text{CO(+ R'CHOHR'')} \qquad \text{(Eq. 7)}$$

It should be pointed out that neither of these two schemes have been substantiated, and they are mentioned solely to show that reactions of the type in Eq. 5 are feasible stoichiometrically.

At first thought, reactions such as Eqs. 4 and 5 would not seem to differ widely. RCOOH could dissolve in Q_1 and justify the Bawn-type kinetics which apply to such a situation. But in that case it should not matter if the materials were ground or not. It is noted from Table II that grinding gives an increased decomposition rate (0.057 *versus* 0.036 hr^{-1} for 40% acid and 0.107 *versus* 0.049 hr^{-1} for 20% acid). Hence, contact points between the alkoxyfuroic acid and the microcrystalline cellulose must be involved. A model which accounts for this is:

1. At contact points (the number of which is denoted N in the following) a reaction of the type shown in Eq. 5 takes place giving at least one liquid decomposition product (*e.g.*, Q_1).
2. The furoic acid will dissolve in the Q_1 to the extent of its solubility (S moles per mole of Q_1) and will start covering the surface (a, cm^2) of the microcrystalline cellulose.
3. The reaction then accelerates because of increased contact points between the (now dissolved) furoic acid and the microcrystalline cellulose.
4. Due to crowding there will, eventually, be a deceleration period.

It might be argued that the external surface of the microcrystalline cellulose would be insufficient to account for the total decomposition. There are, however, two "types" of surface present in microcrystalline cellulose: nitrogen adsorption gives low surface areas, whereas water isotherms give surface areas 100 times as large (19–22).

By the decomposition at a contact point, it is assumed that the decomposition, creating one Q_1 molecule, will dislodge (dissolve) S molecules of RCOOH at the contact point. If the initial number of contact points is N_0 and if there is a reaction possibility of α at each contact point,

Table III—Late-Period Data Treated According to Eq. 24

Derivative	Furoic Acid, %	Temperature	$\ln(1-x) = -K't + D$ Slope ($-K'$)	Intercept (D)	R^2 [a]	$\phi L_0/N_0$
C_{14}	60	90°	−.061	1.70	0.998	1.50
C_{14}	40[b]	90°	−0.55	0.68	0.967	0.67
C_{14}	80	90°	−0.036	1.06	0.946	4.00
C_{14}	40	90°	−0.041	0.82	0.99	0.67
C_{14}	20[c]	90°	−0.037	−0.20	0.875	0.21
C_{14}	20	90°	−0.021	−0.42	0.895	0.25
C_{14}	30[d]	90°	−0.052	1.18	0.989	0.43
C_{14}	10	90°	−0.038	0.0031	0.979	0.11
C_{14}	47[d]	90°	−0.11	3.6	0.987	0.89[f]
C_{14}	18[d]	90°	−0.017	−0.16	0.943	0.22
C_{14}	40[e]	90°	−0.034	1.28	0.970	0.67
C_{14}	20[e]	90°	−0.038	0.97	0.999	0.25
C_8	20	90°	−0.020	0.60	0.998	
C_8	40	90°	−0.016	0.44	0.955	
C_{14}	40	85°	−0.010	1.23	0.995	
C_{14}	40	95°	−0.081	1.51	0.993	
C_{14}	40	100°	−0.39	1.05	0.984	

[a] Coefficient of correlation squared. [b] Ground in ball mill. [c] Hand ground with a mortar and pestle. [d] Applied as a methanolic solution. [e] Applied as a solution in acetone. [f] Data not included in D *versus* $\phi L_0/N_0$ correlation.

then:

$$dN/dt = \alpha \cdot (S-1) \cdot N \qquad \text{(Eq. 8)}$$

since, when α molecules react, $\alpha \cdot S$ new contact points are created, and one (the one at which the reaction takes place) is lost.

At some point in time there will arise the distinct probability of "overcrowding," *i.e.*, saturated Q_1 will start getting in contact with sites already reacted (containing Q_2 and not native microcrystalline cellulose). If this probability is proportional to N, with proportionality constant β [similar to a termination probability in a Prout–Tompkins-type reaction (12)], then Eq. 8 becomes:

$$dN/dt = q \cdot N \qquad \text{(Eq. 9)}$$

where:

$$q = \alpha \cdot (S-1) - \beta \qquad \text{(Eq. 10)}$$

There would be an initial value of α denoted α_0, and initially the value of β would be zero. In Prout–Tompkins reactions it takes considerable time before β becomes sizable. However, in the model proposed here, the external surface is relatively small (compared with the total surface) so that the crowding may be assumed to occur rapidly, and if it is assumed that β has a finite value from the onset, then considering $\alpha = \alpha_0$ and $\beta = \beta_0$ throughout the process may be acceptable. This allows integration of Eq. 9, which with imposition of initial conditions yields:

$$N = N_0 \cdot e^{qt} \qquad \text{(Eq. 11)}$$

Since the rate of decomposition is proportional to the number of contact points at a given time t, then denoting by L the number of molecules of alkoxyfuroic acid that are intact at time t:

$$dL/dt = -\gamma \cdot N \qquad \text{(Eq. 12)}$$

where γ is a constant. From the definition of L it follows that:

$$x = (L_0 - L)/L_0 \qquad \text{(Eq. 13)}$$

This inserted in Eq. 12 yields:

$$dx/dt = -(1/L_0)dL/dt \qquad \text{(Eq. 14)}$$

which inserted in Eq. 12 gives:

$$dx/dt = (1/L_0) \cdot \gamma \cdot N \qquad \text{(Eq. 15)}$$

Substituting Eq. 11 into Eq. 15 then gives:

$$dx/dt = (\gamma N_0/L_0)e^{qt} \qquad \text{(Eq. 16)}$$

Integration of this (with imposition of initial conditions) yields:

$$x = (\gamma N_0/\{L_0 q\})(e^{qt} - 1) \qquad \text{(Eq. 17)}$$

If:

$$A = \{L_0 q/(\gamma N_0)\} \qquad \text{(Eq. 18)}$$

then the logarithmic form of Eq. 18 is identical to the Bawn equation (Eq. 1):

$$\ln(1 + Ax) = qt \qquad \text{(Eq. 19)}$$

Eq. 19 differs from Eq. 1 in the sense that the intercept is zero. It is seen from Table II, that this indeed is the case: all the intercepts listed fail to differ significantly from zero. q is hence equal to K in Eq. 1 (Table II).

Even though Eq. 19 is of the general form of a Bawn equation, the argumentation leading to its derivation is quite different. The fact that the data fit Eq. 19 is no proof of the proposed model. In fact, a model can never be proven correct, one can only fail to show that it contradicts a particular set of data, and this, in itself, does not guarantee that other models (not thought of) might not prove to be better. To lend credence to a model it is worthwhile to ascertain that it is consistent in as many respects as can be thought of.

There are two distinct cases in the aforementioned model: (*a*) the number of surface sites of the microcrystalline cellulose (N_0) is larger than the initial number of alkoxyfuroic acid molecules (L_0), or (*b*) the opposite is the case. The former (*a*) is the case in this study. In general a model has a certain domain in which it applies, and beyond which other mechanisms take over. In the case in point, there will be a given point in time, t', at which all the furoic acid will have dissolved; *i.e.*, beyond this point there is no more solid furoic acid in the system, it is all dissolved, and adsorbed at sites on the microcrystalline cellulose.

If there are L' intact furoic acid molecules left at t', then $(L_0 - L')$ molecules of Q_0 will have been formed, so that (by definition of S):

$$S = L'/(L_0 - L') \qquad \text{(Eq. 20)}$$

or:

$$L' = L_0 S/(1 + S) \qquad \text{(Eq. 21)}$$

After t' the rate of decrease in number of furoic acid molecules would simply be proportional to the number of intact furoic acid molecules, *i.e.*:

$$dL/dt = -K' \cdot L \qquad \text{(Eq. 22)}$$

since there is no longer a termination probability. (The molecules are visualized as situated at microcrystalline cellulose sites with a probability of K' of reacting.) Integrating this and imposing that $L = L'$ at $t = t'$ then gives:

$$\ln L = -K'(t - t') + \ln[SL_0/(1 + S)] \qquad \text{(Eq. 23)}$$

or:

$$(L/L_0) = (1 - x) = [S/(1 + S)] \cdot e^{-K'(t-t')} \qquad \text{(Eq. 24)}$$

The logarithmic form of this is:

$$\ln(1 - x) = -K' \cdot t + D \qquad \text{(Eq. 25)}$$

where:

$$D = K't' + \ln[S/(1 + S)] \qquad \text{(Eq. 26)}$$

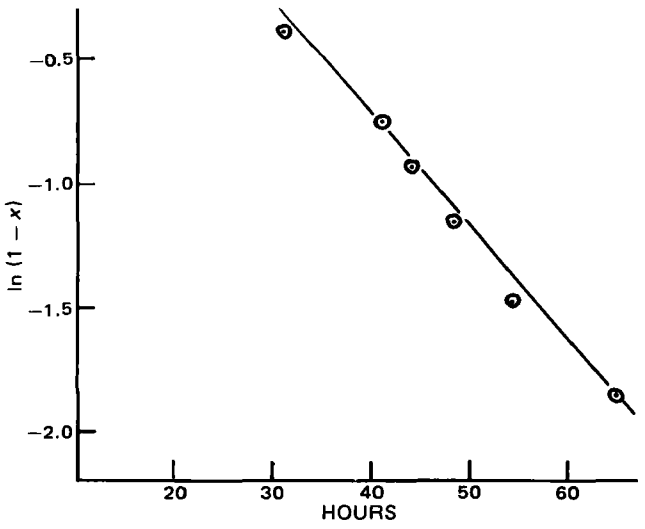

Figure 4—*The late phase of decomposition, which is supposed to be first order. ln(1 − x) is plotted* versus *time for a C_{14} alkoxyfuroic acid–microcrystalline cellulose mixture (40:60).*

Hence the latter part of the curve should be an exponential decay curve. Data treated in this fashion are shown in Fig. 4, and least-squares fit values are shown in Table III.

Precision in this range is, of course, less than the remainder of the data, since all the x values are between 0.8 and 1.0. Nevertheless fits are good (as judged by visual inspection of the figure, as well as from correlation coefficients in the table).

At a particular temperature, the solubility S is constant. It is noted that at time t' (Eq. 17):

$$(L_0 - L')/L_0 = x' = \{\gamma N_0/(L_0 q)\} \cdot (e^{qt'} - 1) \qquad \text{(Eq. 27)}$$

This may be rearranged to read:

$$t' = (1/q) \cdot \{1 + \ln[(L_0 - L') \cdot q/(\gamma \cdot N_0)]\} \sim (1/q) \cdot \ln(L_0/N_0) + (1/q) \cdot \ln(q/\gamma) \qquad \text{(Eq. 28)}$$

where the approximation $e^{qt'} \gg 1$[5] and $L' \ll L_0$. N_0 is proportional to the amount of microcrystalline cellulose (M_1,g) and L_0 is proportional to the amount of furoic acid (M_0,g). Hence (L_0/N_0) is proportional to M_2/M_1, *i.e.*:

$$M_2/M_1 = \phi \cdot (L_0/N_0) \qquad \text{(Eq. 29)}$$

where ϕ is a constant. When Eqs. 28 and 29 are inserted in Eq. 26, the following expression emerges:

$$D = (K'/q)[(\ln(M_2/M_1) - \ln q + \ln(\gamma\phi)] + \ln(S/\{1 + S\}) \qquad \text{(Eq. 30)}$$

If S is sizable (as in the case of the pure furoic acids), then $\ln\{S/(1 + S)\}$ is approximately zero, so that Eq. 29, may be written (in rearranged form):

$$(D \cdot q/K') - \ln q = \ln(M_2/M_1) + \ln(\gamma\phi) \qquad \text{(Eq. 31)}$$

A plot of $(D \cdot q/K') - \ln q$ as a function of $\ln(M_2/M_1)$ should therefore be linear. The values of these two parameters are shown in Table IV, and a plot according to Eq. 31 is shown in Fig. 5. It should again be stressed that the extraction of information from the data at this point is at the limit of precision, but that it is done to check the model for consistency, not to obtain values of parameters. It is seen from Fig. 5 that a fairly good straight line ensues. The least-squares fit is:

$$(D \cdot q/K') - \ln q = 0.7 \ln(M_2/M_1) + 3.9 \qquad \text{(Eq. 32)}$$

The 95% confidence limits on the slope are ± 0.4, so that 1.0 is in this interval, hence Eq. 31 is not contradicted. Aside from operating at the limit of precision, the confidence limits on the slope are large because only five points are involved. In this treatment the milled samples were omitted for reasons mentioned earlier, and the solvent-deposited samples were omitted as well, because they appear to give lower rate constants

[5] For the data in Fig. 3, for instance, $q = 0.036$ and $t' = 50$ so that $\exp(qt') = 6$.

Table IV—ln A as a Function of $\ln(qM_2/M_1)$ [a]

Derivative	Furoic Acid, %	M_2/M_1	A	ln A	$\ln(qM_2/M_1)$
C_{14}	60	1.50	28.25	3.34	−2.31
C_{14}	40[b]	0.67	7.85	2.06	−3.27
C_{14}	80	4.00	10.75	2.37	−1.97
C_{14}	40	0.67	6.75	1.91	−3.72
C_{14}	20[c]	0.25	15.09	2.71	−3.62
C_{14}	20	0.25	5.65	1.73	−4.40
C_{14}	30[d]	0.43	9.11	2.21	−3.99
C_{14}	10	0.11	0.86	−0.15	−6.34
C_{14}	47[d]	0.90	10.66	2.37	−3.28
C_{14}	18[d]	0.23	0.86	−0.15	−6.30
C_{14}	40[e]	0.67	3.87	1.35	−4.48
C_{14}	20[e]	0.25	1.62	0.48	−5.73

[a] Data treated according to Eq. 31, least-squares fit: $\ln A = 0.73 \cdot \ln(qM_2/M_1) + 4.68$ with a correlation coefficient of 0.93. [b] Ground with a ball mill. [c] Hand ground with a mortar and pestle. [d] Applied as a methanolic solution. [e] Applied as a solution in acetone.

as shown in Table II (0.13 *versus* 0.049 hr^{-1} for 20% acid in acetone, 0.017 *versus* 0.036 hr^{-1} for 40% acid in acetone, and 0.042 *versus* a prorated 0.046 for 47% acid in methanol).

A further consistency check exists in the following consideration: Eq. 18 suggests that the parameter A in Eq. 19 (listed in Table III) should be proportional to q and to the ratio M_2/M_1. In logarithmic form Eq. 18 becomes:

$$\ln A = \ln(qL_0/N_0) - \ln\gamma = \ln(qM_2/M_1) - \ln(\phi/\gamma) \qquad \text{(Eq. 33)}$$

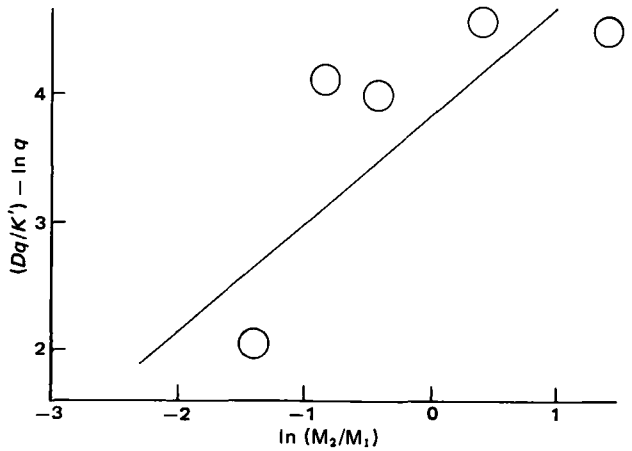

Figure 5—*Eq. 31 may be written: (Dq/K′) = ln (qM₂/M₁) + ln(φγ); the data from Table IV are presented in this fashion. Data from Table IV plotted according to Eq. 31.*

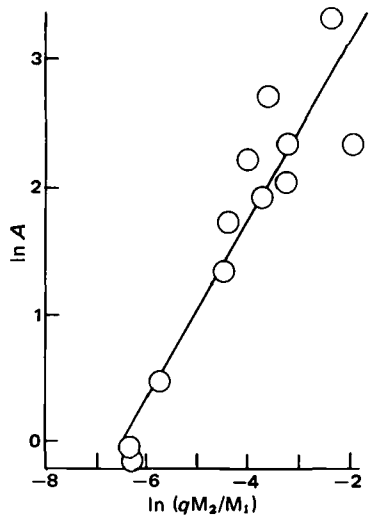

Figure 6—*The floating parameter, A, according to Eq. 33 should be a linear function of ln(qM₂/M₁); the data from Table IV are shown in this fashion.*

Table V—Temperature Dependence of K Values of C_{14} Derivative–Microcrystalline Cellulose Mixtures [a]

Temperature	1000/T	K (q)	ln K(ln q)	K'	ln K'
85°	2.792	0.0039	−5.55	0.0104	−4.56
90°	2.754	0.0360	−3.32	0.0405	−3.21
95°	2.716	0.0688	−2.67	0.0807	−2.52
100°	2.680	0.5836	−0.54	0.3940	−0.93

[a] Least-squares fit according to Eq. 33 for $K(q)$ $R^2 = -0.980$, slope = −41.88, and intercept = 111.55; for K', $R^2 = -0.989$, slope = −30.92, and intercept = 81.77.

where Eq. 30 has been introduced for the last step. Values of q are found in Table II, and values of $\ln(qM_2/M_1)$ are listed in the last column of Table III. A plot according to Eq. 33 is shown in Fig. 6. Linearity is plausible from the figure, and the correlation coefficient (0.93) is of satisfactory magnitude. The least-squares fit equation is:

$$\ln A = 0.73 \ln(qM_2/M_1) + 4.68 \qquad \text{(Eq. 34)}$$

The slope, again, does not differ significantly from unity. The values of (ϕ-γ) from Figs. 5 and 6 should be identical but as shown they differ, but (*a*) there is no actual value in obtaining the figures (other than ascertaining that they are of reasonable orders of magnitude), and (*b*) it should be stressed again, that they are obtained at the limit of precision. The restraints on ϕ and γ are that ϕ be positive and (from the argumentation leading to Eq. 12) that γ be between zero and one. The consequences of the model and the data, therefore, do not lead to contradiction in this respect either.

As a final check, the temperature dependence of the K and K' values is according to an Arrhenius equation, *i.e.*:

$$\ln K = -(E_a/R)(1/T) + \ln Z \qquad \text{(Eq. 35)}$$

where E_a is activation energy, R the gas constant, T the absolute temperature, and Z a collision factor. One composition was tested at four temperatures; the data are shown in Table V and graphically in Fig. 7. The least-squares fit parameters of these data according to Eq. 33 are shown as well. The values of E_a are 5.0 and 3.72 kJ/mole, respectively. These values are much lower than for the pure compound and are in the range expected for solution kinetics and chemisorption.

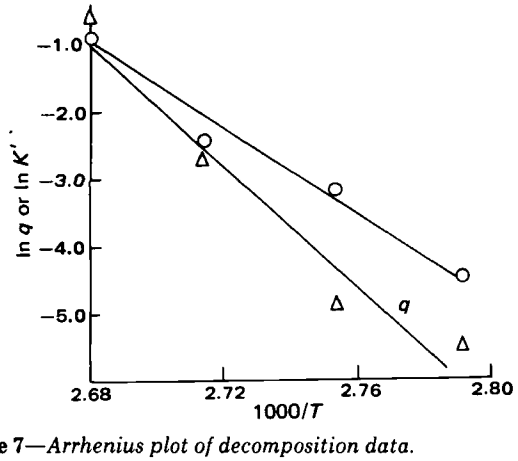

Figure 7—*Arrhenius plot of decomposition data.*

CONCLUSIONS

If microcrystalline cellulose is mixed with an alkoxyfuroic acid, an interaction takes place that could result from a direct reaction of the two components. A liquid decomposition product is formed and this serves as a carrier to increase the number of contact points and (as long as solid alkoxyfuroic acid is present) accelerate the reaction. Once all solid alkoxyfuroic acid is dissolved, the reaction becomes a reaction of adsorbed alkoxyfuroic acid.

REFERENCES

(1) A. Troup and H. Mitchner, *J. Pharm. Sci.*, **53**, 375 (1964).

(2) A. Jacobs, A. Dilatush, S. Weinstein, and J. Windheuser, *J. Pharm. Sci.*, **55**, 893 (1966).

(3) J. Carstensen, M. Osadca, and S. Rubin, *J. Pharm. Sci.*, **58**, 549 (1969).

(4) J. T. Carstensen and R. Kothari, *J. Pharm. Sci.*, **70**, 1095 (1981).

(5) J. T. Carstensen and R. Kothari, *J. Pharm. Sci.*, **69**, 123 (1980).

(6) J. T. Carstensen and M. N. Musa, *J. Pharm. Sci.*, **61**, 1112 (1972).

(7) J. T. Carstensen and P. Pothisiri, *J. Pharm. Sci.*, **64**, 37 (1975).

(8) S. Brunauer, P. Emmett, and E. Teller, *J. Am. Chem. Soc.*, **60**, 309 (1938).

(9) J. T. Carstensen, "Radiolysis of Gaseous Ammonia," Ph.D. Thesis Stevens Institute of Technology, 1967.

(10) C. E. H. Bawn, in "Chemistry of the Solid State," W. E. Garner, Ed., Butterworths, London, England, 1955, p. 254.

(11) P. Pothisiri and J. T. Carstensen, *J. Pharm. Sci.*, **64**, 1931 (1975).

(12) E. G. Prout and F. C. Tompkins, *Trans. Faraday Soc.*, **40**, 488 (1944).

(13) Y. Machida and T. Nagai, *Chem. Pharm. Bull.*, **22**, 2346 (1974).

(14) K. Takayama, N. Nambu, and T. Nagai, *Chem. Pharm. Bull.*, **25**, 879 (1977).

(15) K. Takayama, N. Nambu, and T. Nagai, *Chem. Pharm. Bull.*, **25**, 2608 (1977).

(16) W. Jander, *Z. Anorg. Chem.*, **163**, 1 (1927).

(17) R. P. Rastogi and N. B. Singh, *J. Phys. Chem.*, **70**, 3315 (1966).

(18) P. Burkart, J. Bandisch, and C. Ruscher, *Tappi*, **52**, 693 (1969).

(19) R. G. Hollenbeck, G. E. Peck, and D. O. Kildsig, *J. Pharm. Sci.*, **67**, 1599 (1978).

(20) K. Marshall, D. Sixsmith, and N. G. Stanley-Wood, *J. Pharm. Pharmacol.*, **24**, Suppl., 138p (1972).

(21) Y. Nakai, E. Fukuoka, S. Nakajima, and J. Hasegawa, *Chem. Pharm. Bull.*, **25**, 96, (1977).

(22) Y. Nakai, S. Nakajima, K. Yamamoto, K. Terada, and T. Konno, *Chem. Pharm. Bull.*, **28**, 652 (1980).

ACKNOWLEDGMENTS

Abstracted in part from a dissertation submitted by R. C. Kothari to the University of Wisconsin in partial fulfillment of the Doctor of Philosophy degree requirements.

Supported in part by a research grant from Hoffmann-La Roche, Inc., Nutley, NJ 07110.

The authors thank Dr. J. Sheridan, Hoffmann-La Roche, Nutley, N.J. and Drs. M. A. Zoglio and R. A. Parker, Merrell-Dow Laboratories, Cincinnati, Ohio for technical assistance.

Studies on Drug Metabolism by Use of Isotopes XXVII: Urinary Metabolites of Rutin in Rats and the Role of Intestinal Microflora in the Metabolism of Rutin

SHIGEO BABA[x], TAKASHI FURUTA, MINORU FUJIOKA, and TSUYOSHI GOROMARU

Received February 25, 1982, from *Tokyo College of Pharmacy, 1432-1 Horinouchi, Hachioji, Tokyo 192-03, Japan.* Accepted for publication August 17, 1982.

Abstract □ Analysis of urinary metabolites of orally administered rutin (I) labeled with deuterium ([2′,5′,6′-^{2}H]rutin, rutin-*d*) was carried out by GLC–MS. In rat urine, 3-hydroxyphenylacetic acid (III), 3-methoxy-4-hydroxyphenylacetic acid (IV), 3,4-dihydroxyphenylacetic acid (V), 3,4-dihydroxytoluene (VI), and 3-(*m*-hydroxyphenyl)propionic acid (VIII) were identified as rutin metabolites and were differentiated from the corresponding endogeneous compounds. Unchanged I and quercetin (II) were not present in the urine. Rutin-*d* was injected intraperitoneally in rats, administered orally to neomycin-treated rats, and incubated *in vitro* with the intestinal contents of rats. The experiments suggested the involvement of intestinal microflora in the metabolism of orally administered I.

Keyphrases □ Rutin—metabolites in rat urine, GLC–MS analysis, role of intestinal microflora □ Metabolites—rutin, analysis in rat urine, role of intestinal microflora □ Intestinal microflora—role in rutin metabolism, *in vitro* analysis with rat intestinal contents, GLC–MS detection

The metabolic fate of orally administered [2′,5′,6′-^{2}H]rutin (rutin-*d*) in humans was elucidated using GLC–MS (1, 2). 3-Hydroxyphenylacetic acid (III), 3-methoxy-4-hydroxyphenylacetic acid (IV), 3,4-dihydroxyphenylacetic acid (V), 3,4-dihydroxytoluene (VI), and β-*m*-hydroxyphenylhydracrylic acid (VII) were identified as urinary metabolites of rutin (I) and were differentiated from the corresponding endogenous compounds. All of these urinary metabolites were formed *via* reduction of the double bond of the γ-pyranone ring; III and VII were formed *via* dehydroxylation at the 4′-position of the B-ring.

The metabolism of I has been studied extensively in animals. In rat urine, III, IV, and V were identified as rutin metabolites after oral administration of I (3). Evidence for the involvement of the intestinal microflora in the metabolism of I was suggested by some investigators (4–8). These authors reported that anaerobic incubation of I with extracts of rat intestinal contents resulted in the formation of ring-fission metabolites (III and VIII). The intestinal origin of these metabolites was also demonstrated indirectly by the fact that excretion of the phenolic acids in the urine was suppressed when I was administered orally to neomycin-treated or germ-free rats (8, 9). However, an accurate determination of III–V derived from administered I is not possible, because the phenolic acids in question are also endogenous metabolites excreted in the ordinary urine and feces.

A radioactive isotope tracer technique is useful for the metabolic studies. Several radioactive metabolites were found in the urine after oral administration of [G-^{3}H]I in rats, but the structures were not elucidated (10). A mass chromatographic method using I labeled with stable isotopes is superior to a radioactive tracer technique in the structural elucidation of I metabolites. This report identifies the urinary metabolites of I in rats and elucidates the role of the intestinal microflora in the metabolism of I using a stable isotope tracer technique.

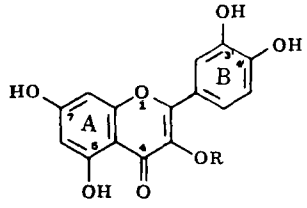

I: R = rutinose
II: R = H

EXPERIMENTAL[1]

Materials—Rutin[2] (I), quercetin[2] (II), 3-hydroxyphenylacetic acid[2] (III), 3-methoxy-4-hydroxyphenylacetic acid[2] (IV), 3,4-dihydroxyphenylacetic acid[2] (V), 3,4-dihydroxytoluene[3] (VI), 3-(3,4-dihydroxyphenyl)propionic acid[4] (IX), *p*-hydroxyphenyllactic acid[5] (X), neomycin sulfate[6], yeast extract[7], and peptone[7] were obtained commercially.

[2′,5′,6′-^{2}H]Rutin (Rutin-*d*)—A solution of NaOH (0.58 g) and I (6.0 g) in D_2O[8] (60.0 g) was heated at 95° for 8 hr in a sealed tube in a nitrogen atmosphere. The mixture was lyophilized, and D_2O (60.0 g) was added. The solution was heated for 8 hr in a similar manner and was acidified with 10% AcOH (200 ml). The resultant yellow solid was collected, washed with H_2O, dried, and then chromatographed using cross-linked dextran gel[9] with CH_3OH as eluant. Recrystallization from CH_3OH–H_2O (1:1) gave [2′,5′,6′,6,8-^{2}H]rutin as yellow needles (4.80 g). To a solution of NaOH (0.64 g) and H_2O (50.0 g) was added [2′,5′,6′,6,8-^{2}H]rutin (4.80 g). The mixture was stirred for 1 hr at 25° and then was acidified with 10% AcOH (150 ml). After repeating this procedure, the crude solid was purified as above for [2′,5′,6′,6,8-^{2}H]rutin to give [2′,5′,6′-^{2}H]rutin (rutin-*d*), 3.60 g (60.0% yield), mp 193°; ^{1}H-NMR(CD_3OD): δ 1.15 (d, 3, J = 6.0 Hz, rhamnosyl-CH_3), 6.16 (d, 1, J = 2.5 Hz, 6-CH), and 6.38 ppm (d, 1, J = 2.5 Hz, 8-CH). The ^{1}H-NMR spectrum showed that the isotopic composition (d_1, d_2, and d_3) was 1:6:3.

β-*m*-Hydroxyphenylhydracrylic Acid (VII)—To a solution of *m*-benzyloxyphenylhydracrylic acid (11) (1.0 g) in EtOH (70 ml) was added 5% Pd-C (0.25 g). The solution was stirred under a hydrogen atmosphere for 3 hr. The uptake of hydrogen was ~90 ml (theoretical 82 ml). The catalyst was removed by filtration. The filtrate was concentrated to dryness under reduced pressure, and the residue was crystallized from *n*-hexane–Et_2O (1:1) to give 0.65 g (97.1% yield). Recrystallization from *n*-hexane–EtOAc (1:1) gave V, 0.50 g (75% yield), mp 158–159° dec. [lit. (11) 159°]; ^{1}H-NMR (DMSO-d_6): δ 6.50–7.20 (m, 4, ArH), 4.84 (t, 1, J = 6.0 Hz, 3-CH), 2.48 ppm (d, 2, J = 6.0 Hz, 2-CH_2), and OH exchangeable; MS: m/z 182 (M^+).

[1] Melting points were determined in open-glass capillaries and are uncorrected. ^{1}H-NMR spectra were determined on a JEOL JM-MH-100 spectrometer using deuterated methanol for rutin-*d* and deuterated dimethyl sulfoxide for VII and VIII as solvents, with tetramethylsilane as the internal standard. Elemental analyses were performed by Analytical Center, Tokyo College of Pharmacy, Tokyo, Japan.

[2] Nakarai Chemicals Ltd., Kyoto, Japan.

[3] Wako Pure Chemical Industries, Tokyo, Japan.

[4] Aldrich Chemical Co., Milwaukee, Wis.

[5] Tokyo Chemical Industry, Tokyo, Japan.

[6] P-L Biochemicals, Inc., Milwaukee, Wis.

[7] Difco Laboratories, Detroit, Mich.

[8] Deuterium content ≥99.95%; E. Merck, Darmstadt, West Germany.

[9] Sephadex LH-20; Pharmacia Fine Chemicals, Uppsala, Sweden.

0022-3549/83/1000-1155$01.00/0

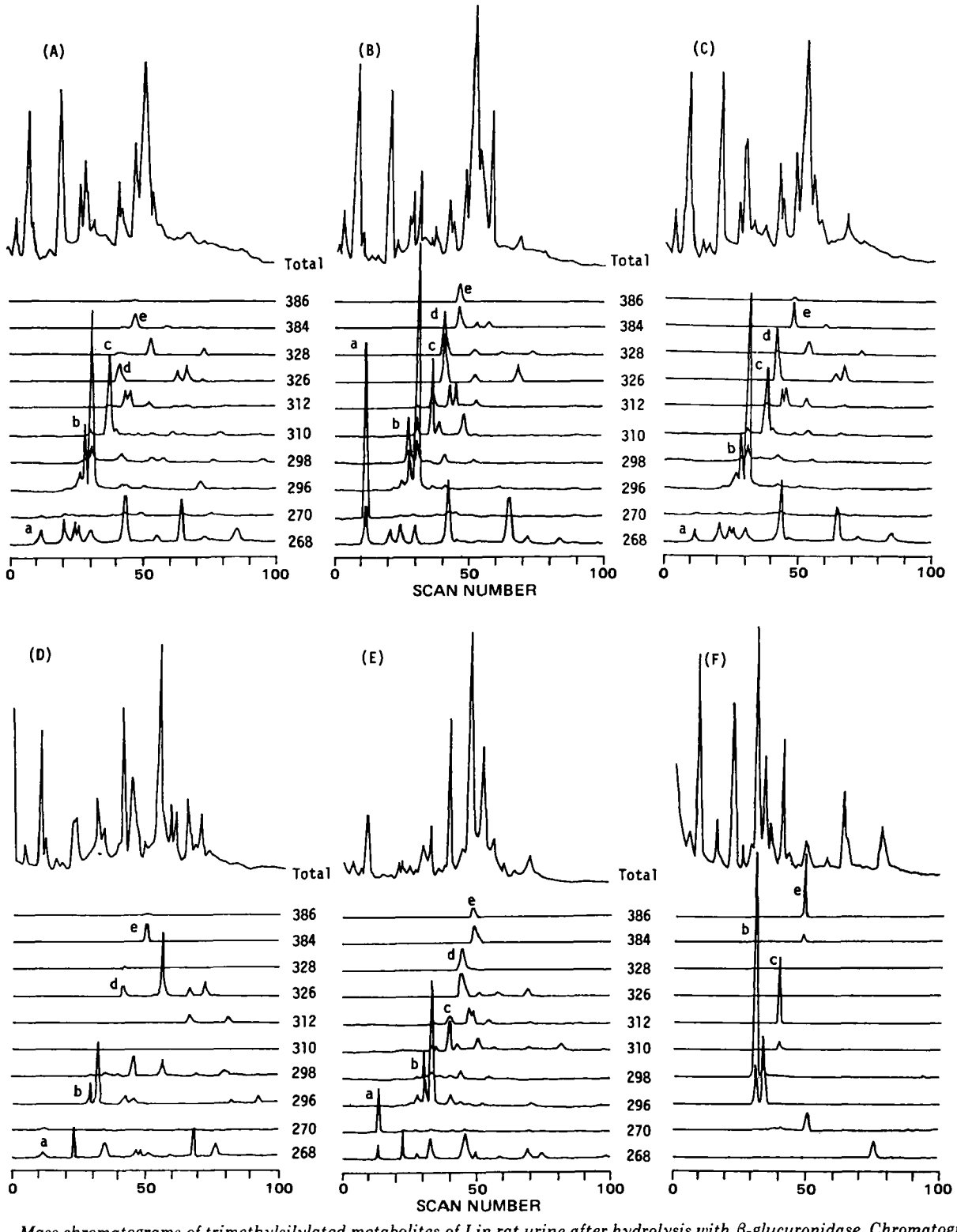

Figure 1—*Mass chromatograms of trimethylsilylated metabolites of I in rat urine after hydrolysis with β-glucuronidase. Chromatograms were obtained from the 24-hr urine of rats prior to (A) and after (B) oral administration of rutin-d and after intraperitoneal injection of rutin-d (C) before neomycin treatment. Chromatograms also were obtained from the 24-hr urine after oral administration of rutin-d in rats on the 2nd (D) and 14th (E) days after neomycin treatment. Chromatogram F was obtained from the incubation mixture of rutin-d and rat intestinal contents. Key: (a) VI [M^+:268, $(M+2)^+$:270]; (b) III [M^+:296, $(M+2)^+$:298]; (c) VIII [M^+:310, $(M+2)^+$:312]; (d) IV [M^+:326, $(M+2)^+$:328]; (e) V [M^+:384, $(M+2)^+$:386].*

Anal.—Calc. for $C_9H_{10}O_4$: C, 59.34; H, 5.53. Found: C, 59.38; H, 5.43.

3-(*m*-Hydroxyphenyl)propionic Acid (VIII)—To a solution of *trans*-*m*-hydroxycinnamic acid[5] (1.0 g) in EtOH (70 ml) was added 5% Pd-C (0.30 g). The solution was stirred under a hydrogen atmosphere for 2 hr. The uptake of hydrogen was ~150 ml (theoretical 137 ml). The catalyst was removed by filtration. The filtrate was concentrated under reduced pressure to give 1.0 g (100% yield) of VIII which was recrystallized from Et_2O–benzene (1:1) to give white needles (VIII), 0.94 g (94% yield), mp 111°; ^{1}H-NMR (DMSO-d_6): δ 6.50–7.15 (m, 4, ArH), 2.40–2.84 ppm (A_2B_2 4, CH_2CH_2), and exchangeable OH; MS: *m/z* 166 (M^+).

Anal.—Calc. for $C_9H_{10}O_3$: C, 65.05; H, 6.07. Found: C, 65.15; H, 6.02.

GLC–MS—A GLC–mass spectrometer[10] and a data processing system[11] connected to a minicomputer[12] were used. The GLC system employed a 2 m × 3-mm i.d. glass column packed with 2% OV-105 on 60–80 mesh Chromosorb W[13]; it was packed with 1.5% OV-1 on 80–100 mesh Shimalite[3] for analysis of II. The columns were preconditioned with a helium flow of 30 ml/min at 230° (OV-105) and 280° (OV-1) for 24 hr, or until the baseline was stable. The column, flash heater, and separator temperatures were 160°, 180°, and 280°, respectively. The helium flow rate was 20 ml/min. The mass spectometer employed an ionization-source temperature of 310° and ionization energy of 20 eV.

One minute following injection of the sample, automatic magnet scanning was initiated, covering an m/z range of 50–500 every 8 sec. All scanning data were stored in the data processing system. Mass chromatograms were obtained on a digital plotter by monitoring the molecular ions of the $d_0(M^+)$ and $d_2[(M + 2)^+]$ forms of the trimethylsilylated derivatives of possible metabolites of I.

Drug Administration and Urine Collection—Three male Wistar albino rats, weighing 180–220 g, orally received 100 mg of rutin-*d*/kg. Urine was collected for 24 hr prior to and 24 hr after oral administration of rutin-*d*. Seven days later each animal was injected intraperitoneally with rutin-*d* (20 mg/kg). Urine was collected for 24 hr after the administration.

To inhibit the action of intestinal microflora, neomycin sulfate (100 mg/kg) was orally administered twice a day for 4 days to an additional three rats. Rutin-*d* (100 mg/kg) was administered orally to the rats on the 2nd and 14th day after treatment with neomycin ended. Urine was collected for 24 hr after each administration of rutin-*d*. Urine samples were diluted with distilled water to 30 ml and were kept frozen until analysis.

***In Vitro* Experiments**—The incubation medium was composed of 0.5% (w/v) yeast extract and 0.5% (w/v) peptone in 0.1 *M* phosphate buffer (pH 7.4). The rat intestinal contents were well mixed with 50 ml of the medium. The resulting suspension was centrifuged at low speed (500× *g*) for 1 min. To 5 ml of the supernatant thus obtained was added 3.0 mg of rutin-*d*. The mixture was incubated for 12 hr at 37° under anaerobic conditions.

Identification of I Metabolites by TLC—Urine samples (10 ml) collected prior to and after rutin-*d* administration were incubated at 37° for 24 hr with 10 ml of 0.1 *M* acetate buffer (pH 5.0) containing 3000 U of β-glucuronidase[14]. The incubation mixture was lyophilized and suspended in CH_3OH (10 ml). The suspension was centrifuged (1500× *g*) and the supernatant layer mixed with Et_2O (10 ml). The resulting suspension was centrifuged, and the precipitate was dissolved in CH_3OH (0.5 ml). A 0.1-ml volume of this solution was subjected to TLC[15]. Control urine (10 ml), collected prior to the rutin-*d* administration, was mixed with 200 μg of I and a sample (0.1 ml) was subjected to the TLC procedure. The TLC plate was developed with 1-butanol–AcOH–H_2O (4:1:2) and the spots were visualized by aluminum chloride (12), R_f 0.45 (I).

Identification of I Metabolites by GLC–MS—Urine samples (10 ml) collected prior to and after rutin-*d* administration were incubated at 37° for 24 hr in 10 ml of 0.1 *M* acetate buffer (pH 5.0) containing 3000 U of β-glucuronidase. Portions (10 ml) of urine obtained prior to and after the rutin-*d* administration and the incubation samples were subjected to the separation and extraction procedures without β-glucuronidase hydrolysis. Urine and incubation samples were acidified with 10% HCl (pH 1.0) and extracted with ether. The ether layer was concentrated to dryness under reduced pressure. The residue was dissolved in dry pyridine (0.1 ml), and *N,O*-bis(trimethylsilyl)acetamide[5] (0.05 ml) was added. The silylated derivatives were injected in the GLC–MS.

RESULTS AND DISCUSSION

The urine samples (10 ml) collected prior to and after I administration were subjected to TLC after extraction and separation procedures. The TLC results revealed that I was not present in the urine. To a 10-ml portion of the urine collected prior to the administration was added 200 μg of I; this urine sample was also subjected to TLC as above and I was detected. The results showed that the excretion of I in the urine after the I administration to rats was >20 μg/ml and suggested that orally administered I might be completely metabolized, as in humans (1).

[10] LKB-9000; Shimadzu Seisakusho Ltd., Kyoto, Japan.
[11] GCMSPAC-300; Shimadzu Seisakusho Ltd., Kyoto, Japan.
[12] OKITAC-4300; Oki Electric Industry Co., Tokyo, Japan.
[13] Nishio Industry Co., Ltd., Tokyo, Japan.
[14] Tokyo Zoki Kagaku Co., Ltd., Tokyo, Japan.
[15] Kieselgel $60F_{254}$; E. Merck, Darmstadt, West Germany.

Table I—Presence of Urinary Metabolites of Rutin in Rats and *In Vitro* with Rat Intestinal Contents [a]

Metabolite	Untreated Rats[b] po	Untreated Rats[b] ip	Neomycin-Treated Rats[b] After 2 Days	Neomycin-Treated Rats[b] After 14 Days	*In Vitro*[c]
III	+	—	—	+	+
IV	+	—	—	+	—
V	+	—	—	+	+
VI	+	—	—	+	—
VIII	+	—	—	+	+
I	—	—	—	—	recovered
II	—	—	—	—	—

[a] Urine and incubation samples obtained after the extraction and separation procedures were analyzed by GLC–MS or TLC. Key: (+) metabolite was detected; (—) metabolite was not detected. [b] Rutin-*d* was administered orally (po) or intraperitoneally (ip) to untreated rats and orally to neomycin-treated rats on the 2nd and 14th day after neomycin treatment ended. [c] Rutin-*d* was incubated with rat intestinal contents under anaerobic conditions.

The isotopic composition (d_1, d_2, and d_3) in rutin-*d* was 1:6:3. Therefore, particular attention was paid to the d_2 form for the determination of I metabolites by GLC–MS. The urine samples collected prior to and after the rutin-*d* administration were subjected to silylation with *N,O*-bis(trimethylsilyl)acetamide and analyzed by the GLC–MS computer system. Mass chromatograms were obtained by monitoring the molecular ions of the $d_0(M^+)$ and $d_2[(M + 2)^+]$ forms of the silylated derivatives of possible I metabolites. A metabolite was identified by examining the presence of duplicate peaks at the same retention time in the mass chromatogram.

Typical mass chromatograms obtained from the urine after hydrolysis with β-glucuronidase are given in Fig. 1A and B. The ratios of the peak intensities $[(M + 2)^+/M^+]$ shown in Fig. 1A were practically the same as those estimated from control urine. On the other hand, the ratios of the peak intensities $[(M + 2)^+/M^+]$ were larger in peaks a–e in Fig. 1B than those in the peaks shown in Fig. 1A, indicating the increment of the peak intensity in each $(M + 2)^+$ peak. These findings made it evident that orally administered rutin-*d* was metabolized to give five metabolites which were also present in the urine as endogenous materials.

These metabolites were identified as III (peak b), IV (peak d), V (peak e), VI (peak a), and VII (peak c). Identification was made by comparing the mass spectra and GLC retention times of the respective mass chromatogram peaks with the corresponding silylated authentic compounds. The five metabolites identified in the urine after hydrolysis with β-glucuronidase were also found in the urine without β-glucuronidase treatment. Four of these metabolites, *i.e.*, III–VI, were the same as those found in human urine. β-*m*-Hydroxyphenylhydracrylic acid (VII), detected in human urine, 3-(3,4-dihydroxyphenyl)propionic acid (IX), *p*-hydroxyphenyllactic acid (X), and β-*p*-hydroxyphenylhydracrylic acid (XI) were excluded from the metabolites of rutin-*d* by the mass spectra of the corresponding authentic compounds or the results of one investigation (13). Quercetin, an aglycone of I, was not found in the urine. It was impossible to follow the metabolic change occurring in the A-ring on which no atoms were deuterium labeled.

Rutin-*d* was injected intraperitoneally in rats on the 7th day after oral administration of rutin-*d*. The urine samples from the rats injected with rutin-*d* were subjected to the GLC–MS analysis. The mass chromatogram (Fig. 1C) thus obtained was similar to that obtained prior to oral administration of rutin-*d* (Fig. 1A). The five metabolites detected in urine after the oral administration of rutin-*d* were not excreted in the urine after the intraperitoneal injection of rutin-*d* (Fig. 1B and C). The results indicated that orally administered I must be metabolized by intestinal microflora or by enzymes in the intestinal walls. Petrakis *et al.* (14) injected [G-^{14}C]quercetin into rats intraperitoneally and found radioactive vanillic acid only in the urine. In the case of the rutin-*d* injection, this metabolite, though endogenously present, could not to be found in the urine.

The absorption of I in the GI tract has been investigated (10, 15–19). It has been reported that [G-^{3}H]I (10) and [G-^{14}C]II (14) are absorbed very slowly from the GI tract when administered orally to rats. Because of the slow absorption of I and II by the intestines, the intestinal microflora play a significant role in the metabolism of orally administered I.

Rutin-*d* was administered to another group of rats orally. The mass chromatogram thus obtained was similar to that shown in Fig. 1B and showed the presence of five metabolites derived from rutin-*d*. The rats then received neomycin orally twice a day for 4 days to inhibit the action of the intestinal microflora. Rutin-*d* was administered to the rats on the

2nd day after treatment with neomycin ended. The mass chromatogram is given in Fig. 1D. In peaks a, b, d, and e in Fig. 1D, the ratios of the peak intensities $[(M + 2)^+/M^+]$ were much smaller than those of the corresponding peaks in the mass chromatogram obtained when rutin-*d* was administered to untreated rats (Fig. 1B). In addition, peak c did not appear in Fig. 1D. Rutin-*d* was also administered to rats on the 14th day after neomycin treatment when the action of the intestinal microflora had been restored. In the mass chromatogram thus obtained (Fig. 1E), the $[(M + 2)^+/M^+]$ ratios were larger than those in the mass chromatogram obtained from neomycin-treated rats (Fig. 1D). The five metabolites were detected in the untreated rats. They were reduced or disappeared in the neomycin-treated rats and were increased on the 14th day after neomycin treatment. The results obtained from the intraperitoneal injection and the subsequent neomycin-treatment experiments showed that intestinal microflora greatly influence the metabolism of orally administered I.

Rutin-*d* was incubated with extracts of rat intestinal contents under anaerobic conditions. As shown in the mass chromatogram (Fig. 1F) thus obtained, three metabolites, *i.e.*, III (peak b), V (peak e), and VIII (peak c), appeared. Compound II and unchanged I were also found in the incubation mixture. The *in vitro* experiments suggested direct involvement of the intestinal microflora in the metabolism of I, even though all of the metabolites detected in the urine after oral administration of rutin-*d* were not found. The lack of formation of metabolites IV and VI in the mixture indicated that they were excreted in the urine *via* methylation or decarboxylation by enzymes in the intestinal walls or in other tissues after the absorption of orally administered I from the GI tract.

It has been reported that I was metabolized to give phenolic acids such as III, IV, VIII, *etc.* by the isolated perfused rat liver (19). These phenolic acids should be excreted in the urine *via* liver metabolism if I is absorbed as such from the GI tract after oral administration of rutin-*d* in neomycin-treated rats. However, these metabolites were not found in the urine from neomycin-treated rats (Fig. 1D), and neither I nor II was present. It is then reasonable to assume that orally administered I could not be absorbed from the GI tract *per se*. 3,4-Dihydroxyphenyl[carboxy-^{14}C]acetic acid (V), when administered to rats orally, was almost completely excreted in the urine in the form of III, IV, and V (20). Thus, I must be metabolized to the phenolic acids by intestinal microflora, with subsequent absorption from the GI tract.

In this study, five metabolites (III–VI and VIII) derived from orally administered rutin-*d* were differentiated from these compounds endogenously present in the urine and successfully identified by the mass chromatographic method. In addition, the involvement of intestinal microflora in the metabolism of I was investigated by this method (Table I). It is possible that the human intestinal microflora may also play a significant role in the formation of urinary metabolites of I (III–VII) in humans.

REFERENCES

(1) S. Baba, T. Furuta, M. Horie, and H. Nakagawa, *J. Pharm. Sci.*, **70**, 780 (1981).

(2) K. Hiraoka, T. Miyamoto, S. Baba, and T. Furuta, *J. Labelled Compd. Radiopharm.*, **18**, 613 (1981).

(3) A. N. Booth, C. W. Murray, F. T. Jones, and F. DeEds, *J. Biol. Chem.*, **233**, 251 (1956).

(4) A. N. Booth and R. T. Williams, *Biochem. J.*, **88**, 66P (1963).

(5) R. R. Scheline, *Acta Pharmacol. Toxicol.*, **26**, 332 (1968).

(6) R. R. Scheline, *J. Pharm. Sci.*, **57**, 2021 (1968).

(7) R. R. Scheline, *Pharmacol. Rev.*, **25**, 451 (1973).

(8) A. Barrow and L. A. Griffiths, *Xenobiotica*, **4**, 743 (1974).

(9) L. A. Griffiths and A. Barrow, *Biochem. J.*, **130**, 1161 (1972).

(10) O. Tamemasa, R. Goto, and S. Ogura, *Pharmacometrics*, **12**, 193 (1976).

(11) M. D. Armstrong and K. N. F. Shaw, *J. Biol. Chem.*, **225**, 269 (1957).

(12) A. Sturm and H. Scheja, *J. Chromatogr.*, **16**, 194 (1964).

(13) S. K. Wadman, C. Van Der Heiden, D. Ketting, J. P. Kamerling, and J. F. G. Vliegenthart, *Clin. Chim. Acta*, **47**, 307 (1973).

(14) P. L. Petrakis, A. G. Kallianos, S. H. Wender, and M. R. Shetlar, *Arch. Biochem. Biophys.*, **85**, 264 (1959).

(15) T. Fukuda, *Arch. Exp. Pathol. Pharmakol.*, **164**, 685 (1932).

(16) J. B. Field and P. E. Pekers, *Am. J. Med. Sci.*, **218**, 1 (1949).

(17) W. L. Porter, D. F. Dickel, and J. F. Couch, *Arch Biochem.*, **21**, 273 (1949).

(18) W. G. Clark and E. M. MacKay, *J. Am. Med. Assoc.*, **143**, 1411 (1950).

(19) O. Takacs, S. Benko, L. Varga, A. Antal, and M. Gabor, *Angiologica*, **9**, 175 (1972).

(20) J. C. Dacre, R. R. Scheline, and R. T. Williams, *J. Pharm. Pharmacol.*, **20**, 619 (1968).

Antitumor Agents LXII: Synthesis and Biological Evaluation of Podophyllotoxin Esters and Related Derivatives

RON K. LEVY, IRIS H. HALL, and KUO-HSIUNG LEE ˣ

Received June 11, 1982, from the *Department of Medicinal Chemistry, School of Pharmacy, University of North Carolina at Chapel Hill, Chapel Hill, NC 27514.* Accepted for publication August 17, 1982.

Abstract □ Synthetic esters of the C-4 hydroxyl group of podophyllotoxin (I) were prepared. In addition, esters were synthesized using the diol system of tetrahydropyranyl podophyllol (XV), produced by reducing the lactone ring of tetrahydropyranyl podophyllotoxin with lithium aluminum hydride. Six compounds, the acrylate (IV), 3,3-dimethyl acrylate (V), phenoxyacetate (IX), and ethyl adipate (XI) of I as well as podophyllol (XIV) and tetrahydropyranyl podophyllol dimesylate (XVIII), showed significant activity when tested using the P-388 lymphocytic leukemia screen at 3 mg/kg/day. None of the esters showed higher activity than that shown by the parent molecule I when tested at the same dosage level.

Keyphrases □ Podophyllotoxin—esters, synthesis, antileukemic activity in mice □ Synthesis—podophyllotoxin esters, antileukemic activity in mice □ Antileukemic agents—potential, podophyllotoxin esters, synthesis

The development of teniposide (VM-26) and etoposide (VP-16-213), two glucopyranosyl derivatives related to the lignan podophyllotoxin (I), as clinically effective anticancer drugs has been reviewed recently (1). An examination of the structural features of teniposide and etoposide indicated that a free hydroxyl group at C-4 in epipodophyllotoxin is not essential for potent activity. Thus, it was considered that further modification of the C-4 hydroxyl group of I or epipodophyllotoxin could yield additional potent antitumor agents. In view of the importance of an

0022-3549/83/1000-1158$01.00/0

2nd day after treatment with neomycin ended. The mass chromatogram is given in Fig. 1D. In peaks a, b, d, and e in Fig. 1D, the ratios of the peak intensities $[(M + 2)^+/M^+]$ were much smaller than those of the corresponding peaks in the mass chromatogram obtained when rutin-*d* was administered to untreated rats (Fig. 1B). In addition, peak c did not appear in Fig. 1D. Rutin-*d* was also administered to rats on the 14th day after neomycin treatment when the action of the intestinal microflora had been restored. In the mass chromatogram thus obtained (Fig. 1E), the $[(M + 2)^+/M^+]$ ratios were larger than those in the mass chromatogram obtained from neomycin-treated rats (Fig. 1D). The five metabolites were detected in the untreated rats. They were reduced or disappeared in the neomycin-treated rats and were increased on the 14th day after neomycin treatment. The results obtained from the intraperitoneal injection and the subsequent neomycin-treatment experiments showed that intestinal microflora greatly influence the metabolism of orally administered I.

Rutin-*d* was incubated with extracts of rat intestinal contents under anaerobic conditions. As shown in the mass chromatogram (Fig. 1F) thus obtained, three metabolites, *i.e.*, III (peak b), V (peak e), and VIII (peak c), appeared. Compound II and unchanged I were also found in the incubation mixture. The *in vitro* experiments suggested direct involvement of the intestinal microflora in the metabolism of I, even though all of the metabolites detected in the urine after oral administration of rutin-*d* were not found. The lack of formation of metabolites IV and VI in the mixture indicated that they were excreted in the urine *via* methylation or decarboxylation by enzymes in the intestinal walls or in other tissues after the absorption of orally administered I from the GI tract.

It has been reported that I was metabolized to give phenolic acids such as III, IV, VIII, *etc.* by the isolated perfused rat liver (19). These phenolic acids should be excreted in the urine *via* liver metabolism if I is absorbed as such from the GI tract after oral administration of rutin-*d* in neomycin-treated rats. However, these metabolites were not found in the urine from neomycin-treated rats (Fig. 1D), and neither I nor II was present. It is then reasonable to assume that orally administered I could not be absorbed from the GI tract *per se*. 3,4-Dihydroxyphenyl[carboxy-^{14}C]acetic acid (V), when administered to rats orally, was almost completely excreted in the urine in the form of III, IV, and V (20). Thus, I must be metabolized to the phenolic acids by intestinal microflora, with subsequent absorption from the GI tract.

In this study, five metabolites (III–VI and VIII) derived from orally administered rutin-*d* were differentiated from these compounds endogenously present in the urine and successfully identified by the mass chromatographic method. In addition, the involvement of intestinal microflora in the metabolism of I was investigated by this method (Table I). It is possible that the human intestinal microflora may also play a significant role in the formation of urinary metabolites of I (III–VII) in humans.

REFERENCES

(1) S. Baba, T. Furuta, M. Horie, and H. Nakagawa, *J. Pharm. Sci.*, **70**, 780 (1981).

(2) K. Hiraoka, T. Miyamoto, S. Baba, and T. Furuta, *J. Labelled Compd. Radiopharm.*, **18**, 613 (1981).

(3) A. N. Booth, C. W. Murray, F. T. Jones, and F. DeEds, *J. Biol. Chem.*, **233**, 251 (1956).

(4) A. N. Booth and R. T. Williams, *Biochem. J.*, **88**, 66P (1963).

(5) R. R. Scheline, *Acta Pharmacol. Toxicol.*, **26**, 332 (1968).

(6) R. R. Scheline, *J. Pharm. Sci.*, **57**, 2021 (1968).

(7) R. R. Scheline, *Pharmacol. Rev.*, **25**, 451 (1973).

(8) A. Barrow and L. A. Griffiths, *Xenobiotica*, **4**, 743 (1974).

(9) L. A. Griffiths and A. Barrow, *Biochem. J.*, **130**, 1161 (1972).

(10) O. Tamemasa, R. Goto, and S. Ogura, *Pharmacometrics*, **12**, 193 (1976).

(11) M. D. Armstrong and K. N. F. Shaw, *J. Biol. Chem.*, **225**, 269 (1957).

(12) A. Sturm and H. Scheja, *J. Chromatogr.*, **16**, 194 (1964).

(13) S. K. Wadman, C. Van Der Heiden, D. Ketting, J. P. Kamerling, and J. F. G. Vliegenthart, *Clin. Chim. Acta*, **47**, 307 (1973).

(14) P. L. Petrakis, A. G. Kallianos, S. H. Wender, and M. R. Shetlar, *Arch. Biochem. Biophys.*, **85**, 264 (1959).

(15) T. Fukuda, *Arch. Exp. Pathol. Pharmakol.*, **164**, 685 (1932).

(16) J. B. Field and P. E. Pekers, *Am. J. Med. Sci.*, **218**, 1 (1949).

(17) W. L. Porter, D. F. Dickel, and J. F. Couch, *Arch Biochem.*, **21**, 273 (1949).

(18) W. G. Clark and E. M. MacKay, *J. Am. Med. Assoc.*, **143**, 1411 (1950).

(19) O. Takacs, S. Benko, L. Varga, A. Antal, and M. Gabor, *Angiologica*, **9**, 175 (1972).

(20) J. C. Dacre, R. R. Scheline, and R. T. Williams, *J. Pharm. Pharmacol.*, **20**, 619 (1968).

Antitumor Agents LXII: Synthesis and Biological Evaluation of Podophyllotoxin Esters and Related Derivatives

RON K. LEVY, IRIS H. HALL, and KUO-HSIUNG LEE ˣ

Received June 11, 1982, from the *Department of Medicinal Chemistry, School of Pharmacy, University of North Carolina at Chapel Hill, Chapel Hill, NC 27514.* Accepted for publication August 17, 1982.

Abstract □ Synthetic esters of the C-4 hydroxyl group of podophyllotoxin (I) were prepared. In addition, esters were synthesized using the diol system of tetrahydropyranyl podophyllol (XV), produced by reducing the lactone ring of tetrahydropyranyl podophyllotoxin with lithium aluminum hydride. Six compounds, the acrylate (IV), 3,3-dimethyl acrylate (V), phenoxyacetate (IX), and ethyl adipate (XI) of I as well as podophyllol (XIV) and tetrahydropyranyl podophyllol dimesylate (XVIII), showed significant activity when tested using the P-388 lymphocytic leukemia screen at 3 mg/kg/day. None of the esters showed higher activity than that shown by the parent molecule I when tested at the same dosage level.

Keyphrases □ Podophyllotoxin—esters, synthesis, antileukemic activity in mice □ Synthesis—podophyllotoxin esters, antileukemic activity in mice □ Antileukemic agents—potential, podophyllotoxin esters, synthesis

The development of teniposide (VM-26) and etoposide (VP-16-213), two glucopyranosyl derivatives related to the lignan podophyllotoxin (I), as clinically effective anticancer drugs has been reviewed recently (1). An examination of the structural features of teniposide and etoposide indicated that a free hydroxyl group at C-4 in epipodophyllotoxin is not essential for potent activity. Thus, it was considered that further modification of the C-4 hydroxyl group of I or epipodophyllotoxin could yield additional potent antitumor agents. In view of the importance of an

0022-3549/83/1000-1158$01.00/0

ester group in the cytotoxicity and antileukemic activity of compounds in certain classes (2–5), a series of C-4 hydroxyl esters of I were prepared and examined for their antileukemic activity against *in vivo* P-388 lymphocytic leukemia cell growth. The effect of the ester group on the antileukemic activity of I has not yet been studied (1). In addition, modification of the podophyllotoxin nucleus by substituting an ester moiety at the diol system of tetrahydropyranyl podophyllol (XV), as well as the antileukemic activity of the resulting products are reported.

RESULTS AND DISCUSSION

Several esters of podophyllotoxin (I) and tetrahydropyranyl podophyllol (XV) were prepared by a general method and assayed for *in vivo* antileukemic activity against P-388 lymphocytic leukemia growth in mice according to the standard National Cancer Institute procedures (6). The antileukemic activity of I–XIX are shown in Table I and are compared to podophyllotoxin (I) at the same dosage levels. The maximum observed T/C% value of 171 for I at 3 mg/kg/day compares favorably with that reported in the literature (7). This dosage was therefore chosen for a study of the structure–activity relationship of the various esters.

Generally, every compound tested showed a significant decrease in antileukemic activity compared with I when administered at 3 mg/kg/day. Compounds II, III, VI–VIII, X, XII, XIII, XV–XVII, and XIX were found to be inactive. Compounds which showed significant (T/C ≥ 120%) (6, 8) antileukemic activity included IV, V, IX, XI, XIV, and XVIII with respective T/C% values of 135, 121, 133, 120, 120, and 130 at 3 mg/kg/day. These data indicate that the introduction of an ester moiety into I and XV does not enhance the antileukemic activity (P-388), but in general causes a loss of activity.

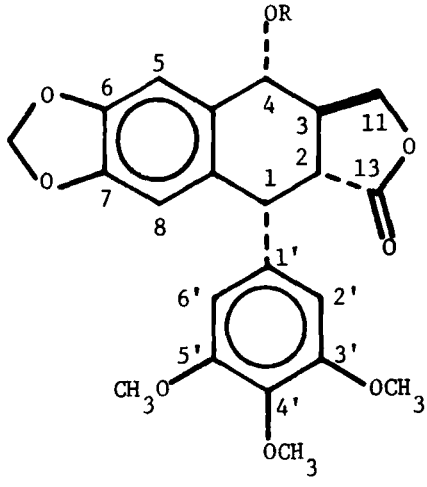

I : R = H (podophyllotoxin)

II : R = $COCH_3$

III : R = $COCH_2CH_2CH_3$

IV : R = $COCH{=}CH_2$

V : R = $COCH{=}C(CH_3)_2$

VI : R = CO– 

VII : R = CO– 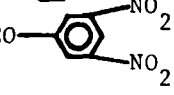

VIII : R = $COCH_2CH_2$– 

IX : R = $COCH_2O$– 

X : R = $COCH_2COOCH_2CH_3$

XI : R = $CO(CH_2)_4COOCH_2CH_3$

XII : R = $COCH_2CH_2COO$-podophyllotoxin

XIII : R = 

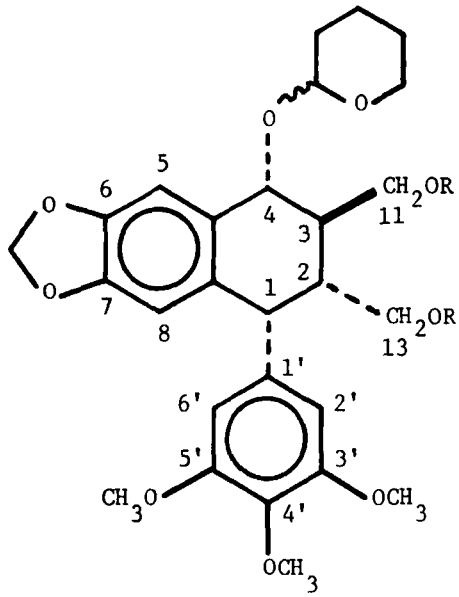

XIV : R = H, OH replaces 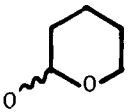

(podophyllol)

XV : R = H

XVI : R = $COCH_2Br$

XVII : R = $COCH_2CH_2Br$

XVIII : R = SO_2CH_3

XIX : R = SO_2– 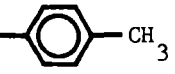

EXPERIMENTAL[1]

Podophyllotoxin (I)—Podophyllotoxin was isolated from the chloroform extract of *Podophyllum peltatum*[2] according to literature methods (9, 10).

[1] Unless otherwise specified, microanalyses were performed by M-H. W. Laboratories, Phoenix, Ariz. or Integral Microlab, Inc., Raleigh, N.C. Mass spectral data were recorded using an A.E.I. MS-902 mass spectrometer. Melting points were determined on a Thomas-Hoover melting point apparatus. IR spectra were recorded in chloroform on a Perkin-Elmer 257 grating spectrophotometer. ^{1}H-NMR spectra were measured in deuterated chloroform either on a JEOL C-60HL or a JEOL FX-60 NMR spectrometer. All NMR data are given in parts per million and reported as downfield from the internal standard, tetramethylsilane. The abbreviations s, d, t, q, and m refer to single, doublet, triplet, quartet, and multiplet, respectively. Silica gel refers either to Mallinckrodt Silicar CC-7 (200–325 mesh) or Merck Silica gel 60 GF-254. TLC refers to precoated plates available from Analtech, which were developed in 15:1 chloroform–methanol. Visualization of TLC spots was performed in one or more of the following manners: (*a*) iodine vapor; (*b*) spraying with 40% sulfuric acid or 1% ceric sulfate in 10% sulfuric acid followed by heating; or (*c*) viewing under UV light.

[2] Purchased from Dr. Madis Laboratories Inc., South Hackensack, N.J.

Table I—Antileukemic Activity of Podophyllotoxinyl Esters and Related Compounds Against the P-388 Lymphocytic Leukemia in BDF_1 Male Mice (~22 g) Dosed on Days 1–9

Compound	Dose, mg/kg/day ip	Survival Treated/Control, days[a]	T/C %[b]
I	0.5	12.1/10.2	119
	1	15.0/10.2	147
	2	12.6/10.2	124
	3	17.4/10.2	171
	5	11.6/10.2	114
	10	7.1/10.2	70
II	3	11.5/10.2	113
	5	12.2/10.2	120
III	3	11.1/10.2	109
	5	10.2/10.2	100
IV	3	13.8/10.2	135
	5	13.6/10.2	133
V	3	12.3/10.2	121
VI	3	11.4/10.2	112
	5	11.3/10.2	111
VII	3	10.7/10.2	105
	5	9.6/10.2	98
VIII	3	11.8/10.2	116
IX	3	13.6/10.2	133
	5	11.5/10.2	113
X	3	9.7/10.2	99
XI	3	12.2/10.2	120
XII	3	11.6/10.2	118
	5	9.6/10.2	98
XIII	3	10.3/10.2	105
XIV	1.5	10.4/10.2	106
	3	11.8/10.2	120
	4.5	11.0/10.2	108
XV	3	10.4/10.2	106
	5	11.4/10.2	116
XVI	3	4.5/10.2	46[c]
XVII	3	11.4/10.2	116
XVIII	3	12.7/10.2	130
	5	10.5/10.2	103
XIX	3	11.2/10.2	114
	5	12.0/10.2	118
5-Fluorouracil	25	18.0/9.66	186
0.05% Polysorbate	—	10.2/10.2	100

[a] Average value. [b] A compound is active if it exhibits a T/C ≥ 120% (6, 8). [c] Toxic.

Synthesis of Esters—Except for bis(podophyllotoxinyl) succinate (XII), all compounds were synthesized by the following general procedures: To 200 mg (0.48 mmole) of podophyllotoxin in 10 ml of dry benzene and 5 ml of pyridine was added 2.4 mmoles of the appropriate acid chloride. The mixture was stirred at room temperature until TLC indicated that the reaction was complete. At that time, 5 ml of 5% sulfuric acid was added in a dropwise manner and the mixture was stirred for an additional hour. The organic layer was then removed, and the aqueous layer was extracted twice with chloroform. The organic layers were combined, dried over magnesium sulfate, filtered, and then evaporated *in vacuo*. The residue was column chromatographed on silica gel eluted with chloroform. The first fraction collected contained the desired compound with analytical data as specified.

Podophyllotoxinyl Acetate (II)—Colorless needles (175 mg, 80% from EtOH), mp 177–179° [lit. mp 179–181° (11), 204° (12), and 209–210° (13)]; IR (nujol): 1775 (γ-lactone), 1715 (ester), and 1230 (acetate) cm^{-1}; ^{1}H-NMR ($CDCl_3$): δ 1.98 (3, s, $OCOCH_3$), 2.70–2.90 (2, m, H-2 and H-3), 3.78 (6, s, OCH_3-3′ and OCH_3-5′), 3.81 (3, s, OCH_3-4′), 4.00–4.70 (4, unresolved m, H-1, H-4, and H-11), 5.98 (2, s, OCH_2O), 6.38 (2, s, H-2′ and H-6′), 6.52 (1, s, H-8), and 6.77 ppm (1, s, H-5).

Anal.—Calc. for $C_{24}H_{24}O_9$: *m/z* 456.1418 (M^+). Found: *m/z* 456.1424.

Podophyllotoxinyl Butyrate (III)—White amorphous solid (217 mg, 93% yield), mp 57–61° (sintered at 44–46°); R_f 0.62; IR: 1770 (γ-lactone), 1735, and 1235 (ester) cm^{-1}; ^{1}H-NMR: δ 1.01 (3, t, J = 7.0 Hz, CH_2CH_3), 1.40–2.00 (2, m, $CH_2CH_2CH_3$), 2.44 (2, t, J = 7.0 Hz, $CH_2CH_2CH_3$), 2.75–3.05 (2, m, H-2 and H-3), 3.78 (6, s, OCH_3-3′ and OCH_3-5′), 3.83 (3, s, OCH_3-4′), 4.00–4.70 (4, m, H-1, H-4 and H-11), 5.98 (2, s, OCH_2O), 6.39 (2, s, H-2′ and H-6′), 6.53 (1, s, H-8), and 6.75 ppm (1, s, H-5).

Anal.—Calc. for $C_{26}H_{28}O_9$: *m/z* 484.1732 (M^+). Found: *m/z* 484.1739.

Podophyllotoxinyl Acrylate (IV)—White amorphous powder (150 mg, 66% yield), mp 86–90° (sintered at 68°); R_f 0.64; IR: 1770 (γ-lactone), 1720 (ester), 1410, 1290, 995, and 935 (terminal olefin) cm^{-1}; ^{1}H-NMR: δ 2.80–3.10 (2, m, H-2 and H-3), 3.78 (6, s, OCH_3-3′ and OCH_3-5′), 3.81 (3, s, OCH_3-4′), 4.00–4.70 (4, unresolved m, H-1, H-4, and H-11), 6.04 (2, s, OCH_2O), 6.53 (1, s, H-8), 6.80 (1, s, H-5), 5.98 (2, m, $C{=}CH_2$), 6.41 (2, s, H-2′ and H-6′), and 6.15–6.65 ppm (1, overlapped m, $OCH{=}CH_2$).

Anal.—Calc. for $C_{25}H_{24}O_9$: C, 64.10; H, 5.13. Found: C, 64.11; H, 5.45.

Podophyllotoxinyl 3,3-Dimethyl Acrylate (V)—Colorless oil (66 mg, 27% yield); R_f 0.64; IR: 1765 (γ-lactone), 1700, 1230, and 1120 (acrylate) cm^{-1}; ^{1}H-NMR: δ 1.95 (3, d, J = 1.2 Hz, $=C{-}CH_3$), 2.22 (3, d, J = 1.2 Hz, $=C{-}CH_3$), 2.70–3.05 (2, m, H-2 and H-3), 3.78 (6, s, OCH_3-3′ and OCH_3-5′), 3.82 (3, s, OCH_3-4′), 4.15–4.70 (4, m, H-1, H-4, and H-11), 5.75 [1, m, $CH{=}C(CH_3)_2$], 5.98 (2, s, OCH_2O), 6.39 (2, s, H-2′ and H-6′), 6.53 (1, s, H-8), and 7.78 ppm (1, s, H-5).

Anal.—Calc. for $C_{27}H_{28}O_9$: C, 65.32; H, 5.64. Found: C, 65.68; H, 5.71.

Podophyllotoxinyl Benzoate (VI)—White amorphous solid (197 mg, 70% yield), mp 72–74° (sintered at 55–57°) [lit. (14) mp 113–117° as needles from EtOH]; R_f 0.65; IR:1770 (γ-lactone), 1710, 1250, 1120 (benzoate), 750, and 710 (monosubstituted aromatic ring) cm^{-1}; ^{1}H-NMR: δ 2.90–3.10 (2, m, H-2 and H-3), 3.69 (6, s, OCH_3-3′ and OCH_3-5′), 3.81 (3, s, OCH_3-4′), 4.25–4.75 (4, m, H-1, H-4, and H-11), 6.00 (1, s, H-8), 6.88 (1, s, H-5), and 7.30–8.40 ppm (5, m, COC_6H_5).

Anal.—Calc. for $C_{29}H_{26}O_9$: *m/z* 518.1576 (M^+). Found: *m/z* 518.1572.

Podophyllotoxinyl 3,5-Dinitrobenzoate (VII)—Yellow powder (110 mg, 37% yield), mp 153–156° (sintered at 149°); R_f 0.64; IR: 1775 (γ-lactone), 1730 (ester), 1540, and 1340 (aromatic nitro group) cm^{-1}; ^{1}H-NMR: δ 2.90–3.20 (2, m, H-2 and H-3), 3.83 (9, s, OCH_3-3′, OCH_3-4′, and OCH_3-5′), 4.20–4.80 (4, m, H-1, H-4, and H-11), 6.04 (2, s, OCH_2O), 6.45 (2, s, H-2′ and H-6′), 6.63 (1, s, H-8), 6.80 (1, s, H-5), and 9.01–9.41 ppm [3, m, $C_6H_3(NO_2)_2$].

Anal.—Calc. for $C_{29}H_{24}N_2O_{13}$: *m/z* 608.1275 (M^+). Found: *m/z* 608.1269.

Podophyllotoxinyl Hydrocinnamate (VIII)—Colorless oil (171 mg, 65% yield); R_f 0.62; IR: 1770 (γ-lactone), 1725, and 1235 (ester) cm^{-1}; ^{1}H-NMR: δ 2.70–3.10 (6, m, $COCH_2CH_2$-Ph, H-2, and H-3), 3.75 (6, s, OCH_3-3′ and OCH_3-5′), 3.81 (3, s, OCH_3-4′), 3.90–4.70 (4, m, H-1, H-4, and H-11), 5.94 (2, s, OCH_2O), 6.35 (2, s, H-2′ and H-6′), 6.50 (2, br s, H-5 and H-8), and 7.22 ppm (5, s, C_6H_5).

Anal.—Calc. for $C_{31}H_{30}O_9$: *m/z* 546.1889 (M^+). Found: *m/z* 546.1897.

Podophyllotoxinyl Phenoxyacetate (IX)—White amorphous solid (252 mg, 95% yield), mp 71–74° (sintered at 59–62°); R_f 0.65; IR: 1765 (γ-lactone), 1730, 1240 (ester), and 1040 (aromatic ether) cm^{-1}; ^{1}H-NMR: δ 2.80–3.10 (2, m, H-2 and H-3), 3.75 (6, s, OCH_3-3′ and OCH_3-5′), 3.82 (3, s, OCH_3-4′), 4.00–4.70 (4, m, H-1, H-4, and H-11), 4.76 (2, s, $COCH_2O$), 5.98 (2, s, OCH_2O), 6.36 (2, s, H-2′ and H-6′), 6.52 (1, s, H-8), 6.62 (1, s, H-5), and 6.70–7.50 ppm (5, m, OC_6H_5).

Anal.—Calc. for $C_{30}H_{28}O_{10}$: *m/z* 548.1683 (M^+). Found: *m/z* 548.1685.

Podophyllotoxinyl Ethyl Malonate (X)—White amorphous compound (169 mg, 64% yield), mp 68–70° (sintered at 54°); IR: 1775 (γ-lactone), 1730, and 1745 (slight shoulder) (esters) cm^{-1}; ^{1}H-NMR: δ 1.20 (3, t, J = 7.0 Hz, OCH_2CH_3), 2.70–3.00 (2, m, H-2 and H-3), 3.43 (2, s, $COCH_2CO$), 3.67 (6, s, OCH_3-3′ and OCH_3-5′), 3.43 (3, s, OCH_3-4′), 4.15 (2, overlapped q, J = 7.0 Hz, OCH_2CH_3), 4.00–4.65 [4, m (overlapped by q), H-1, H-4, and H-11], 5.90 (2, s, OCH_2O), 6.30 (2, s, H-2′ and H-6′), 6.45 (1, s, H-8), and 6.76 ppm (1, s, H-5).

Anal.—Calc. for $C_{27}H_{28}O_{11}$: *m/z* 528.1629 (M^+). Found: *m/z* 528.1625.

Podophyllotoxinyl Ethyl Adipate (XI)—Colorless oil (72 mg, 26% yield); IR:1770 (γ-lactone), 1720, and 1235 (ester) cm^{-1}; ^{1}H-NMR: δ 1.28 (3, t, J = 7.0 Hz, OCH_2CH_3), 1.50–2.00 (4, m, $CH_2CH_2CH_2CH_2$), 2.00–2.65 (4, m, $COCH_2(CH_2)_2CH_2CO$), 2.75–3.00 (2, m, H-2 and H-3), 3.78 (6, s, OCH_3-3′ and OCH_3-5′), 3.83 (3, s, OCH_3-4′), 4.15 (2, q, J = 7.0 Hz, OCH_2CH_3), 4.00–4.70 (4, m, H-1, H-4, and H-11), 6.00 (2, s, OCH_2O), 6.40 (2, s, H-2′ and H-6′), 6.54 (1, s, H-8), and 6.75 ppm (1, s, H-5).

Anal.—Calc. for $C_{30}H_{34}O_{11}$: *m/z* 570.2101 (M^+). Found: *m/z* 570.2106.

Bis(podophyllotoxinyl) Succinate (XII)—To 200 mg (0.48 mmole)

of podophyllotoxin (I) dissolved in 10 ml of dry benzene was added 100 mg (0.65 mmole) of succinyl chloride in 10 ml of benzene. The mixture was refluxed until TLC indicated the reaction was complete. Ten milliliters of water was added and the reaction was stirred for an additional hour, after which time the organic layer was removed, washed twice with saturated sodium bicarbonate solution, dried over magnesium sulfate, filtered, and then evaporated *in vacuo*. The oily residue was dried under high vacuum to give 97 mg (44%) of XII, mp 154–157°; IR:1765 (γ-lactone) and 1735 (ester) cm^{-1}; ^{1}H-NMR: δ 2.80 (4, br s, $COCH_2CH_2CO$), 2.70–2.95 (4, m, two H-2 and H-3), 3.77 (12, s, two OCH_3 at C-3′ and C-5′), 3.82 (6, s, two OCH_3 at C-4′), 4.20–4.70 (8, m, two H-1, H-4, and H-11), 5.98 (4, br s, two OCH_2O), 6.39 (4, s, two H-2′ and H-6′), 6.53 (2, two H-8), and 6.81 ppm (2, s, two H-5). Reactions attempted using a small amount of pyridine to improve the yield of XII were unsuccessful.

Anal.—Calc. for $C_{48}H_{46}O_{18}$: *m/z* 910.2680 (M^+). Found: *m/z* 910.2691.

Tetrahydropyranyl Podophyllotoxin (XIII)—Podophyllotoxin (200 mg, 0.48 mmole) was suspended in 10 ml of anhydrous ether and stirred at room temperature. *p*-Toluenesulfonic acid monohydrate (8 mg) and 530 mg (6 mmoles) of dihydropyran were added. As the reaction continued, the product dissolved in the ether, leaving a colorless solution. When TLC showed that the reaction was complete, the ether solution was washed twice with 5 ml of saturated sodium bicarbonate followed by water, dried over magnesium sulfate, filtered, and then evaporated *in vacuo*. Petroleum ether caused XIII, a white amorphous compound (185 mg 77% yield), to precipitate out of an ether solution of the resulting residue, observed mp 93–95° (effervescing from 65°) [lit. (15) mp 90–100°]; R_f 0.51; IR: 1775 (γ-lactone), 1130, and 1075 (aliphatic ether) cm^{-1}; ^{1}H-NMR: δ 1.65 [6, m, $C(CH_2)_3C$ (THP)], 2.83 (2, m, H-2 and H-3), 3.75 (6, s, OCH_3-3′ and OCH_3-5′), 3.80 (3, s, OCH_3-4′), 3.30–5.00 [7, overlapped br m, H-1, H-4, H-11, $—OCH_2$ (THP) and O—CH—O (THP)], 5.96 (2, s, OCH_2O), 6.40 (2, s, H-2′ and H-6′), 6.84 (1, s, H-8), and 7.12 ppm (1, s, H-5).

Anal.—Calc. for $C_{27}H_{30}O_9$: *m/z* 498.1889 (M^+). Found: *m/z* 498.1892.

Podophyllol (XIV)—This was prepared from podophyllotoxin by lithium aluminum hydride reduction according to a literature method (16).

Tetrahydropyranyl Podophyllol (XV)—Tetrahydropyranyl podophyllotoxin (XIII) (440 mg, 0.88 mmole) was dissolved in 10 ml of dry ether. This solution was added dropwise to an ice-cold suspension of 44 mg (1.1 mmoles) of 95% lithium aluminum hydride and stirred at room temperature. When TLC indicated completion, the reaction was cooled to 0° with ice, and a few drops of water were added slowly. After the initial vigorous reaction subsided, an additional 10 ml of water was added slowly, and the entire mixture was stirred for 1 hr. The mixture was filtered through a pad of diatomaceous earth[3] to remove the solids, and the aqueous layer was separated from the organic layer. The aqueous layer was extracted twice with ether and the organic phase was washed with water, dried over magnesium sulfate, filtered, and evaporated *in vacuo*, to give 416 mg (93%) of a white amorphous solid (XV), mp 61–63° (sintered at 41–42°) [lit. (15) mp 75–90°]; R_f 0.67; IR: 3200–3600 (OH), 1130 (ether), and 1040 (primary OH) cm^{-1}; ^{1}H-NMR: δ 1.45–2.50 [8, m, H-2, H-3, and $—C(CH_2)_3C—$ (THP)], 3.75 (6, s, OCH_3-3′ and OCH_3-5′), 3.82 (3, s, OCH_3-4′), 5.90 (2, s, OCH_2O), 6.33 (2, s, H-2′ and H-6′), 6.40 (1, s, H-8), 6.78 (1, s, H-5), and 3.00–5.00 ppm [9, overlapped m, H-1, H-4, H-11, H-13, $—OCH_2$ (THP), and —OCHO— (THP)].

Anal.—Calc. for $C_{27}H_{34}O_9$: *m/z* 502.2201 (M^+). Found: *m/z* 502.2206.

Tetrahydropyranyl Podophyllol Di-(2-bromoacetate) (XVI)—White oily gummy solid (157 mg, 53% yield); R_f 0.66; IR: 1740 (ester) and 1235 (CH_2Br) cm^{-1}; ^{1}H-NMR: δ 1.65 [6, m, $C(CH_2)_3C$ (THP)], 2.20–2.70 (2, m, H-2 and H-3), 3.78 (6, s, OCH_3-3′ and OCH_3-5′), 3.83 (3, s, OCH_3-4′), 3.76 (4, br s, $COCH_2Br$), 3.00–5.08 [9 (exclusive of above), m, H-1, H-4, CH_2OCO, CH_2O (THP), and OCHO (THP)], 5.91 (2, s, OCH_2O), and 6.10–6.80 ppm (4, m, H-5, H-8, H-2′, and H-6′).

Anal.—Calc. for $C_{31}H_{36}Br_2O_{11}$: *m/z* 742.0624 (M^+). Found: *m/z* 586 (corresponds to $[M - 2\,Br]^+$). M^+ was not observed, but M+2 and M+4 peaks were both observed indicating the presence of two bromine atoms.

Tetrahydropyranyl Podophyllol Di-(3-bromopropionate) (XVII)—Colorless oil (85 mg, 39% yield); R_f 0.72; IR: 1735 (ester) and 1215 (alkyl bromide) cm^{-1}; ^{1}H-NMR: δ 1.65 [6, m, $(CH_2)_3C$ (THP)], 2.80 (4, m, two $OCOCH_2CH_2$), 2.30–3.10 (2, m, H-2 and H-3), 3.58 (4, overlapped t, two CH_2Br), 3.79 (6, s, OCH_3-3′ and OCH_3-5′), 3.83 (3, s, OCH_3-4′), 3.00–5.00 [9 (exclusive of above), m, H-1, H-4, CH_2OCO, CH_2O (THP), and OCHO (THP)], 5.91 (2, s, OCH_2O), and 6.10–6.85 ppm (4, m, H-5, H-8, H-2′, and H-6′).

Anal.—Calc. for $C_{33}H_{40}Br_2O_{11}$: *m/z* 770.0937 (M^+). Found: *m/z* 691 (corresponds to $[M - Br]^+$). Although M^+ was not observed, M+2 and M+4 were also detected indicating the presence of two bromine atoms.

Tetrahydropyranyl Podophyllol Dimesylate (XVIII)—White amorphous solid (90 mg, 79.5% yield), mp 47–50° (dec.); R_f 0.72; IR: 1370, 1245, and 1175 (SO_2) cm^{-1}; ^{1}H-NMR: δ 1.65 [6, m, $C—(CH_2)_3—C$ (THP)], 3.01 (3, s, $SO_2—CH_3$), 3.19 (3, s, SO_2CH_3), 2.00–3.00 (2, m, H-2 and H-3), 3.78 (6, s, OCH_3-3′ and OCH_3-5′), 3.82 (3, s, OCH_3-4′), and 5.92 ppm (2, s, OCH_2O).

Anal.—Calc. for $C_{29}H_{38}O_{13}S_2$: C, 52.88; H, 5.81; S, 9.75. Found: C, 52.97; H, 5.85; S, 9.85.

Tetrahydropyranyl Podophyllol Ditosylate (XIX)—White amorphous solid (384 mg, 57% yield), mp 70–72° (sintered at 56–58°) [lit. (15) mp 76–88°]; R_f 0.77; IR: 1360, 1235, and 1187 (SO_2) cm^{-1}; ^{1}H-NMR: δ 1.58 [6, m, $C—(CH_2)_3—C$ (THP)], 2.45 (6, s, $ArCH_3$), 2.00–3.00 (2, m, H-2 and H-3), 3.00–5.00 [9 (exclusive of below), m, H-1, H-4, $CH_2O—S$, $—OCH_2$ (THP), and OCHO (THP)], 3.75 (6, s, OCH_3-3′ and OCH_3-5′), 3.82 (3, s, OCH_3-4′), 5.88 (2, s, OCH_2O), 6.30 (2, s, H-2′ and H-6′), 6.20–7.00 [2 (exclusive of above), m, H-5 and H-8], and 6.50 ppm (4, q, J = 8.5 Hz, $SO_2C_6H_4CH_3$).

Anal.—Calc. for $C_{41}H_{46}O_{13}S_2$: *m/z* 810.2381 (M^+). Found: *m/z* 810.2376.

Biological Assay—The antileukemic activity was assessed against the P-388 lymphocytic leukemia growth in BDF_1 male mice (~22 g). In this screen, 10^6 cells were implanted on day 0. The test compounds were administered intraperitoneally from day 1 to day 9. T/C values were calculated according to the protocol of the National Institutes of Health (14). 5-Fluorouracil was used as the internal standard in the screen.

[3] Celite.

REFERENCES

(1) I. Jardine, in "Anticancer Agents Based on Natural Product Models," J. M. Cassady and J. D. Douros, Eds., Academic, New York, N.Y., 1980, Chap. 9, and literature cited therein.

(2) K.-H. Lee, R. Meck, C. Piantadosi, and E. S. Huang, *J. Med. Chem.*, **16**, 299 (1973).

(3) I. H. Hall, K.-H. Lee, M. Okano, D. Sims, T. Ibuka, Y. F. Liou, and Y. Imakura, *J. Pharm. Sci.*, **70**, 1147 (1981).

(4) K.-H. Lee, T. Ibuka, D. Sims, O. Muraoka, H. Kiyokawa, I. H. Hall, and H. L. Kim, *J. Med. Chem.*, **24**, 924 (1981).

(5) K.-H. Lee, M. Okano, I. H. Hall, D. A. Brent, and B. Soltmann, *J. Pharm. Sci.*, **71**, 338 (1982).

(6) R. I. Geran, N. H. Greenberg, M. M. MacDonald, A. M. Schumacher, and B. J. Abbott, *Cancer Chemother. Rep., Part 3*, **3**, 1 (1972).

(7) J. L. Hartwell and B. J. Abbott, *Adv. Pharmacol. Chemother.*, **7**, 117 (1969).

(8) J. Douros and M. Suffness, in "New Drugs in Cancer Chemotherapy," S. K. Carter, Y. Sakurai, and H. Umezawa, Eds., Springer-Verlag, New York, N.Y., 1981, p. 153.

(9) M. V. Nadkarni and J. L. Hartwell, *J. Am. Chem. Soc.*, **75**, 1308 (1952).

(10) J. L. Hartwell and W. E. Detty, *J. Am. Chem. Soc.*, **72**, 246 (1950).

(11) W. Borsche and J. Niemann, *Ann*, **494**, 126 (1932).

(12) E. Spath, F. Wessely, and L. Kornfeld, *Chem. Ber.*, **65**, 1536 (1932).

(13) J. L. Hartwell and A. W. Schrecker, *J. Am. Chem. Soc.*, **72**, 3320 (1950).

(14) J. L. Hartwell and A. W. Schrecker, *J. Am. Chem. Soc.*, **73**, 2909 (1951).

(15) W. J. Gensler, C. D. Murthy, and M. H. Trammell, *J. Med. Chem.*, **20**, 635 (1977).

(16) N. L. Drake and E. H. Price, *J. Am. Chem. Soc.*, **73**, 201 (1951).

ACKNOWLEDGMENTS

Supported by U.S. Public Health Service Research Grant CA-17625 awarded to K.-H. Lee.

The authors thank Mr. Fred Williams of the Research Triangle Center for Mass Spectrometry for the electron-impact mass spectra data.

Part LXI of this series is H. Nozaki, H. Suzuki, K.-H. Lee, and A. T. McPhail, *J. Chem. Soc. Chem. Commun.*, 1048 (1982).

Simultaneous Determination of Tegafur and 5-Fluorouracil in Serum by GLC Using Nitrogen-Sensitive Detection

NOBUO KAWABATA *, SEIYU SUGIYAMA *x, TSUKASA KUWAMURA *, YOSHICHIKA ODAKA *, and TETSUO SATOH ‡

Received November 30, 1981, from the **Central Research Laboratory, SS Pharmaceutical Co., Ltd., Narita, Chiba 286, Japan*, and ‡*Laboratory of Biochemical Pharmacology and Biotoxicology, Department of Drug Evaluation and Toxicological Sciences, Faculty of Pharmaceutical Sciences, Chiba University, 1-33 Yayoicho, Chiba 280, Japan.* Accepted for publication August 4, 1982.

Abstract □ A sensitive assay of both tegafur (I) and 5-fluorouracil (5-FU) using GLC with a nitrogen–phosphorus-sensitive detector is described. The drugs were extracted from rabbit serum with ethyl acetate and methylated with diazomethane. Linearity was obtained over the concentration ranges of 3.13–200 μg/ml for I and 0.0313–2 μg/ml and 10–50 ng/ml for 5-FU. The detection limits of I and 5-FU in serum were 50 and 8 ng/ml, respectively. The serum concentrations of the drugs determined by the present method closely agreed with those obtained by spectrophotometry for I and microbial assay for 5-FU.

Keyphrases □ Tegafur—simultaneous determination with 5-fluorouracil, rabbit serum, GLC using nitrogen-sensitive detection □ 5-Fluorouracil—simultaneous determination with tegafur, rabbit serum, GLC using nitrogen-sensitive detection □ GLC—nitrogen-sensitive detection, tegafur and 5-fluorouracil, simultaneous determination in rabbit serum

Tegafur [5-fluoro-1-(tetrahydro-2-furyl)uracil (I)], a prodrug of 5-fluorouracil (5-FU), is widely used as an antitumor agent (1–3). Various assays for I and/or 5-FU in biological fluids, such as spectrophotometry (4), microbial (4, 5), GLC (6–15), GLC–mass spectrometry (6, 16–20), and high-performance liquid chromatography (HPLC) (20–30), have been reported. All of these methods either lack adequate sensitivity and specificity and/or involve complicated and lengthy procedures. This paper describes a highly sensitive GLC method using a nitrogen–phosphorus-sensitive detector for simultaneously determining I and 5-FU.

EXPERIMENTAL

Materials—Tegafur (I)[1], 5-fluorouracil (5-FU)[2], and orotic acid[2] were used as received. Ethereal diazomethane solution was prepared according to the method of Arndt (31). All other chemicals and solvents were analytical reagent grade.

GLC Determination—The serum sample (1 ml) was adjusted to pH 6.3 with 0.1 ml of 0.5 *M* NaH_2PO_4 and extracted with 8 ml of ethyl acetate. After centrifugation at 2500 rpm for 10 min, the organic layer was removed and then evaporated to dryness under vacuum at room temperature. (With the lower concentration of 5-FU, <30 ng/ml, it was necessary to extract the serum sample with 8 ml of ethyl acetate twice.) The residue was dissolved in 0.1 ml of 30-μg/ml methanolic orotic acid and then 0.1 ml of ethereal diazomethane was added. The mixture was allowed to stand at room temperature for 30 min and then was evaporated to dryness under vacuum at room temperature. The residue was dissolved in 100 μl of acetone, and 1–2 μl of this solution was injected into a gas chromatograph[3] equipped with a nitrogen–phosphorus-sensitive detector for the measurement of I and 5-FU.

A 2 m × 3-mm i.d. glass column packed with 1% PEG-HT on 60–80 mesh Uniport HP[4] was used for the chromatography. The temperatures of the injection port, column, and detector were 300°, 175°, and 300°, respectively. Helium, the carrier gas, was maintained at a flow rate of 20 ml/min. The flow rates of air and hydrogen were optimized at 60 and 3 ml/min, respectively.

The sensitivities for the measurement of 5-FU and I were set at 1 × 16 and 10 × 32, respectively. The serum concentrations of I were ~100 times higher than those of 5-FU, so the sensitivity of the instrument was lowered to 1/20 for I after 5-FU and orotic acid were detected. Quantitation was carried out by studying the calibration curves obtained by plotting the ratio of the peak area of the methylated derivative of I to that of orotic acid, or the ratio of the peak height of the methylated derivative of 5-FU to that of orotic acid against the concentrations of these two compounds.

Analysis of Methylated Derivative Structures by GLC-Mass Spectrometry (MS)—A 0.1-ml aliquot of I, 5-FU, or orotic acid in acetone solution (1000 μg/ml) was added to 0.1 ml of ethereal diazomethane. After standing for 30 min at room temperature, the mixture was evaporated to dryness under vacuum at room temperature. The residue was dissolved in 100 μl of acetone, and 1 μl of this solution was injected into a gas chromatograph–mass spectrometer[5].

A 1 m × 3-mm i.d. glass column packed with 3% OV-17 on 80–100 mesh Chromosorb W HP[4] was used. The temperatures of the injection port, column, and separator were 260°, 200°, and 220°, respectively. The flow rate of helium, the carrier gas, was 30 ml/min. Electron-impact mass spectra were measured with 70-eV ionization energy, 60-μA ionization current, and 3500-V acceleration voltage.

Spectrophotometric and Microbial Determination—The assays were conducted according to the method of Yasuda *et al.* (4). Concentrations of I were measured by UV absorption at 270 nm after extraction from serum samples with chloroform at pH 2.0. The aqueous phase was assayed microbiologically after the pH was adjusted to 7.0.

Drug Administration—Male albino rabbits weighing 2.0–2.5 kg were used. Animals were administered I in a 1 *M* sodium carbonate solution (pH 9.0) at a dose level of 50 mg/kg iv. Blood samples were taken from the ear vein at appropriate time intervals up to 8 hr after drug administration and were centrifuged after coagulation. The serum obtained was frozen at −20° for subsequent analysis.

RESULTS

Identification of Methylated Derivatives of I, 5-FU, and Orotic Acid by GLC–MS—The MS data for the methylated derivatives of I, 5-FU, and orotic acid are shown in Table I. The structures of these methylated derivatives were shown to be 1-(tetrahydro-2-furyl)-3-*N*-methyl-5-fluorouracil (II), 1,3-dimethyl-5-fluorouracil (III), and methyl 1,3-dimethylorotate (IV), respectively.

Calibration Curves—For the construction of calibration curves, blank rabbit serum was spiked with known amounts of I and 5-FU and subjected to the GLC determination procedure described above. The calibration curves obtained from serum were $y = 0.0251x + 0.0462$ ($r = 0.9988$) for I, $y = 0.8615x + 0.0082$ ($r = 0.9991$) for 5-FU, and $y = 0.0036x + 0.0013$ ($r = 0.9981$) for the lower concentration of 5-FU over the concentration ranges of 3.13–200 μg/ml, 0.0313–2 μg/ml, and 10–50 ng/ml, respectively.

These calibration curves were compared with those obtained with the samples of I or 5-FU dissolved in acetone without the extraction step. Linear relationships were obtained in samples both from the serum and those dissolved in acetone. The mean recoveries of I and 5-FU from the serum were 99 and 75%, respectively. The detection limits of I and 5-FU

[1] Aldrich Chemical Co., Milwaukee, Wis.
[2] Sigma Chemical Co., St. Louis, Mo.
[3] Model 5710A, Hewlett-Packard, Avondale, Pa.
[4] Gaschro Kogyo, Tokyo, Japan.
[5] Shimadzu-LKB 9000B, Kyoto, Japan.

0022-3549/83/1000-1162$01.00/0

Table I—Mass Spectral Data for Methylated Derivatives of I, 5-Fluorouracil, and Orotic Acid

Methylated Derivative	*m/z* (Relative Intensity)	Probable Assignment
1-(Tetrahydro-2-furyl)-3-*N*-methyl-5-fluorouracil	214 (9.8)	M^+
	144 (13.0)	$(M—\overline{CHCH_2CH_2CH_2O}+H)$
	71 (100.0)	$\overline{CH_2CH_2CH_2CH=O}^+$
	43 (48.5)	C_2F^+
1,3-Dimethyl-5-fluorouracil	158 (100.0)	M^+
	101 (34.4)	$(M—CH_3NCO)^+$
	73 (38.4)	$(M—CH_3NCO—CO)^+$
	42 (46.1)	$CH_3—\dot{N}\equiv CH$
Methyl 1,3-dimethyl-orotate	198 (92.3)	M^+
	82 (100.0)	$(M—COOCH_3—CH_3NCO)^+$

in the serum were 50 and 30 ng/ml, respectively. When the extraction procedure was performed twice (the lower concentration of 5-FU), the mean recovery increased to 94% with a detection limit of 8 ng/ml. The limits per injection of I and 5-FU on the column were 50 and 8 pg, respectively. In the triplicate determinations of the serum samples containing various concentrations of I or 5-FU, the coefficients of variation (*CV*) indicated high accuracy and good reproducibility (Table II).

GLC Chromatogram—A typical chromatogram, obtained with the serum sample taken at 2 hr after intravenous administration of I at a dose level of 50 mg/kg, is shown in Fig. 1. The retention times of III, IV, and II were 7.2, 12.4, and 24.0 min, respectively. An unknown endogenous component was detected in the serum with a retention time of 6.0 min, but this peak was well separated from the analyzing compounds. In addition to this peak originating from the endogenous component, another peak with a retention time of 16.4 min was detected in the serum after the administration of I, which might be one of the metabolites of I.

Serum Concentrations of I and 5-FU—The mean serum concentrations of I and 5-FU as a function of time obtained by the present GLC nitrogen–phosphorus-detector method, the spectrophotometric assay method, and the microbial assay method after administration of I at a dose level of 50 mg/kg iv are shown in Fig. 2. Slightly higher concentrations of 5-FU were obtained by the microbial assay method, especially at low levels, than by the present method. The mean serum concentration of I obtained by the present method declined gradually with an elimination half-life of 2.8 hr (Table III). For 5-FU, the peak of serum concentration was at 2 hr after the administration of I, and the elimination half-life was 2.3 hr (Table III).

DISCUSSION

Compound I has been widely used in cancer chemotherapy as a prodrug of 5-FU and is less toxic than 5-FU (32, 33). Compound I is slowly metabolized primarily in the liver to 5-FU. The hepatic microsomal drug-metabolizing enzymes such as cytochrome P_{450} may play a very significant role in this activation (1).

As reported previously (16, 34), when 5-FU is administered, it is rapidly eliminated from the blood with an elimination half-life of 10–30 min. But in the case of the administration of I, 5-FU is released little by little from I for a fairly long period *in vivo*. Various sensitive assay methods for blood

Table II—Accuracy and Reproducibility of GLC Nitrogen–Phosphorus-Detector Analysis of I and 5-Fluorouracil Added to Rabbit Serum

	Amount Added, μg/ml	Amount Found, μg/ml[a]	*CV*, %
I	3	3.1 ± 0.3	9.7
	50	51.3 ± 1.2	2.3
	200	200.0 ± 11.2	5.6
5-Fluorouracil	0.01	0.0100 ± 0.0001[b]	1.0
	0.03	0.0279 ± 0.0003[b]	1.1
	0.05	0.047 ± 0.001[b]	2.1
	0.50	0.51 ± 0.02	3.9
	2.00	2.00 ± 0.03	1.5

[a] Mean ± *SD* of three determinations. [b] Extracted twice.

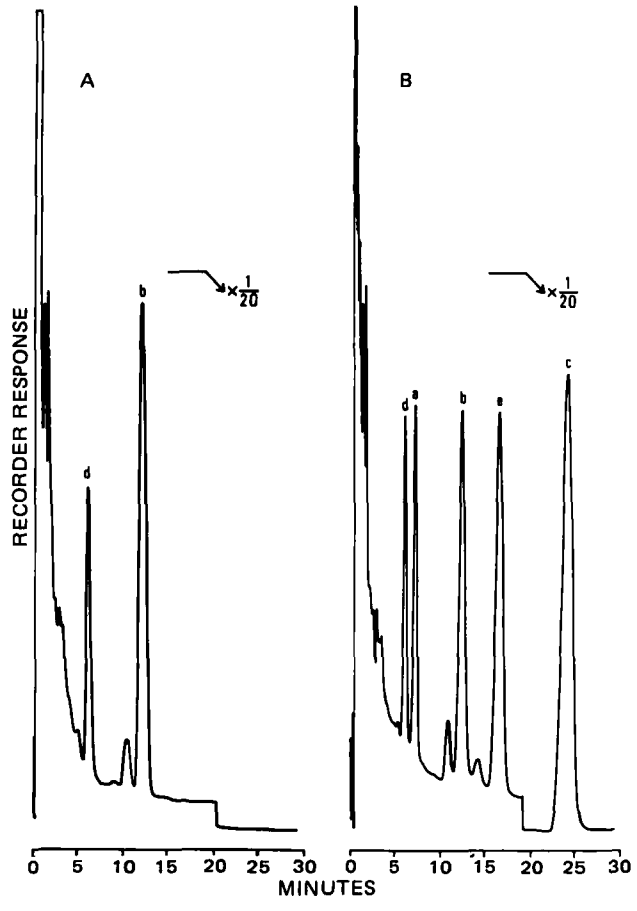

Figure 1—*Typical chromatogram of blank rabbit serum (A) and rabbit serum collected at 2 hr after intravenous administration of I at a dose level of 50 mg/kg (B). Key: (a) 5-FU, 0.5 μg/ml; (b) orotic acid; (c) I, 50 μg/ml; (d) endogenous component; (e) unknown metabolite.*

concentrations of I and 5-FU have been investigated. However, there have been no reports showing simultaneous measurement of the amount of I and 5-FU in biological fluids, except for an HPLC method (24, 27) which resulted in poor separation of 5-FU from the endogenous components. In the present study, I and 5-FU could be detected simultaneously in

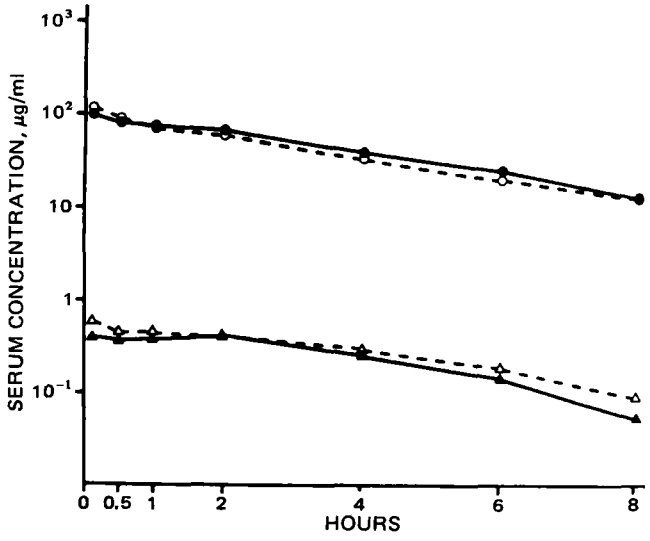

Figure 2—*Mean serum concentrations of I and 5-FU obtained from five rabbits after intravenous administration of I at a dose level of 50 mg/kg. Key: (●), I by the GLC nitrogen–phosphorus-detector method; (○), I by the spectrophotometric method; (▲), 5-FU by the GLC nitrogen–phosphorus-detector method; (△), 5-FU by the microbial assay method.*

Table III—Pharmacokinetic Parameters of I and 5-Fluorouracil Obtained in Rabbits after Intravenous Administration of I at a Dose Level of 50 mg/kg

Rabbit	β[a], hr^{-1}		$t_{1/2}$[b], hr		$AUC_{0-\infty}$[c], hr · μg/ml		V_{CL}[d], liter/kg/hr	$V_{d\beta}$[e], liter/kg
	I	5-FU	I	5-FU	I	5-FU	I	I
1	0.62	0.54	1.1	1.3	279.8	1.71	0.18	0.29
2	0.21	0.17	3.3	4.1	431.5	1.66	0.12	0.56
3	0.11	0.33	6.3	2.1	802.1	1.52	0.06	0.57
4	0.63	0.44	1.1	1.6	234.0	3.06	0.21	0.34
5	0.32	0.29	2.2	2.4	430.1	2.81	0.12	0.37
Mean	0.38	0.35	2.8	2.3	435.5	2.15	0.14	0.43
±*SD*	±0.24	±0.14	±2.2	±1.1	±223.2	±0.72	±0.06	±0.13

[a] β = first-order elimination rate constant. [b] $t_{1/2}$ = biological half-life calculated by $0.693/\beta$. [c] $AUC_{0-\infty}$ = area under the serum concentration–time curve calculated by the trapezoidal rule. [d] V_{CL} = total body clearance, calculated by dose/AUC. [e] $V_{d\beta}$ = volume of distribution during the elimination phase calculated by V_{CL}/β.

serum with high sensitivity and well separated from the endogenous components by the GLC nitrogen–phosphorus-detector method.

5-FU was extracted from serum using the method described in a previous paper (6), on the basis of a pK_a of 8.1 to minimize the concomitant extraction of other acidic compounds contained in the serum that might interfere with the chromatographic assay procedure. Ethyl acetate was used for the extraction solvent. The recoveries of I and 5-FU from serum were 99 and 75%, respectively, which are slightly higher than the values reported by previous investigators (27) who obtained 85 and 60% for I and 5-FU, respectively, using HPLC. The detection limits of I and 5-FU in serum were 50 and 30 ng/ml, respectively. In the case of the lower concentration of 5-FU, the recovery rate increased to 94% by extracting twice with a detection limit of 8 ng/ml in serum. The determinations of the serum samples were conducted in triplicate on the same day using various concentrations of I or 5-FU, covering the range expected for *in vivo* experiments. The results obtained here indicated a satisfactory reproducibility as judged by the coefficients of variation (*CV*).

Compound I and 5-FU cannot be detected with high sensitivity by GLC if not converted to appropriate derivatives. Many derivatizing reagents have been reported (8, 11, 14, 15). When these reagents are injected directly into the GLC after the derivatizing reaction is completed, the peaks of the reagents become broad, and the detector may be contaminated, resulting in shortened column life. The separation of the compounds from the reagents used is difficult. It was reported that the trimethylsilylation of I causes the decomposition of I with 10–30% formation of the trimethylsilylated derivative of 5-FU (6, 13). For these reasons, I and 5-FU were subjected to quantitative methylation with diazomethane, which could be removed after the reaction was complete. No decomposition of I to 5-FU was observed during methylation, and the sample was stable at −20° for ~10 days without any decrease in the methylated derivatives of I and 5-FU. Even if decomposition of the methylated derivative of I occurred, the subsequent conversion to the methylated derivative of 5-FU could not occur because of the removal of diazomethane after derivatization. The calibration curves obtained with these methylated derivatives showed good linearity.

Previous investigators (8, 14) used thymine as an internal standard. However, thymine did not separate completely from 5-FU, either then or in the present study. Therefore, orotic acid was used instead of thymine in the present study; orotic acid showed a satisfactory separation from I, 5-FU, and other endogenous components in serum.

Compound I and 5-FU concentrations in rabbit serum after intravenous administration of I at a dose level of 50 mg/kg could be measured as the methylated derivatives by the present method using a column packed with 1% PEG-HT on Uniport HP. The pharmacokinetic parameters are summarized in Table III; the $t_{1/2}$, V_{CL}, and $V_{d\beta}$ of I were 2.8 hr, 0.14 liter/kg/hr, and 0.43 liter/kg, respectively. These values are fairly consistent with those reported by Au and Sadée (26) who obtained $t_{1/2}$ = 1.4–2.1 hr, V_{CL} = 0.18–0.20 liter/kg/hr, and $V_{d\beta}$ = 0.40–0.54 liter/kg in rabbit plasma by HPLC after intravenous administration of I at a dose level of 60 mg/kg. The elimination half-life of 5-FU derived from I was 2.3 hr, almost equivalent to the value of 2.6 hr in the dog (34).

Good correlations were obtained between the concentrations of I and 5-FU obtained by the present method and by the spectrophotometric assay method (I) ($y = 1.1243x - 6.4795$, $r = 0.9717$) or by the microbial assay method (5-FU) ($y = 0.9265x + 0.0936$, $r = 0.9081$), approximating a theoretical slope of 45°. The 5-FU concentrations obtained by the microbial assay method were slightly higher than those obtained by the present method, especially in the low concentrations, suggesting that the accuracy of the microbial assay method is not as good at low 5-FU levels. 5-FU released *in vivo* is further metabolized to other antibacterial compounds such as 5-fluorouridine, 5-fluorouridine-5′-monophosphate, 5-fluoro-2′-deoxyuridine, 5-fluoro-2′-deoxyuridine-5′-monophosphate, *etc.*, which may result in the higher concentrations obtained by the microbial assay method than those by the present method.

In the present studies, an unknown compound with a retention time of 16.4 min was detected, probably a dehydrogenated metabolite of I as reported in previous papers (24, 27). Dehydrogenated I is more labile than I and could be decomposed to 5-FU *in vivo* (27). But nonenzymatic decomposition of dehydrogenated I was not detected after incubation in 0.1 *M* phosphate buffer (pH 6.0) at 25° (27). On the other hand, in a previous study (6) I was decomposed 0.03% to 5-FU during analysis employing an evaporation procedure under nitrogen at 50° after extraction. Since I is thermally labile, the analytical procedure should be conducted at as low a temperature as possible. In the present study, the overall procedure was carried out at room temperature, resulting in no decomposition of I to 5-FU. This perhaps prevents decomposition of dehydrogenated I, which causes the increased concentration of 5-FU. Furthermore, no decrease of the peak possibly corresponding to the methylated derivative of dehydrogenated I was observed during the analysis. Investigation of valid evidence of this unknown compound as dehydrogenated I is in progress.

REFERENCES

(1) A. M. Cohen, *Drug Metab. Dispos.*, **3**, 303 (1975).

(2) J. P. Horwitz, J. J. McCormick, K. D. Philips, V. M. Maher, J. R. Otto, D. Kessel, and J. Zemlicka, *Cancer Res.*, **35**, 1301 (1975).

(3) S. Fujimoto *et al. Cancer Res.*, **36**, 33 (1976).

(4) I. Yasuda, T. Togo, N. Saimi, S. Watanabe, K. Harima, and T. Suzue, *Chemotherapy*, **21**, 1171 (1973).

(5) H. Fujita, K. Ogawa, T. Sawabe, and K. Kimura, *Gan no Rinsho*, **18**, 911 (1972).

(6) A. T. Wu, H.-J. Schwandt, C. Finn, and W. Sadée, *Res. Commun. Chem. Pathol. Pharmacol.*, **14**, 89 (1976).

(7) C. Pantarotto, R. Fanelli, S. Filippeschi, T. Facchinetti, F. Spreafico, and M. Salmona, *Anal. Biochem.*, **97**, 232 (1979).

(8) H. W. Van Den Berg, R. F. Murphy, R. Hunter, and D. T. Elmore, *J. Chromatogr.*, **145**, 311 (1978).

(9) O. Driessen, D. De Vos, and P. J. A. Timmermans, *J. Chromatogr.*, **162**, 451 (1979).

(10) J. J. Windheuser, J. J. Sutter, and E. Auen, *J. Pharm. Sci.*, **61**, 301 (1972).

(11) J. L. Cohen and P. B. Brennan, *J. Pharm. Sci.*, **62**, 572 (1973).

(12) K. V. Rao, K. Killion, and Y. Tanrikut, *J. Pharm. Sci.*, **63**, 1328 (1974).

(13) E. B. Hills, V. C. Godefroi, I. A. O'Leary, M. Burke, D. Andrzejewski, W. Brukwinski, and J. P. Horwitz, *J. Pharm. Sci.*, **66**, 1497 (1977).

(14) R. E. Finch, M. R. Bending, and A. F. Lant, *J. Pharm. Sci.*, **67**, 1489 (1978).

(15) A. P. DeLeenheer and M. Cl. Cosyns-Duyck, *J. Pharm. Sci.*, **68**, 1174 (1979).

(16) C. Finn and W. Sadée, *Cancer Chemother. Rep. Part 1*, **59**, 279 (1975).

(17) B. L. Hillcoat, *Br. J. Clin. Pharmacol.*, **3**, 135 (1976).

(18) C. Pantarotto, A. Martini, G. Belvedere, A. Bossi, M. G. Donelli, and A. Frigerio, *J. Chromatogr.*, **99**, 519 (1974).

(19) D. B. Lakings and R. H. Adamson, *J. Chromatogr.*, **146**, 512 (1978).

(20) T. Marunaka, Y. Umeno, K. Yoshida, M. Nagamachi, Y. Minami, and S. Fujii, *J. Pharm. Sci.*, **69**, 1296 (1980).

(21) J. A. Benvenuto, K. Lu, and T. L. Loo, *J. Chromatogr.*, **134**, 219 (1977).
(22) N. Hobara and A. Watanabe, *J. Chromatogr.*, **146**, 518 (1978).
(23) J. L. Cohen and R. E. Brown, *J. Chromatogr.*, **151**, 237 (1978).
(24) A. T. Wu, J. L. Au, and W. Sadée, *Cancer Res.*, **38**, 210 (1978).
(25) J. A. Benvenuto, K. Lu, S. W. Hall, R. S. Benjamin, and T. L. Loo, *Cancer Res.*, **38**, 3867 (1978).
(26) J. L. Au and W. Sadée, *Cancer Res.*, **40**, 2814 (1980).
(27) J. L. Au, A. T. Wu, M. A. Friedman, and W. Sadée, *Cancer Treat. Rep.*, **63**, 343 (1979).
(28) A. R. Buckpitt and M. R. Boyd, *Anal. Biochem.*, **106**, 432 (1980).
(29) L. S. F. Hsu and T. C. Marrs, *Ann. Clin. Biochem.*, **11**, 272 (1980).
(30) W. E. Wung and S. B. Howell, *Clin. Chem.*, **26**, 1704 (1980).
(31) F. Arndt, *Org. Synth.*, **15**, 3 (1935).
(32) S. Germane and A. Kimenis, *Eksp. Klin. Farmakoter.*, **1**, 85 (1970).
(33) M. I. Kravchenko, A. Zidermane, and A. Zibere, *Eksp. Klin. Farmakoter.*, **1**, 93 (1970).
(34) K. Lu, T. L. Loo, J. A. Benvenuto, R. S. Benjamin, M. Valdivieso, and E. J. Freireich, *Pharmacologist*, **17**, 202 (1975) (Abstract).

Comparative Assays for Doxepin and Desmethyldoxepin Using High-Performance Liquid Chromatography and High-Performance Thin-Layer Chromatography

R. D. FAULKNER and C. LEE ˣ

Received July 12, 1982, from the *Department of Pharmaceutics, College of Pharmacy, University of Houston, Houston TX 77030.* Accepted for publication September 1, 1982.

Abstract □ Two chromatographic methods, high-performance liquid chromatography (HPLC) and high-performance thin-layer chromatography (HPTLC) were compared for sensitivity and reproducibility in the analysis of the tricyclic antidepressant doxepin and its metabolite, desmethyldoxepin, in plasma. The HPLC procedure yielded a better reproducibility, as reflected by the coefficient of variation, and a higher sensitivity, as reflected by the minimum detectable quantity. The application of these methods for therapeutic and subtherapeutic monitoring of plasma levels of the drug is described.

Keyphrases □ Doxepin—high-performance thin-layer and liquid chromatographic methods, comparison, human plasma, desmethyldoxepin metabolite □ High-performance liquid chromatography—doxepin and desmethyldoxepin in human plasma, comparison with high-performance thin-layer chromatography □ Thin-layer chromatography—high-performance, doxepin and desmethyldoxepin in human plasma, comparison with high-performance liquid chromatography

Doxepin (I) is a tricyclic antidepressant commonly prescribed for the treatment of endogenous depression. Increasing evidence of a correlation between the total tricyclic plasma level [doxepin plus desmethyldoxepin (II)] and the antidepressant effect suggests that monitoring tricyclic plasma levels may be beneficial in the clinical management of depression.

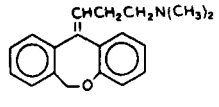

I

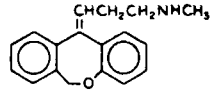

II

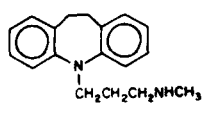

III

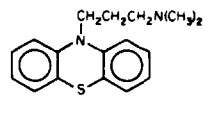

IV

Several assay methods for I and II have been reported, including GLC (1–3), radioimmunoassay (4), GC–mass fragmentography (5), and high-performance liquid chromatography (HPLC) (6–9). Most of these methods either require extensive sample preparation or lack the necessary specificity and sensitivity for pharmacokinetic studies. This paper compares two chromatographic procedures, HPLC and high-performance thin-layer chromatography (HPTLC), for sensitivity and reproducibility in the analysis of I and II in plasma. Desipramine (III) and promazine (IV) were used as internal standards in HPLC and HPTLC, respectively.

EXPERIMENTAL

Materials—A high-performance liquid chromatograph[1] equipped with a variable-wavelength UV detector[2], a sample loop injection valve[3], and a 5-μm octadecylsilane column[4] (150 mm × 4.6-mm i.d.) was used for HPLC analyses. A scanning spectrophotometer–densitometer[5] was used for HPTLC measurements.

Doxepin[6], desmethyldoxepin[6], desipramine[7], and promazine[8] were obtained as hydrochloride salts. Toluene[9], chloroform[9], pentane[9], and 2-propanol[9] were reagent grade and were glass-distilled before use. HPLC-grade acetonitrile[10] and reagent-grade *N*-nonylamine[11] were used as supplied. All glassware used for samples or extracts were silylated with hexamethyldisilazine at elevated temperature and reduced pressure. Working standard solutions were prepared in the following strengths: I, 1 μg/ml; II, 1 μg/ml; III, 2μg/ml; IV, 1 μg/ml.

HPLC Procedures—Analyses were performed using a modified procedure of Kabra *et al.* (10). Plasma standards were prepared by spiking known quantities of I and II in 1 ml of plasma containing 0.1 μg of desipramine internal standard (III). To the spiked plasma samples were added 0.25 ml of saturated sodium carbonate and 4.5 ml of pentane. The sample mixture was rotated for 45 min and then centrifuged. The pentane phase was transferred into a silylated conical vial[12] and back-extracted with 0.1 ml of 0.1 *N* HCl. The organic layer was discarded, and aliquots of the aqueous phase were injected into the liquid chromatograph. The mobile phase was 45% acetonitrile in 0.01 *M* phosphate buffer containing 600 ppm of *N*-nonylamine (pH 3.1). The deaerated and fil-

[1] ConstaMetric IIG; Laboratory Data Control, Riviera Beach, Fla.
[2] Spectromonitor III; Laboratory Data Control, Riviera Beach, Fla.
[3] Model SV-7; Glenco Scientific Inc., Houston, Tex.
[4] Spherisorb; Custom LC Inc., Houston, Tex.
[5] Zeiss Instruments, New York, N.Y.
[6] Pennwalt Corp., Rochester, N.Y.
[7] USV Pharmaceutical Corp., Tuckahoe, N.Y.
[8] SKF Laboratories, Philadelphia, Pa.
[9] Fisher Scientific, Fair Lawn, N.J.
[10] MCB Mfg. Chemicals Inc., Cincinnati, Ohio.
[11] Aldrich Chemical Co., Milwaukee, Wis.
[12] Reacti-Vial; Pierce Chemical Co., Rockford, Ill.

0022-3549/83/1000-1165$01.00/0

(21) J. A. Benvenuto, K. Lu, and T. L. Loo, *J. Chromatogr.*, **134**, 219 (1977).
(22) N. Hobara and A. Watanabe, *J. Chromatogr.*, **146**, 518 (1978).
(23) J. L. Cohen and R. E. Brown, *J. Chromatogr.*, **151**, 237 (1978).
(24) A. T. Wu, J. L. Au, and W. Sadée, *Cancer Res.*, **38**, 210 (1978).
(25) J. A. Benvenuto, K. Lu, S. W. Hall, R. S. Benjamin, and T. L. Loo, *Cancer Res.*, **38**, 3867 (1978).
(26) J. L. Au and W. Sadée, *Cancer Res.*, **40**, 2814 (1980).
(27) J. L. Au, A. T. Wu, M. A. Friedman, and W. Sadée, *Cancer Treat. Rep.*, **63**, 343 (1979).
(28) A. R. Buckpitt and M. R. Boyd, *Anal. Biochem.*, **106**, 432 (1980).
(29) L. S. F. Hsu and T. C. Marrs, *Ann. Clin. Biochem.*, **11**, 272 (1980).
(30) W. E. Wung and S. B. Howell, *Clin. Chem.*, **26**, 1704 (1980).
(31) F. Arndt, *Org. Synth.*, **15**, 3 (1935).
(32) S. Germane and A. Kimenis, *Eksp. Klin. Farmakoter.*, **1**, 85 (1970).
(33) M. I. Kravchenko, A. Zidermane, and A. Zibere, *Eksp. Klin. Farmakoter.*, **1**, 93 (1970).
(34) K. Lu, T. L. Loo, J. A. Benvenuto, R. S. Benjamin, M. Valdivieso, and E. J. Freireich, *Pharmacologist*, **17**, 202 (1975) (Abstract).

Comparative Assays for Doxepin and Desmethyldoxepin Using High-Performance Liquid Chromatography and High-Performance Thin-Layer Chromatography

R. D. FAULKNER and C. LEE ˣ

Received July 12, 1982, from the *Department of Pharmaceutics, College of Pharmacy, University of Houston, Houston TX 77030.* Accepted for publication September 1, 1982.

Abstract □ Two chromatographic methods, high-performance liquid chromatography (HPLC) and high-performance thin-layer chromatography (HPTLC) were compared for sensitivity and reproducibility in the analysis of the tricyclic antidepressant doxepin and its metabolite, desmethyldoxepin, in plasma. The HPLC procedure yielded a better reproducibility, as reflected by the coefficient of variation, and a higher sensitivity, as reflected by the minimum detectable quantity. The application of these methods for therapeutic and subtherapeutic monitoring of plasma levels of the drug is described.

Keyphrases □ Doxepin—high-performance thin-layer and liquid chromatographic methods, comparison, human plasma, desmethyldoxepin metabolite □ High-performance liquid chromatography—doxepin and desmethyldoxepin in human plasma, comparison with high-performance thin-layer chromatography □ Thin-layer chromatography—high-performance, doxepin and desmethyldoxepin in human plasma, comparison with high-performance liquid chromatography

Doxepin (I) is a tricyclic antidepressant commonly prescribed for the treatment of endogenous depression. Increasing evidence of a correlation between the total tricyclic plasma level [doxepin plus desmethyldoxepin (II)] and the antidepressant effect suggests that monitoring tricyclic plasma levels may be beneficial in the clinical management of depression.

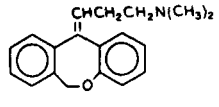

I

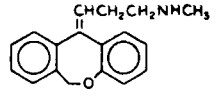

II

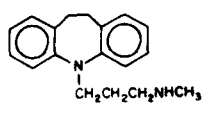

III

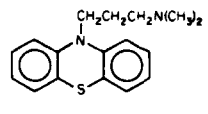

IV

Several assay methods for I and II have been reported, including GLC (1–3), radioimmunoassay (4), GC–mass fragmentography (5), and high-performance liquid chromatography (HPLC) (6–9). Most of these methods either require extensive sample preparation or lack the necessary specificity and sensitivity for pharmacokinetic studies. This paper compares two chromatographic procedures, HPLC and high-performance thin-layer chromatography (HPTLC), for sensitivity and reproducibility in the analysis of I and II in plasma. Desipramine (III) and promazine (IV) were used as internal standards in HPLC and HPTLC, respectively.

EXPERIMENTAL

Materials—A high-performance liquid chromatograph[1] equipped with a variable-wavelength UV detector[2], a sample loop injection valve[3], and a 5-μm octadecylsilane column[4] (150 mm × 4.6-mm i.d.) was used for HPLC analyses. A scanning spectrophotometer–densitometer[5] was used for HPTLC measurements.

Doxepin[6], desmethyldoxepin[6], desipramine[7], and promazine[8] were obtained as hydrochloride salts. Toluene[9], chloroform[9], pentane[9], and 2-propanol[9] were reagent grade and were glass-distilled before use. HPLC-grade acetonitrile[10] and reagent-grade *N*-nonylamine[11] were used as supplied. All glassware used for samples or extracts were silylated with hexamethyldisilazine at elevated temperature and reduced pressure. Working standard solutions were prepared in the following strengths: I, 1 μg/ml; II, 1 μg/ml; III, 2μg/ml; IV, 1 μg/ml.

HPLC Procedures—Analyses were performed using a modified procedure of Kabra *et al.* (10). Plasma standards were prepared by spiking known quantities of I and II in 1 ml of plasma containing 0.1 μg of desipramine internal standard (III). To the spiked plasma samples were added 0.25 ml of saturated sodium carbonate and 4.5 ml of pentane. The sample mixture was rotated for 45 min and then centrifuged. The pentane phase was transferred into a silylated conical vial[12] and back-extracted with 0.1 ml of 0.1 *N* HCl. The organic layer was discarded, and aliquots of the aqueous phase were injected into the liquid chromatograph. The mobile phase was 45% acetonitrile in 0.01 *M* phosphate buffer containing 600 ppm of *N*-nonylamine (pH 3.1). The deaerated and fil-

[1] ConstaMetric IIG; Laboratory Data Control, Riviera Beach, Fla.
[2] Spectromonitor III; Laboratory Data Control, Riviera Beach, Fla.
[3] Model SV-7; Glenco Scientific Inc., Houston, Tex.
[4] Spherisorb; Custom LC Inc., Houston, Tex.
[5] Zeiss Instruments, New York, N.Y.
[6] Pennwalt Corp., Rochester, N.Y.
[7] USV Pharmaceutical Corp., Tuckahoe, N.Y.
[8] SKF Laboratories, Philadelphia, Pa.
[9] Fisher Scientific, Fair Lawn, N.J.
[10] MCB Mfg. Chemicals Inc., Cincinnati, Ohio.
[11] Aldrich Chemical Co., Milwaukee, Wis.
[12] Reacti-Vial; Pierce Chemical Co., Rockford, Ill.

0022-3549/83/1000-1165$01.00/0

Table I—HPLC Determinations of Peak Height Ratios in Plasma [a]

Amount, ng	Ratio of I/III			Ratio of II/III		
	Mean[b]	SD	CV[c]	Mean[b]	SD	CV[c]
10	0.182	0.018	9.9	0.227	0.025	10.9
20	0.338	0.019	5.9	0.394	0.038	9.6
40	0.653	0.035	5.5	0.733	0.041	5.6
60	1.012	0.061	6.0	1.152	0.066	5.7
100	1.572	0.065	4.1	1.800	0.073	4.0

[a] Absorbance measured at 200 nm. [b] Mean of six determinations. [c] Coefficient of variation.

tered mobile phase was pumped through the column at 2.5 ml/min, and the effluents were detected at 200 and 240 nm.

HPTLC Procedures—Analyses were performed following a modified procedure of Fenimore *et al.* (11). To plasma standards containing various amounts of I and II were added 50 ng of promazine internal standard (IV), 0.25 ml of saturated sodium carbonate, and 4.5 ml of pentane. The mixture was gently shaken for 45 min and then centrifuged. The aqueous layer was frozen in an acetone–dry ice bath, and the organic phase was decanted into a silylated conical vial. After complete evaporation of the organic phase, the residue was dissolved in 60 μl of heptane–ethanol (3:1), and 50 μl of the reconstituted sample was spotted onto the HPTLC plate[13]. Development of the plate was carried out in a twin-trough chamber[14] using two solvent systems: toluene–chloroform–2-propanol (20:20:10) and toluene–chloroform–2-propanol–ammonium hydroxide (20:20:10:1). The developed plates were air dried prior to UV scanning.

RESULTS AND DISCUSSION

Figure 1 shows representative liquid chromatograms of a control plasma blank, plasma spiked with III, and plasma to which I, II, and III were added. The retention times were 4.6, 3.3, and 6.3 min for I, II, and III, respectively. As indicated in Fig. 1a, no interfering peaks were found in the control plasma.

The peak height ratios obtained following HPLC analyses of I and II in control plasma are summarized in Table I. The calibration curves were characterized by linear regression equations of $y = 0.0156x + 0.0345$, $r^2 = 0.9981$ for I, and $y = 0.0177x + 0.0480$, $r^2 = 0.9983$ for II. The reproducibility in concentration measurements, as reflected by the coefficient of variation, was 6.3 ± 2.2% for I and 7.2 ± 2.9% for II. The lower detection limit was 5 ng for both I and II.

Figure 2 depicts the thin-layer chromatograms of a control plasma blank, plasma to which promazine internal standard (IV) was added, and

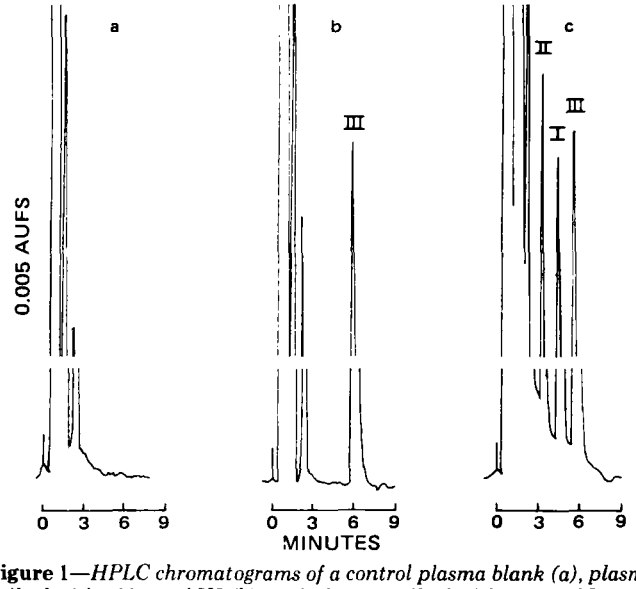

Figure 1—*HPLC chromatograms of a control plasma blank (a), plasma spiked with 100 ng of III (b), and plasma spiked with 60 ng of I, 60 ng of II, and 100 ng of III (c).*

[13] Silica Gel 60; E. Merck, Darmstadt, GFR.
[14] Camag Inc., New Berlin, Wis.

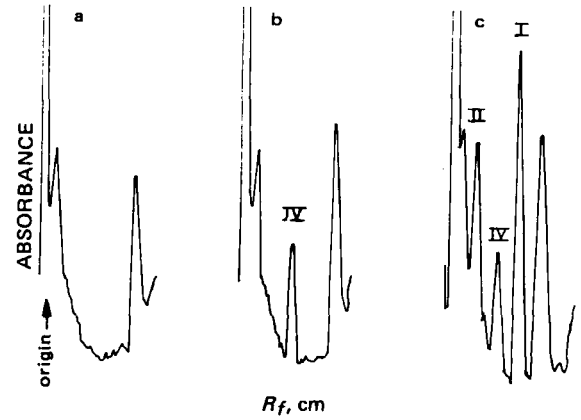

Figure 2—*HPTLC chromatograms of a control plasma blank (a), plasma spiked with 50 ng of IV (b), plasma spiked with 60 ng of I, 60 ng of II, and 50 ng of IV (c).*

Table II—HPTLC Determinations of Peak Height Ratios in Plasma [a]

Amount, ng	Ratio of I/IV			Ratio of II/IV		
	Mean[b]	SD	CV[c]	Mean[b]	SD	CV[c]
10	0.142	0.015	10.6	—[d]	—	—
20	0.232	0.012	5.2	0.097	0.013	12.8
40	0.513	0.027	5.3	0.198	0.020	10.2
60	0.627	0.031	4.9	0.342	0.027	7.8
100	1.040	0.065	6.3	0.550	0.047	8.5

[a] Absorbance measured at 240 nm. [b] Mean of four determinations. [c] Coefficient of variation. [d] II not distinguishable from baseline at 10 ng.

plasma with added I, II, and IV. No interfering signals were detected in the blank plasma at R_f values of 1.6 cm for I, 0.6 cm for II, and 1.0 cm for IV.

The peak height ratios derived at 240 nm following HPTLC analyses of various amounts of I and II in control human plasma are presented in Table II. In the 10 to 100-ng range, the assay reproducibility was 6.5 ± 2.4% for I and 9.8 ± 2.2% for II. Typical calibration curves were characterized by $y = 0.0099x + 0.0551$, $r^2 = 0.9951$ for I, and $y = 0.0057x - 0.0190$, $r^2 = 0.9980$ for II. The sensitivity of measurements was 10 ng for I and 20 ng for II at 200 nm, which decreased to 20 ng for I and 30 ng for II at 240 nm.

Since a common internal standard was not available for both chromatographic procedures, each method requires its own internal standard.

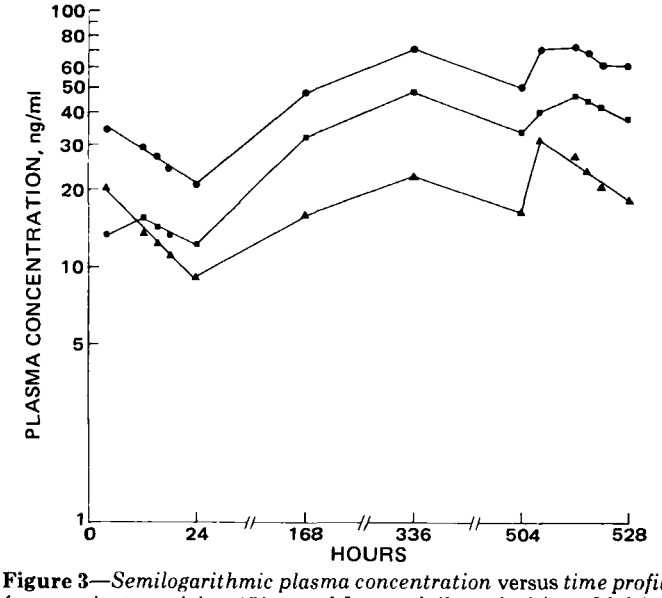

Figure 3—*Semilogarithmic plasma concentration* versus *time profile for a patient receiving 150 mg of I once daily at bedtime. Multiple samples were collected for the 24-hr periods following the 1st and 21st doses. Key: (▲) I; (■) II; (●) I and II.*

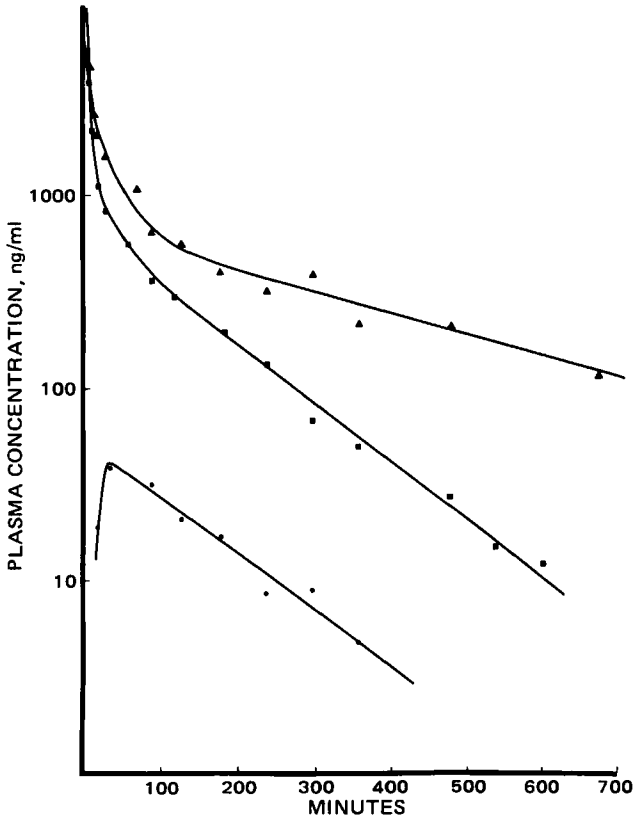

Figure 4—*Semilogarithmic plasma concentration* versus *time plots for I and II in a normal dog following intravenous administrations of 50 mg of I and 50 mg of II on two occasions separated by 2 weeks. Key: (▲) I; (●) II generated from I; (■) II given as a separate dose.*

Promazine was selected as the internal standard for HPTLC method because of the proximity of its R_f value to that of I and II. Similarly, desipramine was used in the HPLC procedure because of its relatively short retention time: 6 min as opposed to 13 min for promazine.

When both chromatographic procedures were compared for detection sensitivity at 200 nm on an equivalent weight basis, the HPLC method appeared to be superior. Since back-extraction was carried out in the HPLC procedure, which could conceivably reduce the extraction recovery, the lower sensitivity of the HPTLC method could not be attributed to the extraction process. One possibility is that the HPLC mobile phase favors the UV absorbance for I and II compared with the silica gel of the HPTLC plate.

In an attempt to compare the reproducibility of the HPTLC procedure at two different wavelengths (200 and 240 nm), coefficients of variation were determined: 10.3 ± 5.0% for I and 12.4 ± 5.6% for II at 200 nm as opposed to 6.5 ± 2.4% for I and 9.8 ± 2.2% for II at 240 nm. The reproducibility was less impressive at 200 nm; however, it was comparable with HPLC at 240 nm. The detecting sensitivity, on the other hand, notably decreased at the longer wavelength.

Figure 3 shows the plasma concentration *versus* time plot for a patient receiving 150 mg of I once daily at bedtime. Multiple samples were collected for 24-hr following the 1st and the 21st doses. Half-lives of I and II were 17.3 and 35.5 hr, respectively, after the first dose, and 23.8 and 40.6 hr following the last dose. It is not clear, based on this patient study, whether multiple dosing of I alters its metabolism.

Figure 4 presents plasma concentration *versus* time plots for a normal dog intravenously administered a 50-mg dose of I and a 50-mg dose of II on two occasions separated by 2 weeks. The β-phase half-life of I in the dog, 2.5 hr, was considerably shorter than that of the depressed human, 17.2 hr. In contrast to the human, the dog exhibited a shorter half-life for II than for I [17.3/35.5 (I/II) in the human *versus* 3.3/2.1 in the dog]. In addition, the dog presented a substantially lower fraction of II in the plasma. These observations suggest an interspecies difference in the metabolic and excretory patterns of I between dogs and humans.

In summary, for measurements of therapeutic levels of I and II in plasma, both HPLC and HPTLC provide adequate sensitivity and reproducibility. The HPLC method offers a higher detection sensitivity and is suggested for pharmacokinetic studies in which subtherapeutic concentrations are to be measured. On the other hand, the HPTLC procedure offers a greater processing capacity and a shorter turnaround time, which are preferred in a clinical setting for the routine monitoring of tricyclic plasma levels.

REFERENCES

(1) L. A. Gifford, P. Turner, and C. M. B. Pare, *J. Chromatogr.*, **105,** 107 (1975).

(2) M. T. Rosseel, M. G. Bogaert, and M. Claeys, *Fresenius Z. Anal. Chem.*, **290,** 158 (1978).

(3) J. E. O'Brien and O. N. Hinsuark, *J. Pharm. Sci.*, **65,** 1068 (1976).

(4) R. Virtanen, J. S. Salonen, M. Scheinin, E. Iisaho, and V. Mattila, *Acta Pharmacol. Toxicol.*, **47,** 274 (1980).

(5) J. T. Biggs, W. H. Holland, S. Chang, P. P. Hipps, and W. R. Sherman, *J. Pharm. Sci.*, **65,** 261 (1976).

(6) F. L. Vandemark, R. F. Adams, and G. J. Schmidt, *Clin. Chem.*, **24,** 87 (1978).

(7) S. H. Y. Wong and T. McCauley, *J. Liq. Chromatogr.*, **4,** 849 (1981).

(8) J. E. Wallace, E. L. Shimek, Jr., and S. C. Harris, *J. Anal. Toxicol.*, **5,** 20 (1981).

(9) H. F. Proeless, H. J. Lohmann, and D. G. Miles, *Clin. Chem.* **24,** 1948 (1978).

(10) P. M. Kabra, N. A. Mar, and L. J. Marton, *Clin. Chim. Acta*, **111,** 123 (1981).

(11) D. C. Fenimore, C. M. Davis, J. H. Whitford, and C. A. Harrington, *Anal. Chem.*, **48,** 2289 (1976).

ACKNOWLEDGMENTS

This work was presented at the APhA Academy of Pharmaceutical Sciences meeting in Las Vegas, April 1982.

The authors wish to thank Dr. C. M. Davis for granting us permission to use the HPTLC equipment at the Texas Research Institute of Mental Sciences.

Determinations of Tiodazosin and Levulinic Acid from Tablets by High-Performance Liquid Chromatography

B. C. PROSSER, B. J. FLOOR, A. E. KLEIN, and N. MUHAMMAD ˣ

Received July 15, 1982, from the *Analytical Research and Development Department, Bristol Laboratories—Division of Bristol-Myers Co., Syracuse, NY 13201.* Accepted for publication September 7, 1982.

Abstract □ Specific assays of tiodazosin and levulinic acid from tablet preparations were developed using high-performance liquid chromatography. Tiodazosin was determined with acetonitrile 50% (v/v) in pH 5.7 acetate buffer on a 300 × 3.9-mm i.d. microparticulate C-18 column using 254 nm detection with butylparaben as the internal standard. Levulinic acid was determined at 280 nm with 1 *N* acetic acid on a 300 × 3.9-mm i.d. microparticulate phenyl column using an external standard. The assays were run sequentially. The relative standard deviations of sample variability (2σ, $n = 6$) and recoveries from synthetic preparation were ±1.6 and ~95%, respectively, for both assays.

Keyphrases □ Tiodazosin—tablets, high-performance liquid chromatographic assay, sequential with levulinic acid □ Levulinic acid—in tiodazosin tablets, sequential high-performance liquid chromatographic assay □ High-performance liquid chromatography—tiodazosin and levulinic acid from tablets, sequential assay

Tiodasozin, 1-(4-amino-6,7-dimethoxy-2-quinazolinyl) -4- [[5-(methylthio) -1,3,4- oxadiazol-2-yl]carbonyl]-piperazine (I), is an orally active hypertensive agent currently undergoing clinical trials. It is formulated in tablets with levulinic acid (4-oxopentanoic acid). A reported high-performance liquid chromatographic (HPLC) assay method for tiodazosin (1) is limited to biological samples and involves work-up procedures and a fluorescence detection system that would not be suitable for the dosage form.

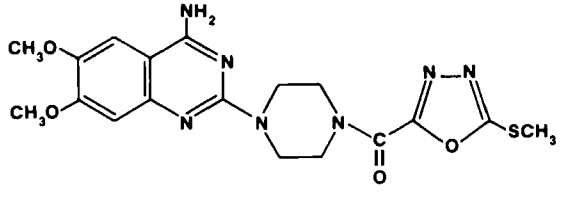

I

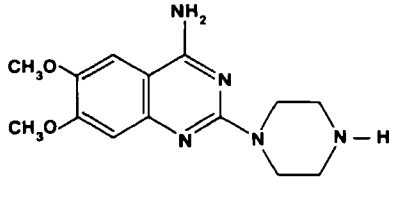

II

Levulinic acid has been quantitatively assayed as the methyl ester by GC (2). This method was found to be unsuitable, however, for the acid in the presence of the tablet excipients due to the incompleteness of the derivatization reaction. A simplified analytical method that does not employ derivatization is described in this study. The method utilizes the relatively weak UV absorptivity of the acid in methanol (3), which is ~20 liters/mole·cm at the 270-nm UV maxima and 15 liters/mole·cm at 280 nm.

Two simple HPLC procedures for the quantitative assay of tiodazosin and levulinic acid are described in the present report. The methods are accurate and specific in the presence of the tablet matrix ingredients.

EXPERIMENTAL

Apparatus—A modular HPLC system consisting of a pump[1], a septumless loop injector[2], and a fixed-wavelength detector[3] was used. Peak elution times and areas were obtained with a reporting integrator system[4].

Reagents and Materials—Tiodazosin[5] and levulinic acid[6] were used without further purification. Sodium acetate[7] and glacial acetic acid[7] were ACS reagent grade. Butylparaben NF[8] was used as received. Acetonitrile[9] was obtained as distilled-in-glass chromatographic grade, and water was distilled and deionized.

Sample Preparation—Ten tablets of tiodazosin were accurately weighed and then ground and blended to a uniform fine powder. A portion of the powdered blend was accurately weighed for each assay.

Tiodazosin Assay—*Chromatographic Conditions*—A stainless steel

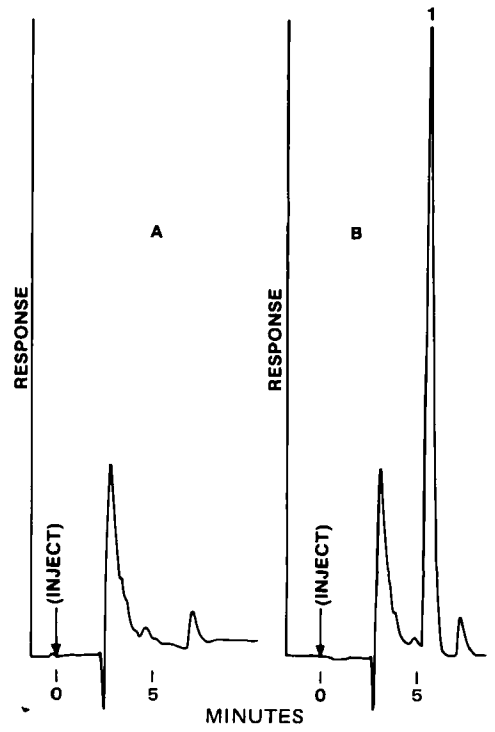

Figure 1—*Representative chromatograms from the levulinic acid assay. Key: (A) placebo with no levulinic acid present; (B) typical tablet sample with levulinic acid (1).*

[1] Model 6000A; Waters Associates, Milford, Mass.
[2] Model 7120; Rheodyne, Berkeley, Calif.
[3] Model 440; Waters Associates, Milford, Mass.
[4] HP-3354 Laboratory Automation System; Hewlett-Packard, Avondale, Pa.
[5] Bristol Reference Standard; Bristol Laboratories, Syracuse, N.Y.
[6] Sigma Chemical Co., Saint Louis, Mo.
[7] Fisher Scientific, Fair Lawn, N.J.
[8] Pfaultz and Bauer, Inc., Stamford, Conn.
[9] Burdick and Jackson, Muskegon, Mich.

0022-3549/83/1000-1168$01.00/0

HPLC column (30 cm × 3.9-mm i.d.) prepacked with bonded octadecylsilane on silica[10] (10% loading by weight, 10-μm mean particle size) was used with a mobile phase of 50% by volume acetonitrile in 0.1 *M* sodium acetate, previously adjusted to pH 5.7 with glacial acetic acid. A flow rate of 1.5 ml/min and a loop injection volume of 20 μl were employed with the detector set at 254 nm.

Standard Solution—A solution of butylparaben in acetonitrile was prepared at a concentration of 100 μg/ml for use as an internal standard. A stock solution of tiodazosin reference material was prepared at a concentration of 50 μg/ml in mobile phase, and a 5-ml aliquot of this stock solution together with 5 ml of the internal standard solution were transferred to a 50-ml volumetric flask and diluted to volume with mobile phase for use as a standard.

Analytical Procedure—The powdered tablet sample equivalent to a theoretical level of ~5 mg of tiodazosin was transferred to a 100-ml volumetric flask. A 50-ml portion of mobile phase was added, the solution sonicated[11] for 5 min, and diluted to volume with mobile phase. A portion of this solution was filtered[12], discarding the first few milliliters, and a 5-ml portion of the filtrate was transferred to a 50-ml volumetric flask. The internal standard (5 ml) was added, and the solution was diluted to volume with mobile phase. Successive injections of the standard and sample solutions were made onto the chromatographic system at room temperature. The peak areas generated were applied to the calculation of milligrams tiodazosin per average tablet weight (ATW) using the formulas:

$$\text{Factor (F) for Tiodazosin} = \frac{\text{Peak Area Internal Standard} \times \text{mg/ml Tiodazosin Standard} \times \text{Purity of Standard}}{\text{Peak Area Tiodazosin Standard} \times \text{mg/ml Internal Standard}}$$

$$\text{mg Tiodazosin per ATW} = \frac{\text{F} \times 1000 \times \text{mg/ml Internal Standard} \times \text{Peak Area Tiodazosin} \times \text{mg per ATW}}{\text{Peak Area Internal Standard} \times \text{mg Sample}}$$

Levulinic Acid Assay—*Chromatographic Conditions*—A prepacked bonded phenyl on silica[13] (10% loading by weight, 10-μm mean particle size) HPLC column (30 cm × 3.9-mm i.d. stainless steel) was employed with a mobile phase of 1.0 *N* acetic acid. The mobile phase was filtered through a 0.45-μm membrane filter[14] prior to use. A flow rate of 1.0 ml/min and a loop injection volume of 200 μl were used with the detector set at 280 nm.

Standard Solution—A standard levulinic acid solution was prepared containing 0.26–0.30 mg of the acid per milliliter of mobile phase. To ensure noninterference, a 500-mg portion of placebo tablet granulation (containing all the tiodazosin tablet excipients) was mixed with 10 ml of the mobile phase. The resulting suspension was filtered[15], and an aliquot was injected into the chromatographic system.

Analytical Procedure—The powdered tablet sample, equivalent to one average tablet weight, was transferred to a 20-ml vial, 10 ml of mobile phase was added, the vial capped, and the suspension was mixed by shaking mechanically for 15 min in a reciprocating shaker. The contents of the vial was filtered[15] prior to chromatographic injection. Successive injections of the standard and sample were made at room temperature. The levulinic acid peak areas were used for the calculation of milligrams levulinic acid per ATW using the formulas:

$$\text{Factor (F) for Levulinic Acid} = \frac{\text{mg/ml Levulinic Acid Standard} \times 10 \times \text{Purity of Standard}}{\text{Peak Area Levulinic Acid}}$$

$$\text{mg Levulinic Acid per ATW} = \frac{\text{F} \times \text{Peak Area Levulinic Acid} \times \text{mg per ATW}}{\text{mg Sample}}$$

RESULTS AND DISCUSSION

The described HPLC method elutes levulinic acid in ~5.8 min and employs the relatively weak UV absorption of the acid at ~280 nm for determinations at concentration levels of $\geq 3 \times 10^{-4}$ *M*. The relatively larger injection volume of 200 μl was required for detectability of levulinic acid below the millimolar level. Figure 1 shows representative chromatograms for a placebo with no levulinic acid and a typical tablet sample.

The tiodazosin content can be determined sequentially from the same powdered tablet sample by employing the described, independent assay procedure. Figure 2 shows a typical chromatogram for this assay, with tiodazosin eluting at ~3.2 min and the internal standard at ~5.8 min. The total analysis time for a typical tablet sample is ~7 min.

Standard linearity was checked over the range 1.00–10.00 mg/ml for tiodazosin and 0.03–1.5 mg/ml for levulinic acid. Both compounds responded linearly over the stated concentration ranges, with least-squares regression analysis of the peak area responses producing correlation coefficients >0.999 in both cases. The difference in the slopes of the regression lines for levulinic acid in the presence of a placebo granulation compared with that in the absence of the placebo was <1% of the mean slope value. This implies a levulinic acid recovery of ~99% from the placebo matrix.

Chromatographic variability was determined by six identical injections of the standard preparations of tablet samples with a label claim of either 10 mg of tiodazosin or 7 mg of levulinic acid. Relative standard deviations (2*s*%) for chromatographic variability and sample variability are ±0.50

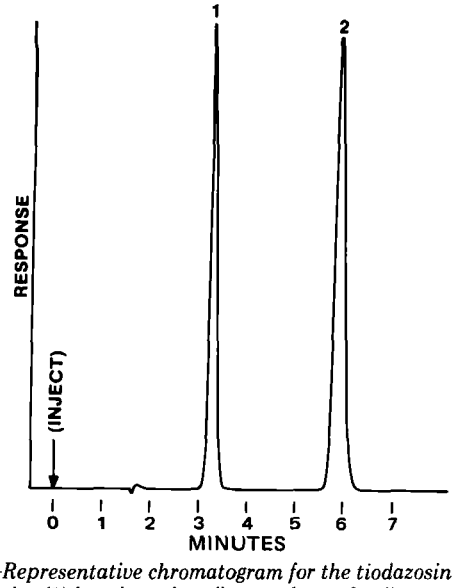

Figure 2—*Representative chromatogram for the tiodazosin assay. Key: (1) tiodazosin; (2) butylparaben (internal standard).*

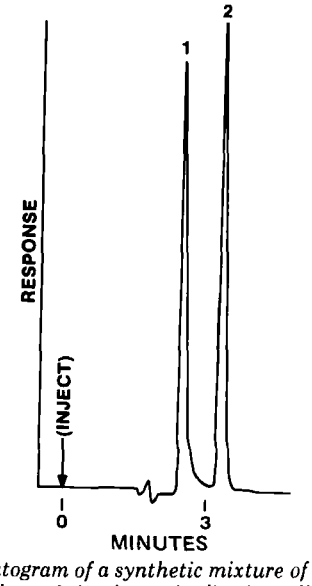

Figure 3—*Chromatogram of a synthetic mixture of tiodazosin (2) and 4-amino-6,7-dimethoxy-2-(1-piperazinyl)quinazoline (1).*

[10] μ-Bondapak C_{18}; Waters Associates, Milford, Mass.
[11] Model B52H; Ultrasonic Bath, Branson Co., Shelton, Conn.
[12] No. 6 Filter Paper; Whatman, Clifton, N.J.
[13] μ-Bondapak Phenyl; Waters Associates, Milford, Mass.
[14] Type HA; Millipore Corp., Bedford, Mass.
[15] No. 576 Filter Paper; Schleicher and Schuell, Keene, N.H.

and ±1.6% for the tiodazosin assay or ±1.8 and ±1.6% for the levulinic acid assay.

Accuracy of the assays was determined by recoveries of individual tiodazosin additions to spiked placebo formulation equivalent to 1, 2, 5, 10, and 20 mg of tiodazosin per tablet. Recoveries for the five spiked samples ranged from 95.7 to 99.3% with a mean recovery of 96.7% (s = ±1.8%), calculated from the regression line generated from the linearity study. The spiking of levulinic acid over the concentration range from 0.5 to 1.5 mg per tablet into a placebo matrix produced recovery results, calculated using the regression line generated in the absence of the placebo, of 87.5% at the 0.5-mg level, 95.6% at the 5-mg level, and 99.6% at the 15-mg level.

The forced degradation of 1-mg tiodazosin tablets under conditions of heat (100° for 20 hr), light (~15 W at 300 nm for 1 week), acid (1 N HCl for 20 hr), and base (1 N NaOH for 20 hr) was performed to test the specificity of the tiodazosin assay method. Absorbance ratios were calculated from chromatograms generated at 220, 254, or 340 nm from both undegraded and degraded samples. No apparent interference was observed from any of the degraded samples, and the relative standard deviations of the 254/220-nm and 254/340-nm absorbance ratios was ±1.2 and ±0.7%, respectively. For the levulinic acid assay, no apparent interferences were observed for degraded samples, where the degradation conditions were adjusted to produce a maximum acid degradation of 10%.

Specificity of the tiodazosin method was also demonstrated by the resolution of the principal known decomposition product, 4-amino-6,7-dimethoxy-2-(1-piperazinyl)quinazoline (II), from the active drug under the assay conditions. A chromatographic tracing of a mixture of I and II is shown in Fig. 3. The results of typical tablet blend analyses gave mean recoveries of 103% for tiodazosin and 99.7% for levulinic acid based on the label claims for a nominal 10 mg of tiodazosin per tablet level. In summary, the reverse-phase HPLC methods described in this paper provide simple, rapid, and quantitative methods for the determination of tiodazosin and levulinic acid from the tablet matrix.

REFERENCES

(1) B. A. Mico, R. A. Baughman, Jr., and L. Z. Benet, *J. Chromatogr.*, **230**, 203 (1982).

(2) E. W. Robb and J. J. Westbrook III, *Anal. Chem.*, **35**, 1644 (1963).

(3) J. H. Turner, P. A. Rebers, P. L. Barrick, and R. H. Cotton, *Anal. Chem.*, **26**, 899 (1954).

General Definition of Valence Delta-Values for Molecular Connectivity

LEMONT B. KIER *ˣ and LOWELL H. HALL ‡

Received March 31, 1982 from the **Department of Pharmaceutical Chemistry, Virginia Commonwealth University, Richmond, VA 23298* and the ‡*Department of Chemistry, Eastern Nazarene College, Quincy, MA 02170.* Accepted for publication August 26, 1982.

Abstract □ The molecular connectivity valence delta-values have been defined in terms of the count of nonhydrogen valence electrons on a valence-state atom as screened from the nucleus by the core electrons. The core is defined as the nonvalence electrons minus 1. This general definition expresses the valence delta-values for second and third quantum level atoms and halogens. Valence delta-values have been derived for higher oxidation states of sulfur and phosphorus. The internal consistency of these delta-values is tested by their ability to closely correlate molar refraction values with $^1\chi^v$. It is found that a second variable, the count of the number of α hydrogen atoms, greatly increases the quality of the correlation. Some biological SAR applications reveal the general utility of these findings.

Keyphrases □ Molecular connectivity—valence delta-values, definition, applications to structure–activity relationships, comparison with molecular refractivity □ Structure–activity relationships—applications of molecular connectivity valence delta-values, comparison with molecular refractivity □ Molecular refractivity—comparison with molecular connectivity valence delta-values, structure–activity relationships

A major advance in the general applicability of molecular connectivity arose from the introduction of valence molecular connectivity indexes by Kier and Hall (1, 2). This innovation made it possible to encode information about heteroatoms and unsaturated features and to correlate this with the relative differences in properties among such molecules. The subsequent use of valence molecular connectivity has been summarized (3).

BACKGROUND

Early Estimates of δ^v—In the initial description of the valence connectivity delta a bonded atom was described by a count of the valence electrons other than those bonding hydrogen (1). This value, designated δ_i^v for atom i was incorporated into the valence connectivity index, $^1\chi^v$, using the same algorithm as for the simple connectivity index, $^1\chi^v = \Sigma(\delta_i^v\delta_j^v)^{-1/2}$. The structural information encoded in the simple δ, a count of σ bonds (electrons) other than those bonding hydrogen, and the δ^v-value was evident from an inspection of a matrix of the two values (3). The sum of the delta-values ($\delta^v + \delta$) for a hybrid atom relates closely to estimates of the hybrid atom volume. It was also shown that the difference between the delta-values ($\delta^v - \delta$) for a hybrid atom is a count of π and lone-pair electrons, referred to as "exterjacent" to describe their relationship to internuclear axes. A count of exterjacent electrons on an atom in its hybrid state, within a quantum level, bears a close relationship to the Mulliken–Jaffe electronegativity (3).

In the earliest consideration of heteroatoms (1), the δ^v-values for second quantum level atoms were verified by relating the calculated $^1\chi^v$ values to molar refraction (MR) data for substituted benzenes (4). The correlation was good, however the experimental value of fluorobenzene presented a problem. The fact that it has a value of 0.4 less than benzene led to the rejection of the logical $\delta_F^v = 7$ and to the derivation of an empirical value of −20. Thus the $(\delta_i^v\delta_F^v)^{-1/2}$ would have a negative value. This subtraction of the modest value of this term in the calculation of $^1\chi^v$ permitted a fairly accurate reproduction of the effect of fluorine in molecules as far as certain physical property values. Using the same approach, empirical values were derived for the other halogens (1) and sulfur (2). These are shown in Table I, column 1.

The Quantum Level Effect on δ^v—Following these initial empirical assignments of higher level atom δ^v-values, a fundamental significance for these numbers was sought. This led to the realization that the empirical δ^v-values for Cl, Br, I, and S were close to the numbers derived by a general expression:

$$\delta^v = \frac{Z^v - h}{Z - Z^v} \qquad \text{(Eq. 1)}$$

where h is the count of hydrogen atoms, Z^v is the count of valence electrons, and Z is the count of all electrons (5). The value $Z - Z^v$ is the count of all nonvalence electrons on the atom; thus, it constitutes information on the principal quantum number of the atom. The denominator in Eq. 1 may be viewed as simulating a radial dimension or a valence orbital screening factor associated with the particular quantum level. Indeed this influence on the valence electrons has been approximated by the use

0022-3549/83/1000-1170$01.00/0

and ±1.6% for the tiodazosin assay or ±1.8 and ±1.6% for the levulinic acid assay.

Accuracy of the assays was determined by recoveries of individual tiodazosin additions to spiked placebo formulation equivalent to 1, 2, 5, 10, and 20 mg of tiodazosin per tablet. Recoveries for the five spiked samples ranged from 95.7 to 99.3% with a mean recovery of 96.7% (s = ±1.8%), calculated from the regression line generated from the linearity study. The spiking of levulinic acid over the concentration range from 0.5 to 1.5 mg per tablet into a placebo matrix produced recovery results, calculated using the regression line generated in the absence of the placebo, of 87.5% at the 0.5-mg level, 95.6% at the 5-mg level, and 99.6% at the 15-mg level.

The forced degradation of 1-mg tiodazosin tablets under conditions of heat (100° for 20 hr), light (~15 W at 300 nm for 1 week), acid (1 N HCl for 20 hr), and base (1 N NaOH for 20 hr) was performed to test the specificity of the tiodazosin assay method. Absorbance ratios were calculated from chromatograms generated at 220, 254, or 340 nm from both undegraded and degraded samples. No apparent interference was observed from any of the degraded samples, and the relative standard deviations of the 254/220-nm and 254/340-nm absorbance ratios was ±1.2 and ±0.7%, respectively. For the levulinic acid assay, no apparent interferences were observed for degraded samples, where the degradation conditions were adjusted to produce a maximum acid degradation of 10%.

Specificity of the tiodazosin method was also demonstrated by the resolution of the principal known decomposition product, 4-amino-6,7-dimethoxy-2-(1-piperazinyl)quinazoline (II), from the active drug under the assay conditions. A chromatographic tracing of a mixture of I and II is shown in Fig. 3. The results of typical tablet blend analyses gave mean recoveries of 103% for tiodazosin and 99.7% for levulinic acid based on the label claims for a nominal 10 mg of tiodazosin per tablet level. In summary, the reverse-phase HPLC methods described in this paper provide simple, rapid, and quantitative methods for the determination of tiodazosin and levulinic acid from the tablet matrix.

REFERENCES

(1) B. A. Mico, R. A. Baughman, Jr., and L. Z. Benet, *J. Chromatogr.*, **230**, 203 (1982).

(2) E. W. Robb and J. J. Westbrook III, *Anal. Chem.*, **35**, 1644 (1963).

(3) J. H. Turner, P. A. Rebers, P. L. Barrick, and R. H. Cotton, *Anal. Chem.*, **26**, 899 (1954).

General Definition of Valence Delta-Values for Molecular Connectivity

LEMONT B. KIER *ˣ and LOWELL H. HALL ‡

Received March 31, 1982 from the **Department of Pharmaceutical Chemistry, Virginia Commonwealth University, Richmond, VA 23298* and the ‡*Department of Chemistry, Eastern Nazarene College, Quincy, MA 02170.* Accepted for publication August 26, 1982.

Abstract □ The molecular connectivity valence delta-values have been defined in terms of the count of nonhydrogen valence electrons on a valence-state atom as screened from the nucleus by the core electrons. The core is defined as the nonvalence electrons minus 1. This general definition expresses the valence delta-values for second and third quantum level atoms and halogens. Valence delta-values have been derived for higher oxidation states of sulfur and phosphorus. The internal consistency of these delta-values is tested by their ability to closely correlate molar refraction values with $^1\chi^v$. It is found that a second variable, the count of the number of α hydrogen atoms, greatly increases the quality of the correlation. Some biological SAR applications reveal the general utility of these findings.

Keyphrases □ Molecular connectivity—valence delta-values, definition, applications to structure–activity relationships, comparison with molecular refractivity □ Structure–activity relationships—applications of molecular connectivity valence delta-values, comparison with molecular refractivity □ Molecular refractivity—comparison with molecular connectivity valence delta-values, structure–activity relationships

A major advance in the general applicability of molecular connectivity arose from the introduction of valence molecular connectivity indexes by Kier and Hall (1, 2). This innovation made it possible to encode information about heteroatoms and unsaturated features and to correlate this with the relative differences in properties among such molecules. The subsequent use of valence molecular connectivity has been summarized (3).

BACKGROUND

Early Estimates of δ^v—In the initial description of the valence connectivity delta a bonded atom was described by a count of the valence electrons other than those bonding hydrogen (1). This value, designated δ_i^v for atom i was incorporated into the valence connectivity index, $^1\chi^v$, using the same algorithm as for the simple connectivity index, $^1\chi^v = \Sigma(\delta_i^v\delta_j^v)^{-1/2}$. The structural information encoded in the simple δ, a count of σ bonds (electrons) other than those bonding hydrogen, and the δ^v-value was evident from an inspection of a matrix of the two values (3). The sum of the delta-values ($\delta^v + \delta$) for a hybrid atom relates closely to estimates of the hybrid atom volume. It was also shown that the difference between the delta-values ($\delta^v - \delta$) for a hybrid atom is a count of π and lone-pair electrons, referred to as "exterjacent" to describe their relationship to internuclear axes. A count of exterjacent electrons on an atom in its hybrid state, within a quantum level, bears a close relationship to the Mulliken–Jaffe electronegativity (3).

In the earliest consideration of heteroatoms (1), the δ^v-values for second quantum level atoms were verified by relating the calculated $^1\chi^v$ values to molar refraction (MR) data for substituted benzenes (4). The correlation was good, however the experimental value of fluorobenzene presented a problem. The fact that it has a value of 0.4 less than benzene led to the rejection of the logical $\delta_F^v = 7$ and to the derivation of an empirical value of −20. Thus the $(\delta_i^v\delta_F^v)^{-1/2}$ would have a negative value. This subtraction of the modest value of this term in the calculation of $^1\chi^v$ permitted a fairly accurate reproduction of the effect of fluorine in molecules as far as certain physical property values. Using the same approach, empirical values were derived for the other halogens (1) and sulfur (2). These are shown in Table I, column 1.

The Quantum Level Effect on δ^v—Following these initial empirical assignments of higher level atom δ^v-values, a fundamental significance for these numbers was sought. This led to the realization that the empirical δ^v-values for Cl, Br, I, and S were close to the numbers derived by a general expression:

$$\delta^v = \frac{Z^v - h}{Z - Z^v} \qquad \text{(Eq. 1)}$$

where h is the count of hydrogen atoms, Z^v is the count of valence electrons, and Z is the count of all electrons (5). The value $Z - Z^v$ is the count of all nonvalence electrons on the atom; thus, it constitutes information on the principal quantum number of the atom. The denominator in Eq. 1 may be viewed as simulating a radial dimension or a valence orbital screening factor associated with the particular quantum level. Indeed this influence on the valence electrons has been approximated by the use

0022-3549/83/1000-1170$01.00/0

Table I—δ^v-Values for Third Quantum Level Atoms and Halogens

Atom	δ^{va}	δ^{vb}	δ^c
F	−20		7
Cl	0.690	0.70	0.78
Br	0.250	0.25	0.26
I	0.085	0.15	0.16
—S—	0.944	0.60	0.67
	—	—	0.56
—SO—	—	—	1.33
—SO_2—	—	—	2.67
—S—S—	—	—	0.89
	—	—	2.22

[a] Data from Refs. 1 and 2. [b] Data calculated using Eq. 1 of Ref. 5. [c] Calculated using Eq. 2.

(6) of the atomic radius (r), the use (7) of r^2, or the use (8, 9) of the square of the quantum number (N^2) in estimating orbital electronegativity or boundary potentials. The values derived from the use of Eq. 1 are listed in Table I, column 2.

Equation 1 now may be viewed as an attempt to simultaneously model two characteristics of valence orbitals: the distance from the nucleus and their boundary potential or electronegativity. The value of $^1\chi^v$ derived from these delta-values contains information related to both of these properties. Recent applications of this information to molecular volume (10), orbital electronegativity (3), and molecular polarity (11) have been published.

THEORETICAL

General Equation for δ^v—The generality of Eq. 1 within the third quantum level is evident; however, it does not correctly describe the previously established δ^v-values for second quantum level atoms. The value $Z - Z^v = 2$ is not correct in Eq. 1 for these atoms. The denominator term $Z - Z^v - 1$ reproduces the δ^v-values for C, N, and O in their various valence states. This is equivalent to counting (or weighting) the pair of $1s^2$ electrons of oxygen as one. To make this count of screening electrons equivalent for both the second and third quantum levels, a general expression for δ^v is necessary:

$$\delta^v = \frac{Z^v - h}{Z - Z^v - 1} \qquad \text{(Eq. 2)}$$

This count of screening electrons, $(Z - Z^v - 1)$, can be explained in two ways. First, there can be invoked an assumption of a difference in the screening contributions of the $1s^2$ electrons relative to the contributions of 2s and 2p electrons. This is a notion embodied in Slater's rules for the same structural characteristic (12). A second explanation arises from the fact that hydrogen atoms are suppressed in formulating δ^v. Thus, the hydrogen electron structure may be viewed as the zero-value reference structure in the count of screening electrons. From this basis, oxygen would have a count of one screening electron while sulfur would have a count of nine electrons. The values of δ^v using Eq. 2 differ very little from those derived from Eq. 1 (Table I, column 3).

The Special Case of Fluorine—The estimation of electronegativity from $\delta^v - \delta$, or a count of exterjacent electrons (3), for the second quantum level leads to the relationship:

$$\epsilon_M(\text{eV}) = 2.05(\delta^v - \delta) + 6.99 \qquad \text{(Eq. 3)}$$

The assumption that fluorine is sp^3 hybridized results in $\delta^v = 7$ and $\delta^v - \delta = 6$. From Eq. 3, this electronic structure predicts an electronegativity for fluorine in its bonding state of 19.3 eV. Hinze and Jaffe report an electronegativity of only 12.18 eV using $s^2p^2p^2p$ as the bonding state of the atom (13). Considerable work confirms the assumption that bound fluorine has little or no sp^3 character. Recalculating $\delta^v - \delta$ for fluorine from the unhybridized structure gives a value of 4 which, from Eq. 3, predicts an electronegativity of 15.2 eV. To reproduce the Mulliken–Jaffe fluorine electronegativity of 12.18 eV would require fluorine to have a δ^v-value of 3.5, corresponding to a fractional hybridization of the valence electrons.

The matter is further complicated by the awareness that in calculating electronegativities, Hinze and Jaffe (13) used ground-state ionization potentials and electron affinities; thus, the actual promotion process may not be faithfully reproduced by their model in the case of fluorine. A comparison of other electronegativity scales suggests that the value of 19 eV is not unreasonable in the Mulliken–Jaffe scale. Fully aware of these complications, we adopt at this time, the nonempirical value of 7 for δ^v_F.

Third Quantum Level Atom Deltas—Applying Eq. 3 to third-level atoms, chlorine, sulfur, and phosphorus atoms have values of 0.78, 0.67, and 0.55, respectively, for δ^v (when there are no bonded hydrogens). These are listed in column 3 of Table I.

The higher oxidation states of sulfur and phosphorus present a new

Table II—Molecules for MR Calculation

Subset	Number in Subset
Alkyl fluorides	9
Alkyl chlorides	9
Alkyl bromides	9
Alkyl iodides	6
Alkanols	6
Dialkyl ethers	6
Alkylamines	6
Alkylnitriles	6
Alkylthiols	8
Dialkyl sulfides	9
Alkylphosphines	10
Dialkyl sulfites	4
Dialkyl sulfates	3
Dialkyl disulfides	5
Trialkyl phosphates	5
Total	101

Table III—Binding of Phenyl Glycosides

para-Substituent	−Log M_{50}[a]	$^1\chi^v$
OH	2.32	0.224
CH_3O	2.40	0.612
C_2H_5O	2.46	1.200
C_4H_9O	2.59	2.200
CH_3	2.29	0.500
C_2H_5	2.46	1.061
C_3H_7	2.51	1.561
sec-Bu	2.58	1.981
tert-Bu	2.63	1.750
H	2.23	0.000
F	2.26	0.189
Cl	2.36	0.566
Br	2.38	0.981
I	2.44	1.250
—$COCH_3$	2.50	0.954
—COC_2H_5	2.56	1.515
CN	2.35	0.474
NO_2	2.34	0.589
NH_2	2.25	0.289

[a] Data taken from Ref. 17.

Table IV—Physicochemical Data for 7-R-4-Hydroxyquinoline-3-Carboxylic Acids and Relationships of Cell Inhibition Potency and χ

R	MDH pI_{50}[a]	$^1\chi^v$	MR[b]
Cl	2.44	0.586	0.603
F	1.98	0.189	0.092
$COCH_3$	3.04	0.954	1.118
$N(CH_3)_2$	3.32	1.118	1.555
$OCH_2C_6H_5$	4.49	2.757	3.174
$OCH_2C_6H_3$-3,4-Cl_2	5.32	3.717	4.174
NO_2	2.72	0.589	0.736
$CONH_2$	3.13	0.743	0.981
COOH	2.97	0.678	0.605
SO_2CH_3	3.18	1.419	1.349
OH	3.31	0.224	0.285
SO_2NH_2	3.02	1.161	1.228
SO_3^-	2.67	1.058	0.971

[a] Data taken from Ref. 18. [b] Data taken from Hansch *et al.*, *J. Med. Chem.*, **16**, 1207 (1973).

Table V—Local Anesthetic Activity of *N*-[(*N'*,*N'*-Disubstituted-amino)acetyl]arylamines

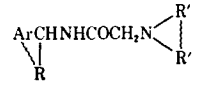

Ar—CH(R)—	—N(R')R'	$^0\chi^v$	pAD		
			Observed[a]	Calculated	Residual
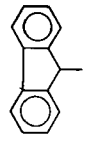	$(C_2H_5)_2$	13.22	1.82	1.75	0.06
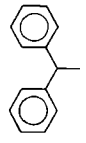	$(C_2H_5)_2$	13.38	1.82	1.73	0.08
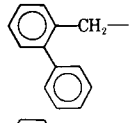	$(C_2H_5)_2$	13.43	1.82	1.73	0.08
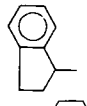	$(C_2H_5)_2$	11.33	1.45	1.48	−0.03
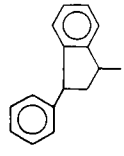	$(C_2H_5)_2$	14.58	1.55	1.43	0.11
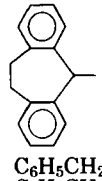	$(C_2H_5)_2$	14.63	1.25	1.41	−0.16
$C_6H_5CH_2$—	$(C_2H_5)_2$	10.25	0.93	0.96	−0.03
$C_6H_5CH_2$—	$(n\text{-}C_3H_7)_2$	12.03	1.75	1.68	0.06
$C_6H_5CH_2$—	$(n\text{-}C_4H_9)_2$	12.95	1.80	1.76	0.03
$C_6H_5CH_2$—		9.53	0.71	0.46	0.24
$C_6H_5CH_2$—		10.21	0.73	0.95	−0.22
$C_6H_5CH_2$—		9.94	0.73	0.76	−0.03
$C_6H_5CH_2$—	$(n\text{-}C_5H_{11})_2$	14.36	1.53	1.51[b]	0.01
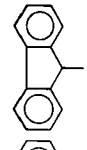	$(n\text{-}C_3H_7)_2$	13.30	1.68	1.74[b]	−0.06
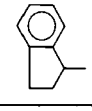	$(n\text{-}C_3H_7)_2$	12.74	1.89	1.76[b]	0.12

[a] Data taken from Ref. 19. [b] Predicted value.

problem. Vogel has shown that the fragment contributions to the molar refraction made by —S—, —SO—, and —SO_2— are nearly identical at 7.92, 7.98, and 7.84, respectively (14). This suggests that the groups —SO— and —SO_2— may be described by the same δ^v used for —S—. It also indicates that the value of δ_S^S for the sulfur atom in each of these groups would be different than the δ_S^S for a sulfide sulfur atom. One may choose the expedient of adopting $\delta_S^S = 0.67$ for —S—, —SO—, and —SO_2—, which subsumes the presence of the oxygen atom(s). The assumption implies that the volume occupied by each sulfur lone-pair orbital is the same as the volume occupied by each oxygen atom bonded to sulfur in —SO— and —SO_2—. This is what Vogel's molar refraction fragment values reveal. The use of $\delta_S^S = 0.67$ as a group value for all three classes of sulfur compounds accurately reproduces MR data for these molecules.

A more useful alternative is to explicitly consider the oxygens bonded to sulfur in SO and SO_2 and to derive from theory, or to calculate empirically, values of δ_S^S in each oxidation state. From molar refractivities of several sulfites and sulfates, averaged values have been found which are close to:

$$\delta^v(\text{S in SO}) = 2\delta^v(\text{—S—}) = 12/9 = 1.333 \quad \text{(Eq. 4)}$$

$$\delta^v(\text{S in } SO_2) = 4\delta^v(\text{—S—}) = 24/9 = 2.666 \quad \text{(Eq. 5)}$$

The theoretical justification for these values is evident from the relative contribution of each sulfur atom to the volume and the relative polarity of one and two S—O bonds. From molar refractivity values, one can also derive a δ^v-value for each sulfur in the disulfide group. This is close to δ^v(S in—S—S—) = 8/9 = 0.888. Finally, the δ^v for phosphorus in orthophosphates is described by δ^v(P in PO) = $4\delta^v(-\underset{|}{P}-) = 20/9 = 2.222$.

It is generally accepted that these S—O and P—O bonds are semipolar. As a consequence, one could expect an appreciably different (increased) value for the δ^v-value for S and P relative to the values in alkyl analogues, reflecting the increased valence state electronegativity.

DISCUSSION

Test of δ^v-Values—A meaningful way of evaluating the interrelationship of the δ^v-values is to relate the molar refraction (MR) values for a mixed group of molecules to molecular connectivity indices. If the δ^v-values encode structural information in an accurate manner among atoms in the second and third quantum levels, it is to be expected that the first-order valence connectivity index, $^1\chi^v$, should bear a close relationship to this physical property. These values have been tested on a set of single function molecules, embracing the important, covalent bonding atoms in the second and third quantum level. These are classified by heteroatom in Table II. (Specific entries are available on request.) Using the δ^v-values shown in column 3 of Table I, the relationship is found to be:

$$MR = 8.444\,^1\chi^v + 5.360$$
$$r = 0.979, s = 2.39, n = 101, F = 2327 \quad \text{(Eq. 6)}$$

It came to our attention in the course of the study on third quantum level atoms that an additional structural feature is important in influencing the MR-value. This feature is the number of hydrogen atoms α to certain heteroatoms, which cannot be accounted for in the δ^v description of the heteroatoms. It was found in the case of the halides beyond fluorine, sulfides and disulfides, and secondary and tertiary phosphines, that the MR-value is diminished roughly in proportion to the number of α hydrogens. The inclusion of the count of α hydrogens for these atoms makes a marked improvement in the correlation with MR:

$$MR = 9.042\,^1\chi^v - 1.286\alpha H + 4.777$$
$$r = 0.996, s = 1.038, n = 101, F = 6397 \quad \text{(Eq. 7)}$$

The αH term is independent of the $^1\chi^v$ index and describes a structural feature not encoded in $^1\chi^v$ or the values of δ^v used in its calculation. It is further of note that the coefficient of the αH term in Eq. 7 is close to the Vogel estimate of the hydrogen contribution to molar refraction (14). This analysis constitutes a valid test of the δ^v-value internal relationship. The correlation with MR-values leads to a degree of confidence in the δ^v-values, and they are proposed for use at this time.

Biological Applications—This demonstrated ability of $^1\chi^v$ to relate to MR stimulates the test of $^1\chi^v$ in biological studies in which MR has been used in property–activity analyses. There has been some recent interest in MR as a surrogate for molecular structure in structure–activity relationship (SAR) analyses (15). In several of these studies, values of MR for substituent groups have been employed. These have been derived from MR-values of whole molecules by partitioning (14). The absolute values of these substituent contributions may vary depending on the method of calculation, although the correlation of values is usually good. A few examples of χ *versus* activity illustrate the capability of this index.

Binding of Substituted Phenyl Glycosides to Concanavalin A—Loonteins *et al.* (17) have reported a study of glycosides binding to the hemagglutinin, concanavalin. Hansch and Leo have shown that MR of the substituent groups on the phenyl ring of the glycosides correlates well with the binding parameters, M_{50} (16).

$$\log M_{50} = 0.0188\,MR + 2.23$$
$$r = 0.954, s = 0.038, n = 19 \quad \text{(Eq. 8)}$$

A single connectivity index $^1\chi^v$, correlates with log M_{50} almost as well:

$$\log M_{50} = 0.181\,^1\chi^v + 2.246$$
$$r = 0.945, s = 0.041, n = 19 \quad \text{(Eq. 9)}$$

The influence of heteroatoms is directly apparent from Eq. 9 as is molecular size (Table III). A second connectivity index would certainly contain more information about influential structure; however, the quality of the data would probably not be compatible with this further refinement.

Quinoline Carboxylic Acids as Cell Respiration Inhibitors—Shah and Coats (18) have reported on a series of 7-substituted 4-hydroxyquinoline-3-carboxylic acids as cell respiration inhibitors. They reported a correlation of inhibitory potency (pI_{50}) and MR:

$$pI_{50} = 0.70MR + 2.29$$
$$r = 0.935, s = 0.318, n = 19 \quad \text{(Eq. 10)}$$

Using $^1\chi^v$ reveals a relationship:

$$pI_{50} = 0.785\,^1\chi^v + 2.82$$
$$r = 0.916, s = 0.360, n = 19 \quad \text{(Eq. 11)}$$

The results are in Table IV. The role of heteroatoms and group size is clearly encoded in the $^1\chi^v$ index.

Local Anesthetic Activity of Arylamines—In a recent study by Heymans *et al.* (19), a series of arylamines were tested for local anesthetic potency (pAD).

$$pAD = 0.497MR - 0.0028(MR)^2 - 20.02$$
$$r = 0.951, s = 0.16, n = 12 \quad \text{(Eq. 12)}$$

Using $^0\chi^v$ in a quadratic equation, we find a relationship:

$$pAD = 2.99\,^0\chi^v - 0.116(^0\chi^v)^2 - 17.5$$
$$r = 0.964, s = 0.14, n = 12 \quad \text{(Eq. 13)}$$

The equation is of sufficient quality to predict the activity of three additional compounds, as shown by the last three entries in Table V.

CONCLUSION

The interpretation of structural influence on activity from an MR *versus* activity relationship is not direct. In contrast, a connectivity index *versus* activity relationship permits a direct assessment of the important structural features influencing activity. Further, it is possible to make predictions of structures with favorable characteristics from a good χ *versus* activity equation. Finally, the use of molecular connectivity in structural quantitation makes it possible to employ more than one index, all of which have a logical and consistent derivation from structure and which guide the investigator to an interpretation of structure, meeting the objectives of the study.

This study presents new delta-values for the higher oxidation states of sulfur and phosphorus, atoms which occur on occasion in biological studies. These findings have broadened the utility of χ^v indices.

It has been shown that valence molecular connectivity indices, calculated from delta-values derived in a consistent manner, can closely reproduce molecular properties such as molar refraction. This leads to the direct correlation of biological activity with valence connectivity indices rather than attempting to relate them to molar refraction.

REFERENCES

(1) L. B. Kier and L. H. Hall, *J. Pharm. Sci.*, **65**, 1806 (1976).

(2) L. B. Kier and L. H. Hall, "Molecular Connectivity in Chemistry and Drug Research," Academic, New York, N.Y., 1976.

(3) L. B. Kier and L. H. Hall, *J. Pharm. Sci.*, **70**, 583 (1981).

(4) F. E. Norrington, R. M. Hyde, S. G. Williams, and R. Wooten, *J. Med. Chem.*, **18**, 604 (1975).

(5) L. B. Kier and L. H. Hall, *Eur. J. Med. Chem.*, **12**, 307 (1977).

(6) W. Gordy, *Phys. Rev.*, **69**, 604 (1946).

(7) A. L. Allred and E. G. Rochow, *J. Inorg. Nucl. Chem.*, **5**, 264 (1958).

(8) C. E. Sun, *J. Chinese Chem. Soc.*, **10**, 77 (1943).

(9) S. T. Li, *J. Chinese Chem. Soc.*, **10**, 167, 169 (1943).

(10) L. H. Hall and L. B. Kier, *Eur. J. Med. Chem.*, **16**, 399 (1981).

(11) L. B. Kier, *J. Pharm. Sci.*, **70**, 930 (1981).

(12) J. C. Slater, *Phys. Rev.*, **36**, 57 (1930).

(13) J. Hinze and H. H. Jaffe, *J. Am. Chem. Soc.*, **84**, 540 (1962).

(14) A. I. Vogel, *J. Chem. Soc.*, **1948**, 1833.

(15) W. J. Dunn III, *Eur. J. Med. Chem.*, **12**, 109 (1977).

(16) C. Hansch and A. Leo, "Substituent Constants for Correlation Analysis in Chemistry and Biology," Wiley, New York, N.Y., 1979.

(17) F. G. Loonteins, P. van Wauwe, R. deGussern, and C. K. deBruyne, *Carbohydr. Res.*, **30**, 51 (1973).

(18) K. J. Shah and E. A. Coats, *J. Med. Chem.*, **20**, 1001 (1977).

(19) F. Heymans, L. Le Therizen, and J. J. Godfroid, *J. Med. Chem.*, **23**, 184 (1980).

Maintenance-Dose Prediction Based on a Single Determination of Concentration: Dose of Parent Drug Required to Give a Desired Steady-State Concentration of Metabolite

JOHN M. WILSON and JOHN T. SLATTERY ˣ

Received April 16, 1982, from the *School of Pharmacy, Department of Pharmaceutics, University of Washington, Seattle, WA 98195.* Accepted for publication August 27, 1982.

Abstract □ A method for predicting the maintenance dose of parent drug required to give a desired steady-state concentration of metabolite, using a single determination of metabolite concentration in serum following the first dose of parent drug, is described. Clinical evidence that such a method is feasible for the drug–metabolite pair imipramine–desipramine has been reported. The error inherent in an estimation of maintenance dose based on a single determination of metabolite concentration is a function of sampling time and the first-order elimination rate constants for parent drug and metabolite (K and k_m, respectively). The method is applicable to drug–metabolite pairs in general by selecting the sampling time (t^*) to give minimum error: $t^* = 1/\bar{k}_m + 1.3/\bar{K}$, when $\bar{k}_m \leq \bar{K}$, and $t^* = 1/\bar{K} + 1.3/\bar{k}_m$, when $\bar{k}_m > \bar{K}$ (bars denote population mean value). The error expected to be encountered in the application of the method to specific drug–metabolite pairs can be analyzed by the graphical methods described.

Keyphrases □ Imipramine—steady-state concentration of desipramine in serum, maintenance dose, single-point prediction method, pharmacokinetics □ Desipramine—steady-state concentration in serum with imipramine administration, maintenance dose, single-point prediction method, pharmacokinetics □ Pharmacokinetics—single-point prediction method for desired steady-state concentration, maintenance dose, drug–metabolite pairs

The use of a single determination of drug concentration in serum at some time after the initial dose to predict the maintenance dose required to give a desired steady-state concentration has become quite popular since Cooper *et al.* (1, 2) first reported its use for lithium in 1973. The method has been applied to drugs with long half-lives [nortriptyline (3–5) and imipramine (6)] as well as drugs with short half-lives [chloramphenicol (7, 8) and theophylline (7, 9)]. A theoretical basis for such a relationship has been described, showing that the method is capable of giving accurate estimates of the maintenance dose needed if the sample is obtained at the appropriate time (10). The error of the method was shown to be a function of the elimination rate constant for the drug in the individual patient. It was later shown that the optimum sampling time (t^*) was equal to $1/\bar{K}$, where $\bar{K}$ is the mean value of the elimination rate constant for parent drug in the population (11).

There have been two instances in which data suggest that the single-point method can be used to predict the maintenance dose of parent drug to give a desired steady-state concentration of metabolite following administration of the parent drug: chloramphenicol following dosing with the succinate ester (7, 8) and desipramine following dosing with the parent drug imipramine (6). In the first case, the optimal sampling time for predicting the maintenance dose was found to be 6 hr, corresponding to the inverse of the mean metabolite elimination rate constant ($1/\bar{k}_m$). In the second case, that of imipramine–desipramine, no optimal sampling time was presented; a good correlation ($r = 0.92$) was noted between the logarithm of the steady-state desipramine concentration and the logarithm of the desipramine concentration obtained 24 hr after a single dose of imipramine. In the imipramine–desipramine case, $1/\bar{k}_m$ would indicate an optimal sampling time of 33 hr. Prediction on the basis of imipramine elimination would suggest a sampling time of 13 hr.

The strength of the correlation between the concentration determined in a single serum sample obtained 24 hr after the first dose and the eventual steady-state concentration of desipramine following administration of imipramine, and the demonstrated success of single-point dose prediction with chloramphenicol suggested that a theoretical framework could be developed to predict the dose of parent drug necessary to achieve a desired concentration of metabolite at steady-state. This report describes the framework and uses it to examine the error inherent in the method, under optimal conditions.

THEORETICAL

The development of an equation relating the maintenance dose of parent drug (D_m) needed to obtain a desired steady-state concentration of metabolite ($C_{ss,m}$) to the concentration of metabolite in serum (C^*_m) at time t^* after administration of an initial dose of parent drug (D^*) proceeds in much the same manner as previously described for parent drug maintenance-dose prediction (10, 11). For simplicity, the kinetics of all species are assumed to conform to linear one-compartment behavior; intravenous injection of the parent drug is also assumed. The general scheme for the elimination of drug is given in Scheme I. Under these conditions, the concentration of metabolite at a specific time after administration of the parent drug is given by:

$$C^*_m = \frac{k_f D^*}{V_m(K - k_m)}(e^{-k_m t^*} - e^{-K t^*}) \qquad \text{(Eq. 1)}$$

where V_m is the apparent volume of distribution of the metabolite and K and k_m are the elimination rate constants for parent drug and metabolite, respectively.

The average concentration of metabolite at steady state is:

$$\bar{C}_{ss,m} = \frac{k_f D_m}{K V_m k_m \tau} \qquad \text{(Eq. 2)}$$

where k_f is the formation rate constant of metabolite from parent drug

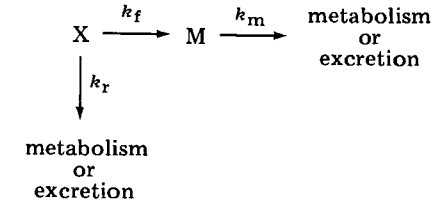

Scheme I—Model for single-point dose prediction. Key: (X) parent drug; (M) metabolite; (k) first-order rate constant; (subscript r) remainder; (subscript f) formation; (subscript m) metabolite.

0022-3549/83/1000-1174$01.00/0

and τ is the dosing interval. The ratio $\overline{C}_{ss,m}/C^*_m$ is therefore:

$$\frac{\overline{C}_{ss,m}}{C^*_m} = \frac{D_m(K - k_m)}{Kk_m\tau D^*(e^{-k_m t^*} - e^{-Kt^*})} \quad \text{(Eq. 3)}$$

The relationship between the maintenance dose and the single concentration determined after the initial dose is:

$$\frac{1}{D_m} = \left[\frac{K - k_m}{\overline{C}_{ss,m}D^*\tau Kk_m(e^{-k_m t^*} - e^{-Kt^*})}\right] C^*_m \quad \text{(Eq. 4)}$$

The term in brackets can be represented by a proportionality factor, Ψ_m:

$$\frac{1}{D_m} = \Psi_m C^*_m \quad \text{(Eq. 5)}$$

where:

$$\Psi_m = \frac{K - k_m}{\overline{C}_{ss,m}D^*\tau Kk_m(e^{-k_m t^*} - e^{-Kt^*})} \quad \text{(Eq. 6)}$$

It should be realized that Ψ_m varies among individuals only as a function of K and k_m; $\overline{C}_{ss,m}$, D^*, t^*, and τ are chosen and held constant for all individuals. The proportionality factor, Ψ_m, is independent of the fraction of dose metabolized to the metabolite of interest (or to other metabolites) and the formation rate constant of the metabolite. The rate constants K and k_m might be more appropriately written as the ratio of clearance to volume of distribution, but the rate constants are written because clearance and volume of distribution do not appear in Ψ_m except as the ratio, K or k_m. This has been addressed in greater detail in the case of single-point parent drug maintenance-dose prediction (11). Since the maintenance dose is determined for an average steady-state concentration, it can be varied if the dosing rate (D_m/τ) is kept constant.

When $K \gg k_m$, as in the case of a prodrug, Ψ_m as defined in Eq. 6 reduces to:

$$\Psi_{m,K\gg km} = \frac{e^{k_m t^*}}{\overline{C}_{ss,m}D^*\tau k_m} \quad \text{(Eq. 7)}$$

which more appropriately defines the proportionality factor Ψ previously described for the metabolite chloramphenicol of the prodrug chloramphenicol succinate. When parameter values are substituted, $\Psi_m = \Psi$ as previously defined (10). It is also of interest to note the definition of Ψ_m at the opposite extreme, namely where $k_m \gg K$:

$$\Psi_{m,km\gg K} = \frac{e^{Kt^*}}{\overline{C}_{ss,m}D^*\tau K} \quad \text{(Eq. 8)}$$

As described previously for parent drug (10), Eq. 5 will serve to predict accurate values of D_m when Ψ_m remains reasonably constant throughout the population. Thus, t^* must be chosen in such a manner to result in minimum variability of Ψ_m as a function of K and k_m. This, by definition, will be the optimum value of t^*. When the sample is obtained at the optimum t^*, a population average value of Ψ_m will have the best chance of working for maintenance-dose prediction purposes.

Figure 1 shows how t^* can be chosen such that Ψ_m is kept reasonably constant as K and k_m vary through the population. Ranges of K and k_m approximate population values for imipramine–desipramine (6). In this figure $\Psi_m/\overline{\Psi}_m$ is plotted to allow direct comparison between the plots. $\overline{\Psi}_m$ is the average value of Ψ_m throughout the population. Also, the lowest values of the axes are at the far right corner in each plot; this departure from convention is made to afford the clearest view of the surface. Among the three values of t^* examined the optimum value of t^* (to the nearest hour) is 48 hr (Fig. 1b) where the plot of $\Psi_m/\overline{\Psi}_m$ is relatively flat compared to t^* = 36 hr (Fig. 1a) and t^* = 60 hr (Fig. 1c). In this case, the maximum error is an ~25% overprediction of dose at low values of k_m in combination with low values of K.

Figure 1 also shows that the greatest error of the method is encountered at the extremes of the values of K and k_m[1]. As the range of values considered here is exceeded, the error will increase (see below). However, if a Gaussian distribution of these rate constants is assumed, it is evident that a very small fraction of the population will be represented by these extreme values. Thus, the method can be expected to work well for a very large majority of the population.

Optimization of Sampling Time—The optimum time for obtaining the sample for maintenance-dose prediction can be determined by constructing plots such as those in Fig. 1 and selecting as t^* the sampling time

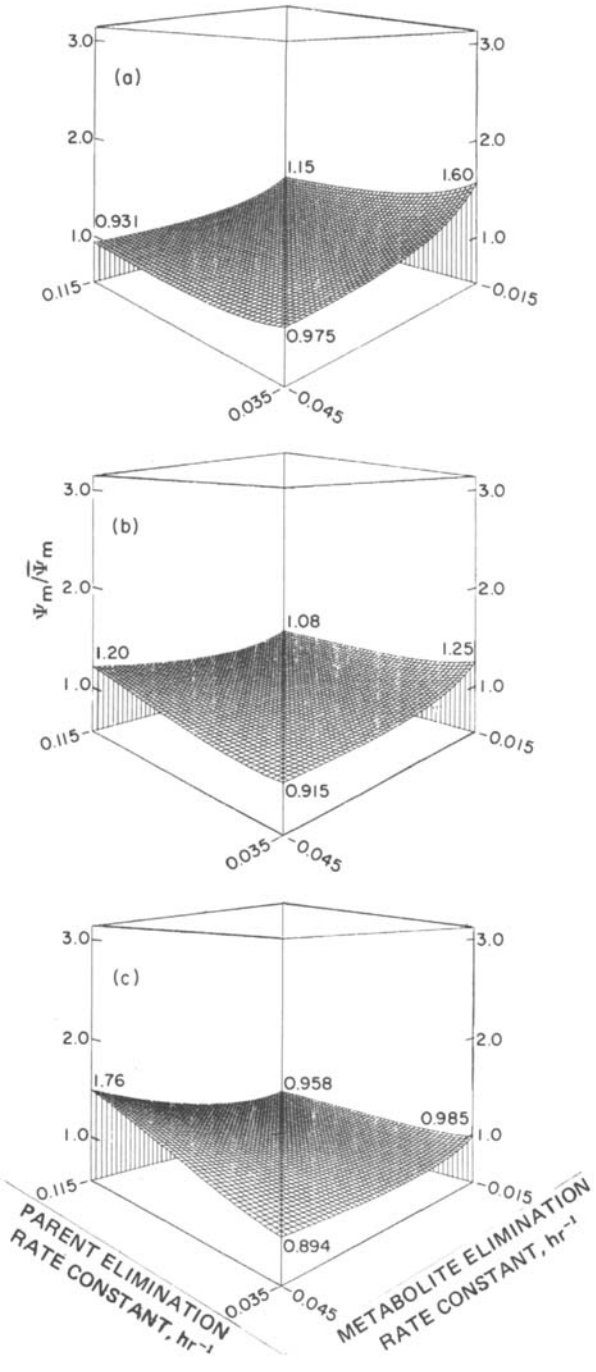

Figure 1—*Relationships between $\Psi_m/\overline{\Psi}_m$ and the elimination rate constants for metabolite (k_m) and parent drug (K) for the parent drug–metabolite pair imipramine–desipramine at t* = 36 (a), 48 (b), and 60 hr (c). The optimum value of t*, 48 hr, gives the most nearly planar surface. The lowest values of all axes appear at the far right corner of each figure.*

which gives the least variability in $\Psi_m/\overline{\Psi}_m$ as a function of K and k_m. This is rather cumbersome and time consuming because of the need for accurate three-dimensional plotting capability.

The problem can be simplified to two dimensions. Ψ_m is a ratio, and the variables K and k_m appear in both the numerator and denominator. For Ψ_m to be constant throughout a population, the numerator and denominator must change in proportion to one another since K and k_m assume different values from one individual to another. A plot of the numerator of Ψ_m (Eq. 6) *versus* its denominator should be as nearly linear as possible at the optimum choice of t^*. Since the value of Ψ_m varies among individuals as a function of K and k_m only, $D^*\tau\overline{C}_{ss,m}$ can be assigned a value of 1 for the purpose of sampling time optimization.

Figure 2 shows such plots for the case of imipramine–desipramine.

[1] In Fig. 1, error is reflected by the degree of curvature of the surface. If there was no inherent error, every individual would have the same value of Ψ_m and $\Psi_m/\overline{\Psi}_m$ would equal 1 at all combinations of K and k_m. As the surface becomes more curved, error increases.

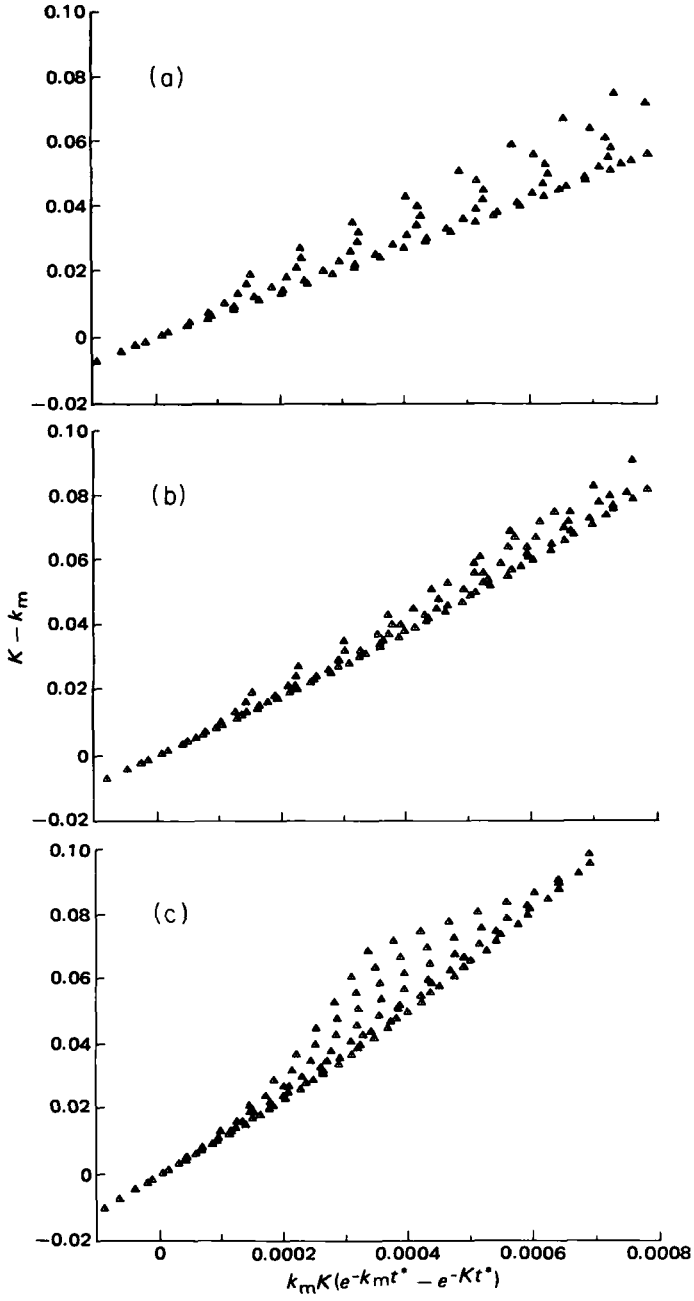

Figure 2—*Plots of the numerator of Eq. 6* versus *the denominator for the parent drug–metabolite pair imipramine–desipramine at* t* = *36 (a), 48 (b), and 60 hr (c). The optimum value of* t* *has the minimum scatter of points, which can be judged numerically as described in the text. This plot represents an alternative optimization method to Fig. 1.*

Points are chosen in this plot by selecting values of K and k_m in nested loops at fixed intervals; plots a, b, and c in Fig. 2 correspond to the respective three-dimensional plots in Fig. 1. The plots in Fig. 2 take the form of scatter plots because of the complex nature of the variability of the numerator and denominator of Ψ_m as a function of K and k_m. Figure 2 shows minimum scatter for $t^* = 48$ hr (Fig. 2b); more scatter is evident for $t^* = 36$ and 60 hr in Fig. 2a and c, respectively. Thus, the outcome of optimization schemes shown in Figs. 1 and 2 is the same.

It is not necessary to rely on a visual comparison of plots to select optimum values of t^* for a given set of values of K and k_m. Since a plot of the numerator of Eq. 6 *versus* the denominator will have a slope equal to Ψ_m, the optimum t^* will result in minimum scatter about a regression line. Measures of relative goodness of fit can therefore be used for optimization purposes. This method has been used for the case of imipramine–desipramine, and 48 hr was again obtained for the optimum value of t^*. Agreement was verified to an accuracy of 1 hr. The coefficients of

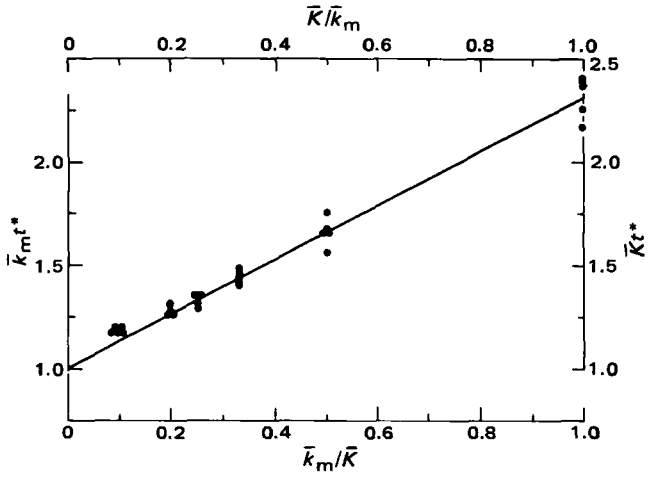

Figure 3—*Relationship between optimum* t* *and the ratio of mean elimination rate constant values. If* $\bar{K} > \bar{k}_m$, *read* $\bar{k}_m$t* *from the left axis from the point on the line corresponding to the appropriate value of the ratio* $\bar{k}_m/\bar{K}$; *if* $\bar{k}_m > \bar{K}$, *read* $\bar{K}$t* *corresponding to the value of the ratio* $\bar{K}/\bar{k}_m$ *from the axis on the right. Equation of line:* $y = 1 + 1.3x$.

variation of the slopes of the plots in Fig. 2 (as %) are 24.7, 12.7, and 22.2 for $t^* = 36$, 48, and 60 hr, respectively.

In the case of maintenance-dose prediction for the parent drug, it was possible to arrive at a simple calculation for the optimum value of t^*; *i.e.*, $t^* = 1/K$ where K is the population mean elimination rate constant for the parent drug. The case of maintenance dose of parent drug to give a desired metabolite concentration at steady state is analytically somewhat more complex. However, using either of the techniques described above, a general solution can be obtained.

In the course of these investigations, we determined the optimum value of t^* for a number of combinations of K and $\bar{k}_m$ (bars denote mean). It was apparent that as the ratio of $\bar{k}_m/K$ increased, the optimum value of t^* increased. Previous experience indicated that a plot of optimum t^* as a function of the ratio $\bar{k}_m/K$ would not be linear and its slope at any point would be a function of the absolute values of $\bar{k}_m$ and K. We therefore constructed a plot of $\bar{k}_m t^*$ as a function of the ratio $\bar{k}_m/K$ and found it to be linear and to serve for predictive purposes whenever $K \geq \bar{k}_m$. A plot of this empirical relationship is shown in Fig. 3. The points in the plot represent the results of optimizations using the technique described above for various ranges of K and k_m. In this figure, t^* could be calculated by reading the value of $\bar{k}_m t^*$ of the left vertical axis for a given value of $\bar{k}_m/K$ when $K \geq k_m$. Conversely, when $k_m > K$, $\bar{K}t^*$ can be read off the plot corresponding to a given value of $\bar{K}/\bar{k}_m$. Thus, given the population mean value of K and k_m, the optimum value of t^* can be estimated from the regression coefficients of Fig. 3. For $\bar{K} \geq \bar{k}_m$:

$$\bar{k}_m t^* = 1 + 1.3\bar{k}_m/\bar{K} \qquad \text{(Eq. 9)}$$

or

$$t^* = \frac{1}{\bar{k}_m} + \frac{1.3}{\bar{K}} \qquad \text{(Eq. 10)}$$

and when $\bar{k}_m > \bar{K}$:

$$\bar{K}t^* = 1 + 1.3\bar{K}/\bar{k}_m \qquad \text{(Eq. 11)}$$

or

$$t^* = \frac{1}{\bar{K}} + \frac{1.3}{\bar{k}_m} \qquad \text{(Eq. 12)}$$

In the case of a prodrug, $K \gg k_m$ and Eq. 9 becomes $t^* \simeq 1/\bar{k}_m$, which is the clinical observation with chloramphenicol when the prodrug, chloramphenicol succinate, is given (8).

The slope of the line in Fig. 3 varies slightly with the range of rate constant values encountered for a particular drug–metabolite pair; *i.e.*, the optimum value of t^* is slightly affected by the range of K and k_m encountered. Figure 4, where $\bar{k}_m/\bar{K} = 0.5$, shows this effect. t^* (44 hr) is optimized for a fourfold variability in K and k_m and is 4 hr too long for a threefold range and 1 hr too early for a fivefold range. Such an effect has been noted by others when considering t^* in the case of parent drug (12). In Figure 5, where $\bar{k}_m/\bar{K} = 0.1$, this effect is not evident. Thus, use of Fig. 3 or Eqs. 9–12 gives an approximate value for optimum t^*; other

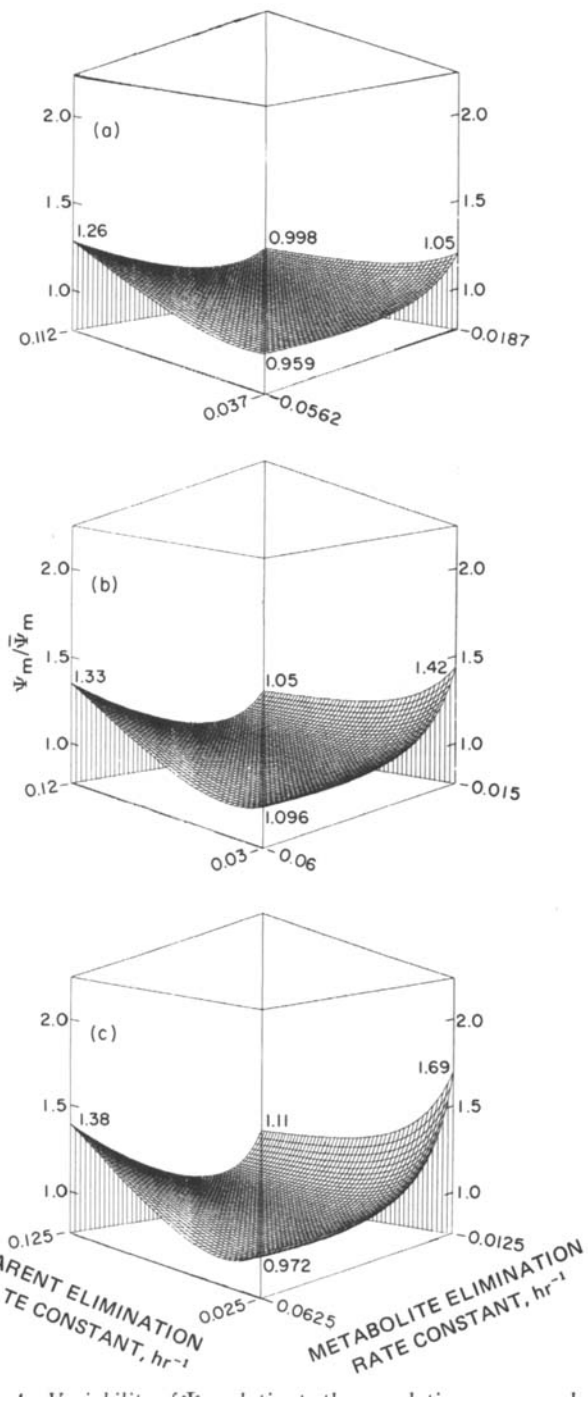

Figure 4—*Variability of Ψ_m relative to the population average value, $\bar{\Psi}_m$, as the range of* K *and* k_m *increases, $\bar{k}_m/\bar{K}$ = 0.5. Range of rate constant values for* k_m *and* K*: (a) threefold; (b) fourfold; (c) fivefold. The lowest values of all axes appear at the far right corner of each figure.*

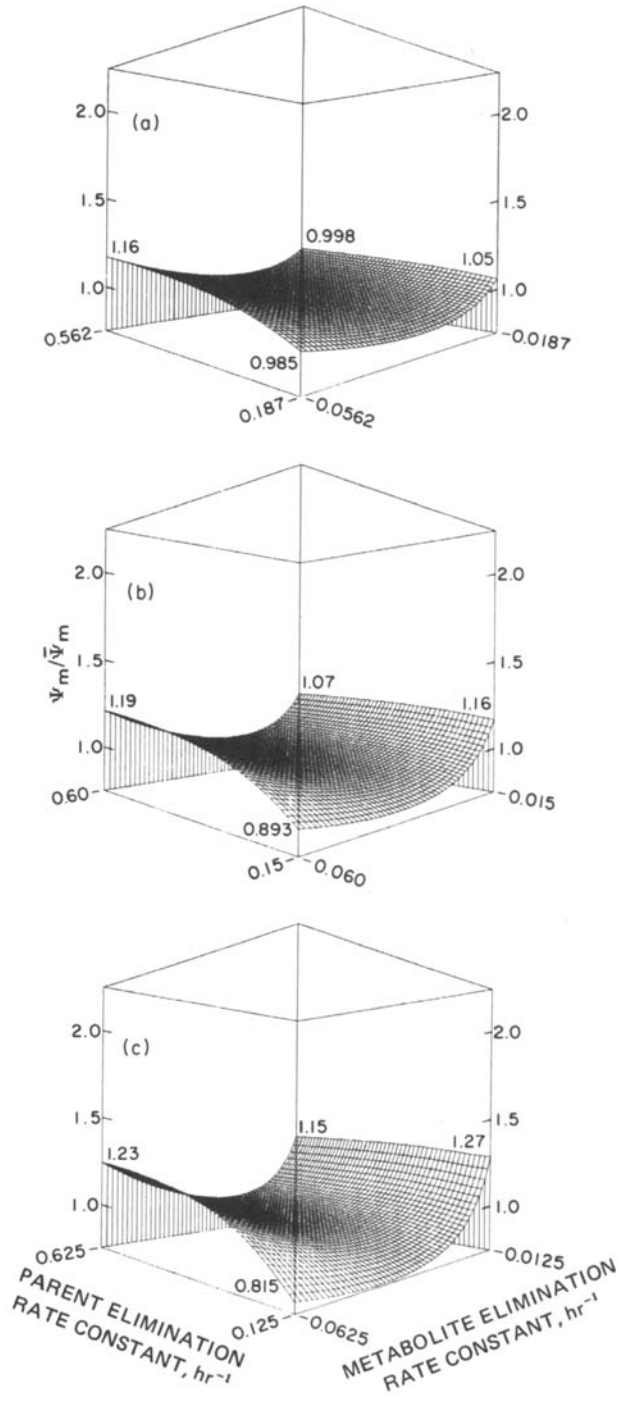

Figure 5—*Variability of Ψ_m relative to the population average value, $\bar{\Psi}_m$, as the range of* K *and* k_m *increases, $\bar{k}_m/\bar{K}$ = 0.1. Range of rate constant values for* k_m *and* K*: (a) threefold; (b) fourfold; (c) fivefold. The lowest values of all axes appear at the far right corner of each figure.*

methods would give more accurate results. Figure 3 and Eqs. 9–12 will give a quick indication as to the possibility of choosing a clinically convenient or feasible sampling time for a particular drug–metabolite pair.

Analysis of Error—Although the optimum value of t^* can be read directly from Fig. 3 or calculated from Eqs. 9–12, that information does not give any insight into the *error* of the method. A direct indication of the magnitude and source of inherent error is obtained from the three-dimensional plots of the type used for optimization in Fig. 1.

These plots for arbitrary cases are presented in Figs. 4 and 5 for cases with $\bar{k}_m/\bar{K}$ = 0.5 and $\bar{k}_m/\bar{K}$ = 0.1, respectively. Actual values of the rate constants cover ranges of three-, four-, and fivefold, respectively, in plots a, b, and c of both figures. Error is greatest as the extreme values of K and k_m are approached in Fig. 4, where the ranges of the two elimination rate constants overlap. Accordingly, as the range is increased, the maximum error increases from 27% at threefold to 69% at fivefold. These errors would result in an overprediction of maintenance dose of the same magnitude.

In Fig. 5 ($\bar{k}_m/\bar{K}$ = 0.1), the ranges of K and k_m do not overlap and at large values of K, the error in maintenance-dose prediction is a function of k_m only and independent of K, as required by Eq. 7. As in Fig. 4, error increases as the range of K and k_m increases, but as the ratio of $\bar{k}_m/\bar{K}$ decreases, the error of the method decreases and is less sensitive to increases in the range of elimination rate constant values.

Neither of these figures gives an indication of the role of the distribution of values of the elimination rate constants in the population. If the

distribution was assumed to be Gaussian, a small fraction of the population would be represented by the values of elimination rate constants at the extreme of the range. Very few individuals would be subjected to the maximum error of the method. Figs. 4 and 5 represent error patterns of specific cases for certain values of K and k_m; they have not been constructed to represent general cases. For any given case, similar plots should be constructed to evaluate error.

DISCUSSION

The optimum sampling time for determining the maintenance dose of parent drug required to give a desired steady-state concentration of metabolite for the drug–metabolite pair imipramine–desipramine indicated by this analysis is 48 hr. A linear relationship between the log of the 24-hr concentration of desipramine following the first dose of imipramine and the log of the eventual steady-state concentration of the drug, if the same dose is kept constant and administered daily, has been found clinically (6). The mathematical basis for relating these two concentrations arises from a rearrangement of Eq. 6 that gives rise to a proportionality factor with the general behavior of Ψ_m (10). The results of the present analysis suggest that the relationship between concentration at 24 hr and eventual steady-state concentration would be curvilinear. A log–log transformation might linearize such a plot. It is expected that a sample collected 48 hr after the first dose would appear to be linearly related to the eventual steady-state concentration.

There are two critical considerations in applying this method to any drug–metabolite pair: (*a*) the error which will be encountered as a function of the elimination kinetics of the pair and (*b*) the possibility that the elimination kinetics may dictate a value of t^* that is not clinically feasible. The variability of Ψ_m is a function of the elimination kinetics of the pair in the population and cannot be overcome when single-point prediction schemes are used. Thus, a poor estimate of maintenance dose will always be obtained for some fraction of the population. When the optimum value of t^* is not used because it is too short to be clinically convenient and a longer time is adopted, the error of the method increases but in a somewhat conservative manner. Patients who eliminate the drug and metabolite slowly will tend to be underdosed and those who eliminate the drug quickly (requiring a relatively larger maintenance dose) tend to be overdosed. This situation is perhaps more tolerable than the converse: when a t^* shorter than the optimum is adopted, patients who eliminate the drug most slowly will tend to be overdosed and those who eliminate it more quickly will tend to be underdosed. Another observation may be more to the point: when the optimum value of t^* is not used, the relationship between $1/D_m$ and C^*_m will become less well-characterized by a straight line. If the curvilinear nature of the relationship can be taken into account, reasonably accurate dose prediction may still be possible.

Single-point dose prediction methods appear to be applicable to most drugs and their metabolites. However, the optimum sampling time for the dose required to give a desired steady-state concentration of the parent drug may be quite different than that required to give a target metabolite concentration. If dosage prediction is warranted for a particular drug (10) and the kinetics of the drug are linear, it appears likely that a single-point method could be developed to suit using the techniques described here. However, it must be remembered that the predicted dose is an estimate that must be confirmed by obtaining samples at steady state.

REFERENCES

(1) T. B. Cooper, P. E. E. Bergner, and G. M. Simpson, *Am. J. Psychol.*, **130**, 601 (1973).

(2) T. B. Cooper and G. M. Simpson, *Am. J. Psychol.*, **133**, 440 (1976).

(3) T. B. Cooper and G. M. Simpson, *Am. J. Psychol.*, **135**, 333 (1978).

(4) R. Braithwaite, S. Montgomery, and S. Dawling, *Clin. Pharmacol. Ther.*, **23**, 303 (1978).

(5) S. A. Montgomery, A. McAuley, D. B. Montgomery, R. A. Braithwaite, and D. S. Dawling, *Clin. Pharmacokinet.*, **4**, 129 (1979).

(6) D. J. Brunswick, J. D. Amsterdam, N. Mendels, and S. L. Stern, *Clin. Pharmacol. Ther.*, **25**, 605 (1979).

(7) J. R. Koup, C. M. Sack, A. L. Smith, and M. Gibaldi, *Clin. Pharmacokinet.*, **4**, 460 (1979).

(8) J. R. Koup, C. M. Sack, A. L. Smith, N. N. Neely, and M. Gibaldi, *Clin. Pharmacokinet.*, **6**, 83 (1981).

(9) G. Shapiro, J. R. Koup, C. T. Furukawa, W. E. Pierson, and M. Gibaldi, *Pediatrics*, **69**, 70 (1982).

(10) J. T. Slattery, M. Gibaldi, and J. R. Koup, *Clin. Pharmacokinet.*, **5**, 377 (1980).

(11) J. T. Slattery, *J. Pharm. Sci.*, **70**, 1174 (1981).

(12) J. D. Unadkat and M. Rowland, *Ther. Drug Monit.*, **4**, 201 (1982).

ACKNOWLEDGMENTS

This work was supported in part by National Institutes of Health Predoctoral Training Grant GM 07750 (J.M.W.).

Bayesian Approach to Bioequivalence Assessment: An Example

H. FLUEHLER *x, A. P. GRIEVE *, D. MANDALLAZ ‡, J. MAU §, and H. A. MOSER *

Received February 22, 1982, from the **Scientific Computing Centre, CIBA-GEIGY AG, Basel, Switzerland;* ‡*Essex Chemie AG, Luzern, Switzerland;* and §*Rheinisch-Westfälische TH, Aachen, West Germany.* Accepted for publication August 26, 1982.

Abstract □ The statistical methods required for a Bayesian analysis of bioequivalence are outlined and numerically illustrated. The analysis consists of the calculation of the posterior probability, given the experimental results, that the ratio of true means of a new and a standard formulation of a drug with respect to some biological response lies in a given interval. Nomograms helpful for the calculation of these probabilities are provided.

Keyphrases □ Bioequivalence—assessment by Bayesian analysis, statistical methods, example and nomograms □ Bayesian analysis—bioequivalence assessment, statistical methods, example, and nomograms

Comparative bioavailability studies serve to investigate the pharmaceutical properties of two or more formulations of the same drug. Decisions on whether two formulations are bioequivalent are usually made by comparing biological responses such as area under the plasma concentration curve or the maximum peak concentration. Since in many instances the objective of a bioavailability study is not to show a difference between formulations, but rather to investigate whether any difference is of practical importance, Westlake (1) and Metzler (2) suggest that hypothesis tests of no difference are of little value.

In this paper the statistical methods needed to perform a Bayesian analysis of bioequivalence given by Mandallaz and Mau (3) are outlined. This method has been illustrated

0022-3549/83/1000-1178$01.00/0

distribution was assumed to be Gaussian, a small fraction of the population would be represented by the values of elimination rate constants at the extreme of the range. Very few individuals would be subjected to the maximum error of the method. Figs. 4 and 5 represent error patterns of specific cases for certain values of K and k_m; they have not been constructed to represent general cases. For any given case, similar plots should be constructed to evaluate error.

DISCUSSION

The optimum sampling time for determining the maintenance dose of parent drug required to give a desired steady-state concentration of metabolite for the drug–metabolite pair imipramine–desipramine indicated by this analysis is 48 hr. A linear relationship between the log of the 24-hr concentration of desipramine following the first dose of imipramine and the log of the eventual steady-state concentration of the drug, if the same dose is kept constant and administered daily, has been found clinically (6). The mathematical basis for relating these two concentrations arises from a rearrangement of Eq. 6 that gives rise to a proportionality factor with the general behavior of Ψ_m (10). The results of the present analysis suggest that the relationship between concentration at 24 hr and eventual steady-state concentration would be curvilinear. A log–log transformation might linearize such a plot. It is expected that a sample collected 48 hr after the first dose would appear to be linearly related to the eventual steady-state concentration.

There are two critical considerations in applying this method to any drug–metabolite pair: (*a*) the error which will be encountered as a function of the elimination kinetics of the pair and (*b*) the possibility that the elimination kinetics may dictate a value of t^* that is not clinically feasible. The variability of Ψ_m is a function of the elimination kinetics of the pair in the population and cannot be overcome when single-point prediction schemes are used. Thus, a poor estimate of maintenance dose will always be obtained for some fraction of the population. When the optimum value of t^* is not used because it is too short to be clinically convenient and a longer time is adopted, the error of the method increases but in a somewhat conservative manner. Patients who eliminate the drug and metabolite slowly will tend to be underdosed and those who eliminate the drug quickly (requiring a relatively larger maintenance dose) tend to be overdosed. This situation is perhaps more tolerable than the converse: when a t^* shorter than the optimum is adopted, patients who eliminate the drug most slowly will tend to be overdosed and those who eliminate it more quickly will tend to be underdosed. Another observation may be more to the point: when the optimum value of t^* is not used, the relationship between $1/D_m$ and C^*_m will become less well-characterized by a straight line. If the curvilinear nature of the relationship can be taken into account, reasonably accurate dose prediction may still be possible.

Single-point dose prediction methods appear to be applicable to most drugs and their metabolites. However, the optimum sampling time for the dose required to give a desired steady-state concentration of the parent drug may be quite different than that required to give a target metabolite concentration. If dosage prediction is warranted for a particular drug (10) and the kinetics of the drug are linear, it appears likely that a single-point method could be developed to suit using the techniques described here. However, it must be remembered that the predicted dose is an estimate that must be confirmed by obtaining samples at steady state.

REFERENCES

(1) T. B. Cooper, P. E. E. Bergner, and G. M. Simpson, *Am. J. Psychol.*, **130**, 601 (1973).

(2) T. B. Cooper and G. M. Simpson, *Am. J. Psychol.*, **133**, 440 (1976).

(3) T. B. Cooper and G. M. Simpson, *Am. J. Psychol.*, **135**, 333 (1978).

(4) R. Braithwaite, S. Montgomery, and S. Dawling, *Clin. Pharmacol. Ther.*, **23**, 303 (1978).

(5) S. A. Montgomery, A. McAuley, D. B. Montgomery, R. A. Braithwaite, and D. S. Dawling, *Clin. Pharmacokinet.*, **4**, 129 (1979).

(6) D. J. Brunswick, J. D. Amsterdam, N. Mendels, and S. L. Stern, *Clin. Pharmacol. Ther.*, **25**, 605 (1979).

(7) J. R. Koup, C. M. Sack, A. L. Smith, and M. Gibaldi, *Clin. Pharmacokinet.*, **4**, 460 (1979).

(8) J. R. Koup, C. M. Sack, A. L. Smith, N. N. Neely, and M. Gibaldi, *Clin. Pharmacokinet.*, **6**, 83 (1981).

(9) G. Shapiro, J. R. Koup, C. T. Furukawa, W. E. Pierson, and M. Gibaldi, *Pediatrics*, **69**, 70 (1982).

(10) J. T. Slattery, M. Gibaldi, and J. R. Koup, *Clin. Pharmacokinet.*, **5**, 377 (1980).

(11) J. T. Slattery, *J. Pharm. Sci.*, **70**, 1174 (1981).

(12) J. D. Unadkat and M. Rowland, *Ther. Drug Monit.*, **4**, 201 (1982).

ACKNOWLEDGMENTS

This work was supported in part by National Institutes of Health Predoctoral Training Grant GM 07750 (J.M.W.).

Bayesian Approach to Bioequivalence Assessment: An Example

H. FLUEHLER *x, A. P. GRIEVE *, D. MANDALLAZ ‡, J. MAU §, and H. A. MOSER *

Received February 22, 1982, from the **Scientific Computing Centre, CIBA-GEIGY AG, Basel, Switzerland;* ‡*Essex Chemie AG, Luzern, Switzerland;* and §*Rheinisch-Westfälische TH, Aachen, West Germany.* Accepted for publication August 26, 1982.

Abstract □ The statistical methods required for a Bayesian analysis of bioequivalence are outlined and numerically illustrated. The analysis consists of the calculation of the posterior probability, given the experimental results, that the ratio of true means of a new and a standard formulation of a drug with respect to some biological response lies in a given interval. Nomograms helpful for the calculation of these probabilities are provided.

Keyphrases □ Bioequivalence—assessment by Bayesian analysis, statistical methods, example and nomograms □ Bayesian analysis—bioequivalence assessment, statistical methods, example, and nomograms

Comparative bioavailability studies serve to investigate the pharmaceutical properties of two or more formulations of the same drug. Decisions on whether two formulations are bioequivalent are usually made by comparing biological responses such as area under the plasma concentration curve or the maximum peak concentration. Since in many instances the objective of a bioavailability study is not to show a difference between formulations, but rather to investigate whether any difference is of practical importance, Westlake (1) and Metzler (2) suggest that hypothesis tests of no difference are of little value.

In this paper the statistical methods needed to perform a Bayesian analysis of bioequivalence given by Mandallaz and Mau (3) are outlined. This method has been illustrated

0022-3549/83/1000-1178$01.00/0

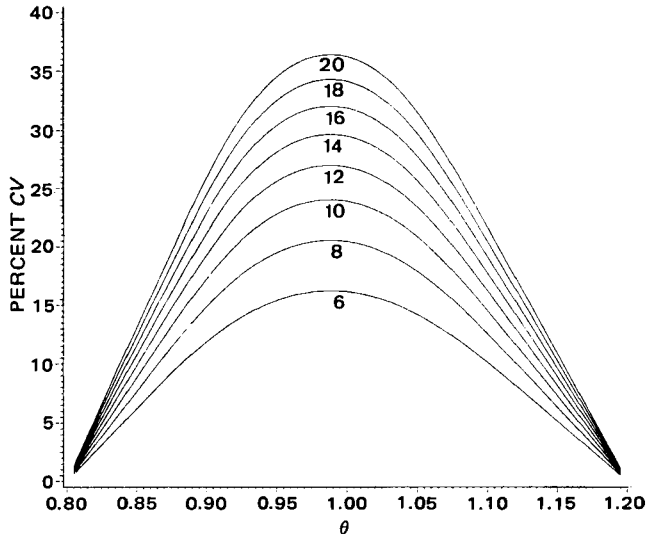

Figure 1—*Values of observed ratios and percent* CV *giving a posterior probability of 0.90 that the true ratio lies between 0.8 and 1.2 for various values of* n.

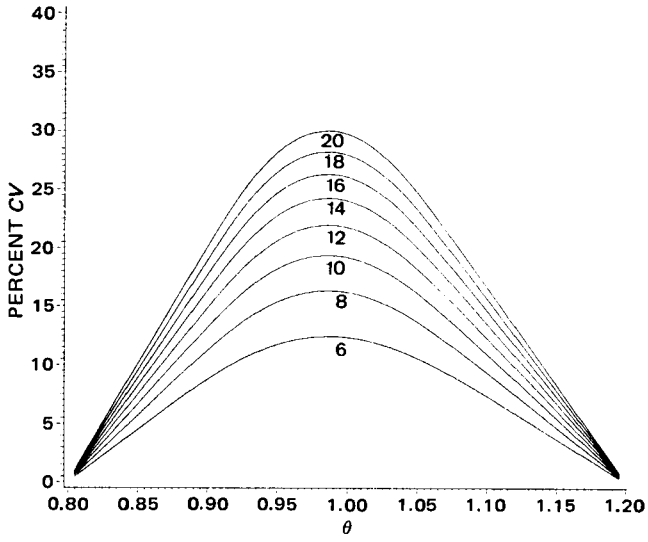

Figure 2—*Values of observed ratios and percent* CV *giving a posterior probability of 0.95 that the true ratio lies between 0.8 and 1.2 for various values of* n.

by Fluehler *et al.* (4) using historical data. The numerical calculations required are illustrated by an example. Readers interested in a general introduction to statistical considerations involved in bioequivalence assessment are referred to Metzler (2) or Westlake (1). An alternative Bayesian approach has been developed by Selwyn *et al.* (5).

THEORETICAL

It is assumed that a new formulation of a drug has been developed and that it is to be compared with the standard formulation of the drug. The comparison will focus on the area under the blood concentration curve (AUC) and the maximum concentration of that curve (C_{max}). If the ratio, θ, of the true means of the new to the standard formulation of the chosen measure (AUC or C_{max}) lies between given limits r_1 and r_2, that is:

$$r_1 \leq \theta \leq r_2 \qquad \text{(Eq. 1)}$$

then the formulations are said to be bioequivalent. The choice of r_1 and r_2 is made on medical and/or regulatory grounds. Thus, for AUC, one might set $r_1 = 0.8$ and $r_2 = 1.2$, which correspond to the AUC of the new formulation differing by at most ±20% from that of the standard formulation. It should be noted that r_1 and r_2 need not be the same for AUC and C_{max} and in general they need not be symmetric about 1.

To provide evidence for or against the bioequivalence statement given in Eq. 1, estimates of the true means of either AUC or C_{max} for both formulations and an estimate of their variance are needed. Because of the large intersubject variation with respect to the absorption, distribution, and elimination of a drug, the crossover design is usually considered the most appropriate for comparative bioavailability studies. In such a design each of n subjects receives each formulation with a sufficiently large time lag to ensure an adequate washout period. The statistical model for a two-way crossover design is:

$$x_{ijk} = \mu + \xi_i + \pi_j + \phi_k + \epsilon_{ijk} \qquad \text{(Eq. 2)}$$

where x_{ijk} are the observed values, μ is the overall mean, ξ_i is the ith subject effect ($i = 1, \ldots, n$), π_j is the jth period effect ($j = 1, 2$), ϕ_k is the kth formulation effect ($k = 1, 2$), and ϵ_{ijk} are experimental errors associated with the x_{ijk} values, which are assumed to be independently normally distributed with zero means and common variance σ^2.

The AUC values are assumed to be normally distributed according to the model in Eq. 2. The C_{max} values, however, are assumed to be log-normally distributed so that $\ln(C_{max})$, instead of C_{max}, obeys the aforementioned model. The analysis of variance (ANOVA) for the crossover design is outlined in basic statistical texts, *e.g.*, Cochran and Cox (6). The error mean square from the ANOVA gives an estimate of the experimental error variance.

A Bayesian approach (3, 4) is used to investigate bioavailability defined in Eq. 1. In this approach the posterior distribution of θ given the experimental results is obtained, from which the posterior probability that θ lies between r_1 and r_2 is calculated; if this probability is large enough, bioequivalence is accepted. The advantage of a Bayesian approach is that the whole distribution of θ may be examined either through the posterior distribution itself or by calculating the cumulative distribution function.

The posterior probability that θ lies between r_1 and r_2 is calculated by:

$$Pr(r_1 \leq \theta \leq r_2) = \int_B^A t_\nu(\tau)d\tau \qquad \text{(Eq. 3)}$$

where $t_\nu(\tau)$ is the density function of Student's t distribution with ν degrees of freedom (DF) and ν is the number of DF of the error mean square (MSQ) from the ANOVA. The integration limits for AUC, normally distributed data, are given by:

$$A = \frac{(\hat{\theta} - r_1)n^{1/2}}{CV(1 + r_1^2)^{1/2}} \qquad \text{(Eq. 4)}$$

$$B = \frac{(\hat{\theta} - r_2)n^{1/2}}{CV(1 + r_2^2)^{1/2}} \qquad \text{(Eq. 5)}$$

with

$$\hat{\theta} = \frac{\bar{X}_{NEW}}{\bar{X}_{STD}} \qquad \text{(Eq. 6)}$$

$$CV = \frac{S}{\bar{X}_{STD}} \qquad \text{(Eq. 7)}$$

$$S = \sqrt{\text{Error (MSQ) from ANOVA}} \qquad \text{(Eq. 8)}$$

$\bar{X}_{NEW}$ and $\bar{X}_{STD}$ are the observed arithmetic formulation means; n is the number of subjects. The integration limits for C_{max}, log-normally distributed data, are given by:

$$A = \frac{[\bar{X}_{NEW} - \bar{X}_{STD} - \ln(r_1)]n^{1/2}}{2^{1/2}S} \qquad \text{(Eq. 9)}$$

$$B = \frac{[\bar{X}_{NEW} - \bar{X}_{STD} - \ln(r_2)]n^{1/2}}{2^{1/2}S} \qquad \text{(Eq. 10)}$$

where now $\bar{X}_{NEW}$ and $\bar{X}_{STD}$ denote the observed arithmetic means of the log-transformed C_{max} values. The cumulative posterior distribution function $Pr(\theta < \theta_0)$, is calculated by setting $r_1 = 0$ and $r_2 = \theta_0$ in Eq. 3.

Alternative methods of displaying information from the posterior distribution are available. Fluehler *et al.* (4) show how Eq. 3 may be used to display posterior probabilities of given intervals in histogram form, while the posterior density function itself may be calculated from the results of Mandallaz and Mau (3).

Although the calculation of the posterior probabilities are straightforward, the nomograms shown in Figs. 1 and 2 are useful tools for the practitioner using the normal model (Eqs. 3–8). In these nomograms the bioequivalence range was chosen to be 0.8–1.2, although nomograms for

Table I—Comparative Bioavailability Study

Number of Subjects	Standard Formulation				New Formulation			
	Period	AUC	C_{max}	$\ln(C_{max})$	Period	AUC	C_{max}	$\ln(C_{max})$
1	2	144.57	296.11	5.6907	1	115.21	67.97	4.2190
2	1	98.17	146.69	4.9883	2	106.60	92.63	4.5286
3	1	121.87	259.37	5.5583	2	129.70	97.75	4.5824
4	2	30.20	197.36	5.2850	1	52.85	196.53	5.2808
5	2	131.51	281.37	5.6397	1	59.42	59.71	4.0895
6	1	104.17	179.14	5.1882	2	152.76	54.99	4.0072
7	1	71.54	251.37	5.5269	2	31.24	93.11	4.5337
8	2	71.98	233.29	5.4523	1	108.22	109.26	4.6938
9	2	78.83	173.61	5.1568	1	82.05	152.18	5.0251
10	1	140.48	227.56	5.4274	2	101.10	177.09	5.1767
11	2	75.27	211.85	5.3559	1	58.72	100.70	4.6121
12	1	111.56	225.71	5.4192	2	83.27	172.22	5.1488
Mean	—	98.35	223.62	5.3907	—	90.10	114.51	4.6581

Table II—ANOVA for the Observed AUC

Source	*DF*	SSQ	MSQ
Subject	11	19570.1	1779.1
Period	1	6.8	6.8
Formulation	1	408.4	408.4
Error	10	6904.2	690.4
Total	23	26889.5	—

Table III—ANOVA for the Observed $\ln(C_{max})$

Source	*DF*	SSQ	MSQ
Subject	11	1.0101	0.0918
Period	1	0.0117	0.0117
Formulation	1	3.2201	3.2201
Error	10	1.4661	0.1466
Total	23	5.7079	—

other ranges and for the log-normal model can be produced. The nomograms give the sample sizes required to achieve posterior probabilities of 0.90 and 0.95 as a function of the observed ratio and percentage coefficient of variation ($100 \times CV$). For instance, suppose an experiment with 12 subjects was carried out and an observed ratio of 1.1 with an observed coefficient of variation of 15% was obtained. From Fig. 2 it is seen that, with this data, a sample size of between 16 and 18 is necessary to achieve a posterior probability of 0.95. However Fig. 1 shows that 12 subjects yield, with the same data, a posterior probability >0.90.

RESULTS

The theoretical results presented are now illustrated by an example. Assume that a slow-release formulation of a drug (NEW) has been developed with the aim of producing markedly lower peak concentrations than the standard drug (STD), while at the same time delivering a similar amount of active ingredient to the circulation. Medical considerations, therefore, lead to the following conditions for bioequivalence:

$$\text{AUC: } 0.8 \le \theta \le 1.2 \qquad \text{(Eq. 11)}$$

and

$$C_{max}\text{: } \theta \le 0.6 \qquad \text{(Eq. 12)}$$

A comparative bioavailability study with 12 subjects is conducted in a two-period crossover design. The design information and observed data [AUC, C_{max}, and $\ln(C_{max})$] are shown in Table I, together with the formulation mean values. The analyses of variance used to estimate the experimental errors are given in Tables II and III for AUC and $\ln(C_{max})$, respectively. The validity of the assumed model (Eq. 2) may be verified by examination of the ANOVA residuals. Interested readers will find appropriate procedures in Belsley *et al.* (7).

Bioequivalence Assessment with Respect to AUC—The estimated ratio, given by Eq. 6 is $\hat{\theta} = 90.10/98.35 = 0.916$. The estimated experimental error from the ANOVA (Table II) is 690.4, so that the estimated coefficient of variation (CV) given by Eq. 7 is $\sqrt{690.4}/98.35 = 0.267$. The posterior probability that θ lies in the interval 0.8–1.2 (Eq. 11) may then be calculated from Eqs. 3–5 to give $Pr(0.8 \le \theta \le 1.2) = 0.846$. The cumulative posterior distribution function is shown in Fig. 3; this may also be used, as illustrated, to calculate the probability of the bioequivalence condition.

Bioequivalence Assessment with Respect to C_{max}—The estimated ratio for log-normally distributed data (3) is given by:

$$\hat{\theta} = \exp[\overline{\ln(C_{max})_{NEW}} - \overline{\ln(C_{max})_{STD}}]$$
$$= \exp[4.658 - 5.391] = 0.481 \qquad \text{(Eq. 13)}$$

The estimated error standard deviation from the ANOVA (Table III) is $S = \sqrt{0.147} = 0.383$. The posterior probability that $\theta \le 0.6$ (Eq. 12) may then be calculated from Eqs. 3, 9, and 10 to give $Pr(\theta \le 0.6) = 0.906$. The cumulative posterior distribution function for θ is shown in Fig. 4.

DISCUSSION

Analysis of the example presented shows the main advantages of a Bayesian approach over previous approaches:

1. Earlier methods for bioequivalence assessment consisted of testing the null hypothesis of no difference between formulations. In the present example this null hypothesis would be rejected for C_{max} since the F-ratio in the ANOVA (Table III) is large, but not for AUC, since the F-ratio in the ANOVA (Table II) is small.
2. The assessment of the bioequivalence condition with respect to AUC for the specified interval 0.8–1.2 (Eq. 11) yielded a posterior probability of 0.846. There is, therefore, not enough evidence for claiming bioequivalence. However, the calculation of the cumulative distribution function allows other aspects of interest to be investigated. Thus it may

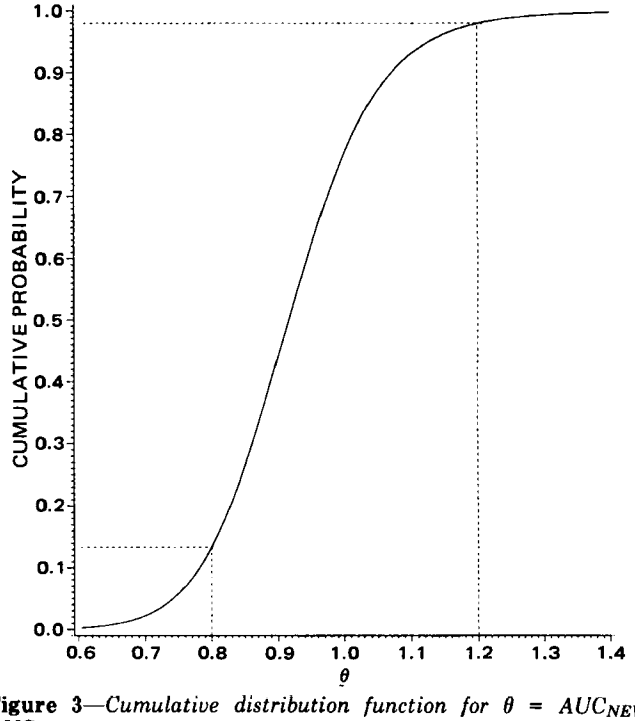

Figure 3—*Cumulative distribution function for* $\theta = AUC_{NEW}/AUC_{STD}$.

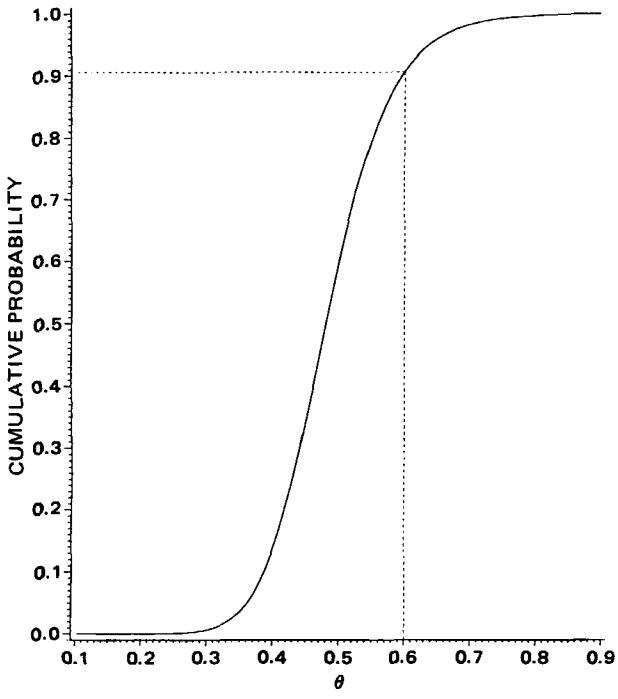

Figure 4—*Cumulative distribution function for* $\theta = (C_{max})_{NEW}/(C_{max})_{STD}$.

be of interest to know the probability that θ is >0.8. This may be read from Fig. 3 and is 0.866—a probability which still might not be high enough to state bioequivalence. In addition it might be desirable to know the probability of θ being >0.7, which also may be read from Fig. 3 and is 0.98.

3. The assessment with respect to C_{max}, that θ is <0.6 (Eq. 12) yielded a posterior probability of 0.906. Similarly it might be desirable to know the probability of θ being >0.7. This probability can be read from Fig. 4 and is 0.02.

4. The method of symmetrical confidence limits proposed by Westlake (1) causes the loss of information since it gives the false impression that the ratio is symmetric about 1. As Mandallez and Mau (3) have shown, the symmetric confidence interval approach may give exactly the same 95% confidence intervals for two sets of data while having completely different posterior distributions for θ, because of the differing variances and locations of the posterior distributions.

REFERENCES

(1) W. J. Westlake, *Biometrics*, **35**, 273 (1979).

(2) C. M. Metzler, *Biometrics*, **30**, 309 (1974).

(3) D. Mandallaz and J. Mau, *Biometrics*, **37**, 213 (1981).

(4) H. Fluehler, J. Hirtz, and H. A. Moser, *J. Pharmacokinet. Biopharm.*, **9**, 235 (1981).

(5) M. R. Selwyn, A. P. Dempster, and N. R. Hall, *Biometrics*, **37**, 11 (1981).

(6) W. G. Cochran and G. M. Cox, "Experimental Design," Wiley, New York, N.Y., 1957.

(7) D. A. Belsley, E. Kuh, and R. E. Welsch, "Regression Diagnostics," Wiley, New York, N.Y., 1980.

In Vivo and *In Vitro* Release of Macromolecules from Polymeric Drug Delivery Systems

L. R. BROWN *‡, C. L. WEI *‡, and R. LANGER *x

Received January 26, 1982, from the **Department of Nutrition and Food Science, Massachusetts Institute of Technology, Cambridge, MA 02139* and ‡*Department of Surgery, Children's Hospital Medical Center, Boston, MA 02115.* Accepted for publication August 30, 1982.

Abstract □ *In vivo* release rates of a macromolecule from an ethylene–vinyl acetate copolymer have been shown to be indistinguishable from those of identical implants tested *in vitro*. The studies were conducted for ~2 months, and two different techniques were used to assess release rates. One of these techniques, using [^{3}H]inulin as a marker, may be particularly useful in future studies assessing *in vivo* release rates from drug delivery systems. The appearance of [^{3}H]inulin in the urine of rats bearing implants allowed continuous monitoring of release. A histological evaluation of tissue sections surrounding polymer implanted for 7 months showed no inflammatory cell reaction.

Keyphrases □ Drug delivery systems—ethylene–vinyl acetate copolymer matrix, inulin, release kinetics, *in vitro–in vivo* comparison □ Ethylene–vinyl acetate copolymer—sustained release of inulin, release kinetics, *in vitro–in vivo* comparison □ Inulin—sustained release using polymeric matrices, release kinetics, *in vitro–in vivo* comparison

Since the first report that biocompatible polymers such as ethylene–vinyl acetate copolymer could be used for the controlled release of macromolecules (mol. wt. > 1000) (1), these systems have been used by different investigators in biological (2–11), ophthalmological (12–17), neurological (18, 19),and microbiological research (20, 21). Macromolecules such as enzymes (22), antigens (23), and insulin (24) have been released in biologically active form for up to 6 months *in vivo*. Extensive studies *in vitro* have demonstrated that the release rates of drugs from these devices can be adjusted over a 2000-fold range by simple alterations in the fabrication procedures of the macromolecule–polymer matrices (25).

The macromolecules incorporated into these polymer matrices are usually proteins. Thus, once released *in vivo*, they are degraded to amino acids and recycled to other body proteins. Neither the native proteins nor their metabolites are excreted. For this reason, it has been difficult to directly measure the absolute release rates of such macromolecules *in vivo*. We now report two new methods to measure *in vivo* release which demonstrate that release kinetics from ethylene–vinyl acetate copolymer implants *in vivo* are indistinguishable from identical implants tested *in vitro*. In one method, release rates of ^{14}C-labeled proteins were determined by assaying the remaining radiolabeled protein in the implants at various time points *in vivo* and *in vitro*. In the second method, the use of the polysaccharide inulin, which is totally excreted (26, 27), permitted direct *in vivo* monitoring of release kinetics by collecting urine and assaying for inulin. These studies should enable investigators to employ ethylene–vinyl acetate copolymer matrices with the knowledge that predetermined *in vitro* release kinetics will be followed *in vivo*.

0022-3549/83/1000-1181$01.00/0

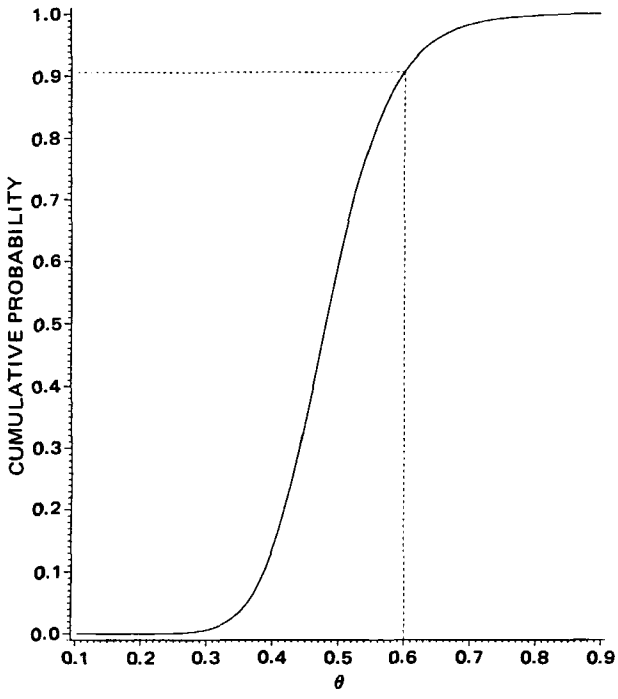

Figure 4—*Cumulative distribution function for* $\theta = (C_{max})_{NEW}/(C_{max})_{STD}$.

be of interest to know the probability that θ is >0.8. This may be read from Fig. 3 and is 0.866—a probability which still might not be high enough to state bioequivalence. In addition it might be desirable to know the probability of θ being >0.7, which also may be read from Fig. 3 and is 0.98.

3. The assessment with respect to C_{max}, that θ is <0.6 (Eq. 12) yielded a posterior probability of 0.906. Similarly it might be desirable to know the probability of θ being >0.7. This probability can be read from Fig. 4 and is 0.02.

4. The method of symmetrical confidence limits proposed by Westlake (1) causes the loss of information since it gives the false impression that the ratio is symmetric about 1. As Mandallez and Mau (3) have shown, the symmetric confidence interval approach may give exactly the same 95% confidence intervals for two sets of data while having completely different posterior distributions for θ, because of the differing variances and locations of the posterior distributions.

REFERENCES

(1) W. J. Westlake, *Biometrics*, **35**, 273 (1979).

(2) C. M. Metzler, *Biometrics*, **30**, 309 (1974).

(3) D. Mandallaz and J. Mau, *Biometrics*, **37**, 213 (1981).

(4) H. Fluehler, J. Hirtz, and H. A. Moser, *J. Pharmacokinet. Biopharm.*, **9**, 235 (1981).

(5) M. R. Selwyn, A. P. Dempster, and N. R. Hall, *Biometrics*, **37**, 11 (1981).

(6) W. G. Cochran and G. M. Cox, "Experimental Design," Wiley, New York, N.Y., 1957.

(7) D. A. Belsley, E. Kuh, and R. E. Welsch, "Regression Diagnostics," Wiley, New York, N.Y., 1980.

In Vivo and *In Vitro* Release of Macromolecules from Polymeric Drug Delivery Systems

L. R. BROWN *‡, C. L. WEI *‡, and R. LANGER *x

Received January 26, 1982, from the **Department of Nutrition and Food Science, Massachusetts Institute of Technology, Cambridge, MA 02139* and ‡*Department of Surgery, Children's Hospital Medical Center, Boston, MA 02115.* Accepted for publication August 30, 1982.

Abstract □ *In vivo* release rates of a macromolecule from an ethylene–vinyl acetate copolymer have been shown to be indistinguishable from those of identical implants tested *in vitro*. The studies were conducted for ~2 months, and two different techniques were used to assess release rates. One of these techniques, using [^{3}H]inulin as a marker, may be particularly useful in future studies assessing *in vivo* release rates from drug delivery systems. The appearance of [^{3}H]inulin in the urine of rats bearing implants allowed continuous monitoring of release. A histological evaluation of tissue sections surrounding polymer implanted for 7 months showed no inflammatory cell reaction.

Keyphrases □ Drug delivery systems—ethylene–vinyl acetate copolymer matrix, inulin, release kinetics, *in vitro–in vivo* comparison □ Ethylene–vinyl acetate copolymer—sustained release of inulin, release kinetics, *in vitro–in vivo* comparison □ Inulin—sustained release using polymeric matrices, release kinetics, *in vitro–in vivo* comparison

Since the first report that biocompatible polymers such as ethylene–vinyl acetate copolymer could be used for the controlled release of macromolecules (mol. wt. > 1000) (1), these systems have been used by different investigators in biological (2–11), ophthalmological (12–17), neurological (18, 19),and microbiological research (20, 21). Macromolecules such as enzymes (22), antigens (23), and insulin (24) have been released in biologically active form for up to 6 months *in vivo*. Extensive studies *in vitro* have demonstrated that the release rates of drugs from these devices can be adjusted over a 2000-fold range by simple alterations in the fabrication procedures of the macromolecule–polymer matrices (25).

The macromolecules incorporated into these polymer matrices are usually proteins. Thus, once released *in vivo*, they are degraded to amino acids and recycled to other body proteins. Neither the native proteins nor their metabolites are excreted. For this reason, it has been difficult to directly measure the absolute release rates of such macromolecules *in vivo*. We now report two new methods to measure *in vivo* release which demonstrate that release kinetics from ethylene–vinyl acetate copolymer implants *in vivo* are indistinguishable from identical implants tested *in vitro*. In one method, release rates of ^{14}C-labeled proteins were determined by assaying the remaining radiolabeled protein in the implants at various time points *in vivo* and *in vitro*. In the second method, the use of the polysaccharide inulin, which is totally excreted (26, 27), permitted direct *in vivo* monitoring of release kinetics by collecting urine and assaying for inulin. These studies should enable investigators to employ ethylene–vinyl acetate copolymer matrices with the knowledge that predetermined *in vitro* release kinetics will be followed *in vivo*.

0022-3549/83/1000-1181$01.00/0

EXPERIMENTAL

Isotope Preparation—Bovine serum albumin[1] (12.2 g) was dissolved in 100 ml of double glass-distilled water. [^{14}C]Methyl bovine serum albumin[2] (1 μCi) was added, and the solution was stirred for 1 hr at 23° with a magnetic stirrer[3]. The solution was then lyophilized[4] yielding a final specific activity for the [^{14}C]methyl bovine serum albumin of 0.082 nCi/mg. β-Lactoglobulin A[1] (6.02 g) was dissolved in 100 ml of double glass-distilled water, and 5 μCi of [^{14}C]methyl β-lactoglobulin A[2] was added. The solution was then lyophilized yielding a final specific activity for [^{14}C]methyl β-lactoglobulin A of 0.83 nCi/mg. Inulin[1] (1.43 g) was suspended in 50 ml of reagent-grade acetone[5] in an Erlenmeyer flask. [^{3}H]Inulin[2] (5 mCi) was added, and the suspension was stirred for 1 hr at 23° with a magnetic stirrer. The suspension was collected on filter paper[6] in a Büchner funnel, rinsing the flask with acetone to remove residual [^{3}H]inulin. The [^{3}H]inulin was collected and dried overnight in a dessicator; the resulting specific activity was 3.44 μCi/mg.

Matrix Preparation—Ethylene–vinyl acetate copolymer[7] was rinsed with water and alcohol to remove inflammatory impurities (2) and dissolved in methylene chloride. The three radioactive macromolecule powders were pulverized with a spatula to produce a normal distribution of particle sizes. As a safety precaution, the powders were not sieved to varying particle size ranges as is often done (25), due to the aerosol effect of shaking radioactive powders.

Fifteen milliliters of 10% (w/v) polymer solution was added to each of six glass vials[8] containing 807 ± 3.1 mg of the pulverized [^{14}C]methyl bovine serum albumin. The polymer–protein mixture was poured into a rectangular mold precooled to −80° and then freeze-dried, at −20° (25). The resulting matrices were 35% (w/w) loaded with [^{14}C]methyl bovine serum albumin. Sixty-seven 1 cm × 1-cm squares were excised from the six slabs (25) with a surgical scalpel blade[9]. The mean weight and standard deviation of the 67 matrices were 67.9 ± 2.9 mg.

Fifteen milliliters of 10% (w/v) polymer solution was added to each of five glass vials containing 989.0 ± 74.0 mg of pulverized [^{14}C]methyl β-lactoglobulin A. The procedure for matrix formation was followed as above, yielding five 40% loaded (w/w) protein polymer matrix slabs. Sixty-seven 0.8 cm × 0.8-cm squares were excised from the five slabs. The mean weight and standard deviation of the 67 matrices were 44.5 ± 1.2 mg.

Fifteen milliliters of 5% (w/v) polymer solution was added to each of three glass vials containing 568 ± 25.4 mg of [^{3}H]inulin. Three 44% loaded (w/w) [^{3}H]inulin polymer matrices were formed. Twenty-nine 1 cm × 1-cm squares were excised from the three slabs. The mean weight and standard deviation of the 29 matrices were 82.00 ± 8.0 mg.

Release of Macromolecules—Kinetic studies, both *in vitro* and *in vivo*, were conducted on the release of three radioactively labeled macromolecules: [^{14}C]methyl bovine serum albumin (mol. wt. 68,000), [^{14}C]methyl β-lactoglobulin A (mol. wt. 18,000), and [^{3}H]inulin (mol. wt. 5200). For the *in vitro* studies, 30 of each set of the ^{14}C-labeled protein–polymer squares and 12 [^{3}H]inulin–polymer squares were placed in glass vials containing 5 ml of sterile phosphate-buffered saline[10] (pH 7.4) and 0.1% sodium azide[5] (release media). The vials were placed on a shaker[11] at 37°. At various time points during the experiment, five polymer squares were removed from the release experiment for the determination of unreleased ^{14}C-labeled protein in the polymer matrices using an isotope recovery method (see below). The remaining polymer squares were transferred to fresh release media to continue the *in vitro* release.

For the *in vivo* studies, 30 ^{14}C-labeled protein–polymer squares identical to those used *in vitro* were implanted into 100- to 150-mg male CD rats[12]. The polymer squares were implanted by making a 2-cm incision in the lower abdominal area of the rat with a scalpel. A pair of sterile round-edged scissors was then used to create a pocket in the subcutaneous tissue ~5 cm from the incision. The polymer square was placed into the pocket with sterile forceps. The wound was closed with animal wound clips[13]. Five polymer squares were removed at the same time points as in the *in vitro* experiments for the determination of unreleased ^{14}C-labeled protein in the polymer matrices.

Thirteen [^{3}H]inulin polymer matrices were implanted into 100- to 150-g male CD rats in the manner described above. The rats were housed in metabolism cages[14] for the duration of the experiment. Urine was collected daily in 15-ml graduated collection tubes[15]. The urine volumes were read directly off the graduated urine collection tubes.

Release Kinetics—*Isotope Recovery Method*—Release rates for the ^{14}C-labeled protein experiments were determined by assaying the remaining radiolabeled bovine serum albumin or β-lactoglobulin A in each polymer square. At various time points during the experiment, five polymer squares were removed from both the rats and the release media. They were placed in scintillation vials, lyophilized to remove residual water, and dissolved in 1 ml of xylene[16]. When the polymer dissolved, the unreleased macromolecule precipitated to the bottom of the vial. One milliliter of distilled water was added to the vial to dissolve the precipitate. Ten milliliters of xylene-based scintillation fluor[17] was added to the dissolved precipitate, and the radioactivity was measured by liquid scintillation counting[18]. The radioactivity remaining in the matrix at any given time was subtracted from the average amount of radioactivity remaining at the previous time point; release rates are expressed as dpm/hr. The procedure described above was used to dissolve the polymer and to precipitate unreleased [^{3}H]inulin in each of two polymer squares at each time point. Then, 10 ml of warm distilled water (70–80°) was added to the dissolved [^{3}H]inulin–polymer matrix to solubilize the inulin precipitate. A 200-μl aliquot of water was then removed and counted[18].

Before the start of the ^{14}C-labeled protein release experiments, 7 of the 67 polymer squares were assayed by the above method to establish the initial dpm per polymer matrix. In a similar manner 4 of the 29 [^{3}H]inulin–polymer squares were assayed to determine the mean dpm per polymer matrix.

Isotope Release Method—In the *in vitro* studies, the amount of radiolabeled macromolecule released was determined by removing a 250-μl aliquot from the release media, adding 4 ml of scintillation fluor, and counting the solution[18]. For the *in vivo* studies [^{3}H]inulin–polymer matrix squares were implanted into five rats housed in metabolism cages. Urine was collected and measured daily. A 250-μl aliquot of urine was added to 4 ml of scintillation fluor plus 400 μl of distilled water in a glass miniscintillation vial[19] and the solution was counted[18]. The channels ratio method of quench correction was used to determine the counting efficiency of the urine samples (28).

Statistics—*In vivo* and *in vitro* release rates were compared by an analysis of covariance on a log transformation of the release rate data (29). The natural logarithms of the release rates and times were calculated. This transformation resulted in a linear relationship for each data set with r^2 ranging from 0.89 to 0.96 for the regression lines. The *in vivo* and *in vitro* regression lines were then compared as follows: The mean square error from the regression model with a separate slope and intercept for each trial condition (there were three trial conditions for bovine serum albumin, three trial conditions for β-lactoglobulin A, and two trial conditions for inulin) was compared with the mean square error for the regression model with common slopes and intercepts for all trial conditions pertaining to a specific macromolecule. The resulting test statistic was compared to the F distribution (30). The regression lines were considered indistinguishable if $p > 0.05$.

Histology—Histology was performed on tissues surrounding washed (2) ethylene–vinyl acetate copolymer subcutaneous implants containing bovine serum albumin after 7 months. The polymer matrices were implanted into male CD rats. An unwashed industrial grade ethylene–vinyl acetate copolymer[7] was used as a control to exhibit an inflammatory response. Sections (5 μm) were prepared using hematoxylin and eosin staining.

RESULTS

Comparison of Release Rates of ^{14}C-Labeled Proteins *In Vitro* and *In Vivo*—Figure 1 compares the release rates of the 35% loaded (w/w) [^{14}C]methyl bovine serum albumin–polymer matrices *in vivo* and *in vitro* as measured by the recovery of unreleased protein in the polymer and as measured directly in the *in vitro* release media. Throughout the

[1] Sigma Chemical Co., St. Louis, Mo.
[2] New England Nuclear, Boston, Mass.
[3] Model PC-35 magnetic stirrer; Corning Glass Works, Corning, N.Y.
[4] Virtis #10-148 lyophilizer; The Virtis Co., Gardinier, N.Y.
[5] Fisher Scientific Co., Fair Lawn, N.J.
[6] Grade 595 filter paper; Schleicher and Schnell, Keene, N.H.
[7] Elvax 40P; Dupont Chemical Co., Wilmington, Del.
[8] Wheaton Scientific Co., Millville, N.J.
[9] No. 10 blade; Bard-Parker, Rutherford, N.J.
[10] Grand Island Biological Co., Grand Island, N.Y.
[11] Clinical Rotating Apparatus, set at speed 3; Arthur H. Thomas, Philadelphia, Pa.
[12] Charles River Breeding Laboratories, Wilmington, Mass.
[13] Autoclip Kit; Clay Adams, Parsippany, N.J.
[14] Econo Metabolism Unit; Scientific Products, McGaw Park, Ill.
[15] No. 2095 graduated centrifuge tube; Falcon, Oxnard, Calif.
[16] Mallinckrodt Inc., Paris, Ky.
[17] Aquasol 2; New England Nuclear, Boston, Mass.
[18] Packard Model 3320 Liquid Scintillation Counter; Packard Instruments, Co., Inc., Downers Grove, Ill.
[19] Rochester Scientific, Rochester, N.Y.

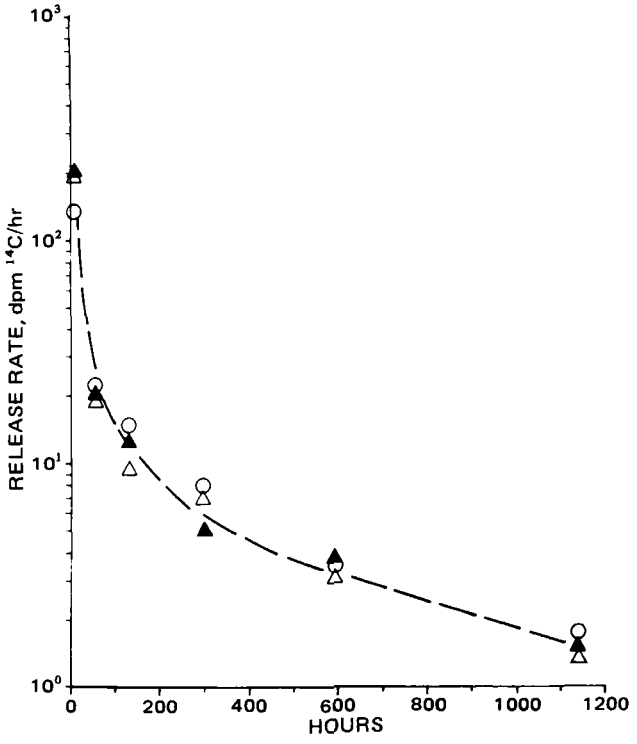

Figure 1—In vivo *and* in vitro *comparison of release rates from 35% loaded (w/w) [^{14}C]methyl bovine serum albumin polymer matrices. Each point represents the average release of five polymer squares. Key: (▲) in vivo recovery; (△) in vitro recovery; (○) in vitro release.*

experiment, *in vivo* and *in vitro* release rates were not statistically different ($p > 0.05$). Figure 2 shows that the release rates of 40% loaded (w/w) [^{14}C]methyl β-lactoglobulin A–polymer matrices *in vivo* and *in vitro* also were not statistically different ($p > 0.05$). At each time point

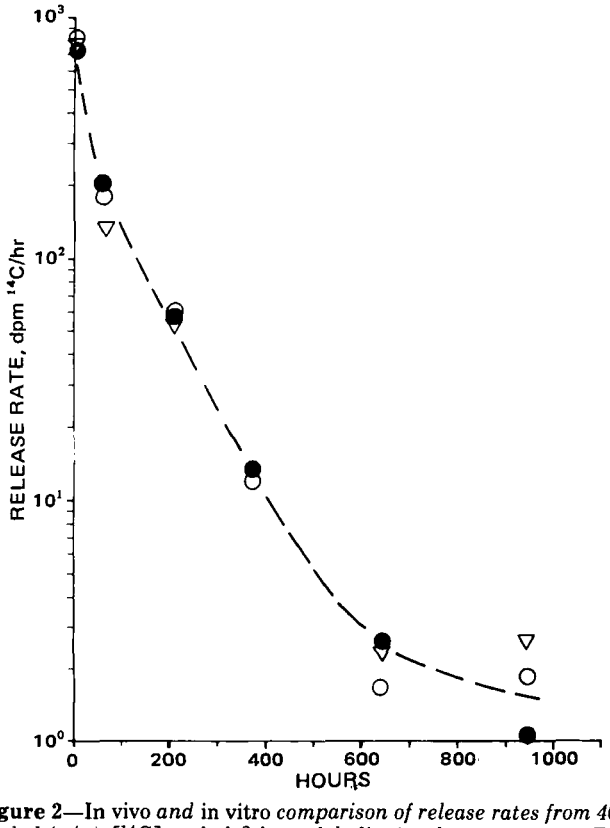

Figure 2—In vivo *and* in vitro *comparison of release rates from 40% loaded (w/w) [^{14}C]methyl β-lactoglobulin A polymer matrices. Each point represents the average of five polymer squares. Key: (○) in vitro recovery; (●) in vitro release; (▽) in vivo recovery.*

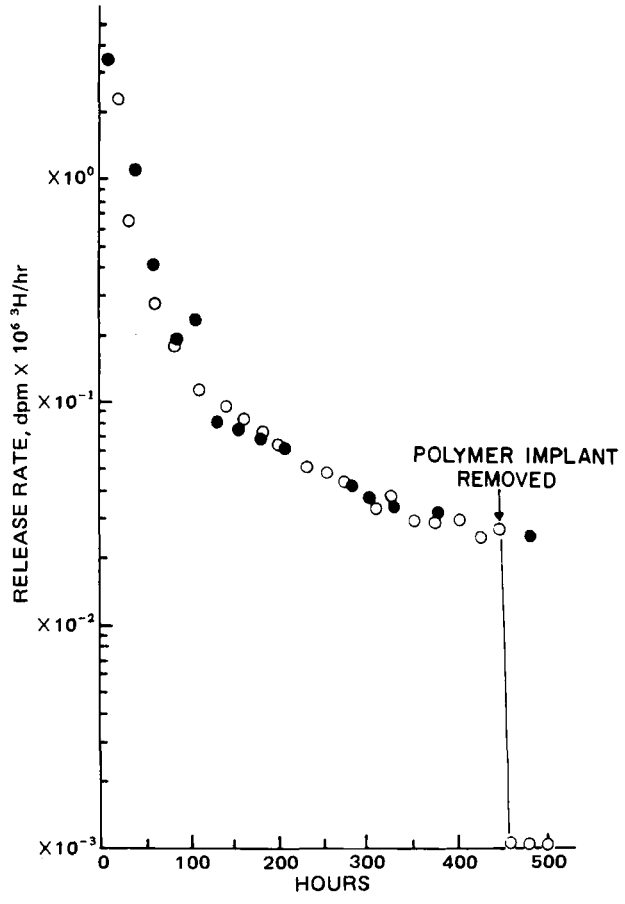

Figure 3—In vivo *and* in vitro *comparison of release rates from 44% loaded (w/w) [^{3}H]inulin. Each* in vivo *point (○) represents the average release rate obtained by the collection of urine from five rats. Each* in vitro *point (●) represents the average release rate from four polymer squares into phosphate-buffered saline. The polymer squares were removed from the rats after 450 hr.*

the recovered and released radioactivity were totaled for each polymer square. Complete material balance was demonstrated as this total equaled (±7%) the initial amount of radioactivity incorporated into each polymer square. The material balance can also be seen by the equivalent *in vitro* release rates obtained by both the recovery and release methods (Figs. 1 and 2).

Comparison of [^{3}H]Inulin Release *In Vivo* and *In Vitro*—Figure 3 compares the release rates of [^{3}H]inulin analyzed directly by the collection of urine from five implanted rats and four polymer squares releasing *in vitro*. Release rates *in vivo* and *in vitro* were indistinguishable ($p > 0.05$). As an internal control, the polymer implants were removed from the rats at 450 hr into the experiment. The rats were placed in the metabolism cages for an additional 50 hr. Within 4.5 hr after the explant of the polymer, recovery of [^{3}H]inulin dropped 51-fold as measured in the urine of the animals. Release rates decreased for the remainder of the experiment (Fig. 3). An additional experiment was conducted over a 1500-hr period with a smaller sample size and showed an *in vitro–in vivo* relationship similar to the above (data not shown).

The possibility of artifacts in the amount of inulin recovered due to tritium exchange with surrounding aqueous media was checked by lyophilizing a known amount of [^{3}H]inulin. If exchange did occur, the water removed during the lyophilization procedure would cause a reduction in the dpm in the sample. No such reduction in the amount of radioactivity was observed, confirming that tritium exchange did not occur.

In a separate experiment, the recovery of unreleased [^{3}H]inulin from polymer matrices releasing *in vivo* and *in vitro* was compared at five different time points over a 30-day period. The amounts of [^{3}H]inulin recovered at various times in both cases were not statistically different ($p > 0.05$).

Histology—Figure 4A shows the tissue response to the washed (2) polymer implants containing bovine serum albumin which were removed after 7 months. The polymer implant (P) was surrounded by a very thin capsule of connective tissue. There was no inflamatory reaction, and the

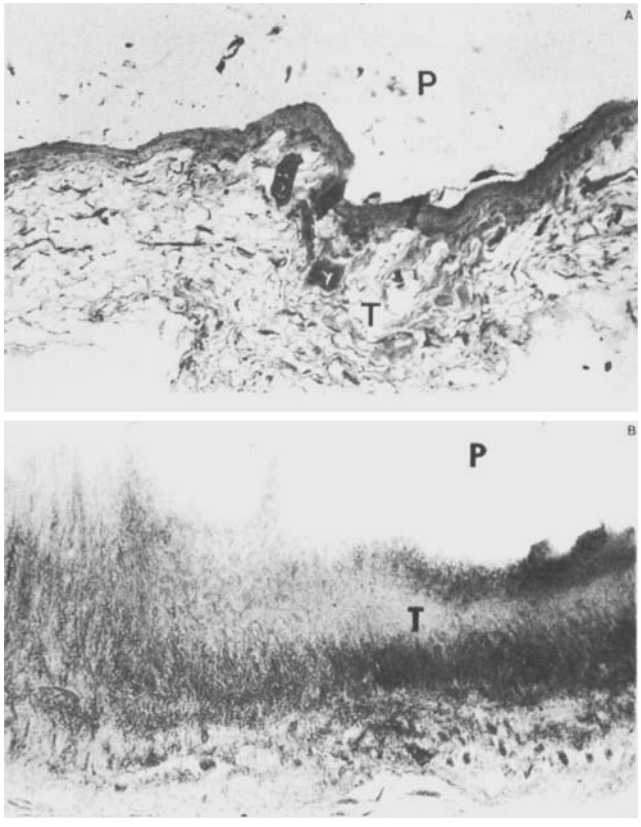

Figure 4—*(A) The washed implant (P) is surrounded by a thin capsule of dense connective tissue (T). There is virtually no inflammatory reaction, and the adjacent loose connective tissue is normal. Original magnification 100×. (B) The tissue (T) surrounding the control unwashed implant (P) shows an extensive inflammatory reaction. The granulation tissue is thick and shows multiple layers, some infiltrated with abundant polymorphonuclear leukocytes. Original magnification 100×.*

adjacent loose connective tissue was normal. As a control, unwashed polymer resulted in tissue sections that showed an extensive inflammatory reaction. The granulation tissue surrounding the control polymer was thick and showed multiple layers, some infiltrated with abundant polymorphonuclear leukocytes (Fig. 4B).

DISCUSSION

These results demonstrate that *in vivo* release kinetics of a particular macromolecule from ethylene–vinyl acetate copolymer matrices closely follow *in vitro* release kinetics of identical implants under physiological conditions. These studies were carried out for three macromolecules with a wide range of molecular weights (5200–68,000) and loadings (35–44%).

Many macromolecules incorporated into the ethylene–vinyl acetate copolymer matrix are proteins or other biological substances (2–25) that are metabolized and redistributed into other body tissues. In these cases, *in vivo* release rates cannot be measured directly. To circumvent this problem, a procedure had to be developed for the recovery of radioactively labeled macromolecules from the ethylene–vinyl acetate copolymer matrix. The implants were removed from the experimental animals, or from the release media in the *in vitro* studies. The squares were first lyophilized to improve the solubility of the polymer in xylene. Xylene was the solvent of choice for two reasons:

1. On dissolution of the polymer, the protein remaining in the polymer precipitated to the bottom of the glass vial. The addition of water to dissolve the precipitated protein was facilitated by the greater density of water compared with xylene. Thus, the ethylene–vinyl acetate copolymer in xylene floated on the upper organic phase, while the water dissolved the precipitated protein in the bottom aqueous phase.
2. The scintillation fluor used to count the radioactivity in the dissolved polymer was a xylene-based fluor. Thus, it was completely compatible with both the xylene–ethylene–vinyl acetate copolymer phase and the aqueous phase. This resulted in a homogeneous translucent emulsion, suitable for liquid scintillation counting. Control studies demonstrated that there was no quenching due to the polymer in the scintillation fluor.

Using this technique, *in vivo* release rates of ^{14}C-labeled proteins were shown to be statistically indistinguishable from *in vitro* release rates with identical implants (Figs. 1 and 2). However, this technique had several disadvantages: (*a*) the need for a large sample size of polymer matrices and animals (30 rats were used in each experiment), (*b*) the use of long half-life ^{14}C-labeled proteins, and (*c*) the inability to directly measure release rates from polymer implants *in vivo*.

In contrast to the proteins, the polysaccharide inulin (mol. wt. 5200) is not metabolized *in vivo* nor reabsorbed by the kidney tubules. Once absorbed into the bloodstream, inulin is totally excreted in the urine (26, 27). Thus, inulin seemed to be an ideal model drug with which to measure *in vivo* release directly by simply collecting urine from [^3H]inulin–polymer-implanted rats housed in metabolism cages. Figure 3 clearly demonstrated that *in vivo* and *in vitro* release rates of [^3H]inulin are indistinguishable. The value of using inulin as a model drug to compare *in vivo* and *in vitro* macromolecule release was shown by its nearly instantaneous appearance in the urine after polymer implantation. When the polymer implant was removed after 450 hr (Fig. 3), release rates dropped 51-fold within 4.5 hr. This was further evidence that inulin release was only associated with the presence of the polymer implant. In addition, the use of [^3H]inulin allowed the continuous monitoring of release *in vivo*. The use of five rats in this experiment *versus* the 30 rats needed for the ^{14}C-labeled protein recovery experiments provided for a simpler experiment design.

The continuous decrease in release rates of macromolecules from the ethylene–vinyl acetate copolymer matrix is predictable from the flat-slab geometry used in these experiments (31). It has been suggested that release occurs through a porous network of tortuous channels created by the powdered drug during the fabrication procedure of the polymer matrix (32). Thus, drug release rates decrease due to increasing diffusion distance through the pores of the matrix as time increases. Constant release rates have been obtained with appropriate geometric design (33). The relationship of *in vivo* and *in vitro* release rates are now being studied for these alternative geometries.

The excellent biocompatibility of washed ethylene–vinyl acetate copolymer was demonstrated by a 7-month polymer implant into subcutaneous rat tissue (Fig. 4). This is consistent with previous studies in which this polymer was shown to be inert in rabbit corneal implants (34). It is conceivable that other polymers may either be subject to bioerosion or induce significant fibrous encapsulation that could cause *in vivo* and *in vitro* release rates to differ. Thus, ethylene–vinyl acetate copolymer may prove to be a useful standard for judging other polymers with respect to biocompatibility and *in vivo* release kinetics.

The results presented here demonstrate that *in vivo* release kinetics are statistically indistinguishable from *in vitro* release kinetics using identical implants for macromolecules with a wide range of molecular weights and loadings. The implication is that a desired *in vivo* release rate could be manipulated through *in vitro* testing. This is of particular importance if these polymer matrices are to be used experimentally (24) or clinically for the delivery of macromolecules such as insulin. Furthermore, the inulin–polymer model establishes a methodology that can be easily applied for *in vivo–in vitro* comparisons for any controlled-release system. Tracer amounts of inulin could be mixed with any drug to monitor the continual effectiveness of an implant in animals or humans. Small implantable sustained-release inulin–polymer matrices may also be useful for extended studies of glomerular filtration. These data show that *in vivo* release can be accounted for by the same mechanisms operating *in vitro;* this should now make possible the further development and increased use of ethylene–vinyl acetate copolymer drug delivery systems.

REFERENCES

(1) R. Langer and J. Folkman, *Nature* (*London*), **263,** 797 (1976).

(2) R. Langer, *Methods Enzymol.*, **73,** 57 (1981).

(3) K. Falterman, D. Ausprunk, and M. Klein, *Surg. Forum*, **27,** 358 (1976).

(4) R. Langer, H. Brem, M. Klein, K. Falterman, and J. Folkman, *Science*, **193,** 70 (1976).

(5) P. Polverini, R. Cotran, M. Gimbrone, and E. Unanue, *Nature* (*London*), **269,** 804 (1977).

(6) A. M. Schor, S. L. Schor, and S. Kumar, *Int. J. Cancer*, **24,** 225 (1979).

(7) J. Gross, R. G. Azizkhan, C. Biswas, R. R. Bruns, D. S. T. Hsieh, and J. Folkman, *Proc. Natl. Acad. Sci. USA*, **78,** 1176 (1981).

(8) R. McAuslan and G. A. Gole, *Trans. Ophthalmol. Soc.*, **100**, 354 (1980).
(9) M. E. Plishkin, S. M. Ginsberg, and N. Carp, *Transplantation*, **29**, 255 (1980).
(10) D. Ausprunk, K. Falterman, and J. Folkman, *Lab. Invest.*, **38**, 284 (1978).
(11) B. M. Glaser, P. A. D'Amore, R. G. Michels, A. Patz, and A. Fenselau, *J. Cell Biol.*, **84**, 298 (1980).
(12) B. M. Glaser, P. A. D'Amore, R. G. Michels, S. K. Brunson, A. H. Fenselau, T. Rice, and A. Patz, *Ophthalmology* (Rochester, MN), **87**, 440 (1980).
(13) B. M. Glaser, P. A. D'Amore, G. A. Lutty, A. H. Fenselau, R. G. Michels, and A. Patz, *Trans. Ophthalmol. Soc.*, **100**, 369 (1980).
(14) A. Patz, S. Brem, D. Finkelstein, C. H. Chen, G. Lutty, A. Bennett, W. R. Coughlin, and J. Gardner, *Ophthalmology* (Rochester, MN), **85**, 626 (1978).
(15) S. Brem, I. Preis, R. Langer, H. Brem, J. Folkman, and A. Patz, *Am. J. Ophthalmol.*, **84**, 323 (1977).
(16) D. Gospodarowicz, H. Bialecki, and T. K. Thakral, *Exp. Eye Res.*, **28**, 501 (1979).
(17) D. Ben Ezra, *Surg. Ophthalmol.*, **24**, 167 (1979).
(18) M. Moskowitz, M. Mayberg, and R. Langer, *Brain Res.*, **212**, 460 (1981).
(19) M. Mayberg, R. Langer, N. Zervas, and M. Moskowitz, *Science*, **213**, 228 (1981).
(20) R. Langer, M. Fefferman, P. Gryska, and K. Bergman, *Can. J. Microbiol.*, **26**, 362 (1980).
(21) M. L. Hedblom and J. Adler, *J. Bacteriol.*, **144**, 1048 (1980).
(22) R. Langer and J. Folkman, in "Polymeric Delivery Systems," R. J. Kostelnik, Ed., Gordon and Breach, New York, N.Y., 1978, pp. 175–196.
(23) I. Preis and R. Langer, *J. Immunol. Meth.*, **28**, 193 (1979).
(24) H. Creque, R. Langer, and J. Folkman, *Diabetes*, **29**, 37 (1980).
(25) W. Rhine, D. Hsieh, and R. Langer, *J. Pharm. Sci.*, **69**, 265 (1980).
(26) H. W. Smith, in "Principles of Renal Physiology," Oxford University Press, New York, N.Y., 1956, pp. 26–73.
(27) Y. Gutman, C. W. Gattschalk, and W. T. Lassiter, *Science*, **147**, 753 (1965).
(28) V. W. Andreucci, in "Manual of Renal Micropuncture," Idelson Publishers, Naples, Italy, 1978, p. 303.
(29) B. W. Brown and M. Hollander, in "Statistics, A Biomedical Introduction," Wiley, New York, N.Y., 1977, p. 275.
(30) J. Neter and W. Wasserman, in "Applied Linear Statistical Models. Regression, Analysis of Variance and Experimental Design." Richard D. Irwin, Homewood, Ill., 1974, p. 160.
(31) T. Higuchi, *J. Pharm. Sci.*, **52**, 1145, (1963).
(32) R. Langer, W. Rhine, D. Hsieh, and R. Bawa, in "Controlled Release of Bioactive Materials," R. Baker, Ed., Academic, New York, N.Y., 1980, p. 83.
(33) D. S. T. Hsieh, W. D. Rhine, and R. Langer, *J. Pharm. Sci.*, **72**, 17 (1983).
(34) R. Langer, H. Brem, and D. Tapper, *J. Biomed. Mat. Res.*, **15**, 267 1981.

ACKNOWLEDGMENTS

This work was supported by grants from the Juvenile Diabetes Foundation, the American Diabetes Association, and the National Institutes of Health (GM 26698).

The authors thank Christian Haudenschild, Jeffrey Stoff, Julie Glowacki, Judith Sudhalter, Robert Muller, William Rand, Dean Hsieh, Annette LaRocca, Nancy Healey, and Heidi Bobeck.

Absorption of Triazolam from Pelleted Drug–Diet Mixtures by the Mouse: Quantitation of α-Hydroxytriazolam in Urine

WADE J. ADAMS ˣ, PAUL A. BOMBARDT, and ROBERT A. CODE

Received January 6, 1982, from *Pharmaceutical Research and Development, The Upjohn Company, Kalamazoo, MI 49001.* Accepted for publication September 14, 1982.

Abstract □ The absorption of triazolam from pelleted drug–diet mixtures by mice under steady-state conditions was determined for doses up to 150 mg/kg/day by measuring α-hydroxytriazolam, the principal urinary metabolite of triazolam in the mouse, in urine samples collected over a 24-hour period. Following β-glucuronide glucuronosohydrolase hydrolysis of the urine, quantitation of α-hydroxytriazolam was accomplished using a specific reverse-phase liquid chromatographic method which utilized UV detection at 214 nm. Assay precision was >2.7% (*CV*) over the concentration range of interest. Statistical analysis of the excretion data indicated that the mathematical relationship between the triazolam dose and the quantity of α-hydroxytriazolam excreted was linear for female mice and nonlinear for male mice. Triazolam absorption, as reflected by α-hydroxytriazolam urinary excretion data, increased with triazolam dose.

Keyphrases □ Triazolam—absorption from drug–diet mixtures by mice, determination by metabolite excretion in urine, α-hydroxytriazolam □ α-Hydroxytriazolam—urinary excretion, use to measure triazolam absorption in mice, drug–diet mixtures □ Absorption—triazolam in mice, drug–diet mixtures, measurement by α-hydroxytriazolam excretion in urine

The incorporation of drugs into the laboratory diet of mice and rats is a convenient and commonly used method of administering drugs in chronic toxicology studies since it eliminates the need for time-consuming daily administration of aqueous solutions or suspensions by gavage. In addition to its convenience, this mode of administration also eliminates the daily trauma and danger of pulmonary complications associated with dosing by gavage. As is well known, however, the administration of a drug in a carrier, such as laboratory diet, may affect drug absorption. Information concerning the absorption of a drug from the carrier over the range of dosages administered in toxicological studies may be useful, if not essential, in assessing the significance of study results. It should also be noted that the Food and Drug Administration's recently instituted Good Laboratory Practice regulations may require that the degree of absorption of a drug from a carrier be determined (1).

Several methods have been reported for determining the relative absorption of drugs following administration of pulverized drug–diet mixtures. Van Harken and Hottendorf (2) determined the exposure of rats to cefatrizine, under steady-state conditions, by comparing the area

0022-3549/83/1000-1185$01.00/0

(8) R. McAuslan and G. A. Gole, *Trans. Ophthalmol. Soc.*, **100**, 354 (1980).
(9) M. E. Plishkin, S. M. Ginsberg, and N. Carp, *Transplantation*, **29**, 255 (1980).
(10) D. Ausprunk, K. Falterman, and J. Folkman, *Lab. Invest.*, **38**, 284 (1978).
(11) B. M. Glaser, P. A. D'Amore, R. G. Michels, A. Patz, and A. Fenselau, *J. Cell Biol.*, **84**, 298 (1980).
(12) B. M. Glaser, P. A. D'Amore, R. G. Michels, S. K. Brunson, A. H. Fenselau, T. Rice, and A. Patz, *Ophthalmology* (Rochester, MN), **87**, 440 (1980).
(13) B. M. Glaser, P. A. D'Amore, G. A. Lutty, A. H. Fenselau, R. G. Michels, and A. Patz, *Trans. Ophthalmol. Soc.*, **100**, 369 (1980).
(14) A. Patz, S. Brem, D. Finkelstein, C. H. Chen, G. Lutty, A. Bennett, W. R. Coughlin, and J. Gardner, *Ophthalmology* (Rochester, MN), **85**, 626 (1978).
(15) S. Brem, I. Preis, R. Langer, H. Brem, J. Folkman, and A. Patz, *Am. J. Ophthalmol.*, **84**, 323 (1977).
(16) D. Gospodarowicz, H. Bialecki, and T. K. Thakral, *Exp. Eye Res.*, **28**, 501 (1979).
(17) D. Ben Ezra, *Surg. Ophthalmol.*, **24**, 167 (1979).
(18) M. Moskowitz, M. Mayberg, and R. Langer, *Brain Res.*, **212**, 460 (1981).
(19) M. Mayberg, R. Langer, N. Zervas, and M. Moskowitz, *Science*, **213**, 228 (1981).
(20) R. Langer, M. Fefferman, P. Gryska, and K. Bergman, *Can. J. Microbiol.*, **26**, 362 (1980).
(21) M. L. Hedblom and J. Adler, *J. Bacteriol.*, **144**, 1048 (1980).
(22) R. Langer and J. Folkman, in "Polymeric Delivery Systems," R. J. Kostelnik, Ed., Gordon and Breach, New York, N.Y., 1978, pp. 175–196.
(23) I. Preis and R. Langer, *J. Immunol. Meth.*, **28**, 193 (1979).
(24) H. Creque, R. Langer, and J. Folkman, *Diabetes*, **29**, 37 (1980).
(25) W. Rhine, D. Hsieh, and R. Langer, *J. Pharm. Sci.*, **69**, 265 (1980).
(26) H. W. Smith, in "Principles of Renal Physiology," Oxford University Press, New York, N.Y., 1956, pp. 26–73.
(27) Y. Gutman, C. W. Gattschalk, and W. T. Lassiter, *Science*, **147**, 753 (1965).
(28) V. W. Andreucci, in "Manual of Renal Micropuncture," Idelson Publishers, Naples, Italy, 1978, p. 303.
(29) B. W. Brown and M. Hollander, in "Statistics, A Biomedical Introduction," Wiley, New York, N.Y., 1977, p. 275.
(30) J. Neter and W. Wasserman, in "Applied Linear Statistical Models. Regression, Analysis of Variance and Experimental Design." Richard D. Irwin, Homewood, Ill., 1974, p. 160.
(31) T. Higuchi, *J. Pharm. Sci.*, **52**, 1145, (1963).
(32) R. Langer, W. Rhine, D. Hsieh, and R. Bawa, in "Controlled Release of Bioactive Materials," R. Baker, Ed., Academic, New York, N.Y., 1980, p. 83.
(33) D. S. T. Hsieh, W. D. Rhine, and R. Langer, *J. Pharm. Sci.*, **72**, 17 (1983).
(34) R. Langer, H. Brem, and D. Tapper, *J. Biomed. Mat. Res.*, **15**, 267 1981.

ACKNOWLEDGMENTS

This work was supported by grants from the Juvenile Diabetes Foundation, the American Diabetes Association, and the National Institutes of Health (GM 26698).

The authors thank Christian Haudenschild, Jeffrey Stoff, Julie Glowacki, Judith Sudhalter, Robert Muller, William Rand, Dean Hsieh, Annette LaRocca, Nancy Healey, and Heidi Bobeck.

Absorption of Triazolam from Pelleted Drug–Diet Mixtures by the Mouse: Quantitation of α-Hydroxytriazolam in Urine

WADE J. ADAMS ˣ, PAUL A. BOMBARDT, and ROBERT A. CODE

Received January 6, 1982, from *Pharmaceutical Research and Development, The Upjohn Company, Kalamazoo, MI 49001.* Accepted for publication September 14, 1982.

Abstract □ The absorption of triazolam from pelleted drug–diet mixtures by mice under steady-state conditions was determined for doses up to 150 mg/kg/day by measuring α-hydroxytriazolam, the principal urinary metabolite of triazolam in the mouse, in urine samples collected over a 24-hour period. Following β-glucuronide glucuronosohydrolase hydrolysis of the urine, quantitation of α-hydroxytriazolam was accomplished using a specific reverse-phase liquid chromatographic method which utilized UV detection at 214 nm. Assay precision was >2.7% (*CV*) over the concentration range of interest. Statistical analysis of the excretion data indicated that the mathematical relationship between the triazolam dose and the quantity of α-hydroxytriazolam excreted was linear for female mice and nonlinear for male mice. Triazolam absorption, as reflected by α-hydroxytriazolam urinary excretion data, increased with triazolam dose.

Keyphrases □ Triazolam—absorption from drug–diet mixtures by mice, determination by metabolite excretion in urine, α-hydroxytriazolam □ α-Hydroxytriazolam—urinary excretion, use to measure triazolam absorption in mice, drug–diet mixtures □ Absorption—triazolam in mice, drug–diet mixtures, measurement by α-hydroxytriazolam excretion in urine

The incorporation of drugs into the laboratory diet of mice and rats is a convenient and commonly used method of administering drugs in chronic toxicology studies since it eliminates the need for time-consuming daily administration of aqueous solutions or suspensions by gavage. In addition to its convenience, this mode of administration also eliminates the daily trauma and danger of pulmonary complications associated with dosing by gavage. As is well known, however, the administration of a drug in a carrier, such as laboratory diet, may affect drug absorption. Information concerning the absorption of a drug from the carrier over the range of dosages administered in toxicological studies may be useful, if not essential, in assessing the significance of study results. It should also be noted that the Food and Drug Administration's recently instituted Good Laboratory Practice regulations may require that the degree of absorption of a drug from a carrier be determined (1).

Several methods have been reported for determining the relative absorption of drugs following administration of pulverized drug–diet mixtures. Van Harken and Hottendorf (2) determined the exposure of rats to cefatrizine, under steady-state conditions, by comparing the area

0022-3549/83/1000-1185$01.00/0

under the 24-hr plasma concentration–time curves of the antibiotic after feeding a pulverized cefatrizine–diet mixture *ad libitum* and administering a suspension of the drug once daily. Although satisfactory results were obtained, the authors indicated that it was a very laborious procedure that required a team of technicians working overnight to collect the blood samples. This procedure also places the animals under a great deal of stress, particularly if a sufficient number of blood samples are collected to characterize the blood level profile adequately, and the analysis of a large number of samples is required. To overcome these problems, Smyth *et al.* (3) studied the absorption of several drugs in rats by comparing the urinary excretion of radioactivity after feeding radiolabeled drug–diet mixtures and administering a solution/suspension of each drug. Difficulties may be encountered using this procedure also, since incorporation of radiolabeled drug into the diet using the same techniques that were used to prepare drug–diet mixtures for the corresponding toxicological study may not be possible. In addition, adequate quantities of radiolabeled drug must be available.

The present report describes a study of the absorption of triazolam[1] (I), a potent new hypnotic with a short duration of action (4), from pelleted drug–diet mixtures by mice under steady-state conditions. The extent of triazolam absorption was determined by quantitating α-hydroxytriazolam, 8-chloro-6-(2-chlorophenyl)-1-(hydroxymethyl) - 4*H*-*s*-triazolo[4,3 - *a*][1,4]benzodiazepine (I-a), the principal urinary metabolite of triazolam in the mouse[2], in 0 to 24-hr urine samples following β-glucuronide glucuronosohydrolase hydrolysis.

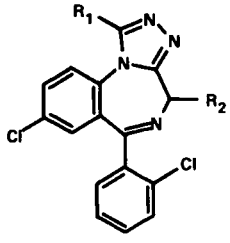

I

I: R_1=CH_3, R_2=H; triazolam

I-a: R_1=CH_2OH, R_2=H; α-hydroxytriazolam

I-b: R_1=CH_2OH; R_2=OH; α, 4-dihydroxytriazolam

I-c: R_1=H, R_2=H; 1-demethyltriazolam

I-d: R_1=CH_3, R_2=OH; 4-hydroxytriazolam

EXPERIMENTAL

Study Protocol—One week prior to the termination of a 24-month carcinogenicity study of triazolam in $B_6C_3F_1$ mice, three male and three female mice were randomly selected from among surviving mice in each dosage group of the study and placed in individual stainless steel metabolism cages equipped with urine and feces separators. As in the carcinogenicity study, water and pelleted food[3] containing sufficient drug to provide approximately 0-, 10-, 30-, and 100-mg/kg/day triazolam doses were provided *ad libitum* to mice in each dosage group. The potency, content uniformity, and stability of the pelleted triazolam–diet mixtures were determined using a high-performance liquid chromatographic (HPLC) assay[4]. Food consumption was measured daily by weighing tared feed cups. Following a 2-day acclimatization period, urine samples were collected over two consecutive 24-hr periods in screw-capped vials fitted with aluminum-lined caps. Any urine remaining in the cages was rinsed into the containers with deionized water. The samples were stored at −20°.

Reagents—The solvents used in the study were distilled-in-glass UV grade[5]. Analytical reagent-grade inorganic chemicals[6] were prepared in distilled, deionized water. The reference standard, α-hydroxytriazolam, and the internal standard, alprazolam (8-chloro-1-methyl-6-phenyl-4*H*-*s*-triazolo[4,3-*a*][1,4]benzodiazepine), were used without further purification[7]. The β-D-glucuronide glucuronosohydrolase preparation[8] (E.C. 3.2.1.31) was used as received.

Standards—A 20-μg/ml stock solution of α-hydroxytriazolam was prepared by dissolving an accurately weighed sample of the reference standard in acetonitrile. Calibration curve standards containing 20, 14, 10, 7, 5, 3, 2, 1, and 0.5 μg/ml of α-hydroxytriazolam were prepared by making appropriate dilutions of the stock solution with acetonitrile. A 1-μg/ml working internal standard solution was prepared by dissolving the reference standard, alprazolam, in acetonitrile.

Calibration Curves—Calibration curves were prepared each day of sample analysis to establish the linearity and reproducibility of the method. One-milliliter aliquots of the internal standard and the appropriate calibration curve standard were added to 16 × 125-mm screw-capped culture tubes fitted with polytef-lined caps, and the acetonitrile was evaporated to dryness at 50° under a gentle stream of dry nitrogen[9]. A 500-μl aliquot of blank mouse urine was added to each tube prior to enzymatic hydrolysis.

Sample Preparation—One milliliter of internal standard was added to 16 × 125-mm screw-capped culture tubes fitted with polytef-lined caps, and the acetonitrile was evaporated to dryness at 50° under a gentle stream of dry nitrogen. The urine samples were thoroughly mixed, and 500-, 175-, and 50-μl aliquots of the samples collected from animals administered 0 and ~10, ~30, and ~100 mg/kg/day of triazolam, respectively, were transferred to the sample tubes for analysis. The 175- and 50-μl samples were diluted to 500-μl with 0.05 *M* acetate buffer (pH 4.5) prior to enzymatic hydrolysis.

Enzymatic Hydrolysis—The calibration curve standards and unknowns were hydrolyzed in a water bath[10] at 37° for 24 hr following addition of 100 μl of 2 *M* acetate buffer (pH 4.5) and 400 μl of 0.05 *M* acetate buffer (pH 4.5) containing 30,000 Fishman units of β-D-glucuronide glucuronosohydrolase.

Extraction—The hydrolyzed samples were buffered with 2 ml of 4 *M* NaOH and extracted twice with 5-ml aliquots of methylene chloride–toluene (1:1, v/v) for 15 min at 280 cpm on a two-speed reciprocating shaker[11]. Following centrifugation for 10 min at 2000 rpm, the organic phase was transferred to 15-ml conical tubes and evaporated to dryness at 50° under a gentle stream of dry nitrogen. The resulting residues were reconstituted in 4 ml of chromatographic mobile phase, thoroughly mixed on a high-speed vortex mixer[12], and chromatographed (250-μl samples).

Chromatographic Analysis—A constant-flow liquid chromatograph[13] equipped with a loop injection valve[14] and a 214-nm UV detector[15] was used for the analysis. The samples were chromatographed on a commercially prepared reverse-phase column[16], thermostated[17] at 50°, using a mobile phase containing water–acetonitrile (7:3, v/v) at a flow rate of 2.0 ml/min. Under these chromatographic conditions the retention times of the α-hydroxytriazolam and internal standard were ~9.5 and 14 min, respectively.

Mass Spectrometry—Chromatographic fractions collected at the retention times of major peaks in chromatograms of enzymatically hydrolyzed urine extracts were lyophilized, and electron-impact mass spectra (EI/MS) (70 eV) were recorded using a magnetic sector mass spectrometer[18].

[1] Halcion; The Upjohn Co., Kalamazoo, MI 49001.
[2] E. G. Daniels, R. L. VanEyk, and J. E. Stafford, unpublished data.
[3] 5003M Purina Laboratory Chow; Ralston Purina Co., St. Louis, Mo.
[4] W. J. Adams and P. A. Bombardt, unpublished data.
[5] Burdick & Jackson Laboratories, Muskegon, Mich.
[6] Mallinckrodt, St. Louis, Mo.
[7] Pharmaceutical Research & Development Laboratories, The Upjohn Co., Kalamazoo, Mich.
[8] Sigma Chemical Co., St. Louis, MO 63178.
[9] Multivap Analytical Evaporator; Organomation Associates, Shrewsbury, Mass.
[10] Model 3005-7 Sample Thermostat; Chicago Apparatus Co., Chicago, Ill.
[11] Eberbach and Sons, Ann Arbor, Mich.
[12] Lab-Line Instruments, Melrose Park, Ill.
[13] Model 6000A; Waters Associates, Milford, Mass.
[14] Model CV-6-HP_{ax}; Valco Instruments, Houston, Tex.
[15] Model 1203 UV Monitor; Laboratory Data Control, Riviera Beach, Fla.
[16] Brownlee Labs RP-5A; Rheodyne, Inc., Berkeley, Calif.
[17] LAUDA K-2/R Circulating Water Bath; Brinkmann Instruments, Westbury, NY 11590
[18] Model CH7A; Varian MAT, Bremen, W. Germany.

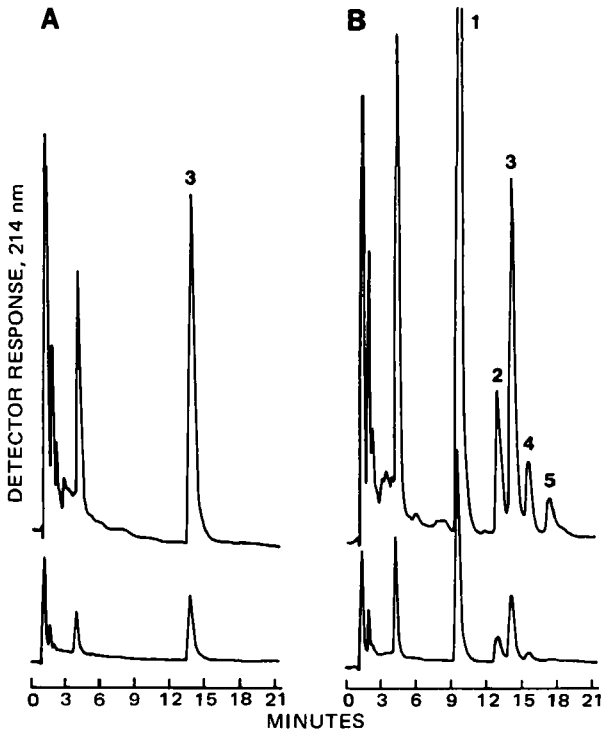

Figure 1—*Chromatograms of extracts of hydrolyzed mouse urine from (A) a control mouse and (B) a mouse administered ~10 mg/kg triazolam. Key: (1) α-hydroxytriazolam; (2) 1-demethyltriazolam; (3) internal standard; (4) triazolam; and (5) 5-chloro-2-(3-methyl-4H-1,2,4-triazol-4-yl)-2′-chlorobenzophenone.*

Calculations—The α-hydroxytriazolam concentrations of the unknown samples were calculated from peak height ratios using the slope computed by linear regression analysis of the unweighted calibration curve data. Peak height ratios were calculated by dividing the α-hydroxytriazolam peak heights by the internal standard peak heights. The quantity of α-hydroxytriazolam excreted over a 24-hr period, expressed as milligrams of α-hydroxytriazolam per kilogram of body weight, was calculated from the α-hydroxytriazolam concentration, the volume of urine collected over the 24-hr period, and the mean body weight.

The triazolam dose received by each animal, expressed as milligrams of triazolam per kilogram of body weight, was calculated from the quantity of food consumed over the 24-hr period in which the urines were collected and the mean body weight. No attempt was made to correct the diet consumption data for the amount of food dropped through the bottom of the cage. The quantity of food dropped into the urine appeared to be small and evenly distributed among the dosage groups.

Statistical Analysis—Statistical analyses of the experimental data were performed using the SAS statistical analysis programs (5) and NONLIN (6), a computer program for parameter estimation in nonlinear situations.

RESULTS AND DISCUSSION

The measurement of drug levels in the blood following single- or multiple-dose administration of drugs is the experimental approach most frequently used in relative bioavailability studies in humans and large animals, where sequential sampling at precisely known times is possible. This approach is also feasible for bolus drug administration to mice, but has the disadvantage of requiring the sacrifice of several mice at each time point for which data are needed. In the case of *ad libitum* administration of drug–diet mixtures to mice or rats, however, drug ingestion occurs over an extended period instead of precisely known times; therefore, it is difficult and extremely laborious to obtain reliable estimates of relative bioavailability by analysis of blood samples.

An alternative to the determination of relative bioavailability from drug levels in the blood is the measurement of the urinary excretion of intact drug or of a principal drug metabolite (7). A recent single-dose metabolism study of [^{14}C]triazolam in $B_6C_3F_1$ mice established that although there is no urinary excretion of intact drug, ~17% of the orally administered dose of triazolam is excreted in the urine as α-hydroxytriazolam[2]. Excretion of all drug-related materials was complete within 72 hr. Under the chronic-dosing conditions of this study, α-hydroxytriazolam was the major extractable metabolite. Therefore, quantitation of α-hydroxytriazolam in 24-hr urine samples under steady-state conditions was the logical experimental approach for the determination of the relative bioavailability of triazolam in mice. An HPLC method utilizing UV detection was developed for the quantitation of α-hydroxytriazolam in mouse urine.

Table I—Chromatographic Retention Times of Triazolam and Selected Triazolam Metabolites [a]

Compound	Retention Time, min[b]
I	15.5
I-a	9.5
I-b	6.0
I-c	12.8
I-d	10.6
II	11.9
II-a	17.4
II-b	10.0

[a] Samples chromatographed on a 5-μm LiChrosorb RP-8 reverse-phase column thermostated at 50° using a mobile phase containing water–acetonitrile (7:3, v/v): at a flow rate of 2.0 ml/min. [b] The void volume of the column was 1.2 ml.

Chromatographic Analysis—Resolution of α-hydroxytriazolam and the internal standard from coextracted endogenous interferences was accomplished using a 5-μm LiChrosorb RP-8 reverse-phase column thermostated at 50° and a mobile phase containing water–acetonitrile (7:3, v/v) at a flow rate of 2.0 ml/min. Thermostating the column at 50° reduced column back-pressure and shortened the retention times of the compounds of interest. Typical chromatograms of extracts of urine from a control mouse and from a mouse administered ~10 mg/kg/day of triazolam are shown in Fig. 1. The internal standard was added to both samples. The α-hydroxytriazolam and internal standard eluted at ~9.5 and 14.0 min, respectively.

Comparison of chromatograms of urine extracts from control and triazolam-dosed mice indicated that significant quantities of triazolam and several metabolites in addition to α-hydroxytriazolam had been extracted from the urine of the triazolam-dosed mice. Although triazolam was not detected in the urine of mice in the recently conducted metabolism study[2], its presence in the urine samples collected in this study was not unexpected, since it was apparent that all collected urine samples had been contaminated with small pieces of pelleted food which had dropped through the bottom of the cage. The triazolam eluted at ~15.5 min and did not interfere in the analysis. Chromatography of authentic samples of triazolam metabolites that had been identified in mice[2], rats[2,19], dogs (8), or humans (9) provided tentative evidence that the metabolites eluting at ~6.0, 11.9, 12.8, and 17.4 min were α,4-dihydroxytriazolam (I-b), 5-chloro-2-(3-hydroxymethyl-5-methyl-4*H*-1,2,4-triazol-4-yl)-2′-chlorobenzophenone (II), 1-demethyltriazolam (I-c), and 5-chloro-2-(3-methyl-4*H*-1,2,4-triazol-4-yl)-2′-chlorobenzophenone (II-a), respectively (Table I). Direct-inlet MS characterization of chromatographic

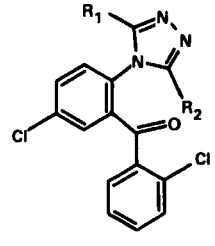

II

II: R_1=CH_3, R_2=CH_2OH; 5-chloro-2-(3-hydroxymethyl-5-methyl-4H-1,2,4-triazol-4-yl)-2′-chlorobenzophenone

II-a: R_1=CH_3, R_2=H; 5-chloro-2-(3-methyl-4H-1,2,4-triazol-4-yl)-2′-chlorobenzophenone

II-b: R_1=CH_2OH, R_2=H; 5-chloro-2-(3-hydroxymethyl-4H-1,2,4-triazol-4-yl)-2′-chlorobenzophenone

[19] F. S. Eberts and R. C. Meeks, unpublished data.

Table II—Abbreviated Electron-Impact Mass Spectra of Triazolam, Selected Triazolam Metabolites, and Lyophilized Chromatographic Fractions

Compound	$M^{+\cdot}$	Six Most Intense Ions for $m/z > 100$, % Relative Abundance
Peak 1[a]	—	360(66), 358(100), 330(35), 328(50), 323(32), 318(33)
I-a	358(100)	360(65), 330(39), 329(32), 328(58), 323(27), 239(33)
II-b	347(13)	320(65), 318(100), 312(54), 284(41), 139(55), 111(50)
Peak 2[b]	—	328(52), 293(30), 265(20), 236(29), 137(18), 111(33)
I-c	328(100)	330(66), 329(30), 293(62), 265(28), 239(20), 137(27)
Peak 4[c]	—	344(66), 342(100), 315(61), 314(31), 313(87), 238(67)
I	342(81)	344(55), 315(69), 314(34), 313(100), 239(34), 238(84)
Peak 5[d]	—	331(19), 296(63), 268(19), 236(16), 183(19), 139(31)
II-a	331(31)	298(35), 296(100), 268(32), 139(47), 127(27), 111(41)

[a] Figure 1, peak 1; 9–11 min fraction. [b] Figure 1, peak 2; 12.5–13.8 min fraction. [c] Figure 1, peak 4; 15.3–16.6 min fraction. [d] Figure 1, peak 5; 17.0–19.0 min fraction.

fractions collected at the retention times of major peaks in the chromatograms confirmed the presence of α-hydroxytriazolam (Table II, peak 1), 1-demethyltriazolam (Table II, peak 2), triazolam (Table II, peak 4), and 5-chloro-2-(3-methyl-4*H*-1,2,4-triazol-4-yl)-2′-chlorobenzophenone (Table II, peak 5) in extracts of the enzymatically hydrolyzed urine. No attempt was made to confirm the identity of minor metabolites. However, a minor metabolite that eluted as a shoulder on the trailing edge of the α-hydroxytriazolam peak in some chromatograms was collected in the same chromatographic fraction as α-hydroxytriazolam (Fig. 1; peak 1, 9–11 min) and was tentatively identified as 5-chloro-2-(3-hydroxymethyl-4*H*-1,2,4-triazol-4-yl)-2′-chlorobenzophenone (II-b). In addition to α-hydroxytriazolam, 4-hydroxytriazolam (I-d) and α,4-dihydroxytriazolam were also isolated from urine and identified by GC/MS in the recently conducted metabolism study of triazolam in the mouse[2]; 5-chloro-2-(3-methyl-4*H*-1,2,4-triazol-4-yl)-2′-chlorobenzophenone was tentatively identified. The low extraction efficiencies of 4-hydroxytriazolam and α,4-dihydroxytriazolam in toluene–methylene chloride (1:1, v/v) precluded isolation of sufficient quantities of these metabolites to allow confirmation by MS in the present study.

Assay Recovery—The absolute recovery of α-hydroxytriazolam from hydrolyzed urine was determined by comparing the slopes of standard curves for which the α-hydroxytriazolam standards were added prior to and following the extraction step in the sample preparation procedure. Alprazolam was added as an external standard in the recovery experiments.

Extraction of the hydrolyzed urine with toluene provided excellent recoveries of triazolam, as had been found in previously developed analytical methods for triazolam in serum (10, 11); however, the recovery of α-hydroxytriazolam was <30%. Addition of methylene chloride to the toluene (1:1, v/v) increased the recovery to 94.5 ± 2.7% and provided an extract that was free of endogenous interferences. Furthermore, the recoveries of the internal standard, triazolam, 5-chloro-2-(3-hydroxymethyl-5-methyl-4*H*-1,2,4-triazol-4-yl)-2′-chlorobenzophenone, and 5-chloro-2-(3-methyl-4*H*-1,2,4-triazol-4-yl)-2′-chlorobenzophenone were all >90%. However, the recoveries of α,4-dihydroxytriazolam and 4-hydroxytriazolam were <3 and 45%, respectively.

Assay Linearity and Precision—The linearity and precision of the method were established by analyzing standard curve samples on each day that unknowns were analyzed. Linear regression analysis of calibration curve data indicated no significant deviations from linearity ($r^2 \geq 0.9962$, $n = 3$) for α-hydroxytriazolam concentrations ranging from 0.5 to 20 μg/ml. The standard curve intercepts were not significantly different from zero ($p > 0.05$) for all three curves.

An estimate of the interassay reproducibility and precision was obtained by comparison of standard curves prepared over a 3-day period. The slopes of the three curves ranged from 1.0703 to 1.2145 ml/μg with a mean slope ± percent relative standard deviation of 1.1563 ± 0.0097 ml/μg and a mean correlation coefficient (r^2) of 0.9994. The percent relative standard deviations of the interassay ordinate values for the three curves were ± 3.3, 3.4, 3.2, 4.9, 8.4, 3.6, 6.3, 10.8, and 5.7 for concentrations (abscissa) of 0.5, 1.0, 2.0, 3.0, 5.1, 7.1, 10.2, 14.3, and 20.4 μg/ml, respectively. The limit of detection of the method was ~6 ng/ml (0.5 ng on-column; signal/noise, 3/1).

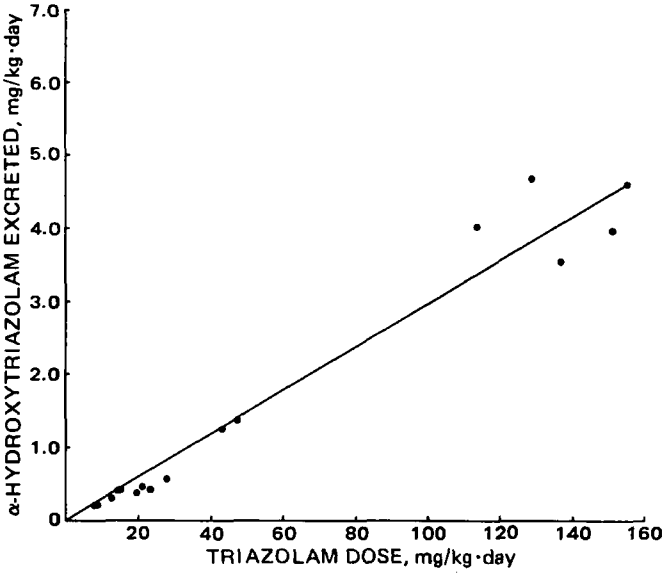

Figure 2—*Plot of the α-hydroxytriazolam excretion data for female mice. The solid line is a plot of the theoretical model which gave the best fit of the experimental data;* $E = C_1(dose)$, *where* E *represents the milligrams of α-hydroxytriazolam excreted per kilogram body weight per day and* $C_1 = 0.0298 \pm 0.0011$ *(ESD) mg of α-hydroxytriazolam/mg of triazolam.*

Triazolam Absorption—Plots of the quantity of α-hydroxytriazolam excreted in urine over a 24-hr period *versus* triazolam dose for the female and male mice are shown in Figs. 2 and 3, respectively. Regression analysis of the female excretion data (5) indicated that the quantity of α-hydroxytriazolam excreted (E) was proportional to the triazolam dose. That is, coefficients for the $n = 0, 2, 3, 4$, *etc.* terms in the polynomial expression, $E = \sum_{n=0}^{N} C_n \cdot (\text{dose})^n$, were not statistically significant ($p > 0.05$). The root-mean-square (RMS) deviation for the linear function, $E = C_1 \cdot (\text{dose})$, was 0.301 mg of α-hydroxytriazolam/kg·day, with $C_1 = 0.0298 \pm 0.0011$ (*ESD*) mg of α-hydroxytriazolam/mg of triazolam. Regression analysis of the male α-hydroxytriazolam excretion data (5), assuming dose proportionality, indicated that the slope of the line, 0.0428 ± 0.0047 (*ESD*) mg of α-hydroxytriazolam/mg of triazolam, was greater than that found for the female excretion data. More important, however, a distinct

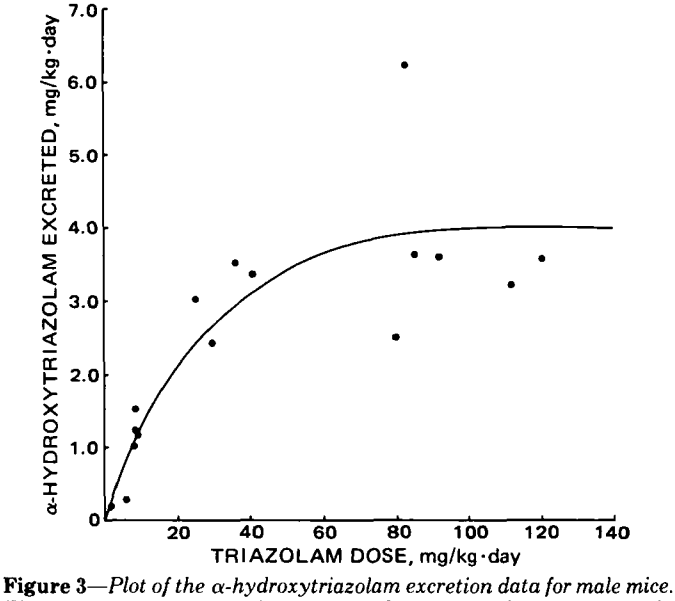

Figure 3—*Plot of the α-hydroxytriazolam excretion data for male mice. The solid line represents the theoretical model which gave the best fit of the experimental data:* $E = A[1 - e^{-B(\text{dose})}]$, *where* E *represents the milligrams of α-hydroxytriazolam excreted per kg body weight per day,* $A = 4.02 \pm 0.40$ *(ESD) mg of α-hydroxytriazolam/kg-day, and* $B = 0.038 \pm 0.010$ *(ESD) kg·day/mg.*

nonlinear trend in the male excretion data was apparent, reflected in the RMS deviation (1.162 mg of α-hydroxytriazolam/kg·day) which was nearly four times greater than that for the female data. A plausible nonlinear model of the male excretion data is one in which the quantity of α-hydroxytriazolam excreted approaches an asymptotic value with increasing doses of triazolam. An exponential function of the dose was adopted, $E = A[1 - e^{-B \cdot (\text{dose})}]$, where A and B are adjustable parameters. The best fit parameters for the male excretion data, estimated using NONLIN (6), were $A = 4.02 \pm 0.40$ mg of α-hydroxytriazolam/kg·day and $B = 0.038 \pm 0.010$ kg·day/mg; the associated RMS deviation was 0.70 mg of α-hydroxytriazolam/kg·day, a significantly better fit of the experimental data than that afforded by the one-parameter linear model ($F_{\text{statistic}} = 34.6$; $n = 22$).

In conclusion, triazolam absorption, as reflected by α-hydroxytriazolam urinary excretion data for female and male mice, increased with triazolam dose. The quantity of α-hydroxytriazolam excreted by female mice was proportional to the triazolam dose, while the male excretion data were adequately represented by a model which predicts that the quantity of α-hydroxytriazolam excreted approaches an asymptotic value with increasing doses of triazolam.

REFERENCES

(1) *Fed. Regist.*, **43**, (247), 60018, December 22, 1978.

(2) D. R. Van Harken and G. H. Hottendorf, *Toxicol. Appl. Pharmacol.*, **43**, 407 (1978).

(3) R. D. Smyth, R. C. Gaver, K. A. Dandekar, D. R. Van Harken, and G. H. Hottendorf, *Toxicol. Appl. Pharmacol.*, **50**, 493 (1979).

(4) J. B. Hester, A. D. Rudzik, and B. V. Kamdar, *J. Med. Chem.*, **14**, 1078 (1972).

(5) J. H. Goodnight, in "SAS User's Guide," J. T. Helwig and K. A. Council, Eds., SAS Institute, Raleigh, N.C., 1979, pp. 237–263.

(6) C. M. Metzler, "NONLIN, A Computer Program for Parameter Estimation in Nonlinear Situations," The Upjohn Co., Kalamazoo, Mich., 1969.

(7) J. G. Wagner, "Fundamentals of Clinical Pharmacokinetics," Drug Intelligence Publications, Hamilton, Ill., 1975, p. 349.

(8) F. S. Eberts, Jr., *Drug Metab. Dispos.*, **5**, 547 (1977).

(9) F. S. Eberts, Jr., Y. Philopoulos, L. M. Reineke, and R. W. Vliek, *Clin. Pharmacol. Ther.*, **29**, 81 (1981).

(10) W. J. Adams, *Anal. Lett.*, **12**, 657 (1979).

(11) W. J. Adams, U. M. Rykert, and P. A. Bombardt, *Anal. Lett.*, **13**, 149 (1980).

ACKNOWLEDGMENTS

Presented in part at the 31st National Meeting of the APhA Academy of Pharmaceutical Sciences held in Orlando, Fla. in 1981.

The authors wish to thank A. A. Forist and D. G. Kaiser for their assistance in developing the study protocol, E. G. Daniels for helpful discussions concerning triazolam metabolism in the mouse; H. Ko, H. S. Greenberg, and C. M. Metzler for helpful discussions concerning modeling and statistical analysis of the excretion data; and S. Yoder for typing this manuscript.

Mechanisms of Potassium Chloride Release from Compressed, Hydrophilic, Polymeric Matrices: Effect of Entrapped Air

R. W. KORSMEYER ‡, R. GURNY *x, E. DOELKER *, P. BURI *, and N. A. PEPPAS ‡

Received June 28, 1982, from the *School of Pharmacy, University of Geneva, CH-1211 Geneva 4, Switzerland and the ‡ School of Chemical Engineering, Purdue University, West Lafayette, IN 47907. Accepted for publication September 14, 1982.

Abstract □ The release of potassium chloride from hydroxypropyl methylcellulose matrices was investigated for tablets prepared with several different compression forces. It was determined that the release kinetics for these systems deviates significantly from the classical $t^{1/2}$ dependence. This behavior was attributed to air entrapped in the matrix during preparation. Removal of the air prior to release restored the traditional $t^{1/2}$ behavior.

Keyphrases □ Potassium chloride—release from hydroxypropyl methylcellulose matrices, effect of entrapped air, kinetics □ Matrices, hydroxypropyl methylcellulose—release of potassium chloride, effect of entrapped air, kinetics □ Kinetics—release of potassium chloride from hydroxypropyl methylcellulose matrices, effects of entrapped air

Compressed, hydrophilic, polymeric matrices provide a convenient method for achieving sustained release of highly water-soluble drugs (1, 2). Release profiles are usually analyzed using equations derived by T. Higuchi (3) and W. Higuchi (4) and adapted by Lapidus and Lordi (5, 6). However, such systems often exhibit complex kinetics (7, 8) that are poorly explained by these traditional models of drug release. Modeling efforts in this area may be assisted by better understanding of the physical factors that contribute to (*a*) the swelling of the polymeric matrix due to transport of the penetrating species into the porous system and (*b*) the initial dissolution and release of the incorporated drug.

The goal of this work was to investigate some of the factors affecting the overall release behavior, especially the importance of entrapped air in the porous structure. The model system chosen consisted of potassium chloride as the water-soluble drug and hydroxypropyl methylcellulose as the hydrophilic polymer. Some of the technological factors influencing the overall potassium chloride release profile in this system have been analyzed by Salomon *et al.* (9–11). Their studies revealed that the release deviates significantly from the traditional $t^{1/2}$ dependence called for by the Higuchi and Lapidus–Lordi models during the early stages of the experiments. Even improved mathematical models especially developed for this system (12) could not fully describe the release behavior. To investigate this physical phenomenon more thoroughly, the experimental procedure of Salomon *et al.* (9–11) was followed with improved time resolution.

EXPERIMENTAL

Materials—The materials used were potassium chloride[1] (water solubility, 332 mg/cm³ at 37°) and hydroxypropyl methylcellulose[2]. This polymer had the following characteristics according to the manufacturer:

[1] Ph. Helv./Ph. Eur. grade; Siegfried, Zofingen, Switzerland.
[2] Methocel K 15M Premium; Dow Chemical Co., Midland, MI 48640.

0022-3549/83/1000-1189$01.00/0

nonlinear trend in the male excretion data was apparent, reflected in the RMS deviation (1.162 mg of α-hydroxytriazolam/kg·day) which was nearly four times greater than that for the female data. A plausible nonlinear model of the male excretion data is one in which the quantity of α-hydroxytriazolam excreted approaches an asymptotic value with increasing doses of triazolam. An exponential function of the dose was adopted, $E = A[1 - e^{-B \cdot (\text{dose})}]$, where A and B are adjustable parameters. The best fit parameters for the male excretion data, estimated using NONLIN (6), were $A = 4.02 \pm 0.40$ mg of α-hydroxytriazolam/kg·day and $B = 0.038 \pm 0.010$ kg·day/mg; the associated RMS deviation was 0.70 mg of α-hydroxytriazolam/kg·day, a significantly better fit of the experimental data than that afforded by the one-parameter linear model ($F_{\text{statistic}} = 34.6$; $n = 22$).

In conclusion, triazolam absorption, as reflected by α-hydroxytriazolam urinary excretion data for female and male mice, increased with triazolam dose. The quantity of α-hydroxytriazolam excreted by female mice was proportional to the triazolam dose, while the male excretion data were adequately represented by a model which predicts that the quantity of α-hydroxytriazolam excreted approaches an asymptotic value with increasing doses of triazolam.

REFERENCES

(1) *Fed. Regist.*, **43**, (247), 60018, December 22, 1978.

(2) D. R. Van Harken and G. H. Hottendorf, *Toxicol. Appl. Pharmacol.*, **43**, 407 (1978).

(3) R. D. Smyth, R. C. Gaver, K. A. Dandekar, D. R. Van Harken, and G. H. Hottendorf, *Toxicol. Appl. Pharmacol.*, **50**, 493 (1979).

(4) J. B. Hester, A. D. Rudzik, and B. V. Kamdar, *J. Med. Chem.*, **14**, 1078 (1972).

(5) J. H. Goodnight, in "SAS User's Guide," J. T. Helwig and K. A. Council, Eds., SAS Institute, Raleigh, N.C., 1979, pp. 237–263.

(6) C. M. Metzler, "NONLIN, A Computer Program for Parameter Estimation in Nonlinear Situations," The Upjohn Co., Kalamazoo, Mich., 1969.

(7) J. G. Wagner, "Fundamentals of Clinical Pharmacokinetics," Drug Intelligence Publications, Hamilton, Ill., 1975, p. 349.

(8) F. S. Eberts, Jr., *Drug Metab. Dispos.*, **5**, 547 (1977).

(9) F. S. Eberts, Jr., Y. Philopoulos, L. M. Reineke, and R. W. Vliek, *Clin. Pharmacol. Ther.*, **29**, 81 (1981).

(10) W. J. Adams, *Anal. Lett.*, **12**, 657 (1979).

(11) W. J. Adams, U. M. Rykert, and P. A. Bombardt, *Anal. Lett.*, **13**, 149 (1980).

ACKNOWLEDGMENTS

Presented in part at the 31st National Meeting of the APhA Academy of Pharmaceutical Sciences held in Orlando, Fla. in 1981.

The authors wish to thank A. A. Forist and D. G. Kaiser for their assistance in developing the study protocol, E. G. Daniels for helpful discussions concerning triazolam metabolism in the mouse; H. Ko, H. S. Greenberg, and C. M. Metzler for helpful discussions concerning modeling and statistical analysis of the excretion data; and S. Yoder for typing this manuscript.

Mechanisms of Potassium Chloride Release from Compressed, Hydrophilic, Polymeric Matrices: Effect of Entrapped Air

R. W. KORSMEYER ‡, R. GURNY *x, E. DOELKER *, P. BURI *, and N. A. PEPPAS ‡

Received June 28, 1982, from the *School of Pharmacy, University of Geneva, CH-1211 Geneva 4, Switzerland and the ‡ School of Chemical Engineering, Purdue University, West Lafayette, IN 47907. Accepted for publication September 14, 1982.

Abstract □ The release of potassium chloride from hydroxypropyl methylcellulose matrices was investigated for tablets prepared with several different compression forces. It was determined that the release kinetics for these systems deviates significantly from the classical $t^{1/2}$ dependence. This behavior was attributed to air entrapped in the matrix during preparation. Removal of the air prior to release restored the traditional $t^{1/2}$ behavior.

Keyphrases □ Potassium chloride—release from hydroxypropyl methylcellulose matrices, effect of entrapped air, kinetics □ Matrices, hydroxypropyl methylcellulose—release of potassium chloride, effect of entrapped air, kinetics □ Kinetics—release of potassium chloride from hydroxypropyl methylcellulose matrices, effects of entrapped air

Compressed, hydrophilic, polymeric matrices provide a convenient method for achieving sustained release of highly water-soluble drugs (1, 2). Release profiles are usually analyzed using equations derived by T. Higuchi (3) and W. Higuchi (4) and adapted by Lapidus and Lordi (5, 6). However, such systems often exhibit complex kinetics (7, 8) that are poorly explained by these traditional models of drug release. Modeling efforts in this area may be assisted by better understanding of the physical factors that contribute to (*a*) the swelling of the polymeric matrix due to transport of the penetrating species into the porous system and (*b*) the initial dissolution and release of the incorporated drug.

The goal of this work was to investigate some of the factors affecting the overall release behavior, especially the importance of entrapped air in the porous structure. The model system chosen consisted of potassium chloride as the water-soluble drug and hydroxypropyl methylcellulose as the hydrophilic polymer. Some of the technological factors influencing the overall potassium chloride release profile in this system have been analyzed by Salomon *et al.* (9–11). Their studies revealed that the release deviates significantly from the traditional $t^{1/2}$ dependence called for by the Higuchi and Lapidus–Lordi models during the early stages of the experiments. Even improved mathematical models especially developed for this system (12) could not fully describe the release behavior. To investigate this physical phenomenon more thoroughly, the experimental procedure of Salomon *et al.* (9–11) was followed with improved time resolution.

EXPERIMENTAL

Materials—The materials used were potassium chloride[1] (water solubility, 332 mg/cm³ at 37°) and hydroxypropyl methylcellulose[2]. This polymer had the following characteristics according to the manufacturer:

[1] Ph. Helv./Ph. Eur. grade; Siegfried, Zofingen, Switzerland.
[2] Methocel K 15M Premium; Dow Chemical Co., Midland, MI 48640.

0022-3549/83/1000-1189$01.00/0

Table I—Physical Characteristics of Investigated Tablets [a]

Compression Force, kN	Pressure, MPa	Thickness, mm	Apparent Density, g/cm³	Void Fraction	Mean Pore Diameter, μm
5	28	2.75 ± 0.09	1.025 ± 0.043	0.385 ± 0.026	6.25 ± 1.30
10	56	2.37 ± 0.04	1.208 ± 0.004	0.275 ± 0.003	2.22 ± 0.14
27	150	2.10 ± 0.04	1.370 ± 0.008	0.178 ± 0.005	0.36 ± 0.04
50	280	2.05 ± 0.02	1.390 ± 0.019	0.166 ± 0.011	0.25 ± 0.12

[a] Average of three experiments (± *SD*).

number average molecular weight $\overline{M}_n$ = 120,000, intrinsic viscosity [η] = 11.0 dl/g, number average degree of polymerization $\overline{DP}_n$ = 650, viscosity of a 2% solution at 20° η = 150 poises, and degree of substitution 19–24% methoxy and 4–12% hydroxypropoxy (based on total weight of polymer). In addition, this resin is completely amorphous and remained so during these experiments, as verified by X-ray diffraction.

Diffusion Experiments—Equal amounts by weight of potassium chloride and hydroxypropyl methylcellulose of particle size 63–100 μm were combined using a tridimensional mixer[3]. A 500-mg portion of the resulting mixture was compressed with the desired force (5,10, 27, or 50 kN corresponding to pressure of 28, 56, 150, and 280 MPa, respectively) in a 15-mm acrylic die on a hydraulic press[4] equipped with flat-faced punches. The tablet was left within the die and one face was sealed with a plastic stopper. The assembly was then placed in 500 ml of distilled water at 37° as described previously (9, 11). The release of potassium chloride was followed by continuous monitoring of the conductivity[5] of the release medium. Tablets prepared in the same manner as those used in the release experiments were characterized using the method of Gupte (13) (see Table I).

Samples were also prepared at 28 and 280 MPa using the same procedure as before but removing the air entrapped in the tablets by a modification of the technique developed by Desai *et al.* (14). The tablet holder was placed in a filter flask which was sealed, placed in a 37° water bath, and evacuated to a pressure of 0.03–0.06 mm Hg. Distilled water (500 cm³) was aspired into the flask, stirring begun, and the contents circulated through the conductivity cell as above.

RESULTS AND DISCUSSION

The results of the release experiments are summarized in graphical form in Fig. 1, which represents the fractional release, M_t/M_∞, as a function of time. The most striking feature is the increase in release rate after 1.4–4.0 hr (depending on the pressure used). In addition, the release from tablets compressed at 280 MPa is significantly faster than the others, in the range of $M_t/M_\infty < 0.2$. For $M_t/M_\infty > 0.2$, the release rate from all tablets except those compressed at 28 MPa is quite similar.

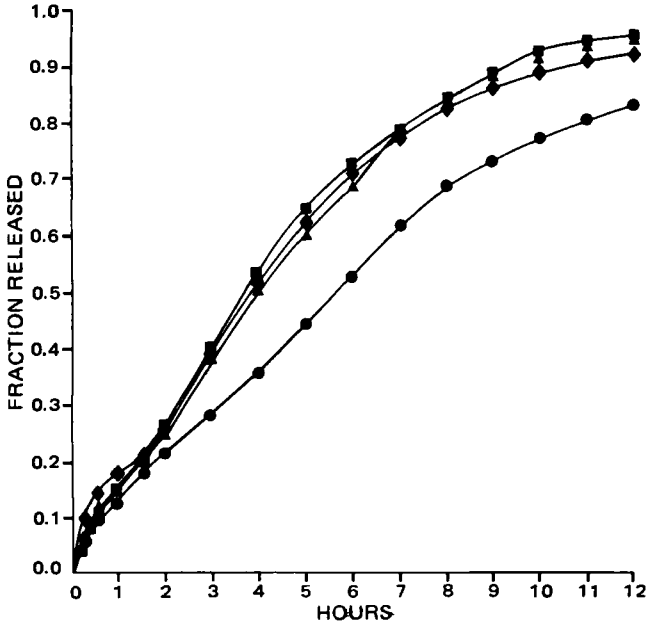

Figure 1—*Potassium chloride release profiles from tablets prepared at different pressures. Key: (●) 28 MPa; (■) 56 MPa; (▲) 150 MPa; (◆) 280 MPa.*

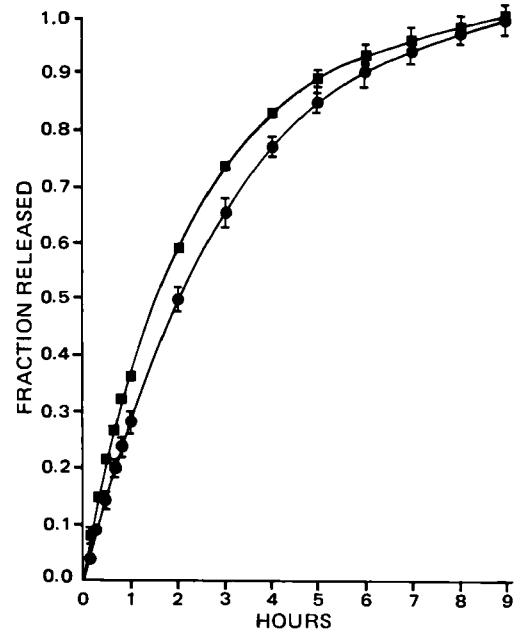

Figure 2—*Potassium chloride release profiles from evacuated tablets prepared at 28 MPa (●) and 280 MPa (■).*

In the systems studied, the release rate was found to vary inversely with tablet porosity and mean pore diameter. Since the opposite effect is normally expected, one must infer that release is not governed by the traditional porous-diffusion mechanism. One possible explanation is that air trapped within the tablets acts as a transport barrier. Consequently, as the initial porosity of the tablets increases, the initial air content increases leading to slower release of the drug.

To test this assumption, a new series of experiments using tablets prepared at the two extreme pressures was undertaken utilizing the modification of the technique developed by Desai *et al.* for polyethylene matrices (14) (Fig. 2). This technique effectively eliminated all observed anomalies in the release rate. Moreover, only a small difference was observed between the tablets prepared at 28 MPa and those prepared at 280 MPa. The release behavior could be fitted well to the equation:

$$\frac{M_t}{M_\infty} = a + bt^{1/2} \qquad \text{(Eq. 1)}$$

for values of $M_t/M_\infty \leq 0.6$.

When the experimental data were fitted to Eq. 1, the average values obtained for the coefficients *a* and *b* and the corresponding lag times were as shown in Table II. The fact that the values of the intercept, *a*, are not equal to zero could reasonably be attributed to the time lag associated with tablet swelling, although the physical manipulation of the equipment at the beginning of each experiment introduces uncertainty at these very short times.

Table II—Fitting of Release Data from Fig. 2 to a Square-Root of Time Release Behavior

Pressure, MPa	Intercept (*a*)	Slope (*b*), $hr^{-1/2}$	Time lag, hr	*r*
28	−0.181 ± 0.0009	0.476 ± 0.032	0.145	0.996–0.998
280	−0.127 ± 0.017	0.502 ± 0.014	0.064	0.998–0.999

[3] Turbula mixer model T2A; Bachofen, Basle, Switzerland.
[4] Specac, Sidcup, England.
[5] E518 conductivity meter; Metrohm, Herisau, Switzerland.

Table III—Characteristic Time of Increase in Release Rate Due to Entrapped Air as a Function of Void Fraction of the Tablets

Pressure, MPa	Void Fraction	Characteristic Time, hr
28	0.385	3.5–4.0
56	0.275	1.9–2.5
150	0.178	1.7–1.8
280	0.166	1.4–1.5

Even though the values of the volume and porosity of these tablets are continuously changing during swelling and release, owing to the short time-scale of the experiment, the changes are not large and therefore one may obtain an approximate value for the effective solute diffusivity D' by use of an equation adapted by Lapidus and Lordi (6):

$$\frac{M_t}{M_\infty} = \frac{S}{M_\infty}\left[D'\epsilon C_s\left(\frac{2M_\infty}{V} - \epsilon C_s\right)\right]^{1/2} t^{1/2} \qquad \text{(Eq. 2)}$$

where S is the surface area available for release (1.767 cm^2), V is the volume of the tablet (0.477 cm^3 at 28 MPa and 0.362 cm^3 at 280 MPa), C_s is the solubility of the active agent (332 mg/cm^3), ϵ is the tablet porosity (0.17 at 280 MPa and 0.38 at 28 MPa), and D' is expressed as D/τ, where τ is the tortuosity of the matrix and D is the effective diffusivity of the drug. Using these values, D' could be calculated from the slope of the plot of M_t/M_∞ *versus* $t^{1/2}$ yielding $D' = 1.04 \times 10^{-5}$ cm^2/sec for systems prepared at 28 MPa and $D' = 1.83 \times 10^{-5}$ cm^2/sec for systems prepared at 280 MPa.

The unusual release behavior of compressed hydroxypropyl methylcellulose tablets is attributed to the entrapped air. The characteristic time at which the increase in release rate is observed can be roughly correlated with the initial tablet porosity (Table III), although the observed increase was sharp only for systems prepared at 150 and 280 MPa. The correlation of this characteristic time with tablet void volume may be interpreted as representing pore filling with gradual displacement of entrained air (see Fig. 3). It is observed that air continues to escape from the tablet throughout most of the drug release. After ~2 hr a nonflat moving front has been formed at the polymer–water interface (Fig. 3c). On complete release of the drug (Fig. 3d), the tablet is not at mechanical equilibrium, although swollen. The outermost portion of the tablet is transparent, but a large amount of air remains entrapped.

Consequently, the inflection in the release curves does not represent the point at which all the air has been displaced, but probably a point at which the pressure of the entrained air (which is compressed as water enters the tablet) equals the pressure of the incoming water. The air then escapes gradually through the pores of the tablet, aided by the softening of the polymer as it absorbs water.

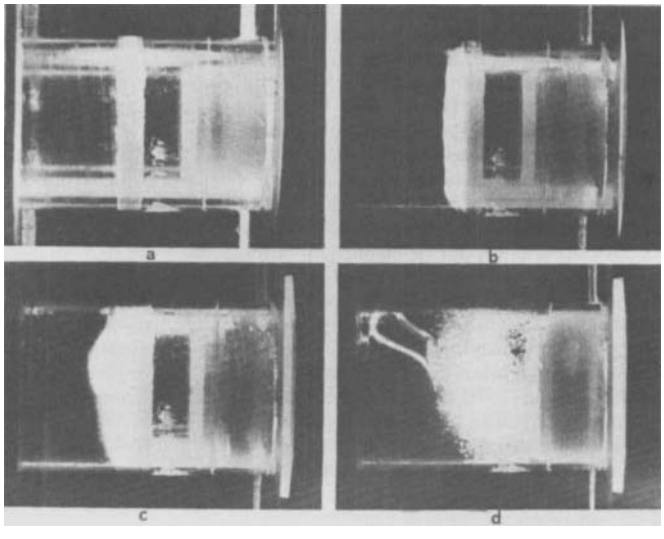

Figure 3—*Sequential swelling of potassium chloride–hydroxypropyl methylcellulose systems at* t = *0 (a),* t = *0.17 hr (b)* t = *2.50 hr (c), and* t = *24 hr [complete potassium chloride release (d)].*

Table IV—Fitting of Release Data from Fig. 1 to Eq. 3 for $M_t/M_\infty \leq 0.7$

Pressure, MPa	Intercept (a)	Slope (b), hr^{-1}	r
28	0.034	0.083	0.998
56	0.019	0.125	0.999
150	0.030	0.113	0.997
280	0.045	0.118	0.994

In contrast, when the tablets are evacuated prior to the introduction of water, the water is forced into the pores rather quickly by atmospheric pressure, as calculated by standard equations for flow in porous media (15). This results in the introduction of a saturated aqueous phase throughout the tablet at the beginning of the experiment. Release then proceeds by a purely diffusive mechanism. An additional simplification effected by this treatment in the case of hydroxypropyl methylcellulose is that potassium chloride release occurs quickly relative to the swelling so that volume changes of the tablet are less important.

It is interesting to observe that the effect of the entrained air is to improve the release profile as compared with traditional $t^{1/2}$ release. For example, although the release profiles are obviously not truly linear with time, the release curve may be fitted to:

$$\frac{M_t}{M_\infty} = a + bt \qquad \text{(Eq. 3)}$$

with $r > 0.99$ up to $M_t/M_\infty = 0.7$, as shown in Table IV. These systems therefore represent an approximation to zero-order release kinetics, although no physical significance should be given at this point to the values of the intercept and the slope reported.

We can conclude that air entrapped during preparation can have a significant effect on the release of drugs from hydrophilic matrices such as hydroxypropyl methylcellulose. This factor is therefore an important consideration in the design of *in vitro* release experiments.

REFERENCES

(1) H. E. Huber, L. B. Dale, and G. L. Christenson, *J. Pharm. Sci.*, **55,** 974 (1966).

(2) H. E. Huber and G. L. Christenson, *J. Pharm. Sci.*, **57,** 164 (1968).

(3) T. Higuchi, *J. Pharm. Sci.*, **52,** 1145 (1963).

(4) W. I. Higuchi, *J. Pharm. Sci.*, **51,** 802 (1962).

(5) H. Lapidus and N. G. Lordi, *J. Pharm. Sci.*, **55,** 840 (1966).

(6) H. Lapidus and N. G. Lordi, *J. Pharm. Sci.*, **57,** 1292 (1968).

(7) M. Bamba, F. Puisieux, J. P. Marty, and J. T. Carstensen, *Int. J. Pharm.*, **2,** 307 (1979).

(8) M. Bamba, F. Puisieux, M. P. Marty,and J. T. Carstensen, *Int. J. Pharm.*, **3,** 87 (1979).

(9) J. L. Salomon, E. Doelker, and P. Buri, *Pharm. Acta Helv.*, **54,** 82 (1979).

(10) J. L. Salomon, P. Vuagnat, E. Doelker, and P. Buri, *Pharm. Acta Helv.*, **54,** 86 (1979).

(11) J. L. Salomon, E. Doelker, and P. Buri, *Pharm. Ind.*, **41,** 799 (1979).

(12) N. A. Peppas, R. Gurny, E. Doelker, and P. Buri, *J. Membr. Sci.*, **7,** 241 (1980).

(13) A. R. Gupte, *Acta Pharm. Technol.*, **22,** 153 (1976).

(14) S. J. Desai, P. Singh, A. P. Simonelli, and W. I. Higuchi, *J. Pharm. Sci.*, **55,** 1235 (1966).

(15) R. A. Greenkorn and D. P. Kessler, "Transfer Operations," McGraw Hill, New York, N.Y., 1972.

ACKNOWLEDGMENTS

The authors thank Dr. H. D. Flack of the Crystallography Group of the University of Geneva for the useful discussions on X-ray diffraction measurements.

Antihyperlipidemic Activity of Saccharin Analogues in Rodents

I. H. HALL ˣ, P. JOSÉE VOORSTAD, JAMES M. CHAPMAN, Jr., and GEORGE H. COCOLAS

Received January 28, 1982, from the *Division of Medicinal Chemistry, School of Pharmacy, University of North Carolina, Chapel Hill, NC 27514.* Accepted for publication August 27, 1982.

Abstract □ Saccharin analogues were observed to be potent antihyperlipidemic agents at 20 mg/kg/day in rodents, significantly reducing both serum cholesterol and triglyceride levels in both normal and atherogenic mice. The saccharin analogues suppressed *in vitro* and *in vivo* liver enzymatic activity of acetyl-CoA synthetase, citrate lyase, and mitochondrial citrate exchange leading to a reduction of available cytoplasmic acetyl-CoA, which is required for the synthesis of cholesterol and fatty acids. Liver acetyl-CoA carboxylase, phosphatidate phosphohydralase, and glycerol-3-phosphate acyl transferase activities were markedly reduced by the saccharin analogues. Suppression of these enzymes would lead to a reduction of triglyceride synthesis. The saccharin analogues accelerated bile excretion of cholesterol metabolites and increased the fecal excretion of the cholesterol, triglycerides, neutral lipids, and phospholipids. The liver and plasma lipoprotein lipid content (including cholesterol, triglycerides, and neutral lipids) was markedly reduced by the saccharin analogues, whereas phospholipid content was elevated. The reduction of lipid content of serum chylomicron, very low-density, low-density, and high-density lipoprotein fractions by the saccharin analogues indicates that these agents may be useful in controlling hyperlipidemic diseases where specific lipoprotein fractions are elevated.

Keyphrases □ Saccharin—analogues, antihyperlipidemic activity, cholesterol and triglyceride reduction □ Antihyperlipidemic agents—saccharin analogues, cholesterol and triglyceride reduction □ Cholesterol—antihyperlipidemic effect of saccharin analogues □ Triglycerides—antihyperlipidemic effect of saccharin analogues

The antihyperlipidemic activity of saccharin and 1-*N*-(*o*-benzosulfimido)butan-3-one has been reported previously (1) in mice at 20 mg/kg/day ip. Saccharin afforded a 33% reduction in serum cholesterol after 16 days and a 49% reduction in serum triglyceride levels after 14 days, whereas 1-*N*-(*o*-benzosulfimido)butan-3-one resulted in a 38% reduction of serum cholesterol and a 49% reduction of serum triglyceride levels (1). Saccharin derivatives were examined for their hypolipidemic effects because of their structural similarity to phthalimide (2) and *N*-phenyl-bridged isoindoline ketones (3), which have been reported previously to have hypolipidemic action in rodents. The purpose of this study was to examine the antihyperlipidemic activity of saccharin and its derivatives in detail, as well as their mode of action on cellular lipid metabolism in rodents.

EXPERIMENTAL

Source of Compounds—Saccharin was purchased commercially[1]. The syntheses and chemical characterizations of 1-*N*-(*o*-benzosulfimido)butan-3-one(1) and 3-*N*-(*o*-benzosulfimido)propionic acid have been reported previously (2).

Antihyperlipidemic Screens in Normal Rodents—Compounds were suspended in 1% carboxymethylcellulose–water and administered to male CF_1 mice (~25 g in weight) intraperitoneally or Holtzman male rats (~200 g in weight) orally by an intubation needle for 16 days. On days 9 and 16, blood was obtained by tail vein bleeding, and the serum was separated by centrifugation for 3 min. The serum cholesterol levels were determined by a modification of the Liebermann–Burchard reaction (4). Serum was also collected on day 14, and the triglyceride content was determined using a commercial kit[2].

Testing in Atherogenic Mice—Male CF_1 mice (~25 g) were placed on a commercial diet[3] that contained butterfat (400 g), cellulose[4] (60 g), cholesterol (53 g), choline dihydrogen citrate (4 g), salt mixture oil[5] (40 g), sodium cholate (20 g), sucrose (223 g), vitamin-free casein (200 g), and total vitamin supplement for a 2-week period. After the cholesterol and triglyceride levels were assayed and observed to be elevated, the mice were administered test drugs at 20 mg/kg/day for an additional 2-week period. Serum cholesterol and triglyceride levels were measured after 14 days of drug administration.

Animal Weights and Food Intake—Periodic animal weights were obtained during the experiments and expressed as a percentage of the animal's weight on day 0. After dosing for 16 days with test drugs, selected organs were excised, trimmed of fat, and weighed. The organ weights were expressed as a percentage of the total body weight of the animal. The average food intake[6] in g/rat/day was determined over the 16-day dosing period.

Toxicity Studies—The acute toxicity (LD_{50} value) (5) was determined in male CF_1 mice by administering test drugs intraperitoneally from 100 mg to 2 g/kg as a single dose. The number of deaths recorded in the group over 7 days was determined for each dosage.

Enzymatic Studies—*In vitro* enzymatic studies were determined using 10% homogenates of male CF_1 mouse liver with 2.5 μmoles of the test drugs and male Holtzman rat livers with 0.100–10 m*M* concentration of the test drugs. *In vivo* enzymatic studies were determined using 10% homogenates of liver from male CF_1 mice obtained after administering the agents for 16 days at a dose of 10–60 mg/kg/day. The liver homogenates for both *in vitro* and *in vivo* studies were prepared in 0.25 *M* sucrose and 0.001 *M* EDTA[(ethylenedinitrilo)tetraacetic acid].

Acetyl-CoA synthetase (6) and adenosine triphosphate-dependent citrate lyase (7) activities were determined spectrophotometrically at 540 nm as the hydroxamate of acetyl-CoA formed after 30 min at 37°. Mitochondrial citrate exchange was determined by the procedure of Robinson *et al.* (8, 9) using sodium [^{14}C]bicarbonate (41 mCi/mmole) incorporated into mitochondrial [^{14}C]citrate after isolating the mitochondria (9000×*g* for 10 min) from the homogenates. The exchange of the [^{14}C]citrate was determined after incubating the mitochondrial fraction, which was loaded with labeled citrate, and the test drugs for 10 min. Then the radioactivity was measured in the mitochondrial and supernatant fractions in scintillation fluid[7] and expressed as a percentage. Cholesterol side-chain oxidation was determined by the method of Kritchevsky and Tepper (10) using [26-^{14}C]cholesterol (50 mCi/mmole) and mitochondria isolated from rat liver homogenates. After an 18-hr incubation at 37° with the test drugs, the generated $^{14}CO_2$ was trapped in the center well in [2-[2-(*p*-1,1,3,3-tetramethylbutylcresoxy)ethoxy]-ethyl]dimethylbenzylammonium hydroxide[8] and counted[7]. 3-Hydroxy-3-methylglutaryl-CoA reductase (HMG-CoA reductase) was measured using [1-^{14}C]acetate (56 Ci/mmole) using a postmitochondrial supernatant (9000×*g* for 20 min) incubated for 60 min at 37° (11). The digitonide derivative of cholesterol was isolated and counted (12). Acetyl CoA carboxylase activity was measured by the method of Greenspan and Lowenstein (13). Initially, the enzyme had to be polymerized for 30 min at 37°, and then the assay mixture containing sodium [^{14}C]bicarbonate (41.0 mCi/mmole) was added and incubated for 30 min at 37° with the test drugs. Fatty acid synthetase activity was determined by the method

[1] Ruger Chemical Co., Inc.

[2] Hycel Triglyceride Test Kit; Fisher Scientific Co.
[3] Basal Atherogenic Test Diet; U.S. Biochemical Corp.
[4] Celufil.
[5] Wesson.
[6] Wayne Blox Rodent Chow.
[7] Fisher Scintiverse in a Packard Scintillation Counter.
[8] Hyamine hydroxide; New England Nuclear.

0022-3549/83/1000-1192$01.00/0

Table I—Effects of Saccharin Analogues on Serum Cholesterol and Triglyceride Levels of Male Holtzman Rats and Male CF_1 Mice [a]

Compound	Rats: Dose, mg/kg/day	Rats: Serum Cholesterol Day 9	Rats: Serum Cholesterol Day 16	Rats: Serum Triglyceride Day 14	Mice: Dose, mg/kg/day	Mice: Serum Cholesterol Day 9	Mice: Serum Cholesterol Day 16	Mice: Serum Triglyceride Day 14
Control (1% carboxymethylcellulose)		100 ± 9[d]	100 ± 7[e]	100 ± 8[f]		100 ± 5[g]	100 ± 6[h]	100 ± 6[i]
Saccharin					10	81 ± 8[b]	76 ± 4[b]	47 ± 4[b]
	20	65 ± 6[b]	56 ± 7[b]	55 ± 6[b]	20	77 ± 6[b]	68 ± 7[b]	48 ± 6[b]
					40	66 ± 5[b]	65 ± 3[b]	54 ± 3[b]
					60	63 ± 5[b]	62 ± 4[b]	61 ± 4[b]
1-*N*-(*o*-Benzosulfimido)butan-3-one	20	64 ± 5[b]	56 ± 6[b]	65 ± 6[b]	20	60 ± 8[b]	62 ± 6[b]	51 ± 7[b]
3-*N*-(*o*-Benzosulfimido)propionic Acid					10	85 ± 6[c]	76 ± 7[b]	84 ± 5[b]
	20	72 ± 6[b]	63 ± 7[b]	48 ± 7[b]	20	70 ± 7[b]	56 ± 7[b]	58 ± 5[b]
					40	77 ± 6[b]	65 ± 5[b]	60 ± 4[b]
					60	68 ± 8[b]	62 ± 6[b]	58 ± 5[b]

[a] Expressed as percentage of control (mean ± *SD*); $n = 6$. [b] $p \leq 0.001$ [c] $p \leq 0.005$. [d] 73 ± 7 mg%. [e] 78 ± 6 mg%. [f] 110 ± 9 mg%. [g] 118 ± 6 mg%. [h] 122 ± 7 mg%. [i] 137 ± 8 mg%.

of Brady *et al.* (14) using [2-^{14}C]malonyl-CoA (37.5 mCi/mmole) incorporated into newly synthesized fatty acids, which were extracted with ether and counted. Acyl transferase activity was determined with L-[2-^{3}H]glycerol-3-phosphate (7.1 Ci/mmole) and the microsomal fraction of the liver homogenates (15). The reaction was terminated after 10 min, and the lipids were extracted with chloroform–methanol (1:2) containing 1% concentrated HCl and counted. Phosphatidate phosphohydralase activity was measured as the inorganic phosphate released after 30 min from phosphatidic acid by the method of Mavis *et al.* (16). The released inorganic phosphate after development with ascorbic acid and ammonium molybdate was determined at 820 nm.

The *in vitro* oxidative phosphorylation process in male CF_1 mouse liver was also examined with an oxygen electrode[9] connected to an oxygraph[10] at 37°. The reaction vessel typically contained 55 μmoles of sucrose, 22 μmoles of monobasic potassium phosphate, 22 μmoles of potassium chloride, 90 μmoles of succinate or 60 μmoles of α-ketoglutarate as substrate, 2 μmoles of adenosine triphosphate, and 2.5 μmoles of the test compounds in a total volume of 1.8 ml. After the basal metabolic (state 4) rate was obtained, 0.257 μmole of adenosine diphosphate was added to obtain the adenosine diphosphate-stimulated respiration (state 3) rate (17). The rates were calculated as μl of oxygen consumed/mg of liver/hr.

Liver, Small Intestine, and Fecal Lipid Extraction—In male CF_1 mice that had been administered test drugs for 16 days, the liver, small intestine, and fecal materials (24-hr collection) were removed and a 10% homogenate in 0.25 *M* sucrose and 0.001 *M* EDTA was prepared. An aliquot (2 ml) of the homogenate was extracted by the methods of Floch *et al.* (18) and Bligh and Dyer (19) and the number of milligrams of lipid weighed. The lipid was taken up in methylene chloride, and the cholesterol level (4), triglyceride levels[11], neutral lipid content (20), and phospholipid content (21) were determined.

[^{14}C]Cholesterol Distribution in Mice and Rats—Male CF_1 mice (~25 g) were administered test agents intraperitoneally for 14 days and rats were administered test agents orally. On day 13, 10 μCi of [4-^{14}C]-cholesterol (52.5 mCi/mmole) was administered intraperitoneally in mice and orally in rats, and feces were collected for 0–6, 6–12, and 12–24 hr postadministration. Twenty-four hours after cholesterol administration, the major organs were excised and samples of blood, chyme, and urine were obtained. Homogenates (10%) were prepared of the tissues which were combusted[12] and counted. Some tissue samples were plated on filter paper[13], dried, and digested for 24 hr in base[8] at 40° and counted. Results were expressed as dpm/mg of wet tissue and dpm/mg of total organ.

Cholesterol Absorption Study—Male Holtzman rats (~400 g) were administered test drug intraperitoneally for 14 days at 20 mg/kg/day. On day 13, 10 μCi of [1,2-^{3}H]cholesterol (40.7 Ci/mmole) was administered to the rat orally. Twenty-four hours later, the blood was collected and the serum was separated by centrifugation (22). Both the serum and the precipitate were counted.

Bile Cannulation Study—Male Holtzman rats (~400 g) were treated with test drugs at 20 mg/kg/day orally for 14 days. The rats were anesthetized with chlorpromazine[14] (25 mg/kg) followed after 30 min by pentobarbital[15] (22 mg/kg ip). The duodenum section of the small intestine was isolated and ligatures were placed around the pyloric sphincter and at a site distally approximately one-third of the way down the duodenum. Sterile isotonic saline was injected into the sectioned off duodenum segment. The saline expanded the duodenum and the common bile duct. After the bile duct was identified, a loose ligature was placed around the duct, an incision was made, the plastic tubing[16] was introduced into the duct. Once past the ligature, the tubing was tied in place and the ligatures around the duodenum were removed. When bile was freely moving down the cannulated tube, [1,2-^{3}H]cholesterol (40.7 Ci/mmole) was injected intravenously into the rats. The bile was collected over the next 6 hr and measured (in ml). Aliquots were counted as well as analyzed for cholesterol content (4).

Plasma Lipoprotein Fractions—Male Holtzman rats (~400 g) were administered test drugs at 20 mg/kg/day for 14 days. On day 14, blood was collected from the abdominal aorta. Serum was separated from whole blood by centrifugation at 3500 rpm. Aliquots (3 ml) were separated by density gradient ultracentrifugation according to the methods of Hatch and Lees (23) and Havel *et al.* (24) into the chylomicrons, very low-density lipoproteins, high-density lipoproteins, and low-density lipoproteins. Each of the fractions was analyzed for cholesterol (4), triglyceride[11], neutral lipids (20), phospholipids (21), and protein levels (25).

RESULTS

Saccharin, 1-*N*-(*o*-benzosulfimido)butan-3-one, and 3-*N*-(*o*-benzosulfimido)propionic acid markedly reduced the serum lipid levels in normal rodents after intraperitoneal administration. In CF_1 mice, saccharin afforded a 38% reduction of serum cholesterol after 16 days of dosing at the 60-mg/kg dose (Table I). In the triglyceride screen in mice, the 10- and 20-mg/kg doses resulted in a reduction of 53 and 52%, respectively. Saccharin was also active as a hypolipidemic agent orally in rats at 20 mg/kg, suppressing serum cholesterol levels 44% and serum triglyceride levels 45%. 3-*N*-(*o*-Benzosulfimido)propionic acid was active in the mouse screen. The maximum suppression of serum cholesterol levels in mice was at 20 mg/kg/day, with 44% reduction. In the triglyceride screen, the 20-, 40-, and 60-mg/kg/day doses caused >40% reduction. 3-*N*-(*o*-Benzosulfimido)propionic acid was active orally in the rat. The serum cholesterol levels were suppressed 37% at 20 mg/kg/day in the rat, while triglyceride levels were suppressed 52%. 1-*N*-(*o*-Benzosulfimido)-butan-3-one in the mouse screen reduced serum cholesterol 38% and triglyceride 49%, whereas in the rat, serum cholesterol was reduced 44% and triglyceride level was reduced 35%. In mice that had been rendered atherogenic by a high lipid diet, after 2 weeks of administration it can be observed that saccharin and the propionic analogue suppressed the induced cholesterol levels by >170% resulting in serum cholesterol only slightly above normal levels (Table II). In the triglyceride screen, levels

[9] Clark oxygen electrode for measuring pO_2 tension.
[10] Gilson Instruments.
[11] Bio-Dynamics/bmc Triglyceride Kit.
[12] Packard Tissue Oxidizer.
[13] Whatman No. 1.
[14] Thorazine, chlorpromazine hydrochloride; Smith, Kline and French Laboratories.
[15] Nembutal, sodium pentobarbital; Abbott Laboratories.
[16] PE-10 Intramedic polyethylene tubing.

Table II—Effects of Saccharin Analogues on Serum Cholesterol and Triglyceride Levels in Normal and Atherogenic Mice [a]

Compound	Serum Cholesterol		Serum Triglyceride	
	2-Week Diet +	14-Day Dosing	2-Week Diet +	14-Day Dosing
Control (1% Carboxymethylcellulose)	100 ± 6[d]	100 ± 7[e]	100 ± 5[f]	100 ± 4[g]
Control Atherogenic Diet	289 ± 9[b]	290 ± 9[b]	131 ± 3[b]	131 ± 5[b]
Saccharin (20 mg/kg/day)	289 ± 9[b]	116 ± 6[c]	131 ± 6[b]	100 ± 4
3-*N*-(*o*-Benzosulfimido)propionic Acid (20 mg/kg/day)	290 ± 10[b]	119 ± 7[c]	129 ± 8[b]	88 ± 5[c]

[a] Expressed as percentage of control (mean ± *SD*); $n = 6$. [b] $p \leq 0.001$ as related to 1% carboxymethylcellulose values. [c] $p \leq 0.005$. [d] 118 ± 6 mg%. [e] 122 ± 7 mg%. [f] 136 ± 7 mg%. [g] 139 ± 5 mg%.

Table III—Effect of Saccharin Derivatives on the Weight of Major Organs and Body Weight of Rats After 16 Days of Dosing at 20 mg/kg/day

Compound	Mean Weight on Day Zero, g	Body Weight Increase on Day 16, %	Food Consumption, gm/day
Control (1% carboxymethylcellulose)	439 ± 8	138 ± 3	22.5
Saccharin	378 ± 9	141 ± 4	19.0
3-*N*-(*o*-Benzosulfimido)propionic Acid	421 ± 8	139 ± 3	20.5

	Percent of Total Body Weight				
	Liver	Lung	Heart	Kidney	Spleen
Control (1% carboxymethylcellulose)	3.46 ± 0.83	0.48 ± 0.04	0.34 ± 0.03	0.71 ± 0.09	0.25 ± 0.05
Saccharin	3.12 ± 0.95	0.50 ± 0.03	0.34 ± 0.04	0.66 ± 0.08	0.21 ± 0.06
Weight of organ, g	15.21 ± 3.59	2.10 ± 0.17	1.51 ± 0.13	3.12 ± 0.39	1.11 ± 0.22

	Brain	Adrenal	Stomach	Small Intestine	Large Intestine
Control (1% carboxymethylcellulose)	0.36 ± 0.04	0.011 ± 0.005	0.68 ± 0.22	2.35 ± 0.65	1.09 ± 0.22
Saccharin	0.34 ± 0.06	0.014 ± 0.008	0.83 ± 0.28	2.28 ± 0.53	1.19 ± 0.18
Weight of organ, g	1.59 ± 0.17	0.047 ± 0.021	2.99 ± 0.96	10.32 ± 2.86	4.78 ± 0.97

[a] Mean ± *SD*; $n = 6$.

Table IV—*In Vitro* Effects of Saccharin Analogues on Mouse Liver Enzyme Activities at 2.5 μmoles [a]

Compound	Mitochondrial Citrate Exchange	Acetyl-CoA Synthetase	Citrate Lyase	HMG-CoA Reductase	Cholesterol Side-Chain Oxidation
Control (1% carboxymethylcellulose)	100 ± 10[c]	100 ± 11[d]	100 ± 9[e]	100 ± 7[f]	100 ± 8[g]
Saccharin	7 ± 5[b]	61 ± 7[b]	65 ± 6[b]	71 ± 7[b]	94 ± 6
1-*N*-(*o*-Benzosulfimido)butan-3-one	7 ± 6[b]	74 ± 9[b]	47 ± 8[b]	98 ± 5	72 ± 4[b]
3-*N*-(*o*-Benzosulfimido)propionic Acid	20 ± 7[b]	53 ± 7[b]	—	95 ± 5	61 ± 3[b]

	Acetyl-CoA Carboxylase	Fatty Acid Synthetase	Phosphatidate Phosphohydrolase	Acyl Transferase
Control (1% carboxymethylcellulose)	100 ± 6[h]	100 ± 7[i]	100 ± 7[j]	100 ± 8[k]
Saccharin	9 ± 2[b]	93 ± 5	52 ± 5[b]	15 ± 3[b]
1-*N*-(*o*-Benzosulfimido)butan-3-one	12 ± 3[b]	104 ± 7	61 ± 4[b]	25 ± 6[b]
3-*N*-(*o*-Benzosulfimido)propionic Acid	43 ± 5[b]	98 ± 6	49 ± 5[b]	8 ± 4[b]

	α-Ketoglutarate		Succinate	
	State 4	State 3	State 4	State 3
Control (1% carboxymethylcellulose)	100 ± 6[l]	100 ± 7[m]	100 ± 5[n]	100 ± 6[o]
Saccharin	69 ± 6[b]	68 ± 4[b]	78 ± 6[b]	65 ± 3[b]
1-*N*-(*o*-Benzosulfimido)butan-3-one	82 ± 7[c]	80 ± 3[b]	64 ± 5[b]	63 ± 4[b]
3-*N*-(*o*-Benzosulfimido)propionic Acid	77 ± 7	61 ± 4[b]	76 ± 5[b]	66 ± 5[b]

[a] Expressed as percentage of control (mean ± *SD*); $n = 6$. [b] $p \leq 0.001$. [c] 30.8 ± 3.1 mg% exchange of mitochondrial citrate. [d] 28.5 ± 3.14 mg of acetyl-CoA formed/g wet tissue/30 min. [e] 30.5 ± 2.74 mg of citrate hydrolyzed/g wet tissue/30 min. [f] 384,900 ± 26,943 dpm cholesterol formed/g wet tissue/60 min. [g] 6080 ± 5.58 dpm CO_2 formed/g wet tissue/18 hr. [h] 32,010 ± 1921 dpm/g wet tissue/30 min. [i] 37,656 ± 2635 dpm/g wet tissue/30 min. [j] 16.70 ± 1.16 μg Pi/g wet tissue/15 min. [k] 537,800 ± 43,024 dpm triglyceride formed/g wet tissue/10 min. [l] 3.51 ± 0.21 μl of oxygen consumed/hr/mg of tissue. [m] 5.21 ± 0.36 μl of oxygen consumed/hr/mg of tissue. [n] 5.92 ± 0.30 μl of oxygen consumed/hr/mg of tissue. [o] 11.31 ± 0.67 μl of oxygen consumed/hr/mg of tissue.

were reduced to normal levels by saccharin and 12% below normal (control) levels by the propionic acid derivative.

Saccharin and the propionic acid derivative did not affect the daily food intake over the 16-day dosing period, nor was the increase in body weight significantly different from the control rats (Table III). The acute toxicity studies demonstrated that the LD_{50} values in mice as a single intraperitoneal injection exceeded 2 g/kg which was the limit of solubility of the agents in carboxymethylcellulose. *In vitro* enzymatic studies of liver from CF_1 mice at 2.5 μmoles of the test agents, demonstrated that mitochondrial [^{14}C]citrate exchange was inhibited markedly by all three agents: 93% by saccharin and the butanone derivative and 80% by the propionic acid derivative (Table IV). Acetyl-CoA synthetase activity was suppressed 26–47% by these agents. Saccharin suppressed citrate lyase activity 35%, and the butanone derivatives suppressed citrate lyase activity 53%. HMG-CoA reductase activity was inhibited 29% by saccharin, but was essentially unaffected by the other two compounds. Cholesterol side-chain oxidation was inhibited 28% by the butanone derivative and 30% by the propionic analogue, but was unaffected by saccharin. Saccharin was more active and caused a 91% reduction of acetyl-CoA carboxylase activity; butanone caused 38% reduction, whereas 3-*N*-(*o*-benzsulfimido)propionic acid caused only 57% reduction. Fatty acid synthetase activity was not affected by any of the saccharin agents. Phosphatidate phosphohydralase activity was reduced 39–51%, and acyl transferase activity was reduced 75–92% by these test agents.

The saccharin agents suppressed basal respiration (state 4) rates. When succinate was used as substrate, saccharin derivatives reduced basal respiration 22–36%. When α-ketoglutarate was used as substrate, a reduction of 18–31% in basal respiration occurred. For the adenosine diphosphate-stimulated respiration (state 3) rate using succinate as substrate, a reduction of 34–37% was observed; with α-ketoglutarate substrate, a reduction of 20–39% was noted.

ID_{50} values obtained for *in vitro* enzymatic studies on rat liver ho-

Table V—*In Vivo* Effects of Saccharin Analogues on CF_1 Male Mouse Liver Enzyme Activities After 16 Days of Administration [a]

Compound	Dose, mg/kg/day	Acetyl-CoA Synthetase	HMG-CoA Reductase	Acetyl-CoA Carboxylase	Fatty Acid Synthetase	Phosphatidate Phosphohydralase	Liver Lipids
Control (1% carboxymethylcellulose)	—	100 ± 7[d]	100 ± 6[e]	100 ± 5[f]	100 ± 6[g]	100 ± 8[h]	100 ± 9[i]
Saccharin	10	73 ± 6[b]	80 ± 7[b]	41 ± 3[b]	73 ± 7[b]	30 ± 4[b]	57 ± 5[b]
	20	75 ± 6[b]	76 ± 6[b]	44 ± 4[b]	85 ± 7[c]	45 ± 3[b]	48 ± 4[b]
	40	71 ± 7[b]	77 ± 6[b]	56 ± 7[b]	85 ± 5[c]	82 ± 5[c]	54 ± 5[b]
	60	77 ± 5[b]	85 ± 6[c]	68 ± 6[b]	88 ± 5[c]	102 ± 7	61 ± 6[b]
3-*N*-(*o*-Benzosulfimido)propionic Acid	10	80 ± 5[b]	82 ± 8[c]	55 ± 4[b]	79 ± 6[b]	63 ± 5[b]	84 ± 6[c]
	20	71 ± 4[b]	75 ± 3[b]	45 ± 3[b]	83 ± 5[b]	73 ± 4[b]	58 ± 6[b]
	40	66 ± 5[b]	79 ± 5[b]	52 ± 5[b]	83 ± 6[c]	83 ± 6[c]	60 ± 7[b]
	60	64 ± 7[b]	72 ± 4[b]	72 ± 4[b]	78 ± 6[b]	93 ± 5	58 ± 6[b]

[a] Expressed as percentage of control (mean ± *SD*); $n = 6$. [b] $p \leq 0.001$. [c] $p \leq 0.005$. [d] 28.5 ± 3.14 mg of acetyl-CoA formed/g wet tissue/30 min. [e] 384,900 ± 26,943 dpm cholesterol formed/g wet tissue/60 min. [f] 32,010 ± 1921 dpm/g wet tissue/30 min. [g] 37,656 ± 2635 dpm/g wet tissue/30 min. [h] 16.70 ± 1.16 μg Pi/g wet tissue/15 min. [i] 79.5 ± 5.56 mg/g wet tissue.

Table VI—Effects of Saccharin Analogues on Liver and Small Intestinal Lipid Content After 16 Days of Dosing [a]

Compound	Dose, mg/kg/day	Lipid, mg	Cholesterol	Neutral Lipids	Triglyceride	Phospholipids
				Liver, % of control		
Control (1% carboxymethylcellulose)	—	100 ± 6	100 ± 7[d]	100 ± 4[e]	100 ± 5[f]	100 ± 8[g]
Saccharin	10	47 ± 4[b]	34 ± 5[b]	19 ± 3[b]	54 ± 4[b]	116 ± 7[c]
	20	48 ± 6	55 ± 5[b]	20 ± 2[b]	28 ± 3[b]	105 ± 6[c]
	40	54 ± 3[b]	63 ± 4[b]	13 ± 3[b]	54 ± 3[b]	120 ± 6[c]
	60	61 ± 4[b]	60 ± 7[b]	32 ± 4[b]	64 ± 4[b]	129 ± 9[b]
3-*N*-(*o*-Benzosulfimido)propionic Acid	10	84 ± 5[c]	51 ± 5[b]	63 ± 3[b]	75 ± 4[b]	129 ± 9[b]
	20	58 ± 5[b]	54 ± 5[b]	41 ± 5[b]	74 ± 7[b]	126 ± 5[b]
	40	60 ± 4[b]	58 ± 4[b]	81 ± 3[b]	49 ± 3[b]	99 ± 6
	60	58 ± 5[b]	52 ± 6[b]	105 ± 6	83 ± 8[b]	96 ± 7
				Small Intestine, % of control		
Control (1% carboxymethylcellulose)	—	100 ± 5	100 ± 7[h]	100 ± 5[i]	100 ± 6[j]	100 ± 8[k]
Saccharin	10	85 ± 4[b]	104 ± 8	78 ± 7[b]	74 ± 4[b]	97 ± 7
	20	53 ± 3[b]	157 ± 9[b]	130 ± 7[b]	29 ± 3[b]	111 ± 8
	40	75 ± 5[b]	175 ± 9[b]	70 ± 8[b]	59 ± 5[b]	114 ± 6[c]

[a] Mean ± *SD*; $n = 6$. [b] $p \leq 0.001$. [c] $p \leq 0.005$. [d] 12.24 ± 0.86 mg cholesterol/g tissue. [e] 28.35 ± 1.13 mg neutral lipid/g tissue. [f] 4.77 ± 0.24 mg triglyceride/g tissue. [g] 4.39 ± 0.35 mg phospholipid (P)/g tissue. [h] 7.81 ± 0.54 mg cholesterol/g tissue. [i] 7.18 ± 0.36 mg neutral lipid/g tissue. [j] 1.06 ± 0.06 mg triglyceride/g tissue. [k] 2.02 ± 0.16 mg phospholipid (P)/g tissue.

Table VII—Effects of Saccharin on the Fecal Excretion of Lipids After Administration for 16 Days [a]

Compound	Lipid, mg/g	Cholesterol	Neutral Lipids	Triglyceride	Phospholipids
			0 to 6-hr Fecal Sample, % of control		
Control (1% carboxymethylcellulose)	100 ± 6	100 ± 7[d]	100 ± 7[e]	100 ± 6[f]	100 ± 5[g]
Saccharin					
10 mg/kg/day	100 ± 7	115 ± 6[c]	107 ± 6	100 ± 5	113 ± 6
20 mg/kg/day	174 ± 9[b]	166 ± 8[b]	159 ± 5[b]	146 ± 8[b]	140 ± 8[b]
40 mg/kg/day	91 ± 5	74 ± 5[b]	114 ± 7	133 ± 7[b]	114 ± 6[c]
			6 to 12-hr Sample, % of control		
Control (1% carboxymethylcellulose)	100 ± 6	100 ± 7[h]	100 ± 8[i]	100 ± 6[j]	100 ± 6[k]
Saccharin					
10 mg/kg/day	118 ± 9[c]	108 ± 8	91 ± 7	90 ± 5	108 ± 5
20 mg/kg/day	131 ± 7[b]	115 ± 7[b]	105 ± 7	150 ± 7[b]	143 ± 8[b]
40 mg/kg/day	110 ± 6	100 ± 6	104 ± 8	108 ± 7	133 ± 7[b]
			12 to 24-hr Sample, % of control		
Control (1% carboxymethylcellulose)	100 ± 7	100 ± 8[l]	100 ± 6[m]	100 ± 7[n]	100 ± 6[o]
Saccharin					
10 mg/kg/day	124 ± 8[b]	102 ± 7	143 ± 7[b]	225 ± 12[b]	120 ± 7[b]
20 mg/kg/day	141 ± 8[b]	105 ± 6	143 ± 8[b]	277 ± 10[b]	120 ± 5[b]
40 mg/kg/day	126 ± 6[b]	100 ± 7	150 ± 8[b]	255 ± 9[b]	111 ± 6[c]

[a] Mean ± *SD*; $n = 6$. [b] ≤ 0.001. [c] $p \leq 0.005$. [d] 19.77 ± 1.38 mg/g. [e] 17.62 ± 1.23 mg/g. [f] 1.74 ± 0.10 mg/g. [g] 1.85 ± 0.09 mg/g. [h] 29.47 ± 2.06 mg/g. [i] 33.94 ± 2.72 mg/g. [j] 1.86 ± 0.11 mg/g. [k] 1.61 ± 0.10 mg/g. [l] 28.47 ± 2.27 mg/g. [m] 33.94 ± 2.04 mg/g. [n] 1.86 ± 0.13 mg/g. [o] 1.39 ± 0.08 mg/g.

mogenate were calculated from a semilogarithmic plot. In the acetyl-CoA synthetase assay, saccharin afforded an $ID_{50} \simeq 6.61$ m*M*. For the acetyl-CoA carboxylase assay, an $ID_{50} \simeq 1.26$ m*M* was obtained for saccharin, and an $ID_{50} \simeq 1.36$ m*M* was obtained for the propionic acid derivative. For the phosphatidate phosphohydralase assay, saccharin afforded an $ID_{50} \simeq 3.56$ m*M* and the propionic acid derivative an $ID_{50} \simeq 1.68$ m*M*. For the acyl transferase assay, saccharin gave an ID_{50} value of 3.26 m*M* and the propionic analogue gave a value of 1.93 m*M*.

In vivo studies on the enzymatic activities of liver from mice treated with test agents for 16 days showed that saccharin at doses from 10 to 60 mg/kg suppressed acetyl-CoA synthetase activity ~25% (Table V). *In vivo* HMG-CoA reductase activity was suppressed 23–24% at 20 and 40 mg/kg/day. Acetyl-CoA carboxylase activity was suppressed maximally at the lower doses; *i.e.*, 10 and 20 mg/kg/day afforded a 50–56% reduction. Fatty acid synthetase activity was not affected by *in vivo* administration of the drugs. Phosphatidate phosphohydralase activity was reduced 70% by saccharin at 10 mg/kg/day and 55% at 20 mg/kg/day. Liver lipids were reduced 53–39% by *in vivo* administration of 10–60 mg/kg/day of saccharin. 3-*N*-(*o*-Benzosulfimido)propionic acid *in vivo* administration resulted in a dose-related reduction of acetyl-CoA synthetase activity, with 60 mg/kg/day causing the maximum inhibition, *i.e.*, 36%. HMG-Co-A reductase activity was reduced 25 and 28% at 20 and 60 mg/kg/day, respectively. The propionic acid derivative caused marked reduction of acetyl-CoA carboxylase activity, with 20 mg/kg/day resulting in the maximum inhibition of 55%. Fatty acid synthetase activity was not affected by the propionic acid analogue. Phosphatidate phosphohydralase

Table VIII—[^{3}H]Cholesterol Content 24 hr After Intraperitoneal Injection of 10 μCi in CF_1 Mice Administered Saccharin for 16 Days at 20 mg/kg/day with Imides

Organ	Control		Saccharin	
	Total dpm[a]	Tritium Recovered, %	Total dpm[a]	Tritium Recovered, %
Brain	8305 ± 306	0.124	8048 ± 417	0.120
Lung	33949 ± 1982	0.506	30113 ± 1147	0.449
Heart	23774 ± 2112	0.354	7645 ± 902	0.114
Liver	436066 ± 4508	6.502	365175 ± 3721	5.445
Spleen	54303 ± 3291	0.810	57878 ± 2886	0.863
Kidney	82954 ± 1789	1.237	61030 ± 948	0.910
Stomach	266464 ± 5621	3.973	161898 ± 3277	2.414
Small intestine	607318 ± 9241	9.056	63445 ± 1112	9.460
Large intestine	791297 ± 7432	11.799	319288 ± 6456	8.614
Subtotal		34.361		28.389
Feces				
0–6 hr	374855 ± 14399	5.589	1738384 ± 18451	25.920
6–12 hr	2126220 ± 27861	31.703	1542185 ± 22231	22.995
12–24 hr	1901108 ± 36986	28.333	1524749 ± 28564	22.735
Total excreted in feces in 24 hr		65.625		71.650
Plasma/ml	256730 ± 5366		197092 ± 5382	

[a] Mean ± *SD*; $n = 6$.

Table IX—Effects of Saccharin on [^{3}H]Cholesterol Distribution in Holtzman Rats After 14 Days of Dosing[a]

Organ	Control		Saccharin	
	Total Organ dpm[b]	Recovery, %	Total Organ dpm[b]	Recovery, %
Brain	42412 ± 1171	1.21	43591 ± 986	1.26
Heart	37638 ± 3215	1.07	20412 ± 1836	0.59
Lung	100584 ± 7431	2.87	70230 ± 3233	2.02
Liver	901785 ± 7886	25.77	451828 ± 3954	13.06
Spleen	67760 ± 1431	1.93	69885 ± 1879	2.02
Kidney	69192 ± 986	1.97	59505 ± 1203	1.72
Stomach	127446 ± 8321	3.64	70230 ± 6121	2.03
Small intestine	851406 ± 70012	24.33	919916 ± 53202	26.59
Large intestine	246924 ± 12104	7.05	468088 ± 29998	13.53
Chyme	163977 ± 8421	4.68	444908 ± 12562	12.86
Feces	889892 ± 43265	25.43	841037 ± 12008	24.31
Total	3499016		3459630	

[a] At 20 mg/kg/day. [b] Mean ± *SD*; $n = 6$.

activity was reduced 37 and 27% at 10 and 20 mg/kg/day, respectively.

Liver lipids were reduced by the propionic acid derivative, with doses >20 mg/kg/day causing at least 50% reduction. The liver cholesterol and neutral lipids, including triglyceride levels, were reduced by saccharin and the propionic acid derivative (Table VI). Saccharin at 10 mg/kg reduced liver cholesterol levels 66% and at 20 mg/kg caused 45% reduction. Liver neutral lipid levels at 20–40 mg/kg were reduced >80% by saccharin. Liver triglyceride levels were reduced maximally at 20 mg/kg of saccharin, resulting in 72% reduction. Liver phospholipid levels were elevated significantly by saccharin at 40 and 60 mg/kg/day. The propionic acid analogue at all doses employed caused >40% reduction of liver cholesterol content. Liver neutral lipids were reduced 50% at 20 mg/kg/day by the propionic acid derivative, whereas liver triglyceride levels were reduced 51% at 40 mg/kg/day. Liver phospholipid levels were elevated at the lower doses (*i.e.*, 10 and 20 mg/kg/day) by the propionic acid analogue. Extracted lipids from the small intestine of mice treated for 16 days with saccharin at 20 mg/kg/day showed a reduction of triglyceride, but an elevation of cholesterol and neutral lipids. The phospholipid content was essentially not altered in the small intestine tissue.

Table X—Effect of Saccharin on Bile Secretion and Cholesterol Absorption in Rats After Administration of Saccharin for 15 Days[a]

	Bile Secretion Over 6 Hr		
	Bile flow, ml/hr	Total cpm for 6 hr	Cholesterol Content, mg%
Control (1% carboxymethylcellulose)	0.560 ± 0.042	1016 ± 81	111 ± 8
Saccharin (20 mg/kg/day)	0.675 ± 0.036	1858 ± 129[c]	194 ± 10[c]

	[^{3}H]Cholesterol Absorption 24 Hr After Administration	
	Plasma dpm[b]	Percent of Control
Control (1% carboxymethylcellulose)	14280 ± 385	100 ± 5
Saccharin (20 mg/kg/day)	9568 ± 463[c]	67 ± 5[c]

[a] Mean ± *SD*; $n = 6$. [b] Plasma volume assumed to be 17 ml for rats. [c] $p \leq 0.001$.

Examination of the lipid content of the fecal material (Table VII) excreted after administration of saccharin at 20 mg/kg/day indicated that the amount of lipid per gram of fecal material as well as cholesterol, triglyceride, and phospholipid contents were elevated in 0 to 6-, 6 to 12-, and 12 to 24-hr fecal collections. The fecal triglyceride content was markedly increased in the 12 to 24-hr sample. The distribution study in mice with [^{3}H]cholesterol (Table VIII) indicated that the cholesterol in bile was elevated 5.5 to 25.92% of the total recovered cholesterol content in the 0 to 6-hr fecal sample. The excretion of cholesterol in the feces tended to equilibrate over the 24-hr period so that the control mice excreted 65.5% of the cholesterol or bile acids in 24 hr, whereas the saccharin-treated mice excreted 71.6% of the labeled cholesterol or bile acids. From Table VIII, it can also be seen that after administration of saccharin, there was less accumulation of radiolabeled cholesterol in the major organs (brain, lung, heart, liver, kidney, stomach, and large intestine) compared with the control. Increases in labeled cholesterol were observed in the spleen and small intestines. The distribution of cholesterol in rats after 14 days of saccharin administration, again showed that there was no accumulation of cholesterol in the major organs (Table IX). Higher concentrations of cholesterol were found in the intestine and chyme after oral administration of the labeled cholesterol compared with control values.

The cannulation studies (Table X) demonstrate that after saccharin administration, there is an increase in bile flow from 0.560 to 0.675 ml/hr with an increase in cholesterol content, *i.e.*, 82% in dpm and 75% increase in mg%. After administering saccharin for 14 days to rats, it can be observed that there was a 33% reduction of cholesterol absorption from the gut over a 24-hr period.

The lipoprotein fractions of rat blood (Table XI) collected after a 2-week administration of saccharin demonstrated that cholesterol, neutral lipid, and triglyceride contents were reduced in the chylomicrons and very low-density, low-density, and high-density lipoprotein fractions. The phospholipid content of the individual fractions was not reduced significantly in all fractions; in fact, the high-density lipoprotein fraction showed a 148% increase in phospholipid content. The protein content of all fractions was reduced; particularly significant were the chylomicron, very low-density, and high-density lipoprotein fractions.

Data are expressed in the Tables I–XI as percent of control ± the standard deviation. The probable significant level (p) between each test group and the control group was determined by the Student's t test.

DISCUSSION

Saccharin, 1-*N*-(*o*-benzosulfimido)butan-3-one, and 3-*N*-(*o*-benzosulfimido)propionic acid were demonstrated to be very potent antihyperlipidemic agents in rodents at 20 mg/kg/day. The dosage required to induce reductions of plasma lipids was low compared with clofibrate

Table XI—Effect of Saccharin on Lipoprotein Fractions of Blood from Holtzman Rats After 14 Days of Dosing [a]

Compound	Cholesterol	Neutral Lipids	Triglyceride	Phospholipids	Protein
			Chylomicrons		
Control (1% carboxymethylcellulose)	100 ± 9[b]	100 ± 8[c]	100 ± 6[d]	100 ± 10[e]	100 ± 7[f]
Saccharin (20 mg/kg/day)	30 ± 4[v]	36 ± 5[v]	51 ± 6[v]	112 ± 9	61 ± 6[v]
			Very Low-Density Lipoproteins		
Control (1% carboxymethylcellulose)	100 ± 8[g]	100 ± 9[h]	100 ± 7[i]	100 ± 8[j]	100 ± 8[k]
Saccharin (20 mg/kg/day)	61 ± 7[v]	21 ± 4[v]	49 ± 5[v]	86 ± 9	64 ± 5[v]
			Low-Density Lipoproteins		
Control (1% carboxymethylcellulose)	100 ± 9[l]	100 ± 7[m]	100 ± 8[n]	100 ± 7[o]	100 ± 8[p]
Saccharin (20 mg/kg/day)	38 ± 4[v]	59 ± 6[v]	65 ± 6[v]	83 ± 8[w]	84 ± 9[w]
			High-Density Lipoproteins		
Control (1% carboxymethylcellulose)	100 ± 8[q]	100 ± 9[r]	100 ± 4[s]	100 ± 6[t]	100 ± 8[u]
Saccharin (20 mg/kg/day)	58 ± 6[v]	66 ± 7[v]	79 ± 8[v]	248 ± 12[v]	29 ± 4[v]

[a] Expressed as percent of control (mean ± *SD*); $m = 6$. [b] 337 ± 30 μg/ml. [c] 67 ± 5.6 μg/ml. [d] 420 ± 25 μg/ml. [e] 145 ± 15 μg/ml. [f] 3.0 ± 0.2 μg/ml. [g] 190 ± 15 μg/ml. [h] 98 ± 9 μg/ml. [i] 221 ± 15 μg/ml. [j] 26 ± 2 μg/ml. [k] 50 ± 4 μg/ml. [l] 210 ± 19 μg/ml. [m] 10 ± 0.7 μg/ml. [n] 45.1 ± 3.6 μg/ml. [o] 41 ± 3 μg/ml. [p] 0.681 ± 0.54 μg/ml. [q] 544 ± 44 μg/ml. [r] 620 ± 56 μg/ml. [s] 27 ± 1 μg/ml. [t] 153 ± 9 μg/ml. [u] 5.68 ± 0.45 μg/ml. [v] $p \leq 0.001$. [w] $p \leq 0.005$.

(100–200 mg/kg), which induces only marginal changes (15–20%) in serum and liver cholesterol and total lipid levels (26). The dose required for antihyperlipidemic activity of the saccharin analogues was in a safe therapeutic range compared with the observed LD_{50} values. The saccharin analogues were observed to be equally effective in rats and mice by either the oral or intraperitoneal administration routes. The agents were markedly effective in atherogenic mice in lowering the blood lipids, which approached normal levels after 2 weeks of drug administration.

The saccharin analogue did not bring about this reduction of lipids due to suppression of appetite in rats. Rather, saccharin analogues suppressed key enzymes in the early synthesis of cholesterol and fatty acids and in the synthesis of triglycerides. The enzymes include acetyl-CoA synthetase, citrate lyase, and mitochondrial citrate exchange. All of the enzymes play a role in synthesizing cytoplasmic acetyl-CoA, an intermediate precursor in cholesterol and fatty acid syntheses. The inhibition of these enzymes appeared to be related more with the suppression of serum cholesterol levels. The inhibition of mitochondrial citrate exchange by the saccharin analogues is a key regulatory site for the conversion of excess carbohydrates in the diet to lipids for storage. The inhibition of the acetyl-CoA carboxylase enzyme by saccharin analogues reduces the available fatty acids for triglyceride and cholesterol ester syntheses. The suppression of the acyl transferase and phosphatidate phosphohydralase enzymes correlates with the reduction of serum triglyceride levels, since the former enzyme is responsible for the addition of fatty acid to glycerol-3-phosphate for *de novo* triglyceride synthesis and the latter enzyme allows the synthesis of triglycerides from phospholipids. The same enzymes were inhibited in both rat and mice livers. Furthermore, the same enzymes were inhibited *in vivo* after 16 days of dosing with the saccharin analogues in mice. The ID_{50} estimates obtained from the rat liver enzyme assay are realistic values considering the dose required in the *in vivo* hydrolipidemic screen.

Clofibrate has been shown to accelerate basal respiration (state 4) and to inhibit adenosine diphosphate-stimulated respiration, thus uncoupling oxidative phosphorylation and reducing available energy for synthetic process in the cell (17). This may be due to the detergent-type effect of clofibrate. The saccharin analogues did not uncouple oxidative phosphorylation. They did reduce both states 3 and 4 respiration, interfering with the availability of adenosine triphosphate for enzymatic reaction, which requires energy.

It is interesting to note that the lipids being removed from the plasma compartment are not deposited in the major organs. Clearly the cholesterol, neutral lipids, and triglyceride levels are being reduced in the liver; however, the phospholipid content is elevated, probably indicative of inhibition of phosphatidate phosphohydralase activity by the saccharin analogues. In the treated animal, there was no indication of major changes in the body weight or major organ weights after administering the agents for 16 days. Rather, the cholesterol or bile acids were excreted in the bile at a fast rate and were cleared in the feces at an early time segment. Saccharin did decrease cholesterol absorption from the gut, which may explain the reduction of cholesterol in the tissues and the increase in the small intestine and feces.

Human chylomicrons and very low-density lipoproteins contain a high concentration of triglycerides. The low- and high-density lipoprotein fractions contain high concentrations of cholesterol ester and phospholipids. The saccharin analogues in the future may be helpful in Type I hyperlipidemic disease which is a state of hyperchylomicronemia. Types IIa, IIb, IV, and V hyperlipidemic states have increased levels of either low-density or very low-density lipoproteins, or both. Saccharin analogues were shown to suppress both of these lipoprotein fractions.

It would appear that saccharin analogues are more potent antihyperlipidemic agents in rodents than many of the current agents on the market today. A relatively low dose of the analogues was required to observe the lipid-lowering effect. It has been reported previously (1) that no deleterious side effects were observed in the rodent after short-term administration of these agents.

REFERENCES

(1) I. H Hall, J. M. Chapman, and G. H. Cocolas, *J. Pharm. Sci.*, **70,** 326 (1981).

(2) J. M. Chapman, G. H. Cocolas, and I. H. Hall, *J. Med. Chem.*, **28,** 243 (1983).

(3) J. W. H. Watthey, J. Berndt, B. J. Henrici, S. Lausten, and M. Miller, "Abstracts," American Chemical Society Meeting 173rd, MEDI 12 (1977).

(4) A. T. Nessu, J. V. Pastewka, and A. C. Peacock, *Clin. Chim. Acta*, **10,** 229 (1964).

(5) J. T. Litchfield, Jr. and F. Wilcoxon, *J. Pharmacol. Exp. Ther.*, **96,** 99 (1949).

(6) A. G. Goodridge, *J. Biol. Chem.*, **248,** 4218 (1973).

(7) M. Hoffman, L. Weiss, and O. H. Wieland, *Anal. Biochem.*, **84,** 441 (1978).

(8) B. H. Robinson, G. R. Williams, M. L. Halperin, and C. C. Leznoff, *Eur. J. Biochem.*, **15,** 263 (1970).

(9) B. H. Robinson and G. R. Williams, *Biochim. Biophys. Acta*, **216,** 63 (1970).

(10) D. Kritchevsky and S. A. Tepper, *Atherosclerosis*, **18,** 93 (1973).

(11) G. T. Haven, J. R. Krzemien, and T. T. Nguyen, *Res. Commun. Chem. Pathol. Pharmacol.*, **6,** 253 (1973).

(12) F. Wada, K. Hirata, and Y. Sakameto, *J. Biochem. (Tokyo)*, **65,** 71 (1969).

(13) M. D. Greenspan and J. M. Lowenstein, *J. Biol. Chem.*, **243,** 6273 (1968).

(14) R. O. Brady, R. M. Bradley, and E. G. Trams, *J. Biol. Chem.*, **235,** 3093 (1960).

(15) R. G. Lamb, S. D. Wyrick, and C. Piantadosi, *Atherosclerosis*, **27,** 147 (1977).

(16) R. D. Mavis, J. N. Finkelstein, and B. P. Hall, *J. Lipid. Res.*, **19,** 467 (1978).

(17) I. Hall and G. L. Carlson, *J. Med. Chem.*, **19,** 1257 (1976).

(18) J. Folch, M. Lees, and G. H. C. Stanley, *J. Biol. Chem.*, **226,** 497 (1957).

(19) E. G. Bligh and W. J. Dyer, *Can. J. Biochem. Physiol.*, **37,** 911 (1959).

(20) J. H. Bragdon, *J. Biol. Chem.*, **190,** 513 (1951).

(21) C. P. Stewart and E. B. Henday, *Biochem. J.*, **29,** 1683 (1935).

(22) A. Adam, J. van Cantfort, and J. Gielen, *Lipids*, **11,** 610 (1976).

(23) F. T. Hatch and R. S. Lees, *Adv. Lipid Res.*, **6,** 33 (1968).

(24) R. J. Havel, H. A. Eder, and J. H. Bragdon, *J. Clin. Invest.*, **34**, 1395 (1955).
(25) O. H. Lowry, N. J. Rosebrough, A. L. Farr, and R. J. Randall, *J. Biol. Chem.*, **193**, 265 (1951).
(26) J. M. Thorp and W. S. Waring, *Nature (London)*, **194**, 948 (1962).

ACKNOWLEDGMENTS

Supported by Grant HL25680 from the National Heart, Lung, and Blood Institute, National Institutes of Health.

The authors wish to thank Melba Gibson, Jerry McKee, and Mary Dorsey for their technical assistance.

Photostability of Solid-State Ubidecarenone at Ordinary and Elevated Temperatures under Exaggerated UV Irradiation

YOSHIHISA MATSUDA ˣ **and REIKO MASAHARA**

Received June 15, 1982, from the *Kobe Women's College of Pharmacy, Higashinada, Kobe 658, Japan.* Accepted for publication September 1, 1982.

Abstract □ The photostability of ubidecarenone was investigated. Two irradiation apparatus, a grating monochromator and a high-pressure mercury vapor lamp, were employed at ordinary and elevated temperatures. Both physicochemical and chemical stabilities were significantly affected by irradiation wavelength, with UV light causing the greatest changes. The degree of degradation was a function of the light absorption properties of the substrate and markedly increased when the absorption became >30%. The photolytic degradation followed apparent first-order kinetics at all wavelengths and was promoted with temperature elevation. The Arrhenius plot gave an activation energy in the solid state different from that in the liquid state. These activation energies linearly decreased with increasing intensity of UV light.

Keyphrases □ Ubidecarenone—photostability, ordinary and elevated temperatures, exaggerated UV irradiation, activation energies □ Photostability—solid-state ubidecarenone, ordinary and elevated temperatures, exaggerated UV irradiation, activation energies □ Degradation—ubidecarenone photostability, ordinary and elevated temperatures, exaggerated UV irradiation

Preformulation study is of prime importance in the rational development of dosage forms for drug substances labile against various environmental factors. In designing a solid dosage form, it is necessary to know the inherent stability of the drug substance. There have been many reports concerning the behavior of organic compounds when subjected to heat or moisture. Photochemical mechanisms of solid-state reactions also have been reviewed (1), but not from the viewpoint of stabilization. Because of the complexity of photochemical reactions, there has been very little reported on the photostability of solid dosage forms (2–9).

Ubidecarenone [2,3-dimethoxy-5-methyl-6-decaprenylbenzoquinone (I)], a lipid-soluble benzoquinone derivative with a melting point of ~48° (10), is widely used in Japan for the treatment of angina. It is a yellow or orange crystalline powder; on exposure to light, I gradually decomposes and the color changes to dark yellow (10). The dosage forms commercially available are tablets, granules, and hard or soft gelatin capsules; these are photo-protected with a package system using light-resistant films.

The objective of the present investigation was to obtain useful informations on the behavior of I in the presence of light and heat under ordinary and accelerated storage conditions as the first step toward photostabilization.

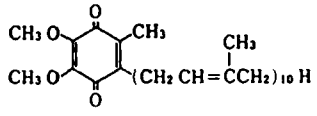

I

Emphasis was placed on the photostability of the drug itself.

EXPERIMENTAL

Samples—Ubidecarenone, 170 mg, was accurately weighed and compressed into a flat-faced tablet 15 mm in diameter, using a compression-tension testing machine[1]. To keep the surface condition constant, a fixed compression force of 200 kg was used. Tablets were used for the quantification of appearance change by light irradiation. For the kinetic study 50 mg of ubidecarenone was dissolved in 50 ml of *n*-hexane–ether (1:1). Sixty microliters was placed on a quartz-glass plate (26 × 38 mm) and evaporated at room temperature. The oily sample was then cooled to 0–4° for 24 hr and allowed to crystallize. A 60-μg sample (<70 μm in diameter) was dispersed over the plate to illuminate all molecules as uniformly as possible. Samples were stored over silica gel in a desiccator in the dark until the irradiation test.

UV Irradiation—Two irradiation apparatus were employed. To investigate the effect of irradiation wavelength on the appearance change or photolytic degradation, a grating monochromator[2] with a 5-kW xenon lamp adjusted for 290–500 nm, a 5- to 21-nm intervals, was used (8). A band width of 5 nm was employed at all wavelengths. The amount of energy irradiated to each sample was calculated from the counts of the integrating photometer attached to the monochromator. Tablets or crystalline samples were attached to the front of the sample holder of the monochromator and exposed to UV rays. Elevation of temperature in the monochromator was prevented by a cooling water jacket surrounding the light source; the surface of samples was maintained at 25°.

In the accelerated irradiation test at ordinary and elevated temperature, the samples were placed in a thermostated jacket (Fig. 1). Water at the prescribed temperature was allowed to circulate through the jacket, and the temperature in the sample chamber was monitored with a thermocouple sensor. The jacket was placed in a fading tester[3] equipped with a 400-W mercury vapor lamp for color fading, as reported previously (11), and exposed to UV rays. The distance between the light source and the sample was 30 cm. The temperature in the fading tester was maintained below 27° by a constant-operating fan. To control the UV intensity irradiated to the sample, several optical filters[4] having various light transmission properties were attached to the front of the sample chamber.

[1] Autograph model IS-5000; Shimadzu Co., Kyoto, Japan.
[2] Model CRM-50; Japan Spectroscopic Co., Tokyo, Japan.
[3] Model MH-1; Mitsubishi Electric Co., Tokyo, Japan.
[4] Toshiba Kasei Kogyo Co., Tokyo, Japan.

0022-3549/83/1000-1198$01.00/0

(24) R. J. Havel, H. A. Eder, and J. H. Bragdon, *J. Clin. Invest.*, **34**, 1395 (1955).
(25) O. H. Lowry, N. J. Rosebrough, A. L. Farr, and R. J. Randall, *J. Biol. Chem.*, **193**, 265 (1951).
(26) J. M. Thorp and W. S. Waring, *Nature (London)*, **194**, 948 (1962).

ACKNOWLEDGMENTS

Supported by Grant HL25680 from the National Heart, Lung, and Blood Institute, National Institutes of Health.

The authors wish to thank Melba Gibson, Jerry McKee, and Mary Dorsey for their technical assistance.

Photostability of Solid-State Ubidecarenone at Ordinary and Elevated Temperatures under Exaggerated UV Irradiation

YOSHIHISA MATSUDA ˣ **and REIKO MASAHARA**

Received June 15, 1982, from the *Kobe Women's College of Pharmacy, Higashinada, Kobe 658, Japan.* Accepted for publication September 1, 1982.

Abstract □ The photostability of ubidecarenone was investigated. Two irradiation apparatus, a grating monochromator and a high-pressure mercury vapor lamp, were employed at ordinary and elevated temperatures. Both physicochemical and chemical stabilities were significantly affected by irradiation wavelength, with UV light causing the greatest changes. The degree of degradation was a function of the light absorption properties of the substrate and markedly increased when the absorption became >30%. The photolytic degradation followed apparent first-order kinetics at all wavelengths and was promoted with temperature elevation. The Arrhenius plot gave an activation energy in the solid state different from that in the liquid state. These activation energies linearly decreased with increasing intensity of UV light.

Keyphrases □ Ubidecarenone—photostability, ordinary and elevated temperatures, exaggerated UV irradiation, activation energies □ Photostability—solid-state ubidecarenone, ordinary and elevated temperatures, exaggerated UV irradiation, activation energies □ Degradation—ubidecarenone photostability, ordinary and elevated temperatures, exaggerated UV irradiation

Preformulation study is of prime importance in the rational development of dosage forms for drug substances labile against various environmental factors. In designing a solid dosage form, it is necessary to know the inherent stability of the drug substance. There have been many reports concerning the behavior of organic compounds when subjected to heat or moisture. Photochemical mechanisms of solid-state reactions also have been reviewed (1), but not from the viewpoint of stabilization. Because of the complexity of photochemical reactions, there has been very little reported on the photostability of solid dosage forms (2–9).

Ubidecarenone [2,3-dimethoxy-5-methyl-6-decaprenylbenzoquinone (I)], a lipid-soluble benzoquinone derivative with a melting point of ~48° (10), is widely used in Japan for the treatment of angina. It is a yellow or orange crystalline powder; on exposure to light, I gradually decomposes and the color changes to dark yellow (10). The dosage forms commercially available are tablets, granules, and hard or soft gelatin capsules; these are photo-protected with a package system using light-resistant films.

The objective of the present investigation was to obtain useful informations on the behavior of I in the presence of light and heat under ordinary and accelerated storage conditions as the first step toward photostabilization.

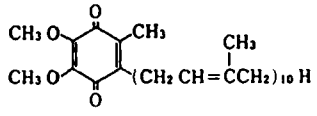

I

Emphasis was placed on the photostability of the drug itself.

EXPERIMENTAL

Samples—Ubidecarenone, 170 mg, was accurately weighed and compressed into a flat-faced tablet 15 mm in diameter, using a compression-tension testing machine[1]. To keep the surface condition constant, a fixed compression force of 200 kg was used. Tablets were used for the quantification of appearance change by light irradiation. For the kinetic study 50 mg of ubidecarenone was dissolved in 50 ml of *n*-hexane–ether (1:1). Sixty microliters was placed on a quartz-glass plate (26 × 38 mm) and evaporated at room temperature. The oily sample was then cooled to 0–4° for 24 hr and allowed to crystallize. A 60-μg sample (<70 μm in diameter) was dispersed over the plate to illuminate all molecules as uniformly as possible. Samples were stored over silica gel in a desiccator in the dark until the irradiation test.

UV Irradiation—Two irradiation apparatus were employed. To investigate the effect of irradiation wavelength on the appearance change or photolytic degradation, a grating monochromator[2] with a 5-kW xenon lamp adjusted for 290–500 nm, a 5- to 21-nm intervals, was used (8). A band width of 5 nm was employed at all wavelengths. The amount of energy irradiated to each sample was calculated from the counts of the integrating photometer attached to the monochromator. Tablets or crystalline samples were attached to the front of the sample holder of the monochromator and exposed to UV rays. Elevation of temperature in the monochromator was prevented by a cooling water jacket surrounding the light source; the surface of samples was maintained at 25°.

In the accelerated irradiation test at ordinary and elevated temperature, the samples were placed in a thermostated jacket (Fig. 1). Water at the prescribed temperature was allowed to circulate through the jacket, and the temperature in the sample chamber was monitored with a thermocouple sensor. The jacket was placed in a fading tester[3] equipped with a 400-W mercury vapor lamp for color fading, as reported previously (11), and exposed to UV rays. The distance between the light source and the sample was 30 cm. The temperature in the fading tester was maintained below 27° by a constant-operating fan. To control the UV intensity irradiated to the sample, several optical filters[4] having various light transmission properties were attached to the front of the sample chamber.

[1] Autograph model IS-5000; Shimadzu Co., Kyoto, Japan.
[2] Model CRM-50; Japan Spectroscopic Co., Tokyo, Japan.
[3] Model MH-1; Mitsubishi Electric Co., Tokyo, Japan.
[4] Toshiba Kasei Kogyo Co., Tokyo, Japan.

0022-3549/83/1000-1198$01.00/0

Table I—Irradiation Energies after 1 hr of Irradiation Through Various Glass Optical Filters

Filter	Irradiation Energy (300–400 nm), erg/cm^2
None	1.21×10^8
UV-25	1.02×10^8
UV-D25	9.97×10^7
UV-35	7.60×10^7
VY-42	2.09×10^5

The irradiation energies (300–400 nm) through these filters at the surface of a sample were measured with a UV intensity meter[5] (Table I). Samples were withdrawn from the monochromator or fading tester at designated time intervals for tristimulus colorimetry or high-performance liquid chromatographic (HPLC) analysis.

Colorimetric Measurements—To follow a quantitative change in surface color of the sample, a color and color difference meter[6] equipped with a halogen lamp as the light source was employed, and the surface color of the tablets in the L,a,b coordinate system was measured as reported previously (11). The Hunter's color difference ΔE (12) before and after irradiation was calculated to evaluate color darkening. After the measurement, samples were returned to the monochromator and irradiation was continued.

Absorption Measurements—At every irradiation, UV absorption spectra [semi-integral attenuance spectra (13)] of the sample powders in the gas phase were measured by a multipurpose recording spectrophotometer[7] with an end-on type photomultiplier. Air was used as the absorption control in accordance with the method described previously (5).

HPLC Analysis—A liquid chromatograph[8] equipped with a fixed-wavelength UV detector[9] was used for HPLC analysis. Ubidecarenone was quantified at 254 nm. The prepacked column[10] (30 cm × 3.9-mm i.d.) was operated at ambient temperature at a flow rate of 1.4 ml/min. The mobile phase consisted of a solvent system of n-hexane–ether (85:15). The internal standard solution of benzophenone was prepared at a concentration of 100 μg/ml. All solvents and reagents were HPLC and analytical grade, respectively, and were used as received.

After irradiation, samples on the plate were washed several times with ether, 30 μl of the internal standard solution was added, and the mixed solution was evaporated to dryness under vacuum. The residue was then dissolved in 300 μl of n-hexane–ether (1:1); 2 μl of this solution was injected onto the chromatograph with a 10-μl syringe by the on-flow technique. A typical chromatogram of the sample obtained after 15-min irradiation is shown in Fig. 2. The amount of ubidecarenone was the mean of three determinations.

RESULTS AND DISCUSSION

Color Darkening of the Tablet Surface—The coloration reaction of solid pharmaceutical preparations by light may be localized on the surface, differing from that of liquid preparations in which all drug molecules take part in the reaction. It is nevertheless possible to qualitatively estimate the photostability of the drug by the extent of coloration or color fading.

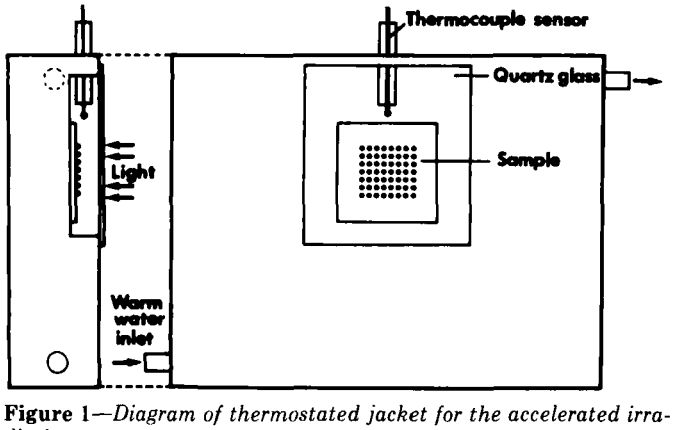

Figure 1—*Diagram of thermostated jacket for the accelerated irradiation test.*

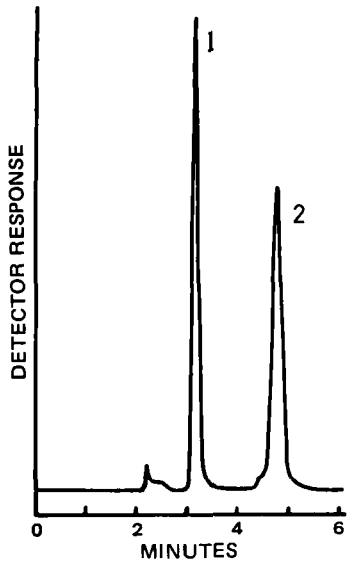

Figure 2—*Typical chromatogram of photodegraded ubidecarenone. Key: (1) benzophenone (internal standard); (2) ubidecarenone.*

Figure 3 shows the action spectrum for color darkening of a tablet surface irradiated under an intensity of 3.49×10^8 erg/cm^2. The color difference (ΔE) increased with decreasing irradiation wavelength and reached its maximum at ~350 nm. The color darkening was observed also in the visible region over 400 nm and resulted in a significant color difference even at ~450 nm. Above 480 nm, ΔE remained <2 NBS units, indicating that apparent color darkening did not occur in this wavelength region in view of the relationship between visual perception and color difference (14). Such behavior in coloration was strikingly different from the results obtained for sulfisomidine (8) and indomethacin (15), which were photostable against visible light. The photostability of ubidecarenone over a wide range of irradiation wavelength suggests that the selection of a desirable light source and the optimization of illumination conditions are necessary for studying the photoreaction of pharmaceuticals.

The process of these color changes was examined under irradiation with a mercury vapor lamp, and the change in ΔE against time was followed up to the maximum irradiation energy of 2.62×10^8 erg/cm^2 (after 120-min irradiation). For the kinetic interpretation of this process, the increase in ΔE against time may be expressed as (9):

$$\frac{d\Delta E}{dt} = k(\Delta E)^n \qquad \text{(Eq. 1)}$$

where t and k are irradiation time and the color-darkening rate constant, respectively, and n is constant. Integrating Eq. 1 under the initial condition ($\Delta E = 0$ at $t = 0$), we obtain:

$$\log \Delta E = \frac{1}{1-n} \log t + \frac{1}{1-n} \log [(1-n)k] \quad (n \neq 1) \qquad \text{(Eq. 2)}$$

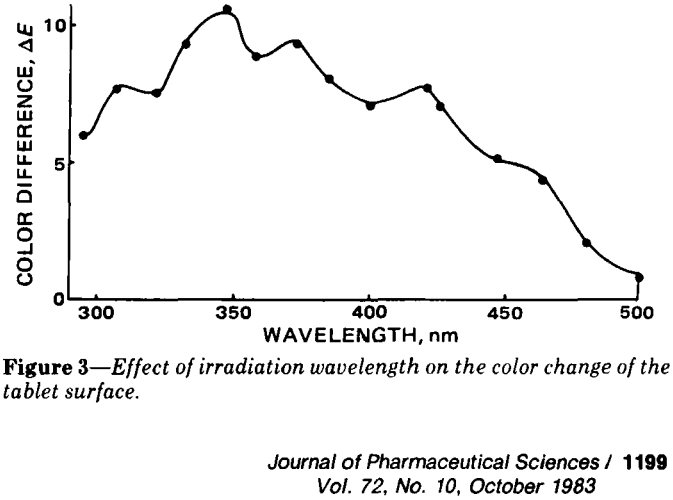

Figure 3—*Effect of irradiation wavelength on the color change of the tablet surface.*

[5] Model UVR-365, Tokyo Optical Instruments Co., Tokyo, Japan.
[6] Model ND-101, Nippon Denshoku Co., Tokyo, Japan.
[7] Model MPS-50L, Shimadzu Co., Kyoto, Japan.
[8] Model LC-3A, Shimadzu Co., Kyoto, Japan.
[9] Model SPD-2A, Shimadzu Co., Kyoto, Japan.
[10] μPorasil, Waters Associates, Milford, MA 01757.

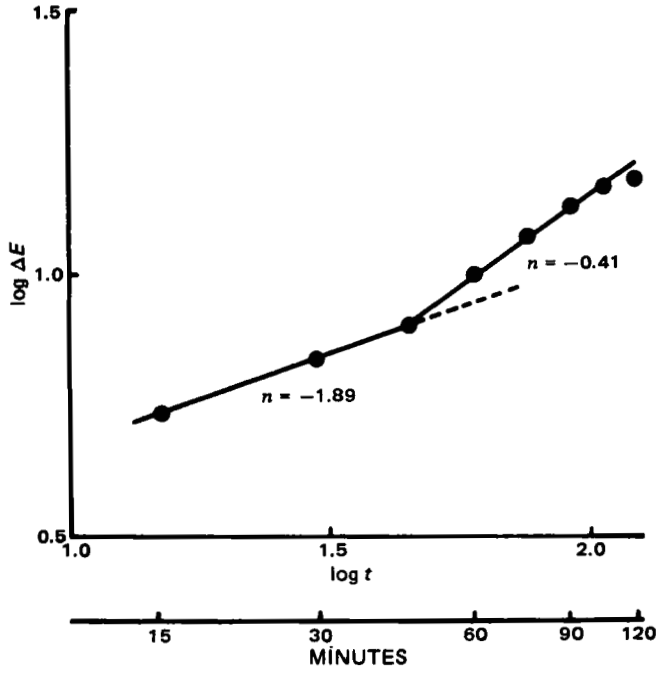

Figure 4—*Double-logarithmic plot for the color change process (cf. Eq. 2).*

Equation 2 indicates that a linear relationship with a slope of $1/(1 - n)$ should hold between ΔE and t on the double-logarithmic scale. The double-logarithmic plot of the color darkening process gave two excellent straight lines with different slopes (Fig. 4); the color darkening rate in the latter period was much higher than that in the earlier period of irradiation.

Physicochemical Change of Crystals—The results shown in Fig. 4 suggest that the mechanism of color darkening may undergo a change during the process of irradiation. The color darkening may be attributable to change in the surface condition of the tablet in addition to structural change of the drug molecules. Figure 5 shows photomicrographs of ubidecarenone crystals irradiated for various times. No change in appearance of the wrinkled surface was observed up to 30 min of irradiation, but after 50 min liquefaction of the surface layer of crystals began and gradually extended inward. After 90 min all crystals were liquefied to oily droplets. This may be due to the formation of a photoproduct with a lower melting point than the original substance. These physicochemical changes must affect the UV absorption properties of solid-state samples. Figure 6 shows the absorption spectra obtained under the same irradiation condition as Fig. 5. The spectrum of the original state before irradiation gave an absorption maximum and minimum at 278 and 236 nm, respectively. As

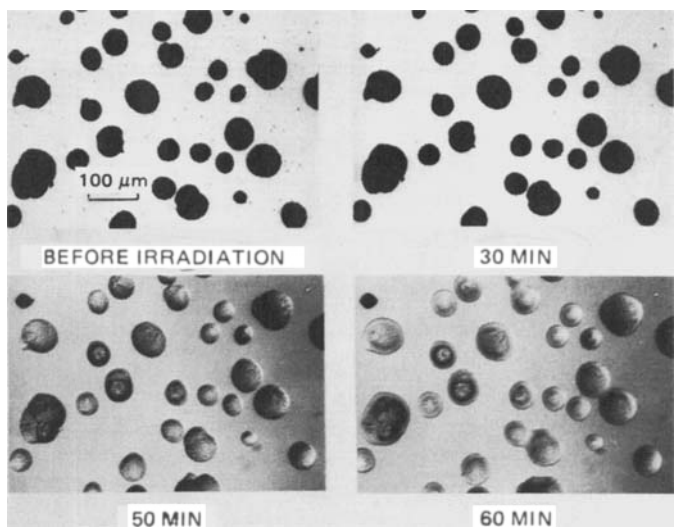

Figure 5—*Liquefaction of ubidecarenone crystals irradiated using a mercury vapor lamp.*

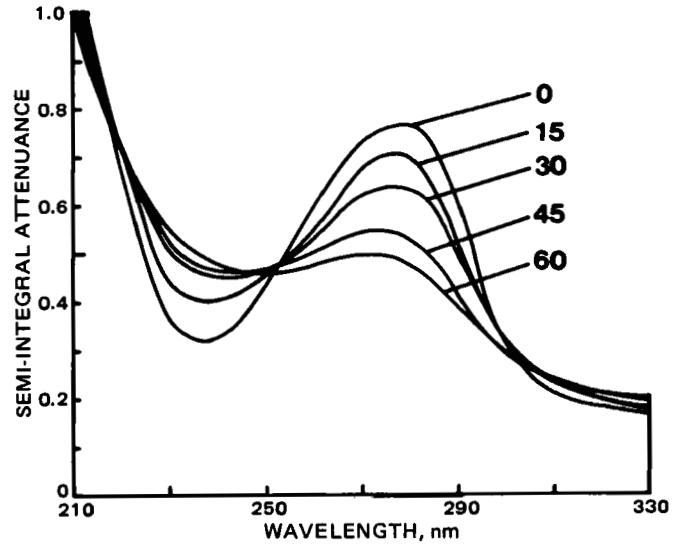

Figure 6—*Effect of irradiation time on the absorption spectrum of solid-state ubidecarenone. Numbers on the graph refer to irradiation time in minutes.*

the irradiation time proceeded, the absorption curve showed a flattening tendency, increase in the minimum and decrease in the maximum. The isosbestic points were confirmed at 254 and 300 nm up to 30 min of irradiation. After 45 min, however, these points were not obtained, and the absorption maximum and minimum shifted to shorter and longer wavelengths, respectively. The disappearance of isosbestic points after 45 min was closely related to the alteration in color-darkening rate (Fig. 4) and the beginning of liquefaction (Fig. 5). The presence and absence of isosbestic points suggest occurrence of a photochemical reaction on the crystal surface.

Photolytic Degradation at Various Irradiation Wavelengths—The photolytic degradation is also believed to be affected by irradiation wavelength. Figure 7 shows the semilogarithmic plot of percent remaining ubidecarenone against irradiation energy at several representative wavelengths. Good linear relationships existed between both parameters at every wavelength, indicating that the photolytic degradation followed apparent first-order kinetics. The irradiation energy was directly proportional to time. Even under the same irradiation energy, the degree

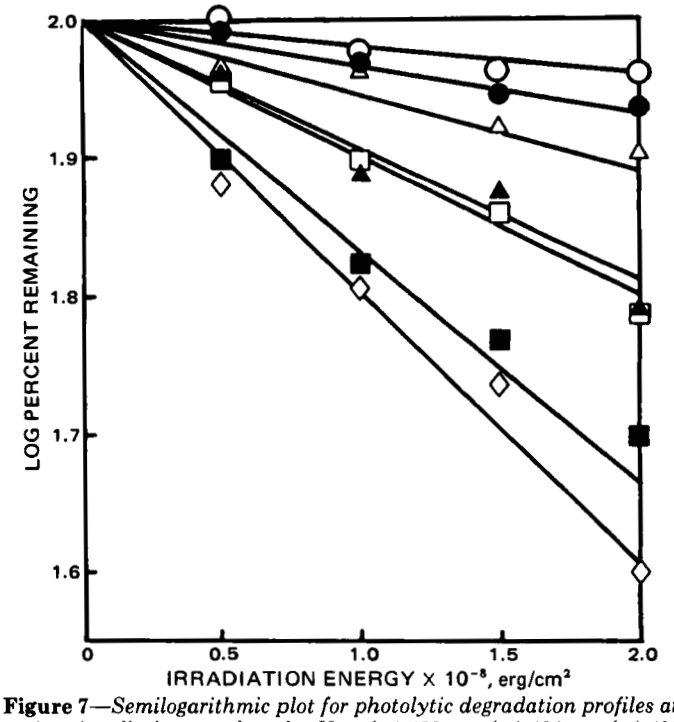

Figure 7—*Semilogarithmic plot for photolytic degradation profiles at various irradiation wavelengths. Key: (○) 480 nm; (●) 464 nm; (△) 426 nm; (▲) 400 nm; (□) 373 nm; (■) 347 nm; (◇) 290 nm.*

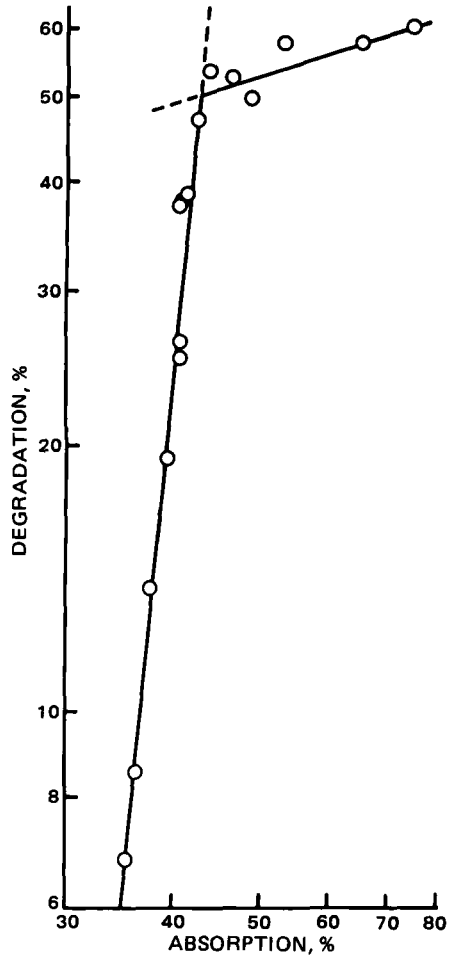

Figure 8—*Relationship between percent degradation and percent absorption of irradiated light energy.*

of degradation varied largely depending on the wavelength: it increased with decreasing irradiation wavelength. According to Grottus–Draper's law, only the light absorbed by a substrate can subject it to chemical change. Therefore, the results obtained in Fig. 7 may be attributed to the fact that the semi-integral attenuance increased with decreasing wavelength above 290 nm, as recognized in Fig. 6.

Supposing that the intensity of reflected light at the surface of substrate is negligibly low compared with that of light either absorbed by or transmitted through the substrate, the absorbance may be replaced

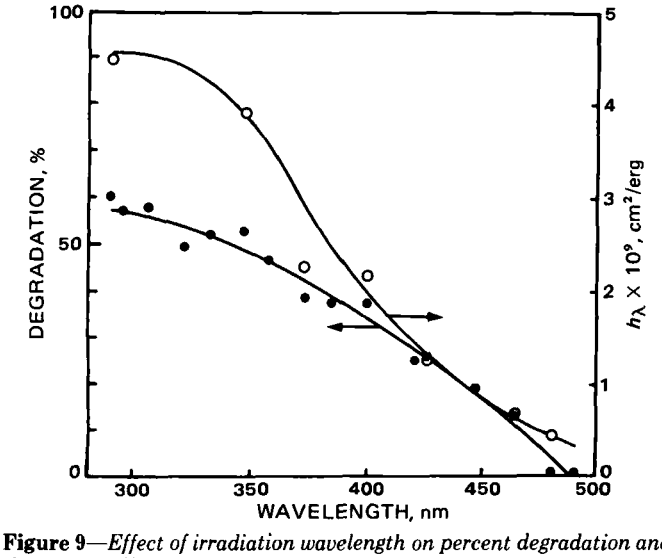

Figure 9—*Effect of irradiation wavelength on percent degradation and the energy efficiency constant,* h_λ.

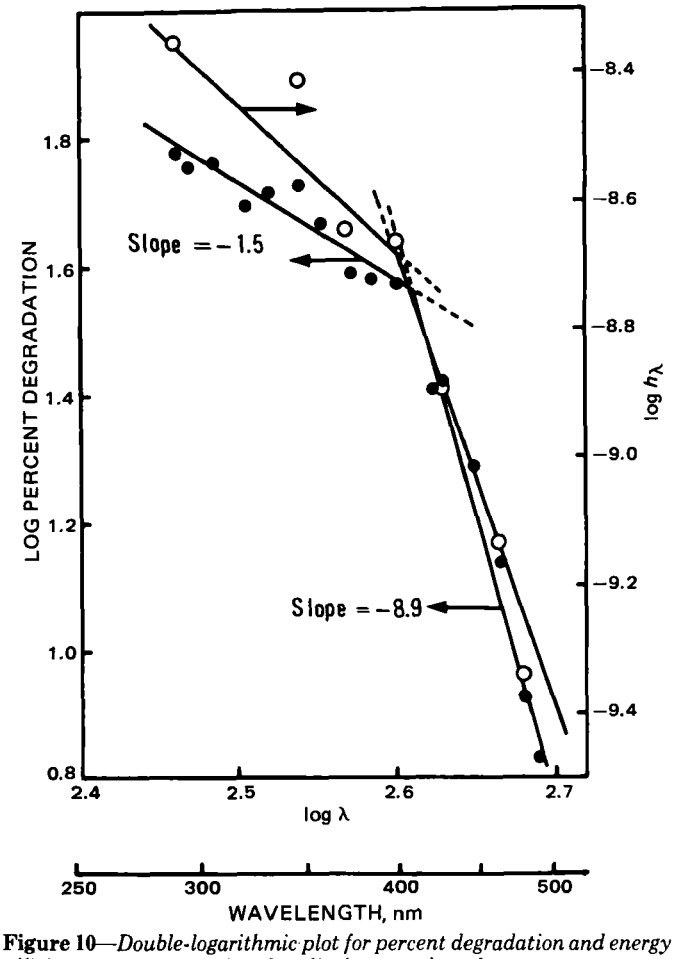

Figure 10—*Double-logarithmic plot for percent degradation and energy efficiency constant against irradiation wavelength.*

with semi-integral attenuance, ${}_pE_t$. The percent absorption, A, is then given by:

$$A\ (\%) = 100 - 10^{\log T} \qquad \text{(Eq. 3)}$$

where, $\log T = 2 - {}_pE_t$. Thus, the quantitative relationship between the degree of degradation and light absorption can be given as in Fig. 8; the percent degradation under the same irradiation energy of 2.0×10^8 erg/cm^2 in the range of 290–500 nm is plotted in this graph against percent absorption at that irradiation wavelength, using ${}_pE_t$ values of the original curve before irradiation in Fig. 6. It is clear that the percent degradation is quite sensitive to light absorption in the region of lower percent absorption, whereas it is less sensitive for higher percent absorption: the critical point existed at ~43% absorption. Photolytic degradation could no longer take place below 30% absorption. This result indicates that the absorption of light by ubidecarenone is not necessarily effective in producing degradation. In such a situation after a molecule had absorbed a quantum of light energy, it might collide with other molecules to raise their kinetic energy, resulting in only an elevation of the system temperature.

The slope of each line in Fig. 7 is equivalent to a degradation rate constant with a unit of min^{-1} at one irradiation wavelength. However, due to the spectral irradiation energy distribution of the light source, the required irradiation time differs depending on the irradiation wavelength even though under the same irradiation energy. It is not, therefore, reasonable to regard the slope as the degradation rate constant. In this case, an energy efficiency constant, h_λ, with a unit of cm^2/erg is used for convenience. Figure 9 shows the dependencies of the percent degradation and the energy efficiency constant obtained from Fig. 7 on the irradiation wavelength under the irradiation energy of 2.0×10^8 erg/cm^2. The percent degradation decreased with increasing wavelength, and no degradation occurred >480 nm. This pattern was in agreement with that of appearance change in Fig. 3. The energy efficiency constant was also reduced significantly with increasing irradiation wavelength. These parameters were replotted on the double-logarithmic scale (Fig. 10). For all parameters, good regression lines with an intersection at ~410 nm were estab-

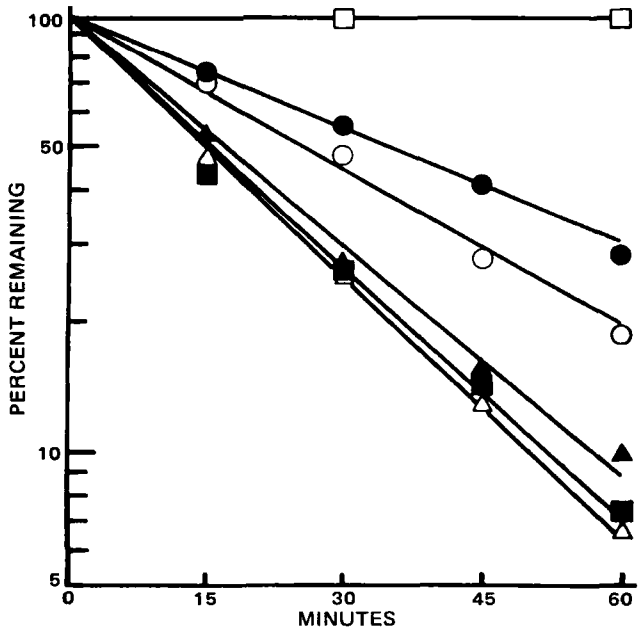

Figure 11—*Semilogarithmic plot for photolytic degradation profiles at various temperatures. Key: (□) 60° in the dark; (●) 25°; (○) 35°; (▲) 45°; (■) 55°; (△) 60°.*

lished over the whole range of wavelengths, but the slopes in two wavelength regions differed markedly. On the basis of this fact, we can deduce that though ubidecarenone is highly degraded by UV light, the effect of irradiation wavelength is much greater in the visible region than in the UV region.

Effect of Temperature on Photolytic Degradation—In examining the photostability of solid drugs with low melting point, it is of value to know how the photostability will be affected by temperature, as drugs stored at higher than melting point may degrade. Very little has been reported concerning the effect of temperature in photochemical reactions. In such cases the contributions of elevated temperature were promotive (16) or repressive (17–19) to the reaction.

Figure 11 shows the semilogarithmic plot of percent residual ubidecarenone against irradiation time at various temperatures. The time

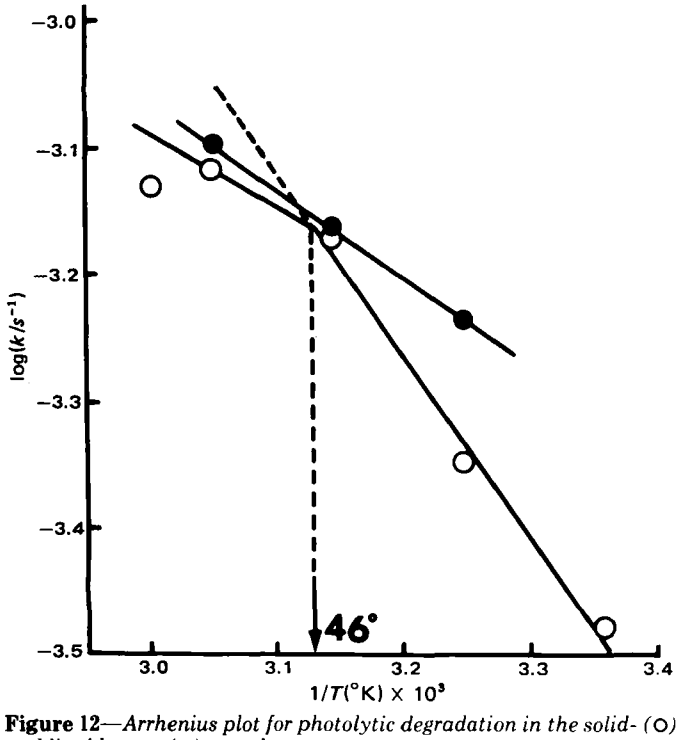

Figure 12—*Arrhenius plot for photolytic degradation in the solid- (○) and liquid-state (●) samples.*

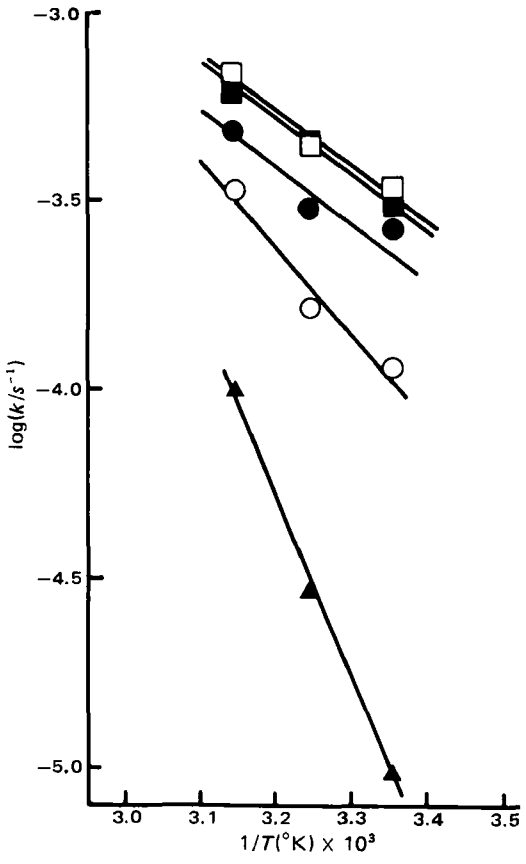

Figure 13—*Arrhenius plot for the photolytic degradation of ubidecarenone covered with various optical filters (see Table I). Key: (□) without filter; (■) UV-25; (●) UV-D25; (○) UV-35; (▲) VY-42.*

dependency of degradation was confirmed to follow apparent first-order kinetics at every temperature, as expected from Fig. 7. The degradation was significantly accelerated by elevation of temperature. It was evident that even at 60°, no degradation occurred at all in the dark, which suggests that the thermal reaction by itself cannot participate in the chemical degradation.

These degradation rate constants are given as an Arrhenius plot in Fig. 12. In the case of a liquid-state sample which was not allowed to recrystallize, the plots gave only one satisfactory line over the whole range of temperatures. In contrast, the plots for a solid sample gave two straight lines with different slopes; a critical temperature of 46° obtained as an intersection of two lines agreed with the initiating temperature for melting on the differential thermal analysis (DTA) curve of the sample. The slopes of these lines, therefore, indicate the activation energies for photodegradation in the solid and liquid states. The line in the range of temperatures higher than the melting point was adjacent and parallel to that of the liquid-state sample, giving an activation energy of 3.14 kcal/mole, which was much lower than that of 6.67 kcal/mole in the solid state. The liquid-state sample was far more prone to photodegradation than the solid sample. The difference in the activation energy depending on the existing states of sample seems to rely on the mobility of molecules subjected to the reaction in addition to the light absorption properties. In any case, these activation energies were much lower than the reported activation energies for typical drug decomposition in the liquid phase (20). It is worthy to note that reactions with such low activation energy take place so readily that photostable pharmaceutical preparations may not be able to be formulated without extreme care.

Under the various irradiation energies using several optical filters (Table I), the time dependency of degradation was examined at 25°, 35°, and 45°. The results are summarized as an Arrhenius plot in Fig. 13. This graph reveals a thermodynamic relationship between the tendency of degradation and UV intensity. As expected from the foregoing discussions, the higher the UV intensity, the more rapid the degradation. In contrast, the effect of temperature on the degradation rate constant was more significant with decreasing UV intensity. The ratios of the degradation rate constant for the sample without a filter to that for the sample covered with a VY-42 filter at 25° and 45° were 34.5 and 8.6, respectively.

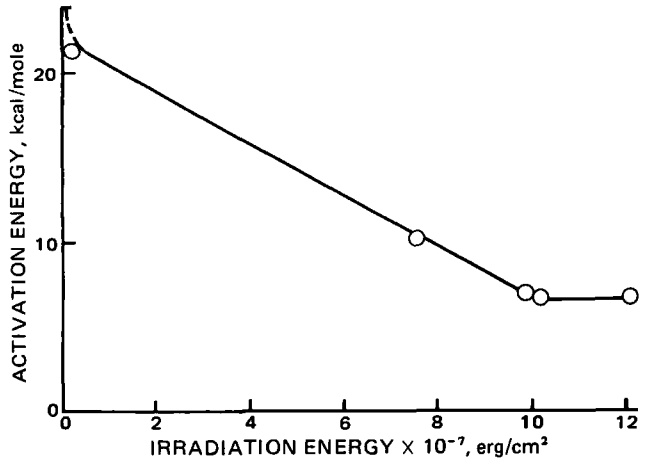

Figure 14—*Effect of UV intensity on the activation energy.*

These values were smaller by one or two orders of magnitude in comparison with the UV intensity ratio of 579, irradiated on each sample. In this respect, the elevation of temperature could be verified again to have a synergistic effect on the chemical degradation of ubidecarenone. The effect of UV irradiation energy on the activation energy calculated from the slope of each regression line is shown in Fig. 14. The activation energy linearly decreased up to $\sim 1.0 \times 10^8$ erg/cm^2; with values larger than this it was no longer dependent on the UV intensity. It should be pointed out that even under very low intensity (in the case of filter VY-42), the activation energy approached a finite value of 21.3 kcal/mole, which is within the usual range of activation energies for hydrolysis or oxidation (21).

REFERENCES

(1) S. R. Byrn, *J. Pharm. Sci.*, **65**, 1 (1976).

(2) T. Eble and E. R. Garrett, *J. Am. Pharm. Assoc., Sci. Ed.*, **43**, 536 (1954).

(3) L. J. DeMerre and C. Wilson, *J. Am. Pharm. Assoc., Sci. Ed.*, **45**, 129 (1956).

(4) E. E. Kaminski, R. M. Cohn, J. L. McGuire, and J. T. Carstensen, *J. Pharm. Sci.*, **68**, 368 (1979).

(5) Y. Matsuda and Y. Minamida, *Chem. Pharm. Bull.*, **24**, 2228 (1976).

(6) Y. Matsuda, H. Inouye, and R. Nakanishi, *J. Pharm. Sci.*, **67**, 196 (1978).

(7) Y. Matsuda and M. Mihara, *Chem. Pharm. Bull.*, **26**, 2649 (1978).

(8) Y. Matsuda and M. Itoh, *Asian J. Pharm. Sci.*, **1**, 107 (1979).

(9) Y. Matsuda and R. Masahara, *Yakugaku Zasshi*, **100**, 953 (1980).

(10) "Shin-iyakuhin no Kikaku-Shikenho Kaisetsu," Society of Japanese Pharmacopeia ed., Yakugyo Zihosha Co., Tokyo, Japan, 1978, p. 123.

(11) Y. Matsuda and Y. Minamida, *Yakugaku Zasshi*, **96**, 425 (1976).

(12) R. S. Hunter, *J. Opt. Soc. Am.*, **38**, 661 (1948).

(13) K. Shibata, "Spectrophotometry and Spectrophotometer" (in Japanese), Kohdansha Co., Tokyo, Japan, 1974, p. 159.

(14) E. I. Stearms, *Am. Dyestuff Rep.*, **40**, 563 (1951).

(15) Y. Matsuda, T. Itooka, and Y. Mitsuhashi, *Chem. Pharm. Bull.*, **28**, 2665 (1980).

(16) H. E. Zimmerman and W. R. Elser, *J. Am. Chem. Soc.*, **91**, 887 (1969).

(17) O. L. Chapman and R. D. Lusa, *J. Am. Chem. Soc.*, **92**, 6352 (1970).

(18) J. Saltiel, J. T. D'Agostino, O. L. Chapman, and R. D. Lusa, *J. Am. Chem. Soc.*, **93**, 2804 (1971).

(19) P. de Mayo, *Acc. Chem. Res.*, **4**, 41 (1971).

(20) R. E. Notari and S. M. Caiola, *J. Pharm. Sci.*, **58**, 1203 (1969).

(21) L. Kennon, *J. Pharm. Sci.*, **53**, 815 (1964).

ACKNOWLEDGMENTS

Presented before the Pharmaceutical Manufacturing Section at the 101st Annual Meeting of the Pharmaceutical Society of Japan, Kumamoto, Japan, April 1981.

The authors thank Eisai Co. Ltd. for providing samples of ubidecarenone and are indebted to Dr. Y. Ichimura for valuable discussion.

Determination of Busulfan in Plasma by GC–MS with Selected-Ion Monitoring

HANS EHRSSON ˣ **and MOUSTAPHA HASSAN**

Received May 25, 1982, from *Karolinska Apoteket, Box 60024, S-104 01 Stockholm, Sweden.* Accepted for publication September 15, 1982.

Abstract □ A GC–MS technique with selected-ion monitoring is described for the determination of busulfan in plasma. Busulfan is extracted from plasma with methylene chloride and converted to 1,4-diiodobutane. Analysis by GC–MS with selected-ion monitoring (m/z 183) gave a relative standard deviation of ±4.3% (n = 5) at the 10-ng/ml level.

Keyphrases □ Busulfan—determination in human plasma, GC–MS with selected-ion monitoring of 1,4-diiodobutane □ GC–MS analysis—selected-ion monitoring, determination of busulfan in human plasma

The alkylating agent, busulfan, 1,4-butanediol dimethanesulfonate, is the drug of choice in the treatment of chronic myeologenous leukemia. The drug has been in clinical use since the 1950's, but the fate of the drug in humans has only been studied by administering radioactively labeled compound and measuring total radioactivity in plasma and urine (1, 2). This paper describes the conversion of busulfan to 1,4-diiodobutane, and the subsequent quantitation of this material by GC–MS with selected-ion monitoring.

EXPERIMENTAL

Synthesis of 1,5-Pentanediol Dimethanesulfonate (Internal Standard)—Methanesulfonic anhydride (9 g) was added carefully to a stirred mixture of 1,5-pentanediol (5.5 g) in pyridine–methylene chloride (40 ml, 1:1). After stirring overnight at 25° the mixture was filtered, and the organic phase was washed with water. The organic phase was evaporated to ~5 ml and left at 4° for 48 hr. The crystals which formed were separated, washed with ice-cold water, and dried (yield: 9%); mp 35° [lit. (3) 34–35°]. The compound was identified by GC–MS[1] after conversion to the corresponding 1,5-diiodo derivative according to the procedure given below. There were prominent peaks at m/z 324 (M^+, 8%), 199 (5), 197 (53), 169 (5), 155 (26), 70 (8), and 69 (100).

Conversion of Busulfan to 1,4-Diiodobutane—Busulfan was con-

[1] LKB 2091; the ionizing energy was 70 eV.

0022-3549/83/1000-1203$01.00/0

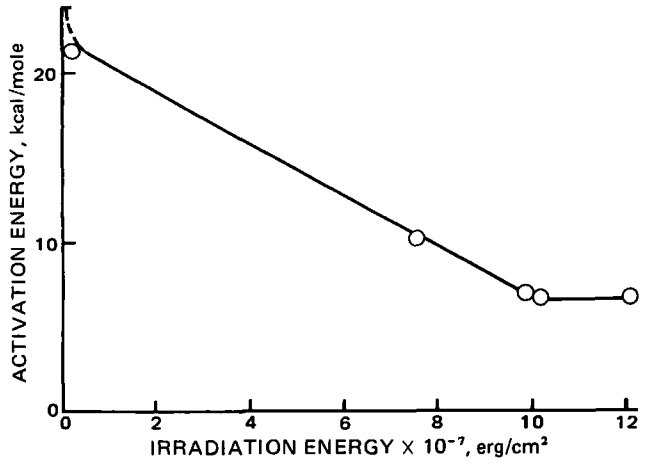

Figure 14—*Effect of UV intensity on the activation energy.*

These values were smaller by one or two orders of magnitude in comparison with the UV intensity ratio of 579, irradiated on each sample. In this respect, the elevation of temperature could be verified again to have a synergistic effect on the chemical degradation of ubidecarenone. The effect of UV irradiation energy on the activation energy calculated from the slope of each regression line is shown in Fig. 14. The activation energy linearly decreased up to $\sim 1.0 \times 10^8$ erg/cm^2; with values larger than this it was no longer dependent on the UV intensity. It should be pointed out that even under very low intensity (in the case of filter VY-42), the activation energy approached a finite value of 21.3 kcal/mole, which is within the usual range of activation energies for hydrolysis or oxidation (21).

REFERENCES

(1) S. R. Byrn, *J. Pharm. Sci.*, **65**, 1 (1976).

(2) T. Eble and E. R. Garrett, *J. Am. Pharm. Assoc., Sci. Ed.*, **43**, 536 (1954).

(3) L. J. DeMerre and C. Wilson, *J. Am. Pharm. Assoc., Sci. Ed.*, **45**, 129 (1956).

(4) E. E. Kaminski, R. M. Cohn, J. L. McGuire, and J. T. Carstensen, *J. Pharm. Sci.*, **68**, 368 (1979).

(5) Y. Matsuda and Y. Minamida, *Chem. Pharm. Bull.*, **24**, 2228 (1976).

(6) Y. Matsuda, H. Inouye, and R. Nakanishi, *J. Pharm. Sci.*, **67**, 196 (1978).

(7) Y. Matsuda and M. Mihara, *Chem. Pharm. Bull.*, **26**, 2649 (1978).

(8) Y. Matsuda and M. Itoh, *Asian J. Pharm. Sci.*, **1**, 107 (1979).

(9) Y. Matsuda and R. Masahara, *Yakugaku Zasshi*, **100**, 953 (1980).

(10) "Shin-iyakuhin no Kikaku-Shikenho Kaisetsu," Society of Japanese Pharmacopeia ed., Yakugyo Zihosha Co., Tokyo, Japan, 1978, p. 123.

(11) Y. Matsuda and Y. Minamida, *Yakugaku Zasshi*, **96**, 425 (1976).

(12) R. S. Hunter, *J. Opt. Soc. Am.*, **38**, 661 (1948).

(13) K. Shibata, "Spectrophotometry and Spectrophotometer" (in Japanese), Kohdansha Co., Tokyo, Japan, 1974, p. 159.

(14) E. I. Stearms, *Am. Dyestuff Rep.*, **40**, 563 (1951).

(15) Y. Matsuda, T. Itooka, and Y. Mitsuhashi, *Chem. Pharm. Bull.*, **28**, 2665 (1980).

(16) H. E. Zimmerman and W. R. Elser, *J. Am. Chem. Soc.*, **91**, 887 (1969).

(17) O. L. Chapman and R. D. Lusa, *J. Am. Chem. Soc.*, **92**, 6352 (1970).

(18) J. Saltiel, J. T. D'Agostino, O. L. Chapman, and R. D. Lusa, *J. Am. Chem. Soc.*, **93**, 2804 (1971).

(19) P. de Mayo, *Acc. Chem. Res.*, **4**, 41 (1971).

(20) R. E. Notari and S. M. Caiola, *J. Pharm. Sci.*, **58**, 1203 (1969).

(21) L. Kennon, *J. Pharm. Sci.*, **53**, 815 (1964).

ACKNOWLEDGMENTS

Presented before the Pharmaceutical Manufacturing Section at the 101st Annual Meeting of the Pharmaceutical Society of Japan, Kumamoto, Japan, April 1981.

The authors thank Eisai Co. Ltd. for providing samples of ubidecarenone and are indebted to Dr. Y. Ichimura for valuable discussion.

Determination of Busulfan in Plasma by GC–MS with Selected-Ion Monitoring

HANS EHRSSON ˣ **and MOUSTAPHA HASSAN**

Received May 25, 1982, from *Karolinska Apoteket, Box 60024, S-104 01 Stockholm, Sweden.* Accepted for publication September 15, 1982.

Abstract □ A GC–MS technique with selected-ion monitoring is described for the determination of busulfan in plasma. Busulfan is extracted from plasma with methylene chloride and converted to 1,4-diiodobutane. Analysis by GC–MS with selected-ion monitoring (m/z 183) gave a relative standard deviation of ±4.3% (n = 5) at the 10-ng/ml level.

Keyphrases □ Busulfan—determination in human plasma, GC–MS with selected-ion monitoring of 1,4-diiodobutane □ GC–MS analysis—selected-ion monitoring, determination of busulfan in human plasma

The alkylating agent, busulfan, 1,4-butanediol dimethanesulfonate, is the drug of choice in the treatment of chronic myeologenous leukemia. The drug has been in clinical use since the 1950's, but the fate of the drug in humans has only been studied by administering radioactively labeled compound and measuring total radioactivity in plasma and urine (1, 2). This paper describes the conversion of busulfan to 1,4-diiodobutane, and the subsequent quantitation of this material by GC–MS with selected-ion monitoring.

EXPERIMENTAL

Synthesis of 1,5-Pentanediol Dimethanesulfonate (Internal Standard)—Methanesulfonic anhydride (9 g) was added carefully to a stirred mixture of 1,5-pentanediol (5.5 g) in pyridine–methylene chloride (40 ml, 1:1). After stirring overnight at 25° the mixture was filtered, and the organic phase was washed with water. The organic phase was evaporated to ~5 ml and left at 4° for 48 hr. The crystals which formed were separated, washed with ice-cold water, and dried (yield: 9%); mp 35° [lit. (3) 34–35°]. The compound was identified by GC–MS[1] after conversion to the corresponding 1,5-diiodo derivative according to the procedure given below. There were prominent peaks at m/z 324 (M^+, 8%), 199 (5), 197 (53), 169 (5), 155 (26), 70 (8), and 69 (100).

Conversion of Busulfan to 1,4-Diiodobutane—Busulfan was con-

[1] LKB 2091; the ionizing energy was 70 eV.

0022-3549/83/1000-1203$01.00/0

Table I—Stability of Busulfan at 37.0° [a]

Medium	$t_{1/2}$ (±SE), hr
Whole blood	8.7 ± 0.4 (n = 10)
Plasma	12.2 ± 0.1 (n = 10)
Phosphate buffer (pH 7.0)	16.0 ± 0.7 (n = 7)

[a] Busulfan concentration: 2.8×10^{-4} M.

verted to 1,4-diiodobutane using 1 M sodium iodide in acetone (0.1 ml), with a reaction time of 20 min at 70°. After addition of n-hexane (0.05 ml) and water (0.1 ml), an aliquot (1–2 μl of hexane) was removed for analysis.

Determination of Partition Coefficient—The distribution of busulfan was studied using phosphate buffer (pH 7.0, μ = 0.1) as the aqueous phase and methylene chloride as the organic phase with an equilibrium time of 30 min at 25.0 ± 0.1°. The concentration of busulfan in the organic phase was determined after addition of the internal standard, evaporation, and conversion to 1,4-diiodobutane as above. The concentration of busulfan in the aqueous phase was determined after transfer into methylene chloride by extraction of the aqueous phase three times with equal volumes of the solvent. The analyses were performed by GC–FID[2].

Determination of Rate Constants for the Formation of 4-iodo-1-butanol Methanesulfonate (I) and 1,4-Diiodobutane—At appropriate times 1.00-ml samples were withdrawn from an acetone solution of busulfan (4×10^{-3} M) in 1 M sodium iodide at 50.0 ± 0.5°. The reaction was stopped by rapid cooling (−70°), and the acetone was evaporated to near dryness. The residue was mixed with 1.00 ml of methylene chloride and 1.00 ml of water. The concentration of 1,4-diiodobutane was determined by mixing 0.100 ml of the organic phase with 1,5-diiodopentane and analyzing by GC–FID. The concentrations of busulfan and I were determined using the following procedure. The methylene chloride phase (0.500 ml) was evaporated to dryness, the residue was mixed with 0.500 ml of ethanol–water (1:1), and an aliquot (0.100 ml) was injected into the liquid chromatograph[3]. The fractions containing busulfan and I were collected, mixed with the internal standard and extracted with methylene chloride. The organic phase was evaporated to dryness, and busulfan and I were converted to 1,4-diiodobutane and analyzed by GC.

The mass spectrum of I was consistent with the expected structure. Peaks were located at m/z 278 (M^+, 1%), 183 (1), 151 (10), 86 (13), 84 (20), 79 (14), 56 (5), 55 (100), and 51 (9). The mass spectrum of the prepared 1,4-diiodobutane was identical with that of a commercially available reference compound. Peaks were located at m/z 310 (M^+, 2%), 184 (5), 183 (81), 155 (10), 137 (8), 135 (8), 56 (10), and 55 (100).

Determination of Busulfan in Plasma—Plasma (1.00 ml) was mixed with 0.100 ml of the internal standard (1.00 μg/ml) in acetone and extracted with methylene chloride (4.00 ml) for 30 min using a mechanical shaker (100 strokes/min). The organic phase was separated and evaporated to dryness, and the derivatization was performed using the aforementioned procedure. The analysis was carried out by GLC–MS[4] focusing at m/z 183 (1,4-diiodobutane) and m/z 197 (1,5-diiodopentane).

RESULTS AND DISCUSSION

Stability of Busulfan—The stability of busulfan in whole blood and plasma is lower than in phosphate buffer, pH 7.0 (Table I). Busulfan differs in this respect from the nitrogen mustards, chlorambucil and melphalan, where an increased stability has been observed in samples containing albumin (4, 5). The stability of busulfan was also studied in plasma at a concentration of 4×10^{-7} M and was not significantly different from that observed at 2.8×10^{-4} M. The degradation of busulfan in human blood samples was minimized by rapidly cooling the blood to 4° and freezing the plasma fraction (−20°) within 1 hr after the blood collection.

Extraction—Methylene chloride was used in the extraction of busulfan because of its favorable extraction properties (k_d = 28.7) and high

[2] Varian 3700; the column (1.5-m × 2-mm i.d.) was packed with 10% SP-2401 on 100–120 Supelcoport and was operated at 130°.

[3] The column (150-mm × 4-mm i.d.) was packed with LiChrosorb RP-8. Ethanol–water (1:1) was used as the mobile phase. The detection was performed by an Altex model 153 detector measured at 254 nm (1,4-diiodobutane and I) and by an LDC Refracto Monitor III (busulfan). The capacity factors were 0.3 (busulfan), 0.9 (I), and 4.6 (1,4-diiodobutane).

[4] LKB 2091 with an ionizing energy of 70 eV. The column (1.5-m × 2-mm i.d.) was packed with 10% SP-2401 on 100–120 Supelcoport and was operated at 140° using a helium flow rate of 20 ml/min. The injector and the ion source temperatures were 230° and 270°, respectively.

Table II—GC of busulfan [a]

Busulfan Injected, μg	Peak Height Ratio[b]	Column Temperature
1	0.80 ± 0.11	190°
0.2	0.23 ± 0.04	190°
1	0.97 ± 0.09	175°
0.2	0.44 ± 0.13	175°

[a] The column was 3% OV-17 on 100–120 Gas Chrom Q (1.5 m) with injector and detector (FID) temperatures of 210° and 270°, respectively. The carrier gas flow was adjusted to give the same retention time (5.2 min) for busulfan at 190° and 175°. [b] The mean peak height ratio of busulfan to 9-bromophenanthrene (±SD; n = 6). The busulfan–9-bromophenanthrene ratio was kept constant.

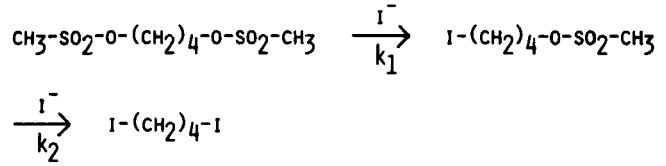

Scheme I—Reaction of busulfan with sodium iodide.

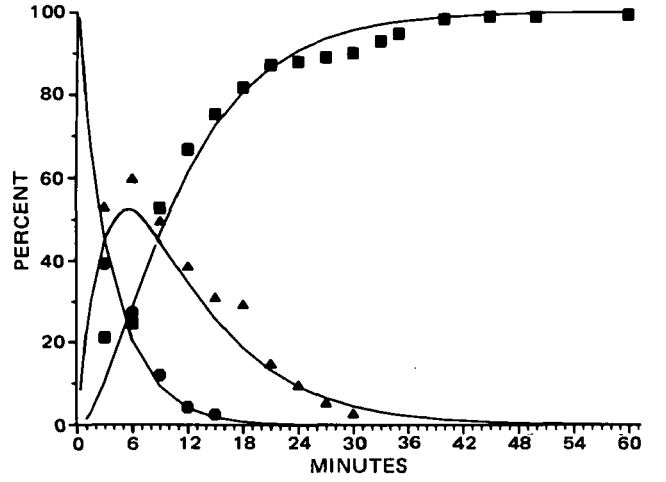

Figure 1—*Time course for the reaction of busulfan with 1 M sodium iodide in acetone at 50°. The solid lines are constructed from the rate constants obtained by nonlinear regression analysis. Key: (●) busulfan; (▲) 4-iodo-1-butanol methanesulfonate; (■) 1,4-diiodobutane.*

Figure 2—*Chromatogram obtained from plasma containing 10 ng of busulfan/ml using selected-ion monitoring with a 1.5-m column packed with 10% SP-2401 at 140°. Key: (A) busulfan as 1,4-diiodobutane; (B) 1,5-pentanediol dimethanesulfonate as 1,5-diiodopentane.*

volatility, being readily evaporated prior to the derivatization step. Using a V_{org}/V_{aq} ratio of 4.98 ± 1% of busulfan (n = 5) was extracted from plasma (busulfan concentration 50 ng/ml).

GC of Intact Busulfan—The peak height ratios of busulfan to 9-bromophenanthrene obtained after injections of different amounts of the compounds at two column temperatures were drastically reduced when lower amounts of busulfan were chromatographed; in all cases poor precision was obtained (Table II). Analysis of busulfan at the lower temperature (175°), keeping the retention time the same by adjustment of the carrier gas flow, gave the highest peak height ratio, which indicates that the results obtained are primarily due to degradation of busulfan in the chromatographic system and not to adsorption phenomena (6). This assumption is also supported by the fact that when using different batches of OV-17 column packing material, multiple asymmetric peaks were occasionally observed.

Conversion of Busulfan to 1,4-Diiodobutane—The reaction of busulfan with sodium iodide proceeds according to Scheme I. The reaction was performed in acetone since nucleophilic substitution reactions are known to be rapid in this solvent (7). The time course for busulfan, I, and 1,4-diiodobutane using 1 M sodium iodide in acetone is given in Fig. 1. Evaluation of the apparent first-order rate constants by nonlinear regression analysis gave $k_1 = 0.266 \pm 0.013$ and $k_2 = 0.124 \pm 0.008$ min^{-1}. Since the ratio between the constants is ~2, it follows that the methanesulfonate ester group of busulfan and that of I have similar reactivity (3). A quantitative reaction was obtained after 20 min using 1 M sodium iodide and a temperature of 70°.

Chromatographic Properties—1,4-Diiodobutane had excellent GC properties giving a symmetric peak (Fig. 2). No indications of decomposition in the chromatographic system were observed.

Detection, Selectivity, and Precision—The minimum detectable concentration (MDC) value obtained by electron-capture detection (ECD) was ~10 times lower than that obtained by selected-ion monitoring (SIM), 0.6×10^{-16} and 5.7×10^{-16} mole/sec, respectively[5]. However, analysis of plasma samples revealed that the higher sensitivity of the ECD could not be utilized because of interfering peaks in the chromatograms. The blanks varied considerably between patients and, in most cases, it was not possible to perform quantitations <10 ng/ml. Since the plasma peaks after administration of therapeutic doses (2 mg) of busulfan are 20–30 ng/ml, meaningful pharmacokinetic studies require determinations in the low nanogram range. A chromatogram obtained from plasma using SIM is given in Fig. 2. The standard curve obtained from plasma using SIM was linear within the range studied (10–400 ng/ml). A least-squares analysis gave a correlation coefficient of 0.9997, a slope of $2.12 \times 10^{-2} \pm 0.03 \times 10^{-2}$, and an intercept of $4.7 \times 10^{-2} \pm 7.6 \times 10^{-2}$. The relative standard deviation was ±2.6% at 100 ng/ml and ±4.3% at 10 ng/ml (n = 5).

[5] Signal to noise ratio = 3. ECD: A Varian ^{63}Ni-detector (DC) operating at a foil temperature of 200°. SIM: LKB 2091, focusing at m/z 183 (70 eV).

REFERENCES

(1) M. V. Nadkarni, E. G. Trams, and P. K. Smith, *Cancer Res.*, **19**, 713 (1959).

(2) H. Vodopick, H. E. Hamilton, and H. L. Jackson, *J. Lab. Clin. Med.*, **73**, 266 (1969).

(3) R. F. Hudson, G. M. Timmis, and R. D. Marshall, *Biochem. Pharmacol.*, **1**, 48 (1958).

(4) H. Ehrsson, U. Lönroth, I. Wallin, M. Ehrnebo, and S. O. Nilsson, *J. Pharm. Pharmacol.*, **33**, 313 (1981).

(5) H. Ehrsson and U. Lönroth, *J. Pharm. Sci.*, **71**, 826 (1982).

(6) K. Grob, *J. High Resol. Chromatogr.*, **3**, 585 (1980).

(7) A. J. Parker, *Chem. Rev.*, **69**, 1 (1969).

ACKNOWLEDGMENTS

The authors thank Dr. S. O. Nilsson for performing the nonlinear regression analysis.

Steroidal Thiourea and Thiazoline Derivatives: Synthesis and *In Vitro* Effects on Bovine Pancreatic Ribonuclease Activity

EL-SEBAII A. IBRAHIM *, A.-MOHSEN M. E. OMAR *x, N. S. HABIB *, OMAIMA M. ABOULWAFA *, S. M. EL-SEWEDY ‡, and J. BOURDAIS §

Received February 24, 1982, from the **Pharmaceutical Chemistry Department, Faculty of Pharmacy*, the ‡*Department of Applied Medical Chemistry, Medical Research Institute, University of Alexandria, Egypt* and the §*Laboratorie de Chimie des Hétérocycles d'Intérêt Biologique, Université d'Aix-Marseille II, Faculté de Medecine Nord, 13326 Marseille, Cédex 15, France.* Accepted for publication August 16, 1982.

Abstract □ Two novel series of steroidal derivatives containing various thiourea and substituted thiazoline moieties attached to the 2- or 4-position of estrone were synthesized and examined for *in vitro* effect on bovine pancreatic ribonuclease activity. All compounds studied exhibited a catabolic activity. The steroidal thiazoline derivatives were more potent activators of ribonuclease than the steroidal thioureas.

Keyphrases □ Steroids—thiourea and thiazoline derivatives, synthesis, *in vitro* effect on bovine pancreatic ribonuclease activity □ Synthesis—steroidal thiourea and thiazoline derivatives, *in vitro* effect on bovine pancreatic ribonuclease activity □ Catabolic activity—steroidal thiourea and thiazoline derivatives, *in vitro*, bovine pancreatic ribonuclease activity

Recent reports from this laboratory have described the synthesis and pharmacological properties of a variety of androgenic and estrogenic thiosemicarbazones (1), acylhydrazones (2–5), and several steroidal heterocycles (6, 7). Further interest in structure–activity relationships (SAR) of steroidal heterocyclics prompted the preparation of XVIII–XXXII (Scheme I) to evaluate the changes in the endocrinological activity caused when the 2- or 4-position of estrone-3-methyl ether is blocked by variously substituted thiazoline moieties. Some of the steroidal thioureas (VIII–XVI), prepared as starting materials, and the thiazoline derivatives were found to possess catabolic-like properties as indicated from their *in vitro* effect on the activity of bovine pancreatic ribonuclease.

RESULTS AND DISCUSSION

Synthesis—The designed compounds (XVIII–XXXII) were prepared in accordance with the sequence of reactions shown in Scheme I. The 2-

0022-3549/83/1000-1205$01.00/0

volatility, being readily evaporated prior to the derivatization step. Using a V_{org}/V_{aq} ratio of 4.98 ± 1% of busulfan (n = 5) was extracted from plasma (busulfan concentration 50 ng/ml).

GC of Intact Busulfan—The peak height ratios of busulfan to 9-bromophenanthrene obtained after injections of different amounts of the compounds at two column temperatures were drastically reduced when lower amounts of busulfan were chromatographed; in all cases poor precision was obtained (Table II). Analysis of busulfan at the lower temperature (175°), keeping the retention time the same by adjustment of the carrier gas flow, gave the highest peak height ratio, which indicates that the results obtained are primarily due to degradation of busulfan in the chromatographic system and not to adsorption phenomena (6). This assumption is also supported by the fact that when using different batches of OV-17 column packing material, multiple asymmetric peaks were occasionally observed.

Conversion of Busulfan to 1,4-Diiodobutane—The reaction of busulfan with sodium iodide proceeds according to Scheme I. The reaction was performed in acetone since nucleophilic substitution reactions are known to be rapid in this solvent (7). The time course for busulfan, I, and 1,4-diiodobutane using 1 M sodium iodide in acetone is given in Fig. 1. Evaluation of the apparent first-order rate constants by nonlinear regression analysis gave $k_1 = 0.266 \pm 0.013$ and $k_2 = 0.124 \pm 0.008$ min^{-1}. Since the ratio between the constants is ~2, it follows that the methanesulfonate ester group of busulfan and that of I have similar reactivity (3). A quantitative reaction was obtained after 20 min using 1 M sodium iodide and a temperature of 70°.

Chromatographic Properties—1,4-Diiodobutane had excellent GC properties giving a symmetric peak (Fig. 2). No indications of decomposition in the chromatographic system were observed.

Detection, Selectivity, and Precision—The minimum detectable concentration (MDC) value obtained by electron-capture detection (ECD) was ~10 times lower than that obtained by selected-ion monitoring (SIM), 0.6×10^{-16} and 5.7×10^{-16} mole/sec, respectively[5]. However, analysis of plasma samples revealed that the higher sensitivity of the ECD could not be utilized because of interfering peaks in the chromatograms. The blanks varied considerably between patients and, in most cases, it was not possible to perform quantitations <10 ng/ml. Since the plasma peaks after administration of therapeutic doses (2 mg) of busulfan are 20–30 ng/ml, meaningful pharmacokinetic studies require determinations in the low nanogram range. A chromatogram obtained from plasma using SIM is given in Fig. 2. The standard curve obtained from plasma using SIM was linear within the range studied (10–400 ng/ml). A least-squares analysis gave a correlation coefficient of 0.9997, a slope of $2.12 \times 10^{-2} \pm 0.03 \times 10^{-2}$, and an intercept of $4.7 \times 10^{-2} \pm 7.6 \times 10^{-2}$. The relative standard deviation was ±2.6% at 100 ng/ml and ±4.3% at 10 ng/ml (n = 5).

[5] Signal to noise ratio = 3. ECD: A Varian ^{63}Ni-detector (DC) operating at a foil temperature of 200°. SIM: LKB 2091, focusing at m/z 183 (70 eV).

REFERENCES

(1) M. V. Nadkarni, E. G. Trams, and P. K. Smith, *Cancer Res.*, **19**, 713 (1959).

(2) H. Vodopick, H. E. Hamilton, and H. L. Jackson, *J. Lab. Clin. Med.*, **73**, 266 (1969).

(3) R. F. Hudson, G. M. Timmis, and R. D. Marshall, *Biochem. Pharmacol.*, **1**, 48 (1958).

(4) H. Ehrsson, U. Lönroth, I. Wallin, M. Ehrnebo, and S. O. Nilsson, *J. Pharm. Pharmacol.*, **33**, 313 (1981).

(5) H. Ehrsson and U. Lönroth, *J. Pharm. Sci.*, **71**, 826 (1982).

(6) K. Grob, *J. High Resol. Chromatogr.*, **3**, 585 (1980).

(7) A. J. Parker, *Chem. Rev.*, **69**, 1 (1969).

ACKNOWLEDGMENTS

The authors thank Dr. S. O. Nilsson for performing the nonlinear regression analysis.

Steroidal Thiourea and Thiazoline Derivatives: Synthesis and *In Vitro* Effects on Bovine Pancreatic Ribonuclease Activity

EL-SEBAII A. IBRAHIM *, A.-MOHSEN M. E. OMAR *x, N. S. HABIB *, OMAIMA M. ABOULWAFA *, S. M. EL-SEWEDY ‡, and J. BOURDAIS §

Received February 24, 1982, from the **Pharmaceutical Chemistry Department, Faculty of Pharmacy*, the ‡*Department of Applied Medical Chemistry, Medical Research Institute, University of Alexandria, Egypt* and the §*Laboratorie de Chimie des Hétérocycles d'Intérêt Biologique, Université d'Aix-Marseille II, Faculté de Medecine Nord, 13326 Marseille, Cédex 15, France.* Accepted for publication August 16, 1982.

Abstract □ Two novel series of steroidal derivatives containing various thiourea and substituted thiazoline moieties attached to the 2- or 4-position of estrone were synthesized and examined for *in vitro* effect on bovine pancreatic ribonuclease activity. All compounds studied exhibited a catabolic activity. The steroidal thiazoline derivatives were more potent activators of ribonuclease than the steroidal thioureas.

Keyphrases □ Steroids—thiourea and thiazoline derivatives, synthesis, *in vitro* effect on bovine pancreatic ribonuclease activity □ Synthesis—steroidal thiourea and thiazoline derivatives, *in vitro* effect on bovine pancreatic ribonuclease activity □ Catabolic activity—steroidal thiourea and thiazoline derivatives, *in vitro*, bovine pancreatic ribonuclease activity

Recent reports from this laboratory have described the synthesis and pharmacological properties of a variety of androgenic and estrogenic thiosemicarbazones (1), acylhydrazones (2–5), and several steroidal heterocycles (6, 7). Further interest in structure–activity relationships (SAR) of steroidal heterocyclics prompted the preparation of XVIII–XXXII (Scheme I) to evaluate the changes in the endocrinological activity caused when the 2- or 4-position of estrone-3-methyl ether is blocked by variously substituted thiazoline moieties. Some of the steroidal thioureas (VIII–XVI), prepared as starting materials, and the thiazoline derivatives were found to possess catabolic-like properties as indicated from their *in vitro* effect on the activity of bovine pancreatic ribonuclease.

RESULTS AND DISCUSSION

Synthesis—The designed compounds (XVIII–XXXII) were prepared in accordance with the sequence of reactions shown in Scheme I. The 2-

0022-3549/83/1000-1205$01.00/0

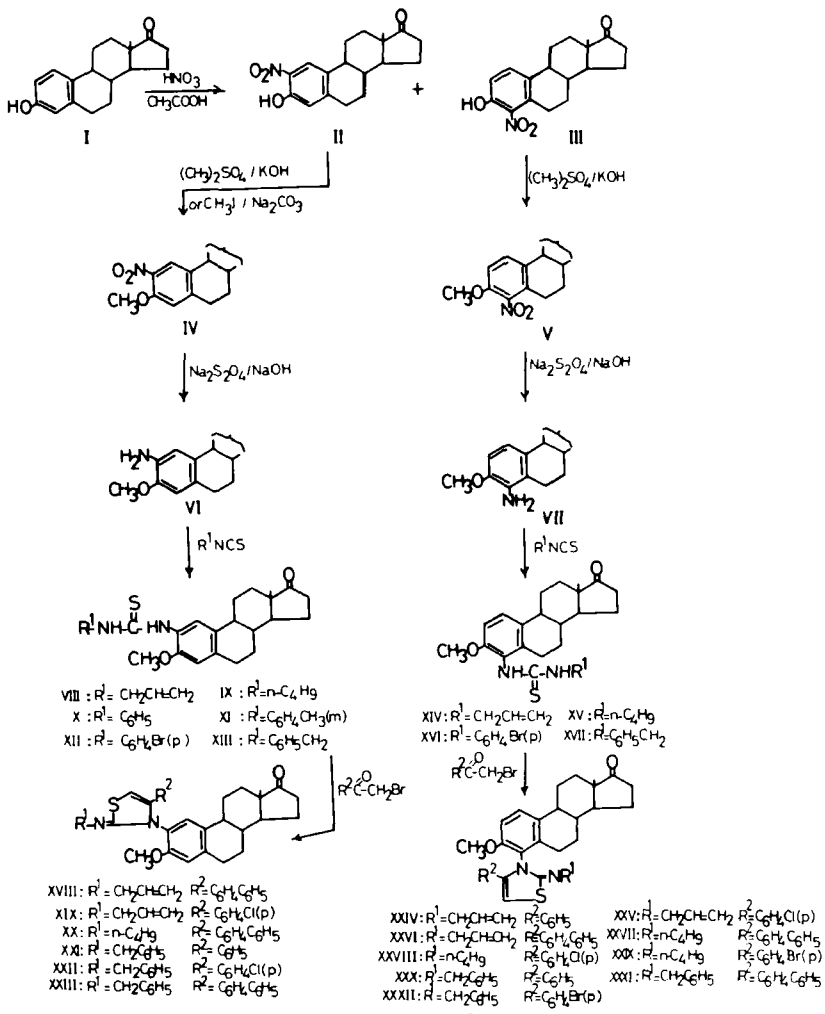

Scheme I

and 4-mononitroestrones (II and III), prepared by nitration of estrone (I) with a mixture of nitric acid and acetic acid (8), were methylated to the corresponding 3-methyl ethers (IV and V) using dimethyl sulfate and potassium hydroxide (9) or methyl iodide and sodium carbonate (10). The products were reduced by sodium dithionite in alkaline medium (9) to give the required 2-amino- (VI) and 4-aminoestrone-3-methyl (VII) ethers in good yields.

Treatment of the amines (VI and VII) with the appropriate alkyl, aryl, or aralkylisothiocyanate derivatives in absolute ethanol (11) gave, respectively, the *N*-substituted *N'*-(3-methoxy-17-oxoestra-1,3,5(10)-trien-2-yl)thioureas (VIII–XIII) and *N*-substituted *N'*-(3-methoxy-17-oxoestra-1,3,5(10)-trien-4-yl)thioureas (XIV–XVII) (Table I). The reaction of VIII, IX, XIII–XV, and XVII, in which R^1 was an alkyl or aralkyl function, with the selected phenacyl bromide in refluxing absolute ethanol (12) proceeded smoothly and gave high yields of the required 2-(2',4'-disubstituted thiazolin-3'-yl)-3-methoxyestra-1,3,5(10)-trien-17-ones (XVIII–XXIII) and the corresponding 4-(2',4'-disubstituted thiazolin-3'-yl)-3-methoxyestra-1,3,5(10)-trien-17-ones (XXIV–XXXII) (Table II). When R^1 was an aryl moiety, as in X–XII and XVI, the reaction with phenacyl bromide gave a mixture of two products that could not be separated. In addition, in one case, when IX was treated with *p*-chlorophenacyl bromide, the *S*-alkylpseudothiourea hydrobromide salt (XXXIII) was obtained (Scheme II).

The products were identified by elemental analyses, IR, UV, and ^{1}H-NMR spectra and, for representative examples, by mass spectra (Tables I, II, and III). The UV spectra showed two absorption maxima at 245–253 and 290–295 nm for VIII and XIII, a single absorption maximum at 276–286 nm for X–XII, and two absorption maxima at 244–251 and 277–282 nm for the thioureas XIV–XVII. The steroidal thiazolines, on the other hand, showed one absorption maximum at ~295 nm for XIX and XXI, while XXV and XXX absorbed at 288 nm. The remainder of the thiazoline derivatives showed two absorption maxima, sometimes as a shoulder, at 256–266 and 290–320 nm. The addition of hydrochloric acid caused a hypsochromic shift of the absorption maxima of all thiazoline derivatives (Tables I and II).

^{1}H-NMR spectra of the steroidal thiourea derivatives (Table I) showed the signals for the common protons of the C_{18}—CH_3, C_3—OCH_3, C_1—H, C_2—H, and C_4—H of the steroidal nucleus (13) at the expected chemical shift. The N—H proton attached to ring A of estrone resonated downfield between 7.25 and 7.97 ppm and was shown as a singlet disappearing on deuteration. The chemical shift of the other N—H proton was dependent on the nature of the substituent present. In the allyl (VIII and XIV), butyl (IX and XV), and benzyl (XIII and XVII) derivatives, the proton was shown at a multiplet at 5.65–6.25 ppm, while in the *p*-bromophenylthiourea (XII), it appeared as a singlet at 7.88 ppm. The ^{1}H-NMR spectra of the steroidal thiazolines (XVIII–XXXI), on the other hand, lacked the signals due to N—H protons, but showed a singlet between 5.72 and 5.83 ppm for the thiazoline C_5—H (13). The chemical shifts of the other protons were almost the same as those of the thiourea derivatives (Table III).

The ^{1}H-NMR spectrum of the steroidal pseudothiourea derivative (XXXIII) did not show the signal of the butyl-NH proton, indicating that this proton was involved in the enolization of the thiourea (IX) from the thione to the thiol form. In addition, the absence of a distinct signal for the two methylenic protons of the S—CH_2—CO function suggested that enolization of XXXIIIa to XXXIIIb had taken place (Scheme II). As a result, the olefinic C—H proton has been identified at low field at ~6.56 ppm while the OH proton was included in the fingerprint area of the steroidal skeleton.

The mass spectra of XV and XVII, as representative examples of the synthesized thioureas, showed the molecular ion peak at *m/z* 414 and 448, respectively (Scheme III). A common fragmentation pattern of these compounds was found to be the elimination of the 3-OCH_3 group followed by cyclization of the produced ion to give the base peak A at *m/z* 383 for the butyl derivative and 417 for the benzyl derivative (Scheme III, Pathway 1). In accordance with Pathway 2, the compounds underwent

Table I—Synthesized *N*-Substituted *N'*-(3-Methoxy-17-oxoestra-1,3,5(10)-trien-2-yl)thioureas (VIII–XIII) and *N*-Substituted *N'*-(3-Methoxy-17-oxoestra-1,3,5(10)-trien-4-yl)thioureas (XIV–XVII)

Compound	Reaction Conditions	Yield, %	Melting Point[a]	Molecular Formula	Analysis, %	Calc.	Found	UV ethanol λ_{max} (log ϵ)	^{1}H-NMR (δ), ppm
VIII	Reflux (1 hr)	95	169–171°	$C_{23}H_{30}N_2O_2S$	C	69.32	68.99	247 (4.212), 291 (3.892)	0.9 (s, 3, C_{18}—CH_3), 3.8 (s, 3, OCH_3), 4.28 (m, 2, allyl H), 5.09 (m, 1, allyl H), 5.23 (m, 1, allyl H), 5.7–6.2 (group of singlets, 2, allyl H and NH, disappearing on deuteration), 6.69 (s, 1, C_4—H), 7.24 (s, 1, C_1—H), 7.97 (s, 1, steroidal NH, disappearing on deuteration)
					H	7.59	7.76		
					N	7.03	6.60		
IX	Reflux (1 hr)	90	101–103°	$C_{24}H_{34}N_2O_2S$	C	69.53	69.50	245 (4.273), 290 (3.968)	0.89 (s, 3, C_{18}—CH_3), 0.90 (t, 3H, J = 6 Hz, CH_2CH_3), 3.59 (m, 2, CH_2—CH_2NH), 3.78 (s, 3, OCH_3), 6.04 (m, 1, CH_2NH, disappearing on deuteration), 6.66 (s, 1, C_4—H), 7.19 (s, 1, C_1—H), 7.4 (s, 1, steroidal NH, disappearing on deuteration)
					H	8.27	8.30		
					N	6.76	6.70		
X	Room temperature (overnight)	90	169–171°	$C_{26}H_{30}N_2O_2S$	C	71.86	71.50	276 (4.285)	
					H	6.98	7.10		
					N	6.45	6.30		
XI	Room temperature (overnight)	93	166–168°	$C_{27}H_{32}N_2O_2S$	C	72.29	72.10	279 (4.324)	
					H	7.19	7.10		
					N	6.25	6.50		
XII	Reflux (30 min)	87	193–195°	$C_{26}H_{29}BrN_2O_2S$	C	60.81	61.14	286(4.279)	0.87 (s, 3, C_{18}—CH_3), 3.77 (s, 3, OCH_3), 6.63 (s, 1, C_4—H), 7.2 (s, 1, C_1—H), 7.25 (d, 2, J = 9 Hz, aromatic H), 7.48 (d, 2, J = 9 Hz, aromatic H), 7.88 (s, 1, BrC_6H_4NH, disappearing on deuteration), 7.92 (s, 1, steroidal NH, disappearing on deuteration)
					H	5.65	6.01		
					N	5.45	5.10		
XIII	Reflux (10 min)	90	152–154°	$C_{27}H_{32}N_2O_2S$	C	72.29	72.17	253 (4.233), 295 (3.893)	0.82 (s, 3, C_{18}—CH_3), 3.73 (s, 3, OCH_3), 4.8 (t, 2H, J = 5 Hz, $CH_2C_6H_5$, becoming a doublet at 4.85 on deuteration), 6.25 (m, 1, $C_6H_5CH_2NH$, disappearing on deuteration), 6.61 (s, 1, C_4—H), 7.12 (s, 1, C_1—H), 7.28 (s, 5, aromatic H), 7.52 (s, 1, steroidal NH, disappearing on deuteration)
					H	7.19	7.13		
					N	6.25	6.38		
XIV	Reflux (3.5 hr)	98	181–183°	$C_{23}H_{30}N_2O_2S$	C	69.32	69.40	251 (4.253), 282 (3.609)	0.9 (s, 3, C_{18}—CH_3), 3.80 (s, 3, OCH_3), 4.26 (m, 2, allyl H), 5.04 (m, 1, allyl H), 5.16 and 5.22 (2 m, 1, allyl H), 5.65–6.06 (m, 2, allyl H+, CH_2NH, becoming a group of singlets at 5.69–6.14 for allyl H after deuteration), 6.82 (d, 1, J = 9 Hz, C_2—H), 7.3 (d, 2, J = 9 Hz, C_1—H + steroidal NH, becoming 1H after deuteration)
					H	7.59	7.67		
					N	7.03	7.20		
XV	Reflux (3 hr)	98	162–164°	$C_{24}H_{34}N_2O_2S$	C	69.53	69.58	245 (4.331), 281 (3.707)	0.88 (t, 3, J = 6 Hz, CH_2CH_3), 0.89 (s, 3, C_{18}—CH_3), 3.54 (q, 2, J = 6 Hz and 12 Hz, $NHCH_2$, becoming a triplet on deuteration at 3.58, J = 6 Hz), 3.77 (s, 3, OCH_3), 5.67 (t, 1, J = 6 Hz, CH_2NH, disappearing on deuteration), 6.8 (d, 1, J = 9 Hz, C_2—H), 7.27 (d, 2, J = 9 Hz, C_1—H +steroidal NH, becoming 1H after deuteration)
					H	8.27	8.38		
					N	6.76	6.95		
XVI	Reflux (1 hr)	76	149–151°	$C_{26}H_{29}BrN_2O_2S$	C	60.81	61.10	244sh (4.276), 277 (4.340)	
					H	5.65	5.78		
					N	5.45	5.70		
XVII	Reflux (3 hr)	93	215–217°	$C_{27}H_{32}N_2O_2S$	C	72.29	72.29	244 (4.233), 280 (3.482)	0.89 (s, 3, C_{18}—CH_3), 3.77 (s, 3, OCH_3), 4.88 (m, 2, $CH_2C_6H_5$), 5.91 (m, 1, benzyl NH, disappearing on deuteration), 6.81 (d, 1, J = 9 Hz, C_2—H), 7.25–7.38 (m, 2, C_1—H + steroidal NH, overlapping with aromatic H), 7.31 (s, 5, aromatic H)
					H	7.19	7.29		
					N	6.25	6.40		

[a] The products were crystallized from benzene–light petroleum except XII and XVII which were crystallized from ethanol–benzene.

cleavage of C_6 and C_7 from the steroidal nucleus to give ion B at m/z 385 and 419, which on losing the thiourea function gave ion C at m/z 256. The thiourea functions in XV and XVII were found to undergo elimination of hydrogen sulfide giving the carbodiimide ion D, at m/z 380 and 414, fission of the isothiocyanate function (14) giving ion E at m/z 299, and cleavage of a butyl or benzylamino function to yield ion F at m/z 341. Ion E in turn, lost an NH function giving ion G at m/z 284, while ion F cleaved sulfur to give the isocyanide ion H at m/z 309.

Table II—Synthesized 2-(2′,4′-Disubstituted thiazolin-3′-yl)-3-methoxyestra-1,3,5(10)-trien-17-ones (XVIII–XXIII) and 4-(2′,4′-Disubstituted thiazolin-3′-yl)-3-methoxyestra-1,3,5(10)-trien-17-ones (XXIV–XXXII)

Compound	Reflux Time	Yield, %	Melting Point[a]	Molecular Formula	Analysis, %[b] C	H	N	UV λ_{max} (log ϵ)[c]
XVIII	30 min	76	183–185° (ethanol–benzene)	$C_{37}H_{38}N_2O_2S \cdot \frac{1}{2} H_2O$	76.15 76.52	6.68 6.97	4.80 5.12	264 (4.614), 300 (4.374)/ 278 (4.633)
XIX	30 min	67	122–124° (aqueous ethanol)	$C_{31}H_{33}ClN_2O_2S$	69.85 69.42	6.19 6.13	5.25 5.35	296 (4.194)/ 288sh (4.599), 264 (4.303)
XX	1.5 hr	74	129–131° (ethanol)	$C_{38}H_{42}N_2O_2S$	77.26 77.07	7.17 7.36	4.74 4.98	266 (4.570), 300sh (4.326)/ 278 (4.589)
XXI	30 min	78	217–219° (benzene–light petr.)	$C_{35}H_{36}N_2O_2S$	76.62 76.41	6.61 6.75	5.11 5.22	295 (4.177)/ 262 (4.253), 290sh (4.156)
XXII	1 hr	85	130–132° (methanol)	$C_{35}H_{35}ClN_2O_2S$	72.10 72.14	6.00 6.26	4.80 5.02	300 (4.252)/ 260sh (4.280), 266 (4.307)
XXIII	30 min	83	124–126° (ethanol)	$C_{41}H_{40}N_2O_2S$	78.82 78.40	6.45 6.69	4.48 4.63	256 (4.596), 296 (4.374)/ 271 (4.619)
XXIV	1 hr	96	138–140° (aqueous methanol)	$C_{31}H_{34}N_2O_2S$	74.67 74.47	6.87 7.22	5.62 5.83	288 (4.149)/ 266 (4.201)
XXV	1 hr	86	155–157° (aqueous ethanol)	$C_{31}H_{33}ClN_2O_2S \cdot \frac{1}{2} H_2O$	68.69 69.18	6.27 6.57	5.17 5.65	266sh (4.272), 290 (4.196)/ 226sh (4.635), 268 (4.404)
XXVI	1 hr	80	145–147° (aqueous ethanol)	$C_{37}H_{38}N_2O_2S$	77.32 77.21	6.67 6.84	4.87 4.96	258 (4.594), 320sh (5.034)/ 270 (4.622)
XXVII	1.5 hr	74	125–127° (aqueous ethanol)	$C_{38}H_{42}N_2O_2S$	77.26 77.52	7.17 7.29	4.74 4.80	258 (4.612), 320sh (5.027)/ 270 (4.632)
XXVIII	2 hr	83	114–116° (aqueous ethanol)	$C_{32}H_{37}ClN_2O_2S$	70.00 69.69	6.74 7.06	5.10 5.24	262 sh (4.287), 289 (4.225)/ 220 (4.659), 263 (4.411)
XXIX	2 hr	63	118–120° (aqueous ethanol)	$C_{32}H_{37}BrN_2O_2S$	64.75 64.84	6.23 6.33	4.72 4.81	231 sh (4.604), 265sh (4.201) 290 (4.104)/ 231 (4.536), 268 (4.225)
XXX	1.5 hr	82	126–128° (aqueous ethanol)	$C_{35}H_{36}N_2O_2S$	76.62 76.67	6.61 6.80	5.11 5.42	288 (4.080)/ 269 (4.212)
XXXI	1.5 hr	79	233–235° (ethanol–benzene)	$C_{41}H_{40}N_2O_2S$	78.82 78.54	6.45 6.52	4.48 5.00	263 (4.100), 300 sh (4.563)/ 282 (4.602)
XXXII	1.5 hr	82	154–156° (aqueous ethanol)	$C_{35}H_{35}BrN_2O_2S$	66.98 66.59	5.58 5.60	4.46 4.31	277 sh (4.632), 289 (4.176)/ 265 (4.376)

[a] With crystallization solvent in parentheses. [b] The first row are calculated values; the second row are the values found. [c] Using ethanol/using ethanol + HCl.

The mass spectrum of 2-(2′-benzylamino-4′-biphenylthiazolin-3′-yl)-3-methoxyestra-1,3,5(10)-trien-17-one (XXIII) showed the molecular ion peak at *m/z* 624 (Scheme IV). In accordance with Pathway 1 (Scheme IV), the fragmentation of the molecule was found to be elimination of an ethylene function from ring B and three hydrogens giving ion A at *m/z* 593. This pathway was confirmed by the appearance of the metastable peak at 563.75. In Pathway 2, the molecule fragmented through elimination of a benzyl function to yield ion B at *m/z* 533, while in Pathway 3 the biphenyl group of the thiazoline moiety was eliminated and ring D removed to give ion C, as the base peak, at *m/z* 373. Ion C, in turn, was found to undergo cleavage through removal of the phenyl group of the benzyl moiety, a thioketene function from the thiazoline ring, and the methoxyl group and then cyclized to ion D at *m/z* 209. The removal of only the phenyl and thioketene moieties from ion C gave the carbodiimide ion F at *m/z* 238, which after cleaving carbon and a methyl radical produced ions G and H at *m/z* 226 and 211, respectively. The spectra of all examined compounds have also shown the different ions corresponding to the reported fragmentation of the steroidal nucleus (15), as well as those of susbstituted thiazoline ring (16–18) (Table III).

Biological Screening—Compounds VIII, X, XVI–XVIII, XX, XXII, XXV, XXIX, and XXX were tested *in vitro* for possible anabolic–catabolic activity by measuring their effect on the activity of bovine pancreatic ribonuclease, as previously reported (7, 19). The results (Table IV) indicated that the steroidal thiazoline derivatives caused a more potent activation of the enzyme than the corresponding steroidal thioureas. In addition, the fact that the thiourea XVI and the thiazolines XXV and XXX caused the highest percentage activation of the enzyme suggested that substitution, especially with the bulky thiazoline moieties, in the 2-position of estrone greatly hinders the binding of the hormonal derivative with the enzyme. The high percentage of enzyme activation caused by the pseudothiourea XXXIII has been attributed to its high polar structure and malleability in spatial arrangement, which allows maximum contact with the enzyme. The thiazoline derivatives XVIII and XXV, having allyl and biphenyl or *p*-chlorophenyl moieties in the heterocyclic ring, as well as XXX, containing the benzyl and phenyl groups, and the steroidal pseudothiourea XXXIII are most likely to possess catabolic activity being the most potent activators of the enzyme. Such a property, effective in suppressing cancer metastasis (20, 21), has recommended such compounds for evaluation for anticancer activity. Compared with these results, the correlative studies from this laboratory indicated that the fusion of a substituted oxazole or oxazoline ring to the 2,3- or 3,4-positions of estrone causes the products to induce a mild or similar percentage of enzyme activation (6, 7).

EXPERIMENTAL[1]

Steroidal Thiourea Derivatives (VIII–XVII)—A solution of the steroidal amines VI and VII (9) (200 mg, 0.66 mmole) and the selected alkyl, aryl, or aralkylisothiocyanate derivative (1.5 *M* equivalent) in ethanol (20 ml) was left at room temperature or heated under reflux as specified in Table I. Ethanol was removed under reduced pressure, and the residue was covered with light petroleum and stored in the refrigerator for 1 hr. The solvent was decanted, and the residue was treated with fresh light petroleum and scratched to deposit the solid. This was filtered, crystallized from the proper solvent, and identified by elemental analysis and IR, UV, and ^{1}H-NMR spectra (Table I). IR (mineral oil): ν 3380–3140 (N—H), 1735–1710 (C=O), 1605–1585 and 1500–1480 (C=C, aromatic), 1535–1520, 1340–1310, 1190–1170, and 950–905 (N—C=S amide I, II, III, and IV bands, respectively), and 1290–1240 and 1080–1050 cm^{-1} (C—O—C). The mass spectrum of XV showed *m/z* (relative abundance %): M^+ at 414(18), 385(10), 384(28), 383(100), 382(15), 381(47), 380(55), 342(22), 341(98), 324(3), 309(10), 300(18), 299(78), 298(6), 285(10), 284(18), 283(5), 256(10), 243(12), 231(10), 230(12), 228(6), 217(17), 216(7), 215(6), 213(5), 212(6), 211(7), 199(7), 198(10), 197(6), 186(10), 185(8), 184(11), 175(8), 174(10), 173(11), 172(13), 171(10), 160(13), 159(10), 158(17), 147(8), 146(15), 145(6), 144(8), 143(10), 142(8), 141(11), 131(12), 130(3), 129(13), 128(17), 116(12), 115(30), 103(12), 102(5), 97(10), 81(8), 79(8), 72(5), 57(25), 55(23), 53(12), and 41(43); the mass spectrum of XVII showed *m/z* (relative abundance %): M^+ at 448(15), 419(10), 418(32), 417(100), 416(13), 415(42), 414(48), 342(4), 341(17), 309(2), 300(10), 299(37), 298(4), 285(3), 284(8), 283(3), 256(3), 243(3), 231(3), 230(3), 228(3), 217(4), 216(3), 215(3), 213(4), 212(4), 211(6), 199(5), 198(6), 197(42), 186(6), 185(5), 184(7), 175(5), 174(6), 173(6), 172(8), 171(6), 165(6), 160(10), 159(5), 158(10), 149(3), 147(4), 146(8), 145(4), 144(6), 143(7), 142(6), 141(72), 131(8), 130(12), 129(10), 128(12), 117(7), 107(6), 106(27), 97(5), 92(18), 91(100), 79(13), 78(7), 77(7), and 41(23).

[1] All melting points are uncorrected. IR spectra were measured as Nujol mulls on a Beckmann 4210 IR Spectrophotometer, and UV spectra for ethanol solution were measured on a Shimadzu double-beam spectrophotometer (Model UV-200S). ^{1}H-NMR and mass spectra were measured on a Perkin-Elmer R32 and an AEI-MS-50, respectively.

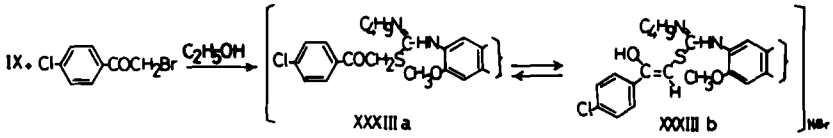

Scheme II

2- and 4-(2′,4′-Disubstituted thiazoline-3′-yl)-3-methoxyestra-1,3,5(10)-trien-17-ones (XVIII–XXXII)—A mixture of the thiourea derivatives (VIII, IX, XIII–XV, and XVII) (200 mg) and the molar equivalent of substituted phenacyl bromide in absolute ethanol (10 ml) was heated under reflux for the specified time (Table II). Ethanol was removed under reduced pressure, and the oily residue was dissolved in chloroform (75 ml). The solution was washed with water (3 × 50 ml), dried (anhydrous sodium sulfate), and evaporated to give an oily residue. On scratching with light petroleum, the products deposited in solid form; they were crystallized from the proper solvents and identified by elemental analysis and IR, UV, ^{1}H-NMR, and mass spectra (Tables II and III). IR (mineral oil): ν 1735–1725 (C=O), 1620–1610 (C=N), 1595–1560 and 1500–1490 (C=C, aromatic), and 1265–1235 and 1090–1075 cm^{-1} (C—O—C).

Table III—^{1}H-NMR and Mass Spectral Data of the Steroidal Thiazoline Derivatives

Compound	^{1}H-NMR (δ), ppm	Mass Spectrum, *m/z* (Relative Abundance, %)
XVIII	0.9 (s, distorted, 3, C_{18}—CH_3), 3.81 (s, 3, OCH_3), 4.51 (m, 2, allyl H), 4.94 (m, 1, allyl H), 5.16 (m, 1, allyl H), 5.6–6.2 (group of singlets, 1, allyl H), 5.8 (s, 1, thiazoline H), 6.67 (s, 1, C_4—H), 7.0 (s, 1, C_1—H), 7.3–7.75 (m, 9, aryl H)	
XIX	0.9 (s, 3, C_{18}—CH_3), 3.8 (s, 3, OCH_3), 4.46 (m, 2, allyl H), 4.95 (m, 1, allyl H), 5.2 (m, 1, allyl H), 5.6–6.2 (group of singlets, 1, allyl H), 5.78 (s, 1, thiazoline H), 6.64 (s, 1, C_4—H), 7.0 (s, 1, C_1—H), 7.35 (s, 4, aryl H)	534(45), 533(40), 532(100), 531(13), 520(5), 519(13), 518(10), 517(29), 505(5), 504(15), 503(45), 502(38), 501(100), 494(2), 493(5), 492(6), 491(10), 324(11), 323(33), 322 (9), 298(9), 297(8), 296(4), 236(5), 225(4), 224(5), 223(8), 211(5), 210(6), 209(6), 199(4), 198(4), 197(5), 196(8), 194(2), 186(4), 185(5), 184(5), 173(5), 172(5), 171(5), 170(6), 169(6), 168(15), 160(11), 159(63), 158(4), 155(5), 143(4), 141(6), 140(3), 138(5), 136(5), 134(8), 133(5), 130(4), 129(8), 128(8), 116(5), 115(10), 103(4), 97(4), 55(11), 41(50).
XX	0.84 (t, 3, J = 7 Hz, CH_2—CH_3), 0.9 (s, 3, C_{18}—CH_3), 3.8 (s, 3, OCH_3), 3.88 (m, 2, N—CH_2—), 5.75 (s, 1, thiazoline H), 6.65 (s, 1, C_4—H), 7.0 (s, 1, C_1—H), 7.25–7.75 (group of multiplets, 9, aryl h)	
XXI	0.9 (s, 3, C_{18}—CH_3), 3.76 (s, 3, OCH_3), 5.1 (s, 2, —$CH_2C_6H_5$), 5.73 (s, 1, thiazoline H), 6.64 (s, 1, C_4—H), 6.98 (s, 1, C_1—H), 7.04–7.40 (group of multiplets, 10, aryl H)	
XXII	0.9 (s, 3, C_{18}—CH_3), 3.75 (s, 3, OCH_3), 5.08 (s, 2, —$CH_2C_6H_5$), 5.73 (s, 1, thiazoline H), 6.64 (s, 1, C_4—H), 6.96 (s, 1, C_1—H), 7.03–7.33 (group of multiplets, 9, aryl H)	
XXIII	0.9 (s, 3, C_{18}—CH_3), 3.78 (s, 3, OCH_3), 5.15 (s, 2, —$CH_2C_6H_5$), 5.8 (s, 1, thiazoline H), 6.65 (s, 1, C_4—H), 6.99 (s, 1, C_1—H), 7.19 (s, 5, phenyl H), 7.22–7.66 (group of multiplets, 9, aryl H)	625(19), 624(40), 595(4), 594(10), 593(22), 534(10), 533(14), 395(2), 374(29), 373(100), 371(4), 370(6), 369(23), 297(5), 296(3), 238(6), 226(2), 225(3), 224(13), 211(9), 210(24), 209(6), 208(3), 199(2), 198(2), 197(6), 184(4), 181(8), 180(4), 179(6), 178(13), 172(2), 171(2), 167(4), 161(8), 159(2), 158(2), 153(4), 141(3), 129(5), 128(4), 116(3), 115(6), 107(3), 106(5), 105(5), 97(3), 92(14), 91(67), 77(4), 41(9).
XXIV	0.9 (s, 3, C_{18}—CH_3), 3.8 (s, 3, OCH_3), 4.5 (m, 2, allyl H), 4.99 (m, 1, allyl H), 5.21 (m, 1, allyl H), 5.76 (s, 1, thiazoline H), 5.72–6.06 (group of singlets, 1, allyl H), 6.81 (d, 1, J = 9 Hz, C_2—H), 7.05 (d, 1, J = 9 Hz, C_1—H), 7.45 (s, 5, aryl H)	
XXVI	0.9 (s, 3, C_{18}—CH_3), 3.82 (s, 3, OCH_3), 4.57 (m, 2, allyl H), 5.06 (m, 1, allyl H), 5.22 (m, 1, allyl H), 5.81 (s, 1, thiazoline H), 5.8–6.35 (group of singlets, 1, allyl H), 6.82 (d, 1, J = 9 Hz, C_2—H), 7.07 (d, 1, J = 9 Hz, C_1—H), 7.4–7.82 (m, 9, aryl H)	
XXVII	0.73 (t, 3, J = 7 Hz, CH_2—CH_3), 0.91 (s, 3, C_{18}—CH_3), 3.82 (s, 3, OCH_3), 3.98 (t, 2, J = 7 Hz, —N—CH_2—), 5.77 (s, 1, thiazoline H), 6.85 (d, 1, J = 9 Hz, C_2—H), 7.08 (d, 1, J = 9 Hz, C_1—H), 7.39–7.82 (m, 9, aryl H)	
XXVIII	0.8 (t, 3, J = 7 Hz, CH_2CH_3), 0.91 (s, 3, C_{18}—CH_3), 3.82 (s, 3, OCH_3), 3.91 (t, 2, J = 7 Hz, N—CH_2—), 5.75 (s, 1, thiazoline H), 6.85 (d, 1, J = 9 Hz, C_2—H), 7.91 (d, 1, J = 9 Hz, C_1—H), 7.45 (m, 4, aryl H)	550(46), 549(39), 548(100), 547(8), 535(2), 533(6), 521(3), 520(3), 519(8), 518(5), 517(13), 515(6), 495(8), 495(24), 493(21), 492(55), 491(4), 480(2), 479(4), 478(4), 477(12), 475(9), 464(2), 463(5), 462(4), 461(10), 339(5), 338(5), 322(6), 321(6), 309(8), 298(9), 297(33), 296(6), 290(4), 282(9), 252(14), 250(18), 211(6), 210(12), 209(6), 198(6), 196(18), 194(11), 186(4), 185(4), 184(6), 174(4), 173(4), 172(5), 171(6), 170(4), 169(9), 168(8), 160(4), 159(3), 158(5), 157(4), 155(4), 143(4), 141(4), 140(8), 138(24), 136(5), 134(12), 133(5), 129(6), 128(5), 116(3), 115(7), 103(3), 97(5), 57(12), 55(14), 41(52).
XXIX	0.74 (t, 3, J = 7 Hz, CH_2CH_3), 0.91 (s, 3, C_{18}—CH_3), 3.82 (s, 3, OCH_3), 3.91 (t, 2, J = 7 Hz, —N—CH_2—), 5.72 (s, 1, thiazoline H), 6.85 (d, 1, J = 9 Hz, C_2—H), 7.08 (d, 1, J = 9 Hz, C_1—H), 7.31 (d, 2, J = 9 Hz, aryl H), 7.65 (d, 2, J = 9 Hz, aryl H)	
XXXI	0.9 (s, 3, C_{18}—CH_3), 3.81 (s, 3, OCH_3), 5.21 (s, 2, —$CH_2C_6H_5$), 5.83 (s, 1, thiazoline H), 6.81 (d, 1, J = 9 Hz, C_2—H), 7.03 (d, 1, J = 9, Hz, C_1—H), 7.29 (s, 5, $CH_2C_6H_5$), 7.2–7.72 (m, 9, biphenyl H)	625(18), 624(36), 596(4), 595(14), 594(39), 593(84), 535(13), 533(3), 395(20), 374(3), 373(8), 370(2), 369(5), 297(2), 238(11), 226(13), 225(3), 224(3), 211(8), 210(20), 209(6), 208(3), 198(2), 197(4), 184(3), 181(3), 180(4), 179(5), 178(16), 172(2), 167(4), 153(3), 141(3), 129(3), 128(9), 116(2), 115(5), 107(1), 106(1), 97(2), 92(13), 91(100), 77(3), 41(6).

Table IV—In Vitro Effects of the Synthesized Steroidal Thiourea and Thiazoline Derivatives on the Activity of Bovine Pancreatic Ribonuclease

Compound		Molar Concentration of the Products (M)			
		10^{-6}	10^{-7}	10^{-8}	10^{-9}
I	Mean ± SE[a]	219.6 ± 10.03	225.4 ± 20.04	231.2 ± 14.4	230 ± 17.02
	% Activation	12.46	15.61	18.57	17.98
	p Value	>0.05	>0.05	>0.05	>0.05
	Control		(200.2 ± 14.2)		
VIII	Mean ± SE	278.2 ± 8.12	298.6 ± 26.8	274.6 ± 25.1	286.3 ± 18.6
	% Activation	39.20	49.22	37.50	43.12
	p Value	<0.001	<0.001	<0.05	<0.001
X	Mean ± SE	276.2 ± 25.1	256.5 ± 12.2	254.6 ± 18.2	282.4 ± 13.2
	% Activation	37.98	28.12	27.21	41.26
	p Value	<0.01	<0.01	<0.01	<0.001
XVI	Mean ± SE	259.2 ± 14.4	360.6 ± 10.6	438.3 ± 15.4	464.1 ± 24.8
	% Activation	29.5	80.2	119.2	132.3
	p Value	<0.01	<0.001	<0.001	<0.001
XVII	Mean ± SE	202.2 ± 19.2	223.6 ± 12.8	205.3 ± 12.3	234.6 ± 12.9
	% Activation	0.99	11.68	2.55	17.18
	p Value	>0.05	>0.05	>0.05	>0.05
	Control		(195 ± 15.2)		
XVIII	Mean ± SE	384 ± 18.2	322 ± 10.4	377 ± 21.3	375 ± 20.3
	% Activation	96.92	95.90	93.33	92.30
	p Value	<0.001	<0.001	<0.001	<0.001
XX	Mean ± SE	280 ± 11.5	275 ± 19.4	268 ± 13.2	325 ± 19.6
	% Activation	44.06	41.10	37.20	66.66
	p Value	>0.05	>0.05	>0.05	>0.01
XXII	Mean ± SE	246 ± 22.32	260 ± 28.3	295 ± 21.2	323 ± 16.6
	% Activation	26.57	33.39	51.77	65.99
	p Value	>0.05	<0.05	<0.01	<0.01
XXV	Mean ± SE	362 ± 25.5	402 ± 14.6	379 ± 16.2	467 ± 13.2
	% Activation	85.64	106.15	94.16	139.49
	p Value	<0.001	<0.001	<0.001	<0.001
XXIX	Mean ± SE	206 ± 22.2	196 ± 11.3	206 ± 20.6	198 ± 13.5
	% Activation	5.64	0.51	5.64	1.54
	p Value	>0.05	>0.05	>0.05	>0.05
XXX	Mean ± SE	314 ± 13.2	405 ± 17.3	453 ± 16.2	512 ± 22.3
	% Activation	61.03	107.69	132.31	162.56
	p Value	<0.001	<0.001	<0.001	<0.001
XXXIII	Mean ± SE	450 ± 26.1	528 ± 14.3	246 ± 26.3	227 ± 24.1
	% Activation	130.77	170.77	26.15	16.41
	p Value	<0.001	<0.001	>0.05	>0.05

[a] The ribonuclease activity is expressed in units as the mean value ± standard error.

***N*-(3-Methoxy-17-oxoestra-1,3,5(10)-trien-2-yl)-*S*-(*p*-chlorophenacyl)-*N'*-butyl-pseudothiourea Hydrobromide (XXXIII)**—A mixture of equimolar amounts of *N*-butyl-*N'*-(3-methoxy-17-oxoestra-1,3,5(10)-trien-2-yl)thiourea (IX) (200 mg) and 4-chlorophenacyl bromide in absolute ethanol (10 ml) was heated under reflux for 2 hr. The ethanol was evaporated to dryness, and the oily residue was dissolved in chloroform (75 ml) and washed with water (3 × 50 ml). The chloroform layer was dried (anhydrous sodium sulfate) and evaporated to dryness; the product was scratched with light petroleum to give a solid which was filtered and dried. Crystallization from benzene–light petroleum gave 160 mg (60% yield) of a yellowish amorphous solid, mp 208–210° (dec). IR (mineral oil): ν 3400 (N—H broad), 1735 (C=O), 1620 (C=N), 1590 and 1500 (C=C, aromatic), and 1255 and 1090 cm^{-1} (C—O—C); UV (ethanol): λ_{max} (log ϵ) 300 (4.209); UV (ethanol–HCl): λ_{max} (log ϵ) 228 sh (4.585), 266 (4.272), and 295 sh (4.107); ^{1}H-NMR ($CDCl_3$): δ 0.85 (t, 3, J = 6 Hz, butyl-CH_3, overlapping with the singlet of C_{18}—CH_3), 0.88 (s,

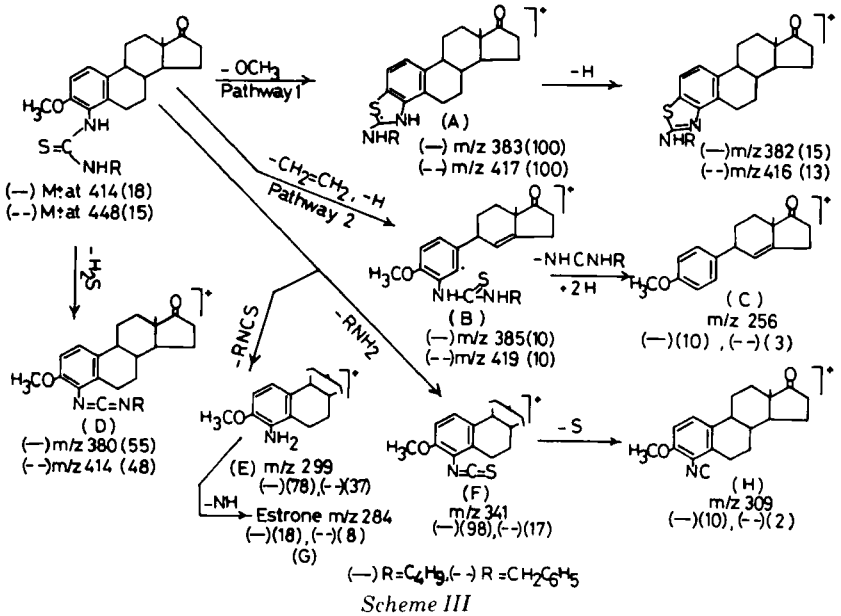

Scheme III

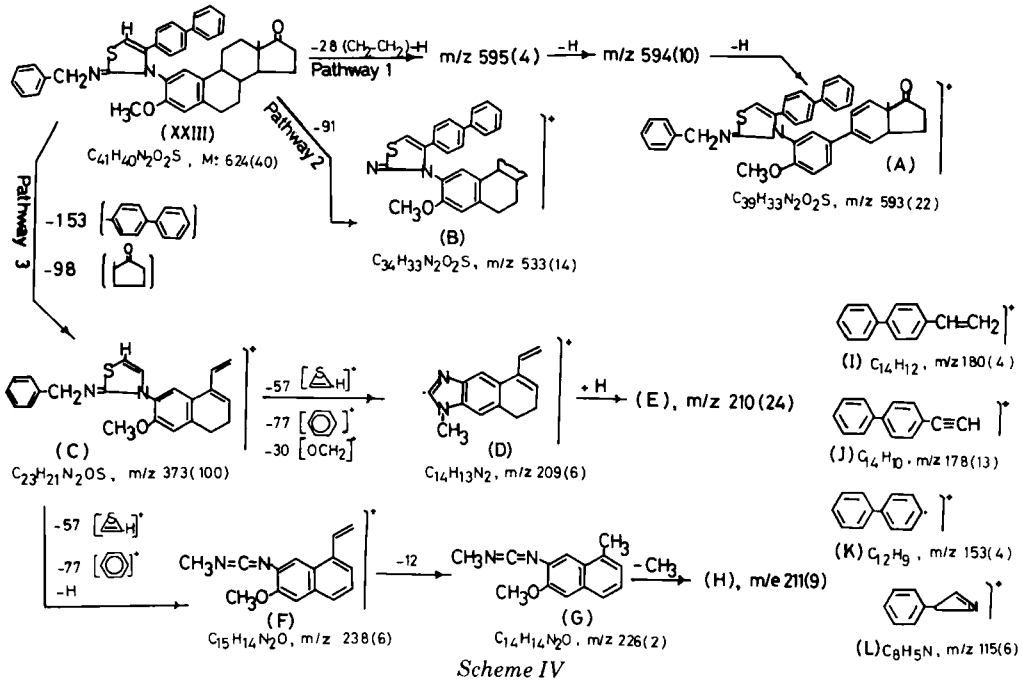

Scheme IV

3, C_{18}—CH_3), 3.79 (s, 3, OCH_3), 4.61 (t, 2, J = 6 Hz, —CH_2N—), 6.56 (s, 1, S—C*H*=C—OH), 6.7 (s, 1, C_4—H), 7.28 (s, 1, C_1—H), and 7.47 (m, 5, 4 aromatic protons + steroidal N—H).

Anal. —Calc. for $C_{32}H_{40}BrClN_2O_2S \cdot \frac{1}{2} H_2O$: C, 59.03; H, 6.30; N, 4.30. Found: C, 59.19; H, 6.88; N, 4.67.

***In Vitro* Anabolic–Catabolic Activities**—Four sets of solutions and media (7) were used in the evaluation procedures. After mixing the components of each set, the tubes were incubated at 37° for 15 min and then treated with 4 ml of ethanol–glacial acetic acid (15:1, v/v) to terminate the reaction. After storage for 1 hr in the refrigerator, the tubes were centrifuged for 15 min and the clear supernatants were measured spectrophotometrically at 260 nm. The results of the effect of VIII, X, XVI–XVIII, XX, XXII, XXV–XXIX, XXX, and XXXIII on the activity of bovine pancreatic ribonuclease are shown in Table IV.

REFERENCES

(1) A.-Mohsen M. E. Omar, S. M. El-Khawass, A. B. Makar, N. M. Bakry, and T. T. Daabees, *Pharmazie*, **33**, 577 (1978).

(2) A.-Mohsen M. E. Omar and F. A. Ashour, *Pharmazie*, **33**, 747 (1979).

(3) S. M. El-Khawass, A.-Mohsen M. E. Omar, T. T. Daabees, and F. M. Sharaby, *Pharmazie*, **35**, 143 (1980).

(4) A.-Mohsen M. E. Omar, A. M. Farghaly, A. A. B. Hazzaa, and N. H. Eshba, *Pharmazie*, **35**, 809 (1980).

(5) El-Sebaii A. Ibrahim, A.-Mohsen M. E. Omar, M. A. Khalil, A. B. Makar, and T. T. Daabees, *Pharmazie*, **35**, 810 (1980).

(6) El-Sebaii A. Ibrahim, A.-Mohsen M. E. Omar, N. S. Habib, and Omaima M. AboulWafa, *J. Heterocycl. Chem.*, **19**, 761 (1982).

(7) A.-Mohsen M. E. Omar and Omaima M. AboulWafa, *J. Pharm. Sci.*, **71**, 983 (1982).

(8) R. A. Pickering and H. Werbin, *J. Am. Chem. Soc.*, **80**, 680 (1958).

(9) S. Kraychy, *J. Am. Chem. Soc.*, **81**, 1702 (1959).

(10) A. J. Tomson and J. P. Horwitz, *J. Org. Chem.*, **24**, 2056 (1959).

(11) A.-Mohsen M. E. Omar, N. S. Habib, and Omaima M. AboulWafa, *Pharmazie*, **32**, 758 (1977).

(12) A.-Mohsen M. E. Omar, S. A. Shams-El-Din, A. A. Ghobashy, and M. A. Khalil, *Eur. J. Med. Chem.*, **16**, 77 (1981).

(13) E. R. Clark, A.-Mohsen M. E. Omar, and G. Prestwich, *J. Med. Chem.*, **20**, 1096 (1977).

(14) A.-Mohsen M. E. Omar, A. M. Farghaly, A. A. B. Hazzaa, N. H. Eshba, F. M. Sharaby, and T. T. Daabees, *J. Pharm. Sci.*, **70**, 1075 (1981).

(15) C. Djerassi, J. M. Wilson, H. Budzikiewicz, and J. W. Chamberlain, *J. Am. Chem. Soc.*, **84**, 4544 (1962).

(16) H. Ogura, S. Sugimoto, and T. Itoh, *Org. Mass Spectrom.*, **3**, 1341 (1970).

(17) G. M. Clarke, R. Grigg, and D. H. Williams, *J. Chem. Soc. (B)*, **1966**, 339.

(18) M. J. Rix and B. R. Webster, *Org. Mass Spectrom.*, **5**, 311 (1971).

(19) S. M. El-Sewedy, E. A. El-Basiouni, and S. T. Assar, *Biochem. Pharm.*, **27**, 1831 (1978).

(20) A. Graffi and W. Arnold, *Acta Biol. Med. Ger.*, **30**, 15 (1973).

(21) Taik Koo Yun, XI International Cancer Congress, Florence, 1974, Panel 15.

ACKNOWLEDGMENTS

Presented in part at the Symposium on Chemistry in Developing Countries, New York, N.Y., August 1981.

Supported in part by Pharco Pharmaceuticals, Cairo, Egypt. The authors thank Shering AG, Berlin, West Germany, for the donation of estrone. Thanks are also due to Dr. E. Dorme and Mrs. Cabaret, Université de Paris-sud, Orsay, and Dr. D. C. Das, Institut de Chimie des Substances Naturelles, Gif-Sur-Yvette, France, for the microanalytical, ^{1}H-NMR, and mass spectral data.

High-Performance Liquid Chromatographic Determination of Cyproheptadine Hydrochloride in Tablet Formulations

GREGORY W. BURROWS ˣ **and CHERYL L. ALLIGER**

Received November 6, 1981, from the *Analytical Chemistry Department, Food and Drug Research Laboratories, Inc., Waverly, NY 14892.* Accepted for publication August 26, 1982

Abstract □ A high-performance liquid chromatographic method is described which determines cyproheptadine hydrochloride in tablet formulations. Tablets were dissolved in water–acetonitrile (50:50) and analyzed using an octadecylsilane column with a mobile phase of 85% acetonitrile and 15% of an aqueous solution of 0.01 *M* 1-octanesulfonic acid, 0.5% triethylamine, and 1% acetic acid using UV absorbance detection at 280 nm.

Keyphrases □ Cyproheptadine hydrochloride–high-performance liquid chromatography, tablet formulations □ High-performance liquid chromatography—cyproheptadine hydrochloride in tablet formulations

Cyproheptadine hydrochloride, an oral antihistamic agent used in the treatment of perennial and seasonal rhinitis and other allergic reactions (1), is formulated in various ways. In this analysis, cyproheptadine was separated from vitamins, plant extracts, and fillers. The standard spectrophotometric analysis described in USP XX (2) proved unsatisfactory with these formulations. Excipients coeluting from the silica gel column caused an elevated absorbance and erroneous assay.

Various authors have described separations of antihistamines and cyproheptadine hydrochloride by GLC (3, 4) and reverse-phase high-performance liquid chromatography (HPLC) (5, 6). A buffered, normal phase, ion-paired separation has also been reported (7). The purpose of this study was to develop a chromatographic analysis to separate a complex mixture of ingredients in a tablet formulation.

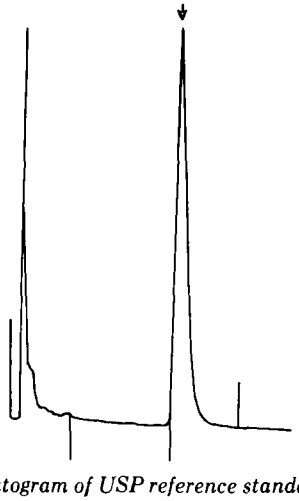

Figure 1—*Chromatogram of USP reference standard cyproheptadine hydrochloride.*

EXPERIMENTAL

The high-performance liquid chromatograph[1] with an octadecylsilane column[2] was used for all separations. The detector was equipped with a 280-nm filter and set at 0.05 AUFS. Mobile phase at ambient temperature was pumped at 2 ml/min. (500–1000 psi) until the baseline was stable.

Chemicals and Reagents—Acetonitrile[3] was HPLC grade, 1-octanesulfonic acid[4] and glacial acetic acid[5] were reagent grade, triethylamine[5] was reagent grade and redistilled in glass, and cyproheptadine HCl[6] was USP reference standard.

Mobile Phase—The mobile phase was delivered using two pumps and a solvent programmer. The programmer was set to pump a mixture of 85% acetonitrile and 15% aqueous phase. The aqueous phase consisted of a solution of 0.01 *M* 1-octanesulfonic acid, 0.5% triethylamine, and 1% acetic acid.

Standard Curve—Standard solutions were prepared to concentrations ranging from 26.68 to 80.04 μg/ml representing results of 40 to 120% of theoretical. A plot of concentration *versus* area was linear (correlation coefficient = 0.99997). The line equation is $y = mx + b$, where m (slope) = 1.06×10^7 and b (intercept) = -0.005×10^7. Run on 3 successive days, the average slope had an *RSD* of 0.43%.

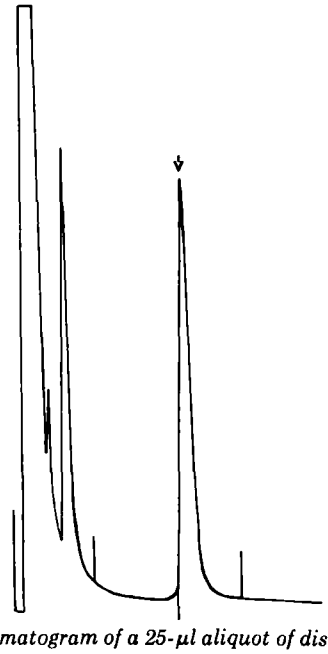

Figure 2—*Chromatogram of a 25-μl aliquot of dissolved tablets.*

[1] Model 204 Chromatograph with two M6000A pumps, Model 660 Solvent programmer, U6K Universal Injector, M730 data module, M440 UV detector, Waters Associates, Milford, Mass.
[2] 5 mm (10 μm) Radial Pak A, Waters Associates, Milford, Mass.
[3] J. T. Baker Chemical Co., Phillipsburg, NJ 08865
[4] Eastman Kodak Co., Rochester, NY 14650
[5] Fisher Scientific Co., Fair Lawn, NJ 07410
[6] U.S. Pharmacopeial Convention, Inc., Rockville, MD 20852

0022-3549/83/1000-1212$01.00/0

Table I—Dissolution of Cyproheptadine Hydrochloride

Dissolution Medium	Sample Identification	Peak[a] Area ($\times 10^6$)	Cyproheptadine Hydrochloride Available, %
Distilled water	USP reference standard	6.859	100
Distilled water	Cyproheptadine hydrochloride (used in tablet formulation)	6.410	93.4
Distilled water	Blank powder	None detected	
Simulated gastric fluid	USP reference standard	2.973	43.3
Simulated gastric fluid	Tablets	2.932	42.7
Simulated intestinal fluid	USP reference standard	3.369	49.1
Simulated intestinal fluid	Tablets	0.784	11.4

[a] One determination each.

Analytical Procedure—Five tablets (each containing approximately 0.7 mg cyproheptadine hydrochloride) were placed in a 50-ml volumetric flask. Twenty-five ml 50:50 (v/v) acetonitrile–water was added and swirled until the tablets were completely dissolved and then brought to volume with acetonitrile–water. The amount of cyproheptadine in the tablets was calculated from the linear regression of the standard curve.

A solution of powdered excipients without cyproheptadine hydrochloride was prepared at a concentration equal to five tablets in a 50-ml solution. No interferences from other ingredients or contaminants in the analysis were detected in the blank solution.

Three samples of the powdered excipient spiked with cyproheptadine gave recoveries of 100.4, 100.0, and 99.8% (mean = 100.1 ± 0.3%).

RESULTS AND DISCUSSION

Cyproheptadine (a weak aliphatic base) pairs with octanesulfonate in a weakly acidic mobile phase. A mobile phase of acetonitrile–aqueous solution (85:15) (0.01 *M* octanesulfonic acid, 1% acetic acid, 0.5% triethylamine) gave the best separation (Fig. 1) with cyproheptadine resolved from other ingredients (Fig. 2) with no interferences from contaminants or excipients.

Table II—Assays of Three Production Lots

No. Lot	Theoretical Concentration, mg/tablet	Obtained Concentration, mg/tablet Replicate Analyses 1	2	3	Mean	*SD*
1	0.667	0.639	0.635	0.637	0.637	0.002
2	0.667	0.649	0.628	0.667	0.648	0.020
3	0.667	0.616	0.653	0.627	0.632	0.019

A comparison of analyses of cyproheptadine dissolved in distilled, deionized water, simulated gastric fluid [USP XX (2)], and simulated intestinal fluid [USP XX (2)] showed irregular results (Table I). Preliminary results indicate that dissolution is slow in the simulated fluids with total release times of several hours.

Since water appeared to be the best dissolution solvent, a mixture of acetonitrile–water was used, which made the resultant solution more compatible with the mobile phase. The assay of three production lots of tablets was measured to be 95.5, 97.2, and 94.8% of theoretical content (Table II). The method precision by triplicate assays was 0.3, 3.1, and 3.0%, respectively.

REFERENCES

(1) "Physicians Desk Reference," 35th ed. Medical Economics Co., Oradell, N.J.

(2) "The United States Pharmacopeia XX/The National Formulary XV," 20th rev., U.S. Pharmacopeial Convention, Rockville, Md., 1980, p. 193–194.

(3) A. W. Missen, Rep.—*N.Z. Dep. Sci. Ind. Res., Chem Div. Rep.*, ISS C. D. 2282, 36 (1979).

(4) E. C. G. Clarke, "Isolation and Identification of Drugs," Vol. I, Pharmaceutical Press, London, 1974, p. 278.

(5) B. B. Wheals, *J. Chromatogr.*, **187**, 65 (1980).

(6) D. L. Massaret and M. R. Detavernier, *J. Chromatogr.*, **187**, 139 (1980).

(7) D. L. Massaret and G. Hoogewijis, *Anal. Lett.*, **13**, 389 (1980).

ACKNOWLEDGMENTS

Acknowledgment is given to the sponsor for funding of this work and giving permission to publish. Details of the formulation have been omitted to protect client confidentiality.

Synthesis and Anticonvulsant Testing of 4-Phenylsemicarbazides

MILTON J. KORNET ˣ and JOHN YEOU-RUOH CHU

Abstract □ A series of compounds based on the semicarbazide structure have been synthesized. Anticonvulsant activity was found in a majority of the compounds using both the maximal electroshock seizure and the subcutaneous pentylenetetrazol seizure threshold tests. Activity of the compounds was weaker than the 1,1,2-trisubstituted semicarbazides previously reported.

Keyphrases □ 4-Phenylsemicarbazides—synthesis and anticonvulsant activity □ Anticonvulsants—synthesis of 4-phenylsemicarbazides

Earlier work (1–5) on the synthesis and anticonvulsant activity of 4-phenylsemicarbazides was concerned primarily with compounds in which N-1 and N-2 are fully substituted by alkyl or aryl residues. To obtain additional information regarding structure–activity relationships for these types of compounds, it was desirable to prepare the series of compounds represented by III. This series differs from all of the previous series in that the compounds contain a hydrogen atom at N-2. This series includes 2-methyl, 2,6-dimethyl, and 2-chloro-6-methyl substituents in the aromatic ring since such substitution generally proved to be optimal in the previous series of 4-phenylsemicarbazides studied (1, 3).

RESULTS AND DISCUSSION

1,1-Disubstituted hydrazines (II) readily added to aryl isocyanates (I) and afforded III in good yields (Scheme I, Table I). Several different 1,1-disubstituted hydrazines were used (Table I) including the cage-like compound, 3-amino-3-azabicyclo[3.2.2]nonane. The latter compound

0022-3549/83/1000-1213$01.00/0

Table I—Dissolution of Cyproheptadine Hydrochloride

Dissolution Medium	Sample Identification	Peak[a] Area ($\times 10^6$)	Cyproheptadine Hydrochloride Available, %
Distilled water	USP reference standard	6.859	100
Distilled water	Cyproheptadine hydrochloride (used in tablet formulation)	6.410	93.4
Distilled water	Blank powder	None detected	
Simulated gastric fluid	USP reference standard	2.973	43.3
Simulated gastric fluid	Tablets	2.932	42.7
Simulated intestinal fluid	USP reference standard	3.369	49.1
Simulated intestinal fluid	Tablets	0.784	11.4

[a] One determination each.

Analytical Procedure—Five tablets (each containing approximately 0.7 mg cyproheptadine hydrochloride) were placed in a 50-ml volumetric flask. Twenty-five ml 50:50 (v/v) acetonitrile–water was added and swirled until the tablets were completely dissolved and then brought to volume with acetonitrile–water. The amount of cyproheptadine in the tablets was calculated from the linear regression of the standard curve.

A solution of powdered excipients without cyproheptadine hydrochloride was prepared at a concentration equal to five tablets in a 50-ml solution. No interferences from other ingredients or contaminants in the analysis were detected in the blank solution.

Three samples of the powdered excipient spiked with cyproheptadine gave recoveries of 100.4, 100.0, and 99.8% (mean = 100.1 ± 0.3%).

RESULTS AND DISCUSSION

Cyproheptadine (a weak aliphatic base) pairs with octanesulfonate in a weakly acidic mobile phase. A mobile phase of acetonitrile–aqueous solution (85:15) (0.01 *M* octanesulfonic acid, 1% acetic acid, 0.5% triethylamine) gave the best separation (Fig. 1) with cyproheptadine resolved from other ingredients (Fig. 2) with no interferences from contaminants or excipients.

Table II—Assays of Three Production Lots

No. Lot	Theoretical Concentration, mg/tablet	Obtained Concentration, mg/tablet Replicate Analyses 1	2	3	Mean	*SD*
1	0.667	0.639	0.635	0.637	0.637	0.002
2	0.667	0.649	0.628	0.667	0.648	0.020
3	0.667	0.616	0.653	0.627	0.632	0.019

A comparison of analyses of cyproheptadine dissolved in distilled, deionized water, simulated gastric fluid [USP XX (2)], and simulated intestinal fluid [USP XX (2)] showed irregular results (Table I). Preliminary results indicate that dissolution is slow in the simulated fluids with total release times of several hours.

Since water appeared to be the best dissolution solvent, a mixture of acetonitrile–water was used, which made the resultant solution more compatible with the mobile phase. The assay of three production lots of tablets was measured to be 95.5, 97.2, and 94.8% of theoretical content (Table II). The method precision by triplicate assays was 0.3, 3.1, and 3.0%, respectively.

REFERENCES

(1) "Physicians Desk Reference," 35th ed. Medical Economics Co., Oradell, N.J.

(2) "The United States Pharmacopeia XX/The National Formulary XV," 20th rev., U.S. Pharmacopeial Convention, Rockville, Md., 1980, p. 193–194.

(3) A. W. Missen, Rep.—*N.Z. Dep. Sci. Ind. Res., Chem Div. Rep.*, ISS C. D. 2282, 36 (1979).

(4) E. C. G. Clarke, "Isolation and Identification of Drugs," Vol. I, Pharmaceutical Press, London, 1974, p. 278.

(5) B. B. Wheals, *J. Chromatogr.*, **187**, 65 (1980).

(6) D. L. Massaret and M. R. Detavernier, *J. Chromatogr.*, **187**, 139 (1980).

(7) D. L. Massaret and G. Hoogewijis, *Anal. Lett.*, **13**, 389 (1980).

ACKNOWLEDGMENTS

Acknowledgment is given to the sponsor for funding of this work and giving permission to publish. Details of the formulation have been omitted to protect client confidentiality.

Synthesis and Anticonvulsant Testing of 4-Phenylsemicarbazides

MILTON J. KORNET ˣ and JOHN YEOU-RUOH CHU

Abstract □ A series of compounds based on the semicarbazide structure have been synthesized. Anticonvulsant activity was found in a majority of the compounds using both the maximal electroshock seizure and the subcutaneous pentylenetetrazol seizure threshold tests. Activity of the compounds was weaker than the 1,1,2-trisubstituted semicarbazides previously reported.

Keyphrases □ 4-Phenylsemicarbazides—synthesis and anticonvulsant activity □ Anticonvulsants—synthesis of 4-phenylsemicarbazides

Earlier work (1–5) on the synthesis and anticonvulsant activity of 4-phenylsemicarbazides was concerned primarily with compounds in which N-1 and N-2 are fully substituted by alkyl or aryl residues. To obtain additional information regarding structure–activity relationships for these types of compounds, it was desirable to prepare the series of compounds represented by III. This series differs from all of the previous series in that the compounds contain a hydrogen atom at N-2. This series includes 2-methyl, 2,6-dimethyl, and 2-chloro-6-methyl substituents in the aromatic ring since such substitution generally proved to be optimal in the previous series of 4-phenylsemicarbazides studied (1, 3).

RESULTS AND DISCUSSION

1,1-Disubstituted hydrazines (II) readily added to aryl isocyanates (I) and afforded III in good yields (Scheme I, Table I). Several different 1,1-disubstituted hydrazines were used (Table I) including the cage-like compound, 3-amino-3-azabicyclo[3.2.2]nonane. The latter compound

0022-3549/83/1000-1213$01.00/0

Table I—Physical Properties of 4-Phenylsemicarbazides

Compound	X	R	Melting Point	Yield, %	Recrystallization Solvent[a]	Formula	Analysis, % Calc.	Found
IIIa	o-CH_3	$N(CH_3)_2$	140–142°[b]	93	A	$C_{10}H_{15}N_3O$	C 62.15	
							H 7.82	
							N 21.74	
IIIb	2,6-$(CH_3)_2$	$N(CH_3)_2$	156–158°	91	A	$C_{11}H_{17}N_3O$	C 63.74	63.44
							H 8.27	8.28
							N 20.27	20.24
IIIc	2-Cl,6-CH_3	$N(CH_3)_2$	149.5–151°	93	A	$C_{10}H_{14}ClN_3O$	C 52.75	52.55
							H 6.20	6.31
							N 18.45	18.16
IIId	o-CH_3	$N(CH_2)_4$	147–148°	50	A	$C_{12}H_{17}N_3O$	C 65.73	65.54
							H 7.81	8.05
							N 19.16	19.43
IIIe	2,6-$(CH_3)_2$	$N(CH_2)_4$	189–190°	62	A	$C_{13}H_{19}N_3O$	C 66.92	66.80
							H 8.21	8.17
							N 18.01	18.25
IIIf	2-Cl,6-CH_3	$N(CH_2)_4$	157–158°	73	A	$C_{12}H_{16}ClN_3O$	C 56.81	56.60
							H 6.36	6.49
							N 16.56	16.20
IIIg	o-CH_3	$N(CH_2)_5$	153–155.5°	77	A	$C_{13}H_{19}N_3O$	C 66.92	66.80
							H 8.21	8.04
							N 18.01	17.89
IIIh	2,6-$(CH_3)_2$	$N(CH_2)_5$	197–199°	79	B	$C_{14}H_{21}N_3O$	C 67.98	67.70
							H 8.56	8.56
							N 16.99	16.67
IIIi	2-Cl,6-CH_3	$N(CH_2)_5$	173–175°	80	A	$C_{13}H_{18}ClN_3O$	C 58.32	58.02
							H 6.78	6.50
							N 15.69	15.39
IIIj	o-CH_3	$N(CH_2CH_2)_2O$	187–189°	86	B	$C_{12}H_{17}N_3O_2$	C 61.26	60.99
							H 7.28	7.15
							N 17.86	17.59
IIIk	2,6-$(CH_3)_2$	$N(CH_2CH_2)_2O$	222–223°	82	B	$C_{13}H_{19}N_3O_2$	C 62.63	62.35
							H 7.68	7.48
							N 16.85	16.57
IIIl	2-Cl,6-CH_3	$N(CH_2CH_2)_2O$	204–206°	78	B	$C_{12}H_{16}ClN_3O_2$	C 53.44	53.14
							H 5.98	5.90
							N 15.58	15.38
IIIm	o-CH_3	$N(CH_2)_6$	122–124°	88	A	$C_{14}H_{21}N_3O$	C 67.98	67.77
							H 8.56	8.61
							N 16.99	16.91
IIIn	2,6-$(CH_3)_2$	$N(CH_2)_6$	162–164°	92	A	$C_{15}H_{23}N_3O$	C 68.93	68.67
							H 8.87	8.67
							N 16.08	15.80
IIIo	2-Cl,6-CH_3	$N(CH_2)_6$	127.5–129.5°	92	A	$C_{14}H_{20}ClN_3O$	C 59.68	59.38
							H 7.15	7.02
							N 14.91	14.79
IIIp	2-Cl,6-CH_3	$N(CH_2CH_2)_2NCH_3$	196–198°	27	A	$C_{13}H_{19}ClN_4O$	C 55.22	54.99
							H 6.77	6.90
							N 19.81	19.65
IIIq	o-CH_3	$N[CH_2CH(CH_2CH_2)]_2$	199–201°	82	A	$C_{16}H_{23}N_3O$	C 70.30	70.04
							H 8.48	8.65
							N 15.37	15.26
IIIr	2,6-$(CH_3)_2$	$N[CH_2CH(CH_2CH_2)]_2$	218–220°	73	A	$C_{17}H_{25}N_3O$	C 71.05	71.22
							H 8.77	8.57
							N 14.62	14.48
IIIs	2-Cl,6-CH_3	$N[CH_2CH(CH_2CH_2)]_2$	244–246°	73	A	$C_{16}H_{22}ClN_3O$	C 62.43	62.17
							H 7.20	7.10
							N 13.65	13.63
IIIt	2,6-$(CH_3)_2$	$N(CH_3)CH_2CO_2C_2H_5$	112–114°	79	A	$C_{14}H_{21}N_3O_3$	C 60.20	60.38
							H 7.58	7.34
							N 15.04	15.26

[a] A, ethyl acetate; B, ethyl acetate–methanol. [b] M. Wilcox, *J. Med. Chem.*, 11, 171 (1968) reported mp, 142–143°.

was obtained in two steps *via* the intermediate *N*-nitroso derivative from commercially available 3-azabicyclo[3.2.2]nonane (6). Additionally, ethyl (1-methylhydrazino)acetate was prepared from methylhydrazine and ethyl bromoacetate (7).

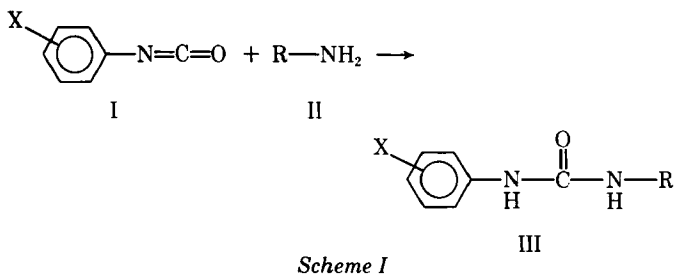

Scheme I

Compounds IIIa–IIIt were tested in the maximal electroshock seizure (MES) and subcutaneous pentylenetetrazol seizure threshold (scMet) tests for anticonvulsant activity and in the rotorod test for neurotoxicity in male Carworth Farms No. 1 mice by reported procedures (1). In the MES test, compounds IIIb, IIId, IIIg, IIIi, IIIj, IIIk, IIIl, and IIIn exhibited activity at 300 mg/kg at 30 min. Only IIIb showed toxicity at this dosage level. Compounds IIIb, IIIc, and IIIh showed activity at the same dosage at 4 hr. Compound IIIc was the only compound active at 100 mg/kg (30 min).

Five compounds (IIIb, IIIg, IIIh, IIIi, and IIIm) were active in the scMet test at 300 mg/kg at 30 min. Compound IIIh was also active at this same dosage at 4 hr. Two compounds underwent further testing. Compounds IIIc and IIIh exhibited MES ED_{50} = 76 (61–90, 95% C.I. [confidence interval]) and 282 (244–319, 95% C.I.) mg/kg; scMet ED_{50} = 222 (146–326, 95% C.I.) and 424 (240–695, 95% C.I.) mg/kg and TD_{50} = 210 (165–272, 95% C.I.) and 528 (390–698, 95% C.I.) mg/kg, respectively.

These data indicate that 4-phenylsemicarbazides derived from 1,1-dialkylated hydrazines possess anticonvulsant activity; however, it is of a lower order than that shown by 4-phenylsemicarbazides derived from 1,1,2-trialkylated hydrazines (1, 3). The cage compounds IIIq, IIIr, and IIIs were uniformly inactive and these results are consistent with the poor activity found for other cage compounds (4, 5).

EXPERIMENTAL[1]

Ethyl (1-Methylhydrazino)acetate—A solution of 16.7 g (0.1 mole) of ethyl bromoacetate in 17 ml of benzene was added dropwise with magnetic stirring over a 90-min period to a solution of 9.2 g (0.2 mole) of methylhydrazine in 50 ml of benzene. After the reaction mixture had stirred overnight at room temperature, the benzene phase was decanted and the salt residue was washed three times with 15 ml of benzene. The benzene was distilled through a 1-ft Vigreux column at 42 mm Hg. The residue was then distilled and afforded 8.82 g (67%) of a colorless oil, bp 88° (21 mm); IR (film): 1740 cm^{-1} (C=O).

Anal.—Calc. for $C_5H_{12}N_2O$: C, 45.44; H, 9.15; N, 21.20. Found: C, 45.29; H, 9.26; N, 21.31.

[1] Melting points were determined on a Thomas-Hoover melting point apparatus and are uncorrected. The IR spectra were taken on a Perkin-Elmer 700 spectrophotometer as either liquid films or potassium bromide pellets. NMR spectra were recorded on a Varian EM-360 or T-60 spectrometer, using tetramethylsilane as the internal reference. Mass spectra were obtained on a RMU-7 double-focusing spectrometer by Hitachi/Perkin-Elmer. Elemental analyses were performed by Baron Consulting Co., Orange, Conn. All compounds exhibited ^{1}H-NMR and mass spectra consistent with the structures shown.

4-Phenylsemicarbazides (III)—Compound IIIb was prepared by the dropwise addition of a solution of 2.66 g (0.0180 mole) of 2,6-dimethylphenyl isocyanate (I) in 6 ml of dry benzene to a solution of 1.20 g (0.020 mole) of 1,1-dimethylhydrazine in 10 ml of dry benzene at room temperature. After ~10 min heat was evolved. The mixture was heated for 2.5 h in an oil bath (85°). The solvent was evaporated under reduced pressure, and the residue was recrystallized from ethyl acetate and gave 3.40 g (91%) of white crystalline product, mp 156–158°.

REFERENCES

(1) M. J. Kornet, *J. Pharm. Sci.*, **67**, 1471 (1978).

(2) M. J. Kornet and R. Joyce Garrett, *J. Pharm. Sci.*, **68**, 377 (1979).

(3) M. J. Kornet and J. Chu, *J. Heterocycl. Chem.*, **18**, 293 (1981).

(4) M. J. Kornet and J. Chu, *J. Heterocycl. Chem.*, **19**, 697 (1982).

press.

(5) M. J. Kornet and J. Chu, *J. Pharm. Sci.*, **72**, 94 (1983).

(6) E. Schenker, Fr. 1,514,454; through *Chem. Abstr.*, **70**, 106529q (1969).

(7) R. B. Moffett, G. N. Evenson, and P. F. Von Voigtlander, *J. Heterocycl. Chem.*, **14**, 1231 (1977).

ACKNOWLEDGMENTS

The authors are grateful to the Antiepileptic Drug Development Program of the National Institutes of Health for the anticonvulsant activity data and to NIH for grant support for this investigation.

Investigation of the β-Cyclodextrin–Hydrocortisone Inclusion Compound

SYLVAN G. FRANK ˣ and DALIA R. KAVALIUNAS *

Received March 25, 1982, from the *Division of Pharmaceutics and Pharmaceutical Chemistry, College of Pharmacy, The Ohio State University, Columbus, OH 43210.* Accepted for publication September 8, 1982.

*Present Address: Vicks Division, Richardson-Merrell Inc., Wilton, CT 06897.

Abstract □ The formation of an inclusion compound by β-cyclodextrin with hydrocortisone has been studied by proton magnetic resonance (^{1}H-NMR) and phase solubility analysis. The magnitude of the chemical shifts of the interior and exterior β-cyclodextrin protons in the presence of hydrocortisone indicated that hydrocortisone is included within the β-cyclodextrin cavity and probably interacts with protons on the edge of the torus. The overall stoichiometry of the inclusion compound was not a single, simple relationship, but was unusual in that it was variable and apparently dependent on the relative amounts of hydrocortisone and β-cyclodextrin in the system.

Keyphrases □ Inclusion complexes—β-cyclodextrin–hydrocortisone, phase solubility analyses, ^{1}H-NMR □ β-Cyclodextrin–hydrocortisone—inclusion complexes, phase solubility analyses, ^{1}H-NMR □ Phase solubility analyses—β-cyclodextrin–hydrocortisone, ^{1}H-NMR

The formation of an inclusion compound by dinoprostone (prostaglandin E_2) with β-cyclodextrin has been reported earlier (1). From phase solubility analysis and ^{1}H-NMR spectroscopy it was concluded that a 1:1 complex formed, with the dinoprostone molecule partially included within the β-cyclodextrin cavity and the remainder of the molecule extended to the exterior of the torus.

In the present study attention has been directed to the formation of an inclusion complex between hydrocortisone and β-cyclodextrin. Such an inclusion compound by itself is not necessarily unique; however, these initial studies indicated that an unusual dependence apparently existed between the stoichiometry of the interaction and the concentration of β-cyclodextrin.

EXPERIMENTAL

The experimental procedure was similar to that employed previously (1). β-Cyclodextrin[1] was recrystallized twice from distilled water and dried under vacuum at 60°; hydrocortisone USP[2], was used as received; and water was double-distilled and deionized. Samples for ^{1}H-NMR spectroscopy were prepared by saturating a 2% w/v solution of β-cyclodextrin in D_2O[3] with hydrocortisone. Excess complex was allowed to precipitate and the supernatant solution of the inclusion compound was decanted. ^{1}H-NMR spectra at 100 MHz[4] were determined on the supernatant in standard 5-mm tubes.

Samples for phase solubility analysis were prepared by placing excess quantities of hydrocortisone (0.021, 0.040, or 0.060 g) with increasing amounts of β-cyclodextrin into 20-ml culture tubes containing 10 ml of water. The samples were sealed (with screw caps[5]) and rotated end-over-end at ~41 rpm for 24 hr in a thermostated water bath at 30 ± 0.1°. Aliquots of the supernatant were filtered through a prerinsed membrane filter (0.45 μm)[6] and spectrophotometrically assayed at 248 nm.

[1] Nutritional Biochemicals, Inc.
[2] Calbiochem.
[3] Bio-Rad Laboratories (99.85 mole % D_2O).
[4] Varian XL-100 NMR spectrometer.
[5] Teflon lined.
[6] Millipore Corp., Type HA.

0022-3549/83/1000-1215$01.00/0

These data indicate that 4-phenylsemicarbazides derived from 1,1-dialkylated hydrazines possess anticonvulsant activity; however, it is of a lower order than that shown by 4-phenylsemicarbazides derived from 1,1,2-trialkylated hydrazines (1, 3). The cage compounds IIIq, IIIr, and IIIs were uniformly inactive and these results are consistent with the poor activity found for other cage compounds (4, 5).

EXPERIMENTAL[1]

Ethyl (1-Methylhydrazino)acetate—A solution of 16.7 g (0.1 mole) of ethyl bromoacetate in 17 ml of benzene was added dropwise with magnetic stirring over a 90-min period to a solution of 9.2 g (0.2 mole) of methylhydrazine in 50 ml of benzene. After the reaction mixture had stirred overnight at room temperature, the benzene phase was decanted and the salt residue was washed three times with 15 ml of benzene. The benzene was distilled through a 1-ft Vigreux column at 42 mm Hg. The residue was then distilled and afforded 8.82 g (67%) of a colorless oil, bp 88° (21 mm); IR (film): 1740 cm^{-1} (C=O).

Anal.—Calc. for $C_5H_{12}N_2O$: C, 45.44; H, 9.15; N, 21.20. Found: C, 45.29; H, 9.26; N, 21.31.

[1] Melting points were determined on a Thomas-Hoover melting point apparatus and are uncorrected. The IR spectra were taken on a Perkin-Elmer 700 spectrophotometer as either liquid films or potassium bromide pellets. NMR spectra were recorded on a Varian EM-360 or T-60 spectrometer, using tetramethylsilane as the internal reference. Mass spectra were obtained on a RMU-7 double-focusing spectrometer by Hitachi/Perkin-Elmer. Elemental analyses were performed by Baron Consulting Co., Orange, Conn. All compounds exhibited ^{1}H-NMR and mass spectra consistent with the structures shown.

4-Phenylsemicarbazides (III)—Compound IIIb was prepared by the dropwise addition of a solution of 2.66 g (0.0180 mole) of 2,6-dimethylphenyl isocyanate (I) in 6 ml of dry benzene to a solution of 1.20 g (0.020 mole) of 1,1-dimethylhydrazine in 10 ml of dry benzene at room temperature. After ~10 min heat was evolved. The mixture was heated for 2.5 h in an oil bath (85°). The solvent was evaporated under reduced pressure, and the residue was recrystallized from ethyl acetate and gave 3.40 g (91%) of white crystalline product, mp 156–158°.

REFERENCES

(1) M. J. Kornet, *J. Pharm. Sci.*, **67**, 1471 (1978).

(2) M. J. Kornet and R. Joyce Garrett, *J. Pharm. Sci.*, **68**, 377 (1979).

(3) M. J. Kornet and J. Chu, *J. Heterocycl. Chem.*, **18**, 293 (1981).

(4) M. J. Kornet and J. Chu, *J. Heterocycl. Chem.*, **19**, 697 (1982).

press.

(5) M. J. Kornet and J. Chu, *J. Pharm. Sci.*, **72**, 94 (1983).

(6) E. Schenker, Fr. 1,514,454; through *Chem. Abstr.*, **70**, 106529q (1969).

(7) R. B. Moffett, G. N. Evenson, and P. F. Von Voigtlander, *J. Heterocycl. Chem.*, **14**, 1231 (1977).

ACKNOWLEDGMENTS

The authors are grateful to the Antiepileptic Drug Development Program of the National Institutes of Health for the anticonvulsant activity data and to NIH for grant support for this investigation.

Investigation of the β-Cyclodextrin–Hydrocortisone Inclusion Compound

SYLVAN G. FRANK ˣ and DALIA R. KAVALIUNAS *

Received March 25, 1982, from the *Division of Pharmaceutics and Pharmaceutical Chemistry, College of Pharmacy, The Ohio State University, Columbus, OH 43210.* Accepted for publication September 8, 1982.

*Present Address: Vicks Division, Richardson-Merrell Inc., Wilton, CT 06897.

Abstract □ The formation of an inclusion compound by β-cyclodextrin with hydrocortisone has been studied by proton magnetic resonance (^{1}H-NMR) and phase solubility analysis. The magnitude of the chemical shifts of the interior and exterior β-cyclodextrin protons in the presence of hydrocortisone indicated that hydrocortisone is included within the β-cyclodextrin cavity and probably interacts with protons on the edge of the torus. The overall stoichiometry of the inclusion compound was not a single, simple relationship, but was unusual in that it was variable and apparently dependent on the relative amounts of hydrocortisone and β-cyclodextrin in the system.

Keyphrases □ Inclusion complexes—β-cyclodextrin–hydrocortisone, phase solubility analyses, ^{1}H-NMR □ β-Cyclodextrin–hydrocortisone—inclusion complexes, phase solubility analyses, ^{1}H-NMR □ Phase solubility analyses—β-cyclodextrin–hydrocortisone, ^{1}H-NMR

The formation of an inclusion compound by dinoprostone (prostaglandin E_2) with β-cyclodextrin has been reported earlier (1). From phase solubility analysis and ^{1}H-NMR spectroscopy it was concluded that a 1:1 complex formed, with the dinoprostone molecule partially included within the β-cyclodextrin cavity and the remainder of the molecule extended to the exterior of the torus.

In the present study attention has been directed to the formation of an inclusion complex between hydrocortisone and β-cyclodextrin. Such an inclusion compound by itself is not necessarily unique; however, these initial studies indicated that an unusual dependence apparently existed between the stoichiometry of the interaction and the concentration of β-cyclodextrin.

EXPERIMENTAL

The experimental procedure was similar to that employed previously (1). β-Cyclodextrin[1] was recrystallized twice from distilled water and dried under vacuum at 60°; hydrocortisone USP[2], was used as received; and water was double-distilled and deionized. Samples for ^{1}H-NMR spectroscopy were prepared by saturating a 2% w/v solution of β-cyclodextrin in D_2O[3] with hydrocortisone. Excess complex was allowed to precipitate and the supernatant solution of the inclusion compound was decanted. ^{1}H-NMR spectra at 100 MHz[4] were determined on the supernatant in standard 5-mm tubes.

Samples for phase solubility analysis were prepared by placing excess quantities of hydrocortisone (0.021, 0.040, or 0.060 g) with increasing amounts of β-cyclodextrin into 20-ml culture tubes containing 10 ml of water. The samples were sealed (with screw caps[5]) and rotated end-over-end at ~41 rpm for 24 hr in a thermostated water bath at 30 ± 0.1°. Aliquots of the supernatant were filtered through a prerinsed membrane filter (0.45 μm)[6] and spectrophotometrically assayed at 248 nm.

[1] Nutritional Biochemicals, Inc.
[2] Calbiochem.
[3] Bio-Rad Laboratories (99.85 mole % D_2O).
[4] Varian XL-100 NMR spectrometer.
[5] Teflon lined.
[6] Millipore Corp., Type HA.

0022-3549/83/1000-1215$01.00/0

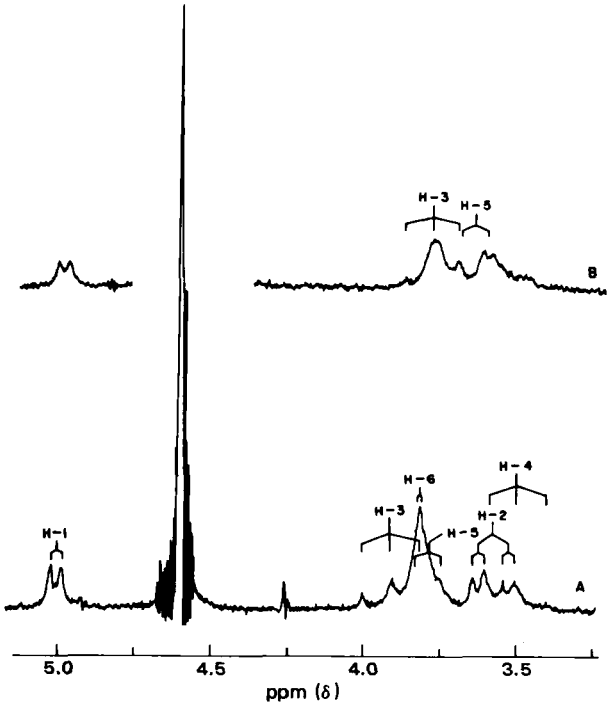

Figure 1—*^{1}H-NMR spectra of β-cyclodextrin (A) and the β-cyclodextrin–hydrocortisone inclusion compound (B) in D_2O.*

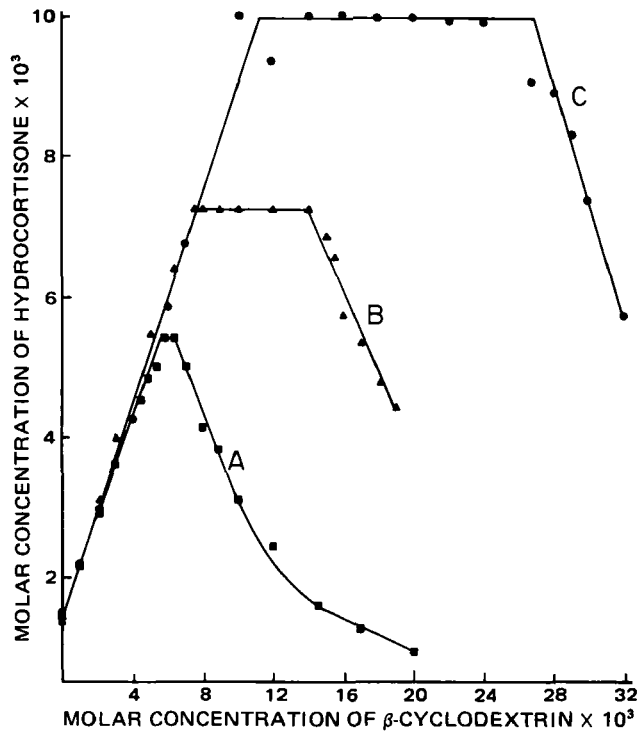

Figure 2—*Phase solubility diagram of β-cyclodextrin–hydrocortisone inclusion compounds at 30 ± 0.1°. Concentrations of hydrocortisone in excess of its solubility (per 10 ml of solution) and the stoichiometries of the soluble complexes (in moles of β-cyclodextrin/mole of hydrocortisone) were: A, 0.021 g and 1.4; B, 0.040 g and 1.7; and C, 0.060 g and 2.4, respectively.*

RESULTS AND DISCUSSION

The ^{1}H-NMR spectra of β-cyclodextrin and of the β-cyclodextrin–hydrocortisone inclusion compound are shown in Fig. 1. The β-cyclodextrin spectrum (Fig. 1A) is presented as a continuous spectrum; however, the spectrum of the inclusion compound (Fig. 1B) is broken for ease in comparison of the two spectra. Except for the HDO and HOH peaks, at ~4.6 ppm in both spectra, all of the peaks shown in Fig. 1 are those of β-cyclodextrin. In the case of the β-cyclodextrin–hydrocortisone inclusion compound, the hydrocortisone protons would be expected to appear further upfield, but due to their low concentration they were not detected.

From NMR and X-ray studies, the glucose units of β-cyclodextrin have been found to be in the C-1 chair configuration (2, 3), with primary and secondary hydroxyl groups around the opening of the torus. H-1, H-2, and H-4 are on the exterior and H-3, H-5, and possibly H-6 are located within the cavity. Other studies have shown that H-3 and H-5 undergo shielding by the guest component upon inclusion compound formation (3).

In the presence of hydrocortisone, the β-cyclodextrin spectrum is shifted upfield and reduced in magnitude due to the lower solubility of the inclusion compound compared with that of β-cyclodextrin alone. Similar behavior was found earlier for the dinoprostone–β-cyclodextrin systems (1). The anomeric hydrogens, H-1, appear as a doublet at the farthest downfield position and are gauche, whereas the rest of the β-cyclodextrin protons are axial. Due to their fixed position, the HDO and HOH peaks were used as internal standards in the measurement of the chemical shifts of the β-cyclodextrin protons in the presence of hydrocortisone, relative to their positions in the absence of hydrocortisone. Still farther upfield is a sideband (Fig. 1A), followed by a group of peaks corresponding to the remaining β-cyclodextrin protons. The sideband appeared only in the β-cyclodextrin spectrum.

The chemical shifts of the β-cyclodextrin protons in the presence of hydrocortisone are given in Table I. The H-3 and H-5 protons, which are located within the β-cyclodextrin cavity, show significant chemical shifts, and therefore underwent the greatest shielding effect due to the presence of the guest component. By contrast, H-1 and H-6 show much lower shifts, indicating a lower probability of interaction with hydrocortisone. The greater chemical shift of the H-5 protons compared with that of the H-3 protons suggest that on the ^{1}H-NMR time scale, more hydrocortisone entered the cavity from the H-5 side of the torus than from the H-3 side. Inclusion compounds of this type can be expected to occur by penetration from either side; however, complexes formed with hydrocortisone partially included on the H-5 side are apparently in greatest abundance. Although the stoichiometry of the β-cyclodextrin–hydrocortisone complex cannot be determined conclusively from ^{1}H-NMR observations, the strong chemical shifts of H-3 and H-5 suggest that the included portion of one hydrocortisone molecule fits snugly within the cavity, in close proximity to these protons. This observation is supported by a CPK space-filling model of the inclusion compound, which suggests that more than one molecule of hydrocortisone per molecule of β-cyclodextrin (each partially within the cavity) would result in a poor fit of either guest molecule, giving a very loosely bound complex.

Table I—Hydrocortisone-Induced Chemical Shifts of β-Cyclodextrin Protons

Proton	Δδ, ppm
H-1	0.03
H-2	0.01
H-3	0.11
H-4	0.01
H-5	0.13
H-6	0.02

Phase solubility analysis indicated, however, that the inclusion compound was not of simple 1:1 stoichiometry, but that the nature of the complex apparently was dependent on the total amount of hydrocortisone present relative to that of β-cyclodextrin (Fig. 2). While the general characteristics of portions of the phase solubility diagram in Fig. 2 follow that of the *p*-aminobenzoic acid–caffeine system reported by Higuchi and Lach (4), the molar concentration of hydrocortisone at the plateau region anomalously increased as the total amount of hydrocortisone increased. The approximate stoichiometries of the three β-cyclodextrin–hydrocortisone inclusion compounds represented by curves A, B, and C in Fig. 2 are 1.4, 1.7, and 2.4 molecules of β-cyclodextrin per molecule of hydrocortisone, respectively. Obviously these are difficult systems to interpret, and additional studies are in order to confirm the nature of the complex(es) and the mechanism of formation.

REFERENCES

(1) S. G. Frank and M. J. Cho, *J. Pharm. Sci.*, **67**, 1665 (1978).

(2) A. Hybl, R. E. Rundle, and D. E. Williams, *J. Am. Chem. Soc.*, **87**, 2779 (1965).

(3) A. L. Thakkar and P. V. Demarco, *J. Pharm. Sci.*, **60**, 652 (1971).

(4) T. Higuchi and J. L. Lach, *J. Am. Pharm. Assoc., Sci. Ed.*, **43**, 465 (1954).

ACKNOWLEDGMENTS

The authors wish to thank The Upjohn Company for assistance with the ^{1}H-NMR spectroscopy.

Metabolism of Cathinone to *d*-Norpseudoephedrine in Humans

A. N. GUANTAI and C. K. MAITAI ˣ

Received August 7, 1981, from the *Department of Pharmacy, University of Nairobi, Nairobi, Kenya.* Accepted for publication September 16, 1982.

Abstract □ Cathinone, a potent psychostimulant isolated from young shoots of *Catha edulis* was given to four human volunteers. Examination of urine collected from the volunteers at predetermined intervals showed the presence of unchanged cathinone, *d*-norpseudoephedrine, and two unidentified basic substances. The observed biotransformation of cathinone to the less potent psychostimulant, *d*-norpseudoephedrine involves reduction of a ketone group to alcohol, a common metabolic pathway in humans.

Keyphrases □ Cathinone—metabolism to *d*-norpseudoephedrine in humans □ *Catha edulis*—metabolism in humans

Catha edulis Forsk grows well in several countries of Eastern, Central, and Southern Africa. Because of the psychostimulant and mental dependence associated with habitual chewing of young shoots of this plant, it has been investigated extensively. Although chemical investigation of *C. edulis* goes back to the 19th century, the most significant result was obtained by Wolfes in 1930 (1) when he isolated and identified *d*-norpseudoephedrine, a CNS stimulant with amphetamine-like properties. There was some controversy as to whether the amount of *d*-norpseudoephedrine present in *Catha* material could account wholly for the observed psychostimulant effect, thus providing impetus for further chemical investigation (2). Several years later, a second phenylalkylamine closely related to *d*-norpseudoephedrine was isolated and named "cathinone" (3). This compound is a much more potent psychostimulant than *d*-norpseudoephedrine, and has attracted much attention as a potential drug of abuse (4).

The excretion of *d*-norpseudoephedrine in human urine has been investigated (5). In preliminary investigations involving known habitual chewers of *C. edulis*, *d*-norpseudoephedrine was shown to be the major compound present in urine when it was collected several hours after chewing *C. edulis*. Since cathinone is a major constituent of the young shoots of *C. edulis*, it seemed odd that it was absent or present only in trace amounts in several urine samples examined. A literature survey showed that the fate of cathinone in humans has not been investigated and accordingly this work was undertaken.

EXPERIMENTAL

Collection of Urine Samples—Four volunteers who had never chewed the material before participated in the experiment. Two volunteers were given 16 mg of cathinone extracted from young shoots of *C. edula* by preparatory TLC (3, 6), while the other two were given 16 mg of synthetic cathinone. All four volunteers had only milk for breakfast. Urine samples were collected at the following intervals: 0 (control), 0–4, 4–8, 8–12, 12–15, and 15–24 hr. Each urine sample was examined for the presence of cathinone and related substances as described below.

Examination of Urine for Cathinone, *d*-Norpseudoephedrine, and Related Basic Substances— Approximately 40 ml of urine was taken, 2–3 ml of strong lead acetate solution (7) was added, and after thorough mixing the precipitated proteins were removed by centrifugation. The supernatant was acidified to pH 5–6 with 0.1 *N* sulfuric acid and any precipitate removed by centrifugation. The acidified urine sample was extracted with chloroform, four times to remove acids and neutrals. The aqueous urine portion was then alkalinized (pH 9) using dilute ammonia solution and extracted with 4 × 100 ml of chloroform. The combined chloroform was distilled off at 40° using a rotary evaporator and the residue examined by TLC.

Examination of residue for *d*-norpseudoephedrine, cathinone, and related basic substances using TLC was carried out as follows. The residues were taken up in 2 ml of chloroform and ~10 μl was spotted on TLC plates coated with silica gel[1], and activated at 100° for 1 hr. Cathinone and *d*-norpseudoephedrine were spotted on the same TLC plates as the basic residues from urine. The plates were developed in either of the following solvent systems: (*A*) ethyl acetate–methanol–ammonia (17:2:1) or (*B*) cyclohexane–chloroform–diethylamine (5:4:1). Usually the plates were developed for 35–45 min. After development the plates were examined under UV light, then sprayed with 0.3% ninhydrin solution (8) after which they were heated at 105° for 10 min. The intensity of fluorescence under UV light and that of color after spraying with ninhydrin solution were judged on a 3-point scale as shown in the results. Where cathinone or *d*-norpseudoephedrine (or both) was not detected, the chloroform basic residue was concentrated almost to dryness and the experiment repeated.

The presence of *d*-norpseudoephedrine and cathinone in the basic residue extracted from urine was also investigated with a gas–liquid chromatograph[2] equipped with a flame ionization detector. The GLC column used was glass, 4-mm i.d. × 1.5 m long, packed with nonacid washed Chromosorb W (100–200 mesh)[3] coated with 1% polyethylene glycol 20 *M* (carbowax 20 *M*)[4]. The column was conditioned for 8–10 hr at 230°. The experimental operating conditions were as follows: hydrogen pressure, 1.4 kg/cm^2; condensed air pressure, 0.65 kg/cm^2; nitrogen flow rate 30 ml/min; column temperature programmed from 80–200° at 5°/min and finally left at 200° for 10 min; chart speed, 1 cm/2 min. The retention times and peaks were recorded[5].

For quantitative analysis, the areas under the curves were measured by the method of triangulation (9) and compared with areas obtained with standard solutions of cathinone and *d*-norpseudoephedrine. The standard solutions were prepared by dissolving 5 mg of either cathinone or *d*-norpseudoephedrine in 40 ml of control urine and subjecting this to the same extraction procedure as the experimental urine. It was then assumed that the percentage recovery of both compounds from experi-

[1] GF254, Merck & Co.
[2] Pye Unicam Series 104.
[3] Sigma Chemical Co.
[4] British Drug House.
[5] Pye Unicam linear recorder, type AR55.

0022-3549/83/1000-1217$01.00/0

(3) A. L. Thakkar and P. V. Demarco, *J. Pharm. Sci.*, **60**, 652 (1971).

(4) T. Higuchi and J. L. Lach, *J. Am. Pharm. Assoc., Sci. Ed.*, **43**, 465 (1954).

ACKNOWLEDGMENTS

The authors wish to thank The Upjohn Company for assistance with the ^{1}H-NMR spectroscopy.

Metabolism of Cathinone to *d*-Norpseudoephedrine in Humans

A. N. GUANTAI and C. K. MAITAI ˣ

Received August 7, 1981, from the *Department of Pharmacy, University of Nairobi, Nairobi, Kenya.* Accepted for publication September 16, 1982.

Abstract □ Cathinone, a potent psychostimulant isolated from young shoots of *Catha edulis* was given to four human volunteers. Examination of urine collected from the volunteers at predetermined intervals showed the presence of unchanged cathinone, *d*-norpseudoephedrine, and two unidentified basic substances. The observed biotransformation of cathinone to the less potent psychostimulant, *d*-norpseudoephedrine involves reduction of a ketone group to alcohol, a common metabolic pathway in humans.

Keyphrases □ Cathinone—metabolism to *d*-norpseudoephedrine in humans □ *Catha edulis*—metabolism in humans

Catha edulis Forsk grows well in several countries of Eastern, Central, and Southern Africa. Because of the psychostimulant and mental dependence associated with habitual chewing of young shoots of this plant, it has been investigated extensively. Although chemical investigation of *C. edulis* goes back to the 19th century, the most significant result was obtained by Wolfes in 1930 (1) when he isolated and identified *d*-norpseudoephedrine, a CNS stimulant with amphetamine-like properties. There was some controversy as to whether the amount of *d*-norpseudoephedrine present in *Catha* material could account wholly for the observed psychostimulant effect, thus providing impetus for further chemical investigation (2). Several years later, a second phenylalkylamine closely related to *d*-norpseudoephedrine was isolated and named "cathinone" (3). This compound is a much more potent psychostimulant than *d*-norpseudoephedrine, and has attracted much attention as a potential drug of abuse (4).

The excretion of *d*-norpseudoephedrine in human urine has been investigated (5). In preliminary investigations involving known habitual chewers of *C. edulis*, *d*-norpseudoephedrine was shown to be the major compound present in urine when it was collected several hours after chewing *C. edulis*. Since cathinone is a major constituent of the young shoots of *C. edulis*, it seemed odd that it was absent or present only in trace amounts in several urine samples examined. A literature survey showed that the fate of cathinone in humans has not been investigated and accordingly this work was undertaken.

EXPERIMENTAL

Collection of Urine Samples—Four volunteers who had never chewed the material before participated in the experiment. Two volunteers were given 16 mg of cathinone extracted from young shoots of *C. edula* by preparatory TLC (3, 6), while the other two were given 16 mg of synthetic cathinone. All four volunteers had only milk for breakfast. Urine samples were collected at the following intervals: 0 (control), 0–4, 4–8, 8–12, 12–15, and 15–24 hr. Each urine sample was examined for the presence of cathinone and related substances as described below.

Examination of Urine for Cathinone, *d*-Norpseudoephedrine, and Related Basic Substances— Approximately 40 ml of urine was taken, 2–3 ml of strong lead acetate solution (7) was added, and after thorough mixing the precipitated proteins were removed by centrifugation. The supernatant was acidified to pH 5–6 with 0.1 *N* sulfuric acid and any precipitate removed by centrifugation. The acidified urine sample was extracted with chloroform, four times to remove acids and neutrals. The aqueous urine portion was then alkalinized (pH 9) using dilute ammonia solution and extracted with 4 × 100 ml of chloroform. The combined chloroform was distilled off at 40° using a rotary evaporator and the residue examined by TLC.

Examination of residue for *d*-norpseudoephedrine, cathinone, and related basic substances using TLC was carried out as follows. The residues were taken up in 2 ml of chloroform and ~10 μl was spotted on TLC plates coated with silica gel[1], and activated at 100° for 1 hr. Cathinone and *d*-norpseudoephedrine were spotted on the same TLC plates as the basic residues from urine. The plates were developed in either of the following solvent systems: (*A*) ethyl acetate–methanol–ammonia (17:2:1) or (*B*) cyclohexane–chloroform–diethylamine (5:4:1). Usually the plates were developed for 35–45 min. After development the plates were examined under UV light, then sprayed with 0.3% ninhydrin solution (8) after which they were heated at 105° for 10 min. The intensity of fluorescence under UV light and that of color after spraying with ninhydrin solution were judged on a 3-point scale as shown in the results. Where cathinone or *d*-norpseudoephedrine (or both) was not detected, the chloroform basic residue was concentrated almost to dryness and the experiment repeated.

The presence of *d*-norpseudoephedrine and cathinone in the basic residue extracted from urine was also investigated with a gas–liquid chromatograph[2] equipped with a flame ionization detector. The GLC column used was glass, 4-mm i.d. × 1.5 m long, packed with nonacid washed Chromosorb W (100–200 mesh)[3] coated with 1% polyethylene glycol 20 *M* (carbowax 20 *M*)[4]. The column was conditioned for 8–10 hr at 230°. The experimental operating conditions were as follows: hydrogen pressure, 1.4 kg/cm^2; condensed air pressure, 0.65 kg/cm^2; nitrogen flow rate 30 ml/min; column temperature programmed from 80–200° at 5°/min and finally left at 200° for 10 min; chart speed, 1 cm/2 min. The retention times and peaks were recorded[5].

For quantitative analysis, the areas under the curves were measured by the method of triangulation (9) and compared with areas obtained with standard solutions of cathinone and *d*-norpseudoephedrine. The standard solutions were prepared by dissolving 5 mg of either cathinone or *d*-norpseudoephedrine in 40 ml of control urine and subjecting this to the same extraction procedure as the experimental urine. It was then assumed that the percentage recovery of both compounds from experi-

[1] GF254, Merck & Co.
[2] Pye Unicam Series 104.
[3] Sigma Chemical Co.
[4] British Drug House.
[5] Pye Unicam linear recorder, type AR55.

0022-3549/83/1000-1217$01.00/0

Table I—TLC Examination of Basic Residue from Urine of Volunteers who had Ingested Cathinone[a]

Urine Sample	Collection Time, hr[b]	Substance Detected Cathinone	Substance Detected *d*-norpseudoephedrine
1	0 (control)	none	none
2	0–4	++[c]	++
3	4–8	++	++
4	8–12	+[d]	++
5	12–15	0[e]	+
6	15–24	0	+

[a] Two unidentified substances in trace amount, associated with cathinone were observed in samples 2, 3, 4 and 5. The R_f values of unidentified substances in solvent system *A* were 0.71 and 0.85. [b] After ingestion of cathinone. [c] ++ = Easily detected. [d] + = Trace amount. [e] 0 = not detected.

mental and control urine was approximately the same. Control experiments had shown recovery of >90% under the standardized conditions.

RESULTS

Both cathinone and *d*-norpseudoephedrine separated well in solvent systems *A* and *B*, the R_f values being as follows: *A*-cathinone 0.55, *d*-norpseudoephedrine 0.42; *B*-cathinone 0.38, *d*-norpseudoephedrine 0.47. Results of TLC are summarized in Table I. Results of GLC were in agreement with those obtained with TLC. With GLC only one *d*-norpseudoephedrine peak was observed at 165° (retention time 7.5 min) while the major cathinone peak was observed at 151° (retention time 5.1 min). Another peak associated with cathinone appeared at 145° (retention time 3.7 min). The results were fairly reproducible, and it was possible to calculate the amount of cathinone and *d*-norpseudoephedrine excreted in the urine. There was no significant variation in the excretion pattern of either cathinone or *d*-norpseudoephedrine in the four volunteers even when the experiment was repeated after 4 weeks. The amount of cathinone and *d*-norpseudoephedrine recovered from the urine of each of the volunteers agreed to within 20% and the results are summarized in Table II.

DISCUSSION

Results obtained in the present study show that some of the cathinone ingested by humans is metabolized to *d*-norpseudoephedrine and possibly two other unidentified metabolites. Metabolism of cathinone to *d*-norpseudoephedrine involves reduction of a ketone group to alcohol, a fairly common metabolic pathway in humans, catalyzed by liver microsomal enzymes. In several drugs (*e.g.*, cortisone and warfarin) reduction of a ketone or aldehyde to an alcohol is often associated with significant change in potency. Usually both the parent drug and the metabolite will contribute to the biological activity, the net result often being determined by such pharmacokinetic parameters as the rate of elimination. The finding that little, if any cathinone is excreted in human urine after 15 hr, may be important in forensic toxicology since *d*-norpseudoephedrine, also present in *C. edulis*, is known to be excreted over a much longer period.

Table II—Amount of Cathinone and *d*-Norpseudoephedrine Excreted in Human Urine (Result of GLC)

Urine Sample(s)	Cathinone Recovered, mg	*d*-norpseudoephedrine Recovered, mg
2 (0–4 hr after ingestion of cathinone)	0.72 ± 0.12 (4.4% of amount ingested)	3.2 ± 0.3 (equivalent to 20% ingested cathinone)
3, 4, 5, 6 (4–24 hr after ingestion of cathinone)	1.04 ± 0.08 (6.5% of amount ingested)	9.9 ± 0.6 (equivalent to 61.9% ingested cathinone)
2, 3, 4, 5, 6 (0–24 hr)	1.765 (11% of amount ingested)	13.12 (equivalent to 81.9% ingested cathinone)

REFERENCES

(1) O. Wolfes, *Arch. Pharm.*, **268**, 81 (1930).

(2) H. Friebel and R. Brilla, *Naturwissenschaft*, **50**, 354 (1963).

(3) United Nations Document MNAR/11/75, GE 75-12624 (1975) (prepared by United Nations Division of Narcotic Drugs, Geneva).

(4) D. W. Peterson, C. K. Maitai, and S. B. Sparber *Life Sci.*, **27**, 2143 (1980).

(5) C. K. Maitai and G. M. Mugera *J. Pharm. Sci.*, **64**, 702 (1975).

(6) A. N. Guantai, MSc thesis, Nairobi University, Kenya, 1982 (p. 40).

(7) "British Pharmacopoeia," Appendix IA, (A30), Her Majesty's Stationery Office, London, 1973.

(8) E. Stahl, "Thin Layer Chromatography, Laboratory Handbook," 2nd ed., George Allen and Unwin (London) 1969 p. 889.

(9) H. P. Birchfield and E. E. Storrs, "Biochemical Application of Gas Chromatography," Academic, New York, N.Y., 1962, p. 122.

ACKNOWLEDGMENTS

The authors wish to thank Ms. Esme Lumsden of the United Nations Division of Narcotic Drugs for a sample of cathinone. The authors wish to thank Prof. S. Talalaj for identifying the plant material used in the present work. A specimen of the plant is deposited in the Department of Pharmacy, University of Nairobi.

Nonparametric Pharmacokinetic Calculations: One-Compartment Open Model

WILLIAM H. SHELVER ˣ and FRED F. FARRIS

Received May 25, 1982, from *North Dakota State University, Department of Pharmaceutical Sciences, College of Pharmacy, Fargo, ND 58105.* Accepted for publication September 8, 1982.

Abstract □ A nonparametric method suitable for estimation of parameters in nonlinear problems was developed for one-compartment pharmacokinetic data. The method was tested by running 500 simulations with various types of error and comparing the results with a standard nonlinear regression computation. The nonparametric method was superior to nonlinear regression techniques if the assumptions for the error structure of the regression were not true.

Keyphrases □ One-compartment pharmacokinetic model—nonparametric method, comparison with standard nonlinear regression procedure, estimation of parameter

Calculating the parameters of a pharmacokinetic model containing more than one exponential term requires the use of either the method of residuals (sometimes referred to as stripping or feathering) or one of various nonlinear regression techniques. As they have been applied classically, both general techniques have proven somewhat

0022-3549/83/1000-1218$01.00/0

Table I—TLC Examination of Basic Residue from Urine of Volunteers who had Ingested Cathinone[a]

Urine Sample	Collection Time, hr[b]	Substance Detected Cathinone	Substance Detected *d*-norpseudoephedrine
1	0 (control)	none	none
2	0–4	++[c]	++
3	4–8	++	++
4	8–12	+[d]	++
5	12–15	0[e]	+
6	15–24	0	+

[a] Two unidentified substances in trace amount, associated with cathinone were observed in samples 2, 3, 4 and 5. The R_f values of unidentified substances in solvent system *A* were 0.71 and 0.85. [b] After ingestion of cathinone. [c] ++ = Easily detected. [d] + = Trace amount. [e] 0 = not detected.

mental and control urine was approximately the same. Control experiments had shown recovery of >90% under the standardized conditions.

RESULTS

Both cathinone and *d*-norpseudoephedrine separated well in solvent systems *A* and *B*, the R_f values being as follows: *A*-cathinone 0.55, *d*-norpseudoephedrine 0.42; *B*-cathinone 0.38, *d*-norpseudoephedrine 0.47. Results of TLC are summarized in Table I. Results of GLC were in agreement with those obtained with TLC. With GLC only one *d*-norpseudoephedrine peak was observed at 165° (retention time 7.5 min) while the major cathinone peak was observed at 151° (retention time 5.1 min). Another peak associated with cathinone appeared at 145° (retention time 3.7 min). The results were fairly reproducible, and it was possible to calculate the amount of cathinone and *d*-norpseudoephedrine excreted in the urine. There was no significant variation in the excretion pattern of either cathinone or *d*-norpseudoephedrine in the four volunteers even when the experiment was repeated after 4 weeks. The amount of cathinone and *d*-norpseudoephedrine recovered from the urine of each of the volunteers agreed to within 20% and the results are summarized in Table II.

DISCUSSION

Results obtained in the present study show that some of the cathinone ingested by humans is metabolized to *d*-norpseudoephedrine and possibly two other unidentified metabolites. Metabolism of cathinone to *d*-norpseudoephedrine involves reduction of a ketone group to alcohol, a fairly common metabolic pathway in humans, catalyzed by liver microsomal enzymes. In several drugs (*e.g.*, cortisone and warfarin) reduction of a ketone or aldehyde to an alcohol is often associated with significant change in potency. Usually both the parent drug and the metabolite will contribute to the biological activity, the net result often being determined by such pharmacokinetic parameters as the rate of elimination. The finding that little, if any cathinone is excreted in human urine after 15 hr, may be important in forensic toxicology since *d*-norpseudoephedrine, also present in *C. edulis*, is known to be excreted over a much longer period.

Table II—Amount of Cathinone and *d*-Norpseudoephedrine Excreted in Human Urine (Result of GLC)

Urine Sample(s)	Cathinone Recovered, mg	*d*-norpseudoephedrine Recovered, mg
2 (0–4 hr after ingestion of cathinone)	0.72 ± 0.12 (4.4% of amount ingested)	3.2 ± 0.3 (equivalent to 20% ingested cathinone)
3, 4, 5, 6 (4–24 hr after ingestion of cathinone)	1.04 ± 0.08 (6.5% of amount ingested)	9.9 ± 0.6 (equivalent to 61.9% ingested cathinone)
2, 3, 4, 5, 6 (0–24 hr)	1.765 (11% of amount ingested)	13.12 (equivalent to 81.9% ingested cathinone)

REFERENCES

(1) O. Wolfes, *Arch. Pharm.*, **268**, 81 (1930).

(2) H. Friebel and R. Brilla, *Naturwissenschaft*, **50**, 354 (1963).

(3) United Nations Document MNAR/11/75, GE 75-12624 (1975) (prepared by United Nations Division of Narcotic Drugs, Geneva).

(4) D. W. Peterson, C. K. Maitai, and S. B. Sparber *Life Sci.*, **27**, 2143 (1980).

(5) C. K. Maitai and G. M. Mugera *J. Pharm. Sci.*, **64**, 702 (1975).

(6) A. N. Guantai, MSc thesis, Nairobi University, Kenya, 1982 (p. 40).

(7) "British Pharmacopoeia," Appendix IA, (A30), Her Majesty's Stationery Office, London, 1973.

(8) E. Stahl, "Thin Layer Chromatography, Laboratory Handbook," 2nd ed., George Allen and Unwin (London) 1969 p. 889.

(9) H. P. Birchfield and E. E. Storrs, "Biochemical Application of Gas Chromatography," Academic, New York, N.Y., 1962, p. 122.

ACKNOWLEDGMENTS

The authors wish to thank Ms. Esme Lumsden of the United Nations Division of Narcotic Drugs for a sample of cathinone. The authors wish to thank Prof. S. Talalaj for identifying the plant material used in the present work. A specimen of the plant is deposited in the Department of Pharmacy, University of Nairobi.

Nonparametric Pharmacokinetic Calculations: One-Compartment Open Model

WILLIAM H. SHELVER ˣ and FRED F. FARRIS

Received May 25, 1982, from *North Dakota State University, Department of Pharmaceutical Sciences, College of Pharmacy, Fargo, ND 58105.* Accepted for publication September 8, 1982.

Abstract □ A nonparametric method suitable for estimation of parameters in nonlinear problems was developed for one-compartment pharmacokinetic data. The method was tested by running 500 simulations with various types of error and comparing the results with a standard nonlinear regression computation. The nonparametric method was superior to nonlinear regression techniques if the assumptions for the error structure of the regression were not true.

Keyphrases □ One-compartment pharmacokinetic model—nonparametric method, comparison with standard nonlinear regression procedure, estimation of parameter

Calculating the parameters of a pharmacokinetic model containing more than one exponential term requires the use of either the method of residuals (sometimes referred to as stripping or feathering) or one of various nonlinear regression techniques. As they have been applied classically, both general techniques have proven somewhat

0022-3549/83/1000-1218$01.00/0

Table I—Mean and Coefficient of Variation of Parameter Estimates from 500 Simulations Using a One-Compartment Pharmacokinetic Model with Data of Constant Variance and Containing One Randomly Selected Outlier of Increasing Magnitude [a]

Outlier Magnitude	Marquardt Nonlinear Regression [b]			Nonparametric [b]		
	k_a	K	FD/V	k_a	K	FD/V
1	2.00	0.200	3.00	2.00	0.200	3.00
	(2.67)	(2.04)	(0.99)	(3.04)	(2.55)	(1.11)
2	2.00	0.200	3.00	2.00	0.200	3.00
	(3.13)	(2.39)	(1.17)	(3.43)	(2.82)	(1.24)
4	2.00	0.200	3.00	1.99	0.200	3.01
	(4.57)	(3.58)	(1.74)	(4.17)	(3.00)	(1.37)
6	2.00	0.200	3.00	1.99	0.201	3.01
	(6.33)	(4.79)	(2.40)	(4.66)	(3.02)	(1.46)
8	2.00	0.201	3.01	1.98	0.201	3.01
	(8.26)	(6.21)	(3.11)	(5.31)	(3.05)	(1.48)

[a] Variance = 0.2, k_a = 2, K = 0.2, FD/V = 3.0, the outlier randomly selected from one of the seven points with a variance from 1 × 0.2 (no outlier) to 8 × 0.2. The concentrations were computed at t = 0.5, 1.0, 1.5, 2.0, 4.0, 8.0, and 12 hr. [b] Numbers in parentheses are coefficients of variation.

unsatisfactory. The method of residuals lacks objectivity and may be theoretically biased, and the nonlinear regression techniques may fail to converge under certain circumstances (1).

Recently, several investigators have examined the use of nonparametric methods and have found them to be superior to parametric regression techniques in the analysis of enzyme kinetic (2) and receptor-binding data (3). Indeed, some statisticians are beginning to question the general application of conventional regression procedures. Endrenyi and Tang (4) found that a nonparametric method was superior to conventional linear regression techniques when applied to the analysis of a single exponential kinetic model. Koup (5) used a similar technique, in combination with the method of residuals, to solve for the parameters in a biexponential model using a nonparametric method to determine the best fit for the terminal portion of the curve. The second linear component was determined by the method of residuals and the appropriate parameters ascertained. It was found that, for his system, the nonparametric results were markedly superior for two constants and slightly inferior for the remaining two constants.

The purpose of this paper is to formulate a nonparametric method for the solution of nonlinear equations. The method is tested by its performance with a conventional nonlinear regression technique, using data with different error structures and in the presence of outliers of increasing importance.

BACKGROUND

In 1974, Eisenthal and Cornish-Bowden (6) developed a nonparametric method for processing enzymatic data. The method, frequently referred to as a "direct linear plot," was originally devised as a graphical procedure for estimating enzyme kinetic parameters. Basically it involves plotting all possible sets of data in parameter space. This plot leads to a series of line intersections, where each intersecting point represents a different estimate of the desired parameters. The median value of this series of parameters is then selected as the best estimate. Since medians rather than means are used, the method is extremely resistant to the effects of outliers, providing at least the majority of points are good. In searching the literature, no reference applying this nonparametric technique to determine the parameters of nonlinear equations was found.

One approach is to divide the experimental data into sets, which allows the determination of the desired parameters and the estimation of the parameter values for each set. The selected nonparametric technique is then applied to the resultant list of estimates. The most complex problem is determining the parameter estimates for each set. This can be accomplished by using numerical solutions to solve the nonlinear equations. Application of this technique to the one-compartment, first-order absorption pharmacokinetic model follows.

THEORETICAL

The one-compartment, first-order absorption model in pharmacokinetics is described by the general equation:

$$C = \frac{FD}{V}\frac{k_a}{k_a - K}(e^{-Kt} - e^{-k_a t}) \qquad \text{(Eq. 1)}$$

where C corresponds to the plasma drug concentration at time t, F is the fraction of dose absorbed, D is the dose, V is the volume of distribution, and k_a and K are the absorption and elimination rate constants, respectively. If FD/V is treated as a single value, then the equation can be solved once we know the three parameters FD/V, K and k_a. The determination of three parameters requires the solution of three simultaneous equations of the form:

$$C_1 = \frac{FD}{V}\frac{k_a}{k_a - K}(e^{-Kt_1} - e^{-k_a t_1}) \qquad \text{(Eq. 2)}$$

$$C_2 = \frac{FD}{V}\frac{k_a}{k_a - K}(e^{-Kt_2} - e^{-k_a t_2}) \qquad \text{(Eq. 3)}$$

$$C_3 = \frac{FD}{V}\frac{k_a}{k_a - K}(e^{-Kt_3} - e^{-k_a t_3}) \qquad \text{(Eq. 4)}$$

Equations 2–4 are generated by substituting the values for three data points (time and concentation) into the general equation (Eq. 1). Unfortunately, the nonlinear nature of these equations makes them difficult to solve algebraically. To simplify the problem, ratios of the above equations were taken to give Eqs. 5 and 6:

$$\frac{C_1}{C_2} = \frac{e^{-Kt_1} - e^{-k_a t_1}}{e^{-Kt_2} - e^{-k_a t_2}} = R_1 \qquad \text{(Eq. 5)}$$

$$\frac{C_2}{C_3} = \frac{e^{-Kt_2} - e^{-k_a t_2}}{e^{-Kt_3} - e^{-k_a t_3}} = R_2 \qquad \text{(Eq. 6)}$$

This step eliminates FD/V from the equations, and yields two equations and two unknowns which can be solved using the Newton-Raphson method (7) for approximating the roots of simultaneous equations. This technique uses expressions in the form of those shown in Eqs. 7 and 8:

$$X = X_0 - \frac{\frac{F\partial G}{\partial Y} - \frac{G\partial F}{\partial Y}}{\frac{\partial G}{\partial Y}\frac{\partial F}{\partial X} - \frac{\partial F}{\partial Y}\frac{\partial G}{\partial X}} \qquad \text{(Eq. 7)}$$

$$Y = Y_0 + \frac{\frac{F\partial G}{\partial X} - \frac{G\partial F}{\partial Y}}{\frac{\partial G}{\partial Y}\frac{\partial F}{\partial X} - \frac{\partial F}{\partial Y}\frac{\partial G}{\partial X}} \qquad \text{(Eq. 8)}$$

where X is unknown 1, *i.e.*, K_1; Y is unknown 2, *i.e.*, k_{a_1}, and F and G are Eqs. 5 and 6. Once the appropriate partial derivatives are taken then the parameters K and k_a are estimated by iteration until they do not change significantly. The third parameter, FD/V, is then determined by substituting the estimated values of K and k_a into Eq. 9.

$$FD/V = \frac{C(k_a - K)}{k_a(e^{-Kt} - e^{-k_a t})} \qquad \text{(Eq. 9)}$$

The above process gives one set of parameter estimates corresponding to the use of one set of three data points. Another combination of three

Table II—Mean and Coefficient of Variation of Parameter Estimates from 500 Simulations Using a One-Compartment Pharmacokinetic Model with Data of Constant Coefficient of Variation and Containing One Randomly Selected Outlier of Increasing Magnitude[a]

Outlier Magnitude	Marquardt Nonlinear Regression[b]			Nonparametric[b]		
	k_a	K	FD/V	k_a	K	FD/V
1	2.03	0.201	3.01	1.918	0.204	3.06
	(12.30)	(5.74)	(4.51)	(11.76)	(3.77)	(4.42)
2	2.03	0.201	3.02	1.90	0.205	3.08
	(14.59)	(6.87)	(5.41)	(13.23)	(4.49)	(5.31)
4	2.06	0.203	3.03	1.86	0.206	3.11
	(26.49)	(10.32)	(7.90)	(15.74)	(5.68)	(5.74)
6	2.52	0.206	3.05	1.85	0.208	3.12
	(191.78)	(17.33)	(10.86)	(17.77)	(6.61)	(6.09)
8	81.67	0.206	3.06	1.84	0.208	3.14
	(2116.61)	(17.06)	(12.38)	(17.36)	(6.81)	(7.35)

[a] Coefficient of variation = 5%, $k_a = 2$, $K = 0.2$, $FD/V = 3.0$, the outlier randomly selected from one of the seven points with a coefficient of variation from $1 \times 0.05 \times C$ (no outlier) to $8 \times 0.05 \times C$. The concentrations were computed at $t = 0.5$, 1.0, 1.5, 2.0, 4.0, 8.0, and 12 hr. [b] Numbers in parentheses are coefficients of variation.

data points is selected and the procedure repeated to give a new set of parameter estimates. The process is again repeated until all possible combinations of data have been used. In the present paper, seven data points (seven time and concentration combinations) were used. This gave a list of 35 estimates (all combinations of seven items taken three at a time). The median value from each list was then selected as the best estimate for that particular parameter. If desired, confidence limits can be obtained by the method of Cornish-Bowden *et al.* (8).

In their comparison of methods of analyzing enzyme kinetic data, Atkins and Nimmo (2) emphasize the importance of thoroughly testing new methods by simulation before applying them in practice. To test the present method, 500 simulations were performed as described in the *Experimental* section.

EXPERIMENTAL

To provide an adequate test for the method, two computer programs[1] were formulated to generate data and determine parameters. Both programs generated data by taking assumed constants ($k_a = 2.00$, $FD/V = 3.00$ and $K = 0.200$), calculating the concentration seven times ($t = 0.5$, 1.0, 1.5, 2.0, 4.0, 8.0, and 12.0), and adding randomly generated, normally distributed error with a mean of 0 and a variance of one times either a percentage (5%) of the generated concentration (constant coefficient of variation) or a constant (0.02) (constant variance), depending on the error structure desired. Both programs generated the same set of data points. Outliers were produced by randomly selecting one of the times and multiplying the error added to the term by a constant (1, 2, 4, 6, or 8). The outlier concentration thus generated had a larger error than the rest of the points. One program analyzed the data by a standard nonlinear regression procedure (9), and the other program utilized the proposed nonparametric method. Five hundred simulations were carried out and the average of each parameter was computed along with the coefficient of variation and other summary statistics.

RESULTS AND DISCUSSION

The use of nonweighted, nonlinear regression assumes a constant variance and, as expected in the nonlinear regression technique, performed well with this error structure when no outliers or only a small outlier was present (Table I). As the size of the outlier was increased, the nonparametric method demonstrated its superiority by showing a much smaller coefficient of variation. The presence of one outlier with a variance eight times the variance of the other points gave coefficients of variation for the nonlinear regression twice the corresponding nonparametric coefficients of variation. Neither computational procedure demonstrated appreciable bias.

When an error structure with a constant coefficient of variation was analyzed (Table II) (which violates the assumptions of nonweighted, nonlinear regression), the nonparametric method was slightly superior when no outliers were present, and markedly superior when outliers reached moderate size with regard to coefficients of variation. Although a weighted nonlinear regression would have improved the performance of the nonlinear regression technique, the proper use of weighting is nearly impossible in practice because of lack of knowledge of the appropriate weights. Consequently, the superiority of the nonparametric method is clearly demonstrated. The nonparametric method demonstrated a slight bias.

The nonparametric method is not a panacea for all the ills of pharmacokinetic data processing because of two concerns. Since all possible sets of three data points are utilized in the calculations, a problem exists if these data points do not contain the proper information. For example, the later points in a collection do not contain information concerning k_a if the data are collected after the absorption phase is essentially complete. Consequently, k_a values computed from the later data points will be essentially meaningless and will probably be represented at the extremes of the distribution. Should a sufficient number of these occur, the median may be affected. A second deficiency of the nonparametric method arises from data points too close together. This problem is similar to determining the slope of a line using two points close together. The slope in the case of the line, or the parameter estimates in the case of the nonparametric method, will be determined more by error than by the location of the points. For our simulation, we chose a conventional experimental design, with points selected at short intervals at the onset to ensure a reasonable determination of k_a, and the time period extending over sufficient time to ensure adequate determination of K (roughly 3.5 half-lives). While this experimental design is not optimum for either nonlinear regression or nonparametric determinations, it approximates data normally used for the determination of nonparametric parameters, without straining either computational technology.

Occasionally the nonparametric method will not converge because of either excessive error in the points or too little information for calculating one of the parameters. In our computer program, if the estimated parameter is 100 or 0.01 times the original estimate, the iteration is stopped and the values of 0.01 times or 100 times the original estimate are assigned. This places these values at the extremes (where they would normally be), and the median is relatively unaffected. The Newton–Raphson method is unstable if the estimate is not close to the true value, so the above safeguard prevents instability of the computer program during the simulations. In actual practice, although these results would produce outliers and hence not affect the results, a different algorithm might be beneficial.

In conclusion, the utility of a nonparametric technique for the determination of parameters of nonlinear equations is demonstrated. As anticipated, the nonparametric technique outperforms conventional nonlinear regression computations unless the error structure coincides with the weighting used for the nonlinear regression technique. The general method developed is anticipated to be applicable to other nonlinear problems although appropriate numerical techniques for solving simultaneous nonlinear equations must be developed for the particular model under examination.

[1] The programs were written using the Statistical Analysis System (SAS) version 79.5 run utilizing North Dakota State University Computer System.

REFERENCES

(1) K. T. Muir and S. Riegelman, *J. Pharmacokinet. Biopharm.*, **7**, 685 (1979).

(2) G. L. Atkins and I. A. Nimmo, *Biochem. J.*, **149**, 775 (1975).

(3) N. A. C. Cressie and D. D. Keightley, *Biometrics*, **37**, 235 (1981).

(4) L. Endrenyi and H. Tang, *Comput. Biomed. Res.*, **13**, 430 (1980).

(5) L. R. Koup, *J. Pharm. Sci.*, **70**, 1093 (1981).
(6) R. Eisenthal and A. Cornish-Bowden, *Biochem. J.*, **139**, 715 (1974).
(7) S. D. Conte and C. deBoor, "Elementary Numerical Analysis—An Algorithm Approach," McGraw-Hill, New York, N.Y., 1972, p. 84.
(8) A. Cornish-Bowden, W. R. Porter, and W. F. Traper, *J. Theor. Biol.*, **74**, 163 (1978).
(9) D. W. Marquardt, *J. Soc. Ind. Appl. Math.*, **2**, 431 (1963).

Comparison of UV and Fluorescence Spectrophotometry for the Quantification of a Potent Myotonia Inducer: Anthracene-9-carboxylic Acid, in Plasma, Urine, and Saline Perfusion Fluids

ARTURO VILLEGAS-NAVARRO *¶x, ANTONIO MORALES-AGUILERA *¶, and ARTEMISA POSADA-RETANA ‡

Received August 16, 1982, from the * Departamento de Farmacologia del Centro de Investigación y Estudios Avanzados del Instituto Politécnico Nacional Apartado Postal 14-740 07000 México, D.F. and the ‡ Sección de Control Analítico de Medicamentos, Centro de Investigación y Estudios Avanzados del Instituto Politécnico Nacional, Apartado Postal 14-740 07000 México, D.F. Accepted for publication September 7, 1982. ¶ Present address: Unidad de Investigación Biomédica del Noreste Apartado Postal 020-E 64720 Monterrey, Nuevo León, México

Abstract □ UV and fluorescence spectrophotometry were used to establish the analytical profile of a potent myotonia inducer, anthracene-9-carboxylic acid (I). UV spectrophotometry is useful for the determination of I when it is dissolved in physiological solutions (Ringer's, Tyrode's, *etc*). In these fluids there is a linear relationship between UV absorption and I concentration between 500 and 2000 ng/ml ($2.25–9.0 \times 10^{-6}$ *M*). However, in biological fluids there are interferences in the UV absorption due to organic substances. On the other hand, fluorescence spectrophotometry is more sensitive than UV for determinations in plasma and urine. Within the range of 200–1000 ng/ml ($0.9–4.5 \times 10^{-6}$ *M*) fluorescence intensity increases linearly with concentration. Furthermore, when both emission and excitation spectra are combined there are no interferences due to organic substances normally present in those fluids. An extraction procedure of I from plasma and urine is also described, and the importance of I determinations in relation to the problem of this myotonia-inducing aromatic monocarboxylic acid is discussed.

Keyphrases □ Fluorescence spectrophotometry—comparison of UV for quantification of a potent myotonia inducer

Several classes of chemical agents can produce, both *in vivo* and *in vitro*, changes in the function of mammalian skeletal muscle resembling the condition known as myotonia congenita in humans and in goats (1, 2). These agents include the veratrum alkaloids (3), the substitution of chloride ion by other ions that do not cross the muscle membrane (4, 5), a group of hypocholesterolemic substances (6, 7), clofibric acid that reduces the triglyceride levels (8), and other aromatic monocarboxylic acids (9–11). All these substances act directly on the membrane of mammalian skeletal muscle. However, an increasing number of studies in recent years (12–14) have confirmed the early proposal of Bryant and Morales-Aguilera (15) that aromatic monocarboxylic acids induce in mammalian muscle fibers a state that more closely resembles naturally occurring myotonia congenita than do the other agents. Bryant and Morales-Aguilera (15) and Palade and Barchi (16) showed that anthracene-9-carboxylic acid (I) is the most potent inducer of myotonia among the tested aromatic monocarboxylic acids and also that these substances very specifically block the chloride channel. The availability of chemical agents whose effects resemble the naturally occurring condition is important in the development of animal models that can give information as to the mechanisms of the disease. With the exception of clofibric acid (17), there is a lack of quantitative studies regarding the *in vivo* kinetics of the myotonia-inducing aromatic monocarboxylic acids. Also, methods are not available for their chemical determination in biological fluids. In this paper we report UV and fluorescence spectrophotometric methods for I determination and compare them in blood, plasma, urine, and saline perfusates, covering most of the present analytical needs of biomedical researchers interested in the study of myotonia induced by I.

EXPERIMENTAL

Determination of I by UV Spectrophotometry—*Sodium Bicarbonate Buffer*—Fifty milligrams of I[1] and 1.5 g of sodium bicarbonate were placed in a 100-ml volumetric flask and brought to volume with water. Since I is almost insoluble in water (the concentration of a saturated water solution is 1.88×10^{-4} *M*), it was necessary to alkalinize the medium with sodium hydroxide to pH 8–9 (22°)[2] and stir vigorously for at least 20 min. This solution has 320 mosm[3]. By successive dilutions of the isotonic alkaline solution of I the following concentrations were obtained: 0.5, 1.0, 1.5, and 2.0 μg/ml. The absorbance of these solutions was measured relative to an isotonic solution blank at 255 nm[4]. These solutions are unstable in light, so it is necessary to proceed immediately; the solutions must be protected from light.

Chloroform—A 50-mg volume of I was placed in a 100-ml volumetric flask, and brought to volume with chloroform. The dilutions to 0.5, 1.0, 1.5, and 2.0 μg/ml were made with the same solvent. Their absorbance was measured *versus* a chloroform blank at 255 nm.

Excitation/Emission Spectrum of I in Chloroform—In a 50-ml volumetric flask, 25 mg of I was added, brought to volume with chloroform, and diluted to a final concentration of 10 μg/ml. The spectra of excitation and emission were obtained in a spectrophotofluorometer[5], and the results are shown in Fig. 1. The excitation spectrum exhibits a clear absorption peak at 355 nm. This wavelength was used subsequently for excitation of the samples. The fluorescence spectrum manifests an enhanced emission at 470 nm, and the peak at this wavelength was used to quantify I in blood, plasma, and urine.

[1] Aldrich Chemical Co.
[2] Coleman Instruments Model 37-A Ph Meter.
[3] Wescor Model 5100 Osmometer.
[4] Unicam Sp 800 Spectrophotometer.
[5] Aminco-Bowman.

0022-3549/83/1000-1221$01.00/0

(5) L. R. Koup, *J. Pharm. Sci.*, **70**, 1093 (1981).
(6) R. Eisenthal and A. Cornish-Bowden, *Biochem. J.*, **139**, 715 (1974).
(7) S. D. Conte and C. deBoor, "Elementary Numerical Analysis—An Algorithm Approach," McGraw-Hill, New York, N.Y., 1972, p. 84.
(8) A. Cornish-Bowden, W. R. Porter, and W. F. Traper, *J. Theor. Biol.*, **74**, 163 (1978).
(9) D. W. Marquardt, *J. Soc. Ind. Appl. Math.*, **2**, 431 (1963).

Comparison of UV and Fluorescence Spectrophotometry for the Quantification of a Potent Myotonia Inducer: Anthracene-9-carboxylic Acid, in Plasma, Urine, and Saline Perfusion Fluids

ARTURO VILLEGAS-NAVARRO *¶x, ANTONIO MORALES-AGUILERA *¶, and ARTEMISA POSADA-RETANA ‡

Received August 16, 1982, from the * Departamento de Farmacologia del Centro de Investigación y Estudios Avanzados del Instituto Politécnico Nacional Apartado Postal 14-740 07000 México, D.F. and the ‡ Sección de Control Analítico de Medicamentos, Centro de Investigación y Estudios Avanzados del Instituto Politécnico Nacional, Apartado Postal 14-740 07000 México, D.F. Accepted for publication September 7, 1982. ¶ Present address: Unidad de Investigación Biomédica del Noreste Apartado Postal 020-E 64720 Monterrey, Nuevo León, México

Abstract □ UV and fluorescence spectrophotometry were used to establish the analytical profile of a potent myotonia inducer, anthracene-9-carboxylic acid (I). UV spectrophotometry is useful for the determination of I when it is dissolved in physiological solutions (Ringer's, Tyrode's, *etc*). In these fluids there is a linear relationship between UV absorption and I concentration between 500 and 2000 ng/ml ($2.25–9.0 \times 10^{-6}$ *M*). However, in biological fluids there are interferences in the UV absorption due to organic substances. On the other hand, fluorescence spectrophotometry is more sensitive than UV for determinations in plasma and urine. Within the range of 200–1000 ng/ml ($0.9–4.5 \times 10^{-6}$ *M*) fluorescence intensity increases linearly with concentration. Furthermore, when both emission and excitation spectra are combined there are no interferences due to organic substances normally present in those fluids. An extraction procedure of I from plasma and urine is also described, and the importance of I determinations in relation to the problem of this myotonia-inducing aromatic monocarboxylic acid is discussed.

Keyphrases □ Fluorescence spectrophotometry—comparison of UV for quantification of a potent myotonia inducer

Several classes of chemical agents can produce, both *in vivo* and *in vitro*, changes in the function of mammalian skeletal muscle resembling the condition known as myotonia congenita in humans and in goats (1, 2). These agents include the veratrum alkaloids (3), the substitution of chloride ion by other ions that do not cross the muscle membrane (4, 5), a group of hypocholesterolemic substances (6, 7), clofibric acid that reduces the triglyceride levels (8), and other aromatic monocarboxylic acids (9–11). All these substances act directly on the membrane of mammalian skeletal muscle. However, an increasing number of studies in recent years (12–14) have confirmed the early proposal of Bryant and Morales-Aguilera (15) that aromatic monocarboxylic acids induce in mammalian muscle fibers a state that more closely resembles naturally occurring myotonia congenita than do the other agents. Bryant and Morales-Aguilera (15) and Palade and Barchi (16) showed that anthracene-9-carboxylic acid (I) is the most potent inducer of myotonia among the tested aromatic monocarboxylic acids and also that these substances very specifically block the chloride channel. The availability of chemical agents whose effects resemble the naturally occurring condition is important in the development of animal models that can give information as to the mechanisms of the disease. With the exception of clofibric acid (17), there is a lack of quantitative studies regarding the *in vivo* kinetics of the myotonia-inducing aromatic monocarboxylic acids. Also, methods are not available for their chemical determination in biological fluids. In this paper we report UV and fluorescence spectrophotometric methods for I determination and compare them in blood, plasma, urine, and saline perfusates, covering most of the present analytical needs of biomedical researchers interested in the study of myotonia induced by I.

EXPERIMENTAL

Determination of I by UV Spectrophotometry—*Sodium Bicarbonate Buffer*—Fifty milligrams of I[1] and 1.5 g of sodium bicarbonate were placed in a 100-ml volumetric flask and brought to volume with water. Since I is almost insoluble in water (the concentration of a saturated water solution is 1.88×10^{-4} *M*), it was necessary to alkalinize the medium with sodium hydroxide to pH 8–9 (22°)[2] and stir vigorously for at least 20 min. This solution has 320 mosm[3]. By successive dilutions of the isotonic alkaline solution of I the following concentrations were obtained: 0.5, 1.0, 1.5, and 2.0 μg/ml. The absorbance of these solutions was measured relative to an isotonic solution blank at 255 nm[4]. These solutions are unstable in light, so it is necessary to proceed immediately; the solutions must be protected from light.

Chloroform—A 50-mg volume of I was placed in a 100-ml volumetric flask, and brought to volume with chloroform. The dilutions to 0.5, 1.0, 1.5, and 2.0 μg/ml were made with the same solvent. Their absorbance was measured *versus* a chloroform blank at 255 nm.

Excitation/Emission Spectrum of I in Chloroform—In a 50-ml volumetric flask, 25 mg of I was added, brought to volume with chloroform, and diluted to a final concentration of 10 μg/ml. The spectra of excitation and emission were obtained in a spectrophotofluorometer[5], and the results are shown in Fig. 1. The excitation spectrum exhibits a clear absorption peak at 355 nm. This wavelength was used subsequently for excitation of the samples. The fluorescence spectrum manifests an enhanced emission at 470 nm, and the peak at this wavelength was used to quantify I in blood, plasma, and urine.

[1] Aldrich Chemical Co.
[2] Coleman Instruments Model 37-A Ph Meter.
[3] Wescor Model 5100 Osmometer.
[4] Unicam Sp 800 Spectrophotometer.
[5] Aminco-Bowman.

0022-3549/83/1000-1221$01.00/0

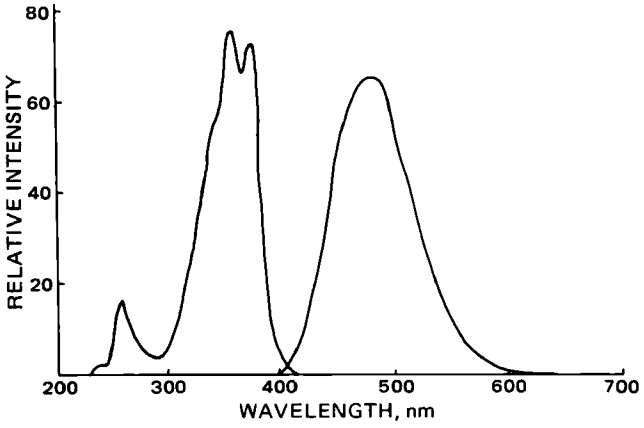

Figure 1—*Wavelength maxima for excitation (left) and emission (right) of I in chloroform (10 μg/ml).*

Standard Curve—Twenty-five milligrams of I was dissolved in chloroform and diluted to 50 ml in a volumetric flask, and then diluted with chloroform to the following concentrations: 0.2, 0.4, 0.6, 0.8, 1.0, and 1.25 μg/ml. The emission spectrum was determined for each dilution, and the intensity of fluorescence was plotted *versus* I concentration.

Spectrophotofluorometric Quantification of I in Blood, Plasma, and Urine of Rabbits—*Stock Standard*—Fifty milligrams of I and 0.75 g of sodium bicarbonate were dissolved in water and adjusted to 50 ml in a volumetric flask. This solution had 320 mosm and the pH was 8.5.

Blood, Plasma, and Urine Samples—With a syringe containing an anticoagulant[6] 10 ml of blood was drawn from the marginal vein of the ear from each of nine healthy New Zealand White rabbits. Plasma was obtained from 5 ml of this blood by centrifugation at 2000 rpm during 10 min[7]. The urine of the rabbits was collected by a catheter placed in the urinary bladder[8] and diluted 10-fold with water before analyses.

Sample Preparation—Two milliliters of whole blood were pipetted into a 15-ml centrifuge tube and mixed with 2 ml of stock standard previously diluted 10-fold. The plasma and urine were prepared in the same way.

Extraction Procedure—To 1.0 ml of blood, plasma, or urine prepared sample was added 0.5 ml of 3 *M* HCl, 0.5 g of sodium chloride, and 50 ml of chloroform in a Erlenmeyer flask. The contents were ultrasonicated[9] for 15 min, then centrifuged (full speed for about 10 min) to separate the immiscible liquid. The water layer was removed and the fluorescence of I was determinated in chloroform. The reproducibility of the assay was assessed by calculating the standard deviation of the mean value of the individual determinations.

RESULTS AND DISCUSSION

Solubility of I in chloroform is greater than in methanol or water. Therefore it is easier to work with chloroformic solutions since the extraction of I from biological fluids is faster and more efficient with this solvent.

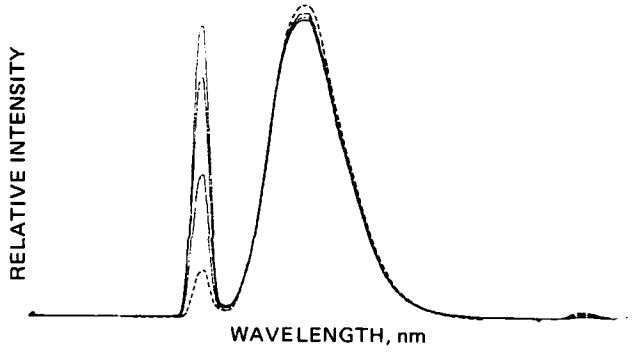

Figure 2—*Emission spectra of chloroform-extracted I from a plasma sample (n = 3). The dotted line corresponds to the standard.*

[6] Heparin, Sigma Chemical Co.
[7] Phillips-Drucker, Model L-7011 Centrifuge.
[8] Foley catheter, No. 8.
[9] Ultrasonic cleaner, Tank Unit.

Table I—Percent of Recovery of Added I [a]

Sample	Urine	Plasma	Whole Blood
1	98.0	96.0	59.0
2	100.0	96.6	60.6
3	101.2	97.7	52.1
4	101.3	98.4	72.2
5	102.0	98.4	74.1
6	101.3	100.7	76.8
7	100.5	97.8	61.3
8	105.0	102.1	63.3
9	105.0	102.1	63.3
Mean ± *SD*	101.0 ± 2	98.0 ± 2	66.5 ± 6

[a] To each of nine samples there was added 50.0 μg of I/ml. Standard curve for I using 1.0 μg/ml as a reference.

UV Spectrophotometry—Concentrations of I in sodium bicarbonate buffer and chloroform were determined by measuring the increase in absorbance at 255 nm. With the procedure for measuring I by UV detection, the peak height and the amount of I in the standards as well as in the sample are linearly related to concentration in the two solvents. The absorbance is directly proportional to I concentration of 0.5 to 2.0 μg/ml ($r^2 = 0.99$). The use of UV spectrophotometry for the determination of I is convenient when saline-perfused preparations are used because the composition of the saline solutions (Ringer's, Tyrode's, Locke's, *etc*) does not interfere with the readings. The detection limits of this method are 0.5–2.0 μg/ml ($2.25–9.0 \times 10^{-6}$ *M*). This range is within the one found in saline-perfused preparations (10^{-6}–10^{-4} *M*). In other words, in those preparations it is possible to quantify directly or after one dilution the I concentration by UV detection. On the other hand, in the case of chloroform extracts of normal blood, plasma, and urine, some constituents of those fluids gave large interfering peaks near, or at the point of maximal I absorbance in UV, interfering with its quantification. Furthermore, urine is often contaminated with blood.

Spectrophotofluorometric Determination of I—Excitation and emission spectra of I in chloroform were established because these data were not found in the literature (Fig. 1). The fluorescence spectrum obtained by this laboratory is similar to the one reported by Werner and Hercules in ethanol, although the absorption spectrum is different (18). There is a linear relationship over the range of 0.2–1.0 μg/ml, whereas higher concentrations are off because of self-quenching (19).

Compound Recovery—Table I shows the quantitative results obtained by spectrophotofluorometry for blood, plasma, and urine samples obtained from nine rabbits. The percent recovery of I added to samples and extracted with chloroform was in whole blood, plasma, and urine, 66.5 ± 7%, 98.0 ± 1%, and 101.0 ± 2%, respectively. Figure 2 shows the spectrum of a sample of plasma analyzed in triplicate. Similar results were obtained with urine (Table I).

UV Spectrophotometric *versus* Spectrophotofluorometric Assay—The sensitivity of these two formes of detection of I in chloroform were compared. The spectrophotofluorometric detection limit was found to be 200 ng/ml. The spectrophotometric UV limit was 500 ng/ml. Thus, the fluorometric method is at least twice as sensitive.

The recovery of I from plasma and urine averages 98.0 ± 1% and 101.0 ± 2%, respectively. These results indicate that the fluorometric method for plasma and urine is precise at low concentrations (Table I). However, the fluorometric method is not satisfactory for whole blood because recovery of added purified I averages only 66.5 ± 7% for whole blood.

Sensitivity—The detection limit of the fluorometric method lies in the nanogram range. This sensitivity is satisfactory because lower concentrations of I do not affect biological preparations *in vitro* (14, 15). *In vivo* a 8.0-mg/kg dose of I administered intraperitoneally to rats or intravenously to goats or rabbits elicits a clear myotonic state as well as "percussion myotonia" and the "warm-up" phenomenon. Pharmacokinetic studies in rabbits (20) shows that the same dose (8 mg/kg) produces at 1 and 120 min plasma concentrations of 1.63×10^{-4} and 1.0×10^{-5} *M*, respectively. These concentrations are similar to the ones found as active *in vitro*, and can be determined by the fluorometric method. Furthermore, the emission spectra of the chloroformic extracts of plasma and urine are clean (Fig. 2).

Specificity—To rule out interferences from other substances present in plasma or urine, we performed determinations in blank samples (without I) and found no fluorescence at the wavelength used with this method. Therefore, the method is also specific for I. Under the assay conditions which we have described, the precision and the sensitivity of the present method was found to be reliable for I determinations in some

biological liquids. It is possible to perform 14 assays in ~3 hr including reagent blanks, standards, and controls. Thus, our method should be suitable both for research in pharmacology and in a chemistry laboratory.

REFERENCES

(1) R. J. Lipicky, S. H. Bryant, and J. H. Salmon, *J. Clin. Invest.*, **50**, 2091 (1971).
(2) G. L. Brown and A. M. Harvey, *Brain*, **62**, 341 (1939).
(3) O. Krayer and G. H. Acheson, *Physiol. Rev.*, **26**, 383 (1946).
(4) H. Lüllman, *Arch. Exp. Pathol. Pharmakol.*, **240**, 351 (1961).
(5) K. G. Morgan, R. K. Entrikin, and S. H. Bryant, *Am J. Physiol.*, **229**, 1155 (1975).
(6) N. Winer, J. M. Martt, J. E. Somers, L. Wolcott, H. E. Dale, and T. W. Burns, *J. Lab. Clin. Med.*, **66**, 758 (1965).
(7) N. Winer, D. M. Klachko, R. D. Baer, P. L. Langley, and T. W. Burns, *Science*, **153**, 312 (1966).
(8) M. M. Best and C. H. Duncan, *Circulation*, **28**, 690 (1963).
(9) J. Pohl and E. Hesse, *Klin. Wschr.*, **4**, 343 (1925).
(10) R. G. Smith, *J. Pharmacol. Exp. Ther.*, **54**, 87 (1935).
(11) R. B. Moffett and A. H. Tang, *J. Med. Chem.*, **11**, 1020 (1968).
(12) M. B. Laskowski and W. D. Dettbarn, *Annu. Rev. Pharmacol. Toxicol.*, **17**, 387 (1977).
(13) H. Kwieciński, *CRC Crit. Rev. Toxicol.*, **8**, 279 (1981).
(14) K. Mrożek, H. Kwieciński, and A. Kamińska, *Acta Physiol. Pol.*, **25**, 321 (1974).
(15) S. H. Bryant and A. Morales-Aguilera, *J. Physiol.*, **219**, 367 (1971).
(16) P. T. Palade and R. L. Barchi, *J. Gen. Physiol.*, **69**, 879 (1977).
(17) T. Taylor and L. F. Chasseaud, *J. Pharm. Sci.*, **66**, 1638 (1977).
(18) T. C. Werner and D. M. Hercules, *J. Phys. Chem.*, **73**, 2005 (1969).
(19) I. B. Berlman, "Handbook of Fluorescence Spectra of Aromatic Molecules," Academic, London, 1965, pp. 1–37.
(20) A. Villegas-Navarro, "Farmacocinética del ácido 9-antracencarboxílico en el conejo," M.Sc. Thesis, Centro de Investigación y Estudios Avanzados, Instituto Politécnico Nacional, México, D.F. 1977.

Determination of Azobenzene and Hydrazobenzene in Phenylbutazone and Sulfinpyrazone Products by High-Performance Liquid Chromatography

F. MATSUI ˣ, E. G. LOVERING, N. M. CURRAN, and J. R. WATSON †

Received April 28, 1982, from the *Bureau of Drug Research, Health Protection Branch, Health and Welfare Canada, Tunney's Pasture, Ottawa, Ontario K1A OL2.* Accepted for publication August 27, 1982. † Deceased.

Abstract □ A high-performance liquid chromatographic method has been developed for the simultaneous determination of azobenzene and hydrazobenzene in phenylbutazone and sulfinpyrazone raw materials and formulations. The drug raw material or formulation is shaken with 1 *N* NaOH and *n*-hexane and centrifuged. The *n*-hexane layer is injected into a chromatograph equipped with a 10-μm cyano-amino bonded phase column. Azobenzene and hydrazobenzene are detected at 313 and 254 nm, respectively; the sensitivities are ~1 and 2 ppm, respectively, in the raw materials and formulations.

Keyphrases □ Azobenzene—determination in phenylbutazone and sulfinpyrazone products by high-performance liquid chromagraphy □ Hydrazobenzene—determination in phenylbutazone and sulfinpyrazone products by high-performance liquid chromatography □ High-performance liquid chromatography—determination of azobenzene and hydrazobenzene in phenylbutazone and sulfinpyrazone products

Hydrazobenzene is an intermediate in the manufacture of phenylbutazone and sulfinpyrazone (1). These drugs may be contaminated with hydrazobenzene as a result of incomplete clean up after manufacture or if the drugs degrade by hydrolytic ring opening and subsequent cleavage of the residual amido function (2). Azobenzene forms readily by autoxidation of hydrazobenzene (2); its presence in drugs may be due to the use of impure hydrazobenzene during manufacture or to the oxidation of hydrazobenzene (2). Recent work indicates that hydrazobenzene is a carcinogen in rats and mice (3) and that azobenzene is a carcinogen in rats, but not in mice (4).

There appear to be few available methods for the determination of azo- and hydrazobenzene. Hydrazobenzene (5) and azobenzene (6, 7) have been detected in phenylbutazone formulations by TLC, and a high-performance liquid chromatography (HPLC) method for the determination of hydrazobenzene in aqueous media (8) has been reported. An HPLC method for the simultaneous determination of azo- and hydrazobenzene in phenylbutazone and sulfinpyrazone drug raw materials and formulations is described here.

EXPERIMENTAL

Materials—Azobenzene[1], hydrazobenzene[2] (1,2-diphenylhydrazine), sodium hydroxide[3], HPLC-grade *n*-hexane[4], and absolute ethanol[5] were used as received. All solvents were flushed with nitrogen prior to use.

Apparatus—The liquid chromatograph consisted of a single-piston metering pump[6], an injector[7] equipped with a 100-μl sample loop, a dual-channel UV detector[8] (254 nm, 0.02 AUFS and 313 nm, 0.05 AUFS) and two 10-mV strip chart recorders[9] (chart speed of 0.5 cm/min). A Partisil-10 PAC[10] analytical column (25 cm × 4.6-mm i.d.) and a Porasil 400[11] (37–75 μm) precolumn (10 cm × 4 mm-i.d.) were used at ambient temperature with a mobile phase flow rate of 2 ml/min. The mobile phase was a solution of 2.5% absolute ethanol in *n*-hexane (v/v) flushed with nitrogen.

Calibration Curves—*Azobenzene*—A solution of azobenzene in

[1] Pfaltz and Bauer Inc., Stamford, Conn.
[2] Aldrich Chemical Co., Milwaukee, Wis.
[3] Analytical Reagent Grade.
[4] Burdick and Jackson Laboratories, Muskegon, Mich.
[5] Consolidated Alcohols Ltd., Toronto, Ont.
[6] Model 110A; Altex Scientific, Berkeley, Calif.
[7] Model CV-6-UHPa-N_{60}; Valco Instruments Co., Houston, Tex.
[8] Model 440; Waters Associates, Milford, Mass.
[9] Linear Instruments Corp., Irvine, Calif.
[10] Whatman Inc., Clifton, N.J. (Cyano-amino polar phase bonded to silica gel).
[11] Waters Associates, Milford, Mass.

0022-3549/83/1000-1223$01.00/0

biological liquids. It is possible to perform 14 assays in ~3 hr including reagent blanks, standards, and controls. Thus, our method should be suitable both for research in pharmacology and in a chemistry laboratory.

REFERENCES

(1) R. J. Lipicky, S. H. Bryant, and J. H. Salmon, *J. Clin. Invest.*, **50**, 2091 (1971).
(2) G. L. Brown and A. M. Harvey, *Brain*, **62**, 341 (1939).
(3) O. Krayer and G. H. Acheson, *Physiol. Rev.*, **26**, 383 (1946).
(4) H. Lüllman, *Arch. Exp. Pathol. Pharmakol.*, **240**, 351 (1961).
(5) K. G. Morgan, R. K. Entrikin, and S. H. Bryant, *Am J. Physiol.*, **229**, 1155 (1975).
(6) N. Winer, J. M. Martt, J. E. Somers, L. Wolcott, H. E. Dale, and T. W. Burns, *J. Lab. Clin. Med.*, **66**, 758 (1965).
(7) N. Winer, D. M. Klachko, R. D. Baer, P. L. Langley, and T. W. Burns, *Science*, **153**, 312 (1966).
(8) M. M. Best and C. H. Duncan, *Circulation*, **28**, 690 (1963).
(9) J. Pohl and E. Hesse, *Klin. Wschr.*, **4**, 343 (1925).
(10) R. G. Smith, *J. Pharmacol. Exp. Ther.*, **54**, 87 (1935).
(11) R. B. Moffett and A. H. Tang, *J. Med. Chem.*, **11**, 1020 (1968).
(12) M. B. Laskowski and W. D. Dettbarn, *Annu. Rev. Pharmacol. Toxicol.*, **17**, 387 (1977).
(13) H. Kwieciński, *CRC Crit. Rev. Toxicol.*, **8**, 279 (1981).
(14) K. Mrożek, H. Kwieciński, and A. Kamińska, *Acta Physiol. Pol.*, **25**, 321 (1974).
(15) S. H. Bryant and A. Morales-Aguilera, *J. Physiol.*, **219**, 367 (1971).
(16) P. T. Palade and R. L. Barchi, *J. Gen. Physiol.*, **69**, 879 (1977).
(17) T. Taylor and L. F. Chasseaud, *J. Pharm. Sci.*, **66**, 1638 (1977).
(18) T. C. Werner and D. M. Hercules, *J. Phys. Chem.*, **73**, 2005 (1969).
(19) I. B. Berlman, "Handbook of Fluorescence Spectra of Aromatic Molecules," Academic, London, 1965, pp. 1–37.
(20) A. Villegas-Navarro, "Farmacocinética del ácido 9-antracencarboxílico en el conejo," M.Sc. Thesis, Centro de Investigación y Estudios Avanzados, Instituto Politécnico Nacional, México, D.F. 1977.

Determination of Azobenzene and Hydrazobenzene in Phenylbutazone and Sulfinpyrazone Products by High-Performance Liquid Chromatography

F. MATSUI ˣ, E. G. LOVERING, N. M. CURRAN, and J. R. WATSON †

Received April 28, 1982, from the *Bureau of Drug Research, Health Protection Branch, Health and Welfare Canada, Tunney's Pasture, Ottawa, Ontario K1A OL2.* Accepted for publication August 27, 1982. † Deceased.

Abstract □ A high-performance liquid chromatographic method has been developed for the simultaneous determination of azobenzene and hydrazobenzene in phenylbutazone and sulfinpyrazone raw materials and formulations. The drug raw material or formulation is shaken with 1 *N* NaOH and *n*-hexane and centrifuged. The *n*-hexane layer is injected into a chromatograph equipped with a 10-μm cyano-amino bonded phase column. Azobenzene and hydrazobenzene are detected at 313 and 254 nm, respectively; the sensitivities are ~1 and 2 ppm, respectively, in the raw materials and formulations.

Keyphrases □ Azobenzene—determination in phenylbutazone and sulfinpyrazone products by high-performance liquid chromagraphy □ Hydrazobenzene—determination in phenylbutazone and sulfinpyrazone products by high-performance liquid chromatography □ High-performance liquid chromatography—determination of azobenzene and hydrazobenzene in phenylbutazone and sulfinpyrazone products

Hydrazobenzene is an intermediate in the manufacture of phenylbutazone and sulfinpyrazone (1). These drugs may be contaminated with hydrazobenzene as a result of incomplete clean up after manufacture or if the drugs degrade by hydrolytic ring opening and subsequent cleavage of the residual amido function (2). Azobenzene forms readily by autoxidation of hydrazobenzene (2); its presence in drugs may be due to the use of impure hydrazobenzene during manufacture or to the oxidation of hydrazobenzene (2). Recent work indicates that hydrazobenzene is a carcinogen in rats and mice (3) and that azobenzene is a carcinogen in rats, but not in mice (4).

There appear to be few available methods for the determination of azo- and hydrazobenzene. Hydrazobenzene (5) and azobenzene (6, 7) have been detected in phenylbutazone formulations by TLC, and a high-performance liquid chromatography (HPLC) method for the determination of hydrazobenzene in aqueous media (8) has been reported. An HPLC method for the simultaneous determination of azo- and hydrazobenzene in phenylbutazone and sulfinpyrazone drug raw materials and formulations is described here.

EXPERIMENTAL

Materials—Azobenzene[1], hydrazobenzene[2] (1,2-diphenylhydrazine), sodium hydroxide[3], HPLC-grade *n*-hexane[4], and absolute ethanol[5] were used as received. All solvents were flushed with nitrogen prior to use.

Apparatus—The liquid chromatograph consisted of a single-piston metering pump[6], an injector[7] equipped with a 100-μl sample loop, a dual-channel UV detector[8] (254 nm, 0.02 AUFS and 313 nm, 0.05 AUFS) and two 10-mV strip chart recorders[9] (chart speed of 0.5 cm/min). A Partisil-10 PAC[10] analytical column (25 cm × 4.6-mm i.d.) and a Porasil 400[11] (37–75 μm) precolumn (10 cm × 4 mm-i.d.) were used at ambient temperature with a mobile phase flow rate of 2 ml/min. The mobile phase was a solution of 2.5% absolute ethanol in *n*-hexane (v/v) flushed with nitrogen.

Calibration Curves—*Azobenzene*—A solution of azobenzene in

[1] Pfaltz and Bauer Inc., Stamford, Conn.
[2] Aldrich Chemical Co., Milwaukee, Wis.
[3] Analytical Reagent Grade.
[4] Burdick and Jackson Laboratories, Muskegon, Mich.
[5] Consolidated Alcohols Ltd., Toronto, Ont.
[6] Model 110A; Altex Scientific, Berkeley, Calif.
[7] Model CV-6-UHPa-N_{60}; Valco Instruments Co., Houston, Tex.
[8] Model 440; Waters Associates, Milford, Mass.
[9] Linear Instruments Corp., Irvine, Calif.
[10] Whatman Inc., Clifton, N.J. (Cyano-amino polar phase bonded to silica gel).
[11] Waters Associates, Milford, Mass.

0022-3549/83/1000-1223$01.00/0

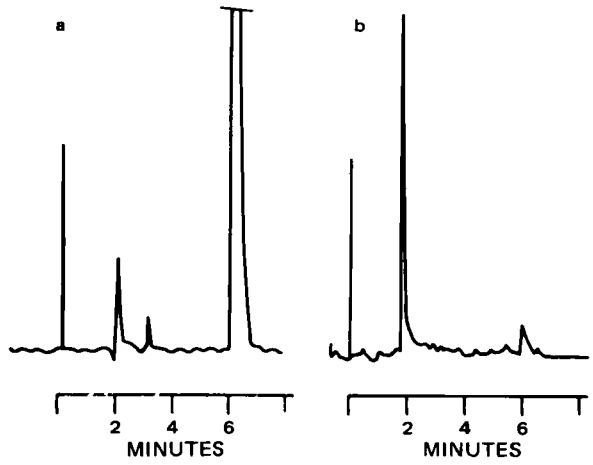

Figure 1—*Chromatograms of azobenzene (2.0 min) and hydrazobenzene (6.1 min). Key: (a) detection at 254 nm, (b) detection at 313 nm.*

n-hexane (1.6 μg/ml) was diluted with the same solvent to obtain five standard solutions ranging from 0.048 to 0.80 μg/ml. Duplicate 100-μl aliquots representing on-column amounts of 0.0048–0.080 μg of azobenzene were chromatographed at 313 nm with the signal attenuated to 0.05 AUFS.

Hydrazobenzene—A solution of hydrazobenzene in *n*-hexane (1.6 μg/ml) was diluted with the same solvent to obtain five standard solutions ranging from 0.10 to 1.6 μg/ml. Duplicate 100-μl aliquots representing on-column amounts of 0.010–0.160 μg of hydrazobenzene were chromatographed at 254 nm with the signal attenuated to 0.02 AUFS.

Daily Calibration—Two standard solutions of each compound (azo- and hydrazobenzene) were prepared fresh each day. The concentrations of the standards were such that the on-column levels were ~0.006 and 0.060 μg for azobenzene and ~0.016 and 0.120 μg for hydrazobenzene.

System Check Sample—Powdered, well-mixed composites were prepared from 50 capsules (or tablets) of phenylbutazone or sulfinpyrazone products which were known to contain azobenzene and hydrazobenzene. These were analyzed periodically to check the reproducibility of the chromatographic system and the sampling procedures.

Analysis of Phenylbutazone or Sulfinpyrazone Preparations—Phenylbutazone or sulfinpyrazone drug raw material (100 mg), or an aliquot of a composite of powdered tablets or capsule contents equivalent to 100 mg of the drug substance, was shaken with 10.0 ml of 1 *N* NaOH just long enough to wet the solid mass. To this was added 5.0 ml of *n*-hexane, and the mixture was shaken for 5 min on a horizontal shaker. After centrifuging at 4000 rpm for 1 min, the upper organic layer containing the azobenzene and/or hydrazobenzene was immediately separated from the aqueous phase containing the drug. Duplicate 100-μl aliquots of the organic phase were chromatographed with the 254- and 313-nm detectors in series. When the peak for the azobenzene and/or hydrazobenzene was off-scale, the sample was diluted with *n*-hexane and injected again. Quantitation was by the peak height technique for both impurities. Calibration standards of azobenzene and hydrazobenzene in *n*-hexane were used as the external reference solutions.

RESULTS AND DISCUSSION

During development of the method it was found that some sulfinpyrazone samples contained an impurity which was eluted at 1.8 min and was incompletely resolved from azobenzene at 2.0 min. This impurity was shown to be toluene by GC–MS. Toluene and azobenzene were resolved at retention times of 2.8 and 4.0 min, respectively, by elimination of ethanol from the mobile phase. This, however, delayed the elution of hydrazobenzene to such an extent that there was an unacceptable loss of sensitivity. Therefore, ethanol was retained in the mobile phase and the azobenzene was quantitated at 313 nm, where absorption by toluene is insignificant. The hydrazobenzene, which was eluted at 4.9 min, was quantitated by measurements at 254 nm. Typical chromatograms at both wavelengths are presented in Fig. 1.

Hydrazobenzene is reported to be oxidized readily in solvents such as benzene, methylene chloride, and methanol (8). In *n*-hexane in equilibrium with the atmosphere, hydrazobenzene was oxidized to azobenzene at a rate of ~5%/hr at room temperature. In nitrogen-flushed *n*-hexane there was no increase in the azobenzene level during the first 30 min and only a 4% conversion after ~2 hr. In addition it was found that azo- and hydrazobenzene in the nitrogen-flushed calibration solutions were stable over a period of 1 hr, as indicated by the constancy of the response factors of the five calibration solutions. Over the period of the extraction neither drug was degraded sufficiently to cause detectable increases in the azo- and hydrazobenzene levels. For phenylbutazone, the levels began to increase after 15 min, but no change was observed in sulfinpyrazone after 50 min.

The reproducibility of the procedure used for the extraction of azo- and hydrazobenzene from formulations was investigated using phenylbutazone and sulfinpyrazone formulations known to contain azo- and hydrazobenzene. Using 10 ml of 1 *N* NaOH and 5 ml of *n*-hexane as provided for by the method, the extraction of both contaminants was invariant between 50 and 250 mg of phenylbutazone and 50 and 150 mg of sulfinpyrazone. Increasing the amount of *n*-hexane used in the extraction from 5 to 10 and 5 to 20 ml for sulfinpyrazone and phenylbutazone, respectively, had no effect on the amounts of azo- and hydrazobenzene detected. The partition of azo- and hydrazobenzene into *n*-hexane from sodium hydroxide solution is virtually complete. This was demonstrated by shaking a solution of the contaminants dissolved in *n*-hexane with 1 *N* NaOH. There was no detectable change in the observed levels of azo- and hydrazobenzene after shaking with the base. Drug raw materials and formulations were spiked with known amounts of azo- and hydrazobenzene. Recoveries ranged between 85 and 110%.

The response of the chromatographic system was linear from 4 to 70 ng of azobenzene on-column, with an intercept that did not vary significantly from zero. The relative standard deviation of the ratio of the peak height to the weight of azobenzene was 2.3% for five calibration points. For hydrazobenzene the linear range was from 10 to 150 ng with a corresponding relative standard deviation of 3.5%. These ranges would correspond to azo- and hydrazobenzene levels of 2–35 ppm and 5–75 ppm, respectively, in 100 mg of drug when assayed by the procedure described in this paper. The chromatographic reproducibilities were established by injecting six aliquots of each of two solutions of azo- and hydrazobenzene. On-column amounts of 0.0057 and 0.032 μg of azobenzene gave relative standard deviations of the peak height–weight ratio of 2.34 and 0.53%, respectively. For hydrazobenzene, the relative standard deviations were 5.99 and 3.12% for on-column quantities of 0.0737 and 0.145 μg, respectively. The reproducibility of the assay for azo- and hydrazobenzene in formulations of phenylbutazone and sulfinpyrazone ranged between 4 and 13%, in general agreement with recoveries from the spiked samples.

The minimum detectable amounts of azobenzene and hydrazobenzene on column are ~1.5 and 4 ng, respectively. These levels corresponded to ~1 and 2 ppm of azobenzene and hydrazobenzene, respectively, for an on-column equivalent of 2000 μg of the drug. The minimum quantifiable levels were about twice these amounts.

REFERENCES

(1) D. Lednicer and L. A. Mitscher, "Organic Chemistry of Drug Synthesis," Wiley, New York, N.Y., 1977, p. 234.

(2) D. V. C. Awang, A. A. Vincent, and F. Matsui, *J. Pharm. Sci.*, **62**, 1673 (1973).

(3) National Cancer Institute Carcinogenesis Technical Report Series No. 92, 1978.

(4) National Cancer Institute Carcinogenesis Technical Report Series No. 154, 1979.

(5) I. J. McGilveray, *Med. Serv. J. Can.*, **23**, 233 (1967).

(6) H. Fabre and B. Mandrou, *J. Pharm. Sci.*, **70**, 460 (1981).

(7) F. Matsui, D. L. Robertson, P. Lafontaine, H. Kolasinski, and E. G. Lovering, *J. Pharm. Sci.*, **67**, 646 (1978).

(8) R. M. Riggin and C. C. Howard, *Anal. Chem.*, **51**, 210 (1979).

Increased Cytotoxicity of N^6-(Δ^2-Isopentenyl)adenosine in Combination with Pentostatin Against L-1210 Leukemia Cells

BRUCE HACKER and YUNIK CHANG ˣ

Received June 4, 1982, from the *College of Pharmacy, University of Oklahoma, Oklahoma City, OK 73190.* Accepted for publication September 21, 1982.

Abstract □ Pentostatin (I), a tight-binding inhibitor of adenosine deaminase, was evaluated in combination with the partially effective antitumor nucleoside N^6-(Δ^2-isopentenyl)adenosine (II) for cytotoxic activity against cultured L-1210 lymphocytic mouse leukemia cells. Although I alone (≤ 10 μg/ml) was ineffective, it significantly potentiated and prolonged the cytotoxic and cytostatic activities of II. The combination of I (2–10 μg/ml) with II (25 μg/ml) resulted in inhibition of cellular proliferation (80–96%) within 24 hr with maintenance at that level for an extended period of time due to the continued ability of I to prevent the facile deamination of the allylic side chain of II. This type of adjuvant chemoprotection has potential use for other labile oncologic agents.

Keyphrases □ Pentostatin—potentiation of N^6-(Δ^2-isopentenyl)-adenosine, cytotoxicity, mouse L-1210 leukemia cells □ N^6-(Δ^2-isopentenyl)adenosine—potentiation by pentostatin, cytotoxicity, mouse L-1210 leukemia cells □ Cytotoxicity—N^6-(Δ^2-isopentenyl)adenosine, potentiation by pentostatin, mouse L-1210 leukemia cells

Since its initial characterization by Woo *et al.* (1), pentostatin (2′-deoxycoformycin) (I), the tight-binding inhibitor of adenosine deaminase, has been shown to possess both antilymphocytic (2) and immunosuppressive activity (3) in several animal test systems. The ability of I to oppose or block the enzymatic deamination of several adenosine analogues to inactive forms (4) prompted clinical interest and utilization of the drug in the treatment of human chronic and acute lymphocytic leukemia. Recent studies have shown that I is of particular use in the treatment of acute lymphoblastic leukemia (5), as well as for chronic T-cell lymphocytic leukemia (6). Of special interest has been combination of I with the antiviral and antitumor agent vidarabine (7).

Other studies have revealed the existence of a correlation between the cytotoxicity of I and the accumulation of deoxyadenosine-5′-triphosphate in acute lymphocytic leukemia (8, 9), as well as the ratio of deoxyadenosine-5′-triphosphate to adenosine-5′-triphosphate in red blood cells. Another adenosine nucleoside analogue N^6-(Δ^2-isopentenyl)adenosine (II), used in the present investigation, has also been shown previously to possess growth-inhibitory effects on sarcoma-180 cells as well as some cytostatic action in treating human myeloblastic leukemia (10). Its immunosuppressive activity (11) has been linked to its ability to block the transport of preformed nucleosides at the level of transmembrane translocation in several mammalian species (11, 12). Moreover, it has been possible to prepare a serologically specific antibody to II (13).

Despite their potential for treating human leukemias, use of II and other adenosine antimetabolites has been limited due to their susceptibility to enzymatic degradation and subsequent inactivation by an enzyme system related to adenosine deaminase [N^6-(Δ^2-isopentenyl)-adenosine-aminohydrolase (14)]. This difficulty has been overcome, in great measure, by release of II at a controllable and predictable rate from a silicone rubber monolithic polymer matrix (15–17). This represented a successful attempt to match the rate of release of II against the aminohydrolase activity in tumor cells. The present study using I was begun to establish a means of preventing the degradation of II, thereby potentiating and prolonging its effectiveness against L-1210 leukemia cells.

EXPERIMENTAL

Drug Agents—The preparation of N^6-(Δ^2-isopentenyl)adenosine (II) was conducted as described elsewhere (11, 12, 16). Pentostatin [(*R*)-3-(2-deoxy-β-D-*erythro*-pentofuranosyl)-3,6,7,8-tetrahydroimidazo-[4,5-*d*][1,3]diazepin-8-ol; I] was supplied[1]. Both agents were stored at −20° over silica gel.

Culturing of L-1210 Cells and Determination of Cell Number—Mouse lymphocytic leukemia cells (L-1210) were routinely cultured under sterile conditions in a 5% carbon dioxide atmosphere at 37°, with transfer during the mid-log phase of growth into 5 ml of fresh medium[2] (RPMI 1640 supplemented with L-glutamine plus 10% fetal calf serum) as described elsewhere (16), using wide-mouth culture flasks[3] to accommodate silicone polymeric membranes when used. Total cell number and viability values were determined using Turk's solution and trypan blue exclusion, respectively (16). Aliquots of each cell suspension, to which II and/or I was added at time zero, were aseptically removed for the determination of cell number and for centrifugation–filtration[4] to yield cell-free filtrates for high-performance liquid chromatographic (HPLC) determinations.

Analysis of I and II Content in Cell Growth Medium—High performance liquid chromatography using two reverse-phase columns[5] eluted with varying methanolic solutions, as described in part previously (15, 16), was used to determine the stability and metabolism of both nucleoside drug agents in the cell culture medium at various intervals. This was accomplished during continuous incubation conditions by removal of aliquots (0.05–0.20 ml) for centrifugation–filtration (16).

Determination of the Cytotoxicity of I and II—Solutions of I or II were freshly prepared by dissolving the drugs in RPMI 1640 without serum, with sterile-filtration followed by aseptic addition at time zero.[6] At appropriate times thereafter, aliquots of each cell suspension were removed for determination of cell number, viability, and/or required analytical studies (16).

RESULTS AND DISCUSSION

Adenosine deaminase and a related aminohydrolase for II not only have important roles in normal catabolic pathways for adenine nucleosides, but are capable of deaminating N^6-(Δ^2-isopentenyl)adenosine (II) (14). Deamination of II to inosine greatly reduces its ability to interfere with nucleic precursor transport and synthesis (11, 12) and its immunosuppressive activity (11, 13), thereby diminishing its chemotherapeutic potential as an anticancer agent (10). The present investigation demonstrates that a natural product, the potent adenosine deaminase inhibitor pentostatin (1–9), can potentiate and prolong the antileukemic effect of

[1] Natural Products Branch, Division of Cancer Treatment, National Cancer Institute, Bethesda, Md.
[2] Grand Island Biological Co., Grand Island, N.Y.
[3] Corning no. 25100; 25 ml.
[4] Bioanalytical System, Inc., West Lafayette, Ind.
[5] Micropak MCH-10, Varian Instruments Co., Palo Alto, Calif.; Zorbax ODS, Dupont Co., Wilmington, Del.
[6] Millex SLG-S0250S, Millipore Filter Co., Bedford, Mass.

0022-3549/83/1000-1225$01.00/0

Table I—Effects of Pentostatin and N^6-(Δ^2-Isopentenyl)adenosine on the Proliferation of L-1210 Leukemia Cells in Culture [a]

	Compound Added [b]						
	None	I		II		I plus II	
Time, hr [c]	Cells/ml × 10^{-5}	Cells/ml × 10^{-5}	Inhibition, %	Cells/ml × 10^{-5}	Inhibition, %	Cells/ml × 10^{-5}	Inhibition, %
24	3 ± 0.5 [d]	3 ± 0.5	0	0.8 ± 0	73	0.5 ± 0	83
48	14.5 ± 1.0	14 ± 0.8	3.2	4.5 ± 0.5	69	2.8 ± 0.5	81
72	34 ± 1.0	33.5 ± 1.0	1.5	11.1 ± 1.0	68	4.5 ± 0.5	86
96	42 ± 1.5	41 ± 2.0	2.4	14.2 ± 1.0	66	9 ± 1.0	79
144	50 ± 1.5	48 ± 2.0	4.0	22 ± 1.0	56	7.5 ± 1.0	85

[a] Each T-flask initially contained 2 × 10^5 L-1210 mouse leukemia cells per milliliter (100% viability by trypan blue exclusion) in 5 ml of growth medium (RPMI 1640 plus 10% fetal calf serum). Experiments were conducted using 2 or 3 replicates for each type of determination. [b] Additions (0.1–0.3 ml) of each agent dissolved in RPMI 1640 medium followed by sterile filtration were made at time zero to yield final concentrations of I (2 μg/ml) and/or II (25 μg/ml). [c] Aliquots (0.1–0.2 ml) of each cell suspension were removed aseptically at various time intervals for the following determinations: total cell count using Turk's solution, cell viability (trypan blue exclusion), and HPLC (15, 16). [d] Mean ± *SD*.

II against cultured L-1210 cells (Table I). Although I alone (≤10 μg/ml) does not interfere with L-1210 cellular proliferation, it is capable of enhancing the antileukemic effects of II (25 μg/ml). At an optimal concentration of 5–10 μg/ml, I in combination with II results in almost total cell death (96%) within 24 hr. The few remaining cells have viability values of 40–50%. The most impressive effect of I (2 μg/ml) is its ability to prevent the cytotoxic capacity of II from declining at longer intervals of incubation time, when L-1210 leukemia cells are in the stationary phase of growth. This effect is discernible at concentrations of as low as 0.2 μg/ml[7]. These results suggest that inhibition of N^6-(Δ^2-isopentenyl)-adenosine-aminohydrolase prevents the inactivation of II, thereby enhancing and prolonging its effectiveness as an antitumor drug agent. In other recent studies (15–17), it has been demonstrated that the usefulness of II against L-1210 cells may also be potentiated by controlled release of this nucleoside from a polymeric silicone matrix.

REFERENCES

(1) P. W. K. Woo, H. W. Dion, S. M. Lange, L. F. Dahl, and L. J. Durham, *J. Heterocycl. Chem.*, **11**, 641 (1974).

(2) C. E. Cass and H. Au Yeung, *Cancer Res.*, **36**, 1486 (1976).

(3) M. M. Chassin, M. A. Chirigos, D. G. Johns, and R. Adamson, *N. Engl. J. Med.*, **296**, 1232 (1977).

(4) J. F. Smyth, R. M. Paine, and A. L. Jackman, *Cancer Chemother. Pharmacol.*, **5**, 93 (1980).

(5) D. G. Poplack, S. E. Sallan, G. Rivera, J. Holcenberg, S. B. Murphy, J. Blatt, J. M. Lipton, P. Venner, D. L. Glaubiger, R. Ungerleider, and D. Johns, *Cancer Res.*, **41**, 3343 (1981).

(6) A. Yu, B. Bakay, S. Matsumoto, W. Nyhan, M. Green, and I. Royston, *Proc. Am. Assoc. Cancer Res.*, **22**, 226 (1981).

(7) G. A. LePage, L. S. Worth, and A. P. Kimball, *Cancer Res.*, **36**, 1481 (1976).

(8) C. A. Koller and B. S. Mitchell, *Proc. Am. Assoc. Cancer Res.*, **22**, 221 (1981).

(9) R. L. Wortmann, J. Holcenberg, and D. C. Poplack, *Cancer Treat. Rep.*, **66**, 387 (1982).

(10) J. T. Grace, M. T. Hakala, R. H. Hall, and J. Blakeslee, *Proc. Am. Assoc. Cancer Res.*, **8**, 23 (1967).

(11) B.Hacker and T. L. Feldbush, *Cancer*, **27**, 1384 (1971).

(12) D. Hare and B. Hacker, *Physiol. Chem. Phys.*, **4**, 275 (1972).

(13) B. Hacker, H. Van Vunakis, and L. Levine, *J. Immunol.*, **108**, 1726 (1972).

(14) R. H. Hall and G. Mintsioulis, *J. Biochem.*, **73**, 739 (1973).

(15) B. Hacker and Y. Chang, *Proc. Am. Pharm. Assoc. Acad. Pharm. Sci.*, **11**, 136 (1981).

(16) Y. Chang and B. Hacker, *J. Pharm. Sci.*, **71**, 328 (1982).

(17) B. Hacker and Y. Chang, *J. Pharm. Sci.*, **72**, 902 (1983).

[7] B. Hacker, unpublished results.

Arylidenepyruvic Acid Thiosemicarbazone and Thiazoline Derivatives As Potential Antimicrobial Agents

A.-MOHSEN M. E. OMAR *x, IBRAHIM M. LABOUTA *, M. GABR KASEM *, and J. BOURDAIS ‡

Received May 25, 1982, from the **Pharmaceutical Chemistry Department, Faculty of Pharmacy, University of Alexandria, Egypt* and ‡*Laboratoire de Chimie des Hétérocycles d'Intérêt Biologique, Université d'Aix-Marseille II, Faculté de Médecine Nord, 13326 Marseille, Cedex 15, France.* Accepted for publication August 16, 1982.

Abstract □ Two novel series of arylidenepyruvic acid thiosemicarbazone and thiazoline derivatives were synthesized and evaluated as potential antimicrobial agents. These substances did not exhibit any significant antibacterial effects when tested against a variety of microorganisms.

Keyphrases □ Antimicrobial agents, potential—arylidenepyruvic acid thiosemicarbazone and thiazoline derivatives, synthesis, evaluation for antibacterial activity □ Arylidenepyruvic acids—thiosemicarbazones and thiazolines derivatives, synthesis, antimicrobial effects.

The introduction of a thiosemicarbazone moiety to alter the pharmacological activity of a variety of biologically active compounds has been demonstrated recently in several studies from this laboratory (1–5). Continuing such studies, the thiosemicarbazones (II–XIV) derived from various arylidenepyruvic acids and the corresponding thiazolines (XV–XXVII, Scheme I) were synthesized and tested for antimicrobial activity.

RESULTS AND DISCUSSION

Chemistry—The thio compounds (II–XXVII) were prepared as shown in Scheme I. A mixture of pyruvic acid or the properly substituted arylidenepyruvic acid (I), prepared through Claisen condensation of pyruvic acid and various aryl aldehydes (6), and an equivalent amount of 4-substituted 3-thiosemicarbazide was heated under reflux in aqueous acetic acid. The products (II–XIV) which separated on concentrating and cooling the mixtures, were crystallized from ethanol. The reaction of these

0022-3549/83/1000-1226$01.00/0

Table I—Effects of Pentostatin and N^6-(Δ^2-Isopentenyl)adenosine on the Proliferation of L-1210 Leukemia Cells in Culture [a]

	Compound Added [b]						
	None	I		II		I plus II	
Time, hr [c]	Cells/ml × 10^{-5}	Cells/ml × 10^{-5}	Inhibition, %	Cells/ml × 10^{-5}	Inhibition, %	Cells/ml × 10^{-5}	Inhibition, %
24	3 ± 0.5 [d]	3 ± 0.5	0	0.8 ± 0	73	0.5 ± 0	83
48	14.5 ± 1.0	14 ± 0.8	3.2	4.5 ± 0.5	69	2.8 ± 0.5	81
72	34 ± 1.0	33.5 ± 1.0	1.5	11.1 ± 1.0	68	4.5 ± 0.5	86
96	42 ± 1.5	41 ± 2.0	2.4	14.2 ± 1.0	66	9 ± 1.0	79
144	50 ± 1.5	48 ± 2.0	4.0	22 ± 1.0	56	7.5 ± 1.0	85

[a] Each T-flask initially contained 2 × 10^5 L-1210 mouse leukemia cells per milliliter (100% viability by trypan blue exclusion) in 5 ml of growth medium (RPMI 1640 plus 10% fetal calf serum). Experiments were conducted using 2 or 3 replicates for each type of determination. [b] Additions (0.1–0.3 ml) of each agent dissolved in RPMI 1640 medium followed by sterile filtration were made at time zero to yield final concentrations of I (2 μg/ml) and/or II (25 μg/ml). [c] Aliquots (0.1–0.2 ml) of each cell suspension were removed aseptically at various time intervals for the following determinations: total cell count using Turk's solution, cell viability (trypan blue exclusion), and HPLC (15, 16). [d] Mean ± *SD*.

II against cultured L-1210 cells (Table I). Although I alone (≤10 μg/ml) does not interfere with L-1210 cellular proliferation, it is capable of enhancing the antileukemic effects of II (25 μg/ml). At an optimal concentration of 5–10 μg/ml, I in combination with II results in almost total cell death (96%) within 24 hr. The few remaining cells have viability values of 40–50%. The most impressive effect of I (2 μg/ml) is its ability to prevent the cytotoxic capacity of II from declining at longer intervals of incubation time, when L-1210 leukemia cells are in the stationary phase of growth. This effect is discernible at concentrations of as low as 0.2 μg/ml[7]. These results suggest that inhibition of N^6-(Δ^2-isopentenyl)-adenosine-aminohydrolase prevents the inactivation of II, thereby enhancing and prolonging its effectiveness as an antitumor drug agent. In other recent studies (15–17), it has been demonstrated that the usefulness of II against L-1210 cells may also be potentiated by controlled release of this nucleoside from a polymeric silicone matrix.

REFERENCES

(1) P. W. K. Woo, H. W. Dion, S. M. Lange, L. F. Dahl, and L. J. Durham, *J. Heterocycl. Chem.*, **11**, 641 (1974).

(2) C. E. Cass and H. Au Yeung, *Cancer Res.*, **36**, 1486 (1976).

(3) M. M. Chassin, M. A. Chirigos, D. G. Johns, and R. Adamson, *N. Engl. J. Med.*, **296**, 1232 (1977).

(4) J. F. Smyth, R. M. Paine, and A. L. Jackman, *Cancer Chemother. Pharmacol.*, **5**, 93 (1980).

(5) D. G. Poplack, S. E. Sallan, G. Rivera, J. Holcenberg, S. B. Murphy, J. Blatt, J. M. Lipton, P. Venner, D. L. Glaubiger, R. Ungerleider, and D. Johns, *Cancer Res.*, **41**, 3343 (1981).

(6) A. Yu, B. Bakay, S. Matsumoto, W. Nyhan, M. Green, and I. Royston, *Proc. Am. Assoc. Cancer Res.*, **22**, 226 (1981).

(7) G. A. LePage, L. S. Worth, and A. P. Kimball, *Cancer Res.*, **36**, 1481 (1976).

(8) C. A. Koller and B. S. Mitchell, *Proc. Am. Assoc. Cancer Res.*, **22**, 221 (1981).

(9) R. L. Wortmann, J. Holcenberg, and D. C. Poplack, *Cancer Treat. Rep.*, **66**, 387 (1982).

(10) J. T. Grace, M. T. Hakala, R. H. Hall, and J. Blakeslee, *Proc. Am. Assoc. Cancer Res.*, **8**, 23 (1967).

(11) B.Hacker and T. L. Feldbush, *Cancer*, **27**, 1384 (1971).

(12) D. Hare and B. Hacker, *Physiol. Chem. Phys.*, **4**, 275 (1972).

(13) B. Hacker, H. Van Vunakis, and L. Levine, *J. Immunol.*, **108**, 1726 (1972).

(14) R. H. Hall and G. Mintsioulis, *J. Biochem.*, **73**, 739 (1973).

(15) B. Hacker and Y. Chang, *Proc. Am. Pharm. Assoc. Acad. Pharm. Sci.*, **11**, 136 (1981).

(16) Y. Chang and B. Hacker, *J. Pharm. Sci.*, **71**, 328 (1982).

(17) B. Hacker and Y. Chang, *J. Pharm. Sci.*, **72**, 902 (1983).

[7] B. Hacker, unpublished results.

Arylidenepyruvic Acid Thiosemicarbazone and Thiazoline Derivatives As Potential Antimicrobial Agents

A.-MOHSEN M. E. OMAR *x, IBRAHIM M. LABOUTA *, M. GABR KASEM *, and J. BOURDAIS ‡

Received May 25, 1982, from the **Pharmaceutical Chemistry Department, Faculty of Pharmacy, University of Alexandria, Egypt* and ‡*Laboratoire de Chimie des Hétérocycles d'Intérêt Biologique, Université d'Aix-Marseille II, Faculté de Médecine Nord, 13326 Marseille, Cedex 15, France.* Accepted for publication August 16, 1982.

Abstract □ Two novel series of arylidenepyruvic acid thiosemicarbazone and thiazoline derivatives were synthesized and evaluated as potential antimicrobial agents. These substances did not exhibit any significant antibacterial effects when tested against a variety of microorganisms.

Keyphrases □ Antimicrobial agents, potential—arylidenepyruvic acid thiosemicarbazone and thiazoline derivatives, synthesis, evaluation for antibacterial activity □ Arylidenepyruvic acids—thiosemicarbazones and thiazolines derivatives, synthesis, antimicrobial effects.

The introduction of a thiosemicarbazone moiety to alter the pharmacological activity of a variety of biologically active compounds has been demonstrated recently in several studies from this laboratory (1–5). Continuing such studies, the thiosemicarbazones (II–XIV) derived from various arylidenepyruvic acids and the corresponding thiazolines (XV–XXVII, Scheme I) were synthesized and tested for antimicrobial activity.

RESULTS AND DISCUSSION

Chemistry—The thio compounds (II–XXVII) were prepared as shown in Scheme I. A mixture of pyruvic acid or the properly substituted arylidenepyruvic acid (I), prepared through Claisen condensation of pyruvic acid and various aryl aldehydes (6), and an equivalent amount of 4-substituted 3-thiosemicarbazide was heated under reflux in aqueous acetic acid. The products (II–XIV) which separated on concentrating and cooling the mixtures, were crystallized from ethanol. The reaction of these

0022-3549/83/1000-1226$01.00/0

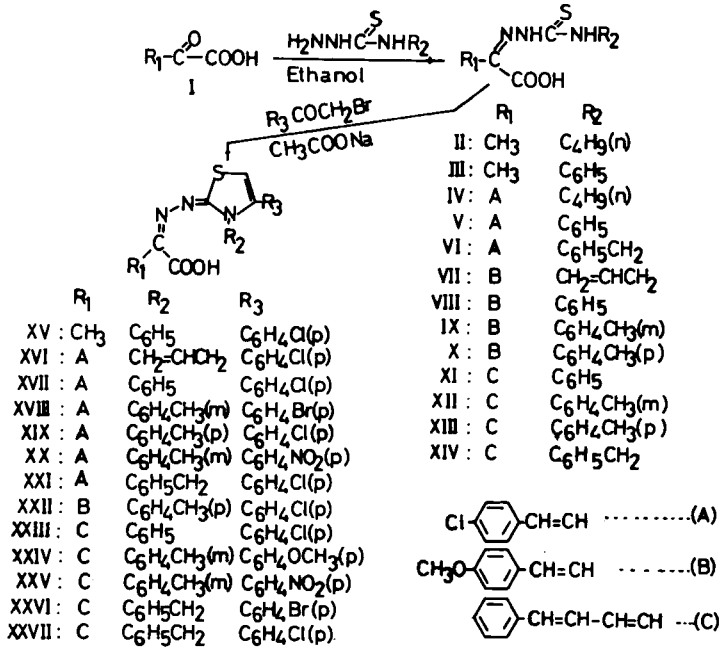

Scheme I

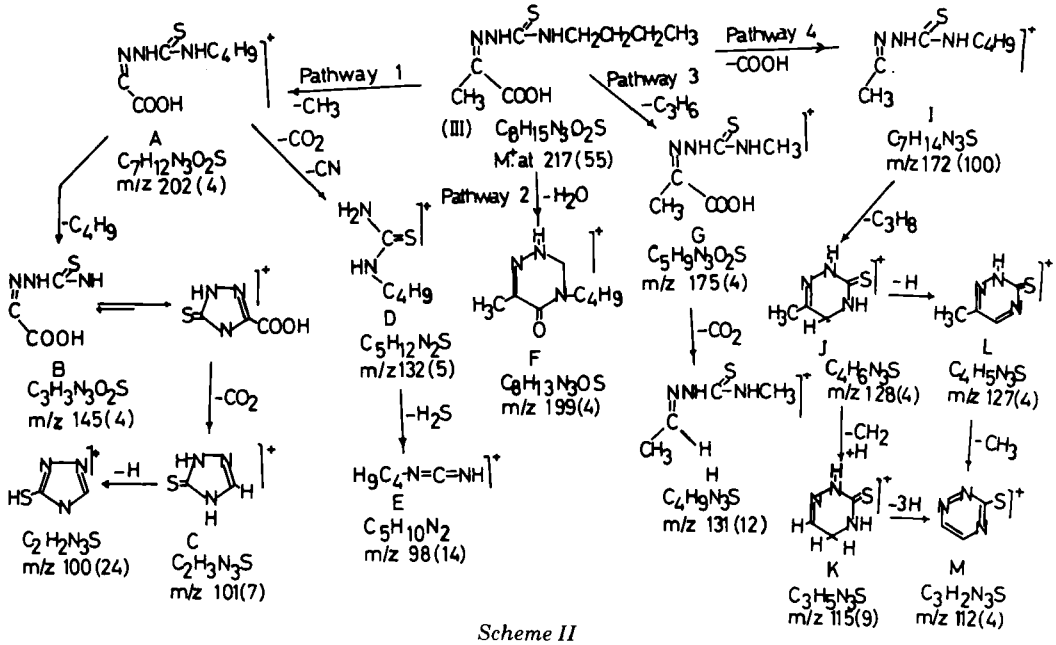

Scheme II

thiosemicarbazones with phenacyl bromide or the appropriately substituted phenacyl bromide and sodium acetate under reflux in ethanol yielded the arylidenepyruvic acid thiazoline derivatives (XV–XXVII).

The structure of the products was confirmed by IR and, for some representative examples, by ^{1}H-NMR spectral data. The IR spectra of the thiosemicarbazones (II–XIV) showed the bands characterizing the OH, NH, C=O, C=N, and NCS groups. Compounds XV–XXVII, on the other hand, lacked the NH absorption while showing absorption for C=O and C=N groups. The ^{1}H-NMR spectrum of III showed the CH_3 protons as a singlet at 2.21, the aromatic protons as a multiplet between 7.1 and 7.9, and the two NH and COOH protons as two singlets at 10.92 and 11.24 ppm, respectively. The spectrum of V showed the aromatic and the unsaturated side-chain protons as a multiplet between 7.0 and 8.1, while the protons of the COOH and the two NH functions appeared as singlets (disappearing on deuteration) at 10.92, 12.15, and 12.8 ppm, respectively. The spectra of the thiazolines XV and XXIV lacked the NH protons and showed the triazoline proton at 6.79 ppm.

The mass spectrum of III, as a representative example, showed the molecular ion peak at *m/z* 217 (Scheme II). This indicated that the molecule had undergone cleavage of a methyl group from the pyruvic acid portion to give ion *A* at *m/z* 202, (pathway 1). Ion *A* eliminated a butyl group forming the triazole ion *B*, at *m/z* 145, which eliminated carbon dioxide to give ion *C* at *m/z* 101. In an alternate way, ion *A* was found to eliminate carbon dioxide and a cyanide function to form the butylthiourea ion *D*, at *m/z* 132, which lost hydrogen sulfide to yield the carbodiimide ion *E* at *m/z* 98. In pathway 2, the molecule lost water to produce the triazine ion *F*, at *m/z* 199, while in pathway 3, the successive loss of propane and carbon dioxide gave ions *G* and *H* at *m/z* 175 and 131, respectively. The loss of a carboxylic function from the main product III (pathway 4) gave ion *I*, as the base peak, at *m/z* 172. This ion on losing propane gave ion *J*, at *m/z* 128, which on elimination of methylene and acceptance of hydrogen gave the triazine ion *K* at *m/z* 115. The loss of hydrogen from ion *J* followed by cleavage of the methyl group produced ions *L* and *M* at *m/z* 127 and 112, respectively.

Antimicrobial Screening—Using the serial dilution method in nutrient agar[1], all the products in concentrations of 100, 10, and 1 μg/ml were found to be inactive against *Escherichia coli* (NCTC 10418), *Klebsiella aerogenes* A, *Pseudomonas aeruginosa* (NCTC 10662), *Serratia mar-*

[1] The tests were performed in accordance with the protocol of antimicrobial screening of the Chemotherapeutic Research Centre, Beecham Pharmaceuticals, Brockham Park, Betchworth, Surrey, RH3 7AJ, United Kingdom.

Table I—Synthesized Thiosemicarbazones (II–XIV) and Thiazolines (XV–XXVII)

Compound	Yield, %	Melting Point	Molecular Formula	Analysis, %[a] C	H	N
II	92	197°	$C_8H_{15}N_3O_2S$	44.23 43.87	6.96 7.21	19.35 19.63
III	93	191–192°	$C_{10}H_{11}N_3O_2S$	50.63 50.74	4.67 4.77	17.72 17.93
IV	93	173–174°	$C_{15}H_{18}ClN_3O_2S$	53.02 53.30	5.30 5.40	12.37 12.72
V	91	185–186°	$C_{17}H_{14}ClN_3O_2S$	56.74 57.05	3.89 4.02	11.68 11.87
VI	95	194° (dec.)	$C_{18}H_{16}ClN_3O_2S$	57.83 57.73	4.28 4.34	11.24 11.47
VII	91	131–132°	$C_{15}H_{17}N_3O_3S$	56.42 56.69	5.37 5.53	13.16 13.01
VIII	94	183–184°	$C_{18}H_{17}N_3O_3S$	60.84 60.64	4.82 4.62	11.83 11.56
IX	93	254–255°	$C_{19}H_{19}N_3O_3S$	61.78 62.10	5.19 5.40	11.38 11.28
X	95	217–218°	$C_{19}H_{19}N_3O_3S$	61.78 61.72	5.19 5.48	11.38 11.62
XI	91	198° (dec.)	$C_{19}H_{17}N_3O_2S$	64.95 65.19	4.88 4.81	11.96 11.38
XII	93	168–169°	$C_{20}H_{19}N_3O_2S$	65.74 65.38	5.24 5.47	11.50 11.65
XIII	92	187–188°	$C_{20}H_{19}N_3O_2S$	65.74 65.38	5.24 5.10	11.50 11.69
XIV	95	204°	$C_{20}H_{19}N_3O_2S$	65.74 65.61	5.24 5.31	11.59 11.63
XV	75	148–149°	$C_{18}H_{13}ClN_3O_2S$	58.24 58.12	3.50 3.87	11.33 11.28
XVI	68	179–181°	$C_{22}H_{17}Cl_2N_3O_2S$	57.64 57.44	3.71 4.10	9.17 9.19
XVII	68	197°	$C_{25}H_{17}Cl_2N_3O_2S$	60.72 60.51	3.44 3.78	8.50 8.85
XVIII	68	251–253°	$C_{25}H_{19}BrClN_3O_2S$	56.47 56.53	3.43 3.57	7.60 7.89
XIX	68	193–195°	$C_{26}H_{19}Cl_2N_3O_2S$	61.41 61.23	3.74 3.71	8.26 8.11
XX	64	179–180°	$C_{26}H_{19}ClN_4O_4S$	60.17 60.46	3.60 3.93	10.80 10.56
XXI	72	207–209°	$C_{26}H_{19}Cl_2N_3O_2S$	61.41 61.20	3.74 3.83	8.26 8.05
XXII	70	181–183°	$C_{27}H_{22}ClN_3O_3S$	64.34 64.12	4.36 4.54	8.34 8.19
XXIII	69	220°	$C_{27}H_{20}ClN_3O_2S$	66.73 66.57	4.12 4.38	8.56 8.54
XXIV	72	118–120°	$C_{29}H_{25}N_3O_3S$	70.29 70.53	5.90 5.72	8.48 8.64
XXV	65	212–214°	$C_{28}H_{22}N_4O_4S$	65.87 64.68	4.34 4.37	10.98 10.67
XXVI	70	198–199°	$C_{28}H_{22}BrN_3O_2S$	61.76 61.43	4.04 4.36	7.72 7.33
XXVII	70	195–196°	$C_{28}H_{22}ClN_3O_2S$	67.26 67.17	4.40 4.62	8.41 8.65

[a] Calc. over found.

cescene (US32), *Staphylococcus aureus* Oxford, and *Candida albicans* (W97). Such inactivity, despite the antifungal and antimicrobial properties reported for arylidenepyruvic acid (7) and a variety of thiosemicarbazones (8–13), has been attributed to the bulk of the thiosemicarbazone moieties and the electronic changes caused by the presence of these groups on the α-carbon of the various arylidenepyruvic acids used. In the thiazoline derivatives (XV–XXVII), in which the 3- and 4-substituents were selected to fulfill the maximum requirement for hydrophobic π, electronic δ, and steric E_s factors in accordance with Topliss (14), the inactivity was assumed to be due to the bulky arylidenepyruvic acid hydrazone chains which, through intramolecular association with the remainder of the molecule, have hindered the permeability of tested compounds.

EXPERIMENTAL[2]

Substituted Thiosemicarbazone Arylidenepyruvic Acid Derivatives (II–XIV)—Equimolar amounts of pyruvic acid or the appropriately substituted arylidenepyruvic acid (I) (6) and the selected substituted thiosemicarbazides were heated under reflux in 80% aqueous acetic acid for 15–20 min. The mixtures were partially concentrated *in vacuo*, cooled, and the separated products recrystallized from ethanol. The yield and physical data of the products are recorded in Table I. IR (mineral oil): 3520–3420 (OH), 3360–3200 (NH), 1750–1690 (C=O), 1660–1580 (C=N and C=C), 1550–1515, 1315–1240, 1175–1157, and 970–930 cm^{-1} (NCS amide I, II, III, and IV bands, respectively). ^{1}H-NMR (III, DMSO-d_6): δ 2.21 (s, 3, CH_3), 7.1–7.9 (m, 5, Ar-H), and 10.92 and 11.24 ppm (2s, broad, 3, 2 × NH + COOH, disappearing on deuteration). ^{1}H-NMR (V, DMSO-d_6): δ 7.0–7.3 (m, 2, ethylene-H), 7.68 (s, 5, Ar-H), 7.5–8.1 (m, 4, Ar-H), and 10.9, 12.15, and 12.8 ppm (3s, 3, 2 × NH + COOH, disappearing on deuteration). Mass spectrum for III: *m/z* (relative abundance %) M^+ at 217 (65), 202 (4), 199 (4), 174 (22), 172 (100), 171 (4), 145 (4), 144 (5), 132 (5), 131 (12), 130 (20), 129 (4), 128 (4), 127 (4), 117 (4), 116 (59), 115 (9), 112 (4), 101 (7), 100 (24), 98 (14), 96 (31), 89 (13), 88 (59), 75 (19), 74 (11), 73 (14), 72 (61), and 70 (13).

Arylidenepyruvic Acid (3,4-Disubstituted 4-Thiazolin-2-ylidene)hydrazones (XV–XXVII)—An equimolar amount of the thiosemicarbazone derivatives (II–XIV) and phenacyl bromide or substituted phenacyl bromide and sodium acetate was heated under reflux in ethanol for 2–4 hr. The mixture was cooled, diluted with water, and the product removed by filtration. Recrystallization from ethanol or 90% aqueous ethanol gave XV–XXVII. The yields and physical constants of the synthesized thiazolines are recorded in Table I. IR (mineral oil): 3400–3200 (OH, associated), 1740–1660 (C=O), and 1620–1570 cm^{-1} (C=N and C=C).

REFERENCES

(1) A.-Mohsen M. E. Omar and N. S. Habib, *Pharmazie*, **33**, 81 (1978).

(2) A.-Mohsen M. E. Omar, S. M. El-Khawass, A. B. Makar, N. M. Bakry, and T. T. Daabees, *Pharmazie*, **33**, 577 (1978).

(3) El-Sebaii A. Ibrahim, A.-Mohsen M. E. Omar, M. A. Khalil, M. A. Makar, M. T. I. Soliman, and T. T. Daabees, *Pharmazie*, **35**, 80 (1980).

(4) A.-Mohsen M. E. Omar, S. A. Shams El-Dine, A. A. Ghobashy, and M. A. Khalil, *Eur. J. Med. Chem.*, **16**, 77 (1981).

(5) A.-Mohsen M. E. Omar, A. M. Farghaly, A. A. B. Hazzaa, N. H. Eshba, F. M. Sharabi, and T. T. Daabees, *J. Pharm. Sci.*, **70**, 1075 (1981).

(6) I. M. Roushdi, El-Sebaii A. Ibrahim, R. M. Shafik, and F. S. G. Soliman, *Pharmazie*, **27**, 731 (1972).

(7) E. Friedmann, *Nature (London)*, **135**, 108 (1935).

(8) H. R. Wilson, G. R. Revankan, and R. L. Tolman, *J. Med. Chem.*, **17**, 760 (1974).

(9) P. M. Sadler, *J. Org. Chem.*, **26**, 1315 (1961).

(10) W. H. Wagner and E. Winkelmann, *Arzneim.-Forsch.*, **22**, 1713 (1972).

(11) E. Winkelmann and H. Rolly, *Arzneim.-Forsch.*, **22**, 1704 (1972).

(12) D. J. Jones, R. Slack, S. Squires, and K. R. H. Wooldridge, *J. Med. Chem.*, **8**, 676 (1965).

(13) E. Winkelmann, W. H. Wagner, and H. Wirth, *Arzneim.-Forsch.*, **27**, 950 (1977).

(14) J. G. Topliss, *J. Med. Chem.*, **15**, 1006 (1972).

ACKNOWLEDGMENTS

Supported in part by Pharco Pharmaceuticals, Cairo, Egypt.

The authors thank the members of the Chemotherapeutic Research Centre, Beecham Pharmaceuticals, Brockham Park, Betchworth, Surrey, RH3 7 AJ, United Kingdom, for the antimicrobial screening.

[2] Melting points were determined in open capillaries and are uncorrected. IR spectra were measured on a Beckmann 4210 IR Spectrophotometer. ^{1}H-NMR spectra were determined on Varian A60, while the mass spectra were recorded on EAI.MS-50.

Models of Hepatic Drug Elimination

Keyphrases □ Hepatic drug clearance—saturation kinetics, sinusoidal perfusion model, venous equilibrium model □ Heterogeneity of organ extraction—intrahepatic shunts

To the Editor:

In a recent communication (1) Morgan and Raymond identify observable quantities which would help to discriminate between two models of drug uptake by the intact liver: the venous equilibration model (2) and the undistributed sinusoidal perfusion model (3, 4). Several comments are necessary in light of recent results.

In the case of hepatic elimination of galactose, the two models have already been refuted experimentally: the first at 0.01 (5) and the second at 0.002 (6, 7) levels of statistical significance. To be so decisive, these experiments involved substrate concentrations across the entire Michaelis–Menten range, whereas Morgan and Raymond (1) confine their considerations to the limiting forms of the models at substrate concentrations so low that the hepatic uptake kinetics become linear (first order).

The quantitative results which refute the undistributed sinusoidal perfusion model give strong support to the distributed sinusoidal perfusion model (7, 8) not discussed by Morgan and Raymond (1). Michaelis–Menten uptake by a single perfused sinusoid is treated the same in the undistributed (4) and distributed (8) models, but the distributed model drops the biologically incredible assumption that all sinusoids extract equally: it incorporates and quantifies functional heterogeneity of sinusoids and its effect on organ uptake.

Envisage an intact liver with hepatic blood flow rate F and, for some enzyme–substrate combination, the Michaelis constants, V_{max} and K_m (intrinsic hepatic clearance V_{max}/K_m), resulting in a steady uptake rate:

$$V = F(C_i - C_o) \qquad \text{(Eq. 1)}$$

when the substrate concentration is C_i at the inlet and C_o at the outlet of the liver. For N sinusoids acting in parallel, the undistributed model asserts that the corresponding quantities for each sinusoid are:

$$f = F/N = \bar{f},\ v_{max} = V_{max}/N = \bar{v}_{max},\ v = V/N = \bar{v} \qquad \text{(Eq. 2)}$$

By contrast, the distributed model works with statistical dispersions of v_{max} and f (about their means $\bar{v}_{max}$ and $\bar{f}$) over the assembly of sinusoids comprising a liver. It is, in fact, the dispersion of the ratio v_{max}/f that controls deviations from the undistributed model in the context of uptake (7).

Now, let an arbitrary distribution of v_{max}/f over the sinusoids of an intact liver have the variance σ^2. A remarkable feature of Michaelis–Menten kinetics [and of more general saturation kinetics (7, 9)] is that when it is put in the hepatic setting, the rate of uptake by an undistributed liver, $V(\sigma^2 = 0)$, is always greater than the rate of uptake by a distributed liver, $V(\sigma^2)$, which has the same values of the macroscopic parameters F, V_{max}, K_m. The rate $V(\sigma^2 = 0)$ is thus an *upper limit* of the rate $V(\sigma^2)$; it is remarkably close in some cases (7, 10). There is also a lower limit of $V(\sigma^2)$ valid for any shape of the v_{max}/f distribution (7). For Michaelis–Menten kinetics:

$$V(\sigma^2 = 0) \geqq V(\sigma^2) \geqq V(\sigma^2 = 0) - 2F\sigma^2/(27K_m) \qquad \text{(Eq. 3)}$$

This exact result will suffice to indicate how functional heterogeneity of the intact liver can be studied in terms of the distributed model. A clinically interesting problem of this kind is the quantification of intrahepatic shunts (8), since such shunts are kinetically equivalent to a fraction of sinusoids with $v_{max} = 0, f \neq 0$.

The study by Keiding and Chiarantini (5) went beyond merely refuting the venous equilibration model: it set a calculable upper limit on the possible values of σ^2 in the rat liver (10). An altogether different attempt at discriminating between the venous equilibration model and the undistributed perfusion model has been made by Pang and Gillette using the hepatic conversion of a substrate into a metabolite, which is in turn conjugated in liver cells (11). When suitably interpreted, the results of the experiment neither refute nor confirm the sinusoidal perfusion model, but rather give information about functional heterogeneity of the liver along the blood flow [zones of liver function (12 and references therein)].

The aforementioned comments emphasize the fruitfulness of the controversy touched upon recently (1), which is surely a sufficient consolation for the refutation of both the contending models.

(1) D. J. Morgan and K. Raymond, *J. Pharm. Sci.*, **71**, 600 (1982).
(2) M. Rowland, L. Z. Benet, and G. G. Graham, *J. Pharmacokinet. Biopharm.*, **1**, 123 (1973).
(3) K. Winkler, S. Keiding, and N. Tygstrup, in "The Liver," G. Paumgartner and R. Preisig, Eds., Karger, Basel, Switzerland, 1973, pp. 145–155.
(4) L. Bass, S. Keiding, K. Winkler, and N. Tygstrup, *J. Theor. Biol.*, **61**, 393 (1976).
(5) S. Keiding and E. Chiarantini, *J. Pharmacol. Exp. Ther.*, **205**, 465 (1978).
(6) S. Keiding, S. Johansen, K. Winkler, K. Tønnesen, and N. Tygstrup, *Am. J. Physiol.*, **230**, 1302 (1976).
(7) L. Bass and P. J. Robinson, *Microvasc. Res.*, **22**, 43 (1981).
(8) L. Bass, P. J. Robinson, and A. J. Bracken, *J. Theor. Biol.*, **72**, 161 (1978).
(9) S. Johansen and S. Keiding, *J. Theor. Biol.*, **89**, 549 (1981).
(10) L. Bass and P. J. Robinson, *J. Theor. Biol.*, **81**, 761 (1979).
(11) K. S. Pang and J. R. Gillette, *J. Pharmacol. Exp. Ther.*, **207**, 178 (1978).
(12) L. Bass, *Gastroenterology*, **81**, 976 (1981).

Ludvik Bass
Department of Mathematics
University of Queensland
St. Lucia 4067
Australia

Received November 30, 1982.
Accepted for publication May 11, 1983.

0022-3549/83/1000-1229$01.00/0

Models of Hepatic Drug Elimination: A Response

Keyphrases □ Hepatic drug clearance—sinusoidal perfusion model, venous equilibrium model

To the Editor:

Although the distributed sinusoidal perfusion model of hepatic elimination described by Bass (1) appears more physiologically realistic than the two previous models, the statement that these latter models have been refuted experimentally should be challenged. First, the data on which this statement is based arise from only two studies (2, 3) and are not as conclusive as implied (1). The study design used in one of these studies (2) has already been acknowledged as not very useful for discriminating among the models in an earlier publication (4). In the other study (3) hepatic venous outflow concentrations of galactose were examined in the perfused rat liver under the influence of two perfusate flow rates (11 ml/min for 50 min, followed by 7 ml/min for 40 min, followed by 11 ml/min for 40 min). The sinusoidal models predict a lowering of the outflow substrate concentration at the lower flow rate, while the venous equilibrium model predicts no change in the outflow substrate concentration. A significant drop in outflow concentration was reported (3), but this was largely determined by averaging the data from the two periods of higher flow even though in about half the 10 experiments the outflow concentration during the second period was considerably greater than the outflow concentration during the first period.

One of the reviewers of this report has highlighted this fact by showing that a paired t test of outflow concentration during the two 11-ml/min flow periods, which were separated by 40 min of perfusion at 7 ml/min (or a constant flow of 11 ml/min in the three control studies), yields a statistically significant difference at the $p < 0.05$ level ($t = 2.19$ $DF = 12$). Similarly, when inflow concentration from these two time periods with a flow at 11 ml/min are tested, a statistically significant difference $p < 0.05$ ($t = 2.24$, $DF = 12$) is observed. One assumption necessary to ensure the legitimacy of all of the calculations performed by Bass is that the liver preparation is physiologically stable over the course of the experiment. Specifically, if a liver is infused with substrate at a constant rate, inflow and outflow concentrations should depend only on hepatic blood flow rate (*i.e.* V_{max} and K_m should not vary as a function of time).

Comparing the first two flow periods only (11 ml/min and 7 ml/min), during which the preparation is more reliable, the outflow of galactose concentrations actually increased in three experiments, decreased by no more than that of control livers (about 10%) in two livers, and decreased more substantially in the other five. Thus, the data could be viewed as inconclusive. Bass has also used the data from the earlier study (3) to support the distributed sinusoidal model (4) which predicts an increase in the logarithmic average of perfusate inflow and outflow concentrations of substrate with decreasing flow. The logarithmic average concentration, however, increased in only 5 of the 10 experiments, the mean change being 0.0009 mM ($SD = 0.0267$), a change of barely 1%: again not conclusive.

The other point that should be made is that the published data on lidocaine (5) supporting the venous equilibrium model have never been refuted by further experimentation with that drug. The studies with galactose cannot be assumed to automatically hold for all other substrates because the experiments were carried out under Michaelis–Menten conditions, galactose is an endogenous substance, and the zone of the liver in which a substance is eliminated (6) may dictate which model applies. For example, a substance, such as galactose, that is eliminated in the periportal region may be expected to follow the distributed sinusoidal model, whereas the venous equilibrium model may be appropriate for drugs that are eliminated in the centrilobular region where the enzymes for drug biotransformation are predominant (6). Therefore, in view of the functional hepatocellular heterogeneity it is naive to assume that all observed phenomena can be explained in terms of a single model as suggested (1). Models will, however, have served their function if they provide inspiration for further experimentation, as suggested previously (7), that ultimately results in more refined and physiologically meaningful models.

(1) L. Bass, *J. Pharm. Sci.*, **72**, 1229 (1983).
(2) S. Keiding, S. Johansen, K. Winkler, K. Tønnesen, and N. Tygstrup, *Am. J. Physiol.*, **230**, 1302 (1976).
(3) S. Keiding and E. Chiarantini, *J. Pharmacol. Exp. Ther.*, **205**, 465 (1978).
(4) L. Bass and P. J. Robinson, *J. Theor. Biol.*, **81**, 761 (1979).
(5) K. S. Pang and M. Rowland, *J. Pharmacokinet. Biopharm.*, **5**, 655 (1977).
(6) K. Jungermann and N. Katz, *Hepatology*, **2**, 385 (1982).
(7) D. J. Morgan and K. Raymond, *J. Pharm. Sci.*, **71**, 600 (1982).

Denis J. Morgan
Victorian College of Pharmacy
Parkville
Victoria, Australia, 3052

Received January 11, 1983.
Accepted for publication June 6, 1983.

Hepatic Extraction of Free Fatty Acids in Pregnant and Nonpregnant Female Rats

Keyphrases □ Free fatty acids—hepatic extraction □ Plasma protein binding—role of free fatty acids □ Hepatic drug clearance, intrinsic—role of drug protein binding and influence of free fatty acids

To the Editor:

Plasma protein binding can have important effects on the metabolic and excretory clearance of drugs (1, 2). Free fatty acids, whose concentrations in plasma can vary appreciably due to stress, diet, and other physiological variables (3), can competitively inhibit the plasma protein binding of many drugs (4, 5). Wiegand and Levy (6) have pointed out previously that extensive hepatic extraction of a protein binding inhibitor could cause an increase in the steady-state plasma concentration of unbound drug, with little or no effect on the concentration of total (free plus bound) drug, if the plasma protein binding of the drug

0022-3549/83/1000-1230$01.00/0

Models of Hepatic Drug Elimination: A Response

Keyphrases □ Hepatic drug clearance—sinusoidal perfusion model, venous equilibrium model

To the Editor:

Although the distributed sinusoidal perfusion model of hepatic elimination described by Bass (1) appears more physiologically realistic than the two previous models, the statement that these latter models have been refuted experimentally should be challenged. First, the data on which this statement is based arise from only two studies (2, 3) and are not as conclusive as implied (1). The study design used in one of these studies (2) has already been acknowledged as not very useful for discriminating among the models in an earlier publication (4). In the other study (3) hepatic venous outflow concentrations of galactose were examined in the perfused rat liver under the influence of two perfusate flow rates (11 ml/min for 50 min, followed by 7 ml/min for 40 min, followed by 11 ml/min for 40 min). The sinusoidal models predict a lowering of the outflow substrate concentration at the lower flow rate, while the venous equilibrium model predicts no change in the outflow substrate concentration. A significant drop in outflow concentration was reported (3), but this was largely determined by averaging the data from the two periods of higher flow even though in about half the 10 experiments the outflow concentration during the second period was considerably greater than the outflow concentration during the first period.

One of the reviewers of this report has highlighted this fact by showing that a paired t test of outflow concentration during the two 11-ml/min flow periods, which were separated by 40 min of perfusion at 7 ml/min (or a constant flow of 11 ml/min in the three control studies), yields a statistically significant difference at the $p < 0.05$ level ($t = 2.19$ $DF = 12$). Similarly, when inflow concentration from these two time periods with a flow at 11 ml/min are tested, a statistically significant difference $p < 0.05$ ($t = 2.24$, $DF = 12$) is observed. One assumption necessary to ensure the legitimacy of all of the calculations performed by Bass is that the liver preparation is physiologically stable over the course of the experiment. Specifically, if a liver is infused with substrate at a constant rate, inflow and outflow concentrations should depend only on hepatic blood flow rate (*i.e.* V_{max} and K_m should not vary as a function of time).

Comparing the first two flow periods only (11 ml/min and 7 ml/min), during which the preparation is more reliable, the outflow of galactose concentrations actually increased in three experiments, decreased by no more than that of control livers (about 10%) in two livers, and decreased more substantially in the other five. Thus, the data could be viewed as inconclusive. Bass has also used the data from the earlier study (3) to support the distributed sinusoidal model (4) which predicts an increase in the logarithmic average of perfusate inflow and outflow concentrations of substrate with decreasing flow. The logarithmic average concentration, however, increased in only 5 of the 10 experiments, the mean change being 0.0009 mM ($SD = 0.0267$), a change of barely 1%: again not conclusive.

The other point that should be made is that the published data on lidocaine (5) supporting the venous equilibrium model have never been refuted by further experimentation with that drug. The studies with galactose cannot be assumed to automatically hold for all other substrates because the experiments were carried out under Michaelis–Menten conditions, galactose is an endogenous substance, and the zone of the liver in which a substance is eliminated (6) may dictate which model applies. For example, a substance, such as galactose, that is eliminated in the periportal region may be expected to follow the distributed sinusoidal model, whereas the venous equilibrium model may be appropriate for drugs that are eliminated in the centrilobular region where the enzymes for drug biotransformation are predominant (6). Therefore, in view of the functional hepatocellular heterogeneity it is naive to assume that all observed phenomena can be explained in terms of a single model as suggested (1). Models will, however, have served their function if they provide inspiration for further experimentation, as suggested previously (7), that ultimately results in more refined and physiologically meaningful models.

(1) L. Bass, *J. Pharm. Sci.*, **72**, 1229 (1983).
(2) S. Keiding, S. Johansen, K. Winkler, K. Tønnesen, and N. Tygstrup, *Am. J. Physiol.*, **230**, 1302 (1976).
(3) S. Keiding and E. Chiarantini, *J. Pharmacol. Exp. Ther.*, **205**, 465 (1978).
(4) L. Bass and P. J. Robinson, *J. Theor. Biol.*, **81**, 761 (1979).
(5) K. S. Pang and M. Rowland, *J. Pharmacokinet. Biopharm.*, **5**, 655 (1977).
(6) K. Jungermann and N. Katz, *Hepatology*, **2**, 385 (1982).
(7) D. J. Morgan and K. Raymond, *J. Pharm. Sci.*, **71**, 600 (1982).

Denis J. Morgan
Victorian College of Pharmacy
Parkville
Victoria, Australia, 3052

Received January 11, 1983.
Accepted for publication June 6, 1983.

Hepatic Extraction of Free Fatty Acids in Pregnant and Nonpregnant Female Rats

Keyphrases □ Free fatty acids—hepatic extraction □ Plasma protein binding—role of free fatty acids □ Hepatic drug clearance, intrinsic—role of drug protein binding and influence of free fatty acids

To the Editor:

Plasma protein binding can have important effects on the metabolic and excretory clearance of drugs (1, 2). Free fatty acids, whose concentrations in plasma can vary appreciably due to stress, diet, and other physiological variables (3), can competitively inhibit the plasma protein binding of many drugs (4, 5). Wiegand and Levy (6) have pointed out previously that extensive hepatic extraction of a protein binding inhibitor could cause an increase in the steady-state plasma concentration of unbound drug, with little or no effect on the concentration of total (free plus bound) drug, if the plasma protein binding of the drug

0022-3549/83/1000-1230$01.00/0

Table I—Hepatic Extraction of Free Fatty Acids in Pregnant and Nonpregnant Female Rats [a]

	Pregnant			Nonpregnant		
	Venous Plasma Conc., μM		Hepatic	Venous Plasma Conc., μM		Hepatic
	Hepatic	Femoral	Extraction Ratio	Hepatic	Femoral	Extraction Ratio
Palmitic	87.1 ± 16.4	144 ± 28	0.391 ± 0.068	96.1 ± 12.4	149 ± 28	0.347 ± 0.087
Stearic	36.2 ± 7.8	51.4 ± 11.5	0.293 ± 0.078	44.9 ± 2.9[b]	54.1 ± 4.6	0.164 ± 0.102
Oleic	95.1 ± 14.6	170 ± 30	0.434 ± 0.081	105 ± 17	177 ± 43	0.391 ± 0.122
Linoleic	56.8 ± 10.7	113 ± 21	0.484 ± 0.113	76.2 ± 20.0	157 ± 51	0.504 ± 0.070

[a] Results are reported as mean ± SD, $n = 5$. [b] Significantly different from corresponding value in pregnant rats ($p < 0.05$).

is decreased with increasing inhibitor concentration. Such a change in drug concentration, apart from its pharmacodynamic implications (6), could be interpreted as a decrease in the drug's intrinsic clearance. Based on these considerations, we have determined the hepatic extraction of the four major endogenous free fatty acids in rats. Since the hepatic extraction of compounds is affected by their plasma protein binding and intrinsic hepatic clearance, studies were conducted also on pregnant rats, because pregnancy is associated with decreased plasma albumin concentration and decreased activity of certain oxidative metabolic processes (7, 8).

Female Sprague–Dawley rats (same age), both nonpregnant (≃200 g) and 20-days pregnant, had a cannula inserted in the femoral vein under ether anesthesia. The liver was then exposed through a midline abdominal incision. The liver lobules were reflected with wet gauze and the hepatic vein was clamped near its junction with the vena cava to avoid mixing blood from the liver with blood from the general circulation. Either 1 or 2 ml of blood was obtained from the hepatic vein by direct insertion of a 22-gauge hypodermic needle pointing toward the liver (9). Simultaneously, a blood sample from the femoral vein was obtained through the indwelling cannula. The blood was collected in plastic syringes containing EDTA (≃2 mg/ml of blood) and the plasma separated by centrifugation. The plasma was extracted into hexane within 5 min after blood collection, and the concentrations of the free fatty acids (as their methyl esters) were determined by GC by the method of Brunk and Swanson (10), but using smaller sample volumes and n-heptadecanoic acid rather than n-pentadecanoic acid as the internal standard.

The results of the study are summarized in Table I. The concentrations of the four major endogenous free fatty acids were considerably lower in hepatic venous plasma than in plasma from blood taken from the femoral vein. Linoleic acid was most extensively extracted, while the hepatic extraction of stearic acid was least pronounced. Plasma from pregnant rats is subject to rapid *in vitro* lipolysis which was minimized by rapid extraction of the plasma with organic solvent (11). Under these conditions the fatty acid concentrations in plasma of pregnant rats were similar to those in plasma of nonpregnant animals. There was no significant difference between pregnant and nonpregnant animals with respect to the hepatic extraction ratio of the individual free fatty acids. Hepatic vein–femoral vein albumin concentration ratios, determined in another experiment, were (mean ± SD) 1.03 ± 0.13, n = 4, for pregnant rats and 0.998 ± 0.056, n = 11, for nonpregnant animals.

The hepatic extraction values reported here are based on net concentration differences caused by hepatic extraction, and by hepatic output of free fatty acids synthesized by the liver (12). A contribution by extrahepatic tissues to the observed net concentration changes is also possible since solute concentrations in the femoral venous blood may not be the same as the concentrations in blood entering the liver (13). However, the femoral vein sampling site is appropriate because the usual pharmacokinetic studies involve blood sampling from a peripheral vein.

It has been reported (9) that ether anesthesia caused liver blood flow in rats to decrease from an average of 60.5 to 33.8 ml/min/kg. Unless ether anesthesia also causes a corresponding decrease in the intrinsic hepatic clearance of fatty acids, the extraction ratios reported here may be somewhat higher than the hepatic extraction ratios in nonanesthetized rats.

It is customary to determine the intrinsic clearance of drugs on the basis of the infusion rate and the steady-state concentration of unbound drug in plasma of blood taken from a peripheral vein. If the plasma protein binding of the drug is inhibited by free fatty acids in a concentration-dependent manner, then the free fraction of the drug in the blood entering the liver (and in the systemic circulation) is higher than that in blood leaving the liver, due to the decrease of the free fatty acid concentrations across the liver. Under these conditions, estimates of a drug's intrinsic clearance may be lower than the true value. This is particularly troublesome since free fatty acids are known to inhibit certain drug biotransformation processes (14, 15). An apparent decrease in the intrinsic clearance of a drug due to elevation of free fatty acids (5, 16) may represent the combined effects of metabolic inhibition and a change in plasma protein binding in the blood as it passes through the liver.

(1) G. Levy and A. Yacobi, *J. Pharm. Sci.*, **63**, 805 (1974).

(2) G. Levy, *J. Pharm. Sci.*, **69**, 482 (1980).

(3) R. G. McDonald-Gibson, M. Young, and F. E. Hytten, *Br. J. Obstet. Gynaecol.*, **82**, 460 (1975).

(4) W. J. Jusko and M. Gretch, *Drug Metab. Rev.*, **5**, 43 (1976).

(5) I. Johno, M.-Y. Huang, and R. H. Levy, *Epilepsia*, **23**, 649 (1982).

(6) U. W. Wiegand and G. Levy, *J. Pharm. Sci.*, **69**, 480 (1980).

(7) M. Dean, B. Stock, and G. Levy, *Clin. Pharmacol. Ther.*, **28**, 253 (1980).

(8) R. Kato, *Xenobiotica*, **7**, 25 (1977).

(9) M. Yokota, T. Iga, S. Awazu, and M. Hanano, *J. Appl. Physiol.*, **41**, 439 (1976).

(10) S. D. Brunk and J. R. Swanson, *Clin. Chem.*, **27**, 924 (1981).

(11) R. C. Chou, Ph.D. Thesis, State University of New York at Buffalo, 1983.

(12) L. Hummel, T. Zimmermann, H. Schenk, A. Schwartze, W. Schirrmeister, and H. Wagner, *Acta Biol. Med. Ger.*, **37**, 259 (1978).

(13) W. E. Connor and J. W. Eckstein, *J. Clin. Invest.*, **38**, 1746 (1959).

(14) R. P. Di Augustine and J. R. Fouts, *Biochem. J.*, **115**, 547 (1969).

(15) M. Lang, *Gen. Pharmacol.*, **7**, 415 (1976).

(16) L. A. Bowdle, I. H. Patel, R. H. Levy, and A. J. Wilensky, *Eur. J. Clin. Pharmacol.*, **23**, 343, 1982.

Ruby C. Chou
Ulf W. Wiegand
David M. Soda
Gerhard Levy ˣ
Department of Pharmaceutics
School of Pharmacy
State University of New York at Buffalo
Amherst, NY 14260

Received April 11, 1983.
Accepted for publication June 22, 1983.

Supported in part by Grant GM 20852 from the National Institute of General Medical Sciences, National Institutes of Health.

Albumin Binding and Hepatic Uptake: The Importance of Model Selection

Keyphrases □ Albumin—effect on removal of taurocholate by the liver □ Taurocholate—removal by liver, albumin

To the Editor:

Dr. Colburn's letter to the *Journal* in March 1982 (1) purports to invalidate a conclusion we published earlier in the *Journal of Clinical Investigation* (2) concerning the role of albumin binding on the removal of taurocholate by the perfused rat liver. Having just learned of Colburn's communication we offer the following rebuttal. Better late than never!

The observations we reported (which are not in contention) show that the extraction fraction of taurocholate declines only slightly when the perfusate albumin concentration is increased, even though this maneuver reduces the free (unbound) fraction of taurocholate by a factor of five. The table shows the data for rat livers perfused at the same flow rate and with the same total concentration of taurocholate (18 μM).

Albumin Concentration (g/dl)	Free Fraction of Taurocholate in Perfusate	Taurocholate Extraction Fraction
0.5	0.57	0.97
5.0	0.11	0.86

The objective of the experiment was to learn what these numbers imply about the apparent rate constant for hepatic uptake, given that the low concentration of taurocholate ensures that both the binding reaction in extracellular fluid and the removal process are operating far removed from saturation and that the binding reaction is fast enough compared with the removal rate to be considered at equilibrium. These stipulations are also not in contention. Instead the controversy focuses on the choice of an appropriate model with which to interpret the data.

Colburn prefers to model the extracellular fluid as a single homogeneous compartment in which each liver cell is exposed to the same taurocholate concentration—the so-called "lumped" or "venous equilibrium model." In this case the steady-state conservation equation is:

$$Fu_0 = \psi VKu_v + Fu_v \qquad \text{(Eq. 1)}$$

in which ψ is the free fraction, F is perfusate flow, K is the rate constant for removal of free taurocholate, and V is the extracellular volume. The terms, u_0 and u_v, in Eq. 1 are the inflow and outflow concentrations of total taurocholate, respectively. Rearranging Eq. 1 yields:

$$K = FE/[\psi V(1 - E)] \qquad \text{(Eq. 2)}$$

in which the extraction fraction, E, is $(u_0 - u_v)/u_0$. Equation 2 is the one suggested by Wilkinson and Shand (3) to whom Colburn appeals for support.

We have preferred to use a so-called "distributed" model accounting for the decline in taurocholate concentration that occurs along each sinusoid. The conservation relation for a single sinusoid is in this case:

$$F\frac{du}{dx} = -\psi\gamma Ku \qquad \text{(Eq. 3)}$$

where x is the sinusoidal volume running from $x = 0$ at the portal inlet to $x = V$ at the hepatic venous outlet and γ is the ratio of the sinusoidal volume to the volume of the Disse space divided by the sinusoidal volume. The solution to Eq. 3 is:

$$K = -F\ln(1 - E)/\psi\gamma V \qquad \text{(Eq. 4)}$$

If one now computes the ratio of the K values from the observations made with high and low concentrations of albumin, the results are strikingly different depending on the choice of the model.

$\frac{K \text{ at high albumin}}{K \text{ at low albumin}}$	Lumped Model	Distributed Model
	0.98	2.9

The interest in these calculations derives from the fact that both models are constructed on the conventional teaching that only free taurocholate is available for removal. If we accept Colburn's model this assumption appears confirmed because the calculations yield the expected identity of the rate constants. If we accept the distributed model, however, the data contradict the conventional teaching because in this case the rate constants differ by nearly a factor of three. The direction of the discrepancy is such that liver cells appear to enjoy some special mechanism for enhancing the dissociation of the albumin–ligand complex—in effect making more free taurocholate available to liver cells than the conventional teaching would predict. There is, in fact, a growing body of additional evidence to support this conclusion (4–7), but our concern here is with the question of which model to accept.

Those who choose the Colburn model will have to decide where the change from u_0 to u_v occurs. Plainly it cannot be attributed to the removal of taurocholate by hepatocytes because the model requires that all liver cells be exposed to the same concentration. Alternative choices that the drop in concentration occurs in the presinusoidal portal circulation or in the postsinusoidal hepatic veins would not only be anatomic nonsense but would imply that the calculated rate constant has nothing whatever to do with the transport function of liver cells. On this basis we conclude that although Colburn's analysis of the data appears to confirm a widely held preconception, it is physiologically irrelevant. His model simply does not describe a real liver.

0022-3549/83/1000-1232$01.00/0

Ruby C. Chou
Ulf W. Wiegand
David M. Soda
Gerhard Levy ˣ
Department of Pharmaceutics
School of Pharmacy
State University of New York at Buffalo
Amherst, NY 14260

Received April 11, 1983.
Accepted for publication June 22, 1983.

Supported in part by Grant GM 20852 from the National Institute of General Medical Sciences, National Institutes of Health.

Albumin Binding and Hepatic Uptake: The Importance of Model Selection

Keyphrases □ Albumin—effect on removal of taurocholate by the liver □ Taurocholate—removal by liver, albumin

To the Editor:

Dr. Colburn's letter to the *Journal* in March 1982 (1) purports to invalidate a conclusion we published earlier in the *Journal of Clinical Investigation* (2) concerning the role of albumin binding on the removal of taurocholate by the perfused rat liver. Having just learned of Colburn's communication we offer the following rebuttal. Better late than never!

The observations we reported (which are not in contention) show that the extraction fraction of taurocholate declines only slightly when the perfusate albumin concentration is increased, even though this maneuver reduces the free (unbound) fraction of taurocholate by a factor of five. The table shows the data for rat livers perfused at the same flow rate and with the same total concentration of taurocholate (18 μM).

Albumin Concentration (g/dl)	Free Fraction of Taurocholate in Perfusate	Taurocholate Extraction Fraction
0.5	0.57	0.97
5.0	0.11	0.86

The objective of the experiment was to learn what these numbers imply about the apparent rate constant for hepatic uptake, given that the low concentration of taurocholate ensures that both the binding reaction in extracellular fluid and the removal process are operating far removed from saturation and that the binding reaction is fast enough compared with the removal rate to be considered at equilibrium. These stipulations are also not in contention. Instead the controversy focuses on the choice of an appropriate model with which to interpret the data.

Colburn prefers to model the extracellular fluid as a single homogeneous compartment in which each liver cell is exposed to the same taurocholate concentration—the so-called "lumped" or "venous equilibrium model." In this case the steady-state conservation equation is:

$$Fu_0 = \psi VKu_v + Fu_v \qquad \text{(Eq. 1)}$$

in which ψ is the free fraction, F is perfusate flow, K is the rate constant for removal of free taurocholate, and V is the extracellular volume. The terms, u_0 and u_v, in Eq. 1 are the inflow and outflow concentrations of total taurocholate, respectively. Rearranging Eq. 1 yields:

$$K = FE/[\psi V(1 - E)] \qquad \text{(Eq. 2)}$$

in which the extraction fraction, E, is $(u_0 - u_v)/u_0$. Equation 2 is the one suggested by Wilkinson and Shand (3) to whom Colburn appeals for support.

We have preferred to use a so-called "distributed" model accounting for the decline in taurocholate concentration that occurs along each sinusoid. The conservation relation for a single sinusoid is in this case:

$$F\frac{du}{dx} = -\psi\gamma Ku \qquad \text{(Eq. 3)}$$

where x is the sinusoidal volume running from $x = 0$ at the portal inlet to $x = V$ at the hepatic venous outlet and γ is the ratio of the sinusoidal volume to the volume of the Disse space divided by the sinusoidal volume. The solution to Eq. 3 is:

$$K = -F\ln(1 - E)/\psi\gamma V \qquad \text{(Eq. 4)}$$

If one now computes the ratio of the K values from the observations made with high and low concentrations of albumin, the results are strikingly different depending on the choice of the model.

$\frac{K \text{ at high albumin}}{K \text{ at low albumin}}$	Lumped Model	Distributed Model
	0.98	2.9

The interest in these calculations derives from the fact that both models are constructed on the conventional teaching that only free taurocholate is available for removal. If we accept Colburn's model this assumption appears confirmed because the calculations yield the expected identity of the rate constants. If we accept the distributed model, however, the data contradict the conventional teaching because in this case the rate constants differ by nearly a factor of three. The direction of the discrepancy is such that liver cells appear to enjoy some special mechanism for enhancing the dissociation of the albumin–ligand complex—in effect making more free taurocholate available to liver cells than the conventional teaching would predict. There is, in fact, a growing body of additional evidence to support this conclusion (4–7), but our concern here is with the question of which model to accept.

Those who choose the Colburn model will have to decide where the change from u_0 to u_v occurs. Plainly it cannot be attributed to the removal of taurocholate by hepatocytes because the model requires that all liver cells be exposed to the same concentration. Alternative choices that the drop in concentration occurs in the presinusoidal portal circulation or in the postsinusoidal hepatic veins would not only be anatomic nonsense but would imply that the calculated rate constant has nothing whatever to do with the transport function of liver cells. On this basis we conclude that although Colburn's analysis of the data appears to confirm a widely held preconception, it is physiologically irrelevant. His model simply does not describe a real liver.

0022-3549/83/1000-1232$01.00/0

The distributed model, though possibly oversimplified as well, is certainly a much better representation of the physiological facts. It may even be correct, because on closer inspection (2, 4) the distributed model turns out to be free of restrictive assumptions that the sinusoids are of uniform bore or that each liver cell has the same transport capacity. The interpretation moreover is virtually independent of variations in the distribution of flow to a large population of sinusoids.

Compartmental analysis is a powerful tool for gaining new physiological insights. Its utility, however, depends critically on the validity of the underlying assumptions. If these are wrong so will be the results. The worst of this is that model-dependent interpretations of the data can rarely, if ever, be used to validate the preconceptions on which the model was constructed. We suggest that Colburn may wish to reconsider the simplistic assumptions on which his model rests before taking too seriously the conclusions that flow from it.

(1) W. A. Colburn, *J. Pharm. Sci.*, **71**, 373 (1982).
(2) E. L. Forker and B. A. Luxon, *J. Clin. Invest.*, **67**, 1517 (1981).
(3) G. R. Wilkinson and D. G. Shand, *Clin. Pharmacol. Ther.*, **18**, 377 (1975).
(4) E. L. Forker, B. A. Luxon, M. Snell, and N. Shurmantine, *J. Pharm. Exp. Ther.*, **223**(2), 342 (1982).
(5) R. Weisiger, J. Gollan, and R. Ockner, *Science*, **211**, 1048 (1981).
(6) E. L. Forker, and B. A. Luxon, *J. Clin. Invest.*, in press, 1983.
(7) J. Barnhart, W. Hardison, B. Witt, and R. Berk, *Am. J. Physiol.*, in press, 1983.

E. L. Forker ˣ
B. A. Luxon
Department of Medicine
University of Missouri-Columbia
Columbia, MO 65212

Received May 2, 1983.
Accepted for publication June 30, 1983.

Albumin Binding and Hepatic Uptake: The Importance of Model Selection—A Response

Keyphrases □ Albumin—effect on removal of taurocholate by the liver □ Taurocholate—removal by liver, albumin

To the Editor:

Forker and Luxon have written an interesting rebuttal to my earlier communication (1). However, it only serves to confuse the issue even more.

Forker and Luxon presented data in their original report, which they interpreted using the parallel tube or "distributed" model (2). They concluded that albumin helps mediate the removal of taurocholate from a perfused liver preparation. Using the same data, I presented an alternate interpretation using the widely used and accepted well-stirred, venous equilibrium or "lumped" model. I concluded that albumin does not mediate taurocholate removal.

In their rebuttal (3) Forker and Luxon attempt to lend physiological credence to the parallel tube model at the expense of the well-stirred model. Neither model is physiologically realistic in that the liver is neither a well-stirred beaker nor is it a series of parallel tubes.

The theoretical basis for each of these two models has been developed and discussed in depth (4–6). Although the well-stirred model has been shown to be more predictive than the parallel tube model, in some cases (7–8) it would seem that neither model holds a universally distinct advantage over the other and that attributing physiological meaning to parallel tube model-based conclusions, which contradict previous work in the area, would seem unjustified without further substantiation. Unless the data are unequivocal, parsimony should rule, and if a model must be chosen the one that is time proven (7–9) should prevail.

(1) W. A. Colburn, *J. Pharm. Sci.*, **71**, 373 (1982).
(2) E. L. Forker and B. A. Luxon, *J. Clin. Invest.*, **67**, 1517 (1981).
(3) E. L. Forker and B. A. Luxon, *J. Pharm. Sci.*, **72**, 1232 (1983).
(4) J. R. Gillette, in "Concepts in Biochemical Pharmacology, J. R. Gillette and J. R. Mitchell, Eds., Part 3, Springer-Verlag, New York, N.Y., 1975, pp. 35–85.
(5) G. R. Wilkinson in "The Effect of Disease States on Drug Pharmacokinetics," L. Z. Benet, Ed., American Pharmaceutical Association, Washington, D.C., 1976, pp. 13–22.
(6) K. S. Pang and M. Rowland, *J. Pharmacokinet. Biopharm.*, **5**, 625 (1977).
(7) K. S. Pang and M. Rowland, *J. Pharmacokinet. Biopharm.*, **5**, 655 (1977).
(8) K. S. Pang and M. Rowland, *J. Pharmacokinet. Biopharm.*, **5**, 681 (1977).
(9) A. B. Ahmad, P. N. Bennett, and M. Rowland, *J. Pharm. Pharmacol.*, **35**, 219 (1983).

Wayne A. Colburn
Department of Pharmacokinetics and Biopharmaceutics
Hoffmann-La Roche Inc.
Nutley, NJ 07110

Received May 20. 1983.
Accepted for publication June 30, 1983.

0022-3549/83/1000-1233$01.00/0

The distributed model, though possibly oversimplified as well, is certainly a much better representation of the physiological facts. It may even be correct, because on closer inspection (2, 4) the distributed model turns out to be free of restrictive assumptions that the sinusoids are of uniform bore or that each liver cell has the same transport capacity. The interpretation moreover is virtually independent of variations in the distribution of flow to a large population of sinusoids.

Compartmental analysis is a powerful tool for gaining new physiological insights. Its utility, however, depends critically on the validity of the underlying assumptions. If these are wrong so will be the results. The worst of this is that model-dependent interpretations of the data can rarely, if ever, be used to validate the preconceptions on which the model was constructed. We suggest that Colburn may wish to reconsider the simplistic assumptions on which his model rests before taking too seriously the conclusions that flow from it.

(1) W. A. Colburn, *J. Pharm. Sci.*, **71**, 373 (1982).
(2) E. L. Forker and B. A. Luxon, *J. Clin. Invest.*, **67**, 1517 (1981).
(3) G. R. Wilkinson and D. G. Shand, *Clin. Pharmacol. Ther.*, **18**, 377 (1975).
(4) E. L. Forker, B. A. Luxon, M. Snell, and N. Shurmantine, *J. Pharm. Exp. Ther.*, **223**(2), 342 (1982).
(5) R. Weisiger, J. Gollan, and R. Ockner, *Science*, **211**, 1048 (1981).
(6) E. L. Forker, and B. A. Luxon, *J. Clin. Invest.*, in press, 1983.
(7) J. Barnhart, W. Hardison, B. Witt, and R. Berk, *Am. J. Physiol.*, in press, 1983.

E. L. Forker ˣ
B. A. Luxon
Department of Medicine
University of Missouri-Columbia
Columbia, MO 65212

Received May 2, 1983.
Accepted for publication June 30, 1983.

Albumin Binding and Hepatic Uptake: The Importance of Model Selection—A Response

Keyphrases □ Albumin—effect on removal of taurocholate by the liver □ Taurocholate—removal by liver, albumin

To the Editor:

Forker and Luxon have written an interesting rebuttal to my earlier communication (1). However, it only serves to confuse the issue even more.

Forker and Luxon presented data in their original report, which they interpreted using the parallel tube or "distributed" model (2). They concluded that albumin helps mediate the removal of taurocholate from a perfused liver preparation. Using the same data, I presented an alternate interpretation using the widely used and accepted well-stirred, venous equilibrium or "lumped" model. I concluded that albumin does not mediate taurocholate removal.

In their rebuttal (3) Forker and Luxon attempt to lend physiological credence to the parallel tube model at the expense of the well-stirred model. Neither model is physiologically realistic in that the liver is neither a well-stirred beaker nor is it a series of parallel tubes.

The theoretical basis for each of these two models has been developed and discussed in depth (4–6). Although the well-stirred model has been shown to be more predictive than the parallel tube model, in some cases (7–8) it would seem that neither model holds a universally distinct advantage over the other and that attributing physiological meaning to parallel tube model-based conclusions, which contradict previous work in the area, would seem unjustified without further substantiation. Unless the data are unequivocal, parsimony should rule, and if a model must be chosen the one that is time proven (7–9) should prevail.

(1) W. A. Colburn, *J. Pharm. Sci.*, **71**, 373 (1982).
(2) E. L. Forker and B. A. Luxon, *J. Clin. Invest.*, **67**, 1517 (1981).
(3) E. L. Forker and B. A. Luxon, *J. Pharm. Sci.*, **72**, 1232 (1983).
(4) J. R. Gillette, in "Concepts in Biochemical Pharmacology, J. R. Gillette and J. R. Mitchell, Eds., Part 3, Springer-Verlag, New York, N.Y., 1975, pp. 35–85.
(5) G. R. Wilkinson in "The Effect of Disease States on Drug Pharmacokinetics," L. Z. Benet, Ed., American Pharmaceutical Association, Washington, D.C., 1976, pp. 13–22.
(6) K. S. Pang and M. Rowland, *J. Pharmacokinet. Biopharm.*, **5**, 625 (1977).
(7) K. S. Pang and M. Rowland, *J. Pharmacokinet. Biopharm.*, **5**, 655 (1977).
(8) K. S. Pang and M. Rowland, *J. Pharmacokinet. Biopharm.*, **5**, 681 (1977).
(9) A. B. Ahmad, P. N. Bennett, and M. Rowland, *J. Pharm. Pharmacol.*, **35**, 219 (1983).

Wayne A. Colburn
Department of Pharmacokinetics and Biopharmaceutics
Hoffmann-La Roche Inc.
Nutley, NJ 07110

Received May 20. 1983.
Accepted for publication June 30, 1983.

0022-3549/83/1000-1233$01.00/0

REVIEWS

Proceedings of the First International Symposium on Cyclodextrins. (Budapest, Hungary, 30 September–2 October 1981). Edited by J. SZEJTLI. D. Reidel Publishing Co., 1300AA Dordrecht, Holland. (U.S. Distributor, Kluwer Boston, Inc., 190 Old Derby St., Hingham, MA 02043.) 1982. 544 pp. 17 × 24 cm. Price $84.50.

The cyclodextrins (cycloamyloses) are cyclic oligomers of D-glucose produced by the action of cyclodextrin glycosyltransferases on starch. The products consisting of 6, 7, and 8 glucose units are called α-, β-, and γ-cyclodextrins, respectively; these substances are commercially available, and have attracted the interest of many researchers because the cyclodextrin molecule possesses a cavity of molecular dimensions and is capable of forming an inclusion complex, by acting as the "host," with "guest" species small enough to enter the cavity. In the autumn of 1981, a conference was held in Budapest, Hungary at which workers in the cyclodextrin field presented their results; this book is the proceedings of the conference.

The symposium, and the book, was organized into six parts: Chemistry and Production of Cyclodextrins (7 papers); Enzymology, Toxicology, and Metabolism (10); Cyclodextrin Complexes (16); Cyclodextrin Derivatives (8); Cyclodextrins in Pharmaceuticals (13); and Applications of Cyclodextrins in Foods, Agriculture, and Other Industries (9). Most of the commercial production and applications research is being carried out in Hungary and Japan, and these countries were well represented at the symposium. Only two U.S. laboratories presented papers, so the book does not give a balanced view of the world-wide activity in the field.

Many of the papers will interest pharmaceutical researchers, because the cyclodextrins' capability of forming inclusion complexes can alter the effective properties of a guest drug molecule. This "molecular encapsulation" can affect drug solubility, volatility, dissolution rate, chemical reactivity, and even biological activity. Although cyclodextrins are unlikely ever to become widely used formulation ingredients, it is probable that they will merit occasional specialized application, and laboratories working with drug delivery systems will find this book a useful introduction to current ideas, literature, and workers in the field.

Reviewed by Kenneth A. Connors
School of Pharmacy
University of Wisconsin
Madison, WI 53706

Formulation of Veterinary Dosage Forms. Edited by JACK BLODINGER. Marcel Dekker, New York, NY 10016. 1983. 316 pp. 15 × 23 cm. Price $48.50 (20% higher outside the U.S. and Canada).

This book is a member of a continuing set, which until now collectively comprises 17 volumes of text books and monographs entitled "Drugs and Pharmaceutical Sciences." As stated in the preface of this volume, the book describes the types of drug formulations administered to animals, the art and science used in their development, and the techniques needed to administer them so as to ensure optimum efficacy.

The first five chapters of this volume cover the details of all phases of veterinary dosage formulation from initial development to final stability testing. They are "The Basis For Selection Of The Dosage Form," "Specialized Dose Dispensing Equipment," "Formulation of Drug Dosage Forms For Animals," "Formulation of Drugs For Administration *Via* Feed Or Drinking Water," and "Stability Studies Of Veterinary Formulation." The sixth chapter, "Regulatory Clearance," is well placed at the end and covers the requirements for registration of animal health products in the United States, Australia, Brazil, the European Economic Community, and Japan.

Each chapter is written by an expert on the subject in a crisp, authoritative, and comprehensive manner. Useful details on the development of drug forms for animals which differ from those known in the human field are presented in a logical and succinct manner. Each chapter is well referenced through 1980. The index is extensive and good, providing the reader with cross-referencing to both specific and broad general categories.

This book fills a previous void, and anyone actively involved in formulation of veterinary dosage forms will find it to be of great value.

Reviewed by Samir A. Hanna
Analytical Research and Development
Bristol Laboratories
Syracuse, NY 13201

Radioimmunoassay and Related Procedures in Medicine–1982. Proceedings series; International Atomic Energy Agency. 1983. 823 pp. 15 × 24 cm.

This volume resulted from an international symposium on radioimmunoassay and related procedures in medicine held in Vienna, Austria in June 1982. The symposium was organized and the book edited by the International Atomic Energy Agency. The volume consists of 9 review papers, abstracts of 65 presentations, 23 poster presentations, and edited summaries of the discussions. Areas that were reviewed and had original research presentations include: reagents and separation procedures, assays for free hormones, receptors, biological substances, and drugs. Other areas covered include data processing, intralaboratory control, automation, external surveillance of assay performance, assay services in developing countries, public health, and clinical applications and alternatives to radioassays.

The review papers in this volume are relatively complete discussions of specialized topics in radioimmunoassay technology. The scientific and poster presentations are sufficiently detailed that meaningful scientific information on methods, results, and discussion can be extracted. Because of the large cross section of radioimmunoassay concepts and technology that are covered in this volume, potential readers should carefully examine the specific topics of review or original research to be certain that individual areas of interest are present prior to purchasing or reading this book.

Reviewed by Donald R. Stanski
Department of Clinical Pharmacology
Stanford University School of Medicine
Stanford, CA 94305

Central Analgetics. Edited by DANIEL LEDNICER. Wiley-Interscience, New York, N.Y., 1982. 219 pp. 15 × 23 cm. Price $47.50.

Central Analgetics is the inaugural volume in the *Chemistry and Pharmacology of Drugs* series under the editorship of Daniel Lednicer. This book provides for the first time a comprehensive collection of reviews of the physiology, pharmacology, and chemistry involved in the transmission of pain, as well as its alleviation by drug therapy.

The book is divided into four chapters, each contributed by an author active in the forefront of the field chosen for critical review. In the first chapter, by J. S. Mohrland, basic physiology of pain is outlined; this includes the complex network of neural pathways, transmitters, and modulators which interact prior to the sensation of pain. Of special interest are discussions pertaining to the interplay between pain stimuli and other central nervous system functions. The second chapter, by P. F. Von Voigtlander, is a compilation of animal models, both *in vivo* and *in vitro*, which have proven usefulness in predicting clinically effective analgetics. In examining the various test methods for abuse potential, dysphoria, and other side effects, the author also presents an overview of current concepts of opioid receptors, thus adding new dimensions and greater depth to his discussions. Chapter 3, by J. S. Morley, deals with

REVIEWS

Proceedings of the First International Symposium on Cyclodextrins. (Budapest, Hungary, 30 September–2 October 1981). Edited by J. SZEJTLI. D. Reidel Publishing Co., 1300AA Dordrecht, Holland. (U.S. Distributor, Kluwer Boston, Inc., 190 Old Derby St., Hingham, MA 02043.) 1982. 544 pp. 17 × 24 cm. Price $84.50.

The cyclodextrins (cycloamyloses) are cyclic oligomers of D-glucose produced by the action of cyclodextrin glycosyltransferases on starch. The products consisting of 6, 7, and 8 glucose units are called α-, β-, and γ-cyclodextrins, respectively; these substances are commercially available, and have attracted the interest of many researchers because the cyclodextrin molecule possesses a cavity of molecular dimensions and is capable of forming an inclusion complex, by acting as the "host," with "guest" species small enough to enter the cavity. In the autumn of 1981, a conference was held in Budapest, Hungary at which workers in the cyclodextrin field presented their results; this book is the proceedings of the conference.

The symposium, and the book, was organized into six parts: Chemistry and Production of Cyclodextrins (7 papers); Enzymology, Toxicology, and Metabolism (10); Cyclodextrin Complexes (16); Cyclodextrin Derivatives (8); Cyclodextrins in Pharmaceuticals (13); and Applications of Cyclodextrins in Foods, Agriculture, and Other Industries (9). Most of the commercial production and applications research is being carried out in Hungary and Japan, and these countries were well represented at the symposium. Only two U.S. laboratories presented papers, so the book does not give a balanced view of the world-wide activity in the field.

Many of the papers will interest pharmaceutical researchers, because the cyclodextrins' capability of forming inclusion complexes can alter the effective properties of a guest drug molecule. This "molecular encapsulation" can affect drug solubility, volatility, dissolution rate, chemical reactivity, and even biological activity. Although cyclodextrins are unlikely ever to become widely used formulation ingredients, it is probable that they will merit occasional specialized application, and laboratories working with drug delivery systems will find this book a useful introduction to current ideas, literature, and workers in the field.

Reviewed by Kenneth A. Connors
School of Pharmacy
University of Wisconsin
Madison, WI 53706

Formulation of Veterinary Dosage Forms. Edited by JACK BLODINGER. Marcel Dekker, New York, NY 10016. 1983. 316 pp. 15 × 23 cm. Price $48.50 (20% higher outside the U.S. and Canada).

This book is a member of a continuing set, which until now collectively comprises 17 volumes of text books and monographs entitled "Drugs and Pharmaceutical Sciences." As stated in the preface of this volume, the book describes the types of drug formulations administered to animals, the art and science used in their development, and the techniques needed to administer them so as to ensure optimum efficacy.

The first five chapters of this volume cover the details of all phases of veterinary dosage formulation from initial development to final stability testing. They are "The Basis For Selection Of The Dosage Form," "Specialized Dose Dispensing Equipment," "Formulation of Drug Dosage Forms For Animals," "Formulation of Drugs For Administration *Via* Feed Or Drinking Water," and "Stability Studies Of Veterinary Formulation." The sixth chapter, "Regulatory Clearance," is well placed at the end and covers the requirements for registration of animal health products in the United States, Australia, Brazil, the European Economic Community, and Japan.

Each chapter is written by an expert on the subject in a crisp, authoritative, and comprehensive manner. Useful details on the development of drug forms for animals which differ from those known in the human field are presented in a logical and succinct manner. Each chapter is well referenced through 1980. The index is extensive and good, providing the reader with cross-referencing to both specific and broad general categories.

This book fills a previous void, and anyone actively involved in formulation of veterinary dosage forms will find it to be of great value.

Reviewed by Samir A. Hanna
Analytical Research and Development
Bristol Laboratories
Syracuse, NY 13201

Radioimmunoassay and Related Procedures in Medicine–1982. Proceedings series; International Atomic Energy Agency. 1983. 823 pp. 15 × 24 cm.

This volume resulted from an international symposium on radioimmunoassay and related procedures in medicine held in Vienna, Austria in June 1982. The symposium was organized and the book edited by the International Atomic Energy Agency. The volume consists of 9 review papers, abstracts of 65 presentations, 23 poster presentations, and edited summaries of the discussions. Areas that were reviewed and had original research presentations include: reagents and separation procedures, assays for free hormones, receptors, biological substances, and drugs. Other areas covered include data processing, intralaboratory control, automation, external surveillance of assay performance, assay services in developing countries, public health, and clinical applications and alternatives to radioassays.

The review papers in this volume are relatively complete discussions of specialized topics in radioimmunoassay technology. The scientific and poster presentations are sufficiently detailed that meaningful scientific information on methods, results, and discussion can be extracted. Because of the large cross section of radioimmunoassay concepts and technology that are covered in this volume, potential readers should carefully examine the specific topics of review or original research to be certain that individual areas of interest are present prior to purchasing or reading this book.

Reviewed by Donald R. Stanski
Department of Clinical Pharmacology
Stanford University School of Medicine
Stanford, CA 94305

Central Analgetics. Edited by DANIEL LEDNICER. Wiley-Interscience, New York, N.Y., 1982. 219 pp. 15 × 23 cm. Price $47.50.

Central Analgetics is the inaugural volume in the *Chemistry and Pharmacology of Drugs* series under the editorship of Daniel Lednicer. This book provides for the first time a comprehensive collection of reviews of the physiology, pharmacology, and chemistry involved in the transmission of pain, as well as its alleviation by drug therapy.

The book is divided into four chapters, each contributed by an author active in the forefront of the field chosen for critical review. In the first chapter, by J. S. Mohrland, basic physiology of pain is outlined; this includes the complex network of neural pathways, transmitters, and modulators which interact prior to the sensation of pain. Of special interest are discussions pertaining to the interplay between pain stimuli and other central nervous system functions. The second chapter, by P. F. Von Voigtlander, is a compilation of animal models, both *in vivo* and *in vitro*, which have proven usefulness in predicting clinically effective analgetics. In examining the various test methods for abuse potential, dysphoria, and other side effects, the author also presents an overview of current concepts of opioid receptors, thus adding new dimensions and greater depth to his discussions. Chapter 3, by J. S. Morley, deals with

REVIEWS

Proceedings of the First International Symposium on Cyclodextrins. (Budapest, Hungary, 30 September–2 October 1981). Edited by J. SZEJTLI. D. Reidel Publishing Co., 1300AA Dordrecht, Holland. (U.S. Distributor, Kluwer Boston, Inc., 190 Old Derby St., Hingham, MA 02043.) 1982. 544 pp. 17 × 24 cm. Price $84.50.

The cyclodextrins (cycloamyloses) are cyclic oligomers of D-glucose produced by the action of cyclodextrin glycosyltransferases on starch. The products consisting of 6, 7, and 8 glucose units are called α-, β-, and γ-cyclodextrins, respectively; these substances are commercially available, and have attracted the interest of many researchers because the cyclodextrin molecule possesses a cavity of molecular dimensions and is capable of forming an inclusion complex, by acting as the "host," with "guest" species small enough to enter the cavity. In the autumn of 1981, a conference was held in Budapest, Hungary at which workers in the cyclodextrin field presented their results; this book is the proceedings of the conference.

The symposium, and the book, was organized into six parts: Chemistry and Production of Cyclodextrins (7 papers); Enzymology, Toxicology, and Metabolism (10); Cyclodextrin Complexes (16); Cyclodextrin Derivatives (8); Cyclodextrins in Pharmaceuticals (13); and Applications of Cyclodextrins in Foods, Agriculture, and Other Industries (9). Most of the commercial production and applications research is being carried out in Hungary and Japan, and these countries were well represented at the symposium. Only two U.S. laboratories presented papers, so the book does not give a balanced view of the world-wide activity in the field.

Many of the papers will interest pharmaceutical researchers, because the cyclodextrins' capability of forming inclusion complexes can alter the effective properties of a guest drug molecule. This "molecular encapsulation" can affect drug solubility, volatility, dissolution rate, chemical reactivity, and even biological activity. Although cyclodextrins are unlikely ever to become widely used formulation ingredients, it is probable that they will merit occasional specialized application, and laboratories working with drug delivery systems will find this book a useful introduction to current ideas, literature, and workers in the field.

Reviewed by Kenneth A. Connors
School of Pharmacy
University of Wisconsin
Madison, WI 53706

Formulation of Veterinary Dosage Forms. Edited by JACK BLODINGER. Marcel Dekker, New York, NY 10016. 1983. 316 pp. 15 × 23 cm. Price $48.50 (20% higher outside the U.S. and Canada).

This book is a member of a continuing set, which until now collectively comprises 17 volumes of text books and monographs entitled "Drugs and Pharmaceutical Sciences." As stated in the preface of this volume, the book describes the types of drug formulations administered to animals, the art and science used in their development, and the techniques needed to administer them so as to ensure optimum efficacy.

The first five chapters of this volume cover the details of all phases of veterinary dosage formulation from initial development to final stability testing. They are "The Basis For Selection Of The Dosage Form," "Specialized Dose Dispensing Equipment," "Formulation of Drug Dosage Forms For Animals," "Formulation of Drugs For Administration *Via* Feed Or Drinking Water," and "Stability Studies Of Veterinary Formulation." The sixth chapter, "Regulatory Clearance," is well placed at the end and covers the requirements for registration of animal health products in the United States, Australia, Brazil, the European Economic Community, and Japan.

Each chapter is written by an expert on the subject in a crisp, authoritative, and comprehensive manner. Useful details on the development of drug forms for animals which differ from those known in the human field are presented in a logical and succinct manner. Each chapter is well referenced through 1980. The index is extensive and good, providing the reader with cross-referencing to both specific and broad general categories.

This book fills a previous void, and anyone actively involved in formulation of veterinary dosage forms will find it to be of great value.

Reviewed by Samir A. Hanna
Analytical Research and Development
Bristol Laboratories
Syracuse, NY 13201

Radioimmunoassay and Related Procedures in Medicine–1982. Proceedings series; International Atomic Energy Agency. 1983. 823 pp. 15 × 24 cm.

This volume resulted from an international symposium on radioimmunoassay and related procedures in medicine held in Vienna, Austria in June 1982. The symposium was organized and the book edited by the International Atomic Energy Agency. The volume consists of 9 review papers, abstracts of 65 presentations, 23 poster presentations, and edited summaries of the discussions. Areas that were reviewed and had original research presentations include: reagents and separation procedures, assays for free hormones, receptors, biological substances, and drugs. Other areas covered include data processing, intralaboratory control, automation, external surveillance of assay performance, assay services in developing countries, public health, and clinical applications and alternatives to radioassays.

The review papers in this volume are relatively complete discussions of specialized topics in radioimmunoassay technology. The scientific and poster presentations are sufficiently detailed that meaningful scientific information on methods, results, and discussion can be extracted. Because of the large cross section of radioimmunoassay concepts and technology that are covered in this volume, potential readers should carefully examine the specific topics of review or original research to be certain that individual areas of interest are present prior to purchasing or reading this book.

Reviewed by Donald R. Stanski
Department of Clinical Pharmacology
Stanford University School of Medicine
Stanford, CA 94305

Central Analgetics. Edited by DANIEL LEDNICER. Wiley-Interscience, New York, N.Y., 1982. 219 pp. 15 × 23 cm. Price $47.50.

Central Analgetics is the inaugural volume in the *Chemistry and Pharmacology of Drugs* series under the editorship of Daniel Lednicer. This book provides for the first time a comprehensive collection of reviews of the physiology, pharmacology, and chemistry involved in the transmission of pain, as well as its alleviation by drug therapy.

The book is divided into four chapters, each contributed by an author active in the forefront of the field chosen for critical review. In the first chapter, by J. S. Mohrland, basic physiology of pain is outlined; this includes the complex network of neural pathways, transmitters, and modulators which interact prior to the sensation of pain. Of special interest are discussions pertaining to the interplay between pain stimuli and other central nervous system functions. The second chapter, by P. F. Von Voigtlander, is a compilation of animal models, both *in vivo* and *in vitro*, which have proven usefulness in predicting clinically effective analgetics. In examining the various test methods for abuse potential, dysphoria, and other side effects, the author also presents an overview of current concepts of opioid receptors, thus adding new dimensions and greater depth to his discussions. Chapter 3, by J. S. Morley, deals with

REVIEWS

Proceedings of the First International Symposium on Cyclodextrins. (Budapest, Hungary, 30 September–2 October 1981). Edited by J. SZEJTLI. D. Reidel Publishing Co., 1300AA Dordrecht, Holland. (U.S. Distributor, Kluwer Boston, Inc., 190 Old Derby St., Hingham, MA 02043.) 1982. 544 pp. 17 × 24 cm. Price $84.50.

The cyclodextrins (cycloamyloses) are cyclic oligomers of D-glucose produced by the action of cyclodextrin glycosyltransferases on starch. The products consisting of 6, 7, and 8 glucose units are called α-, β-, and γ-cyclodextrins, respectively; these substances are commercially available, and have attracted the interest of many researchers because the cyclodextrin molecule possesses a cavity of molecular dimensions and is capable of forming an inclusion complex, by acting as the "host," with "guest" species small enough to enter the cavity. In the autumn of 1981, a conference was held in Budapest, Hungary at which workers in the cyclodextrin field presented their results; this book is the proceedings of the conference.

The symposium, and the book, was organized into six parts: Chemistry and Production of Cyclodextrins (7 papers); Enzymology, Toxicology, and Metabolism (10); Cyclodextrin Complexes (16); Cyclodextrin Derivatives (8); Cyclodextrins in Pharmaceuticals (13); and Applications of Cyclodextrins in Foods, Agriculture, and Other Industries (9). Most of the commercial production and applications research is being carried out in Hungary and Japan, and these countries were well represented at the symposium. Only two U.S. laboratories presented papers, so the book does not give a balanced view of the world-wide activity in the field.

Many of the papers will interest pharmaceutical researchers, because the cyclodextrins' capability of forming inclusion complexes can alter the effective properties of a guest drug molecule. This "molecular encapsulation" can affect drug solubility, volatility, dissolution rate, chemical reactivity, and even biological activity. Although cyclodextrins are unlikely ever to become widely used formulation ingredients, it is probable that they will merit occasional specialized application, and laboratories working with drug delivery systems will find this book a useful introduction to current ideas, literature, and workers in the field.

Reviewed by Kenneth A. Connors
School of Pharmacy
University of Wisconsin
Madison, WI 53706

Formulation of Veterinary Dosage Forms. Edited by JACK BLODINGER. Marcel Dekker, New York, NY 10016. 1983. 316 pp. 15 × 23 cm. Price $48.50 (20% higher outside the U.S. and Canada).

This book is a member of a continuing set, which until now collectively comprises 17 volumes of text books and monographs entitled "Drugs and Pharmaceutical Sciences." As stated in the preface of this volume, the book describes the types of drug formulations administered to animals, the art and science used in their development, and the techniques needed to administer them so as to ensure optimum efficacy.

The first five chapters of this volume cover the details of all phases of veterinary dosage formulation from initial development to final stability testing. They are "The Basis For Selection Of The Dosage Form," "Specialized Dose Dispensing Equipment," "Formulation of Drug Dosage Forms For Animals," "Formulation of Drugs For Administration *Via* Feed Or Drinking Water," and "Stability Studies Of Veterinary Formulation." The sixth chapter, "Regulatory Clearance," is well placed at the end and covers the requirements for registration of animal health products in the United States, Australia, Brazil, the European Economic Community, and Japan.

Each chapter is written by an expert on the subject in a crisp, authoritative, and comprehensive manner. Useful details on the development of drug forms for animals which differ from those known in the human field are presented in a logical and succinct manner. Each chapter is well referenced through 1980. The index is extensive and good, providing the reader with cross-referencing to both specific and broad general categories.

This book fills a previous void, and anyone actively involved in formulation of veterinary dosage forms will find it to be of great value.

Reviewed by Samir A. Hanna
Analytical Research and Development
Bristol Laboratories
Syracuse, NY 13201

Radioimmunoassay and Related Procedures in Medicine–1982. Proceedings series; International Atomic Energy Agency. 1983. 823 pp. 15 × 24 cm.

This volume resulted from an international symposium on radioimmunoassay and related procedures in medicine held in Vienna, Austria in June 1982. The symposium was organized and the book edited by the International Atomic Energy Agency. The volume consists of 9 review papers, abstracts of 65 presentations, 23 poster presentations, and edited summaries of the discussions. Areas that were reviewed and had original research presentations include: reagents and separation procedures, assays for free hormones, receptors, biological substances, and drugs. Other areas covered include data processing, intralaboratory control, automation, external surveillance of assay performance, assay services in developing countries, public health, and clinical applications and alternatives to radioassays.

The review papers in this volume are relatively complete discussions of specialized topics in radioimmunoassay technology. The scientific and poster presentations are sufficiently detailed that meaningful scientific information on methods, results, and discussion can be extracted. Because of the large cross section of radioimmunoassay concepts and technology that are covered in this volume, potential readers should carefully examine the specific topics of review or original research to be certain that individual areas of interest are present prior to purchasing or reading this book.

Reviewed by Donald R. Stanski
Department of Clinical Pharmacology
Stanford University School of Medicine
Stanford, CA 94305

Central Analgetics. Edited by DANIEL LEDNICER. Wiley-Interscience, New York, N.Y., 1982. 219 pp. 15 × 23 cm. Price $47.50.

Central Analgetics is the inaugural volume in the *Chemistry and Pharmacology of Drugs* series under the editorship of Daniel Lednicer. This book provides for the first time a comprehensive collection of reviews of the physiology, pharmacology, and chemistry involved in the transmission of pain, as well as its alleviation by drug therapy.

The book is divided into four chapters, each contributed by an author active in the forefront of the field chosen for critical review. In the first chapter, by J. S. Mohrland, basic physiology of pain is outlined; this includes the complex network of neural pathways, transmitters, and modulators which interact prior to the sensation of pain. Of special interest are discussions pertaining to the interplay between pain stimuli and other central nervous system functions. The second chapter, by P. F. Von Voigtlander, is a compilation of animal models, both *in vivo* and *in vitro*, which have proven usefulness in predicting clinically effective analgetics. In examining the various test methods for abuse potential, dysphoria, and other side effects, the author also presents an overview of current concepts of opioid receptors, thus adding new dimensions and greater depth to his discussions. Chapter 3, by J. S. Morley, deals with

one of the most interesting aspects of analgesic research: the endogenous, pain-regulating peptides and their synthetic analogues. This chapter should be of prime interest to those who seek the new challenges (and opportunities) of designing enkephalin releasers, metabolic inhibitors, as well as antagonists for substance P as analgetics of the future. The book concludes with a chapter by D. Lednicer on the evolution and SAR of major synthetic analgetics based on morphine. Although a good portion of the material treated in this chapter is historical in nature, it nonetheless serves as a useful guide to medicinal chemists and pharmacologists who are embarking on analgesic research. One minor blemish in this otherwise comprehensive coverage lies in the omission of some recently disclosed tricyclic analgetics, which deviate considerably from the partial morphine derivatives, both in structure and in activity profile.

Overall, the quality of production of this volume is excellent; figures and structures are clearly drawn and errors are minimal. It is a fine reference book which fulfills its purpose.

Reviewed by Helen H. Ong
Chemical Research Department
Hoechst-Roussel Pharmaceuticals Inc.
Somerville, NJ 08876

Chromatography of Alkaloids, Part A: Thin-Layer Chromatography. (*Journal of Chromatography*, Vol. 23A). By A. BAERHEIM SVENDSEN and R. VERPOORTE. Elsevier Science Publishing Co., New York, NY 10017. 1982. 533 pp. 16 × 24 cm. Price $104.25 (Dfl. 245).

Although this is the twenty-third volume in a continuing series which began in 1973 with the publication of "Chromatography of Antibiotics" (Volume 1), this is the first volume that is exclusively devoted to the discussion of the chromatography of alkaloids. Because of the large amount of information available, it was decided to publish this volume in two parts: Part A (thin-layer chromatography) and Part B (gas-liquid and high-performance liquid chromatography).

The book is divided into two major portions entitled a "General Part" and a "Special Part." The "General Part," consists of four chapters covering about 60 pages. Chapter 1 includes a discussion of adsorbents, solvent systems, development techniques, sample application, and several tables describing solvent classification and selectivity. Chapter 2 presents a discussion of the various methods of detection, including reagents, tables with color reactions, and a consideration of nonalkaloidal components capable of eliciting false-positive reactions with Dragendorff Reagent. Chapter 3 consists of a general consideration of thin-layer chromatographic separation and identification of alkaloids. This chapter also discusses the use of various reagents, solvent systems, fluorescence, ion-pair adsorption, and ion-exchange thin-layer chromatography. Finally, Chapter 4 includes a discussion of isolation methods and artifact formation resulting from different isolation techniques.

The "Special Part" of the book consists of 17 chapters, about 420 pages, which are devoted to the following classes of alkaloids: pyrrolidine, pyrrolizidine, pyridine, piperidine, quinolizidine, tropane, quinoline, phenethylamine and isoquinoline-derived, indole, steroidal, and miscellaneous. Each chapter consists of an extensive discussion of adsorbents, developing solvents, R_f values, detecting reagents, and references and is richly endowed with tables.

The Appendix alphabetically lists the 106 different reagents that have been discussed throughout the book and includes detailed instructions for their preparation. Finally, the Index is composed of a Subject Index, which contains general topics and classes, and a Compound Index, which contains only compounds.

This is a well-referenced and richly tabled book which should be extremely useful to anyone involved with the detection, isolation/separation, and identification of alkaloids from any source. It is not highly theoretical, nor is it intended to be, and is a practical work which addresses the subject concisely. The price is steep for the individual scientist, but certainly departmental, school, and institutional libraries would want this book in their collection.

Reviewed by Paul L. Schiff, Jr.
Department of Pharmacognosy School of Pharmacy
University of Pittsburgh
Pittsburgh, PA 15261

Controlled Release Delivery Systems. Edited by THEODORE J. ROSEMAN and S. Z. MANSDORF. Marcel Dekker, Inc., 270 Madison Ave., New York, N.Y. 10016. 1983. 402 pp. 15 × 23 cm. Price $57.50 (20% higher outside the U.S. and Canada).

The book, which contains 25 chapters, describes the proceedings of the Eighth International Symposium on Controlled Release of Bioactive Materials held in Fort Lauderdale, Florida, July 26–29, 1981. The editors of the book are recognized leaders in the field of polymeric controlled-release systems, and the authors selected to contribute full-length manuscripts represent a broad international array of experts in this area.

The topics covered in the book range from biomedical applications to agricultural uses for release vehicles for pesticides and herbicides. Heavy emphasis is placed on polymeric delivery systems with only one chapter on the use of prodrugs and one on liposomes. Subjects covered in the book include liposomes, microencapsulation, reservoir and monolithic devices, biodegradable and swellable matrices, prodrugs, and a contribution on magnetically controlled polymeric systems. All chapters contain a discussion section and all are adequately referenced. A subject index is also included.

This is a useful book, providing a reader with an overview of the various applications in controlled-release technology. It cannot be recommended for an individual seeking an in-depth discussion on any one given subject. However, it is well written and serves to elucidate the current status of this rapidly growing field.

Reviewed by Kenneth J. Widder
Molecular Biosystems, Inc.
San Diego, CA 92121

NOTICES

Advances in Steroid Analysis. Edited by S. GOROG. Elsevier Scientific Publishing Co., 52 Vanderbilt Ave., New York, NY 10017. 1982. 551 pp. 16 × 24 cm. Price $104.75 (Dfl. 225.00).

Analytical Profiles of Drug Substances. Vol. II. Edited by KLAUS FLOREY, Academic Press, 111 5th Ave., New York, NY 10003. 1982. 665 pp. 15 × 23 cm.

Application of Pharmacokinetics to Patient Care. Edited by CHARLES A. WALKER and LAMBROS P. TTERLIKKIS. Praeger, 521 Fifth Ave., New York, NY 10175. 1982. 175 pp. 15 × 24 cm. Price $26.50.

Assessing Causes of Adverse Drug Reactions. (*With Special Reference to Standardized Methods*). Editor JAN VENULET. Coeditors: GARRY-CLAUDE BERNEKER and ANTONIO G. CIUCCI. Academic Press, 111 Fifth Ave., New York, NY 10003. 1982. 223 pp. 15 × 23 cm.

Benzodiazepines. A Handbook. (*Basic Data, Analytical Methods, Pharmacokinetics and Comprehensive Literature*). By HAROLD SCHULTZ, Springer-Verlag New York Inc., 175 5th Ave., New York, NY 10010. 1982. 439 pp. 19 × 27 cm. Price $88.00.

British National Formulary, Number 4 (*1982*). Publications of the Pharmaceutical Society of Great Britain. 1 Lambeth High Street, London, SE1 7JN, England. 1982. 454 pp. 13 × 22. Price £4.50.

Cancer Mortality by Occupation and Social Class 1851–1971. (IARC Scientific Publications No. 36) Office of Population Censuses and Surveys, Studies on Medical and Population Subjects No. 44. By W. P. D. LOGAN, Her Majesty's Stationary Office, London, and Lyons International Agency for Research on Cancer. 1982. 253 pp. 20 × 30 cm. Price $30.00 (Sw Fr. 60).

Chromatographic Separation and Extraction with Foamed Plastics and Rubbers. By G. J. MOODY and J. D. R. THOMAS. Marcel Dekker, Inc., 270 Madison Ave., New York, NY 10016. 1982. 139 pp. 14 × 23 cm. Price $29.75. (20% higher outside the U.S. and Canada).

Critical Stability Constants. Vol. 5. First Supplement. By ARTHUR E. MARTELL and ROBERT M. SMITH. Plenum Publishing Corp., 233 Spring St., New York, NY 10013. 1982. 604 pp. 21 × 28 cm. Price $69.50.

Crown Compounds. (*Their Characteristics and Applications.*) By MICHIO HIRAOKA. Elsevier Scientific Publishing Co., 52 Vanderbilt Ave., New York, NY 10017. 1982. 275 pp. 16 × 25 cm. Price $83.75. (Dfl. 180.00).

one of the most interesting aspects of analgesic research: the endogenous, pain-regulating peptides and their synthetic analogues. This chapter should be of prime interest to those who seek the new challenges (and opportunities) of designing enkephalin releasers, metabolic inhibitors, as well as antagonists for substance P as analgetics of the future. The book concludes with a chapter by D. Lednicer on the evolution and SAR of major synthetic analgetics based on morphine. Although a good portion of the material treated in this chapter is historical in nature, it nonetheless serves as a useful guide to medicinal chemists and pharmacologists who are embarking on analgesic research. One minor blemish in this otherwise comprehensive coverage lies in the omission of some recently disclosed tricyclic analgetics, which deviate considerably from the partial morphine derivatives, both in structure and in activity profile.

Overall, the quality of production of this volume is excellent; figures and structures are clearly drawn and errors are minimal. It is a fine reference book which fulfills its purpose.

Reviewed by Helen H. Ong
Chemical Research Department
Hoechst-Roussel Pharmaceuticals Inc.
Somerville, NJ 08876

Chromatography of Alkaloids, Part A: Thin-Layer Chromatography. (*Journal of Chromatography*, Vol. 23A). By A. BAERHEIM SVENDSEN and R. VERPOORTE. Elsevier Science Publishing Co., New York, NY 10017. 1982. 533 pp. 16 × 24 cm. Price $104.25 (Dfl. 245).

Although this is the twenty-third volume in a continuing series which began in 1973 with the publication of "Chromatography of Antibiotics" (Volume 1), this is the first volume that is exclusively devoted to the discussion of the chromatography of alkaloids. Because of the large amount of information available, it was decided to publish this volume in two parts: Part A (thin-layer chromatography) and Part B (gas-liquid and high-performance liquid chromatography).

The book is divided into two major portions entitled a "General Part" and a "Special Part." The "General Part," consists of four chapters covering about 60 pages. Chapter 1 includes a discussion of adsorbents, solvent systems, development techniques, sample application, and several tables describing solvent classification and selectivity. Chapter 2 presents a discussion of the various methods of detection, including reagents, tables with color reactions, and a consideration of nonalkaloidal components capable of eliciting false-positive reactions with Dragendorff Reagent. Chapter 3 consists of a general consideration of thin-layer chromatographic separation and identification of alkaloids. This chapter also discusses the use of various reagents, solvent systems, fluorescence, ion-pair adsorption, and ion-exchange thin-layer chromatography. Finally, Chapter 4 includes a discussion of isolation methods and artifact formation resulting from different isolation techniques.

The "Special Part" of the book consists of 17 chapters, about 420 pages, which are devoted to the following classes of alkaloids: pyrrolidine, pyrrolizidine, pyridine, piperidine, quinolizidine, tropane, quinoline, phenethylamine and isoquinoline-derived, indole, steroidal, and miscellaneous. Each chapter consists of an extensive discussion of adsorbents, developing solvents, R_f values, detecting reagents, and references and is richly endowed with tables.

The Appendix alphabetically lists the 106 different reagents that have been discussed throughout the book and includes detailed instructions for their preparation. Finally, the Index is composed of a Subject Index, which contains general topics and classes, and a Compound Index, which contains only compounds.

This is a well-referenced and richly tabled book which should be extremely useful to anyone involved with the detection, isolation/separation, and identification of alkaloids from any source. It is not highly theoretical, nor is it intended to be, and is a practical work which addresses the subject concisely. The price is steep for the individual scientist, but certainly departmental, school, and institutional libraries would want this book in their collection.

Reviewed by Paul L. Schiff, Jr.
Department of Pharmacognosy School of Pharmacy
University of Pittsburgh
Pittsburgh, PA 15261

Controlled Release Delivery Systems. Edited by THEODORE J. ROSEMAN and S. Z. MANSDORF. Marcel Dekker, Inc., 270 Madison Ave., New York, N.Y. 10016. 1983. 402 pp. 15 × 23 cm. Price $57.50 (20% higher outside the U.S. and Canada).

The book, which contains 25 chapters, describes the proceedings of the Eighth International Symposium on Controlled Release of Bioactive Materials held in Fort Lauderdale, Florida, July 26–29, 1981. The editors of the book are recognized leaders in the field of polymeric controlled-release systems, and the authors selected to contribute full-length manuscripts represent a broad international array of experts in this area.

The topics covered in the book range from biomedical applications to agricultural uses for release vehicles for pesticides and herbicides. Heavy emphasis is placed on polymeric delivery systems with only one chapter on the use of prodrugs and one on liposomes. Subjects covered in the book include liposomes, microencapsulation, reservoir and monolithic devices, biodegradable and swellable matrices, prodrugs, and a contribution on magnetically controlled polymeric systems. All chapters contain a discussion section and all are adequately referenced. A subject index is also included.

This is a useful book, providing a reader with an overview of the various applications in controlled-release technology. It cannot be recommended for an individual seeking an in-depth discussion on any one given subject. However, it is well written and serves to elucidate the current status of this rapidly growing field.

Reviewed by Kenneth J. Widder
Molecular Biosystems, Inc.
San Diego, CA 92121

NOTICES

Advances in Steroid Analysis. Edited by S. GOROG. Elsevier Scientific Publishing Co., 52 Vanderbilt Ave., New York, NY 10017. 1982. 551 pp. 16 × 24 cm. Price $104.75 (Dfl. 225.00).

Analytical Profiles of Drug Substances. Vol. II. Edited by KLAUS FLOREY, Academic Press, 111 5th Ave., New York, NY 10003. 1982. 665 pp. 15 × 23 cm.

Application of Pharmacokinetics to Patient Care. Edited by CHARLES A. WALKER and LAMBROS P. TTERLIKKIS. Praeger, 521 Fifth Ave., New York, NY 10175. 1982. 175 pp. 15 × 24 cm. Price $26.50.

Assessing Causes of Adverse Drug Reactions. (*With Special Reference to Standardized Methods*). Editor JAN VENULET. Coeditors: GARRY-CLAUDE BERNEKER and ANTONIO G. CIUCCI. Academic Press, 111 Fifth Ave., New York, NY 10003. 1982. 223 pp. 15 × 23 cm.

Benzodiazepines. A Handbook. (*Basic Data, Analytical Methods, Pharmacokinetics and Comprehensive Literature*). By HAROLD SCHULTZ, Springer-Verlag New York Inc., 175 5th Ave., New York, NY 10010. 1982. 439 pp. 19 × 27 cm. Price $88.00.

British National Formulary, Number 4 (*1982*). Publications of the Pharmaceutical Society of Great Britain. 1 Lambeth High Street, London, SE1 7JN, England. 1982. 454 pp. 13 × 22. Price £4.50.

Cancer Mortality by Occupation and Social Class 1851–1971. (IARC Scientific Publications No. 36) Office of Population Censuses and Surveys, Studies on Medical and Population Subjects No. 44. By W. P. D. LOGAN, Her Majesty's Stationary Office, London, and Lyons International Agency for Research on Cancer. 1982. 253 pp. 20 × 30 cm. Price $30.00 (Sw Fr. 60).

Chromatographic Separation and Extraction with Foamed Plastics and Rubbers. By G. J. MOODY and J. D. R. THOMAS. Marcel Dekker, Inc., 270 Madison Ave., New York, NY 10016. 1982. 139 pp. 14 × 23 cm. Price $29.75. (20% higher outside the U.S. and Canada).

Critical Stability Constants. Vol. 5. First Supplement. By ARTHUR E. MARTELL and ROBERT M. SMITH. Plenum Publishing Corp., 233 Spring St., New York, NY 10013. 1982. 604 pp. 21 × 28 cm. Price $69.50.

Crown Compounds. (*Their Characteristics and Applications.*) By MICHIO HIRAOKA. Elsevier Scientific Publishing Co., 52 Vanderbilt Ave., New York, NY 10017. 1982. 275 pp. 16 × 25 cm. Price $83.75. (Dfl. 180.00).

one of the most interesting aspects of analgesic research: the endogenous, pain-regulating peptides and their synthetic analogues. This chapter should be of prime interest to those who seek the new challenges (and opportunities) of designing enkephalin releasers, metabolic inhibitors, as well as antagonists for substance P as analgetics of the future. The book concludes with a chapter by D. Lednicer on the evolution and SAR of major synthetic analgetics based on morphine. Although a good portion of the material treated in this chapter is historical in nature, it nonetheless serves as a useful guide to medicinal chemists and pharmacologists who are embarking on analgesic research. One minor blemish in this otherwise comprehensive coverage lies in the omission of some recently disclosed tricyclic analgetics, which deviate considerably from the partial morphine derivatives, both in structure and in activity profile.

Overall, the quality of production of this volume is excellent; figures and structures are clearly drawn and errors are minimal. It is a fine reference book which fulfills its purpose.

Reviewed by Helen H. Ong
Chemical Research Department
Hoechst-Roussel Pharmaceuticals Inc.
Somerville, NJ 08876

Chromatography of Alkaloids, Part A: Thin-Layer Chromatography. (*Journal of Chromatography*, Vol. 23A). By A. BAERHEIM SVENDSEN and R. VERPOORTE. Elsevier Science Publishing Co., New York, NY 10017. 1982. 533 pp. 16 × 24 cm. Price $104.25 (Dfl. 245).

Although this is the twenty-third volume in a continuing series which began in 1973 with the publication of "Chromatography of Antibiotics" (Volume 1), this is the first volume that is exclusively devoted to the discussion of the chromatography of alkaloids. Because of the large amount of information available, it was decided to publish this volume in two parts: Part A (thin-layer chromatography) and Part B (gas-liquid and high-performance liquid chromatography).

The book is divided into two major portions entitled a "General Part" and a "Special Part." The "General Part," consists of four chapters covering about 60 pages. Chapter 1 includes a discussion of adsorbents, solvent systems, development techniques, sample application, and several tables describing solvent classification and selectivity. Chapter 2 presents a discussion of the various methods of detection, including reagents, tables with color reactions, and a consideration of nonalkaloidal components capable of eliciting false-positive reactions with Dragendorff Reagent. Chapter 3 consists of a general consideration of thin-layer chromatographic separation and identification of alkaloids. This chapter also discusses the use of various reagents, solvent systems, fluorescence, ion-pair adsorption, and ion-exchange thin-layer chromatography. Finally, Chapter 4 includes a discussion of isolation methods and artifact formation resulting from different isolation techniques.

The "Special Part" of the book consists of 17 chapters, about 420 pages, which are devoted to the following classes of alkaloids: pyrrolidine, pyrrolizidine, pyridine, piperidine, quinolizidine, tropane, quinoline, phenethylamine and isoquinoline-derived, indole, steroidal, and miscellaneous. Each chapter consists of an extensive discussion of adsorbents, developing solvents, R_f values, detecting reagents, and references and is richly endowed with tables.

The Appendix alphabetically lists the 106 different reagents that have been discussed throughout the book and includes detailed instructions for their preparation. Finally, the Index is composed of a Subject Index, which contains general topics and classes, and a Compound Index, which contains only compounds.

This is a well-referenced and richly tabled book which should be extremely useful to anyone involved with the detection, isolation/separation, and identification of alkaloids from any source. It is not highly theoretical, nor is it intended to be, and is a practical work which addresses the subject concisely. The price is steep for the individual scientist, but certainly departmental, school, and institutional libraries would want this book in their collection.

Reviewed by Paul L. Schiff, Jr.
Department of Pharmacognosy School of Pharmacy
University of Pittsburgh
Pittsburgh, PA 15261

Controlled Release Delivery Systems. Edited by THEODORE J. ROSEMAN and S. Z. MANSDORF. Marcel Dekker, Inc., 270 Madison Ave., New York, N.Y. 10016. 1983. 402 pp. 15 × 23 cm. Price $57.50 (20% higher outside the U.S. and Canada).

The book, which contains 25 chapters, describes the proceedings of the Eighth International Symposium on Controlled Release of Bioactive Materials held in Fort Lauderdale, Florida, July 26–29, 1981. The editors of the book are recognized leaders in the field of polymeric controlled-release systems, and the authors selected to contribute full-length manuscripts represent a broad international array of experts in this area.

The topics covered in the book range from biomedical applications to agricultural uses for release vehicles for pesticides and herbicides. Heavy emphasis is placed on polymeric delivery systems with only one chapter on the use of prodrugs and one on liposomes. Subjects covered in the book include liposomes, microencapsulation, reservoir and monolithic devices, biodegradable and swellable matrices, prodrugs, and a contribution on magnetically controlled polymeric systems. All chapters contain a discussion section and all are adequately referenced. A subject index is also included.

This is a useful book, providing a reader with an overview of the various applications in controlled-release technology. It cannot be recommended for an individual seeking an in-depth discussion on any one given subject. However, it is well written and serves to elucidate the current status of this rapidly growing field.

Reviewed by Kenneth J. Widder
Molecular Biosystems, Inc.
San Diego, CA 92121

NOTICES

Advances in Steroid Analysis. Edited by S. GOROG. Elsevier Scientific Publishing Co., 52 Vanderbilt Ave., New York, NY 10017. 1982. 551 pp. 16 × 24 cm. Price $104.75 (Dfl. 225.00).

Analytical Profiles of Drug Substances. Vol. II. Edited by KLAUS FLOREY, Academic Press, 111 5th Ave., New York, NY 10003. 1982. 665 pp. 15 × 23 cm.

Application of Pharmacokinetics to Patient Care. Edited by CHARLES A. WALKER and LAMBROS P. TTERLIKKIS. Praeger, 521 Fifth Ave., New York, NY 10175. 1982. 175 pp. 15 × 24 cm. Price $26.50.

Assessing Causes of Adverse Drug Reactions. (*With Special Reference to Standardized Methods*). Editor JAN VENULET. Coeditors: GARRY-CLAUDE BERNEKER and ANTONIO G. CIUCCI. Academic Press, 111 Fifth Ave., New York, NY 10003. 1982. 223 pp. 15 × 23 cm.

Benzodiazepines. A Handbook. (*Basic Data, Analytical Methods, Pharmacokinetics and Comprehensive Literature*). By HAROLD SCHULTZ, Springer-Verlag New York Inc., 175 5th Ave., New York, NY 10010. 1982. 439 pp. 19 × 27 cm. Price $88.00.

British National Formulary, Number 4 (*1982*). Publications of the Pharmaceutical Society of Great Britain. 1 Lambeth High Street, London, SE1 7JN, England. 1982. 454 pp. 13 × 22. Price £4.50.

Cancer Mortality by Occupation and Social Class 1851–1971. (IARC Scientific Publications No. 36) Office of Population Censuses and Surveys, Studies on Medical and Population Subjects No. 44. By W. P. D. LOGAN, Her Majesty's Stationary Office, London, and Lyons International Agency for Research on Cancer. 1982. 253 pp. 20 × 30 cm. Price $30.00 (Sw Fr. 60).

Chromatographic Separation and Extraction with Foamed Plastics and Rubbers. By G. J. MOODY and J. D. R. THOMAS. Marcel Dekker, Inc., 270 Madison Ave., New York, NY 10016. 1982. 139 pp. 14 × 23 cm. Price $29.75. (20% higher outside the U.S. and Canada).

Critical Stability Constants. Vol. 5. First Supplement. By ARTHUR E. MARTELL and ROBERT M. SMITH. Plenum Publishing Corp., 233 Spring St., New York, NY 10013. 1982. 604 pp. 21 × 28 cm. Price $69.50.

Crown Compounds. (*Their Characteristics and Applications.*) By MICHIO HIRAOKA. Elsevier Scientific Publishing Co., 52 Vanderbilt Ave., New York, NY 10017. 1982. 275 pp. 16 × 25 cm. Price $83.75. (Dfl. 180.00).

one of the most interesting aspects of analgesic research: the endogenous, pain-regulating peptides and their synthetic analogues. This chapter should be of prime interest to those who seek the new challenges (and opportunities) of designing enkephalin releasers, metabolic inhibitors, as well as antagonists for substance P as analgetics of the future. The book concludes with a chapter by D. Lednicer on the evolution and SAR of major synthetic analgetics based on morphine. Although a good portion of the material treated in this chapter is historical in nature, it nonetheless serves as a useful guide to medicinal chemists and pharmacologists who are embarking on analgesic research. One minor blemish in this otherwise comprehensive coverage lies in the omission of some recently disclosed tricyclic analgetics, which deviate considerably from the partial morphine derivatives, both in structure and in activity profile.

Overall, the quality of production of this volume is excellent; figures and structures are clearly drawn and errors are minimal. It is a fine reference book which fulfills its purpose.

Reviewed by Helen H. Ong
Chemical Research Department
Hoechst-Roussel Pharmaceuticals Inc.
Somerville, NJ 08876

Chromatography of Alkaloids, Part A: Thin-Layer Chromatography. (*Journal of Chromatography*, Vol. 23A). By A. BAERHEIM SVENDSEN and R. VERPOORTE. Elsevier Science Publishing Co., New York, NY 10017. 1982. 533 pp. 16 × 24 cm. Price $104.25 (Dfl. 245).

Although this is the twenty-third volume in a continuing series which began in 1973 with the publication of "Chromatography of Antibiotics" (Volume 1), this is the first volume that is exclusively devoted to the discussion of the chromatography of alkaloids. Because of the large amount of information available, it was decided to publish this volume in two parts: Part A (thin-layer chromatography) and Part B (gas-liquid and high-performance liquid chromatography).

The book is divided into two major portions entitled a "General Part" and a "Special Part." The "General Part," consists of four chapters covering about 60 pages. Chapter 1 includes a discussion of adsorbents, solvent systems, development techniques, sample application, and several tables describing solvent classification and selectivity. Chapter 2 presents a discussion of the various methods of detection, including reagents, tables with color reactions, and a consideration of nonalkaloidal components capable of eliciting false-positive reactions with Dragendorff Reagent. Chapter 3 consists of a general consideration of thin-layer chromatographic separation and identification of alkaloids. This chapter also discusses the use of various reagents, solvent systems, fluorescence, ion-pair adsorption, and ion-exchange thin-layer chromatography. Finally, Chapter 4 includes a discussion of isolation methods and artifact formation resulting from different isolation techniques.

The "Special Part" of the book consists of 17 chapters, about 420 pages, which are devoted to the following classes of alkaloids: pyrrolidine, pyrrolizidine, pyridine, piperidine, quinolizidine, tropane, quinoline, phenethylamine and isoquinoline-derived, indole, steroidal, and miscellaneous. Each chapter consists of an extensive discussion of adsorbents, developing solvents, R_f values, detecting reagents, and references and is richly endowed with tables.

The Appendix alphabetically lists the 106 different reagents that have been discussed throughout the book and includes detailed instructions for their preparation. Finally, the Index is composed of a Subject Index, which contains general topics and classes, and a Compound Index, which contains only compounds.

This is a well-referenced and richly tabled book which should be extremely useful to anyone involved with the detection, isolation/separation, and identification of alkaloids from any source. It is not highly theoretical, nor is it intended to be, and is a practical work which addresses the subject concisely. The price is steep for the individual scientist, but certainly departmental, school, and institutional libraries would want this book in their collection.

Reviewed by Paul L. Schiff, Jr.
Department of Pharmacognosy School of Pharmacy
University of Pittsburgh
Pittsburgh, PA 15261

Controlled Release Delivery Systems. Edited by THEODORE J. ROSEMAN and S. Z. MANSDORF. Marcel Dekker, Inc., 270 Madison Ave., New York, N.Y. 10016. 1983. 402 pp. 15 × 23 cm. Price $57.50 (20% higher outside the U.S. and Canada).

The book, which contains 25 chapters, describes the proceedings of the Eighth International Symposium on Controlled Release of Bioactive Materials held in Fort Lauderdale, Florida, July 26–29, 1981. The editors of the book are recognized leaders in the field of polymeric controlled-release systems, and the authors selected to contribute full-length manuscripts represent a broad international array of experts in this area.

The topics covered in the book range from biomedical applications to agricultural uses for release vehicles for pesticides and herbicides. Heavy emphasis is placed on polymeric delivery systems with only one chapter on the use of prodrugs and one on liposomes. Subjects covered in the book include liposomes, microencapsulation, reservoir and monolithic devices, biodegradable and swellable matrices, prodrugs, and a contribution on magnetically controlled polymeric systems. All chapters contain a discussion section and all are adequately referenced. A subject index is also included.

This is a useful book, providing a reader with an overview of the various applications in controlled-release technology. It cannot be recommended for an individual seeking an in-depth discussion on any one given subject. However, it is well written and serves to elucidate the current status of this rapidly growing field.

Reviewed by Kenneth J. Widder
Molecular Biosystems, Inc.
San Diego, CA 92121

NOTICES

Advances in Steroid Analysis. Edited by S. GOROG. Elsevier Scientific Publishing Co., 52 Vanderbilt Ave., New York, NY 10017. 1982. 551 pp. 16 × 24 cm. Price $104.75 (Dfl. 225.00).

Analytical Profiles of Drug Substances. Vol. II. Edited by KLAUS FLOREY, Academic Press, 111 5th Ave., New York, NY 10003. 1982. 665 pp. 15 × 23 cm.

Application of Pharmacokinetics to Patient Care. Edited by CHARLES A. WALKER and LAMBROS P. TTERLIKKIS. Praeger, 521 Fifth Ave., New York, NY 10175. 1982. 175 pp. 15 × 24 cm. Price $26.50.

Assessing Causes of Adverse Drug Reactions. (*With Special Reference to Standardized Methods*). Editor JAN VENULET. Coeditors: GARRY-CLAUDE BERNEKER and ANTONIO G. CIUCCI. Academic Press, 111 Fifth Ave., New York, NY 10003. 1982. 223 pp. 15 × 23 cm.

Benzodiazepines. A Handbook. (*Basic Data, Analytical Methods, Pharmacokinetics and Comprehensive Literature*). By HAROLD SCHULTZ, Springer-Verlag New York Inc., 175 5th Ave., New York, NY 10010. 1982. 439 pp. 19 × 27 cm. Price $88.00.

British National Formulary, Number 4 (*1982*). Publications of the Pharmaceutical Society of Great Britain. 1 Lambeth High Street, London, SE1 7JN, England. 1982. 454 pp. 13 × 22. Price £4.50.

Cancer Mortality by Occupation and Social Class 1851–1971. (IARC Scientific Publications No. 36) Office of Population Censuses and Surveys, Studies on Medical and Population Subjects No. 44. By W. P. D. LOGAN, Her Majesty's Stationary Office, London, and Lyons International Agency for Research on Cancer. 1982. 253 pp. 20 × 30 cm. Price $30.00 (Sw Fr. 60).

Chromatographic Separation and Extraction with Foamed Plastics and Rubbers. By G. J. MOODY and J. D. R. THOMAS. Marcel Dekker, Inc., 270 Madison Ave., New York, NY 10016. 1982. 139 pp. 14 × 23 cm. Price $29.75. (20% higher outside the U.S. and Canada).

Critical Stability Constants. Vol. 5. First Supplement. By ARTHUR E. MARTELL and ROBERT M. SMITH. Plenum Publishing Corp., 233 Spring St., New York, NY 10013. 1982. 604 pp. 21 × 28 cm. Price $69.50.

Crown Compounds. (*Their Characteristics and Applications.*) By MICHIO HIRAOKA. Elsevier Scientific Publishing Co., 52 Vanderbilt Ave., New York, NY 10017. 1982. 275 pp. 16 × 25 cm. Price $83.75. (Dfl. 180.00).

Cyclodextrins and Their Inclusion Complexes. By J. SZEJTLI. Heyden & Son, Inc., 247 S. 41st Street, Philadelphia, PA 19104. 182. 296 pp. 16 × 24 cm. Price $35.00.

Drugs and Nursing Implications. 4th Ed. By LAURA E. GOVONI and JANICE E. HAYES. Appleton-Century-Crofts, 292 Madison Ave., New York, NY 10017. 1982. 1143 pp. 15 × 23 cm.

Drug Therapy in Obstetrics and Gynecology. Edited by WILLIAM F. RAYBURN and FREDERICK P. ZUSPAN. Appleton-Century-Crofts, 292 Madison Ave., New York, NY 10017. 1982. 399 pp. 17 × 24 cm. Price $38.50.

Dynamics of Biological Membranes. (Influence on Synthesis, Structure and Function). By M. D. HOUSLAY and K. K. STANLEY. John Wiley & Sons, One Wiley Drive, Somerset, NJ 08873. 1982. 330 pp. 15 × 23 cm. Price $54.95.

Environmental Health Criteria 18: Arsenic. Health & Biomedical Information Programme, World Health Organization, 1211 Geneva 27, Switzerland, 174 pp. 13 × 21 cm.

Environmental Health Criteria 19: Hydrogen Sulfide. Health & Biomedical Information Programme, World Health Organization, 1211 Geneva 27, Switzerland. 1982. 60 pp. 14 × 21 cm. Price Sw Fr. 6.

Field Guide to the Detection and Control of Xerophthalmia. 2nd Ed. By ALFRED SOMMER. World Health Organization, Health and Biomedical Information Programme, 1211 Geneva 27, Switzerland. 1982. 58 pp. 15 × 24 cm. Price Sw Fr. 10.

Flavonoids and Bioflavonoids, 1981. Studies In Organic Chemistry II. (Proceedings of the International Bioflavonoids Symposium—6th Hungarian Bioflavonoid Symposium, Munich, FRG 9-6-81). Edited by L. FARKAS, M. GABOR, F. KALLAY, and H. WAGNER. Elsevier Scientific Publishing Co., 52 Vanderbilt Ave., New York, NY 10017. 1982. 534 pp. 16 × 24 cm. Price $104.75. (Dfl. 225).

From Genetic Experimentation to Biotechnology—The Critical Transition. Edited by WILLIAM J. WHELAN and SANDRA BLACK. John Wiley & Sons, Inc., One Wiley Drive, Somerset, NJ 08873. 1982. 266 pp. 15 × 23 cm. Price $39.95.

IARC Monographs on the Evaluation of the Carcinogenic Risk of Chemicals to Humans. Vol. 27: Some Aromatic Amines, Anthraquinones and Nitroso Compounds, and Inorganic Fluorides Used in Drinking Water and Dental Preparations. Lyons, International Agency for Research on Cancer. 1982. 341 pp. 17 × 24 cm. Price Sw Fr. 40.

IARC Monographs on the Evaluation of the Carcinogenic Risk of Chemicals to Humans. Vol. 28: The Rubber Industry. Health & Biomedical Information Programme, World Health Organization, 1211 Geneva 27, Switzerland. 486 pp. 17 × 24 cm. Price Sw Fr. 70.

Immune Regulation. (Evolutionary and Biological Significance). Edited by LAURENS N. RUBEN and M. ERIC GERSHWIN. Dekker, 270 Madison Ave., New York, NY 10016. 331 pp. 15 × 23 cm. Price $45.00 (20% higher outside U.S. and Canada.)

Index Nominum 1982. 11th Ed. Edited and published by the Laboratory of the Swiss Pharmaceutical Society of Zurich. Drug Intelligence Publications, Inc., 1241 Broadway, Hamilton, IL 62341. 1982. 1006 pp. 20 × 30 cm. Price $140.00.

Laboratory Decontamination and Destruction of Carcinogens in Laboratory Wastes: Some Nitrosamines. Editors: M. CASTEGNARO. G. EISENBRAND, G. ELLEN, L. KEEFER, D. KLEIN, E. B. SANSONE, D. SPINCER, G. TELLING & K. WEBB. Health & Biomedical Information Programme, World Health Organization, 1211 Geneva 27, Switzerland. 1982. 73 pp. 17 × 24 cm. Price $10.00 (Sw Fr. 18).

Legislative Action to Combat the World Smoking Epidemic. By RUTH ROEMER. Health & Biomedical Information Programme, World Health Organization, 1211 Geneva 27, Switzerland. 131 pp. 15 × 24 cm. Price Sw Fr. 17.

Literature Guide to the GLC of Body Fluids. By AUSTIN W. SIGNEUR. Plenum, 233 Spring Street, New York, NY 10013. 1982. 385 pp. 21 × 27 cm. Price $85.00.

Macromolecular Chemistry, Vol. 2. A Review of the Literature Published during 1979 and 1980. Reporters: A. D. JENKINS and J. F. KENNEDY. The Royal Society of Chemistry, Burlington House, London WIV OBN, England. 1982, 425 pp. 13 × 22 cm. Price $117.00 (£59.00)

Methods in Environmental Virology. Edited by CHARLES P. GERBA and SAGAR M. GOYAL. Dekker, 270 Madison Ave., New York, NY 10016. 1982. 378 pp. 15 × 23 cm. Price $59.50 (20% higher outside the U.S. and Canada).

The Natural Coumarins: (Occurrence, Chemistry, and Biochemistry). By ROBERT D. H. MURRAY, JESUS MENDEZ, and STEWART A. BROWN. Wiley. One Wiley Drive, Somerset, NJ 08873. 1982. 702 pp. 17 × 25 cm. Price $162.00.

Orphan Drugs. Edited by FRED E. KARCH. Dekker, 270 Madison Ave., New York, NY 10016. 1982. 210 pp. 15 × 23 cm. Price $49.50. (20% higher outside the U.S. and Canada).

Patents For Chemists. By PHILIP W. GRUBB. Oxford University Press, 200 Madison Ave., New York, NY 10016. 1982. 273 pp. 15 × 23 cm. Price $39.95.

Pharmacology of Histamine Receptors. Edited by C. R. GANELLIN and M. E. PARSONS. John Wright-PSG Inc., Littleton, MA 01460. 1982. 521 pp. 15 × 24 cm. Price $69.50.

Problems of Drug Dependence, NIDA Research Monograph 41. (Proceedings of the 43rd Annual Scientific Meeting, The Committee on Problems of Drug Dependence, Inc). 1982. National Institute on Drug Abuse, Division of Research, 5600 Fishers Lane, Rockville, MD 20857. 561 pp. 14 × 23 cm.

Quality Assurance in Diagnostic Radiology. Geneva, World Health Organization Health & Biomedical Information Programme, World Health Organization, 1211 Geneva 27, Switzerland. 1982. 65 pp. 15 × 14 cm. Price Sw Fr. 11.

Recent Developments in Cardiac Muscle Pharmacology. Edited by SHOJI SHIBATA and LESLIE E. BAILEY. Igaku-Shoin Medical Publishers, Inc., 1140 Avenue of the Americas, New York, NY 10036. 1982. 128 pp. 17 × 26 cm. Price $29.50.

Steric Effects in Biomolecules. Studies in Physical and Theoretical Chemistry. Vol. 18. (Proceedings of the International Symposium. Eger, Hungary, 10/5-8, 1981). Edited by G. NARAY-SZABO. Elsevier Scientific Publishing Co., 52 Vanderbilt Ave., New York, NY 10017. 1982. 416 pp. 16 × 24 cm. Price $107.00 (Dfl. 230.00).

1982 Year Book of Drug Therapy. Edited by LEO E. HOLLISTER and LOUIS C. LASAGNA. Year Book Medical Publishers, 35 East Wacker Drive, Chicago, IL 60601. 1982. 437 pp. 15 × 23 cm. Price $40.00.

NEW JOURNALS

Journal of Carbohydrate Chemistry. Edited by DONALD E. KELLY. Dekker, 270 Madison Ave., New York, NY 10016. 1982. 128 pp. 14 × 23 cm. Price $75.00 (Institutional); $37.50 (Individual). Add postage ($6.30, surface; $12.75, airmail) outside the U.S.

Journal of Toxicology. Vol. 1 No. 1: Cutaneous and Ocular Toxicology. Edited by EDWARD M. JACKSON, Dekker, 270 Madison Ave., New York, NY 10016. 1982. 88 pp. 17 × 26 cm. Price $111.50 (Institutional), $55.75 (Individual). Add postage ($8.40, surface; $11.20, airmail) outside the U.S.

Improving the Reliability of Clinical Investigators

[Editor's note: The May 1983 editorial triggered an exchange of letters between former FDA Commissioner Jere E. Goyan and the author of the editorial, Edward G. Feldmann. In the interest of stimulating further thought on the important subject dealt with in the editorial, they have agreed to publication of their correspondence which follows herewith.]

Goyan letter to Feldmann, dated June 2, 1983:

Just a note to let you know that I read your editorial[1] entitled "The 'Weak Link' in Drug Research." I was somewhat astonished at your analysis and conclusions but understand your concerns. Indeed, one of the biggest shocks of my life was the opportunity to review some of the proposed disciplinary actions against clinical investigators. It is distressing to learn that many of the people in the "white hats" are at least somewhat gray, if not black. However, I am a little hard pressed to understand what alternatives we might have in this regard. It seems to me that we are going to have to make use of clinical investigators in academic settings, but unfortunately we may have to devote more resources to their policing. In any case, it was as usual a very provocative and worthwhile editorial.

Jere E. Goyan
Dean, School of Pharmacy
University of California
San Francisco, CA 94143

Received June 6, 1983.

[1] E. G. Feldmann, *J. Pharm., Sci.*, **72**, 463 (1983).

Feldmann letter to Goyan, dated June 7, 1983:

Last week I attended an FDA retirement dinner and reception and had an opportunity to chat with various FDA staff members from new drug officers to enforcement/compliance people to legal staff, and I was frankly surprised at how many of them apparently had read the editorial, brought it up in conversation with me, and expressed their personal concerns regarding the reliability of clinical investigators and their data submitted in support of NDAs. It was quite apparent to me that I had hit a responsive chord among the FDA staff.

I fully understand your comments as to the difficulty in identifying alternatives to our present system. I am not sure that I have any magical answers either, and for that reason did not attempt to include any in the editorial.

However, it would seem to me that arrangements could be worked out which would involve individuals (clinical investigators) who are *employees* of drug firms being based physically at hospitals or in academic settings which would enable them to conduct investigations in much the same environment and with the same basic *modus operandi* that is presently utilized—the only significant difference being that rather than functioning as independent contractors, they would actually be employed by the drug company involved.

In a sense, it might be argued that this kind of arrangement would result in somewhat less "independence" or "independent authority" on the part of the clinical investigator. Although that argument (for "independence") sounds good in theory, in practice there appear to be certain drawbacks:

(a) The company, *per se*, is not responsible for the actions of the clinical investigator, and it can readily disclaim responsibility if there is any "hanky panky."

(b) A conscientious drug firm has its hands tied and cannot have complete access to the data to the degree that it would have if the investigator were a paid employee; hence, it cannot fully assure itself of the completeness, adequacy, and suitability of the data.

(c) Under the present system, independent investigators feel pressured to provide favorable reports to their sponsoring or contracting companies if they hope to generate future "business." However, if they were on the regular payroll, they would have no more pressure in this regard than other comparable departments within the firm, such as the other divisions within the research and development department.

(d) The clinical investigations could be made a much more intimate part of the comprehensive NDA in that they would be simply another part of the company's overall research effort rather than a separate sort of "appendage" to the NDA, as many of them are currently.

I realize that some may object to such an arrangement in that it tends to reduce "academic freedom." On the other side of the coin, however, it also tends to result in better cooperation and interchange between industry and academia—a goal or objective that we frequently hear and read is being currently encouraged. As I noted above, I am not sure this is either the preferred or even a feasible idea, but it is one alternative to our present system.

Edward G. Feldmann
American Pharmaceutical Association
Washington, DC 20037

Received June 8, 1983.

Goyan letter to Feldmann, dated June 14, 1983:

Thank you for your letter of June 7. I hope you will see fit to publish your thoughts, as outlined in the letter, in the *Journal* in the near future. They are both interesting and provocative and may well be the way of the future. In any case, you have struck a responsive chord in a number of us, and I, for one, would like to see some sort of debate initiated in this regard.

Jere E. Goyan
Dean, School of Pharmacy
University of California
San Francisco, CA 94143

Received June 17, 1983.

Kavanagh letter to Feldman

Your editorial "The Weak Link in New Drug Research" [1] points to an old problem well known to drug makers which is now receiving public attention. I see no way to improve the quality of clinical testing and its evaluation. My reasons are the following.

These observations are based on approximately 28 years of experience with two drug companies and rely on material provided to me by employees of other companies. In general, the opinion among scientists employed by drug companies is that physicians make very poor directors of research, at any level, since they have neither the aptitude for scientific work nor the training as scientists. My experience leads me to agree with this opinion.

A physician from Parke-Davis said in 1960 that he envied Eli Lilly and Co. because it had its own clinical facilities, in operation since 1926. This in-house clinical facility was to evaluate clinical reports submitted by outside physicians who were clinically evaluating Lilly products. The availability of this monitoring function should make clinical investigations more efficient.

Here are some specific examples. Around 1960, pediatricians in San Francisco were treating neonates routinely with 20 mg/kg chloramphenicol (twice the dose recommended by Parke-Davis for adults), and approximately one-third of the infants died. Parke-Davis, of course, was blamed. Another drug company informed me they could use only about one-third of the results from their contracted clinical studies. An analyst for another company visited six clinicians who were studying a new antibiotic and found that only one was using an assay that would give meaningful data. During the study of a new antibiotic, an assay laboratory found interfering material in the urine of patients being treated with the new antibiotic. Paper chromatography revealed as many as seven foreign antibiotics in the urine samples. The physicians were amazed that the laboratory discovered they were using more than one drug.

I wonder how much of this kind of information ever gets back to anyone in charge of clinical testing. What could be done with the

information? Obviously, this system of testing is expensive, time consuming, and frustrating for the drug companies, but what can they do as long as physicians dominate clinical testing?

The basic problem with clinical testing is the assumption that physicians are scientists. There is no reason to expect a physician to be a scientist.

Clinical testing will improve only when properly qualified people do the work. The physicians who are members of a testing team should be selected for scientific aptitude and then given the needed training. The team should include a physician, a pharmacist (preferably Pharm.D.), an experienced technical writer (to help organize data and prepare the reports), and such other support personnel as needed for that particular study. In the case of antibiotic testing, the team should include someone experienced in the principles and practices of using a microbiological assay for antibiotics (these people are rare).

One reason I am pessimistic about the possibility of improving clinical testing is the difficulty in getting physicians to give up the power they now possess. The ego problem could be minimized by selecting the physician members from among those who have a Ph.D. degree in a related subject such as zoology or physiology. Their previous experience in a laboratory would assure their understanding the importance of scientific protocol, the awareness that correlation and cause are not synonymous, and the effects of genetic makeup of the patients on results.

Many more examples could be given, but these are sufficient to indicate what some of the problems are. Obviously, no drug firm would dare make public these complaints. The firms doing the research are dependent on the good will of physicians for their success.

Frederick Kavanagh
Corvallis, Oregon 97330

Received August 9, 1983.

[1] E. G. Feldmann, *J. Pharm. Sci.*, **72**, 463 (1983).

Pharmaceutical Analysis and Control Award

Members of the Pharmaceutical Analysis and Control (PAC) Section of the APhA Academy of Pharmaceutical Sciences are concerned about the paucity of students choosing to study pharmaceutical analysis at the doctoral level. As a means of promoting graduate study in this discipline, the PAC Section is offering an undergraduate award in pharmaceutical analysis for 1984. Applications are currently being invited from undergraduate students enrolled in the last two years of baccalaureate or equivalent degree programs in accredited schools or colleges of pharmacy and departments of chemistry who have demonstrated interest and potential for a career in pharmaceutical analysis. The Award will consist of scholarship support ($1,000) for a ten-week summer period or equivalent (NLT 400 hrs) of laboratory research in pharmaceutical analysis. Applications are due in the Academy Office by December 31, 1983. Notice of awards will be mailed by March 31, 1984. Application instructions and application forms are available by calling or writing: APhA Academy of Pharmaceutical Sciences, Undergraduate Award in Pharmaceutical Analysis, 2215 Constitution Avenue, N.W., Washington, D.C., 20037, (202) 628-4410.

We encourage faculty and students to apply for the PAC Award in Pharmaceutical Analysis. Thank you.

Robert V. Smith, Ph.D.
Chairman Elect,
PAC Section, APhA Academy of Pharmaceutical Sciences

Received August 18, 1983.

information? Obviously, this system of testing is expensive, time consuming, and frustrating for the drug companies, but what can they do as long as physicians dominate clinical testing?

The basic problem with clinical testing is the assumption that physicians are scientists. There is no reason to expect a physician to be a scientist.

Clinical testing will improve only when properly qualified people do the work. The physicians who are members of a testing team should be selected for scientific aptitude and then given the needed training. The team should include a physician, a pharmacist (preferably Pharm.D.), an experienced technical writer (to help organize data and prepare the reports), and such other support personnel as needed for that particular study. In the case of antibiotic testing, the team should include someone experienced in the principles and practices of using a microbiological assay for antibiotics (these people are rare).

One reason I am pessimistic about the possibility of improving clinical testing is the difficulty in getting physicians to give up the power they now possess. The ego problem could be minimized by selecting the physician members from among those who have a Ph.D. degree in a related subject such as zoology or physiology. Their previous experience in a laboratory would assure their understanding the importance of scientific protocol, the awareness that correlation and cause are not synonymous, and the effects of genetic makeup of the patients on results.

Many more examples could be given, but these are sufficient to indicate what some of the problems are. Obviously, no drug firm would dare make public these complaints. The firms doing the research are dependent on the good will of physicians for their success.

Frederick Kavanagh
Corvallis, Oregon 97330

Received August 9, 1983.

[1] E. G. Feldmann, *J. Pharm. Sci.*, **72**, 463 (1983).

Pharmaceutical Analysis and Control Award

Members of the Pharmaceutical Analysis and Control (PAC) Section of the APhA Academy of Pharmaceutical Sciences are concerned about the paucity of students choosing to study pharmaceutical analysis at the doctoral level. As a means of promoting graduate study in this discipline, the PAC Section is offering an undergraduate award in pharmaceutical analysis for 1984. Applications are currently being invited from undergraduate students enrolled in the last two years of baccalaureate or equivalent degree programs in accredited schools or colleges of pharmacy and departments of chemistry who have demonstrated interest and potential for a career in pharmaceutical analysis. The Award will consist of scholarship support ($1,000) for a ten-week summer period or equivalent (NLT 400 hrs) of laboratory research in pharmaceutical analysis. Applications are due in the Academy Office by December 31, 1983. Notice of awards will be mailed by March 31, 1984. Application instructions and application forms are available by calling or writing: APhA Academy of Pharmaceutical Sciences, Undergraduate Award in Pharmaceutical Analysis, 2215 Constitution Avenue, N.W., Washington, D.C., 20037, (202) 628-4410.

We encourage faculty and students to apply for the PAC Award in Pharmaceutical Analysis. Thank you.

Robert V. Smith, Ph.D.
Chairman Elect,
PAC Section, APhA Academy of Pharmaceutical Sciences

Received August 18, 1983.

November 1983
Volume 72 Number 11

JOURNAL OF PHARMACEUTICAL SCIENCES

A publication of the American Pharmaceutical Association

The *Journal of Pharmaceutical Sciences* (ISSN 0022-3549) is published monthly by the American Pharmaceutical Association (APhA) at 2215 Constitution Ave., N.W., Washington, DC 20037. Second-class postage paid at Washington, D.C. and at additional mailing office.

Offices—Editorial, Advertising, and Subscription: 2215 Constitution Ave., N.W., Washington, DC 20037. All Journal staff may be contacted at this address. Printing: 20th & Northampton Streets, Easton, PA 18042.

Annual Subscriptions—United States and foreign, industrial and government institutions $75; educational institutions $75; individuals *for personal use only* $40; single copies $10. APhA and SAPhA members may subscribe to *J. Pharm. Sci.* for $20.00 per year. All foreign subscriptions add $10 for postage. Subscription rates are subject to change without notice.

Claims—Missing numbers will not be supplied if dues or subscriptions are in arrears for more than 60 days or if claims are received more than 60 days after the date of the issue, or if loss was due to failure to give notice of change of address. APhA cannot accept responsibility for foreign delivery when its records indicate shipment was made.

Change of Address—Members and subscribers should notify at once both the Post Office and APhA of any change of address.

Photocopying—The code at the foot of the first page of an article indicates that APhA has granted permission for copying of the article beyond the limits permitted by Sections 107 and 108 of the U.S. Copyright Law provided that the copier sends the per copy fee stated in the code to the Copyright Clearance Center, Inc., 21 Congress St., Salem, MA 01970. Copies may be made for personal or internal use only and not for general distribution.

Microfilm—Available from University Microfilms International, 300 N. Zeeb Road, Ann Arbor, MI 48106.

Keeping Current With Technology

"Technology." Over the years, we have all heard and used this term many times. But yet, during the past year or two, it has virtually burst onto the contemporary scene with a whole new dimension and depth of meaning.

To compare the technology in our daily lives of five years ago *versus* that of today, is almost like comparing flight by hot air balloon to flight by supersonic jet aircraft. Simply put, recent changes in technology have been that great.

Every facet of our lives from work to play, to recreation, to personal living has been affected, and the developments have occurred with astonishing swiftness. Indeed, the rate of change has been as mind-boggling as the degree of change.

For example, just about a year ago, video games arrived and mushroomed with such attraction and public acceptance that investment counselors were touting the stock of all their manufacturers, the games were by far the biggest seller of the 1982 Christmas season, and video game parlors were popping up in almost every neighborhood shopping center. But now, less than a year later, we just heard a report that video games have peaked in popularity, and predictions are that the games, their franchise operations, and their manufacturers will soon experience a severe decline that will be every bit as rapid and intense as their recent, rocketing popularity.

One of the most innovative and revolutionary computer manufacturers, Osborne Computer Corporation, had a similar rapid ascendancy as it carved out a major share of the computer market of two to four years ago. But just as this column was being written, business and financial reports in the public press are describing the sudden demise of that company. It went from one of the most popular growth stocks to filing for bankruptcy within the short period of approximately six months. In explanation, a security analyst said that "time had simply passed them by." Their relatively small, portable units were a dramatic breakthrough compared with the large, floor model consoles previously available; but, in turn, those table model units were made equally obsolete by the much smaller, lighter, and more portable units that competitors came out with just a few months later.

In the pharmaceutical field, the impact of rapidly changing technology is almost as dramatic.

At a corporate level, there have been some mergers and acquisitions that at first seem strange, but upon reflection make a great deal of sense. Witness the marriage of Smith Kline & French Laboratories, and Beckman Instruments Company. Ten years ago, we could never have visualized any common denominator between a "Spansule® Capsule" and a "DU Spectrophotometer." But today is a completely different story.

And at the level of drug dosage forms, we increasingly hear of "new drug delivery systems." Time-release implants, transdermal absorption, nasal administration, implanted drug pumps, and various other approaches to *in vivo* biological drug delivery are no longer either dreams, speculations, or theory, but are now being routinely used in patients.

Again, the suddenness of this change is literally breathtaking. Scientists and practitioners who were up-to-date a few short years ago, today find themselves embarrassingly obsolescent if they have not kept abreast of these developments.

For this reason in particular, the American Pharmaceutical Association and its subdivisions—including the Academy of Pharmaceutical Sciences—have chosen the theme of "Technology 2000" for the APhA and APS Annual Meeting to be held May 5–10, 1984, in Montreal, P.Q., Canada.

All aspects of the meeting—from exhibitors, to general sessions, to special presentations—will focus on and emphasize technology, its recent advances, and its impact on current pharmaceutical research, development, and practice. With respect to exhibits in particular, a special effort is being put forth to attract technology-oriented exhibitors so that the Exposition at the 1984 Annual Meeting will constitute a convenient, ready-made opportunity to see first-hand the most up-to-date equipment being put through its paces in providing modern technological benefits.

All of these offerings should go far in assisting the meeting registrants to put this new technology into mental perspective and to relate it to the way that pharmacy will be practiced and pharmaceutical research will be conducted in the 21st century.

We strongly urge all of our readers to plan to attend the 1984 Annual Meeting in order that, individually, they will not find themselves suffering the fate of some of the recently high-flying computer manufacturers who suddenly found to their dismay that "time had simply passed them by."

—EDWARD G. FELDMANN
American Pharmaceutical Association
Washington, DC 20037

0022-3549/83/1100-1237$01.00/0

JOURNAL OF PHARMACEUTICAL SCIENCES

NOVEMBER 1983
VOLUME 72 NUMBER 11

RESEARCH ARTICLES

Physiologically Based Pharmacokinetic Model for β-Lactam Antibiotics I: Tissue Distribution and Elimination in Rats

AKIRA TSUJI *x, TAKAYOSHI YOSHIKAWA *, KAZUNORI NISHIDE *, HIDEMI MINAMI *, MOTONOBU KIMURA *, EMI NAKASHIMA *, TETSUYA TERASAKI *, ETSUKO MIYAMOTO *¶, CHARLES H. NIGHTINGALE §, and TSUKINAKA YAMANA ‡

Received April 5, 1982, from the *Faculty of Pharmaceutical Sciences and ‡Hospital Pharmacy, Kanazawa University, Kanazawa 920, Japan and §Hartford Hospital, Hartford, CT 06115 and University of Connecticut, School of Pharmacy, Storrs, CT 06268. Accepted for publication September 2, 1982. ¶Present address: School of Pharmacy, Hokuriku University, Kanazawa 920-11, Japan.

Abstract □ The disposition characteristics of β-lactam antibiotics in rats were investigated, and a physiologically based pharmacokinetic model capable of predicting the tissue distribution and elimination kinetics of these drugs was developed. Protein-binding parameters in rat serum were determined by equilibrium dialysis. Linear binding was found for penicillin G, methicillin, dicloxacillin, and ampicillin; however, nonlinear binding was observed for penicillin V and cefazolin. After intravenous bolus dosing, cefazolin was recovered almost completely in urine and bile, while for the penicillins, penicilloic acid was found to be the major metabolite. Biliary excretion of cefazolin followed Michaelis-Menten kinetics, and no significant inhibition of urinary secretion was observed after probenecid administration. The renal clearance of unbound drug was 0.82 ml/min with a reabsorption ratio (R) of 0.22. Tubular secretion was inhibited for the penicillins by probenecid plasma concentrations of 50 μg/ml, resulting in an R-value of 0.32. Erythrocyte uptake, serum protein binding, and tissue-to-plasma partition coefficient (K_p) were measured. Theoretical K_p values were calculated and found to be in good agreement with the K_p values for three of the antibiotics. Plasma and tissue concentrations (lung, heart, muscle, skin, gut, bone, liver, and kidney) were measured as a function of time at various doses for inulin and cefazolin in rats after an intravenous bolus dose, and were found to be in reasonable agreement with concentrations predicted by the model. These correlations demonstrate that the proposed model can accurately describe the plasma and tissue contributions of inulin and cefazolin in the rat and suggest that this model could have utility in predicting drug distribution in humans.

Keyphrases □ β-Lactam antibiotics—protein binding and metabolism, rats, pharmacokinetics, physiologically based model □ Pharmacokinetics—β-lactam antibiotics, protein binding and metabolism in rats, physiologically based model □ Metabolism—β-lactam antibiotics in rats, pharmacokinetics, physiologically based model

Serum or plasma levels of antibiotics are often used as indices of pharmacological efficacy. However, since bacterial infections are generally localized in the extravascular space, it is important to know the antibiotic concentration in the interstitial fluid. Numerous pharmacokinetic studies on penicillins and cephalosporins have been published (1–6); however, few compare kinetically the levels of these antibiotics in plasma and tissues. Physiologically based pharmacokinetic models (7–12) have been developed using data obtained from animals such as tissue binding or tissue-to-plasma partition coefficients (K_p). Some of these studies have been used successfully to predict both plasma and tissue levels in humans (7–9, 11). Recently, Greene *et al.* (13) reported that using serum protein binding and renal clearance data, the novel physiological pharmacokinetics of cephalosporins could be adapted to predict plasma concentration–time profiles after bolus intravenous injections in humans.

This study describes the metabolism and tissue binding behavior of several β-lactam antibiotics in rats, establishes a mathematical model for the interpretation of tissue distribution and elimination kinetics of these antibiotics, and describes the use of inulin as a model drug for verification of the present model.

EXPERIMENTAL

Materials—Penicillin G potassium (1595 U/mg)[1], methicillin sodium (843 μg/mg)[2], penicillin V potassium (1490 U/mg)[1], propicillin potassium (888 μg/mg)[3], dicloxacillin sodium (884 μg/mg)[1], ampicillin sodium (959 μg/mg)[3], 6-aminopenicillanic acid (97.6% pure)[1], cefazolin sodium (945

[1] Meiji Seika Kaisha, Tokyo, Japan.
[2] Banyu Pharmaceutical Co., Tokyo, Japan.
[3] Takeda Chemical Industries, Osaka, Japan.

0022-3549/83/1100-1239$01.00/0

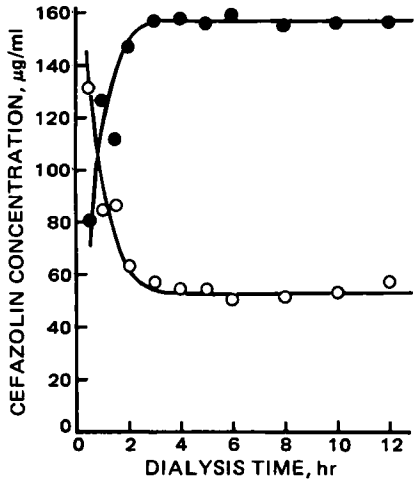

Figure 1—*Cefazolin concentrations in buffer (○) and rat serum (●) compartments at 37° during the protein binding experiment. The initial concentration of cefazolin in the buffer compartment was 200 μg/ml.*

μg/mg)[4], *and indocyanine green*[5] were used as received. [^{14}C]Cefazolin[4] with a specific activity of 2.04 μCi/mg was supplied, and [^{14}C]inulin (2.4 μCi/mg) was purchased from a commercial source[6]. Unless otherwise specified, the radiolabeled drug was used in conjunction with a cold carrier.

Solutions of the penicilloic acids of dicloxacillin, propicillin, penicillin V, ampicillin, and 6-aminopenicillanic acid were prepared according to the method of Schwartz and Delduce (14). All other chemicals were reagent grade and were used without further purification.

Animals—Male albino Wistar rats, weighing ~240 g, and a 9-kg beagle dog were fasted for 20 hr prior to the experiment, with free access to water. The rats were anesthetized with urethane (1.3 g/kg ip) ~1 hr prior to surgery. The dog was anesthetized with sodium pentobarbital[7] administered intravenously at a dose of 25 mg/kg.

Intravenous Bolus Injection—The ureters and bile ducts of rats were catheterized with polyethylene tubing[8], and the drugs were injected (over 5 sec) through the femoral vein. The β-lactam antibiotics or inulin were dissolved in 0.5 ml of normal saline. For the plasma and tissue concentration studies, blood samples (~0.2 ml) were withdrawn from the jugular vein at designated times after drug administration and collected in heparinized tubes. The blood was centrifuged at 3000 rpm, and plasma

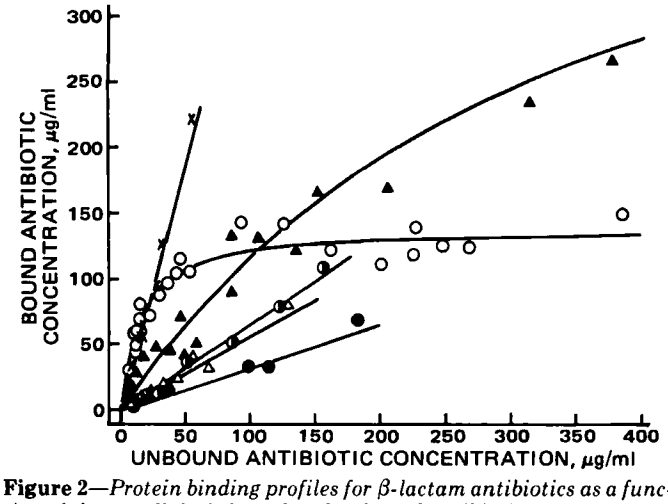

Figure 2—*Protein binding profiles for β-lactam antibiotics as a function of the postdialysis bound and unbound antibiotic concentrations at 37°. The points represent the experimental values, and the solid lines were generated from Eq. 1 or Eq. 2; the binding parameters are listed in Table I. Key: (●) methicillin; (△) penicillin G; (◑) ampicillin; (○) cefazolin; (▲) penicillin V; (X) dicloxacillin.*

[4] Fujisawa Pharmaceutical Co., Osaka, Japan.
[5] Daiichi Seiyaku Co., Tokyo, Japan.
[6] New England Nuclear Co., Boston, Mass.
[7] Nembutal; Dainihon Pharmaceutical Co., Osaka, Japan.
[8] Type PE-10; Clay Adams, Becton Dickinson, Co., Parsippany, N.J.

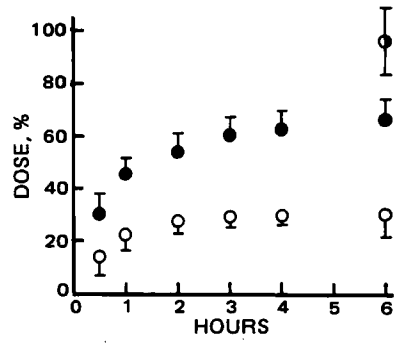

Figure 3—*Time courses of the percent of cefazolin recovered in bile (○) and urine (●) after a 100-mg/kg iv bolus dose to rats. Each point represents the mean of four rats, the vertical bars representing the standard deviations. Total recovery (◑), as the intact cefazolin 6 hr after the administration, was 95.7 ± 13.0%.*

separated. The total blood volume taken from any rat in a single experiment was ≤1.6 ml.

For tissue sampling, the rats were sacrificed, and the lung, heart, skeletal muscle, bone, gut (from duodenum to the cecum), liver, and kidney were quickly excised, rinsed with ice-cold saline, blotted dry, and weighed. These tissues were homogenized with a two- to fivefold excess of isotonic phosphate buffer (pH 7.4) in a polytef homogenizer. The entire skin was stripped from the rat carcass. Sections of the skin from the flank regions were sampled and cut into small pieces. Bone samples were taken from the femoral and foreleg portions and crushed. The chips of skin and bone were weighed and extracted with isotonic phosphate buffer (pH 7.4) by shaking for 4 hr. The fluids were then centrifuged at 3000 rpm for 10 min, and the supernatant was removed for microbiological assay of cefazolin and for the colorimetric assay of inulin.

In the experiments using radioactive drugs, the rats were injected with a 10- to 200-mg/kg dose of cefazolin or a 20-mg/kg dose of inulin, each of which contained radiolabeled drug. The excised tissue samples were rinsed with ice-cold saline and blotted dry. One-half of the dry tissue was used for analysis.

Determination of Hepatic Blood Flow—The hepatic blood flow of rats under urethane or ether anesthesia was estimated using the method of Yokota *et al.* (15). A priming dose of indocyanine green was injected into the femoral vein of the rat and immediately followed by a constant infusion[9] of the dye into the opposite femoral vein at a rate of 13–27 μg/min, yielding a steady-state plasma level of ~10 μg/ml. Three blood samples (0.2 ml each) were simultaneously withdrawn from the hepatic vein and femoral artery every 10 min starting 60 min after the initiation of the dye injection. The plasma was separated by centrifugation and stored at 4° until assayed. Aliquots (50–100 μl) of the plasma were diluted 10- to 20-fold with distilled water and quantified by measurement of the absorbance at 800 nm[10]. Hematocrits (Hct, %) were measured[11] using the first and last arterial and hepatic venous blood samples, and averaged. The hepatic plasma and blood flows were calculated with the equation of Bradley *et al.* (16).

Determination of Tissue-to-Plasma Partition Coefficients—The equilibrium tissue-to-plasma concentration ratios, K_p, of penicillin V, dicloxacillin, cefazolin, and [^{14}C]inulin were obtained experimentally for each of the tissues used in the pharmacokinetic model. Solutions of the penicillins, cefazolin with or without added [^{14}C]cefazolin, and inulin containing [^{14}C]inulin prepared with saline were infused[9] at a rate of 0.5 ml/hr through the femoral vein of rats. Based on the preliminary experimental data collected after intravenous bolus injection of each drug, a priming dose was administered to quickly attain a steady-state condition.

Blood samples were withdrawn periodically through the jugular vein. After 2 or 3 hr of infusion, blood samples from the femoral artery, renal vein, and hepatic vein were taken. The animals were sacrificed immediately by exsanguination *via* the carotid artery. Tissue samples taken at the steady-state plasma level were prepared in the same manner as described above for bolus-dose experiments.

The distribution of antibiotics into erythrocytes and bone marrow were studied under the conditions described above. In addition, a beagle dog was infused with cefazolin at a rate of 180 mg/hr, without a priming dose,

[9] Infusion pump model KN; Natsume Seisakusho Co., Tokyo, Japan.
[10] Double-beam spectrophotometer, UV-200; Shimadzu, Kyoto, Japan.
[11] Hematocrit MC-200; Hitachi Koki Co., Tokyo, Japan.

Table I—Binding Parameters [a] of β-Lactam Antibiotics with Rat Serum Protein

β-Lactam Antibiotic	n [b]	$10^{-4} K_B$ [b], M^{-1}	$10^{-4} K_{B,app}$ [c], M^{-1}
Penicillin G	—	—	1.132 ± 0.048
Penicillin V	2.78 ± 0.26	0.109 ± 0.014	—
Methicillin	—	—	0.656 ± 0.070
Ampicillin	—	—	1.322 ± 0.048
Dicloxacillin	—	—	7.434 ± 0.448
Cefazolin	0.63 ± 0.03	2.980 ± 0.479	—

[a] The binding parameters were determined by the equilibrium dialysis method at 37°. An albumin concentration of 5.00×10^{-4} M was used for calculation. [b] Defined by Eq. 1. [c] Defined by Eq. 2.

over a 10-hr period. After achievement of steady-state levels, aliquots of blood were withdrawn periodically through a cannula inserted into the saphenous vein of the dog. Bone marrow fluids were withdrawn periodically from a portion of femoral bone using the usual puncture technique. The hematocrits of the blood samples were determined[11]. Antibiotic concentrations of the whole blood and whole bone marrow were determined after hemolysis with an equivalent volume of distilled water. The results were used to estimate the partition coefficients of these antibiotics between plasma and erythrocytes and between plasma and bone marrow.

Determination of Renal and Hepatic Clearances—Intravenous infusions were performed to measure the renal and hepatic clearances of penicillin G or cefazolin at steady state in rats. In the renal clearance measurements, the femoral artery, femoral vein, left renal vein, and ureters were cannulated. Antibiotic solutions containing inulin to estimate the glomerular filtration rate (GFR) were prepared with 3% mannitol and infused[9] at a rate of 3.7 ml/hr through the femoral vein using a priming dose for each drug. After constant urine flow and steady-state levels of the antibiotic and inulin were achieved, urine was collected over 30-min intervals and blood was withdrawn through the femoral artery and renal vein at the midpoint of the urine collection period. The renal excretion rate (dX_u/dt) was calculated from $dX_u/dt = C_u UF$, where C_u and UF indicate the urine concentration of drug and urine flow in ml/min, respectively.

The inhibitory effect of probenecid on the tubular secretion of penicillin G and cefazolin were examined as follows. Probenecid was dissolved in aqueous sodium hydroxide and then neutralized with hydrochloric acid. A 3% mannitol solution containing penicillin G, cefazolin, or inulin, and probenecid was infused at a rate of 3.7 ml/hr. In each experiment, the steady-state plasma concentration of probenecid was assayed.

The procedure used to measure the hepatic clearance of cefazolin, was essentially the same as that described for determining hepatic plasma flow. At steady state, the total plasma concentration (bound and unbound) of cefazolin in the femoral artery, hepatic vein, and bile were determined by microbiological assay.

Determination of Serum Protein Binding—Acrylic resin plates with four compartments of 5 mm depth and 25 mm diameter were used for the dialysis studies. Two plates were joined tightly, holding a cellulose membrane[12] between them. An 0.8-ml aliquots of rat serum was put into one compartment and, unless otherwise specified, 0.8 ml of pH 7.4 isotonic phosphate buffer containing an appropriate concentration of antibiotic was put into the other compartment. The plates were incubated for 6 hr at 37°. After appropriate dilution of equilibrated samples with the isotonic phosphate buffer, the antibiotic concentrations in both compartments were measured by microbiological assay. The concentration of the antibiotic bound to serum protein was obtained by subtracting the concentration of unbound drug from the total drug concentration. When the effect of the buffer component on the binding ratio was investigated, the following solutions were used instead of isotonic phosphate buffer: Tris-hydrochloride buffer (pH 7.4), 0.067 M phosphate buffer (pH 7.4), and protein-free rat serum obtained by ultrafiltration[13] of pooled serum.

Paper Chromatography—Paper chromatography was conducted in a cold room according to the method of Thomas (17). The developing solvent was n-butyl alcohol–pyridine–water (1:1:1). A portion of the urine or bile sample was treated with 1 N NaOH for 20 min at room temperature followed by neutralization with 1 N HCl, and 10 μl was spotted on the paper[14]. Ten microliters of the untreated portion was spotted directly on the paper. The chromatograms were visualized by spraying with 1% starch in acetic acid–0.1 N I_2–4% KI (50:3:1). For detection of intact penicillin V, the paper was sprayed with 0.1 N NaOH and after 20 min sprayed with 0.1 N HCl. Standard samples of each penicillin and penicilloic acid were prepared using normal urine and bile and were chromatographed similarly as a reference marker.

Table II—Urinary and Biliary Recoveries (Percent of Dose) of Penicillin V and Its Metabolites after Intravenous Administration in Rats [a]

Compound	Urine, %	Bile, %	Total, %
Penicillin V	13.8 ± 6.6	29.5 ± 3.1	43.3 ± 7.3
Phenoxymethylpenicilloic acid	17.1 ± 2.2	18.7 ± 1.0	35.8 ± 2.4
6-Aminopenicillanic acid and its penicilloic acid	6.9 ± 2.8	15.1 ± 2.0	22.0 ± 3.4
Total			101.1 ± 8.4

[a] The urine and bile collection periods were 0–9 hr and the dose was 100 mg/kg. Each point represents the mean of three rats ± SD.

Analytical Procedures—*Microbiological Assay*—Plasma, urine, bile, and tissue samples from rats administered β-lactam antibiotics were assayed (unless otherwise specified) by the microbiological paper disk diffusion method using *Sarcina lutea*[15], *Staphylococcus aureus*[16], or *Bacillus subtilis*[17] as the test organism. In the determination of drug distribution into erythrocytes, blood samples used for plasma quantification were hemolyzed with an equal volume of distilled water and analyzed. Calculation of the antibiotic concentration was made from standard curves prepared using pooled blood, urine, bile, and the corresponding tissue homogenates. The accuracy of the microbiological assay was ±5%.

Spectrofluorometric Assay—Spectrofluorometric methods were utilized for simultaneous analysis of a penicillin and the penicilloic acid metabolite in whole blood, urine, and bile. The blood was hemolyzed with an equal volume of distilled water. The analytical method employed for samples taken after intravenous administration of penicillin V, propicillin, or dicloxacillin was based on the formation of a fluorescent Schiff-base resulting from the reaction between penicilloaldehyde and 0.1% 5-dimethylaminonaphthalene-1-sulfonylhydrazine. After acylation with phenoxyacetic anhydride at pH 9.0, 6-aminopenicillanic acid and its cleaved β-lactam ring product were assayed as described previously[18] (18). The method of Miyazaki *et al.* (19) was used for quantification of ampicillin. The accuracy of the fluorometry assay was ±4%.

Radiochemical Assay—The radioactivity of [^{14}C]cefazolin and [^{14}C]inulin in plasma was determined by direct liquid scintillation counting[19]. Triplicate 50–250-μl aliquots of plasma were added to glass counting vials containing 10 ml of dioxane-based scintillation fluid. Quenching was corrected by the external standard method. Tissue samples after intravenous bolus dosing or constant infusion were oxidized[20] to $^{14}CO_2$, and radioactivity was determined by liquid scintillation counting[19].

Determination of Inulin—The method used for the determination of inulin in plasma, urine, and lung tissue was a modified form of the colorimetric assay developed by Waugh (20). Reagents and standard solutions of inulin were prepared as described previously (20). Samples of plasma (0.1 ml), 0.3 ml of distilled water, and 0.1 ml of zinc sulfate reagent were added to centrifuge tubes, followed by the addition (with continuous agitation) of 0.1 ml of 0.5 N NaOH. After centrifugation at 3000 rpm for 10 min, the supernatant was removed for analysis. Urine was assayed by adding 0.5 ml of zinc sulfate reagent and 0.5 ml of 0.5 N NaOH to 1.0 ml of urine, yielding a protein-free supernatant. For tissue sample assay, the tissue was cut into small pieces. The chips were weighed and extracted with saline by shaking for 4 hr. The fluids were then centrifuged at 3000 rpm for 10 min, and the supernatant was analyzed.

Aliquots (0.2 ml) of the supernatant from plasma, urine, or tissue samples were placed in a test tube, 0.2 ml of 1.8 N NaOH was added, and

[12] VisKing; Ethyl Corp.
[13] Amicon MMC, Lexington, Mass.
[14] Toyo Roshi No. 50, 2 × 40 cm; Toyo Roshi Co., Tokyo, Japan.
[15] IFO 12708; Institute for Fermentation, Osaka, Japan. The strain was derived from ATCC 9341.
[16] IFO 12732; Institute for Fermentation, Osaka, Japan. The strain was derived from ATCC 6538P.
[17] IFO 3134; Institute for Fermentation, Osaka, Japan. The strain was derived from ATCC 6633.
[18] In a previous paper (18), the concentration of 5-dimethylaminonaphthalene-1-sulfonylhydrazine reagent was erroneously referred to as 10%. The correct concentration is 0.1%. The full paper on the detailed procedure and the results are in preparation.
[19] Model LSC-671; Aloka Co., Tokyo, Japan.
[20] Sample oxidizer, Model 306; Packard Instruments, Downers Grove, Ill.

Table III—Urinary and Biliary Recoveries (Percent of Dose) of Penicillins and Their Penicilloic Acids after Intravenous Administration in Rats [a]

Penicillin	Intact Penicillin, %			Penicilloic Acid, %		
	Urine	Bile	Total	Urine	Bile	Total
Penicillin G [b]	30.0 ± 13.8	25.7 ± 3.6	55.7 ± 14.3	3.7 ± 1.0	12.9 ± 2.9	16.6 ± 3.1
Propicillin	19.1 ± 11.1	24.2 ± 2.4	43.3 ± 11.4	4.4 ± 1.3	21.0 ± 2.0	25.4 ± 2.4
Dicloxacillin	9.6 ± 6.0	14.4 ± 7.1	24.0 ± 9.3	5.5 ± 3.1	24.4 ± 3.4	29.9 ± 4.6
Ampicillin	34.9 ± 13.2	19.5 ± 2.3	54.4 ± 13.4	3.2 ± 1.4	9.9 ± 4.1	13.1 ± 4.3

[a] The urine and bile collection periods were 0–3 hr; the dose was 100 mg/kg. Each point represents the mean of three rats ± *SD*. [b] The urine and bile collection periods were 0–24 hr; the dose was 100 mg/kg. Each point represents the mean of eight rats ± *SD*.

the mixture was heated at 100° for 10 min. The mixture was cooled and 3 ml of 70% (v/v) H_2SO_4 and 0.3 ml of cysteine–tryptophan reagent was added. After heating at 50° for 25 min, the solution was cooled to room temperature and the color was evaluated against a blank[11] at 515 nm.

Determination of Probenecid—Concentrations of probenecid in plasma and urine were determined by a high-performance liquid chromatographic (HPLC) assay (21). Samples were prepared as described previously (21), but the chromatographic conditions were modified slightly. A reverse-phase column[21] (25 cm × 4.6-mm i.d.), packed in this laboratory, was used in conjunction with a chromatograph[22] equipped with a variable-wavelength detector[23]. The mobile phase was acetonitrile–0.014 *M* pH 6.0 phosphate buffer (3:7). The column and solvent were kept at ambient temperature. A flow rate of 2.5 ml/min was used, yielding an operating pressure of 110 kg/cm^2. The spectrophotometric detector had an 8-μl flow cell and was operated at 254 nm; the injection volume was 50 μl. Complete peak resolution was obtained with a retention time of 4 min. Peak heights were used for quantification; standard curves were generated by blank plasma and urine samples spiked with varying amounts of probenecid as described previously (21).

Data Analysis—The data were analyzed using a digital computer[24]. The program used for the physiologically based pharmacokinetic models was designed in-house by incorporating the NUMINT program, a subroutine in NONLIN (22).

RESULTS

Serum Protein Binding—Cefazolin diffused rapidly from the buffer compartment into the serum compartment (Fig. 1). Equilibrium was established within 4 hr and was maintained for the 12-hr duration of the experiment. The effect of buffer components on the binding behavior of cefazolin was also examined. The percentage of cefazolin bound at a total concentration of 70 μg/ml was determined to be 85.6 ± 3.4, 86.8 ± 3.6, 88.3 ± 1.8, and 85.1 ± 3.0 in isotonic phosphate buffer (pH 7.4), 0.067 *M* phosphate buffer (pH 7.4), Tris-hydrochloride buffer, and protein-free rat serum, respectively. These differences were not statistically significant.

Figure 2 illustrates the protein binding profiles for each of the studied β-lactam antibiotics as a function of the postdialysis antibiotic concentration. The protein binding behavior varied among antibiotics. Nonlinear protein binding was observed for cefazolin and penicillin V, whereas apparent linear binding was found for penicillin G, methicillin, dicloxacillin, and ampicillin. Assuming that albumin is the sole binding protein for β-lactam antibiotics, then:

$$C_B = \frac{nPK_BC_F}{1 + K_BC_F} \qquad \text{(Eq. 1)}$$

where C_B and C_F are the concentrations of antibiotic bound and unbound with serum protein, n is the number of binding sites on the albumin molecule, K_B is the affinity constant for albumin, and P is the albumin concentration (mol. wt. 69,000) in serum. (Measured values for P averaged 5.0×10^{-4} *M*.) The nonlinear least-squares regression computer program, NONLIN, was used to fit the data to Eq. 1. In the case of linear binding, simplification of Eq. 1 yields:

$$C_B = K_{B,app}PC_F \qquad \text{(Eq. 2)}$$

where $K_{B,app}$ is the apparent affinity constant for albumin. The binding parameters are presented in Table I.

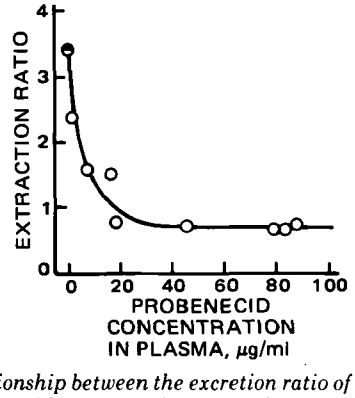

Figure 4—*Relationship between the excretion ratio of penicillin G and the plasma probenecid concentration at steady state after the constant and simultaneous infusion of penicillin G, probenecid, and inulin to rats. The point for the control experiment without probenecid (●) represents the mean value (3.41 ± 0.96) of five rats.*

Metabolic Elimination After Intravenous Bolus Injection—Paper chromatography of rat urine and bile samples after the intravenous administration of penicillin V detected penicilloic acid (R_f 0.72) and the β-lactam ring-cleaved product of 6-aminopenicillanic acid (R_f 0.35). English *et al.* (23) previously found 6-aminopenicillanic acid as well as penicilloic acid in urine after intravenous and oral administration of some penicillins in animal species. Table II shows that unchanged penicillin V (43%), penicilloic acid (36%), and the sum of 6-aminopenicillanic acid and the β-lactam ring-cleaved product (22%) were excreted over 9 hr both in urine and bile after a single dose of penicillin V. Total recovery in urine and bile was 101 ± 8%. The penicilloic acids were found to be the major metabolites of penicillin G, propicillin, dicloxacillin, and ampicillin (Table III). Kind *et al.* (24) demonstrated that penicillin G and ampicillin were inactivated at different rates by isolated rat liver cells; this suggests a metabolic route for these compounds.

Cafazolin, on the other hand, was recovered almost completely in the intact form in urine and bile after intravenous single-dose administration in rats (Fig. 3). Nishida *et al.* (25) have shown that the amount of recovered cefazolin in 24-hr urine and bile samples were 81 and 17%, respectively, after intramuscular administration to rats. These results show that the metabolism of cefazolin is negligible in rats, similar to other species including the human (5).

Extraction of Antibiotics from the Circulation by Kidney and

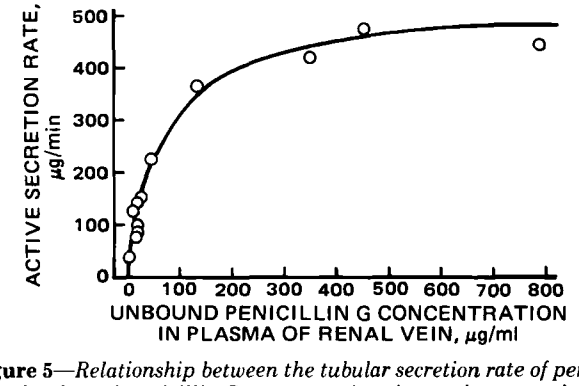

Figure 5—*Relationship between the tubular secretion rate of penicillin G and unbound penicillin G concentrations in renal venous plasma at steady state after the constant and simultaneous infusion of penicillin G and inulin to rats. The points represent the experimental values; the solid line was generated from Eq. 5 and the Michaelis–Menten kinetic parameters of Vu = 530.1 μg/min and $K_{m,u}$ = 69.6 μg/ml.*

[21] Lichrosorb Rp-8, 10-μm particle size; E. Merck AG, Darmstadt, W. Germany.
[22] Model TRIROTAR-II; Japan Spectroscopic Co., Tokyo, Japan.
[23] Model UVIDEC 100-III; Japan Spectroscopic Co., Tokyo, Japan.
[24] FACOM M-170F; at the Data Processing Center, Kanazawa University, Kanazawa, Japan.

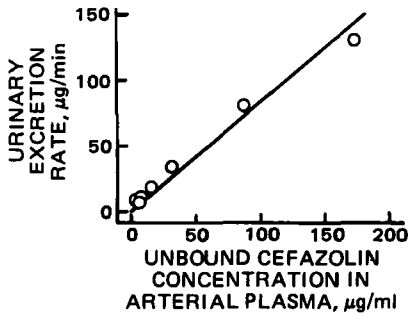

Figure 6—*Relationship between the urinary excretion rate of cefazolin and the unbound cefazolin concentration in arterial plasma at steady state after the constant and simultaneous infusion of cefazolin and inulin to rats. The renal clearance was evaluated from the slope of the line drawn through the experimental points.*

Liver—*Renal Clearance*—To clarify the renal excretion mechanism of β-lactam antibiotics in rats, the renal clearances of penicillin G and cefazolin were measured. Studies on the relationship between serum protein binding and the renal clearance of drugs are limited. Recently, Levy (26) suggested that the renal tubular secretion rate is a function of the concentration of free drug in the renal venous plasma except for the case of blood flow rate-limited secretion. Hori *et al.* (27) demonstrated that the tubular secretion of sulfathiazole is dependent on the unbound sulfathiazole in plasma. If the renal excretion rate of β-lactam antibiotics is governed by the sum of the rates of glomerular filtration (G) [which is dependent on the unbound antibiotic in the arterial plasma ($C_{F,p}$)] and the capacity-limited tubular secretion (S) [which, in turn, depends on the unbound antibiotic concentration ($C_{F,kd}$) in the renal venous plasma], then the rate expression for urinary excretion may be written as:

$$\frac{dX_u}{dt} = (G + S)(1 - R) \quad \text{(Eq. 3)}$$

$$G = GFR \cdot C_{F,p} \quad \text{(Eq. 4)}$$

$$S = \frac{Vu \cdot C_{F,kd}}{K_{m,u} + C_{F,kd}} \quad \text{(Eq. 5)}$$

where R, Vu, and $K_{m,u}$ represent the reabsorption fraction, the maximum rate of tubular secretion, and the Michaelis constant, respectively, and X_u is the amount of antibiotic excreted in the urine.

It was reported that some β-lactam antibiotics are actively secreted into renal tubules in rats, dogs, rabbits, and humans, and that the secretion is completely inhibited by probenecid (4–6). A preliminary experiment was performed to examine the effect of probenecid on the secretion of penicillin G in the rat kidney. The ratio of plasma renal clearance of penicillin G to inulin clearance (the conventional measure of overall renal excretion) was 2.19 ± 0.62 (n = 5) during the control period, where penicillin G was infused at a rate of 12.5 mg/hr. The clearance ratio decreased dramatically (79%) to 0.46 (n = 1) in the period of simultaneous infusion of probenecid at a rate of 2.4 mg/hr. To obtain more precise information for the tubular secretion and reabsorption of penicillins, probenecid was simultaneously infused with penicillin G and inulin to achieve various steady-state probenecid levels. The plots of the steady-state excretion ratio, $(dX_u/dt)_{ss}/G_{ss}$, *versus* the steady-state plasma concentration of probenecid (Fig. 4) show that as the plasma concentration of probenecid increased, the excretion ratio of penicillin G decreased markedly. There was no significant change in the serum protein binding of penicillin G in the presence of probenecid. It is obvious from these results that penicillin G is actively secreted in rats. Since a complete inhibition of the tubular secretion of this antibiotic was attained at >50-μg/ml probenecid levels in plasma, the reabsorption fraction of penicillin G could be obtained from the mean of the data of $(dX_u/dt)_{ss}/G_{ss}$ at >50-μg/ml probenecid levels. This was found to be 0.33 ± 0.03 (n = 4). Decreasing the urine flow by 85% did not significantly change the reabsorption fraction (0.32 ± 0.15, n = 4) of penicillin G in rats, although urine flow rate is known to be one of the factors influencing the tubular reabsorption of drugs (27).

The secretion rate was, therefore, calculated for the data under steady-state conditions and without the administration of probenecid using:

$$S_{ss} = \left(\frac{dX_u}{dt}\right)_{ss}/(1 - R) - GFR(C_{F,p})_{ss} \quad \text{(Eq. 6)}$$

The relationship between the unbound concentration in the renal venous plasma at steady state $(C_{F,kd})_{ss}$ and the steady-state secretion rate S_{ss} of penicillin G (Fig. 5) clearly indicates the saturable secretion of penicillin G. The Michaelis–Menten kinetic parameters for penicillin G tubular secretion, obtained by NONLIN, were Vu = 530.1 ± 49.4 μg/min and $K_{m,u}$ = 69.6 ± 13.8 μg/ml.

Similar experiments were also made for cefazolin. The observed ratio of plasma renal clearance to inulin clearance was 0.35 ± 0.04 (n = 4) in the control period. After probenecid infusion, the value was 0.31 ± 0.03 (n = 4) (probenecid steady-state plasma level of 88 μg/ml), with the differences being statistically insignificant. The results indicate a negligible contribution of the tubular secretion of cefazolin in rats. When the steady-state excretion rates, $(dX_u/dt)_{ss}$, were plotted *versus* the unbound cefazolin concentrations, $(C_{F,p})_{ss}$, there was a linear relationship with a zero intercept and a slope of 0.82 ml/min (Fig. 6). By employing a GFR value of 1.06 ± 0.15 ml/min (n = 4), the R-value for cefazolin was determined to be 0.22. These results demonstrate that cefazolin is excreted mainly by glomerular filtration and then reabsorbed in part by the renal tubules.

Hepatic Clearance—Cefazolin was infused into rats with bile fistules to achieve various steady-state plasma levels. Since metabolism of cefazolin was found to be negligible (as described in a previous section), the steady-state biliary secretion rate, $(dX_{bi}/dt)_{ss}$, may be attributed to the uptake of this antibiotic into hepatocytes or biliary secretion itself. If the hepatic uptake is not the rate-limiting step and the biliary secretion rate is capacity limited, the rate can be described by a Michaelis–Menten equation:

$$\left(\frac{dX_{bi}}{dt}\right)_{ss} = \frac{V_{bi}(C_{F,1v})_{ss}}{K_{m,bi} + (C_{F,1v})_{ss}} \quad \text{(Eq. 7)}$$

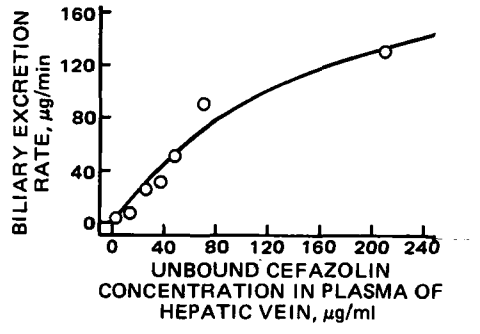

Figure 7—*Relationship between the biliary excretion rate of cefazolin and unbound cefazolin concentrations in hepatic venous plasma at steady state after the constant infusion of cefazolin to rats. The points represent the experimental values; the solid line was generated from Eq. 7 and the Michaelis–Menten kinetic parameters of* V_{bi} = 238.8 μg/min *and* $K_{m,bi}$ = 163.3 μg/ml.

Table IV—Tissue-to-Plasma Partition Coefficients (Kp) of β-Lactam Antibiotics for Various Tissues of Rats

Tissue	K_p[a] Penicillin V	Dicloxacillin	Cefazolin
Lung	0.157 ± 0.078 (n = 14)	0.123 ± 0.027 (n = 5)	0.154 ± 0.078 (n = 8)
Heart	0.095 ± 0.024 (n = 12)	0.074 ± 0.014 (n = 4)	0.101 ± 0.022 (n = 15)
Muscle	0.062 ± 0.017 (n = 10)	0.051 ± 0.014 (n = 4)	0.077 ± 0.029 (n = 18)
Bone	—	—	0.111 ± 0.021 (n = 15)
Skin	—	—	0.303 ± 0.058 (n = 11)
Spleen	0.096 ± 0.020 (n = 12)	0.088 ± 0.031 (n = 5)	—
Gut	0.966 ± 0.452 (n = 14)	1.357 ± 0.590 (n = 12)	0.114 ± 0.029 (n = 10)
Liver	0.250 ± 0.052 (n = 12)[b]	0.430 ± 0.287 (n = 9)[c]	0.788 ± 0.354 (n = 10)[b]
Kidney	3.70 ± 0.87 (n = 14)[b]	1.27 ± 0.44 (n = 10)[c]	2.79 ± 1.05 (n = 10)[b]

[a] The value of K_p is the ratio of tissue concentration to the venous outflow plasma concentration at steady state, as defined by Eq. 8. [b] Corrected by using the corresponding plasma flow rate and the elimination clearance according to the technique described by Chen and Gross (28). [c] Apparent value calculated from the ratio of tissue concentration to the arterial plasma concentration at steady state.

Table V—*In Vivo* Uptake of β-Lactam Antibiotics into Erythrocytes of Rats

β-Lactam Antibiotic	No. of Experiments	Rat Weight, g	$(C_{T,p})_{ss}$,[a] μg/ml	$(C_{WB})_{ss}$,[b] μg/ml	Hematocrit, %	K_p[c]
Penicillin G	4	255 ± 5	105.9 ± 13.3	48.8 ± 5.0	54.8 ± 2.1	0.016
Penicillin V	3	242 ± 1	29.8 ± 4.2	12.0 ± 3.2	51.3 ± 4.6	0
Methicillin	3	254 ± 10	63.1 ± 9.0	31.2 ± 2.8	51.7 ± 2.2	0.022
Dicloxacillin	3	241 ± 2	36.6 ± 9.4	17.4 ± 3.3	51.1 ± 3.3	0
Ampicillin	3	243 ± 2	99.9 ± 14.4	44.5 ± 7.4	52.2 ± 2.5	0
Cephaloridine	4	240 ± 5	52.0 ± 8.4	26.3 ± 3.2	51.5 ± 2.8	0.040
Cefazolin	3	238 ± 2	77.5 ± 12.3	32.9 ± 2.9	53.2 ± 3.4	0

[a] Total antibiotic concentration in arterial plasma at steady state. [b] Total antibiotic concentration in whole blood at steady state. [c] Mean value calculated from Eq. 9. All negative K_p values were listed as zero.

where V_{bi} and $K_{m,bi}$ represent the maximum rate and Michaelis constant, respectively, for the biliary secretion, and $(C_{F,1v})_{ss}$ represents the free antibiotic concentration in hepatic venous plasma at steady state.

Plotting the relationship between $(dX_{bi}/dt)_{ss}$ and $(C_{F,1v})_{ss}$ yielded a convex curvature (Fig. 7). The values of V_{bi} and $K_{m,bi}$ were 238.8 ± 56.8 μg/min and 163.3 ± 65.4 μg/ml, respectively, using NONLIN according to Eq. 7. The magnitudes of the apparent renal clearance of 0.82 ml/min and the biliary secretion parameters of V_{bi} and $K_{m,bi}$ predict that at high cefazolin free levels, urinary excretion is superior to biliary secretion, and at low levels both excretions may be comparable.

Tissue-to-Plasma Partition Coefficient—The steady-state tissue-to-plasma concentration ratios, K_p, of penicillin V, dicloxacillin, and *cefazolin were measured* experimentally for each rat tissue compartment (Table IV). The K_p for any organ is defined by:

$$K_{p,i} = \frac{(C_{T,i})_{ss}}{(C_{F,i} + C_{B,i})_{ss}} \quad \text{(Eq. 8)}$$

where $(C_{T,i})_{ss}$ and $(C_{F,i} + C_{B,i})_{ss}$ represent the total antibiotic concentration in a whole tissue (excluding blood) and total antibiotic concentration in the tissue venous plasma, respectively, at steady state. For noneliminating organs, the steady-state arterial plasma concentration, $(C_{T,p})_{ss}$, was used for the calculation as $(C_{T,p})_{ss} = (C_{F,i} + C_{B,i})_{ss}$. When an antibiotic concentration in the venous plasma of kidney or liver was not measured, the K_p value was corrected by using the corresponding plasma flow rate and clearance, as suggested by Chen and Gross (28).

The K_p values of β-lactam antibiotics in all tissues except gut and kidney were found to be <1. The antibiotics studied were highly concentrated in the kidney, which is the major eliminating organ. Penicillin V and dicloxacillin exhibited extremely higher K_p values in gut tissue than cefazolin. This phenomenon may be the result of an extensive contribution of enterohepatic recirculation of the former two antibiotics (12). Because of the almost negligible intestinal absorption of cefazolin in rats (29), cefazolin provided the true K_p value for gut tissue.

Distribution of several β-lactam antibiotics into erythrocytes was evaluated by measuring the steady-state concentrations in whole blood and plasma of rats. The K_p value for erythrocytes was calculated from:

$$K_p = 1 + \left[\frac{(C_{WB})_{ss}}{(C_{T,p})_{ss}} - 1\right] \Big/ (\text{Hct}/100) \quad \text{(Eq. 9)}$$

where $(C_{WB})_{ss}$ is the whole blood concentration at steady state. The results (Table V) indicate negligible distribution of β-lactam antibiotics into the rat erythrocyte compartment. Nishida *et al.* (30) previously demonstrated that distribution of penicillins into rabbit erythrocytes was <3% or negligible after intravenous bolus administration; their results are consistent with our observations.

Development of the Physiologically Based Pharmacokinetic Model—Figure 8 is a diagrammatic representation of a noneliminating organ subdivided anatomically into three fluid compartments: (*a*) the capillary blood volume, (*b*) the interstitial fluid, and (*c*) the intracellular space. In formulating the kinetics of β-lactam antibiotics in these tissues (except the liver and kidney), the following assumptions, based on the experimental evidence described in the previous and subsequent sections, were made.

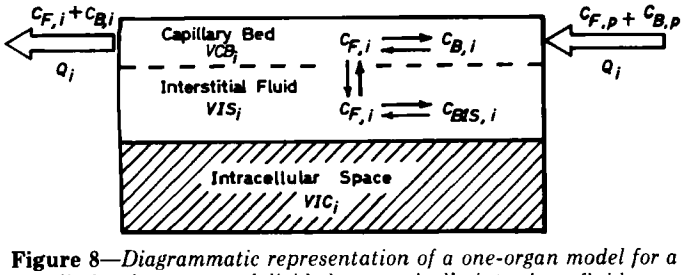

Figure 8—*Diagrammatic representation of a one-organ model for a noneliminating organ subdivided anatomically into three fluid compartments.*

1. Free and bound antibiotics entering with arterial plasma mix with the antibiotics in the tissue capillary bed.
2. Only the mixed antibiotics in the capillary bed, which is free from plasma protein binding, can diffuse rapidly in the tissue (except bone).
3. Entrance into the intracellular space by the antibiotic is negligible; therefore, the diffused antibiotic is restricted to the interstitial fluid of the tissue.
4. The antibiotic diffused into the interstitial fluid can bind only with albumin existing in this compartment, in a similar manner as with plasma albumin.
5. Bone tissue is divided into three compartments consisting of capillary bed, bone marrow, and bone cortex. The bone marrow-to-plasma ratio is assumed to be 1. The antibiotic binds in the bone marrow exactly as in the plasma, and only unbound antibiotics can diffuse into the bone cortex fluid space.
6. A well-mixed state exists in the capillary bed, interstitial fluid, and bone regions.
7. Free and bound antibiotic concentrations in venous plasma leaving the tissues are the same as those in the capillary bed.

From the above assumptions regarding the distribution of β-lactam antibiotics in noneliminating organs (except bone), a mass balance equation can be expressed as:

$$VCB_i\left(\frac{dC_{F,i}}{dt} + \frac{dC_{B,i}}{dt}\right) + VIS_i\left(\frac{dC_{F,i}}{dt} + \frac{dC_{BIS,i}}{dt}\right) = Q_i(C_{F,p} + C_{B,p}) - Q_i(C_{F,i} + C_{B,i}) \quad \text{(Eq. 10)}$$

The nomenclature for this equation and others is given in Appendix I (Glossary). The two terms of the left-hand side of Eq. 10 represent the accumulation rates of free and bound antibiotics in the capillary bed and interstitial fluid, respectively. Differentiation of the plasma binding equations (Eqs. 1 and 2) yields:

$$\frac{dC_{B,i}}{dt} = \alpha_i \frac{dC_{F,i}}{dt} \quad \text{(Eq. 11)}$$

In the case of nonlinear binding behavior:

$$\alpha_i = \frac{nPK_B}{(1 + K_B C_{F,i})^2} \quad \text{(Eq. 12)}$$

Similarly, linear binding yields:

$$\alpha_i = K_{B,app}P \quad \text{(Eq. 13)}$$

Taking the tissue-to-plasma albumin concentration ratio, AR_i, for *i*-type tissue and using assumption 4, Eq. 10 can be simplified to:

$$[VCB_i(1 + \alpha_i) + VIS_i(1 + \alpha_i AR_i)]\frac{dC_{F,i}}{dt} = Q_i[(1 + \beta_p)C_{F,p} - (1 + \beta_i)C_{F,i}] \quad \text{(Eq. 14)}$$

where β_i can be defined for the nonlinear binding case as:

$$\beta_i = \frac{nPK_B}{1 + K_B C_{F,i}} \quad \text{(Eq. 15)}$$

and in the linear binding case, $\beta_i = \alpha_i$. If assumption 5 is valid, the mass

Table VI—Hepatic Blood Flow by a Continuous Indocyanine Green Infusion Method in Anesthetized Rats [a]

Anesthesia	No. of Experiments	Body Weight, g	Liver Weight, g	Hematocrit, %	$Q_{p,1v}$[b]/100 g body, ml/min	$Q_{p,1v}$[b]/liver, ml/min	$Q_{b,1v}$[c]/100 g body, ml/min	$Q_{b,1v}$[c]/liver, ml/min
Urethane	4	245 ± 7	7.4 ± 0.6	52.0 ± 3.9	1.52 ± 0.29	0.50 ± 0.10	3.17 ± 0.66	1.04 ± 0.23
Ether	3	246 ± 2	7.3 ± 0.1	46.0 ± 1.0	2.24 ± 1.10	0.75 ± 0.36	4.15 ± 2.04	1.39 ± 0.67
Ether[d]	5	308 ± 8	11.7 ± 1.7	41.0 ± 5.0	1.99 ± 0.46	0.53 ± 0.11	3.38 ± 0.73	0.90 ± 0.17
Control[d]	4	312 ± 8	12.3 ± 1.6	39.0 ± 4.0	3.69 ± 0.51	0.93 ± 0.07	6.05 ± 0.74	1.53 ± 0.06

[a] Each point represents the mean ± *SD*. [b] Hepatic plasma flow. [c] Hepatic blood flow which was calculated from: $Q_{b,1v} = Q_{p,1v}/(1 - \text{Hematocrit}/100)$. [d] Data taken from Yokota *et al.* (15).

balance in the bone compartment can be written as Eq. II-5 (Appendix II).

In the mathematical description for the eliminating organs such as the liver and kidney, K_p values were employed to predict the tissue concentrations, because uptake and accumulation of antibiotics into the intracellular spaces appeared to be difficult to evaluate at the present time. Okada *et al.* (31) demonstrated recently that the extent of binding of cefazolin, cephaloridine, cephalexin, and cloxacillin with 90% of liver and kidney homogenates was 2~65% for rats and beagle dogs, and that the tissue binding appears to be unrelated to the binding of the drugs to serum albumin. β-Lactam antibiotics are highly protein-bound with the water-soluble hepatic and renal intracellular protein, ligandin (32). The binding between the drugs and ligandin may correlate with their hepatic and renal uptakes from plasma.

A full diagram of blood circulation through various tissues is represented in Fig. 9. All pertinent tissues for which antibiotic concentrations are known, except for carcass (fat and others), have been included. The plasma flow of the liver (Table VI) and the tissue volumes of the heart, liver, and kidney used for the calculations were experimental values determined in this laboratory. The organ flow rates, except for the liver, and volumes of the other tissues were taken from published physiological values (8, 10, 33–35), adjusted to reflect the size of the animals studied. Sapirstein *et al.* (34) determined that in rats, bronchial blood flow constituted only 3% of cardiac output. Based on this simulation study, the contribution of the bronchial circulation to antibiotic distribution into lung tissue was assumed to be negligible. The physiological parameters employed in this study are listed in Table VII.

Binding to the Interstitial Protein—If assumptions 2 and 3 are valid for β-lactam antibiotics in noneliminating organs (except bone), the following mass balance equation can be written:

$$C_{T,i} = IS_i(C_{F,i} + C_{BIS,i}) \qquad \text{(Eq. 16)}$$

where IS is the interstitial space expressed by:

$$IS_i = \frac{VIS_i}{VIS_i + VIC_i} \qquad \text{(Eq. 17)}$$

From assumption 3, for the antibiotics showing nonlinear serum protein binding behavior, Eq. 1 can be written as:

$$C_{BIS,i} = \frac{n \cdot AR_i \cdot PK_B C_{F,i}}{1 + K_B C_{F,i}} \qquad \text{(Eq. 18)}$$

Since $C_{F,i} = C_{F,p}$ in noneliminating organ regions, except bone, at steady state, Eqs. 16 and 18 can be expressed as:

$$(C_{T,i})_{ss} = IS_i \cdot \left[1 + \frac{n \cdot AR_i \cdot PK_B}{1 + K_B(C_{F,p})_{ss}}\right](C_{F,p})_{ss} \qquad \text{(Eq. 19)}$$

Similarly in the case of linear binding:

$$(C_{T,i})_{ss} = IS_i \cdot (1 + AR_i \cdot PK_{B,app})(C_{F,p})_{ss} \qquad \text{(Eq. 20)}$$

The interstitial space (IS_i) of lung, heart, skin, bone, gut, and liver in rats was estimated from the distribution of inulin or [^{14}C]inulin. The value of IS_i for each tissue was calculated as the ratio of tissue to plasma concentrations at steady state (Table VIII). The interstitial water content of most tissues was 10–20%. The IS value of skin, however, was 30% of the blood-free organ, much higher than that found in the other tissues studied. Our results were consistent with those reported by Higaki and Fujimoto (36) using data after intravenous bolus injection of [^{14}C]inulin in kidney-ligated rats, but were less than IS values evaluated (37) from the mannitol and thiosulfate spaces. The reason for larger spaces determined by the latter two compounds may be due to their partial distribution into the intracellular compartment.

Cefazolin seems to be a good model to test the validity of Eq. 19 or 20, because of its remarkable nonlinear binding characteristics with rat albumin. Figure 10 illustrates plots of the steady-state tissue concentration $(C_{T,i})_{ss}$ *versus* the steady-state arterial plasma free concentration $(C_{F,p})_{ss}$ obtained for heart, muscle, skin, and gut.

When we used the AR_i values of 0.5, 0.6, and 0.9 reported (37) for heart, muscle, and gut, respectively, the curves generated from Eq. 19 using the binding parameters of cefazolin listed in Table I and the corresponding interstitial space in Table VIII were in good agreement with the experimental tissue levels of cefazolin. Katz *et al.* (37) demonstrated that AR values for muscle and skin were ~0.55, but the interstitial albumin content of skin and gut was twice that of muscle in rats. Rothschild *et al.* (38) found that most of the extravascular albumin was located in the skin in humans, and the concentration of albumin in the extravascular and extracellular skin approaches that in the plasma. The high level of albumin in skin is likely to be related to the high interstitial space of this tissue (Table VIII). The observed skin levels fit well with the curves generated from Eq. 19 with the reasonable assumption of AR = 1. Figure 10 clearly indicates that the free concentration of cefazolin in plasma at <20 μg/ml had a greater effect on the tissue levels than did cefazolin plasma concentrations >50 μg/ml. This is a result of the nonlinear binding with rat plasma albumin and is described by Eq. 19.

Little basic information has been reported concerning antibiotic concentrations in bone, especially bone marrow. Pitkin *et al.* (39) found that cefazolin levels were detected in bone and bone marrow of normal rabbits dosed intramuscularly even in the absence of detectable levels in serum. However, the concentration ratio of bone cortex to bone marrow of this antibiotic was ~0.05 (39). More recently, it was found (40) that the concentrations of cefazolin in bone marrow were equal to or exceeded that in serum 60 min after the administration of 50 mg/kg iv in rabbits. Because bone marrow sampling was difficult in rats, we used a beagle dog to evaluate assumption 5. The results (Table IX) indicate that the observed cefazolin levels in whole bone marrow, although somewhat scattered, were almost equal to the whole blood levels at steady state. Since the mean whole blood levels were well described using Eq. 9 with the mean steady-state plasma levels and hematocrit of 41% (assuming K_p

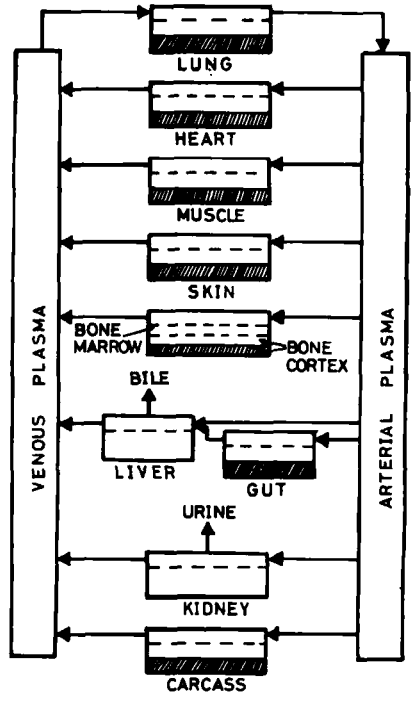

Figure 9—*Physiological pharmacokinetic model fully diagramming the blood circulation through various tissues.*

Table VII—Physiological Parameters for 240-g Rats [a]

Tissue	Total Tissue Volume (V), ml	Interstitial Fluid Volume (VIS)[b], ml	Plasma Volume in Capillary Bed (VCB)[c], ml	Plasma Flow Rate (Q), ml/min	Tissue-to-Plasma Albumin Ratio (AR)
Venous blood pool	2.9	—	1.4[d]	30.0	1.0
Arterial blood pool	1.5	—	0.8[d]	30.0	1.0
Lung	1.6	0.3	0.3	30.0	0.5
Heart	1.0[e]	0.1	0.2	0.8	0.5
Muscle	108.0	13.0	0.7	3.6	0.6
Skin	43.0	13.0	0.2	2.4	1.0
Bone	26.0	3.0	1.1[f]	0.8	1.0[g]
Gut	16.0	1.5	3.0	2.6	0.9
Liver	8.0[e]	1.3	1.0	3.7	0.5
Kidney	2.0[e]	0.4	2.5	7.3	0.5
Carcass (fat, others)	14.0	2.0	0.1	11.4	0.5

[a] Based on the values in Refs. 8, 10, 33–35, and 37. [b] Calculated from the equation: $VIS = V \times$ (Inulin space). The inulin spaces for various tissues except kidney and carcass are listed in Table VIII. For kidney tissue, the inulin space of 19.6% is reported in Ref. 36. For carcass, 15% inulin space was assumed. [c] Estimated from the values reported in Refs. 10 and 56 under the assumption that rats, dogs, and humans have the same ratio of blood volume in capillary bed-to-tissue volume without blood. [d] 50% hematocrit was assumed. [e] Determined experimentally in this laboratory. [f] Including bone marrow. [g] Bone marrow.

= 0), it is safe to conclude that the bone marrow-to-plasma concentration ratio was almost unity, consistent with previous observations in humans (41, 42).

The validity of Eq. 19 or 20 was also tested by comparing the K_p values observed for dicloxacillin and penicillin V as well as cefazolin (Table IV) and those calculated by combining Eqs. 1, 8, and 19:

$$(K_{p,i})_{calc} = IS_i \frac{1 + K_B(C_{F,p})_{ss} + n \cdot AR_i \cdot PK_B}{1 + K_B(C_{F,p})_{ss} + nPK_B} \quad \text{(Eq. 21)}$$

or Eqs. 2, 18, and 20:

$$(K_{p,i})_{calc} = IS_i \frac{1 + AR_i \cdot PK_{B,app}}{1 + PK_{B,app}} \quad \text{(Eq. 22)}$$

For bone tissue, Eq. 21 may be rewritten using assumption 5 for the nonlinear binding case:

$$(K_{p,bn})_{calc} = \frac{IS_{bn}[1 + K_B(C_{F,p})_{ss}] + S_{bnm}nPK_B}{1 + K_B(C_{F,p})_{ss} + nPK_B} \quad \text{(Eq. 23)}$$

where IS_{bn} and S_{bnm} represent inulin space and bone marrow space, respectively, in bone tissue. The AR values of lung and S_{bnm} were assumed to be 0.5 and 0.038 (Table VII), respectively; the binding parameters were taken from Table I. There is a good agreement between observed (Table IV) and calculated K_p values in all cases (Fig. 11), indicating that assumptions 3–5 made for tissue distribution of β-lactam antibiotics are reasonable and applicable, at least for noneliminating organs.

Application to Tissue Distribution Kinetics of Inulin—Prior to testing the validity of the physiologically based pharmacokinetic model developed for the body distribution of β-lactam antibiotics, the model was used to simulate the tissue distribution kinetics of inulin in rats. Since inulin is known to be excreted almost completely by glomerular filtration and its distribution is restricted only to plasma and tissue interstitial fluid, the present model has an intrinsic ability to predict the concentration–time profiles of inulin in any tissue.

In the adaptation of this model to a compound having a large molecular size such as inulin, however, the capillary wall permeability must be handled somewhat differently. The capillary walls in lung, heart, muscle, skin, and gut are composed of an interlocking mosaic of endothelial cells with slits (43). Therefore, the restricted transport of inulin through the capillary walls in these tissues does not allow the instantaneous establishment of the equilibrium of inulin between the capillary bed and interstitial fluid. Such a restricted transport of inulin has been apparently described by Fick's law of diffusion (43c–45). The mass balance equations for lung, muscle, skin, and gut tissues are shown in Appendix III. By using values of 20 ml/min/100 g of tissue for lung and heart, 10 ml/min/100 g of tissue for gut, and 2 ml/min/100 g of tissue for muscle and skin as the permeability constants K_i (44, 45); 1.20 ml/min as the GFR (determined for 240-g rats from repeated experimental trials in our laboratory); and the tissue volumes and plasma flows listed in Table VII, the 16 differential equations were solved numerically by a digital computer. The results of the simulations are shown in Figs. 12 and 13. The predicted curves, except for muscle, are in good agreement with the mean values of the experimentally determined tissue levels of inulin after a 20-mg/kg dose and the plasma levels after both 20- and 200-mg/kg iv doses. The predicted peak inulin concentrations for the poorly perfused muscle and skin are reached relatively late, *i.e.*, 10–15 min after the bolus administration. However, the experimental concentration–time profiles in muscle and skin did not show such slow appearance of inulin. This may be the result of a more rapid uptake of inulin into the muscle and skin interstitial fluids from the capillary walls in rats than that reported for rabbits and dogs (44).

Application to Tissue Distribution Kinetics of Cefazolin—The differential equations described for cefazolin in Appendix II were solved numerically by incorporating various constants listed in Tables I, IV, and VII. Figures 14 and 15 show the predicted and observed concentration profiles for plasma, lung, heart, muscle, skin, bone, liver, and kidney tissues after the intravenous bolus injection of cefazolin to the urethane-anesthetized rats. Figure 16 also compares the simulation results from the model and the experimental tissue levels of plasma, muscle, skin, and kidney 60 min after the administration of cefazolin at various doses. As seen in these figures, there was reasonable agreement between the model predictions and the experimental concentrations in plasma and in various tissues at any time after any dose.

The physiological parameters in Table VII are statistical average values, and the plasma flow rates (except for liver) are those under unanesthetized conditions. It is, therefore, necessary to test the stability of the present model by comparing the numerical results derived from standard values for all parameters with the numerical results derived

Table VIII—[^{14}C]Inulin Space of Various Tissue of Rats

Tissue	Steady-State Concentration, μg/ml or μg/g						Inulin Space[a], %
	Experiment 1	Experiment 2	Experiment 3				
Plasma	13.6 ± 0.2	16.4 ± 0.7	20.5 ± 1.6				100.0
Heart	1.77	2.05	2.36				12.3 ± 0.8
Muscle	1.94	1.46	2.58				11.9 ± 2.8
Skin	4.07	4.50	6.66				29.9 ± 2.6
Bone	2.14	2.42	3.13				15.2 ± 0.5
Gut	1.35	1.70	1.65				9.6 ± 1.2
Liver	2.37	2.87	3.22				16.9 ± 1.0
	Experiment 4	Experiment 5	Experiment 6	Experiment 7	Experiment 8	Experiment 9	
Plasma[b]	220.6	256.6	288.0	383.8	463.6	499.0	100.0
Lung[b]	43.1	49.6	64.8	78.3	96.4	99.8	20.4 ± 1.2

[a] Defined by 100 × ratio of tissue-to-plasma concentration at steady state. [b] Experiments without [^{14}C]inulin. Inulin concentrations in plasma and the lung tissue were determined by a colorimetric assay described in the text.

Table IX—Cefazolin Concentrations in Plasma, Whole Blood, and Whole Bone Marrow After Constant Infusion [a] of Cefazolin in a 9-kg Beagle Dog

	Concentration, μg/ml												
	Time, min												
	380	385	410	415	420	450	470	477	483	500	507	517	Mean ± *SD*
Plasma	67.6	—	54.5	—	53.3	74.8	82.2	—	95.6	65.3	—	60.0	69.2 ± 14.5
Whole blood	—	—	—	—	44.9	45.5	—	—	41.3	—	—	39.1	42.7 ± 3.0
Whole bone marrow	—	27.9	—	57.7	—	—	—	41.5	—	—	61.5	—	47.2 ± 15.5
Hematocrit, %	—	—	—	—	41.0	41.6	—	—	42.5	—	—	42.1	41.8 ± 0.6

[a] Infusion was carried out at a rate of 180 mg/hr without a priming dose.

from ±10% variation of standard values for each of the parameters. Such variation in any body region of the tissue, capillary volumes, and plasma flow rates did not significantly affect the simulation results, indicating that the model is quite stable within ±10% of the physiological parameters.

DISCUSSION

The binding of antimicrobial agents to plasma protein and tissues is considered to be an important factor in antimicrobial activity and pharmacokinetics. Much of the research effort has been directed toward determining the binding to plasma protein, uptake by erythrocytes, and the extravascular binding of β-lactam antibiotics. Nevertheless, the data are still incomplete in certain aspects: the published reports are sometimes in conflict. This study investigates the full disposition characteristics of β-lactam antibiotics in rats and describes a pharmacokinetic model that is capable of predicting tissue distribution and elimination kinetics not only in rats, but also in other species including humans.

β-Lactam antibiotics bind to serum protein, mainly albumin, in a reversible manner (46). It is generally accepted that such a binding equilibrium occurs within microseconds. Greene *et al.* (47) confirmed the rapid binding of cefazolin to canine serum, the binding equilibrium being attained as fast as the sample could be ultrafiltered. There is a general lack of agreement in the literature regarding the extent of binding for β-lactam antibiotics obtained from experiments carried out by different methods and even by the same method. The equilibrium dialysis method is known to be very reliable for determining quantitative binding of stable drugs, but has disadvantages for unstable drugs due to the time requirement to complete the diffusion equilibrium processes. However, use of microdiffusion cells in this study achieved the complete diffusion equilibrium within 4 hr (Fig. 1).

The serum protein binding ratio of β-lactam antibiotics varies with the species of animal and the total concentration of antibiotic. Shimizu (48) compared the protein binding of penicillins and cephalosporins in the sera of different animals using centrifugal ultrafiltration techniques. The extent of binding of cefazolin was ≥90% in humans, rabbits, and rats (equivalent to that of dicloxacillin), but only ~50% in dogs, horses, and bovines. The percent of cefazolin bound to human serum albumin significantly decreased with increases in the total antibiotic concentration (48). Similar results were obtained in this study using rat serum. The free fraction of cefazolin is 11% at 10 μg/ml, 20% at 100 μg/ml, and 41% at 200 μg/ml. Since the free fraction more than doubled between 10 and 100 μg/ml and increased by a factor of >4 between 10 and 200 μg/ml, the

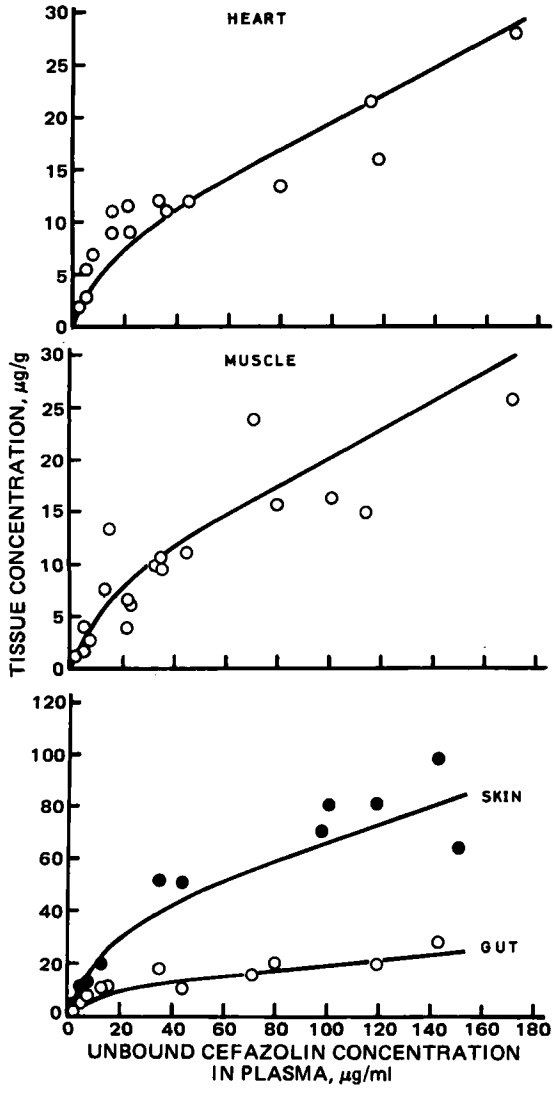

Figure 10—*Relationship between cefazolin concentration in the heart, muscle, skin, and gut tissues and the unbound cefazolin concentration in plasma at steady state after the constant infusion of cefazolin to rats. The points represent the experimental values; the solid lines were generated from Eq. 19 and the various parameters listed in Tables I, VII, and VIII.*

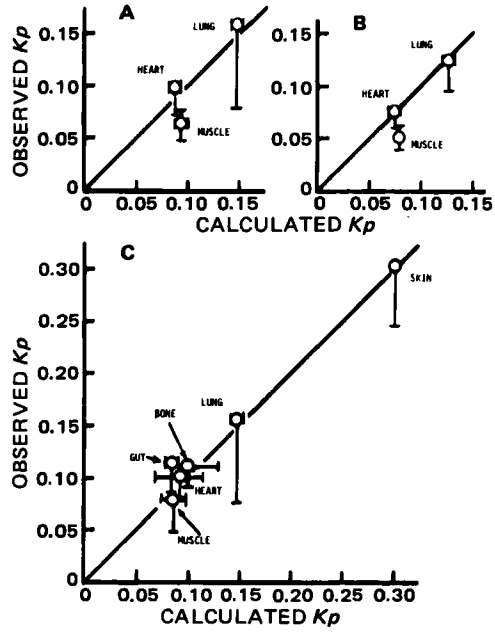

Figure 11—*Relationship between the observed K_p values of penicillin V (A), dicloxacillin (B), and cefazolin (C) for various tissues and the theoretical K_p values calculated from Eq. 21 or 23 and the various parameters listed in Tables I, VII, and VIII. The bars represent the standard deviation of the experimental values and the lower and upper limits of the theoretical values.*

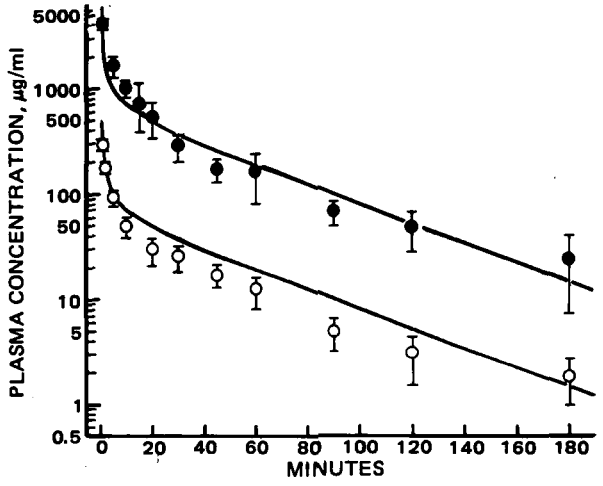

Figure 12—*Model-predicted (lines)* versus *observed (points) plasma inulin concentrations after 20- (○) and 200-mg/kg (●) intravenous bolus doses to rats. Each point represents the mean of 3–8 rats; bars represent the standard deviations.*

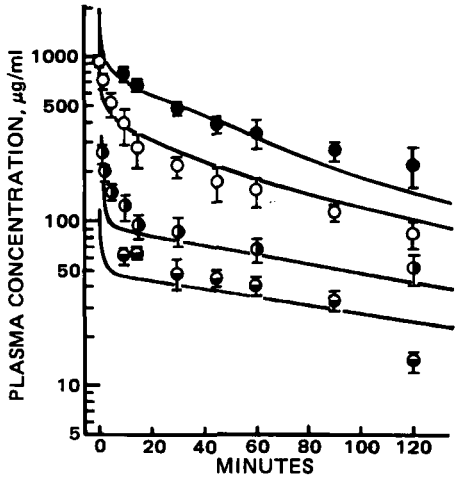

Figure 14—*Model-predicted (lines)* versus *observed (points) plasma cefazolin concentrations after 10- (◒), 20- (◑), 100- (○), and 200-mg/kg (●) intravenous bolus doses to rats. Each point represents the mean of 3–9 rats; bars represent the standard deviations.*

distribution of cefazolin into tissue regions in rats will change radically. Other β-lactam antibiotics studied did not show such a remarkable nonlinear binding behavior.

The binding behavior of β-lactam antibiotics could be explained by the nonlinear binding equation (Eq. 1), where the magnitude of the binding constant (K_B) and the drug concentration (C_F) are very important parameters. If K_B is sufficiently small, Eq. 1 becomes Eq. 2, which expresses an apparent linear binding. Nayler (49) reported that the apparent binding constant of penicillins in human serum correlated quantitatively with the lipophilicity of the antibiotics. The experimental results shown in Fig. 2 and Table I demonstrate that the extent of binding of the five penicillins studied in rat serum correlates qualitatively with their lipophilicity. Dicloxacillin, which is the most lipophilic, has the largest $K_{B,app}$ value, whereas the more hydrophilic methicillin has a smaller $K_{B,app}$ value.

The mechanism of hepatic elimination of β-lactam antibiotics is not clearly understood. Although the penicillin derivatives studied were subjected to extensive metabolism to the penicilloic acids (4), cefazolin did not exhibit such metabolism in rats. The reason for the resistance of cefazolin to metabolic degradation is not clear, but similar results have been reported in other species including humans (5, 6).

The processes concerned with the transport of drugs into bile have been studied (50). Although passive diffusion may play a part in the transport of drug into bile, it is generally believed that active transport is the primary process (50). The biliary secretion of some penicillins and cephalosporins in rats have been studied by Ryrfeldt (51) and Wright and Line

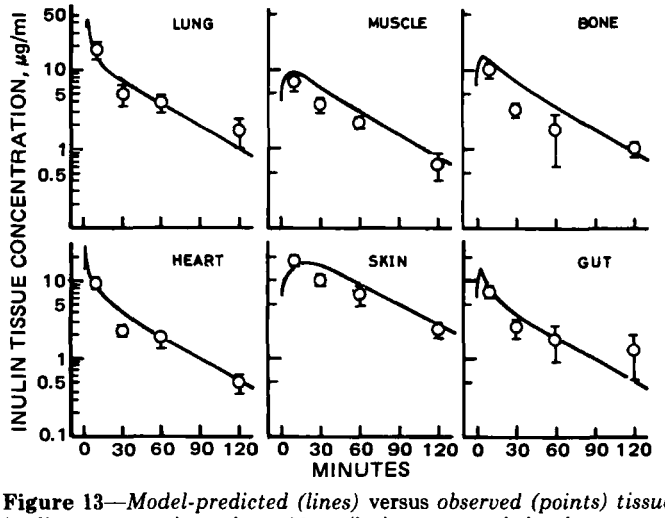

Figure 13—*Model-predicted (lines)* versus *observed (points) tissue inulin concentrations after a 20-mg/kg intravenous bolus dose to rats. Each point represents the mean of 3–5 rats; bars represent the standard deviations.*

(52). However, quantitative reports on the biliary excretion rate are limited. Previously, the biliary excretion of penicillin V was characterized by Michaelis–Menten kinetics (12). A similar capacity-limited excretion into bile was also observed for cefazolin, using Eq. 7.

The renal excretion of β-lactam antibiotics has been studied extensively. Using the micropuncture technique, Bergeron *et al.* (53) reported that penicillin G was excreted from plasma by glomerular filtration and active secretion from the proximal tubules, and that the respective contribution ratios were ~35 and 65%. The present study utilizing the net inhibitory effect of probenecid on the renal excretion of penicillin G into rat urine showed 35% glomerular filtration and 65% tubular secretion, consistent with the result of Bergeron *et al.* (53). On the other hand, the rate of cefazolin excretion into urine was unaffected by probenecid. The results indicate that the renal tubular secretion of cefazolin plays a minor role in the renal elimination process in rats. Our conclusion obtained for this antibiotic does not agree with the recent finding by Yamazaki *et al.* (54), who predicted a significant contribution of tubular secretion of cefazolin in rats. This apparent discrepancy cannot be explained completely by the difference in the protein binding ratio determined in both laboratories and needs to be investigated further. Therefore, until such time when a reliable urinary excretion mechanism of β-lactam antibiotics is established, we adopted the apparent renal clearance value of 0.82 ml/min (dependent on the unbound concentration in the arterial plasma) in this pharmacokinetic prediction for cefazolin in rats.

The kinetic behavior of antibiotics in an infected tissue fluid is important for antimicrobial chemotherapy. Classical approaches are usually based on the curve-fitting of plasma concentration data with multiexponential equations to construct the necessary compartment models. Sometimes, the compartments and parameters thus estimated have no physiological reality in the species being investigated. Therefore, it is difficult to use classical pharmacokinetics to interpret the differences between animal and human experiments.

To overcome this difficulty, physiological pharmacokinetic models have been developed and adapted for some drugs by several workers (7–12). These models are based on experimental data regarding tissue binding or tissue-to-plasma (or blood) partition coefficients (K_p) in laboratory animals, as with penicillin V (12). This approach has the potential advantages of predicting tissue drug levels and reflecting the variations in drug binding with different tissues of the animals investigated. However, because there are sometimes substantial differences in K_p values among species (11) and the property of K_p in each tissue is often obscure, this approach does not always allow us to predict the tissue concentration–time profiles of drugs in other species, *i.e.*, humans.

Our present goal was to make possible *a priori* predictions of β-lactam antibiotic levels in organs of any species, based on the knowledge of parameters easily determined for human subjects as well as experimental animals. This study was designed to use cefazolin, which exhibits interesting nonlinear binding with serum proteins and simpler elimination characteristics in rats than the other β-lactam antibiotics.

One of the key points in solving this problem is to clarify the exact nature of the K_p values of β-lactam antibiotics for various tissues. Peterson *et al.* (55) determined the binding of some β-lactam antibiotics

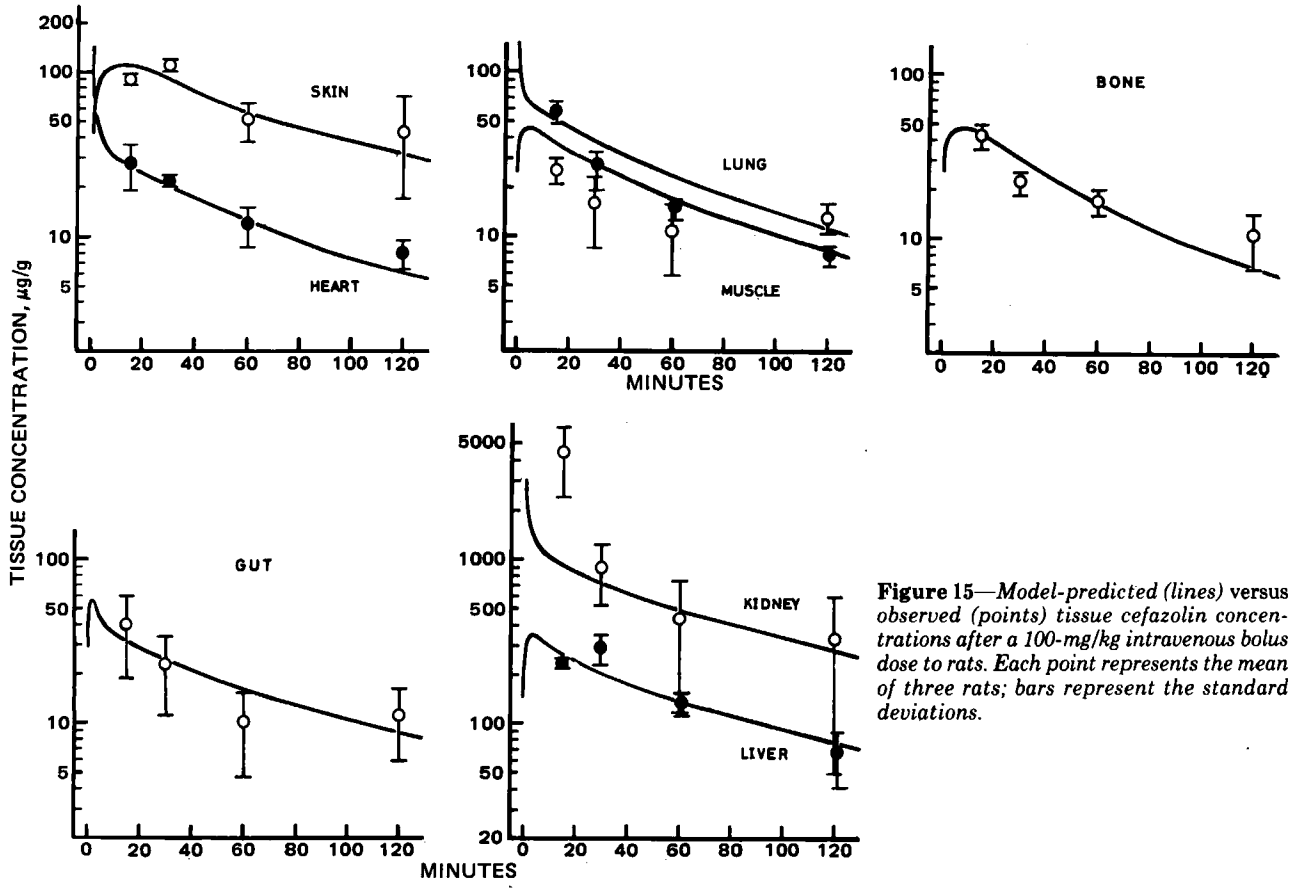

Figure 15—*Model-predicted (lines)* versus *observed (points) tissue cefazolin concentrations after a 100-mg/kg intravenous bolus dose to rats. Each point represents the mean of three rats; bars represent the standard deviations.*

in dilute homogenates of canine tissues and employed the results to predict the apparent volume of distribution after intravenous administration in dogs. The question may be raised whether binding data obtained *in vitro* with tissue homogenates are applicable to *in vivo* conditions. For a drug that is unable to penetrate into the tissue intracellular space, binding to tissue apparently was not the sole factor responsible for *in vivo* accumulation of the drug. With β-lactam antibiotics, however, due to the experimental difficulty in assessing the extent of antibiotic penetration into cells, the conclusions obtained from the various animal model studies differed among investigators. By determining the steady-state plasma and tissue levels of cefazolin in rats, we obtained evidence in support of our claim that this antibiotic cannot enter erythrocytes and tissue cells of noneliminating organs, and that albumin existing in these tissue interstitial fluids play a major role in determining antibiotic levels in various tissues. On this basis, the K_p values of β-lactam antibiotics could be successfully interpreted for not only cefazolin, but also penicillin V and dicloxacillin.

Despite the use of simplifying assumptions in formulating the antibiotic distribution in physiologically and anatomically complex body regions, there was a reasonably close fit between the simulation from the present model and the experimental tissue levels after intravenous bolus administration of cefazolin in rats. The simulations demonstrate that the tissue distribution of cefazolin in rats is complete within 15 min even in the slowly perfused muscle, skin, and bone tissues. The observed high cefazolin level in skin compared with the levels in the other noneliminating tissues is due to the higher content of albumin and the larger interstitial space. The time course of cefazolin in skin was also nicely predicted by the present pharmacokinetic model based on the assumption that albumin concentration in the skin interstitial fluid is equal to that in plasma. In addition to the examination for β-lactam antibiotics, this model could predict the tissue distribution profiles of inulin. The model, incorporating the slow diffusion of a large molecule from capillary membranes into the interstitial fluids of lung, heart, muscle, skin, and gut tissues, was able to adequately represent the concentrations of inulin in plasma and various tissues. As seen in Fig. 13, inulin in skin showed a markedly different behavior from cefazolin, and the concentration–time profile in skin was almost identical with those in heart, muscle, bone, and gut; this is the consequence of the lack of binding of inulin with albumin. This result supports the assumption made for the skin compartment in the present work.

Although our model was able to provide a good prediction of intravenous dosing data of cefazolin and inulin in rats, there are still a number of deficiencies. First, it is necessary to identify the magnitude of uptake clearance of antibiotics into hepatocytes compared with hepatic plasma flow rate. Second, we need to more fully characterize the kinetics and mechanisms not only of active transport into tubular cells and reabsorption from tubules in the kidney, but also biliary secretion and metabolism in the liver for the β-lactam antibiotics. The proposed model, nevertheless, is capable of predicting tissue concentrations as a function of time after a single bolus dose in normal animals and should be useful in predicting these levels in animals where renal and hepatic function, albumin concentration, extravascular space, and blood flow are altered due to disease states.

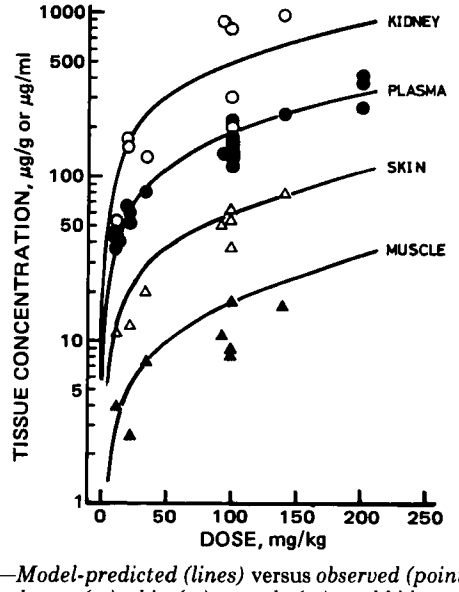

Figure 16—*Model-predicted (lines)* versus *observed (points) concentrations in plasma (●), skin (△), muscle (▲), and kidney (○) 60 min after intravenous bolus injections at various doses to rats.*

APPENDIX I: GLOSSARY

AR = Tissue-to-plasma albumin ratio
C_B = Bound concentration in plasma, μg/ml
C_{BIS} = Bound concentration in tissue interstitial fluid, μg/ml
C_F = Free concentration in plasma or in tissue interstitial fluid, μg/ml
C_T = Total concentration in tissue, μg/ml or μg/g
GFR = Glomerular filtration rate, ml/min
$I(t)$ = Dose input function, min^{-1}
IS = Tissue interstitial space
K = Permeability constant from capillary wall to interstitial fluid, ml/min
K_m = Michaelis constant, μg/ml
K_p = Tissue-to-plasma partition coefficient
P = Albumin concentration in serum, M
Q = Plasma flow rate, ml/min
R = Reabsorption ratio
UF = Urine flow rate, ml/min
V = Volume of tissue (excluding equilibrium blood), ml
∇_{bi} = Maximum rate of biliary secretion, μg/min
VCB = Plasma volume in capillary bed of tissue, ml
VIC = Volume of tissue intracellular water, ml
VIS = Volume of tissue interstitial fluid, ml
α = Coefficient in the differentiation of the plasma protein binding
β = *Bound-to-unbound* concentration ratio

Subscripts
b = blood
p = arterial plasma
u = urine
bi = bile
vp = venous plasma
lg = lung
lgi = lung interstitial fluid
ht = heart
hti = heart interstitial fluid
ms = muscle
msi = muscle interstitial fluid
sk = skin
ski = skin interstitial fluid
bn = bone
bnm = bone marrow
bnc = bone cortex
gt = gut
gti = gut interstitial fluid
cr = carcass
lv = liver
kd = kidney
wb = whole blood
ss = steady state

APPENDIX II: MODEL EQUATIONS FOR CEFAZOLIN

Venous plasma:

$$V_{vp}(1+\alpha_{vp})\frac{dC_{F,vp}}{dt} = Q_{ht}(1+\beta_{ht})C_{F,ht} + Q_{ms}(1+\beta_{ms})C_{F,ms} + Q_{sk}(1+\beta_{sk})C_{F,sk} + Q_{bn}(1+\beta_{bn})C_{F,bn} + Q_{cr}(1+\beta_{cr})C_{F,cr} + Q_{lv}(1+\beta_{lv})C_{F,lv} + Q_{kd}(1+\beta_{kd})C_{F,kd} - (Q_{ht}+Q_{ms}+Q_{sk}+Q_{bn}+Q_{cr}+Q_{lv}+Q_{kd})(1+\beta_{vp})C_{F,vp} + \text{Dose}\cdot I(t) \quad \text{(Eq. II-1)}$$

Arterial plasma:

$$V_p(1+\alpha_p)\frac{dC_{F,p}}{dt} = (Q_{ht}+Q_{ms}+Q_{sk}+Q_{bn}+Q_{cr}+Q_{lv}+Q_{kd}) \times [(1+\beta_{lg})C_{F,lg} - (1+\beta_p)C_{F,p}] \quad \text{(Eq. II-2)}$$

Lung:

$$[VCB_{lg}(1+\alpha_{lg}) + VIS_{lg}(1+\alpha_{lg}AR_{lg})]\frac{dC_{F,lg}}{dt} = (Q_{ht}+Q_{ms}+Q_{sk}+Q_{bn}+Q_{cr}+Q_{lv}+Q_{kd})[(1+\beta_{vp})C_{F,vp} - (1+\beta_{lg})C_{F,lg}] \quad \text{(Eq. II-3)}$$

Heart:

$$[VCB_{ht}(1+\alpha_{ht}) + VIS_{ht}(1+\alpha_{ht}AR_{ht})]\frac{dC_{F,ht}}{dt} = Q_{ht}[(1+\beta_p)C_{F,p} - (1+\beta_{ht})C_{F,ht}] \quad \text{(Eq. II-4)}$$

Muscle:

$$[VCB_{ms}(1+\alpha_{ms}) + VIS_{ms}(1+\alpha_{ms}AR_{ms})]\frac{dC_{F,ms}}{dt} = Q_{ms}[(1+\beta_p)C_{F,p} - (1+\beta_{ms})C_{F,ms}] \quad \text{(Eq. II-5)}$$

Skin:

$$[VCB_{sk}(1+\alpha_{sk}) + VIS_{sk}(1+\alpha_{sk}AR_{sk})]\frac{dC_{F,sk}}{dt} = Q_{sk}[(1+\beta_p)C_{F,p} - (1+\beta_{sk})C_{F,sk}] \quad \text{(Eq. II-6)}$$

Bone:

$$[(VCB_{bn}+V_{bnm})(1+\alpha_{bn}) + VIS_{bnc}]\frac{dC_{F,bn}}{dt} = Q_{bn}[(1+\beta_p)C_{F,p} - (1+\beta_{bn})C_{F,bn}] \quad \text{(Eq. II-7)}$$

Carcass:

$$[VCB_{cr}(1+\alpha_{cr}) + VIS_{cr}(1+\alpha_{cr}AR_{cr})]\frac{dC_{F,cr}}{dt} = Q_{cr}[(1+\beta_p)C_{F,p} - (1+\beta_{cr})C_{F,cr}] \quad \text{(Eq. II-8)}$$

Liver:

$$[(1+\alpha_{lv})(VCB_{lv}+V_{lv}K_{p,lv})]\frac{dC_{F,lv}}{dt} = (Q_{lv}-Q_{gt})(1+\beta_p)C_{F,p} + Q_{gt}(1+\beta_{gt})C_{F,gt} - Q_{lv}(1+\beta_{lv})C_{F,lv} - \frac{V_{biCF,lv}}{K_{m,bi}+C_{F,lv}} \quad \text{(Eq. II-9)}$$

Gut tissue:

$$[VCB_{gt}(1+\alpha_{gt}) + VIS_{gt}(1+\alpha_{gt}AR_{gt})]\frac{dC_{F,gt}}{dt} = Q_{gt}[(1+\beta_p)C_{F,p} - (1+\beta_{gt})C_{F,gt}] \quad \text{(Eq. II-10)}$$

Kidney:

$$[(1+\alpha_{kd})(VCB_{kd}+V_{kd}K_{p,kd})]\frac{dC_{F,kd}}{dt} = Q_{kd}[(1+\beta_p)C_{F,p} - (1+\beta_{kd})C_{F,kd}] - GFR(1-R)C_{F,p} \quad \text{(Eq. II-11)}$$

where the dose input function can be calculated as the function of the reciprocal of the injection time, λ (7):

$$I(t) = 30\lambda(\lambda t)^2(1-\lambda t)^2 \quad \text{(Eq. II-12)}$$

The values of α_i and β_i are defined by Eqs. 12 and 15, respectively, in the text.

Total concentration in plasma and total tissue concentration corresponding to the observed values in i-type tissue, except liver and kidney, can be calculated from Eqs. II-13 and II-14, respectively:

$$C_{T,p} = (1+\beta_p)C_{F,p} \quad \text{(Eq. II-13)}$$

$$C_{T,i} = IS_i(1+\beta_i AR_i)C_{F,i} \quad \text{(Eq. II-14)}$$

Calculation of total tissue concentration in liver and kidney is made from:

$$C_{T,i} = (1+\beta_i)K_{pi}C_{F,i} \quad (i = \text{liver, kidney}) \quad \text{(Eq. II-15)}$$

APPENDIX III: MODEL EQUATIONS FOR INULIN

Instead of Eqs. II-3 to II-6 and II-10 in Appendix II, the following mass balance equations can be written for the lung, heart, muscle, skin, and gut regions (see text).

Lung:

$$VCB_{lg}\frac{dC_{F,lg}}{dt} = Q_{lg}(C_{F,pv} - C_{F,lg}) - K_{lg}(C_{F,lg} - C_{F,lgi}) \quad \text{(Eq. III-1)}$$

$$VIS_{lg}\frac{dC_{F,lgi}}{dt} = K_{lg}(C_{F,lg} - C_{F,lgi}) \qquad \text{(Eq. III-2)}$$

Heart:

$$VCB_{ht}\frac{dC_{F,ht}}{dt} = Q_{ht}(C_{F,p} - C_{F,ht}) - K_{ht}(C_{F,ht} - C_{F,hti}) \qquad \text{(Eq. III-3)}$$

$$VIS_{ht}\frac{dC_{F,hti}}{dt} = K_{ht}(C_{F,ht} - C_{F,hti}) \qquad \text{(Eq. III-4)}$$

Muscle:

$$VCB_{ms}\frac{dC_{F,ms}}{dt} = Q_{ms}(C_{F,p} - C_{F,ms}) - K_{ms}(C_{F,ms} - C_{F,msi}) \qquad \text{(Eq. III-5)}$$

$$VIS_{ms}\frac{dC_{F,msi}}{dt} = K_{ms}(C_{F,ms} - C_{F,msi}) \qquad \text{(Eq. III-6)}$$

Skin:

$$VCB_{sk}\frac{dC_{F,sk}}{dt} = Q_{sk}(C_{F,p} - C_{F,sk}) - K_{sk}(C_{F,sk} - C_{F,ski}) \qquad \text{(Eq. III-7)}$$

$$VIS_{sk}\frac{dC_{F,ski}}{dt} = K_{sk}(C_{F,sk} - C_{F,ski}) \qquad \text{(Eq. III-8)}$$

Gut:

$$VCB_{gt}\frac{dC_{F,gt}}{dt} = Q_{gt}(C_{F,p} - C_{F,gt}) - K_{gt}(C_{F,gt} - C_{F,gti}) \qquad \text{(Eq. III-9)}$$

$$VIS_{gt}\frac{dC_{F,gti}}{dt} = K_{gt}(C_{F,gt} - C_{F,gti}) \qquad \text{(Eq. III-10)}$$

Elimination of inulin was negligible in the liver and occurs in the kidney through glomerular filtration, where negligible reabsorption (R = 0) can be assumed. Because there is no binding of inulin with any protein, $\alpha_i = 0$ and $\beta_i = 0$, then $C_{T,i} = IS_iC_{F,i}$ in every tissue region.

REFERENCES

(1) M. Gibaldi, M. A. Schwartz, and M. E. Plaut, *Antimicrob. Agents Chemother.—1968*, **1969**, 378.

(2) L. W. Dittert, W. O. Griffen, Jr., J. C. LaPiana, F. J. Shaifeld, and J. T. Doluisio, *Antimicrob. Agents Chemother.—1969*, **1970**, 42.

(3) R. E. Notari, "Biopharmaceutics and Pharmacokinetics, an Introduction," 2nd ed., Dekker, New York, N.Y., 1975, (References cited therein).

(4) T. Bergan, *Antibiot. Chemother.*, **25**, 1 (1978) (References cited therein).

(5) C. H. Nightingale, D. S. Greene, and R. Quintiliani, *J. Pharm. Sci.*, **64**, 1899 (1975) (References cited therein).

(6) J. M. Brogard, F. Comte, and M. Pinget, *Antibiot. Chemother.*, **25**, 123 (1978) (References cited therein).

(7) K. B. Bischoff and R. L. Dedrick, *J. Pharm. Sci.*, **57**, 1346 (1968).

(8) K. B. Bischoff, R. L. Dedrick, D. S. Zaharko, and J. A. Longstreth, *J. Pharm. Sci.*, **60**, 1128 (1971).

(9) N. Benowitz, R. P. Forsyth, K. L. Melmon, and M. Rowland, *Clin. Pharmacol. Ther.*, **16**, 87 (1974).

(10) C. N. Chen and J. D. Andrade, *J. Pharm. Sci.*, **65**, 717 (1976).

(11) L. I. Harrison and M. Gibaldi, *J. Pharm. Sci.*, **66**, 1679 (1977).

(12) A. Tsuji, E. Miyamoto, T. Terasaki, and T. Yamana, *J. Pharm. Pharmacol.*, **31**, 116 (1979).

(13) D. S. Greene, R. Quintiliani, and C. H. Nightingale, *J. Pharm. Sci.*, **67**, 191 (1978).

(14) M. A. Schwartz and A. J. Delduce, *J. Pharm. Sci.*, **58**, 1137 (1969).

(15) M. Yokota, T. Iga, S. Awazu, and M. Hamano, *J. Appl. Physiol.*, **41**, 439 (1976).

(16) S. E. Bradley, F. J. Ingelfinger, G. P. Bradley, and J. J. Curry, *J. Clin. Invest.*, **24**, 890 (1945).

(17) R. Thomas, *Nature (London)*, **191**, 1161 (1961).

(18) A. Tsuji, E. Miyamoto, and T. Yamana, *J. Pharm. Pharmacol.*, **30**, 811 (1978).

(19) K. Miyazaki, O. Ogino, and T. Arita, *Chem. Pharm. Bull.* **12**, 413 (1964).

(20) W. H. Waugh, *Clin. Chem.*, **23**, 639 (1977).

(21) R. K. Harle and T. Cowen, *Analyst*, **103**, 492 (1978).

(22) C. M. Metzler, "NONLIN, A Computer Program for Parameter Estimation in Nonlinear Systems," Technical Report 7292/69/7292/005, The Upjohn Co., Kalamazoo, Mich., 1969.

(23) A. R. English, H. T. Huang, and B. A. Sobin, *Proc. Soc. Exp. Biol. Med.*, **104**, 405 (1960).

(24) A. C. Kind, H. N. Beaty, L. F. Fenster, and W. M. M. Kirby, *J. Lab. Clin. Med.*, **71**, 728 (1968).

(25) M. Nishida, T. Matsubara, T. Murakawa, Y. Mine, Y. Yokota, S. Goto, and S. Kuwahara, *J. Antibiot.*, **23**, 184 (1970).

(26) G. Levy, *J. Pharm. Sci.*, **69**, 482 (1980).

(27) (*a*) R. Hori, K. Sunayashiki, and A. Kamiya, *J. Pharm. Sci.*, **65**, 463 (1976); (*b*) R. Hori, K. Sunayashiki, and A. Kamiya, *Chem. Pharm. Bull.*, **26**, 740 (1978) (References cited therein).

(28) H. S. G. Chen and J. F. Gross, *J. Pharmacokinet. Biopharm.*, **7**, 117 (1979).

(29) A. Tsuji, E. Miyamoto, O. Kubo, and T. Yamana, *J. Pharm. Sci.*, **68**, 812 (1979).

(30) M. Nishida, T. Matsubara, T. Uemura, T. Murakawa, and Y. Yokota, *Jpn. J. Antibiot.*, **23**, 217 (1970).

(31) N. Okada, H. Sakamoto, S. Nakamoto, Y. Yokota, T. Murakawa, and M. Nishida, *Chemotherapy (Tokyo)*, **25**, 392 (1977).

(32) (*a*) M. L. Kornguth, R. A. Monson, and C. M. Kunin, *J. Infect. Dis.*, **129**, 552 (1974); (*b*) R. Kirsch, G. Fleischner, K. Kamisaka, and I. M. Arias, *J. Clin. Invest.*, **55**, 1009 (1975).

(33) L. Jansky and J. S. Hart, *Can. J. Physiol. Pharmacol.*, **46**, 653 (1968).

(34) L. A. Sapirstein, E. H. Sapirstein, and A. Bredemeyer, *Circ. Res.*, **8**, 135 (1960).

(35) R. L. Dedrick, D. S. Zaharko, and R. J. Lutz, *J. Pharm. Sci.*, **62**, 882 (1973).

(36) K. Higaki and M. Fujimoto, *J. Physiol. Soc. Jpn.*, **31**, 164 (1969).

(37) J. Katz, G. Bonorris, S. Golden, and A. L. Sellers, *Clin. Sci.*, **39**, 705 (1970).

(38) M. A. Rothschild, A. Bauman, R. S. Yalow, and S. A. Berson, *J. Clin. Invest.*, **34**, 1334 (1955).

(39) D. H. Pitkin, C. Sachs, I. Zajac, and P. Actor, *Antimicrob. Agents Chemother.*, **11**, 760 (1977).

(40) E. Dingeldein and H. Wahlig, *Arzneim.-Forsch, Drug Res.*, **29**, 400 (1979).

(41) T. Shidou, *Jpn. J. Antibiot.*, **29**, 999 (1976).

(42) M. Kawashima and T. Torisu, *Jpn. J. Antibiot.*, **30**, 278 (1977).

(43) (*a*) G. Majino, in "Handbook of Physiology," Sect. 2, vol. III, W. F. Hamilton and P. Dow, Eds., American Physiological Society, Washington, D.C., 1963, p. 1035; (*b*) J. G. Luft, in "The Inflammatory Process," B. W. Zweifach, L. Grant, and R. T. McCluskey, Eds., Academic, New York, N.Y., 1965, p. 121; (*c*) E. M. Penkin, *Circ. Res.*, **41**, 735 (1977).

(44) L. E. Wittners, Jr., M. Bartlett, and J. A. Johnson, *Microvas. Res.*, **11**, 67 (1976).

(45) (*a*) W. P. Paaske and P. Sejrsen, *Acta Physiol. Scand.*, **100**, 437 (1977); (*b*) W. P. Paaske, *Physiologist*, **23**, 75 (1980).

(46) G. N. Rolinson and R. Sutherland, *Brit. J. Pharmacol.*, **25**, 638 (1965).

(47) D. S. Greene, R. Quintiliani, and C. H. Nightingale, *J. Pharm. Sci.*, **66**, 1663 (1977).

(48) T. Shimizu, *Jpn. J. Antibiot.*, **27**, 296 (1974).

(49) J. H. C. Nayler, in "Advances in Drug Research," vol. 7, N. J. Harper and A. B. Simmonds, Eds., Academic, New York, N.Y., 1973, p. 1.

(50) C. T. Ashworth and E. Sanders, *Am. J. Pathol.*, **37**, 343 (1960).

(51) A. Ryrfeldt, *Acta Pharmacol. Toxicol.*, **32**, Suppl., III, 1 (1973).

(52) W. E. Wright and V. D. Line, *Antimicrob. Agents Chemother.*, **17**, 842 (1980).

(53) M. G. Bergeron, F. J. Gennari, M. Barza, L. Weistein, and S. Cortell, *J. Infect. Dis.*, **132**, 374 (1975).

(54) I. Yamazaki, Y. Shirakawa, and T. Fugono, *J. Antibiot.*, **34**, 1055 (1981).

(55) L. R. Peterson, D. N. Gerding, D. McLinn, and W. H. Hall, *J. Antimicrob. Chemother.*, **5**, 219 (1979).

(56) W. W. Mapleson, *J. Appl. Physiol.*, **18**, 197 (1963).

ACKNOWLEDGMENTS

Presented in part at the 12th Symposium on Drug Metabolism and Action, Kanazawa, Japan, Oct. 8–9, 1980.

The authors are indebted to Dr. Shinobu Nakamura, School of Medicine, Kanazawa University, for the bone marrow sampling and helpful discussions. Thanks are also given to Mr. H. Nakamura, Miss Y. Yoshida, Miss K. Narizuka, Miss H. Hironaka, Miss M. Nishikawa, Miss M. Uwagawa, and Mr. H. Mizuo for their excellent assistance in the experimental work and to Fujisawa Pharmaceutical Co., Osaka, Japan for the supply of [^{14}C]cefazolin.

Solution Activity Product (K_{FAP}) and Simultaneous Demineralization–Remineralization in Bovine Tooth Enamel and Hydroxyapatite Pellets

JEFFREY L. FOX *‡¶ˣ, BALA V. IYER *‡, WILLIAM I. HIGUCHI *‡¶, and JOHN J. HEFFERREN §

Received May 17, 1982, from the **Dental Research Institute* and the ‡*College of Pharmacy, The University of Michigan, Ann Arbor, MI 48109* and the §*American Dental Association Health Foundation.* Accepted for publication August 26, 1982. ¶Present address: Dept. of Pharmaceutics, University of Utah, Salt Lake City, UT 84112.

Abstract □ The effects of changing the ion activity product of the remineralization solution at pH 4.5 (pK_{FAP} 108–118) on the remineralization behavior of demineralized bovine tooth enamel and hydroxyapatite pellets have been studied. Solutions containing calcium-45, phosphate, and fluoride in acetate buffers were used. The ^{45}Ca/F molar ratios indicated the formation of fluoridated hydroxyapatite in the enamel or the pellet when the pK_{FAP} values for remineralizing solutions were <112. When the pK_{FAP} values were >112, the ^{45}Ca/F ratios were found to be ≪5. Also, when the pK_{FAP} values were large (>112), the remineralization patterns based on the fluoride distribution in the tooth (or pellet) were found to be different than when the pK_{FAP} values were small (<112). The hypothesis that a pK_{FAP} value of 112 is the demarcation between remineralization only and simultaneous dissolution–remineralization has been proposed based on these results.

Keyphrases □ Tooth enamel—bovine, demineralization and remineralization, effect of bulk solution activity product □ Hydroxyapatite—pellets, demineralization and remineralization, effect of bulk solution activity product □ Remineralization—demineralized bovine tooth enamel, hydroxyapatite pellets, effect of bulk solution activity product

Previous studies conducted in these laboratories (1) indicated that both bovine tooth enamel and hydroxyapatite pellets could be extensively remineralized in a fluoride-containing remineralizing solution after prior demineralization treatments for various lengths of time. After 3 or 6 hr of prior demineralization in a partially saturated acetate buffer at pH 4.5, fluoride uptake levels on the order of 1000 ppm were found after remineralization, at depths up to ~50 μm from the surface. The stoichiometry of the remineralized phase was shown to be fluoridated hydroxyapatite rather than calcium fluoride based on the ^{45}Ca/F ratio and determination by X-ray diffraction analysis. All of the remineralization studies (1) were conducted in solutions at an ionic product ($K_{FAP} = a^{10}_{Ca^{2+}} a^{6}_{PO_4^{3-}} a^{2}_{F^-}$) of $\sim 1 \times 10^{-108}$.

The purpose of the present study was to investigate the influence of varying the K_{FAP} value for the remineralizing solution. A case of special interest was where the K_{FAP} values are $>10^{-120}$, the solubility product for fluorapatite (2), but $<10^{-114}$, the ion activity product value below which dissolution takes place with hydroxyapatite pellets (3). A question of great interest was how the concomittant dissolution of hydroxyapatite, if it were to occur, would influence the remineralization behavior in this K_{FAP} region.

EXPERIMENTAL

Materials—*Bovine Teeth*—Teeth from 8-week-old strictly kosher calves were obtained from packing houses in the Chicago area. From these incisors, only those without any visible surface defects and with a reasonably flat surface were used for the experiments. The labial surfaces of these selected teeth were then ground with rotating sandpaper (No. 400 first, then No. 600) to remove the pellicle.

Hydroxyapatite Pellet—Synthetic hydroxyapatite crystals prepared using the procedure developed by Moreno (4) were used in the preparation of the pellets. Approximately 50 mg of hydroxyapatite, preequilibrated in a humidity chamber containing saturated potassium nitrate aqueous solution to maintain the humidity at ~67%, was compressed in a 0.62-cm diameter die with a force of 4540 kg using a laboratory press[1].

Preparation of Buffer Solutions—As in a previous study (1) a solution ~16% saturated (on a molar basis) with respect to the thermodynamic solubility of hydroxyapatite was used for demineralization. The solution was a 0.1 *M* acetate buffer containing 3.5 m*M* each of total calcium and phosphate. The pH was adjusted to 4.5 with sodium hydroxide and the ionic strength to 0.5 *M* by the addition of sodium chloride. For remineralization 0.1 *M* acetate buffers (pH 4.5) containing differing amounts of total calcium and phosphate depending on the desired bulk solution activity product ($K_{FAP} = a^{10}_{Ca^{2+}} a^{6}_{PO_4^{3-}} a^{2}_{F^-}$) as shown in Table I, were employed. These solutions also contained 10 ppm of fluoride and sodium chloride to adjust the ionic strength to 0.5 *M*. All the chemicals used for the preparation of buffer solutions were analytical grade. A predetermined amount of calcium-45 as $^{45}CaCl_2$ in water[2] was added to these solutions.

Demineralization—A bovine tooth was covered with dental inlay wax except for a 0.25-cm^2 area in the labial surface. In the pellet experiments, a hydroxyapatite pellet was completely covered with inlay wax except for one exposed surface (area, 0.25 cm^2). The tooth or pellet was then demineralized in the 16% partially saturated buffer solution for a period of 6 and 3 hr, respectively, after attaching a thin glass rod to each (length, ~14 cm). The glass rod was used to ensure careful handling during demineralization and remineralization. The use of 6 and 3 hr as the demineralization times was based on previous experimental results (1) which clearly indicated that the demineralizing solution was not saturated

[1] Carver Press.
[2] New England Nuclear, Boston, Mass.

0022-3549/83/1100-1252$01.00/0

ACKNOWLEDGMENTS

Presented in part at the 12th Symposium on Drug Metabolism and Action, Kanazawa, Japan, Oct. 8–9, 1980.

The authors are indebted to Dr. Shinobu Nakamura, School of Medicine, Kanazawa University, for the bone marrow sampling and helpful discussions. Thanks are also given to Mr. H. Nakamura, Miss Y. Yoshida, Miss K. Narizuka, Miss H. Hironaka, Miss M. Nishikawa, Miss M. Uwagawa, and Mr. H. Mizuo for their excellent assistance in the experimental work and to Fujisawa Pharmaceutical Co., Osaka, Japan for the supply of [^{14}C]cefazolin.

Solution Activity Product (K_{FAP}) and Simultaneous Demineralization–Remineralization in Bovine Tooth Enamel and Hydroxyapatite Pellets

JEFFREY L. FOX *‡¶ˣ, BALA V. IYER *‡, WILLIAM I. HIGUCHI *‡¶, and JOHN J. HEFFERREN §

Received May 17, 1982, from the **Dental Research Institute* and the ‡*College of Pharmacy, The University of Michigan, Ann Arbor, MI 48109* and the §*American Dental Association Health Foundation.* Accepted for publication August 26, 1982. ¶Present address: Dept. of Pharmaceutics, University of Utah, Salt Lake City, UT 84112.

Abstract □ The effects of changing the ion activity product of the remineralization solution at pH 4.5 (pK_{FAP} 108–118) on the remineralization behavior of demineralized bovine tooth enamel and hydroxyapatite pellets have been studied. Solutions containing calcium-45, phosphate, and fluoride in acetate buffers were used. The ^{45}Ca/F molar ratios indicated the formation of fluoridated hydroxyapatite in the enamel or the pellet when the pK_{FAP} values for remineralizing solutions were <112. When the pK_{FAP} values were >112, the ^{45}Ca/F ratios were found to be ≪5. Also, when the pK_{FAP} values were large (>112), the remineralization patterns based on the fluoride distribution in the tooth (or pellet) were found to be different than when the pK_{FAP} values were small (<112). The hypothesis that a pK_{FAP} value of 112 is the demarcation between remineralization only and simultaneous dissolution–remineralization has been proposed based on these results.

Keyphrases □ Tooth enamel—bovine, demineralization and remineralization, effect of bulk solution activity product □ Hydroxyapatite—pellets, demineralization and remineralization, effect of bulk solution activity product □ Remineralization—demineralized bovine tooth enamel, hydroxyapatite pellets, effect of bulk solution activity product

Previous studies conducted in these laboratories (1) indicated that both bovine tooth enamel and hydroxyapatite pellets could be extensively remineralized in a fluoride-containing remineralizing solution after prior demineralization treatments for various lengths of time. After 3 or 6 hr of prior demineralization in a partially saturated acetate buffer at pH 4.5, fluoride uptake levels on the order of 1000 ppm were found after remineralization, at depths up to ~50 μm from the surface. The stoichiometry of the remineralized phase was shown to be fluoridated hydroxyapatite rather than calcium fluoride based on the ^{45}Ca/F ratio and determination by X-ray diffraction analysis. All of the remineralization studies (1) were conducted in solutions at an ionic product ($K_{FAP} = a^{10}_{Ca^{2+}} a^{6}_{PO_4^{3-}} a^{2}_{F^-}$) of $\sim 1 \times 10^{-108}$.

The purpose of the present study was to investigate the influence of varying the K_{FAP} value for the remineralizing solution. A case of special interest was where the K_{FAP} values are $>10^{-120}$, the solubility product for fluorapatite (2), but $<10^{-114}$, the ion activity product value below which dissolution takes place with hydroxyapatite pellets (3). A question of great interest was how the concomittant dissolution of hydroxyapatite, if it were to occur, would influence the remineralization behavior in this K_{FAP} region.

EXPERIMENTAL

Materials—*Bovine Teeth*—Teeth from 8-week-old strictly kosher calves were obtained from packing houses in the Chicago area. From these incisors, only those without any visible surface defects and with a reasonably flat surface were used for the experiments. The labial surfaces of these selected teeth were then ground with rotating sandpaper (No. 400 first, then No. 600) to remove the pellicle.

Hydroxyapatite Pellet—Synthetic hydroxyapatite crystals prepared using the procedure developed by Moreno (4) were used in the preparation of the pellets. Approximately 50 mg of hydroxyapatite, preequilibrated in a humidity chamber containing saturated potassium nitrate aqueous solution to maintain the humidity at ~67%, was compressed in a 0.62-cm diameter die with a force of 4540 kg using a laboratory press[1].

Preparation of Buffer Solutions—As in a previous study (1) a solution ~16% saturated (on a molar basis) with respect to the thermodynamic solubility of hydroxyapatite was used for demineralization. The solution was a 0.1 *M* acetate buffer containing 3.5 m*M* each of total calcium and phosphate. The pH was adjusted to 4.5 with sodium hydroxide and the ionic strength to 0.5 *M* by the addition of sodium chloride. For remineralization 0.1 *M* acetate buffers (pH 4.5) containing differing amounts of total calcium and phosphate depending on the desired bulk solution activity product ($K_{FAP} = a^{10}_{Ca^{2+}} a^{6}_{PO_4^{3-}} a^{2}_{F^-}$) as shown in Table I, were employed. These solutions also contained 10 ppm of fluoride and sodium chloride to adjust the ionic strength to 0.5 *M*. All the chemicals used for the preparation of buffer solutions were analytical grade. A predetermined amount of calcium-45 as $^{45}CaCl_2$ in water[2] was added to these solutions.

Demineralization—A bovine tooth was covered with dental inlay wax except for a 0.25-cm^2 area in the labial surface. In the pellet experiments, a hydroxyapatite pellet was completely covered with inlay wax except for one exposed surface (area, 0.25 cm^2). The tooth or pellet was then demineralized in the 16% partially saturated buffer solution for a period of 6 and 3 hr, respectively, after attaching a thin glass rod to each (length, ~14 cm). The glass rod was used to ensure careful handling during demineralization and remineralization. The use of 6 and 3 hr as the demineralization times was based on previous experimental results (1) which clearly indicated that the demineralizing solution was not saturated

[1] Carver Press.
[2] New England Nuclear, Boston, Mass.

0022-3549/83/1100-1252$01.00/0

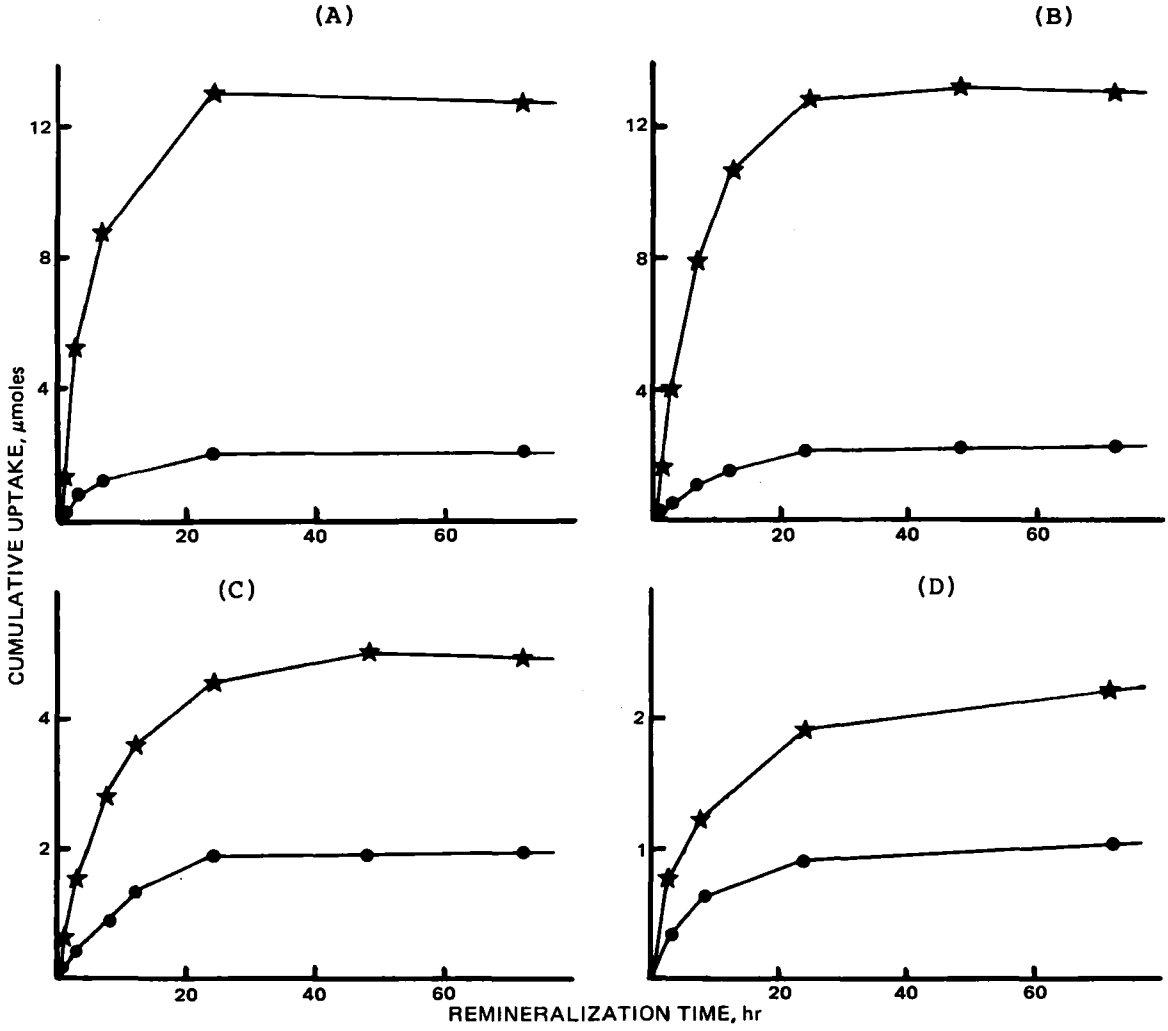

Figure 1—*Effect of remineralization time on the cumulative uptake of calcium-45 (★) and fluoride (●) ions in demineralized bovine tooth. Key: pK_{FAP} (A) 108; (B) 110; (C) 114; (D) 118.*

with respect to hydroxyapatite during that period. During demineralization the solution was shaken gently with a wrist action shaker[3] and kept at 30°. The volume of the buffer solution used was kept at 10 ml.

Remineralization—The demineralized tooth or pellet was washed completely with double-distilled water and dried. It was then subjected to the remineralization treatment for a period of 1–72 hr. During remineralization the solution was shaken gently in the wrist action shaker and kept at 30° as the remineralization proceeded.

Etching—The remineralized sample was thoroughly washed with double-distilled water and dried. The enamel was then etched in 1 ml of 0.5 *M* perchloric acid for successive periods of 30, 30, 120, 200, and 250 sec; the surface was washed with 1 ml of water after each etching and the washings were collected with the 0.5 *M* perchloric acid used for etching. In the case of pellets, the same procedure was repeated except the etchings were done for successive periods of 30, 30, 120, 200, 250, and 600 sec.

Analytical Techniques for the Estimation of Phosphate, Fluoride, and Calcium-45—Phosphate concentrations of the etching solutions were determined by the method of Gee *et al.* (5) in which the phospho-ammonium-molybdate complex formed was reduced by stannous chloride. The absorbance of the resulting blue solution was determined after 15 min at 720 nm[4]. Fluoride concentrations were determined by a fluoride ion electrode[5] using a low level total ionic strength-adjusting buffer. Concentrations of calcium-45 were determined using a scintillation counter[6].

Calculation of Layer Depth—The depth of the etched layers of the teeth were calculated from the amounts of phosphate removed from the etched layers, assuming the density of samples to be 2.95 g/ml. It was expected that this density value would be too large an estimate for the actual density near the surface; however, it is a convenient way to present the data and was adopted for this reason.

[3] Burrell Co., Pittsburgh, Pa.
[4] Model 25 Spectrophotometer; Beckman Instruments, Fullerton, Calif.
[5] Model 94-09; Orion Co., Cambridge, Mass.
[6] Model 9000 Liquid Scintillation System; Beckman Instruments, Fullerton, Calif.

RESULTS AND DISCUSSION

Effect of Remineralization Time—To determine the effect of remineralization time, bovine teeth demineralized for 6 hr were remin-

Table I—Calcium, Phosphate, and Fluoride Concentrations in Remineralizing Solutions Corresponding to Various pK_{FAP} Values [a]

pK_{FAP}	Ion Concentration Ca^{2+}, m*M*	PO_4^{3-}, m*M*	F^-, ppm	Ca/P Ratio
108	12.00	12.00	10	1.0
110	9.23	9.23	10	1.0
112	6.87	6.87	10	1.0
114	5.13	5.13	10	1.0
116	3.83	3.83	10	1.0
118	2.86	2.86	10	1.0
114	12.17	1.22	10	10.0
116	9.09	0.91	10	10.0
118	6.80	0.68	10	10.0
114	2.85	14.23	10	0.20
116	2.12	10.59	10	0.20
118	1.58	7.90	10	0.20
116	16.74	0.33	10	50.00
116	0.96	47.77	10	0.02

[a] pH 4.5, 0.5 μ, 0.1 *M* acetate buffer.

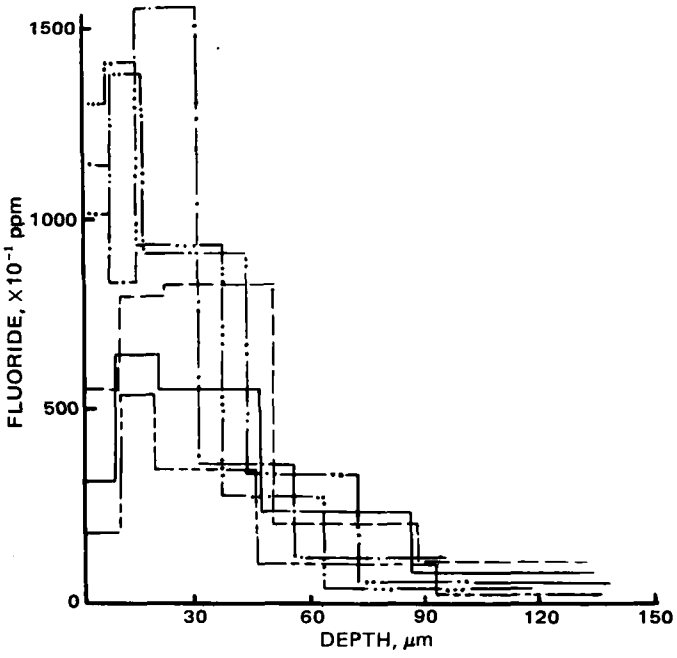

Figure 2—*The influence of driving force pK_{FAP} on the fluoride uptake of demineralized bovine teeth (pH 4.5, μ = 0.5, 0.1 M acetate buffer, Ca/P ratio = 1). Key: pK_{FAP} (— • • • —) 108; (— • • —) 110; (— • —) 112; (- - -) 114; (—) 116; (— - - —) 118.*

eralized for a period of 1–72 hr. For the purpose of remineralization, solutions with pK_{FAP} values of 108, 110, 114, and 118 were used. The effect of remineralization time on cumulative calcium-45 and fluoride uptake is shown in Fig. 1. These cumulative calcium-45 and fluoride uptake values were determined by summing the respective values obtained for each successive layer. Figure 1 clearly indicates that the remineralization is essentially complete in 24 hr except in the case where the remineralizing solution had a pK_{FAP} value of 118. In this case there was a slight increase in calcium-45 and fluoride concentrations from 24 to 72 hr of remineralization.

Effect of pK_{FAP} on Remineralization—To study the effect of the bulk solution activity product on remineralization, the remineralization studies were carried out by varying the pK_{FAP} values from 108 to 118. It was not possible to prepare a solution with a pK_{FAP} value <108 at pH 4.5 due to spontaneous precipitation during the pH adjustment. Calculations suggest that this may be due to the precipitation of dicalcium phosphate dihydrate.

All of the remineralization studies were carried out for a period of 24 hr. The cumulative uptake of calcium-45 and fluoride, and the ^{45}Ca/F molar ratio for each remineralized enamel layer and corresponding pK_{FAP} values, are shown in Table II. Calcium-45 uptake appeared to be constant at each pK_{FAP} value. Fluoride levels remained relatively constant until a pK_{FAP} of ~114 and seemed to drop somewhat at 116 and 118 (Table II). The ^{45}Ca/F molar ratios were near or somewhat above 5, which indicated the formation of fluoridated hydroxyapatite when the remineralizing solution had a pK_{FAP} of 108 or 110. At the larger pK_{FAP} values, however, the ratios decreased, reaching a value of 2.1 at pK_{FAP} 118.

A point of primary interest in this study was to determine the remineralization behavior when the pK_{FAP} value was >114. An attempt was made to determine whether the drop in the ^{45}Ca/F ratio at the higher pK_{FAP} values might be related to the system undergoing simultaneous dissolution of hydroxyapatite and remineralization (or recrystallization) of fluoroapatite[7]. The hypothesis that the deposited material in the enamel surface region actually had a Ca/F ratio of 10:2 was tested by varying the calcium-45 specific activity in the remineralizing solution. This was achieved by varying the bulk solution Ca/P ratios from 50 to 0.02 in the pK_{FAP} range of 114–118. As can be seen from Table III, there was an increase in the ^{45}Ca/F molar ratio with an increase in bulk solution Ca/P ratio and a decrease in the ^{45}Ca/F ratio with a decrease in Ca/P ratio in the remineralizing solution for the same pK_{FAP} value. This supported the idea that the deposited material in the enamel surface region actually had a Ca/F molar ratio close to 10:2 and that a simultaneous dissolution–remineralization process is occurring above a certain pK_{FAP} value. The results obtained were tested by correcting the results for the microenvironmental calcium-45 specific activity at the tooth surface as calculated by an approximate computer model. The details of the model parameters are as shown in the *Appendix*. The results obtained by assuming a surface pK_{FAP} of 110 at appropriate bulk solution concentration seemed to fit very well with the experimental values obtained. The theoretical values obtained from the model parameters are indicated in the last columns of Tables II and III.

Figure 2 gives the enamel fluoride concentration profiles for the bovine teeth experiments. While, as pointed out above, the cumulative uptakes are all of the same order of magnitude, it is seen that the remineralization pattern when the pK_{FAP} values are large is different from that when the pK_{FAP} values are small. At a pK_{FAP} of 108, there is significantly more remineralization near the tooth surface (~10–15 μm) than when the pK_{FAP} values of the solutions were large. These results are generally in agreement with a quantitative microradiographic study recently completed in these laboratories (7).

Hydroxyapatite pellets remineralized for 24 hr after 3 hr of demineralization were tested for calcium-45 and fluoride uptake as shown in Table IV. These results show that, as in the case of the bovine teeth experiments, calcium-45 uptake decreased with increasing pK_{FAP}, with no notable decrease in the fluoride uptake. The ^{45}Ca/F molar ratios also dropped below 5 with increasing pK_{FAP} of the remineralizing solutions, as was obtained in the case of bovine teeth.

Consideration of all the experimental results at pH 4.5 clearly indicates that the pK_{FAP} value of the remineralizing solution is the most important variable in determining the course of remineralization, with a pK_{FAP} of 112 being the demarcation between remineralization only and simulta-

Table II—Effect of pK_{FAP} on Bovine Tooth Remineralization [a]

pK_{FAP}	Calcium-45, μmoles	Fluoride, μmoles	^{45}Ca/F Ratio	
			Observed	Theoretical
108	13.1, 13.7[b]	1.92, 1.85	6.8, 7.4	—
110	12.5, 13.2	2.2, 2.6	5.7, 5.1	—
112	8.2, 8.0	2.0, 2.1	4.1, 3.9	3.87
114	4.5, 5.4	1.9, 2.0	2.4, 2.7	2.95
116	3.4, 2.8	1.6, 1.5	2.2, 1.9	2.24
118	1.9, 1.8	0.90, 0.85	2.1, 2.1	1.69

[a] At pH 4.5, Ca/P = 1.0, fluoride concentration = 10 ppm. [b] Duplicate values.

Table III—Effect of Ca/P Ratio on Bovine Tooth Remineralization [a]

pK_{FAP}	Ca/P Ratio	Calcium-45, μmoles	Fluoride, μmoles	^{45}Ca/F Ratio	
				Observed	Theoretical
114	10	6.2, 5.4[b]	1.7, 1.6	3.7, 3.4	4.01
114	0.2	2.5, 2.2	1.3, 1.2	1.94, 1.88	2.48
116	50	7.4, 6.4	1.72, 1.52	4.3, 4.2	4.3
116	10	4.0, 4.4	1.3, 1.2	3.0, 3.6	3.44
116	0.2	2.3, 2.0	1.2, 1.16	1.9, 1.7	1.74
116	0.02	1.0, 1.1	0.64, 0.66	1.6, 1.8	1.44
118	10	2.2, 2.5	0.9, 1.1	2.5, 2.3	2.86
118	0.2	1.2, 1.6	0.96, 0.95	1.2, 1.7	1.23

[a] At pH 4.5, fluoride concentration = 10 ppm, with 0.5 μ, 0.1 *M* acetate buffer. [b] Duplicate values.

Table IV—Hydroxyapatite Pellet Remineralization

pK_{FAP}	Calcium-45, μmoles	Fluoride, μmoles	^{45}Ca/F Ratio
108	7.7, 7.1[b]	1.2, 1.1	6.6, 6.1
110	7.0, 7.4	1.0, 1.1	6.8, 6.6
112	5.9, 5.4	0.9, 0.8	6.4, 6.5
114	5.0, 5.5	0.9, 1.0	5.6, 5.4
116	3.9, 2.6	1.0, 0.8	3.9, 3.5
118	3.0, 3.0	1.0, 1.1	3.1, 2.7

[a] At pH 4.5, fluoride concentration 10 ppm, Ca/P ratio = 1. [b] Duplicate values.

[7] Although the conditions and the nature of the experiments were different, Thiradilok and Feagin (6) observed that remineralization and dissolution–remineralization occur under different conditions in bovine enamel experiments. For example, when calcium, phosphate, and fluoride were all present in the remineralizing solutions (pH 7), remineralization was found to occur. However, if only calcium and fluoride or only phosphate and fluoride were present (and therefore the solution was initially unsaturated with respect to hydroxyapatite) these investigators found both dissolution and remineralization may take place. Their findings therefore are generally in good agreement with the present results.

neous dissolution–remineralization. Further experimental studies are in progress to determine whether the present conclusions regarding the "critical" pK_{FAP} value applies under other conditions (*e.g.*, at other pH values of the remineralizing solution). Also the similarities between the hydroxyapatite pellet experiments and bovine and human teeth studies are being evaluated further.

APPENDIX

Estimation of Calcium-45 Specific Activity at the Bovine Enamel Surface During Simultaneous Demineralization–Remineralization

It has been shown previously (3) that a hydroxyapatite pellet dissolves in the presence of partially saturated buffer containing fluoride when the solution is unsaturated with respect to a pK_{FAP} of ~114. In this dissolution situation, the solution concentration of calcium is higher in the pellet and at the hydroxyapatite surface than in the bulk solution, whereas the fluoride gradient goes the other way, favoring uptake of fluoride from the solution.

In this paper, bovine enamel was studied under similar conditions with the partially saturated bulk solution containing both calcium-45 and fluoride, and the uptake of both species was monitored. If it is assumed that bovine enamel behaves similarly to hydroxyapatite, then when the bulk solution has a pK_{FAP} of >112, the calcium concentration will be higher at the enamel surface since its apparent solubility under these conditions is governed by a pK_{FAP} of ~112. The result is that calcium-45 coming to the surface from the bulk solution will be diluted out by the higher "cold" calcium supplied by hydroxyapatite demineralization. Thus, at sites where calcium and fluoride uptake occurs, it would be expected that measuring uptake of calcium-45 would give too low a value for the calcium uptake as a result of the dilution of calcium-45 by "cold" calcium. The dilution of calcium-45 has been estimated and therefore the expected $^{45}Ca/F$ uptake ratio (assuming total Ca/F uptake is 10:2) was calculated by using a physical model incorporating the following assumptions:

1. The bovine enamel is assumed to dissolve stoichiometrically.
2. Fluoride and calcium-45 concentrations at the enamel surface are assumed equal to the bulk concentrations.
3. At the enamel surface a suitable expression for describing the surface solution ion activity product is:

$$K_{FAP} = 10^{-110} \text{ or } K_{HAP}(a^{10}_{Ca}a^{6}_{PO_4}a^{2}_{OH}) = 10^{-122}$$

4. The remineralization process in the enamel occurs with the ratio of deposited total Ca/F being 10:2.

Using this model, the expected $^{45}Ca/F$ uptake ratios have been calculated and seem to agree quite well with the experimental results over a range of bulk solution K_{FAP} values and for solution Ca/P ratios from 1:50 to 50:1.

REFERENCES

(1) M. Yonese, J. L. Fox, N. Nambu, J. J. Hefferren, and W. I. Higuchi, *J. Pharm. Sci.*, **70**, 904 (1981).

(2) W. E. Brown, T. M. Gregory, and L. C. Chow, *Caries Res.*, **11**, 118 (1977).

(3) M. B. Fawzi, Ph.D. Thesis, The University of Michigan, Ann Arbor, Mich. (1976).

(4) E. C. Moreno, T. M. Gregory, and E. W. Brown, *J. Res. Natl. Bur. Std.*, **72A**, 773 (1968).

(5) A. Gee, L. Domingues, and V. Deitz, *Anal. Chem.*, **26**, 1487 (1954).

(6) S. Thiradilok, Ph.D. Thesis, University of Alabama, Birmingham, Ala. (1977).

(7) D. H. Bergstrom, J. L. Fox, and W. I. Higuchi, *J. Pharm. Sci.*, in press.

ACKNOWLEDGMENTS

This project was supported by Grants DE04600 and DE01830 from the National Institute of Dental Research.

Analysis of Monobutyryl and Dibutyryl Derivatives of Adenosine 3′,5′-Monophosphate in Biological Samples Using Isocratic Ion Pair High-Performance Liquid Chromatography

VAL H. SCHAEFFER *, ASAAD N. MASOUD *‡ˣ, and ROBERT J. RUBIN *

Received June 17, 1982, from the **Division of Toxicology, Department of Environmental Health Sciences* and ‡*Department of Anesthesiology/Critical Care Medicine, Johns Hopkins Medical Institutions, Baltimore, MD 21205.* Accepted for publication September 1, 1982.

Abstract □ Adenosine 3′,5′-monophosphate (cyclic AMP), its dibutyryl and monobutyryl derivatives, and a number of other naturally occurring adenine-containing compounds were separated by isocratic ion pair high-performance liquid chromatography. A mobile phase consisting of 30% methanol in 0.1 *M* KH_2PO_4 (pH 4.0) containing 1 m*M* tetramethylammonium hydroxide as the counterion was used to separate the butyryl derivatives. To sufficiently separate cyclic AMP from other adenine-containing compounds, a mobile phase containing 6% methanol in the same aqueous buffer plus counterion was used. Extraction of these cyclic nucleotides from deproteinized biological samples using disposable reverse-phase extraction columns is described. This not only eliminated lipophilic contaminants, but also served to concentrate the samples. The outlined procedures were used to determine the concentrations of the butyryl derivatives in lung tissue and perfusate following a 35-min lung perfusion with 100 μM N^6-$O^{2'}$-dibutyryl cyclic AMP. The role of this technique in the analysis of cyclic nucleotide derivatives as compared with conventional assay procedures is discussed.

Keyphrases □ Adenosine 3′,5′-monophosphate—dibutyryl and monobutyryl derivatives, lung tissue and perfusate, separation by isocratic ion pair high-performance liquid chromatography □ Analogues—dibutyryl and monobutyryl cyclic AMP, lung tissue and perfusate, separation by isocratic ion pair high-performance liquid chromatography □ High-performance liquid chromatography—ion pair, isocratic, cyclic AMP and its dibutyryl and monobutyryl derivatives, lung tissue and perfusate

Analogues of adenosine 3′,5′-monophosphate (cyclic AMP) were first synthesized to selectively mimic the effects of this cyclic nucleotide in various biological systems. The most extensively used analogue has been N^6-$O^{2'}$-dibutyryl cyclic AMP (1). In most instances the dibutyryl derivative has proved to be more biologically active when

0022-3549/83/1100-1255$01.00/0

neous dissolution–remineralization. Further experimental studies are in progress to determine whether the present conclusions regarding the "critical" pK_{FAP} value applies under other conditions (*e.g.*, at other pH values of the remineralizing solution). Also the similarities between the hydroxyapatite pellet experiments and bovine and human teeth studies are being evaluated further.

APPENDIX

Estimation of Calcium-45 Specific Activity at the Bovine Enamel Surface During Simultaneous Demineralization–Remineralization

It has been shown previously (3) that a hydroxyapatite pellet dissolves in the presence of partially saturated buffer containing fluoride when the solution is unsaturated with respect to a pK_{FAP} of ~114. In this dissolution situation, the solution concentration of calcium is higher in the pellet and at the hydroxyapatite surface than in the bulk solution, whereas the fluoride gradient goes the other way, favoring uptake of fluoride from the solution.

In this paper, bovine enamel was studied under similar conditions with the partially saturated bulk solution containing both calcium-45 and fluoride, and the uptake of both species was monitored. If it is assumed that bovine enamel behaves similarly to hydroxyapatite, then when the bulk solution has a pK_{FAP} of >112, the calcium concentration will be higher at the enamel surface since its apparent solubility under these conditions is governed by a pK_{FAP} of ~112. The result is that calcium-45 coming to the surface from the bulk solution will be diluted out by the higher "cold" calcium supplied by hydroxyapatite demineralization. Thus, at sites where calcium and fluoride uptake occurs, it would be expected that measuring uptake of calcium-45 would give too low a value for the calcium uptake as a result of the dilution of calcium-45 by "cold" calcium. The dilution of calcium-45 has been estimated and therefore the expected $^{45}Ca/F$ uptake ratio (assuming total Ca/F uptake is 10:2) was calculated by using a physical model incorporating the following assumptions:

1. The bovine enamel is assumed to dissolve stoichiometrically.
2. Fluoride and calcium-45 concentrations at the enamel surface are assumed equal to the bulk concentrations.
3. At the enamel surface a suitable expression for describing the surface solution ion activity product is:

$$K_{FAP} = 10^{-110} \text{ or } K_{HAP}(a^{10}_{Ca}a^{6}_{PO_4}a^{2}_{OH}) = 10^{-122}$$

4. The remineralization process in the enamel occurs with the ratio of deposited total Ca/F being 10:2.

Using this model, the expected $^{45}Ca/F$ uptake ratios have been calculated and seem to agree quite well with the experimental results over a range of bulk solution K_{FAP} values and for solution Ca/P ratios from 1:50 to 50:1.

REFERENCES

(1) M. Yonese, J. L. Fox, N. Nambu, J. J. Hefferren, and W. I. Higuchi, *J. Pharm. Sci.*, **70**, 904 (1981).

(2) W. E. Brown, T. M. Gregory, and L. C. Chow, *Caries Res.*, **11**, 118 (1977).

(3) M. B. Fawzi, Ph.D. Thesis, The University of Michigan, Ann Arbor, Mich. (1976).

(4) E. C. Moreno, T. M. Gregory, and E. W. Brown, *J. Res. Natl. Bur. Std.*, **72A**, 773 (1968).

(5) A. Gee, L. Domingues, and V. Deitz, *Anal. Chem.*, **26**, 1487 (1954).

(6) S. Thiradilok, Ph.D. Thesis, University of Alabama, Birmingham, Ala. (1977).

(7) D. H. Bergstrom, J. L. Fox, and W. I. Higuchi, *J. Pharm. Sci.*, in press.

ACKNOWLEDGMENTS

This project was supported by Grants DE04600 and DE01830 from the National Institute of Dental Research.

Analysis of Monobutyryl and Dibutyryl Derivatives of Adenosine 3′,5′-Monophosphate in Biological Samples Using Isocratic Ion Pair High-Performance Liquid Chromatography

VAL H. SCHAEFFER *, ASAAD N. MASOUD *‡ˣ, and ROBERT J. RUBIN *

Received June 17, 1982, from the **Division of Toxicology, Department of Environmental Health Sciences* and ‡*Department of Anesthesiology/Critical Care Medicine, Johns Hopkins Medical Institutions, Baltimore, MD 21205.* Accepted for publication September 1, 1982.

Abstract □ Adenosine 3′,5′-monophosphate (cyclic AMP), its dibutyryl and monobutyryl derivatives, and a number of other naturally occurring adenine-containing compounds were separated by isocratic ion pair high-performance liquid chromatography. A mobile phase consisting of 30% methanol in 0.1 *M* KH_2PO_4 (pH 4.0) containing 1 m*M* tetramethylammonium hydroxide as the counterion was used to separate the butyryl derivatives. To sufficiently separate cyclic AMP from other adenine-containing compounds, a mobile phase containing 6% methanol in the same aqueous buffer plus counterion was used. Extraction of these cyclic nucleotides from deproteinized biological samples using disposable reverse-phase extraction columns is described. This not only eliminated lipophilic contaminants, but also served to concentrate the samples. The outlined procedures were used to determine the concentrations of the butyryl derivatives in lung tissue and perfusate following a 35-min lung perfusion with 100 μM N^6-$O^{2'}$-dibutyryl cyclic AMP. The role of this technique in the analysis of cyclic nucleotide derivatives as compared with conventional assay procedures is discussed.

Keyphrases □ Adenosine 3′,5′-monophosphate—dibutyryl and monobutyryl derivatives, lung tissue and perfusate, separation by isocratic ion pair high-performance liquid chromatography □ Analogues—dibutyryl and monobutyryl cyclic AMP, lung tissue and perfusate, separation by isocratic ion pair high-performance liquid chromatography □ High-performance liquid chromatography—ion pair, isocratic, cyclic AMP and its dibutyryl and monobutyryl derivatives, lung tissue and perfusate

Analogues of adenosine 3′,5′-monophosphate (cyclic AMP) were first synthesized to selectively mimic the effects of this cyclic nucleotide in various biological systems. The most extensively used analogue has been N^6-$O^{2'}$-dibutyryl cyclic AMP (1). In most instances the dibutyryl derivative has proved to be more biologically active when

0022-3549/83/1100-1255$01.00/0

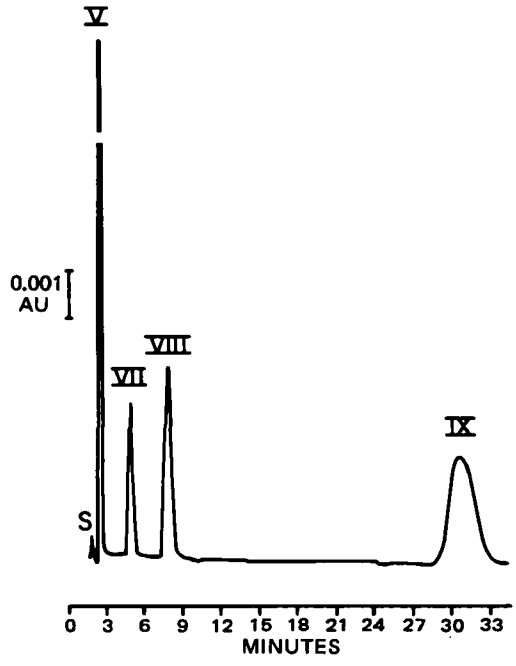

Figure 1—*Chromatogram of a mixture containing reference compounds V (346 pmole), VII (215 pmole), VIII (256 pmole), and IX (1000 pmole). Mobile phase was 30% methanol in 0.1 M KH_2PO_4–1 mM $(CH_3)_4NOH$. Other chromatographic conditions are as described under* Experimental.

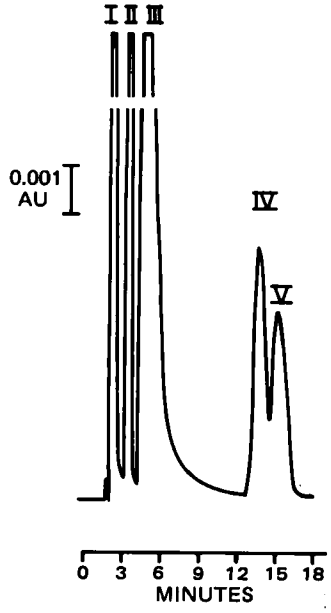

Figure 2—*Chromatogram of a mixture containing reference compounds I (500 pmole), II (1000 pmole), III (1200 pmole), IV (300 pmole), and V (285 pmole). Mobile phase was 6% methanol in 0.1 M KH_2PO_4–1 mM $(CH_3)_4NOH$. Other chromatographic conditions are as described under* Experimental.

administered *in vivo* than the unsubstituted cyclic nucleotide, presumably due to its increased lipophilicity (2). It is generally agreed that the dibutyryl cyclic nucleotide is metabolized by most cells to its two monobutyryl derivatives, N^6-monobutyryl cyclic AMP and $O^{2'}$-monobutyryl cyclic AMP (3).

Although the use of these particular cyclic nucleotide analogues has become widespread, the predominant analytical methods for determining the compounds still rely on paper chromatography and TLC (4, 5). These techniques are time consuming and lack the sensitivity and specificity necessary for highly complex mixtures such as biological samples. In recent years, separation by high-performance liquid chromatography (HPLC) has been described (6, 7). The systematic analysis of these compounds in biological extracts, however, has not been reported.

This paper describes the separation of dibutyryl cyclic AMP, its monobutyryl derivatives, cyclic AMP, and several selected adenine nucleotides, nucleosides, and bases most likely to be present in biological samples, using an isocratic ion pair HPLC system. Extraction and quantitation of these compounds from both a rat lung perfusate and lung tissue is also described.

Table I—Mean k' Values for the Four Cyclic Nucleotides Using Three Different Mobile Phases [a]

Compound	k' Mobile Phase A[b]	Mobile Phase B[c]	Mobile Phase C[d]
V	8.05 ± 0.20	0.33 ± 0.01	0.24 ± 0.01
VII	—[e]	6.79 ± 0.13	1.52 ± 0.02
VIII	—	—	3.07 ± 0.03
IX	—	—	14.97 ± 2.00

[a] k' is defined as $(t_R - t_0)/t_0$ where t_R = retention time of the compound and t_0 = retention time of unretained material (solvent front). k' values are the mean ± *SD* of five determinations representing day-to-day variation. [b] 6% Methanol in 0.1 *M* KH_2PO_4–1 m*M* $(CH_3)_4NOH$ (pH 4). [c] 20% Methanol in 0.1 *M* KH_2PO_4–1 m*M* $(CH_3)_4NOH$ (pH 4). [d] 30% Methanol in 0.1 *M* KH_2PO_4–1 m*M* $(CH_3)_4NOH$ (pH 4). [e] — not eluted.

EXPERIMENTAL

Reagents and Reference Standards—The following compounds were used as chromatographic standards: adenosine 5′-diphosphate sodium salt (I) from equine muscle[1], adenosine 5′-monophosphate sodium crystals[1] (II), assay 99%, adenine[2] (III), adenosine[2] (IV), adenosine 3′,5′-monophosphate sodium crystals[1] (V), theophylline[1] (VI), N^6-monobutyryladenosine 3′,5′-monophosphate sodium salt[1] (VII), $O^{2'}$-monobutyryladenosine 3′,5′-monophosphate sodium salt[1] (VIII), and N^6,$O^{2'}$-dibutyryladenosine 3′,5′-monophosphate sodium salt[1] (IX). All compounds are numbered according to their order of elution.

The following reagents were also used: bovine albumin fraction V[1] (96–99% pure), phosphoric acid[3] (85% pure), tetramethylammonium hydroxide pentahydrate[3], potassium phosphate[3] (reagent grade), 60% perchloric acid[4] (reagent grade), potassium hydroxide[5], and glass-distilled methanol[6]. In-house water was filtered, passed through a reverse osmosis system, glass-distilled, and then demineralized.

Stock solutions of reference standards were prepared at 100 μg/ml in purified water and stored frozen. The stock solutions were diluted to prepare various working standards for chromatography.

HPLC Apparatus and Procedures—The apparatus was similar to that described previously (8). This included an injector equipped with 20-μl loop[7] and a reciprocating pump[8], a 5000-psi gauge, a 1-m pulse damper, a reverse-phase 250 × 4-mm column packed in our laboratory with RP-18[9] (10 μm), and a UV variable-wavelength detector[10].

An aqueous stock solution was prepared containing 1 *M* KH_2PO_4 and 10 m*M* tetramethylammonium hydroxide adjusted to pH 4.0 with phosphoric acid (14.7 *M*). All mobile phases contained a 10-fold dilution of this stock solution, resulting in a final concentration in all mobile phases of 0.1 *M* KH_2PO_4 and 1 m*M* tetramethylammonium hydroxide (pH 4.0). Three mobile phases were used isocratically in this research,

[1] Sigma Chemical Co., St. Louis, Mo. I: grade IX, 97% pure, lot 109C7130; II: 99% pure, lot 87C7170; V: 99% pure, lot 109C7020; VI: lot 16C0135; VII: 97% pure, lot 040F7220; VIII 97% pure, lot 040F7220; IX: 96% pure, lot 100F7340.
[2] National Cancer Institute, Bethesda, Md.
[3] MCB Laboratories, Cincinnati, Ohio.
[4] B&A Laboratories.
[5] Fisher Scientific Co.
[6] Burdick and Jackson, Muskegon, Mich.
[7] Model 7010; Rheodyne.
[8] Model 396; Milton-Roy.
[9] E. Merck Laboratories.
[10] Model Spectro-Monitor III; Laboratory Data Control.

Table II—Cyclic Nucleotide Extraction From Perfusate Using Octadecylsilane Disposable Columns [a]

Compound	Recovery, % 30% Methanol	75% Methanol
V	78 ± 2	—[b]
VII	9 + 1	69 ± 4
VIII	—	78 ± 2
IX	—	76 ± 2

[a] Control perfusate was spiked with the compounds. Following deproteinization with 0.6 *N* perchloric acid and neutralization, supernatant was passed through a C-18 disposable extraction column (1 ml). The column was eluted with 0.5 ml 30% methanol in 0.1 *M* KH_2PO_4–1 m*M* $(CH_3)_4NOH$ (pH 4) followed by 0.5 ml of 75% methanol in 0.1 *M* KH_2PO_4–1 m*M* $(CH_3)_4NOH$ (pH 4). These 0.5-ml eluates were collected separately and analyzed by HPLC. [b] — not detected.

all of which varied in the methanol concentration: (A) 6% methanol, (B) 20% methanol, and (C) 30% methanol. All mobile phases were filtered through a 0.22-μm membrane filter[11], then deaerated under vacuum prior to use. An aqueous buffer containing 45% methanol was used following chromatography of all tissue extracts to elute strongly retained contaminants. The column was stored in water–methanol (9:1) at the end of each day. The flow rate was 1.2 ml/min., the detector was set at 254 nm with either 0.02 or 0.01 AUFS, and the recorder chart speed was 0.25 cm/min. The void volume, determined by introducing pure methanol on the column, was 1.95 ml.

Preparation of Biological Samples—Perfusate and tissue samples were obtained following perfusion of Krebs–Henseleit buffer supplemented with 4.5% bovine albumin, 0.1 m*M* dibutyryl derivative (IX), and 0.2 m*M* theophylline (VI) through a recirculating isolated rat lung preparation for 35 min. After the perfusion, the lungs were immediately frozen in liquid nitrogen, and both the lung tissue and perfusate were stored at −60° until further preparation.

Approximately 1 g of lung tissue was homogenized at 4° with three volumes of 0.6 *N* perchloric acid. The precipitate was removed following centrifugation at 12,000×*g*, and the supernatant was neutralized with 10 *N* KOH. In a similar manner, aliquots of perfusate (0.5 ml) were deproteinized directly by addition of 50 μl of 6 *N* perchloric acid, and the resulting supernatant fraction was neutralized with 10 *N* KOH.

The total supernatant fraction was passed through 1-ml octadecylsilane (C-18) disposable extraction columns[12]. These columns were conditioned

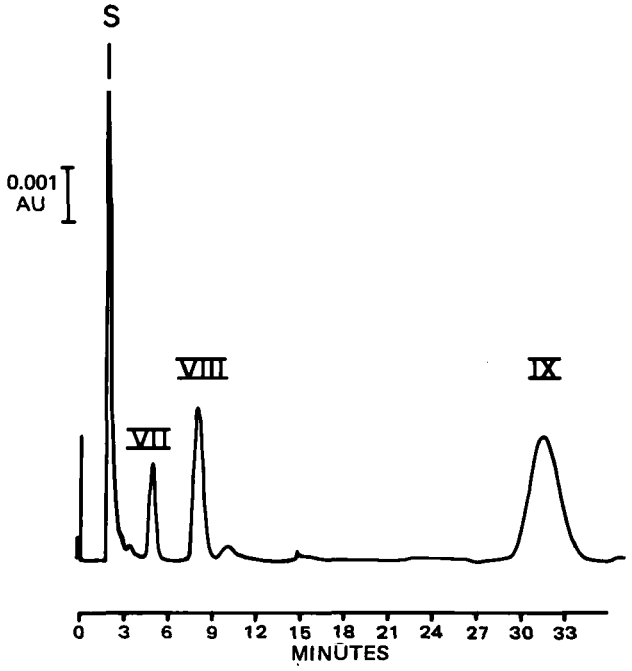

Figure 3—*Krebs buffer supplemented with 100 μM dibutyryl cyclic AMP was subjected to a 35-min sham perfusion, deproteinized in 0.6 N perchloric acid, and extracted on a C-18 disposable column (see text). Mobile phase used was 30% methanol in 0.1 M KH_2PO_4–1 mM $(CH_3)_4NOH$. Other chromatographic conditions are as described under* Experimental. *Key: (S) solvent front.*

[11] Type GS; Millipore Corp.
[12] J. T. Baker, Phillipsburg, N.J.

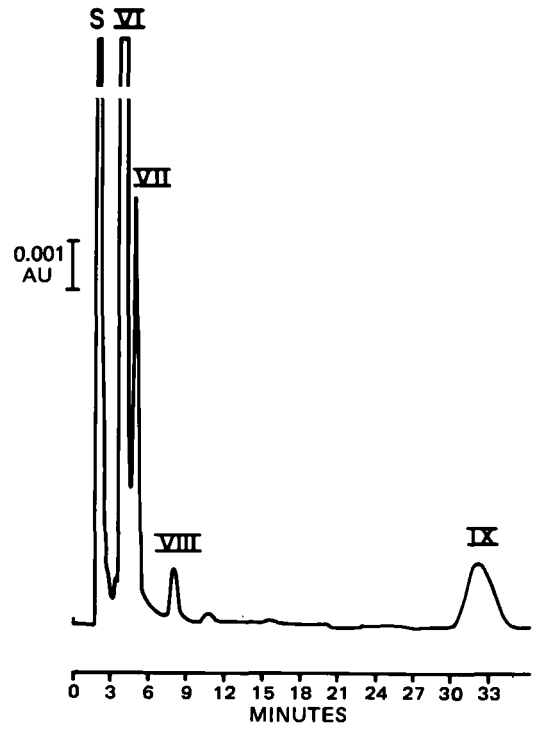

Figure 4—*Krebs buffer supplemented with 100 μM dibutyryl cyclic AMP and 200 μM theophylline was subjected to 35-min lung perfusion, deproteinized in 0.6* N *perchloric acid, and extracted on a C-18 disposable column (see text). Mobile phase was 30% methanol in 0.1* M KH_2PO_4–1 mM $(CH_3)_4NOH$. *Other chromatographic conditions are as described in* Experimental. *Key: (S) solvent front.*

by the introduction of several volumes of methanol followed by reequilibration with several volumes of the aqueous buffer, 0.1 *M* KH_2PO_4–1 m*M* tetramethylammonium hydroxide (pH 4.0). After sample introduction, the columns were first eluted with 0.5 ml of mobile phase C followed by 0.5 ml of 75% methanol in aqueous buffer. Each 0.5-ml fraction was separately collected for HPLC.

RESULTS

Chromatography of Cyclic AMP and Derivatives—Figure 1 illustrates the separation of cyclic AMP and its butyryl derivatives using mobile phase C (30% methanol). The dibutyryl derivative (IX), $O^{2'}$-monobutyryl derivative (VIII), and in most cases the N^6-monobutyryl derivative (VII) were sufficiently retained for analysis in biological samples. However, the unsubstituted cyclic nucleotide (V) eluted too close to the solvent front for adequate separation from the many other nucleotides, nucleosides, and nucleobases eluting at the solvent front and present in biological samples (data not shown). Figure 2 shows the separation of V from four other adenine-containing compounds using mobile phase A (6% methanol). Under these chromatographic conditions, the order of elution is as follows: nucleotide diphosphates, nucleotide monophosphates, nucleobases, nucleosides, and cyclic nucleotides, which possess the longest retention time. Nucleotide triphosphates elute before the diphosphates (data not shown). Since adenosine (IV) is the most retained of the common nucleosides found in biological systems using reverse-phase liquid chromatography (9, 10), all other biological nucleotides, nucleosides, and bases would presumably elute prior to V. Therefore, this procedure theoretically should produce a method suitable for cyclic AMP analysis in biological samples.

The *k'* values of the four cyclic nucleotide derivatives using three different mobile phases are presented in Table I. Mobile phase A was chosen for determinations of V in biological samples. Both mobile phases B and C were used for the analysis of VII. Compounds VIII and IX were separated using mobile phase C. Standard deviations reflect variation due, for the most part, to different batches of mobile phases, fluctuation in room temperature, and the degree of column equilibration with the mobile phase.

Extraction of Cyclic Nucleotides from Biological Samples—To purify the deproteinized biological material of lipophilic impurities that might shorten the useful lifetime of the chromatographic column, the

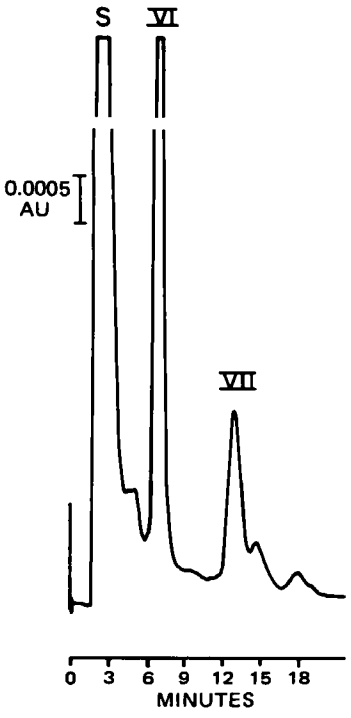

Figure 5—*Lung tissue following 35-min perfusion with 100 μM dibutyryl cyclic AMP and 200 μM theophylline was homogenized, deproteinized with 0.6* N *perchloric acid, and extracted on a C-18 disposable column (see text). Mobile phase was 20% methanol in 0.1* M KH_2PO_4*-1 m*M $(CH_3)_4NOH$*. Other chromatographic conditions are as described under* Experimental. *Key: (S) solvent front.*

Figure 6—*Lung tissue following 35-min perfusion with an unsupplemented Krebs perfusate was homogenized, deproteinized with 0.6* N *perchloric acid, and extracted on a C-18 disposable column (see text). Mobile phase used was 20% methanol in 0.1* M KH_2PO_4*-1 m*M $(CH_3)_4NOH$*. Other chromatographic conditions are as described under* Experimental.

samples were passed through the C-18 disposable extraction column described earlier. This purification procedure has two additional features that make it extremely attractive. First of all, it served to concentrate cyclic nucleotides by as much as sixfold. Secondly, a separation of V from the butyryl derivatives was accomplished.

Table II shows that 30% methanol in buffer will result in the elution of 78% of V from a lung perfusion medium, while most of VII, VIII, and IX are retained on the extraction column. Application of 75% methanol in buffer will then elute retained cyclic nucleotide analogues (69–78%). Initial elution using <30% methanol produces less recovery of V in the first fraction collected. Percentages of methanol <75% used in the second elution also results in less recovery of the butyryl derivatives. Greater than 75% methanol on the other hand causes increased elution of lipophilic impurities. Thus, the fraction eluted with 30% methanol in buffer was used for the analysis of V, while the butyryl derivatives were analyzed using the fraction eluted with 75% methanol buffer.

Analysis of Cyclic Nucleotides in Biological Samples—A perfusate containing 100 *μM* dibutyryl derivative (no theophylline) was circulated for 35 min in the perfusion apparatus in the absence of a lung. After deproteinization, the perfusate was extracted by the above procedure. The fraction eluted from the column with 30% methanol in buffer was analyzed by HPLC using mobile phase A and was calculated to contain 3.7 ± 1.00 μmoles of V/ml. The HPLC analysis of the 75% methanol fraction from the column using mobile phase C is shown in Fig. 3. It was calculated that each milliliter of the original sham perfusate contained 12.2 ± 0.8 μmoles of VII, 12.0 ± 0.7 μmoles of VIII, and 62.5 ± 2.6 μmoles of IX. Since only small amounts of impurities were found in the commercial supply of IX, these data reflect decomposition during deproteinization.

Figure 4 is a representative chromatogram of a similar perfusate following a 35-min perfusion through a lung. The additional presence of VI (k' = 1.0) should be noted. The perfusate analysis revealed that the concentration of the original dibutyryl derivative had fallen by 55%. Thirteen percent of the initial concentration of IX was recovered as VII. The remaining fraction had presumably entered the intracellular spaces of the lung and been metabolized.

Lung tissue following the 35-min perfusion with or without the dibutyryl derivative was also analyzed by the aforementioned procedures. Chromatographic data using mobile phase C revealed very small amounts of IX (1 nmole/g, wet weight) and VIII (0.5 nmole/g, wet weight) in tissue exposed to IX. The high theophylline content relative to the amounts of VII interfered with the determination of VII in these tissue extracts. To eliminate this problem, mobile phase B was used to analyze VII in lung tissue. Figures 5 and 6 are chromatograms of the tissue perfused with and without the dibutyryl derivative. Compounds VI and VII are well separated under these conditions (Fig. 5). Control tissues do not contain peaks that interfere with either VI or VII (Fig. 6). Following perfusion with 100 *μM* dibutyryl derivative, 10.55 ± 4.87 nmole/g (wet weight) of the monobutyryl derivative (VII) could be recovered from the lung tissue.

Analysis of the unsubstituted cyclic nucleotide (V) in lung tissue exposed to the dibutyryl derivative using mobile phase A was complicated by the fact that control lungs produced a complex chromatogram with one or more peaks coeluting with V. However, extracts of the tissue treated with IX do not consistently differ from unexposed tissue in the region in which V elutes. These results suggest that perfusion with the dibutyryl derivative does not result in significant accumulation of the unsubstituted cyclic nucleotide. However, this can not be established unequivocally until V is separated from the coeluting material.

DISCUSSION

The most common assay techniques for cyclic AMP in biological samples are radioimmunoassay, first described by Steiner *et al.* (11) and modified by Cailla and colleagues (12), and a competitive protein binding assay originally described by Gilman (13) and Brown *et al.* (14). These extremely sensitive methods (<0.1 pmole) appear to be more sensitive than current chromatographic techniques and also eliminate the necessity for complex separations from other nucleotides present in most cellular extracts. Unfortunately, the specificity of these assay systems is no longer adequate when cyclic nucleotide analogues are involved. For example, the affinity of the N^6-butyryl derivative (VII) for the cyclic AMP-dependent binding protein is ~30% of that for cyclic AMP itself (15). The $O^{2'}$-butyryl and dibutyryl derivatives have an even higher affinity than the unsubstituted cyclic nucleotide for the cyclic AMP-specific antibody (12). Therefore, these assay systems are not useful for determining the distribution of the butyryl derivatives.

The methods described here to separate the cyclic nucleotide derivatives do not have the problem of specificity inherent in the more conventional assay systems, since the butyryl groups caused a marked increase in lipophilicity making them easily separable from the parent compound and other nucleotides by HPLC. Although the chromatographic procedure as described here can only detect these compounds to the 0.01–0.1 nmole level, more sensitive UV detection settings, in-

creased amounts injected, and the use of larger extraction columns for trace enrichment of the samples may provide sensitivity comparable to that of the more conventional assays. The separation of cyclic AMP from other biological substances using a simple isocratic HPLC system may be a difficult task. However, the use of gradient elution with a reverse-phase column (10) or the use of ion-exchange chromatography may separate V from the coeluting compound(s) (16).

It should also be pointed out that the chromatogram in Fig. 2 is a good example of the extra dimension offered to the chromatographic process by ion pairing. All compounds analyzed with mobile phase A eluted in the reverse order of their polarity as expected in conventional reverse-phase chromatography. The only exceptions were V and IV. Although V is slightly less hydrophobic than IV, it has a greater retention under the conditions used due to the presence of tetramethylammonium hydroxide. The interaction of the tetramethyammonium cation with the negatively charged V increases its retention. On the other hand, the positively charged IV is not affected by this cation (7). The result is that while IV and V coelute without this cation, its presence causes V to elute after IV so that separation of these two compounds can be achieved.

By the use of the methods described here, it has been shown that the N^6-butyryl derivative is the major product formed following the perfusion of rat lung with dibutyryl cyclic AMP. It is estimated that ~24% of the dibutyryl derivative taken up by the lung during the perfusion period can be recovered as the N^6-monobutyryl analogue from the perfusate and lung compartments. The remaining portion has most likely been further metabolized to the straight-chain monophosphate by the action of phosphodiesterase, since it is not recovered in the lung as the unmetabolized dibutyryl cyclic AMP. We have also shown that 35-min perfusion with 100 μM dibutyryl derivative results in a sevenfold increase in the cyclic AMP content of the lung measured by the protein binding assay of Gilman (13) (data not shown). HPLC analysis reveals that 90% of this increased protein binding can be attributed to the formation of the N^6-butyryl derivative in the lung tissue.

In light of recent findings that different cyclic nucleotide analogues can selectively activate different isozymes of protein kinase (17, 18), it has become important to know the intracellular distribution of these analogues following treatment with cyclic nucleotide derivatives. This analytical procedure provides a specific, sensitive, and simple method for measuring dibutyryl cyclic AMP and its metabolites in biological systems. This technique can potentially be applied for analysis of many of the other cyclic nucleotide analogues. Also, not only can it be used for perfusion studies, but could also be adapted to cell culture and whole animal experiments.

REFERENCES

(1) G. A. Robison, R. W. Butcher, and E. W. Sutherland, *Ann. Rev. Biochem.*, **37**, 149 (1968).

(2) T. Posternak, E. W. Sutherland, and W. F. Henion, *Biochem. Biophys. Acta*, **65**, 558 (1962).

(3) E. Kaukel, K. Mundhenk, and H. Huz, *Eur. J. Biochem.*, **27**, 197 (1972).

(4) E. W. Sutherland and T. W. Rall, *J. Am. Chem. Soc.*, **79**, 3607 (1957).

(5) J. P. Miller, K. H. Boswell, K. Muneyama, L. W. Simon, R. K. Robins, and D. A. Shuman, *Biochemistry*, **12**, 1010 (1973).

(6) J. C. L. V. Luang, N. N. Quang, and G. Hazebroucq, *Adv. Biosci.*, **24**, 201 (1979).

(7) P. J. M. Van Haastert, *J. Chromatogr.*, **210**, 229 (1981).

(8) M. I. Al-Moslih, G. R. Dubes, and A. N. Masoud, *HRC&CC.*, **4**, 173 (1981).

(9) F. S. Anderson and R. C. Murphy, *J. Chromatogr.*, **121**, 251 (1976).

(10) N. E. Hoffman and J. C. Liao, *Anal. Chem.*, **49**, 2231 (1977).

(11) A. L. Steiner, C. W. Parker, and D. M. Kipnis, *J. Biol. Chem.*, **247**, 1106 (1972).

(12) H. L. Cailla, M. S. Racine-Weisbach, and M. A. Delaage, *Anal. Biochem.*, **56**, 394 (1973).

(13) A. G. Gilman, *Proc. Natl. Acad. Sci. USA*, **67**, 305 (1970).

(14) B. L. Brown, J. D. M. Albano, R. P. Ekins, and A. M. Schierzi, *Biochem. J.*, **121**, 561 (1971).

(15) F. A. Nelson and B. M. Birch, *J. Biol. Chem.*, **248**, 8361 (1973).

(16) D. S. Hsu and S. S. Chen, *J. Chromatogr.*, **192**, 193 (1980).

(17) T. S. Yagura, C. C. Sigman, P. A. Sturm, E. J. Reist, H. L. Johnson, and J. P. Miller, *Biochem. Biophys. Res. Commun.*, **92**, 463 (1980).

(18) T. S. Yagura and J. P. Miller, *Biochemistry*, **20**, 879 (1981).

ACKNOWLEDGMENTS

This work was supported by NIH Grants ES 00093 and ES 07067.

The authors would like to thank Ms. Monica Cotner for typing the manuscript.

Subnanogram Quantitation of Chlorpromazine in Plasma by High-Performance Liquid Chromatography with Electrochemical Detection

J. K. COOPER, G. McKAY, and K. K. MIDHA ˣ

Received March 23, 1982, from the *College of Pharmacy, University of Saskatchewan, Saskatoon, Saskatchewan, S7N OWO Canada.* Accepted for publication September 17, 1982.

Abstract □ A specific and sensitive high-performance liquid chromatographic (HPLC) method for the quantitative determination of subnanogram levels of chlorpromazine in plasma is described. Following extraction of chlorpromazine and the internal standard, prochlorperazine, HPLC analysis is carried out on a cyano column with a mobile phase consisting of 0.1 *M* ammonium acetate in acetonitrile (10:90 v/v). The use of oxidative thin-layer amperometric detection allowed the quantitation of 0.25 ng of chlorpromazine/ml of plasma with a coefficient of variation of 5.1%. The HPLC method has adequate sensitivity to follow plasma concentration–time profiles up to 24 hr following low single oral doses of chlorpromazine in healthy volunteers.

Keyphrases □ Chlorpromazine—human plasma, high-performance liquid chromatographic determination of subnanogram levels, electrochemical detection □ High-performance liquid chromatography—electrochemical detection, subnanogram levels, chlorpromazine, human plasma

Chlorpromazine is the most widely used phenothiazine antipsychotic agent. It is extensively metabolized (1–6) both systematically and presystemically (7, 8) to numerous metabolites, some of which are psychoactive. The quantitative analysis of chlorpromazine in plasma or serum has been achieved by several methods which include GLC–

0022-3549/83/1100-1259$01.00/0

creased amounts injected, and the use of larger extraction columns for trace enrichment of the samples may provide sensitivity comparable to that of the more conventional assays. The separation of cyclic AMP from other biological substances using a simple isocratic HPLC system may be a difficult task. However, the use of gradient elution with a reverse-phase column (10) or the use of ion-exchange chromatography may separate V from the coeluting compound(s) (16).

It should also be pointed out that the chromatogram in Fig. 2 is a good example of the extra dimension offered to the chromatographic process by ion pairing. All compounds analyzed with mobile phase A eluted in the reverse order of their polarity as expected in conventional reverse-phase chromatography. The only exceptions were V and IV. Although V is slightly less hydrophobic than IV, it has a greater retention under the conditions used due to the presence of tetramethylammonium hydroxide. The interaction of the tetramethyammonium cation with the negatively charged V increases its retention. On the other hand, the positively charged IV is not affected by this cation (7). The result is that while IV and V coelute without this cation, its presence causes V to elute after IV so that separation of these two compounds can be achieved.

By the use of the methods described here, it has been shown that the N^6-butyryl derivative is the major product formed following the perfusion of rat lung with dibutyryl cyclic AMP. It is estimated that ~24% of the dibutyryl derivative taken up by the lung during the perfusion period can be recovered as the N^6-monobutyryl analogue from the perfusate and lung compartments. The remaining portion has most likely been further metabolized to the straight-chain monophosphate by the action of phosphodiesterase, since it is not recovered in the lung as the unmetabolized dibutyryl cyclic AMP. We have also shown that 35-min perfusion with 100 μM dibutyryl derivative results in a sevenfold increase in the cyclic AMP content of the lung measured by the protein binding assay of Gilman (13) (data not shown). HPLC analysis reveals that 90% of this increased protein binding can be attributed to the formation of the N^6-butyryl derivative in the lung tissue.

In light of recent findings that different cyclic nucleotide analogues can selectively activate different isozymes of protein kinase (17, 18), it has become important to know the intracellular distribution of these analogues following treatment with cyclic nucleotide derivatives. This analytical procedure provides a specific, sensitive, and simple method for measuring dibutyryl cyclic AMP and its metabolites in biological systems. This technique can potentially be applied for analysis of many of the other cyclic nucleotide analogues. Also, not only can it be used for perfusion studies, but could also be adapted to cell culture and whole animal experiments.

REFERENCES

(1) G. A. Robison, R. W. Butcher, and E. W. Sutherland, *Ann. Rev. Biochem.*, **37**, 149 (1968).

(2) T. Posternak, E. W. Sutherland, and W. F. Henion, *Biochem. Biophys. Acta*, **65**, 558 (1962).

(3) E. Kaukel, K. Mundhenk, and H. Huz, *Eur. J. Biochem.*, **27**, 197 (1972).

(4) E. W. Sutherland and T. W. Rall, *J. Am. Chem. Soc.*, **79**, 3607 (1957).

(5) J. P. Miller, K. H. Boswell, K. Muneyama, L. W. Simon, R. K. Robins, and D. A. Shuman, *Biochemistry*, **12**, 1010 (1973).

(6) J. C. L. V. Luang, N. N. Quang, and G. Hazebroucq, *Adv. Biosci.*, **24**, 201 (1979).

(7) P. J. M. Van Haastert, *J. Chromatogr.*, **210**, 229 (1981).

(8) M. I. Al-Moslih, G. R. Dubes, and A. N. Masoud, *HRC&CC.*, **4**, 173 (1981).

(9) F. S. Anderson and R. C. Murphy, *J. Chromatogr.*, **121**, 251 (1976).

(10) N. E. Hoffman and J. C. Liao, *Anal. Chem.*, **49**, 2231 (1977).

(11) A. L. Steiner, C. W. Parker, and D. M. Kipnis, *J. Biol. Chem.*, **247**, 1106 (1972).

(12) H. L. Cailla, M. S. Racine-Weisbach, and M. A. Delaage, *Anal. Biochem.*, **56**, 394 (1973).

(13) A. G. Gilman, *Proc. Natl. Acad. Sci. USA*, **67**, 305 (1970).

(14) B. L. Brown, J. D. M. Albano, R. P. Ekins, and A. M. Schierzi, *Biochem. J.*, **121**, 561 (1971).

(15) F. A. Nelson and B. M. Birch, *J. Biol. Chem.*, **248**, 8361 (1973).

(16) D. S. Hsu and S. S. Chen, *J. Chromatogr.*, **192**, 193 (1980).

(17) T. S. Yagura, C. C. Sigman, P. A. Sturm, E. J. Reist, H. L. Johnson, and J. P. Miller, *Biochem. Biophys. Res. Commun.*, **92**, 463 (1980).

(18) T. S. Yagura and J. P. Miller, *Biochemistry*, **20**, 879 (1981).

ACKNOWLEDGMENTS

This work was supported by NIH Grants ES 00093 and ES 07067.

The authors would like to thank Ms. Monica Cotner for typing the manuscript.

Subnanogram Quantitation of Chlorpromazine in Plasma by High-Performance Liquid Chromatography with Electrochemical Detection

J. K. COOPER, G. McKAY, and K. K. MIDHA ˣ

Received March 23, 1982, from the *College of Pharmacy, University of Saskatchewan, Saskatoon, Saskatchewan, S7N OWO Canada.* Accepted for publication September 17, 1982.

Abstract □ A specific and sensitive high-performance liquid chromatographic (HPLC) method for the quantitative determination of subnanogram levels of chlorpromazine in plasma is described. Following extraction of chlorpromazine and the internal standard, prochlorperazine, HPLC analysis is carried out on a cyano column with a mobile phase consisting of 0.1 *M* ammonium acetate in acetonitrile (10:90 v/v). The use of oxidative thin-layer amperometric detection allowed the quantitation of 0.25 ng of chlorpromazine/ml of plasma with a coefficient of variation of 5.1%. The HPLC method has adequate sensitivity to follow plasma concentration–time profiles up to 24 hr following low single oral doses of chlorpromazine in healthy volunteers.

Keyphrases □ Chlorpromazine—human plasma, high-performance liquid chromatographic determination of subnanogram levels, electrochemical detection □ High-performance liquid chromatography—electrochemical detection, subnanogram levels, chlorpromazine, human plasma

Chlorpromazine is the most widely used phenothiazine antipsychotic agent. It is extensively metabolized (1–6) both systematically and presystemically (7, 8) to numerous metabolites, some of which are psychoactive. The quantitative analysis of chlorpromazine in plasma or serum has been achieved by several methods which include GLC–

0022-3549/83/1100-1259$01.00/0

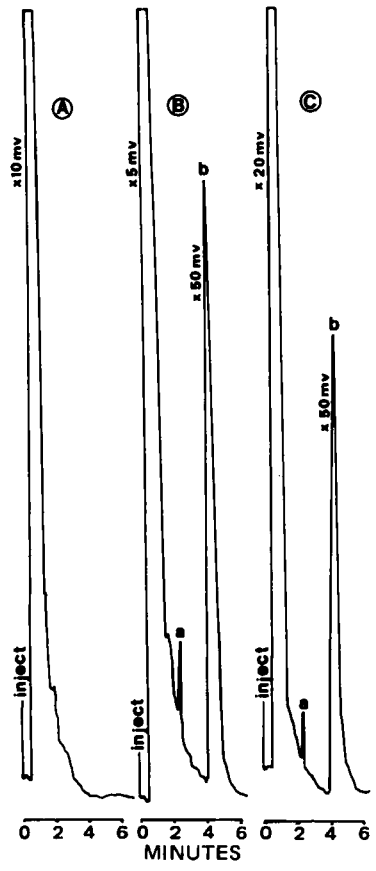

Figure 1—*Chromatograms of plasma extracted as outlined in* Experimental *with recorded sensitivity changes. Key: (A) blank plasma; (B) spiked plasma containing chlorpromazine (peak a, 0.5 ng/ml) and prochlorperazine (peak b, 50 ng/ml); (C) plasma sample 10 hr postdose from a volunteer (73.0 kg) who received 2 × 25-mg tablets orally of chlorpromazine hydrochloride. Chlorpromazine (peak a, 1.70 ng/ml) and prochlorperazine (peak b, 50 ng/ml).*

ECD (9), radioassay (10), radioimmunoassay (11, 12), fluorometry (13), GLC–NPD (14, 15), GLC–MS (1, 16, 17), and high-performance liquid chromatography (HPLC) (18–21).

HPLC methods, in general, are facile, easy to adopt, and are well suited for the therapeutic monitoring of drugs. Two of the HPLC procedures for chlorpromazine quantitation employ UV detection (18, 19), and the more sensitive (1 ng/ml) of these methods (18) was applicable to plasma level determinations in volunteers receiving chlorpromazine intravenously. Administration of chlorpromazine orally in low doses (25–50 mg), however, results in plasma levels that are generally in the subnanogram range at the end of the plasma concentration–time curve (7). Therefore, more sensitive analytical methods are needed to study the pharmacokinetics of this drug following low single oral doses. The development of such a method was achieved using electrochemical detection coupled with an improved extraction procedure that gave a greater recovery of the drug from plasma. Oxidative thin-layer amperometric detection (electrochemical detection) of chlorpromazine was investigated by Curry and Brown (20) and showed promise, but details of the assay were lacking. The procedure of Murakami *et al.* (21) was based on a reverse-phase HPLC system in which the extraction procedure was complex and plasma concentrations <1 ng/ml were not determined. The normal-phase HPLC method described here is simple, sensitive, and requires no specially treated glassware or apparatus. The improvement in the recovery of chlorpromazine from plasma was achieved by modification of an extraction procedure used for trifluoperazine (22).

Table I—HPLC Estimation of Chlorpromazine Added to Plasma [a]

Amount Added, ng	*n*	Mean Peak Height Ratio × 5	*SD*	*CV*[b]
0.25	5	0.0348	0.0018	5.10
0.50	5	0.0667	0.0031	4.60
1.0	5	0.1330	0.0036	2.71
2.5	5	0.3317	0.0071	2.14
5.0	5	0.6853	0.0292	4.26
10.0	5	1.3843	0.0276	1.99

[a] $y = mx + b$, where $m = 0.1368$ and $b = 0.0027$. [b] Mean = 3.47, $r = 0.999$.

EXPERIMENTAL

Materials—All solvents used both for extraction and in the HPLC mobile phase were HPLC grade[1]. Chlorpromazine hydrochloride[2], prochlorperazine mesylate[3], and 25-mg chlorpromazine tablets[4] were used as received. All other chemicals were commercial analytical grade.

HPLC—A liquid chromatographic pump[5] and valve loop injector[6] with a 500-μl sample loop was connected to an electrochemical detector[7]. The detector was fitted with a glassy carbon electrode and set at +0.9 V in the oxidation mode with a fixed 10-nA feed connected to a recorder[8]. All changes in attenuation were made only with the recorder to avoid baseline stabilization problems. The column (250 mm × 4.6-mm i.d.) was packed with 10-μm Spherisorb CN[9]. The mobile phase consisted of 0.1 *M* ammonium acetate–acetonitrile (1:9) and was deaerated before use by filtration[10]. The column was maintained at ambient temperature with a flow rate of 4 ml/min.

Preparation of Stock Solutions and Standard Curves—A stock solution of the internal standard, prochlorperazine mesylate (100 μg/ml, calculated as free base), was prepared monthly in double-distilled deionized water. The solution was stored in the dark at 4°. Daily dilutions were made in double-distilled deionized water to give a 100-ng/ml working solution. An aqueous solution of chlorpromazine hydrochloride (100 μg/ml, calculated as free base) was prepared monthly in double-distilled deionized water and stored as described for the internal standard. Daily dilutions of 100 ng/ml were made in 1:1 water–plasma and microliter amounts were added to give chlorpromazine concentrations of 0.25, 0.5, 1.0, 2.5, and 10 ng/ml in plasma.

Extraction of Samples—Plasma samples were extracted by a modification of a GLC–MS method developed for trifluoperazine (22). To a test tube[11] were added 2 ml of plasma and 1 ml of aqueous internal standard (prochlorperazine, 100 ng/ml). The sample was mixed[12] for 10 sec, and 0.5 ml of saturated sodium carbonate was then added. The sample was again mixed, and 5 ml of 3% isopropyl alcohol in pentane was added. The sample was capped and mixed for 20 min[13] and then centrifuged[14] at 1725×*g* for 5 min. The upper organic layer was transferred by Pasteur pipet to a clean 10-ml tube, and the extraction was repeated with another 5 ml of 3% isopropyl alcohol in pentane. The organic extracts were combined and a few antibumping granules[15] were added. The sample was evaporated to dryness at 65°[16]. To the cooled tube was added 200 μl of

[1] Caledon Laboratories, Georgetown, Ontario, Canada.
[2] Poulenc Ltd., Montreal, Quebec, Canada.
[3] Sandoz Pharmaceutical, Dorval, Quebec, Canada.
[4] Smith Kline & French, Philadelphia, Pa.
[5] Waters model M45; Waters Associates, Mississauga, Ontario, Canada.
[6] Rheodyne model 7125; Technical Marketing Associates, Calgary, Alberta, Canada.
[7] Model LC4A; Bioanalytical Systems through Technical Marketing Associates, Calgary, Alberta, Canada.
[8] Perkin-Elmer model 56; Perkin-Elmer, Montreal, Quebec, Canada.
[9] Beckman Instruments, Toronto, Ontario, Canada.
[10] Millipore Corp., Bedford, Mass.
[11] Polytef-lined screw-capped (13 × 100-mm) tubes; Corning Glass, Corning, N.Y.
[12] Vortex-Genie; Fisher Scientific Co., Edmonton, Alberta, Canada.
[13] Büchler Evapomix; Fisher Scientific Co., Edmonton, Alberta, Canada.
[14] TJ6 Centrifuge; Beckman Instruments, Toronto, Ontario, Canada.
[15] BDH Chemicals, Toronto, Ontario, Canada.
[16] Thermolyne Dri-Bath; Fisher Scientific Co., Edmonton, Alberta, Canada.

Table II—Recovery of Chlorpromazine and Prochlorperazine from Plasma

Drug	Amount Added to 1 ml of Plasma, ng	n	Mean Amount Recovered, ng	Recovery, %[a]
Chlorpromazine	5.00	10	4.31	86.12 ± 2.26
	1.00	10	0.86	85.76 ± 2.90
Prochlorperazine	50.00	7	43.16	86.31 ± 1.33

[a] Mean ± *SD*.

HPLC-grade acetonitrile, the sample was mixed for 20 sec, and aliquots of 100 μl were injected into the chromatograph.

Plasma Level Study—Three healthy male volunteers weighing 73.0, 77.8, and 87.8 kg participated in the study, which was performed under medical supervision. Each volunteer was administered orally two 25-mg tablets of a commercial formulation of chlorpromazine with 250 ml of water. No xanthine-containing beverage was allowed during the study and no alcoholic beverages were allowed 24 hr before and 24 hr after the last blood sample. A lemon–lime beverage (200 ml) was provided 2 hr after dosing, and a standard lunch at 4.5 hr. Blood samples (10 ml each) were obtained at 0, 0.5, 1, 2, 3, 4, 6, 8, 10, 12, 15, and 24 hr following ingestion of the drug. The samples were collected by means of venipuncture into heparinized evacuated tubes[17] taking care to not allow the blood to come in contact with the rubber stopper[18]. After centrifugation the plasma was removed and stored at −20° until analysis; subsequently, thawed samples were stored at 4°.

Recovery Study—For the determination of the recovery of chlorpromazine and the internal standard, blank plasma was spiked at 1 and 5 ng/ml for chlorpromazine and 50 ng/ml for prochlorperazine. The samples were extracted as described and peak heights were compared with those obtained for absolute injection of the same amounts of chlorpromazine and prochlorperazine in acetonitrile.

Quantitation—Standard curves were constructed by chromatographing spiked plasma standards and plotting the peak height ratio of the drug to the internal standard *versus* the concentration of the drug. Unknown samples were analyzed along with calibration standards, and concentrations were determined by comparison of the peak height ratios to the standard curve obtained for that day. Patient samples above the stated linear range of 10 ng/ml were diluted as required with fresh blank control plasma and reanalyzed.

RESULTS AND DISCUSSION

Figure 1A shows a typical chromatogram of an extract of fresh blank plasma, and Fig. 1B shows a chromatogram obtained when the method was applied to spiked plasma containing 0.5 ng/ml of chlorpromazine and 50 ng/ml of the internal standard. Chlorpromazine and the internal standard gave well-separated sharp symmetrical peaks with retention times of 2.4 and 4.4 min, respectively. There were no extraneous peaks in chromatograms obtained for blank control plasma. Figure 1C shows a 10-hr postdose plasma sample (2 ml) of a volunteer (73.0 kg) who received 50 mg of chlorpromazine hydrochloride orally; the chlorpromazine concentration was estimated to be 1.7 ng/ml in this sample.

Mass spectral analysis of collected peaks from extracts of pooled plasma from volunteers and spiked samples were found to be identical and gave no evidence of possible interferences. The known metabolites of chlorpromazine either eluted in the same order and relative retention times as in the previous HPLC method using UV detection (18) or did not give any response with electrochemical detection. The use of a more concentrated ammonium acetate buffer increased the retention time of chlorpromazine by 2 min over that observed in the earlier study. This change in retention time resolved the peak due to chlorpromazine from components that eluted in the void volume. When the concentration of acetonitrile was decreased to 70%, no significant change in the retention time of chlorpromazine was observed; however, there was a significant decrease in the signal-to-noise ratio. Also, separation of chlorpromazine metabolites is best carried out using a 90% acetonitrile-based mobile phase. Linear extraction of chlorpromazine at low concentrations was observed to be a problem during the development of the HPLC–UV procedure reported from this laboratory (18). To correct this problem an extraction scheme was developed that provided linearity, but resulted in low recoveries: 34.5%. In the present method using 3% isopropyl alcohol in pentane increased the recovery to 86%, and produced reproducible results over the concentration range of 0.25–10.0 ng/ml. Furthermore, the use of the alternate detection system, electrochemical detection, allowed the quantitation of subnanogram amounts of chlorpromazine in plasma. In addition, no problems of occlusion, as observed in the HPLC–UV procedure (18), were encountered since deproteinization was unnecessary, and loss of drug due to adsorption to glass surfaces was not evident.

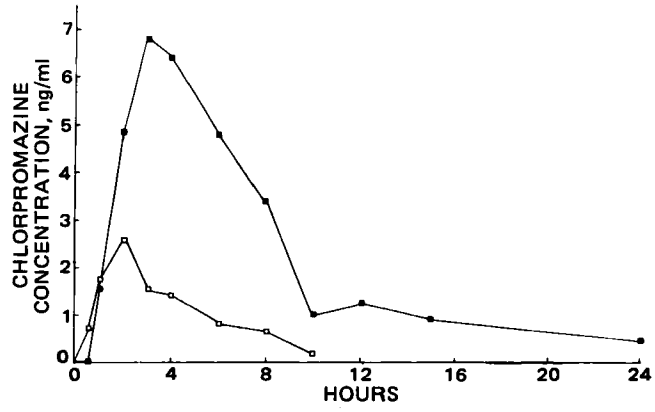

Figure 2—*Plasma concentration–time profiles for two volunteers (A = 77.8 kg, B = 87.8 kg) after each received a single oral dose of chlorpromazine (2 × 25-mg) tablets. Key: (■) volunteer A; (□) volunteer B.*

The electrochemical detector provides at least a 10-fold increase in sensitivity; this finding is in agreement with Curry and Brown (20). An apparent limitation of electrochemical detection is the presence of wide solvent fronts, which may be due to the response of endogenous materials coextracted from plasma. This limitation prevents operation of the detector at its lowest limits of detection. Despite this problem it is evident from Fig. 1B, where no appreciable interferences are observed with the recorder operated at 5 mV, that 0.5-ng amounts of drug can be measured.

Table I shows a composite standard curve obtained from the quantitation of chlorpromazine in plasma. The curve is linear in the range of 0.25–10 ng/ml. The ratio of chlorpromazine to prochlorperazine plotted against chlorpromazine concentration gave a straight line, which passed through the origin with a correlation coefficient of 0.999, a mean slope value of 0.1368, and an overall mean coefficient of variation of 3.47%. The limit of detection of this assay is ~0.1 ng/ml in plasma, and the limit of accurate quantitation is 0.25 ng/ml when 2-ml plasma samples are used. It is adequate for following plasma concentration–time profiles in patients receiving low oral doses of chlorpromazine.

The overall recoveries of chlorpromazine and the internal standard are shown in Table II. Results are based on at least 10 determinations at the 5- and 1-ng/ml levels for chlorpromazine and 7 determinations at the 50-ng/ml level for the internal standard. Mean recoveries of 85.94 ± 2.58% and 86.31 ± 1.33% were obtained for chlorpromazine and the internal standard (prochlorperazine), respectively. Application of this method is shown in Fig. 2, where plasma concentration *versus* time profiles are shown for two healthy male volunteers each receiving 2 × 25-mg tablets of chlorpromazine hydrochloride. Intersubject variability in plasma levels, as shown in Fig. 2, makes it clear that analysis of chlorpromazine should be carried out with the most sensitive procedure available especially when low oral doses are administered.

The described HPLC method is simple, requiring minimum sample handling and time. It is sensitive enough for single- as well as multiple-dose pharmacokinetic or bioavailability studies of low oral doses of chlorpromazine. Furthermore, multiple-dose studies and therapeutic monitoring could be carried out with smaller plasma sample volumes than previously required.

[17] Vacutainers; Becton, Dickinson & Co., Mississauga, Ontario, Canada.

[18] Necessary to avoid distortions in plasma chlorpromazine concentrations (23).

REFERENCES

(1) J. C. Craig, L. D. Gruenke, B. A. Hitzeman, J. Holaday, and H. H. Loh, *Dev. Neurosci. (Amsterdam)*, **7**, 129 (1980).

(2) G. Alfredsson, F.-A. Wiesel, and P. Skett, *Psychopharmacology (Berlin)*, **53**, 13 (1977).

(3) G. Alfredsson, G. Sedvall, F.-A. Wiesel, and B. Wode-Helgodt, *Dev. Neurosci. (Amsterdam)*, **7**, 199 (1980).

(4) B. Wode-Helgodt and G. Alfredsson, *Psychopharmacology (Berlin)*, **73**, 55 (1981).
(5) B. S. Binney and G. K. Aghajanian, *Life Sci.*, **15**, 309 (1974).
(6) S. Lal and T. L. Sourkes, *Eur. J. Pharmacol.*, **17**, 283 (1972).
(7) J. C. K. Loo, K. K. Midha, and I. J. McGilveray, *Commun. Psychopharmacol.*, **4**, 121 (1980).
(8) S. H. Curry, in "Antipsychotic Drugs: Pharmacodynamics and Pharmacokinetics," G. Sedvall, B. Uvnäs, and Y. Zotterman, Eds., Pergamon, Oxford, 1976, pp. 343–352.
(9) S. H. Curry, *Psychopharmacol. Commun.*, **2**, 1 (1976).
(10) D. H. Efron, S. R. Harris, A. A. Manian, and L. E. Gaudette, *Psychopharmacologia*, **19**, 207 (1971).
(11) K. K. Midha, J. C. K. Loo, J. W. Hubbard, M. L. Rowe, and I. J. McGilveray, *Clin. Chem. (Winston-Salem, N.C.)*, **25**, 166 (1979).
(12) K. Kawashima, R. Dixon, and S. Spector, *Eur. J. Pharmacol.*, **32**, 195 (1975).
(13) P. N. Kaul, L. R. Whitfield, and M. L. Clark, *J. Pharm. Sci.*, **65**, 689 (1976).
(14) H. Dekirmenjian, J. I. Javaid, B. Duslak, and J. M. Davis, *J. Chromatogr.*, **160**, 291 (1978).
(15) R. N. Gupta, G. Bartolucci, and G. Molnar, *Clin. Chim. Acta.*, **109**, 351 (1981).
(16) G. Alfredsson, B. Wode-Helgodt, and G. Sedvall, *Psychopharmacology (Berlin)*, **48**, 123 (1976).
(17) C.-G. Hammar, B. Holmstedt, and R. Ryhage, *Anal. Biochem.*, **25**, 532 (1968).
(18) K. K. Midha, J. K. Cooper, I. J. McGilveray, A. G. Butterfield, and J. W. Hubbard, *J. Pharm. Sci.*, **70**, 1043 (1981).
(19) D. Stevenson and E. Reid, *Anal. Lett.*, **14**, 741 (1981).
(20) S. H. Curry and E. A. Brown, *IRCS Med. Sci. Libr. Compend.*, **9**, 166 (1981).
(21) K. Murakami, K. Murakami, T. Ueno, J. Hijikata, K. Shirasawa, and T. Muto, *J. Chromatogr.*, **227**, 103 (1982).
(22) K. K. Midha, R. M. H. Roscoe, K. Hall, E. M. Hawes, J. K. Cooper, G. McKay, and H. U. Shetty, *Biomed. Mass Spectrom.*, **9**, 186 (1982).
(23) K. K. Midha, J. C. K. Loo, and M. L. Rowe, *Res. Comun. Psychol. Psychiatry Behav.*, **4**, 193 (1979).

ACKNOWLEDGMENTS

The authors thank Dr. E. M. Hawes for helpful discussions and Mr. K. Hall for mass spectral analysis. The postdoctoral award from Saskatchewan Health Research Board to G. McKay is gratefully acknowledged.

Maintenance-Dose Prediction Based on a Single Determination of Concentration: General Applicability to Two-Compartment Drugs with Reference to Lithium

CHERYL L. ZIMMERMAN and JOHN T. SLATTERY[x]

Received April 16, 1982, from the *School of Pharmacy, Department of Pharmaceutics, University of Washington, Seattle, WA 98195.* Accepted for publication September 21, 1982.

Abstract □ A general approach to the selection of the maintenance dose (D_m) required to give a desired steady-state concentration of drug based on a single determination of concentration after a test dose (C^*) is extended to drugs with two-compartment pharmacokinetic characteristics. Using the equation developed, the value of the proportionality factor relating $1/D_m$ to C^* was found to be within 3.2% of the value calculated from a published nomogram for lithium. The inherent error is shown to be a function of the value of the hybrid rate constants α and β, as well as the value of an intercompartmental transfer rate constant, k_{21}, in an individual.

Keyphrases □ Dose, maintenance—steady-state concentration, prediction by single determination of concentration, two-compartment pharmacokinetics, lithium □ Concentration, steady-state—maintenance dose, prediction by single determination of concentration, two-compartment pharmacokinetics, lithium □ Pharmacokinetics—two-compartment, maintenance dose for steady-state concentration, prediction by single determination of concentration, lithium

In 1973, Cooper *et al.* observed a correlation ($r = 0.972$) between the serum lithium concentration obtained 24 hr after the administration of a 600-mg dose of lithium carbonate and the eventual steady-state concentration if that dose were continued three times a day (1). From that observation, they constructed a nomogram that predicted the maintenance dose required to achieve a therapeutic steady-state concentration of lithium in plasma (0.6–1.2 meq/liter) based on the concentration determined 24 hr after administration of a test dose of the drug. The same group published a report 2 years later confirming the success of the method (2).

Similar techniques have since been proposed for drugs with widely differing pharmacokinetic characteristics (3–9). Montgomery *et al.* (5) proposed that blood samples taken 24 or 48 hr after an oral test dose of nortriptyline could adequately predict steady-state concentrations of that drug using a justification similar to that used by Cooper *et al.* Koup *et al.* suggested that a strong correlation between steady-state levels and drug concentrations 6 hr after administering a single dose of chloramphenicol or theophylline would exist based on a series of pharmacokinetic simulations (7), and later provided clinical data to support the method (8). The appropriate sampling times for those drugs seemed to correspond to their average half-life in the population. It thus became apparent that this approach to maintenance-dose prediction could be applied to many drugs, and that its successful use depended on implicit knowledge of the individual pharmacokinetic characteristics of a drug within the population.

A theoretical framework was provided to explain and evaluate the empirical clinical observations. The theory was founded on the essential clinical observation that there existed an optimal time at which a blood sample could be obtained from an individual, in which the concentration

0022-3549/83/1100-1262$01.00/0

(4) B. Wode-Helgodt and G. Alfredsson, *Psychopharmacology (Berlin)*, **73**, 55 (1981).
(5) B. S. Binney and G. K. Aghajanian, *Life Sci.*, **15**, 309 (1974).
(6) S. Lal and T. L. Sourkes, *Eur. J. Pharmacol.*, **17**, 283 (1972).
(7) J. C. K. Loo, K. K. Midha, and I. J. McGilveray, *Commun. Psychopharmacol.*, **4**, 121 (1980).
(8) S. H. Curry, in "Antipsychotic Drugs: Pharmacodynamics and Pharmacokinetics," G. Sedvall, B. Uvnäs, and Y. Zotterman, Eds., Pergamon, Oxford, 1976, pp. 343–352.
(9) S. H. Curry, *Psychopharmacol. Commun.*, **2**, 1 (1976).
(10) D. H. Efron, S. R. Harris, A. A. Manian, and L. E. Gaudette, *Psychopharmacologia*, **19**, 207 (1971).
(11) K. K. Midha, J. C. K. Loo, J. W. Hubbard, M. L. Rowe, and I. J. McGilveray, *Clin. Chem. (Winston-Salem, N.C.)*, **25**, 166 (1979).
(12) K. Kawashima, R. Dixon, and S. Spector, *Eur. J. Pharmacol.*, **32**, 195 (1975).
(13) P. N. Kaul, L. R. Whitfield, and M. L. Clark, *J. Pharm. Sci.*, **65**, 689 (1976).
(14) H. Dekirmenjian, J. I. Javaid, B. Duslak, and J. M. Davis, *J. Chromatogr.*, **160**, 291 (1978).
(15) R. N. Gupta, G. Bartolucci, and G. Molnar, *Clin. Chim. Acta.*, **109**, 351 (1981).
(16) G. Alfredsson, B. Wode-Helgodt, and G. Sedvall, *Psychopharmacology (Berlin)*, **48**, 123 (1976).
(17) C.-G. Hammar, B. Holmstedt, and R. Ryhage, *Anal. Biochem.*, **25**, 532 (1968).
(18) K. K. Midha, J. K. Cooper, I. J. McGilveray, A. G. Butterfield, and J. W. Hubbard, *J. Pharm. Sci.*, **70**, 1043 (1981).
(19) D. Stevenson and E. Reid, *Anal. Lett.*, **14**, 741 (1981).
(20) S. H. Curry and E. A. Brown, *IRCS Med. Sci. Libr. Compend.*, **9**, 166 (1981).
(21) K. Murakami, K. Murakami, T. Ueno, J. Hijikata, K. Shirasawa, and T. Muto, *J. Chromatogr.*, **227**, 103 (1982).
(22) K. K. Midha, R. M. H. Roscoe, K. Hall, E. M. Hawes, J. K. Cooper, G. McKay, and H. U. Shetty, *Biomed. Mass Spectrom.*, **9**, 186 (1982).
(23) K. K. Midha, J. C. K. Loo, and M. L. Rowe, *Res. Comun. Psychol. Psychiatry Behav.*, **4**, 193 (1979).

ACKNOWLEDGMENTS

The authors thank Dr. E. M. Hawes for helpful discussions and Mr. K. Hall for mass spectral analysis. The postdoctoral award from Saskatchewan Health Research Board to G. McKay is gratefully acknowledged.

Maintenance-Dose Prediction Based on a Single Determination of Concentration: General Applicability to Two-Compartment Drugs with Reference to Lithium

CHERYL L. ZIMMERMAN and JOHN T. SLATTERY[x]

Received April 16, 1982, from the *School of Pharmacy, Department of Pharmaceutics, University of Washington, Seattle, WA 98195.* Accepted for publication September 21, 1982.

Abstract □ A general approach to the selection of the maintenance dose (D_m) required to give a desired steady-state concentration of drug based on a single determination of concentration after a test dose (C^*) is extended to drugs with two-compartment pharmacokinetic characteristics. Using the equation developed, the value of the proportionality factor relating $1/D_m$ to C^* was found to be within 3.2% of the value calculated from a published nomogram for lithium. The inherent error is shown to be a function of the value of the hybrid rate constants α and β, as well as the value of an intercompartmental transfer rate constant, k_{21}, in an individual.

Keyphrases □ Dose, maintenance—steady-state concentration, prediction by single determination of concentration, two-compartment pharmacokinetics, lithium □ Concentration, steady-state—maintenance dose, prediction by single determination of concentration, two-compartment pharmacokinetics, lithium □ Pharmacokinetics—two-compartment, maintenance dose for steady-state concentration, prediction by single determination of concentration, lithium

In 1973, Cooper *et al.* observed a correlation ($r = 0.972$) between the serum lithium concentration obtained 24 hr after the administration of a 600-mg dose of lithium carbonate and the eventual steady-state concentration if that dose were continued three times a day (1). From that observation, they constructed a nomogram that predicted the maintenance dose required to achieve a therapeutic steady-state concentration of lithium in plasma (0.6–1.2 meq/liter) based on the concentration determined 24 hr after administration of a test dose of the drug. The same group published a report 2 years later confirming the success of the method (2).

Similar techniques have since been proposed for drugs with widely differing pharmacokinetic characteristics (3–9). Montgomery *et al.* (5) proposed that blood samples taken 24 or 48 hr after an oral test dose of nortriptyline could adequately predict steady-state concentrations of that drug using a justification similar to that used by Cooper *et al.* Koup *et al.* suggested that a strong correlation between steady-state levels and drug concentrations 6 hr after administering a single dose of chloramphenicol or theophylline would exist based on a series of pharmacokinetic simulations (7), and later provided clinical data to support the method (8). The appropriate sampling times for those drugs seemed to correspond to their average half-life in the population. It thus became apparent that this approach to maintenance-dose prediction could be applied to many drugs, and that its successful use depended on implicit knowledge of the individual pharmacokinetic characteristics of a drug within the population.

A theoretical framework was provided to explain and evaluate the empirical clinical observations. The theory was founded on the essential clinical observation that there existed an optimal time at which a blood sample could be obtained from an individual, in which the concentration

0022-3549/83/1100-1262$01.00/0

of drug would be related to the eventual steady-state concentration by a proportionality factor that could be regarded as being constant throughout the population (10, 11). The theory is consistent with the clinical observations made with chloramphenicol and theophylline. However, the theory suggested that the optimum sampling time for lithium would be ~16 hr after administration of the first dose of drug. The sampling time used clinically (with great success) was 24 hr. Thus, it was possible that the theory did not account for all factors in sampling time optimization. The most obvious shortcoming of the theory was that it was developed for drugs with one-compartment pharmacokinetic characteristics; lithium is a two-compartment drug. It is apparently necessary to extend the theoretical analysis to drugs with biexponential plasma concentration–time profiles, conventionally described by a two-compartment model.

The purpose of this report is to expand the theory to drugs with two-compartment characteristics and to evaluate the source and magnitude of error inherent in the method when it is employed under optimal conditions. We do not report a new dosing method.

THEORETICAL

The development of an expression that relates the maintenance dose (D_m) required to give a desired average steady-state concentration ($\overline{C}_{ss}$) to the concentration in plasma (C^*) at some time (t^*) after the first dose (D^*) for a drug with two-compartment pharmacokinetic characteristics is very similar to the development of the analogous expression for a one-compartment drug (10). Equations pertaining to the intravenous administration of the two-compartment drug will be used even though lithium itself is given orally. If, as in the case of lithium, absorption is rapid relative to distribution and elimination and the bioavailability does not vary between doses, the conclusions based on intravenous dosing will be valid for oral dosing as well. It is also assumed that the values of pharmacokinetic parameters describing the deposition of the drug do not change between the single dose and steady state.

The average concentration of a drug in plasma at steady state $\overline{C}_{ss}$, is defined as:

$$\overline{C}_{ss} = \frac{\int_0^{\infty} C\,dt}{\tau} \qquad \text{(Eq. 1)}$$

where C is the concentration of drug in plasma, t is time, and τ is the time between doses. For a drug with linear, two-compartment kinetics, Eq. 1 can be expressed as:

$$\overline{C}_{ss} = \frac{D_m(\alpha - k_{21})}{\alpha\tau V_c(\alpha - \beta)} + \frac{D_m(k_{21} - \beta)}{\beta\tau V_c(\alpha - \beta)} \qquad \text{(Eq. 2)}$$

where V_c is the volume of the central compartment, α and β are hybrid distribution- and elimination-phase rate constants, respectively, and k_{21} is a first-order rate constant for transfer of drug from the peripheral to the central compartment (12).

The concentration of drug following a single dose is:

$$C^* = \frac{D^*}{V_c}\left[\frac{(\alpha - k_{21})}{(\alpha - \beta)}e^{-\alpha t^*} + \frac{(k_{21} - \beta)}{(\alpha - \beta)}e^{-\beta t^*}\right] \qquad \text{(Eq. 3)}$$

The ratio $\overline{C}_{ss}/C^*$ is therefore:

$$\frac{\overline{C}_{ss}}{C^*} = \frac{D_m}{D^*\tau\alpha\beta}\left[\frac{k_{21}(\alpha - \beta)}{(\alpha - k_{21})e^{-\alpha t^*} + (k_{21} - \beta)e^{-\beta t^*}}\right] \qquad \text{(Eq. 4)}$$

By a rearrangement of Eq. 4, the maintenance dose can be related to C^* by a proportionality factor, ψ:

$$\frac{1}{D_m} = \psi C^* \qquad \text{(Eq. 5)}$$

where

$$\psi = \frac{k_{21}(\alpha - \beta)}{\overline{C}_{ss}\alpha\beta\tau D^*[(\alpha - k_{21})e^{-\alpha t^*} + (k_{21} - \beta)e^{-\beta t^*}]} \qquad \text{(Eq. 6)}$$

Equation 6 shows that the proportionality factor ψ relating maintenance dose to C^* is a complex function of α, β, and k_{21} in an individual. α and β are functions of the intercompartmental transfer and elimination rate microconstants, k_{12}, k_{21}, and k_{10} (12). Equations 5 and 6 will serve as an appropriate means of calculating maintenance dose for a drug with two-compartment behavior when ψ is relatively constant throughout the population, *i.e.*, when each individual's value of ψ is close to the population's mean value of ψ ($\overline{\psi}$). The values of the pharmacokinetic parameters k_{12}, k_{21}, and k_{10} (and therefore α and β) vary among individuals, and one can exert no control over them. The choice of $\overline{C}_{ss}$, τ, and D will depend on the drug used and will have no effect on the variability of ψ between individuals. By the choice of an appropriate value for t^*, the variability of ψ throughout the population can be minimized (10, 11).

Choice of Optimum Sampling Time (t^*)—In selecting the optimum sampling time for a one-compartment drug, the expression for ψ was recast in terms of clearance (CL) and volume of distribution (V). The partial first derivatives of ψ with respect to these independent variables were set at zero, and the resulting expressions were simultaneously solved for time. ψ was found to be minimally affected by interindividual variations in CL and V when t^* was $1/\overline{K}$, where $\overline{K}$ is the mean (or median) value of the elimination rate constant in the population (11). In attempting to do the same for ψ in the multicompartment case (Eq. 6), an explicit value for t^* was not found. Therefore, numerical approximation techniques were used to estimate a value of t^* at which variability of ψ throughout the population was minimal. This approach (described below) has the important benefit of allowing the examination of the behavior of ψ as it approaches its optimum, which provides some insight into the error of the method. By definition, the optimum value of t^* will be that value which produces the minimum variability of ψ throughout the population.

The optimum sampling time (t^*) was selected using parameter values for lithium based on data published by Amdisen (13) and Neilson-Kudsk and Amdisen (14). Fourfold ranges of α and k_{21} centered around mean values of 0.888 and 0.375 hr^{-1}, respectively, were considered. This encompassed the mean $\pm 2SD$ for both parameters. A histogram of β values was constructed from a published histogram of lithium half-life values in 226 patients. The fivefold range of β values was centered about a mean value of 0.065 hr^{-1}; this encompassed the mean $\pm 4SD$ for β. The broader range was used for β because preliminary studies showed that error was most sensitive to changes in β; it was therefore important to cover the entire range of values reported. A program was written to calculate ψ at a given t^* for 125 combinations of α, β, and k_{21}. The numerator of Eq. 6 was plotted against its denominator for various values of t^*. The slope of this plot is $\overline{\psi}$. The coefficient of variation of the estimate of the slope for the best-fit straight line was calculated for each t^* plot. Plots representing the analysis for t^* = 12, 16, 20, and 24 hr are shown in Fig. 1.

The t^* that gives the smallest amount of variation around the regression line, as measured by the smallest coefficient of variation of the slope[1] (or ψ) for the given ranges of α, β, and k_{21}, is the optimum sampling time. In this case, t^* = 16 hr shows the least amount of variation (29.9%) when compared with t^* = 12 hr (37.4%), t^* = 20 hr (33.0%), and t^* = 24 hr (43.8%). A value of 16 ± 1 hr is the optimum sampling time; the other values were chosen for illustrative purposes. This process could be summarized as a plot of the coefficient of variation of the slope *versus* time (which would actually be a plot of the relative variance of ψ as a function of time), where the minimum would represent the optimum sampling time.

Analysis of Error—The use of optimum t^* will give a minimum error in single-point dose prediction methods, but the choice itself does not give an indication of the magnitude or the source of error involved. It has been possible in previous descriptions of one-point maintenance-dose estimation to graphically examine the error of the method by plotting $\psi/\overline{\psi}$ as a function of the variables that determine the value of ψ (11, 16). In this case, $\psi/\overline{\psi}$ would be plotted as a function of α, β, and k_{21} and would therefore be four-dimensional. Such an approach would be helpful, however, if a majority of the variability of ψ among individuals was a function of only one or two of these parameters, allowing a two- or three-dimensional plot to be constructed.

Our investigations of the lithium case have shown that the majority of the variability in ψ through the population was a function of β rather than α or k_{21}. Thus, it would be possible to construct a plot of $\psi/\overline{\psi}$ *versus* β to more closely examine the influence of the major determinant of error. To view the whole problem, however, it is necessary to somehow incor-

[1] Percent coefficient of variation = (standard deviation/mean) × 100. Mean and standard deviation of the slope of the regression line were calculated according to standard methods (15).

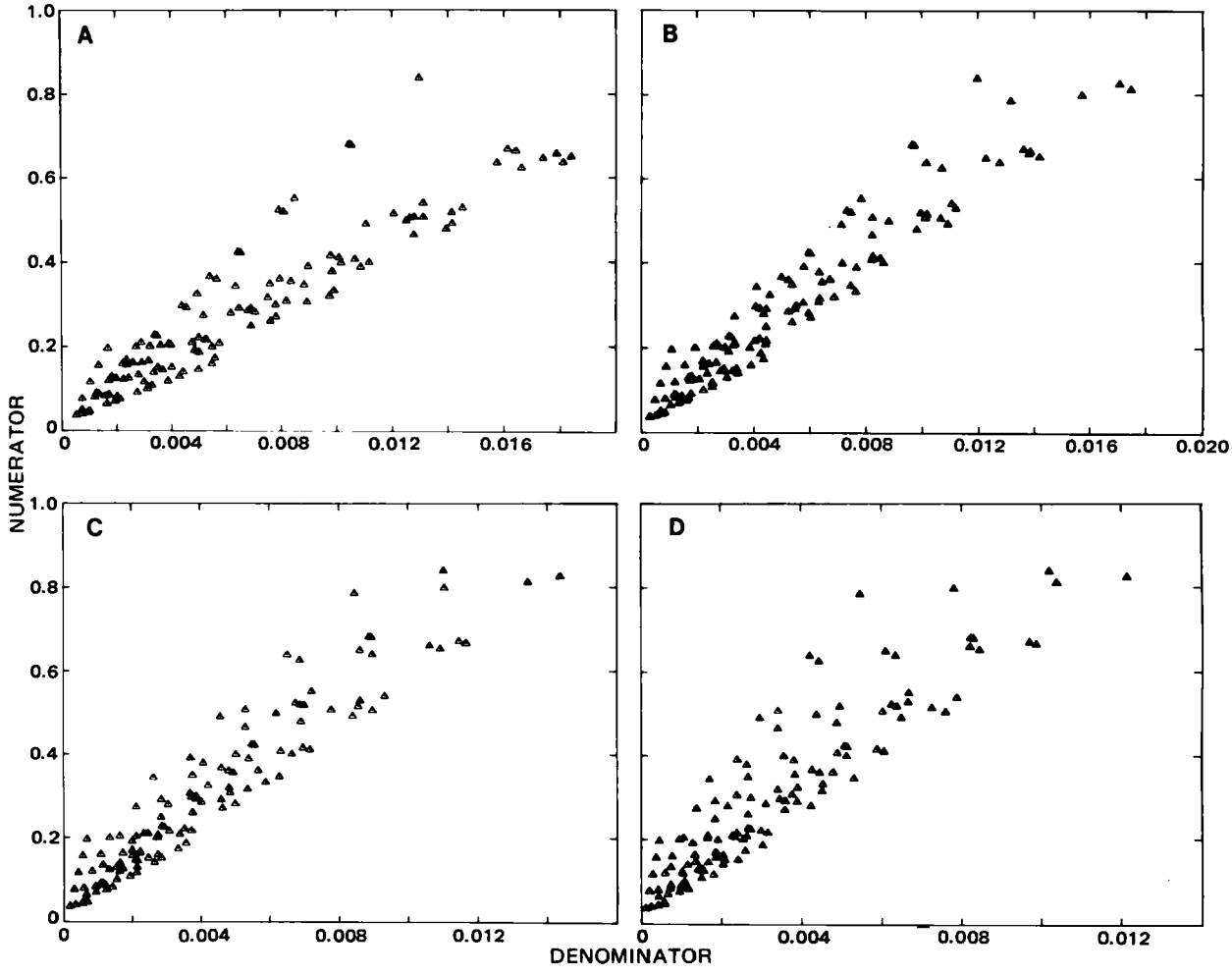

Figure 1—*Optimization of sampling time (t*) for lithium. The numerator of Eq. 6 is plotted* versus *the denominator for values of* α, β, *and* k_{21} *covering the range encountered through the population for lithium (13, 14). The minimum relative scatter is observed for the optimum value of* t*, *16 hr. Key: (A)* t* = *12 hr; (B)* t* = *16 hr; (C)* t* = *20 hr; (D)* t* = *24 hr.*

porate a depiction of the added error due to interindividual variation in α and k_{21}. This was accomplished by random selection of 100 values of α and k_{21} from a normal distribution (based on literature values of mean and standard deviation) for each value of β and calculating the value of $\psi/\overline{\psi}$ for each combination of α, β, and k_{21}. Figure 2 shows the mean values of $\psi/\overline{\psi}$ for each value of β and the magnitude of error due to interindividual variation in β alone, which is analogous to the graphical analysis of error for one-compartment drugs. With t^* = 16 hr, the departure of the plot of $\psi/\overline{\psi}$ from a value of 1 is minimal through the range of values of β covered in the plot. (If ψ did not vary through the population, $\psi/\overline{\psi}$ would always equal 1 and there would be no inherent error in the method.) Values of t^* at 12 and 24 hr give maximum errors of 50–60% at opposite extremes of β, and t^* = 20 hr gives a maximum error of ~40%. When t^* = 16 hr, the maximum error is ~25%.

A more complete analysis of error is obtained from the plots in Fig. 3. The mean value of $\psi/\overline{\psi}$ is again plotted as a function of β, but in this case the mean value is bracketed by ±2 *SD*, as calculated from the aforementioned 100 random combinations of α and k_{21} selected based on published values of their respective mean and standard deviation (13, 14). The maximum error expected to be encountered, taking the variability in ψ due to α and k_{21} into account, is ~40% for t^* = 16 hr and ~100% for t^* = 24 hr. Both of these errors would cause an overdose in patients with unusually large values of β, *i.e.*, individuals with unusually short half-life values.

This method of evaluation of error does not indicate the maximum error which could be encountered in the method, but it does indicate the maximum to be expected in ~95% of the population. Unusual patients could encounter greater error.

Comparison of Theory with a Published Nomogram—The single-point dose prediction for lithium proposed by Cooper *et al.* (1, 2) can be used as a basis for determining the validity of the equations developed here. Their nomogram consisted of seven maintenance doses recommended for seven respective ranges of C^*. Using that nomogram and Eq. 5, a value of ψ was calculated for each value of D_m and the mean C^* for which that dose was recommended. The mean of these values was 6.21 ml/meq·mg. Using Eq. 6; mean values of α, β, and k_{21}; and values of $\overline{C}_{ss}$, t^*, and D^* used by Cooper *et al.* in constructing the nomogram, the value calculated for $\overline{\psi}$ was 6.02 ml/meq·mg. Thus, Eq. 6 and literature data allowed the calculation of a value of ψ within 3.2% of the value found in the clinical experiment.

The agreement between the value of ψ implicitly used by Cooper *et al.* and that calculated using Eq. 6 and literature values of α, β, and k_{21} would seem to indicate that the theory is quantitatively valid. How then can the discrepancy between the optimum sampling time indicated by the theoretical analysis (16 hr) and the sampling time used by Cooper *et al.* (24 hr) in their successful nomogram be reconciled? The choice of optimum sampling time as described above is based on the assumed use of a constant value of ψ throughout the population.

The values of ψ corresponding to the higher ranges of C^* in the nomogram were quite close to one another (coefficient of variation, 11%). However, the value of ψ calculated for the lowest range of C^* for which dosing recommendations were made (mean of this range is 0.025 meq/liter) is 2.12 times the mean value for the higher ranges of concentration.

Patients with low values of concentration will tend to have larger values of β (shorter half-life values) than the population average. The theoretical analysis (Fig. 3) shows that patients with large values of β will tend to be overdosed using the population average value of ψ if the sample to be used for dose prediction purposes is obtained at 24 hr. The published nomogram corrects for this by using a larger value of ψ for these individuals, which reduces the recommended maintenance dose by approximately one-half of what it would be if the value of ψ used in other concentration ranges was retained. The published nomogram, therefore, corrects the error that would be encountered if a constant value of ψ were used

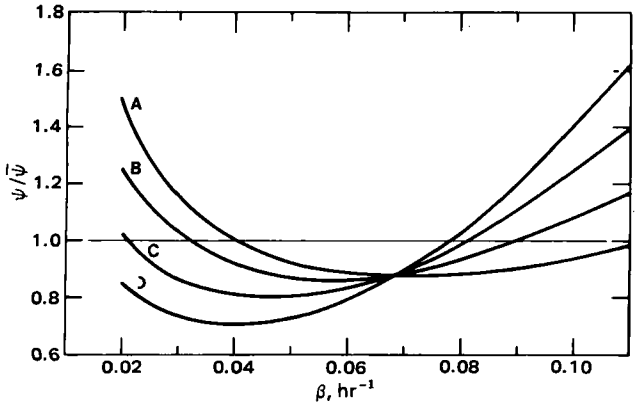

Figure 2—*Relationship between $\psi/\bar{\psi}$ and β for different values of sampling time (t*). α and k_{21} are kept constant at values of 0.888 and 0.375 hr^{-1}, respectively. Key: (A) t* = 12 hr; (B) t* = 16 hr; (C) t* = 20 hr; (D) t* = 24 hr.*

throughout the population by empirically raising the value of ψ in patients who would otherwise tend to be overdosed.

DISCUSSION

The principal purpose of this paper is to examine the single-point maintenance-dose prediction method proposed by Cooper *et al.* for lithium. A more flexible approach has since been described by Sheiner and Beal (17). The single-point method and the Bayesian approach to maintenance-dose selection (17) introduced by Sheiner and Beal have in common a dependence on the knowledge of the distribution of pharmacokinetic parameter values within the population. The Bayesian approach makes use of demographic and pathological information, which is particularly important in the selection of the first dose and in changing the dose as blood level data are obtained. The same sort of information could be incorporated into a single-point method where ψ, t^*, and D^* would be chosen with respect to disease and other factors that affect the relevant pharmacokinetic parameters.

The Bayesian method has additional advantages in that it does not require a sample to be obtained at a particular time and it adjusts the dose as follow-up concentration data are obtained. This method would probably give a more accurate prediction of maintenance dose earlier and with a minimal number of blood samples if the sample was obtained at the time after the first dose which gave the most information about clearance. The optimum t^* considered here and elsewhere (11) corresponds to a blood sample which will serve as the most accurate predictor of maintenance dose required to achieve a desired average concentration at steady state. The proportionality factor between dosing rate and steady-state concentration is clearance. It has been shown empirically and can be shown mathematically that a concentration obtained at t^* will also contain the most information about clearance.

The theory described here is based on the development of a relationship between $1/D_m$ and C^*, which can be described with minimum error by assuming a constant value of a proportionality factor (ψ) throughout the population. If this is done, the error of the method will increase as the extremes of parameter values are approached. A recent report described a case in which a patient with an unusually long half-life and unusually large volume of distribution of lithium was given a dose of lithium carbonate for maintenance of a steady-state concentration of 0.8–1.1 meq/liter which actually led to a steady-state concentration of 2.6 meq/liter and symptoms of toxicity (18). A complete characterization of the pharmacokinetics of lithium in the patient led to the readjustment of his dose to 1050 mg of lithium carbonate (he was given 1800 mg on the basis of the nomogram). Use of this dose led to the attainment of the target steady-state concentration. Substitution of his pharmacokinetic parameter values calculated from the concentration–time plot presented in the report into Eq. 6 led to the calculation of a maintenance dose in close agreement to the 1050-mg dose calculated by classical means. Thus, the failure of the nomogram to predict the correct dose required by this patient was due to his unusual values of β as well as α and k_{21} (all were unusually low). This case illustrates an important limitation of all single-point dose prediction methods: patients with unusual pharmacokinetic parameter values will be improperly dosed. Such methods should therefore be used only as an aid to the selection of a dose that will allow the attainment of a therapeutic concentration of drug with a minimum

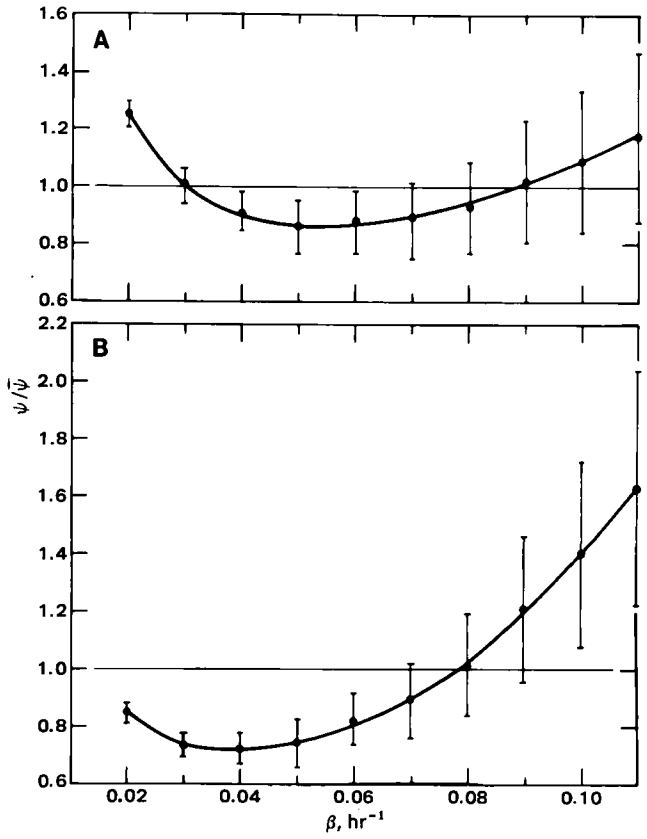

Figure 3—*Relationship between $\psi/\bar{\psi}$ and β for t* = 16 hr (A) and t* = 24 hr (B). Values of α and k_{21} were randomly selected from distributions described in the literature. Bars encompass mean (0) ± 2 SD of the value of the ratio due to variation in the values of α and k_{21}.*

of dosage adjustment. The appropriateness of the dose selected should be confirmed by the determination of concentration after the patient reaches steady state.

The key to the optimization of sampling time described here is the assumption that a single value of ψ will be used for dose prediction purposes for all individuals. The nomogram described by Cooper *et al.* is based on a sampling time 50% longer than the optimum if a constant value of ψ is used. The nomogram is successful because the nonlinearity of the relationship between $1/D_m$ and C^*, when C^* is determined 24 hr after the test dose, is accounted for by using a larger value of ψ in patients with low values of C^*. Such an approach should be possible with other drugs to the extent that low values of C^* correlate with large values of β, rather than large values of volume of distribution. If a low value of C^* is mostly a function of a large volume of distribution, an error due to this parameter will be introduced, which may increase the error beyond that which would be encountered if a constant value of ψ were used.

The theoretically optimum t^* has been shown previously to be the reciprocal of the population mean elimination rate constant based on equations developed for drugs that exhibit a monoexponential decline in plasma concentration. With such drugs, the optimum t^* is, therefore, equal to the harmonic mean of mean residence time (19) in the population. Since mean residence time is a model-independent parameter (its calculation assumes linear kinetics with elimination occurring from the central compartment), it is expected that the harmonic mean of the mean residence time would also be the optimum sampling time for maintenance-dose prediction or estimation of clearance for drugs that exhibit a biexponential decline in plasma concentration.

REFERENCES

(1) T. B. Cooper, P. E. Bergner, and G. M. Simpson, *Am. J. Psych.*, **130**, 601 (1973).

(2) T. B. Cooper and G. M. Simpson, *Am J. Psych.*, **133**, 440 (1976).

(3) T. B. Cooper and G. M. Simpson, *Am J. Psych.*, **135**, 333 (1978).

(4) R. Braithwaite, S. Montgomery, and S. Dawling, *Clin. Pharmacol. Ther.* **23**, 303 (1978).
(5) S. A. Montgomery, R. McAuley, D. B. Montgomery, R. A. Braithwaite, and S. Dawling, *Clin. Pharmacokinet.*, **4**, 129 (1979).
(6) D. J. Brunswick, J. D. Amsterdam, J. Mendels, and S. L. Stern, *Clin. Pharmacol. Ther.*, **25**, 605 (1979).
(7) J. R. Koup, C. M. Sack, A. L. Smith, and M. Gibaldi, *Clin. Pharmacokinet.*, **4**, 460 (1979).
(8) J. R. Koup, C. M. Sack, A. L. Smith, N. N. Neely, and M. Gibaldi, *Clin. Pharmacokinet.*, **6**, 83 (1981).
(9) G. G. Shapiro, J. R. Koup, C. T. Furukawa, W. E. Pierson, M. Gibaldi, D. Futuay, and C. W. Bierman, *Pediatrics*, **69**, 70 (1982).
(10) J. T. Slattery, M. Gibaldi, J. R. Koup, *Clin. Pharmacokinet.*, **5**, 377 (1980).
(11) J. T. Slattery, *J. Pharm. Sci.*, **70**, 1174 (1981).
(12) "Pharmacokinetics," M. Gibaldi and D. Perrier Eds, Dekker, New York, N.Y., 1975, pp. 48–60.
(13) A. Amidsen, *Dan. Med. Bull.*, **22**, 277 (1975).
(14) F. Nielsen-Kudsk and A. Amdisen, *Eur. J. Clin. Pharmacol.*, **16**, 271 (1979).
(15) "Applied Regression Analysis and Other Multivariable Methods," D. G. Kleinbaum and L. L. Kupper, Eds., Duxbury Press, North Scituate, Mass., 1978, pp. 37–50.
(16) J. M. Wilson and J. T. Slattery, *J. Pharm. Sci.*, **72**, in press.
(17) L. B. Scheiner, S. Beal, B. Rosenberg, and V. V. Marathe, *Clin. Pharmacol. Ther.*, **26**, 294 (1979).
(18) F. Gengo, J. Timko, J. D'Antonio, T. A. Ramsey, A. Frazer, and J. Mendels, *J. Clin. Psych.*, **41**, 319 (1980).
(19) J. H. Oppenheimer, H. L. Schwartz, and M. I. Surks, *J. Clin. Endocrin. Metab.*, **41**, 319 (1975).

Corneal Penetration Behavior of β-Blocking Agents I: Physicochemical Factors

RONALD D. SCHOENWALD ˣ and HONG-SHIAN HUANG *

Received July 26, 1982, from the *Pharmaceutics Division, College of Pharmacy, University of Iowa, Iowa City, IA 52242.* Accepted for publication September 16, 1982. *Present Address: National Defense Medical Center, Taipei, Taiwan 107, ROC.

Abstract □ Rabbit corneas were excised and mounted in a chamber to determine the permeability characteristics of a group of β-blocking agents which varied in octanol–water partitioning over a fourfold logarithmic range. From the permeability rate at steady state, permeability coefficients (pH 7.65) were determined. For each drug the distribution coefficient and pK_a were measured, permitting the partition coefficients to be estimated. Various correlations were determined for the log permeability coefficient as a sum of log functions of the partition (or distribution) coefficient, molecular weight, and/or degree of ionization. The best fit, as judged by a high correlation coefficient ($r = 0.9756$) and lack of systematic deviation, was represented by: $\log P_T = 0.623 \log DC - 0.108(\log DC)^2 - 5.0268$.

Keyphrases □ β-Blocking agents—permeability characteristics, excised rabbit corneas, physicochemical factors □ Permeability—β-blocking agents, excised rabbit corneas, physicochemical factors □ Ophthalmic drugs—β-blocking agents, corneal permeability, rabbits, physicochemical factors

Whenever an ophthalmic drug is applied topically to the eye, only a small amount (<10%) actually penetrates the cornea and reaches the internal eye tissues (1–3). Precorneal factors, such as rapid drainage by the nasolacrimal apparatus and noncorneal absorption, account for the poor absorption (4). As a result, optimal absorption depends on achieving a rapid penetration rate across the cornea to minimize the competing, but nonabsorptive rate factors. Rapid penetration either permits a lower dose to be administered or, in the case of an inactive drug, leads to the development of a clinically effective drug.

The penetration potential of a drug with regard to its chemical structure can be assessed by the use of the partition coefficient of the drug. This has been shown for the cornea by Schoenwald and Ward (5) and by Mosher and Mikkelson (6). Schoenwald and Ward (5) determined the permeability rates across excised rabbit corneas for 11 steroids. Permeability coefficients for each steroid were calculated, and their logarithms were plotted against their respective log octanol–water partition coefficients. A parabolic relationship fit the data, with optimal permeability observed at a log partition coefficient of 2.9. Likewise, Mosher and Mikkelson (6) determined the *in vitro* corneal transport of *n*-alkyl-*p*-aminobenzoate ester homologues. For this series a parabolic equation also fit the data; optimal permeability was observed at a log partition coefficient of 2.5–2.6 (*n*-propyl homologue).

Although relative potency is a significant factor, a rapid penetration rate can contribute significantly to effectiveness. For example, prednisolone acetate (1% ophthalmic suspension) has been ranked as the most effective topical anti-inflammatory agent when the epithelium of the inflamed cornea is intact (7), whereas prednisolone (equally potent orally) is not effective topically. The prodrug di-

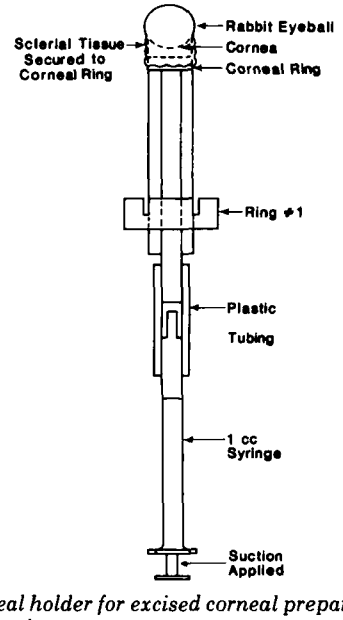

Figure 1—*Corneal holder for excised corneal preparation used in the permeability experiment.*

0022-3549/83/1100-1266$01.00/0

(4) R. Braithwaite, S. Montgomery, and S. Dawling, *Clin. Pharmacol. Ther.* **23**, 303 (1978).
(5) S. A. Montgomery, R. McAuley, D. B. Montgomery, R. A. Braithwaite, and S. Dawling, *Clin. Pharmacokinet.*, **4**, 129 (1979).
(6) D. J. Brunswick, J. D. Amsterdam, J. Mendels, and S. L. Stern, *Clin. Pharmacol. Ther.*, **25**, 605 (1979).
(7) J. R. Koup, C. M. Sack, A. L. Smith, and M. Gibaldi, *Clin. Pharmacokinet.*, **4**, 460 (1979).
(8) J. R. Koup, C. M. Sack, A. L. Smith, N. N. Neely, and M. Gibaldi, *Clin. Pharmacokinet.*, **6**, 83 (1981).
(9) G. G. Shapiro, J. R. Koup, C. T. Furukawa, W. E. Pierson, M. Gibaldi, D. Futuay, and C. W. Bierman, *Pediatrics*, **69**, 70 (1982).
(10) J. T. Slattery, M. Gibaldi, J. R. Koup, *Clin. Pharmacokinet.*, **5**, 377 (1980).
(11) J. T. Slattery, *J. Pharm. Sci.*, **70**, 1174 (1981).
(12) "Pharmacokinetics," M. Gibaldi and D. Perrier Eds, Dekker, New York, N.Y., 1975, pp. 48–60.
(13) A. Amidsen, *Dan. Med. Bull.*, **22**, 277 (1975).
(14) F. Nielsen-Kudsk and A. Amdisen, *Eur. J. Clin. Pharmacol.*, **16**, 271 (1979).
(15) "Applied Regression Analysis and Other Multivariable Methods," D. G. Kleinbaum and L. L. Kupper, Eds., Duxbury Press, North Scituate, Mass., 1978, pp. 37–50.
(16) J. M. Wilson and J. T. Slattery, *J. Pharm. Sci.*, **72**, in press.
(17) L. B. Scheiner, S. Beal, B. Rosenberg, and V. V. Marathe, *Clin. Pharmacol. Ther.*, **26**, 294 (1979).
(18) F. Gengo, J. Timko, J. D'Antonio, T. A. Ramsey, A. Frazer, and J. Mendels, *J. Clin. Psych.*, **41**, 319 (1980).
(19) J. H. Oppenheimer, H. L. Schwartz, and M. I. Surks, *J. Clin. Endocrin. Metab.*, **41**, 319 (1975).

Corneal Penetration Behavior of β-Blocking Agents I: Physicochemical Factors

RONALD D. SCHOENWALD ˣ and HONG-SHIAN HUANG *

Received July 26, 1982, from the *Pharmaceutics Division, College of Pharmacy, University of Iowa, Iowa City, IA 52242.* Accepted for publication September 16, 1982. *Present Address: National Defense Medical Center, Taipei, Taiwan 107, ROC.

Abstract □ Rabbit corneas were excised and mounted in a chamber to determine the permeability characteristics of a group of β-blocking agents which varied in octanol–water partitioning over a fourfold logarithmic range. From the permeability rate at steady state, permeability coefficients (pH 7.65) were determined. For each drug the distribution coefficient and pK_a were measured, permitting the partition coefficients to be estimated. Various correlations were determined for the log permeability coefficient as a sum of log functions of the partition (or distribution) coefficient, molecular weight, and/or degree of ionization. The best fit, as judged by a high correlation coefficient ($r = 0.9756$) and lack of systematic deviation, was represented by: $\log P_T = 0.623 \log DC - 0.108(\log DC)^2 - 5.0268$.

Keyphrases □ β-Blocking agents—permeability characteristics, excised rabbit corneas, physicochemical factors □ Permeability—β-blocking agents, excised rabbit corneas, physicochemical factors □ Ophthalmic drugs—β-blocking agents, corneal permeability, rabbits, physicochemical factors

Whenever an ophthalmic drug is applied topically to the eye, only a small amount (<10%) actually penetrates the cornea and reaches the internal eye tissues (1–3). Precorneal factors, such as rapid drainage by the nasolacrimal apparatus and noncorneal absorption, account for the poor absorption (4). As a result, optimal absorption depends on achieving a rapid penetration rate across the cornea to minimize the competing, but nonabsorptive rate factors. Rapid penetration either permits a lower dose to be administered or, in the case of an inactive drug, leads to the development of a clinically effective drug.

The penetration potential of a drug with regard to its chemical structure can be assessed by the use of the partition coefficient of the drug. This has been shown for the cornea by Schoenwald and Ward (5) and by Mosher and Mikkelson (6). Schoenwald and Ward (5) determined the permeability rates across excised rabbit corneas for 11 steroids. Permeability coefficients for each steroid were calculated, and their logarithms were plotted against their respective log octanol–water partition coefficients. A parabolic relationship fit the data, with optimal permeability observed at a log partition coefficient of 2.9. Likewise, Mosher and Mikkelson (6) determined the *in vitro* corneal transport of *n*-alkyl-*p*-aminobenzoate ester homologues. For this series a parabolic equation also fit the data; optimal permeability was observed at a log partition coefficient of 2.5–2.6 (*n*-propyl homologue).

Although relative potency is a significant factor, a rapid penetration rate can contribute significantly to effectiveness. For example, prednisolone acetate (1% ophthalmic suspension) has been ranked as the most effective topical anti-inflammatory agent when the epithelium of the inflamed cornea is intact (7), whereas prednisolone (equally potent orally) is not effective topically. The prodrug di-

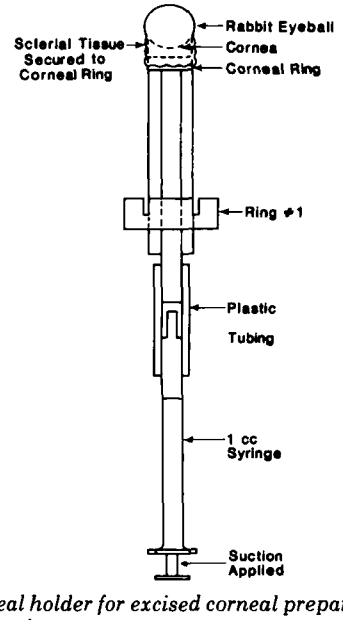

Figure 1—*Corneal holder for excised corneal preparation used in the permeability experiment.*

0022-3549/83/1100-1266$01.00/0

Table I—Chemical Structures, pK_a, and Partition Coefficients of β-Blocking Agents

Structure	Compound	pK_a	PC[a]
Very lipophilic:			
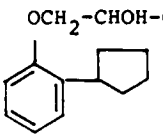	Penbutolol	9.26	14,200.0
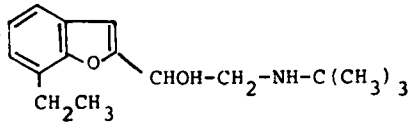	Bufuralol	8.97	4,460.0
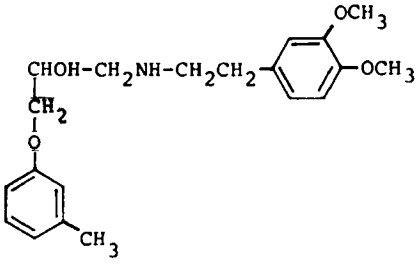	Bevantolol	8.38	1010.0
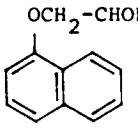	Propranolol	9.23	1640.0
Lipophilic:			
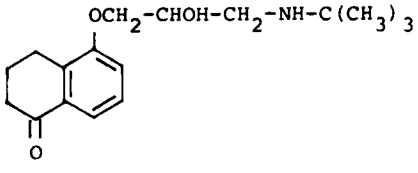	Levbunolol	9.32	249.0
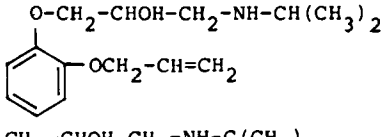	Oxprenolol	9.32	235.0
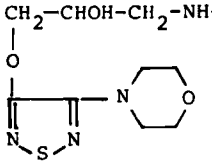	Timolol	9.21	82.0
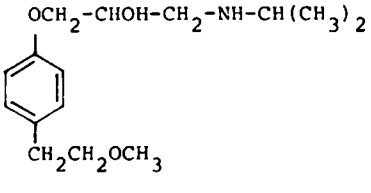	Metoprolol	9.24	76.0
Hydrophilic:			
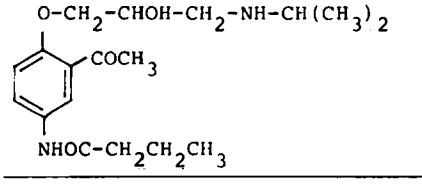	Acebutolol	9.20	59.0

continued

Table I—*Continued*

Structure	Compound	pK_a	PC[a]
Hydrophilic:			
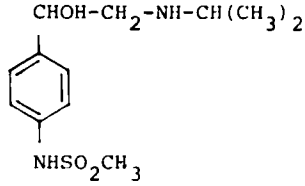	Sotalol	pK_{a1} = 8.15 pK_{a2} = 9.65	0.24
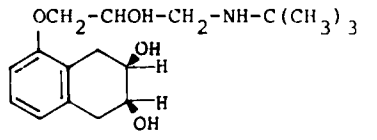	Nadolol	9.39	8.5
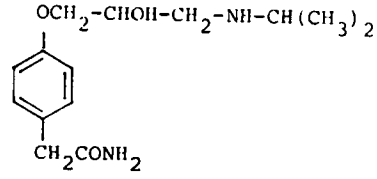	Atenolol	9.32	1.46

[a] Octanol–aqueous partition coefficient; the distribution coefficient was determined at pH 7.4 and 35° and converted through Eq. 2 to PC.

pivefrin is another example of a drug with improved corneal penetration when compared with the parent drug, epinephrine (8). A more rapid penetration rate for the prodrug has led to use of a reduced dosage and the observation of less ocular side effects.

The β-blocking agent timolol was introduced commercially to treat glaucoma following topical instillation of eye drops. Propranolol (9), atenolol (10), metoprolol (11), and practolol (10) also lower intraocular pressure, whereas nadolol and sotalol appear not to (12), even though nadolol is approximately equal in potency to propranolol. The purpose of this study was to compare the permeability of a series of β-blocking agents with a fourfold range in partitioning behavior across excised rabbit corneas to determine if optimal permeability can be identified.

EXPERIMENTAL

Drugs—β-Blocking agents used in the experiments included acebutolol hydrochloride[1], atenolol[2], beventolol hydrochloride[3], bufuralol hydrochloride[4], levbunolol hydrochloride[3], metoprolol tartrate[5], nadolol[6], oxyprenolol hydrochloride[5], penbutolol sulfate[7], propranolol hydrochloride[8], sotalol hydrochloride[9], and timolol maleate[10]. Structures of each drug are shown in Table I.

Potentiometric Titration Method for the Determination of pK_a—A pH meter[11] connected to a titrator[12] and equipped with a combination electrode[13] was used. The titrator was equipped with a 1.0-ml, syringe-type buret and was used for all titrations in the study. The buret was attached to a delivery tip capable of accurately metering 0.005

[1] May & Baker LTD Research Laboratories.
[2] Stuart Pharmaceuticals, Division of ICI Americas Inc., Wilmington, Del.
[3] Warner-Lambert Company, Pharmaceutical Research Division, Ann Arbor, Mich.
[4] Roche Products LTD, Research Department.
[5] CIBA Pharmaceutical Co., Division of CIBA-GEIGY Corp., Summit, N.J.
[6] E. R. Squibb & Sons, Inc., Princeton, N.J.
[7] Hoechst-Roussel Pharmaceuticals, Inc., Somerville, N.J.
[8] Ayerst Laboratories, Inc., New York, N.Y.
[9] Mead Johnson & Company, Evansville, Ind.
[10] Merck Sharp & Dohme Research Lab, Division of Merck & Co., Inc., Rahway, N.J.
[11] Model 620, Fisher Accumet pH meter.
[12] Metrohm Multi-Dosimat E415, Herisau, Switzerland.
[13] Metrohm AG 9100, Herisau, Switzerland.

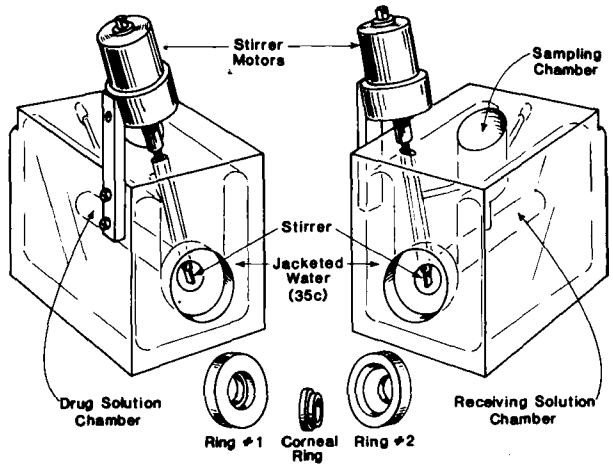

Figure 2—*Modified perfusion chamber with the installation of two stirrers; the corneal rings and chambers are also pictured.*

ml of titrant into the titration cell. The cell had a capacity of 50 ml and was surrounded by a jacket through which 35° water was circulating. A 0.29-mg/ml solution (1 m*M*) of a salt of each β-blocking agent was prepared for titration. In the event that the drug species was a free base, an equivalent amount of hydrochloric acid was added. For some highly lipophilic drugs, such as penbutolol and bufuralol, a concentration as low as 100 μg/ml was used to prevent precipitation during drug titration.

An aliquot (25–40 ml) of drug solution was accurately transferred to the titration cell, maintained at 35°. Nitrogen continuously flowed over the sample solution to prevent carbon dioxide absorption from the surrounding air. At each titration interval, a volume of 0.005–0.02 ml of titrant was added while stirring. For the majority of β-blocking agents, which have pK_a values of 8–9.4 at 35°, the titration usually started at pH ~6 and ended at pH 10 or 11. A modified Gran plot was used to determine the K_a for each compound (13) with the exception of sotalol, which contained two K_a values determined by the Speakman method (14).

Determination of Distribution Coefficients (15)—Sorensen's phosphate buffer (pH 7.38) was prepared from monobasic potassium phosphate and dibasic sodium phosphate. The buffer and octanol were mutually saturated at 35° before use. The distribution coefficient at 35° was determined by dissolving drug in the aqueous-buffer phase and shaking intermittently with octanol at 35° for 5 hr to reach a distribution equilibrium. The volume ratio of octanol and buffer depended on the lipophilicity of the drug. The volumes of each phase were chosen so that drug concentration in the aqueous phase, before and after extraction, could be measured by high-performance liquid chromatography (HPLC). Centrifugation was used to separate the two phases.

The distribution coefficient (DC) was calculated by:

$$DC = \frac{(C_b - C_a)V_w}{C_b V_o} \qquad \text{(Eq. 1)}$$

where C_b and C_a represent the concentrations in the aqueous-buffer phase before and after distribution, respectively; V_w represents the volume of the aqueous phase; and V_o, the volume of the octanol phase. The partition coefficient (PC) was calculated from the distribution coefficient by:

$$PC = DC\left(1 + \frac{1}{\text{antilog}\,(pH - pK_a)}\right) \qquad \text{(Eq. 2)}$$

The pH was measured from the buffered phase at 35° after distribution was complete. All distribution coefficients reported here were measured at pH 7.4, but through the use of Eq. 2 were converted to pH 7.65, the pH of the excised corneal experiments.

Excised Cornea Procedure—Male New Zealand White rabbits[14], weighing 1.6–2.0 kg each, were sacrificed by injecting a bolus of air into the marginal ear vein. The intact eye, along with the lids and conjunctival sac, was then enucleated. The exposed cornea of the enucleated eye was carefully placed on a corneal holder, which maintained the cornea curvature and held the eye in place (5, 16, 17). Various tissues of the eye were dissected leaving the cornea, a small ring of scleral tissue, and the palpebral conjunctiva, which was tied to the corneal ring (Fig. 1).

The conjunctival and scleral tissue served as a gasket and permitted the cornea to be suspended within the corneal ring, which was then positioned between rings 1 and 2 and placed in the center of the perfusion chamber. The chamber was made from acrylic plastic[15] and was jacketed to maintain the cornea and the perfusion solution at 35° (5, 16, 17).

Bicarbonated Ringer's solution was modified (17) to preserve tissue integrity of an excised cornea over 6 hr and used throughout the perfusion studies. It was prepared in two parts: Part I was composed of sodium chloride (12.4 g/liter), potassium chloride (0.716 g/liter), monobasic sodium phosphate monohydrate (0.206 g/liter), and sodium bicarbonate (4.908 g/liter); part II was composed of calcium chloride dihydrate (0.230 g/liter), magnesium chloride hexahydrate (0.318 g/liter), glucose (1.80 g/liter), and oxidized glutathione[16] (0.184 g/liter). Both parts were stored in the refrigerator and were used in ~3 weeks to prevent mold growth. Equal volumes of parts I and II were mixed prior to use.

Within 20–40 min of death, the cornea was mounted and clamped between two cylindrical compartments of the perfusion chamber. A measured volume (7.0 ml) of bicarbonated Ringer's solution was added first to the endothelial side as the receiving solution to prevent the cornea from buckling. An equal volume of solution containing a β-blocking agent was then added to the epithelial side as the drug solution. The perfusion chamber system was designed in such a way that the height of the receiving solution was slightly higher than that of the drug solution to ensure that the cornea would not buckle during the course of the experiment. A mixture of O_2–CO_2 (95:5) was bubbled through the fluids in both chambers for 10 min to achieve a pH of 7.65 before being added to the perfusion chamber. Circulation of fluid inside each half chamber was induced immediately by bubbling the same gas mixture through at a rate of three to five bubbles/sec to maintain the solution at a constant pH of 7.65.

Samples ranged from 0.1 to 0.5 ml depending on the assay sensitivity of each drug. Samples were withdrawn from the receiving chamber (*i.e.*, endothelial side) over a 4-hr period. An equal volume of solution was immediately added to the receiving solution to maintain a constant volume. The first sample was withdrawn within 2 min after starting the permeation and served as a control to detect leakage and rapid penetration. Subsequent samples were taken approximately every 40 min through the 4-hr period.

The sampling method for the corneal permeability experiments of levbunolol and nadolol varied from other drugs in that equal volumes of solutions (0.1 ml) were removed from both sides of cornea. In this way, equal volumes on both sides were maintained throughout the experiment.

After each permeability experiment, the cornea was trimmed of excess scleral tissue and conjunctiva, weighed, and dried in an oven overnight at 103°. After each cornea was dried, it was reweighed so that the hydration level of the wet cornea could be determined. The normal cornea has a hydration level of 76–80% (18). If manipulation of the cornea or if the drug itself led to damage of the epithelium and/or endothelium, then the hydration level would rise (83–92%) and the data were discarded.

Determination of Aqueous Diffusional Layer Resistance in the Perfusion Chamber—Fluid circulation in the chamber was provided

Table II—Experimental Conditions for the HPLC Assay of β-Blocking Agents

Drug	Column[a]	Wavelength, nm	Methanol, %[b]	Flow Rate, ml/min
Acebutolol	A	254	20, 38	2
Atenolol	A	254	20, 7.5	2
Bevantolol	B	254	28, 30	2
Bufuralol	B	254	28, 30	2
Levbunolol	B	254	28, 47	2
Metoprolol	A	280	35, 35	2
Nadolol	A	254	20, 31	2
Oxprenolol	B	280	22, 15	2.5
Penbutolol	B	254	25, 62.2	2
Propranolol	B	254	28, 23	2
Sotalol	A	254	42[c], 30	2.5
Timolol	A	254	42[c], 30	2.5

[a] (A) μ-Bondapak C18; (B) μ-Bondapak CN. Waters Associates, Milford, Mass. [b] The two numbers represent the percentage of methanol in the mobile phase for partitioning and corneal permeability determinations, respectively; the aqueous phase contained 1.5% acetic acid and was adjusted to pH 4 by sodium hydroxide. [c] The aqueous phase consisted of 58% 0.005 *M* heptanesulfonic acid and 1% acetic acid; the flow rate was 2.0 ml/min for these conditions.

[14] Morrison Rabbitry, West Branch, Iowa.

[15] Medical Research Instruments, University of Iowa, Iowa City, Iowa.

[16] Aldrich Chemical Co., Inc., Milwaukee, Wis.

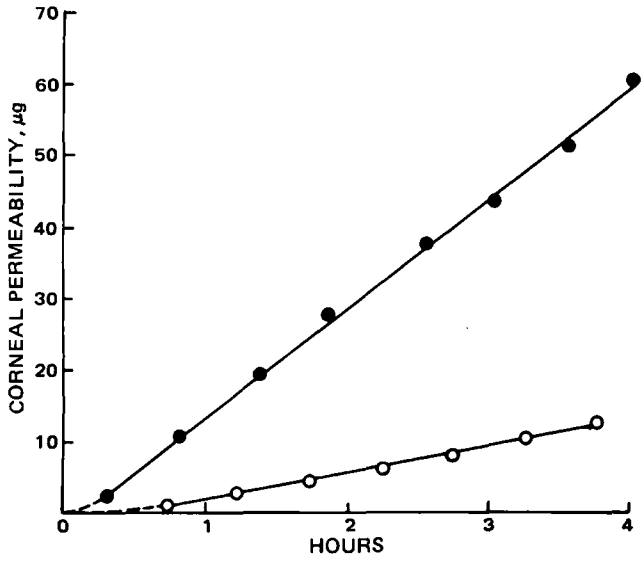

Figure 3—*Permeability rate of propranolol (●) and atenolol (○) across single excised rabbit corneas including linear regression lines; the initial concentrations for propranolol and atenolol were 85 and 2000 μg/ml, respectively.*

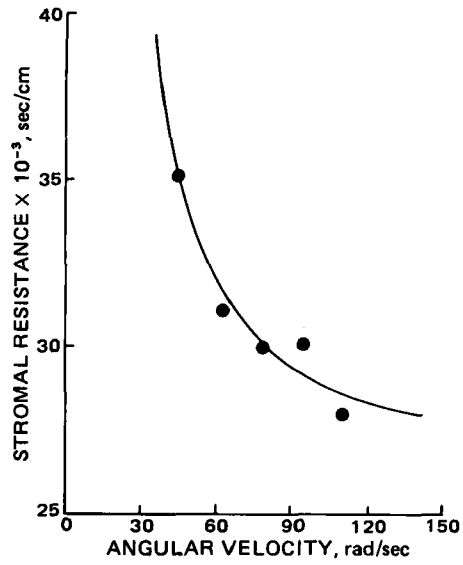

Figure 4—*Nonlinear regression results of the diffusional resistance of atenolol to stirring rate through excised rabbit stromal preparations. Each point is the average of 3–6 determinations; standard deviations were ≤10% of the mean.*

by maintaining a rate of three to five gas bubbles/sec. This maintains good mixing within each half chamber, as can be shown by adding a drop of colored solution into either half of the chamber and observing the homogeneous color that occurs in <1 min. However, to accurately determine the resistance of the cornea, it was necessary to detect and measure the magnitude of aqueous diffusional layer resistance, R_{aq}; consequently, the stirring was modified for these experiments.

The perfusion chamber was modified by installing two stirrers, one on each side of the cornea, with the center of each stirrer affixed 1 cm from the center of the corneal ring. Figure 2 depicts the modified perfusion chamber and rings used in mounting the cornea. In preliminary experiments it was observed that different rates of stirring induced varying degrees of swelling due to mechanical injury of the epithelium and endothelium.

An important purpose of the epithelium and endothelium is to control the thickness of the cornea by maintaining hydration levels at ~ 78%. By completely removing the epithelium and endothelium, the remaining stromal layer reached a constant and maximal thickness within the first 30 min of stirring such that subsequent changes in the stirring rate had no effect. The epithelium was removed by scraping with the blunt end of a scalpel blade. The endothelium was gently rubbed off with a cotton-tipped applicator (19). The removal of endothelium could be detected with the aid of a dissecting microscope. The epithelium was removed immediately following enucleation; the endothelium was removed just prior to mounting in the perfusion chamber. Atenolol (500 μg/ml) was chosen as the diffusing substance for these experiments. Since the aqueous diffusional barrier is independent of drug, these results were interpreted for the other β-blocking agents as well.

Once drug was placed adjacent to the cornea, the stirring speed was increased in steps every 30 min over a 4-hr period. The apparent permeability coefficients were determined for each 30-min increment. A sample was removed for atenolol analysis at the beginning and end of each 30-min period; both samples were used to calculate the permeability coefficient for each stirring speed. To minimize biological variability, each cornea was used to generate five or six permeability coefficients over a period of 4 hr.

Drug Assay—An HPLC method was used for analysis of each drug. The HPLC system included an injector[17], solvent delivery system, UV-absorption detector[17], column[18], and recorder[19]. The injector was equipped with different-sized loops, ranging from 50 μl to 200 ml, which enabled the injection of an accurate volume of sample solution. A solution of known concentration was used as an external standard. Each sample solution was divided so that two injections could be made and the results averaged.

[17] Model 7125 injector; Rheodyne, Cotati, CA 94928.
[18] M-6000 A solvent delivery system, Model 440 absorbance detector, μ-Bondapak C18, and μ-Bondapak CN Columns; Waters Associates, Milford, MA 01757.
[19] Model 5211-1; OmniScribe; Houston Instruments, Austin, Tex.

The mobile phases consisted of varying ratios of methanol and deaerated, deionized water containing 1.5% acetic acid, adjusted to pH 4 using sodium hydroxide. One exception was the mobile phase for sotalol and timolol, which utilized 0.005 *M* heptanesulfonic acid (to increase retention time) and 1% acetic acid. Table II lists the types of columns used, wavelengths at which UV measurements were made, methanol content of the mobile phase, and mobile phase flow rate. Methanol percentages in the mobile phases varied depending on whether partitioning or permeability experiments had been conducted. Drug solutions withdrawn from the endothelial side following corneal permeability contain polar extracts from the cornea which were eluted from the column within 1–3 min. In all experiments the retention times for the drugs were between 4 and 12 min. Linearity existed over the concentrations employed for each β-blocking agent (correlation coefficients >0.99).

Calculation of Permeability Coefficients—The apparent permeability coefficient (P_{app}, cm/sec) was determined by (19):

$$P_{app} = \frac{\Delta Q}{\Delta t(3600)AC_0} \qquad \text{(Eq. 3)}$$

where the term $\Delta Q/\Delta t$ is the permeability rate (*i.e.*, steady-state flux, μg/hr) of drug across each excised cornea, C_0 is the initial drug concentration (μg/ml), A is the corneal surface area (cm²), and 3600 is the conversion of hours to seconds. Corrections of C_0 were made to account for the sample volume removed over time and subsequently replaced with blank solution.

The corneal thickness increases with hydration, and the permeability coefficient is inversely proportional to barrier thickness. Therefore, it was important to determine corneal thicknesses. For a 2-kg rabbit, the corneal thickness (h) can be determined by:

$$h\ (\text{cm}) = \frac{0.42 + \text{H}}{100} \qquad \text{(Eq. 4)}$$

where H is the mg of water/mg of dry tissue (20). When stromal thicknesses were swollen due to epithelial and endothelial removal, the stroma resistances, $R_{str,swl}$, that were used to assess the aqueous diffusional barrier were corrected to the normal stromal thickness as existing in intact cornea (*i.e.*, $R_{str,int}$) by:

$$R_{str,int} = R_{str,swl}\left(\frac{h_{int}}{h_{swl}}\right) \qquad \text{(Eq. 5)}$$

where subscripts int and swl represent intact cornea and swollen stroma, respectively.

RESULTS AND DISCUSSION

The pK_a and partition coefficients of each β-blocking agent are listed in Table I. Although the aromatic substituents varied substantially for the series, these were too far removed from the amino group to exert much

of an effect on the pK_a values. Therefore, most pK_a values were within a narrow range (8.97–9.65). The pK_a of bevantolol was slightly lower (8.38) because of the electron-withdrawing effect of the ethoxybenzyl substituent. Sotalol has two pK_a values, 8.15 and 9.72, which are close to one another and compare reasonably well to the values of 8.30 and 9.80 published by Garrett and Schnelle (21) using the potentiometric titration method at 25°. The anilino group in sotalol acts as a weak acid as a result of the electron-withdrawing effect of the neighboring sulfonyl group. Ionization of the anilino group accounts for spectral shifts (21) and correlates with the pK_a of 8.15. The second pK_a, 9.72, was then assigned to the protonated amine group in the alkyl side chain of sotalol.

The distribution coefficients obtained from the extraction method using octanol and Sorenson's buffer varied over a fourfold log range. The range in partitioning behavior of the series is a consequence of the differences in aromatic substitution. The partitioning results permitted the compounds to be grouped as very lipophilic, lipophilic, or hydrophilic, classifications which were predictable from structural considerations. In addition to the amino group, the hydrophilic compounds also contained relatively polar substituents on the aromatic ring. Therefore, hydrogen bonding interactions with water are greater for atenolol and acebutolol, which contain amido groups, for nadolol, which contains a dihydroxy function and for sotalol, which contains a sulfonamido moiety. The very lipophilic compounds, on the other hand, contain hydrophobic substituents. The cyclopentyl group on the benzene ring gives penbutolol a high distribution and partition coefficient, whereas the furanyl group imparts lipophilicity to bufuralol. The ethoxybenzyl substituent in bevantolol not only lowers its pK_a, but also increases its lipophilicity. The high partition coefficient of propranolol is a result of the high lipophilic contribution of naphthalene. Based on the partitioning results of the very lipophilic and hydrophilic compounds, the remaining compounds (levbunolol, oxyprenolol, timolol, and metoprolol) appear to contain substituents of an intermediate nature as far as polarity.

Corneal Permeability—The permeability coefficients of each β-blocking agent were obtained by linear regression of the steady-state flux. Figure 3 shows a plot of Q *versus* t for propranolol and atenolol across excised rabbit corneas. The data points closely fit the least-square regression line once steady state has been reached. The lag time, defined by the linear intercept on the time axis, is related to the time required to reach steady-state permeation; more specifically, it is inversely related to the permeability coefficient. Consequently, the more rapidly penetrating compounds will have a shorter lag time and a greater steady-state flux. The slope of the straight line ($\Delta Q/\Delta t$), was substituted into Eq. 3 to obtain the apparent permeability coefficient. The apparent permeability coefficient also contains any aqueous diffusional layers that may exist on each side of the cornea.

Mathematical Model Relating Stirring Rate to Aqueous Diffusional Layer Resistance—The total diffusional resistance, R_{app}, through a multilayered barrier is represented by (22):

$$R_{app} = \frac{1}{P_{app}} = \sum_{i=1}^{n} R_i = \sum \frac{h_i}{D_i A(\mathrm{PC})_i} \qquad \text{(Eq. 6)}$$

where i represents each homogeneous barrier in series, n represents the total number of barriers, h represents barrier thickness, A represents surface area, D represents the diffusion coefficient, and PC represents the partition coefficient (22). With regard to significant diffusional layers, the rabbit cornea possesses two main tissue types: the lipophilic epithelium and endothelium, and the hydrophilic stroma. Assuming the existence of an aqueous diffusional barrier, the apparent resistance of the cornea can be considered as layers in series (23, 24) or:

$$R_{app} = \frac{1}{P_{app}} = R_{epi} + R_{str} + R_{endo} + R_{aq} \qquad \text{(Eq. 7)}$$

or

$$R_{app} = R_T + R_{aq} \qquad \text{(Eq. 8)}$$

where R_{aq} represents the sum of aqueous diffusional resistances on each side of the cornea and R_T represents the sum of the resistances of the corneal layers (epithelium, stroma, and endothelium).

According to the Nernst theory (25), there is a thin layer of static liquid of thickness h_{aq} immediately adjacent to a solid body. Outside of the static liquid layer is the well-stirred bulk solution. Experimental determinations have shown that the aqueous diffusional layer thickness, h_{aq}, can be expressed as:

$$h_{aq} = V^{-n} \qquad \text{(Eq. 9)}$$

where V is the velocity of the moving liquid. The exponent n depends on the experimental conditions ranging from $n = 0.33$ to ≥ 1. The thickness measurements representing the diffusional layer are apparent and not real. For example, experimental measurements have shown that the liquid retains its mobility down to a distance from the solid surface smaller than h_{aq}. Despite the fact that the Nernst theory may not exactly represent the diffusional behavior at the interface of liquid and solid, it can be used empirically to calculate R_{aq} (25).

In determining the resistance of the β-blocking agents across excised rabbit corneas within the stirred perfusion chamber, the following equation, which combines Eqs. 6–9, was considered:

$$R_{app} = R_{str} + \frac{h_{aq1}}{DA(\mathrm{PC})} + \frac{h_{aq2}}{DA(\mathrm{PC})} \qquad \text{(Eq. 10)}$$

where h_{aq1} and h_{aq2} are the aqueous diffusional layer thicknesses on each side of the mounted cornea at a given stirring rate, and R_{str} represents the membrane resistance for the stroma. R_{app} is measured experimentally at a specific stirring rate, *i.e.*, $1/P_{app}$.

By assigning $h_{aq} = h_{aq1} + h_{aq2}$ and substituting V^{-n} for h_{aq}, then Eq. 10 can be expressed as:

$$R_{app} = R_{str} + \frac{V^{-n}}{DA(\mathrm{PC})} \qquad \text{(Eq. 11)}$$

In the modified perfusion chamber, the stirrer is at the center of a circle 1 cm in diameter which contacts tangentially with the membrane and the perfusion chamber wall. Assuming that the liquid velocity tangential to the membrane, V, is proportional to the angular velocity of stirring, v, then Eq. 9 becomes:

$$R_{app} = R_{str} + \frac{(mv)^{-n}}{DA(\mathrm{PC})} \qquad \text{(Eq. 12)}$$

where m is a proportionality factor between the liquid velocity (cm/sec) and the angular velocity (rad/sec)[20]. To perform the nonlinear regression analysis the diffusion coefficient (D) was approximated by 1×10^{-5} cm²/sec, an appropriate estimate for compounds of 200–300 molecular weight (22); PC was assigned a value of 1 for the aqueous system, and A was assigned a value 1.087 cm², which represented the surface area of the cornea used throughout the study. The remaining unknown parameter values (R_T, m, and n) were determined from the nonlinear regression analysis[21]. Figure 4 shows the results for atenolol permeation through excised stromal preparations with stirring rates varying from 425 to 1050 rpm. The computer-generated parameter values substituted into Eq. 10 become:

$$R_{app} = 26.8 \times 10^3 + 100{,}000\ (0.1006v)^{-1.67} \qquad \text{(Eq. 13)}$$

where 26.8×10^3 sec/cm represents the intrinsic stromal resistance, R_{str}. The apparent stromal resistance to atenolol permeation was 30.5×10^3 sec/cm. This latter value represents the experimental conditions for the perfusion chamber when stirred with the bubbling action of O_2–CO_2. The difference between the two resistances ($R_{app} - R_{str}$) is 3.7×10^3 sec/cm and represents the aqueous diffusional layer resistance, R_{aq}. This value was used in determining the intrinsic membrane resistances for the other β-blocking agents.

Permeability *versus* Partitioning Correlations—Figure 5 shows a plot of log P_T [22] against log PC; Table III contains the calculated parameter values. The data, although somewhat scattered, shows a plateau region for the very lipophilic compounds (propranolol, bufuralol, bevantolol, and penbutolol). The rate-determining factor responsible for the plateau region is not a result of the aqueous diffusion layer, since its contribution was subtracted from the experimentally determined permeability coefficients. The permeability rate is probably controlled by the hydrophilic stroma for these very lipophilic compounds. The relatively poor permeability shown for the hydrophilic compounds nadolol and sotalol possibly explains their poor potential for lowering intraocular pressure.

Multiple regression analyses[23] (26) were performed on the data to find the best set of parameters to describe the change in log P_T with a change in either log PC or log DC. Although the ranges in molecular weight and pK_a were relatively narrow for the β-blocking agents selected for study,

[20] rpm was converted to rad/sec by: rad/sec = rpm$(2\pi)/60$.

[21] Nonlinear regression was performed using the BMDP3R programs on an IBM370, at the University of Iowa Computer Center, University of Iowa, Iowa City, IA 52242.

[22] P_T represents the permeability coefficient across the intact excised rabbit cornea; $P_T = 1/R_T$.

[23] Multiple linear regression was performed using the BMDP1R, BMDP2R, and BMDP9R regression programs on an IBM370 computer.

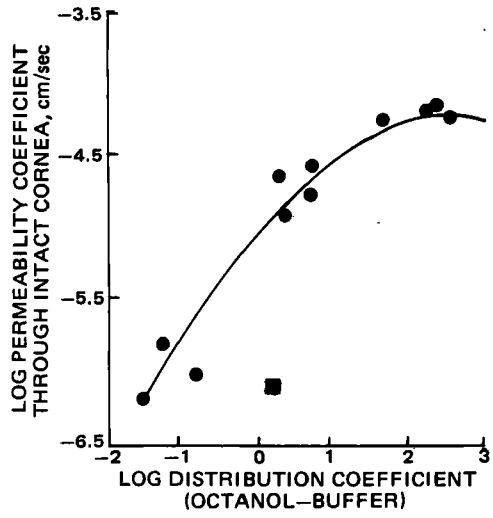

Figure 5—*Log–log plot of permeability coefficient (pH 7.65) and distribution coefficient (pH 7.65). The regression curve is represented by: log P_T = 0.623 log DC − 0.108 (log DC)^2 − 5.0268, where r = 0.9756 and* n = *11; acebutolol (■) is included in the figure, but not in the regression curve.*

a log MW term and a log DI[24] term were included in the analysis. Molecular weight (MW) is inversely related to diffusion and has been shown to improve correlations of this type (27, 28). Because of the plateau region (Fig. 5), a (log PC)^2 or (log DC)^2 term was also included. All possible subsets were analyzed, beginning with the intercept plus one parameter, then the intercept plus two parameters, *etc.*, up to the single set representing the intercept plus the maximum of four parameters. The correlation coefficient (r) and systematic deviation were used as the criteria to judge the best fit. The best fit for log P_T was represented as a function of all the parameters:

$$\log P_T = 1.01 \log PC - 0.115(\log PC)^2 - 5.64 \log MW - 10.4 \log DI + 7.27 \quad \text{(Eq. 14)}$$

$$r = 0.9272 \qquad p = 0.0041 \qquad n = 12$$

Both molecular weight and degree of ionization showed the expected inverse relationship to permeability. However, with either the molecular weight or degree of ionization term omitted from the regression analysis, the correlation coefficient was reduced only minimally to 0.8989 or 0.8678, respectively. With both molecular weight and degree of ionization removed, the correlation coefficient was 0.8560. With only the log PC term and the intercept, the regression analysis yielded a correlation coefficient of 0.8523. This latter linear regression line, however, shows systematic deviation at the plateau region and was not considered an acceptable fit to the data.

When DC was substituted for PC the multiple regression analyses produced an equally good fit:

$$\log P_T = 0.681 \log DC - 0.123(\log DC)^2 - 5.04 \log MW - 2.64 \log DI + 7.22 \quad \text{(Eq. 15)}$$

$$r = 0.9282 \qquad p = 0.0040 \qquad n = 12$$

When the degree of ionization was removed from consideration in Eq. 15, the correlation coefficient was reduced slightly to 0.9223. The lack of improvement from considering the degree of ionization is understandable, since the distribution and permeability coefficients represent the data at the same pH. By excluding the molecular weight term and (log DC)^2, the correlation coefficient was 0.8908 illustrating the small, but necessary, contribution of the squared term when systematic deviation is considered.

The hydrophilic acebutolol deviated the most from any regression line. By considering acebutolol as an outlier and excluding it from the regression analysis, the correlation coefficients increased. For example, the best regression lines yielded:

$$\log P_T = 0.972 \log PC - 0.112(\log PC)^2 - 2.71 \log MW - 9.26 \log DI + 0.219 \quad \text{(Eq. 16)}$$

[24] DI represents degree of ionization and was calculated from: DI = 1/[1 + antilog (pH − pK_a)].

Table III—Permeability Coefficients and Physical Constants of β-Blocking Agents[a]

Drug	log P_T, cm/sec	log DC	log PC	log MW	log DI
Penbutolol	−4.22	2.53	4.15	2.46	−0.0106
Bufuralol	−4.14	2.31	3.65	2.44	−0.0200
Bevantolol	−4.17	2.19	3.00	2.50	−0.0740
Propranolol	−4.24	1.62	3.21	2.41	−0.0114
Levbunolol	−4.76	0.72	2.40	2.51	−0.0092
Oxprenolol	−4.56	0.69	2.37	2.42	−0.0092
Timolol	−4.91	0.34	1.91	2.49	−0.0119
Metoprolol	−4.62	0.28	1.88	2.50	−0.0110
Acebutolol	−6.07	0.20	1.77	2.52	−0.0119
Nadolol	−5.99	−0.82	0.93	2.49	−0.0079
Sotalol	−5.79	−1.25	−0.62	2.43	−0.0040
Atenolol	−6.17	−1.52	0.16	2.42	−0.0092

[a] P_T represents the permeability coefficient across the intact excised rabbit cornea; DC represents distribution coefficient; PC represents partition coefficient; MW represents molecular weight; DI represents degree of ionization.

$$r = 0.9696 \qquad p = 0.0008 \qquad n = 11$$

$$\log P_T = 0.623 \log DC - 0.108(\log DC)^2 - 5.0268 \quad \text{(Eq. 17)}$$

$$r = 0.9756 \qquad p < 0.00009 \qquad n = 11$$

Equation 17 predicts an optimum log DC value of 2.88, determined by setting d log P_T/d log DC equal to zero and solving for log DC. However, there is no experimental evidence that a parabola would best describe the data. Compounds of greater lipophilicity than penbutolol could not be obtained to test this phenomenon.

Although correlations of this type are helpful in predicting useful molecular modifications, extrapolation to *in vivo* ophthalmic bioavailability must take into consideration solubility, the short residence time of instilled drops in the eye, and rapid metabolism or poor distribution to the target tissue. For example, a drug may have ideal partitioning behavior, but if it is not soluble, its concentration in tears will be too low to achieve an adequate penetration rate since the penetration rate is equal to the permeability coefficient multiplied by tear concentration. If a suspension is formulated because of the poor drug solubility, expulsion of the particles by the eye may take place before solubilization occurs, resulting in lower bioavailability.

REFERENCES

(1) R. Lazare and M. Horlington, *Exp. Eye Res.*, **21**, 281 (1975).

(2) T. F. Patton and J. R. Robinson, *J. Pharm. Sci.*, **65**, 1295 (1976).

(3) H. Benson, *Arch Ophthalmol.*, **91**, 313 (1974).

(4) V. H.-L. Lee and J. R. Robinson, *J. Pharm. Sci.*, **68**, 673 (1979).

(5) R. D. Schoenwald and R. L. Ward, *J. Pharm. Sci.*, **67**, 786 (1978).

(6) G. L. Mosher and T. J. Mikkelson, *Int. J. Pharm.*, **2**, 239 (1979).

(7) H. M. Leibowitz and A. Kupferman, *Invest. Ophthalmol.*, **13**, 757 (1974).

(8) A. I. Mandell and S. M. Podos, "Dipivalyl Epinephrine (DPE): A New Pro-Drug in the Treatment of Glaucoma," in "Symposium of Ocular Therapy," Vol. 10, Wiley, 1977.

(9) J. Vale, A. C. Gibbs, and C. I. Phillips, *Br. J. Ophthalmol.*, **56**, 770 (1972).

(10) K. Wettrell, *Acta Ophthalmol., Suppl.*, 134 (1977).

(11) N. V. Neilsen, *Acta Ophthalmol.*, **59**, 495 (1981).

(12) M. V. W. Bergamini, J. Anderson, V. J. Rajadhyaksha, and R. Schoenwald, "Diacetyl Nadolol and Triacetyl Nadolol: Potential Prodrugs of Nadolol with Ocular Beta Blocking Activity," presented at the Association for Research and Vision in Ophthalmology meeting, Sarasata, Fla., May 1982.

(13) F. J. C. Rossotti and H. Rossotti, Jr. *Chem. Ed.*, **42**, 375 (1965).

(14) J. C. Speakman, *J. Am. Chem. Soc.*, **62**, 855 (1940).

(15) C. Hansch, in "Strategy of Drug Design," Appendix I W. P. Purcell, G. E. Bass and J. M. Clayton, Eds, Wiley, New York, N.Y., 1973.

(16) H. F. Edelhauser, J. R. Hoffert and P. O. Fromm, *Invest. Ophthalmol.*, **4**, 290 (1965).

(17) W. J. O'Brien and H. F. Edelhauser, *Invest. Ophthalmol. Visual Sci.*, **16**, 1093 (1977).

(18) D. M. Maurice and M. V. Riley, in "Biochemistry of the Eye," C. N. Graymore, Ed., Academic, London and New York, 1970, pp. 6–16.
(19) J. H. Kim, K. Green, M. Martinez, and D. Paton, *Exp. Eye Res.*, **12**, 231 (1971).
(20) B. O. Hedbys and S. Mishima, *Exp. Eye Res.*, **5**, 221 (1966).
(21) E. R. Garrett and K. Schnelle, *J. Pharm. Sci.*, **60**, 833 (1971).
(22) G. L. Flynn, S. H. Yalkowsky, and T. J. Roseman, *J. Pharm. Sci.*, **63**, 479 (1974).
(23) I. Fatt in "Physiology of the Eye," Butterworth, Woburn, Mass., 1978, pp. 114–121.
(24) R. D. Schoenwald and J. A. Houseman, *Biopharm. Drug Dispos.*, (1982), in press.
(25) V. G. Levich, in "Physicochemical Hydrodynamics," Prentice Hall, Englewood Cliffs, N.J., 1962, pp. 40–46.
(26) N. Draper and H. Smith, in "Applied Regression Analysis," 2nd ed., Wiley, New York, N.Y., 1981, pp. 294–312.
(27) E. J. Lien and P. H. Wang, *J. Pharm. Sci.*, **69**, 648 (1980).
(28) E. J. Lien, A. A. Alhaider, and V. H.-L. Lee, Jr. *Parenter. Sci. Technol.*, **36**, 86 (1982).

ACKNOWLEDGMENTS

This work was abstracted in part from a doctoral dissertation submitted by H. S. Huang and supported in part by Allergan Pharmaceuticals, Irvine, CA 92713.

Corneal Penetration Behavior of β-Blocking Agents II: Assessment of Barrier Contributions

HONG-SHIAN HUANG *, RONALD D. SCHOENWALD ˣ, and JOHN L. LACH

Received July 26, 1982, from the *Pharmaceutics Division, College of Pharmacy, University of Iowa, Iowa City, IA 52242.* Accepted for publication September 16, 1982. *Present Address: National Defense Medical Center, P.O. Box 8244-14, Taipei, Taiwan 107, ROC.

Abstract □ Rabbit corneas were excised and mounted in a chamber to determine the permeability characteristics of a group of β-blocking agents. By measuring the permeability rate of each drug across intact cornea, stroma alone, epithelium–stroma, and stroma–endothelium, it was possible to determine the resistance to penetration for each corneal layer. The reciprocal of the sum of resistances for the epithelium, stroma, and endothelium equaled the experimentally determined permeability coefficient for the intact cornea (104 ± 6.0%). Thus, the penetration of β-blocking agents through the excised rabbit cornea could be treated as three barriers in series. For hydrophilic compounds, the epithelium was the rate-determining barrier. The endothelium offered less resistance, whereas the stroma offered only very minimal resistance. The lipophilic compounds penetrated the excised cornea more rapidly. However, the stroma became rate-determining for the most lipophilic compounds (penbutolol, bufuralol, bevantolol, and propranolol). Although the octanol–buffer (pH 7.65) distribution coefficient of these compounds varied over a fourfold logarithmic range, the permeability coefficient was considered nearly constant [3.4×10^{-5} (±0.34) cm/sec] for stroma. Also, the ratios of tortuosity to porosity for the stromal layer were 1.58 ± 0.15. These results suggest that drug diffuses through an aqueous media of gel-like mucopolysaccharide interspersed by a matrix of collagen fibrils. From further analyses intra- and intercellular pathways for epithelium and endothelium were added to the model resulting in a sigmoidal representation of permeability coefficient *versus* distribution coefficient. However, the intercellular (pore) pathway could not be adequately quantified because of the variation in the data for very hydrophilic compounds.

Keyphrases □ β-Blocking agents—permeability characteristics, excised rabbit corneas, barrier contributions □ Permeability—β-blocking agents, excised rabbit corneas, barrier contributions □ Ophthalmic drugs—β-blocking agents, corneal permeability, rabbits, barrier contributions

To optimize the penetration rate of drugs across biological membranes, quantitative multiple regression analyses are conducted to relate permeability to various physicochemical factors (1–3). These factors are often related through a sum of log terms, including partition coefficient, molecular weight, and degree of ionization. With the use of a digital computer and the appropriate algorithms, the regression analysis can be performed by a stepwise addition or deletion of each term or by comparing all possible subsets of the terms (4). In this way the significance of each term can be ascertained. Once all relevant physiochemical properties have been defined, an optimal chemical structure can be proposed. This semiempirical approach, however, does not characterize the biological limitations imposed by the membrane, such as the significance of parallel aqueous pore pathways or limiting diffusional layers.

The permeability coefficients (P_T) of 12 β-blocking agents through excised rabbit corneas mounted in a perfusion chamber at pH 7.65 were determined in the previous paper (5). Through multiple regression analyses (excluding one outlier), log P_T could be related to partitioning factors by:

$$\log P_T = 0.6228 \log DC - 0.1081(\log DC)^2 - 5.03$$
$$r = 0.9756 \quad p < 0.00009 \quad n = 11 \qquad \text{(Eq. 1)}$$

where DC represents the octanol–buffer (pH 7.65) distribution coefficient. Neither a log molecular weight term nor a log degree of ionization term significantly improved the correlation. The parabolic equation represented in Eq. 1 predicted optimal penetrability at a log DC value of 2.88, the apex of the parabola. However, the experimental data (log P_T *versus* log DC) was curvilinear, leveling off to a plateau such that the asymptotic transport model of Ho *et al.* (6) could be applied. It is the purpose of this study to determine the limiting biological factors governing the steady-state flux of β-blocking agents across the multilayered excised rabbit cornea.

EXPERIMENTAL

Drugs—β-Blocking agents used in the experiments were acebutolol hydrochloride[1], atenolol[2], bevantolol hydrochloride[3], bufuralol hydrochloride[4], levbunolol hydrochloride[3], metoprolol tartrate[5], nadolol[6],

[1] May & Baker LTD Research Laboratories.
[2] Stuart Pharmaceuticals, Division of ICI Americas Inc., Wilmington, Del.
[3] Warner-Lambert Co., Pharmaceutical Research Division, Ann Arbor, Mich.
[4] Roche Products LTD, Research Department.
[5] CIBA Pharmaceutical Co., Division of CIBA-GEIGY Corp., Summit, N.J.
[6] E. R. Squibb & Sons, Inc., Princeton, N.J.

0022-3549/83/1100-1272$01.00/0

(18) D. M. Maurice and M. V. Riley, in "Biochemistry of the Eye," C. N. Graymore, Ed., Academic, London and New York, 1970, pp. 6–16.
(19) J. H. Kim, K. Green, M. Martinez, and D. Paton, *Exp. Eye Res.*, **12**, 231 (1971).
(20) B. O. Hedbys and S. Mishima, *Exp. Eye Res.*, **5**, 221 (1966).
(21) E. R. Garrett and K. Schnelle, *J. Pharm. Sci.*, **60**, 833 (1971).
(22) G. L. Flynn, S. H. Yalkowsky, and T. J. Roseman, *J. Pharm. Sci.*, **63**, 479 (1974).
(23) I. Fatt in "Physiology of the Eye," Butterworth, Woburn, Mass., 1978, pp. 114–121.
(24) R. D. Schoenwald and J. A. Houseman, *Biopharm. Drug Dispos.*, (1982), in press.
(25) V. G. Levich, in "Physicochemical Hydrodynamics," Prentice Hall, Englewood Cliffs, N.J., 1962, pp. 40–46.
(26) N. Draper and H. Smith, in "Applied Regression Analysis," 2nd ed., Wiley, New York, N.Y., 1981, pp. 294–312.
(27) E. J. Lien and P. H. Wang, *J. Pharm. Sci.*, **69**, 648 (1980).
(28) E. J. Lien, A. A. Alhaider, and V. H.-L. Lee, Jr. *Parenter. Sci. Technol.*, **36**, 86 (1982).

ACKNOWLEDGMENTS

This work was abstracted in part from a doctoral dissertation submitted by H. S. Huang and supported in part by Allergan Pharmaceuticals, Irvine, CA 92713.

Corneal Penetration Behavior of β-Blocking Agents II: Assessment of Barrier Contributions

HONG-SHIAN HUANG *, RONALD D. SCHOENWALD ˣ, and JOHN L. LACH

Received July 26, 1982, from the *Pharmaceutics Division, College of Pharmacy, University of Iowa, Iowa City, IA 52242.* Accepted for publication September 16, 1982. *Present Address: National Defense Medical Center, P.O. Box 8244-14, Taipei, Taiwan 107, ROC.

Abstract □ Rabbit corneas were excised and mounted in a chamber to determine the permeability characteristics of a group of β-blocking agents. By measuring the permeability rate of each drug across intact cornea, stroma alone, epithelium–stroma, and stroma–endothelium, it was possible to determine the resistance to penetration for each corneal layer. The reciprocal of the sum of resistances for the epithelium, stroma, and endothelium equaled the experimentally determined permeability coefficient for the intact cornea (104 ± 6.0%). Thus, the penetration of β-blocking agents through the excised rabbit cornea could be treated as three barriers in series. For hydrophilic compounds, the epithelium was the rate-determining barrier. The endothelium offered less resistance, whereas the stroma offered only very minimal resistance. The lipophilic compounds penetrated the excised cornea more rapidly. However, the stroma became rate-determining for the most lipophilic compounds (penbutolol, bufuralol, bevantolol, and propranolol). Although the octanol–buffer (pH 7.65) distribution coefficient of these compounds varied over a fourfold logarithmic range, the permeability coefficient was considered nearly constant [3.4×10^{-5} (±0.34) cm/sec] for stroma. Also, the ratios of tortuosity to porosity for the stromal layer were 1.58 ± 0.15. These results suggest that drug diffuses through an aqueous media of gel-like mucopolysaccharide interspersed by a matrix of collagen fibrils. From further analyses intra- and intercellular pathways for epithelium and endothelium were added to the model resulting in a sigmoidal representation of permeability coefficient *versus* distribution coefficient. However, the intercellular (pore) pathway could not be adequately quantified because of the variation in the data for very hydrophilic compounds.

Keyphrases □ β-Blocking agents—permeability characteristics, excised rabbit corneas, barrier contributions □ Permeability—β-blocking agents, excised rabbit corneas, barrier contributions □ Ophthalmic drugs—β-blocking agents, corneal permeability, rabbits, barrier contributions

To optimize the penetration rate of drugs across biological membranes, quantitative multiple regression analyses are conducted to relate permeability to various physicochemical factors (1–3). These factors are often related through a sum of log terms, including partition coefficient, molecular weight, and degree of ionization. With the use of a digital computer and the appropriate algorithms, the regression analysis can be performed by a stepwise addition or deletion of each term or by comparing all possible subsets of the terms (4). In this way the significance of each term can be ascertained. Once all relevant physiochemical properties have been defined, an optimal chemical structure can be proposed. This semiempirical approach, however, does not characterize the biological limitations imposed by the membrane, such as the significance of parallel aqueous pore pathways or limiting diffusional layers.

The permeability coefficients (P_T) of 12 β-blocking agents through excised rabbit corneas mounted in a perfusion chamber at pH 7.65 were determined in the previous paper (5). Through multiple regression analyses (excluding one outlier), log P_T could be related to partitioning factors by:

$$\log P_T = 0.6228 \log DC - 0.1081(\log DC)^2 - 5.03$$
$$r = 0.9756 \quad p < 0.00009 \quad n = 11 \qquad \text{(Eq. 1)}$$

where DC represents the octanol–buffer (pH 7.65) distribution coefficient. Neither a log molecular weight term nor a log degree of ionization term significantly improved the correlation. The parabolic equation represented in Eq. 1 predicted optimal penetrability at a log DC value of 2.88, the apex of the parabola. However, the experimental data (log P_T *versus* log DC) was curvilinear, leveling off to a plateau such that the asymptotic transport model of Ho *et al.* (6) could be applied. It is the purpose of this study to determine the limiting biological factors governing the steady-state flux of β-blocking agents across the multilayered excised rabbit cornea.

EXPERIMENTAL

Drugs—β-Blocking agents used in the experiments were acebutolol hydrochloride[1], atenolol[2], bevantolol hydrochloride[3], bufuralol hydrochloride[4], levbunolol hydrochloride[3], metoprolol tartrate[5], nadolol[6],

[1] May & Baker LTD Research Laboratories.
[2] Stuart Pharmaceuticals, Division of ICI Americas Inc., Wilmington, Del.
[3] Warner-Lambert Co., Pharmaceutical Research Division, Ann Arbor, Mich.
[4] Roche Products LTD, Research Department.
[5] CIBA Pharmaceutical Co., Division of CIBA-GEIGY Corp., Summit, N.J.
[6] E. R. Squibb & Sons, Inc., Princeton, N.J.

0022-3549/83/1100-1272$01.00/0

Table I—Permeability Coefficients and Hydration Levels for the Permeation of β-Blocking Agents Across Excised Corneal Preparations [a]

β-Blocking Agent	Intact Cornea		Stromal and Endothelial Layers		Epithelial and Stromal Layers		Stroma Only	
	P_{app} [b]	HL [c]	P_{app} [b]	HL [c]	P_{app} [b]	HL [c]	P_{app} [b]	HL [c]
Penbutolol	44.9(5.1)	80.3(1.4)	29.4(5.4)	90.4(0.5)	—	—	—	—
Bufuralol	57.0(6.8)	79.7(1.1)	40.2(1.7)	90.5(0.3)	48.1(0.3)	89.5(0.7)	39.5(1.7)	92.5(1.0)
Bevantolol	53.9(5.0)	79.4(0.7)	34.0(2.7)	90.1(0.4)	45.1(4.6)	90.2(0.5)	34.3(2.3)	93.0(0.4)
Propranolol	47.6(1.7)	79.5(0.4)	31.2(1.2)	89.4(0.7)	39.3(5.1)	90.3(0.3)	35.1(1.6)	91.7(0.3)
Levbunolol	16.4(1.4)	81.5(1.3)	25.3(1.7)	90.3(0.9)	—	—	—	—
Oxprenolol	25.1(1.2)	79.6(1.1)	31.0(1.1)	88.3(0.2)	26.1(1.6)	89.9(0.2)	36.7(4.0)	91.9(0.2)
Timolol	11.7(1.3)	77.4(2.9)	25.6(1.3)	87.8(0.6)	—	—	—	—
Metoprolol	22.0(1.6)	79.0(0.7)	28.2(2.5)	87.5(0.3)	23.0(0.9)	89.0(0.3)	33.7(1.0)	91.9(0.5)
Acebutolol	0.85(0.06)	76.3(0.90)	9.33(0.91)	86.1(2.5)	0.97(0.060)	89.9(0.5)	30.0(2.1)	92.6(0.3)
Sotalol	1.60(0.40)	77.5(1.5)	18.3(1.8)	90.9(0.8)	—	—	—	—
Nadolol	1.03(0.12)	77.1(0.7)	15.0(0.7)	91.3(1.4)	—	—	—	—
Atenolol	0.67(0.10)	77.0(1.7)	15.7(1.1)	91.7(0.4)	0.64(0.27)	87.6(0.5)	32.8(2.0)	92.0(0.2)

[a] Standard deviation in parentheses. [b] Apparent permeability coefficient (10^{-6} cm/sec); n = 4–8 for each determination. [c] Hydration level (percent of water in excised cornea following permeation experiment).

oxyprenolol hydrochloride[5], penbutolol sulfate[7], propranolol hydrochloride[8], sotalol hydrochloride[9], and timolol maleate[10]. The distribution coefficients used in this study, as well as the general procedure for determining the coefficients, were described in the previous paper (5).

Excised Cornea Procedure—Male New Zealand White rabbits[11], weighing 1.6–2.0 kg each, were sacrificed by injecting a bolus of air into the marginal ear vein. The experimental procedure for excising and mounting the corneas in the perfusion chamber were described previously (5). Four different corneal preparations were used in the permeability experiments: the intact cornea, stroma, epithelium–stroma, and endothelium–stroma.

The epithelium and/or endothelium was removed before mounting in the perfusion chamber. The entire epithelium was removed immediately after enucleation by scraping with the blunt end of a scalpel blade. The endothelium was removed after excising the cornea and attaching it to the corneal ring, but just prior to mounting in the perfusion chamber. It was removed by carefully and gently rubbing the endothelial surface with a cotton-tipped applicator (7, 8). The removal of endothelium could be detected with the aid of a dissecting microscope. Whenever a particular corneal layer was removed, the remaining layers were left undisturbed. Solutions used during the permeability experiments as well as sampling procedure, assay methodology, and permeability coefficient calculations were described in the previous paper (5).

Corneal Thickness—Following each permeability experiment, the corneal preparations were weighed and dried in an oven at 103° for 8–12 hr. The dried corneal mass was weighed so that the hydration level of the cornea during steady state could be determined. For a 2-kg rabbit the thickness of the cornea can be determined by:

$$q(\text{cm}) = \frac{0.42 + \text{H}}{100} \qquad \text{(Eq. 2)}$$

where H represents mg of water/mg of dry tissue (9).

The rabbit cornea can be divided into three distinct diffusional layers. The outer (epithelium), consisting of 6–10 cellular layers, is the most lipophilic. The inner layer, which is also lipophilic, consists of a single layer of endothelial cells. The middle layer (stroma) is a hydrophilic layer which accounts for 90% of the corneal thickness. The epithelium and endothelium control hydration and therefore normal thickness; however, when the cornea swells it is the stromal layer only which collects fluid and swells. Consequently, for a 2-kg rabbit the epithelial and endothelial thicknesses remain constant at 0.00385 and 0.0005 cm, respectively (10). From these values and from the experimentally determined hydration levels, Eq. 2 was used to correct for differences in stromal thickness for all corneal preparations. One particular result of stromal swelling is that its thickness but not its diameter increases, which is the reason for the linear form of Eq. 2.

Calculation of Corneal Layer Resistances—The total diffusional resistance, R_{app}, through the multilayered cornea is represented by (11):

$$R_{app} = \frac{1}{P_{app}} = \sum_{i=1}^{n} R_i = \sum \frac{h_i}{D_i A (\text{PC})_i} \qquad \text{(Eq. 3)}$$

where P_{app} is the experimentally measured permeability coefficient, i is the designation for each homogeneous barrier in a series of n barriers, h is the barrier thickness, A its surface area, D represents the effective diffusion coefficient, and PC represents the effective partition coefficient between the barrier and its adjacent phase.

The calculated permeability coefficients were converted to their reciprocals and expressed as resistances. Including the aqueous diffusional barrier, the apparent resistance of the excised cornea can be represented as a sum of barriers in a series:

$$R_{app} = R_T + R_{aq} \qquad \text{(Eq. 4)}$$

and

$$R_T = R_{epi} + R_{str} + R_{endo} \qquad \text{(Eq. 5)}$$

where R_{aq} is the sum of the aqueous diffusional resistances on each side of the cornea in the perfusion chamber and R_T is the sum of resistances of the significant layers of the cornea (epithelium, stroma, and endothelium).

The resistance of the aqueous diffusional layer in the perfusion chamber was 3.7×10^3 sec/cm using O_2–CO_2 gas (5:95) to induce stirring. R_{aq} was determined for atenolol by comparing the permeability coefficient of the drug at different stirring rates using a modified perfusion chamber equipped with a stainless steel stirrer (5); R_{aq} was then deducted from the apparent resistances to obtain the intrinsic resistance for intact cornea, stroma, epithelium–stroma, and stroma–endothelium for all compounds.

The thicknesses varied for each corneal preparation depending on whether the cornea was intact or the epithelium and/or endothelium was removed. To apply Eq. 5, resistances were corrected for experimentally induced differences in thicknesses. Since resistance is directly proportional to barrier thickness, the resistances could be corrected to the normal stromal thickness as existing in the intact cornea ($R_{str,int}$) by:

$$R_{str,int} = R_{str,swl}\left(\frac{h_{int}}{h_{swl}}\right) \qquad \text{(Eq. 6)}$$

Table II—Calculated Log Distribution Coefficients and Log Permeability Coefficients [a] for Epithelium, Stroma, Endothelium, and Intact Cornea

β-Blocking Agent	Log P_{epi}	Log P_{str}	Log P_{endo}	Log P_T [b]	Log DC [c]
Penbutolol	−2.23	−3.84	−3.94	−4.22	2.53
Bufuralol	−3.39	−3.80	−3.64	−4.14	2.31
Bevantolol	−3.05	−3.84	−3.90	−4.17	2.19
Propranolol	−3.11	−3.91	−3.97	−4.24	1.62
Levbunolol	−4.52	−3.89	−4.19	−4.76	0.72
Oxprenolol	−4.22	−3.87	−4.10	−4.56	0.69
Timolol	−4.74	−3.90	−4.27	−4.91	0.34
Metoprolol	−4.34	−3.92	−4.19	−4.62	0.28
Acebutolol	−6.00	−3.93	−4.95	−6.07	0.20
Nadolol	−5.95	−3.93	−4.58	−5.99	−0.82
Sotalol	−5.77	−3.95	−4.38	−5.79	−1.25
Atenolol	−6.22	−3.93	−4.53	−6.17	−1.52

[a] Permeability coefficients have the dimensions of cm/sec (n = 4–8 for each determination. [b] P_T represents the permeability coefficient for the excised intact cornea (n = 4–8); R_{aq} has been subtracted. [c] DC represents the distribution coefficient between octanol and Sorensen's buffer at pH 7.65.

[7] Hoechst-Roussel Pharmaceuticals, Inc., Somerville, N.J.
[8] Ayerst Laboratories, Inc., New York, N.Y.
[9] Mead Johnson & Company, Evansville, Ind.
[10] Merck Sharp & Dohme Research Lab, Division of Merck & Co., Inc., Rahway, N.J.
[11] Morrison Rabbitry, West Branch, Iowa.

Table III—Comparison of the Excised Intact Corneal Resistance to the Total Resistance of the Three Corneal Composite Layers Obtained Separately From Various Corneal Preparations

β-Blocking Agent	$R_{epi} + R_{str} + R_{endo}$[a], 10^3 sec/cm	R_T[b] (Intact Cornea), 10^3 sec/cm	$(R_{epi} + R_{str} + R_{endo})/R_T$, %
Bufuralol	13.6	13.8	98.6
Bevantolol	16.4	14.9	110.0
Propranolol	19.1	17.3	110.0
Oxprenolol	37.2	36.1	103.0
Metoprolol	45.5	41.8	109.0
Acebutolol	1104.5	1177.3	93.8
Atenolol	1584.6	1491.3	106.0
			Average 104 ± 6%

[a] Determined from epithelium–stroma, stroma–endothelium, and stroma corneal preparations (n = 4–8). [b] Determined from intact corneas (n = 4–8).

where h is the stromal thickness and the subscripts int and swl represent intact cornea and swollen stroma, respectively. Equation 6 was also used for another purpose: R_{epi} could be calculated by subtracting $R_{str,swl}$ from $R_{epi/str}$. Although the stroma was swollen in both preparations, their thicknesses were not exactly equal; therefore, the $R_{str,swl}$ value was first adjusted to the same stromal thickness as occurred for $R_{epi/str}$. This was done using the hydration levels and Eqs. 2 and 6. By the same procedure R_{endo} was calculated from the resistance value experimentally determined for the stroma–endothelium corneal preparation.

RESULTS AND DISCUSSION

The permeability coefficients were obtained by linear regression of the quantity of drug penetrating the corneal preparation over time after steady state had been reached. Table I lists the averaged permeability coefficient of each β-blocking agent for intact cornea, stroma, epithelium–stroma, and stroma–endothelium; Table I also lists the hydration levels obtained for each corneal preparation. Excised intact cornea maintained its transparency and rarely exceeded a hydration level of 80% after 4 hr of permeation. If the drug concentration was above a certain level (which varied for each drug), swelling occurred and consequently the hydration level increased. This was a result of cationic drug interaction with the cornea. For each drug a concentration was used that did not induce intact corneal swelling. For stroma, epithelium–stroma, and stroma–endothelium, swelling could not be avoided since the removal of the epithelium and/or endothelium caused the swelling and not the drug. It was determined in preliminary experiments that swelling, and hence stromal thickness, gradually increased over time reaching 95% of maximum in 0.45, 1.0, and 0.30 hr for stroma, epithelium–stroma, and stroma–endothelium corneal preparations, respectively.

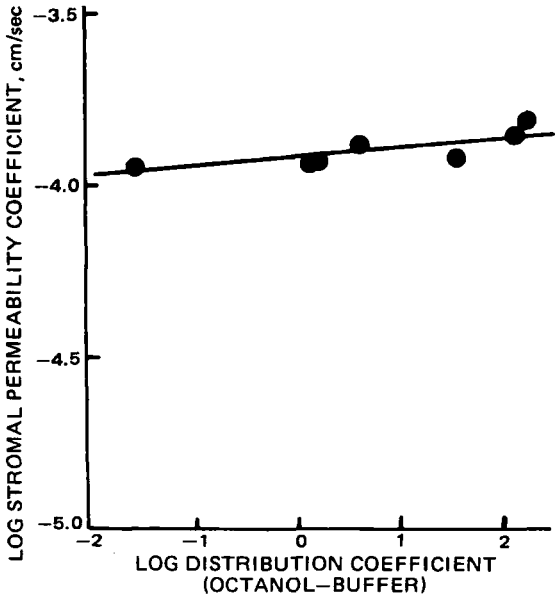

Figure 1—*Log–log plot of permeability coefficient through stroma (P_{str}) corrected to intact corneal thickness* versus *distribution coefficient (octanol–Sorenson's buffer, pH 7.65) for seven β-blocking agents. Linear regression: slope = 0.0292, intercept = −3.9098, and r = 0.8062.*

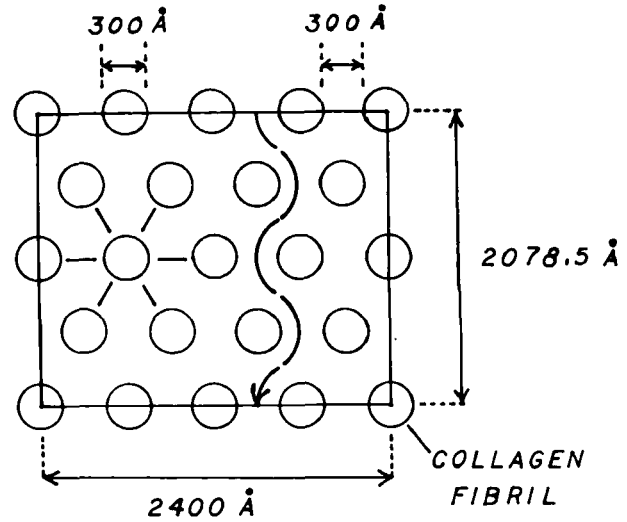

Figure 2—*Arrangement of collagen fibrils geometrically interspersed in the stroma as proposed to calculate the ratio of tortuosity to porosity (= 1.56) from stromal diffusion. The curved arrow between the fibrils represents the diffusional pathway of least resistance.*

Table II lists the calculated log values of R_{str}, R_{epi}, and R_{endo}. R_{str} was determined from $R_{str,swl}$ by correcting for thickness differences (Eq. 6) to the resistance expected in a normal cornea with a hydration level of 78.7%, the average obtained for all determinations of intact cornea (n = 43). Table III shows a comparison between the resistances of excised intact corneas, each determined from separate experiments, and that of the sum of three composite layers (Eq. 5) estimated from the various corneal preparations. Good agreement (106 ± 4%) exists for the seven β-blocking agents for which complete data were generated. These results indicate that the penetration of β-blocking agents through the excised rabbit cornea could be treated as three barriers in series.

Stromal Diffusion—Figure 1 represents a plot of log P_{str} *versus* log DC for the seven drugs for which complete permeability data were calculated. The plot shows a good linear relationship with a slope near zero (slope = 0.0292, intercept = 3.91, r = 0.778) indicating P_{str} is generally independent of DC. This is not surprising since the stroma contains 76–80% water. The remainder is composed mostly of collagen fibers and mucopolysaccharide, the latter of which is hydrophilic and responsible for the high water content of the stroma (10). Considering the large range of lipophilic/hydrophilic character covered by the seven drugs (over four log units), the results strongly suggest that drug is diffusing through the aqueous mucopolysaccharide medium of the stroma which is interspersed by a matrix of collagen fibers. The collagen fibrils, 300 Å in diameter, are arranged nearly parallel to one another with a fairly regular open spacing of ~300 Å between fibrils (10). The fibrils probably provide a high resistance to penetration and increase the diffusional path length as opposed to free diffusion through the aqueous stromal medium. Mathematically, resistance through the stroma can be defined by[12]:

$$R_{str} = \frac{h_{str}}{D_{str}(PC)} \qquad \text{(Eq. 7)}$$

where D_{str}, the effective diffusion coefficient in the stroma, can be expanded to (11):

$$D_{str} = \frac{D_{aq}\epsilon}{\tau} \qquad \text{(Eq. 8)}$$

In this equation, ϵ is the porosity (dimensionless) or volume fraction of the stroma, D_{aq} is the aqueous diffusion coefficient, and τ is the tortuosity (dimensionless) imposed by the geometrical arrangement of the stromal matrix. By combining Eqs. 7 and 8 and assuming PC as unity, stromal resistance can be defined by:

$$R_{str} = \frac{h_{str}\tau}{D_{aq}\epsilon} \qquad \text{(Eq. 9)}$$

[12] Equation 7 does not contain the A term in the denominator as shown in Eq. 3 because it is incorporated into the calculation of R_{str}; A = 1.087 cm² for 2-kg rabbits.

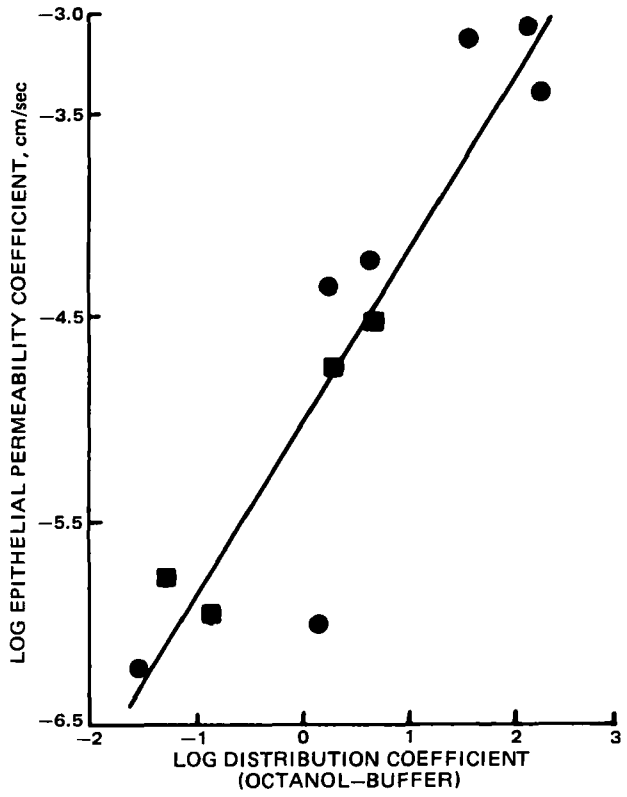

Figure 3—*Log–log plot of permeability coefficient through epithelium (P_{epi}) versus distribution coefficient (octanol–Sorensen's buffer, pH 7.65) for 11 β-blocking agents. Key: (●) determined from various corneal preparations, (■) calculated by difference using Eq. 5, regression results from Fig. 1, and permeability coefficient for intact cornea (penbutolol not shown). Linear regression: slope = 0.8505, intercept = −5.033 and* r = *0.9207.*

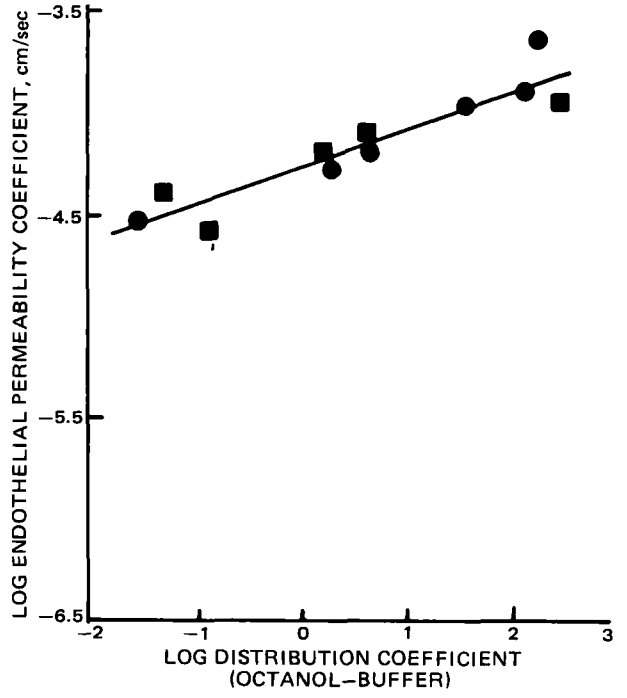

Figure 4—*Log–log plot of permeability coefficient through endothelium (P_{endo}) versus distribution coefficient (octanol–Sorensen's buffer, pH 7.65) for 11 β-blocking agents. Key: (●) determined from various corneal preparations (acebutolol not shown), (■) calculated by difference using Fig. 1 and permeability coefficient for intact cornea. Linear regression: slope = 0.1843, intercept = −4.2724, and* r = *0.9283.*

The collagen structure of the stroma can be depicted as in Fig. 2. Assuming that the average diffusional path of least resistance is midway between the geometrically arranged collagen fibrils, the porosity and tortuosity can be estimated as 0.773 and 1.21, respectively, resulting in a τ/ϵ ratio of 1.56.

In Eq. 9 both R_{str} and h_{str} are known from the experimental data. The averaged resistance for a normal stromal thickness of 0.03725 cm (78.7% hydration) is 7.83×10^3 sec/cm. To estimate D_{aq} for Eq. 9, the Sutherland–Einstein equation[13] and the well-established aqueous diffusion coefficient for benzoic acid (MW = 122), 1.1×10^5 cm²/sec at 25° (11), were used. After correcting for molecular weight, the β-blocking agents yielded an average diffusion coefficient of 7.5×10^{-6} cm²/sec in water. Temperature and viscosity differences between water and stromal medium were not included in the correction, although they should compensate for one another. These estimations yielded a τ/ϵ value of 1.58 for normal stroma. Therefore, good agreement exists between the τ/ϵ value for stroma predicted from geometrical considerations of collagen in Fig. 2, neglecting the mucopolysaccharide contribution to viscosity or structure.

Maurice (12) described a factor referred to as an obstruction of the stroma to diffusion or more specifically, as "how many times diffusion in tissue is slower than diffusion in saline at the same temperature." This factor is similar to the τ/ϵ ratio in Eqs. 7–9. Values for ^{134}Cs, ^{82}Br, and ^{24}Na ranged from 1.9 to 2.7, which agree fairly well with our value of 1.58 considering that the molecules studied and the methods used are quite different.

[13] The Sutherland-Einstein equation is:

$$D = \frac{RT}{6T\eta N}\left(\frac{4N}{3M\upsilon}\right)^{1/3}$$

where D is the diffusion coefficient, R is the gas constant, T is the temperature, N is Avogadro's number, M is the molecular weight, υ is the partial specific volume, and η is viscosity of the solvent. Assuming D is proportional to $(1/M)^{1/3}$ and that all other parameters remain unchanged, then the value D_{aq} for β-blocking agents with an average molecular weight of 288 is: $D_{aq} = (1.1 \times 10^{-5})(122/288)^{1/3} = 7.5 \times 10^{-6}$ cm²/sec.

Epithelial Diffusion—Figure 3 represents a linear plot of log P_{epi} *versus* log DC. Five drugs (penbutolol, levbunolol, timolol, nadolol, and sotalol) lack the permeability data for stroma and epithelium–stroma preparations so that individual resistances could not be directly calculated for all layers. However, because of the excellent fit between permeability and partitioning for seven of the drugs shown in Fig. 1, predictions for R_{str} could be obtained from the known DC value. Using the experimentally determined permeability data for intact cornea, R_T was calculated. Consequently R_{epi} could be determined from Eq. 5 by difference for the five drugs lacking the appropriate experimental data. The R_{epi} value for penbutolol was over one log unit from the least-squares fitted line (slope = 0.8505, intercept = −5.033, and r = 0.9207). Its deviation could be a consequence of the very small percentage contribution of the P_{epi} value estimated for penbutolol and, therefore, the large potential for error when taking its reciprocal. It is interesting to note that the slope in Fig. 3 is only slightly <1, suggesting that the lipophilic character of the epithelium is only slightly lower than octanol (a slope of 1 would indicate identical partitioning behavior).

Endothelial Diffusion—Figure 4 represents a plot of log P_{endo} *versus* log DC for all of the drugs except acebutolol, which had an outlying value. The R_{endo} value of acebutolol was small compared to R_{epi} and may have been subject to a relatively large error. The linear regression analysis

Table IV—Percent Contribution of the Resistance of Individual Corneal Layers to the Total Corneal Resistance

β-Blocking Agent	R_{epi}/R_T, %	R_{str}/R_T, %	R_{endo}/R_T, %	Log DC[a]
Penbutolol	1.0	46.0	53.0	2.53
Bufuralol	18.0	50.0	32.0	2.31
Bevantolol	7.0	44.0	49.0	2.19
Propranolol	7.0	45.0	48.0	1.62
Levbunolol	58.0	15.0	27.0	0.72
Oxprenolol	45.0	21.0	34.0	0.69
Timolol	68.0	9.0	23.0	0.34
Metoprolol	48.0	18.0	34.0	0.28
Acebutolol	91.0	1.0	8.0	0.20
Nadolol	95.0	1.0	4.0	−0.82
Sotalol	95.0	1.0	4.0	−1.25
Atenolol	97.5	0.5	2.0	−1.52

[a] The distribution coefficient is between octanol and Sorensen's buffer at pH 7.65, which is also the pH of the permeability experiments.

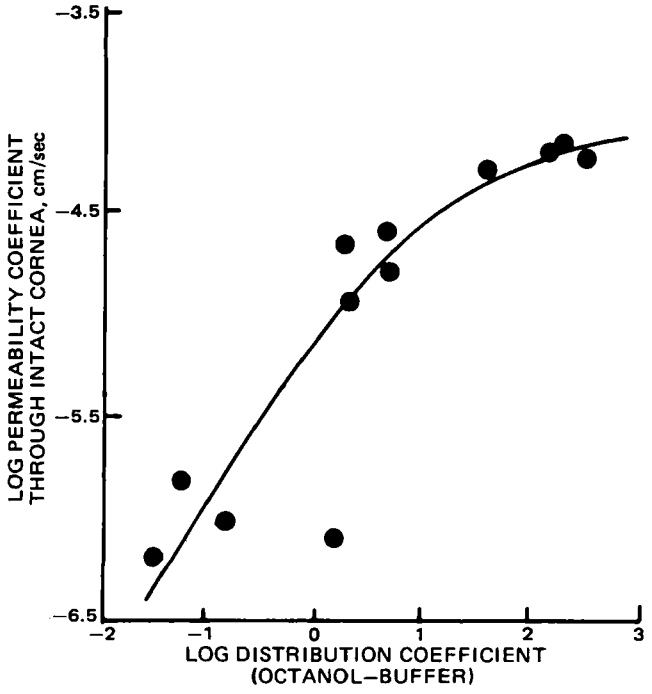

Figure 5—*Log–log plot of theoretical curve fitted to experimentally determined permeability coefficients through intact cornea (●) versus distribution coefficient (octanol–Sorensen's buffer, pH 7.65) for 12 β-blocking agents; computer-generated curve represents the sum of three composite corneal layers according to Eq. 20.*

produced a line with a slope and intercept intermediate between epithelial and stromal data (slope = 0.1843, intercept = −4.272, and r = 0.9282).

The intercepts from the linear regression in Figs. 2–4 represent the log P_T value for a compound with a log DC of zero. The permeability coefficients, in units of 10^{-6} cm/sec, are 9.27, 53.46, and 123.03, respectively, for epithelium, endothelium, and stroma for a compound whose DC equals 1. For a compound with this partitioning behavior, the epithelium is the rate-determining barrier. A β-blocking agent must be considerably more lipophilic before another layer becomes rate determining.

Relative Layer Contributions—Table IV shows the percent contribution of the resistances from each corneal layer to the total corneal resistance according to Eq. 5. The percent contribution of epithelial resistance increases as the drug lipophilicity decreases. Conversely, resistance decreases for stroma and endothelium as the lipophilicity of the drug decreases. Stroma is hydrophilic and expected to behave in this manner. However, the endothelium is considered lipophilic due to its cellular composition. Because the endothelium is only one cell thick and therefore does not present the tortuosity of the multilayered epithelium, it is possible that intercellular (pore) transport becomes significant for the more hydrophilic compounds.

For the most lipophilic compounds (penbutolol, bufuralol, bevantolol and propranolol), the stroma and endothelium offer the greater resistance. For the other more hydrophilic compounds, the epithelium is the most significant barrier to penetration.

Diffusional Model Relating DC to P_T—The total diffusional resistance, R_T, through the three-layer corneal membrane was generalized in Eq. 3, but can be expanded according to Eq. 5 to:

$$P_T = \frac{1}{R_T} = \frac{1}{\frac{h_1}{D_1(\mathrm{PC})_1} + \frac{h_2}{D_2(\mathrm{PC})_2} + \frac{h_3}{D_3(\mathrm{PC})_3}} \qquad \text{(Eq. 10)}$$

where all terms have been previously defined; for simplicity, the numerical subscripts 1, 2, and 3 are used for the epithelial, stromal, and endothelial layers, respectively. An attempt was made to determine if each corneal layer, with its own effective partition coefficient (PC), could be related to the distribution coefficient of an octanol–buffer (pH 7.65) system according to:

$$(\mathrm{PC})_i = \gamma_i(\mathrm{DC})^a \qquad \text{(Eq. 11)}$$

where γ is a proportionality constant and a represents a measure of the sensitivity of the biological partition coefficient (PC) of layer i to the *in vitro* distribution coefficient (DC).

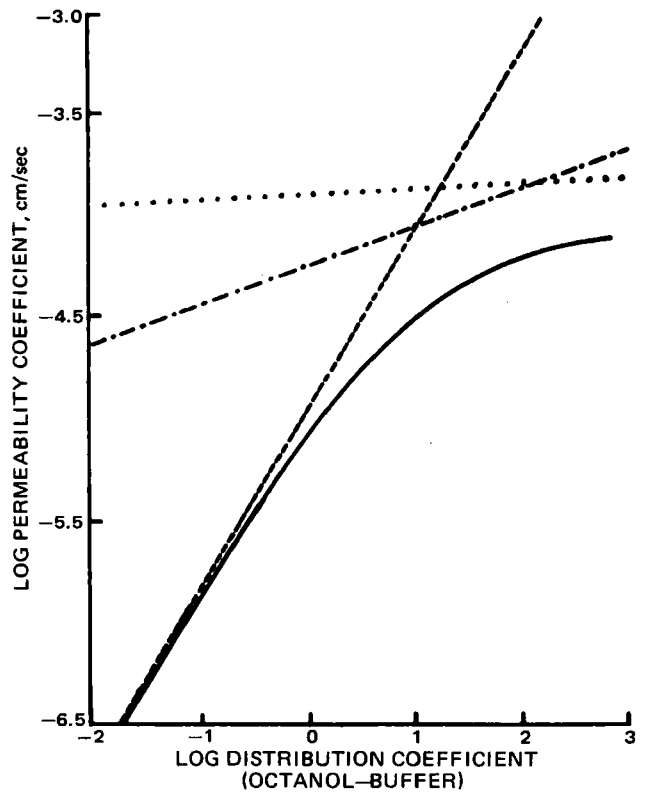

Figure 6—*Computer-generated log–log plots of permeability coefficient for intact cornea and three separate corneal layers* versus *distribution coefficient (octanol–Sorensen's buffer, pH 7.65). Key: (- - -) epithelium, (· · ·) stroma, (— · —) endothelium, (——) intact cornea generated from Eq. 20.*

The basis for use of Eq. 11 comes from the work of Collander (13), who studied the partition of organic compounds between higher alcohols and water. He found that there was a linear relationship among the log partition coefficients in two different solvent systems:

$$\log \mathrm{PC}_{S2} = a \cdot \log(\mathrm{PC}_{S1}) + b \qquad \text{(Eq. 12)}$$

where S1 and S2 represent two different solvent systems each containing water as the polar phase, but with different nonpolar phases. The octanol–water system has been used as a reference system for correlation to *in vivo* responses (14, 15). When other systems are used, conversion to the octanol–water system can be achieved through Eq. 12. Equation 11 can be converted to a form identical to Eq. 12, where S1 in Eq. 11 represents octanol–buffer (pH 7.65) and S2 represents a membrane–water system. Equation 11 can be substituted into Eq. 10 to give:

$$P_T = \frac{1}{\frac{h_1}{D_1\gamma_1(\mathrm{DC})^{a_1}} + \frac{h_2}{D_2\gamma_2(DC)^{a_2}} + \frac{h_3}{D_3\gamma_3(DC)^{a_3}}} \qquad \text{(Eq. 13)}$$

Combining fractions and rearranging gives:

$$P_T = \frac{(D_1\gamma_1/h_1)(\mathrm{DC})^{a_1}}{1 + (h_2D_1\gamma_1/h_1D_2\gamma_2)(\mathrm{DC})^{a_1-a_2} + (h_3D_1\gamma_1/h_1D_3\gamma_3)(\mathrm{DC})^{a_1-a_3}} \qquad \text{(Eq. 14)}$$

and combining constants leads to:

$$P_T = \frac{dx^e}{1 + fx^g + ix^j} \qquad \text{(Eq. 15)}$$

where x = DC, $d = D_1\gamma_1/h_1$, $e = a_1$, $f = h_2D_1\gamma_1/h_1D_2\gamma_2$, $g = a_1 - a_2$, $i = h_3D_1\gamma_1/h_1D_3\gamma_3$, and $j = a_1 - a_3$. For a single epithelial layer, $h_2 = h_3 = 0$ and Eq. 13 becomes:

$$P_{epi} = \frac{1}{R_{epi}} = \frac{D_1\gamma_1(\mathrm{DC})^{a_1}}{h_1} \qquad \text{(Eq. 16)}$$

Similarly:

$$P_{str} = \frac{1}{R_{str}} = \frac{D_2\gamma_2(\mathrm{DC})^{a_2}}{h_2} \qquad \text{(Eq. 17)}$$

Table V—Nonlinear Least-Squares Best Fit of the Relationship Between Permeability Coefficient and Distribution Coefficient (Octanol–Buffer) [a]

Corneal Layer	f_hP_h 10^{-6} cm/sec	$f_lD\gamma/h$, 10^{-6} cm/sec	a	Weight	RMS[b]	r[c]	DF[d]
Endothelium	15.19	21.380	0.3298	$(1/P)^{0.85}$	32.7	−0.275	9
	10.60	31.410	0.2709	$(1/P)^{0.50}$	138.2	−0.431	9
Epithelium	0.60[e]	9.346	0.7885	$(1/P)^{0.85}$	243.2	0.225	9
	0.60[e]	25.290	0.6152	$(1/P)^{0.50}$	2007.7	0.101	9

[a] Results apply to three barriers in series with parallel pathways assigned to epithelium and endothelium only; see Eq. 23 for an explanation of the symbols. [b] Residual mean square calculated by dividing residual sum of squares by degrees of freedom. [c] Correlation coefficient. [d] Degrees of freedom. [e] A fixed value for computer fitting represents the permeability coefficient from the most hydrophilic drug, atenolol.

and

$$P_{endo} = \frac{1}{R_{endo}} = \frac{D_3\gamma_3(DC)^{a3}}{h_3} \qquad \text{(Eq. 18)}$$

Equations 16–18 can be linearly rearranged to yield:

$$\log P_i = a_i \log (DC) + \log \frac{D_i\gamma_i}{n_i} \qquad \text{(Eq. 19)}$$

Equation 19 indicates that for a single corneal layer, the plot of log P_i *versus* log DC will show a linear relationship with a slope a_i and an intercept equal to log $D_i\gamma_i/h_i$. This requires that all drugs used in the plot have the same diffusion coefficient within layer i.

By substituting the intercepts and slopes from the log P_i *versus* log DC plots of the three corneal layers into Eq. 15, the following equation was obtained:

$$P_T = \frac{(9.27 \times 10^{-6})(DC)^{0.8505}}{1 + 0.0753(DC)^{0.8216} + 0.1734(DC)^{0.6662}} \qquad \text{(Eq. 20)}$$

Equation 20 is exactly the same form as Eq. 15. Figure 5 shows that the experimental data corresponding to the log P_T *versus* log DC plot for intact corneal permeability fits the curve represented by Eq. 20. The excellent fit further justifies our theoretical basis regarding corneal penetration through three composite layers acting as a sum of barriers in series.

Figure 6 is a combination of all the log P_i *versus* log DC curves for permeation through intact cornea, epithelium, stroma, and endothelium. It clearly shows that the permeabilities are rate determined by the epithelium for the four hydrophilic compounds (atenolol, sotalol, nadolol, and acebutolol). There are four intermediate lipophilic compounds (*i.e.*, metoprolol, timolol, oxyprenolol, and levbunolol) whose permeabilities are controlled by epithelium, endothelium, and stroma, in that order. The most lipophilic compounds fall on the plateau range, with their permeabilities controlled by endothelium and stroma; these compounds include propranolol, bufuralol, bevantolol, and penbutolol. It is interesting to note that linear processes (Fig. 6) can be added to produce curvilinear results. This occurs because of the small slope values (a in Eq. 19) of stroma and endothelium; therefore, a plateau is reached for the most lipophilic compounds.

The only outlier in Fig. 5 is acebutolol, for which the experimental permeability coefficient falls significantly below the theoretical curve represented by Eq. 20. By applying the Sutherland–Einstein equation to correct for the difference in molecular weight between acebutolol (336.4) and the remaining 11 β-blocking agents (289.6), the diffusion coefficient of acebutolol was found to be only 5% lower than the average. When the 5% correction is applied, the permeability coefficient is still significantly below the computer-generated line of best fit. Figures 3 and 4 indicate that log P_{epi} and log P_{endo} for acebutolol deviate from the observed trend, shown by their respective plots against log DC. This suggests that the decreased permeability coefficients of acebutolol through epithelium and endothelium, and not the stroma, account for the deviation of the experimental data from the curve. It was thought that acebutolol might cause a physiological or structural change in the epithelial or endothelial layers such that the permeation decreases. However, the experimental hydration level obtained following intact corneal permeability was within the normal range, suggesting that the corneal layers had not been altered in permeability. Still another possibility for the deviation for acebutolol may lie in its partitioning behavior. From a structural point of view, acebutolol may show exceptional hydrogen bonding ability compared to the other 11 β-blocking agents. The fact that the acebutolol structure contains acetyl, amide, and tertiary amine groups indicates that significantly more hydrogen bonding could occur compared with the other compounds, possibly leading to the deviation of acebutolol in Fig. 5.

Intercellular (or Aqueous Pore) Pathways in the Epithelial and Endothelial Layers—When two or more independent diffusional pathways exist in a given diffusional medium, the total permeability coefficient at steady state is (11):

$$P_T = f_1P_1 + f_2P_2 + \ldots + f_nP_n \qquad \text{(Eq. 21)}$$

where $f_1, f_2, \ldots f_n$ define the fractional areas of each route and $P_1, P_2, \ldots P_n$ are the individual permeability coefficients through each pathway. It has been suggested that there are two parallel pathways occurring for the diffusion of drugs across biological membranes (6, 16). One pathway is represented by hydrophilic channels that consist of pores or intercellular spaces, whereas the other pathway is represented by lipophilic transport across lipoid-like cell membranes. Hydrophilic molecules with low lipophilic partitioning behavior (low DC) are logically thought to diffuse through the hydrophilic channels, the path of least resistance. Applying these concepts to either the epithelium or endothelium, Eq. 21 becomes:

$$P_i = f_hP_h + f_lP_l \qquad \text{(Eq. 22)}$$

where subscripts h and l refer to hydrophilic and lipophilic transport, respectively. Since the hydrophilic channels are mostly filled with water, the diffusion coefficients for the β-blocking agents should approximate the diffusion coefficient in water for an average molecular weight of 288. The DC value for each drug can be assumed equal to 1. P_h becomes a

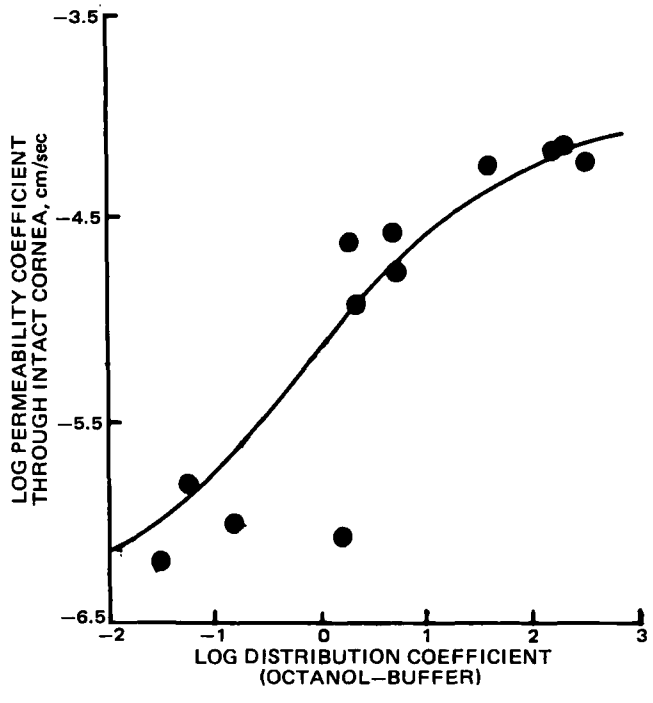

Figure 7—*Log–log plot of permeability coefficient* versus *distribution coefficient (octanol–Sorensen's buffer, pH 7.65). The theoretical curve represents the model with three barriers in series as well as intra- and intercellular parallel pathways for epithelium and endothelium. Key: (●) intact corneal permeability data, (—) computer-generated sigmoidal curve representing parallel pathways according to Eq. 24.*

[14] Nonlinear regression was performed using the BMDP3R program on an IBM370 computer.

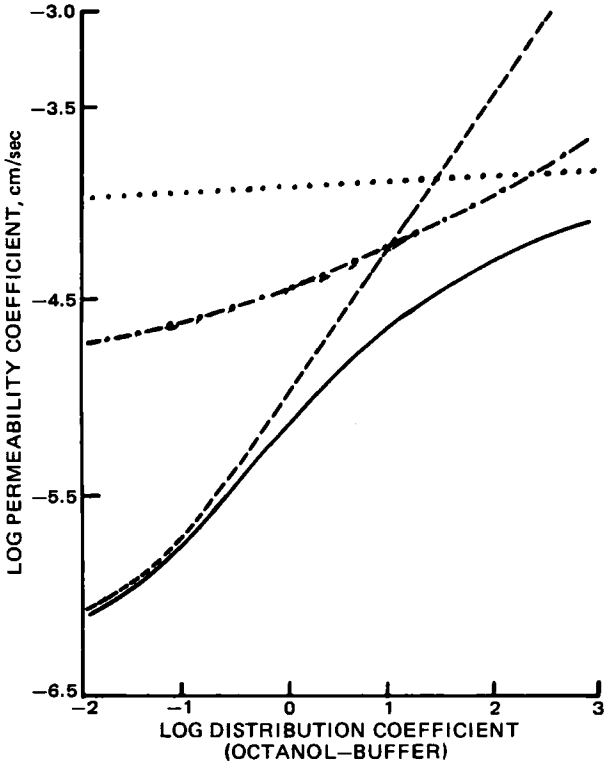

Figure 8—*Computer-generated log–log plots of permeability coefficient for intact cornea and three separate corneal layers* versus *distribution coefficient using (octanol–Sorensen's buffer, pH 7.65). The model includes intra- and intercellular pathways for epithelium and endothelium. Key: (- - -) epithelium, (· · ·) stroma, (-·-) endothelium, (—) intact cornea generated from Eq. 24.*

constant, but P_l is dependent on DC; thus, by combining Eqs. 3, 11, and 22 for either epithelial or endothelial transport:

$$P_i = f_h P_h + \frac{f_l D \gamma_i (\mathrm{DC})^{a_i}}{h_i} \qquad \text{(Eq. 23)}$$

Equation 23 can be fit by nonlinear regression[14] to either P_{epi} or P_{endo} *versus* DC to obtain estimates of $f_h P_h$ and $f_l D\gamma_i/h_i$.

Parallel Endothelial Pathways—Electron micrographs show that the boundries of adjoining endothelial cells are separated by ~200 Å (10). Based on an average endothelial thickness of 4.5 μm, as well as an experimentally determined P_{endo} of 2×10^{-5} cm/sec and a diffusion coefficient of 1.7×10^{-5} cm²/sec for ^{24}Na, Maurice (10, 17) estimated f_h in the endothelium to be 1/1720. Setting P_h equal to $D(\mathrm{PC})/h$ and assuming that PC = 1, h = 4.5 μm, and $D = 7.5 \times 10^{-6}$ cm²/sec[13], P_h becomes 1.7×10^{-2} cm/sec and $f_h P_h$ becomes 9.7×10^{-6} cm/sec. Therefore, 9.7×10^{-6} cm/sec was used as an initial estimate for the nonlinear fit to Eq. 23 for P_{endo} *versus* DC. Since f_l is nearly unity, the initial estimates for $D\gamma/h$ and a were obtained from the linear fit of log P_{endo} *versus* log DC (Fig. 4).

Weighting factors were used in the nonlinear fitting procedure since $f_h P_h$ is more likely determined by the hydrophilic compounds, which have much lower permeability and distribution coefficients than those of the lipophilic compounds. Table V shows the results of the computer fit for the endothelium. Using the weights of $(1/P_3)^{0.85}$ or $(1/P_3)^{0.5}$ the final estimates of $f_h P_h$ are reasonably close to the theoretically derived initial estimate. However, if the endothelial permeability coefficient for acebutolol, which is extremely low, is again taken as an outlier and discarded for the computer fitting, then $f_h P_h$ decreases to ~0. Consequently, a strict interpretation of the results is tenuous based on the variability of the data. The intercellular pathway for the endothelium cannot be confirmed from our nonlinear regression analysis unless a greater number of data points in the hydrophilic range are used.

Parallel Epithelial Pathways—Since the epithelium has 5–10 cellular layers, its intercellular pathway should have a large tortuosity and small area fraction. The epithelial permeability coefficient for the most hydrophilic drug, atenolol, is only 0.6×10^{-6} cm/sec. Assuming atenolol traversed the epithelium predominately through pores, the value of 0.6×10^{-6} cm/sec was assigned as an initial estimate for $f_h P_h$ for the nonlinear regression of epithelial permeation. The initial estimates for $D\gamma/h$ and a were obtained from the linear fit of log P_{epi} *versus* log DC (Fig. 3).

Despite the uncertainty defining the intercellular pathway, the computer fitting using Eq. 23 provides useful information for both epithelial and endothelial layers. As pointed out previously, the a-value indicates the sensitivity of the respective corneal layer to the change in the lipophilicity/hydrophilicity character of the penetrating drug. As shown in Table V, the slope values (a) are <0.35 for the endothelium. In contrast, the epithelium has a-values 2 times as high as that calculated for the endothelium. The results indicate that compared with endothelium, the epithelium is more sensitive to the lipophilicity of permeating compounds. These conclusions are consistent with the results of the linear regression fits of log P_i *versus* log DC.

The hydrophilic stroma contains very low cell counts and, therefore, the intercellular pathway model did not apply. The log P_{str} *versus* log DC data was fitted by linear regression. The parameter values from the line of best fit as well as those from the P_i *versus* DC nonlinear curve-fitting procedure were used to construct the following:

$$P_T = \frac{1}{\dfrac{10^6}{0.6 + 9.346 \cdot (\mathrm{DC})^{0.7885}} + \dfrac{10^6}{123.03 \cdot (\mathrm{DC})^{0.0289}} + \dfrac{10^6}{15.19 + 21.38 \cdot (\mathrm{DC})^{0.3298}}} \qquad \text{(Eq. 24)}$$

where the three terms in the denominator on the right-hand side represent the permeability coefficient through epithelium, stroma, and endothelium, respectively. According to Eq. 24, the computer-generated curve of log P_T *versus* log DC (Fig. 7) describes the experimental permeability coefficients through intact cornea. The lower limit of the curve represents the intercellular pathway while the plateau is controlled by the endothelium and stroma, overall resulting in a sigmoidal curve. Figure 8 shows the computer-fitted curves for stroma, endothelium, epithelium, and intact cornea. Unlike the linear log P_{str} *versus* log DC plot for stroma, the curves for epithelium and endothelium in Fig. 8 approach a minimum in the hydrophilic range.

Because of the variability in the log P_i values for the hydrophilic compounds, Figs. 7 and 8 do not describe the data any better than Figs. 5 and 6. Nevertheless, the sigmoidal curve obtained in Figs. 7 and 8 resemble the intestinal absorption profile proposed by Ho *et al.* (6) for similar data. These authors showed that a sigmoidal relationship existed between the rates of absorption and lipophilicity. Diffusion through the aqueous pore pathway in the intestine accounted for the lower limiting value represented by the most hydrophilic compounds, whereas at high lipophilicity, the absorption rate reached a plateau controlled by the aqueous boundary layer adjacent to the intestinal absorptive cell membrane. Corneal penetration rate, on the other hand, is limited for lipophilic β-blocking agents by the stroma, which is primarily an aqueous barrier on the cornea; however, the hydrophilic stromal barrier is a physiologically real and permanent barrier located within the cornea. Both Figs. 5 and 7 show that stroma and endothelium control the corneal permeation of lipophilic compounds in the absence of an aqueous diffusional (or boundary) layer.

REFERENCES

(1) E. J. Lien, in "Drug Design," Vol. V, E. J. Ariens, Ed., Academic, New York, N.Y., 1975, pp. 82–132.

(2) E. J. Lien and P. H. Wang, *J. Pharm. Sci.*, **69**, 648 (1980).

(3) E. J. Lien, A. A. Alhaider, and V. H. L. Lee, Jr. *Parenter. Sci. Technol.*, **36**, 86 (1982).

(4) N. Draper and H. Smith, in "Applied Regression Analysis," 2nd ed., Wiley, New York, N.Y., 1981, pp. 294–312.

(5) R. D. Schoenwald and H. S. Huang, *J. Pharm. Sci.*, **72**, 1266 (1983).

(6) N. F. H. Ho, J. Y. Park, W. Morozowich, and W. I. Higuchi, in "Design of Biopharmaceutical Properties through Prodrugs and Analogs," E. B. Roche, Ed., Am Pharm Assoc, Washington, D.C., 1977, pp. 136–227.

(7) J. H. Kim, K. Green, M. Martinez, and D. Paton, *Exp. Eye Res.*, **12**, 231 (1971).

(8) R. D. Schoenwald and J. A. Houseman, *Biopharm. Drug Dispos.*, **3**, 231 (1982).

(9) B. O. Hedbys and S. Mishima, *Exp. Eye Res.*, **5**, 221 (1966).

(10) I. Fatt, in "Physiology of the Eye," Butterworth, Woburn, Mass.,

1978, pp. 92–188.
(11) G. L. Flynn, S. H. Yalkowsky, and T. J. Roseman, *J. Pharm. Sci.*, 63, 479 (1974).
(12) D. M. Maurice, in "The Structure of the Eye," G. K. Smelser, Ed., Academic, New York and London, 1960, pp. 381–391.
(13) R. Collander, *Acta Chem. Scand.*, 5, 774 (1951).
(14) R. N. Smith, C. Hansch, and M. M. Ames, *J. Pharm. Sci.*, 64, 599 (1975).
(15) A. Leo, C. Hansch, and D. Elkins, *Chem. Rev.*, 71, 525 (1971).
(16) W. D. Stein, "Theoretical and Experimental Biology," Vol. 6, Academic, New York and London, 1967, pp. 73–74, 106–125.
(17) D. M. Maurice in "The Eye," Vol. 1, 2nd ed., H. Davson, Ed., Academic, New York, N.Y., 1969, pp. 6–8, 534–557.

ACKNOWLEDGMENTS

This work was abstracted from a doctoral dissertation submitted by H. S. Huang and was supported in part by Allergan Pharmaceuticals, Irvine, Calif.

The authors express their sincere thanks to Associate Professor Douglas Flanagan for his suggestions.

Corneal Penetration Behavior of β-Blocking Agents III: *In Vitro–In Vivo* Correlations

HONG-SHIAN HUANG *, RONALD D. SCHOENWALD ˣ, and JOHN L. LACH

Received July 26, 1982, from the *Pharmaceutics Division, College of Pharmacy, University of Iowa, Iowa City, IA 52242.* Accepted for publication September 4, 1982. *Present address: National Defense Medical Center, P.O. Box 8244-14, Taipei, Taiwan 107, ROC.

Abstract □ Aqueous humor levels were determined over time after the topical administration to rabbit eyes of 1% isotonic buffered (pH 7.3) solutions of three β-blocking agents, acebutolol hydrochloride, timolol maleate, and bufuralol hydrochloride (arranged in order of increasing lipophilicity). Corneal permeability coefficients, determined from a previous *in vitro* study, were inversely related to the observed time to peak for the three drugs, as expected. Two of the drugs, bufuralol and timolol, did not give the expected rank order for C_{max} and AUC, which could result from differences in distribution and/or elimination processes. Aqueous boundary layers were postulated for *in vivo* corneal permeability which suggested that bufuralol and timolol may have nearly identical effective permeability coefficients *in vivo*.

Keyphrases □ Permeability—acebutolol, timolol, bufuralol, excised rabbit corneas, pharmacokinetics, *in vitro–in vivo* correlations □ Acebutolol—corneal permeability in rabbits, pharmacokinetics, *in vitro–in vivo* correlations □ Timolol—corneal permeability in rabbits, pharmacokinetics, *in vitro–in vivo* correlations □ Bufuralol—corneal permeability in rabbits, pharmacokinetics, *in vitro–in vivo* correlations

In a previous report (1) the penetration behavior of 12 β-blocking agents measured across excised rabbit corneas was correlated with partitioning, which varied over a fourfold logarithmic range. Optimal penetration (log permeability coefficient) reached a maximum at a log distribution coefficient (octanol–buffer, pH 7.65) of ~2–3. Subsequent results (2) showed that a plateau was reached because the stroma, and to a lesser extent the endothelium, became the rate-controlling barrier for the most lipophilic compounds, while the epithelium acted as a rate-determining barrier for the hydrophilic compounds.

The purpose of this study was to determine if the corneal permeability coefficients of three compounds ranging widely in lipophilicity could be correlated with parameters obtained from the aqueous humor–time profile. The three drugs (in descending lipophilic order: bufuralol, timolol, and acebutolol) were administered as 1% isotonic, buffered (pH 7.3) solutions.

EXPERIMENTAL

Reagents and Materials—Isotonic, buffered (pH 7.3), 1% w/v solutions of acebutolol hydrochloride, timolol maleate, and bufuralol hydrochloride were prepared separately[1]. The reagents used for aqueous humor extraction and subsequent high-performance liquid chromatographic (HPL) assay were reagent- or UV spectrophotometry-grade chemicals. New Zealand White rabbits, 2 months of age and of either sex, weighing 1.6–2.0 kg were used for the experiments.

Topical Administration and Aqueous Humor Sampling—The rabbits were administered drug with their heads in an upright position while resting in a restraining box. The rabbits were returned to their cages when the sampling interval was >1 hr. A 50-μl volume was instilled onto the cornea of each eye while the lower lid was gently pulled away from the eye globe to form a pocket. The lower eyelid was held against the upper lid for 20 sec after instillation. Second and third instillations were given 2 and 4 min after the first application. The multiple-dose regimen was designed to give aqueous humor concentrations above the sensitivity of the assay. This especially applies to acebutolol hydrochloride, since its permeability was found to be the lowest.

At various postinstillation times, rabbits were sacrificed by a rapid injection of ~25 ml of air into the marginal ear vein. Each cornea was then quickly rinsed with 1 ml of normal saline solution to get rid of residual drug. The aqueous humor samples were withdrawn by puncture with a 26-gauge 0.95-cm needle attached to a 0.5-ml disposable syringe[2] through the corneal–scleral junction into the anterior chamber. The same syringe was used for the opposite eye of each rabbit in order to pool the aqueous humor of both eyes.

The sampling times for each drug are listed in Table I; each value represents an average of 4–12 rabbit eyes. The aqueous humor samples were left in the syringes and were assayed within a few hours. Although rabbit aqueous humor sample volumes varied from animal to animal (ranging from 0.25 to 0.35 ml), a constant volume of sample was used in the assay for each drug.

Extraction and Analyses—A mixer[3] was used to facilitate the mixing and extraction. In 10-ml, glass centrifuge tubes, aqueous humor samples of 0.25 ml were mixed with 0.1 ml of 0.5 *N* NaOH, extracted with 2.0 ml of methylene chloride, and centrifuged. After discarding the aqueous layer, the organic phase was extracted with 1.0 ml of 0.05 *N* sulfuric acid. The acidic aqueous phase was used for HPLC assay of acebutolol.

A 0.30-ml volume of aqueous humor sample was mixed with 0.1 ml of 1 *N* NaOH and extracted with 5 ml of heptane containing 4% isoamyl alcohol in a 10-ml glass centrifuge tube. No centrifugation was necessary

[1] 1% Acebutolol (as hydrochloride salt) contained the following vehicle ingredients: 0.184 g of $NaH_2PO_4 \cdot H_2O$, 0.758 g of Na_2HPO_4, and 0.288 g of NaCl/100 ml of solution. 1% Timolol (as maleate salt) contained the following vehicle ingredients: 0.947 g of Na_2HPO_4, 0.265 g of NaOH, and 0.332 g of NaCl/100 ml of solution. 1% Bufuralol (as hydrochloride salt) contained the following vehicle ingredients: 0.184 g of $NaH_2PO_4 \cdot H_2O$, 0.758 g of Na_2HPO_4, and 0.242 g of NaCl (1.0 g bufuralol hydrochloride)/100 ml of solution.

[2] Glaspack B-D, sterile disposable glass syringe; Becton, Dickinson, and Co., Rutherford, N.J.

[3] Vortex genie mixer, S8223; Scientific Products.

0022-3549/83/1100-1279$01.00/0

1978, pp. 92–188.
(11) G. L. Flynn, S. H. Yalkowsky, and T. J. Roseman, *J. Pharm. Sci.*, 63, 479 (1974).
(12) D. M. Maurice, in "The Structure of the Eye," G. K. Smelser, Ed., Academic, New York and London, 1960, pp. 381–391.
(13) R. Collander, *Acta Chem. Scand.*, 5, 774 (1951).
(14) R. N. Smith, C. Hansch, and M. M. Ames, *J. Pharm. Sci.*, 64, 599 (1975).
(15) A. Leo, C. Hansch, and D. Elkins, *Chem. Rev.*, 71, 525 (1971).
(16) W. D. Stein, "Theoretical and Experimental Biology," Vol. 6, Academic, New York and London, 1967, pp. 73–74, 106–125.
(17) D. M. Maurice in "The Eye," Vol. 1, 2nd ed., H. Davson, Ed., Academic, New York, N.Y., 1969, pp. 6–8, 534–557.

ACKNOWLEDGMENTS

This work was abstracted from a doctoral dissertation submitted by H. S. Huang and was supported in part by Allergan Pharmaceuticals, Irvine, Calif.

The authors express their sincere thanks to Associate Professor Douglas Flanagan for his suggestions.

Corneal Penetration Behavior of β-Blocking Agents III: *In Vitro–In Vivo* Correlations

HONG-SHIAN HUANG *, RONALD D. SCHOENWALD ˣ, and JOHN L. LACH

Received July 26, 1982, from the *Pharmaceutics Division, College of Pharmacy, University of Iowa, Iowa City, IA 52242.* Accepted for publication September 4, 1982. *Present address: National Defense Medical Center, P.O. Box 8244-14, Taipei, Taiwan 107, ROC.

Abstract □ Aqueous humor levels were determined over time after the topical administration to rabbit eyes of 1% isotonic buffered (pH 7.3) solutions of three β-blocking agents, acebutolol hydrochloride, timolol maleate, and bufuralol hydrochloride (arranged in order of increasing lipophilicity). Corneal permeability coefficients, determined from a previous *in vitro* study, were inversely related to the observed time to peak for the three drugs, as expected. Two of the drugs, bufuralol and timolol, did not give the expected rank order for C_{max} and AUC, which could result from differences in distribution and/or elimination processes. Aqueous boundary layers were postulated for *in vivo* corneal permeability which suggested that bufuralol and timolol may have nearly identical effective permeability coefficients *in vivo*.

Keyphrases □ Permeability—acebutolol, timolol, bufuralol, excised rabbit corneas, pharmacokinetics, *in vitro–in vivo* correlations □ Acebutolol—corneal permeability in rabbits, pharmacokinetics, *in vitro–in vivo* correlations □ Timolol—corneal permeability in rabbits, pharmacokinetics, *in vitro–in vivo* correlations □ Bufuralol—corneal permeability in rabbits, pharmacokinetics, *in vitro–in vivo* correlations

In a previous report (1) the penetration behavior of 12 β-blocking agents measured across excised rabbit corneas was correlated with partitioning, which varied over a fourfold logarithmic range. Optimal penetration (log permeability coefficient) reached a maximum at a log distribution coefficient (octanol–buffer, pH 7.65) of ~2–3. Subsequent results (2) showed that a plateau was reached because the stroma, and to a lesser extent the endothelium, became the rate-controlling barrier for the most lipophilic compounds, while the epithelium acted as a rate-determining barrier for the hydrophilic compounds.

The purpose of this study was to determine if the corneal permeability coefficients of three compounds ranging widely in lipophilicity could be correlated with parameters obtained from the aqueous humor–time profile. The three drugs (in descending lipophilic order: bufuralol, timolol, and acebutolol) were administered as 1% isotonic, buffered (pH 7.3) solutions.

EXPERIMENTAL

Reagents and Materials—Isotonic, buffered (pH 7.3), 1% w/v solutions of acebutolol hydrochloride, timolol maleate, and bufuralol hydrochloride were prepared separately[1]. The reagents used for aqueous humor extraction and subsequent high-performance liquid chromatographic (HPL) assay were reagent- or UV spectrophotometry-grade chemicals. New Zealand White rabbits, 2 months of age and of either sex, weighing 1.6–2.0 kg were used for the experiments.

Topical Administration and Aqueous Humor Sampling—The rabbits were administered drug with their heads in an upright position while resting in a restraining box. The rabbits were returned to their cages when the sampling interval was >1 hr. A 50-μl volume was instilled onto the cornea of each eye while the lower lid was gently pulled away from the eye globe to form a pocket. The lower eyelid was held against the upper lid for 20 sec after instillation. Second and third instillations were given 2 and 4 min after the first application. The multiple-dose regimen was designed to give aqueous humor concentrations above the sensitivity of the assay. This especially applies to acebutolol hydrochloride, since its permeability was found to be the lowest.

At various postinstillation times, rabbits were sacrificed by a rapid injection of ~25 ml of air into the marginal ear vein. Each cornea was then quickly rinsed with 1 ml of normal saline solution to get rid of residual drug. The aqueous humor samples were withdrawn by puncture with a 26-gauge 0.95-cm needle attached to a 0.5-ml disposable syringe[2] through the corneal–scleral junction into the anterior chamber. The same syringe was used for the opposite eye of each rabbit in order to pool the aqueous humor of both eyes.

The sampling times for each drug are listed in Table I; each value represents an average of 4–12 rabbit eyes. The aqueous humor samples were left in the syringes and were assayed within a few hours. Although rabbit aqueous humor sample volumes varied from animal to animal (ranging from 0.25 to 0.35 ml), a constant volume of sample was used in the assay for each drug.

Extraction and Analyses—A mixer[3] was used to facilitate the mixing and extraction. In 10-ml, glass centrifuge tubes, aqueous humor samples of 0.25 ml were mixed with 0.1 ml of 0.5 *N* NaOH, extracted with 2.0 ml of methylene chloride, and centrifuged. After discarding the aqueous layer, the organic phase was extracted with 1.0 ml of 0.05 *N* sulfuric acid. The acidic aqueous phase was used for HPLC assay of acebutolol.

A 0.30-ml volume of aqueous humor sample was mixed with 0.1 ml of 1 *N* NaOH and extracted with 5 ml of heptane containing 4% isoamyl alcohol in a 10-ml glass centrifuge tube. No centrifugation was necessary

[1] 1% Acebutolol (as hydrochloride salt) contained the following vehicle ingredients: 0.184 g of $NaH_2PO_4 \cdot H_2O$, 0.758 g of Na_2HPO_4, and 0.288 g of NaCl/100 ml of solution. 1% Timolol (as maleate salt) contained the following vehicle ingredients: 0.947 g of Na_2HPO_4, 0.265 g of NaOH, and 0.332 g of NaCl/100 ml of solution. 1% Bufuralol (as hydrochloride salt) contained the following vehicle ingredients: 0.184 g of $NaH_2PO_4 \cdot H_2O$, 0.758 g of Na_2HPO_4, and 0.242 g of NaCl (1.0 g bufuralol hydrochloride)/100 ml of solution.

[2] Glaspack B-D, sterile disposable glass syringe; Becton, Dickinson, and Co., Rutherford, N.J.

[3] Vortex genie mixer, S8223; Scientific Products.

0022-3549/83/1100-1279$01.00/0

Table I—Aqueous Humor Concentrations of Acebutolol, Timolol, and Bufuralol after Multiple Instillations in Rabbit Eyes of 50 μl of an Isotonic, Buffered (pH 7.3), 1% Solution at 0, 2, and 4 min [a]

Time, min	Aqueous Humor Concentration, μg/ml		
	Acebutolol	Timolol	Bufuralol
7	—	—	20.6 (3.35)
10	0.023 (0.015)	11.3 (0.46)	22.9 (4.22)
20	0.270 (0.014)	—	18.3 (2.71)
25	—	30.7 (3.31)	—
30	0.380 (0.053)	—	7.39 (3.96)
40	—	16.2 (6.26)	4.15 (1.25)
55	0.910 (0.203)	—	1.15 (0.57)
60	—	8.67 (1.02)	—
85	1.260 (0.280)	—	0.33 (0.11)
120	1.120 (0.180)	4.05 (1.08)	0.084 (0.028)
180	0.590 (0.150)	1.66 (1.06)	0.063 (0.014)

[a] Values in parentheses represent one standard deviation.

as the two layers separated completely. A 4-ml volume of the heptane layer was transferred to 1.0 ml of 0.1 *N* HCl in another 10-ml glass tube and mixed. The acidic aqueous layer was then assayed for timolol by HPLC.

Aqueous humor samples of 0.25 ml from bufuralol-treated rabbits were placed into a 10-ml glass centrifuge tube, alkalinized with 0.1 ml of 0.5 *N* NaOH, and extracted with 0.5 ml of heptane containing 1.5% isoamyl alcohol. After centrifugation, 0.4 ml of the heptane layer was transferred to a 4-ml glass vial, extracted with 0.5 ml of 0.1 *N* HCl; and then assayed by HPLC for bufuralol concentration.

Aqueous humor blanks obtained from control rabbits were spiked with various quantities of each drug and extracted by the methods described above. The slopes of the calibration curves were used for calculation of drug concentrations in the unknown aqueous humor samples.

The HPLC system[4] was equipped with an injector[5] consisting of different-sized loops ranging from 50 to 200 μl, which enabled the injection of an accurate sample volume. Each sample was divided so that two injections could be made and the results averaged. The mobile phase for

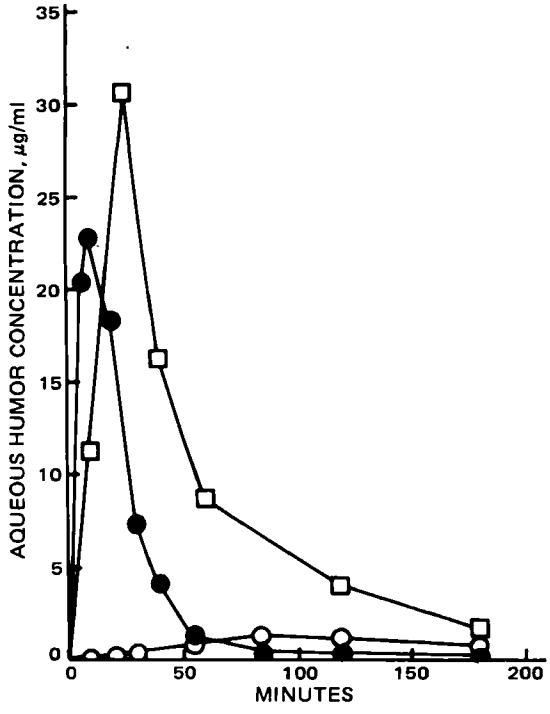

Figure 1—*Aqueous humor concentration–time profiles for three β-blocking agents following multiple instillations in rabbit eyes of 50 μl of an isotonic, buffered (pH 7.3), 1% solution at 0, 2, and 4 min. Key: (□) timolol; (●) bufuralol; (○) acebutolol.*

[4] M-6000A solvent delivery system, Model 440 absorbance detector, μ-Bondapak C18 (acebutolol and timolol) and μ-Bondapak CN (bufuralol) columns, Waters Associates, Milford, MA 01575; Omniscribe Model 5211-1 recorder, Houston Instruments, Austin, Tex.

[5] Model 7125 injector; Rheodyne, Cotati, CA 94928.

Table II—Aqueous Humor Concentration in Comparison with the Excised Corneal Permeability Coefficient and Distribution Coefficient [a]

Drug	t_p[b], min	C_{max}[b], μg/ml	AUC[c], min·μg/ml	P_T[d], 10^{-6} cm/sec	Log DC[e] (octanol–buffer)
Bufuralol	10	22.86	603	57.00	2.31
Timolol	25	30.65	1525	11.70	0.34
Acebutolol	85	1.26	176	0.85	0.20

[a] 50 μl of a 1%, isotonic, buffered (p 7.3) solution was topically administered to rabbit eyes at 0, 2, and 4 min. [b] Time to peak (t_p) and peak concentration (C_{max}). [c] Area under the curve up to last sampling point (180 min). [d] Intrinsic corneal permeability coefficient obtained from *in vitro* permeability experiments (1, 2). [e] Log distribution coefficient between octanol and buffer (pH 7.65) (1, 2).

acebutolol and bufuralol consisted of methanol and 1.5% acetic acid in deaerated, deionized water adjusted to pH 4 with sodium hydroxide (3:7 and 7:18, respectively). For timolol the mobile phase contained 42% methanol and 58% 0.005 *M* heptanesulfonic acid in 1% acetic acid solution adjusted to pH 4. For all three drugs the flow rate was 2.0 ml/min (1). The assay sensitivity for acebutolol and bufuralol was 25 ng/ml; the assay sensitivity for timolol was 50 ng/ml.

Permeability and Distribution Coefficients—The procedures for determining these coefficients, as well as the reported values for each drug used in this study, were reported in the previous papers (1, 2). Both coefficients were determined at pH 7.65.

RESULTS AND DISCUSSION

Following the topical administration of 50 μl of isotonic, buffered (pH 7.3) 1% drug solutions to rabbit eyes at 0, 2, and 4 min; the aqueous humor concentrations at various times were measured. Table I and Fig. 1 list the results obtained for acebutolol, timolol, and bufuralol.

Table II lists the peak concentration (C_{max}), time to peak (t_p), the area under the aqueous humor–time curve through 180 min (AUC), excised corneal permeability coefficient (P_T), and the log distribution coefficient (log DC). A correlation exists between t_p and P_T (and DC). Excluding elimination considerations, the more slowly the drug penetrates, the greater t_p becomes; theoretically, this will occur as the lipophilicity of

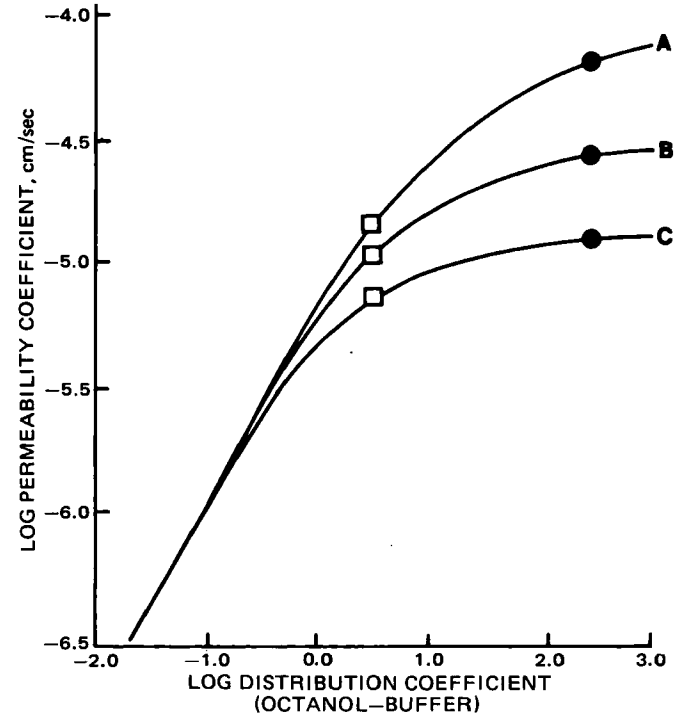

Figure 2—*Simulated curves for the log–log plot of permeability coefficient* versus *distribution coefficient (octanol–buffer, pH 7.65) for intact cornea in the presence of various postulated thicknesses of aqueous humor diffusional layers. Key: (A) none, (B) 0.15 cm, (C) 0.45 cm; (●) bufuralol; (□) timolol.*

the drug decreases. Acebutolol has the lowest cornea permeability coefficient and, thus, has the longest t_p (85 min). Bufuralol has the shortest t_p (10 min), whereas timolol has an intermediate t_p of 25 min. Acebutolol has the lowest C_{max} and AUC; these results are expected for a hydrophilic drug which does not rapidly penetrate the cornea. Although bufuralol is much more lipophilic than timolol, its C_{max} and AUC are actually less than the values reported for timolol (Table II).

These drugs differ structurally and therefore could vary not only in penetration, but also in distribution, metabolism, and excretion processes. Consequently, C_{max}, t_p, and AUC may not necessarily correlate perfectly to the permeability coefficient. The t_p value is perhaps the parameter most likely to show a perfect correlation. This is reasoned from the work of Makoid and Robinson (3), who determined the ophthalmic pharmacokinetics of pilocarpine topically applied to the rabbit eye. From their work an equation was developed for t_p:

$$t_p = \frac{\ln \frac{k_{10}}{k_{23}}}{k_{10} - k_{23}} \qquad \text{(Eq. 1)}$$

where k_{10} is the precorneal loss rate constant and k_{23} is the loss rate constant from cornea to aqueous humor. The permeability coefficient would be directly related to k_{23}. Equation 1 assumes that k_{10} is much larger than uptake into the epithelium of the cornea from the precorneal area. This assumption applies to most, if not all, ophthalmic drugs, since k_{10} is a function of scleral absorption as well as drainage rate, the latter being relatively large for aqueous solutions. The drainage rate would be expected to be the same for each β-blocking agent at the same pH and osmolarity.

Both C_{max} and AUC are a function of distribution to corneal tissue and elimination from the eye in addition to penetration. A smaller AUC or C_{max} may result from a larger volume of distribution within the eye and/or from a more rapid elimination from the aqueous humor. For drugs with large differences in P_T, such that this factor predominates, perfect correlations between P_T and C_{max} or AUC may be more likely. However, if aqueous boundary layers are significant this may not be true. Aqueous boundary layers have been shown to play an important role in intestinal absorption. For high lipophilic compounds, the absorption rate assumes a plateau with a maximal rate; intestinal absorption is limited by the rate of diffusion through the aqueous diffusional barrier adjacent to the mucous membrane.

Aside from disposition considerations, drug permeation across the cornea *in vivo* may be significantly hindered by the diffusional layers on both sides of the cornea. The aqueous boundary layer adjacent to the endothelium and within the anterior chamber may be large. The physiological aqueous volume of the rabbit is 287 μl with a turnover rate of ~1%/min (4, 5). It is difficult to estimate the effective diffusional layer thickness in aqueous humor that would exist in the presence of this turnover rate. It is possible that a turnover rate of 1% would have a negligible mixing effect on the aqueous humor compared with the stirring in the modified perfusion chamber. For example purposes let us assume that the entire anterior chamber volume is a barrier. Since the aqueous diffusional layer represents the entire sampling volume for drug analysis, only half of the aqueous humor thickness can be used as the diffusional layer. As a result, the diffusional layer is estimated to be ~0.15 cm[6].

In the precorneal region the thickness of the tear film ($6–7 \times 10^{-4}$ cm) could also serve as an aqueous boundary layer (6). Although blinking of the eyelid mixes the drug with the tear film, it may also reduce the size of an aqueous boundary layer to below the thickness of the tear film. Regardless, it is probably small and not significant in size compared with the potential aqueous barrier in the anterior chamber.

To show the effect of a postulated *in vivo* aqueous boundary layer in addition to corneal layer resistances, curves were simulated for the log–log plot of permeability coefficient *versus* distribution coefficient. These curves[7] are shown in Fig. 2 for intact cornea in the presence of postulated aqueous boundary layers of 0, 0.15, and 0.45 cm. As the aqueous boundary layer increases, the plateau region in curves B and C occur at a lower distribution coefficient. Also, the maximum log permeability coefficient is greatly reduced. Therefore, if we consider these additional boundary resistances, which may exist *in vivo*, it is likely that the log P_T[8] *versus* log DC curve would form a plateau at lower log DC values than calculated from the *in vitro* experiments (1, 2). This suggests that timolol and bufuralol may have nearly identical effective permeability coefficients *in vivo*. Although the results shown in Fig. 2 may not explain the lack of a perfect correlation between the *in vitro* permeability and distribution coefficients for two of the drugs, it should be realized that another prodrug more lipophilic than timolol may not increase the penetration rate.

REFERENCES

(1) R. D. Schoenwald and H. S. Huang, *J. Pharm. Sci.*, **72**, 1266 (1983).

(2) H. S. Huang, R. D. Schoenwald, and J. L. Lach, *J. Pharm. Sci.*, **72**, 1272 (1983).

(3) M. C. Makoid and J. R. Robinson, *J. Pharm. Sci.*, **68**, 435 (1979).

(4) T. J. Mikkelson, S. S. Chrai, and J. R. Robinson, *J. Pharm. Sci.*, **62**, 1648 (1973).

(5) J. M. Conrad and J. R. Robinson, *J. Pharm. Sci.*, **66**, 219 (1977).

(6) I. Fatt in "Physiology of the Eye," Butterworth, Woburn, Mass., 1978, p. 206.

ACKNOWLEDGMENTS

This work was abstracted in part from a doctoral dissertation submitted by Hong-Shian Huang to the Graduate College, University of Iowa.

The study was supported in part by Allergan Pharmaceuticals, Irvine, Calif.

[6] The anterior chamber can be assumed crudely to represent a cylinder with a radius r, a height h, and a volume V equal to 287 μl or ~0.3 cm^3. Since $V = \pi r^2 h$, h is calculated to be 0.15 cm.

[7] The curves in Fig. 2 were generated from Eq. 20 in Ref. 2 with the additional consideration of an R_{aq} = 0.15 and 0.45. Equation 20 in Ref. 2 equates the permeability coefficient to the sum of the reciprocal of the resistances of each boundary layer.

[8] P_T represents the intrinsic permeability coefficient for excised corneas for which the *in vitro* R_{aq} was substracted.

Anti-inflammatory Agents III: Structure–Activity Relationships of Brusatol and Related Quassinoids

I. H. HALL ˣ, K. H. LEE, Y. IMAKURA, M. OKANO, and A. JOHNSON

Received June 14, 1982, from the *Division of Medicinal Chemistry, School of Pharmacy, University of North Carolina, Chapel Hill, NC 27514.* Accepted for publication September 21, 1982.

Abstract □ A series of quassinoids were observed to be potent inhibitors of induced inflammation and arthritis in rodents. Brusatol afforded the most potent activity followed by brucein-D. A 3-hydroxy-Δ^3-2-oxo moiety in brusatol or a 1-hydroxy-Δ^3-2-oxo moiety in brucein-D, as well as a C-15 ester-bearing δ-lactone ring in brusatol and C-11 and C-12 free hydroxyl groups are required in both quassinoids for potent anti-inflammatory activity. Preliminary studies indicate that one of the modes of action of quassinoids as anti-inflammatory agents is to stabilize lysosomal membranes, reducing the release of hydrolytic enzymes that cause damage to surrounding tissues.

Keyphrases □ Anti-inflammatory agents—potential, brusatol and related quassinoids, structure–activity relationships □ Brusatol—related quassinoids, anti-inflammatory potential, structure–activity relationships □ Structure–activity relationships—brusatol and related quassinoids, anti-inflammatory potential

Previously, a series of pseudoguaianolides and germacranolides were reported to possess potent anti-inflammatory and antiarthritic activity in rodents (1, 2). Common to all of these compounds is the inclusion within their structure of an α-methylene-γ-lactone moiety which is a γ-lactone enone system. Those compounds containing an α-methylene-γ-lactone were ~2–4 times more potent than indomethacin in rodent screens. Since quassinoids contain a cyclohexanone enone system within their structure in addition to a δ-lactone ring, a study was undertaken to investigate a series of quassinoids and their ester derivatives for anti-inflammatory activity. Furthermore, brusatol-producing *Brucea javanica* and other quassinoid-producing species, such as *Simaba cedron*, have been observed to have anti-inflammatory activity (3, 4).

Bruceantin is an antineoplastic agent used in clinical trials in humans. Previous studies have shown that brusatol (I) and bruceantin (II) suppress oxidative phosphorylation of P-388 lymphocytic leukemia cells (5) and inhibit lysosomal hydrolytic enzymatic activities, *e.g.*, cathepsin and ribonuclease (6). Aspirin-type anti-inflammatory agents uncouple oxidative phosphorylation, and corticosteroids stabilize lysosomal membranes. Thus, both modes of action are important to anti-inflammatory activity.

EXPERIMENTAL

Source of Compounds—Bruceoside-A (X), brucein-D (XIII), and brucein-E (XIV) were originally isolated from *B. javanica* (7). Brusatol (I) was obtained either by treating bruceoside-A (X) with 3 *N* H_2SO_4–methanol (1:1) to hydrolyze the glycosidic linkage (7, 8) or directly from the chloroform extract of *B. javanica*. Bruceantin (II) and bruceolide (III) were obtained from bruceoside-A by a synthetic procedure (9). The chemical synthesis, purification, and physical characteristics of a series

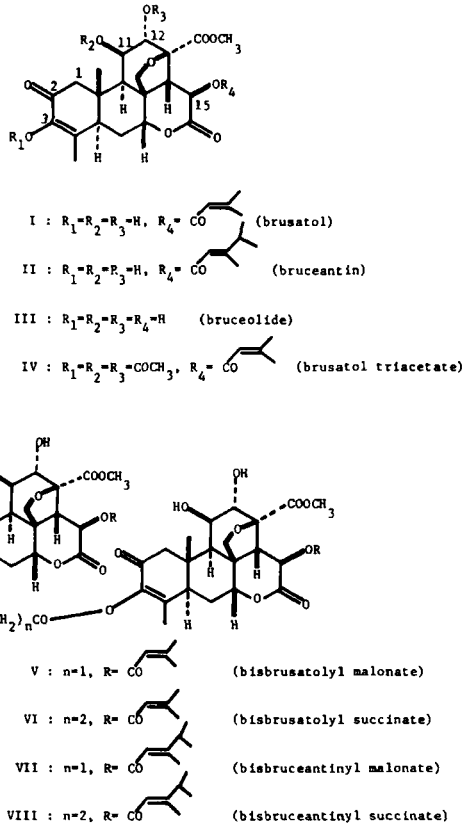

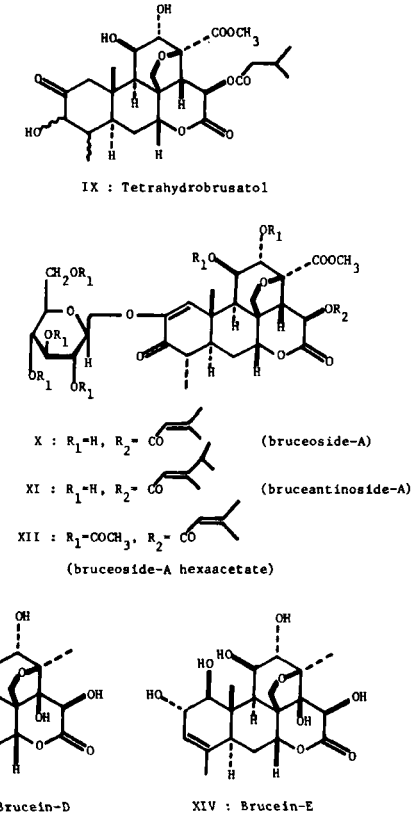

0022-3549/83/1100-1282$01.00/0

Table I—Anti-inflammatory Activity of Quassinoids in Male Rats [a]

Compound	Percent of Control	
	0.25 mg/kg, Administered Twice	1 mg/kg, Administered Twice
I Brusatol	33 ± 4[b]	18 ± 3[b]
II Bruceantin	51 ± 6[b]	25 ± 4[b]
III Bruceolide	71 ± 6[b]	60 ± 5[b]
IV Brusatol triacetate	81 ± 7[b]	70 ± 8[b]
V Bisbrusatolyl malonate	62 ± 5[b]	60 ± 4[b]
VI Bisbrusatolyl succinate	72 ± 8[b]	70 ± 8[b]
VII Bisbruceantinyl malonate	72 ± 9[b]	62 ± 9[b]
VIII Bisbruceantinyl succinate	69 ± 8[b]	60 ± 7[b]
IX Tetrahydrobrusatol	69 ± 5[b]	54 ± 6[b]
X Bruceoside-A	83 ± 8	68 ± 7[b]
XI Bruceantinoside-A	98 ± 10	72 ± 9[b]
XII Bruceoside-A-hexacetate	73 ± 6[b]	65 ± 5[b]
XIII Brucein-D	64 ± 5[b]	37 ± 5[b]
XIV Brucein-E	78 ± 4[b]	66 ± 6[b]
Indomethacin (10 mg/kg, administered twice)	—	27 ± 6[b]
Phenylbutazone (50 mg/kg, administered twice)	—	53 ± 5[b]
Control (0.05% polysorbate 80)	100 ± 10	100 ± 9

[a] Mean ± *SD;* six animals per group. [b] Significant, $p \leq 0.001$.

of brusatolyl and bisbrusatolyl esters (IV–VI) (10), two bisbruceantinyl esters (VII and VIII) (11) and tetrahydrobrusatol (IX) (10) have been reported previously by this laboratory. Bruceantinoside-A (XI) was isolated from *Brucea antidysenterica* by a published procedure (12), and bruceoside-A hexaacetate (XII) was synthesized from bruceoside-A (8).

Anti-inflammatory Screen—Sprague–Dawley male rats (~160 g) were administered test compounds at 0.25 and 1.0 mg/kg in 0.05% polysorbate 80–water at 3 hr and again at 30 min prior to injection of 0.2 ml of 1% carrageenan in saline into the plantar surface of the right hindfoot. Isotonic saline was injected into the left hindfoot, which served as a baseline. After 3 hr, both feet were excised at the tibiotarsal (ankle) joint according to a modified method (13), resulting in an average net weight increase of 0.655 g for the control animals. Indomethacin and phenylbutazone were used as standards.

Antiarthritic Screen—Male Sprague–Dawley rats (~160 g) were injected at the base of the tail with 0.2 ml of light mineral oil containing 1 mg of dried *Mycobacterium butyricum* and 0.4 mg of digitonin. The test drugs were administered on days 3–20 at 0.25 and 0.50 mg/kg/day ip. Animals were sacrificed on day 21, and the feet were excised and weighed (14). The control animals achieved an average net weight increase of 0.830 g.

Writhing Reflex—The writhing reflex also was utilized as an analgesic test. Mice were administered the test drugs at 0.25, 0.5, and 1.0 mg/kg ip 20 min prior to the administration of 0.5 ml of 0.6% acetic acid (15). After 5 min, the number of stretches, characterized by repeated contractures, was counted for 10 min. The control mice averaged 78 stretch reflexes/10 min.

Cell Preparation—Metabolic studies were conducted on CF_1 male mouse (~30 g) liver homogenates. Homogenates (10%) were prepared using a pestle in 0.25 *M* sucrose and 0.001 *M* EDTA (ethylenediaminetetraacetic acid) at pH 7.2.

Oxidative Phosphorylation Studies—Basal and adenosine diphosphate-stimulated respirations of the 10% liver homogenates of CF_1 male mice were measured using succinate or α-ketoglutarate as the substrate (16). The reaction vessel contained sucrose (55 μmoles), potassium chloride (22 μmoles), dibasic potassium phosphate (22 μmoles), sodium succinate (90 μmoles) or α-ketoglutarate (60 μmoles), and the test compounds (brusatol, bruceantin, and bruceoside-A) at 25, 50, and 100 μ*M* in 0.05% polysorbate 80–water in a total volume of 1.8 ml.

Oxygen consumption was measured using a Clark electrode connected to an oxygraph. After the basal metabolism (state 4) level was obtained, 0.257 μmole of adenosine diphosphate was added to obtain the adenosine diphosphate-stimulated respiration rate (state 3). The respiration rate was calculated in microliters of oxygen consumed per hour per milligram of wet weight of CF_1 mouse liver homogenate. *In vivo* oxidative phosphorylation studies were conducted on male mice and rats treated with

Table II—Effects of Quassinoids on the Writhing Reflex of Male Mice [a]

Compound	Dose, mg/kg	Percent of Control
I Brusatol	0.3	61 ± 5[b]
	0.6	42 ± 4[b]
	1.2	71 ± 6[b]
II Bruceantin	0.6	63 ± 7[b]
X Bruceoside-A	0.6	65 ± 8[b]
Indomethacin	10	43 ± 7[b]
Control (0.05% polysorbate 80)	—	100 ± 6

[a] Mean ± *SD;* six animals per group. [b] Significant, $p \leq 0.001$.

brusatol at 0.25 mg/kg/day for 3 days. Animals were sacrificed on day 4, and liver homogenates were prepared for the respiration studies.

Lysosomal Hydrolytic Enzymatic Activities—Free and total acid phosphatase activities were studied using 0.1 *M* β-glycerol phosphate in pH 5.0, 0.1 *M* acetate buffer incubated with CF_1 mouse liver homogenates for 30 min (17). The test drugs were incubated *in vitro* at 25, 50, and 100 μ*M* in 0.05% polysorbate 80–water. The total enzymatic activity was obtained by treating the liver homogenates with 0.02% alkylphenoxypolyethoxyethanol 100 to release the bound hydrolytic enzymes from the lysosomal membrane. The reaction was terminated with 10% trichloroacetic acid, and the mixture was centrifuged. Inorganic phosphate was determined by the method of Chen *et al.* (18). Free, total, and percent released acid phosphatase activities were calculated after correcting for the blank values.

Free and total cathepsin activities were determined in an analogous manner on mouse liver homogenates with 2% azocasein as the substrate in pH 5.0, 0.1 *M* acetate buffer (19). The supernatant was assayed for acid-soluble peptide fragments at 366 nm. Free, total, and percent released cathepsin activities were calculated after correcting for the blank values.

Prostaglandin Synthetase Activity—The incubation medium of Tomlinson *et al.* (20) was used to determine the [^{3}H]prostaglandin formation from [^{3}H]arachidonic acid (86.2 Ci/mmole) and 10 mg of purified commercial prostaglandin synthetase from bovine seminal vesicles. After 1 hr at 37°, the reaction was terminated with 1 *N* HCl, and the mixture was extracted with ether and evaporated. The residue was dissolved in ethyl acetate and spotted on silica gel TLC plates, which were eluted with chloroform–methanol–water–acetic acid (90:8:1:0.8) (21). The plates were dried and developed in iodine vapor; with the use of prostaglandin standards, the appropriate areas were scraped and counted for tritium content. Indomethacin was used as an internal standard at 10^{-4} and 10^{-6} *M*. Quassinoids were tested at 25, 50, and 100 μ*M* final concentrations.

RESULTS AND DISCUSSION

In Tables I–VI the values are presented as percent of control ± the standard deviation. The number of animals in each group was six.

The quassinoids demonstrated significant anti-inflammatory activity at 0.25 and 1 mg/kg in Sprague–Dawley rats (Table I). When tested at 1 mg/kg, all of the quassinoids showed at least 30% reduction of inflammation. Brusatol (I) was the most potent compound, demonstrating higher activity at 1 mg/kg than indomethacin at 10 mg/kg. The hydroxy enone ring-A system (as seen in I, II, and XIII) and an ester group attached to C-15 of the δ-lactone ring of I and II are required for potent anti-inflammatory activity, as either reduction of the ring-A enone olefinic bond or removal of the C-15 ester group (as in IX and III, respectively) led to decreased activity. Esterification of the hydroxyl groups at C-3, C-11, and C-12 or glucosidation of the hydroxyl group at C-2 gave rise to less active compounds (*e.g.*, IV, V–VIII, and X–XII). In addition, a reduction of the ring-A enone carbonyl group of XIII to an α-glycol (XIV) also caused a diminution in activity. Thus, the structural requirement for the potent anti-inflammatory activity of the foregoing brusatol-related quassinoids may include either a 3-hydroxy-Δ^3-2-oxo

Table III—Effects of Quassinoids on Chronic Adjuvant-Induced Arthritis in Male Rats [a]

Compound	Dose, mg/kg	Percent of Control
I Brusatol	0.25	51 ± 6[b]
	0.50	49 ± 6[b]
Indomethacin	10	55 ± 5[b]
Control (0.05% polysorbate 80)	—	100 ± 9

[a] Mean ± *SD*, six animals per group. [b] Significant $p \leq 0.001$.

Table IV—Effects of Quassinoids on the Oxidative Phosphorylation Process of Male Mouse Liver Homogenates [a]

Compound	Percent of Control			
	Succinate		α-Ketoglutarate	
	State 4	State 3	State 4	State 3
In vitro				
I Brusatol, 100 μM	101 ± 8	93 ± 8	96 ± 7	95 ± 9
II Bruceantin, 100 μM	97 ± 7	95 ± 6	93 ± 4	97 ± 6
X Bruceoside-A, 100 μM	95 ± 4	96 ± 7	89 ± 7	93 ± 6
Control (0.05% polysorbate 80)	100 ± 12[b]	100 ± 12[c]	100 ± 9[d]	100 ± 11[e]
In vivo				
I Brusatol, 0.25 mg/kg/day	95 ± 5	98 ± 6	97 ± 5	92 ± 8
Control (0.05% polysorbate 80)	100 ± 12[b]	100 ± 8[c]	100 ± 11[d]	100 ± 13[e]

[a] Mean ± *SD*; six animals per group. [b] 5.92 μl O_2 consumed/hr/mg of wet tissue. [c] 11.31 μl O_2 consumed/hr/mg of wet tissue. [d] 3.51 μl O_2 consumed/hr/mg of wet tissue. [e] 5.21 μl O_2 consumed/hr/mg of wet tissue.

moiety in ring-A for I or a 1-hydroxy-Δ^3-2-oxo moiety in ring-A of XIII, a C-15 ester bearing δ-lactone ring-D of I, and the free hydroxyl groups at C-11 and C-12.

Brusatol at 0.6 mg/kg appeared to be as potent as indomethacin at 10 mg/kg in reducing the writhing reflex in mice, which is a test for irritant or inflammation pain (Table II). After 3 weeks administration, brusatol effectively reduced induced chronic arthritis in rats at 0.25 and 0.50 mg/kg/day, which was comparable to the activity of indomethacin at 10 mg/kg/day (Table III).

Although an in-depth mode of action study was not carried out, preliminary data (Table IV) indicates that brusatol and bruceantin did not uncouple oxidative phosphorylation of liver mitochondria with succinate as substrate (which is a flavin adenine dinucleotide dehydrogenase) or with α-ketoglutarate (a nicotinic adenine dinucleotide-linked dehydrogenase) in both the *in vitro* and *in vivo* studies. It has been noted before that quassinoids uncouple oxidative phosphorylation of P-388 lymphocytic leukemia cells, but not liver cells (3). The quassinoids tested did not inhibit prostaglandin synthesis using an isolated enzyme system (Table V); however, indomethacin did effectively inhibit prostaglandin synthesis in this system. Brusatol and bruceantin reduced the release of hydrolytic enzymes from lysosomes of the liver (Table VI). Both acid phosphatase and cathepsin release was inhibited significantly. Brusatol and bruceantin inhibited acid phosphatase release 49 and 60%, respectively, at 100 μM. Cathepsin activity was inhibited 78% by brusatol at 25 μM and 30% by bruceantin at 100 μM. Elevated cathepsin activity has previously been related to the inflammation process, and suppression of the enzymatic activity has been linked to anti-inflammatory action (22). The margin of inhibition of free lysosomal enzyme release by the quassinoid is sufficient to account for the anti-inflammatory activity observed. Quassinoids have been observed to inhibit other lysosomal enzymes in P-388 cells (4).

Other studies have established that the antineoplastic activity of quassinoids is linked directly to their ability to suppress the elongation step of protein by blocking the peptidyl synthetase reaction of P-388 cells. The inhibition of protein synthesis may be important in the rapid proliferation of lymphocytes and polymorphonuclear neutrophils during the inflammation process. Therefore, this mode of action cannot be excluded as a mode for the anti-inflammatory action of quassinoids.

Table V—*In Vitro* Effects of Quassinoids on Prostaglandin Synthetase Activity [a]

Compound	dpm of Prostaglandin Formed/hr	Percent of Control
I Brusatol		
25 μM	61377 ± 3387	102 ± 6
50 μM	63278 ± 3511	104 ± 6
100 μM	63114 ± 3109	108 ± 5
II Bruceantin, 100 μM	64392 ± 3686	107 ± 6
Indomethacin	36482 ± 2033[b]	60 ± 3[b]
Control (0.05% polysorbate 80)	60389 ± 3453	100 ± 6

[a] Mean ± *SD*; six animals per group. Conversion from [^{3}H]arachidonic acid to prostaglandins = 69.9%. [b] Significant, $p \leq 0.001$.

Table VI—*In Vitro* Effects of Quassinoids on Male Mouse Liver Lysosomal Hydrolytic Enzymes [a]

Compound	Percent of Control	
	Free Acid Phosphatase Activity	Free Cathepsin Activity
I Brusatol		
25 μM	72 ± 6[d]	22 ± 3[d]
50 μM	65 ± 6[d]	66 ± 7[d]
100 μM	51 ± 5[d]	73 ± 6[d]
II Bruceantin, 100 μM	40 ± 4[d]	64 ± 5[d]
Control (0.05% polysorbate 80)	100 ± 8[b]	100 ± 6[c]

[a] Mean ± *SD*; six animals per group. [b] 0.753 mg of phosphate released/hr/g wet tissue. [c] 2.688 mg of amino acids released/hr/g wet tissue. [d] Significant, $p \leq 0.001$.

REFERENCES

(1) I. H. Hall, K. H. Lee, C. O. Starnes, Y. Sumida, R. Y. Wu, T. G. Waddell, J. W. Cochran, and K. G. Gerhart, *J. Pharm. Sci.*, **68**, 537 (1979).

(2) I. H. Hall, C. O. Starnes, Jr., K. H. Lee, and T. G. Waddell, *J. Pharm. Sci.*, **69**, 537 (1980).

(3) T. A. Geissman, *Annu. Rev. Pharmacol.*, **4**, 305 (1964).

(4) "Chung Yao Ta Tzu Tien," Vol. 2, Shanghai Ko Hseuh Chi Shu Press, Hong Kong, 1978, p. 1643.

(5) S. A. ElGebaly, I. H. Hall, K. H. Lee, Y. Sumida, Y. Imakura, and R. Y. Wu, *J. Pharm. Sci.*, **68**, 887 (1979).

(6) I. H. Hall, K. H. Lee, S. A. ElGebaly, Y. Imakura, Y. Sumida, and R. Y. Wu, *J. Pharm. Sci.*, **68**, 883 (1979).

(7) K. H. Lee, Y. Imakura, and H. C. Huang, *J. Chem. Soc. Chem. Commun.*, **69**, (1979).

(8) K. H. Lee, Y. Imakura, Y. Sumida, R. Y. Wu, I. H. Hall, and H. C. Huang, *J. Org. Chem.*, **44**, 2180 (1979).

(9) M. Okano and K. H. Lee, *J. Org. Chem.*, **46**, 118 (1981).

(10) K. H. Lee, M. Okano, I. H. Hall, D. A. Brent, and B. Saltmann, *J. Pharm. Sci.*, **71**, 338 (1982).

(11) I. H. Hall, K. H. Lee, M. Okano, D. Sims, T. Ibuka, Y. F. Liou, and Y. Imakura, *J. Pharm. Sci.*, **70**, 1147 (1981).

(12) M. Okano, K. H. Lee, and I. H. Hall, *J. Natl. Prod.*, **44**, 470 (1981).

(13) A. P. Roszkowski, W. H. Rooks, A. Tomolonis, and L. M. Miller, *J. Pharmacol. Exp. Ther.*, **179**, 114 (1971).

(14) B. H. Waksman, C. M. Pearson, and J. T. Sharp, *J. Immunol.*, **85**, 403 (1960).

(15) R. Vingar, J. F. Traux, and J. L. Selph, *Eur. J. Pharmacol.*, **37**, 23 (1976).

(16) I. H. Hall and G. L. Carlson, *J. Med. Chem.*, **19**, 1257 (1976).

(17) R. Gianetto and C. deDuve, *Biochem. J.*, **59**, 433 (1955).

(18) P. S. Chen, T. Y. Toribara, and H. Warner, *Anal. Chem.*, **28**, 1756 (1956).

(19) W. D. Schleuning and H. Fritz, *Methods Enzymol.*, **XLV**, 330 (1976).

(20) R. V. Tomlinson, H. J. Ringold, M. C. Qureshi, and E. Forchielli, *Biochem. Biophy. Res. Commun.*, **46**, 552 (1972).

(21) M. Glatt, H. Kälin, K. Watner, and K. Borene, *Agents Action*, **7**, 321 (1977).

(22) O. Rojas-Espinosa and A. M. Dannenberg in "Inflammation and Anti-inflammatory Therapy," G. Katona and J. R. Blengio, Eds., Spectrum, New York, N.Y., 1974, p. 31.

ACKNOWLEDGMENTS

Supported in part by U.S. Public Health Service Research Grant CA-17625 awarded to K. H. Lee and I. H. Hall.

Parts I and II are References 1 and 2, respectively.

Plant Anticancer Agents XXVII: Antileukemic and Cytotoxic Constituents of *Dirca occidentalis* (Thymelaeaceae)

MOHAMMED M. BADAWI, SUKHDEV S. HANDA, A. DOUGLAS KINGHORN[x], GEOFFREY A. CORDELL, and NORMAN R. FARNSWORTH

Received August 12, 1982, from the *Department of Pharmacognosy and Pharmacology, College of Pharmacy, University of Illinois at the Medical Center, Chicago, IL 60612.* Accepted for publication September 7, 1982.

Abstract □ Two antileukemic daphnane esters, Pimelea factor P_2 (I) and the new compound dircin (II), were isolated from the twigs and flowers of *Dirca occidentalis* A. Gray (Thymelaeaceae). Three lignans, (−)-medioresinol (III), (+)-syringaresinol (IV), and (−)-lariciresinol (V), as well as the coumarin daphnoretin (VI), were found to be additional cytotoxic constitents of this taxon.

Keyphrases □ *Dirca occidentalis* (Thymelaeaceae)—isolation of antileukemic and cytotoxic constituents, daphnane esters and lignans, identification □ Daphnane esters—isolation from *Dirca occidentalis* (Thymelaeaceae), identification, antileukemic and cytotoxic potential □ Lignans—isolation from *Dirca occidentalis* (Thymelaeaceae), identification, antileukemic and cytotoxic potential □ Antileukemic agents—potential, daphnane esters and lignans isolated from *Dirca occidentalis* (Thymelaeaceae), cytotoxicity

Dirca occidentalis, one of two species representing a small genus in the family Thymelaeaceae indigenous to North America (1), is native to the Pacific States, where it is known by the colloquial name of western leatherwood (2). Although no laboratory studies appear to have been performed on either *D. occidentalis* or *Dirca palustris* L., the bark of *D. palustris* is highly vesicant to the skin and produces severe vomiting and purgation when ingested (3, 4).

In a continuing search for anticancer agents of plant origin[1], our attention turned to *D. occidentalis* after a chloroform extract of a combined sample of the twigs and flowers was found to display significant *in vivo* and *in vitro* activity against the P-388 lymphocytic leukemia system[2] when tested according to standard protocols (6). In this paper, we report the isolation and identification of two antileukemic daphnane ester principles from this plant, Pimelea factor P_2 (I) and the novel compound dircin (II). In addition, four other cytotoxic constituents were isolated, namely, the lignans (−)-medioresinol (III), (+)-syringaresinol (IV), and (−)-lariciresinol (V) and the coumarin daphnoretin (VI).

DISCUSSION

The molecular mass of dircin (II) was determined as 696 daltons by field-desorption mass spectrometry, a value consistent with a molecular formula of $C_{39}H_{52}O_{11}$. Comparison of the spectroscopic data (UV, IR, ^{1}H-NMR, MS) obtained for this isolate with those of Pimelea factor P_2 (I) and other 1α-alkyldaphnane derivatives (7–9), suggested that II is an acetoxy derivative of Pimelea factor P_2 (I). Thus, observations of

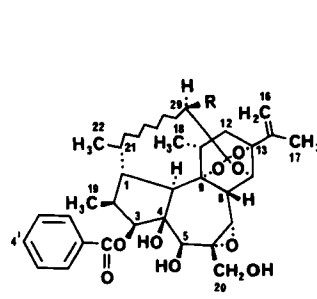

I: R = H
II: R = $OCOCH_3$

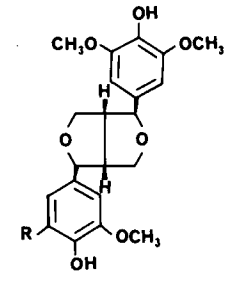

III: R = H
IV: R = OCH_3

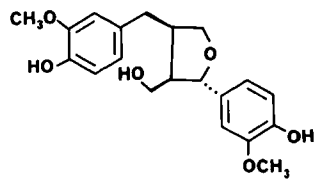

V

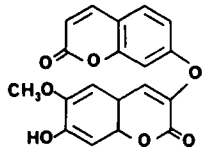

VI

similar chemical shifts in the ^{1}H-NMR spectra of I and II permitted the assignment in the latter compound of methyl groups attached to C-2, C-11, and C-21; an isopropenyl group at C-13; a C-6α,C-7α-epoxide bridge; a C-9α,C-13α,C-14α-orthoester function; a 1α-alkyl chain; and a benzoate ester substituent at C-3. The remaining sites for possible esterification by an acetate group are at hydroxy groups attached to C-4, C-5, C-20, or at some other site in the molecule. The first of these alternatives was ruled out because esterification of this tertiary hydroxy group is unlikely, and no C-4-esterified tigliane or daphnane esters have been found as natural products to date (10). In addition, no resonance shifts in the ^{1}H-NMR spectrum of II relative to that of I for the protons adjacent to C-4 suggested such ester substitution. Likewise, a lack of esterification at either C-5 or C-20 in II was evident from the observation of resonances at δ 4.05 and 3.81 ppm, respectively (7–9). Since no signal assignable for a C-12 methine proton was present in the ^{1}H-NMR spectrum of II at ~δ 5.00 ppm (11, 12), such as that observed at δ 4.93 ppm in the ^{1}H-NMR spectrum of the positional isomer of II, linifolin a (12β-acetoxy-Pimelea factor P_2) (8), by a process of elimination the acetate group was placed in the alkyl chain of II. Similarities in the ^{1}H-NMR resonances assigned for the C-16 methylene protons in II(δ 4.88, 5.07 ppm) with those in the 29β-hydroxylated 1α-alkyldaphnane ester gnidimacrin (δ 4.85, 5.09) [a structure established by X-ray crystallography (9)] suggested the presence of a 29β-acetoxy function in II. In support of this the C-16 methylene protons in Pimelea factor P_2 (I), with no electronegative group substitution at C-29 on the alkyl chain, were found to resonate in a slightly upfield position at δ 4.85 and 4.96 ppm. The observation of the C-29 methine proton chemical shift at δ 5.28 ppm as a doublet in the ^{1}H-NMR spectrum of II suggested that coupling was apparent with only the *cis*-oriented C-28 methylene proton.

The structural assignment proposed here for dircin (II) is tentative, since the limited amounts of this isolate obtained in this investigation did not permit selective hydrolysis experiments to be performed to confirm the relative positions of ester substitution. However, support for our assignment of dircin as II may be gathered from the fact that all 3-esterified 1α-alkyldaphnane esters isolated to date from plants of the

[1] For the previous article in this series, see Ref. 5.

[2] Plant extracts, fractions, and isolates were tested under the auspices of the Drug Research and Development Program of the National Cancer Institute. A compound is considered active *in vivo* if it exhibits a prolongation of life in excess of 125% and is regarded as cytotoxic if the ED_{50} is ≤4 μg/ml. In *in vivo* testing, samples were administered intraperitoneally to six CD_2F_1 male tumor-bearing mice over a 10-day period. Evaluation was carried out by comparison of survival times with control tumor-bearing animal groups.

0022-3549/83/1100-1285$01.00/0

Table I—Antileukemic and Cytotoxic Activity of *Dirca occidentalis* Isolates [a]

Compound	NSC Number	P-388 Screen *In Vivo* Dose, μg/kg	*In Vivo* % T/C	*In Vitro* ED_{50}, μg/ml
Pimelea factor P_2 (I)	334694	400	147	0.0000012
		200	127	
		100	110	
		50	116	
		25	110	
Dircin (II)	334696	125	156	0.00000025
		62.5	147	
		31.3	125	
(−)-Medioresinol (III)	329245	NT[b]		0.33
(+)-Syringaresinol (IV)	329246	2000	100	0.41
		1000	108	
		500	107	
		250	96	
(−)-Lariciresinol (V)	329247	NT[b]		0.23
Daphnoretin (VI)	291852	2000	107	3.5
		1000	100	
		500	95	
		250	100	

[a] Tested according to standard protocols (6). [b] NT = not tested.

Thymelaeaceae have been found to possess a benzoate group at C-3 (7–10). Dircin (II) is thus assigned as 29β-acetoxy-Pimelea factor P_2, being the 29β-acetate ester of the parent structure 1,2,6,7-tetrahydro-5,29-dihydroxy-21-methyl-6α,7α-epoxy-1α-nonylresiniferonol-30-oic acid (10).

Daphnane esters (8–14), lignans (15, 16), and coumarins (5, 15) have all been found previously as antileukemic and/or cytotoxic constituents of plants in the family Thymelaeaceae. It is pertinent to point out that while Pimelea factor P_2 (linifolin b) was determined in an earlier investigation to be devoid of activity against the P-388 lymphocytic leukemia system *in vivo* (8), this compound was shown to be active against this test system at the higher dose levels used in this study (Table I). Dircin (II), the most potent of the compounds isolated from *D. occidentalis* (Table I), exhibits somewhat less intense activity in the P-388 test system than demonstrated by the 1α-alkyldaphnane esters gnidimacrin and gnidimacrin 20-palmitate, which were isolated from *Gnidia subcordata* Meisn (9). However, the previously demonstrated skin-irritant and mouse skin tumor-promoting activities of Pimelea factor P_2 (I) and other daphnane esters (10) may very well act to restrict the development of I and II as clinically useful anticancer agents.

EXPERIMENTAL[3]

Plant Material—The twigs and flowers of *D. occidentalis* A. Gray (Thymelaeaceae) were collected in California in August 1977[4].

Extraction and Fractionation—The air-dried, milled plant material (12.5 kg) was defatted with petroleum ether (bp 60–80°), with the marc being extracted with methanol. On removal of solvent *in vacuo*, the residue was partitioned between water and chloroform. Biological activity was concentrated in both the petroleum ether extract, which was not examined further, and the chloroform extract, which was active against the P-388 lymphocytic leukemia test system both *in vivo* (T/C 144% at 1.87 mg/kg) and *in vitro* (ED_{50} 0.21 μg/ml).

A portion (90 g) of the dried chloroform extract was chromatographed on silica gel[5] (2 kg), with 2-liter fractions being collected and pooled on the basis of similar TLC profiles. Fraction F037 (17 g), obtained by elution with chloroform–methanol (9:1), exhibited an ED_{50} of 0.07 μg/ml in the P-388 cell culture system, while combined fractions F040–F042 (2.2 g), eluted with chloroform–methanol (19:1 and 17:3), were also found to be cytotoxic (P-388, ED_{50} 0.043, 0.18, 0.14 μg/ml, respectively).

Fraction F037 was rechromatographed on silica gel[5] (820 g), and eluted with chloroform and chloroform–methanol mixtures of increasing polarity, to afford 50 fractions (500 ml each). Crystals of daphnoretin (VI, 50 mg, 0.000092%), (−)-medioresinol (III, 6 mg, 0.000011%) and (+)-syringaresinol (IV, 18 mg, 0.000033%) were successively obtained during this separation on elution with chloroform–methanol (99:1). However, the more polar fractions F060–F064 (1.2 g) were highly cytotoxic (P-388, ED_{50} 1.9×10^{-4}–4.8×10^{-6} μg/ml), and were rechromatographed on silica gel[5] (40 g). Fractions eluted with chloroform–methanol (9:1) were pooled (0.9 g) and subjected to low-pressure column chromatography on octylsilyl silica gel contained in a prepacked column[6], using solvent systems composed of water–acetonitrile–methanol mixtures of decreasing polarity. Two daphnane esters were obtained as a result of this separation and were purified by preparative TLC on silica gel G plates[5], developed with benzene–ethyl acetate–hexane–ether (3:3:1:1), as follows: Pimelea factor P_2 (I, R_f 0.49, 3 mg, 0.000005%) and dircin (II, R_f 0.36, 4 mg). Further quantities of II were obtained by workup of other active fractions from the chloroform extract of *D. occidentalis*, in a manner similar to that described above, to produce a total of 32 mg (0.000059%) of this compound.

Fractions F040–F042 were similarly chromatographed on silica gel[5] eluted with chloroform–methanol mixtures. (−)-Lariciresinol (V, 10 mg, 0.000018%) was eluted with chloroform–methanol (19:1) and was purified by recrystallization from acetone–hexane (1:1).

Characterization of Biologically Active Isolates—The resinous Pimelea factor P_2 (I) exhibited the following spectral data. IR ν_{max} ($CHCl_3$): 3500, 1740, 1580, 1420, 1365, and 1235 cm^{-1}; UV λ_{max} (MeOH) (log ε): 229 (3.85) and 279 (3.10) nm; ^{1}H-NMR (60 MHz): δ 0.83 (d, 3, J = 6.4 Hz, 18-CH_3), 1.04 (d, 3, J = 6.5 Hz, 19-CH_3), 1.47 (d, 3, J = 3.5 Hz, 22-CH_3), 1.73 (bs, 3, 17-CH_3), 2.90 (d, 1, J = 2.7 Hz, 8-H), 3.11 (d, 1, J = 11.0 Hz, 10-H), 3.34 (s, 1, 7-H), 3.85 (bs, 2, 20-H_2), 4.10 (s, 1, H-5), 4.27 (d, 1, J = 2.7 Hz, 14-H), 4.85 and 4.96 (two bs, 1 each, 16-H_2), 5.09 (d, 1, J = 4.0 Hz, 3-H), and 7.45–8.05 ppm (m, 5, aromatic H); MS (20 eV): *m/z* 638 (M^+, 12%), 607 (11), 595 (24), 480 (11), 475 (13), 467 (16), 327 (11), 309 (10), 279 (13), 269 (15), 265 (10), 203 (11), 176 (19), 163 (16), 161 (41), 149 (22), 121 (16), and 105 (100). These data are in agreement with those reported for Pimelea factor P_2 (Daphnopsis factor R_1) (7) and linifolin b (8). Identity was established as Pimelea factor P_2 by direct comparison with an authentic sample[7] (^{1}H-NMR, MS, co-TLC).

The resinous isolate dircin (II), $[\alpha]_D^{25}$ + 9.0° (*c* 0.07, $CHCl_3$), exhibited the following spectral data. IR ν_{max} ($CHCl_3$): 3500, 1700, 1450, 1360, and 1270 cm^{-1}; UV λ_{max} (MeOH) (log ε): 228 (3.91) and 278 (3.10) nm; ^{1}H-NMR (400 MHz): δ 0.98 (d, 3, J = 7.5 Hz, 18-CH_3), 1.08 (d, 3, J = 7 Hz, 19-CH_3), 1.32 (d, 3, J = 7.5 Hz, 22-CH_3), 1.77 (bs, 3, 17-CH_3), 2.04 (s, 3, —OCOCH_3), 2.95 (d, 1, J = 12 Hz, 10-H), 2.96 (d, 1, J = 3 Hz, 8-H), 3.32 (s, 1, 7-H), 3.81 (ABq, 2, J_{AB} = 12 Hz, 20-H_2), 4.05 (s, 1, H-5), 4.19 (d, 1, J = 3 Hz, 14-H), 4.88 (d, 1, J = 6 Hz, H-3), 4.88 and 5.07 (two bs, 1 each, 16-H_2), 5.28 (d, 1, J = 8 Hz, 29-H), 7.50 (t, 2, J = 8 Hz, 3′- and 5′-H), 7.63 (t, 1, J = 7.5 Hz, 4′-H), and 8.06 ppm (dd, 2, J = 1.5 and 7.5 Hz, 2′- and 6′-H); MS (20 eV): *m/z* 696 (M^+, 2%), 678 (2), 647 (2), 592 (1), 561 (2), 556 (3), 533 (3), 467 (4), 403 (4), 368 (3), 363 (3), 345 (4), 327 (6), 309 (6), 299 (3), 297 (3), 281 (9), 205 (12), 203 (5), 189 (9), 188 (9), 177 (9), 176 (16), 161 (19), 148 (15), 147 (13), 133 (10), 123 (11), 122 (20), and 105 (100); field-desorption MS: MH^+ observed at *m/z* 697.

(−)-Medioresinol (III), mp 155–160°, $[\alpha]_D^{25}$−17.0° (*c* 0.14, $CHCl_3$) [lit. (17) (+)-medioresinol, mp 175–176°, $[\alpha]_D$ +57.4° ($CHCl_3$)], exhibited the following spectral data. IR ν_{max} (KBr): 3450, 3090, 1600, 1505, 1445, 1415, 1355, 1270, 1235, 1190, 1145, 1095, 1045, 945, and 780 cm^{-1}; UV λ_{max} (95% EtOH) (log ε): 220 sh (4.58), 232 (4.13), and 280 (3.58) nm; ^{1}H-NMR (60 MHz): δ 3.01–3.16 (m, 2, 8- and 8′-H), 3.88 (s, 9, 3 × —OCH_3), 3.76–3.98 and 4.13–4.30 (m, 4, 9- and 9′-H_2), 4.73 (dm, 2, J = 4.0 Hz, 7- and 7′-H), 5.48 (s, 1, phenolic OH), 5.59 (s, 1, phenolic OH), 6.58 (s, 2, 2- and 6-H), and 6.86 ppm (m, 3, 2′-, 5′-, and 6′-H); MS: *m/z* 388 (M^+, 100%), 358 (8), 235 (8), 210 (17), 206 (19), 193 (23), 182 (38), 181 (48), 180 (21), 167 (33), 163 (21), 161 (19), 154 (17), 151 (48), 137 (35), 124 (10), and 123 (10). These spectral data are in agreement with those published for (+)-medioresinol (17), and III exhibited identical TLC migration data to an authentic sample of (+)-medioresinol[8]. (−)-Medioresinol has not been isolated from a plant source previously.

[3] Melting points were determined by means of a Kofler hot-plate apparatus and are uncorrected. Specific rotations were measured on a Perkin-Elmer 241 polarimeter. The UV spectra were obtained with a Beckman DB-G spectrophotometer and IR spectra on a Beckman model 18-A spectrophotometer, with polystyrene calibration at 1601 cm^{-1}. ^{1}H-NMR spectra were recorded in $CDCl_3$ with a Varian T-60A instrument operating at 60 MHz, equipped with a Nicolet Model TT-7 attachment. Tetramethylsilane was used as an internal standard, and chemical shifts are reported in δ (ppm). Low-resolution mass spectra were obtained with a Varian MAT-112S double-focusing spectrometer, operating at 70 eV.

[4] Plant material was collected and identified by staff of the Economic Botany Laboratory, BARC-East, U.S.D.A., Science and Education Administration, Beltsville, Md. A voucher specimen representing this collection has been deposited in the Herbarium of the National Arboretum, Washington, D.C.

[5] E. Merck, Darmstadt, W. Germany.

[6] Lobar, size B, containing LiChoprep RP-8 (40–63 μm); manufactured by E. Merck, Darmstadt, W. Germany.

[7] An authentic sample of Pimelea factor P_2 and a copy of its ^{1}H-NMR spectrum were kindly supplied by Professor E. Hecker.

[8] Authentic samples of (+)-medioresinol and (±)-syringaresinol were kindly provided by Dr. H. Fujimoto.

(+)-Syringaresinol (IV), mp 173–175°, $[\alpha]_D^{25}$+12.8° (*c* 0.05, $CHCl_3$) [lit. (17) mp 171–173°, $[\alpha]_D$ +19.0° ($CHCl_3$)], exhibited the following spectral data. IR ν_{max} (KBr): 3450, 3080, 1600, 1510, 1445, 1415, 1370, 1190, 1100, 980, 840, and 730 cm^{-1}; UV λ_{max} (95% EtOH) (log ϵ): 220 sh (4.16), 239 (4.05), and 273 (3.27) nm; ^{1}H-NMR (60 MHz): δ 3.07 (m, 2, 8- and 8′-H), 3.89 (s, 12, 4 × —OCH_3), 3.80–3.99 and 4.16–4.42 (m, 4, 9- and 9′-H_2), 4.73 (d,2, J = 4.0 Hz, 7- and 7′-H), 5.54 (s, 2, 4- and 4′-H), and 6.58 ppm (s, 4, 2-, 6-, 2′-, and 6′-H); MS: *m/z* 418 (M^+, 100%), 403 (3), 358 (3), 280 (4), 251 (5), 235 (11), 210 (16), 193 (25), 182 (41), 181 (65), 167 (56), 161 (18), 154 (17), and 151 (19). These spectral data are in agreement with those reported for (+)- and (±)-syringaresinol (17, 18), and the identification of IV as (+)-syringaresinol was confirmed by direct comparison (MS, co-TLC) with an authentic sample of (±)-syringaresinol.

(−)-Lariciresinol (V), mp 160–162°, $[\alpha]_D^{25}$−17.8° (*c* 1.4, acetone), exhibited the following spectral properties. IR ν_{max} (KBr): 3320, 3090, 1510, 1460, 1420, 1230, 1035, and 845 cm^{-1}; UV λ_{max} (MeOH) (log ϵ): 232 (4.17) and 283 (4.02) nm; ^{1}H-NMR (60 MHz): δ 2.2–3.0 (m, 4, 7-H_2, 8- and 8′-H), 3.5–4.1 (m, 4, 9- and 9′-H_2), 3.70 (s, 3, —OCH_3), 3.82 (s, 3, —OCH_3), 4.78 (d, 1, J = 6.2 Hz, 7′-H), 5.61 (m, 2, phenolic OH), and 6.70–6.83 ppm (m, 6, aromatic H); MS: *m/z* 360 (M^+, 62%), 345 (4), 329 (1), 252 (8), 236 (11), 194 (22), 180 (12), 175 (10), 167 (11), 153 (31), 151 (47), 137 (100), and 122 (17). These spectral data are similar to those expressed previously for (+)-lariciresinol (19), and V was closely comparable to an authentic sample[9] of (+)-lariciresinol (MS, co-TLC). The (−)-enantiomer of this lignan does not appear to have been obtained previously from a plant source.

Daphnoretin (VI), mp 243–244°, exhibited the following spectral data. IR ν_{max} (KBr): 3400, 3080, 1722, 1715, 1618, 1585, 1565, 1280, 1245, 1085, 840, and 757 cm^{-1}; UV λ_{max} (MeOH) (log ϵ): 230 (4.13), 267 (3.80), 325 (4.17), and 343 (4.22) nm; ^{1}H-NMR (60 MHz, DMSO-d_6): δ 3.83 (s, 3, —OCH_3), 6.35 (d, 1, J = 9.5 Hz, 3′-H), 7.03–7.78 (m, 5, aromatic H), 7.85 (s, 1, 4-H), and 8.01 (d, 1, J = 9.5 Hz, 4′-H); MS: *m/z* 352 (M^+, 100%), 337 (4), 324 (5), 309 (11), 262 (5), 179 (25), 167 (20), and 89 (18). Compound VI was identified as daphnoretin on the basis of consistency of the above data with published spectral data for this compound (15, 20–22), and confirmation of this identity was made by direct comparison with an authentic sample[10].

Biological Activity of the Isolates—The activities of isolates I–VI from *D. occidentalis* against the P-388 lymphocytic leukemia test system, *in vivo* and *in vitro*, are shown in Table I.

[9] An authentic sample of (+)-lariciresinol was donated by Dr. S. F. Fonseca.

[10] Daphnoretin was isolated in our laboratory previously from *Peddia fischeri* (5).

REFERENCES

(1) J. C. Willis, in "A Dictionary of the Flowering Plants and Ferns," 8th ed., H. K. Airy-Shaw, Ed., University Press, Cambridge, England, 1973, p. 377.

(2) L. Abrams, "Illustrated Flora of the Pacific States (Washington, Oregon, California), vol. III, Geraniaceae to Scrophulariaceae," Stanford University Press, Stanford, Calif. 1951, p. 163.

(3) K. F. Lampe and R. Fagerström, "Plant Toxicity and Dermatitis. A Manual for Physicians," Williams & Wilkins, Baltimore, Md., 1968, p. 31.

(4) "The Dispensatory of the United States of America," 19th ed., H. C. Wood, J. P. Remington, and S. P. Sadtler, Eds., J. B. Lippencott, Philadelphia, Pa., 1907, p. 1474.

(5) S. S. Handa, A. D. Kinghorn, G. A. Cordell, and N. R. Farnsworth, *J. Nat. Prod.*, **46**, 248 (1983).

(6) R. I. Geran, N. H. Greenberg, M. M. McDonald, A. M. Schumacher, and B. J. Abbott, *Cancer Chemother. Rep.*, **3**(2), 1 (1972).

(7) S. Zayed, W. Adolf, A. Hafez, and E. Hecker, *Tetrahedron Lett.*, **1977**, 3481.

(8) M. I. Tyler and M. E. H. Howden, *Tetrahedron Lett.*, **1981**, 689.

(9) S. M. Kupchan, Y. Shizuri, T. Murae, J. G. Sweeny, H. R. Haynes, M.-S. Shen, J. C. Barrick, R. F. Bryan. D. van der Helm, and K. K. Wu, *J. Am. Chem. Soc.*, **98**, 5719 (1976).

(10) E. Hecker, in "Carcinogenesis, Vol. 2. Mechanisms of Tumor Promotion and Cocarcinogenesis," T. J. Slaga, A. Sivak, and R. K. Boutwell, Eds., Raven, New York, N.Y., 1978, p. 11.

(11) S. M. Kupchan, J. G. Sweeny, R. L. Baxter, T. Murae, V. A. Zimmerly, and B. R. Sickles, *J. Am. Chem. Soc.*, **97**, 672 (1975).

(12) S. M. Kupchan, Y. Shizuri, W. C. Sumner, Jr., H. R. Haynes, A. P. Leighton, and B. R. Sickles, *J. Org. Chem.*, **41**, 3850 (1976).

(13) S. M. Kupchan and R. L. Baxter, *Science*, **187**, 652 (1975).

(14) R. Kasai, K.-H. Lee, and H.-C. Huang, *Phytochemistry*, **20**, 2592 (1981).

(15) K.-H. Lee, K. Tagahara, H. Suzuki, R.-Y. Wu, M. Haruna, I. H. Hall, H.-C. Huang, K. Ito, T. Iida, and J.-S. Lai, *J. Nat. Prod.*, **44**, 530 (1981).

(16) S. J. Torrance, J. J. Hoffmann, and J. R. Cole, *J. Pharm. Sci.*, **68**, 664 (1979).

(17) H. Fujimoto and T. Higuchi, *Mokuzai Gakkaishi*, **23**, 405 (1977).

(18) L. H. Briggs, R. C. Cambie, and R. A. F. Couch, *J. Chem. Soc. (C)*, **1968**, 3042.

(19) R. Anderson, T. Popoff, and O. Theander, *Acta Chem. Scand. B*, **29**, 835 (1975).

(20) R. Tschesche, U. Schacht, and G. Legler, *Justus Liebigs Ann., Chem.*, **662**, 113 (1963).

(21) P. L. Majumder, G. C. Sengupta, B. N. Dinda, and A. Chatterjee, *Phytochemistry*, **13**, 1929 (1974).

(22) M. Williams and J. M. Cassady, *J. Pharm. Sci.*, **65**, 912 (1976).

ACKNOWLEDGMENTS

This work was carried out under contract CM-97295 with the Division of Cancer Treatment, National Cancer Institute, National Institutes of Health, Bethesda, Md. The authors would like to thank the Economic Botany Laboratory, BARC-East, U.S.D.A., Science and Education Administration, Beltsville, Md. (funded by the National Cancer Institute), for the provision and identification of the plant material.

Thanks are also due to: Professor Dr. E. Hecker, Deutsches Krebsforschungszentrum, Heidelberg, W. Germany, for Pimelea factor P_2 and a copy of its ^{1}H-NMR spectrum; Dr. H. Fujimoto, Kyoto University, Japan, for (+)-medioresinol and (±)-syringaresinol; Dr. S. F. Fonseca, Universidade Estadual de Campinas, Brazil, for (+)-lariciresinol; Professor J. P. Kutney, University of British Columbia, for the highfield ^{1}H-NMR spectrum; Dr. C. E. Costello, Mass Spectrometry, Massachusetts Institute of Technology, for the field-desorption mass spectral data; and to Dr. C. T. Che and Mr. D. D. McPherson, University of Illinois at the Medical Center, for ^{1}H-NMR and mass spectral data, respectively.

Demethylation of Imipramine by Enteric Bacteria

ALICE M. CLARK *, ROBERT T. CLINTON *,
JOHN K. BAKER ‡, and CHARLES D. HUFFORD *x

Received March 19, 1982, from the *Department of Pharmacognosy and the ‡Department of Medicinal Chemistry, School of Pharmacy, University of Mississippi, University, MS 38677. Accepted for publication September 30, 1982.

Abstract □ The ability of a number of aerobic and anaerobic bacteria to *N*-demethylate imipramine (I) to desipramine (II) has been investigated. Of the bacteria investigated, almost half were known inhabitants of the human GI tract. More than half of the enteric bacteria studied were capable of *N*-demethylating imipramine (I) to desipramine (II) to some extent in at least one medium. It was found that the medium in which the organism was grown had a significant effect on the *N*-demethylase activity observed.

Keyphrases □ Imipramine—*N*-demethylation to desipramine, microbial transformation, enteric bacteria □ Microbial transformation—imipramine, *N*-demethylation to desipramine, enteric bacteria □ Desipramine—microbial *N*-demethylation of imipramine, enteric bacteria

Imipramine (I) is a widely used tricyclic antidepressant whose metabolism, distribution, and excretion has been studied in detail (1–5). Desipramine (II) is a biologically active metabolite of imipramine which is formed by hepatic as well as by extrahepatic metabolism (6). A major site of extrahepatic metabolism has been shown to be the GI contents (6). It has also been shown that demethylation of I does not occur during passage across the intestinal wall (7). The role of the GI microflora in drug metabolism has been reviewed and has been shown to be a significant factor with many drugs (8–11). The microbial metabolism of imipramine using a number of fungi has also been shown to parallel the mammalian metabolism of imipramine (12). This study examined the metabolism of imipramine by bacteria, many of which are known to be inhabitants of the human GI tract.

EXPERIMENTAL

Imipramine hydrochloride (I)[1] was shown to be free of desipramine (II) and iminodibenzyl (III), known contaminants of some commercial samples of imipramine (13), by high-performance liquid chromatographic (HPLC) and TLC analyses. Desipramine hydrochloride was also shown to be pure by HPLC and TLC analyses. All solvents used for HPLC analysis were reagent grade quality.

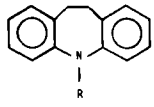

I: R = $(CH_2)_3N(CH_3)_2$
II: R = $(CH_2)_3NHCH_3$
III: R = H

Fermentation Screening Procedures for Aerobic Bacteria—Aerobic bacterial stock cultures were maintained on nutrient agar[2] and eugon agar[3] at 4° and transferred every 4–6 months. Screening for the demethylation of imipramine to desipramine was carried out in four different media. Three of the media used were complex media; the fourth was a defined medium. The media used were: eugon broth[3] (medium A); 5 g of dextrose, 2 g of corn steep liquor, 5 g of yeast extract, 1 g of peptone, and 1 liter of distilled water (medium B); 20 g of dextrose, 5 g of peptone, 5 g of tryptone, 2.5 g of $CaCO_3$, and 1 liter of distilled water (medium C); and 780 ml of basal salts solution (14) [containing 1.5 g of KH_2PO_4, 7.0 g of $(NH_4)_2HPO_4$, 0.5 g of $MgSO_4 \cdot 7H_2O$, 0.3 g of $CaCl_2 \cdot 2H_2O$, 0.04 g of $MnSO_4 \cdot 4H_2O$, 0.025 g of $FeSO_4 \cdot 7H_2O$, 0.002 g of ammonium molybdate, and 1 liter of distilled water], 100 ml of amino acid solution (containing 0.38 g of DL-alanine, 0.89 g of DL-aspartic acid, 0.30 g of L-arginine hydrochloride, 0.02 g of L-cystine, 0.140 g of L-glutamic acid, 0.17 g of glycine, 0.24 g of L-histidine hydrochloride, 0.76 g of DL-isoleucine, 0.57 g of L-leucine, 0.24 g of L-lysine hydrochloride, 0.06 g of DL-methionine, 0.11 g of L-proline, 0.12 g of DL-serine, 0.10 g of DL-threonine, 0.06 g of L-tyrosine, 0.15 g of DL-valine, and 100 ml of distilled water), 20 ml of vitamin solution (15) (containing 5.0 μg of biotin, 10.0 μg of folic acid, 0.5 mg of riboflavin, 2.5 mg of thiamine hydrochloride, 2.5 mg of pyridoxal hydrochloride, 2.5 mg of calcium pantothenate, 2.5 mg of nicotinic acid, and 100 ml of distilled water), and 100 ml of glucose solution (30%, w/v) (medium D).

A two-stage fermentation procedure was utilized as previously described (12). For screening in media A–C, the cultures were grown in 25 ml of medium held in 125-ml Erlenmeyer flasks. The cultures were incubated at 37° and 250 rpm. Imipramine hydrochloride was added to 24-hr-old stage II cultures as a 5% solution in dimethylformamide to give a final concentration of 200 μg/ml of medium. The cultures were incubated for 6 days and assayed for desipramine formation at 3 and 6 days after substrate addition. The samples were adjusted to pH 8 and extracted with three equal volumes of chloroform. The combined chloroform layers were dried and evaporated, and the residues were analyzed by TLC and HPLC.

For screening in medium D, the cultures were grown in 10 ml of medium held in 50-ml Erlenmeyer flasks, incubated at 250 rpm and 37°. Imipramine hydrochloride was added to sterile medium D prior to inoculation of stage II cultures. The substrate was added as a 1% dimethylformamide solution to give a final concentration of 100 μg/ml of medium. The stage II cultures, containing substrate, were incubated for 48 hr. Each whole culture was adjusted to pH 8 and extracted with an equal volume of dichloromethane, and the dichloromethane extracts were evaporated and analyzed by TLC and HPLC.

Fermentation Screening Procedures for Anaerobic Bacteria—Stock cultures of anaerobic bacteria were maintained in appropriate agar or broth media in disposable anaerobic systems[4]. Screening for desipramine production was carried out in 10 ml of either brain heart infusion broth[3] or medium E which consisted of 20 g of peptone, 10 g of yeast extract, 5 g of glucose, 5 g of maltose, 0.5 g of cysteine, 40 ml of salts solution, and 4 ml of a 0.025% aqueous solution of resazurin per liter of distilled water. The salts solution consisted of 0.1 g of K_2HPO_4, 0.1 g of KH_2PO_4, 1.0 g of $NaHCO_3$, 0.2 g of NaCl, 0.02 g of $CaCl_2$, 0.02 g of $MgSO_4$, trace amounts of ammonium molybdate and $CoCl_2 \cdot 6H_2O$, and 0.3 ml of 50% H_2SO_4 per 200 ml of distilled water. Each medium was dispersed into 16 × 125-mm screw-cap test tubes (10 ml/tube) and sterilized by autoclaving at 121° and 15 psi for 20 min. After sterilization each medium was supplemented with 100 μg of imipramine hydrochloride/ml of medium.

The sterile medium containing imipramine was inoculated from stock cultures of anaerobic bacteria (0.05 ml broth culture/10 ml sterile medium). The cultures were incubated at 37° under anaerobic conditions[4] for 7 days, at which time the whole cultures were extracted and analyzed as described for aerobic cultures grown in medium D.

Control Studies—Culture controls consisted of fermentation blanks in which each organism was grown under identical conditions as biotransformation cultures, but without substrate. The cultures were extracted and analyzed as described for the biotransformation cultures.

Substrate controls were necessary to establish the stability of the substrate to the fermentation conditions used. Therefore, substrate controls were obtained for each set of medium and incubation conditions used. Substrate controls for aerobic cultures grown in media A–C were

[1] Sigma Chemical Co.
[2] Difco Laboratories, Detroit, Mich.
[3] BBL Microbiology Systems, Cockeysville, Md.
[4] GasPak Disposable Anaerobic System; BBL Microbiology Systems, Cockeysville, Md.

0022-3549/83/1100-1288$01.00/0

obtained by growing stage II cultures of two representative organisms (*Escherichia coli* 10536 and *Bacillus cereus* v. *fluorescens* 13024) in each medium for 7 days (250 rpm, 37°). The cultures were then sterilized by autoclaving. Imipramine hydrochloride (200 μg/ml of medium) was added to the sterilized cultures, which were incubated an additional 6 days at 37° and 250 rpm. The sterilized substrate control cultures were then extracted and analyzed as described for aerobic cultures grown in media A–C. Five cultures of *E. coli* 10536 and two cultures of *B. cereus* v. *fluorescens* 13824 were used to determine medium A control values. For medium B control values, five cultures of *E. coli* 10536 and three cultures of *B. cereus* v. *fluorescens* 13824 were used. For medium C five cultures of each organism were used. Three cultures of *B. cereus* v. *fluorescens* grown in medium A and two cultures grown in medium B became contaminated after sterilization and addition of imipramine, and therefore could not be used in calculating control values. In addition, substrate controls consisting of sterile media (A–C) containing imipramine (200 μg/ml) were prepared and incubated at 250 rpm and 37° for 6 days (five determinations/medium). Each substrate control was extracted and analyzed as described for growing cultures. In addition, substrate controls consisting of sterile medium D containing imipramine (100 μg/ml of medium) were prepared and incubated at 250 rpm and 37° for 48 hr (five determinations). Each substrate control was extracted and analyzed as described for aerobic cultures grown in medium D.

Substrate controls for anaerobic media were obtained by growing each of the seven anaerobic bacteria in media without imipramine for 7 days. The cultures were then sterilized by autoclaving. After cooling, imipramine hydrochloride was added (100 μg/ml of medium) and incubation under anaerobic conditions[4] (37°) was continued an additional 7 days. The substrate control cultures were then extracted and analyzed as described for aerobic cultures grown in medium D.

TLC Analyses—Culture extracts were redissolved in 100 μl of chloroform or dichloromethane, and 6-μl aliquots of the solutions were spotted on precoated silica gel G TLC plates[5]. The plates were developed in ethyl acetate–methanol–ammonium hydroxide (81:15:4) and visualized by UV light and by spraying with diazotized *p*-nitroaniline followed by spraying with concentrated hydrochloric acid. The R_f values and colors for imipramine and desipramine are 0.57 (blue) and 0.29 (blue), respectively.

HPLC Analyses—Quantitative analyses of the culture extracts were accomplished on a silica column[6] using an HPLC pump[7], a microsyringe-loaded loop injector[8], and a UV detector[9]. The mobile phase consisted of methanol–2 *N* ammonia–1 *N* ammonium nitrate (27:2:1) and was used at a flow rate of 1.0 ml/min. Culture extracts were redissolved in 400 μl of methanol, and 5-μl aliquots of the solutions were injected for HPLC. Quantitation of desipramine in culture extracts was accomplished by comparison of the peak heights in culture extracts with the peak heights of standard samples of desipramine at known concentrations.

For aerobic cultures grown in complex media (A–C), desipramine levels were considered significant if the level exceeded the sterilized control value plus four times the standard deviation for that medium. Thus, for medium A, levels <0.56% were not considered significant and for media B and C, levels <0.59% and 0.64%, respectively, were not considered significant. For aerobic cultures grown in medium D, a sterilized control value was established for each organism. In these cases, yields of desipramine that exceeded 3 times the control value were considered significant. The same criterion was used for determining significant *N*-demethylase activity among anaerobic bacteria.

RESULTS AND DISCUSSION

Imipramine (I) was subjected to biotransformation screening using 29 aerobic and 7 anaerobic bacteria. Of the aerobic bacteria, nine are known to be inhabitants of the human GI tract; these organisms were screened in three complex media (media A–C) and one defined medium (D). The remaining 20 aerobic bacteria were screened in the three complex media (A–C). All seven anaerobic bacteria were screened for their ability to *N*-demethylate imipramine in two complex media: brain heart infusion broth and medium E. Cultures grown in the presence of imipramine were extracted with either dichloromethane or chloroform, and the extracts were analyzed by TLC and HPLC. The results of these studies are summarized in Tables I–III.

[5] Brinkmann Instruments, Inc., Westbury, N.Y.
[6] μPorasil; Waters Associates, Milford, Mass.
[7] Model M-6000; Waters Associates, Milford, Mass.
[8] Model U6-K; Waters Associates, Milford, Mass.
[9] Model 440; Waters Associates, Milford Mass.

Table I—Yields of Desipramine by Aerobic Bacteria in Complex Media [a]

Bacterium (ATCC number)	Medium A	Medium B	Medium C
Arthrobacter species (19140)	0.29	0.15	0.16
Arthrobacter species (21237)	0.90[b]	0.70[b]	0.70[b]
Bacillus cereus v. *fluorescens* (13824)	0.95[b]	1.20[b]	1.80[b]
Bacillus megaterium (9885)	1.10[b]	0.20	1.10[b]
Bacillus subtilis (6633)	0.20	0.05	0.40
Corynebacterium species (14887)	—[c]	—[c]	—[c]
Enterobacter aerogenes (13048)[d]	0.17	0.08	0.31
Escherichia coli (27165)[d]	0.34	0.11	0.23
E. coli (10536)	1.58[b]	0.22	1.78[b]
Flavobacterium oxydans (1245)	0.52	0.40	0.60
Klebsiella pneumoniae (27889)[d]	0.10	0.79[b]	0.35
K. pneumoniae (29016)[d]	0.70[b]	0.29	0.21
Mycobacterium cuneatum (21498)	—[c]	—[c]	—[c]
Mycobacterium smegmatis (607)	—[c]	—[c]	—[c]
M. smegmatis (14468)	0.05	0.10	0.20
Nocardia corallina (19070)	0.70[b]	0.05	0.05
N. corallina (19071)	0.62[b]	0.50	0.25
N. corallina (19148)	0.60[b]	0.40	0.20
Nocardia minima (19150)	0.46	0.71[b]	0.30
Nocardia petroleophila (15777)	0.55	0.70[b]	0.67[b]
Proteus vulgaris (27973)[d]	0.50	0.30	0.40
Pseudomonas aeruginosa (14205)[d]	0.80[b]	0.40	0.30
P. aeruginosa (15442)	0.35	0.35	0.23
Pseudomonas desmolytica (15005)	—[c]	—[c]	—[c]
Pseudomonas species (19286)	0.79[b]	0.61[b]	0.10
Staphylococcus aureus (6538)	0.79[b]	0.50	<0.10
S. aureus (14458)[d]	0.46	0.20	0.34
Streptococcus faecalis (6569)[d]	0.50	0.50	0.71[b]
Streptococcus faecium (6056)[d]	1.12[b]	0.13	0.36
Control (sterilized)[e]	0.32 ± 0.06	0.31 ± 0.07	0.28 ± 0.09
Control[f]	0.26 ± 0.08	0.10 ± 0.03	0.07 ± 0.02

[a] Yields are expressed as percent yield on a mole basis. [b] Considered as significant *N*-demethylase activity, based on a minimum value of the sterilized control value plus 4 times the standard deviation. [c] These cultures were not analyzed by HPLC since TLC analysis showed no desipramine. [d] Known inhabitants of the gut. [e] Sterilized control values are expressed as the average (±*SD*) of 7–10 determinations using sterilized cultures of two representative organisms, *E. coli* 10536 and *B. cereus* v. *fluorescens* 13824, grown in each of the three media. [f] Simple control values are expressed as the average (±*SD*) of five determinations in which imipramine was incubated in each of the sterile media for 6 days.

The quantitative results obtained from HPLC analyses of aerobic bacteria grown in complex media (A–C) containing imipramine are shown in Table I. The results obtained from HPLC analyses of aerobic gut bacteria grown in the defined medium (D) containing imipramine are shown in Table II. Twelve of the twenty-nine organisms screened were capable of *N*-demethylation in medium A. In media B and C, six of the bacteria screened could *N*-demethylate imipramine (Table I). In total, 16 of the 29 aerobic bacteria screened, including 5 of the 9 gut bacteria, were capable of *N*-demethylating imipramine to some extent in at least one of the complex media (Table I).

Two additional gut bacteria, which were incapable of *N*-methylation in the complex media, were shown to *N*-demethylate imipramine when grown in medium D (Table II). One organism, *Streptococcus faecalis* 6569 would not grow in medium D. Only two aerobic gut bacteria, *Klebsiella pneumoniae* 29016 and *Streptococcus faecium* 6056, were capable of *N*-demethylation in both complex (A) and defined media (D).

A number of anaerobic bacteria were also screened for their ability to *N*-demethylate imipramine (I). A total of seven anaerobes known to inhabit the GI tract of the human were screened for *N*-demethylase activity in two complex media. The results of these studies are shown in Table III. Only one anaerobe, *Fusobacterium fusiforme* 23726 showed signifi-

Table II—Yields of Desipramine by Aerobic Gut Bacteria in Defined Medium [a]

Bacterium (ATCC number)	Yields of Desipramine	
	Growing Cultures	Control Cultures[b]
Enterobacter aerogenes (13048)	0.72	0.60
Escherichia coli (27165)	2.02[c]	0.67
Klebsiella pneumoniae (27889)	2.19	1.23
K. pneumoniae (29016)	1.12[c]	0.22
Proteus vulgaris (27973)	1.77[c]	0.52
Pseudomonas aeruginosa (14205)	2.20	1.58
Staphylococcus aureus (14458)	0.55	0.19
Streptococcus faecalis (6569)	—[d]	—[d]
Streptococcus faecium (6056)	1.60[c]	0.52

[a] Yields are expressed as percent yield on a mole basis. [b] Simple substrate controls consisting of sterile medium containing imipramine showed an average percent yield of desipramine of 0.17 ± 0.05 after 48 hr of incubation. [c] Considered as significant *N*-demethylase activity, based on a minimum value of 3 times the control value. [d] No growth in this medium.

cant *N*-demethylase activity in medium E. However, in brain heart infusion medium, four of the seven anaerobes (*Bacteroides eggerthii* 27754, *Bifidobacterium longum* 15707, *Clostridium paraperfringens* 27640, and *Lactobacillus catenaforme* 25644) were capable of *N*-demethylation. It is interesting to note that *F. fusiforme* 23726 did not show *N*-demethylase activity in brain heart infusion medium. Therefore, as with the aerobic bacteria, it appears that the choice of medium is important in demonstrating *N*-demethylase activity in anaerobic bacteria.

Table III—Yields of Desipramine from Anaerobic Bacteria in Complex Media [a]

Bacterium (ATCC number)	Yield of Desipramine			
	Growing Cultures in Medium E	Control Cultures in Medium E	Growing Cultures in Brain Heart Infusion Medium	Control Cultures in Brain Heart Infusion Medium
Bacteroides eggerthii (27754)	0.58	0.55	1.28[b]	0.31
Bifidobacterium adolescentis (15703)	0.80	0.65	0.53	0.26
Bifidobacterium bifidum (15696)	0.66	0.34	0.68	0.47
Bifidobacterium longum (15707)	0.48	0.26	1.73[b]	0.45
Clostridium paraperfringens (27640)	0.52	0.42	0.78[b]	0.22
Fusobacterium fusiforme (23726)	0.78[b]	0.21	0.39	0.24
Lactobacillus catenaforme (25644)	0.60	0.42	0.81[b]	0.21

[a] Yields are expressed as percent yield on a mole basis. [b] Considered as significant *N*-demethylase activity, based on a minimum value of 3 times the control value.

Based on these studies, it appears that *N*-demethylase activity was common among bacteria. Of particular interest were the enteric bacteria, both aerobic and anaerobic. A high percentage of the gut bacteria screened were capable of *N*-demethylation of imipramine to desipramine. Among the anaerobic bacteria, five of seven were capable of *N*-demethylating imipramine to desipramine as were seven of nine aerobic gut bacteria. The medium in which the organism was grown appeared to have a significant influence on the *N*-demethylase activity. Since it is known that considerable variability exists in response to imipramine therapy, the variable *N*-demethylation of imipramine may be an important consideration (16). A similar situation occurs with digoxin in which the gut flora metabolizes the drug to biologically inactive metabolites in some patients, lowering their plasma levels of digoxin (17).

REFERENCES

(1) J. V. Dingell, F. Sulser, and J. R. Gillette, *J Pharmacol. Exp. Ther.*, **143,** 14 (1964).

(2) J. L. Crammer and B. Scott, *Psychopharmacologia*, **8,** 461 (1966).

(3) M. H. Bickel and M. Baggioline. *Biochem. Pharmacol.*, **15,** 1155 (1966).

(4) M. H. Bickel and H. J. Weder, *Arch. Int. Pharmacodyn. Ther.*, **173,** 433 (1968).

(5) J. Christiansen and L. F. Gam, *J. Pharm. Pharmacol.*, **25,** 604 (1973).

(6) R. Minder, F. Schnetzer and M. H. Bickel, *Naunyn-Schmiedebergs Arch. Pharmak.*, **268,** 334 (1971).

(7) H. Dencker, S. V. Dencker, A. Green, and A. Nagy, *Clin. Pharmacol. Ther.*, **19,** 584 (1976).

(8) R. R. Scheline, *Pharmacol. Rev.*, **25,** 451 (1972).

(9) R. R. Scheline, "Mammalian Metabolism of Plant Xenobiotics," Academic, New York, N.Y., 1978.

(10) J. Caldwell and G. M. Hawksworth, *J. Pharm. Pharmacol.*, **25,** 422 (1972).

(11) G. E. Smith and L. A. Griffiths, *Xenobiotica*, **4,** 477 (1974).

(12) C. D. Hufford, G. A. Capiton, A. M. Clark, and J. K. Baker, *J. Pharm. Sci.*, **70,** 151 (1981).

(13) J. J. Saady, N. Narashimhachari, and R. O. Friedel, *Clin. Chem.*, **27,** 343 (1981).

(14) H. Proom and B. C. J. G. Knight, *J. Gen. Microbiol.*, **13,** 474 (1955).

(15) P. J. Coloe and N. J. Hayward, *J. Med. Microbiol.*, **9,** 211 (1976).

(16) J. Amsterdam, D. Brunswick, and J. Mendels, *Am. J. Psychiatry*, **137,** 653 (1981).

(17) J. Lindenbaum, D. G. Rund, V. P. Butter, Jr., D. Tse-Eng, and J. R. Saha, *N. Engl. J. Med.*, **305,** 789 (1981).

ACKNOWLEDGMENTS

This work was supported in part by the Committee on Faculty Research, University of Mississippi, and the Research Institute of Pharmaceutical Sciences, School of Pharmacy, University of Mississippi.

The authors are grateful for the sample of desipramine hydrochloride provided by Merrell-National Laboratories. They also thank Mrs. Claudia Ann Perrier for technical assistance.

Microbial Transformations of Natural Antitumor Agents XXII: Conversion of Bouvardin to *O*-Desmethylbouvardin and Bouvardin Catechol

RICHARD J. PETROSKI *, ROBERT B. BATES ‡, GARY S. LINZ ‡, and JOHN P. ROSAZZA *x

Received July 19, 1982, from the **Division of Medicinal Chemistry and Natural Products, College of Pharmacy, The University of Iowa, Iowa City, IA 52242* and the ‡*Department of Chemistry, College of Liberal Arts, University of Arizona, Tucson, AZ 85721.* Accepted for publication September 9, 1982.

Abstract □ Bouvardin is a cyclic hexapeptide antitumor agent which undergoes two major microbial transformation reactions. Screening with 220 cultures revealed 17 different strains capable of producing *O*-desmethylbouvardin in good yield. *O*-Desmethylbouvardin was isolated and characterized from preparative scale incubations with *Streptomyces rutgersensis* NRRL B-1256. Four aspergilli and one streptomycete formed bouvardin catechol when *O*-desmethylbouvardin was used as substrate. Bouvardin catechol was isolated and characterized from a preparative scale incubation with *Aspergillus ochraceous* UI 398.

Keyphrases □ Bouvardin—conversion to *O*-desmethylbouvardin and bouvardin catechol, microbial transformation, *Streptomyces rutgersensis, Aspergillus ochraceous* □ Microbial transformation—bouvardin to *O*-desmethylbouvardin and bouvardin catechol, *Streptomyces rutgersensis, Aspergillus ochraceous* □ Metabolites—bouvardin, microbial transformation to *O*-desmethylbouvardin and bouvardin catechol, *Streptomyces rutgersensis, Aspergillus ochraceous*

Bouvardin (I), a novel cyclic hexapeptide antitumor agent isolated from the plant *Bouvardia ternifolia* (Rubiaceae) (1), has demonstrated antitumor activity against the P-388 lymphocytic leukemia test system and against B-16 melanoma (1). Modification of bouvardin by synthetic methods appeared to be difficult; thus, this material was deemed an excellent candidate for microbiological modification (2). This report describes microbial transformation experiments of bouvardin which afforded two major metabolites, *O*-desmethylbouvardin (II) and bouvardin catechol (III).

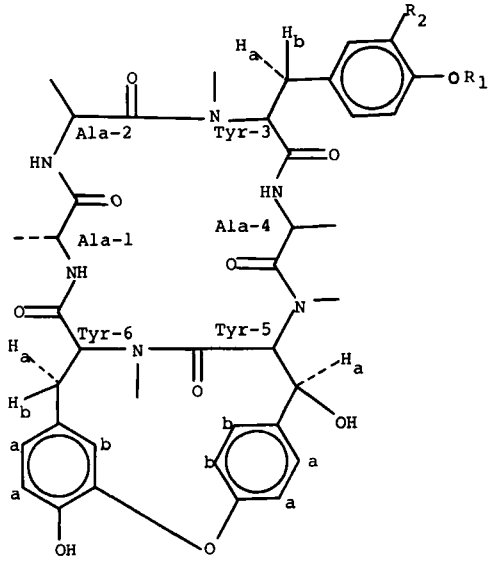

I: $R_1 = CH_3$, $R_2 = H$
II: $R_1 = R_2 = H$
III: $R_1 = H$, $R_2 = OH$

EXPERIMENTAL

Melting points were determined in open-ended capillary tubes and are corrected. UV spectra[1] were measured in ethanol solutions, and IR spectra[2] were determined in potassium bromide pellets. ^{1}H-NMR spectra[3] were obtained in $CDCl_3$ using tetramethylsilane as an internal standard. ^{13}C-NMR spectra were obtained in DMSO-d_6 at 90 MHz with an instrument operating at 22.635 MHz. Assignments for appropriate carbon signals were confirmed by use of off-resonance noise decoupling and delayed decoupling techniques to indicate multiplicities of carbons due to carbon-proton splittings. Low-resolution mass spectra[4] were obtained using a direct-inlet probe, and high-resolution and field-desorption mass spectra were provided through the mass spectral facility of the Massachusetts Institute of Technology, Cambridge, Mass.

Chromatography—TLC was performed on buffered 0.25-mm layers of silica gel GF_{254} on glass plates. Plates were prepared by spreading a slurry of 25 g of silica gel GF_{254} in 50 ml of 4% aqueous KH_2PO_4. After air drying, plates were uniformly deactivated by predevelopment with methyl ethyl ketone saturated with water. Plates were developed with methylene chloride–methanol–water (90:10:0.5 or 85:10:0.5), and developed chromatograms were visualized by fluorescence quenching under 254-nm UV light, or by spraying with Dragendorff's reagent (3) or with ceric ammonium sulfate reagent [1% $Ce(NH_4)_4(SO_4)_4$ in 50% H_3PO_4] and warming the sprayed plates with a heat gun.

Bouvardin (I)—Bouvardin was obtained[5] as a crystalline compound which possessed the following physical properties: mp 240–241°; UV (EtOH): 278 (ϵ 3780) and 284 nm (3370); IR: 3620 (OH phenolic), 1680 (amide C=O), and 1245 cm^{-1} (C—O—C); ^{1}H-NMR: see Table I; mass spectrum (field-desorption): m/z 772 for $C_{40}H_{48}N_6O_{10}$; high-resolution mass spectral fragments obtained by electron-impact spectroscopy: see Table II. ^{13}C-NMR spectral data was obtained on a DMSO-d_6 solution of bouvardin and was identical to that reported by Bates *et al.* (4).

Fermentation Procedure—All cultures are maintained in the University of Iowa, College of Pharmacy culture collection. Cultures were grown according to the usual two-stage fermentation procedure used in these laboratories (5) in a soybean meal–glucose medium of the following composition: 5 g of soybean meal; 20 g of glucose, 5 g of yeast extract, 5 g of sodium chloride, 5 g of dibasic potassium phosphate, and 1000 ml of distilled water; the pH was adjusted to 7.0 with 6 *N* HCl. Nutrient broth[6] was employed in the cultivation of bacterial strains. Media were sterilized in an autoclave at 121° for 15 min prior to use.

Fermentations were conducted on rotary shakers[7] operating at 250 rpm and describing a 2.5-cm orbital stroke at 27° in steel-capped Delong culture flasks containing one-fifth of their volumes of culture medium. Fermentations were initiated by suspending the surface growth from slants in 5 ml of sterile medium and by using the resulting suspension to inoculate stage I cultures. Thick 72-hr stage I cultures were used to inoculate stage II fermentations; the inoculum volume consisted of 10% of the volume of medium held in the stage II culture flasks. Bouvardin was added as substrate to 24-hr stage II cultures in a dimethylformamide solution, and the progress of microbial transformation reactions was monitored by TLC. For this, 4-ml samples were withdrawn at various time intervals, adjusted to pH 6.5 by the addition of 1 ml of 2 *M* pH 6.3

[1] Model SP1800; Pye Unicam Ltd., Cambridge, England.
[2] Perkin-Elmer Model 267, Norwalk, Conn.
[3] Bruker Model WM250 or Bruker FX90Q, USA Bruker Instruments, Inc., Billerica, MA 01821.
[4] Model 3200; Finnigan Corp., Sunnyvale Calif.
[5] National Cancer Institute, DTP, DCT, Silver Spring, MD 20910.
[6] Difco Laboratories, Detroit, Mich.
[7] Model G-25; New Brunswick Scientific Co., Edison, N.J.

0022-3549/83/1100-1291$01.00/0

Table I—^{1}H-NMR [a] Chemical Shifts (δ) and Coupling Constants (Hz) for Bouvardin (I), *O*-Desmethylbouvardin (II), and Bouvardin Catechol (III) in $CDCl_3$

	I	II	III
Ala-4β	1.08d (6.6)	1.10	1.09
Ala-1β	1.30d (7.0)	1.30	1.31
Ala-2β	1.37d (6.9)	1.37	1.37
Tyr-6-N-Me	2.74s	2.74	2.74
Tyr-3-N-Me	2.87s	2.88	2.91
Tyr-6β_a	2.91dd (18.8, 3)	2.90	2.90
Tyr-6β_b	3.12dd (18.8, 10.8)	3.11	3.12
Tyr-5-N-Me	3.33s	3.33	3.33
Tyr-3β	3.35m	3.35m	~3.31m
Tyr-3α	3.62dd (9.2, 5.9)	3.61	3.62
Tyr-3-O-Me	3.80s	—	—
Tyr-6δ_b	4.35d (1.8)	4.35	4.36
Tyr-6α	4.37m	4.33	4.34
Ala-1α	4.38 ~ p (7)	4.37	4.38
Ala-2α	4.76 ~ p (7)	4.77	4.77
Ala-4α	4.90 ~ p (7)	4.89	4.89
Tyr-5β_a	5.08dd (10.2, 1.8)	5.07	5.07
Tyr-5α	5.36d (1.8)	5.36	5.37
Tyr-6-OH	5.58s	5.61	5.79
Ala-1-NH	6.00d (7.1)	6.05	6.16
Ala-4-NH	6.44d (7.7)	6.44	6.47
Tyr-5-OH	6.50d (10.2)	6.51	6.52
Tyr-6δ_a	6.51dd (8.1, 1.8)	6.53	6.54
Ala-2-NH	6.65d (7.9)	6.66	6.68
Tyr-3ϵ	6.81 ~ d (8.7)	6.78	6.81d (7.4)
Tyr-6ϵ_a	6.84d (8.1)	6.84	6.84
Tyr-5ϵ_b	6.95dd (8.7, 2.2)	6.97	6.97
Tyr-3δ	7.05 ~ d (8.5)	7.01	6.53dd (7.4, 2.0)
Tyr-5ϵ_a	7.23dd (8.5, 2.2)	7.25	7.25
Tyr-5δ_b	7.38dd (8.5, 2.2)	7.39	7.39
Tyr-5δ_a	7.50dd (8.7, 2.2)	7.51	7.51
Tyr-3-OH	—	4.88s	6.40, 6.43s

[a] 250 MHz.

Table II—High-Resolution Electron-Impact Mass Spectral Fragments Obtained With Bouvardin (I), *O*-Desmethylbouvardin (II), and Bouvardin Catechol (III)

Empirical Formula	Calculated Mass	Observed Mass (Percent Relative Abundance)		
		I	II	III
C_6H_6O	94.04186	94.04336 (11.91)	94.04286 (87.83)	94.04137(51.29)
C_7H_7O	107.04969	107.04907 (17.44)	107.04833 (100)	107.04845 (56.71)
$C_6H_6O_2$	110.03678	—	110.03544 (16.61)	110.03977 (80.49)
$C_5H_8N_2O$	112.06366	112.06352 (21.23)	112.06363 (55.39)	112.06323 (61.88)
$C_7H_7O_2$	123.04460	—	123.04436 (5.86)	123.04994 (100)
$C_7H_{10}N_2O$	138.07931	138.07939 (27.92)	138.07909 (66.82)	138.08114 (78.14)
C_8H_9O	121.06534	121.06343 (100)	121.06391 (45.05)	—
$C_{14}H_{13}O_2$	213.09155	213.09087 (1.0)	213.09246 (73.50)	213.09072 (1.4)

phosphate buffer, and extracted with 1 ml of ethyl acetate. Approximately 30 μl of the extracts were spotted onto TLC plates for analysis.

Small-scale fermentations were used to screen 220 microorganisms for their abilities to metabolize bouvardin. Screening experiments were conducted in 125-ml steel-capped Delong flasks in 25 ml of medium, and 10 mg of bouvardin was added to each culture. Initial screening results were confirmed in a second experiment with control cultures containing no substrate and with autoclaved cultures incubated with bouvardin.

Preparation of *O*-Desmethylbouvardin (II) from Bouvardin by *Streptomyces rutgersensis* (NRRL) B-1256)—*S. rutgersensis* was grown in 500- or 1000-ml culture flasks, and a total of 3.36 g of I in 22.4 ml of dimethylformamide was evenly dispensed to a final concentration of 0.6 mg of bouvardin/ml of culture medium in the 24-hr stage II cultures. Conversions of bouvardin to one major metabolite commenced within 24 hr and neared completion after 12 days of incubation (TLC). Cells were separated from the fermentation beer by filtration, and the combined filtrates were adjusted to pH 6.5 with 10% aqueous KOH. The filtrate (5.5 liters) was extracted exhaustively with ethyl acetate (2 × 2.5 liters) and then with ethyl acetate–2-propanol (9:1, 2 × 2 liters). The extracts were combined, dried over anhydrous sodium sulfate, filtered, and evaporated to a thick oily residue. This residue was triturated with water to remove the dimethylformamide, and the resulting suspension was filtered through a sintered glass funnel to collect the bouvardin-containing solids. The crude product (4.57 g) was purified by column chromatography on silica gel[8] (90 g, 3 × 35 cm) using a solvent system of methylene chloride–methanol–water (90:10:0.5) at a flow rate of 0.7 ml/min; 20-ml fractions were collected. Fractions 17–24 contained bouvardin (0.49 g), while fractions 25–42 provided *O*-desmethylbouvardin (II) (2.53 g, 79% yield). Recrystallization of the metabolite from ethyl acetate yielded the analytical sample (1.91 g): mp 224.5–227.0°; UV: 239.5 (6850), 278 (3540), and 280 nm (3560); IR: 3380 (OH phenolic), 1680 (amide C=O), and 1245 cm^{-1} (C—O—C); ^{1}H-NMR; see Table I; mass spectrum (field-desorption): *m/z* 797 ($M + K^+$), 781 ($M + Na^+$), 758 (M^+ for $C_{39}H_{46}N_6O_{10}$), and 740 ($M - H_2O$); electron-impact mass spectral data: see Table II.

Preparation of Bouvardin Catechol (III) from *O*-Desmethylbouvardin (II) by *Aspergillus ochraceous*—*A. ochraceous* (UI 398) was grown in 12, 1-liter Delong culture flasks for the stage II incubation. A total of 960 mg of II was dissolved in 9.6 ml of dimethylformamide and dispensed evenly among the cultures to give a final *O*-desmethylbouvardin concentration of 0.4 mg/ml in culture medium. Ascorbic acid (500 mg in 4 ml of H_2O) was added to each flask at 48 hr after addition of *O*-desmethylbouvardin, when TLC analyses first indicated the presence of III (6). After 96 hr, TLC estimation indicated an 80% conversion of II to III, and the fermentation was harvested.

Cells were separated from the medium by filtration through cheesecloth, and the cells were extracted with ethyl acetate (200 ml). This extract was later combined with culture filtrate extracts. The filtrate (2000 ml) was extracted with ethyl acetate (3 × 1 liter) and then with ethyl acetate–2-propanol (9:1, 1 liter). After drying the combined extracts over anhydrous sodium sulfate, evaporation yielded an oily residue (800 mg), which was dissolved in methylene chloride–methanol–water (90:10:0.5, 5 ml) and applied to silica gel column (90 g, 3 × 35 cm). The column was

[8] Baker 3405; J. T. Baker Chemical Co., Phillipsburg, N.J.

eluted at a flow rate of 0.7 ml/min while 20-ml fractions were collected. After 50 fractions, the solvent was changed to methylene chloride–methanol–water (90:20:0.5) for an additional 30 fractions. Fractions 14–24 contained unreacted *O*-desmethylbouvardin (II) (164 mg), fractions 25 and 26 contained a mixture of II and III (49 mg), and fractions 27–55 contained bouvardin catechol (III) (280 mg, 34.5% yield based on substrate utilized). The crude bouvardin catechol was dissolved in methyl ethyl ketone (10 ml), and 50 ml of hexane was added to precipitate 262 mg of the catechol (III) from solution. This material was collected by filtration and gave the following physical data: mp 221–223°; UV: 284 nm (2740); IR: 3350 (broad, OH phenolic), 1650 (amide C=O), and 1270 cm^{-1} (C—O—C); ^{1}H-NMR: see Table I; mass spectrum (field-desorption): *m/z* 797 ($M + Na^+$) and 774 (M^+ for $C_{39}H_{46}N_6O_{11}$); electron-impact spectrum: see Table II. The Arnow's test was positive, indicative of a catechol moiety in the structure of the metabolite (7).

RESULTS AND DISCUSSION

Compounds such as bouvardin whose structural complexity render total synthesis or chemical modification difficult are excellent substrates for microbiological modification (2). The present study was designed to provide metabolites of bouvardin in sufficient quantity for biological evaluation to extend the structure–activity relationships of the antitumor peptide. Small-scale screening experiments with 220 cultures resulted in the identification of 17 microorganisms which accumulated the same major metabolite (Table III). The metabolite was produced in consistently high yield (TLC) by *S. rutgersensis* (NRRL B-1256), and this organism was selected for preparative-scale fermentation to obtain sufficient amounts of the metabolite for structure elucidation and biological testing. The metabolite was obtained in 79% yield in the preparative-scale incubation, and ^{1}H-NMR and mass spectral measurements supported its structure as *O*-desmethylbouvardin (II).

The ^{1}H-NMR spectrum of the metabolite was identical to that of bouvardin, except for the absence of the signal for the methoxyl group protons of the tyrosine-3 residue (Table I) and the presence of a new hydroxyl signal at 4.48 ppm. Similarly, the signal for the methoxyl carbon atom of bouvardin, which resonates at 55.494 ppm, was absent in the ^{13}C-NMR spectrum of the metabolite. Field-desorption mass spectral measurement provided a molecular ion of *m/z* 758 for the metabolite *versus m/z* 772 for bouvardin. While the electron-impact mass spectrum failed to provide ions at higher mass, the base peak of the metabolite spectrum was at *m/z* 107.04833 for C_7H_7O (Table II). This peak is derived from the *N*-methyltyrosine-3 residue of the metabolite. In bouvardin, the base peak exists at *m/z* 121.06343 for C_8H_9O, the methoxylated aromatic ring derived from the tyrosine-3 amino acid residue. These data strongly support the structure of the major bouvardin metabolite as *O*-desmethylbouvardin (II).

Since II could be efficiently produced by microbial transformation of bouvardin, this metabolite was also utilized as a substrate in microbial transformation experiments. *O*-Desmethylbouvardin (II) was screened with 10 cultures known to accomplish aromatic hydroxylation. Of the cultures examined, *Aspergillus alliaceus* (NRRL 315), *A. ochraceous* (UI 398). *A. ochraceous* (NRRL 1008), and *Streptomyces griseus* (UI 1158) provided the same more polar (TLC) metabolite of II. *A. ochraceous* UI 398 gave the highest and most consistent yields of the new metabolite, and it was used in a preparative-scale incubation. In the preparative-scale fermentation, ascorbic acid was employed to prevent possible degradation of the phenolic starting material and the presumed catechol metabolite that was being formed. A similar approach was utilized in the microbial oxidation of *N*-blocked tyrosine residues to form *N*-blocked levodopa derivatives (6). Following solvent extraction and chromatography, the metabolite was obtained in 34.5% yield and was identified as bouvardin catechol by spectral and chemical methods.

A positive Arnow's test suggested that the metabolite possessed a catechol moiety in its structure (7). While the metabolite gave a positive test, *O*-desmethylbouvardin and bouvardin were negative. Field-desorption mass spectrometry indicated a molecular weight of 774 for the metabolite, consistent with the addition of a single oxygen atom to *O*-desmethylbouvardin. The base peak in the electron-impact spectrum (Table II) of the metabolite was at *m/z* 123.04461 for $C_7H_7O_2$, which would be expected if an oxygen atom had been introduced into the tyrosine-3 residue of *O*-desmethylbouvardin. This fragment is supported by the presence of a characteristic catechol fragment at *m/z* 110.03977 for $C_6H_6O_2$, which was intense in the spectrum of the metabolite but relatively insignificant in the spectrum of *O*-desmethylbouvardin or bouvardin (Table II).

A detailed analysis of the ^{1}H- and ^{13}C-NMR spectral properties of bouvardin has been made (4); this provided a useful tool in establishing the structure of the new bouvardin metabolite. The 250-MHz ^{1}H-NMR spectrum of the metabolite strongly supported its proposed structure as bouvardin catechol (III). All of the resonances of the metabolite were virtually identical for I, II, and III except for signals attributed to the aromatic protons of the tyrosine-3 moiety and for OH and NH absorptions which moved farther downfield in the spectrum of III due to concentration differences. The tyrosine-3 absorption changed in the expected ways for III. The aromatic absorption pattern for this metabolite resembled that of 4-methyl catechol (8) as a typical ABX system with protons for the Tyr-3δ [6.53 ppm (dd, J = 7.4 and 2.0 Hz) and 6.70 ppm (d, J = 2.0 Hz)] and Tyr-3ϵ [6.81 ppm (d, J = 7.4 Hz)] possessing the appropriate coupling constants. These data confirm the structure of the metabolite as that of bouvardin catechol (III).

Table III—Cultures[a] Producing *O*-Desmethylbouvardin (II) from Bouvardin (I).

Corynebacterium mediolarum (ATCC 14004)
Cyathus striatus (UI 356)
Gelasinospora autosteria (UIGA)
Hansenula species (UI-HCY)
Helicostylum piriforme (QM 6944)
Lentodium squamulosum (UI 1566)
Mycobacterium fortuitum (UI 53378)
Nannizzia cajetana (−) (UI 1128)
Phanerochaete chrysosporium (UI 446)
Poria monticola (UI 332)
Pseudomonas putida (ATCC 17453)
Sepedonium chrysospermum (ATCC 13378)
Sordaria bomboidee (UI 183)
Streptomyces rimosus (NRRL 2234)
S. rimosus (ATCC 14673)
Streptomyces rutgersensis (NRRL B-1256)
Unidentified Yeast (UI 1477)

[a] ATCC, American Type Culture Collection, Rockville, Md.; NRRL, Northern Regional Research Laboratories, Peoria, Ill. UI, University of Iowa, College of Pharmacy Culture Collection, Iowa City, Iowa; QM Quartermaster Culture Collection, U.S. Army Laboratories, Natick, Mass.

Additional attempts were made to modify bouvardin by employing cultures known to form peptide antibiotics containing α,β-unsaturation or dehydro-amino acid moieties in their structural backbones. It was reasoned that formation of the dehydro-moieties could occur as late biosynthetic reactions in the formation of antibiotics such as mikamycin (9), subtilin (10), dehydro-*N*-benzyloxycarbonyl-L-tryptophan (11), glycocinnamoyl-spermidines (12), antibiotic A32390A (13), telomycin (14), stendomycin (15), trichostatin C (16), and ostreogrycin (17), and that the introduction of this type of functionality into bouvardin could result in enhanced or novel antitumor activity. Cultures were grown in nutrient broth with and without supplements of phenylalanine, alanine, or tyrosine as possible inducers of enzymes capable of dehydrogenating amino acids (11). None of the antibiotic-producing cultures formed novel derivatives of bouvardin. In these experiments, *Nocardia* species (NRRL 5646), *Streptomyces hygroscopicus* (ATCC 32431), and *Actinoplanes philippinensis* (NRRL 5462) formed *O*-desmethylbouvardin from bouvardin, albeit in lower yields than *S. rutgersensis*.

Bouvardin and its metabolites, *O*-desmethylbouvardin (II) and bouvardin catechol (III) were submitted to the National Cancer Institute for biological testing *versus* the P-388 leukemia test system. None of the metabolites were active, thus indicating that the *O*-desmethylation and further hydroxylation reactions are bioinactivation processes.

REFERENCES

(1) S. D. Jolad, J. J. Hoffmann, S. J. Torrance, R. M. Wiedhopf, J. R. Cole, S. K. Arora, R. B. Bates, R. L. Gargiulo, and G. R. Kriek, *J. Am. Chem. Soc.*, **99**, 9040 (1977).

(2) J. P. Rosazza, in "Anticancer Agents Based on Natural Product Models," J. Cassady and J. Douros, Eds., Academic, New York, N.Y., 1981, pp. 437–463.

(3) E. Stahl, "Thin Layer Chromatography," 2nd ed., Springer-Verlag, New York, N.Y., 1969, p. 873 (No. 94, only solution A was used).

(4) R. B. Bates, J. R. Cole, J. R. Hoffmann, G. R. Kreik, G. S. Linz, and S. J. Torrance *J. Am. Chem. Soc.*, in press.

(5) R. E. Betts, D. E. Walters, and J. P. Rosazza, *J. Med. Chem.*, **17**, 599 (1975).

(6) C. J. Sih, P. Foss, J. Rosazza, and M. Lemberger, *J. Am. Chem. Soc.*, **91**, 6204 (1969).

(7) L. E. Arnow, *J. Biol. Chem.*, **118**, 531 (1937).
(8) Sadtler Standard NMR Spectra No. 6065.
(9) R. L. Hamill, *J. Antibiot.*, **29**, 76 (1976).
(10) E. Gross and H. H. Kiltz, *Biochem. Biophys. Res. Commun.*, **50**, 559 (1973).
(11) P. J. Davis, M. Gustafson, and J. P. Rosazza, *Biochim. Biophys. Acta*, **385**, 133 (1975).
(12) H. D. Tresner, J. H. Korshalla, A. A. Fantini, J. D. Korshalla, J. D. Kirby, J. J. Goodman, R. A. Kele, A. J. Shay, and D. B. Borders, *J. Antibiot.*, **31**, 394 (1978).
(13) L. D. Boeck, M. M. Hoehn, T. H. Sands, and R. W. Wetzel, *J. Antibiot.*, **31**, 19 (1978).
(14) J. C. Sheehan, D. Mania, S. Nakamura, J. A. Stock, and K. Maeda, *J. Am. Chem. Soc.*, **90**, 462 (1968).
(15) R. Q. Thompson and M. S. Hughes, *J. Antibiot., Ser. A.*, **16**, 187 (1963).
(16) N. Tsuji and M. Kobayashi, *J. Antibiot.*, **31**, 939 (1978).
(17) G. R. Delbierre, F. W. Eastwood, G. E. Grean, D. G. I. Kingston, P. S. Sarin, Lord Todd, and D. H. Williams, *J. Chem. Soc. C*, **1966**, 1653.

ACKNOWLEDGMENTS

The authors wish to acknowledge financial support for this work through NCI-CM-77176 funded through the National Cancer Institute.

We thank the mass spectrometry laboratories, Department of Chemistry, Massachusetts Institute of Technology, for mass spectral services provided.

Prodrugs as Drug Delivery Systems XXV: Hydrolysis of Oxazolidines—A Potential New Prodrug Type

MARIANNE JOHANSEN and HANS BUNDGAARD ˣ

Received September 7, 1982, from the *Royal Danish School of Pharmacy, Departments of Pharmaceutics and Pharmaceutical Chemistry AD, DK-2100 Copenhagen, Denmark.* Accepted for publication September 30, 1982.

Abstract □ The hydrolysis kinetics of several oxazolidines derived from (−)-ephedrine and various aldehydes and ketones were studied to assess their suitability as prodrug forms for β-amino alcohols and/or carbonyl-containing compounds. The oxazolidines were found to undergo a facile and complete hydrolysis in the pH range of 1–11 at 37°. The hydrolysis rates were subject to general acid–base catalysis by buffer substances and depended strongly on pH. Most oxazolidines showed sigmoidal pH–rate profiles with maximum rates at pH > 7–7.5. At pH 7.40 and 37° the following half-lives of hydrolysis for the various ephedrine oxazolidines were found: 5 sec (formaldehyde), 18 sec (propionaldehyde), 5 min (benzaldehyde), 5 sec (salicylaldehyde), 30 min (pivalaldehyde), 4 min (acetone), and 6 min (cyclohexanone). The reaction rates in neutral and basic solutions were shown to decrease with increasing steric effects of the substituents derived from the carbonyl component and to decrease with increasing basicity of the oxazolidines. The oxazolidines are weaker bases (pK_a 5.2–6.9) than the parent β-amino alcohol and more lipophilic at physiological pH. It is suggested that oxazolidines can be considered as potentially useful prodrug candidates for drugs containing a β-amino alcohol moiety or carbonyl groups.

Keyphrases □ Ephedrine—oxazolidine derivatives, potential prodrugs for β-amino alcohols and carbonyl-containing compounds □ Oxazolidines—potential prodrugs for β-amino alcohols and carbonyl-containing compounds, ephedrine □ Prodrugs—potential, oxazolidine derivatives, for β-amino alcohols and carbonyl-containing compounds, ephedrine

Bioreversible derivatization of drug substances to produce prodrugs with altered physicochemical properties can improve substantially both drug efficacy and safety (1–3). As a part of current studies involving new chemical approaches (4, 5), an investigation was carried out to obtain prodrug candidates for the β-amino alcohol moiety and/or carbonyl groups (aldehydes and ketones). There are several drugs containing a β-amino alcohol moiety (*e.g.*, various sympathomimetic amines and β-blockers) which may exhibit delivery problems, *e.g.*, due to unfavorable solubility or lipophilicity characteristics. For this moiety no prodrug types have apparently been described, and likewise, only few bioreversible derivatives of carbonyl-containing drugs have been explored (6, 7). We recently suggested (8) that oxazolidines should be considered as potentially useful prodrug candidates for β-amino alcohols or drugs containing carbonyl groups. Oxazolidines (II and III) derived from (−)-ephedrine (I) and benzaldehyde or salicylaldehyde were found to undergo a facile and quantitative hydrolysis in the pH range of 1–11, the half-lives of hydrolysis at pH 7.4 and 37° being 5 min (II) and 5 sec (III). To further explore the potential of oxazolidines as prodrug types and to delineate some structure–activity relationships, this study has been extended to include oxazolidines derived from (−)-ephedrine and the ketones acetone and cyclohexanone, as well as the aliphatic aldehydes formaldehyde, propionaldehyde, and pivalaldehyde. In the present paper the kinetics of hydrolysis of these oxazolidines (IV–VIII) are described along with data for the lipophilicity of the compounds.

EXPERIMENTAL

Chemicals—The oxazolidines IV–VIII were prepared by treating (−)-ephedrine[1] with the appropriate aldehyde or ketone, according to previously described procedures (9–11), and these materials were purified by distillation *in vacuo*. The boiling or melting points observed agreed with those previously reported (9–11), and satisfactory elemental analysis data (C, H, and N) were obtained. Buffer substances and all chemicals or solvents were of reagent grade.

Kinetic Studies—All rate studies were performed in aqueous buffer solutions at 37.0 ± 0.2°. The buffers used were hydrochloric acid, formate, acetate, phosphate, borate, and carbonate solutions. A constant ionic strength (μ) of 0.5 was maintained for each buffer by adding a calculated amount of potassium chloride. The rates of hydrolysis were followed by one or more of three methods depending on the reaction rate.

Direct UV spectrophotometry—In this method the progress of decomposition of the oxazolidines was followed spectrophotometrically[2] by recording the decrease in absorbance at 220 nm. At this wavelength the absorption of substrate and products differed maximally. Reactions were performed in 2.5-ml aliquot portions of buffer solutions in a thermostated quartz cell and were initiated by adding 20 μl of a stock solution of the oxazolidines in acetonitrile to give a final concentration of ~5×10^{-4} *M*. Rate constants were calculated from the slopes of linear plots of log ($A_t - A_\infty$) against time, where A_t and A_∞ are the absorbance

[1] AG Fluka, Switzerland.
[2] Zeiss PMQ II equipped with a thermostated cell compartment.

0022-3549/83/1100-1294$01.00/0

(7) L. E. Arnow, *J. Biol. Chem.*, **118**, 531 (1937).
(8) Sadtler Standard NMR Spectra No. 6065.
(9) R. L. Hamill, *J. Antibiot.*, **29**, 76 (1976).
(10) E. Gross and H. H. Kiltz, *Biochem. Biophys. Res. Commun.*, **50**, 559 (1973).
(11) P. J. Davis, M. Gustafson, and J. P. Rosazza, *Biochim. Biophys. Acta*, **385**, 133 (1975).
(12) H. D. Tresner, J. H. Korshalla, A. A. Fantini, J. D. Korshalla, J. D. Kirby, J. J. Goodman, R. A. Kele, A. J. Shay, and D. B. Borders, *J. Antibiot.*, **31**, 394 (1978).
(13) L. D. Boeck, M. M. Hoehn, T. H. Sands, and R. W. Wetzel, *J. Antibiot.*, **31**, 19 (1978).
(14) J. C. Sheehan, D. Mania, S. Nakamura, J. A. Stock, and K. Maeda, *J. Am. Chem. Soc.*, **90**, 462 (1968).
(15) R. Q. Thompson and M. S. Hughes, *J. Antibiot., Ser. A.*, **16**, 187 (1963).
(16) N. Tsuji and M. Kobayashi, *J. Antibiot.*, **31**, 939 (1978).
(17) G. R. Delbierre, F. W. Eastwood, G. E. Grean, D. G. I. Kingston, P. S. Sarin, Lord Todd, and D. H. Williams, *J. Chem. Soc. C*, **1966**, 1653.

ACKNOWLEDGMENTS

The authors wish to acknowledge financial support for this work through NCI-CM-77176 funded through the National Cancer Institute.

We thank the mass spectrometry laboratories, Department of Chemistry, Massachusetts Institute of Technology, for mass spectral services provided.

Prodrugs as Drug Delivery Systems XXV: Hydrolysis of Oxazolidines—A Potential New Prodrug Type

MARIANNE JOHANSEN and HANS BUNDGAARD ˣ

Received September 7, 1982, from the *Royal Danish School of Pharmacy, Departments of Pharmaceutics and Pharmaceutical Chemistry AD, DK-2100 Copenhagen, Denmark.* Accepted for publication September 30, 1982.

Abstract □ The hydrolysis kinetics of several oxazolidines derived from (−)-ephedrine and various aldehydes and ketones were studied to assess their suitability as prodrug forms for β-amino alcohols and/or carbonyl-containing compounds. The oxazolidines were found to undergo a facile and complete hydrolysis in the pH range of 1–11 at 37°. The hydrolysis rates were subject to general acid–base catalysis by buffer substances and depended strongly on pH. Most oxazolidines showed sigmoidal pH–rate profiles with maximum rates at pH > 7–7.5. At pH 7.40 and 37° the following half-lives of hydrolysis for the various ephedrine oxazolidines were found: 5 sec (formaldehyde), 18 sec (propionaldehyde), 5 min (benzaldehyde), 5 sec (salicylaldehyde), 30 min (pivalaldehyde), 4 min (acetone), and 6 min (cyclohexanone). The reaction rates in neutral and basic solutions were shown to decrease with increasing steric effects of the substituents derived from the carbonyl component and to decrease with increasing basicity of the oxazolidines. The oxazolidines are weaker bases (pK_a 5.2–6.9) than the parent β-amino alcohol and more lipophilic at physiological pH. It is suggested that oxazolidines can be considered as potentially useful prodrug candidates for drugs containing a β-amino alcohol moiety or carbonyl groups.

Keyphrases □ Ephedrine—oxazolidine derivatives, potential prodrugs for β-amino alcohols and carbonyl-containing compounds □ Oxazolidines—potential prodrugs for β-amino alcohols and carbonyl-containing compounds, ephedrine □ Prodrugs—potential, oxazolidine derivatives, for β-amino alcohols and carbonyl-containing compounds, ephedrine

Bioreversible derivatization of drug substances to produce prodrugs with altered physicochemical properties can improve substantially both drug efficacy and safety (1–3). As a part of current studies involving new chemical approaches (4, 5), an investigation was carried out to obtain prodrug candidates for the β-amino alcohol moiety and/or carbonyl groups (aldehydes and ketones). There are several drugs containing a β-amino alcohol moiety (*e.g.*, various sympathomimetic amines and β-blockers) which may exhibit delivery problems, *e.g.*, due to unfavorable solubility or lipophilicity characteristics. For this moiety no prodrug types have apparently been described, and likewise, only few bioreversible derivatives of carbonyl-containing drugs have been explored (6, 7). We recently suggested (8) that oxazolidines should be considered as potentially useful prodrug candidates for β-amino alcohols or drugs containing carbonyl groups. Oxazolidines (II and III) derived from (−)-ephedrine (I) and benzaldehyde or salicylaldehyde were found to undergo a facile and quantitative hydrolysis in the pH range of 1–11, the half-lives of hydrolysis at pH 7.4 and 37° being 5 min (II) and 5 sec (III). To further explore the potential of oxazolidines as prodrug types and to delineate some structure–activity relationships, this study has been extended to include oxazolidines derived from (−)-ephedrine and the ketones acetone and cyclohexanone, as well as the aliphatic aldehydes formaldehyde, propionaldehyde, and pivalaldehyde. In the present paper the kinetics of hydrolysis of these oxazolidines (IV–VIII) are described along with data for the lipophilicity of the compounds.

EXPERIMENTAL

Chemicals—The oxazolidines IV–VIII were prepared by treating (−)-ephedrine[1] with the appropriate aldehyde or ketone, according to previously described procedures (9–11), and these materials were purified by distillation *in vacuo*. The boiling or melting points observed agreed with those previously reported (9–11), and satisfactory elemental analysis data (C, H, and N) were obtained. Buffer substances and all chemicals or solvents were of reagent grade.

Kinetic Studies—All rate studies were performed in aqueous buffer solutions at 37.0 ± 0.2°. The buffers used were hydrochloric acid, formate, acetate, phosphate, borate, and carbonate solutions. A constant ionic strength (μ) of 0.5 was maintained for each buffer by adding a calculated amount of potassium chloride. The rates of hydrolysis were followed by one or more of three methods depending on the reaction rate.

Direct UV spectrophotometry—In this method the progress of decomposition of the oxazolidines was followed spectrophotometrically[2] by recording the decrease in absorbance at 220 nm. At this wavelength the absorption of substrate and products differed maximally. Reactions were performed in 2.5-ml aliquot portions of buffer solutions in a thermostated quartz cell and were initiated by adding 20 μl of a stock solution of the oxazolidines in acetonitrile to give a final concentration of ~5×10^{-4} *M*. Rate constants were calculated from the slopes of linear plots of log ($A_t - A_\infty$) against time, where A_t and A_∞ are the absorbance

[1] AG Fluka, Switzerland.
[2] Zeiss PMQ II equipped with a thermostated cell compartment.

0022-3549/83/1100-1294$01.00/0

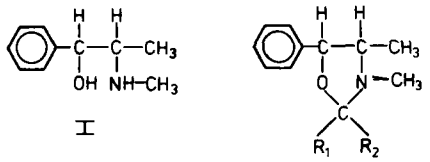

I

II 

III 

IV H H

V C_2H_5 H

VI CH_3 CH_3

VII 

VIII $(CH_3)_3C$ H

readings at time t and at infinity (*i.e.*, when no further changes in absorbance occurred), respectively.

Trapping of Carbonyl Product—The rates of hydrolysis of IV and VII were measured at some pH values (pH 3–6) by trapping the formaldehyde or cyclohexanone formed with semicarbazide and following the increase in absorbance of the semicarbazone at 235 nm (12, 13). Semicarbazide hydrochloride was included in the buffer solutions at a concentration of 5×10^{-3} *M*. The concentration of the trapping reagent (and pH range) was such that there was no induction period in the observed pseudo first-order rate plots, *i.e.*, trapping of carbonyl compound was fast relative to its formation. The semicarbazide had no significant influence on the reaction rate in the concentration used; at higher concentrations a slight catalytic effect was noted. The initial oxazolidine concentration was ~2×10^{-4} *M*, and the reactions were performed either directly in a thermostated cuvette or in flasks kept in a water bath. Pseudo first-order rate constants were determined from plots of log $(A_\infty - A_t)$ against time; in all cases stable end points (A_∞) were observed.

High-Performance Liquid Chromatography (HPLC)—Slower reactions were usually followed using an HPLC method. The apparatus[3] used was equipped with a variable-wavelength UV detector (8-μl, 1-cm flow cells), a 10-μl loop injection valve, and a reverse-phase column[4] (4.0 mm × 25 cm). The mobile phase consisted of methanol–0.04 *M* potassium dihydrogen phosphate (7:3 v/v). The flow rate was 1.6 ml/min, and the column effluent was monitored at 215 or 220 nm. Under these conditions the oxazolidines were separated from ephedrine and both could readily be determined (Fig. 1). Quantitation of the compounds was done from measurement of the peak heights in relation to those of standards chromatographed under the same conditions. In the kinetic runs, buffer solutions containing the oxazolidines at initial concentrations of ~0.5 mg/ml were kept at 37°, and aliquots were removed at suitable intervals and chromatographed. First-order rate constants for the hydrolysis were determined from the slopes of linear plots of the logarithm of residual oxazolidine against time.

Measurement of Partition Coefficients—The partition coefficients of the oxazolidine derivatives VI, VII, and VIII were determined in an octanol–phosphate buffer (0.05 *M*, pH 7.40) system as previously described (8). The solute concentration in the octanol phase was determined by the aforementioned HPLC method before and after partition, the equilibrium being obtained after mixing the two phases for only 3 min at 20° (for stability reasons). For each compound, determinations were carried out in triplicate, and the log P values thereby obtained were reproducible to within ±6%.

RESULTS AND DISCUSSION

Kinetics of Hydrolysis—The kinetics of decomposition of the oxazolidines IV–VII were studied in aqueous solution at 37° over the pH range of 0.5–11. At constant pH and temperature the hydrolysis displayed strict first-order kinetics for >3 half-lives, and in all kinetic runs followed by HPLC, ephedrine was found to be liberated in stoichiometric amounts. As described above, different experimental methods were used to follow the reactions. In several cases the rate of hydrolysis of oxazolidines at a given pH was determined using more than one of the methods and, as seen from the examples given in Table I, the values of the pseudo first-order rate constants (k_{obs}) derived were in favorable agreement.

The hydrolysis of the oxazolidines was found to be subject to significant buffer catalysis, as has previously been observed for II (8). The hydrolysis rates showed in all cases a linear dependence on buffer concentration, as illustrated in Fig. 2 for the degradation of oxazolidine VI in phosphate buffers.

The influence of pH on the hydrolysis rate is shown in Fig. 3, where the logarithms of the k_{obs} values at zero buffer concentration (k_0, obtained

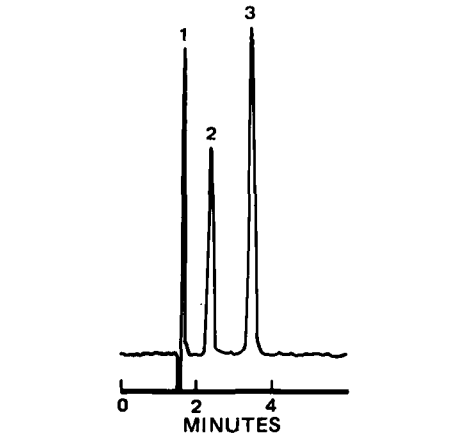

Figure 1—*Chromatogram of a partially degraded aqueous solution of VI. Key: (1) solvent front; (2) (−)-ephedrine; (3) VI.*

Table I—Pseudo First-Order Rate Constants (k_{obs}, min^{-1}) for the Hydrolysis of Various Oxazolidines [a] as Determined by Different Methods

Compound	Buffer	Method[b] A	B	C
V	0.05 *M* formate (pH 3.15)	0.10	—	0.11
VI	0.05 *M* phosphate (pH 7.40)	0.21	—	0.22
VII	0.1 *M* acetate (pH 5.55)	0.016	0.017	0.015

[a] μ = 0.5; 37°. [b] (A) Direct UV spectrophotometry; (B) trapping of carbonyl product with semicarbazide; (C) HPLC of oxazolidine.

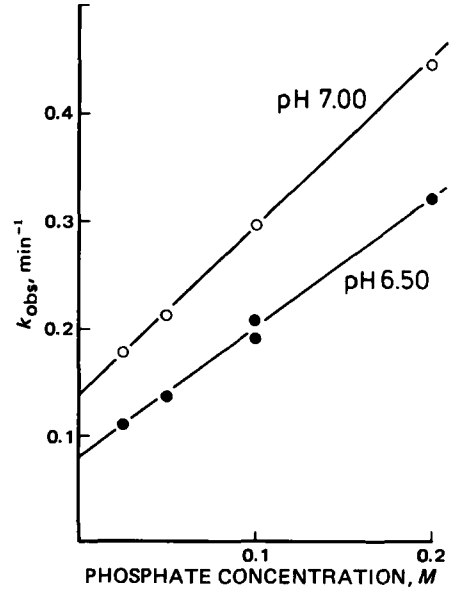

Figure 2—*Effect of phosphate buffer concentration on the pseudo first-order rate constant for the hydrolysis of VI (μ = 0.5; 37°).*

[3] Spectra-Physics Model 3500B.

[4] LiChrosorb RP-8 reverse-phase column; E. Merck, Darmstadt, West Germany.

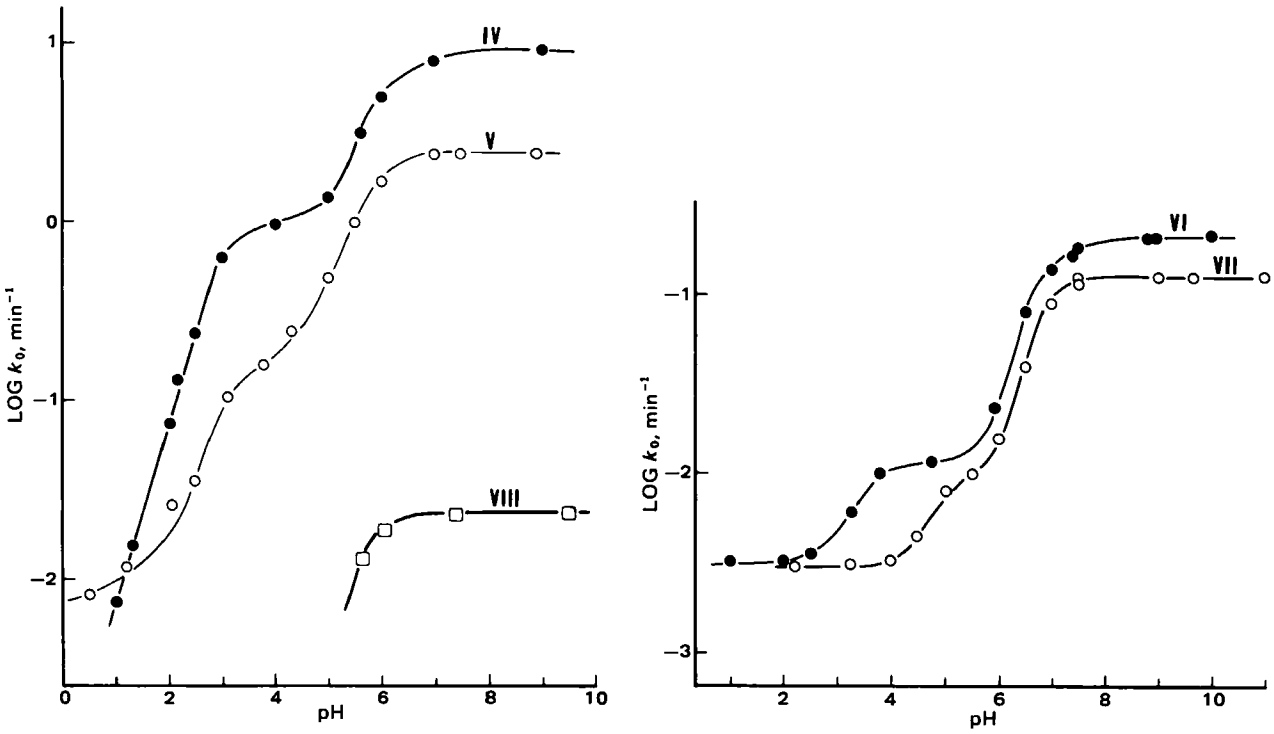

Figure 3—*The pH-rate profiles for the hydrolysis of the oxazolidines IV–VIII at 37° (μ = 0.5).*

by extrapolation of plots such as those in Fig. 2 to zero buffer concentration) are plotted against pH. The k_0 values at pH < 2.2 were obtained directly from runs in hydrochloric acid solution.

Previous studies (14–16) have shown that the hydrolysis occurs in two separate reaction stages: reversible ring opening to give a cationic Schiff base species followed by hydrolysis of this intermediate to give the β-amino alcohol and the carbonyl component (Scheme I). These studies involving various 2-(substituted phenyl)-3-ethyloxazolidines, 2-[4-(dimethylamino)styryl]-3-phenyloxazolidine, and 2-(4-methylphenyl)-2,3-dimethyloxazolidine led to the proposed reaction scheme in which the ring opening proceeding with C—O bond breaking is subject to hydrogen ion catalysis as well as a possible unimolecular C—O bond breaking or a water-catalyzed ring opening. The cationic Schiff base intermediate formed is in equilibrium with the oxazolidine and undergoes both spontaneous and hydroxide-ion-catalyzed hydrolysis.

A similar mechanism may be involved in the hydrolysis of the oxazolidines IV–VIII. For these derivatives, however, no build up of a Schiff base intermediate occurs. Using UV spectrophotometry no such intermediate could be detected in the pH range studied, and furthermore, no lag time was observed in the rate of appearance of ephedrine as determined by HPLC. Thus, if formed, the Schiff base intermediate must be present in small steady-state concentrations. A similar conclusion was also reached in case of hydrolysis of the benzaldehyde derivative II (8). The sigmoidal pH-rate profiles obtained for the oxazolidines studied indicate, on the other hand, that such an intermediate may be involved in the reaction pathway and that a change of the rate-determining step in the overall reaction with pH is taking place. In weakly acid to basic solution (pH > 5.5–6), the rate-determining step in the overall hydrolysis of the oxazolidines is suggested to involve a unimolecular or water-catalyzed breakdown of the free base form of the oxazolidines. Letting k_1 be the apparent first-order rate constant for this process and K_a the apparent ionization constant of the protonated oxazolidines, the expression for k_0 would be:

$$k_0 = \frac{k_1 K_a}{a_H + K_a} \qquad \text{(Eq. 1)}$$

where a_H is the hydrogen ion activity. In Fig. 3 the lines at pH > 5.5–6 were constructed from Eq. 1 and the rate constants and pK_a values given in Table I. It is seen that the experimental data obtained in this pH region fit very satisfactorily to Eq. 1. Further support for this interpretation of the kinetic data is provided by the identical pK_a values obtained kinetically and by potentiometric titration for the oxazolidines VI and VII (Table II). Due to their facile hydrolysis the pK_a values of IV and V could not be determined titrimetrically. It should be added, however, that other kinetically equivalent reactions, *e.g.*, hydroxide-ion-catalyzed hydrolysis of protonated oxazolidine, can equally account for the observed k_0–pH relationship in neutral and alkaline solutions.

As seen from Fig. 4 the oxazolidine derived from benzaldehyde (II) behaves quite differently from those from the aliphatic aldehydes (IV and V). The hydrolysis of this oxazolidine shows a bell-shaped pH–rate profile as previously reported (8). In contrast the pH–rate profile for the corresponding oxazolidine from salicylaldehyde (III) (8) is sigmoidal, as are those for IV, V, and VIII. The rate data for III at pH > 4 were analyzed in terms of Eq. 1, and the k_1 and pK_a values derived are included in Table I.

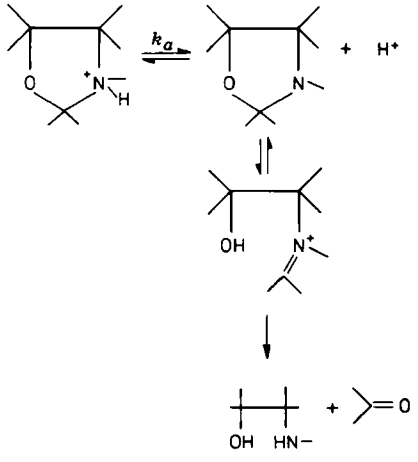

Scheme I

Table II—Rate Data for the Hydrolysis of Various Oxazolidines and pK_a Values[a]

Oxazolidine	k_1, min^{-1}	pK_a[b]	
II	—	—	(5.6)[c]
III	9.1	5.2	
IV	9.1	6.0	
V	2.4	5.9	
VI	0.21	6.9	(6.9)[c]
VII	0.13	6.9	(6.9)[c]
VIII	0.023	5.9	

[a] μ = 0.5; 37°. [b] Kinetically determined values; the values listed in parentheses were determined titrimetrically. [c] Values taken from Ref. 17.

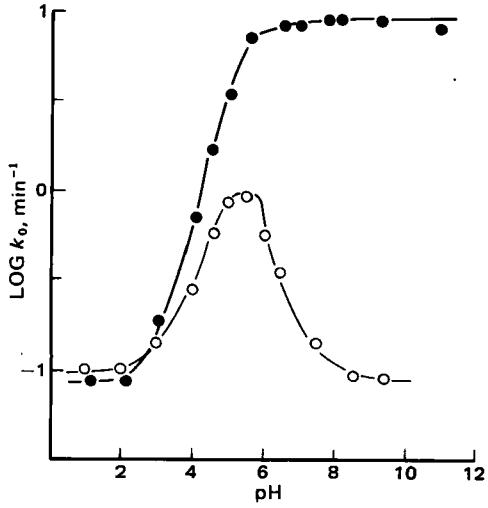

Figure 4—*The pH–rate profiles for the hydrolysis of the oxazolidines II (○) and III (●) at 37° (μ = 0.5). (Taken from Ref. 8.)*

The pK_a values derived for the oxazolidines are substantially smaller than the pK_a value (9.6) for ephedrine. The difference can most likely be attributed to the presence of the electronegative ring oxygen atom in the oxazolidines, *cf.*, the difference in the pK_a values for piperidine (11.1) and morpholine (8.3).

Lipophilicity of the Oxazolidines—The apparent partition coefficients ($P = C_{octanol}/C_{aqueous}$) for the oxazolidines VI–VIII were measured using an octanol–aqueous buffer system, using 0.05 *M* phosphate buffer, pH 7.40. The values found for log P were 0.92 (VI), 1.83 (VII), and 1.68 (VIII). The log P values for the free base forms of the compounds can be calculated from these values when correction is made for the degree of ionization at pH 7.4; the values thus obtained are 1.04 (VI), 1.94 (VII), and 1.69 (VIII). The log P value for the benzaldehyde derivative (II) was previously reported to be 1.58 at pH > 7. The log P value for ephedrine (pK_a 9.6) in a similar octanol–phosphate buffer (pH 7.4) system has been reported to be −1.35, with a log P value of 1.02 for the free base form (18). These results show that the oxazolidines prepared from acetone, cyclohexanone, or benzaldehyde are more lipophilic than the parent ephedrine, especially at physiological pH where the oxazolidines are largely in the free base form and ephedrine is largely protonated. Due to stability reasons the log P values for the oxazolidines III–V could not be experimentally determined, but could be estimated on the basis of hydrophobic substituent constants (19) and the values for derivatives described above.

Structural Effects on Reaction Rate—The rate data obtained show that the structure of the carbonyl component has a pronounced effect on the rate of oxazolidine hydrolysis in both acidic, neutral, and alkaline

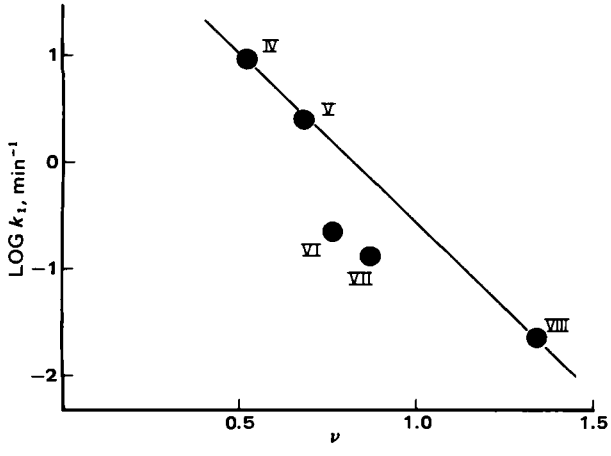

Figure 5—*Plot of log* k_1 *against the steric substituent parameter ν for various oxazolidines. The correlation plot was made for IV, V, and VIII possessing the same* pK_a *values. The ν values used refer to the moiety of the oxazolidines derived from the carbonyl compounds including the ring carbon atom in the oxazolidines, e.g., for IV and VI the ν values are those for methyl and isopropyl, respectively.*

Table III—Half-lives of Hydrolysis of Various Oxazolidines at pH 1 and 7.4 [a]

Oxazolidine	$t_{1/2}$, min	
	pH 1	pH 7.4
II[b]	7	5.0
III[b]	8	0.08
IV	96	0.08
V	70	0.3
VI	220	4.0
VII	230	5.9
VIII	—	30

[a] μ = 0.5; 37°. [b] The rate data are from a previous study (8).

solutions. Considering the rate constant k_1 and accordingly, the hydrolysis rate in weakly acidic to basic aqueous solutions, the structural effects appear to involve both electrical and steric effects. The oxazolidines derived from the three aliphatic aldehydes (IV, V, and VIII) possess almost the same pK_a values (Table II), and the variation of the rates of hydrolysis of these derivatives can be accounted for in terms of different steric properties of the aldehyde part. As seen in Fig. 5, an excellent linear correlation exists between log k_1 and the steric substituent parameter ν (20). The regression equation between log k_1 and ν for these oxazolidines is given by:

$$\log k_1 = -3.2\nu + 2.6 \quad (k_1 \text{ in } \text{min}^{-1};\ 37°) \qquad \text{(Eq. 2)}$$

This result implies that the reactivity of oxazolidines in neutral and basic solutions decreases with increasing steric effects within the carbonyl moiety. As seen from Fig. 5 such a correlation also appears to hold for oxazolidines derived from ketones, although only rate data for two derivatives have been obtained. The decreased reactivity of the ketone–oxazolidines as compared to the aldehyde–oxazolidines (Fig. 5) may most likely be due to differences in the pK_a values of the oxazolidines, *i.e.*, increased pK_a results in decreased reactivity. As previously suggested (8) the considerably greater reactivity of III compared with II may be attributed to some kind of intramolecular catalysis by the *ortho*-situated hydroxyl group in III. It is obvious, however, that the present data are insufficient to delineate the structural factors (steric and electrical), both within the aldehyde or ketone part and the amino alcohol moiety, that may influence the stability of oxazolidines.

Consideration of Oxazolidines as Prodrug Types—The results obtained extend the previous suggestion (8) that oxazolidines may have potential as prodrug forms for β-amino alcohols or carbonyl-containing compounds. The derivatives undergo a quantitative conversion to the parent compounds in aqueous solution with rates highly dependent on pH. As shown in Table III the decomposition of the oxazolidines at pH 7.4 and 37° is quite rapid, whereas a greater stability is achieved in acid solutions. These rates might not be expected to change much *in vivo*. The oxazolidines are much weaker bases than the parent β-amino alcohol, and this results in higher lipophilicity at physiological pH. Such increased lipophilicity may become advantageous in situations where delivery problems for β-amino alcohol-type drugs are due to low lipophilicity. Thus, by appropriate selection of the carbonyl moiety of oxazolidines it may be feasible to obtain prodrugs of β-amino alcohols with varying physicochemical properties, such as lipophilicity and rate of drug release, and hence to control and modify the delivery and overall activity characteristics of the parent drugs. In considering oxazolidines as prodrug candidates for carbonyl-containing substances, their weakly basic character may also be advantageous in that the transformation of such substances into oxazolidines introduces a readily ionizable moiety, which may allow the preparation of derivatives with increased aqueous solubilities at acidic pH values. For example, a potentially useful purpose of transforming a carbonyl-containing drug substance into a bioreversible oxazolidine derivative could be to enhance its dissolution behavior in an effort to improve the oral bioavailability.

REFERENCES

(1) V. Stella, in "Pro-drugs as Novel Drug Delivery Systems," T. Higuchi and V. Stella, Eds., American Chemical Society, Washington, D.C., 1975, p. 1.

(2) A. A. Sinkula and S. H. Yalkowsky, *J. Pharm. Sci.*, **64**, 181 (1975).

(3) V. Stella, T. J. Mikkelson, and J. D. Pipkin, in "Drug Delivery Systems: Characteristics and Biochemical Applications," R. L. Juliano,

Ed., Oxford University Press, New York and Oxford, 1980, p. 112.
(4) H. Bundgaard, M. Johansen, V. Stella, and M. Cortese, *Int. J. Pharm.*, **10**, 181 (1982).
(5) H. Bundgaard, in "Optimization of Drug Delivery, Alfred Benzon Symposium 17," H. Bundgaard, A. B. Hansen, and H. Kofod, Eds., Munksgaard, Copenhagen, 1982, p. 178.
(6) J. P. Patel and A. J. Repta, *Int. J. Pharm.*, **9**, 29 (1981).
(7) A. J. Repta, M. J. Hageman, and J. P. Patel, *Int. J. Pharm.*, **10**, 239 (1982).
(8) H. Bundgaard and M. Johansen, *Int. J. Pharm.*, **10**, 165 (1982).
(9) H. Pfanz and G. Kirchner, *Justus Liebigs Ann. Chem.*, **614**, 149 (1958).
(10) J. B. Hyne, *J. Am. Chem. Soc.*, **81**, 6058 (1959).
(11) A. H. Beckett, G. R. Jones, and D. A. Hollingsbee, *J. Pharm. Pharmacol.*, **30**, 15 (1978).
(12) R. P. Bell and P. G. Evans, *Proc. R. Soc. London, Ser. A*, **291**, 297 (1966).
(13) H. Bundgaard and M. Johansen, *Int. J. Pharm.*, **5**, 67 (1980).
(14) T. H. Fife and L. Hagopian, *J. Am. Chem. Soc.*, **90**, 1007 (1968).
(15) T. H. Fife and J. E. C. Hutchins, *J. Org. Chem.*, **45**, 2099 (1980).
(16) R. A. McClelland and R. Somani, *J. Org. Chem.*, **46**, 4345 (1981).
(17) S. A. Soliman, *Can. J. Pharm. Sci.*, **8**, 132 (1973).
(18) P.-H. Wang and E. J. Lien, *J. Pharm. Sci.*, **69**, 662 (1980).
(19) C. Hansch and A. Leo, "Substituent Constants for Correlation Analysis in Chemistry and Biology," Wiley, New York, N.Y., 1979.
(20) M. Charton, in "Design of Biopharmaceutical Properties through Prodrugs and Analogs," E. B. Roche, Ed., American Pharmaceutical Association, Washington, D.C., 1977, p. 228.

Determinants of Bumetanide Response in the Dog: Effect of Indomethacin

DAVID E. SMITH ˣ and HENRY S. H. LAU

Received July 1, 1982, from the *College of Pharmacy, The University of Michigan, Ann Arbor, MI 48109.* Accepted for publication September 16, 1982.

Abstract □ Four male unanesthetized dogs each weighing 22.0–29.0 kg received 0.250 mg/kg iv of bumetanide before (treatment I) and after (treatment II) indomethacin pretreatment. Lactated Ringer's solution was administered intravenously throughout both treatments at a flow rate of 2 ml/min to avoid fluid and electrolyte depletion. Unchanged bumetanide and indomethacin concentrations were analyzed using high-performance liquid chromatography. Sodium was measured by flame photometry and creatinine by colorimetry. Indomethacin pretreatment did not significantly change the pharmacokinetics of bumetanide, affecting neither the total amount of drug nor time course of drug delivered into the urine. In contrast, indomethacin pretreatment resulted in a dramatic reduction in the 4-hr sodium excretion and urine volume. Therefore, a pharmacokinetic interaction may be eliminated as a possible mechanism for the attenuation, by indomethacin, of the natriuretic and diuretic response of bumetanide. Instead, it appears that indomethacin diminishes the response to bumetanide *via* prostaglandin inhibition.

Keyphrases □ Bumetanide—pharmacokinetics, sodium excretion, dogs, effect of indomethacin pretreatment □ Indomethacin—pretreatment, effect on sodium excretion, pharmacokinetics of bumetanide, dogs □ Pharmacokinetics—bumetanide, sodium excretion, pharmacokinetics in the dog, effect of indomethacin pretreatment

Bumetanide [3-(butylamino)-4-phenoxy-5-sulfamoylbenzoic acid] is a high-ceiling diuretic with pharmacological action similar to that of furosemide (1–3). The diuretic appears to act primarily at the medullary portion of the ascending limb of the loop of Henle, where it inhibits solute reabsorption, although inhibition of sodium transport in the proximal nephron also occurs (4–7). In addition, bumetanide induces intrarenal hemodynamic changes (8–12). Since bumetanide is highly bound to plasma proteins (13, 14), the drug gains access to the kidney lumen predominantly at the pars recta of the proximal tubule *via* the nonspecific organic acid secretory pathway (1, 13).

Indomethacin has been shown recently to attenuate the natriuretic and diuretic response to bumetanide in experimental animals (12), healthy volunteers (15, 16), and patients (17). These authors proposed that indomethacin, a potent inhibitor of prostaglandin synthetase, interferes with the prostaglandin-mediated effect of bumetanide. However, it is also possible that indomethacin may compete with bumetanide (both drugs are weak organic acids) for active secretion into the lumen of the kidney tubule, thereby modifying either the total amount of diuretic delivered to its active site or the time course of drug delivery. Since previous investigators (12, 15–17) did not measure concentrations and/or amounts of bumetanide in the plasma and urine, this alternative hypothesis (pharmacokinetic interaction) cannot be eliminated. Therefore, the present investigation was undertaken to clarify the mechanism by which indomethacin diminishes the pharmacodynamic response to bumetanide.

EXPERIMENTAL

Materials—An aqueous solution dosage form of bumetanide[1] was prepared using 0.4 *N* NaOH immediately prior to use. Indomethacin capsules[2] were obtained commercially. Indomethacin powder[3] was used as received. All other chemicals and solvents were reagent grade or better, as previously reported (18).

Methods—Four male, mongrel, conditioned, unanesthetized dogs weighing 22.0–29.0 kg received 0.250 mg/kg of bumetanide before (treatment I) and after (treatment II) pretreatment with indomethacin. Each dog was fasted the night before and throughout the entire study period. Bumetanide was administered intravenously over a 3-min infusion[4] period, with the beginning of the infusion being considered as time zero. A 100-mg dose of indomethacin (two 50-mg capsules) was ingested the night before (11:00 to 11:30 p.m.) and on the study day (60 min prior to bumetanide administration). An interval of at least 1 week elapsed between studies, and identical lots for each drug were used throughout.

Heparinized scalp vein needles[5] were placed in the forelegs of each dog:

[1] Lot A-29; Hoffmann-La Roche, Inc., Nutley, N.J.
[2] Lot D2520; Merck Sharp and Dohme, West Point, Pa.
[3] Merck Sharp and Dohme, Rahway, N.J.
[4] Harvard Compact Infusion Pump; Harvard Apparatus Co., Inc., South Natick, Mass.
[5] E-Z Set—PRN Intermittent Infusion Set; The Deseret Co., Sandy, Utah.

0022-3549/83/1100-1298$01.00/0

Ed., Oxford University Press, New York and Oxford, 1980, p. 112.
(4) H. Bundgaard, M. Johansen, V. Stella, and M. Cortese, *Int. J. Pharm.*, **10**, 181 (1982).
(5) H. Bundgaard, in "Optimization of Drug Delivery, Alfred Benzon Symposium 17," H. Bundgaard, A. B. Hansen, and H. Kofod, Eds., Munksgaard, Copenhagen, 1982, p. 178.
(6) J. P. Patel and A. J. Repta, *Int. J. Pharm.*, **9**, 29 (1981).
(7) A. J. Repta, M. J. Hageman, and J. P. Patel, *Int. J. Pharm.*, **10**, 239 (1982).
(8) H. Bundgaard and M. Johansen, *Int. J. Pharm.*, **10**, 165 (1982).
(9) H. Pfanz and G. Kirchner, *Justus Liebigs Ann. Chem.*, **614**, 149 (1958).
(10) J. B. Hyne, *J. Am. Chem. Soc.*, **81**, 6058 (1959).
(11) A. H. Beckett, G. R. Jones, and D. A. Hollingsbee, *J. Pharm. Pharmacol.*, **30**, 15 (1978).
(12) R. P. Bell and P. G. Evans, *Proc. R. Soc. London, Ser. A*, **291**, 297 (1966).
(13) H. Bundgaard and M. Johansen, *Int. J. Pharm.*, **5**, 67 (1980).
(14) T. H. Fife and L. Hagopian, *J. Am. Chem. Soc.*, **90**, 1007 (1968).
(15) T. H. Fife and J. E. C. Hutchins, *J. Org. Chem.*, **45**, 2099 (1980).
(16) R. A. McClelland and R. Somani, *J. Org. Chem.*, **46**, 4345 (1981).
(17) S. A. Soliman, *Can. J. Pharm. Sci.*, **8**, 132 (1973).
(18) P.-H. Wang and E. J. Lien, *J. Pharm. Sci.*, **69**, 662 (1980).
(19) C. Hansch and A. Leo, "Substituent Constants for Correlation Analysis in Chemistry and Biology," Wiley, New York, N.Y., 1979.
(20) M. Charton, in "Design of Biopharmaceutical Properties through Prodrugs and Analogs," E. B. Roche, Ed., American Pharmaceutical Association, Washington, D.C., 1977, p. 228.

Determinants of Bumetanide Response in the Dog: Effect of Indomethacin

DAVID E. SMITH ˣ and HENRY S. H. LAU

Received July 1, 1982, from the *College of Pharmacy, The University of Michigan, Ann Arbor, MI 48109.* Accepted for publication September 16, 1982.

Abstract □ Four male unanesthetized dogs each weighing 22.0–29.0 kg received 0.250 mg/kg iv of bumetanide before (treatment I) and after (treatment II) indomethacin pretreatment. Lactated Ringer's solution was administered intravenously throughout both treatments at a flow rate of 2 ml/min to avoid fluid and electrolyte depletion. Unchanged bumetanide and indomethacin concentrations were analyzed using high-performance liquid chromatography. Sodium was measured by flame photometry and creatinine by colorimetry. Indomethacin pretreatment did not significantly change the pharmacokinetics of bumetanide, affecting neither the total amount of drug nor time course of drug delivered into the urine. In contrast, indomethacin pretreatment resulted in a dramatic reduction in the 4-hr sodium excretion and urine volume. Therefore, a pharmacokinetic interaction may be eliminated as a possible mechanism for the attenuation, by indomethacin, of the natriuretic and diuretic response of bumetanide. Instead, it appears that indomethacin diminishes the response to bumetanide *via* prostaglandin inhibition.

Keyphrases □ Bumetanide—pharmacokinetics, sodium excretion, dogs, effect of indomethacin pretreatment □ Indomethacin—pretreatment, effect on sodium excretion, pharmacokinetics of bumetanide, dogs □ Pharmacokinetics—bumetanide, sodium excretion, pharmacokinetics in the dog, effect of indomethacin pretreatment

Bumetanide [3-(butylamino)-4-phenoxy-5-sulfamoylbenzoic acid] is a high-ceiling diuretic with pharmacological action similar to that of furosemide (1–3). The diuretic appears to act primarily at the medullary portion of the ascending limb of the loop of Henle, where it inhibits solute reabsorption, although inhibition of sodium transport in the proximal nephron also occurs (4–7). In addition, bumetanide induces intrarenal hemodynamic changes (8–12). Since bumetanide is highly bound to plasma proteins (13, 14), the drug gains access to the kidney lumen predominantly at the pars recta of the proximal tubule *via* the nonspecific organic acid secretory pathway (1, 13).

Indomethacin has been shown recently to attenuate the natriuretic and diuretic response to bumetanide in experimental animals (12), healthy volunteers (15, 16), and patients (17). These authors proposed that indomethacin, a potent inhibitor of prostaglandin synthetase, interferes with the prostaglandin-mediated effect of bumetanide. However, it is also possible that indomethacin may compete with bumetanide (both drugs are weak organic acids) for active secretion into the lumen of the kidney tubule, thereby modifying either the total amount of diuretic delivered to its active site or the time course of drug delivery. Since previous investigators (12, 15–17) did not measure concentrations and/or amounts of bumetanide in the plasma and urine, this alternative hypothesis (pharmacokinetic interaction) cannot be eliminated. Therefore, the present investigation was undertaken to clarify the mechanism by which indomethacin diminishes the pharmacodynamic response to bumetanide.

EXPERIMENTAL

Materials—An aqueous solution dosage form of bumetanide[1] was prepared using 0.4 *N* NaOH immediately prior to use. Indomethacin capsules[2] were obtained commercially. Indomethacin powder[3] was used as received. All other chemicals and solvents were reagent grade or better, as previously reported (18).

Methods—Four male, mongrel, conditioned, unanesthetized dogs weighing 22.0–29.0 kg received 0.250 mg/kg of bumetanide before (treatment I) and after (treatment II) pretreatment with indomethacin. Each dog was fasted the night before and throughout the entire study period. Bumetanide was administered intravenously over a 3-min infusion[4] period, with the beginning of the infusion being considered as time zero. A 100-mg dose of indomethacin (two 50-mg capsules) was ingested the night before (11:00 to 11:30 p.m.) and on the study day (60 min prior to bumetanide administration). An interval of at least 1 week elapsed between studies, and identical lots for each drug were used throughout.

Heparinized scalp vein needles[5] were placed in the forelegs of each dog:

[1] Lot A-29; Hoffmann-La Roche, Inc., Nutley, N.J.
[2] Lot D2520; Merck Sharp and Dohme, West Point, Pa.
[3] Merck Sharp and Dohme, Rahway, N.J.
[4] Harvard Compact Infusion Pump; Harvard Apparatus Co., Inc., South Natick, Mass.
[5] E-Z Set—PRN Intermittent Infusion Set; The Deseret Co., Sandy, Utah.

0022-3549/83/1100-1298$01.00/0

one was used for administration of bumetanide and replacement fluids, the other for obtaining blood samples. Blood samples (3 ml) were collected just prior to bumetanide dose (blank) and at 3, 5, 10, 20, 30, 45, 60, 80, 100, 120, 150, 180, 210, and 240 min. Voided urine was collected *via* an indwelling bladder catheter[6] just prior to bumetanide dosing (blank) and at 20, 40, 80, 120, 180, and 240 min. The bladder was flushed with 2 × 5 ml of air at the end of each urine collection to ensure a complete catch. Lactated Ringer's solution ws administered intravenously throughout the entire study period of both treatments at a flow rate of 2 ml/min to avoid fluid and electrolyte depletion. All 4-hr plasma samples showed normal sodium concentrations.

Assays—Plasma and urine samples containing bumetanide, with and without indomethacin pretreatment, were analyzed by a high-performance liquid chromatographic (HPLC) method as described previously (18). Plasma samples (0.20 ml) containing indomethacin were prepared and analyzed in a similar fashion to that of bumetanide. A 50- μl aliquot of acetophenone (0.025 mg/ml) was used as the internal standard, and the solvent system (50% acetonitrile in 0.015 *M* phosphoric acid aqueous solution, adjusted to pH 5.0 with 4 *N* NaOH) was pumped isocratically at a flow rate of 2.0 ml/min at ambient temperature. Both indomethacin and acetophenone were measured using UV detection at 254 nm (0.01 AUFS). The voltage spans on the dual-pen recorder were set at 10 mV for indomethacin and at 50 mV for acetophenone. Using the mobile phase described above, indomethacin and acetophenone had retention times in plasma of 9.0 and 4.5 min, respectively (Fig. 1). A representative standard curve of indomethacin–acetophenone peak height ratio over the indomethacin plasma concentration range (0.25–5.00 μg/ml) resulted in the following linear least-squares regression equation: $y = 0.232x - 0.003$; $r^2 = 0.999$.

Plasma and urine samples were measured for sodium with a flame photometer[7]. Creatinine was determined colorimetrically using a commercial kit[8].

Calculations—Plasma concentration–time curves of bumetanide were fitted (equally weighted) to the general polyexponential equation for post constant-rate infusion data (19):

$$C_p = \sum_{i=1}^{n} Yi\, e^{-\lambda i t} \qquad \text{(Eq. 1)}$$

where C_p represents the plasma concentration at time t, Yi is the coefficient of the ith exponential term for post constant-rate intravenous infusion data, and λi is the exponent of the ith exponential term. The values of the coefficients and exponential terms in Eq. 1 were obtained using a nonlinear least-squares regression program[9] and a microcomputer[10]. Initial estimates were obtained using the RSTRIP[9] program. The number of exponents (n) needed for each data set were determined by the application of Akaike's information criterion (20).

Since:

$$Yi = \sum_{i=1}^{n} (1 - e^{\lambda i T}) Ci/(-\lambda i T) \qquad \text{(Eq. 2)}$$

and T is the constant-rate infusion time and Ci is the coefficient of the ith exponential term for bolus intravenous data, Eq. 1 can be rearranged (19) to:

$$C_p = \sum_{i=1}^{n} (1 - e^{\lambda i T})\, Ci\, e^{-\lambda i t}/(-\lambda i T) \qquad \text{(Eq. 3)}$$

Once the values of the coefficients and exponential terms in Eq. 1 are determined by computer fitting, the values of Ci in Eq. 3 can be calculated.

The following pharmacokinetic parameters were calculated using standard equations (19, 21):

$$V_1 = D/\sum_{i=1}^{n} Ci \qquad \text{(Eq. 4)}$$

$$Vd_{ss} = D \sum_{i=1}^{n} Ci/\lambda i^2 \Big/ \left(\sum_{i=1}^{n} Ci/\lambda i\right)^2 \qquad \text{(Eq. 5)}$$

$$Vd_{area} = D/\left(\lambda_1 \sum_{i=1}^{n} Ci/\lambda i\right) \qquad \text{(Eq. 6)}$$

[6] Swan-Ganz Flow-Directed Monitoring Catheter, Model 93-111-7F; American Edwards Laboratories, Santa Ana, Calif.
[7] Model 455; Corning Medical and Scientific, Medfield, Mass.
[8] Sigma Chemical Co., St. Louis, Mo.
[9] Personal communication, Dr. J. L. Fox, College of Pharmacy, The University of Michigan, Ann Arbor, Mich.
[10] Apple II Plus Computer; Apple Computer Inc., Cupertino, Calif.

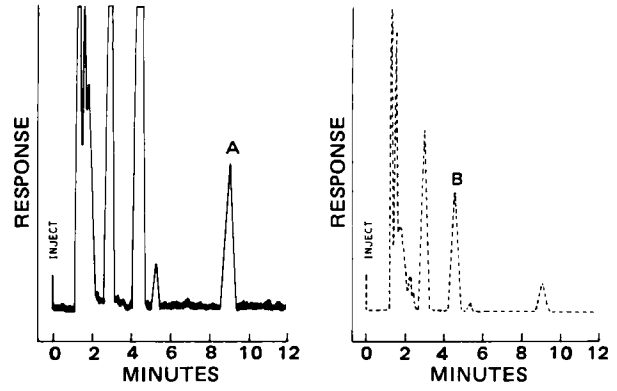

Figure 1—*Chromatograms for plasma spiked with indomethacin (A) and the internal standard (B), acetophenone, using UV detection (254 nm). Voltage spans on the dual-pen recorder were 10 mV (—) and 50 mV (- - - - -).*

$$CL_p = D/\sum_{i=1}^{n} Ci/\lambda i \qquad \text{(Eq. 7)}$$

$$CL_r = Ae^{\infty} \Big/ \sum_{i=1}^{n} Ci/\lambda i \qquad \text{(Eq. 8)}$$

$$CL_{nr} = CL_p - CL_r \qquad \text{(Eq. 9)}$$

$$t_{1/2} = 0.693/\lambda_1 \qquad \text{(Eq. 10)}$$

$$K_{10} = CL_p/V_1 \qquad \text{(Eq. 11)}$$

$$fe = Ae^{\infty}/D \qquad \text{(Eq. 12)}$$

In Eqs. 4–12, V_1 is the volume of the central compartment; Vd_{ss} is the volume of distribution at steady state; Vd_{area} is that volume which, when multiplied by C_p in the log-linear phase is equal to the amount of drug in the body; D is the intravenous dose (equal to the product of the zero-order infusion rate and the length of infusion); C_1 and λ_1 are the coefficient and exponent, respectively, such that λ_1 is the smallest of the λi values of the polyexponential equation; CL_p is the total plasma clearance; CL_r is the renal clearance; CL_{nr} is the nonrenal clearance; Ae^{∞} is the amount of unchanged drug recovered in the urine at time infinity; $t_{1/2}$ is the biological half-life; K_{10} is the first-order elimination rate constant from the central compartment; and fe is the fraction of the available dose excreted unchanged in the urine. Creatinine clearance (CL_{cr}) was calculated by dividing the urinary excretion rate of creatinine by its plasma concentration at the midpoint of the urine collection period.

Data throughout the study are expressed as mean ± *SD*, unless otherwise indicated. Statistical differences were determined by a paired t test. A p value of <0.05 was considered to be significant.

RESULTS

Plasma concentrations of bumetanide over 4 hr were fitted to a biexponential equation for six data sets and to a triexponential equation for two data sets (Table I). The goodness of the fit, as determined by R^2 and the correlation, was ≥0.991.

The pharmacokinetics of bumetanide before (treatment I) and after (treatment II) indomethacin pretreatment are presented in Table II. None of the pharmacokinetic parameters evaluated were statistically different between treatments. This is demonstrated by the virtually superimposable plasma concentration–time profiles (Fig. 2) and the urinary excretion rate–time profiles (Fig. 3) observed between treatments I and II. Mean plasma concentrations of indomethacin ranged from 0.62 to 4.36 μg/ml during the study period, well above the plasma concentrations of bumetanide (Fig. 2).

The effects of indomethacin on bumetanide-induced diuresis and natriuresis are presented in Table III. Pharmacodynamic data are reported as electrolyte excretion rate and cumulative excretion (as opposed to fractional excretion), since sodium concentrations and creatinine clearances did not differ between treatments (CL_{cr} = 2.49 ± 0.24 ml/min·kg for treatment I *versus* 2.33 ± 0.32 ml/min·kg for treatment II; $p > 0.50$). Indomethacin pretreatment results in a dramatic reduction in urine volume (1060 ± 77 ml/4 hr for treatment I *versus* 543 ± 115 ml/4 hr for treatment II; $p < 0.005$) as well as sodium excretion (121 ± 17 meq/4 hr for treatment I *versus* 62.4 ± 21.3 meq/4 hr for treatment II; $p < 0.005$). Analyses of the sodium excretion rate over time show that the

Table I—Coefficients and Exponential Terms of Bumetanide Obtained Using Biexponential and Triexponential Equations

Dog	Treatment[a]	Biexponential Equation C_1, ng/ml	C_2, ng/ml	λ_1, min^{-1}	λ_2, min^{-1}	R^2 [b]	Correlation[c]
1	I	120	1855	0.0095	0.1150	0.991	0.994
2	I	119	1634	0.0102	0.1016	0.997	0.998
3	I	125	1978	0.0125	0.1166	0.996	0.997
	II	173	2289	0.0169	0.1028	0.992	0.995
4	I	164	1187	0.0134	0.1265	0.995	0.996
	II	110	1188	0.0122	0.1130	0.996	0.997

Dog	Treatment	Triexponential Equation C_1, ng/ml	C_2, ng/ml	C_3, ng/ml	λ_1, min^{-1}	λ_2, min^{-1}	λ_3, min^{-1}	R^2 [b]	Correlation[c]
1	II	49.5	529	1355	0.0081	0.0414	0.1604	0.999	0.999
2	II	106	647	1839	0.0102	0.0578	0.2020	0.999	0.999

[a] (I) bumetanide before indomethacin pretreatment; (II) bumetanide after indomethacin pretreatment. [b] $R^2 = [\Sigma(Obs)^2 - \Sigma(Dev)^2]/\Sigma(Obs)^2$. [c] Correlation between the calculated and observed plasma concentrations.

Table II—Pharmacokinetics of Bumetanide Before and After Indomethacin Pretreatment

Dog	Treatment[a]	Weight kg	CL_p, ml/min·kg	V_1, ml/kg	Vd_{ss}, ml/kg	Vd_{area}, ml/kg	$t_{1/2}$, min	K_{10}, min^{-1}	CL_r, ml/min·kg	CL_{nr}, ml/min·kg	fe
1	I	24.0	8.70	127	443	913	72.7	0.0685	3.81	4.89	0.438
	II	27.0	9.13	129	375	1134	86.0	0.0708	2.98	6.15	0.327
2	I	22.0	9.03	143	421	881	67.6	0.0631	4.12	4.91	0.456
	II	23.5	8.13	96	335	800	68.2	0.0847	3.55	4.58	0.437
3	I	22.5	9.28	119	324	741	55.3	0.0780	4.45	4.83	0.480
	II	24.0	7.69	102	195	455	41.0	0.0754	3.03	4.66	0.394
4	I	27.0	11.6	185	528	866	51.7	0.0627	5.82	5.78	0.504
	II	29.0	12.8	193	547	1053	57.0	0.0663	2.96	9.86	0.232
Mean (*SD*)	I	23.9 (2.2)	9.65 (1.32)	144 (29)	429 (84)	850 (75)	61.8 (9.9)	0.0681 (0.0071)	4.55 (0.89)	5.10 (0.45)	0.470 (0.029)
Mean (*SD*)	II	25.9 (2.6)	9.44 (2.32)	130 (44)	363 (145)	860 (305)	63.0 (18.9)	0.0743 (0.0079)	3.13 (0.28)	6.31 (2.47)	0.348 (0.089)
Level of Significance[b]		S ($p < 0.02$)	NS ($p < 0.50$)	NS ($p > 0.20$)	NS ($p > 0.10$)	NS ($p > 0.50$)	NS ($p > 0.50$)	NS ($p > 0.20$)	NS ($p > 0.05$)	NS ($p > 0.20$)	NS ($p > 0.10$)

[a] (I) bumetanide before indomethacin pretreatment; (II) bumetanide after indomethacin pretreatment. [b] (S) significant; (NS) not significant.

Table III—Effects of Indomethacin on Bumetanide Diuresis and Natriuresis

Dog	Treatment[a]	Urine Volume, ml/4 hr	Sodium Excretion, meq/4 hr
1	I	1131	123
	II	467	48.6
2	I	1028	116
	II	625	78.0
3	I	967	103
	II	424	40.0
4	I	1115	143
	II	657	83.1
Mean (*SD*)	I	1060 (77)	121 (17)
Mean (*SD*)	II	543 (115)	62.4 (21.3)
Level of Significance[b]		S ($p < 0.005$)	S ($p < 0.005$)

[a] (I) bumetanide before indomethacin pretreatment; (II) bumetanide after indomethacin pretreatment. [b] (S) significant.

inhibiting effect of indomethacin was most pronounced during the initial 40–60 min (Fig. 4).

DISCUSSION

Several studies have shown that indomethacin decreases the cumulative response to bumetanide in experimental animals (12), healthy volunteers, (15, 16), and patients (17). Mechanisms consistent with this attenuated response include the inhibition, by indomethacin, of prostaglandin-induced changes in renal hemodynamics and direct tubular effects, as well as competition between bumetanide and indomethacin for active tubular transport into the kidney lumen. Previous investigators (12, 15–17) only considered the mechanism involving prostaglandin inhibition, since concentrations and/or amounts of bumetanide in the plasma and urine were not determined.

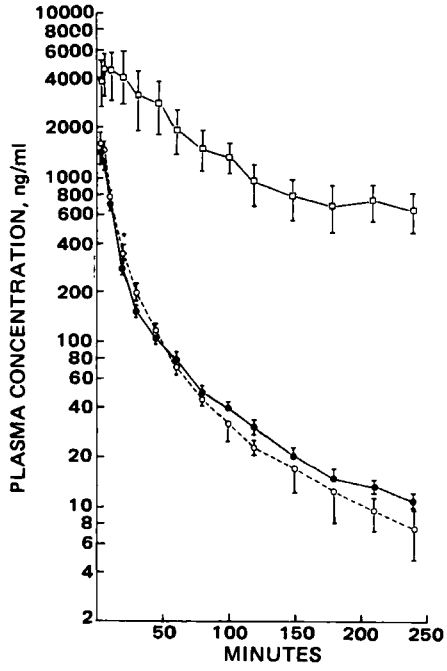

Figure 2—*Plasma concentration* versus *time plots of bumetanide alone (●), bumetanide after indomethacin pretreatment (○), and indomethacin (□). Data are expressed as the mean ± SEM (n = 4). Asterisks denote statistical differences between the treatments.*

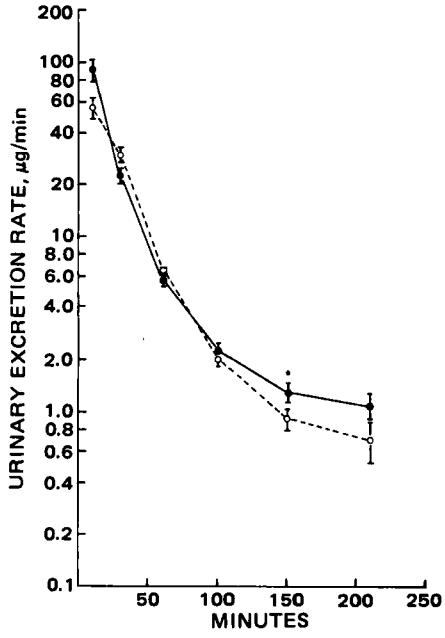

Figure 3—*Urinary excretion rate* versus *midpoint time plots of bumetanide alone (●) and bumetanide after indomethacin pretreatment (○). Data are expressed as the mean ± SEM (n = 4). Asterisks denote statistical differences between the treatments.*

In the present investigation, indomethacin pretreatment did not significantly change the pharmacokinetics of bumetanide (Table II), affecting neither the total amount of drug nor time course of drug delivered into the urine. Although *fe* was reduced ~25% in the presence of indomethacin, the extent of this change was minimal compared with the marked effect of indomethacin on bumetanide-induced natriuresis and diuresis (~50% reduction).

Figures 5 and 6 demonstrate the effect of indomethacin on the dose–response curves of bumetanide. Indomethacin decreased the maximal response (sodium excretion rate) to bumetanide when the dose was expressed as either plasma concentration (Fig. 5) or urinary excretion rate (Fig. 6). These effects are consistent with those of a noncompetitive inhibition, presumably that of prostaglandin synthesis. The effect of indomethacin on bumetanide-induced natriuresis and diuresis could not be explained by normalizing the response to creatinine clearance. This finding is in agreement with previous studies by Brater *et al.* (15) and Olsen (12). Brater *et al.* (15) reported that unlike furosemide, indomethacin decreased the increment in fractional sodium excretion due to bumetanide in healthy volunteers. Olsen (12) observed that absolute

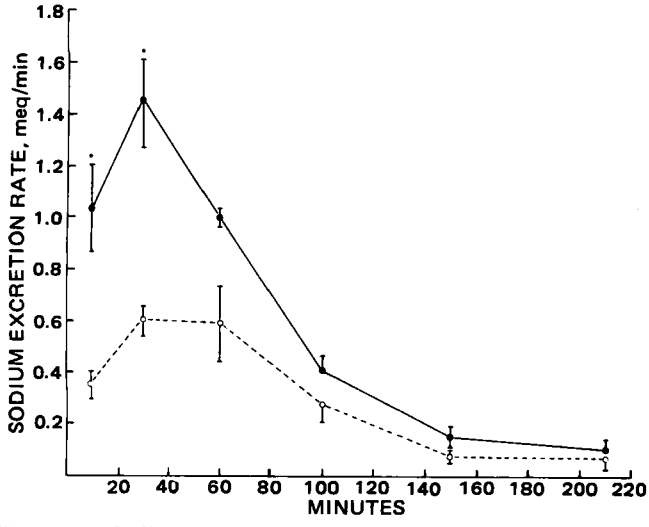

Figure 4—*Sodium excretion rate* versus *midpoint time plots of bumetanide alone (●) and bumetanide after indomethacin pretreatment (○). Data are expressed as the mean ± SEM (n = 4). Asterisks denote statistical differences between the treatments.*

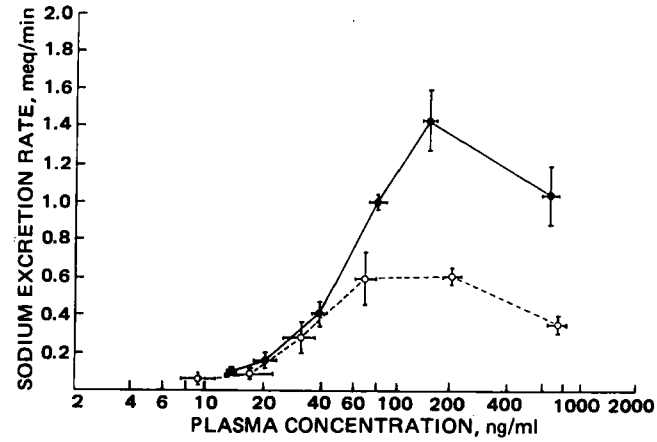

Figure 5—*Sodium excretion rate* versus *plasma concentration plots of bumetanide alone (●) and bumetanide after indomethacin pretreatment (○). Data are expressed as the mean ± SEM (n = 4).*

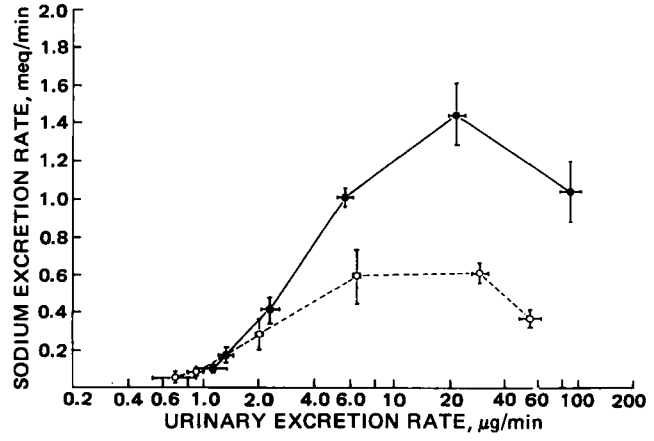

Figure 6—*Sodium excretion rate* versus *urinary excretion rate plots of bumetanide alone (●) and bumetanide after indomethacin pretreatment (○). Data are expressed as the mean ± SEM (n = 4).*

and fractional sodium excretions after bumetanide were significantly lower in indomethacin-pretreated dogs compared with nonpretreated dogs at a time when neither renal blood flow nor glomerular filtration rate were significantly different.

The present study and that of previous investigators (12, 15) suggest that indomethacin affects the pharmacodynamic response to bumetanide by a mechanism other than prostaglandin-mediated changes in renal hemodynamics. Although speculative, renal prostaglandins may be involved in the regulation of medullary tonicity and solute excretion at a tubular level. This hypothesis is supported by an *in vitro* study in the isolated, perfused segments of rabbit nephrons (22), which demonstrated that dinoprostone inhibits net chloride transport across the medullary thick ascending limb of the loop of Henle, but had no effect on the cortical segment. This is consistent with the mechanism of action of bumetanide, which is inhibition of active chloride reabsorption in the ascending limb of the loop of Henle.

The present study demonstrated that indomethacin had no significant effect on the disposition of bumetanide. Therefore, a pharmacokinetic interaction may be eliminated as a possible mechanism for the attenuation, by indomethacin, of the natriuretic and diuretic response of bumetanide. Instead, it appears that indomethacin diminishes the response to bumetanide *via* prostaglandin inhibition, although the precise nature of this interaction remains unclear.

REFERENCES

(1) H. H. Frey, *Postgrad. Med. J. Suppl.*, **51**, 14 (1975).

(2) U. B. Olsen, *Acta Pharmacol. Toxicol. Suppl.* **III**, 3 (1977).

(3) M. Cohen, *J. Clin. Pharmacol.*, **21**, 537 (1981).

(4) E. Bourke, M. J. A. Asbury, S. O'Sullivan, and P. B. B. Gatenby, *Eur. J. Pharmacol.*, **23**, 283 (1973).

(5) S. Jayakumar and J. B. Puschett, *J. Pharmacol. Exp. Ther.*, **201**, 251 (1977).

(6) M. Imai, *Eur. J. Pharmacol.*, **41**, 409 (1977).
(7) S. G. Karlander, R. Henning, and O. Lundvall, *Eur. J. Clin. Pharmacol.*, **6**, 220 (1973).
(8) A. C. Bollerup, B. Hesse, and B. Sigurd, *Acta Pharmacol. Toxicol.*, **34**, 305 (1974).
(9) K. L. Duchin and D. E. Hutcheon, *J. Pharmacol. Exp. Ther.*, **204**, 135 (1978).
(10) T. Higashio, Y. Abe, and K. Yamamoto, *J. Pharmacol. Exp. Ther.*, **207**, 212 (1978).
(11) U. B. Olsen and I. Ahnfelt-Rønne, *Acta Physiol. Scand.*, **97**, 251 (1976).
(12) U. B. Olsen, *Acta Pharmacol. Toxicol.*, **37**, 65 (1975).
(13) E. H. Østergaard, M. P. Magnussen, C. K. Nielsen, E. Eilertsen, and H. H. Frey, *Arzneim.-Forsch.*, **22**, 66 (1972).
(14) M. R. Cohen, E. Hinsch, R. Vergona, J. Ryan, S. J. Kolis, and M. A. Schwartz, *J. Pharmacol. Exp. Ther.*, **197**, 697 (1976).
(15) C. Brater, P. Chennavasin, J. M. Beck, and W. R. Fox, *Clin. Pharmacol. Ther.*, **27**, 421 (1980).
(16) J. Kaufman, R. Hamburger, J. Matheson, and W. Flamenbaum, *J. Clin. Pharmacol.*, **21**, 663 (1981).
(17) R. Pedrinelli, A. Magagna, F. Arzilli, P. Sassano, and A. Salvetti, *Clin. Pharmacol. Ther.*, **28**, 722 (1980).
(18) D. E. Smith, *J. Pharm. Sci.*, **71**, 520 (1982).
(19) J. G. Wagner, *J. Pharmacokinet. Biopharm.*, **5**, 161 (1977).
(20) K. Yamaoka, T. Nakagawa, and T. Uno, *J. Pharmacokinet. Biopharm.*, **6**, 165 (1978).
(21) J. G. Wagner, "Fundamentals of Clinical Pharmacokinetics," Drug Intelligence Publications, Hamilton, Ill., 1975, pp. 38, 83, 349.
(22) J. B. Stokes, *J. Clin. Invest.*, **64**, 495 (1979).

ACKNOWLEDGMENTS

Supported in part by a Biomedical Research Support Grant from the College of Pharmacy and a Faculty Research Rackham Grant, The University of Michigan. During the course of this work H. S. H. Lau was supported as an NIH Predoctoral Scholar on NIH Training Grant GM 07767-04.

The authors thank Dr. J. L. Fox for the availability of his computer programs and expertise.

Contamination of Injectable Solutions with 2-Mercaptobenzothiazole Leached from Rubber Closures

JOHN C. REEPMEYER ˣ **and YVONNE H. JUHL**

Received June 18, 1982, from the *Food and Drug Administration, National Center for Drug Analysis, St. Louis, MO 63101.* Accepted for publication October 27, 1982.

Abstract □ An impurity, discovered in a sample of digoxin injectable solution commercially packaged in a syringe for single-dose delivery, was found to originate from the rubber closure of the syringe and was identified as 2-mercaptobenzothiazole, a common accelerator for rubber vulcanization. Several similarly packaged injectable solutions of a variety of drugs from various manufacturers were examined and over half contained 2-mercaptobenzothiazole. The compound was identified by UV spectrophotometry (including a pH-dependent shift in its absorbance maximum), by mass spectrometry, and by comparison with standard 2-mercaptobenzothiazole using silica gel and reverse-phase high-performance liquid chromatography (HPLC). The presence of this impurity in injectable solutions may have implications with regard to toxicity and may interfere with the assay of digoxin injectable solution by HPLC.

Keyphrases □ Injectable formulations—contamination by 2-mercaptobenzothiazole leached from rubber closures, single-dose syringes, syringe cartridges □ 2-Mercaptobenzothiazole—contaminant of injectable solutions, leached from rubber closures, single-dose syringes, syringe cartridges □ Drug packaging—injectable solutions, single-dose syringes, and syringe cartridges, contamination by 2-mercaptobenzothiazole leached from rubber closures

During the assay for digoxin in injectable solutions by reverse-phase high-performance liquid chromatography (HPLC) conducted according to the USP method (1), an impurity was discovered in a sample commercially packaged in a syringe for a single-dose delivery. The small variation in mobile phase compositions permitted by the method produced considerable differences in resolution of digoxin from its contaminant and differences in the digoxin assays. When the mobile phase composition was varied, a significant difference was observed between the change in retention time of digoxin and that of the impurity, which implied that the impurity was structurally unrelated to digoxin. The origin, identification, and significance of this impurity are discussed in this report.

EXPERIMENTAL

Reverse-Phase HPLC—For the analysis of digoxin injectable solutions, the HPLC system consisted of a liquid chromatograph[1], a variable-wavelength detector[2] set at 218 nm and 0.2 AUFS, a recorder–integrator[3] with a chart speed of 0.5 cm/min, and an automatic injector[4] set to inject 20 μl. A reverse-phase C18 column[5] and a mobile phase of 30% aqueous acetonitrile[6] were used; the flow rate was 2.0 ml/min. The digoxin injectable solution samples were used undiluted (0.25 mg/ml). To determine if the contaminant in the digoxin injectable solution was a cardiac glycoside related to digoxin, samples of digoxigenin mono- and bisdigitoxoside[7], digoxigenin[7], and diginatin[7] were chromatographed twice, with 26 and 30% acetonitrile as mobile phases, and were compared by retention time to the impurity.

Concomitant Use of HPLC and UV Spectrophotometry—To obtain a full UV spectrum of chromatographically pure compound, the column effluent was passed first through a detector[8], fixed at 254 nm and connected to a recorder[9] to produce a chromatogram and then through a 10-mm flow cell positioned in a rapid-scanning spectrophotometer[10] to produce the spectrum. As the mobile phase passed through the flow cell, UV spectra were recorded every 2 sec until the intensity of the signal reached a maximum, at which time the solvent flow from the column was diverted, locking the sample in the flow cell. This permitted repetitive scanning of the sample and produced a smooth spectrum of the com-

[1] Model 204 liquid chromatograph; Waters Associates, Millipore Corp., Milford, MA 01757.
[2] Model 450 variable-wavelength detector; Waters Associates.
[3] Data Module; Waters Associates.
[4] WISP 710B; Waters Associates.
[5] μBondapak C-18, 10-μm particle size, 300 mm (length) × 3.9 mm (i.d.); Waters Associates.
[6] For the chromatographic column used in this work, 30% acetonitrile was preferred over 26% acetonitrile (the concentration recommended by the USP) because elution time was shortened without chromatographic interference from related cardiac glycosides. With 30% acetonitrile, the system suitability requirements of the USP (1) were met.
[7] Burroughs Wellcome Co., Inc., Research Triangle Park, NC 27709.
[8] Model 440 absorbance detector; Waters Associates.
[9] Model 3390A Reporting Integrator; Hewlett-Packard Co., Palo Alto, CA 94304.
[10] Model 8450A UV/visible spectrophotometer; Hewlett-Packard Co.

0022-3549/83/1100-1302$01.00/0

(6) M. Imai, *Eur. J. Pharmacol.*, **41**, 409 (1977).
(7) S. G. Karlander, R. Henning, and O. Lundvall, *Eur. J. Clin. Pharmacol.*, **6**, 220 (1973).
(8) A. C. Bollerup, B. Hesse, and B. Sigurd, *Acta Pharmacol. Toxicol.*, **34**, 305 (1974).
(9) K. L. Duchin and D. E. Hutcheon, *J. Pharmacol. Exp. Ther.*, **204**, 135 (1978).
(10) T. Higashio, Y. Abe, and K. Yamamoto, *J. Pharmacol. Exp. Ther.*, **207**, 212 (1978).
(11) U. B. Olsen and I. Ahnfelt-Rønne, *Acta Physiol. Scand.*, **97**, 251 (1976).
(12) U. B. Olsen, *Acta Pharmacol. Toxicol.*, **37**, 65 (1975).
(13) E. H. Østergaard, M. P. Magnussen, C. K. Nielsen, E. Eilertsen, and H. H. Frey, *Arzneim.-Forsch.*, **22**, 66 (1972).
(14) M. R. Cohen, E. Hinsch, R. Vergona, J. Ryan, S. J. Kolis, and M. A. Schwartz, *J. Pharmacol. Exp. Ther.*, **197**, 697 (1976).
(15) C. Brater, P. Chennavasin, J. M. Beck, and W. R. Fox, *Clin. Pharmacol. Ther.*, **27**, 421 (1980).
(16) J. Kaufman, R. Hamburger, J. Matheson, and W. Flamenbaum, *J. Clin. Pharmacol.*, **21**, 663 (1981).
(17) R. Pedrinelli, A. Magagna, F. Arzilli, P. Sassano, and A. Salvetti, *Clin. Pharmacol. Ther.*, **28**, 722 (1980).
(18) D. E. Smith, *J. Pharm. Sci.*, **71**, 520 (1982).
(19) J. G. Wagner, *J. Pharmacokinet. Biopharm.*, **5**, 161 (1977).
(20) K. Yamaoka, T. Nakagawa, and T. Uno, *J. Pharmacokinet. Biopharm.*, **6**, 165 (1978).
(21) J. G. Wagner, "Fundamentals of Clinical Pharmacokinetics," Drug Intelligence Publications, Hamilton, Ill., 1975, pp. 38, 83, 349.
(22) J. B. Stokes, *J. Clin. Invest.*, **64**, 495 (1979).

ACKNOWLEDGMENTS

Supported in part by a Biomedical Research Support Grant from the College of Pharmacy and a Faculty Research Rackham Grant, The University of Michigan. During the course of this work H. S. H. Lau was supported as an NIH Predoctoral Scholar on NIH Training Grant GM 07767-04.

The authors thank Dr. J. L. Fox for the availability of his computer programs and expertise.

Contamination of Injectable Solutions with 2-Mercaptobenzothiazole Leached from Rubber Closures

JOHN C. REEPMEYER ˣ **and YVONNE H. JUHL**

Received June 18, 1982, from the *Food and Drug Administration, National Center for Drug Analysis, St. Louis, MO 63101.* Accepted for publication October 27, 1982.

Abstract □ An impurity, discovered in a sample of digoxin injectable solution commercially packaged in a syringe for single-dose delivery, was found to originate from the rubber closure of the syringe and was identified as 2-mercaptobenzothiazole, a common accelerator for rubber vulcanization. Several similarly packaged injectable solutions of a variety of drugs from various manufacturers were examined and over half contained 2-mercaptobenzothiazole. The compound was identified by UV spectrophotometry (including a pH-dependent shift in its absorbance maximum), by mass spectrometry, and by comparison with standard 2-mercaptobenzothiazole using silica gel and reverse-phase high-performance liquid chromatography (HPLC). The presence of this impurity in injectable solutions may have implications with regard to toxicity and may interfere with the assay of digoxin injectable solution by HPLC.

Keyphrases □ Injectable formulations—contamination by 2-mercaptobenzothiazole leached from rubber closures, single-dose syringes, syringe cartridges □ 2-Mercaptobenzothiazole—contaminant of injectable solutions, leached from rubber closures, single-dose syringes, syringe cartridges □ Drug packaging—injectable solutions, single-dose syringes, and syringe cartridges, contamination by 2-mercaptobenzothiazole leached from rubber closures

During the assay for digoxin in injectable solutions by reverse-phase high-performance liquid chromatography (HPLC) conducted according to the USP method (1), an impurity was discovered in a sample commercially packaged in a syringe for a single-dose delivery. The small variation in mobile phase compositions permitted by the method produced considerable differences in resolution of digoxin from its contaminant and differences in the digoxin assays. When the mobile phase composition was varied, a significant difference was observed between the change in retention time of digoxin and that of the impurity, which implied that the impurity was structurally unrelated to digoxin. The origin, identification, and significance of this impurity are discussed in this report.

EXPERIMENTAL

Reverse-Phase HPLC—For the analysis of digoxin injectable solutions, the HPLC system consisted of a liquid chromatograph[1], a variable-wavelength detector[2] set at 218 nm and 0.2 AUFS, a recorder–integrator[3] with a chart speed of 0.5 cm/min, and an automatic injector[4] set to inject 20 μl. A reverse-phase C18 column[5] and a mobile phase of 30% aqueous acetonitrile[6] were used; the flow rate was 2.0 ml/min. The digoxin injectable solution samples were used undiluted (0.25 mg/ml). To determine if the contaminant in the digoxin injectable solution was a cardiac glycoside related to digoxin, samples of digoxigenin mono- and bisdigitoxoside[7], digoxigenin[7], and diginatin[7] were chromatographed twice, with 26 and 30% acetonitrile as mobile phases, and were compared by retention time to the impurity.

Concomitant Use of HPLC and UV Spectrophotometry—To obtain a full UV spectrum of chromatographically pure compound, the column effluent was passed first through a detector[8], fixed at 254 nm and connected to a recorder[9] to produce a chromatogram and then through a 10-mm flow cell positioned in a rapid-scanning spectrophotometer[10] to produce the spectrum. As the mobile phase passed through the flow cell, UV spectra were recorded every 2 sec until the intensity of the signal reached a maximum, at which time the solvent flow from the column was diverted, locking the sample in the flow cell. This permitted repetitive scanning of the sample and produced a smooth spectrum of the com-

[1] Model 204 liquid chromatograph; Waters Associates, Millipore Corp., Milford, MA 01757.
[2] Model 450 variable-wavelength detector; Waters Associates.
[3] Data Module; Waters Associates.
[4] WISP 710B; Waters Associates.
[5] μBondapak C-18, 10-μm particle size, 300 mm (length) × 3.9 mm (i.d.); Waters Associates.
[6] For the chromatographic column used in this work, 30% acetonitrile was preferred over 26% acetonitrile (the concentration recommended by the USP) because elution time was shortened without chromatographic interference from related cardiac glycosides. With 30% acetonitrile, the system suitability requirements of the USP (1) were met.
[7] Burroughs Wellcome Co., Inc., Research Triangle Park, NC 27709.
[8] Model 440 absorbance detector; Waters Associates.
[9] Model 3390A Reporting Integrator; Hewlett-Packard Co., Palo Alto, CA 94304.
[10] Model 8450A UV/visible spectrophotometer; Hewlett-Packard Co.

0022-3549/83/1100-1302$01.00/0

pound even at extremely low concentrations[11]. In this manner, a full spectrum of any or all compounds in a chromatogram could be generated. Samples were injected manually[12].

The UV spectrum of the impurity was obtained in this manner by injecting the digoxin injectable solution. Small variations seen in the absorbance maximum of the impurity seemed to coincide with slight variations in the mobile phase composition. To determine if this variation in the absorbance maximum was due to small changes in pH, a fraction of eluant containing the impurity was collected from the column into a microcell and treated with small aliquots of 2 *N* NaOH, 1 *N* HCl, and pH 8 buffer solution. The absorbance maximum was measured at various pH values.

Extraction of Digoxin Injectable Solution—The contents of one 2-ml syringe of digoxin injectable solution was mixed with 2 ml of 1 *N* HCl and extracted with two 5-ml portions of chloroform. The aqueous acidic solution was made strongly basic with 2 *N* NaOH and extracted with two additional 5-ml portions of chloroform. A 400-μl aliquot from each of the four chloroform extracts was evaporated to dryness under a nitrogen stream; the residue from each was dissolved in 100 μl of 30% aqueous acetonitrile and analyzed by HPLC and UV spectroscopy using the method described above. Only the first chloroform extract contained the impurity. This solution was then extracted with 10 ml of 1 *N* NaOH. The aqueous solution was acidified with 2 *N* HCl to pH 1 and extracted with 5 ml of chloroform. The impurity was found only in this final chloroform extract.

Extraction of Container Parts—An empty digoxin injection container was separated into three parts: the rubber sheath which covered the needle, the glass barrel with its attached needle, and the rubber closure. Each part was submerged in a mixture of propylene glycol–ethanol–water (40:10:50), the solvent mixture used for the injection medium, and heated in an oil bath maintained at 60° for 2 weeks[13]. Extracts were examined for the presence of the impurity by HPLC.

Mass Spectroscopy—Since larger quantities of contaminant were available from the rubber parts of the injection container than from the injectable solution, the rubber sheath was selected as a source of a sample of the compound for mass spectroscopy. To avoid contamination of the compound with propylene glycol, one of the three solvents in the mixture originally used to extract the compound from the rubber sheath, other extraction solvents were sought: dilute NaOH solution was found to be suitable.

A 4-mm section of the rubber sheath was placed in 2 ml of 1 *N* NaOH in a tightly capped reaction vial and heated for 3 days in an oil bath maintained at 65°. The aqueous solution was extracted with two 3-ml portions of dichloromethane, acidified with 2 *N* HCl, and extracted with two 2.5-ml portions of dichloromethane. The latter two extracts were combined, and a 100-μl aliquot was analyzed by the aforementioned combination of HPLC and UV spectrophotometry. The solution contained a compound which appeared to be reasonably pure by HPLC and had a UV spectrum characteristic of the impurity. The dichloromethane solution was evaporated to dryness under a stream of dry nitrogen. Electron-impact mass spectra for this compound and for 2-mercaptobenzothiazole[14] (I), a compound suspected to be the impurity based on the prevailing evidence, were obtained by direct probe on a mass spectrometer[15].

Comparison of the Impurity to Standard I by HPLC and UV Spectrophotometry—A slice of rubber closure (55 mg) was placed in 5 ml of 0.5 *N* NaOH in a tightly stoppered container and heated at 50° for 24 hr. The solution was diluted with a mixture of CH_3CN–H_2O–HOAc (50:47:3), which produced a solution of pH 7, and injected onto the reverse-phase column. The rubber sheath (125 mg) was treated similarly. The extracted compound was compared to standard I by retention time and by the UV spectrum measured using the technique described above.

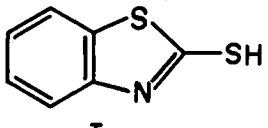

I

A mobile phase consisting of CH_3CN–H_2O–HOAc (260:740:0.03) provided an amount of acetic acid that was sufficiently high (the mobile phase was pH 4) to suppress ionization of the compound, but sufficiently low to prevent its interference in the UV spectrum of the compound.

A 100-μl portion of the digoxin injectable solution sample was mixed with 120 μl of the mobile phase, and a 200-μl aliquot was chromatographed. The impurity, which was separated from digoxin, was collected from the column and examined in both acid and base by UV spectrophotometry. Standard I was treated similarly, and its spectra were compared to those of the impurity.

Silica Gel HPLC and UV Spectrophotometry—Four different digoxin (0.25 mg/ml) and two sodium phenobarbital (65 and 130 mg/ml) injectable solution samples were extracted with organic solvents by the method described below to provide samples for silica gel chromatography. Because of its high concentration relative to the contaminant in the injectable solutions, it was necessary to eliminate most of the phenobarbital to avoid column overload and to allow resolution of the impurity from phenobarbital. Both phenobarbital and I are weakly acidic compounds, which eliminated simple base extraction as a means of separation. 1-Chlorobutane had the lowest reported distribution coefficient (K = 0.4) for phenobarbital (2), and therefore it was the solvent of choice for elimination of phenobarbital. Water (4 ml; 8 ml for sodium phenobarbital at 130 mg/ml), 1-chlorobutane (5 ml), the injectable solution (1–1.5 ml), and 0.5 *N* HCl (1 ml) were shaken in a 30-ml separatory funnel. The upper (chlorobutane) layer was separated, washed with four 5-ml portions of 0.5 *N* HCl, and evaporated to dryness. The residue was partitioned between 3 ml of 0.1 *N* NaOH and 3 ml of heptane. The aqueous base was acidified with 1 *N* HCl and extracted with 4 ml of CH_2Cl_2. The organic solvent was evaporated; the residue was dissolved in 200 μl of mobile solvent, and the entire amount was chromatographed. The contaminant was separated on a silica gel column[16] with a mobile phase consisting of heptane–isopropyl alcohol containing 1% water–acetic acid (990:10:0.3). The column effluent was passed through a rapid-scanning spectrophotometer, as previously described.

Examination of Various Injectable Drug Solutions—Samples from several manufacturers of injectable solutions of digoxin, sodium phenobarbital, epinephrine, lidocaine hydrochloride, mepivacaine hydrochloride, pilocarpine hydrochloride, and dexamethasone sodium phosphate, each packaged in a single-dose delivery syringe or syringe cartridge where the solution was in contact with a rubber closure, were examined for the presence of I by reverse-phase HPLC with a mobile phase of CH_3CN–H_2O–HOAc (260:740:0.3). Each injectable solution (200 μl), except for sodium phenobarbital, was used undiluted. With phenobarbital injectable solutions, I was not resolved from the drug during HPLC; therefore, it was necessary to perform a preliminary extraction by the procedure described above.

As each injectable solution was chromatographed, the fraction of eluate containing a compound with a retention time equal to that of standard I was collected in a microcell. The UV spectrum was recorded at pH 4 (the mobile phase pH) and again at pH 11 or 12 after the addition of 10–20 μl of 1 *N* NaOH. Spectra were normalized at their absorbance maxima (323 or 322 nm in acid; 311 or 310 nm in base) for direct comparison to the spectra of the standard.

Quantitation—Each of the various injectable drug solutions was quantitatively analyzed for I. The HPLC system was the same as that used in the analysis of digoxin injectable solution, except that the variable-wavelength detector was set to 323 nm and 0.04 AUFS and the mobile phase consisted of 30% acetonitrile and 1% acetic acid in water. Injectable solution samples were used directly without dilution. The standard solution was prepared by dissolving I in 50% ethanol to give a concentration of 4 or 8 μg/ml. The injection volume for samples and standard was 40 μl. Linearity for I was established. Repeatability was examined by making seven successive injections of I standard solution and measuring peak area. The relative standard deviation was 0.25%.

Interference with Digoxin Assay—Three samples of digoxin injectable solution known to contain I were assayed for digoxin by the HPLC method specified in the USP (1) with 31% CH_3CN, a mobile phase in which I coeluted with digoxin, and with 29% CH_3CN, a mobile phase in which I was separated from digoxin. The percent of the label claim was determined in each case.

RESULTS

Origin and Identity of the Contaminant—The chromatogram of the contaminated digoxin injectable solution is shown in Fig. 1; the mobile

[11] Good spectra were obtained at absorbance readings as low as 0.01 AUFS. At higher concentrations, smooth spectra were obtained with continuous flow through the flowcell.

[12] U6K injector; Waters Associates.

[13] Undoubtedly, this was far in excess of the time required for extraction. The extraction process was simply left unattended.

[14] Aldrich Chemical Co., Milwaukee, WI 53233.

[15] LKB 9000 mass spectrometer; LKB Instruments, Inc., Rockville, MD 20852.

[16] LiChrosorb Si60, 10-μm particle size, 250 mm (length) × 4.6 mm (i.d.); EM Laboratories, Inc., Elmsford, NY 10523.

Figure 1—*Chromatogram of a commercial sample of digoxin injectable solution showing the contaminant, 2-mercaptobenzothiazole (A), and digoxin (B). The mobile phase was 29% acetonitrile; the detector was set at 218 nm.*

phase was 29% acetonitrile. When a mobile phase of 26% acetonitrile was used to obtain the chromatograms of cardiac glycosides related to digoxin, the impurity had a retention time within 0.1 min of that of diginatin. However, in 30% acetonitrile, diginatin and the impurity were well separated with retention times of 5.30 and 7.70 min, respectively.

The UV spectrum of chromatographically purified contaminant had a λ_{max} that varied from 320 to 316 nm, corresponding to slight variations in the mobile phase composition. This implied that the impurity was devoid of an unsaturated butyrolactone chromophore and was unrelated

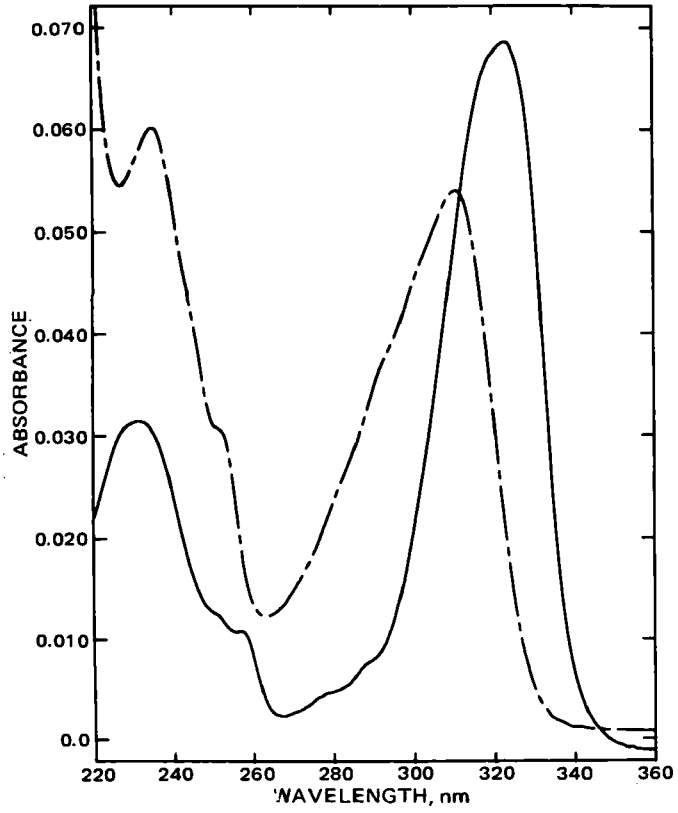

Figure 2—*UV spectra of 2-mercaptobenzothiazole in acetonitrile–water at pH 4 (—) and at pH 12 (— — — — —).*

Table I—Qualitative and Quantitative Analysis of 2-Mercaptobenzothiazole (I) in Various Injectable Drug Solutions [a]

Manufacturer	λ_{max} of Contaminant, nm (pH)[b]	Amount Found, μg/ml[c]
	Standard I	
—	323 or 322 (4); 311 or 310 (12)	—
	Dexamethasone Sodium Phosphate (4 mg/ml)	
A	—	0
B	323 (4); 307 (12)[d]	1.1
B	323 (4); 311 (12)	7.9
	Digoxin (0.25 mg/ml)	
A	323 (4); 311 (11)	8.2
A	323 (4); 311 (12)	4.6, 7.5, 8.6
A	323 (4); 311 (12)	2.9, 6.5, 6.2
A	323 (4); 311 (12)	6.6
	Epinephrine (1:1000)	
A	323 (4); 311 (12)	9.7
A	323 (4); 311 (12)	11.1
A	323 (4); 311 (12)	11.6
	Lidocaine Hydrochloride (2%)	
C[e]	—	0
C	323 (4); 311 (12)[d]	1.0, 0, 0
D	323 (4); 310 (12)	2.8
E[e]	—	0
	Mepivacaine Hydrochloride (2%)	
C	—	0
D	323 (4); 310 (12)	1.5
D	323 (4); 310 (12)	3.5, 3.1, 3.5
	Pilocarpine Hydrochloride (4%)	
F	323 (4); 310 (12)[d]	1.0
F	323 (4); 307 (12)[d]	0.7
	Sodium Phenobarbital (60 mg/ml)	
A	323 (4); 311 (11)	3.2
	Sodium Phenobarbital (130 mg/ml)	
A	323 (4); 311 (12)	3.4
G	323 (4); 311 (12)	5.1

[a] Each injectable solution listed represents a different lot. Some samples were past their expiration date. [b] Unless otherwise noted, normalized spectra were practically superimposable with those of standard I. [c] Multiple values represent individual analyses of injectable solutions of the same lot but from different containers. [d] UV spectrum was distorted especially at shorter wavelengths due to interfering substances. [e] Three lots from this manufacturer were free of I.

to digoxin. When measured as a function of pH, the absorbance maximum shifted from 311 nm in base to 323 nm in acid, with the greatest shift occurring at pH ~6–7, indicating that the compound was ionic or ionizable. The impurity was partitioned from dilute hydrochloric acid into chloroform and from chloroform into aqueous base. This partitioning behavior, in conjunction with the observed pH profile, showed that the impurity was an acidic compound with an estimated pK_a of 6–7.

The rubber sheath and rubber closure extracts contained a compound with a retention time and a UV spectrum that matched those of the impurity in the digoxin injectable solution; the glass barrel extract did not. Thus, the impurity originated from the rubber parts of the syringe, and since the injection medium had limited, if any, contact with the rubber sheath which covered the needle, the contaminant was undoubtedly leached from the rubber closure.

2-Mercaptobenzothiazole (I), a compound commonly used as an accelerator in the vulcanization of rubber, contains a weakly acidic aromatic thiol group[17] and has an absorbance maximum at 320 nm (4), making it a prime candidate for the structure of the contaminant. The electron-impact mass spectrum for standard I and for the compound extracted from the rubber sheath matched very closely, each with a very strong molecular ion at m/z 167 (base peak). The impurity in the digoxin in-

[17] The acidic dissociation constant of I has been determined spectrophotometrically to be 6.93 in 40% aqueous ethanol at 27° (3).

Table II—Assay of Digoxin Injectable Formulation Samples by HPLC With and Without Interference from 2-Mercaptobenzothiazole (I)

	Mobile Phase				
	29% CH_3CN		31% CH_3CN		
Sample	Retention Time, min[a]	Assay[b]	Retention Time, min[c]	Assay[b]	Difference[b]
1	7.55	—			
	8.75	95.3	5.90	106.4	11.1
2	7.30	—			
	8.75	96.1	5.95	116.5	20.4
3	7.15	—			
	8.70	95.7	5.95	106.3	10.6

[a] The first peak was due to the impurity (I); drift in retention time was due to incomplete column equilibration. The compound of longer retention time was digoxin. [b] Percent of label claim. [c] Digoxin and I eluted together as a single peak.

jectable solution and the compounds extracted from the rubber sheath and rubber closure had the same retention time and the same UV spectrum as standard I. The UV spectra of the standard had absorbance maxima at 323 and 311 nm at pH 4 and pH 12, respectively (Fig. 2). These maxima were also oberved for the impurity when treated similarly.

Examination of Other Drug Injectable Solution Samples—Efforts to establish the source and identity of the impurity had been conducted on one digoxin injectable solution sample. Since the contaminant was found to originate from the rubber closure of the injection syringe, one would expect other drug samples packaged in this or a similar type of container to contain the contaminant also. Results of the qualitative and quantitative analysis of all drug injectable formulation samples examined are given in Table I. Fortunately, in most of the drug samples that were examined qualitatively by HPLC and by UV spectrophotometry, the injection ingredients did not interfere with the identification of I.

In some instances, the contaminant peak was not completely resolved from the tail or leading edge of the drug or excipient peaks, and some distortion was evident in the UV spectrum of the collected sample. This distortion occurred only in a few samples containing low levels of I (Table I) and, even in these cases, the distortion occurred generally in the shorter wavelengths of the spectrum; the peak at 323 nm (in acid) was unaffected, and the peak normally at 310 nm (in base) was sometimes shifted slightly toward shorter wavelengths. When there was no chromatographic interference, spectra of the isolated contaminant normalized at their absorbance maxima (323 nm in acid, 311 nm in base) were practically superimposable with those of the standard. In the case of sodium phenobarbital, I was completely submerged under one large phenobarbital absorption peak, necessitating removal of the drug by a preliminary extraction.

During quantitative analysis of the various drug samples when the detector was set to 323 nm, the only peak observed in the chromatogram, other than peaks occasionally seen at or near the solvent front, was the peak corresponding to I. 2-Mercaptobenzothiazole (I) was found in over half of the injectable solutions examined.

Silica Gel HPLC—Silica gel HPLC was performed on four digoxin and two sodium phenobarbital injectable solutions to complement the evidence provided by reverse-phase HPLC. Each sample contained a compound with a retention time between 6.10 and 6.22 min, which compared well with retention times of 6.09 and 6.19 min for duplicate injections of standard I. The spectrum of each sample and standard had an absorbance maximum at 327 nm, although the spectra of the impurity from phenobarbital samples were distorted by the presence of interfering compounds that were poorly resolved by HPLC.

Interference with Digoxin Assay—In reverse-phase HPLC, I was influenced less significantly by changes in the mobile phase than digoxin. Thus, in 29% CH_3CN I eluted before digoxin, in 31% CH_3CN the compounds coeluted, and in 34% CH_3CN digoxin eluted before I. Coelution of these two compounds during digoxin assay would give erroneously high assay values. Table II shows that the true assay results were raised by 10.6, 11.1, and 20.4% for three digoxin samples due to interference from I.

DISCUSSION

After the contaminant in the digoxin injectable formulation was identified, it was thought that this compound, being acidic, would be found at higher concentrations in injectable solutions of high pH, such as sodium phenobarbital; this proved not to be the case. The digoxin injectable solution medium consisted of 40% propylene glycol, 10% alcohol, and 50% water at neutral pH; sodium phenobarbital and dexamethasone sodium phosphate injectable solutions were weakly basic aqueous solutions; and epinephrine, lidocaine hydrochloride, and mepivacaine hydrochloride were weakly acidic aqueous solutions. A comparison of the amounts of I found in the injectable solutions (Table I) showed that the concentration of the impurity had no apparent dependence on the composition or pH of the solution medium and undoubtedly was more dependent on the level of the compound in the rubber closure. The concentration of I varied from lot to lot of a particular drug solution, and even from one container to the next within the same lot.

There are literature reports describing the extraction of I and related compounds from rubber materials. Various types of rubber were extracted with solvents simulating those found in food products, and all but chloroprene were found to contain I, its zinc salt, or 2,2-dithiobis-(benzothiazole), all apparently assayed as I by GC (5). The compound has also been extracted into water from rubber articles that come in contact with foods (6, 7). Two compounds related to I, 2-(methylmercapto)benzothiazole (8) and 2-(2-hydroxyethylmercapto)benzothiazole (9), have been extracted into aqueous media from the rubber closures of disposable syringes. The latter compound reportedly arose from a reaction between I and ethylene oxide, a compound used during the sterilization of the disposable syringes.

The official method of analysis for digoxin injectable solution (1) specifies reverse-phase HPLC with acetonitrile–water as the mobile phase. Unfortunately, if I were present in the digoxin solution, it might elute from the column together with digoxin and raise the apparent analytical result.

A literature survey was conducted for known toxicological properties of I. The compound was shown to be an allergen in rubber-induced skin sensitivity (10, 11). Mutagenic activity of I was observed in fruit flies (12), and slight mutagenic activity was produced in cultured cells from Chinese hamsters by a rubber extract containing I and other vulcanizing accelerators (7). One study revealed that the compound may produce neoplasms in mice (13), although the results of that study were inconclusive, and the amounts of the compound used in that study were much greater than the amounts found in the injectable solutions.

In conclusion, it appears that I is a common contaminant for a variety of injectable drug solutions packaged in single-dose injection syringes or syringe cartridges with rubber closures. It may pose problems as an analytical or toxicological contaminant.

REFERENCES

(1) "The United States Pharmacopeia," 20th rev., second supplement, United States Pharmacopeial Convention, Rockville, Md., 1980, pp. 58–59.

(2) M. K. C. Chao, K. S. Albert, and S. A. Fusari, in "Analytical Profiles of Drug Substances," vol. 7, K. Florey, Ed., Academic, New York, N.Y., 1978, pp. 374–375.

(3) J. P. Danehy and K. N. Parameswaran, *J. Chem. Eng. Data*, **13**, 386 (1968).

(4) "Organic Electronic Spectral Data," vol. IV, J. P. Phillips and F. C. Nachod, Eds., Wiley, New York, N.Y., 1963, p. 102.

(5) G. Salvatore and A. Sampaolo, *Rass. Chim.*, **25**, 54 (1973); through *Chem. Abstr.*, **79**, 77074r (1973).

(6) B. Zyszczynska-Florian, *Rocz. Panstw. Zakl. Hig.*, **25**, 63 (1974); through *Chem. Abstr.*, **81**, 38627v (1974).

(7) T. Baba, *Osaka Shiritsu Daigaku Igaku Zasshi*, **29**, 807 (1980); through *Chem. Abstr.*, **95**, 148799z (1981).

(8) M. A. Inchiosa, Jr., *J. Pharm. Sci.*, **54**, 1379 (1965).

(9) M. C. Petersen, J. Vine, J. J. Ashley, and R. L. Nation, *J. Pharm. Sci.*, **70**, 1139 (1981).

(10) F. Saito and Y. Yamatuta, *Nippon Hifuka Gakkai Zasshi*, **82**, 763 (1972); through *Chem. Abstr.*, **78**, 150970r (1973).

(11) A. A. Anton'ev and I. V. Gerasimenko, *Vestn. Dermatol. Venerol.*, 56 (1976); through *Chem. Abstr.*, **85**, 129775r (1976).

(12) Y. A. Revazova, *Toksikol. Nov. Khim. Veshchestv, Vnedryaemykh Rezin. Shinnuyu Prom.*, 196 (1968); through *Chem. Abstr.*, **71**, 47071e (1969).

(13) National Technical Information Service, PB 223-159; through "Registry of Toxic Effects of Chemical Substances," 1978 ed., R. J. Lewis, Sr., Ed., National Institute for Occupational Safety and Health, Cincinnati, Ohio, 1979, p. 228.

Analysis of Folinic Acid in Human Serum Using High-Performance Liquid Chromatography with Amperometric Detection

B. K. BIRMINGHAM * and D. S. GREENE ‡x

Received April 22, 1982, from the **Department of Pharmacy, College of Pharmacy, University of Rhode Island, Kingston, RI 02881* and *‡Bio Research Laboratories, Ltd., Scientific Affairs Division, Senneville, Quebec H9X 3R3, Canada.* Accepted for publication September 23, 1982.

Abstract □ An assay for the separation and quantification of folinic acid in serum was developed using high-performance liquid chromatography with electrochemical detection. Folinic acid was extracted from serum using a C18 minicolumn treated with dibasic ammonium phosphate. The drug was eluted from this column with methanol, which was evaporated under a nitrogen stream at 50°. The mobile phase, pH 3.5 ammonium phosphate buffer–methanol–acetonitrile (93:4:3), was pumped at a flow rate of 3.0 ml/min. The recovery of folinic acid added to human serum was 101.11 ± 8.5% (mean ± *SD*). A plot of folinic acid peak height as a function of concentration was linear over the range of 2.5×10^{-7} to 2.5×10^{-6} *M*. Neither methotrexate nor other reduced folates interfered with the analysis of folinic acid. Sample preparation and analysis can be completed within 2 min of sample collection.

Keyphrases □ Folinic acid—analysis by high-performance liquid chromatography, amperometric detection, human serum □ High-performance liquid chromatography—amperometric detection, folinic acid and other folates, human serum

Folinic acid, *N*-[*p*-[[(2-amino-5-formyl-5,6,7,8-tetrahydro-4-hydroxy-6-pteridinyl)-methyl]amino]benzoyl]-L-glutamic acid, is a reduced folate used to prevent or reduce the toxicity associated with high-dose methotrexate therapy for the treatment of neoplastic disease (1). The optimization of folinic acid dosage regimens necessitates an understanding of its disposition; however, studies characterizing the pharmacokinetics of this compound have been hampered by the lack of a rapid, sensitive, and specific assay method. Previously reported methods for folinic acid quantification include microbiological assay (2), radiochemical assay (3), radioimmunology (4), and spectrophotometry (5). The application of these techniques to pharmacokinetic studies is somewhat limited since spectrophotometric methods are not sufficiently sensitive, differential microbiological assays are generally not precise, and radiochemical and radioimmunologic techniques may suffer from a lack of specificity.

A high-performance liquid chromatographic (HPLC) assay employing electrochemical detection, suitable for the routine analysis of folinic acid, has been designed and is free from interference from folic acid, dihydrofolic acid, 5-methyl tetrahydrofolic acid, and methotrexate. This assay has been applied to the quantification of folinic acid in human serum.

EXPERIMENTAL

Reagents—Folinic acid[1], 5-methyltetrahydrofolic acid[2], dibasic ammonium phosphate[3], methanol[4], acetonitrile[4], EDTA[5] (disodium ethylenediaminetetraacetic acid), and phosphoric acid[3] were used as received.

HPLC System—A liquid chromatograph consisting of a solvent delivery system[6], a fixed-loop injector[7] with a 100-μl loop, a microparticulate radially compressed reverse-phase column[8], an electronic noise filter[9], and an electrochemical detector with a 5-mm diameter glassy carbon electrode[10] was used. The temperature of the column was adjusted by placing the column in a constant-temperature oven[11]. Data were collected and analyzed using an electronic integrator/recorder[12].

The mobile phase consisted of 0.5 *M* ammonium phosphate buffer–methanol–acetonitrile (93:4:3) with pH adjusted to either 3.5 or 5.5. The pH of the mobile phase used for characterization of the system was 5.5; the pH was decreased to 3.5 when serum samples were analyzed, to increase resolution. EDTA (10 m*M*) was added to decrease background electrical noise. The mobile phase was prepared daily, filtered, and deaerated before use. Double-distilled, deionized water was used for the preparation of all solutions.

Electrochemical Characteristics of the Folate Analogues—The oxidation characteristics of folinic acid were evaluated using the mobile phase at a pH of 5.5 and a flow rate of 3.0 ml/min. The concentration of folinic acid was 1.0×10^{-6} *M*. Applied potentials were adjusted between +0.3 and +0.9 V. A 30-min equilibration period was necessary following each change in applied potential to reestablish a suitable baseline.

Extraction—Ascorbic acid (1 mg/ml) was added to all serum samples immediately after collection to prevent drug degradation. Folinic acid was extracted from serum using reverse-phase C18 disposable cartridges[13]. The cartridges were activated using 10 ml of methanol followed by 10 ml of 5 m*M* ammonium phosphate buffer, pH 5.5. One milliliter of serum was then pushed through the cartridge followed by 3 ml of 5 m*M* ammonium phosphate buffer, pH 5.5. The effluent was discarded. The outlet end of the cartridge was then connected to a vacuum and the cartridge was dried for 5 min, after which time the drug was eluted with 2 ml of methanol. The eluant was collected and evaporated at 50° under a nitrogen stream in a sample concentrator[14]. The evaporated samples were stored at −4°; samples were reconstituted in 500 μl of mobile phase before being assayed.

Recovery Studies—The recovery of folinic acid in serum was determined by comparison of peak heights of drug prepared in mobile phase to peak heights obtained after extraction from serum. A standard curve was constructed by plotting peak height as a function of concentration for extracted serum samples containing known amounts of folinic acid over the range of 2.5×10^{-7} to 2.5×10^{-6} *M*. The data were analyzed using a linear regression program on a programmable calculator. Concentrations of all samples were calculated using the resulting regression coefficients.

RESULTS AND DISCUSSION

Figure 1 is a plot of detector response (log peak height) as a function of applied potential for folinic acid. The threshold for the oxidation of this compound was +0.4 V. An increase in applied potential resulted in an increase in generated current until a plateau was reached at +0.7 V. It was not possible to characterize response at >+0.9 V due to an extremely high background current, presumably caused by the oxidation of components in the mobile phase.

[1] Lederle Laboratories, Pearl River, N.Y.
[2] Sigma Chemical, St. Louis, Mo.
[3] Fisher Scientific, Fair Lawn, N.J.
[4] Waters Associates, Milford, Mass.
[5] Allied Chemical, Morristown, N.J.
[6] Model 6000A; Waters Associates, Milford, Mass.
[7] Model 7120; Rheodyne Inc., Cotati, Calif.
[8] RCSS C18 Column; Waters Associates, Milford, Mass.
[9] Model SC102; Foxboro Instruments, New Haven, Conn.
[10] Model LC-2A; BioAnalytical Systems, West Lafayette, Ind.
[11] Model 15; Thelco, Inc., New York, N.Y.
[12] Model 720; Waters Associates, Milford, Mass.
[13] C^{18} SEP-PAK; Waters Associates, Milford, Mass.
[14] Model 190; Fisher Scientific, Fair Lawn, N.J.

0022-3549/83/1100-1306$01.00/0

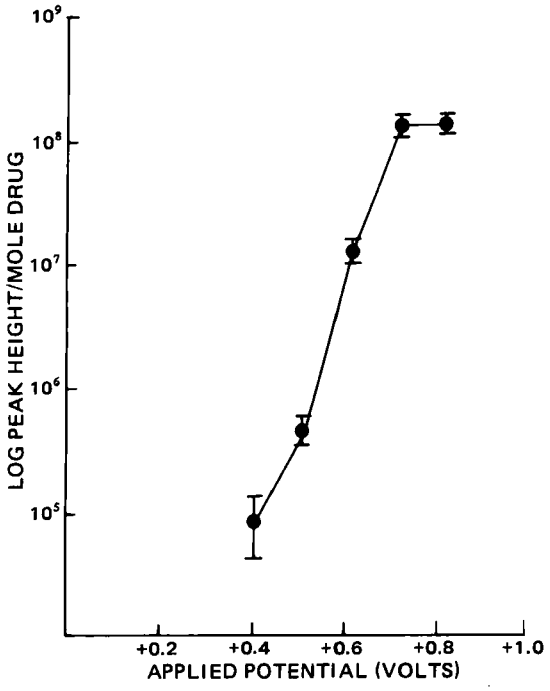

Figure 1—*Detector response as a function of applied potential for folinic acid.*

High electrolyte concentrations are necessary in mobile phases when electrochemical detection is used in order to reduce resistance and increase the current at the electrode surface. Varying concentrations of electrolyte may also affect the diffusion coefficient of the electroactive species, limiting the current at the electrode. The effect of varying ammonium phosphate concentrations, at a constant pH of 5.5, on detector response (Fig. 2) was determined for folinic acid. There was a constant increase in response with increasing salt concentration until a plateau was reached at 0.01 *M*.

The effect of buffer concentration on the retention of folinic acid was also characterized. Figure 3 describes the retention time for folinic acid as a function of ammonium phosphate concentration (pH 5.5). It is evident that as buffer concentration increases, there is a corresponding increase in retention time.

The general effect of mobile phase velocity on the diffusion layer thickness within the electrochemical cell and the resulting effect on current yield has been reported (6). The optimal flow rate, in terms of detector response, was determined by plotting response (measured as peak height) as a function of flow rate (Fig. 4) for folinic acid. It is apparent that the peak height decreases with increasing flow rate between 1.0 and 7.0 ml/min.

Investigation of the effect of flow rate on retention (Fig. 5) showed that significant deviations from linearity occur as flow rate increases. Both the capacity and selectivity of the radially compressed column decreased with increases in flow rate. A log–log transformation (Fig. 5 inset) of the data, however, was linear. These findings are in general agreement with studies of flow control in HPLC reported by Schrinker (7).

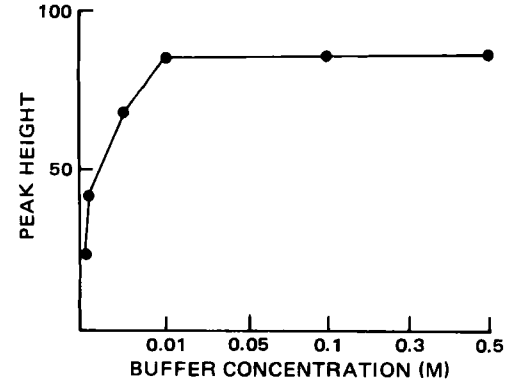

Figure 2—*Detector response as a function of mobile phase salt concentration (pH 5.5).*

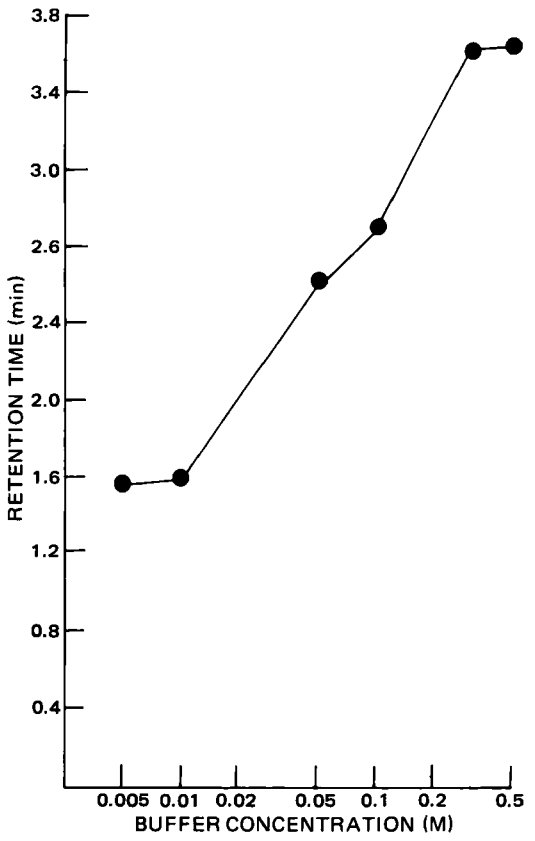

Figure 3—*Effect of buffer concentration on folinic acid retention.*

It has been reported by Gilpin and Sisco (8) that both normal and bonded phases may be affected by temperature, and that variations in capacity >25% have been reported with temperature changes of ≤1°. Because of the high efficiency and reactivity associated with radially compressed columns, the effect of temperature on the retention time of folinic acid was investigated. Table I reports the retention times for folinic acid over a range of temperatures between 20° and 50°. A decrease in retention time (capacity) with increasing temperature was observed; however, the resolution of the system actually improved at higher temperatures. This can best be explained by the decrease in folinic acid peak width.

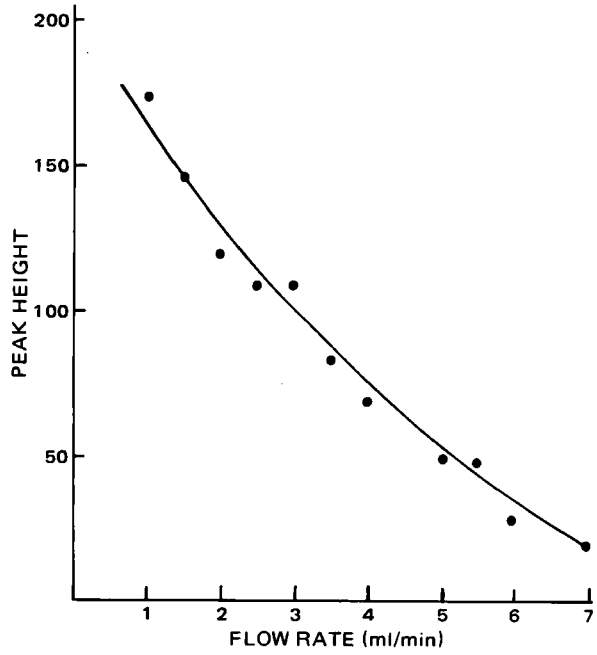

Figure 4—*Detector response to folinic acid as a function of mobile phase flow rate.*

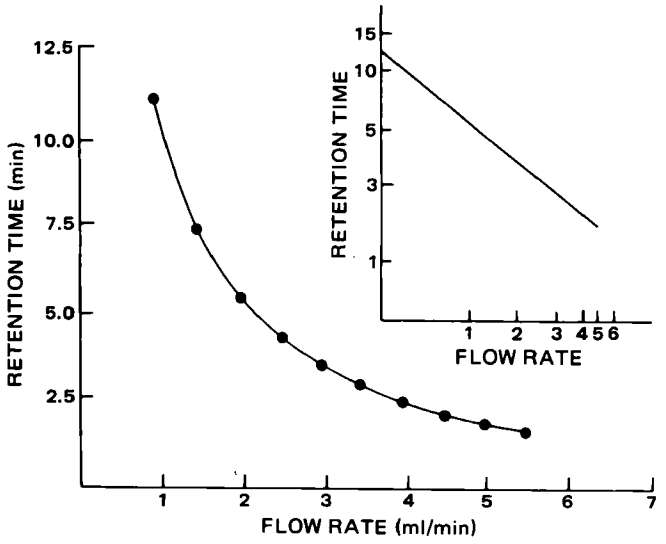

Figure 5—*Retention time as a function of flow rate for folinic acid. The inset is the log–log transformation of the graph.*

Temperature fluctuations were found to affect daily chromatographic results. Ambient temperatures varied as much as 10° during the course of the day, causing as much as 20% changes in observed retention times for folate compounds using the same mobile phase. The installation of a constant-temperature oven circumvented the effect of temperature changes on the system. Column temperatures were held constant at 40°, and the retention time was found to be reproducible within the 5% limits of the system.

Figure 6 is a plot of the retention of folinic acid as a function of pH. The mobile phase flow rate was 3.0 ml/min, and the ammonium phosphate concentration was 0.5 *M*. It was evident from examination of this figure that pH has a significant effect on folinic acid retention.

The extraction and recovery of folinic acid added to pooled human serum was virtually complete. The recovery of drug over the concentration range of 2.5×10^{-7} to 2.5×10^{-6} *M* ranged from 94 to 117% with a mean value of 101%. Folinic acid-spiked serum samples were found to be stable for 2 months when stored at −4°. However, after extraction, samples were only stable for 2 days. A plot of calculated folinic acid concentration as a function of actual concentration in spiked serum

Table I—Effect of Temperature on Folinic Acid Retention

Temperature	Retention Time, min
20°	4.60
30°	4.13
40°	3.50
50°	2.68

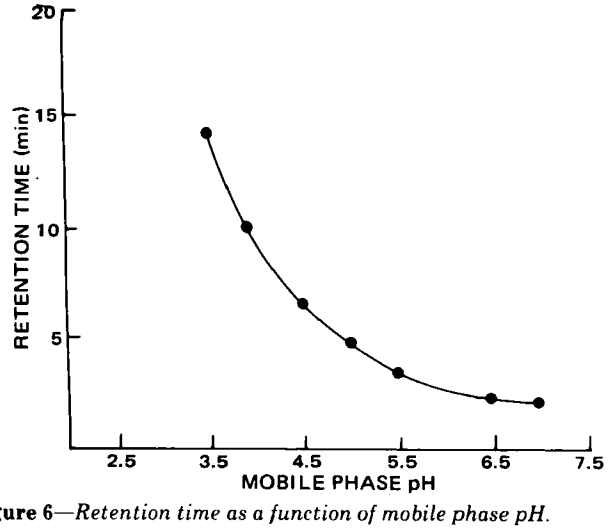

Figure 6—*Retention time as a function of mobile phase pH.*

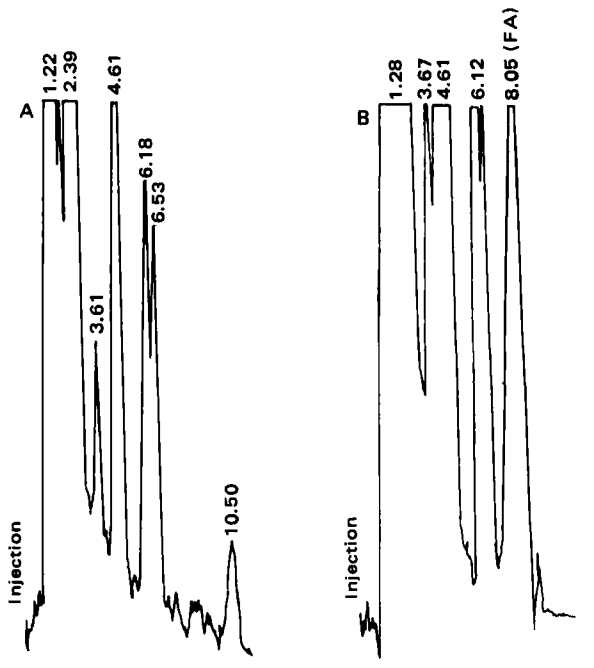

Figure 7—*Chromatograms from subject KB using chromatographic conditions described in the text. Numbers above peaks represent retention time in minutes. Key: (A) serum blank; (B) serum sample collected 5 min after intravenous injection of 10 mg of folinic acid; (FA) folinic acid (concentration 7.3×10^{-6} M).*

samples was linear ($r = 0.99$; slope = 1.02). The slope was not significantly different from 1.0 (Student's t test, $p > 0.05$) and the intercept was not significantly different from 0 (Student's t test, $p > 0.05$). To improve the resolution between folinic acid and other eluting components of the sample matrix, it was necessary to decrease the pH of the mobile phase from 5.5 to 3.5. The retention time for folinic acid under these conditions was 8.05 min. The compound was completely resolved from neighboring peaks at 6.53 and 10.50 min in all samples. The column capacity for folinic acid was 7.13; the efficiency of the column was calculated to be 530 plates. Figure 7A is a representative chromatogram of a drug-free serum sample; Fig. 7B shows a chromatogram obtained from a serum sample collected 5 min after the injection of 10 mg iv of folinic acid to the same 80-kg human volunteer.

Folic acid, dihydrofolic acid, and 5-methyltetrahydrofolic acid analyzed under these conditions had retention times of 4–6 min; therefore, these compounds did not interfere with folinic acid. Detection of methotrexate under these chromatographic conditions requires an applied potential of >+0.9 V. Therefore, the presence of methotrexate in serum samples obtained from patients receiving high-dose methotrexate therapy should not interfere with the analysis of folinic acid.

Figure 8 is a semilogarithmic plot of the data obtained following rapid

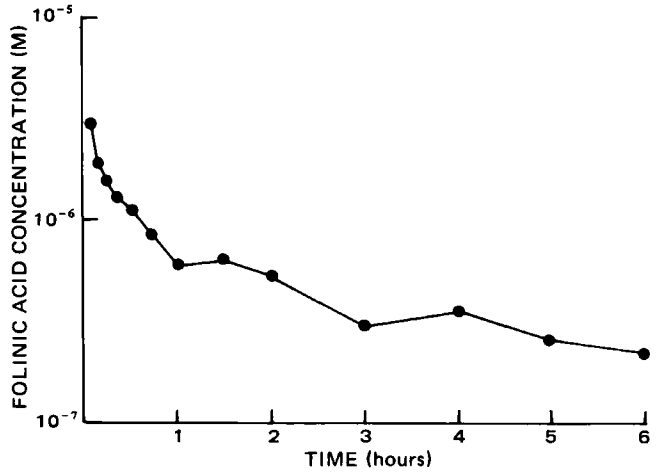

Figure 8—*Folinic acid concentration as a function of time following the intravenous administration of 10 mg of drug.*

intravenous administration of a 10-mg dose of folinic acid to a healthy 57-kg volunteer. These data are similar to those reported by Rothenberg *et al.* (3) following the administration of folinic acid to two healthy subjects. The disposition of folinic acid was characterized by a two-compartment open model. The peak plasma concentration was 3.5×10^{-6} *M*. The distribution and elimination half-lives were 0.27 and 3.7 hr, respectively. These half-lives are different from those obtained by Mehta *et al.* (2) using a microbiological assay, probably because the HPLC assay reported here and the assay of Rothenberg *et al.* (3) do not differentiate the stereoisomers, whereas the microbiological assay measures only the *l* isomer.

REFERENCES

(1) R. K. Blakely, "The Biochemistry of Folic Acid and Related Pteridines," A. Neuberger and E. L. Tatum, Eds., North Holland Publishing, Amsterdam, 1969.

(2) B. M. Mehta, W. H. Conti, and H. Gisolfi, *Cancer Treat. Rep.*, **62**, 345 (1978).

(3) S. P. Rothenberg, M. Da Costa, and Z. Rosenberg, *Anal. Biochem.*, **93**, 483 (1979).

(4) V. Raso, *Cancer Treat. Rep.*, **61**, 585 (1977).

(5) S. K. Chapman, B. C. Greene, and R. R. Streiff, *J. Chromatogr.*, **145**, 302 (1978).

(6) P. T. Kissinger, *Anal. Chem.*, **49**, 447a (1977).

(7) H. Shrinker, *Am. Lab.*, **10**, 111 (1978).

(8) R. K. Gilpin and W. R. Sisco, *J. Chromatogr.*, **194**, 285 (1980).

ACKNOWLEDGMENTS

Supported in part by U.S. Public Health Service Grants (National Cancer Institute) CA-25312, 13943, and 20892.

Plasmolysis, Red Blood Cell Partitioning, and Plasma Protein Binding of Etofibrate, Clofibrate, and Their Degradation Products

PAUL ALTMAYER and EDWARD R. GARRETT ˣ

Received May 24, 1982, from *The Beehive, College of Pharmacy, J. Hillis Miller Health Center, University of Florida, Gainesville, FL 32610.* Accepted for publication September 8, 1982.

Abstract □ Etofibrate (I), the ethylene glycol diester of clofibric and nicotinic acids, degrades almost equally through both half-esters with half-lives of ~10 and 1 min in fresh dog and human plasma, respectively. The nicotinate V degrades with half-lives of ~12 hr and 50 min in fresh dog and human plasma, respectively. Ester III and clofibrate VI degrade by saturable Michaelis–Menten kinetics in fresh human plasma, with similar maximum initial rates and respective terminal first-order half-lives of 12 and 26 min. Tetraethyl pyrophosphate at 100 μg/ml inhibited human plasma and red blood cell esterases permitting plasma protein binding and red blood cell partitioning studies. The red blood cell–plasma water partition coefficient was 5.4 for 0.2–80 μg/ml of I. Clofibrate (VI) showed a saturable erythrocyte partitioning that decreased from 7.8 (10 μg/ml) to 1 (50 μg/ml). The strong binding of I and VI to ultrafiltration membranes necessitated the determination of their plasma protein binding by the method of variable plasma concentrations of erythrocyte suspensions to give 96.6% (0.2–80 μg/ml) and 98.2% (13.6–108.4 μg/ml) binding, respectively. Methods for the determination of the parameters of saturable and nonsaturable plasma protein binding for unstable and membrane-binding drugs by the method of variable plasma concentrations in partitioning erythrocyte suspensions are presented.

Keyphrases □ Etofibrate—degradation products, plasmolysis, red blood cell partitioning, plasma protein binding □ Clofibrate—degradation products, plasmolysis, red blood cell partitioning, plasma protein binding □ Plasmolysis—etofibrate, clofibrate, degradation products □ Red blood cell partitioning—etofibrate, clofibrate, degradation products □ Plasma protein binding—etofibrate, clofibrate, degradation products

Clofibric acid derivatives and nicotinic acid are well established therapeutic agents for the treatment of hyperlipidemia, a major risk factor in coronary artery disease (1, 2). Etofibrate [2-nicotinoyloxyethyl 2-(4-chlorophenoxy)-2-methylpropionate, (I)], the ethylene glycol diester of clofibric and nicotinic acids, is effective in lowering triglycerides and cholesterol in controlled clinical trials (3, 4). The greater lipid-lowering effect of etofibrate in rats than simultaneously administered equimolar amounts of clofibric and nicotinic acids permitted the postulation that both etofibrate and/or its derived half-esters may have pharmacological activity (5). It was reported (6) that both half-esters were detectable after incubation of rat microsomes with etofibrate and that they appeared to be more stable in biological fluids than their etofibrate precursor.

The solution stabilities of etofibrate (I), clofibrate (VI), and derived monoesters were reported previously (7). The possible solvolytic routes are given in Schemes I and II. Conditions were established for optimal extractions and log k–pH profiles for solution solvolyses were constructed for various temperatures using specific high-performance liquid chromatographic (HPLC) assays. Preliminary studies in fresh dog plasma (7) indicated that a considerable fraction of etofibrate rapidly hydrolyzed in dog plasma to produce the ethylene glycol ester of clofibric acid (III), which also hydrolyzed rapidly. This is in contrast to other reported studies in diluted human blood (8).

This paper reports on the human red blood cell–plasma partitioning and human plasma protein binding of etofibrate (I), clofibrate (VI), and their degradation products using the esterase inhibitor, tetraethyl pyrophosphate. Improved HPLC assays of higher sensitivity were applied to complete studies of the human and dog plasmolytic routes and degradation rates. In addition, complete methods for the determination of the parameters of saturable and nonsaturable plasma protein binding for unstable and membrane-bound drugs by the method of variable plasma concentrations in partitioning erythrocyte suspensions are presented.

EXPERIMENTAL

Methods—Acetic acid[1], sodium acetate[1], dibasic sodium phosphate[1], monobasic potassium phosphate[1], *tert*-butyl alcohol[2], sodium chloride[2],

[1] Mallinckrodt Inc., Parris, KY 40361.
[2] Fisher Scientific Co., Fair Lawn, NJ 07410.

0022-3549/83/1100-1309$01.00/0

intravenous administration of a 10-mg dose of folinic acid to a healthy 57-kg volunteer. These data are similar to those reported by Rothenberg *et al.* (3) following the administration of folinic acid to two healthy subjects. The disposition of folinic acid was characterized by a two-compartment open model. The peak plasma concentration was 3.5×10^{-6} *M*. The distribution and elimination half-lives were 0.27 and 3.7 hr, respectively. These half-lives are different from those obtained by Mehta *et al.* (2) using a microbiological assay, probably because the HPLC assay reported here and the assay of Rothenberg *et al.* (3) do not differentiate the stereoisomers, whereas the microbiological assay measures only the *l* isomer.

REFERENCES

(1) R. K. Blakely, "The Biochemistry of Folic Acid and Related Pteridines," A. Neuberger and E. L. Tatum, Eds., North Holland Publishing, Amsterdam, 1969.

(2) B. M. Mehta, W. H. Conti, and H. Gisolfi, *Cancer Treat. Rep.*, **62**, 345 (1978).

(3) S. P. Rothenberg, M. Da Costa, and Z. Rosenberg, *Anal. Biochem.*, **93**, 483 (1979).

(4) V. Raso, *Cancer Treat. Rep.*, **61**, 585 (1977).

(5) S. K. Chapman, B. C. Greene, and R. R. Streiff, *J. Chromatogr.*, **145**, 302 (1978).

(6) P. T. Kissinger, *Anal. Chem.*, **49**, 447a (1977).

(7) H. Shrinker, *Am. Lab.*, **10**, 111 (1978).

(8) R. K. Gilpin and W. R. Sisco, *J. Chromatogr.*, **194**, 285 (1980).

ACKNOWLEDGMENTS

Supported in part by U.S. Public Health Service Grants (National Cancer Institute) CA-25312, 13943, and 20892.

Plasmolysis, Red Blood Cell Partitioning, and Plasma Protein Binding of Etofibrate, Clofibrate, and Their Degradation Products

PAUL ALTMAYER and EDWARD R. GARRETT ˣ

Received May 24, 1982, from *The Beehive, College of Pharmacy, J. Hillis Miller Health Center, University of Florida, Gainesville, FL 32610.* Accepted for publication September 8, 1982.

Abstract □ Etofibrate (I), the ethylene glycol diester of clofibric and nicotinic acids, degrades almost equally through both half-esters with half-lives of ~10 and 1 min in fresh dog and human plasma, respectively. The nicotinate V degrades with half-lives of ~12 hr and 50 min in fresh dog and human plasma, respectively. Ester III and clofibrate VI degrade by saturable Michaelis–Menten kinetics in fresh human plasma, with similar maximum initial rates and respective terminal first-order half-lives of 12 and 26 min. Tetraethyl pyrophosphate at 100 μg/ml inhibited human plasma and red blood cell esterases permitting plasma protein binding and red blood cell partitioning studies. The red blood cell–plasma water partition coefficient was 5.4 for 0.2–80 μg/ml of I. Clofibrate (VI) showed a saturable erythrocyte partitioning that decreased from 7.8 (10 μg/ml) to 1 (50 μg/ml). The strong binding of I and VI to ultrafiltration membranes necessitated the determination of their plasma protein binding by the method of variable plasma concentrations of erythrocyte suspensions to give 96.6% (0.2–80 μg/ml) and 98.2% (13.6–108.4 μg/ml) binding, respectively. Methods for the determination of the parameters of saturable and nonsaturable plasma protein binding for unstable and membrane-binding drugs by the method of variable plasma concentrations in partitioning erythrocyte suspensions are presented.

Keyphrases □ Etofibrate—degradation products, plasmolysis, red blood cell partitioning, plasma protein binding □ Clofibrate—degradation products, plasmolysis, red blood cell partitioning, plasma protein binding □ Plasmolysis—etofibrate, clofibrate, degradation products □ Red blood cell partitioning—etofibrate, clofibrate, degradation products □ Plasma protein binding—etofibrate, clofibrate, degradation products

Clofibric acid derivatives and nicotinic acid are well established therapeutic agents for the treatment of hyperlipidemia, a major risk factor in coronary artery disease (1, 2). Etofibrate [2-nicotinoyloxyethyl 2-(4-chlorophenoxy)-2-methylpropionate, (I)], the ethylene glycol diester of clofibric and nicotinic acids, is effective in lowering triglycerides and cholesterol in controlled clinical trials (3, 4). The greater lipid-lowering effect of etofibrate in rats than simultaneously administered equimolar amounts of clofibric and nicotinic acids permitted the postulation that both etofibrate and/or its derived half-esters may have pharmacological activity (5). It was reported (6) that both half-esters were detectable after incubation of rat microsomes with etofibrate and that they appeared to be more stable in biological fluids than their etofibrate precursor.

The solution stabilities of etofibrate (I), clofibrate (VI), and derived monoesters were reported previously (7). The possible solvolytic routes are given in Schemes I and II. Conditions were established for optimal extractions and log k–pH profiles for solution solvolyses were constructed for various temperatures using specific high-performance liquid chromatographic (HPLC) assays. Preliminary studies in fresh dog plasma (7) indicated that a considerable fraction of etofibrate rapidly hydrolyzed in dog plasma to produce the ethylene glycol ester of clofibric acid (III), which also hydrolyzed rapidly. This is in contrast to other reported studies in diluted human blood (8).

This paper reports on the human red blood cell–plasma partitioning and human plasma protein binding of etofibrate (I), clofibrate (VI), and their degradation products using the esterase inhibitor, tetraethyl pyrophosphate. Improved HPLC assays of higher sensitivity were applied to complete studies of the human and dog plasmolytic routes and degradation rates. In addition, complete methods for the determination of the parameters of saturable and nonsaturable plasma protein binding for unstable and membrane-bound drugs by the method of variable plasma concentrations in partitioning erythrocyte suspensions are presented.

EXPERIMENTAL

Methods—Acetic acid[1], sodium acetate[1], dibasic sodium phosphate[1], monobasic potassium phosphate[1], *tert*-butyl alcohol[2], sodium chloride[2],

[1] Mallinckrodt Inc., Parris, KY 40361.
[2] Fisher Scientific Co., Fair Lawn, NJ 07410.

0022-3549/83/1100-1309$01.00/0

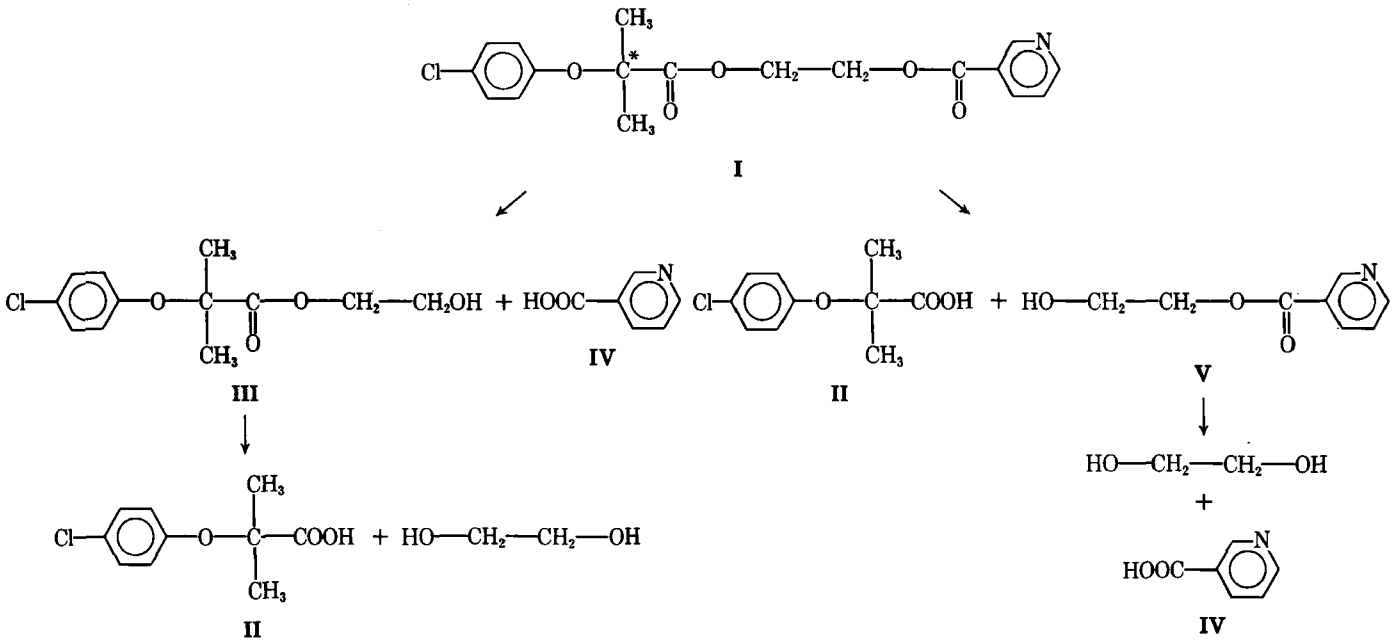

Scheme I—Pathways of etofibrate hydrolysis. (*) ^{14}C atom of radiolabeled etofibrate.

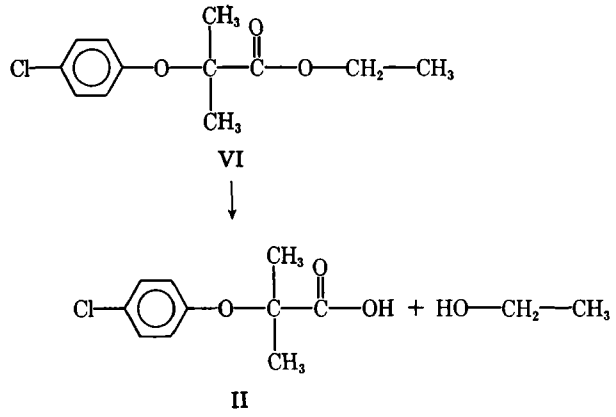

Scheme II—Pathway of clofibrate hydrolysis.

tetrabutylammonium phosphate[3], and volumetric concentrations of hydrochloric acid[4] were analytical grade. Chloroform[2], ethyl acetate[1], methanol[2], and acetonitrile[2] were HPLC or UV grade. The following also were used: sodium chloride injection USP[5], sodium heparin injection USP[6], and disposable syringes[7]. Tetraethyl pyrophosphate[8] was used as enzyme inhibitor. Thymol[2] and phenylurea[4] were internal standards for the HPLC systems. Etofibrate[9] (I), clofibric acid[9] (II), 2-hydroxyethyl 2-(4-chlorophenoxy)-2-methylpropionate[9] (III), nicotinic acid[9] (IV), 2-hydroxyethyl nicotinate[9] (V), and clofibrate[9] (VI) were used as received. For protein-binding studies, ultrafiltration cones[10], cone supports[11] and tubes[10], molecular filters[11], and a sample filtration assembly[11] were used.

Specifically ^{14}C-labeled etofibrate[9] (Scheme I) was used for plasma protein binding and red blood cell partition studies. A toluene-based scintillation[12] cocktail was used in the radioactive assay.

Apparatus—The HPLC system consisted of single pump[13], a radial compression module[14] equipped with a C_8 or C_{18} column[13] (8 mm i.d.), and an automatic injector[15]. The variable-wavelength UV detector[16] was set at 225 or 254 nm, with a strip chart recorder[17]. Radioactivity was assayed with a liquid scintillation counter[18]. A laboratory centrifuge was used[19].

HPLC Procedures—Three HPLC systems were used: System A for I, II, and III; System B for IV and V; and System C for VI.

System A—Prepared solutions of 0.05 *M* sodium acetate were adjusted to a measured pH 3.75 with 0.05 *M* acetic acid. The mobile phase was a mixture of this buffer and acetonitrile (50:50). The flow rate of 2 ml/min gave almost no back pressure (0–500 psi) on the C_8 column. The wavelength of the UV detector was 225 nm.

System B—The mobile phase was a mixture of an aqueous solution of 0.008 *M* tetrabutylammonium phosphate and methanol (25:75). The flow rate of 2 ml/min produced a back pressure of 400–700 psi with the C_{18} column. The wavelength of the UV detection was 254 nm.

System C—The mobile phase was a mixture of 0.05 *M* acetate buffer (pH 3.75) and acetonitrile (37:63). The flow rate of 2.2 ml/min gave a back-pressure of 1100 psi on the C_{18} column. The wavelength of the UV detector was 225 nm.

HPLC Analytical Methods in Plasma for I, II, and III—*Extraction Procedure (Method a)*—Aliquots (0.2 or 0.5 ml) of fresh, heparinized dog or human plasma were adjusted to pH 2.5 with 25 or 62.5 μl of 1 *N* HCl and extracted with 2 or 5 ml of chloroform for 10 min with slow shaking. Aliquots (1.6 or 4 ml) of the organic phase were evaporated to dryness under a nitrogen stream. The residue was reconstituted with mobile phase containing the internal standard (thymol), and 50 μl was injected into HPLC system A.

Acetonitrile Deproteinization (Method b)—An equal volume of acetonitrile containing the internal standard (thymol) was added to a plasma sample, vortexed at high speed for 30 sec, and centrifuged at 3000 rpm for 10 min. A 50-μl aliquot of the supernatant was injected into HPLC system A.

HPLC Analytical Methods in Plasma for IV and V—*Extraction Procedure (Method c)*—Fresh plasma (0.5 ml) was adjusted to pH 2 with 65 μl of 1 *N* HCl and extracted with 2 ml of an ethyl acetate–*tert*-butyl alcohol mixture (50:50) for 10 min with slow shaking. After centrifugation for 10 min at 3000 rpm, 1.8 ml of the organic phase was evaporated under a nitrogen stream. The residue was reconstituted with mobile phase containing phenylurea as an internal standard, and 50 μl was injected into HPLC system B.

Acetonitrile Deproteinization (Method d)—Acetonitrile (2 or 2.5 ml) was added to plasma (0.2 or 0.5 ml). The mixture was vortexed for 30 sec and centrifuged for 10 min at 3000 rpm. Aliquots of the clear supernatant

[3] Eastman Kodak Co., Rochester NY 14650.
[4] Ricca Chemical Co., Arlington, TX 76012.
[5] McGaw Laboratories, Irvine, CA 92714.
[6] The Upjohn Co., Kalamazoo, MI 49001.
[7] Monoject, Division of Sherwood Medical, A Brunswick Co., St. Louis, MO 63103.
[8] Chemical Procurement Laboratories, College Point, N.Y.
[9] Merz & Co., Frankfurt am Main, West Germany.
[10] Type 2100 CF-50; Amicon Corp., Lexington, MA 02173.
[11] Types PTGC and PSAC; Millipore Corp., Bedford, MA 01730.
[12] ScintiVerse; Fisher Scientific Co., Fair Lawn, NJ 07410.
[13] Model M 6000A; Waters Associates, Milford, MA 01751.
[14] Waters Associates, Milford, MA 01751.
[15] Model Wisp 710A; Waters Associates, Milford, MA 01751.
[16] LC 75 Spectrophotometer; Perkin-Elmer, Norwalk CT 06856.
[17] Fisher recordall series 5000; Fisher Scientific Co., Pittsburgh, PA 15219.
[18] Tricarb 460 CD; Packard Instrument Co. Inc., Downers Grove IL 60515.
[19] International Equipment Co., Needham Heights, MA 02194.

(1 or 2.5 ml) were evaporated to dryness under a nitrogen stream. The residue was reconstituted with mobile phase containing phenylurea as internal standard, and 50 μl was injected into HPLC system B.

HPLC Analytical Methods in Plasma for VI (Method e)—Appropriate volumes of acetonitrile containing the internal standard (etofibrate) were added to 0.2 or 0.5 ml of plasma. The mixture was vortexed and centrifuged at 3000 rpm for 10 min. Aliquots of the clear supernatant were injected into HPLC system C.

Purification of Radiolabeled Etofibrate—^{14}C-Labeled etofibrate (0.03 mg), of presumed specific activity 1.47×10^8 dpm/mg, was dissolved in 1 ml of acetonitrile. A 100-μl aliquot, mixed with 10 ml of scintillation fluid[12] was dark-adapted for 12 hr before liquid scintillation counting. The ^{14}C-labeled etofibrate in acetonitrile solution (100 μl) was injected into HPLC system A, monitored by the UV detector, and the eluant was collected in 30-sec intervals for 20 min. Scintillation fluid (10 ml) was added to each collection before counting. Approximately 20% of the counts of the injected sample lay outside the etofibrate fraction (retention time range: 8–13 min) identified by its UV peak. The ^{14}C-labeled etofibrate was purified by combining the collected etofibrate fractions obtained by repetitive injections of 100-μl aliquots into the chromatograph and extracting twice with chloroform. An aliquot (500 μl) of the aqueous phase was counted and showed no significant radioactivity (39 cpm), indicating complete extraction. The chloroform extract was evaporated under a nitrogen stream and the residue reconstituted in acetonitrile. A 50-μl aliquot of this purified ^{14}C-labeled etofibrate solution was injected into the chromatograph, and the 30-sec fractions of eluant (up to 20 min) were counted; 94.4% of the total injected radioactivity was in the etofibrate collection. The amount of etofibrate in the assayed sample was determined against a calibration curve prepared from unlabeled drug in the same system. Thus, the specific activity of the purified [^{14}C]etofibrate could be calculated (1.253×10^5 dpm/μg).

Plasmolysis Studies of I, III, V, and VI—Fresh human and dog plasma were used. The blood was centrifuged for 15 min at 3000 rpm immediately after blood withdrawal into a heparinized syringe. The plasma stability studies were performed in a water bath at 37.5° for human and 38.5° for dog plasma. The plasma was spiked with a known amount of III or V in phosphate buffer (pH 7.4) for the respective studies of their degradation. Since clofibrate (VI) had poor aqueous solubility, it was added to plasma in methanol solution (1–20 μl in 3 ml of plasma). Etofibrate in 0.05 *M* HCl was added to plasma. Aliquots (0.2 or 0.5 ml) of plasma were removed at intervals and added to tubes containing acetonitrile (methods b, d, and e) or extraction solvents (methods a and c) and immediately vortexed or shaken before assay.

The kinetics of plasmolysis were studied with and without the enzyme inhibitor tetraethyl pyrophosphate (usually 90–117 μg/ml of plasma or blood). The stability of etofibrate and clofibrate was also studied in fresh human whole blood inhibited by tetraethyl pyrophosphate. The solutions of tetraethyl pyrophosphate in phosphate buffer (pH 7.4) had to be prepared freshly before each study because of its instability. The plasma of spiked blood was assayed after separation from erythrocytes by centrifugation for 4 min at 5000 rpm.

Red Blood Cell–Buffer Partition Studies—Fresh human heparinized blood was centrifuged for 15 min at 3000 rpm and the plasma removed. Isoosmotic phosphate buffer (pH 7.4) was added to the packed red blood cells with gentle mixing. The slurry was centrifuged for 10 min at 2000 rpm, and the separated buffer was discarded; this procedure was repeated three times. A phosphate-buffered solution of tetraethyl pyrophosphate (11.7 mg/μl) was added to the packed red blood cells to give ~90 μg/ml of the inhibitor. Aliquots of this red blood cell suspension were added to previously assayed spiked phosphate buffer. The mixture was mixed carefully and allowed to equilibrate for 25 min. A hematocrit was taken, and the tube was centrifuged for 10 min at 2000 rpm. An aliquot (200 or 500 μl) of the supernatant buffer was removed for analysis. The red blood cell–phosphate buffer partition coefficients were determined as a function of drug concentration and time.

Binding to Ultrafiltration Membranes—The binding of I, VI, and their degradation products to three commonly used ultrafiltration membranes was studied[10,11]. Solutions of isoosmotic phosphate buffer (pH 7.4) were prepared with 10 μg/ml of I, VI, and their degradation products, separately and in mixture. An aliquot was taken for analysis, and 5 ml was filtered through the ultrafiltration assembly in 500-μl amounts. Aliquots (200 μl) of each sequential filtration were analyzed for drug.

Plasma Protein Binding—*Compounds II–V by the Ultrafiltration Method*—Appropriate volumes of stock solutions of II–V in acetonitrile were evaporated under a nitrogen stream to dryness. A phosphate buffer solution of tetraethyl pyrophosphate was added to 22 ml of fresh human heparinized plasma to give 95.7 μg/ml, and 8 ml of plasma was used to redissolve the compounds. Additional plasma was added to give five different drug concentrations, and the plasma samples were assayed. These plasma samples (4 ml) were filtered through pretreated ultrafiltration cones for 3 min at 3000 rpm. The first 0.8 ml of ultrafiltrate was discarded, and the next 0.5 ml was assayed. The filtration cones were pretreated by filtering 2 ml of phosphate buffer containing concentrations of drugs similar to those of the subsequently filtered plasma, *i.e.*, 5, 10, 20, 50, and 100 μg/ml with subsequent filtering of 4.0 ml of plain buffer on the premise that this latter filtration would remove the nonirreversibly bound material that would introduce error into the binding study.

Etofibrate (I) and Clofibrate (VI) by the Method of Variable Plasma Concentrations—Fresh heparinized human blood was centrifuged for 15 min at 3000 rpm. The plasma was transferred to a stoppered tube. The red blood cells were washed three times with isoosmotic phosphate buffer (pH 7.4), and the buffer phases were discarded.

The desired mixtures of acetonitrile and ^{14}C-labeled and unlabeled etofibrate in acetonitrile in a centrifuge tube were dried under a nitrogen stream. The residues were reconstituted in 40 μl of isotonic ethanol–buffer (50:50). Appropriate amounts of plasma (inhibited by 100 μg/ml of tetraethyl pyrophosphate) and isotonic phosphate buffer (pH 7.4) were mixed to give from 0 to 100% of etofibrate in each pseudoplasma. The pseudoplasma samples (1.0 ml of each) were added to the amounts of dried I needed to give concentrations of 0.2, 2.0, 8.0, 16.0, 40.0, and 80.0 μg/ml. An aliquot (200 μl) was mixed with 10 ml of scintillation fluid and counted. An aliquot (0.5 ml) of a red blood cell suspension containing 100 μg/ml of tetraethyl pyrophosphate was added to each pseudoplasma and gently mixed. Hematocrits were taken and the pseudoblood was allowed to equilibrate for 20 min. The pseudoblood samples were centrifuged for 10 min at 3000 rpm, and 200 μl of the pseudoplasma, mixed with 10 ml of a scintillation fluid, were counted by liquid scintillation.

The clofibrate protein binding was studied similarly with 20 μl of a methanolic solution containing 15, 30, 60, and 120 μg of VI added to separate 1.0-ml pseudoplasma samples before the addition of the red blood cells. The samples were analyzed by HPLC method e using mobile phase C.

RESULTS AND DISCUSSION

Reverse-Phase HPLC Assays—*Compounds I, II, and III*—HPLC system A with analytical method a using chloroform extraction, evaporation, and reconstitution provided a chromatogram (Fig. 1A) for analyses of I (retention time, 10.8 min), III (4.7 min), and II (3.4 min) in mixtures. The internal standard, thymol, had a retention time of 7.3 min. The average of the standard errors of estimate (65–185 ng/ml, $n = 8$), of the concentration of I was 99 ng/ml of plasma for the 0.4- to 20-μg/ml assay range. The average of standard errors of estimate for III (46–126 ng/ml, $n = 5$) was 102 ng/ml of plasma for the 0.4- to 10-μg/ml assay range. The average of standard errors of estimate for II (27–121 ng/ml, $n = 5$) was 72 ng/ml of plasma for the 0.4- to 10-μg/ml assay range. This HPLC system had advantages over those reported previously (1) in that mixtures of I, II, and III in plasma could be assayed simultaneously.

Compounds IV and V—The ion-pair methodology of HPLC system B with analytical method c using ethyl acetate–*tert*-butyl alcohol extraction, evaporation, and reconstitution provided chromatographic separation of V (retention time, 6.3 min) from IV (10 min) and from plasma interferences. The internal standard, phenylurea, had a retention time of 7.5 min (Fig. 1B). The average of standard errors of estimate for V (40–92 ng/ml, $n = 5$) was 67 ng/ml of plasma for the 0.4- to 10-μg/ml assay range, and for IV (49–172 ng/ml, $n = 5$) the average was 102 ng/ml of plasma for the same assay range. Specific assays for IV and V from plasma were not given previously (7), since plasma components interfered with their detection in the prior evaluated HPLC procedures.

Compound VI—HPLC system C with plasma deproteinization by analytical method e provided 225-nm UV detection of VI with a retention time of 6.1 min; the internal standard, I.S., had a retention time of 4.5 min (Fig. 1C). The standard error of estimate of VI in the 0.4- to 4-μg/ml plasma range was 51 ng/ml.

Plasmolysis of Etofibrate and Its Intermediate Solvolytic Products in Fresh Dog Plasma—Preliminary studies of the stability of etofibrate in fresh dog plasma (7) indicated apparent half-lives of 4.4–6.9 min at 37.5°: 4.4 min at an initial concentration of 3.6×10^{-5} *M*, 6.9 min at 5.9×10^{-5} *M*, and 5.7 min at 1.19×10^{-4} *M*. A repeat study in fresh dog plasma at 5.4×10^{-5} *M* (19.5 μg/ml) and 38.5° using the aforementioned HPLC assays showed a half-life of 10.6 min (Fig. 2A).

Another study (Fig. 2B) in fresh dog plasma at 3.6×10^{-5} *M* (13.3 μg/ml) showed a biphasic degradation of etofibrate at 38.5° that could

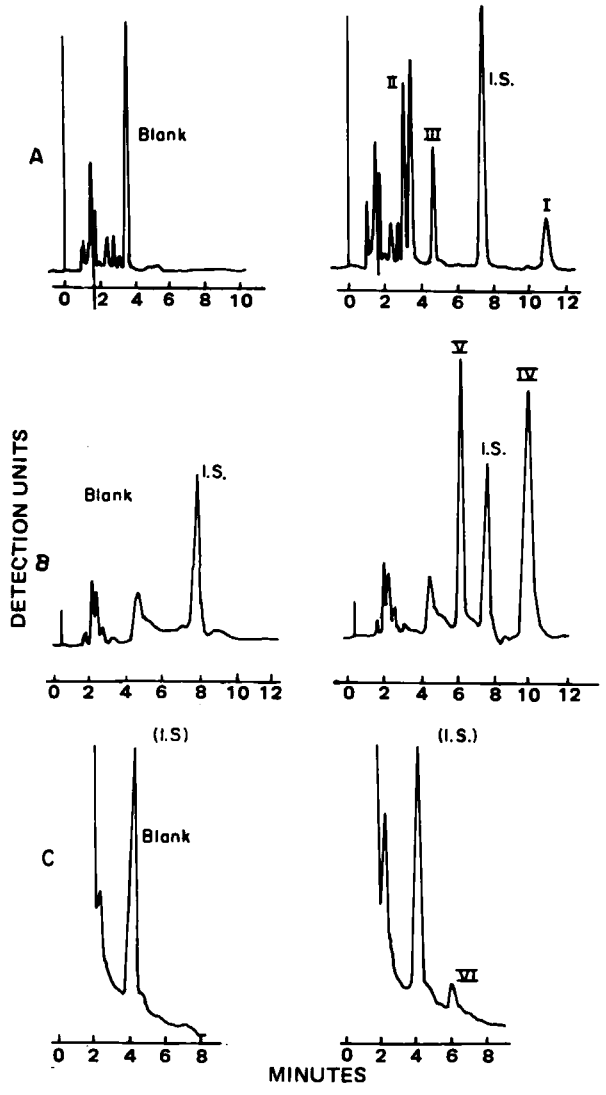

Figure 1—*Reverse-phase chromatograms of clofibric acid esters and their solvolytic products. Key: (A) Detection at 225 nm of plasma blank and plasma containing 2 μg/ml each of I, II, and III, extracted with chloroform (method a, system A). The injection volume was 50 μl; the internal standard was thymol (I.S.). (B) Detection at 254 nm of plasma blank and plasma containing 4.1 μg/ml of IV and V (method d, system B). The internal standard was phenylurea (I.S.); the injection volume was 50 μl. (C) Detection at 225 nm of plasma blank containing phenylurea as internal standard and plasma containing 0.8 μg/ml of VI (method c, system C) with 50 μl injected.*

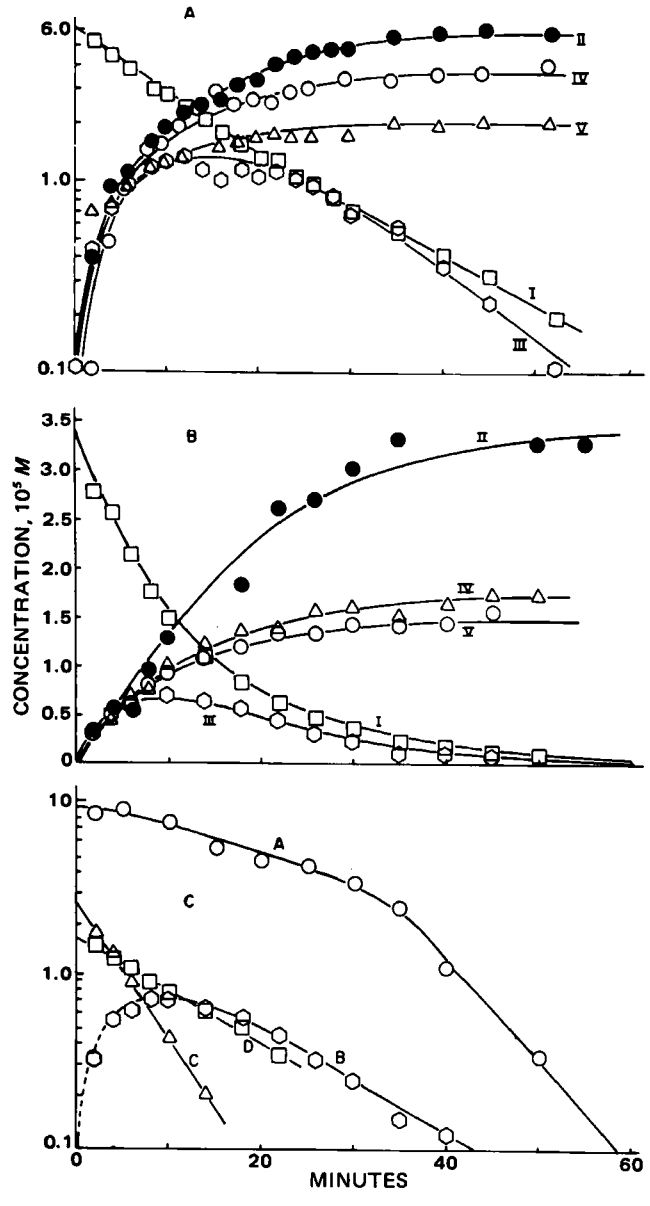

Figure 2—*(A) Semilogarithmic plots against time for 5.4 × 10^{-5} M (19.5 μg/ml) etofibrate (I) and its solvolytic products, II, III, IV, and V, in dog plasma at 38.5°. The apparent half-lives of I and III were 10.6 and 9.9 min, respectively. (B) Cartesian plots against time for 3.6 × 10^{-5} M I and its degradation products in dog plasma at 38.5°. The lines represent the predicted concentrations according to Eqs. 1 (I), 4 (V), 5 (III), 6 (IV), and 7 (II). The values used for the parameters were: f = 0.55, k_3 = 0.16616 min^{-1}, k_4 = 0.00096 min^{-1}, k = 0.07558 min^{-1}, and $[I]_0$ = 3.3 × 10^{-6} M. (C) Semilogarithmic plot against time of the III data resulting from I solvolysis in dog plasma (Fig. 2B). Curve B was calculated according to Eq. 5 with f = 0.55, k_3 = 0.166 min^{-1}, k = 0.0756 min^{-1}, $[I]_0$ = 3.3 × 10^{-6} M. Curve A shows a terminal half-life of 5.6 min for 8.08 × 10^{-5} M III in the same plasma. The appearing rate constant for III was calculated from the slope of the feathered line (curve C); the half-life of this process is 4.2 min. The appearing half-life of IV (12 min) was calculated from the slope of the sigma minus plot (curve D) of log ([IV]60 − [IV]) where $[IV]_{60}$ was the concentration of IV at 60 min.*

be fitted to $10^5 p = 14.5\, e^{-0.1438t} + 20.5\, e^{-0.058t}$ where p is in moles/liter and t is in min. The terminal half-life was 11.9 min; the apparent half-life of the first phase was 4.8 min, in the range of the half-life estimated previously (7) using assays of lower sensitivity.

The ester III previously showed apparent terminal half-lives of 11.2 min (initial etofibrate concentration of 5.9 × 10^{-5} *M*) and 5.8 min (initial etofibrate concentration of 1.19 × 10^{-4} *M*). Ester III, spiked at 4.23 × 10^{-5} *M* in fresh dog plasma had an apparent half-life of 11.5 min in the preliminary studies at 37.5° (7) and, in a present study at 8.08 × 10^{-5} *M*, of 5.6 min at 38.5° (curve A, Fig. 2C). This latter study used the greater analytical sensitivities given in this paper; the terminal phase was observed below 2.5 × 10^{-5} *M*, whereas in the preliminary study (7) the half-life was estimated from concentrations down to this value. The plasmolysis of III appears to be a saturable process (Fig. 2C). The terminal phase of the generated III in these present studies with 5.4 × 10^{-5} *M* (Fig. 2A) and 3.6 × 10^{-5} *M* (Fig. 2B and C) etofibrate in fresh dog plasma at 38.5° showed respective half-lives of 9.9, and 9.6 min. These values were well in excess of the aqueous solvolyses of these compounds, which were ~6 and 12 days at pH 7.4 and 40° for I and III, respectively.

The terminal half-lives (9.6–9.9 min) of III generated from etofibrate exceeded the terminal half-life of 5.6 min for spiked 8.08 × 10^{-5} *M* III in fresh dog plasma (Fig. 2C) and were close to the 10.6–11.9-min terminal half-lives for etofibrate. When the curve for III generated from etofibrate degradation was feathered, the resulting half-life for the appearance of III was determined as 4.2 min (curve C, Fig. 2C), close to the half-life for the loss of spiked III in plasma, indicating a probable "flip-flop."

The intermediary nicotinate (V), was more stable in fresh dog plasma than I and II (compare Figs. 2 and 3). The apparent half-life was 12.0 hr

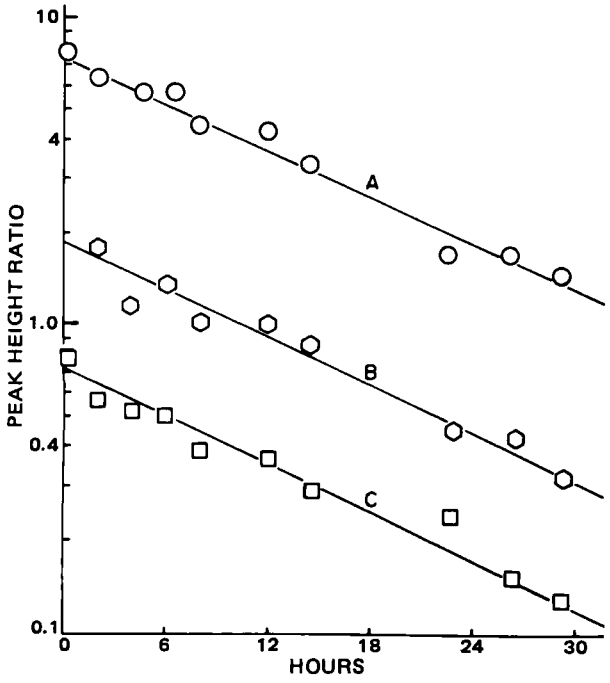

Figure 3—*Semilogarithmic plots of the peak height ratios (HPLC) of V with respect to phenylurea (internal standard) against time for the degradation in fresh dog plasma at 38.5°. Key: (A)* $C_0 = 99\ \mu g/ml$, $t_{1/2} = 12.1\ hr$; *(B)* $C_0 = 49.5\ \mu g/ml$, $t_{1/2} = 12.0\ hr$; *(C)* $C_0 = 12.4\ \mu g/ml$, $t_{1/2} = 11.9\ hr$.

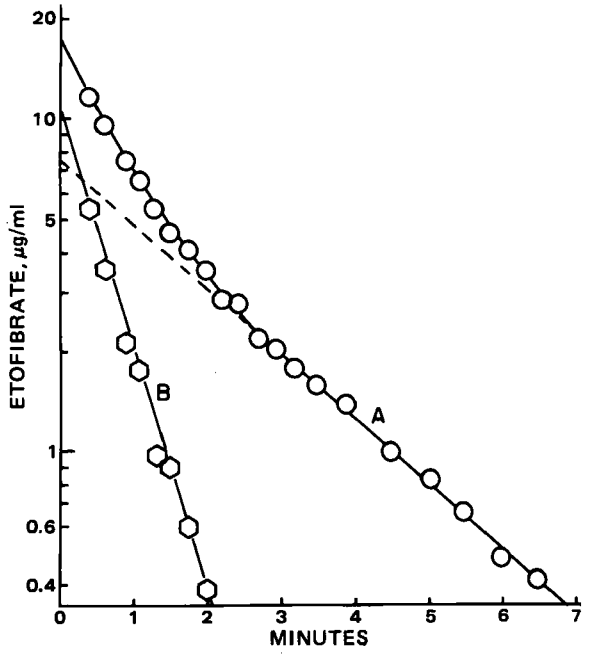

Figure 4—*Semilogarithmic plot (A) of the degradation of 18.09 μg/ml of I in heparinized human plasma at 37.5° which conforms to* C *(μg/ml)* $= 10.5\ e^{-1.59t} + 7.5\ e^{-0.444t}$ *where* t *is in minutes, and feathered curve (B) to characterize the first exponential.*

at 38.5° and was independent of the initial concentration (between 12.4 and 99 μg/ml).

The "flip-flop" phenomenon should not be, and was not, evident here, since the rate of generation of the nicotinate V is very much faster than its degradation. The slope of the semilogarithmic plot of amount of nicotinic acid not-yet-formed against time (sigma minus plot) gave an apparent half-life of ~12 min, equivalent to that for the disappearance of etofibrate and the assigned half-life for the appearance of ester III (estimated from the feathered curve of III against time).

To fit the solvolysis of etofibrate in plasma according to the model given in Scheme III, the concentration–time data from the plasmolysis of I could be reasonably approximated by a monoexponential function of the form:

$$[I] = [I]_0 \cdot e^{-kt} \qquad \text{(Eq. 1)}$$

If the products of etofibrate solvolysis were only V and II, and if no III were generated, the concentration of V could be calculated from the expression (9):

$$[V'] = [I]_0 \frac{k}{k_4 - k}\left[e^{-kt} - e^{-k_4 t}\right] \qquad \text{(Eq. 2)}$$

where $[I]_0$ is the initial concentration, [V'] is the nicotinic acid monoglycolate concentration on the presumption that I is only degrading through the V route, k is the first-order elimination rate constant for I degradation, and k_4 is the first-order rate constant for the plasmolysis of V. The ratio of experimentally observed [V] to calculated [V'] is:

$$f = [V]/[V'] \qquad \text{(Eq. 3)}$$

which was 0.55 for the studies given in Fig. 2B and C, and f is the fraction of I going through the V route. Thus the fraction of I going through the III route is $1 - f = 0.45$.

If the degradation of III can be approximated by a first-order rate constant k_3, the following set of equations describes the time course of all possible solvolysis products as a function of the initial etofibrate concentration $[I]_0$:

$$[V] = [I]_0 \cdot \frac{fk}{k_4 - k}\left[e^{-kt} - e^{-k_4 t}\right] \qquad \text{(Eq. 4)}$$

$$[III] = [I]_0 \cdot \frac{(1-f)k_3}{k - k_3}\left[e^{-k_3 t} - e^{-kt}\right] \qquad \text{(Eq. 5)}$$

$$[IV] = [I]_0 \cdot (1-f)(1 - e^{-kt}) + [I]_0 f\left[1 - \frac{1}{k - k_4}\left(ke^{-k_4 t} - k_4 e^{-kt}\right)\right] \qquad \text{(Eq. 6)}$$

$$[II] = [I]_0 \cdot f(1 - e^{-kt}) + [I]_0 \cdot (1-f) \times \left[1 - \frac{1}{k_3 - k}\left(k_3 e^{-kt} - ke^{-k_3 t}\right)\right] \qquad \text{(Eq. 7)}$$

The lines through the experimental values in Fig. 2B and C were drawn on the basis of concentrations calculated from Eqs. 4–7 using the parameters given in the legend of the figures. The good agreement of the experimental data and calculated curves supports Scheme III and confirms the "flip-flop" phenomenon for the III curve.

Etofibrate Solvolysis in Human Plasma—A typical curve for the degradation of etofibrate in fresh heparinized human plasma is shown in Fig. 4 for 18.8 μg/ml and showed even more pronounced biphasic character than was observed in fresh dog plasma. The terminal half-life was 1.54 min at 37.5°; the half-life of the earlier phase, obtained by feathering, was 0.44 min. The nonlinearity of such semilogarithmic plots occurred with various other initial concentrations (8, 16, and 40 μg/ml) with similar terminal half-lives of 1.7 min at 38.5°. This indicated no dose dependency. An additional study at 18.7 μg of etofibrate/ml at 13° showed a biphasic curve also, with a terminal half-life of 7.7 min. The initial phase had a half-life of 0.4 min, and $10^5 p = 1.31\ e^{-1.67t} + 3.71\ e^{-0.096t}$ where p is in moles/liter and t is in min.

Since a possible explanation of this unexpected biphasic phenomenon could be the inhibition of an enzymatic process by formed solvolytic products, the solvolyses of 21.5 μg/ml of etofibrate were repeated in the same fresh human plasma in the absence and presence of 23.8 μg/ml of II, III, IV, or V added 20 sec before the addition of etofibrate. There were no significant differences in the etofibrate degradations, with terminal half-lives of 1.7 min in the same plasma with or without any of these added compounds. Thus, product inhibition or slowing of an enzymic process could not be concluded.

An alternative explanation could be the decay of enzymic activity with time or its irreversible inactivation by the substrate. If these were true, reinoculation of plasma with fresh substrate would give decreasing rates

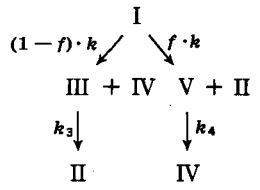

Scheme III—Model of etofibrate plasmolysis.

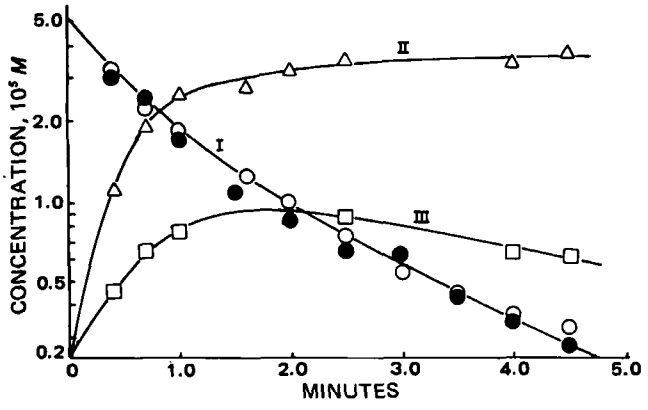

Figure 5—*Semilogarithmic plots of concentrations of I, II, and III with time. Ten minutes after the degradation of 19.77 μg/ml of I in the fresh human plasma at 37.5° (○), 20.17 μg/ml of I (●) was added and its time course monitored.*

or possibly eliminate the biphasic nature. Ten minutes after 19.77 μg/ml of etofibrate was added to fresh human plasma and subsequently degraded at 37.5°, 20.17 μg/ml of etofibrate was again added and its time course monitored (Fig. 5). There was no significant difference between the time courses of the sequential studies of etofibrate degradation in the same human plasma. Both showed terminal half-lives of 1.5 min in this plasma.

Etofibrate showed significantly shorter terminal half-lives of degradation (1.5–1.7 min) in fresh human plasma than in fresh dog plasma (5–10 min). In the several human plasma studies, 50 ± 5% of the degrading etofibrate produced the more stable nicotinate V and the remainder went through the route involving ester III.

2-Hydroxyethyl Nicotinate (V) Stability in Human Plasma—The ester, V, showed apparent first-order degradation in fresh human plasma with half-lives of 45–55 min, which were not significantly affected by concentration in the 2- to 21-μg/ml range (Fig. 6). These half-lives were more shorter than the 12-hr half-life observed in dog plasma (Fig. 3).

2-Hydroxyethyl 2-(4-chlorophenoxy)-2-methylpropionate (III) Stability in Human Plasma—The ester, III, did not degrade by first-order processes at all concentrations in fresh human plasma. Semilogarithmic plots of concentrations with time were not linear; they showed the decreasing convex curve typical of saturable processes (10).

Such saturable processes can be described by:

$$-dC/dt = \frac{\upsilon_{max} C}{K_m + C} \qquad \text{(Eq. 8)}$$

where preliminary estimates of υ_{max} can be made from the initial slope at high concentrations of linear plots of concentration against time (Fig. 7) and the υ_{max} and K_m values can be estimated from the terminal slopes

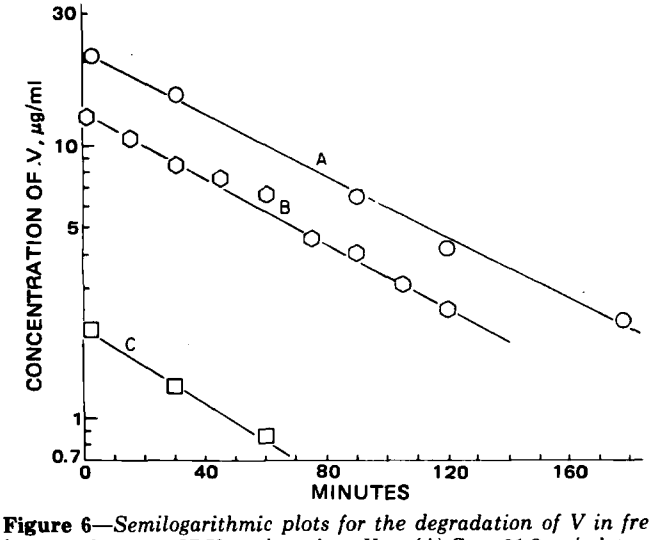

Figure 6—*Semilogarithmic plots for the degradation of V in fresh human plasma at 37.5° against time. Key: (A) C_0 = 21.3 μg/ml, $t_{1/2}$ = 54.5 min; (B) C_0 = 13.4 μg/ml, $t_{1/2}$ = 50.9 min; (C) C_0 = 2.1 μg/ml, $t_{1/2}$ = 45.4 min.*

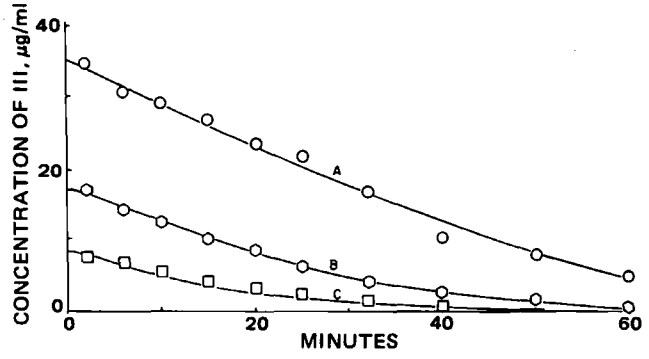

Figure 7—*Plots of concentrations of III with time in fresh human plasma at 37.5° fitted to the Michaelis–Menten equation $-dC/dt = v_{max}C/(K_m + C)$ with v_{max} = 0.77 μg/ml/min and K_m = 8 μg/ml. The initial concentrations of III were 35.2 (A), 17.5 (B), and 8.5 μg/ml (C).*

of ln C against time. The times for various concentrations (C) can be calculated from the integrated form of the Michaelis–Menten equation (Eq. 8):

$$-(K_m \ln C/C_0 + C - C_0)/\upsilon_{max} = t \qquad \text{(Eq. 9)}$$

where C_0 is the initial concentration and C the concentration at any time, t. All of the experimentally observed time courses for 8.5-, 17.5-, and 35.2-μg/ml initial concentrations of III in human plasma could be fitted by Eq. 9 with K_m = 8 μg/ml and υ_{max} = 0.77 μg/ml/min (Fig. 7) to demonstrate the validity of this equation and the postulation of saturable enzymic solvolysis for these initial concentrations. The apparent terminal half-life of III can be calculated from $0.693/(\upsilon_{max}/K_m)$ = 0.693/(0.77/8) = 7.2 min and was close to the half-life for the solvolysis of III in fresh dog plasma.

Clofibrate (VI) Stability in Human Plasma—Clofibrate demonstrated solvolysis in human plasma by a similar saturable enzymic process (Fig. 8), which agreed with the previously indicated saturable kinetics in dog plasma (7). The values of the parameters of Eqs. 8 and 9, υ_{max} = 0.77 μg/ml/min, K_m = 28 μg/ml, $t_{1/2} = 0.693K_m/\upsilon_{max}$ = 25.2 min, fitted the data for plasma level–time studies for initial clofibrate concentrations in human plasma of 125, 55.5, 12, and 6.1 μg/ml (Fig. 8). The identical υ_{max} of 0.77 μg/ml/min for clofibrate and ester III with the different K_m values could indicate solvolyses of these compounds by the same enzyme system, but with different affinities.

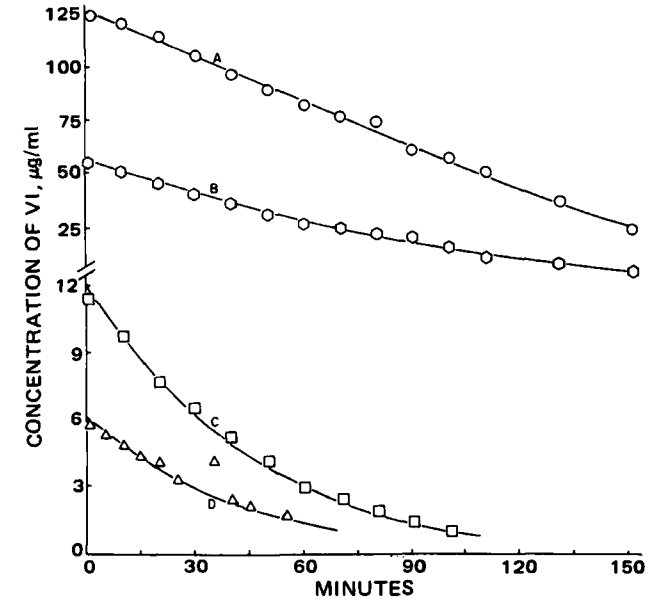

Figure 8—*Plots of VI concentrations with time in fresh human plasma at 37.5° fitted to the Michaelis–Menten equation $-dC/dt = v_{max}C/(K_m + C)$ with v_{max} = 0.77 μg/ml/min and K_m = 28 μg/ml. The initial concentrations were 125 (A), 55.5 (B), 12 (C), and 6.1 μg/ml (D). The apparent half-life of the apparent first-order terminal phase of curve C was 25.9 min.*

Table I—Red Blood Cell–Buffer Partitioning of Etofibrate (I), Clofibric Acid (II), 2-Hydroxyethyl 2-(4-Chlorophenoxy)-2-methylpropionate (III), Nicotinic Acid (IV), and 2-Hydroxyethyl Nicotinate (V)

Compound	Assay Procedures[a]	Tetraethyl Pyrophosphate Concentration, μg/ml[b]	Drug Concentration Range, μg/ml[c]	n	D (Average ± SD)
I	LSC[e]	89.5	0.2–80	6	5.46 ± 0.30
I[d]	Aa	117	1.15–1.265	5	6.03 ± 0.36
III	Aa	117	1.25–22.86	5	3.23 ± 0.22
III[d]	Aa	117	1.36–23.30	5	3.06 ± 0.34
II	Aa	117	1.57–35.38	4	1.98 ± 0.19
II	Aa	0	1.55 ± 35.22	5	2.21 ± 0.23
II[d]	Aa	117	1.56–29.98	5	2.30 ± 0.20
IV	Bd	0	2.10–50.48	5	0.97 ± 0.21
IV	Bd	117	1.66–47.34	5	1.25 ± 0.44
IV[d]	Bd	117	2.24–49.09	5	1.00 ± 0.13
V	Bd	117	2.53–35.05	4	1.09 ± 0.41
V[d]	Bd	117	1.39–35.13	5	1.07 ± 0.29

[a] Capital letter designates the HPLC system; small letter designates the method of preparation for analysis as given in *Experimental*. [b] Concentration of tetraethyl pyrophosphate in the RBC suspension. [c] Drug concentration in buffer after equilibration with red blood cells. [d] Studies effected by simultaneous spiking with I, II, III, IV, and V. [e] Radiolabeled etofibrate was studied and assayed by liquid scintillation counting (LSC).

Inhibition of Clofibric Acid Ester Plasmolysis—The plasmolysis of heroin had been inhibited by the addition of 100 μg/ml of tetraethyl pyrophosphate, a compound that did not hemolyze red blood cells when added to blood nor denature proteins (11). This enzyme inhibitor was also used to inhibit the hydrolysis of clofibric acid esters in human blood and plasma (Fig. 9). The plasmolyses of etofibrate (I), (curves A and B), ester III, (curve C), and clofibrate (VI) (curves D and E) were suppressed for at least 1 hr by adding tetraethyl pyrophosphate to blood or plasma, in contrast with the ready solvolyses of these compounds in uninhibited human plasma (I, curve H; III, curve F; VI, curve G). The use of tetraethyl pyrophosphate as a plasmolysis inhibitor thus provided a method to ascertain the red blood cell partitioning and plasma protein binding of these highly unstable clofibric acid esters in human plasma.

Tetraethyl pyrophosphate showed different patterns in dog and human plasma. Tetraethyl pyrophosphate (137.5 μg/ml) in fresh dog plasma suppressed the solvolysis of I for only 10–12 min (Fig. 10, curves A, B, and E), in contrast with the inhibition in fresh human plasma for at least 130 min (Fig. 10, curve D). Increased (7.5×) tetraethyl pyrophosphate concentrations (963.3 μg/ml) did not even double the time of complete plasmolysis inhibition (Fig. 10, curve C). The solvolysis after 22 min increased to an apparent half-life of 58.2 min, similar to the half-life observed with 128.9 μg/ml of tetraethyl pyrophosphate.

Red Blood Cell–Buffer Partitioning—*Etofibrate and its Solvolytic Products*—The red blood cell–plasma partition coefficient of a drug (*D*), on the presumption that only unbound drug in the plasma can diffuse into the red blood cells, can be defined (12) as:

$$D = [A_{RBC}]/[A_p^u] = \{[A_B]/[A_p^u](1 - H) - [A_p^b]/[A_p^u] - 1\}(1 - H)/H \quad \text{(Eq. 10)}$$

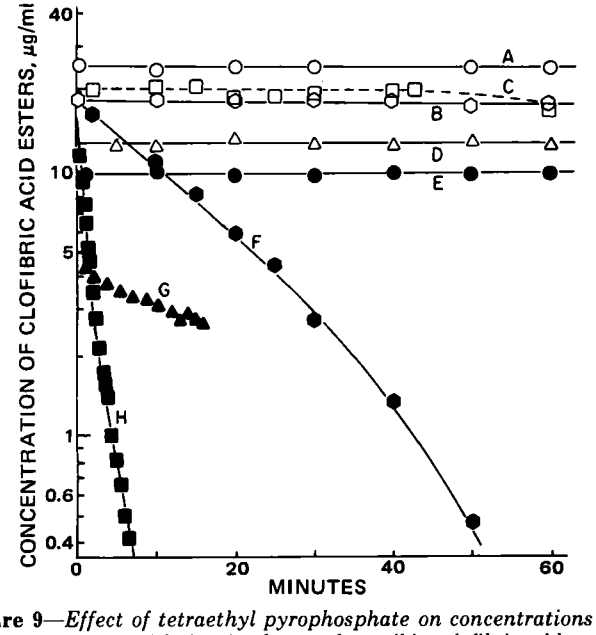

Figure 9—*Effect of tetraethyl pyrophosphate on concentrations of clofibric acid esters with time in plasma after spiking clofibric acid esters in fresh human blood or plasma. Key: (A) fresh human whole blood containing 102.4 μg/ml of tetraethyl pyrophosphate spiked with 18.24 μg/ml of I; (B) fresh human plasma containing 102.4 μg/ml of tetraethyl pyrophosphate spiked with 18.24 μg/ml of I; (C) fresh human plasma containing 47.2 μg/ml of tetraethyl pyrophosphate spiked with 19.84 μg/ml of III; (D) fresh human whole blood containing 99.5 μg/ml of tetraethyl pyrophosphate spiked with 12.65 μg/ml of VI; (E) fresh human plasma containing 101.4 μg/ml tetraethyl pyrophosphate spiked with 9.9 μg/ml of VI; (F) III degradation (C_0 = 16.5 μg/ml) in uninhibited human plasma; (G) VI degradation (C_0 = 4.5 μg/ml) in uninhibited human plasma; (H) I degradation (C_0 = 18.24 μg/ml) in uninhibited human plasma.*

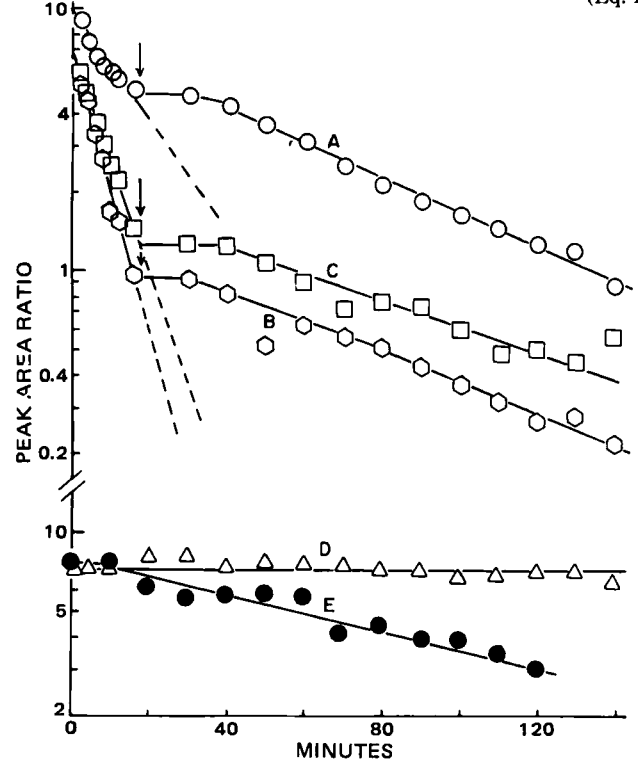

Figure 10—*Effect of tetraethyl pyrophosphate on the solvolysis of I. Key: (A) One-day-old dog plasma spiked with 30.3 μg/ml of I at room temperatuare. After 18 min (arrow) 128.9 μg/ml of tetraethyl pyrophosphate was added. (B) Fresh dog plasma spiked with 20.2 μg/ml of I at 38.5°. After 18 min (arrow) 128.9 μg/ml of tetraethyl pyrophosphate was added, and the test tube was kept at room temperature. (C) Identical to B, except 963.3 μg/ml of tetraethyl pyrophosphate was added. (D) Fresh human plasma containing 137.5 μg/ml of tetraethyl pyrophosphate spiked with 20 μg/ml of I. (E) Identical to D, except dog plasma was used.*

Table II—Human Plasma Protein Binding of Clofibric Acid (II), the 2-Hydroxyethyl Ester (III), Nicotinic Acid (IV), and the 2-Hydroxyethyl Ester[a] (V) by the Ultrafiltration Method

Compound	C_p, μg/ml[b]	C_{pw}, μg/ml[c]	Percent Bound	Average Percent Bound ± *SD* (*SEM*)
II	19.71	0.30	98.48	
	45.18	1.38	96.95	97.20 ± 1.18 (0.68)
	101.97	3.92	96.16	
III	4.96	0.91	81.65	
	10.24	1.59	84.47	
	20.21	2.97	85.30	83.17 ± 1.65 (0.74)
	48.28	8.33	82.75	
	105.16	19.25	81.69	
V	4.66	3.98	14.59	
	9.20	9.08	1.30	
	18.86	17.55	6.95	6.0 ± 6.3 (3.2)
	47.29	46.75	1.14	
IV	6.42	5.93	7.63	
	13.57	11.13	17.98	
	30.84	26.72	13.36	12.6 ± 4.3 (2.2)
	79.32	70.30	11.37	

[a] Tetraethyl pyrophosphate (95.7 μg/ml) was added to plasma before spiking with drug. [b] Drug concentration in plasma before filtration. [c] Drug concentration in ultrafiltrate (plasma water).

where $[A_{RBC}]$ is the total drug concentration in the red blood cells; $[A_p]$, $[A_p^u]$, and $[A_p^b]$ are the respective drug concentrations in plasma, plasma water (*i.e.*, unbound to plasma proteins), and bound to plasma proteins; $[A_B]$ is the total concentration of a drug in whole blood or red blood cell suspension; and H is the hematocrit. The value of $[A_p^b]$ is zero in red blood cell–buffer suspensions.

Etofibrate, clofibrate, and its solvolytic products showed rapid equilibration between buffer and human red blood cells. The apparent partition coefficients, D, did not change with time after the 3 min needed for mixing and subsequent centrifugation. There was no significant concentration dependency of the partition coefficient in the studied concentration ranges (Table I). There was no significant difference between the partition coefficients for the nonsolvolyzable clofibric and nicotinic acids with or without the presence of the enzyme inhibitor tetraethyl pyrophosphate, indicating the noninterference of this compound with the partitioning. The partition coefficients for etofibrate, clofibric acid, and ester III were much greater than unity (Table I), demonstrating specific binding to erythrocytes, greatly in excess of that which would be anticipated from simple volume partitioning.

Clofibrate—The red blood cell–buffer partition coefficient, D, for clofibrate was concentration dependent. It decreased with increasing clofibrate concentration, indicating saturable partitioning into the red blood cells, from 7.8 at 10 μg/ml to 1 at 50 μg/ml.

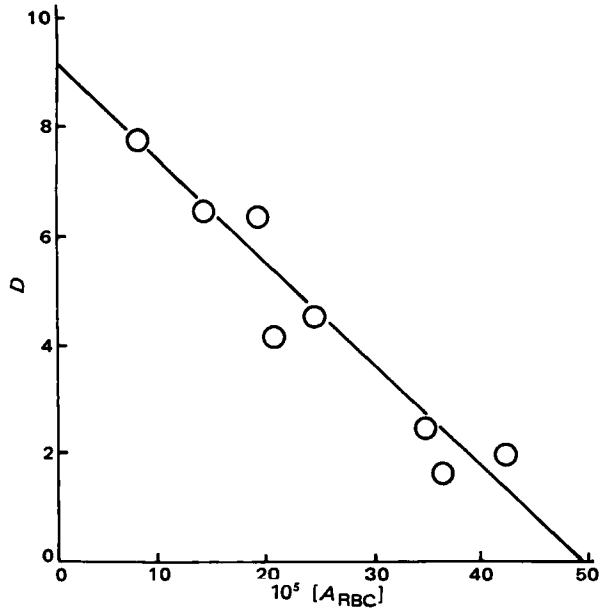

Figure 1—*Modified Scatchard plot for the presumed saturable binding or partitioning (D) of clofibrate to red blood cells from the buffer suspension against the clofibrate concentration in the buffer removed by binding to the red blood cells, [A_{RBC}]. The fitted line was calculated by least-square regression:* $D = 9.185 - 1.92 \times 10^4 [A_{RBC}]$.

The interaction between a ligand and a class of receptors can be formulated as (12):

$$n[A_p^u] + [R] \overset{K}{\rightleftharpoons} [A_nR] \qquad \text{(Eq. 11)}$$

where $[A_p^u]$ is the concentration of free or unbound drug in the buffer phase of the suspension, $[A_{RBC}] = [A_p] - [A_p^u]$ is the concentration of bound ligand to the receptor (erythrocyte) where $[A_p]$ would be the concentration of drug in the buffer phase if there were no binding to the receptor, K is the association constant for the binding of a molecule of drug to one of the equivalent n binding sites of the receptor, and $[R]$ is the concentration of the receptors.

The modified Scatchard equation can be derived on the premise of only one class of n equivalent binding sites (13):

$$D = \frac{[A_R]}{[A_p^u]} = nK[R] - K[A_{RBC}] \qquad \text{(Eq. 12)}$$

and shows that plots of the apparent partition coefficient (D) against the drug concentration in the continuous phase that had been removed to bind the receptors should be linear if there were only one class of n equivalent binding sites per receptor (red blood cell) so that saturable binding was manifested. Such a plot is given in Fig. 11 for a hematocrit of 0.24 at room temperature. The negative of the slope is $K = 1.92 \times 10^4$ M^{-1}. The intercept, $nK[R]$, is 9.185; the number of binding sites $n[R]$ on the postulation of a volume of a red blood cell of 90 μm^3 and 1.11×10^{10} cells/ml of packed red blood cells permits the calculation of the number of binding sites per red blood cell as 4.3×10^{-17} moles/single red blood cell.

Plasma Protein Binding by Ultrafiltration—When isotonic phosphate buffer, pH 7.4, containing 10 μg/ml of etofibrate, clofibrate, or their potential solvolytic products was ultrafiltered, nicotinate V and the clofibric and nicotinic acids showed no significant binding to the filter membranes. The concentration in the first and successive 0.5 ml of filtrate was the same as the initial concentration in the buffer to be filtered (Fig. 12). Etofibrate bound strongly to the membrane. Although the concentration in successive 0.5 ml filtrates of the 5-ml aliquot showed increasing concentrations, a maximum of only 39.8% of the filtered concentration could be recovered in the last 0.5 ml of ultrafiltrate (Fig. 12A). Although the ultrafiltrate showed increased concentrations of etofibrate if the membrane prefiltered 3 ml of 100 μg/ml etofibrate, the concentration recovery was still incomplete (Fig. 12B). Further attempts were made to saturate the membrane with prefiltration of larger concentrations and volumes of etofibrate solutions. However, the variability among successive filtrates and filtrations was too great. The cone filter[10] was chosen rather than the molecular filters[11] for the ultrafiltration studies because it showed the lowest binding for the investigated compounds, particularly for the ester III.

The percentages of drug bound to human plasma proteins by this ul-

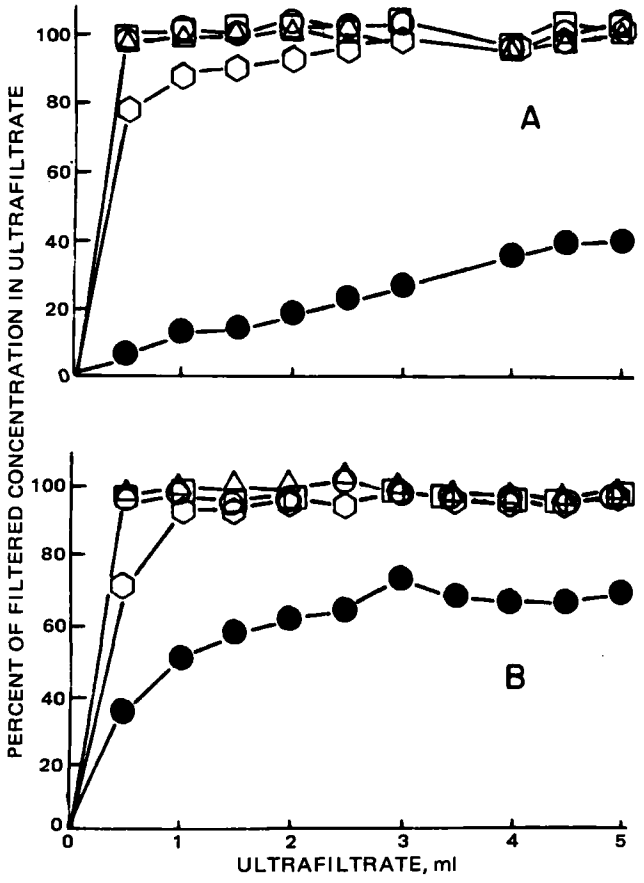

Figure 12—*Percent recovery of ultrafiltrate concentrations of I (●), II (□), III (○), IV (△), and V (○) in 5 ml of pH 7.4 isotonic phosphate buffer in each successive 0.5-ml filtrate. Key: (A) Each drug was filtered separately without membrane pretreatment. (B) The membranes were pretreated by prefiltering 2 ml of buffer containing 100 μg/ml of compound. The excess was rinsed with isotonic buffer.*

trafiltration technique for those compounds that do not show excessive binding to the ultrafiltration membranes are given in Table II. There was no apparent concentration dependence for the protein binding of clofibric acid (II) and ester III, with 97.2 ± 1.2 and 83.2 ± 1.7%, respectively. The results from protein binding studies of nicotinic acid (IV) and the nicotinate V had greater variability, 6.0 ± 6.3 and 12.6 ± 4.3%, respectively. If the study at the lower concentration of 5.9 μg/ml were omitted, the ester

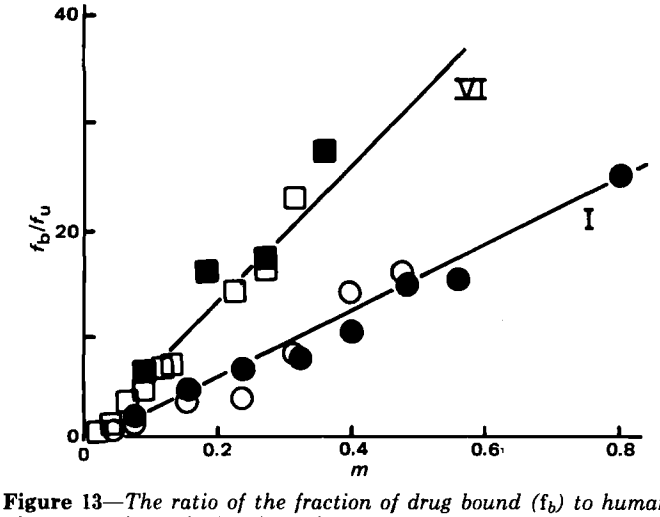

Figure 13—*The ratio of the fraction of drug bound (f_b) to human plasma proteins to the fraction unbound (f_u) as a function of the fraction (m) of normal plasma in pseudoplasma. The intercepts are zero. The slopes are 30 for I at 0.2 μg/ml (●) and 80 μg/ml (○) and 60 for VI at 13.9 μg/ml (■) and 108.4 μg/ml (□).*

Table III—Percent Plasma Protein Binding (100*f*) of Etofibrate and Clofibrate by the Method of Erythrocyte Suspension in Variable Plasma Concentrations, *H* = 0.25

	μg/ml[a]	$S \pm SEM_S$[b]	Percent Bound $(100f) \pm SEM$[c]
Etofibrate[d]	0.212	30.03 ± 1.04	96.78 ± 0.11
	2.19	30.52 ± 1.14	96.83 ± 0.12
	8.12	32.56 ± 0.97	97.03 ± 0.09
	15.8	30.60 ± 1.70	96.84 ± 0.17
	39.2	32.04 ± 1.48	96.97 ± 0.14
	79.7	30.9 ± 2.73	96.87 ± 0.27
Average ± *SD*			96.89 ± 0.09
Clofibrate[e]	13.6	57.32 ± 5.20	98.29 ± 0.16
	13.9	58.87 ± 3.42	98.33 ± 0.10
	27.1	53.51 ± 1.19	98.16 ± 0.04
	54.2	48.13 ± 1.86	97.96 ± 0.08
	108.4	62.1 ± 11.6	98.42 ± 0.03
Average ± *SD*			98.23 ± 0.18

[a] Total plasma concentration of drug before partitioning into red blood cells. [b] Slope of the plot of $f/(1-f)$ *versus* m. [c] $f = S/(1+S)$; *SEM* of $100f$ is $100\{|(S + SEM_S)/(1 + S + SEM_S)] - [(S - SEM_S)/(1 + S - SEM_S)]|/2$. [d] Radioactivity of labeled compound was assayed in red blood cell-equilibrated plasma. The tetraethyl pyrophosphate concentration was 89.5 μg/ml in the red blood cell suspension and 99.45 μg/ml in the plasma. [e] HPLC assay C-d of red blood cell-equilibrated plasma was used. The tetraethyl pyrophosphate concentration was 117 μg/ml in the red blood cell suspension and 115.84 μg/ml in the plasma.

V showed a possible concentration ratio dependence of protein binding.

Human Plasma Protein Binding of Etofibrate and Clofibrate by the Method of Variable Plasma Concentrations in Erythrocyte Suspensions—The high binding of etofibrate and clofibrate to ultrafiltration membranes prevented their use in the determination of plasma protein binding. The instability of these compounds in plasma 1 hr after enzyme inhibition of plasma with tetraethyl pyrophosphate prevented the use of such traditional methods as ultracentrifugation and equilibrium dialysis to determine plasma protein binding. Tetraethyl pyrophosphate undergoes degradation by solvolysis with time.

A method that uses the partitioning of plasma-unbound drug into erythrocytes with varying plasma concentrations to determine plasma protein binding was developed previously by Garrett and Hunt (14) and applied to the nonsaturable protein binding of tetrahydrocannabinol. The method was also applied to the determination of the plasma protein binding of papaverine (15) and methadone (16). In the latter case it was clearly shown that protein binding determined by this technique gave the same results (66% plasma protein binding) as the more conventional ultracentrifugation method. Synthetic blood samples are prepared with known hematocrit, varying fractions of plasma and plasma water (or pH 7.4 phosphate buffer), and known concentrations of drug. The drug-equilibrated erythrocytes are separated from the pseudoblood samples by centrifugation and the pseudoplasma samples are analyzed for their concentrations.

The total amount of drug, A_{tot}, added to pseudoplasma was confirmed by assay and washed red blood cells were added to give an hematocrit of H. From the assayed pseudoplasma concentrations $[A_p]$ of volume $V_p = V_{tot}(1 - H)$, centrifugally separated from a pseudoblood of hematocrit H and volume V_{tot}, the amount of drug partitioned into the red blood cells, A_{RBC}, was calculated:

$$A_{RBC} = A_{tot} - V_p[A_p] \qquad \text{(Eq. 13)}$$

where $[A_{RBC}] = A_{RBC}/V_{RBC}$ and $V_{RBC} = HV_{tot}$. Thus, the fraction (f) of drug in plasma that is unbound to plasma proteins can be calculated from the assayed, separated plasma concentration of drug, $[A_p]$, by:

$$f = 1 - \frac{[A_p^u]}{[A_p]} = 1 - \frac{[A_{RBC}]}{D[A_p]} = 1 - \frac{(A_{tot} - V_p[A_p])}{DHV_{tot}[A_p]} \qquad \text{(Eq. 14)}$$

where D is the partition coefficient for red blood cell–plasma water (or buffer) (Eq. 10). In the special case for clofibrate this partition coefficient was a function of the red blood cell concentration:

$$D = 9.185 - 1.92 \times 10^{-4}[A_{RBC}] \qquad \text{(Eq. 15)}$$

The method is extremely sensitive and particularly useful when both the plasma protein binding and red blood cell–plasma water partition coefficient are high.

In the cases of both etofibrate and clofibrate, plots of the fraction of drug bound to plasma protein, against the fraction of plasma, m, in

pseudoplasma were superimposable for all plasma and unbound drug in plasma concentrations [A_p^u]. Plots (Fig. 13) of $f/(1-f)$ against m are linear for all [A_p^u] and pass through the origin with slopes of S. The fraction of drug bound to 100% plasma when $m = 1$ can then be calculated (Table III). The human plasma protein binding of etofibrate is 96.89 ± 0.09% (*SD*) for plasma concentrations in the 0.2- to 80-μg/ml range. The human plasma protein binding of clofibrate is 98.23 ± 0.18% (*SD*) for plasma concentrations in the 14- to 108-μg/ml range.

REFERENCES

(1) S. C. Grundy, E. H. Ahrens, G. Scalen, P. H. Schreibman, and P. J. Nestel, *J. Lipid Res.*, **13**, 531 (1972).

(2) B. J. Kudchodkar, H. S. Sodhi, L. Horlick, and D. T. Mason, *Clin. Pharmacol. Ther.*, **24**, 354 (1978).

(3) J. Schneider and H. Kaffarnik, *Fortschr. Med.*, **94**, 785 (1976).

(4) H. Kaffarnik, J. Schneider, and W. Haase, *Dtsch. Med. Wochenschr.*, **100**, 2486 (1975).

(5) W. Sterner and A. Schultz, *Arzneim.-Forsch. (Drug Res.)*, **24**, 1990 (1974).

(6) M. Kummer, W. Schatton, H. Linde, and H. Oelschlaeger, *Pharm. Ztg.*, **124**, 1312 (1979).

(7) E. R. Garrett and M. R. Gardner, *J. Pharm. Sci.*, **71**, 14 (1982).

(8) H. Oelschlaeger, D. Rothley, M. Ewert, and P. Nachev, *Arzneim.-Forsch. (Drug Res.)*, **30**, 984 (1980).

(9) E. R. Garrett, *J. Am. Chem. Soc.*, **80**, 4049 (1958).

(10) E. R. Garrett, J. Brès, and K. Schnelle, *J. Pharmacokinet. Biopharm.*, **2(1)**, 43 (1974).

(11) E. R. Garrett and T. Gürkan, *J. Pharm. Sci.*, **68**, 26 (1979).

(12) E. R. Garrett and H. J. Lambert, *J. Pharm. Sci.*, **62**, 550 (1973).

(13) M. C. Meyer and D. E. Guttman, *J. Pharm. Sci.*, **57**, 895 (1968).

(14) E. R. Garrett and C. A. Hunt, *J. Pharm. Sci.*, **63**, 1056 (1974).

(15) E. R. Garrett, H. Roseboom, J. R. Green Jr., and W. Schuermann, *Int. J. Clin. Pharmacol.*, **16**, 193 (1978).

(16) H. Derendorf and E. R. Garrett, *J. Pharm. Sci.*, **72**, 630 (1983).

ACKNOWLEDGMENT

Supported in part by a grant from Merz and Co., Frankfurt (Main), West Germany.

Pharmacokinetic Model for Diazepam and its Major Metabolite Desmethyldiazepam Following Diazepam Administration

M. L. JACK and W. A. COLBURN ˣ

Received April 22, 1982, from the *Department of Pharmacokinetics and Biopharmaceutics, Hoffmann-La Roche Inc., Nutley, NJ 07110.* Accepted for publication September 29, 1982.

Abstract □ A five-compartment open model was used to simulate the blood concentration profiles of diazepam and its metabolite, desmethyldiazepam, following single- and multiple-dose administrations of diazepam. The parameter estimates for diazepam were previously reported literature values. The parameter estimates for the metabolite were calculated from literature values of blood concentrations of desmethyldiazepam following the administration of clorazepate. The five-compartment open model suggests that ~50% of the administered diazepam is biotransformed to desmethyldiazepam, and that the elimination profile of the metabolite is not altered by the presence of the drug. The model may also be readily adapted to predict the concentrations of diazepam and desmethyldiazepam in cerebrospinal fluid following the administration of diazepam by simply correcting the blood or plasma concentrations of the drug and metabolite for the degree of plasma protein binding.

Keyphrases □ Diazepam—desmethyldiazepam, pharmacokinetics, single- and multiple-dose administrations, five-compartment open model, blood, CSF □ Desmethyldiazepam—diazepam, pharmacokinetics, single- and multiple-dose administrations, five-compartment open model, blood, CSF □ Pharmacokinetics—diazepam, desmethyldiazepam, single- and multiple-dose administrations, five-compartment open model, blood, CSF

Diazepam (7-chloro-1,3-dihydro-1-methyl-5-phenyl-2*H*-1,4-benzodiazepin-2-one) is effective in the symptomatic relief of tension and anxiety, as well as for the relief of skeletal muscle spasms (1–5). Desmethyldiazepam, the major metabolite of diazepam, is the pharmacologically active metabolite of the prodrugs clorazepate and prazepam, which are also used as anxiolytic agents (6–8).

Diazepam pharmacokinetics have been described previously by a three-compartment model by Kaplan *et al.* (6) and Moolenaar *et al.* (9). Several investigators have described the pharmacokinetic profile of desmethyldiazepam following oral administration of the prodrug clorazepate in terms of a two-compartment open model (8, 10–12). The present report combines the three-compartment open model for diazepam and the two-compartment open model for desmethyldiazepam to define the pharmacokinetic profiles of diazepam and its metabolite following single- and multiple-dose administrations of the drug.

EXPERIMENTAL

Clinical Protocol—The data used in this study were previously reported by Kaplan *et al.* (study A) (6). Briefly, four healthy male volunteers, ages 25–43, each received single 10-mg doses of diazepam administered intravenously and orally 1 week apart. Commencing 1 week thereafter, each subject received a 10-mg oral dose of the drug every 24 hr for 15 days. The subjects were fasted for 7 hr prior to receiving the single-dose administrations, and food was withheld for 1 hr postadministration.

Blood specimens were obtained 1, 2.5, 5, 10, 20, 30, and 45 min and at 1, 1.5, 2, 3, 4, 6, 8, 12, 24, 30, and 48 hr following intravenous administration, and at 0.25, 0.5, 0.75, 1, 1.5, 2, 3, 4, 6, 8, 12, 24, 30, and 48 hr following the single-dose oral administration. Following chronic administration, blood samples were obtained 0 (predose), 0.5, 1, 2, 4, and 24 hr postadministration on day 1; 1, 2, and 24 hr postadministration on days 2–11; 1 and 2 hr postadministration on day 12 and at 0 (predose), 1, 2, 4, 6, 8, 12, 24, 30, 36, 48, 72, 96, 120, 144, 168, 192, and 216 hr postadministration on day 15.

Analytical Method—Blood specimens were analyzed for diazepam and desmethyldiazepam by the electron-capture GLC procedure of de Silva and Puglisi (13), with a sensitivity of 10 and 20 ng/ml, respectively, for each component using a 1-ml specimen.

Pharmacokinetic Model—The five-compartment open model used to describe the pharmacokinetic profiles of diazepam and its major me-

0022-3549/83/1100-1318$01.00/0

pseudoplasma were superimposable for all plasma and unbound drug in plasma concentrations [A_p^u]. Plots (Fig. 13) of $f/(1-f)$ against m are linear for all [A_p^u] and pass through the origin with slopes of S. The fraction of drug bound to 100% plasma when $m = 1$ can then be calculated (Table III). The human plasma protein binding of etofibrate is 96.89 ± 0.09% (*SD*) for plasma concentrations in the 0.2- to 80-μg/ml range. The human plasma protein binding of clofibrate is 98.23 ± 0.18% (*SD*) for plasma concentrations in the 14- to 108-μg/ml range.

REFERENCES

(1) S. C. Grundy, E. H. Ahrens, G. Scalen, P. H. Schreibman, and P. J. Nestel, *J. Lipid Res.*, **13**, 531 (1972).

(2) B. J. Kudchodkar, H. S. Sodhi, L. Horlick, and D. T. Mason, *Clin. Pharmacol. Ther.*, **24**, 354 (1978).

(3) J. Schneider and H. Kaffarnik, *Fortschr. Med.*, **94**, 785 (1976).

(4) H. Kaffarnik, J. Schneider, and W. Haase, *Dtsch. Med. Wochenschr.*, **100**, 2486 (1975).

(5) W. Sterner and A. Schultz, *Arzneim.-Forsch. (Drug Res.)*, **24**, 1990 (1974).

(6) M. Kummer, W. Schatton, H. Linde, and H. Oelschlaeger, *Pharm. Ztg.*, **124**, 1312 (1979).

(7) E. R. Garrett and M. R. Gardner, *J. Pharm. Sci.*, **71**, 14 (1982).

(8) H. Oelschlaeger, D. Rothley, M. Ewert, and P. Nachev, *Arzneim.-Forsch. (Drug Res.)*, **30**, 984 (1980).

(9) E. R. Garrett, *J. Am. Chem. Soc.*, **80**, 4049 (1958).

(10) E. R. Garrett, J. Brès, and K. Schnelle, *J. Pharmacokinet. Biopharm.*, **2(1)**, 43 (1974).

(11) E. R. Garrett and T. Gürkan, *J. Pharm. Sci.*, **68**, 26 (1979).

(12) E. R. Garrett and H. J. Lambert, *J. Pharm. Sci.*, **62**, 550 (1973).

(13) M. C. Meyer and D. E. Guttman, *J. Pharm. Sci.*, **57**, 895 (1968).

(14) E. R. Garrett and C. A. Hunt, *J. Pharm. Sci.*, **63**, 1056 (1974).

(15) E. R. Garrett, H. Roseboom, J. R. Green Jr., and W. Schuermann, *Int. J. Clin. Pharmacol.*, **16**, 193 (1978).

(16) H. Derendorf and E. R. Garrett, *J. Pharm. Sci.*, **72**, 630 (1983).

ACKNOWLEDGMENT

Supported in part by a grant from Merz and Co., Frankfurt (Main), West Germany.

Pharmacokinetic Model for Diazepam and its Major Metabolite Desmethyldiazepam Following Diazepam Administration

M. L. JACK and W. A. COLBURN ˣ

Received April 22, 1982, from the *Department of Pharmacokinetics and Biopharmaceutics, Hoffmann-La Roche Inc., Nutley, NJ 07110.* Accepted for publication September 29, 1982.

Abstract □ A five-compartment open model was used to simulate the blood concentration profiles of diazepam and its metabolite, desmethyldiazepam, following single- and multiple-dose administrations of diazepam. The parameter estimates for diazepam were previously reported literature values. The parameter estimates for the metabolite were calculated from literature values of blood concentrations of desmethyldiazepam following the administration of clorazepate. The five-compartment open model suggests that ~50% of the administered diazepam is biotransformed to desmethyldiazepam, and that the elimination profile of the metabolite is not altered by the presence of the drug. The model may also be readily adapted to predict the concentrations of diazepam and desmethyldiazepam in cerebrospinal fluid following the administration of diazepam by simply correcting the blood or plasma concentrations of the drug and metabolite for the degree of plasma protein binding.

Keyphrases □ Diazepam—desmethyldiazepam, pharmacokinetics, single- and multiple-dose administrations, five-compartment open model, blood, CSF □ Desmethyldiazepam—diazepam, pharmacokinetics, single- and multiple-dose administrations, five-compartment open model, blood, CSF □ Pharmacokinetics—diazepam, desmethyldiazepam, single- and multiple-dose administrations, five-compartment open model, blood, CSF

Diazepam (7-chloro-1,3-dihydro-1-methyl-5-phenyl-2*H*-1,4-benzodiazepin-2-one) is effective in the symptomatic relief of tension and anxiety, as well as for the relief of skeletal muscle spasms (1–5). Desmethyldiazepam, the major metabolite of diazepam, is the pharmacologically active metabolite of the prodrugs clorazepate and prazepam, which are also used as anxiolytic agents (6–8).

Diazepam pharmacokinetics have been described previously by a three-compartment model by Kaplan *et al.* (6) and Moolenaar *et al.* (9). Several investigators have described the pharmacokinetic profile of desmethyldiazepam following oral administration of the prodrug clorazepate in terms of a two-compartment open model (8, 10–12). The present report combines the three-compartment open model for diazepam and the two-compartment open model for desmethyldiazepam to define the pharmacokinetic profiles of diazepam and its metabolite following single- and multiple-dose administrations of the drug.

EXPERIMENTAL

Clinical Protocol—The data used in this study were previously reported by Kaplan *et al.* (study A) (6). Briefly, four healthy male volunteers, ages 25–43, each received single 10-mg doses of diazepam administered intravenously and orally 1 week apart. Commencing 1 week thereafter, each subject received a 10-mg oral dose of the drug every 24 hr for 15 days. The subjects were fasted for 7 hr prior to receiving the single-dose administrations, and food was withheld for 1 hr postadministration.

Blood specimens were obtained 1, 2.5, 5, 10, 20, 30, and 45 min and at 1, 1.5, 2, 3, 4, 6, 8, 12, 24, 30, and 48 hr following intravenous administration, and at 0.25, 0.5, 0.75, 1, 1.5, 2, 3, 4, 6, 8, 12, 24, 30, and 48 hr following the single-dose oral administration. Following chronic administration, blood samples were obtained 0 (predose), 0.5, 1, 2, 4, and 24 hr postadministration on day 1; 1, 2, and 24 hr postadministration on days 2–11; 1 and 2 hr postadministration on day 12 and at 0 (predose), 1, 2, 4, 6, 8, 12, 24, 30, 36, 48, 72, 96, 120, 144, 168, 192, and 216 hr postadministration on day 15.

Analytical Method—Blood specimens were analyzed for diazepam and desmethyldiazepam by the electron-capture GLC procedure of de Silva and Puglisi (13), with a sensitivity of 10 and 20 ng/ml, respectively, for each component using a 1-ml specimen.

Pharmacokinetic Model—The five-compartment open model used to describe the pharmacokinetic profiles of diazepam and its major me-

0022-3549/83/1100-1318$01.00/0

Table I—Pharmacokinetic Parameters Obtained Following the Single-Dose Administration of 15 mg of Clorazepate Dipotassium to Six Normal Subjects

Parameter	Study B[a]				Study C[b]		Mean ± SD[c]
	1	2	3	4	1	2	
A, ng/ml	177.9	446.7	236.1	962.8	800.8	130.1	459.1 ± 349
α, hr^{-1}	1.13	0.56	1.32	1.42	1.11	0.60	1.02 ± 0.36
B, ng/ml	85.0	79.2	116.7	92.6	65.3	72.4	85.2 ± 181
β, hr^{-1}	0.017	0.010	0.017	0.016	0.013	0.014	0.015 ± 0.003
K_a, hr^{-1}	3.4	0.71	3.6	1.84	1.58	3.43	2.43 ± 1.21
V_{cDD}, l	48.7	58.6	37.3	40.8	33.1	55.3	45.6 ± 10.2
K_{12}, hr^{-1}	0.628	0.287	0.710	0.952	0.819	0.333	0.622 ± 0.265
K_{21}, hr^{-1}	0.480	0.259	0.583	0.430	0.250	0.251	0.376 ± 0.143
K_{Mel}, hr^{-1}	0.041	0.023	0.039	0.054	0.056	0.033	0.041 ± 0.013

[a] Taken from Ref. 7. [b] Taken from Ref. 15. [c] Mean values used as estimates in the pharmacokinetic model.

tabolite, desmethyldiazepam, is presented in Fig. 1. Equations for the blood concentration–time profiles of drug and metabolite were derived by the method of Kaplan *et al.* (14). The pharmacokinetic parameters previously reported in study A were used as the estimates for diazepam (6). Desmethyldiazepam blood concentration–time data following administration of clorazepate, previously reported by Abruzzo *et al.* (study B) (7) and Brooks *et al.* (study C) (15) were fitted using NONLIN (16) to obtain parameter estimates for the metabolite disposition (Table I). The parameters K_{21} and K_{12} in Table I are identical to K_{54} and K_{45} in the present model.

Parameter estimates for K_{14}, the rate of formation of the metabolite following diazepam administration, had not been previously reported in the literature. Initial estimates of K_{14} were obtained based on the fraction (f_m) of diazepam metabolized to desmethyldiazepam calculated both following single-dose and chronic-dose administrations of the drug. To estimate the amount of diazepam biotransformed to desmethyldiazepam following single-dose intravenous and oral administrations, the mean area under the blood concentration–time curve from time 0 to infinity ($AUC_{0\to\infty}$ for desmethyldiazepam in four subjects (Study A) were calculated (Table II). The AUC were determined using the trapezoidal-rule for the blood concentration–time curve from 0 to 48 hr postadministration. The area from 48 hr to infinity was then calculated by dividing the last observed blood concentrations of the metabolite by the overall elimination rate constant (β) for desmethyldiazepam, which was determined following chronic administration of diazepam in the same subjects (6). The mean $AUC_{0\to\infty}$ for desmethyldiazepam following single-dose oral administration of 15 mg of clorazepate (studies B and C), which was used as a standard area representing 10 mg of systemically available metabolite are presented in Table II. The ratio of the desmethyldiazepam $AUC_{0\to\infty}$ for each subject in study A, divided by the mean $AUC_{0\to\infty}$ for the six subjects in studies B and C were used to estimate the fraction (f_m) of diazepam metabolized to desmethyldiazepam in study A. K_{14} is then calculated by multiplying the total elimination rate (K_{TOT}) of the drug by the estimated fraction (f_m) metabolized. K_{TOT} was previously reported as K_{el} in study A (6). K_{14} and the fraction (f_m) of diazepam metabolized to desmethyldiazepam for the four subjects in study A based on the single-dose administration of the drug are reported in Table II.

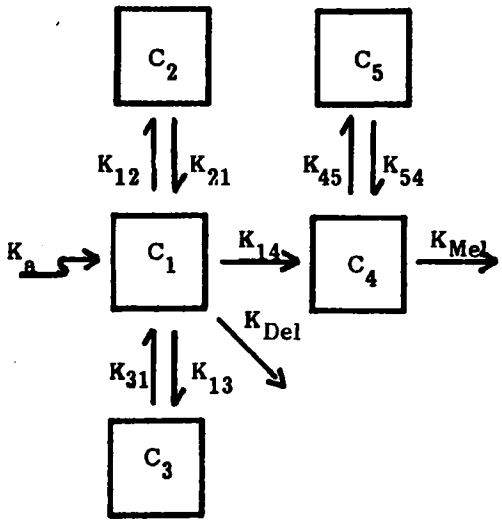

Figure 1—*Five-compartment open pharmacokinetic model used to describe the physiological disposition characteristics of diazepam and its metabolite, desmethyldiazepam.* C_1, C_2, *and* C_3 *are the concentrations of diazepam in the respective compartments;* C_4 *and* C_5 *are the concentrations of desmethyldiazepam in the respective compartments.* K_a *is the first-order absorption rate constant of diazepam;* K_{12}, K_{21}, K_{13}, K_{31}, K_{45}, *and* K_{54} *are the transfer coefficients between compartments;* K_{TOT} *is the total elimination rate of diazepam;* K_{14} *is the rate of metabolism of diazepam to desmethyldiazepam;* K_{Mel} *is the elimination rate of desmethyldiazepam; and* K_{Del} *is the rate of elimination of diazepam via pathways other than metabolism to desmethyldiazepam,* $K_{TOT} = (K_{14} + K_{Del})$.

The pharmacokinetic parameters for diazepam and its metabolite at steady state may also be used to estimate K_{14} and the fraction (f_m) of the drug metabolized to desmethyldiazepam. The differential equations describing the rate of change of desmethyldiazepam concentrations in the central (C_4) and peripheral (C_5) compartments, respectively, following the administration of diazepam based on Fig. 1 may be expressed as:

$$\frac{dC_4}{dt} = C_1K_{14} + K_{54}C_5 - (K_{45} + K_{Mel})C_4 \qquad \text{(Eq. 1)}$$

$$\frac{dC_5}{dt} = C_4K_{45} - C_5K_{54} \qquad \text{(Eq. 2)}$$

At steady state, both dC_4/dt and dC_5/dt equal zero and, based on Eq. 2, C_4K_{45} is equal to C_5K_{54}. Substituting for C_5K_{54} in Eq. 1, C_1K_{14} is then equal to $\overline{C}_4^{ss}K_{Mel}$ at steady state. The conversion of steady-state concentrations of diazepam and desmethyldiazepam to amounts is obtained by multiplying the concentrations by the volume of their respective compartments. Therefore, K_{14} may be expressed as:

$$K_{14} = \frac{\overline{C}_4^{ss} \cdot K_{Mel} \cdot V_{cDD}}{\overline{C}_1^{ss} \cdot V_{cD}} \qquad \text{(Eq. 3)}$$

where V_{cD} and V_{cDD} are the volumes of compartments 1 and 4, and $\overline{C}_4^{ss}$ and $\overline{C}_1^{ss}$ are the steady-state concentrations in compartments 1 and 4 respectively. V_{cD} was previously reported for each subject in study A, and the mean V_{cDD} and K_{Mel} for desmethyldiazepam (Table I) were used in Eq. 3. The average of the mean steady-state blood concentration ($\overline{C}_1^{ss}$) and $\overline{C}_4^{ss}$ from study A (for the drug and metabolite, respectively) following once daily chronic administration of diazepam are reported in Table III. The blood concentrations on days 8–12 and 15 were used to calculate the average of the mean $\overline{C}_1^{ss}$ for diazepam, and blood concentrations on days 11, 12, and 15 were used to determine the average of the mean $\overline{C}_4^{ss}$ for

Table II—Area ($AUC_{0\to\infty}$) Under the Blood Concentration–Time Curves of Desmethyldiazepam Following the Administration of 10 mg of Diazepam [a] or 15 mg of Clorazepate Dipotassium [b] to Normal Subjects

Subject	Studies		f_m[c]	K_{14}[d]
	A	B and C		
1	3864	5014	0.64	0.07
2	3076	7643	0.51	0.12
3	3272	6782	0.55	0.04
4	4015	5720	0.67	0.09
5	—	5350	—	—
6	—	5501	—	—
Mean ±SD		6003 ±1003		

[a] Study A; taken from Ref. 6. [b] Studies B and C; taken from Refs. 7 and 15, respectively. [c] f_m = $AUC_{0\to\infty}$ (study I)/$AUC_{0\to\infty}$ (mean). [d] $K_{14} = K_{TOT}$-f_m; K_{TOT} is reported for each subject in Ref. 6.

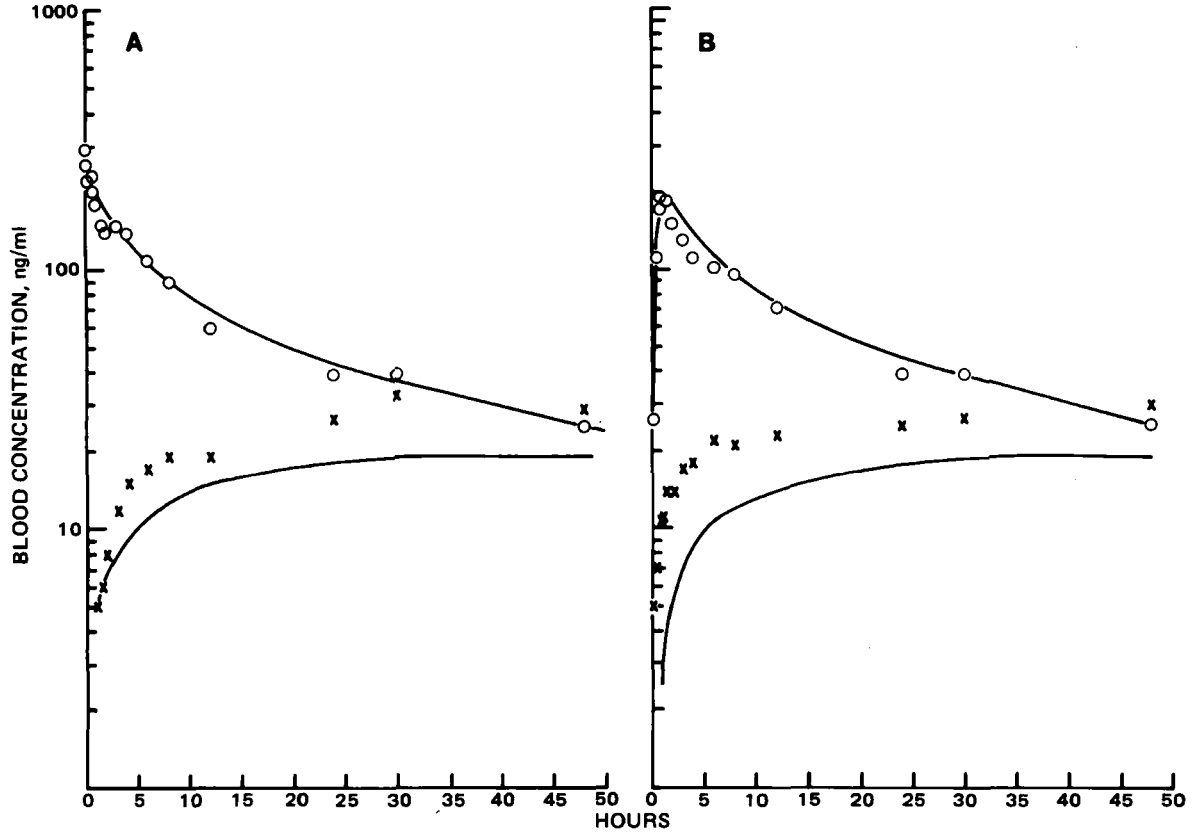

Figure 2—*Blood concentration–time profiles of diazepam (○) and desmethyldiazepam (×) following 10-mg intravenous (A) and oral (B) administrations of diazepam to a normal subject (solid lines represent simulated diazepam and desmethyldiazepam blood concentration–time profiles).*

desmethyldiazepam. The resulting K_{14} values calculated using Eq. 3 are reported in Table III. The fraction (f_m) is then calculated by:

$$f_m = \frac{K_{14}}{K_{TOT}} \qquad \text{(Eq. 4)}$$

where K_{TOT} was previously reported as K_{e1} in study A (6).

The mean K_{14} values from Tables II and III for each subject were used as initial parameter estimates for the pharmacokinetic model in Fig. 1. The blood concentration–time data for diazepam and desmethyldiazepam following single-dose intravenous and oral, and chronic oral administrations were then simulated using the initial parameter estimates previously described.

RESULTS AND DISCUSSION

Model for Blood Concentration–Time Data—The simulated and experimental blood concentration–time profiles of diazepam and desmethyldiazepam following single intravenous and oral doses in one subject are presented in Fig. 2. The corresponding simulated and experimental drug and metabolite blood concentrations following the chronic oral administration of diazepam are presented for the same subject in Fig. 3.

Support for the proposed model required coincidence of simulated and experimental blood concentration–time profiles for diazepam and its metabolite following single-dose intravenous and oral, and chronic oral administrations of the drug to normal subjects. Good agreement was observed between experimental data points and the simulated blood concentration of diazepam in the four subjects from study A. The desmethyldiazepam blood concentrations following chronic dosing were in good agreement with the simulated blood concentrations as shown in Fig. 3B. The simulated blood concentrations of the metabolite following single-dose administration of diazepam are lower than the observed blood concentrations. Such findings may reflect intersubject variability and/or residual amounts of desmethyldiazepam from a previous dose due to the 1-week washout period between doses and the half-life of the metabolite. These findings indicate that the five-compartment open model for diazepam and desmethyldiazepam adequately describe the pharmacokinetic profiles of the drug and its metabolite following diazepam administration. Since the same parameter estimates sufficiently described both the single-dose and chronic-dose blood–concentration time profiles of diazepam and desmethyldiazepam, it may be concluded that there was no enzyme induction or inhibition of the drug in this study.

The pharmacokinetic profiles of diazepam and its metabolite following administration of diazepam and profiles of desmethyldiazepam following administration of its prodrugs have been reported by numerous investigators. However, there are no studies in the literature comparing the pharmacokinetic profiles of desmethyldiazepam when formed as a metabolite of diazepam or as a metabolite of clorazepate in the same subjects. In determining the pharmacokinetic profile of the metabolite following clorazepate administration, it was assumed that clorazepate, at normal GI pH, is completely hydrolyzed to desmethyldiazepam, and that the resulting desmethyldiazepam was completely absorbed (10). Therefore,

Table III—Pharmacokinetic Parameters Resulting from the Five-Compartment Model in Four Subjects From Study A [a]

Subject	$\bar{C}_1^{ss}$, μg/ml	$\bar{C}_4^{ss}$, μg/ml	V_{cD}	V_{cDD} [b]	K_{Mel}, hr^{-1}	K_{14}, hr^{-1}	f_m
1	0.17	0.15	29.8	45.6	0.041	0.06	0.50
2	0.14	0.11	17.4	45.6	0.041	0.08	0.37
3	0.17	0.12	32.6	45.6	0.041	0.04	0.47
4	0.16	0.12	20.0	45.6	0.041	0.07	0.51

[a] Study A is from Ref. 6, Headings refer to the mean steady-state concentrations of diazepam ($\bar{C}_1^{ss}$) and desmethyldiazepam ($\bar{C}_4^{ss}$), volumes of compartments 1 (V_{cD}) and 4 (V_{cDD}), elimination rate of desmethyldiazepam (K_{Mel}, mean values from Table I), formation rate of desmethyldiazepam (K_{14}, calculated using Eq. 3), and the fraction (f_m, K_{14}/K_{TOT}) of diazepam metabolized to desmethyldiazepam.

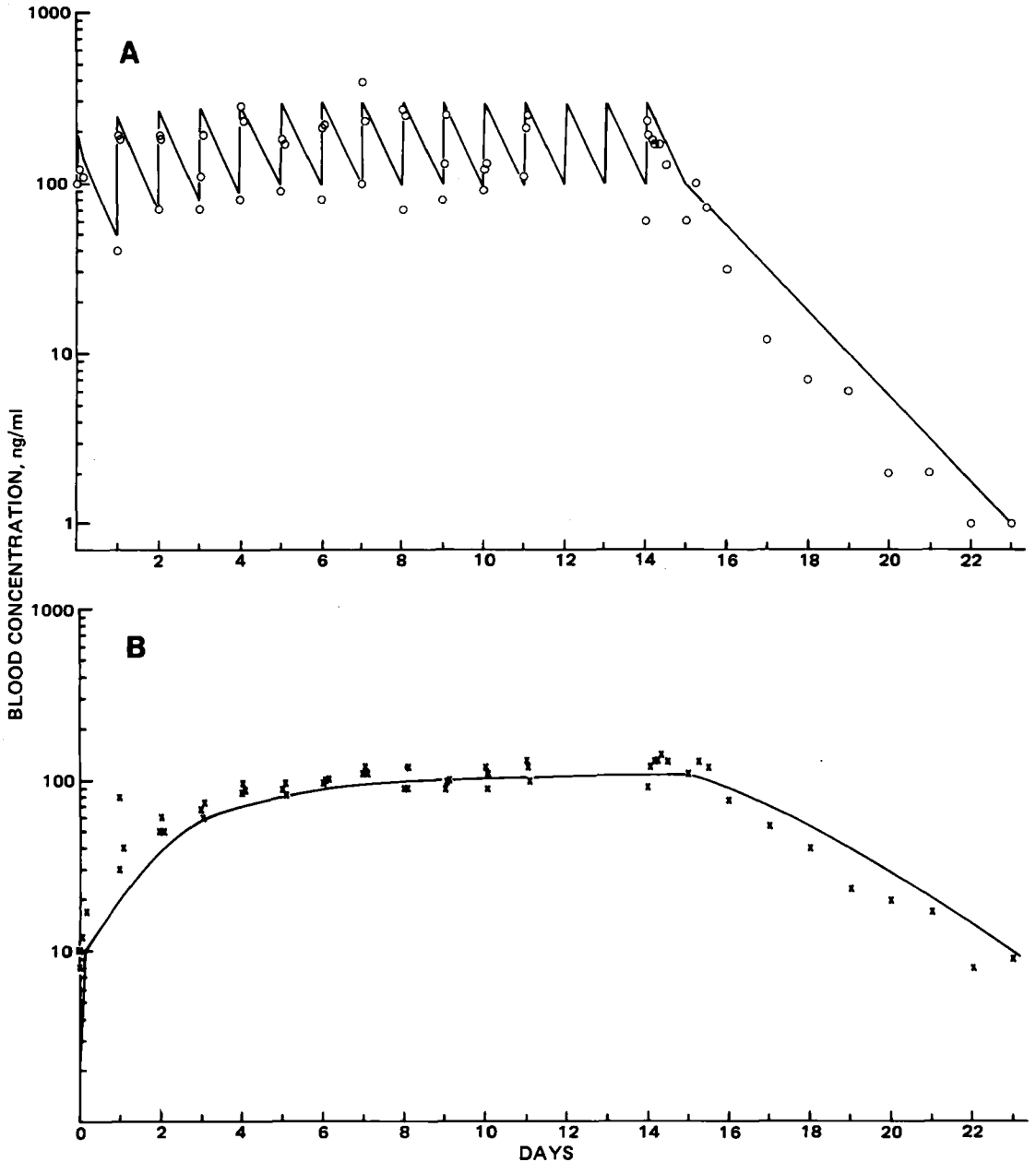

Figure 3—*Blood concentration–time profile of diazepam (A) and desmethyldiazepam (B) following once daily oral administration of 10 mg of diazepam for 15 days to a normal subject (solid lines represent simulated diazepam and desmethyldiazepam blood concentration–time profiles).*

the mean values of the desmethyldiazepam pharmacokinetic parameters following the administration of clorazepate to a normal subject population were used as parameter estimates.

Based on the initial estimates of the metabolite pharmacokinetic parameters, following clorazepate administration, the fraction (f_m) of diazepam metabolized to desmethyldiazepam was estimated to be ~0.5 by two different methods. Similar results were reported by Dasberg (17) following the chronic administration of 5 mg of diazepam and desmethyldiazepam to the same subjects in a double-blind, cross-over study. Similar results were also obtained in the cat following single-dose administration of both the drug and metabolite (18).

Model Adapted for Cerebrospinal Fluid Concentration–Time Data—This five-compartment open model may be readily adapted to predict the concentrations of diazepam and desmethyldiazepam in cerebrospinal fluid (CSF) following the administration of diazepam. Greenblatt *et al.* (19), Hallstrom *et al.* (20), Kanto *et al.* (21), and Hendel (22) have shown that the concentrations of the drug and its metabolite in CSF are in equilibrium with the unbound plasma concentrations of these compounds for the time course of the plasma concentration profile. Therefore by correcting the plasma concentrations of diazepam for protein binding, the CSF concentrations, which are presumed to reflect drug concentrations at the site of action, may be predicted.

Following single-dose administration, the concentrations of diazepam and desmethyldiazepam in CSF were simulated and are shown in Fig. 4. The model indicates that the concentration of the drug is greater than the concentration of the metabolite in CSF for the first 24 hr postadministration, suggesting that the clinical effects observed following a single-dose administration of diazepam must be attributed primarily to

Table IV—Observed and Calculated CSF Concentrations (ng/ml) of Diazepam and Desmethyldiazepam in Five Patients Following Long-Term Diazepam Therapy

Subject	Observed		Calculated
	Diazepam	Desmethyldiazepam	Desmethyldiazepam
1	22	56	55
2	30	49	75
3	14	39	35
4	21	42	50
5	28	68	70

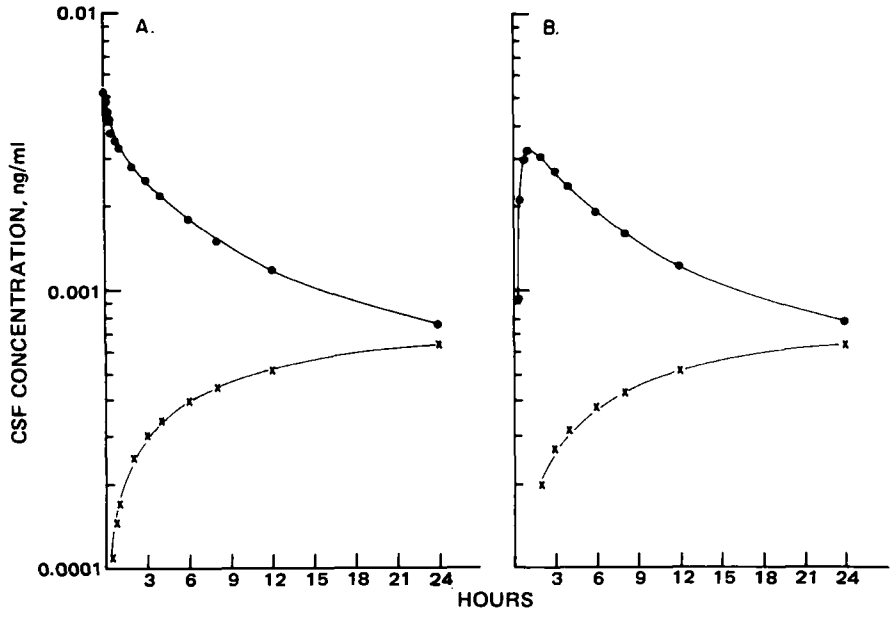

Figure 4—*Simulated CSF concentration–time profiles of diazepam (●) and desmethyldiazepam (×) following single-dose 10-mg intravenous (A) and oral (B) administrations of diazepam to a normal subject.*

diazepam and not desmethyldiazepam. Following chronic administration, the concentration of the metabolite in CSF at steady state will be equivalent to or greater than the concentration of the drug in CSF (Fig. 5). Therefore, at steady state the desmethyldiazepam will contribute significantly to the pharmacological activity observed following chronic administration of diazepam.

Hendel has reported that desmethyldiazepam accumulates in the CSF of patients treated with diazepam for several months (22). However, the metabolite CSF concentrations were calculated using the five-compartment model with the reported drug CSF concentrations in these patients corrected by the factor 2.52 (Table IV). This factor is the result of the product of 1.26 and 2; 1.26 is the relative accumulation factor for desmethyldiazepam with respect to diazepam in plasma at steady state as reported by Greenblatt *et al.* (23), and 2 is the difference in desmethyldiazepam free fraction compared with diazepam free fraction (24). The calculated CSF concentrations of metabolite at steady state are in good agreement with the observed CSF concentrations, suggesting that accumulation of this metabolite following chronic administration of diazepam is predictable.

CONCLUSION

A five-compartment open model describing the pharmacokinetic profile of diazepam and its metabolite, desmethyldiazepam, following the administration of diazepam has been developed. The pharmacokinetic parameters for desmethyldiazepam obtained following the oral administration of clorazepate adequately described the pharmacokinetics of this metabolite following diazepam administration. The parameter estimates and model simulations suggest that ~50% of the administered diazepam dose is metabolized to desmethyldiazepam. This finding suggests that the formation rate for the metabolite is approximately one-half of the total elimination rate for the drug; *i.e.*, $K_{14} = 0.06\ hr^{-1}$ whereas $K_{TOT} = 0.12\ hr^{-1}$. Overall, the single-dose pharmacokinetic parameters of diazepam following its administration and the single-dose

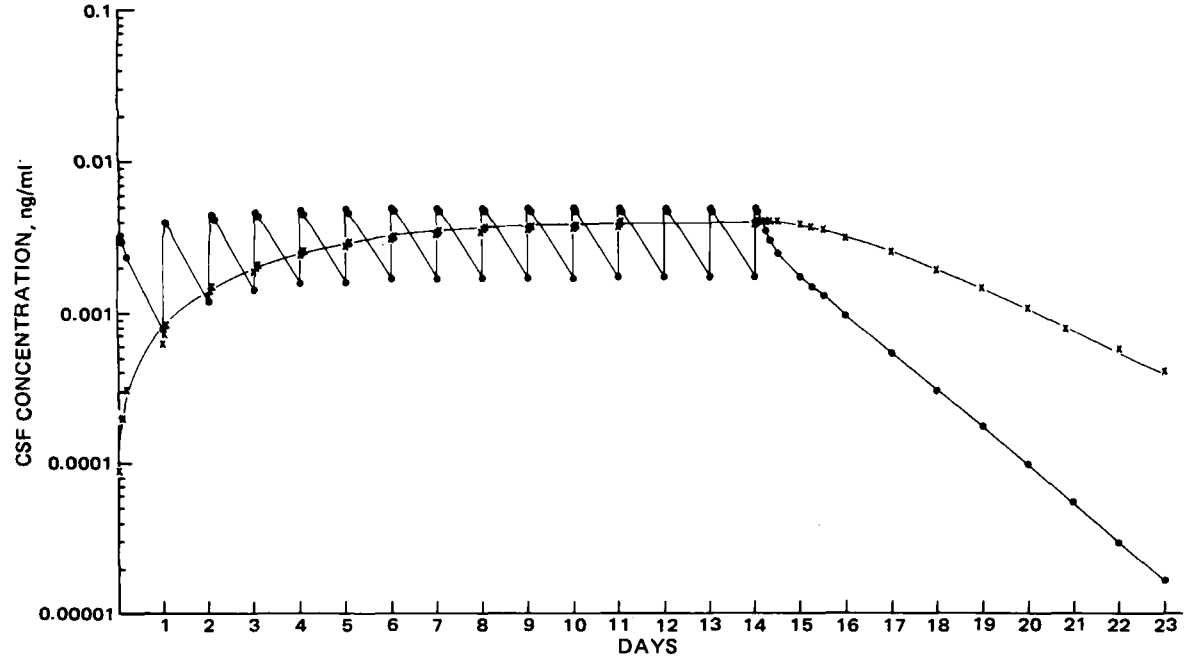

Figure 5—*Simulated CSF concentration–time profiles of diazepam (●) and desmethyldiazepam (×) following once daily chronic oral administration of 10 mg of diazepam for 15 days to a normal subject.*

pharmacokinetics of desmethyldiazepam following the administration of clorazepate can be used to describe the blood concentration–time profiles of diazepam and desmethyldiazepam following both single-dose and chronic administration of the drug, suggesting that there is no enzyme induction or inhibition of diazepam metabolism following multiple-dose administration. This model has also been adapted to predict the concentrations of diazepam and desmethyldiazepam in CSF following the administration of diazepam.

REFERENCES

(1) L. O. Randall, G. A. Heise, W. Schallek, R. E. Bagdon, R. Banziger, A. Boris, R. A. Moe, and W. B. Abrams, *Curr. Ther. Res. Clin. Exp.*, **3**, 405 (1961).

(2) F. P. Pignataro, *Curr. Ther. Res. Clin. Exp.*, **4**, 389 (1963).

(3) A. Di Francesco, *Am. J. Psychiat.*, **119**, 989 (1963).

(4) H. M. Beerman, *Am. J. Psychiat.*, **120**, 870 (1964).

(5) R. A. Katz, J. H. Aldes, and M. Rector, *J. Neuropsychiat.*, Suppl. 3, S91 (1962).

(6) S. A. Kaplan, M. L. Jack, K. Alexander, and R. E. Weinfeld, *J. Pharm. Sci.*, **62**, 1789 (1973).

(7) C. W. Abruzzo, T. Macasieb, R. E. Weinfeld, J. A. Rider, and S. A. Kaplan, *J. Pharmacokinet. Biopharm.*, **5**, 377 (1977).

(8) D. J. Greenblatt, *J. Pharm. Sci.*, **67**, 427 (1978).

(9) F. Moolenaar, S. Bakker, J. Visser, and T. Huizinga, *Int. J. Pharm.*, **5**, 127 (1980).

(10) A. J. Wilensky, R. H. Levy, A. S. Troupin, L. Noretti-Ojemann, and P. Friel, *Clin. Pharmacol. Ther.*, **24**, 22 (1978).

(11) P. J. Carrigan, G. C. Chao, W. M. Barker, D. J. Hoffman, and A. H. C. Chun, *J. Clin. Pharmacol.*, **17**, 18 (1977).

(12) A. H. C. Chun, P. J. Carrigan, D. J. Hoffman, R. P. Kershner, and J. D. Stuart, *Clin. Pharmacol. Ther.*, **22**, 329 (1977).

(13) J. A. F. de Silva and C. V. Puglisi, *Annal. Chem.*, **42**, 1725 (1970).

(14) S. A. Kaplan, M. Lewis, M. A. Schwartz, E. Postma, S. Cotler, C. W. Abruzzo, T. L. Lee, and R. E. Weinfeld, *J. Pharm. Sci.*, **59**, 1569 (1970).

(15) M. A. Brooks, M. R. Hackman, R. E. Weinfeld, and T. Macasieb, *J. Chromatogr.*, **135**, 123 (1977).

(16) C. M. Metzler, G. L. Elfring, and A. J. Mc Ewen, *Biometrics*, **30**, 562 (1974).

(17) H. M. Dasberg, *Psychopharmacologia*, **43**, 191 (1975).

(18) S. Cotler, J. Gustafson, and W. A. Colburn, *J. Pharm. Sci.*, in press.

(19) D. J. Greenblatt, H. R. Ochs, and B. L. Lloyd, *Psychopharmacology*, **70**, 89 (1980).

(20) C. Hallstrom, M. H. Lader, and S. H. Curry, *Br. J. Clin. Pharmacol.*, **9**, 333 (1980).

(21) J. Kanto, L. Kangas, and T. Siirtola, *Acta. Pharmacol. Toxicol.*, **36**, 328 (1975).

(22) J. Hendel, *Acta Pharmacol. Toxicol.*, **37**, 17 (1975).

(23) D. J. Greenblatt, T. P. Laughren, M. D. Allen, J. S. Harmatz, and R. I. Shader, *Br. J. Clin. Pharmacol.*, **11**, 35 (1981).

(24) M. D. Allen and D. J. Greenblatt, *J. Clin. Pharmacol.*, **20**, 639 (1980).

In Vivo Release of Norethindrone Coupled to a Biodegradable Poly(α-amino acid) Drug Delivery System

M. A. ZUPON *, S. M. FANG ˣ, J. M. CHRISTENSEN ‡, and R. V. PETERSEN

Received November 23, 1981, from the *Department of Pharmaceutics, College of Pharmacy, University of Utah, Salt Lake City, UT 84112.* Accepted for publication October 5, 1982. Present addresses: *Division of Product Development, Schering-Plough Corp., Bloomfield, NJ 07003 and ‡School of Pharmacy, Oregon State University, Corvallis, OR 97331.

Abstract □ The *in vivo* release of norethindrone from a biodegradable steroid–polymer conjugate was studied in rats. The drug–polymer conjugate, consisting of [^{3}H]norethindrone coupled *via* a 17-carbonate bond to poly-N^5-(3-hydroxypropyl)-L-glutamine was administered to female rats by subcutaneous injection. The *in vivo* release of steroid, determined by measuring the daily radioactivity output in urine and feces, was fairly constant though it showed a gradual decrease during the 9-month study period. The data indicate that this biodegradable norethindrone–polymer conjugate is a potential candidate for the controlled delivery of norethindrone to effect long-term contraception.

Keyphrases □ Norethindrone—sustained release, biodegradable steroid–polymer conjugate, *in vivo* release rate □ Delivery systems—sustained release of norethindrone, biodegradable steroid–polymer conjugate, *in vivo* release rate □ Contraceptives—norethindrone, sustained release, biodegradable steroid–polymer conjugate, *in vivo* release rate

Although controlled release of drugs at uniform predictable rates from various drug dosage forms has been an object of considerable research for many years, the use of synthetic polymeric materials in the design of controlled-release devices is of recent origin. Of major interest has been the incorporation of contraceptive progestins into various polymers to form controlled, sustained-release drug delivery systems. The use of monolithic devices of poly(dimethylsiloxane) with progestins has been the subject of numerous reports (1–8). These devices, however, have the disadvantage of requiring implantation and removal. Furthermore, significant foreign-body reactions were observed in tissues surrounding these implants, which may be the cause of difficulty in achieving prolonged, constant release of progestins from these devices. Alternatively, the "Uterine Progesterone System" has been the subject of several studies (9–11). The safety and effectiveness of this device has been well established (9, 10, 12). Hydrogel polymers, *e.g.*, poly(hydroxyethyl methacrylate), have also been used to prepare sustained-release devices for progestins (13, 14) with favorable results.

Recently, biodegradable polymers as carriers for controlled, sustained release of various drugs have been evaluated. These polymers are synthesized from monomers which are composed of normal body constituents or which exhibit good compatibility with the body physiology. Various biodegradable polymers have been prepared for the controlled release of contraceptive steroids (15–19). The materials employed for these studies are poly(lactic acid) (15, 16), glutamic acid–leucine copolymer (17), and polyesters of homo- or copolymers of glycolide, DL-lactide, ϵ-caprolactone, or DL-ϵ-decalactone (18). Studies on the *in vitro* and *in vivo* hydrolysis of homopolymers of δ-benzyl-L-glutamate have been reported (20, 21). The

0022-3549/83/1100-1323$01.00/0

pharmacokinetics of desmethyldiazepam following the administration of clorazepate can be used to describe the blood concentration–time profiles of diazepam and desmethyldiazepam following both single-dose and chronic administration of the drug, suggesting that there is no enzyme induction or inhibition of diazepam metabolism following multiple-dose administration. This model has also been adapted to predict the concentrations of diazepam and desmethyldiazepam in CSF following the administration of diazepam.

REFERENCES

(1) L. O. Randall, G. A. Heise, W. Schallek, R. E. Bagdon, R. Banziger, A. Boris, R. A. Moe, and W. B. Abrams, *Curr. Ther. Res. Clin. Exp.*, **3**, 405 (1961).

(2) F. P. Pignataro, *Curr. Ther. Res. Clin. Exp.*, **4**, 389 (1963).

(3) A. Di Francesco, *Am. J. Psychiat.*, **119**, 989 (1963).

(4) H. M. Beerman, *Am. J. Psychiat.*, **120**, 870 (1964).

(5) R. A. Katz, J. H. Aldes, and M. Rector, *J. Neuropsychiat.*, Suppl. 3, S91 (1962).

(6) S. A. Kaplan, M. L. Jack, K. Alexander, and R. E. Weinfeld, *J. Pharm. Sci.*, **62**, 1789 (1973).

(7) C. W. Abruzzo, T. Macasieb, R. E. Weinfeld, J. A. Rider, and S. A. Kaplan, *J. Pharmacokinet. Biopharm.*, **5**, 377 (1977).

(8) D. J. Greenblatt, *J. Pharm. Sci.*, **67**, 427 (1978).

(9) F. Moolenaar, S. Bakker, J. Visser, and T. Huizinga, *Int. J. Pharm.*, **5**, 127 (1980).

(10) A. J. Wilensky, R. H. Levy, A. S. Troupin, L. Noretti-Ojemann, and P. Friel, *Clin. Pharmacol. Ther.*, **24**, 22 (1978).

(11) P. J. Carrigan, G. C. Chao, W. M. Barker, D. J. Hoffman, and A. H. C. Chun, *J. Clin. Pharmacol.*, **17**, 18 (1977).

(12) A. H. C. Chun, P. J. Carrigan, D. J. Hoffman, R. P. Kershner, and J. D. Stuart, *Clin. Pharmacol. Ther.*, **22**, 329 (1977).

(13) J. A. F. de Silva and C. V. Puglisi, *Annal. Chem.*, **42**, 1725 (1970).

(14) S. A. Kaplan, M. Lewis, M. A. Schwartz, E. Postma, S. Cotler, C. W. Abruzzo, T. L. Lee, and R. E. Weinfeld, *J. Pharm. Sci.*, **59**, 1569 (1970).

(15) M. A. Brooks, M. R. Hackman, R. E. Weinfeld, and T. Macasieb, *J. Chromatogr.*, **135**, 123 (1977).

(16) C. M. Metzler, G. L. Elfring, and A. J. Mc Ewen, *Biometrics*, **30**, 562 (1974).

(17) H. M. Dasberg, *Psychopharmacologia*, **43**, 191 (1975).

(18) S. Cotler, J. Gustafson, and W. A. Colburn, *J. Pharm. Sci.*, in press.

(19) D. J. Greenblatt, H. R. Ochs, and B. L. Lloyd, *Psychopharmacology*, **70**, 89 (1980).

(20) C. Hallstrom, M. H. Lader, and S. H. Curry, *Br. J. Clin. Pharmacol.*, **9**, 333 (1980).

(21) J. Kanto, L. Kangas, and T. Siirtola, *Acta. Pharmacol. Toxicol.*, **36**, 328 (1975).

(22) J. Hendel, *Acta Pharmacol. Toxicol.*, **37**, 17 (1975).

(23) D. J. Greenblatt, T. P. Laughren, M. D. Allen, J. S. Harmatz, and R. I. Shader, *Br. J. Clin. Pharmacol.*, **11**, 35 (1981).

(24) M. D. Allen and D. J. Greenblatt, *J. Clin. Pharmacol.*, **20**, 639 (1980).

In Vivo Release of Norethindrone Coupled to a Biodegradable Poly(α-amino acid) Drug Delivery System

M. A. ZUPON *, S. M. FANG ˣ, J. M. CHRISTENSEN ‡, and R. V. PETERSEN

Received November 23, 1981, from the *Department of Pharmaceutics, College of Pharmacy, University of Utah, Salt Lake City, UT 84112.* Accepted for publication October 5, 1982. Present addresses: *Division of Product Development, Schering-Plough Corp., Bloomfield, NJ 07003 and ‡School of Pharmacy, Oregon State University, Corvallis, OR 97331.

Abstract □ The *in vivo* release of norethindrone from a biodegradable steroid–polymer conjugate was studied in rats. The drug–polymer conjugate, consisting of [^{3}H]norethindrone coupled *via* a 17-carbonate bond to poly-N^5-(3-hydroxypropyl)-L-glutamine was administered to female rats by subcutaneous injection. The *in vivo* release of steroid, determined by measuring the daily radioactivity output in urine and feces, was fairly constant though it showed a gradual decrease during the 9-month study period. The data indicate that this biodegradable norethindrone–polymer conjugate is a potential candidate for the controlled delivery of norethindrone to effect long-term contraception.

Keyphrases □ Norethindrone—sustained release, biodegradable steroid–polymer conjugate, *in vivo* release rate □ Delivery systems—sustained release of norethindrone, biodegradable steroid–polymer conjugate, *in vivo* release rate □ Contraceptives—norethindrone, sustained release, biodegradable steroid–polymer conjugate, *in vivo* release rate

Although controlled release of drugs at uniform predictable rates from various drug dosage forms has been an object of considerable research for many years, the use of synthetic polymeric materials in the design of controlled-release devices is of recent origin. Of major interest has been the incorporation of contraceptive progestins into various polymers to form controlled, sustained-release drug delivery systems. The use of monolithic devices of poly(dimethylsiloxane) with progestins has been the subject of numerous reports (1–8). These devices, however, have the disadvantage of requiring implantation and removal. Furthermore, significant foreign-body reactions were observed in tissues surrounding these implants, which may be the cause of difficulty in achieving prolonged, constant release of progestins from these devices. Alternatively, the "Uterine Progesterone System" has been the subject of several studies (9–11). The safety and effectiveness of this device has been well established (9, 10, 12). Hydrogel polymers, *e.g.*, poly(hydroxyethyl methacrylate), have also been used to prepare sustained-release devices for progestins (13, 14) with favorable results.

Recently, biodegradable polymers as carriers for controlled, sustained release of various drugs have been evaluated. These polymers are synthesized from monomers which are composed of normal body constituents or which exhibit good compatibility with the body physiology. Various biodegradable polymers have been prepared for the controlled release of contraceptive steroids (15–19). The materials employed for these studies are poly(lactic acid) (15, 16), glutamic acid–leucine copolymer (17), and polyesters of homo- or copolymers of glycolide, DL-lactide, ϵ-caprolactone, or DL-ϵ-decalactone (18). Studies on the *in vitro* and *in vivo* hydrolysis of homopolymers of δ-benzyl-L-glutamate have been reported (20, 21). The

0022-3549/83/1100-1323$01.00/0

Table I—Characteristics of Norethindrone–Polymer Conjugate

	Batch A	Batch B
Degree of Norethindrone Coupling	39%	60%
Particle Size	N.D.[a]	100 ± 80 μm
Molecular Weight[b]	N.D.[a]	230,000

[a] Not Determined. [b] The molecular weight of poly-N^5-(3-hydroxypropyl)-L-glutamine. The norethindrone–polymer conjugate does not have enough solubility to render a determination of the molecular weight.

results indicated they could be favorable materials for the sustained release of contraceptive steroids.

In this laboratory, a drug delivery system consisting of norethindrone covalently coupled to poly-N^5-(3-hydroxypropyl)-L-glutamine was recently prepared (22). This drug delivery system should be ideally suited for the controlled release of norethindrone. The polymeric device is biogradable leaving no empty shell for removal at the end of the drug therapy. The hydrolytic product, L-glutamic acid, is a normal body constituent and should show compatibility with the body tissues. Furthermore, the steroid, which is covalently bonded to the biodegradable polymer by a labile bond, may be released in concert with the gradual erosion of the polymer backbone around the surface of the polymer particle. A sustained release of steroid may thus be achieved without the involvement of any diffusion process.

EXPERIMENTAL

Reagents—Tritium-labeled norethindrone and [^{14}C]testosterone obtained for a commercial source[1] were purified by TLC before use. The stability of the tritium atoms in [^{3}H]norethindrone was evaluated by repetitively placing the labeled drug in an ethanol–water (1:1) solution at 25° for 24 hr followed by vacuum distillation of the solution. The extent of exchange between the tritium atoms of the steroid and the hydrogen atoms of the medium was assessed by measuring the radioactivity associated with the distillates. The tritium atoms in [^{3}H]norethindrone were found to be quite stable. Only a negligible amount of radioactivity was found in the distillates: 0.15 and 0.012% in the first and second distillates, respectively.

Polymeric Drug Delivery System—The norethindrone–polymer conjugate consists of norethindrone covalently coupled to poly-N^5-(3-hydroxypropyl)-L-glutamine through the 17-carbonate bond (22):

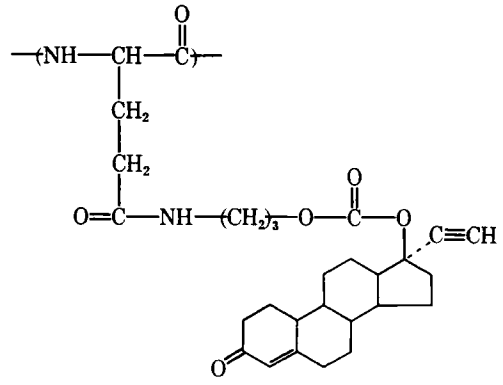

Two batches of the compound (A and B) were obtained (Table I). Batch A was administered to two rats (A_1 and A_2) at doses of 4.9 and 10 mg, respectively, while 10 mg of batch B was administered to each of five rats.

Biological Half-Life of Norethindrone in Rats—Female Sprague–Dawley rats (200–240 g) were anesthetized with sodium pentobarbital (0.3 mg/g of body weight). An ~3-cm incision was made on the abdominal wall to expose the inferior vena cava. A catheter was placed into the inferior vena cava to inject and withdraw samples. Tritium-labeled norethindrone solution (1.88 μg/25 μCi/0.1 ml Ringer's solution) was injected into the vein, and 0.3 ml of blood was withdrawn at 30-min intervals with a syringe previously rinsed with heparin. Each 0.3-ml blood sample was replaced with 0.3 ml of Ringer's solution to restore blood volume. A portion (0.1 ml) of each 0.3-ml blood sample was pipetted into a conical centrifuge tube containing 5 μl each of nonlabeled norethindrone (1×10^{-3} *M*) and testosterone (1×10^{-3} *M*) and a known amount of [^{14}C]testosterone, which served as the internal standard. The blood sample was centrifuged, and the plasma was transferred to another tube. The cellular fraction was extracted four times with 0.3-ml portions of Ringer's solution, which was then combined with the plasma fraction. The above procedures were carried out quickly at 0–4° to prevent any metabolism of the internal standard. The combined plasma fraction was immediately extracted four times with 2-ml aliquots of methylene chloride. The methylene chloride fractions were pooled and evaporated to dryness under a nitrogen stream. The residue, after being dissolved in 100 μl of methanol, was spotted on a silica gel TLC plate. The plate was eluted with a benzene–ethyl acetate solution (4:1), and the spots corresponding to the parent drug and internal standard were isolated and placed into scintillation vials. To each fraction was added 12 ml of a scintillation fluor cocktail[2], and the radioactivity was measured in a scintillation counter[3]. The efficiency of recovery for norethindrone was normalized according to the amount of recovery of the internal standard, [^{14}C]testosterone, from the TLC plate.

The biological half-life of the total radioactivity, which represents the parent drug and all metabolites, was determined by measuring the radioactivity in 0.1-ml aliquots of the blood sample after treatment with 2 ml of a tissue solubilizer[4] and 0.5 ml of benzoyl peroxide solution (12% in toluene).

***In Vivo* Steroid Release Rate Determination**—The tritiated norethindrone–polymer conjugate (10 mg as a fine powder) was placed in 5 ml of sterile Ringer's solution and let stand overnight. The next day, the supernatant was decanted off, and the precipitate was rinsed several times with sterile Ringer's solution. A small amount of the resulting suspension was plated onto sheep's blood and trypticase soy-base agar plates and incubated for 48 hr at 37° for sterility testing. No colonies were found on the agar plates.

Mature female Sprague–Dawley rats, weighing 210–225 g, were each injected subcutaneously with 0.5 ml of the suspension into the dorsal side just below the neck. The rats were then placed in individual metabolism cages, and their feces and urine were collected at 24-hr intervals for at least 14 days following implantation. Thereafter, the biological samples were collected three times a week, 2 days apart.

The total volume of urine was measured, and a 1-ml aliquot of urine was sampled. To the urine sample, 0.6 ml of water and 12 ml of a scintillation fluor cocktail were added, and the radioactivity in each sample was counted in a scintillation counter. The total amount of fecal matter collected from each metabolism cage was weighed and put in an oven at 60° for ~12 hr until dry. The dry mass was then weighed and pulverized to an homogenous mixture of fine powders in a blender. Two aliquots of the dried fecal matter (0.2 g/sample) were accurately weighed and placed in separate glass scintillation vials. To each vial was added 0.3 ml of 70% perchloric acid and 0.6 ml of 30% hydrogen peroxide to effect complete digestion. The vials were then tightly sealed and incubated for 12 hr at 60° in a shaking water bath until all the fecal matter was completely solubilized. After the digestion, the vials were cooled for 30 min at room temperature before adding 12 ml of a scintillation fluor cocktail[5]. The vials were then kept in a dark place for at least 24 hr before they were counted in a scintillation counter. This procedure effectively minimized chemiluminescence. With this digestion procedure, no appreciable loss of radioactivity due to the processing was observed. These data were used to calculate the daily and cumulative output of radioactivity in the urine and feces.

RESULTS AND DISCUSSION

If the release of [^{3}H]norethindrone from the steroid–polymer conjugate approximates a zero-order kinetic process, the amount of total radioactivity in the body would gradually build up to an eventual steady-state value as shown in the following equation:

$$Q_b = (k_0/k_{el})(1 - e^{-k_{el}t}) \qquad \text{(Eq. 1)}$$

where Q_b is the amount of the total radioactivity in the body, k_0 is the

[1] New England Nuclear Corp., Boston, Mass.

[2] Formula 950A; New England Nuclear Corp., Boston, Mass.
[3] Model LS9000; Beckman Instruments, Inc., Irvine, Calif.
[4] Protosol; New England Nuclear Corp., Boston, Mass.
[5] Biofluor; New England Nuclear Corp., Boston, Mass.

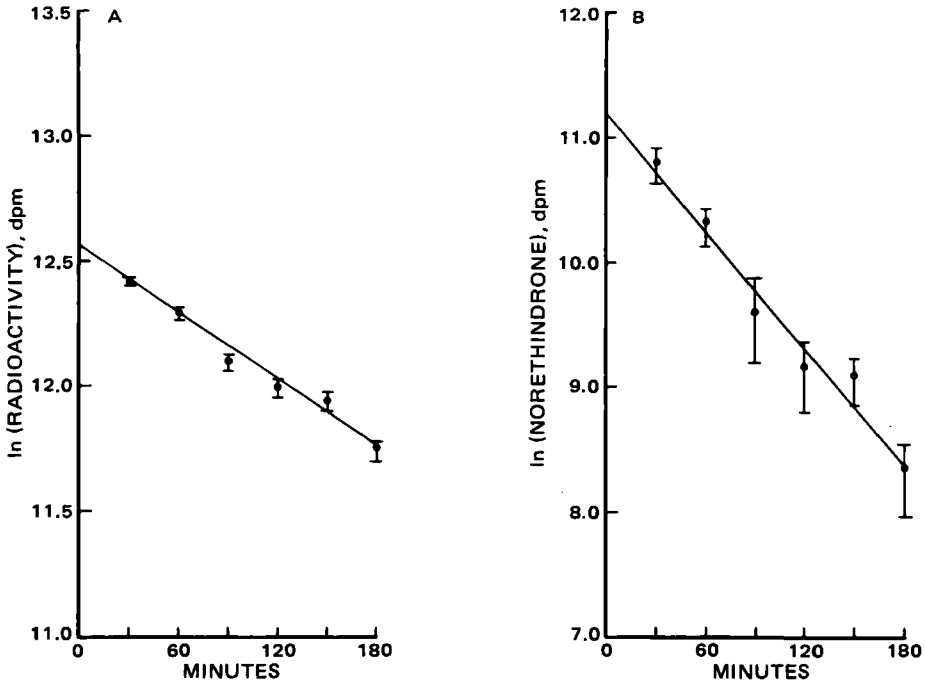

Figure 1—*Semilogarithmic plot of the elimination of total radioactivity (A) or [^{3}H]norethindrone (B) in female Sprague–Dawley rats. Values were determined after intravenous injection of [^{3}H]norethindrone (mean ± SD, n = 6).*

steroid release rate from the steroid–polymer conjugate, and k_{el} is the elimination rate of the total radioactivity. Since the amount of the total radioactivity excreted in the urine and feces (Q_{ex}) equals $k_{el} \cdot Q_b$, then:

$$Q_{ex} = k_0(1 - e^{-k_{el}t}) \qquad \text{(Eq. 2)}$$

and at steady state ($t \rightarrow \infty$):

$$Q_{ex} = k_0 \qquad \text{(Eq. 3)}$$

Equation 3 states that at steady state the amount of the total radioactivity excreted from the body is the same as that of the total radioactivity released from the steroid–polymer conjugate. The rate of the daily output of radioactivity in urine and feces at steady state is, therefore, a valid indication of the daily release rate of steroid from the biodegradable drug delivery system.

Since the above argument is valid only under steady-state conditions, it is necessary to know exactly when steady state is achieved in female rats. From Eq. 1, it can be shown that the time required to reach 95% of steady state is:

$$t_{0.95} = 4.3 \times t_{1/2} \qquad \text{(Eq. 4)}$$

The biological half-life of norethindrone in female rats was found to be 44 min (Fig. 1B), which agrees with that reported earlier by Back *et al.* (23). The elimination of the total radioactivity from rats after the intravenous injection of [^{3}H]norethindrone, however, was slower than that for parent [^{3}H]norethindrone. The half-life for the total radioactivity elimination was 161 min (Fig. 1A). This means that if the norethindrone–polymer conjugate releases norethindrone at a constant zero-order rate after its injection, it will take ~12 hr before the *in vivo* release rate in the urine and feces would reach a constant steady-state value.

Following intravenous and subcutaneous injection of [^{3}H]norethin-

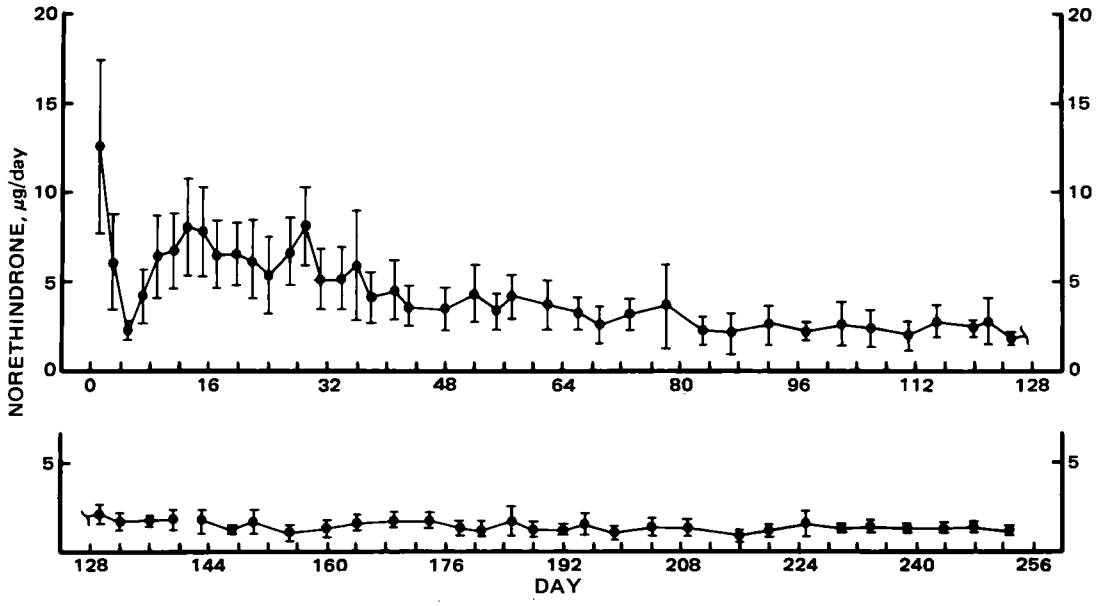

Figure 2—*Daily excretion of radioactivity in urine and feces. Norethindrone–polymer conjugate, batch B (10 mg), containing [^{3}H]norethindrone was injected subcutaneously into female Sprague–Dawley rats. The radioactivity excreted in the urine and feces was measured at various times after the administration (mean ± SD, n = 5).*

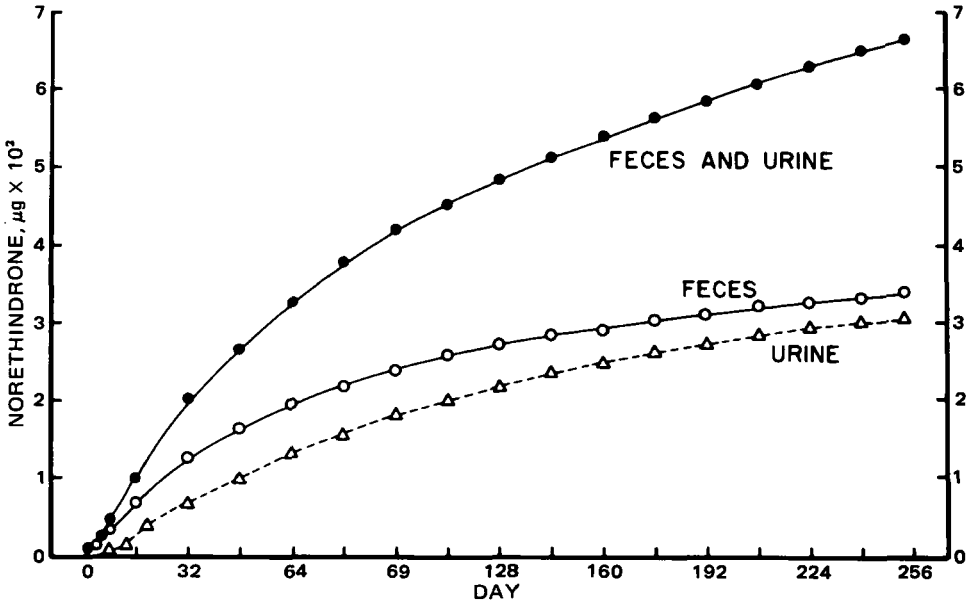

Figure 3—*Cumulative excretion of radioactivity in urine and feces. Norethindrone–polymer conjugate, batch B (10 mg), containing [³H]norethindrone was injected subcutaneously into female Sprague–Dawley rats. The total radioactivity excreted in the urine and feces at various times after the administration is presented (mean, n = 5).*

drone to female Sprague–Dawley rats, it was observed that ~50–60% of the total radioactivity was excreted in the feces. A similar pattern was observed in rats administered the norethindrone–polymer conjugate.

Figures 2 and 3 show the *in vivo* steroid release rate profile for batch B; similar results were observed with batch A. In all animals administered [³H]norethindrone–polymer conjugate (either batch A or B), the release rate profile was characterized by a slight burst of radioactivity release immediately after the injection, followed by a fairly constant release rate for a period up to 10 months. However, a gradual decrease in the rate of steroid release over this long period was evident.

The average *in vivo* release rate of steroid for batch B from day 17 through day 253 was 0.37 μg of norethindrone/mg of norethindrone–polymer conjugate/day. For batch A, the *in vivo* steroid release rate from day 22 through day 292, expressed as μg of norethindrone/mg of norethindrone–polymer conjugate/day, was 0.27 and 0.26 for rats A_1 and A_2, respectively. The daily steroid release from these two animals administered batch A at two different doses were essentially equivalent. The daily steroid release rates from the five animals administered batch B were also very similar, as evidenced from the relatively small standard deviation (Fig. 2). Additionally, both batches A and B appeared to show similar long-term steroid release profiles throughout the study period.

The work measured the *in vivo* release of norethindrone which was covalently coupled to a biodegradable polyglutamate polymer. The system showed a fairly constant release of steroid for a time period in excess of 9 months. A slight decrease in the amount of norethindrone release was evident, however, over this long period.

The data showed that the norethindrone–polymer conjugate is a potential candidate for the controlled delivery of norethindrone to effect long-term contraception. Variation of parameters (*e.g.*, molecular weight, particle size, degree of norethindrone coupling, and the length of spacer group of the steroid–polymer conjugate) may result in products capable of achieving a specified *in vivo* duration and rate of steroid release.

REFERENCES

(1) L. L. Dogle and T. H. Clew, *Am. J. Obstet. Gynecol.*, **101**, 564 (1968).

(2) G. Benaginano, M. Ermini, C. C. Chang, K. Sundaram, and F. A. Kincl, *Acta Endocrinol.*, **63**, 29 (1970).

(3) A. Scommegna, A. Theresita, M. Luna, R. Rao, and W. P. Dmowski, *Obstet. Gynecol.*, **43**, 769 (1974).

(4) G. Benaginao, M. Ermini, L. Carenza, and G. Rotfini, *Acta Endocrinol.*, **73**, 335 (1973).

(5) S. El-Mahgoub, *Am. J. Obstet. Gynecol.*, **123**, 133 (1975).

(6) C. G. Nilsson and T. Luukkainen, *Contraception*, **15**, 295 (1977).

(7) D. R. Mishell, D. E. Moore, S. Roy, P. F. Brenner, and M. A. Page, *Am. J. Obstet. Gynecol.*, **130**, 55 (1978).

(8) F. G. Burton, W. E. Skiens, N. R. Gordon, J. T. Veal, D. R. Kalkwarf, and G. W. Duncan, *Contraception*, **17**, 221 (1978).

(9) A. Rosado, J. J. Hicks, R. Aznar, and E. Mercado, *Contraception*, **9**, 39 (1974).

(10) J. Martinez-Manautou, *J. Steroid Biochem.*, **6**, 889 (1975).

(11) K. Hagenfeldt and B. M. Landgren, *J. Steroid Biochem.*, **6**, 895 (1975).

(12) P. F. Brenner, D. L. Cooper, and D. R. Mishell, *Am. J. Obstet. Gynecol.*, **121**, 704 (1975).

(13) Y. W. Chein and E. P. K. Lau, *J. Pharm. Sci.*, **65**, 488 (1976).

(14) S. Z. Song, J. R. Cardinal, S. H. Kim, and S. W. Kim, *J. Pharm. Sci.*, **70**, 216 (1981).

(15) T. M. Jackanicz, H. A. Nash, D. L. Wise, and J. B. Gregory, *Contraception*, **8**, 227 (1973).

(16) C. G. Nilsson, F. D. B. Johansson, T. M. Jackanicz, and T. Luukkainen, *Am. J. Obstet. Gynecol.*, **122**, 90 (1975).

(17) K. R. Sidman, W. D. Steber, and A. W. Burg, in "Drug Delivery Systems," H. L. Gabelnick, Ed., U.S. Department of Health, Education and Welfare, National Institutes of Health, Bethesda, Md., 1976, pp. 120–141.

(18) C. Pitt, D. Christensen, R. Jeffcoat, G. L. Kimnol, A. Schindler, M. E. Wall, and R. A. Zweidinger, in "Drug Delivery Systems," H. L. Gabelnick, Ed., U.S. Department of Health, Education and Welfare, National Institutes of Health, Bethesda, Md., 1976, pp. 141–193.

(19) H. Gabelnick, "Annual Report Summary," NICHD Contract Summary, U.S. Department of Health, Education and Welfare, National Institutes of Health, Bethesda, Md., 1977.

(20) J. M. Anderson, A. Hiltner, K. Schodt, and R. Woods, *J. Biomed. Mater. Res. Symp.*, **3**, 25 (1972).

(21) J. M. Anderson, D. F. Gibbons, R. L. Martin, A. Hiltner, and R. Woods, *J. Biomed. Mater. Res. Symp.*, **5**, 197 (1974).

(22) J. Feijen, D. Gregonis, C. Anderson, R. V. Petersen, and J. Anderson, *J. Pharm. Sci.*, **69**, 871 (1980).

(23) J. D. Back, A. M. Breckinridge, F. E. Crawford, M. L. Orme, P. H. Rowe, and E. Smith, *J. Pharmacol. Exp. Ther.*, **207**, 555 (1978).

ACKNOWLEDGMENTS

This study was supported by NICHD-Contract No. N01-HD-7-2823.

The authors gratefully acknowledge Dr. D. E. Gregonis, Dr. J. Feijen, Dr. S. W. Kim, and Dr. J. M. Anderson for providing the compounds used in this study and their helpful discussion in the preparation of this manuscript. The authors also acknoweldge the technical assistance of Mr. Steve Himebaugh.

Comparative Study of Topological and Linear Free Energy-Related Parameters for the Prediction of GC Retention Indices

L. BUYDENS *, D. COOMANS *, M. VANBELLE *, D. L. MASSART *x, and R. VANDEN DRIESSCHE ‡

Received November 12, 1981, from the *Farmaceutisch Instituut and the ‡Laboratorium van Farmakologie, Vrije Universiteit Brussel, Laarbeeklaan 103, B-1090 Brussels, Belgium. Accepted for publication October 5, 1982.

Abstract □ The different molecular connectivity indices were considered as to their capacity for describing GC retention indices of a data set consisting of molecules of different chemical families. $^1\chi$ describes best the chromatographic behavior on nonpolar stationary phases, whereas $^3\chi_p$ in combination with an electronic parameter (σ) yields the best results when using the polar stationary phases.

Keyphrases □ Molecular connectivity—correlation to GC retention indices, polar and nonpolar stationary phases, topological and linear free-energy parameters □ GC retention indices—correlation to molecular connectivity, polar and nonpolar stationary phases, topological and linear free-energy parameters □ Topology—correlation of GC retention indices and molecular connectivity, linear free energy parameters, polar and nonpolar stationary phases

The pharmacological action of drugs results from the interaction of the molecules with receptor sites. These interactions are often described in terms of structural parameters (1–3). GC retention indices, which result from the interaction of the molecules with the stationary phase, have been shown (4–8) to be related to the various structural parameters used to describe drug–receptor interactions. Therefore, the GC behavior of the molecules can be used as a simple model for methodological studies of structure–activity relationships.

Relating GC behavior to structural parameters such as the molecular connectivity ($^1\chi$) or the combination of $^1\chi$ with physicochemical parameters such as σ and π (5, 7), leads to satisfactory results when one studies molecules of a single chemical family such as the alcohols, alkanes, or the methyl esters of fatty acids (5, 7). For molecules of different families, especially using more polar stationary phases, the results show that the parameters used do not satisfactorily describe the GC behavior (5). Therefore, use of additional parameters that describe the variance unexplained by the other variables is necessary.

This paper investigates to what extent the additional higher-order terms of the molecular connectivity permit better results. For this purpose the higher-order terms are included in a statistical treatment together with the previously used structural parameters (5).

THEORETICAL

The parameters used are the valence molecular connectivity indices (hereafter called connectivity indices) the Wiener number (W), Hosoya's index (Z), Hansch's constant (π), and Hammett's constant (σ). The full definitions and calculations for these parameters can be found elsewhere (1–3, 9, 10).

To calculate the connectivity parameters the molecule is displayed in skeletal form. To each of the i atoms a value, δ_i, is assigned according to the difference between the number of valence electrons and the number of hydrogen atoms suppressed. An example using 2-methyl-1-butanol (I) is given in Fig. 1.

The respective connectivity indices are calculated by means of the following equations. For the zero-order term ($^0\chi$):

$$^0\chi = \sum_1^i (\delta_i)^{-1/2} \qquad \text{(Eq. 1)}$$

where δ_i represent the δ-values of the i atoms. For the 2-methyl-1-butanol example, $^0\chi = (2/\sqrt{1}) + (2/\sqrt{2}) + (1/\sqrt{3}) + (1/\sqrt{5}) = 4.439$. For the first-order term ($^1\chi$):

$$^1\chi = \sum_i^N (\delta_i\delta_j)^{-1/2} \qquad \text{(Eq. 2)}$$

where $\delta_{i,j}$ are the δ-values of the adjacent atoms i and j, and N is the number of bonds in the molecule. Using 2-methyl-1-butanol, $^1\chi = (1/\sqrt{1\times2})\ (2/\sqrt{2\times3}) + (1/\sqrt{1\times3}) + (1/\sqrt{2\times5}) = 2.417$. For the second-order term ($^2\chi$):

$$^2\chi = \sum^M (\delta_i\delta_j\delta_k)^{-1/2} \qquad \text{(Eq. 3)}$$

where $\delta_{i,j,k}$ are the δ-values of the atoms of two adjacent bonds, and M is the number of adjacent bonds pairs in the molecule. For the 2-methyl-1-butanol example, $^2\chi = (1/\sqrt{1\times2\times3}) + (1/\sqrt{2\times3\times1}) + (1/\sqrt{1\times3\times2}) + (1/\sqrt{3\times2\times5}) + (1/\sqrt{2\times2\times3}) = 1.696$. For the third-order path term ($^3\chi_p$):

$$^3\chi_p = \sum^P (\delta_i\delta_j\delta_k\delta_l)^{-1/2} \qquad \text{(Eq. 4)}$$

where $\delta_{i,j,k,l}$ are the δ-values for the atoms of three adjacent bonds forming the butane skeleton (C—C—C—C) and p is the number of three adjacent bonds forming the butane skeleton in the molecule. Using 2-methyl-1-butanol, $^3\chi_p = (1/\sqrt{1\times2\times3\times1}) + (1/\sqrt{1\times2\times3\times2}) + (1/\sqrt{2\times3\times2\times5}) + (1/\sqrt{1\times3\times2\times5}) = 1.009$. For the third-order cluster term ($^3\chi_c$):

$$^3\chi_c = \sum^Q (\delta_i\delta_j\delta_k\delta_l)^{-1/2} \qquad \text{(Eq. 5)}$$

where $\delta_{i,j,k,l}$ are the δ-values for the atoms of three adjacent bonds forming the isobutane skeleton, and Q is the number of isobutane groups in the molecule. For 2-methyl-1-butanol: $^3\chi_c = (1/\sqrt{2\times3\times2\times1}) = 0.289$.

The Wiener number (W) and Hosoya's index (Z) are also topological parameters. Formulas for their calculation can be found elsewhere (3, 11). Because the molecules considered herein are all aliphatic molecules the σ scale, derived from the hydrolysis of aliphatic acid esters was used (1, 2, 10).

EXPERIMENTAL

The different parameters were calculated for ~100 compounds[1] belonging to different families (alkanes, alkenes, alcohols, aldehydes, ketones, and esters). Retention indices (12) on four stationary phases of different polarity were used: squalane and SE-30 were used as the nonpolar phases, while ethylene glycol was of intermediate polarity and di-

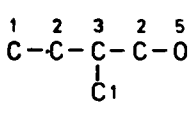

Figure 1—*δ-Values for the atoms of 2-methyl-1-butanol (I). δ-Values of the respective atoms are given above (beside) the atoms.*

[1] Furnished on request.

0022-3549/83/1100-1327$01.00/0

Table I—Correlation Coefficients Between Parameters

	$^0\chi$	$^1\chi$	$^2\chi$	$^3\chi_p$	$^3\chi_c$	W	Z	π	σ
$^0\chi$	1.000								
$^1\chi$	0.956	1.000							
$^2\chi$	0.812	0.688	1.000						
$^3\chi_p$	0.757	0.786	0.650	1.000					
$^3\chi_c$	0.348	0.134	0.789	0.250	1.000				
W	0.869	0.861	0.559	0.525	0.064	1.000			
Z	0.802	0.831	0.457	0.528	−0.040	0.950	1.000		
π	0.685	0.721	0.545	0.474	0.179	0.617	0.536	1.000	
σ	−0.335	−0.345	−0.309	−0.362	−0.410	−0.102	−0.029	−0.742	1.000

ethylene glycol succinate was used as the polar phase. The molecular connectivity indices were calculated with a microcomputer[2] using a program developed in-house.

Multiple regressions were calculated following a stepwise regression procedure using the SPSS program (13). The independent variables were introduced in the multiple regression equation only if they met certain statistical criteria. The variable that accounts for the largest amount of variance in the dependent variable (with the highest correlation coefficient) was used first in the regression equation. The variable that explains the greatest amount of variance not accounted for by the variables already in the equation entered the regression equation in the following step. Correlation studies between the different connectivity indices were also carried out using the SPSS program (13).

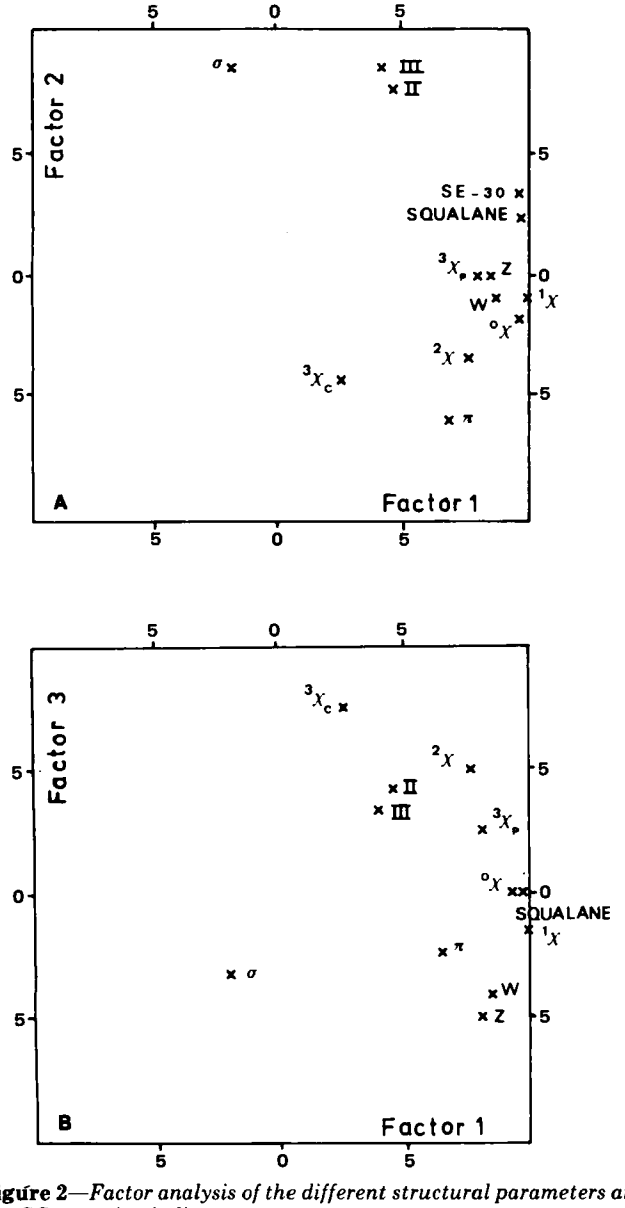

Figure 2—*Factor analysis of the different structural parameters and the GC retention indices.*

[2] Apple II computer.

RESULTS AND DISCUSSION

To find the relationship between the different connectivity indices, correlation coefficients between these indices were calculated. The different structural features necessary to calculate all the connectivity indices are not present in all molecules. Therefore, some of the indices are not different from zero for all the molecules of the basic set. The correlation coefficients are calculated only for the molecules with a non-zero value for the indices. A subset was chosen to compare the different indices such that the indices compared are all different from zero for all the molecules of the subset. The resulting correlation matrix is shown in Table I.

The results show that the parameters W and Z correlate best with the zero- and first-order terms of the molecular connectivity. The parameter σ, as expected, is completely different from the other variables, since its correlation coefficient with the other variables is nearly zero. The correlation between the connectivity indices decreases for the higher-order terms. $^3\chi_c$ does not correlate with the path connectivity term. These results, in agreement with those of Kier and Hall (3), suggest that the higher-order terms of the molecular connectivity contain different information which can indeed improve the regression equation.

Regression equations were calculated for the retention indices on the four stationary phases using these parameters. The equations are of the general form:

$$(RI)_i = a + bx_{1i} + cx_{2i} + dx_{3i} + \ldots + e_i \qquad \text{(Eq. 6)}$$

where RI is the retention index and $x_{1i}, \ldots, x_{3i}$ are the values for the different structural parameters for compound i. The results are given in Table II; the multiple correlation (MR) and the simple correlation (SR) coefficients are given. The multiple correlation coefficient is the correlation coefficient of the regression equation with all variables entered up to the considered step.

Table II—Correlation Coefficients of the Stepwise Regression Equations for the Total Data Set [a]

Stationary Phase	Parameter	Multiple Correlation	Simple Correlation
Nonpolar			
Squalane	$^1\chi$	0.91	0.91
	π	0.94	0.47
SE-30	$^1\chi$	0.84	0.84
	π	0.92	0.37
Polar			
Diethylene glycol succinate			
	σ	0.50	0.50
	$^3\chi_p$	0.68	0.25
	Z	0.71	0.07
	$^1\chi$	0.72	0.10
	$^0\chi$	0.74	0.04
	$^2\chi$	0.85	0.03
Polyethylene glycol			
	σ	0.37	0.37
	$^3\chi_p$	0.64	0.35
	W	0.67	0.07
	$^1\chi$	0.70	0.19
	$^2\chi$	0.72	0.138
	$^0\chi$	0.83	0.125

Table III—Correlation Coefficients of the Stepwise Regression Equation for the Data Set Without Outliers

Stationary Phase	Parameter	Multiple Correlation	Simple Correlation
Nonpolar			
Squalane[a]	$^1\chi$	0.94	0.94
	π	0.97	0.50
	σ	0.97	0.14
	Z	0.98	0.77
SE-30[b]	$^1\chi$	0.91	0.91
	π	0.96	0.42
	σ	0.98	0.11
	Z	0.98	0.76
Polar			
Diethylene glycol succinate[c]	σ	0.45	0.45
	$^3\chi_p$	0.76	0.41
	Z	0.82	0.09
	$^1\chi$	0.87	0.26
	π	0.89	−0.34
	$^0\chi$	0.90	0.21
	$^2\chi$	0.97	0.18
Polyethylene glycol[c]	$^3\chi_p$	0.52	0.52
	σ	0.73	0.28
	Z	0.78	0.14
	$^1\chi$	0.83	0.36
	π	0.85	−0.20
	$^0\chi$	0.86	0.30
	$^2\chi$	0.95	0.29

[a] $N = 48$. [b] $N = 45$. [c] $N = 44$.

For the nonpolar stationary phases, the topological parameter $^1\chi$ describes best the behavior; this is in agreement with earlier results (5). For the more polar stationary phases, the most important parameter in the earlier study was σ, describing electronic effects (5). In the present study σ also appeared first (Table II). This is not surprising, since the interaction with the more polar stationary phases are much more specific. The second most important parameter was the $^3\chi_p$ term. This means that once the electronic effects are filtered out of the total variance, $^3\chi_p$ describes best the residual steric influences on the chromatographic behavior of the more polar stationary phases.

As stated above, the higher-order terms of the molecular connectivity parameters cannot be computed for all 100 substances in the original data set. To derive the effect of the inclusion of $^3\chi_p$ in the set variables, the multiple regression was carried out with and without $^3\chi_p$ [*i.e.*, with the variables of our earlier study (5)]. It is clear that $^3\chi_p$ does indeed improve the correlation coefficient, since the correlation coefficient obtained with the two first variables introduced in the regression equation increased from 0.57 (without $^3\chi_p$) to 0.68 (with $^3\chi_p$) for diethylene glycol succinate. The results for the polar phases are improved by including the higher-order term $^3\chi_p$. They are, however, still worse than those for the nonpolar stationary phases.

To see which effects are not explained by the parameters included in the regression equation, the molecules whose chromatographic behavior is not well described with the regression equation, *i.e.*, the molecules which have a large residual (e in Eq. 6), can be examined. The greatest residuals are found for molecules that contain more than one functional group, such as an hydroxyl and a keto group or two keto groups. The results of the regression equations without these outliers are shown in Table III. For the nonpolar stationary phases, the results are satisfactory. For the most polar stationary phase (diethylene glycol succinate), the most important parameter is still the electronic parameter σ, followed by $^3\chi_p$. For the mediumly polar polyethylene glycol, the first parameter entered is now $^3\chi_p$, followed by σ. In both cases the results are improved by omitting the outliers.

$^1\chi$ is entered as the first topological parameter in the regression equation for the apolar stationary phases, while $^3\chi_p$ is used for the polar stationary phases. More information about the intercorrelation between the parameters and the retention indices can be obtained by factor analysis. Factor analysis reduces the total amount of variables to a few fundamental variables (factors or latent variables) which are a linear combination of the original variables. These new variables are chosen so that as much of the total variance as possible is explained. Up to this point, the retention indices were considered as dependent variables and π, σ, and the topological parameters as independent variables. This means that the retention indices were predicted or explained by means of the structural parameters. However, both the retention indices and the structural parameters can be thought of as variables containing information about the structural aspects and, therefore, about possible interactions of the molecules. Factor analysis can show which variables (structural parameters and retention indices) contain analogous information (*i.e.*, are related to each other).

Factor analysis of the data set, without the outliers, resulted in the extraction of three important factors, explaining respectively 55, 20, and 13% of the total variance. Figure 2A shows that the topological parameters form a cluster near the cluster of the nonpolar stationary phases in the two-dimensional space of the first two factors. This cluster is rather distant from the cluster of the two polar stationary phases. The only parameter in the neighborhood of the polar phases is σ. These results are analogous to those of an earlier study (5). The topological parameters best describe the chromatographic behavior on the nonpolar stationary phases. In the plane of the first and third factor (Fig. 2B), however, the topological parameter $^3\chi_p$ is situated near the polar phases, which means that in the three-dimensional space the parameters σ and $^3\chi_p$ are most closely related to the polar stationary phases. The other topological parameters are still best related to the nonpolar phases. This shows that the steric effects determining the GC behavior are different for polar and nonpolar stationary phases. For the nonpolar phases, the lower-order connectivity terms are sufficient to account for these effects. For the more polar stationary phases, a better description of the molecules is necessary to describe the chromatographic behavior; this can be provided by means of the higher-order term $^3\chi_p$. It is, however, not the $^3\chi_c$ term that improves the regression equation. A reason for this could be the fact that $^3\chi_c$ describes only part of the molecule, while $^3\chi_p$ gives a more general idea of the whole molecule.

From these results it can be concluded that the GC behavior of molecules from different chemical families can be described satisfactorily by means of a general topological parameter on nonpolar stationary phases, since these interactions are quite nonspecific. For the more polar phases a higher-order term of the molecular connectivity, $^3\chi_p$, and an electronic parameter, σ, are required, since these interactions are quite specific (dipole–dipole interactions, hydrogen bonding, *etc.*). It should, however, be pointed out that these results are obtained for molecules containing only one functional group. The interpretation of the chromatographic behavior of molecules with more than one functional group is more difficult. A reason for this could be that the resultant electronic effect of two functional groups is not described sufficiently by σ. Electronic parameters, such as the dipole moment, could possibly improve these results. It is also known that two functional groups influence the partition coefficient of the molecules in a different way than each functional group separately (2, 14).

REFERENCES

(1) C. Hansch, "Drug Design," vol. 1, E. J. Ariens, Ed., Academic, New York, N.Y., 1971, chap. 2.

(2) Y. C. Martin, "Quantitative Drug Design: A Critical Introduction," Dekker, New York and Basel, 1978.

(3) L. B. Kier and L. H. Hall, "Molecular Connectivity in Chemistry and Drug Research," Academic, New York, N.Y., 1976.

(4) Y. Michotte and D. L. Massart, *J. Pharm. Sci.*, **66**, 1630 (1977).

(5) L. Buydens and D. L. Massart, *Anal. Chem.*, **53**, 1990 (1981).

(6) T. R. McGregor, *J. Chromatogr. Sci.*, **17**, 314 (1979).

(7) L. B. Kier and L. H. Hall, *J. Pharm. Sci.*, **68**, 120 (1979).

(8) J. S. Millership and A. D. Woolfson, *J. Pharm. Pharmacol.*, **30**, 483 (1978).

(9) L. B. Kier and L. H. Hall, *J. Pharm. Sci.*, **70**, 583 (1981).

(10) J. Shorter, "Correlation Analysis—Recent Advances," N. B. Chapman and J. Shorter, Eds., Plenum, New York, N.Y., 1978.

(11) G. L. Amidon and S. T. Anik, *J. Pharm. Sci.*, **65**, 801 (1976).

(12) W. O. McReynolds, "Gas Chromatographic Retention Data," Preston Technical Abstracts Co., Illinois, 1966.

(13) N. H. Nie, C. H. Hull, J. G. Jenkins, K. Stenbrenner, and D. H. Bent, "SPSS-Statistical Package for the Social Sciences," 2nd ed., McGraw-Hill, New York, N.Y., 1975.

(14) R. F. Rekker, "Quantitative Structure-Activity Analysis," R. Franke and P. Oehme, Eds., Akademie-Verlag, Berlin, 1978.

ACKNOWLEDGMENTS

The authors thank the Fonds voor Geneeskundig Wetenschappelijk Onderzoek for financial assistance.

Stability-Indicating High-Performance Liquid Chromatographic Assay for Oxazepam Tablets and Capsules

VAN D. REIF ˣ **and NICHOLAS J. DEANGELIS**

Received July 23, 1982, from the *Analytical Research and Development Subdivision, Wyeth Laboratories, Inc., Philadelphia, PA 19101.* Accepted for publication September 17, 1982.

Abstract □ A stability-indicating high-performance liquid chromatographic (HPLC) assay for oxazepam in capsules and tablets was developed. The material was extracted with 2% aqueous methanol and chromatographed on a C18 reverse-phase column, which was eluted with methanol–water–acetic acid (60:40:1). A wavelength of 254 was used for detection. This assay separated oxazepam from all degradation products mentioned in the literature or observed in stress-degraded samples. Degradation products could be detected at the 0.1% level. Degradation of oxazepam to 6-chloro-4-phenyl-2-quinazolinecarboxaldehyde and 2-amino-5-chlorobenzophenone was observed after either acid or base treatment. Acidic conditions also afforded 2′-benzoyl-4′-chloroglyoxanilide and 6-chloro-4-phenyl-2(1*H*)-quinazolinone.

Keyphrases □ Oxazepam—analysis, high-performance liquid chromatography, stability, tablets, capsules □ High-performance liquid chromatography—oxazepam capsules and tablets, stability-indicating analysis □ Sedatives—oxazepam, high-performance liquid chromatographic analysis, tablets, capsules, stability indicating

Various methods have been described for the determination of oxazepam (I), a 1,4-benzodiazepine tranquilizer. The current official method (1) employs UV spectrophotometric determination after extraction with ethanol. Increased selectivity was observed using polarographic detection (2, 3), which is dependent on reduction of the intact 4,5-azomethine bond. During GLC analysis, oxazepam decomposes to 6-chloro-4-phenyl-2-quinazolinecarboxaldehyde, II (4, 5). GLC methods, therefore, have been based on measurement of either II or 2-amino-5-chlorobenzophenone (III), which is formed by prior hydrolysis of oxazepam (6). High-performance liquid chromatographic (HPLC) methods have been described for detection and quantitation of I in biological fluids (7–11) and in mixtures of benzodiazepines (12–15). However, a selective chromatographic method for dosage forms in the presence of degradation products has not been published. This report describes the development of a specific and precise HPLC method for oxazepam tablets and capsules. Degradation products were isolated and identified to validate method specificity.

The hydrolysis of I to a benzophenone (III) was reported in 1964 (16). Formation of the aldehyde (II) after heat treatment (4, 5) and under acidic conditions (17) has been described, along with proposed mechanisms. Han *et al.* (18) reported the tentative identification of two intermediates of oxazepam hydrolysis. The interpretation of kinetic data obtained by UV measurements was, in part, substantiated by the isolation of these components. One, a prominent acid degradation product (IV) was designated as the initial product of 4,5-azomethine hydrolysis. The other (V) was predominant in base, but formed also in acid, and was designated as the product of 1,2-amide bond hydrolysis. However, neither degradation product when isolated, gave a mass spectral parent peak that corresponded to the mass of the assigned structure.

Two potential degradation products, 7-chloro-5-phenyl-4,5-dihydro-2*H*-benzodiazepine-2,3-(1*H*)-dione (VI) and 6-chloro-3,4-dihydro-4-phenyl-2-quinazolinecarboxylic acid (VII), were prepared from I by treatment with strong base (19). Two other potential degradation products, 2′-benzoyl-4′-chloroglyoxanilide (VIII) and 6-chloro-4-phenyl-2(1*H*)-quinazolinone (IX), have been reported as metabolites (20).

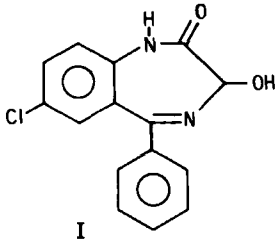

I

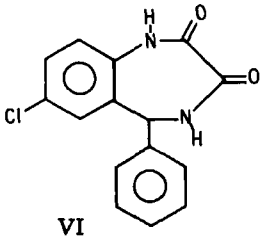

VI

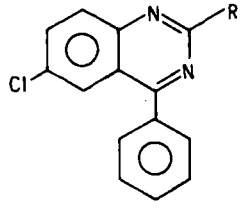

II: R = CHO
X: R = CH_2OH

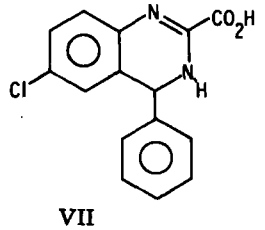

VII

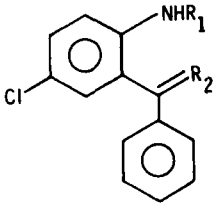

III: R_1 = H R_2 = O
VIII: R_1 = COCHO R_2 = O
IV: R_1 = COCHOH—NH_2 R_2 = O
V: R_1 = H R_2 = N—CHOH—CO_2H

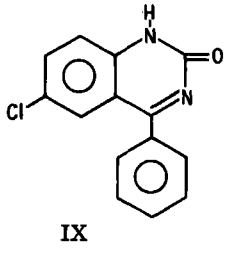

IX

EXPERIMENTAL

Materials—The following reference compounds were synthesized according to literature procedures: II (17); VI and VII (19); and (IX) (21). Compounds VIII[1] and X[2] were obtained in-house. The mass spectra for X gave the predicted monochlorinated parent peaks at *m/z* 270 and 272, and the melting point was the same as reported (22). The melting point and IR spectra for VIII corresponded to reported data (23). Compounds I[3] and III[4] were obtained commercially.

[1] C. O. Tio, Drug Disposition Section, Wyeth Laboratories, Inc.
[2] C. L. Robinson, Chemical Development Section, Wyeth Laboratories, Inc.
[3] Wyeth Laboratories, Inc., Philadelphia, Pa.
[4] Aldrich Chemical Co., Milwaukee, Wis.

0022-3549/83/1100-1330$01.00/0

Table I—Chromatographic Separation of Impurities and Degradation Products

Compound	HPLC[a] Retention Time, min	TLC[b] R_f
VI (Dione)	3.6	0.20
VII (Carboxylic Acid)	4.5	0
I (Oxazepam)	5.6	0.22
IX (Quinazolinone)	8.2	0.51[c]
VIII (Glyoxanilide)	11.2	0.54
II (Aldehyde)	11.8	0.76
X (Alcohol)	12.4	0.68[c]
III (Benzophenone)	18.4	0.83[d]

[a] Assay system, Chromegabond C18, E. S. Industries. [b] Chloroform–toluene–methanol (52:45:7); silica gel GF, visualization by shortwave UV. [c] Distinguished by blue fluorescence under long wavelength UV. [d] Distinguished by yellow spot with visible light.

Oxazepam Degradation—Hydrolysis conditions and TLC procedures were similar to those reported previously (18). The following 0.1 *M* buffers at 80° were used: hydrochloric acid, pH 5.5 phosphate, pH 3.2 acetate, and sodium hydroxide. Aliquots of hydrolyzed solutions were also withdrawn and analyzed directly by HPLC. TLC spots were extracted with methanol and were analyzed by HPLC and mass spectra for further identification.

Assay—The chromatograph[5] was equipped with a UV detector[6] set at 254 nm. A fixed-loop septumless injector[7] with a 10-μl loop was used in conjunction with 10-μm microparticulate reverse-phase columns[8], 25–30 cm × 4.6-mm i.d. The mobile phase consisted of methanol–water–acetic acid (60:40:1) with a 2-ml/min flow rate. An electronic integrator[9] was used for area determinations; peak heights were determined manually.

The system suitability was tested by dissolving ~10 mg of oxazepam and 15 mg of II in 250 ml of methanol; 10 μl of this solution was chromatographed using the assay conditions. The resolution factor (24) between oxazepam and II is ≥5.0. Unsuitable resolution can often be improved by a slight reduction of the mobile phase methanol concentration.

The standard was prepared by dissolving a quantity of oxazepam standard[10] in methanol–water (49:1) to give a known concentration of ~0.1 mg/ml. Samples were prepared by emptying ≥20 capsules and determining the average weight, or by weighing ≥20 finely powdered tablets. An accurately weighed portion of the powder containing ~25 mg of oxazepam was transferred to a 250-ml volumetric flask, 5 ml of water was added, and the flask was swirled to wet the powder. Approximately 200 ml of methanol was added, the solution was sonicated[11] for 5 min, stirred for 30 min, and diluted to volume with methanol. A portion was centrifuged to provide a clear solution for injection into the chromatograph.

Degradation Determination—Degradation was determined in the dosage forms with a 0.1% limit of detection. Methanol (10 ml) was added to a portion of capsule or tablet powder containing ~25 mg of oxazepam. The suspension was sonicated for 10 min and then centrifuged. Using the above HPLC conditions, 10 μl of the supernatant was injected into the chromatograph within 30 min after preparation. (After 1 hr, 0.1% of II, due to degradation of I in the methanol solution, may be detected.) The detector sensitivity was adjusted to give standard peak heights of ≥10 mm. Standards were prepared in methanol at a concentration of ~5 μg/ml.

RESULTS AND DISCUSSION

Oxazepam Degradation—With the use of similar hydrolysis and TLC conditions, three degradation products, comparable to those originally reported by Han *et al.* (18), were observed. The pH conditions necessary for their formation and the TLC R_f values matched the original data. As reported, the ultimate hydrolysis product, the benzophenone (III), was observed after either acid or base treatment. Consistent with the original results, a second degradation product, which formed with ease in acid, had a mass spectral parent peak at *m/z* 287. However, this substance was identified by TLC R_f as the glyoxanilide (VIII) and not as the initial hydrolysis product, IV, as originally stated. When eluted from the TLC plate, this acid degradation product also had the same HPLC retention time as VIII reference material (Table I), and its mass spectrum was the same as a metabolite previously identified (20) as VIII. The third degradation product, predominant in base, was identified as the aldehyde (II) by comparison of mass spectra and chromatographic retention with reference material (Table I). No degradation products were observed that could be identified as IV or V.

A yellow TLC band at R_f 0.93, identified as the Schiff-base dimer of II and III, was also observed in chloroform extracts of both acidic and basic hydrolyses solutions. A mass spectrum of the extracted TLC band gave peaks at *m/z* 231, 268, and 481, corresponding to parent peaks for

[5] Constametric II, Laboratory Data Control.
[6] Spectroflow Monitor SF-770, Schoeffel.
[7] Rheodyne 70-10.
[8] Chromegabond C18, E. S. Industries; μ-Bondapak C18, Waters Associates; Zorbax ODS (15 cm × 4.6 mm), DuPont; and Partisil ODS-3, Whatman.
[9] SP4100, Spectraphysics.
[10] USP Reference Standards, Rockville, MD 20852.
[11] Branson Ultrasonic Bath, Branson Cleaning Equipment Co., Shelton, Conn.

Table II—Method Reproducibility and Recovery

Oxazepam Product	Precision[a]
10-mg Capsule	98 ± 0.9 (height) 98 ± 1.3 (area)
30-mg Capsule	97 ± 1.9 (height) 97 ± 1.9 (area)
15-mg Tablet	99 ± 0.72 (height) 99 ± 0.35 (area)

	Recovery, %	
Composition[b]	10 parts oxazepam	30 parts oxazepam
A	99	101
B	99	101
C	101	99

[a] Average percent of label claim ± *RSD*; $n = 5$. [b] A: lactose–Ac Di Sol–stearic acid–methylcellulose (300:6:3:60) and oxazepam (10 or 30); B: dicalcium phosphate dihydrate–polacrilin potassium–starch–magnesium stearate (300:6:6:3) and oxazepam (10 or 30); C: Avicel–alginic acid–sodium starch glycolate–talc (300:6:6:3) and oxazepam (10 or 30).

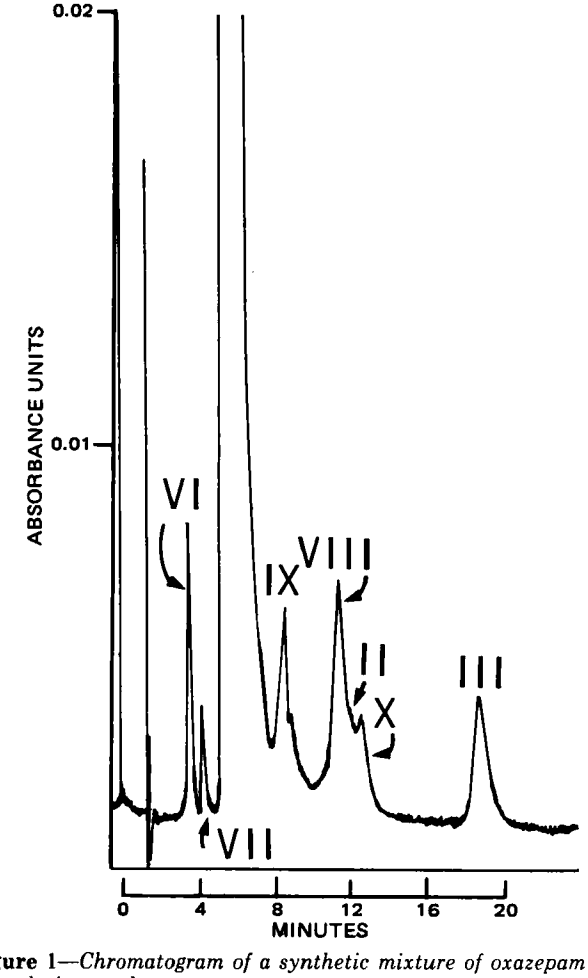

Figure 1—*Chromatogram of a synthetic mixture of oxazepam and degradation products.*

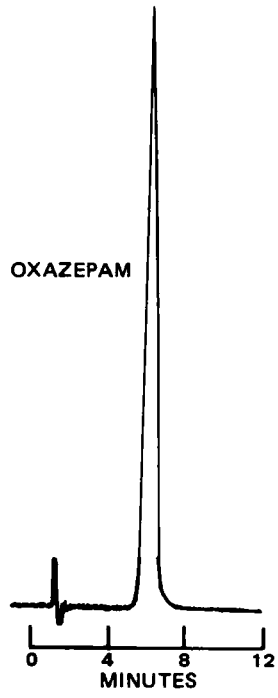

Figure 2—*Typical assay chromatogram.*

the benzophenone (III), the aldehyde (II), and the Schiff-base, respectively. Rechromatography of the extracted band gave, in addition to a spot at R_f 0.93, spots corresponding to II and III indicating that the dimer was not stable. HPLC gave only peaks corresponding to II and III. Further evidence for Schiff-base formation was the fact that the band at R_f 0.93 was obtained from chloroform standard solutions containing both II and III, but not from solutions containing II or III alone.

The quinazoline alcohol (X), the dione (VI), and the quinazolinecarboxylic acid (VII) were observed as relatively minor base-degradation products. The quinazolinone (IX) formed under either acidic or basic conditions. During method development, extraction of product composites with 0.1 *N* HCl–methanol (2:98) yielded low assays with rapid formation of IX.

The aldehyde, II, was the most prominent degradation product under stress conditions in the dosage forms. However, <0.5% was present in samples stored at room temperature for 5 years or at 45° for 6 months.

Assay—Precision data, obtained by replicate assays of commercial samples, and recovery data for synthetic mixtures of I and three combinations of commonly used excipients are reported in Table II. Placebo interference due to each mixture was <0.1% for the method. Linearity was checked by assaying solutions in the 0.06- to 0.12-mg/ml range. The chromatographic response was linear to the highest concentration tested.

The HPLC system separated I from all of the degradation products reported in the literature or observed in decomposed solutions (Table I). A separation of oxazepam from degradation products at levels of ~0.5% is shown in Fig. 1. Similar separations were achieved on the four different commercial columns tested, with the differences being minor variations in the resolution of individual impurities from each other. The columns tested passed the system suitability test. A typical assay chromatogram is shown in Fig. 2.

REFERENCES

(1) "The United States Pharmacopeia," 20th rev., United States Pharmacopeial Convention, Rockville, Md., 1980, p. 570.

(2) F. R. Fazzari and O. H. Riggleman, *J. Pharm. Sci.*, **58**, 1530 (1969).

(3) M. A. Brooks, J. J. Bel Bruno, J. A. F. DeSilva, and M. R. Hackman, *Anal. Chim. Acta*, **74**, 367 (1975).

(4) W. Sadee and E. van der Kleijn, *J. Pharm. Sci.*, **60**, 135 (1971).

(5) A. Forgione, P. Martelli, F. Marcucci, R. Fanelli, E. Mussini, and G. C. Jommi, *J. Chromatogr.*, **59**, 163 (1971).

(6) J. A. F. DeSilva, B. A. Koechlin, and G. Bader, *J. Pharm. Sci.*, **55**, 692 (1966).

(7) M. D. Osselton, M. D. Hammond, and P. J. Twitchett, *J. Pharm. Pharmacol.*, **29**, 460 (1977).

(8) E. Grassi, G. L. Passetti, and A. Trebbi, *J. Chromatogr.*, **144**, 132 (1977).

(9) P. M. Kabra, G. L. Stevens, and L. J. Marton, *J. Chromatogr.*, **150**, 355 (1978).

(10) T. B. Vree, A. M. Baars, Y. A. Hekster, E. van der Kleijn, and W. J. O'Reilly, *J. Chromatogr.*, **162**, 605 (1979).

(11) U. R. Tjaden, M. T. Meeles, C. P. Thys, and M. van der Kaay, *J. Chromatogr.*, **181**, 227 (1980).

(12) D. H. Rodgers, *J. Chromatogr. Sci.*, **12**, 742 (1974).

(13) C. Gonnet and J. L. Rocca, *J. Chromatogr.*, **120**, 419 (1976).

(14) F. Taylor Noggle, Jr. and C. R. Clark, *J. Assoc. Off. Anal. Chem.*, **62**, 799 (1979).

(15) J. K. Baker, R. E. Skelton, and C. Ma, *J. Chromatogr.*, **168**, 417 (1979).

(16) J. A. F. DeSilva, M. A. Schwartz, V. Stefanovic, J. Kaplan, and L. D'Arconte, *Anal. Chem.*, **36**, 2099 (1964).

(17) S. C. Bell and S. J. Childress, *J. Org. Chem.*, **29**, 506 (1964).

(18) W. W. Han, G. J. Yakatan, and D. D. Maness, *J. Pharm. Sci.*, **66**, 573 (1977).

(19) S. C. Bell and S. J. Childress, *J. Org. Chem.*, **27**, 1691 (1962).

(20) S. F. Sisenwine, C. O. Tio, S. K. Shrader, and H. W. Ruelius, *Arzneim.-Forsch.*, **22**, 682 (1972).

(21) T. S. Sulkowski and S. J. Childress, *J. Org. Chem.*, **27**, 4424 (1962).

(22) P. N. Giraldi, A. Fojanesi, G. P. Tosolini, E. Dradi, and W. Logemann, *J. Heterocycl. Chem.*, **7**, 1429 (1970).

(23) U.S. Patent 3,899,527 (Aug. 12, 1975) to R. J. McCaully (American Home Products).

(24) "The United States Pharmacopeia," 20th rev., United States Pharmacopeial Convention, Rockville, Md., 1980, p. 945.

ACKNOWLEDGMENTS

Presented in part at the Pharmaceutical Analysis and Control Section, APhA Academy of Pharmaceutical Sciences meeting in Washington, D.C., May 1980.

Complex Formation Between α-Cyclodextrin and 4-Substituted Phenols Studied by Potentiometric and Competitive Spectrophotometric Methods

SHU-FEN LIN and KENNETH A. CONNORS ˣ

Received February 11, 1982, from the *School of Pharmacy, University of Wisconsin, Madison, WI 53706.* Accepted for publication October 8, 1982.

Abstract □ Stability constants for complex formation between α-cyclodextrin and the conjugate acid and base forms of nine phenols were measured in aqueous solution at 25°. The potentiometric method, in which the apparent acid dissociation constant of the phenol is measured as a function of cyclodextrin concentration, was supplemented by a modified version of a competitive spectrophotometric methyl orange method. For all phenols, the 1:1 stability constant for the conjugate base form (K_{11b}) was larger than K_{11a} for the conjugate acid form. Finite K_{12b} values were found for phenols whose 4-substituents could tolerate a positive charge by electron delocalization. Complex stability, as measured by K_{11a} and K_{11b}, increases with electron density and polarizability at the 4-substituent. It is concluded that the 4-substituent is the sole or predominant site of binding for both the conjugate acid and base forms of the phenols. The general result that K_{11b} is greater than K_{11a} for any phenol is accounted for by relative delocalization of charge in the anion and neutral species.

Keyphrases □ α-Cyclodextrin—complex formation with 4-substituted phenols, stability constants, potentiometric and competitive spectrophotometric methods □ 4-Substituted phenols—complex formation with α-cyclodextrin, stability constants, potentiometric and competitive spectrophotometric methods □ Competitive spectrophotometry—with methyl orange, α-cyclodextrin–4-substituted phenol complexation, stability constants, comparison with potentiometric methods

In an earlier paper (1), the potentiometric method for studying cyclodextrin complexes was applied to a series of 4-substituted benzoic acids. This method has now been used to investigate the complexing of α-cyclodextrin with 4-substituted phenols.

THEORETICAL

Potentiometric Method—The theory of the method was described earlier (1); only a summary of the points pertinent to the present application is given here. The symbolism is identical with that used in the prior treatment (1).

The procedure is to measure the apparent dissociation constant (pK_a') of the phenol (substrate) at total concentration S_t in the presence of a total concentration L_t of α-cyclodextrin (the ligand), L_t being varied from zero up to nearly its solubility limit. The quantity $\Delta pK_a'$ is defined by:

$$\Delta pK_a' = pK_a' - pK_a \qquad \text{(Eq. 1)}$$

where pK_a is the dissociation constant when $L_t = 0$. The theory of the method (1), for a system that may contain 1:1 (SL) and 1:2 (SL_2) complexes of both the conjugate acid and base forms of the substrate, shows that $\Delta pK_a'$ is related to the complex stability constants by:

$$\Delta pK_a' = \log C = \log\left(\frac{1 + K_{11a}[L] + K_{11a}K_{12a}[L]^2}{1 + K_{11b}[L] + K_{11b}K_{12b}[L]^2}\right) \qquad \text{(Eq. 2)}$$

where K_{11a}, K_{12a}, K_{11b}, and K_{12b} are stepwise complex stability constants, the numerical subscripts indicating stoichiometry and the letters the conjugate acid–base form, and [L] is the equilibrium (unbound) concentration of ligand. For carboxylic acids it appears to be a general result that $\Delta pK_a'$ is a positive quantity (1–3); hence, C is greater than unity. For phenols, however, $\Delta pK_a'$ is negative, so C is smaller than one, and it becomes more convenient to work with its reciprocal C'. The basic relationship is then:

$$C' = \frac{1 + K_{11b}[L] + K_{11b}K_{12b}[L]^2}{1 + K_{11a}[L] + K_{11a}K_{12a}[L]^2} \qquad \text{(Eq. 3)}$$

All of the systems here can be described as special cases of Eq. 3. The particular case to which a system belongs is diagnosed by plotting C' against L_t; then, an appropriate linearized plotting form is applied to extract stability constant estimates. Since $L_t \neq [L]$, the free concentration [L] is calculated, and iterations are made until the stability constant estimates converge. The four special cases of Eq. 3, the linear plotting forms, and the equations for the calculation of [L] are:

Case I:

$$C' = \frac{1 + K_{11b}[L]}{1 + K_{11a}[L]} \qquad \text{(Eq. 4)}$$

$$\frac{C' - 1}{[L]} = K_{11b} - C'K_{11a} \qquad \text{(Eq. 5)}$$

$$[L] = L_t - \frac{S_t}{X + 1} \qquad \text{(Eq. 6)}$$

where:

$$X = \frac{(C' + 1)(R' - C')}{(C' - 1)(R' + C')} \qquad \text{(Eq. 7)}$$

and $R' = K_{11b}/K_{11a}$.

Case II:

$$C' = 1 + K_{11b}[L] \qquad \text{(Eq. 8)}$$

$$[L] = L_t - \frac{(C' - 1)}{2C'} S_t \qquad \text{(Eq. 9)}$$

Case III:

$$C' = 1 + K_{11b}[L] + K_{11b}K_{12b}[L]^2 \qquad \text{(Eq. 10)}$$

$$\frac{C' - 1}{[L]} = K_{11b} + K_{11b}K_{12b}[L] \qquad \text{(Eq. 11)}$$

$$[L] = \frac{2C'(L_t - S_t) + 2S_t}{2C' - S_tK_{11b}} \qquad \text{(Eq. 12)}$$

Case IV:

$$C' = \frac{1 + K_{11b}[L] + K_{11b}K_{12b}[L]^2}{1 + K_{11a}[L]} \qquad \text{(Eq. 13)}$$

$$\frac{C' - 1}{[L]} + C'K_{11a} = K_{11b} + K_{11b}K_{12b}[L] \qquad \text{(Eq. 14)}$$

$$K_{11a}[L]^2 + \left[1 + S_tK_{11a}\left(\frac{3}{2} - \frac{R'}{2C'}\right) - L_tK_{11a}\right][L] - \left[L_t - \frac{S_t(C' - 1)}{C'}\right] = 0 \qquad \text{(Eq. 15)}$$

To make the case IV linear plot according to Eq. 14, K_{11a} must be known. For case IV systems, K_{11a} was determined by a competitive spectrophotometric method as described in the following section.

Competitive Indicator Method—In 1953 Broser (4) showed that methyl orange and α-cyclodextrin form a complex in acidic solution, the complexed form of the indicator absorbing light much less intensely than the free form. If a third solute, capable of forming a cyclodextrin complex, is added to the solution, some of the complexed indicator will be competitively displaced, with a corresponding increase in the absorption intensity. This is the basis of the competitive methyl orange spectrophotometric method, which was used by Lautsch *et al.* (5) to study adrenalin–α-cyclodextrin complex formation. Casu and Ravà applied this method to measure K_{11a} values for many substituted benzoic acid substrates (6). The stability constants reported by these workers were, however, not in good agreement with those found potentiometrically in this laboratory (1). For this reason, the methyl orange method has been reexamined and modified as follows.

0022-3549/83/1100-1333$01.00/0

Let S represent the substrate of interest, L the cyclodextrin, and I the indicator. The competitive complexation equilibrium is shown in Scheme I:

$$IL + S \rightleftarrows SL + I$$

Scheme I

Mass balance equations on the substrate, ligand, and indicator are:

$$S_t = [S] + [SL] \quad \text{(Eq. 16)}$$

$$L_t = [L] + [SL] + [IL] \quad \text{(Eq. 17)}$$

$$I_t = [I] + [IL] \quad \text{(Eq. 18)}$$

(It is, in general, not permissible to neglect the [IL] term in Eq. 17.) Stability constants for the complexes SL and IL are defined, where 1:1 stoichiometry is assumed, as:

$$K_{11S} = \frac{[SL]}{[S][L]} \quad \text{(Eq. 20)}$$

$$K_{11I} = \frac{[IL]}{[I][L]} \quad \text{(Eq. 21)}$$

In the systems of present interest, where the substrate is the conjugate acid form of a phenol, K_{11S} is equivalent to K_{11a}.

Eqs. 16–21 are combined to give:

$$L_t = [L] + \frac{K_{11S}[L]S_t}{1 + K_{11S}[L]} + \frac{K_{11I}[L]I_t}{1 + K_{11I}[L]} \quad \text{(Eq. 22)}$$

Defining the indicator ratio $Q = [I]/[IL]$ allows Eq. 21 to be written as $K_{11I} = 1/Q[L]$, which, substituted into Eq. 22, gives:

$$L_t = \frac{1}{QK_{11I}} + \frac{S_tK_{11S}}{QK_{11I} + K_{11S}} + \frac{I_t}{Q + 1} \quad \text{(Eq. 23)}$$

The quantity P is defined as:

$$P = L_t - \frac{1}{QK_{11I}} - \frac{I_t}{Q + 1} \quad \text{(Eq. 24)}$$

Therefore, Eq. 23 may be written:

$$P = \frac{S_tK_{11S}}{QK_{11I} + K_{11S}}$$

or

$$\frac{S_t}{P} = \frac{K_{11I}}{K_{11S}}Q + 1 \quad \text{(Eq. 25)}$$

The indicator ratio Q can be measured by means of:

$$Q = \frac{\epsilon - \epsilon_{IL}}{\epsilon_I - \epsilon} \quad \text{(Eq. 26)}$$

where ϵ_I and ϵ_{IL} are the molar absorptivities of free and complexed indicator, respectively, and ϵ is the apparent molar absorptivity in any solvent containing both forms. If the total indicator concentration is constant in all solutions, the absorptivities can be replaced by absorbances.

K_{11I} can be obtained by independent measurements on solutions of indicator and ligand by the conventional spectrophotometric method. Eq. 25 therefore provides a graphical approach to determining K_{11S} by plotting S_t/P against Q, where P is obtained using Eq. 24.

The possible formation of a substrate–indicator complex (SI) has been analyzed (7) for its effect on the determination of K_{11S}. It was found that such an effect can be minimized if S_t and [I] are small; [I] is small when Q is small, when I_t is small, or when L_t is large. Another complicating factor is self-association of the indicator. DeVylder and DeKeukeleire (8) observed self-association of methyl orange in pH 2.2 aqueous solutions at indicator concentrations $>10^{-4}$ M. In the present work I_t was 1.67×10^{-5} M; hence, self-association could be neglected.

According to Eq. 25, the best estimate of K_{11S} should be possible if K_{11I} is approximately equal to K_{11S}, for then the slope will be approximately one. The method may therefore be useful for a wide range of substrates if indicators are identified with appropriate K_{11I} values.

EXPERIMENTAL

Materials—α-Cyclodextrin[1] was dried at 95° for 48 hr. Methyl orange[2] was recrystallized from water, then washed with ethanol followed by ether (9); its molar absorptivity in 0.08 M HCl at 508 nm was 4.82×10^4. Solid phenols[3] were recrystallized until their melting points agreed with literature values. 4-Methoxyphenol was distilled under reduced pressure; bp 111°/2 mm Hg, mp 55°. Water was redistilled from alkaline permanganate.

Potentiometric Studies—A stock solution of the phenol was prepared such that its final diluted total concentration (S_t) would be 0.003–0.004 M, and the phenol was half-neutralized with 0.10 M NaOH. The solution was brought to the mark with 0.10 M NaCl.

α-Cyclodextrin was weighed into 5-ml volumetric flasks in amounts that covered its full solubility range. Portions (4.0 ml) of the phenol stock solution were pipetted into each flask, and the solutions were brought to volume with 0.10 M NaCl. They were equilibrated at 25.0; to ensure adequate mixing, a 10-mm stirring bar was added and was driven by a submerged water-driven magnetic stirrer. The solution was transferred to a 5-ml test tube, and the combination pH electrode was lowered into the solution, which was protected from contact with the atmosphere. The pH was measured[4], and pK_a' was calculated using:

$$pK_a' = pH - \log \frac{b + [H^+] - [OH^-]}{S_t - (b + [H^+] - [OH^-])} \quad \text{(Eq. 27)}$$

where b is the added concentration of sodium hydroxide; in these studies $b = S_t/2$. Reproducibility on duplicate solutions was 0.003 pH unit or better. All studies were at 25.0° and ionic strength 0.10 M.

Competitive Methyl Orange Spectrophotometric Method—Portions (4.0 ml) of a stock solution containing 4.185×10^{-5} M methyl orange in 0.20 M HCl were pipetted into 10.0-ml volumetric flasks containing 2.0 ml of 0.01 M α-cyclodextrin aqueous solution. Substrate (phenol) solutions at variable concentrations such that the final substrate concentrations (S_t) were from 2.0×10^{-3} M to 1.38×10^{-2} M were added to the flasks, and the solutions were brought to volume. The reference solution was prepared with the same concentration of α-cyclodextrin in 0.08 M HCl. The final solutions were equilibrated at 25.0°, and absorbances were read[5] at 508 nm in 1-cm cells. For calculating Q by Eq. 26, the molar absorptivities were measured in 0.08 M HCl at 508 nm, giving $\epsilon_I = 4.82 \times 10^4$ and $\epsilon_{IL} = 8.72 \times 10^2$. The stability constant K_{11I} for the 1:1 complex of methyl orange with α-cyclodextrin at 25.0° in 0.08 M HCl was determined by the conventional Benesi–Hildebrand spectrophotometric method (10); K_{11I} was found to be 672.9 M^{-1} (standard deviation 5.0 M^{-1}).

RESULTS

Nine phenols were studied by the potentiometric method. 4-Cyanophenol and 4-nitrophenol could be described as case I systems; Fig. 1 shows the plot of C' against L_t for the 4-cyanophenol–α-cyclodextrin system, and Fig. 2 is the corresponding plot according to Eq. 5. Phenol, 4-methylphenol, and 4-fluorophenol were case II systems, as indicated for 4-methylphenol in Fig. 3. The C' *versus* L_t plot for 4-methoxyphenol (Fig. 4) shows that it is a case III system; Fig. 5 is the linearized plot according to Eq. 11 for this system. 4-Iodophenol, 4-bromophenol, and 4-chlorophenol showed case IV behavior, as seen in Fig. 6 for 4-chlorophenol.

For case IV systems, an independent study is necessary to determine K_{11a} for use in Eq. 14. The UV absorption spectra of these compounds were not significantly altered by the presence of α-cyclodextrin, so simple UV spectrophotometry did not provide a method for measuring K_{11a}. The competitive methyl orange spectrophotometric method was therefore used. Since the potentiometric data showed that these were case IV systems, evidently $K_{12a} = 0$, and only 1:1 stoichiometry need be considered for the conjugate acid forms of the substrates. The studies were made at constant L_t and varying S_t. Figure 7 is the plot according to Eq. 25 for the 4-chlorophenol–methyl orange–α-cyclodextrin system. Figure 8 shows the linear plot of Eq. 14 for 4-chlorophenol, in which the K_{11a} value determined from Fig. 7 has been used to construct the ordinate values.

The validity of the assignments of case I systems was tested by treating them according to case IV equation (Eq. 14), which should give a slope of zero for a case I system. Similarly, case II assignments were tested by plotting according to the case III equation. The stability constants are listed in Table I. The K_{12b} values for the methoxy, iodo, bromo, and chloro compounds are clearly significant; these are the case III and IV systems. The K_{12b} values evaluated for the case I and II systems are not significantly different from zero, except for phenol. However, the corre-

[1] Sigma Chemical Co. (Lot 29C-0425).
[2] Eastman Organic Chemicals.
[3] Aldrich Chemical Co. These compounds were purified by A. B. Wong.
[4] Orion 701A pH meter equipped with a Sargent-Welch S30072-15 electrode.
[5] On Cary Model 14 or Perkin-Elmer Model 559 spectrophotometers.

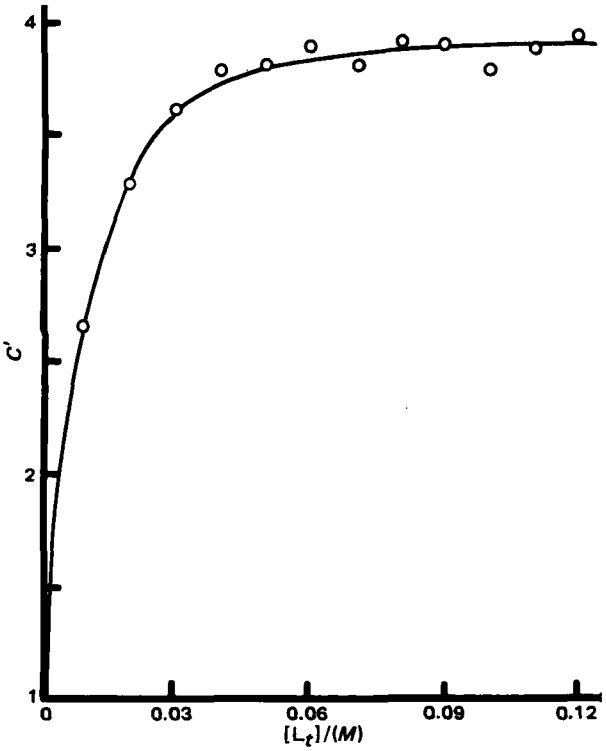

Figure 1—*Plot of C′ against L_t for 4-cyanophenol–α-cyclodextrin, a case I system.*

lation coefficient was 0.998 for the case II linear plot, whereas it was 0.553 for treatment as a case III system; hence, phenol is better described as a case II system, with K_{12b} equal to zero.

DISCUSSION

Competitive Indicator Method—To test the competitive methyl orange spectrophotometric method, it was applied to the determination of K_{11a} for 4-nitrophenol, which can be measured by several techniques. Table II lists stability constants for the 4-nitrophenol–α-cyclodextrin

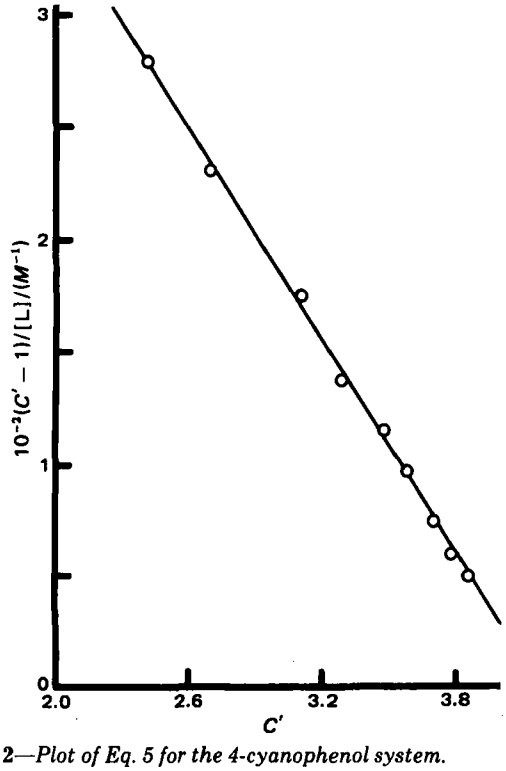

Figure 2—*Plot of Eq. 5 for the 4-cyanophenol system.*

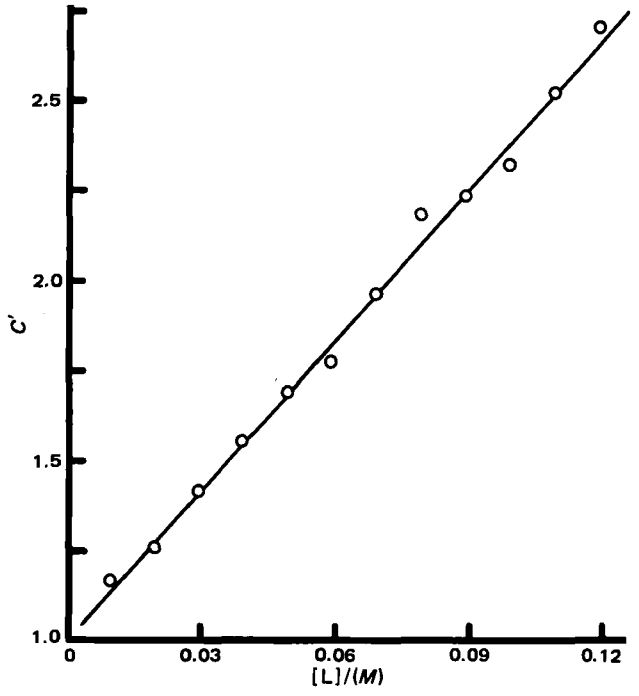

Figure 3—*Plot of Eq. 8 for the 4-methylphenol system.*

system determined in this work and as reported by other investigators. It is clear that the methyl orange method gives a result consistent with other methods. The methyl orange method was also applied to the benzoic acid–α-cyclodextrin system, yielding K_{11a} = 810 M^{-1}. This is significantly lower than the value 1050 M^{-1} reported by Casu and Ravà (6) for this system studied by their version of the competitive methyl orange method (which neglects the [IL] term in Eq. 17), but is consistent with recent values determined by other methods (1).

The method as described, using methyl orange as the indicator, is applicable only in an acidic solution, but with other indicators it may be useful under other conditions. The plot according to Eq. 25 should yield an intercept of unity, and this was verified in the present applications. When K_{11I} is approximately equal to K_{11S}, competition to displace the

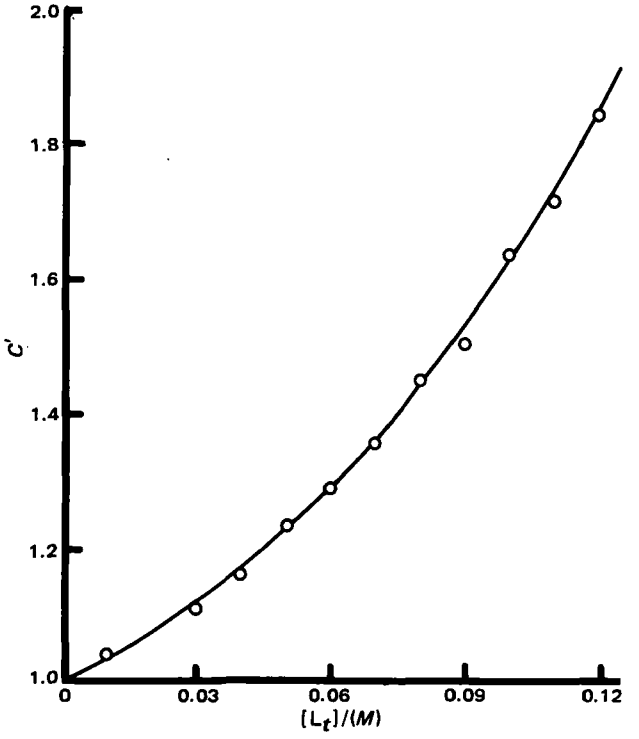

Figure 4—*Plot of C′ against L_t for 4-methoxyphenol, a case III system.*

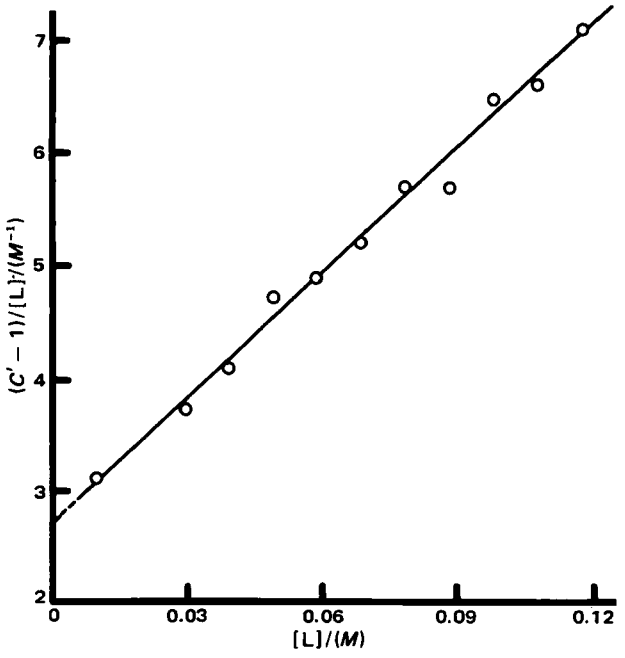

Figure 5—*Plot of Eq. 11 for the 4-methoxyphenol system.*

indicator requires that L_t and S_t be of comparable magnitude, although L_t can be much larger than I_t. If K_{11S} is much larger than K_{11I}, a smaller concentration of substrate would suffice to displace the indicator from its complex. Equation 25 can accommodate changes in both S_t and L_t in an experiment, but it was found convenient to hold L_t constant and to vary S_t.

Binding Sites and Complex Stability—These phenolic compounds can be viewed as substrates having two possible binding sites, namely the hydroxyl group and the 4-substituted moiety, that can interact with the cavity of the α-cyclodextrin. A model for such a system was described earlier (1, 18). For a two-binding site substrate that forms only 1:1 and 1:2 complexes, the experimental stability constants K_{11} and K_{12} are related to the binding site stability constants by:

$$K_{11} = K_X + K_Y \qquad \text{(Eq. 28)}$$

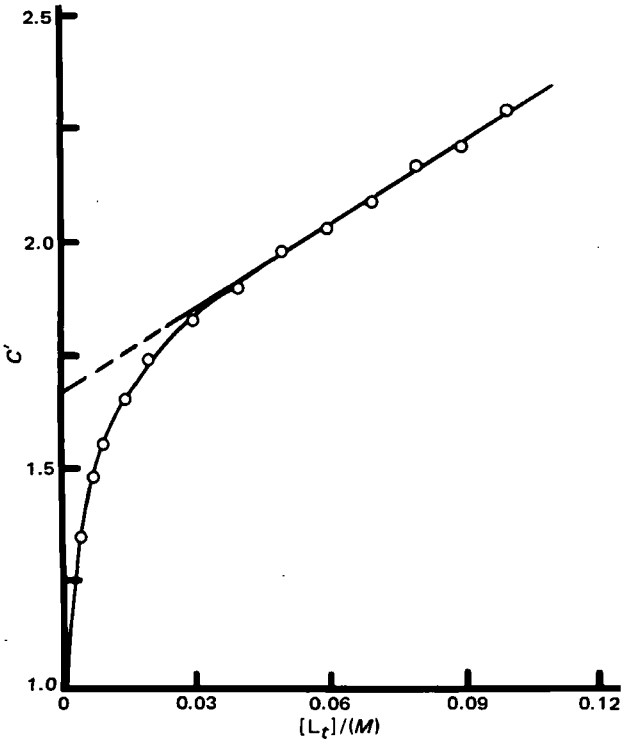

Figure 6—*Plot of C′ against L_t for 4-chlorophenol, a case IV system.*

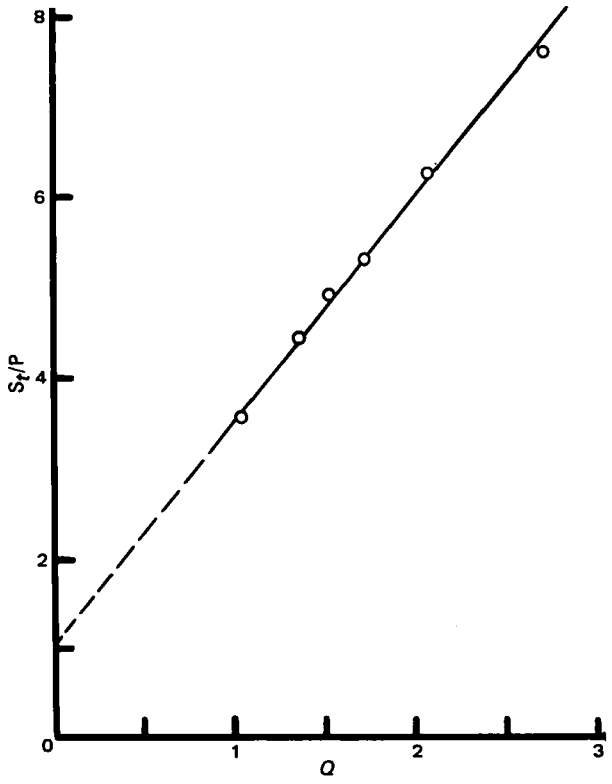

Figure 7—*Plot of Eq. 25 for the 4-chlorophenol–methyl orange–α-cyclodextrin system.*

$$K_{12} = \frac{aK_XK_Y}{K_{11}} \qquad \text{(Eq. 29)}$$

In these relationships K_X and K_Y are 1:1 stability constants for binding to sites X and Y, and a is a parameter that measures interaction between the two sites in a 1:2 complex. Such a two-site substrate is therefore capable of forming two isomeric 1:1 complexes and one 1:2 complex. This model leads to interpretations in terms of binding sites. The derivation

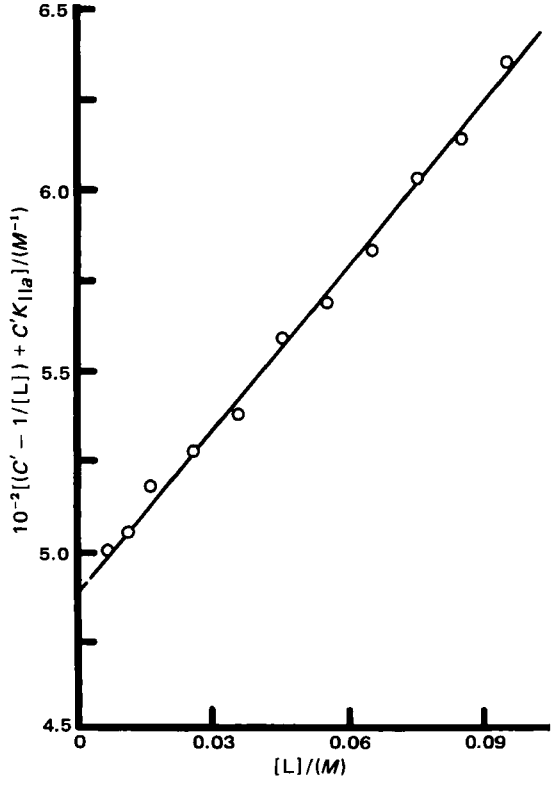

Figure 8—*Plot of Eq. 14 for the 4-chlorophenol system.*

Table I—Stability Constants for α-Cyclodextrin Complexes of 4-Substituted Phenols at 25° [a]

4-Substituent	K_{11b}, M^{-1}	K_{12b}, M^{-1}	K_{11a}, M^{-1}
OCH_3	2.7 (0.10)	13.3 (0.68)	0
CH_3	13.9 (0.34)	−0.08 (0.36)	0
H	10.9 (0.19)	0.46 (0.21)	0
COO^- [b]	—	—	16.6 (0.23)
F	15.6 (0.70)	−1.00 (0.95)	0
I	3955 (26.3)	2.4 (0.09)	2316 (65.5)
Cl	487.9 (1.6)	3.1 (0.06)	272 (9.9)
Br	1221 (7.4)	4.7 (0.09)	704 (31.8)
COOH [b]	—	—	1130 (7.7)
CN	662 (9.0)	0.09 (0.08)	158.3 (2.7)
NO_2	2408 (87.6)	−0.14 (0.16)	245 (10.2)

[a] Standard deviations in parentheses. [b] Taken from Ref. 1.

of Eq. 29 is given elsewhere (1), and the significance of a has also been discussed previously (1).

Whether a cyclodextrin interacts with a binding site is largely dependent on the size and shape of the site; but if the site can enter the cyclodextrin cavity to form an inclusion complex, the strength of the complex will be controlled mainly by the electron density, the polarizability, and the polarity of the binding site. Increases in site electron density and polarizability will tend to increase complex stability, whereas high polarity will decrease complex stability (in a polar solvent). In a series of closely related substrates, the trend of complex stabilities with these factors may therefore give information about the binding sites. In this way Hammett plots of K_{11a} and K_{11b} for 4-substituted benzoic acids (1) led to the conclusion that K_{11a} describes mainly binding to the carboxylic acid site, whereas K_{11b} describes binding solely at the 4-substituent site.

This approach will be used to discuss the data in Table I. It is postulated that complex stability in a series is primarily determined by site electron density, modified by polarizability and polarity. The substrates in Table I are arranged in order of increasing Hammett substituent constant σ for the 4-substituent; σ is a measure of the electron-attracting ability of the substituent. For both K_{11a} and K_{11b} the same rough trend is seen, namely an increase in complex stability with increasing electron density at the 4-substituent. These data therefore suggest that the primary binding site, for both the conjugate acid and the conjugate base forms of the substrates, is the 4-substituent end of the molecule.

The correlations of K_{11a} and K_{11b} with σ are obviously not closely followed, the halogens I and Br having complex-strengthening effects not accounted for by their σ values. But these substituents have high polarizabilities, which will tend to increase complex stability; K_{11a} and K_{11b} can be well correlated by:

$$\log K_{11a} = -0.96 + 0.12R_D - 0.10\mu \qquad \text{(Eq. 30)}$$

$$\log K_{11b} = -1.41 + 5.33\sigma + 0.15R_D - 0.81\mu \qquad \text{(Eq. 31)}$$

where R_D is the molar refraction of $X—C_6H_5$ and μ is the dipole moment of $X—C_6H_4—OH$[6]. These correlations have no theoretical significance, but they suggest that this interpretation is reasonable.

If K_{11b} and K_{11a} describe binding at the 4-substituent, then K_{12b} and K_{12a} describe binding at the hydroxyl site, because the 1:2 complex is formed by adding a second cyclodextrin to the 1:1 complex. But K_{12a} is zero for all systems, leading to the conclusion that no significant binding occurs at the phenolic hydroxyl site; this conclusion applies also to those phenolate substrates for which K_{12b} is zero. There exist, however, some finite K_{12b} values, and it is notable that in each of these substrates (the methoxy, iodo, chloro, and bromo compounds) the 4-substituent can tolerate a positive charge by electron release through resonance delocalization; this may sufficiently counter the electron release of the phenolate site to allow significant binding at that site.

K_{11a} for the phenol $^-OOC—C_6H_4—OH$ is evidently the same quantity as K_{11b} for the benzoic acid anion $HO—C_6H_4—COO^-$. When this was discussed as a benzoate (1), it was concluded that the carboxylate site binding was negligible, leaving binding at the phenolic site to account for the observed binding. On the other hand, it has been concluded here that binding at the hydroxyl site in phenols is probably negligible. This inconsistency suggests that it may not always be permissible to make a common assignment of binding mode to all of the members of a series. In this case, the negative charge on the carboxylate may oppose the usual electron release by the hydroxyl group, leaving the hydroxyl site susceptible to binding.

[6] The correlation coefficients are 0.99 for both equations. The standard deviations are 0.06 in log K_{11a} and 0.13 in log K_{11b}.

Table II—Comparison of Stability Constants for the 4-Nitrophenol–α-Cyclodextrin System [a]

Method	K_{11b}, M^{-1}	K_{11a}, M^{-1}	Reference
Spectrophotometry	2230	290	11
Thermometry	—	126	12
Potentiometry	2200	200	2
Spectrophotometry	2512	190	13
Polarography	2439	—	14
Potentiometry	2143	211	15
Spectrophotometry	2720	250	16
Potentiometry	2382	270	17
Potentiometry	2408	245	This work
Spectrophotometry [b]	—	249	This work
Competitive spectrophotometry [c]	—	249	This work

[a] At 25°; ionic strengths differ. [b] Studied at 317 nm. [c] Methyl orange method described herein.

Effect of Phenol Ionization on Complex Stability—It is a general result that K_{11b} is greater than K_{11a} for the cyclodextrin complexes of phenols (Table I); that is, the anionic form of the substrate "partitions" into the relatively nonpolar cyclodextrin cavity more favorably than does the un-ionized form. This unexpected behavior (which is the reverse of the situation seen with carboxylic acid substrates) has been discussed for the particular case of 4-nitrophenol by several authors. Dunn and Bernhard (19) accounted for the greater stability of the 4-nitrophenoxide–α-cyclodextrin complex in terms of a stronger dispersion force field between the included nitrophenoxide and the interior of the cavity. These authors assumed that the nitro end of the substrate was inserted into the cavity. Bergeron and Channing (20) have shown that this is in fact the geometry of the complex. Benzoic acid, on the other hand, complexes with the carboxylic acid end of the molecule penetrating the cavity (1, 15, 21). Bergeron *et al.* (21) have called attention to this difference in substrate–ligand orientation and have related it to the corresponding difference in relative stabilities of the neutral and charged complexes. Their argument is that, if induced dipole–dipole interaction is primarily responsible for binding, the nitrophenolate will be more strongly bound than is the neutral phenol.

It is not necessary to specify the types of forces responsible for binding to account generally for the result that $K_{11b} > K_{11a}$. This result is surprising only if an ion is regarded as a point charge. But a phenolate ion is decidedly not a point charge on the molecular scale. The concept described in the preceding section, namely that complex stability is determined by *binding site* electron density, polarizability, and polarity, will be applied to the phenol and phenolate complexes with cyclodextrin.

Neutral phenols are highly dipolar species, especially those with electron-withdrawing 4-substituents, as revealed by their dipole moments, which can be accounted for by electron delocalization as shown in Scheme II.

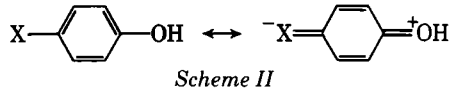

Scheme II

Electron density is increased at the 4-substituent and is decreased at the hydroxyl group; moreover the polarizability of the hydroxyl group is decreased. Thus, complexing with the cyclodextrin cavity should occur at the 4-substituent site rather than at the hydroxyl site, and this is consistent with the trend of K_{11a} values as discussed above.

On ionization of the hydroxyl group, delocalization disperses the excess electronic charge as in Scheme III.

Scheme III

The electron density at the 4-substituent is greater in the anion than in the neutral form, hence the complex stability at this binding site is greater in the anion. As shown above, K_{11a} represents solely binding at the 4-substituent, and K_{11b} represents predominantly 4-substituent binding. (Those substrates with finite K_{12b} values include, in K_{11b}, a small contribution from binding at the hydroxyl site, according to Eq. 28.) Therefore, K_{11b} will be larger than K_{11a}. Moreover, the increased charge density on the oxygen in the phenolate species actually may lead to some binding at this site, which in the current context is actually less polar than the hydroxyl group in the neutral substrate. Localized negative charge

(as in carboxylic acid anions) may be destabilizing, positive charge (as in protonated amines) will always be destabilizing, but delocalized negative charge (as in phenol anions) may be stabilizing.

REFERENCES

(1) K. A. Connors, S.-F. Lin, and A. B. Wong, *J. Pharm. Sci.*, **71**, 217 (1982).

(2) K. A. Connors and J. M. Lipari, *J. Pharm. Sci.*, **65**, 379 (1976).

(3) K. A. Connors and T. W. Rosanske, *J. Pharm. Sci.*, **69**, 173 (1980).

(4) W. Broser, *Z. Naturforsch.*, **8B**, 722 (1953).

(5) V. W. Lautsch, W. Bandel, and W. Broser, *Z. Naturforsch.*, **11B**, 282 (1956).

(6) B. Casu and L. Ravà, *Ric. Sci.*, **36**, 733 (1966).

(7) S.-F. Lin, Ph.D. Thesis, University of Wisconsin-Madison, 1981.

(8) M. DeVylder and D. DeKeukeleire, *Bull. Soc. Chim. Belg.*, **87**, 9, 497 (1978).

(9) D. D. Perrin, W. L. F. Armarego, and D. R. Perrin, "Purification of Laboratory Chemicals," Pergamon, Long Island City, N.Y., 1966.

(10) H. A. Benesi and J. H. Hildebrand, *J. Am. Chem. Soc.*, **71**, 2703 (1949).

(11) F. Cramer, W. Saenger, and H.-Ch. Spatz, *J. Am. Chem. Soc.*, **89**, 14 (1967).

(12) E. A. Lewis and L. D. Hansen, *J. Chem. Soc., Perkin Trans. II*, **1973**, 2081.

(13) R. J. Bergeron, M. A. Channing, G. J. Gibeily, and D. M. Pillor, *J. Am. Chem. Soc.*, **99**, 5146 (1977).

(14) T. Osa, T. Matsue, and M. Fujihara, *Heterocycles*, **6**, 1833 (1977).

(15) R. I. Gelb, L. M. Schwartz, R. F. Johnson, and D. A. Laufer, *J. Am. Chem. Soc.*, **101**, 1869 (1979).

(16) T. W. Rosanske, Ph.D. Thesis, University of Wisconsin-Madison, 1979.

(17) A. B. Wong, Ph.D. Thesis, University of Wisconsin-Madison, 1980.

(18) T. W. Rosanske and K. A. Connors, *J. Pharm. Sci.*, **69**, 564 (1980).

(19) M. F. Dunn and S. A. Bernhard, in "Investigation of Rates and Mechanisms of Reactions," Part I, (Vol. VI of "Techniques of Chemistry"), E. S. Lewis, Ed., Wiley, New York, N.Y., 1974, p. 624.

(20) R. J. Bergeron and M. A. Channing, *J. Am. Chem. Soc.*, **101**, 2511 (1979).

(21) R. J. Bergeron, M. A. Channing, and K. A. McGovern, *J. Am. Chem. Soc.*, **100**, 2878 (1978).

ACKNOWLEDGMENTS

This study was supported in part by a grant from The Upjohn Company. Preliminary studies by Dr. Albert B. Wong are gratefully acknowledged.

Improvement of the Oral Bioavailability of Digitalis Glycosides by Cyclodextrin Complexation

KANETO UEKAMA *x, TOSHIO FUJINAGA *, FUMITOSHI HIRAYAMA *, MASAKI OTAGIRI *, MASAKI YAMASAKI ‡, HAKARU SEO §, TSUYOSHI HASHIMOTO §, and MICHIO TSURUOKA §

Received January 6, 1982, from the **Faculty of Pharmaceutical Sciences, Kumamoto University, 5-1, Oe-honmachi, Kumamoto 862, Japan,* ‡*Department of Biochemistry, Medical School, Kumamoto University, 2-2-1, Honjo, Kumamoto 860, Japan,* and §*Department of Pharmacy, Miyazaki Medical College Hospital, 5200 Kiyotake-cho, Miyazaki-gun, Miyazaki 889-16, Japan.* Accepted for publication September 1, 1982.

Abstract □ Inclusion complexes of the digitalis glycosides digitoxin, digoxin, and methyl digoxin with three cyclodextrins (α-, β-, γ-homologues) in water and in the solid state were studied by a solubility method, IR and ^{1}H-NMR spectroscopy, and X-ray diffractometry. Solid complexes (in a molar ratio of 1:4) of the digitalis glycosides with γ-cyclodextrin were prepared and their *in vivo* absorption examined. The rapidly dissolving form of the γ-cyclodextrin complex significantly increased plasma levels of digoxin (~5.4-fold) after oral administration to dogs.

Keyphrases □ Bioavailability—oral, digoxin, digitoxin, methyl digoxin, complexation with cyclodextrins □ Digoxin—complexation with cyclodextrins, oral bioavailability, digitoxin, methyl digoxin □ Cyclodextrins—complexation with digitalis glycosides, oral bioavailability, digoxin, digitoxin, methyl digoxin

The bioavailability of the digitalis glycosides from commercial tablets varies significantly (1–3). The main cause of this variability appears to be related to such factors as low water solubility (4–6) and chemical instability in acidic media (7–9). Cyclodextrins have been used extensively to improve various physicochemical properties of drug molecules (10–12) by forming inclusion complexes in which the drug molecules are included in the relatively hydrophobic cavity of the cyclodextrins (13).

The present study describes the inclusion complexes of the digitalis glycosides digitoxin, digoxin, and methyl digoxin with the three cyclodextrins (α-, β-, γ-homologues). Complex formation in water and in the solid state was studied by a solubility method, IR and ^{1}H-NMR spectroscopy, and X-ray diffractometry. Plasma levels of digoxin were determined after the oral administration of the digoxin–γ-cyclodextrin complex to dogs.

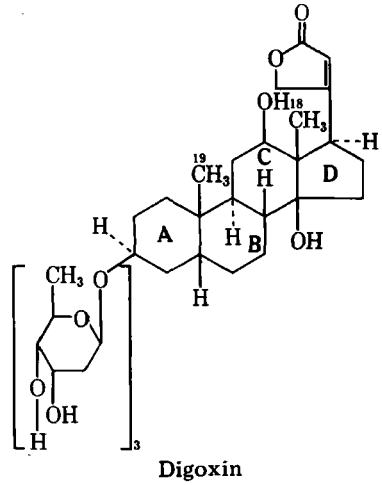

Digoxin

0022-3549/83/1100-1338$01.00/0

(as in carboxylic acid anions) may be destabilizing, positive charge (as in protonated amines) will always be destabilizing, but delocalized negative charge (as in phenol anions) may be stabilizing.

REFERENCES

(1) K. A. Connors, S.-F. Lin, and A. B. Wong, *J. Pharm. Sci.*, **71**, 217 (1982).

(2) K. A. Connors and J. M. Lipari, *J. Pharm. Sci.*, **65**, 379 (1976).

(3) K. A. Connors and T. W. Rosanske, *J. Pharm. Sci.*, **69**, 173 (1980).

(4) W. Broser, *Z. Naturforsch.*, **8B**, 722 (1953).

(5) V. W. Lautsch, W. Bandel, and W. Broser, *Z. Naturforsch.*, **11B**, 282 (1956).

(6) B. Casu and L. Ravà, *Ric. Sci.*, **36**, 733 (1966).

(7) S.-F. Lin, Ph.D. Thesis, University of Wisconsin-Madison, 1981.

(8) M. DeVylder and D. DeKeukeleire, *Bull. Soc. Chim. Belg.*, **87**, 9, 497 (1978).

(9) D. D. Perrin, W. L. F. Armarego, and D. R. Perrin, "Purification of Laboratory Chemicals," Pergamon, Long Island City, N.Y., 1966.

(10) H. A. Benesi and J. H. Hildebrand, *J. Am. Chem. Soc.*, **71**, 2703 (1949).

(11) F. Cramer, W. Saenger, and H.-Ch. Spatz, *J. Am. Chem. Soc.*, **89**, 14 (1967).

(12) E. A. Lewis and L. D. Hansen, *J. Chem. Soc., Perkin Trans. II*, **1973**, 2081.

(13) R. J. Bergeron, M. A. Channing, G. J. Gibeily, and D. M. Pillor, *J. Am. Chem. Soc.*, **99**, 5146 (1977).

(14) T. Osa, T. Matsue, and M. Fujihara, *Heterocycles*, **6**, 1833 (1977).

(15) R. I. Gelb, L. M. Schwartz, R. F. Johnson, and D. A. Laufer, *J. Am. Chem. Soc.*, **101**, 1869 (1979).

(16) T. W. Rosanske, Ph.D. Thesis, University of Wisconsin-Madison, 1979.

(17) A. B. Wong, Ph.D. Thesis, University of Wisconsin-Madison, 1980.

(18) T. W. Rosanske and K. A. Connors, *J. Pharm. Sci.*, **69**, 564 (1980).

(19) M. F. Dunn and S. A. Bernhard, in "Investigation of Rates and Mechanisms of Reactions," Part I, (Vol. VI of "Techniques of Chemistry"), E. S. Lewis, Ed., Wiley, New York, N.Y., 1974, p. 624.

(20) R. J. Bergeron and M. A. Channing, *J. Am. Chem. Soc.*, **101**, 2511 (1979).

(21) R. J. Bergeron, M. A. Channing, and K. A. McGovern, *J. Am. Chem. Soc.*, **100**, 2878 (1978).

ACKNOWLEDGMENTS

This study was supported in part by a grant from The Upjohn Company. Preliminary studies by Dr. Albert B. Wong are gratefully acknowledged.

Improvement of the Oral Bioavailability of Digitalis Glycosides by Cyclodextrin Complexation

KANETO UEKAMA *x, TOSHIO FUJINAGA *, FUMITOSHI HIRAYAMA *, MASAKI OTAGIRI *, MASAKI YAMASAKI ‡, HAKARU SEO §, TSUYOSHI HASHIMOTO §, and MICHIO TSURUOKA §

Received January 6, 1982, from the **Faculty of Pharmaceutical Sciences, Kumamoto University, 5-1, Oe-honmachi, Kumamoto 862, Japan,* ‡*Department of Biochemistry, Medical School, Kumamoto University, 2-2-1, Honjo, Kumamoto 860, Japan,* and §*Department of Pharmacy, Miyazaki Medical College Hospital, 5200 Kiyotake-cho, Miyazaki-gun, Miyazaki 889-16, Japan.* Accepted for publication September 1, 1982.

Abstract □ Inclusion complexes of the digitalis glycosides digitoxin, digoxin, and methyl digoxin with three cyclodextrins (α-, β-, γ-homologues) in water and in the solid state were studied by a solubility method, IR and ^{1}H-NMR spectroscopy, and X-ray diffractometry. Solid complexes (in a molar ratio of 1:4) of the digitalis glycosides with γ-cyclodextrin were prepared and their *in vivo* absorption examined. The rapidly dissolving form of the γ-cyclodextrin complex significantly increased plasma levels of digoxin (~5.4-fold) after oral administration to dogs.

Keyphrases □ Bioavailability—oral, digoxin, digitoxin, methyl digoxin, complexation with cyclodextrins □ Digoxin—complexation with cyclodextrins, oral bioavailability, digitoxin, methyl digoxin □ Cyclodextrins—complexation with digitalis glycosides, oral bioavailability, digoxin, digitoxin, methyl digoxin

The bioavailability of the digitalis glycosides from commercial tablets varies significantly (1–3). The main cause of this variability appears to be related to such factors as low water solubility (4–6) and chemical instability in acidic media (7–9). Cyclodextrins have been used extensively to improve various physicochemical properties of drug molecules (10–12) by forming inclusion complexes in which the drug molecules are included in the relatively hydrophobic cavity of the cyclodextrins (13).

The present study describes the inclusion complexes of the digitalis glycosides digitoxin, digoxin, and methyl digoxin with the three cyclodextrins (α-, β-, γ-homologues). Complex formation in water and in the solid state was studied by a solubility method, IR and ^{1}H-NMR spectroscopy, and X-ray diffractometry. Plasma levels of digoxin were determined after the oral administration of the digoxin–γ-cyclodextrin complex to dogs.

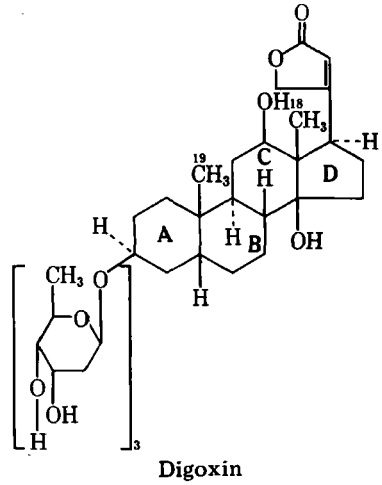

Digoxin

0022-3549/83/1100-1338$01.00/0

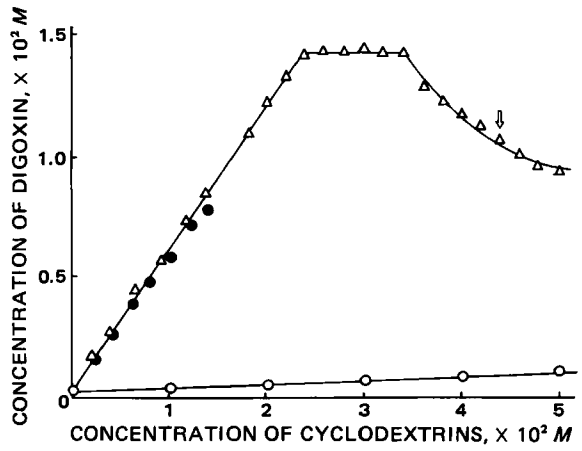

Figure 1—*Phase solubility diagrams of the digoxin–cyclodextrin systems in water at 25°. Key: (○) α-cyclodextrin; (●) β-cyclodextrin; and (△) γ-cyclodextrin. The arrow indicates the experimental conditions for the preparation of solid γ-cyclodextrin complexes (see* text*).*

EXPERIMENTAL

Materials—Digitoxin[1], digoxin[2], methyl digoxin[2], and the α-, β-, and γ-cyclodextrins[3] were used as supplied. All other materials and solvents were analytical reagent grade. Deionized double-distilled water was used.

Solubility Studies—Solubility measurements were carried out according to Higuchi and Lach (14). Excess amounts of digitalis glycosides were added to an aqueous solution containing various concentrations of cyclodextrins and were shaken at 25 ± 0.5°. After equilibrium was reached (~7 days), an aliquot was centrifuged and pipetted through a cotton filter. A 0.5-ml aliquot was diluted with ethanol–water (1:1, v/v) and analyzed spectrophotometrically[4]. An apparent stability constant, K', was calculated from the initial linear portion of the phase solubility diagram according to the following (15):

$$K' = \frac{\text{slope}}{\text{intercept} \cdot (1 - \text{slope})}$$

Preparation of Solid Complexes—The solid complexes were prepared by mixing appropriate amounts of the cyclodextrin and digitalis glycoside in water. Appropriate mixtures were chosen by examining the descending curvature of the B_s-type phase solubility diagram (see Fig. 1). For example, 3.25 g of digoxin and 14.3 g of γ-cyclodextrin were added to 250 ml of water, and the mixture was stirred at 25° for 7 days. The complex, which precipitated as a microcrystalline powder, was removed by filtration and dried under vacuum at 60° for 48 hr. This powder corresponded to a 1:4 digoxin–γ-cyclodextrin complex, which had a molecular weight of 5965.

Spectroscopic Studies—The IR spectra[5] were measured as potassium bromide pellets. ^{1}H-NMR spectra[6] were measured in D_2O using Fourier transform methodology (16). An average of 6000 accumulations with 8192 data points were made at a sweep width of 2000 Hz. The ^{1}H-chemical shifts were assigned values based on the external standard 3-(trimethylsilyl)propanesulfonic acid sodium salt with an accuracy of ±0.0012 ppm. The powder X-ray diffraction spectra[7] were obtained by scanning at 1°/min in terms of 2θ angle.

Dissolution Studies—The digoxin powder (150 mg, 100 mesh) was compressed into a cylindrical tablet (diameter 10 mm) at a pressure of ~200 kg/cm^2. The release of drug was measured using a rotating disk apparatus (17) in 0.05 M KCl–HCl solution (pH 1.52) at 37°. At appropriate intervals, 1-ml samples were removed, extracted with chloroform, and assayed by high-performance liquid chromatography (HPLC). The dissolution behavior of 1:4 digitalis glycoside–γ-cyclodextrin complexes (150 mg, 100 mesh) was examined in a similar manner.

HPLC Analysis—The chromatograph[8] was operated at a flow rate of 0.7 ml/min. The separation utilized a column[9] (40 mm × 25 cm) with methanol–water (58:42) as a mobile phase, and the eluant was monitored spectrophotometrically at 220 nm. Components were quantitated by measuring peak heights and comparing the height with an internal standard containing a known amount of prednisolone[2].

***In Vivo* Absorption Studies**—Six female beagle dogs, with an average weight of 11 kg, were used. A tablet was administered orally with 20 ml of water after an overnight fast at intervals of at least 1 week. The administration sequence was based on a crossover matrix designed to minimize any residual or cumulative effects of the preceding dose. The formulations of the tablets were as follows: 98–99% (w/w) lactose as a diluent, 1.0% (w/w) magnesium stearate as a lubricant, and 0.1% (w/w) digoxin or 0.76% (w/w) digoxin–γ-cyclodextrin complex. Plasma samples were obtained at timed intervals, and digoxin concentrations were determined by enzyme immunoassay[10] (18).

Table I—Apparent Stability Constants (M^{-1}) of Digitalis Glycoside–Cyclodextrin Complexes Determined by the Solubility Method in Water at 25°

Digitalis Glycoside	Cyclodextrin α	Cyclodextrin β	Cyclodextrin γ
Digoxin	180	11200	12200
Digitoxin	290	17000	63600
Methyl digoxin	400	11400	13600

RESULTS AND DISCUSSION

Solubility Study—The complexing behavior of digitalis glycosides with cyclodextrins in water was studied by a solubility method. The phase solubility diagrams obtained for digoxin with three cyclodextrins in water are shown in Fig. 1. In the case of α-cyclodextrin, the solubility of digoxin increased slightly in a linear fashion as a function of the α-cyclodextrin concentration, and the resulting solubility curve can be classified as type A_L (15). The solubility plot for the β-cyclodextrin system is qualitatively similar to that for α-cyclodextrin, where a large increase in digoxin solubility was obtained within the solubility limit of β-cyclodextrin (~1.6 × 10^{-2} M). On the other hand, γ-cyclodextrin showed a typical B_S-type solubility curve (15), where the initial ascending portion is followed by a plateau region and then a decrease in total digoxin solubility accompanied by precipitation of a microcrystalline complex. Although the shape of solubility curves in Fig. 1 cannot be completely explained in terms of a stoichiometric relationship (19), an apparent stability constant (K'), as a tentative measure of inclusion complexation, was estimated from the equation based on the assumption that a 1:1 complex is initially formed. Table I summarizes the K' values for digitalis glycoside–cyclodextrin systems calculated from the initial ascending portion of solubility diagrams. The cavity size dependencies of the present systems were clearly noted from the magnitude of K' values (γ- > β- > α-cyclodextrin).

Since the digitalis glycoside molecule is too large to be included within the cyclodextrin cavity, it is reasonable to assume that at least one complex with a stoichiometric host-to-guest molecular ratio greater than one may be formed, in particular for the higher concentrations of cyclodextrin. To gain insight into the stoichiometry of the γ-cyclodextrin system, the solid material that precipitated beyond the plateau region was analyzed (19). The analysis of the digoxin–γ-cyclodextrin system gave the following results for 10^2L_t (the total concentration of γ-cyclodextrin) and X_s (the mole fraction of digoxin in the solid): 3.6, 0.20; 4.0, 0.20; 4.2, 0.20; 4.4, 0.20; 4.8, 0.20; and 5.0, 0.20. These data indicate that 1:4 complex formation of digoxin with γ-cyclodextrin predominate beyond the plateau region, while the lower-order complexes (*i.e.*, 1:1, 1:2, and 1:3) may be formed around the initial increasing portion of the solubility diagram (Fig. 1). Similar results were obtained for γ-cyclodextrin with digitoxin and methyl digoxin. Since only the 1:4 solid complex was isolated from the descending curvature of the B_S-type solubility diagram (probably because of limited solubility), this form was used for further study.

NMR Study—^{1}H-NMR techniques (200 MHz) were employed to examine the inclusion mode in aqueous solution. Table II summarizes a typical example of the effects of cyclodextrins on some ^{1}H-chemical shifts (18-methyl and 19-methyl) of digoxin (20). Unfortunately, the other proton signals were too weak to be quantitatively analyzed under the experimental conditions used. In the presence of cyclodextrins, both

[1] Shionogi Pharmaceutical Co. Ltd., Osaka, Japan.
[2] Mitsubishi Yuka Pharmaceutical Co. Ltd., Ibaraki, Japan.
[3] Nippon Shokuhin Kako Ltd., Tokyo, Japan.
[4] Hitachi 556S; Hitachi Ltd., Tokyo, Japan.
[5] JEOL JIR-40; JEOL Ltd., Tokyo, Japan.
[6] JEOL JNM-FX 200; JEOL Ltd., Tokyo, Japan.
[7] Rigaku Denki Geiger Flex 2012; Rigaku Denki Co. Ltd., Tokyo, Japan.
[8] ATTO HSLC-013-4; ATTO Co., Tokyo, Japan.
[9] LiChrosorb RP-18 (5 μm); E. Merck, Darmstadt, West Germany.
[10] Digoxin batch assay Emit cad.; Syva Co., U.S.A.

Table II—Effects of Cyclodextrins on ^{1}H-Chemical Shifts of Some Digoxin Protons in Deuterium Oxide [a]

Protons[b]	Without Cyclodextrins	^{1}H Increment[c] with Cyclodextrins, ppm		
		α	β	γ
18-Methyl	0.772	0.038	0.055	0.040
19-Methyl	0.932	0.017	0.198	0.081

[a] Concentrations of digoxin and cyclodextrins were 1.0×10^{-4} *M* and 4.0×10^{-4} *M*, respectively. [b] Assigned according to Ref. 20. [c] The values are positive if any upfield shift of the resonance occurs.

signals moved downfield probably due to the steric perturbation through inclusion complexation (21). Interestingly, the downfield shift of the 19-methyl signal was apparently greater than that of the 18-methyl signal, particularly for β-cyclodextrin. This suggests that the A-ring moiety of the digoxin molecule may strongly interact with β-cyclodextrin. The magnitude of the downfield shifts of both methyl protons decreased in the order of β- > γ- > α-cyclodextrin. The effect of digoxin on ^{1}H-chemical shifts of cyclodextrins was also examined. All cyclodextrin protons located within or near the cavity (*e.g.*, H-3, H-5, or H-6) experienced a shielding effect, where the magnitude of the upfield shift decreased in the order of β- > γ- > α-cyclodextrin. These NMR data indicate that the digoxin molecule is located at the entrance of the α-cyclodextrin cavity, could penetrate further into the β-cyclodextrin cavity, and is loosely bound to γ-cyclodextrin.

Since β-cyclodextrin induced a chemical shift change that was the largest among the three cyclodextrins (Table II), ^{1}H-chemical shift displacements ($\Delta\delta$) of the 19-methyl signal of digoxin on addition of β-cyclodextrin were quantitatively examined. Figure 2 shows the plots of molar ratio of β-cyclodextrin–digoxin *versus* change in chemical shift (δ) of the 19-methyl signal. Above a molar ratio of 4 for β-cyclodextrin–digoxin, no further substantial changes of the chemical shifts occur. This suggests that the stoichiometric equivalence point is reached to form 1:4 complexes of digoxin with β-cyclodextrin. A similar stoichiometric relationship was expected for digoxin–γ-cyclodextrin, which is consistent with the result of the solubility study. Inspection of a space-filling molecular model[11] shows that four molecules of β- or γ-cyclodextrin are available for the complete inclusion of the digoxin; digoxin fits tightly into β-cyclodextrin channels and more loosely into the larger interior space of γ-cyclodextrin channels.

Evidences of Complex Formation in Solid State—To confirm the complexation of cyclodextrins with digitalis glycosides in the solid state, X-ray diffractometry and IR spectroscopy were employed and compared with the corresponding physical mixtures in the same molar ratio. Figure 3 shows the powder X-ray diffraction patterns of the digoxin–γ-cyclodextrin complex and their physical mixture. The diffraction pattern of the physical mixture was simply the superposition of each component, while that of γ-cyclodextrin complex was apparently different from each constituent and constituted a new solid phase. The γ-cyclodextrin complex gave a somewhat diffuse diffraction pattern, suggesting that it is less crystalline than the physical mixture. Figure 4 shows the IR spectra of the digoxin–γ-cyclodextrin complex in the carbonyl-stretching region of the C-23 carbonyl group in digoxin (22). In the case of the γ-cyclodextrin complex, the 1720 cm^{-1} band was found to shift to 1743 cm^{-1},

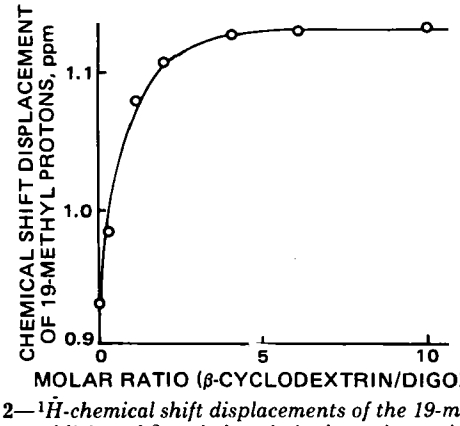

Figure 2—*^{1}H-chemical shift displacements of the 19-methyl signal of digoxin on addition of β-cyclodextrin in deuterium oxide.*

[11] Corey–Pauling–Koltun molecular model.

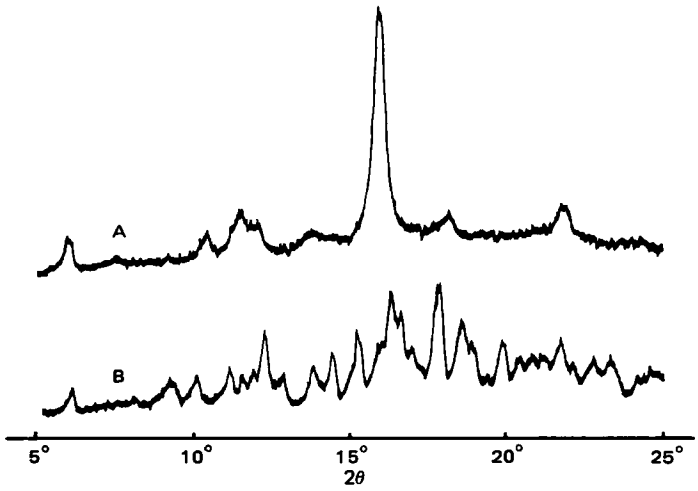

Figure 3—*Powder X-ray diffraction patterns of the digoxin–γ-cyclodextrin system. Key: (A) 1:4 complex of digoxin with γ-cyclodextrin; (B) physical mixture of digoxin and γ-cyclodextrin in 1:4 molar ratio.*

suggesting the dissociation of the intermolecular hydrogen bonds of digoxin through inclusion complexation. Similar results were obtained for other glycoside–γ-cyclodextrin systems. These data clearly indicate that the digitalis glycoside–γ-cyclodextrin complexes exist in the solid state.

Dissolution Behavior of Inclusion Complex—Figure 5 shows a typical example of the dissolution profiles of digoxin and 1:4 digoxin–γ-cyclodextrin complex from the rotating disk with constant surface area in acidic medium (pH 1.52) at 37°, where intact digoxin was quantitatively determined by HPLC. It is evident that the complexed form of digoxin dissolved much more rapidly (~100-fold) than digoxin itself. Similar results were obtained for other digitalis glycoside–γ-cyclodextrin systems. The observed increase in rate may be due to an increase in solubility and/or a decrease in crystallinity of the drug by inclusion complexation (23). It is interesting to note that the dissolution profile of the complex showed a negative curvature with time. This dissolution data may provide evidence for a complicated system, *i.e.*, decrease in concentration of intact digoxin due to acid hydrolysis or change in the tablet surface of the complexed digoxin during the dissolution process. This preliminary study revealed that γ-cyclodextrin significantly retarded the hydrolysis of digoxin in an acidic medium, which is described in detail in a separate paper (24). It seems most likely that the digoxin is precipitating on the surface of the tablet as it dissociates resulting in negative curvature of the dissolution curve, since the NMR data in Table II suggested that the inclusion of digoxin into the γ-cyclodextrin cavity is not tight. Although the complex appears to dissociate rather quickly after dissolution, the initial decrease in dissolution rate together with improved chemical stability in acidic medium suggests that the γ-cyclodextrin complexes of digitalis glycosides may have good oral bioavailability.

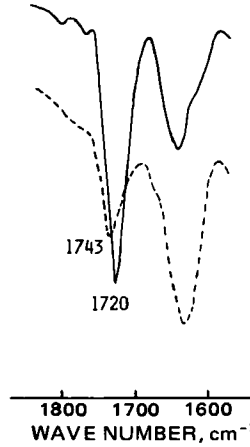

Figure 4—*IR spectra of the digoxin–γ-cyclodextrin system, measured by the potassium bromide disk method. Key: (- - - -) 1:4 complex of digoxin with γ-cyclodextrin; (—) physical mixture of digoxin and γ-cyclodextrin in 1:4 molar ratio.*

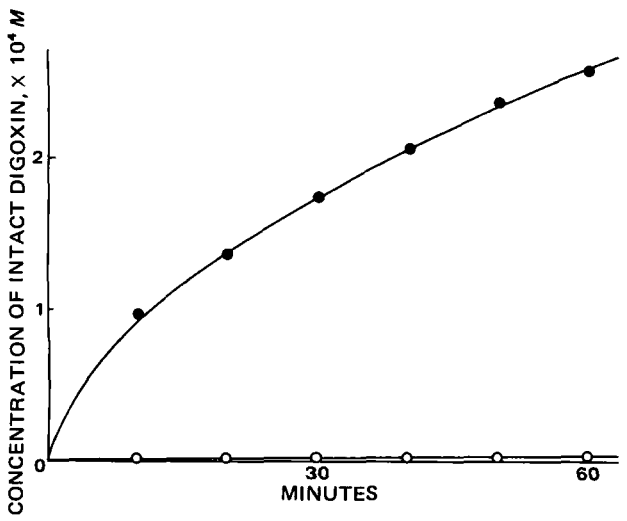

Figure 5—*Dissolution curves of digoxin and its γ-cyclodextrin complex in acidic medium (pH 1.52) at 37°, measured by the rotating disk method. Key: (○) digoxin; (●) 1:4 complex of digoxin with γ-cyclodextrin.*

Bioavailability of Digoxin–γ-Cyclodextrin Complex—The *in vivo* absorption study was undertaken to find out if the *in vitro* dissolution enhancement of digoxin from its γ-cyclodextrin complex increases the GI absorption of the drug. Finely powdered digoxin and its γ-cyclodextrin complex were compressed to tablets (average weight 50 mg) to give a final digoxin content of 0.1 or 0.05%. Figure 6 shows the mean plasma levels of digoxin following the oral administration of tablets to dogs, where the concentration of digoxin in the plasma sample was determined by enzyme immunoassay (18). When equivalent doses of digoxin (100 μg) were administered to dogs, the γ-cyclodextrin complex attained maximum plasma levels of 0.90 ± 0.14 mg/liter at 45 min, which was ~3 times higher than that of digoxin alone (25). The area under the plasma concentration–time curve (AUC) of the complex up to 24 hr was found to be 5.4 times as much as that of digoxin alone. Furthermore, the AUC of the γ-cyclodextrin complex containing 50 μg of digoxin was also found to be superior to that of 100 μg of digoxin alone. Therefore, the enhanced bioavailability of digoxin by γ-cyclodextrin complexation suggests that the complex offers a decrease in dose and fewer side effects in oral digitalis glycoside therapy. It should be noted also that the 1:4 complexation of digitalis glycosides with γ-cyclodextrin results in an ~8-fold increase in the molecular weight of the drug, which may facilitate the pharmaceutical preparation, particularly the content uniformity test.

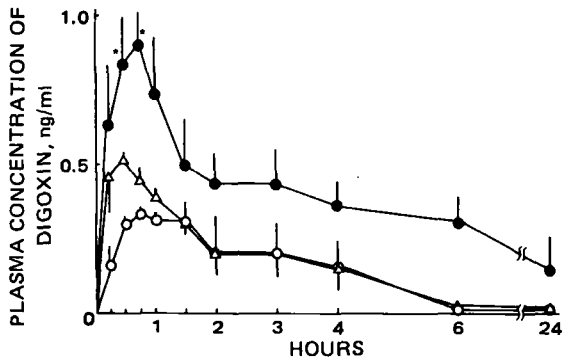

Figure 6—*Plasma levels of digoxin following the oral administrations of tablets containing digoxin or 1:4 digoxin–γ-cyclodextrin complex to dogs. Each point represents the mean ±SE of six dogs. Key: (○) 100-μg digoxin tablet; (●) γ-cyclodextrin complex tablet containing 100 μg of digoxin; (△) γ-cyclodextrin complex tablet containing 50 μg of digoxin; (*) $p < 0.01$, (●) versus (○).*

REFERENCES

(1) J. Lindenbaum, M. H. Mellow, M. O. Blackstone, and V. P. Butler, Jr., *N. Engl. J. Med.*, **285**, 1344 (1971).

(2) V. Manninen, J. Melin, and G. Hartel, *Lancet*, **ii**, 934 (1972).

(3) T. R. D. Shaw, M. R. Howard, and J. Hammer, *Lancet*, **ii**, 303 (1972).

(4) T. Higuchi and M. Ikeda, *J. Pharm. Sci.*, **63**, 809 (1974).

(5) R. K. Reddy, S. A. Khalil, and M. W. Gouda, *J. Pharm. Sci.*, **65**, 1753 (1976).

(6) W. L. Chiou and L. E. Kyle, *J. Pharm. Sci.*, **68**, 1224 (1979).

(7) L. A. Sternson and R. D. Shaffer, *J. Pharm. Sci.*, **67**, 327 (1978).

(8) S. A. H. Khalil and S. El-Masry, *J. Pharm. Sci.*, **67**, 1358 (1978).

(9) T. Sonobe, S. Hasumi, T. Yoshino, Y. Kobayashi, H. Kawata, and T. Nagai, *J. Pharm. Sci.*, **69**, 410 (1980).

(10) A. L. Thakkar, P. B. Kuehn, J. H. Perrin, and W. L. Wilham, *J. Pharm. Sci.*, **61**, 1841 (1972).

(11) J. Cohen and J. L. Lach, *J. Pharm. Sci.*, **52**, 132 (1963).

(12) K. Uekama, *Yakugaku Zasshi*, **101**, 857 (1981).

(13) W. Saenger, *Angew. Chem. Int. Ed. Engl.*, **19**, 344 (1980).

(14) T. Higuchi and J. L. Lach, *J. Am. Pharm. Assoc., Sci. Ed.*, **43**, 349 (1954).

(15) T. Higuchi and K. A. Connors, *Adv. Anal. Chem. Instr.*, **4**, 117 (1965).

(16) K. Müllen and P. S. Pregosin, "Fourier Transform NMR Techniques: A Practical Approach," Academic, London, 1976.

(17) H. Nogami, T. Nagai, and A. Suzuki, *Chem. Pharm. Bull.*, **14**, 329 (1966).

(18) R. H. Drost, T. A. Plomp, A. J. Teunissen, A. H. J. Maas, and R. A A. Maes, *Clin. Chim. Acta*, **79**, 557 (1977).

(19) T. W. Rosanske and K. A. Connors, *J. Pharm. Sci.*, **69**, 564 (1980).

(20) H. W. Voigtländer and G. Balsam, *Arch. Pharm.*, **301**, 208 (1968).

(21) B. V. Cheney, *J. Am. Chem. Soc.*, **90**, 5386 (1968).

(22) L. S. Porubcan, G. S. Born, J. L. White, and S. L. Hem, *J. Pharm. Sci.*, **68**, 358 (1979).

(23) K. Uekama, T. Fujinaga, F. Hirayama, M. Otagiri, and M. Yamasaki, *Int. J. Pharm.*, **10**, 1 (1982).

(24) K. Uekama, T. Fujinaga, F. Hirayama, M. Otagiri, Y. Kurono, and K. Ikeda, *J. Pharm. Pharmacol.*, in press.

(25) K. Uekama, T. Fijinaga, M. Otagiri, H. Seo, and M. Tsuruoka, *J. Pharm. Dyn.*, **4**, 735 (1981).

ACKNOWLEDGMENTS

Supported by a Grant-in-Aid for Scientific Research from the Ministry of Education, Science and Culture, Japan.

The authors are grateful to Professor K. Asahina and Dr. Y. Kanaya, Tokyo College of Pharmacy, for the preparation of tablets.

Capillary GLC Assay for Carbinoxamine and Hydrocodone in Human Serum Using Nitrogen-Sensitive Detection

D. J. HOFFMAN ˣ, M. J. LEVEQUE, and T. THOMSON

Received July 21, 1982, from the *Pharmaceutical Products Division, Abbott Laboratories, North Chicago, IL 60064.* Accepted for publication October 5, 1982

Abstract □ Capillary gas chromatography using an open tubular fused silica column and NP-FID was applied to the simultaneous analysis of the antihistamine, carbinoxamine, and the antitussive, hydrocodone, in human serum. Carbinoxamine and hydrocodone were extracted into methylene chloride–2-propanol (9:1) under alkaline conditions along with their respective internal standards, brompheniramine and *N*-ethylhydrocodone. The basic drugs were back-extracted into 0.1 *N* sulfuric acid and reextracted into benzene after making the aqueous phase alkaline with potassium hydroxide. The benzene extracts were evaporated to dryness and the residues were reconstituted with 40 μl of *n*-nonyl alcohol–methanol (19:1). Samples (1–2 μl) were injected onto the capillary column in the splitless mode (solvent effect) at 185° and the temperature programmed to 250°. Calibration curves using spiked serum standards were linear to at least 20 ng/ml for both drugs. Coefficients of variation averaged ±6.1% for carbinoxamine and ±5.0% for hydrocodone in the 2–15 ng/ml range. Sensitivity was estimated to be ~0.2 ng/ml for a 2-ml serum sample. Serum levels of carbinoxamine and hydrocodone were determined in a human volunteer administered these drugs.

Keyphrases □ GLC assay—carbinoxamine and hydrocodone in human serum, nitrogen sensitive detection □ Carbinoxamine—GLC assay, nitrogen sensitive detection □ Hydrocodone—GLC assay, nitrogen sensitive detection □ Nitrogen sensitive detection—GLC assay for carbinoxamine and hydrocodone in human serum

Carbinoxamine, 2-[(4-chlorophenyl)-2-pyridinylmethoxy]-*N*,*N*-dimethylethanamine, is an antihistamine structurally related to chlorpheniramine. Quantitative methods for determining carbinoxamine in biological fluids have not been published. However, several methods have been published for chlorpheniramine. These methods include GLC–MS (1, 2), GLC–electron-capture detection (3), GLC–nitrogen-sensitive detection (4, 5) and high-performance liquid chromatography (HPLC) (6, 7).

Hydrocodone, 4,5α-epoxy-3-methoxy-17-methylmorphinan-6-one, is a widely used antitussive agent. A method to determine hydrocodone in serum using GLC–electron-capture detection has been described by Barnhart and Caldwell (8) using the pentafluorophenylhydrazone derivative. The purpose of this investigation was to develop a specific and sensitive capillary GLC method for the simultaneous determination of carbinoxamine and hydrocodone in human serum.

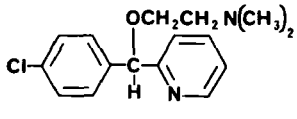

CARBINOXAMINE

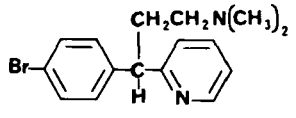

BROMPHENIRAMINE (INTERNAL STANDARD)

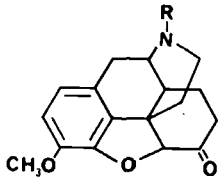

R = -CH_3 HYDROCODONE
R = -C_2H_5 N-ETHYLHYDROCODONE (INT.STD.)

EXPERIMENTAL

Chemicals—Carbinoxamine maleate, hydrocodone bitartrate, and brompheniramine maleate were USP reference standards. Reagent grade potassium hydroxide, sulfuric acid, hydrochloric acid, and 2-propanol were used without further purification[1]. Methylene chloride, benzene, and methanol were glass distilled[2]. *n*-Nonyl alcohol[3] was distilled in glass and the fraction boiling between 214°–215° was used.

Instrumentation—The GLC analyses were performed on a gas chromatograph[4] equipped with a capillary injection system[5] and a nitrogen-sensitive detector. Separations were performed on a 10–12 m × 0.25-mm i.d. fused silica open tubular column wall-coated with SE-30[6]. The film thickness was 0.25 μm. The flow rate of the helium carrier gas was adjusted to give partition ratios (k) of ~4.6 and 8 for carbinoxamine and hydrocodone, respectively, under the chromatographic conditions described below. Linear flow rates were in the 30–40-cm/sec range. The initial oven temperature was 185°. After 1.1 min at 185° it was programmed to increase at 25°/min for 0.9 min and then at 10°/min until it reached 250° where it was held for 1 min. The temperature of the nitrogen-specific detector was 300°, with hydrogen and air flow rates of 3.0 and 50 ml/min, respectively. The injection port temperature was 260°. A 8 cm × 2-mm i.d. fused silica splitless liner was used with a purge activation time of 0.9 min. The computing integrator had a slope sensitivity of 0.1 and an attenuation of 2^3 or 2^2.

Preparation of the Hydrocodone Internal Standard—The internal standard for hydrocodone, 4,5-epoxy-3-methoxy-17-ethylmorphinan-6-one, herein referred to as *N*-ethylhydrocodone, was synthesized from dihydronorcodeinone by the method of Clark and Woodbridge (9). Dihydronorcodeinone was synthesized from hydrocodone using the cyanogen bromide method of Clark *et al.* (10).

Preparation of Serum Standards—About 35 mg of carbinoxamine maleate and 37.5 mg of hydrocodone bitartrate reference standards were accurately weighed into a 50-ml volumetric flask and dissolved in water. A secondary aqueous standard was made in water to a final concentration of ~10 μg/ml as the free base. Working serum standards at 15, 10, 5, and 2 ng/ml were prepared by adding 75, 50, 25, and 10 μl of the secondary standard to a 50-ml volumetric flask and adjusting to volume with drug-free serum. The serum should be checked by the analytical procedure for interferences, since antihistamines are available in common nonprescription cold preparations. Internal standards, brompheniramine and *N*-ethylhydrocodone, were prepared in the same solution of 0.01 *N* HCl at 40 ng/ml.

Extraction Procedure—To a screw-cap test tube was added 2 ml of serum sample or standard, 1 ml of internal standard solution, 1 ml of 2 *N* KOH, and 6 ml of methylene chloride–2-propanol (9:1). The test tube

[1] Mallinckrodt reagent grade.
[2] Burdick and Jackson.
[3] Eastman Chemical Co.
[4] Hewlett-Packard Model 5840A.
[5] Hewlett-Packard Model 18835B.
[6] J & W Scientific, Inc.

0022-3549/83/1100-1342$01.00/0

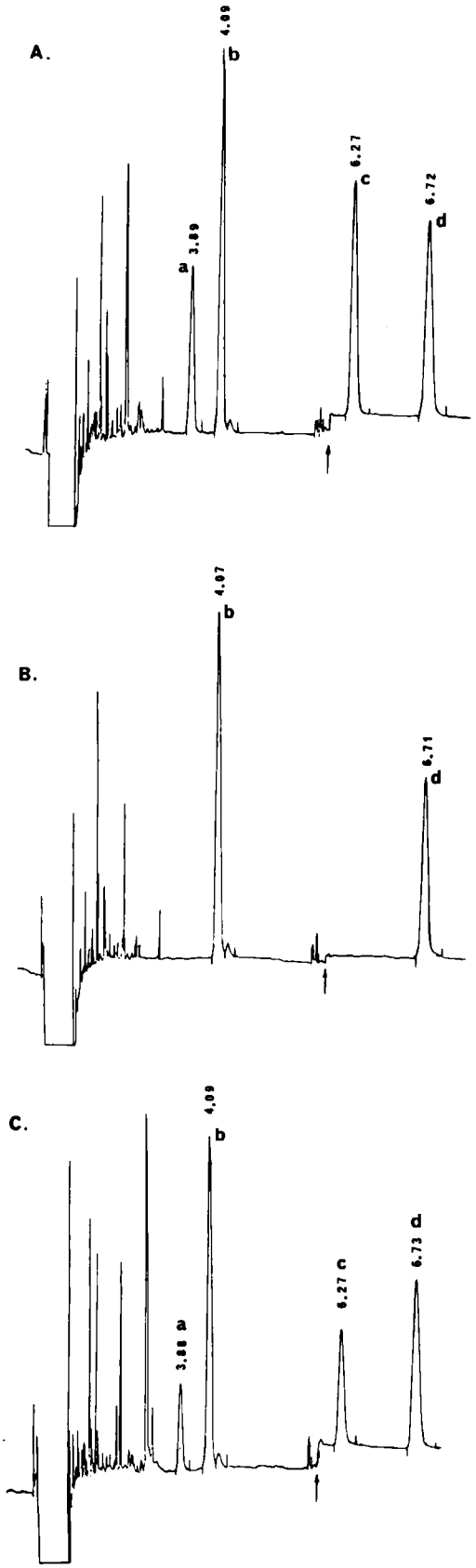

Figure 1—*Chromatograms of serum extracts. Key: (A) Serum standard containing 10 ng/ml of carbinoxamine and hydrocodone; (B) Serum sample of human volunteer prior to drug administration; (C) Serum sample of human volunteer 4.5 hr postdose with 5 mg of hydrocodone bitartrate and 4 mg of carbinoxamine maleate; (a) carbinoxamine; (b) brompheniramine; (c) hydrocodone; (d) N-ethylhydrocodone. Arrow denotes attenuation change from 2^3 to 2^2.*

Table I—Analytical Precision of the Determination of Carbinoxamine and Hydrocodone in Spiked Human Serum

Concentration, ng/ml	Peak Area Ratio[a] (n = 4)	Calculated Concentration, ng/ml[a]	*RSD*
Carbinoxamine			
0	0	0.5	—
2	0.122 ± 0.012	1.97 ± 0.19	9.6
5	0.302 ± 0.019	4.81 ± 0.29	6.1
10	0.651 ± 0.030	10.3 ± 0.48	4.7
15	0.940 ± 0.038	14.9 ± 0.61	4.1
Hydrocodone			
0	0	−0.006	—
2	0.221 ± 0.16	2.03 ± 0.15	7.4
5	0.530 ± 0.032	4.87 ± 0.29	6.0
10	1.11 ± 0.038	10.2 ± 0.36	3.5
15	1.62 ± 0.050	14.9 ± 0.46	3.1

[a] Mean ± *SD*.

was capped and shaken at a moderate rate (150 cpm) on a reciprocal shaker[7] for 10 min. After centrifugation[8] at 2500 rpm for 5 min at 2–5°, the upper aqueous phase was discarded by aspiration. The organic phase was decanted into a clean test tube containing 2 ml of 0.1 *N* sulfuric acid and capped. After shaking and centrifuging the upper aqueous layer was transferred to a test tube containing 0.3 ml 2 *N* KOH and 2 ml of benzene. The sample was vigorously mixed[9] for 10 sec and centrifuged. Avoiding any aqueous phase, the benzene layer was transferred with a pipet freshly rinsed with absolute ethanol to a conical screw-cap test tube. The sample was evaporated to dryness at 35°–40° with a gentle stream of dry, filtered air. The residue was constituted with 40 μl of 5% methanol in *n*-nonyl alcohol and the entire test tube wall was rinsed with the solvent and centrifuged. A 2–3 μl aliquot was injected into the GLC using the splitless injection technique.

Injection Technique—Since injections were made in the splitless mode, using the solvent effect (11), the injection process was slow. The sample was loaded into a 10-μl syringe followed by air to the 1-μl mark. The purge flow was eliminated and the septum was pierced by the syringe needle. The needle was heated for 5–10 sec in the injection port and the sample injected at a rate of ~1 μl/sec. The syringe needle was left in the injection port for 5 sec after sample introduction.

Calculations—Calibration curves of peak area ratios (carbinoxamine–brompheniramine and hydrocodone–*N*-ethylhydrocodone) *versus* serum carbinoxamine or hydrocodone concentrations were linear to at least 20 ng/ml. Unknowns were calculated from a least-squares linear regression fit to known carbinoxamine and hydrocodone serum standards.

RESULTS AND DISCUSSION

Capillary GLC is inherently more sensitive than conventional GLC because of the higher amount of detectable substance passing through the detector per unit of time. Sensitivity is of particular importance in the analysis of drugs such as carbinoxamine and hydrocodone where peak serum concentrations are typically in the 5–15-ng/ml range.

Chromatographic peaks of carbinoxamine and hydrocodone were symmetrical and well resolved from serum coextractives, as shown in Fig. 1. It was necessary to use two internal standards because of the different extraction and chromatographic properties of carbinoxamine and hydrocodone. Brompheniramine was chosen as the internal standard for carbinoxamine because it eluted in a clean chromatographic region and was completely resolved from carbinoxamine. Chlorpheniramine, which elutes just prior to carbinoxamine, was not used because of its more common presence in pharmaceutical antihistamine preparations. This method could be used to determine serum chlorpheniramine levels. Either carbinoxamine or brompheniramine would suffice as an internal standard for a chlorpheniramine assay.

The precision of both assays is shown in Table I. In the concentration range of 2–15 ng/ml the coefficients of variation ranged from 4.1 to 9.6% for carbinoxamine and from 3.1 to 7.4% for hydrocodone. Extraction efficiencies averaged 71.2 ± 2.8% and 78.4 ± 2.5% for carbinoxamine and hydrocodone, respectively, at 10 ng/ml.

[7] Eberbach Corp.
[8] Sorvall RC-3B, DuPont, Inc.
[9] Maxi Mix Model M-16715, Thermolyne, Sybron Corp.

Table II—Analysis of Spiked Serum Samples of Carbinoxamine and Hydrocodone at Low Concentration

Concentration, ng/ml	Peak Area Ratios[a]	
	Carbinoxamine/IS	Hydrocodone/IS
0.2	0.0065 ± .0018 (28.2%)[b]	0.0088 ± .002 (25.9%)
0.5	0.0206 ± .0042 (20.3%)	0.0423 ± .0061 (14.4%)
1.0	0.0736 ± .0075 (10.2%)	0.091 ± .0079 (8.7%)

[a] Mean ± *SD*; $n = 4$. [b] Coefficient of variation (%).

Calibration curves of peak area ratios *versus* concentration in serum were linear up to at least 20 ng/ml. Assay sensitivity or the minimum quantifiable concentration was evaluated by determining the assay precision in the 0.2–1.0-ng/ml range. By defining the sensitivity as that concentration of drug that has a ±25% *CV*, the sensitivity for both carbinoxamine and hydrocodone is ~0.2 ng/ml using a 2-ml sample volume (Table II).

To assess the validity of this analytical procedure, serum samples from a human volunteer were assayed. The serum carbinoxamine and hydrocodone concentrations from a human volunteer orally administered, under fasted conditions, a solution containing 4 mg of carbinoxamine maleate and 5 mg of hydrocodone bitartrate are shown in Table III. Typical chromatograms from a human volunteer are also shown in Fig. 1. This assay provides the precision and sensitivity to conduct pharmacokinetic and bioavailability studies in humans receiving a single oral dose of carbinoxamine maleate and hydrocodone bitartrate.

Table III—Serum Carbinoxamine and Hydrocodone Concentrations after Oral Administration of 4 mg of Carbinoxamine Maleate and 5 mg of Hydrocodone Bitartrate to a Human Volunteer

Time Postdose, hr	Serum Concentration, ng/ml	
	Carbinoxamine	Hydrocodone
0	0	0
0.5	1.1	4.6
1	3.8	9.1
1.5	4.6	10.7
2	8.0	10.4
3	7.5	7.5
4.5	6.3	4.3
6	5.5	4.2
9	3.2	1.7
12	1.7	0.6
24	1.1	0
36	0.7	0

REFERENCES

(1) J. A. Thompson and F. H. Leffert, *J. Pharm. Sci.*, **69**, 707 (1980).

(2) J. A. Thompson, D. C. Bloedow, and F. H. Leffert, *J. Pharm. Sci.*, **70**, 1284 (1981).

(3) J. W. Barnhart and J. D. Johnson, *Anal. Chem.*, **49**, 1085 (1977).

(4) H. T. Smith, J. T. Jacob, and R. G. Achari, *J. Chromatogr. Sci.*, **16**, 561 (1978).

(5) J. E. O'Brien, O. Hinsvark, W. Bryant, L. Amsel, and F. E. Leaders, *Anal. Lett.*, **10**, 1163 (1977).

(6) C. M. Lai, R. G. Stoll, Z. M. Look, and A. Yacobi, *J. Pharm. Sci.*, **68**, 1243 (1979).

(7) N. K. Athanikar, G. W. Peng, R. L. Nation, S. M. Huang, and W. L. Chiou, *J. Chromatogr.*, **162**, 367 (1979).

(8) J. W. Barnhart and W. J. Caldwell, *J. Chromatogr.*, **130**, 243 (1977).

(9) R. L. Clark and N. J. Woodbridge, U.S. Pat. 2,741,617, April 10, 1956.

(10) R. L. Clark, A. A. Pessolano, J. Weijlard, and K. Pfister, *J. Am. Chem. Soc.*, **75**, 4963 (1953).

(11) K. Grob and G. Grob, *J. Chromatogr. Sci.*, **7**, 584 (1969).

ACKNOWLEDGMENTS

Presented at the 31st National Meeting of The Academy of Pharmaceutical Sciences in Orlando, Florida, November 1981.

The authors thank Dr. A. H. C. Chun and the Ross Laboratories Division of Abbott Laboratories for supplying the human serum samples.

Hypolipidemic Activity of Phthalimide Derivatives IV: Further Chemical Modification and Investigation of the Hypolipidemic Activity of *N*-Substituted Imides

JAMES M. CHAPMAN, Jr., GEORGE H. COCOLAS, and I. H. HALL ˣ

Received June 14, 1982, from the *Division of Medicinal Chemistry, School of Pharmacy, University of North Carolina, Chapel Hill, NC 27154.* Accepted for publication September 24, 1982.

Abstract □ A further investigation of *N*-substituted derivatives of phthalimide for hypolipidemic activity has revealed that the chain length, as well as the type of substitution on the *N*-alkyl chain of phthalimide is critical for biological activity. In these studies the hypolipidemic activity was not improved by extending the chain length beyond five carbon atoms in the alkyl and alkanoic acid series. Imido nitrogen substituents, other than alkanoic acids, methyl ketones, and alkyl groups, caused a reduction in hypolipidemic activity, *e.g.*, hydroxy, amino, hydroxymethyl, or carbethoxy. Reduction of the keto group in the side chain to an alcohol, as well as forming derivatives of the keto group, did not improve the hypolipidemic activity with the exception of 1-*N*-phthalimidobutan-3-one semicarbazone. This compound demonstrated improved hypocholesterolemic activity over phthalimide and 1-*N*-phthalimidobutan-3-one. Substitution of the 3-position of the aromatic moiety of phthalimide with an amino or nitro group, as well as substituting a pyridine or cyclohexyl ring for the phenyl ring, led to the loss of hypolipidemic activity.

Keyphrases □ Phthalimide—*N*-substituted derivatives, synthesis, hypolipidemic activity, mice, structure–activity relationships □ Hypolipidemic agents—potential, *N*-substituted derivatives of phthalimide, structure–activity relationships, mice □ Structure–activity relationships—*N*-substituted phthalimide derivatives, hypolipidemic activity, mice

Previously, it was shown that phthalimide (I) is a potent hypolipidemic agent in rodents. Serum cholesterol levels were reduced 43% in mice after administration for 16 days at 20 mg/kg/day. Serum triglyceride levels were also reduced 56% after 14 days of administration in mice at the same dose. The phthalimide derivatives were more potent

0022-3549/83/1100-1344$01.00/0

Table II—Analysis of Spiked Serum Samples of Carbinoxamine and Hydrocodone at Low Concentration

Concentration, ng/ml	Peak Area Ratios[a]	
	Carbinoxamine/IS	Hydrocodone/IS
0.2	0.0065 ± .0018 (28.2%)[b]	0.0088 ± .002 (25.9%)
0.5	0.0206 ± .0042 (20.3%)	0.0423 ± .0061 (14.4%)
1.0	0.0736 ± .0075 (10.2%)	0.091 ± .0079 (8.7%)

[a] Mean ± *SD*; $n = 4$. [b] Coefficient of variation (%).

Calibration curves of peak area ratios *versus* concentration in serum were linear up to at least 20 ng/ml. Assay sensitivity or the minimum quantifiable concentration was evaluated by determining the assay precision in the 0.2–1.0-ng/ml range. By defining the sensitivity as that concentration of drug that has a ±25% *CV*, the sensitivity for both carbinoxamine and hydrocodone is ~0.2 ng/ml using a 2-ml sample volume (Table II).

To assess the validity of this analytical procedure, serum samples from a human volunteer were assayed. The serum carbinoxamine and hydrocodone concentrations from a human volunteer orally administered, under fasted conditions, a solution containing 4 mg of carbinoxamine maleate and 5 mg of hydrocodone bitartrate are shown in Table III. Typical chromatograms from a human volunteer are also shown in Fig. 1. This assay provides the precision and sensitivity to conduct pharmacokinetic and bioavailability studies in humans receiving a single oral dose of carbinoxamine maleate and hydrocodone bitartrate.

Table III—Serum Carbinoxamine and Hydrocodone Concentrations after Oral Administration of 4 mg of Carbinoxamine Maleate and 5 mg of Hydrocodone Bitartrate to a Human Volunteer

Time Postdose, hr	Serum Concentration, ng/ml	
	Carbinoxamine	Hydrocodone
0	0	0
0.5	1.1	4.6
1	3.8	9.1
1.5	4.6	10.7
2	8.0	10.4
3	7.5	7.5
4.5	6.3	4.3
6	5.5	4.2
9	3.2	1.7
12	1.7	0.6
24	1.1	0
36	0.7	0

REFERENCES

(1) J. A. Thompson and F. H. Leffert, *J. Pharm. Sci.*, **69**, 707 (1980).

(2) J. A. Thompson, D. C. Bloedow, and F. H. Leffert, *J. Pharm. Sci.*, **70**, 1284 (1981).

(3) J. W. Barnhart and J. D. Johnson, *Anal. Chem.*, **49**, 1085 (1977).

(4) H. T. Smith, J. T. Jacob, and R. G. Achari, *J. Chromatogr. Sci.*, **16**, 561 (1978).

(5) J. E. O'Brien, O. Hinsvark, W. Bryant, L. Amsel, and F. E. Leaders, *Anal. Lett.*, **10**, 1163 (1977).

(6) C. M. Lai, R. G. Stoll, Z. M. Look, and A. Yacobi, *J. Pharm. Sci.*, **68**, 1243 (1979).

(7) N. K. Athanikar, G. W. Peng, R. L. Nation, S. M. Huang, and W. L. Chiou, *J. Chromatogr.*, **162**, 367 (1979).

(8) J. W. Barnhart and W. J. Caldwell, *J. Chromatogr.*, **130**, 243 (1977).

(9) R. L. Clark and N. J. Woodbridge, U.S. Pat. 2,741,617, April 10, 1956.

(10) R. L. Clark, A. A. Pessolano, J. Weijlard, and K. Pfister, *J. Am. Chem. Soc.*, **75**, 4963 (1953).

(11) K. Grob and G. Grob, *J. Chromatogr. Sci.*, **7**, 584 (1969).

ACKNOWLEDGMENTS

Presented at the 31st National Meeting of The Academy of Pharmaceutical Sciences in Orlando, Florida, November 1981.

The authors thank Dr. A. H. C. Chun and the Ross Laboratories Division of Abbott Laboratories for supplying the human serum samples.

Hypolipidemic Activity of Phthalimide Derivatives IV: Further Chemical Modification and Investigation of the Hypolipidemic Activity of *N*-Substituted Imides

JAMES M. CHAPMAN, Jr., GEORGE H. COCOLAS, and I. H. HALL ˣ

Received June 14, 1982, from the *Division of Medicinal Chemistry, School of Pharmacy, University of North Carolina, Chapel Hill, NC 27154.* Accepted for publication September 24, 1982.

Abstract □ A further investigation of *N*-substituted derivatives of phthalimide for hypolipidemic activity has revealed that the chain length, as well as the type of substitution on the *N*-alkyl chain of phthalimide is critical for biological activity. In these studies the hypolipidemic activity was not improved by extending the chain length beyond five carbon atoms in the alkyl and alkanoic acid series. Imido nitrogen substituents, other than alkanoic acids, methyl ketones, and alkyl groups, caused a reduction in hypolipidemic activity, *e.g.*, hydroxy, amino, hydroxymethyl, or carbethoxy. Reduction of the keto group in the side chain to an alcohol, as well as forming derivatives of the keto group, did not improve the hypolipidemic activity with the exception of 1-*N*-phthalimidobutan-3-one semicarbazone. This compound demonstrated improved hypocholesterolemic activity over phthalimide and 1-*N*-phthalimidobutan-3-one. Substitution of the 3-position of the aromatic moiety of phthalimide with an amino or nitro group, as well as substituting a pyridine or cyclohexyl ring for the phenyl ring, led to the loss of hypolipidemic activity.

Keyphrases □ Phthalimide—*N*-substituted derivatives, synthesis, hypolipidemic activity, mice, structure–activity relationships □ Hypolipidemic agents—potential, *N*-substituted derivatives of phthalimide, structure–activity relationships, mice □ Structure–activity relationships—*N*-substituted phthalimide derivatives, hypolipidemic activity, mice

Previously, it was shown that phthalimide (I) is a potent hypolipidemic agent in rodents. Serum cholesterol levels were reduced 43% in mice after administration for 16 days at 20 mg/kg/day. Serum triglyceride levels were also reduced 56% after 14 days of administration in mice at the same dose. The phthalimide derivatives were more potent

0022-3549/83/1100-1344$01.00/0

Table I—Hypolipidemic Activity of Miscellaneous *N*-Substituted Cyclic Imides in Male Mice at 20 mg/kg/day ip

	Compound	Percent of Control[a] Day 14 Serum Triglyceride	Day 9 Serum Cholesterol	Day 16 Serum Cholesterol
I	Phthalimide	44 ± 8[b]	63 ± 8[b]	57 ± 7[b]
II	*N*-Hydroxyphthalimide	66 ± 5[b]	100 ± 11	70 ± 6[b]
III	*N*-Hydroxymethylphthalimide	54 ± 7[b]	79 ● 9[b]	75 ± 9[b]
IV	*N*-Aminophthalimide	81 ± 6[b]	94 ± 10	89 ± 9
V	1-*N*-Phthalimidopropan-2-one	48 ± 10	80 ± 16[c]	67 ± 12[b]
VI	1-*N*-Phthalimidopropan-2-ol	55 ± 5[b]	69 ± 8[b]	62 ± 4[b]
VII	1-*N*-Phthalimidobutan-2-one	69 ± 12[b]	64 ± 7[b]	65 ± 5[b]
VIII	1-*N*-Phthalimidobutan-2-ol	64 ± 4	88 ± 4	72 ± 7
IX	1-*N*-Phthalimidobutan-3-one	58 ± 7[b]	67 ± 11[b]	63 ± 7[b]
X	1-*N*-Phthalimidobutan-3-ol	98 ± 12	96 ± 5	88 ± 7
XI	1-*N*-Phthalimidobutan-3-ketoxime	84 ± 9[b]	89 ± 6[e]	73 ± 5[b]
XII	1-*N*-Phthalimidobutan-3-ketoxime acetate	91 ± 11	81 ± 7[b]	96 ± 5
XIII	1-*N*-Phthalimidobutan-3-semicarbazone	75 ± 6[b]	57 ± 6[b]	43 ± 4[b]
XIV	*N*-n-Butylphthalimide	82 ± 16[c]	72 ± 10[b]	54 ± 6[b]
XV	*N*-*n*-Butyl-3-aminophthalimide	72 ± 10	85 ± 7[b]	82 ± 6[b]
XVI	*N*-n-Butyl-3-nitrophthalimide	88 ± 9[c]	100 ± 9	81 ± 4[b]
XVII	*N*-*n*-Butyl-pyridyl-2,3-dicarboximide	86 ± 5[b]	99 ± 6	75 ± 5[b]
XVIII	*N*-*n*-Butyl-*cis*-1,2-cyclohexyldicarboximide	81 ± 8[b]	98 ± 7	83 ± 8[b]
XIX	8-*N*-Phthalimidooctanoic acid	87 ± 4[b]	78 ± 8[b]	65 ± 2[b]
XX	12-*N*-Phthalimidodecanoic acid	89 ± 4[b]	95 ± 9	75 ± 7[b]
XXI	1-*N*-Phthalimido-3-phenyl-2-propene	77 ± 7[b]	89 ± 9[c]	74 ± 3[b]
XXII	α-(*N*-Phthalimido)ethylphenyl ketone	98 ± 5	84 ± 5[b]	73 ± 6[b]
XXIII	*N*-Carbethoxyphthalimide	113 ± 9	80 ± 6[b]	80 ± 6[b]
XXIV	*N*-*n*-Octadecylphthalimide	92 ± 6	96 ± 12	91 ± 9
XXV	*N*-(Phthalimidomethyl)acetamide	59 ± 6[b]	67 ± 3[b]	70 ± 7[b]
XXVI	Isatin	92 ± 7	87 ± 8[c]	77 ± 7[b]
	1% Carboxymethylcellulose	100 ± 6	100 ± 5[d]	100 ± 8[e]

[a] Mean ± *SD*; $n = 6$. [b] $p \leq 0.001$. [c] $p \leq 0.010$. [d] Control value 132 ± 7 mg%. [e] Control value 128 dl/liter.

than clofibrate, and preliminary experiments suggested they were nontoxic. Further investigation of SAR requirements for hypolipidemic activity of phthalimides was undertaken by substituting the nitrogen of the imide ring with a series of alkyl, methyl ketone, carboxylic acid, and acetate ester substituents of varying chain lengths (1).

The previous study revealed that alkyl substitutions of four carbon atoms or an oxygen atom substituted for one carbon atom afforded the best hypolipidemic activity in mice. Consequently, a number of other chemical modifications of phthalimides were undertaken. Many of these compounds were chemical probes to investigate the potential hypolipidemic activity and do not represent a full series of compounds for complete SAR analysis.

RESULTS AND DISCUSSION

Substitution of the phthalimido nitrogen with a hydroxyl group (II), a hydroxymethyl group (III), or an amino group (IV) resulted in compounds with decreased hypolipidemic activity compared with the parent molecule, phthalimide, in both the serum cholesterol and triglyceride screens. It may be noted that *N*-hydroxyphthalimide (II) reduced serum triglyceride levels 36%, whereas phthalimide reduced triglyceride levels 56%. Reduction of *N*-phthalimidopropan-2-one (V) and *N*-phthalimidobutan-2-one (VII) to the corresponding alkanols (VI and VIII) resulted in compounds which showed essentially no difference in hypolipidemic activity. However, reduction of 1-*N*-phthalimidobutan-3-one (IX) to 1-*N*-phthalimidobutan-3-ol (X) resulted in loss of hypolipidemic activity. Derivatization of the carbonyl group of the ketone moiety in 1-*N*-phthalimidobutan-3-one (IX) as in the ketoxime (XI), the ketoxime acetate (XII), and the semicarbazone of the ketone produced varied results in hypolipidemic activity. Compounds XI and XII did not significantly lower serum cholesterol and triglyceride levels in mice, but the semicarbazone (XIII) reduced serum cholesterol levels 47% and serum triglyceride levels 25%. This magnitude of reduction of serum cholesterol levels by the semicarbazone demonstrated that it was one of the more potent imide derivatives in the hypocholesterolemic screen in mice.

Substitution of an amino (XV) or nitro group (XVI) at the 3-position of the phenyl ring of *N*-*n*-butylphthalimide or substitution of the aromatic moiety of phthalimide by a pyridine (XVII) or cyclohexyl (XVIII) moiety resulted in no change in hypotriglyceridemic activity; however, there was a marked reduction in biological activity in the cholesterol screen. Elongation of the *N*-alkyl substitution on the imido nitrogen in the *N*-phthalimido alkanoic acid series led to a decrease in hypolipidemic activity. Previously, we have shown that *N*-substituted alkanoic acid series, from acetic to caproic, were potent as hypolipidemic agents in mice. Interestingly, the pharmacological data for these compounds demonstrated that the shorter the side chain, the higher the hypotriglyceridemic activity and the longer the side chain, the higher the hypocholesterolemic activity. However, the two acids tested in this present study were less active in both screens compared with those in the original series.

Random substitution of the side chain, *e.g.*, 1-*N*-phthalimido-3-phenyl-2-propene (XXI) and α-(*N*-phthalimido)ethylphenyl ketone (XXII), resulted in compounds which retained moderate (>25%) hypocholesterolemic activity, but only XXI demonstrated any hypotriglyceridemic activity (~23%). *N*-Carbethoxyphthalimide was essentially inactive in both screens.

We have previously synthesized a homologous series of *N*-*n*-alkylphthalimides, including the methyl through octyl derivatives. The butyl analogue showed the most potent activity with decreasing activity displayed by the pentyl through octyl derivatives. Further chain elongation, *e.g.*, *N*-*n*-octadecylphthalimide (XXIV), afforded a compound essentially devoid of hypolipidemic activity.

Substitution of a nitrogen for a methylene group of 1-*N*-phthalimidobutan-3-one (IX) resulted in XXV, which was active as a hypolipidemic agent lowering serum triglyceride levels 41% and serum cholesterol levels 30%. Isatin (XXVI), an isomer of phthalimide, demonstrated no hypotriglyceridemic activity and only moderate hypocholesterolemic activity (~23%).

Whereas the compounds presented here were generally no more potent than the ones previously reported in this series (1), they do demonstrate chemical modifications that will probably not result in the development of a potent hypolipidemic imide.

EXPERIMENTAL

Chemistry—Melting points were determined using a melting point apparatus[1] and are uncorrected. NMR data were obtained utilizing a 60-MHz spectrometer[2]. Compounds I, II, IV, XXIII, and XXVI were obtained from a commercial source[3] and were tested without further

[1] Mel Temp.
[2] JEOL C 60 HL.
[3] Aldrich Chemical Co., Milwaukee, Wis.

purification. Syntheses of I, III, V, IX, and XIV were reported previously (1).

Compounds VI, XVI–XX, and XXIV—Equimolar amounts (0.006–0.15 mole) of the appropriate anhydride and amine were refluxed overnight in 75–200 ml of toluene, collecting the water of reaction by azeotropic distillation. The toluene was removed *in vacuo*, and the residue was distilled or recrystallized.

1-N-*Phthalimidopropan-2-ol* (*VI*)—The amount obtained was 26.7 g (72% yield) (ethanol-ligroine); mp 89–91.5° [lit. (2) mp 88–90°].

N-n-*Butyl-3-nitrophthalimide* (*XVI*)—The amount obtained was 19.0 g (62% crude yield) (ethanol); mp 69–70° [lit. (3) mp 71–72°].

Anal.—Calc. for $C_{12}H_{12}N_2O_4$: C, 58.06; H, 4.87. Found: C, 58.21; H, 4.82.

N-n-*Butylpyridyl-2,3-dicarboximide* (*XVII*)—The amount obtained was 0.52 g (8% yield) (ethanol–H_2O); mp 84–85°. ^{1}H-NMR ($CDCl_3$): 7.72–9.19 (m, 3, aromatic), 3.81 (t, 2, N—CH_2), and 0.75–2.02 ppm (m, 7, —$CH_2CH_2CH_3$).

Anal.—Calc. for $C_{11}H_{12}N_2O_2$: C, 64.69; H, 5.92. Found: C, 64.59; H, 5.95.

N-n-*Butyl*-cis-*1,2-cyclohexyldicarboximide* (*XVIII*)—The amount obtained was 12.9 g (62% yield); bp 119–123°/0.27–0.68 mm Hg [lit. (4) bp 115–118°/2 mm Hg].

Anal.—Calc. for $C_{12}H_{19}NO_2$ C, 68.87; H, 9.15. Found: C, 68.96; H, 9.32.

8-N-*Phthalimidooctanoic Acid* (*XIX*)—The amount obtained was 1.0 g (55% yield) (hexane); mp 89–90°; ^{1}H-NMR ($CDCl_3$): 7.63–8.07 (m, 4, aromatic), 3.77 (t, 2, N—CH_2), 2.45 (t, 2, CH_2CO_2), and 1.15–2.01 ppm [m, 10, $(CH_2)_5CH_2CO_2$].

Anal.—Calc. for $C_{16}H_{19}NO_4$: C, 66.42; H, 6.62; N, 4.84. Found: C, 66.24; H, 6.42, N, 4.83.

12-N-*Phthalimidodecanoic Acid* (*XX*)—The amount obtained was 2.5 g (36% yield) (hexane); mp 87–88°; ^{1}H-NMR ($CDCl_3$): 7.50–7.96 (m, 4, aromatic), 3.68 (t, 2, N—CH_2), 2.20 (t, 2, CH_2CO_2), and 1.10–1.88 ppm [m, 18, $(CH_2)_9CH_2CO_2$].

Anal.—Calc. for $C_{20}H_{27}NO_4$: C, 69.54; H, 7.88; N, 4.06. Found: C, 69.61; H, 8.12; N, 3.94.

N-n-*Octadecylphthalimide* (*XXIV*)—The amount obtained was 28.1 g (70% yield) (ethanol); mp 78–79° [lit. (5) mp 80–81°].

Anal.—Calc. for $C_{26}H_{41}NO_2$: C, 78.15; H, 10.34. Found: C, 78.10; H, 10.61.

1-*N*-Phthalimidobutan-2-one (VII) and 1-*N*-Phthalimidobutan-2-ol (VIII)—1-Amino-2-butanol (3.95 g, 0.044 mole), prepared from 1,2-epoxybutane by the procedure of de Montmollin and Achermann (6), was dissolved in 100 ml of toluene, and 6.5 g (0.044 mole) of phthalic anhydride was added. The mixture was refluxed for 2 hr, collecting the water formed in the reaction by azeotropic distillation. The toluene was removed *in vacuo*, and the residue was recrystallized from isopropyl alcohol to afford 4.0 g (41%) of 1-*N*-phthalimidobutan-2-ol (VIII), mp 71–71.5°. ^{1}H-NMR ($CDCl_3$): 7.72–8.10 (m, 4, aromatic), 3.76–4.00 (m, 3, CH_2CH(OH)—), 2.32–2.54 (br s, 1, OH), 1.38–1.88 (m, 2, —CH_2CH_3), and 1.05 (t, 3, CH_3).

Anal. Calc. for $C_{12}H_{13}NO_3$: C, 66.35; H, 5.10. Found: C, 66.58; H, 5.11.

1-*N*-Phthalimidobutan-2-ol (2.02 g, 0.009 mole) in 18 ml of CH_2Cl_2 was added to 2.98 g (0.014 mole) of pyridinium chlorochromate suspended in 20 ml of CH_2Cl_2. The mixture was stirred 2.5 hr, 50 ml of ether was added, and the supernatant was decanted and filtered. Evaporation of the filtrate and repeated recrystallization from water gave 0.27 g (14%) of 1-*N*-phthalimidobutan-2-one (VII), mp 107–108° [lit. (7) mp 107–108°].

Anal.—Calc. for $C_{13}H_{12}NO_3$: C, 66.74; H, 5.98. Found: C, 65.70; H, 5.98.

1-*N*-Phthalimidobutan-3-ol (X)—1-*N*-Phthalimidobutan-3-one (9.78 g, 0.045 mole) was added to a mixture of 32.31 g (0.158 mole) aluminum isopropoxide in 300 ml of isopropyl alcohol. The mixture was refluxed for 6 hr (at this time it gave a negative test for acetone with 2,4-dinitrophenylhydrazine). The isopropyl alcohol was removed *in vacuo*, 450 ml of 0.16 *N* HCl was added, and the mixture extracted with ethyl acetate. Evaporation of the organic phase *in vacuo* yielded a yellow oil which on distillation gave 5.6 g (49%) of 1-*N*-phthalimidobutan-3-ol, mp 58–60° [lit. (8) mp 48°].

Anal.—Calc. for $C_{12}H_{13}NO_8$: C, 65.74; H, 5.98. Found: C, 66.00; H, 5.92.

1-*N*-Phthalimidobutan-3-ketoxime (XI)—1-*N*-Phthalmidobutan-3-one (5.0 g, 0.023 mole) was suspended in 25 ml of ethanol, and 5.0 g of hydroxylamine hydrochloride was added, followed by 25 ml of pyridine. The mixture was refluxed 3 hr, the volatile material removed *in vacuo*, and the residue was recrystallized from ethanol to yield 0.62 g (12%) of 1-*N*-phthalimidobutan-3-ketoxime, mp 179° [lit. (9) mp 178°].

Anal.—Calc. for $C_{12}H_{12}N_2O_3$: C, 62.06; H, 5.20. Found: C, 62.31; H, 4.94.

1-*N*-Phthalimidobutan-3-ketoxime Acetate (XII)—1-*N*-Phthalimidobutan-3-ketoxime (1.0 g, 0.013 mole) was refluxed for 4 hr in 90 ml of acetic anhydride. The volatile material was removed *in vacuo*, and the residue was recrystallized from water to give 0.22 g (18%) of 1-*N*-phthalimidobutan-3-ketoxime acetate, mp 110–112°; ^{1}H-NMR (acetone-d_6): 7.98 (s, 4, aromatic), 4.02 (t, 2, N—CH_2), 2.73 (t, 2, CH_2C=N), 2.10 (s, 3, CH_3), and 2.02 ppm (s, 3, CH_3).

Anal.—Calc. for $C_{14}H_{14}N_2O_4$: C, 61.31; H, 5.15. Found: C, 61.50; H, 4.98.

1-*N*-Phthalimidobutan-3-semicarbazone (XIII)—1-*N*-Phthalimidobutan-3-one (4.0 g, 0.018 mole) was added to a solution of 4.0 g (0.035 mole) of semicarbazide hydrochloride and 6.0 g of sodium acetate in 40 ml of ethanol and 22 ml of water. The mixture was warmed until it became milky white and was then allowed to stand for 3 hr; 40 ml of water was added, and the precipitate was collected and recrystallized from methanol to give 1.98 g (40%) of 1-*N*-phthalimidobutan-3-semicarbazone, mp 221–223° [lit. (10) mp 202–203°].

Anal.—Calc. for $C_{13}H_{14}N_4O_3$: C, 56.93; H, 5.15. Found: C, 57.13; H, 5.07.

***N*-*n*-Butyl-3-aminophthalimide (XV)**—*N*-*n*-Butyl-3-nitrophthalimide (XVI) (12.4 g, 0.5 mole) was dissolved in 300 ml of ethanol, added to 4 g of 10% Pd-C, and shaken for 10 min under hydrogen in a low-pressure apparatus[4] (60 psig). The catalyst was removed by filtration, the solvent was evaporated *in vacuo*, and the residue was recrystallized from ethanol–water to give 8.05 g (73%) of *N*-*n*-butyl-3-aminophthalimide, mp 67–70°; ^{1}H-NMR ($CDCl_3$): 6.83–7.62 (m, 3, aromatic), 5.38 (s, 2, NH_2), 3.67 (t, 2, N—CH_2), and 0.75–1.95 ppm (m, 7, $CH_2CH_2CH_3$).

Anal.—Calc. for $C_{12}H_{14}N_2O_2$: C, 66.04; H. 6.47. Found: C, 66.00; H, 6.40.

1-*N*-Phthalimido-3-phenyl-2-propene (XXI)—This compound was prepared by refluxing equimolar amounts of potassium phthalimide and cinnamyl bromide in absolute ethanol for 12 hr. The solvent was removed under reduced pressure, and the residue was washed with water. The residual water-insoluble product was collected by filtration and then recrystallized from toluene to give XXI, in 65% yield, mp 160–161°.

Anal.—Calc. for $C_{17}H_{13}NO_2$: C, 77.55; H, 4.98; N, 5.32. Found: C, 77.78; H, 5.09; N, 5.39.

α-(*N*-Phthalimido)ethylphenyl Ketone (XXII)—An equimolar amount of potassium phthalimide and α-bromopropiophenone in ethyl alcohol were refluxed for 5 hr. The solvent was removed under reduced pressure, and the residue was washed with water and then recrystallized from toluene–petroleum ether to give XXII in 60% yield, mp 88–89°.

Anal.—Calc. for $C_{17}H_{13}NO_3$: C, 73.11; H, 4.69; N, 5.02. Found: C, 73.27; H, 4.72; N, 5.00.

***N*-(Phthalimidomethyl)acetamide (XXV)**—Utilizing the procedure of Buc (11), 8.85 g (0.05 mole) of *N*-hydroxymethylphthalimide and 3.5 ml (0.066 mole) of acetonitrile were added to 50 ml of concentrated sulfuric acid. The mixture was stirred for 22 hr, 250 ml of ice was added, and the precipitate was collected and recrystallized from ethanol to give 3.5 g (33%) of XXV, mp 224–227° [lit. (11) mp 213–214.5°].

Anal.—Calc. for $C_{11}H_{10}N_2O_3$: C, 60.57; H, 4.59. Found: C, 60.58; H, 4.59.

Biological Studies—All compounds were tested at 20 mg/kg/day and administered intraperitoneally to male mice at 11:00 a.m. On days 9 and 16, the blood was collected via the tail vein. The blood samples were collected between 8:00 and 9:30 a.m. in alkali-free nonheparinized microcapillary tubes, which were centrifuged for 3 min to obtain the serum (12). Duplicate 25-μl samples of nonhemolyzed serum were used to determine the milligram percent serum cholesterol levels by a modification of the Liebermann–Burchard reaction. Using a separate group of mice, which were bled on day 14, serum triglyceride levels (in dl/liter) were measured using duplicate samples of 50 μl[5].

REFERENCES

(1) J. M. Chapman, Jr., G. H. Cocolas, and I. H. Hall, *J. Med. Chem.*, **22**, 1399 (1979).

(2) S. Gabriel and H. Ohle, *J. Chem. Soc.*, **112**, I, 563 (1917).

[4] Parr Shaker.

[5] Hycel Triglyceride Test; Hycel, Inc., 1975.

(3) A. Yoshida and M. Shindo, *Japan Kokai*, **78 40**, 787 (1978); *Chem. Abstr.*, **89**, P109552v (1978).
(4) M. S. Newman, B. J. Magerlein, and W. B. Wheatley, *J. Am. Chem. Soc.* **68**, 2113 (1946).
(5) W. Wood, *J. Chem. Soc.*, **1956**, 3327.
(6) M. de Montmollin and F. Achermann, *Helv. Chim. Acta*, **12**, 874 (1929).
(7) N. Rabjohn and E. R. Rogier, *J. Org. Chem.*, **11**, 781 (1946).
(8) R. Robinson and H. Suginome, *J. Chem. Soc.*, **1932**, 304.
(9) O. Wichterle and M. Hudlicky, *Coll. Czech. Chem. Commun.*, **12**, 101 (1947); *Chem. Abstr.*, **41**, 4149e (1947).
(10) H. Irai, S. Shima, and N. Murata, *Kogyo Kaguku Zasshi*, **62**, 82 (1959); *Chem. Abstr.*, **58**, 5659b (1963).
(11) S. R. Buc, *J. Am. Chem. Soc.*, **69**, 254 (1974).
(12) A. T. Ness, J. V. Pastewka, and A. C. Peacock, *Clin. Chem. Acta*, **10**, 229 (1964).

ACKNOWLEDGMENTS

Supported by Grant HL25680, National Heart, Lung, and Blood Institute, National Institutes of Health.

We thank Melba Gibson and Greg Webb for their technical assistance on this project.

High-Performance Liquid Chromatographic Stability-Indicating Assay for Naphazoline and Tetrahydrozoline in Ophthalmic Preparations

JOHN BAUER ˣ and SUZANNE KROGH

Received July 12, 1982, from the *Pharmaceutical Products Division, Abbott Laboratories, North Chicago, IL 60064.* Accepted for publication October 5, 1982.

Abstract □ A high-performance liquid chromatographic (HPLC) analysis for tetrahydrozoline and naphazoline in ophthalmic solutions is presented. The analysis allows a more reproducible, direct stability-indicating assay than the colorimetric methods generally employed. The HPLC system is so designed that a variety of ophthalmic solutions containing either naphazoline or tetrahydrozoline can be analyzed concomitantly.

Keyphrases □ High-performance liquid chromatography—stability-indicating assay, ophthalmic preparation, naphazoline, tetrahydrozoline □ Naphazoline—high-performance liquid chromatographic stability-indicating assay, ophthalmic preparation □ Tetrahydrozoline—high-performance liquid chromatographic stability-indicating assay

Tetrahydrozoline (I) and naphazoline (II) are sympathomimetic agents used in the majority of commercially available occular decongestants. The current analytical methodologies are either colorimetric or ultraviolet. Tetrahydrozoline analysis involves color development with either sodium nitroprusside (1, 2) or bromophenol blue (2). Naphazoline is presently assayed by either UV-absorption spectroscopy (3) or colorimetry (1).

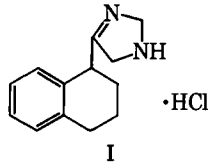

I

2-(1,2,3,4-Tetrahydro-1-naphthyl)-2-imidazoline, monohydrochloride

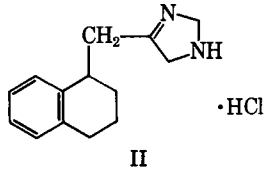

II

2(1-Naphthylmethyl)-2-imidazoline, monohydrochloride

These methods generally involve isolation steps as well as color development times and are subject to interferences. The high-performance liquid chromatographic (HPLC) procedure developed in our laboratory is a direct stability-indicating assay for tetrahydrozoline and naphazoline in ophthalmic solutions.

EXPERIMENTAL

Materials—Methanol[1], citric acid[2], sodium citrate[3], and perchloric acid[4] were used as received. Tetrahydrozoline and naphazoline were USP reference standards. A high-performance liquid chromatograph[5] and a UV visible spectrophotometer[6] were used. A microparticulate octadecylsilane column[7] was used. The temperature was ambient and the flow rate 2.0 ml/min. The analytical wavelength was 265 nm. Injection volume was 20 μl.

Mobile Phase—Six grams of sodium citrate dihydrate and 4 g of anhydrous citric acid were added to 700 ml of water and mixed until dissolved; 7 ml of perchloric acid was added and the pH determined. The pH was adjusted to 2.2 ± 0.2 by further addition of perchloric acid. A 300-ml volume of methanol was added, the solution mixed thoroughly, filtered through a 0.45-μm filter, and deaerated for ~10 min.

Tetrahydrozoline Internal Standard Solution—A solution containing ~150 mg of tetrahydrozoline hydrochloride was prepared by dissolving and diluting to volume with distilled water to 100 ml (~1.5 mg/ml).

Naphazoline Internal Standard Solution—A preparation of ~40 mg of naphazoline in 100 ml of water was prepared and diluted 1/10 with water for use as the internal standard solution (~0.04 mg/ml).

Naphazoline Standard—Approximately 120 mg of naphazoline hydrochloride was weighed accurately into a 100-ml volumetric flask and dissolved and diluted to volume with distilled water. A 5.0-ml volume of this solution was pipetted into a 50-ml volumetric flask and diluted to volume with distilled water (~0.12 mg/ml); 5.0 ml of this solution was pipetted into a 10-ml volumetric flask and diluted to volume with tetrahydrozoline internal standard solution.

[1] Methanol, Burdick and Jackson or equivalent spectrophotometric grade.
[2] Citric acid anhydrous AR Grade.
[3] Sodium citrate dihydrate AR Grade.
[4] Perchloric acid (60%), Fisher Scientific.
[5] Waters Model 6000A Liquid Chromatography Pump; Rheodyne Model 7120 Injector with 20-μl loop; DuPont variable-wavelength detector; Hewlett-Packard 3385A Recording Integrator.
[6] Varian/Cary 219 UV Spectrophotometer.
[7] Waters μBondapak C_{18} liquid chromatographic column.

0022-3549/83/1100-1347$01.00/0

(3) A. Yoshida and M. Shindo, *Japan Kokai*, **78 40**, 787 (1978); *Chem. Abstr.*, **89**, P109552v (1978).
(4) M. S. Newman, B. J. Magerlein, and W. B. Wheatley, *J. Am. Chem. Soc.* **68**, 2113 (1946).
(5) W. Wood, *J. Chem. Soc.*, **1956**, 3327.
(6) M. de Montmollin and F. Achermann, *Helv. Chim. Acta*, **12**, 874 (1929).
(7) N. Rabjohn and E. R. Rogier, *J. Org. Chem.*, **11**, 781 (1946).
(8) R. Robinson and H. Suginome, *J. Chem. Soc.*, **1932**, 304.
(9) O. Wichterle and M. Hudlicky, *Coll. Czech. Chem. Commun.*, **12**, 101 (1947); *Chem. Abstr.*, **41**, 4149e (1947).
(10) H. Irai, S. Shima, and N. Murata, *Kogyo Kaguku Zasshi*, **62**, 82 (1959); *Chem. Abstr.*, **58**, 5659b (1963).
(11) S. R. Buc, *J. Am. Chem. Soc.*, **69**, 254 (1974).
(12) A. T. Ness, J. V. Pastewka, and A. C. Peacock, *Clin. Chem. Acta*, **10**, 229 (1964).

ACKNOWLEDGMENTS

Supported by Grant HL25680, National Heart, Lung, and Blood Institute, National Institutes of Health.

We thank Melba Gibson and Greg Webb for their technical assistance on this project.

High-Performance Liquid Chromatographic Stability-Indicating Assay for Naphazoline and Tetrahydrozoline in Ophthalmic Preparations

JOHN BAUER ˣ and SUZANNE KROGH

Received July 12, 1982, from the *Pharmaceutical Products Division, Abbott Laboratories, North Chicago, IL 60064.* Accepted for publication October 5, 1982.

Abstract □ A high-performance liquid chromatographic (HPLC) analysis for tetrahydrozoline and naphazoline in ophthalmic solutions is presented. The analysis allows a more reproducible, direct stability-indicating assay than the colorimetric methods generally employed. The HPLC system is so designed that a variety of ophthalmic solutions containing either naphazoline or tetrahydrozoline can be analyzed concomitantly.

Keyphrases □ High-performance liquid chromatography—stability-indicating assay, ophthalmic preparation, naphazoline, tetrahydrozoline □ Naphazoline—high-performance liquid chromatographic stability-indicating assay, ophthalmic preparation □ Tetrahydrozoline—high-performance liquid chromatographic stability-indicating assay

Tetrahydrozoline (I) and naphazoline (II) are sympathomimetic agents used in the majority of commercially available occular decongestants. The current analytical methodologies are either colorimetric or ultraviolet. Tetrahydrozoline analysis involves color development with either sodium nitroprusside (1, 2) or bromophenol blue (2). Naphazoline is presently assayed by either UV-absorption spectroscopy (3) or colorimetry (1).

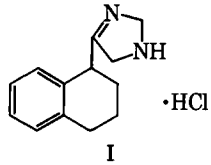

I

2-(1,2,3,4-Tetrahydro-1-naphthyl)-2-imidazoline, monohydrochloride

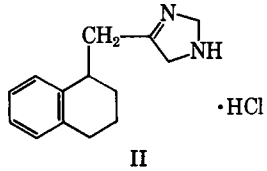

II

2(1-Naphthylmethyl)-2-imidazoline, monohydrochloride

These methods generally involve isolation steps as well as color development times and are subject to interferences. The high-performance liquid chromatographic (HPLC) procedure developed in our laboratory is a direct stability-indicating assay for tetrahydrozoline and naphazoline in ophthalmic solutions.

EXPERIMENTAL

Materials—Methanol[1], citric acid[2], sodium citrate[3], and perchloric acid[4] were used as received. Tetrahydrozoline and naphazoline were USP reference standards. A high-performance liquid chromatograph[5] and a UV visible spectrophotometer[6] were used. A microparticulate octadecylsilane column[7] was used. The temperature was ambient and the flow rate 2.0 ml/min. The analytical wavelength was 265 nm. Injection volume was 20 μl.

Mobile Phase—Six grams of sodium citrate dihydrate and 4 g of anhydrous citric acid were added to 700 ml of water and mixed until dissolved; 7 ml of perchloric acid was added and the pH determined. The pH was adjusted to 2.2 ± 0.2 by further addition of perchloric acid. A 300-ml volume of methanol was added, the solution mixed thoroughly, filtered through a 0.45-μm filter, and deaerated for ~10 min.

Tetrahydrozoline Internal Standard Solution—A solution containing ~150 mg of tetrahydrozoline hydrochloride was prepared by dissolving and diluting to volume with distilled water to 100 ml (~1.5 mg/ml).

Naphazoline Internal Standard Solution—A preparation of ~40 mg of naphazoline in 100 ml of water was prepared and diluted 1/10 with water for use as the internal standard solution (~0.04 mg/ml).

Naphazoline Standard—Approximately 120 mg of naphazoline hydrochloride was weighed accurately into a 100-ml volumetric flask and dissolved and diluted to volume with distilled water. A 5.0-ml volume of this solution was pipetted into a 50-ml volumetric flask and diluted to volume with distilled water (~0.12 mg/ml); 5.0 ml of this solution was pipetted into a 10-ml volumetric flask and diluted to volume with tetrahydrozoline internal standard solution.

[1] Methanol, Burdick and Jackson or equivalent spectrophotometric grade.
[2] Citric acid anhydrous AR Grade.
[3] Sodium citrate dihydrate AR Grade.
[4] Perchloric acid (60%), Fisher Scientific.
[5] Waters Model 6000A Liquid Chromatography Pump; Rheodyne Model 7120 Injector with 20-μl loop; DuPont variable-wavelength detector; Hewlett-Packard 3385A Recording Integrator.
[6] Varian/Cary 219 UV Spectrophotometer.
[7] Waters μBondapak C_{18} liquid chromatographic column.

0022-3549/83/1100-1347$01.00/0

Table I—Comparison of Tetrahydrozoline Assays

Sample No.	Run No.	HPLC Analysis	Colorimetric Analysis (Sodium Nitroprusside)
1	1	99.5	99.5
	2	99.0	96.7
2	1	97.4	99.5
	2	97.6	99.9
3	1	98.4	99.5
	2	99.0	101.3
4	1	97.3	97.5
	2	97.7	98.1

Table II—Comparison of Naphazoline Assays

Sample No.	Run No.	HPLC Analysis	Colorimetric Analysis (Sodium Nitroprusside)
1	1	100.8	106.8
	2	100.1	97.8
2	1	103.8	102.3
	2	103.4	107.8
3	1	98.2	104.5
	2	99.9	104.5
4	1	102.4	106.1
	2	102.5	105.2

Table III—Precision of Naphazoline and Tetrahydrozoline Analyses

	Naphazoline, mg/ml Found	Tetrahydrozoline, mg/ml Found
	0.1210	0.524
	0.1210	0.524
	0.1200	0.508
	0.1180	0.518
	0.1204	0.508
	0.1228	0.515
	0.1218	0.515
	0.1228	0.510
	0.1225	0.513
	0.1228	0.506
Mean	0.1212	0.514
SD	±0.0016	±0.006
RSD	±1.33%	±1.2%

Tetrahydrozoline Standard—Approximately 100 mg of tetrahydrozoline was accurately weighed into a 100-ml volumetric flask, dissolved, and diluted to volume with distilled water. A 25.0-ml volume of this solution was pipetted into a 50-ml volumetric flask and diluted to volume with distilled water (~0.5 mg/ml); 5.0 ml of this solution was pipetted into a 10-ml volumetric flask and diluted to volume with naphazoline internal standard solution.

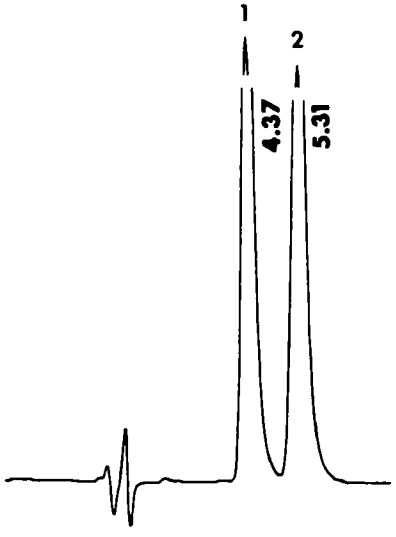

Figure 1—*Typical chromatogram of (1) naphazoline and (2) tetrahydrozoline.*

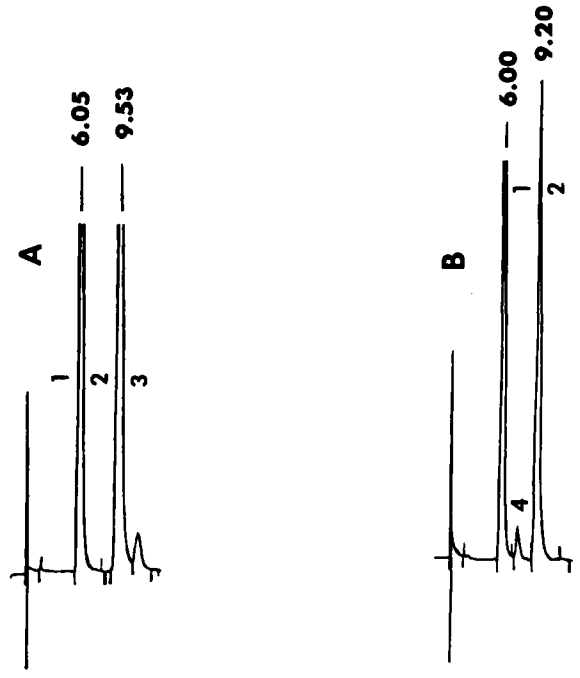

Figure 2—*Separation of degradation products of (A) naphazoline preparation and (B) tetrahydrozoline preparation. Key: (1) tetrahydrozoline, (2) naphazoline, (3) N-(2-aminoethyl)-1,2,3,4-tetrahydro-1-naphthylamine, and (4) N-(2-aminoethyl)-1-(1-naphthyl)acetamide.*

Sample Procedure—A 5.0-ml volume of the sample was pipetted into a 10-ml volumetric flask and diluted to volume with the appropriate internal standard solution.

RESULTS AND DISCUSSION

The HPLC analysis is, in the majority of cases, more reproducible than the sodium nitroprusside colorimetric methods for tetrahydrozoline and naphazoline (Tables I and II). In addition the use of naphazoline as the internal standard for tetrahydrozoline and tetrahydrozoline as the internal standard for naphazoline allows direct analysis of a variety of ophthalmic solutions using a single eluant system.

The precision data for the HPLC analysis (Table III) and the comparative study (Tables I and II) demonstrate that the HPLC analysis is better than the colorimetric techniques, which in our laboratories gave standard deviations of 1.5% for naphazoline and 2.8% for tetrahydrozoline.

A typical chormatogram is shown in Fig. 1. Both tetrahydrozoline and naphazoline can be separated from their respective degradation products, *N*-(2-aminoethyl)-1,2,3,4-tetrahydro-1-napthylamine (III) and *N*-(2-aminoethyl)-1-(1-napthyl)acetamide (IV) (Fig. 2). These components can be quantitated separately if desired, although appropriate corrections for extinction coefficient differences must be used.

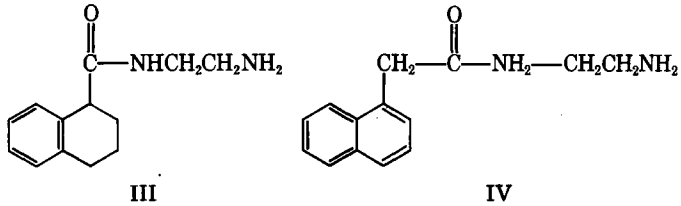

III IV

Both compounds III and IV have been isolated from the HPLC system and identified spectroscopically. The response for both tetrahydrozoline and naphazoline is linear. The naphazoline response from 0.02 to 0.1 mg/ml gave a correlation coefficient of 0.9999, n = 1.0019 (4). Tetrahydrozoline response gave a correlation coefficient of 0.9999 between 0.1 and 0.5 mg/ml, n = 1.0029. The analysis is applicable to a variety of ophthalmic solutions[8].

The HPLC assay presented constitutes a direct, stability-indicating

[8] Clear Eyes, Naphcon, 20/20, Murine Plus, Visine, Visine AC, Soothe.

analysis for either of the two major sympathomimetic agents in use in topical ocular decongestants. The technique is more reproducible than the present colorimetric assay and does not suffer from the time restraints and interferences possible in colorimetric assays. The HPLC method presented can be easily automated and allows analysis of a variety of ophthalmic solutions on a single HPLC system.

REFERENCES

(1) S. C. Slack and W. J. Moder, *J. Am. Pharm. Assoc., Sci. Ed.* **46**, 742 (1957).

(2) "United States Pharmacopeia," 20th rev., U.S. Pharmacopeial Convention, Rockville, Md., 1980, p. 783.

(3) "United States Pharmacopeia," 20th rev., U.S. Pharmacopeial Convention, Rockville, Md., 1980, p. 543.

(4) E. M. Gindler, *Clin. Chem.*, **25**, 337 (1979).

ACKNOWLEDGMENTS

The authors thank Ms. Diane Horgen and Mr. Joseph Martin for assistance in preparation of this paper.

Stability-Indicating Assay, Dissolution, and Content Uniformity of Sodium Levothyroxine in Tablets

STEVEN L. RICHHEIMER ˣ and TAHANI M. AMER

Received July 19, 1982, from the *Stability Laboratory, Pharmaceutical Basics, Inc., Denver, CO 80223.* Accepted for publication October 14, 1982.

Abstract □ A reverse-phase high-performance liquid chromatographic (HPLC) method for determining sodium levothyroxine in tablet formulations is described. The sodium levothyroxine was extracted from tablets using a mobile phase consisting of 60% acetonitrile and 40% aqueous buffer. After centrifugation 200 μl of the solution was chromatographed on a 10-μm C_{18} column. The method gave accurate results when tested against the USP method, by the standard additions method, and by the spiked-placebo method. The method can also be used to determine content uniformity and dissolution of sodium levothyroxine tablets.

Keyphrases □ Sodium levothyroxine—stability-indicating assay, dissolution, content uniformity, tablets □ Dissolution—sodium levothyroxine, stability-indicating assay, content uniformity, tablets □ Content uniformity—sodium levothyroxine, stability-indicating assay, dissolution, tablets □ Stability—assay of sodium levothyroxine in tablets, dissolution, content uniformity

Sodium levothyroxine (I) tablets are widely prescribed in thyroid replacement therapy, with a wide range of doses available (25–300 μg/tablet). The USP XX method of assay consists of a lengthy ignition and oxidation to iodate followed by titration of the liberated iodine (1). The method is neither stability indicating nor sensitive enough to be used for content uniformity and dissolution determinations.

A number of other assay procedures based on liquid chromatography have appeared in the literature (2–13). This report describes a new reverse-phase liquid chromatographic (HPLC) assay method that adequately separates I from degradation products and can be used for the identification, content uniformity analysis, and dissolution testing of I in tablets.

EXPERIMENTAL

Reagents and Materials—Sodium levothyroxine[1] (I) was assayed by the USP XX procedure (14); sodium liothyronine[1] and 3,5-diiodo-L-thyronine[2] were used as received. Reagents used were analytical reagent grade. The levothyroxine sodium tablets (USP) were obtained commercially from four sources[3–6].

Apparatus—The high-performance liquid chromatograph[7] was equipped with a variable-wavelength UV detector[8], a strip-chart recorder[9], an electronic integrator[10], and a 200-μl loop-type injector[11]. Commercial 10-μm C_{18} columns[12] (30 cm × 4 mm i.d.) were used at am-

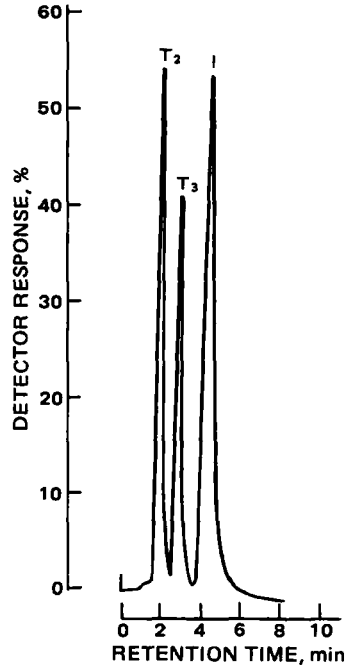

Figure 1—*Chromatogram of sodium levothyroxine (I, 20 μg/ml) with added sodium liothyronine (T_3, 10 μg/ml), and 3,5-diiodo-L-thyronine (T_2, 10 μg/ml).*

[1] Sanabo Gesellschaft, Kundle, Austria.
[2] Sigma Chemical Co., St. Louis, Mo.
[3] Armour Pharmaceutical Co., Phoenix, Ariz.
[4] Flint, Division of Baxter-Travenol, Morton Grove, Ill.
[5] Lederle Laboratories, Pearl River, N.Y.
[6] Pharmaceutical Basics, Inc., Denver, Co.
[7] Model 5020, Varian Associates, Palo Alto, Calif.
[8] Model UV-50, Varian Associates, Palo Alto, Calif.
[9] Model 1005, Beckman Instruments, Fullerton, Calif.
[10] Model CDS-111L, Varian Associates, Palo Alto, Calif.
[11] Model CV-6-UHPa-N60, Valco Instruments Co., Houston, Tex.
[12] Model MCH-10, Varian Associates, Palo Alto, Calif.; μBondapak C18, Waters Associates, Milford, Mass.

0022-3549/83/1100-1349$01.00/0

analysis for either of the two major sympathomimetic agents in use in topical ocular decongestants. The technique is more reproducible than the present colorimetric assay and does not suffer from the time restraints and interferences possible in colorimetric assays. The HPLC method presented can be easily automated and allows analysis of a variety of ophthalmic solutions on a single HPLC system.

REFERENCES

(1) S. C. Slack and W. J. Moder, *J. Am. Pharm. Assoc., Sci. Ed.* **46**, 742 (1957).

(2) "United States Pharmacopeia," 20th rev., U.S. Pharmacopeial Convention, Rockville, Md., 1980, p. 783.

(3) "United States Pharmacopeia," 20th rev., U.S. Pharmacopeial Convention, Rockville, Md., 1980, p. 543.

(4) E. M. Gindler, *Clin. Chem.*, **25**, 337 (1979).

ACKNOWLEDGMENTS

The authors thank Ms. Diane Horgen and Mr. Joseph Martin for assistance in preparation of this paper.

Stability-Indicating Assay, Dissolution, and Content Uniformity of Sodium Levothyroxine in Tablets

STEVEN L. RICHHEIMER ˣ and TAHANI M. AMER

Received July 19, 1982, from the *Stability Laboratory, Pharmaceutical Basics, Inc., Denver, CO 80223.* Accepted for publication October 14, 1982.

Abstract □ A reverse-phase high-performance liquid chromatographic (HPLC) method for determining sodium levothyroxine in tablet formulations is described. The sodium levothyroxine was extracted from tablets using a mobile phase consisting of 60% acetonitrile and 40% aqueous buffer. After centrifugation 200 μl of the solution was chromatographed on a 10-μm C_{18} column. The method gave accurate results when tested against the USP method, by the standard additions method, and by the spiked-placebo method. The method can also be used to determine content uniformity and dissolution of sodium levothyroxine tablets.

Keyphrases □ Sodium levothyroxine—stability-indicating assay, dissolution, content uniformity, tablets □ Dissolution—sodium levothyroxine, stability-indicating assay, content uniformity, tablets □ Content uniformity—sodium levothyroxine, stability-indicating assay, dissolution, tablets □ Stability—assay of sodium levothyroxine in tablets, dissolution, content uniformity

Sodium levothyroxine (I) tablets are widely prescribed in thyroid replacement therapy, with a wide range of doses available (25–300 μg/tablet). The USP XX method of assay consists of a lengthy ignition and oxidation to iodate followed by titration of the liberated iodine (1). The method is neither stability indicating nor sensitive enough to be used for content uniformity and dissolution determinations.

A number of other assay procedures based on liquid chromatography have appeared in the literature (2–13). This report describes a new reverse-phase liquid chromatographic (HPLC) assay method that adequately separates I from degradation products and can be used for the identification, content uniformity analysis, and dissolution testing of I in tablets.

EXPERIMENTAL

Reagents and Materials—Sodium levothyroxine[1] (I) was assayed by the USP XX procedure (14); sodium liothyronine[1] and 3,5-diiodo-L-thyronine[2] were used as received. Reagents used were analytical reagent grade. The levothyroxine sodium tablets (USP) were obtained commercially from four sources[3–6].

Apparatus—The high-performance liquid chromatograph[7] was equipped with a variable-wavelength UV detector[8], a strip-chart recorder[9], an electronic integrator[10], and a 200-μl loop-type injector[11]. Commercial 10-μm C_{18} columns[12] (30 cm × 4 mm i.d.) were used at am-

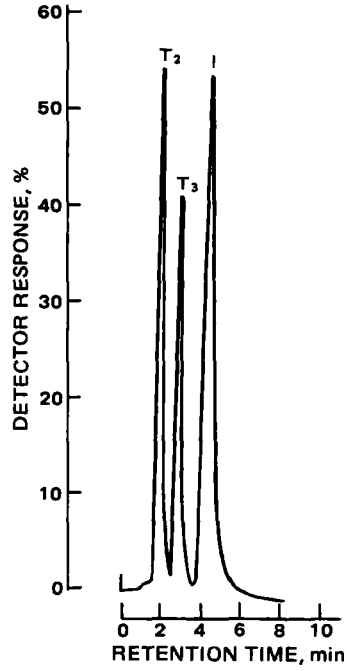

Figure 1—*Chromatogram of sodium levothyroxine (I, 20 μg/ml) with added sodium liothyronine (T_3, 10 μg/ml), and 3,5-diiodo-L-thyronine (T_2, 10 μg/ml).*

[1] Sanabo Gesellschaft, Kundle, Austria.
[2] Sigma Chemical Co., St. Louis, Mo.
[3] Armour Pharmaceutical Co., Phoenix, Ariz.
[4] Flint, Division of Baxter-Travenol, Morton Grove, Ill.
[5] Lederle Laboratories, Pearl River, N.Y.
[6] Pharmaceutical Basics, Inc., Denver, Co.
[7] Model 5020, Varian Associates, Palo Alto, Calif.
[8] Model UV-50, Varian Associates, Palo Alto, Calif.
[9] Model 1005, Beckman Instruments, Fullerton, Calif.
[10] Model CDS-111L, Varian Associates, Palo Alto, Calif.
[11] Model CV-6-UHPa-N60, Valco Instruments Co., Houston, Tex.
[12] Model MCH-10, Varian Associates, Palo Alto, Calif.; μBondapak C18, Waters Associates, Milford, Mass.

0022-3549/83/1100-1349$01.00/0

Table I—Comparison of the USP XX and HPLC Assay for a 100-μg Tablet

	USP XX	HPLC
Number of Determinations	8	8
Mean, %	101.3	100.7
Range, %	104.5–98.8	101.8–99.1
Percent *RSD*	2.21	0.85

bient temperature. A stainless steel column (4 cm × 4 mm i.d.) packed with a 40-μm C_{18} pellicular material[13] was used both as a guard column and in place of the injection loop for dissolution studies. Dissolutions were performed on a commercial dissolution apparatus[14] using the USP-rotating-paddle method.

Chromatographic Conditions—The mobile phase was a mixture of 60% acetonitrile and 40% pH 3.0 aqueous buffer containing 0.005 *M* 1-octanesulfonic acid and 0.005 *M* tetramethylammonium chloride. The acetonitrile was reduced to 50% for columns with less retentive packing material[13]. Flow rate was 2 ml/min, and the detector was at 230 nm and 0.08 AUFS.

Standard Preparation—The levothyroxine reference standard[15] (19.5 mg) or I (20 mg) was dissolved in 100.0 ml of mobile phase. The stock solution could be stored for several months in darkness at 4°. Working standards were prepared daily from the stock solution by dilution with the mobile phase.

Sample Preparation—Twenty tablets were weighed and finely powdered. A portion of powder equivalent to 200 μg of I was transferred to a glass-stoppered centrifuge tube. Mobile phase (10.0 ml) was added, and the mixture was sonicated for 5 min and then centrifuged. The supernatant was then filtered through a 0.45-μm membrane filter[16] if it was not free of particulate matter. For content uniformity analyses, one tablet was placed in a centrifuge tube and enough mobile phase was added to make the final concentration 20 μg/ml (except 25- and 50-μg tablets, 5- and 10-μg/ml were acceptable). The tablet was sonicated until completely disintegrated, and the solution was analyzed using the composite assay, reducing the standard concentration where applicable.

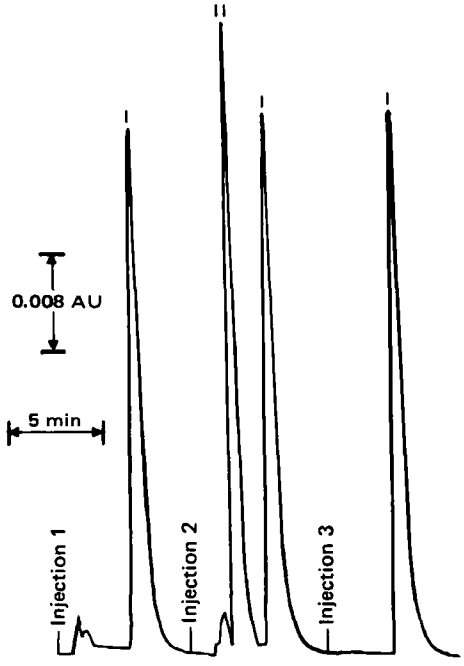

Figure 2—*Typical chromatograms for the assay of sodium levothyroxine. The mobile phase is 60% acetonitrile and 40% pH 3.0 buffer. Key: injection 1: 200-μg tablet from manufacturer B; injection 2: 100-μg tablet from manufacturer A (II is an excipient peak); and injection 3: standard, 20 μg/ml.*

[13] Vydac RP 201SC, Varian Associates, Palo Alto, Calif.
[14] Model 725115, Hanson Research, Northridge, Calif.
[15] United States Pharmacopeial Convention, Rockville, Md.
[16] Acrodisc CR, 25mm, Gelman Sciences, Ann Arbor, Mich.

Table II—Comparison of the USP XX and HPLC Assays for I in Tablets Stored at Elevated Temperatures

Manufacturer	Potency, μg	Storage Days	Temperature[a], °	USP XX, %	HPLC, %
A	100	21	60	101.3	70.9
A	300	21	60	100.0	74.0
A	100	91	40	101.0	74.3
B	100	21	60	104.8	41.1
B	300	21	60	102.4	48.0
B	100	91	40	105.2	34.3
C	100	1	80	108.3	13.4
D	100	21	60	100.0	67.0
D	300	91	40	100.7	67.1

[a] All samples stored at ambient humidity.

Assay Procedure—Standard and sample preparations (200 μl) were injected into the liquid chromatograph. Either peak areas or peak heights were measured. Compound I was quantitated by comparing the peak response of the sample to that of the standard.

Dissolution Procedure—Phosphate buffer (500 ml, pH 7.5, 0.05 *M*) at 37 ± 0.5° was used with the USP rotating-paddle method at 50 rpm. A 20-ml aliquot of the mixture was withdrawn after 30 min and filtered through a 0.45-μm membrane filter. A portion of the filtrate equivalent to 1 μg of I (0.25 μg for 25-μg tablets) was passed through a 4 cm × 4-mm guard column with C_{18} packing attached to the sampling valve. The column was rinsed with 1 ml of water and injected onto the liquid chromatograph under the same conditions specified for the assay. Similarly, 1.0 ml of a standard (1 μg/ml of I) in dissolution medium (0.25 μg/ml for 25-μg tablets) was injected. The amount of I dissolved was quantitated by comparing the peak areas obtained for the standard and sample chromatograms.

RESULTS AND DISCUSSION

Chromatography and Specificity—Various mobile phases were investigated; however, the equimolar combination of 1-octanesulfonate and tetramethylammonium chloride with acetonitrile was found to give the sharpest peak for I, as well as providing adequate separation of I from degradation products and tablet excipients. Figure 1 shows a typical chromatographic separation of I from liothyronine (T_3) and 3,5-diiodo-L-thyronine (T_2). Figure 2 shows typical chromatograms obtained in the assay of two brands of tablets and a standard. Extraction of I by the mobile phase was quantitative, as evidenced by recovery experiments using whole tablets and I in combination with individual tablet excipients. Incomplete extraction of I in the presence of magnesium stearate was observed using several other extracting solvents (100% acetonitrile, ammoniacal methanol, and 60:40 acetonitrile–water). It is possible that I forms an insoluble ion-pair complex with the stearate which is inhibited in the presence of 1-octanesulfonate and tetramethylammonium chloride but not other extracting solvents.

The specificity of the method was further tested by degrading samples of I (20–200 μg/ml) by irradiation, hydrolysis, oxidation, and heat and assaying the resulting solutions by the proposed method. Short-wavelength UV (24 hr) caused 100% degradation, while refluxing with 0.1 *N* HCl or 0.1 *N* NaOH (16 hr) caused 41.1 and 43.4% degradation, respectively. Oxidation with 0.01 *M* H_2O_2 and 0.01 *M* Fe^{2+} (16 hr) caused 97% degradation. Thermal degradation of I at 80° combined with tablet excipients was 17–87% in 24 hr depending on the formulation. In every case the unidentified degradation products eluted before the I peak and did not interfere with the analysis of I.

Comparison to the USP Method and Reproducibility—A new lot (<1 month since manufacture) of 100-μg tablets of I was assayed re-

Table III—Recovery of Sodium Levothyroxine (I) Added to Tablet Formulations

Manufacturer	Stated Potency, μg	Unspiked I/Tablet	Amt. of I Added, μg	Amt. of I Measured, μg	Recovery[a], %
A	25	24.0	12.5	35.6	97.5
A	300	281.0	150.1	429.4	99.6
B	25	22.2	12.5	33.6	96.9
B	200	195.7	100.9	297.9	100.4
C	100	89.5	50.4	140.8	100.6
D	200	196.7	100.9	297.6	100.0

[a] Percent Recovery = [measured I/(unspiked I + added I)] × 100.

peatedly by the USP XX method and by the proposed method. The results (Table I) indicate that the two methods are in close agreement for this lot and that reproducibility is good (*RSD* = 0.85%). However, samples stored at elevated temperatures (Table II) for even short periods of time gave higher assay results by the USP XX method than by HPLC due to degradation of I in the tablet formulations.

Recovery of I Added to Spiked Placebo Mixtures and Linearity—The effectiveness of the extraction step and accuracy of the method was tested by adding I in an amount corresponding to 50–125% of the label claim to several powdered placebo mixtures (25-, 100-, 200-, and 300-μg tablets). A plot of the amount of I added *versus* the amount recovered indicates that the slopes are unity within experimental error (1.000 ± 0.008), that the intercepts are near zero (0.40 ± 0.76), and that the correlation coefficients are unity (1.000). Recoveries for the 20 spiked samples tested (five for each potency) ranged from 98.1 to 100.6% (average: 100.0%; *RSD* = 0.53). In each case a placebo blank was also run which showed no interfering peaks. These data indicate that the method is linear and accurate between 50 and 125% for the tablet formulations tested. Both peak area and peak height gave equally accurate results.

The method was also tested by spiking several different commercially available tablets with additional I. Tablet potencies ranged from 25 to 300 μg, and in each case 50% of the label amount of I was added. The results (Table III) indicate that complete recovery was obtained for all formulations tested.

The linearity of the method was further tested by chromatographing a series of seven standard solutions ranging in concentration from 5 to 35 μg/ml. Plots of both peak area and peak height *versus* concentration were linear (correlation coefficients = 0.9999) and showed no bias (intercepts were 0.0 ± 0.75%). These results indicate that an external standard (equivalent to 20 μg/ml of I) can be used to analyze samples varying in concentration over a sevenfold range.

Content Uniformity and Dissolution Studies—The applicability of the method for content uniformity determinations was tested by assaying 10 individual 25-μg tablets from manufacturer A. The mean value of 95.9% agreed well with a composite assay for this lot of 96.0%, and the variation (2.60% high to 2.61% low) was close to the weight variation for the same 10 tablets (2.04–1.86%).

The accuracy of the dissolution method was tested by determining the recovery of varying amount of I added to dissolution medium (0.05 *M* phosphate buffer, pH 7.5) plus tablet excipients. The results (Table IV) indicate that recovery is quantitative in the range of 30–100% (0.3–1.0 μg); reproducibility using peak area was also good (*RSD* = 1.3%, $n = 8$). Retention of I on the guard column was complete, since washing with 10 times the normal amount of dissolution medium did not reduce the amount of I recovered (although the peak was broadened). Results using commercially available tablets (100 μg) varied from 36.2 to 68.4% dissolved using the method depending on manufacturer and were significantly lower with water (−39%) and 0.1 *N* HCl (−28%) as the dissolution media.

Several studies have shown differences in the potency and/or bioavailability of sodium levothyroxine preparations (15–17). Reported differences in bioavailability may be due to the use of subpotent tablets in the study, since several of the lots tested by the proposed HPLC method from more than one manufacturer were found to be well below the USP minimum of 90.0% of label claim. Since the stability of I in different formulations varies considerably, it is possible that the differences in potencies occur not at the time of manufacture but on aging. Unfortunately the USP method, which measures only total iodine, does not provide a specific or meaningful method for the determination of the stability of I in dosage forms. The proposed method is accurate, reproducible, and specific for I and adequately quantitates I in the presence of degradation products. In addition the method can be applied to identification, content uniformity, and dissolution of I in tablets. Official adoption of an HPLC method for the assay of sodium levothyroxine tablets will go a long way toward providing a better standardized and uniform product with a well-established shelf life.

Table IV—Sodium Levothyroxine (I) Dissolution–Recovery Study

Sample	Amount of I added, μg	Amount of I measured, μg[a]	Recovery, %
30	30.0	30.3	101.0
50	50.0	50.0	100.0
70	70.0	69.2	98.9
100	100.0	98.6	98.6

[a] 500 ml of dissolution medium was used and 5.0 ml passed through guard column prior to injection (0.3–1.0 μg injected).

REFERENCES

(1) "The United States Pharmacopeia," 20th rev., U.S. Pharmacopeial Convention, Rockville, Md., 1980, p. 447.

(2) R. S. Rapaka, P. W. Knight, and U. K. Prasan, *J. Pharm. Sci.*, **70**, 131 (1981).

(3) E. P. Lankmayr, B. Maichin, G. Knapp, and F. Nachtmann, *J. Chromatogr.*, **224**, 239 (1981).

(4) D. J. Smith, M. Biesemeyer, and C. Yaciw, *J. Chromatogr. Sci.*, **19**, 72 (1981).

(5) F. Nachtmann, *Acta Pharm. Tech.*, Suppl., July, 1979, p. 145.

(6) R. S. Rapaka, P. W. Knight, V. P. Shah, and V. K. Prasad, *Anal. Lett.*, **12**, 1201 (1979).

(7) D. J. Smith and J. H. Graham, *J. Assoc. Off. Anal. Chem.*, **62**, 818 (1979).

(8) M. T. Hearn, W. S. Hancock, and C. A. Bishop, *J. Chromatogr.*, **157**, 337 (1978).

(9) W. A. Dark and L. W. Grossman, Jr., *Applications Highlights* AH-139, Waters Associates Inc., Milford, Mass.

(10) B. L. Karger, S. C. Su, S. Marchese, and B.-A. Persson, *J. Chromatogr. Sci.*, **12**, 678 (1974).

(11) U. R. Cieri and J. C. Illuminati, *J. Assoc. Off. Anal. Chem.*, **60**, 628 (1977).

(12) G. G. Skellern, M. Mahmoudian, and B. I. Knight, *J. Chromatogr.*, **179**, 213 (1979).

(13) N. M. Alexander and M. Nishimoto, *Clin. Chem.*, **25**, 1757 (1979).

(14) "The United States Pharmacopeia," 20th rev., U.S. Pharmacopeial Convention, Rockville, Md., 1980, p. 446.

(15) S. Stoffer and W. E. Szpunar, *J. Am. Med. Assoc.*, **244**, 1704 (1980).

(16) R. W. Rees-Jones and P. R. Larsen, *J. Am. Med. Assoc.*, **243**, 549 (1980).

(17) A. Ramos-Gabatin, J. M. Jacobson, and R. L. Young, *J. Am. Med. Assoc.*, **247**, 203 (1982).

In Vivo Evaluation of the Michaelis–Menten Constant For a Medium Extraction Ratio Drug: Application to Cinromide in the Rhesus Monkey

ELIZABETH A. LANE * **and RENÉ H. LEVY** ˣ

Received August 27, 1982, from the *University of Washington, Department of Pharmaceutics, Seattle, WA 98195.* Accepted for publication October 14, 1982. *Present address: Laboratory of Chemical Pharmacology, National Heart, Lung and Blood Institute, Bethesda, MD 20205.

Abstract □ The dose-dependent nonlinearity of the clearance of cinromide, a medium extraction ratio drug, has been established in two monkeys. Special problems encountered in evaluation of nonlinearity of such drugs were resolved by the experimental design: cinromide was infused to steady state *via* the portal vein. A linearized form of the Michaelis–Menten equation was used to determine v_{max} and K_m. In addition, cinromide was administered to one of the monkeys *via* a femoral vein to verify the overestimation of K_m by administration at a peripheral venous site.

Keyphrases □ Cinromide—*in vivo* evaluation of Michaelis–Menten constant, medium extraction ratio drug, application to the rhesus monkey □ Michaelis–Menten constant—*in vivo* evaluation, medium extraction ratio drug, application to cinromide in the rhesus monkey □ Medium extraction ratio drug—*in vivo* evaluation of Michaelis-Menten constant, application to cinromide in the rhesus monkey

The accurate determination of *in vivo* Michaelis–Menten parameters is dependent on a number of considerations. For any drug it is a function of the compartmental model to which the data are fitted (1). For drugs with medium or high extraction ratios, the relationship between site of administration and site of elimination is important (2). For example, it has been pointed out that an overestimation of the Michaelis–Menten constant (K_m) is theoretically expected for drugs with high hepatic extraction ratios administered by a peripheral venous site (3). Oral administration presents the advantage of an estimation of intrinsic clearance, but it allows no control over the rate of absorption. Furthermore, it requires an independent determination of fraction absorbed. A review of the literature indicates that the problems associated with the *in vivo* determination of Michaelis–Menten parameters for a medium or high extraction ratio drug have not yet been resolved.

An investigation of the pharmacokinetic characteristics of cinromide in the rhesus monkey established that this drug has a medium extraction ratio (4). Administration of this drug by intravenous (femoral vein) infusion at three zero-order rates for 5 hr suggested the presence of nonlinearity. At the highest infusion rate (~100 mg/hr) steady state was achieved within 5 hr (half-life = 0.92 ± 0.23 hr) in only two of the five monkeys, and the postinfusion half-life of cinromide was significantly longer after the highest infusion rate (4). The object of the present study was to establish the nonlinearity of cinromide and to attempt an *in vivo* determination of Michaelis–Menten parameters. The experimental design was based on the following considerations: (*a*) the problems of extraction ratio, site of administration, and fraction absorbed were resolved by placement of a catheter in the hepatoportal vein; (*b*) the bias of compartmental models was avoided, and the rate of presentation of the drug to the liver was controlled by selection of a steady-state approach.

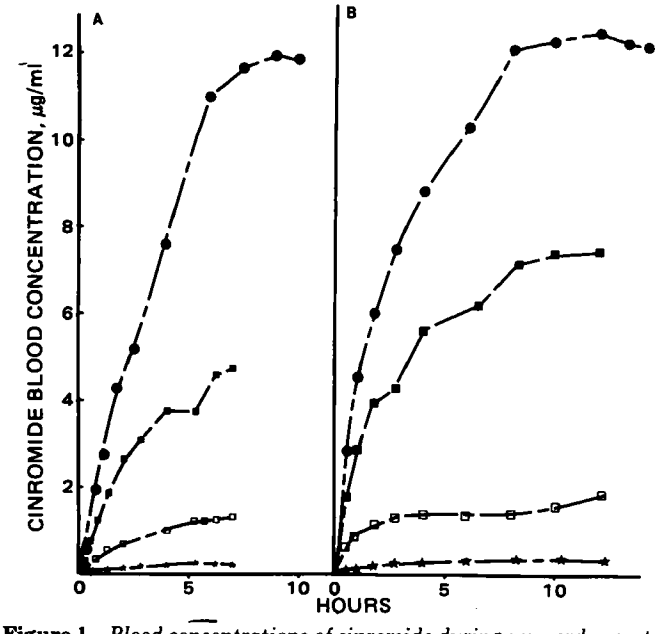

Figure 1—*Blood concentrations of cinromide during zero-order portal vein infusions. Key: (A) Monkey 306 dosed at (★) 11.5, (□) 34.0, (■) 70.0, and (●) 93.3 mg/hr; (B) monkey 307 dosed at (★) 12.3, (□) 30.6, (■) 69.9, and (●) 85.6 mg/hr.*

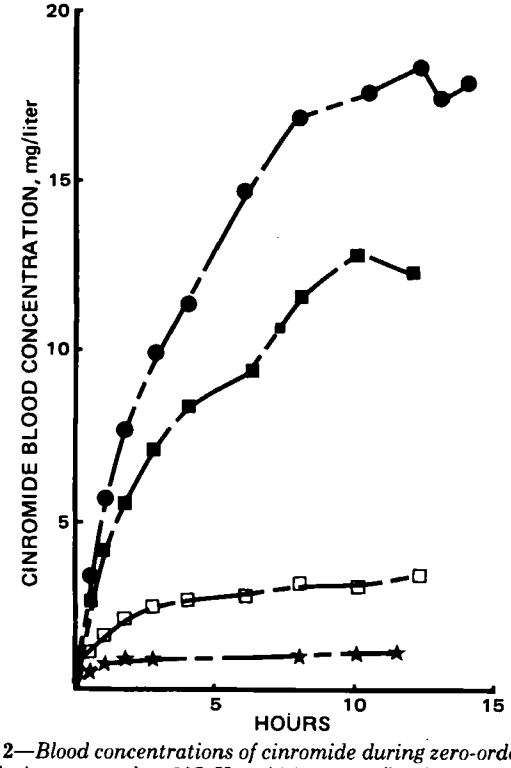

Figure 2—*Blood concentrations of cinromide during zero-order femoral vein infusions to monkey 307. Key: (★) 15.2 mg/hr; (□) 32.8 mg/hr; (■) 76.6 mg/hr; (●) 90.2 mg/hr.*

0022-3549/83/1100-1352$01.00/0

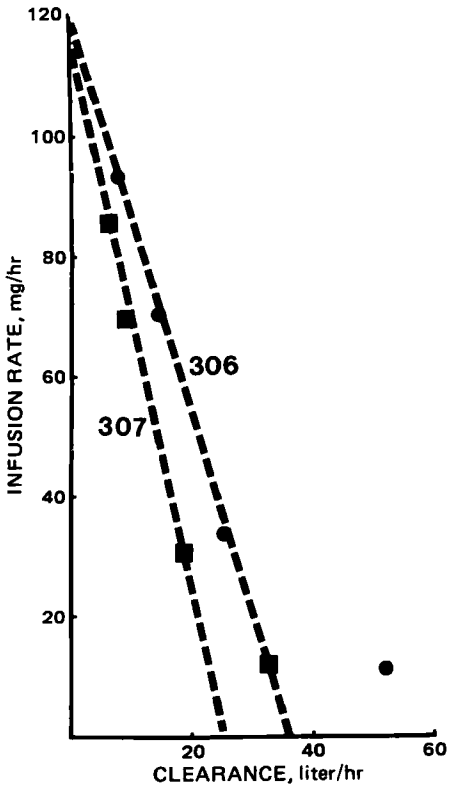

Figure 3—*Graphic evaluation of Michaelis–Menten constants for cinromide administered* via the *portal vein.*

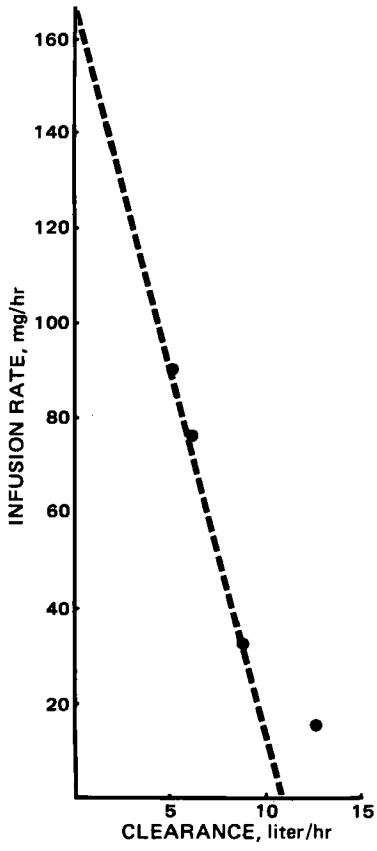

Figure 4—*Graphic evaluation of Michaelis–Menten constants for cinromide administered* via *a femoral vein (nonportal route) to monkey 307.*

EXPERIMENTAL

Two male rhesus monkeys [306 (5.7 kg) and 307 (7.9 kg)] were conditioned in primate chairs prior to the beginning of this study. Two catheters were surgically implanted in each monkey; one in the portal vein and one in the jugular vein. Patency of catheters was assured by infusion of saline (1 ml/hr). The monkeys were maintained on fresh fruit and monkey food.

Cinromide[1] was administered in 60% polyethylene glycol 400 solution by constant-rate infusion at 4 ml/hr *via* the portal vein. Four different concentrations of cinromide were infused to give dosage rates of ~10-, 30-, 70-, and 90-mg/hr. Infusions were aimed at achieving steady state and were maintained for at least 7 hr for the 10-, 30-, and 70-mg/hr doses, and at least 10 hr for the 90-mg/hr dose rate. Eleven blood samples were collected *via* the jugular vein catheter during each infusion. Blood samples were analyzed by high-performance liquid chromatography (HPLC) as previously described (4). To verify the effect of administration route on determination of the Michaelis–Menten constant, cinromide was administered to one monkey (307) *via* a femoral vein at the same four infusion rates.

RESULTS AND DISCUSSION

The concentrations achieved by four portal vein infusions to two monkeys are shown in Fig. 1. In every case, steady state appears to have been achieved. In both monkeys, the increase in steady-state concentration was more than proportional to the increase in infusion rate, illustrating the decrease in intrinsic clearance with increase in dose rate. A sevenfold increase in dosing rate corresponded to a 30-fold increase in steady-state concentration. The concentrations achieved by infusion of cinromide at the same rates *via* a femoral vein into monkey 307 are shown in Fig. 2. A sixfold increase in dosing rate corresponded to a 15-fold increase in steady-state concentration. Thus, the nonlinearity of cinromide was less pronounced when administered *via* the femoral vein than when administered *via* the portal vein. These results demonstrate the buffering effect of blood flow on systemic clearance.

Determination of parameters from the data of Figs. 1 and 2 was based on the following theoretical considerations. For a low extraction ratio drug, the dose-dependent clearance (CL) may be expressed as:

$$CL = \frac{R_0}{C^*} = \sum_{i=1}^{n} \frac{v_{\max_i}}{K_{m_i} + C^*} \qquad \text{(Eq. 1)}$$

where C^* is the steady-state total drug concentration, R_0 is the drug infusion rate, $v_{\max_i}$ is the maximum velocity of the reaction for the ith enzyme, and K_{m_i} is the Michaelis constant for the ith enzyme, uncorrected for blood protein binding. It is also assumed that the free fraction in blood is constant.

Most commonly a single $v_{\max}$ and K_m are evaluated as if a single enzyme is responsible for the elimination of the drug. If the drug is eliminated by more than one enzyme having similar values of K_m, they cannot be distinguished by this approach (5). A useful linear transformation of this relationship (Eq. 1) has been applied to phenytoin (6) and other drugs:

$$R_0 = v_{\max_1} - K_{m_1} \frac{R_0}{C^*} \qquad \text{(Eq. 2)}$$

For a medium to high extraction ratio drug eliminated only in the liver, it is appropriate to apply the above equations when drug is administered by a portal route. When drug is administered *via* a peripheral vein and the well-stirred model of the liver is assumed, the clearance is related to the Michaelis–Menten parameters by:

$$CL = \frac{R_0}{C^*} = \frac{Q_H \sum_{i=1}^{n} \frac{v_{\max_i}}{K_{m_i} + C^*}}{Q_H + \sum_{i=1}^{n} \frac{v_{\max_i}}{K_{m_i} + C^*}} \qquad \text{(Eq. 3)}$$

where Q_H is the liver blood flow. If drug is eliminated by a single enzyme, Eq. 3 may be rearranged to give:

$$R_0 = v_{\max_1} - \left(K_{m_1} + \frac{v_{\max_1}}{Q_H}\right) \frac{R_0}{C^*} \qquad \text{(Eq. 4)}$$

Comparison of Eqs. 2 and 4 demonstrates that the evaluation of K_m is dependent on administration route, while the determination of $v_{\max}$ is independent. When drug is administered by a peripheral venous site, K_m is overestimated by the value of $v_{\max}/Q_H$, as suggested by other authors (3).

The data from the portal vein infusions were plotted according to the

[1] Supplied by Burroughs Wellcome Co., Research Triangle Park, N.C.

linearized form of the Michaelis–Menten equation (Eq. 2). These data appeared to be nonlinear for both monkeys (Fig. 3). This nonlinearity is of the type observed in cases involving two saturable pathways with different values of K_m (5). Nonlinear least-squares fitting of data to acquire the best estimates of parameters requires at least one more datum point than the number of parameters to be estimated. In this case, there are only four data points to estimate four parameters; therefore, no estimates of the parameters for the pathway having the lower K_m were attempted. The v_{max} and K_m for the higher capacity pathway could be approximated by fitting the data from the three higher infusion rates to a straight line. The values of v_{max} and K_m were 120 mg/hr and 3.35 mg/liter for monkey 306 and 114 mg/hr and 4.43 mg/liter for monkey 307. A plot of data from the femoral vein infusions according to the linearized form of the Michaelis–Menten equation shows nonlinearity similar to that of the portal vein data (Fig. 4). The estimated values of v_{max} and K_m are 170 mg/hr and 15.6 mg/liter, respectively.

These values of v_{max} and K_m for femoral vein administration may be compared with those obtained for the same monkey dosed *via* the portal vein. The observed difference in v_{max} was not expected. It may be a result of the metabolism of cinromide by more than one enzyme, as indicated by the nonlinearity of the data from all four infusions. Also, the clearance values obtained from the three higher infusion rates into the femoral vein span a narrow range (5.1 to 9.3 liter/hr), which can result in uncertainty in the intercept. According to theory (Eqs. 2 and 4) the value of K_m obtained by femoral vein administration (15.6 mg/liter) should exceed that obtained by portal vein administration (4.4 mg/liter) by the ratio v_{max}/Q_H. This ratio can be roughly estimated if the hepatic blood flow in monkey 307 is calculated using the portal and femoral infusion data and the equation of Wilkinson and Shand (7). Although this equation was developed for a dose-independent intrinsic clearance, it can be applied in the dose-dependent case, provided that the steady-state concentration of drug at the enzyme is equal for the two routes of administration. This is accomplished by the administration of drug by the femoral and portal routes at equal rates. The average value obtained from the four pairs of infusions was 21.0 ± 2.8 liter/hr. Division of the two values of v_{max} from monkey 307 by this value of blood flow yields 5.4 and 8.4 mg/liter, within 50–70% of the difference between the two values of K_m (11.2 mg/liter). This calculation is compatible with the theoretical prediction. Equality between these two estimates of the difference in K_m arising from route of administration is not expected, since the determination of K_m, v_{max}, and Q_H involve error. In fact, the degree of compatibility suggests that the well-stirred model of the liver can be used to explain the effects of administration route on the disposition of cinromide.

The dose-dependent nonlinearity of cinromide, a medium extraction ratio drug, has been demonstrated. Catheterization of the portal vein for chronic drug administration provided a means of evaluating the intrinsic clearance of cinromide independently of hepatic blood flow and, thereby, a means of examining the dose dependence of cinromide. Comparison of values obtained for the whole body Michaelis–Menten constant for the peripheral and portal routes of administration confirmed the theoretically predicted effects of flow limitation on clearance.

REFERENCES

(1) A. J. Sedman and J. G. Wagner, *J. Pharmacokinet. Biopharm.*, **2**, 161 (1974).

2 J. L. Rheingold, R. E. Lindstrom, and P. K. Wilkinson, *J. Pharmacokinet. Biopharm.*, **9**, 261 (1981).

(3) K. S. Pang, M. Rowland, and T. N. Tozer, *Drug. Metab. Dispos.*, **6**, 197 (1978).

(4) E. A. Lane and R. H. Levy, *J. Pharm. Sci.*, **72**, 493 (1983).

(5) A. J. Sedman and J. G. Wagner, *J. Pharmacokinet. Biopharm.*, **2**, 149 (1974).

(6) T. M. Ludden, D. W. Hawkins, J. P. Allen, and F. Hoffman, *Lancet*, **i**, 307 (1976).

(7) G. R. Wilkinson and D. G. Shand, *Clin. Pharmacol. Ther.*, **18**, 377 (1975).

ACKNOWLEDGMENTS

This study was supported in part by NINCDS Research Contract N01-NS-1-2282. E. A. Lane was supported by National Institutes of Health National Research Service Awards GM-07348 and GM-07750 from the National Institute of General Medical Sciences.

The authors acknowledge the work of Ms. Sally Nickelson in animal surgery and maintenance.

Tick Repellents II: *N*-Substituted Azacyclopentanones and Azacyclopentenones

W. A. SKINNER ˣ, U. ROSENTRETER*, and T. ELWARD

Received May 10, 1982, from *Life Sciences Division, SRI International, Menlo Park, CA 94025.* Accepted for publication September 3, 1982. *Present address: Waldstrasse 11, 5600 Wuppertal 1, West Germany.

Abstract □ Several *N*-substituted azacyclopentanones and azacyclopentenones were synthesized and evaluated as repellents for the brown dog tick *Rhipicephalus sanguineus*. Several of these compounds were more effective in our test system than were the standard repellents, *N,N*-diethyl-*m*-toluamide and butopyranoxyl.

Keyphrases □ *N*-Substituted azacyclopentanones—synthesis, structure–activity relationships, evaluation as tick repellents □ *N*-Substituted azacyclopentenones—synthesis, structure–activity relationships, evaluation as tick repellents □ Tick repellents—potential, *N*-substituted azacyclopentanones and azacyclopentenones, synthesis

Tick-borne diseases still represent a problem and the need for a safe means of controlling ticks exists. Compounds useful for repelling mosquitoes are not necessarily those that are the most effective for ticks. Screening of repellents for ticks required the development of a rapid, simple assay system, which has been completed in our laboratories. This method, which was described previously (1), involved the use of a plastic vial containing the ticks with a filter paper cap impregnated with the test substance. The common behavior of ticks to travel upward is used to compare the control behavior with that in a vial treated at the top with repellent.

Most repellents reported for ticks have been amides or esters (2). We decided to explore azacyclopentanones and azacyclopentenones as a group of cyclic amides for their ability to repel the brown dog tick, *Rhipicephalus sanguineus*.

Compounds reported in Tables I–III were prepared by the methods described in *Experimental* for selected compounds.

EXPERIMENTAL[1]

Preparation of 1-Decyl-azacyclopentane-2-one (Ib)—A mixture of 22.1 g of 1-bromodecane (0.1 mole), 8.5 g (0.1 mole) of 2-pyrrolidone,

[1] Elemental analyses were performed by the Microanalytical Laboratory, Department of Chemistry, Stanford University, Stanford, Calif.

0022-3549/83/1100-1354$01.00/0

linearized form of the Michaelis–Menten equation (Eq. 2). These data appeared to be nonlinear for both monkeys (Fig. 3). This nonlinearity is of the type observed in cases involving two saturable pathways with different values of K_m (5). Nonlinear least-squares fitting of data to acquire the best estimates of parameters requires at least one more datum point than the number of parameters to be estimated. In this case, there are only four data points to estimate four parameters; therefore, no estimates of the parameters for the pathway having the lower K_m were attempted. The v_{max} and K_m for the higher capacity pathway could be approximated by fitting the data from the three higher infusion rates to a straight line. The values of v_{max} and K_m were 120 mg/hr and 3.35 mg/liter for monkey 306 and 114 mg/hr and 4.43 mg/liter for monkey 307. A plot of data from the femoral vein infusions according to the linearized form of the Michaelis–Menten equation shows nonlinearity similar to that of the portal vein data (Fig. 4). The estimated values of v_{max} and K_m are 170 mg/hr and 15.6 mg/liter, respectively.

These values of v_{max} and K_m for femoral vein administration may be compared with those obtained for the same monkey dosed *via* the portal vein. The observed difference in v_{max} was not expected. It may be a result of the metabolism of cinromide by more than one enzyme, as indicated by the nonlinearity of the data from all four infusions. Also, the clearance values obtained from the three higher infusion rates into the femoral vein span a narrow range (5.1 to 9.3 liter/hr), which can result in uncertainty in the intercept. According to theory (Eqs. 2 and 4) the value of K_m obtained by femoral vein administration (15.6 mg/liter) should exceed that obtained by portal vein administration (4.4 mg/liter) by the ratio v_{max}/Q_H. This ratio can be roughly estimated if the hepatic blood flow in monkey 307 is calculated using the portal and femoral infusion data and the equation of Wilkinson and Shand (7). Although this equation was developed for a dose-independent intrinsic clearance, it can be applied in the dose-dependent case, provided that the steady-state concentration of drug at the enzyme is equal for the two routes of administration. This is accomplished by the administration of drug by the femoral and portal routes at equal rates. The average value obtained from the four pairs of infusions was 21.0 ± 2.8 liter/hr. Division of the two values of v_{max} from monkey 307 by this value of blood flow yields 5.4 and 8.4 mg/liter, within 50–70% of the difference between the two values of K_m (11.2 mg/liter). This calculation is compatible with the theoretical prediction. Equality between these two estimates of the difference in K_m arising from route of administration is not expected, since the determination of K_m, v_{max}, and Q_H involve error. In fact, the degree of compatibility suggests that the well-stirred model of the liver can be used to explain the effects of administration route on the disposition of cinromide.

The dose-dependent nonlinearity of cinromide, a medium extraction ratio drug, has been demonstrated. Catheterization of the portal vein for chronic drug administration provided a means of evaluating the intrinsic clearance of cinromide independently of hepatic blood flow and, thereby, a means of examining the dose dependence of cinromide. Comparison of values obtained for the whole body Michaelis–Menten constant for the peripheral and portal routes of administration confirmed the theoretically predicted effects of flow limitation on clearance.

REFERENCES

(1) A. J. Sedman and J. G. Wagner, *J. Pharmacokinet. Biopharm.*, **2**, 161 (1974).

2 J. L. Rheingold, R. E. Lindstrom, and P. K. Wilkinson, *J. Pharmacokinet. Biopharm.*, **9**, 261 (1981).

(3) K. S. Pang, M. Rowland, and T. N. Tozer, *Drug. Metab. Dispos.*, **6**, 197 (1978).

(4) E. A. Lane and R. H. Levy, *J. Pharm. Sci.*, **72**, 493 (1983).

(5) A. J. Sedman and J. G. Wagner, *J. Pharmacokinet. Biopharm.*, **2**, 149 (1974).

(6) T. M. Ludden, D. W. Hawkins, J. P. Allen, and F. Hoffman, *Lancet*, **i**, 307 (1976).

(7) G. R. Wilkinson and D. G. Shand, *Clin. Pharmacol. Ther.*, **18**, 377 (1975).

ACKNOWLEDGMENTS

This study was supported in part by NINCDS Research Contract N01-NS-1-2282. E. A. Lane was supported by National Institutes of Health National Research Service Awards GM-07348 and GM-07750 from the National Institute of General Medical Sciences.

The authors acknowledge the work of Ms. Sally Nickelson in animal surgery and maintenance.

Tick Repellents II: *N*-Substituted Azacyclopentanones and Azacyclopentenones

W. A. SKINNER ˣ, U. ROSENTRETER*, and T. ELWARD

Received May 10, 1982, from *Life Sciences Division, SRI International, Menlo Park, CA 94025.* Accepted for publication September 3, 1982. *Present address: Waldstrasse 11, 5600 Wuppertal 1, West Germany.

Abstract □ Several *N*-substituted azacyclopentanones and azacyclopentenones were synthesized and evaluated as repellents for the brown dog tick *Rhipicephalus sanguineus*. Several of these compounds were more effective in our test system than were the standard repellents, *N,N*-diethyl-*m*-toluamide and butopyranoxyl.

Keyphrases □ *N*-Substituted azacyclopentanones—synthesis, structure–activity relationships, evaluation as tick repellents □ *N*-Substituted azacyclopentenones—synthesis, structure–activity relationships, evaluation as tick repellents □ Tick repellents—potential, *N*-substituted azacyclopentanones and azacyclopentenones, synthesis

Tick-borne diseases still represent a problem and the need for a safe means of controlling ticks exists. Compounds useful for repelling mosquitoes are not necessarily those that are the most effective for ticks. Screening of repellents for ticks required the development of a rapid, simple assay system, which has been completed in our laboratories. This method, which was described previously (1), involved the use of a plastic vial containing the ticks with a filter paper cap impregnated with the test substance. The common behavior of ticks to travel upward is used to compare the control behavior with that in a vial treated at the top with repellent.

Most repellents reported for ticks have been amides or esters (2). We decided to explore azacyclopentanones and azacyclopentenones as a group of cyclic amides for their ability to repel the brown dog tick, *Rhipicephalus sanguineus*.

Compounds reported in Tables I–III were prepared by the methods described in *Experimental* for selected compounds.

EXPERIMENTAL[1]

Preparation of 1-Decyl-azacyclopentane-2-one (Ib)—A mixture of 22.1 g of 1-bromodecane (0.1 mole), 8.5 g (0.1 mole) of 2-pyrrolidone,

[1] Elemental analyses were performed by the Microanalytical Laboratory, Department of Chemistry, Stanford University, Stanford, Calif.

0022-3549/83/1100-1354$01.00/0

Table I—1-Alkyl-azacyclopentane-2-ones

Compound	R	Boiling Point/ 0.5 mm Hg[a]	Yield, %	I.R. (C=O), cm^{-1}	Formula	Analysis, % Calc.	Analysis, % Found	Tick Repellency at 0.44 mg/cm², %
Ia	C_8H_{17}	110°	85	1690	$C_{12}H_{23}NO$	C 73.04 H 11.75 N 7.10	72.86 11.64 7.11	78[b]
Ib	$C_{10}H_{21}$	122°	78	1690	$C_{14}H_{27}NO$	C 74.61 H 12.08 N 6.21	74.49 11.94 6.21	25
Ic	$C_{12}H_{15}$	150°	91	1690	$C_{16}H_{31}NO$	C 75.83 H 12.33 N 5.53	75.96 12.59 5.46	20
N,N-diethyl-*m*-toluamide								32
Butopyranoxyl								48
Solvent control								7%
Nontreated control								9%

[a] Boiling points normalized to 0.5 mm Hg for direct comparison. [b] 25% at 0.29 mg/cm² and 20% at 0.19 mg/cm².

and 11.2 g (0.1 mole) of potassium *tert*-butoxide was stirred in 100 ml of anhydrous dimethyl sulfoxide for 1 hr. The dimethyl sulfoxide was removed under reduced pressure, the residue dissolved in 100 ml of ether, and washed with water (2 times). After drying the organic phase with anhydrous magnesium sulfate and removing the solvent under reduced pressure, the oily residue was distilled *in vacuo*. The first fraction, (bp 140–147°/1.2 mm Hg), was discarded. The second fraction gave 17.4 g of product, bp 148°/1.2 mm Hg.

1-Ethyl-5-octyl-azacyclopent-4-ene-2-one (IIe)—A solution of octylmagnesium bromide was prepared by adding in a dropwise manner, 34.2 g (0.177 mole) of 1-bromooctane in 10 ml of ether to 6.5 g (0.268 g-atom) of magnesium in 10 ml of ether and then heating at reflux for 3 hr. The Grignard reagent was added over a 2-hr period to a solution of 15 g (0.118 mole) of *N*-ethyl-succinimide in 50 ml of anhydrous tetrahydrofuran. The mixture was allowed to stand at room temperature for 2 days, and then was poured into a mixture of ice and 10% sulfuric acid. After separation of the organic layer, the aqueous phase was extracted twice with 50 ml of ether. The combined organic phases were washed with saturated sodium hydrogen carbonate and dried over anhydrous sodium sulfate. The solvent was removed under reduced pressure, and the residue was evaporatively distilled to give 10 g of a yellow oil, 120° air bath temperature/0.9 mm Hg. A second fractional distillation using a Vigreux column yielded 6.6 g of product, bp 130°/1.0 mm Hg.

1-Ethyl-5-octyl-azacyclopentane-2-one (IIIb)—1-Ethyl-5-octyl-azacyclopent-4-ene-2-one, (5.3 g, 0.0238 mole) in 25 ml of ethanol was hydrogenated under atmospheric pressure with 0.5 g of 10% Pd-C. After the uptake of hydrogen was completed, the catalyst was removed by filtration, the solvent evaporated, and the residue distilled to give 5 g of product, bp 130°/0.9 mm Hg.

The tick repellency assay was as previously described (1).

RESULTS AND DISCUSSION

A comparison of the tick repellency of the azacyclopentanones with *N,N*-diethyl-*m*-toluamide and butopyranoxyl at 0.44 mg/cm² shows that a number of these substances are considerably more repellent than the standard compounds (Tables I–III). In the 1-alkyl-azacyclopentane-2-one series, the *n*-octyl derivative is outstanding. The boiling point of 110°/0.5 mm Hg corresponds closely to that of *N,N*-diethyl-*m*-toluamide, whereas the *n*-decyl and dodecyl compounds are considerably higher boiling derivatives and are probably too nonvolatile for optimum repellency.

In the 1-ethyl-5-alkyl-azacyclopentane-4-ene-2-one series, the *n*-pentyl, -hexyl, -heptyl, -octyl, and -decyl derivatives are all outstanding as tick repellents. The maximum activity is reached with the *n*-hexyl derivative (bp 110°/0.5 mm Hg). However, a comparison of the *n*-hexyl derivative with the *n*-octyl derivative in the 1-alkyl-azacyclopentane-2-one series, where the boiling points are identical, reveals that the unsaturation in the ring leads to enhanced repellency.

In the last series explored, 1-ethyl-5-alkyl-azacyclopentane-2-ones, the *n*-octyl and *n*-decyl derivatives have improved repellency over *N,N*-diethyl-*m*-toluamide with the *n*-octyl derivative, boiling point of 120°/0.5 mm Hg, being the best. Comparison of this series with the aza-

Table II—1-Ethyl-5-alkyl-azacyclopent-4-ene-2-one

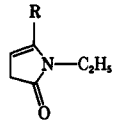

Compound	R	Boiling Point/ 0.5 mm Hg	Yield, %	I.R., cm^{-1}	Formula	Analysis, % Calc.	Analysis, % Found	Tick Repellency at 0.44 mg/cm², %
IIa	C_4H_9	86°	36.5	(C=O) 1720 (C=C) 1670	$C_{10}H_{17}NO$	C 71.81 H 10.25 N 8.37	C 71.42 H 10.16 N 8.38	25
IIb	C_5H_{11}	94°	39.0	(C=O) 1720 (C=C) 1670	$C_{11}H_{19}NO$	C 72.89 H 10.56 N 7.73	C 73.15 H 10.74 N 7.43	60
IIc	C_6H_{13}	110°	31.0	(C=O) 1720 (C=C) 1670	$C_{12}H_{21}NO$	C 73.80 H 10.84 N 7.17	C 73.66 H 10.69 N 7.14	100[a]
IId	C_7H_{15}	118°	36.0	(C=O) 1720 (C=C) 1670	$C_{13}H_{23}NO$	C 74.59 H 11.07 N 6.69	C 74.41 H 11.04 N 6.68	95
IIe	C_8H_{17}	125°	25.0	(C=O) 1720 (C=C) 1670	$C_{14}H_{25}NO$	C 75.28 H 11.28 N 6.27	C 75.34 H 11.33 N 6.18	98[b]
IIf	$C_{10}H_{21}$	142°	20.0	(C=O) 1720 (C=C) 1620	$C_{16}H_{29}NO$	C 76.44 H 11.63 N 5.57	C 76.25 H 11.42 N 5.29	98[c]

[a] 93% at 0.29 mg/cm² and 63% at 0.19 mg/cm². [b] 82% at 0.29 mg/cm² and 47% at 0.19 mg/cm². [c] 77% at 0.29 mg/cm² and 20% at 0.19 mg/cm².

Table III—1-Ethyl-5-alkyl-azacyclopentane-2-ones

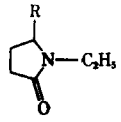

Compound	R	Boiling Point/ 0.5 mm Hg	Yield, %	I.R. (C=O), cm^{-1}	Formula	Analysis, % Calc.	Analysis, % Found	Tick Repellency at 0.44 mg/cm^2, %
IIIa	C_6H_{13}	110°	89	1690	$C_{12}H_{23}NO$	C 73.04 H 11.75 N 7.10	C 73.26 H 11.97 N 6.99	25
IIIb	C_8H_{17}	120°	94	1690	$C_{14}H_{27}NO$	C 74.61 H 12.08 N 6.21	C 74.94 H 12.09 N 6.11	75[a]
IIIc	$C_{10}H_{21}$	154°	90	1690	$C_{16}H_{31}NO$	C 75.83 H 12.33 N 5.33	C 76.07 H 12.44 N 5.41	40

[a] 55% at 0.29 mg/cm^2.

cyclopentene series again indicates the importance of unsaturation as an enhancer of repellency toward the tick in this series of compounds.

REFERENCES

(1) W. A. Skinner, U. Rosentreter, and T. Elward, *J. Pharm. Sci.*, 71, 837 (1982).

(2) W. A. Skinner and H. L. Johnson, in "Drug Design," Vol. X, H. J. Ariens, Ed., Academic, New York, N.Y., 1980, p. 278.

ACKNOWLEDGMENTS

Supported by SRI International's Institute Research and Development Program.

Synthesis and Antileukemic Activity of 2-(2-Methylthio-2-aminovinyl)-1-methylquinolinium Iodides

WILLIAM O. FOYE ˣ, YOUNG HO KIM *, and JOEL M. KAUFFMAN ‡

Received July 19, 1982, from the *Samuel M. Best Research Laboratory, Massachusetts College of Pharmacy and Allied Health Sciences, Boston, MA 02115.* Accepted for publication October 13, 1982. Present address: *U.E.C. Co., Ltd., Hanyang Building, Chung-ku, Seoul, Korea and ‡Department of Chemistry, Philadelphia College of Pharmacy and Science, Philadelphia, PA 19104.

Abstract □ Reaction of 2-bis(2-methylthio)vinyl-1-methylquinolinium iodide with several heterocyclic aliphatic amines at 30–70° resulted in replacement of one methylthio group to give the title compounds. Reaction with pyrrolidine gave an unidentified product lacking sulfur. Antileukemic screening against P-388 lymphocytic leukemia showed positive activity only with the 6-methyl-morpholino derivative, whereas the 6-unsubstituted morpholino derivative was inactive. This result is in contrast to previous testing results with the 2-bis(2-methylthio)vinyl compounds where both 6-substituted and 6-unsubstituted derivatives showed activity.

Keyphrases □ 2-(2-Methyl-2-aminovinyl)-1-methylquinolinium iodides—synthesis, antileukemic activity in mice □ Synthesis—2-(2-methyl-2-aminovinyl)-1-methylquinolinium iodides, antileukemic activity in mice □ Antileukemia agents—potential, 2-(2-methyl-2-aminovinyl)-1-methylquinolinium iodides, synthesis, P-388 screen in mice

A series of 6-substituted-1-methylquinolinium-2-dithioacetic acid zwitterions (I) (1, 2) has shown appreciable antileukemic activity against P-388 lymphocytic leukemia in mice. An attempt to find compounds having better solubilities, in both water and organic solvents, led to the synthesis of the derived 2-bis(2-methylthio)vinyl-1-methylquinolinium iodides (II) (3). The latter compounds had comparable antileukemic activity, but at lower dose levels than found for the zwitterions. The 6-unsubstituted derivative, however, had activity equal to or better than that of the 6-substituted compounds. Compounds with electron-attracting and electron-releasing 6-substituents were equally active in this series.

Another type of derivative of the dithioacetic acid zwitterion structure (I), which should show improved solubility properties, is the 2-methylthio-2-aminovinyl compound (III) (3). Accordingly, a series of these compounds, using several heterocyclic amines, was prepared for anticancer screening. With the exception of the previously prepared morpholino derivative where a 6-methyl substituent was included, the 6-position was left unsubstituted.

Leukemia cell culture studies were carried out with the 6-methyl derivative of II, but no effects on cell cycle traverse were observed (4). This indicated that a metabolic conversion of the bis(methylthio)vinyl compounds, and most likely their dithioacetic acid precursors as well, is required for antileukemic activity. A study of DNA-binding specificity and RNA polymerase-inhibitory activity showed that the bis(methylthio)vinyl compounds (II), as well as the 2-methylthio-2-morpholinovinyl derivative (III, R = CH_3), had DNA-binding ability involving

0022-3549/83/1100-1356$01.00/0

Table III—1-Ethyl-5-alkyl-azacyclopentane-2-ones

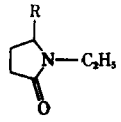

Compound	R	Boiling Point/ 0.5 mm Hg	Yield, %	I.R. (C=O), cm^{-1}	Formula	Analysis, % Calc.	Analysis, % Found	Tick Repellency at 0.44 mg/cm^2, %
IIIa	C_6H_{13}	110°	89	1690	$C_{12}H_{23}NO$	C 73.04 H 11.75 N 7.10	C 73.26 H 11.97 N 6.99	25
IIIb	C_8H_{17}	120°	94	1690	$C_{14}H_{27}NO$	C 74.61 H 12.08 N 6.21	C 74.94 H 12.09 N 6.11	75[a]
IIIc	$C_{10}H_{21}$	154°	90	1690	$C_{16}H_{31}NO$	C 75.83 H 12.33 N 5.33	C 76.07 H 12.44 N 5.41	40

[a] 55% at 0.29 mg/cm^2.

cyclopentene series again indicates the importance of unsaturation as an enhancer of repellency toward the tick in this series of compounds.

REFERENCES

(1) W. A. Skinner, U. Rosentreter, and T. Elward, *J. Pharm. Sci.*, 71, 837 (1982).

(2) W. A. Skinner and H. L. Johnson, in "Drug Design," Vol. X, H. J. Ariens, Ed., Academic, New York, N.Y., 1980, p. 278.

ACKNOWLEDGMENTS

Supported by SRI International's Institute Research and Development Program.

Synthesis and Antileukemic Activity of 2-(2-Methylthio-2-aminovinyl)-1-methylquinolinium Iodides

WILLIAM O. FOYE ˣ, YOUNG HO KIM *, and JOEL M. KAUFFMAN ‡

Received July 19, 1982, from the *Samuel M. Best Research Laboratory, Massachusetts College of Pharmacy and Allied Health Sciences, Boston, MA 02115.* Accepted for publication October 13, 1982. Present address: *U.E.C. Co., Ltd., Hanyang Building, Chung-ku, Seoul, Korea and ‡Department of Chemistry, Philadelphia College of Pharmacy and Science, Philadelphia, PA 19104.

Abstract □ Reaction of 2-bis(2-methylthio)vinyl-1-methylquinolinium iodide with several heterocyclic aliphatic amines at 30–70° resulted in replacement of one methylthio group to give the title compounds. Reaction with pyrrolidine gave an unidentified product lacking sulfur. Antileukemic screening against P-388 lymphocytic leukemia showed positive activity only with the 6-methyl-morpholino derivative, whereas the 6-unsubstituted morpholino derivative was inactive. This result is in contrast to previous testing results with the 2-bis(2-methylthio)vinyl compounds where both 6-substituted and 6-unsubstituted derivatives showed activity.

Keyphrases □ 2-(2-Methyl-2-aminovinyl)-1-methylquinolinium iodides—synthesis, antileukemic activity in mice □ Synthesis—2-(2-methyl-2-aminovinyl)-1-methylquinolinium iodides, antileukemic activity in mice □ Antileukemia agents—potential, 2-(2-methyl-2-aminovinyl)-1-methylquinolinium iodides, synthesis, P-388 screen in mice

A series of 6-substituted-1-methylquinolinium-2-dithioacetic acid zwitterions (I) (1, 2) has shown appreciable antileukemic activity against P-388 lymphocytic leukemia in mice. An attempt to find compounds having better solubilities, in both water and organic solvents, led to the synthesis of the derived 2-bis(2-methylthio)vinyl-1-methylquinolinium iodides (II) (3). The latter compounds had comparable antileukemic activity, but at lower dose levels than found for the zwitterions. The 6-unsubstituted derivative, however, had activity equal to or better than that of the 6-substituted compounds. Compounds with electron-attracting and electron-releasing 6-substituents were equally active in this series.

Another type of derivative of the dithioacetic acid zwitterion structure (I), which should show improved solubility properties, is the 2-methylthio-2-aminovinyl compound (III) (3). Accordingly, a series of these compounds, using several heterocyclic amines, was prepared for anticancer screening. With the exception of the previously prepared morpholino derivative where a 6-methyl substituent was included, the 6-position was left unsubstituted.

Leukemia cell culture studies were carried out with the 6-methyl derivative of II, but no effects on cell cycle traverse were observed (4). This indicated that a metabolic conversion of the bis(methylthio)vinyl compounds, and most likely their dithioacetic acid precursors as well, is required for antileukemic activity. A study of DNA-binding specificity and RNA polymerase-inhibitory activity showed that the bis(methylthio)vinyl compounds (II), as well as the 2-methylthio-2-morpholinovinyl derivative (III, R = CH_3), had DNA-binding ability involving

0022-3549/83/1100-1356$01.00/0

one binding function and inhibited RNA polymerase to a somewhat lower degree than was shown by chloroquine (5). It was believed that the function responsible for binding to DNA is the active methylene (V) resulting from loss of the bis(methylthio)methinyl moiety (4).

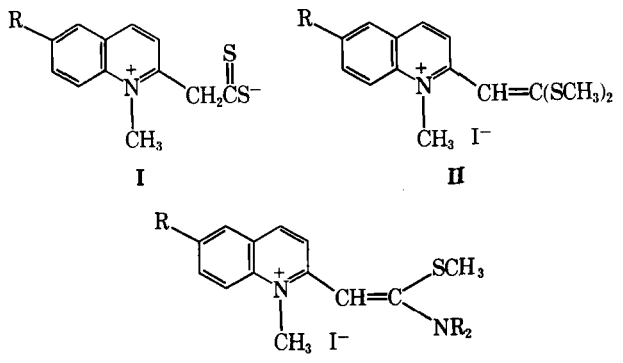

I II III

DISCUSSION

Chemistry—The 2-methylthio-2-aminovinyl-1-methylquinolinium iodides (III) were prepared from the 2-bis(2-methylthio)vinyl-1-methylquinolinium iodides (II) by reaction with the appropriate amine at 30–70°, according to the previous procedure (3). The bis(methylthio)vinyl compounds were obtained from the reaction of the dithioacetic acid zwitterions (I) by reaction with methyl iodide (6, 7); the monomethyl esters of the dithioacetic acids were never isolated in these reactions. In actual practice, preparing a solution of the methylene base (V) in dry toluene, followed by reaction with carbon disulfide in toluene, and treatment with iodomethane in dimethyl formamide, was found to be superior to isolating the intermediate zwitterion (I). The synthetic route is indicated in Scheme I.

The reaction mixtures were examined for by-products, but only the original methiodide (IV) was found. Since the method of preparation precludes the carrying along of the methiodide because it is insoluble in toluene, and there was no chromatographic or other evidence that the products contained any of the active antileukemic compound II (R = H), any antileukemic activity found should be due to structure III.

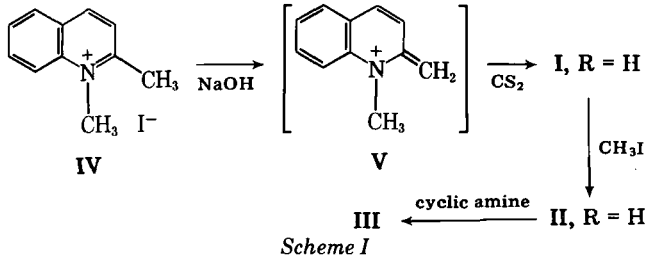

IV V

Scheme I

The NMR spectra of III generally agreed with the spectrum of the morpholino derivative already described (3). The *S*-methyl protons appeared as a singlet at δ 2.6 ppm, and the *N*-methyl peak appeared as a singlet at δ 4.1 ppm. The vinyl proton, at δ 5.5–5.6 ppm, was shielded to a considerable extent, compared with its position at δ 6.76 ppm in the bis(methylthio) compound.

It has already been pointed out (3) that this shielding provided an indication for a *trans* arrangement of the amino function, with partial involvement of charge on the morpholino nitrogen. Calculations by the Tobey–Simon Rule (8) agreed with a *trans* structure.

The reduced heterocyclic amines employed in this synthesis gave variable yields of crystalline products. In the case of 2-methylpiperazine, only a 14% yield was realized, probably due to steric hindrance of the methyl. It is assumed that the nitrogen at the greater distance from the methyl was involved in replacing *S*-methyl, since less steric hindrance would result in the product. Reaction with pyrrolidine gave a product having no sulfur whose structure was not that of a nucleophilic replacement of the bis(methylthio)methinyl moiety by pyrrole. Nucleophilic replacement of the bis(methylthio)methinyl moiety by amines has been observed by Mizuyama *et al.* (9).

Table I—Antileukemic Activity in Mice[a]

Structure III NR_2	R	Dose, mg/kg[b]	Weight Difference[c], g	Median Survival Time, T/C%[d] Test 1	Test 2
—N O	CH_3	6.25	−3.2, −3.4	141	149
		3.13	−1.7, −1.5	130	119
—N O	H	25.00	−2.6, −2.2	121	110
		12.50	−2.1, −0.9	119	105
—N S	H	6.25	−1.9	113	—
		3.13	−1.4	113	—
—N	H	1.56	−2.8	116	—
		0.78	−0.5	109	—
—N N—CH_3	H	25.00	−0.9	102	—
		12.50	−1.1	98	—

[a] CD_2F_1 mice were inoculated with P-388 lymphocytic leukemia cells. [b] Drugs were administered intraperitoneally on days 1, 5, and 9. [c] Test group minus control group. [d] A T/C% value of ≥125 is considered a positive result.

Antileukemia Test Results—Antileukemia testing was performed at the National Cancer Institute using P-388 lymphocytic leukemia in mice according to their protocol (10). Details regarding dose and survival time are listed in Table I.

Positive activity was shown in this series only by the *N*-morpholino-6-methyl derivative (3). The *N*-morpholino derivative lacking the 6-methyl was inactive. This result is in contrast with testing data for the dithioacetic acid zwitterions (2) and the bis(methylthio)vinyl derivatives (3) where activity was found with both the 6-substituted and 6-unsubstituted derivatives. It is possible that in this (methylthioamino)vinyl series, the antileukemic activity does not depend on the formation of the active methylene compound (V) but on binding to nucleic acid or other macromolecules involving the morpholine moiety. Equilibrium binding constants to calf thymus DNA for several of the bis(methylthio)vinyl derivatives were lower than for the *N*-morpholino-6-methyl compound (5). Also, the (methylthioamino)vinyl group, a tautomeric form of a thioamide, should be more stable to hydrolysis than the ketene thioacetals.

EXPERIMENTAL[1]

1-Methyl-2-[2-methylthio-2-(1-morpholino)vinyl]-quinolinium Iodide—To a suspension of 2-bis(2-methylthio)vinyl-1-methylquinolinium iodide (2.70 g, 0.007 mole) (2), in 50 ml of dimethylformamide was added an equimolar amount of morpholine (0.61 g, 0.007 mole). The mixture was stirred at 70° for 2 hr and then at 50° for 17 hr. The reaction was monitored by TLC (chloroform–methanol, 95:5). After it was cooled, the mixture was diluted with toluene (300 ml) and stored at 0°.

The precipitate was collected and dissolved in acetone, treated twice with charcoal, and the solvent was evaporated. The orange crystalline product was recrystallized from absolute ethanol to give 1.8 g (60%), m.p. 198–200°. ^{1}H-NMR: δ 2.60 (s, 3, SCH_3), 3.70 (s, br, 8, morpholino), 4.09 (s, 3, NCH_3), 5.59 (s, 1, vinyl), and 7.6–8.2 ppm (m, 6, aromatic).

Anal.—Calc. for $C_{17}H_{21}IN_2OS$: C, 47.67; H, 4.94; N, 6.54; S, 7.48. Found: C, 47.52; H, 5.07; N, 6.43; S, 7.59.

1-Methyl-2-[2-methylthio-2-(4-thiomorpholino)vinyl]-quinolinium Iodide—To a suspension of II (R = H) (2.72 g, 0.007 mole) in 50 ml of dimethylformamide was added freshly distilled thiomorpholine (1.33 g, 0.013 mole), and the mixture was stirred at 35° for 4 days. The reaction was monitored by TLC (chloroform–methanol 9:1). It was diluted with anhydrous ether (200 ml) and stored at 0° for 2 hr.

The precipitate was collected and recrystallized twice from 1-propanol using charcoal, giving 2.0 g (69%) of orange crystals, m.p. 203–205°.

[1] Melting points were determined in capillaries with a Mel-Temp block and are uncorrected. ^{1}H-NMR spectra were obtained with a Varian T-60 spectrometer using DMSO-d_6 as solvent and tetramethylsilane as internal standard. IR spectra were obtained with a Perkin–Elmer model 457A grating spectrophotometer using KBr pellets. Elemental analyses were done by F. B. Strauss, Oxford, England. TLC was carried out using silica gel plates, and products were detected by exposure to iodine vapor. Organic reagents were supplied by Aldrich Chemical Co. or Eastman Organic Chemicals.

^{1}H-NMR: δ 2.60 (s, 3), 2.9 (d, br, 4), 4.0 (d, br, 4), 4.10 (s, 3), 5.60 (s, 1), and 7.6–8.2 ppm (m, 6).

Anal.—Calc. for $C_{17}H_{21}IN_2S_2$: C, 45.94; H, 4.76; N, 6.30. Found: C, 45.59; H, 4.79; N, 6.32.

1-Methyl-2 - [2-methylthio-2-(1-piperidino)vinyl] - quinolinium Iodide—To a suspension of II (R = H) (2.72 g, 0.007 mole) in 25 ml of dimethyl sulfoxide was added freshly distilled piperidine (1.0 g, 0.012 mole), and the mixture was stirred at 30° for 5 days. It was treated as in the previous procedure, and the crude precipitate was dissolved in 1-propanol (300 ml), treated with charcoal, and filtered while hot. This procedure was repeated three times, and the combined filtrates were evaporated to dryness under reduced pressure. The residue was recrystallized from 2-propanol to give 2.70 g (90%) of orange crystals, m.p. 195–196°. ^{1}H-NMR: δ 1.75 (s, 6), 2.63 (s, br, 3), 3.81 (s, br, 4), 4.10 (s, 3), 5.55 (s, 1), and 7.6–8.2 ppm (m, 6).

Anal.—Calc. for $C_{18}H_{23}IN_2S$: C, 50.70; H, 5.43; N, 6.57. Found: C, 50.93; H, 5.23; N, 6.38.

1-Methyl-2-[2-methylthio-2-(4-methyl-1-piperazino)vinyl]-quinolinium Iodide—Following the previous procedure, II (R = H) (1.20 g, 0.0031 mole) in dimethyl sulfoxide (25 ml) was treated with 1-methylpiperazine (0.35 g, 0.0035 mole). The product was recrystallized from acetic acid and again from absolute ethanol to give 0.63 g (48%) of orange crystals, m.p. 188–191°. ^{1}H-NMR: δ 2.58 (s, 3), 2.95 (s, 3), 3.40 (br, 4), 3.83 (br, 4), 4.10 (s, 3), 5.80 (s, 1), and 7.6–8.2 ppm (m, 6).

Anal.—Calc. for $C_{18}H_{24}IN_3S$: C, 48.98; H, 5.48; N, 9.52; S, 7.26. Found: C, 49.00; H, 5.49; N, 9.29; S, 7.30.

1-Methyl-2-[2-methylthio-2-(3-methyl-1-piperazino)vinyl]-quinolinium Iodide—Following the previous procedure, II (R = H) (2.72 g, 0.007 mole) in dimethyl sulfoxide (25 ml) was treated with 2-methylpiperazine (0.70 g, 0.007 mole). The thick, oily product crystallized on long storage in the refrigerator. It was recrystallized from absolute ethanol and ether to give 0.41 g (14%) of orange-brown crystals,m.p. 188–190°. ^{1}H-NMR: δ 2.13 (s, 3), 2.58 (s, 3), 3.40–3.70 (br, 7), 4.10 (s, 3), 5.58 (s, 1), and 7.6–8.2 ppm (m, 6).

Anal.—Calc. for $C_{19}H_{24}IN_3S$: C, 48.98; H, 5.48; N, 9.52; S, 7.26. Found: C, 48.83; H, 5.58; N, 9.11; S, 7.08.

REFERENCES

(1) W. O. Foye, Y. J. Lee, K. A. Shah, and J. M. Kauffman, *J. Pharm. Sci.*, **67**, 962 (1978).

(2) W. O. Foye and J. M. Kauffman, *J. Pharm. Sci.*, **68**, 336 (1979).

(3) W. O. Foye and J. M. Kauffman, *J. Pharm. Sci.*, **69**, 477 (1980).

(4) W. O. Foye, J. M. Kauffman, and R. Ganapathi, "Current Chemotherapy and Infectious Disease," Vol. II, Proc. 11th Int. Congress of Chemotherapy and 19th Intersc. Conf. on Antimicrobial Agents and Chemotherapy (1979), pp. 1629–1631, 1980.

(5) W. O. Foye, O. Vajragupta, and S.K. Sengupta, *J. Pharm. Sci.*, **71**, 253 (1982).

(6) R. Gompper, B. Wetzel, and W. Elser, *Tetrahedron Lett.*, **53**, 5519 (1968).

(7) K. Mizuyama, Y. Tominaga, Y. Matsuda, and G. Kobayashi, *Yakugaku Zasshi*, **94**, 702 (1974).

(8) R. M. Silverstein, G. C. Bassler, and T. C. Morrill, "Spectrometric Identification of Organic Compounds," 3rd ed., Wiley, New York, N.Y., 1974, p. 223.

(9) K. Mizuyama, Y. Tominaga, Y. Matsuda, and G. Kobayashi, *Yakugaku Zasshi*, **95**, 290 (1975).

(10) R. I. Geran, N. H. Greenberg, M. M. MacDonald, A. M. Schumacher, and B. J. Abbott, *Cancer Chemother. Rep.*, Part 3, **3**, 1 (1972).

ACKNOWLEDGMENTS

Supported by funds from the John R. and Marie K. Sawyer Memorial Fund, Massachusetts College of Pharmacy and Allied Health Sciences.

Quantitative Analysis of Ethchlorvynol in a Capsule Dosage Form by NMR Spectroscopy

KAREN B. FEKETY ˣ **and THOMAS MEDWICK**

Received July 19, 1982, from the *College of Pharmacy, Rutgers University, Piscataway, NJ 08854.* Accepted for publication October 14, 1982.

Abstract □ A quantitative ^{1}H-NMR procedure is described for measuring ethchlorvynol in capsules. Deuterochloroform is used as the solvent, and hexamethylenetetramine as the internal standard; the analysis is based on the comparison of the area of the AB peak system of ethchlorvynol with the area of the hexamethylenetetramine singlet. The ^{1}H-NMR method yields results that are precise to within 1% and agree well with results of the more cumbersome and less specific USP titrimetric procedure.

Keyphrases □ Ethchlorvynol—NMR quantitative analysis, capsule dosage form □ NMR quantitative analysis—ethchlorvynol, capsule dosage form

Ethchlorvynol (I), a nonbarbiturate hypnotic, is a tertiary acetylenic carbinol (1-chloro-3-ethyl-1-penten-4-yn-3-ol). The official USP XX procedure for the analytical determination of this drug substance, both alone and in its pharmaceutical dosage form, is based on the reaction of I with excess silver nitrate, producing the silver acetylide and nitric acid (1, 2). The resultant acid is immediately titrated with ~0.05 *N* NaOH; however, end point determination with the methyl red–methylene blue indicator is hampered by the precipitation of the silver acetylide. According to the official procedure, capsules must be weighed, carefully opened, emptied, and reweighed, with the difference taken as the capsule contents. The difficult end point and sample manipulations often lead to poor results.

Although there are several procedures published for the determination of I in biological fluids (3–8), there are only two other published methods for its determination in the pharmaceutical dosage form. Davidson (9), proposed a GLC analysis, accepted by the AOAC (10), and that uses 1,3-dichloro-2-propanol as an internal standard; a standard deviation range of 1.3–2.9% on assays of known solutions and the 500-mg capsule dosage form is reported. Drawbacks inherent in this procedure include the need for column preparation and overnight conditioning and the necessity of injecting a I standard (purified by vacuum distillation and quantified by the USP XX titrimetric procedure) along with the unknown solutions. Rizk and associates (11) proposed a colorimetric method for the determination of certain monosubstituted acetylenic hypnotic drugs, including I. In this procedure, silver acetylide

0022-3549/83/1100-1358$01.00/0

^{1}H-NMR: δ 2.60 (s, 3), 2.9 (d, br, 4), 4.0 (d, br, 4), 4.10 (s, 3), 5.60 (s, 1), and 7.6–8.2 ppm (m, 6).

Anal.—Calc. for $C_{17}H_{21}IN_2S_2$: C, 45.94; H, 4.76; N, 6.30. Found: C, 45.59; H, 4.79; N, 6.32.

1-Methyl-2 - [2-methylthio-2-(1-piperidino)vinyl] - quinolinium Iodide—To a suspension of II (R = H) (2.72 g, 0.007 mole) in 25 ml of dimethyl sulfoxide was added freshly distilled piperidine (1.0 g, 0.012 mole), and the mixture was stirred at 30° for 5 days. It was treated as in the previous procedure, and the crude precipitate was dissolved in 1-propanol (300 ml), treated with charcoal, and filtered while hot. This procedure was repeated three times, and the combined filtrates were evaporated to dryness under reduced pressure. The residue was recrystallized from 2-propanol to give 2.70 g (90%) of orange crystals, m.p. 195–196°. ^{1}H-NMR: δ 1.75 (s, 6), 2.63 (s, br, 3), 3.81 (s, br, 4), 4.10 (s, 3), 5.55 (s, 1), and 7.6–8.2 ppm (m, 6).

Anal.—Calc. for $C_{18}H_{23}IN_2S$: C, 50.70; H, 5.43; N, 6.57. Found: C, 50.93; H, 5.23; N, 6.38.

1-Methyl-2-[2-methylthio-2-(4-methyl-1-piperazino)vinyl]-quinolinium Iodide—Following the previous procedure, II (R = H) (1.20 g, 0.0031 mole) in dimethyl sulfoxide (25 ml) was treated with 1-methylpiperazine (0.35 g, 0.0035 mole). The product was recrystallized from acetic acid and again from absolute ethanol to give 0.63 g (48%) of orange crystals, m.p. 188–191°. ^{1}H-NMR: δ 2.58 (s, 3), 2.95 (s, 3), 3.40 (br, 4), 3.83 (br, 4), 4.10 (s, 3), 5.80 (s, 1), and 7.6–8.2 ppm (m, 6).

Anal.—Calc. for $C_{18}H_{24}IN_3S$: C, 48.98; H, 5.48; N, 9.52; S, 7.26. Found: C, 49.00; H, 5.49; N, 9.29; S, 7.30.

1-Methyl-2-[2-methylthio-2-(3-methyl-1-piperazino)vinyl]-quinolinium Iodide—Following the previous procedure, II (R = H) (2.72 g, 0.007 mole) in dimethyl sulfoxide (25 ml) was treated with 2-methylpiperazine (0.70 g, 0.007 mole). The thick, oily product crystallized on long storage in the refrigerator. It was recrystallized from absolute ethanol and ether to give 0.41 g (14%) of orange-brown crystals,m.p. 188–190°. ^{1}H-NMR: δ 2.13 (s, 3), 2.58 (s, 3), 3.40–3.70 (br, 7), 4.10 (s, 3), 5.58 (s, 1), and 7.6–8.2 ppm (m, 6).

Anal.—Calc. for $C_{19}H_{24}IN_3S$: C, 48.98; H, 5.48; N, 9.52; S, 7.26. Found: C, 48.83; H, 5.58; N, 9.11; S, 7.08.

REFERENCES

(1) W. O. Foye, Y. J. Lee, K. A. Shah, and J. M. Kauffman, *J. Pharm. Sci.*, **67**, 962 (1978).

(2) W. O. Foye and J. M. Kauffman, *J. Pharm. Sci.*, **68**, 336 (1979).

(3) W. O. Foye and J. M. Kauffman, *J. Pharm. Sci.*, **69**, 477 (1980).

(4) W. O. Foye, J. M. Kauffman, and R. Ganapathi, "Current Chemotherapy and Infectious Disease," Vol. II, Proc. 11th Int. Congress of Chemotherapy and 19th Intersc. Conf. on Antimicrobial Agents and Chemotherapy (1979), pp. 1629–1631, 1980.

(5) W. O. Foye, O. Vajragupta, and S.K. Sengupta, *J. Pharm. Sci.*, **71**, 253 (1982).

(6) R. Gompper, B. Wetzel, and W. Elser, *Tetrahedron Lett.*, **53**, 5519 (1968).

(7) K. Mizuyama, Y. Tominaga, Y. Matsuda, and G. Kobayashi, *Yakugaku Zasshi*, **94**, 702 (1974).

(8) R. M. Silverstein, G. C. Bassler, and T. C. Morrill, "Spectrometric Identification of Organic Compounds," 3rd ed., Wiley, New York, N.Y., 1974, p. 223.

(9) K. Mizuyama, Y. Tominaga, Y. Matsuda, and G. Kobayashi, *Yakugaku Zasshi*, **95**, 290 (1975).

(10) R. I. Geran, N. H. Greenberg, M. M. MacDonald, A. M. Schumacher, and B. J. Abbott, *Cancer Chemother. Rep.*, Part 3, **3**, 1 (1972).

ACKNOWLEDGMENTS

Supported by funds from the John R. and Marie K. Sawyer Memorial Fund, Massachusetts College of Pharmacy and Allied Health Sciences.

Quantitative Analysis of Ethchlorvynol in a Capsule Dosage Form by NMR Spectroscopy

KAREN B. FEKETY ˣ **and THOMAS MEDWICK**

Received July 19, 1982, from the *College of Pharmacy, Rutgers University, Piscataway, NJ 08854.* Accepted for publication October 14, 1982.

Abstract □ A quantitative ^{1}H-NMR procedure is described for measuring ethchlorvynol in capsules. Deuterochloroform is used as the solvent, and hexamethylenetetramine as the internal standard; the analysis is based on the comparison of the area of the AB peak system of ethchlorvynol with the area of the hexamethylenetetramine singlet. The ^{1}H-NMR method yields results that are precise to within 1% and agree well with results of the more cumbersome and less specific USP titrimetric procedure.

Keyphrases □ Ethchlorvynol—NMR quantitative analysis, capsule dosage form □ NMR quantitative analysis—ethchlorvynol, capsule dosage form

Ethchlorvynol (I), a nonbarbiturate hypnotic, is a tertiary acetylenic carbinol (1-chloro-3-ethyl-1-penten-4-yn-3-ol). The official USP XX procedure for the analytical determination of this drug substance, both alone and in its pharmaceutical dosage form, is based on the reaction of I with excess silver nitrate, producing the silver acetylide and nitric acid (1, 2). The resultant acid is immediately titrated with ~0.05 *N* NaOH; however, end point determination with the methyl red–methylene blue indicator is hampered by the precipitation of the silver acetylide. According to the official procedure, capsules must be weighed, carefully opened, emptied, and reweighed, with the difference taken as the capsule contents. The difficult end point and sample manipulations often lead to poor results.

Although there are several procedures published for the determination of I in biological fluids (3–8), there are only two other published methods for its determination in the pharmaceutical dosage form. Davidson (9), proposed a GLC analysis, accepted by the AOAC (10), and that uses 1,3-dichloro-2-propanol as an internal standard; a standard deviation range of 1.3–2.9% on assays of known solutions and the 500-mg capsule dosage form is reported. Drawbacks inherent in this procedure include the need for column preparation and overnight conditioning and the necessity of injecting a I standard (purified by vacuum distillation and quantified by the USP XX titrimetric procedure) along with the unknown solutions. Rizk and associates (11) proposed a colorimetric method for the determination of certain monosubstituted acetylenic hypnotic drugs, including I. In this procedure, silver acetylide

0022-3549/83/1100-1358$01.00/0

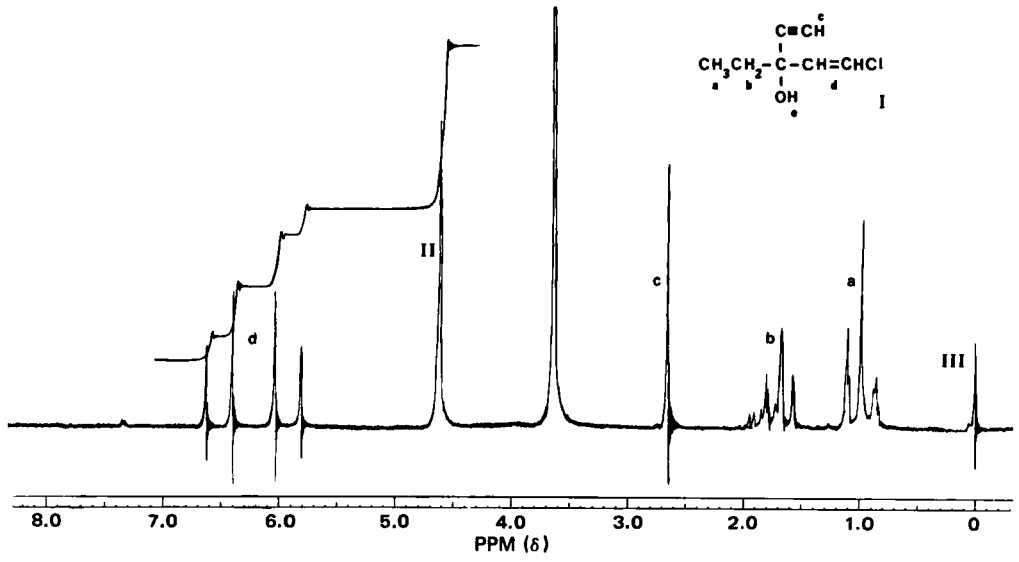

Figure 1—*^{1}H-NMR spectrum of ethchlorvynol in deuterochloroform. Key: (II) hexamethylenetetramine (internal standard); (III) tetramethylsilane.*

is formed and extracted into 4-methyl-2-pentanone, and after acidification, an equivalent amount of silver ions is liberated and assayed colorimetrically as silver dithizonate (λ_{max} = 472 nm). Although the method claims a standard deviation of 1.5–2.9%, it is complicated by the need for a calibration curve for silver nitrate and an involved extraction procedure.

The procedure proposed in this study utilizes quantitative ^{1}H-NMR. Rucker and Natarajan (12) used NMR spectroscopy to quantitatively determine nine sedatives (including I) in mixtures using calibration curves obtained from the responses of standard solutions. However, this study describes the use of an internal standard, which results in a simple, rapid, specific, precise, and accurate analytical method.

EXPERIMENTAL

Materials—The following were used: internal standard, hexamethylenetetramine (methenamine USP), 100.05%, 30 mesh (II)[1]; reference standard, tetramethylsilane (III)[2]; solvent, deuterochloroform, 99.8% D[3] (IV). Ethchlorvynol capsules, 500 mg and 750 mg, were obtained from commercial sources.

Procedure—An individual capsule of I was placed into a suitable glass-stoppered vessel for cutting (*e.g.*, a weighing bottle). With a dissecting scalpel, the capsule was cut cleanly in half, and the blade was rinsed with a few drops of IV to ensure recovery of the entire capsule contents. The appropriate amount of accurately weighed II (~80 mg for a 500-mg capsule and 120 mg for a 750-mg capsule) was added to the container, followed by ~3 ml of IV. The container was stoppered and shaken to ensure complete dissolution of II. The solution was transferred to a glass syringe fitted with a filter apparatus[4], and ~0.5 ml was filtered directly into a standard 5-mm analytical NMR tube. A drop of III was added as needed to reference the peak field positions to 0 ppm on the δ scale. The tube was placed into an NMR spectrometer[5], and the spectrum was obtained adjusting the spin rate so that no spinning side bands interfered with the peaks of interest. The peaks were integrated at 5.81, 6.05, 6.40, and 6.62 ppm and the singlet at 4.65 ppm, not fewer than five times, taking care to avoid saturation.

[1] Merck and Co., Rahway, N.J.
[2] Aldrich Chemical Co., Milwaukee, Wis.
[3] Sci-Graphics, Wayne, N.J.
[4] A Millipore HA filter type 0.45 μm and a 2-ml B-D Yale Luerlok glass syringe.
[5] A Varian A-60 NMR spectrometer, equipped with a V-6031 variable temperature probe having a six-turn insert was used. All spectra were scanned at a probe temperature of 42°.

The amount of I per capsule was calculated as follows:

$$\text{mg of I/capsule} = \text{mg of II} \times (\text{Au/As}) \times (\text{Eu/Es})$$

where Au is the integral value representing I (5.81, 6.05, 6.40, and 6.62 ppm), As is the integral representing II (4.65 ppm), Eu is the proton equivalent weight of I (FW/2 = 72.305), and Es is the proton equivalent weight of II (FW/12 = 11.683).

RESULTS AND DISCUSSION

The solubility of ethchlorvynol (I) and hexamethylenetetramine (II) in deuterochloroform (IV) and the insolubility of the capsule shell makes this solvent a good choice for this ^{1}H-NMR procedure. Although the actual formulation of the dosage form is unknown to the authors, the only peak not ascribable to I occurs at 3.60 ppm and does not interfere with the spectrum of I. Filtration of the solution removes undissolved material, since the unfiltered samples leave difficult-to-remove beadlets in the NMR tube. Filtering the sample does not affect the analytical results, as evidenced by studies of samples before and after filtration.

The ^{1}H-NMR spectrum for I with the addition of II is seen in Fig. 1. The assignments made in this work are in agreement with the limited assignments made by Rucker and Natarajan (12) for the ^{1}H-NMR spectrum of I. For I, the resonances, characteristic of an AB system (d) at δ 5.81, 6.06, 6.40, and 6.62 ppm, correspond to the olefinic protons in the molecule. The methylene protons (b) are not chemically equivalent because of the adjacent asymmetric carbon atom, and therefore are split into 2 quartets (band center δ 1.67 ppm) by the methyl protons; the methyl protons (a) are seen as a triplet centered at δ 1.00 ppm. The acetylenic hydrogen (c) resonates as a singlet at δ 2.62 ppm. The broad based peak at δ 3.60 ppm appears to be a consequence of the formulation and may be a polar material that exchanges with the hydroxyl proton (e) of I. Compound II exhibits only one resonance signal at δ 4.65 ppm, since all 12 of its protons are equivalent. Finally, a very small peak from an impurity in IV is seen at δ 7.32 ppm. All chemical shifts are measured with respect to III at 0 ppm.

The quantitative analysis of I is based on the integration of the area of the AB system quartet which is compared with the area arising from the singlet for II. Summaries of the analyses of a series of both the 500- and 750-mg commercial capsules appear in Tables I and II, respectively. As the results indicate, the ^{1}H-NMR method is both precise, with a relative standard deviation of ~1%, and accurate, as evidenced by the good agreement of the ^{1}H-NMR results in comparison with samples analyzed by the official USP procedure.

The potential value of the proposed ^{1}H-NMR procedure in the analysis of dosage forms of I is established by these measurements, with no evidence of interference from other capsule components or the capsule shell. Blank systems including only the solvent and the capsule shell, with and without the internal standard, showed that no signals are derived from the capsule shell ingredients. This analytical measurement by quantitative ^{1}H-NMR circumvents the lengthy manipulations inherent in the

Table I—Analysis of 500-mg Ethchlorvynol Capsules

Sample	^{1}H-NMR			USP	
	Internal Standard Added, mg	Ethchlorvynol, mg	Percent of Label Claim	Ethchlorvynol, mg	Percent of Label Claim
1	86.86	480.50	96.1	492.33	98.5
2	77.19	473.05	94.6	494.00	98.8
3	81.17	487.33	97.4	485.40	97.1
4	80.74	485.74	97.1	484.33	96.9
5	83.57	482.37	96.5	489.31	97.9
6	79.03	487.01	97.4	484.00	96.8
7	86.72	486.56	97.3	485.61	97.1
8	89.43	487.02	97.4	479.77	96.0
9	81.53	480.53	96.1	491.95	98.4
10	82.92	475.73	95.1	488.74	97.8
Mean		482.58	96.6	487.54	97.5
SD		± 5.10	± 1.02	± 4.47	± 0.89

Table II—Analysis of 750-mg Ethchlorvynol Capsules

Sample	^{1}H-NMR			USP	
	Internal Standard Added, mg	Ethchlorvynol, mg	Percent of Label Claim	Ethchlorvynol, mg	Percent of Label Claim
1	116.71	724.00	96.5	719.05	95.9
2	116.89	738.97	98.5	725.27	96.7
3	116.46	712.64	95.0	714.47	95.2
4	120.73	726.72	96.9	720.82	96.1
5	117.53	722.34	96.3	724.43	96.6
6	119.77	731.19	97.4	717.44	95.7
7	119.35	724.57	96.6	720.28	96.1
8	116.33	722.19	96.3	724.24	96.6
9	118.54	724.07	96.5	728.65	97.2
10	118.83	723.38	96.5	719.65	96.0
Mean		725.01	96.7	721.43	96.2
SD		± 6.73	± 0.89	± 4.20	± 0.57

USP procedure, and avoids the necessity of a reference standard of I, as in the procedure of Rucker and Natarajan (12). In brief, the method is more specific and appears superior to the existing analyses.

REFERENCES

(1) "The United States Pharmacopeia," 20th rev., U.S. Pharmacopeial Convention, Rockville, Md., 1980, p. 305.

(2) N. D. Cheronis and T. S. Ma, "Organic Functional Group Analysis," Wiley-Interscience, New York, N.Y., 1964, p. 385.

(3) D. W. Robinson, *J. Pharm. Sci.*, **57**, 185 (1968).

(4) P. F. Gibson and N. Wright, *J. Pharm. Sci.*, **61**, 169 (1972).

(5) E. J. Algeri, G. G. Katsas, and M. A. Luongo, *Am. J. Clin. Pathol.*, **38**, 125 (1962).

(6) C. S. Frings and P. S. Cohen, *Am. J. Clin. Pathol.*, **54**, 833 (1970).

(7) J. E. Wallace, W. J. Wilson, and E. V. Cahoe, *J. Forensic Sci.*, **9**, 342 (1964).

(8) J. E. Wallace, H. E. Hamilton, J. Ariloff, and K. Blum, *Clin. Chem.*, **20**, 159 (1974).

(9) A. W. Davidson, *J. Assoc. Off. Anal. Chem.*, **53**, 834 (1970).

(10) "Official Methods of Analysis," 13th ed., AOAC, Washington, D.C., 1980, sec. 37.100–37.104.

(11) M. S. Rizk, M. I. Walash, and A. Elbrashy, *J. Assoc. Off. Anal. Chem.*, **63**, 88 (1980).

(12) G. Rucker and P. N. Natarajan, *Arch. Pharm.*, **300**, 276 (1967).

ACKNOWLEDGMENTS

Taken in part from the thesis submitted by Karen B. Fekety to the Graduate School, Rutgers University in partial fulfillment of the requirements for the degree of Master of Science.

Gratitude is extended to the New Jersey Pharmaceutical Quality Control Association for granting to Karen B. Fekety their Summer Fellowship for 1982.

2,3-Dihydro-4*H*-1-benzopyran-4-one *O*-Carbamoyloximes, a Series of Gastric Antisecretory Agents

GEORGE C. WRIGHT ˣ, THOMAS J. SCHWAN, MARVIN M. GOLDENBERG, and RONALD E. WHITE

Received May 28, 1982, from the *Division of Biological and Chemical Research, Research and Development, Norwich Eaton Pharmaceuticals, Inc., Norwich, NY 13815.* Accepted for publication September 3, 1982.

Abstract □ A series of 2,3-dihydro-4*H*-1-benzopyran-4-one *O*-carbamoyloximes were synthesized and evaluated for gastric antisecretory activity in a pylorus-ligated rat model. Various substituents in the 6-position did not afford any compounds more active than I.

Keyphrases □ 2,3-Dihydro-4*H*-1-benzopyran-4-one *O*-carbamoyloximes—synthesis, antisecretory activity, pylorus-ligated rats □ Antisecretory agents, gastric—potential, 2,3-dihydro-4*H*-1-benzopyran-4-one *O*-carbamoyloxime series, synthesis, evaluation in pylorus-ligated rats □ Synthesis—2,3-dihydro-4*H*-1-benzopyran-4-one *O*-carbamoyloxime series, gastric antisecretory activity, pylorus-ligated rats

To identify novel agents acting on the GI tract, 10 members of a series of 2,3-dihydro-4*H*-1-benzopyran-4-one *O*-carbamoyloximes were synthesized and evaluated for gastric antisecretory activity (1).

RESULTS AND DISCUSSION

Chemistry—Eight compounds (I–VI, VIII, and IX; Table I) were prepared by the reaction of the appropriate oxime XI with the isocyanate XII (Scheme I). The amine VII (Table I) was obtained by catalytic hydrogenation of the corresponding nitro compound VI (Table I, Scheme I), while acid-catalyzed reaction of XIII with potassium cyanate gave X (Scheme I).

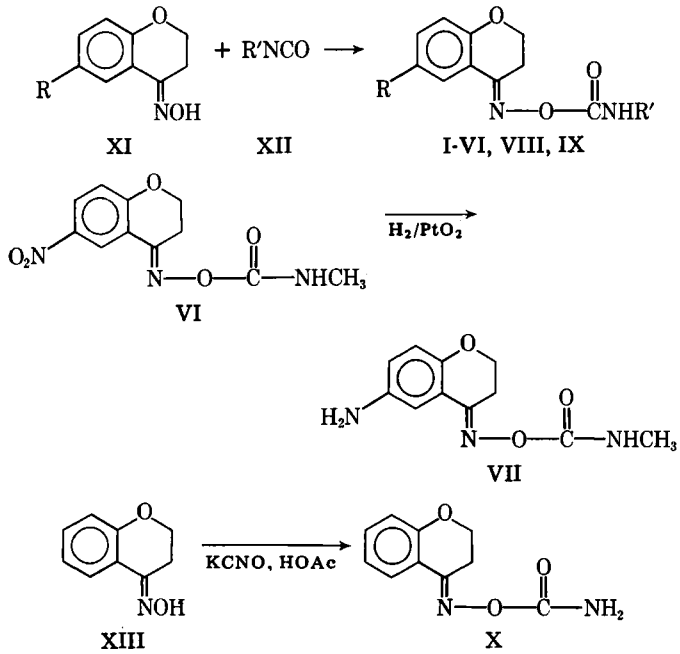

Scheme I

The intermediate oximes XIa–d (Table II) were prepared from the corresponding 2,3-dihydro-4*H*-benzopyran-4-ones (XIV) (Scheme II), which were synthesized by ring closure of the corresponding 3-phenoxypropanoic acids (XV) with polyphosphoric acid, as described by Parham and Huestis (2).

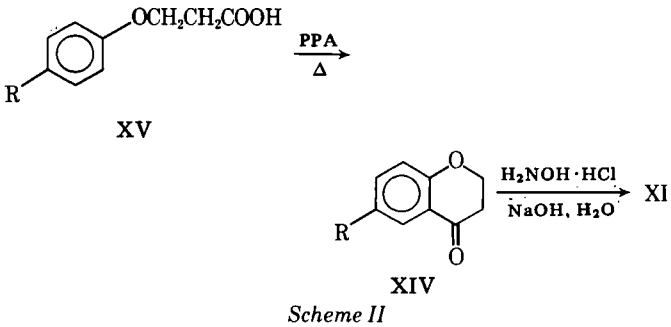

Scheme II

Pharmacology—Compounds I–V and VII exhibited marked antagonism of total gastric acid output in pylorus-ligated rats. Compounds VIII–X showed moderate antagonism, while VI was inactive (Table III). Dose–response determinations of the 10 compounds revealed that I was most potent in inhibiting total gastric acid output as exemplified by a low ID_{50} value of 5.7 mg/kg p.o. Compounds II–V were also active in reducing gastric acid output with ID_{50} values of 22.1–22.7 mg/kg p.o. No evidence of toxicity was noted at their respective ID_{50} values.

EXPERIMENTAL[1]

Synthesis—*2,3-Dihydro-6-nitro-4*H*-1-benzopyran-4-one Oxime (XI d)*—To a solution of hydroxylamine hydrochloride (79 g, 1.14 moles) in water (770 ml) were added 10% NaOH (619 ml) and 2,3-dihydro-6-nitro-4*H*-benzopyran-4-one (150 g, 0.78 mole) (3, 4). Sufficient ethanol–ether (95:5) (750 ml) was added to give a solution at reflux. The mixture was refluxed for 25 min, cooled to 50° over 2 hr, and the resultant tan crystals were collected by filtration and washed with ethanol–ether (95:5) to give 60 g, mp 173–178°. Recrystallization from benzene gave material with a melting point of 185–186° in 27% yield.

*2,3-Dihydro-6-nitro-4*H*-1-benzopyran-4-one O-(Methylaminocarbonyl)oxime (VI)*—A mixture of XI d (19 g, 0.09 mole) and benzene was refluxed for 45 min in a flask equipped with a Dean Stark trap. Heating was discontinued and *N,N*-diethylethanamine (0.5 ml) was added, followed by a solution of methyl isocyanate (7.3 g, 0.10 mole) in benzene (30 ml). The mixture was refluxed for 3 hr and then stored at room temperature for 3 days. The material was collected by filtration, stirred in absolute ethanol (150 ml), and cooled overnight to give, after filtration, 16 g of VI.

An analytical sample was prepared by recrystallization from absolute ethanol (Table I); IR (mineral oil): 2.98 (NH) and 5.73 μm (C=O); ^{1}H-NMR: 2.80 (d, 3, CH_3, collapsed to singlet on exchange with D_2O), 3.10 and 4.45 (2 t, J = 6.4 Hz, 4, CH_2CH_2), 6.21 (d, J = 9.2 Hz, 1, aromatic), 7.27 (dd, $J_{5,7}$ = 2.7 Hz, $J_{7,8}$ = 9.2 Hz, 1, aromatic), 7.98 (d, J = 2.7 Hz, 1, aromatic), and 6.77 ppm (broad, 1, NH, exchanged with D_2O).

Similarly prepared were I–IV, VIII, and IX (Table I). In the case of V, filtration of the reaction mixture provided the product directly (Table I).

*6-Amino-2,3-dihydro-4*H*-1-benzopyran-4-one O-(Methylaminocarbonyl)oxime Hydrochloride (VII)*—A mixture of VI (4.0 g, 0.016 mole) and ethanol (400 ml) was shaken with hydrogen in the presence of platinum oxide (0.20 g) until the theoretical quantity of hydrogen was consumed (21 hr). The catalyst was removed by filtration, and the filtrate was cooled in an ice bath and treated with ethanolic hydrogen chloride.

[1] Melting points were determined on a Mel-Temp apparatus, and those below 230° were corrected. IR spectra were determined as Nujol mulls on a Perkin-Elmer 137B spectrophotometer, and NMR spectra were determined on a Varian A-60A spectrometer in dimethyl sulfoxide-d_6 with tetramethylsilane as an internal standard.

0022-3549/83/1100-1361$01.00/0

Table I—Physical and Analytical Data for 2,3-Dihydro-4*H*-1-benzopyran-4-one *O*-Carbamoyloximes

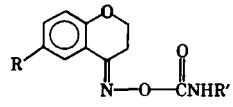

Compound	R	R′	Recrystallization Solvent	Melting Point	Yield, %	Formula	Elemental Analysis, % Calc.	Found
I	H	CH_3	2-propanol	125–126°	88	$C_{11}H_{12}N_2O_3$	C 59.99	59.76
							H 5.49	5.59
							N 12.72	12.69
II	CH_3O	C_2H_5	2-propanol	97–98°	83	$C_{13}H_{16}N_2O_4$	C 59.08	59.21
							H 6.10	6.16
							N 10.60	10.56
III	H	C_2H_5	2-propanol	110–111°	79	$C_{12}H_{14}N_2O_3$	C 61.53	61.44
							H 6.02	5.92
							N 11.96	11.98
IV	CH_3O	CH_3	2-propanol	119–120°	59	$C_{12}H_{14}N_2O_4$	C 57.59	57.55
							H 5.64	5.66
							N 11.20	11.20
V	Cl	CH_3	benzene	182–184	80	$C_{11}H_{11}ClN_2O_3$	C 51.68	51.50
							H 4.35	4.23
							N 11.00	10.80
VI	NO_2	CH_3	ethanol	204–207°	67	$C_{11}H_{11}N_3O_5$	C 49.81	49.80
							H 4.18	4.24
							N 15.85	15.65
VII	NH_2	CH_3	methanol	194–199°	58	$C_{11}H_{13}N_3O_3 \cdot HCl$	C 48.62	48.46
							H 5.19	5.18
							N 15.47	15.13
VIII	H	$CH_2CH{=}CH_2$	toluene	83–86°	73	$C_{13}H_{14}N_2O_3$	C 63.40	63.38
							H 5.73	5.81
							N 11.38	11.40
IX	H	$CH_2CH_2CH_3$	toluene	80–82°	68	$C_{13}H_{16}N_2O_3$	C 62.89	62.78
							H 6.50	6.67
							N 11.28	10.96
X	H	H	toluene	120–122°	44	$C_{10}H_{10}N_2O_3$	C 58.25	58.59
							H 4.89	4.77
							N 13.58	13.45

Table II—Physical and Analytical Data for 2,3-Dihydro-4*H*-1-benzopyran-4-one Oximes

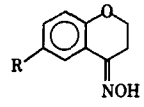

Compound	R	Melting Point	Yield, %	IR, μm OH	^{1}H-NMR, ppm	Empirical Formula	Elemental Analysis, % Calc.	Found
XI a	H	140–142° (lit. 138°)[b]	97	3.10				
XI b	CH_3O	120–121° (lit. 120°)[b]	99	3.10				
XI c	Cl[a]	127–128°	55	3.15	2.85 and 4.25 (2 t, J = 6.4 Hz, 4, CH_2CH_2), 6.99 (d, J = 9.4 1, aromatic), 7.35 (dd, $J_{5,7}$ = 2,2 Hz, $J_{7,8}$ = 9.4 Hz, 1, aromatic), 7.78 (d, J = 2.2 Hz, 1, aromatic), 11.55 (s, 1, exchanged with D_2O)	$C_9H_8ClNO_2$	C 54.70	54.83
							H 4.08	4.06
							N 7.09	6.88
XI d	NO_2	185–186°	27	3.08	3.00 and 4.48 (2 t, J = 6.4 Hz, 4, CH_2CH_2), 7.30 (d, J = 9.4 Hz, 1, aromatic), 8.30 (dd, $J_{5,7}$ = 3.2 Hz, $J_{7,8}$ = 9.4 Hz, 1, aromatic), 8.77 (d, J = 3.2 Hz, 1, aromatic), 11.87 (s, 1, exchanged with D_2O)	$C_9H_8N_2O_4$	C 51.92	51.92
							H 3.87	3.79
							N 13.46	13.34

[a] For intermediate 6-chloro-2,3-dihydro-4*H*-1-benzopyran-4-one, see Ref. 3 and 4. [b] See Ref. 1.

The solution was concentrated to a volume of 70 ml and cooled. The product was removed by filtration. IR (mineral oil): 2.90 (NH_2) and 5.70 μm (C=O); ^{1}H-NMR: 2.73 (d, 3, CH_3, collapsed to singlet in D_2O), 3.00 and 4.30 (2 t, J = 6.4 Hz, 4, CH_2CH_2), 7.07 (d, J = 9.0 Hz, 1, aromatic), 7.48 (dd, $J_{5,7}$ = 2.7 Hz, $J_{7,8}$ = 8.8 Hz, 1, aromatic), 8.06 (d, J = 2.7 Hz, 1, aromatic), 7.7 (broad, 2, NH_2, exchanged with D_2O), and 6.82 ppm (broad, 2, NH and HCl).

*2,3-Dihydro-4*H*-1-benzopyran-4-one O-(Aminocarbonyl)oxime* (*X*)—To a solution of the oxime (XI a) (8.15 g, 0.05 mole) in glacial acetic acid (175 ml) at ambient temperature was added a solution of potassium cyanate (4.05 g, 0.05 mole) in water (20 ml). The solution was stirred at ambient temperature for 48 hr, diluted with 200 ml of water, and extracted with chloroform (2 × 150 ml). The combined extracts were dried (magnesium sulfate), concentrated to dryness *in vacuo*, and the residue was recrystallized from methylbenzene (40 ml) to give the product (Table I); IR (mineral oil): 2.83 and 2.90 (NH_2) and 5.67 μm (C=O); ^{1}H-NMR: 3.01 and 4.28 (2 t, J = 6.8 Hz, 4, CH_2CH_2), 7.27 (m, 4, aromatic and NH_2), and 8.22 ppm (d, J = 2.0 Hz, 2, aromatic).

Pharmacology—Male Sprague–Dawley rats, each weighing 180–210 g and previously fasted for 24 hr, were used in the modified, standard pylorus-ligated gastric secretory model. All compounds were given perorally, as suspensions in 0.5% methyl cellulose[2], 1 hr prior to pylorus

[2] Methocel.

Table III—Effect of Compounds I–X on Gastric Secretion in the Pylorus-Ligated Rat

	No. of Rats	Dose mg/kg p.o.	Volume of Gastric Secretions: ml/100 g Body Wt.	Volume of Gastric Secretions: Mean Percent of Control[b]	Total Gastric Acid Output: meq/100 g Body Wt.	Total Gastric Acid Output: Mean Percent of Control[b]	ID_{50}[c], mg/kg p.o. (95% Confidence Limits)
Control[a]	5		3.01 ± 0.79		0.18 ± 0.059		
I	3	50	1.99 ± 0.33	66	0.096 ± 0.028	53	5.7 (1.0–21.0)
Control[a]	5		3.44 ± 0.89		0.23 ± 0.076		
II	3	100	2.30 ± 0.50	67	0.097 ± 0.035	42	22.1 (11.7–37.0)
Control[a]	5		4.65 ± 0.71		0.31 ± 0.066		
III	3	100	1.78 ± 0.20	38	0.063 ± 0.0050	20	26.7 (19.2–31.0)
Control[a]	5		3.46 ± 0.60		0.21 ± 0.060		
IV	3	100	2.24 ± 0.63	65	0.12 ± 0.041	57	24.7 (19.2–31.0)
Control[a]	5		1.85 ± 0.62		0.095 ± 0.052		
V		100	0.83 ± 0.12	45	0.057 ± 0.012	60	25.9 (11.9–50.7)
Control[a]	5		5.00 ± 0.76		0.31 ± 0.083		
VI		100	4.07 ± 1.16	81	0.37 ± 0.12	121	—
Control[a]	5		5.00 ± 1.27		0.31 ± 0.083		
VII	3	100	1.78 ± 0.58	36	0.14 ± 0.064	45	>180
Control[a]	5		5.62 ± 0.18		0.61 ± 0.049		
VIII	3	100	1.34 ± 0.21	24	0.062 ± 0.010	10	57.4 (51.6–64.9)
IX	3	100	1.48 ± 0.29	26	0.073 ± 0.017	12	43.4 (24.4–111.3)
X	3	100	2.22 ± 0.055	39	0.014 ± 0.091	23	50.4 (30.1–127.1)

[a] The control values were obtained by peroral administration of 0.50% methylcellulose solution to a group of rats at 1 ml/100 g % body weight. [b] Compared to control (nondrug-treated) reading 4 hr after pylorus-ligation of rat stomach. [c] The dose eliciting 50% inhibition of total gastric acid output; calculated from data obtained at doses of 10, 30, and 100 mg/kg p.o., by method of linear regression analysis (5) of the dose–response curve.

ligation. Under light ether anesthesia, the rat stomach was ligated at the pylorus region. The conscious rat was sacrificed by a chloroform overdose 4 hr after ligation. The stomach was carefully excised and its contents drained into a centrifuge tube. Samples were centrifuged to separate secretions from debris, and gastric fluid volume was read and recorded. Titration was performed on a sample aliquot of 1 ml diluted to a volume of 5 ml using distilled water. The titrant used was 0.1 *N* NaOH. Acid concentration in the stomach was determined by titration to pH 7. Total gastric acid output was calculated as the product of volume of gastric secretions and acid concentration for each compound tested.

REFERENCES

(1) G. C. Wright, T. J. Schwan, and M. M. Goldenberg, U.S. Pat. 4,169,097, Sept. 25, 1979.

(2) W. E. Parham and L. D. Huestis, *J. Am. Chem. Soc.*, **84**, 813 (1962).

(3) C. D. Hurd and S. Hayao, *J. Am. Chem. Soc.*, **76**, 5065 (1954).

(4) T. L. Gresham, J. E. Jansen, F. W. Shaver, R. A. Bankert, W. L. Beears, and M. G. Prendergast, *J. Am. Chem. Soc.*, **71**, 661 (1949).

(5) H. A. Graybill, "An Introduction to Linear Statistical Models," Vol. 1, McGraw Hill, New York, N.Y., 1961.

Effect of Nutrient Depletion on the Sensitivity of *Pseudomonas cepacia* to Antimicrobial Agents

R. M. COZENS * **and M. R. W. BROWN** ˣ

Received June 28, 1982, from the *Microbiology Research Group, Department of Pharmacy, University of Aston in Birmingham, Birmingham B4 7ET, England.* Accepted for publication October 7, 1982.

* Present address: CIBA-GEIGY Ltd., Infectious Diseases Research, Basle, CH-4002 Switzerland.

Abstract □ *Pseudomonas cepacia* depleted of various nutrients showed marked variation in sensitivity to cetrimide, chlorhexidine, and benzalkonium chloride. In all cases cells depleted of magnesium were the most resistant. It is proposed that these observations may be due to alterations of the envelope of *P. cepacia* in response to changes in the growth environment. This may have profound implications for investigations of the resistance of this organism both *in vivo* and *in vitro*.

Keyphrases □ Nutrient depletion—effect of senstivity of *Pseudomonas cepacia* to antimicrobial agents □ Antimicrobial agents—effect of nutrient depletion on sensitivity of *Pseudomonas cepacia* □ *Pseudomonas cepacia*—effect of nutrient depletion on sensitivity to antimicrobial agents

Pseudomonas cepacia, previously considered as only a plant pathogen, has, in the last decade, been implicated in nosocomial infections with increasing frequency (1–3). The organism is more resistant to most useful antimicrobial agents than other Gram-negative bacteria. It is capable of survival and even multiplication in quaternary ammonium compounds (2, 4, 5) and will multiply in distilled or deionized water (6, 7).

0022-3549/83/1100-1363$01.00/0

Table III—Effect of Compounds I–X on Gastric Secretion in the Pylorus-Ligated Rat

	No. of Rats	Dose mg/kg p.o.	Volume of Gastric Secretions: ml/100 g Body Wt.	Volume of Gastric Secretions: Mean Percent of Control[b]	Total Gastric Acid Output: meq/100 g Body Wt.	Total Gastric Acid Output: Mean Percent of Control[b]	ID_{50}[c], mg/kg p.o. (95% Confidence Limits)
Control[a]	5		3.01 ± 0.79		0.18 ± 0.059		
I	3	50	1.99 ± 0.33	66	0.096 ± 0.028	53	5.7 (1.0–21.0)
Control[a]	5		3.44 ± 0.89		0.23 ± 0.076		
II	3	100	2.30 ± 0.50	67	0.097 ± 0.035	42	22.1 (11.7–37.0)
Control[a]	5		4.65 ± 0.71		0.31 ± 0.066		
III	3	100	1.78 ± 0.20	38	0.063 ± 0.0050	20	26.7 (19.2–31.0)
Control[a]	5		3.46 ± 0.60		0.21 ± 0.060		
IV	3	100	2.24 ± 0.63	65	0.12 ± 0.041	57	24.7 (19.2–31.0)
Control[a]	5		1.85 ± 0.62		0.095 ± 0.052		
V		100	0.83 ± 0.12	45	0.057 ± 0.012	60	25.9 (11.9–50.7)
Control[a]	5		5.00 ± 0.76		0.31 ± 0.083		
VI		100	4.07 ± 1.16	81	0.37 ± 0.12	121	—
Control[a]	5		5.00 ± 1.27		0.31 ± 0.083		
VII	3	100	1.78 ± 0.58	36	0.14 ± 0.064	45	>180
Control[a]	5		5.62 ± 0.18		0.61 ± 0.049		
VIII	3	100	1.34 ± 0.21	24	0.062 ± 0.010	10	57.4 (51.6–64.9)
IX	3	100	1.48 ± 0.29	26	0.073 ± 0.017	12	43.4 (24.4–111.3)
X	3	100	2.22 ± 0.055	39	0.014 ± 0.091	23	50.4 (30.1–127.1)

[a] The control values were obtained by peroral administration of 0.50% methylcellulose solution to a group of rats at 1 ml/100 g % body weight. [b] Compared to control (nondrug-treated) reading 4 hr after pylorus-ligation of rat stomach. [c] The dose eliciting 50% inhibition of total gastric acid output; calculated from data obtained at doses of 10, 30, and 100 mg/kg p.o., by method of linear regression analysis (5) of the dose–response curve.

ligation. Under light ether anesthesia, the rat stomach was ligated at the pylorus region. The conscious rat was sacrificed by a chloroform overdose 4 hr after ligation. The stomach was carefully excised and its contents drained into a centrifuge tube. Samples were centrifuged to separate secretions from debris, and gastric fluid volume was read and recorded. Titration was performed on a sample aliquot of 1 ml diluted to a volume of 5 ml using distilled water. The titrant used was 0.1 *N* NaOH. Acid concentration in the stomach was determined by titration to pH 7. Total gastric acid output was calculated as the product of volume of gastric secretions and acid concentration for each compound tested.

REFERENCES

(1) G. C. Wright, T. J. Schwan, and M. M. Goldenberg, U.S. Pat. 4,169,097, Sept. 25, 1979.

(2) W. E. Parham and L. D. Huestis, *J. Am. Chem. Soc.*, **84**, 813 (1962).

(3) C. D. Hurd and S. Hayao, *J. Am. Chem. Soc.*, **76**, 5065 (1954).

(4) T. L. Gresham, J. E. Jansen, F. W. Shaver, R. A. Bankert, W. L. Beears, and M. G. Prendergast, *J. Am. Chem. Soc.*, **71**, 661 (1949).

(5) H. A. Graybill, "An Introduction to Linear Statistical Models," Vol. 1, McGraw Hill, New York, N.Y., 1961.

Effect of Nutrient Depletion on the Sensitivity of *Pseudomonas cepacia* to Antimicrobial Agents

R. M. COZENS * **and M. R. W. BROWN** ˣ

Received June 28, 1982, from the *Microbiology Research Group, Department of Pharmacy, University of Aston in Birmingham, Birmingham B4 7ET, England.* Accepted for publication October 7, 1982.

* Present address: CIBA-GEIGY Ltd., Infectious Diseases Research, Basle, CH-4002 Switzerland.

Abstract □ *Pseudomonas cepacia* depleted of various nutrients showed marked variation in sensitivity to cetrimide, chlorhexidine, and benzalkonium chloride. In all cases cells depleted of magnesium were the most resistant. It is proposed that these observations may be due to alterations of the envelope of *P. cepacia* in response to changes in the growth environment. This may have profound implications for investigations of the resistance of this organism both *in vivo* and *in vitro*.

Keyphrases □ Nutrient depletion—effect of senstivity of *Pseudomonas cepacia* to antimicrobial agents □ Antimicrobial agents—effect of nutrient depletion on sensitivity of *Pseudomonas cepacia* □ *Pseudomonas cepacia*—effect of nutrient depletion on sensitivity to antimicrobial agents

Pseudomonas cepacia, previously considered as only a plant pathogen, has, in the last decade, been implicated in nosocomial infections with increasing frequency (1–3). The organism is more resistant to most useful antimicrobial agents than other Gram-negative bacteria. It is capable of survival and even multiplication in quaternary ammonium compounds (2, 4, 5) and will multiply in distilled or deionized water (6, 7).

0022-3549/83/1100-1363$01.00/0

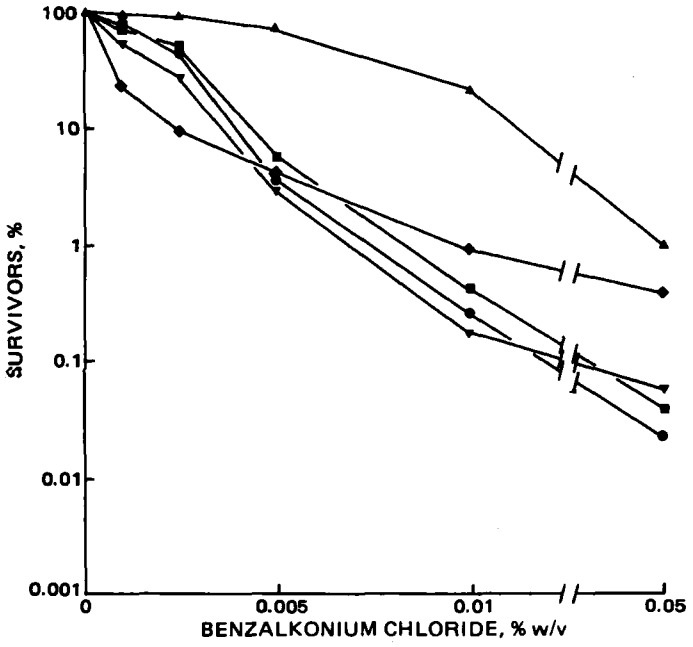

Figure 1—*The effect of benzalkonium chloride on cells of* P. cepacia *depleted of glucose (●), magnesium (▲), and ammonium (■), phosphate (◆), and ferrous ions (▼).*

The relationship between susceptibility to antimicrobial agents and the growth environment has been recognized for some time (8). Brown (9) has emphasized the need for the use of nutritionally defined cultures for the investigation of the response of bacteria to antimicrobial agents and host defense mechanisms. As *P. cepacia* in its natural environment or as a contaminant of disinfectant solutions is probably depleted of an essential nutrient (9), the use of cultures depleted in this way would possibly be more relevant in investigations of the extreme resistance of this organism. This paper describes the effect of nutrient depletion on the resistance of *P. cepacia* to some common antimicrobial agents.

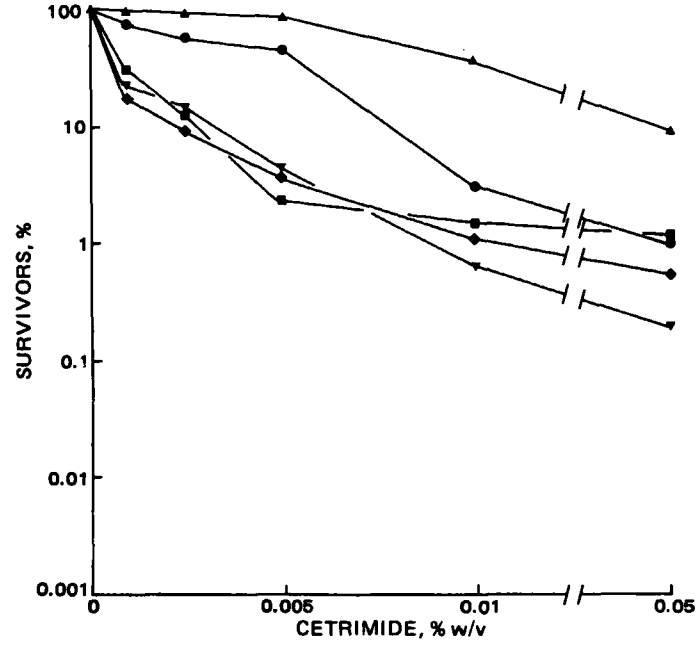

Figure 2—*The effect of cetrimide on cells of* P. cepacia *depleted of various nutrients (see Fig. 1 for key).*

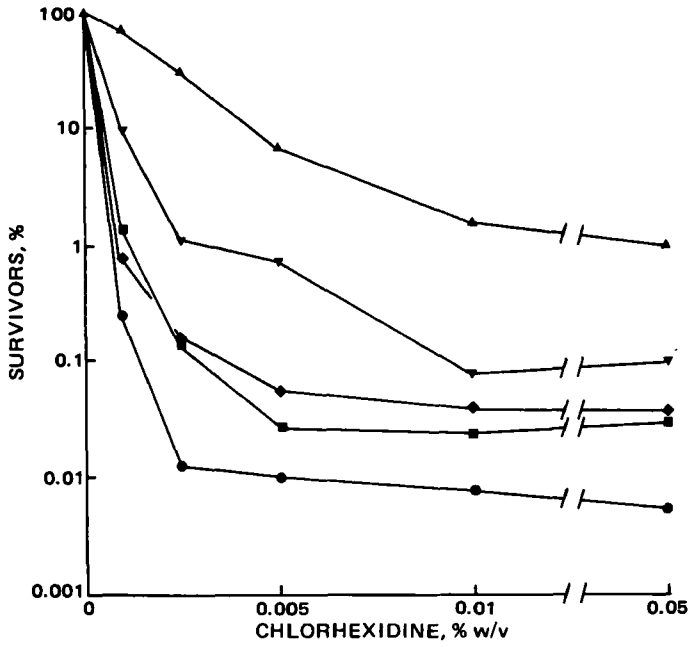

Figure 3—*The effect of chlorhexidine on cells of* P. cepacia *depleted of various nutrients (see Fig. 1 for key).*

EXPERIMENTAL

Organism—*Pseudomonas cepacia* NCTC 10661 was used throughout. Cultures were maintained by monthly subculture on nutrient agar slopes stored at 4°. The basic medium contained 20 m*M* of glucose, 12 m*M* of $(NH_4)_2SO_4$, 1.2 m*M* of K_2HPO_4, 3.2 m*M* of $MgSO_4 \cdot 7H_2O$, 0.02 m*M* of $FeSO_4 \cdot 7H_2O$, 3 m*M* of NaCl, 3 m*M* of KCl, and 50 m*M* of 3-(*N*-morpholino)propanesulfonic acid (I), pH 7.4. Chemicals[1] were of the purest grade available.

For nutrient depletion studies the concentrations were separately adjusted: 2.0 m*M* of glucose, 0.5 m*M* of $(NH_4)_2SO_4$, 0.1 m*M* of K_2HPO_4, 0.01 m*M* of $MgSO_4 \cdot 7H_2O$, and no added iron to give the respective depletions. These concentrations allowed the cultures to reach maximum exponential phase at A_{470} = 0.5. Cultures (25 ml) were grown in baffled 100-ml Erlenmeyer flasks at 37° in a reciprocal shaking water bath at 120 throws/min.

Resistance to Antibacterial Agents—Cells grown under various nutrient depletions, as described above, were harvested by centrifugation, washed twice in saline buffered with I (pH 7.4) and finally resuspended to a A_{470} = 1.0. Cell suspension (0.1 ml) was added to 9.9 ml of various concentrations of drug (cetrimide[1], benzalkonium chloride[2], chlorhexidine gluconate[3]) prepared in saline buffered with (I). After 15 min at 37° samples were removed, the drugs inactivated by dilution in lecithin–polysorbate 80 broth, and suitable dilutions were incorporated into pour plates of nutrient agar. The plates were incubated for 36 hr at 37° before counting the resulting colonies.

RESULTS AND DISCUSSION

Figures 1–3 show the variation in sensitivity to antibacterial agents when the depleting nutrient was altered. In all cases, cells depleted of magnesium showed the greatest resistance to the action of these agents. Of the other depletions examined, the resistances against benzalkonium chloride and cetrimide showed little variation. Chlorhexidine showed a wider spread of activity, with glucose-depleted cells being the most sensitive.

Al-Hiti and Gilbert (10) have shown that those organisms specified for use in the USP XIX test for the effectiveness of antimicrobial preservatives exhibited a changed sensitivity to chlorhexidine diacetate and benzalkonium chloride, when depleted of different nutrients. The results described here show that *P. cepacia* exhibits similar changes in sensitivity to antimicrobial agents caused by different nutrient depletions.

[1] BDH Chemicals, Poole, UK. Listed in The British Pharmacopoeia as mainly tetradecyltrimethylammonium bromide with smaller amounts of dodecyl- and hexadecyltrimethylammonium bromide.
[2] Sigma, Poole, UK.
[3] ICI Ltd., Macclesfield, UK.

The cell envelope, and particularly the outer membrane, of Gram-negative bacteria is known to change in response to changes in the growth environment (8, 11, 12). It is therefore likely that these changes in resistance may reflect changes in the cell envelope which either prevent access of the drug to the site of action or alter the site of action such that the drugs show decreased activity. Little is known about the cell envelope of *P. cepacia*. The lipopolysaccharide is atypical, not containing 2-keto-3-deoxyoctonate and with several quantitative differences in the sugar moieties (13). The cellular fatty acid compositions (mostly derived from the envelope phospholipids) of *P. cepacia* and *Pseudomonas aeruginosa* differ in that the former has proportionately more cyclopropane fatty acids than does the latter (14).

REFERENCES

(1) D. G. J. Bassett, K. J. Stokes, and W. R. G. Thomas, *Lancet*, **i**, 1188 (1970).

(2) P. C. Hardy, G. M. Ederer, and J. M. Matsen, *N. Engl. J. Med.*, **282**, 33 (1970).

(3) I. Phillips, S. Eykyn, M. A. Curtis, and J. J. S. Snell, *Lancet* **i**, 375 (1971).

(4) F. W. Adair, S. G. Geftic, and J. Gelzer, *Appl. Microbiol.*, **60**, 299 (1969).

(5) S. G. Geftic, H. Heymann, and F. W. Adair, *Appl. Env. Microbiol.*, **37**, 505 (1979).

(6) L. A. Carson, M. S. Favero, W. W. Bond, and N. J. Petersen, *Appl. Microbiol.*, **25**, 476 (1973).

(7) S. M. Gelbart, G. E. Reinhardt, and H. B. Greenless, *J. Clin. Microbiol.*, **3**, 62 (1976).

(8) J. Melling and M. R. W. Brown, in "Resistance of *Pseudomonas aeruginosa*," M. R. W. Brown, Ed., Wiley, London, England, 1975, p. 35.

(9) M. R. W. Brown, *J. Antimicrob. Chemother.*, **3**, 198 (1977).

(10) M. M. A. Al-Hiti and P. Gilbert, *J. Appl. Bacteriol.*, **49**, 119 (1980).

(11) D. C. Ellwood and D. W. Tempest, *Adv. Micro. Physiol.*, **7**, 83 (1972).

(12) P. Gilbert and M. R. W. Brown, *J. Bacteriol.*, **133**, 1066 (1978).

(13) J. M. Maniello, H. Heymann, and F. W. Adair, *J. Gen. Microbiol.*, **112**, 397 (1979).

(14) S. Ikemoto, H. Kuraishi, K. Komagata, R. Azuma, T. Suto, and H. Murooka, *J. Gen. Appl. Microbiol.*, **24**, 199 (1978).

COMMUNICATIONS

Mean Hepatic Transit Time in the Determination of Mean Absorption Time

Keyphrases □ Mean hepatic transit time—determination of mean absorption time, pharmacokinetics □ Mean absorption time—determination by mean hepatic transit time, pharmacokinetics □ Pharmacokinetics—mean hepatic transit time, mean absorption time, mean residence time

To the Editor:

In recent studies the statistical moment theory has been employed to estimate mean absorption time (MAT) of drugs (1–5). The MAT has been defined as the mean time of a molecule (1) or the mean residence time (MRT) of all molecules (2) from a dosage form (such as solution or tablet) spent at the input site (GI lumen in the case of oral administration) before being absorbed into the general circulation. The MAT after oral administration has been calculated based on the following equation (1–5):

$$MAT = MRT_{po} - MRT_{iv} \qquad \text{(Eq. 1)}$$

where MRT_{po} is the MRT of the orally absorbed drug molecules in the body, and MRT_{iv} is the MRT of intravenously (usually from a peripheral vein in the leg or arm) administered drug molecules in the body. Both plasma and urinary excretion data have been proposed to estimate the MRT_{po} and MRT_{iv}. When a solution dosage form is studied, the calculated MAT has been referred to as mean intrinsic absorption time (5). When both solution and solid dosage forms are evaluated, the difference in their MRT may be considered to equal the mean *in vivo* dissolution time (MDT) from the solid dosage form. This is based on the assumption that once released from the solid dosage form, it is subject to the same influence as the drug administered in solution (1–3).

The main purpose of this communication is to discuss a complication in using Eq. 1 to determine the MAT. Its potential significance in absorption rate calculations and hepatic clearance studies will also be briefly mentioned. In analogy to the above assumption requirement in the determination of MDT, use of Eq. 1 must also require that the orally absorbed drug is handled in the body exactly the same way as that administered intravenously. This demand apparently can not be met because the orally absorbed drug has to pass through the GI wall and then the liver before entering the heart, while the intravenously administered drug can be carried almost instantaneously from the injection site to the heart before being distributed to the rest of body. The mean time to pass through the GI wall and liver can be called mean GI wall transit time, MTT_{GI}, and mean hepatic transit time, MTT_h, respectively. The portal circulation between the GI wall and liver is extremely fast and can be ignored. Therefore, Eq. 1 can be modified to:

$$MAT = MRT_{po} - MRT_{iv} - MTT_{GI} - MTT_h \qquad \text{(Eq. 2)}$$

The MTT in a tissue or organ during a single passage can be determined directly by instantaneous injection of a compound into the affluent blood and monitoring of effluent blood concentration, C_{out}, under the single-pass nonrecirculating condition (6–8):

$$MTT = \frac{\int_0^\infty tC_{out}dt}{\int_0^\infty C_{out}dt} \qquad \text{(Eq. 3)}$$

0022-3549/83/1100-1365$01.00/0

The cell envelope, and particularly the outer membrane, of Gram-negative bacteria is known to change in response to changes in the growth environment (8, 11, 12). It is therefore likely that these changes in resistance may reflect changes in the cell envelope which either prevent access of the drug to the site of action or alter the site of action such that the drugs show decreased activity. Little is known about the cell envelope of *P. cepacia*. The lipopolysaccharide is atypical, not containing 2-keto-3-deoxyoctonate and with several quantitative differences in the sugar moieties (13). The cellular fatty acid compositions (mostly derived from the envelope phospholipids) of *P. cepacia* and *Pseudomonas aeruginosa* differ in that the former has proportionately more cyclopropane fatty acids than does the latter (14).

REFERENCES

(1) D. G. J. Bassett, K. J. Stokes, and W. R. G. Thomas, *Lancet*, **i**, 1188 (1970).

(2) P. C. Hardy, G. M. Ederer, and J. M. Matsen, *N. Engl. J. Med.*, **282**, 33 (1970).

(3) I. Phillips, S. Eykyn, M. A. Curtis, and J. J. S. Snell, *Lancet* **i**, 375 (1971).

(4) F. W. Adair, S. G. Geftic, and J. Gelzer, *Appl. Microbiol.*, **60**, 299 (1969).

(5) S. G. Geftic, H. Heymann, and F. W. Adair, *Appl. Env. Microbiol.*, **37**, 505 (1979).

(6) L. A. Carson, M. S. Favero, W. W. Bond, and N. J. Petersen, *Appl. Microbiol.*, **25**, 476 (1973).

(7) S. M. Gelbart, G. E. Reinhardt, and H. B. Greenless, *J. Clin. Microbiol.*, **3**, 62 (1976).

(8) J. Melling and M. R. W. Brown, in "Resistance of *Pseudomonas aeruginosa*," M. R. W. Brown, Ed., Wiley, London, England, 1975, p. 35.

(9) M. R. W. Brown, *J. Antimicrob. Chemother.*, **3**, 198 (1977).

(10) M. M. A. Al-Hiti and P. Gilbert, *J. Appl. Bacteriol.*, **49**, 119 (1980).

(11) D. C. Ellwood and D. W. Tempest, *Adv. Micro. Physiol.*, **7**, 83 (1972).

(12) P. Gilbert and M. R. W. Brown, *J. Bacteriol.*, **133**, 1066 (1978).

(13) J. M. Maniello, H. Heymann, and F. W. Adair, *J. Gen. Microbiol.*, **112**, 397 (1979).

(14) S. Ikemoto, H. Kuraishi, K. Komagata, R. Azuma, T. Suto, and H. Murooka, *J. Gen. Appl. Microbiol.*, **24**, 199 (1978).

COMMUNICATIONS

Mean Hepatic Transit Time in the Determination of Mean Absorption Time

Keyphrases □ Mean hepatic transit time—determination of mean absorption time, pharmacokinetics □ Mean absorption time—determination by mean hepatic transit time, pharmacokinetics □ Pharmacokinetics—mean hepatic transit time, mean absorption time, mean residence time

To the Editor:

In recent studies the statistical moment theory has been employed to estimate mean absorption time (MAT) of drugs (1–5). The MAT has been defined as the mean time of a molecule (1) or the mean residence time (MRT) of all molecules (2) from a dosage form (such as solution or tablet) spent at the input site (GI lumen in the case of oral administration) before being absorbed into the general circulation. The MAT after oral administration has been calculated based on the following equation (1–5):

$$MAT = MRT_{po} - MRT_{iv} \qquad \text{(Eq. 1)}$$

where MRT_{po} is the MRT of the orally absorbed drug molecules in the body, and MRT_{iv} is the MRT of intravenously (usually from a peripheral vein in the leg or arm) administered drug molecules in the body. Both plasma and urinary excretion data have been proposed to estimate the MRT_{po} and MRT_{iv}. When a solution dosage form is studied, the calculated MAT has been referred to as mean intrinsic absorption time (5). When both solution and solid dosage forms are evaluated, the difference in their MRT may be considered to equal the mean *in vivo* dissolution time (MDT) from the solid dosage form. This is based on the assumption that once released from the solid dosage form, it is subject to the same influence as the drug administered in solution (1–3).

The main purpose of this communication is to discuss a complication in using Eq. 1 to determine the MAT. Its potential significance in absorption rate calculations and hepatic clearance studies will also be briefly mentioned. In analogy to the above assumption requirement in the determination of MDT, use of Eq. 1 must also require that the orally absorbed drug is handled in the body exactly the same way as that administered intravenously. This demand apparently can not be met because the orally absorbed drug has to pass through the GI wall and then the liver before entering the heart, while the intravenously administered drug can be carried almost instantaneously from the injection site to the heart before being distributed to the rest of body. The mean time to pass through the GI wall and liver can be called mean GI wall transit time, MTT_{GI}, and mean hepatic transit time, MTT_h, respectively. The portal circulation between the GI wall and liver is extremely fast and can be ignored. Therefore, Eq. 1 can be modified to:

$$MAT = MRT_{po} - MRT_{iv} - MTT_{GI} - MTT_h \qquad \text{(Eq. 2)}$$

The MTT in a tissue or organ during a single passage can be determined directly by instantaneous injection of a compound into the affluent blood and monitoring of effluent blood concentration, C_{out}, under the single-pass nonrecirculating condition (6–8):

$$MTT = \frac{\int_0^\infty tC_{out}dt}{\int_0^\infty C_{out}dt} \qquad \text{(Eq. 3)}$$

0022-3549/83/1100-1365$01.00/0

In linear pharmacokinetics it can also be estimated by (6–9):

$$MTT = V_{ss}/Q \qquad \text{(Eq. 4)}$$

where V_{ss} is the apparent (effective) steady-state volume of distribution of the tissue or organ for a given drug and Q is the blood flow rate through that tissue or organ. In view of the fast blood flow through the small section (with a limited tissue mass during each passage) of major GI absorption sites (usually in the small intestine) the MTT_{GI} may be expected to be relatively short or negligible for most drugs except those with extremely high binding property. Furthermore, the precise location and fraction absorbed at each location usually can not be ascertained. Therefore, under most circumstances the MTT_{GI} probably can be ignored.

The V_{ss} for the liver may be estimated by (10, 11):

$$V_{ss} = V_b + R_h V_h \qquad \text{(Eq. 5)}$$

where V_b is the volume of blood in the liver, R_h is the hepatic tissue–venous blood partition coefficient of drug, and V_h is the hepatic tissue volume (excluding blood). For a normal 70-kg human adult the V_b, V_h, and Q_h can be assumed to be 0.37, 1.5, and 1.58 liters/min, respectively (12, 13). Substitution of the above values into Eqs. 4 and 5 will result in the following equation for estimating the MTT_h for various drugs in human adults:

$$MTT_h \text{ in min} = (0.37 + 1.5R_h)/1.58 \qquad \text{(Eq. 6)}$$

The actual determination of R_h values in normal humans is extremely difficult or virtually impossible under practical circumstances. In view of the many reported successes in interspecies scaling in pharmacokinetic studies (11, 13–15) R_h values of several drugs in animals reported or estimated from the literature (15–18) will be used here for the purpose of illustration; as an approximation, the drug is also assumed to be instantaneously (19, 20) and evenly distributed in whole blood. The results of the calculation are summarized in Table I. The MTT_h obtained ranged from 0.52 min for tolbutamide to 977 min (16.3 hr) for chloroquine. The unusually long transit times estimated here for chloroquine and hydroxychloroquine (12.8 hr) during a single passage through the liver are somewhat of a surprise. These results indicate that for chloroquine and hydroxychloroquine it may take an average of more than 10 hr before they are transported from the liver by the blood stream or before they are metabolized by the liver following absorption. The MTT_h for the blood across the liver, on the other hand, can be estimated to be only 0.234 min (0.37/1.58) or 14 sec, which is only slightly higher than the values of 8.4 and 9.0 sec, reported earlier in the dog (7) and rat (21), respectively. It should be noted that the blood MTT across hepatic sinusoids, where diffusion of drug into hepatocytes for biotransformation and/or biliary excretion takes place, could be 36% shorter (7).

Table I—Mean Hepatic Transit Times (MTT_h) of Several Drugs in Humans Estimated Based on the Hepatic Tissue–Plasma Concentration Ratios (R_h) Obtained from Animal Studies

Drug[a]	Animal Species for R_h value	R_h	MTT_h (min)
Sulfobromophthalein (15)	Rat	7.0	6.9
Digoxin (15)	Dog	15.8	15.2
Dactinomycin (15)	Dog	32.2	30.8
Doxorubicin (15)	Rabbit	60.4	57.6[c]
Tolbutamide (16)	Rat	0.30	0.52
Chlorpheniramine (10, 17)[b]	Rabbit	31.4	30.0
Chloroquine (18)	Rat	1029.0	977.0[d]
Hydroxychloroquine (18)	Rat	811.0	770.0[d]

[a] Number in parentheses is reference number. [b] Correction was made for hepatic extraction ratio of 0.89 (17) based on ref. 11. [c] An actual value of 57 min was calculated for the rat based on the rat liver perfusion data (see text for detail). [d] These values might be considerably overestimated (see text for detail).

The possibility of a long MTT_h (57.6 min) for doxorubicin in humans (Table I) seems to be substantiated by results of analysis of rat (200–250 g of body weight) liver perfusion data recently reported by Skibba *et al.* (22). The plasma level (μg/ml) *versus* time (min) profile in the reservoir following a bolus dose of 2250 μg of doxorubicin could be approximated by the following biexponential equation, $1.2e^{-0.0711t} + 2.1e^{-0.0041t}$. The estimated V_{ss} based on the standard method (23) was 1003 ml. Since the reservoir had a volume of 150 ml the V_{ss} for the liver should be 853 ml. With that estimated V_{ss} and a Q of 15 ml/min used in their study, one could estimate the MTT_h (based on Eq. 4) to be 57 min.

The true MTT_h of chloroquine in humans might be considerably shorter than estimated here if its distribution between plasma and red blood cells could take place very rapidly, since its concentration in red blood cells has been shown to be much higher (~10 times) than that in plasma (24). The uptake of chloroquine by human red blood cells has been shown to follow saturable kinetics and not to be "instantaneous" (25). Therefore, it appears reasonable to assume that the estimated MTT_h for chloroquine shown in Table I might be either slightly or markedly overestimated. This probably was the case with hydroxychloroquine as well.

The above concepts and findings may be of importance in our study of MAT and the process of GI absorption. They indicate that the conventional method (Eq. 1) may significantly overestimate the true MAT. For digoxin, dactinomycin, doxorubicin, chlorpheniramine, and chloroquine, these overestimations might be 16, 32, 60, 30, and 977 min, respectively (Table I). In theory, the MRT_{po} should be always greater than the MRT_{iv}, even if all the drug is instantaneously absorbed through the GI tract. The degree of differences may vary tremendously with drugs that depends largely on their R_h values (Table I), although the size of the liver and the blood flow may also be important. In this regard it is of interest to point out that in patients with congestive heart failure, hepatic flow might be greatly reduced, and the volume of blood in the liver greatly increased [*i.e.*, up to one extra liter (26)]. Therefore, hepatic transit time for drugs or blood might be much longer than in normal subjects. It is likely that a drug with a larger steady-state volume of distribution in the body would tend to have a longer MTT_h.

It appears that in theory the MTT_h should also be a function of the hepatic extraction ratio, as shown for ethanol (27). For example, when the extraction ratio is unity, no drug molecules will be transported to the general circulation. Therefore, the calculated MTT_h will be zero.

When all drug molecules diffusing out of the hepatic sinusoids are eliminated through biotransformation and/or biliary excretion, the MTT_h for those remaining molecules will essentially equal that for blood. On the other hand, the MTT_h would become the longest for a given drug when the extraction ratio is zero (*i.e.*, no hepatic elimination). Under this condition, transit times for those molecules penetrating hepatic tissues deeply and/or binding strongly hepatic tissues will all be "counted" in the determination of MTT_h for all molecules. Therefore, the data presented in Table I probably represent average values with "normal" hepatic functions.

The MRT analysis has been regarded generally as being model independent. However, it has been shown recently that it might be subject to the influence of the blood-sampling site (28, 29). Although disposition kinetics in the whole body are best represented by systemic arterial data, use of venous data in the MDT analysis should be satisfactory as long as the same site is used for blood sampling throughout the study; this is also true with the MAT analysis shown in Eq. 1 or 2.

In the calculation of MRT_{iv} plasma-level data are most often described by polyexponential equations assuming that the injected drug is instantaneously and homogeneously (kinetically speaking) distributed to the plasma (central) compartment or initial volume of distribution. Such a concept has been questioned recently (29–33). Its potential effect on the determination of MRT_{iv} and MAT seems apparent.

The concept of hepatic first-pass transit times discussed in this communication may also be important in the evaluation of rates of oral absorption using conventional compartmental or deconvolution methods (34–38). This is consistent with an early study (39) which suggested that in the oral absorption rate calculation the calculated rate is based on the same reference sampling point (such as from an arm vein) between intravenous and oral studies. Since one is really only interested in the rate of absorption across the GI membrane, the conventional methods of calculation (34–38) may tend to underestimate the true rate of absorption due to the first "stop" or "trap" in the liver. The extensive trapping in and subsequent slow release from the liver apparently could account for the peculiar peripheral venous plasma level profile of doxorubicin following 30 min of constant intraarterial hepatic infusion to a patient (40). Plasma levels at 10 and 30 min after the beginning of peripheral intravenous infusion of the same dose 3 days later could be estimated (Fig. 1 of ref. 40) to be ~12 and 7 times higher than from the first infusion. The plasma level from intrahepatic infusion started to rise only 60 min after the end of infusion and was 3.3 times higher than from the intravenous infusion 90 min later. Using the 10-min data, the conventional methods would predict the rate of intraarterial infusion or absorption to be only one-twelfth the intravenous infusion. In other words, the infusion or absorption rate could be underestimated by about 92%. This phenomenon might also have occurred in the three dogs receiving portal venous dosing of propranolol in a previous study (41). The infusion rate was repeatedly reduced by ~two-thirds every 7.5 min for 45 min. Systemic arterial propranolol levels were the lowest at the end of the highest rate of infusion (Fig. 5 of ref. 41). One dog peaked at 30 min, another at 60 min, and a third dog plateaued between 20 and 40 min. On the other hand, the highest plasma concentrations were found in the other two dogs studied almost immediately after the same highest rate of infusion (41). The maximum difference at the end of the highest infusion among the five dogs studied could be estimated to be ~150-fold. This dramatic difference was probably primarily a result of the difference in hepatic transit time during the first passage since the plasma levels were quite similar during later periods. Unusually extensive uptake of propranolol by the liver following oral or hepatic portal administration (up to 10 mg/kg) to rats has also been reported (42, 43). The uptake has also been shown (42, 43) to be dependent on the route and dose of administration, thus further complicating the MAT calculation using Eq. 1 or 2.

The concepts of hepatic transit times discussed in this communication also may be useful in the design and evaluation of intrahepatic administration regimens and in the study of hepatic clearance of drugs. The importance of finite hepatic blood transit times and metabolite transfer times in metabolism has been extensively discussed recently (21, 44).

(1) D. J. Cutler, *J. Pharm. Pharmacol.*, **30**, 476 (1978).

(2) K. Yamaoka, T. Nakagawa, and T. Uno, *J. Pharmacokinet. Biopharm.*, **6**, 547 (1978).

(3) S. Riegelman and P. Collier, *J. Pharmacokinet. Biopharm.*, **8**, 509 (1980).

(4) Y. Tanigawara, K. Yamaoka, T. Nakagawa, and T. Uno, *Chem. Pharm. Bull.*, **30**, 2174 (1982).

(5) Y. Tanigawara, K. Yamaoka, T. Nakagawa, and T. Uno, *J. Pharm. Sci.*, **71**, 1129 (1982).

(6) P. Meier and K. L. Zierler, *J. Appl. Physiol.*, **6**, 731 (1954).

(7) C. A. Goresky, *Am. J. Physiol.*, **204**, 626 (1963).

(8) J. B. Bassingthwaighte, *Science*, **167**, 1347 (1970).

(9) J. M. van Rossum, J. Burgers, G. van Lingen, and J. de Bie, *Trends Pharmacol. Sci.*, **4**, 27 (1983).

(10) S. M. Huang and W. L. Chiou, *J. Pharmacokinet. Biopharm.*, **9**, 711 (1981) (references therein).

(11) G. Lam, M. L. Chen, and W. L. Chiou, *J. Pharm. Sci.*, **71**, 454 (1982) (references therein).

(12) W. W. Mapleson, *J. Appl. Physiol.*, **18**, 197 (1963).

(13) R. H. Smith, D. H. Hunt, A. B. Seifen, A. Ferrari, and D. S. Thompson, *J. Pharm. Sci.*, **68**, 1016 (1979).

(14) H. Boxenbaum, *J. Pharmacokinet. Biopharm.*, **10**, 201 (1982).

(15) H. S. G. Chen and J. F. Gross, *J. Pharmacokinet. Biopharm.*, **7**, 117 (1979).

(16) O. Sugita, Y. Sawada, Y. Sugiyama, T. Iga, and M. Hanano, *J. Pharmacokinet. Biopharm.*, **10**, 297 (1982).

(17) S. M. Huang, Y. C. Huang, and W. L. Chiou, *J. Pharmacokinet. Biopharm.*, **9**, 725 (1981).

(18) E. W. McChesney, W. F. Banks, Jr., and R. J. Fabian, *Toxicol. Appl. Pharmacol.*, **10**, 501 (1967).

(19) M. G. Lee, M. L. Chen, and W. L. Chiou, *Res. Commun. Chem. Pathol. Pharmacol.*, **34**, 17 (1981).

(20) M. L. Chen, M. G. Lee, and W. L. Chiou, *J. Pharm. Sci.*, **72**, 572 (1983).

(21) K. S. Pang, L. Waller, M. G. Horning, and K. K. Chan, *J. Pharmacol. Exp. Ther.*, **222**, 14 (1982).

(22) J. L. Skibba, F. E. Jones, and R. E. Condon, *Cancer Treat. Rep.*, **66**, 1357 (1982).

(23) W. L. Chiou, *Int. J. Clin. Pharmacol. Ther. Toxicol.*, **20**, 255 (1982).

(24) S. A. Adelusi, A. H. Dawodu, and L. A. Salako, *Br. J. Clin. Pharmacol.*, **14**, 483 (1982).

(25) A. Yayon and H. Ginsberg, *Anal. Biochem.*, **107**, 322 (1980).

(26) A. C. Guyton, "Textbook of Medical Physiology," W. B. Saunders, Philadelphia, Pa., 1971, p. 369.

(27) C. A. Goresky, E. R. Gordon, and G. G. Bach, *Am. J. Physiol.*, **244**, G198 (1983).

(28) W. L. Chiou, G. Lam, M. L. Chen, and M. G. Lee, *Res. Commun. Chem. Pathol. Pharmacol.*, **35**, 17 (1982).

(29) M. L. Chen, G. Lam, M. G. Lee, and W. L. Chiou, *J. Pharm. Sci.*, **71**, 1386 (1982).
(30) W. L. Chiou, G. Lam, M. L. Chen, and M. G. Lee, *J. Pharm. Sci.*, **70**, 1037 (1981).
(31) W. L. Chiou and G. Lam, *Int. J. Clin. Pharmacol. Ther. Toxicol.*, **20**, 197 (1982).
(32) S. Bojholm, O. B. Paulson, and H. Flachs, *Clin. Pharmacol. Ther.*, **32**, 478 (1982).
(33) J. D. Huang and S. Øie, *J. Pharm. Sci.*, **71**, 1421 (1982).
(34) J. C. K. Loo and S. Riegelman, *J. Pharm. Sci.*, **57**, 918 (1968) (references therein).
(35) A. E. Till, L. Z. Benet, and K. C. Kavan, *J. Pharmacokinet. Biopharm.*, **2**, 525 (1974) (references therein).
(36) P. Veng-Pedersen, *J. Pharmacokinet. Biopharm.*, **8**, 463 (1980) (references therein).
(37) W. L. Chiou, *J. Pharm. Sci.*, **69**, 57 (1980) (references therein).
(38) D. Cutler, *Pharmacol. Ther.*, **4**, 123 (1981) (references therein).
(39) M. Rowland, L. Z. Benet, and G. G. Graham, *J. Pharmacokinet. Biopharm.*, **1**, 123 (1973).
(40) Y. N. Lee, K. K. Chan, P. A. Harris, and J. L. Cohen, *Cancer*, **45**, 2231 (1980).
(41) C. F. George, M. L. Orme, P. Buranapong, D. Macerlean, A. M. Breckenridge, and C. T. Dollery, *J. Pharmacokinet. Biopharm.*, **4**, 17 (1976).
(42) D. S. Shand and R. E. Rangno, *Pharmacology*, **7**, 159 (1972).
(43) T. Rikihisa, T. Ohkuama, M. Mori, M. Otsuka, and T. Suzuki, *Chem. Pharm. Bull.*, **29**, 2035 (1981).
(44) K. S. Pang, *Drug Metab. Rev.*, **14**, 61 (1983).

Win L. Chiou
Department of Pharmacodynamics
College of Pharmacy
University of Illinois at Chicago
Chicago, IL 60612

Received March 15, 1983.
Accepted for publication July 19, 1983.
This research was supported in part by a grant from the National Cancer Institute, CA-29754-03.

Errors in Estimating the Unbound Fraction of Drugs Due to the Volume Shift in Equilibrium Dialysis

Keyphrases □ Equilibrium dialysis—volume shift, unbound fraction of drug □ Unbound fraction of drugs—equilibrium dialysis, volume shift

To the Editor:

Equilibrium dialysis is commonly used to estimate serum protein binding of drugs. Consideration of the influence of the volume shift on the unbound fraction has, however, not been addressed until recently (1). The water flux from the buffer side to the serum side during dialysis causes binding protein dilution as well as an overestimation of the unbound fraction. The overestimation is dependent on the extent of the volume shift, the unbound fraction of drugs, and the concentration dependency of binding. Correction for the volume shift is important when the volume shift is substantial and when the unbound fraction of drugs is small.

The molarity of macromolecules in undiluted serum sample is ~1 m*M*, which gives 0.025 atm (263 mm H_2O) of osmotic pressure at 37°. The pressure causes water to migrate from the buffer side to the serum side (1) and expands the dialysis membrane. Because the serum sample is not completely restrained in the dialysis cells and the dialysis membrane, the hydrostatic pressure due to the volume shift is always less than the osmotic pressure. Osmotic equilibrium is actually never reached in this type of equilibrium dialysis. The extent of the volume shift depends on the time used for dialysis. Tozer *et al.* (1) reported an average volume shift of 31% in 16-hr dialysis. Using the same type of dialysis cells and dialysis membrane, we experienced an average volume shift of 10% in 4–6 hr of dialysis. Undue water flux can be avoided by a judicious choice of equilibration time.

Assuming that binding follows the law of mass action, the unbound fraction (f_u) of a drug that has multiple binding sites on a serum binding protein can be expressed as follows:

$$f_u = 1 \Big/ \left[1 + \mathrm{Pt} \sum_{i=1}^{n} 1/(C_u + K\mathrm{d}_i)\right] \qquad \text{(Eq. 1)}$$

where $K\mathrm{d}_i$ is the dissociation constant for binding site i, Pt is the total concentration of binding sites, and C_u is the measured unbound drug concentration. The extent of the volume shift can be defined as the ratio of serum volume before (V_s) and after ($V_{s'}$) dialysis and expressed as:

$$\mathrm{F} = V_s/V_{s'} = \mathrm{Pt}'/\mathrm{Pt} \qquad \text{(Eq. 2)}$$

where Pt′ is the concentration of binding sites after dialysis. In assessing the importance of the volume shift correction, the unbound fractions, with and without water flux correction, need to be compared. Assuming the unbound concentration to be the same with and without a water flux, the unbound fraction without correction for volume shift ($f_{u'}$) is related to the unbound fraction with volume shift correction by:

$$f_{u'} = f_u/[\mathrm{F} \cdot (1 - f_u) + f_u] \qquad \text{(Eq. 3)}$$

or

$$f_u = f_{u'} \cdot \mathrm{F}/(f_{u'} \cdot \mathrm{F} + 1 - f_{u'}) \qquad \text{(Eq. 4)}$$

(See *Appendix* for derivation.) Neglecting the volume shift, the fractional error [$\mathrm{E} = (f_{u'} - f_u)/f_u$] in calculating the unbound fraction is:

$$\mathrm{E} = (1 - \mathrm{F}) \cdot (1 - f_u)/[\mathrm{F} \cdot (1 - f_u) + f_u] \qquad \text{(Eq. 5)}$$

or

$$\mathrm{E} = (1 - \mathrm{F}) \cdot (1 - f_{u'})/\mathrm{F} \qquad \text{(Eq. 6)}$$

It is apparent from Eqs. 5 and 6 that when the volume shift is <10% (F > 0.9), the error introduced in neglecting volume shift is <11%, which is not critical in comparison with other errors in the protein binding determination. However, if the volume shift is >10% and the unbound fraction calculated without the volume shift correction is <0.9, the volume shift should always be considered in calculating the unbound fraction. Equation 4 can be used for the volume shift correction provided that the binding is not concentration dependent in the measured concentration range.

When equilibrium dialysis is used to determine the unbound fraction of a drug with concentration-dependent binding, the transfer of drug from the serum side to the buffer side causes a decrease in the drug concentration on the serum side with a subsequent decrease in the unbound fraction of the drug (1, 2). The complicated correction

0022-3549/83/1100-1368$01.00/0

(29) M. L. Chen, G. Lam, M. G. Lee, and W. L. Chiou, *J. Pharm. Sci.*, **71**, 1386 (1982).
(30) W. L. Chiou, G. Lam, M. L. Chen, and M. G. Lee, *J. Pharm. Sci.*, **70**, 1037 (1981).
(31) W. L. Chiou and G. Lam, *Int. J. Clin. Pharmacol. Ther. Toxicol.*, **20**, 197 (1982).
(32) S. Bojholm, O. B. Paulson, and H. Flachs, *Clin. Pharmacol. Ther.*, **32**, 478 (1982).
(33) J. D. Huang and S. Øie, *J. Pharm. Sci.*, **71**, 1421 (1982).
(34) J. C. K. Loo and S. Riegelman, *J. Pharm. Sci.*, **57**, 918 (1968) (references therein).
(35) A. E. Till, L. Z. Benet, and K. C. Kavan, *J. Pharmacokinet. Biopharm.*, **2**, 525 (1974) (references therein).
(36) P. Veng-Pedersen, *J. Pharmacokinet. Biopharm.*, **8**, 463 (1980) (references therein).
(37) W. L. Chiou, *J. Pharm. Sci.*, **69**, 57 (1980) (references therein).
(38) D. Cutler, *Pharmacol. Ther.*, **4**, 123 (1981) (references therein).
(39) M. Rowland, L. Z. Benet, and G. G. Graham, *J. Pharmacokinet. Biopharm.*, **1**, 123 (1973).
(40) Y. N. Lee, K. K. Chan, P. A. Harris, and J. L. Cohen, *Cancer*, **45**, 2231 (1980).
(41) C. F. George, M. L. Orme, P. Buranapong, D. Macerlean, A. M. Breckenridge, and C. T. Dollery, *J. Pharmacokinet. Biopharm.*, **4**, 17 (1976).
(42) D. S. Shand and R. E. Rangno, *Pharmacology*, **7**, 159 (1972).
(43) T. Rikihisa, T. Ohkuama, M. Mori, M. Otsuka, and T. Suzuki, *Chem. Pharm. Bull.*, **29**, 2035 (1981).
(44) K. S. Pang, *Drug Metab. Rev.*, **14**, 61 (1983).

Win L. Chiou
Department of Pharmacodynamics
College of Pharmacy
University of Illinois at Chicago
Chicago, IL 60612

Received March 15, 1983.
Accepted for publication July 19, 1983.
This research was supported in part by a grant from the National Cancer Institute, CA-29754-03.

Errors in Estimating the Unbound Fraction of Drugs Due to the Volume Shift in Equilibrium Dialysis

Keyphrases □ Equilibrium dialysis—volume shift, unbound fraction of drug □ Unbound fraction of drugs—equilibrium dialysis, volume shift

To the Editor:

Equilibrium dialysis is commonly used to estimate serum protein binding of drugs. Consideration of the influence of the volume shift on the unbound fraction has, however, not been addressed until recently (1). The water flux from the buffer side to the serum side during dialysis causes binding protein dilution as well as an overestimation of the unbound fraction. The overestimation is dependent on the extent of the volume shift, the unbound fraction of drugs, and the concentration dependency of binding. Correction for the volume shift is important when the volume shift is substantial and when the unbound fraction of drugs is small.

The molarity of macromolecules in undiluted serum sample is ~1 m*M*, which gives 0.025 atm (263 mm H_2O) of osmotic pressure at 37°. The pressure causes water to migrate from the buffer side to the serum side (1) and expands the dialysis membrane. Because the serum sample is not completely restrained in the dialysis cells and the dialysis membrane, the hydrostatic pressure due to the volume shift is always less than the osmotic pressure. Osmotic equilibrium is actually never reached in this type of equilibrium dialysis. The extent of the volume shift depends on the time used for dialysis. Tozer *et al.* (1) reported an average volume shift of 31% in 16-hr dialysis. Using the same type of dialysis cells and dialysis membrane, we experienced an average volume shift of 10% in 4–6 hr of dialysis. Undue water flux can be avoided by a judicious choice of equilibration time.

Assuming that binding follows the law of mass action, the unbound fraction (f_u) of a drug that has multiple binding sites on a serum binding protein can be expressed as follows:

$$f_u = 1 \Big/ \left[1 + \mathrm{Pt} \sum_{i=1}^{n} 1/(C_u + K\mathrm{d}_i)\right] \qquad \text{(Eq. 1)}$$

where $K\mathrm{d}_i$ is the dissociation constant for binding site i, Pt is the total concentration of binding sites, and C_u is the measured unbound drug concentration. The extent of the volume shift can be defined as the ratio of serum volume before (V_s) and after ($V_{s'}$) dialysis and expressed as:

$$\mathrm{F} = V_s/V_{s'} = \mathrm{Pt}'/\mathrm{Pt} \qquad \text{(Eq. 2)}$$

where Pt′ is the concentration of binding sites after dialysis. In assessing the importance of the volume shift correction, the unbound fractions, with and without water flux correction, need to be compared. Assuming the unbound concentration to be the same with and without a water flux, the unbound fraction without correction for volume shift ($f_{u'}$) is related to the unbound fraction with volume shift correction by:

$$f_{u'} = f_u/[\mathrm{F} \cdot (1 - f_u) + f_u] \qquad \text{(Eq. 3)}$$

or

$$f_u = f_{u'} \cdot \mathrm{F}/(f_{u'} \cdot \mathrm{F} + 1 - f_{u'}) \qquad \text{(Eq. 4)}$$

(See *Appendix* for derivation.) Neglecting the volume shift, the fractional error [$\mathrm{E} = (f_{u'} - f_u)/f_u$] in calculating the unbound fraction is:

$$\mathrm{E} = (1 - \mathrm{F}) \cdot (1 - f_u)/[\mathrm{F} \cdot (1 - f_u) + f_u] \qquad \text{(Eq. 5)}$$

or

$$\mathrm{E} = (1 - \mathrm{F}) \cdot (1 - f_{u'})/\mathrm{F} \qquad \text{(Eq. 6)}$$

It is apparent from Eqs. 5 and 6 that when the volume shift is <10% (F > 0.9), the error introduced in neglecting volume shift is <11%, which is not critical in comparison with other errors in the protein binding determination. However, if the volume shift is >10% and the unbound fraction calculated without the volume shift correction is <0.9, the volume shift should always be considered in calculating the unbound fraction. Equation 4 can be used for the volume shift correction provided that the binding is not concentration dependent in the measured concentration range.

When equilibrium dialysis is used to determine the unbound fraction of a drug with concentration-dependent binding, the transfer of drug from the serum side to the buffer side causes a decrease in the drug concentration on the serum side with a subsequent decrease in the unbound fraction of the drug (1, 2). The complicated correction

0022-3549/83/1100-1368$01.00/0

method suggested by Tozer *et al.*, which corrects for both the volume shift and concentration-dependent binding, becomes necessary in calculating unbound fraction of a concentration-dependent binding drug such as prednisolone (1).

Although Eqs. 3 and 4 were derived under the assumption that drugs bind to a single-binding protein with multiple binding sites, the equations can be used as a good approximation to the correct unbound fractions for drugs that bind to two or more different binding proteins. For example, for a drug with two classes of binding sites, one having high capacity (600 μM) but low affinity (Kd = 100 μM), and the other having low capacity (20 μM) but high affinity (Kd = 1 μM), shows an unbound fraction of 0.04 at 0.1 μM drug concentration (Eq. 3A). A 30% volume shift gives a 40% error in unbound fraction ($f_{u'}$ = 0.056, Eq. 4A). Equation 4 can be used to convert $f_{u'}$ to f_u with good accuracy (f_u calculated = 0.04).

The extent of volume shift is usually determined by measuring the sample volume before and after equilibrium dialysis. Practically, it is not easy to determine the sample volume accurately after dialysis. It would be advisable instead to measure the binding protein concentration before and after dialysis and apply for correction calculations.

APPENDIX

The unbound fraction of a drug is by definition:

$$f_u = C_u \Big/ \left(C_u + \sum_{i=1}^{n} Cb_i\right) \qquad \text{(Eq. 1A)}$$

where $\sum_{i=1}^{n} Cb_i$ is the sum of concentrations of drugs bound to different binding sites. Based on the law of mass action, Cb_i can be expressed as:

$$Cb_i = C_u \cdot Pt_i/(Kd_i + C_u) \qquad \text{(Eq. 2A)}$$

and Eq. 1A can be written as:

$$f_u = 1 \Big/ \left[1 + \sum_{i=1}^{n} Pt_i/(Kd_i + C_u)\right] \qquad \text{(Eq. 3A)}$$

and

$$f_{u'} = 1 \Big/ \left[1 + \sum_{i=1}^{n} Pt_{i'}/(Kd_i + C_u)\right] \qquad \text{(Eq. 4A)}$$

Assuming a single binding protein with multiple binding sites, Eq. 3A can be simplified to be Eq. 1 and $f_{u'}$ is equal to:

$$f_{u'} = 1 \Big/ \left[1 + Pt' \sum_{i=1}^{n} 1/(C_u + Kd_i)\right] \qquad \text{(Eq. 5A)}$$

Letting

$$S = \sum_{i=1}^{n} 1/(C_u + Kd_i) \qquad \text{(Eq. 6A)}$$

Eq. 1 can be rearranged to:

$$S = (1 - f_u)/(f_u \cdot Pt) \qquad \text{(Eq. 7A)}$$

Substituting Eq. 7A into Eq. 5A, gives:

$$f_{u'} = 1/[1 + Pt' \cdot (1 - f_u)/(f_u \cdot Pt)] \qquad \text{(Eq. 8A)}$$

where Pt'/Pt is equal to F (Eq. 2). Substituting F into Eq. 8A gives Eq. 3. Similarly, Eq. 5A can be rearranged to:

$$S = (1 - f_{u'})/(f_{u'} \cdot Pt') \qquad \text{(Eq. 9A)}$$

Substituting Eqs. 2 and 9A into Eq. 1, Eq. 4 is derived.

(1) T. N. Tozer, J. G. Gambertolio, D. E. Furst, D. S. Avery, and N. H. G. Holford, *J. Pharm. Sci.*, in press (1983).

(2) H. L. Behm and J. G. Wagner, *Res. Commun. Chem. Pathol. Pharmacol.*, **26**, 145 (1979).

Jin-ding Huang
National Taiwan University
School of Pharmacy
Taipei, Taiwan
Republic of China

Received May 16, 1983.
Accepted for publication July 28, 1983.

Rate of Recovery from Fazadinium: Relationship to the Rate of Decline of its Plasma Concentration

Keyphrases □ Fazadinium—rate of recovery, relationship to plasma concentration, pharmacokinetics □ Pharmacokinetics—fazadinium, rate of recovery, relationship to plasma concentration

To the Editor:

Fazadinium bromide, introduced into anesthetic practice in 1972, is of clinical interest as a short-acting neuromuscular blocking agent. An approach is presented here which strongly suggests that the differences in the rate of recovery from the neuromuscular blocking effects of fazadinium are solely dependent on the pharmacokinetics of the relaxant. This approach is not new in that it was first presented on theoretical grounds more than a decade ago and utilized with recovery data for succinylcholine in both neonates and adults (1, 2).

If the claim (3) that fazadinium is eliminated by apparent first-order kinetics is true, and if it can be assumed that its metabolite(s) are inactive (4), then the duration (t) of the neuromuscular blocking action of fazadinium and the rate of decline (R) of the effect (paralysis) in the linear (20–80% or 25–75%) range can be related according to the following equations, as derived for succinylcholine (1, 2):

$$t = (2.3/k_{10})(\log A^0 - \log A_{min}) \qquad \text{(Eq. 1)}$$

$$R = m(k_{10}/2.3) \qquad \text{(Eq. 2)}$$

Table I—Pharmacokinetic Analysis of Recovery from the Neuromuscular Blocking Effects of Fazadinium [a]

Patient	Duration (t)[b], min	Rate of Decline (R)[c], % min^{-1}	$t \times R$, %	$k_{app\ 25\text{–}75}$[d], min^{-1}
3	14	3.57	49.98	−0.0382
4	22	2.27	49.94	−0.0286
5	24	2.08	49.92	−0.0210
1	26	1.92	49.92	−0.0251
2	27	1.85	49.95	−0.0219
6	34	1.47	49.98	−0.0149

[a] Based on data from ref. 3. [b] Time interval when the twitch height was depressed between 25 and 75% of its control value: between 75 and 25% muscle paralysis. [c] Rate of recovery in the 75–25% paralysis range. [d] $k_{app\ 25\text{–}75} = (\log C_{25} - \log C_{75}/t_{25} - t_{75})$ where C and t are the plasma concentrations and times respectively at 25 and 75% effect levels.

0022-3549/83/1100-1369$01.00/0

method suggested by Tozer *et al.*, which corrects for both the volume shift and concentration-dependent binding, becomes necessary in calculating unbound fraction of a concentration-dependent binding drug such as prednisolone (1).

Although Eqs. 3 and 4 were derived under the assumption that drugs bind to a single-binding protein with multiple binding sites, the equations can be used as a good approximation to the correct unbound fractions for drugs that bind to two or more different binding proteins. For example, for a drug with two classes of binding sites, one having high capacity (600 μM) but low affinity (Kd = 100 μM), and the other having low capacity (20 μM) but high affinity (Kd = 1 μM), shows an unbound fraction of 0.04 at 0.1 μM drug concentration (Eq. 3A). A 30% volume shift gives a 40% error in unbound fraction ($f_{u'}$ = 0.056, Eq. 4A). Equation 4 can be used to convert $f_{u'}$ to f_u with good accuracy (f_u calculated = 0.04).

The extent of volume shift is usually determined by measuring the sample volume before and after equilibrium dialysis. Practically, it is not easy to determine the sample volume accurately after dialysis. It would be advisable instead to measure the binding protein concentration before and after dialysis and apply for correction calculations.

APPENDIX

The unbound fraction of a drug is by definition:

$$f_u = C_u \Big/ \left(C_u + \sum_{i=1}^{n} Cb_i\right) \qquad \text{(Eq. 1A)}$$

where $\sum_{i=1}^{n} Cb_i$ is the sum of concentrations of drugs bound to different binding sites. Based on the law of mass action, Cb_i can be expressed as:

$$Cb_i = C_u \cdot Pt_i/(Kd_i + C_u) \qquad \text{(Eq. 2A)}$$

and Eq. 1A can be written as:

$$f_u = 1 \Big/ \left[1 + \sum_{i=1}^{n} Pt_i/(Kd_i + C_u)\right] \qquad \text{(Eq. 3A)}$$

and

$$f_{u'} = 1 \Big/ \left[1 + \sum_{i=1}^{n} Pt_{i'}/(Kd_i + C_u)\right] \qquad \text{(Eq. 4A)}$$

Assuming a single binding protein with multiple binding sites, Eq. 3A can be simplified to be Eq. 1 and $f_{u'}$ is equal to:

$$f_{u'} = 1 \Big/ \left[1 + Pt' \sum_{i=1}^{n} 1/(C_u + Kd_i)\right] \qquad \text{(Eq. 5A)}$$

Letting

$$S = \sum_{i=1}^{n} 1/(C_u + Kd_i) \qquad \text{(Eq. 6A)}$$

Eq. 1 can be rearranged to:

$$S = (1 - f_u)/(f_u \cdot Pt) \qquad \text{(Eq. 7A)}$$

Substituting Eq. 7A into Eq. 5A, gives:

$$f_{u'} = 1/[1 + Pt' \cdot (1 - f_u)/(f_u \cdot Pt)] \qquad \text{(Eq. 8A)}$$

where Pt'/Pt is equal to F (Eq. 2). Substituting F into Eq. 8A gives Eq. 3. Similarly, Eq. 5A can be rearranged to:

$$S = (1 - f_{u'})/(f_{u'} \cdot Pt') \qquad \text{(Eq. 9A)}$$

Substituting Eqs. 2 and 9A into Eq. 1, Eq. 4 is derived.

(1) T. N. Tozer, J. G. Gambertolio, D. E. Furst, D. S. Avery, and N. H. G. Holford, *J. Pharm. Sci.*, in press (1983).

(2) H. L. Behm and J. G. Wagner, *Res. Commun. Chem. Pathol. Pharmacol.*, **26**, 145 (1979).

Jin-ding Huang
National Taiwan University
School of Pharmacy
Taipei, Taiwan
Republic of China

Received May 16, 1983.
Accepted for publication July 28, 1983.

Rate of Recovery from Fazadinium: Relationship to the Rate of Decline of its Plasma Concentration

Keyphrases □ Fazadinium—rate of recovery, relationship to plasma concentration, pharmacokinetics □ Pharmacokinetics—fazadinium, rate of recovery, relationship to plasma concentration

To the Editor:

Fazadinium bromide, introduced into anesthetic practice in 1972, is of clinical interest as a short-acting neuromuscular blocking agent. An approach is presented here which strongly suggests that the differences in the rate of recovery from the neuromuscular blocking effects of fazadinium are solely dependent on the pharmacokinetics of the relaxant. This approach is not new in that it was first presented on theoretical grounds more than a decade ago and utilized with recovery data for succinylcholine in both neonates and adults (1, 2).

If the claim (3) that fazadinium is eliminated by apparent first-order kinetics is true, and if it can be assumed that its metabolite(s) are inactive (4), then the duration (t) of the neuromuscular blocking action of fazadinium and the rate of decline (R) of the effect (paralysis) in the linear (20–80% or 25–75%) range can be related according to the following equations, as derived for succinylcholine (1, 2):

$$t = (2.3/k_{10})(\log A^0 - \log A_{min}) \qquad \text{(Eq. 1)}$$

$$R = m(k_{10}/2.3) \qquad \text{(Eq. 2)}$$

Table I—Pharmacokinetic Analysis of Recovery from the Neuromuscular Blocking Effects of Fazadinium [a]

Patient	Duration (t)[b], min	Rate of Decline (R)[c], % min^{-1}	$t \times R$, %	$k_{app\ 25\text{–}75}$[d], min^{-1}
3	14	3.57	49.98	−0.0382
4	22	2.27	49.94	−0.0286
5	24	2.08	49.92	−0.0210
1	26	1.92	49.92	−0.0251
2	27	1.85	49.95	−0.0219
6	34	1.47	49.98	−0.0149

[a] Based on data from ref. 3. [b] Time interval when the twitch height was depressed between 25 and 75% of its control value: between 75 and 25% muscle paralysis. [c] Rate of recovery in the 75–25% paralysis range. [d] $k_{app\ 25\text{–}75} = (\log C_{25} - \log C_{75}/t_{25} - t_{75})$ where C and t are the plasma concentrations and times respectively at 25 and 75% effect levels.

0022-3549/83/1100-1369$01.00/0

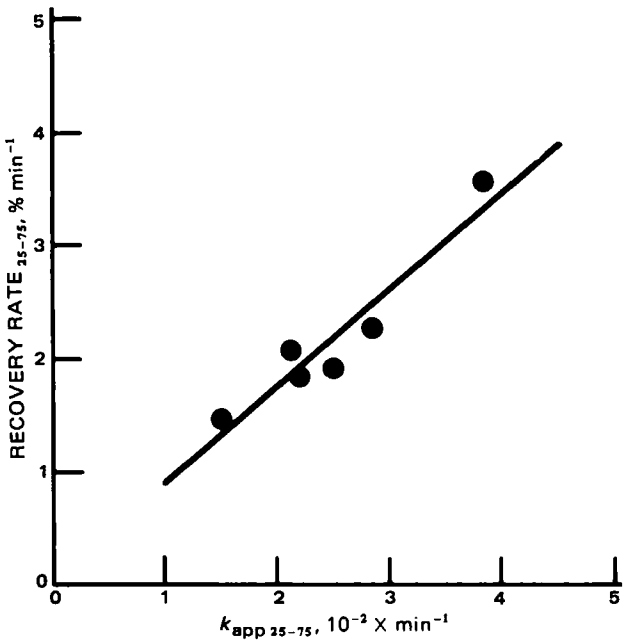

Figure 1—*Relationship between the rate of recovery from the neuromuscular blocking effects of fazadinium and the calculated* $k_{app\ 25-75}$. *Individual patient data are shown as solid circles while the solid line represents the linear regression line* ($r^2 = 0.897$, $p < 0.005$).

$$t \times R = m(\log A^0 - \log A_{min}) \qquad \text{(Eq. 3)}$$

where k_{10} is the apparent first-order rate constant for drug elimination from its site of action, A_{min} is the minimum effective dose, and m is the slope of the log dose (A^0) response relationship for the relaxant. Thus, according to the above three equations, four pharmacokinetic factors determine the duration and rate of decline of effect, with three of these terms (m, A^0, and A_{min}) appearing on the right side of Eq. 3, while k_{10} is implicit on the left-hand side but cancels out as such. Thus, in a group of patients given the same drug dose but showing different durations of effect, the product of duration (t) and rate of decline (R) of effect will yield a constant value if the differences in the observed time course of effect are solely the result of differences in k_{10}, the elimination rate constant. If, however, the values of $t \times R$ differ between the patients, then it must be concluded that these patients differ with respect to m and/or A_{min} and/or k_{10}.

The results obtained from the six patients in the study by D'Hollander *et al.* (3) are listed in Table I, with the numerical designations used by these authors but in order of increasing duration of effect. It can be seen that although the six patients differed in the duration (t) and the rate of decline (R) from the effects of fazadinium, the $t \times R$ values were identical for all the patients, implying that the differences in the rate of recovery from the neuromuscular effects of fazadinium in these six patients were solely due to a difference in the rate of elimination of the relaxant from the body. This claim is further supported by the finding that $k_{app\ 25-75}$, the apparent rate of decline of the (log) plasma concentration, which is a measure of the elimination rate of the relaxant during the linear (25–75%) phase of recovery, was different in each of the six patients and there was an excellent linear relationship between the *rate* of recovery from fazadinium and the calculated $k_{app\ 25-75}$ (Fig. 1).

(1) G. Levy, *Anesthesiology*, **32**, 551 (1970).
(2) G. Levy, *Br. J. Anaesth.*, **42**, 979 (1970).
(3) A. A. D'Hollander, P. Duvaldestin, D. Henzel, C. Delcroix, and J. M. Desmonts, *Br. J. Anaesth.*, **53**, 853 (1981).
(4) B. Srinivasan, C. Wahdi, and B. Pleuvry, *J. Pharm. Pharmacol.*, **25**, 657 (1973).

Iqbal M. Ramzan
Department of Pharmaceutics
State University of New York at Buffalo
Amherst, NY 14260

Received April 29, 1983.
Accepted for publication August 16, 1983.

BOOKS

REVIEWS

Pharmacokinetics, 2nd Ed. By MILO GIBALDI and DONALD PERRIER. Marcel Dekker, 270 Madison Avenue, New York, NY 11016. 1982. 494 pp. 16 × 23 cm. Price: $34.50 (20% higher outside the U.S. and Canada).

The second edition of this now classic text detailing the mathematical description of pharmacokinetics has been greatly expanded and updated over the previous edition. One of the most important new aspects to be presented is the comprehensive discussion of clearance concepts, flow models, and physiological modeling, which has given the new text a much broader scope while at the same time introduces the reader to new concepts presented over the last few years. In addition, an overview depicting the usefulness of statistical moments in pharmacokinetics is presented, a concept being explored extensively in the pharmacokinetic literature today which should prove useful to both the established researcher and the student. The new material added to the text is, in general, approached (as is the mark of these authors) in a detailed, step-by-step procedure that renders the work especially useful to novices and subsequently makes it an important teaching tool.

It is important to note that not only have new chapters and topics been added, but that the majority of the original text has undergone revision, expansion, and addition of new material. The majority of the equations have been generalized, thereby making them useful in a variety of models. Although the generalization makes the edition slightly less useful as a reference book for pharmacokinetic relationships, it is most illustrative for teaching purposes in demonstrating the generalities of kinetic models. Without too much effort, the generalized equations can readily be converted to relationships that can be applied in specific situations. The authors have also added a more philosophical overview to the various concepts that increase the understanding of many of the equations and relationships presented.

Other interesting additions to the second edition are the kinetics of irreversible pharmacological response, product inhibition aspects of nonlinear kinetics, and various aspects of protein binding in relation in pharmacokinetics. Although the discussion dealing with protein binding is often divergent from what this reviewer believes to be a rational development of the relationship between protein binding and pharmacokinetics, it is a valuable and instructive addition, especially in lieu of the paucity of such discussions.

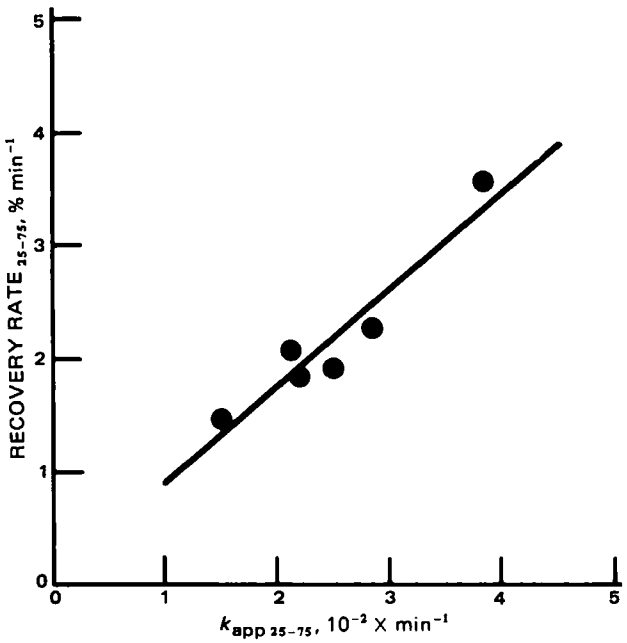

Figure 1—*Relationship between the rate of recovery from the neuromuscular blocking effects of fazadinium and the calculated* $k_{app\ 25-75}$. *Individual patient data are shown as solid circles while the solid line represents the linear regression line* ($r^2 = 0.897$, $p < 0.005$).

$$t \times R = m(\log A^0 - \log A_{min}) \qquad \text{(Eq. 3)}$$

where k_{10} is the apparent first-order rate constant for drug elimination from its site of action, A_{min} is the minimum effective dose, and m is the slope of the log dose (A^0) response relationship for the relaxant. Thus, according to the above three equations, four pharmacokinetic factors determine the duration and rate of decline of effect, with three of these terms (m, A^0, and A_{min}) appearing on the right side of Eq. 3, while k_{10} is implicit on the left-hand side but cancels out as such. Thus, in a group of patients given the same drug dose but showing different durations of effect, the product of duration (t) and rate of decline (R) of effect will yield a constant value if the differences in the observed time course of effect are solely the result of differences in k_{10}, the elimination rate constant. If, however, the values of $t \times R$ differ between the patients, then it must be concluded that these patients differ with respect to m and/or A_{min} and/or k_{10}.

The results obtained from the six patients in the study by D'Hollander *et al.* (3) are listed in Table I, with the numerical designations used by these authors but in order of increasing duration of effect. It can be seen that although the six patients differed in the duration (t) and the rate of decline (R) from the effects of fazadinium, the $t \times R$ values were identical for all the patients, implying that the differences in the rate of recovery from the neuromuscular effects of fazadinium in these six patients were solely due to a difference in the rate of elimination of the relaxant from the body. This claim is further supported by the finding that $k_{app\ 25-75}$, the apparent rate of decline of the (log) plasma concentration, which is a measure of the elimination rate of the relaxant during the linear (25–75%) phase of recovery, was different in each of the six patients and there was an excellent linear relationship between the *rate* of recovery from fazadinium and the calculated $k_{app\ 25-75}$ (Fig. 1).

(1) G. Levy, *Anesthesiology*, **32**, 551 (1970).
(2) G. Levy, *Br. J. Anaesth.*, **42**, 979 (1970).
(3) A. A. D'Hollander, P. Duvaldestin, D. Henzel, C. Delcroix, and J. M. Desmonts, *Br. J. Anaesth.*, **53**, 853 (1981).
(4) B. Srinivasan, C. Wahdi, and B. Pleuvry, *J. Pharm. Pharmacol.*, **25**, 657 (1973).

Iqbal M. Ramzan
Department of Pharmaceutics
State University of New York at Buffalo
Amherst, NY 14260

Received April 29, 1983.
Accepted for publication August 16, 1983.

BOOKS

REVIEWS

Pharmacokinetics, 2nd Ed. By MILO GIBALDI and DONALD PERRIER. Marcel Dekker, 270 Madison Avenue, New York, NY 11016. 1982. 494 pp. 16 × 23 cm. Price: $34.50 (20% higher outside the U.S. and Canada).

The second edition of this now classic text detailing the mathematical description of pharmacokinetics has been greatly expanded and updated over the previous edition. One of the most important new aspects to be presented is the comprehensive discussion of clearance concepts, flow models, and physiological modeling, which has given the new text a much broader scope while at the same time introduces the reader to new concepts presented over the last few years. In addition, an overview depicting the usefulness of statistical moments in pharmacokinetics is presented, a concept being explored extensively in the pharmacokinetic literature today which should prove useful to both the established researcher and the student. The new material added to the text is, in general, approached (as is the mark of these authors) in a detailed, step-by-step procedure that renders the work especially useful to novices and subsequently makes it an important teaching tool.

It is important to note that not only have new chapters and topics been added, but that the majority of the original text has undergone revision, expansion, and addition of new material. The majority of the equations have been generalized, thereby making them useful in a variety of models. Although the generalization makes the edition slightly less useful as a reference book for pharmacokinetic relationships, it is most illustrative for teaching purposes in demonstrating the generalities of kinetic models. Without too much effort, the generalized equations can readily be converted to relationships that can be applied in specific situations. The authors have also added a more philosophical overview to the various concepts that increase the understanding of many of the equations and relationships presented.

Other interesting additions to the second edition are the kinetics of irreversible pharmacological response, product inhibition aspects of nonlinear kinetics, and various aspects of protein binding in relation in pharmacokinetics. Although the discussion dealing with protein binding is often divergent from what this reviewer believes to be a rational development of the relationship between protein binding and pharmacokinetics, it is a valuable and instructive addition, especially in lieu of the paucity of such discussions.

After extensive scrutinization this reviewer can find only a few areas that may be considered for changes in future editions: 1. The use of natural logarithms instead of log to the base of 10. This will remove the always difficult task by students of deciding when to use the correction factor 2.303. 2. The use of the current concept of clearance throughout the book, not just in segments; *i.e.*, treating clearance as a fundamental pharmacokinetic parameter throughout the book rather than being dependent on volume of distribution and fractional rates (*i.e.*, elimination rate constant).

In summary, this is a substantially expanded version of the first edition, and as a comprehensive and logically developed text, it will probably enjoy an even higher readership than its predecessor. A must for all pharmacokineticists.

Reviewed by Svein Øie
Department of Pharmacy
School of Pharmacy
University of California
San Francisco, CA 94143

Chromatography and Mass Spectrometry in Biomedical Sciences 2. (Analytical Chemistry Symposia Series 14). Edited by A. FRIGERIO. Elsevier/North Holland, 52 Vanderbilt Avenue, New York, N.Y. 10017. 1983. 506 pp. 16 × 24 cm. Price $106.50 (Dfl. 250).

This book contains the proceedings of the International Conference on Chromatography and Mass Spectrometry in Biomedical Sciences, held in Bordighera, Italy, in June 1982. There are five plenary lectures on five topics. Three of these lectures are on techniques such as combined gas chromatography–Fourier transform infrared spectroscopy, quantitative ion-exchange thin-layer chromatography, and tandem mass spectrometry (MS–MS). They represent the state of the art on each of the techniques and are well written. The other two plenary lectures are on "Recent Applications of Mass Spectrometry to Cannabinoid Studies" and "Chromatographic Techniques for Determination of Some Calcium Antagonist Drugs in Biological Fluids." Both of these presentations, as well as the previous three lectures, are worth reading. The rest of the papers presented or given as poster sessions at this meeting are widely varied, from drug studies to environmental analysis, where the techniques applied include the use of radioimmunoassay, high-performance liquid chromatography, thin-layer chromatography, gas chromatography, and combined techniques of gas chromatography–mass spectrometry. Like any other conference there are some good papers, some average in quality, and some which do not add anything new to the use of chromatography and mass spectrometry in the biomedical or environmental fields.

Since this book covers a very broad spectrum of techniques and subjects, it can not be recommended for anyone seeking an in-depth discussion on any particular subject. It certainly can be recommended for those who want an overview of the state of the art and current thinking of chromatography and mass spectrometry.

Reviewed by Kamal K. Midha
College of Pharmacy
University of Saskatchewan
Saskatoon S7N 0W0, Saskatchewan, Canada

New Drug Parade: A Historical Minireview 1954–1982. By PAUL DE HAEN. Paul de Haen International, Inc., 2750 S. Shoshone Street, Englewood, CO 80110. 1983. 22 × 28 cm. Price $25.00.

New Drug Review: A Historical Minireview offers a statistical and descriptive tabulation of major new drug introductions in the United States from 1954 to present, including single chemical entities, duplicate single products, combination products, and new dosage forms. Major drugs introduced each year are listed by trade name, generic name, manufacturer, therapeutic use, chemical class, and foreign developer. The listed drugs have been selected on the basis of chemical innovation and therapeutic advantages.

In addition to the statistical and descriptive information, the publication includes brief comments for each year on such significant events as the state of research, trends in the pharmaceutical industry, and the relationship between the industry and governmental agencies. Also included are pertinent references to the original reports in *Drug and Cosmetic Industry* and secondary citations of the press comments, editorials, and reprint history. Following the individual information for each year is an overview of the entire period, including summary statistics.

—Staff Review

NOTICES

Basic Documents, 33rd Ed. World Health Organization, Geneva, Switzerland. 1983. 176 pp. 16 × 24 cm. Price Sw. Fr. 12.

Cancer Incidence in Five Continents, Vol. IV. (IARC Scientific Publications No. 42). Edited by J. A. H. WATERHOUSE, C. S. MUIR, K. SHANMUGARATNAM, and J. POWELL. World Health Organization, 1211 Geneva 27, Switzerland. 1982. 812 pp. 22 × 30 cm. Price $50.00 (Sw. Fr. 100).

Cancer Incidence in Singapore 1968–1977. By K. SHANMUGARATNAM, H. P. LEE, and N. E. DAY. World Health Organization, International Agency for Research on Cancer, Singapore Cancer Registry, Lyon, France. 1983. 171 pp. 21 × 29.8 cm. Price $15.00 (Sw. Fr. 30).

Catalog of Teratogenic Agents, 4th Ed. By THOMAS H. SHEPARD. The Johns Hopkins University Press, Baltimore, MD 21218. 1983. 529 pp. 16 × 24 cm. Price $35.00.

Chronopharmakologie—Tagesrhythmen und Arzneimittelwirkung, By BJORN LEMMER. Wissenschaftliche Verlagsgesellschaft mbH Stuttgart, Birkenwaldstrasse 44, 7000 Stuttgart 1, West Germany. 1983. 100 pp. 15.5 × 23 cm. Price DM 29.

Circular Dichroic Spectroscopy: Excition Coupling in Organic Stereochemistry. By NOBUYUKI HARADA and KOJI NAKANISHI. University Science Books, 20 Edgehill Road, Mill Valley, CA 94941. 1983. 460 pp. 21 × 24 cm. Price $32.00.

Complying With FDA Good Manufacturing Practice Requirements: How to Develop Your GMP/QA Manual. By JOHN J. RIORDAN and WILLIAM COTLIAR. Association for the Advancement of Medical Instrumentation, 1901 N. Fort Myer Drive, Arlington, VA 22209. 1983. 201 pp. 22 × 28 cm. Price $65.00 ($50.00 for AAMI members.)

Depressive Disorders in Different Countries. World Health Organization, Geneva, Switzerland. 1983. 150 pp. 16 × 24 cm. Price Sw. Fr. 17.

Dermal and Transdermal Absorption. Edited by RAINER BRANDAU and BARBEL H. LIPPOLD. Wissenschaftliche Verlagsgesellschaft mbH, Postfach 40, D-7000 Stuttgart 1, West Germany. 1982. 257 pp. 15 × 23 cm. Price DM 88, fur Bezieher, DM 70.50 der Reihe.

Drug Benefit Formulary, No. 19, July 1983. PARCOST Comparative Drug Index. The Ministry of Health, Ontario, Canada. 1983. 214 pp. 14.8 × 20.9 cm. Price $1.00.

Drug Treatment in Obstetrics: A Handbook of Prescribing. By R. S. LEDWARD and D. F. HAWKINS. Methuen, 733 Third Avenue, New York, NY 10017. 1983. 262 pp. 12.4 × 18.6 cm. Price $29.00 (cloth), $13.95 (paperback).

Drug Utilization in Norway During the 1970s—Increases, Inequalities, Innovations. Edited by SOLVEIG SAKSHAUG, MARIT ANDREW, PETER F. HJORT, PETER KNUT M. LUNDR, and KARE ØYDVIN. Norwegian Medicinal Depot, P.O. Box 100, Vietvet, Oslo 5, Norway. 1983. 271 pp. 15 × 21 cm. Paperback.

Eleventh Annual Report, 1982: World Health Organization Special Programme of Research Development and Research Training in Human Reproduction. World Health Organization, Geneva, Switzerland. 1982. 159 pp. 18.5 × 24 cm.

Environmental Carcinogens—Selected Methods for Analysis, Vol. 5: Mycotoxins. (IARC Scientific Publications No. 44). Editor-in-Chief, H. EGAN. World Health Organization, 1211 Geneva 27, Switzerland. 1982. 455 pp. 19 × 25 cm. Price $30.00 (Sw. Fr. 60).

After extensive scrutinization this reviewer can find only a few areas that may be considered for changes in future editions: 1. The use of natural logarithms instead of log to the base of 10. This will remove the always difficult task by students of deciding when to use the correction factor 2.303. 2. The use of the current concept of clearance throughout the book, not just in segments; *i.e.*, treating clearance as a fundamental pharmacokinetic parameter throughout the book rather than being dependent on volume of distribution and fractional rates (*i.e.*, elimination rate constant).

In summary, this is a substantially expanded version of the first edition, and as a comprehensive and logically developed text, it will probably enjoy an even higher readership than its predecessor. A must for all pharmacokineticists.

Reviewed by Svein Øie
Department of Pharmacy
School of Pharmacy
University of California
San Francisco, CA 94143

Chromatography and Mass Spectrometry in Biomedical Sciences 2. (Analytical Chemistry Symposia Series 14). Edited by A. FRIGERIO. Elsevier/North Holland, 52 Vanderbilt Avenue, New York, N.Y. 10017. 1983. 506 pp. 16 × 24 cm. Price $106.50 (Dfl. 250).

This book contains the proceedings of the International Conference on Chromatography and Mass Spectrometry in Biomedical Sciences, held in Bordighera, Italy, in June 1982. There are five plenary lectures on five topics. Three of these lectures are on techniques such as combined gas chromatography–Fourier transform infrared spectroscopy, quantitative ion-exchange thin-layer chromatography, and tandem mass spectrometry (MS–MS). They represent the state of the art on each of the techniques and are well written. The other two plenary lectures are on "Recent Applications of Mass Spectrometry to Cannabinoid Studies" and "Chromatographic Techniques for Determination of Some Calcium Antagonist Drugs in Biological Fluids." Both of these presentations, as well as the previous three lectures, are worth reading. The rest of the papers presented or given as poster sessions at this meeting are widely varied, from drug studies to environmental analysis, where the techniques applied include the use of radioimmunoassay, high-performance liquid chromatography, thin-layer chromatography, gas chromatography, and combined techniques of gas chromatography–mass spectrometry. Like any other conference there are some good papers, some average in quality, and some which do not add anything new to the use of chromatography and mass spectrometry in the biomedical or environmental fields.

Since this book covers a very broad spectrum of techniques and subjects, it can not be recommended for anyone seeking an in-depth discussion on any particular subject. It certainly can be recommended for those who want an overview of the state of the art and current thinking of chromatography and mass spectrometry.

Reviewed by Kamal K. Midha
College of Pharmacy
University of Saskatchewan
Saskatoon S7N 0W0, Saskatchewan, Canada

New Drug Parade: A Historical Minireview 1954–1982. By PAUL DE HAEN. Paul de Haen International, Inc., 2750 S. Shoshone Street, Englewood, CO 80110. 1983. 22 × 28 cm. Price $25.00.

New Drug Review: A Historical Minireview offers a statistical and descriptive tabulation of major new drug introductions in the United States from 1954 to present, including single chemical entities, duplicate single products, combination products, and new dosage forms. Major drugs introduced each year are listed by trade name, generic name, manufacturer, therapeutic use, chemical class, and foreign developer. The listed drugs have been selected on the basis of chemical innovation and therapeutic advantages.

In addition to the statistical and descriptive information, the publication includes brief comments for each year on such significant events as the state of research, trends in the pharmaceutical industry, and the relationship between the industry and governmental agencies. Also included are pertinent references to the original reports in *Drug and Cosmetic Industry* and secondary citations of the press comments, editorials, and reprint history. Following the individual information for each year is an overview of the entire period, including summary statistics.

—Staff Review

NOTICES

Basic Documents, 33rd Ed. World Health Organization, Geneva, Switzerland. 1983. 176 pp. 16 × 24 cm. Price Sw. Fr. 12.

Cancer Incidence in Five Continents, Vol. IV. (IARC Scientific Publications No. 42). Edited by J. A. H. WATERHOUSE, C. S. MUIR, K. SHANMUGARATNAM, and J. POWELL. World Health Organization, 1211 Geneva 27, Switzerland. 1982. 812 pp. 22 × 30 cm. Price $50.00 (Sw. Fr. 100).

Cancer Incidence in Singapore 1968–1977. By K. SHANMUGARATNAM, H. P. LEE, and N. E. DAY. World Health Organization, International Agency for Research on Cancer, Singapore Cancer Registry, Lyon, France. 1983. 171 pp. 21 × 29.8 cm. Price $15.00 (Sw. Fr. 30).

Catalog of Teratogenic Agents, 4th Ed. By THOMAS H. SHEPARD. The Johns Hopkins University Press, Baltimore, MD 21218. 1983. 529 pp. 16 × 24 cm. Price $35.00.

Chronopharmakologie—Tagesrhythmen und Arzneimittelwirkung, By BJORN LEMMER. Wissenschaftliche Verlagsgesellschaft mbH Stuttgart, Birkenwaldstrasse 44, 7000 Stuttgart 1, West Germany. 1983. 100 pp. 15.5 × 23 cm. Price DM 29.

Circular Dichroic Spectroscopy: Excition Coupling in Organic Stereochemistry. By NOBUYUKI HARADA and KOJI NAKANISHI. University Science Books, 20 Edgehill Road, Mill Valley, CA 94941. 1983. 460 pp. 21 × 24 cm. Price $32.00.

Complying With FDA Good Manufacturing Practice Requirements: How to Develop Your GMP/QA Manual. By JOHN J. RIORDAN and WILLIAM COTLIAR. Association for the Advancement of Medical Instrumentation, 1901 N. Fort Myer Drive, Arlington, VA 22209. 1983. 201 pp. 22 × 28 cm. Price $65.00 ($50.00 for AAMI members.)

Depressive Disorders in Different Countries. World Health Organization, Geneva, Switzerland. 1983. 150 pp. 16 × 24 cm. Price Sw. Fr. 17.

Dermal and Transdermal Absorption. Edited by RAINER BRANDAU and BARBEL H. LIPPOLD. Wissenschaftliche Verlagsgesellschaft mbH, Postfach 40, D-7000 Stuttgart 1, West Germany. 1982. 257 pp. 15 × 23 cm. Price DM 88, fur Bezieher, DM 70.50 der Reihe.

Drug Benefit Formulary, No. 19, July 1983. PARCOST Comparative Drug Index. The Ministry of Health, Ontario, Canada. 1983. 214 pp. 14.8 × 20.9 cm. Price $1.00.

Drug Treatment in Obstetrics: A Handbook of Prescribing. By R. S. LEDWARD and D. F. HAWKINS. Methuen, 733 Third Avenue, New York, NY 10017. 1983. 262 pp. 12.4 × 18.6 cm. Price $29.00 (cloth), $13.95 (paperback).

Drug Utilization in Norway During the 1970s—Increases, Inequalities, Innovations. Edited by SOLVEIG SAKSHAUG, MARIT ANDREW, PETER F. HJORT, PETER KNUT M. LUNDR, and KARE ØYDVIN. Norwegian Medicinal Depot, P.O. Box 100, Vietvet, Oslo 5, Norway. 1983. 271 pp. 15 × 21 cm. Paperback.

Eleventh Annual Report, 1982: World Health Organization Special Programme of Research Development and Research Training in Human Reproduction. World Health Organization, Geneva, Switzerland. 1982. 159 pp. 18.5 × 24 cm.

Environmental Carcinogens—Selected Methods for Analysis, Vol. 5: Mycotoxins. (IARC Scientific Publications No. 44). Editor-in-Chief, H. EGAN. World Health Organization, 1211 Geneva 27, Switzerland. 1982. 455 pp. 19 × 25 cm. Price $30.00 (Sw. Fr. 60).

After extensive scrutinization this reviewer can find only a few areas that may be considered for changes in future editions: 1. The use of natural logarithms instead of log to the base of 10. This will remove the always difficult task by students of deciding when to use the correction factor 2.303. 2. The use of the current concept of clearance throughout the book, not just in segments; *i.e.*, treating clearance as a fundamental pharmacokinetic parameter throughout the book rather than being dependent on volume of distribution and fractional rates (*i.e.*, elimination rate constant).

In summary, this is a substantially expanded version of the first edition, and as a comprehensive and logically developed text, it will probably enjoy an even higher readership than its predecessor. A must for all pharmacokineticists.

Reviewed by Svein Øie
Department of Pharmacy
School of Pharmacy
University of California
San Francisco, CA 94143

Chromatography and Mass Spectrometry in Biomedical Sciences 2. (Analytical Chemistry Symposia Series 14). Edited by A. FRIGERIO. Elsevier/North Holland, 52 Vanderbilt Avenue, New York, N.Y. 10017. 1983. 506 pp. 16 × 24 cm. Price $106.50 (Dfl. 250).

This book contains the proceedings of the International Conference on Chromatography and Mass Spectrometry in Biomedical Sciences, held in Bordighera, Italy, in June 1982. There are five plenary lectures on five topics. Three of these lectures are on techniques such as combined gas chromatography–Fourier transform infrared spectroscopy, quantitative ion-exchange thin-layer chromatography, and tandem mass spectrometry (MS–MS). They represent the state of the art on each of the techniques and are well written. The other two plenary lectures are on "Recent Applications of Mass Spectrometry to Cannabinoid Studies" and "Chromatographic Techniques for Determination of Some Calcium Antagonist Drugs in Biological Fluids." Both of these presentations, as well as the previous three lectures, are worth reading. The rest of the papers presented or given as poster sessions at this meeting are widely varied, from drug studies to environmental analysis, where the techniques applied include the use of radioimmunoassay, high-performance liquid chromatography, thin-layer chromatography, gas chromatography, and combined techniques of gas chromatography–mass spectrometry. Like any other conference there are some good papers, some average in quality, and some which do not add anything new to the use of chromatography and mass spectrometry in the biomedical or environmental fields.

Since this book covers a very broad spectrum of techniques and subjects, it can not be recommended for anyone seeking an in-depth discussion on any particular subject. It certainly can be recommended for those who want an overview of the state of the art and current thinking of chromatography and mass spectrometry.

Reviewed by Kamal K. Midha
College of Pharmacy
University of Saskatchewan
Saskatoon S7N 0W0, Saskatchewan, Canada

New Drug Parade: A Historical Minireview 1954–1982. By PAUL DE HAEN. Paul de Haen International, Inc., 2750 S. Shoshone Street, Englewood, CO 80110. 1983. 22 × 28 cm. Price $25.00.

New Drug Review: A Historical Minireview offers a statistical and descriptive tabulation of major new drug introductions in the United States from 1954 to present, including single chemical entities, duplicate single products, combination products, and new dosage forms. Major drugs introduced each year are listed by trade name, generic name, manufacturer, therapeutic use, chemical class, and foreign developer. The listed drugs have been selected on the basis of chemical innovation and therapeutic advantages.

In addition to the statistical and descriptive information, the publication includes brief comments for each year on such significant events as the state of research, trends in the pharmaceutical industry, and the relationship between the industry and governmental agencies. Also included are pertinent references to the original reports in *Drug and Cosmetic Industry* and secondary citations of the press comments, editorials, and reprint history. Following the individual information for each year is an overview of the entire period, including summary statistics.

—Staff Review

NOTICES

Basic Documents, 33rd Ed. World Health Organization, Geneva, Switzerland. 1983. 176 pp. 16 × 24 cm. Price Sw. Fr. 12.

Cancer Incidence in Five Continents, Vol. IV. (IARC Scientific Publications No. 42). Edited by J. A. H. WATERHOUSE, C. S. MUIR, K. SHANMUGARATNAM, and J. POWELL. World Health Organization, 1211 Geneva 27, Switzerland. 1982. 812 pp. 22 × 30 cm. Price $50.00 (Sw. Fr. 100).

Cancer Incidence in Singapore 1968–1977. By K. SHANMUGARATNAM, H. P. LEE, and N. E. DAY. World Health Organization, International Agency for Research on Cancer, Singapore Cancer Registry, Lyon, France. 1983. 171 pp. 21 × 29.8 cm. Price $15.00 (Sw. Fr. 30).

Catalog of Teratogenic Agents, 4th Ed. By THOMAS H. SHEPARD. The Johns Hopkins University Press, Baltimore, MD 21218. 1983. 529 pp. 16 × 24 cm. Price $35.00.

Chronopharmakologie—Tagesrhythmen und Arzneimittelwirkung, By BJORN LEMMER. Wissenschaftliche Verlagsgesellschaft mbH Stuttgart, Birkenwaldstrasse 44, 7000 Stuttgart 1, West Germany. 1983. 100 pp. 15.5 × 23 cm. Price DM 29.

Circular Dichroic Spectroscopy: Excition Coupling in Organic Stereochemistry. By NOBUYUKI HARADA and KOJI NAKANISHI. University Science Books, 20 Edgehill Road, Mill Valley, CA 94941. 1983. 460 pp. 21 × 24 cm. Price $32.00.

Complying With FDA Good Manufacturing Practice Requirements: How to Develop Your GMP/QA Manual. By JOHN J. RIORDAN and WILLIAM COTLIAR. Association for the Advancement of Medical Instrumentation, 1901 N. Fort Myer Drive, Arlington, VA 22209. 1983. 201 pp. 22 × 28 cm. Price $65.00 ($50.00 for AAMI members.)

Depressive Disorders in Different Countries. World Health Organization, Geneva, Switzerland. 1983. 150 pp. 16 × 24 cm. Price Sw. Fr. 17.

Dermal and Transdermal Absorption. Edited by RAINER BRANDAU and BARBEL H. LIPPOLD. Wissenschaftliche Verlagsgesellschaft mbH, Postfach 40, D-7000 Stuttgart 1, West Germany. 1982. 257 pp. 15 × 23 cm. Price DM 88, fur Bezieher, DM 70.50 der Reihe.

Drug Benefit Formulary, No. 19, July 1983. PARCOST Comparative Drug Index. The Ministry of Health, Ontario, Canada. 1983. 214 pp. 14.8 × 20.9 cm. Price $1.00.

Drug Treatment in Obstetrics: A Handbook of Prescribing. By R. S. LEDWARD and D. F. HAWKINS. Methuen, 733 Third Avenue, New York, NY 10017. 1983. 262 pp. 12.4 × 18.6 cm. Price $29.00 (cloth), $13.95 (paperback).

Drug Utilization in Norway During the 1970s—Increases, Inequalities, Innovations. Edited by SOLVEIG SAKSHAUG, MARIT ANDREW, PETER F. HJORT, PETER KNUT M. LUNDR, and KARE ØYDVIN. Norwegian Medicinal Depot, P.O. Box 100, Vietvet, Oslo 5, Norway. 1983. 271 pp. 15 × 21 cm. Paperback.

Eleventh Annual Report, 1982: World Health Organization Special Programme of Research Development and Research Training in Human Reproduction. World Health Organization, Geneva, Switzerland. 1982. 159 pp. 18.5 × 24 cm.

Environmental Carcinogens—Selected Methods for Analysis, Vol. 5: Mycotoxins. (IARC Scientific Publications No. 44). Editor-in-Chief, H. EGAN. World Health Organization, 1211 Geneva 27, Switzerland. 1982. 455 pp. 19 × 25 cm. Price $30.00 (Sw. Fr. 60).

After extensive scrutinization this reviewer can find only a few areas that may be considered for changes in future editions: 1. The use of natural logarithms instead of log to the base of 10. This will remove the always difficult task by students of deciding when to use the correction factor 2.303. 2. The use of the current concept of clearance throughout the book, not just in segments; *i.e.*, treating clearance as a fundamental pharmacokinetic parameter throughout the book rather than being dependent on volume of distribution and fractional rates (*i.e.*, elimination rate constant).

In summary, this is a substantially expanded version of the first edition, and as a comprehensive and logically developed text, it will probably enjoy an even higher readership than its predecessor. A must for all pharmacokineticists.

Reviewed by Svein Øie
Department of Pharmacy
School of Pharmacy
University of California
San Francisco, CA 94143

Chromatography and Mass Spectrometry in Biomedical Sciences 2. (Analytical Chemistry Symposia Series 14). Edited by A. FRIGERIO. Elsevier/North Holland, 52 Vanderbilt Avenue, New York, N.Y. 10017. 1983. 506 pp. 16 × 24 cm. Price $106.50 (Dfl. 250).

This book contains the proceedings of the International Conference on Chromatography and Mass Spectrometry in Biomedical Sciences, held in Bordighera, Italy, in June 1982. There are five plenary lectures on five topics. Three of these lectures are on techniques such as combined gas chromatography–Fourier transform infrared spectroscopy, quantitative ion-exchange thin-layer chromatography, and tandem mass spectrometry (MS–MS). They represent the state of the art on each of the techniques and are well written. The other two plenary lectures are on "Recent Applications of Mass Spectrometry to Cannabinoid Studies" and "Chromatographic Techniques for Determination of Some Calcium Antagonist Drugs in Biological Fluids." Both of these presentations, as well as the previous three lectures, are worth reading. The rest of the papers presented or given as poster sessions at this meeting are widely varied, from drug studies to environmental analysis, where the techniques applied include the use of radioimmunoassay, high-performance liquid chromatography, thin-layer chromatography, gas chromatography, and combined techniques of gas chromatography–mass spectrometry. Like any other conference there are some good papers, some average in quality, and some which do not add anything new to the use of chromatography and mass spectrometry in the biomedical or environmental fields.

Since this book covers a very broad spectrum of techniques and subjects, it can not be recommended for anyone seeking an in-depth discussion on any particular subject. It certainly can be recommended for those who want an overview of the state of the art and current thinking of chromatography and mass spectrometry.

Reviewed by Kamal K. Midha
College of Pharmacy
University of Saskatchewan
Saskatoon S7N 0W0, Saskatchewan, Canada

New Drug Parade: A Historical Minireview 1954–1982. By PAUL DE HAEN. Paul de Haen International, Inc., 2750 S. Shoshone Street, Englewood, CO 80110. 1983. 22 × 28 cm. Price $25.00.

New Drug Review: A Historical Minireview offers a statistical and descriptive tabulation of major new drug introductions in the United States from 1954 to present, including single chemical entities, duplicate single products, combination products, and new dosage forms. Major drugs introduced each year are listed by trade name, generic name, manufacturer, therapeutic use, chemical class, and foreign developer. The listed drugs have been selected on the basis of chemical innovation and therapeutic advantages.

In addition to the statistical and descriptive information, the publication includes brief comments for each year on such significant events as the state of research, trends in the pharmaceutical industry, and the relationship between the industry and governmental agencies. Also included are pertinent references to the original reports in *Drug and Cosmetic Industry* and secondary citations of the press comments, editorials, and reprint history. Following the individual information for each year is an overview of the entire period, including summary statistics.

—Staff Review

NOTICES

Basic Documents, 33rd Ed. World Health Organization, Geneva, Switzerland. 1983. 176 pp. 16 × 24 cm. Price Sw. Fr. 12.

Cancer Incidence in Five Continents, Vol. IV. (IARC Scientific Publications No. 42). Edited by J. A. H. WATERHOUSE, C. S. MUIR, K. SHANMUGARATNAM, and J. POWELL. World Health Organization, 1211 Geneva 27, Switzerland. 1982. 812 pp. 22 × 30 cm. Price $50.00 (Sw. Fr. 100).

Cancer Incidence in Singapore 1968–1977. By K. SHANMUGARATNAM, H. P. LEE, and N. E. DAY. World Health Organization, International Agency for Research on Cancer, Singapore Cancer Registry, Lyon, France. 1983. 171 pp. 21 × 29.8 cm. Price $15.00 (Sw. Fr. 30).

Catalog of Teratogenic Agents, 4th Ed. By THOMAS H. SHEPARD. The Johns Hopkins University Press, Baltimore, MD 21218. 1983. 529 pp. 16 × 24 cm. Price $35.00.

Chronopharmakologie—Tagesrhythmen und Arzneimittelwirkung, By BJORN LEMMER. Wissenschaftliche Verlagsgesellschaft mbH Stuttgart, Birkenwaldstrasse 44, 7000 Stuttgart 1, West Germany. 1983. 100 pp. 15.5 × 23 cm. Price DM 29.

Circular Dichroic Spectroscopy: Excition Coupling in Organic Stereochemistry. By NOBUYUKI HARADA and KOJI NAKANISHI. University Science Books, 20 Edgehill Road, Mill Valley, CA 94941. 1983. 460 pp. 21 × 24 cm. Price $32.00.

Complying With FDA Good Manufacturing Practice Requirements: How to Develop Your GMP/QA Manual. By JOHN J. RIORDAN and WILLIAM COTLIAR. Association for the Advancement of Medical Instrumentation, 1901 N. Fort Myer Drive, Arlington, VA 22209. 1983. 201 pp. 22 × 28 cm. Price $65.00 ($50.00 for AAMI members.)

Depressive Disorders in Different Countries. World Health Organization, Geneva, Switzerland. 1983. 150 pp. 16 × 24 cm. Price Sw. Fr. 17.

Dermal and Transdermal Absorption. Edited by RAINER BRANDAU and BARBEL H. LIPPOLD. Wissenschaftliche Verlagsgesellschaft mbH, Postfach 40, D-7000 Stuttgart 1, West Germany. 1982. 257 pp. 15 × 23 cm. Price DM 88, fur Bezieher, DM 70.50 der Reihe.

Drug Benefit Formulary, No. 19, July 1983. PARCOST Comparative Drug Index. The Ministry of Health, Ontario, Canada. 1983. 214 pp. 14.8 × 20.9 cm. Price $1.00.

Drug Treatment in Obstetrics: A Handbook of Prescribing. By R. S. LEDWARD and D. F. HAWKINS. Methuen, 733 Third Avenue, New York, NY 10017. 1983. 262 pp. 12.4 × 18.6 cm. Price $29.00 (cloth), $13.95 (paperback).

Drug Utilization in Norway During the 1970s—Increases, Inequalities, Innovations. Edited by SOLVEIG SAKSHAUG, MARIT ANDREW, PETER F. HJORT, PETER KNUT M. LUNDR, and KARE ØYDVIN. Norwegian Medicinal Depot, P.O. Box 100, Vietvet, Oslo 5, Norway. 1983. 271 pp. 15 × 21 cm. Paperback.

Eleventh Annual Report, 1982: World Health Organization Special Programme of Research Development and Research Training in Human Reproduction. World Health Organization, Geneva, Switzerland. 1982. 159 pp. 18.5 × 24 cm.

Environmental Carcinogens—Selected Methods for Analysis, Vol. 5: Mycotoxins. (IARC Scientific Publications No. 44). Editor-in-Chief, H. EGAN. World Health Organization, 1211 Geneva 27, Switzerland. 1982. 455 pp. 19 × 25 cm. Price $30.00 (Sw. Fr. 60).

Environmental Carcinogens—Selected Methods of Analysis, Vol. 6: N-Nitroso Compounds. Edited by H. EGAN. World Health Organization, International Agency for Research on Cancer, Lyon, France. 1983. 508 pp. 18.5 × 24.5 cm. Price $40.00 (Sw. Fr. 80).

Environmental Health Criteria 22: Ultrasound. Published under the joint sponsorship of the United Nations Environment Programme, the World Health Organization, and the International Radiation Protection Association. World Health Organization, Geneva, Switzerland. 1982. 199 pp. 14 × 21 cm. Price Sw. Fr. 16.

Environmental Health Criteria 23: Lasers and Optical Radiation. Published under the joint sponsorship of the United Nations Environment Programme, the World Health Organization, and the International Radiation Protection Association. World Health Organization, Geneva, Switzerland. 1982. 154 pp. 14 × 21 cm. Price Sw. Fr. 13.

Environmental Health Criteria 24: Titanium. Published under the joint sponsorship of the United Nations Environment Programme, the International Labour Organization, and the World Health Organization. World Health Organization, Geneva, Switzerland. 1982. 68 pp. 14 × 21 cm. Price Sw. Fr. 11.

Environmental Health Criteria 25: Selected Radionuclides. Published under the joint sponsorship of the United Nations Environment Programme, the International Labour Organization, and the World Health Organization. World Health Organization, Geneva, Switzerland. 1983. 237 pp. 14 × 21 cm. Price Sw. Fr. 18.

The Essential Guide to Nonprescription Drugs. By DAVID R. ZIMMERMAN. Harper and Row, 10 East 53rd Street, New York NY 10022. 1983. 886 pp. 15 × 24 cm. Price $10.95 (paperback).

The Fischer Indole Synthesis. By B. ROBINSON. Wiley, One Wiley Drive, Somerset, NJ 08873. 1983. 923 pp. 16 × 24 cm. Price $200.00.

A Handbook on Drug and Alcohol Abuse: The Biomedical Aspects (2nd Ed.). By FREDRICK G. HOFFMAN. Oxford University Press, 200 Madison Avenue, New York, NY 10016. 1983. 329 pp. 15.3 × 22.9 cm. Price $27.50 (Cloth), $14.95 (paperback).

Handbook of Metal Ligand Heats and Related Thermodynamic Quantities, 3rd Ed., Revised and Expanded. By JAMES J. CHRISTENSEN and REED M. IZATT. Dekker, 270 Madison Avenue, New York, NY 10016. 1983. 800 pp. 18 × 26 cm. Price $95.00 (20% higher outside the U.S. and Canada).

Handbook of Resolutions and Decisions of the World Health Assembly and the Executive Board, Vol. II, 5th Ed. (1973–1982). World Health Organization, Geneva, Switzerland. 1983. 366 pp. 21 × 29.8 cm. Price Sw. Fr. 16.

Handbook of the Spinal Cord, Vol. 1: Pharmacology. Edited by ROBERT A. DAVIDOFF. Dekker, 270 Madison Avenue, New York, NY 10016. 1983. 560 pp. 16 × 24 cm. Price $69.75 (20% higher outside the U.S. and Canada).

IARC Monographs on the Evaluation of the Carcinogenic Risk of Chemicals to Humans, Vol. 30: Miscellaneous Pesticides. International Agency for Research on Cancer, World Health Organization, Lyon, France. 1982. 424 pp. 18 × 24 com. Price $30.00 (Sw. Fr. 60).

Index Plantarum Medicinalium Totius Mundi Eorumque Synonymorum. By GIUSEPPE PENSO. Organizzazione Editoriale Medico Farmaceutica s.r.l., Via Edolo 42, 20125 Milano, Italy. 1983. 1027 pp. 17 × 25 cm.

International Nonproprietary Names (INN) For Pharmaceutical Substances: Cumulative List No. 6. World Health Organization, Geneva, Switzerland. 1982. 494 pp. 18 × 24 cm. Price Sw. Fr. 55.

Kinetic Methods in Chemical Analysis. Application of Computers in Analytical Chemistry. (Comprehensive Analytical Chemistry, Vol. XVIII). By M. KOPANICA, V. STARA, and K. ECKSCHLAGER. Elsevier Scientific, P.O. Box 330, 1000 AH Amsterdam, The Netherlands. 1983. 446 pp. 16 × 23 cm. Price $110.00 (Dfl. 275.00).

Laboratory Decontamination and Destruction of Carcinogens in Laboratory Wastes: Some Polycyclic Aromatic Hydrocarbons. (IARC Scientific Publication No. 49). Edited by M. CASTEGNARO, G. GRIMMER, O. HUTZINGER, W. KARCHER, H. KUNTE, M. LAFONTAINE, E. B. SANSONE, G. TELLING, and S. P. TUCKER. International Agency for Research on Cancer, 150 cours Albert-Thomas, 69372 Lyon Cedex 08, France. 1983. 81 pp. 18 × 24 cm. Price $10.00 (Sw. Fr. 20).

Manual of Dermatological Therapeutics. By KENNETH ARNDT. Little, Brown and Co., Medical Division, 34 Beacon Street, Boston, MA 02106. 1983. 347 pp. 14.5 × 22 cm. Price $15.95.

Measuring Change in Nutritional Status. World Health Organization, Geneva, Switzerland. 1983. 101 pp. 21 × 29.8 cm. Price Sw. Fr. 14.

Medical Applications of Clinical Nutrition. Edited by JEFFREY BLAND. Keats Publishing, 27 Pine Street, New Canaan, CT 06840. 1983. 321 pp. 16 × 24 cm. Price $25.00.

Myasthenia Gravis. Edited by E. X. ALBUQUERQUE and A. T. EL-DEFRAWI. Methuen, 733 Third Avenue, New York, NY 10017. 1983. 500 pp. 16 × 24 cm. Price $75.00.

The New Regulatory Climate—Working Effectively With the FDA. Association for the Advancement of Medical Instrumentation, 1901 N. Fort Myer Drive, Suite 602, Arlington, VA 22209. 1983. 90 pp. 22 × 28 cm. Price $40.00 ($25.00 for AAMI members).

Nuclear Power: Management of High-Level Radioactive Waste. (WHO Regional Publications, European Series No. 13). World Health Organization, Regional Office for Europe, Copenhagen, Denmark. 1982. 63 pp. 16 × 24 cm. Price Sw. Fr. 10.

Particle Size Analysis, 1981. Edited by N. STANLEY-WOOD and T. ALLEN. Wiley, One Wiley Drive, Somerset, NJ 08873. 1983. 461 pp. 17 × 26 cm. Price $74.95.

Trace Elements, Hair Analysis and Nutrition. By RICHARD A. PASSWATER and ELMER M. CRANTON. Keats Publishing, 27 Pine Street, New Canaan, CT 06840. 1983. 385 pp. 15.4 × 22.9 cm. Price $14.95 (paperback), $18.95 (cloth). (Received by *American Pharmacy.*)

Twentieth Century Druggist: Memoirs. By CHARLES W. ROBINSON. Galen Press, 18 North Humberside HU17 8AX, United Kingdom. 1983. 244 pp. 15 × 21 cm. Price $12.00 (£6.50 UK, £7.50 rest of the world).

The Use of Essential Drugs. (World Health Organization Technical Report Series No. 685). World Health Organization, Geneva, Switzerland. 1983. 46 pp. 11 × 17 cm. Price Sw. Fr. 4.

Vacation Certificate Requirements For International Travel and Health Advice to Travellers, 1983. World Health Organization, Geneva, Switzerland. 1983. 70 pp. 15 × 21 cm. Price Sw. Fr. 12.

1983 Year Book of Drug Therapy. Edited by LEO E. HOLLISTER and LOUIS LASAGNA. Year Book Medical Publishers, Chicago, IL 60601. 1983. 428 pp. 16 × 24 cm. Price $39.95.

NEW JOURNALS

Acta Farmaceutica Bonaerense, (Vol. 1, No. 1: 1982). Publicacion del Colegio de Farmaceuticos de la Provincia de Buenos Aires (Argentina). 1982. 67 pp. 18 × 25.7 cm.

International Pharmaceutical Technology and Product Manufacture Abstracts, (Vol. 1, No. 1: July 1983). Chidwell University Press Ltd., P.O. Box 78, London NW11 OPG, England. 44 pp. 15 × 21 cm. Price $160.00 (£80). Published quarterly.

Journal of Environmental Sciences and Health, Part C: Environmental Carcinogenesis Reviews, (Vol. C1, No. 1: 1983.) JOSEPH C. ARGOS, MARY F. ARGUS, and YIN TAK WOO, Eds. Dekker Journals, 270 Madison Avenue, New York, NY 10016. 1983. 135 pp. 15.2 × 23 cm. Price $219.50 per annum ($109.75 professionals and students).

Journal of Industrial Irradiation Technology, (Vol. 1, No. 1: 1983). RICHARD BRADLEY, Ed. Dekker, 270 Madison Avenue, New York, NY 10016. 1983. 103 pp. 15 × 23 cm. Price $95.00 (institutional), $47.50 (individual); add $9.20 (surface), $14.40 (airmail Europe), or $17.60 (airmail Asia) for postage outside the U.S.

Journal of Pharmaceutical and Biomedical Analysis, (Vol. 1, No. 1: 1983). ANTHONY FELL and JAMES N. MILLER, Eds. Pergamon, Headington Hill Hall, Oxford 0X3 0BW, U.K. 1983. 123 pp. 18.4 × 24.8 cm. Price $60.00 per annum.

Journal of Social and Administrative Pharmacy, (Vol. 1, No. 1: 1983). RUNE WESTERLING, Ed. Swedish Pharmaceutical Press, P.O. Box 1136, S-111 81 Stockholm, Sweden. 1983. 48 pp. 17 × 24.5 cm. Price $22.00 per annum.

Pharmazeutische Zeitung Scientific Edition, (Vol. 1: 1983). EVE-MARIE WOLF and GERD E. BAUER, Eds. Deutsches Apothekerhaus, Beethovenplatz 1–3, 6000 Frankfurt am Main, West Germany. 1983. 22 pp. 21 × 29 cm. Published weekly.

Solvent Extraction and Ion Exchange, (Vol. 1, No. 1: 1983). E. PHILIP HORWITZ and JAMES D. NAVRATIL, Eds. Dekker, 270 Madison Ave., New York, NY 10016. 1983. 239 pp. 15 × 22.8 cm. Price $450.00 per annum ($225.00 professionals and students).

Adverse Drug Reaction Reporting

After reading your comments in the June 10th issue of *Apharmacy Weekly*[1], regarding the adverse drug reaction reporting system, I felt that it was necessary to write you regarding this matter. Our company has been greatly concerned with this problem for many years. We have been constantly trying to find an effective system for reporting adverse drug reactions to the pharmacy department and participating in a national data collection program.

It has been our experience that the principal obstacle to the adverse drug reaction program is the physician. In the hospital setting, no physician wants to have an entry on a patient's chart stating that the patient experienced an adverse drug reaction. This is due to the fear of civil liability. In our efforts to have this information placed on the chart by a nurse, both pharmacy and nursing have been criticized for "diagnosing" or "practicing medicine."

I believe our experience is directly related to the surprising fact that Johnson and Johnson knew of nearly twice as many instances of adverse drug reactions from the prescription medication, Zomax, as the FDA had known. I would not be surprised to discover that this information, which the company had acquired, was verbal feedback from the physicians to the sales representatives, rather than a written report directly from the physicians. It appears that the fear of legal liability is having a very strong impact on the practice of medicine and our ADR reporting system problem is just one symptom of this.

Until this problem is resolved, it is my belief that it will be a continuing problem and present great difficulties in developing an effective reporting system. This situation will continue in spite of the efforts of JCAH surveyors, who constantly stress the necessity of accurate charting the patient's history and the response to therapy, and our own efforts in trying to have this information placed in the chart within the nursing notes, as a nursing diagnosis of a "suspected" adverse drug reaction. In addition to this, we are informing the medical staff through the pharmacy and therapeutics committee of their potential liability for failure to report adverse drug reactions in the patient's medical history and chart. This legal liability would result if the patient suffers a repeat adverse drug reaction with possible injury and mortality during subsequent hospitalization.

In summary, we continue to search for and would greatly enjoy your support in finding a system for reporting adverse drug reactions which could achieve the necessary physician support to ensure it's success.

William (Bill) Springfield
Director, Pharmacy Operations
Central Division
AMI Pharmacy Management Services
Houston, TX 77060

Received June 27, 1983.

[1] *Apharmacy Weekly*, **22**, 91 (1983). See also E. G. Feldmann, *J. Pharm. Sci.*, **72**, 585 (1983).

Postscript:

Since I am in agreement with your concern with the problem of adverse drug reaction reporting, I am agreeable to using my letter in the "Open Forum Page" of the *Journal*. I hope it will stimulate more thought and discussion toward an effective method for reporting in our clinical settings. Hopefully, each pharmacy practitioner will begin to view themselves as members of the research and development process and communicate this attitude to physicians in such a manner that it becomes contagious within their ranks also.

December 1983
Volume 72 Number 12

JOURNAL OF PHARMACEUTICAL SCIENCES

A publication of the American Pharmaceutical Association

The *Journal of Pharmaceutical Sciences* (ISSN 0022-3549) is published monthly by the American Pharmaceutical Association (APhA) at 2215 Constitution Ave., N.W., Washington, DC 20037. Second-class postage paid at Washington, D.C. and at additional mailing office.

Offices—Editorial, Advertising, and Subscription: 2215 Constitution Ave., N.W., Washington, DC 20037. All Journal staff may be contacted at this address. Printing: 20th & Northampton Streets, Easton, PA 18042.

Annual Subscriptions—United States and foreign, industrial and government institutions $75; educational institutions $75; individuals *for personal use only* $40; single copies $10. APhA and SAPhA members may subscribe to *J. Pharm. Sci.* for $20.00 per year. All foreign subscriptions add $10 for postage. Subscription rates are subject to change without notice.

Claims—Missing numbers will not be supplied if dues or subscriptions are in arrears for more than 60 days or if claims are received more than 60 days after the date of the issue, or if loss was due to failure to give notice of change of address. APhA cannot accept responsibility for foreign delivery when its records indicate shipment was made.

Change of Address—Members and subscribers should notify at once both the Post Office and APhA of any change of address.

Microfilm—Available from University Microfilms International, 300 N. Zeeb Road, Ann Arbor, MI 48106.

New Era for Nonprescription Drugs

The law says that drugs must be "safe and effective" if they are to be legally on the market.

But it was not always so.

Specifically, less than 50 years ago, it was neither a legal requirement nor an actuality that drugs in the American marketplace were generally safe and effective.

The Federal Food, Drug, and Cosmetic Act of 1938 formally established safety as a condition of drug approval and marketing. The Drug Amendments of 1962 did likewise regarding drug effectiveness.

However, it takes more than just a vote in Congress and the signature of a President to transform the objective into the reality. Recognizing that the criteria of safety and effectiveness could be applied rather readily in evaluating *new* drugs as a condition of their approval by the federal Food and Drug Administration, it remained to develop some system for the review and evaluation of those drugs *already* on the market—particularly, for the effectiveness evaluation of pre-1962 drugs.

And so it was in the mid-1960's that the FDA—working along with the National Academy of Sciences/National Research Council—undertook the Drug Efficiency Study Implementation (DESI). This was a massive program over a 10-year period to evaluate the effectiveness of virtually all drug products marketed prior to 1962.

Very early in this project, it became evident that the complete task was impossible and certain limitations would need to be applied. The most fundamental of these adjustments was the decision to concentrate on the prescription drug products, of which there were almost 10,000, and to set aside the nonprescription drug products, which numbered over 300,000. In view of the fact that not only was a much smaller and manageable a universe involved, but also that the drugs were more important in the sense of being used to treat more serious health problems and conditions, this decision made a great deal of sense to all concerned.

And eventually, the DESI project ground to its inevitable conclusion, with many products forced off the market, others reformulated, and still others relabeled as to claims and conditions for use. Although the process was long and stressful, the general consensus appears to be that the net result has been beneficial to the public health and welfare, and that both consumers and health care professionals now can have a high level of confidence that prescription drug products will perform in accord with their claims.

But what about those several hundred thousand nonprescription drug products?

Under law, they must be just as safe and effective for their labeled purposes and claims as their prescription legend cousins. The only real difference between these two drug classes is that the former are judged to be suitable for use without professional supervision, while the latter—for one reason or another—are judged to necessitate such professional practitioner involvement.

As the DESI project was proceeding on track during the very late 60's and early 70's, the FDA concluded that the nonprescription drugs would require a different approach logistically. Instead of considering them on a product-by-product basis, the FDA decided to approach the project on a drug active ingredient basis. With active ingredients totaling less than a thousand, in contrast to the several hundred thousand products, this alternative was clearly more practical and manageable.

And so was conceived the FDA's "OTC Drug Review" which has now been in process for some 11 to 12 years, depending upon when one regards the starting date to have occurred. In contrast to the DESI project, in which the FDA contracted with the NAS-NRC to conduct the fact-finding aspect, the OTC Drug Review was organized and operated by FDA itself. A series of 17 advisory panels—composed of about 250 outside nongovernment drug experts—were established with each panel responsible for a particular therapeutic or pharmacologic class of drugs. The panels, which were staffed by FDA, reviewed 20,000 volumes of data, held 508 meetings over 1,047 days, and participated in innumerable phone conferences, exchanges of correspondence, and other activities relating to their deliberations.

On October 7 of this year, the FDA and its parent Department of Health and Human Services, proudly announced that a most important milestone had been reached in this monumental project. The 58th, and last, report of the advisory panels was publicly released.

Although agency officials pointed out that much work still remains to be done to convert the final panel recommendations into regulatory action, they emphasized that major strides had already been made "in improved products, greater safety, and reduced medical costs."

HHS Secretary Margaret M. Heckler concluded her statement with the comment that, "The review has begun to transform the nonprescription drug market." And the accompanying FDA summary cited ample statistics and examples to document her assessment.

What impact will this all have on pharmacy and the pharmaceutical sciences?

Nonprescription drugs and drug products have long had an image of being nothing more than harmless, ineffective nostrums at best, and potentially harmful quack remedies at worst.

But the FDA's OTC Drug Review has changed that. The products on the market now and in the future have been established as safe and effective. And professional organizations have been making great efforts to educate practitioners and the public in the proper selection and use of such products.

In particular, the American Pharmaceutical Association has contributed enormously in this regard through publication of its highly respected *Handbook of Nonprescription Drugs*, which is now in its 7th Edition. APhA has also been conducting a whole host of other efforts, including workshops and seminars, to support an active and effective role for the pharmacist with regard to self-medication by the public.

And in recent years the nonprescription drug industry has generally assumed a high sense of public responsibility for the products it produces as well as their proper use. Indeed, the Proprietary Association, which is the major trade organization of nonprescription drug manufacturers, currently is closely cooperating with APhA in efforts to produce a consumer version of APhA's *Handbook*.

Finally, the general public today is much more health conscious than ever before; it has a keen interest in knowing as much as possible about self-treatment; and it wants to feel confident that the therapeutic agents it uses are safe and reliable.

Consequently, the entire picture as to contemporary perceptions and attitudes regarding nonprescription drugs is dramatically different from that which prevailed just a few short years ago. And the resultant shift in emphasis will greatly affect not only pharmacy practitioners but also pharmaceutical educators and scientists as well.

—EDWARD G. FELDMANN
American Pharmaceutical Association
Washington, DC 20037

0022-3549/83/1200-1373$01.00/0

JOURNAL OF PHARMACEUTICAL SCIENCES

DECEMBER 1983
VOLUME 72 NUMBER 12

LITERATURE SURVEY

Drug Delivery to Local Subcutaneous Structures Following Topical Administration

RICHARD H. GUY ˣ and HOWARD I. MAIBACH

Received October 26, 1982, from the *School of Pharmacy and Department of Dermatology, School of Medicine, University of California–San Francisco, San Francisco, CA 94143.*

Keyphrases □ Topical administration—drug delivery to local subcutaneous tissues, literature survey □ Drug delivery—local subcutaneous tissues *via* topical administration, literature survey

This article brings together a collection of results and observations which demonstrate the achievement of significant drug delivery to local subcutaneous structures following topical administration. It is probably no exaggeration to say that the concept of using the transdermal route to advantageously reach lower tissue, such as the muscle beneath the subcutaneous fat, goes directly against conventional thought. Indeed, the cutaneous microvasculature has long been offered as an excellent example of a classical "sink" phenomenon; that is, following penetration through the stratum corneum, epidermis, and upper dermis, it has been held that the permeating species will then pass into one of the small blood vessels forming the microcapillary network and hence be systemically diluted in the circulatory system. The argument seems totally reasonable: the stratum corneum is an excellent barrier to the passage into the body of many substances that contact with the skin. Thus, in the large majority of cases, drug arrival beneath the stratum corneum is slow such that the concentration of material at this point is invariably very much less than that present on the skin surface. These conditions are precisely those implicit in a "sink" situation and, coupled with the extensive dermal capillary matrix, it is not surprising that further penetration into the tissue has been considered unlikely.

On closer perusal of the literature, however, it becomes apparent that a small but significant number of reports exist which show that deeper penetration can take place and that subcutaneous drug levels can be achieved following topical application which cannot be reached after parenteral or oral administration of the active agent. This brief review gathers the results available in the (admittedly) diverse sources to reanalyze conventional thought and to stimulate inquiry into this important aspect of drug input *via* the skin.

SUBCUTANEOUS DRUG DELIVERY: EXPERIMENTAL OBSERVATIONS

Over the last 15 years, there have appeared several communications which address the question of local subcutaneous drug delivery following topical dosing. These encompass a diverse array of chemical substances such as dimethyl sulfoxide, a salicylate derivative, steroids, and commonly used organophosphorous pesticides. In almost all cases, the studies have involved animal models since excision of tissue and its analysis is possible. However, evidence has been found that the same deeper penetration from the skin surface occurs in humans; further, *a priori*, there is no reason to suggest that the animal experiments performed are not good qualitative predictors, at least of the behavior expected in humans. It is believed, therefore, that the following discussion provides tantalizing and somewhat novel information on the potential of the topical route for the delivery of chemotherapeutic agents.

In 1968, Gorog and Kovacs (1) studied the anti-inflammatory properties of dimethyl sulfoxide (DMSO) in rats. It was found that carrageenan-induced rat paw edema was improved by both oral and topical DMSO therapy. Furthermore, and of greater relevance, arthritis induced by Mycobacterium adjuvant was inhibited to a greater degree by topical, rather than oral, DMSO administration. In the same way, DMSO applied to the skin of rats had an inhibitory effect on arthritis produced experimentally by 6-sulfanilamidazole. These early data, therefore, argue strongly for local deep penetration of the solvent.

A more detailed investigation on the disposition of topically applied ^{3}H-labeled escin was performed in mice and rats by Lang (2). The radioactive compound was ap-

0022-3549/83/1200-1375$01.00/0

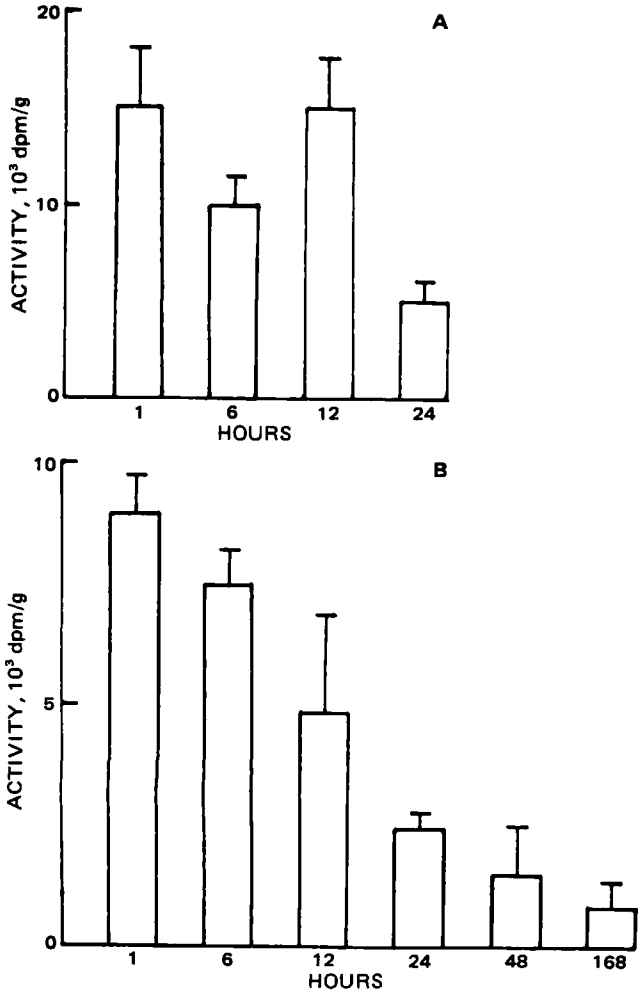

Figure 1—*Radioactivity in mouse (A) and rat (B) back muscles at various times after cutaneous application of [^{3}H]escin. (Data taken from Ref. 2.)*

plied to the backs of animals, and tissue distribution was subsequently evaluated at various times by organ dissection after sacrifice. The tissues monitored were the back muscles, blood, liver, kidney, heart, lungs, spleen, testes, brain, leg muscle, femur, and stomach lining. In the mouse the amount of activity detected in the back muscle beneath the skin application site exceeded by 20–100 times the amount detected in any of the other regions. A similar pattern of behavior, though less pronounced (10–30 times greater in the back muscle) was observed in the rat. The time course of disposition to the back muscle in the two species is shown in Fig. 1. It is apparent that significant levels of escin are present in the deeper local tissue over prolonged periods of time. A further observation reported in this paper (and elsewhere) also implies that all material penetrating the upper skin layers is not immediately subjected to a sink condition. Measurements were made of activity residing in the skin beneath the application site and in several skin strips 0.5 cm wide at distances of 1–5 cm from the center of the application zone. The data (Fig. 2) for the mouse clearly show that radial movement of drug within the skin is an additional transport pathway to the expected capillary uptake process. It should be pointed out that implied radial movement within the skin has been reported on other occasions. It is a common observation

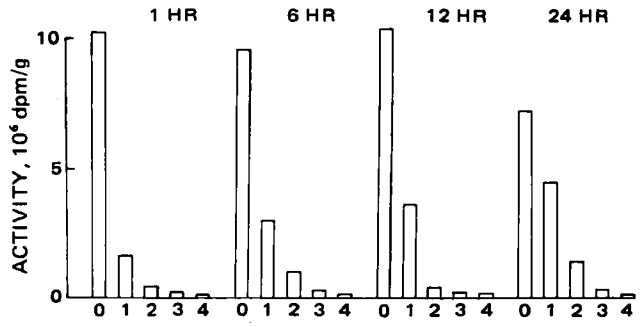

Figure 2—*Radioactivity located in several skin areas at various times after cutaneous application of [^{3}H]escin to the mouse. Column 0 corresponds to skin directly under the application site. Columns 1, 2, 3, and 4 refer to skin strips at 0.5-cm intervals away from the contact zone. (Data taken from Ref. 2.)*

that topical vasodilators capable of producing visible erythema induce a redness on the skin surface that expands with time beyond the region of application (3). As an example, the work by Fountain *et al.* (4) with the methyl ester of nicotinic acid may be cited (Fig. 3); recently, this line of investigation has been pursued in a more quantitative sense (5), and the radial transport of methyl nicotinate absorbed into the skin has been measured as a function of drug concentration and time (Table I). The rapidity of the outward movement implies that passive diffusion cannot be the mechanism involved, and it has been suggested that the cutaneous vasculature must participate. However, it is evident, whatever the mechanism, that the role of the microcirculation in this case is not merely depletive. It is also true that radial movement within the skin as assessed by visual detection of a pharmacological response is not limited to vasodilation, but has also been witnessed with the opposite effect produced by corticosteroids (6). Thus, the evidence for lateral transport prior to removal by dermal capillaries seems quite firm.

The most extensive study of local subcutaneous delivery of chemical substances was by Marty *et al.* (7–11) who

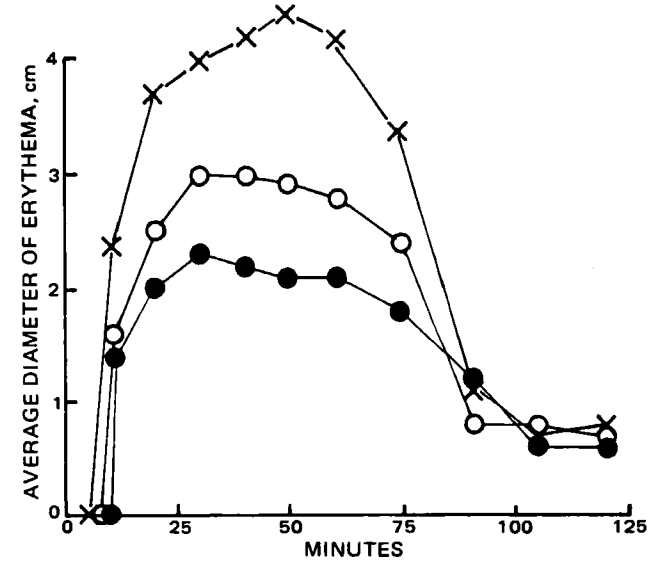

Figure 3—*Lateral movement of methyl nicotinate in the skin as assessed by erythematous area. The drug was applied in aqueous solution at ambient temperature (25°). Each data point is the average of five readings from various sites. Key: methyl nicotinate concentration (×) 1.0%; (○) 0.5%; (●) 0.25%. (Data from ref. 5.)*

Table I—Radial Transport of Methyl Nicotinate in the Dermis as a Function of Time (t) for Two Topically Applied Concentrations (C) with Various Application Durations (t_1)[a]

Erythematous Reaction to Methyl Nicotinate[b]					
C = 997 mM			C = 100 mM		
t_1, sec	t, min	A, cm^2	t_1, sec	t, min	A, cm^2
15	2.25	1.4	120	2.5	1.4
	4	7.5		6	2.7
	7	13.9		9.5	5.9
	10	18.4		15	7.1
30	2.75	3.5	600	4	2.4
	4	5.5		7	4.6
	5	11.4		11	8.7
	6	14.4		16	11.2
	7	15.7	1200	6	2.6
	10.5	18.8		8	7.7
60	2	4.5		12	11.6
	3	7.7		18	14.7
	5	15.4		23	19.1
	8	23.1			
	14	25.8			

[a] Data taken from Ref. 5. Methyl nicotinate was applied in aqueous solution to a skin surface area of 0.79 cm^2. [b] A = area of erythema.

attempted to explain the localized and deep therapeutic effect of certain dermatological preparations. These authors demonstrated, in each case, that percutaneous absorption was accompanied by diffusion and retention in the connective and muscle tissues located beneath the administration area. Alcoholic or propylene glycol solutions of radiolabeled thyroxine, triiodothyronine, estradiol, dexamethasone, and diisopropyl fluorophosphate were applied to the shorn abdomen or back of Sprague–Dawley rats, and the contact zones were protected and covered for periods of between 0.5 and 6 hr (7). At the end of the test the rat was killed and blood was drawn from the carotid artery. The site of skin application was dissected and fragments of subcutaneous tissue, muscle, and brown interscapular fat were removed from below the contact area. Samples of liver, kidneys, and part of the muscle from a rear paw were also collected and weighed.

Liquid scintillation counting was used to determine the radioactive concentrations in the various organs; the results were converted to amounts of drug present in nanograms per gram of tissue (Table II). For thyroxine, after 1 hr, the levels in plasma, liver, kidneys, and skeletal muscle were not significantly different. Beneath the application area, the radioactive concentration was 100 times greater in the subcutaneous tissue than in the plasma. The subjacent muscle showed the same phenomenon though of less intensity. The ratio (concentration in muscle below the application zone/concentration in paw muscle) increased substantially with time (4.2 at 30 min, 8.6 at 60 min, and 14.3 at 2 hr). Triiodothyronine gave similar results with considerable retention in the subcutaneous region and deeper muscle. Liver and kidney levels matched the plasma concentration. Estradiol showed the greatest retention in the subcutis and muscle below the application area (20 and 40 times the plasma level, respectively). The ratio of the skin muscle concentration to the paw muscle concentration was 17. Dexamethasone showed the lowest penetration rate, and enhanced drug delivery to the subjacent tissue was barely significant. Absorption of diisopropyl fluorophosphate was greatest, on the other hand, but resulted in little local muscle retention over that found elsewhere. In general, however, the authors showed accumulation in local skin muscle under the application zone.

It was suggested that this enhancement corresponded to molecular diffusion in the deep direction independent of the level of vascular perfusion (the latter being anatomically distinct for the regions of viable epidermis, dermis, and subjacent muscle). Further, the authors implied that, contrary to accepted concepts (12), the blood supply to the dermis is *not* capable of resorbing certain chemicals proportionately to their penetration through the epidermis. Thus, the substrate accumulates with time and is able to diffuse to deeper tissue. To support their hypothesis, Marty *et al.* (7) drew attention to the fact that both dexamethasone (a poorly absorbed substance with low solubility in water) and diisopropyl fluorophosphate (soluble in water and oil) show little accumulation, suggesting that the blood supply is able to transport these substances away in solution relatively efficiently. Conversely, the poorly water soluble thyroxine, triiodothyronine, and estradiol show much diminished resorption by the microvasculature and establish significant levels further into the tissue with increasing contact time.

In two subsequent reports (8, 9), the disposition of tritiated dexamethasone in mice and rats following topical application was compared with oral administration. Pro-

Table II—Distribution of Various Substances in Different Tissues in the Rat after Application to the Skin[a]

Penetrating Species/Amount Deposited, μg	Experiment Duration, hr	Tissue Concentration, ng/g						Significance of Difference Between A and B
		Plasma	Liver	Kidneys	Subcutaneous Tissue[b]	Muscle under Application Zone (A)	Paw Muscle (B)	
[^{125}I]Thyroxine/400 (N = 7, 6, 5)	0.5	0.7 ± 0.2	1.1 ± 0.4	2.1 ± 0.6	55 ± 11	3.8 ± 1.0	1.0 ± 0.5	$p < 0.05$
	1	1.60 ± 0.5	2.9 ± 1.2	2.6 ± 0.7	132 ± 42	8.0 ± 2.4	1.5 ± 0.6	$p < 0.05$
	2	4.0 ± 0.9	3.9 ± 1.8	5.6 ± 0.7	178 ± 45	23 ± 2.3	1.6 ± 0.2	$p < 0.01$
[^{125}I]Triiodothyronine/400 (N = 6,6)	1	2.5 ± 0.2	3.6 ± 0.7	5 ± 1	111 ± 15	10 ± 3	2.5 ± 0.9	$p < 0.05$
	2	3.9 ± 0.3	5 ± 1	8.3 ± 2.2	240 ± 70	23 ± 4.4	2.0 ± 0.4	$p < 0.01$
[^{3}H]Estradiol/110 (N = 6)	2	1.0 ± 0.3	4 ± 1.5	2.2 ± 0.4	370 ± 87	42 ± 15	2.4 ± 0.6	$p < 0.01$
[^{3}H]Dexamethasone/100 (N = 12, 5, 5)	2	0.19 ± 0.06	1.05 ± 0.33	0.65 ± 0.14	8.1 ± 2.1	0.75 ± 0.14	0.27 ± 0.08	$p < 0.05$
	4	0.19 ± 0.03	1.52 ± 0.30	0.67 ± 0.20	5.2 ± 0.9	0.7 ± 0.3	0.25 ± 0.01	$p = 0.05$
	6	0.34 ± 0.10	1.0 ± 0.1	1.44 ± 0.60	4.8 ± 0.6	1.6 ± 0.6	0.42 ± 0.15	N.S.
[^{3}H]Diisopropyl fluorophosphate/20,000 (N = 7)	3	1210 ± 114	3100 ± 640	8500 ± 2400	35800 ± 15000	2450 ± 1000	590 ± 150	$p < 0.05$

[a] Data taken from Ref. 7. [b] All values significantly different from those in plasma, $p < 0.01$.

Table III—Percutaneous Absorption of [^{3}H]Dexamethasone in Mice [a]

Application Duration, hr [b]	Tissue Concentration, ng/g: Subcutaneous Tissue	Abdominal Muscle	Homogenized Mouse
1	49 ± 19 [c]	4.1 ± 1.3 [c]	0.90 ± 0.14
2	69 ± 10 [c]	12 ± 3.5 [c]	2.6 ± 1.7
4	97 ± 30 [c]	29 ± 13 [d]	3.3 ± 1.0

[a] Data taken from Refs. 8 and 9. Dose applied = 19 μg/cm^2. [b] N = 5 at 1 hr; N = 6 at 2 and 4 hr. [c] Significance of difference between tissue and homogenized mouse, $p < 0.05$. [d] Significance of difference between tissue and homogenized mouse, $p < 0.01$.

cedures similar to those described in the previous study (7) were used; Tables III and IV summarize the results. It is plain that observations consistent with those of the earlier work were found; for example, in mice, under the area of topical application, the levels of radioactivity in subcutaneous tissue and in the lower muscle were 30 and 10 times higher, respectively, than in other tissues. Levels and distribution were quite different following oral administration; the plasma concentration was higher and large amounts were located in liver and kidney. Such a pattern of behavior (topical *versus* oral) was intimated to be of potential importance in terms of the metabolic inactivation of the administered chemical.

Further investigation into the fixation of topically applied materials in the superficial structures of the skin, and its importance in problems of decontamination and bioavailability, was then conducted (10, 11). The materials studied were diisopropyl fluorophosphate, malathion, parathion, estradiol, and progesterone. Comparable methodology was employed in the rat and mouse animal models (Tables V, VI, and VII). In the mouse, the amount of diisopropyl fluorophosphate found in the abdominal muscle under the application region and in the local vicinity represented ~28% (105 μg) of the total quantity absorbed; the remaining 72% was diluted in almost the entire animal. Malathion produced similar observations with 36% of the absorbed chemical being located in subcutaneous tissue at or near to the application zone. The subjacent tissue showed malathion levels of the order of 1000 μg/g compared with the animal carcass concentration

Table VII—Distribution of Diisopropyl Fluorophosphate, Malathion, and Parathion in Rat Tissues after Percutaneous Application [a]

Tissue	Tissue Concentration, μg/g: Diisopropyl Fluorophosphate	Malathion	Parathion
Subcutaneous tissue	130 ± 25 [b]	145 ± 20 [b]	155 ± 60 [b]
Muscle beneath zone	14 ± 2 [b]	2.5 ± 0.6	1.45 ± 0.45 [c]
Paw muscle	4.0 ± 1.5	1.7 ± 0.6	—[d]
Blood	1.3 ± 0.3	3.6 ± 0.6	0.4 ± 0.1
Liver	4.1 ± 0.5 [b]	1.4 ± 0.2	0.10 ± 0.02 [c]
Plasma	2.3 ± 0.7	—[d]	—[d]
Kidney	8.9 ± 1.5 [b]	2.3 ± 0.7	0.20 ± 0.03

[a] Data taken from Ref. 10; 100 μl was applied over a surface area of 5 cm^2 for 3 hr. N = 7 for diisopropyl fluorophosphate, N = 8 for malathion and parathion. [b] Significance of the difference between blood and tissue concentrations, $p < 0.01$. [c] Significance of the difference between blood and tissue concentrations, $p < 0.05$. [d] —, Not detectable.

Table IV—Tissue Concentrations of [^{3}H]Dexamethasone Following Topical and Oral Administration to Rats [a]

Route	Time, hr [b]	Tissue Concentration, ng/g: Plasma	Subcutaneous Tissue	Abdominal Muscle	Leg Muscle	Liver	Kidneys
Topical	2	0.19 ± 0.06	8.1 ± 2.1 [c]	0.77 ± 0.14 [c]	0.27 ± 0.08	1.05 ± 0.30	0.65 ± 0.14
	4	0.19 ± 0.03	5.2 ± 0.9 [c]	0.68 ± 0.30 [d]	0.25 ± 0.04	1.52 ± 0.30	0.67 ± 0.20
	6	0.34 ± 0.10	4.9 ± 0.5 [c]	1.6 ± 0.6 [c]	0.43 ± 0.15	0.99 ± 0.10	1.44 ± 0.50
Oral	1	22 ± 1	13 ± 2	11.5 ± 1.3	11.6 ± 1.7	145 ± 9	44 ± 6
	4	19 ± 0.5	8.1 ± 1.6	8.9 ± 0.4	9.5 ± 0.7	168 ± 27	36 ± 3
	24	2.7 ± 0.4	1.6 ± 0.5	1.50 ± 0.35	1.5 ± 0.3	11 ± 1.6	3.6 ± 0.6

[a] Data taken from Refs. 8 and 9. The topical dose was 19 μg/cm^2; the oral dose was 40 μg/kg. N = 5 for all times except t = 2 hr (topical) for which N = 12. [b] Time = duration of application (topical) or survival time (oral). [c] Significance of difference between tissue and plasma, $p < 0.05$. [d] Significance of difference between tissue and plasma, $p < 0.01$.

Table V—Percutaneous Absorption of [^{3}H]Diisopropyl Fluorophosphate, [^{35}S]Malathion, and [^{35}S]Parathion in the Mouse [a]

Penetrating Species [b]	Quantities of the Applied Dose Found in Tissues: Muscle Under and Circumscribed at Application Area, μg	%	Mouse Carcass, μg	%	Overall Absorption, μg	%
Diisopropyl fluorophosphate	105 ± 10	1.05 ± 0.10	250 ± 60	2.5 ± 0.6	355 ± 70	3.5 ± 0.7
Malathion	60 ± 10	0.50 ± 0.08	110 ± 25	0.9 ± 0.2	170 ± 40	1.4 ± 0.3
Parathion	50 ± 8	0.40 ± 0.06	130 ± 25	1.0 ± 0.2	180 ± 20	1.4 ± 0.2

[a] Data taken from Ref. 10; 10 μl was applied over a surface area of 1 cm^2 for 1 hr. [b] N = 6 for diisopropyl fluorophosphate and parathion, N = 7 for malathion.

Table VI—Tissue Concentrations of Diisopropyl Fluorophosphate, Malathion, and Parathion after Absorption in the Mouse [a]

Penetrating Species [b]	Tissue Concentration, μg/g: Muscle Under Application Area (M_1)	Circumscribed Muscle (M_2)	Carcass (B)	M_1/B	M_2/B
Diisopropyl fluorophosphate	3920 ± 520	1610 ± 610 [c]	11 ± 3.5	355	145
Malathion	1880 ± 570	650 ± 200 [d]	3.4 ± 0.8	550	190
Parathion	2140 ± 730	530 ± 180 [e]	4.0 ± 0.7	535	130

[a] Data taken from Ref. 10; 10 μl was applied over a surface area of 1 cm^2 for 1 hr. [b] N = 6 for diisopropyl fluorophosphate and parathion, N = 7 for malathion. [c] Significance of the difference between M_1 and M_2 (by the paired series method), $p < 0.001$. [d] Significance of the difference between M_1 and M_2 (by the paired series method), $p < 0.02$. [e] Significance of the difference between M_1 and M_2 (by the paired series method), $p < 0.05$.

Table VIII—Skin Absorption of Estradiol and Progesterone in the Mouse [a]

Steroid	Concentration, μg/g	Conc. in Tissue Under Application Zone, ng/g		Conc. in Whole Crushed Mouse, ng/g
		Subcutaneous	Muscle	
Estradiol	600	1695 ± 350	804 ± 191	43 ± 8
Progesterone	5000	43,600 ± 1100	9350 ± 2900	342 ± 52

[a] Data taken from Ref. 11.

Table IX—Local Concentrations of Steroids in Subcutaneous Tissue Beneath the Application Zone on the Skin after 2 hr [a]

Species	Steroid/Conc., %	Reference Conc.[b] (S), ng/g	Concentration Ratio (Tissue/S)	
			Subcutaneous	Muscle
Mouse	Estradiol/0.06	43 ± 8	39	19
Rat[c]	Estradiol/0.06	1.93 ± 0.18	75	11
Mouse	Progesterone/0.5	342 ± 52	125	27
Rat	Progesterone/0.5	15.1 ± 1.1	200	19

[a] Data taken from Ref. 11. [b] The reference concentration for the mouse is that in the whole crushed carcass after local excision; for the rat, the reference is plasma concentration. [c] After subcutaneous injection (10 μg/kg), S = 0.88 ± 0.05 and tissue/S = 2 (subcutaneous) and 0.75 (muscle).

of <5 μg/g. The data for parathion paralleled those for malathion quite closely. With the same substances in the rat, essentially the same pattern of behavior was found (Table VII). It is apparent, therefore, that the organophosphorous pesticides represent another class of compound for which subcutaneous fixation takes place.

For the steroids estradiol and progesterone (11) (Tables VIII and IX), accumulation was again found in the connective tissue of the abdominal muscle in the region under application. The effect was not seen after subcutaneous administration (Table IX). As before, the authors argued that the results demonstrate slow exchanges between blood and tissue such that the steroids are not removed efficiently as they diffuse in the intercellular fluids. Their observations were emphasized to be distinct from the classic "reservoir" effect noted for this class of compound (13–15), but it was suggested that the latter would mean that the likelihood of deeper penetration was increased. It was concluded that the data constitute pharmacokinetic proof contributing to the confirmation of local subcutaneous pharmacological effects of topically administered hormones.

Finally, in a recent paper (16) Rabinowitz *et al.* have studied the local, articular, and systemic absorption of oral and topical salicylates in dogs and humans using radioisotope techniques. Specifically, tissue disposition following oral [^{14}C]aspirin was compared with that after topical administration of triethanolamine [^{14}C]salicylate. In the canine model, one group of five beagles received per os a 500-mg capsule of [^{14}C]aspirin; a second group received 10 g of ^{14}C-labeled triethanolamine salicylate cream applied to the shaved right knee. Urine and blood samples were taken at 30 and 60 min, and the animals were then killed and tissue samples were analyzed. In the human model, six subjects with seropositive adult-onset rheumatoid arthritis and active knee synovitis were studied. Each subject was dosed, on separate occasions, orally with a [^{14}C]aspirin capsule and topically with 10 g of triethanolamine [^{14}C]salicylate cream to one knee; 2–6 weeks elapsed between the two administrations. Blood and urine samples were taken pretreatment and at 60 and 120 min postdose. At 120 min a synovial fluid aspiration was performed, taking care to avoid sample contamination from the application site. Patients were also asked to rate their subjective pain relief after the two medications.

Table X—[^{14}C]Salicylate Tissue Concentrations after Oral and Topical Salicylate Administration to Dogs [a]

Tissue	[^{14}C]Salicylate Concentration, μg/g	
	Oral	Topical
Blood		
30 min	34.80 ± 2.33	2.60 ± 0.02
60 min	30.60 ± 0.24	0.22 ± 0.02
Urine	12.57 ± 5.16	0.16 ± 0.09
Skin	0.64 ± 0.09	312.20 ± 40.80
Muscle	1.76 ± 0.16	38.20 ± 5.16
Fascia	1.04 ± 0.28	16.40 ± 1.96
Fat pad	1.00 ± 0.10	5.60 ± 1.20
Tendon	0.20 ± 0.03	3.00 ± 0.44
Ligament	0.50 ± 0.16	2.00 ± 0.20
Cartilage	0.43 ± 0.03	1.62 ± 0.49
Synovial fluid	1.00 ± 0.10	0.80 ± 0.12
Synovium	0.62 ± 0.10	0.74 ± 0.12

[a] Data taken from Ref. 16; all values are mean ± *SEM*.

Blood levels achieved in dogs after topical dosing were 10–100 times lower than those after oral administration of an equimolecular quantity of salicylate (Table X). However, the topical route resulted in higher local salicylate levels: the skin level was, expectedly, highest, but superior levels were seen in all local deeper tissues (ligament, tendon, cartilage, fascia, fat). The adjacent muscle showed 20 times more radioactivity after topical than oral administration.

Despite blood level differences spanning orders of magnitude (oral ≫ topical), topical dosing in humans produced 60% of the salicylate level in synovial fluid found after oral aspirin administration (Table XI). Subjective improvement was reported by two-thirds of the study group for both salicylate administration routes. Hence, once again, topical delivery is seen to produce high local subcutaneous levels of drug despite appreciably reduced blood concentrations. Direct deep penetration is thus the mechanism implicated. The authors of this study concluded that the lipid solubility of triethanolamine salicylate permits it to remain localized and to be slowly absorbed into the blood. This suggested a desirable feature for providing pain relief of local discomfort without systemic side effects. Parenthetically, a study[1] performed in the rabbit using two commercial preparations[2] of triethanolamine salicylate found as much salicylate in the muscle beneath the application site as in the same tissue

[1] A. Fujii, L. G. Nutine, and E. S. Cook, personal communication.
[2] Asperheat and Aspercreme; Thompson Medical Co., Inc., New York, N.Y.

Table XI—[^{14}C]Salicylate Concentrations in Blood, Urine, and Synovial Fluid 1 and 2 hr after Oral and Topical Salicylate Administration to Humans [a]

Tissue	[^{14}C]Salicylate Concentration, μg/ml			
	Oral		Topical	
	1 hr	2 hr	1 hr	2 hr
Blood	10.27 ± 1.04	10.33 ± 1.06	0.03 ± 0.00	0.08 ± 0.01
Urine	0.64 ± 0.13	1.45 ± 0.27	0.02 ± 0.01	0.18 ± 0.06
Synovial fluid	0.29 ± 0.03	0.40 ± 0.08	0.16 ± 0.02	0.25 ± 0.04

[a] Data taken from Ref. 16. All values are mean ± *SEM*; $N = 6$ for $t = 1$ hr, $N = 4$ for $t = 2$ hr.

following oral dosing of aspirin. Also, a double-blind investigation carried out by Golden (17) using similar salicylate preparations[2] on 40 patients again indicated that equally effective subjective pain relief could be attained using topical triethanolamine salicylate as with oral aspirin. The topical delivery route was suggested to offer a superior alternative in the alleviation of certain rheumatic conditions.

CONCLUSIONS

The experimental work summarized in this survey leaves little doubt that the principle of subcutaneous delivery of topically applied substances is established. Together with the observations of lateral movement of penetrating materials within the dermis, it is apparent that the vascular supply of the skin is not always a perfect "sink." The limited data available is teasing and implies that deeper penetration may be a far more ubiquitous phenomenon than had ever been thought possible; in a sense, the behavior has rarely been seen (and hence assumed not to exist) because few have bothered to look for it. As with all research, additional studies will provide further clarification and delineation of these issues. For example, further kinetic information and, hence, the residence times of various penetrating species as a function of depth into the tissue, and the quantity of material present subcutaneously, await clearer assessment. More information is required about the amount of applied substance absorbed and what fraction of that amount is localized in the deeper tissues. In terms of a complete overview of percutaneous absorption as a drug delivery process, it is important that the aspects discussed here are not ignored. As for practical applications, the clinical one is self-evident and, even on the basis of the results reviewed here, has been repeatedly alluded to by the workers involved: deeper penetration can concentrate more active compound in local affected muscular tissue than can practical alternative administration routes. Better (or at least equivalent) therapy is possible, therefore, without systemic distribution of the drug, *i.e.*, significant blood levels, and possible side effects. The ramifications of this potential in terms of pharmacology and pharmacokinetics warrant further study.

ADDENDUM

Since the submission of this article two further examples of local deep penetration after topical administration have been brought to our attention. Areh (Ph.D. thesis, Massachusetts College of Pharmacy and Allied Health Science, 1982) prepared a number of salicylate derivatives and demonstrated, in rabbits, that therapeutic levels could be achieved in local muscle tissue after transdermal delivery. Wada *et al.* [*J. Pharm. Pharmacol.*, **34**, 467 (1982)] considered the percutaneous absorption and anti-inflammatory activity of indomethacin administered in a topical ointment to rats. They found that the drug concentration in the muscle of the treated paw was very high and ~10 times that in the tissue of any other paw and 7 times that in the blood.

REFERENCES

(1) P. Gorog and I. B. Kovacs, *Curr. Ther. Res.*, **10**, 485 (1968).

(2) V. W. Lang, *Arzneim.-Forsch.*, **24**, 71 (1974).

(3) S. Shuster, *Br. J. Dermatol.*, **106**, 235 (1982).

(4) R. B. Fountain, B. S. Baker, J. W. Hadgraft, and I. Sarkany, *Br. J. Dermatol.*, **81**, 202 (1969).

(5) R. H. Guy and H. I. Maibach, *Arch. Dermatol. Res.*, **273**, 91 (1982); W. J. Albery, R. H. Guy, and J. Hadgraft, *Int. J. Pharm.*, **15**, 125 (1983).

(6) H. Osamura, *J. Dermatol.*, **9**, 45 (1982).

(7) M. James, J.-P. Marty, and J. Wepierre, *C. R. Hebd. Seances Acad. Sci. Ser. D*, **278**, 2063 (1974).

(8) M. James, J.-P. Marty, and J. Wepierre, *C. R. Hebd. Seances Acad. Sci. Ser. D*, **281**, 1525 (1975).

(9) M. James, J.-P. Marty, and J. Wepierre, *Eur. J. Drug Metab. Pharmacokinet.*, **2**, 69 (1976).

(10) J.-P. Marty, Ph.D. thesis, Université de Paris-Sud, Paris, France, 1976.

(11) J.-P. Marty, M. James, N. Hajo, and J. Wepierre, in "Percutaneous Penetration of Steroids," P. Mauvais-Jarvais, Ed., Academic, New York, N.Y., 1980, pp. 205–218.

(12) R. T. Tregear, "Physical Functions of Skin," Academic, London, 1966, pp. 1–52.

(13) F. D. Malkinson and E. H. Ferguson, *J. Invest. Dermatol.*, **25**, 281 (1955).

(14) A. W. McKenzie and R. B. Stoughton, *Arch. Dermatol.*, **86**, 608 (1962).

(15) C. F. H. Vickers, *Arch. Dermatol.*, **88**, 20 (1963).

(16) J. L. Rabinowitz, E. S. Feldman, A. Weinberger, and H. R. Schumacher, *J. Clin. Pharmacol.*, **22**, 42 (1982).

(17) E. L. Golden, *Curr. Ther. Res.*, **24**, 524 (1978).

ACKNOWLEDGMENTS

This work was supported in part by NIH grant 1-R03-OH01830-01.

Moisture Sorption Kinetics for Water-Soluble Substances I: Theoretical Considerations of Heat Transport Control

L. VAN CAMPEN *, G. L. AMIDON ‡, and G. ZOGRAFI ˣ

Received June 9, 1982, from the *School of Pharmacy, University of Wisconsin-Madison, Madison, WI 53706.* Accepted for publication October 22, 1982. Present addresses: *Boehringer Ingelheim Ltd., Ridgefield, CT 06877 and ‡College of Pharmacy, University of Michigan, Ann Arbor, MI 48104.

Abstract □ A model based on heat transport control was developed to describe the uptake of water on a deliquescent solid in an atmosphere of pure water vapor. The model assumes the presence of a saturated liquid film on the surface of the solid. The decrease in the vapor pressure of water over the surface, brought about by the colligative effect of solid dissolved in the liquid film, is effectively offset by the increase in temperature of the film (and the solid) caused by the heat released on condensation of the water vapor. The thermal transients die out quickly and a steady-state analysis is valid. At steady state the temperature of the liquid film (and solid) is that temperature at which the vapor pressure of water above the saturated solution is equal to the chamber pressure. Consequently, water uptake occurs at a rate that depends on the heat flux away from the surface. The water uptake rate, W'_h, is constant at a given relative humidity and is described by an equation of the form $W'_h = (C + F)\cdot\ln(RH_i/RH_o)$, where C and F are conductive and radiative coefficients, RH_i the chamber relative humidity, and RH_o the relative humidity at and above which continuous water uptake (deliquescence) occurs. The model contains no adjustable parameters and can thus be directly tested against experimental results.

Keyphrases □ Sorption—moisture, water-soluble substances, kinetics, heat transport control, theoretical model with water vapor atmosphere □ Kinetics—moisture sorption of water-soluble substances, heat transport control, theoretical model with water vapor atmosphere □ Deliquescence—water-soluble substances, sorption kinetics, heat transport control, theoretical model with water vapor atmosphere

The interaction of water with pharmaceutical materials plays a fundamental role in many aspects of drug product development, from synthetic design and dosage form selection to effective product packaging and drug bioavailability. The affinity that a substance has for sorbing water from its vapor state is generally referred to as hygroscopicity. Since adsorption or condensation is not an entropically favored process, the water–solid interaction must provide a sufficient enthalpic driving force if such sorption is to occur. Even the relatively weak binding of physisorption, for which the heat of adsorption is comparable to the heat of condensation, can provide this driving force over a large range in relative humidity. At higher relative humidities, multilayer adsorption can occur (1). For water-soluble substances, dissolution of the molecules at the solid surface can occur once such multilayer adsorption is established. Chikazawa, Kanazawa, and others have shown that as few as two layers of adsorbed water can effect hydrated ion formation at relative humidities 30–40% below that humidity associated with the equilibrium water vapor pressure over a saturated solution of the solid (2, 3). This critical relative humidity, or RH_o, characteristic of the solid is that point above which the adsorbed water assumes the character of bulk solution or condensate. Water activity of the condensate is depressed as a result of the solute present, and the phenomenon of deliquescence is thereby triggered.

Figure 1 shows a schematic representation of the deliquescent process for a soluble drug particle. Suppose that water vapor at a bulk atmosphere relative humidity, RH_i, adsorbs onto the solid surface of the particle. If this humidity is above the RH_o of the drug, further adsorption will occur spontaneously and the thickness of the condensate film will grow. Solid will continue to dissolve and saturate the film, maintaining the relative humidity at the surface at RH_o. To reach equilibrium with the atmosphere at RH_i, total dissolution and some degree of solution dilution must occur. To predict deliquescent behavior *a priori* requires an understanding of what fundamental factors, chemical and environmental, control the kinetics of the process. Despite the practical consequences of deliquescent hygroscopic behavior, only limited investigations of sorption kinetics above RH_o have appeared in the literature (4–8), all using an empirical expression to describe the phenomenon. The purpose of the present study, therefore, was to gain a more quantitative understanding of deliquescence.

BACKGROUND

Consider the overall picture of what processes are operating to control deliquescence in the presence of an inert atmosphere such as air, where adsorption of vapor onto any solid surface involves the simultaneous transport of both mass and heat (9–16). While there may exist additional heat effects, these two processes are at least coupled by the heat of water condensation released per unit mass transported from the vapor to the condensed phase. This is expressed by:

$$W' \cdot \Delta H = Q \qquad \text{(Eq. 1)}$$

where $W' = dW/dt$ = rate of mass transport (vapor condensation), W is the sample weight at time t, ΔH is the heat generated per unit mass condensed, and Q is the heat flux from the surface at which condensation occurs. The extent to which either process limits or controls the rate of condensation depends on the molecular diffusivities and thermal prop-

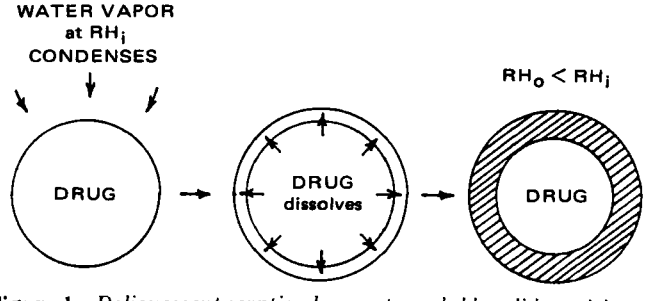

Figure 1—*Deliquescent sorption by a water-soluble solid particle.*

0022-3549/83/1200-1381$01.00/0

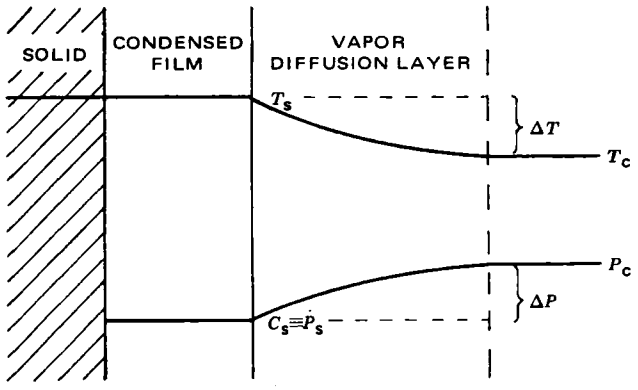

Figure 2—*Thermal and pressure gradients existing at a soluble solid surface covered with condensed water.*

erties of all phases in the condensing system. For hygroscopic moisture uptake by a solid exhibiting substantial water solubility, such as that illustrated in Fig. 1, this system consists of three phases: pure, undissolved solid; a liquid film of condensate in which solid has dissolved; and water vapor in an atmosphere of inert gas. It follows then that there exist two interfaces over which transport must occur: solid–liquid and liquid–vapor. A closer examination of this condensation system is given in Fig. 2, in which:

$$P_c = RH_i\left(\frac{P_0}{100}\right) \qquad \text{(Eq. 2)}$$

where P_c is equal to the bulk water vapor pressure in the atmosphere, and

$$P_s = RH_o\left(\frac{P_0}{100}\right) \qquad \text{(Eq. 3)}$$

where P_s is equal to the water vapor pressure in equilibrium over a saturated solution of the solid; P_0 represents the pressure of pure water vapor at bulk atmosphere temperature, T_c, and C_s and T_s represent the water vapor concentration and the temperature at the surface, respectively. Possible steady-state thermal and pressure gradients are indicated in Fig. 2. Steady-state sorption implies that the driving force for uptake, whether thermal or diffusive, has reached a constant value, *i.e.*, W' is constant.

The zero pressure (or concentration) gradient shown within the liquid film in Fig. 2 is consistent with the assumption that film saturation is maintained throughout steady-state moisture uptake. The likelihood of a zero gradient in temperature within the solid and liquid phases will be substantiated shortly in the discussion of non-steady-state heat transport.

The thermodynamic basis for hygroscopic uptake lies in the difference between P_s and P_c in the vicinity of the saturated film surface. Water vapor will condense progressively on the surface as long as $P_s < P_c$. Three general cases exist when sorption occurs, each implying a different extent to which heat or mass transport controls uptake.

Case *i*: Mass Transport Control (Isothermal), $\Delta T = 0$, $\Delta P = \Delta P_{max}$—Heat generated upon condensation is rapidly transported away from the liquid–vapor interface so as to render the system effectively isothermal throughout the course of steady-state uptake. The pressure difference, ΔP, is maximized since P_s at T_c is less than P_s at T_s for any $T_s > T_c$. The rate of uptake, W', is then proportional to ΔP and the surface area over which uptake occurs.

Case *ii*: Heat Transport Control (Isobaric), $\Delta T = \Delta T_{max}$, $\Delta P = 0$—Heat generated upon condensation is sufficient to maintain the liquid–vapor interface at a temperature T_s, elevated above that of the bulk atmosphere maintained externally at T_c. The temperature difference, $\Delta T = T_s - T_c$, is exactly that necessary to raise P_s at T_c to P_s at T_s such that P_s at T_s equals P_c at T_c. In this case, W' is proportional to ΔT by virtue of its explicit dependence on the heat flux as given in Eq. 1.

Case *iii*: Mass–Heat Transport in Balance, $0 < \Delta T < \Delta T_{max}$, $0 < \Delta P < \Delta P_{max}$—The gradients depicted in Fig. 2 exemplify this intermediate situation. Because neither ΔP nor ΔT is constrained to zero, there exists no unique ΔP–ΔT combination which can be predicted *a priori* to satisfy the requirements of steady-state condensation without knowledge of both the thermal and diffusive characteristics of the system.

In considering the three cases given above, it is apparent that for water uptake from an atmosphere of pure water vapor, diffusion barriers to transport in the vapor phase cannot exist. In the absence of a second gas component, resistance to transport can arise only from the collision of water molecules against one another, which in itself would not generate a measurable gradient in water vapor pressure, *i.e*, "nature abhors a vacuum." Consequently, the role of heat transport can be tested explicitly by deriving appropriate equations for case *ii* and testing the model with experimental studies using an atmosphere of pure water vapor. The present paper, therefore, reports a theoretical model for case *ii*; the second paper of this series (17) presents a test of this model with experimental studies, and the third paper describes water uptake in an inert atmosphere such as air (18).

THEORETICAL

The sample undergoing sorption is considered to be a compressed circular disk situated symmetrically near the hemispherical base of a cylindrical chamber, a configuration chosen for its experimental feasibility. Figure 3 illustrates the geometry that must be considered in discussing the transport of heat within this system. Regarding the development of a local temperature gradient within the sample disk itself, the disk may be considered to behave as a planar slab if its diameter far exceeds its thickness. With respect to any transport external to the sample or the surface of its developing film, a hollow-sphere geometry will be assumed, consistent with the radial nature of the transport occurring between the disk and the surrounding chamber. Here the sample is represented by a hypothetical inner sphere of radius $r = a$ such that it is equivalent in surface area to that of the sample itself; the chamber then behaves as an outer sphere of radius $r = b$ at which surface the temperature is maintained at T_c. Presuming the disk and chamber to behave as concentric spheres allows a more manageable mathematical treatment of transport occuring in the system. The more rigorous approach of using disk-to-sphere or disk-to-hemisphere transport geometries is unnecessarily complex for two reasons. First, the isotherm surfaces that exist during steady-state heat transport from a disk to a surrounding sphere take on spherical shape as distance from the disk increases, behaving much like a hollow-sphere system when the disk diameter is small relative to the outside sphere. Second, and more practically, the errors associated with predicting transport as if within a closed sphere should have a constant effect for any sample tested in this configuration. Thus, the legitimate theoretical comparison of the hygroscopic behavior of different materials can be made despite these approximations.

Upon condensation, heat is generated at the film surface by two primary sources (in the absence of auxiliary reactions, *e.g.*, hydration, *etc.*): heat of condensation, releasing $\Delta H_v = 0.58$ cal/mg of water condensed; and heat of dissolution, approximately equal to the product of the solubility, C_{sat}, and the heat of solution, ΔH_{soln}. For a number of nonhydrating alkali halide salts, $C_{sat} \cdot \Delta H_{soln}$ is unlikely to exceed an approximate value of 0.04 cal/mg of water; for such compounds the contribution of the heat of dissolution to the heat generated on condensation can be considered negligible, such that $\Delta H = -\Delta H_v$ in Eq. 1.

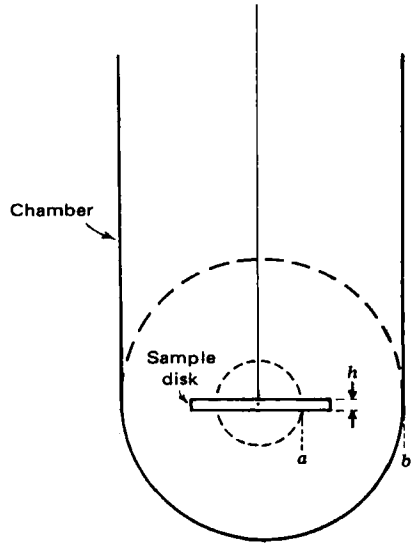

Figure 3—*Chamber and sample geometry; slab and hollow-sphere model.*

Table I—Physical Constants for the Transport Model in an Atmosphere of Pure Water Vapor

Symbols	Constants
a, cm	0.5[a]
b, cm	2.0[a]
M_w, mg/mole	1.8×10^4
k, cal/cm·sec·deg	4.26×10^{-5}
α, cm²/sec	4.13
ΔH, cal/mole	−10,500[b]
ΔH_v, cal/mole	10,500
R, cal/deg·mole	1.987
T_c, °K	298
σ, cal/cm²·sec·deg⁴	1.36×10^{-12}
e	0.95[c]

[a] Theoretically arbitrary in value; these particular values have been assigned in this case for their consistency with an available experimental apparatus. [b] The assumption is made here that the heat of condensation predominates over all other possible heat effects such that the latter are neglected. [c] Film surface emissivity approximated by value given for pure water (20).

Heat transport away from the surface limits the rate of condensation; thus, uptake depends on the thermal properties of the system. There exist two primary heat sinks in the system described in Fig. 3: the atmosphere surrounding the sample and the sample itself. Heat transport to and through these media can occur *via* three basic mechanisms: conduction inward through the sample or radially outward through the atmosphere; convection, a term used here (in the absence of forced convection) to designate the extra heat transport that occurs as a result of the radially inward bulk flow of water vapor that feeds the condensation process; and radiation from the hypothetical surface $r = a$ to surface $r = b$.

A general expression for heat flux, Q, reflecting the three mechanisms of heat transport (19) is:

$$Q = q_{cond} + q_{conv} + q_{rad} \quad \text{(Eq. 4)}$$

where

$$q_{cond} = -4\pi r^2 \cdot k \frac{dT}{dr} \quad \text{(Eq. 5)}$$

$$q_{conv} = W' C_p (T_s - T) \quad \text{(Eq. 6)}$$

$$q_{rad} = A\sigma e (T_s^4 - T_c^4) \quad \text{(Eq. 7)}$$

and k is the thermal conductivity of the medium, C_p is the specific heat capacity of the medium, A is the sample surface area $= 4\pi a^2$, σ is the Stefan–Boltzmann constant, and e is the emissivity of the sample surface. Table I contains the physical constants of interest.

Before discussing the quantitative implications of steady-state uptake for heat transport-controlled condensation, it is necessary to estimate the time required to establish steady-state thermal gradients within the system, *i.e.*, within both the solid disk and the surrounding atmosphere. In doing so the assumption is made that thermal conductivity, thermal diffusivity, and specific heat values are independent of water vapor concentration and temperature.

Non-Steady-State Heat Transport—*Sample Disk*—Only conduction need be considered for heat transport within the sample disk. The time-dependent temperature distribution for a slab of thickness, h, whose parallel surfaces are subjected to a sudden change in temperature has already been determined in the literature (21, 22). The sample disk can be assumed to behave according to this model if edge effects are neglected. Specifically, the disk region bounded by $-h/2 < z < +h/2$ is subjected to the boundary conditions that $T = T_c$ for all z at $t = 0$ and $T = T_s$ at $z = \pm h/2$ for $t > 0$. The temperature profile describing one-half of the (symmetrical) slab for $z = 0$ to $z = h/2$ is given by (21):

$$T = T_s + \frac{4}{h} \sum_{n=0}^{\infty} \exp[-\alpha(2n+1)^2\pi^2 t/h^2] \cos\frac{(2n+1)\pi z}{h} \cdot \left[\frac{h(-1)^{n+1}T_s}{(2n+1)\pi} + T_c \int_0^{h/2} \cos\frac{(2n+1)\pi z'}{h} dz'\right] \quad \text{(Eq. 8)}$$

where α is the thermal diffusivity of the solid slab. In dimensionless terms this can be written (21, 22):

$$T^* = 1 - \frac{4}{\pi} \sum_{n=0}^{\infty} \frac{(-1)^n}{2n+1} \cdot \exp[-(2n+1)^2\pi^2 t^*/4] \cos\frac{(2n+1)\pi z^*}{2} \quad \text{(Eq. 9)}$$

in which:

$$T^* = \frac{T - T_c}{T_s - T_c} \quad \text{(Eq. 10)}$$

$$z^* = \frac{z}{h/2} \quad \text{(Eq. 11)}$$

$$t^* = \frac{\alpha t}{(h/2)^2} \quad \text{(Eq. 12)}$$

From Eq. 9 it can be shown (21, 22) that the center ($z = 0$) of such a slab reaches 97% of its equilibrium value by dimensionless time, $t^* = 1.5$, from which real time can be calculated. For example, the center portion of a (relatively) thin solid disk of potassium chloride crystal of $\alpha = 0.056$ cm²/sec and a thickness $h = 0.06$ cm should attain ~97% of its final temperature change, ΔT, within 0.03 sec. Thus, one could predict that thermal equilibrium should be rapidly established within such materials as the alkali halide salts. Furthermore, the heat required to raise, for example, a 150-mg sample of potassium chloride ($C_p = 0.162$ cal/g·deg) by a $\Delta T = 5°$ is 0.12 cal. Since heat is released at the disk surface at the rate of 0.58 cal/mg of water vapor condensed, the role of such a disk as a significant heat sink over the course of substantial steady-state uptake can be considered negligible.

Atmosphere—The time required to establish a steady-state temperature gradient external to the disk surface depends on the non-steady-state component of heat transport radially outward from the sample. Such heat transport through the atmosphere can occur *via* all three mechanisms identified earlier, and indeed they all contribute to maintaining the steady-state gradient. If the water vapor atmosphere is considered transparent to radiation, however, only conduction and convection will contribute to the establishment of the gradient. Since the effect of convection on maintaining the steady state will be shown to be negligible in the following discussion, only conductive flux will be considered in the non-steady-state gradient development.

The solution for the time-dependent temperature distribution in the atmosphere is readily accessible from the non-steady-state mass and heat transport equations developed in Appendix I. In terms of dimensionless variables where T^* is defined in Eq. 10 and the analogous distance and time variables are defined as:

$$r^* = \frac{r - a}{b - a} \quad \text{(Eq. 13)}$$

and

$$t^* = \frac{\alpha t}{(b-a)^2} \quad \text{(Eq. 14)}$$

the expression for T^*, as taken from Eq. A8, becomes:

$$T^* = \left[\frac{1}{r^*(b/a - 1) + 1}\right] \cdot \left[1 - r^* - \frac{2}{\pi} \sum_{n=1}^{\infty} \frac{1}{n} \sin n\pi r^* \cdot \exp(-n^2\pi^2 t^*)\right] \quad \text{(Eq. 15)}$$

This function is described in Fig. 4 where $\Pi^* = T^*$. For condensation in vacuum (where $b - a = 1.5$ cm) the time required to reach $t^* = 0.5$ is only 0.28 sec. If air were present, steady-state gradients would essentially be attained within 5.6 sec given an estimated value of $\alpha = 0.214$ cm²/sec for humid air[1]. As apparent earlier for the disk, it can be concluded that a steady thermal state is rapidly established within the atmosphere relative to the time scale of extended uptake.

The time required for the conductive heat flux, and therefore uptake rate, to reach a steady-state level at surface $r = a$ can be calculated using Eq. A21. For the example above, these lag times equal (−)0.047 sec and (−)0.94 sec in vacuum and in air, respectively. These times are consistent with the development of the temperature gradients as established in Fig. 4. At surface $r = b$, lag times are calculated using Eq. A25, and for the vacuum and air systems equal 0.94 sec and 1.9 sec, respectively.

Steady-State Heat Transport—Steady-state moisture uptake requires a constant heat flux, by virtue of the coupling in Eq. 1; this, in turn, implies the maintenance of a constant ΔT. The ΔT necessary to raise P_s at T_c to P_s at T_s such that it equals P_c at T_c, as implied by heat transport control, can by first approximation be estimated by the Clausius–Cla-

[1] Since heat transfer will also contribute to sorption kinetics in air, and since the effect of air will be discussed in the third paper in this series (18), lag times in reaching steady state both in vacuum and air are included at this point for comparison purposes, as developed in Appendix I. This value for humid air was estimated using C_p values of water vapor and air weighted by mole fraction and thermal conductivity (k) values for water vapor and air, as taken from Table I and as calculated using the Lindsay and Bromley modification of the Wassiljewa equation (23), respectively.

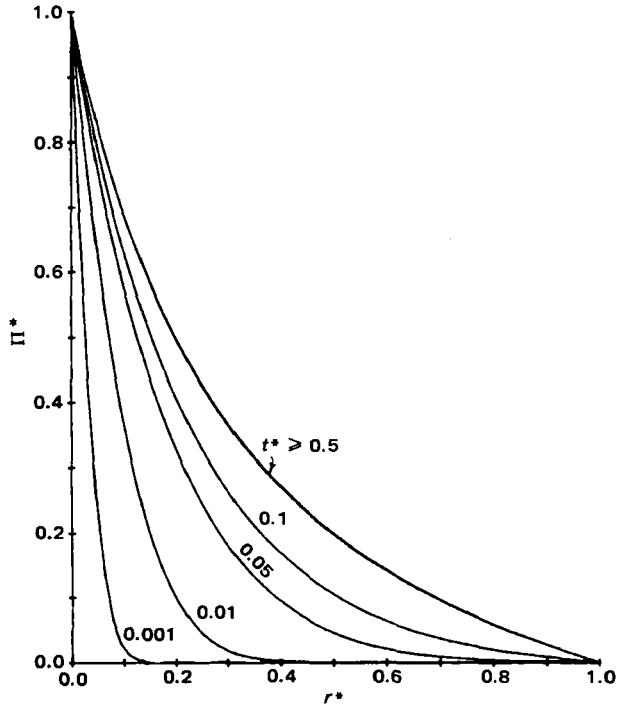

Figure 4—*Gradient in* Π* *at various* t* *values for a hollow sphere,* a < r < b, where b/a = 4.

peyron equation as developed below:

$$\ln \frac{P_s(T_s)}{P_s(T_c)} = \ln \frac{P_c(T_c)}{P_s(T_c)} \quad \text{(Eq. 16)}$$

$$= \ln \frac{RH_i}{RH_o} \quad \text{(Eq. 17)}$$

such that:

$$\ln \frac{RH_i}{RH_o} = \frac{\Delta H_v}{RT_sT_c}(T_s - T_c) \quad \text{(Eq. 18)}$$

where ΔH_v is the heat of vaporization and R is the gas constant. Solving for ΔT, one obtains:

$$T_s - T_c = \frac{RT_c^2 \ln \frac{RH_i}{RH_o}}{\Delta H_v - RT_c \ln \frac{RH_i}{RH_0}} \quad \text{(Eq. 19)}$$

For several nonhydrating alkali halide salts whose solubility and RH_o dependence on temperature are known (24, 25), ΔT as defined above is observed to vary from 0–15°, depending on the ratio of $RH_i(T_c)$ to $RH_o(T_c)$. Use of the Clausius–Clapeyron equation to estimate these ΔT values for saturated salt solutions is subject to two sources of error: the small temperature dependence of the heat of vaporization of pure water and, more significantly, the effect of the salt and its (temperature-dependent) solubility on water activity and the heat of vaporization. Despite these errors, Eq. 19 predicts ΔT values equal to 100–110% of those actually observed (24, 25) for saturated solutions of the alkali halides.

The evaluation of transient-state heat flux within and heat capacity of the sample disk suggests that the disk has a negligible effect on the maintenance of ΔT. Of primary importance, then, is the radial heat flow within the hollow-sphere system. From Eqs. 4–7 this steady-state flux can be expressed as:

$$Q = -4\pi r^2 \cdot k \frac{dT}{dr} + W'C_p(T_s - T) + A\sigma e(T_s^4 - T_c^4) \quad \text{(Eq. 20)}$$

During steady-state flux:

$$\frac{dQ}{dr} = 0 \quad \text{(Eq. 21)}$$

Therefore:

$$0 = 4\pi k \frac{d}{dr}\left(r^2 \frac{dT}{dr}\right) + W'C_p \frac{dT}{dr} \quad \text{(Eq. 22)}$$

where the derivative of the radiation term vanishes under the assumption that the atmosphere is transparent to radiative flux. Differentiating the product term and rearranging leads to:

$$\frac{d^2T}{dr^2} + \left(\frac{2}{r} + \frac{W'C_p}{4\pi kr^2}\right)\frac{dT}{dr} = 0 \quad \text{(Eq. 23)}$$

Solving the equation by reduction of order and then applying the boundary conditions, $T = T_s$ at $r = a$ and $T = T_c$ at $r = b$, one arrives at the expression:

$$T = \frac{T_s\left[\exp\left(\frac{W'C_p}{4\pi kr}\right) - \exp\left(\frac{W'C_p}{4\pi kb}\right)\right] - T_c\left[\exp\left(\frac{W'C_p}{4\pi kr}\right) - \exp\left(\frac{W'C_p}{4\pi ka}\right)\right]}{\left[\exp\left(\frac{W'C_p}{4\pi ka}\right) - \exp\left(\frac{W'C_p}{4\pi kb}\right)\right]} \quad \text{(Eq. 24)}$$

Expressed in terms of T^* as defined in Eq. 10:

$$T^* = \frac{1 - \exp\left[\frac{W'C_p}{4\pi k}\left(\frac{1}{r} - \frac{1}{b}\right)\right]}{1 - \exp\left[\frac{W'C_p}{4\pi k}\left(\frac{1}{a} - \frac{1}{b}\right)\right]} \quad \text{(Eq. 25)}$$

The above expressions describe the steady-state temperature gradient within the hollow sphere as maintained by both conduction and convection. Convection is used here to denote the heat transport that occurs in raising the temperature of the water vapor surrounding the sample to T_s just prior to its condensation. It will be shown that this convective component of the flux has essentially no effect on the temperature gradient given W' values of experimental magnitude. Neglecting the convective term, Eq. 22 becomes:

$$0 = 4\pi k \frac{d}{dr}\left(r^2 \frac{dT}{dr}\right) \quad \text{(Eq. 26)}$$

This leads to a second-order differential equation whose solution over the same boundary conditions is:

$$T = (T_s - T_c)\frac{a}{r}\left(\frac{b - r}{b - a}\right) \quad \text{(Eq. 27)}$$

or

$$T^* = \frac{a}{r}\left(\frac{b - r}{b - a}\right) \quad \text{(Eq. 28)}$$

As expected, this is the same gradient described by Eq. (A4) as $t \to \infty$. As the term $W'C_p/4\pi k$ increases, convection is more likely to influence the temperature profile. Yet even at a relatively high uptake rate of W' = 2 mg/min in the vacuum system, for which the value of $C_p/4\pi k$ = 837 cm·sec/g, the temperature gradient remains effectively indistinguishable from the steady-state profile exhibited in Fig. 4, in which convection was neglected. Consistent with this result, it has been shown (26) that convection contributes negligibly (<2%) to the overall steady-state heat flux from the surface $r = a$. This flux is then given by:

$$Q\Big|_{r=a} = -4\pi ka^2 \frac{dT}{dr}\Big|_{r=a} + q_{rad} \quad \text{(Eq. 29)}$$

$$= -4\pi ka^2(T_s - T_c)\frac{dT^*}{dr}\Big|_{r=a} + q_{rad} \quad \text{(Eq. 30)}$$

which on substituting Eqs. 7 and 28 yields:

$$Q\Big|_{r=a} = \frac{4\pi kab}{b - a}(T_s - T_c) + 4\pi a^2\sigma e(T_s^4 - T_c^4) \quad \text{(Eq. 31)}$$

Recalling Eq. 1, the uptake rate may easily be expressed in terms of T_s by utilizing the above equation. It is of greater interest, however, to determine the direct dependence of W', the dependent experimental variable, on RH_i, the independent variable. An expression relating ΔT to RH_i is given by Eq. 19. A comparable expression for $\Delta(T^4)$ is required for substitution into the radiation term. From Eq. 19 the solution for T_s can be raised to the fourth power and simplified by dropping all terms contributing <2% (for RH_i/RH_o ratios <2.7) to the resulting overall polynomial. This leads to an approximate expression for $\Delta(T^4)$ similar in form to that for ΔT:

$$T_s^4 - T_c^4 = \frac{4RT_c^5 \ln \frac{RH_i}{RH_o}}{\Delta H_v - 4RT_c \ln \frac{RH_i}{RH_o}} \quad \text{(Eq. 32)}$$

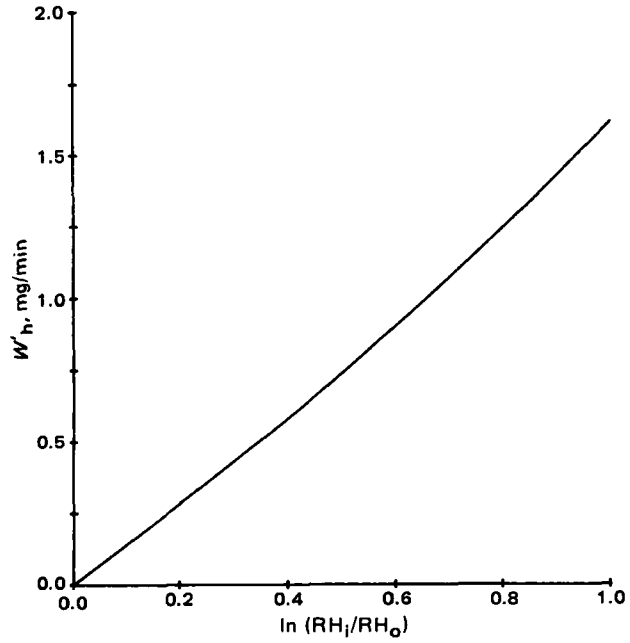

Figure 5—*Theoretical* W'_h versus *ln* (RH_i/RH_o) *as predicted by Eq. 33.*

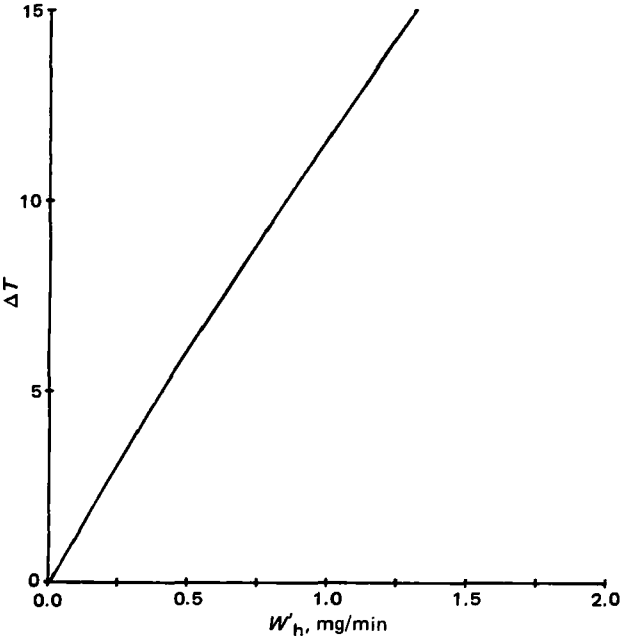

Figure 6—*Relationship between* ΔT *and* W'_h *for heat transport-controlled sorption (see Table I).*

Substituting Eqs. 19 and 32 into Eq. 31, then combining with Eq. 1, one arrives at a final equation for the dependence of W', or W'_h to indicate heat transport control, on RH_i:

$$W' = W'_h = \left[\frac{60M_w \cdot 4\pi kab}{\Delta H(b-a)}\left(\frac{RT_c^2}{\Delta H_v - RT_c \ln \frac{RH_i}{RH_o}}\right) + \frac{60M_w \cdot 4\pi a^2 \sigma e}{\Delta H}\left(\frac{4RT_c^5}{\Delta H_v - 4RT_c \ln \frac{RH_i}{RH_o}}\right)\right] \cdot \ln \frac{RH_i}{RH_o} \quad \text{(Eq. 33)}$$

where the factor $60M_w$ simply converts W'_h from mole/sec to mg/min. More simply:

$$W'_h = (C + F) \ln \frac{RH_i}{RH_o} \quad \text{(Eq. 34)}$$

where C and F represent the conduction and radiative terms, respectively, in Eq. 33 and are themselves weakly dependent on ln (RH_i/RH_o). Interestingly, C and F, *i.e.*, conduction and radiation, contribute almost equally to heat transport in an atmosphere of pure water vapor.

Eq. 33 allows *a priori* prediction of heat transport-controlled uptake rates for condensation systems whose geometry is well defined and whose physical properties are known. Furthermore, the curve so predicted and shown in Fig. 5 represents a unique curve for W'_h as a function of ln (RH_i/RH_o) that should be common to all materials, regardless of their RH_o values, given the same sample and chamber geometry.

Since ΔT is a unique function of ln (RH_i/RH_o) by virtue of the Clausius–Clapeyron relation and W'_h is also a unique function of ln(RH_i/RH_o), ΔT and W'_h should be interdependent if condensation is indeed proceeding under thermal control. Again using the parameters listed in Table I, the predicted graph of ΔT *versus* W'_h is given in Fig. 6.

SUMMARY

A heat transport control model for water uptake by solids has been developed for the case of a water-soluble solid immersed in an atmosphere of pure water vapor. The model is based on the fact that the heat of condensation of water released during water uptake must be transported to the surroundings. In an atmosphere of pure water vapor, where diffusion does not occur, this heat flux limits the rate of condensation.

Development of a non-steady-state model indicates that the non-steady time period is very short. Thus, a steady-state model is appropriate for time periods of pharmaceutical interest. The equations for heat transport (conduction, convection, and radiation) when combined with the Clausius–Clapeyron equation lead to an equation which predicts the water uptake rate with no adjustable parameters (Eq. 33). The results of the analysis indicate that the convection term is of minor importance and that conduction and radiation control heat flux to comparable degrees.

APPENDIX I: NON-STEADY STATE

The non-steady-state solution referred to previously is developed herein. Since non-steady-state considerations are of interest both here and in subsequent papers, which include mass transport considerations, a general solution is developed for both heat and mass transport. Because of the analogous behavior of mass diffusion and (conductive) heat flow, the general parameter, Π, will be used to represent either concentration (C) or temperature (T). Similarly, the symbol, τ, will be used to represent a general diffusivity in place of D or α.

The general equation for radial diffusion with a constant diffusion coefficient is:

$$\frac{\partial \Pi}{\partial t} = \tau \left[\frac{1}{r^2}\frac{\partial}{\partial r}\left(r^2 \frac{\partial \Pi}{\partial r}\right)\right] \quad \text{(Eq. A1)}$$

The solution to this equation describes the time dependence of either the concentration distribution for mass diffusion or the temperature distribution for conductive heat flux in which all velocity gradients associated with convection and viscous dissipation have been assumed to be equal to zero (27). For the hollow-sphere system in which $a < r < b$, subjected to the boundary conditions $\Pi = \Pi_c$ for all r at $t = 0$, $\Pi = \Pi_s$ at $r = a$, and $\Pi = \Pi_c$ at $r = b$ for $t > 0$, Π is described by the function (28):

$$\Pi = \frac{a\Pi_s}{r} + \frac{(b\Pi_c - a\Pi_s)(r-a)}{r(b-a)} + \frac{2}{\pi r}\sum_{n=1}^{\infty}\left\{\frac{b\Pi_c\cos n\pi - a\Pi_s}{n} \cdot \sin\frac{n\pi(r-a)}{b-a}\cdot\exp[-\tau n^2\pi^2 t/(b-a)^2]\right\} + \frac{2\Pi_c}{r(b-a)}\sum_{n=1}^{\infty}\left\{\sin\frac{n\pi(r-a)}{b-a}\cdot\exp[-\tau n^2\pi^2 t/(b-a)^2] \cdot\int_a^b r'\sin\frac{n\pi(r'-a)}{b-a}\,dr'\right\} \quad \text{(Eq. A2)}$$

Given that Π^* is defined as:

$$\Pi^* = \frac{\Pi - \Pi_c}{\Pi_s - \Pi_c} \quad \text{(Eq. A3)}$$

it can be shown that the nature of Eq. A1 does not change if expressed in dimensionless terms, *i.e.*, Π^* can be substituted for Π in Eq. A1. Thus, the solution expressed by Eq. A2 for Π is readily adapted to a solution for Π^* according to Eq. A3. Because the boundary conditions are redefined as $\Pi^* = 1$ at $r = a$ ($\Pi = \Pi_s$) and $\Pi^* = 0$ at $r = b$ ($\Pi = \Pi_c$), however, the solution for Π^* simplifies to:

$$\Pi^* = \frac{a}{r} + \frac{(-a)(r-a)}{r(b-a)} + \frac{2}{\pi r}\sum_{n=1}^{\infty}\left\{\frac{-a}{n}\sin\frac{n\pi(r-a)}{b-a}\cdot\exp[-\tau n^2\pi^2 t/(b-a)^2]\right\} \quad \text{(Eq. A4)}$$

where the fourth term vanishes when expressed in dimensionless form. Then, allowing:

$$t^* = \frac{\tau t}{(b-a)^2} \quad \text{(Eq. A5)}$$

and

$$r^* = \frac{r-a}{b-a} \quad \text{(Eq. A6)}$$

where then

$$\frac{a}{r} = \frac{1}{r^*(b/a-1)+1} \quad \text{(Eq. A7)}$$

and substituting these new variables into Eq. A4, the expression for Π^* further simplifies to:

$$\Pi^* = \left[\frac{1}{r^*(b/a-1)+1}\right]\left[1 - r^* - \frac{2}{\pi}\sum_{n=1}^{\infty}\frac{1}{n}\sin n\pi r^* \cdot\exp(-n^2\pi^2 t^*)\right] \quad \text{(Eq. A8)}$$

The time course to developing a steady-state Π^* gradient over r^* can then be plotted for various t^* values at a given ratio of b/a. Figure 4 presents such a plot for $b/a = 4$, where the incremented value of n was truncated at $n = 20$. Discontinuities observed in the $t^* = 0.001$ plot at $\Pi^* \sim 0$ would not have appeared if n were to have been truncated at an even higher value. It is clear from Fig. 4 that the gradient at $t^* = 0.5$ is virtually indistinguishable from the $t^* = \infty$ curve.

To determine the time required for the actual flux, and hence uptake rate, to reach a steady-state level, the time dependence of the flux must be evaluated. Total mass flux from the surface $r = a$ over time t is given by:

$$W_t\Big|_{r=a} = \int_0^t -D\frac{\partial C}{\partial r}\Big|_{r=a}\,dt' \quad \text{(Eq. A9)}$$

The term ρC_p must be introduced into the analoguos expression for heat flux:

$$Q_t\Big|_{r=a} = \int_0^t -\rho C_p\cdot\alpha\frac{\partial T}{\partial r}\Big|_{r=a}\,dt' \quad \text{(Eq. A10)}$$

or

$$Q_t\Big|_{r=a} = \int_0^t -k\frac{\partial T}{\partial r}\Big|_{r=a}\,dt' \quad \text{(Eq. A11)}$$

where k is the thermal conductivity of the medium in the hollow sphere. Because of the introduction of the additional parameter k and the potential confusion of its appearance with α in the solution to Eq. A11, the flux associated with heat conduction, rather than mass diffusion, will be solved for in the following development.

In terms of T^*, r, and t, where T^* is defined by Eq. 10 and is consistent with the definition of Π^*:

$$Q_t\Big|_{r=a} = -k(T_s - T_c)\int_0^t\frac{\partial T^*}{\partial r}\Big|_{r=a}\,dt' \quad \text{(Eq. A12)}$$

Allowing S to represent the summation term in Eq. A8 in which $\Pi^* = T^*$,

$$\frac{\partial T^*}{\partial r}\Big|_{r=a} = -\frac{1}{a} - \frac{1}{b-a} + \frac{\partial S}{\partial r}\Big|_{r=a} \quad \text{(Eq. A13)}$$

where:

$$\frac{\partial S}{\partial r}\Big|_{r=a} = -\frac{2a}{\pi r}\Big|_{r=a}\frac{\partial}{\partial r}\sum_{n=1}^{\infty}\left\{\frac{1}{n}\sin\frac{n\pi(r-a)}{b-a}\cdot\exp[-\alpha n^2\pi^2 t/(b-a)^2]\right\}\Big|_{r=a} + \frac{2a}{\pi r^2}\sum_{n=1}^{\infty}\left\{\frac{1}{n}\sin\frac{n\pi(r-a)}{b-a}\cdot\exp[-\alpha n^2\pi^2 t/(b-a)^2]\right\}\Big|_{r=a} \quad \text{(Eq. A14)}$$

$$= -\frac{2}{b-a}\sum_{n=1}^{\infty}\exp[-\alpha n^2\pi^2 t/(b-a)^2] \quad \text{(Eq. A15)}$$

Then:

$$\int_0^t\frac{\partial T^*}{\partial r}\Big|_{r=a}\,dt' = -\frac{bt}{a(b-a)} - \frac{2}{b-a}\cdot\int_0^t\sum_{n=1}^{\infty}\exp[-\alpha n^2\pi^2 t'/(b-a)^2]\,dt' \quad \text{(Eq. A16)}$$

$$= -\frac{bt}{a(b-a)} - \frac{2(b-a)}{\alpha\pi^2}\left\{\sum_{n=1}^{\infty}\frac{1}{n^2} - \sum_{n=1}^{\infty}\frac{1}{n^2}\cdot\exp[-\alpha n^2\pi^2 t/(b-a)^2]\right\}\Big| \quad \text{(Eq. A17)}$$

Since:

$$\sum_{n=1}^{\infty}\frac{1}{n^2} = \frac{\pi^2}{6} \quad \text{(Eq. A18)}$$

then

$$Q_t\Big|_{r=a} = k(T_s - T_c)\left\{\frac{bt}{a(b-a)} + \frac{b-a}{3\alpha} - \frac{2(b-a)}{\alpha\pi^2} \cdot \sum_{n=1}^{\infty}\frac{1}{n^2}\cdot\exp[-\alpha n^2\pi^2 t/(b-a)^2]\right\} \quad \text{(Eq. A19)}$$

As $t \to \infty$, the total conductive flux from surface $r = a$ becomes:

$$Q_{t\infty}\Big|_{r=a} = k(T_s - T_c)\left[\frac{b}{a(b-a)}\right]\left[t + \frac{a(b-a)^2}{3\alpha b}\right] \quad \text{(Eq. A20)}$$

revealing a lag time to steady-state flux of:

$$t_{\text{lag},r=a} = -\frac{a(b-a)^2}{3\alpha b} \quad \text{(Eq. A21)}$$

The total heat flux at the surface $r = b$ over time t can be similarly evaluated. In this case:

$$\frac{\partial T^*}{\partial r}\Big|_{r=b} = -\frac{a}{b(b-a)} + \frac{\partial S}{\partial r}\Big|_{r=b} \quad \text{(Eq. A22)}$$

which leads to:

$$Q_t\Big|_{r=b} = k(T_s - T_c)\left\{\frac{at}{b(b-a)} - \frac{a(b-a)}{6\alpha b} - \frac{2a(b-a)}{b\alpha\pi^2} \cdot \sum_{n=1}^{\infty}\frac{(-1)^n}{n^2}\cdot\exp[-\alpha n^2\pi^2 t/(b-a)^2]\right\} \quad \text{(Eq. A23)}$$

As $t \to \infty$, the total conductive flux to surface $r = b$ becomes:

$$Q_{t\infty}\Big|_{r=b} = k(T_s - T_c)\left[\frac{a}{b(b-a)}\right]\left[t - \frac{(b-a)^2}{6\alpha}\right] \quad \text{(Eq. A24)}$$

revealing a lag time to steady-state flux at the outside surface of:

$$t_{\text{lag},r=b} = \frac{(b-a)^2}{6\alpha} \quad \text{(Eq. A25)}$$

Note that the final equations given above for total heat flux and the lag times to steady state at either surface $r = a$ or $r = b$ (Eqs. A19, A21, A23, and A25) can be readily converted to the analogous expressions in time-dependent mass flux by replacing Q_t and T by W_t and C, respectively, and by replacing both α and k by D.

APPENDIX II: GLOSSARY

- a effective sample radius, radius of hypothetical inner sphere
- A surface area
- b chamber radius
- c subscript, chamber
- C concentration
- C conduction term
- C_p heat capacity
- C_s surface concentration
- C_{sat} saturation solubility
- D (vapor) diffusion coefficient
- e emissivity
- F radiation term
- h thickness of sample disk
- ΔH heat generated or consumed per unit moisture condensed
- ΔH_{soln} heat of solution
- ΔH_v heat of vaporization
- k thermal conductivity
- M_w molecular weight of water
- P water vapor pressure
- P_c pressure in atmosphere (chamber)
- P_0 pressure of pure water vapor at given temperature
- P_s pressure at sample surface
- ΔP pressure difference
- ΔP_{max} maximum pressure difference, taken as $P_c - P_s$
- q_{cond} conductive heat flux
- q_{conv} convective heat flux
- q_{rad} radiative heat flux
- Q heat flux
- Q_t quantity of heat flow in time t
- r radius
- r^* dimensionless radius
- R gas constant
- RH_i relative humidity in atmosphere
- RH_o critical relative humidity of a substance associated with the relative humidity in equilibrium over a saturated solution of the substance
- s subscript, at the sample surface
- S series term
- t time
- t^* dimensionless time variable
- $t_{lag,r=a}$ lag time to steady-state flux at surface $r = a$
- T temperature
- T_c temperature in chamber, *i.e.*, at temperature-controlled wall of chamber
- T_s temperature at sample surface
- T^* dimensionless temperature variable
- ΔT temperature difference
- ΔT_{max} maximum temperature difference, taken as $T_s - T_c$
- W sample weight
- W' sorption rate
- W'_h sorption rate associated with heat transport control
- z slab thickness
- z^* dimensionless slab thickness
- α thermal diffusivity
- Π general mass or heat quantity, non-steady state
- Π^* dimensionless non-steady-state general mass on heat quantity variable
- σ Stefan–Boltzmann constant
- τ diffusivity

REFERENCES

(1) A. W. Adamson, "Physical Chemistry of Surfaces," 3rd ed. Wiley-Interscience, New York, N.Y. 1976, p. 548.

(2) M. Chikazawa, M. Kaiho, and T. Kanazawa, *Nippon Kagaku Kaishi*, **1972,** 874 (1972).

(3) T. Kanazawa, M. Chikazawa, M. Kaiho, and T. Fujimaki, *Nippon Kagaku Kaishi*, **1973,** 1669 (1973).

(4) R. Yamamoto and T. Takahashi, *J. Pharm. Soc. Jpn.*, **76,** 7 (1956).

(5) J. T. Carstensen, "Pharmaceutics of Solids and Solid Dosage Forms," Wiley, New York, N.Y., 1977, pp. 11–15.

(6) L. Van Campen, "An Approach to the Evaluation of Hygroscopicity for Pharmaceutical Solids, " M.S. Thesis, University of Wisconsin–Madison (1979).
(7) L. Van Campen, G. Zografi, and J. T. Carstensen, *Int. J. Pharm.*, **5**, 1 (1980).
(8) A. S. Mikulinski and R. I. Rubinstein, *J. Phys. Chem. (USSR)*, **9**, 431 (1937).
(9) T. K. Sherwood, *Ind. Eng. Chem.*, **21**, 976 (1929).
(10) E. R. Gilliland, *Ind. Eng. Chem.*, **30**, 506 (1938).
(11) C. B. Shepherd, C. Hadlock, and R. C. Brewer, *Ind. Eng. Chem.*, **30**, 388 (1938).
(12) G. King and A. B. D. Cassie, *Trans. Faraday Soc.*, **36**, 445 (1940).
(13) A. B. D. Cassie, *Trans. Faraday Soc.* **36**, 453 (1940).
(14) A. B. D. Cassie and S. Baxter, *Trans. Faraday Soc.*, **36**, 458 (1940).
(15) A. A. Armstrong, Jr. and V. Stannett, *Die Makromol. Chem.*, **90**, 145 (1966).
(16) D. M. Ruthven, L.-K. Lee, and H. Yucel, *AIChE J.*, **26**, 16 (1980).
(17) L. Van Campen, G. L. Amidon, and G. Zografi, *J. Pharm. Sci.*, **72**, 1388 (1983).
(18) L. Van Campen, G. L. Amidon, and G. Zografi, *J. Pharm. Sci.*, **72**, 1394 (1983).
(19) R. B. Bird, W. E. Stewart, and E. N. Lightfoot, "Transport Phenomena," Wiley, New York, N.Y., 1960, p. 505.
(20) R. B. Bird, W. E. Stewart, and E. N. Lightfoot, "Transport Phenomena," Wiley, New York, N.Y., 1960, p. 432.
(21) H. S. Carslaw and J. C. Jaeger, "Conduction of Heat in Solids," 2nd ed., Clarendon Press, Oxford, England 1959, pp. 100–101.
(22) C. Crank, "The Mathematics of Diffusion," 2nd ed., Oxford University Press, England, 1975 pp. 47–50.
(23) R. C. Reid, J. M. Prausnitz, and T. K. Sherwood, "The Properties of Gases and Liquids," 3rd ed., McGraw-Hill, New York, N.Y. 1977, pp. 508–509.
(24) P. H. Stahl, "Feuchtigkeit und Trocken in der Pharmazeutischen Technologie," Steinkopff, Darmstadt, W. G., 1980, p. 183.
(25) S. Gal, "Die Methodik der Wasserdampf-Sorptionsmessungen," Springer-Verlag, Berlin, W. G., 1967, p. 41.
(26) L. Van Campen, "Moisture Sorption Kinetics for Water-Soluble Substances," Ph.D. Thesis, University of Wisconsin–Madison (1981).
(27) R. B. Bird, W. E. Stewart, and E. N. Lightfoot, "Transport Phenomena," Wiley, New York, N.Y., 1960, p. 319.
(28) H. S. Carslaw and J. C. Jaeger, "Conduction of Heat in Solids," 2nd ed., Clarendon Press, Oxford, England, 1959, p. 246.

ACKNOWLEDGMENTS

Submitted by L. Van Campen to the University of Wisconsin–Madison in 1981, in partial fulfillment of the doctor of philosophy degree requirements.

L. V. C. expresses appreciation for graduate fellowship support to the American Foundation for Pharmaceutical Education and Merck Sharp and Dohme Research Laboratories.

Moisture Sorption Kinetics for Water-Soluble Substances II: Experimental Verification of Heat Transport Control

L. VAN CAMPEN*, G. L. AMIDON‡, and G. ZOGRAFI×

Received June 9, 1982, from the *School of Pharmacy, University of Wisconsin–Madison, Madison, WI 53706.* Accepted for publication October 22, 1982. Present Addresses: * Boehringer Ingelheim Ltd., Ridgefield, CT 06877 and ‡ College of Pharmacy, University of Michigan, Ann Arbor, MI 48104.

Abstract □ The rates of water sorption as a function of relative humidity for water-soluble substances exhibiting deliquescence have been measured in an atmosphere of pure water vapor. The substances studied included a series of alkali halides, choline halides, and sugars. The results were compared with a theoretical model, previously described, which relates the rate of water uptake to the transport of heat produced during the process away from the surface. Taking into account the heat of water vapor condensation, heat of solution, and heat of hydration, when hydration occurs, the model allows excellent *a priori* prediction of water uptake rates as a function of relative humidity.

Keyphrases □ Sorption—kinetics, alkali halides, choline halides, and sugars in a water vapor atmosphere, application of theoretical model □ Kinetics—moisture sorption, alkali halides, choline halides, and sugars in a water vapor atmosphere, application of theoretical model □ Deliquescence—sorption kinetics, alkali halides, choline halides, and sugars in a water vapor atmosphere, application of theoretical model

A quantitative treatment for the kinetics of water vapor sorption onto water-soluble solids which exhibit deliquescence has been developed in the preceding paper (1). The treatment was confined to situations where the rate is determined solely by the kinetics of heat transfer away from the surface to the atmosphere surrounding the solid. It was assumed that the resultant film of aqueous solution is saturated with respect to the dissolved solid throughout the process.

The model essentially says that heat generated upon condensation of water vapor, and any other heat change occurring during sorption, maintains the liquid–vapor interface at a temperature, T_s, elevated above that of the bulk atmosphere, externally maintained at T_c. The water vapor pressure over the saturated film, therefore, rises with temperature until the pressure difference between surface and atmosphere becomes infinitesimal, and remains so during steady-state uptake. The ability of the system to transfer heat away from the surface is assumed to limit the sorption rate. This sorption rate, W_h', was shown to depend on the relative humidity of the atmosphere, RH_i, and that in equilibrium with the saturated aqueous film around the solid, RH_o, as described by the equation:

$$W_h' = \left[\frac{60M_w \cdot 4\pi kab}{\Delta H(b-a)}\left(\frac{RT_c^2}{\Delta H_v - RT_c \ln \frac{RH_i}{RH_o}}\right) + \frac{60M_w \cdot 4\pi a^2 \sigma e}{\Delta H} \times \left(\frac{4RT_c^5}{\Delta H_v - 4RT_c \ln \frac{RH_i}{RH_o}}\right)\right] \cdot \ln \frac{RH_i}{RH_o} \quad \text{(Eq. 1)}$$

0022-3549/83/1200-1388$01.00/0

(6) L. Van Campen, "An Approach to the Evaluation of Hygroscopicity for Pharmaceutical Solids, " M.S. Thesis, University of Wisconsin–Madison (1979).
(7) L. Van Campen, G. Zografi, and J. T. Carstensen, *Int. J. Pharm.*, **5**, 1 (1980).
(8) A. S. Mikulinski and R. I. Rubinstein, *J. Phys. Chem. (USSR)*, **9**, 431 (1937).
(9) T. K. Sherwood, *Ind. Eng. Chem.*, **21**, 976 (1929).
(10) E. R. Gilliland, *Ind. Eng. Chem.*, **30**, 506 (1938).
(11) C. B. Shepherd, C. Hadlock, and R. C. Brewer, *Ind. Eng. Chem.*, **30**, 388 (1938).
(12) G. King and A. B. D. Cassie, *Trans. Faraday Soc.*, **36**, 445 (1940).
(13) A. B. D. Cassie, *Trans. Faraday Soc.* **36**, 453 (1940).
(14) A. B. D. Cassie and S. Baxter, *Trans. Faraday Soc.*, **36**, 458 (1940).
(15) A. A. Armstrong, Jr. and V. Stannett, *Die Makromol. Chem.*, **90**, 145 (1966).
(16) D. M. Ruthven, L.-K. Lee, and H. Yucel, *AIChE J.*, **26**, 16 (1980).
(17) L. Van Campen, G. L. Amidon, and G. Zografi, *J. Pharm. Sci.*, **72**, 1388 (1983).
(18) L. Van Campen, G. L. Amidon, and G. Zografi, *J. Pharm. Sci.*, **72**, 1394 (1983).
(19) R. B. Bird, W. E. Stewart, and E. N. Lightfoot, "Transport Phenomena," Wiley, New York, N.Y., 1960, p. 505.
(20) R. B. Bird, W. E. Stewart, and E. N. Lightfoot, "Transport Phenomena," Wiley, New York, N.Y., 1960, p. 432.
(21) H. S. Carslaw and J. C. Jaeger, "Conduction of Heat in Solids," 2nd ed., Clarendon Press, Oxford, England 1959, pp. 100–101.
(22) C. Crank, "The Mathematics of Diffusion," 2nd ed., Oxford University Press, England, 1975 pp. 47–50.
(23) R. C. Reid, J. M. Prausnitz, and T. K. Sherwood, "The Properties of Gases and Liquids," 3rd ed., McGraw-Hill, New York, N.Y. 1977, pp. 508–509.
(24) P. H. Stahl, "Feuchtigkeit und Trocken in der Pharmazeutischen Technologie," Steinkopff, Darmstadt, W. G., 1980, p. 183.
(25) S. Gal, "Die Methodik der Wasserdampf-Sorptionsmessungen," Springer-Verlag, Berlin, W. G., 1967, p. 41.
(26) L. Van Campen, "Moisture Sorption Kinetics for Water-Soluble Substances," Ph.D. Thesis, University of Wisconsin–Madison (1981).
(27) R. B. Bird, W. E. Stewart, and E. N. Lightfoot, "Transport Phenomena," Wiley, New York, N.Y., 1960, p. 319.
(28) H. S. Carslaw and J. C. Jaeger, "Conduction of Heat in Solids," 2nd ed., Clarendon Press, Oxford, England, 1959, p. 246.

ACKNOWLEDGMENTS

Submitted by L. Van Campen to the University of Wisconsin–Madison in 1981, in partial fulfillment of the doctor of philosophy degree requirements.

L. V. C. expresses appreciation for graduate fellowship support to the American Foundation for Pharmaceutical Education and Merck Sharp and Dohme Research Laboratories.

Moisture Sorption Kinetics for Water-Soluble Substances II: Experimental Verification of Heat Transport Control

L. VAN CAMPEN*, G. L. AMIDON‡, and G. ZOGRAFI×

Received June 9, 1982, from the *School of Pharmacy, University of Wisconsin–Madison, Madison, WI 53706.* Accepted for publication October 22, 1982. Present Addresses: * Boehringer Ingelheim Ltd., Ridgefield, CT 06877 and ‡ College of Pharmacy, University of Michigan, Ann Arbor, MI 48104.

Abstract □ The rates of water sorption as a function of relative humidity for water-soluble substances exhibiting deliquescence have been measured in an atmosphere of pure water vapor. The substances studied included a series of alkali halides, choline halides, and sugars. The results were compared with a theoretical model, previously described, which relates the rate of water uptake to the transport of heat produced during the process away from the surface. Taking into account the heat of water vapor condensation, heat of solution, and heat of hydration, when hydration occurs, the model allows excellent *a priori* prediction of water uptake rates as a function of relative humidity.

Keyphrases □ Sorption—kinetics, alkali halides, choline halides, and sugars in a water vapor atmosphere, application of theoretical model □ Kinetics—moisture sorption, alkali halides, choline halides, and sugars in a water vapor atmosphere, application of theoretical model □ Deliquescence—sorption kinetics, alkali halides, choline halides, and sugars in a water vapor atmosphere, application of theoretical model

A quantitative treatment for the kinetics of water vapor sorption onto water-soluble solids which exhibit deliquescence has been developed in the preceding paper (1). The treatment was confined to situations where the rate is determined solely by the kinetics of heat transfer away from the surface to the atmosphere surrounding the solid. It was assumed that the resultant film of aqueous solution is saturated with respect to the dissolved solid throughout the process.

The model essentially says that heat generated upon condensation of water vapor, and any other heat change occurring during sorption, maintains the liquid–vapor interface at a temperature, T_s, elevated above that of the bulk atmosphere, externally maintained at T_c. The water vapor pressure over the saturated film, therefore, rises with temperature until the pressure difference between surface and atmosphere becomes infinitesimal, and remains so during steady-state uptake. The ability of the system to transfer heat away from the surface is assumed to limit the sorption rate. This sorption rate, W_h', was shown to depend on the relative humidity of the atmosphere, RH_i, and that in equilibrium with the saturated aqueous film around the solid, RH_o, as described by the equation:

$$W_h' = \left[\frac{60M_w \cdot 4\pi kab}{\Delta H(b-a)}\left(\frac{RT_c^2}{\Delta H_v - RT_c \ln \frac{RH_i}{RH_o}}\right) + \frac{60M_w \cdot 4\pi a^2 \sigma e}{\Delta H} \times \left(\frac{4RT_c^5}{\Delta H_v - 4RT_c \ln \frac{RH_i}{RH_o}}\right)\right] \cdot \ln \frac{RH_i}{RH_o} \quad \text{(Eq. 1)}$$

0022-3549/83/1200-1388$01.00/0

where the various symbols represent parameters defined in the preceding paper (1).

Since all of these parameters are either available in the literature or experimentally determinable, it is possible to use Eq. 1 to predict the value of W_h' for various values of RH_i and for solids of varying RH_o. In this paper we present experimental studies of water sorption kinetics under vacuum conditions, where diffusion of water vapor is not a consideration and where heat transport control would be expected to predominate.

EXPERIMENTAL

Materials—Potassium chloride[1], potassium bromide[2], potassium iodide[3], sodium chloride[4], anhydrous sodium bromide[1], choline chloride[5], choline bromide[5], choline iodide[5], tetrabutylammonium bromide[6], sucrose[7], fructose[5], D-glucose monohydrate[1], and anhydrous D-glucose[3] were all reagent grade and were used as received. The dihydrate of sodium bromide was prepared by dissolving a maximum amount of the anhydrous form in boiling distilled water, filtering the hot solution, and cooling to room temperature. The crystals were collected and dried on filter paper. Loss on drying indicated that the crystals contained 100.6% of the theoretical water content. All samples of the dihydrate were stored over their own saturated solution since it would effloresce at any relative humidity <57.7%. Manipulation of the more hygroscopic compounds, such as choline chloride, was performed within a plastic inflatible glove bag[8] in which a relative humidity of <15% could be maintained under nitrogen. Such compounds were stored in partially evacuated desiccators over anhydrous calcium sulfate[9].

Equipment and Procedures—The apparatus, consisting of an electrobalance associated with a vacuum system, and the general procedures used to measure sorption kinetics have been described in considerable detail elsewhere (2). In the studies reported here, silicone diffusion pump oil[10] was used as the oil manometer fluid because of its low vapor pressure (2.3×10^{-6} torr) and suitable viscosity (42 cps) at 25°. A chromel–alumel thermocouple, calibrated to 0.1° in vacuum against an external reference thermocouple kept at 25.0 ± 0.05°, was installed within the sample chamber and positioned in the vicinity of the solid sample surface. A vacuum of 10^{-2} torr was maintained and various relative humidities were provided from chambers containing different saturated inorganic salt solutions (2). Temperature of the sample chamber atmosphere was maintained at 25 ± 0.05° by a thermostated water jacket.

All studies were carried out using solid samples compressed into disks since the well-defined geometry could be expressed in terms of the hollow-sphere geometry used in the development of the theoretical model (1). These disks were prepared by compressing 300 mg of powder on a hydraulic press at 66 kN over a 1-min interval between two 1.91 cm flat-faced punches. The disks were generally cut in half with a razor blade to provide two samples per disk. The alkali halides were oven dried at temperatures >150° and ground to a fine powder before compression. The choline halides and sugars were not subjected to elevated temperatures, but were powdered by grinding under sub-RH_o conditions at 25°–27°.

Solubility and Heat of Solution—The molal solubilities at 25° for all compounds studied are listed in Table I. Because of their extremely high solubilities, values for the three choline halides, not previously reported, were determined in this study by a visual method. Known quantities of distilled water and choline halide were added in various proportions of 2-ml glass ampules which were then sealed with plastic film and equilibrated at constant temperature. After equilibration, the molal solubility was estimated by bracketing the point of saturation.

The heats of solution for the various compounds are also listed in Table I. All values were taken from the references cited or were determined as part of this study from the temperature coefficient of solubility and the application of the van't Hoff equation or by solution calorimetry. A value of 3.26 kcal/mole from the literature for choline chloride (3) is in reasonably close agreement with an estimate of 2.6 kcal/mole from solubility considering the difficulty of handling the extremely hygroscopic choline chloride samples, its high solubility, and the method used to determine solubility. The general direction and magnitude of change in going from choline chloride to choline bromide is very similar to that seen for the chloride and bromide salts of a related quaternary ammonium ion reported in the literature (3).

Table I—Aqueous Solubility and Heats of Solution for Various Deliquescent Solids at 25°

Compound	C_{sat}, m (Ref. No.)	ΔH_{soln}, kcal/mole
Potassium chloride	4.81 (4)	4.115 (5)
Potassium bromide	5.65 (4)	4.750 (5)
Potassium iodide	8.86 (4)	4.860 (5)
Sodium chloride	6.14 (4)	0.928 (5)
Sodium bromide		
Anhydrous	—	0.58 (5)
Dihydrate	9.12 (4)	4.57 (5)
Choline iodide	14.0[a]	9.900[a]
Choline bromide	25.9[a]	4.800[a]
Choline chloride	32.2[a]	3.260 (3)
Tetrabutylammonium bromide	26.4 (6)	−2.050 (7)
Sucrose	6.18 (5)	1.319 (5)
Glucose		
Monohydrate	5.5 (8)	5.272[b]
Anhydrous	5.0 (8)	2.620[b]
Fructose	18.5 (9)	2.222[b]

[a] Determined from solubility in this study. [b] Determined calorimetrically in the laboratory of Professor S. Lindenbaum, University of Kansas.

RESULTS

Rate of Moisture Sorption—The rate of moisture sorption was estimated from the slope of the earliest portion of the water uptake *versus* time curve exhibiting extended linearity under stable RH_i conditions (2). In all cases, the time required to reach steady state was consistent with theoretical estimates (1). For the alkali halides (except sodium bromide), choline chloride, and sucrose, linear uptake of the disks was observed over very long time intervals (*i.e.*, hours) and appeared independent of percent weight gained until sufficient moisture had been sorbed so as to cause distortion of the disk and drop formation on the bottom surface of the disk. For these materials, multiple data points could be collected for the same sample by subjecting it to successive increments (or decrements) in RH_i. For the other compounds a fresh sample was used for each RH_i.

Normalization of Disk Surface Area—Most disk samples were halved for testing as indicated in *Experimental*. Because the semicircular disks were not exact halves owing to slight crumbling or asymmetric cutting, there existed differences in surface areas between sample disks. Since the facial surface area-to-weight ratio of a partial disk is theoretically equal to the known facial surface area-to-weight ratio of the whole disk, the facial surface area of the sample could be normalized to that of a perfect semicircular disk by comparing its weight with one half that of the whole disk from which it was prepared. Edge effects on the resulting normalization factor are negligible. Since the uptake rate is approximately proportional to disk surface area over the small changes in area corrected for in this normalization, the weight ratio factor could then be directly applied to the observed sorption rate data. Thus the normalized rate, W_n', for a half disk, is calculated by:

$$W_n' = W_{obs}' \cdot \frac{0.5\ (W_0, \text{whole disk})}{(W_0, \text{half disk})} \qquad \text{(Eq. 2)}$$

In Fig. 1 rates of sorption, W', are plotted *versus* relative humidity before and after normalization for potassium bromide disks intentionally cut to ⅓ and ⅔ sizes. In all cases normalization puts points closer to a straight line[11] going through RH_o for potassium bromide.

Effect of Varying Compression Pressure—Disks of potassium bromide (300 mg) compressed at 66, 44, 22, and 6.6 kN force were compared for their sorption characteristics. The disks were halved for testing.

[1] J. T. Baker Chemical Co.
[2] Allied Chemical.
[3] Mallinckrodt Chemical Works.
[4] Fisher Scientific Co.
[5] Sigma Chemical Co.
[6] Aldrich Chemical Co.
[7] Mann Research Labs.
[8] Model X-27-27; Instruments for Research and Industry.
[9] Drierite, Indicating; W. A. Hammond Drierite Co.
[10] DC704; Dow Corning.

[11] While theoretically incorrect (1), the linear plot is a reasonable approximation for the W' function at the high RH_i and small ΔRH_i values that pertain to potassium bromide and, thus, serves adequately to illustrate the success of normalization.

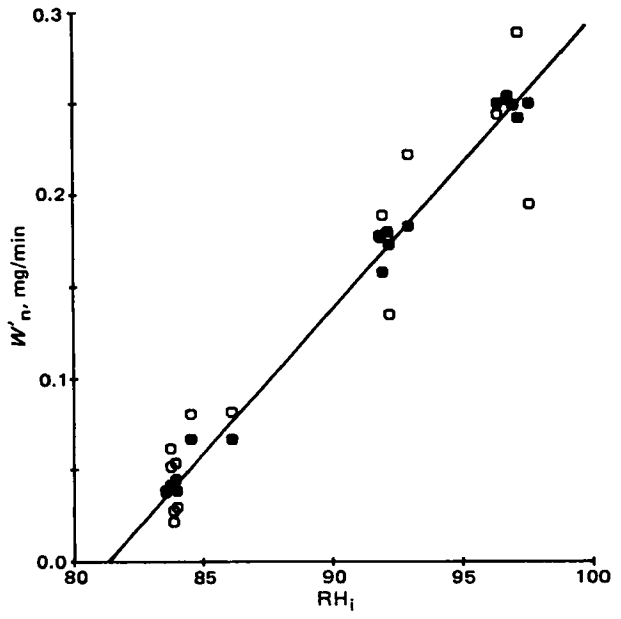

Figure 1—*Effect of normalization on treating observed W′ data for potassium bromide disks of varying size. Key: (○) observed W′; (●) W_n'.*

On the basis of weight, disk dimensions, and the density of pure potassium bromide, porosity of the disks ranged from ~4% (at 66 kN) to 25% (at 6.6 kN). Each sample was subjected to successive RH_i levels. The results are given in Fig. 2. It is clear from this plot that sorption rate did not depend significantly on disk porosity. It could, therefore, be inferred that lack of *density uniformity* in the disk is of no consequence to sorption, other than its potential effect on the normalization factor. The apparent reason porosity plays no role in sorption is that a film of (saturated) solution builds immediately during initial uptake, providing a smooth surface for continued sorption regardless of the internal porous structure of the disk.

Effect of Varying Disk Size—Heat transport-controlled sorption governed by Eq. 1 has a complex dependence on the effective disk (inner sphere) radius a. For a whole disk of real diameter 1.905 cm and average thickness 0.6 mm, $A = 4\pi a^2 = 2\pi(1.905/2)^2 + \pi(1.905)\,(0.06) = 6.06\ cm^2$, or $a = 0.69$ cm. As the disk is cut, the value of radius a does not fall by simple proportion. Accordingly, W' should not be expected to fall proportionally with decreasing disk size. From the expression given for W_h' by Eq. 1, one can write that:

$$W_h' = C' \cdot \frac{ab}{(b-a)} + F' \cdot a^2 \qquad \text{(Eq. 3)}$$

where C′ and F′ are conduction and radiation coefficients defined to reflect the dependence of W_h' on the characteristic disk dimension, a, pertaining to the hollow-sphere geometry of the system. If conduction and radiation contribute equally to heat transfer (1), then C′ = F′, and:

$$W_h' = C'\left(\frac{a}{1-a/b} + a^2\right) \qquad \text{(Eq. 4)}$$

The theoretical dependence of W_h' on disk W size is calculated according to Eq. 4, the results of which are summarized in Table II. A value of b = 2.05 cm was used for these calculations and for all subsequent calculations using Eq. 1 and related equations where b appears.

Table II—Predicted Sorption Rate Dependence on Disk Size

Disk Size	a[a] cm	W_h' (Eq. 4)	W_h'/W_h' at ½ disk
Whole	0.694	1.53 C′	1.72
⅔	0.567	1.10 C′	1.24
½	0.491	0.89 C′	1.00
⅓	0.401	0.66 C′	0.74

[a] Calculated neglecting edge effects for partial disks.

The sorption rates plotted for partial disks of potassium bromide in Fig. 1 to illustrate the normalization method are plotted again in Fig. 3, this time normalized to their appropriate facial surface area fraction, *e.g.*, ⅓, ⅔. Linear curves[11] for uptake by a whole disk, ⅔ disk, and ⅓ disk are drawn in Fig. 3 with appropriate theoretical slopes relative to the half disk, according to Table II. Excellent agreement is obtained between these curves and the observed (normalized) sorption rates, substantiating the appropriateness of the heat transport model expressed by Eq. 1, in general, and the relation between W' and disk size expressed by Eq. 4, specifically.

Effect of Varying the Initial Weight, W_0—Unless the heat capacity of the sample plays a significant role in the control of the sorption process, varying W_0 for a given disk size should have little or no effect on uptake rates. Again, W' should be expected to depend more on overall disk surface area than volume or weight of solid. Sorption by whole disks and half disks of potassium bromide of differing W_0 is compared in Fig. 4. The half-disk data have been normalized as usual according to Eq. 2. From the results in this plot[11], it can be concluded that W' is indeed relatively independent of W_0. Based on all of the preceding results, the sample preparation chosen for characterizing the sorption characteristics of

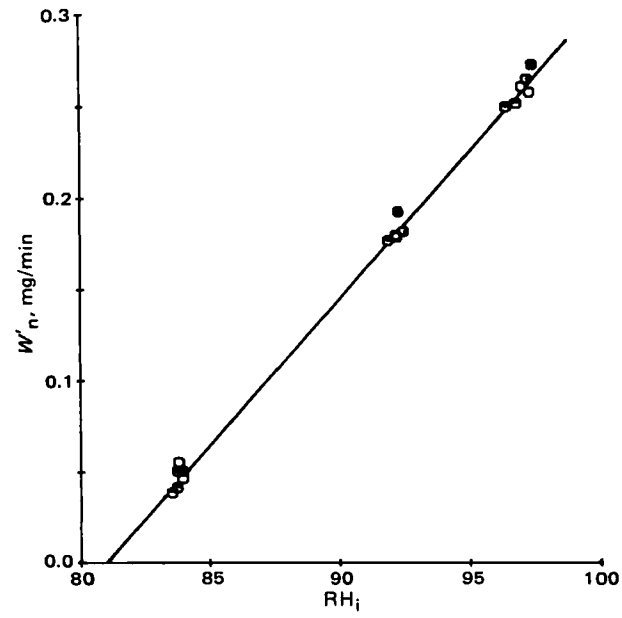

Figure 2—*Effect of compression pressure on sorption rates for potassium bromide disks. Compression pressure: (◑) 6.6 kN; (●) 22 kN; (○) 44 kN; (◒) 66 kN.*

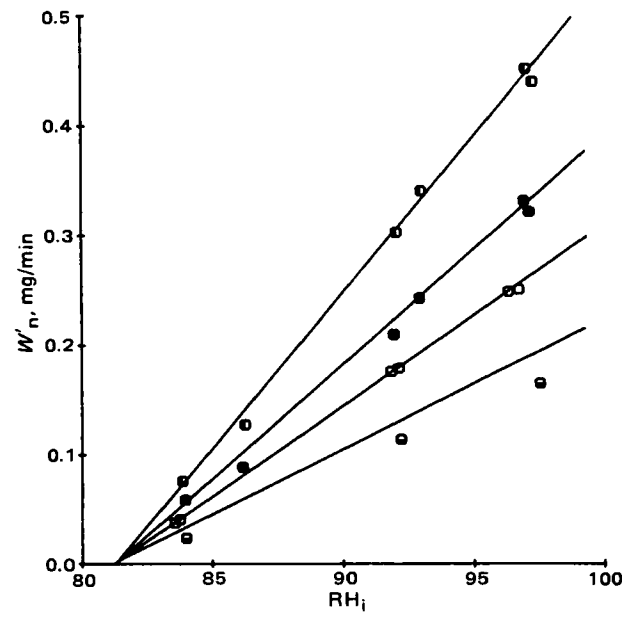

Figure 3—*Dependence of sorption rate for potassium bromide disks on disk size; data normalized to appropriate partial disk surface area. Key: (◒) ⅓ disk; (○) ½ disk; (●) ⅔ disk; (◐) whole disk.*

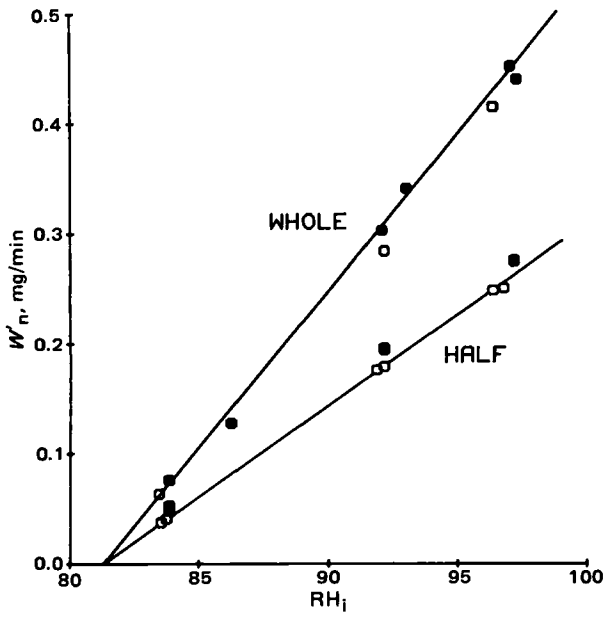

Figure 4—*Dependence of sorption rate for potassium bromide disks on disk* W_0 *for given approximate size. Key: (○)* W_0 *~150 mg; (●)* W_0 *~300 mg.*

various compounds in vacuum was that of a halved disk of W_{00} = 150 mg placed directly on the open wire stirrup.

Temperatures Changes at the Surface—Simultaneous measurement of temperature in the vicinity of the solid surface using the thermocouple allowed the estimation of ΔT, the temperature difference between the atmosphere (25°) and the point near the surface where the thermocouple was positioned. Since a substantial gradient in temperature is predicted to exist at the surface by the heat transport model, direct measurement of such gradients would provide some additional support for such a model. Consequently, the bimetallic junction of the thermocouple installed in the sample chamber was adjusted to hang over the sample disk within 0.5 mm of the top surface. Measurements of temperature taken at varying heights above the sample, >0.5 mm, allowed some definition of the temperature gradients created during the process of water sorption. Although exact fit to theory was not expected because the thermocouple could not be positioned exactly at the disk surface

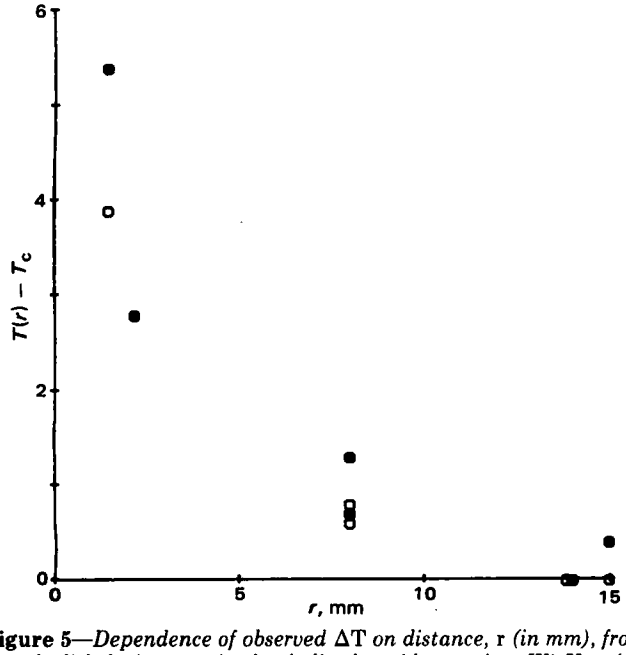

Figure 5—*Dependence of observed* ΔT *on distance,* r *(in mm), from sample disk during sorption by choline bromide at a given* W'. *Key: (●)* W' *~1.3 mg/min (*RH_i *~75); (○)* W' *~0.9 mg/min (*RH_i *~64).*

Table III—Values of ΔH and RH_o Used in Calculating Rates of Water Sorption from Eq. 1

Compound	ΔH kcal/mole	RH_o
Potassium chloride	−10.140	84.3
Potassium bromide	−10.020	80.7
Potassium iodide	−9.725	68.3
Sodium chloride	−10.400	75.3
Sodium bromide		
Anhydrous	−10.520	57.7
Dihydrate	−9.414	57.7
Choline iodide	−8.003	72.5
Choline bromide	−8.260	40.6
Choline chloride	−8.609	23.0
Tetrabutylammonium bromide	−11.475	61.0
Sucrose	−10.350	84.3
Glucose		
Monohydrate	−9.974	81.3
Anhydrous	−10.260	81.3
Fructose	−9.759	64.0

where the temperature gradient is steepest in its decline, it was possible to show that ΔT exists, and that it falls off at increasing distance from the surface. This is seen in Fig. 5 for choline bromide at two rates of sorption, *i.e.*, two values of RH_i. Figure 6 also shows the distance-dependent temperature difference for choline bromide and potassium iodide and also shows that an increase in uptake rate at any position of the thermocouple is generally associated with an increasing temperature difference. Similar observations were made with the other compounds studied.

Prediction of Water Uptake Rates—To test Eq. 1 quantitatively, steady-state uptake rates were determined at various values of RH_o. Table III lists the values of RH_o and ΔH used to obtain theoretical plots from Eq. 1. Other constants were as described in the preceding paper (1). The value of ΔH, unless otherwise specified, was calculated using the heat of condensation of water vapor (ΔH_c, which is −10.5 kcal/mole), the heat of solution (ΔH_{soln}), and the aqueous molal solubility (C_{sat}) as follows:

$$\Delta H = \Delta H_c + (C_{sat} \cdot \Delta H_{soln})/55.5 \qquad \text{(Eq. 5)}$$

where C_{sat} has units of moles of solute/1000 g of water, and ΔH_{soln} is in kilocalories per mole. The number 55.5 converts values into appropriate units. In the case of anhydrous potassium bromide and anhydrous glucose, the value of RH_o used was that of the hydrated form and ΔH was estimated by including the heat of hydration along with the heat of

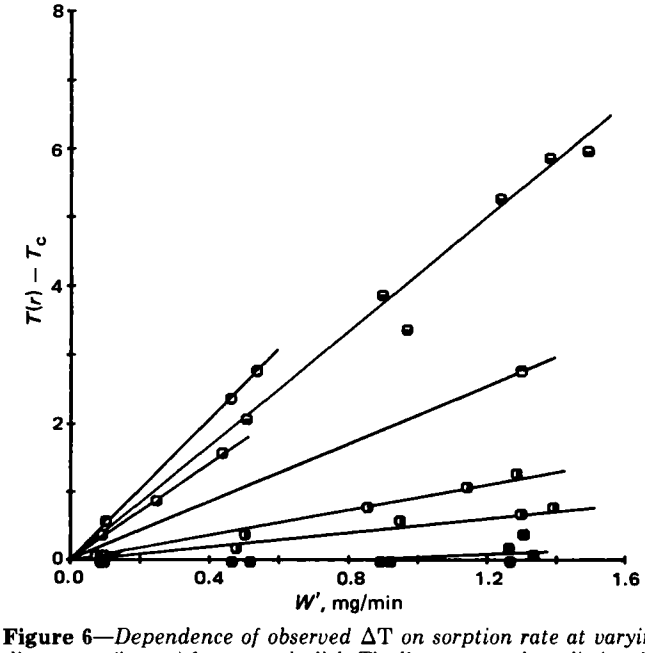

Figure 6—*Dependence of observed* ΔT *on sorption rate at varying distances* r *(in mm) from sample disk. The lines serve only to distinguish data from a given sorption run. Choline bromide: (●)* r *~15; (◑)* r *~8; (◒)* r *~2; (◒)* r *~1. Potassium iodide: (◕)* r *~1; (◐)* r *~0.5.*

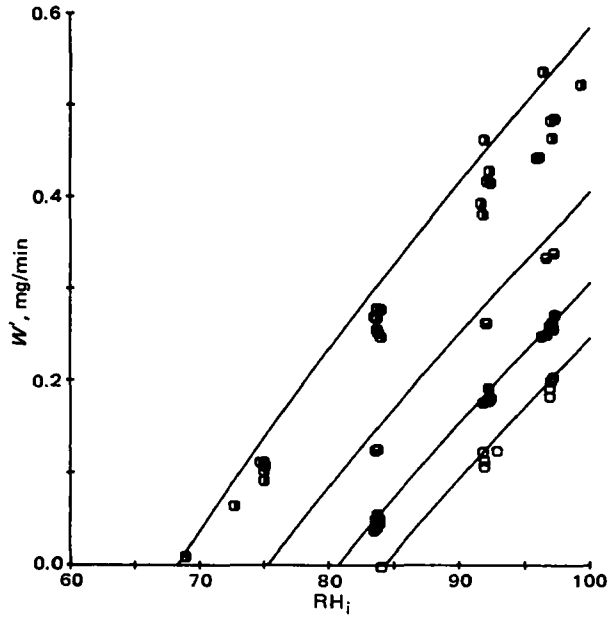

Figure 7—*Sorption rates for disks of alkali halides as a function of RH_i. The lines are the theoretical sorption curves plotted for W′ according to Eq. 1. Key (◑) potassium iodide; (◒) sodium chloride; (●) potassium bromide; (○) potassium chloride.*

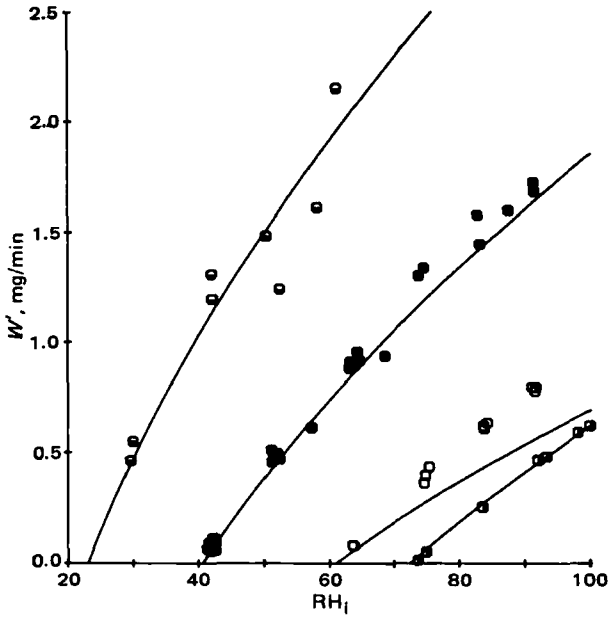

Figure 9—*Sorption rates for disks of quaternary ammonium halides as a function of RH_i. The lines are the theoretical sorption curves plotted for W′ according to Eq. 1. Key: (◒) choline chloride; (●) choline bromide; (◑); choline iodide; (○) tetrabutylammonium bromide.*

condensation and heat of solution, using Eq. 5. Figures 7–10 present theoretical graphs with experimental data for the heat transport-controlled W' (W_h') *versus* RH_i.

DISCUSSION

The results of experimental studies on water uptake rates of deliquescent substances in an atmosphere of pure water vapor, with the exception of tetrabutylammonium bromide and anhydrous glucose, provide excellent confirmation of the heat transport model described in the preceding paper (1). Thus, it appears possible to predict rates of uptake in a vacuum for most solids *a priori*, knowing their RH_0, solubility in water, and heat of solution, all experimentally determinable parameters. If crystalline hydrates can form, as in the case of sodium bromide, anhydrous glucose, and perhaps tetrabutylammonium bromide, the contribution of heat changes, attributable to hydration, however, must also be considered.

Fit of the model to solids varying very greatly in rates of water uptake, having also a broad range of solubilities and values of RH_0 and ΔH_{soln}, supports the important assumption that mass transport in the aqueous film surrounding the solid does not become rate limiting in determining the concentration of material dissolved in the film. In this regard, it is interesting to note that for systems having saturated solutions with viscosities 15–200 times that of water, agreement between theory and experiment for sorption rates was excellent. Analysis of the results using anhydrous sodium bromide and its dihydrate suggests the following picture. Below the value of RH_0 for the hydrate, water vapor can be taken up by the anhydrous form to form the hydrate. When RH_0 for the hydrate is exceeded, the hydrate layer dissolves in the liquid film to begin the

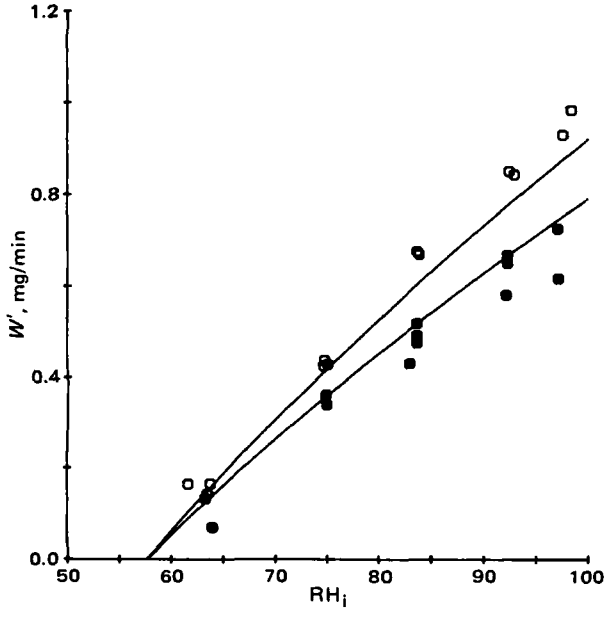

Figure 8—*Sorption rates for disks of the anhydrous (●) and dihydrate (○) forms of sodium bromide as a function of RH_i. The lines are the theoretical sorption curves plotted for W′ according to Eq. 1.*

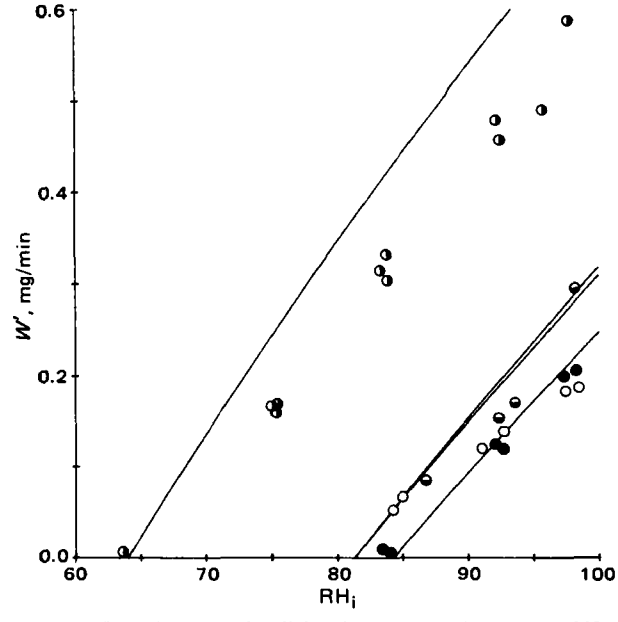

Figure 10—*Sorption rates for disks of sugars as a function of RH_i. The lines are the theoretical sorption curves plotted for W′ according to Eq. 1, where higher and lower curves intercepting RH_i = 81.3 represent W′ for the monhydrate and anhydrous forms of glucose, respectively. Key: (◒) fructose; (●) glucose · H_2O; (◐) glucose; (○) sucrose.*

process of deliquescence. This exposes more anhydrous crystal surface which quickly forms the hydrate. The heat released by hydrate formation increases the overall heat released, and this slows down the rate of water uptake relative to that observed with the hydrated crystal (see Fig. 8). The key to this picture is the rapid formation of the crystalline hydrate at the solid–liquid interface relative to the rate of heat transport and water uptake.

The significant lack of fit to the theoretical plot >84% RH_i for anhydrous glucose (Fig. 10) as opposed to the excellent fit for the monohydrate form of glucose, suggests strongly that the simple picture of rapid crystalline hydrate formation is not applicable. Rather, it appears that at higher RH_i values other kinetic processes, yet to be determined, are assuming greater significance. That the situation can be more complicated in some cases is seen with tetrabutylammonium bromide (Fig. 9) where the values predicted using only the heat of condensation of water and the reported heat of solution (7) are very different than those experimentally observed. In the case of tetrabutylammonium halide, the large cation has the tendency to exist in unusual states of hydration both in aqueous solution and in the crystalline form. In solution, tetrabutylammonium ions exhibit significant amounts of water structuring, leading to what has been termed "caging" of water around the cationic group (10, 11); this degree of structuring will decrease with increasing temperature. This strong tendency for hydration is also reflected in the formation by tetrabutylammonium salts of well-defined crystalline hydrates, having hydration numbers of 32 (12, 13). These hydrates are assumed to be of the clathrate type, similar in character to gas hydrates. Here, the cation acts as a guest in a host cavity created by water molecules and the anion. Evidence for polymorphism in these crystalline systems has also been reported (14).

Considering what takes place during the deliquescent process, any number of processes of structure formation or breaking in this system can contribute to ΔT and the net heat which must be transported away from the surface. If crystalline hydrate formation, as described for sodium bromide and glucose, predominates, we might expect a much slower rate than is actually observed. However, if water structuring in solution was being broken down, for example, as the temperature in the film increased, the net heat released would be much less than predicted from the heat of solution and this would lead to faster rates. In such a complex process involving higher degrees of ordering, there is also the possibility that simple equilibrium conditions are not reached and that incomplete hydration or slow rates of change during rapid water uptake affect the final rate of heat released and hence water uptake. It is interesting to note in this regard that the data obtained with tetrabutylammonium bromide can be fitted excellently if we assume a ΔH_{soln} of ~4.0 kcal/mole, which is close to the values of ΔH_{soln} for choline chloride and choline bromide, both of which have molal solubilities close to that of tetrabutylammonium bromide. This suggests the possibility that the part of the equilibrium heat of solution attributable to the unusual hydration properties of this ion is not making a contribution to the overall kinetic process. This certainly points out the importance of knowing as much as possible about the molecular nature of such complex water vapor–solid interactions when attempting to interpret the overall mechanisms of hygroscopicity. Fortunately, the behavior of many water-soluble species of pharmaceutical interest, exemplified by all of the other compounds studied, are much less complicated than tetrabutylammonium bromide.

CONCLUSIONS

A theoretical model for heat transport-controlled water uptake by deliquescent solids has been experimentally tested in an environment of pure water vapor (vacuum) where resistance to mass transport in the vapor phase would not be expected to be a factor. Studies with alkali halide salts, sugars, and choline salts provide excellent agreement with theory. As long as all heat-producing or -consuming processes are taken into account, knowing only solubility, various heat changes, and RH_0, it is possible to predict *a priori* the rate of water uptake for deliquescent substances as a function of RH_i, the chamber relative humidity.

REFERENCES

(1) L. Van Campen, G. L. Amidon, and G. Zografi, *J. Pharm. Sci.*, **72,** 1381 (1983).

(2) L. Van Campen, G. Zografi, and J. T. Carstensen, *Intern. J. Pharm.*, **5,** 1 (1980).

(3) G. E. Boyd, J. W. Chase, and F. Vaslow, *J. Phys. Chem.*, **71,** 573 (1967).

(4) R. C. Weast (Ed.), "Handbook of Chemistry and Physics," 57th ed., Chemical Rubber Co. Press, Cleveland, Ohio, 1976–77.

(5) E. W. Washburn (Ed.), "International Critical Tables of Numerical Data Physics, Chemistry and Technology," McGraw Hill, New York, N.Y. 1926.

(6) S. Lindenbaum and G. E. Boyd, *J. Phys. Chem.*, **68,** 911 (1964).

(7) C. V. Krishnan and H. L. Friedman, *J. Phys. Chem.*, **73,** 3934 (1969).

(8) "The Merck Index," 9th ed., Merck & Co., Inc., Rahway, N.J. 1976.

(9) "Martindale, The Extra Pharmacopeia," 27th ed., The Pharmaceutical Press, London, 1977.

(10) H. S. Frank and W. Y. Wen, *Dis. Faraday Soc.*, **24,** 133 (1957).

(11) W. Y. Wen, in "Water and Aqueous Solutions," R. A. Horne, Ed. Wiley–Interscience, New York, N.Y., 1972, p. 613.

(12) D. L. Fowler, W. V. Lobenstein, D. B. Pall, and C. A. Kraus, *J. Am. Chem. Soc.*, **62,** 1140 (1940).

(13) R. McMullan and G. A. Jeffrey, *J. Chem. Phys.*, **31,** 1231 (1959).

(14) W. Y. Wen, Ph.D Thesis, University of Pittsburgh, (1957).

ACKNOWLEDGMENTS

Submitted by L. Van Campen to the University of Wisconsin–Madison in 1981, in partial fulfillment of the doctor of philosophy degree requirements.

The authors wish to thank Mark Kontny, James Kou, Vincente Alonso-Perez, and Kevin Johnson for their excellent technical assistance and are grateful to S. Lindenbaum for the use of his solution calorimeter. L.V.C. wishes to thank the American Foundation for Pharmaceutical Education and Merck Sharp and Dohme Research Laboratories for providing graduate fellowship support.

Moisture Sorption Kinetics for Water-Soluble Substances III: Theoretical and Experimental Studies in Air

L. VAN CAMPEN *, G. L. AMIDON ‡, and G. ZOGRAFI ˣ

Received June 9, 1982, from the *School of Pharmacy, University of Wisconsin-Madison, Madison, WI 53706.* Accepted for publication October 22, 1982. Present addresses: *Boehringer Ingelheim Ltd., Ridgefield, CT 06877 and ‡College of Pharmacy, University of Michigan, Ann Arbor, MI 48104.

Abstract □ As an extension of the model of heat transport control developed for the kinetics of water sorption by water-soluble substances from an atmosphere of pure water vapor, equations have been developed to account for limitations of diffusion on mass transport of water vapor when air is present. Although the inability to determine the vapor diffusion layer thickness prevents using these equations to predict sorption behavior *a priori*, minimum water sorption rates can be calculated by assuming a diffusion layer thickness equal to the sample chamber radius. Combining heat transport and mass transport produces equations which describe very well the observed sorption by three water-soluble salts in one atmosphere of air. As in the absence of air, sorption rates are predicted and observed to be constant at a given atmospheric relative humidity.

Keyphrases □ Sorption—moisture, water-soluble substances, kinetics, theoretical model with air atmosphere, application to potassium bromide, potassium iodide, and choline iodide □ Kinetics—moisture sorption by water-soluble substances, theoretical model with air atmosphere, application to potassium bromide, potassium iodide, and choline iodide □ Deliquescence—kinetics of water sorption, theoretical model with air atmosphere, application to potassium bromide, potassium iodide, and choline iodide

In the first paper in this series (1) a theoretical model for the kinetics of water sorption by water-soluble solids exhibiting deliquescence was developed based on a heat transport control model. This model was tested successfully for water sorption from an atmosphere of pure water vapor over wide ranges of relative humidity in the second paper (2). In the present paper, this work is extended to include water sorption kinetics from an atmosphere containing air at approximately 1 atm of pressure. In such a case, one would expect the effects of diffusion through air on the mass transport of water vapor to influence the overall process. A model for water sorption in air is developed herein, first by assuming that only mass transport occurs and then by combining this with the heat transport model previously developed (1). Within the constraints of applying a mass transport model *a priori*, several water sorption experiments in an atmosphere of air have been performed to illustrate the potential importance of mass and heat transport in such a process.

THEORETICAL

Mass Transport Model (Isothermal)—As described in detail in the first paper (1) the thermodynamic basis for water uptake by water-soluble solids lies in the difference between equilibrium water vapor pressure, P_s, over the saturated solution of the solid and that in the atmosphere surrounding the solid, P_c. As seen in Fig. 1, when the heat sinks surrounding the liquid–vapor interface are sufficient in efficiency and capacity so as to maintain the system isothermal at T_c ($\Delta T = 0$), the rate of steady-state uptake is directly proportional to the constant water vapor pressure difference, $\Delta P = P_c - P_s$, over the vapor diffusion layer adjacent to the liquid–vapor interface. Expressed in terms of relative humidity, this difference becomes:

$$(100)\frac{\Delta P}{P_0} = RH_i - RH_o \qquad \text{(Eq. 1)}$$

where RH_i is the independent variable in a moisture-uptake experiment.

The radial diffusive flux of water vapor through a nondiffusing gas can be described by the following expression:

$$W'_{sp} = x_w W'_{sp} - M_w c D \frac{dx_w}{dr} \qquad \text{(Eq. 2)}$$

where W'_{sp} is the mass of water vapor transported in the z-direction per unit time per unit area, x_w is the mole fraction of water vapor in the atmosphere, M_w is the molecular weight of water, c is the total molar concentration in the atmosphere, and D is the binary diffusion coefficient of water vapor in the atmosphere. The first term in the right-hand side of Eq. 2 pertains to the mass flux of water vapor resulting from bulk fluid motion (where that of the inert gas is considered negligble) and the second term results from the diffusive mass flux of vapor superimposed on the bulk flow. Solving for W'_{sp} and expressing x_w in terms of pressure P, assuming gas ideality such that:

$$x_w = P/(P + P_i) \qquad \text{(Eq. 3)}$$

where P_i is inert gas pressure, one obtains:

$$W'_{sp} = -\frac{M_w c D}{P_T - P}\frac{dP}{dr} \qquad \text{(Eq. 4)}$$

where P_T represents the total (water vapor and inert gas) pressure. Here it is assumed that the temperature dependence of relative humidity is independent of the partial pressure of any inert gas present (3), and that the diffusion coefficient is independent of water vapor concentration and temperature.

Steady-state radial diffusion requires that:

$$\frac{d}{dr}(r^2 W'_{sp}) = 0 \qquad \text{(Eq. 5)}$$

Substitution of the expression for mass flux, W'_{sp}, from Eq. 4 then gives:

$$\frac{d}{dr}\left(r^2 \frac{M_w c D}{P_T - P}\frac{dP}{dr}\right) = 0 \qquad \text{(Eq. 6)}$$

When this expression is integrated over the boundary conditions for a hollow sphere[1], given as $P = P_s$ at $r = a$ and $P = P_c$ at $r = a'$, where $a' - a = \delta$ = effective thickness of the vapor diffusion layer, the following

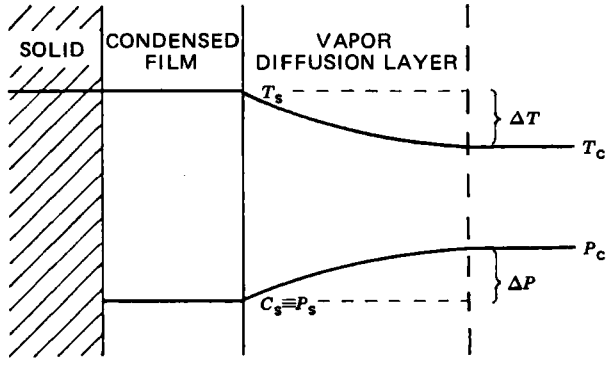

Figure 1—*Thermal and pressure gradients existing at a soluble solid surface covered with condensed water.*

[1] A hollow-sphere geometry was chosen earlier (1) for the development of the heat transport control model, and hence, it will also be carried through in this series of derivations.

0022-3549/83/1200-1394$01.00/0

relation is obtained:

$$\ln (P_T - P) = \left(\frac{\frac{1}{r} - \frac{1}{a}}{\frac{1}{a'} - \frac{1}{a}}\right) \ln \left(\frac{P_T - P_c}{P_T - P_s}\right) + \ln (P_T - P_s) \quad \text{(Eq. 7)}$$

From Eq. 4, the mass flux at surface $r = a$ is given as:

$$W'_{sp}\Big|_{r=a} = M_w c D \left.\frac{d \ln (P_T - P)}{dr}\right|_{r=a} \quad \text{(Eq. 8)}$$

for which the derivative is evaluated on the basis of Eq. 7 to yield:

$$W'_{sp}\Big|_{r=a} = -M_w c D \left(\frac{1}{\frac{a^2}{a'} - a}\right) \ln \left(\frac{P_T - P_c}{P_T - P_s}\right) \quad \text{(Eq. 9)}$$

Since mass is conserved, the mass flux across any spherical surface in the system is:

$$W' = 4\pi a^2 W'_{sp}\Big|_{r=a} \quad \text{(Eq. 10)}$$

$$= \left(\frac{4\pi M_w c D}{\frac{1}{a} - \frac{1}{a'}}\right) \ln \left(\frac{P_T - P_c}{P_T - P_s}\right) \quad \text{(Eq. 11)}$$

or, rearranged and expressed in terms of relative humidity:

$$W' = W'_m = -\left(\frac{60 \cdot 4\pi M_w c D}{\frac{1}{a} - \frac{1}{a'}}\right) \ln \left(\frac{100(P_T/P_0) - RH_o}{100(P_T/P_0) - RH_i}\right) \quad \text{(Eq. 12)}$$

where a factor of 60 has been included to convert W' (or W'_m to indicate mass transport control) to units of mg/min, given that M_w has units of mg/mole, c has units of mole/cm^3, and D has units of cm^2/sec. This equation is then the solution for steady-state radial mass diffusion in a hollow sphere. The negative sign for W' in Eq. 12 when $RH_o < RH_i$ reflects water vapor diffusion in the negative r-direction, consistent with the condensation process.

In the case where $P \ll P_T$, integration of Eq. 4 over the same boundary conditions followed by the evaluation of dP/dr at $r = a$ in the same manner given above, leads to the analogous expression for W'_m:

$$W'_m = -\frac{60 \cdot 4\pi M_w c D P_0}{100 P_T \left(\frac{1}{a} - \frac{1}{a'}\right)} (RH_i - RH_o) \quad \text{(Eq. 13)}$$

In addressing the question of the time required to reach steady state, the solution for the time-dependent radial pressure gradient in the atmosphere is readily obtained from the non-steady-state mass transport equations developed in Appendix I of the first paper in this series (1). From this, the time required for the steady-state diffusion expressed by Eq. 13 to establish itself can be determined. In terms of dimensionless concentration, pressure, or relative humidity (at a given constant temperature), this solution comes directly from Eq. A8 in Appendix I of Ref. 1:

$$C^* = P^* = RH^* = \left[\frac{1}{r^*(a'/a - 1) + 1}\right] \times \left[1 - r^* - \frac{2}{\pi} \sum_{n=1}^{\infty} \frac{1}{n} \sin n\pi r^* \cdot \exp(-n^2\pi^2 t^*)\right] \quad \text{(Eq. 14)}$$

where C^*, P^*, and RH^* are all defined analogously with the definition of Π^*, and where:

$$t^* = \frac{Dt}{(a' - a)^2} \quad \text{(Eq. 15)}$$

and

$$r^* = \frac{r - a}{a' - a} \quad \text{(Eq. 16)}$$

This function is described in Fig. 6 of Ref. 1 where $\Pi^* = C^*$ and $a' = b$. Since the time to steady state increases as $a' \to b$, allowing $a' = b$ should result in a conservative estimate of the time required for the pressure gradient to establish itself. In 1 atm of air, the time then required to reach $t^* = 0.5$ is only 4.3 sec using the constants given in Table I. Thus, even at the likely maximum diffusion layer thickness of 2 cm, pressure gradients within the system should be rapidly established relative to the time scale of extended uptake.

Table I—Physical Constants for the Transport Model in 1 atm of Air

Symbols	Constants
a, cm	0.5[a]
b, cm	2.05
P_0, atm	3.12×10^{-4}
P_T, atm	1
M_w, mg/mole	1.8×10^4
D, cm^2/sec	0.258[b]
c, moles/cm^3	4.09×10^{-5}
k, cal/cm · sec · deg	6.22×10^{-5} [c]
α, cm^2/sec	0.214[d]
ΔH_v, cal/mole	10500
R, cal/deg · mole	1.987
T_c, °K	298
σ, cal/cm^2·sec·deg^4	1.36×10^{-12}
e	0.95[e]

[a] Characteristic disk thickness unique to each compound examined; range = 0.492–0.512 cm. [b] Calculated according to Ref. 5 for water vapor in the presence of a nonpolar inert gas. [c] Calculated using the Lindsay and Bromley modification of the Wassiljewa equation (6). [d] Used in calculations were C_p values weighted by mole fraction and k as indicated above. [e] Film surface emissivity approximated by value given for pure water (7).

The time required for the mass flux to reach a steady-state level can be calculated from the lag time at surface $r = a$ whose solution is given by the analogous form of Eq. A21 (*cf.* Ref. 1) for mass diffusion:

$$t_{lag,r=a} = -\frac{a(a' - a)^2}{3Da'} \quad \text{(Eq. 17)}$$

For the example above, this lag time equals (−)0.72 sec, where again the value of a' is taken to its extreme value of $b = 2$ cm. At surface $r = b$, a lag time of 1.4 sec is calculated using the analogous form of Eq. A25 (*cf.* Ref. 1) for $a' = b$:

$$t_{lag,r=b} = \frac{(b - a)^2}{6D} \quad \text{(Eq. 18)}$$

It is clear from these results that in the system containing air, the measurement of steady-state uptake rates should not be precluded by the transient effects associated with the establishment of the steady-state pressure gradient driving the uptake.

Combined Mass–Heat Transport Model—The uptake rate W' in air is explicitly dependent on the difference in relative humidity, $RH_i - RH_o$, as described by Eq. 13 when condensation is limited by water vapor diffusion to the sample. When the process is limited by heat transport, however, W' exhibits only an implicit dependence on this difference as given below in Eq. 19, developed earlier (1):

$$W'_h = \left[\frac{60 M_w \cdot 4\pi k a b}{\Delta H (b - a)} \left(\frac{R T_c^2}{\Delta H_v - R T_c \ln \frac{RH_i}{RH_o}}\right) + \frac{60 M_w \cdot 4\pi a^2 \sigma e}{\Delta H} \left(\frac{4 R T_c^5}{\Delta H_v - 4 R T_c \ln \frac{RH_i}{RH_o}}\right)\right] \cdot \ln \frac{RH_i}{RH_o} \quad \text{(Eq. 19)}$$

When heat and mass transport are in balance, these equations must be solved simultaneously, since in this case neither the humidity difference (now $< RH_i - RH_o$) which drives mass transport, nor ΔT (now $< \Delta T_{max}$ as estimated by the Clausius–Clapeyron relation in Eq. 20 below) which drives heat transport, can be predicted *a priori*. As before (1):

$$\Delta T_{max} = \frac{R T_c^2 \ln \frac{RH_i}{RH_o}}{\Delta H_v - R T_c \ln \frac{RH_i}{RH_o}} \quad \text{(Eq. 20)}$$

Scheme I illustrates the interrelationship between the effective difference in relative humidity, $\Delta RH = RH_i - RH_s$, where RH_s is the effective relative humidity (relative to P_0 at 25°) at the sample surface, and

the experimentally controlled $\Delta RH = RH_i - RH_o$. The Clausius–Clapeyron equation now relates RH_o to RH_s, where the analogous form of Eq. 20 becomes:

$$\begin{array}{ccccc} & \text{Clausius–Clapeyron Equation} & & & \\ P_s^{(T_c)} & \longrightarrow & P_s^{(T_s)} & < & P_c^{(T_c)} \\ \| & & \| & & \| \\ RH_o & < & RH_s & < & RH_i \end{array}$$

Scheme I

$$\Delta T = T_s - T_c = \frac{RT_c^2 \ln \frac{RH_s}{RH_o}}{\Delta H_v - RT_c \ln \frac{RH_s}{RH_o}} \quad \text{(Eq. 21)}$$

Accounting for Eq. 21 in deriving an equation for the dependence of W' on ΔT as in Eq. 19, one obtains:

$$W' = \left[\frac{60M_w \cdot 4\pi kab}{\Delta H(b-a)}\left(\frac{RT_c^2}{\Delta H_v - RT_c \ln \frac{RH_s}{RH_o}}\right) + \frac{60M_w \cdot 4\pi a^2 \sigma e}{\Delta H}\left(\frac{4RT_c^5}{\Delta H_v - 4RT_c \ln \frac{RH_s}{RH_o}}\right)\right] \cdot \ln \frac{RH_s}{RH_o} \quad \text{(Eq. 22)}$$

The analogous transformation for mass transport (when $P \ll P_T$) as given by Eq. 13 becomes:

$$W' = -\frac{60 \cdot 4\pi M_w c D P_0}{100 P_T \left(\frac{1}{a} - \frac{1}{a'}\right)}(RH_i - RH_s) \quad \text{(Eq. 23)}$$

$$= -k_m A(RH_i - RH_s) \quad \text{(Eq. 24)}$$

where k_m, is a mass transport coefficient for diffusive flux over area $A = 4\pi a^2$, is given by:

$$k_m = \frac{60M_w c D P_0}{100 P_T \left(a - \frac{a^2}{a'}\right)} \quad \text{(Eq. 25)}$$

Since neither T_s nor RH_s is known in Eqs. 21–23, however, the above expressions for W' are not useful in their present form. Furthermore, because of the complex logarithmic dependence of W' on RH_s in Eq. 22 and linear dependence in Eq. 23, RH_s cannot be eliminated analytically from their simultaneous solution. For predictive purposes, therefore, it becomes worthwhile to introduce two approximations.

The first useful approximation entails linearizing the relationship between temperature and relative humidity in Eq. 21. This can be accomplished by establishing an empirical relation based on P_0-values covering an experimentally appropriate range in T_s and T_c. Consider moisture sorption by common alkali halide salts: according to the above model, heat transport-controlled sorption is predicted to occur over a $\Delta T < 10°$ at $T_c = 298°K$. Assuming that the water vapor pressure over a salt solution has the same temperature dependence as that over pure water, the variation of P_0 between 298°K and 303°K on conversion to relative humidity yields the following predictive equation for RH_s as a function of T_s:

$$RH_s - RH_o = 0.0679 \cdot RH_o(T_s - T_c) \quad \text{(Eq. 26)}$$

For sodium chloride this relation overestimates the reported value for RH_s at $T_s = 302.4°K$ (4) by only 0.5%.

The second useful approximation addresses the dependence of the radiation term on $\Delta(T^4)$. Allowing:

$$T_s^4 - T_c^4 = 4T_c^3(T_s - T_c) \quad \text{(Eq. 27)}$$

where $T_c = 298°K$ and $T_s = 313°K$, this approximation underestimates the value of $\Delta(T^4)$ by <7.5% even at an extreme ΔT of 15°.

The combination of Eqs. 1 and 31 from Ref. 1 with Eq. 27 (above), *including the units* conversion factor of $60M_w$, leads to a simpler expression for the dependence of W' on ΔT:

$$W' = \left[\frac{60M_w \cdot 4\pi kab}{\Delta H(b-a)} + \frac{4T_c^3 \cdot 60M_w \cdot 4\pi a^2 \sigma e}{\Delta H}\right] \cdot \Delta T \quad \text{(Eq. 28)}$$

Substituting for ΔT from Eq. 26 gives:

$$W' = k_h A(RH_s - RH_o) \quad \text{(Eq. 29)}$$

where k_h is a heat transport coefficient for heat flux over the surface of area $A = 4\pi a^2$, and is given by:

$$k_h = -\frac{14.72}{RH_o}\left[\frac{60M_w kb}{a\Delta H(b-a)} + \frac{4T_c^3 \cdot 60M_w \sigma e}{\Delta H}\right] \quad \text{(Eq. 30)}$$

Solving for RH_s in Eq. 29 and substituting the result into Eq. 24, one obtains:

$$W' = -k_m A(RH_i - RH_o + W'/k_h A) \quad \text{(Eq. 31)}$$

On rearranging, a final equation for W' is obtained in which the effects of both heat and mass transport (for systems in which $P \ll P_T$) are accounted for:

$$W' = W'_{mh} = -\frac{k_m k_h}{k_m + k_h} A(RH_i - RH_o) \quad \text{(Eq. 32)}$$

or

$$W'_{mh} = -\frac{60M_w \cdot 4\pi c D P_0(RH_i - RH_o)}{100P_T\left(\frac{1}{a} - \frac{1}{a'}\right) - \frac{cDP_0 \cdot \Delta H(b-a)RH_o}{14.72[kab + 4T_c^3 a^2 \sigma e(b-a)]}} \quad \text{(Eq. 33)}$$

The contribution of the mass–heat transport coupling is reflected by the demoninator of this equation: as the second term vanishes, as for a system with $k = \infty$ where $\Delta T \to 0$, the mass transport control relation of Eq. 13 remains. Conversely, as the vapor diffusion layer becomes infinitesimal as $a' \to a$, Eq. 33 reduces to an expression similar in form to Eq. 28 wherein the logarithmic dependence of ΔT on RH_i has been effectively linearized.

EXPERIMENTAL

Materials—The sources and treatment of potassium iodide, potassium bromide, and choline iodide have been presented in the preceding paper (2).

Methods—The preparation of disks, the apparatus used, and the method of treating data were described in the preceding paper (2), with one important change instituted in the present study. The very slow diffusion of water vapor from the relative humidity chambers to the sample through an atmosphere of air precluded use of the chambers as described previously. Therefore, a small volume of saturated salt solution, containing an excess of salt, whose RH_o equalled the desired RH_i, was placed directly into the sample tube. The tube was capped and shaken for several minutes prior to use to accelerate humidity equilibrium. The chamber was then rapidly set in place around the loaded sample, with air thus present at a pressure of approximately 1 atm.

To assure that the value of RH_i in the chamber containing air was known and constant during a run, an electronic humidity sensor[2] was installed within the sample chamber. This consisted of a thin rectangular block of cross-linked polystyrene copolymer. The impedance changes caused by sorption and desorption of water were measured by an AC bridge circuit, capable of measuring a maximum value of 1.1 MΩ. Calibration was carried out by exposing the sensor, placed in the sample chamber at atmospheric air pressure, to known relative humidities. The temperature change, ΔT, near the sample surface was also monitored with a thermocouple, as previously described (2).

RESULTS

Since the diffusion layer thickness, δ, is unknown, neither Eq. 13 nor Eq. 33 can be used to predict *a priori* uptake rates for a given system. In the case where a' approaches the radius of the sample tube, b, and hence where $\delta = b - a$, the diffusional barrier would be maximized such that the rate of water sorption would be at a minimum value of W'. Using appropriate values of the various parameters needed to apply Eqs. 13 (for W'_m) and 33 (for W'_{mh}) found in Table I, and also using parameters in Table I needed to apply Eq. 19 for W'_h for the heat transport model in an atmosphere of air, three theoretical plots can be produced to describe

[2] Phys-Chemical Research Corp.

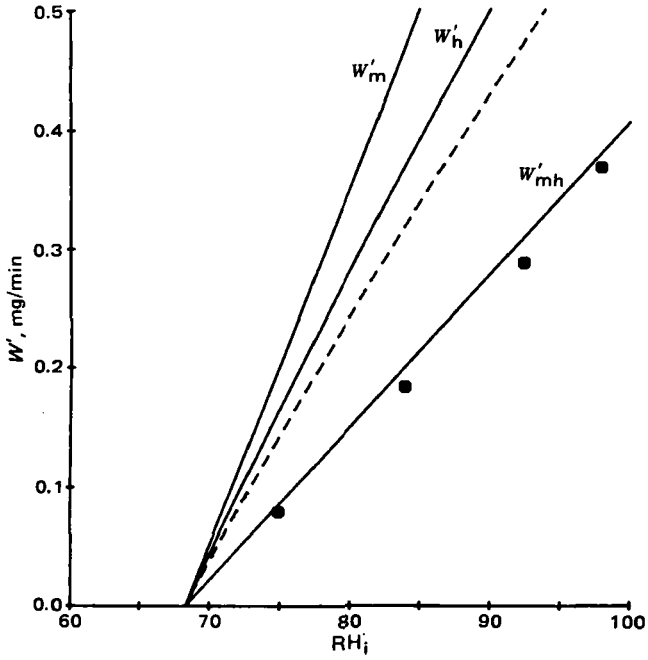

Figure 2—*Sorption rates in 1 atm air for disks of potassium iodide as a function of RH. The solid lines are theoretical sorption curves for* W'_m, W'_h *(air), and* W'_{mh} *plotted according to Eqs. 13, 19, and 33, respectively. The dashed line presents the corresponding theoretical curve for heat transport-controlled sorption in the absence of inert gas.*

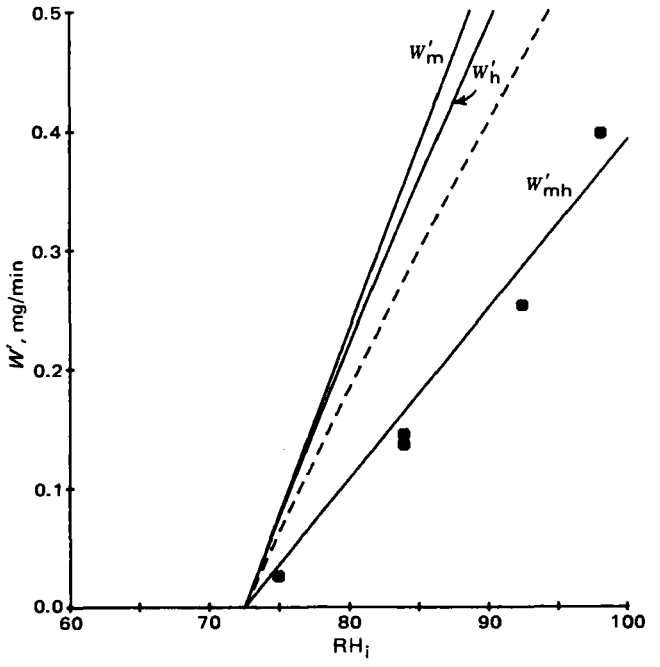

Figure 4—*Sorption rates in 1 atm of air for disks of choline iodide as a function of RH. The solid lines are theoretical sorption curves for* W'_m, W'_h *(air), and* W'_{mh} *plotted according to Eqs. 13, 19 and 33, respectively. The dashed line presents the corresponding theoretical curve for heat transport-controlled sorption in the absence of inert gas.*

water sorption rates as a function of RH_i. Figures 2–4 present comparisons of these theoretical curves with experimental results for potassium iodide, potassium bromide, and choline iodide, respectively. For the sake of further comparison, the corresponding theoretical plots as shown in the preceding paper (2) for water sorption in the absence of any inert gas, where heat transport strictly controls uptake, are also included in each case.

From the theoretical plots, it is clear that mass transport over a vapor diffusion layer of finite thickness is expected to limit the rates of water uptake relative to the case where only heat transport control is operating. It can be seen also that in the absence of resistance to mass transport, heat transport is sufficiently faster in air than in vacuum so that it alone would allow much higher rates of sorption. Hence any observed reduction in sorption rates in air relative to a vacuum must be a consequence of the mass transport component.

It is interesting to note that in all three cases shown in Figs. 1–4, the observed data are best described by the combined mass–heat transport model expressed by Eq. 33 when the vapor diffusion layer is assumed to be equal to the chamber dimension. Furthermore, measured ΔT values associated with sorption in air were observed to be depressed as much as 30–50% relative to values obtained at the same RH_i under an atmosphere of pure water vapor. This result is consistent with the lower ΔT value predicted for sorption controlled by both mass and heat transport.

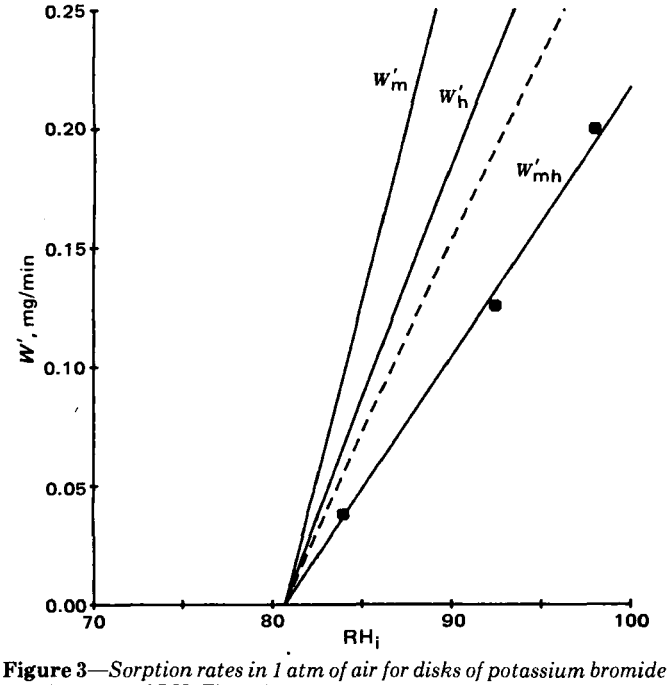

Figure 3—*Sorption rates in 1 atm of air for disks of potassium bromide as a function of RH. The solid lines are theoretical sorption curves for* W'_m, W'_h *(air), and* W'_{mh} *plotted according to Eqs. 13, 19 and 33, respectively. The dashed line presents the corresponding theoretical curve for heat transport-controlled sorption in the absence of inert gas.*

DISCUSSION

The results of studies in air, and previous work in an atmosphere of pure water vapor (1, 2), clearly indicate the importance of heat transport and mass transport as underlying mechanisms in the process of water sorption by water-soluble substances. The study of sorption in a vacuum provides a convenient approach for carrying out fundamental studies which demonstrate the importance of heat transport in these systems. Since convective flow of water vapor in the absence of an inert gas is rapid, constant pressure is immediately established throughout the chamber, making uncontrolled geometrical factors arising from equipment design relatively unimportant. In contrast, diffusional resistance to water vapor flow in air, from source to sample, retards the establishment of steady-state sorption and renders the system highly sensitive to the geometry of the sample chamber. To overcome this problem requires equipment design which emphasizes better control of vapor delivery to the solid surface. Even though our experimental results agree well with the combined heat–mass transport model, assuming minimum uptake at $\delta = b - a$, the present apparatus does not allow for flexibility in varying geometric factors.

Given the constraints of undetermined geometric factors which control mass transport of vapor, equations derived to include both heat and mass transport mechanisms are very successful in accounting for observations made when water sorption takes place in an atmosphere consisting of air and water vapor. The importance of heat transport, not previously discussed in the context of water uptake by deliquescent substances, seems

firmly established from both previous studies of sorption in the absence of air (1, 2) as well as the present study in which the moderating effects of diffusion are evident.

APPENDIX: GLOSSARY[3]

a' radius of sphere bounded by outside radius of vapor diffusion layer
c molar gas concentration; also subscript denoting "chamber"
C^* dimensionless concentration variable
k_h mass transport coefficient associated with heat transport-controlled aspect of sorption
k_m mass transport coefficient associated with mass transport-controlled aspect of sorption
P_i pressure of inert gas
P_T total pressure
P^* dimensionless pressure variable
RH_s unknown relative humidity at the sample surface associated with conditions of balanced heat and mass transport in which the two processes control sorption to a similar degree
RH^* dimensionless relative humidity variable
W_{sp} sorption rate per unit surface area
W_m sorption rate associated with mass transport control
W_{mh} sorption rate associated with the combined control of both heat and mass transport
x_w mole fraction water vapor
δ vapor diffusion layer thickness

[3] Refer to the first paper in this series (1) for the majority of symbol identification. Listed here are only those symbols introduced in the present paper.

REFERENCES

(1) L. Van Campen, G. L. Amidon, and G. Zografi, *J. Pharm. Sci.*, **72,** 1381 (1983).
(2) L. Van Campen, G. L. Amidon, and G. Zografi, *J. Pharm. Sci.*, **72,** 1388 (1983).
(3) S. Gal, "Die Methodik der Wasserdampf-Sorption-messungen," Springer-Verlag, Berlin, 1967, p. 21.
(4) M. M. Markowitz and D. A. Boryta, *J. Chem. Eng. Data*, **6,** 16 (1961).
(5) R. B. Bird, W. E. Stewart, and E. N. Lightfoot, "Transport Phenomena," Wiley, New York, N.Y., 1960, p. 505.
(6) R. C. Reid, J. M. Prausnitz, and T. K. Sherwood, "The Properties of Gases and Liquids," 3rd ed., McGraw-Hill, New York, N.Y., 1977, pp. 508–509.
(7) R. B. Bird, W. E. Stewart, and E. N. Lightfoot, "Transport Phenomena," Wiley, New York, N.Y., 1960, p. 432.

ACKNOWLEDGMENTS

Submitted by L. Van Campen to the University of Wisconsin–Madison in 1981, in partial fulfillment of the doctor of philosophy degree requirements.

L.V.C. expresses appreciation for graduate fellowship support to the American Foundation for Pharmaceutical Education and Merck Sharp and Dohme Research Laboratories.

Quantitative Determination of Benzoyl Peroxide by High-Performance Liquid Chromatography and Comparison to the Iodometric Method

NEHRU GADDIPATI ˣ, FRANK VOLPE, and G. ANTHONY

Received June 14, 1982, from the *Quality Services Department, R&D Division, Revlon Health Care Group, Tuckahoe, NY 10707.* Accepted for publication October 14, 1982.

Abstract □ A selective high-performance liquid chromatographic (HPLC) procedure for the quantitative determination of benzoyl peroxide in pharmaceutical dosage forms is described. Benzoyl peroxide was dissolved or extracted in the presence of an internal standard, acenaphthylene. The specificity of the stability-indicating HPLC and iodometric procedures are presented for benzoyl peroxide.

Keyphrases □ Benzoyl peroxide—degradation products, stability-indicating high-performance liquid chromatography, comparison with iodometric procedures □ High-performance liquid chromatography—stability indicating, benzoyl peroxide and its degradation products, commercial formulations, comparison with iodometric procedures □ Degradation products—benzoyl peroxide, stability-indicating high-performance liquid chromatography in commercial formulations.

Benzoyl peroxide (dibenzoyl peroxide), active against acne-causing bacteria, is widely used in pharmaceutical preparations as an antibacterial and keratolytic agent (1). Analytical methods currently available include spectrophotometry (2), polarography (2), TLC (3), titrimetry (4), and high-performance liquid chromatography (HPLC) (5, 6).

BACKGROUND

Benzoyl peroxide is a chemically reactive molecule which readily decomposes in various solvents (7) to give compounds such as biphenyl, phenyl benzoate, benzoic acid, benzene, 4-biphenylcarboxylic acid, homophthalic acid, homoterephthalic acid, and carbon dioxide (8). Daley *et al.* reported a selective titrimetric procedure (9), modifying the conventionally utilized iodometric method. They proposed the addition of phenyl sulfide prior to the titration to eliminate potential interferences caused by the presence of hydroperoxide impurities such as perbenzoic acid. This iodometric procedure has been accepted as the USP method for analysis of benzoyl peroxide lotion (10). Oliveri-Vigh and Hainsworth proposed an HPLC procedure that is selective in the presence of benzoic acid and benzaldehyde (5). Burton *et al.* proposed a similar HPLC procedure specific for analysis of benzoyl peroxide in gels and lotions in the presence of benzoic acid and perbenzoic acid (6); this procedure has been adopted as the USP method for analysis of benzoyl peroxide gel (11).

Analyses of benzoyl peroxide using Burton *et al.*'s procedure or the compendial HPLC procedure (6, 11) may give less accurate results, because this method depends on the use of an homogeneous reference standard. The aforementioned analytical procedures utilize aqueous benzoyl peroxide as the reference material to prepare the standard solutions. Aqueous benzoyl peroxide (70% benzoyl peroxide) is a heterogenous mixture which is nonuniform in its water content, typically varying

0022-3549/83/1200-1398$01.00/0

firmly established from both previous studies of sorption in the absence of air (1, 2) as well as the present study in which the moderating effects of diffusion are evident.

APPENDIX: GLOSSARY[3]

a' radius of sphere bounded by outside radius of vapor diffusion layer
c molar gas concentration; also subscript denoting "chamber"
C^* dimensionless concentration variable
k_h mass transport coefficient associated with heat transport-controlled aspect of sorption
k_m mass transport coefficient associated with mass transport-controlled aspect of sorption
P_i pressure of inert gas
P_T total pressure
P^* dimensionless pressure variable
RH_s unknown relative humidity at the sample surface associated with conditions of balanced heat and mass transport in which the two processes control sorption to a similar degree
RH^* dimensionless relative humidity variable
W_{sp} sorption rate per unit surface area
W_m sorption rate associated with mass transport control
W_{mh} sorption rate associated with the combined control of both heat and mass transport
x_w mole fraction water vapor
δ vapor diffusion layer thickness

[3] Refer to the first paper in this series (1) for the majority of symbol identification. Listed here are only those symbols introduced in the present paper.

REFERENCES

(1) L. Van Campen, G. L. Amidon, and G. Zografi, *J. Pharm. Sci.*, **72,** 1381 (1983).
(2) L. Van Campen, G. L. Amidon, and G. Zografi, *J. Pharm. Sci.*, **72,** 1388 (1983).
(3) S. Gal, "Die Methodik der Wasserdampf-Sorption-messungen," Springer-Verlag, Berlin, 1967, p. 21.
(4) M. M. Markowitz and D. A. Boryta, *J. Chem. Eng. Data*, **6,** 16 (1961).
(5) R. B. Bird, W. E. Stewart, and E. N. Lightfoot, "Transport Phenomena," Wiley, New York, N.Y., 1960, p. 505.
(6) R. C. Reid, J. M. Prausnitz, and T. K. Sherwood, "The Properties of Gases and Liquids," 3rd ed., McGraw-Hill, New York, N.Y., 1977, pp. 508–509.
(7) R. B. Bird, W. E. Stewart, and E. N. Lightfoot, "Transport Phenomena," Wiley, New York, N.Y., 1960, p. 432.

ACKNOWLEDGMENTS

Submitted by L. Van Campen to the University of Wisconsin–Madison in 1981, in partial fulfillment of the doctor of philosophy degree requirements.

L.V.C. expresses appreciation for graduate fellowship support to the American Foundation for Pharmaceutical Education and Merck Sharp and Dohme Research Laboratories.

Quantitative Determination of Benzoyl Peroxide by High-Performance Liquid Chromatography and Comparison to the Iodometric Method

NEHRU GADDIPATI ˣ, FRANK VOLPE, and G. ANTHONY

Received June 14, 1982, from the *Quality Services Department, R&D Division, Revlon Health Care Group, Tuckahoe, NY 10707.* Accepted for publication October 14, 1982.

Abstract □ A selective high-performance liquid chromatographic (HPLC) procedure for the quantitative determination of benzoyl peroxide in pharmaceutical dosage forms is described. Benzoyl peroxide was dissolved or extracted in the presence of an internal standard, acenaphthylene. The specificity of the stability-indicating HPLC and iodometric procedures are presented for benzoyl peroxide.

Keyphrases □ Benzoyl peroxide—degradation products, stability-indicating high-performance liquid chromatography, comparison with iodometric procedures □ High-performance liquid chromatography—stability indicating, benzoyl peroxide and its degradation products, commercial formulations, comparison with iodometric procedures □ Degradation products—benzoyl peroxide, stability-indicating high-performance liquid chromatography in commercial formulations.

Benzoyl peroxide (dibenzoyl peroxide), active against acne-causing bacteria, is widely used in pharmaceutical preparations as an antibacterial and keratolytic agent (1). Analytical methods currently available include spectrophotometry (2), polarography (2), TLC (3), titrimetry (4), and high-performance liquid chromatography (HPLC) (5, 6).

BACKGROUND

Benzoyl peroxide is a chemically reactive molecule which readily decomposes in various solvents (7) to give compounds such as biphenyl, phenyl benzoate, benzoic acid, benzene, 4-biphenylcarboxylic acid, homophthalic acid, homoterephthalic acid, and carbon dioxide (8). Daley *et al.* reported a selective titrimetric procedure (9), modifying the conventionally utilized iodometric method. They proposed the addition of phenyl sulfide prior to the titration to eliminate potential interferences caused by the presence of hydroperoxide impurities such as perbenzoic acid. This iodometric procedure has been accepted as the USP method for analysis of benzoyl peroxide lotion (10). Oliveri-Vigh and Hainsworth proposed an HPLC procedure that is selective in the presence of benzoic acid and benzaldehyde (5). Burton *et al.* proposed a similar HPLC procedure specific for analysis of benzoyl peroxide in gels and lotions in the presence of benzoic acid and perbenzoic acid (6); this procedure has been adopted as the USP method for analysis of benzoyl peroxide gel (11).

Analyses of benzoyl peroxide using Burton *et al.*'s procedure or the compendial HPLC procedure (6, 11) may give less accurate results, because this method depends on the use of an homogeneous reference standard. The aforementioned analytical procedures utilize aqueous benzoyl peroxide as the reference material to prepare the standard solutions. Aqueous benzoyl peroxide (70% benzoyl peroxide) is a heterogenous mixture which is nonuniform in its water content, typically varying

0022-3549/83/1200-1398$01.00/0

by a few percent from sample to sample. The specification in the pharmacopeia for aqueous benzoyl peroxide provides a range of not less than 65% and not more than 82% of $C_{14}H_{10}O_4$ (12).

Standard preparation in the proposed HPLC procedure has been designed to eliminate the inaccuracies associated with the use of a nonhomogeneous reference material like aqueous benzoyl peroxide. The HPLC procedure described in this paper is specific, provides the direct and accurate determination needed to evaluate the stability of pharmaceutical products containing benzoyl peroxide, and has the added advantages of detecting and quantifying degradation products.

EXPERIMENTAL

Apparatus and Reagents—A high-performance liquid chromatograph[1] equipped with an automatic sampler system[2], a reverse-phase column[3], and a variable-wavelength spectrophotometric detector[4] interfaced to an electronic integrator[5] was used. Aqueous benzoyl peroxide[6], acenaphthylene[7], homophthalic acid[7], 4-biphenylcarboxylic acid[7], benzaldehyde[7], phenyl benzoate[7], biphenyl[7], *o*-terphenyl[7], *p*-terphenyl[7], benzoic acid[8], benzene[8], acetone[8], UV-grade methanol and acetonitrile[9], reagent-grade potassium iodide and sodium thiosulfate[10], and phenyl sulfide[11] were used as received.

HPLC Assay—*Chromatographic Conditions*—The mobile phase consisted of methanol–water (75:25, v/v) filtered through a 0.45-μm membrane filter[12]. The flow rate of the mobile phase was set at 1.0 ml/min. The injection volume for the standard and sample preparations was maintained at 20 μl, and the column effluent was monitored by UV absorption at 238 nm (maximum absorbance for benzoyl peroxide).

Procedure—A stock solution of internal standard was prepared by dissolving acenaphthylene in acetonitrile at a concentration of 2.0 mg/ml. A reference standard stock solution was prepared by dissolving ~360 mg of aqueous benzoyl peroxide in 100 ml of acetonitrile. The potency of the reference standard stock solution was determined by pipetting a 10.0-ml aliquot and measuring the amount of benzoyl peroxide by the compendial iodometric procedure described under the monograph of benzoyl peroxide lotion (12), except that acetonitrile was substituted for acetone. A 20.0-ml aliquot of the reference standard stock solution was diluted to 100 ml with acetonitrile for the HPLC standard stock solution. A standard pair solution of benzoyl peroxide (0.05 mg/ml) and acenaphthylene (0.20 mg/ml) was prepared by mixing 10.0 ml of the internal standard stock solution and 10.0 ml of the HPLC standard stock solution, and diluting to 100 ml with acetonitrile.

Sample solutions were made by accurately weighing a sample equivalent to 50 mg of benzoyl peroxide into a 100-ml volumetric flask, sonicating for 15 min in 70 ml of acetonitrile, and then diluting to volume with acetonitrile. Sample pair solutions were prepared by mixing 10.0 ml of the internal standard solution and 10.0 ml of the sample solution in a 100 ml-volumetric flask and diluting this to volume with acetonitrile. All solutions were filtered through 0.45-μm membrane filter[13].

Compendial Titrimetric Assay—A reference standard stock solution was prepared by dissolving 250 mg of benzoyl peroxide in 100.0 ml of acetone. Aliquots (10.0 ml) of the reference standard stock solution were assayed in the presence of postulated degradation compounds for specificity evaluation, and in the presence of placebo ingredients for synthetic recovery studies for the lotion and wash formulations of benzoyl peroxide. Reference standard solutions and benzoyl peroxide formulations (cream, lotion, gel, and wash) were assayed by the pharmacopeial procedure described under the monograph for benzoyl peroxide lotion.

RESULTS AND DISCUSSIONS

Assay Selectivity—*HPLC Procedure*—A stability-indicating method must be able to discriminate between degradation products and the active ingredient. Preferably, a stability-indicating procedure should also quantitatively demonstrate the inverse relationship between the decrease in the active ingredient and increase in the degradation products. To show that a method is stability-indicating, routes of degradation products may be postulated and tested in the assay system for interference. The specificity of the HPLC system has been demonstrated (Fig. 1), and the retention times of the postulated degradation compounds are listed in Table I. Analyses of the synthetic placebos for benzoyl peroxide lotion and wash formulations by the proposed HPLC method showed no chromatographic peaks at the retention times of benzoyl peroxide and acenaphthylene (internal standard). A typical chromatogram of the standard pair mixture is shown in Fig. 2.

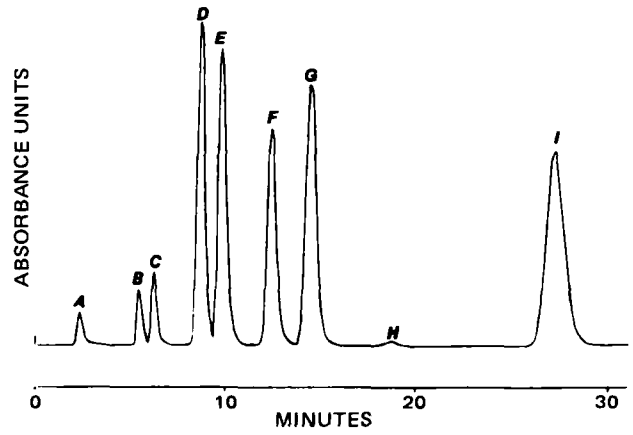

Figure 1—*High-performance liquid chromatogram of benzoyl peroxide and its decomposition products. Key: (A,B) degradation products of benzoyl peroxide in methanol; (C) benzene; (D) phenyl benzoate; (E) benzoyl peroxide; (F) acenaphthylene (internal standard); (G) biphenyl; (H) impurity from acenaphthylene; (I) o-terphenyl.*

Compendial Titrimetric Procedure—The compendial iodometric procedure involves a sodium thiosulfate titration of liberated iodine, resulting from the oxidation of potassium iodide by benzoyl peroxide. Phenyl sulfide is added prior to the introduction of potassium iodide to prevent the liberation of free iodine by the reduction of hydroperoxide impurities such as perbenzoic acid. To determine the influence of adding phenyl sulfide, benzoyl peroxide solution was tested with varying quantities of phenyl sulfide, and a linear relationship was observed between the decrease in recovery and amount of phenyl sulfide added. The regression equation (n = 7) for the volume of titrant consumed (y) for 18 mg of benzoyl peroxide and the amount of phenyl sulfide added (x, expressed in milliliters) was $y = 21.3867 + (-0.9134)(x)$. The coefficient of determination was 0.995, $CV = 0.25\%$, and at the 95% confidence interval the slope and intercept were -0.9134 ± 0.074 and 21.387 ± 0.078, respectively. To challenge the specificity of this method, benzoyl peroxide samples were analyzed in the presence of postulated degradation products; the data (Table II) demonstrate specificity of the iodometric procedure.

Statistical Evaluation—*HPLC Procedure*—Quantitation was based on the benzoyl peroxide–internal standard peak ratio. With these ratios, the linearity between detector response at 238 nm and the amount of active ingredient injected was established for concentrations between 13.5 and 76.4 μg of benzoyl peroxide. The regression equation (n = 9) for the benzoyl peroxide–internal standard peak area ratio (y) and the

Table I—Location of the Degradation Compounds of Benzoyl Peroxide as a Function of Retention Time

Compounds	Retention Time, min
Homophthalic acid	2.20
Benzoic acid	2.76
4-Biphenylcarboxylic acid	3.38
Phenol	3.65
Benzaldehyde	4.12
Benzene	6.00
Phenyl benzoate	8.46
Benzoyl peroxide (active)	9.46
Acenaphthylene (internal standard)	11.96
Biphenyl	13.87
o-Terphenyl	25.82
p-Terphenyl	55.94

[1] Model 6000 Solvent Delivery System, Waters Associates, Milford, Mass.
[2] Intelligence Sampler System 710A, Waters Associates, Milford, Mass.
[3] μBondapak C_{18}, 3.9-mm i.d. × 30-cm, Waters Associates, Milford, Mass.
[4] Model 450 Variable-Wavelength Absorbance Detector, Waters Associates, Milford, Mass.
[5] Model 3385 A, Hewlett-Packard, Paramus, N.J.
[6] Penn Walt Corp., Rochester, N.Y.
[7] Aldrich Chemical Co., Inc., Metuchen, N.J.
[8] J. T. Baker Chemical Co., Phillipsburg, N.J.
[9] Burdick and Jackson Laboratories, Muskegon, Mich.
[10] Fisher Scientific Co., Fair Lawn, N.J.
[11] Eastman Kodak Co., Rochester, N.Y.; Pfaltz and Bauer, Stamford, Conn.
[12] Type OE-67, Schleicher and Schuell, Inc., Keene, N.H.
[13] Type RC-55, Schleicher and Schuell, Inc., Keene, N.H.

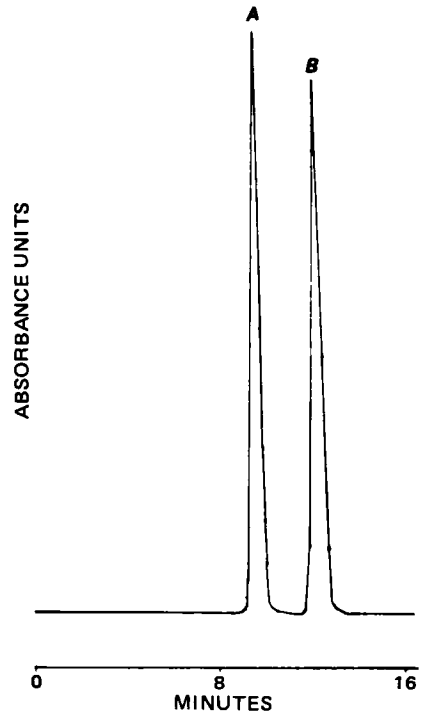

Figure 2—*High-performance liquid chromatogram of benzoyl peroxide. Key: (A) Benzoyl peroxide; (B) acenaphthylene (internal standard).*

Table II—Recovery of I[a] in the Presence of Postulated Degradation Products

Degradation Product	Amount Added[b], mg	Benzoyl Peroxide Found, mg	Recovery, %
Homophthalic acid	3.7	25.5	98.5
Benzoic acid	2.5	25.5	98.5
4-Biphenylcarboxylic acid	4.0	25.6	99.2
Phenol	1.9	25.5	98.5
Benzene	0.3	26.0	100.4
Phenyl benzoate	3.9	26.2	101.2
Biphenyl	3.3	26.2	101.2
o-Terphenyl	4.7	26.0	100.4
p-Terphenyl	4.7	26.2	101.2

[a] Each aliquot contained 25.9 mg. [b] Equivalent to ~20% decomposition assuming a 1:1 stoichiometry.

amount of benzoyl peroxide injected (x, expressed as μg/ml) was $y = (1.104 \times 10^{-3}) + (1.953 \times 10^{-2})(x)$. The coefficient of determination was 0.9999, $CV = 0.74\%$, and at the 95% confidence interval the slope and intercept were 0.0195 ± 0.0002 and 0.0011 ± 0.0072, respectively. The response factor ratios, defined as the area ratio (acenaphthylene/benzoyl peroxide) times the concentration ratio (benzoyl peroxide/acenaphthalene) were quite constant for all concentrations. Precision was demonstrated by a relative standard deviation of 0.4% for 16 replicate injections. The results of the analyses of mixtures consisting of the addition of active ingredient to wash and lotion placebo mixtures demonstrate the accuracy of the proposed method with average recoveries of 99.5 and 99.7%, respectively.

Compendial Titrimetric Procedure—Linearity was obtained by the iodometric procedure between 2.0 and 81.4 mg of benzoyl peroxide. The regression equation ($n = 11$) for the volume of titrant consumed (y) and the amount of benzoyl peroxide (x, expressed in milligrams) were $y = (9.151 \times 10^{-2}) + 0.8107x$. The coefficient of determination was 0.9999, $CV = 0.73\%$, and at the 95% confidence interval the slope and intercept were 0.8107 ± 0.0055 and 0.915 ± 0.2422, respectively. Precision of this USP titration method was demonstrated by a relative standard deviation of 0.3% for seven replicate analyses. The analytical results of active and placebo mixtures for wash and lotion formulations demonstrate the accuracy of the iodometric procedure with average recoveries of 99.8 and 100.2%, respectively.

Table III—HPLC and USP Iodometric Analyses of Commercial Formulations of Lotion, Cream, Wash, and Gel

Formulation	Dosage Claimed, mg of I/g	HPLC, mg of I/g	USP Iodometric, mg of I/g
Lotion	100	105.6	106.2
	100	100.5	103.3
	100	107.9	105.3
	50	48.4	50.1
	50	58.0	56.6
	50	45.3	45.8
Cream	100	110.0	109.0
	100	98.5	95.1
Wash	100	103.3	103.0
	100	108.0	107.4
	50	57.0	55.1
	40	41.7	41.2
Gel	50	54.8	54.7

CONCLUSIONS

In five determinations of aqueous benzoyl peroxide using the USP iodometric determination, the benzoyl peroxide ranged from 66.9 to 73.5% ($CV = 4.25\%$) indicating the nonhomogenous distribution of water in the benzoyl peroxide raw material. Therefore, the utilization of aqueous benzoyl peroxide as the reference standard in HPLC analysis affects the analytical performance based on the homogeneity of the material. Standard preparation in the aforementioned HPLC procedure has been designed to compensate for the variability of water content in aqueous benzoyl peroxide.

The experimental data shown in Table III were obtained on randomly selected samples of benzoyl peroxide lotion, wash, cream, and gel formulations. Each sample was analyzed by the HPLC and the USP iodometric procedures. The results from both methods are comparable, and the procedures are precise, accurate, and specific for determination of benzoyl peroxide in commercial formulations. The HPLC procedure presented in this paper is stability indicating, capable of detecting and quantifying the decomposition products of benzoyl peroxide, and adopts a new technique for the standard preparation to improve the precision, accuracy, and reproducibility of the analysis for benzoyl peroxide formulations.

REFERENCES

(1) "Physician's Desk Reference for Non-Prescription Drugs," 2nd ed., Medical Economics Co., Oradell, N.J., 1981.

(2) M. P. Gruber and R. W. Klein, *J. Pharm. Sci.*, **56**, 1505 (1967).

(3) D. L. Simmons, H. S. L. Woo, J. J. Liston, and R. J. Ranz, *Can. J. Pharm. Sci.*, **2**, 101 (1967).

(4) D. H. Wheeler, *J. Am. Oil Chem. Soc.*, **25**, 144 (1948).

(5) S. Oliveri-Vigh and F. T. Hainsworth III, *J. Pharm. Sci.*, **67**, 1035 (1978).

(6) F. W. Burton, R. R. Gadde, and W. L. McKenzie, *J. Pharm. Sci.*, **68**, 280 (1979).

(7) K. Nozaki and P. D. Bartlett, *J. Am. Chem. Soc.*, **68**, 1686 (1946).

(8) J. K. Kochi, B. M. Graybill, and M. Kurtz, *J. Am. Chem. Soc.*, **82**, 5257 (1964).

(9) R. E. Daley, J. J. Lomzer, and L. Chafetz, *J. Pharm. Sci.*, **64**, 1999 (1975).

(10) "Third Supplement to the United States Pharmacopeia, 19th Rev.," U.S. Pharmacopeial Convention, Rockville, Md., 1975.

(11) "Second Supplement to the United States Pharmacopeia, 20th Rev.," U.S. Pharmacopeial Convention, Rockville, Md., 1981.

(12) "United States Pharmacopeia, 20th Rev.," U.S. Pharmacopeial Convention, Rockville, Md., 1980.

ACKNOWLEDGMENTS

The authors express their gratitude to Mr. J. Shastri and to Ms. N. Medalla for their assistance in evaluating the benzoyl peroxide formulations.

Effects of Preservatives, Steroids, and Ethylenediaminetetraacetate on the Antimicrobial Activity of Sulfacetamide

R. D. HOULSBY, M. GHAJAR ˣ, and L. CHAVEZ

Received August 13, 1982, from the *Microbiology Department, CooperVision Pharmaceuticals, Inc., Mountain View, CA 94043.* Accepted for publication October 14, 1983.

Abstract □ The effect of EDTA (ethylenediaminetetraacetate), steroids, and preservatives on the antimicrobial activity of 10% sodium sulfacetamide solutions was evaluated in this study by kill rate and minimum inhibitory concentration (MIC) using five representative microorganisms. The results indicate that thimerosal-preserved sulfacetamide solutions containing EDTA are more effective against *Pseudomonas aeruginosa*, *Serratia marcescens*, *Staphylococcus epidermidis*, and *Candida albicans* than similar paraben-preserved solutions. Furthermore, the addition of EDTA improves the kill rate, but not the MIC, for the *Pseudomonas*, *Serratia*, and *Candida* species regardless of the preservative. The combination of a steroid with sulfacetamide does not affect its antimicrobial activity.

Keyphrases □ Ophthalmic solutions—sulfacetamide, antimicrobial activity, effects of EDTA, steroids, preservatives □ Sulfacetamide—ophthalmic solutions, antimicrobial activity, effects of EDTA, steroids, preservatives □ Antimicrobial activity—of sulfacetamide in ophthalmic solutions, effects of EDTA, steroids, preservatives

Sodium sulfacetamide is an antimicrobial agent which prevents the growth and division of bacteria by interfering with the uptake of *p*-aminobenzoic acid. *p*-Aminobenzoic acid is required for folic acid synthesis which, in turn, is required for synthesis of purines and the pyrimidine, thymine, the building blocks of DNA. The competitive inhibition of *p*-aminobenzoic acid by sulfacetamide is reduced by some local anesthetics, such as tetracaine, that are derivatives of *p*-aminobenzoic acid (1). It has also been reported that the presence of sodium metabisulfite inhibits the antimicrobial activity of sodium sulfacetamide (2).

Sulfacetamide is the least sensitizing member of the sulfonamide group of antibiotics (3). It has been widely used during the past 25 years to treat blepharitis (4), pustular acne, and seborrheic dermatitis (5), and has also been used prophylactically following cataract surgery (6). It is effective against streptococci (except enterococci), pneumococci, *Bacillus anthracis*, *Corynebacterium diphtheriae*, *Clamydia trachomatis*, and some strains of *Haemophilus influenzae*, *Yersinia*, *Nocardia*, and *Actinomyces*. Many strains of *Neisseria* and *Enterobacteriaceae* have acquired resistance to this drug.

Sodium sulfacetamide solutions for ophthalmic use usually contain preservatives. Richards and McBride (2) showed that the inclusion of preservative systems decreases the sterilization time of sulfacetamide solutions from 5 hr to <15 min when challenged with 10^6 colony-forming units/ml of *Pseudomonas aeruginosa* 6750. The preservative systems included either chlorhexidine and phenylethyl alcohol, phenylmercuric nitrate and phenylethyl alcohol, or chlorocresol and phenylethyl alcohol, with or without EDTA (ethylenediaminetetraacetate).

The purpose of the present study was to determine the effects of prednisolone sodium phosphate, EDTA, thimerosal, and methyl- and propylparaben on the *in vitro* antimicrobial activity of solutions containing sodium sulfacetamide. The antimicrobial activities of the solutions tested were determined by kill rate and minimum inhibitory concentration (MIC) techniques using five test microorganisms: *Pseudomonas aeruginosa*, *Serratia marcescens*, *Staphylococcus epidermidis*, *Candida albicans*, and spores of *Aspergillus fumigatus*.

EXPERIMENTAL

Commercially available 10% sodium sulfacetamide solutions were obtained from pharmaceutical distributors; two experimental formulations were prepared in-house. The ingredients of each solution are listed in Table I. Both standard strains and clinical isolates were used as test microorganisms. The standard strains included *P. aeruginosa* 15442[1], *S. marcescens* 14041[1], *St. epidermidis* 17917[1], *C. albicans* 10231[1], and *A. fumigatus* 10894[1]. The clinical isolates of *P. aeruginosa* were SUH-51278[2] and H-23778[2]. Microbiological growth media included trypticase soy agar[3], trypticase soy broth[3], D/E neutralizing agar[4], and Sabouraud dextrose agar[4]. Other chemicals used in this study included APHA phosphate buffer[3], polysorbate 80[5], and sodium chloride[6].

Microbial cultures were prepared by inoculating 10-ml aliquots of trypticase soy broth with stock bacterial and yeast cultures maintained on either trypticase soy agar or Sabouraud dextrose agar slants and incubated for 18–24 hr at 32–34°. The second 24-hr cultures were harvested by centrifugation, washed three times in phosphate-buffered saline (centrifuged between each wash), and resuspended in sterile distilled water. The suspension of cells was further diluted to give an optical density at 500 nm, corresponding to ~10^6 colony-forming units/ml of test sample. Fungal spores were harvested from Sabouraud dextrose agar plates, washed five times in distilled water (centrifuged between each wash), and diluted to ~10^6 colony-forming units/ml of test sample.

To determine the death rate kinetics, the experiment was initiated by the addition of 0.1 ml of the standardized cultures to 20 ml of each test solution. The microbes were recovered between 1 min and 6 hr, diluted, and cultured in pour plates of D/E medium. The recovery plates were incubated for a maximum of 5 days at 30–35° followed by 5 days at room temperature. The experiments were repeated if recovery times or sample dilutions were inappropriate for the test microbe. The kill rate was expressed as a D-value, the time in minutes required to reduce the number of viable microorganisms by 90% (one log). The D-values were calculated from the best-fitting straight lines determined by linear regression. Thus, a lower D-value indicates a more rapid kill. All recoveries were validated by standard procedures.

MIC values were evaluated using microtiter plates with four overlapping concentrations of each solution, run in duplicate. After incubating the plates for 48 hr at 32–34°, the wells were scored as true positive (turbid), true negative (no turbidity), or plus–minus (very slight turbidity). The MIC was determined by calculating the geometric mean ($\bar{G}$) of the highest concentration of test solution to give a true positive, the lowest concentration to give a true negative, and the two median concentrations to give a plus–minus:

$$\bar{G} = (\text{highest positive value} \times \text{two median plus–minus values} \times \text{lowest negative value})^{1/4}$$

If only one median plus–minus value is used, the cube root of the product is taken; if no plus–minus values are used, the square root of the product is taken.

[1] American Type Culture Collection.
[2] Stanford University Hospital, Palo Alto, Calif.
[3] Baltimore Biological Laboratories, Cockeysville, Md.
[4] Difco Laboratories, Detroit, Mich.
[5] U.S. Biochemical Corp., Cleveland, Ohio.
[6] Fisher Scientific Co., Fair Lawn, N.J.

0022-3549/83/1200-1401$01.00/0

Table I—Composition of Sulfacetamide Solutions

Sulfacetamide Solution[a]	Preservative	EDTA[b]	Steroid[c]
A	Thimerosal, 0.01%	—	—
B	Methylparaben, 0.05%; propylparaben, 0.01%	—	—
A′	Thimerosal, 0.01%	0.1%	—
C	Methylparaben, 0.02%; propylparaben, 0.005%	—	0.25%
C′	Methylparaben, 0.02%; propylparaben, 0.005%	0.1%	0.25%

[a] 10% sulfacetamide as active ingredient. [b] The disodium salt. [c] Prednisolone sodium phosphate.

RESULTS

The kill rates of *P. aeruginosa*, *S. marcescens*, *St. epidermidis*, *C. albicans*, and *A. fumigatus* (spores) exposed to two ophthalmic solutions each formulated with 10% sodium sulfacetamide are presented in Table II. The data indicate that the sulfacetamide products are most rapidly bactericidal against *Pseudomonas*, (D = 168 min), slightly bactericidal against *Serratia* (D = 1318 min) and *Candida* (D = 2972 min), and not bactericidal against *Staphylococcus* or fungicidal against spores of *Aspergillus*. The large standard error associated with the D-value for *Serratia* is due to the preservative effect, as seen in Table III. Sulfacetamide solutions preserved with thimerosal are more rapidly bactericidal against *Serratia* than those preserved with parabens (Table III), resulting in lower D-values (faster kill rates). Since ocular anti-infective agents are washed out of the eye by natural tearing, solutions with low D-values would be more effective in controlling infection than those with high D-values.

Table II—Average Kill Rate (D-value) for Two Ophthalmic Solutions[a] Each Formulated with 10% Sodium Sulfacetamide

Microorganism	Number of Determinations	Average D-value[b] for Solutions A and B, min
Pseudomonas aeruginosa (four strains)	17	168 ± 17
Serratia marcescens	4	1318 ± 543
Staphylococcus epidermidis	4	NE[c]
Candida albicans	4	2972 ± 48
Aspergillus fumigatus	6	NE[c]

[a] Both solutions contain 10% sodium sulfacetamide; one was preserved with 0.01% thimerosal (solution A) and one with parabens (solution B). Neither product contains steroids or EDTA. [b] Mean ± *SE*. [c] NE = no significant effect observed during 6 hr of exposure.

Table III—Effect of Preservative Contained in 10% Sodium Sulfacetamide Solutions[a] on the Kill Rate (D-value) of *Serratia marcescens*

Solution	D-Value, min[b] Thimerosal Preservative	D-Value, min[b] Paraben Preservatives
A	436 ± 136	—
B	—	2200 ± 438
A + B	1318 ± 543	

[a] Neither solution contains steroids or EDTA. [b] Mean ± *SE*.

Table IV—MIC Values for Thimerosal- and Paraben-Preserved Sulfacetamide Solutions[a]

Microorganism	Solution A (Thimerosal)	Solution B (Parabens)
Pseudomonas aeruginosa	1.1	1.8
Serratia marcescens	0.4	1.5
Staphylococcus epidermidis	0.2	29.6
Candida albicans	2.0	≥50.0
Aspergillus fumigatus	2.8	6.5

[a] Expressed as %.

Table V—Effect of Steroids on the Kill Rate (D-value) of 10% Sodium Sulfacetamide as Formulated in Two Ophthalmic Solutions[a] Against Several Microorganisms

Microorganism	D-Value, min[b] Solution B (Without Steroid)	D-Value, min[b] Solution C (With Steroid)
Pseudomonas aeruginosa (four strains)	186 ± 28	235 ± 48
Serratia marcescens	2200 ± 438	1218 ± 184
Staphylococcus epidermidis	NE[c]	NE[c]
Candida albicans	2938 ± 56	NE[c]
Aspergillus fumigatus (spores)	1935 ± 136	NE[c]

[a] Both solutions contain 10% sodium sulfacetamide preserved with parabens; neither contain EDTA. [b] Mean ± *SEM*. [c] NE = no significant effect observed during 6 hr of exposure.

Table VI—MIC Values[a] for Steroidal and Nonsteroidal Sodium Sulfacetamide Solutions

Microorganism	Solution B (Without Steroid)	Solution C (With Steroid)
Pseudomonas aeruginosa	1.8	1.5
Serratia marcescens	1.5	1.6
Staphylococcus epidermidis	29.6	41.8
Candida albicans	≥50.0	≥50.0
Aspergillus fumigatus	6.5	6.8

[a] Expressed as percent.

Table VII—Effect of EDTA on the Kill Rate of Sulfacetamide Solutions Preserved with Either Thimerosal or Parabens

Preserved with 0.01% Thimerosal

Microorganism	D-value, min Product A[a]	D-value, min Product A′[b]
Pseudomonas aeruginosa (four strains)	148 ± 19	13 ± 1
Serratia marcescens	436 ± 136	247 ± 49
Staphylococcus epidermidis	1764 ± 306	2848 ± 600
Candida albicans	3006 ± 31	1459 ± 70
Aspergillus fumigatus (spores)	NE[c]	NE[c]

Preserved with Parabens

Microorganism	D-value, min Product C[a]	D-value, min Product C′[b]
Pseudomonas aeruginosa (four strains)	235 ± 48	35 ± 5
Serratia marcescens	1218 ± 184	637 ± 62
Staphylococcus epidermidis	NE[c]	NE[c]
Candida albicans	NE[c]	1612 ± 373
Aspergillus fumigatus (spores)	NE[c]	NE[c]

[a] Without EDTA. [b] With EDTA. [c] NE = no significant effect observed during 6 hr of exposure.

Table VIII—Effect of EDTA on the MIC Values of Sulfacetamide Solutions Preserved With Either Thimerosal or Parabens

Preserved with Thimerosal

Microorganism	Solution A[a]	Solution A′[b]
Pseudomonas aeruginosa	1.1	1.3
Serratia marcescens	0.4	0.4
Staphylococcus epidermidis	0.2	0.1
Candida albicans	2.0	3.1
Aspergillus fumigatus	2.8	0.3

Preserved with Parabens

Microorganism	Product C[a]	Product C′[b]
Pseudomonas aeruginosa	1.5	1.7
Serratia marcescens	1.6	2.0
Staphylococcus epidermidis	41.8	29.8
Candida albicans	≥50.0	≥50.0
Aspergillus fumigatus	6.8	7.4

[a] Without EDTA. [b] With EDTA.

The same anti-infective solutions were compared by MIC values in Table IV. The MIC values represent the bacteriostatic effect of each solution expressed as the percent of product required to inhibit growth; the lower the MIC, the more the test solution can be diluted and still inhibit microbial proliferation. Sulfacetamide solutions preserved with thimerosal have MIC values ranging from 0.2 to 2.8 for the five test microorganisms. The solutions preserved with parabens exhibit slightly higher MIC values for *Pseudomonas*, *Serratia*, and spores of *Aspergillus* (1.5–6.5) and significantly higher MIC values for *Staphylococcus* and *Candida* (19.6 and 5.0, respectively).

The effect of steroids and EDTA on the antimicrobial efficacy of the solutions was evaluated using the kill rate and MIC methods. The kill rates appear to be unaffected by the presence of steroids (Table V). The MIC values agree with this observation (Table VI). However, the addition of 0.1% EDTA to the sulfacetamide solutions significantly reduced the D-value for *Pseudomonas*, *Serratia*, and *Candida* regardless of the preservative (Table VII). This increase in antimicrobial activity, as indicated by smaller D-values, is not reflected by significantly different MIC values (Table VIII).

DISCUSSION

The results of both kill rate and MIC methods used to evaluate ophthalmic anti-infective solutions provide a better understanding of the antimicrobial effects of sulfacetamide and the clinical use of products containing this drug. Both methods indicate greater antimicrobial activity when thimerosal is used as the solution preservative than that seen with parabens: the kill rate for *Serratia* is increased and the MIC values for *Staphylococcus*, *Candida*, and possibly *Aspergillus* are decreased. The results using both methods also indicate that the addition of steroids to sulfacetamide formulations does not affect kill rates or MIC values.

However, only one method could detect the effect of EDTA on the antimicrobial activity of sulfacetamide. The kill rate for *Pseudomonas*, *Serratia*, and possibly *Candida* increased with the addition of EDTA, yet no differences in MIC values were observed. Thus, evaluation of antimicrobial activity using just one technique may not be adequate in determining the efficacy of ocular anti-infective products. MIC values are routinely used to evaluate the microbial sensitivity of parenterally administered antibiotics, yet this method of evaluation may miss interactions of other agents important in ocular therapy. This study shows that sulfacetamide solutions containing EDTA and thimerosal as preservatives are more effective against the organisms tested than sulfacetamide solutions containing paraben preservatives *without* EDTA. The antipseudomonal activity of thimerosal-preserved sulfacetamide solutions is particularly interesting, since they are usually not considered effective against this microorganism.

REFERENCES

(1) G. Hopkins, *Optician*, **183**, 20 (1982).

(2) R. M. E. Richards and R. J. McBride, *J. Pharm. Pharmacol.*, **24**, 159P (1972).

(3) "AMA Drug Evaluations," 3rd. ed., Publishing Sciences Group, Littleton, Mass., 1977, p. 964.

(4) I. Abboud, *Bull, Ophthalmol. Soc., Egypt*, **75**, 539 (1972).

(5) S. Olansky, *Cutis*, **19**, 852 (1977).

(6) M. Roumem and I. Isakow, *Ophthalmologica*, **197**, 42 (1977).

High-Performance Liquid Chromatographic Analysis of Diflunisal in Plasma and Urine: Application to Pharmacokinetic Studies in Two Normal Volunteers

J. E. RAY ˣ and R. O. DAY

Received May 17, 1982, from the *Department of Clinical Pharmacology, St. Vincent's Hospital, Darlinghurst, New South Wales, 2010, Australia.* Accepted for publication October 19, 1982.

Abstract □ A high-performance liquid chromatographic (HPLC) assay with fluorescence detection has been developed for the determination of diflunisal in plasma and urine. The plasma or urine, containing naproxen as the internal standard, was extracted with ether–hexane (1:1). The samples were analyzed on a microparticulate column, and the compounds were eluted using a mobile phase of 0.05 *M* phosphate buffer (pH 3) and methanol. Plasma samples were analyzed from two healthy male subjects who received a 250- and 750-mg oral dose of diflunisal 3 weeks apart. The data were analyzed according to a two-compartment open model. There was a disproportionate increase in the area under the plasma concentration–time curves (AUC 750 mg/AUC 250 mg was 3.84 for subject A and 4.22 for subject B) and a reduction in plasma clearance after the 750-mg dose of diflunisal. These data suggest that the kinetics of diflunisal may be dose dependent.

Keyphrases □ Diflunisal—high-performance liquid chromatographic analysis, plasma and urine, application to pharmacokinetic studies □ High-performance liquid chromatography—analysis of diflunisal in plasma and urine, application to pharmacokinetic studies □ Pharmacokinetics—diflunisal, high-performance liquid chromatographic analysis, plasma and urine

Diflunisal, 2′,4′-difluoro-4-hydroxy-3-biphenylcarboxylic acid, a salicylic acid derivative with analgesic and anti-inflammatory activity (1, 2), has been assayed in biological fluids by a fluorescence method (3). This assay procedure lacks the specificity of GLC and high-performance liquid chromatography (HPLC) (4). The more tedious GLC method (3) has been superseded by HPLC assays (4–6), but these methods have thus far been relatively insensitive.

The pharmacokinetics of diflunisal have been investigated, but these studies have used either the nonspecific fluorescence assay to measure plasma concentrations (3, 7–9) or the relatively insensitive HPLC procedures (10) which necessitated the administration of high doses (750 mg) of diflunisal. This paper reports the development of a sensitive and specific HPLC assay for quantitating diflunisal in plasma or urine and its application to a preliminary study of the pharmacokinetics of diflunisal in humans.

EXPERIMENTAL

Chemicals and Reagents—Diflunisal[1] and naproxen[2] were the reference and internal standards, respectively. Stock solutions of these

[1] Dolobid; Merck Sharp & Dohme, Sydney, Australia.
[2] Syntex, Sydney, Australia.

0022-3549/83/1200-1403$01.00/0

The same anti-infective solutions were compared by MIC values in Table IV. The MIC values represent the bacteriostatic effect of each solution expressed as the percent of product required to inhibit growth; the lower the MIC, the more the test solution can be diluted and still inhibit microbial proliferation. Sulfacetamide solutions preserved with thimerosal have MIC values ranging from 0.2 to 2.8 for the five test microorganisms. The solutions preserved with parabens exhibit slightly higher MIC values for *Pseudomonas*, *Serratia*, and spores of *Aspergillus* (1.5–6.5) and significantly higher MIC values for *Staphylococcus* and *Candida* (19.6 and 5.0, respectively).

The effect of steroids and EDTA on the antimicrobial efficacy of the solutions was evaluated using the kill rate and MIC methods. The kill rates appear to be unaffected by the presence of steroids (Table V). The MIC values agree with this observation (Table VI). However, the addition of 0.1% EDTA to the sulfacetamide solutions significantly reduced the D-value for *Pseudomonas*, *Serratia*, and *Candida* regardless of the preservative (Table VII). This increase in antimicrobial activity, as indicated by smaller D-values, is not reflected by significantly different MIC values (Table VIII).

DISCUSSION

The results of both kill rate and MIC methods used to evaluate ophthalmic anti-infective solutions provide a better understanding of the antimicrobial effects of sulfacetamide and the clinical use of products containing this drug. Both methods indicate greater antimicrobial activity when thimerosal is used as the solution preservative than that seen with parabens: the kill rate for *Serratia* is increased and the MIC values for *Staphylococcus*, *Candida*, and possibly *Aspergillus* are decreased. The results using both methods also indicate that the addition of steroids to sulfacetamide formulations does not affect kill rates or MIC values.

However, only one method could detect the effect of EDTA on the antimicrobial activity of sulfacetamide. The kill rate for *Pseudomonas*, *Serratia*, and possibly *Candida* increased with the addition of EDTA, yet no differences in MIC values were observed. Thus, evaluation of antimicrobial activity using just one technique may not be adequate in determining the efficacy of ocular anti-infective products. MIC values are routinely used to evaluate the microbial sensitivity of parenterally administered antibiotics, yet this method of evaluation may miss interactions of other agents important in ocular therapy. This study shows that sulfacetamide solutions containing EDTA and thimerosal as preservatives are more effective against the organisms tested than sulfacetamide solutions containing paraben preservatives *without* EDTA. The antipseudomonal activity of thimerosal-preserved sulfacetamide solutions is particularly interesting, since they are usually not considered effective against this microorganism.

REFERENCES

(1) G. Hopkins, *Optician*, **183**, 20 (1982).

(2) R. M. E. Richards and R. J. McBride, *J. Pharm. Pharmacol.*, **24**, 159P (1972).

(3) "AMA Drug Evaluations," 3rd. ed., Publishing Sciences Group, Littleton, Mass., 1977, p. 964.

(4) I. Abboud, *Bull, Ophthalmol. Soc., Egypt*, **75**, 539 (1972).

(5) S. Olansky, *Cutis*, **19**, 852 (1977).

(6) M. Roumem and I. Isakow, *Ophthalmologica*, **197**, 42 (1977).

High-Performance Liquid Chromatographic Analysis of Diflunisal in Plasma and Urine: Application to Pharmacokinetic Studies in Two Normal Volunteers

J. E. RAY ˣ and R. O. DAY

Received May 17, 1982, from the *Department of Clinical Pharmacology, St. Vincent's Hospital, Darlinghurst, New South Wales, 2010, Australia.* Accepted for publication October 19, 1982.

Abstract □ A high-performance liquid chromatographic (HPLC) assay with fluorescence detection has been developed for the determination of diflunisal in plasma and urine. The plasma or urine, containing naproxen as the internal standard, was extracted with ether–hexane (1:1). The samples were analyzed on a microparticulate column, and the compounds were eluted using a mobile phase of 0.05 *M* phosphate buffer (pH 3) and methanol. Plasma samples were analyzed from two healthy male subjects who received a 250- and 750-mg oral dose of diflunisal 3 weeks apart. The data were analyzed according to a two-compartment open model. There was a disproportionate increase in the area under the plasma concentration–time curves (AUC 750 mg/AUC 250 mg was 3.84 for subject A and 4.22 for subject B) and a reduction in plasma clearance after the 750-mg dose of diflunisal. These data suggest that the kinetics of diflunisal may be dose dependent.

Keyphrases □ Diflunisal—high-performance liquid chromatographic analysis, plasma and urine, application to pharmacokinetic studies □ High-performance liquid chromatography—analysis of diflunisal in plasma and urine, application to pharmacokinetic studies □ Pharmacokinetics—diflunisal, high-performance liquid chromatographic analysis, plasma and urine

Diflunisal, 2′,4′-difluoro-4-hydroxy-3-biphenylcarboxylic acid, a salicylic acid derivative with analgesic and anti-inflammatory activity (1, 2), has been assayed in biological fluids by a fluorescence method (3). This assay procedure lacks the specificity of GLC and high-performance liquid chromatography (HPLC) (4). The more tedious GLC method (3) has been superseded by HPLC assays (4–6), but these methods have thus far been relatively insensitive.

The pharmacokinetics of diflunisal have been investigated, but these studies have used either the nonspecific fluorescence assay to measure plasma concentrations (3, 7–9) or the relatively insensitive HPLC procedures (10) which necessitated the administration of high doses (750 mg) of diflunisal. This paper reports the development of a sensitive and specific HPLC assay for quantitating diflunisal in plasma or urine and its application to a preliminary study of the pharmacokinetics of diflunisal in humans.

EXPERIMENTAL

Chemicals and Reagents—Diflunisal[1] and naproxen[2] were the reference and internal standards, respectively. Stock solutions of these

[1] Dolobid; Merck Sharp & Dohme, Sydney, Australia.
[2] Syntex, Sydney, Australia.

0022-3549/83/1200-1403$01.00/0

compounds were prepared daily by dissolving the drugs in acetone[3]. Chromatographic-grade hexane[4] and methanol[5] were used, while all other reagents were analytical grade. Ether[6] was distilled in glass.

Extraction Procedure—The plasma or urine containing the internal standard was extracted according to the method of Van Loenhout *et al.* (6) with the following modifications: (*a*) to achieve adequate recovery of diflunisal from urine, samples were extracted twice with 5 ml of ether–hexane (1:1), and (*b*) the residue remaining after evaporation of the ether–hexane was resuspended in the HPLC mobile phase.

Clinical Study—Single 250- and 750-mg doses of diflunisal were administered to two healthy male subjects. The doses were not randomized, and the same formulation was used in both studies. Subjects fasted overnight before the drug administration and continued fasting until 4 hr postdose. All doses were administered at 8:00 a.m. and the tablets were swallowed whole with 200 ml of water. Venous blood samples were drawn into potassium oxalate–sodium fluoride[7] tubes before drug administration and at 0.5, 1, 1.5, 2, 2.5, 4, 5, 6, 8, 10, 12, 18, 24, 30, 36, 42, 48, 60, and 72 hr after the drug was given.

Instrumentation—Assays were carried out using a constant-flow high-performance liquid chromatograph[8]. It consisted of a solvent delivery system[9], an autosampler injector[10] with a pneumatic-actuated injection valve fitted with a 20-μl sample loop[11], a microparticulate reverse-phase column[12] (5 μm; 25 cm × 4.6-mm i.d.), a guard column[13], and a spectrophotofluorometer[14] with the excitation monochromotor set at 315 nm and the fluorescence emission at 389 nm (cutoff filter).

Chromatography—The compounds in plasma were eluted with a mobile phase of 64% methanol in 0.05 *M* phosphate buffer (pH 3), prepared from monobasic sodium phosphate with the pH adjusted using sulfuric acid. The column temperature was 50° and the flow rate was 1 ml/min. The same conditions were used to analyze urine samples, but a linear gradient (10 min) from 60% methanol in 0.05 *M* phosphate buffer (pH 3) to 70% methanol in phosphate buffer was necessary to move the diflunisal and naproxen peaks from interfering peaks at the solvent front.

Pharmacokinetic Analysis—The data were analyzed assuming a two-compartment open model with delayed absorption (11) and were fitted to the appropriate triexponential equation using a nonlinear regression analysis program (12). The equation fitted was:

$$C_1 = Ae^{-\alpha(t-t_0)} + Be^{-\beta(t-t_0)} - Ce^{-k_a(t-t_0)}$$

where C_1 is the plasma concentration, t the time after the dose, t_0 the lag time, and k_a the apparent first-order absorption rate constant. A, B, α, and β are constants related to model parameters (11); A and B are also related to the dose (D) and the fraction of the dose that reaches the systemic circulation (f). Initial estimates of these parameters were obtained graphically using the method of residuals (11). The volume of distribution V_d (area), the total body clearance (CL), and area under the curve (AUC) were estimated as described by Wagner (11).

RESULTS AND DISCUSSION

Assay—Reverse-phase HPLC with fluorescence detection was an effective method of quantitating diflunisal in human plasma and urine. Typical chromatograms obtained from blank plasma, blank urine, plasma containing diflunisal and naproxen (internal standard), and urine containing diflunisal and naproxen are shown in Fig. 1. Interference by endogenous substances did not occur from either drug-free plasma or urine (Fig. 1).

The standard curve for diflunisal was linear over the concentration range of 0.05–100 μg/ml in both plasma and urine. The correlation coefficient for the standard curves over this concentration range was >0.999 (n = 4). The coefficient of variation was <5% for all concentrations measured (Table I), and the sensitivity of the method was 50 ng/ml. Under the assay conditions described, acetylsalicylic acid and salicylic acid had elution times of 2.9 and 3.1 min, respectively, and did not interfere with the diflunisal or naproxen peaks.

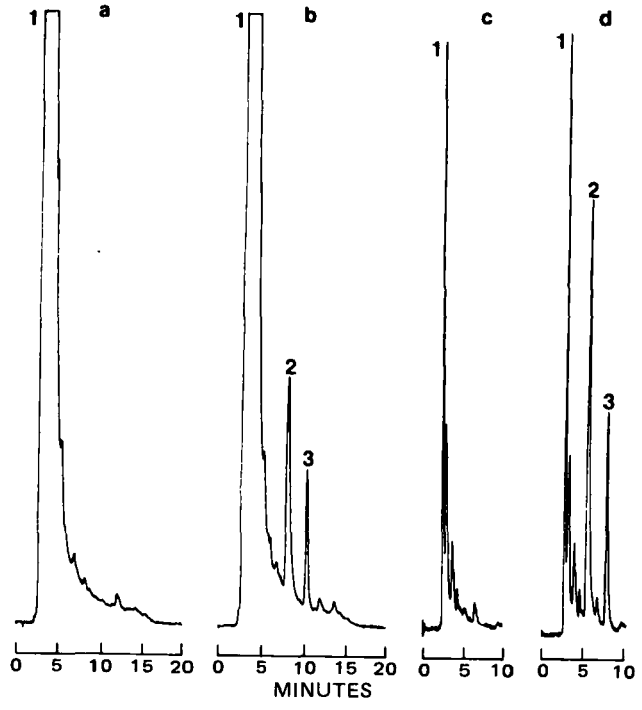

Figure 1—*Chromatograms of blank urine (a), spiked (200 ng/ml) urine (b), blank plasma (c), and spiked (200 ng/ml) plasma (d). Key: (1) solvent front; (2) diflunisal; (3) naproxen (internal standard).*

The method described was sufficiently sensitive to detect plasma concentrations of diflunisal for 80 hr after oral doses of 250 and 750 mg of the drug. The procedure has marked advantages over previous methods in both sensitivity (4–6) and specificity (3). The use of identical extraction and similar chromatographic conditions for the detection of diflunisal in plasma and urine makes the method simple and convenient for pharmacokinetic studies.

Pharmacokinetics—After the 250-mg dose of diflunisal, peak concentrations of 39.6 and 33.9 μg/ml were reached at 3.5 and 2.1 hr, respectively (Fig. 2). The pharmacokinetic data were analyzed according to a two-compartment open model although the elimination phase in subject B (250-mg dose) was not strictly linear. Agreement between the computer-generated curves and the experimental values was good. The various phramacokinetic parameters are shown in Table II. The half-lives of the initial α phase were 1.7 and 0.9 hr, while those of the β phase were 10.8 and 9.8 hr for the two subjects. The total body clearance was 8.6 and

Table I—Recovery and Reproducibility of the Diflunisal Assay [a]

Concentration, μg/ml	CV, %	Recovery, %
	Plasma	
0.050	4.2	97.4
0.075	3.0	96.2
0.100	2.7	97.8
0.150	2.6	97.9
0.200	2.7	97.6
10	4.8	105.0
25	3.2	98.1
50	4.2	94.3
100	2.2	99.9
	Urine	
0.050	2.1	101.0
0.075	2.6	96.8
0.100	2.4	97.9
0.150	3.5	98.9
0.200	2.1	98.4
10	4.0	96.1
25	2.7	103.3
50	1.6	97.2
100	2.4	98.9

[a] Number of estimations = 4.

[3] Hopkin & Williams, Ajax Chemicals, Sydney, Australia.
[4] Unichrom Reagents, Ajax Chemicals, Sydney, Australia.
[5] Waters Associates, Sydney, Australia.
[6] Ajax Chemicals, Sydney, Australia.
[7] Venoject; Kimble-Terumo, Inc., Elkton, Md.
[8] Varian Pty. Ltd., Sydney, Australia.
[9] Model 5000; Varian Pty Ltd., Sydney, Australia.
[10] Model 8055; Varian Pty Ltd., Sydney, Australia.
[11] Model 7126; Rheodyne, Cotati, Calif.
[12] Ultrasphere-ODS; Altex, Berkeley, Calif.
[13] Lichrosorb RP-8 (Cartridge); Brownlee Labs. Inc., Santa Clara, Calif.
[14] Model FS970; Schoeffel Instruments, Westwood, N.J.

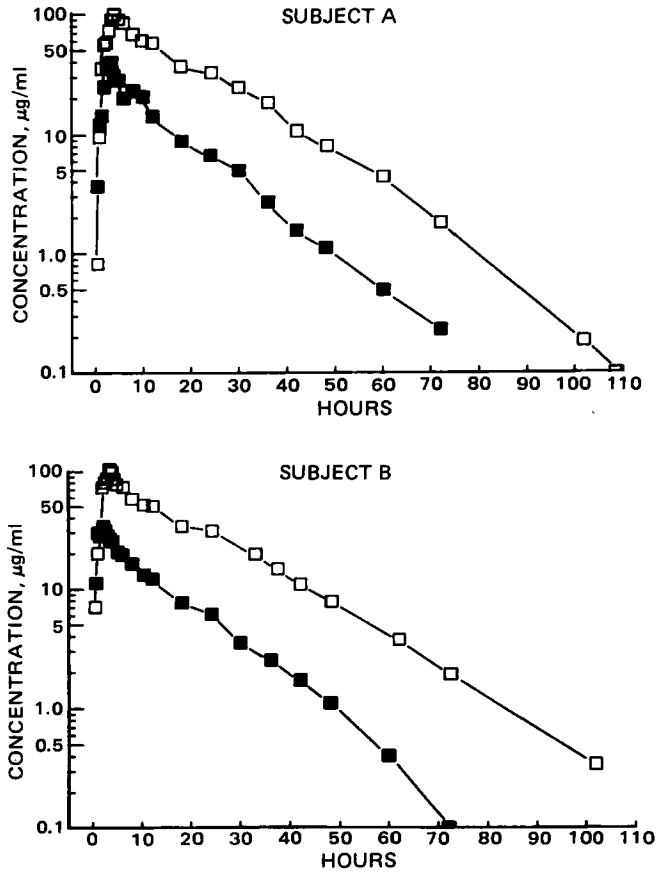

Figure 2—*Diflunisal plasma concentrations in two normal male subjects after a single 250-mg oral dose (■) and a single 750-mg oral dose (□).*

Table II—Plasma Pharmacokinetic Parameters in Two Normal Subjects After a 250-mg Oral Dose

Parameter	Subject A	Subject B
Lag time, hr	0.5	0.4
Peak time, hr	3.5	2.1
k_a, hr^{-1}	0.5	1.7
$t_{1/2,\alpha}$, hr	1.7	0.9
$t_{1/2,\beta}$, hr	10.8	9.8
V_d (area), liters[a]	14.1	8.6
CL, ml/min	8.6	10.0
$AUC_{0-\infty}$, μg·hr/ml	482.2	415.5

[a] Calculation assumes $f = 1$ (7).

10.0 ml of plasma/min. The volume of distribution was 14.1 and 8.6 liters. These data are in good agreement with those previously obtained after a 500-mg oral dose (7). The volume of distribution and clearance of diflunisal are low, but similar to other nonsteroidal anti-inflammatory drugs (13). Pharmacokinetic parameters were not estimated after the 750-mg oral doses of diflunisal in the two subjects because the log plasma concentration–time curves suggested a nonlinear elimination phase.

It has been suggested that diflunisal exhibits dose-dependent kinetics (3, 7, 8). Tocco *et al.* showed that the AUC values for [^{14}C]diflunisal in plasma of healthy volunteers were ~18 times higher after a 500-mg dose when compared with a 50-mg dose of diflunisal (3). Further, these authors reported a shorter elimination half-life (6 hr) after a 50-mg oral dose, compared with an elimination half-life of 10.8 hr after a 500-mg oral dose. However, these data are difficult to interpret because the assays lacked specificity. Dresse *et al.* (8) administered 500 mg of diflunisal twice a day for 8 days to 10 male volunteers and suggested that the elimination of diflunisal might be nonlinear for plasma concentrations >10 μg/ml. A third study, in which a nonspecific fluorescence assay was used, reported that the plasma elimination half-life of diflunisal decreased with declining plasma concentration, again suggesting nonlinear elimination of the drug (7).

Table III—Plasma Pharmacokinetic Parameters in Two Normal Subjects After a 750-mg Oral Dose

Parameter	Subject A	Subject B
Peak time, hr	4.0	3.5
Peak concentration, μg/ml	99.0	99.3
CL, ml/min	6.74	7.13
$AUC_{0-\infty}$, μg·hr/ml	1855	1752
AUC 750 mg/AUC 250 mg	3.84[a]	4.22[b]

[a] This ratio is significantly different from 3.0 ($p < 0.05$), one-sample t test. The one-sample t test is used to find the probability that the mean of a single sample of a population is different than an hypothesized value (15). [b] This ratio is significantly different from 3.0 ($p < 0.01$), one-sample t test.

The pharmacokinetics of diflunisal after 250- and 750-mg oral doses of the drug are shown in Tables II and III. There was a disproportionate increase in the plasma concentration–time AUC (Table III) and a reduction in plasma clearance (Tables II and III) when comparing the 750-mg oral dose of diflunisal with the 250-mg oral dose. Visual inspection of the plasma–concentration time curve for subject A suggests nonlinear elimination of the drug following the 750-mg dose of diflunisal. However, this phenomenon is not apparent in subject B.

The elimination of diflunisal is almost exclusively dependent on glucuronidation of the parent compound to ether glucuronide (64%) and ester glucuronide (20%), which are excreted in the urine (3). Pharmacokinetic studies with sodium salicylate, a compound structurally similar to diflunisal, have demonstrated that humans have a limited capacity for salicyl phenolic glucuronide formation (14), while the salicyl acyl glucuronide formation follows a first-order process (14). Data in normal volunteers suggest that the diflunisal phenolic glucuronide formation may be capacity limited (3). The data obtained from our study suggest that the kinetics of diflunisal may be dose dependent, but further study is needed to confirm this.

REFERENCES

(1) C. A. Stone, C. G. Van Arman, V. J. Lotti, D. H. Minsker, E. A. Risley, W. J. Bagdon, D. L. Bokelman, R. D. Jensen, B. Mendlowski, C. L. Tate, H. M. Peck, R. E. Zwickey, and S. E. McKinney, *Br. J. Clin. Pharmacol.*, **4**, 19S (1977).

(2) S. L. Steelman, K. F. Tempero, and V. J. Cirillo, *Clin. Ther.*, **1(A)**, 1 (1978).

(3) D. J. Tocco, G. O. Breault, A. G. Zacchei, S. L. Steelman, and C. V. Perrier, *Drug Metab. Dispos.*, **3(6)**, 453 (1975).

(4) M. Balali-Mood, I. S. King, and L. F. Prescott, *J. Chromatogr.*, **229**, 234 (1982).

(5) L. F. Prescott, I. S. King, L. Brown, M. Balali-Mood, and P. I. Adriaenssmens, *Proc. Analyt. Div. Chem. Soc.*, **16**, 300 (1979).

(6) J. W. A. Van Loenhout, H. C. J. Ketelaars, F. W. J. Gribnau, C. A. M. Van Ginneken, and Y. Tan, *J. Chromatogr.*, **182**, 487 (1980).

(7) R. Verbeeck, T. B. Tjandramaga, A. Mullie, R. Verbesselt, R. Verberckmoes, and P. J. Schepper, *Br. J. Clin. Pharmacol.*, **7**, 273 (1979).

(8) A. Dresse, D. Delapierre, and G. Baudinet, "Diflunisal," (Royal Society of Medicine, International Congress and Symposium Series No. 6), Academic Press/Royal Society of Medicine, London 1979, p. 21–23.

(9) A Dresse, M. A. Gerard, A. Lays, K. F. Tempero, and L. Verhaest, *Pharm. Acta. Helv.*, **53(6)**, 177 (1978).

(10) M. Balali-Mood and L. F. Prescott, *Br. J. Clin. Pharmacol.*, **10**, 163 (1980).

(11) J. G. Wagner, "Fundamentals of Clinical Pharmacokinetics," 1st ed., Drug Intelligence Publications, Hamilton, Ill., 1975, p. 102.

(12) P. Veng-Pederson, *J. Pharmacokinet. Biopharm.*, **5**, 513 (1977).

(13) G. D. Champion and G. G. Graham, *Aust. N.Z. J. Med.*, (Suppl 1), **8**, 94 (1978).

(14) G. Levy, T. Tsuchiya, and L. P. Amsel, *Clin. Pharmacol. Ther.*, **13**, 258 (1972).

(15) "Tektronix Manual, Plot 50: Statistics," Vol. 1, Tektronix, Inc., Beaveston, Ore. 1975, p. 3.1.

ACKNOWLEDGMENTS

The authors greatly appreciate the support of Merck Sharp and Dohme (Australia) Pty Ltd and thank Miss G. Wallace for typing this manuscript.

Decomposition of Thimerosal in Aqueous Solution and its Determination by High-Performance Liquid Chromatography

M. J. READER ˣ **and C. B. LINES**

Received August 2, 1982, from the *Central Analytical Laboratories (Chemical), The Wellcome Foundation Limited, Temple Hill, Dartford, Kent, DA1 5AH, United Kingdom.* Accepted for publication October 14, 1982.

Abstract □ Studies on the decomposition of thimerosal in aqueous solution have confirmed that thiosalicylic acid and ethylmercuric hydroxide are the initial products. On prolonged reaction, thiosalicylic acid was oxidized to 2,2′-dithiosalicylic acid, while ethylmercuric hydroxide was reduced to elemental mercury. As a result, a specific, reverse-phase high-performance liquid chromatographic assay has been developed for thimerosal in the presence of its decomposition products. By comparison, an existing colorimetric assay procedure employing dithizone was shown to be not fully specific. The presence of sodium chloride in the solution accelerated the decomposition of thimerosal. There was evidence that thimerosal was sorbed onto plastic containers on storage.

Keyphrases □ Thimerosal—degradation products, aqueous solutions, effect of sodium chloride, high-performance liquid chromatography □ Ophthalmic solutions—thimerosal decomposition in aqueous solutions, effect of sodium chloride, high-performance liquid chromatography □ High-performance liquid chromatography—thimerosal and its degradation products, aqueous solutions, effect of sodium chloride

Thimerosal, ethyl (sodium *o*-mercaptobenzoato)mercury (I), is widely used in pharmaceutical preparations, such as eyedrops, as an antibacterial and antifungal preservative. However, it is known to be unstable in aqueous solution (1, 2). It has also been reported that the presence of halides can have an adverse influence on the stability of I (3–5), and that I can be lost from solutions stored in plastic containers (6). The object of this study was to identify the decomposition products of thimerosal in aqueous solution under various conditions and, hence, develop a specific analytical method for the intact preservative in stored test solutions.

The decomposition of I in aqueous solution has been studied previously (2), and it was shown that the major products were thiosalicylic acid (II) and ethylmercuric hydroxide (III). Compound II can also undergo irreversible oxidation to 2,2′-dithiosalicylic acid (IV) (7). Hydrolysis in the presence of halide ions gave ethylmercuric halide (V) rather than the hydroxide (4).

Chemical assay procedures previously reported for the analysis of I have included UV spectrophotometry (8), polarography (9, 10), and colorimetry (11–13). None of these methods were fully specific for I in the presence of decomposition products, particularly the colorimetric assay, which is sensitive to all mercury-containing species present in the solution. Therefore, it was decided to seek a high-performance liquid chromatographic (HPLC) method for the analysis of I. A previously reported anion exchange HPLC method (14) was considered to be unsuitable for the assay of I in pharmaceutical preparations due to poor peak shape, while another method (15) failed to provide adequate resolution of I from its decomposition products. A more recent method (16) using radial-compression HPLC gave imprecise assays and did not satisfactorily resolve the degradation products of I from each other. The HPLC method described here gave resolution of I from its major decomposition products and has been used to assay I in test solutions and pharmaceutical vehicles.

EXPERIMENTAL

Compounds and Reagents—The following compounds were obtained commercially and used without further purification: thimerosal[1], ethylmercuric chloride[2], thiosalicylic acid[3], and 2,2′-dithiosalicylic acid[4]. All other reagents and solvents were analytical reagent grade[1]. Ethylmercuric hydroxide was synthesized by a published method (17).

High-Performance Liquid Chromatography—*Equipment*—A constant-flow pump[5] was used to deliver the eluant to a stainless steel column packed with 10-μm silica particles bonded with octadecylsilane[6]. Injections were made with a rotary valve injector[7] equipped with a 25-μl loop. No attempt was made to control the column temperature. A variable-wavelength detector[8] set at 222 nm was employed at an attenuation of 0.5 AUFS for 0.01% (w/v) solutions of thimerosal and at 0.05 AUFS for 0.001% (w/v) solutions.

Chromatographic Conditions—The mobile phase consisted of a mixture of methanol–water–phosphoric acid in a ratio of 60:50:1.0. The pressure at a flow rate of 2.6 ml min^{-1} was 1800 psig. Separations were effected isocratically at ambient temperature, and quantification was carried out by comparison of the areas of peaks obtained from test solutions with the area of the peak obtained from a standard thimerosal solution (Fig. 1).

Thin-Layer Chromatography—TLC was carried out on prepared silica gel plates[9] (20 cm × 20 cm × 0.25 mm) with mixtures of chloroform–methanol (1:1) (system A) or butanone–ethanol–acetic acid (70:30:0.1) (system B) as the developing solvents; loadings of thimerosal were usually 50 or 100 μg. Components were detected by viewing under UV light at 254 nm and visualized by spraying with a 0.05% (w/v) solution of diphenylthiocarbazone (dithizone) in chloroform.

Dithizone Colorimetric Assay—A volume of the test solution equivalent to 0.1 mg of I was transferred by pipet to a separator containing 0.5 *M* sulfuric acid (20 ml) and glacial acetic acid (20 ml). Ten percent sodium hydroxide (30 ml) was added followed by toluene (15 ml) and dithizone solution (1 ml). The mixture was shaken and allowed to settle. Most of the aqueous (lower) phase was removed and discarded. Anhydrous sodium sulfate (1 g) was added to the remaining emulsion, which was then filtered through a phase separating paper[10]. The color of the clear solution was measured in a 1-cm cell at 475 nm against a reagent blank on a spectrophotometer[11]. This was compared with the color formed from an aliquot of a standard thimerosal solution (10 ml; 0.001% w/v) treated in an identical manner.

Preparation of Dithizone and Thimerosal Solutions—Dithizone (64 mg) was dissolved in chloroform (100 ml); 10 ml of this solution was diluted to 100 ml with chloroform. Thimerosal (100 mg) was dissolved in water (100 ml). Two successive dilutions of 10 ml to 100 ml were made to obtain the standard solution.

[1] BDH Chemicals Ltd., Poole, England.
[2] Cambrian Chemicals, Croydon, England.
[3] Aldrich Chemical Co., Milwaukee, Wis.
[4] Aldrich Chemical Co., Ltd., Gillingham, Dorset, England.
[5] Model CE 210, Cecil Instruments Ltd., Cambridge, England.
[6] Spherisorb 10 ODS, Phase Separations Ltd., Clwyd, Wales.
[7] Rheodyne Inc., Cotati, Calif.
[8] Model CE 212, Cecil Instruments Ltd., Cambridge, England.
[9] Silica gel 60 F_{254} (Merck) BDH Chemicals Ltd., Poole, England.
[10] $1P_5$, Whatman Lab. Sales Ltd., Maidstone, Kent, England.
[11] Model SP8-1000, Pye Unicam Ltd., Cambridge, England.

0022-3549/83/1200-1406$01.00/0

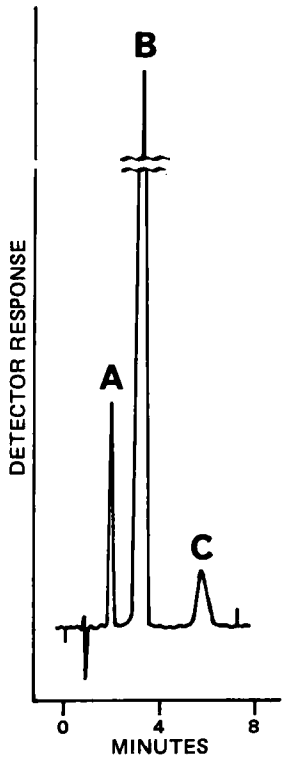

Figure 1—*Chromatogram of thiosalicylic acid (A), thimerosal (B), and 2,2′-dithiosalicylic acid (C).*

Hydrolysis of Thiomerosal in Aqueous Solution and in Saline—Solutions of thimerosal at a concentration of 0.5% in water and in 0.8% saline were heated under reflux and samples were removed at convenient intervals for TLC analysis. After 1 week, TLC (system B) showed one secondary spot at R_f 0.69 (nonabsorbing UV 254; yellow with dithizone) plus unreacted thimerosal (R_f 0.43). Neither solution contained any thimerosal after 3 weeks, but TLC now showed two major spots at R_f 0.23 and 0.30. The spot at R_f 0.69 was absent.

Both solutions were then cooled and acidified with hydrochloric acid to give white precipitates which were extracted into chloroform. The aqueous phases still contained insoluble materials which were filtered off, washed with water, and dried to give white solids, mp 283° (from the aqueous reaction) and 288° (from the saline reaction) identified as 2,2′-dithiosalicylic acid (IV) [lit. (2) mp 287–290°]. IR analysis gave an intense band at 1690 cm^{-1} due to the C=O stretching of an aromatic carboxylic acid. UV analysis showed two maxima at 252 and 313 nm in ethanol–0.1 *M* NaOH. TLC of the chloroform extracts showed two spots at R_f 0.23 and 0.30. Droplets of elemental mercury were also found in both solutions.

Stability in 0.8% Saline—*Thiosalicylic Acid*—A 0.2% solution of thiosalicylic acid in 0.8% saline was refluxed for 6 days. TLC (system B) showed complete conversion to IV (R_f 0.23); this was confirmed by UV analysis.

Ethylmercuric Chloride—A 0.2% solution/suspension of ethylmercuric chloride in 0.8% saline was refluxed for 6 days and monitored by TLC (system B). There was no indication of decomposition during this period and no visible formation of metallic mercury in the reaction vessel.

Interaction of Thiosalicylic Acid and Ethylmercuric Compounds in Aqueous Solution—Thiosalicylic acid (0.16 g, 1 mmole) and ethylmercuric chloride (0.27 g, 1 mmole) in water (20 ml) containing 1 *M* NaOH (1 ml) were refluxed for 1 week. TLC (system B) showed the formation of IV (R_f 0.23) and loss of ethylmercuric chloride (R_f 0.69). There was also deposition of metallic mercury. A parallel experiment with thiosalicylic acid (0.16 g, 1 mmole) and ethylmercuric hydroxide (0.25 g, 1 mmole) in 0.8% saline (20 ml) containing 1 *M* NaOH (1 ml) gave similar results.

RESULTS AND DISCUSSION

Decomposition Studies—The formation of II and III, or ethylmercuric chloride (V) in the presence of chloride ions, in the hydrolysis of I in water and 0.8% saline has been confirmed by TLC (Table I). No I and III (or V) remained after refluxing for 3 weeks, and the major products were shown to be II and IV by TLC and spectroscopic analysis. Mercury was also deposited from these solutions. The reaction shown in Scheme I represents the decomposition pathway of I under aqueous conditions. Compounds II and IV have been named and represented as the free carboxylic acids throughout, although in aqueous solution they will usually be present as their sodium salts.

Table I—R_f Values and Response to the Spray Reagent on TLC of I–V

Compound	R_f Values System A	R_f Values System B	Color with Dithizone
Thimerosal (I)	0.54	0.43	Yellow
Ethylmercuric chloride (V)	0.76	0.69	Lemon yellow
Ethylmercuric hydroxide (III)	0.70	0.65	Lemon yellow
Thiosalicylic acid (II)	0.40	0.29	Faint mauve[a]
2,2′-Dithiosalicylic acid (IV)	0.30	0.23	Faint mauve-pink[a]

[a] Color develops on standing.

It has been demonstrated that II oxidized to IV on heating in 0.8% saline. Compound V alone, when heated in 0.8% saline, failed to degrade to mercury. However equimolar mixtures of II and III, and of II and V, have been shown to interact when heated in aqueous solution. As II was oxidized to IV, the ethylmercuric compounds (III and V) were correspondingly reduced to metallic mercury.

Analytical Studies—During the development of a reverse-phase HPLC method various water–methanol mixtures were tried and the pH of the eluant was controlled using phosphoric acid to reduce the effect of peak tailing. The eluant allowed monitoring at 222 nm, the UV absorption maximum of thimerosal at this pH. The mobile phase chosen for the analysis gave the following k' values: thiosalicylic acid, 1.5; thimerosal, 3.0; 2,2′-dithiosalicylic acid, 6.0. The effect of decreasing the proportion of methanol relative to water in the mobile phase was to increase the retention of all three components resulting in a high overall analysis time, while an increase in the methanol–water ratio impaired the resolution of thimerosal and thiosalicylic acid.

A standard calibration curve for thimerosal was constructed using a stock solution of 102 μg/ml and three solutions of 61.2, 40.8, and 20.4 μg/ml prepared by dilution of the stock solution. The $y = mx + c$ linear regression equation gave a slope of 1844, and intercept of 1577, and was linear in the range of 20.4–102 μg/ml (the corresponding integrator response ranging from 38,741 to 189,527). The plot gave a Pearson's correlation coefficient of 0.99998 ($p < 0.01$).

It was considered that the good fit and linearity of the calibration plot (which also passed very close to the origin) together with the good reproducibility of the method (coefficient of variation, 0.7%) allowed analysis to be carried out using drug peak areas alone and obviated the need for an internal standard. The limits of detection when 25-μl injections of solutions were made with a detector attenuation of 0.05 AUFS were 0.2 μg/ml for thiosalicylic acid and 0.1 μg/ml for thimerosal.

The HPLC procedure was used to assay thimerosal in samples of 0.01% aqueous solutions after storage in various containers for 24 months at

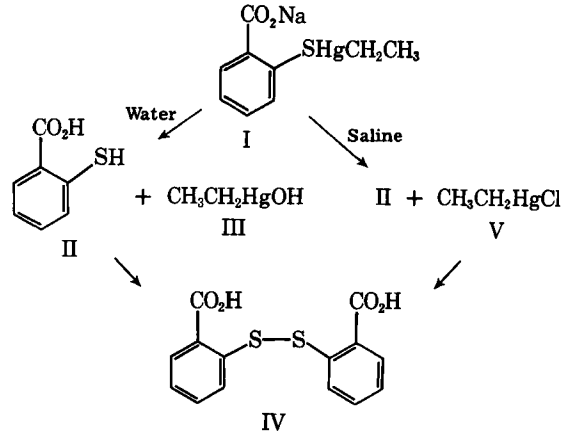

Scheme I—Reaction scheme for the decomposition of thimerosal in aqueous solution.

Table II—Results of HPLC and Dithizone Analyses of 0.01% Aqueous Thimerosal Solutions Stored for 2 Years at 5°, 25°, 37°, and 50° in Glass and Plastic Containers

Container	Temp, °	Recovery of Thimerosal, %				Thiosalicylic Acid, %			
		HPLC		Dithizone		Found		Calculated[a]	
		A[b]	B[b]	A	B	A	B	A	B
Glass ampules	5	100.5	97.6	99.6	98.1	4.8	3.4	0.0	2.4
	25	85.9	88.2	97.2	97.3	15.9	12.6	14.2	11.8
	37	80.4	80.4	95.4	94.5	20.8	18.9	19.7	19.7
	50	40.0	38.9	74.2	71.7	53.5	44.1	60.1	61.2
Glass ampules (autoclaved)	5	55.7	82.9	87.4	99.5	26.5	18.5	44.4	17.1
	25	66.5	63.8	89.5	97.7	24.6	24.1	33.6	36.2
	37	24.4	80.7	88.1	94.7	64.3	18.1	75.6	19.4
	50	9.3	29.1	59.7	74.9	56.2	49.3	90.6	70.9
Polyethylene bottles	5	95.1	99.6	95.8	100.0	5.5	3.8	5.0	0.5
	25	79.4	85.1	87.4	89.9	11.2	11.1	20.5	15.0
	37	67.3	65.1	76.5	69.1	15.0	16.8	32.8	34.9
	50	34.3	0.0	36.4	6.9	9.1	10.0	65.6	100.0
Polypropylene bottles	5	95.5		97.4		5.2		4.5	
	25	77.8		89.5		16.4		22.3	
	37	69.6		71.2		23.2		30.5	
	50	0.0		18.3		39.4		100.0	
Polyethylene containers	5	94.5		98.5		3.6		5.5	
	25	68.3		12.8		14.5		31.8	
	37	0.0		12.0		30.1		100.0	

[a] This figure represents the amount of thiosalicylic acid expected from the decomposition indicated by the HPLC assay of thimerosal. [b] A and B refer to assay values on two separate samples.

5°, 25°, 37°, and 50°. The containers included glass ampules, one-half of which were autoclaved at 120° for 20 min before the start of the storage test (the other half were not autoclaved) and three types of plastic containers. The results, together with those obtained colorimetrically using dithizone, are given in Table II.

After storage, the solutions in glass ampules that were not autoclaved showed HPLC assays lower than those obtained by the dithizone method. This trend was even more marked in those solutions which had been previously autoclaved. These figures are a reflection of the greater specificity of the HPLC method compared with the colorimetric assay.

The level of thimerosal after storage in plastic containers was found to be lower than that found in glass ampules especially at higher storage temperatures. There was, in general, fairly good agreement between the two assay methods for plastic containers. From the HPLC assay of solutions in plastic containers, it is clear that thimerosal is lost from solution by hydrolysis and by some form of sorption onto the containers; these effects increase with temperature. In plastic containers at 25° there was also less thiosalicylic acid detected than would have been anticipated from the thimerosal levels; this trend became more marked at 37° and 50°, providing a further indication of sorption of thimerosal onto the container. By comparison, in glass containers there was reasonably good mass balance between thimerosal decomposed and thiosalicylic acid formed up to 37°, less so at 50°. The sorption of organomercury compounds, including thimerosal, onto the surface of plastic containers has been noted previously (6, 18) and was shown to be dependent on storage temperature and time for a given plastic.

Table III—Results of the HPLC Assays of Thimerosal Solutions in Water and in Saline Stored for 15 days at 5°, 25°, and 50° in Glass Containers

Initial Thimerosal Concentration, %	Temp, °	Time, days	HPLC Assay of Thimerosal, %	
			Water	0.8% Saline
0.001	5	8	100.8	32.5
	25		101.8	<5
	50		28.9	<5
	5	15	105.2	30.3
	25		96.5	<5
	50		44.6	NA[a]
0.01	5	8	103.3	69.1
	25		99.7	50.0
	50		95.1	50.2
	5	15	95.6	69.2
	25		104.3	59.0
	50		NA[a]	NA[a]
0.1	5	8	104.7	98.6
	25		97.6	96.6
	50		99.9	92.0
	5	15	88.2	89.3
	25		79.4	72.8
	50		76.8	NA[a]

[a] NA = not analyzed.

Since ophthalmic pharmaceutical formulations are commonly rendered isotonic with the fluids in the eye using sodium chloride, the effect of this salt on the stability of thimerosal in aqueous solution was investigated. Thimerosal was stored as 0.1, 0.01, and 0.001% solutions in water and 0.8% saline at 5°, 25°, and 50° for up to 15 days. HPLC analysis was carried out after 8 and 15 days (Table III).

In water, thimerosal was stable except when stored at 50° at the lowest concentration (0.001%), the assay dropping to 30–40%. This effect of the initial concentration of thimerosal became even more marked in saline. After 8 days at 0.001% initial concentration, there was no thimerosal remaining at 25° and 50° and only ~30% at 5°. These figures present a disturbing picture, since they mirror what could be expected in ophthalmic formulations where thimerosal is very often present at concentrations of 0.001% in the presence of 0.8% saline. At 0.01 and 0.1% initial concentrations, sodium chloride had a less dramatic effect on the assay, but decomposition of thimerosal was still much faster in its presence.

In view of these findings on the effect of sodium chloride on the stability of thimerosal, equivalent pharmaceutical vehicles containing thimerosal at an initial concentration of 0.001% and 0.8% sodium chloride were prepared and stored at 5° for 3 months. HPLC assay showed no thimerosal (<10%) remaining, while the dithizone method gave satisfactory assay values of 101.3 and 102.3% of the labelled strength for two such samples. These figures further reflect the specificity of the HPLC method compared with the colorimetric procedure.

It was reported (5) that there was only 30% thimerosal remaining after storage in 0.4% aqueous sodium chloride, and in an equivalent pharmaceutical vehicle containing sodium chloride, for 2 months at 70°. However these findings were based on the semispecific UV or colorimetric methods for the assay of thimerosal and would seem to be somewhat optimistic. If the data in Table III together with that obtained from an equivalent pharmaceutical vehicle are considered, a much more pessimistic picture is presented of the stability of thimerosal in saline solution and, thus, in pharmaceutical preparations containing sodium chloride.

The exact reasons for the marked effect of sodium chloride on the decomposition of thimerosal are not clear at present. It is well known that chloride and other halides have a marked affinity to coordinate with mercury(II) compounds, and this could be a contributory factor in the detrimental effect of sodium chloride on the stability of thimerosal in solution. There is some evidence to show that the decomposition of thimerosal in water to thiosalicylic acid and ethylmercuric hydroxide is a reversible reaction. The effect of chloride could be to disturb this equilibrium by reaction with the ethylmercuric hydroxide to give ethylmercuric chloride, which does not react nearly as readily with thiosalicylic acid in neutral solution to give thimerosal.

Further investigations will be needed to substantiate this mechanism of the action of chloride ions and other anionic species. What is evident

from these investigations is that the use of sodium chloride as an isotonic agent with thimerosal as preservative in ophthalmic preparations is open to question.

REFERENCES

(1) K. Tsuji, Y. Yamawaki, and Y. Miyazaki, *Arch. Pract. Pharm.*, **24,** 110 (1951).

(2) F. Tanaka and M. Mitsuno, *Ann. Rept. Takeda Research Lab.*, **10,** 65 (1951).

(3) K. Horworka, B. Horworka, and R. Meyer, *Pharmazie*, **28,** 136 (1973).

(4) E. Lüdtke and R. Pohloudek-Fabini, *Pharmazie*, **32,** 625 (1977).

(5) E. Lüdtke, H. Darsow, and R. Pohloudek-Fabini, *Pharmazie*, **32,** 99 (1977).

(6) N. E. Richardson, D. J. G. Davies, B. J. Meakin, and D. A. Norton, *J. Pharm. Pharmacol.*, **29,** 717 (1977).

(7) M. J. Kharasch, U.S. Pat. 2,012,820 (1935).

(8) F. Neuwald and G. Schmitzek, *Pharm. Ztg.*, **112,** 1308 (1967).

(9) E. B. Beyer, *J. Assoc. Off. Anal. Chem.*, **52,** 844, (1969).

(10) T. Omura, S. Morishita, and Y. Ueda, *Bunseki Kagaku*, **19,** 941 (1970).

(11) A. R. Neurath, *Cesk. Farm.*, **10,** 75 (1961).

(12) J. Viska and A. Okac, *Cesk. Farm.*, **15,** 356 (1966).

(13) J. Viska and A. Okac, *Cesk. Farm.*, **16,** 29 (1967).

(14) C. C. Fu and M. J. Sibley, *J. Pharm. Sci.*, **66,** 738 (1977).

(15) R. C. Meyer and L. B. Cohn, *J. Pharm. Sci.*, **67,** 1636 (1978).

(16) S. W. Lam, R. C. Meyer, and L. T. Takahashi, *J. Parent. Sci. Technol.*, **35,** 262 (1981).

(17) K. H. Slotta and K. R. Jacobi, *J. Prakt. Chem.*, **120,** 283 (1929).

(18) G. C. Kondos, *Pharm. Prax.*, **12,** 257 (1977).

Bioavailability of Propylthiouracil in Humans

H. P. RINGHAND *, W. A. RITSCHEL *x, M. C. MEYER ‡, A. B. STRAUGHN ‡, and B. E. CABANA §

Received April 4, 1982, from the **College of Pharmacy, University of Cincinnati Medical Center, Cincinnati, OH 45267,* ‡*Department of Pharmaceutics, College of Pharmacy, University of Tennessee, Memphis, TN 38163,* and the §*Food and Drug Administration, Division of Biopharmaceutics, Rockville, MD 20852.* Accepted for publication October 6, 1982.

Abstract □ Single lots of five commercially available 50-mg propylthiouracil formulations were evaluated *in vitro* and *in vivo*. Each product met the USP XIX specifications for drug content, content uniformity, and disintegration time. However, major differences were noted among products in their rate and extent of dissolution. Statistically significant differences ($p < 0.05$) were observed *in vivo* among the drug formulations at all but one of the sampling times, as determined from crossover blood level studies in 12 healthy male volunteers. The differences among the areas under the plasma level–time curves for the various products were not statistically significant. No statistically significant correlations were found between the *in vitro* and *in vivo* parameters studied.

Keyphrases □ Propylthiouracil—human plasma levels *in vivo*, bioavailability, correlation with *in vitro* dissolution □ Bioavailability—propylthiouracil, human plasma, correlation with *in vitro* dissolution □ Dissolution, *in vitro*—propylthiouracil, correlation with *in vivo* bioavailability, humans

Propylthiouracil, a thyrostatic drug that inhibits the synthesis of hormones within the thyroid gland and reduces the conversion of thyroxine (T_4) to the more potent triiodothyronine, T_3, in the peripheral tissues (1), is prescribed for the chronic treatment of hyperthyroidism and the preparation of hyperthyroid patients for surgery. While differences in bioavailability among propylthiouracil formulations have not been documented, propylthiouracil has been included in several lists of drugs with potential or actual differences in bioavailability (2, 3). The present study involved a crossover comparison to assess the relative bioavailability of five currently marketed products.

EXPERIMENTAL

Product Selection—Five single lots of 50-mg propylthiouracil tablets from separate manufacturers were evaluated; the individual products are identified in Table I. The sixth formulation, a solution of propylthiouracil, was utilized as a reference and was prepared as follows.

A stock solution of sucrose–glycerin was prepared by combining 6.5 g of sucrose with 12.5 ml of glycerin, diluting to 500 ml with distilled water. The day before each study a sucrose–glycerin–citric acid solution was prepared by adding 2.0 ml of 0.5 *M* citric acid to 95.4 ml of the sucrose–glycerin stock solution. On the day of each study the propylthiouracil reference solution was freshly prepared using USP propylthiouracil powder[1]. A 150-mg quantity of the powdered propylthiouracil was accurately weighed and dissolved in 6 ml of 0.2 *M* NaOH. The resulting solution was then diluted immediately with 24 ml of the sucrose–glycerin–citric acid solution and administered to the subject.

Clinical Study Protocol—Twelve male volunteers[2] underwent urinalysis and hematological and blood chemistry[3] testing to ensure that they were in good health. Also included in the initial medical evaluation was a T_4 determination by radioimmunoassay, T_3 uptake, and free thyroxine blood study. As a precaution against possible side effects of the propylthiouracil, the white blood cell and differential count, as well as prothrombin time, were monitored at the midpoint of the 6-week study. The subjects ranged in age from 20 to 25 years, in height from 172 to 198 cm, and in weight from 72 to 93 kg; all were considered to be of normal weight for their height (4).

The sequence of dose administration was based on a crossover matrix, designed to minimize the influence of any residual or cumulative effects of the preceding doses (5). Each subject received three 50-mg tablets or reference solution equivalent to 150 mg of propylthiouracil once a week for 6 weeks. The propylthiouracil formulations were administered with 200 ml of water in the morning following an overnight fast[4]. No food and water were permitted for 4 hr after ingestion of the dose. The subjects were instructed to avoid any food high in fat content on days of testing to minimize analytical problems associated with excessive lipids in the plasma. While the subjects were not sequestered on the days of testing they were instructed to avoid undue exercise. Subjects were also cautioned to avoid any other medication during the 6-week period of the study.

[1] USP propylthiouracil powder was provided by Lederle Labs.

[2] Staff and students of the University of Tennessee Center for the Health Sciences. Written informed consent was obtained.

[3] SMA 18/90.

[4] A standardized meal was not required prior to fasting.

0022-3549/83/1200-1409$01.00/0

from these investigations is that the use of sodium chloride as an isotonic agent with thimerosal as preservative in ophthalmic preparations is open to question.

REFERENCES

(1) K. Tsuji, Y. Yamawaki, and Y. Miyazaki, *Arch. Pract. Pharm.*, **24,** 110 (1951).

(2) F. Tanaka and M. Mitsuno, *Ann. Rept. Takeda Research Lab.*, **10,** 65 (1951).

(3) K. Horworka, B. Horworka, and R. Meyer, *Pharmazie*, **28,** 136 (1973).

(4) E. Lüdtke and R. Pohloudek-Fabini, *Pharmazie*, **32,** 625 (1977).

(5) E. Lüdtke, H. Darsow, and R. Pohloudek-Fabini, *Pharmazie*, **32,** 99 (1977).

(6) N. E. Richardson, D. J. G. Davies, B. J. Meakin, and D. A. Norton, *J. Pharm. Pharmacol.*, **29,** 717 (1977).

(7) M. J. Kharasch, U.S. Pat. 2,012,820 (1935).

(8) F. Neuwald and G. Schmitzek, *Pharm. Ztg.*, **112,** 1308 (1967).

(9) E. B. Beyer, *J. Assoc. Off. Anal. Chem.*, **52,** 844, (1969).

(10) T. Omura, S. Morishita, and Y. Ueda, *Bunseki Kagaku*, **19,** 941 (1970).

(11) A. R. Neurath, *Cesk. Farm.*, **10,** 75 (1961).

(12) J. Viska and A. Okac, *Cesk. Farm.*, **15,** 356 (1966).

(13) J. Viska and A. Okac, *Cesk. Farm.*, **16,** 29 (1967).

(14) C. C. Fu and M. J. Sibley, *J. Pharm. Sci.*, **66,** 738 (1977).

(15) R. C. Meyer and L. B. Cohn, *J. Pharm. Sci.*, **67,** 1636 (1978).

(16) S. W. Lam, R. C. Meyer, and L. T. Takahashi, *J. Parent. Sci. Technol.*, **35,** 262 (1981).

(17) K. H. Slotta and K. R. Jacobi, *J. Prakt. Chem.*, **120,** 283 (1929).

(18) G. C. Kondos, *Pharm. Prax.*, **12,** 257 (1977).

Bioavailability of Propylthiouracil in Humans

H. P. RINGHAND *, W. A. RITSCHEL *x, M. C. MEYER ‡, A. B. STRAUGHN ‡, and B. E. CABANA §

Received April 4, 1982, from the **College of Pharmacy, University of Cincinnati Medical Center, Cincinnati, OH 45267,* ‡*Department of Pharmaceutics, College of Pharmacy, University of Tennessee, Memphis, TN 38163,* and the §*Food and Drug Administration, Division of Biopharmaceutics, Rockville, MD 20852.* Accepted for publication October 6, 1982.

Abstract □ Single lots of five commercially available 50-mg propylthiouracil formulations were evaluated *in vitro* and *in vivo*. Each product met the USP XIX specifications for drug content, content uniformity, and disintegration time. However, major differences were noted among products in their rate and extent of dissolution. Statistically significant differences ($p < 0.05$) were observed *in vivo* among the drug formulations at all but one of the sampling times, as determined from crossover blood level studies in 12 healthy male volunteers. The differences among the areas under the plasma level–time curves for the various products were not statistically significant. No statistically significant correlations were found between the *in vitro* and *in vivo* parameters studied.

Keyphrases □ Propylthiouracil—human plasma levels *in vivo*, bioavailability, correlation with *in vitro* dissolution □ Bioavailability—propylthiouracil, human plasma, correlation with *in vitro* dissolution □ Dissolution, *in vitro*—propylthiouracil, correlation with *in vivo* bioavailability, humans

Propylthiouracil, a thyrostatic drug that inhibits the synthesis of hormones within the thyroid gland and reduces the conversion of thyroxine (T_4) to the more potent triiodothyronine, T_3, in the peripheral tissues (1), is prescribed for the chronic treatment of hyperthyroidism and the preparation of hyperthyroid patients for surgery. While differences in bioavailability among propylthiouracil formulations have not been documented, propylthiouracil has been included in several lists of drugs with potential or actual differences in bioavailability (2, 3). The present study involved a crossover comparison to assess the relative bioavailability of five currently marketed products.

EXPERIMENTAL

Product Selection—Five single lots of 50-mg propylthiouracil tablets from separate manufacturers were evaluated; the individual products are identified in Table I. The sixth formulation, a solution of propylthiouracil, was utilized as a reference and was prepared as follows.

A stock solution of sucrose–glycerin was prepared by combining 6.5 g of sucrose with 12.5 ml of glycerin, diluting to 500 ml with distilled water. The day before each study a sucrose–glycerin–citric acid solution was prepared by adding 2.0 ml of 0.5 *M* citric acid to 95.4 ml of the sucrose–glycerin stock solution. On the day of each study the propylthiouracil reference solution was freshly prepared using USP propylthiouracil powder[1]. A 150-mg quantity of the powdered propylthiouracil was accurately weighed and dissolved in 6 ml of 0.2 *M* NaOH. The resulting solution was then diluted immediately with 24 ml of the sucrose–glycerin–citric acid solution and administered to the subject.

Clinical Study Protocol—Twelve male volunteers[2] underwent urinalysis and hematological and blood chemistry[3] testing to ensure that they were in good health. Also included in the initial medical evaluation was a T_4 determination by radioimmunoassay, T_3 uptake, and free thyroxine blood study. As a precaution against possible side effects of the propylthiouracil, the white blood cell and differential count, as well as prothrombin time, were monitored at the midpoint of the 6-week study. The subjects ranged in age from 20 to 25 years, in height from 172 to 198 cm, and in weight from 72 to 93 kg; all were considered to be of normal weight for their height (4).

The sequence of dose administration was based on a crossover matrix, designed to minimize the influence of any residual or cumulative effects of the preceding doses (5). Each subject received three 50-mg tablets or reference solution equivalent to 150 mg of propylthiouracil once a week for 6 weeks. The propylthiouracil formulations were administered with 200 ml of water in the morning following an overnight fast[4]. No food and water were permitted for 4 hr after ingestion of the dose. The subjects were instructed to avoid any food high in fat content on days of testing to minimize analytical problems associated with excessive lipids in the plasma. While the subjects were not sequestered on the days of testing they were instructed to avoid undue exercise. Subjects were also cautioned to avoid any other medication during the 6-week period of the study.

[1] USP propylthiouracil powder was provided by Lederle Labs.

[2] Staff and students of the University of Tennessee Center for the Health Sciences. Written informed consent was obtained.

[3] SMA 18/90.

[4] A standardized meal was not required prior to fasting.

0022-3549/83/1200-1409$01.00/0

Table I—*In Vitro* Test Results for 50-mg Propylthiouracil Products [a]

Product	Assay, % of Label Claim	Content Uniformity, Mean % of Label Claim (*SD*)[b]	Dissolution Profile, Mean % of Label Claim (*SD*)[c] 0.1 *N* HCl 5 min	0.1 *N* HCl 20 min	0.1 *N* HCl 60 min	Water 5 min	Water 20 min	Water 60 min
1	—	—	—	—	—	—	—	—
2	102.0	104.0 (1.0)	2.5 (0.2)	8.7 (0.5)	20.6 (1.0)	3.0 (0.3)	10.0 (1.1)	24.6 (2.0)
3	101.0	102.0 (1.5)	3.3 (0.8)	12.5 (0.6)	27.4 (0.6)	3.2 (0.7)	10.0 (0.9)	21.3 (1.9)
4	99.8	104.0 (1.6)	50.3 (12.5)	77.3 (12.4)	88.3 (11.0)	57.7 (9.6)	86.8 (10.1)	94.2 (8.1)
5	102.0	102.0 (1.6)	25.8 (3.2)	87.8 (5.5)	102.1 (2.7)	26.2 (5.4)	54.4 (9.7)	80.8 (10.2)
6	100.0	99.8 (2.5)	4.6 (0.9)	21.3 (5.6)	53.8 (11.1)	5.3 (1.4)	23.1 (5.3)	58.6 (11.8)

[a] Manufacturer and lot numbers are as follows: (1) propylthiouracil reference solution prepared as described in the text; (2) Eli Lilly, OAF 35B; (3) Lederle, 461-260; (4) Parke-Davis, TB 299; (5) Mylan, 1005410; (6) Richlyn, 29327. All products were obtained from FDA regional offices. [b] Means are based on 10 determinations (*SD*). [c] Means are based on six determinations (*SD*).

Table II—Mean Plasma Levels of Propylthiouracil in 12 Subjects Following Ingestion of a Single 150-mg Dose

Product[a]	Propylthiouracil Plasma Levels at Each Sampling Time, μg/ml 0.33 hr	0.67 hr	1.0 hr	1.5 hr	2.0 hr	3.0 hr	4.0 hr	6.0 hr	8.0 hr
1	3.04 (64.5)[b]	3.94 (20.6)	3.53 (15.7)	2.80 (19.9)	2.27 (23.4)	1.48 (33.1)	0.97 (40.9)	0.42 (80.5)	0.17 (96.9)
2	0.10 (130.0)	0.47 (62.1)	0.86 (44.8)	1.80 (37.9)	2.62 (25.1)	2.55 (22.0)	1.73 (24.4)	0.76 (42.0)	0.31 (52.0)
3	0.82 (146.3)	2.57 (73.2)	2.55 (59.7)	2.54 (38.7)	2.53 (41.3)	2.04 (38.1)	1.51 (60.6)	0.59 (56.1)	0.24 (60.4)
4	1.78 (77.4)	3.29 (42.0)	3.44 (23.6)	3.06 (19.0)	2.48 (18.8)	1.75 (32.7)	1.15 (37.5)	0.49 (40.3)	0.19 (57.6)
5	1.35 (84.1)	2.65 (25.9)	2.95 (20.2)	3.04 (17.1)	2.66 (20.3)	1.86 (25.4)	1.24 (27.8)	0.51 (41.1)	0.21 (43.1)
6	1.13 (92.4)	3.08 (53.2)	3.22 (39.5)	3.14 (25.1)	2.64 (19.5)	1.79 (21.1)	1.20 (35.0)	0.45 (43.7)	0.20 (48.1)

[a] See Table I for product information. [b] Values in parentheses represent the coefficient of variation, *i.e.*, *SD* × 100/mean.

Blood samples (7 ml) were collected in heparinized containers prior to ingestion of the dose and at 0.33, 0.66, 1, 1.5, 2, 3, 4, 6, and 8 hr post-administration. The blood samples were immediately centrifuged, and the plasma fractions were removed and frozen until assayed. All analyses were completed within 4 days from the time of sampling.

Assay of Plasma Samples—The determination of propylthiouracil concentrations was performed using a high-performance liquid chromatographic (HPLC) method developed by Ringhand and Ritschel (6). A 3.0-ml plasma sample was added to 0.5 g of ammonium sulfate and mixed vigorously for 1 min. The mixture was extracted for 10 min with 15.0 ml of chloroform. After centrifugation, a 10.0-ml aliquot of the chloroform layer was removed and mixed with 1.0 ml of a 1.75-μg/ml methylthiouracil internal standard solution and evaporated to dryness.

The residue was dissolved in 250 ml of mobile solvent, acetic acid–methanol–water (10:75:915), and 25 μl was injected into the chromatograph[5]. The chromatograph was equipped with a fixed-wavelength 280-nm detector and a stainless steel column, 25 cm × 3.1-mm i.d., packed with an octadecylsilane reverse-phase support[6]. A flow rate of 2.3 ml/min was used. Plasma propylthiouracil concentrations were determined from standard curves of propylthiouracil/methylthiouracil peak height ratio *versus* propylthiouracil concentration, prepared over a range of 0.1–5.0 μg/ml using pooled human plasma.

***In Vitro* Tests**—The USP XIX product assay, content uniformity, and tablet disintegration were performed on each product (7). Dissolution profiles were determined for each product on six individual tablets in two different media: water and 0.1 *N* HCl. Tests were performed using the USP Dissolution Apparatus 2 (8) maintained at 50 rpm and a temperature of 37 ± 0.5°[7]. Samples (10 ml) were taken at 5, 20, and 60 min. The liquid level was maintained by adding 10-ml aliquots of dissolution medium to replace the sample aliquots as they were taken.

Statistical Analysis—The relative bioavailability of the five propylthiouracil products was determined using the following parameters:

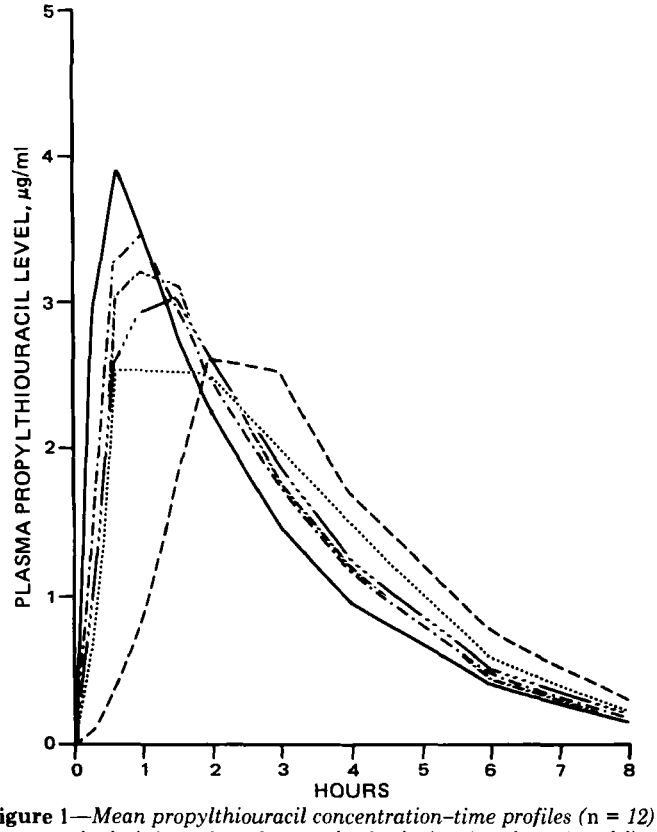

Figure 1—*Mean propylthiouracil concentration–time profiles (n = 12) on peroral administration of a standard solution (product 1) and five different commercially available propylthiouracil tablet preparations (products 2–6). Key: (————) product 1; (— — — — — —) product 2; (·····) product 3; (— · — · — · —) product 4; (▬ ▬ ▬ ▬) product 5; (▬ ▬ ▬ ▬) product 6.*

[5] Model 202/401; Waters Associates, Milford, Mass.
[6] Spherisorb 10 μm; Spectra-Physics, Santa Clara, Calif.
[7] 33710-S1 Body for Reaction Kettle—1000 ml, Kimble Glass Co., Vineland, N.J., was substituted for the dissolution vessel described.

Table III—Significance Levels for Differences Between Subjects, Weeks, and Drugs

Parameter	F Ratio Test (p Value) Subject Groups	Weeks	Drugs
Plasma Concentration			
20 min	0.218	0.814	<0.001
40 min	0.259	0.806	<0.001
1.0 hr	0.238	0.622	<0.001
1.5 hr	0.014	0.676	<0.001
2.0 hr	0.019	0.221	0.304
3.0 hr	0.076	0.009	<0.001
4.0 hr	0.053	0.362	0.001
6.0 hr	0.293	0.672	0.004
8.0 hr	0.272	0.218	0.002
Peak plasma concentration	0.038	0.787	<0.001
Time to peak plasma concentration	0.120	0.724	<0.001
AUC			
0–8 hr	0.072	0.046	0.803
$0 \rightarrow \infty$	0.110	0.031	0.766

Table IV—Newman-Keuls *A Posteriori* Test for Significant Product Differences in Parameters Studied

Parameter	Product Ranking (Lowest to Highest)[a]					
Peak concentration	2	5	3	4	6	1
Time to peak concentration	1	6	4	5	3	2
AUC						
0–8 hr	2	1	6	5	3	4
$0 \rightarrow \infty$	2	1	6	5	4	3
Plasma concentration						
20 min	2	3	6	5	4	1
40 min	2	3	5	6	4	1
1.0 hr	2	3	5	6	4	1
1.5 hr	2	3	1	5	4	6
2.0 hr	1	4	3	2	6	5
3.0 hr	1	4	6	5	3	2
4.0 hr	1	4	6	5	3	2
6.0 hr	1	6	4	5	3	2
8.0 hr	1	4	6	5	3	2

[a] Products underlined by a common line not found to differ significantly ($p > 0.05$). See Table I for product information.

plasma concentrations at each sampling time, time of peak plasma concentration, peak plasma concentration, and area under the plasma concentration–time curve (AUC). A three-way analysis of variance (9) and the Newman-Keuls *a posteriori* test (10) were used to analyze for differences among products, subjects, and weeks.

RESULTS AND DISCUSSION

Table I summarizes the results of the *in vitro* tests. Each of the five products met the USP XIX requirements for drug content, disintegration, and content uniformity. However, major differences were observed for the rate and extent of dissolution of the different drug products[8].

The average plasma concentrations for each product at each sampling time are summarized in Table II and illustrated graphically in Fig. 1. The statistical analyses of differences among subject groups, weeks, and test products at each sampling time are given in Tables III and IV. Significant differences ($p < 0.05$) in plasma levels were observed among the products at all sampling times except at 2 hr. The Newman-Keuls analysis found

[8] USP XIX does not include a dissolution requirement for propylthiouracil tablets.

Table V—Propylthiouracil Bioavailability Parameters[a]

Product[b]	Peak Plasma Concentration, μg/ml	Time to Peak Plasma Concentration, hr	AUC (0–8 hr), μg·hr/ml	AUC ($0 \rightarrow \infty$), μg·hr/ml
1	4.32	0.61	10.84	11.29
	(18.7)	(46.4)	(24.6)	(27.9)
2	2.77	2.50	10.39	11.09
	(18.6)	(20.7)	(17.9)	(18.6)
3	3.83	1.61	11.07	11.71
	(22.6)	(72.5)	(21.5)	(21.8)
4	3.98	1.10	11.16	11.61
	(20.5)	(65.0)	(19.2)	(19.8)
5	3.38	1.15	11.04	11.57
	(15.9)	(43.2)	(17.7)	(18.6)
6	3.98	1.06	11.00	11.38
	(21.9)	(51.2)	(15.0)	(15.7)

[a] Each value represents the mean of 12 subjects. *RSD* (*SD* × 100/mean) is given in parentheses. [b] See Table I for product information.

no significant differences among products 3–6 at any of the sampling times. All observed differences were due to products 1 and 2 being different from one or more of the other dosage forms.

The mean values of peak concentration, time to peak concentration, $AUC_{0-8\ hr}$ and $AUC_{0\rightarrow\infty}$ are summarized in Table V; the statistical analyses of differences among these parameters are given in Tables III and IV. There were no significant differences ($p < 0.05$) among products for either $AUC_{0-8\ hr}$ or $AUC_{0\rightarrow\infty}$. The ranges for both AUC values represented a difference of <7%.

The mean time (0.6 hr) for product 1, the reference solution, to reach peak concentration was significantly different from the 2.5 and 1.6 hr required to reach peak concentration for products 2 and 3, respectively. The mean time to reach peak concentration was significantly longer for product 2 than for all other products.

Since the products exhibited equal AUC values, products demonstrating the longest times to reach peak concentration would be expected to have lower peak concentrations. This was observed as product 1, the product exhibiting the shortest time to peak concentration had the greatest peak plasma concentration (4.23 μg/ml). In addition, product 2 (which demonstrated the longest time to peak concentration) had the lowest peak concentration (2.77 μg/ml).

It is evident that product 2 exhibited a significantly slower rate of absorption than the other four tablet products (products 3–6). As a result product 2 cannot be considered to be bioequivalent to those dosage forms. The clinical significance of this apparent slower absorption of product 2, or conversely the more rapid absorption of products 3–6, is not known.

To substantiate the ability of the study to detect significant differences among the parameters, a power analysis was applied to the data (Table VI). Because of the large variability obtained for the plasma levels of propylthiouracil at each sampling time, a subject population in excess of 30 would have been required for a 20% difference to be significant (p

Table VI—Power Analysis[a]

Parameter	Minimum Number of Subjects for 20% Differences	Minimum Detectable Difference, %
Plasma concentration		
20 min	>30	55.5
40 min	>30	41.8
1.0 hr	>30	41.1
1.5 hr	>30	34.4
2.0 hr	16–19	25.9
3.0 hr	10–11	18.6
4.0 hr	>30	35.6
6.0 hr	>30	41.2
8.0 hr	>30	39.1
Peak plasma concentration	16–19	23.7
Time to peak plasma concentration	>30	40.8
AUC		
0–8 hr	6–7	14.0
$0 \rightarrow \infty$	6–7	14.5

[a] $\alpha = 0.05$, $\beta = 0.2$.

< 0.05) at all but two of the sampling times. Nevertheless, significant differences were observed since actual differences exceeded 20%.

The relative standard deviation for the mean peak plasma concentration was <25%, and the number of subjects necessary to detect a 20% difference was 16–17. Statistically significant differences were observed for this parameter, since actual differences were >50%. Similarly, it would have taken >30 subjects to detect a 20% difference in time to reach peak plasma concentration. However, significant differences were observed because actual differences exceeded 200%. No significant differences were seen among the products for $AUC_{0-8\ hr}$ or $AUC_{0\to\infty}$, although the power of the study was adequate to detect differences of 14.5%.

There was a perfect rank-order correlation of the mean percent of drug dissolved at 5 min in both acid and water for products 2–6 and the propylthiouracil plasma concentration observed at 20 min. The best correlations were found between the mean percent dissolved in water at 5, 20, and 60 min and the plasma propylthiouracil concentration at 20 min, with correlation coefficients of 0.81, 0.86, and 0.89, respectively. Corresponding correlation coefficients of 0.82, 0.80, and 0.85 were found for dissolution data obtained in acid. Attempts to relate either peak plasma propylthiouracil concentration or time to peak concentration were less successful. Correlation coefficients describing peak concentration and any of the dissolution values were all <0.42. The best correlation with time to peak concentration was with the percent dissolved at 60 min in either water or acid ($r = 0.75$). It is apparent the results of the dissolution studies were not useful in providing generally applicable correlations with *in vivo* data. However product 2, which exhibited the longest time to achieve peak concentration, was somewhat more slowly dissolved in acid at each sampling time compared with the other more rapidly absorbed dosage forms.

REFERENCES

(1) A. Melander, E. Wahlin, K. Danielson, and A. Hanson, *Acta Med. Scand.*, **201**, 41 (1979).

(2) "Public Health Service, Approved Drug Products with Proposed Therapeutic Equivalence Evaluations," Food and Drug Administration, Rockville, Md., January 1979, p. 114.

(3) *Fed. Regist.*, **42**, January 7, 1977, p. 1649.

(4) *Anonymous*, *Statist. Bull. Metrop. Life Insur. Co.*, **58**, 1 (1977).

(5) E. G. Williams, *Aust. J. Sci. Res. A.*, **2**, 149 (1949).

(6) H. P. Ringhand and W. A. Ritschel, *J. Pharm. Sci.*, **68**, 1461 (1979).

(7) "The United States Pharmacopeia," 19th Rev., U.S. Pharmacopeial Convention, Rockville, Md., 1975, p. 423.

(8) Fourth Supplement to USP XIX and NF XIV. U.S. Pharmacopeial Convention, Inc., Rockville, Md., 1978, pp. 194–195.

(9) B. J. Winer, "Statistical Principles in Experimental Design," 2nd ed., McGraw-Hill, New York, N.Y., 1962, p. 452.

(10) B. J. Winer, "Statistical Principles in Experimental Design," 2nd ed., McGraw-Hill, New York, N.Y., 1962, p. 191.

Pharmacokinetic Profile of Intravenous Liposomal Triamcinolone Acetonide in the Rabbit

ISAAC ABRAHAM ˣ, JANE C. HILCHIE, and MICHAEL MEZEI

Received June 15, 1981, from the *College of Pharmacy, Dalhousie University, Halifax, Nova Scotia, Canada.* Accepted for publication October 8, 1982.

Abstract □ The pharmacokinetics of triamcinolone[2-^{14}C]acetonide, encapsulated in neutral multilamellar liposomes, and a control preparation of the steroid in a 3:1 solution of polyethylene glycol–water was investigated in the rabbit after single intravenous bolus injections. Blood samples were obtained at various times up to 7 hr postinjection and assayed for the drug by liquid scintillation counting. Blood drug concentration–time data showed biexponential decay and were analyzed by nonlinear, least-squares regression analysis to obtain the initial (time zero) drug concentration $[(C_b)_0]$ and the initial (fast, α) and terminal (slow, β) disposition rate constants. From these estimates the central compartment volume (V_c) and the respective half-lives $[(t_{1/2})_\alpha, (t_{1/2})_\beta]$ of the fast and slow disposition phases were calculated. The total body clearance (CL_T) and the apparent distribution volume (Vd) were obtained by nonparametric analysis. Significant differences were observed between the liposome-encapsulated dosage form and the solution of the steroid in β and Vd_β. While β for the liposomal form was smaller than that for the solution, the apparent Vd was larger with the liposome-encapsulated drug. There was no difference in the total body clearance of the drug in the two dosage forms. Results of the study suggest that when administered by the intravenous route, liposome-encapsulated drug may exhibit extensive tissue distribution and a prolonged half-life.

Keyphrases □ Triamcinolone acetonide—liposomal encapsulation, pharmacokinetics, rabbits □ Dosage forms—liposomal encapsulation, triamcinolone acetonide, pharmacokinetics, rabbits □ Pharmacokinetics—liposome-encapsulated triamcinolone acetonide, rabbits

In recent years liposomes—artificial phospholipid vesicles—have gained increasing attention as a potential drug delivery system (1). A common objective for the choice of liposomes as drug carriers is the desire to ensure selective distribution or localization of therapeutic agents in specific organ tissues (2–4). By this means, high concentrations of an agent in an organ of interest can be attained while reducing potential toxicity to other organs, which can result from indiscriminate dispersion of the agent in the body. Notable successes have been reported with liposomal preparations in the treatment of arthritic joints (3, 5) and experimental leishmaniasis (6) and in the alleviation of respiratory distress syndrome in infants (7). However, reports on the formal pharmacokinetic analyses of liposome-encapsulated drugs are rather scanty.

Unlike many drug delivery systems that are designed to release the active component (drug) instantly *in vivo*, the liposome-encapsulated dosage form in circulation may remain as a single phospholipid vesicle for relatively long periods. In this instance the pharmacokinetic behavior of the encapsulated drug will largely be determined by the disposition characteristics of the liposomal entity. Several physical and chemical factors of the liposome can, therefore, potentially influence the disposition of liposome-entrapped drug. Such factors include vesicle size, surface charge, and lipid composition.

As interest in the clinical application of liposomes as drug carriers grows, there is need to gain more information about the pharmacokinetics of drugs and, hence, their

0022-3549/83/1200-1412$01.00/0

< 0.05) at all but two of the sampling times. Nevertheless, significant differences were observed since actual differences exceeded 20%.

The relative standard deviation for the mean peak plasma concentration was <25%, and the number of subjects necessary to detect a 20% difference was 16–17. Statistically significant differences were observed for this parameter, since actual differences were >50%. Similarly, it would have taken >30 subjects to detect a 20% difference in time to reach peak plasma concentration. However, significant differences were observed because actual differences exceeded 200%. No significant differences were seen among the products for $AUC_{0-8\ hr}$ or $AUC_{0\to\infty}$, although the power of the study was adequate to detect differences of 14.5%.

There was a perfect rank-order correlation of the mean percent of drug dissolved at 5 min in both acid and water for products 2–6 and the propylthiouracil plasma concentration observed at 20 min. The best correlations were found between the mean percent dissolved in water at 5, 20, and 60 min and the plasma propylthiouracil concentration at 20 min, with correlation coefficients of 0.81, 0.86, and 0.89, respectively. Corresponding correlation coefficients of 0.82, 0.80, and 0.85 were found for dissolution data obtained in acid. Attempts to relate either peak plasma propylthiouracil concentration or time to peak concentration were less successful. Correlation coefficients describing peak concentration and any of the dissolution values were all <0.42. The best correlation with time to peak concentration was with the percent dissolved at 60 min in either water or acid ($r = 0.75$). It is apparent the results of the dissolution studies were not useful in providing generally applicable correlations with *in vivo* data. However product 2, which exhibited the longest time to achieve peak concentration, was somewhat more slowly dissolved in acid at each sampling time compared with the other more rapidly absorbed dosage forms.

REFERENCES

(1) A. Melander, E. Wahlin, K. Danielson, and A. Hanson, *Acta Med. Scand.*, **201**, 41 (1979).

(2) "Public Health Service, Approved Drug Products with Proposed Therapeutic Equivalence Evaluations," Food and Drug Administration, Rockville, Md., January 1979, p. 114.

(3) *Fed. Regist.*, **42**, January 7, 1977, p. 1649.

(4) *Anonymous*, *Statist. Bull. Metrop. Life Insur. Co.*, **58**, 1 (1977).

(5) E. G. Williams, *Aust. J. Sci. Res. A.*, **2**, 149 (1949).

(6) H. P. Ringhand and W. A. Ritschel, *J. Pharm. Sci.*, **68**, 1461 (1979).

(7) "The United States Pharmacopeia," 19th Rev., U.S. Pharmacopeial Convention, Rockville, Md., 1975, p. 423.

(8) Fourth Supplement to USP XIX and NF XIV. U.S. Pharmacopeial Convention, Inc., Rockville, Md., 1978, pp. 194–195.

(9) B. J. Winer, "Statistical Principles in Experimental Design," 2nd ed., McGraw-Hill, New York, N.Y., 1962, p. 452.

(10) B. J. Winer, "Statistical Principles in Experimental Design," 2nd ed., McGraw-Hill, New York, N.Y., 1962, p. 191.

Pharmacokinetic Profile of Intravenous Liposomal Triamcinolone Acetonide in the Rabbit

ISAAC ABRAHAM ˣ, JANE C. HILCHIE, and MICHAEL MEZEI

Received June 15, 1981, from the *College of Pharmacy, Dalhousie University, Halifax, Nova Scotia, Canada.* Accepted for publication October 8, 1982.

Abstract □ The pharmacokinetics of triamcinolone[2-^{14}C]acetonide, encapsulated in neutral multilamellar liposomes, and a control preparation of the steroid in a 3:1 solution of polyethylene glycol–water was investigated in the rabbit after single intravenous bolus injections. Blood samples were obtained at various times up to 7 hr postinjection and assayed for the drug by liquid scintillation counting. Blood drug concentration–time data showed biexponential decay and were analyzed by nonlinear, least-squares regression analysis to obtain the initial (time zero) drug concentration $[(C_b)_0]$ and the initial (fast, α) and terminal (slow, β) disposition rate constants. From these estimates the central compartment volume (V_c) and the respective half-lives $[(t_{1/2})_\alpha, (t_{1/2})_\beta]$ of the fast and slow disposition phases were calculated. The total body clearance (CL_T) and the apparent distribution volume (Vd) were obtained by nonparametric analysis. Significant differences were observed between the liposome-encapsulated dosage form and the solution of the steroid in β and Vd_β. While β for the liposomal form was smaller than that for the solution, the apparent Vd was larger with the liposome-encapsulated drug. There was no difference in the total body clearance of the drug in the two dosage forms. Results of the study suggest that when administered by the intravenous route, liposome-encapsulated drug may exhibit extensive tissue distribution and a prolonged half-life.

Keyphrases □ Triamcinolone acetonide—liposomal encapsulation, pharmacokinetics, rabbits □ Dosage forms—liposomal encapsulation, triamcinolone acetonide, pharmacokinetics, rabbits □ Pharmacokinetics—liposome-encapsulated triamcinolone acetonide, rabbits

In recent years liposomes—artificial phospholipid vesicles—have gained increasing attention as a potential drug delivery system (1). A common objective for the choice of liposomes as drug carriers is the desire to ensure selective distribution or localization of therapeutic agents in specific organ tissues (2–4). By this means, high concentrations of an agent in an organ of interest can be attained while reducing potential toxicity to other organs, which can result from indiscriminate dispersion of the agent in the body. Notable successes have been reported with liposomal preparations in the treatment of arthritic joints (3, 5) and experimental leishmaniasis (6) and in the alleviation of respiratory distress syndrome in infants (7). However, reports on the formal pharmacokinetic analyses of liposome-encapsulated drugs are rather scanty.

Unlike many drug delivery systems that are designed to release the active component (drug) instantly *in vivo*, the liposome-encapsulated dosage form in circulation may remain as a single phospholipid vesicle for relatively long periods. In this instance the pharmacokinetic behavior of the encapsulated drug will largely be determined by the disposition characteristics of the liposomal entity. Several physical and chemical factors of the liposome can, therefore, potentially influence the disposition of liposome-entrapped drug. Such factors include vesicle size, surface charge, and lipid composition.

As interest in the clinical application of liposomes as drug carriers grows, there is need to gain more information about the pharmacokinetics of drugs and, hence, their

0022-3549/83/1200-1412$01.00/0

therapeutic fate when entrapped in such phospholipid vesicles. The objective of the present study was to characterize the pharmacokinetics of a model compound, triamcinolone [2-^{14}C]acetonide, entrapped in neutral multilamellar liposomes after rapid intravenous injection in the rabbit.

EXPERIMENTAL

Liposomal Triamcinolone—Neutral, multilamellar liposomes containing triamcinolone[1], dipalmitoyl DL-α-phosphatidylcholine[2], and cholesterol[2] in the respective mole ratio of 0.5:1.1:0.5 were prepared as previously described (4). The volume of the final liposomal suspension was adjusted with the dispersion medium (8 m*M* $CaCl_2$) so that a 0.3-ml dose contained the desired radioactivity (12 μCi). Over 80% of the liposomes obtained by the procedure were shown by microscopic size distribution to have a mean diameter of 9 μm (range 7–11 μm) (8). Each batch of liposomes was used within 3 days of preparation, and daily microscopic examination of the liposomes showed no apparent lysis of the vesicles.

A control preparation of unencapsulated triamcinolone was prepared as a solution in polyethylene glycol 400–water (3:1) so that a 0.3-ml dose contained the desired radioactivity (12 μCi). The clear control solution of triamcinolone had approximately the same viscosity as the liposomal suspension as determined, visually, by their flow pattern.

Intravenous Administration of Liposomal and Control Triamcinolone Preparations—The hair on the ear lobes of male New Zealand White rabbits (3–4 kg) was removed with an animal hair clipper[3]. An infusion set[4] equipped with a 21-gauge (0.8-mm) hypodermic needle and a winged adapter was inserted into the central artery of one ear lobe to facilitate sampling of blood for drug analysis. The patency of the set was maintained by intermittent flushing with heparinized sodium chloride injection (100 IU/ml).

After removing 0.5 ml of arterial blood as a control sample, a single 0.3-ml dose of the triamcinolone preparation in a 1-ml tuberculin syringe[5] was administered by rapid intravenous injection *via* the marginal vein of the opposite ear lobe. Following administration of the dose, serial 0.5-ml blood samples were obtained over a 7-hr period *via* the catheterized ear artery. The blood samples were placed in glass tubes[6] containing 0.5 ml of citrated buffer solution as anticoagulant. The samples were frozen (−10°) until analyzed.

Quantitation of Triamcinolone in Whole Blood—Five milliliters of ethanol (95%) was added to the citrated blood (0.5 ml) in the stoppered collection tube. The mixture was vortexed at high speed for 2 min and centrifuged at 1000×*g* for 5 min at room temperature. The supernatant was decanted into a 50-ml Erlenmeyer flask, and the pellet was resuspended in another 5-ml aliquot of ethanol; the process was repeated four more times. The combined ethanolic extracts were evaporated to dryness over a boiling water bath. The residue was redissolved in 15 ml of methylene chloride and transferred to a 20-ml glass counting vial. The methylene chloride was allowed to evaporate to dryness overnight at room temperature. The residue was redissolved in 10 ml of Bray's solution[7], 0.5 ml of glacial acetic acid was added, and then the radioactivity was determined by liquid scintillation counting[8].

The blood triamcinolone concentration of each sample was calculated from the radioactivity and the specific activity of the administered preparation after correction for background values (determined using a blank). Over the triamcinolone concentration range of ~15–960 ng/ml, this extraction procedure resulted in ~80% recovery of equivalent radioactivity from whole blood spiked with the drug.

Data Analysis—Blood triamcinolone concentration (C_b) *versus* time (t) data after a single intravenous bolus injection were fitted to the following with the aid of the least-squares regression analysis program, NONLIN (9):

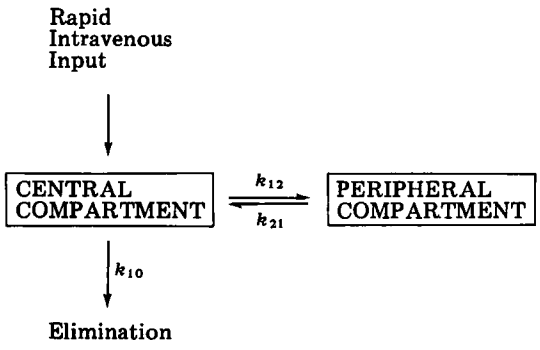

Figure 1—*A representation of the two-compartment open model system.*

$$C_b = Ae^{-\alpha t} + Be^{-\beta t} \quad \text{(Eq. 1)}$$

Initial estimates of A, B, α, and β were obtained with the CSTRIP program (10). In Eq. 1, α and β are first-order disposition rate constants, while A and B represent appropriate concentration constants. The two-compartment open model system with elimination from the central compartment (Fig. 1) was assumed.

The central compartment volume (V_c) was estimated by:

$$V_c = \text{Dose}/(C_b)_0 \quad \text{(Eq. 2)}$$

where $(C_b)_0 = (A + B)$. The intercompartmental transfer rate constants, k_{21} and k_{12}, and the elimination rate constant, k_{10}, were calculated from:

$$k_{21} = (A\beta + B\alpha)/(C_b)_0 \quad \text{(Eq. 3)}$$

$$k_{10} = \alpha\beta/k_{21} \quad \text{(Eq. 4)}$$

$$k_{12} = (\alpha + \beta) - (k_{21} + k_{10}) \quad \text{(Eq. 5)}$$

The total body clearance (CL_T) was calculated using:

$$CL_T = \frac{\text{Dose}}{\int_0^\infty C_b \cdot dt} \quad \text{(Eq. 6)}$$

where $\int_0^\infty C_b \cdot dt$ is the total area under the blood drug concentration–time curve and was estimated by the trapezoidal rule to obtain the area up to the last measured blood triamcinolone concentration (C_b^*). The area beyond C_b^* was computed by dividing C_b^* by β. The apparent volume of distribution (Vd_β) was determined by the relationship:

$$Vd_\beta = CL_T/\beta \quad \text{(Eq. 7)}$$

Half-life values for the fast disposition phase $(t_{1/2})_\alpha$ and terminal phase $(t_{1/2})_\beta$ were calculated using:

$$(t_{1/2})_\alpha = 0.693/\alpha \quad \text{(Eq. 8)}$$

$$(t_{1/2})_\beta = 0.693/\beta \quad \text{(Eq. 9)}$$

The unpaired, two-tailed Student's t test was used to assess the significance of the observed differences in the pharmacokinetic parameters between the control and liposomal triamcinolone preparations. A $p_{0.05}$ significance level was used.

RESULTS AND DISCUSSION

Figure 2 illustrates characteristic dose-normalized blood concentration–time curves for the control and liposomal triamcinolone dosage forms in two separate rabbits after single intravenous bolus injections. Relative to the control preparation, a characteristic feature of all liposomal curves was a more rapid initial disposition phase followed by a slower, more sustained terminal phase. A comparison of the mean pharmacokinetic constants (±*SEM*) for the control and liposomes is presented in Table I.

It has been reported (11) that triamcinolone hexacetonide administered orally to cats and dogs did not undergo significant deacetonization or de-esterification. Earlier in this laboratory it was determined that 90% of the intravenous dose of triamcinolone acetonide was excreted unchanged in the urine by rabbits (8). Recently we found that the total radioactivity of the ethanolic solution from whole blood obtained from

[1] New England Nuclear, Boston, Mass.
[2] Sigma Chemical Co., St. Louis, Mo.
[3] Oster, Milwaukee, Wis.
[4] Butterfly, Abbott Ireland Ltd., Sligo, Ireland.
[5] Plastipak, Becton, Dickinson & Co. Canada Ltd., Mississauga, Ont.
[6] Venoject, Kimble-Terumo, Elkton, Md.
[7] Bray's scintillation counting solution: Omnifluor (New England Nuclear, Boston, Mass.), 0.8 g; naphthalene, 6 g; ethylene glycol, 2 ml; methanol, 10 ml; and 1,4-dioxane to 100 ml.
[8] Beckman Spectrometer Model LS 3133T.

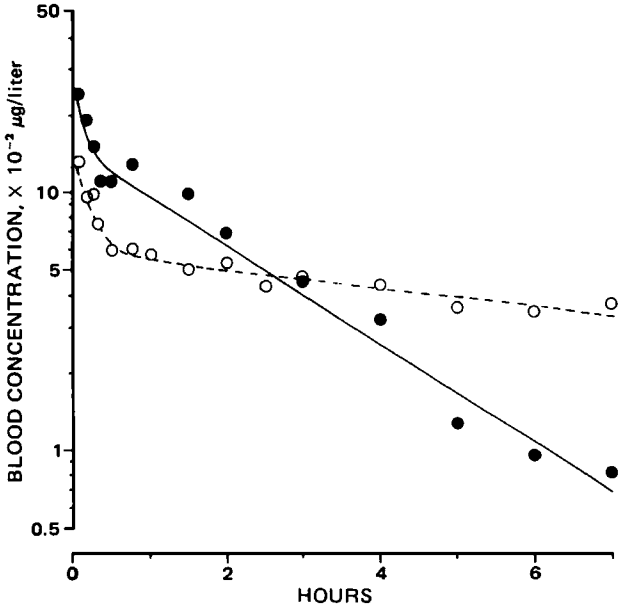

Figure 2—*Dose-normalized blood levels of triamcinolone following single intravenous bolus injections of control (●) and liposomal (○) preparations in two separate rabbits.*

rabbits receiving intravenous triamcinolone was comparable with the radioactivity determined after the ethanolic solution was subjected to ethyl acetate extraction of the intact drug. These findings indicate that the ^{14}C-label on the ketal ring of triamcinolone acetonide is a stable tracer for disposition studies. They also suggest that the total radioactivity of the ethanolic solution from whole blood represented, essentially, the unchanged drug.

Compared with the control, the overall apparent distribution of triamcinolone in the liposomal form was more extensive. On the average, V_c increased by (1.8 − 0.7) liter/kg = 1.1 liter/kg (Table I), while Vd_β changed by (7.09 − 1.41) liter/kg = 5.68 liter/kg when the liposomal form of the drug was used. These volume increases suggest that, within both the central and peripheral compartments, liposome-entrapped drug reached organ tissues that were not normally accessible to the unencapsulated triamcinolone. It has been observed (12) that in plasma and other calcium-containing media, negatively charged liposomes aggregate to form larger particles; these particles are then rapidly removed from the circulatory system by the reticuloendothelial system (RES), of which the liver and spleen are major components. It has also been reported that subfractionation of livers of animals receiving liposomes showed that liposome-entrapped enzymes were localized chiefly in the lysosomal fraction (13). It is thus apparent that cells of the RES, particularly the Kupffer cells in the liver, play a major role in the removal of liposomes from the circulatory system, although electron microscopic evidence also indicates that hepatic parenchymal cells may be involved in liposomal clearance (14). A two-stage mechanism for liposomal removal from circulatory system has been proposed (15, 16) in which the Kupffer cells are thought to be responsible for the rapid phase of liposomal removal from the blood while the slower disappearance phase is attributable to the liver parenchymal cells. Therefore, it may be deduced that the liver and spleen could be regarded as part of the central compartment because of their high vascularity, ease of blood perfusion, and relatively high content of Kupffer cells. In addition, the liver parenchyma could be considered as part of the peripheral compartment.

The increase in the apparent volume of distribution with the liposomes and the concomitant increase in α and k_{12} relative to the control dosage form (Table I) suggest that liposomes potentially increase the rate and extent of entrapped drug distribution relative to the unencapsulated form of the drug. The relative constancy of the liposomal curve terminal slope (Fig. 2) suggests that any rapid initial accumulation of liposomes in the liver and other organs of the RES does not result in significant lysis of the vesicles. Since the liver does not metabolize triamcinolone as such (8, 11), any significant lysis of liposomes in the liver and subsequent release of drug would have resulted in a change in the slope of the terminal portion of the liposomal curve, which would then have declined in a fashion somewhat parallel to the terminal portion of the control curve. It is possible that the majority of liposomes (particularly the smaller vesicles) accumulating in the liver were held in the relatively open and fenestrated endothelium of the liver capillaries (1). It is not unlikely for small intact liposomes held in this type of hepatic vasculature architecture to reenter the circulatory system and sustain triamcinolone levels. Assuming that they do accumulate rapidly in the liver and are able to reenter the circulatory system liposomes could prove beneficial not only as drug carriers for targeting the liver and other organ tissues of the RES with therapeutic agents, but also as a potential intravascular depot system.

There was no significant difference in the mean clearances (0.73 ± 0.17 and 0.57 ± 0.06 liter/hr/kg, respectively) of triamcinolone from the liposomal and solution dosage forms. From the relationship between CL_T, Vd_β and β (Eq. 7), it is seen that an increase in Vd_β and a concurrent decrease in β tend to offset each other and thereby minimize potential changes in CL_T. However the apparent similarity of CL_T values observed in this study underlie the fact that there may not be a fundamental change in the clearance mechanisms of triamcinolone in the rabbit whether the steroid is administered in the liposomal or solution form. Similarities in the k_{10} (Table I) tend to support this view.

Due to technical difficulties it was not possible to administer equal amounts of triamcinolone in the two dosage forms. In the control studies, two of the doses employed were 263 and 803 µg. At these dose levels the respective areas under the blood drug concentration–time curves were 200 and 579 µg/hr/liter; CL_T values were 0.44 and 0.42 liter/hr/kg; and β values were 0.34 and 0.42 hr^{-1}, respectively. These etimates do not indicate that triamcinolone *per se* exhibits dose-dependent pharmacokinetics in the rabbit over the dose range employed in this study. It is, therefore, doubtful that the observed differences in the pharmacokinetics were due to differences in the dose administered in the two dosage forms.

Probably an ideal control dosage form in this study would have been a physical admixture of all the components in the liposomal dosage form, *i.e.* triamcinolone, phospholipids, cholesterol, and the dispersing liquid (8 m*M* aqueous calcium chloride). However, triamcinolone is insoluble in aqueous media; a control preparation which might contain triamcinolone crystals would be unsuitable for intravenous administration. Moreover, the presence of drug crystals in the control raises another

Table I—Mean Pharmacokinetic Parameters for Control and Liposomal Triamcinolone after Single Intravenous Injections in the Rabbit

Parameter	Mean (± *SEM*) Control[a]	Mean (± *SEM*) Liposomal[b]	*t* Test[c]	Significance Level
Dose, µg	769 (128.80)	314 (26.12)	—	—
$(C_b)_0$, µg/liter	326.83 (55.8)	365 (13.76)	—	—
α, hr^{-1}	9.22 (4.36)	17.57 (5.01)	1.575	NS[d]
β, hr^{-1}	0.41 (0.04)	0.13 (0.03)	5.754	$p < 0.001$
$(t_{1/2})_\alpha$, hr	0.23 (0.09)	0.07 (0.02)	1.879	NS
$(t_{1/2})_\beta$, hr	1.72 (0.14)	9.03 (3.35)	1.964	NS
V_c, liter/kg	0.70 (0.06)	1.80 (0.57)	1.722	NS
Vd_β, liter·kg	1.41 (0.16)	7.09 (1.88)	2.715	$p < 0.005$
k_{21}, hr^{-1}	3.48 (1.19)	3.14 (0.39)	0.292	NS
k_{12}, hr^{-1}	5.30 (3.20)	13.76 (4.52)	1.487	NS
k_{10}, hr^{-1}	0.86 (0.14)	0.78 (0.27)	0.249	NS
CL_T, liter/hr/kg	0.57 (0.06)	0.73 (0.17)	0.822	NS

[a] $n = 5$; [b] $n = 6$. [c] Critical $t_{0.05} = 2.262$. [d] NS—not significant at $p_{0.05}$.

objection in that the drug may not be presented in the same physical state, since in the liposomal triamcinolone is present as a molecular dispersion in lipid micelles (17). Under these circumstances the possibility of a dissolution-dependent disposition of triamcinolone in the control preparation would seriously affect the pharmacokinetic comparison of the two dosage forms. Finally, a physical admixture of drug, lipids, and calcium chloride solution could, potentially, promote the spontaneous formation of an undetermined number of liposomes when agitated. If this happened, the control would not be totally free of drug-containing liposomes. Thus, while the triamcinolone solution in polyethylene glycol–water used in this study may not be qualitatively similar to the liposomal dosage form, it was designed to present the model compound in an intravenous dosage form that was miscible with plasma water. The comparison of the pharmacokinetics of triamcinolone in liposomal and solution dosage forms is, thus, analogous to other comparative studies (*e.g.*, bioavailability) of a therapeutic agent in different formulations which may not (and often do not) contain the same excipients. If it is assumed that the presence in blood of exogenous lipids (used in the preparation of the liposomes) and polyethylene glycol in the concentrations used did not influence blood flow rate significantly, then the differences in β and Vd_β observed in this study are due probably to the favorable physicochemical properties (especially lipid solubility) of the liposomal entity.

Results of the present study indicate that liposome-encapsulated triamcinolone enhances tissue distribution of the drug in the rabbit. The results also suggest that, given by the intravenous route, neutral multilamellar liposomes could serve as carriers for chemotherapeutic agents whose efficacy depends on sustained blood levels and deep tissue distribution.

REFERENCES

(1) R. L. Juliano and D. Layton, in "Drug Delivery Systems," R. L. Juliano, Ed., Oxford University Press, New York, N.Y., 1980, chap. 6.

(2) Y. E. Rahman, E. A. Cerny, S. L. Tollakson, B. J. Wright, S. L. Nance, and J. F. Thompson, *Proc. Soc. Exp. Biol. Med.*, **146**, 1173 (1974).

(3) M. M. Jonah, E. A. Cerny, and Y. E. Rahman, *Biochim. Biophys. Acta*, **541**, 321 (1978).

(4) M. Mezei and V. Gulasekharam, *Life Sci.*, **26**, 1473 (1980).

(5) N. C. Phillips, D. P. Page Thomas, C. G. Knight, and J. T. Dingle, *Ann. Rheum. Dis.*, **38**, 535 (1979).

(6) C. A. Alving, E. A. Steck, W. L. Hanson, P. S. Loizeaux, W. L. Chapman, Jr., and V. B. Waits, *Life Sci.*, **22**, 1021 (1978).

(7) H. Ivey, S. Roth, and J. Kattwinkel, *Pediatr. Res.*, **11**, 573 (1977).

(8) V. Gulaskharam, "Liposomes for Selective Delivery of Drugs in Topical Routes of Administration." Master of Science thesis, Dalhousie University, Halifax, Nova Scotia, 1980.

(9) C. M. Metzler, G. L. Elfring, and A. J. McEwen, *Biometrics*, **30**, 562 (1974).

(10) A. J. Sedman and J. G. Wagner, *J. Pharm. Sci.*, **65**, 1006 (1976).

(11) V. Zbinovsky and P. Chrekian, in "Analytical Drug Profiles," Vol. 6, K. Florey, Ed., Academic, New York, N.Y., 1977, pp. 579–598.

(12) R. L. Juliano and D. Stamp, *Biochem. Biophys. Res. Commun.*, **63**, 651 (1975).

(13) G. Gregoriadis and B. E. Ryman, *Biochem. J.*, **129**, 123 (1972).

(14) Y. E. Rahman and B. J. Wright, *J. Cell Biol.*, **65**, 112 (1975).

(15) G. Gregoriadis and D. E. Neerunjun, *Eur. J. Biochem.*, **47**, 179 (1974).

(16) G. Sherphof, F. Roerdink, M. Waite, and J. Parks, *Biochim. Biophys. Acta*, **542**, 296 (1978).

(17) F. J. T. Fildes and J. E. Oliver, *J. Pharm. Pharmacol.*, **30**, 337 (1978).

ACKNOWLEDGMENTS

This project was supported by the Medical Research Council of Canada (Grant MA 6664).

The authors are particularly grateful to Dr. C. T. Ueda and Mrs. Jeannetta G. Nickols, University of Nebraska Medical Center, for the use of their computer facilities, Mrs. Anne Fenton of the Dalhousie University Animal Care Facility for her technical assistance, and Mrs. Annette Cook for her excellent secretarial work.

Acrylic Microspheres *In Vivo* IX: Blood Elimination Kinetics and Organ Distribution of Microparticles with Different Surface Characteristics

PER ARTURSON ‡, TIMO LAAKSO *, and PETER EDMAN *x

Received May 10, 1982, from the **Division of Pharmacy, Department of Drugs, National Board of Health and Welfare, S-751 25 Uppsala, Sweden* and ‡*Department of Pharmaceutical Biochemistry, Biomedical Center, University of Uppsala, S-751 23 Uppsala, Sweden.* Accepted for publication September 24, 1982.

Abstract □ The elimination of microparticles from blood after intravenous injection is dependent on the surface characteristics of the particles. The half-life in blood increases from 44 to 84 min after modification of surface-localized human serum albumin with polyethylene glycol. Irrespective of the surface properties, particles are localized in the reticuloendothelial system, mainly in the liver and spleen. In preimmunized mice, the distribution of particles is somewhat altered, *i.e.*, the liver and lung uptake is significantly higher in preimmunized animals than in untreated animals. The rate of phagocytosis of particles with different surface characteristics has also been studied *in vitro* with isolated mouse peritoneal macrophages. This technique gives a good correlation with the *in vivo* results; thus particles with a short half-life in mice are rapidly phagocytosed by the macrophages *in vitro*.

Keyphrases □ Microparticles—polyacrylamide, blood elimination kinetics, organ distribution, effect of surface characteristics, mice □ Elimination—polyacrylamide microparticles from blood, kinetics, organ distribution, effect of surface characteristics, mice □ Delivery systems—polyacrylamide microparticles, blood elimination, kinetics, organ distribution, mice

Immobilized systems in the form of small beads or particles have recently been introduced as carriers of enzymes *in vivo* (1). Some of these systems are characterized as biodegradable (*e.g.*, liposomes), while others are slowly metabolized (*e.g.*, acrylic particles). Irrespective of the type of particles, these systems show great promise as a tool for "active targeting" of enzymes and other macromolecules to specific cells or organs in the body. However, one of the

0022-3549/83/1200-1415$01.00/0

objection in that the drug may not be presented in the same physical state, since in the liposomal triamcinolone is present as a molecular dispersion in lipid micelles (17). Under these circumstances the possibility of a dissolution-dependent disposition of triamcinolone in the control preparation would seriously affect the pharmacokinetic comparison of the two dosage forms. Finally, a physical admixture of drug, lipids, and calcium chloride solution could, potentially, promote the spontaneous formation of an undetermined number of liposomes when agitated. If this happened, the control would not be totally free of drug-containing liposomes. Thus, while the triamcinolone solution in polyethylene glycol–water used in this study may not be qualitatively similar to the liposomal dosage form, it was designed to present the model compound in an intravenous dosage form that was miscible with plasma water. The comparison of the pharmacokinetics of triamcinolone in liposomal and solution dosage forms is, thus, analogous to other comparative studies (*e.g.*, bioavailability) of a therapeutic agent in different formulations which may not (and often do not) contain the same excipients. If it is assumed that the presence in blood of exogenous lipids (used in the preparation of the liposomes) and polyethylene glycol in the concentrations used did not influence blood flow rate significantly, then the differences in β and Vd_β observed in this study are due probably to the favorable physicochemical properties (especially lipid solubility) of the liposomal entity.

Results of the present study indicate that liposome-encapsulated triamcinolone enhances tissue distribution of the drug in the rabbit. The results also suggest that, given by the intravenous route, neutral multilamellar liposomes could serve as carriers for chemotherapeutic agents whose efficacy depends on sustained blood levels and deep tissue distribution.

REFERENCES

(1) R. L. Juliano and D. Layton, in "Drug Delivery Systems," R. L. Juliano, Ed., Oxford University Press, New York, N.Y., 1980, chap. 6.

(2) Y. E. Rahman, E. A. Cerny, S. L. Tollakson, B. J. Wright, S. L. Nance, and J. F. Thompson, *Proc. Soc. Exp. Biol. Med.*, **146**, 1173 (1974).

(3) M. M. Jonah, E. A. Cerny, and Y. E. Rahman, *Biochim. Biophys. Acta*, **541**, 321 (1978).

(4) M. Mezei and V. Gulasekharam, *Life Sci.*, **26**, 1473 (1980).

(5) N. C. Phillips, D. P. Page Thomas, C. G. Knight, and J. T. Dingle, *Ann. Rheum. Dis.*, **38**, 535 (1979).

(6) C. A. Alving, E. A. Steck, W. L. Hanson, P. S. Loizeaux, W. L. Chapman, Jr., and V. B. Waits, *Life Sci.*, **22**, 1021 (1978).

(7) H. Ivey, S. Roth, and J. Kattwinkel, *Pediatr. Res.*, **11**, 573 (1977).

(8) V. Gulaskharam, "Liposomes for Selective Delivery of Drugs in Topical Routes of Administration." Master of Science thesis, Dalhousie University, Halifax, Nova Scotia, 1980.

(9) C. M. Metzler, G. L. Elfring, and A. J. McEwen, *Biometrics*, **30**, 562 (1974).

(10) A. J. Sedman and J. G. Wagner, *J. Pharm. Sci.*, **65**, 1006 (1976).

(11) V. Zbinovsky and P. Chrekian, in "Analytical Drug Profiles," Vol. 6, K. Florey, Ed., Academic, New York, N.Y., 1977, pp. 579–598.

(12) R. L. Juliano and D. Stamp, *Biochem. Biophys. Res. Commun.*, **63**, 651 (1975).

(13) G. Gregoriadis and B. E. Ryman, *Biochem. J.*, **129**, 123 (1972).

(14) Y. E. Rahman and B. J. Wright, *J. Cell Biol.*, **65**, 112 (1975).

(15) G. Gregoriadis and D. E. Neerunjun, *Eur. J. Biochem.*, **47**, 179 (1974).

(16) G. Sherphof, F. Roerdink, M. Waite, and J. Parks, *Biochim. Biophys. Acta*, **542**, 296 (1978).

(17) F. J. T. Fildes and J. E. Oliver, *J. Pharm. Pharmacol.*, **30**, 337 (1978).

ACKNOWLEDGMENTS

This project was supported by the Medical Research Council of Canada (Grant MA 6664).

The authors are particularly grateful to Dr. C. T. Ueda and Mrs. Jeannetta G. Nickols, University of Nebraska Medical Center, for the use of their computer facilities, Mrs. Anne Fenton of the Dalhousie University Animal Care Facility for her technical assistance, and Mrs. Annette Cook for her excellent secretarial work.

Acrylic Microspheres *In Vivo* IX: Blood Elimination Kinetics and Organ Distribution of Microparticles with Different Surface Characteristics

PER ARTURSON ‡, TIMO LAAKSO *, and PETER EDMAN *x

Received May 10, 1982, from the **Division of Pharmacy, Department of Drugs, National Board of Health and Welfare, S-751 25 Uppsala, Sweden* and ‡*Department of Pharmaceutical Biochemistry, Biomedical Center, University of Uppsala, S-751 23 Uppsala, Sweden.* Accepted for publication September 24, 1982.

Abstract □ The elimination of microparticles from blood after intravenous injection is dependent on the surface characteristics of the particles. The half-life in blood increases from 44 to 84 min after modification of surface-localized human serum albumin with polyethylene glycol. Irrespective of the surface properties, particles are localized in the reticuloendothelial system, mainly in the liver and spleen. In preimmunized mice, the distribution of particles is somewhat altered, *i.e.*, the liver and lung uptake is significantly higher in preimmunized animals than in untreated animals. The rate of phagocytosis of particles with different surface characteristics has also been studied *in vitro* with isolated mouse peritoneal macrophages. This technique gives a good correlation with the *in vivo* results; thus particles with a short half-life in mice are rapidly phagocytosed by the macrophages *in vitro*.

Keyphrases □ Microparticles—polyacrylamide, blood elimination kinetics, organ distribution, effect of surface characteristics, mice □ Elimination—polyacrylamide microparticles from blood, kinetics, organ distribution, effect of surface characteristics, mice □ Delivery systems—polyacrylamide microparticles, blood elimination, kinetics, organ distribution, mice

Immobilized systems in the form of small beads or particles have recently been introduced as carriers of enzymes *in vivo* (1). Some of these systems are characterized as biodegradable (*e.g.*, liposomes), while others are slowly metabolized (*e.g.*, acrylic particles). Irrespective of the type of particles, these systems show great promise as a tool for "active targeting" of enzymes and other macromolecules to specific cells or organs in the body. However, one of the

0022-3549/83/1200-1415$01.00/0

drawbacks of using such particles as a carrier system is the lack of "directability," because the reticuloendothelial system (RES), mainly the liver, spleen, and bone marrow, dominates the uptake of intravenously injected particles. It is well recognized that this uptake must be circumvented to realize the dream of "active targeting" using particulate carrier systems.

Within a few hours after intravenously injecting massive amounts of particles, none are left free in the circulatory system [*e.g.*, microparticles of polyacrylamide have a half-life of 40–60 min in blood (2)]. This efficacy in identifying the foreign nature of such particles in the presence of particles that are normal to blood must depend on surface characteristics. The present study investigates the possibility of changing the rate of phagocytosis of the microparticles in order to make them more suitable as carriers for enzymes.

EXPERIMENTAL

Materials—Human serum albumin[1], IgG[1], rabbit anti-(human serum albumin) globulin[2], L-asparaginase[3], polyethylene glycol monoethyl ether[4] (mol. wt. 1900), [^{14}C]salicylic acid[5], and [^{14}C]paraformaldehyde[5] were used without further purification. Acrylamide[6], *N,N'*-methylenebisacrylamide[6], *N,N,N',N'*-tetramethylethylenediamine[7], tris(hydroxymethyl)aminomethane[7], and other chemicals were analytical grade.

Preparation of Microparticles—Microparticles[8] were prepared and characterized using a reported method (1). A solution of acrylamide (6% w/v) and *N,N'*-methylenebisacrylamide (2% w/v) in 0.1 *M* KCl–0.005 *M* sodium phosphate buffer (pH 7.4), which also contained the protein to be immobilized, was homogenized in an organic phase consisting of toluene–chloroform (4:1 v/v). Ten milliliters of the aqueous phase was emulsified with an homogenizer in 200 ml of the organic phase with a detergent[9] immediately after the catalyst system, consisting of *N,N,N',N'*-tetramethylethylenediamine and ammonium persulfate, had been added to the monomer solution. For the experiments described, microparticles were prepared from human serum albumin, L-asparaginase, or polyethylene glycol-modified human serum albumin by dissolving 0.5–2 g, 96 mg, or 0.5 g of the substrate, respectively, in 10 ml of the monomer solution. After polymerization, the microparticles were freed from the organic phase by repeated washings with buffer and physiological saline. Prior to injection, the particles were carefully dispersed in physiological saline.

^{14}C-Labeled particles were prepared as described by Sjöholm and Edman (2). Radioactivity was measured by liquid scintillation counting. The counting efficiency was calculated with an external standard.

Functional Capacity of Immobilized Human Serum Albumin—The functional capacity of albumin in microparticles was determined as previously described (3). Microparticles with albumin were incubated with [^{14}C]salicylic acid. The amount of albumin binding with salicylic acid was calculated from the binding degree and from a standard curve derived by equilibrium dialysis with different albumin concentrations.

Preparation of Tissue Samples for the Determination of the Distribution of Microparticles—^{14}C-Labeled microparticles in physiological saline (0.2 ml) were injected intravenously or intraperitoneally in the mice. The dose corresponded to 0.5 mg of lyophilized microparticles. The different particles used are specified in Table I. After 6 hr, 24 hr, 1, and 2 weeks, five animals were killed by cervical dislocation. Five mice which were not given any microparticles were used as a control group. The organs were immediately removed, weighed, and prepared for radioactivity measurements. The whole spleen, both lungs, one kidney, and 0.2–0.3 g of the liver were each dissolved in 2 ml of a tissue solubilizer[10] in a counting vial. After treatment at 40° for 12 hr (yielding a clear solution), 2-propanol (0.4 ml) and 30% hydrogen peroxide (0.8 ml) were added to minimize color quenching. A scintillation cocktail[11] (10 ml) was then added, and the samples were counted after adapting to the dark and appropriate temperature.

Determination of the Disappearance Rate of Microparticles from the Circulatory System—Male mice[12] weighing 18–22 g were used. The microparticles (0.5 mg dry weight) were injected intravenously in the tail vein, in a total volume of 0.2 ml. The characteristics of the particles used are summarized in Tables I and II.

Blood samples (75 μl) were collected with a heparinized microtube from the orbital plexus 5, 10, 15, 20, 30, 45, 60, 90, 120, 240, and 300 min after dosing. Only two blood samples were drawn from each mouse; thus, the cumulative blood volume withdrawn never exceeded 10% of the total blood volume. Background values were obtained in the same manner from animals not given microparticles. The animals were unrestrained and had free access to food and water.

The whole blood was digested with 1 ml of a solution consisting of tissue solubilizer[10] and 2-propanol (1:1) in a counting vial. Hydrogen peroxide (30%, 0.5 ml,) was added and the vial was left at 40° for 15 min. A scintillation cocktail[11] was then added and after appropriate equilibration to darkness and temperature, the samples were counted in the liquid scintillation counter.

Assay of Native and Immobilized L-Asparaginase—L-Asparaginase activity was determined from the amount of ammonia produced by reaction with the substrate, L-asparagine, at 37° as earlier described (1). After addition of the ammonia color reagent, the absorbance was determined at 500 nm. Appropriate enzyme and substrate blanks were included in all assays. A standard curve was prepared with known amounts of ammonium sulfate. One unit of activity is defined as the amount of enzyme catalyzing the formation of 1.0 μmole of ammonia/min at 37°.

Autoradiography—Whole-body autoradiography was performed using the method of Ullberg (4). The ^{14}C-labeled microparticles in 0.2 ml of physiological saline were injected in the tail vein. After 24 hr the animals were anesthetized with ether and killed by immersion in hexane–solid carbon dioxide (−78°). With an aqueous gel of carboxymethylcellulose as the medium, the mice were mounted on a large microtome stage. Several 20- or 60-μm saggital sections were cut through the whole body and fixed on adhesive tape. The sections were cut at −15 to −20° and freeze-dried. The slices were pressed against photographic films, which were exposed for up to 6 months. After developing, the films were compared with the corresponding tissue sections.

Determination of Particle Size—The size of the particles was measured from photographs taken by scanning electron microscopy as described by Höglund and Morein (5). The particles were fixed at 4° with glutaric dialdehyde for ~20 hr. Postfixation was done in neutralized 1% osmium tetroxide for 1 hr. The samples were rinsed in saline and freeze-dried. The dehydrated specimens were coated with palladium–gold alloy in an evaporator and analyzed in a scanning electron microscope[13] at 30-keV accelerating voltage.

Immunization Procedures—The mice were injected with L-asparaginase (5 IU) in native form intramuscularly and/or subcutaneously. The enzyme was administered in Freund's complete or incomplete adjuvant. The animals received booster injections after 5, 10, 20, and 30 days. Blood was collected from the orbital plexus and centrifuged at 4° to obtain serum. Each mouse received a total dose of 20–25 IU of L-asparaginase during the study. The antibody titer was assayed by double immunodiffusion in agar gel as described by Ouchterlony (6).

Preparation of Polyethylene Glycol-Modified Human Serum Albumin—Covalent attachment of monomethoxy polyethylene glycol (mol. wt. 1900) to human serum albumin was effected using the procedure of Abuchowski *et al.* (7). Cyanuric chloride (5.5 g, 0.03 mmole) was dissolved in 400 ml of anhydrous toluene and monomethoxy polyethylene glycol (mol. wt. 1900) (19 g, 0.01 mmole) was added to the solution. The 2-*O*-methoxypolyethylene glycol-4,6-dichloro-*s*-triazine (activated polyethylene glycol) formed was precipitated several times with petroleum ether until it was free of cyanuric chloride. The activated polyethylene glycol was coupled to human serum albumin by dissolving the two reactants in sodium borate buffer (0.1 *M*, pH 9.2). The reaction was allowed to proceed for 2 hr at 4°. The fraction of modified primary amino groups was determined by the trinitrobenzenesulfonate method of Ha-

[1] KABI AB, Stockholm, Sweden.
[2] DAKO AB, Copenhagen, Denmark.
[3] Crasnitin; obtained as a gift from Bayer (Sverige).
[4] Aldrich Europe Co.
[5] Amersham, England.
[6] Eastman Kodak Co.
[7] Sigma Chemical Co.
[8] U.S. Patent 4,061,966.
[9] Pluronic F 68.
[10] Soluene 350, Packard Instrument Co.
[11] Dimilume 30, Packard Instrument Co.
[12] NMRI strain.
[13] JSM-U3 microscope, JEOL.

Table I—Characteristics of the Microparticles

Preparation	Protein Immobilized	mg of Protein Incorporated / mg of Dry Particles[a]	Size Distribution[b] <300 nm	301–750 nm	751–1050 nm	1051–1800 nm	Mean Particle Diameter, nm
I	None	—	30%	49%	11%	10%	520
II	None	—	9%	26%	36%	29%	860
III	Human serum albumin	0.05[c]	33%	64%	3%	—	290
IV	Human serum albumin	0.17[c]	not determined				
V	Polyethylene glycol-modified human serum albumin	0.13[d]	21%	70%	9%	—	370
VI	L-Asparaginase	0.02	not determined				

[a] The dry weight of the microparticles was determined after lyophilization. [b] Particle diameter. The size distribution was determined by scanning electron microscopy; 350–550 particles were counted from each preparation. [c] The values were obtained by determination of the functional capacity of albumin as described in the text. [d] The high degree of polyethylene glycol substitution changed the functional capacity of the albumin used. The amount of protein incorporated was therefore determined by amino acid analysis.

beeb (8). Protein concentrations were determined by the biuret method (9), since the method by Lowry *et al.* (10) gives erroneously high values with polyethylene glycol-modified albumin (7). A double immunodiffusion test was used (6) to study the interaction between polyethylene glycol-modified human serum albumin and rabbit anti-(human serum albumin).

Cultivation of Mouse Peritoneal Macrophages—Cells from the peritoneal cavity of unstimulated adult male mice were harvested with 3 ml of cold (4°) phosphate-buffered saline. The cells were further suspended in 10 ml of cold (4°) buffer and mildly spun down at 180×*g* for 10 min. The pellet was resuspended in a nutrient medium[14] containing 10 m*M* 4-(2-hydroxyethyl)-1-piperazineethanesulfonic acid, pH 7.4. The medium was supplemented with benzylpenicillin (100 U/ml), streptomycin (10 μg/ml), and 20% fetal calf serum. The cells were seeded on 50-mm plastic petri dishes and cultured at 37° in 5% CO_2 in air at 85% humidity. After incubation for 45 min, nonadherent cells were removed by washing with buffer, and 5 ml of fresh medium was added. The cells were incubated for an additional 24 hr before use.

Measurement of Phagocytosis of Microparticles—^{14}C-Labeled microparticles (0.25 mg dry weight in 50 μl of phosphate-buffered saline) with a radioactivity of ~50,000 dpm were added to a petri dish containing 1–2 × 10^6 mouse peritoneal macrophages, and the phagocytosis was studied at 37° or 0°. After 2, 4, and 6 hr, the tissue culture medium was aspirated, and the tissue cultures were rinsed with saline (0.154 *M* NaCl) six times to remove unattached microparticles. The contents of the dried dishes were digested for 8 hr at room temperature in 1.5 ml of 0.5 *M* NaOH (11). A 100-μl portion of the digest was removed by aspiration for protein determination; the rest was quantitatively transferred to a liquid scintillation vial, and the radioactivity was determined.

Estimation of the Rate of Particle Aggregation—A light-scattering spectroscopy instrument[15] capable of estimating the size of particles, aggregates, or other particulate matter within the size range of 0.10–3 μm was used to measure the relative size of different microparticle batches and to follow the aggregation of microparticles in the presence of specific antisera. Microparticles and protein solutions were diluted in phosphate-buffered saline, which was passed through a membrane filter (pore size 0.22 μm) prior to use. In a typical experiment, particles of the same size containing human serum albumin, L-asparaginase, or no protein at all were diluted to the same absorption at 450 nm. The initial value for 450 μl of the sample was recorded by the instrument and 100 μl of a solution of antiserum [*i.e.*, rabbit anti-(human albumin serum) containing 3.6 mg of IgG/ml] or buffer was added with subsequent recording of the light scattering. All measurements were done in triplicate.

RESULTS

Blood Clearance of Microparticles with Different Surface Characteristics—When a protein is immobilized in microparticles, it will not only be localized within the gel structure but will also protrude from the matrix and, thus, will be partly localized on the surface of the microparticles (12). To investigate if surface-localized protein would influence the survival of microparticles in blood, four different preparations were made (Table I). After intravenous injection the blood life span of microparticles was followed with time (Fig. 1). In Table II some experimental values calculated from the curves in Fig. 1 are summarized. The experimental points obtained during the first 90 min were fitted to a straight line by linear regression (with time as the independent variable and the concentration in the circulatory system as the dependent variable). The 5-min values were omitted, since the initial mixing in the whole blood volume apparently was not complete at this time. From the slope of the line, k, the half life ($t_{1/2}$) was estimated from the expression:

Table II—Blood Elimination Parameters of the Microparticles[a]

Preparation	$t_{1/2}$, min	V_d, ml	CL, ml/min
I	61	2.6	0.024
III	44	2.1	0.034
IV	33	2.5	0.052
V	84	2.5	0.020
Mean ± *SEM*		2.4 ± 0.1	

[a] Half-lives, distribution volumes, and clearance values.

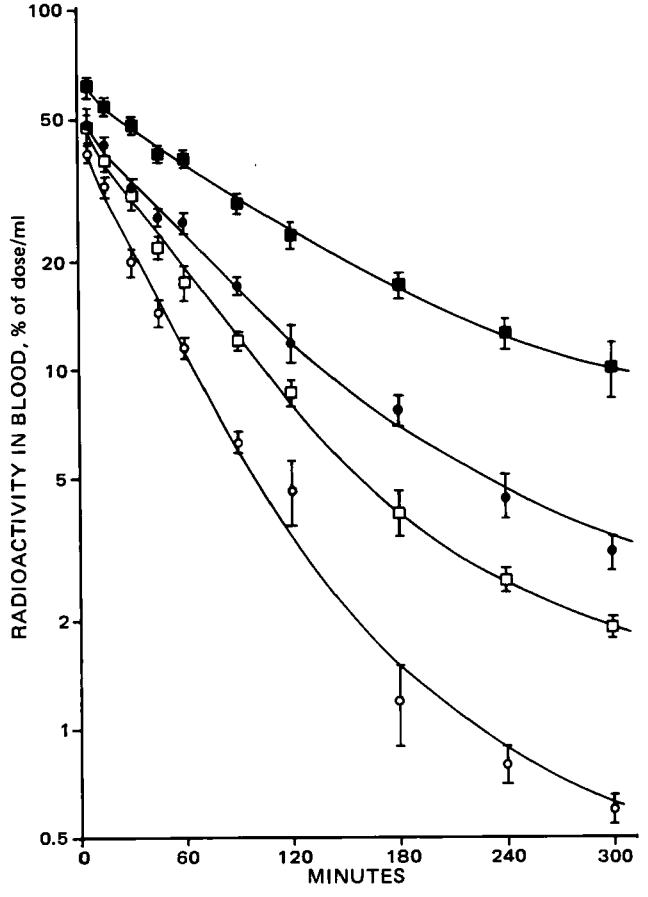

Figure 1—*Disappearance of ^{14}C-labeled microparticles from blood after intravenous injection in mice. Radioactivity is calculated in percent of the total dose (log scale) retained in 1 ml of blood. Key: (●) empty particles; (○) particles containing 0.17 mg of albumin/mg of particles; (□) particles containing 0.05 mg of albumin/mg of particles; and (■) particles containing polyethylene glycol-modified albumin.*

[14] F-10 medium, GIBCO BIO-CULT.
[15] Nanosizer, Coulter, England.

$$t_{1/2} = \frac{\log 2}{k} \quad \text{(Eq. 1)}$$

From the intercept on the y-axis (C_0^g) and the dose given, the apparent volume of distribution, V_d, was calculated:

$$V_d = \frac{\text{dose}}{C_0^g} \quad \text{(Eq. 2)}$$

From $t_{1/2}$ and V_d, the clearance from the blood was estimated according to:

$$CL = \frac{0.693 \times V_d}{t_{1/2}} \quad \text{(Eq. 3)}$$

Intravenously injected empty microparticles (I) were rapidly cleared from the circulatory system with a half-life of 61 min. Particles with immobilized human serum albumin (0.05 mg of protein/mg of lyophilized particles, III), were eliminated with a half-life of 44 min. The elimination rate was further accelerated when the protein content in the particles was increased; *e.g.*, particles with 0.17 mg of protein/mg of dry weight (IV) were eliminated from the circulatory system with a half-life of 33 min.

In an attempt to block the influence of the surface-localized proteins on the extraction rate of particles from the circulatory system, polyethylene glycol-modified human serum albumin was immobilized (V). Seventy percent of the primary amino groups of albumin were derivatized with activated polyethylene glycol. The antigenicity of the derivative was checked by double immunodiffusion. In accordance with the results of Abuchowski *et al.* (7), no precipitation occurred when ≥50% of the primary amino groups were modified. As a consequence, the survival time of these particles in blood was significantly prolonged ($t_{1/2}$ = 84 min) as compared with albumin-containing particles (33 min).

Distribution of Microparticles with Different Surface Characteristics—The distribution pattern of the microparticles was followed quantitatively in mice for 2 weeks after intravenous injection (Table III). The surface properties of the microparticles had no effect on the gross distribution pattern. The microparticles were concentrated in the spleen and liver, and initially also in the lungs. These results agree with those found earlier with empty polyacrylamide particles (2) except for the lung uptake. Earlier, only small amounts of radioactivity were found in the lungs after injection of massive doses (4.1 mg) of empty microparticles in mice. In this study, 4–30% of the radioactivity was found in the lungs 6 hr after injection. However, in 24 hr a redistribution could be seen, with elimination of radioactivity from the lungs and a corresponding uptake of radioactivity in the liver.

The differences in the results between this and the previous study (2) were thought to be an effect of the microparticle size, since larger particles were used in this study. In the earlier study, the mean particle size was estimated to 0.25 μm compared with mean values of 0.29–0.86 μm in this study (Table I). The effect of the particle size on the organ distribution was checked by comparing two preparations of empty microparticles with mean diameters of 0.52 and 0.86 μm (I and II, respectively). As expected, the batch with the larger particles was retained to a greater extent in the lungs than the batch with the smaller mean particle diameter. Thus, 6 hr after intravenous injection, 30% of II and 9% of I were found in the lungs. Two weeks after the injection of small microparticles (I), no radioactivity was detected in the lungs, while 10% of the large microparticles (II) still remained in the lungs.

Uptake of Microparticles by Mouse Peritoneal Macrophages—The dependence of the elimination rate of microparticles from blood in mice on the proteins immobilized in the microparticles was also studied *in vitro*. A system with mouse macrophages was designed, in which the phagocytosis of ^{14}C-labeled microparticles with different immobilized proteins was followed. A nontoxic dose (0.25 mg dry weight of particles) was added to a monolayer of the macrophages cultivated in a petri dish. The extent of phagocytosis was estimated from the radioactivity content in the macrophages after different time periods and related to the protein content, which represents a measure of viable cells. The dose chosen was the lowest found to give the maximal uptake in ~1–2 × 10^6 cells.

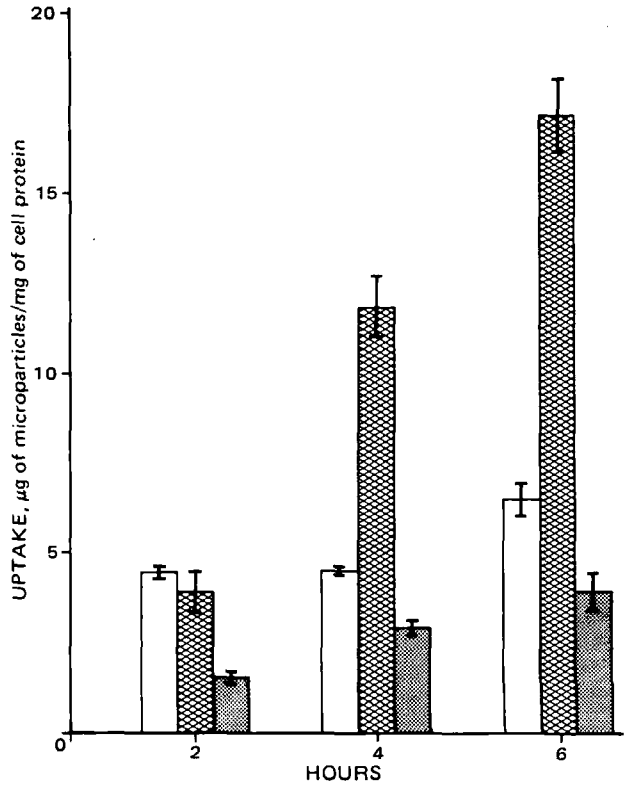

Figure 2—*Rates of uptake of microparticles with different surface characteristics by mouse peritoneal macrophages. All values represent the mean ± SEM of triplicate incubations, corrected for unspecific interaction between cells and particles. The uptake was calculated as the amount of microparticles (μg)/mg of cell protein. Key: (□) ^{14}C-Labeled empty microparticles (I); (▨) albumin-containing particles (IV); (■) particles with polyethylene glycol-modified albumin (V).*

The results from the cell studies are summarized in Fig. 2. The rate of uptake of empty microparticles was slower than that of particles containing human serum albumin, but faster than that of particles in which the amino groups of albumin had been chemically modified with polyethylene glycol. The unspecific adsorption of particles to the macrophages, as measured at 0°, was low and insignificant. As is apparent, the results correlate well with those found in the *in vivo* studies.

Disappearance Rate from Blood of Microparticles with L-Asparaginase in Preimmunized Mice—The mice were immunized with

Table III—Organ Distribution of Microparticles with Different Surface Characteristics [a]

Time, days	Organ	Preparation I	III	IV	V
0.25	Liver	38.4 ± 1.2	57.1 ± 1.4	47.3 ± 1.2	48.4 ± 2.5
	Spleen	8.3 ± 0.3	17.4 ± 1.0	13.2 ± 0.5	16.5 ± 0.4
	Lung	30.5 ± 0.9	9.9 ± 0.4	15.3 ± 0.4	3.6 ± 0.2
1	Liver	42.3 ± 1.6	61.7 ± 0.9	54.1 ± 2.1	56.5 ± 2.2
	Spleen	8.8 ± 0.4	13.9 ± 0.8	12.9 ± 0.4	16.2 ± 0.4
	Lung	19.6 ± 0.5	2.4 ± 0.5	6.1 ± 0.7	2.4 ± 0.2
7	Liver	65.2 ± 1.3	65.7 ± 3.1	63.0 ± 1.2	60.9 ± 1.1
	Spleen	10.7 ± 0.1	13.0 ± 0.4	12.7 ± 0.6	13.6 ± 0.9
	Lung	7.3 ± 0.9	0.6 ± 0.09	2.6 ± 0.3	0.2 ± 0.02
14	Liver	62.1 ± 2.1	62.5 ± 0.8	53.9 ± 1.0	54.8 ± 1.1
	Spleen	9.6 ± 0.6	12.0 ± 0.6	9.7 ± 0.3	13.1 ± 0.2
	Lung	10.3 ± 0.9	0.5 ± 0.03	2.8 ± 0.2	0.1 ± 0.01

[a] *Distribution of microparticles after intravenous injection in mice. Each value is expressed as percent of the injected dose and represents the mean ±SEM of five animals.*

Table IV—Organ Distribution of Microparticles Containing L-Asparaginase [a]

Time, days	Organ	Untreated Mice	Immunized Mice
0.25	Liver	41.2 ± 0.2	49.4 ± 2.7
	Spleen	17.6 ± 1.0	4.6 ± 0.2
	Lung	5.7 ± 0.4	12.3 ± 2.7
1	Liver	43.3 ± 0.9	53.2 ± 1.9
	Spleen	13.6 ± 1.0	9.6 ± 0.3
	Lung	1.8 ± 0.2	7.2 ± 1.3
7	Liver	43.0 ± 3.5	54.6 ± 4.1
	Spleen	10.3 ± 1.0	9.6 ± 1.5
	Lung	0.0	0.3 ± 0.03
14	Liver	36.4 ± 2.5	46.3 ± 2.6
	Spleen	7.9 ± 1.0	12.2 ± 2.1
	Lung	0.3 ± 0.03	0.3 ± 0.02

[a] Distribution of ^{14}C-labeled microparticles containing L-asparaginase after intravenous injection in preimmunized and untreated mice. The figures show means ±*SEM* obtained from four or five animals.

soluble L-asparaginase as described above. The antibody titer, as detected by double immunodiffusion according to Ouchterlony (6), was 1:1 to 1:2. Only small doses of microparticles with L-asparaginase could be given. After intravenous injection of 0.5 mg of particles containing 1.2 IU of L-asparaginase, three of eight mice died within 15–20 min. After half the original dose (0.25 mg dry weight of microparticles) was administered, 3 of 18 mice died. The microparticles were very rapidly cleared from the circulatory system with a half-life of <10 min.

The quantitative distribution of the particles in surviving mice was followed in the liver, spleen, and lungs over a period of 2 weeks (Table IV). The values obtained from the lungs of preimmunized mice 6 hr postinjection showed that 12% of the injected dose was found in this organ compared with 6% in the controls (nonimmunized mice). The liver uptake of the injected dose was 8–11% greater for preimmunized animals during the entire study.

After intraperitoneal injection in preimmunized mice, the microparticles were localized in the lymph nodes draining the peritoneal cavity and the central lymphatic vessels, as shown by the autoradiogram (Fig. 3) taken 1 day after injection. The quantitative distribution of the L-asparaginase-containing particles in different organs was followed over a period of 1 week. The total recovery was low, 7% of the injected dose being found in the liver and spleen after 6 hr compared with 17% in the controls. After 1 week, 26 and 35% of the injected dose was recovered in these organs in preimmunized and nonimmunized animals, respectively.

The high lung uptake of L-asparaginase particles after intravenous injection in preimmunized mice is probably due to aggregate formation between the particles and circulating antibodies. To study the rate of formation of particle aggregates, an *in vitro* system was set up to simulate the interaction between specific antibodies and particles containing the corresponding antigen. In this study, anti-(human serum albumin) and albumin particles were used to simulate the *in vivo* condition and the particle size was followed with a light-scattering spectroscope (Fig. 4). As expected, incubation with the specific antibody gave a rapid increase in particle size. The apparent mean diameter increased from 0.6 to 2 μm after a 15-min incubation with the specific antibody and to >3 μm after 60 min. There was no interaction between anti-(human albumin globulin) and empty particles or with particles containing L-asparaginase under the conditions used. Furthermore, the interaction between the albumin particles and anti-albumin serum was inhibited by adding soluble human serum albumin to the solution.

Reticuloendothelial System (RES) Blockade—The capacity of the RES to phagocytose foreign particles from the circulation and an attempt to block such phagocytosis were investigated by repeated intravenous injections of empty polyacrylamide microparticles. In the first study, 0.5 mg of unlabeled empty particles was injected intravenously, and after 6 half-lives a second 0.5 mg dose of ^{14}C-labeled particles was injected. The second study was performed by injecting 2.5 mg (dry weight) particles, with the second dose (0.5 mg) given 16 hr later. This time point was chosen for two reasons. First, there are no particles in the blood after 16 hr. Second, it is known (13) that 24 hr after injection of particles there is an increasing number of phagocytosing cells in the RES, especially in the liver, signifying that the phagocytic capacity is increased. Considering these facts, we chose a time point between 6–24 hr, namely 16 hr.

Irrespective of the size of the first dose (0.5 or 2.5 mg), the RES retained its capacity to extract particles from the blood. Moreover, the blood clearance and organ uptake of microparticles in blockaded animals were almost the same as in normal animals. Thus, the liver and spleen uptake in blockaded animals corresponded to 60–70% of the injected dose, whereas the uptake in the lungs was increased to ~10–15% of the dose. The half-life ($t_{1/2}$) of the particles in blood was 50–60 min in the blockaded animals, the same as in untreated animals.

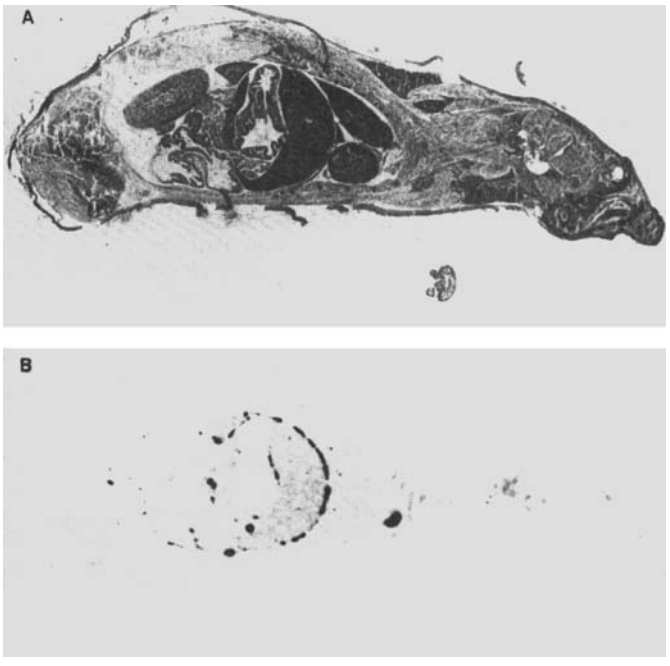

Figure 3—*Whole body autoradiogram (B) of a mouse 1 day after intraperitoneal injection of ^{14}C-labeled microparticles containing L-asparaginase (50,000 dpm in 0.5 mg). The mouse was immunized against L-asparaginase. (A) Corresponding tissue section, 20 μm.*

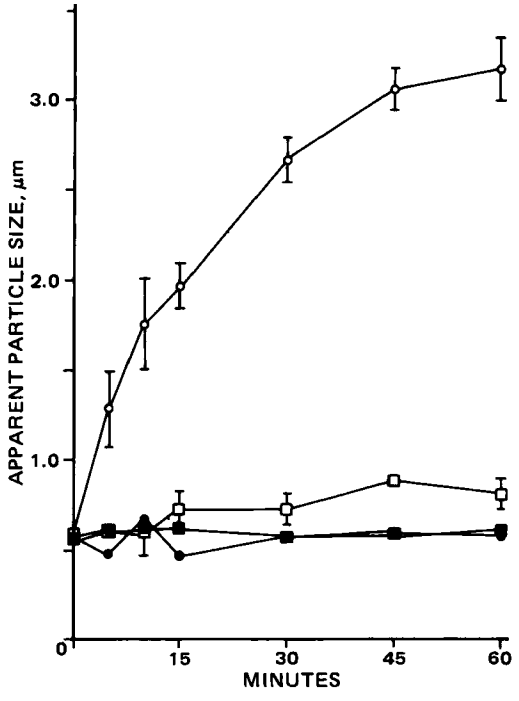

Figure 4—*Interaction between antialbumin globulin and particles with immobilized proteins. The immobilized proteins were albumin (○) and L-asparaginase (□); empty particles (●) were used as controls. In one study (■), albumin particles and antialbumin globulin were incubated in a solution containing free albumin (2×10^{-4} M). The interaction was measured as an increase in the apparent particle size. All values are mean ± SD from triplicate determinations.*

DISCUSSION

When immobilized in acrylic microparticles, proteins are partly entrapped within the polymeric network and partly fixed in the polymer threads forming the particles (12). As a consequence, a fraction of the immobilized macromolecules are localized on the surface and protrude from the particles. This phenomenon has been utilized to detect specific cell-surface receptors and for cell separation purposes after immobilization of appropriate cell-reactive agents in the microparticles (14).

Microparticles containing proteins are rapidly cleared from the circulatory system after intravenous injection. Furthermore, the rate of elimination from the incubation is significantly affected by the protein immobilized in the particles and depends on the amount of protein localized on the particle surface. The results indicate that the phagocytosis of the microparticles apparently is mediated by some receptor mechanism that makes it possible for the macrophages in the RES to discriminate between different surface characteristics and also to estimate the extent of the foreign nature of the particles. The data in Fig. 1, moreover, show that the "estrangement" of the microparticles mediated by the surface-localized proteins can be camouflaged by polyethylene glycol, manifested as an increased circulating lifetime. As a result of the modification with polyethylene glycol, the half-life of microparticles with human serum albumin in blood is increased from 33 to 84 min. This dramatic change may be due to different effects imparted by the modification of the surface properties: a decrease in the foreign nature, changed affinity for water, increased size, or a combination of these effects. The work of Abuchowski *et al.* (7) has shown that polyethylene glycol alters the immunological properties of bovine serum albumin and increases the circulating time of bovine catalase in mice. Polyethylene glycol has also been used in conjugates with antigen to suppress reaginic antibody response (15). It is thus evident that important determinants on the surface are quenched by the modification. However, the long half-life, which significantly exceeded that of microparticles containing no protein ($t_{1/2}$ = 61 min), indicates that other factors may also be involved, *e.g.*, physicochemical surface properties. In this case, the changed size distribution of the microparticles cannot be of any significance, as the size of the particles containing the modified albumin was approximately the same.

The survival time of microparticles in blood was drastically decreased in preimmunized mice, which in this case was a result of aggregation and a concomitant accelerated phagocytosis by the macrophages of the RES, especially the Kupffer cells. The liver uptake of the injected dose was 10% greater in immunized mice as compared with the controls. A plausible explanation to this difference is that Kupffer cells phagocytose larger particles in preference to smaller ones (16). *In vitro* experiments with particles containing albumin and anti-albumin globulin support such an interpretation. Thus, the apparent mean diameter of the particles increased from <1 μm to 3 μm within 15 min. A higher lung uptake in immunized animals gives further support to this hypothesis.

In the experiments presented only modest changes of the tissue distribution were observed, although a substantial change in the clearance rate of different particles was detected. This indicates that the RES, especially the liver and spleen, has an important and dominating role in particle clearance. It is likely that this phenomenon is representative for all particulate matter of submicron size.

Many papers describe attempts to block the RES (17, 18). These studies have shown that the capacity of the RES to eliminate foreign particles from the circulatory system is high. It was, moreover, necessary to inject massive and toxic doses of particles, ghost red blood cells, or liposomes to obtain a blockade. Pretreatment of mice with 0.5 mg of particles, which is the threshold dose required to produce morphological changes in the liver and spleen, did not affect the rate of elimination of subsequently injected particles. However, the practical use of an RES blockade is limited, because the treatment impairs the innate immunity of the recipient.

The results clearly demonstrate that alteration of the surface characteristics of the microparticles can lead to an increased circulation time *in vivo*. The finding is important because it constitutes a means of designing a carrier for macromolecular drugs in order to actively target drugs to specific cells in the vascular system *in vivo*.

REFERENCES

(1) P. Edman and I. Sjöholm, *J. Pharmacol. Exp. Ther.*, **211,** 663 (1979).

(2) I. Sjöholm and P. Edman, *J. Pharmacol. Exp. Ther.*, **211,** 656 (1979).

(3) I. Sjöholm, B. Ekman, A. Kober, I. Ljungstedt-Pählman, B. Weiving, and T. Sjödin, *Mol. Pharmacol.*, **16,** 767 (1979).

(4) S. Ullberg, in "Proceedings of the 2nd UN International Conference on the Peaceful Uses of Atomic Energy," vol. 24, Geneva, 1958, pp. 248.

(5) S. Höglund and B. Morein, *J. Gen. Virol.*, **21,** 359 (1973).

(6) O. Ouchterlony, in "Handbook of Experimental Immunology," D. M. Weir, Ed., Blockwell Scientific Publications, Oxford, 1967, p. 655.

(7) A. Abuchowski, T. van Es, C. Palczuk and F. F. Davis, *J. Biol. Chem.*, **252,** 3578 (1977).

(8) A. F. S. A. Habeeb, *Anal. Biochem.*, **14,** 328 (1966).

(9) A. G. Gornall, C. J. Bardawill, and M. M. David, *J. Biol. Chem.*, **177,** 751 (1949).

(10) O. H. Lowry, N. I. Rosebrough, A. L. Farr, and R. J. Randall, *J. Biol. Chem.*, **193,** 265 (1951).

(11) R. H. Michell, S. J. Pancake, J. Noseworthy, and M. L. Karnovsky, *J. Cell. Biol.*, **40,** 216 (1969).

(12) B. Ekman and I. Sjöholm, *Nature (London)* **257,** 825 (1975).

(13) R. L. Souhami and I. W. B. Bradfield, *J. Rest. Soc.*, **16,** 75 (1974).

(14) I. Ljungstedt, B. Ekman, and I. Sjöholm, *Biochem. J.*, **170,** 161 (1978).

(15) W. Y. Lee and A. H. Sehon, *Nature (London)* **267,** 618 (1977).

(16) F. B. D. Scott, H. S. Williams, and P. M. Marriott, *Br. J. Exp. Pathol.*, **48,** 411 (1967).

(17) R. L. Souhami, H. M. Patel, and B. E. Ryman, *Biochim. Biophys. Acta*, **674,** 354 (1981).

(18) Y. I. Kao and R. L. Juliano, *Biochim., Biophys. Acta*, **677,** 453 (1981).

ACKNOWLEDGMENTS

This work was supported by the Swedish Medical Research Council, the Swedish Board for Technical Development, and the I. F. Foundation for Pharmaceutical Research.

We thank Miss Siv Larsson and Mrs. Elisabet Tidare for technical assistance. We acknowledge with thanks stimulating discussions with Professor Ingvar Sjöholm.

Determination of Concentration-Dependent Water Diffusivity in a Keratinous Membrane

MAW-SHENG WU

Received July 6, 1982, from the *Personal Care Division, The Gillette Company, Boston, MA 02106.* Accepted for publication October 22, 1982.

Abstract □ A permeation method was developed to determine water diffusivity, $D(C)$, as a function of water concentration (C) in a keratinous membrane. The method involved the determination of a series of mean diffusivities ($\overline{D}$) and mean concentrations ($\overline{C}$) in the membrane. $\overline{D}$ was obtained from $\overline{D} = F\,H(C_o - C_h)$, where F was the flux at steady state, H was the membrane thickness, and C_o and C_h were the water concentrations in the membrane at the donor and receptor sides, respectively. The difference between C_o and C_h was kept small in each experiment. Therefore, as a first approximation, $\overline{C}$ was equal to $(C_o + C_h)/2$. After successive approximations, an empirical equation was found to provide the best fit to $\overline{D}$ *versus* $\overline{C}$ and to give the best convergence between the assumed and calculated $\overline{C}$; the equation was taken as $D(C)$. $D(C)$ for water in fetal hog periderm was found to be: $D(C) = 1.0 \times 10^{-18} + 9.70 \times 10^{-9}\,C^{0.69}$.

Keyphrases □ Diffusivity—water in keratinous membranes, determination using concentration, fetal hog periderm, topical formulations □ Topical formulations—determination of water diffusivity using concentration, keratinous membranes, fetal hog periderm □ Permeability—topically applied formulations, determination of diffusivity using concentration, keratinous membranes

Passive transport of matter through a biological membrane is usually governed by Fick's law. In most cases, a constant diffusion coefficient for transported material (penetrant) can adequately describe the diffusion process. However, on some occasions, especially when the penetrant is also a solvent or plasticizer for the membrane, the diffusion coefficient could be a function of the concentration of the penetrant (1).

Permeability of a topically applied drug sometimes is influenced by the hydration state of the stratum corneum (2). Therefore, knowing the water concentration profile in the stratum corneum would be helpful in studying the percutaneous absorption of the drug. *In vivo*, water is not evenly distributed across the thickness of the tissue: a concentration gradient exists. On the dermal side of the stratum corneum, the tissue is fully hydrated, whereas on the skin surface, the water concentration is much lower and is regulated by the ambient condition. Therefore, transpiration of water through the stratum corneum is inevitably due to the concentration gradient. From the rate of transpiration and Fick's diffusion equation, one may obtain the water concentration profile in the stratum corneum and thus, the amount of water at different sites within the tissue, if the diffusivity of water in the stratum corneum is known.

Methods have been developed to determine diffusivity as a function of concentration (3). The most commonly used sorption–desorption method, devised by Crank and Park (4), is based on the mass of the membrane as the frame of reference. To obtain a concentration profile across the thickness of a membrane, one may have to use the volume of the membrane as the frame of reference. However, if the change in the volume of mixing between the penetrant and the membrane varies with the concentration, as is the case with water in the stratum corneum (5), then converting a system based on the mass to one based on volume as the reference coordinate could be very difficult, if not impossible.

A method to determine the diffusivity of water in a keratinous membrane is reported here. The method considers the concentration variations of water in the membrane as well as concentration-dependent volume change of the membrane. Fetal hog periderm was chosen as the model tissue for the keratinous membrane as it is easy to obtain in large quantities and is free from the hair usually accompanying stratum corneum.

THEORETICAL

In diffusion-controlled transpiration, if the diffusion follows Fick's laws, then the rate of transpiration (flux) could be expressed by Fick's first law:

$$F = -D\frac{dC}{dx} \qquad \text{(Eq. 1)}$$

where F is the flux (*i.e.*, the rate of transpiration of water across any place in a keratinous membrane), C is the concentration of the diffusion substance (*e.g.*, water), x is the position along the direction of diffusion (position along the thickness of the membrane), and D is the diffusivity of the penetrant. Since D may be dependent on the concentration (C), D is rewritten as $D(C)$ to illustrate the relationship between these parameters. The flux, F, at steady state may be further expressed in an integrated form of Eq. 1 (6):

$$F = \frac{1}{H}\int_{C_h}^{C_o} D(C)dC \qquad \text{(Eq. 2)}$$

where H is the thickness of the membrane and C_h and C_o are the penetrant concentrations in the membrane at the receptor and donor sides, respectively.

The mean diffusivity $\overline{D}$, at the mean concentration $\overline{C}$, is defined as:

$$\overline{D} = \left[\int_{C_h}^{C_o} D(C)dC\right] \Big/ (C_o - C_h) \qquad \text{(Eq. 3)}$$

and by substituting Eq. 2 into Eq. 3, $\overline{D}$ becomes:

$$\overline{D} = FH/C_o - C_h) \qquad \text{(Eq. 4)}$$

$\overline{D}$ may be readily calculated from Eq. 4 using the measurements of F, H, C_o, and C_h. Furthermore, if the difference between C_o and C_h is small, then the mean concentration, $\overline{C}$, can be expressed as:

$$\overline{C} = (C_o + C_h)/2 \qquad \text{(Eq. 5)}$$

Therefore, as a first approximation to determine the empirical equation for $D(C)$, a series of permeation experiments in various concentration ranges can be conducted by keeping the difference of C_o and C_h small in each experiment. From the experimental results, a series of $\overline{D}$ and $\overline{C}$ can be calculated. Plotting $\overline{D}$ *versus* $\overline{C}$, an empirical equation for $D(C)$ which gives the best fit to the experimental data can be determined.

This equation is then inserted into Eq. 1, which can be integrated to give C as a function of x (or *vice versa*). The curve of C *versus* x, *i.e.*, the water distribution profile across the thickness of the membrane, is then integrated to obtain the area under the curve. This area, divided by the membrane thickness (H), yields the mean concentration ($\overline{C}$) of water in the membrane. These calculated values of $\overline{C}$ are then compared with the values of $\overline{C}$ used to obtain $D(C)$. If the assumed and calculated values

0022-3549/83/1200-1421$01.00/0

of $\overline{C}$ are not equal, then the assumed values are adjusted to obtain a new empirical equation for $D(C)$. The adjusted values are again compared with the calculated values. This process is repeated until the two sets of numbers are equal or converge. If more than one functional form for $D(C)$ is obtained from the first approximation, the functional form which results in the best convergence and provides the best fit to the experimental data will prevail in the iteration and is the best equation for $D(C)$.

In the previous calculation, the thickness of the membrane, H, is a known parameter. Its value lies between H_h and H_o (the membrane thickness when the water concentrations in the membrane are C_h and C_o, respectively). Although the relationship between H and C is not known, it may be assumed that:

$$H = (H_o + H_h)/2 \qquad \text{(Eq. 6)}$$

because the difference between C_o and C_h is small.

EXPERIMENTAL

Tissue Preparation—Fetal hog skin was obtained from a commercial source[1]. The periderm was prepared using a procedure reported for human stratum corneum (7). A whole fetal hog skin was immersed in a 60° water bath for ~1 min. The skin was then taken out of the bath, and the periderm was carefully peeled from the tissue.

Determination of Rate of Water Loss (F)—Measurement of the rate of water loss, *i.e.*, the flux (F), through the periderm was carried out using diffusion cells. The cell was half filled with a saturated salt solution to produce a constant relative humidity inside the cell and, hence, a constant water concentration (C_o) at the donor side of the membrane. The cell was placed in a desiccator filled with another saturated salt solution to produce a lower relative humidity outside of the cell and therefore, a constant water concentration (C_h) at the receptor side of the membrane. The desiccator was placed in a constant temperature room at 21°. The rate of water loss at steady state was obtained gravimetrically when the rate became constant. The experiments were carried out in small relative humidity ranges of 0–12%, 12–23%, 23–33%, 33–44%, 44–57%, 57–75%, 75–85%, 75–100%, and 85–100%. The salts used were phosphorous pentoxide, lithium chloride, potassium acetate, magnesium chloride, potassium carbonate, potassium bromide, sodium chloride, and potassium chloride for relative humidities of 0, 12, 23, 33, 44, 57, 75, and 85%, respectively.

Volume of the Membrane—Volumes of the membranes at various relative humidities were determined using air comparison pycnometry (8).

Determination of Water Concentration—Dry periderm was equilibrated in a desiccator at a constant humidity maintained by a saturated salt solution. After each tissue reached a constant weight, the weights of the tissues were taken and, from the weight gain and the volume of each tissue, the concentrations of water in the membranes at various relative humidities were determined.

Determination of Membrane Thickness—The thickness of the membrane at various humidities was obtained from the weight per area and the density of the tissue at each humidity. To do this, a sheet of periderm was placed on a sheet of aluminum foil. This was done by floating the tissue in water and carefully raising the aluminum foil beneath the tissue to bring the tissue out of the water. The tissue was free of wrinkles and could expand and contract freely. The tissue with the aluminum foil was then dried and put in a desiccator with a constant relative humidity. The desiccator and a microbalance were placed in a humidity chamber having the same relative humidity as the desiccator. After the tissue was equilibrated, a piece of the tissue–aluminum foil was cut and its weight was determined with the balance. The tissue was then removed from the aluminum foil, and the weight of the aluminum foil was determined. From the weight difference, the weight of the tissue was obtained; from the weight of the aluminum foil alone and a predetermined weight–area correlation curve for the aluminum, the area of the tissue was determined. Thus, the weight per unit area of periderm at each humidity could be determined.

RESULTS AND DISCUSSION

The rates of water loss (F) at various experimental conditions are listed in Table I. Table II shows the water concentration and the membrane thickness at the various relative humidities of interest. Large standard deviations were found in the rate of water loss and in the thickness measurements. These deviations are probably due to the large variation of the tissue sample used. The water concentration data are fairly consistent. Because each fetal hog provided <0.2 g of the dry periderm, at least 10 animals were required for each volume determination. Inherent variations in the tissues were probably balanced by the large sample size to produce the fairly consistent data in the water concentrations. The mean water diffusivityes, $\overline{D}$, obtained here (4×10^{-10} to 3.2×10^{-9} cm²/sec) are in the range of that for human stratum corneum (9).

From the plot of $\overline{D}$ *versus* $\overline{C}$, four functional forms can be found to provide a reasonable fit to the experimental data (Fig. 1). The four functional forms are $D(C) = D_o - Ae^{-BC}$, $D(C) = D_o + AC^B$, $D(C) = D_o + Ae^{BC}$, and $D(C) = D_o + AC/(1 + BC)$, where D_o, A, and B are constants.

Table I—Rate of Water Loss Through Fetal Hog Periderm at 21° and Various Relative Humidities

Experimental Condition (% RH_h − % RH_o)[a]	Rate of Water Loss, g/cm² sec × 10^8
0–12	0.95 ± 0.17 (6)[b]
12–23	1.69 ± 0.83 (7)
23–33	2.36 ± 1.08 (7)
33–44	3.88 ± 1.92 (9)
44–57	6.98 ± 1.92 (9)
57–75	10.73 ± 4.87 (11)
75–85	8.64 ± 0.55 (6)
75–100	20.54 ± 6.02 (6)
85–100	11.89 ± 4.43 (11)

[a] % RH_h and % RH_o were the relative humidity conditions under which C_h and C_o were determined. [b] Number of samples in parentheses.

Table II—Water Concentration and Thickness of Fetal Hog Periderm at Various Relative Humidities

Relative Humidity, %	Water Concentration, g/cm³	Membrane Thickness, cm × 10^4
0	0	10.1 ± 3.31
12	0.024	10.3 ± 4.92
23	0.043	10.5 ± 1.50
33	0.059	10.6 ± 3.31
44	0.084	10.9 ± 2.40
57	0.116	11.4 ± 2.32
75	0.173	11.8 ± 4.54
85	0.223	16.5 ± 5.95
100	0.290	24.3 ± 9.86

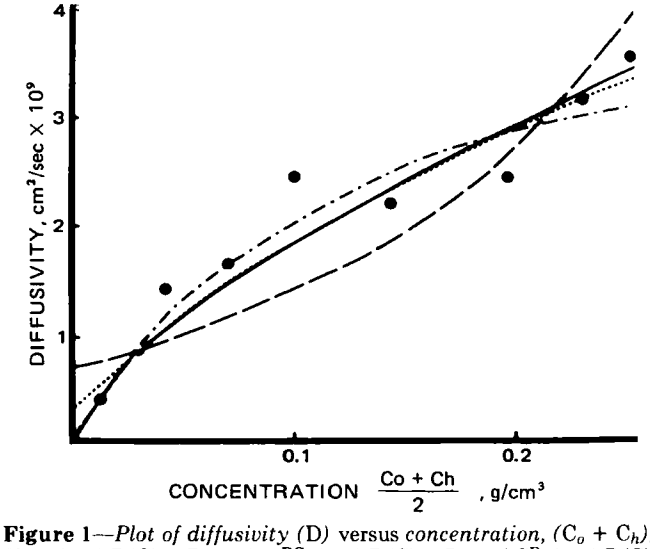

Figure 1—*Plot of diffusivity* (D) versus *concentration*, $(C_o + C_h)/2$. *Key:* (·····) $D(C) = D_o - Ae^{-BC}$; (——) $D(C) = D_o + AC^B$; (- - -) $D(C) = D_o + Ae^{BC}$; (-·-·-) $D(C) = D_o + AC/(1 + BC)$.

[1] Texas Biological Inc., Dallas, Tex.

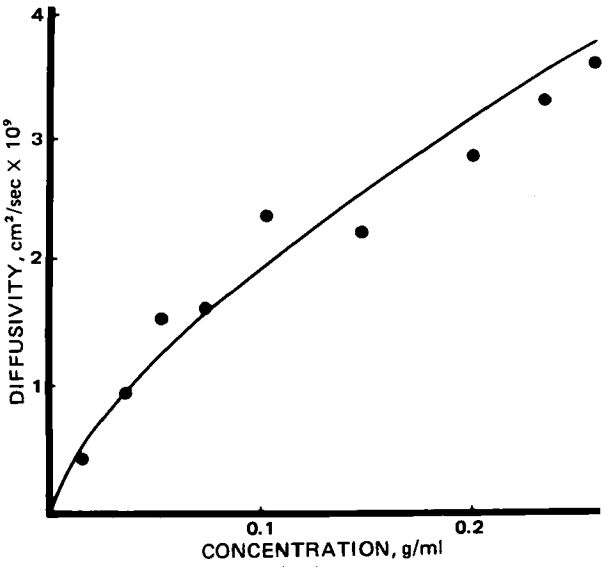

Figure 2—*Comparison of experimental data and the diffusivity equation. Key: (●) experimental data; (—)* $D(C) = 1.0 \times 10^{-18} + 9.70 \times 10^{-9} C^{0.69}$.

A computer was used to carry out the successive iterations. In the calculation, the equations were linearized. The value of D_o was determined by trial and error; values for B and A were obtained from the slope and the intercept of the linearized equation. In the iteration, the concentrations used were restricted between C_h and C_o. At the end of the iteration, $D(C) = D_o + AC^B$ was found to give the best convergence of the assumed and calculated mean concentrations and to provide the best fit to the experimental data (Fig. 2). The final equation for $D(C)$ is:

$$D(C) = 1.0 \times 10^{-18} + 9.70 \times 10^{-9} C^{0.69} \quad \text{(Eq. 7)}$$

The large standard deviation associated with the measured thickness, H (Table II), raised concern about the appropriateness of the approximation for H. Therefore, the iteration process was altered. The mean water concentration $\overline{C}$, was fixed as $(C_o + C_h)/2$ while the assumed values for H were adjusted in the iteration until they converged with the calculated values. The resulting equation is shown below:

$$D(C) = 1.0 \times 10^{-18} + 10.0 \times 10^{-9} C^{0.72} \quad \text{(Eq. 8)}$$

Comparison of Eq. 8 with Eq. 7 shows that they are not significantly different. Therefore, Eq. 7 is a reasonable representation for the diffusivity of water in fetal hog periderm.

The method developed here provides an alternative way to obtain the diffusivity as a function of the penetrant concentration. With the appropriate experimental designs and the data analyses mentioned herein, this method can circumvent some of the difficulties associated with the other methods of obtaining diffusivity.

REFERENCES

(1) H. Fijuita, *Adv. Polymer Sci.*, **3**, 1 (1961).

(2) B. Idson, *J. Pharm. Sci.*, **64**, 901 (1975).

(3) J. Crank and G. S. Park, "Diffusion in Polymers," Academic, New York, N.Y., 1968, p. 15.

(4) J. Crank and G. S. Park, *Trans. Faraday Soc.*, **45**, 240 (1949).

(5) R. J. Scheuplein and L. J. Morgan, *Nature (London)*, **214**, 456 (1966).

(6) J. Crank "The Mathematics of Diffusion," 2nd ed., Oxford University Press, Oxford, 1975, p. 191.

(7) I. H. Blank, R. J. Scheuplein, and P. J. MacFlane, *J. Invest. Dermatol.*, **49**, 582 (1967).

(8) M. Wu, *J. Soc. Cosmet. Chem.*, **33**, 85 (1982).

(9) R. J. Scheuplein and I. H. Blank, *Physiol. Rev.*, **51**, 702 (1971).

High-Performance Liquid Chromatographic Assay for Etomidate in Human Plasma: Results of Preliminary Clinical Studies Using Etomidate for Hypnosis in Total Intravenous Anesthesia

MICHAEL J. AVRAM ˣ, ROBERT J. FRAGEN, HARRY W. LINDE

Received July 19, 1982, from *Northwestern University Medical School, Department of Anesthesia, Chicago, IL 60611.* Accepted for publication November 2, 1982.

Abstract □ A sensitive and specific high-performance liquid chromatographic assay was developed for the measurement of etomidate in human plasma following extraction of the drug and the internal standard. Using 0.5-ml aliquots of plasma, the assay was linear in the concentration range of 20–2000 ng of etomidate/ml of plasma. This method was used to evaluate a preliminary clinical study of an etomidate infusion regimen for hypnosis in a total intravenous anesthesia protocol in 23 patients. The average duration of the infusion was 30 min, and awakening and alertness occurred 20 and 36 min after the termination of the infusion, respectively, at the respective plasma concentrations of 297 and 214 ng/ml. These results and this assay will be used to design and evaluate an improved etomidate infusion regimen.

Key phrases □ Etomidate—high-performance liquid chromatography, human plasma, infusion, hypnosis in total intravenous anesthesia □ Hypnotic agents—etomidate, infusion, hypnosis in total intravenous anesthesia, high-performance liquid chromatography, human plasma □ High-performance liquid chromatography—etomidate, human plasma, infusion, hypnosis in total intravenous anesthesia

Etomidate, a carboxylated imidazole, is an hypnotic agent which rapidly produces sleep after intravenous administration (1) and has only a minimal and transient effect on respiration (2) and no effect on cardiovascular stability (3). Etomidate is primarily metabolized in the liver by ester hydrolysis to the inactive carboxylic acid (4, 5). Recovery of consciousness is rapid due to both redistribution and metabolism of the drug (6). These properties suggest that an etomidate infusion would be suitable for the maintenance of hypnosis in a totally intravenous anesthesia regimen.

Several methods for the measurement of etomidate in plasma have been reported, but these use instrumentation that may not be readily available and require the extraction of relatively large volumes of plasma. The method of Wynants *et al.* (7) uses GC with an alkali flame ionization detector (AFID) and is sensitive to 10 ng/ml but requires the extraction of 3 ml of plasma. Van Hamme *et al.* (8) reported a GC–MS assay that is sensitive to 1 ng/ml using extracts of 1–4 ml of plasma. Sensitivity to 5 ng/ml was achieved by De Boer *et al.* (9) using capillary GC with an nitrogen–phosphorus detector. A GC–AFID method was also developed by Haring *et al.* (10) which requires the extraction of only 1 ml of plasma, but is sensitive to only 30 ng/ml.

It was the purpose of the present study to develop a simple yet sensitive high-performance liquid chromatographic (HPLC) method for measuring plasma etomidate concentrations. This method was then used to measure the plasma etomidate concentrations in blood samples obtained during an infusion of etomidate for hypnosis in a totally intravenous anesthesia regimen and up to 6 hr postinfusion. The resulting plasma concentration *versus* time curves were then used to evaluate the infusion protocol and determine the plasma etomidate concentrations at awakening and alertness under the conditions of the anesthetic.

EXPERIMENTAL

Reagents—Etomidate sulfate [*R*-(+)-ethyl 1-(α-methylbenzyl)imidazole-5-carboxylate sulfate], propoxate hydrochloride [*R*-(+)-propyl 1-(α-methylbenzyl)imidazole-5-carboxylate hydrochloride], *R*-(+)-1-(α-methylbenzyl)imidazole-5-carboxylic acid, mandelic acid, and hippuric acid were used as received[1]. All organic solvents were LC[2] or analytical[3] grade. The sulfuric acid, ammonium hydroxide, sodium hydroxide, and sodium borate were analytical grade[4].

Instrumentation—Plasma etomidate concentrations were measured using a constant-flow HPLC system consisting of a solvent delivery system[5], a universal injector[6], a radial compression separation unit[7] liquid chromatography cartridge and cartridge insert packed with 10-μm CN resin[8], and a fixed-wavelength UV detector fitted with a 254-nm wavelength kit[9]. The chromatograms were recorded, the peaks were identified and integrated, and the concentrations were reported on the basis of the internal standard area ratio method by a reporting integrator[10].

Extraction—Five-milliliter blood samples were obtained by syringe through a 16-gauge polytef catheter, previously inserted in an arm vein in each patient, at appropriate time intervals (described below) and transferred to heparinized blood collection tubes[11]. The plasma samples were removed after centrifugation of the blood for 10 min at 2000 rpm and stored at −30° until extracted in duplicate according to a modification of the procedures of Wynants *et al.* (7) and Van Hamme *et al.* (8).

A 500-μl aliquot of plasma, 50 μl of a 3.423-μg/ml ethanolic solution of propoxate hydrochloride and 100 μl of 0.05 *M* borate buffer (pH 10) were added to a conical centrifuge tube and mixed. This mixture was extracted twice with 3.0 ml of hexane–ether (9:1, v/v) by mixing for 5 min on a slowly rotating mixer. The mixtures were centrifuged for 5 min at 2000 rpm, and the hexane–ether layers were transferred to a conical centrifuge tube containing 3.0 ml of 0.5 *M* H_2SO_4 and mixed for 5 min. The mixture was centrifuged for 5 min at 2000 rpm, and the hexane–ether layer was removed and discarded. The acidic aqueous extract was washed with 3.0 ml of hexane–ether for 5 min; the mixture was centrifuged for 5 min at 2000 rpm and the hexane–ether layer was removed and discarded. The acid extract was made basic by adding 1 ml of 3 *M* NH_4OH. This solution was extracted with 4 ml of methylene chloride, and then centrifuged for 5 min at 2000 rpm. The organic phase was evaporated to dryness under reduced pressure at 30° [12], and the residual material was reconstituted with 100 μl of methanol; 15 to 30 μl was injected into the HPLC. Recovery was evaluated by comparing the etomidate–propoxate area ratios for standards containing 2000, 200, and 20 ng of etomidate

[1] Courtesy of Janssen Pharmaceutica, Beerse, Belgium.
[2] Waters Associates, Milford, Mass.
[3] Mallinckrodt, Inc., Paris, Ky.
[4] Mallinckrodt, Inc. or J. T. Baker, Phillipsburg, N.J.
[5] Waters Associates Model M-45.
[6] Waters Associates Model U6K.
[7] Waters Associates Model RCM-100.
[8] Waters Associates Radial-PAK CN and CN Guard-PAK.
[9] Waters Associates Model 440.
[10] Model 3390A; Hewlett-Packard, Avondale, Pa.
[11] Model A3206KA; Becton, Dickinson and Co., Rutherford, N.J.
[12] Model R-110; Buchi/Brinkmann, Westbury, N.Y.

0022-3549/83/1200-1424$01.00/0

(as the base)/ml of plasma in which the internal standard solution was added after the extraction to those in which it was added before the extraction.

Chromatography—The HPLC system was as described above; the mobile phase was methanol–water (54:46) delivered at 1.8 ml/min. The etomidate concentrations, in terms of free base, were determined by the internal standard area ratio method.

The linearity, accuracy, and precision of the assay were assessed by the measurement of the etomidate concentration of replicate plasma standards made by adding known amounts of etomidate from stock solutions to blank human plasma. These plasma standards contained 20, 50, 100, 200, 500, 1000, and 2000 ng/ml of etomidate as the base.

Clinical Study—Twenty-three women scheduled to have minor gynecologic surgery, but otherwise in good health, participated in this institutionally approved study after giving informed consent. The patients were premedicated with morphine sulfate (0.1 mg/kg im) 60–90 min prior to induction of anesthesia. An intravenous infusion of 5% dextrose in Ringer's lactate was started through a 20-gauge polytef catheter into a large vein of the arm opposite that used for blood sampling; drugs were administered intravenously through this tubing at the injection site closest to the catheter. Three to five minutes prior to the induction of anesthesia, fentanyl (100 μg iv) and droperidol (2.5 mg iv) were administered. Anesthesia was induced with 0.3 mg/kg of etomidate (a 2-mg/ml solution in propylene glycol) administered intravenously over 1 min. Maintenance of hypnosis was accomplished with a continuous intravenous infusion of 0.1% etomidate (1 ml of a 125-mg/ml etomidate solution in 10% ethyl alcohol diluted to 125 ml with 0.9% NaCl or 5% dextrose in water) by an infusion pump at a rate 0.1 mg/kg/min for the first 10 min then at 0.01 mg/kg/min for the remainder of the anesthesia. Further analgesia was provided, when necessary, using fentanyl (50 μg iv). Pancuronium was given, when necessary, to facilitate tracheal intubation and for muscle relaxation and was reversed at the end of the operation by pyridostigmine (10 mg iv) and glycopyrrolate (0.4 mg iv). Patients were ventilated with oxygen or oxygen-enriched air.

The times to awakening and alertness were determined as the time from discontinuing the etomidate infusion to the time the patients responded to verbal stimuli and the time the patients were oriented in time and place, respectively. Once they were alert, they were asked to attempt to arise and walk beside their bed every 15 min until they were able to walk unaided for a distance of ~2 m.

Blood samples were obtained 1, 2, 5, 10, 15, 30, and 45 min into the etomidate infusion and 5, 10, 15, 30, 45, 60, 75, 90, 120, 180, 240, and 360 min postinfusion. Plasma etomidate concentrations at awakening and alertness were determined, when necessary, by interpolation of the plasma concentration *versus* time curves for each patient. The elimination half-life was determined by a log-linear regression analysis of the plasma concentration *versus* time relationship during the elimination phase.

RESULTS AND DISCUSSION

Chromatographic Assay—Chromatograms of extracts of the 2000-ng/ml and the 20-ng/ml plasma etomidate standards are illustrated in Fig. 1. The carboxylic acid metabolities of etomidate eluted in <1.2 min, well before the esters etomidate and propoxate, and therefore did not interfere with the assay. None of the drugs administered concomitantly in the present protocol were found to interfere with the assay.

The accuracy and precision of the HPLC technique was evaluated by measuring the concentration of etomidate in spiked plasma standards six times each over the period of a week (Table I). A linear regression analysis of the standard etomidate concentrations from 20 to 2000 ng/ml *versus* etomidate–propoxate area ratios verified the linearity of the extracted standard curve ($r = 0.999$; $y = 267.9x + 3.5$). The average recoveries for four replicate samples at 2000, 200, and 20 ng/ml were 82.4, 82.6, and 82.4%, respectively.

Clinical Study—The average (±*SD*) age and weight of the patients were 35 (±10) years and 64 (±12) kg, respectively. No patient complained of pain on injection and no signs of venous irritation were observed. All patients fell asleep rapidly, remained asleep throughout the operation, and had no recall of operative events. Mild, almost imperceptible, myoclonia occurred at induction in two patients, but lasted less than 15 sec in each case. There were no clinically significant side effects during maintenance, and changes in blood pressure and heart rate occurred only in relation to the administration of other drugs and surgical stimulation. Awakening was complicated in six patients by the desire to turn to the lateral position, muscle twitching, restlessness, or hypertonus in the period between first awakening and complete alertness. Postoperative nausea or vomiting was observed in four patients.

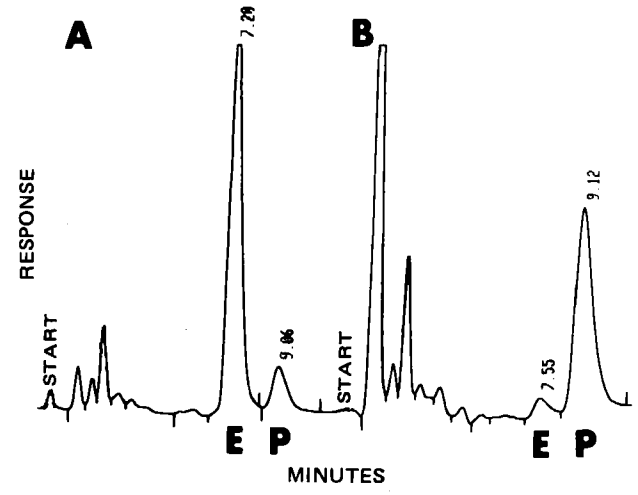

Figure 1—*Chromatograms of etomidate (E) standards extracted from blank plasma with the internal standard propoxate (P). Key: (A) plasma sample containing 2000 ng of etomidate/ml; (B) plasma sample containing 20 ng of etomidate/ml. The retention times for the peaks are as indicated.*

Table I—Accuracy and Precision for the Plasma Etomidate Assay [a]

Etomidate Added, ng/ml	Etomidate Measured, ng/ml [b]	Mean Error, ng/ml	Relative Error, %	*CV*, %
20	23.6 ± 3.2	3.6	18.	13.6
50	53.0 ± 4.1	3.0	6.0	7.7
100	102.5 ± 8.5	2.5	2.5	8.3
200	205.6 ± 6.5	5.6	2.8	3.2
500	494.7 ± 11.1	5.3	1.1	2.2
1000	984.0 ± 36.0	16.0	1.6	3.7
2000	2008.0 ± 51.0	8.0	0.4	2.5

[a] $n = 6$. [b] Mean ± *SD*.

A typical plasma etomidate concentration *versus* time curve during and after the infusion is shown in Fig. 2, and pertinent clinical results for the 23 patients are listed in Table II. The average length of anesthesia in these patients was 30 (±26) min, and they awoke at an average of 20 (±9) min after the end of the etomidate infusion. The mean plasma etomidate concentration on awakening was 297 (±74) ng/ml; Schüttler

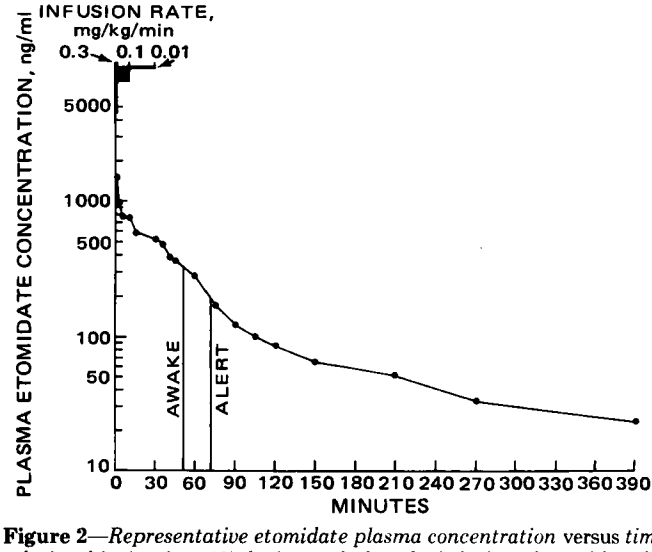

Figure 2—*Representative etomidate plasma concentration* versus *time relationship (patient 10) during and after the infusion of etomidate for hypnosis in total intravenous anesthesia. The rates and duration of the infusion as well as the times of and plasma concentrations at awakening and alertness are indicated.*

Table II—Time and Plasma Etomidate Concentrations at the End of the Infusion, Awakening, and Alertness and Elimination Half-Life of Etomidate

Patient	Age, year	Weight, kg	Infusion		Awakening		Alertness		Elimination Half-Life, hr
			Duration, min	Plasma Conc. at End, ng/ml	Postinfusion Time, min	Plasma Conc., ng/ml	Postinfusion Time, min	Plasma Conc., ng/ml	
1	26	50	46	473	8	280	25	195	1.1
2	27	57	22	650	15	424	40	290	4.2
3	32	54	24	584	28	240	58	155	2.7
4	29	74	18	1178	12	410	42	200	—[a]
5	46	63	22	430	19	310	26	270	3.5
6	32	68	18	897	24	390	39	270	—[a]
7	25	57	23	303	6	210	7	190	—[a]
8	27	56	45	448	15	200	18	170	5.0
9	27	60	18	528	12	310	22	220	4.7
10	29	54	31	525	21	310	41	190	2.6
11	29	70	136	509	34	170	—[a]	—[a]	—[a]
12	44	74	14	2948	22	350	52	170	1.9
13	32	60	45	411	18	220	25	160	6.2
14	32	67	49	282	21	220	51	145	3.3
15	30	50	42	540	16	300	26	270	2.0
16	45	61	18	521	10	338	25	180	—[a]
17	44	85	18	1091	13	370	25	270	1.0
18	41	61	17	625	15	235	30	180	—[a]
19	27	52	22	729	26	375	44	270	2.9
20	28	56	25	1152	33	370	41	310	2.9
21	41	58	10	2885	25	265	36	215	3.4
22	65	90	15	1572	38	220	43	210	3.0
23	46	90	20	1020	39	310	72	170	5.5
Mean (±*SD*)	35 (±10)	64 (±12)	30 (±26)	883 (±718)	20 (±9)	297 (±73)	36 (±15)	214 (±50)	3.3 (±1.5)

[a] —Not determined.

et al. (11), using the analytical method of Wynants *et al.* (7), found the minimal plasma etomidate concentration producing an hypnotic effect to be ~300 ng/ml. The patients were alert an average of 36 (±15) min after the end of the etomidate infusion, and this was associated with an average plasma etomidate concentration of 214 (±50) ng/ml. The patients were able to walk unaided for ~2 m an average of 87 (±29) min following the termination of the infusion. The elimination half-life was 3.3 (±1.5) hr, which is longer than that of Schüttler *et al.* (11) but shorter than that of Van Hamme *et al.* (12). The patients generally remained drowsy for 4–6 hr after leaving the recovery room.

While these results demonstrate that anesthesia can be satisfactorily accomplished with an etomidate infusion and bolus injections of fentanyl, droperidol, and pancuronium, the present protocol is not optimal. An etomidate infusion regimen for hypnosis in totally intravenous anesthesia should be designed to maintain plasma concentrations above the awakening concentration while avoiding dose-related side effects and keeping awakening time under 10 min regardless of the duration of anesthesia. This could theoretically be accomplished using the plasma etomidate data of the present study and the etomidate pharmacokinetic data from the intravenous bolus study of Van Hamme *et al.* (12). The HPLC method reported here could then be easily used to evaluate such a designed infusion regimen.

REFERENCES

(1) J. M. Gooding and G. Corssen, *Anesth. Analg.*, **55**, 286 (1976).

(2) M. Morgan, J. Lumley, and J. G. Whitwam, *Br. J. Anaesth.*, **49**, 233 (1977).

(3) J. M. Gooding and G. Corssen, *Anesth. Analg.*, **56**, 717 (1977).

(4) J. J. P. Heykants, W. E. G. Meuldermans, L. J. M. Michiels, P. J. Lewi, and P. A. J. Janssen, *Arch. Int. Pharmacodyn.*, **216**, 113 (1975).

(5) M. M. Ghoneim and M. J. Van Hamme, *Anesthesiology*, **50**, 227 (1979).

(6) G. De Ruiter, D. T. Popescu, A. G. De Boer, J. B. Smeekens, and D. D. Breimer, *Arch. Int. Pharmacodyn.*, **249**, 180 (1981).

(7) J. Wynants, R. Woestenborghs, and J. Heykants, "A Gas Chromatographic Assay Method for Etomidate in Human Plasma," Biological Research Report R 26,490/13, Janssen Research Products Information Service, Janssen Pharmaceutica, B-2340 Beerse, Belgium, Dec. 1974.

(8) M. J. Van Hamme, J. J. Ambre, and M. M. Ghoneim, *J. Pharm. Sci.*, **66**, 1344 (1977).

(9) A. G. De Boer, J. B. Smeekens, and D. D. Breimer, *J. Chromatogr.*, **162**, 591 (1979).

(10) C. M. M. Haring, I. C. Dijkhuis, and B. van Dijk, *Acta Anaesthesiol. Belg.*, **31**, 107 (1980).

(11) J. Schüttler, M. Stoeckel, M. Wilms, H. Schwilden, and P. M. Lauwen, *Anaesthesist*, **29**, 662 (1980).

(12) M. J. Van Hamme, J. J. Ambre, and M. M. Ghoneim, *Anesthesiology*, **49**, 274 (1978).

ACKNOWLEDGMENTS

This study was supported in part by a grant from Janssen R&D, Inc.

The authors wish to thank Mohammad R. Majlessi for his excellent technical support, Peggy J. Collins for her assiduous clerical assistance, and Janssen Pharmaceutica for generously providing samples of the pure standard.

Effect of Inorganic Additives on Solutions of Nonionic Surfactants V: Emulsion Stability

HANS SCHOTT ˣ and ALAN E. ROYCE

Received June 14, 1982 from the *School of Pharmacy, Temple University, Philadelphia, PA 19140.* Accepted for publication October 7, 1982.

Abstract □ Electrolytes often break emulsions to which they were added as active ingredients, adjuvants, or impurities. The stability of oil-in-water emulsions containing octoxynol 9 NF as the emulsifier and various added electrolytes was investigated by measuring droplet size, turbidity, and oil separation on storage at various temperatures and in a centrifugal field at 25°. Electrolytes were added to hexadecane emulsions after emulsification (direct addition); alternatively, hexadecane was emulsified in octoxynol 9–electrolyte mixtures (reverse addition). Xylene emulsions were prepared by direct addition only. Hexadecane emulsions containing 0.10% octoxynol 9 were considerably more stable than xylene emulsions containing 0.60% because the surfactant is practically insoluble in hexadecane, but miscible in all proportions with xylene. An emulsifier soluble in the disperse phase as well as the continuous phase evidently forms less stable interfacial films. The electrolytes investigated were sulfuric and hydrochloric acids, magnesium nitrate, and aluminum nitrate, which salt octoxynol 9 in by complexation between its ether groups and their cations; sodium thiocyanate, which salts the surfactant in by destructuring water; and sodium chloride and sodium sulfate, which salt octoxynol 9 out. The addition of these electrolytes at concentrations up to 2 or 3 *m* to hexadecane emulsions produced fast and extensive creaming, little or no flocculation, no coalescence, and only minor changes in droplet size or turbidity on storage at room temperature. The extent of coalescence during centrifugation was actually reduced by the additives. Such stability is unusual. Droplet size and turbidity depended mainly on octoxynol 9 concentration. The greatest decrease in the former and increase in the latter occurred when the concentration was increased from 0.10 to ~0.4%. All emulsions became slightly coarser on storage at 25°. Stability at 50° was impaired by aluminum nitrate and magnesium nitrate and to a lesser extent by sodium sulfate and sodium chloride. Reverse-addition emulsions differentiated better between the electrolytes than direct-addition emulsions. Electrolytes salting octoxynol 9 in, especially by complexation, generally produced the finest and most stable emulsions. Similarly, xylene emulsions were destabilized more by the electrolytes which salted the emulsifier out than by those salting it in. Centrifugation of hexadecane emulsions at 7800×*g* compressed the creamed emulsion layer into a plug of clear, transparent, isotropic gel from which coalesced hexadecane separated slowly on further centrifugation. These semisolid gels contained the hexadecane as discrete, uncoalesced droplets because, on immersion in water or octoxynol 9 solutions with or without electrolytes, they turned opaque, liquefied, and redispersed spontaneously into emulsions of nearly the same average droplet size as the original emulsions.

Keyphrases □ Hexadecane—emulsions with octoxynol 9, stability, effect of added electrolytes □ Xylene—emulsions with octoxynol 9, stability, effect of added electrolytes □ Stability—of hexadecane and xylene emulsions with octoxynol 9, effect of added electrolytes □ Emulsions—hexadecane with octoxynol 9, xylene with octoxynol 9, stability, effect of added electrolytes

The principal effect of electrolytes on aqueous solutions of polyoxyethylated nonionic surfactants consists of salting in or salting out, depending on whether the electrolyte increases or decreases the solubility of the surfactants, raising or lowering their cloud points. Electrolytes in the first category contain either cations capable of forming complexes with the ether groups of the polyoxyethylated moiety of the nonionic surfactants, or large and polarizable anions that break the hydrogen-bonded structure of water. All di- and trivalent cations, plus the hydronium and lithium cation, form complexes with model ethers and increase the solubility of polyoxyethylated surfactants by complexation (1, 2). Only salts of sodium, potassium, ammonium, tetramethylammonium, and cesium tend to salt out the surfactants (1–4) because these cations do not form complexes with the ether oxygen atoms.

Large anions that break the structure of water include iodide, thiocyanate (4, 5), and perchlorate (2) as well as the guanidinium cation (6). Depolymerization of water increases the hydration of the ether linkages of the surfactants through hydrogen bonding by disrupting the hydrogen bonds among the water molecules (1, 2). The salt effects of the anions are in agreement with the Hofmeister or lyotropic series (4).

Salts are frequently incorporated into emulsions for a variety of purposes or occur as impurities. The objective of the present work was to investigate how salting-in and salting-out electrolytes affect the stability of oil-in-water emulsions prepared with a nonionic polyoxyethylated emulsifier. The main variables to be investigated were surfactant concentration, nature and concentration of the electrolytes, temperature, and order of addition. The range of electrolyte concentrations was extended to the high values at which the surfactant is extensively salted in or out.

The surfactant, octoxynol 9, was selected because it is a monograph in the National Formulary and because its interactions with electrolytes have been investigated extensively with regard to cloud point (1–3, 5), micelle formation, and surface properties (7). Moreover, it is used commercially as an emulsifying and suspending agent and as a detergent for hard surfaces and skin.

EXPERIMENTAL

Materials—The surfactant, octoxynol 9 NF[1], is a branched octylphenol with an average of 9–10 ethylene oxide units. It is a viscous, anhydrous liquid with a hydrophilic–lipophilic balance (HLB) of 13.4 and a critical micelle concentration of 0.16 g/liter at 25°.

The oils used were hexadecane[2] and xylene[3]. The electrolytes were ACS reagent grade. The water was double distilled. Electrolyte concentrations are expressed as molality (*m*); the concentrations of oil and octoxynol 9 are expressed as percent (w/w) based on the weight of the water present in the solutions and emulsions as 100%. Thus, a 5.00% octoxynol 9 solution or emulsion contains 5.00 g of octoxynol 9 in 100 g of water.

Emulsification—In the direct-addition procedure, the electrolytes were added in the final stage. Preliminary coarse emulsions containing 50% oil were made in 100-g batches, as illustrated for a hexadecane emulsion with a 0.10% octoxynol 9 content: 1.40 g of a 5.00% octoxynol 9 solution, 65.29 g of water, and 33.31 g of hexadecane were added in this order to a tall-form 200-ml beaker. The octoxynol 9 solution was at least 2 days old to ensure full hydration. The mixture was stirred for 20 min at 30-V input with a mixer equipped with two counter-rotating propel-

[1] Triton X-100, Rohm & Haas Co., Philadelphia, Pa.
[2] Practical grade, Eastman Organic Chemicals.
[3] Purified, J. T. Baker Chemicals.

0022-3549/83/1200-1427$01.00/0

Table I—Effect of Octoxynol 9 Concentration, Storage Temperature, and Emulsion Age on Mean Droplet Size and Specific Turbidity of Hexadecane–Water Emulsions

Emulsion No.	Octoxynol 9 Concentration, %(w/w)	Storage Temperature, °	Emulsion Age, days	D_a[a], μm	D_{vs}[b], μm	$\frac{\tau/C^c}{10^{-3}\text{ cm}}\left(\frac{\text{g of diluted emulsion}}{\text{g of hexadecane}}\right)$
			Direct Addition			
1	0.10	25	0	3.29	5.28	8.05
2	0.10	25	9	3.47	5.26	8.01
3	0.10	25	30	—	—	7.81
4	0.10	25	64	3.49	5.50	7.73
5	0.10	37	22	3.65	5.17	—
6	0.15	25	4	2.26	3.55	13.8
7	0.20	25	1–2	1.96	2.97	15.0
8	0.20	25	7	2.13	3.41	14.6
9	0.20	25	46	2.52	3.57	14.8
10	0.20	50	8	2.26	3.53	14.8
11	0.30	25	6	1.31	2.53	16.2
12	1.0	25	0	0.93	2.21	18.0
			Reverse Addition			
13	0.10	25	1	1.71	3.77	14.9
14	0.10	25	11	2.01	3.42	14.4
15	0.10	25	22	2.40	4.33	14.1
16	0.10	25	57	—	—	13.5

[a] Arithmetic mean diameter. [b] Mean volume-surface diameter defined by Eq. 1. [c] Specific turbidity, derived from Eq. 2.

lers[4]. The stirring conditions were selected because higher speeds and/or longer agitation caused foaming while lower speeds produced coarser droplets. The emulsion was further comminuted by passing it three times through a stainless steel hand-operated homogenizer[5], applying maximum tension to the spring. The second and third pass did not substantially reduce the mean droplet size, but improved the reproducibility.

The finished emulsion was prepared by mixing weighed amounts of a 5.00% aqueous octoxynol 9 solution, water, aqueous electrolyte solution, and homogenized emulsion to give the desired composition. The surfactant concentration was the same, for instance, 0.10%, in the preliminary and the finished emulsion. The oil content was 25% for most finished hexadecane and all finished xylene emulsions. Most hexadecane emulsions contained 0.10 or 0.20% octoxynol 9. Since the xylene emulsions were intrinsically less stable, their octoxynol 9 content was 0.60%. The preliminary coarse xylene emulsions made with the counter-rotating mixer contained, therefore, 8.37 g of a 5.00% octoxynol 9 solution, 58.43 g of water, and 33.20 g of xylene.

The reverse-addition procedure was used for hexadecane emulsions only. The order of mixing of the ingredients was as follows: 5.00% octoxynol 9 solution, water, and aqueous electrolyte solution to give a solution containing 0.10% octoxynol 9 and the desired electrolyte molality. This solution was stored at room temperature for at least 2 days prior to the addition of hexadecane and emulsification. The preliminary coarse emulsion was made in 100-g batches containing 25% hexadecane by stirring for 20 min at 30-V input with the counter-rotating mixer. The emulsification was completed by three passes through the hand-operated homogenizer.

Storage—To characterize the emulsions, various measurements were made on aliquots withdrawn at regular intervals. During the period of investigation, most emulsion samples were stored at 25 ± 0.5°. A few were stored at 50 ± 1°.

Visual Observation of Coalescence—Some xylene emulsions were so unstable that they separated visible amounts of clear oil at room temperature. For quantitative comparison, 55-g emulsion samples were stored in milk-test Babcock bottles; the volume of xylene separated after various storage times at 25° was calculated from its height in the neck.

Higher coalescence rates at elevated temperatures were measured for xylene or hexadecane emulsions by weighing 20- to 23-g emulsion samples into stoppered 25-ml graduated cylinders, immersing the cylinders into constant-temperature baths, and recording the volume of clear oil separated as a function of time. All emulsions used for measuring coalescence rates at elevated temperatures or in a centrifuge at room temperature, which contained 25% hexadecane or xylene, were prepared by direct addition.

Droplet Size Measurements—The method used for microscopic measurements of droplet size is described in a separate publication (8). Prior to the measurements, the emulsions were diluted ~600-fold, using either an octoxynol 9 solution of the same concentration as the emulsion, which was thickened with polyvinyl alcohol, or a warm gelatin solution, which gelled on cooling.

Turbidity Measurements—Emulsions containing 25% hexadecane were opaque. Transmittance was measured as a function of hexadecane concentration after diluting the emulsions to varying degrees. Dilutions, which usually ranged from 200- to 2000-fold, were made with octoxynol 9 solutions having the same surfactant concentration as the emulsions. Emulsions were diluted immediately before measuring their transmittance.

Transmittance measurements were made with a double-beam spectrophotometer[6] and 1-mm quartz cells. Even though the emulsions were "white," their transmittance varied with the wavelength. Unless otherwise specified, the wavelength used was 475 nm.

Centrifugation—The stability of hexadecane emulsions was studied by centrifugation at 25° and 10,000 rpm or 7800× the acceleration of gravity (g) for 65 min, using a thermostated centrifuge[7]. The glass tubes used had a capacity of 12 ml and an inside diameter of 12.5 mm. They were filled with an amount of emulsion containing 1.80 g of hexadecane, which ranged from 9 to 11 g.

Centrifugation separated the emulsions into four layers, which were (from bottom to top) a clear aqueous solution, a white opaque viscous layer of creamed emulsion a few millimeters thick, a clear gel layer with a thickness of up to 18 mm, and a layer of clear hexadecane a few millimeters thick. The tubes were stoppered and stored in a vertical position at 25°. On standing, the gel reverted gradually and almost completely to a white opaque cream over a 15-hr period, separating small amounts of clear hexadecane. The creamed emulsion layer continued to bleed additional small amounts of clear hexadecane for a few hours after the disappearance of the gel. When the oil separation was essentially complete, the clear hexadecane was aspirated quantitatively and weighed. Storage times after emulsification were, therefore, 17–24 hr for emulsions with 0.10% octoxynol 9 and 48 hr for emulsions with 0.20%. Results are expressed as percent hexadecane separated, based on the 1.80 g present in the emulsion samples placed in the centrifuge tubes.

Xylene emulsions, being less stable, were centrifuged at speeds of only 4000–5000 rpm for only 15–30 min to distinguish the effects of different additives. Even though only small amounts of clear gel formed, the centrifuged emulsions were stored for 24 hr at 25° prior to separating and weighing the coalesced xylene.

[4] Brookfield counter-rotating mixer, Brookfield Engineering Laboratories, Stoughton, Mass.

[5] Emulsion homogenizer, Arthur H. Thomas Co., Philadelphia, Pa.

[6] Coleman Model 124.

[7] Beckman Model J-21 preparative centrifuge, equipped with a fixed-angle rotor Type JA-20.

RESULTS

Droplet Size from Microscopic Measurements—Droplet sizes were measured in incremental intervals of 1 μm. The data were used to determine the droplet size distributions. The average droplet sizes were represented by the arithmetic mean diameter, D_a, and the mean volume–surface diameter, D_{vs}:

$$D_{vs} = \sum N_i D_i^3 \Big/ \sum N_i D_i^2 \qquad \text{(Eq. 1)}$$

where D_i is the diameter equal to the midpoint of the ith size interval and N_i the number of droplets in that interval.

The mean volume–surface diameter is inversely related to the specific surface area of the emulsion sample. For a given sample, it is larger than the arithmetic mean diameter because each droplet contributes to the latter only in proportion to the first power of its diameter. The mean volume–surface diameter is influenced to a greater extent by larger droplets and, hence, reflects more effectively increases in droplet size than the arithmetic mean diameter (9).

Table I lists the effects of various experimental variables on the mean droplet size of hexadecane emulsions in the absence of additives. The most influential variable was octoxynol 9 concentration. When it was increased from 0.10 to 0.30%, the D_a and D_{vs} values of freshly prepared emulsions decreased by 61 and 53%, respectively. Another approximately threefold increase in concentration, from 0.30 to 1.0% octoxynol 9, reduced the mean diameters by only 29 and 13%, respectively. Plots of average droplet size *versus* octoxynol 9 concentration level off at ~0.4% (Fig. 1).

Aging of the emulsions at room temperature or at 37° or 50° produced minor, but consistent, increases in droplet size (compare emulsions 1–5 and 7–10). The reverse-addition procedure resulted in smaller droplet sizes than direct addition. This fact is to be expected because, during the preliminary emulsification and the homogenization, the ratio of octoxynol 9 to hexadecane was twice as large in the reverse-addition procedure. Moreover, in the reverse addition, as opposed to direct addition, the entire volume of the emulsion was subjected to homogenization. Furthermore, all emulsions, regardless of the volume fraction of oil, were quite fluid: their relative viscosities were only ~2. Therefore, the shear stress during homogenization of the direct-addition emulsion, which at that point had twice the hexadecane concentration as the reverse-addition emulsion, was not substantially greater. A few hexadecane–water emulsions prepared by direct addition but containing 10% hexadecane had mean diameters comparable with standard 25% hexadecane emulsions prepared under identical conditions.

The purpose of this investigation was to compare the effect of various salting-in and salting-out electrolytes on emulsion stability. Therefore, electrolytes were employed at concentrations corresponding to comparable salting-in and salting-out efficiencies. When their solubilities permitted, the effect of salting-out electrolytes was compared at concentrations at which they lowered the cloud point of octoxynol 9 by 35° in the absence of hexadecane, *i.e.*, from 65° to 30°. Such a concentration is 0.40 *m* for sodium sulfate and 2.20 *m* for sodium chloride.

The effect of salting-in electrolytes was investigated mainly at concentrations at which they raised the cloud point of octoxynol 9 by 30° in the absence of hexadecane. These concentrations are 3.0 *m* for sulfuric and hydrochloric acids and 1.80 *m* for sodium thiocyanate (1). The corresponding magnesium nitrate concentration, 4.25 *m*, is too close to the solubility limit, so this salt was studied at 2.00 *m*. Higher and lower concentrations for all electrolytes were also investigated.

The effect of electrolytes is described first for emulsions stored at 25°. Comparison of the average diameters in Tables I and II illustrates two surprising facts. All hexadecane emulsions were remarkably stable towards electrolytes, even at 1–3 *m* concentrations. Neither salting-in nor salting-out electrolytes produced major changes in droplet size.

Since most emulsions became slightly but consistently coarser on aging, the average diameters were compared for emulsions of approximately the same age. When examining the effect of additives, emulsions were always compared at equal octoxynol 9 concentrations since this was the most important factor affecting droplet size.

For a few emulsions prepared by direct addition, electrolytes actually produced smaller droplets than blank emulsions without additives. For instance, emulsions 17–20 with added electrolytes have smaller D_a and D_{vs} values than emulsion 1 (blank). For most emulsions, the changes in droplet size produced by various additives were minor. The following emulsions have nearly identical values for D_a and D_{vs}, respectively: 6 (blank) and 23 and 24; 7 (blank) and 36, 39, 41, 44, 52, and 59; 8 (blank) and 27, 29, 34, 37, 45, 50, and 55; and 11 (blank) and 62 and 63.

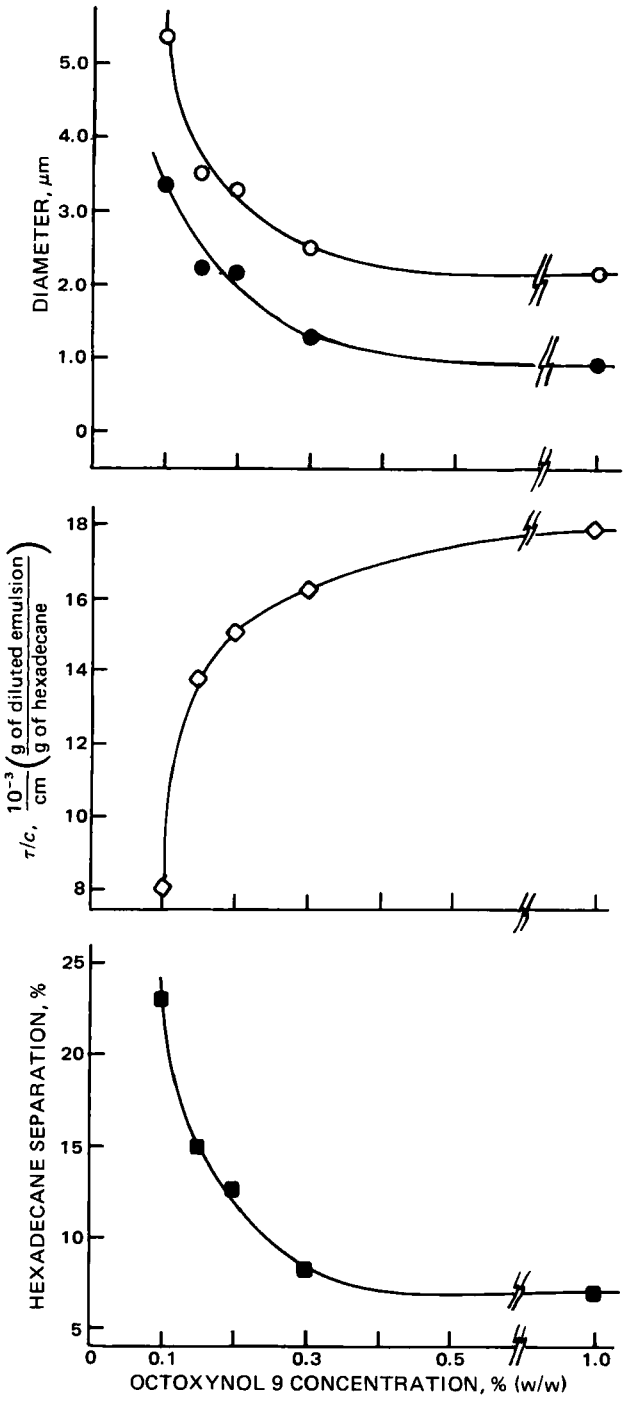

Figure 1—*Effect of octoxynol 9 concentration on mean volume–surface diameter, D_{vs}, arithmetic mean diameter, D_a, specific turbidity, τ/C, and hexadecane separation in the centrifuge. Key: (○) D_{vs}; (●) D_a; (◇) τ/C; (■) hexadecane separation.*

Where additives were investigated at several concentrations, no consistent trend of either increasing or decreasing average droplet sizes with increasing additive concentration are noticeable. This observation holds for the salting-in additives hydrochloric acid (compare emulsions 26, 28, 30, 33, and 36; 27, 29, 31, 34, and 37; and 32, 35, and 38), aluminum nitrate (compare emulsion 39 with 41 and 40 with 43), and magnesium nitrate (compare emulsion 44 with 47 and 46 with 48) as well as for the salting-out additives sodium chloride (compare emulsions 49, 52, and 54; also 51, 53, and 56) and sodium sulfate (compare emulsion 57 with 59).

The difference between the effect of salting-in and salting-out electrolytes on droplet size are clear-cut only in the case of emulsions prepared by reverse addition. Emulsions containing the salting-in complexing electrolytes sulfuric acid and magnesium nitrate had about the

Table II—Effect of Additives on Droplet Size and Specific Turbidity of Hexadecane–Water Emulsions Stored at 25°

Emulsion No.	Octoxynol 9 Concentration, %(w/w)	Additive	Additive Concentration, m	Emulsion Age, days	D_a[a], μm	D_{vs}[b], μm	τ/C[c], 10^{-3} (g of diluted emulsion / g of hexadecane) / cm
			Direct Addition				
17	0.10	H_2SO_4	3.00	0	2.51	4.52	6.89
18		NaSCN	1.50	0	2.74	5.27	7.72
19		NaCl	2.20	0	2.54	4.97	—
20		Na_2SO_4	0.40	0	2.64	4.67	7.77
21				56	—	—	6.53
22				167	3.16	5.06	—
23	0.15	H_2SO_4	3.00	4	2.36	3.68	13.8
24		Na_2SO_4	0.40	4	2.30	3.66	13.8
25	0.20	H_2SO_4	3.00	5	1.97	4.05	14.7
26		HCl	0.10	2	2.44	3.60	15.8
27				9	2.06	3.31	15.3
28			0.50	2	2.62	3.75	16.3
29				9	2.12	3.68	16.3
30			1.00	1	1.51	3.52	15.4
31				9	1.52	3.49	15.3
32				50	2.30	3.94	—
33			2.00	1	1.51	3.21	15.7
34				9	2.40	3.60	15.4
35				50	2.69	4.15	—
36			3.00	1	2.03	3.33	14.7
37				9	2.26	3.44	14.6
38				46	2.31	3.50	14.0
39		$Al(NO_3)_3$	0.50	1	1.94	2.98	16.0
40				48	2.42	3.54	15.6
41			1.40	1	1.90	2.89	14.9
42				9	2.02	2.95	14.8
43				46	2.41	3.15	14.6
44		$Mg(NO_3)_2$	0.50	1	2.05	3.25	14.9
45				9	2.22	3.27	14.9
46				46	2.26	3.35	—
47			2.00	1	1.88	3.09	15.5
48				48	2.37	3.65	15.5
49		NaCl	0.50	1	1.68	2.89	15.7
50				9	2.14	3.46	15.2
51				50	2.74	3.76	—
52			1.20	1	1.94	3.54	15.6
53				48	2.60	3.68	—
54			2.20	1	1.65	2.99	15.5
55				9	2.26	3.71	—
56				50	2.75	4.01	—
57	0.20	Na_2SO_4	0.20	2	2.24	3.45	16.1
58				9	2.39	3.46	16.2
59			0.40	1	1.89	3.19	15.7
60				5	1.91	3.18	15.5
61				48	2.45	3.67	14.2
62	0.30	H_2SO_4	3.00	6	1.35	2.58	16.6
63		Na_2SO_4	0.40	6	1.67	2.88	16.4
64	1.00	H_2SO_4	3.00	3	1.88	2.72	17.9
65				17	2.09	3.16	17.4
66		Na_2SO_4	0.40	3	2.33	2.98	17.7
67				17	2.41	3.09	—
			Reverse Addition				
68	0.10	H_2SO_4	3.00	1	1.67	4.14	7.9
69		$Mg(NO_3)_2$	2.00	1	1.74	3.79	11.2
70				11	1.97	4.30	10.6
71			3.00	1	1.88	2.98	13.6
72		NaSCN	1.50	1	1.91	4.03	11.7
73				11	2.19	5.11	11.0
74		NaCl	2.20	1	2.37	4.08	9.9
75				11	2.86	4.31	9.1
76		Na_2SO_4	0.40	1	2.55	5.16	8.5
77				11	2.61	5.33	7.4
78				63	—	—	6.4

[a] Arithmetic mean diameter. [b] Mean volume–surface diameter defined by Eq. 1. [c] Specific turbidity, derived from Eq. 2.

same D_a and D_{vs} values, respectively, as emulsions without additives [compare emulsion 13 (blank) with 68, 69, and 71; and 14 (blank) with 70].

The two salting-out electrolytes sodium chloride and sodium sulfate produced coarser emulsions by reverse addition than the blanks [compare emulsions 13 (blank) with 74 and 76; and 14 (blank) with 75 and 77]. Sodium thiocyanate, which salts in octoxynol 9 by destructuring water, had an intermediate effect on droplet size (compare emulsions 13 with 72 and 14 with 73).

Emulsions stored above room temperature were gently inverted nearly once a day to redisperse the creamed layer throughout the entire volume. Mean droplet diameters are listed in Table III. As was observed for emulsions prepared by direct addition stored at 25°, both salting-in and salting-out additives produced only minor changes in droplet size [compare emulsions 2 and 4 (blanks) with 79 and 80; also 10 (blank) with 81–95]. Storage at 50° for 22 days (not listed in Table III) resulted in only slightly larger droplet sizes than storage for 7–9 days, with D_a increasing, on the average, 14% and D_{vs} 8%.

Table III—Effect of Additives on Droplet Size and Specific Turbidity of Hexadecane–Water Emulsions Prepared by Direct Addition and Stored at Elevated Temperatures

Emulsion No.	Octoxynol 9 Concentration, %(w/w)[a]	Additive	Additive Concentration, m	Emulsion Age, days	D_a[b], μm	D_{vs}[c], μm	τ/C[d], 10^{-3} cm (g of diluted emulsion / g of hexadecane)
79	0.10 (37°)	H_2SO_4	3.00	22	3.45	5.62	—
80		Na_2SO_4	0.40	22	4.56	6.00	—
81	0.20 (50°)	HCl	0.10	9	1.83	2.82	15.7
82			0.50	9	2.20	3.17	16.1
83			1.00	7	1.95	2.96	15.9
84			2.00	7	1.98	3.22	16.0
85			3.00	7	2.34	3.59	14.8
86		$Al(NO_3)_3$	0.50	7	1.84	2.79	16.1
87			1.40	7	2.12	3.20	14.7
88		$Mg(NO_3)_2$	0.50	7	2.36	3.17	14.8
89			2.00	7	2.13	3.52	15.9
90		Na_2SO_4	0.20	9	2.58	3.52	15.9
91			0.40	7	2.35	3.27	15.7
92				42	—	—	12.7
93		NaCl	0.50	7	2.40	3.55	15.5
94			1.20	7	2.18	3.36	15.6
95			2.20	7	2.13	3.34	14.7

[a] Storage temperature in parentheses. [b] Arithmetic mean diameter. [c] Mean volume–surface diameter defined by Eq. 1. [d] Specific turbidity, derived from Eq. 2.

However, prolonged storage at 50° led to partial coalescence for all emulsions containing 0.20% octoxynol 9, ranging from <5% of the amount of emulsified hexadecane for emulsions without additives and those containing hydrochloric acid or sodium thiocyanate to 25–50% for emulsions containing aluminum nitrate within 250 days (see below).

Most xylene emulsions containing 0.60% octoxynol 9 underwent detectable coalescence within a few days at room temperature, separating at least traces of clear xylene. Moreover, they coalesced considerably on dilution with water. Therefore, xylene emulsions were not characterized by microscopic droplet size measurements.

Turbidity—To include any submicroscopic droplets that may have been present, microscopic droplet size measurements were supplemented by turbidity determinations. Turbidity, τ, is the inverse of the light path length, L, that reduces the intensity of a beam of light to $1/e$ of its original value by scattering or absorption (10):

$$\tau = \frac{\ln(I_0/I_{tr})}{L} \qquad \text{(Eq. 2)}$$

The light intensities I_0 and I_{tr} refer to the incident and transmitted beams, respectively. The turbidities of hexadecane–water emulsions were thus calculated from the measured transmittance values by dividing the natural logarithm of the reciprocal of the transmittance by the path length, which was 0.1 cm.

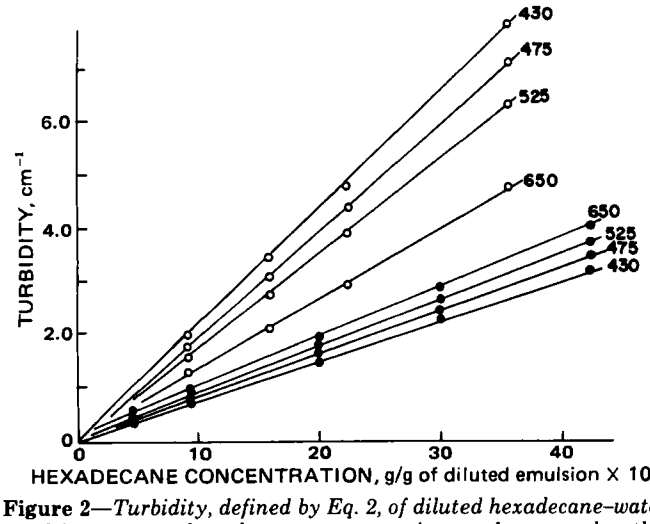

Figure 2—*Turbidity, defined by Eq. 2, of diluted hexadecane–water emulsions* versus *hexadecane concentration at four wavelengths. Numbers on lines designate wavelengths in nanometers. Key: (●) 0.10% octoxynol 9; (○) 1.00% octoxynol 9.*

Plots of turbidity *versus* hexadecane concentration, C, expressed as g of hexadecane/g of diluted emulsion, were straight lines going through the origin. Their slopes equal the specific turbidity, τ/C, expressed in units of (1/cm) (g of diluted emulsion/g of hexadecane). The specific turbidity is, thus, formally analogous to absorptivity, the difference being that the former includes light scattering and absorption whereas the latter, which refers to solutions, involves light absorption only (11).

Specific turbidities were generally calculated from transmittance values at five concentrations by linear regression as the slope of the straight line passing through the origin. Standard deviations of the slope (12) usually ranged from 0.4 to 3%.

At constant oil concentration, smaller droplet sizes result in more opaque emulsions. The specific turbidity is inversely proportional to the mean volume–surface droplet diameter (11, 13, 14) and can be used to assess the effect of additives on the latter.

Figure 2 contains plots of turbidity measured at four wavelengths *versus* hexadecane concentration for two 2-month-old emulsions without additives which were diluted immediately before the transmittance determinations. The upper set of curves represents an emulsion with 1.00% octoxynol 9 (D_{vs} = 2.21 μm) and the lower set represents an emulsion with 0.10% octoxynol 9 (D_{vs} = 5.28 μm). The slopes of the two sets of curves, representing specific turbidity, have the opposite wavelength dependence. The coarser emulsion scattered red light (650 nm) more strongly than violet (430 nm); the specific turbidities increased from violet to blue (475 nm) to green (525 nm) to red. The finer emulsion scattered violet light more strongly than red; the specific turbidities increased from red to green to blue to violet light.

Such a reversal of the wavelength dependence of turbidity is not uncommon. Plots of the total scattering coefficient (K) or of extinction *versus* the droplet size parameter ($\alpha = \pi nD/\lambda$) are sinusoidal (11, 13, 14). In that expression, n is the refractive index of the continuous phase and λ is the wavelength of the light. Hence, for some droplet size ranges, light scattering and turbidity increase as the wavelength increases (a descending branch of the K–α plot). For others, K increases with decreasing λ (an ascending branch).

The reason for selecting blue as the wavelength for subsequent transmittance measurements was that the ratio of the specific turbidities of the two additive-free emulsions containing 1.00 and 0.10% octoxynol 9, respectively, obtained with blue light approaches most closely the inverse ratio of their mean volume–surface diameters. The inverse D_{vs} ratio is 5.28/2.21 = 2.39. The specific turbidity ratios are 1.38, 1.96, 2.37, and 2.84 for red, green, blue, and violet light, respectively. The theoretical inverse D_{vs}–τ/C relationship in the range of droplet sizes encountered in the present work is, thus, most closely obeyed for turbidities measured with the blue light (λ = 475 nm).

It was not possible to measure the transmittance of xylene emulsions. Dilution with an octoxynol 9 solution having the same concentration as the emulsion, namely, 0.60%, reduced the size and number of droplets through micellar solubilization. This octoxynol 9 concentration exceeded the critical micelle concentration almost 40-fold and xylene, as opposed

Table IV—Effect of Additives on the Coalescence of Oil–Water Emulsions Prepared by Direct Addition

Additive	Additive Concentration, *m*	Time to Separate Listed Fraction of Oil Present: Xylene[a] 25°[c] 25%[d]	25°[c] 50%[d]	40°[c] 25%	40°[c] 50%	45°[c] 25%	45°[c] 50%	50°[c] 25%	50°[c] 50%	Hexadecane[b] 98°[c] 25%[d]	98°[c] 50%
—	—	[e]		[f,g]		11.5 day[f]	14 day	[f]		104 min	7.9 hr
NaCl	1.20	24 day	—	4.4 min	5.9 min						
	2.20	4 hr	12 hr	3.8 min	4.0 min	1.2 min	1.6 min	1.1 min	1.5 min	14.1 min	18.0 min
Na_2SO_4	0.20	17 day	—	4.5 min	5.0 min	2.0 min	2.2 min	1.6 min	1.8 min		
	0.40	23 hr	10 day							1.8 min	2.2 min
HCl	1.00	[e]		15.0 min	22.8 min	4.9 min	7.5 min	2.7 min	3.2 min		
	3.00	[e]						3.1 min	3.6 min	103 min	3.6 hr
$Mg(NO_3)_2$	2.00	[e]		18 hr	3 day	57 min	4.0 hr	10.3 min	39.2 min	5.4 min	6.5 min
$Al(NO_3)_3$	1.20	[e]				11 min	55 min	5.6 min	7.7 min	4.9 min	8.2 min
NaSCN	1.50	[e]		62 day[f]	77 day	6.3 hr	25 hr	8.0 min	15.3 min	104 min	5.7 hr

[a] Emulsions contained 0.60% octoxynol 9. [b] Emulsions contained 0.20% octoxynol 9. [c] Storage temperature. [d] Volume of oil separated as clear supernatant under the influence of gravity, expressed as percent of the 25% oil present in emulsion. [e] No oil separation in 24–26 days. [f] Approximately 5% of the oil separated in 17–19 hr. [g] Less than 10% of the oil separated in 80 days.

to hexadecane, is solubilized extensively. Dilution of the xylene emulsions with water resulted in coalescence.

The conclusions derived from the turbidity measurements are similar to those from droplet size determinations, although the inverse proportionality between τ/C and D_{vs} was not always exactly obeyed. The exceptions were caused by changes in droplet size distribution, possibly involving submicroscopic droplets.

The most important factor determining specific turbidity was octoxynol 9 concentration. The major increase in τ/C with increasing surfactant concentration took place at <0.4% (Table I, Fig. 1). Aging produced small, but consistent, decreases in τ/C.

The addition of salting-in and salting-out electrolytes alike produced only minor changes in specific turbidity for emulsions prepared by direct addition. Major differences were observed for emulsions prepared by reverse addition, where emulsions without additives had the highest τ/C values. These values were considerably higher than the τ/C values of direct-addition emulsions without additives having the same 0.10% octoxynol 9 level; they were practically identical with those of direct-addition emulsions containing 0.20% octoxynol 9 (compare emulsion 13 with 1 and 7, and 14 with 2 and 8 in Table I). The near equality of the specific turbidities of the direct-addition blank emulsions containing 0.20% octoxynol 9 and the reverse-addition blank emulsions containing 0.10% octoxynol 9 is ascribed to the fact that both types had the same ratio of octoxynol 9 to hexadecane during the preliminary emulsification and homogenization.

Among the emulsions prepared by reverse addition, those without additives had the highest specific turbidities. Emulsions with sodium thiocyanate and magnesium nitrate (emulsions 69, 71, and 72) had intermediate values, while the remaining additives produced lower specific turbidities that were still larger than those of the corresponding emulsions prepared by direct addition.

Coalescence on Storage—Hexadecane emulsions prepared by direct addition containing 0.20% octoxynol 9 and all additives at the levels listed in Tables III–V were completely stable on storage for 8 months at 25°. Despite extensive creaming, resulting in the separation of concentrated emulsion layers above practically clear aqueous phases, no coalesced hexadecane could be detected. Gentle inversion of the containers readily redispersed the creamed layers, reconstituting intact and uniform emulsions.

Hexadecane emulsions stored at 50° separated cream layers that were viscous. In some samples, coalesced oil became evident after 42 days and more oil separated during the following 80–90 days. During an additional 120–130 days at 50°, the amount of coalesced oil increased only slightly except for emulsions containing aluminum nitrate, which already underwent extensive coalescence during the first 126-day period and which separated substantially more oil subsequently.

The emulsions are ranked below in order of increasing stability. Percentages in parentheses following the formula of the additive represent approximate volumes of coalesced hexadecane, expressed as percent of the total volume of hexadecane in the sample, observed after 126 ± 5 or 250 ± 5 days storage at 50°. When two percentages are listed, the first refers to hexadecane separated after 126 days, the second to separation after 250 days; single percentage values indicate that coalescence did not increase noticeably between 126 and 250 days. Absence of percentage values indicates that, while some hexadecane did coalesce in 126 and 250 days, it amounted to <5%. The ranking on storage at 50° is: 1.40 *m* $Al(NO_3)_3$ (30%, 50%) < 0.50 *m* $Al(NO_3)_3$ (20%, 25%) < 2.00 *m* $Mg(NO_3)_2$ (15%) < 0.50 *m* $Mg(NO_3)_2$ (12%) = 0.50 *m* NaCl (12%) < 0.40 *m* Na_2SO_4 (10%) < 0.20 *m* Na_2SO_4 (8%) < 1.20 *m* NaCl (<5%, 10%) < 2.20 *m* NaCl = blank = 0.10, 0.50, 1.00, 2.00, and 3.00 *m* HCl = 1.50 *m* NaSCN.

Hexadecane emulsions immersed in boiling water were unstable (Table IV). Those without additives, with hydrochloric acid, and with sodium thiocyanate coalesced more slowly than those containing sodium sulfate, aluminum nitrate, magnesium nitrate, and sodium chloride.

Xylene emulsions, despite their higher octoxynol 9 content, had considerably shorter shelf lives than hexadecane emulsions at comparable temperatures. The latter were more stable at 98° than the former at 50°. All four salting-in electrolytes investigated (hydrochloric acid, sodium thiocyanate, magnesium nitrate, and aluminum nitrate) destabilized the xylene emulsions only moderately compared with the blank while both salting-out electrolytes (sodium chloride and sodium sulfate) accelerated their coalescence considerably (Table IV).

Centrifugation Studies—The highest centrifugal speed that the glass tubes could withstand was 10,000 rpm or 7800×*g*. At that speed, 65 min provided optimum discrimination between the variables. Shorter periods, 30 or 45 min, separated smaller amounts of coalesced hexadecane and increased the coefficients of variation. Centrifugation periods of 2 or 4 hr increased the amounts of coalesced hexadecane without enhancing the differences between additives.

The separation of hexadecane did not follow zero-, first-, or second-order kinetics (15) nor the Vold–Mittal empirical equation (16). Therefore, the data presented in Table V are merely the amounts of hexadecane coalesced after 65 min centrifugation, expressed as percent of the total weight of hexadecane in the tube.

When the amount of emulsion containing 25% hexadecane (based on the weight of water) was increased from 7 to 8.5 and to 10 g in preliminary experiments, the percent coalesced hexadecane separated after 65 min centrifugation remained constant for blank emulsions and for emulsions containing each of the various additives. Despite this observation, the measurements presented in Table V were standardized by weighing into each centrifuge tube an amount of emulsion containing 1.80 g of hexadecane.

The driving force that promotes creaming of the emulsions, compression of most of the oil phase into a clear gel layer, and coalescence and separation of oil is directly proportional to the difference in density between the continuous aqueous phase and the oil droplets (10). Hence, at comparable acceleration, the centrifugal force is considerably greater when the aqueous phase is a concentrated and dense electrolyte solution than when no electrolytes were added to the water. To compensate for the increased buoyancy of the oil droplets in dense electrolyte solutions, the percent hexadecane separated (5th column of Table V) was multiplied by the factor $(d_{water} - d_{cetane})/(d_{salt} - d_{cetane})$, where d_{water}, d_{cetane}, and d_{salt} represent the 25° densities of water, of hexadecane (0.771), and of the aqueous electrolyte solutions, respectively. Neglecting the effect of octoxynol 9 on the densities changed the factor by <1%. The corrected hexadecane separation (last column of Table V) shows the intrinsic effects of electrolytes on emulsion stability. This correction generally magnified the trends produced by the various electrolytes shown in the 5th column.

Higher octoxynol 9 concentrations reduced the oil separation because they produced finer emulsions. At comparable octoxynol 9 concentrations, emulsions containing sodium sulfate separated somewhat less

Table V—Effect of Additives and of Octoxynol 9 Concentration on Coalescence of Hexadecane–Water Emulsions in a Centrifugal Field

Octoxynol 9 Concentration, %	Additive	Additive Concentration, *m*	Emulsion Age, days[a]	Hexadecane Separation, %[b]	*N*[c]	Corrected Hexadecane Separation, %[d]
			Direct Addition			
0.10	—	—	0	23.1 ± 1.6	16	23.1
			30	24.3	2	24.3
			153	24.3	2	24.3
	Na_2SO_4	0.005	0	19.3 ± 0.9	6	19.2
		0.10	0	20.6 ± 1.6	8	18.8
		0.20	0	22.4 ± 1.0	8	20.2
		0.40	0	19.2 ± 0.8	8	15.8
			68	19.8	2	16.3
			118	20.7	2	17.0
			153	55.6	2	45.7
	NaCl	0.010	0	23.6	2	23.6
		0.50	0	14.1	2	13.0
		1.50	0	14.1	2	11.2
		1.75	0	16.3	2	12.6
			133	17.1	2	13.2
		2.20	0	19.9	2	14.6
		2.95	0	26.2	2	17.8
	H_2SO_4	0.001	0	23.2	2	23.2
		0.01	0	19.6	2	19.5
		0.10	0	15.7 ± 1.0	6	15.2
		1.00	0	12.1 ± 0.9	4	9.6
		2.00	0	9.0 ± 0.4	4	6.0
		3.00	0	7.3 ± 0.4	7	4.3
		5.00	0	4.5	2	2.2
0.10	HCl	0.002	0	20.7	2	20.7
		0.01	0	16.9 ± 0.2	4	16.8
		1.00	0	15.6 ± 0.5	4	14.4
		2.00	0	15.4 ± 0.4	4	13.4
		3.00	0	15.8 ± 0.8	8	13.0
		4.00	0	14.7	2	11.5
		6.00	0	13.8	2	9.9
	$Mg(NO_3)_2$	0.05	0	13.0	2	12.7
		0.10	0	11.1	2	10.5
		1.50	0	2.7	2	1.6
		2.00	0	5.2 ± 0.2	4	2.8
	NaSCN	0.01	0	26.5 ± 0.7	4	26.4
		0.50	0	13.2 ± 0.9	6	12.1
		1.50	0	14.1 ± 0.6	12	11.2
		3.00	0	14.9 ± 1.0	6	10.1
0.15	—	—	3	15.0	2	15.0
0.20	—	—	1–2	12.7 ± 0.8	10	12.7
			7–8	13.0 ± 1.0	8	13.0
			43	16.1 ± 1.1	4	16.1
			7–8*	15.4 ± 0.7	4	15.4
			43*	17.7 ± 0.8	4	17.7
	Na_2SO_4	0.20	1	9.9 ± 0.7	4	8.9
			7	9.3 ± 0.6	4	8.4
			7*	9.8 ± 0.7	4	
		0.40	8	7.9 ± 0.5	4	6.5
			43	8.8 ± 0.5	4	7.2
			8*	12.4 ± 0.5	4	
			43*	29.5 ± 0.6	4	
0.20	NaCl	0.50	8	8.5 ± 0.4	8	7.8
			43	10.9 ± 0.5	4	10.0
			8*	8.7 ± 0.3	4	
			43*	11.8 ± 0.5	4	
		1.20	8	9.1 ± 0.5	8	7.5
			43	10.4 ± 0.9	4	8.6
			8*	10.5 ± 0.7	4	
			43*	13.0 ± 0.5	4	
		2.20	8	9.1 ± 0.4	8	6.8
			43	10.6 ± 0.1	4	7.8
			8*	18.0 ± 1.0	4	
			43*	20.1 ± 1.1	4	
	HCl	0.50	7	6.0 ± 0.4	8	5.8
			7*	6.9 ± 0.5	4	
		1.00	7	4.3	2	4.0
			43	5.5 ± 0.3	12	5.1
			43*	7.6 ± 0.5	8	
		2.00	8	2.5 ± 0.3	4	2.2
			43	4.6 ± 0.3	4	4.0
			8*	5.6 ± 0.4	4	
			43*	8.9 ± 0.5	4	
	$Mg(NO_3)_2$	0.50	43	9.1 ± 0.8	4	7.4
			43*	10.1 ± 0.6	4	
		2.00	6	3.6	2	2.0
			43	3.8 ± 0.2	4	2.1
			43*	4.6 ± 0.4	4	
	$Al(NO_3)_3$	0.50	6	2.9 ± 0.3	3	2.2
			43	3.3 ± 0.3	8	2.5
			43*	9.2 ± 0.6	4	
		1.40	7	3.9	2	2.1
			43	5.2 ± 0.4	4	2.8
			43*	10.1 ± 0.7	4	
0.30	—	—	3	8.2 ± 0.5	3	8.2
			Reverse Addition			
0.10	—	—	0	16.0 ± 0.9	4	16.0
			11	17.4 ± 1.1	3	17.4
			57	18.6 ± 0.8	3	18.6
	Na_2SO_4	0.40	0	29.8	2	24.5
			11	33.0	2	27.1
			63	40.1	2	33.0
	NaCl	2.20	0	25.0 ± 1.2	4	18.4
			27	35.9 ± 1.3	3	26.4
			63	37.8 ± 1.0	3	27.8
	H_2SO_4	3.00	0	30.0 ± 1.4	4	17.5
	$Mg(NO_3)_2$	2.00	0	21.1 ± 0.6	3	11.4
			11	34.3 ± 2.6	3	18.6
			24	38.0 ± 1.8	3	20.6
		3.00	0	32.6 ± 2.3	3	15.1
	NaSCN	1.50	0	13.3 ± 1.1	4	10.6
			11	14.2 ± 1.2	3	11.3
			62	18.5 ± 1.3	3	14.7

[a] Stored at 25° unless marked by asterisk, indicating storage at 50°. [b] Weight of coalesced hexadecane, expressed as percent of the 1.80 g of hexadecane present per tube, ± SD. [c] Number of measurements. [d] See text for density correction.

hexadecane than emulsions without additives. The extent of hexadecane separation first decreased somewhat and then increased with progressively higher concentrations of sodium chloride at the 0.10% octoxynol 9 level. At the 0.20% level, no significant changes in hexadecane separation were observed beyond 0.50 *m* NaCl.

The salting-in electrolytes lowered the hexadecane separation significantly compared with emulsions without electrolytes of comparable octoxynol 9 concentration, especially those electrolytes which form complexes with octoxynol 9, namely, sulfuric and hydrochloric acids and magnesium and aluminum nitrates. Higher concentrations of these electrolytes resulted in considerably lower hexadecane separation. Only a few percent hexadecane was separated at the highest concentrations of these electrolytes (Table V): 5.00 *m* H_2SO_4, 2.00 *m* HCl only with 0.20% octoxynol 9, 1.50 or 2.00 *m* $Mg(NO_3)_2$, and 0.50 or 1.40 *m* $Al(NO_3)_3$ almost completely prevented coalescence of hexadecane at 7800×*g*. Sodium thiocyanate, which salts in octoxynol 9 by destructuring water, reduced coalescence only slightly.

Aging the emulsions at 25° prior to centrifugation caused small but significant increases in hexadecane separation. Aging at 50° generally produced more extensive separation.

Emulsions without added electrolytes prepared by direct addition separated more hexadecane on centrifugation than emulsions of comparable octoxynol content prepared by reverse addition, in keeping with their smaller droplet size. The presence of all electrolytes except sodium thiocyanate increased the separation of hexadecane during the centrifugation of emulsions prepared by reverse addition when compared with the corresponding emulsions without additives. The salting-out electrolytes sodium chloride and sodium sulfate increased the hexadecane

Table VI—Low-Speed Centrifugation of Xylene–Water Emulsions

Additive	Additive Concentration, *m*	Xylene Separated, %[a]	*N*[b]	Corrected Xylene Separation, %[d]
—	—	0.8 ± 0.2	4	0.8
Na_2SO_4	0.20	19 ± 3	4	17
	0.40[c]	71 ± 3	4	58
NaCl	2.20[c]	80	2	59
HCl	2.00	3.2 ± 0.8	4	2.8
	3.00	4.8 ± 0.7	4	4.0
$Mg(NO_3)_2$	2.00	0.05	2	0.03
$Al(NO_3)_3$	1.40	0.3	2	0.2
NaSCN	1.50	7.6	2	6.0

[a] Weight of coalesced xylene, expressed as percent of the 1.80 g of xylene present per tube, ± SD. [b] Number of measurements. [c] Appreciable separation before centrifugation. [d] See text for density correction.

separation somewhat more for reverse-addition emulsions than for those prepared by direct addition. The major difference between the two types of emulsions occurred with the salting-in complexing electrolytes sulfuric acid and magnesium nitrate, which slightly increased the oil separation during centrifugation of the reverse-addition emulsions while strongly reducing the oil separation of the direct-addition emulsions.

The xylene emulsions employed in the low-speed centrifugation studies of Table VI contained 0.60% octoxynol 9 and were prepared by direct addition. After aging for 30 min at 25°, emulsion quantities containing 1.80 g of xylene were centrifuged for 30 min at 5000 rpm or 1960×*g*. Centrifugation of emulsions containing salting-in complexing electrolytes (hydrochloric acid, magnesium nitrate, and aluminum nitrate) produced a slight amount of clear gel, while the bulk of the emulsified droplets collected in an opaque creamed layer. The other emulsions produced no clear gel at all. Despite this observation, all centrifuged emulsions were stored for 24 hr at 25° prior to removing and weighing the coalesced xylene.

The differences between the effects of the various types of electrolytes during the centrifugation of xylene emulsions were pronounced. Sodium sulfate and sodium chloride, the salting-out electrolytes, caused extensive coalescence. Of the electrolytes which salt the surfactant in by complexation, magnesium nitrate and aluminum nitrate reduced the xylene coalescence even further than the already small extent observed for emulsions without additives, while hydrochloric acid increased it somewhat. Sodium thiocyanate, which salts octoxynol in by destructuring water, caused more extensive coalescence, but still considerably less than the salting-out electrolytes.

Freeze–Thaw Cycles—This technique was not well suited for studying the stability of emulsions containing high concentrations of electrolytes because they creamed rapidly before freezing and because the electrolytes lowered the freezing point of the aqueous phase considerably. Reproducible results were difficult to obtain even when agitating the emulsions while freezing them in a dry ice–acetone mixture. After one freeze–thaw cycle, thawed hexadecane emulsions containing only 0.10% octoxynol 9 were more opaque than emulsions also containing 0.40 *m* Na_2SO_4 or 3.00 *m* H_2SO_4, but the differences between the latter two were only minor. No significant amounts of coalesced hexadecane were observed in any of the thawed emulsions.

DISCUSSION

Shelf Stability—Emulsion stability can be defined in terms of three phenomena: creaming or clearing; flocculation or aggregation; and demulsification, coalescence, or breaking (17). Because of the high density of many of the aqueous electrolyte solutions employed, most emulsions used in this study creamed rapidly. The droplets in the concentrated cream layer preserved their identity, however, and gentle agitation redispersed them throughout the aqueous phase with no change in their size distribution.

Flocculation, another possible measure of instability, was moderate even in the presence of high electrolyte concentrations. By contrast, emulsions stabilized with ionic surfactants are prone to extensive flocculation even at comparatively low electrolyte concentrations, which may lead to coalescence. Instability, as used here, refers to the irreversible coalescence of small droplets into larger drops, resulting eventually in the separation of a clear layer of oil.

Nature of Oil Phase—Hexadecane emulsions prepared by direct addition with high concentrations of salting-in as well as salting-out electrolytes were unusually stable. The differences between the effects of the two types of electrolytes were only minor. Hexadecane emulsions prepared by reverse addition showed some discrimination between electrolytes. Salting-in electrolytes operating through complexation with the ether groups of octoxynol 9 generally increased the emulsion stability, salting-out electrolytes decreased it, while sodium thiocyanate, which salts octoxynol 9 in by destructuring water, was intermediate.

Xylene emulsions prepared by direct addition were considerably less stable than hexadecane emulsions even at a sixfold higher octoxynol 9 level. The electrolyte effects were more pronounced, but qualitatively similar to those observed with reverse-addition hexadecane emulsions.

The large difference in the stability of xylene and hexadecane emulsions based on octoxynol 9 is ascribed to the difference in solubility of the surfactant in the two hydrocarbons. Xylene and octoxynol 9 are miscible in all proportions. The solubility of octoxynol 9 in hexadecane at 25°, determined spectrophotometrically at 277 nm, was ~1.4% (w/v). This value is an upper limit because of the polydispersity of the surfactant and the likelihood that the species with the lowest degree of ethoxylation, *i.e.*, with the highest concentration of the absorbing phenyl group, have the highest solubility in hexadecane and were preferentially extracted from the bulk octoxynol 9.

The fact that octoxynol 9 is miscible in all proportions with the disperse phase as well as the continuous phase of xylene–water emulsions evidently reduced the stability of the interfacial octoxynol 9 films compared with those in hexadecane–water emulsions, where the surfactant is only slightly soluble in the disperse phase. This cause of emulsion instability is unusual because few surfactants are freely soluble in both water and oils.

In the case of xylene–water emulsions, salting-out electrolytes tend to displace octoxynol 9, including the octoxynol 9 forming the interfacial film surrounding the droplets, into the xylene phase. Thereby, these electrolytes were effective in breaking the emulsions. In the case of hexadecane–water emulsions, salting-out electrolytes can displace octoxynol 9 only as far as the hexadecane–water interface, thereby possibly increasing the thickness of the interfacial film. Such a stabilizing effect is probably offset, at least in part, by reduced hydration of the polyoxyethylene moiety of the adsorbed octoxynol 9 film, compressing that film and reducing its effectiveness as a barrier against coalescence. These considerations do not account for the effect of salting-in electrolytes on emulsion stability.

Stabilization Mechanisms and Salt Effects—Nonionic surfactants stabilize aqueous dispersions primarily by steric interactions (18) between the polyoxyethylene moieties of adsorbed surfactant molecules. Electrostatic repulsion plays, at best, a minor role even in the absence of electrolytes (19, 20). At the high and swamping electrolyte concentrations employed in this study, electrostatic forces are unlikely to make any contribution to emulsion stability. Therefore, surface, interfacial, and bulk properties of aqueous solutions of nonionic surfactants containing various electrolytes are examined below for an explanation of the differences between salting-in and salting-out electrolytes, which were especially noticeable in xylene emulsions and in hexadecane emulsions prepared by reverse addition.

The surface areas of polyoxyethylated surfactant molecules adsorbed at air–water or oil–water interfaces depend mainly on the cross-sectional areas of their randomly coiled polyoxyethylene moieties, which are immersed in the aqueous phase (21). Effects of electrolytes on the surface properties of octoxynol 9 and other nonionic surfactants were relatively small (22). In plots of surface tension *versus* the logarithm of concentration, the negative slopes in the region of saturation adsorption were rendered somewhat steeper by the addition of electrolytes at concentrations up to 3 *m*, corresponding to moderate reductions in the surface area per adsorbed surfactant molecule (7). The monolayers of adsorbed surfactant became more closely packed. Salting-in electrolytes produced somewhat larger decreases in surface area than salting-out electrolytes. The largest decreases, observed with cadmium nitrate and sulfuric acid, were 30% (7).

Salting-in electrolytes increased or decreased the plateau surface tensions above the critical micelle concentration by a few dyne/cm at most, and their effectiveness was unrelated to their capacity to raise cloud points (7). Sodium nitrate in concentrations up to 0.1 *M*, calcium nitrate up to 0.01 *M*, and aluminum nitrate up to 10^{-4} *M* produced only minor changes in the interfacial tension of the system chlorobenzene–water containing 1% or 10% of the homogeneous nonionic surfactant hexaoxyethylene glycol monohexadecyl ether (HLB = 10.4) (23).

These observations, which refer to monolayers of surfactants, do not adequately explain the differences between the effects of salting-in and

salting-out electrolytes on emulsion stability. On the other hand, an effect similar to the salt-induced contraction of the polyoxyethylene coils of octoxynol 9 molecules forming interfacial films was observed in bulk with aqueous solutions of high molecular weight polyethylene oxides. Their intrinsic viscosity was reduced by cloud-point-depressing electrolytes, indicating a contraction of their hydrodynamic volume[8] (24). Weaker cloud-point depressants produced smaller reductions in intrinsic viscosity (24), while salting-in electrolytes actually increased the intrinsic viscosity[8].

Another approach to interpreting the effects of electrolytes is in terms of steric stabilization. Steric stabilization of emulsions requires that the free energy change of the overlap interaction between the polyoxyethylene moieties of the surfactant molecules adsorbed on two approaching droplets be positive. The resulting repulsion may overcome the attraction due to London–van der Waals forces (18). The steric repulsion caused by interpenetration of the adsorbed surfactant layers can be ascribed to an entropic (volume restriction) effect due to a decrease in the conformational entropy of the polyoxyethylene chains and/or to a heat of mixing or osmotic effect (18).

It has been suggested that the increase in the heat of hydration and of mixing caused by salts such as sodium thiocyanate, which salt in nonionic surfactants by destructuring water, results in an increase in the enthalpic contribution to the steric barrier against coalescence (25). Electrolytes which salt in octoxynol 9 by complex formation between their cations and the ether groups are likely to cause an increase in the excess osmotic pressure arising from the overlap of the polyoxyethylene layers of two approaching droplets. An equivalent concept is that these electrolytes increase the positive value of the second virial coefficient of aqueous polyoxyethylene solutions, thereby increasing the repulsion between the polyoxyethylene layers surrounding the droplets (*cf.* Eq. 57 of Ref. 18).

The difference in the effects of salting-in and salting-out electrolytes on the stability of hexadecane emulsions prepared by direct and reverse addition indicates that the interfacial octoxynol 9 films were profoundly affected by the order of addition. This behavior, while not unusual in systems that are intrinsically unstable, is not readily explained by steric stabilization. If the interfacial octoxynol 9 film consisted of multilayers, the observed effects could be ascribed to the formation of a liquid crystalline phase at the hexadecane–water interface (26).

In this connection, it is of interest to estimate the thickness of the layer of octoxynol 9 adsorbed at the surface of the hexadecane droplets. The limiting cross-sectional area per octoxynol 9 molecule adsorbed at the isooctane–water interface is obtained from the bottom curve of Fig. 8 of Ref. 27, which is a plot of the interfacial tension, $\gamma_{O/W}$, *versus* the molar concentration, C_2, of octoxynol 9. The plot is linear from 10^{-5} M to the critical micelle concentration, indicating that saturation adsorption prevailed over that concentration range. The equation of the linear portion, obtained by regression analysis from the data points on the graph, is:

$$\gamma_{O/W} = -31.52 - 4.857 \ln C_2 \qquad \text{(Eq. 3)}$$

Using the value of the slope, $d\ \gamma_{O/W}/d \ln C_2 = -4.857$ in the Gibbs adsorption equation results in an area of 84.7 Å^2 per molecule of adsorbed octoxynol 9 at saturation adsorption, *i.e.*, in a close-packed monolayer.

The standard hexadecane emulsions contained 25 g of hexadecane per 100 g of water. Those with 0.10% octoxynol 9 had $D_{vs} = 5.28 \times 10^{-4}$ cm, which corresponds to an interfacial area of 367,000 cm^2. Assuming that all surfactant molecules in excess of the critical micelle concentration (0.016%) are adsorbed at the oil–water interface, 100 g of a 0.10% octoxynol 9 solution contains 0.084 g of surfactant available for adsorption. This amount covers 686,000 cm^2, *i.e.*, enough for 1.87× a monolayer, or nearly a bilayer of close-packed octoxynol 9 molecules.

The curves in Fig. 1 tend to level off at ~0.4% octoxynol 9, corresponding to $D_{vs} = 2.28$ μm. At that point, the amount of octoxynol 9 present exceeds that needed to cover the emulsion droplets with a close-packed monolayer by a factor of 3.7. This value is approximate because the area per octoxynol 9 molecule in an adsorbed multilayer is unlikely to be the same as that in a monolayer. The surfactant films surrounding the droplets, having a thickness of ~4 molecules, could well form a liquid crystalline interphase which, though birefringent, is too thin to be visible under the microscope between crossed polarizer and analyzer.

[8] Hans Schott, unpublished data.

Centrifugal Stability—The first stage in the centrifugation of common oil–water emulsions is the separation of an opaque creamed layer containing all of the oil droplets from a lower clear aqueous layer. Emulsions containing high electrolyte concentrations cream even on standing.

In high centrifugal fields, such as the 7800×g used here, the spherical oil droplets are probably pressed so close together in the cream layer that they become distorted into polyhedra similar to foams. The centrifugal force then squeezes liquid from the flattened aqueous lamellae separating the oil droplets, which drains through Plateau borders. Coalescence occurs on rupture of the interfacial octoxynol 9 films, resulting in the separation of a clear oil layer (28, 29).

In the course of centrifugation of the hexadecane emulsions, the opaque white cream layer changed within minutes almost completely into a new phase, namely, a transparent gel layer, which propagated from the bottom to the top. Coalescence of hexadecane droplets, resulting in the formation of a clear oil supernatant, occurred slowly from this transparent gel plug.

Despite extensive studies of ultracentrifugation of emulsions by Vold's group (15), Garrett (30), and Rehfeld (31), only brief mention is made (30) of a "translucent cream" above the opaque cream layer. The transparent gel observed in the present work apparently was not detected previously because it is as clear as the coalesced oil and, since it consists of almost pure oil, has almost the same refractive index. The boundary between gel and coalesced hexadecane is faint and becomes evident only to the touch, on separating the layers. Thus, it took a preparative rather than an analytical ultracentrifuge to detect the clear gel.

This gel, unlike the viscous opaque cream layers compacted by centrifugation, had a substantial yield value. Its plastic viscosity was low. Even though the gel consisted mainly of hexadecane, water was the continuous phase. When the centrifuge tubes containing hexadecane emulsions were stored after centrifugation, the clear gel plugs reverted to opaque cream layers as the aqueous phase diffused into them from below.

When pieces of gel were immersed in aqueous solutions, they slowly disintegrated to fluid emulsions. The hexadecane droplets preserved their identity and remained intact in these gels, as shown by the following set of experiments. Gels were prepared by centrifuging standard hexadecane emulsions containing 0.20% octoxynol 9 and either no electrolyte, or 2.00 m HCl, or 0.40 m Na_2SO_4. When these gels were redispersed in aqueous media of the same composition as those of the original emulsions, the mean volume–surface diameters of the reconstituted emulsions were 3.66 μm for the blank, 3.38 μm in 2.00 m HCl, and 4.75 μm in 0.40 m Na_2SO_4. These diameters are only 23, 5, and 49% larger, respectively, than the D_{vs} values of the original emulsions (Table II).

The gels were transparent and isotropic; they showed no birefringence when examined between crossed polarizer and analyzer. The individual oil droplets could not be distinguished under the microscope. These facts indicate that the thickness of the aqueous lamellae separating the distorted hexadecane droplets in the gels was considerably smaller than the wavelength of light. Thus, light passing through the clear gels underwent little or no refraction.

The chief driving force for the penetration of water or of aqueous solutions of octoxynol 9 and electrolytes into the gel plugs, transforming them back into cream layers and eventually redispersing them into dilute emulsions, is probably the osmotic or enthalpic component responsible for the steric stabilization of emulsions. Centrifugation of the cream layers squeezed the aqueous lamellae between distorted, polyhedral oil droplets down to a thickness of a few nanometers, causing compression or interpenetration of the polyoxyethylene moieties of the octoxynol 9 molecules adsorbed on adjacent droplets. The aqueous lamellae thus contained a high concentration of polyoxyethylene chains, *i.e.*, they were hypertonic compared with the bulk aqueous phase. Elastic retractive forces tending to expand the compressed polyoxyethylene chains and interfacial tension tending to restore the spherical droplet shape probably contributed somewhat to the penetration of aqueous media into the gel plugs.

In connection with the osmotic effect, it is significant that gels made from emulsions containing 0.20% octoxynol 9 plus 2.00 m HCl were somewhat more stable than gels formed from emulsions containing octoxynol 9 only, whereas gels from emulsions containing 0.20% octoxynol 9 plus 0.40 m Na_2SO_4 were less stable, separating some hexadecane on standing. The former gels probably had somewhat thicker lamellae than gels prepared from emulsions without electrolytes due to the presence of hydrochloric acid molecules bound to the ether groups of octoxynol 9 forming an oxonium compound. The latter gels probably had thinner aqueous lamellae owing to the salting-out effect of sodium sulfate.

The observation that stability measurements by centrifugation and

by the other methods were not in complete agreement is ascribed to the complex sequence of steps occurring during the former. The correlation between long-term shelf stability of emulsions and their resistance to high-speed centrifugation was not sufficiently good to make the latter a reliable technique for predicting the former (32, 33).

REFERENCES

(1) H. Schott, *J. Colloid Interface Sci.*, **43**, 150 (1973).

(2) H. Schott and S. K. Han, *J. Pharm. Sci.*, **64**, 658 (1975).

(3) W. N. Maclay, *J. Colloid Sci.*, **11**, 272 (1956).

(4) M. J. Schick, *J. Colloid Sci.*, **17**, 801 (1962).

(5) H. Schott and S. K. Han, *J. Pharm. Sci.*, **66**, 165 (1977).

(6) M. J. Schick and A. H. Gilbert, *J. Colloid Sci.*, **20**, 464 (1965).

(7) H. Schott and S. K. Han, *J. Pharm. Sci.*, **65**, 975 (1976).

(8) H. Schott and A. E. Royce, *J. Pharm. Sci.*, **72**, 313 (1983).

(9) G. Herdan, "Small Particle Statistics," 2nd ed., Academic, New York, N.Y., 1960, chap. 4.

(10) K. J. Mysels, "Introduction to Colloid Chemistry," Interscience, New York, N.Y., 1959, chaps. 3 and 20.

(11) H. C. van de Hulst, "Light Scattering by Small Particles," Wiley, New York, N.Y., 1957, chaps. 10, 18, and 19.

(12) W. J. Youden, "Statistical Methods for Chemists," Wiley, New York, N.Y., 1951, chap. 5.

(13) G. F. Lothian and F. P. Chappel, *J. Appl. Chem.*, **1**, 475 (1951).

(14) J. D. S. Goulden, *Trans. Faraday Soc.*, **54**, 941 (1958).

(15) R. D. Vold and M. Maletic, *J. Colloid Interface Sci.*, **65**, 390 (1978), and 7 references cited therein.

(16) R. D. Vold and K. L. Mittal, *J. Soc. Cosmet. Chem.*, **23**, 171 (1972).

(17) R. D. Vold and R. C. Groot, *J. Soc. Cosmet. Chem.*, **14**, 233 (1963).

(18) T. Sato and R. Ruch, "Stabilization of Colloidal Dispersions by Polymer Adsorption," Dekker, New York, N.Y., 1980, chap. 3.

(19) P. H. Elworthy and A. T. Florence, *J. Pharm. Pharmacol.*, **21**, 70s (1969).

(20) P. H. Elworthy and A. T. Florence, *J. Pharm. Pharmacol.*, **21**, 79s (1969).

(21) M. J. Schick, S. M. Atlas, and F. R. Eirich, *J. Phys. Chem.*, **66**, 1326 (1962).

(22) L. Hsiao, H. N. Dunning, and P. B. Lorenz, *J. Phys. Chem.*, **60**, 657 (1956).

(23) P. H. Elworthy, A. T. Florence, and J. A. Rogers, *J. Colloid Interface Sci.*, **35**, 23 (1971).

(24) F. E. Bailey and R. W. Callard, *J. Appl. Polymer Sci.*, **1**, 56 (1959).

(25) A. T. Florence, F. Madsen, and F. Puisieux, *J. Pharm. Pharmacol.*, **27**, 385 (1975).

(26) S. Friberg, P. O. Jansson, and E. Cederberg, *J. Colloid Interface Sci.*, **55**, 614 (1976).

(27) E. H. Crook, D. B. Fordyce, and G. F. Trebbi, *J. Phys. Chem.*, **67**, 1987 (1963).

(28) R. D. Vold and R. C. Groot, *J. Phys. Chem.*, **66**, 1969 (1962).

(29) A. U. Hahn and K. L. Mittal, *Colloid Polymer Sci.*, **257**, 959 (1979).

(30) E. R. Garrett, *J. Soc. Cosmet. Chem.*, **21**, 393 (1970), and 3 references cited therein.

(31) S. J. Rehfeld, *J. Colloid Interface Sci.*, **46**, 448 (1974), and 1 reference cited therein.

(32) P. Sherman, *Soap Perfum. Cosmet.*, **44**, 693 (1971).

(33) R. D. Vold and M. C. Acevedo, *J. Am. Oil Chem. Soc.*, **54**, 84 (1977).

ACKNOWLEDGMENTS

Support by the National Institutes of Health under Grant GM 27802 is gratefully acknowledged.

X-ray Structural Studies and Physicochemical Properties of Cimetidine Polymorphism

MEGUMI SHIBATA ˣ, HIROMASA KOKUBO, KAZUHIRO MORIMOTO, KATSUAKI MORISAKA, TOSHIMASA ISHIDA, and MASATOSHI INOUE

Received April 2, 1982, from the *Osaka College of Pharmacy, 2-10-65 Kawai, Matsubara-City, Osaka 580, Japan.* Accepted for publication October 7, 1982.

Abstract □ Four crystalline forms of cimetidine, three anhydrous (forms A, B, and D) and a monohydrate (form C), obtained by slow evaporation of aqueous solutions of varying concentrations were characterized by IR spectroscopy, X-ray powder patterns, dissolution rates in deionized water, and thermal analyses. Among the three anhydrous forms of cimetidine, form A was thermodynamically more stable than the others. The structural conversion of form C into form A on dehydration was confirmed by IR spectroscopy and X-ray powder patterns. The structures of forms C and D were determined using X-ray diffraction. Form D was of spirally curled conformation; it was linked in a head-to-tail arrangement with the neighboring molecules *via* intermolecular hydrogen bonds between the imidazole nitrogen and guanidine nitrogen atoms. Form C was characterized by its folded conformation due to the weak stacking interaction between the imidazole and guanidine moieties; there was stabilization by double hydrogen bond formation with neighboring molecules and *via* water molecules of crystallization. The dissolution rate constant in deionized water for form C was ~1.29, 1.70, and 1.90 times greater than those measured for forms A, D, and B, respectively. There was a similar relationship among the four forms with respect to the rates of inhibition of stress ulceration. Regarding the molecular conformations of the crystalline forms and the rates of inhibition of stress ulceration, the *gauche* orientation of the guanidine group relative to the imidazole ring would be the conformation necessary for effective binding to the histamine H_2-receptor. The compactly folded conformation of form C appears to be optimal for binding to the active site of the receptor and for clinical efficacy.

Keyphrases □ Cimetidine—polymorphic crystalline forms, X-ray structural studies, physicochemical properties □ Polymorphism—cimetidine crystals, X-ray structural studies, physicochemical properties □ Structure—polymorphic crystalline forms of cimetidine, X-ray studies, physicochemical properties

Cimetidine, *N″*-cyano-*N*-methyl-*N′*-[2-[[(5-methyl-1*H*-imidazol-4-yl)methyl]thio]ethyl]guanidine, a specific competitive histamine H_2-receptor antagonist, inhibits the secretion of histamine-stimulated gastric acid. Because of its minimal side effects, it is widely used in the treatment of human peptic ulcers (1). Cimetidine has different crystalline forms (polymorphism) when crystallized under various conditions (2, 3). Since the bioavailability of

0022-3549/83/1200-1436$01.00/0

by the other methods were not in complete agreement is ascribed to the complex sequence of steps occurring during the former. The correlation between long-term shelf stability of emulsions and their resistance to high-speed centrifugation was not sufficiently good to make the latter a reliable technique for predicting the former (32, 33).

REFERENCES

(1) H. Schott, *J. Colloid Interface Sci.*, **43**, 150 (1973).

(2) H. Schott and S. K. Han, *J. Pharm. Sci.*, **64**, 658 (1975).

(3) W. N. Maclay, *J. Colloid Sci.*, **11**, 272 (1956).

(4) M. J. Schick, *J. Colloid Sci.*, **17**, 801 (1962).

(5) H. Schott and S. K. Han, *J. Pharm. Sci.*, **66**, 165 (1977).

(6) M. J. Schick and A. H. Gilbert, *J. Colloid Sci.*, **20**, 464 (1965).

(7) H. Schott and S. K. Han, *J. Pharm. Sci.*, **65**, 975 (1976).

(8) H. Schott and A. E. Royce, *J. Pharm. Sci.*, **72**, 313 (1983).

(9) G. Herdan, "Small Particle Statistics," 2nd ed., Academic, New York, N.Y., 1960, chap. 4.

(10) K. J. Mysels, "Introduction to Colloid Chemistry," Interscience, New York, N.Y., 1959, chaps. 3 and 20.

(11) H. C. van de Hulst, "Light Scattering by Small Particles," Wiley, New York, N.Y., 1957, chaps. 10, 18, and 19.

(12) W. J. Youden, "Statistical Methods for Chemists," Wiley, New York, N.Y., 1951, chap. 5.

(13) G. F. Lothian and F. P. Chappel, *J. Appl. Chem.*, **1**, 475 (1951).

(14) J. D. S. Goulden, *Trans. Faraday Soc.*, **54**, 941 (1958).

(15) R. D. Vold and M. Maletic, *J. Colloid Interface Sci.*, **65**, 390 (1978), and 7 references cited therein.

(16) R. D. Vold and K. L. Mittal, *J. Soc. Cosmet. Chem.*, **23**, 171 (1972).

(17) R. D. Vold and R. C. Groot, *J. Soc. Cosmet. Chem.*, **14**, 233 (1963).

(18) T. Sato and R. Ruch, "Stabilization of Colloidal Dispersions by Polymer Adsorption," Dekker, New York, N.Y., 1980, chap. 3.

(19) P. H. Elworthy and A. T. Florence, *J. Pharm. Pharmacol.*, **21**, 70s (1969).

(20) P. H. Elworthy and A. T. Florence, *J. Pharm. Pharmacol.*, **21**, 79s (1969).

(21) M. J. Schick, S. M. Atlas, and F. R. Eirich, *J. Phys. Chem.*, **66**, 1326 (1962).

(22) L. Hsiao, H. N. Dunning, and P. B. Lorenz, *J. Phys. Chem.*, **60**, 657 (1956).

(23) P. H. Elworthy, A. T. Florence, and J. A. Rogers, *J. Colloid Interface Sci.*, **35**, 23 (1971).

(24) F. E. Bailey and R. W. Callard, *J. Appl. Polymer Sci.*, **1**, 56 (1959).

(25) A. T. Florence, F. Madsen, and F. Puisieux, *J. Pharm. Pharmacol.*, **27**, 385 (1975).

(26) S. Friberg, P. O. Jansson, and E. Cederberg, *J. Colloid Interface Sci.*, **55**, 614 (1976).

(27) E. H. Crook, D. B. Fordyce, and G. F. Trebbi, *J. Phys. Chem.*, **67**, 1987 (1963).

(28) R. D. Vold and R. C. Groot, *J. Phys. Chem.*, **66**, 1969 (1962).

(29) A. U. Hahn and K. L. Mittal, *Colloid Polymer Sci.*, **257**, 959 (1979).

(30) E. R. Garrett, *J. Soc. Cosmet. Chem.*, **21**, 393 (1970), and 3 references cited therein.

(31) S. J. Rehfeld, *J. Colloid Interface Sci.*, **46**, 448 (1974), and 1 reference cited therein.

(32) P. Sherman, *Soap Perfum. Cosmet.*, **44**, 693 (1971).

(33) R. D. Vold and M. C. Acevedo, *J. Am. Oil Chem. Soc.*, **54**, 84 (1977).

ACKNOWLEDGMENTS

Support by the National Institutes of Health under Grant GM 27802 is gratefully acknowledged.

X-ray Structural Studies and Physicochemical Properties of Cimetidine Polymorphism

MEGUMI SHIBATA ˣ, HIROMASA KOKUBO, KAZUHIRO MORIMOTO, KATSUAKI MORISAKA, TOSHIMASA ISHIDA, and MASATOSHI INOUE

Received April 2, 1982, from the *Osaka College of Pharmacy, 2-10-65 Kawai, Matsubara-City, Osaka 580, Japan.* Accepted for publication October 7, 1982.

Abstract □ Four crystalline forms of cimetidine, three anhydrous (forms A, B, and D) and a monohydrate (form C), obtained by slow evaporation of aqueous solutions of varying concentrations were characterized by IR spectroscopy, X-ray powder patterns, dissolution rates in deionized water, and thermal analyses. Among the three anhydrous forms of cimetidine, form A was thermodynamically more stable than the others. The structural conversion of form C into form A on dehydration was confirmed by IR spectroscopy and X-ray powder patterns. The structures of forms C and D were determined using X-ray diffraction. Form D was of spirally curled conformation; it was linked in a head-to-tail arrangement with the neighboring molecules *via* intermolecular hydrogen bonds between the imidazole nitrogen and guanidine nitrogen atoms. Form C was characterized by its folded conformation due to the weak stacking interaction between the imidazole and guanidine moieties; there was stabilization by double hydrogen bond formation with neighboring molecules and *via* water molecules of crystallization. The dissolution rate constant in deionized water for form C was ~1.29, 1.70, and 1.90 times greater than those measured for forms A, D, and B, respectively. There was a similar relationship among the four forms with respect to the rates of inhibition of stress ulceration. Regarding the molecular conformations of the crystalline forms and the rates of inhibition of stress ulceration, the *gauche* orientation of the guanidine group relative to the imidazole ring would be the conformation necessary for effective binding to the histamine H_2-receptor. The compactly folded conformation of form C appears to be optimal for binding to the active site of the receptor and for clinical efficacy.

Keyphrases □ Cimetidine—polymorphic crystalline forms, X-ray structural studies, physicochemical properties □ Polymorphism—cimetidine crystals, X-ray structural studies, physicochemical properties □ Structure—polymorphic crystalline forms of cimetidine, X-ray studies, physicochemical properties

Cimetidine, *N″*-cyano-*N*-methyl-*N′*-[2-[[(5-methyl-1*H*-imidazol-4-yl)methyl]thio]ethyl]guanidine, a specific competitive histamine H_2-receptor antagonist, inhibits the secretion of histamine-stimulated gastric acid. Because of its minimal side effects, it is widely used in the treatment of human peptic ulcers (1). Cimetidine has different crystalline forms (polymorphism) when crystallized under various conditions (2, 3). Since the bioavailability of

0022-3549/83/1200-1436$01.00/0

pharmacologically active compounds is generally dependent on their crystalline forms (4), detection of the most active among the cimetidine crystalline forms is important for understanding the specific stereochemistry of the H_2-receptor and for the effective clinical use of the agent.

This paper reports the physicochemical properties of four cimetidine crystalline forms (A, B, C, and D) obtained from aqueous solutions at different sample concentrations. The different forms were characterized by determining melting points, IR spectra, X-ray powder patterns, thermal behavior, and dissolution rates. The crystal structures of forms C and D were determined by X-ray diffraction.

EXPERIMENTAL

Preparation of Cimetidine Crystalline Forms—The preparation of the crystalline forms of cimetidine has been reported previously (3); crystallization from organic solvents such as acetonitrile produced platelet crystals, and crystallization from aqueous solutions produced three crystalline forms. Four crystalline forms were obtained by slow evaporation of the aqueous solutions; these were platelet (form A), needle (form B), pyramidal (form C), and cubic (form D) crystals. The cimetidine concentrations used for the preparation of crystal forms A, B, C, and D were 80, 10–40, 150, and 2–10 mg/ml, respectively[1]. The solutions were placed inside covered beakers and allowed to evaporate slowly at room temperature (25°; forms A, B, and D) or at 4–6° (form C). After 3–4 weeks, well-formed crystals were obtained; the crystalline forms were confirmed to coincide with those reported previously (3) by comparison of their respective IR spectra.

IR Spectra and Thermal Analyses—IR spectra were measured by using potassium bromide disks[2]. Gravimetry and the calorimetric changes accompanying the thermal decomposition were measured by thermogravimetry (TG) and differential thermal analysis (DTA) instruments[3]. The TG and DTA profiles were measured using 20 mg of powdered samples; the heating rate was 5°/min.

X-ray Powder Patterns—X-ray powder patterns were measured by the permeance method, using a diffractometer[4] and copper Kα radiation. The powder pattern of each crystalline form was measured twice and averaged.

X-ray Data Collection of Crystalline Forms C and D—Preliminary oscillation and Weissenberg photographs showed both crystal systems to be monoclinic (Table I). The density of both crystals was measured by the flotation method in benzene–carbon tetrachloride. A single crystal (0.3 × 0.3 × 0.4 mm, form C; 0.5 × 0.4 × 0.3 mm, form D) was mounted on a computer-controlled four-circle diffractometer[5]. Intensity data on 2305 (form C) and 2138 (form D) independent reflections [$Fo \geq 3\sigma(Fo)$] were obtained using graphite-monochromated copper Kα radiation and the $\omega - 2\theta$ scanning technique ($\sin\theta/\lambda \leq 0.588$ Å^{-1}). The scan speed was 4°/min; the background was measured for 5 sec. The intensity of four standard reflections for the respective crystals, measured every 100 reflections, showed no structural deteriorations due to X-ray irradiation during the measurement of all reflections. Corrections were applied for the Lorentz and polarization factors, but not for the absorption effects.

Structure Determinations and Refinements—The structures of forms C and D were solved by the direct method using the MULTAN 78 program (5). An electron density map using the normalized structure factors (E), computed with the phase set having the highest figure of merit using 180 reflections with $|E| \geq 1.57$ (form C) or 170 reflections with $|E| \geq 1.73$ (form D), gave reasonable positions for all nonhydrogen atoms. The atomic coordinates were refined by the block-diagonal least-squares method with anisotropic temperature factors. The positional parameters of all hydrogen atoms could be determined from a difference Fourier map.

Refinement, including those parameters with isotropic temperature factors, was then continued. The quantity minimized was $\Sigma\omega(|Fo| - |Fc|)^2$; in the final refinement, the following weighting scheme was used: for form C, $w = 0.24$ for $Fo = 0.0$, $w = 1.0$ for $0 < Fo \leq 11.0$, and $w = 1.0/[1.0 + 0.112(Fo - 11.0)]$ for $Fo > 11.0$; for form D, $w = 1.0$ for $0 < Fo \leq 9.0$ and $w = 1.0/[1.0 + 0.235(Fo - 9.0)]$ for $Fo > 9.0$. The final R-value was 0.049 for form C and 0.039 for form D.

The final atomic positional and thermal parameters of form D are given in Tables II and III, respectively[6]. All numerical calculations were performed using the UNICS programs (6)[7]. Atomic scattering factors cited in the *International Tables for X-ray Crystallography* (7) were used.

Measurement of Dissolution Rates of the Four Crystalline Forms in Deionized Water—A schematic drawing of the dissolution apparatus is presented in Fig. 1. Deionized water (46 ml) was introduced into the dissolution chamber outside the cellulose dialysis membrane.[8] Each crystalline form (20 mg, 44–74 μm in diameter), suspended in 4 ml of

Table I—Crystal Data

	Crystalline Form	
	Form C	Form D
	$C_{10}H_{16}N_6S{\cdot}H_2O$	$C_{10}H_{16}N_6S$
Molecular weight	270.35	252.34
Crystal system	Monoclinic	Monoclinic
Space group	Cc	$P2_1/n$
Cell constants		
a(Å)	12.620(5)	7.284(1)
b(Å)	7.772(4)	10.814(2)
c(Å)	14.742(5)	16.172(3)
β(°)	117.76(2)	94.69(1)
V(Å^3)	1342.8(1)	1269.5(4)
Z	4	4
Dm(g·cm^{-3})	1.333(1)	1.310(1)
Dx(g·cm^{-3})	1.337	1.320
μ(Cu-Kα) (cm^{-1})	20.919	21.175
F(0 0 0)	576	536

Table II—Atomic Coordinates of Form D

Atom	x^a	y^a	z^a
S	0.7407(1)	0.7499(0)	0.7395(0)
N(1)	0.5812(2)	0.4240(1)	0.9221(1)
N(2)	0.7377(2)	0.5961(2)	0.9112(1)
N(3)	0.6810(2)	0.6042(1)	0.5648(1)
N(4)	0.5043(2)	0.7121(1)	0.4654(1)
N(5)	0.3763(2)	0.6333(2)	0.5834(1)
N(6)	0.0580(2)	0.6768(2)	0.5290(1)
C(1)	0.7292(3)	0.4908(2)	0.9504(1)
C(2)	0.5861(2)	0.5969(2)	0.8537(1)
C(3)	0.4889(3)	0.4904(2)	0.8597(1)
C(4)	0.3176(3)	0.4432(2)	0.8136(2)
C(5)	0.5465(3)	0.7011(2)	0.7952(1)
C(6)	0.8324(2)	0.6043(2)	0.7072(1)
C(7)	0.7131(2)	0.5349(2)	0.6415(1)
C(8)	0.5185(2)	0.6513(2)	0.5374(1)
C(9)	0.6488(3)	0.7192(2)	0.4096(1)
C(10)	0.2102(2)	0.6590(2)	0.5514(1)
H(N1)	0.540(3)	0.351(2)	0.940(2)
H(N3)	0.775(2)	0.623(2)	0.540(1)
H(N4)	0.412(3)	0.753(2)	0.453(1)
H(1)	0.815(3)	0.468(2)	0.995(1)
H(4a)	0.294(5)	0.490(3)	0.768(2)
H(4b)	0.221(5)	0.423(3)	0.848(2)
H(4c)	0.339(5)	0.364(4)	0.783(3)
H(5a)	0.440(3)	0.676(2)	0.754(1)
H(5b)	0.514(3)	0.775(2)	0.824(1)
H(6a)	0.859(3)	0.550(2)	0.759(1)
H(6b)	0.952(3)	0.631(2)	0.686(1)
H(7a)	0.591(3)	0.515(2)	0.661(1)
H(7b)	0.778(3)	0.460(2)	0.627(1)
H(9a)	0.596(4)	0.757(2)	0.359(2)
H(9b)	0.699(3)	0.637(2)	0.398(1)
H(9c)	0.749(3)	0.766(2)	0.431(1)

[a] *SD* in parentheses.

[1] The reproducibilities of forms A, B, and C were very good, but that of form D could not be warranted.
[2] Model 260-10, Hitachi infrared spectrometer, Japan.
[3] Model M8075, Rigaku Denki Co., Japan.
[4] Microflex, Model 4180D1, Rigaku Denki Co., Japan.
[5] Model AFC-5, Rigaku Denki Co., Japan.

[6] After the present determination and refinements of the form C crystal, an independent determination of this crystal form was reported by B. Prodic-Kojic and Z. Ruzic-Toros (10). Their structure is identical to ours; however, their crystal parameters are somewhat different.
[7] These calculations were carried out on an ACOS-700 computer at the Computation Center of Osaka University.
[8] VisKing tube, Union Carbide Co.

Table III—Anisotropic Thermal Parameters ($\times 10^4$) of the Nonhydrogen Atoms of Form D[a]

Atom	B_{11}	B_{22}	B_{33}	B_{12}	B_{13}	B_{23}
S	259(1)	78(0)	32(0)	−86(1)	30(1)	−2(0)
N(1)	157(3)	73(1)	36(1)	−37(3)	32(2)	3(2)
N(2)	194(3)	86(2)	31(1)	−62(4)	13(2)	−8(2)
N(3)	114(2)	81(1)	25(1)	18(3)	8(2)	5(1)
N(4)	123(3)	80(1)	28(1)	27(3)	4(2)	12(1)
N(5)	122(3)	91(1)	30(1)	9(3)	19(2)	−2(1)
N(6)	120(3)	104(2)	56(1)	15(4)	34(2)	8(2)
C(1)	194(4)	99(2)	33(1)	−38(4)	9(3)	4(2)
C(2)	176(3)	74(2)	28(1)	−31(4)	32(2)	−14(2)
C(3)	173(4)	75(2)	31(1)	−19(4)	29(2)	−18(2)
C(4)	220(5)	115(2)	50(1)	−98(5)	−15(3)	−12(3)
C(5)	213(4)	79(2)	38(1)	−2(4)	35(3)	1(2)
C(6)	157(3)	107(2)	28(1)	7(4)	5(2)	10(2)
C(7)	171(3)	74(2)	29(1)	32(4)	−1(2)	11(2)
C(8)	116(3)	58(1)	25(1)	2(3)	3(2)	−13(1)
C(9)	157(3)	107(2)	27(1)	−9(4)	16(2)	13(2)
C(10)	140(3)	68(1)	35(1)	2(3)	42(2)	−6(2)

[a] The anisotropic temperature factors are expressed in the form: $\exp[-(B_{11}h^2 + B_{22}k^2 + B_{33}l^2 + B_{12}hk + B_{13}hl + B_{23}kl)]$. *SD* in parentheses.

deionized water, was introduced into the membrane. The test solution (550 ml) was placed into the reservoir; the total aqueous solution for measuring the dissolution rate constants was maintained at a volume of 600 ml, in order to retain the sink condition ($C \ll C_s$, where C is the concentration of the used sample and the C_s is the saturated sample).

The dissolution chamber was shaken at 200 strokes/min in an incubator at 37 ± 0.5°. The aqueous solution was circulated with a pump at a flow rate of 9.0 ml/min; the dissolved amount of the drug as a function of time was continuously monitored using a UV spectrophotometer (220 nm).

In addition to this method, the dissolution rate constants of forms A, B, and C were measured by the rotating disk method. These samples were tentatively measured using the compressed disks under several pressures: 454, 908, 1362, 1816, and 2270 kg/cm^2. As the rates of these forms were almost unchanged within the range of 454–2270 kg/cm^2, the experiment was carried out under the pressure that was suitable for making disks. The preparation of the disk samples did not affect the crystalline forms until a pressure of 4540 kg/cm^2 was reached, as verified by IR spectra.

All experiments were carried out under the following conditions. The compressed disk was attached to a holder of matched size in such a manner that only the bottom face of the disk was in contact with the deionized water; the other part of the disk was covered with paraffin. The holder (with disk) was attached to the shaft and set in a flask containing 1000 ml of deionized water; the flask was placed in a constant temperature bath (37 ± 0.5°). The rotating velocity of the disk was 100 rpm. The dissolved amount of the sample was monitored as noted above.

RESULTS AND DISCUSSION

Melting Points and IR Spectra of Four Crystalline Forms—The melting points of the four crystalline forms and their characteristic IR bands are summarized in Table IV. The IR spectra of crystalline forms A, B, C, and D corresponded to forms I, IV, II, and III reported by Pro-

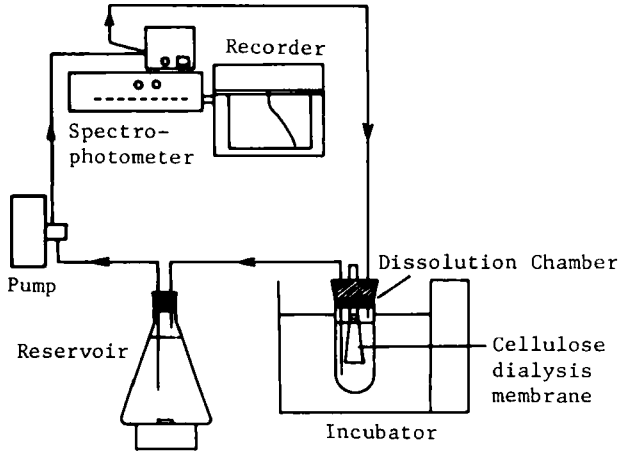

Figure 1—*Schematic drawing of the dissolution apparatus.*

Table IV—Melting Points and IR Spectra of the Four Crystalline Forms

Form	Crystal Form	Melting Point	Characteristic bands, cm^{-1}
A	plate	149–152°	1210 1160 1025 800 765 758 690 670 605 560 540
B	needle	152–154°	2850 1430 1420 1220 1190 1120 1040 650 630 590
C	pyramid	81–83°	3510 3400 3300 1180 1170 1130 1110 880 870 605 470
D	cube	146–147°	3400 3000 2920 2850 1470 1210 1190 1180 1160 1035 515 480

dic-Kojic *et al.* (3). Form C had the characteristic band at 3510 cm^{-1} corresponding to the hydroxyl group; its melting point was lower than that of the other forms, suggesting the presence of water of crystallization. The other crystalline forms, with melting points higher than form C, were anhydrous forms, indicative of the crystalline polymorphism of cimetidine. This point was also confirmed by measuring the X-ray powder patterns (Fig. 2).

DTA and TG Profiles—Figures 3 and 4 show the DTA and TG profiles of the four crystalline forms. In these profiles, the DTA and TG curves represent the thermal change and the percent of weight loss, respectively. In the DTA curves of forms B and D (Fig. 3), the endothermic peaks near 150° corresponded to the respective melting points. Exothermic reactions began near 185°. Although the thermal change behavior was similar, form D appears to be more loosely packed within the crystalline lattice because its endo- and exothermic peaks were smaller than those of form B. This idea is also supported by the difference of their densities [Dm = 1.351(2) g·cm^{-3} for form B and Dm = 1.310(1) g·cm^{-3} for form C].

In the DTA curve of form A (Fig. 4), the endothermic peak near 150° was larger than that of forms B and D. As is obvious from the TG curve below 150°, form A crystal is thermally quite stable; decomposition begins at a temperature >200°. These data suggest that the molecular packing mode of form A is thermodynamically more stable than that of forms B and D.

On the other hand, the DTA and TG curves of form C were very different; there were two endothermic peaks near 80° and 150° in the DTA curve. In the TG curve at 80°, which corresponds to the melting point of this form, the weight loss of one water molecular per cimetidine molecule was observed. Above 80°, the DTA and TG curves of form C were identical to those of form A, suggesting that the structural change of form C to form A was due to the release of water of crystallization. This point was also confirmed by measuring the IR spectra and the X-ray diffraction patterns.

Molecular Structure of Cimetidine in Crystalline Form D—Figure 5 shows the bond lengths and angles of form D with their atomic num-

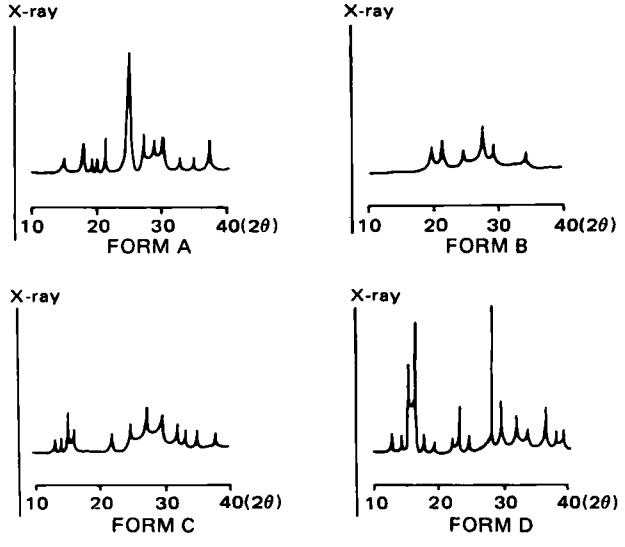

Figure 2—*X-ray powder patterns of the four crystalline forms (20°).*

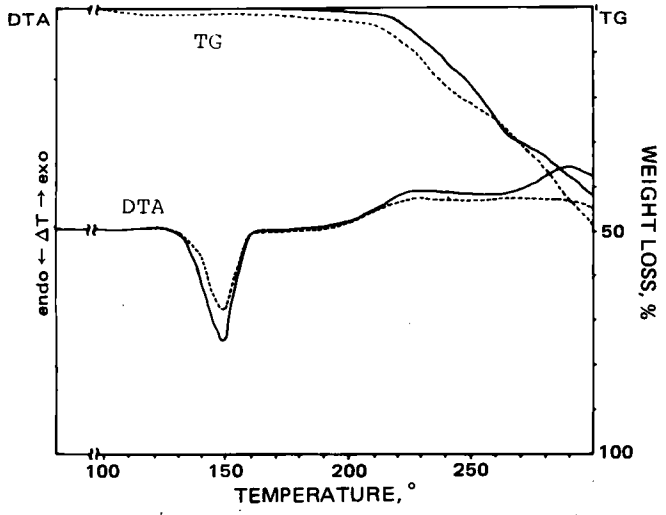

Figure 3—*Differential thermal analysis (DTA) and thermogravimetric (TG) curves of forms B (—) and D (- - - -).*

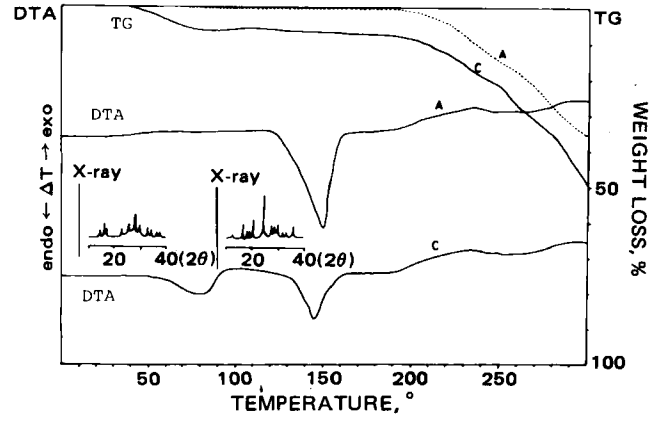

Figure 4—*Differential thermal analysis (DTA) and thermogravimetric (TG) curves of forms A and C. The X-ray powder patterns of form C and dehydrated form C on heating to 100° are also shown (insets).*

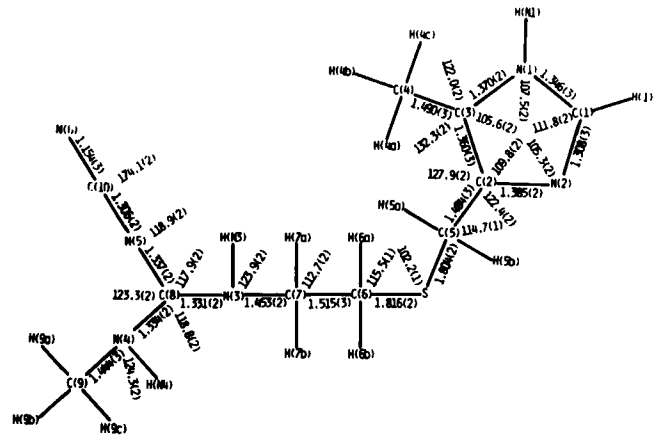

Figure 5—*Bond lengths (Å) and angles (°) of the nonhydrogen atoms of form D (with SD in parentheses).*

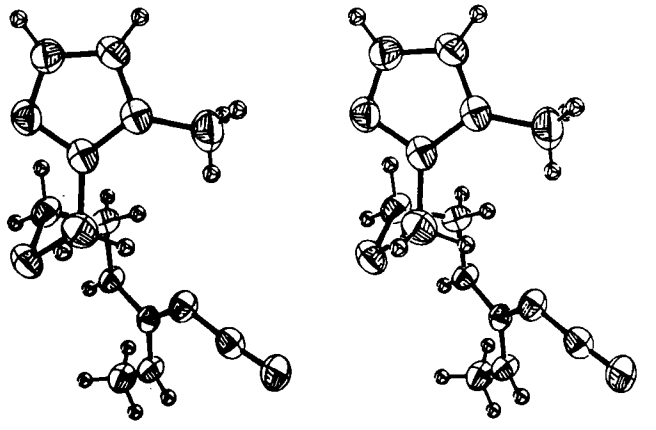

Figure 6—*Stereoscopic drawings of the molecular conformation of form D projected onto the imidazole ring.*

bering. The equations of the least-squares planes for the imidazole ring, C(2)—C(5)—S, S—C(6)—C(7)—N(3), and the guanidine group, the displacement of individual atoms from these planes, and the dihedral angles between the planes are listed in Table V. A stereoscopic drawing of the molecule, projected onto the imidazole ring, is presented in Fig. 6.

Although the observed bond angles were in agreement with those of related histamine H_2-receptor antagonists within their estimated standard errors, the bond length of the thioether linkage in form D, C(5)—S (1.804 Å), was significantly shorter than that of form A (1.828 Å) (8), form

Table V—Optimal Planes and Deviations (Å) of Individual Atoms

Equations of the best planes expressed by $m_1x + m_2y + m_3z = d$ in the orthogonal space

Plane	m_1	m_2	m_3	d
I Imidazole ring	0.60174	−0.43525	−0.66967	−10.13240
II C(2)C(5)S	0.20995	0.65007	0.73029	14.90376
III SC(6)C(7)N(3)	0.93047	0.26603	−0.23191	3.27256
IV Guanidine group	0.18502	0.85315	0.48775	10.79567

Deviations (Å) from the best plane

I Imidazole Ring		II C(2)C(5)S		III SC(6)C(7)N(3)		IV Guanidine Group	
C(1)*	0.004(3)	C(2)*	0.000(0)	S*	−0.008(1)	C(8)*	0.006(2)
C(2)*	−0.002(2)	C(5)*	0.000(0)	C(6)*	0.366(3)	N(3)*	−0.002(2)
C(3)*	0.003(2)	S*	0.000(0)	C(7)*	−0.295(2)	N(4)*	−0.002(2)
N(1)*	−0.003(2)	C(3)	−0.828(3)	N(3)*	0.093(2)	N(5)*	−0.002(2)
N(2)*	−0.004(2)	N(2)	0.888(4)	C(8)	−0.728(3)	C(7)	−0.014(3)
C(4)	0.009(4)	C(6)	−1.255(4)	C(5)	−1.759(2)	C(9)	−0.166(3)
C(5)	0.012(3)					C(10)	−0.232(3)
H(1)	−0.030(23)					N(6)	−0.444(4)
H(N1)	−0.047(27)					H(N3)	0.106(19)
						H(N4)	0.153(20)

Dihedral angles (°) between the best planes

	II	III	IV
I	49.8(1)	52.2(1)	54.1(1)
II		79.4(1)	18.3(1)
III			74.0(1)

[a] Atoms with asterisks define the plane in each case.

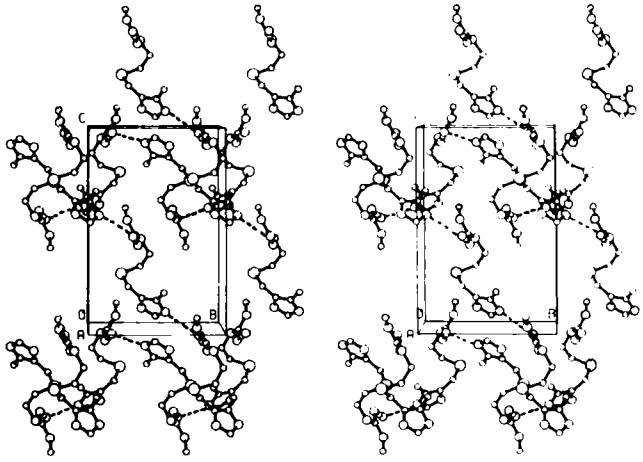

Figure 7—*Stereoscopic drawings of the molecular packing of form D, viewed along the* a*-axis. For the sake of clarity, the hydrogen atoms are omitted. The dotted lines represent the hydrogen bonds.*

C (1.825 Å), metiamide (1.828 Å) (9), and *N*-[2-[(imidazol-4-yl)methylthio]ethyl]-*N″*-methylthiourea (thiaburimamide) (1.829 Å) (9); the C(8)—N(5) bond length of the guanidine group (1.337 Å) is also shorter than that of form A (1.346 Å) and form C (1.343 Å). As in the related molecules, the imidazole ring of this crystal is planar with a maximum shift of 0.004 Å for the C(1) and the N(2) atoms; and C(4) and the C(5) atoms lie almost on this plane. The guanidine group is also planar with a maximum deviation of 0.006 Å for the C(8) atom; the C(7) atom lies essentially on the plane.

As is obvious from Fig. 6, the molecule can be characterized by its spiral-shaped conformation. The dihedral angle between the imidazole ring and the guanidine group is 54.1(1)°; both moieties are linked to each other by the C(5)—S—C(6)—C(7)—N(3) bond sequence manifesting the spirally curled arrangement with an ~360° rotation.

Crystal Packing of Crystalline Form D—The molecular packing viewed down the *a*-axis is shown in Fig. 7; the hydrogen bonding parameters and the short contacts <3.5 Å are listed in Table VI. The molecules are linked *via* intermolecular hydrogen bonds with the imidazole and guanidine nitrogen atoms of neighboring molecules, N(1)—H(N1)···N(6) = 2.988(2) Å and N(3)—H(N3)···N(6) = 2.959(2) Å, thereby forming head-to-tail molecular arrangements in the *b*- and *c*-directions. Many short contacts were observed between neighboring imidazole rings, between neighboring guanidine groups, and between the neighboring imidazole ring and guanidine group. These short contacts stabilize the molecular packing in the crystal.

Molecular and Crystal Structure of Form C—Since the present crystal determination showed the molecular and crystal structure of form C to be identical with that reported by Prodic-Kojic and Ruzic-Toros (10), the structural features observed in the crystal will be presented briefly. The molecular conformation in this crystal is characterized by the folded form resulting from the weak stacking interaction between the imidazole and guanidine moieties. The dihedral angle between both planes is 10.8(2)°; their mean interplanar spacing is 3.676 Å. This conformation is further stabilized by the hydrogen bond formed by the water of crystallization [N(1)···O = 2.383(7) Å, N(6)···O = 3.064(8) Å]. In the crystal packing, the water of crystallization is further hydrogen bonded to the N(2) atom of the neighboring imidazole ring [N(2)···O = 2.800 (7) Å]. The infinite double layers, found by these three hydrogen bonds by water of crystallization and a N(6)···N(3) hydrogen bond [3.034(8) Å], are arranged parallel to the *a*- and *b*-directions and are held together by van der Waals contacts in the *c*-direction.

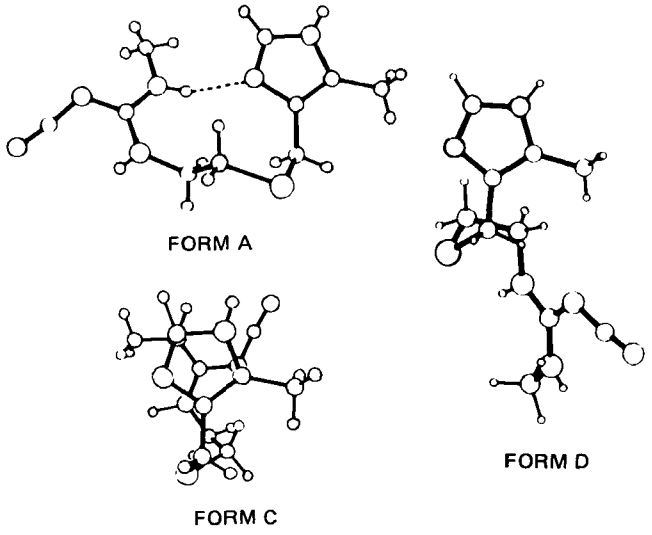

Figure 8—*Comparison of the molecular conformations of forms A, C, and D projected onto the imidazole ring.*

Table VII—Comparison of the Torsion Angle of the Cimetidine Molecule Observed in Crystalline Forms A, C, and D

	Form A	Form C	Form D
N(2)—C(2)—C(5)—S	−73.1	70.5(6)	49.4(2)
C(3)—C(2)—C(5)—S	108.3	−106.6(6)	−129.5(2)
C(2)—C(5)—S—C(6)	61.3	59.8(5)	−45.4(2)
C(5)—S—C(6)—C(7)	61.2	138.5(4)	69.2(2)
S—C(6)—C(7)—N(3)	184.3	68.6(5)	60.7(2)
C(6)—C(7)—N(3)—C(8)	92.1	76.2(7)	110.8(2)
C(7)—N(3)—C(8)—N(4)	−8.8	178.5(5)	−179.1(2)
C(7)—N(3)—C(8)—N(5)	172.6	−2.1(8)	−0.2(2)
N(3)—C(8)—N(4)—C(9)	171.8	1.0(9)	−7.2(3)
N(3)—C(8)—N(5)—C(10)	−12.5	175.5(5)	168.0(2)

Table VIII—Intramolecular Distances (Å) Between the N(2) Atom of the Imidazole Ring and the Nitrogen Atom of the Cyanoguanidine Group

	Form A	Form C	Form D
N(3)	4.090	3.914(7)	5.584(2)
N(4)	2.881	3.836(7)	7.378(2)
N(5)	5.061	4.416(8)	5.737(2)
Orientation between the imidazole ring and the cyanoguanidine group	*gauche*	*gauche*	*trans*

Molecular Conformations Observed in Forms A, C, and D and Their Biological Implications—The molecular conformations and selected torsion angles observed in the crystal structures of forms A, C, and D are presented in Fig. 8 and Table VII. Since forms A, C, and D were

Table VI—Hydrogen Bonds and Short Contacts <3.5 Å [a]

Donor(D)	Acceptor(A)	Distance, Å	Angle, °
		Hydrogen bonds	
N(1)	$N(6)^{I}$	D···A 2.998(2) H···A 2.08(3)	D—H···A 175(2)
N(3)	$N(6)^{II}$	D···A 2.959(2) H···A 2.17(2)	D—H···A 156(1)
		Short contacts (Å) < 3.5 Å	
$N(1)—N(1)^{III}$	3.306(3)	$N(3)—C(8)^{V}$	3.476(2)
$N(1)—C(1)^{III}$	3.312(3)	$N(4)—C(7)^{V}$	3.490(2)
$N(2)—N(4)^{IV}$	2.926(2)	$C(8)—C(8)^{V}$	3.492(2)
$N(2)—N(6)^{IV}$	3.432(2)	$C(9)—N(6)^{II}$	3.447(3)

[a] Roman numerals denote the following equivalent positions relative to the reference molecule at *x,y,z*: (I) 1/2 − *x*, −1/2 + *y*, 3/2 − *z*; (II) 1 + *x,y,z*; (III) 1 − *x*,1 − *y*,2 − *z*; (IV) 1/2 + *x*,3/2 − *y*,1/2 + *z*; (V) 1 − *x*,1 − *y*,1 − *z*. *SD* in parentheses.

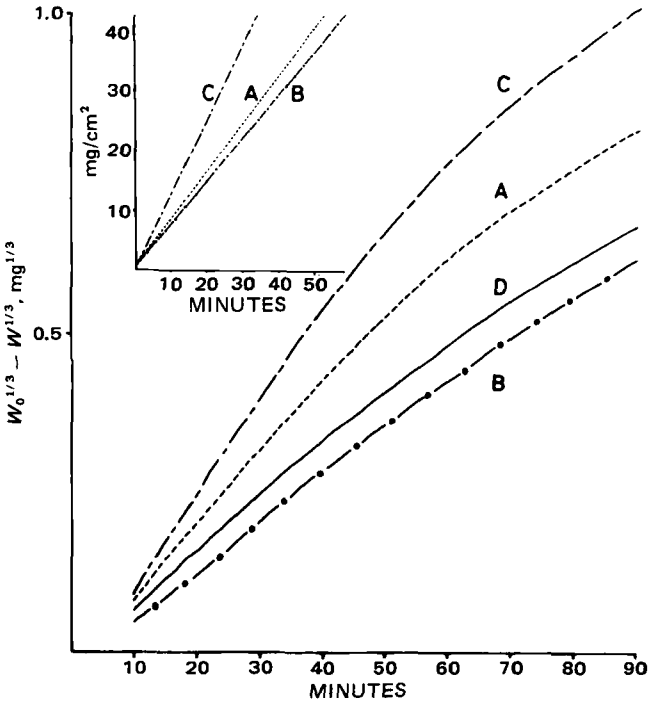

Figure 9—*Dissolution profiles of the four crystalline forms in particle systems and those of the three crystalline forms in disk systems (inset).*

prepared from aqueous solutions at different sample concentrations, the energetic stability of their molecular conformations (Fig. 8) appears to be the same. The conformations of forms A, C, and D are characterized by an intramolecular hydrogen bond formation, leading to the formation of a stable 10-member ring (form A), by a weak stacking interaction between the imidazole and guanidine moieties which is further stabilized by the hydrogen bond formation by water of crystallization (form C), and by a spiral conformation (form D).

Based on extended Hückel molecular orbital calculations of various related agonists, Kier (11) proposed that the conditions necessary for the H_2-receptor activity of histamine are: (*a*) distance between the N(2) atom of the imidazole ring and the nitrogen atom of the side chain is near 3.6 Å and (*b*) the orientation of the nitrogen atoms with respect to the imidazole ring is *gauche*. Durant *et al.* (12) reported that the introduction of an unchanged side chain such as the cyanoguanidine group into the imidazole ring is more effective for binding to the histamine H_2-receptor.

Table VIII lists the intramolecular distances between the N(2) atom of the imidazole ring and the N(3), N(4), or N(5) atom of the cyanoguanidine group, and the orientation between the two moieties in the cimetidine molecules. The *gauche* orientation of the guanidine group with respect to the imidazole ring is observed in forms A and C; their intramolecular N—N distances are in the range of 2.881–5.061 Å for form A and 3.836(7)–4.416(8) Å for form C. On the other hand, form D takes a *trans* orientation; the distance in this form ranges from 5.584(2) to 7.378(2) Å. According to the proposal of Kier (11), the molecular conformation of form A or C would probably be the conformation necessary for effective binding to the histamine H_2-receptor. The conformation of form C, which has an N—N distance of ~3.6 Å and *gauche* orientation, appears to be the most highly preferred conformation for binding to the active site of the receptor, although the energetically stable 10-member ring of form A, effected by an intramolecular hydrogen bond, was also found in the related H_2-receptor antagonists, metiamide (9) and *N*-[4-(imidazol-4-yl)butyl]-*N'*-methylthiourea (burimamide) (13).

Table IX—Effects of Four Crystalline Forms for Stress Ulceration in Rats

Dose, mg/kg	Mean Area of Ulcer, mm^2	Inhibition Rate, %
Control	22.3 ± 4.3	
Form A		
12.5	6.9 ± 2.1	69.3
25.0	5.9 ± 2.4	73.7
50.0	3.4 ± 2.3	84.4
Form B		
12.5	8.7 ± 4.8	60.8
25.0	3.2 ± 1.1	85.5
50.0	3.6 ± 2.2	84.0
Form C		
12.5	2.8 ± 1.7	87.4[a]
25.0	3.2 ± 1.1	85.8
50.0	2.2 ± 0.9	90.4
Form D		
12.5	8.0 ± 2.6	64.1

[a] $p < 0.05$ relative to the same dose of form A or B.

Dissolution Rates of the Four Crystal Forms and Their Efficacy in Preventing Stress Ulceration—The dissolution profiles measured by disk and particle methods are shown in Fig. 9. The rotating disk preparation was carried out under a pressure of 1362 kg/cm^2. The dissolution rate constants of forms A, B, and C were 0.81(6), 0.74(4), and 1.24(6) mg/cm^2/min, respectively; that of form C is ~1.53 and 1.68 times greater than those of forms A and B[9]. In the particle system, the dissolution rate can be expressed in terms of the Hixson–Crowell law (14), $W_0^{1/3} - W^{1/3} = Kt$, where W_0 is the initial weight of drug, W is the undissolved weight at time t, and K is the apparent dissolution rate constant. Up to 40 min, the profiles appear to be linear, suggesting that application of the Hixson–Crowell law is valid for measuring the dissolution rate of cimetidine. The dissolution rate constants of form A, B, C, and D during the 40-min period were 1.16(4), 0.79(1), 1.50(5), and 0.88(6) × 10^{-2} $mg^{1/3}$/min, respectively. The rate constant for form C is ~1.29, 1.70, and 1.90 times greater than those for forms A, D, and B, respectively. The results obtained by these two different methods show clearly that form C is more soluble in deionized water than the other forms. This relationship has also been observed in the difference of their solubilities [5.4(1), 4.7(1), 5.8(1), and 5.0(1) g/liter for forms A, B, C, and D, respectively, at 25°] and in gastric juice[10].

The effect of the four crystalline forms on rat gastric ulcers produced by restraint and water-immersion stress was also examined[11]. The animals received a peroral dose of 12.5, 25.0, or 50.0 mg/kg of the respective crystalline form before water immersion. The inhibition rate of the drug on the development of stress ulcers was calculated as follows:

$$\text{Inhibition rate (\%)} = 100 \times \frac{Mc - Mt}{Mc}$$

where Mc is the mean of the total ulcer area for rats in the control group (n = 12) and Mt is the mean of the total ulcer area in the test groups (n = 6/crystalline form). The Student's t test was used to determine the statistical significance of data obtained in this study. The results are given in Table IX; full details of this experiment will be reported elsewhere. Form C, especially at the lower dose which corresponds to that used clinically, exhibited significant inhibition of stress ulceration; results of the t test at the 12.5-mg/kg dose showed that form C was significantly more effective than forms A, B, and D.

REFERENCES

(1) R. N. Brogden, R. C. Heel, T. M. Speight, and G. S. Avery, *Drugs*, **15**, 93 (1978).

(2) Smith Kline & French, *German Patent Application*, 2742531 (1978).

(3) B. Prodic-Kojic, F. Kajfes, B. Belin, R. Toso, and V. Sunjic, *Gazz. Chim. Ital.*, **109**, 535 (1979).

(4) J. K. Haleblian, *J. Pharm. Sci.*, **64**, 1269 (1975).

(5) P. Main, S. E. Hull, L. Lessinger, G. Germain, J. P. Declerq, and M. M. Woolfson, "A System of Computer Programs for the Automatic Solution of Crystal Structures from X-ray Diffraction Data, MULTAN 78," University of York, England, 1978.

(6) "The Universal Crystallographic Computing System," Library of Programs, Computing Center of Osaka University, Osaka, Japan, 1979.

(7) "International Tables for X-ray Crystallography," vol. IV, Kynoch Press, Birmingham, England, 1974.

[9] The experiment for form D was omitted because of the difficulty in preparing its crystalline form.

[10] H. Kokubo, M. Shibata, K. Morimoto, K. Morisaka, T. Ishida, and M. Inoue, unpublished data.

[11] The inhibition of stress ulceration of form D was examined with only one dose (12.5 mg/kg) because large-scale preparation of this form was very difficult.

(8) E. Hädicke, F. Frickel, and A. Franke, *Chem. Ber.*, 111, 3222 (1978).
(9) K. Prout, S. R. Critchley, C. R. Ganellin, and R. C. Mitchell, *J. Chem. Soc. Perkin Trans. II*, **1977**, 68.
(10) B. Prodic-Kojic and Z. Ruzic-Toros, *Acta Crystallogr.*, **B36**, 1223 (1980).
(11) L. B. Kier, *J. Med. Chem.*, **11**, 441 (1968).
(12) G. J. Durant, C. R. Ganellin, and M. E. Parsons, *J. Med. Chem.*, **18**, 905 (1975).
(13) B. Kamenar, K. Prout, and C. R. Ganellin, *J. Chem. Soc. Perkin Trans. II*, **1973**, 1734.
(14) A. Hixson and J. Crowell, *Ind. Eng. Chem.*, **23**, 923 (1931).

Volume Shifts and Protein Binding Estimates using Equilibrium Dialysis: Application to Prednisolone Binding in Humans

THOMAS N. TOZER, JOHN G. GAMBERTOGLIO ˣ, DANIEL E. FURST, DENIS S. AVERY, and NICHOLAS H. G. HOLFORD

Received November 19, 1981, from the *Schools of Pharmacy and Medicine, University of California, San Francisco, CA 94143.* Accepted for publication October 21, 1982.

Abstract □ Sizable volume shifts can occur during equilibrium dialysis. This net movement of water, presumably caused by the osmotic effect of plasma proteins, reduces the concentration of binding proteins. In this paper the theory of protein binding estimation is extended, equations are developed for calculating the unbound and bound drug concentrations at dialysis equilibrium by correcting for the dilution of the proteins, and the equations are applied to a study of prednisolone. To demonstrate the importance of correcting for the volume shift, the parameters of a model in which prednisolone binds to corticosteroid-binding globulin, a protein with a limited capacity, and albumin were estimated. Unbound and bound concentrations were determined by correcting for both volume shifts (average 31%) and loss of drug to the buffer side, by correcting only for loss of drug to buffer side, and by making no correction at all (the usual method of treating equilibrium dialysis data). The error introduced by neglecting volume shifts was analyzed by comparing the parameter values obtained using the three methods. The results confirm the need to adjust for volume shifts and imply that reported binding constants obtained by equilibrium dialysis may be in error for many substances.

Keyphrases □ Equilibrium dialysis—measurement of protein binding, effect of volume shifts, theoretical model, application to prednisolone in humans □ Protein binding—determined by equilibrium dialysis, effect of volume shifts, theoretical model, application to prednisolone in humans □ Prednisolone—protein binding as determined by equilibrium dialysis, effect of volume shifts, application of theoretical model, humans

Binding of drugs to plasma proteins is important in pharmacokinetics and pharmacodynamics. Equilibrium dialysis is commonly employed for estimation of binding, but it has limitations. With the introduction of translucent cells, it has become evident that sizable volume shifts occur across the dialysis membrane. We have investigated the importance of these volume shifts in the estimation of plasma protein binding parameters and have developed a procedure to correct for them. The procedure is applied to a study of prednisolone in humans.

The binding of prednisolone in plasma is thought to involve two proteins, corticosteroid-binding globulin (transcortin) and albumin. In the range of concentrations associated with therapy (1), the plasma protein binding of prednisolone is concentration dependent largely because of saturable binding to sites on corticosteroid-binding globulin. It has been shown *in vitro* that glucocorticoid activity is a function of unbound concentration and that the activity can be altered by the addition or removal of the globulin (2). Definition of concentration–effect relationships for prednisolone, therefore, requires the ability to estimate unbound prednisolone concentrations. Estimates of unbound concentration *in vivo* can be obtained by measurement of total prednisolone concentration (bound plus unbound) and application of a suitable model for predicting the unbound concentration from the total concentration.

There are several complications in the use of equilibrium dialysis to estimate plasma protein binding. These include binding of drug to the dialysis cell or membrane, transfer of substantial amounts of drug from the plasma to the buffer side of the membrane, and osmotic volume shifts of fluid to the plasma side. Some of these problems have been discussed elsewhere (3). In this paper, a method is described for calculating the magnitude of osmotic volume shifts and for estimating the parameters that reflect binding *in vivo*.

THEORETICAL

Figure 1 is a schematic representation of equilibrium in a dialysis device containing plasma on one side and buffer solution on the other, with and without a volume shift. The volume of the plasma side is increased and the buffer side is decreased, because of a net osmotic transfer of water across the membrane. Osmotic equilibrium may or may not be reached at the time equilibrium is virtually achieved with respect to the drug. The derivations which follow assume conservation of the mass of prednisolone in the system and of the total volume of the two half-cells. Symbols and abbreviations are defined in Appendix I.

Conservation of Volume—The total volume of the cell is unchanged by dialysis; therefore:

$$\underset{\text{(before)}}{V_P + V_B} = \underset{\text{(after)}}{V'_P + V'_B} \qquad \text{(Eq. 1)}$$

Letting δ be the fractional increase in V_P due to osmotic water shift, then:

$$V'_P = V_P(1 + \delta) \qquad \text{(Eq. 2)}$$

and

0022-3549/83/1200-1442$01.00/0

(8) E. Hädicke, F. Frickel, and A. Franke, *Chem. Ber.*, 111, 3222 (1978).
(9) K. Prout, S. R. Critchley, C. R. Ganellin, and R. C. Mitchell, *J. Chem. Soc. Perkin Trans. II*, **1977**, 68.
(10) B. Prodic-Kojic and Z. Ruzic-Toros, *Acta Crystallogr.*, **B36**, 1223 (1980).
(11) L. B. Kier, *J. Med. Chem.*, **11**, 441 (1968).
(12) G. J. Durant, C. R. Ganellin, and M. E. Parsons, *J. Med. Chem.*, **18**, 905 (1975).
(13) B. Kamenar, K. Prout, and C. R. Ganellin, *J. Chem. Soc. Perkin Trans. II*, **1973**, 1734.
(14) A. Hixson and J. Crowell, *Ind. Eng. Chem.*, **23**, 923 (1931).

Volume Shifts and Protein Binding Estimates using Equilibrium Dialysis: Application to Prednisolone Binding in Humans

THOMAS N. TOZER, JOHN G. GAMBERTOGLIO ˣ, DANIEL E. FURST, DENIS S. AVERY, and NICHOLAS H. G. HOLFORD

Received November 19, 1981, from the *Schools of Pharmacy and Medicine, University of California, San Francisco, CA 94143.* Accepted for publication October 21, 1982.

Abstract □ Sizable volume shifts can occur during equilibrium dialysis. This net movement of water, presumably caused by the osmotic effect of plasma proteins, reduces the concentration of binding proteins. In this paper the theory of protein binding estimation is extended, equations are developed for calculating the unbound and bound drug concentrations at dialysis equilibrium by correcting for the dilution of the proteins, and the equations are applied to a study of prednisolone. To demonstrate the importance of correcting for the volume shift, the parameters of a model in which prednisolone binds to corticosteroid-binding globulin, a protein with a limited capacity, and albumin were estimated. Unbound and bound concentrations were determined by correcting for both volume shifts (average 31%) and loss of drug to the buffer side, by correcting only for loss of drug to buffer side, and by making no correction at all (the usual method of treating equilibrium dialysis data). The error introduced by neglecting volume shifts was analyzed by comparing the parameter values obtained using the three methods. The results confirm the need to adjust for volume shifts and imply that reported binding constants obtained by equilibrium dialysis may be in error for many substances.

Keyphrases □ Equilibrium dialysis—measurement of protein binding, effect of volume shifts, theoretical model, application to prednisolone in humans □ Protein binding—determined by equilibrium dialysis, effect of volume shifts, theoretical model, application to prednisolone in humans □ Prednisolone—protein binding as determined by equilibrium dialysis, effect of volume shifts, application of theoretical model, humans

Binding of drugs to plasma proteins is important in pharmacokinetics and pharmacodynamics. Equilibrium dialysis is commonly employed for estimation of binding, but it has limitations. With the introduction of translucent cells, it has become evident that sizable volume shifts occur across the dialysis membrane. We have investigated the importance of these volume shifts in the estimation of plasma protein binding parameters and have developed a procedure to correct for them. The procedure is applied to a study of prednisolone in humans.

The binding of prednisolone in plasma is thought to involve two proteins, corticosteroid-binding globulin (transcortin) and albumin. In the range of concentrations associated with therapy (1), the plasma protein binding of prednisolone is concentration dependent largely because of saturable binding to sites on corticosteroid-binding globulin. It has been shown *in vitro* that glucocorticoid activity is a function of unbound concentration and that the activity can be altered by the addition or removal of the globulin (2). Definition of concentration–effect relationships for prednisolone, therefore, requires the ability to estimate unbound prednisolone concentrations. Estimates of unbound concentration *in vivo* can be obtained by measurement of total prednisolone concentration (bound plus unbound) and application of a suitable model for predicting the unbound concentration from the total concentration.

There are several complications in the use of equilibrium dialysis to estimate plasma protein binding. These include binding of drug to the dialysis cell or membrane, transfer of substantial amounts of drug from the plasma to the buffer side of the membrane, and osmotic volume shifts of fluid to the plasma side. Some of these problems have been discussed elsewhere (3). In this paper, a method is described for calculating the magnitude of osmotic volume shifts and for estimating the parameters that reflect binding *in vivo*.

THEORETICAL

Figure 1 is a schematic representation of equilibrium in a dialysis device containing plasma on one side and buffer solution on the other, with and without a volume shift. The volume of the plasma side is increased and the buffer side is decreased, because of a net osmotic transfer of water across the membrane. Osmotic equilibrium may or may not be reached at the time equilibrium is virtually achieved with respect to the drug. The derivations which follow assume conservation of the mass of prednisolone in the system and of the total volume of the two half-cells. Symbols and abbreviations are defined in Appendix I.

Conservation of Volume—The total volume of the cell is unchanged by dialysis; therefore:

$$\underset{\text{(before)}}{V_P + V_B} = \underset{\text{(after)}}{V'_P + V'_B} \qquad \text{(Eq. 1)}$$

Letting δ be the fractional increase in V_P due to osmotic water shift, then:

$$V'_P = V_P(1 + \delta) \qquad \text{(Eq. 2)}$$

and

0022-3549/83/1200-1442$01.00/0

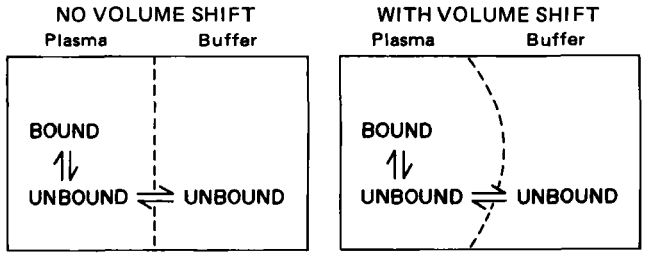

Figure 1—*Schematic diagram of a dialysis cell at equilibrium with respect to drug distribution. Whether there is a volume shift (on right) or not (on left), the unbound concentrations on both sides of the membrane (---) are identical. The amount bound on the plasma side is unchanged, but the bound concentration on the plasma side is decreased as the fluid shifts from the buffer side to the plasma side.*

$$V'_B = V_B - V_P \cdot \delta \qquad \text{(Eq. 3)}$$

Conservation of Mass—The total amount of drug is unchanged by dialysis; therefore $(C_P \cdot V_P + C^*_B \cdot V_B)$ (before) = $(C'_P \cdot V'_P + C'_B \cdot V'_B)$ (after), where C^*_B is the concentration of labeled drug added to the buffer before dialysis. Substituting for V'_P and V'_B using Eqs. 2 and 3 gives $C_P \cdot V_P + C^*_B \cdot V_B = C'_P \cdot V_P(1 + \delta) + C'_B(V_B - V_P \cdot \delta)$. Therefore:

$$C'_P = \frac{C_P \cdot V_P + C^*_B \cdot V_B}{V_P(1 + \delta) + \frac{C'_B}{C'_P}(V_B - V_P \cdot \delta)} \qquad \text{(Eq. 4)}$$

Conservation of Radiolabel—When radiolabeled drug is added to the buffer side before dialysis to produce a concentration of D_B disintegrations/min/ml, then the concentration of radioactivity on the plasma and buffer sides after dialysis are D'_P and D'_B, *i.e.*, $D_B \cdot V_B$ (before) = $(D'_P \cdot V'_P + D'_B \cdot V'_B)$ (after). Substituting for V'_P and V'_B using Eqs. 2 and 3 and solving for δ:

$$\delta = \frac{R \cdot (D_B - D'_B) - D'_P}{D'_P - D'_B} \qquad \text{(Eq. 5)}$$

where R is the ratio of V_B to V_P.

After dialysis, the ratio of unbound drug concentration to total drug concentration (C'_B/C'_P) is the same as the ratio of the radiolabel concentrations (D'_B/D'_P); therefore, Eq. 4 can be simplified by substituting Eq. 5 for δ and by replacing C'_B/C'_P with D'_B/D'_P, giving:

$$C'_P = \frac{(C_P + C^*_B \cdot R)}{R} \cdot \frac{D'_P}{D'_B} \qquad \text{(Eq. 6)}$$

and

$$C'_B = \frac{(C_P + C^*_B \cdot R)}{R} \cdot \frac{D'_B}{D_B} \qquad \text{(Eq. 7)}$$

The bound concentration on the plasma side, C'_{bnd}, is then obtained from the difference between C'_P and C'_B:

$$C'_{bnd} = \frac{(C_P + C^*_B \cdot R)}{R} \cdot \frac{(D'_P - D'_B)}{D_B} \qquad \text{(Eq. 8)}$$

Volume Shift Correction—The amount of drug bound to plasma proteins depends, among other factors, on the amount of binding proteins present and the unbound concentration. At dialysis equilibrium the shift in volume from the buffer side to the plasma side is simply the transfer of buffer solution, containing drug at the unbound concentration, from the buffer to the plasma side as shown in Fig. 1. This transfer does not change the unbound concentration, but the *bound* concentration on the plasma side is decreased by the transfer of fluid. The amount of binding protein is not influenced by the transfer nor is the unbound equilibrium concentration; therefore, the total *amount bound* is the same *with or without* a volume shift.

The theoretical basis of this conclusion has been previously reported (4) for the method of ultrafiltration. In ultrafiltration, plasma filtrate contains drug at the same concentration as that unbound in the plasma. Continued filtration concentrates the protein and the bound drug, but the amount of drug bound remains unchanged. In contrast to ultrafiltration, a volume shift in equilibrium dialysis produces a decrease in the protein and bound drug concentrations as a result of the net transfer of water and unbound drug to the plasma side. In both cases, the concentration of unbound drug remains the same.

Conservation of Amount Bound—The amount bound postdialysis is $C'_{bnd} \cdot V'_P$. From the argument in the previous paragraph, the amount bound if no volume shift had occurred would have been the same. Therefore:

$$C^0_{bnd} \cdot V_P = C'_{bnd} \cdot V'_P \qquad \text{(Eq. 9)}$$

where C^0_{bnd} is the bound drug concentration expected had no volume shift occurred. Substituting for V'_P from Eq. 2 and simplifying:

$$C^0_{bnd} = C'_{bnd}(1 + \delta) \qquad \text{(Eq. 10)}$$

Now substituting for C'_{bnd} from Eq. 8 and for δ from Eq. 5:

$$C^0_{bnd} = \frac{(C_P + C^*_B \cdot R) \cdot [R(D_B - D'_B) - D'_B]}{D_B \cdot R} \qquad \text{(Eq. 11)}$$

Nonlinear Binding—The sum of the estimates of the unbound (Eq. 7) and bound (Eq. 11) concentrations gives the expected total drug concentration in the plasma postdialysis had no volume shift occurred. This value is not the same as the drug concentration in plasma before dialysis, because some drug had been transferred to the buffer during dialysis. To predict the bound and unbound concentrations in the original plasma sample, an appropriate protein binding model, such as the one below (5), must be used:

$$C^0_{bnd} = \frac{CAP_1 \cdot C'_B}{K_{d1} + C'_B} + \frac{CAP_2 \cdot C'_B}{K_{d2} + C'_B} \qquad \text{(Eq. 12)}$$

where CAP_1 and CAP_2 are the binding capacities of two classes of binding protein sites with equilibrium dissociation constants K_{d1} and K_{d2}, respectively. If the concentrations of the binding proteins are measured, CAP_1 and CAP_2 can be expressed as $n_1 \cdot P_1$ and $n_2 \cdot P_2$, where P_1 and P_2 are the concentrations of the binding proteins ($P_1 = P_2$ if both classes of binding sites are on the same protein) and n_1 and n_2 are the numbers of the respective binding sites in each class. If the protein concentrations are not measured, the binding capacities are best expressed as CAP_1 and CAP_2.

If $K_d \gg C'_B$ (as is the case for prednisolone), the model expressed by Eq. 12 reduces to:

$$C^0_{bnd} = \frac{CAP_1 \cdot C'_B}{K_{d1} + C'_B} + S \cdot C'_B \qquad \text{(Eq. 13)}$$

where S is a constant (CAP_2/K_{d2}).

Once the parameters of a model such as Eq. 12 are estimated, the unbound (C_u) and bound (C_{bnd}) concentrations in the original plasma sample can be determined by simultaneous solution of Eq. 13 and the relationship, $C_P = C_{bnd} + C_u$. The unbound and bound concentrations are then:

$$C_u = \frac{C_P - L + \sqrt{(C_P - L)^2 + M \cdot C_P}}{N} \qquad \text{(Eq. 14)}$$

and

$$C_{bnd} = C_P - C_u \qquad \text{(Eq. 15)}$$

where $L = S \cdot K_{d1} + CAP_1 + K_{d1}$, $M = 4 \cdot K_{d1} \cdot (S + 1)$, and $N = 2 \cdot (S + 1)$.

Other Dialysis Systems—The expressions for the unbound (Eq. 7) and bound (Eq. 11) postdialysis concentrations corrected for volume shift are simplified if the initial plasma and buffer volumes are equal, as shown in Appendix II. The relationships for measurement of protein binding when no radiolabel is added are given in Appendix III. Appendix IV provides appropriate relationships for calculating the fraction unbound, a binding parameter commonly used in pharmacokinetics.

Error Introduced by not Recognizing Volume Shifts—The method described above (method I) accounts for volume shifts and for movement of drug from the plasma to the buffer side during dialysis. Behm and Wagner (3) proposed a method for calculating the value of C'_P with the assumption that no volume shift occurs, but accounting for movement of drug from plasma to buffer. On rearrangement and accounting for added radiolabel, their method (method II) becomes:

$$C'_P = \frac{(C_P + C^*_B \cdot R)}{1 + f_u' \cdot R} \qquad \text{(Eq. 16)}$$

where f_u' is the ratio of concentrations of drug (or radiolabel) in the buffer cell to the plasma cell after dialysis (C'_B/C'_P or D'_B/D'_P). Unbound (C'_B) and bound (C'_{bnd}) concentrations are:

$$C'_B = C'_P \cdot f_u' \qquad \text{(Eq. 17)}$$

$$C'_{bnd} = C'_P \cdot (1 - f_u') \qquad \text{(Eq. 18)}$$

A third method (method III) commonly used for protein binding measurements (6), ignores both the volume shift and the shift of drug from the plasma cell to the buffer cell. The unbound and bound concentrations are then given by:

$$C'_B = (C_P + C^*_B \cdot R) \cdot f_u' \quad \text{(Eq. 19)}$$

$$C'_{bnd} = (C_P + C^*_B \cdot R) \cdot (1 - f_u') \quad \text{(Eq. 20)}$$

EXPERIMENTAL

Nine patients who had received kidney transplants volunteered for a comparative bioavailability study of prednisone and prednisolone oral tablets *versus* intravenous prednisolone (1). Plasma samples obtained from this study were stored at −70° before analysis by high-performance liquid chromatography (HPLC) for total prednisolone concentration (7).

The protein binding of prednisolone was determined by equilibrium dialysis, using acrylic plastic equilibrium dialysis cells[1] with a 1-ml maximum capacity/cavity. The membrane employed[2] had a molecular weight cut-off of 12,000–14,000. One-half milliliter of plasma was equilibrated against 0.5 ml of Krebs–Ringer buffer, (pH 7.4, 0.153 *M*), containing 4.5 ng of [6,7-(*n*)-^{3}H]prednisolone (specific activity 43 Ci/mmole)[3]. Dialysis was continued for 16 hr in a shaking incubator[4] at a water temperature of 37°. One-tenth milliliter of dialyzed plasma and 0.1 ml of dialyzed buffer were then transferred to individual glass scintillation vials, to which was added 10 ml of scintillation fluid[5]. After shaking, the vials were counted in a scintillation counter[6]. The counting efficiency was determined by the channels-ratio method of quench correction. Additional correction was made for background counts. The purity (98%) of the radioactive prednisolone was confirmed by TLC and prednisolone was found to be stable in the dialysis cell during the equilibration period.

The bound and unbound concentrations after dialysis were computed after correction for volume shift (method I, Eqs. 7 and 11), by the method proposed by Behm and Wagner (3) (method II, Eqs. 17 and 18), and by the standard method (method III, Eqs. 19 and 20). The fractional increase in the plasma cell volume was calculated using Eq. 5. These calculations were performed using the PROPHET computer system (8). The binding parameters of Eq. 13 were estimated using MKMODEL (9) and unweighted nonlinear least-squares regression (10, 11).

RESULTS AND DISCUSSION

The distribution of volume shifts was estimated from 388 samples used in this study (Fig. 2). The mean volume shift was 0.31 ± 0.15 (mean ± *SD*). There was no correlation between volume shift and predialysis prednisolone concentration. On dialysis of the radiolabel in buffer against an equal volume of buffer, there was no volume shift and negligible binding (<2%) to cell walls or membrane. The binding parameters estimated in the samples from the intravenous and two oral studies by each of the three methods are shown and compared in Table I. The relatively large standard deviations mostly reflect interindividual differences.

Figure 3 shows the fit of the model (Eq. 13) to bound and unbound concentrations obtained by method I from an individual subject. Using average parameter values, graphs of bound against unbound concentrations were simulated (Fig. 4) using MKMODEL (7). In a similar fashion, the unbound concentrations predicted by the binding parameters from each method were plotted as a function of total concentration (Fig. 5). Finally, the unbound fraction was calculated for each method as a function of the total concentration (Fig. 6).

Measurement of drug (or radiolabel) on the plasma side after dialysis is not required when using the volume correction method. However, this measurement can be used to estimate the magnitude of the volume shift. A mean volume shift of 31% was estimated with the aforementioned dialysis conditions. The most likely cause of the shift is the osmotic effect of the impermeable plasma proteins; its magnitude is presumably controlled by the duration of dialysis, the concentration of protein, the area and thickness of the membrane, and other factors that determine the rate of osmotic equilibration.

[1] Technilab Instruments.
[2] Spectrapor No. 2, Spectrum Medical.
[3] Amersham Corp.
[4] Dubnoff Metabolic Shaking Incubator; Precision Scientific Co., Chicago, Ill.
[5] Aquasol, New England Nuclear.
[6] Model 3320, Packard.

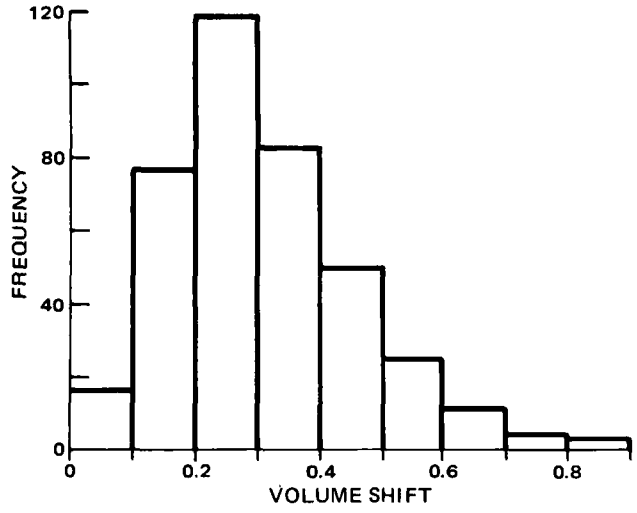

Figure 2—*Distribution of volume shifts (expressed by the fractional increase in V_p) calculated using Eq. 5 for 388 protein binding measurements. The statistics of the distribution are:* N = *388; mean* ± SD = *0.31* ± *0.15; median = 0.29; geometric mean = 0.27; range = 0.005–0.86; skewness = 0.91; kurtosis = 1.03.*

Failure to recognize and compensate for volume shifts in equilibrium dialysis can be a serious source of error. For example, if the volume shift determined in this study had been ignored, the pharmacokinetic parameters, clearance, and volume of distribution based on the unbound concentration, would have been underestimated by ~30%.

We contend that the proposed method (method I) for estimating the concentration of bound and unbound drug after equilibrium dialysis is superior to the other methods. This contention is based on the extension of the theoretical basis for equilibrium dialysis outlined in *Theoretical.*

It is clear from Table I that estimates of protein binding parameters are dependent on the method chosen for calculation of bound and unbound concentrations. The disparity between the predictions based on these parameter estimates, for bound as a function of unbound concentration and for unbound concentration or fraction unbound as a function of total drug concentration, are shown in Figs. 4–6. These differences are largely explained by the failure of methods II and III to account for the shift of fluid between the dialysis chambers.

The proposed method corrects for volume changes whether nonlinear binding is absent or present. The method is potentially required for any substance, drug or hormone, whose binding is estimated by equilibrium dialysis. Furthermore, the results of this study imply that all equilibrium dialysis binding data in the literature may be in error to the extent that volume shifts occurred and were ignored.

APPENDIX I: GLOSSARY OF TERMS

Volume Terms

V_P	Volume before dialysis on plasma side of dialysis cell
V'_P	Volume after dialysis on plasma side of dialysis cell
V_B	Volume before dialysis on buffer side of dialysis cell
V'_B	Volume after dialysis on buffer side of dialysis cell
R	Ratio of V_B to V_P
δ	Fractional increase in V_P due to volume change during dialysis

Concentration Terms

C_P	Total plasma drug concentration before dialysis, including radiolabeled drug if added to plasma
C'_P	Total drug concentration on plasma side after dialysis
C'_B	Drug concentration after dialysis on buffer side (unbound drug concentration on both sides at equilibrium)
C'_{bnd}	Bound drug concentration on plasma side after dialysis
C^0_{bnd}	Bound drug concentration that would have been observed after dialysis if no volume shift had occurred
C_{bnd}	Bound drug concentration in plasma before dialysis
C_u	Unbound drug concentration in plasma before dialysis
C^*_B	Concentration of radiolabelled drug in buffer before dialysis

Table I—Prednisolone Protein Binding Parameters

Method	Binding Capacity (CAP_1), ng/ml		Dissociation Constant (K_{d1}), ng/ml		Nonspecific Binding Constant (S)	
	iv[a]	po[b]	iv[a]	po[b]	iv[a]	po[b]
I	168 ± 52[c]	199 ± 154	18 ± 6	42 ± 73	2.1 ± 0.9	2.3 ± 1.9
II	202 ± 100	205 ± 146	31 ± 21	33 ± 26	1.2 ± 0.5	1.4 ± 1.2
III	241 ± 114	247 ± 183	40 ± 27	41 ± 32	1.3 ± 0.4	1.5 ± 1.2

[a] IV = intravenous prednisolone (N = 9). [b] PO = values for prednisolone following oral prednisone or oral prednisolone (N = 9 for both drugs). [c] Mean ± SD.

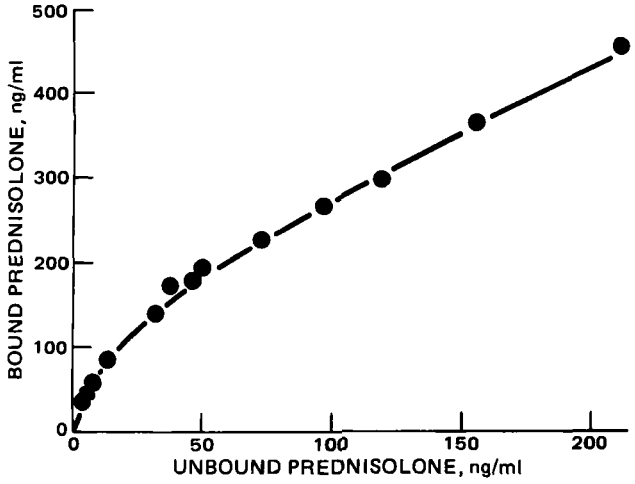

Figure 3—*Typical data of one individual for the determination of binding parameters. The bound concentration was determined by method I (see text) which corrects for volume shifts. The line was obtained by fitting the parameters of Eq. 13 to the data using unweighted nonlinear least-squares regression.*

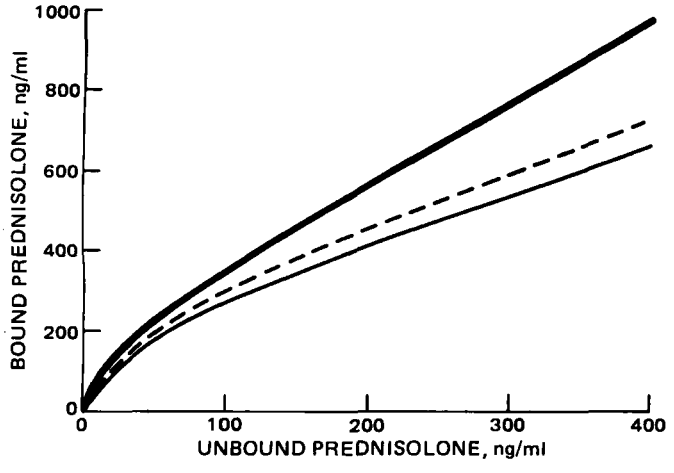

Figure 4—*Simulated relationships between bound and unbound prednisolone concentrations. Parameter values, from fits of individual data to Eq. 13 using the three methods, were averaged for the simulation. The average parameter values for CAP_1, K_{d1}, and S were: (—) method I, 168, 18, 2.1: (—) method II, 202, 31, 1.2; (------) method III, 241, 40, 1.3.*

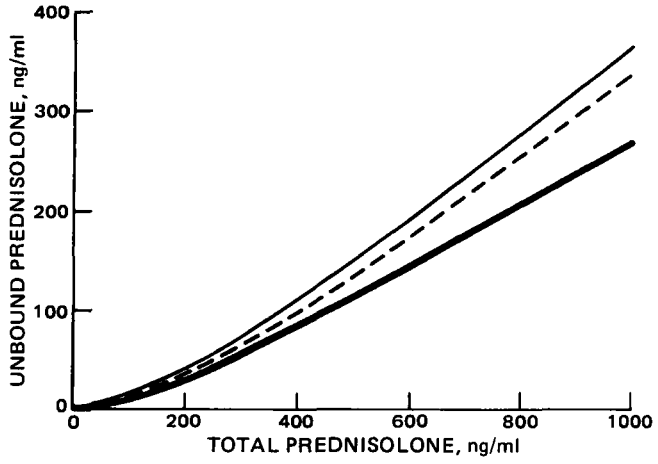

Figure 5—*Simulated relationship between unbound and total prednisolone concentrations using the three methods for determining prednisolone binding. The average parameter values are given in Fig. 4. Key: (—) method I; (—) method II; (---) method III.*

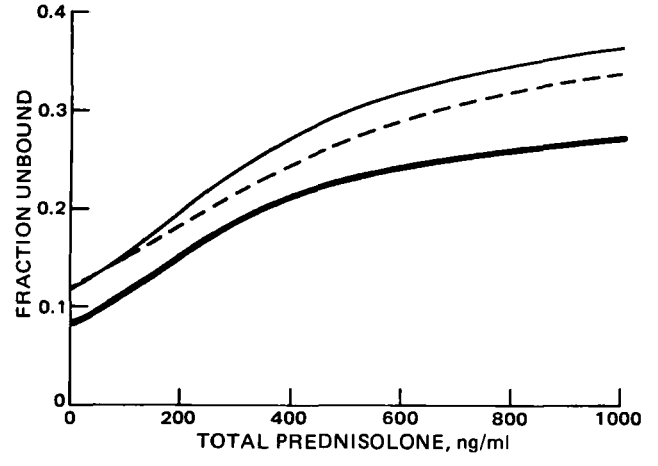

Figure 6—*Simulated relationship between the unbound fraction and the total prednisolone concentration using the three methods for determining prednisolone binding. The average parameter values are given in Fig. 4. Key: (—) method I; (—) method II; (---) method III.*

D_P Radiolabel concentration (dpm/ml) in plasma before dialysis (label added to plasma)

D'_P Radiolabel concentration (dpm/ml) on plasma side after dialysis

D_B Radiolabel concentration (dpm/ml) in buffer before dialysis

D'_B Radiolabel concentration (dpm/ml) on buffer side after dialysis

Binding Parameters

CAP_1, CAP_2 Binding capacities for drug to plasma proteins at two different sites

K_{d1}, K_{d2} Equilibrium dissociation constants for two different sites

S Ratio of CAP_2 to K_{d2}

f_u Ratio of C_u to C_P

f_u' Ratio of C'_B to C'_P

APPENDIX II: EQUAL PREDIALYSIS VOLUMES

In the derivations herein, the volume of the plasma and buffer cell contents are assumed to be unequal at the start of dialysis. It is common practice, as in these studies, to use equal volumes. This simplifies the expressions for unbound (Eq. 7) and bound (Eq. 11) concentrations incorporating the volume correction, that is:

$$C'_B = (C_P + C'_B)\frac{D'_B}{D_B} \qquad \text{(Eq. A1)}$$

$$C^0_{bnd} = C_P + C^*_B - 2 \cdot C'_B \quad \text{(Eq. A2)}$$

APPENDIX III: DIRECT DRUG MEASUREMENT

If concentration of drug (no radiolabel added) is measured, the volume-corrected bound concentration postdialysis is given by:

$$C^0_{bnd} = C_P - C'_B\,(R + 1) \quad \text{(Eq. A3)}$$

From mass balance, $V_P C_P = C'_P \cdot V'_P + C'_B \cdot V'_P$ and using Eqs. 2 and 3, the volume shift δ is:

$$\delta = \frac{C_P - C'_P - R \cdot C'_B}{(C_P - C'_B)} \quad \text{(Eq. A4)}$$

APPENDIX IV: THE FRACTION UNBOUND

Label Added to Buffer—The fraction unbound, f_u', after dialysis and corrected for volume shift, can be calculated from the concentrations of radioactivity in the buffer before and after dialysis. The relationship is:

$$f_u' = \frac{D'_B}{R(D_B - D'_B)} \quad \text{(Eq. A5)}$$

when radiolabel is initially added to the buffer. The relationship is obtained from Eqs. 7 and 11 and the definition of fraction unbound, $f_u' = C'_B/(C^0_{bnd} + C'_B)$. The fraction unbound after dialysis, when no radiolabel is added and drug is initially present in plasma, is:

$$f_u' = \frac{C'_B}{C_P - R \cdot C'_B} \quad \text{(Eq. A6)}$$

This relationship is obtained from Eqs. A3 and A4.

Label Added to Plasma Before Dialysis—Relationships similar to Eqs. 7, 11, and A5, can be derived for the situation in which radiolabel is added to the plasma before dialysis. These relationships, corrected for volume shift, are:

$$C'_B = C_P \cdot \frac{D'_B}{D_P} \quad \text{(Eq. A7)}$$

$$C^0_{bnd} = \frac{C_P \cdot [D_P - D'_B(R + 1)]}{D_P} \quad \text{(Eq. A8)}$$

$$f_u' = \frac{D'_B}{D_P - R \cdot D'_B} \quad \text{(Eq. A9)}$$

where C_P is the drug concentration, including radiolabel, and D_P is the disintegrations per min per ml in the plasma before dialysis.

Fraction Unbound When Nonlinear Binding Occurs—The fractions unbound calculated by Eqs. A5, A6, and A9 are the values expected at the postdialysis total plasma concentration; the fraction unbound in the plasma sample drawn from a subject or patient will be different, because of loss of drug to the buffer side. The fraction unbound in the original sample can then be determined from the unbound and bound concentrations as calculated in Eqs. 14 and 15 and from the definition of f_u, *i.e.*, $f_u = C_u/(C_u + C_{bnd})$.

REFERENCES

(1) J. G. Gambertoglio, F. J. Frey, N. H. G. Holford, J. L. Birnbaum, P. Stanik Lizak, F. Vincenti, N. J. Feduska, O. Salvatierra, Jr., and W. J. C. Amend, Jr., *Kidney Intl.*, **21,** 621 (1982).

(2) P. L. Ballard, in "Glucocorticoid Hormone Action," J. D. Baxter and G. G. Rousseau, Eds., Springer Verlag, New York, N.Y., 1979, pp. 25–48.

(3) J. L. Behm and J. G. Wagner, *Res. Commun. Chem. Pathol. Pharmacol.*, **26,** 145 (1979).

(4) J. A. Sophianopoulos, S. J. Durham, A. J. Sophianopoulos, H. L. Ragsdale, and W. P. Cropper, *Arch. Biochem. Biophys.*, **187,** 132 (1978).

(5) J. G. Wagner, "Fundamentals of Clinical Pharmacokinetics," Drug Intelligence Publications, Hamilton, Ill., 1975, p. 27.

(6) P. A. Routledge, A. Barchowsky, T. D. Bjornsson, B. B. Kitchess, and D. G. Shand, *Clin. Pharmacol. Ther.*, **27,** 347 (1980).

(7) F. J. Frey, B. N. Frey, and L. Z. Benet, *Clin. Chem.*, **25,** 1944 (1979).

(8) W. F. Raub, *Fed. Proc.*, **33,** 2790 (1979).

(9) N. H. G. Holford, *in* "PROPHET Public Procedures," H. M. Perry and J. J. Wood, Eds., Bolt, Beranek, and Newman, Cambridge, Mass., 1982, p. 89.

(10) J. B. Whitlan and K. G. Brown, *Intl. J. Pharmacokinet.*, **5,** 49 (1980).

(11) G. Knott, *Comp. Biomed. Res.*, **10,** 271 (1979).

ACKNOWLEDGMENTS

This work was supported, in part, by Grants AM 27099, GM 16496, GM 28423, and GM 28072 from the National Institutes of Health and by a grant from the Academic Senate Committee on Research, University of California, San Francisco.

Direct Determination of Avermectins in Plasma at Nanogram Levels by High-Performance Liquid Chromatography

JAMES V. PIVNICHNY ˣ, JUNG-SOOK K. SHIM, and LAURIE A. ZIMMERMAN

Received June 16, 1982, from the *Merck Sharp and Dohme Research Laboratories, Rahway, NJ 07065.* Accepted for publication October 21, 1982.

Abstract □ 22,23-Dihydroavermectin B_{1a} (I) is determined in animal plasma over the concentration range 5–60 ng/ml by reverse-phase high-performance liquid chromatography (HPLC) with UV photometric detection. Prior to HPLC the sample is isolated by gravity-fed adsorption column chromatography on Florisil. The Δ^2 isomer of I (designated as compound III) is used as an internal standard, and the conversion of I to this isomer by base hydrolysis is described. An accuracy of 2 ng/ml (mean deviation) and a precision in the range of 1–3 ng/ml (standard deviation) were observed for the method. The limit of detection is 2 ng/ml based on the background observed for normal cattle plasma. The method is applicable to bioavailability studies of I at usual therapeutic concentrations.

Keyphrases □ Avermectins—direct determination in plasma at nanogram levels, high-performance liquid chromatography, isomerization by hydrolysis □ High-performance liquid chromatography—direct determination of avermectins in plasma at nanogram levels, isomerization by hydrolysis □ Isomerization—avermectins in plasma, hydrolysis, direct determination at nanogram levels, high-performance liquid chromatography

The avermectins are disaccharide derivatives of a structurally similar group of pentacyclic 16-membered lactones (1, 2) which function as broad-spectrum antiparasitic agents (3, 4). Studies in a variety of animals (5) have indicated that these compounds are exceptionally potent. Because of this, effective dosage levels are unusually low (typically 0.2 mg/kg), and the concentrations of this drug found in plasma samples from animals treated with such doses are correspondingly low (<100 ng/ml). The analytical procedure originally reported for determining the avermectins in animal plasma (6) is based on conversion of these compounds to fluorescent derivatives followed by high-performance liquid chromatography (HPLC) with fluorometric detection. The derivatization reaction, which involves dehydration using acetic anhydride–pyridine to form a six-membered aromatic ring in conjugation with a butadiene unit, is time consuming and sensitive to minor experimental variations. A recently reported modification of this method applied to cattle and sheep tissue (7) makes use of the catalyst 1-methylimidazole, as developed by Connors and coworkers for the acetylation of hydroxy compounds (8, 9), to decrease both the reaction time and variability.

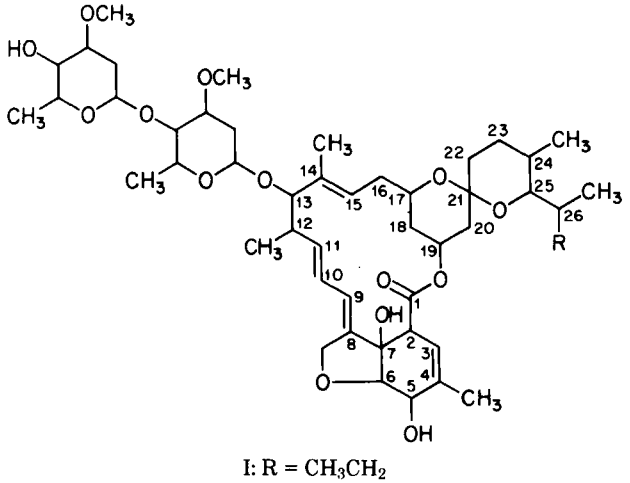

I: R = CH_3CH_2
II: R = CH_3

This report describes a direct HPLC procedure with UV photometric detection for determining the avermectins in animal plasma. The particular avermectin component used, 22,23-dihydroavermectin B_{1a} (I), is one of major pharmaceutical interest. The method requires no derivatization and yet has a detection limit approaching that of the original fluorescence procedure.

EXPERIMENTAL

Instrumentation—A high-performance liquid chromatograph was used which consisted of a pump[1] operated at a constant flow rate of 0.8 ml/min, an automatic sample injector with the capability of handling 0.25-ml sample volumes[2], a prepacked microparticulate octadecylsilyl column[3], and a variable-wavelength photometric detector[4] set at 245 nm. The detector output (0.02 AUFS) was displayed on a strip chart recorder[5], and the column was completely enclosed in a water jacket maintained at 30° with a circulating constant-temperature bath[6].

Reagents—The production and isolation of the avermectins has been previously described (10, 11). The purity of the various lots of I used in this study, each of which contained <10% 22,23-dihydroavermectin B_{1b} (II), was established by HPLC. The conversion of I to its Δ^2 isomer (III) for use as an internal standard is described below. All solvents were either HPLC grade[7] or distilled in glass[8]. Distilled water was further purified by passing through an ultrapure water system[9]. The chromatographic eluant was acetonitrile–methanol–water (53:35:7).

22,23-Dihydroavermectin B_{1a} Δ^2 Isomer (III)—A solution of 20 mg/ml of I in methanol–water (9:1) was mixed with an equal volume of 0.1 *M* KOH in the same solvent. After 4 hr at room temperature, portions of the reaction mixture were injected into the HPLC system described above, and III was collected as a solution in the eluant as it emerged from the detector. A total amount of III in excess of 5 mg was collected from 10 separate 0.1-ml injections. After dilution with methanol, the concentration of III in this solution was determined by comparison of its HPLC peak area to that of I using the assumption that the molar absorptivities for the two compounds are equal at the detector wavelength.

Florisil Columns—Florisil[10], 100–200 mesh, was washed thoroughly with chloroform–ethyl acetate (3:1), dried, and then washed with water

[1] Model 740B; Spectra-Physics, Santa Clara, Calif.
[2] Model 710B WISP; Waters Associates, Milford, Mass.
[3] ZORBAX ODS, 4.6 mm i.d. × 250 mm; DuPont, Wilmington, Del.
[4] Spectromonitor III; Laboratory Data Control, Riviera Beach, Fla.
[5] Model 561; Linear Instruments, Irvine, Calif.
[6] Model FS, Haake Instruments, Saddle Brook, N.J.
[7] Fisher Scientific, Pittsburgh, Pa.
[8] Burdick and Jackson, Muskegon, Mich.
[9] Super-Q; Millipore Corp., Bedford, Mass.
[10] Floridin, Pittsburgh, Pa.

0022-3549/83/1200-1447$01.00/0

and dried overnight at 120°. Glass columns (0.7-cm i.d. × 10 cm) were fabricated with conical funnel tops (6.5-cm diameter) and constricted bottoms. A small plug of silanized glass wool was inserted into each column followed by 0.40 g of Florisil. Each prepared column was rinsed with 10 ml of chloroform immediately before use.

Procedure—A plasma sample was combined with the internal standard by first evaporating 1.00 ml of a 140-ng/ml solution of III in an extraction vessel (50-ml centrifuge tube) at 50° under a stream of dry nitrogen and then adding 5.00 ml of the plasma. The sample was then extracted with three 15-ml portions of ethyl acetate, and the combined extracts were evaporated to dryness as above. The residue was dissolved in 1 ml of chloroform and placed on the Florisil column. Two chloroform rinses (1 ml each) and one additional 10-ml portion of chloroform were added to the column. Elution with 25 ml of chloroform–ethyl acetate (3:1) which had been saturated with water afforded the desired fraction. After evaporating to dryness at 50° with dry nitrogen, this was dissolved in 0.25 ml of methanol–water (19:1).

A 0.10-ml aliquot was injected into the chromatographic system. An analytical reference standard was processed as 1.0 ml of a chloroform solution containing 100 ng/ml of I and 140 ng/ml of III, starting with the Florisil chromatography. Quantitation was by peak height measurement with normalization using the internal standard.

RESULTS AND DISCUSSION

Characterization of the Analytical Method—The suitability of ethyl acetate for extracting the avermectins from animal plasma has previously been demonstrated using radiolabeled I in the original fluorescence HPLC procedure (6). The only modification employed here was the elimination of the initial treatment with ethanol. The Florisil column described in the original method was used here, but a total of 13 ml of chloroform was used to load the column instead of the 6 ml originally used. The additional chloroform removed more potential interfering material from the Florisil column before the desired material was eluted with water-saturated ethyl acetate–chloroform.

Typical chromatograms for a sample of normal cattle plasma supplemented with 40 ng/ml of I and the analytical reference standard are shown in Fig. 1. The sample (I) and the internal standard (III) elute with capacity factors (k') of 8.8 and 11.1, respectively, and are completely resolved from each other as well as from interfering endogenous substances. A small amount of the avermectin component II is apparent in the chromatogram of the analytical reference standard, but any of this which might be in the sample is obscured by extraneous plasma components.

No plasma components, however, interfere significantly with either the sample or the internal standard. This is shown in Fig. 2. Chromatogram A, which was obtained for a sample of drug-free cattle plasma, shows only a small peak eluting at the retention time of I. For this particular sample, the peak corresponds to an apparent drug concentration of 1.5 ng/ml. Chromatogram B was obtained from a plasma sample from an animal which had been dosed with I as described below. The sample was processed through the analytical procedure in the absence of internal standard; nothing can be seen eluting at the retention time of this compound. The peak and shoulder that are seen in this chromatogram eluting with retention times slightly less than that of III are due to extraneous plasma components which have been observed in varying amounts in the plasma of different animals. This case represents the maximum amount of these components encountered for any animal examined in this study, and, in fact, the components are completely absent in the other chromatograms illustrated here.

This analytical method is accurate and precise when applied to samples of cattle plasma containing I in the concentration range of 5–60 ng/ml. When normal cattle plasma was supplemented with I over this range, a mean deviation of 1.7 ng/ml from the expected concentration was observed. Linear least-squares analysis of these found *versus* expected results, which are listed in Table I, yield a coefficient of determination (r^2) of 0.979 with a slope of 0.936 and an intercept of 1.6 ng/ml. Replicate determinations at supplemented levels of 20, 30, 40, and 60 ng/ml indicate within-run precision values in the range of 1–3 ng/ml (standard deviation). Since the data of Table I are the combined results of five individual runs, an indication of between-run precision is given by the standard error of estimate for the least-squares fit. This value is 2.2 ng/ml. Analyses of samples from eight control animals showed an average apparent concentration of 1.1 ng/ml of I with a standard deviation of 0.9 ng/ml, demonstrating that the method is free of interferences at concentrations >5 ng/ml.

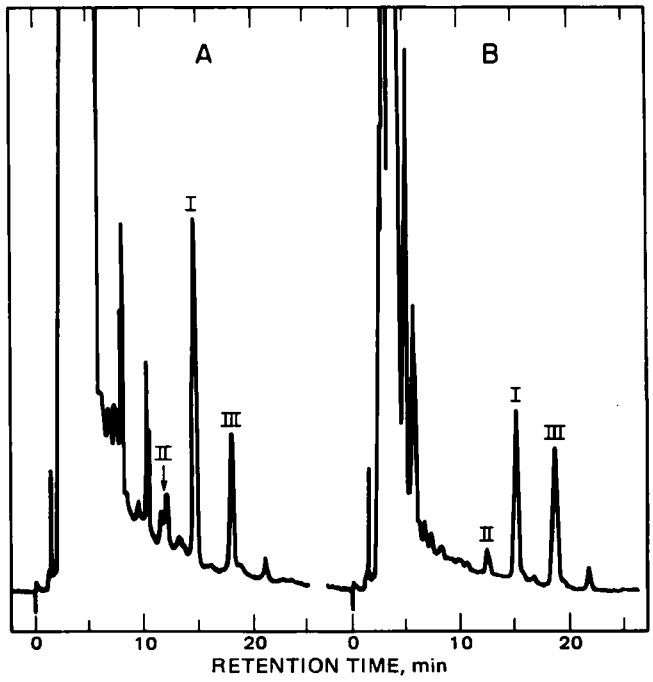

Figure 1—*Chromatograms obtained with this analytical procedure. Key: (A) normal cattle plasma supplemented with 40 ng/ml of I; (B) analytical reference standard corresponding to a sample containing 20 ng/ml of I carried through the procedure.*

The overall recoveries of both sample and internal standard carried through the analytical procedure were ~80%. This was determined by supplementing several 5-ml samples of normal cattle plasma with 100 ng of I and 140 ng of III, processing them through the entire procedure, and comparing the resultant chromatographic signals to those obtained for the same amounts of I and III chromatographed directly. These recovery values are essentially the same as that previously determined for I in the portion of the fluorescence procedure preceding the derivatization reaction (6).

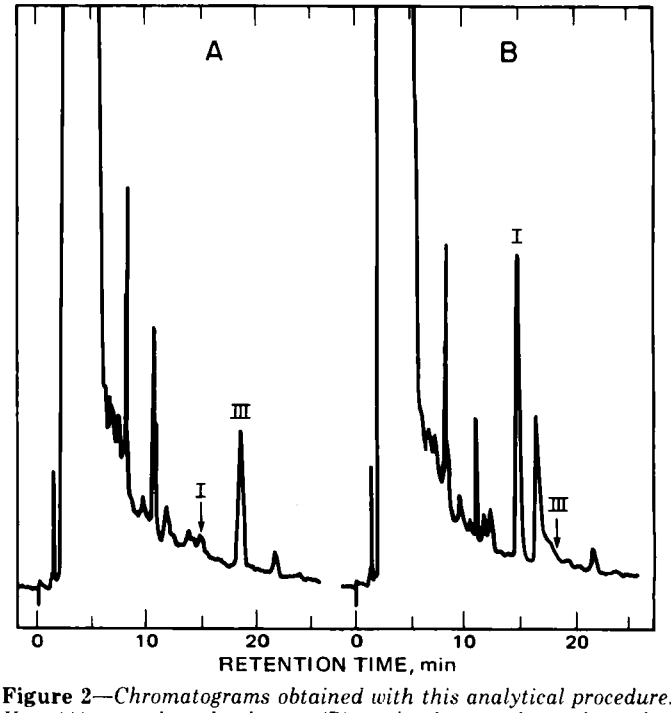

Figure 2—*Chromatograms obtained with this analytical procedure. Key: (A) normal cattle plasma; (B) cattle plasma taken 3 days after dosing with 0.2 mg/kg of I. The internal standard was omitted from the analytical procedure.*

Table I—Accuracy and Precision of the Method Applied to Normal Cattle Plasma Supplemented with Various Amounts of I

Concentration Added, ng/ml	Mean Concentration Determined, ng/ml	Number of Determinations	Standard Deviation ng/ml
5.0	6.0	1	—
15.0	14.4	1	—
20.0	21.5	5	1.0
25.0	25.9	1	—
30.0	30.1	8	0.8
35.0	31.6	1	—
40.0	37.4	8	2.5
45.0	45.8	1	—
55.0	54.9	1	—
60.0	58.1	7	2.8

Application—To further test this analytical procedure, it was applied to plasma samples obtained from an *in vivo* study involving an Angus steer. The animal was dosed subcutaneously with a solution of I at a dosage level of 0.2 mg/kg, and samples were collected over the period of 2 weeks. The observed concentration–time profile is shown in Fig. 3. A maximum concentration of ~70 ng/ml was reached in 1 day, and the elimination phase closely follows first-order decay kinetics as shown by the semilogarithmic insert in the figure. Least-squares fitting of the results covering 1–14 days gives the expression:

$$C = 80.6e^{-0.236t}$$

where C is the concentration in ng/ml and t is time in days. The coefficient of determination (r^2) is 0.993, and the half-life for elimination is 2.9 days.

The Δ^2 Isomer (III)—The avermectins react with hydroxide in methanol–water solutions to give a number of products as shown by the chromatograms of Fig. 4. Starting with I under the conditions chosen here, the predominant initial reaction is an epimerization of the hydrogen at C-2 to form IV. This compound has a slightly greater retention time than I in the chromatographic system, and the amount of IV increases as the amount of I decreases. The eventual result might be complete conversion of I to IV or the establishment of an equilibrium mixture of I and IV were it not for the fact that a third product forms by the shifting of a double bond from the C-3 position to C-2 to produce III.

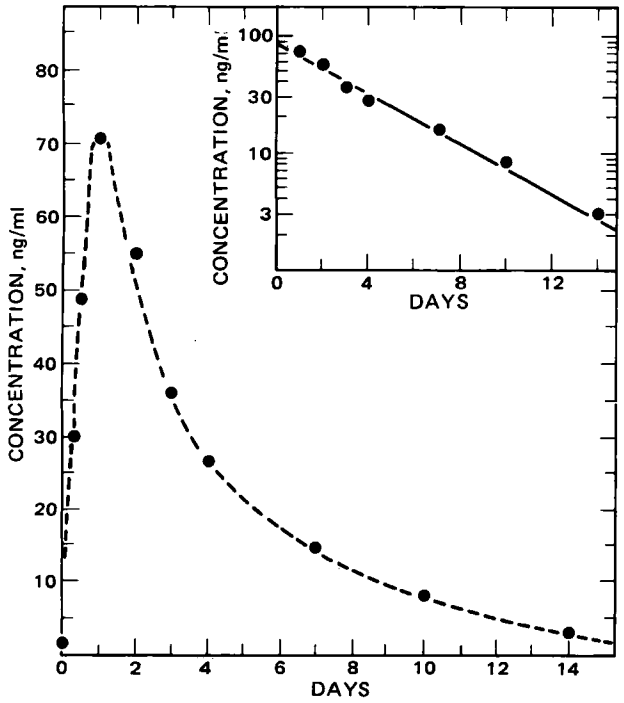

Figure 3—*Plasma concentration of I observed for an Angus steer dosed subcutaneously with I at a level of 0.2 mg/kg. The insert presents the elimination phase data on a logarithmic scale.*

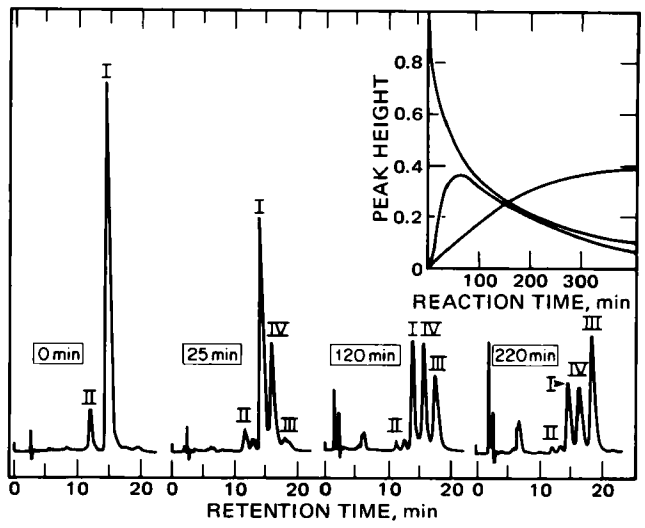

Figure 4—*Chromatograms showing the conversion of I to its 2-epimer and Δ^2 isomer by reaction with 0.05 M KOH in methanol–water (9:1). The inset shows the variation in chromatographic peak heights over the course of the reaction.*

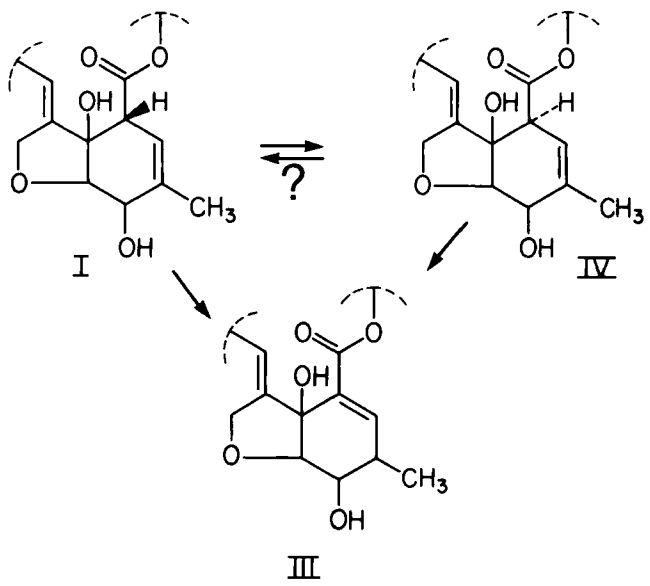

Scheme I

In the chromatographic system, III elutes after IV, and although its concentration increases more slowly than IV early in the reaction, it continues to increase even after IV begins to decrease. Eventually it becomes the predominant product, and at this point it is isolated by semipreparative HPLC. It is not known how stable III is in the basic reaction mixture, but after isolation it is completely stable in methanolic solution at 5° for at least several months. Also, it is not known whether the mechanism is strictly stepwise, that is, I goes to IV which then goes to III, or whether I and IV simultaneously are converted to III as indicated in Scheme I. Compound IV was identified by comparison of its HPLC retention time to that of an authentic sample which had been independently synthesized[11], and III was identified on the basis of its 300-MHz ^{1}H-NMR spectrum[12].

Using III as an internal standard is appropriate since its structure is very similar to that of the sample. That two such large molecules differing

[11] H. Mrozik, Merck Sharp and Dohme Research Laboratories, June 1979, personal communication.

[12] B. H. Arison, Merck Sharp and Dohme Research Laboratories, June 1979, personal communication.

only in the position of a double bond can be so well separated demonstrates that excellent efficiency and selectivity are provided by the chromatographic system. For all steps in the procedure other than HPLC, the two compounds behave identically. In addition, it is advantageous that the internal standard is easily prepared from the sample. The only problem in this situation is that the internal standard may also be a metabolite of the drug; but, this is not the case here. The plasma sample (Fig. 2B) which was analyzed with no internal standard was taken from an animal 3 days after dosing and 2 days after the highest drug concentration had been observed. No peak corresponding to III is present. Similarly, plasma samples taken at later times also show nothing eluting at this retention time.

CONCLUSION

The analytical procedure presented here is a substantial simplification of the original fluorescence derivatization HPLC method. At a typical therapeutic plasma concentration of 40 ng/ml, the observed mean deviation of 1.7 ng/ml corresponds to an accuracy of 4% mean relative error. Similarly, the standard deviation of 2 ng/ml typically observed corresponds to a precision of 5% relative standard deviation. These values are essentially the same as those observed for the fluorescence method. As one would expect, the fluorescence method has a definite advantage with a detection limit of one-tenth that of the direct method. However, the direct method is more rapid and reliable, and with a detection limit of 2 ng/ml, it is entirely suitable for quantitative determination of avermectins in plasma at normally effective dosage levels. Numerous bioavailability studies with both cattle and swine in which peak drug concentrations have ranged from 50 to 100 ng/ml have been successfully conducted in these laboratories using this analytical procedure.

REFERENCES

(1) G. Albers-Schönberg, B. H. Arison, J. C. Chabala, A. W. Douglas, P. Eskola, M. H. Fisher, A. Lusi, H. Mrozik, J. L. Smith, and R. L. Tolman, *J. Am. Chem. Soc.*, **103**, 4216 (1981).

(2) J. P. Springer, B. H. Arison, J. M. Hirshfield, and K. Hoogsteen, *J. Am. Chem. Soc.*, **103**, 4221 (1981).

(3) J. C. Chabala *et al.*, *J. Med. Chem.*, **23**, 1134 (1980).

(4) J. R. Egerton, J. Birnbaum, L. S. Blair, J. C. Chabala, J. Conroy, M. H. Fisher, H. Mrozik, D. A. Ostlind, C. A. Wilkins, and W. C. Campbell, *Br. Vet. J.*, **136**, 88 (1980).

(5) J. R. Egerton, D. A. Ostlind, L. S. Blair, C. H. Eary, D. Suhayda, S. Cifelli, R. F. Riek, and W. C. Campbell, *Antimicrob. Agents Chemother.*, **15**, 372 (1979).

(6) J. W. Tolan, P. Eskola, D. W. Fink, H. Mrozik, and L. A. Zimmerman, *J. Chromatogr.*, **190**, 367 (1980).

(7) P. C. Tway, J. S. Wood, and G. V. Downing, *J. Agric. Food Chem.*, **29**, 1059 (1981).

(8) R. Wachowiak and K. A. Connors, *Anal. Chem.*, **51**, 27 (1979).

(9) K. A. Connors and N. K. Pandit, *Anal. Chem.*, **50**, 1542 (1978).

(10) R. W. Burg *et al.*, *Antimicrob. Agents Chemother.*, **15**, 361 (1979).

(11) T. W. Miller *et al.*, *Antimicrob. Agents Chemother.*, **15**, 368 (1979).

ACKNOWLEDGMENTS

The authors thank J. B. Williams, F. P. Baylis, and their staffs for dosing the animals and providing plasma samples for the bioavailability experiment.

Coil → Helix Transition in Polyadenylic Acid Induced by the Binding of Epinephrine, Norepinephrine, and Isoproterenol: Circular Dichroism Study

HANNA N. BORAZAN ˣ and SONA N. KOUMRIQIAN

Received October 21, 1981, from the *Department of Pharmaceutical Chemistry, College of Pharmacy, University of Baghdad, Baghdad, Republic of Iraq.* Accepted for publication October 19, 1982.

Abstract □ A circular dichroism spectropolarimetric study on the conformation of polyadenylic acid (poly A) in neutral solutions demonstrated a coil → helix transition induced by intercalative binding of critical amounts of epinephrine, norepinephrine, and isoproterenol relative to poly A. Theoretical treatment of the experimental data indicated a first-order kinetic transition in poly A. It was possible to measure transition rate constants of the epinephrine–poly A and norepinephrine–poly A systems and to calculate the activation energies. The results indicate a high level of temperature dependence of the rate constants. The effects can be reversed by increasing ionic strength, indicating the significance of the electrostatic interactions. The importance of the results is discussed in terms of the possible role of the catecholamines as control mechanisms for the poly A-regulated translation of the genetic code on mRNA.

Keyphrases □ Polyadenylic acid—coil → helix transition, intercalative binding of epinephrine, norepinephrine, and isoproterenol, circular dichroism □ Catecholamines—epinephrine, norepinephrine, isoproterenol, intercalative binding to polyadenylic acid, coil → helix transition, circular dichroism □ Coil → helix transition—of polyadenylic acid, induced by catecholamines, intercalative binding of epinephrine, norepinephrine, and isoproterenol, circular dichroism

Most mRNA molecules contain stretches of polyadenylic acid (poly A) at the 3′-end (1), with length of the poly A depending on the evolutionary level of the organism; the larger segments of poly A exist in highly differentiated cells (2). The exact function of this poly A segment is not yet known. Some researchers have proposed that the segments are responsible for increasing the stability of mRNA by inducing a circular structure, while others found that the translation of the genetic code becomes far more efficient in the presence of poly A, attributed to the greater stability of mRNA afforded by poly A (3).

In a continuing effort to study the diversity of the biological effects of adrenergic compounds at the molecular level, the investigation of the possibility that nucleic acids are the target molecules of these drugs was conducted in this laboratory. The present study deals with circular di-

0022-3549/83/1200-1450$01.00/0

only in the position of a double bond can be so well separated demonstrates that excellent efficiency and selectivity are provided by the chromatographic system. For all steps in the procedure other than HPLC, the two compounds behave identically. In addition, it is advantageous that the internal standard is easily prepared from the sample. The only problem in this situation is that the internal standard may also be a metabolite of the drug; but, this is not the case here. The plasma sample (Fig. 2B) which was analyzed with no internal standard was taken from an animal 3 days after dosing and 2 days after the highest drug concentration had been observed. No peak corresponding to III is present. Similarly, plasma samples taken at later times also show nothing eluting at this retention time.

CONCLUSION

The analytical procedure presented here is a substantial simplification of the original fluorescence derivatization HPLC method. At a typical therapeutic plasma concentration of 40 ng/ml, the observed mean deviation of 1.7 ng/ml corresponds to an accuracy of 4% mean relative error. Similarly, the standard deviation of 2 ng/ml typically observed corresponds to a precision of 5% relative standard deviation. These values are essentially the same as those observed for the fluorescence method. As one would expect, the fluorescence method has a definite advantage with a detection limit of one-tenth that of the direct method. However, the direct method is more rapid and reliable, and with a detection limit of 2 ng/ml, it is entirely suitable for quantitative determination of avermectins in plasma at normally effective dosage levels. Numerous bioavailability studies with both cattle and swine in which peak drug concentrations have ranged from 50 to 100 ng/ml have been successfully conducted in these laboratories using this analytical procedure.

REFERENCES

(1) G. Albers-Schönberg, B. H. Arison, J. C. Chabala, A. W. Douglas, P. Eskola, M. H. Fisher, A. Lusi, H. Mrozik, J. L. Smith, and R. L. Tolman, *J. Am. Chem. Soc.*, **103**, 4216 (1981).

(2) J. P. Springer, B. H. Arison, J. M. Hirshfield, and K. Hoogsteen, *J. Am. Chem. Soc.*, **103**, 4221 (1981).

(3) J. C. Chabala *et al.*, *J. Med. Chem.*, **23**, 1134 (1980).

(4) J. R. Egerton, J. Birnbaum, L. S. Blair, J. C. Chabala, J. Conroy, M. H. Fisher, H. Mrozik, D. A. Ostlind, C. A. Wilkins, and W. C. Campbell, *Br. Vet. J.*, **136**, 88 (1980).

(5) J. R. Egerton, D. A. Ostlind, L. S. Blair, C. H. Eary, D. Suhayda, S. Cifelli, R. F. Riek, and W. C. Campbell, *Antimicrob. Agents Chemother.*, **15**, 372 (1979).

(6) J. W. Tolan, P. Eskola, D. W. Fink, H. Mrozik, and L. A. Zimmerman, *J. Chromatogr.*, **190**, 367 (1980).

(7) P. C. Tway, J. S. Wood, and G. V. Downing, *J. Agric. Food Chem.*, **29**, 1059 (1981).

(8) R. Wachowiak and K. A. Connors, *Anal. Chem.*, **51**, 27 (1979).

(9) K. A. Connors and N. K. Pandit, *Anal. Chem.*, **50**, 1542 (1978).

(10) R. W. Burg *et al.*, *Antimicrob. Agents Chemother.*, **15**, 361 (1979).

(11) T. W. Miller *et al.*, *Antimicrob. Agents Chemother.*, **15**, 368 (1979).

ACKNOWLEDGMENTS

The authors thank J. B. Williams, F. P. Baylis, and their staffs for dosing the animals and providing plasma samples for the bioavailability experiment.

Coil → Helix Transition in Polyadenylic Acid Induced by the Binding of Epinephrine, Norepinephrine, and Isoproterenol: Circular Dichroism Study

HANNA N. BORAZAN ˣ and SONA N. KOUMRIQIAN

Received October 21, 1981, from the *Department of Pharmaceutical Chemistry, College of Pharmacy, University of Baghdad, Baghdad, Republic of Iraq.* Accepted for publication October 19, 1982.

Abstract □ A circular dichroism spectropolarimetric study on the conformation of polyadenylic acid (poly A) in neutral solutions demonstrated a coil → helix transition induced by intercalative binding of critical amounts of epinephrine, norepinephrine, and isoproterenol relative to poly A. Theoretical treatment of the experimental data indicated a first-order kinetic transition in poly A. It was possible to measure transition rate constants of the epinephrine–poly A and norepinephrine–poly A systems and to calculate the activation energies. The results indicate a high level of temperature dependence of the rate constants. The effects can be reversed by increasing ionic strength, indicating the significance of the electrostatic interactions. The importance of the results is discussed in terms of the possible role of the catecholamines as control mechanisms for the poly A-regulated translation of the genetic code on mRNA.

Keyphrases □ Polyadenylic acid—coil → helix transition, intercalative binding of epinephrine, norepinephrine, and isoproterenol, circular dichroism □ Catecholamines—epinephrine, norepinephrine, isoproterenol, intercalative binding to polyadenylic acid, coil → helix transition, circular dichroism □ Coil → helix transition—of polyadenylic acid, induced by catecholamines, intercalative binding of epinephrine, norepinephrine, and isoproterenol, circular dichroism

Most mRNA molecules contain stretches of polyadenylic acid (poly A) at the 3′-end (1), with length of the poly A depending on the evolutionary level of the organism; the larger segments of poly A exist in highly differentiated cells (2). The exact function of this poly A segment is not yet known. Some researchers have proposed that the segments are responsible for increasing the stability of mRNA by inducing a circular structure, while others found that the translation of the genetic code becomes far more efficient in the presence of poly A, attributed to the greater stability of mRNA afforded by poly A (3).

In a continuing effort to study the diversity of the biological effects of adrenergic compounds at the molecular level, the investigation of the possibility that nucleic acids are the target molecules of these drugs was conducted in this laboratory. The present study deals with circular di-

0022-3549/83/1200-1450$01.00/0

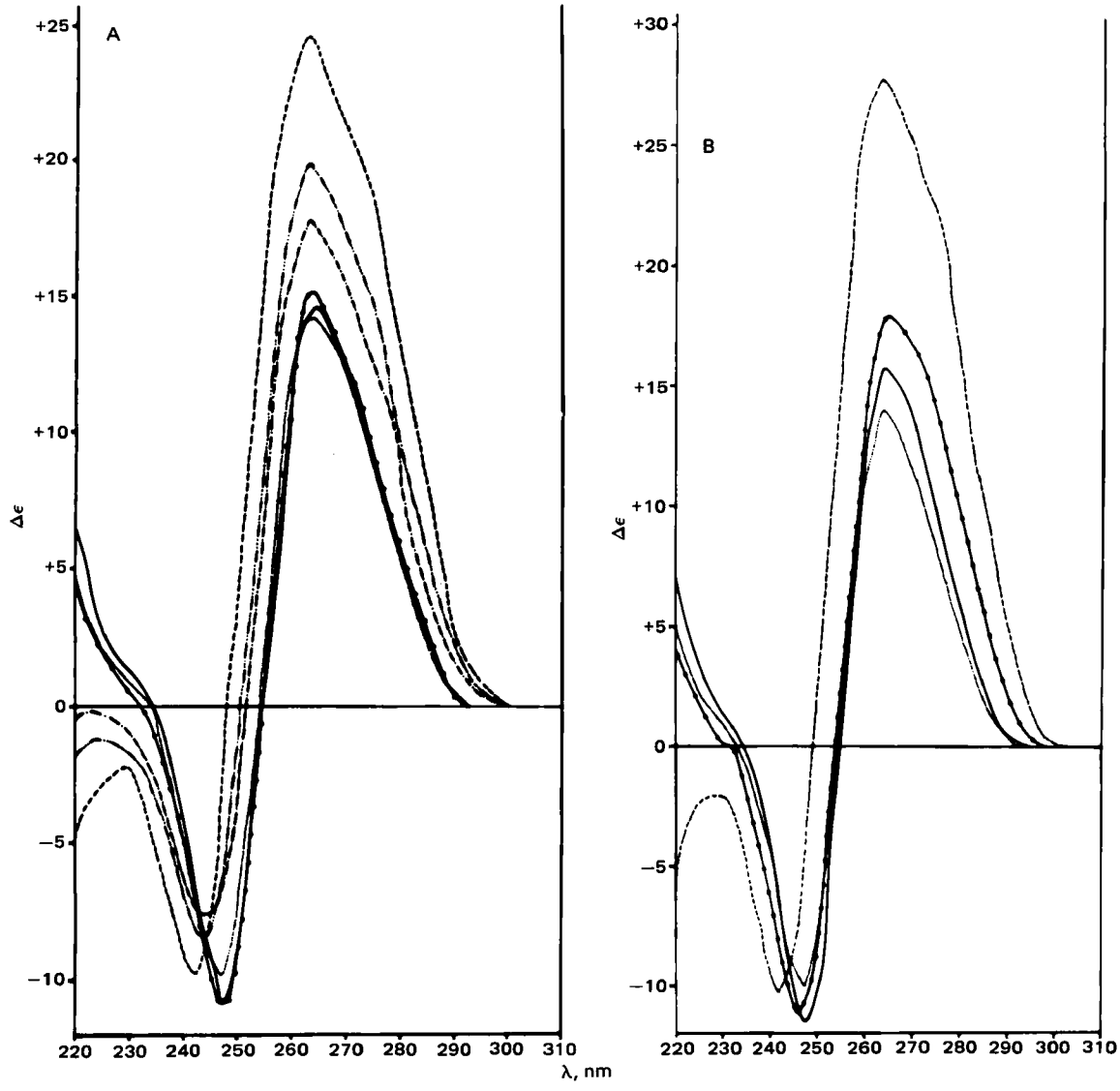

Figure 1—*CD spectra. (A) 5 × 10^{-4} M poly A in the absence (—) and presence of epinephrine hydrogen tartrate at pH 7 (1 mM sodium cacodylate, 1 mM NaCl, and 0.2 mM EDTA), temperature 25°. Key: (. . . . . .) 0.5:1 epinephrine–poly A; (–·–·), (–·· –·· ··), (- - - - - - -) 1:1 epinephrine–poly A at 9, 18, and 126 min, respectively; (–●–●–●–●–●–) effect of increasing ionic strength (0.2 M NaCl) after completion of the transition. The time indicated is at the middle of the scan, speed = 20 nm/min. (B) 5.11 × 10^{-4} M poly A in the absence (—) and presence of 1.022 × 10^{-3} M isoproterenol sulfate at pH 7 (same buffer system as A), temperature 25°. Key: (. . . . . .), (- - - - - - - -) after 7 min and 2 days, respectively; (–●–●–●–) effect of sodium chloride (0.125 M) after the transition is completed.*

chroism (CD) spectropolarimetric investigation of conformational changes in poly A, at pH 7, induced by epinephrine, norepinephrine, and isoproterenol.

EXPERIMENTAL

Polyadenylic acid[1], epinephrine hydrogen tartrate[2], EDTA (disodium ethylenediaminetetraacetate)[2], (+)-tartaric acid[2], norepinephrine[3], sodium cacodylate[3], isoproterenol sulfate dihydrate[4], and sodium chloride[5] were obtained from commercial sources. All chemicals were used without further purification, since they were of the highest commercially available purity.

The prepared solutions contained a fixed concentration of poly A (~5 × 10^{-5} *M*), with varying concentrations of the catecholamines (one-half to twice the concentration of poly A). A value of 10^4 was assumed for the molar absorptivity (ϵ) per nucleotide residue of poly A at 257 nm when preparing standard solutions. The norepinephrine hydrogen tartrate solution was prepared from an equimolar mixture of the acid and the base. The buffer system used was 1 m*M* sodium cacodylate, pH 7, containing 1 m*M* NaCl and 0.2 m*M* EDTA.

Spectroscopic measurements were performed on a spectrophotometer[6] and a circular dichroism spectropolarimeter[7]. All equations used were written on programs and executed on a programmable calculator[8].

The temperature of solutions in the cuvettes (quartz, with a 0.1-cm path length) was maintained constant throughout measurements by using a thermostated cell holder. When working at low temperatures, the spectra were recorded under dry conditions. The experiments were done in a room with subdued lighting to avoid undesired photooxidation of the catecholamines. Each experiment was replicated at least three times.

RESULTS AND DISCUSSION

It is known that poly A in neutral solutions exist in a single-stranded coil conformation (4). This conformation of poly A exhibits a charac-

[1] Boehringer Ingelheim, West Germany.
[2] BDH Chemical Co., Poole, England.
[3] Sigma Chemical Co., St. Louis, Mo.
[4] Aldrich Chemical Co., Milwaukee, Wis.
[5] Evans Medical Co., Ltd., Liverpool, England.

[6] Pye Unicam UV-Visible Spectrophotometer, Model SP8-200.
[7] JASCO CD Spectropolarimeter, Model J-40C.
[8] Hewlett-Packard, Model 9810A.

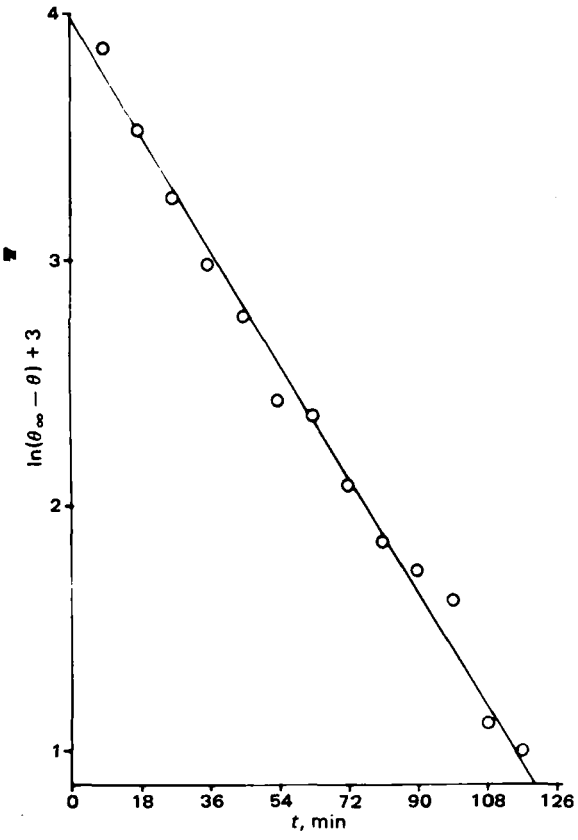

Figure 2—*Ln* $(\theta_\infty - \theta) + 3$ versus t *corresponding to changes in the intensity of the positive band at* λ_{max} *of poly A* (5×10^{-4} M) *in the presence of an equimolar mixture of norepinephrine hydrogen tartrate at pH 7. The conditions are as indicated in Fig. 1.* θ *is expressed in centimeters.*

teristic CD spectrum that is due to ordered base-stacked structures composed of two bands of nearly equal intensities: a positive band with a maximum located at 264 nm and a negative band at 247 nm, with a crossover at 254 nm (5–8).

In the present study, it was found that addition of epinephrine hydrogen tartrate or norepinephrine hydrogen tartrate to poly A at a concentration ratio (amine/poly A) of 0.5 caused a slight reduction of the intensities of the positive and negative bands of the CD spectrum of poly A without altering its shape. This pattern of change could indicate an intercalative binding of the aromatic nucleus between the stacked adenine bases (9, 10). When the concentration ratio was increased to 1.0, an increase in the positive band and a decrease in the negative band of the CD spectrum, as well as shifts in the λ_{max} and λ_{min} toward shorter wavelengths, were observed with time (Fig. 1). After the change was completed, the CD spectrum was composed of two bands, a positive band with a maximum at 263 nm and a negative band with a minimum at 242 nm; at 248 nm the CD signal had a zero value. This spectrum is considered to be identical to that of the double-stranded intertwined helical conformation of poly A existing in acidic solutions, pH 4.8, (5–7). These results indicate a coil → helix transition catalyzed by the binding of epinephrine and norepinephrine.

In order to have a basic understanding of the mechanism of this coil → helix transition, several kinetic models were tested. The best model that seems to be consistent with our experimental data is a first-order transition process in poly A. This led us to the following equation:

$$\ln (\theta_\infty - \theta) = \ln (\theta_\infty - \theta_0) - kt \qquad \text{(Eq. 1)}$$

where θ_0, θ, and θ_∞ represent the ellipticity of the CD signal at times 0, t, and ∞, respectively, and k is the rate constant of the transition. Thus, a plot of ln $(\theta_\infty - \theta)$ *versus* t should lead to a slope of $-k$.

Naturally, the activation energy of the coil → helix transition can be measured in principle according to the Arrhenius equation:

$$\ln k = -\frac{E_a}{RT} + \text{constant} \qquad \text{(Eq. 2)}$$

by plotting ln k *versus* $1/T$. In Eq. 2, E_a is the activation energy, R is the gas constant, and T is the absolute temperature in °K. Representative plots of Eqs. 1 and 2 are shown in Figs. 2 and 3, respectively; the data are summarized in Table I. To minimize errors, the slopes of the curves in Figs. 2 and 3 and those used to calculate the kinetic parameters presented in Table I were calculated by the method of least squares.

Isoproterenol can also induce the coil → helix transition, but this process is very slow. A 2:1 isoproterenol–poly A mixture can bring about the transition completion in >2 days at 25° (Fig. 1B). However, this transition is too slow to enable measurement of k or of the corresponding E_a.

It is evident from Fig. 2 that the transition is a first-order process in poly A when based on measurements of the positive band (264 → 263 nm) and the total peak-to-peak $\lambda_{max} - \lambda_{min}$ amplitude (λ_{min} shifts from 248 to 242 nm). The transition at 4° is a very slow process; it was therefore necessary to leave the solution overnight to bring the transition to completion and to measure θ_∞. Even though the transition occurring at 15° is faster than that at 4°, it was necessary to leave the solution overnight to achieve the most stable double-helical structure. θ_∞ was attained within 2 hr at 25° for both systems.

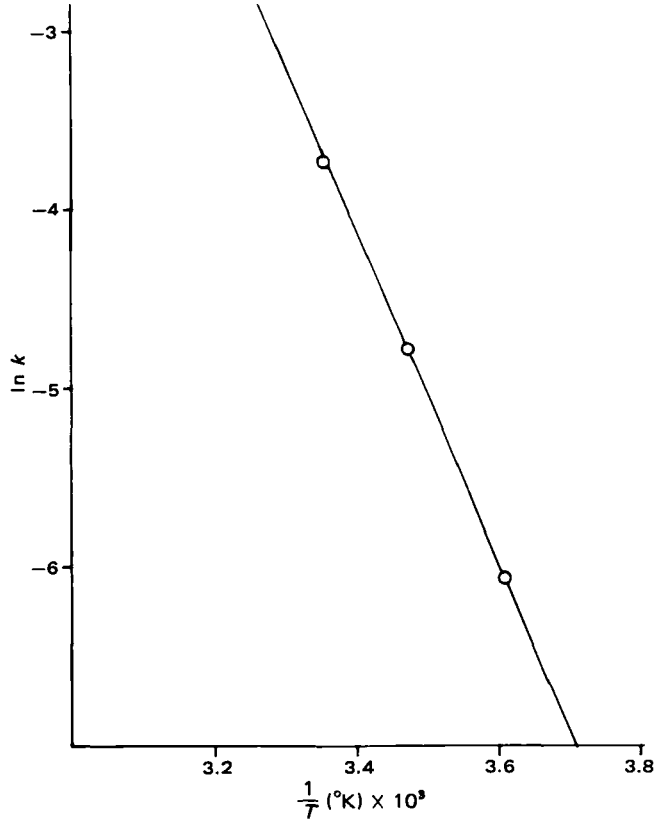

Figure 3—*Ln* k versus *1/*T *for the transition of poly A in the norepinephrine-poly A system based on measurements of the total peak-peak* $(\lambda_{max} - \lambda_{min})$ *amplitude.*

Table I—Rate Constants (k) and Coil → Helix Transition Activation Energies (E_a) of Poly A Based on CD Signals

Temperature ± 1°	Total Peak–Peak Amplitude k, min^{-1} × 10^3	Total Peak–Peak Amplitude E_a, kcal/mole	Positive Amplitude k, min^{-1} × 10^3	Positive Amplitude E_a, kcal/mole
	Epinephrine–Poly A			
4°	3.16		4.02	
15°	9.40	16.408	9.42	16.480
25°	25.50		33.22	
	Norepinephrine–Poly A			
4°	2.31		2.89	
15°	8.45	18.478	8.51	17.104
25°	24.16		25.59	

The positive CD band assumes the stable structure at a faster rate than that of the negative band (as reflected from measurements of the total amplitude) in the case of the epinephrine–poly A system (Table I). In the norepinephrine–poly A system, however, both bands of poly A attain their stable features at approximately the same rate. The activation energy calculated from the changes in the total amplitude and the positive band is very similar in the epinephrine–poly A system, while a slight difference appears to exist in the norepinephrine–poly A (Table I). In comparing both systems, one may observe the high temperature dependence of the rate constants; a change from 4° to 25° can bring about an 8- to 10-fold increase in the rate constant.

The significance of the contributions of electrostatic interactions to the total binding energy was verified by changing the ionic strength of the solutions. It was found that increasing the ionic strength to 0.2 *M* by the addition of sodium chloride had the effect of restoring almost entirely the initial CD spectra of poly A in the three systems (Fig. 1). This can be explained on the basis of competition occurring between sodium ions and the positively charged amino groups existing at pH 7 in the negatively charged phosphate residues. The contribution of other weaker forces to the intercalative binding cannot be neglected, however, since it has been demonstrated (11–13) that adenine can form charge transfer complexes with catechol, epinephrine, and isoproterenol.

The exact geometry of the complexes formed between the catecholamines and poly A in its single- and double-stranded conformations cannot be determined from the CD investigation alone. On the other hand, it should be emphasized that the conformational changes occurring in the poly A molecule cannot be attributed solely to the electrostatic interactions, due to the fact that isopropylamine does not change the CD spectrum of poly A (10). Finally, catecholamines may exert a control mechanism through induction of the coil → helix transition on the regulatory role in genetic code translation which has been hypothesized for the poly A segments present in most mRNA molecules.

REFERENCES

(1) J. D. Watson, "Molecular Biology of the Gene," 3rd ed., Benjamin, Menlo Park, Calif., 1976, pp. 482–483.

(2) R. K. Carlin, *J. Theor. Biol.*, **71**, 323 (1978).

(3) G. Brawerman, *Prog. Nucleic Acid Res. Mol. Biol.*, **17**, 117 (1976).

(4) J. Fresco and P. Doty, *J. Am. Chem. Soc.*, **79**, 3928 (1957).

(5) J. Brahms, *Nature (London)*, **202**, 797 (1964).

(6) J. Brahms, A. M. Michelson, and K. E. Van Holde, *J. Mol. Biol.*, **15**, 467 (1966).

(7) F. H. Wolfe, K. Oikawa, and C. M. Kay, *Can. J. Biochem.*, **47**, 637 (1969).

(8) H. Hashizume and K. Imahori, *J. Biochem.*, **61**, 738 (1967).

(9) M. Durand, J. C. Maurizot, H. N. Borazan, and C. Helene, *Biochemistry*, **14**, 563 (1975).

(10) M. Durand, H. N. Borazan, J. C. Maurizot, J. L. Dimicoli, and C. Helene, *Biochimie*, **58**, 395 (1976).

(11) F. A. Al-Obeidi and H. N. Borazan, *J. Pharm. Sci.*, **65**, 892 (1976).

(12) F. A. Al-Obeidi and H. N. Borazan, *J. Pharm. Sci.*, **65**, 982 (1976).

(13) H. M. Taha, F. A. Al-Obeidi, and H. N. Borazan, *J. Pharm. Sci.*, **68**, 631 (1979).

ACKNOWLEDGMENTS

Abstracted in part from a dissertation submitted by S. N. Koumriqian to the University of Baghdad in partial fulfillment of the Master of Science degree requirements.

The authors thank Dr. Waleed R. Sulaiman, Dean, for his encouragement. They also thank the University of Baghdad for the financial support of this work.

Stability of Triamcinolone Acetonide Solutions as Determined by High-Performance Liquid Chromatography

V. DAS GUPTA

Received July 6, 1982, from the *Department of Pharmaceutics, University of Houston, Houston, TX 77030.* Accepted for publication October 14, 1982.

Abstract □ A stability-indicating assay method based on reverse-phase high-performance liquid chromatography has been developed for the quantitation of triamcinolone acetonide. The method was used to study the stability of triamcinolone acetonide in water–ethanol solutions of varying pH, buffer concentration, and ionic strength. The decomposition of triamcinolone followed pseudo-first-order law and was minimal at pH ~ 3.4. Above pH 5.5, the decomposition increased rapidly and was directly related to phosphate buffer concentration. The decomposition decreased with increasing ionic strength when the pH of the solution was >7. Two new peaks corresponding to decomposition products were noted in the chromatogram; their ratio varied significantly with the composition of the vehicle.

Keyphrases □ Triamcinolone acetonide—decomposition in solution, effect of pH, buffer concentration, and ionic strength, high-performance liquid chromatography □ High-performance liquid chromatography—stability indicating, triamcinolone acetonide and its decomposition products, effect of pH, buffer concentration, and ionic strength □ Stability—triamcinolone in solutions, effect of pH, buffer concentration, and ionic strength, high-performance liquid chromatography

Triamcinolone acetonide (I) is available in different dosage forms such as creams, ointments, and suspensions. Despite its extensive use, little is known about the stability of I in aqueous systems and water-washable ointment bases such as polyethylene glycol ointment base USP (1). In general, corticosteroid decomposition is first order (2) with two parallel routes of decomposition. One route (attack on ring A) produces neutral product(s) and the other (attack on the C-17 side chain) produces acidic product(s).

This study evaluates the stability of triamcinolone acetonide (*a*) in water–ethanol solutions of varying pH with different buffer concentrations and ionic strengths and (*b*) in polyethylene glycol ointment base USP (1) using a stability-indicating reverse-phase high-performance liquid chromatographic (HPLC) assay method developed in our laboratory.

EXPERIMENTAL

Reagents and Chemicals—All reagents and chemicals were either ACS, USP, or NF grade and were used without further purification. Triamcinolone acetonide[1] was used as received.

Chromatographic Conditions—Two columns (30 cm × 4-mm i.d.) were used. One contained a semipolar material[2], the other a nonpolar

[1] E. R. Squibb & Sons, Princeton, N.J.

[2] μBondapak CN; Waters Associates, Milford, Mass.

0022-3549/83/1200-1453$01.00/0

The positive CD band assumes the stable structure at a faster rate than that of the negative band (as reflected from measurements of the total amplitude) in the case of the epinephrine–poly A system (Table I). In the norepinephrine–poly A system, however, both bands of poly A attain their stable features at approximately the same rate. The activation energy calculated from the changes in the total amplitude and the positive band is very similar in the epinephrine–poly A system, while a slight difference appears to exist in the norepinephrine–poly A (Table I). In comparing both systems, one may observe the high temperature dependence of the rate constants; a change from 4° to 25° can bring about an 8- to 10-fold increase in the rate constant.

The significance of the contributions of electrostatic interactions to the total binding energy was verified by changing the ionic strength of the solutions. It was found that increasing the ionic strength to 0.2 *M* by the addition of sodium chloride had the effect of restoring almost entirely the initial CD spectra of poly A in the three systems (Fig. 1). This can be explained on the basis of competition occurring between sodium ions and the positively charged amino groups existing at pH 7 in the negatively charged phosphate residues. The contribution of other weaker forces to the intercalative binding cannot be neglected, however, since it has been demonstrated (11–13) that adenine can form charge transfer complexes with catechol, epinephrine, and isoproterenol.

The exact geometry of the complexes formed between the catecholamines and poly A in its single- and double-stranded conformations cannot be determined from the CD investigation alone. On the other hand, it should be emphasized that the conformational changes occurring in the poly A molecule cannot be attributed solely to the electrostatic interactions, due to the fact that isopropylamine does not change the CD spectrum of poly A (10). Finally, catecholamines may exert a control mechanism through induction of the coil → helix transition on the regulatory role in genetic code translation which has been hypothesized for the poly A segments present in most mRNA molecules.

REFERENCES

(1) J. D. Watson, "Molecular Biology of the Gene," 3rd ed., Benjamin, Menlo Park, Calif., 1976, pp. 482–483.

(2) R. K. Carlin, *J. Theor. Biol.*, **71**, 323 (1978).

(3) G. Brawerman, *Prog. Nucleic Acid Res. Mol. Biol.*, **17**, 117 (1976).

(4) J. Fresco and P. Doty, *J. Am. Chem. Soc.*, **79**, 3928 (1957).

(5) J. Brahms, *Nature (London)*, **202**, 797 (1964).

(6) J. Brahms, A. M. Michelson, and K. E. Van Holde, *J. Mol. Biol.*, **15**, 467 (1966).

(7) F. H. Wolfe, K. Oikawa, and C. M. Kay, *Can. J. Biochem.*, **47**, 637 (1969).

(8) H. Hashizume and K. Imahori, *J. Biochem.*, **61**, 738 (1967).

(9) M. Durand, J. C. Maurizot, H. N. Borazan, and C. Helene, *Biochemistry*, **14**, 563 (1975).

(10) M. Durand, H. N. Borazan, J. C. Maurizot, J. L. Dimicoli, and C. Helene, *Biochimie*, **58**, 395 (1976).

(11) F. A. Al-Obeidi and H. N. Borazan, *J. Pharm. Sci.*, **65**, 892 (1976).

(12) F. A. Al-Obeidi and H. N. Borazan, *J. Pharm. Sci.*, **65**, 982 (1976).

(13) H. M. Taha, F. A. Al-Obeidi, and H. N. Borazan, *J. Pharm. Sci.*, **68**, 631 (1979).

ACKNOWLEDGMENTS

Abstracted in part from a dissertation submitted by S. N. Koumriqian to the University of Baghdad in partial fulfillment of the Master of Science degree requirements.

The authors thank Dr. Waleed R. Sulaiman, Dean, for his encouragement. They also thank the University of Baghdad for the financial support of this work.

Stability of Triamcinolone Acetonide Solutions as Determined by High-Performance Liquid Chromatography

V. DAS GUPTA

Received July 6, 1982, from the *Department of Pharmaceutics, University of Houston, Houston, TX 77030.* Accepted for publication October 14, 1982.

Abstract □ A stability-indicating assay method based on reverse-phase high-performance liquid chromatography has been developed for the quantitation of triamcinolone acetonide. The method was used to study the stability of triamcinolone acetonide in water–ethanol solutions of varying pH, buffer concentration, and ionic strength. The decomposition of triamcinolone followed pseudo-first-order law and was minimal at pH ~ 3.4. Above pH 5.5, the decomposition increased rapidly and was directly related to phosphate buffer concentration. The decomposition decreased with increasing ionic strength when the pH of the solution was >7. Two new peaks corresponding to decomposition products were noted in the chromatogram; their ratio varied significantly with the composition of the vehicle.

Keyphrases □ Triamcinolone acetonide—decomposition in solution, effect of pH, buffer concentration, and ionic strength, high-performance liquid chromatography □ High-performance liquid chromatography—stability indicating, triamcinolone acetonide and its decomposition products, effect of pH, buffer concentration, and ionic strength □ Stability—triamcinolone in solutions, effect of pH, buffer concentration, and ionic strength, high-performance liquid chromatography

Triamcinolone acetonide (I) is available in different dosage forms such as creams, ointments, and suspensions. Despite its extensive use, little is known about the stability of I in aqueous systems and water-washable ointment bases such as polyethylene glycol ointment base USP (1). In general, corticosteroid decomposition is first order (2) with two parallel routes of decomposition. One route (attack on ring A) produces neutral product(s) and the other (attack on the C-17 side chain) produces acidic product(s).

This study evaluates the stability of triamcinolone acetonide (*a*) in water–ethanol solutions of varying pH with different buffer concentrations and ionic strengths and (*b*) in polyethylene glycol ointment base USP (1) using a stability-indicating reverse-phase high-performance liquid chromatographic (HPLC) assay method developed in our laboratory.

EXPERIMENTAL

Reagents and Chemicals—All reagents and chemicals were either ACS, USP, or NF grade and were used without further purification. Triamcinolone acetonide[1] was used as received.

Chromatographic Conditions—Two columns (30 cm × 4-mm i.d.) were used. One contained a semipolar material[2], the other a nonpolar

[1] E. R. Squibb & Sons, Princeton, N.J.

[2] μBondapak CN; Waters Associates, Milford, Mass.

0022-3549/83/1200-1453$01.00/0

Table I—Composition of 0.025% Solutions of Triamcinolone Acetonide Prepared in Ethanol-Water and the Estimated K_{obs} Values

Solution Number	Concentration of Buffer	Buffer	pH of the Buffer Solution[a]	Ionic Strength[b]	Final pH (±0.1)	K_{obs} Value at 25° (Per Day)[c]
1	0.1	HCl	1.5	0.1	1.6	0.0068
2	0.01	HCl	2.0	0.1	2.1	—[d]
3	0.05	Phosphate	3.1	0.1	3.4	—[d]
4	0.05	Phosphate	4.1	0.1	4.5	—[d]
5	0.05	Phosphate	5.1	0.1	5.5	—[d]
6	0.05	Phosphate	6.1	0.1	6.6	0.0095
7	0.05	Phosphate	7.1	0.1	7.5	0.0345
8	0.01	NaOH	11.7	0.1	11.8	3.6
9	0.1	NaOH	12.5	0.1	12.6	18.2
10	0.05	Phosphate	7.2	0.1	7.6	—[e]
11	0.05	Phosphate	7.2	0.2	7.6	—[e]
12	0.05	Phosphate	7.2	0.25	7.6	—[e]
13	0.05	Phosphate	7.2	0.3	7.6	—[e]
14	.075	Phosphate	7.2	0.2	7.6	—[e]
15	0.1	Phosphate	7.2	0.2	7.6	—[e]
16	.05	Phosphate	6.1	0.2	6.6	—[e]
17	0.075	Phosphate	6.1	0.2	6.6	—[e]
18	0.1	Phosphate	6.1	0.2	6.6	—[e]
19	0.2	Phosphate	7.1	—[f]	7.5	0.078
20	0.2	Phosphate[g]	7.1	—[f]	7.4	0.090
21	0.2	Phosphate[g]	7.1	—[f]	7.5	0.108
22	—	—	—	—[f]	6.8	—[e]
23	—	—	—	—[f]	6.9	—[e]
24	—	—	—	—[f]	7.0	—[e]
25	—	—	—	—[f]	7.0	—[e]
26	—	—[g]	—	—[f]	6.2	—[e]
27	—	—[g]	—	—[f]	5.8	—[e]

[a] Each solution contained 25% v/v ethanol except solutions 20 and 21 (10%), 23 (50%), 24 (75%), and 25 (100%). [b] Adjusted with potassium chloride based on the pH of the buffer solutions. [c] The data at 50° are presented in Fig. 4. [d] It was not possible to estimate K_{obs} at 25° since these solutions did not decompose significantly in 8 weeks. [e] Not determined at this temperature. [f] Ionic strength not adjusted. [g] Solutions 20 and 26 contained 15% v/v and 25% v/v glycerin, respectively. Solutions 21 and 27 had 15% v/v and 25% v/v propylene glycol, respectively.

material[3]. The chromatograph[4] was connected to a multiple-wavelength detector[5], a recorder[6], and an integrator[7]. All pH values were determined using a pH meter[8]. Four mobile phases were used:

1. A 0.02 *M* aqueous solution of monobasic potassium phosphate containing 16% v/v of acetonitrile (pH ~4.2).
2. Same as 1 except that the buffering agent was 0.02 *M* ammonium acetate (pH ~7).
3. Same as 1 except that the pH was adjusted to ~2.5 with an 85% aqueous solution of phosphoric acid.
4. Same as 1 except that the acetonitrile concentration was 32% v/v (pH ~4.2).

The flow rate was 2.5 ml/min (3.0 ml/min with mobile phase 4), and the sensitivity was set at 0.04 AUFS (254 nm). The temperature was ambient, and the chart speed was 30.5 cm/hr.

Preparation of Samples—All solutions for stability studies were prepared as presented in Table I using a simple solution method. After the initial data was obtained (pH values and the assays), the solutions were stored at 50 ± 1° (some also at 25 ± 1°) in 60-ml amber-colored bottles[9].

Forty milligrams of I was thoroughly mixed with 19.96 g of polyethylene glycol ointment base USP (1) using the process of trituration. After the initial data was obtained (assay and the pH value of a 1% aqueous solution), the ointment was stored at 50 ± 1° in an opaque white ointment jar[9].

Assay Method—*Preparation of Standard Solutions*—A stock solution of triamcinolone acetonide (I) was prepared by dissolving 100.0 mg of the powder in enough ethanol to make 100 ml. A stock solution of hydrocortisone (the internal standard) of identical concentration was also prepared in ethanol. The standard solution was prepared by mixing 8.0 ml of the stock solution of I and 3.2 ml of hydrocortisone solution with 20 ml of methanol and then bringing the volume to 100 ml with water. The solutions of other concentrations were prepared as needed. Each solution contained identical concentrations of methanol and hydrocortisone.

Assay Solutions—An 8.0-ml quantity of each solution was mixed with 0.8 ml of the stock solution of hydrocortisone and 5 ml of methanol, and the mixture was brought to volume (25 ml) with water. One gram of the ointment was mixed with 5 ml of methanol, 5 ml of water, and 0.8 ml of the hydrocortisone solution. The mixture was stirred until a clear solution was formed and then brought to volume (25 ml) with water.

HPLC Assay Procedure—A 20-μl aliquot of the assay solution was injected into the chomatograph using the described conditions (nonpolar column[3] and mobile phase 4). An identical volume of the appropriate standard solution was injected for comparison after the assay solution eluted. The standard solution contained exactly the same quantity of I as the label claim of the assay solution.

Calculations—Since preliminary investigations indicated that ratios of peak heights of I and the internal standard were directly related to concentrations of I, the results were calculated using:

$$\frac{(R_{ph})_a}{(R_{ph})_s} \times 100 = \text{percent contained in the assay solution} \quad \text{(Eq. 1)}$$

where $(R_{ph})_a$ is the ratio of peak heights of I to the internal standard (hydrocortisone) in the assay solution and $(R_{ph})_s$ is the ratio of the triamcinolone acetonide peak to the internal standard in the standard solution. If the standard solution does not contain an identical concentration of I, the results can be corrected by multiplying the percent found by: Factor = [actual concentration of I (mg/ml) in the standard solution] ÷ [label claim of I (mg/ml) in the assay solution].

When the triamcinolone acetonide peak was too small (<25% of the standard) to quantify accurately, a new assay solution containing a higher concentration of I was injected. Appropriate calculations were then made to determine the exact concentration of I in the assay solution.

RESULTS AND DISCUSSION

Assay Method—The assay method using a nonpolar column and mobile phase 4, containing 0.02 *M* KH_2PO_4 and 32% v/v acetonitrile in water, separated the decomposition products from the intact triamcinolone acetonide and the internal standard (Figs. 1 and 2). The results were reproducible, accurate, and precise with relative standard deviations ranging from 1.6 to 1.9% based on six readings. Before these chromatographic conditions were finalized, mobile phase 1 containing 16% v/v

[3] μBondapak C18; Waters Associates, Milford, Mass.
[4] Model ALC 202 equipped with a U6K universal injector; Waters Associates, Milford, Mass.
[5] Spectroflow monitor SF770; Schoeffel Instruments Corp., Westwood, N.J.
[6] Omniscribe 5213-12; Houston Instruments, Austin, Tex.
[7] Autolab minigrator; Spectra-Physics, Santa Clara, Calif.
[8] Beckman SS-3 Zeromatic; Beckman Instruments, Irvine, Calif.
[9] Brockway Glass Co., Brockway, Pa.

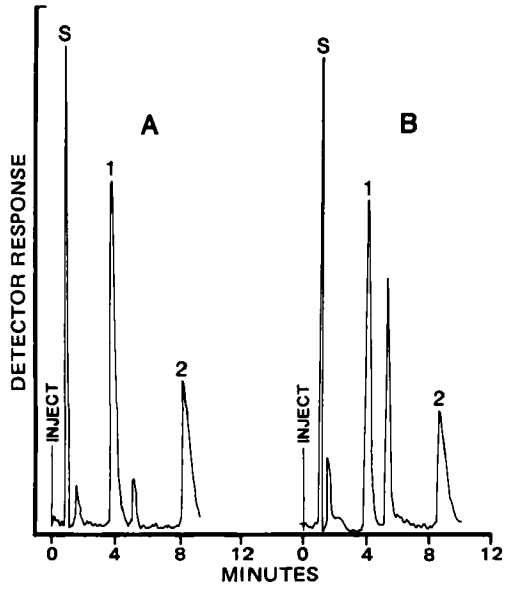

Figure 1—*Typical chromatograms of (A) a standard solution and (B) an 11-day-old solution (solution 19) using a nonpolar column and mobile phase 4. Key: (1) hydrocortisone (internal standard); (2) triamcinolone acetonide; (S) solvent. The two unlabeled peaks are decomposition products.*

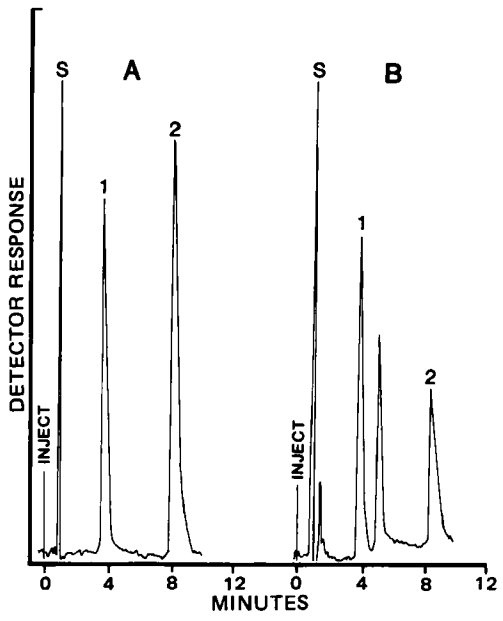

Figure 2—*Typical chromatograms using a nonpolar column and mobile phase 4 of two 11-day-old solutions stored at room temperature. Key: (A) solution 20; (B) solution 21; (1) hydrocortisone (internal standard); (2) triamcinolone acetonide; (S) solvent. All other peaks are decomposition products.*

acetonitrile was tried with a semipolar column. With these chromatographic conditions, the second product of decomposition (the peak between peaks 1 and 2 in Fig. 1B) did not separate from peak 2. Therefore, the results obtained using a semipolar column were erroneous and did not follow first-order kinetics.

Decomposition Products—Corticosteroids usually decompose with two parallel routes of decomposition (2), producing either acidic or neutral products:

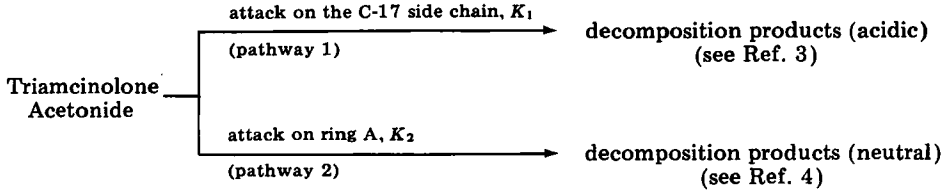

By changing the pH of the mobile phase (mobile phases 1–3), it was possible to decrease (with a mobile phase of higher pH) or increase (with a mobile phase of lower pH) the retention time of the first decomposition product (peak appearing after the solvent peak in Fig. 2). The retention time of the second peak (between peaks 1 and 2 in Fig. 2) was not affected. It appears, therefore, that the first decomposition product peak is from an acidic compound and the second is from a neutral substance.

In an ethanolic solution (solution 19), the peak from the neutral product was higher (Fig. 1B) than the peak from the acidic product. In the presence of glycerin (solution 20), these peaks were smaller and of approximately the same size (Fig. 2A). In propylene glycol (solution 21), the chromatogram (Fig. 2B) was similar to the ethanolic solution chromatogram (Fig. 1B). It is obvious that the ratio of K_1 and K_2 would be different in ethyl alcohol–propylene glycol than in glycerin.

Order of Reaction and Effect of pH—As expected, first-order kinetics were followed (Fig. 3). The rate constants varied with the pH of the buffer solution (Fig. 4) and an optimum pH of stability was estimated to be ~3.4.

Effect of Phosphate Buffer—It is apparent (Fig. 5) that the K_{obs} is directly related to the phosphate concentration. Therefore, triamcinolone acetonide is subject to general acid–base catalysis.

The decomposition of triamcinolone acetonide may be represented by:

$$K_{obs} = K_0 + K_1[H^+] + K_2[OH^-] + K_3[H_2PO_4^-] + K_4[HPO_4^{2-}] \quad \text{(Eq. 2)}$$

At constant pH, $K_1[H^+]$ and $K_2[OH^-]$ are constant and Eq. 2 may be rewritten as:

$$K_{obs} = K + K_3[H_2PO_4^-] + K_4[HPO_4^{2-}] \quad \text{(Eq. 3)}$$

where $K = K_0 + K_1[H^+] + K_2[OH^-]$.

Since the decomposition is first order (Fig. 3), the K_{obs} values were determined using first-order plots, and Eq. 3 may be rearranged as follows:

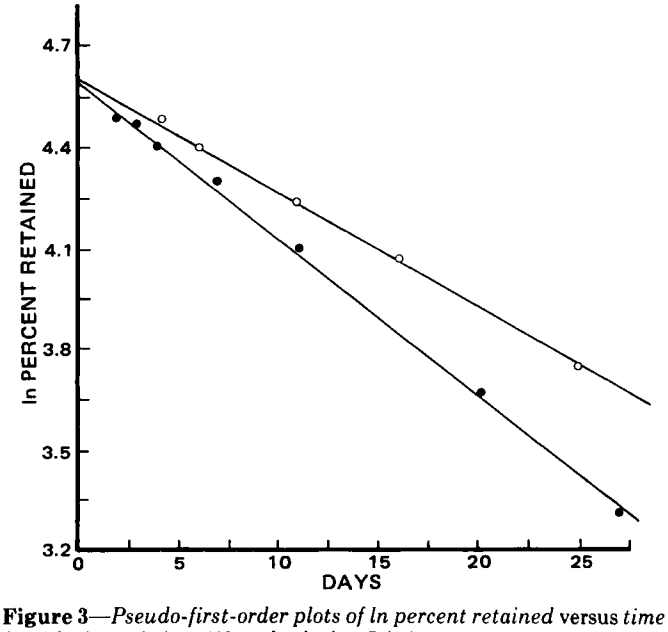

Figure 3—*Pseudo-first-order plots of ln percent retained* versus *time for solution 1 (●) at 50° and solution 7 (○) at 25°.*

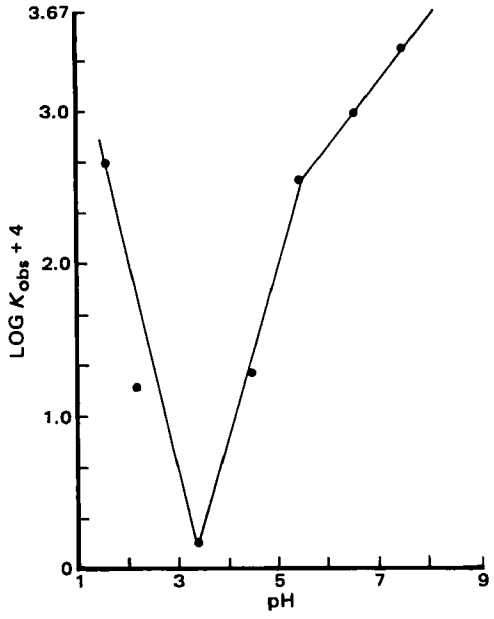

Figure 4—*pH-rate profile curve from* K_{obs} *values at 50°.*

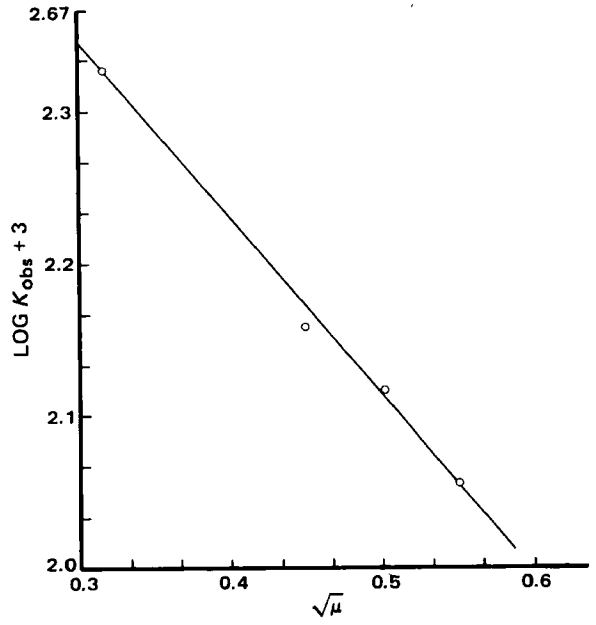

Figure 6—*Plot of log* K_{obs} versus $\sqrt{\mu}$ *at pH 7.6 (solutions 10–13).*

$$K_{obs} = K + [H_2PO_4^-]\left(K_3 + \frac{K_4}{q}\right) \quad \text{(Eq. 4)}$$

where $q = [H_2PO_4^-]/[HPO_4^{2-}]$. On plotting K_{obs} *versus* concentrations of $H_2PO_4^-$, straight lines were obtained (Fig. 5). From the slopes and q values of 3.98 and 0.398 at pH values of 6.6 and 7.6, respectively, the two simultaneous equations were solved for K_3 and K_4. The K_3 and K_4 values were estimated to be 0.575 and 3.79 M^{-1}·day^{-1}. Furthermore, by substituting these values in Eq. 3, K was determined to be negligible.

Effect of Hydrochloric Acid Buffer—In the presence of hydrochloric acid buffer (solution 1), it appears that the major reaction is hydrolysis of triamcinolone acetonide to triamcinolone and acetone. The triamcinolone peak was identified using pure powder and quantified by comparing the peak heights.

Effect of Ionic Strength—From Fig. 6, it is obvious that K_{obs} decreases with increasing ionic strength. Therefore, the reacting ions are probably the protonated form of I and $H_2PO_4^-/HPO_4^{2-}$. However, the slope of the line was ~1.16 *versus* the expected value of ~2.04. This may be due to high ionic strengths, since the equation log K = log K_0 + 1.02 $(Z_A Z_B)\sqrt{\mu}$ was deduced by assuming a value of ≤0.01 (5). In these studies, it was necessary to keep the concentration of buffering agent high in order to maintain constant pH values. Therefore, the ionic strengths were high. The equation cannot be expected to hold at salt concentrations much beyond the range of validity of the Debye–Huckel theory (5).

The other explanation may be that one route of decomposition involves reaction between the undissociated molecule of I and $H_2PO_4^-/HPO_4^{2-}$. If so, this route will not be affected by ionic strength and, hence, the slope will be reduced. Triamcinolone acetonide does decompose at lower pH (~1.6) and higher pH (~12.6) without the presence of phosphate ion. Therefore, H^+ and OH^- also catalyze the reaction only when present in high concentrations. The K_{obs} value at 25° and pH 1.6 was 0.0068 day^{-1} *versus* 18.2 day^{-1} at pH 12.6.

Later, it was determined that at lower pH (solution 1), an increase in ionic strength slightly increased the rate constant in hydrochloric acid buffer. This slight increase may be an experimental error or the difference could be due to a different reaction mechanism in hydrochloric acid buffer *versus* phosphate buffer, as explained above.

Effect of Temperature—As expected, the solutions were much more stable when stored at 25° than at 50°. From the estimated K values, the solutions were stable up to 9 times longer at 25° than at 50°.

Effect of Solvent—The data (solutions 19–21) indicate that ethanol is better than glycerin/propylene glycol for stability of I as long as the same pH is maintained. However, without pH or ionic strength adjustments (solutions 23, 26, 27), glycerin proved better than ethanol/propylene glycol. The estimated K values at 50° were 0.003, 0.004, and 0.007 day^{-1} for solutions 26, 23, and 27, respectively.

In polyethylene glycol ointment base USP (1), K_{obs} was estimated to be 0.008 day^{-1}, which is similar to solution 27 (Table I) which contained 25% v/v propylene glycol. The pH of a 1% aqueous solution of the ointment was 4.2.

In another experiment, an aqueous solution of I (40.0 μg/ml) containing 20% v/v methanol and 0.3% v/v hydrogen peroxide was stored at 50° in a 50-ml volumetric flask. After 5 days, it had decomposed 11.5%.

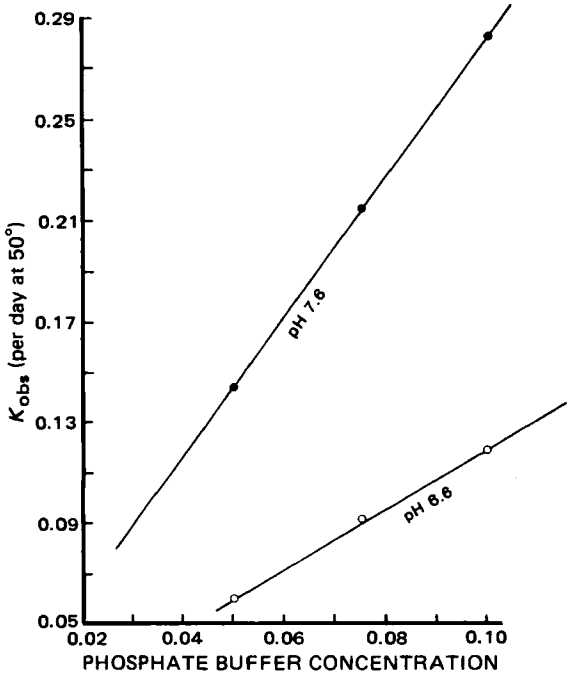

Figure 5—*Plots of* K_{obs} *values* versus *concentrations of phosphate buffer at pH 6.6 (○) and 7.6 (●).*

REFERENCES

(1) "The United States Pharmacopeia," 19th rev., U.S. Pharmacopeial Convention, Rockville, Md., 1975 p. 566.

(2) V. D. Gupta, *J. Pharm. Sci.*, **67**, 299 (1978).

(3) T. Chulski and A. A. Forest, *J. Am. Pharm. Assoc., Sci. Ed.*, **47**, 553 (1958).

(4) A. E. Allen and V. D. Gupta, *J. Pharm. Sci.*, **63**, 107 (1974).

(5) W. J. Moore, "Physical Chemistry," 4th ed., Prentice-Hall, Englewood Cliffs, N.J., 1972, p. 465.

Comparison of Aspirin and Copper Aspirinate with Respect to Gastric Mucosal Damage in the Rat

AGNES A. ALICH *x, VICTORIA J. WELSH *, and LORENTZ E. WITTMERS, JR. ‡

Received July 26, 1982, from the *Department of Chemistry, College of St. Scholastica, Duluth, MN 55811 and the ‡Department of Physiology, School of Medicine, University of Minnesota-Duluth, Duluth, MN 55812. Accepted for publication November 4, 1982.

Abstract □ The copper salt of aspirin has been compared with aspirin in terms of damage to mucosal tissue. Using a protein-bound dye to highlight erosions, it has been found that copper aspirinate is at least as damaging as aspirin itself. This finding is not in agreement with previously published claims. Copper aspirinate produced more widespread superficial erosions and slightly less deep erosions than aspirin alone. Mixtures of the copper(II) ion and aspirin produced results similar to copper aspirinate, suggesting that the hydrolysis products of copper aspirinate, copper(II) ion and aspirin, together may be especially damaging to the mucosa. Copper alone was not damaging, but aspirin alone yielded intermediate results. Short incubation times produced only erosions (no ulcers), which were clearly differentiated into two classes by depth of color. Histological examination verified this classification into superficial and deep erosions.

Keyphrases □ Copper aspirinate—gastric mucosal damage in the rat, protein-bound dye, histology, comparison with aspirin □ Aspirin—gastric mucosal damage in the rat, protein-bound dye, histology, comparison with copper aspirinate □ Ulceration—gastric mucosa, rat, aspirin and copper aspirinate, comparison using protein-bound dye and histology

Gastric mucosal damage induced by the administration of aspirin has been studied for many years. The animal model most often used has been the rat, in which, following exposure to aspirin, numerous ulcers have been found in the corpus (with a few in the antrum) (1, 2). It has been demonstrated that aspirin is absorbed from the corpus and antrum, but not the rumen (3, 4). Buffered aspirin has been shown to produce fewer lesions than aspirin alone (1, 5–7), presumably because the buffered aspirin is not absorbed from the stomach but from the intestine.

In 1976 Sorenson (8, 9) reported that copper aspirinate [tetrakis(acetylsalicylato)-μ-dicopper(II)], the copper salt of acetylsalicylic acid, had a strong antiulcer effect compared with aspirin alone when administered during the period of ulcer development in the Shay rat (10). On the basis of his observations, Sorenson suggested that the copper complex of aspirin may be the pharmacologically active form of this drug. Numerous other researchers then investigated the lesion-producing ability of copper aspirinate in the rat model (11–16). Although some conclusions were drawn supporting Sorenson's claim, these studies leave considerable uncertainty concerning the relative ulcerogenic potential of copper aspirinate and aspirin.

The results presented here are an attempt to make a quantitative comparison of the effect of aspirin and copper aspirinate on the gastric mucosa of the rat, using a protein-bound dye to highlight lesions (17) and histological examination of the tissue to validate the interpretation of the dye observations. With respect to the copper aspirinate, experiments were included to differentiate between the effects of the complex and its hydrolysis products, aspirin and the copper(II) ion. A moderate (pharmacological) dose and short incubation period were used in all experiments. In a separate set of experiments, all compounds were given with a buffer system to assess the effect of the buffer when the drug is prevented from leaving the stomach by ligation of the duodenum.

EXPERIMENTAL

Since lesion formation due to aspirin is altered by the presence of food in the stomach (5, 17), all animals (male Sprague–Dawley-derived rats, 150–300 g body weight) were fasted 24 hr prior to the experiments. Anesthesia was induced with ether and maintained with an intraperitoneal injection of sodium pentobarbital[1] (50 mg/kg of body weight). An endotracheal cannula was inserted through a midline neck incision. The abdomen was opened and the duodenum ligated, care being taken not to obstruct the vascular supply to the stomach. An infant feeding tube was inserted through the esophagus into the stomach, and the stomach was rinsed with 10–15 ml of saline to remove bits of food and other foreign matter. The test suspension (0.5 ml/100 g of body weight) was instilled, and the tube removed. Preliminary experiments indicated that this volume of fluid resulted in an intragastric pressure of <4 cm H_2O when initially administered. The abdomen was closed with wound clips.

The compounds or mixtures employed in these experiments were ground to fine powders, and test suspensions in 0.1% aqueous nonionic surfactant[2] were prepared by sonicating the appropriate amount of the test compound or mixture for 10 min. A nonionic suspending agent was chosen in order to avoid decomposing the copper complex (18). Molar equivalents of the copper(II) ion and aspirin were used in the experiments, as shown in Table I. The suspension volume administered each animal was determined from its body weight (0.5 ml/100 g of body weight). In each case the dose was equivalent to 100 mg aspirin/kg. The suspensions tested were aspirin, copper aspirinate (19), copper sulfate plus aspirin, and copper alone (in the form of copper sulfate). All suspensions were given with and without a buffer. The buffered suspensions contained 3.0 mg/ml of dihydroxyaluminum glycinate[3] and 6.0 mg/ml of magnesium carbonate. This buffer system is the same as that used in a commonly available proprietary product (20).

The suspensions were allowed to incubate in the stomach for 120 min. Ten minutes prior to the end of the incubation period, the animals were given an intravenous (femoral vein) injection of 5% protein-binding dye[4] in saline (17). At 120 min of incubation, the animals were sacrificed. The stomachs were immediately removed, opened along the lesser curvature, and washed with ~10 ml of saline. When necessary, a camel's hair brush was used to remove the mucous layer. The stomachs were pinned over rubber stoppers and examined under a dissecting microscope. Lesions could easily be separated into two groups with well-defined boundaries depending on the intensity of the dye in the tissue. Each of the two groups (one a light blue, the other very dark) was scored by counting the number of lesions (x) in each of five size classes (y). The classes were defined according to Guth *et al.* (2, 21): $y = 1$ (pinpoint lesions), $y = 2$ (lesions <1 mm in diameter), $y = 3$ (lesions 1–2 mm in diameter), $y = 4$ (lesions 2–4 mm in diameter), and $y = 5$ (lesions >4 mm in diameter). A lesion index was computed by:

$$\text{Lesion Index} = \sum_{i=1}^{5} x_i y_i$$

Mean, standard deviation, and standard error were calculated for each group of rats; the number of rats per group ranged from 6 to 17. The stomachs were stored in 10% formalin in saline and recounted after 24

[1] Diabutal; Diamond Labs, Des Moines, Iowa.
[2] Tween 80; ICN Pharmaceuticals, Inc., Cleveland, Ohio.
[3] Dihydroxyaluminum glycinate was generously donated by the Bristol-Meyers Company.
[4] Pontamine Sky Blue 6BX; Pfaltz and Bauer, Stamford, Conn.

0022-3549/83/1200-1457$01.00/0

Table I—Test Suspensions of Drug in 0.1% Aqueous Suspending Medium [a]

Compound	Compound, mg	Aspirin, mmole	Copper, mmole
Aspirin	20.0	0.111	—
Copper aspirinate	23.6	0.111	0.0558
Copper sulfate	13.9	—	0.0558
Copper sulfate/aspirin	13.9/20.0	0.111	0.0558

[a] Per milliliter of suspension. Buffered suspensions also contained 3.0 mg/ml of dihydroxyaluminum glycinate and 6.0 mg/ml of magnesium carbonate (20).

hr. The average of the two values was recorded as the lesion index. The Student's t test (unpaired) was applied as a test of significance ($p < 0.05$).

Representative samples of each type of lesion were taken from the stomach, embedded in paraffin, and stained (hematoxylin–eosin) for histological evaluation. The blocks were sectioned in a serial manner so that the lesions were not missed. The evaluation of the histological material was done under a double-blind procedure.

RESULTS

The lesions outlined by the blue dye were separated into two classes based on two distinct colors of damaged mucosal tissue. Histological examination revealed that the lighter of these were superficial erosions (penetrating less than halfway through the mucosa) and the darker were deep erosions (penetrating more than halfway through the mucosa). No true ulcers were produced in any of these systems. There is excellent agreement between the two methods for rats tested with copper aspirinate or a mixture of copper(II) ion and aspirin, but poor agreement in the experiments involving aspirin alone (Table II). In terms of the lesion index, agreement is good where the index is large, but poor where the index is small.

Figure 1 displays lesion index values calculated by the equation for superficial and deep erosions. In addition to differences in the depth of dye color (due to extent of leakage of the dye–protein complex from

Table II—Agreement of Lesion Grading by Technique [a]

Sample	Treatment	Dye Evaluation	Histological Evaluation [b]	Agree Disagree
1	Copper aspirinate	Superficial	Superficial	Agree
2		Deep	Deep	Agree
3		Superficial	No Lesion	Disagree
4		Superficial	Superficial	Agree
5		Deep	Deep	Agree
6		Superficial	Deep	Disagree
7		Superficial	Superficial	Agree
8		Deep	Deep	Agree
9		Deep	Deep	Agree
10	Copper sulfate plus aspirin	Deep	Deep	Agree
11		Superficial	Deep	Disagree
12		Deep	Deep	Agree
13		Superficial	Superficial	Agree
14		Deep	Deep	Agree
15		Superficial	Superficial	Agree
16	Aspirin	Deep	Superficial	Disagree
17		Deep	Superficial	Disagree
18		Deep	Deep	Agree
19		Deep	Deep	Agree
20		Superficial	None	Disagree
21		Superficial	None	Disagree
22		Deep	Deep	Agree
23		Deep	Superficial	Disagree
24		Superficial	Superficial	Agree
25	Aspirin plus buffer	Deep	Deep	Agree
26		Superficial	None	Disagree
27		Deep	None	Disagree
28		Superficial	Deep	Disagree
29		Deep	Deep	Agree
30		Superficial	Deep	Disagree

[a] In the dye evaluation, assignment was made on the basis of color; in the histological evaluation, on the basis of penetration into the mucosal surface. [b] Superficial lesions extended less than one-half the mucosal thickness; deep lesions penetrated more than one-half the thickness. No lesion penetrated the muscularis mucosa.

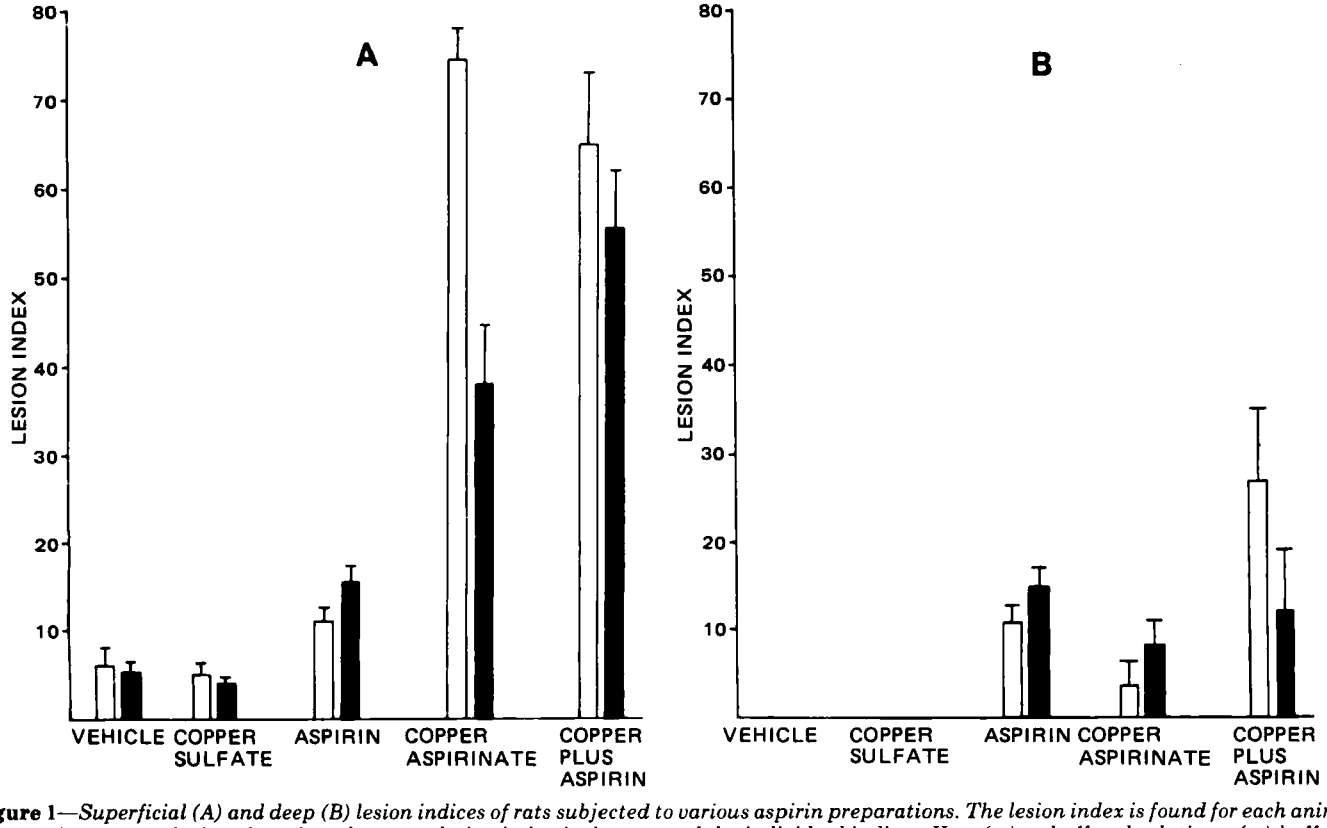

Figure 1—*Superficial (A) and deep (B) lesion indices of rats subjected to various aspirin preparations. The lesion index is found for each animal by summing over each size of erosion; the group lesion index is the mean of the individual indices. Key: (□) unbuffered solutions; (■) buffered solutions. The bars represent +1* SEM.

Table III—Distribution of Superficial Lesions by Size [a]

Test Compound	n		Number of Lesions of Each Size 1	2	3	4	5	Lesion Index
Control	7	Mean	2.36	1.86				6.07
		SEM	0.43	0.89				2.14
Control (buffered)	6	Mean	3.58	0.83				5.25
		SEM	1.23	0.33				1.38
Copper sulfate	8	Mean	3.44	0.75	0.25			5.06
		SEM	0.63	0.37	0.16			1.61
Copper sulfate (buffered)	12	Mean	2.42	1.67				4.08
		SEM	0.59	0.79				0.70
Aspirin	17	Mean	5.94	2.35	0.18			11.18
		SEM	0.95	0.53	0.13			1.89
Aspirin (buffered)	17	Mean	7.50	2.53	0.88	0.06		15.35
		SEM	2.01	0.49	0.32	0.06		2.40
Copper aspirinate	12	Mean	50+	6.58	1.92	0.71	0.62	74.75
		SEM		1.06	0.48	0.35	0.42	3.43
Copper aspirinate (buffered)	10	Mean	7.89	6.39	3.67	1.61	0.45	38.30
		SEM	1.52	1.45	0.71	0.90	0.30	6.26
Copper sulfate plus aspirin	11	Mean	9.68	6.04	3.77	2.91	4.23	65.30
		SEM	1.10	0.88	0.65	1.07	0.98	8.65
Copper sulfate plus aspirin (buffered)	17	Mean	20.26	5.79	3.97	1.74	0.91	55.53
		SEM	4.15	1.06	0.67	0.37	0.27	7.02

[a] The diameter of individual lesions determined the category into which they fell for counting. The mean represents the average number of lesions of each size, and the lesion index is the score obtained by summing.

Table IV—Distribution of Deep Lesions by Size [a]

Test Compound	n		Number of Lesions of Each Size 1	2	3	4	5	Lesion Index
Control	7	Mean						0
		SEM						
Control (buffered)	6	Mean						0
		SEM						
Copper sulfate	8	Mean						0
		SEM						
Copper sulfate (buffered)	12	Mean						0
		SEM						
Aspirin	17	Mean	4.82	2.30	0.38			10.62
		SEM	1.17	0.46	0.17			1.51
Aspirin (buffered)	17	Mean	4.71	3.59	0.55	0.29		14.62
		SEM	1.96	1.26	0.33	0.21		5.44
Copper aspirinate	12	Mean	0.54	0.67	0.21	0.17		3.17
		SEM	0.29	0.40	0.11	0.11		1.05
Copper aspirinate (buffered)	10	Mean	1.44	2.00	0.89			8.11
		SEM	1.44	0.74	0.53			3.06
Copper sulfate plus aspirin	11	Mean	4.36	5.00	2.77	0.77	0.14	26.68
		SEM	1.54	1.45	1.00	0.41	0.14	7.15
Copper sulfate plus aspirin (buffered)	17	Mean	3.85	2.56	0.91	0.03		11.88
		SEM	1.04	0.56	0.32	0.02		2.57

[a] The diameter of individual lesions determined the category into which they fell for counting. The mean represents the average number of lesions of each size, and the lesion index is the score obtained by summing.

damaged blood vessels), deep lesions were small and circular or oval, whereas superficial erosions were irregular in shape and considerably larger. The difference in size is apparent from the comparative lesion indices for the two types of erosions, which are plotted on the same scale in Fig. 1A and B. In general, the presence of the buffer had no significant effect on the extent of damage produced under these experimental conditions.

Copper aspirinate and a mixture of aspirin and copper sulfate caused significant increases over controls in both the superficial and deep lesion indices. Copper aspirinate and copper(II) ion plus aspirin had significantly higher superficial lesion indices than aspirin alone ($p < 0.001$), but were not significantly different from each other. The copper aspirinate deep lesion index was significantly less than the aspirin deep lesion index in the unbuffered systems ($p < 0.001$), but not in the buffered systems.

Tables III and IV contain data from which the lesion indices were calculated. It is clear from this data that the higher superficial lesion index of copper aspirinate and copper(II) ion plus aspirin represent both more and larger erosions than are found for aspirin alone. There does not appear to be a clear difference between the deep erosion data of copper aspirinate and aspirin.

Some deep erosions in categories 3, 4, and 5 were observed to have red or brown centers to which the blue dye had not penetrated; it was initially supposed that these represented ulcers. On histological examination, however, these lesions were found to be erosions, indicating that disruption of the circulation occurs prior to ulcer development. A small number of these appeared in aspirin-treated rats, somewhat more in copper aspirinate-treated rats, and the most in copper-plus-aspirin-treated rats. When copper sulfate was used in the absence of aspirin, the lesion indices were not significantly different from the controls for either superficial or deep erosions.

DISCUSSION

Initial damage to the mucosa from absorption of aspirin is more easily and accurately assessed by the use of a protein-binding dye. Two stages prior to ulcer formation can be clearly distinguished by the loss of the dyed protein into the tissue. The darker blue lesions, as can be seen from the agreement of histological and dye diagnoses (Table II), are deep erosions, penetrating more than halfway through the mucosa. Of the 16 lesions diagnosed as deep by the dye method, 76% were in agreement using the histological diagnosis.

For lesions diagnosed as superficial erosions by the dye method, agreement was poor; less than half were in agreement with the histological diagnosis. Of those that did not agree, the majority were found to have no erosion by the microscopic examination. Thus, the superficial erosions identified by the dye technique included both erosions penetrating less than halfway through the mucosa and pre-erosion lesions which allowed loss of the protein–dye complex from the gastric capillaries. The minimal pathological change necessary to allow the dye to accumulate in the mucosa would be an alteration in capillary permeability of sufficient magnitude to allow transendothelial movement of the protein–dye complex. Robins (22) has shown, by transmission electron microscopy, that the first structural change after administration of aspirin is alteration of the capillary endothelial basement membrane, which leads to the breakdown of small blood vessels before any other cytolytic effects appear. Thus, bleeding (and the loss of the protein–dye complex into the tissue) could occur without gross visible damage to the mucosal structures. Williams *et al.* observed no erosions when copper aspirinate was given to rats, but even after 18 hr, noted that bleeding had occurred (12). Their technique would not have allowed detection of these lesions.

In those experiments in which the superficial lesion index was highest, the correlation between dye and histological evaluation was remarkable. Table II indicates that in copper aspirinate experiments, agreement was 7 of 9, and in copper-plus-aspirin experiments, agreement was 5 of 6. In experiments where the superficial lesion index was low, correlation was poor: for aspirin alone, agreement was 4 of 9, and for buffered aspirin, 2 of 6. Thus, in terms of the calculated superficial lesion indices, the difference between copper aspirinate and aspirin is even larger than it appears to be from Fig. 1A. For the deep lesion index, the only disagreements in diagnosis were overdiagnosis by the dye method in the aspirin and aspirin-plus-buffer classes. Thus, the calculated deep lesion index for aspirin would be less than that indicated in Fig. 1B, whereas those for copper aspirinate and copper-plus-aspirin would be unchanged. It is clear that these data do not support the Sorenson conclusions that copper aspirate is less damaging to stomach mucosa than aspirin.

The Shay rats (10) used by Sorenson are prepared by ligating the duodenum and allowing acid to accumulate in the stomach for 16–19 hr, resulting in ulcer formation. In Sorenson's experiments (8), the aspirin or copper aspirinate was placed in the stomach during the period of ulcer formation. At the end of the experiment, an ulcer index was calculated. The substance was deemed active if the ulcer index was less than that of the controls. Under this protocol, both aspirin and copper aspirinate were reported to be active antiulcer agents, with copper aspirinate much more so than aspirin. These conclusions actually refer to the change in the rate of ulcer formation or healing in the Shay rat model. The excess acid and very long incubation times make Sorenson's results unique and of questionable value in the study of lesion formation by aspirin and related compounds under normal conditions of absorption.

With respect to the other studies in which copper aspirinate was tested, conditions varied greatly (11–16). Williams *et al.* (12) did not fast rats prior to experimentation and did not examine the stomachs for 18 hr after dosing. It has been shown that fed rats develop fewer stomach lesions from aspirin than do fasted rats (5, 17) and that spontaneous healing of lesions begins within 6 hr after damage (5). These authors tallied numbers of erosions, but did not assess size or severity of lesions. They reported that while rats treated with aspirin developed 50% more lesions (histological evaluation of lesion type was not done) than controls, those treated with copper aspirinate developed no erosions (though bleeding was observed). The significance of these data is not clear due to the aforementioned variations in the experimental protocol. Rainsford and Whitehouse (13) reported ulcers formed in groups of five fasted rats given aqueous suspensions of aspirin or copper aspirinate. Those given copper aspirinate were also subjected to cold stress. These authors concluded that since the copper aspirinate-treated rats (with cold stress) did not have significantly more mucosal damage than the aspirin-treated rats, copper aspirinate caused less damage to the mucosa. The data reported in this paper, using larger groups of rats, does not support their conclusions. Boyle *et al.* (11), reporting the percentage of rats having at least one "area of erosion," found that for aspirin alone this figure was ~98% and for copper aspirinate ~15%. Their paper refers to both erosions and ulcers, and it is not clear which were counted. The difference in results is perhaps due to the difference in assessment—the lack of a protein-binding dye to enhance preulcer lesions and a counting formula that did not include both number and size of lesions. Sorenson's results were also tested by Lewis *et al.* (14–16). The rats they used were very young, and it has been shown that juvenile rats do not have the same susceptibilities to aspirin-induced lesions as adult rats (23). Results were about the same for free aspirin as for the copper complex. Observations were made after 6 hr of incubation without magnification or the aid of a dye.

The experiments reported in this paper eliminated as many of these variables as possible. Using a protein-binding dye and summing over both number and sizes of lesions, clear differences appeared between the effects of copper aspirinate and aspirin. Figure 1B shows that copper aspirinate produced fewer deep erosions than aspirin alone although there was apparently a greater disruption of blood flow from copper aspirinate as indicated by the absence of dye in the center of some of these erosions. The difference in the deep lesion indices for these two systems was not significant when buffer was present. The copper aspirinate yielded larger numbers of superficial lesions than aspirin alone (Fig. 1A). The combination of copper plus aspirin caused more deep lesions than either aspirin or copper aspirinate alone, suggesting that it is the hydrolysis products of the copper aspirinate that are the most potent lesion-producing system. The smaller deep lesion index of copper aspirinate *versus* aspirin may be due, in part, to the slow hydrolysis of the complex. The concentration of the hydrolysis products (copper and aspirin) may be sufficient to produce large numbers of superficial lesions, but not enough to produce as many deep lesions as the aspirin alone.

With the exception of one experimental group, in the experimental protocol employed here, the addition of buffer did not result in a significant decrease in lesion formation. Only in the group of animals receiving copper aspirinate did the addition of buffer result in a significant decrease in the formation of deep erosions (Fig. 1B). This should not be interpreted as contradicting the known fact (24) that buffered aspirin is less damaging to stomach mucosa than aspirin alone. In these experiments, the stomach was isolated from the intestinal tract so that the drug was held in the stomach for the duration of the experiment.

The data presented allow several conclusions. First, if one employs protein-bound dye to mark or outline gastric lesions, the severity or type of lesion must be verified by histological methods. The appearance of the dye on the mucosal surface can result from prelesion capillary endothelial damage, erosions, or ulcers. The protocol employed here did not produce ulcers, and it was possible to differentiate between deep and superficial erosions by the color characteristics of the extravasated dye. The dye method includes pre-erosion capillary endothelial damage with superficial erosions. Secondly, the administration of copper aspirinate produced larger numbers and sizes of superficial erosions than did aspirin alone. The frequency of deep erosions was slightly less for copper aspirinate than for aspirin alone. Thirdly, the combination of copper(II) ions and aspirin resulted in a greater effect (a larger deep lesion index) than the copper complex, suggesting that it may be the hydrolysis products of the copper aspirinate complex which cause the more severe gastric mucosal damage. Finally, the addition of a buffer to the preparation resulted in a decrease in lesion formation only in the case of copper aspirinate and only as evaluated from superficial erosions.

REFERENCES

(1) K. D. Rainsford and M. W. Whitehouse, *Life Sci.*, **21,** 371 (1977).

(2) P. H. Guth, D. Aures, and G. Paulsen, *Gastroenterology*, **76,** 88 (1979).

(3) E. Morris, A. A. Nouhaim, T. S. Miya, and J. E. Christian, *J. Pharm. Sci.*, **56,** 896 (1967).

(4) C. H. Morris, J. E. Christian, T. S. Miya, and W. G. Hanson, *J. Pharm. Sci.*, **59,** 325 (1970).

(5) K. W. Anderson in "Salicylates: An International Symposium," A. St. John-Dixon, B. K. Martin, M. J. H. Smith, and P. H. N. Wood, Eds., J. and A. Churchill, Ltd., London, 1963, pp. 217–233.

(6) H. W. Davenport, *Gastroenterology*, **46,** 245 (1964).

(7) K. D. Rainsford, *Gut*, **16,** 514 (1975).

(8) J. R. J. Sorenson, *J. Med. Chem.*, **19,** 135 (1976).

(9) J. R. J. Sorenson, *Inflammation*, **1,** 317 (1976).

(10) H. Shay, S. A. Komarov, S. S. Fels, D. Meranze, M. Gruenstein, and H. Siplet, *Gastroenterology*, **5,** 43 (1945).

(11) E. Boyle, P. C. Freeman, A. C. Goudie, F. R. Mangan, and M. Thompson, *J. Pharm. Pharmacol.*, **28,** 865 (1976).

(12) D. A. Williams, D. T. Walz, and W. O. Foye, *J. Pharm. Sci.*, **65,** 126 (1976).

(13) K. D. Rainsford and M. W. Whitehouse, *J. Pharm. Pharmacol.*, **28,** 83 (1976).

(14) A. J. Lewis, *Agents Actions*, **8,** 244 (1978).

(15) A. J. Lewis, *Br. J. Pharmacol.*, **63,** 413p (1978).

(16) D. H. Brown, W. E. Smith, J. W. Teape, and A. J. Lewis, *J. Med. Chem.*, **23,** 729, (1980).

(17) D. A. Brodie, C. L. Tate, and K. F. Hooke, *Science*, **170**, 183 (1970).
(18) J. R. J. Sorenson, *J. Pharm. Pharmacol.*, **29**, 450 (1977).
(19) A. A. Alich and L. E. Wittmers, Jr., *J. Pharm. Sci.*, **69**, 725 (1980).
(20) B. Huff, Ed., "Physicians Desk Reference," 35th ed., Litton Industries, Oradell, N.J., 1981, p. 735.
(21) P. H. Guth and G. Paulsen, *Digestion*, **19**, 93 (1979).
(22) P. G. Robins, *Br. J. Exp. Pathol.*, **61**, 497 (1980).
(23) G. Wilhelmi and R. Manasse-Gdynia, *Pharmacology*, **8**, 321 (1972).
(24) J. W. D. McDonald in "Acetylsalicylic Acid: New Uses for an Old Drug," Raven, New York, N.Y., 1982, pp. 87–94.

ACKNOWLEDGMENTS

This work was supported in part by Miller-Dwan Medical Center Foundation, the Duluth Clinic Foundation, and the St. Scholastica Faculty Development Fund.

The authors are indebted to Dr. A. C. Aufderheide, Department of Pathology, School of Medicine, University of Minnesota-Duluth, for the histological evaluation of the gastric tissue.

Hemolysis Caused by Cetomacrogol 1000: Evidence for Hydroxyl Radical Participation

RUTH SEGAL ˣ and ILANA MILO-GOLDZWEIG

Received June 1, 1982, from *The Hebrew University of Jerusalem, School of Pharmacy, Department of Pharmacognosy and Natural Products, P.O.B. 12065 Jerusalem, Israel* Accepted for publication October 28, 1982.

Abstract □ The mechanism of cetomacrogol 1000-induced hemolysis was investigated. Previous conclusions that peroxides are involved in the hemolytic process were confirmed. The possibility that hydrogen peroxide, superoxide, hydroxyl radical, or singlet oxygen, which are known to induce hemolysis, are involved in cetomacrogol 1000-induced hemolysis was tested by using specific inhibitors and inactivators. The hydroxyl radical ($OH^{\cdot}$) was shown to be the only apparent oxygen species involved in cetomacrogol 1000-induced hemolysis. Its contribution to the hemolytic potency of the surfactant is ~30%.

Keyphrases □ Cetomacrogol 1000—induction of hemolysis, peroxidation, hydroxyl radical participation, erythrocytes □ Surfactants—cetomacrogol 1000-induced hemolysis, peroxidation, hydroxyl radical participation □ Peroxides—role in surfactant-induced hemolysis, cetomacrogol 1000, hydroxyl radical participation

Polyoxyethylene-derived surfactants are widely used as pharmaceutical aids, although their tendency to form peroxides is well known (1–4) and their deleterious effects on various drugs have been proven (5–7). Like other surface-active compounds, the polyoxyethylene surfactants cause hemolysis when they come in contact with red blood cells (7–9). Results recently published (10) indicate that the hemolytic activity of polyoxyethylene surfactants may be ascribed to their tendency to form peroxides. It should, however, be emphasized that hemolysis is only one form of cytotoxicity.

Peroxidation is believed to be one of the main mechanisms that give rise to membrane damage and cellular death (11–16). Destruction of normal tissue as a consequence of inflammatory reactions is also ascribed to oxygen radicals. The superoxide anion radical ($O_2^{\cdot-}$), hydrogen peroxide, the hydroxyl radical ($OH^{\cdot}$), and the oxygen radicals ($^1O_2$) are highly reactive and can damage most types of cellular polymers. They have been shown to oxidize proteins, peroxidize fatty acids, and cleave polysaccharides *in vitro* (15). All were found to induce lysis of various types of cells (17–19). The abundance of polyunsaturated fatty acids in cell membranes and the facility with which these undergo oxidation are assumed to be the cause of peroxide-induced lysis (20).

Because of the widespread use of these surfactants and the awareness of the pernicious effect of free radicals and especially peroxides, we decided to study the mechanism by which these compounds induce peroxidation, with the ultimate aim of finding potential antidotes to these harmful effects. Their simple structure, easy availability, and the facility with which cell damage can be estimated by means of hemolysis make erythrocytes the ideal model for such research. Cetomacrogol 1000 (polyethylene glycol 1000 monocetyl ether) was chosen as the model polyoxyethylene surfactant in this research.

EXPERIMENTAL

Materials—Cetomacrogol 1000, polyethythelene glycol 1000 monocetyl ether[1], is a solid and, thus, not sensitive to autooxidation (4). Solutions of cetomacrogol 1000 were freshly prepared. Histidine[2], tryptophan[3], mannitol[3], thiourea[4], and digitonin[2] were commercial samples. Hydroquinone[5] was crystallized from benzene prior to use. Catalase[6] was dialyzed against water (specific activity 1.57×10^6 U/ml), superoxide dismutase[3] had a specific activity of 2650 U/mg of protein. Saponin-A was obtained from *Styrax officinalis* (21).

Determination of Hemolytic Activities—All experiments were performed on citrated blood freshly drawn from albino rats. The erythrocytes, freed of plasma by three washings in cold isotonic saline, were diluted with isotonic buffer (3.95 g of $Na_2HPO_4 \cdot 2H_2O$, 0.76 g of KH_2PO_4, 7.2 g of NaCl, *q.s.* to 1000 ml with water; pH adjusted to 7.4) to give a 1% suspension. Varying quantities of hemolysin, dissolved in buffer, were added to 2 ml of the erythrocyte suspension, and the volume was increased to 4 ml with buffer. The components were added in the following order: erythrocyte suspension, buffer, and the hemolyzing agent. The mixtures were incubated for 60 min at 37° in a shaking water bath, and then were centrifuged at $1000 \times g$; the absorbance of the supernatant was determined at 540 nm. The percentage of hemolysis was determined by comparison with a sample in which 100% hemolysis was obtained by the addition of digitonin.

Effect of Inhibitors on Surfactant-Induced Hemolysis—Two sets

[1] Cetomacrogol 1000, A.B.M. Chemical Ltd., England.
[2] E. Merck, Darmstadt, West Germany.
[3] Sigma Chemical Co., St. Lous, Mo.
[4] Riedel-De Haen AG. Seelze-Hannover.
[5] Photographic grade; May and Baker Ltd., Dagenham, England.
[6] Sigma—1000.

0022-3549/83/1200-1461$01.00/0

(17) D. A. Brodie, C. L. Tate, and K. F. Hooke, *Science*, **170**, 183 (1970).
(18) J. R. J. Sorenson, *J. Pharm. Pharmacol.*, **29**, 450 (1977).
(19) A. A. Alich and L. E. Wittmers, Jr., *J. Pharm. Sci.*, **69**, 725 (1980).
(20) B. Huff, Ed., "Physicians Desk Reference," 35th ed., Litton Industries, Oradell, N.J., 1981, p. 735.
(21) P. H. Guth and G. Paulsen, *Digestion*, **19**, 93 (1979).
(22) P. G. Robins, *Br. J. Exp. Pathol.*, **61**, 497 (1980).
(23) G. Wilhelmi and R. Manasse-Gdynia, *Pharmacology*, **8**, 321 (1972).
(24) J. W. D. McDonald in "Acetylsalicylic Acid: New Uses for an Old Drug," Raven, New York, N.Y., 1982, pp. 87–94.

ACKNOWLEDGMENTS

This work was supported in part by Miller-Dwan Medical Center Foundation, the Duluth Clinic Foundation, and the St. Scholastica Faculty Development Fund.

The authors are indebted to Dr. A. C. Aufderheide, Department of Pathology, School of Medicine, University of Minnesota-Duluth, for the histological evaluation of the gastric tissue.

Hemolysis Caused by Cetomacrogol 1000: Evidence for Hydroxyl Radical Participation

RUTH SEGAL ˣ and ILANA MILO-GOLDZWEIG

Received June 1, 1982, from *The Hebrew University of Jerusalem, School of Pharmacy, Department of Pharmacognosy and Natural Products, P.O.B. 12065 Jerusalem, Israel* Accepted for publication October 28, 1982.

Abstract □ The mechanism of cetomacrogol 1000-induced hemolysis was investigated. Previous conclusions that peroxides are involved in the hemolytic process were confirmed. The possibility that hydrogen peroxide, superoxide, hydroxyl radical, or singlet oxygen, which are known to induce hemolysis, are involved in cetomacrogol 1000-induced hemolysis was tested by using specific inhibitors and inactivators. The hydroxyl radical ($OH^{\cdot}$) was shown to be the only apparent oxygen species involved in cetomacrogol 1000-induced hemolysis. Its contribution to the hemolytic potency of the surfactant is ~30%.

Keyphrases □ Cetomacrogol 1000—induction of hemolysis, peroxidation, hydroxyl radical participation, erythrocytes □ Surfactants—cetomacrogol 1000-induced hemolysis, peroxidation, hydroxyl radical participation □ Peroxides—role in surfactant-induced hemolysis, cetomacrogol 1000, hydroxyl radical participation

Polyoxyethylene-derived surfactants are widely used as pharmaceutical aids, although their tendency to form peroxides is well known (1–4) and their deleterious effects on various drugs have been proven (5–7). Like other surface-active compounds, the polyoxyethylene surfactants cause hemolysis when they come in contact with red blood cells (7–9). Results recently published (10) indicate that the hemolytic activity of polyoxyethylene surfactants may be ascribed to their tendency to form peroxides. It should, however, be emphasized that hemolysis is only one form of cytotoxicity.

Peroxidation is believed to be one of the main mechanisms that give rise to membrane damage and cellular death (11–16). Destruction of normal tissue as a consequence of inflammatory reactions is also ascribed to oxygen radicals. The superoxide anion radical ($O_2^{\cdot-}$), hydrogen peroxide, the hydroxyl radical ($OH^{\cdot}$), and the oxygen radicals ($^1O_2$) are highly reactive and can damage most types of cellular polymers. They have been shown to oxidize proteins, peroxidize fatty acids, and cleave polysaccharides *in vitro* (15). All were found to induce lysis of various types of cells (17–19). The abundance of polyunsaturated fatty acids in cell membranes and the facility with which these undergo oxidation are assumed to be the cause of peroxide-induced lysis (20).

Because of the widespread use of these surfactants and the awareness of the pernicious effect of free radicals and especially peroxides, we decided to study the mechanism by which these compounds induce peroxidation, with the ultimate aim of finding potential antidotes to these harmful effects. Their simple structure, easy availability, and the facility with which cell damage can be estimated by means of hemolysis make erythrocytes the ideal model for such research. Cetomacrogol 1000 (polyethylene glycol 1000 monocetyl ether) was chosen as the model polyoxyethylene surfactant in this research.

EXPERIMENTAL

Materials—Cetomacrogol 1000, polyethythelene glycol 1000 monocetyl ether[1], is a solid and, thus, not sensitive to autooxidation (4). Solutions of cetomacrogol 1000 were freshly prepared. Histidine[2], tryptophan[3], mannitol[3], thiourea[4], and digitonin[2] were commercial samples. Hydroquinone[5] was crystallized from benzene prior to use. Catalase[6] was dialyzed against water (specific activity 1.57×10^6 U/ml), superoxide dismutase[3] had a specific activity of 2650 U/mg of protein. Saponin-A was obtained from *Styrax officinalis* (21).

Determination of Hemolytic Activities—All experiments were performed on citrated blood freshly drawn from albino rats. The erythrocytes, freed of plasma by three washings in cold isotonic saline, were diluted with isotonic buffer (3.95 g of $Na_2HPO_4 \cdot 2H_2O$, 0.76 g of KH_2PO_4, 7.2 g of NaCl, *q.s.* to 1000 ml with water; pH adjusted to 7.4) to give a 1% suspension. Varying quantities of hemolysin, dissolved in buffer, were added to 2 ml of the erythrocyte suspension, and the volume was increased to 4 ml with buffer. The components were added in the following order: erythrocyte suspension, buffer, and the hemolyzing agent. The mixtures were incubated for 60 min at 37° in a shaking water bath, and then were centrifuged at $1000 \times g$; the absorbance of the supernatant was determined at 540 nm. The percentage of hemolysis was determined by comparison with a sample in which 100% hemolysis was obtained by the addition of digitonin.

Effect of Inhibitors on Surfactant-Induced Hemolysis—Two sets

[1] Cetomacrogol 1000, A.B.M. Chemical Ltd., England.
[2] E. Merck, Darmstadt, West Germany.
[3] Sigma Chemical Co., St. Lous, Mo.
[4] Riedel-De Haen AG. Seelze-Hannover.
[5] Photographic grade; May and Baker Ltd., Dagenham, England.
[6] Sigma—1000.

0022-3549/83/1200-1461$01.00/0

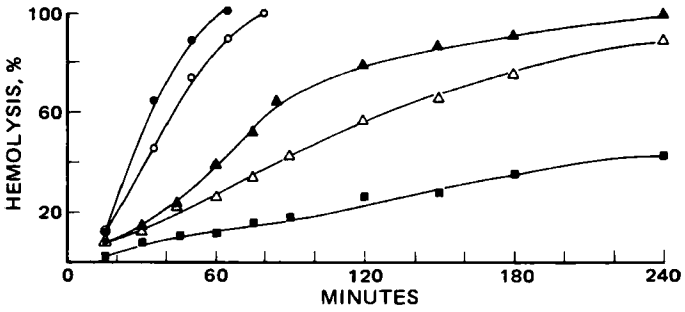

Figure 1—*Time dependence of cetomacrogol 1000-induced hemolysis. Cetomacrogol 1000 concentration: (●) 1.5 × 10⁻⁵ M; (○) 1.3 × 10⁻⁵ M; (▲) 9.5 × 10⁻⁶ M; (△) 7.6 × 10⁻⁶ M; (■) 5.7 × 10⁻⁶ M.*

of experiments were run in parallel: (*a*) a regular hemolysis test and (*b*) the same incubation mixture as in (*a*) but with inhibitor solutions (in buffer) substituting for part of the buffer. The components were added as follows: erythrocytes, buffer, inhibitor, hemolysin. Percentage inhibition was determined as:

$$100 \times \left(1 - \frac{\%\text{ hemolysis with inhibitor}}{\%\text{ hemolysis without inhibitor}}\right)$$

Effect of Visible Light on Cetomacrogol 1000-Induced Hemolysis—Equal volumes of mixtures consisting of erythrocytes, buffer, and cetomacrogol 1000 were introduced into eight test tubes. Four of the test tubes were shielded from light by covering them with aluminium foil. All eight of the test tubes were incubated for 1 hr at 37° and processed as described above.

RESULTS

Figure 1 shows the cetomacrogol 1000-induced hemolysis at various time intervals. The five curves represent different cetomacrogol 1000 concentrations; their shape is in accordance with previous observations that hemolysis produced by polyoxyethylene cetostearyl ethers progresses slowly toward 100% irrespective of the surfactant concentration (10).

To ensure reproducibility of the results and to provide a common basis for comparison of results of different experiments, the extent of the hemolysis was tested after exactly 1 h of incubation at 37°. The percentage of hemolysis was, therefore, reproducible to within 3% hemolysis.

No information is available on the identity of the active tissue-damaging radical produced during autooxidation of the polyoxyethylene surfactants, especially when they are in contact with living cells. We therefore decided to test the inhibitory influence of a variety of enzymes and chemicals which inactivate specific peroxides and radicals known to induce hemolysis. The effectiveness of the various inhibitors was tested at three cetomacrogol 1000 concentrations: 1.3×10^{-5} *M*, 1×10^{-5} *M*, and 7.6×10^{-6} *M*. These concentrations normally cause ~80, 50, and 30% hemolysis within 1 hr.

Catalase—Hydrogen peroxide either by itself or as a precursor of other active radical species is a well-known inducer of tissue damage and hemolysis (20, 22). The enzyme catalase, which catalyzes the conversion of H_2O_2 to O_2 and H_2O, was tested as a potential inhibitor for cetomacrogol 1000-induced hemolysis. The results (Table I) show that catalase had no inhibitory effect on cetomacrogol 1000-induced hemolysis even at levels as high as 625 U/ml.

Superoxide Dismutase—Superoxide radicals (O_2^-), generated enzymatically or photochemically, have been shown to induce lipid peroxidation, to damage membranes, and to kill cells (17, 20). The enzyme superoxide dismutase, which gives rise to the dismutation $O_2^- + O_2^- + 2H^+ \rightarrow H_2O_2 + O_2$ (23), was used to test the possibility of O_2^- being the active hemolyzing agent. No inhibition was obtained with superoxide dismutase (65 U/ml) nor with a superoxide dismutase–catalase mixture. All results are summarized in Table I.

Oxygen Radicals ($^1O_2$)—Hemolysis can be the result of the photosensitized production of $^1O_2$ using either endogenous or exogenous photosensitizers (19). The possibility that singlet oxygen was responsible for the cetomacrogol 1000-induced hemolysis was evaluated by adding specific $^1O_2$ quenchers, *i.e.*, the aromatic amino acids histidine and tryptophan, and hydroquinone (15, 18, 20). The three inhibitors were tested at the highest possible concentrations: hydroquinone at concentrations $>2.5 \times 10^{-4}$ caused damage to the erythrocytes (they turned brown); the maximal concentrations for histidine and tryptophan were those allowed by their solubility.

The results of these experiments are summarized in Table I. Of the three $^1O_2$ quenchers, only histidine caused slight inhibition of hemolysis, while tryptophan and hydroquinone produced no effect at all.

Hydroxyl Radicals—These radicals are very reactive and can interact with unsaturated fatty acids, which are components of the cell membrane, either through hydrogen abstraction or by addition to the unsaturated system (24). Among the oxidizing radicals the hydroxyl radical is the most powerful and most deleterious to the living membrane (25). The role of the hydroxyl radical in the hemolytic effect of cetomacrogol 1000 was tested by the addition of the specific hydroxyl radical quenchers, mannitol and thiourea. Both produced significant inhibition. Inhibition as function of mannitol and thiourea concentration is represented in Figs. 2 and 3, respectively. At high levels of hemolysis, an almost linear correlation between inhibitor concentration and inhibitor effect is observed, whereas at low levels, inhibition increases with inhibitor concentration until a plateau is obtained. In no case does inhibition exceed 35%. The possibility that the inhibition might be due to some nonspecific protective effect of the inhibitors on the red blood cell membranes was eliminated by testing their effect on saponin hemolysis. Digitonin and *Styrax* saponin, two highly potent crystalline compounds, were chosen to represent

Table I—Effect of Catalase, Superoxide Dismutase, Hydroquinone, Tryptophan, and Histidine on Cetomacrogol 1000-Induced Hemolysis

Cetomacrogol 1000 Concentration, *M*	Hemolysis, %	Inhibitor	Inhibitor Concentration	Inhibition, %
1.3×10^{-5}	80 ± 0.2 (5)	Superoxide dismutase	66.2 μg/ml	—
1×10^{-5}	50 ± 0.3 (5)		66.2 μg/ml	—
1.3×10^{-5}	80 ± 0.2 (5)	Catalase	250 μg/ml	—
			625 μg/ml	—
1×10^{-5}	50 ± 0.3 (5)		250 μg/ml	—
			625 μg/ml	—
1.3×10^{-5}	82 ± 0.5 (5)	Hydroquinone	2.2×10^{-4} *M*	—
			2.2×10^{-5} *M*	—
			2.2×10^{-6} *M*	—
1×10^{-5}	51 ± 0 (5)		2.2×10^{-4} *M*	—
1.3×10^{-5}	82 ± 0.5 (5)	Tryptophan	1.3×10^{-2} *M*	—
1×10^{-5}	51 ± 0 (5)		1.3×10^{-2} *M*	—
1.3×10^{-6}	82 ± 0.5 (5)	Histidine	5×10^{-2} *M*	7 ± 1.8 (5)
			2×10^{-2} *M*	7 ± 1.7 (5)
			1×10^{-2} *M*	—
			5×10^{-3} *M*	—
1×10^{-5}	51 ± 0 (5)		5×10^{-2} *M*	16 ± 1.1 (5)
			2×10^{-2} *M*	10 ± 1.5 (5)
			1×10^{-2} *M*	—
			5×10^{-3} *M*	—
7.6 ± 10^{-6}	31 ± 1.2 (5)		5×10^{-2} *M*	21 ± 0.9 (5)
			2×10^{-2} *M*	10 ± 1.2 (5)
			1×10^{-2} *M*	—

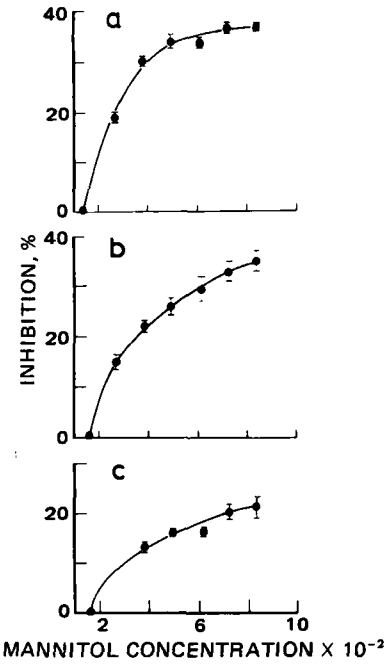

Figure 2—*Inhibition of cetomacrogol 1000-induced hemolysis as a function of mannitol concentration. Key: (a) cetomacrogol 1000, 7.6 × 10^{-6} M; (b) cetomacrogol 1000, 1 × 10^{-5} M; (c) cetomacrol 1000, 1.3 × 10^{-5} M.*

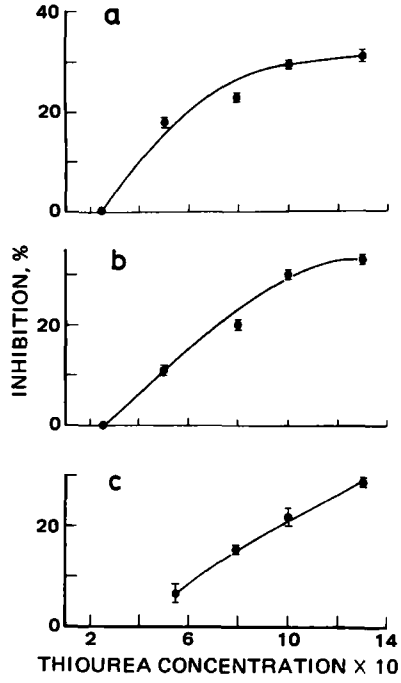

Figure 3—*Inhibition of cetomacrogol 1000-induced hemolysis as a function of thiourea concentration. (a) cetomacrogol 1000, 7.6 × 10^{-6} M; (b) cetomacrogol 1000, 1 × 10^{-5} M; (c) cetomacrogol 1000, 1.3 × 10^{-5} M.*

the saponins. The experiments were performed at two levels of hemolysis (*i.e.*, saponin concentrations). Mannitol and histidine had no effect on saponin hemolysis. Thiourea produced some inhibition at high inhibitor concentrations. However at 1.3 × 10^{-3} *M*, a concentration at which maximal inhibition of cetomacrogol 1000-induced hemolysis was obtained, no effect was observed (Table II).

Free radical reactions are often light catalyzed. We therefore tested whether cetomacrogol 1000-induced hemolysis is promoted by visible light. The experiments were performed at four different surfactant concentrations, and the results are summarized in Table III. They clearly show that the extent of hemolysis is indeed enhanced under the influence of light.

DISCUSSION

The results of the present investigation confirm previous conclusions (10) that the hemolytic activity of polyoxyethylene-derived surface-active agents is to be ascribed, at least in part, to their tendency to form peroxides. Various oxygen radical species and peroxides are known to induce hemolysis as a result of lipid peroxidation (12, 13, 15, 20). Our experiments indicate that in cetomacrogol 1000-induced hemolysis, the hydroxyl radical is strongly involved in the process.

The polyoxyethylene surfactants are polyethers and, therefore, their spontaneous autocatalytic peroxidation has been described as taking place *via* a free radical chain reaction as follows (3):

$$RH + \text{light or catalyst} \rightarrow R\cdot + H\cdot$$

Scheme I—Initiation

$$R\cdot\, O_2 \rightarrow ROO\cdot$$

$$ROO\cdot + RH \rightarrow ROOH + R\cdot$$

Scheme II—Propagation

Free radicals also may be formed by the processes in Scheme III, and removed by those in Scheme IV:

$$ROOH \rightarrow ROO\cdot + H\cdot$$

$$ROOH \rightarrow RO\cdot + \cdot OH$$

$$2ROOH \rightarrow ROO\cdot + RO\cdot + H_2O$$

Scheme III

Table II—Effect of Histidine, Mannitol, and Thiourea on Saponin Hemolysis

Saponin	Saponin Concentration, *M*	Hemolysis, %	Inhibitor	Inhibitor Concentration	Inhibition, %
Styrax saponin	8×10^{-7}	62 ± 0 (5)	Histidine	5×10^{-2}	0 (5)
	6×10^{-7}	46 ± 1 (4)			0 (4)
Digitonin	1.3×10^{-6}	42 ± 1 (5)			0 (5)
	1.0×10^{-6}	25 ± 1 (4)			0 (4)
Styrax saponin	8×10^{-7}	62 ± 0 (5)	Mannitol	1×10^{-1}	0 (5)
	6×10^{-7}	46 ± 1 (4)			0 (4)
Digitonin	1.3×10^{-6}	42 ± 1 (5)			0 (5)
	1.0×10^{-6}	25 ± 1 (4)			0 (4)
Styrax saponin	8×10^{-7}	62 ± 0 (5)	Thiourea	1.3×10^{-1}	48 ± 0 (5)
				6.5×10^{-2}	20 ± 0.3 (5)
				1.3×10^{-2}	0 (5)
	6×10^{-7}	46 ± 1 (4)		6.5×10^{-2}	47 ± 1 (4)
				1.3×10^{-2}	0 (4)
Digitonin	1.3×10^{-6}	42 ± 1 (5)		1.3×10^{-1}	50 ± 1.3 (5)
				6.5×10^{-2}	40 ± 1.5 (5)
				1.3×10^{-2}	0 (5)
	1.5×10^{-6}	58 ± 2 (4)		6.5×10^{-2}	30 ± 1 (4)
				1.3×10^{-2}	0 (4)

Table III—Effect of Visible Light on Cetomacrogol 1000-Induced Hemolysis

Cetomacrogol 1000 Concentration, *M*	Hemolysis in Light, %	Hemolysis in Darkness, %	Inhibition of Hemolysis in Darkness, %
1.3×10^{-5}	80 ± 2 (4)	66 ± 3 (4)	20
1.0 ± 10^{-5}	50 ± 1 (4)	37 ± 2 (4)	26
7.6 ± 10^{-6}	24 ± 2 (4)	18 ± 0.5 (4)	25
5.7 ± 10^{-6}	10 ± 0.5 (4)	8 ± 0.5 (4)	20

$$2RO_2^{\cdot} \xrightarrow{(a)} \text{inactive products}$$

$$RO_2^{\cdot} + R^{\cdot} \xrightarrow{(b)} \text{inactive products}$$

$$2R^{\cdot} \xrightarrow{(c)} \text{inactive products}$$

Scheme IV—Termination

This indicates that hydroxyl radicals may in fact be produced during polyoxyethylene surfactant autooxidation, as suggested by our findings on the active hemolyzing factor. The observation that visible light enhances cetomacrogol 1000-induced hemolysis further substantiates this suggestion.

The concentrations of inhibitors used in the present investigation were high when compared with those used by Kellog and Fridovich (20) to inhibit the hemolysis obtained by xanthine oxidase–acetaldehyde. These authors however used a much lower erythrocyte concentration for their experiments. This difference in the experimental conditions no doubt affects the extent of hemolysis as well as the extent of inhibition obtained by inhibitors.

The shapes of the curves representing the extent of inhibition by mannitol and thiourea as a function of inhibitor concentration are peculiar (Figs. 2 and 3). Although inhibition increases with inhibitor concentration, the curves reach a plateau at ~30% inhibition. The reason for the incomplete inhibition by $OH^{\cdot}$ scavengers may be due to other radicals obtained in the course of the surfactant autooxidation (see Schemes I–IV).

The possibility that histidine might scavenge such radicals seems controvertible since a mixture of histidine–mannitol did not enhance the inhibition beyond that of mannitol alone[7]. The assumption that other peroxide radicals take part in the hemolytic process also seems questionable in view of the fact that experiments conducted under a nitrogen atmosphere also produced only 30% inhibition (10). The high degree of consistency of these results suggests that although surface activity of the polyoxyethylene-derived surfactants could not be correlated with their hemolytic potency, the solubilizing properties of the surfactant contribute to the hemolytic process. Our present experiments suggest that the contribution of the surface activity factor to cetomacrogol 1000-induced hemolysis is ~70%, while the contribution of the $OH^{\cdot}$ radicals is ~30%.

[7] Unpublished results.

REFERENCES

(1) R. Hamburger, E. Azaz, and M. Donbrow, *Pharm. Acta Helv.* **50,** 10 (1975).

(2) J. W. McGinity, J. A. Hill, and A. L. La Via, *J. Pharm. Sci.*, **64,** 356 (1975).

(3) M. Donbrow, E. Azaz, and A. Pillersdorf, *J. Pharm. Sci.*, **67,** 1676 (1978).

(4) M. Donbrow, R. Hamburger, and E. Azaz, *J. Pharm. Pharmacol.*, **27,** 160 (1975).

(5) H. N. Glassman, *Science*, **111,** 688 (1950).

(6) E. Azaz, M. Donbrow, and R. Hamburger, *Pharm. J.*, **211,** 15 (1973).

(7) E. Azaz and R. Segal, *J. Pharm. Pharmacol.* **29,** 322 (1977).

(8) T. Kondo and M. Tomiza *J. Pharm. Sci.*, **57,** 1246 (1968).

(9) B. Y. Zaslavsky, N. N. Ossipov, V. S. Krivich, L. P. Baholdina, and S. V. Rogozhin, *Biochim. Biophys. Acta*, **507,** 1 (1978).

(10) E. Azaz, R. Segal, and I. Milo-Goldzweig, *Biochim. Biophys. Acta*, **646,** 444 (1981).

(11) P. M. Pfeifer and P. B. McCay, *J. Biol. Chem.*, **246,** 6401 (1971).

(12) G. L. Plaa and H. Witschi, *Ann. Rev. Pharmacol. Toxicol.*, **16,** 125 (1976).

(13) T. L. Dormandy, *Lancet*, **i,** 647 (1978).

(14) A. Bendetti, A. F. Casini, M. Ferraly, and M. Comporti, *Biochem. J.*, **180,** 303 (1979).

(15) R. H. Simon, C. H. Scoggin, and D. Patterson, *J. Biol. Chem.*, **256,** 7181 (1981).

(16) M. Kunimoto, K. Inoue, and S. Nojima, *Biochim. Biophys. Acta*, **646,** 169 (1981).

(17) L. Simchovitz and J. Spilberg, *Immunology*, **37,** 301 (1979).

(18) R. Nilsson, G. Swanbeck, and G. Wennersten, *Photochem. Photobiol.*, **22,** 183 (1975).

(19) N. I. Krinski, in "Singlet Oxygen" H. H. Wasserman and R. W. Murray, Eds., Academic New York, N.Y., 1979, p. 597.

(20) E. W. Kellog and I. Fridovich, *J. Biol. Chem.*, **252,** 6721 (1977).

(21) R. Segal, H. Govrin and D. V. Zaitschek, *Tetrahedron Lett.*, **1964,** 527.

(22) M. Naim, B. Gestetner, A. Bondi, and Y. Birk, *J. Agric. Food Chem*, **24,** 11,174 (1976).

(23) I. Fridovich, *Science*, **201,** 875 (1978).

(24) D. C. Nonhebel and J. C. Walton," Free Radical Chemistry," Cambridge University Press, England, 1974, p. 358.

(25) H. A. O. Hill, in "Oxygen Free Radicals and Tissue Damage," Ciba Foundation Symposium 65 Experta Medica, Amsterdam, 1979, p. 5.

Effects of Calcium and Neomycin on Phase Behavior of Phospholipid Bilayers

MADURAI G. GANESAN *, NORMAN D. WEINER *x, and JOCHEN SCHACHT ‡

Received June 25, 1982, from the **College of Pharmacy* and ‡*Kresge Hearing Research Institute, University of Michigan, Ann Arbor, MI 48109.* Accepted for publication October 14, 1982.

Abstract □ Calcium ion (Ca^{2+}, 5 m*M*) caused a large upward shift in the transition temperature (T_c) of dipalmitoyl phosphatidylglycerol liposomes, apparently interacting with external and internal lipid in the bilayer. Neomycin (1 m*M*) caused only a small shift, apparently not penetrating the internal lipid domains. When liposomes were first incubated with Ca^{2+} followed by neomycin, the shift in T_c indicated displacement of Ca^{2+} by the drug. Liposomes of dipalmitoyl phosphatidylcholine or distearoyl phosphatidylcholine did not interact significantly with either cation. In mixed dipalmitoyl phosphatidylcholine–dipalmitoyl phosphatidylglycerol and distearoyl phosphatidylcholine–dipalmitoyl phosphatidylglycerol liposomes, addition of Ca^{2+} or neomycin resulted in phase separation.

Keyphrases □ Calcium—effect on phase behavior of phospholipid bilayers, liposomes, neomycin □ Neomycin—effect on phase behavior of phospholipid bilayers, liposomes, calcium □ Liposomes—effects of calcium and neomycin on phase behavior of phospholipid bilayers □ Phase behavior—effects of calcium and neomycin on phospholipid bilayers, liposomes

Acidic phospholipids have been suggested as the membrane sites responsible for interactions with basic antibiotics in bacteria (1) and mammalian cells (2, 3). In the case of aminoglycoside antibiotics, such interactions have been discussed as mechanisms underlying their nephro- (2) and ototoxicity (3). The aminoglycosides also exert intracellular effects in bacteria and in afflicted eukaryotic cells. The mechanism of cell penetration is not clear. Internalization of aminoglycosides into lysosomes has been reported for the renal cortex (4), but not for other organs. Entry *via* a basic amino acid transport system (5) may be an alternate pathway.

Studies with monomolecular films (6) and liposomes (7) have shown that neomycin and other aminoglycosides affect Ca^{2+} binding to phospholipids, and that the degree of calcium displacement is strongly dependent on the head group of the anionic lipid. Differential scanning calorimetry is a valuable tool in determining physical changes of bilayers resulting from ion or drug interactions with liposomes, *e.g.*, gel-to-liquid phase transitions, phase separation, or membrane fusion (8–11). The present study investigates the actions of Ca^{2+} and neomycin, a highly toxic aminoglycoside, on thermotropic properties of synthetic negatively charged and neutral liposomes with well-defined transition temperatures.

EXPERIMENTAL

Liposomes were prepared from dipalmitoyl L-α-phosphatidylcholine (I), distearoyl L-α-phosphatidylcholine (II), and the ammonium salt of dipalmitoyl L-α-phosphatidyl-DL-glycerol (III)[1]. These lipids showed no impurities by TLC and by analysis of pretransition and main transition peaks of their liposomes.

Lipid samples (15 μmoles) dissolved in chloroform were dried under a nitrogen stream, and residual solvent was removed *in vacuo*. The dried lipid was suspended by vortexing in 10 m*M* tris buffer containing 100 m*M* NaCl and 0.1 m*M* EDTA (ethylenediaminetetraacetic acid), final pH 7.0. The resultant phospholipid concentration was 30 m*M*. Compounds I, III, and I–III (60:40 mole %) were suspended at 42°, II and II–III (60:40 mole %) at 58°. A 60:40 mole % ratio was selected, since at least 40 mole % negatively charged lipid was required to produce clearly defined thermal changes in the presence of Ca^{2+} at concentrations within the physiological range. Aliquots of the liposomal suspensions were incubated with 5 m*M* $CaCl_2$ or 1 m*M* neomycin for 60 min at 25° or 42° or, in the case of II-containing vesicles, at 58°.

Thermograms were obtained with a scanning calorimeter[2]. Aliquots of liposomal suspension (15 μl, containing 0.5–1 μmole of lipid) were transferred to volatile sample pans and properly sealed. Reference sample pans were prepared with the same amount of buffer. Inclusion of Ca^{2+} or neomycin or Ca^{2+}–neomycin mixtures in the reference sample pans did not affect the thermograms. Each sample was scanned between 5° and 70° at a rate of 5°/min and a range of 2 mcal/sec. Indium and water were used as calibration standards.

Phase-transition temperatures (T_c) were determined as the intercept between the slope of the ascending endothermic peaks and the base line. The midpoint value of transition was estimated as the maximal endothermic peak. After each run, the amount of lipid in the sample pan was determined (12). All experiments were repeated on at least three separate preparations.

RESULTS AND DISCUSSION

The thermograms for liposomes containing I or II (Fig. 1a and b) show well-defined sharp transition peaks with a broad pretransition peak. Incubation with Ca^{2+}, neomycin, or Ca^{2+} plus neomycin did not result in any changes in the thermograms. These data are in agreement with our previous monolayer (6) and liposome binding studies (7), which show no interaction between neutral phospholipids and Ca^{2+} or neomycin.

Liposomes containing III (Fig. 2a) have a clear transition peak at 41°. Incubation with Ca^{2+} (Fig. 2b) caused a 14° upward shift in T_c, in good agreement with previous observations (13). The extent of the T_c shift was related to the Ca^{2+} concentration, and 10 m*M* Ca^{2+} resulted in the loss of the transition peak up to 70°. This upward shift has been interpreted as the result of a combination of charge neutralization and specific complexation (13).

Incubation of liposomes containing III with neomycin at 25° (Fig. 2c) broadened the main transition peak of III and split it into two approximately equal components at 40° and 42°. These could represent two distinct domains of phospholipid molecules with different physical properties resulting from shallow perturbation of the bilayer primarily in the region of the phospholipid head-groups (14) and a coexistence between parent and modified phases (15). The split peak caused by neomycin thus suggests an interaction with the outer and lack of interaction

[1] Sigma Chemical Co., St. Louis, Mo.
[2] Perkin-Elmer, Model DSC-2C.

0022-3549/83/1200-1465$01.00/0

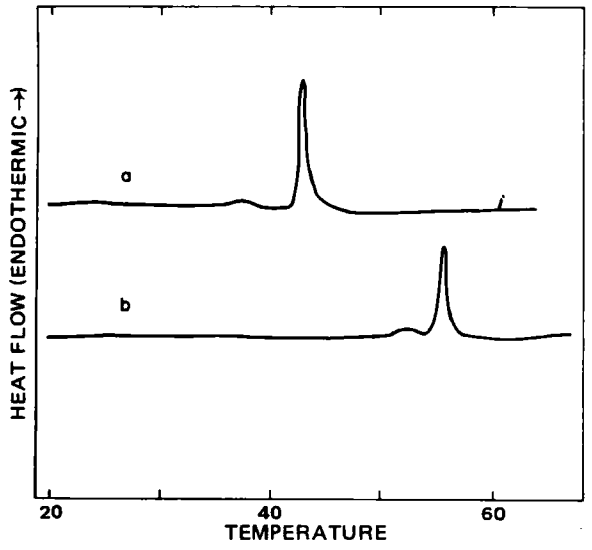

Figure 1—*Thermograms of liposomes containing I (a) and II (b). Conditions of liposome formation and incubation are described in the text.*

with the inner domains of the bilayer. Bilayers which are good permeability barriers to hydrophilic molecules above and below their T_c values (16, 17) are, however, highly permeable at their phase-transition temperature. Incubation of the liposomes with neomycin near their phase-transition temperature could conceivably alter the accessibility of the inner lipid layer. After such treatment at 42°, the split peak still remained (40° and 42°), but the 42° portion of the peak was clearly predominant (Fig. 2d). No such influence of temperature was seen with III and Ca^{2+}. This suggests that Ca^{2+} has access to the inner bilayer regions even when they are in the gel state, while the access of neomycin to the inner regions is limited by and dependent on the fluidity of the membrane. It should be pointed out, however, that the interaction of neomycin with III results in a T_c shift of only ~2°, whereas Ca^{2+} causes a much larger shift, indicating a solidifying effect (13). Thus, the resulting complexes with Ca^{2+} or neomycin have different thermal properties.

In another series of experiments, III was first incubated with Ca^{2+} at 42° and subsequently with neomycin. The resultant thermogram (Fig. 2e) shows the appearance of a distinct transition peak with a midpoint value of 43° and a very small peak at ~55°. Thus, it appears that neomycin, even at a concentration one-fifth that of Ca^{2+}, is essentially reversing the Ca^{2+} effect, *i.e.*, solidification, on the thermal properties of

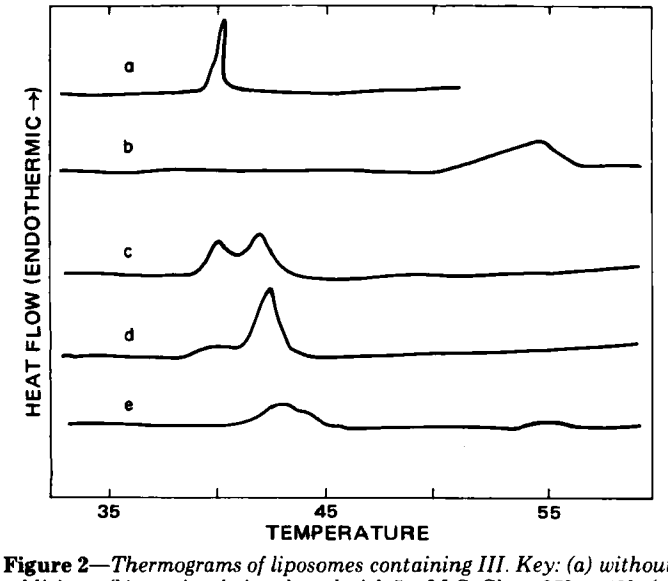

Figure 2—*Thermograms of liposomes containing III. Key: (a) without additions; (b) previously incubated with 5 mM $CaCl_2$ at 25° or 42°; (c) previously incubated with 1 mM neomycin at 25°; (d) previously incubated with 1 mM neomycin at 42°; (e) previously incubated with 5 mM $CaCl_2$ followed by 1 mM neomycin at 42°.*

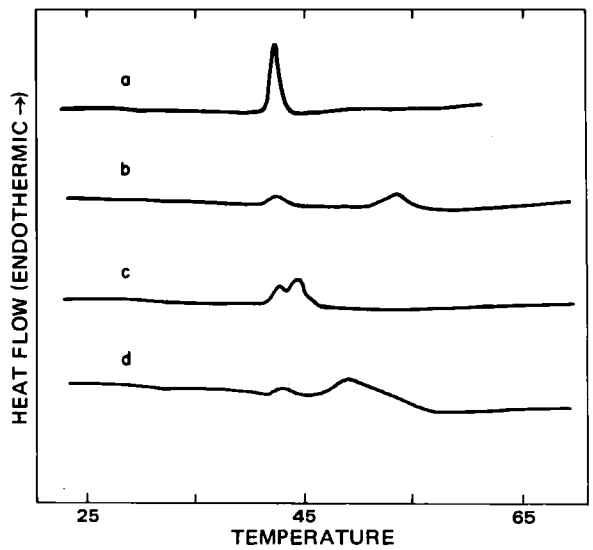

Figure 3—*Thermograms of mixed I–III liposomes (3:2 molar ratio). Key: (a) without additions; (b) incubated with 5 mM $CaCl_2$ at 42°; (c) incubated with 1 mM neomycin at 42°; (d) incubated with 5 mM $CaCl_2$ followed by 1 mM neomycin at 42°.*

the bilayers, indicating displacement of Ca^{2+} by neomycin.

Mixed liposomes containing I–III, 60:40 mole %, show a clear transition peak with a T_c value of 41.5° (Fig. 3a). This value is in agreement with that of Findlay and Barton (18), who pointed out that the almost identical T_c values for pure I, pure III, and I–III mixtures indicate complete miscibility of the components in the bilayer. In this mixed-lipid system, Ca^{2+} caused phase separation (Fig. 3b) with a small, but clearly defined peak at 41° and a major peak at 53°. Since the Ca^{2+}–III ratio is high and since there is free lateral movement of the lipid within the bilayer, the 41° peak should represent a population very rich in I and the 53° peak either a Ca^{2+}–III or a Ca^{2+}–I–III complex. The addition of neomycin to liposomes composed of I–III (Fig. 3c) resulted in a split peak centering at ~42° and 44°, which is shifted upwards ~2° from the split peak observed on incubation of liposomes composed of pure III with neomycin. This is possibly due to the incorporation of I into the neomycin–III complex.

Addition of neomycin to mixed I–III liposomes, preincubated with Ca^{2+} (Fig. 3d), produced a small transition peak at ~42.5° and a larger one at ~49°. Whereas neomycin clearly displaced Ca^{2+} from liposomes containing pure III (Fig. 2e), it appears that the presence of a neutral phospholipid in the bilayer reduced this capability. The appearance of a new peak at 49° may indicate that steric interactions in the Ca^{2+}–I–III complex interfere with neomycin binding.

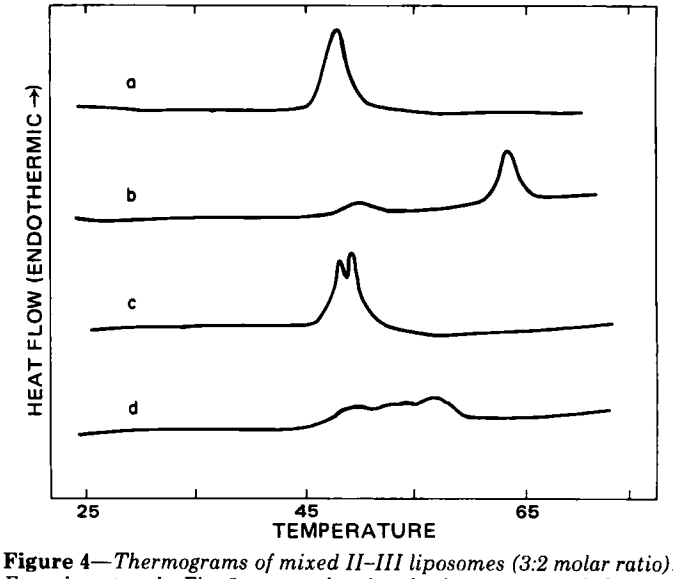

Figure 4—*Thermograms of mixed II–III liposomes (3:2 molar ratio). Experiment as in Fig. 3 except that incubations were carried out at 58°.*

The thermogram for liposomes containing II–III (60:40 mole %) shows a transition peak with a T_c value of 48° (Fig. 4a). This value is intermediate to the T_c values of pure II (57°) and pure III (41.5°), indicating good bilayer mixing. The thermograms after incubation with either Ca^{2+} or neomycin, or both (Fig. 4b, c, and d), are similar to those of liposomes composed of I–III, suggesting that the chain length of the neutral lipid does not drastically influence the overall nature of these interactions.

The displacement of calcium, which has been described for the interaction of the drug with bacteria (19), the neuromuscular junction (20), and inner ear tissues (21), may interfere with normal calcium-dependent physiological functions. The results of this study indicate that these effects may be due, in part, to resultant changes in the thermotropic properties, *i.e.*, degree of fluidity, of the lipid bilayer induced by neomycin.

REFERENCES

(1) M. Teuber and J. R. Miller, *Biochim. Biophys. Acta*, **467**, 280 (1977).

(2) H. D. Humes, N. D. Weiner, and J. Schacht, *INSERM* (Paris), **102**, 333 (1982).

(3) N. D. Weiner and J. Schacht, in "Aminoglycoside Ototoxicity," S. A. Lerner, G. J. Matz, and J. E. Hawkins, Jr., Eds., Little, Brown, Boston, Mass., 1981, pp 113–121.

(4) J. P. Morin, G. Viotte, A. Vanderwalle, F. Van Hoof, P. Tulkens, and J. P. Fillastre, *Kidney Int.*, **18**, 383 (1980).

(5) S. Feldman, C. Josepovitz, M. Scott, E. Pastoriza, and G. J. Kaloyanides, *Fed. Proc. Fed. Am. Soc. Exp. Biol.*, **40**, 647 (1981).

(6) S. Lodhi, N. D. Weiner, and J. Schacht, *Biochim. Biophys. Acta*, **557**, 1 (1979).

(7) M. G. Ganesan, B. Wang, J. Schacht, and N. D. Weiner, *Academy of Pharmaceutical Sciences Abstracts*, **11**, 69 (1981).

(8) D. Papahadjopoulos, W. J. Vail, C. Newton, S. Nir, K. Jacobson, G. Poste, and R. Lazo, *Biochim. Biophys. Acta*, **465**, 579 (1977).

(9) D. Papahadjopoulos, K. Jacobson, G. Poste, and G. Shepherd, *Biochim. Biophys. Acta*, **394**, 504 (1975).

(10) D. Papahadjopoulos, *J. Colloid Interface Sci.*, **58**, 459 (1977).

(11) A. Portis, C. Newton, W. Pangborn, and D. Papahadjopoulos, *Biochemistry*, **18**, 780 (1979).

(12) C. H. Fiske and Y. Subba Row, *J. Biol. Chem.*, **66**, 375 (1925).

(13) D. Papahadjopoulos, *J. Colloid Interface Sci.*, **58**, 459 (1977).

(14) R. F. Barber, B. D. McKersie, R. G. H. Downer, and J. E. Thompson, *Biochim. Biophys. Acta*, **643**, 593 (1981).

(15) R. W. Colman, J. Kuchibhotla, M. K. Jain, and R. K. Murray, Jr., *Biochim. Biophys. Acta*, **467**, 273 (1977).

(16) P. W. M. van Dijck, P. H. J. Th. Ververgaert, A. J. Verkleij, L. L. M. van Deenen, and J. De Gier, *Biochim. Biophys. Acta*, **406**, 465 (1975).

(17) M. C. Blok, L. L. M. van Deenen, and J. De Gier, *Biochim. Biophys. Acta*, **433**, 1 (1976).

(18) E. J. Findlay and P. G. Barton, *Biochemistry*, **17**, 2400 (1978).

(19) C. H. Ramierz-Ronda, R. K. Holmes, and J. P. Sanford, *Antimicrob. Agents Chemother.*, **7**, 239 (1975).

(20) A. P. Corrado, W. A. Prado, and I. Pimenta de Morais, in "Concepts of Membranes in Regulation and Excitation," M. Rocha e Silva, and G. Suarez-Kurtz, Eds., Raven, New York, N.Y., 1975, pp 201–251.

(21) A. Orsulakova, E. Stockhorst, and J. Schacht, *J. Neurochem.*, **26**, 285 (1976).

ACKNOWLEDGMENTS

This work was supported by Research Grant NS-13792 and Program Project Grant NS-05785 from the National Institutes of Health.

Quantitation of Ketoconazole in Biological Fluids Using High-Performance Liquid Chromatography

V. L. PASCUCCI * ˣ, J. BENNETT ‡, P. K. NARANG *, and D. C. CHATTERJI * ¶

Received May 5, 1982, from the **Clinical Pharmacokinetics Research Laboratory, Department of Pharmacy, The Clinical Center, National Institutes of Health, Bethesda, MD 20205* and the ‡*Laboratory of Clinical Investigation, National Institute of Allergy and Infectious Diseases, National Institutes of Health, Bethesda, MD 20205.* Accepted for publication November 2, 1982. ¶Present address: Lyphomed Inc., Melrose Park, IL 60160.

Abstract □ A rapid, specific procedure is described for the quantitation of ketoconazole in biological fluids using high-performance liquid chromatography (HPLC). The procedure involves sample preparation using a reverse-phase C-18 cartridge prior to chromatography and quantitation using peak height ratios (UV absorbance detection, 231 nm) of ketoconazole to the internal standard, phenothiazine. A sensitivity of 0.2 μg/ml was achieved using a 0.5-ml sample. The mean recovery was 86.2%, and overall coefficient of variation of the procedure was 7.1%. This procedure has been used to determine ketoconazole levels in human serum, plasma, CSF, and synovial fluid. A comparison with a microbiological assay is presented, and adaptability of this procedure to quantitation by fluorescence to increase the sensitivity fivefold is discussed.

Keyphrases □ Ketoconazole—quantitation in biological fluids, high-performance liquid chromatography, humans □ High-performance liquid chromatography—quantitation of ketoconazole in biological fluids, humans

Ketoconazole, *cis*-1-acetyl-4-[4[[2-(2,4-dichlorophenyl)-2- (1*H*-imidazol-1-ylmethyl) -1,3-dioxolan-4 - yl] methoxy]phenyl]piperazine, an antifungal agent used to treat a wide variety of superficial and systemic mycoses (1–3), has the advantage over other imidazole derivatives of producing adequate, sustained blood levels following oral administration. Several microbiological assays (4–6) and three high-performance liquid chromatographic (HPLC) methods (7–9) have been described for quantitation of ketoconazole in biological fluids. HPLC techniques have the advantage of direct concentration measurement since the microbiological assays quantitate ketoconazole concentration indirectly as antifungal activity against a test organism. Microbiological procedures lack specificity for ketoconazole; thus, falsely elevated levels may be produced by active metabolites or other concurrently administered antifungal agents.

A rapid and reproducible HPLC method is described which is suitable for quantitation of ketoconazole in biological fluids both for routine monitoring (sensitivity to 0.2 μg/ml using UV detection) or for pharmacokinetic studies

0022-3549/83/1200-1467$01.00/0

The thermogram for liposomes containing II–III (60:40 mole %) shows a transition peak with a T_c value of 48° (Fig. 4a). This value is intermediate to the T_c values of pure II (57°) and pure III (41.5°), indicating good bilayer mixing. The thermograms after incubation with either Ca^{2+} or neomycin, or both (Fig. 4b, c, and d), are similar to those of liposomes composed of I–III, suggesting that the chain length of the neutral lipid does not drastically influence the overall nature of these interactions.

The displacement of calcium, which has been described for the interaction of the drug with bacteria (19), the neuromuscular junction (20), and inner ear tissues (21), may interfere with normal calcium-dependent physiological functions. The results of this study indicate that these effects may be due, in part, to resultant changes in the thermotropic properties, *i.e.*, degree of fluidity, of the lipid bilayer induced by neomycin.

REFERENCES

(1) M. Teuber and J. R. Miller, *Biochim. Biophys. Acta*, **467**, 280 (1977).

(2) H. D. Humes, N. D. Weiner, and J. Schacht, *INSERM* (Paris), **102**, 333 (1982).

(3) N. D. Weiner and J. Schacht, in "Aminoglycoside Ototoxicity," S. A. Lerner, G. J. Matz, and J. E. Hawkins, Jr., Eds., Little, Brown, Boston, Mass., 1981, pp 113–121.

(4) J. P. Morin, G. Viotte, A. Vanderwalle, F. Van Hoof, P. Tulkens, and J. P. Fillastre, *Kidney Int.*, **18**, 383 (1980).

(5) S. Feldman, C. Josepovitz, M. Scott, E. Pastoriza, and G. J. Kaloyanides, *Fed. Proc. Fed. Am. Soc. Exp. Biol.*, **40**, 647 (1981).

(6) S. Lodhi, N. D. Weiner, and J. Schacht, *Biochim. Biophys. Acta*, **557**, 1 (1979).

(7) M. G. Ganesan, B. Wang, J. Schacht, and N. D. Weiner, *Academy of Pharmaceutical Sciences Abstracts*, **11**, 69 (1981).

(8) D. Papahadjopoulos, W. J. Vail, C. Newton, S. Nir, K. Jacobson, G. Poste, and R. Lazo, *Biochim. Biophys. Acta*, **465**, 579 (1977).

(9) D. Papahadjopoulos, K. Jacobson, G. Poste, and G. Shepherd, *Biochim. Biophys. Acta*, **394**, 504 (1975).

(10) D. Papahadjopoulos, *J. Colloid Interface Sci.*, **58**, 459 (1977).

(11) A. Portis, C. Newton, W. Pangborn, and D. Papahadjopoulos, *Biochemistry*, **18**, 780 (1979).

(12) C. H. Fiske and Y. Subba Row, *J. Biol. Chem.*, **66**, 375 (1925).

(13) D. Papahadjopoulos, *J. Colloid Interface Sci.*, **58**, 459 (1977).

(14) R. F. Barber, B. D. McKersie, R. G. H. Downer, and J. E. Thompson, *Biochim. Biophys. Acta*, **643**, 593 (1981).

(15) R. W. Colman, J. Kuchibhotla, M. K. Jain, and R. K. Murray, Jr., *Biochim. Biophys. Acta*, **467**, 273 (1977).

(16) P. W. M. van Dijck, P. H. J. Th. Ververgaert, A. J. Verkleij, L. L. M. van Deenen, and J. De Gier, *Biochim. Biophys. Acta*, **406**, 465 (1975).

(17) M. C. Blok, L. L. M. van Deenen, and J. De Gier, *Biochim. Biophys. Acta*, **433**, 1 (1976).

(18) E. J. Findlay and P. G. Barton, *Biochemistry*, **17**, 2400 (1978).

(19) C. H. Ramierz-Ronda, R. K. Holmes, and J. P. Sanford, *Antimicrob. Agents Chemother.*, **7**, 239 (1975).

(20) A. P. Corrado, W. A. Prado, and I. Pimenta de Morais, in "Concepts of Membranes in Regulation and Excitation," M. Rocha e Silva, and G. Suarez-Kurtz, Eds., Raven, New York, N.Y., 1975, pp 201–251.

(21) A. Orsulakova, E. Stockhorst, and J. Schacht, *J. Neurochem.*, **26**, 285 (1976).

ACKNOWLEDGMENTS

This work was supported by Research Grant NS-13792 and Program Project Grant NS-05785 from the National Institutes of Health.

Quantitation of Ketoconazole in Biological Fluids Using High-Performance Liquid Chromatography

V. L. PASCUCCI * ˣ, J. BENNETT ‡, P. K. NARANG *, and D. C. CHATTERJI * ¶

Received May 5, 1982, from the **Clinical Pharmacokinetics Research Laboratory, Department of Pharmacy, The Clinical Center, National Institutes of Health, Bethesda, MD 20205* and the ‡*Laboratory of Clinical Investigation, National Institute of Allergy and Infectious Diseases, National Institutes of Health, Bethesda, MD 20205.* Accepted for publication November 2, 1982. ¶Present address: Lyphomed Inc., Melrose Park, IL 60160.

Abstract □ A rapid, specific procedure is described for the quantitation of ketoconazole in biological fluids using high-performance liquid chromatography (HPLC). The procedure involves sample preparation using a reverse-phase C-18 cartridge prior to chromatography and quantitation using peak height ratios (UV absorbance detection, 231 nm) of ketoconazole to the internal standard, phenothiazine. A sensitivity of 0.2 μg/ml was achieved using a 0.5-ml sample. The mean recovery was 86.2%, and overall coefficient of variation of the procedure was 7.1%. This procedure has been used to determine ketoconazole levels in human serum, plasma, CSF, and synovial fluid. A comparison with a microbiological assay is presented, and adaptability of this procedure to quantitation by fluorescence to increase the sensitivity fivefold is discussed.

Keyphrases □ Ketoconazole—quantitation in biological fluids, high-performance liquid chromatography, humans □ High-performance liquid chromatography—quantitation of ketoconazole in biological fluids, humans

Ketoconazole, *cis*-1-acetyl-4-[4[[2-(2,4-dichlorophenyl)-2- (1*H*-imidazol-1-ylmethyl) -1,3-dioxolan-4 - yl] methoxy]phenyl]piperazine, an antifungal agent used to treat a wide variety of superficial and systemic mycoses (1–3), has the advantage over other imidazole derivatives of producing adequate, sustained blood levels following oral administration. Several microbiological assays (4–6) and three high-performance liquid chromatographic (HPLC) methods (7–9) have been described for quantitation of ketoconazole in biological fluids. HPLC techniques have the advantage of direct concentration measurement since the microbiological assays quantitate ketoconazole concentration indirectly as antifungal activity against a test organism. Microbiological procedures lack specificity for ketoconazole; thus, falsely elevated levels may be produced by active metabolites or other concurrently administered antifungal agents.

A rapid and reproducible HPLC method is described which is suitable for quantitation of ketoconazole in biological fluids both for routine monitoring (sensitivity to 0.2 μg/ml using UV detection) or for pharmacokinetic studies

0022-3549/83/1200-1467$01.00/0

(sensitivity to 40 ng/ml using fluorescence detection). Comparison of the results obtained using the described method with the values obtained using a microbiological assay (6) is also presented.

EXPERIMENTAL

Materials and Reagents—Ketoconazole[1], (R 41,400), was used in the preparation of spiked serum standards. Phenothiazine[2] was used as the internal standard. Methanol[3] was glass distilled and certified HPLC grade. Water was double-distilled in glass. All HPLC solvents were filtered[4] and then deaerated under reduced pressure prior to use. Reverse-phase C-18 sample cartridges[5] were used in sample preparation.

Chromatographic System and Conditions—The liquid chromatograph was equipped with a UV absorbance detector[6] operated at 231 nm and a solvent delivery system[7]. Alternatively, a spectrofluorometric detector[8] was operated with an excitation wavelength of 206 nm and a 370-nm emission filter. The analytical column[9] (4.6 mm i.d. × 25 cm, 5-μm particle size) was preceded by a 7-cm guard column[10]. The mobile phase consisted of of 75% (v/v) methanol and 25% (v/v) 0.02 *M* monobasic sodium phosphate. The pH of the mobile phase was adjusted to 6.8 with sodium hydroxide. The flow rate was maintained at 1.0 ml/min.

Procedures—Deproteinization and elimination of polar serum constituents were accomplished using C-18 reverse-phase sample preparation cartridges. The cartridges were conditioned by washing with 2.0 ml of methanol followed by 5.0 ml of water. A 0.5-ml aliquot of serum sample or serum standard was placed in a 1.5-ml capped plastic tube[11]. Phenothiazine, 20 μl of a 25-μg/ml solution (for UV detection) or 30 μl of a 100-μg/ml solution (for fluorescence detection), was added to each sample to serve as an internal standard. An alkaline pH was achieved with the addition of 0.125 ml of 0.1 *N* NaOH to each sample. The samples were mixed by inversion, and each was added to a reverse-phase cartridge. Each cartridge was then washed with 6.0 ml of water followed by 2.0 ml of methanol. The eluant from the final 1.5 ml of methanol was collected in a disposable 12- × 75-mm borosilicate culture tube[12] and evaporated to dryness using a gentle air stream at 40°. The residue was reconstituted with 250 μl of methanol–water (1:1) and mixed by vortexing. A 50-μl aliquot was injected onto the HPLC.

Ketoconazole serum standards were prepared by spiking human serum with ketoconazole stock solution (100 μg/ml in methanol) to give final concentrations ranging from 0.5 to 15.0 μg/ml. Ketoconazole was quantitated by comparison of the peak height ratio of the drug to the internal standard using a calibration curve. The peak height ratios were plotted against concentrations of ketoconazole and analyzed by linear regression to generate daily calibration curves. The lower sensitivity limit of the procedure was determined by assaying spiked serum samples at concentrations ranging from 20 ng/ml to 1.0 μg/ml. The sensitivity limit was then defined as the concentration at which the signal-to-noise ratio was 3.

Interday variability was determined by the reproducibility of the daily standard curves ($n \geq 6$) with respect to both their slopes and the calculated values for ketoconazole at various concentrations (0.5, 1.0, 2.0, 5.0, 10.0, and 15.0 μg/ml). The intraday variability was assessed by performing replicate analyses ($N = 6$) using spiked serum samples containing 0.8 and 14.0 μg/ml of ketoconazole. These concentrations were chosen as a representation of the lower (0.8 μg/ml) and higher (14.0 μg/ml) serum concentrations observed in patients receiving ketoconazole for whom routine therapeutic drug monitoring was performed. Aqueous solutions containing known amounts of ketoconazole were compared with spiked serum standards undergoing analysis to calculate the percent recovery at various concentrations. Statistical analyses to determine means, standard deviations, correlation coefficients, coefficients of variation, and linear regressions were performed using a computer[13].

The microbiological assay procedure was performed as described by Drouhet and Dupont (6). The test organism was *Kluyvermyces fragilis* strain 55-1[14].

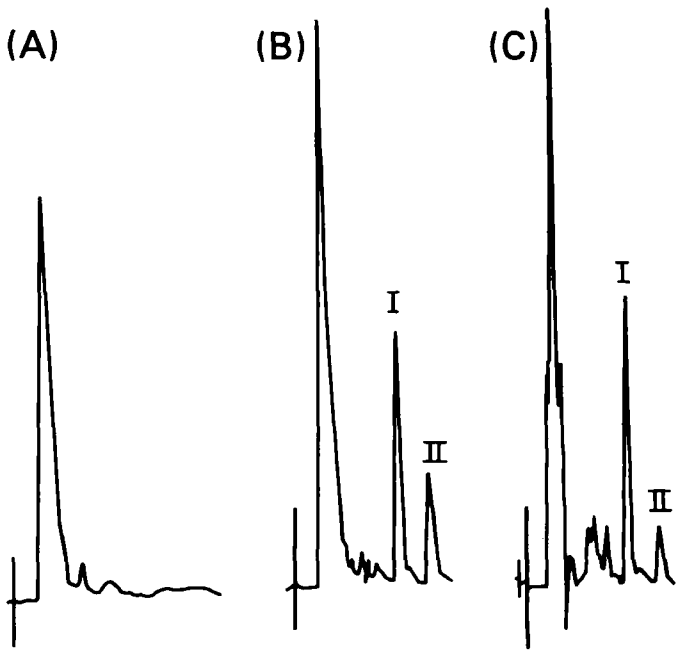

Figure 1—*Representative chromatograms of (A) blank human serum, (B) serum obtained from a patient receiving ketoconazole and spiked with phenothiazine at 0.04 AUFS (observed ketoconazole concentration = 1.13 μg/ml), and (C) human serum spiked with 0.50 μg/ml of ketoconazole (retention time 9.6 min) and phenothiazine (retention time 7.4 min) at 0.04 AUFS. Sample preparation was as described in the text. Key: (I) phenothiazine (internal standard); (II) ketoconazole.*

RESULTS AND DISCUSSION

HPLC Using UV Detection—Representative chromatograms from assayed samples of control human serum, human serum spiked with phenothiazine and ketoconazole, and a serum sample obtained from a patient receiving ketoconazole are shown in Fig. 1. Retention times for phenothiazine and ketoconazole are 7.4 and 9.6 min, respectively. No interfering peaks were observed in the blank serum sample. Miconazole, another imidazole antifungal agent, as well as trifluoperazine, chlorpromazine, diazepam, chlordiazepoxide, doxepin, thiothixene, imipramine, and amitriptyline did not interfere with either the ketoconazole or internal standard peaks. The reverse-phase cartridge separation procedure described helped eliminate several additional peaks which were observed when the serum samples were extracted using various organic solvents.

The standard calibration curves constructed from daily runs of spiked serum standards were linear and highly reproducible. Serum standards containing up to 25 μg/ml have been assayed periodically, and the assay results indicate that the linearity of the curves extends at least to this level. The mean slope of six calibration curves run over a 3-month period was 0.456, with a standard deviation of 0.032; the overall coefficient of variation of the procedure was 7.1%. The correlation coefficient of the six curves was 0.998. Table I lists the results of the interday variability (mean, *SD*, *CV*) from the six runs at each concentration measured. These data indicate the assay procedure is highly reliable and reproducible.

Intraday variability of the method determined from serum standards containing 0.8 and 14.0 μg/ml of ketoconazole was 6.4 and 4.4%, respectively. The average recovery of ketoconazole obtained from the sample preparations over the range of concentrations used in the standard curve was 86.2% (*SD* 4.6%). The recovery of phenothiazine was 91.0% (*SD* 6.4%). Using the described procedure, 0.2-μg/ml concentrations of ketoconazole can be detected while maintaining a signal-to-noise ratio of 3.

[1] Ketoconazole was a gift of Janssen Pharmaceutica, New Brunswick, N.J.
[2] Aldrich Chemical Co., Milwaukee, Wis.
[3] Burdick and Jackson Laboratories, Muskegon, Mich.
[4] 0.45-μm Millipore filter; Millipore Corp., Bedford, Mass.
[5] Waters Associates, Inc., Milford, Mass.
[6] Schoeffel model GM770; Schoeffel Instrument Corp., Westwood, N.J.
[7] Spectra-Physics model 3500B; Spectra-Physics, Santa Clara, Calif.
[8] Schoeffel model FS970; Schoeffel Instrument Corp., Westwood, N.J.
[9] Altex Ultrasphere Octadecylsilane; Beckman Instruments, Inc., Berkeley, Calif.
[10] Guard column packed with C-18 (30–38 μm) particles; Whatman, Inc., Clifton, N.J.
[11] Sarstedt, Princeton, N.J.
[12] Fisher Scientific, Silver Spring, Md.
[13] Hewlett-Packard Model 85; Hewlett-Packard, Corvallis, Or.
[14] Test organism provided by Dr. David A. Stevens, Stanford University.

Table 1—Reproducibility Results from Six Replicate Serum Standard Curves Obtained over a 3-Month Period

Spiked Ketoconazole Concentration, μg/ml	Observed Concentration		
	Mean, μg/ml	*SD*	*CV*, %
0.5	0.56	0.09	16.1
1.0	0.98	0.075	7.7
2.0	2.01	0.14	6.9
5.0	4.98	0.18	3.6
10.0	10.04	0.12	1.2
15.0	15.04	0.08	0.53
Overall Mean			7.1

The procedure presented here has significant advantages over two previously published HPLC procedures (7, 8). The major advantage of our method is the use of an internal standard, which facilitates accurate and precise ketoconazole quantitation. Neither of the previous HPLC methods used internal standardization, although they involved either extraction and concentration procedures (7) or a reverse-phase cartridge filtration procedure (8). In addition, the sample preparation of one of the published methods (7) involves multiple time-consuming extraction steps, whereas the other published procedure (8) does not include the statistical analyses necessary for detailed evaluation. Finally, the sensitivity, efficiency, and overall variability of the procedure presented here compare favorably with the previously published HPLC procedures.

This procedure has been used to successfully analyze various biological fluids from patients receiving ketoconazole, including serum, plasma, CSF, and synovial fluid. Serum samples from several patients receiving 200-, 400-, or 800-mg/day doses of ketoconazole were collected at 2 and 6 hr postdose and analyzed using this procedure. It is apparent that the procedure sensitivity is adequate for such routine therapeutic monitoring. When a single 200-mg dose of ketoconazole is administered to adults, peak levels of 3–4.5 μg/ml are observed, and concentrations at 8 hr postdose are at least 0.2 μg/ml (10). On chronic administration, even higher levels are observed. Our own experience indicates that levels in the patients studied at the stated doses range between 1 and 15 μg/ml. For routine serum level monitoring of ketoconazole at therapeutic doses, the present HPLC method using UV detection has been found to be rapid, reliable, and sensitive.

Comparison with a Microbiological Assay—Serum samples from 32 patients were divided and assayed for ketoconazole by both the HPLC method and a microbiological procedure (6). A comparison of the two procedures is shown graphically in Fig. 1, a plot of the results of the microbiological *versus* the HPLC analyses of the patient samples. Linear regression analysis of the comparative data yields a correlation coefficient of 0.92. However, when a line with a slope of unity that passes through the origin is superimposed on the plot (as in Fig. 2), it can be seen that there is a large amount of scatter as well as a negative deviation of the microbiological assay results from the HPLC results at concentrations >10 μg/ml. The scatter can largely be attributed to the imprecision inherent in the bioassay. (This microbiological procedure had a coefficient of variation of 28% for 18 patients' serum samples run 2–5 times for a total of 56 assays.) However, the general agreement of the results of the two assays suggests that the ketoconazole quantitated in patient samples represents a microbiologically active agent.

HPLC Using Fluorometric Detection—Ketoconazole concentrations may be quantitated using the sample preparation and assay conditions described here with a spectrofluorometric detector as well as a UV absorbance detector. There are two advantages of using fluorescence measurement. First, the reverse-phase cartridge separation procedure is not required for routine monitoring of biological fluids. Using a fluorometric detector, a simple acetonitrile protein precipitation followed by centrifugation and direct injection of the supernatant is an adequate sample preparation to achieve sensitivity equivalent to that seen with cartridge filtration and UV absorbance detection. However, by using the reverse-phase cartridge preparation described, the sensitivity of the HPLC procedure can be increased fivefold, detecting <40 ng/ml of ketoconazole using the spectrofluorometric detector. This enhanced sensitivity is an additional advantage over other HPLC methods, including one procedure which also uses fluorometric detection (9). The increase in sensitivity is a distinct advantage for detailed pharmacokinetic studies of ketoconazole disposition where it is likely that the sensitivity requirements will exceed those of all previously published methods. Data obtained using an unpublished GC procedure for ketoconazole indicate that following a dose of ketoconazole, there is an initial rapid decline in serum levels followed by a much slower elimination phase (10). To fully characterize its biphasic elimination, detection of <100 ng/ml of ketoconazole is required.

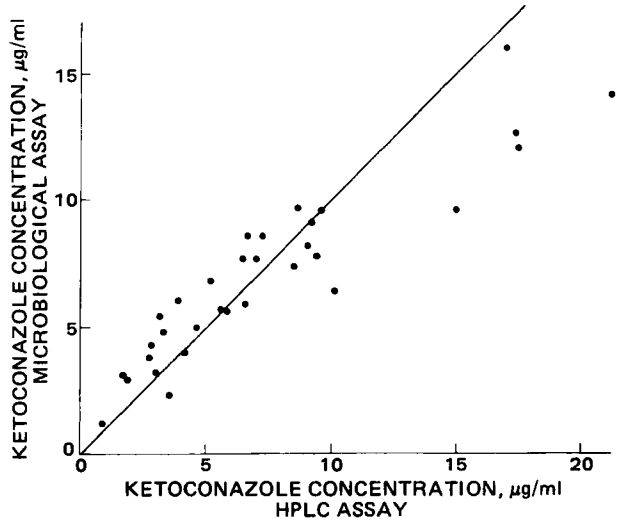

Figure 2—*Comparison of the results of ketoconazole quantitation by microbiological* versus *HPLC analyses. Each point represents parallel determinations of a single patient sample by both methods. The line superimposed on the plot has a slope of unity and passes through the origin.*

In summary, the sensitive, rapid, and reproducible procedure described offers advantages over both microbiological and other HPLC methods. It can be adapted to either UV or fluorometric detectors for routine monitoring of ketoconazole in various biological fluids. Fluorometric detection offers the additional advantage of the increased sensitivity required for application of the procedure to detailed pharmacokinetic studies of ketoconazole disposition.

REFERENCES

(1) F. C. Odds, L. J. R. Milne, J. C. Gentles, and E. H. Ball, *J. Antimicrob. Chemother.*, **6**, 97 (1980).

(2) D. Borelli, J. L. Bran, J. Fuentes, R. Legendre, E. Leiderman, H. B. Levine, A. Restrepo-M., and D. A. Stevens, *Postgrad. Med. J.*, **55**, 657 (1979).

(3) E. W. Gascoigue, G. J. Barton, M. Michaels, W. Mendlermans, and J. Heykants, *Clin. Res. Rev.*, **1**(3), 177 (1981).

(4) Y. M. Clayton and H. J. Wingfield, *Clin. Res. Rev.*, **1**(3), 189 (1981).

(5) R. P. Harvey, R. A. Isenberg, and D. A. Stevens, *Rev. Infect. Dis.*, **2**, 559 (1980).

(6) E. Drouhet and B. Dupont, *Rev. Infect. Dis.*, **2**, 606 (1980).

(7) K. B. Alton, *J. Chromatogr.*, **221**, 337 (1980).

(8) F. A. Andrews, L. R. Peterson, W. H. Beggs, D. Crankshaw, and G. A. Sarosi, *Antimicrob. Agents Chemother.*, **19**, 110 (1981).

(9) S. E. Swezey, K. M. Giacomini, A. Abang, C. Brass, D. A. Stevens, and T. F. Blaschke, *J. Chromatogr.*, **227**, 510 (1982).

(10) H. B. Levine, Ed., "Ketoconazole in the Management of Fungal Disease," ADIS Press, New York, N.Y., 1982, pp. 67, 73.

Quantitation of Amikacin, Kanamycin, Neomycin, and Tobramycin in Pharmaceutical Dosage Forms Using the Hantzsch Reaction

V. DAS GUPTA *×, KENNETH R. STEWART ‡, and JAMES M. GUNTER ‡

Received July 6, 1982, from the *Department of Pharmaceutics, University of Houston, Houston, TX 77030 and the ‡Ben Taub General Hospital Pharmacy, Texas Medical Center Houston, TX 77030. Accepted for publication September 10, 1982.

Abstract □ A spectrophotometric assay method for the quantitative determination of amikacin, kanamycin, neomycin, and tobramycin in pharmaceutical dosage forms has been developed. The method is based on the Hantzsch reaction, forming dihydrolutidine derivatives which can be measured spectrophotometrically. The excipients EDTA, phenol, sodium bisulfite, and sodium citrate do not interfere, while salts of ammonia do interfere. The relative standard deviations based on seven readings were 1.64, 1.88, 2.10, and 1.93% for amikacin, kanamycin, neomycin, and tobramycin, respectively. Assay results have been compared with microbiological assay results provided by the manufacturers. The assay method appears to be stability indicating.

Keyphrases □ Amikacin—quantitation in pharmaceutical dosage forms using the Hantzsch reaction, kanamycin, neomycin, tobramycin □ Kanamycin—quantitation in pharmaceutical dosage forms using the Hantzsch reaction, amikacin, neomycin, tobramycin □ Neomycin—quantitation in pharmaceutical dosage forms using the Hantzsch reaction, amikacin, kanamycin, tobramycin □ Tobramycin—quantitation in pharmaceutical dosage forms using the Hantzsch reaction, amikacin, kanamycin, neomycin

The aminoglycoside antibiotics, amikacin sulfate (I), kanamycin sulfate (II), neomycin sulfate (III), and tobramycin sulfate (IV) are usually quantified by the microbiological procedures established by the Food and Drug Administration (1). The high experimental errors inherent in microbiological assays have been reported previously (2). A spectrophotometric assay technique for I using purified kanamycin acetyltransferase has been reported (3). In addition, a radioimmunoassay procedure for I has been developed (4) and compared with the microbiological assay (5). A previously described spectrofluorometric method (6) involves the purification of I–IV in urine using ion-exchange chromatography followed by formation of the dehydrolutidine derivative. Recently, this methodology, involving the formation of the dehydrolutidine derivative has been extended to provide a colorimetric assay for neomycin sulfate in urine (7). This study reports a spectrophotometric assay technique for the quantitative of amikacin, kanamycin, neomycin, and tobramycin in pharmaceutical dosage forms, based on the formation of the dehydrolutidine derivative (Hantzsch reaction) (7).

EXPERIMENTAL

Chemicals and Reagents—All chemicals and reagents were USP, NF, or ACS quality and were used without further purification. Amikacin sulfate[1], kanamycin sulfate[1], neomycin sulfate[2], and tobramycin sulfate[3] powders were used as received.

Preparation of Stock and Standard Solutions—Stock solutions of I–IV containing 50.0, 40.0, 60.0, 40.0 mg/100 ml (as the free base) in water, respectively, were prepared daily. These stock solutions were diluted further with water to obtain standard solutions as needed. The usual concentrations of I–IV standard solutions were 50.0, 40.0, 60.0, 40.0 μg/ml, respectively.

Preparation of Assay Solutions—All commercial injectable formulations were diluted stepwise with water to obtain antibiotic concentrations similar to the standard solutions. Ten tablets/capsules were weighed, and the tablets or capsule contents were ground to a fine powder. An appropriate quantity of the powder (containing 40–60 mg of the antibiotic) was weighed, mixed with 40 ml of water, brought to volume (100 ml) with water, and mixed thoroughly. The mixture was filtered, rejecting the first 20 ml of the filtrate, and a portion of clear filtrate was diluted further to an appropriate concentration (similar to standard solutions).

Preparation of a Solution of Acetylacetone and Formaldehyde—A buffer solution containing 0.2*M* each of acetic acid, boric acid, and phosphoric acid in water was prepared. The pH of this solution was adjusted to 2.5 (±0.05) with ~1 *N* NaOH, measured by a pH-meter[4]. To a 10-ml portion of the buffer, 0.8 ml of acetylacetone and 1.5 ml of formaldehyde solution (40% in water) were added; the mixture was brought to 30 ml with water and thoroughly mixed. The buffer solution was stable for at least 30 days at room temperature. The reagent was prepared daily.

Assay Procedure—A 2-ml quantity of standard/assay solution was mixed with a 2-ml portion of the acetylacetone–formaldehyde solution in a glass tube. The tube was sealed, placed in a boiling water bath for 20 min, cooled to room temperature, and the contents mixed with 5 ml of water. The absorbance of the solution was measured at 356 nm using a spectrophotometer[5]. A reagent blank was prepared by substituting water for the antibiotic solution.

Calculations—Concentrations were calculated by comparing the absorbance value of the assay solution with that of a standard solution of identical concentration. Since Beer's law (7) was followed:

$$\frac{(A_a)}{(A_s)} \times \text{Actual concentration of the standard solution} = \text{concentration of assay solution found}$$

where (A_a) is the absorbance of the assay solution and (A_s) the absorbance of the standard solution.

Determination of Excipient Interference—To determine the possibility of interference from inactive ingredients, the above assay procedure was followed substituting the inactive ingredient(s) for the antibiotic.

Selectivity of the Method—To determine if the method was stability indicating, solutions of amikacin (50 μg/ml) and tobramycin (40 μg/ml) were mixed with a 250-μg/ml concentration of carbenicillin disodium. Aminoglycoside antibiotics are known to be unstable in the presence of carbenicillin and other penicillins (8). The mixtures of aminoglycoside antibiotics with carbenicillin were stored at 50° and reassayed after 48 hr. Solutions of amikacin, tobramycin, and carbenicillin disodium alone were also stored at 50° for 48 hr and reassayed as controls. The results were calculated as described above, except that the absorbance values were corrected for a slight interference from carbenicillin disodium, measured using a carbenicillin blank.

[1] Supplied by Bristol-Myers Laboratories, Rochester, N.Y.
[2] The Upjohn Co., Kalamazoo, Mich.
[3] Supplied by Eli Lilly and Co., Indianapolis, Ind.
[4] Beckman Zeromatic, SS-3.
[5] Bausch and Lomb Spectronic 20.

0022-3549/83/1200-1470$01.00/0

Table I—Assay Results of Various Dosage Forms

Dosage Form	Label Claim, mg/ml	Antibiotic	Potency Found, % (Based on the Label Claim) Developed Method[a]	Microbiological Method[b]
Injectable				
Lot 1	250	Amikacin	103.7	101.2
Lot 2	250	Amikacin	108.1	104.8
Lot 3	250	Amikacin	104.1	103.6
Lot 4	250	Amikacin	100.6	104.0
Injectable	50	Amikacin	101.7	101.6
Injectable	333.3	Kanamycin	103.6	105.3
Injectable	37.5	Kanamycin	104.2	104.0
Capsule	500	Kanamycin	103.4	101.0
Tablet	350	Neomycin	99.6	100.9
Injectable				
Lot 1	40	Tobramycin	106.3	108.8
Lot 2	40	Tobramycin	104.2	107.5

[a] The relative standard deviations based on seven readings were 1.64, 1.88, 2.1, and 1.93% for I–IV, respectively. [b] As provided by the manufacturers.

RESULTS AND DISCUSSION

The results indicate (Table I) that the method can be used for the quantitation of amikacin, kanamycin, neomycin, and tobramycin in pharmaceutical dosage forms. The relative standard deviations based on seven readings were 1.64, 1.88, 2.10, and 1.93% for amikacin, kanamycin, neomycin, and tobramycin, respectively. It is well known that standard deviations are usually very high when microbiological assay techniques are used.

A 20-min reaction time was determined to be optimal for the completion of the reaction. The reaction usually starts 5–6 min, after the mixture reaches the water bath temperature. The results are highly reproducible and precise (see Table I for standard deviations) when the standard solution is assayed simultaneously with each sample determination. The excipients present in the injectable formulations [EDTA (ethylenediaminetetraacetic acid), phenol, sodium bisulfite, and sodium citrate] did not interfere with the assay procedure (Table II). Also, methylparaben and propylparaben, which are present in injectable formulations of some other aminoglycoside antibiotics, showed no interference (Table II), while salts of ammonia did interfere with the assay procedure (Table II).

Using the recommended wavelength of 356 nm (7) provided a low blank reading and high absorbance value for the dihydrolutidine derivatives. The mechanism of the reaction has been postulated (6). It has been determined that it is not necessary to add all the buffering agents (acetic acid, boric acid, and phosphoric acid) to the solution as recommended (7). Either boric acid or phosphoric acid (0.6 *M*) can be used at pH 2.5. The color that developed was stable for at least 20 min.

Aminoglycoside antibiotics contain amino groups, which react with acetylacetone to form dihydrolutidine derivatives. The method developed appears to be stability indicating (Table III) when applied to the interaction of aminoglycoside antibiotics with penicillins. Tobramycin assayed for only 47.2% of the original after 48 hr of storage at 50° in the presence of carbenicillin disodium, and amikacin assayed for 73.5% in a similar solution. These results are in agreement with an earlier report (8) in which tobramycin was reported to be less stable in the presence of carbenicillin disodium than other aminoglycoside antibiotics, *i.e.*, gentamicin and netilmicin. Tobramycin is also less stable than amikacin in the presence of carbenicillin.

Table II—Effect of Excipients on Absorbance

Inactive Ingredient	Concentration in Solution[a], μg/ml	Absorbance Value Against Blank
EDTA	2.5	0.00
Methyparaben	3.6	0.00
Propylparaben	0.4	0.00
Phenol	10	0.00
Sodium bisulfite	14	0.00
Sodium citrate	5	0.00
Ammonium chloride	14	0.14

[a] These are at least 2 times the concentrations expected in the assay solutions except ammonium chloride, which is not usually added to the dosage forms of these antibiotics.

Table III—Assay Results of Solutions Stored at 50°

Solution Composition	Assay Results (Percent of Label Claim) 0 hr	48 hr
Amikacin (50 μg/ml)	100.5	100.1
Tobramycin (40 μg/ml)	99.8	100.4
Carbenicillin disodium (250 μg/ml)	19.8[a]	14.3[a]
Amikacin (50 μg/ml) and carbenicillin disodium (250 μg/ml)	97.4[b]	73.5[b]
Tobramycin (50 μg/ml) and carbenicillin disodium (250 μg/ml)	97.1[b]	47.2[b]

[a] When assayed as tobramycin, *i.e.*, the assay absorbance value was compared with the absorbance value from a standard solution of tobramycin (40 μg/ml). [b] After correcting for interference from carbenicillin disodium.

REFERENCES

(1) "The United States Pharmacopeia XX"—"National Formulary XV," U.S. Pharmacopeial Convention, Inc., Rockville, Md. 1980, p. 28.

(2) M. Mundell, H. Fischback, and T. Eble, *J. Am. Pharm. Assoc., Sci. Ed.*, **35**, 373 (1946).

(3) E. Scarbrough, J. W. Williams, and D. B. Northrop, *Antimicrob. Agents Chemother.*, **16**, 221 (1979).

(4) J. E. Lewis, J. C. Nelson, and H. A. Elder, *Antimicrob. Agents Chemother.*, **7**, 42 (1975).

(5) P. L. Stevens, L. S. Young, and W. L. Hewitt, *J. Antibiot.*, **29**, 829 (1976).

(6) A. Csiba, *J. Pharm. Pharmacol.*, **31**, 115 (1979).

(7) A. Csiba, *Magy. Kem. Foly.*, **85**, 166 (1979); through *Chem. Abs.* **91**, 35139h (1979).

(8) J. L. Henderson, R. E. Polk, and B. J. Kline, *Am. J. Hosp. Pharm.*, **38**, 1167 (1981).

Minimizing the Aggregation of Neutral Insulin Solutions

R. QUINN and J. D. ANDRADE ˣ

Received November 16, 1981, from the *Department of Bioengineering, University of Utah, Salt Lake City, UT 84112.* Accepted for publication October 21, 1982.

Abstract □ Various solution additives affect the solubility and macroaggregation of insulin in buffered aqueous solutions at physiological pH. The solubility of insulin may be improved with the addition of small amounts of aspartic acid, glutamic acid, EDTA (ethylenediaminetetraacetic acid), lysine, Tris buffer, or bicarbonate buffer. In addition, the propensity of dissolved insulin to reaggregate and precipitate may be inhibited by such additives. Buffered physiological (pH 7.4) saline solutions containing 0.001–0.003 *M* lysine in the presence of 0.005 *M* EDTA or 0.01 *M* lysine in the absence of EDTA improve insulin solubility and are effective in minimizing aggregation. Solutions thus prepared may be suitable for application in intravenous insulin infusion devices and may be useful commercial insulin preparations.

Keyphrases □ Insulin—minimizing aggregation, neutral solutions, lysine, solubility □ Aggregation—minimization, solubility of neutral insulin solutions, lysine solubility □ Lysine—minimizing aggregation of neutral insulin solutions, solubility □ Solubility—minimizing aggregation of neutral insulin solutions, lysine

The tendency of insulin solutions to form macroaggregates is an obstacle in the development of long-term insulin delivery systems (1–5). The macroaggregation of the insulin molecule often limits prolonged infusion to a few days unless the device is regularly flushed during the test period. This problem, as well as a desire to characterize the adsorption of insulin, have led us to search for a physiological solvent or additive that will stabilize insulin solutions. Insulin solubility and prolonged prevention of macroaggregation has been achieved by addition of various agents to dilute insulin solutions (4–8).

EXPERIMENTAL

The Tris buffer contained 0.1 *M* NaCl, 0.005 *M* EDTA (ethylenediaminetetraacetic acid) (Tris-HCl 14.04 g/liter; Tris, 1.34 g/liter)[1]. The phosphate-buffered saline solution was prepared using 1.36 g of Na_2HPO_4, 0.22 g of KH_2PO_4, 0.005 *M* EDTA, and 8.5 g of NaCl/liter (0.01 *M* phosphate and 0.145 *M* NaCl). The pH of both solutions was adjusted to 7.2–7.4, as needed, by addition of 0.1 *M* HCl or 0.1 *M* NaOH. Bicarbonate buffer was prepared using 1.428 g of $NaHCO_3$ and 8.070 g of NaCl diluted to 1 liter. A mixture of 5% CO_2 and compressed air was bubbled through the solution to adjust the pH to 7.4. Amino acids and other additives were added to the buffered solutions in varying concentrations as desired.

Crystalline insulin[2] at a potency of 25.2 U/mg was used in an attempt to regulate solution additives. Many other studies have used commercially available insulin preparations which usually contain additives that influence solubility and aggregation.

Solutions of 1 ml were sealed with paraffin film in 16-ml glass tubes (16 mm × 100 mm) and continuously agitated in a shaking water bath at 100–200 cycles/min and 37°. Solution turbidity was evaluated twice daily. The degree of aggregation of the solution was assessed visually on a five-plus scale: (+) meant clear, no observable particles, and (+++++) meant large aggregates or cloudy. Initially instrumental turbidity measurements were used to assess the degree of aggregation, but because of the macroscopic nature of the aggregate, this method did not accurately reflect the amount of aggregation. "First day" results indicate apparent solubility of insulin after 2–4 hr. The "5–6 day" results indicate degree of aggregation present at that time.

RESULTS

Additives tested were aspartic acid, EDTA, glutamic acid, bicarbonate buffer, ethanol, glycerol, leucine, lysine, and Tris buffer. When increased solubility or prolonged prevention of aggregation was observed, an attempt was made to determine the minimum amount of the additive required to produce the observed result. This was done by serially diluting the additive in the buffered solution while other buffer conditions were held constant. Results are given in Table I.

Ethanol, Glycerol, and Leucine—These three compounds proved to be very unsatisfactory as additives in the concentration range tested (0.001–0.1 *M*). None of the compositions demonstrated delayed onset

Table I—Effect of Additives on Insulin Aggregation

Major Additive	Buffer[a]	pH	EDTA (0.005 *M*)	Insulin Concentration, mg/ml	Effective in Blocking Aggregation?
Lysine (0.0005–0.1 *M*)	PBS	7.4	+	6–10	Yes
Lysine (0.0005–0.1 *M*)	PBS	7.4	–	6	Slight
Lysine (0.001–0.1 *M*)	PBS	9.0	+	6	Yes
Lysine (0.001–0.1 *M*)	PBS	9.0	–	6	Slight
Aspartic Acid (0.00005–0.05 *M*)	PBS	7.4	+	6	No
Aspartic Acid (0.00005–0.05 *M*)	PBS	7.4	–	6	No
Aspartic Acid (0.00005–0.05 *M*)	PBS	3.5	+	3–6	Yes
Aspartic Acid (0.00005–0.05 *M*)	PBS	3.5	–	3–6	Yes
Glutamic Acid (0.00005–0.05 *M*)	PBS	7.4	+	6	No
Glutamic Acid (0.00005–0.05 *M*)	PBS	7.4	–	6	No
Glutamic Acid (0.00005–0.05 *M*)	PBS	3.5	+	3–6	Yes
Glutamic Acid (0.00005–0.05 *M*)	PBS	3.5	–	3–6	Yes
Leucine (0.001–0.1 *M*)	PBS	7.4	+	6	No
Glycerol (0.001–1.0 *M*)	PBS	7.4	+	6	No
Ethanol (0.001–0.1 *M*)	PBS	7.4	+	6	No
Buffer A (0.005–0.1 *M*)[a]	PBS	7.4	+	6	Yes
Buffer A (0.005–0.1 *M*)	PBS	7.4	–	6	No
Buffer A (0.005–0.1 *M*)	Tris	7.4	+	6	Yes
Sodium Bicarbonate	$NaHCO_3$	7.2–7.4	+	0.5	Yes

[a] Key: (PBS) phosphate-buffered saline; (Tris) Tris buffer in 0.1 *M* NaCl.

[1] Chemicals were obtained from Sigma Chemical Co.

[2] Obtained from Calbiochem Behring Corp., La Jolla, Calif.; lot number 003622.

0022-3549/83/1200-1472$01.00/0

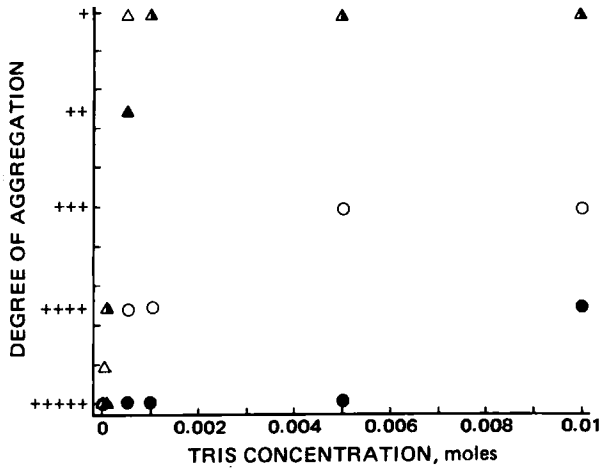

Figure 1—*Comparison of aggregation of insulin in phosphate-buffered saline as a function of Tris concentration. Solution conditions: phosphate-buffered saline, pH 7.2–7.4, temperature 37°, and insulin concentration, 6 mg/ml. Key: Degree of aggregation of solutions with 0.005 M EDTA at 1 (△) and 5 (▲) days; aggregation of solutions without EDTA at 1 (○) and 5 (●) days; (▲) point overlap.*

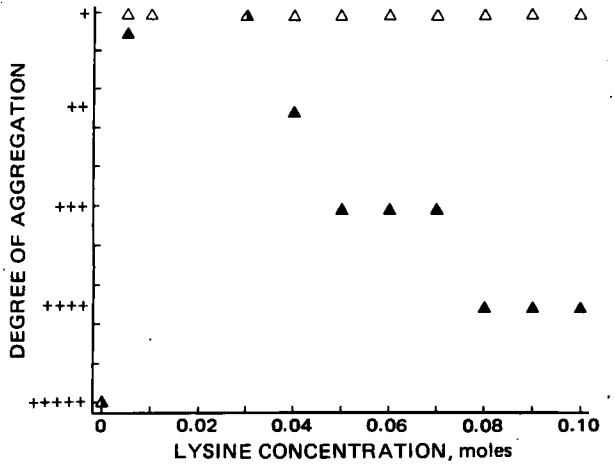

Figure 2—*Concentrations of 0.001–0.01 M lysine in 0.005 M EDTA and phosphate-buffered saline, pH 7.4. Key: degree of aggregation of solutions with 0.005 M EDTA at 1 (△) and 5 (▲) days; (▲) point overlap.*

of aggregation.

Tris Buffer—Phosphate-buffered saline solutions were prepared with and without 0.005 *M* EDTA, at various Tris concentrations (0.001–0.1 *M*). Figure 1 summarizes the aggregation of insulin as a function of Tris concentration in the presence and absence of EDTA, demonstrating that both additives are important in delaying the onset of insulin aggregation.

Lysine—Phosphate-buffered saline solutions containing lysine showed rapid dissolution of insulin, with the dissolution time decreasing as the pH was raised to 8.5–9.0. Solutions containing lysine at pH 7.2–7.4 maintained a clear, unaggregated appearance for 5–6 days. Higher lysine concentrations (0.1–0.01 *M* in 0.005 *M* EDTA) tended to aggregate more than those solutions containing lower lysine concentrations (0.01–0.001 *M*). Lysine (0.001 *M* in 0.005 *M* EDTA) is effective in minimizing aggregation (Fig. 2). However, when 0.005 *M* EDTA was eliminated from the phosphate-buffered saline solution, 0.01 *M* lysine was required to significantly minimize aggregation. Solutions of 0.01 *M* lysine and 0.005 *M* EDTA maintained at 4° without agitation remained not aggregated for periods up to 3 weeks.

Aspartic and Glutamic Acid—Earlier studies in other laboratories (5) showed that glutamic and aspartic acids were important in delaying the onset of aggregate formation. Our studies confirm the results of Bringer *et al.* (5) wherein aggregation was prevented for 6–7 days; however, serial dilution resulted in a decrease in the aggregation time. Aspartic acid proved to be more successful than glutamic acid at blocking insulin aggregation (Table I). It is important to note that due to the acidic nature of these amino acids, the pH of these solutions was 3.5 rather than 7.4. If the solutions were adjusted to pH 7.4, the aggregation was lost. This observation was also noted by Bringer *et al.* (5).

Bicarbonate—Two-milliliter solutions of sodium bicarbonate saturated with insulin were titrated to pH 6.3 with 0.1 *M* HCl, resulting in insulin precipitation. If solutions were back-titrated to pH 7.4 with 0.1 *M* NaOH the insulin remained undissolved. However, if a 5% CO_2–compressed air mixture was bubbled through the solution until pH 7.4 was reached, the insulin redissolved. A similar observation was noted by Lougheed *et al.*, where dissolution times were monitored as a function of bicarbonate concentration (8).

DISCUSSION

These results support the findings of previous researchers that agitation, additives, temperature, pH, and insulin concentration influence the solubility and macroaggregation of insulin. Recent work by Sato *et al.*, demonstrates that urea is effective in minimizing aggregation (9).

Several mechanisms for the prevention of aggregation have been proposed including the possibility of a serum substance (4) that prevents aggregation [newly published data from this group suggests that the bicarbonate concentration is the major factor in mediating insulin solubility (8)]. The chelation effect of the carboxyl groups of amino acids for zinc is believed to block aggregate formation by resulting in a more soluble form of insulin. This data is somewhat supported by the improvement of solubility and prolongation of aggregation time observed in solutions containing EDTA. As a chelating agent, EDTA may compete with insulin for zinc and, therefore, slow aggregate formation (10). Another possible mechanism for minimizing aggregation is that amino acid additives, especially lysine, may interact with the insulin molecule by hydrophobic and ionic means, thereby decreasing insulin–insulin interactions and preventing or slowing the formation of aggregates. More definitive work should be done with detailed analysis of the types of interactions and the conformation of the insulin molecule in these solutions.

Buffered physiological saline solutions containing 0.001 *M* lysine and 0.005 *M* EDTA improve insulin solubility and are effective in delaying the onset of macroaggregation. In the absence of EDTA, 0.01 *M* lysine solutions improve initial solubility and minimize the degree of aggregation. One advantage of the lysine additive is that the solutions are maintained at pH 7.4. A second advantage is that lysine is a common amino acid and is therefore not a synthetic additive.

Results summarized in this study emphasize the importance of additives in improving the solubility and stability of insulin solutions. It should be remembered that the type of insulin and additives used in various insulin preparations influence the properties discussed above, so a comparison of these results with other studies must be done with caution. The only way to accurately assess the contribution of each additive as to its solubility and aggregate-blocking properties is in a study such as this which minimizes the contributions of other solution variables or insulin additives.

REFERENCES

(1) B. Zinman, E. F. Stokes, A. M. Albisser, A. K. Hanna, H. L. Minuk, A. N. Stein, B. S. Leibel, and E. B. Marliss, *Metabolism*, **28**, 511 (1979).

(2) A. M. Albisser, B. S. Leibel, T. G. Ewart, Z. Davidovac, C. K. Botz, and W. Zingy, *Diabetes*, **23**, 389 (1974).

(3) W. D. Lougheed, H. Woulfe-Flanagan, J. R. Clement, and A. M. Albisser, *Diabetologia*, **19**, 1 (1980).

(4) A. M. Albisser, W. D. Lougheed, K. Perlman, and A. Bahoric, *Diabetes*, **29**, 241 (1980).

(5) J. Bringer, A. Heldt, and G. M. Grodsky, *Diabetes*, **30**, 83 (1981).

(6) H. Pekar and G. Frank, *Biochemistry*, **11**, 4013 (1972).

(7) P. D. Jeffrey and J. H. Coates, *Biochemistry*, **5**, 489 (1966).

(8) W. D. Lougheed, U. Fischer, K. Perlman, and A. M. Albisser, *Diabetologia*, **20**, 51 (1981).

(9) S. Sato, C. Ebert, and S. W. Kim, *J. Pharm. Sci.*, **72**, 228 (1983).

(10) T. Blundell, G. Dodson, D. Hodgkin, and D. Mercola, *Adv. Protein Chem.*, **26**, 279 (1972).

ACKNOWLEDGMENTS

Funded by the Kroc Foundation. We thank G. Iwamoto for helpful suggestions in this work.

Michael-Type Reactions of Tenulin, a Biologically Active Sesquiterpene Lactone

THOMAS G. WADDELL ˣ, PAUL H. GEBERT, and DAVID L. TAIT

Received August 9, 1982, from the *Department of Chemistry, University of Tennessee at Chattanooga, Chattanooga, TN 37402.* Accepted for publication November 1, 1982.

Abstract □ The antitumor pseudoguaianolide tenulin has been exposed to a wide variety of biological and model nucleophilic reagents and has been shown to react exclusively with sulfur nucleophiles in a Michael-like fashion. The biological implications of these results are discussed.

Keyphrases □ Tenulin—sesquiterpene lactone, Michael-type reactions, nucleophilic reagents □ Sesquiterpene lactones—tenulin, Michael-type reactions, nucleophilic reagents □ Michael-type reactions—tenulin with nucleophilic reagents, biologically active sesquiterpene lactones

The sesquiterpene lactone tenulin (I) (1) is the major bitter principle of the medicinal herb *Helenium amarum* (2). This compound has received considerable attention with regard to its antitumor (2–5), anti-inflammatory (6, 7), and antihyperlipidemic (8) activity. Recent structure–activity studies have related the biological properties of tenulin to the presence of the cyclopentenone moiety (4, 7, 8). The potential of this unit to act as an electrophile in Michael-like addition reactions is reminiscent of the *in vivo* role of the α-methylene-γ-lactone group (II) as a sulfhydryl (SH) acceptor in cytotoxic natural products (9). Indeed, the efficient Michael-like addition of cysteine (SH) to the tenulin enone has been reported (3). The α-methylene-γ-lactone group is reactive toward a variety of sulfur (9), oxygen (10), and nitrogen (11) nucleophiles. Therefore, it is important to the understanding of the mechanism of action to establish systematically the reactivity and selectivity of the cyclopentenone group of tenulin toward a variety of S, N, and O nucleophilic reagents. Such a study is of broad significance since the cyclopentenone unit appears in several antitumor terpenoids (12, 13).

RESULTS AND DISCUSSION

Table I presents a summary of this work and, for completeness, includes data taken from earlier work (entries 4–8 and 22). Reactions were attempted in aqueous alcohol solutions at room temperature and observed for periods up to 7 days. With the exception of entries 4–8, where spectral methods were used (3), negative reaction results were determined by TLC.

Nucleotides and nucleic acids exposed the cyclopentenone unit of tenulin to various nitrogen and oxygen nucleophiles. However, in no case was any reaction observed. Indeed, cyclopentenone itself does not react with adenosine 5′-monophosphate. Similarly, the amino acids alanine, serine, cysteine, histidine, and lysine contain nitrogen, oxygen, and sulfhydryl nucleophiles. Methanolic solutions of serine, histidine, or lysine (phosphate buffer, pH 7.2), when treated with tenulin, resulted only in the retroaldol conversion of tenulin to isotenulin (III) (14). In striking contrast, the efficient Michael addition of cysteine (SH) to the enone of tenulin (and cyclopentenone) to produce the adduct IV has been reported (3). The results summarized above suggest a strong Michael selectivity of the electrophilic cyclopentenone group for sulfur nucleophiles.

This notion was further tested (entries 14–22) by treating tenulin and cyclopentenone with glutathione (SH) and small model nucleophiles. Tenulin and methylamine interacted in aqueous methanol to produce the Schiff base, tentatively assigned structure V. Compound V was insoluble in water but readily soluble in dilute hydrochloric acid. The IR spectrum showed ν_{max} at 1770 br (γ-lactone and ester) and 1660 cm^{-1} (C=N), but lacked OH and enone absorption. The Schiff base portion of the molecule was confirmed by the UV spectrum where λ_{max} 246 nm (methanol) shifted to 265 nm on addition of two drops of 50% HCl. This bathochromic shift is characteristic of conjugated azomethines (15). An analogous reaction of 2-cyclopentenone with methylamine to form the Schiff base was demonstrated spectrophotometrically (see *Experimental*). Thus, the nucleophilic nitrogen of methylamine prefers the electrophilic carbonyl group of the cyclopentenone unit rather than the β-carbon. Methanol and ethanol do not react with tenulin even at reflux,

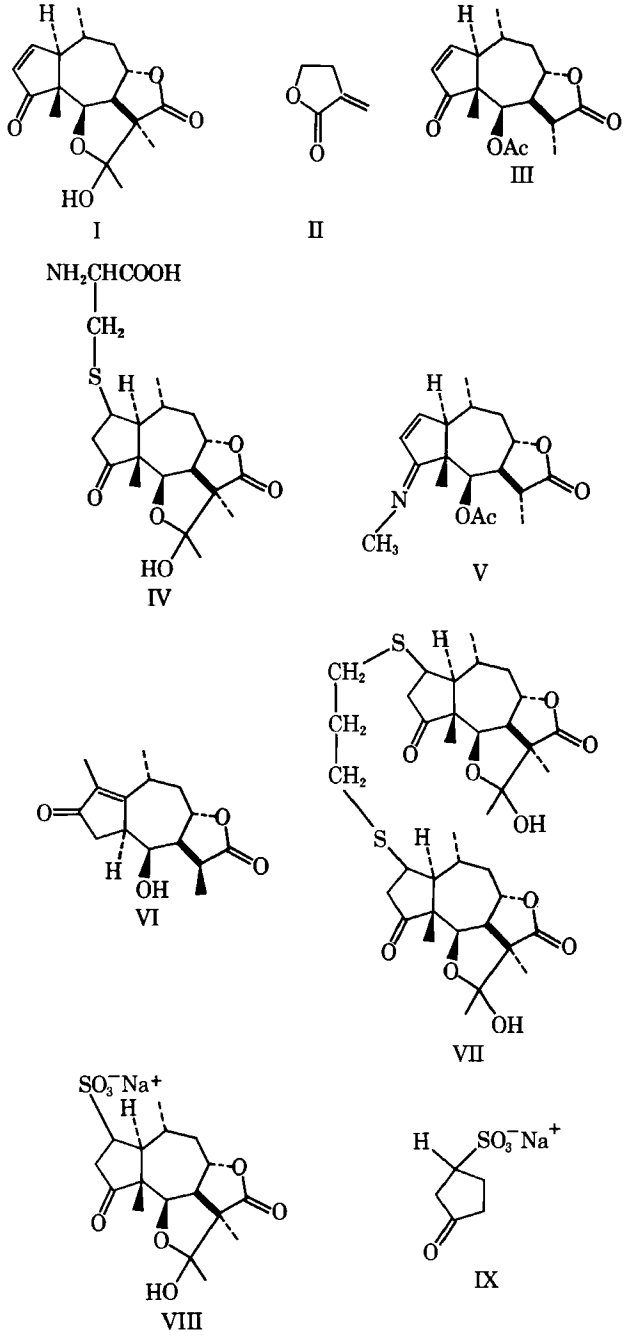

0022-3549/83/1200-1474$01.00/0

Table I—Reactions of Tenulin and 2-Cyclopentenone with Nucleophiles

Entry	Nucleophilic Reagent	With Tenulin	With 2-Cyclopentenone
1	Adenosine 5′-monophosphate	No reaction	No reaction
2	Adenosine	No reaction	
3	Adenine	No reaction	
4	Deoxyguanosine 5′-monophosphate	No reaction (3)	
5	Deoxyguanosine 5′-triphosphate	No reaction (3)	
6	Deoxyadenosine 5′-monophosphate	No reaction (3)	
7	Deoxyadenosine 5′-triphosphate	No reaction (3)	
8	Deoxyribonucleic acid	No reaction (3)	
9	L-Alanine	No reaction	
10	L-Serine	Conversion to isotenulin	
11	L-Cysteine	Michael addition (3)	Michael addition (3)
12	L-Histidine	Conversion to isotenulin	No reaction
13	L-Lysine	Conversion to isotenulin	No reaction
14	Methylamine	Schiff base	Schiff base
15	Sodium methoxide	Skeletal rearrangement	
16	Methanol	No reaction	
17	Ethanol	No reaction	
18	Thiourea	No reaction	No reaction
19	1,3-Propanedithiol	Bis Michael addition	
20	Glutathione (SH)		Michael addition (3)
21	Sodium bisulfite	Michael addition	Michael addition
22	1-Propanethiol		Michael addition (18)

whereas the more reactive sodium methoxide affects the known skeletal rearrangement of tenulin to deacetylneotenulin (VI) (16).

The reactivity of tenulin toward several types of sulfur nucleophiles is summarized in entries 18–22 (Table I). Although the sulfur atom of thiourea has been shown to act as a nucleophile in Michael-like additions (*cf.* 17), this reagent does not react with tenulin or 2-cyclopentenone. In contrast, cyclopentenone does form Michael adducts with the sulfhydryl-containing glutathione (3) and 1-propanethiol (18). The high reactivity of the cyclopentenone toward SH groups is further demonstrated in the reaction of tenulin with one mole equivalent of 1,3-propanedithiol where the major product is the crystalline bis adduct VII, $C_{37}H_{52}O_{10}S_2 \cdot H_2O$. Compound VII showed IR absorption at 3300–3500 (OH), 1780 (γ-lactone), and 1740 cm^{-1} (cyclopentanone). Sulfhydryl absorption near 2550 cm^{-1} was absent. The UV spectrum lacked the characteristic enone absorption of tenulin and chemical analysis for SH (19) was negative.

The known reactivity of sodium bisulfite as a sulfur nucleophile in Michael-like additions (20) prompted the examination of this reagent as a potential nucleophile. The reaction of tenulin with excess sodium bisulfite in aqueous methanol cleanly produced the water-soluble Michael adduct VIII. The IR spectrum of VIII lacked enone carbonyl absorption near 1700 cm^{-1}. A broad band centered at 1740–1770 cm^{-1} indicated γ-lactone and cyclopentanone functional groups. Further evidence for Michael addition was seen in the NMR spectrum of VIII which featured the absence of olefinic proton signals and the presence of a new one proton multiplet at 3.70 ppm (H-2, $HCSO_3Na$). In an analogous manner, 2-cyclopentenone forms the Michael adduct IX when treated with either one or two equivalents of sodium bisulfite.

These experiments have demonstrated that the cyclopentenone unit of tenulin is highly selective for sulfur nucleophiles (SH, bisulfite) in Michael-like addition reactions. This selectivity is not surprising in view of the classification of sulfur and enone as soft Lewis base and Lewis acid, respectively, whereas nitrogen and oxygen nucleophiles are considered to be hard Lewis bases (21).

There are biological implications of this new chemistry of tenulin. The hypothesis that the *in vivo* activity of cyclopentenone-containing natural products may be due to the enone unit alkylating essential sulfhydryl groups of cellular enzymes (3) now stands more firmly with this additional support.

EXPERIMENTAL

Attempted Reactions of Tenulin with Model Nucleophiles—In separate experiments, tenulin (50 mg) was treated with 2 ml of an aqueous methanol solution containing one equivalent of thiourea, adenine, or adenosine. Analogously, in 2 ml of methanol–phosphate buffer (pH 7.2) tenulin was treated with one equivalent of adenosine 5′-monophosphate, L-serine, L-histidine, L-lysine, or L-alanine. Reaction vessels were stoppered, left at room temperature for several days, and monitored by TLC[1]. No reactions were observed. Quantitative yields of tenulin (or isotenulin) were recovered on extraction with chloroform, drying over anhydrous magnesium sulfate, filtration, and evaporation of the filtrate.

Attempted Reactions of 2-Cyclopentenone with Model Nucleophiles—In separate experiments, 2-cyclopentenone (50 mg) was treated with 2 ml of an aqueous methanol solution containing one equivalent of thiourea, L-histidine, L-lysine, or adenosine 5′-monophosphate (in methanol–phosphate buffer, pH 7.2). Reaction vessels were stoppered, left at room temperature for several days, and monitored by TLC. No reactions were observed.

Isotenulin Methylimine (V)—To a solution of 0.051 g (0.17 mmole) of tenulin in 0.5 ml of methanol was added 0.5 ml (excess) of 40% aqueous methylamine. After 2 days at room temperature, the reaction solution was poured into 20 ml of water and extracted twice with 15 ml of chloroform. The combined chloroform extract was dried (magnesium sulfate), filtered, and evaporated to dryness at room temperature. Ether trituration yielded a crystalline compound (8 mg) tentatively assigned as V, mp 155–156° dec.[2] IR[3] ($CHCl_3$): 1770 (γ-lactone and ester) and 1660 cm^{-1} (C=N); UV[4]: 246 nm (MeOH) and 265 nm (MeOH + 2 drops 50% HCl). Compound V was water insoluble but readily soluble in dilute hydrochloric acid.

Deacetylneotenulin (VI)—To a solution of 0.100 g (0.32 mmole) of tenulin in 3 ml of methanol was added dropwise a sodium methoxide solution prepared by dissolving 4 mg (0.17 mmole) of sodium in 2 ml of methanol. After 80 min the reaction mixture was diluted to 50 ml with distilled water and extracted with three 25-ml portions of chloroform. The combined organic layer was dried (magnesium sulfate), filtered, and evaporated to dryness to give 0.075 g (87% yield) of a colorless gum. Ether trituration and recrystallization from acetone–ether gave deacetylneotenulin (VI), mp 242–245° dec. [lit. (22) mp 239–240°]. IR and UV spectra of VI were identical to published data.

Tenulin-1,3-propanedithiol Bis Adduct (VII)—To 0.304 g (0.99 mmole) of tenulin in 2 ml of methanol was added 0.10 ml (0.99 mmole) of 1,3-propanedithiol. The solution was swirled, deoxygenated under a nitrogen stream, sealed, and left at 0° for 3 days. After careful evaporation of the solvent, the yellow oily product was taken up in chloroform–ether whereupon a crystalline solid (136 mg) slowly separated in several crops. Recrystallization from hot methanol gave the bis adduct VII (69 mg, 19% yield), mp 244–248°. IR (nujol): 1780 (γ-lactone) and 1740 cm^{-1} (cyclopentanone); UV(MeOH): 205 mm.

Anal[5].—Calc. for $C_{37}H_{52}O_{10}S_2 \cdot H_2O$: C, 60.14; H, 7.36, S. 8.68. Found: C, 60.27; H, 7.55; S, 9.09.

Tenulin–Sodium Bisulfite Adduct (VIII)—Tenulin (0.052 g, 0.17 mmole) and sodium bisulfite (0.034 g, 0.33 mmole) were dissolved in 1.5 ml of aqueous methanol. After 4 days at room temperature, the reaction solution was allowed to slowly evaporate on a watchglass. The remaining crystalline material was taken up in methanol and filtered through a 1-cm

[1] EM Reagents precoated plates, silica gel 60, 0.25 mm thickness.

[2] Thomas-Hoover apparatus. All melting points are corrected.
[3] Perkin-Elmer 710B.
[4] Hitachi 100-80.
[5] Galbraith Laboratories, Knoxville, Tenn.

column of silica gel. Evaporation of the solvent left a clear oil which crystallized to yield 45 mg (65% yield) of water-soluble VIII, mp gradual dec. up to 108°. IR (nujol): 1740–1770 cm^{-1} (γ-lactone and cyclopentanone). ^{1}H-NMR(CD_3OD)[6]: δ 5.10 (br t, 1, H-8), 4.00 (d, 1, H-6), 3.70 (br, 1, H-2), and 1.20–1.60 ppm (12, 4 Me groups).

2-Cyclopentenone–Sodium Bisulfite Adduct (IX)—2-Cyclopentenone (0.055 g, 0.67 mmole) and sodium bisulfite (0.063 g, 0.61 mmole) were taken up in 2 ml of distilled water. Methanol (0.5 ml) was added after 2 hr at room temperature, the mixture was poured onto a watchglass and the solvent was allowed to evaporate slowly. Recrystallization of the solid residue from methanol–ether yielded 57 mg (46% yield) of the adduct IX, mp 163–166° [lit. (23) mp 165°]. IR (nujol): 1740 cm^{-1} (cyclopentanone). ^{1}H-NMR (D_2O): δ 3.70 (m, 1, $HCSO_3Na$) and 2.10–3.00 ppm (6, complex). Identical results were obtained when this experiment was repeated using a 1:2 molar ratio of ketone to sodium bisulfite.

2-Cyclopentenone Methylimine (Schiff Base)—Excess methylamine was added to a reference 2-cyclopentenone–methanol solution in a UV cuvette. After 18 hr, the $\pi \rightarrow \pi^*$ absorption of the enone carbonyl (310 nm) disappeared. Addition of 2 drops of 50% HCl caused a bathochromic shift in the original $\pi \rightarrow \pi^*$ (230 nm) to 250 nm. A control experiment without methylamine revealed no changes in the original cyclopentenone UV spectrum. The above results are consistent with the formation of the cyclopentenone–methylamine Schiff base (15).

REFERENCES

(1) W. Herz and R. P. Sharma, *J. Org. Chem.*, **40,** 2557 (1975), and references cited therein.

(2) T. G. Waddell, M. B. Ridley, K. D. Evans, and M. E. Green, *J. Tenn. Acad. Sci.*, **54,** 103 (1979).

(3) I. H. Hall, K. H. Lee, E. C. Mar, C. O. Starnes, and T. G. Waddell, *J. Med. Chem.*, **20,** 333 (1977).

(4) T. G. Waddell, A. M. Austin, J. W. Cochran, K. G. Gerhart, I. H. Hall, and K. H. Lee, *J. Pharm. Sci.*, **68,** 715 (1979).

(5) K. H. Lee, I. H. Hall, E. C. Mar, C. O. Starnes, S. A. ElGebaly, T. G. Waddell, R. Hadgraft, C. G. Ruffner, and I. Weidner, *Science*, **196,** 533 (1977).

(6) I. H. Hall, K. H. Lee, C. O. Starnes, Y. Sumida, R. Y. Wu, T. G. Waddell, J. W. Cochran, and K. G. Gerhart, *J. Pharm. Sci.*, **68,** 537 (1979).

(7) I. H. Hall, C. O. Starnes, K. H. Lee, and T. G. Waddell, *J. Pharm. Sci.*, **69,** 537 (1980).

(8) I. H. Hall, K. H. Lee, C. O. Starnes, O. Muraoka, Y. Sumida, and T. G. Waddell, *J. Pharm. Sci.*, **69,** 694 (1980).

(9) S. M. Kupchan, D. C. Feesler, M. A. Eakin, and T. J. Giacobbe, *Science*, **168,** 376 (1970).

(10) S. M. Kupchan, M. Maruyama, R. J. Hemingway, J. C. Hemingway, S. Shibuya, T. Fujita, P. D. Cradwick, A. D. U. Hardy, and G. A. Sim, *J. Am. Chem. Soc.*, **93,** 4914 (1971).

(11) K. H. Lee, H. Furukawa, and E. S. Huang, *J. Med. Chem.*, **15,** 609 (1972).

(12) S. M. Kupchan, Y. Shizuri, W. C. Sumner, R. Haynes, A. P. Leighton, and B. R. Sickles, *J. Org. Chem.*, **41,** 3850 (1976).

(13) K. H. Lee, T. Ibuka, A. Y. McPhail, K. D. Onan, T. A. Geissman, and T. G. Waddell, *Tetrahedron Lett.*, **1974,** 1149.

(14) D. H. R. Barton and P. DeMayo, *J. Chem. Soc.*, **1956,** 142.

(15) R. M. Silverstein, G. C. Bassler, and T. C. Morrill, "Spectrophotometric Identification of Organic Compounds," Wiley, New York, N.Y., 1974, p. 247.

(16) P. Cox and G. Sim, *J. Chem. Soc. Perkin II*, **1976,** 990.

(17) J. Daneke, U. Jahnke, B. Pankow, and H. W. Wanzlick, *Tetrahedron Lett.*, **1970,** 1271.

(18) S. R. Wilson and H. T. Chen, *Bioorg. Chem.*, **9,** 212 (1980).

(19) K. G. Krebbs, D. Heusser, and H. Wimmer, "Thin-layer Chromatography," E. Stahl, Ed., Springer-Verlag, New York, N.Y., 1969, p. 890.

(20) M. Hori, *J. Agr. Chem. Soc. Jpn.*, **18,** 155 (1942).

(21) T. L. Ho, *Chem. Rev.*, **75,** 1 (1975).

(22) W. Herz, W. A. Rohde, K. Rabindran, P. Jayaraman, and N. Viswanathan, *J. Am. Chem. Soc.*, **84,** 3857 (1962).

(23) M. Godchot and F. Taboury, *Compt. Rend.*, **156,** 332 (1913).

[6] JEOL JNM-PMX 60. Chemical shifts are reported as ppm downfield from tetramethylsilane.

ACKNOWLEDGMENTS

Acknowledgment is made to the Donors of the Petroleum Research Fund, administered by the American Chemical Society, for financial support of this work.

The authors thank Mr. Richard Collison for valuable technical assistance.

Quantitative Determination of Hexamidine Isethionate in Pharmaceutical Preparations by High-Performance Liquid Chromatography

P. TAYLOR ˣ, P. D. BRADDOCK, and S. ROSS

Received August 16, 1982, from the *Vick International R & D Laboratories, Egham, Surrey, England.* Accepted for publication November 10, 1982.

Abstract □ Hexamidine isethionate in various pharmaceutical formulations was analyzed quantitatively by high-performance liquid chromatography. The method is rapid, accurate, and precise. Excellent results were obtained from four commercial bases.

Keyphrases □ Hexamidine isethionate—quantitative determination in pharmaceutical preparations, high-performance liquid chromatography □ High-performance liquid chromatography—quantitative determination of hexamidine isethionate, pharmaceutical preparations □ Preparations, pharmaceutical—quantitative determination of hexamidine isethionate by high-performance liquid chromatography

Hexamidine isethionate [4,4′-(hexamethylenedioxy)-dibenzamidine bis(2-hydroxyethanesulfonate)], used as a topical antiseptic in pharmaceutical products, belongs to a group of compounds (aromatic diamidines) which have good antibacterial and antifungal properties (1). Diamidines can be identified in their pure form microscopically (2) and quantified colorimetrically in pharmaceutical preparations using glyoxal sodium bisulfite solution (3). The latter method is nonspecific and subject to interferences. This fact has prompted more recent workers to investigate the use of spectrophotometric (4), GLC (5, 6), and high-performance liquid chromatographic (HPLC) (7) techniques.

The purpose of this study was to develop a rapid HPLC method which would be suitable for the analysis of hexamidine isethionate (I) in pharmaceutical preparations. Validation data are presented for the analysis of a topical cream, and the methodology was found to be applicable to ointments and eyewash solutions.

EXPERIMENTAL

Reagents and Chemicals—The methanol[1] and water[1] used were HPLC grade and the glacial acetic acid[1], chloroform[1], and ether[1] were analytical reagent grade. Hexamidine isethionate[2] was used as received.

Apparatus—The high-pressure solvent pump[3] was connected to a fixed-wavelength detector[4], a fixed-volume injection valve[5], and a recording integrator[6]. The polar column[7] (30 cm × 3.9-mm i.d.) consisted of a monomolecular layer of cyanotrichlorosilane permanently bonded by silicone–carbon bonds to microparticulate silica.

The mobile phase consisted of water–methanol–glacial acetic acid (4:2:1, v/v/v) which was deaerated by vacuum filtration before use. The temperature was ambient, and the flow rate was 1.0 ml/min. The detector sensitivity was 0.02 AUFS (254 nm), the recorder/integrator attenuation was 8, and the chart speed was 0.5 cm/min.

[1] B. D. H. Chemicals, Poole, Dorset, England.
[2] Rhône-Poulenc, Paris, France.
[3] Waters 6000A pump, Waters Associates, Hartford, Cheshire, England.
[4] Waters 440 UV detector, Waters Associates, Hartford, Cheshire, England.
[5] Rheodyne 7125 injection valve, Rheodyne Inc., Berkeley, Calif.
[6] Model 3380A recorder/integrator, Hewlett-Packard, Winnersh, Berkshire, England.
[7] μBondapak-CN, Waters Associates, Hartford, Cheshire, England.

Hexamidine Isethionate Standard Solutions—Standard samples of I in the range of 0–75 mg were accurately weighed into 1000-ml volumetric flasks and diluted to volume with mobile phase. After mixing to dissolve the standards, 10.0-ml aliquots were diluted to 100.0 ml in volumetric flasks using the mobile phase. Twenty microliters of each solution was injected into the HPLC.

Preparation of Samples—*Creams*—Samples of cream (0.5 g) equivalent to 0.5 mg of I were accurately weighed into a 50-ml centrifuge tube and shaken with 40 ml of mobile phase. After centrifugation the supernatant liquid was transferred to a 250-ml separatory funnel, and the process was repeated with a second 40-ml aliquot of mobile phase. The combined extracts were then washed with two 40-ml portions of chloroform, transferred to a 100-ml volumetric flask, and diluted to volume with mobile phase.

Ointments—Samples (0.5 g) equivalent to 0.5 mg of I were first dissolved in 50 ml of hexane and then extracted with two 40-ml aliquots of mobile phase. Treatment was as described above for creams.

Eyewash Solutions—Eyewash solutions were diluted to 200 ml (20-fold) with water, and 20.0 ml of this solution (equivalent to 1 mg of I) was then extracted with three 20-ml aliquots of ether. The ether extracts were discarded, and the aqueous phase was transferred to a 200-ml volumetric flask and diluted to volume with mobile phase. Twenty-microliter aliquots of each sample solution were injected into the HPLC.

Calculations—The peak heights from the injections of the standard hexamidine isethionate solutions were measured manually and plotted as a function of concentration. Since the calibration curve indicated that peak heights were directly related to concentrations (0–0.0075, mg/ml) of I, sample results were calculated by:

$$\frac{(Ph)_a}{(Ph)_s} \times \frac{C}{1000} \times D \times 100 = \%\ \text{w/w (or w/v) of I}$$

where $(Ph)_a$ and $(Ph)_s$ are the peak heights of I in the assay and standard solution chromatograms, respectively, C is the concentration of standard solution of I in mg/ml, and D is the dilution factor.

Reproducibility and Accuracy—Replicate analyses (n = 6) were carried out on a single batch of cream formulated to contain 0.1% w/w of I to test reproducibility of the assay. Known weights of hexamidine isethionate representing levels between 50 and 150% of label claim were added to five 0.5-g samples of placebo cream to check the assay accuracy. After mixing, samples were prepared as described above and injected into the HPLC.

RESULTS AND DISCUSSION

The described method was validated using a topical cream developed in-house. A typical cream sample chromatogram is shown in Fig. 1. Hexamidine isethionate elutes as a sharp peak in <8 min. The calibration curve of the concentration of I *versus* peak height was found to be linear over 0–0.0075 mg/ml and passed very close to the origin (slope = 1.694×10^5, intecept = −1.53, and r = 0.9996). Recovery data from placebo samples with added I indicate that the procedure is quantitative for I over the range 0.25–0.75 mg/0.5 g (Table I). This range corresponds to 50–150% of label for the typical (0.1%, w/w) cream formulations (0.5 mg/0.5 g). The reproducibility of the method was found to be good at 0.9% *RSD* (Table II).

A placebo sample without I when carried through the procedure showed the absence of interferences from formulation excipients, although a small peak which elutes immediately after I could *potentially* interfere should column efficiency deteriorate. However, in this event the positive bias introduced would be small (<2%).

During sample preparation of creams and ointments, it was necessary to extract with chloroform to overcome severe chromatographic inter-

0022-3549/83/1200-1477$01.00/0

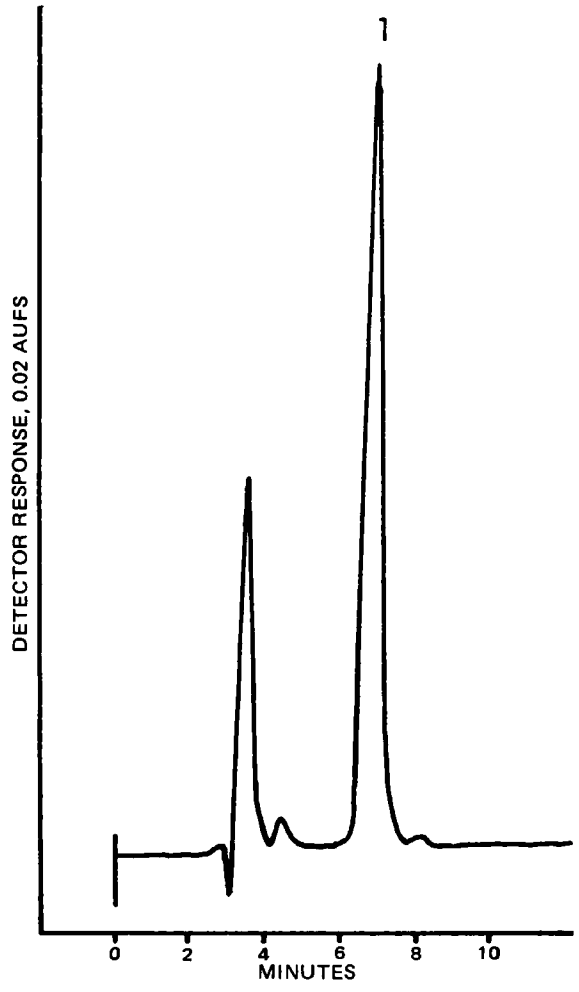

Figure 1—*High-performance liquid chromatogram of a topical oil-in-water cream preparation. Peak 1 is hexamidine isethionate. Other peaks are unidentified components of the cream base.*

ferences. Eyewash solutions required extraction with ether to remove the methylparaben and propylparaben which were included in these formulations. The relatively high concentration of acetic acid used in the mobile phase was essential for adequate resolution and rapid analysis of I. Column stability was satisfactory throughout the experiments, although it was necessary to thoroughly cleanse the chromatograph and column of the corrosive mobile phase between analyses.

The results for the analyses of I in three different dosage forms is given in Table III. In general, results were very close to the label claim. The low result found with ointment 2 could have been due to incomplete extraction from the base.

Table I—Accuracy of the HPLC Assay of Hexamidine Isethionate in a Topical Cream

Added, mg	Found, mg	Recovery, %
0.2525	0.2579	102.1
0.3788	0.3739	98.7
0.5050	0.5043	99.9
0.6313	0.6318	100.1
0.7575	0.7477	98.7

Table II—Reproducibility of the HPLC Assay of Hexamidine Isethionate in a Topical Cream

Sample	Percent w/w
1	0.101
2	0.099
3	0.100
4	0.101
5	0.100
6	0.099
Mean	0.100
SD	8.94×10^{-4}
RSD[a], %	0.894

[a] Relative standard deviation derived from 100 × *SD*/Mean.

Table III—Assay Results for Hexamidine Isethionate in Commercial Dosage Forms

Sample	Claim per Dosage Form, mg/100 g	Hexamidine Isethionate, % of Label Claim
Cream	100	99.9
Ointment 1	100	101.5
Ointment 2	100	83.0
Eyewash solution	100	100.5

REFERENCES

(1) E. B. Schoenbach and E. M. Greenspan, *Medicine*, **27**, 327 (1948).

(2) O. N. Yalcindag, *Sci. Pharm.*, **44**, 328 (1976).

(3) C. W. Ballard, *Quart. J. Pharm.*, **21**, 376 (1948).

(4) S. G. Tiraspolskaya, E. V. Kompantseva, A. S. Bril, and N. A. Kanivets, *Khim. Farm. Zh.*, **11**, 130 (1977).

(5) P. Erdtmansky and T. J. Goehl, *Anal. Chem.*, **47**, 750 (1975).

(6) J. Oszczapowicz, *Pol. J. Chem.*, **52**, 1311 (1978).

(7) D. G. T. Grieg, *Dev. Chromatogr.*, **2**, 147 (1980).

Stability of Mezlocillin Sodium as Determined by High-Performance Liquid Chromatography

V. DAS GUPTA

Received September 13, 1982, from the *College of Pharmacy, University of Houston, Houston, TX 77030.* Accepted for publication October 27, 1982.

Abstract □ The stability of mezlocillin sodium solutions in water with either phosphate buffers or other ingredients used in intravenous admixtures (dextrose, fructose, and sodium chloride) has been studied using a stability-indicating high-performance liquid chromatographic method. This assay shows a relative standard deviation of 1.42% based on six injections. The optimum stability was shown at an approximate pH of 4.8, and solutions in dextrose (5%) and sodium chloride (0.9%) were stable for up to 4 days at 25°, 36 days at 5°, and for 60 days at −10°. When refrigerated, the solutions in 5% fructose and 10% dextrose were as stable as those in 5% dextrose.

Keyphrases □ Mezlocillin sodium—stability, determined by high-performance liquid chromatography □ Stability—mezlocillin sodium, determined by high-performance liquid chromatography □ High-performance liquid chromatography—stability of mezlocillin sodium

Mezlocillin, a new semisynthetic broad-spectrum penicillin antibiotic, commonly administered by intravenous admixture, is effective against a wide variety of microorganisms. Limited information on the stability is available (1): solutions for intravenous use appear to be stable from 24 to 72 hr at controlled room temperature, from 24 to 168 hr under refrigeration, and for 28 days at −12° (1). This investigation studies the stability of mezlocillin sodium at varying pH in some commonly used vehicles for intravenous administration. A stability-indicating high-performance liquid chromatographic (HPLC) method was developed.

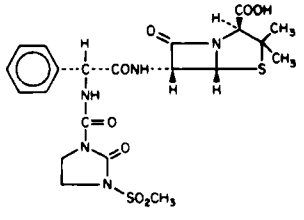

Mezlocillin

EXPERIMENTAL

Materials—All chemicals and reagents were USP, NF, or ACS quality and were used without further purification. Mezlocillin sodium[1] powder was used as received. The liquid chromatograph[2] was equipped with a multiple-wavelength detector[3], a recorder[4], and an integrator[5]. A semipolar[6] column (30 cm long × 4-mm i.d.) was used. The mobile phase contained 0.02 *M* ammonium acetate and 42% (v/v) methanol in water. The flow rate was 2.0 ml/min, the sensitivity was 0.2 AUFS (230 nm), and the chart speed 30.5 cm/hr. The temperature was ambient.

Methods—A standard solution was prepared daily by dissolving 100 mg of mezlocillin sodium in enough water to make 100 ml of the solution. All of the antibiotic solutions were prepared as indicated in Table I using a simple solution method. After the initial data were obtained (physical appearance, pH values[7], and assays), the solutions were stored either at room temperature (25 ± 1°), under refrigeration (5 ± 1°), in the freezer (−10 ± 1°), or at all three temperatures.

Table I—Mezlocillin Solutions Prepared for Stability Studies

Solution	Mezlocillin Sodium, mg/ml	pH (Initial)	Other Ingredient(s)	Ionic Strength[a]
1[b]	10.0	4.8	5% dextrose	—[d]
2[b]	10.0	4.8	0.9% NaCl	—[d]
3[c]	10.0	4.8	5% dextrose	—[d]
4[c]	10.0	4.4	10% dextrose	—[d]
5[c]	10.0	5.2	5% fructose	—[d]
6[c]	1.0	2.9	phosphate buffer, 0.05 *M*	0.2
7[c]	1.0	4.0	phosphate buffer, 0.05 *M*	0.2
8[c]	1.0	4.8	phosphate buffer, 0.05 *M*	0.2
9[c]	1.0	4.8	phosphate buffer, 0.1 *M*	0.2
10[c]	1.0	5.8	phosphate buffer, 0.05 *M*	0.2
11[c]	1.0	6.9	phosphate buffer, 0.05 *M*	0.2
12[c]	1.0	7.8	phosphate buffer, 0.05 *M*	0.2

[a] Adjusted with KCl. [b] Stored in plastic bag; the original plastic Viaflex PL 146 bags from which either 0.9% NaCl or 5% dextrose injection in water was withdrawn for making the solutions. [c] Stored in bottle; sixty-milliliter amber-colored glass bottle; Brockway Glass Co., Brockway, Pa. [d] Ionic strength of this solution was not adjusted.

At appropriate intervals, solutions of mezlocillin were assayed using HPLC. Before analysis, all solutions were diluted with water to an appropriate concentration (identical to the standard solution based on the label claim). Before being diluted, the solutions were brought to room temperature by putting the bags/bottles in tap water. One set of 60-day-old frozen samples was thawed using a microwave oven[8]; the frozen solutions were exposed to microwaves for 3 min.

A 20.0-μl aliquot of the assay solution was injected into the chromatograph using the described conditions. For comparison, an identical volume of the appropriate standard solution was injected after the assay solution eluted.

Calculations—Since preliminary investigations indicated that the peak heights were related directly to the concentrations (range tested: 0.2–1.2 mg/ml), the results were calculated using:

$$\frac{(Ph)_a}{(Ph)_s} = \text{percent of label claim} \qquad \text{(Eq. 1)}$$

where $(Ph)_a$ is the peak height of the assay solution and $(Ph)_s$ is the peak height of a standard solution of identical concentration based on the label claim.

RESULTS AND DISCUSSION

HPLC Assay Method—The method developed is reproducible with a relative standard deviation of 1.42% based on six injections, and separates a number of decomposition products (Fig. 1B and C) from the intact drug (peak 1 in Fig. 1).

It is well documented (2) that at lower pH (~3), the β-lactam moiety undergoes hydrolysis and at higher pH (~8), the side chain undergoes hydrolysis. In Fig. 1B (as compared with Fig. 1A) the additional unidentified peaks are from the hydrolysis of the 3-(methylsulfonyl)-2-oxo-1-imidazolidine ring (see structure of mezlocillin) since the pH of the assay solution was 7.8. In Fig. 1C, the additional peaks are from the hydrolysis of the β-lactam ring. The decomposition of mezlocillin in this

[1] Miles Pharmaceuticals, West Haven, Conn.
[2] Model ALC 202 equipped with U6K universal injector; Waters Associates, Milford, Mass.
[3] Spectroflow monitor SF770; Schoeffel Instrument Corp., Westwood, N.J.
[4] Omniscribe 5313-12; Houston Instruments, Austin, Tex.
[5] Autolab minigrator; Spectra-Physics, Santa Clara, Calif.
[6] Waters Associates μBondapak phenyl (Catalog No. 27198).
[7] All pH values were measured using Beckman Zeromatic SS-3, pH meter.
[8] Amana's Radarrange, Model MR-3.

0022-3549/83/1200-1479$01.00/0

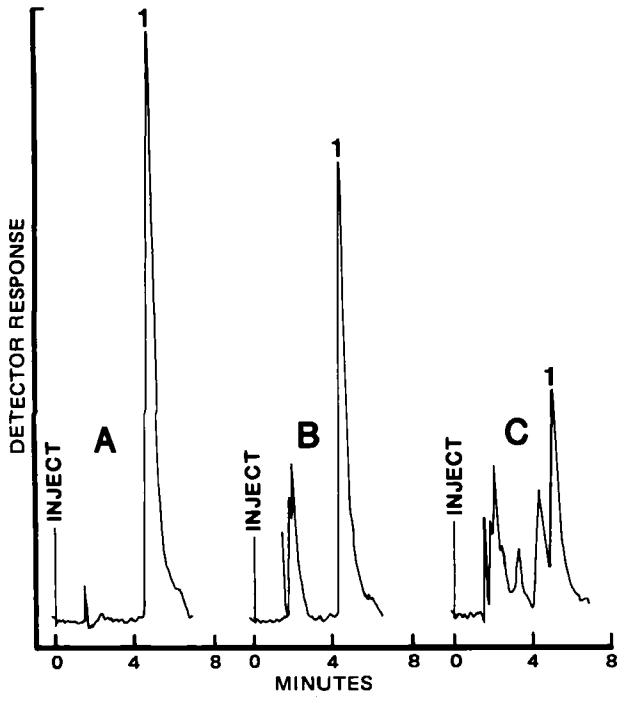

Figure 1—*Typical chromatograms. Peak 1 is from mezlocillin and all others are unidentified. Key: (A) standard solution; (B, C) 4-day old solutions (solutions 12 and 6, respectively) when stored at room temperature.*

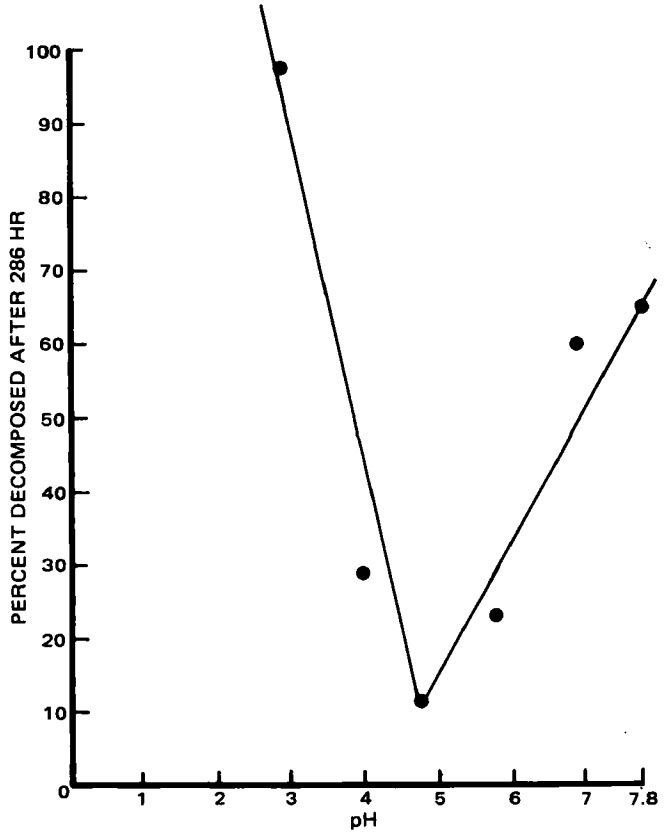

Figure 2—*A pH–rate profile curve from data of solutions 6–12 after 286 hr (~12 days) of storage at room temperature.*

assay solution (pH 2.9) was very fast. It is obvious that decomposition products from the side chain elute immediately after the solvent, while products from β-lactam ring hydrolysis elute immediately before the intact drug (peak 1 in Fig. 1).

The results indicate (Table II, solutions 1 and 2) that the manufacturer's recommended expiration of 48 hr (1) for intravenous solution prepared in 5% dextrose–0.9% NaCl can be extended to 96 hr with a loss in potency of <5%. Under refrigeration, the expiration date may be ex-

Table II—Assay Results and pH Values of Mezlocillin Sodium Solutions at Room Temperature

	Results at 25 ± 1°									
	Day 0		Day 1		Day 4		Day 7		Day 12 (286 hr)	
Solution[a]	pH	Found, %	pH	Found, %	pH	Found, %	pH	Found, %	pH	Found[b], %
1	4.8	100.5	4.7	100.3	4.7	96.3	4.7	90.5	—[c]	—[c]
2	4.8	99.2	4.7	98.8	4.5	96.9	4.5	90.5	—[c]	—[c]
6	2.9	100.6	2.9	80.6	2.9	34.6	2.9	14.0	2.9	2.5
7	4.0	101.1	4.0	100.5	4.0	91.8	4.0	83.3	4.0	71.6
8	4.8	100.9	4.8	100.7	4.8	97.7	4.8	97.2	4.8	89.1
9	4.8	100.6	4.8	101.2	4.8	98.1	4.8	96.9	4.8	87.6
10	5.8	101.3	5.8	101.3	5.8	96.2	5.8	88.6	5.8	77.0
11	6.9	100.6	6.9	100.3	6.9	84.8	6.9	68.3	6.9	40.2
12	7.8	101.0	7.8	100.6	7.8	83.5	7.8	65.2	7.7	35.4

[a] For composition of solution, see Table I. [b] All solutions were clear to the last day of testing. [c] Not determined on this day.

Table III—Assay Results and pH Values of Mezlocillin Sodium Solutions at 5° and −10°

	Results at 5 ± 1°													
	Day 0		Day 1		Day 4		Day 7		Day 14		Day 28		Day 36	
Solution[a]	pH	Found, %	pH	Found, %	pH	Found, %	pH	Found, %	pH	Found, %	pH	Found, %	pH	Found[b], %
1	4.8	100.5	—[c]	—[c]	—[c]	—[c]	4.7	100.1	4.7	100.0	4.7	98.9	4.6	97.8
2	4.8	99.2	—[c]	—[c]	—[c]	—[c]	4.7	99.4	4.7	99.2	4.5	98.3	4.4	96.9
3	4.8	97.8	4.7	97.5	4.7	97.3	—[c]	—[c]	4.7	97.0				
4	4.4	98.0	4.4	97.8	4.4	98.0	—[c]	—[c]	4.4	94.3				
5	5.2	98.0	5.2	98.0	5.2	97.7	—[c]	—[c]	5.1	95.1				

	Results at −10 ± 1°							
	Day 0		Day 28		Day 60		Day 60[d]	
Solution[a]	pH	Found, %	pH	Found, %	pH	Found, %	pH	Found[b], %
1	4.8	100.5	4.8	100.2	4.8	93.5	4.8	93.3
2	4.8	99.2	4.8	99.4	4.7	98.3	4.7	98.3

[a] For composition of solution, see Table I. [b] All solutions were clear to the last day of testing. [c] Not determined on this day. [d] These results are of solutions which were thawed using a microwave oven. For details, see text.

tended (Table III, solutions 1 and 2) to 36 days *versus* 7 days as recommended (1). The loss in potency after a 36-day storage was <3.2%, and the samples were clear. The expiration date for the frozen samples may be extended to 60 days (solutions 1 and 2, Table III) *versus* 28 days as recommended (1) by the manufacturer. There was a loss of <2 and 7% in potency in 60 days for solutions in 0.9% NaCl and 5% dextrose, respectively. There was no significant change in pH values, and the solutions were clear. Furthermore, the frozen samples can be thawed in <4 min using a microwave oven, without any observable decomposition.

It is interesting to point out that the manufacturer has recommended (1) an expiration of 24 hr under refrigeration for solutions in 5% fructose and 10% dextrose *versus* 7 days for solution in 5% dextrose. In our investigations (Table III, solutions 3–5), there was no difference in the stability of these three solutions. No decomposition was found in any sample for up to 4 days under refrigeration, which was also evident from the absence of any additional peak(s) in the chromatograms. After 14 days of storage there was only slightly more decomposition of drug in solutions containing either 10% dextrose or 5% fructose *versus* 5% dextrose (Table III, solutions 3–5). There were no significant changes in pH values, and all solutions were clear.

The optimum pH of stability (Fig. 2) appears to be ~4.8. The phosphate buffer did not catalyze the reaction (solutions 8 and 9, Table III). Trials to treat the data mathematically using first-order equations were not successful, which may be due to the complexity of the reaction as evidenced by a number of new peaks (Fig. 1C) in the chromatogram. The general information about the degradation of penicillins is available in the literature (2, 3).

REFERENCES

(1) "Mezlin, Circular 1878," Miles Pharmaceuticals, West Haven, Conn., Nov. 1981.

(2) K. Shimazaki, M. Ishioka, and M. Suda, *Int. J. Pharm.*, 11, 71 (1982).

(3) K. A. Connors, G. L. Amidon, and L. Kennon, "Chemical Stability of Pharmaceuticals," Wiley, New York, N.Y. 1979, p. 185.

COMMUNICATIONS

Buccal Absorption of Protirelin: An Effective Way to Stimulate Thyrotropin and Prolactin

Keyphrases □ Protirelin—buccal absorption, stimulation of thyrotropin and prolactin, use as a diagnostic tool □ Buccal absorption—evaluation of protirelin, use as a diagnostic tool, measurement of thyrotropin and prolactin stimulation □ Thyrotropin and prolactin stimulation—buccal absorption of protirelin, use as a diagnostic tool

To the Editor:

Most of the biologically active oligopeptides are almost, or completely, inactive if administered perorally. This can be partly attributed to low chemical stability in the course of intestinal passage, and partly to low invasion rates along with rapid plasma degradation. For the same reasons some peptides, like thyrotropin-releasing hormone (TRH) (protirelin), need extremely high peroral doses in order to stimulate biological response. Therefore, intravenous injection is the most common form of peptide administration. However, few studies on nasal (1) and rectal (2) administration have been reported. The purpose of this investigation was to evaluate buccal absorption of protirelin as a model peptide. The major objective was to set the groundwork for future research on buccal peptide delivery and absorption. This study also evaluated buccal protirelin as a diagnostic tool.

Thyroid gland diagnostics by protirelin is mainly a domain of the intravenous test, although some doubts have emerged due to serious side effects (3–5). On the other hand, the peroral protirelin test exhibits only slow response at high doses, and usually needs a 3-hr period to attain maximum stimulation. This is often considered inconvenient for routine clinical diagnostics. Therefore, buccal protirelin could become an appropriate supplement with both intravenous and peroral protirelin, if absorbed properly. This study will show the overall feasibility of buccal protirelin for use in thyroid diagnostics. Buccal absorption will be followed by monitoring thyrotropin and prolactin stimulation.

Ten clinically healthy volunteers, five males and five females, took part in the study. The age range was 23–35 years. For all volunteers an euthyroid state was certified by determinations of triiodothyronine, thyroxine, and thyroxine-binding globulin. The body weights of all volunteers were within normal limits of the ideal body weight according to Broca. All tests were performed beginning at 2 p.m.

For the intravenous test, 200 μg of protirelin[1] was injected in the antecubital vein. Blood samples were taken immediately before and 30 min after injection. For buccal application a polytef disk was prepared with a diameter of ~3.5 cm, corresponding to an area of ~10 cm^2 and a height of 1 cm. The disk had a central circular depression depth of 4 mm, leaving an elevated rim. A previously water-soaked filter paper disk was placed into the depression, and 20 mg of crystalline protirelin[2] was spread onto the filter paper. The protirelin dissolved immediately. Subsequently, the device was put into contact with the buccal mucosa. After 30 min the device was removed, and the mouth was thoroughly washed with tap water. Blood samples were taken at 0, 30, 60, 120, and 180 min *via* a cannula placed into the antecubital vein.

After centrifugation the plasma was separated from the blood and stored at −20° until analysis of thyrotropin and prolactin.

Measurements of thyrotropin[3], prolactin[4], thyroxine-binding globulin[5], triiodothyronine[6], and thyroxine[6] were performed in duplicate using commercially available radioimmunoassays. Standard errors of the radioimmunoassays were from 6 to 8% within kits and from 3 to 9% between kits. A second, but slightly modified, test was per-

[1] Antepan, Henning, D-Berlin.
[2] Hoechst, D-Frankfurt.
[3] TSHK-PR, CIS-CEA-Sorin, I-Saluggia.
[4] PROLK-PR, CIS-CEA-Sorin, I-Saluggia.
[5] RIA-gnost TBG-kit, Behringwerke, D-Marburg.
[6] ARIA II, Becton and Dickinson, Paramus N.J.

0022-3549/83/1200-1481$01.00/0

tended (Table III, solutions 1 and 2) to 36 days *versus* 7 days as recommended (1). The loss in potency after a 36-day storage was <3.2%, and the samples were clear. The expiration date for the frozen samples may be extended to 60 days (solutions 1 and 2, Table III) *versus* 28 days as recommended (1) by the manufacturer. There was a loss of <2 and 7% in potency in 60 days for solutions in 0.9% NaCl and 5% dextrose, respectively. There was no significant change in pH values, and the solutions were clear. Furthermore, the frozen samples can be thawed in <4 min using a microwave oven, without any observable decomposition.

It is interesting to point out that the manufacturer has recommended (1) an expiration of 24 hr under refrigeration for solutions in 5% fructose and 10% dextrose *versus* 7 days for solution in 5% dextrose. In our investigations (Table III, solutions 3–5), there was no difference in the stability of these three solutions. No decomposition was found in any sample for up to 4 days under refrigeration, which was also evident from the absence of any additional peak(s) in the chromatograms. After 14 days of storage there was only slightly more decomposition of drug in solutions containing either 10% dextrose or 5% fructose *versus* 5% dextrose (Table III, solutions 3–5). There were no significant changes in pH values, and all solutions were clear.

The optimum pH of stability (Fig. 2) appears to be ~4.8. The phosphate buffer did not catalyze the reaction (solutions 8 and 9, Table III). Trials to treat the data mathematically using first-order equations were not successful, which may be due to the complexity of the reaction as evidenced by a number of new peaks (Fig. 1C) in the chromatogram. The general information about the degradation of penicillins is available in the literature (2, 3).

REFERENCES

(1) "Mezlin, Circular 1878," Miles Pharmaceuticals, West Haven, Conn., Nov. 1981.

(2) K. Shimazaki, M. Ishioka, and M. Suda, *Int. J. Pharm.*, 11, 71 (1982).

(3) K. A. Connors, G. L. Amidon, and L. Kennon, "Chemical Stability of Pharmaceuticals," Wiley, New York, N.Y. 1979, p. 185.

COMMUNICATIONS

Buccal Absorption of Protirelin: An Effective Way to Stimulate Thyrotropin and Prolactin

Keyphrases □ Protirelin—buccal absorption, stimulation of thyrotropin and prolactin, use as a diagnostic tool □ Buccal absorption—evaluation of protirelin, use as a diagnostic tool, measurement of thyrotropin and prolactin stimulation □ Thyrotropin and prolactin stimulation—buccal absorption of protirelin, use as a diagnostic tool

To the Editor:

Most of the biologically active oligopeptides are almost, or completely, inactive if administered perorally. This can be partly attributed to low chemical stability in the course of intestinal passage, and partly to low invasion rates along with rapid plasma degradation. For the same reasons some peptides, like thyrotropin-releasing hormone (TRH) (protirelin), need extremely high peroral doses in order to stimulate biological response. Therefore, intravenous injection is the most common form of peptide administration. However, few studies on nasal (1) and rectal (2) administration have been reported. The purpose of this investigation was to evaluate buccal absorption of protirelin as a model peptide. The major objective was to set the groundwork for future research on buccal peptide delivery and absorption. This study also evaluated buccal protirelin as a diagnostic tool.

Thyroid gland diagnostics by protirelin is mainly a domain of the intravenous test, although some doubts have emerged due to serious side effects (3–5). On the other hand, the peroral protirelin test exhibits only slow response at high doses, and usually needs a 3-hr period to attain maximum stimulation. This is often considered inconvenient for routine clinical diagnostics. Therefore, buccal protirelin could become an appropriate supplement with both intravenous and peroral protirelin, if absorbed properly. This study will show the overall feasibility of buccal protirelin for use in thyroid diagnostics. Buccal absorption will be followed by monitoring thyrotropin and prolactin stimulation.

Ten clinically healthy volunteers, five males and five females, took part in the study. The age range was 23–35 years. For all volunteers an euthyroid state was certified by determinations of triiodothyronine, thyroxine, and thyroxine-binding globulin. The body weights of all volunteers were within normal limits of the ideal body weight according to Broca. All tests were performed beginning at 2 p.m.

For the intravenous test, 200 μg of protirelin[1] was injected in the antecubital vein. Blood samples were taken immediately before and 30 min after injection. For buccal application a polytef disk was prepared with a diameter of ~3.5 cm, corresponding to an area of ~10 cm^2 and a height of 1 cm. The disk had a central circular depression depth of 4 mm, leaving an elevated rim. A previously water-soaked filter paper disk was placed into the depression, and 20 mg of crystalline protirelin[2] was spread onto the filter paper. The protirelin dissolved immediately. Subsequently, the device was put into contact with the buccal mucosa. After 30 min the device was removed, and the mouth was thoroughly washed with tap water. Blood samples were taken at 0, 30, 60, 120, and 180 min *via* a cannula placed into the antecubital vein.

After centrifugation the plasma was separated from the blood and stored at −20° until analysis of thyrotropin and prolactin.

Measurements of thyrotropin[3], prolactin[4], thyroxine-binding globulin[5], triiodothyronine[6], and thyroxine[6] were performed in duplicate using commercially available radioimmunoassays. Standard errors of the radioimmunoassays were from 6 to 8% within kits and from 3 to 9% between kits. A second, but slightly modified, test was per-

[1] Antepan, Henning, D-Berlin.
[2] Hoechst, D-Frankfurt.
[3] TSHK-PR, CIS-CEA-Sorin, I-Saluggia.
[4] PROLK-PR, CIS-CEA-Sorin, I-Saluggia.
[5] RIA-gnost TBG-kit, Behringwerke, D-Marburg.
[6] ARIA II, Becton and Dickinson, Paramus N.J.

0022-3549/83/1200-1481$01.00/0

Table I—Baseline and Stimulation Levels of Thyrotropin after Buccal Application of Protirelin

Subject[a]	Intravenous Test[b] (min)		Buccal Application[c] (min)					
	0	30	0	15	30	60	120	180
A	1.8	8.9	1.6	—	1.8	4.9	4.1	3.0
A[d]	—	—	1.4	2.1	2.9	5.7	5.4	3.4
B	1.8	7.9	1.7	—	3.3	4.2	4.8	6.8
B[d]	—	—	1.5	1.7	3.0	3.8	2.5	2.7
C	1.8	9.5	1.6	—	4.4	5.5	9.7	12.8
D	1.0	4.0	1.4	—	2.4	3.2	2.4	2.6
E	1.4	4.9	1.2	—	2.5	3.4	2.9	4.9
F	1.9	8.7	1.6	—	4.3	6.2	5.6	4.9
G	4.3	25.1	5.0	—	10.8	17.5	28.0	29.4
H	1.0	4.7	1.1	—	2.8	10.9	5.7	7.2
I	1.7	5.9	0.9	—	5.6	5.0	6.2	7.9
J	3.4	20.3	2.7	—	3.0	6.1	5.0	4.4

[a] A–E = male; F–J = female. [b] Intravenous dose = 0.2 mg of protirelin; plasma levels in μU/ml. [c] Buccal dose = 20 mg of protirelin; plasma levels in μU/ml. [d] Extra test under removal of excess saliva.

Table II—Baseline and Stimulation Levels of Prolactin after Buccal Application of Protirelin

Subject[a]	Intravenous Test[b] (min)		Buccal Application[c] (min)					
	0	30	0	15	30	60	120	180
A	7.6	27.0	7.0	—	13.0	24.4	11.9	10.5
A[d]	—	—	7.1	8.1	14.3	25.3	16.9	10.3
B	10.1	36.0	9.3	—	31.2	22.7	16.5	13.6
B[d]	—	—	6.4	9.5	14.3	13.4	10.1	8.4
C	<3.0	7.6	<3.0	—	<3.0	<3.0	3.6	<3.0
D	3.0	24.5	5.2	—	11.7	14.9	9.8	7.4
E	5.7	23.5	7.3	—	15.8	13.1	7.2	13.1
F	18.2	44.0	5.9	—	26.0	24.6	14.0	12.3
G	11.6	44.0	14.8	—	35.7	31.4	27.6	31.8
H	7.4	17.6	8.4	—	12.3	26.4	10.2	8.3
I	7.8	30.8	6.2	—	31.3	18.1	21.4	12.8
J	38[e]	90[e]	10.5	—	19.7	33.3	16.5	11.0

[a] A–E = male; F–J = female. [b] Intravenous dose = 0.2 mg of protirelin; plasma levels in ng/ml. [c] Buccal dose = 20 mg of protirelin; plasma levels in ng/ml. [d] Extra test under removal of excess saliva. [e] Increased prolactin levels due to metoclopramide medication previous to intravenous test; data excluded from further evaluation; no metoclopramide medication previous to buccal application.

formed with two of the subjects. In addition to the aforementioned procedure, excess saliva was constantly withdrawn by aspiration to prevent undesirable GI absorption of swallowed protirelin, which might stimulate thyrotropin and prolactin after intestinal absorption. Because plasma thyrotropin and prolactin levels of the subject could not be considered normally distributed, the Wilcoxin-Mann-Whitney *U*-test was used for statistical evaluation (6).

The results of the study in terms of the baseline levels and the levels after stimulation by intravenous and buccal application of protirelin are shown in Table I for thyrotropin, and Table II for prolactin. After intravenous application of protirelin, the thyrotropin concentrations increased from a baseline range of 1.0–4.3 μU/ml to a 30-min stimulation range of 4.0–25.1 μU/ml. After buccal application there was a rise from the baseline range of 0.9–5 μU/ml to a 30-min range of 1.8–10.8 μU/ml and to a 60-min range of 3.2–17.5 μU/ml. The subsequent part of the plasma profiles did not show a general tendency among subjects: in some subjects there was a further increase of thyrotropin, whereas in others there was a drop-off. (A graph of the profile is shown in Fig. 1.) The increase from the initial values to the 30-min and the 60-min values is significant, as evidenced by the *U*-test ($p = 0.01$). With respect to prolactin, the intravenous test gave rise to levels in the range of 7.6–44.0 ng/ml after 30 min, with the baseline between 3.0–18.2 ng/ml. In the case of buccal application, the baseline range was 5.2–14.8 ng/ml, whereas upon stimulation prolactin increased to 11.7–35.7 ng/ml after 30 min, and to 13.1–31.4 ng/ml after 60 min. One subject was omitted from further evaluation because several plasma levels were below the limit of analytical sensitivity at 3.0 ng/ml of prolactin. In the subsequent part of the prolactin plasma profiles there was a decrease in levels in all but one subject (see Fig. 1). Like thyrotropin, the increase of prolactin above its baseline level after buccal protirelin application is statistically significant ($p = 0.01$) for the 30-min range, as well as for the 60-min range.

An additional set of data on two subjects showed that an increase of thyrotropin and prolactin levels also could be achieved when the buccal application of protirelin is accompanied by a constant withdrawal of excess saliva from the oral cavity. The values are presented in Table I; for graphical depiction see Fig. 2. It is also interesting to note that following the intravenous test all subjects reported side effects such as nausea, urge to urinate, and facial flushing, but no side effects were observed after buccal protirelin administration.

The conclusion drawn from the presented data is that protirelin is readily absorbed *via* the buccal mucosa, as indicated by a significant stimulation of both thyrotropin and prolactin. The response pattern observed seems to indicate that females exhibit a greater stimulation by protirelin than males do and that peak levels appear more rapidly with prolactin than with thyrotropin. This parallels the typical intravenous stimulation characteristics (3). Compared with the peroral application of protirelin, buccal absorption leads to earlier attainment of maximum thyrotropin and prolactin levels, at half the dose usually taken for the peroral test. Apparently, there is no difference in the maximum increments achieved by both routes of administration, as indicated by comparison with literature data on peroral protirelin stimulation (7).

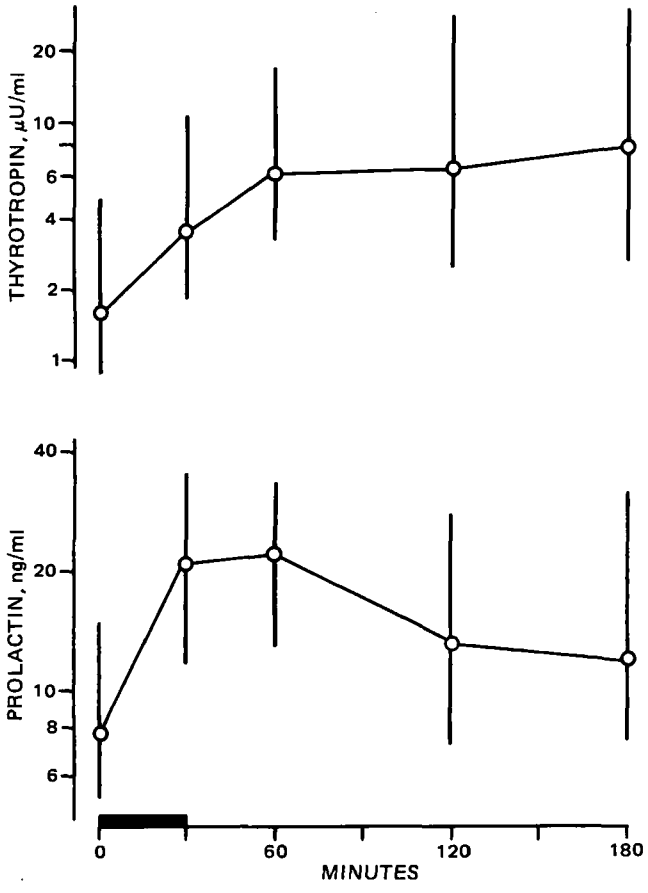

Figure 1—*Plasma thyrotropin and prolactin profiles after buccal application of 20 mg of protirelin. Circles are geometric means of 10 subjects (thyrotropin) and nine subjects (prolactin), respectively. Vertical bars indicate observed range. Horizontal bar indicates time of application.*

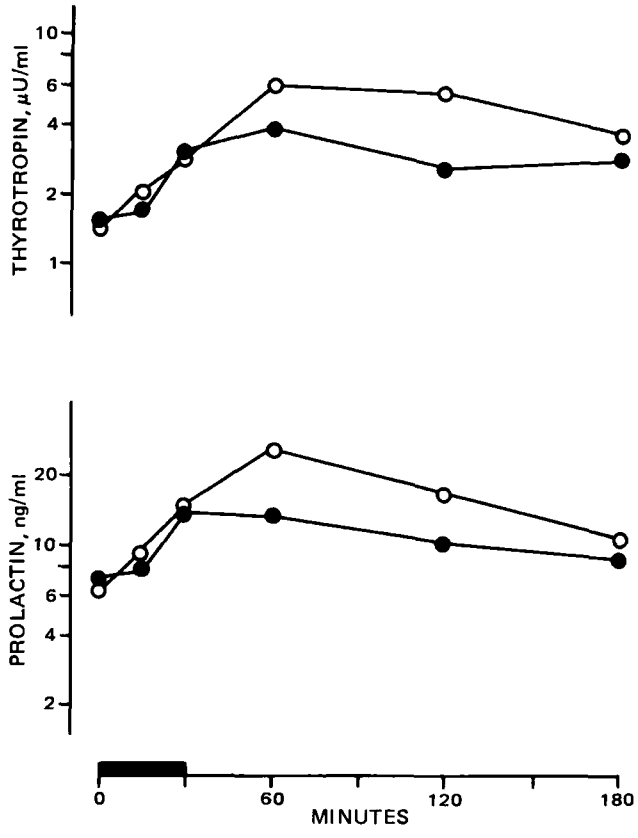

Figure 2—*Plasma thyrotropin and prolactin profiles after buccal application of protirelin under constant withdrawal of excess saliva. Filled and open circles indicate two subjects. Horizontal bar indicates time of application.*

These results also reveal that buccal protirelin administration is a clear alternative to both the peroral and the intravenous tests. As compared with the intravenous test, the obvious advantage of buccal protirelin is the fact that none of the aforementioned side effects were observed. This appears to be due to the lower incremental increase of plasma protirelin and, therefore, to the more moderate stimulation kinetics after buccal administration. In addition, buccal protirelin with a maximum stimulation 30 to 60 min after application, provokes a faster response than the peroral test, which usually requires a period of 2–3 hr to reach its peak (3, 7). We therefore suggest this test be evaluated for diagnostic use. Suitable dosage forms are presently under investigation.

(1) R. Ziegler, G. Holz, F. Raue, and W. Streibl, *Mol. Endocrinol.*, **1**, 293 (1979).

(2) T. Nishihata, J. H. Rytting, T. Higuchi, and L. Caldwell, *J. Pharm. Pharmacol.*, **33**, 334 (1980).

(3) L. J. DeGroot, "Endocrinology," vol. 1, Grune & Stratton, New York, N.Y., 1979, p. 197.

(4) K. Madea, and K. Tanimoto, *Lancet*, **i**, 1058 (1981).

(5) M. Grussendorf, R. VonBlittersdorf, F. Raue, and M. Hüfner, *Acta Endocrinol. (Copenhagen) 99 Suppl.* **246**, 140 (1982).

(6) L. Sachs, "Angewandte Statistik," 5th ed., Springer, Berlin, 1978, p. 230.

(7) P. Bottermann, C. Glogger, and U. Hendergott, *Med. Klin.*, **74**, 1485 (1979).

R. Anders
H. P. Merkle ˣ

Institute of Pharmaceutical Technology and Biopharmaceutics

W. Schurr
R. Ziegler

Department of Internal Medicine (Endocrinology)
University of Heidelberg
D-6900 Heidelberg
Federal Republic Germany

Received December 6, 1982.
Accepted for publication January 13, 1983.
Crystalline thyroliberin was generously supplied by Hoechst AG. Special gratitude is owed to Dr. M. von der Ohe.

Practical Solution to the Michaelis–Menten Equation

Keyphrases □ Michaelis–Menten equation—mathematical solution

To the Editor:

The mathematical solution of the Michaelis–Menten equation apparently only exists in implicit form. The explicit form required in practical usage is obtained by numerical means either using numerical integration or by solving the implicit form using a root-solving algorithm. To avoid this numerical complexity methods have been proposed which are based on a numerical solution in-

0022-3549/83/1200-1483$01.00/0

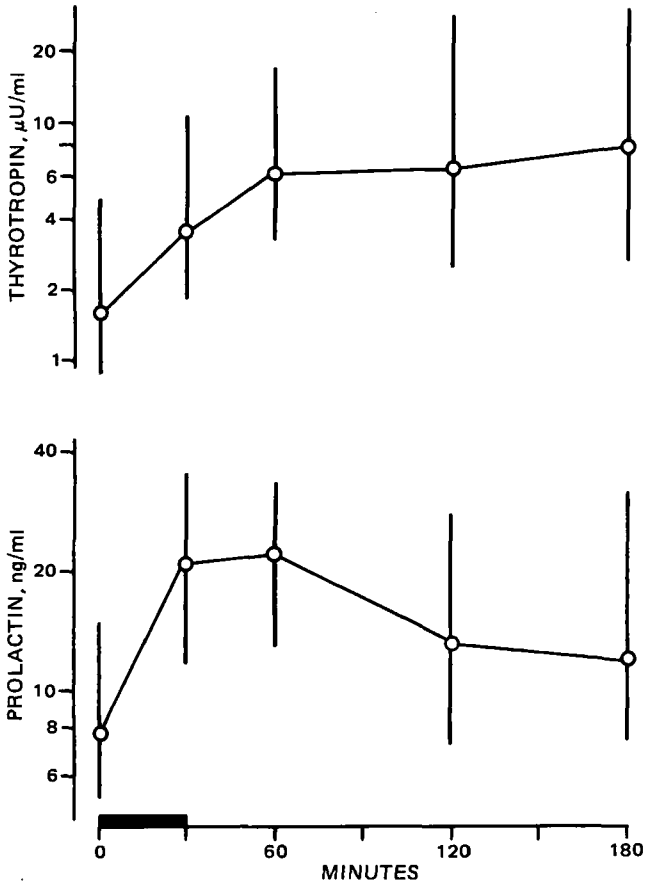

Figure 1—*Plasma thyrotropin and prolactin profiles after buccal application of 20 mg of protirelin. Circles are geometric means of 10 subjects (thyrotropin) and nine subjects (prolactin), respectively. Vertical bars indicate observed range. Horizontal bar indicates time of application.*

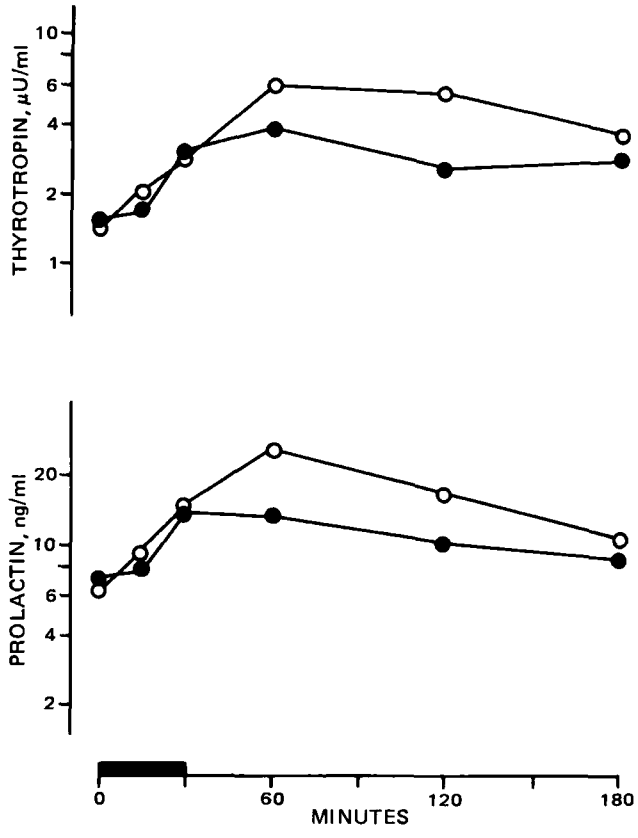

Figure 2—*Plasma thyrotropin and prolactin profiles after buccal application of protirelin under constant withdrawal of excess saliva. Filled and open circles indicate two subjects. Horizontal bar indicates time of application.*

These results also reveal that buccal protirelin administration is a clear alternative to both the peroral and the intravenous tests. As compared with the intravenous test, the obvious advantage of buccal protirelin is the fact that none of the aforementioned side effects were observed. This appears to be due to the lower incremental increase of plasma protirelin and, therefore, to the more moderate stimulation kinetics after buccal administration. In addition, buccal protirelin with a maximum stimulation 30 to 60 min after application, provokes a faster response than the peroral test, which usually requires a period of 2–3 hr to reach its peak (3, 7). We therefore suggest this test be evaluated for diagnostic use. Suitable dosage forms are presently under investigation.

(1) R. Ziegler, G. Holz, F. Raue, and W. Streibl, *Mol. Endocrinol.*, **1**, 293 (1979).

(2) T. Nishihata, J. H. Rytting, T. Higuchi, and L. Caldwell, *J. Pharm. Pharmacol.*, **33**, 334 (1980).

(3) L. J. DeGroot, "Endocrinology," vol. 1, Grune & Stratton, New York, N.Y., 1979, p. 197.

(4) K. Madea, and K. Tanimoto, *Lancet*, **i**, 1058 (1981).

(5) M. Grussendorf, R. VonBlittersdorf, F. Raue, and M. Hüfner, *Acta Endocrinol. (Copenhagen) 99 Suppl.* **246**, 140 (1982).

(6) L. Sachs, "Angewandte Statistik," 5th ed., Springer, Berlin, 1978, p. 230.

(7) P. Bottermann, C. Glogger, and U. Hendergott, *Med. Klin.*, **74**, 1485 (1979).

R. Anders
H. P. Merkle ˣ

Institute of Pharmaceutical Technology and Biopharmaceutics

W. Schurr
R. Ziegler

Department of Internal Medicine (Endocrinology)
University of Heidelberg
D-6900 Heidelberg
Federal Republic Germany

Received December 6, 1982.
Accepted for publication January 13, 1983.
Crystalline thyroliberin was generously supplied by Hoechst AG. Special gratitude is owed to Dr. M. von der Ohe.

Practical Solution to the Michaelis–Menten Equation

Keyphrases □ Michaelis–Menten equation—mathematical solution

To the Editor:

The mathematical solution of the Michaelis–Menten equation apparently only exists in implicit form. The explicit form required in practical usage is obtained by numerical means either using numerical integration or by solving the implicit form using a root-solving algorithm. To avoid this numerical complexity methods have been proposed which are based on a numerical solution in-

0022-3549/83/1200-1483$01.00/0

volving the use of a table of function values (1, 2). Such methods may be useful when operating a nonprogrammable calculator. However, if several calculations are required, such as in plotting curves, the methods become quite tedious and slow because of the repetitive readings of the table values. Furthermore, the published tables are also of limited usefulness because they do not extend far enough to include all values that may occur in clinical practice (1, 2). The following explicit method does not have this limitation. It enables the Michaelis–Menten equation to be evaluated quickly without the use of tables, numerical integration, or iterative techniques.

The solution to the Michaelis–Menten equation:

$$\frac{dC}{dt} = -V_m C/(K_m + C) \qquad \text{(Eq. 1)}$$

is accurately evaluated using the algorithm:

$$C(t) = K_m G(x) \qquad \text{(Eq. 2)}$$

where: $x = V_m t/K_m - C(0)/K_m + \ln [K_m/C(0)]$ (Eq. 3)

The G function in Eq. 2 is for $x \leq -1.9$ evaluated as:

$$G(x) = -x - \ln\left[-x + \frac{a_1 x}{a_2 - x} \ln(-x)\right] \qquad \text{(Eq. 4)}$$

$$a_1 = 0.99419 \qquad \text{(Eq. 5)}$$

$$a_2 = 1.1195 \qquad \text{(Eq. 6)}$$

and for $x > -1.9$:

$$G(x) = \exp\{-x - b_1 \exp(-b_2 x)/[b_3 + \exp(-b_4 x)]\} \qquad \text{(Eq. 7)}$$

$$b_1 = 1.1249 \qquad \text{(Eq. 8)}$$

$$b_2 = 1.0250 \qquad \text{(Eq. 9)}$$

$$b_3 = 0.98405 \qquad \text{(Eq. 10)}$$

$$b_4 = 0.76577 \qquad \text{(Eq. 11)}$$

The maximum global error in the evaluation of the Michaelis–Menten equation using Eq. 2 is 0.078% which is more than sufficient for practical applications.

Derivation—The Michaelis–Menten equation given by Eq. 1 can be transformed by setting:

$$C = K_m y(x) \qquad \text{(Eq. 12)}$$

with x given by Eq. 3. Then:

$$\frac{dC}{dt} = K_m \frac{dy}{dx}\frac{dx}{dt} = K_m \frac{dy}{dx}\frac{V_m}{K_m} = -\frac{V_m K_m y}{K_m + K_m y} \qquad \text{(Eq. 13)}$$

The last equality of Eq. 13 simplifies to:

$$\frac{dy}{dx} = -\frac{y}{1+y} \qquad \text{(Eq. 14)}$$

Separating variables and integration of Eq. 14 gives:

$$\ln y - \ln y_0 + (y - y_0) = -(x - x_0) \qquad \text{(Eq. 15)}$$

or

$$\ln y + y + x = \ln y_0 + y_0 + x_0 \qquad \text{(Eq. 16)}$$

The right-hand side of Eq. 16 is zero since according to Eqs. 12 and 3:

$$\ln y_0 + y_0 + x_0 = \ln [C(0)/K_m] + C(0)/K_m + (-C(0)/K_m + \ln [K_m/C(0)]) = 0 \qquad \text{(Eq. 17)}$$

Thus, Eq. 16 becomes:

$$\ln y(x) + y(x) = -x \qquad \text{(Eq. 18)}$$

Exponentiating both sides yields:

$$y(x) \exp[y(x)] - exp(-x) = 0 \qquad \text{(Eq. 19)}$$

The function $y(x)$ is the same as Toothill's function ϕ and Beal's function F with a change in sign of x; *i.e.*, $y(x) = F(-x) = \phi(-x)$ (1, 2). The implicit, parameterless function $y(x)$ can be approximated in many ways using various standard transcendental functions. The approximation $y(x) \simeq G(x)$ presented (Eqs. 4 and 7) appears to be a reasonable compromise between simplicity and accuracy. It is derived from the following considerations. From Eq. 18 it follows that:

$$y = -x - \ln y \qquad \text{(Eq. 20)}$$

by substituting the right-hand side expression for y on the right-hand side yields:

$$y = -x - \ln(-x - \ln y) \qquad \text{(Eq. 21)}$$

This equation can be used as an approximation for $y(x)$ if a sufficiently accurate approximation for $\ln y$ is used. By empirical numerical means it was found that for $x < 0$ $\ln y$ is quite well approximated by the function:

$$\ln y \simeq \frac{a_1 x}{a_2 - x} \ln(-x) \qquad \text{(Eq. 22)}$$

with a_1 and $a_2 \simeq 1$. Inserting this equation into Eq. 21 yields Eq. 3.

For positive values of x it is more accurate to use Eq. 19 in rearranged form:

$$y = \exp[-x - y] \qquad \text{(Eq. 23)}$$

This equation (Eq. 19) can be used to approximate $y(x)$ when a sufficiently accurate approximation for $y(x)$ is substituted on the right-hand side of Eq. 23. Previous research by the investigators involving empirical approximations of drug level profiles in Michaelis–Menten kinetics suggests that an empirical function of the form:

$$y \simeq b_1 \exp(-b_2 x)/[b_3 + \exp(-b_4 x)] \qquad \text{(Eq. 24)}$$

should be a suitable approximation to use. This was indeed the case. Inserting Eq. 24 into Eq. 23 yields Eq. 7.

The strategy above of expanding and rearranging the functional relationship to be approximated serves the purpose of producing an expression for y which is very little sensitive to errors in the "primary approximation" (*i.e.*, errors in Eqs. 22 and 24). For example, substituting Eq. 22 into Eq. 21 leads to better approximations than substituting into Eq. 20. Similarly the "primary approximation" Eq. 24 may not give sufficiently accurate results by itself. However, when substituted into Eq. 23 an excellent approximation can be obtained.

The constants a_1 and a_2 of Eq. 4 were obtained using FUNFIT (3) by minimizing the sum of squares expression:

$$ss = \sum_i [y(x_i) - G(x_i)]^2 \qquad \text{(Eq. 16)}$$

with x_i ranging from −1.9 to −8.0 in steps of 0.1. The $y(x)$ function was evaluated to an accuracy of at least six significant digits from Eq. 15 using Brent's numerical root-solving algorithm (4). The constants $b_1 - b_4$ of Eq. 7 were similarly evaluated with x_i ranging from −1.9 to 8.0 in steps of 0.1. The switch point $x = -1.9$ in the formula for $G(x)$ was derived empirically from preliminary observations which showed Eq. 4 starts to deviate significantly from $y(x)$ for $x > -1.9$, and the same is the case for Eq. 7 for $x < -1.9$. The maximum relative error $\epsilon = |y(x) - G(x)|/y(x)$ of Eq. 4 with the constants given is 0.078% ($x = -1.9$) in the range $x = -1.9$ to −8.0. From a mathematical analysis of Eq. 4 it can be shown that the relative error will continue to decrease beyond $x = -8$. This was confirmed by evaluating ϵ for $x = -8$ to −20. The maximum relative error for Eq. 7 with the constants given is 0.064% ($x = 2.2$) in the range −1.9–8. The relative error continues to decrease beyond $x = 8$ as expected from Eq. 7, and at about $x = 14$ reaches convergence and starts to oscillate tightly around the "machine precision value."

(1) S. L. Beal, *J. Pharmacokinet. Biopharm.*, **10**, 109 (1982).
(2) J. P. R. Toothill, "Progress in Industrial Microbiology," Vol. 2, Heywood and Company Ltd., London, 1960, p. 105.
(3) P. Veng-Pedersen, *J. Pharmacokinet. Biopharm.*, **5**, 513 (1977).
(4) R. P. Brent, *The Computer Journal*, **14**, 422 (1971).

Peter Veng-Pedersen[x]
Luis Suaréz
Division of Pharmacokinetics
School of Pharmacy and Pharmacal Sciences
Purdue University
West Lafayette, IN 47907

Received January 24, 1983.
Accepted for publication August 23, 1983.

Pan Abrasion and Polymorphism of Titanium Dioxide in Coating Suspensions

Keyphrases □ Tablet-coating suspensions—titanium dioxide, pan abrasion from abrasive components □ Titanium dioxide—in coating suspensions, polymorphic modifications

To the Editor:

It is not generally recognized that aqueous tablet-coating suspensions may contain abrasive components which can cut into the surface of the coating pan causing deposition of metallic particles onto the tablets. Subsequent to a series of film-coating operations in a 24-in. coating pan[1], black specks were observed on the white tablet film coats derived from a commercial batch of color concentrate (Batch A)[2]. This phenomenon was not observed, however, when another batch of color concentrate (Batch B)[2] was employed. Isolation of the foreign material gave a positive test for iron, and it was confirmed that the actual rubbing of tablets coated with either batch against the pan surface produced black smudges. The streaks were, however, less intense on tablets coated with Batch B.

Titanium dioxide, an opacifier used in these aqueous film solutions, can exist in several polymorphic modifications, each with a different hardness (1). Anatase, for example, has a hardness on the Mohs' scale of 5.5–6, whereas rutile is in the range 6–6.5. For comparison, the common oxide of iron, hematite, gives values of 5–6 and magnetite, 5.5–6.5. The pan material itself, stainless steel 304, has a hardness range of 160–400 Brinnell (2). Conversion of the latter scale to the Mohs' scale (3) shows that the upper range lies somewhat below 6 on the Mohs' scale.

The Mohs' scale is a semiquantitative scale of hardness, which is a function of the elastic, plastic, and frictional properties of the surface. Materials with higher Mohs' numbers will scratch or abrade those with lower numbers.

In the range of Mohs' numbers considered here, the scale is linear and relatively sensitive, although hardness values tend to cluster at the high end. Abrasion or wear of the coating pan is essentially a surface phenomenon involving the removal of oxide films. A comparison of the Mohs' numbers shows that rutile is the harder of the two titanium dioxide polymorphs and would be expected to remove material through abrasion more readily than anatase. To confirm whether this could explain the observations, titanium dioxide was extracted from both batches of color concentrate and analyzed by X-ray powder diffraction. Batch A was found to contain 60:40 anatase/rutile in contrast to Batch B which was composed of 90:10 anatase/rutile.

Differences in surface roughness should theoretically not play a major role since, as the number of asperities in the film coating is increased, the number of contacting points would be increased proportionately. More scratches would be produced, but each would be of smaller cross-sectional area. This point was checked by measuring the advancing and receding contact angles of a series of liquids of varying surface tension on the film-coated tablet surfaces (4). There was no significant difference in surface roughness of films produced from either batch.

(1) "Handbook of Chemistry and Physics," 61st ed., CRC Press, Boca Raton, Fla., 1980–1981, pp. B202–207.
(2) R. B. Norden, in "Chemical Engineers' Handbook," 5th ed., R. H. Perry and C. H. Chelton, Eds., McGraw-Hill, New York, N.Y., 1973, chap. 23, p. 39.
(3) G. F. Kinney, "Engineering Properties and Applications of Plastics," Wiley, New York, N.Y.,1957, p. 137.
(4) W. A. Zisman, "Advances in Chemistry Series," #43, R. Gould, Ed., American Chemical Society, 1964, pp. 1–51.

Morton Rosoff
Pai-Chang Sheen[x]
Pharmacy Research and Development
Revlon Health Care Group
Tuckahoe, NY 10707

Received July 28, 1983.
Accepted for publication August 19, 1983.

[1] Accela-Cota, Thomas Engineering, Hoffman Estates, Ill.
[2] Opaspray K-1-7000, Batch A, No. 30345, Batch B No. 29486; Colorcon, West Point, Pa.

0022-3549/83/1200-1485$01.00/0

with x_i ranging from −1.9 to −8.0 in steps of 0.1. The $y(x)$ function was evaluated to an accuracy of at least six significant digits from Eq. 15 using Brent's numerical root-solving algorithm (4). The constants $b_1 - b_4$ of Eq. 7 were similarly evaluated with x_i ranging from −1.9 to 8.0 in steps of 0.1. The switch point $x = -1.9$ in the formula for $G(x)$ was derived empirically from preliminary observations which showed Eq. 4 starts to deviate significantly from $y(x)$ for $x > -1.9$, and the same is the case for Eq. 7 for $x < -1.9$. The maximum relative error $\epsilon = |y(x) - G(x)|/y(x)$ of Eq. 4 with the constants given is 0.078% ($x = -1.9$) in the range $x = -1.9$ to −8.0. From a mathematical analysis of Eq. 4 it can be shown that the relative error will continue to decrease beyond $x = -8$. This was confirmed by evaluating ϵ for $x = -8$ to −20. The maximum relative error for Eq. 7 with the constants given is 0.064% ($x = 2.2$) in the range −1.9–8. The relative error continues to decrease beyond $x = 8$ as expected from Eq. 7, and at about $x = 14$ reaches convergence and starts to oscillate tightly around the "machine precision value."

(1) S. L. Beal, *J. Pharmacokinet. Biopharm.*, **10**, 109 (1982).
(2) J. P. R. Toothill, "Progress in Industrial Microbiology," Vol. 2, Heywood and Company Ltd., London, 1960, p. 105.
(3) P. Veng-Pedersen, *J. Pharmacokinet. Biopharm.*, **5**, 513 (1977).
(4) R. P. Brent, *The Computer Journal*, **14**, 422 (1971).

Peter Veng-Pedersen[x]
Luis Suaréz
Division of Pharmacokinetics
School of Pharmacy and Pharmacal Sciences
Purdue University
West Lafayette, IN 47907

Received January 24, 1983.
Accepted for publication August 23, 1983.

Pan Abrasion and Polymorphism of Titanium Dioxide in Coating Suspensions

Keyphrases □ Tablet-coating suspensions—titanium dioxide, pan abrasion from abrasive components □ Titanium dioxide—in coating suspensions, polymorphic modifications

To the Editor:

It is not generally recognized that aqueous tablet-coating suspensions may contain abrasive components which can cut into the surface of the coating pan causing deposition of metallic particles onto the tablets. Subsequent to a series of film-coating operations in a 24-in. coating pan[1], black specks were observed on the white tablet film coats derived from a commercial batch of color concentrate (Batch A)[2]. This phenomenon was not observed, however, when another batch of color concentrate (Batch B)[2] was employed. Isolation of the foreign material gave a positive test for iron, and it was confirmed that the actual rubbing of tablets coated with either batch against the pan surface produced black smudges. The streaks were, however, less intense on tablets coated with Batch B.

Titanium dioxide, an opacifier used in these aqueous film solutions, can exist in several polymorphic modifications, each with a different hardness (1). Anatase, for example, has a hardness on the Mohs' scale of 5.5–6, whereas rutile is in the range 6–6.5. For comparison, the common oxide of iron, hematite, gives values of 5–6 and magnetite, 5.5–6.5. The pan material itself, stainless steel 304, has a hardness range of 160–400 Brinnell (2). Conversion of the latter scale to the Mohs' scale (3) shows that the upper range lies somewhat below 6 on the Mohs' scale.

The Mohs' scale is a semiquantitative scale of hardness, which is a function of the elastic, plastic, and frictional properties of the surface. Materials with higher Mohs' numbers will scratch or abrade those with lower numbers.

In the range of Mohs' numbers considered here, the scale is linear and relatively sensitive, although hardness values tend to cluster at the high end. Abrasion or wear of the coating pan is essentially a surface phenomenon involving the removal of oxide films. A comparison of the Mohs' numbers shows that rutile is the harder of the two titanium dioxide polymorphs and would be expected to remove material through abrasion more readily than anatase. To confirm whether this could explain the observations, titanium dioxide was extracted from both batches of color concentrate and analyzed by X-ray powder diffraction. Batch A was found to contain 60:40 anatase/rutile in contrast to Batch B which was composed of 90:10 anatase/rutile.

Differences in surface roughness should theoretically not play a major role since, as the number of asperities in the film coating is increased, the number of contacting points would be increased proportionately. More scratches would be produced, but each would be of smaller cross-sectional area. This point was checked by measuring the advancing and receding contact angles of a series of liquids of varying surface tension on the film-coated tablet surfaces (4). There was no significant difference in surface roughness of films produced from either batch.

(1) "Handbook of Chemistry and Physics," 61st ed., CRC Press, Boca Raton, Fla., 1980–1981, pp. B202–207.
(2) R. B. Norden, in "Chemical Engineers' Handbook," 5th ed., R. H. Perry and C. H. Chelton, Eds., McGraw-Hill, New York, N.Y., 1973, chap. 23, p. 39.
(3) G. F. Kinney, "Engineering Properties and Applications of Plastics," Wiley, New York, N.Y.,1957, p. 137.
(4) W. A. Zisman, "Advances in Chemistry Series," #43, R. Gould, Ed., American Chemical Society, 1964, pp. 1–51.

Morton Rosoff
Pai-Chang Sheen[x]
Pharmacy Research and Development
Revlon Health Care Group
Tuckahoe, NY 10707

Received July 28, 1983.
Accepted for publication August 19, 1983.

[1] Accela-Cota, Thomas Engineering, Hoffman Estates, Ill.
[2] Opaspray K-1-7000, Batch A, No. 30345, Batch B No. 29486; Colorcon, West Point, Pa.

0022-3549/83/1200-1485$01.00/0

N-Nitroso Compounds: Occurrence and Biological Effects. Edited by H. BARTSCH, I. K. O'NEILL, M. CASTEGNARO, and M. OKADA. International Agency on Cancer, Health and Biomedical Information Programme, World Health Organization, 1211 Geneva 27, Switzerland, 1982. 753 pp. 17 × 24 cm. Price $55.00 (Sw. Fr. 110).

This volume is comprised of the Proceedings of the 7th International Symposium on *N*-Nitroso Compounds held in Tokyo, September 1981. It includes 73 papers and draws from a wide range of scientific disciplines. Numerous experts present information on the formation, occurrence, and biological effects of *N*-nitroso compounds. Formation of *N*-nitroso compounds within the body is reported by several workers and is discussed in relation to the ingestion of various materials. Data are given on exposure to *N*-nitroso compounds in the general environment and from tobacco usage. New and important developments of methods and approaches are presented that could promote the understanding of basic mechanisms of carcinogenesis and which could also be readily applied to the detection and analysis of *N*-nitroso compounds or their precursors. Also presented are suggestions for possible future research on nitroso compounds. A possible drawback of the book is the limited coverage of nitrosoureas, an important group of compounds in cancer research and treatment.

The papers are short, easy to read, and most present considerable background information. Concise figures and tables are used when appropriate. There is an author index and a thorough subject index. A list of references is given at the end of each chapter to assist readers seeking additional information. This book, written entirely in English, contains an enormous amount of useful information and is recommended as a general reference book to anyone directly involved in work on *N*-nitroso compounds.

Reviewed by George A. Digenis
College of Pharmacy
University of Kentucky
Lexington, KY 40506

Side Effects of Drugs Annual 7. Edited by M. N. G. DUKES. Elsevier Biomedical Press B.V., P.O. Box 1527, 1000 BM Amsterdam, The Netherlands. 1983. 539 pp. 15 × 25 cm. Price $70.25 (Dfl. 165.00).

Adverse reactions to therapeutic agents can result from many and diverse factors. Two reactions of major significance are the abnormal patient reaction to a drug and the development of unexpected toxicity when two or more drugs are administered together. *Side Effects of Drugs Annual*, which has been published annually in January since its inception in 1977, is designed to provide a critical evaluation of the literature and an up-to-date account of recent information relating to these drug reactions and interactions. In this regard, the current *Annual* covers reports published between July 1981 and June 1982. In general, only publications presenting new information are reviewed. The reports which are documented are based on material from the Excerpta Medica Database System, which screens approximately 4000 journals in nearly 20 languages.

Although each *Annual* edition can be used independently, they are best employed as supplements to the most recent edition of the parent reference, *Meyler's Side Effects of Drugs*, an encyclopedic resource that reviews all existing knowledge on adverse reactions. The greatest value of a regularly published supplement is that it permits a continuing discussion of problems associated with the use of drugs; the question of a drug-induced disease raised one year can be followed up in subsequent years as the evidence to confirm or deny its occurrence becomes available. In addition, the *Annual* is published at a time when scattered reports of an iatrogenic disease have appearerd in the medical and pharmaceutical literature, but have not been the subject of critical editorials and other review articles.

Each year an introductory chapter entitled "Side Effects of Drugs Essay" has been published as a forum for the discussion of topics that are of current interest. This year, the essay written by the Chief of the Product Related Disease Division of Canadian Department of Health and Welfare explores drug development and formulation in light of documented adverse reactions, suspected reactions, and mere accusations of the possibility of adverse drug reactions. As noted in the introduction to the essay, its writer has designed it to be controversial with the intention of exposing pitfalls and false conceptions. In addition, beginning in 1980 and continuing with the current edition, a valuable feature entitled "Special Reviews" printed in italic type and identified by the traditional prescription symbol has appeared. These reviews, found in many of the 51 chapters, are critical discussions of controversial areas or the publication of new findings that require revision of existing concepts. Many report the latest developments in issues of continuing concern such as interactions of lithium with other drugs, side effects of β-blockers given prophylactically after myocardial infarction, ketoconazole and the liver, and prediction of anthracycline cardiomyopathy. In addition to discussing the data, each review offers the reader information that is useful clinically in recognizing, evaluating, and managing the specific reaction.

The current edition continues the discussion of drugs used in nonorthodox medicine begun with the first *Side Effects of Drugs Annual*. This year, the authors review the reports of toxicity from herbal remedies as well as updating previous information on laetrile. The chapter on miscellaneous drugs incudes a special review and update on surgical materials and other appliances.

The drugs discussed in *Side Effects of Drugs Annual* are classified according to their pharmacological properties or therapeutic use. They are accessed by consulting an index of drugs, an index of side effects, or an index of interactions. In addition, an index of synonyms enables the reader to identify specific drugs by their foreign brand name, investigational number, chemical name, or abbreviation. To facilitate rapid searching, the three major indices in the current *Annual* provide a complete listing of all references discussed in the previous three volumes of this series. The references in each chapter have been uniquely coded to identify those reports in which (*i*) the information presented is reviewed in some detail; (*ii*) the original citation refers only briefly to the information presented; (*iii*) the original citation presents detailed clinical evidence; and (*iv*) the original citation provides a brief clinical description. The code allows the reader to select the original source most useful in documenting a specific drug-induced side effect.

This is a superb reference which provides an invaluable source of information on adverse drug reactions reported in the literature during a 1-year period. Even though the *Annual* series are not intended to be used as comprehensive references sources, many of the chapters, and in particular the special reviews, make fascinating reading. The major drawback of this reference is its cost, but it should be a part of the collection of medical libraries, drug information centers, and hospital pharmacies, where it would be available to those who dispense as well as those who prescribe drugs.

Reviewed by Arthur I. Jacknowitz
Director, Drug Information Center
West Virginia University
Morgantown, WV 26506

Adapted from a Book Review of *Side Effects of Drug Annual 6* by A. I. Jacknowitz [Am. J. Pharm. Educ., **46**, 317 (1982)], with permission.

Pathology of Tumours in Laboratory Animals, Volume III: Tumours of the Hamster. V. S. TURUSOV, Editor-in-Chief. International Agency for Cancer Research Scientific Publication No. 34. World Health Organization, 1211 Geneva 27, Switzerland. 1983. 461 pp. 18 × 24 cm. Price $40.00 (Sw. Fr. 80).

This volume, sponsored by the World Health Organization, is the third in a series concerning tumors of laboratory rodents, *i.e.*, rat, mouse, and now hamster. The text contains a number of contributions from F. N. Ghadially, A. Cardesa, A. H. Handler, A. D. Kelman, A. Emminger, U.

N-Nitroso Compounds: Occurrence and Biological Effects. Edited by H. BARTSCH, I. K. O'NEILL, M. CASTEGNARO, and M. OKADA. International Agency on Cancer, Health and Biomedical Information Programme, World Health Organization, 1211 Geneva 27, Switzerland, 1982. 753 pp. 17 × 24 cm. Price $55.00 (Sw. Fr. 110).

This volume is comprised of the Proceedings of the 7th International Symposium on *N*-Nitroso Compounds held in Tokyo, September 1981. It includes 73 papers and draws from a wide range of scientific disciplines. Numerous experts present information on the formation, occurrence, and biological effects of *N*-nitroso compounds. Formation of *N*-nitroso compounds within the body is reported by several workers and is discussed in relation to the ingestion of various materials. Data are given on exposure to *N*-nitroso compounds in the general environment and from tobacco usage. New and important developments of methods and approaches are presented that could promote the understanding of basic mechanisms of carcinogenesis and which could also be readily applied to the detection and analysis of *N*-nitroso compounds or their precursors. Also presented are suggestions for possible future research on nitroso compounds. A possible drawback of the book is the limited coverage of nitrosoureas, an important group of compounds in cancer research and treatment.

The papers are short, easy to read, and most present considerable background information. Concise figures and tables are used when appropriate. There is an author index and a thorough subject index. A list of references is given at the end of each chapter to assist readers seeking additional information. This book, written entirely in English, contains an enormous amount of useful information and is recommended as a general reference book to anyone directly involved in work on *N*-nitroso compounds.

Reviewed by George A. Digenis
College of Pharmacy
University of Kentucky
Lexington, KY 40506

Side Effects of Drugs Annual 7. Edited by M. N. G. DUKES. Elsevier Biomedical Press B.V., P.O. Box 1527, 1000 BM Amsterdam, The Netherlands. 1983. 539 pp. 15 × 25 cm. Price $70.25 (Dfl. 165.00).

Adverse reactions to therapeutic agents can result from many and diverse factors. Two reactions of major significance are the abnormal patient reaction to a drug and the development of unexpected toxicity when two or more drugs are administered together. *Side Effects of Drugs Annual*, which has been published annually in January since its inception in 1977, is designed to provide a critical evaluation of the literature and an up-to-date account of recent information relating to these drug reactions and interactions. In this regard, the current *Annual* covers reports published between July 1981 and June 1982. In general, only publications presenting new information are reviewed. The reports which are documented are based on material from the Excerpta Medica Database System, which screens approximately 4000 journals in nearly 20 languages.

Although each *Annual* edition can be used independently, they are best employed as supplements to the most recent edition of the parent reference, *Meyler's Side Effects of Drugs*, an encyclopedic resource that reviews all existing knowledge on adverse reactions. The greatest value of a regularly published supplement is that it permits a continuing discussion of problems associated with the use of drugs; the question of a drug-induced disease raised one year can be followed up in subsequent years as the evidence to confirm or deny its occurrence becomes available. In addition, the *Annual* is published at a time when scattered reports of an iatrogenic disease have appearerd in the medical and pharmaceutical literature, but have not been the subject of critical editorials and other review articles.

Each year an introductory chapter entitled "Side Effects of Drugs Essay" has been published as a forum for the discussion of topics that are of current interest. This year, the essay written by the Chief of the Product Related Disease Division of Canadian Department of Health and Welfare explores drug development and formulation in light of documented adverse reactions, suspected reactions, and mere accusations of the possibility of adverse drug reactions. As noted in the introduction to the essay, its writer has designed it to be controversial with the intention of exposing pitfalls and false conceptions. In addition, beginning in 1980 and continuing with the current edition, a valuable feature entitled "Special Reviews" printed in italic type and identified by the traditional prescription symbol has appeared. These reviews, found in many of the 51 chapters, are critical discussions of controversial areas or the publication of new findings that require revision of existing concepts. Many report the latest developments in issues of continuing concern such as interactions of lithium with other drugs, side effects of β-blockers given prophylactically after myocardial infarction, ketoconazole and the liver, and prediction of anthracycline cardiomyopathy. In addition to discussing the data, each review offers the reader information that is useful clinically in recognizing, evaluating, and managing the specific reaction.

The current edition continues the discussion of drugs used in nonorthodox medicine begun with the first *Side Effects of Drugs Annual*. This year, the authors review the reports of toxicity from herbal remedies as well as updating previous information on laetrile. The chapter on miscellaneous drugs incudes a special review and update on surgical materials and other appliances.

The drugs discussed in *Side Effects of Drugs Annual* are classified according to their pharmacological properties or therapeutic use. They are accessed by consulting an index of drugs, an index of side effects, or an index of interactions. In addition, an index of synonyms enables the reader to identify specific drugs by their foreign brand name, investigational number, chemical name, or abbreviation. To facilitate rapid searching, the three major indices in the current *Annual* provide a complete listing of all references discussed in the previous three volumes of this series. The references in each chapter have been uniquely coded to identify those reports in which (*i*) the information presented is reviewed in some detail; (*ii*) the original citation refers only briefly to the information presented; (*iii*) the original citation presents detailed clinical evidence; and (*iv*) the original citation provides a brief clinical description. The code allows the reader to select the original source most useful in documenting a specific drug-induced side effect.

This is a superb reference which provides an invaluable source of information on adverse drug reactions reported in the literature during a 1-year period. Even though the *Annual* series are not intended to be used as comprehensive references sources, many of the chapters, and in particular the special reviews, make fascinating reading. The major drawback of this reference is its cost, but it should be a part of the collection of medical libraries, drug information centers, and hospital pharmacies, where it would be available to those who dispense as well as those who prescribe drugs.

Reviewed by Arthur I. Jacknowitz
Director, Drug Information Center
West Virginia University
Morgantown, WV 26506

Adapted from a Book Review of *Side Effects of Drug Annual 6* by A. I. Jacknowitz [Am. J. Pharm. Educ., **46**, 317 (1982)], with permission.

Pathology of Tumours in Laboratory Animals, Volume III: Tumours of the Hamster. V. S. TURUSOV, Editor-in-Chief. International Agency for Cancer Research Scientific Publication No. 34. World Health Organization, 1211 Geneva 27, Switzerland. 1983. 461 pp. 18 × 24 cm. Price $40.00 (Sw. Fr. 80).

This volume, sponsored by the World Health Organization, is the third in a series concerning tumors of laboratory rodents, *i.e.*, rat, mouse, and now hamster. The text contains a number of contributions from F. N. Ghadially, A. Cardesa, A. H. Handler, A. D. Kelman, A. Emminger, U.

N-Nitroso Compounds: Occurrence and Biological Effects. Edited by H. BARTSCH, I. K. O'NEILL, M. CASTEGNARO, and M. OKADA. International Agency on Cancer, Health and Biomedical Information Programme, World Health Organization, 1211 Geneva 27, Switzerland, 1982. 753 pp. 17 × 24 cm. Price $55.00 (Sw. Fr. 110).

This volume is comprised of the Proceedings of the 7th International Symposium on *N*-Nitroso Compounds held in Tokyo, September 1981. It includes 73 papers and draws from a wide range of scientific disciplines. Numerous experts present information on the formation, occurrence, and biological effects of *N*-nitroso compounds. Formation of *N*-nitroso compounds within the body is reported by several workers and is discussed in relation to the ingestion of various materials. Data are given on exposure to *N*-nitroso compounds in the general environment and from tobacco usage. New and important developments of methods and approaches are presented that could promote the understanding of basic mechanisms of carcinogenesis and which could also be readily applied to the detection and analysis of *N*-nitroso compounds or their precursors. Also presented are suggestions for possible future research on nitroso compounds. A possible drawback of the book is the limited coverage of nitrosoureas, an important group of compounds in cancer research and treatment.

The papers are short, easy to read, and most present considerable background information. Concise figures and tables are used when appropriate. There is an author index and a thorough subject index. A list of references is given at the end of each chapter to assist readers seeking additional information. This book, written entirely in English, contains an enormous amount of useful information and is recommended as a general reference book to anyone directly involved in work on *N*-nitroso compounds.

Reviewed by George A. Digenis
College of Pharmacy
University of Kentucky
Lexington, KY 40506

Side Effects of Drugs Annual 7. Edited by M. N. G. DUKES. Elsevier Biomedical Press B.V., P.O. Box 1527, 1000 BM Amsterdam, The Netherlands. 1983. 539 pp. 15 × 25 cm. Price $70.25 (Dfl. 165.00).

Adverse reactions to therapeutic agents can result from many and diverse factors. Two reactions of major significance are the abnormal patient reaction to a drug and the development of unexpected toxicity when two or more drugs are administered together. *Side Effects of Drugs Annual*, which has been published annually in January since its inception in 1977, is designed to provide a critical evaluation of the literature and an up-to-date account of recent information relating to these drug reactions and interactions. In this regard, the current *Annual* covers reports published between July 1981 and June 1982. In general, only publications presenting new information are reviewed. The reports which are documented are based on material from the Excerpta Medica Database System, which screens approximately 4000 journals in nearly 20 languages.

Although each *Annual* edition can be used independently, they are best employed as supplements to the most recent edition of the parent reference, *Meyler's Side Effects of Drugs*, an encyclopedic resource that reviews all existing knowledge on adverse reactions. The greatest value of a regularly published supplement is that it permits a continuing discussion of problems associated with the use of drugs; the question of a drug-induced disease raised one year can be followed up in subsequent years as the evidence to confirm or deny its occurrence becomes available. In addition, the *Annual* is published at a time when scattered reports of an iatrogenic disease have appearerd in the medical and pharmaceutical literature, but have not been the subject of critical editorials and other review articles.

Each year an introductory chapter entitled "Side Effects of Drugs Essay" has been published as a forum for the discussion of topics that are of current interest. This year, the essay written by the Chief of the Product Related Disease Division of Canadian Department of Health and Welfare explores drug development and formulation in light of documented adverse reactions, suspected reactions, and mere accusations of the possibility of adverse drug reactions. As noted in the introduction to the essay, its writer has designed it to be controversial with the intention of exposing pitfalls and false conceptions. In addition, beginning in 1980 and continuing with the current edition, a valuable feature entitled "Special Reviews" printed in italic type and identified by the traditional prescription symbol has appeared. These reviews, found in many of the 51 chapters, are critical discussions of controversial areas or the publication of new findings that require revision of existing concepts. Many report the latest developments in issues of continuing concern such as interactions of lithium with other drugs, side effects of β-blockers given prophylactically after myocardial infarction, ketoconazole and the liver, and prediction of anthracycline cardiomyopathy. In addition to discussing the data, each review offers the reader information that is useful clinically in recognizing, evaluating, and managing the specific reaction.

The current edition continues the discussion of drugs used in nonorthodox medicine begun with the first *Side Effects of Drugs Annual*. This year, the authors review the reports of toxicity from herbal remedies as well as updating previous information on laetrile. The chapter on miscellaneous drugs incudes a special review and update on surgical materials and other appliances.

The drugs discussed in *Side Effects of Drugs Annual* are classified according to their pharmacological properties or therapeutic use. They are accessed by consulting an index of drugs, an index of side effects, or an index of interactions. In addition, an index of synonyms enables the reader to identify specific drugs by their foreign brand name, investigational number, chemical name, or abbreviation. To facilitate rapid searching, the three major indices in the current *Annual* provide a complete listing of all references discussed in the previous three volumes of this series. The references in each chapter have been uniquely coded to identify those reports in which (*i*) the information presented is reviewed in some detail; (*ii*) the original citation refers only briefly to the information presented; (*iii*) the original citation presents detailed clinical evidence; and (*iv*) the original citation provides a brief clinical description. The code allows the reader to select the original source most useful in documenting a specific drug-induced side effect.

This is a superb reference which provides an invaluable source of information on adverse drug reactions reported in the literature during a 1-year period. Even though the *Annual* series are not intended to be used as comprehensive references sources, many of the chapters, and in particular the special reviews, make fascinating reading. The major drawback of this reference is its cost, but it should be a part of the collection of medical libraries, drug information centers, and hospital pharmacies, where it would be available to those who dispense as well as those who prescribe drugs.

Reviewed by Arthur I. Jacknowitz
Director, Drug Information Center
West Virginia University
Morgantown, WV 26506

Adapted from a Book Review of *Side Effects of Drug Annual 6* by A. I. Jacknowitz [Am. J. Pharm. Educ., **46**, 317 (1982)], with permission.

Pathology of Tumours in Laboratory Animals, Volume III: Tumours of the Hamster. V. S. TURUSOV, Editor-in-Chief. International Agency for Cancer Research Scientific Publication No. 34. World Health Organization, 1211 Geneva 27, Switzerland. 1983. 461 pp. 18 × 24 cm. Price $40.00 (Sw. Fr. 80).

This volume, sponsored by the World Health Organization, is the third in a series concerning tumors of laboratory rodents, *i.e.*, rat, mouse, and now hamster. The text contains a number of contributions from F. N. Ghadially, A. Cardesa, A. H. Handler, A. D. Kelman, A. Emminger, U.

Mohr, M. Greenblatt, G. Reznik, J. Althoff, F. C. Chesterman, H. Kirkman, R. L. Kempson, A. H. Dodge, L. D. Berman, E. Soto, I. S. Levenbook, O. L. Kolomiyets, M. A. Nikolayeva, P. Straüli, J. Mettler, P. Pour, M. Rustia, H. E. Pogosianz, and O. I. Sokova.

The book was organized, as were the two previous volumes, on an organ approach, giving a description of the individual tumors of each organ based on histological tissue type. Included in each chapter is a discussion of (*a*) normal structure, (*b*) morphology and biology of tumors, (*c*) spontaneous tumors, (*d*) induced tumors, and (*e*) comparative aspects. Included in the normal structure section is a description of the organ's gross anatomy, histological type of tissue, and cell types. The morphology and biology of tumor portion relates the most prevalent types of tumors found in the organ in hamsters based on standard histological classifications of tumors.

The spontaneous tumor section deals with the incidence of a given tumor occurring naturally in various hamster colonies throughout the world. Limited factual records were obviously available to the authors to make their evaluation. The induced-tumor section discusses the ability to induce a specific type of tumor in hamsters with either chemicals, environmental agents, hormones, or radiation. In some cases, the number of successfully induced cancers is included for the reader's perusal.

The portion on comparative aspects relates the probability of a hamster cancer being a good laboratory model in cancer research. Comparisons were made where appropriate, relating similarities of hamster cancers to specific human cancers. Certain hamster tumor models related positively with hormone-, chemical-, or virus-induced cancers in the human.

Each organ chapter contains black and white photographs of examplary tumors from hamsters demonstrating cell types, histology, and morphology points typical to that type of tumor, metastasis, viral inclusions, *etc.* A number of electron micrographs are included. Although expensive, the volume contains no color photographs, which could have enhanced the staining characteristic of the tissue.

The materials in each chapter are well referenced, although the citations are not of recent dates, *i.e.*, 1975–1983. Obviously, attempts were made to collect all available references on a given hamster tumor in this volume. The text is written in a concise, straightforward manner. It is complete and well organized in its treatment of the tumors. This particular volume would not interest most scientists in cancer research, since hamsters are not frequently utilized as tumor-bearing models. Nevertheless, the text is a good reference book and may interest some researchers in the future who wish to develop in hamsters a tumor model that mimics a specific tumor in humans.

Reviewed by Iris Hall,
Division of Medicinal Chemistry and Natural Products
The University of North Carolina at Chapel Hill
Chapel Hill, NC 27514

Manual of Laboratory Pharmacokinetics. By STEPHEN H. CURRY and ROBIN WHELPTON. John Wiley and Sons, One Wiley Drive, Somerset, NJ 08863. 1983. 189 pp. 15 × 23 cm. Price $21.95.

In the preface, the authors state that their purpose in this book was to compile "experiments suitable for use in training laboratory workers in biopharmaceutics, drug metabolism, pharmacokinetics, and related topics." A review of this book must then address the relevance of this book to the pharmaceutical sciences and the degree to which it meets a perceived need.

The changing curricula of pharmacy schools, with an increasing emphasis on clinical relevance in contrast to basic science background of fundamentals, is of concern to many in education. Now with the growing need for pharmacokinetic input to dosage adjustment, the adequacy of the analytical chemistry component of the training becomes a concern. Some schools now seek to emphasize biopharmaceutical applications rather than compendial assays, but this trend is hampered by a scarcity of adequate texts and manuals, especially for instructors who are not personally involved in the biopharmaceutical and pharmacokinetic implications of drug and metabolite assay.

The use of this book as a text in an undergraduate sequence requires the cooperation of instructors in analytical chemistry, pharmacokinetics, and pharmacology. Any student who is exposed to the approach utilized here will be a better "relevant" pharmacist for the knowledge and experience obtained. First-year graduate students, not just in pharmaceutics but also in medicinal chemistry, deserve an exposure to this or an equivalent text if they are not already receiving this knowledge through related biopharmaceutic assay courses and appropriate support pharmaceutics and kinetics.

Each chapter of this book provides good theoretical treatment of the subject matter, has one or more laboratory experiments clearly illustrating the methodology but providing data for pharmacokinetic interpretation, and contains a set of references and reading material. Even more valuable, typical data from each experiment are considered in the Appendix to demonstrate how the data should be presented and interpreted.

A listing of the experiments provides a recognition of the diversity of techniques explored and reviewed. These include: (1) construction of tritium quench correction curve by the channels ratio technique, (2) absorption spectrum of potassium dichromate, (3) fluorescence of quinine, (4) thin-layer chromatography separation of mild analgesic anti-inflammatory drugs, (5) radioimmunoassay of digoxin, (6) measurement of pK_a values of sulfadimidine and its N-4 acetylated metabolite (including preparation), (7) relationship between pH and apparent partition coefficient, (8) tablet dissolution, (9) decomposition of indomethacin, (10) storage of nitroglycerin tablets, (11) Fisher–Parsons approach for the study of drug absorption *in vitro*, (12) determination of K and n for warfarin binding to bovine serum albumin, (13) displacement of warfarin from binding sites on serum proteins, (14) metabolism of drugs by enzymes of the liver microsomal fraction, (15) determination of K_m and V_{max} for butyral-cholinesterase using butyralthiocholine as the substrate, (16) excretion of imipramine and its metabolites by rats housed in metabolism cages (including preparation of imipramine N-oxide), (17) influence of urinary pH on salicylate excretion, (18) pharmacokinetics of sulfadimidine and N^4-acetylsulfadimidine, (19) urinary clearance of these two and determination of acetylator status, (20) kinetics of ethanol elimination with simple measurement of drug effect, (21) measurement of sleeping times in mice, use of drug effect to assess drug metabolism, and pretreated animal differences, (22) turn-over of noradrenaline in rat hearts, and (23) pharmacokinetic models and problems.

An interested student could read this book and its model answers to learn a great deal regarding techniques and methodology without actually having any hands-on experience. Many students deserve the opportunity of studying this book for this reason. In addition many of the faculty of our schools would profit from a similar reading of this book to enhance their background in this area of pharmacy practice. It is sincerely hoped that this and similar books will provide the necessary unification of concepts of fundamental basic sciences with animal and human pharmacology and pharmacokinetics.

Reviewed by John H. Wood
School of Pharmacy
Medical College of Virginia Campus
Virginia Commonwealth University
Richmond, VA 23298

Mohr, M. Greenblatt, G. Reznik, J. Althoff, F. C. Chesterman, H. Kirkman, R. L. Kempson, A. H. Dodge, L. D. Berman, E. Soto, I. S. Levenbook, O. L. Kolomiyets, M. A. Nikolayeva, P. Straüli, J. Mettler, P. Pour, M. Rustia, H. E. Pogosianz, and O. I. Sokova.

The book was organized, as were the two previous volumes, on an organ approach, giving a description of the individual tumors of each organ based on histological tissue type. Included in each chapter is a discussion of (*a*) normal structure, (*b*) morphology and biology of tumors, (*c*) spontaneous tumors, (*d*) induced tumors, and (*e*) comparative aspects. Included in the normal structure section is a description of the organ's gross anatomy, histological type of tissue, and cell types. The morphology and biology of tumor portion relates the most prevalent types of tumors found in the organ in hamsters based on standard histological classifications of tumors.

The spontaneous tumor section deals with the incidence of a given tumor occurring naturally in various hamster colonies throughout the world. Limited factual records were obviously available to the authors to make their evaluation. The induced-tumor section discusses the ability to induce a specific type of tumor in hamsters with either chemicals, environmental agents, hormones, or radiation. In some cases, the number of successfully induced cancers is included for the reader's perusal.

The portion on comparative aspects relates the probability of a hamster cancer being a good laboratory model in cancer research. Comparisons were made where appropriate, relating similarities of hamster cancers to specific human cancers. Certain hamster tumor models related positively with hormone-, chemical-, or virus-induced cancers in the human.

Each organ chapter contains black and white photographs of examplary tumors from hamsters demonstrating cell types, histology, and morphology points typical to that type of tumor, metastasis, viral inclusions, *etc.* A number of electron micrographs are included. Although expensive, the volume contains no color photographs, which could have enhanced the staining characteristic of the tissue.

The materials in each chapter are well referenced, although the citations are not of recent dates, *i.e.*, 1975–1983. Obviously, attempts were made to collect all available references on a given hamster tumor in this volume. The text is written in a concise, straightforward manner. It is complete and well organized in its treatment of the tumors. This particular volume would not interest most scientists in cancer research, since hamsters are not frequently utilized as tumor-bearing models. Nevertheless, the text is a good reference book and may interest some researchers in the future who wish to develop in hamsters a tumor model that mimics a specific tumor in humans.

Reviewed by Iris Hall,
Division of Medicinal Chemistry and Natural Products
The University of North Carolina at Chapel Hill
Chapel Hill, NC 27514

Manual of Laboratory Pharmacokinetics. By STEPHEN H. CURRY and ROBIN WHELPTON. John Wiley and Sons, One Wiley Drive, Somerset, NJ 08863. 1983. 189 pp. 15 × 23 cm. Price $21.95.

In the preface, the authors state that their purpose in this book was to compile "experiments suitable for use in training laboratory workers in biopharmaceutics, drug metabolism, pharmacokinetics, and related topics." A review of this book must then address the relevance of this book to the pharmaceutical sciences and the degree to which it meets a perceived need.

The changing curricula of pharmacy schools, with an increasing emphasis on clinical relevance in contrast to basic science background of fundamentals, is of concern to many in education. Now with the growing need for pharmacokinetic input to dosage adjustment, the adequacy of the analytical chemistry component of the training becomes a concern. Some schools now seek to emphasize biopharmaceutical applications rather than compendial assays, but this trend is hampered by a scarcity of adequate texts and manuals, especially for instructors who are not personally involved in the biopharmaceutical and pharmacokinetic implications of drug and metabolite assay.

The use of this book as a text in an undergraduate sequence requires the cooperation of instructors in analytical chemistry, pharmacokinetics, and pharmacology. Any student who is exposed to the approach utilized here will be a better "relevant" pharmacist for the knowledge and experience obtained. First-year graduate students, not just in pharmaceutics but also in medicinal chemistry, deserve an exposure to this or an equivalent text if they are not already receiving this knowledge through related biopharmaceutic assay courses and appropriate support pharmaceutics and kinetics.

Each chapter of this book provides good theoretical treatment of the subject matter, has one or more laboratory experiments clearly illustrating the methodology but providing data for pharmacokinetic interpretation, and contains a set of references and reading material. Even more valuable, typical data from each experiment are considered in the Appendix to demonstrate how the data should be presented and interpreted.

A listing of the experiments provides a recognition of the diversity of techniques explored and reviewed. These include: (1) construction of tritium quench correction curve by the channels ratio technique, (2) absorption spectrum of potassium dichromate, (3) fluorescence of quinine, (4) thin-layer chromatography separation of mild analgesic anti-inflammatory drugs, (5) radioimmunoassay of digoxin, (6) measurement of pK_a values of sulfadimidine and its N-4 acetylated metabolite (including preparation), (7) relationship between pH and apparent partition coefficient, (8) tablet dissolution, (9) decomposition of indomethacin, (10) storage of nitroglycerin tablets, (11) Fisher–Parsons approach for the study of drug absorption *in vitro*, (12) determination of K and n for warfarin binding to bovine serum albumin, (13) displacement of warfarin from binding sites on serum proteins, (14) metabolism of drugs by enzymes of the liver microsomal fraction, (15) determination of K_m and V_{max} for butyral-cholinesterase using butyralthiocholine as the substrate, (16) excretion of imipramine and its metabolites by rats housed in metabolism cages (including preparation of imipramine N-oxide), (17) influence of urinary pH on salicylate excretion, (18) pharmacokinetics of sulfadimidine and N^4-acetylsulfadimidine, (19) urinary clearance of these two and determination of acetylator status, (20) kinetics of ethanol elimination with simple measurement of drug effect, (21) measurement of sleeping times in mice, use of drug effect to assess drug metabolism, and pretreated animal differences, (22) turn-over of noradrenaline in rat hearts, and (23) pharmacokinetic models and problems.

An interested student could read this book and its model answers to learn a great deal regarding techniques and methodology without actually having any hands-on experience. Many students deserve the opportunity of studying this book for this reason. In addition many of the faculty of our schools would profit from a similar reading of this book to enhance their background in this area of pharmacy practice. It is sincerely hoped that this and similar books will provide the necessary unification of concepts of fundamental basic sciences with animal and human pharmacology and pharmacokinetics.

Reviewed by John H. Wood
School of Pharmacy
Medical College of Virginia Campus
Virginia Commonwealth University
Richmond, VA 23298

ERRATA

In the article titled "Prediction of Stability in Pharmaceutical Preparations XX: Stability Evaluation and Bioanalysis of Cocaine and Benzoylecgonine by High-Performance Liquid Chromatography" (1), the following corrections should be made:

On page 259, Scheme I should appear as shown here:

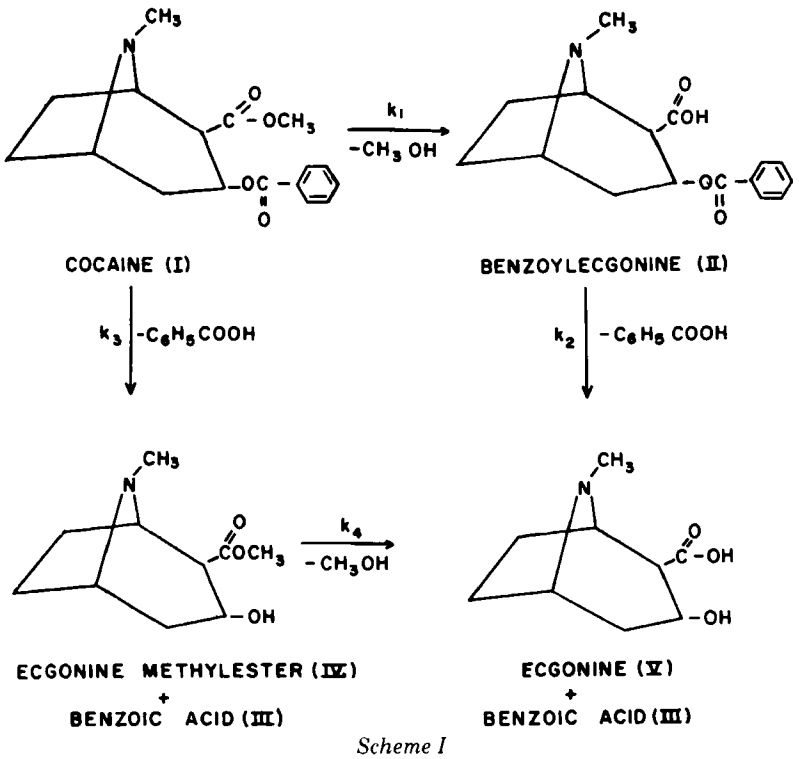

Scheme I

On page 267, Scheme II should appear as shown here:
(1) E. R. Garrett and K. Seyda, *J. Pharm. Sci.*, **72**, 258 (1983).

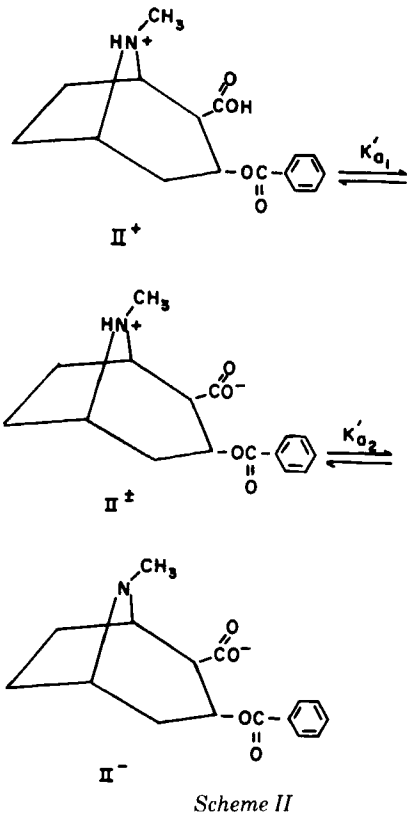

Scheme II

In the article titled "Evaluation of Various N-Substituted Azaspiranedione Derivatives as Potential Antimicrobial Agents" (1), the following should be noted:

On page 184 in Table I and Scheme II, two compounds were given the same number (XIII).

(1) K. R. Scott, P. G. Kennedy, M. Kemp, V. G. Telang, and H. W. Matthews, *J. Pharm. Sci.*, **72**, 183 (1983).

In the book review of "Hormone Drugs" (1), the following correction should be made:

The spelling of the third author's name should be Aubrey S. Outschoorn.

(1) J. M. Rosenberg (reviewer), *J. Pharm. Sci.*, **72**, 720 (1983).

Underscoring the Food-Pharmacy Relationship

I write in support and to underscore the importance of the remarks stated in your editorial "Food and Pharmacy—A Close Relationship" [1]. You have accurately pointed out that recent legislative history has not focused heavily on matters of food safety evaluation. Many of our colleagues in pharmacy and the other basic medical sciences have been deeply involved in drug legislative matters. However, on issues of food safety, I find myself in a somewhat unique, and at times lonesome, position. Many classmates and colleagues in pharmacy and pharmacology are active in appropriate pharmaceutical and pharmacological professional societies, so too it is with other colleagues in the Institute of Food Technologists. However, there are precious few pharmacists and pharmacologists/toxicologists who have looked beyond the world of pharmacy and pharmacology to the potential for the pharmacologic effects of foods. Many of us have tried to point out that numerous problems in toxicology and safety evaluation are common to both foods and drugs. With foods we are often dealing with longer term exposures of test materials administered at levels on the lower portions of the slope of the dose response curve. But the ultimate goal of these researchers is the same—extrapolation of toxicity findings, if any, to man.

The thrust of our testimony before Senator Hatch[2] was to call for an updating of the scientific thinking behind the Delaney Clause to give FDA scientists, specifically, and science in general discretion for scientific judgment as now allowable under the general provisions of the Food, Drug and Cosmetic Act, but not permitted by the absolute strictures of the Delaney Clause. We are not calling for a weakening of food safety laws as some have worried.

It is clear that advances in science and technology referred to by Senator Hatch and mentioned in your editorial, must include studies for the potential for food and drug interactions, both from the standpoint of potential benefits, as well as risks to the consumer, which may be, as you point out, every bit as important and critical as drug–drug interactions.

Unfortunately, ranking minority member Kennedy was not present throughout the hearings. It is hoped, however, that the hearings can and will result in meaningful bipartisan food safety legislation.

Andrew G. Ebert
Research, Development and
Quality Assurance
Pet Incorporated
St. Louis, MO 63116

Received September 14, 1983.

[1] E. G. Feldmann *J. Pharm. Sci.*, **72**, 723 (1983).
[2] Senate Committee on Labor and Human Resources hearing, June 10, 1983, Senator Oran Hatch, Chairman.

Full Disclosure Should Apply to All

I read with interest your editorial in the August issue of the *Journal of Pharmaceutical Sciences*[1]. At the same time I am concerned that you may not be aware that Dr. Jacobson of the Center for Science in the Public Interest (CSPI) is hardly a case study in full disclosure when it comes to addressing the issue of how CSPI is funded.

The American Council on Science and Health (ACSH), a scientific consumer education organization, has carefully documented[2] the secretive and inconsistent activities of CSPI, an organization which owes its existence to the perpetuation of consumer fear of technological advances. We have here a classic example of one living in a glass house and throwing stones. I would be happy to provide copies of the above mentioned article to interested readers.

My point is this—it is just as valid to question the motives of Jacobson and CSPI as it is the motives of scientists who take stands on public issues—and I wish you would have done so.

David B. Roll
Professor of Medicinal Chemistry
Associate Dean for Academic Affairs
The University of Utah
College of Pharmacy
Salt Lake City, UT 84112

Received September 20, 1983.

[1] E. G. Feldmann, *J. Pharm. Sci.*, **72**, 843 (1983).
[2] *ACSH News and Views*, 3(4), 8 (1982).

Author's response:

In quoting Dr. Jacobson, I intended to pass no judgment—nor did I so indicate in my editorial—regarding his personal prejudices, allegiances, or freedom from bias. I know really nothing about the man, but I felt then, as now, that what he wrote was right and proper behavior for all scientists to follow. And as a scientist himself, I would expect Dr. Jacobson to adhere to this same standard of performance along with the rest of us who regard ourselves as scientists.

Edward G. Feldmann
American Pharmaceutical Assoc.
Washington, DC 20037

Underscoring the Food-Pharmacy Relationship

I write in support and to underscore the importance of the remarks stated in your editorial "Food and Pharmacy—A Close Relationship" [1]. You have accurately pointed out that recent legislative history has not focused heavily on matters of food safety evaluation. Many of our colleagues in pharmacy and the other basic medical sciences have been deeply involved in drug legislative matters. However, on issues of food safety, I find myself in a somewhat unique, and at times lonesome, position. Many classmates and colleagues in pharmacy and pharmacology are active in appropriate pharmaceutical and pharmacological professional societies, so too it is with other colleagues in the Institute of Food Technologists. However, there are precious few pharmacists and pharmacologists/toxicologists who have looked beyond the world of pharmacy and pharmacology to the potential for the pharmacologic effects of foods. Many of us have tried to point out that numerous problems in toxicology and safety evaluation are common to both foods and drugs. With foods we are often dealing with longer term exposures of test materials administered at levels on the lower portions of the slope of the dose response curve. But the ultimate goal of these researchers is the same—extrapolation of toxicity findings, if any, to man.

The thrust of our testimony before Senator Hatch[2] was to call for an updating of the scientific thinking behind the Delaney Clause to give FDA scientists, specifically, and science in general discretion for scientific judgment as now allowable under the general provisions of the Food, Drug and Cosmetic Act, but not permitted by the absolute strictures of the Delaney Clause. We are not calling for a weakening of food safety laws as some have worried.

It is clear that advances in science and technology referred to by Senator Hatch and mentioned in your editorial, must include studies for the potential for food and drug interactions, both from the standpoint of potential benefits, as well as risks to the consumer, which may be, as you point out, every bit as important and critical as drug–drug interactions.

Unfortunately, ranking minority member Kennedy was not present throughout the hearings. It is hoped, however, that the hearings can and will result in meaningful bipartisan food safety legislation.

Andrew G. Ebert
Research, Development and
Quality Assurance
Pet Incorporated
St. Louis, MO 63116

Received September 14, 1983.

[1] E. G. Feldmann *J. Pharm. Sci.*, **72**, 723 (1983).
[2] Senate Committee on Labor and Human Resources hearing, June 10, 1983, Senator Oran Hatch, Chairman.

Full Disclosure Should Apply to All

I read with interest your editorial in the August issue of the *Journal of Pharmaceutical Sciences*[1]. At the same time I am concerned that you may not be aware that Dr. Jacobson of the Center for Science in the Public Interest (CSPI) is hardly a case study in full disclosure when it comes to addressing the issue of how CSPI is funded.

The American Council on Science and Health (ACSH), a scientific consumer education organization, has carefully documented[2] the secretive and inconsistent activities of CSPI, an organization which owes its existence to the perpetuation of consumer fear of technological advances. We have here a classic example of one living in a glass house and throwing stones. I would be happy to provide copies of the above mentioned article to interested readers.

My point is this—it is just as valid to question the motives of Jacobson and CSPI as it is the motives of scientists who take stands on public issues—and I wish you would have done so.

David B. Roll
Professor of Medicinal Chemistry
Associate Dean for Academic Affairs
The University of Utah
College of Pharmacy
Salt Lake City, UT 84112

Received September 20, 1983.

[1] E. G. Feldmann, *J. Pharm. Sci.*, **72**, 843 (1983).
[2] *ACSH News and Views*, 3(4), 8 (1982).

Author's response:

In quoting Dr. Jacobson, I intended to pass no judgment—nor did I so indicate in my editorial—regarding his personal prejudices, allegiances, or freedom from bias. I know really nothing about the man, but I felt then, as now, that what he wrote was right and proper behavior for all scientists to follow. And as a scientist himself, I would expect Dr. Jacobson to adhere to this same standard of performance along with the rest of us who regard ourselves as scientists.

Edward G. Feldmann
American Pharmaceutical Assoc.
Washington, DC 20037